Polyhedron Vol. 4, No. 1, pp. 1–14, 1985
Printed in Great Britain.

0277–5387/85 $3.00 + .00
© 1985 Pergamon Press Ltd.

POLYHEDRON REPORT NUMBER 9

CHROMIUM(III) AND THE GLUCOSE TOLERANCE FACTOR

J. BARRETT and P. O.'BRIEN*
Department of Chemistry, Chelsea College, University of London, Manresa Rd., London SW3 6LX, England

and

J. PEDROSA DE JESUS
Department of Chemistry, Universidad Aveiro, Aveiro 3800, Portugal

CONTENTS

1. INTRODUCTION 1
2. CHROMIUM AS A BIOLOGICALLY ESSENTIAL ELEMENT . . . 2
3. TESTING OF GTF 2
4. ISOLATION AND PURIFICATION OF THE GLUCOSE TOLERANCE FACTOR (GTF) 3
5. SYNTHESIS OF THE GLUCOSE TOLERANCE FACTOR (GTF) . . . 6
6. STRUCTURE OF THE GLUCOSE TOLERANCE FACTOR (GTF) . . 6
7. INSULIN 7
8. CHROMIUM(III) CHEMISTRY 7
8.1 Kinetics of substitution reactions. 7
8.2 Thermodynamic studies 8
8.3 Synthetic studies. 9
9. MODE-OF-ACTION OF THE GLUCOSE TOLERANCE FACTOR (GTF) 10
10. CONCLUSIONS. 11
Acknowledgements 12
References. 12

1. INTRODUCTION

Chromium was recognized as an essential trace element in 1955.[1] Rats fed a chromium deficient diet developed an impaired tolerance for intravenous glucose, which could be reversed by an insulin potentiating factor present in brewer's yeast, meat and various other foods. The insulin potentiating factor was found to be a complex of chromium(III)[2] and such substances have been termed Glucose Tolerance Factor(s) (GTFs). Chromium was demonstrated to be essential for humans in 1975.[3]

Chromium has a number of other biological effects, including carcinogenicity[4] and a variety of allergic responses;[5] these are mainly induced by chromium(VI). Chromium is also implicated in protein synthesis and lipid metabolism.[6]

There have been a number of reviews of chromium biochemistry including an extensive article by Mertz,[7] a review of the nutritional role of chromium[8] and several shorter articles mainly concerned with GTF.[9–12] This review will deal solely with those aspects of chromium biochemistry and chemistry relevant to glucose tolerance and discuss both the evidence for and possible structure of GTF, and relevant aspects of the chemistry of chromium(III).

*Author to whom correspondence should be addressed.

2. CHROMIUM AS A BIOLOGICALLY ESSENTIAL ELEMENT

Rats fed a Tolura yeast ration developed a progressive impairment of intravenous glucose tolerance,[1] although this diet was deficient in a number of known essential dietary components, none of these reversed the condition. Brewer's yeast was found to be particularly effective in preventing the syndrome[2] and the unidentified nutritional factor was termed GTF. Purified fractions[13] were capable of both preventing and curing the condition with a single oral dose of 100 mg/100 g of body weight. GTF was found to contain chromium(III) and to become very unstable as the purity increased.

GTF deficient rats were treated with 47 elements[14] of which only chromium(III) restored glucose tolerance. Samples isolated from yeast were much more active than simple substances such as $CrCl_3$ and rather stable complexes such as the tris-acetoacetonate were found to be quite ineffective. Similar effects were found when complexes were incorporated into the diet,[15] or injected intravenously.[16] When injected the optimal dose was much lower at 0.25 mg/100 g of body weight (a neutral solution of chrome alum). As might be expected absorption has an enormous effect on the availability of chromium(III), the kinetic inertness and facile hydrolysis of chromium complexes are probably problems.

The work outlined above rapidly established chromium(III) to be an essential element closely involved with glucose tolerance. It is surprising that, in the period since it's original identification, nothing approaching an exact molecular structure for GTF has emerged. We shall now outline the methods available for the testing, isolation and synthesis of GTF.

3. TESTING OF THE GLUCOSE TOLERANCE FACTOR (GTF)

There is a problem in interpreting studies of chromium(III) complexes which relate to GTF. *In vivo* activity can only be demonstrated by expensive experiments on large numbers of chromium deficient animals. *In vitro* studies are cheaper and more reproducible, but may not actually be related to the *in vivo* mode-of-action of GTF. The vast majority of assay systems involve the potentiation of insulin activity by GTF in isolated fat cells. Mertz has described GTF/chromium(III) as a "true potentiator of the action of the hormone (insulin)".[17] Both insulin and GTF are required in, the *in vivo* and *in vitro* systems to produce maximal effects. The effect of chromium is hence unique and quite distinct from the "insulin mimetic" behaviour of many other metal ions. There is a close relationship between the effects of chromium deficiency *in vivo* and the *in vitro* assays, but there is no hard evidence that the *in vitro* tests are relevant to the mode-of-action of GTF and/or chromium *in vivo*.

The effect of trivalent chromium on glucose uptake by rat epididymal fat tissue was investigated.[15] Four 100 mg pieces of tissue could be obtained from each rat, one of these was used as a control. Tissue samples were then incubated for 2 hr with the chromium complex, glucose and insulin; the absorption of glucose was then determined by chemical or radiochemical assay of that remaining in the medium. The increase in the rate of uptake on the addition of chrome alum varied between + 5% and + 70%, and was particularly marked at low insulin concentrations.

In related studies CO_2 production from isolated epididymal adipose tissue has been measured in the presence of either chromium complexes or purified GTF.[18,19] In this method dose response curves (rate of metabolism vs. insulin concentration) are plotted, chromium(III) complexes and GTF produce steeper dose response curves than insulin alone. This clearly demonstrates that insulin activity is being enhanced, rather than the simple addition of two isolated effects. The effect of purified GTF in this system was much greater than that of any of the synthetic complexes.

A microbiological assay for GTF has been developed,[20] the growth of Flavobacterium rhenanum being linearly dependent on the GTF concentration. Activity was expressed as a regression value (the slope of a plot of growth vs GTF concentration). A linear relationship was obtained between the values obtained by this method and bioassay values obtained from the rat epididymal fat assay.[18]

Quite recently a new assay system has been reported,[21] this allows up to seventy-five assays to be performed using the fat cells of a single rat. Adipocytes were prepared from the epididymal fat pads of chromium(III) deficient rats by the method of Rodbell.[22] Small quantities of these cells were then incubated with the material to be tested and radio-labelled glucose. Carbon dioxide production after 30 min incubation was then measured by trapping the gas in hyamine and

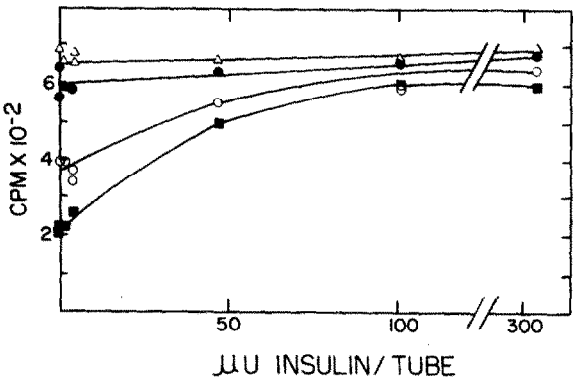


Fig. 1. Effect of yeast extract on insulin stimulation of glocuse oxidation by fat cells. ■, insulin dose response of glucose oxidation by fat cells; ○, levels of insulin + 0.088 mg of yeast extract containing 0.006 ng of chromium; ●, levels of insulin + 0.88 mg of yeast extract containing 0.06 ng of chromium, △, levels of insulin + 1.76 mg of yeast extract containing 0.012 ng of chromium. After Anderson Ref. 21, reproduced with permission.

scintillation counting. Typical results are illustrated in Fig. 1, insulin potentiation being measured as the ratio of the carbon dioxide production at a fixed insulin level in the presence and absence of the chromium complex.

4. ISOLATION AND PURIFICATION OF THE GLUCOSE TOLERANCE FACTOR (GTF)

As mentioned in the introduction highly purified GTF fractions are unstable, the reasons for this are not clear. A number of procedures for the isolation and purification of GTF have appeared. The vast majority of such substances are obtained from yeasts and in particular Brewer's yeast. In this section we shall describe some of the more recent and reliable isolation and purification procedures for GTF(s).

In 1973 Toepfer *et al.* determined the chromium content of a number of food stuffs.[23] Total chromium and alcohol extractable chromium were determined, a significant relationship was found between alcohol extractable chromium and biological activity (as determined by the rat epididymal tissue assay[18]). This is illustrated in Fig. 2. An alcoholic extraction is often the first step in the isolation of GTF.

A partial purification of GTF from brewer's yeast, involving, alcoholic extraction and chromatography on activated charcoal has been described.[24] An increase in the specific activity of GTF of eighty fold was observed. This sample was used to study the binding of GTF to insulin. A sample of ^{51}Cr labelled GTF has been prepared from brewer's yeast grown in a medium containing isotopically labelled chromium.[25] The complex was isolated by extraction with butanol followed by chromatography on Sephadex G-25 and ion exchange chromatography. The ion exchange results suggested that the GTF was a single anionic species. Gel permeation chromatography results pointed to a reversible aggregation of GTF in buffers of low ionic strength. A preliminary amino acid analysis indicated the involvement of leucine or isoleucine, proline, valine, alanine, serine and either glutamic or aspartic acid. This complex was shown to be more readily retained, than simple salts by rats. However it was not tested for GTF activity and has a rather different amino acid composition from other GTF(s). In a related study a number of isotopically labelled chromium(III) complexes, which did not bind to insulin, were isolated.[26]

A detailed procedure for the extraction of GTF from Saccharomyces carlsbergenis has been reported.[27] The extraction procedure was broadly similar to that described above and involved ethanolic extraction, hydrolysis, and ion exchange chromatography. In this work nicotinic acid (I) was detected in the complex both by its characteristic UV and mass spectra. Glycine, glutamic acid and cysteine together with trace amounts of other amino acids were found in the purified sample of GTF. This is probably the most refined GTF yet isolated. Although IR spectra were recorded for this sample no detailed spectroscopic studies were undertaken which is unfortunate as studies of the ligand field spectra might help to suggest likely structures.

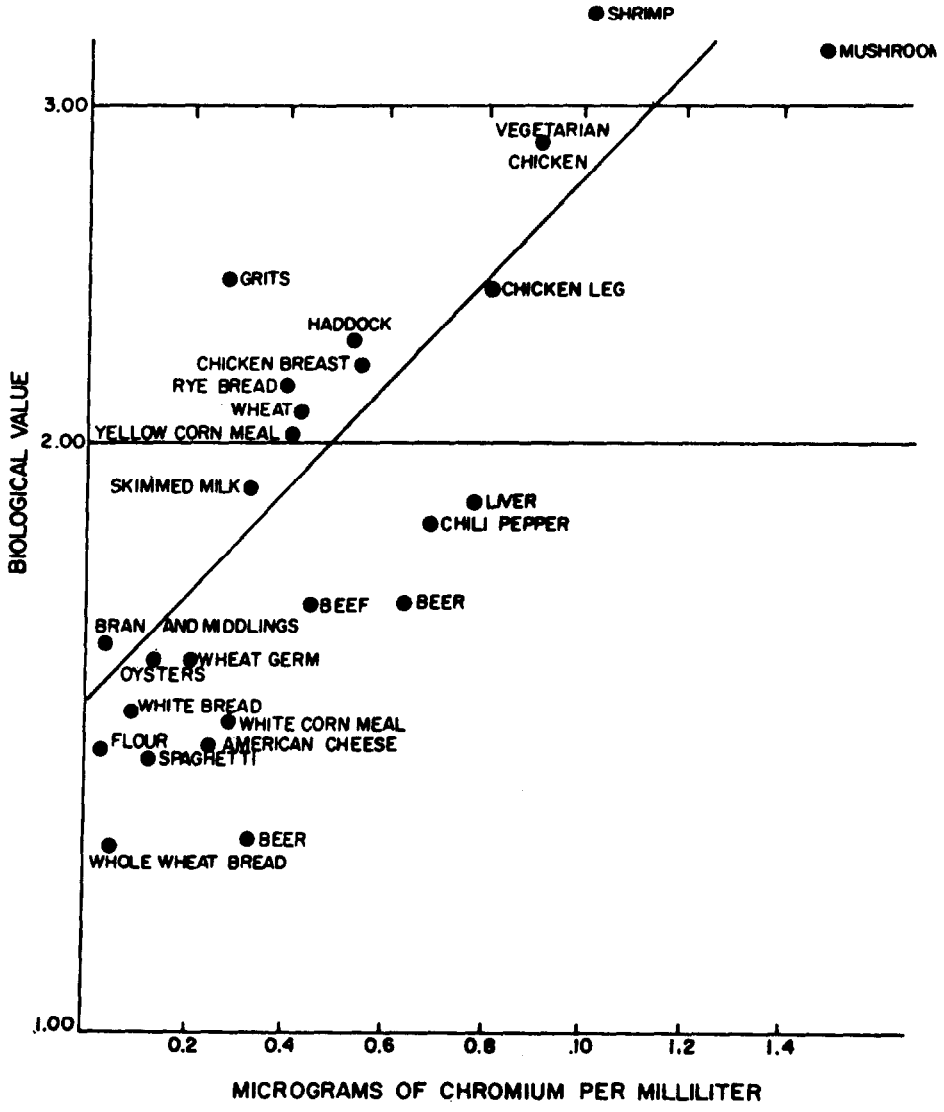
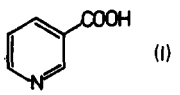


Fig. 2. Relationship between alcohol extractable chromium and biological activity. After Toepfer Ref. 19. Reproduced with permission.



(I)

The isolation of GTF from a yeast extract (Merck) has been described.[28] The procedure involved stirring the extract with 1 : 1 butanol/water, dialysis (3500 molecular weight cut off), and ion-exchange chromatography on DAE-11 cellulose (Cl^-) and Dowex 50W × 8 (H^+). The compound isolated had similar properties to that described by Mertz[27] although no analytical results are provided. The lack of details is unfortunate, a procedure utilizing yeast extracts would eliminate the necessity of cultivating large quantities of yeast to obtain GTF. The extract enhanced carbon dioxide production by several yeast strains investigated, no effect could be observed in experiments on cell free extracts.

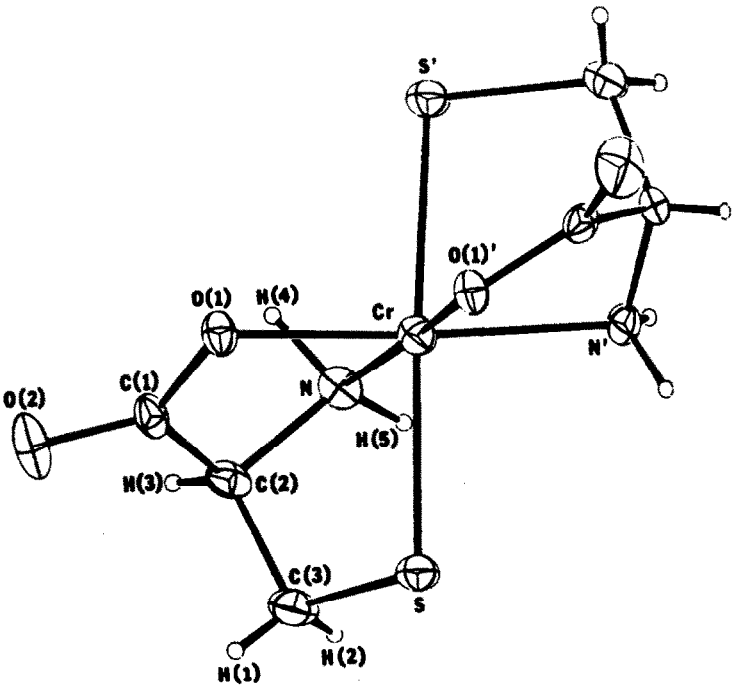
Recently the crystallization of a GTF has been reported,[29] the substance isolated by the Mertz method[27] was further purified by ion-exchange chromatography. Two purple chromium(III) containing fractions were obtained, one of these was successfully crystallized from alcohol/water. A complex of chromium(III) with tryptophan has been isolated from yeasts[30] the authors of this paper suggest that complexes of this ligand may be important in an understanding of GTF.

Finally it has been suggested that chromium(III) may not be an essential component of GTF.[30a,30b] A very thorough chromatographic purification of GTF from Brewer's yeast led to the separation of the Mertz "GTF" into several fractions, including biologically active fractions which contained no chromium(III). However these complexes were tested by monitoring their effect on yeast metabolism, hence the results do not preclude the biological activity of chromium(III) in mammalian systems.

Nicotinic acid is present in the more active GTF preparations isolated from yeasts. The coordination chemistry of this ligand is particularly relevant to glucose tolerance and the presence of this substance is apparently essential for the maximal activity of complexes in *in vitro* tests. The instability of highly purified GTF fractions has frequently been commented on.[7-9] This may be because the substance is stabilized by a protein *in vivo*.

5. SYNTHESIS OF THE GLUCOSE TOLERANCE FACTOR (GTF)

The synthesis and characterization of materials showing biological activity similar to that of GTF isolated from yeast is a logical objective of workers in this area. As already mentioned Mertz found aquo- and similar complexes of chromium to be more active than chelates with strong ligands. An exception to this was an unspecified cysteine complex[31] prepared by C. L. Rollinson which showed marked, but erratic, behaviour in GTF tests. Further investigation of this observation would be interesting, particularly as the crystal structure of a cysteine complex is now known[32] (II).



(II)

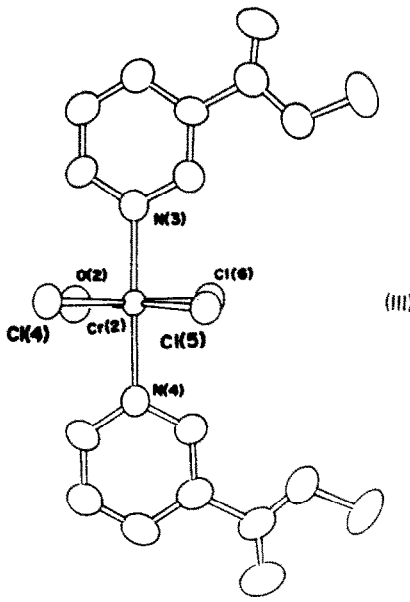
A complex with considerable activity in *in vitro* tests has been synthesised.[27] The preparation involved reacting chromium(III) acetate in 80% alcohol with two equivalents of nicotinic acid followed by the addition of one equivalent, in turn, of glycine, glutamic acid and cysteine. A complex containing nicotinic acid was isolated from the reaction mixture by ion exchange chromatography. The physical properties and biological activity of this complex were very similar to those of GTF isolated from yeast.[27] Although this material is probably a mixture, it should be further investigated as it is one of the most potent synthetic materials as yet obtained.

Anderson *et al* have reported a complex of glutathione/nicotinic acid and chromium(III) to be particularly active in their *in vitro* assay.[21] The complex was described as being purified by *hplc*, however we cannot find the details of the preparation in earlier work from this group.[33,34] This is unfortunate as this is also a species of quite remarkable biological activity.

A ternary complex of nicotinic acid and pyridoxylidene has been prepared. Nicotinic acid is coordinated via the pyridine nitrogen, the biodistribution of this complex was similar to that of GTF.[35] A recent review of the metal ion complexes of glutathione[36] fails to mention the possible

importance of a glutathione/chromium complex in glucose tolerance, the section on chromium concentrates on chromium(VI) chemistry.

The lack of serious synthetic work on GTF is surprising. Recently a number of studies of chromium(III)/nicotinic acid chemistry have appeared, but none of the following work appears to be of any direct relevance to GTF as isolated from yeasts.



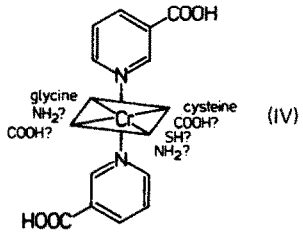
(III)

GTF has been suggested[10] to contain *trans*-nicotinic acid groups, the structure[37] of *trans*-bis(methylnicotinate) aquatrichlorochromium(III) is shown below (III). The Cr–N bond distance is 2.094 Å, which is similar to nitrogen bond lengths in other chromium(III) complexes. The structure of a tri-nuclear chromium(III)/nicotinic acid complex has been reported.[38] The nicotinic acid molecules bridge the chromium atoms via carboxylate oxygens. The structure of this complex is quite different from that proposed for GTF.

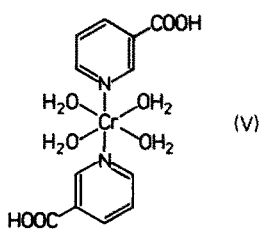
The thermodynamics of the binding of nicotinic acid and its derivatives to di-aqua[N,N′-ethylenebis (salicylideneaminato)] chromium(III) chloride have been investigated.[39] The binding of nicotinic acid to this (labile) complex was not particularly favourable ($K = 7.3$), No suggestions as to the reasons for the apparently essential nature of nicotinic acid in GTF could be made on the basis of this work. Various cobalt(III) complexes of nicotinic acid have been synthesised.[40] A detailed study of the kinetics of ligand substitution in labile chromium(III) Schiff's base complexes has appeared. In these labile complexes a dissociative interchange I_d mechanism was suggested for substitution reactions.[41]

6. STRUCTURE OF THE GLUCOSE TOLERANCE FACTOR (GTF)

The lack of structural information in the papers cited above means that any suggested structure for GTF must be highly speculative. Mertz has suggested[10] that two trans nicotinic acids are coordinated to chromium as illustrated below (IV). The first coordination sphere is completed by the various amino acids involved. Although there is little evidence to support this suggestion it has



(IV)



(V)

attracted support and influenced other workers.[37] One product of the reaction of nicotinic acid and chromium(III) (mole ratio 3 : 1, pH 3.2) has been suggested to be tetra-aquo *trans*-bisnicotinate complex[10] (V). This substance showed some biological activity but no spectral or other characterization was reported. It would be surprising if chloro ligands were not coordinated in this complex.

The view that N-bonded *trans*-nicotinic acids are involved in GTF has recently been challenged,[41a] an O-bonded nicotinic acid complex has been shown to have some biological activity. The biological significance of chromium(III) was suggested to relate to the ability of the relatively hard chromium(III) centre to form stable complexes with the carboxylate group of nicotinic acid. The crucial grouping recognized by the biological system would hence involve the nitrogen of the O-coordinated nicotinic acid.

7. INSULIN

The one unequivocal action of the hormone insulin is its ability to facilitate the transport of glucose across the plasma membranes of muscle and fat cells. There are numerous reviews of the effect and mechanism of action of this hormone.[42] Insulin is believed to exert its primary action (i.e. interact with the receptor) at the membrane of the target cell.

The work of Cuatrecasas[43] demonstrates this elegantly. In the isolated adipocyte model, isotopically labelled insulin covalently bound to Sepharose beads (which are larger than the isolated fat cells), is capable of exerting its full hormonal activity. The association of insulin with its receptor is a simple bimolecular process (dissociation constant 5×10^{-11}). Isotopically labelled insulin could be displaced from the receptor by native insulin but not by oxidised or reduced insulin. This kind of work is of obvious relevance to the mode-of-action of GTF. Detailed studies of GTF or chromium/cell/insulin interactions of the kind described[43] for insulin/cell systems will be needed for a full understanding of the mode-of-action of GTF *in vitro*.

8. CHROMIUM(III) CHEMISTRY

The coordination chemistry of chromium(III) was first investigated by Pfeiffer forming a logical extension to Werner's studies of cobalt(III) complexes. A number of the properties of chromium(III) are rather different from the majority of essential trace elements. Most essential metals are (with the exception of cobalt(III) in vitamin B_{12}) kinetically labile in ligand substitution reactions, chromium(III) complexes are usually fairly inert in ligand substitution reactions. The hydrolysis of chromium(III) is particularly facile and leads to the formation of a number of very stable hydroxy-species. These factors combine to make studies of the thermodynamic stability of chromium(III) quite difficult and consequently rare. In marked contrast the redox stability of the plus three oxidation state ($E^{\ominus} = -0.41$) for chromium(III)/(II) (in aqueous solution),[44a] allows complex formation reactions to be studied; this is quite different from the cobalt(III) system ($E^{\ominus} = +1.84$).[44b] We shall now consider in detail some of the properties of chromium(III) relevant to the chemistry of GTF.

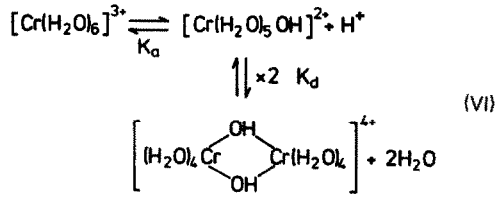
8.1 *Kinetics of substitution reactions*

Chromium(III) has the electronic configuration d^3, crystal (or ligand) field activation energy calculations suggest that such complexes would be kinetically inert.[45] In general this is borne out in practice, the half-life for the exchange of water at the hexaquo-complex is 384 hr (20°C).[46]

Substitution at chromium(III) centres has received a considerable amount of attention[47] because of the possibility of A or I_a.[47] Many chromium(III) formation reactions involve a rate law:[47]

$$k_{obs} = k_i K_{os}[L]/1 + K_{os}[L] \tag{1}$$

k_i is the interchange rate constant, K_{os} is the outer sphere complexation constant and L is the ligand.



(VI)

Such studies are usually held to be carried out under sufficiently acidic conditions that the monohydroxy species of chromium(III) may be ignored. On balance the evidence in the literature seems to favour an associative interchange mechanism (I_a via a tight ion pair derived from the hexaquospecies. The literature reveals some anomalies; in a series of classic papers Hamm *et al.* studied the formation of chromium(III) complexes with dicarboxylic and hydroxy-acids.[48–50] Their kinetic results, (most notably the reaction was zero order in ligand) were originally interpreted in terms of a strictly dissociative process. Basolo and Pearson[51] later suggested that a saturated ion pairing mechanism, (for which eqn (1) becomes $k_{obs} = k_i$) provides a more plausible explanation for Hamm's observations. In marked contrast for the reactions of malonate[52] and oxalate[53] with chromium(III), Banerjea and Chaudhuri found a dependence of reaction rate on ligand concentration. The conditions used in the latter studies were considerably more acidic than those used by Hamm. Complications of rate constants[54] and activation parameters[55,56] for chromium(III) reactions are available, but as exemplified above the situation is far from simple.

The reactions of amino acids with chromium(III) are of relevance to the formation of GTF and absorption of chromium. The reaction with glycine has been studied on several occasions[57,58] and most recently in our laboratory.[59] In the pH range 3.0–3.8 ($I = 0.4$, $NaClO_4$) we have found the reaction to obey the rate law $k_{obs} = k + k'[H]^{-1}$ and be zero order in ligand concentration. The reaction scheme shown in Fig. 3 accounts for our observations, and involves associative interchange within a tight outer-sphere complex for the aquo-species, and a more loosely bound outer-sphere complex for the mono-hydroxy chromium(III) species. In earlier studies of the reactions of chromium(III) with glycine the pH of the reaction was not adequately controlled.

Under certain circumstances ligand substitution in chromium can be rapid and it seems possible that this might provide a mechanism by which chromium(III) could interact with cells/insulin. The ligands involved in GTF are unlikely to promote such lability in adjacent coordination sites. This kind of chemistry is usually associated with rigid (often π-acceptor) ligands which give rise to tetragonal stereochemistries. The rapid rate of reaction of nicotinic acid with chromium(III) Schiff's base complexes has already been mentioned.[41] Other systems in which ligand substitution reactions are rapid include: porphyrin complexes[60–62] and $[Cr(EDTA)H_2O]$[63–65].

8.2 *Thermodynamic studies*

Compared to the majority of transition metals there have been very few studies of the equilibrium between common ligands and chromium(III).[66] There are two major problems involved in measuring equilibrium constants for chromium(III) systems. The kinetic inertness of the

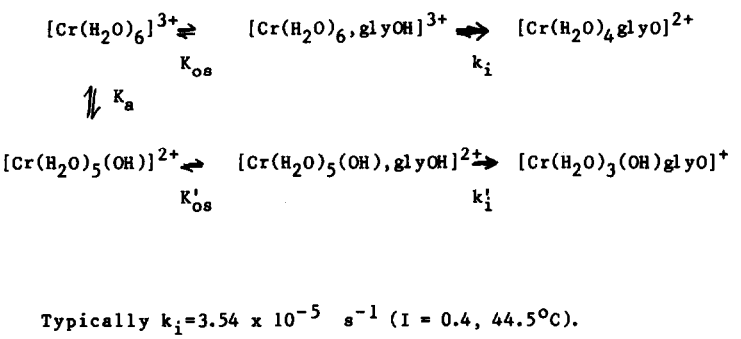


Fig. 3. Scheme for the reaction of chromium(III) and glycine.

hexaquo-complex means that a lengthy equilibration of ligand and metal is required. Secondly the hexaquo complex hydrolyses readily[67a](VI) ($pK_1 = 4.29$ and $K_D = 3.3$, 1M $NaClO_4$, 25°C[67b]) and often effectively irreversibly at higher temperatures. The species formed on the hydrolysis of chromium(III) have recently been studied in some detail.[67b]

Santappa *et al.* have recently studied[68] complexation by a variety of amino acids including aspartic[71] and glutamic acids. Their results together with those of related studies are summarised in Table 1.

Table 1. Typical equilibrium constants*

LIGAND	K_1	K_2	NOTES
L-aspartic acid	12.15	8.98	50°C [68]
L-glutamic acid	11.39	7.57	[68]
α-alanine	8.53	7.44	25°C, [69]
glycine	8.62	7.65	[69]
L-cysteine	8.05	7.45	25°C, [70]
DL-methionine	7.45	6.45	[70]
glycine	7.60	–	40°C, [59] 0.4M $NaClO_4$

* $\log_{10}$ values in 0.1 $NaClO_4$, except reference [59]

8.3 *Synthetic studies*

In this section we shall concentrate on complexes of chromium(III) with those ligands (mainly amino acids) believed to be involved in GTF. In general it has not been realized that these complexes are related to GTF and hence they have not been tested for GTF behaviour.

The preparation of the tris complexes of chromium(III) with the anions of glycine and alanine has been reported on several occasions.[72-79] The isomeric purity of these complexes was first seriously considered by Gillard *et al.*[72] Red insoluble complexes of L-alanine and glycine were found to be *D-β(fac)* and *β(fac)* isomers respectively and were isomorphous with their cobalt(III) analogues. The preparation of the purple *α(mer)* isomer had been claimed by Israily[77] though later workers[72,78] were unable to repeat this preparation. Recently a novel preparation of the *α(mer)* isomer has been reported[78] and characterization by luminescence spectroscopy suggested as a reliable method of judging isomeric purity. The formation of dihydroxy-bridged dimers is a characteristic feature of chromium(III) chemistry and complexes of the kind $[Cr_2(gly)_4(OH)_2]$ originally discovered by Ley[76] have frequently been synthesized.[72,80,81]

There have been a number of synthetic studies of other chromium(III)/amino acid systems.[82-84] In this series of papers a novel solid state synthetic method was developed. Solid hexaammine chromium(III) nitrate was heated with the amino acid, good yields being obtained by this method. Various basic and other amino acids were studied and in all cases *β-(fac)* isomers were obtained.

The complexes of sulphur containing amino acids have been studied and crystal structures for L-cysteine[32] and D-penicillamine[85] complexes determined. The methionine complex of chromium(III) has also been prepared,[86] the red complex has the formula $[Cr(met)_3]$ and is presumably a *β-(fac)* isomer.

The synthesis of aspartic acid complexes has been reported on several occasions,[87,88] in the latter paper three isomers were isolated. Serine complexes have been prepared.[89] Two isomers of

bis(L-histidinato)chromium(III) have been prepared,[90] together with a μ-hydroxy species. Electronic spectra were interpreted with the aid of angular overlap calculations.

Mixed amino acid complexes have been prepared involving aspartic acid and histidine,[91] structures were assigned by comparing CD and other spectra to the related cobalt(III) complexes. In general amino nitrogens were not found trans to each other. Other relevant complexes which have been prepared include mixed amino acid/nitrilotriacetates,[92] a complex of chromium(III) pentammine and glycine[93] and a series of complexes with pyridine carboxylic acids.[94]

Glutathione complexes of chromium(III) have recently been prepared in our laboratory.[95] In these species the chromium is coordinated by both the glycine residue {N,O} and the sulphur of the cysteine components of glutathione. A bis-glutathione complex and mixed complexes with cysteine, glycine and glutamic acid have been prepared. These complexes are being tested for GTF behaviour.

9. MODE-OF-ACTION OF THE GLUCOSE TOLERANCE FACTOR (GTF)

Mertz has listed[7] the following as possible mechanisms by which GTF might act.

1. Chromium may form a complex with insulin in the blood or pancreas.
2. Chromium might inhibit tissue insulinase.
3. The initial binding of insulin to tissue might be enhanced by chromium(III).
4. Chromium could act as a co-factor for a membrane carrier involved in glucose transport.
5. Chromium could act as a catalyst in the initial reaction between insulin and a specific membrane receptor site(s).

There have been remarkably few studies which provide any evidence as to the mode-of-action of GTF, or even the feasibility of Mertz's suggestions outlined above. In order for GTF to effect glucose metabolism it must undergo some specific interaction with the system responsible for glucose uptake and/or metabolism. *In vivo* and *in vitro* results suggest that the most likely mechanism is direct enhancement of insulin activity. The first two of Mertz's suggestions can hence be considered unlikely.

The suggestion that the binding of insulin to receptors is enhanced by chromium has been studied, effectively testing suggestion five above. The binding of insulin to epididymal tissue was only enhanced by about 20%.[96] The formation of a stable GTF/insulin complex has been demonstrated,[19] acylation of the α and ϵ amino groups of insulin inhibited complex formation. The binding constant was not estimated. The synthetic complex of nicotinic acid and glutathione with chromium(III) prepared by Anderson[33,34] binds very strongly to insulin.

A polarographic study of the interactions between chromium/insulin/mitochondria has been reported.[97] A polarographic wave for insulin was attributed to reduction of the disulphide linkage. In the presence of insulin the polarographic wave for the reduction of chromium(III) (1M KCl, pH 7.4, 10^{-4} M Cr(III) of unspecified source) was shifted, indicating complex formation. Three insulin molecules were associated with each chromium(III) and the apparent instability constant was estimated as $10^{-14.5}$ (presumably an overall constant for dissociation of the tris complex). There were also changes in the polarograms of mitochondria and mitrochondria/insulin mixtures in the presence of chromium(III). Insulin reacts with mitochondria by the formation of sulphydryl-disulphide linkages and this reaction is enhanced by the presence of chromium(III). There are suggestions that insulin reacts with its receptor via sulphide linkages.[98,99] The above work supports the suggestion that a possible role for chromium(III) is to facilitate disulphide bond formation by forming an intermediate ternary complex.

The above studies produce no clear suggestion for the mode-of-action of GTF. Obviously the lack of a detailed knowledge of the molecular structure of the factor hampers such work. Perhaps the most attractive hypothesis is that chromium has its own receptor site and that binding to this site potentiates the activity of insulin at a second site (viz. 4 above).

There are a number of features of chromium(III) chemistry which need to be considered.

1. The interaction appears to be rapid, labile substitution positions might be involved. However as pointed out above the ligands involved in GTF are unlikely to promote this kind of chemistry.
2. Nicotinic acid appears to be a near essential component of GTF; unlike other monocarboxylic acid substituted pyridines, nicotinic acid is not capable of acting as an electron transporting bridging ligand in inner-sphere electron transfer reactions.[100] The nature of the coordination of nicotinate in GTF will be crucial to understanding GTF. In a complex containing N-coordinated nicotinate the carboxylate group could be involved in hydrogen bonding to receptor sites.

3. Sulphur containing amino acids also appear to be required and the mode of co-ordination is unknown. If cysteine were coordinated in glycine like mode there would be a free sulphydryl group available for reaction with either insulin or the receptor. The reactivity of such groups in coordinated cysteine has not been investigated.

4. As a consequence of its high charge, ion-pairing is often significant in the reactions of chromium(III).[101] This seems unlikely to be important in GTF as negatively charged ligands are involved in the complex.

The properties of chromium(III) provide no obvious clues as to why this element has evolved a biochemistry so closely related to glucose tolerance. There must be some, as yet, unelucidated explanation for this specific requirement of higher animals for chromium(III).

10. CONCLUSIONS

Chromium deficiency in man and higher animals results in an impairment of intravenous glucose tolerance and diabetes like symptoms. It seems likely that chromium(III) metabolism is abnormal in certain forms of the diabetic condition. We shall now summarise a number of particularly relevant observations.

In a strain of mice with a genetic form of diabetes, glucose tolerance was restored by dosing with purified GTF. In contrast the administration of "inorganic" chromium was ineffective.[102] This work suggests that the ability to absorb chromium and/or synthesise GTF is responsible for the diabetic condition of these animals.

Tissue chromium levels have been shown to decrease with age.[103] This seems particularly relevant to the pregnancy and senile onset forms of diabetes. The heavy demand placed on the mothers body store of chromium(III) has been demonstrated in the laboratory rat; old breeder rats showed impaired glucose tolerance which could be reversed by dosing with chromium.[104] In contrast a recent study[105] of thirty-six pregnant women (including diabetics) found no evidence for abnormal chromium metabolism in gestational diabetes. Mertz has shown[106] that in pregnant rats GTF may be transported across the placenta.

A very limited number of clinical trials involving diabetics have been reported, the results have been summarized by Anderson[8,107] and others.[7] In several cases a favorable response to chromium(III) administration was observed; at present the results are too limited for any conclusions to be drawn. There seems to be some commercial interest in such therapy, a chromium(III) complex of oxobutanol has been patented[108,109] as a dietary supplement and/or therapeutic agent. Chromium metabolism is often disrupted in diabetics, chromium(III) levels in the urine of diabetics are double those in normal subjects.[110]

In conclusion one important aspect of the biochemistry of chromium is its ability to potentiate glucose tolerance. The mechanism by which glucose tolerance is improved is unknown, but seems likely to involve the potentiation of insulin activity by a chromium(III) complex termed GTF. The structure of the complex active in higher animals is unknown. A complex with remarkable biological activity in both *in vivo* and *in vitro* systems has been isolated from Brewer's yeast. GTF isolated from yeasts often contains nicotinic acid and either glutathione or its constituent amino acids. Both GTF and synthetic analogues of GTF have as yet been poorly characterized and there is scope for much more work. Perhaps the most interesting and reliable observation is that complexes which are effective in potentiating the activity of insulin, in *in vitro* models, contain nicotinic acid.

The coordination chemistry of chromium(III) is of crucial importance in glucose tolerance and possibly diabetes. It is surprising that the complexes involved have not been characterized in the 25 yr or so since they were first suggested to exist. This review does not present a comprehensive survey of the biological literature relating to chromium(III) and glucose tolerance, the interested reader is referred to the detailed and excellent articles by Mertz[7,10] and Anderson.[8,107]

Acknowledgements—We should like to thank those authors who have corresponded with us during the preparation of this article. Thanks are also due (P.O'B. and J.P.J.) to the British Council for their support of collaborative work between Aveiro and Chelsea via an "Academic Link".

REFERENCES

1. W. Mertz and K. Schwarz, *Arch. Biochem. Biophys.* 1955, **58**, 504.
2. W. Mertz and K. Schwarz, *Am. J. Physiol.* 1959, **196**, 614.

3. K. N. R. C. Jeejeebhoy, E. B. Chu, G. R. Marliss and A. Bruce-Robinson, *Am. J. Clin. Nutr.* 1977, **30**, 531.
4. (a) K. W. Jennette, *J. Am. Chem. Soc.* 1982, **104**, 874. (b) D. M. L. Goodgame, P. B. Hayman and D. E. Hathaway, *Polyhedron* 1982, **1**, 497.
5. D. Burrows, *Chromium Metabolism and Toxicity*. CRC Press, (1983).
6. E. J. Underwood, *Trace Elements in Human and Animal Nutrition*, 4th Edn, p.258. Academic Press New York (1977).
7. W. Mertz, *Phys. Rev.* 1969, **49**, 163.
8. R. A. Anderson, *The Science of the Total Environment* 1981, **17**, 13.
9. R. A. Anderson and W. Mertz, *TIBS* 1977, **2**, 277.
10. W. Mertz, E. W. Toepfer, E. E. Roginsky and M. M. Polansky, *Fed. Proc.* 1974, **33**, 2275.
11. W. Mertz, *Science* 1981, **213**, 1332.
12. W. Mertz, *Chimica Scripta* 1983, **21**, 145.
13. K. Schwarz and W. Mertz, *Arch. Biochem. Biophys.* 1957, **72**, 515.
14. K. Schwarz and W. Mertz, *Arch. Biochem. Biophys.* 1959, **85**, 292.
15. W. Mertz, E. E. Roginsky and K. Schwarz, *J. Biol. Chem.* 1961, **236**, 318.
16. W. Mertz, E. E. Roginsky and R. C. Reba, *Am. J. Physiol.* 1965, **209**, 489.
17. W. Mertz, *Proc. Nutr. Soc.* 1974, **33**, 307.
18. p. 200 in Ref. 7.
19. W. Mertz and D. E. Thurman, *Fed. Proc.* 1968, **27**, 482.
20. J. Gutierrez, W. Mertz, E. W. Toepfer, M. M. Polansky and E. E. Roginsky, *J. Agric. Food. Chem.* 1974, **22**, 100.
21. R. A. Anderson, J. H. Branter and M. M. Polansky, *J. Agric. Food Chem.* 1978, **26**, 1219.
22. M. Rodbell, *J. Biol. Chem.* 1964, **239**, 375.
23. E. W. Toepfer, W. Mertz, E. E. Roginsky and M. M. Polansky, *J. Agric. Food Chem.* 1973, **21**, 69.
24. G. W. Evans. E. E. Roginsky and W. Mertz, *Biochem. Biophys. Res. Commun.* 1973, **50**, 718.
25. H. J. Votava, C. J. Hahn and G. W. Evans, *Biochem. Biophys. Res. Commun.* 1973, **55**, 312.
26. J. Kumpulaunen, P. Koivistoiner, and S. Lahtinen, *Bioinorg. Chem.* 1978, **8**, 419.
27. E. W. Toepfer, W. Mertz, M. M. Polansky, E. E. Roginsky and W. R. Wolf, *J. Agric. Food Chem.* 1977, **25**, 162.
28. N. Mirsky, A. Weiss and Z. Dori, *J. Bioinorg. Chem.* 1980, **13**, 11.
29. P. P. Nelson and G. G. Briggs, *Fed. Proc.* 1981, **40**, 885.
30. E. Gonzalez–Vergara, J. Hegenauer and P. Saltman, *Fed. Proc.* 1982, **41**, 286.
30. (a) S. J. Haylick, P. D. Buckley and L. F. Blackwell, *J. Inorg. Biochem.* 1983, **18**, 195. (b) S. J. Haylock, P. D. Buckley and L. F. Blackwell, *J. Inorg. Biochem.* 1983, **19**, 105.
31. Unpublished work cited in Ref. 12, p. 215.
32. P. deMeester, D. J. Hodgson, H. C. Freeman and C. J. Moore, *Inorg. Chem.* 1977, **16**, 1494.
33. R. A. Anderson, M. M. Polansky, J. H. Branter and E. E. Roginsky, *Trace Element Metabolism in Man and Animals*. (Edited by M. Kirchgessner), Vol. III, p. 272. Institute fur Ernahrungsphysiologie Universitat Munchen, Freising-Weihenstephen (1978).
34. R. A. Anderson and J. H. Branter, *Fed. Proc.* 1977, **36**, 1123.
35. E. Gonzalez–Vegara, B. C. deGonzalez, J. Hegenauer and P. Saltman, *Ist. J. Chem.* 1981, **21**, 18.
36. D. L. Rabenstein, R. Guevremont and C. A. Evans, *Metal Ions In Biological Systems* (Edited by H. Sigel), Vol. 9, p. 103. Marcel Dekker, New York (1979).
37. J. V. McArdle, E. deLaubenfels, A. L. Shorter and H. L. Ammon, *Polyhedron* 1982, **1**, 471.
38. E. Gonzalez–Vergara, J. Hegenauer, P. Saltman, M. Sabat and J. A. Ibers, *Inorg. Chim. Acta* 1982, **66**, 115.
39. L. E. Gerdom and H. M. Goff, *Inorg. Chem.* 1982, **21**, 3847.
40. T. J. Wierenga and J. I. Legg, *Inorg. Chem.* 1982, **21**, 2881.
41. D. Rajendra Prasad, T. Ramas, D. Ramaswamy and M. Santappa, *Inorg. Chem.* 1982, **21**, 850.
41a. J. A. Cooper, B. F. Anderson, P. D. Buckley and L. F. Blackwell, *Inorg. Chim. Acta* 1984, **91**, 1.
42. (a) M. C. Perry, *Companion to Biochemistry* (Edited by A. T. Bull, J. R. Lagnado, J. O. Thomas and K. F. Tipton) p. 587. Longmans, London (1976). (b) T. Blundell, G. Dodson, D. Hodkin and D. Mercola, *Adv. Protein Chem.* 1972, **26**, 279.
43. (a) P. Cuatrecasas and M. D. Hollenberg, *Adv. Protein Chem.* 1976, **30**, 252. (b) P. Cuatrecasas, *Proc. Natl. Acad. Sci. U.S.A.* 1971, **68**, 1264.
44. F. A. Cotton and G. Wilkinson, *Advanced Inorganic Chemistry*, 4th Edn, a. p. 724, b. p. 768. Wiley Interscience, New York (1980).
45. F. Basolo and R. G. Pearson, *Mechanisms of Inorganic Reactions*, 2nd Edn, p. 145. Wiley, New York (1968).
46. J. Burgess, *Metal Ions in Solution, p.* 317. Ellis Horwood Chichester, U.K. (1978).

47. Ref. 46, Chap. 12, p. 349 and references therein contained.
48. R. E. Hamm and R. E. Davis, *J. Am. Chem. Soc.* 1953, **75**, 3085.
49. R. E. Hamm and R. H. Perkins, *J. Am. Chem. Soc.* 1953, **75**, 2083.
50. R. E. Hamm, R. L. Johnson, R. H. Perkins and R. E. Davis, *J. Am. Chem. Soc.* 1958, **80**, 4469.
51. Ref. 45, p. 197.
52. D. Banerjea and C. Chatterjee, *J. Inorg. Nucl. Chem.* 1969, **31**, 3845.
53. D. Banerjea and S. D. Chaudhuri, *J. Inorg. Nucl. Chem.* 1970, **32**, 1617.
54. J. H. Espenson, *Inorg. Chem.* 1969, **7**, 1554.
55. D. Thusius, *Inorg. Chem.* 1971, **10**, 1106.
56. J. O. Edwards, F. Manacelli and G. Ortagi, *Inorg. Chim. Acta* 1974, **11**, 47.
57. D. Banerjea and S. Chaudhuri, *J. Inorg. Nucl. Chem.* 1968, **30**, 871.
58. I. A. Khan and K. U. Din, *J. Inorg. Nucl. Chem.* 1981, **43**, 1082.
59. M. Abdullah, J. Barrett and P. O'Brien, *J. Chem. Soc., Dalton Trans.*, in press (1984).
60. J. G. Leipoldt, S. S. Basson and D. R. Rabie, *J. Inorg. Nucl Chem.* 1981, **43**, 3239.
61. P. O'Brien and D. A. Sweigart, *Inorg. Chem.* 1982, **21**, 2094.
62. K. R. Ashley, J. G. Leipoldt and V. K. Joshi, *Inorg. Chem.* 1980, **19**, 1608.
63. H. Ogino, T. Watanabe and N. Tanaka, *Chem. Lett.* 1974, 91.
64. Y. Sulfab, R. S. Taylor and A. G. Sykes, *Inorg. Chem.* 1976, **15**, 2388.
65. H. Ogino, M. Shimura and N. Tunaka, *Inorg. Chem.* 1979, **18**, 2497 and references therein.
66. (a) L. G. Sillén and A. E. Martell, Chemical Society Special Publication No. 17 (1964). (b) L. G. Sillén and A. E. Martell, Chemical Society Special Publication No. 25 (1971). (c) D. D. Perrin, *Stability Constants of Metal-Ion Complexes Part B. Organic Ligands.* IUPAC Chemical Data Series No. 22 (1982).
67. (a) See the entries in Ref. 62. (b) H. Stunzi and W. Marty, *Inorg. Chem.* 1983, **22**, 2145.
68. K. Venkatachalapathi, M. S. Nair, D. Ramaswamy and M. Santappa, *J. Chem. Soc., Dalton Trans.* 1982, 291.
69. H. Matsukawa, M. Ohta, S. Takata and R. Tsuchiya, *Bull. Chem. Soc. Jpn.* 1965, **38**, 1235.
70. J. Maslowska and L. Chruscinski, *J. Inorg. Nucl. Chem.* 1981, **43**, 3398.
71. A. Lassocinska, *Roczniki Chem.* 1973, **47**, 889.
72. R. D. Gillard, S. H. Laurie, D. C. Price, D. A. Phipps and C. F. Weick *J. Chem. Soc., Dalton Trans.* 1974, 1385.
73. C. E. Skinner and M. M. Jones, *Inorg. Nucl. Lett.* 1967, **3**, 185.
74. M. Husain, R. Hague and W. U. Malik, *J. Indian Chem. Soc.* 1964, **41**, 394.
75. H. Matsukawa, M. Ota, S. Takata, and R. Tsuchiya, *Bull. Chem. Soc. Japan* 1965, **38**, 1235.
76. H. Ley and K. Ficken, *Berichte.* 1912, **45**, 377.
77. N. Israily, *Compt. Rend. C.* 1966, **262**, 1426.
78. W. M. Wallace and P. E. Hoggard, *Inorg. Chim. Acta* 1982, **65**, L3.
79. H. Mizuochi, A. Uehara, E. Kyuno and R. Tsuchiya, *Bull. Chem. Soc. Japan* 1971, **44**, 1555.
80. A. Earnshaw and J. Lewis, *J. Chem. Soc.* 1961, 396.
81. S. Kallesoe and E. Pederson, *Acta Chem. Scand. B*, 1982, 859.
82. H. Oki and K. Otsuka, *Bull. Chem. Soc. Japan* 1976, **49**, 1841.
83. H. Oki, *Bull. Chem. Soc. Japan* 1977, **50**, 680.
84. H. Oki and Y. Takahashi, *Bull. Chem. Soc. Japan* 1977, **50**, 2288.
85. P. deMeester and D. J. Hodgson, *J. Chem. Soc. Dalton Trans.* 1977, 1604.
86. C. A. McAuliffe, J. V. Quagliano and L. M. Vallarino, *Inorg. Chem.* 1966, **5**, 1996.
87. M. Volshtein, G. G. Motyagina and L. S. Anakhova, *Zhur. Neorg. Khim.* 1956, **1**, 2378. [Chem Abstr. 1957, **52**, 5618e].
88. G. Grouhi-Witte and E. Weiss, Z. Naturforsch. 1976, **31b**, 1190.
89. M. Volstein and G. G. Volstein, *Zhur. Neorg. Khim.* 1959, **4**, 905.
90. P. E. Hoggard, *Inorg. Chem.* 1981, **20**, 415.
91. M. Watabe, H. Yano, Y. Odaka and H. Kobayashi, *Inorg. Chem.* 1981, **20**, 3623.
92. C. L. Sharma, P. K. Jain and T. K. De, *J. Inorg. Nucl. Chem.* 1980, **42**, 1681.
93. T. Ramasami, R. K. Wharton and A. G. Sykes, *Inorg. Chem.* 1975, **14**, 359.
94. B. Chatterjee, *J. Inorg. Nucl. Chem.* 1981, **42**, 2553.
95. M. Abdullah, J. Barrett and P. O'Brien, unpublished results (1983).
96. Ref. 7 p. 203.
97. G. D. Christian, E. C. Knoblock, W. C. Purdy and W. Mertz, *Biochim. Biophys. Acta* 1963, **66**, 420.
98. C. T. O. Fong, L. Silver, E. A. Popenoe and A. F. Debons, *Biochim. Biophysa. Acta* 1962, **56**, 190.
99. W. Mertz and E. E. Roginsky, *J. Biol. Chem.* 1963, **238**, 868.
100. E. S. Gould and H. Taube, *J. Am. Chem. Soc.* 1964, **86**, 1318.
101. See for example N. Fogel, J. M. J. Tai and J. Yarborough, *J. Am. Chem. Soc.* 1962, **84**, 1145.

102. (a) R. J. Doisy, M. S. Jastremski and F. L. Greenstein, *Excerpta Med. Found Int. Congr. Ser.* 1973, **280,** 155. (b) R. J. Doisy, J. H. P. Streeten, J. M. Freiberg and A. J. Schneider, In *Trace elements in Human Health and Disease* (Edited by A. S. Praesad), p. 79. Academic Press, New York (1976).
103. K. M. Hambidge and J. D. Baum, *Am. J. Clin. Nutr.* 1972, **25**, 376, see also Ref. 7. p. 222.
104. W. Mertz, E. E. Roginsky and H. A. Schroeder, *J. Nutr.* 1965, **86**, 107.
105. C. J. Harrison, K. Y. Lei, L. Shenker and C. W. Weber, *Fed. Proc.* 1983, **42**, 926.
106. W. Mertz and E. E. Roginsky, In *Newer Trace Elements in Nutrition* (Edited by W. Mertz and W. E. Cornatzer), Marcel Dekker, New York (1971).
107. R. A. Anderson, *Proc. Chromate Symp. Industrial Health Foundation Inc.*, p. 332 (1981).
108. D. P. Riley, M. M. Anderson and J. J. Rotruck, European Patent Application 81Z00316.8 23/03/81 *Chem. Abstr.* 1981, **96**, 40920p.
109. M. Anderson, D. P. Riley and J. Rotruck, *Fed. Proc.* 1980, **39**, 787.
110. W. K. Cranfield and J. R. Doisy, *Diabetes* 1975, **24**, 106.

Polyhedron Vol. 4, No. 1, pp. 15–21, 1985
Printed in Great Britain.

0277–5387/85 $3.00 + .00
© 1985 Pergamon Press Ltd.

ON THE HYDROLYSIS OF THE TITANIUM(IV) ION IN CHLORIDE MEDIA

LIBERATO CIAVATTA,* DIEGO FERRI and GIUSEPPE RICCIO
Dipartimento di Chimica dell'Università, Via Mezzocannone, 4, 80134 Napoli, Italy

(*Received* 14 *December* 1983; *accepted* 17 *February* 1984)

Abstract—Determinations of the [Ti(IV)]/[Ti(III) ratio in solutions of titanium(IV) chloride equilibrated with $H_2(g)$, at 25°C in 3 M (Na)Cl ionic medium, have indicated the predominance of the $Ti(OH)_2^{2+}$ species in the concentration ranges $0.5 \leq [H^+] \leq 2$ M and $1.5 \times 10^{-3} \leq [Ti(IV)] \leq 0.05$ M. From the equilibrium data the reduction potential has been evaluated

$$Ti(OH)_2^{2+} + 2\,H^+ + e \rightleftharpoons Ti^{3+} + 2H_2O,\ E_{oH} = (7.7 \pm 0.6) \times 10^{-3}\ V.$$

The acidification reactions of $Ti(OH)_2^{2+}$ were also studied in 12 M(Li)Cl medium at 25°C by measuring the redox potential of the Ti(IV)/Ti(III) couple as a function of $[H^+]$. The potentiometric data in the acidity range $0.3 \leq [H^+] \leq 12$ M have been explained by assuming

$$Ti^{4+} + e \rightleftharpoons Ti^{3+},\ E_o = 0.202 \pm 0.002\ V$$

$$Ti^{4+} + H_2O \leftrightharpoons TiOH^{3+} + H^+,\ \log K_{a1} = 0.3 \pm 0.01$$

$$Ti^{4+} + 2H_2O \leftrightharpoons Ti(OH)_2^{2+} + 2H^+,\ \log K_{a1}K_{a2} = 1.38 \pm 0.05.$$

NOTATION

- B total titanium concentration
- B_3 titanium(III) concentration
- B_4 titanium(IV) concentration
- E_0 standard potential of $Ti^{4+} + e \rightleftharpoons Ti^{3+}$
- E_{oH} standard potential of $Ti(OH)_2^{2+} + 2H^+ + e \rightleftharpoons Ti^{3+} + 2H_2O$
- $f(i)$ activity coefficient of the "i" species
- H analytical concentration excess of H^+ assuming as zero level Ti^{4+} and H_2O
- h equilibrium concentration of H^+
- K equilibrium constant for $H^+ + Cl^- \leftrightharpoons HCl$
- K_{an} equilibrium constant for $Ti(OH)_{n-1}^{5-n} + H_2O \rightleftharpoons Ti(OH)_n^{4-n} + H^+$
- $K_{p,q}$ equilibrium constant for reaction (7)
- R B_3/B in solutions equilibrated with hydrogen gas

Concentrations and equilibrium constants are expressed on the molar scale, M, moles/dm^3.

The hydrolysis of the titanium(IV) ion has been studied by a number of investigators but as yet some uncertainties remain on the nature of the protolysis products. Beukenkamp and Herrington,[1] from cation exchange determinations, found that the charge per Ti(IV) atom varies from 1.4 to 1.7 in $HClO_4$ at acidities up to 1.5M. They assumed the equilibrium

$$Ti(OH)_2^{2+} + H_2O \leftrightharpoons Ti(OH)_3^+ + H^+ \qquad (1)$$

with a constant of about $10^{-0.3}$.

Nabivanets,[2] Liberti and Vicedomini,[3] and Magon *et al.*[4] studied the distribution of Ti(IV) to cation exchange resins in the range 0.1–1 M $HClO_4$. On the basis of the distribution decrease with the second power of the acid concentration these authors postulated the presence of $Ti(OH)_2^{2+}$ even though the data are consistent with any doubly charged species as $Ti_2(OH)_6^{2+}$ or $Ti(OH)ClO_4^{2+}$. Nabivanets[2] estimated for equilibrium (1) a constant of $10^{-1.3}$ and also determined that two moles of H^+ are released per mole of Ti(IV) extracted from HCl–$HClO_4$ solutions. Therefore he assumed the presence of $Ti(OH)_2^{2+}$. However his data can be equally well explained by $Ti(OH)Cl^{2+}$ or $TiCl_2^{2+}$ or $Ti(OH)ClO_4^{2+}$.

*Author to whom correspondence should be addressed.

Babko *et al*,[5] and Liberti *et al.*[6] measured the solubility of hydrous TiO_2 in dilute HCl and $HClO_4$, respectively, and interpreted the solubility decrease up to 10^{-2} M H^+ by assuming $Ti(OH)_2^{2+}$. On the other hand Babko *et al.*[5] as well as Nabivanets and Lukachina[7] suggested that the constant solubility, $\sim 10^{-5.5}$ M, in the acidity range from 10^{-7} to 10^{-3} M indicated the formation of $Ti(OH)_4$. From their data Baes and Mesmer[8] estimated for

$$Ti(OH)_2^{2+} + 2H_2O \leftrightharpoons Ti(OH)_4 + 2H^+ \qquad (2)$$

an equilibrium constant of 10^{-5}.

More recently, Einaga,[9] using a glass electrode, has measured at 25°C the hydrogen ion concentration of several titanium(IV) chloride solutions. The [Ti(IV)] ranged from 0.019 to 0.048 molal, the acidity was varied between $10^{-1.1}$ and $10^{-0.7}$ molal and all the solutions were made to contain 2 molal Cl^- by adding NaCl. The accuracy of his measurements was limited by the slow attainment of equilibrium. Einaga explained the data assuming TiO^{2+} as the central group and the reaction

$$8\ TiO^{2+} + 12H_2O \leftrightharpoons (TiO)_8(OH)_{12}^{4+} + 12H^+$$

with a constant (molal scale) of $10^{-1.68}$.

CHOICE OF THE EXPERIMENTAL CONDITIONS AND METHOD OF INVESTIGATION

In this work the redox potential of the Ti(IV)/Ti(III) couple was measured in chloride media of different acidity. The choice of chloride as a solvent salt instead of perchlorate, the favourite of equilibrium analysis chemists for the least complexing tendency of ClO_4^-, was imposed by the appreciable rate at which ClO_4^- is reduced by Ti(III).

Measurements with a glass electrode were not made because at the acidities in question, $h \geq 0.3$ M, the differences $h - H$, even if evaluated from accurate e.m.f. data (0.1 mV), become too uncertain to bear significant information on the nature of the hydrolytic species. At any rate, since the ratio B/H never exceeded 0.05, we could easily find with good approximation expressions $h = h(H, B)$, as shown in the section "Treatment of the data and results".

The interpretation of the potentiometric data is somewhat simplified by the fact that the hydrolysis of the titanium(III) ion, according to Pâris and Gregoire[10] and to Krentzien and Brito,[11] is practically suppressed in our solutions, therefore the $[Ti^{3+}]$ value may always be set equal to B_3.

In the initial stage of the investigation we adopted a 3 M (Na)Cl medium, a level of concentration most often used in studies of the hydrolysis of metal ions.[8] Subsequently, in order to extend the acidity interval, the experiments were carried out in 12 M (Li)Cl. Lithium chloride has a high solubility; additionally its solutions exhibit osmotic coefficients nearly identical to those of HCl.[12] This means that in HCl–LiCl mixtures of constant $[Cl^-]$ the water activity remains essentially unchanged. This is a prerequisite for the constant ionic medium method. The most serious difficulty for the choice of the optimal experimental conditions was represented by the oxidation of the Ti^{3+} ion by water. The reaction is much suppressed by increasing the Cl^- concentration and by decreasing the acidity. It becomes practically negligible at $h < 5$ M in 12 M (Li)Cl. In more acidic solutions the Ti^{3+} oxidation caused drifts in the potentials of platinum electrodes which, however, did not exceed 3×10^{-7} V/s, corresponding to changes in $[Ti^{3+}]$ of about 10^{-9} M/s, in the most unfavourable case; 12 M H^+, 10^{-4} M Ti^{3+}, 2×10^{-3} M Ti(IV). In addition to platinum, which catalyzes the oxidation of Ti^{3+}, gold and mercury electrodes were tested. These did not prove to be inert in our highly complexing media. Therefore the exact B_3 values in the most acidic solutions were determined by analysing samples of the test solution.

On the other hand, the oxidation by water of Ti^{3+} occurs readily in 3 M (Na)Cl media so that rapidly changing potentials were observed with Pt or Hg or Au electrodes. However, good and reproducible determinations could be obtained of B_4/B_3 ratios in titanium solutions equilibrated with hydrogen gas which are equivalent to potentiometric measurements with the Ti(IV)–Ti(III) half-cell. Solutions of Ti(IV) were equilibrated with H_2(g) at 1 atm in presence of finely divided palladium. Then the excess of dissolved H_2 was determined by analysing the Ti(III) content through oxidation with $K_2Cr_2O_7$. In spite of tedious and time-consuming manipulations the "batch" method produces data as accurate as the potentiometric ones provided, as presently, that the B_4/B_3 ratio is not too far from unity.

The test solutions were prepared, just before an experiment initiated, by dilution of stock solutions stored at 4°C. As indicated by the sluggish formation, within a few months, of a precipitate of Ti(IV) hydroxide or oxychloride, the measurements at $h \leq 1$ M were made in supersaturated solutions. Since the amount of solid phase was negligible during the experiment, the results still give a true picture of the equilibria in clear solutions. The coincidence within the limits of experi-

mental error of data obtained by increasing or decreasing B_3 was taken as a criterion for the attainment of real equilibrium in the homogeneous phase.

The potentiometric measurements in 12 M (Li)Cl

Each experiment started by placing a solution of general composition: B M $TiCl_4$, H M HCl, 0.03 M AgCl, $(12 - H - 4B)$ M LiCl, in the cathode compartment of the electrolysis circuit

$$- \quad \text{Pt/TS/12 M LiCl/Ag} \quad + \qquad \text{(C)}$$
$$\text{constant-current supply}$$

and, each ensuing step of electrolysis involved the introduction of a few micromoles of electrons in the test solution, TS, the e.m.f. of cell (R)

$$- \text{RE/TS/Pt} + \qquad \text{(R)}$$

in which

$$\text{RE} = \text{Ag/}10^{-2}\text{M AgCl, 12 M LiCl/12 M LiCl}$$

and

$$\text{TS} = B_4 \text{ M } TiCl_4,\ B_3 \text{ M } TiCl_3,\ 0.03 \text{ M AgCl},\ H \text{ M HCl},\ (12\text{–}H\text{–}4B + B_3)\text{M LiCl},$$

was determined.

The silver(I) in TS served as depolarizer. Silver metal is deposited on the Pt gauze cathode and, due to the appreciable overpotential of the H^+ discharge on silver, no significant amount of current is used to reduce H^+. Silver reacts with Ti(IV) rapidly and quantitatively in solutions where $h < 5$ M and essentially the electrons introduced into TS, except a small amount used to reduce oxidizing impurities, only produce Ti^{3+}. The effect of trace amounts of impurities, mostly oxygen still remaining in TS purged with N_2(g), was accounted for by means of Gran's[13] diagrams, constructed using the data at low levels of B_3. In more acidic solutions the yield of Ti^{3+} decreased with h and was about 90% in 12 M HCl. The actual Ti(III) concentration was ascertained by analysing samples of TS with $K_2Cr_2O_7$.

The e.m.f. of cell (R) can be written at 25°C in V

$$E_R = E_0 + 0.05916 \log \frac{[Ti^{4+}] f(Ti^{4+})}{[Ti^{3+}] f(Ti^{3+})} + E_j - E_{RE} \quad (3)$$

where E_j denotes the liquid junction potential arising at the boundary between TS and 12 M LiCl, and E_{RE} stands for the potential of the reference electrode. The standard states are so defined that f(i)$\rightarrow$1 as the composition of TS tends to 12 M LiCl.

The potential of the reference half-cell, E_{RE}, was determined by measuring the e.m.f. of cell (Q)

$$-\text{RE/}10^{-2}\text{M HCl, 11.99 M LiCl/}H_2\text{(g)/Pt} + \text{(Q)}.$$

In accordance with our definitions, E_Q, the e.m.f. of cell (Q), may be written with good approximation

$$E_Q - 0.05916 \log((10^{-2} - [HCl])/p_{H_2}^{1/2}) = -E_{RE} \quad (4)$$

In eqn (4) $p_{H_2} = p_{atm} - p_{H_2O} - p_{HCl}$. The water vapour pressure was estimated from the osmotic coefficients listed by Robinson and Stokes,[12] while p_{HCl} was obtained by interpolation of data published by Scarano *et al.*[14] The concentration of associated hydrochloric acid was calculated by assuming for $H^+ + Cl^- \rightleftharpoons HCl$ a constant of $10^{-2.32}$. This was deduced as described in "Treatment of the data and results".

In order to determine the liquid junction potential, E_j, and to detect possible changes in E_{RE} the e.m.f. of cell (S)

$$- \text{RE/}10^{-2}\text{M AgCl, } H \text{ M HCl,}$$
$$(12 - H) \text{ M LiCl/Ag} + \qquad \text{(S)}$$

was measured after each series of experiments at the same H level. The e.m.f. of cell (S) is equal to

$$E_S = 0.05916 \log f(Ag^+) + E_j. \quad (5)$$

By subtracting from eqn (3), eqns (4) and (5) and the analytically determined quantity 0.05916 log (B_4/B_3) we may calculate for each point at the same H the function (6)

$$E_0^*(B_4, H) = E_0 + 0.05916 \log \frac{[Ti^{4+}]}{B_4} + 0.05916 \log \frac{f(Ti^{4+})}{f(Ti^{3+}) f(Ag^+)}. \quad (6)$$

The data $E_0^*(B_4, H)$ form the basis of the following calculations. For the correct interpretation of the data some assumptions must be made on the variation of the activity coefficients due to the replacement of Li^+ by H^+. We postulated that no appreciable variation occurs. The validity of this hypothesis was corroborated by confronting the results of the potentiometric work with spectrophotometric measurements in the UV region.

MATERIALS AND ANALYSIS

A series of 0.8 M *titanium(IV) chloride* solutions in 8 M HCl was prepared and analysed as described previously.[15] The solutions were stored at 4°C in a refrigerator in order to freeze reactions leading to precipitation of hydroxides and to minimize HCl losses by volatilization. As periodical analyses indicated, the acid concentration decreased by less than 0.3% in 6 months.

For the determination of the *actual titanium(III) concentration* samples of 10 or 20 cm^3, withdrawn under a nitrogen atmosphere, were added to an excess of deoxygenated $K_2Cr_2O_7$ solution. The oxidation of Ti(III) by Cr(VI) was found to proceed to completion almost instantaneously. The remaining Cr(VI) was treated with NaI and the I_3^- formed was titrated amperometrically with $Na_2S_2O_3$. By this procedure micromolar amounts of I_3^- could be analysed with an uncertainty of $\pm 0.5\%$.

Lithium chloride was made from Li_2CO_3 and HCl Merck of p.a. quality products. First, a 6 M solution was prepared with a small Li_2CO_3 excess. The slightly alkaline solution after boiling was left to stand for a week and then the precipitate of FeOOH and $SiO_2(H_2O)_x$ was filtered off. The acidity was adjusted to 10^{-3} M and the solution was heated to displace CO_2 and to concentrate it further. No Fe(III) and SO_4^{2-} ions could be detected in 14 M stock solutions.

The LiCl concentration was determined by Mohr's method. The low HCl concentration was estimated by coulometric acid-base titrations using a glass electrode as indicator.

Hydrochloric acid p.a. Merck, ~ 38%, was standardized against $KHCO_3$ with an accuracy of 0.1%. The acid concentration was checked periodically to account for losses by volatilization.

Sodium chloride. Baker was dried at 110°C for 2 hr before use.

Silver chloride was precipitated from HCl and $AgNO_3$ p.a. products and was dried at 110°C.

Palladium black, saturated with hydrogen gas, was prepared by cathodic reduction on a large platinum net from $PdCl_2$ in 1 M HCl solution.

Hydrogen as well as *nitrogen*, from commercial cylinders, were passed through activated copper to remove traces of oxygen, then presaturated with the ionic medium and finally led through a sintered glass disc of porosity G4 into the test solution.

EXPERIMENTAL

The e.m.f. measurements were performed at 25.00 ± 0.05°C in a paraffin oil thermostat. The cell arrangement was similar to that described by Forsling *et al.*[16] The Ag, AgCl electrodes, prepared according to Brown,[17] were soaked in 12 M LiCl for 2 days before use. Platinum gauze electrodes were boiled in 1:1 HNO_3 and ignited in alcohol flame. When two Pt electrodes were immersed in the same test solution, they agreed always to within 2×10^{-5} V. For the measurements with cell(Q) palladium coated Pt electrodes were employed. The e.m.f. values of cells(R), (Q) and (S) were measured with a precision of 10^{-5} V using a Dynamco Ltd 2022 digital voltmeter.

Prior to each experiment with cell(R) a stream of purified and presaturated nitrogen gas was led for 1/2 hr through the test solution to purge it of dissolved oxygen. By prolonged scrabbling of the test solutions we have not been able to avoid losses of HCl even when three or four wash bottles had been used. This effect was more pronounced at low acidities when the high viscosity of the solutions makes the attainment of the gas–liquid equilibrium slower. Throughout the measurements the solution was protected by atmospheric contamination by keeping the TS in a six-necked vessel fitted with high vacuum ground glass stoppers. The slight overpressure which develops by temporary temperature rise during electrolysis may cause extrusion of HCl gas if the vessel is not hermetically closed. The small decrease of H, for the removal of HCl by the H_2 flow during the measurements with cell(Q), was accounted for by analysis of the solutions soon after the E_Q value was recorded. The coulometric circuit(C) consisted of a 4 cm^2 platinum net which served as the cathode and a platinum gauze coated with a thick layer of silver which formed the anode. The bridge solution and the anode compartment were placed in a half-cell vessel of the "Wilhelm" type.[16] As the constant-current source a Metrohm E 211 A coulometer was employed. The accuracy and constancy of the current was checked by passing it through a standard resistor and by measuring the resulting potential. The current levels between 0.3 and 3 mA were found to be constant and accurate to within $\pm 0.05\%$. The electrolysis was carried out in steps of no more than 10 μF to minimize temperature increase in the system.

Two identical platinum electrodes, 1 cm long wires, immersed in solution stirred at a constant speed, were employed for the amperometric detection of iodine. The electrodes were connected through a Keithley 168 Autoranging D.D.M. microammeter at a sensitivity of 10^{-7} A, to a source of 0.1 V.

The spectrophotometric measurements were carried out at 25 ± 1°C with an Optika CF4 spectrophotometer using quartz cuvettes. The reference consisted of HCl–LiCl solutions of concentrations

identical to those in the test solutions. The whole absorption spectrum between 200 and 350 nm was recorded but only the absorbancies at 208 nm were used for the calculations. The estimated error in the absorbance is $\pm 5 \times 10^{-3}$.

TREATMENT OF THE DATA AND RESULTS

The excess solubility of $H_2(g)$ *in* 3 M (Na)Cl

In Table 1 the determinations of the ratios [Ti(IV)]/[Ti(III)] in solutions equilibrated with hydrogen gas are summarized in the form of $R(B, H, p_{H_2})$ data.

By assuming that we may set activities equal to molar concentrations[18] and that Ti(IV) species of the most general composition, $Ti_p(OH)_q^{4p-q}$, are present, the equilibrium may be represented by

$$Ti_p(OH)_p^{4p-q} + (p/2)H_2(g) + (q-p)H^+ \quad (7)$$

with equilibrium constant

$$K_{p,q} = [Ti^{3+}]^p[Ti_p(OH)_q^{4p-q}]^{-1} h^{p-q} p_{H_2}^{-p/2}$$

thus

$$R = \frac{B_3}{B_3 + B_4} = \frac{1}{1 + \sum pK_{p,q}^{-1} B_3^{p-1} h^{p-q} p_{H_2}^{-p/2}}. \quad (8)$$

Inspection of Table 1 indicates that, at constant p_{H_2} and h; $\sim H$, R is independent of $B_3(= BR)$, hence, according to (8), $p = 1$. To find q a single species was assumed to predominate and the quantities

$$h = H + qB - (q-1)BR \quad (9)$$

and

$$\log K_{1,q} = \log \frac{R}{1-R} - (q-1)\log h - \frac{1}{2}\log p_{H_2} \quad (10)$$

were calculated for each point with a series of q; 0, 1, 2, 3 and 4. Table 1 shows that no systematic trend of $\log K_{1,q}$ was found with $q = 2$, whereas the deviations for $q \neq 2$ by far exceeded the experimental error. We may thus conclude that in the experimental conditions of Table 1 the predominating Ti(IV) species is the dihydroxotitanium(IV) ion, $Ti(OH)_2^{2+}$.

From the average value of $\log K_{1,2} = 0.13 \pm 0.01$ we calculated for the reduction half-cell

$$Ti(OH)_2^{2+} + 2H^+ + e \rightleftharpoons Ti^{3+} + 2H_2O$$

the standard potential

$$E_{oH} = (7.7 \pm 0.6) \times 10^{-3}\ V.$$

The protolytic equilibria in 12 M (Li)Cl

The $E_0^*(B_4, H)$ data, which form the basis of the following calculations, are given in Table 2.

At each of the H values studied, the E_0^* function proved to remain constant as the Ti(IV) concentration was stepwise decreased within the limits indicated in Table 2. This observation indicates that only mononuclear hydrolysis products are formed. Hence, taking into account the results in 3 M (Na)Cl medium and assuming the constancy of the activity coefficients, we can write from eqn (6)

$$E_0^* = E_0 - 0.05916 \log (1 + K_{a1}h^{-1} + K_{a1}K_{a2}h^{-2}). \quad (11)$$

To evaluate E_0 and the K_{an} values the experimental data recalculated in the form $E_0^*(\log (H - [HCl] + 2B)$ were compared with the normalized[19] form of (11), $Y(\log u)$, where

$$Y = E_0^* - E_0 = -0.05916 \log(1 + Lu + u^2) \quad (12)$$

Table 1. Excess solubility of $H_2(g)$ in 3 M (Na)Cl. $p_{H_2} = 0.980$ atm

$B \times 10^3$, M	H, M	R	$\log K_{1,2}$
10.0	0.463	0.393	0.130
25.2	0.433	0.388	0.131
3.09	1.000	0.570	0.125
10.0	0.980	0.569	0.128
25.2	0.950	0.571	0.135
50.1	0.900	0.571	0.141
10.0	2.000	0.728	0.128
20.0	2.000	0.728	0.125

Table 2. Summary of the conditional standard potentials in 12 M (Li)Cl

$B \times 10^3$, M	H, M	$E_o^* \times 10^3$, V	$B_4 \times 10^3$, M conc. range
2.01	0.331	60.9±0.3	1.4-2
1.00	0.338	61.9±0.3	0.4-1
3.00	1.045	117.4±0.3	1-3
3.00	1.544	135.1±0.3	0.3-3
6.00	3.012	163.3±0.5	0.2-6
2.06	4.315	174.3±0.3	0.1-2
11.5	5.723	181.7±0.2	1-11.5
2.31	7.567	187.3±0.3	0.4-2
25.8	12.09	194.5±0.3	10-25.8
2.02	12.10	193.6±0.5	1-2

$$\log u = \frac{1}{2}\log K_{a1}K_{a2} - \log h \qquad (13)$$

$$\log L = \frac{1}{2}(\log K_{a1} - \log K_{a2}). \qquad (14)$$

For the construction of the experimental plot we introduced the approximation

$$h \sim H - [\mathrm{HCl}] + 2B \qquad (15)$$

which provides reasonable values for h. In fact, since B never exceeded 1% of H, h must be very close to $H - [\mathrm{HCl}]$. The inequality $h > H - [\mathrm{HCl}]$ yields for h the lower limit, while, in accordance with the findings in 3 M (Na)Cl, the upper limit is represented by $h \leq H - [\mathrm{HCl}] + 2B$. We evaluate from the data of Table 2 that the higher and lower h values differ by no more than 0.005 log units. This uncertainty is obviously negligible with respect to other sources of experimental error encountered in the present study.

The extent of association of HCl in LiCl–HCl mixtures was calculated by means of

$$\log K = -2.32 - 0.019\,H. \qquad (16)$$

Equation (16) presumes that, in LiCl–HCl mixtures of 12 M Cl^-, log K varies linearly with H between the values −2.32, valid in 12 M LiCl, and −2.55, relevant to 12 M HCl. The constants were deduced from HCl vapour pressure data, following the approach suggested by Robinson and Bates.[20] For the calculations we employed; density of 12 M LiCl = 1.2543 g/cm^3 (Ref. 21), density of 12 M HCl = 1.179 g/cm^3 (Ref. 22), p_{HCl} in 12 M HCl = 206 torr, value interpolated on the linear plot log p_{HCl} vs log (molality) constructed from data tabulated in International Critical Tables,[23] p_{HCl} in 12 M LiCl = 29.42 × total HCl concentration, torr/M, as evaluated from the study by Scarano *et al.*[14]

An acceptable agreement, within the limits of experimental error, could be found throughout the L range between 0.2 and 0.6, however $L = 0.4$ yielded the best fit. By reading off the differences $E_0^* - Y$ and log $(H - [\mathrm{HCl}] + 2B) - \log u$ in the position of the closest coincidence we computed in accordance with the definitions (12–14)

$$E_0 = 0.202 \pm 0.002\ \mathrm{V} \qquad (17)$$

$$\log K_{a1} = 0.3 \pm 0.1 \qquad (18)$$

$$\log K_{a1}K_{a2} = 1.38 \pm 0.05 \qquad (15)$$

The fit between the model curve and the experimental data is illustrated in Fig. 1.

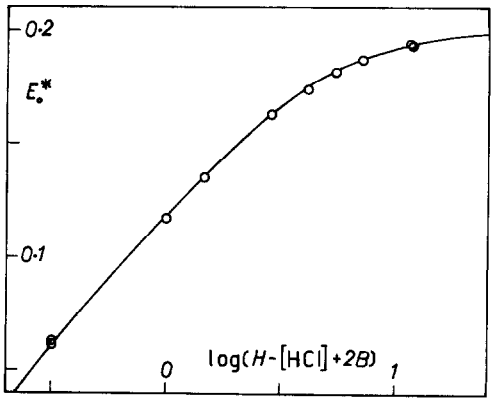


Fig. 1. The conditional standard potential, E_0^*, as a function of log $(H - [\mathrm{HCl}] + 2B)$. The curve has been calculated with the constants given in eqns (17–19).

The calculations hitherto presented are based on the assumption that the activity coefficient quotient in (6) and those included in the K_{an} expressions remain constant when the medium ion Li^+ is substituted by H^+. To get an idea of the plausibility of this hypothesis, the variations with H of the absorbance at 208 nm were interpreted in terms of the K_{an} given above. The measurements of ϵ_M, the absorbance per unit path length (cm) and unit concentration (M), were combined with the analytical data, H and $B = B_4$, and the K_{an} values to construct the function

$$F = \log \epsilon_M + \log (1 + K_{a1}(H - [\mathrm{HCl}] + 2B)^{-1} + k_{a1}K_{a2}(H - [\mathrm{HCl}] + 2B)^{-2}). \qquad (20)$$

Then the graph $F(\log (H - [\mathrm{HCl}] + 2B))$ was confronted with the family of model functions, ϕ (log v), where

$$\phi = F - \log \epsilon(\mathrm{Ti}^{4+}) = \log (1 + \rho v + v^2)$$

$$\log v^2 = \log K_{a1}K_{a2} - 2\log h + \log \epsilon(\mathrm{Ti(OH)_2^{2+}}) - \log \epsilon(\mathrm{Ti}^{4+})$$

$$\log \rho^2 = \log (K_{a1}/K_{a2}) + 2\log \epsilon(\mathrm{TiOH}^{3+}) - \log (\epsilon(\mathrm{Ti}^{4+})\epsilon(\mathrm{Ti(OH)_2}^{2+})).$$

The best agreement, as illustrated in Fig. 2, was found with $\rho = 0.375$. We also derived by translation of the coordinates the values of the molar absorptivities; $\epsilon(\mathrm{Ti}^{4+}) = (5.75 \pm 0.56) \times 10^3$, $\epsilon(\mathrm{TiOH}^{3+}) = (4 \pm 2) \times 10^3$ and $\epsilon(\mathrm{Ti(OH)_2}^{2+}) = (3.2 \pm 0.1) \times 10^3$.

We may thus conclude that the spectrophotometric measurements are satisfactorily explained by assuming the magnitude of K_{a1} and K_{a2} given in (18) and (19) indicating that the activity coefficient

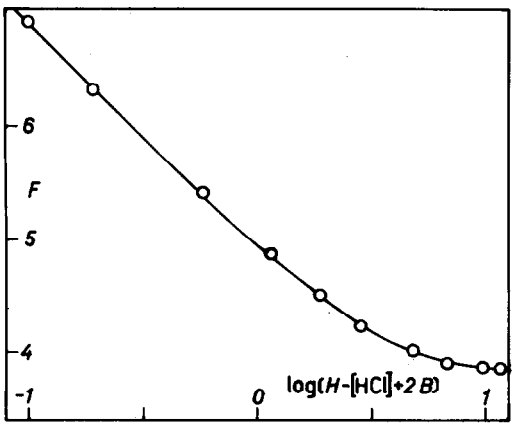


Fig. 2. Spectrophotometric measurements at 208 nm. F, eqn (20), as a function of log $(H - [HCl] + 2B)$. The curve has been calculated with the K_{an} values of eqns (18) and (19) and with the molar absorptivities given in the text.

quotients remain approximately constant when Li^+ is replaced by H^+.

DISCUSSION

We may regard as the most important result of this work the conclusion that in chloride solutions of $h \geq 0.3$ M the Ti^{4+}, $Ti(OH)^{3+}$ and $Ti(OH)_2^{2+}$ species are formed in detectable amounts. The species may contain a number of water molecules and chloride ions which, however, cannot be deduced from equilibrium analysis methods applied in a constant ionic medium.

Evidence for $TiCl_6^{2-}$ and for $TiO_2Cl_4^{4-}$ in concentrated, ≥ 12 M, hydrochloric acid solutions has been obtained from Raman studies. Rumpf[24] assigned three frequences to $TiCl_6^{2-}$. However, Davies and Long[25] have recently reinvestigated the spectra of solutions of molar $Cl^-/Ti(IV)$ ratios 7.3 and 10.6 and have found four reasonably strong lines instead of three, as expected for $TiCl_6^{2-}$ on the basis of octahedral symmetry. These authors in addition to or instead of $TiCl_6^{2-}$ suggested an oxyhalide complex with a highly symmetric structure, as *trans*-$TiO_2Cl_4^{4-}$, on the basis of the relatively low number of Raman lines.

By assuming that the constants in eqns (18) and (19) are valid under the experimental conditions of Davies and Long, ~ 11 M H^+ and ~ 1.6 ÷ 2.7 M Ti(IV), almost 75% of the metal is present as Ti^{4+}, i.e. $TiCl_6^{2-}$, while the remaining 25% is in the form of $Ti(OH)^{3+}$ and $Ti(OH)_2^{2+}$. In reality the *trans*-$TiO_2Cl_4^{4-}$ species suggested by Davies and Long is a mixture of $Ti(OH)^{3+}$ and $Ti(OH)_2^{2+}$ which in a less schematic fashion may be written, respectively, $Ti(OH)(H_2O)Cl_4^-$ and $Ti(OH)_2Cl_4^{2-}$. We may thus infer that the titanium species present in 12 M Cl^- solutions are anionic chloride complexes.

The last conclusion seems in contrast with that of a previous work[15] concerning the investigation of Ti(IV)-F^- complexes in 3 M (Na)Cl media. Then the presence of chloride complexes of Ti(IV) was excluded from the small influence on the equilibrium constants caused by the replacement of Cl^- with ClO_4^-. Evidently, as the fluoride[15] also the chloride complex formation is accomplished within a narrow free-ligand concentration leaving small room for intermediate steps. A magnitude of 10^{-3} for the constant of $Ti(OH)_2^{2+} + 4Cl^- \leftrightharpoons Ti(OH)_2Cl_4^{2-}$ would suffice to have only 7% of Ti(IV) in the form of $Ti(OH)_2Cl_4^{2-}$ at 3 M Cl^-, whereas practically all the metal, 95%, complexed in 12 M Cl^-.

Acknowledgements—This work has been supported by Ministero della Pubblica Istruzione, Roma.

REFERENCES

1. J. Beukenkamp and K. D. Herrington, *J. Am. Chem. Soc.* 1960, **82**, 3025.
2. B. I. Nabivanets, *Russian J. Inorg. Chem.* 1962, **7**, 212.
3. A. Liberti and M. Vicedomini, *Ric. Scient.* 1966, **36**, 851.
4. L. Magon, A. Cassol and R. Portanova, *Gazzetta* 1969, **99**, 933.
5. A. K. Babko, G. I. Gridchina and B. I. Nabivanets, *Russ. J. Inorg. Chem.* 1962, **7**, 66.
6. A. Liberti, V. Chiantella and F. Corigliano, *J. Inorg. Nucl. Chem.* 1963, **25**, 415.
7. B. I. Nabivanets and V. V. Lukachina, *Ukr. Khim. Zh.* 1964, **30**, 1123.
8. C. F. Baes and R. E. Mesmer, *The Hydrolysis of Cations*. Wiley, New York (1976).
9. H. Einaga, *J. Chem. Soc. Dalton Trans.* 1979, 1917.
10. M. R. Pâris and C. Gregoire, *Analyt. Chim. Acta* 1968, **42**, 439.
11. H. Krentzien and F. Brito, *Ion* 1970, **30**, 14, as quoted in Ref. 8.
12. R. A. Robinson and R. H. Stockes, *Electrolyte Solutions*. Butterworths, London (1959).
13. G. Gran, Dissertation. Stockholm (1981).
14. E. Scarano, G. Gay and M. Forina, *Analyt. Chem.* 1971, **43**, 206.
15. L. Ciavatta and A. Pirozzi, *Polyhedron* 1983, **2**, 769.
16. W. Forsling, S. Hietanen and L. G. Sillén, *Acta Chem. Scand.* 1952, **6**, 901.
17. A. S. Brown, *J. Am. Chem. Soc.* 1934, **56**, 646,
18. G. Biedermann and L. G. Sillén, *Arkiv Kemi* 1953, **5**, 425.
19. L. G. Sillén, *Acta Chem. Scand.* 1956, **10**, 186.

20. R. A. Robinson and Roger G. Bates, *Analyt. Chem.* 1971, **43**, 970.
21. *International Critical Tables* 1928, **3**, 77.
22. G. Åkerlöf and J. Teare, *J. Am. Chem. Soc.* 1938, **60**, 1226.
23. *International Critical Tables* 1928, **3**, 301.
24. M. E. P. Rumpf, *Compt. Rend.* 1936, **202**, 950.
25. J. E. D. Davies and D. A. Long, *J. Chem. Soc.* (*A*) 1968, 2560.

Polyhedron Vol. 4, No. 1, pp. 23–27, 1985
Printed in Great Britain.

0277–5387/85 $3.00 + .00
© 1985 Pergamon Press Ltd.

THIOSEMICARBAZIDE COMPLEXES OF ANTIMONY(III) HALIDES

J. MASŁOWSKA*
Institute of General Food Chemistry, Technical University of Łódź, ul. Stefanowskiego 4/10, 90–924 Łódź, Poland

and

K. OPRZĄDEK
Pedagogical Academy, Siedlce, Poland

(*Received*: 25 *July* 1983; *accepted after revision* 17 *February* 1984)

Abstract—Some hitherto unknown complexes of thiosemicarbazide (Htsc) and antimony(III) halides have been synthesized in 1,4-dioxane. The elemental analyses have indicated that these compounds are of the type $Sb(CH_5N_3S)Cl_3$ and $Sb(CH_5N_3S)X_3.C_4H_8O_2$, where X = Br or I. The electronic and vibration spectral analyses have shown that Htsc acts as a bidentate ligand in these complexes, linking through sulphur and "the hydrazine terminal nitrogen" to Sb(III).

Only a few papers have been published on the subject of the synthesis and structure of thiosemicarbazide (Htsc) complexes and an examination of their optical and magnetic properties, and most of them describe the complexes of the transition metal ions.[1–3] Crystallographic studies[1] have shown that Htsc acts as a bidentate ligand with metal ions such as: Cu(II), Ni(II), Co(II), Zn(II) and Fe(III) to form various complexes. Htsc is in the *cis* configuration in such complexes[4] and forms a stable pentagonal chelate ring. In Ag(I) and Hg(II) complexes, e.g. $Ag(Htsc)Cl$,[5,1] $Hg(Htsc)_2Cl_2$ and $Hg(Htsc)_2Br_2$[6] Htsc acts as a monodentate ligand in the *trans* configuration, i.e. the same as the free Htsc molecule. As for the Htsc complexes of the metal ions of the main groups of periodic system, only the complex of Bi(III) is known. This complex $(BiCl_3)_3.4Htsc$ was synthesized by Battaglia *et al.* and the authors have also studied its structure. They showed that it contains an unusual $[Bi_4Cl_{10}(Htsc)_6]^{2+}$ cation.

In the present work are presented the results of the studies of Htsc complexes of Sb(III) as the representative of the main group V of the periodic system. It is well known that Sb(III) ions hydrolize strongly in aqueous solution[8] and that, on the other hand, thiosemicarbazide undergoes protolysis in a strongly acid medium.[9] Because these two processes interfere with complex formation in aqueous solution, we undertook an attempt to synthesize some new Sb(III) complexes of Htsc in a non-aqueous medium.

EXPERIMENTAL

The following chemicals were used: Htsc (p.a.) and $SbCl_3$ (p.a.), both produced by Reachim; $SbBr_3$ (p.a.), produced by Ferak–Berlin; SbI_3, prepared according to[10] and recrystallized from a CCl_4 solution; 1,4–dioxane ($C_4H_8O_2$), purified free from peroxides[11] and distilled before use, and methanol (p.a.), both produced by POCh – Gliwice (Poland).

Electronic spectra were obtained on spectrophotometer Specord, Carl Zeiss Jena in 1 cm quartz cells. IR spectra were obtained on spectrophotometer Specord IR-71, Carl Zeiss Jena, using KBr tablets.

Preparation of $Sb(CH_5N_3S)Cl_3$

0.0025 mole (0.57 g) of $SbCl_3$ was dissolved in 25 cm^3 of 1,4-dioxane. 0.005 mole of Htsc dissolved in 50 cm^3 of 1,4-dioxane was added to the warm solution. The mixture was heated to 50°C under a reflux condenser. The pale yellow solution was left to cool. A white precipitate was obtained which was filtered off, washed with 1,4-dioxane and air-dried first and then dried over P_2O_5 under vacuum (0.79 g of precipitate was obtained; *ca.* 100% yield).

*Author to whom correspondence should be addresesed.

An analogous compound was obtained when methylene chloride with a 5% addition of ethyl alcohol was used as the solvent, but because of the low solubility of Htsc in it, a solution of 0.0025 mole (0.23 g) of Htsc in 200 cm^3 of the solvent was used.

Preparation of $Sb(CH_5N_3S)Br_3.C_4H_8O_2$ *and* $Sb(CH_5N_3S)I_3.C_4H_8O_2$

0.01 mole of SbX_3 (X = Br, I) was dissolved in 100 cm^3 of 1,4-dioxane and simultaneously gently heated. When hot, this solution was added to the previously prepared solution of 0.02 mole (1.8 g) of Htsc in 200 cm^3 of dioxane. The mixture was kept at 50°C for 1 hr and then left at room temperature to crystallize. After 48 hr the precipitate was filtered off, washed by 1,4-dioxane and air-dried first and then dried over P_2O_5 under vacuum. The yield was 95% for $SbBr_3$ and 97% for SbI_3.

RESULTS AND DISCUSSION

Composition and properties of the complexes

In Table 1 there are given the physical properties and elemental analyses of the prepared complexes.

Electronic spectra

The characteristic absorption bands of these complexes in methanol solutions are listed in Table 2. These data indicate that the short-wave band at 204 nm of the ligand Htsc does not, in general, undergo any change when the ligand is bonded to SbX_3, and that the intensity of this band increases as X changes from Cl to I. This region comprises also the characteristic bands of the SbX_3 solutions. Interference of these bands with the absorption band of the ligand may be the reason for the increase in absorption at 204 nm. The other band of thiosemicarbazide at 241 nm undergoes a "blue shift" on complexing in the Cl or Br complexes, but it cannot be observed when X = I because of the intense band due to SbI_3. The intensity decreases on passing from the ligand to the chloro-complex, then increases with the bromo-derivative. Dioxane present in two of the complexes does not absorb in this region.

In the longer wave region a new band of variable intensity occurs at 267 nm, which is not observed in the Htsc spectrum nor in the spectra of the solutions of SbX_3. Because of its position in the longer wave region than the intramolecular Htsc bands and because of its high intensity observed for all the complexes, the new band formed at 267 nm can be attributed to the charge-transfer transition L→M. The curves labelled "mixtures" in Figs. 1(4), 2(4) and 3(4) were obtained after mixing a solution of SbX_3 with solutions of Htsc, and the curves of the complexes (Figs. 1(3), 2(3) and 3(3)) were obtained after dissolving the previously prepared precipitates.

Methanol solutions of the discussed complexes are not stable. After 48 hr there began to precipitate orange deposits of Sb_2S_3 in the solutions if the concentration is $\sim 1.10^{-3}$ mole/dm^3.

IR spectra

Characteristic absorption frequencies of Htsc and its complexes of Sb(III) halides are presented in Table 3. Assignment of the bands was based on

Table 1. Physical properties and elemental analyses of the Sb(III) complexes of thiosemicarbazide prepared in dioxane

Complex	Colour	Melting point °C	Sb %	C %	H %	N %	S %	X %
$Sb(SCN_3H_5)Cl_3$	white	187–189 (decomp.)	38.22 (38.14)	3.30 (3.76)	1.55 (1.57)	13.22 (13.16)	10.52 (10.04)	33.56 (33.32)
$Sb(SCN_3H_5)Br_3.C_4H_8O_2$	white	198–200	22.27 (22.53)	11.75 (11.10)	2.60 (2.40)	8.24 (7.77)	6.69 (5.92)	45.78 (44.35)
$Sb(SCN_3H_5)I_3.C_4H_8O_2$	yellow (dark yellow at 149°)	184–187	17.48 (17.87)	9.37 (8.80)	2.06 (1.91)	6.34 (6.16)	5.01 (4.69)	55.23 (55.87)

The calculated values are in parenthesis.

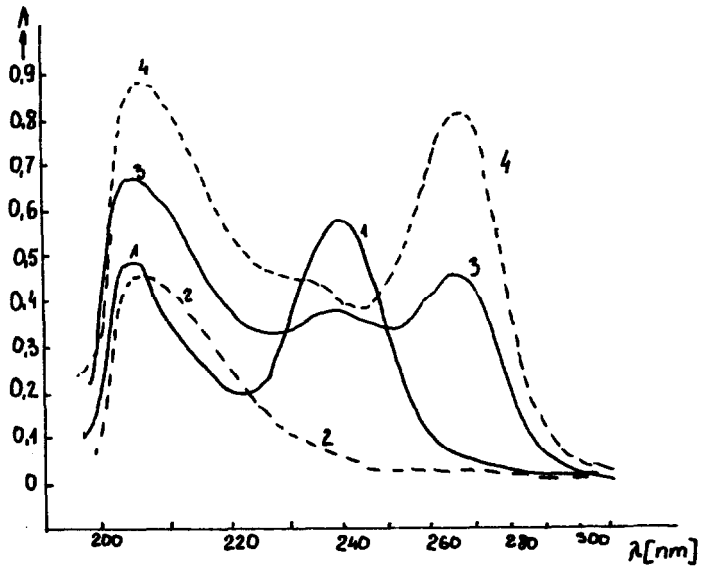


Fig. 1. Electronic spectra in methanol solutions. (1) 5.10^{-5} mole/dm^3 Htsc. (2) 5.10^{-5} mole/dm^3 $SbCl_3$. (3) 5.10^{-5} mole/dm^3 $Sb(Htsc)Cl_3$. (4) Mixture: 5.10^{-5} mole/dm^3 Htsc + 5.10^{-5} mole/dm^3 $SbCl_3$.

the works of Mashima[12] and Adejumobi.[13] In the NH_2 stretching vibration region of the ligand only irregular and not so characteristic changes were observed in the presence of SbX_3. Moreover, CH vibrations are observed in this region.

The $-NH_2$ bending vibrations region (1640 and 1620 cm^{-1} for Htsc), show practically, no change in the complex if its position and intensity are regarded. In this region (1500–1300 cm^{-1}) in the spectrum of Htsc there are observed two characteristic frequencies, which have been attributed to a composite $\nu_{(CN)} + \nu_{(C=S)} + \nu_{(NH_2)}$ vibration at 1480 and 1315 cm^{-1}. When the complex is formed, these bands undergo a 40 cm^{-1} shift to the lower frequencies (the band at 1480 cm^{-1}) and a 70 cm^{-1} shift to the higher frequencies. Similar effects were observed in the complexes: $Ni(Htsc)_2(NO_3)_2$, $Cu(Htsc)_2(NO_3)_2$ and $Zn(Htsc)Cl_2$,[13] in which Htsc

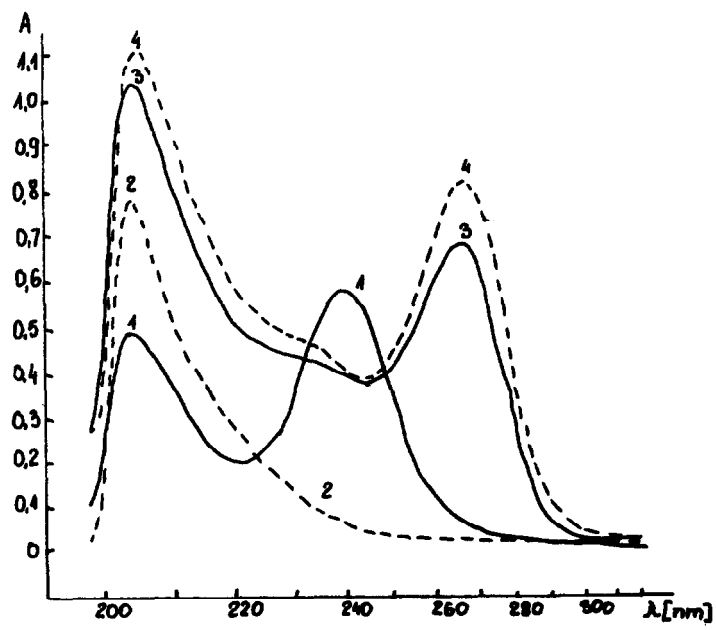


Fig. 2. Electronic spectra in methanol solutions. (1) 5.10^{-5} mole/dm^3 Htsc. (2) 5.10^{-5} mole/dm^3 $SbBr_3$. (3) 5.10^{-5} mole/dm^3 $Sb(Htsc)Br_3.C_4H_8O_2$. (4) Mixture: 5.10^{-5} mole/dm^3 Htsc + 5.10^{-5} mole/dm^3 $SbBr_3$.

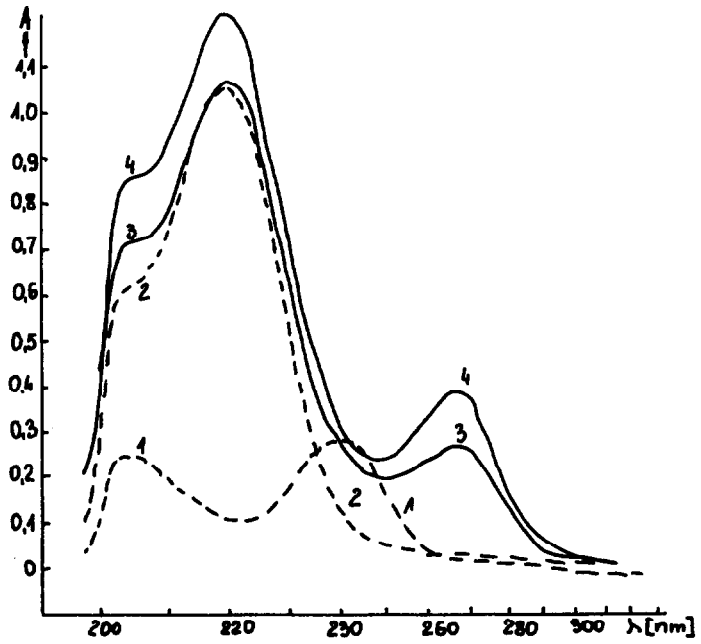


Fig. 3. Electronic spectra in methanol solutions. (1) $2.5.10^{-5}$ mole/dm^3 Htsc. (2) $2.5.10^{-5}$ mole/dm^3 SbI_3. (3) $2.5.10^{-5}$ mole/dm^3 $Sb(Htsc)I_3.C_4H_8O_2$. (4) Mixture: $2.5.10^{-5}$ mole/dm^3 Htsc + $2.5.10^{-5}$ mole/dm^3 SbI_3.

acts as a bidentate ligand, linking through sulphur and the nitrogen atom to the metal ion. Contrary to this, in $HgCl_2(Htsc)_2$ and $HgBr_2(Htsc)_2$ complexes, in which only linking through the sulphur atom occurs,[14] no significant changes in the bands at 1480 and 1315 cm^{-1} were observed.

The two intense bands at 1000 and 800 cm^{-1} in the Htsc spectrum (the second one is attributed mainly to C=S stretching) undergo significant changes in complexes of Sb(III)halides. The 1125–680 cm^{-1} region of $Sb(Htsc)Cl_3$ complexes is almost "blank" and there occurs only a very weak band at 1000 cm^{-1}. Shift of the band at 800 down to 680 cm^{-1} with a considerable decrease in its intensity confirms that the linking occurs through sulphur and the hydrazine nitrogen atom. In the case of complexes in which there is linking via sulphur only, the $\nu_{(C-S)}$ vibration at 800 cm^{-1} is reduced by about 30 cm^{-1}.[6] In the case of Htsc complexes of $SbBr_3$ and SbI_3 there appear sharp and quite intense bands at 860, 890, 1080 and 1040 cm^{-1}. They are the result of the coordination

Table 2. Characteristic absorption bands for $Sb(Htsc)X_3.C_4H_8O_2$ complexes in methanol solutions

Complex	Band I		Band II		Band III	
	λ_{max} (nm)	E	λ_{max} (nm)	E	λ_{max} (nm)	E
Htsc	204	9800	241	11600	-	-
$Sb(Htsc)Cl_3$	205	13400	239	7400	267	9200
$Sb(Htsc)Br_3 \cdot C_4H_8O_2$	204	20800	232.5	8600	267	13600
$Sb(Htsc)I_3 \cdot C_4H_8O_2$	204	28800	220.6	42800	267.5	10400

Table 3. IR absorption frequencies (in cm^{-1}) of $Sb(Htsc)X_3.C_4H_8O_2$ complexes, Htsc = thiosemicarbazide

Assignments	Htsc	$Sb(Htsc)Cl_3$	$Sb(Htsc)Br_3 \cdot C_4H_8O_2$	$Sb(Htsc)I_3 \cdot C_4H_8O_2$
$\nu_{(NH)}$	3350s	3360m		
	3240s			
	3170s	3160		
	3100sh	3040		
	2970m	2950		
$\delta_{(NH_2)}$	1640s	1635s	1635s	1635s
	1620s	1620sh	1620s	1610s
$\nu_{(CN)} + \delta_{(NH_2)}$	1535s	1560m	1570sh	1570m
			1550sh	1550sh
	1505		1530sh	
$\nu_{(CS)} + \nu_{(CN)}$ + $\delta_{(NH_2)}$	1480m	1440s	1445m	1440m
	1315m	1395m	1395m	1380m
amide III band	1280s	1320w	1320w	1320w
			x1300m	x1300m
$\delta_{(NH_2)}$	1220sh	1205m	x1260w	x1255w
			1200w	1195w
	1160s	1125s	1120s	1120s
			x1080m	x1070m
	1000vs	1000vw	x1040w	x1040w
			x 900m	x 890m
			x 860s	x 860s
mainly $\nu_{(CS)}$	800s	680m	690m	675m

x bands assigned to the presence of $C_4H_8O_2$ in the complex,
s - strong, m - medium, w - weak, vw - very weak, sh - shoulder,
ν - stretching, δ - deformation.

of the solvent molecules 1,4-dioxane with the complexes of the type $Sb(Htsc)X_3$ and the formation of the complexes $Sb(Htsc)X_3.C_4H_8O_2$ (X = Br, I).

REFERENCES

1. M. J. Campbell, *Coord. Chem. Rev.* 1975, **15**, 279.
2. U. A. Jayasooriya, D. B. Powell, *Inorg. Chem.* 1982, **21**, 1054.
3. Y. Shibutani, K. Shinra, C. Matsumoto, *J. Inorg. Nucl. Chem.* 1981, **43**, 1395.
4. F. Hansen, R. Groubaek Hazell, *Acta Chem. Scand.* 1969, **23**, 1359.
5. M. Nardelli, G. Fava Gasparri, J. Chierici, *Ric. Sci*, 1965, **35 II-A**, 480.
6. Chung Chieh, L. P. C. Lee, C. Chiu, *Can J. Chem.* 1978, **56**, 2526.
7. L. P. Battaglia, A. Bonamartini Corradi, M. Nardelli, M. E. Tani, *J. Chem. Soc. Dalton Trans.* 1978, 583.
8. Ch. F. Baes, R. E. Mesmer, *The Hydrolysis of Cations*. Wiley - Interscience New York (1976).
9. J. Masłowska, K. Oprządek, *Zeszyty Naukowe Politechniki Łódzkiej* (*Scientific Bulletin of Łódź Technical University*) 1984, **38**, 53.
10. J. Gałecki, *Preparatyka Nieorganiczna* (*Practical Inorganic Chemistry*. WNT, Warszawa (Warsaw), (1964).
11. M. Mąkosza, *Synteza organiczna* (*Organic Synthesis*). PWN, Warszawa (Warsaw) 1972.
12. M. Mashima, *Bull. Chem. Soc. Jpn.* 1964, **37**, 974.
13. A. Adejumobi, D. R. Goddard, *J. Inorg. Nucl. Chem.* 1977, **39**, 910.

Polyhedron Vol. 4, No. 1, pp. 29–31, 1985
Printed in Great Britain.

0277–5387/85 $3.00 + .00
© 1985 Pergamon Press Ltd.

METALLOCYCLOPENTADIENYL DERIVATIVES OF BIVALENT SAMARIUM, EUROPIUM AND YTTERBIUM

GUL'MAMED Z. SULEIMANOV*, YURI S. BOGATCHEV, LEILA T. ABDULLAEVA, IRINA L. ZHURAVLEVA, KHALIL S. KHALILOV, LYUDMILA F. RYBAKOVA and IRINA P. BELETSKAYA
L. Ya. Karpov Institute of Physical Chemistry, Obukha St. 10, Moscow 107120, U.S.S.R.

(*Received* 8 *August* 1983; *accepted after revision* 17 *February* 1984)

Abstract—It has been established that the reaction of metallocyclopentadienyl mercurials with an excess of elemental lanthanides Ln(Ln = Sm, Eu, Yb) in tetrahydrofuran yields substituted cyclopentadienyl derivatives of the metals.

Among the first reported organic derivatives of divalent lanthanides were the bis-cyclopentadienyl derivatives (Cp_2Ln; Ln = Sm, Eu, Yb),[1–3] as well as aryl and alkyl derivatives of the type RLnI(R = ar., alk.; Ln = Sm, Eu, Yb)[4].

Previously, to synthesize divalent cyclopentadienyl derivatives of samarium, europium and ytterbium, we resorted to the following reaction.[5]

$$(C_5H_5)_2Hg + m\,Ln/Hg \longrightarrow (C_5H_5)_2Ln\cdot(THF)_n$$

Ln = Sm, Eu, Yb; $m = 4(5)$; $n = 1$–2.

EXPERIMENTAL

Literature methods were used to prepare $(C_5H_5FeC_5H_4)_2Hg$[6] (1) and $[(OC)_3MnC_5H_4]_2Hg$[7](5). Other chemicals were purchased.

All solvents were dried over $LiAlH_4$ and under an atmosphere of nitrogen prior to use. All reactions were carried out at room temperature in purified solvents under an atmosphere of nitrogen unless it is stated otherwise.

^{1}H NMR spectra were recorded on Bruker WP-200 SY(200.13 MHz) spectrometers and were referenced to internal TMS in C_4D_8O. The IR spectra for (2)–(4) and (6)–(8) were measured on a Perkin–Elmer 580 spectrometer in a CaF_2 cell. The X-Ray fluorescence analyses were made on a VRA-2 spectrometer on the complexes in the form of a tablet.

*Author to whom correspondence should be addressed.

SYNTHESIS OF BIS-FERROCENYL (LANTHANIDE) DERIVATIVES

Bis-ferrocenyl samarium (2). Addition of (0.75 g, 5 mmol) elemental samarium as powder to solution of (1) (0.57 g, 1 mmol) in 50 cm^3 THF. The resulting red solution was stirred at room temperature for 120 hr, filtered (canulla), and THF evaporated to dryness under vacuum. The oily residue was washed with C_6H_6(3 × 10 cm^3) and then extracted with tetrahydrofuran (25 cm^3) filtered, concentrated to *ca.* 10 cm^3 and cooled to −13°C to give deep orange crystals. Yield, 0.06 g, 12%; m.p. 340° (dec.). ^{1}H NMR: $\delta(FeC_5H_5)$:4.280 ppm, $\delta(FeC_5H_4)$:4.305 ppm. IR (Nujol mull)cm^{-1}: 405 m, 478 m, 498 m, 592 vw, 614 w, 722 vw, 798 s, 815 s, 838 vw, 877 m, 890 vw, 995s, 1015s, 1028s, 1064s, 1095m, 1100s, 1141s, 1154s, 1185w, 1219vw. 1250s, 1300 m, 1350w, 1366m, 1375m, 1405m. 1460s, 1515w, 1585vw, 2680vw, 2720s, 2850s, 2920s, 3064m, 3090m.

Similarly, bis-ferrocenyl europium(3) and bis-ferrocenyl ytterbium (4) from (1) and elemental europium(ytterbium).: (3) – ^{1}H NMR: $\delta(FeC_5H_5)$: 4.268 ppm, $\delta(FeC_5H_4)$: 4.318 ppm.; IR(Nujul mull)cm^{-1}: 408m, 475m, 488w, 592w, 610w, 718vw, 792s, 815s, 830w, 855vw, 880m, 890w, 998s, 1010s, 1042m, 1090m, 1105s, 1140s, 1155s, 1194w, 1220vw, 1250s, 1304s, 2682vw, 2720s, 2850s, 2918s, 2922vw, 3062m, 3082m.

(4)-^{1}H NMR: $\delta(FeC_5H_5)$: 4.264 ppm, $\delta(FeC_5H_4)$: 4.151 and 4.458 ppm ($H_{\alpha,\beta}$). IR(Nujol mull)cm^{-1}: 402m, 478m, 590vw, 515w, 725vw, 795s, 815s, 836s, 846w, 880m, 892vw, 995m, 1020s, 1030s, 1040m, 1092m, 1100s, 1140s, 1154s, 1585w, 2682vw, 2720s, 2850s, 2920s, 3060m, 3085m.

SYNTHESIS OF BIS-CYCLOPENTADIENYLMANGANESETRICARBONYL (LANTHANIDE) DERIVATIVES

Bis-cyclopentadienylmanganesetricarbonyl samarium-tetrahydrofuranate (6). Addition of (0.75 g, 5 mmol) elemental samarium as powder to a solution of (5) (0.6 g, 1 mmol) in 25 cm^3 THF. The reaction mixture was stirred at room temperature for 5 hr. After the reaction stopped the yellow solution was decanted and concentrated to *ca.* 5 cm^3 and addition 50 cm^3 *n*-hexane to solution and cooled to −13°C, to give yellow crystals. Yield, 0.46 g, 74%; m.p. 120° (dec). ^{1}H NMR: $\delta(MnC_5H_4)$: 5.185 ppm. IR(Nujol mull)cm^{-1}: ν(C≡O): 1720w, 1780m, 1918s, 2015s; (THF): 1724w, 1768m, 1925s, 2010s.

Similarly, bis-cyclopentadienylmanganesetricarbonyl europium-bis-tetrahydrofuranate(7) and bis-cyclopentadienylmanganese ytterbiumtetrahydrofuranate(8) from (5) elemental europium-(ytterbium). (7)-^{1}H NMR: $\delta(MnC_5H_4)$: 5.208 ppm, IR(THF)cm^{-1}: ν(C≡O): 1724w, 1772m, 1925s, 2012s. (8)-^{1}H NMR: $\delta(MnC_5H_4)$: 5.226 and 4.916 ppm ($H_{\alpha,\beta}$). IR(THF) cm^{-1}: ν(C≡O): 1740w, 1790m, 1942s, 2025s.

RESULTS AND DISCUSSION

Carrying on with the research in this field, the reaction has been extended to π-cyclopentadienyl organometallic derivatives of mercury which have been examined using, by way of example, the reaction between bis-ferrocenyl mercury and bis-cyclopentadienylmanganesetricarbonyl mercury with samarium, europium and ytterbium. It has turned out that bis-ferrocenyl mercury (1) reacts with elemental and amalgamated lanthanides in THF very slowly:

$$\underset{(1)}{[(C_5H_5)Fe(C_5H_4)]_2Hg} + m\,Ln/Hg \longrightarrow \underset{(2)\text{–}(4)}{Ln[(H_4C_5)Fe(C_5H_5)]_2}$$

Ln = Sm(2), Eu(3), Yb(4); m = 4(5).

Moreover, a prolonged heating or boiling of the reaction mixture produced a sparingly soluble compound consisting of Fe, Hg and corresponding lanthanide which were identified by X-ray fluorescence spectroscopy.

However, at room temperature the reaction between bis-cyclopentadienylmanganesetricarbonyl mercury (5) and elemental lanthanides in THF proceeds with, the formation in high yield of the divalent derivatives:

$$\underset{(5)}{[(OC)_3Mn(C_5H_4)]_2Hg} + mLn \longrightarrow \underset{(6)\text{–}(8)}{Ln[(H_4C_5)Mn(CO)_3]]_2\cdot(THF)_n}$$

Ln = Sm(6), Eu(7), Yb(8); m = 4(5); n = 1–2.

Tables 1 and 2 contain the products of reactions.

Likewise, as this was mentioned in the literature,[4,8] the iodides of ferrocene and cyclopentadienylmanganesetricarbonyls react with Sm, Eu and Yb forming divalent derivatives of ferrocene and cyclopentadienylmanganesetricarbonyls of the

Table 1. Reactions of metallocyclopentadienyl mercurials with samarium, europium and ytterbium in tetrahydrofuran

R_2Hg	Metal Ln	Ratio of R_2Hg/Ln	Time (h)	Products	$T_{dec.}$ C°	Yield %
$[(C_5H_5)Fe(C_5H_4)]_2Hg$	Sm	1:5	120	$[(C_5H_5)Fe(C_5H_4)]_2Sm$	340	12
$[(C_5H_5)Fe(C_5H_4)]_2Hg$	Eu	1:4	120	$[(C_5H_5)Fe(C_5H_4)]_2Eu$	348	24
$[(C_5H_5)Fe(C_5H_4)]_2Hg$	Yb	1:4	120	$[(C_5H_5)Fe(C_5H_4)]_2Yb$	375	16
$[(OC)_3Mn(C_5H_4)]_2Hg$	Sm	1:5	5	$[(OC)_3Mn(C_5H_4)]_2Sm\cdot C_4H_8O$	120	74
$[(OC)_3Mn(C_5H_4)]_2Hg$	Eu	1:5	5	$[(OC)_3Mn(C_5H_4)]_2Eu\cdot 2C_4H_8O$	135	66
$[(OC)_3Mn(C_5H_4)]_2Hg$	Yb	1:5	5	$[(OC)_3Mn(C_5H_4)]_2Yb\cdot C_4H_8O$	180	78

Table 2. Analytical data for $[(C_5H_5)Fe(C_5H_4)]_2Ln$ and $[(OC)_3Mn(C_5H_4)]_2Ln\cdot(THF)_n$

Compounds	Found(Required)%			
	C	H	Fe	Mn
$[(C_5H_5)Fe(C_5H_4)]_2Sm$	45.97 (46.08)	3.36 (3.45)	21.15 (21.74)	
$[(C_5H_5)Fe(C_5H_4)]_2Eu$	45.84 (46.18)	3.28 (3.55)	21.06 (21.43)	
$[(C_5H_5)Fe(C_5H_4)]_2Yb$	44.12 (44.24)	3.04 (3.31)	19.85 (20.57)	
$[(OC)_3Mn(C_5H_4)]_2Sm\cdot C_4H_8O$	38.18 (38.23)	2.47 (2.55)		17.36 (17.65)
$[(OC)_3Mn(C_5H_4)]_2Eu\cdot 2C_4H_8O$	40.87 (41.01)	3.16 (3.41)		15.29 (15.63)
$[(OC)_3Mn(C_5H_4)]_2Yb\cdot C_4H_8O$	36.51 (36.88)	2.29 (2.46)		17.77 (16.89)

Grigard reagent type:

$$LMC_5H_4I + Ln \longrightarrow LMC_5H_4LnI \xrightarrow{R\text{-}X} LMC_5H_4\text{-}R + XLnI$$

M = Fe, L = C_5H_5; Ln = Sm, Yb; R = CH_3; X = Cl.
M = Mn, L = 3CO; Ln = Sm, Eu, Yb; R = CH_3, C_6H_5; X = Cl.R = $SiMe_3$, X = Cl.

The yield of ferrocene (cyclopentadienylmanganesetricarbonyl) lanthanides was determined in terms of that of the trimethylsilyl (acyl, benzoyl) derivatives of ferrocene and cyclopentadienylmanganesetricarbonyls. The structure of compounds obtained has been proved by the data acquired with the aid of elemental analysis (Table 2), IR and PMR spectroscopy (shown in the Experimental).

REFERENCES

1. E. O. Fischer, H. Fischer, *J. Organometal. Chem.* 1965, **3**, 181.
2. E. O. Fischer, H. Fischer, *Angew. Chem.* 1964, **76**, 52.
3. F. Calderazzo, P. Papalardo, S. Losi, *J. Inorg. Nucl. Chem.* 1966, **28**, 987.
4. D. F. Evans, G. V. Fazakerley, R. F. Phillips, *J. Chem. Soc., A* 1971, 1931.
5. G. Z. Suleimanov, L. F. Rybakova, Ya. A. Nuriev, T, Kh. Kurbanov and I. P. Beletskaya, *J. Organometal. Chem.* 1982, **235**, C19.
6. A. N. Nesmeynov, E. G. Perevalova, R. V. Golovnya and O. A. Nesmeynaova, *DAN SSSR* 1954, **97**, 459.
7. A. N. Nesmeynav, K. N. Anisimov and Z. P. Valueva, *Izv. AN SSSR, OChN* 1962, 1683.
8. G. Z. Suleimanov, V. I. Bregadze, N. A. Koval'chuk, Kh. S. Khalilov and I. P. Beletskaya, *J. Organometal. Chem.* 1983, **255**, C5.

Polyhedron Vol. 4, No. 1, pp. 33–38, 1985
Printed in Great Britain.

0277–5387/85 $3.00 + .00
© 1985 Pergamon Press Ltd.

Cu(II) COMPLEXES OF N-PROPYL-2-PICOLINAMINE N-OXIDE

GÖZEN ERTEM† and DOUGLAS X. WEST*
Department of Chemistry, Illinois State University, Normal, IL 61761, U.S.A.

(*Received* 7 *December* 1983; *accepted* 17 *February* 1984)

Abstract—Cu(II) complexes have been prepared with N-propyl-2-picolinamine N-oxide (PA) employing the perchlorate, tetrafluoroborate, nitrate, chloride and bromide salts. The following unique solids have been isolated and characterized: $Cu(PA)_2X_2$ ($X = ClO_4^-$, BF_4^- and NO_3^-) and $Cu(PA)X_2$ ($X = Cl^-$, Br^-). Characterization has been accomplished primarily by IR, electronic and ESR measurements of the solid state since considerable alteration of the complexes occurs on dissolution. PA bonds as a bidentate ligand via its N-oxide oxygen and amine nitrogen in all of the complexes. Anion coordination occurs in the halogen complexes and the nitrate ions appear to be bound to Cu(II) as monodentate ligands in $Cu(PA)_2(NO_3)_2$. In addition, there appears to be a rhombic distortion of the CuO_2N_2 chromophore of the perchlorate and tetrafluoroborate solids which is probably due to the steric requirements of the propyl substituents.

A study of the Cu(II) complexes of N-alkyl-[1] and N,N-dialkyl-2-picolinamine N-oxides[2] using the percholate, tetrafluoroborate, nitrate, chloride and bromide salts as starting materials has been carried out in our laboratories. To date we have reported on the N-methyl, N-ethyl, N-isopropyl and N-tert-butyl- complexes among the N-alkyl derivatives (MA, EA, IPA and TBA, respectively). In addition, a parallel study of the Cu(II) complexes of 2-alkyl- and 2-dialkylaminopyridine N-oxides[3] is in progress. Consequently, we are able to compare the potential 5- and 6-membered bidentate rings (i.e. N-oxide oxygen and amine nitrogen functioning as donor atoms) of the two series as well as observe any steric effects caused by increasing the size of the alkyl substituent(s) bonded to the amine nitrogen. In this latter series we noticed several differences between the complexes formed with the propyl derivative compared to the isopropyl derivative.[3] Therefore, we now report the preparation and characterization of five Cu(II) complexes of the title ligand as well as a comparison of the spectral properties to those of the previously isolated Cu(II) complexes of both series of ligands.

†NATO fellow on leave from Istanbul University.

*Author to whom correspondence should be addressed.

EXPERIMENTAL

N-propyl-2-picolinamine N-oxide(PA) was prepared in the same manner as the previous members of this series.[1] The Cu(II) complexes were also prepared as described previously and the instrumentation employed has been described.[1,4]

RESULTS AND DISCUSSION

The compounds isolated in this study are shown in Table 1. Compounds of identical stoichiometry have been isolated with each of the other N-alkyl-2-picolinamine N-oxides.[1] The colors of the solids isolated here are identical to those isolated with EA, but are not similar to IPA since its nitrate, chloride and bromide solids were blue, bright green and dull olive, respectively.[1] Like the other series[1] the perchlorate and tetrafluoroborate solids yield 1:2 electrolytes, the nitrate a 1:1 electrolyte and the halide complexes both are non-electrolytes.[5] Therefore, the two halide compounds might again be expected to be 4-coordinate with the two halogen atoms and a bidentate PA ligand bonding to Cu(II). The perchlorate and tetrafluoroborate solids can probably be considered planar with small interaction between the Cu(II) and the polyatomic anion and similar to the $Cu(MA)_2(ClO_4)_2$. Pavkovic *et al.*[6] have determined the crystal structure of this complex. For the nitrate complex to be a 1:1 electrolyte in solution either there is one coordinated nitrate and one ionic nitrate or two

Table 1. Partial elemental analyses, colors and molar conductivities of Cu(II) complexes of N-propyl-2-picolinamine N-oxide (PA)

Compound	Color	Calculated C	Calculated H	Found C	Found H	Λ[a] ($ohm^{-1}cm^2mol^{-1}$)
$Cu(PA)_2(ClO_4)_2$	violet	36.34	4.74	36.07	4.73	255
$Cu(PA)_2(BF_4)_2$	violet	37.96	4.96	36.82	5.13	262
$Cu(PA)_2(NO_3)_2$	dull blue	41.58	5.43	42.02	5.46	152
$Cu(PA)Cl_2 \cdot H_2O$	yellow green	33.92	5.06	34.04	4.81	38
$Cu(PA)Br_2$	dark violet	27.75	3.62	28.07	4.03	56

[a] ca. 10^{-3}M CH_3CN solutions

weakly coordinated nitrates with one dissociated in solution while the other remains coordinated, or associated electrostatically to the Cu(II) center. Our spectral studies of the previous members of the series[1] suggested the latter to be the case.

Assignments of the important IR bands which aid in the understanding of the Cu(II)-ligand bonding are presented in Table 2. The ν_{NH} of PA is found at somewhat higher energy than IPA and TBA and at much greater energy than MA and EA,[1] and this is an indication that the larger alkyl groups reduce the extent of hydrogen bonding. This hydrogen bonding is intramolecular in contrast to the 2-alkylaminopyridine N-oxides which have intermolecular hydrogen bonding.[7] In the complexes the ν_{NH} band is shifted to lower energy indicating coordination by the amine function. However, the shift for the perchlorate and tetrafluoroborate solids is significantly less than for the rest of the compounds in this study. This same trend occurred in the previously studied compounds[1] and suggests a lack of hydrogen bonding to the tetrahedral polyatomic anions, but significant bonding to the weakly coordinated nitrate ions. Possibly, the lower energies of ν_{NH} in the halo complexes is because the ligand is bound very strongly due to the weaker donor ability of the halogen atoms.

The ν_{NO} is shifted to lower energy in the complexes compared to its position in the ligand's spectrum confirming the coordination of the N-oxide oxygen in the complexes. Consistent with reduced hydrogen bonding of the ligand, ν_{NO} is at higher energy than for other ligands of the series.[1] This band is also at higher energy in the complexes since the magnitude of the shift on complexation is the same. The higher NO bond order is probably due to factors other than weaker CuO bonding since ν_{CuO} in these complexes is little changed from previous studies.[1] Other spectroscopic studies (*vide infra*) show differences in the stereochemistry of these complexes which could account for this difference. Although some increase in the energy of δ_{NO} upon complexation has been observed previously, the greatest increase occurs with the present PA complexes. A metal ion effect similar to

Table 2. IR assignments (cm^{-1}) of N-propyl-2-picolinamine N-oxide (PA) and its Cu(II) complexes

Compound	ν_{NH}	ν_{NO}	$\delta_{CNC(a)}$	$\delta_{CNC(s)}$	δ_{NO}	ν_{Cu-O}	ν_{Cu-N}	ν_{Cu-X}
PA	3340s,b	1258m	1055m	953m	853s			
$Cu(PA)_2(ClO_4)_2$	3288m	1222s	1022m	924m	866m	380m	342m	
$Cu(PA)_2(BF_4)_2$	3318m	1221s	1025m	925m	865m	380m	343m	
$Cu(PA)_2(NO_3)_2$	3210m	1222s	1029m	928m	868m	382m	344m	(280)
$Cu(PA)Cl_2 \cdot H_2O$	3208m	1224s	980m	932m	875m	396m	351m	304sh 290vs
$Cu(PA)Br_2$	3222m	1227s	982m	928m	873m	388m	349m	227s 211s

that of hydrogen bonding[8] as well as the formation of a chelate ring[9] contribute to this increase in energy.

We have tentatively assigned bands at 1055 and 953 cm^{-1} to the antisymmetric and symmetric CNC bending modes of the propylamino groups, respectively. The energies are similar to the analogous bands in the other members of the series[1] for which our assignment was based on the studies of Katritzky and Jones.[10] Upon complexation these bands are both shifted to lower energy further substantiating coordination by the amine function.

In the 300–400 cm^{-1} spectral region each of the complexes has at least two bands. We have assigned the higher energy band to ν_{CuO} fully realizing that bands in this portion of the spectrum are most often combination bands. This is within the 376–421 cm^{-1} range proposed[11] for ν_{MOPy} and identical to our previous assignments[1] although the TBA complexes were at somewhat higher energy (i.e. 400–420 cm^{-1}). Assignment of the lower energy band to ν_{CuN} is consistent with our previous assignments[1] as well as those of others.[12]

It is of interest to note that ν_{CuO} for the 2-alkylaminopyridine N-oxide complexes[3] are generally found at energies near or above 400 cm^{-1} when these ligands are bound as monodentate ligands via the N-oxide oxygen. However, the Cu(II) complexes of 2-dialkylaminopyridine N-oxides[13] in which the ligand functions as a bidentate group, generally have ν_{Cu-O} at energies substantially below 400 cm^{-1}.

Although not shown in Table 2, the IR spectrum of $Cu(PA)_2(ClO_4)_2$ has $\nu_3(ClO_4)$ = 1080 *s,b* and $\nu_4(ClO_4)$ = 630*s* as well as a very weak band at 941 cm^{-1} assignable to $\nu_1(ClO_4)$. The latter band is IR inactive for purely tetrahedral perchlorate and its appearance, along with the lack of splitting of ν_3 and ν_4, suggests non-coordinated, but hydrogen bonded, perchlorate ions. Similarly, the spectrum of $Cu(PA)_2(BF_4)_2$ possesses a strong band at 1060 cm^{-1} and a band of medium intensity at 530 cm^{-1} assignable to ν_3 and ν_4 of BF_4^-, respectively. Based on this assignment there is no indication of coordination of the terafluoroborate ion.

Lever *et al.*[14] suggest that coordinated and ionic nitrate can be distinguished by inspection of the $\nu_1 + \nu_4$ region (i.e. 1700–1800 cm^{-1}) of the spectrum. Weak bands are found at 1785 and 1774 cm^{-1} and the difference of 11 cm^{-1} is within the range of 5–26 cm^{-1} that has been postulated for monodentate nitrate ligand.[14] Since no other bands are observed in this region, it is likely that both nitrates are weakly bound as monodentate ligands. A weak band at 280 cm^{-1} is possibly assignable to ν_{Cu-O} of coordinated nitrato group in agreement with the findings of other workers.[15]

As is shown in Table 2 the chloride and bromide solids both have two bands assigned to copper–halogen stretching frequencies which would be consistent with the cis arrangement expected for the $Cu(PA)X_2$ centers. Additionally, both solids have these bands in energy ranges that would be consistent with terminal rather than bridging halogens.[16] The Br/Cl ratio of the average energies is 0.74 which is consistent with the two compounds having similar structures.[17] Compared to the previous compounds of this series,[1] the average energies of the two bands are generally lower suggesting a steric effect.

We have omitted from Table 3 the intraligand bands in that they provide little information about the bonding of the complexes. Additionally, there

Table 3. Charge transfer (L→M) and *d–d* electronic transitions (kK) for the Cu(II) complexes of N-propyl-2-picolinamine N-oxide (PA)

	Solid State		Solution (CH_3CN)	
Compound	L ⟶ M	d-d	L ⟶ M	d-d
$Cu(PA)_2(ClO_4)_2$	26.46	17.48 14.93sh	27.03	16.26
$Cu(PA)_2(BF_4)_2$	26.46	17.69 15.27sh	26.67	16.34
$Cu(PA)_2(NO_3)_2$	25.25	16.95 14.35sh	27.02	16.26
$Cu(PA)Cl_2 \cdot H_2O$	24.39 (22.22sh)	16.78w (11.24)	26.67 21.74	12.05
$Cu(PA)Br_2$	27.78sh 23.58sh 18.52(Br⟶Cu)	16.13	23.26sh	15.63

is a charge transfer band (*ca.* 31 kK) which we have not included. All of the complexes show a second charge transfer band at *ca.* 26 kK and this has been assigned to an O→Cu(II) transition in agreement with other Cu(II) complexes of substituted pyridine N-oxides.[18] In addition, the two halide solids have at least one additional band at somewhat lower energy than 26 kK due to halogen-to-copper (II) transitions. Accurate assignment of the energies of these bands is difficult because they are shoulders on the higher energy bands mentioned above. However, the Cl→Cu(II) band is generally found in the 20.5–22.5 kK range while the transfer from Br is found at somewhat lower energy. The intensity of the band at 18.52 kK in the solid spectrum of $Cu(PA)Br_2$ suggests it to also be Br→Cu(II) as was suggested for $Cu(MA)Br_2$ and $Cu(EA)Br_2$.[1]

Finally, before discussing the individual compounds it should be noted that there is definitely a change in the nature of the coordination spheres upon dissolution in CH_3CN. There is a loss of the two *d–d* peaks of the reflectance spectra for each of the solids derived from salts of polyatomic anions. This is consistent with a square planar to tetragonally distorted octahedral change in the Cu(II) coordination[19] and is likely achieved by axial bonding of the solvent molecules. In addition, the loss of spectral detail in the compounds of the polyatomic anions is accompanied by a shift to lower energy of the *d–d* band in the halide complexes which also suggests the bonding of additional ligands or possibly, a distortion to a more tetrahedral structure. The remainder of this report will concentrate on the individual compounds including the *d–d* transitions of Table 3 as well as the ESR parameters in Table 4. The IR and other information already discussed will be included only when it is pertinent to the proposed stereochemistry of the compounds.

$Cu(PA)_2(ClO_4)_2$. The *d–d* maximum of the main band, which is generally assigned to transitions to $d_{x^2-y^2}$ from both d_{xz}, d_{yz} and d_{z^2}, at 17.48 kK is consistent with an essentially square planar CuO_2N_2 chromophore.[20] However, since the analogous IPA complex had this band at 18.18 kK and the tetrafluoroborate salt of this study has the band at 17.69 kK, a very weak interaction with the perchlorate anion(s) is not ruled out. Other possibilities are tetrahedral or rhombic distortions of the CuO_2N_2 chromophore. As is shown in Fig. 1 we were unable to accurately assign the lowest magnetic field *g*-value in the powder spectra of either the perchlorate or tetrafluoroborate salt of PA. This is probably due to a rhombic distortion and we have assigned the two other *g*-values as shown in Fig. 1. With the IPA complexes of these two anions the *d–d* band was higher than for the corresponding EA complexes. This higher energy was considered to be due to stronger planar bonding because of the greater steric hindrance of the larger IPA groups preventing interaction of the tetrahedral counter ions with copper in the axial positions. Since the *d–d* bands for PA complexes are even lower than the corresponding EA complexes (e.g. $\nu_{dd} = 17.95$ kK for $Cu(EA)_2(ClO_4)_2$),[1b] the cause of the apparent rhombic distortion is a steric effect of a different nature. We suggest for these complexes that either repulsion between two propyl groups of a Cu(II) center or between Cu(II) centers is more important than repulsion between the propyl groups and the anions. A single crystal X-ray study of either $Cu(PA)_2(ClO_4)_2$ or $Cu(PA)_2(BF_4)_2$ as well as a study of the complexes

Table 4. Powder ESR parameters for the Cu(II) complexes of N-propyl-2-picolin-amine N-oxide (PA)

Compound	Temp.(°K)	$g_{\parallel}$ or g_3	g_2	$g_{\perp}$ or g_1	g_{av}
$Cu(PA)_2(ClO_4)_2$	RT		2.105	2.052	
	77		2.129	2.056	
$Cu(PA)_2(BF_4)_2$	RT		2.096	2.051	
	77		2.118	2.054	
$Cu(PA)_2(NO_3)_2$	RT	2.243		2.054	2.117
	77	2.240		2.054	2.116
$Cu(PA)Cl_2$	RT	2.216		2.099	2.138
	77*	2.211		2.094	2.133
$Cu(PA)Br_2$	RT			g_{iso} =	2.111
	77	2.192		2.077	2.115

*an extra feature at about g = 2.27 is visible.

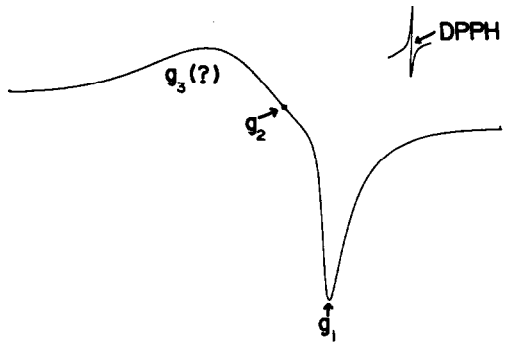


Fig. 1. Powder ESR spectrum of $Cu(PA)_2(ClO_4)_2$ at 77 K.

with the various N-butyl-2-picolinamine N-oxides, which is presently being carried out in our laboratories, should help to confirm our suggestion.

The appearance of the shoulder in the solid reflectance spectrum is indicative of primarily planar bonding[21] rather than the tetragonally distorted octahedral Cu(II) complexes which generally display a single, broad *d–d* band. As is shown in Table 3 dissolution of the complexes in acetonitrile yields spectra with a broad *d–d* band envelope indicating considerable interaction between the solvent and the Cu(II) center with the likely explanation that the CuO_2N_2 chromophore adds solvent molecules in the axial positions. The ESR spectrum of a frozen acetonitrile solution shows a resolved, axial $d_{x^2-y^2}$ ground state spectrum with $g_\parallel = 2.247$, $g_\perp = 2.059$ and $A_\parallel = 166$ G which again suggests axial bonding of the solvent molecules because of the loss of the rhombic spectrum of the solid. Warming this solution, which was frozen immediately upon preparation, gave $g_0 = 2.122$ and $A_0 = 65$ G and, since g_{av} is also equal to 2.122, there is no altering of the nature of the copper (II) site upon freezing. Therefore, we can calculate $A_\perp = 14.5$ G using $A_0 = [(2A_\perp + A_\parallel)3]$. If the solution is allowed to stand for periods of more than an hour, features appear in the frozen solution spectrum which are due to other Cu(II) species and suggest that some substitution for the ligands by solvent molecules occurs.

$Cu(PA)_2(BF_4)_2$. Other than the fact that the tetrafluoroborate salts always have a slightly higher energy maxima for both the main *d–d* band and the low energy shoulder than the corresponding perchlorate solid in this series of complexes, there is little difference between the two solids. Often the $g_\parallel$ value of the powder ESR spectrum is slightly lower and both these differences probably arise from the somewhat poorer donor ability of a fluorine atom compared to an oxygen atom.

$Cu(PA)_2(NO_3)_2$. The IR results indicated that both nitrate ligands were bound in a monodentate fashion to the copper center while the molar conductivity value was indicative of a 1:1 electrolyte. The solid state *d–d* bands are lower in energy than for the previous two solids which can also be indicative of bonding of the anion. Further a typical $d_{x^2-y^2}$ powder ESR spectrum was obtained with $g_\parallel$ in a range more consistent with a tetragonal CuO_2N_2 chromophore[22] than a square planar one.[20]

The same apparent contradiction between the molar conductivity and infrared results was found for $Cu(IPA)_2(NO_3)_2$ and the remaining spectral data for these two solids is virtually identical. We suggest that dissolution does involve dissociation of both nitrate ions from the copper center since the solution *d–d* band is essentially the same as that found for the perchlorate and tetrafluoroborate solutions. The lower conductivity must be a result of some ion pairing probably involving hydrogen bonding, which is not possible with the larger anions. Therefore, both $Cu(PA)_2(NO_3)_2$ and $Cu(IPA)_2(NO_3)_2$ can be considered to be tetragonally elongated octahedral complexes with the nitrate ions weakly coordinated in the axial positions. It is interesting to note that both $Cu(MA)_2(NO_3)_2$ and $Cu(TBA)_2(NO_3)_2$ had "reversed" ESR powder spectra which was suggested to be caused by the presence of inequivalent sites in the unit cell[23] with adjacent copper centers misaligned by 90°[24] for the former[1a] and a compressed octahedron for the latter.[1d] Both of these compounds have molar conductivities that are less than expected for 1:2 electrolytes as well.

$Cu(PA)Cl_2 \cdot H_2O$. Consistent with a broad and weak band centered at 3450 cm^{-1} assignable to a hydrate rather than coordinated water,[25] is an endothermic DSC peak at 124° which is accompanied by a weight loss of 5.2% (Calc. 5.7%). The IR spectrum supports a monomeric $Cu(NO)Cl_2$ chromophore, but the dominance of the intraligand and charge transfer bands in the electronic spectrum makes it difficult to assign the *d–d* bands. The solution electronic and ESR spectra both indicate a substantial change of species (only with methanol were we able to get a sufficiently concentrated solution for the ESR measurement). The powder ESR spectrum has an extremely high value for $g_\perp$, particularly when the rather low value for $g_\parallel$ is considered. Additionally, there is another feature present in the powder spectrum at 77 K (Fig. 2) suggesting either a mixture of monomers or a monomer and a dimer. A third possibility is a cationic species and an anionic species such as $Cu(PA)_2^{2+}$ and $CuCl_4^{2-}$ or $Cu(PA)_2Cl^+$ and $CuCl_3^-$ but the non-electrolytic character in

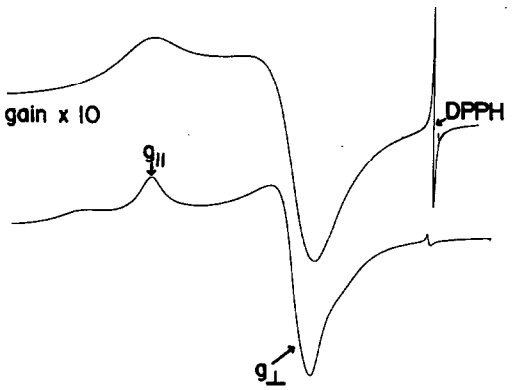


Fig. 2. Powder ESR spectra of $Cu(PA)Cl_2H_2O$ at room temperature (upper) and 77 K (lower).

CH_3CN argues against this possibility. The dominant species, however, is more than likely the 4-coordinate $Cu(PA)Cl_2$ species because the relatively simple IR spectrum is supportive of this structure and a single Cu(II) center.

$Cu(PA)Br_2$. Like $Cu(PA)Br_2$, both $Cu(MA)Br_2$ and $Cu(EA)Br_2$ were violet[1] but $Cu(IPA)Br_2$ and $Cu(TBA)Br_2$ were olive green. The violet color arises from a strong band in the 18 kK region of the visible spectrum. The weak bands at lower energy extending into the near IR are assignable to *d–d* transitions of a tetrahedrally distorted 4-coordinate species. Both $Cu(MA)Br_2$ and $Cu(EA)Br_2$ had rhombic ESR spectra as solids while $Cu(IPA)Br_2$ had an axial spectrum with $g_\parallel = 2.235$, $g_\perp = 2.048$ and $g_{av} = 2.110$. $Cu(PA)Br_2$ has a similar value for g_{av} to the rest of this series but a considerably lower $g_\parallel$ and higher $g_\perp$. This probably is indicative of more covalent bonding of the bromo ligands and the resultant low energy Br→Cu(II) band giving the violet color to $Cu(PA)Br_2$. Recall that $Cu(IPA)Br_2$ is olive green.

In conclusion, PA bonds exclusively as a bidentate ligand via the N-oxide oxygen and the amine nitrogen. While minor differences occur in the spectral properties of the PA complexes when compared to the complexes of MA and EA, these complexes are considerably different from those of IPA. Examples of the differences are the following: a rhombic distortion of the PA complexes with a considerably lower *d–d* band maximum for the perchlorate and tetrafluoroborate salts, the color differences of the nitrate and halogen salts of the two ligands, and the apparent greater covalency of the PA complexes derived from the halogen salts. As indicated earlier we are proceeding to a study of the various N-butyl-2-picolinamine N-oxides to compare with the TBA already reported on[1d] as well as the remainder of the series.[1,2]

REFERENCES

1. D. X. West and R. J. Hartley, *J. Inorg. Nucl. Chem.* 1980, **42**, 1141, 1981, **43**, 963; D. X. West and L. A. McDonald, *J. Inorg. Nucl. Chem.* 1981, **43**, 1507; and D. X. West and K. D. Mariam, *J. Inorg. Nucl. Chem.* 1981, **43**, 2343.
2. D. X. West and R. J. Hartley, *J. Inorg. Nucl. Chem.* 1980, **42**, 711; 1981, **43**, 957.
3. D. X. West and J. S. Sedgwick, *J. Inorg. Nucl. Chem.* 1981, **43**, 2307 and references contained therein.
4. M. Palaniandavar and D. X. West, *Inorg. Chim. Acta* 1983, **71**, 61.
5. W. J. Geary, *Coord. Chem. Rev.* 1971, **7**, 81.
6. S. F. Pavkovic and J. N. Brown, *Acta Cryst.* 1982, **B38**, 274.
7. M. C. R. Symons and D. X. West, unpublished results.
8. S. Kida, J. V. Quaqliano, J. A. Walmsley and S. Y. Tyree, *Spectrochim. Acta* 1963, **19**, 189.
9. C. A. Frank and D. X. West, *J. Inorg. Nucl. Chem.* 1978, **40**, 785.
10. A. R. Katritzky and R. A. Jones, *J. Chem. Soc.* 1959, 3764.
11. T. P. E. Auf der Heyde, C. S. Green, D. S. Needham, D. A. Thornton and G. M. Watkins, *J. Mol. Struct.* 1981, **70**, 121.
12. S. S. Parmer, *Ind. J. Chem.* 1977, **15A**, 459.
13. D. X. West and W-H. Wang, *J. Inorg. Nucl. Chem.*1980, **42**, 985; 1981, 43, 1511.
14. A. B. P. Lever, E. Mantovani and B. S. Ramaswamy, *Can. J. Chem.* 1971, **49**, 1957.
15. R. H. Nutall and D. W. Taylor, *J. Chem. Soc., Chem. Commun.* 1968, 1417.
16. I. S. Ahuja, R. Singh and C. P. Rai, *Trans. Met. Chem.* 1977, **2**, 257; F. A. Devillanova and G. Verani, *Trans. Met. Chem.* 1978, **3**, 42.
17. G. Peyronel and A. C. Fabretti, *J. Coord. Chem.* 1977, **7**, 119.
18. C. A. Frank and D. X. West, *J. Inorg. Nucl. Chem.* 1977, **39**, 793; D. X. West and T. J. Henning, *J. Inorg. Nucl. Chem.* 1978, **40**, 915.
19. J. C. T. Rendell and L. K. Thompson, *Can. J. Chem.* 1979, **57**, 1.
20. H. Yokoi, *Inorg. Chem.* 1978, **17**, 538.
21. S. E. Livingstone and J. E. Oluka, *Trans. Met. Chem.* 1977, **2**, 190.
22. G. Formicka-Kozlowska, H. Kozlowski and B. Jezowska-Trzebiatowska, *Inorg. Chim. Acta* 1977, **25**, 1.
23. W. E. Estes, D. P. Gavel, W. E. Hatfield and D. J. Hodgson, *Inorg. Chem.* 1978, **17**, 1415.
24. A. Murphy, J. Mullane and B. Hathaway, *Inorg. Nucl. Chem. Lett.* 1980, **16**, 129.
25. L. S. Gelfand, L. L. Pytlewski, D. L. Cosgrove, C. M. Mikulski, A. N. Speca and N. M. Karayannis, *Inorg. Chim. Acta* 1979, **32**, 59.

Polyhedron Vol. 4, No. 1, pp. 39–46, 1985
Printed in Great Britain.

0277–5387/85 $3.00 + .00
© 1985 Pergamon Press Ltd.

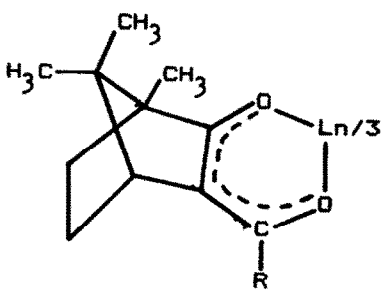
CIRCULARLY POLARIZED LUMINESCENCE STUDIES OF THE ADDUCTS FORMED WITH MIXED-LIGAND Eu(III) β-DIKETONE COMPLEXES AND DIMETHYL SULFOXIDE OR N,N-DIMETHYL FORMAMIDE

HARRY G. BRITTAIN* and C. K. CHAN
Chemistry Department, Seton Hall University, South Orange, NJ 07079, U.S.A.

(*Received* 17 *January* 1984; *accepted* 2 *March* 1984)

Abstract—The adducts formed by $Eu(DK)_2(CDK)$ and $Eu(DK)(CDK)_2$ [DK = achiral β-diketone ligand, and CDK = chiral β-diketone ligand] with either dimethyl sulfoxide (DMSO) or N,N-dimethyl formamide (DMF) have been studied by means of circularly polarized luminescence spectroscopy. While extremely strong stereoselective effects had been observed in earlier studies involving $Eu(CDK)_3$ adducts, analagous phenomena were found to be much smaller in the mixed-ligand compounds. These observations imply that steric interactions involving bulky camphorato ligands are significantly greater than those involving the achiral (and planar) β-diketone ligands.

The determination of enantiomeric purities via NMR spectroscopy involves the use of lanthanide derivatives of chiral β-diketones, many of which are derived from bornan-2-one:



R = $-CF_3$, TFAC
= $-C_3F_7$, HFBC

Applications for the Pr(III) and Eu(III) *tris*-derivatives of TFAC and HFBC have been widespread.[1] In many cases, the lanthanide induced shifts appear to increase in a linear manner as the lanthanide complex is added, but this is not always the case. For instance, the magnitude of the paramagnetic induced shifts has been shown to depend on the stoichiometry of the adduct complex.[2] These dependences are undoubtedly associated with the stereochemical equilibria of the adduct complexes, and any theoretical analysis of induced shifts requires detailed knowledge regarding the adduct in question.

Such information is available from chiroptical studies on the chiral lanthanide compounds, and it has been found that circularly polarized luminescence (CPL) spectroscopy is ideally suited for the stereochemical investigations.[3,4] When either $Eu(TFAC)_3$ [TFAC = (+)-trifluoroacetylcamphor] or $Eu(HFBC)_3$ (HFBC = (+)-3-heptafluoropropylbutyrylcamphor] is dissolved in a non-coordinating solvent, no optical activity can be observed. However, when one forms the adduct complex, strong optical activity is often obtained.[5,6] Similar observations can be made for Tb(III) complexes.[7] This behavior has been studied in detail for sulfoxides, sulfones, and phosphate esters,[8] as well as formamide and acetamide derivatives.[9] Similar results have been noted with Eu(III) derivatives of other chiral β-diketonates.[10]

As a means to study these stereoselective phenomena we have synthesized a series of mixed-ligand Eu(III) complexes containing both chiral and achiral β-diketone ligands, and have reported the chiroptical properties of these in non-coordinating solvents.[11] Compounds having the general formulae $Eu(DK)_2(CDK)$ and $Eu(DK)(CDK)_2$ were prepared, where DK signifies an achiral β-diketone ligand and CDK signifies an inherently chiral β-diketone ligand. It had been noted earlier that adduct formation with the

*Author to whom correspondence should be addressed.

$(EuCDK)_3$ compounds was usually accompanied by the generation of intense optical activity within the Eu(III) emission bands, even though the substrates used to generate the adducts were not chiral. The strongest stereoselective effects were noted in the DMSO adducts,[5,6,8] and the analagous DMF adducts yielded only slightly weaker effects.[5,6,9] Since these effects were thought to result from steric interactions among the bulky camphorato ligands, it was deemed important to observe whether any stereoselectivity could be observed in the DMSO and DMF adducts formed by $Eu(DK)_2(CDK)$ and $Eu(DK)(CDK)_2$. Such studies constitute the present report.

EXPERIMENTAL

The $Eu(DK)_2(CDK)$ and $Eu(DK)(CDK)_2$ compounds used in the present work were prepared as described[11] with the analysis and characterization of these being described therein. In the present work, we shall focus on the compounds where DK = TTFA [4,4,4-trifluoro-1-(2-thienyl)butane-1,3-dionate], DPM [2,2,6,6-tetramethylheptane-3,5-dione], BZAC [benzoylacetone], or DBM [dibenzoylmethane]. As in the earlier works, we will consider only CDK = TFAC or HFBC. The ligands used to prepare the mixed-ligand compounds were used as received from Aldrich. Dimethyl formamide (DMF) and dimethyl sulfoxide (DMSO) were obtained as spectroquality solvents, and were used as received. Stock solutions of each material made up in spectrograde $CHCl_3$, and titrations were carried out in which the substrates were added to $CHCl_3$ solutions of the Eu(III) chelates. These titration procedures have been adequately summarized in our earlier work.[7-10] All measurements were thus performed in $CHCl_3$ solution at room temperature.

All CPL and TL (total luminescence) measurements were obtained on apparatus constructed in our laboratory. In most cases, the 365 nm output of a 200 W Hg–Xe arc lamp was used to excite the complexes. This wavelength was selected by a combination of a 0.1 m grating monochromator and UV-transmitting filters. Measurements of the TL and CPL spectra were carried out simultaneously within the $^5D_0 \rightarrow {}^7F_J$ (J = 0, 1, 2) band systems associated with the Eu(III) ion. The emission was analyzed by a 0.5 m grating monochromator at 5 Å resolution, and it was determined that further increases in resolving power did not yield any significant improvement in the spectral features.

The chiroptical measurements produce two quantities normally measured in arbitrary units. The total luminescence (TL), defined by:

$$I = I_L + I_R \tag{1}$$

and the circularly polarized luminescence, defined by:

$$\Delta I = I_L - I_R. \tag{2}$$

In eqns (1) and (2), I_L and I_R represent the emitted intensities of left- and right-circularly polarized light, respectively. One may remove the unit dependence associated with I and ΔI by taking the ratio of these, and this quantity is termed the luminescence dissymmetry factor:[3]

$$g_{lum} = \Delta I/(1/2)I \tag{3}$$

The g_{lum} factor has theoretical as well as experimental significance in that it may be related to the rotational strength of the transition.[3]

RESULTS AND DISCUSSION

In non-coordinating solvents, one may speak of an $Eu(DK)_3$ compound, but in coordinating solvents one deals with adduct complexes. Upon interaction with a substrate, S, the formation of 1:1 adducts:

$$Eu(DK)_3 + S \rightleftharpoons Eu(DK)_3(S) \tag{4}$$

and 1:2 adducts:

$$Eu(DK)_3 + 2S \rightleftharpoons Eu(DK)_3(S)_2 \tag{5}$$

may be observed. When the substrate is optically active, then chirality may be observed in the f–f emission bands of the Eu(III) ion.[4]

The phenomena associated with the $Eu(CDK)_3$ complexes are more complicated. Since the CDK ligands are inherently chiral, preparation of the $Eu(CDK)_3$ compound results in the formation of four diastereomers. In $CHCl_3$ solution one would anticipate that these would be formed in roughly equivalent amounts, since these compounds are exceedingly labile. The analogous diastereomers of inert transition metal complexes have been resolved,[12,13] and it has been found that the chirality of the Δ isomers is essentially equal in magnitude and opposite in sign to that of the Λ isomers. Thus, in a solution containing equal amounts of the various stereoisomers, one should not be able to observe any optical activity. This has been found to be the case,[5,6] indicating that in non-coordinating solvents the camphorato ligands do not sterically crowd each other. Upon formation of

the adduct complexes:

$$Eu(CDK)_3 + S \rightleftharpoons Eu(CDK)_3(S) \quad (6)$$

$$Eu(CDK)_3 + 2S \rightleftharpoons Eu(CDK)_3(S)_2 \quad (7)$$

one would anticipate that the bulky camphorato ligands would be forced to interact more in the adduct complexes, and the complexes ought to adopt the configurations of lower energy. This process would effectively constitute a partial resolution, and should result in the observation of optical activity within the f–f bands. Such predictions have been verified.[5–10]

The rather low absorptivities of the Eu(III) f–f transitions make the measurement of circular dichroism difficult, but fortunately one may also study f–f optical activity by means of CPL spectroscopy. Excitation of Eu(III) β-diketone complexes by near-UV radiation can result in the observation of strong luminescence in the red region of the spectrum. This emission consists of a series of well-resolved transitions from the excited $^5D_0$ level to the ^7F_J levels of the ground state. We shall henceforth label the spectroscopic transitions by their defining J quantum numbers, and have observed the 0–0 (580 nm), 0–1 (595 nm), and 0–2 (615 nm) bands during the course of our work. CPL within the 0–0 transition is not permitted,[3] but strong CPL was normally observed within the 0–1 and 0–2 transitions.

$Eu(DK)_2(CDK)$ series

In non-coordinating solvents, reasonably strong CPL spectra were obtained for $Eu(DPM)_2(HFBC)$, $Eu(BZAC)_2(HFBC)$, $Eu(DBM)_2(HFBC)$, and $Eu(TTFA)_2(HFBC)$,[11] and the CPL spectra were not found to vary greatly with the identity of the DK ligand. This behavior stands in sharp contrast to that noted for $Eu(TFAC)_3$ or $Eu(HFBC)_3$, where *no* CPL can be obtained in non-coordinating solvents for the reasons just mentioned. With only one chiral ligand present per Eu(III) ion, one would predict that only the vicinal effect would contribute to the metal ion optical activity. This effect represents the chirality resulting when dissymmetry is induced at the Eu(III) ion by the presence of an asymmetric carbon on one of the β-diketone ligands. In the absence of adduct formation, one would not expect to observe significant configurational effects (chirality resulting from the dissymmetric placement of chelate

Table 1. Luminescence dissymmetry factors and CPL wavelength maxima obtained for the $Eu(DK)_2(HFBC)$ compounds, and their DMF and DMSO adducts

DK	$CHCl_3$	DMSO	DMF
a) $^5D_0 \rightarrow {}^7F_1$ $[g_{lum} \times 10^2]$			
BZAC	-4.47 (593)	-2.36 (593)	-2.48 (593)
DBM	-5.33 (593)	-5.54 (593)	-5.77 (593)
DPM	-6.72 (593)	-8.53 (593)	-8.26 (593)
TTFA	-2.02 (593)	-0.75 (589) -0.50 (593)	-2.75 (593)
b) $^5D_0 \rightarrow {}^7F_2$ $[g_{lum} \times 10^3]$			
BZAC	2.96	2.25	3.11
DBM	3.86	4.01	4.12
DPM	10.22	13.4	10.70
TTFA	2.63	2.29 -1.94 3.03	3.56

Notes: All data was obtained in $CHCl_3$ solution, and the dissymmetry factors represent limiting values. The wavelength maxima of the 0-1 CPL bands are given in nanometers.

rings about a metal ion). It should be noted that the $Eu(DK)_2(TFAC)$ compounds could not be studied as the emission intensity of these was too weak to permit the observation of CPL.

The alterations in photophysical parameters upon adduct formation were found to vary somewhat as the DK ligands were varied. When DK = DBM or DPM, it was found that the TL intensities increased only slightly upon formation of the adduct complexes. At the same time, no change was observed in the CPL lineshapes and the intensities of these (as measured by the dissymmetry factors) increased slightly. On the other hand, when DK = BZAC it was found that both the TL and CPL intensities underwent significant decreases upon formation of the DMSO or DMF adducts. As before, the CPL lineshape did not change. The dissymmetry factors obtained for the free complexes and the adducts may be found in Table 1.

Very different behavior was observed in the case of DK = TTFA. A considerable increase in the TL intensity was noted when forming the DMF or DMSO adducts. With DMF, the optical activity was found to increase somewhat, but there was no change in the CPL lineshape. However, when forming the DMSO adduct, a considerable change was observable in the CPL spectrum. Examples of these changes have been provided in Figs. 1 and 2.

The CPL spectra associated with the DMSO adduct appear to consist of a superposition of the DMF lineshapes and the lineshapes of a new

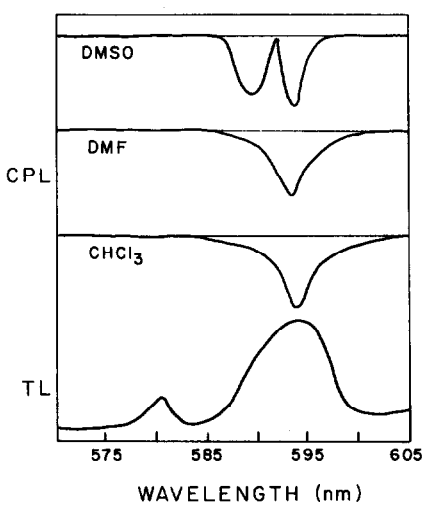


Fig. 1. Circularly polarized luminescence spectra obtained for $Eu(TTFA)_2(HFBC)$ dissolved in $CHCl_3$, and for its DMF and DMSO adducts. The data cover the $^5D_0 \rightarrow {}^7F_0$, $^7F_1$ transitions. The total luminescence lineshape of each compound is essentially the same, and is shown as the lowest trace. The data are shown in arbitrary units.

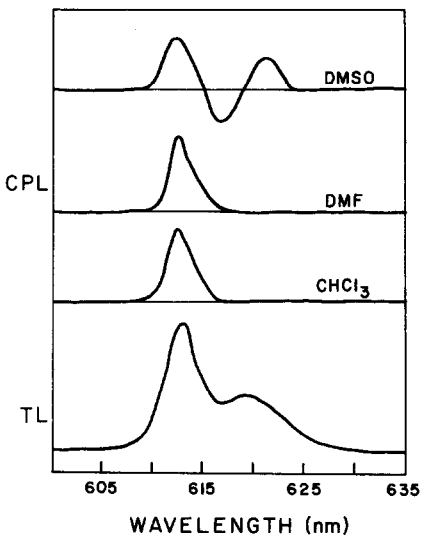


Fig. 2. Circularly polarized luminescence spectra obtained for $Eu(TTFA)_2(HFBC)$ dissolved in $CHCl_3$, and for its DMF and DMSO adducts. The data cover the $^5D_0 \rightarrow {}^7F_2$ transitions. The total luminescence lineshape of each compound is essentially the same, and is shown as the lowest trace.

species. It appears that upon addition of sufficient amounts of DMSO or DMF 1:2 Eu $(CDK)_3$/substrate adducts form.[14] The two substrates could bind *cis* or *trans* to each other depending on the overall steric requirements of the Eu(III) complex, and it is entirely possible that equal amounts of these coexist in the DMSO adduct. The other adducts apparently exhibit much more of a stereochemical preference, and consequently the CPL spectra indicate the presence of only one compound.

$Eu(DK)(CDK)_2$ series

When two chiral β-diketone ligands are bound by a single lanthanide ion, one would expect that a combination of vicinal and configurational effects would play a role in determining the chirality at the metal ion. Depending on the steric requirements of the compounds, a variety of possibilities might result. In non-coordinating solvents, the dissymmetry factors of the $Eu(DK)(CDK)_2$ compounds happened to be smaller than those of the analagous $Eu(DK)_2(CDK)$ compounds, and when DK = BZAC the CPL lineshapes were actually opposite to those of the other complexes.[11] These observations all indicate that the chirality of the $Eu(DK)(CDK)_2$ compounds cannot be taken as a simple summation of two vicinal effects, and indicate that the observed optical activity contains a strong configurational contribution. However, these configurational effects were found to be considerably smaller than those noted in the

DMSO or DMF adducts of $Eu(CDK)_3$ complexes.[5,6]

Formation of the DMF or DMSO adducts of $Eu(DBM)(TFAC)_2$ led to a doubling of the TL intensities, and a marked decrease in the CPL intensities. For the $Eu(DPM)(TFAC)_2$ or $Eu(TTFA)(TFAC)_2$ compounds, formation of the DMSO adducts also led to sizable increases in the TL intensities, but to a total disappearance of the CPL spectra. These results indicate that significant stereochemical alterations can accompany the formation of the adduct complexes in the $Eu(DK)(CDK)_2$ series.

The $Eu(BZAC)(TFAC)_2$ compound was unique in that its CPL spectra were found to be opposite in sign to those of the rest of the $Eu(DK)(TFAC)_2$ series. The DMF adduct of this compound exhibited behavior quite like that of $Eu(DBM)(TFAC)_2$, but formation of the DMSO adduct led to an inversion of the CPL spectra. These effects have been illustrated in Fig. 3 and 4. This latter phenomenon suggests that the decrease in CPL intensities noted with DK = DBM, DPM, or TTFA is associated with formation of significant amounts of adducts whose CPL sign patterns are opposite to those of the parent compounds.

The dissymmetry factors corresponding to the entire series where CDK = TFAC have been collected in Table 2.

The trends observed with the $Eu(DK)(HFBC)_2$ compounds were found to be quite different from

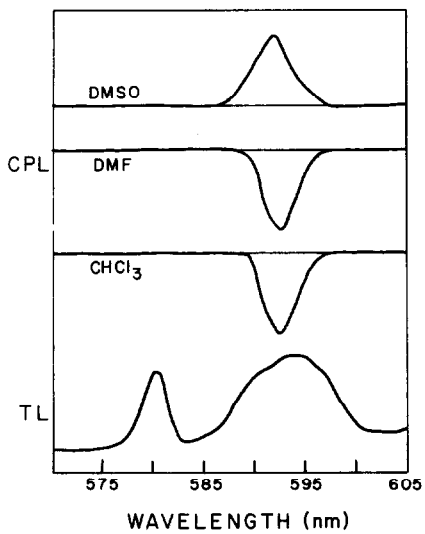


Fig. 3. Circularly polarized luminescence spectra obtained for $Eu(BZAC)(TFAC)_2$ dissolved in $CHCl_3$, and for its DMF and DMSO adducts. The data cover the $^5D_0 \rightarrow {}^7F_0$, $^7F_1$ transitions. The total luminescence lineshape of each compound is essentially the same, and is shown as the lowest trace.

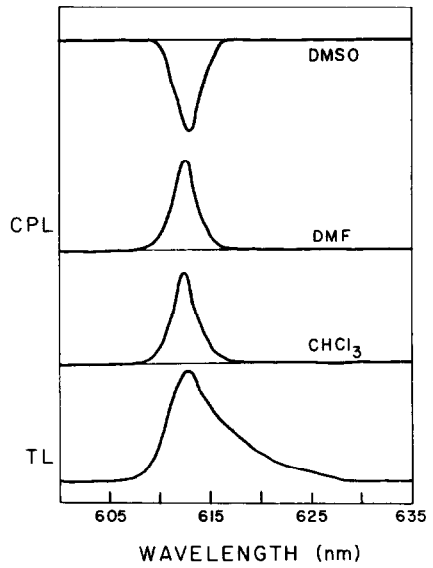


Fig. 4. Circularly polarized luminescence spectra obtained for $Eu(BZAC)(TFAC)_2$ dissolved in $CHCl_3$, and for its DMF and DMSO adducts. The data cover the $^5D_0 \rightarrow {}^7F_2$ transition. The total luminescence lineshape of each compound is essentially the same, and is shown as the lowest trace.

those found for the $Eu(DK)(TFAC)_2$ complexes. With the $Eu(BZAC)(HFBC)_2$, $Eu(DBM)(HFBC)_2$, and $Eu(DPM)(HFBC)_2$ compounds, formation of the DMSO or DMF adducts led to very small changes in the TL intensities. The CPL intensities were found to undergo only small decreases upon formation of the adduct complexes, and the luminescence dissymmetry factors obtained when CDK = HFBC are found in Table 3. Even though the CPL lineshapes obtained for DK = DBM were opposite to those found for DK = BZAC or DPM, the presence of a general trend indicates similar behavior. The decrease in CPL intensity probably reflects the formation of small amounts of a stereoisomer whose chirality is opposite to that of the parent complexes.

The CPL spectrum of $Eu(TTFA)(HFBC)_2$ dissolved in $CHCl_3$ does not resemble that of any of the other $Eu(DK)(HFBC)_2$ complexes, and in fact appears to represent the contributions made by two emitting species. This situation would thus be very much like that seen earlier for $Eu(TTFA)_2(HFBC)$, although the wavelength maxima of the CPL bands were observed to be very different in the two systems.

Formation of the DMF or DMSO adducts of $Eu(TTFA)(HFBC)_2$ led to large enhancements in the TL intensities. While formation of the DMF adduct led to reductions in the CPL intensities, the two CPL peaks were not found to decrease by the same amount. Such an observation would be con-

Table 2. Luminescence dissymmetry factors and CPL wavelength maxima obtained for the $Eu(DK)(TFAC)_2$ compounds, and their DMSO and DMF adducts

DK	$CHCl_3$	DMSO	DMF
a) $^5D_0 \rightarrow {}^7F_1$ $[g_{lum} \times 10^2]$			
BZAC	-7.43 (593)	1.02 (593)	-2.05 (593)
DBM	5.64 (593)	1.78 (593)	2.46 (593)
DPM	3.88 (593)	0.00	0.00
TTFA	1.23 (593)	0.00	0.00
b) $^5D_0 \rightarrow {}^7F_2$ $[g_{lum} \times 10^3]$			
BZAC	5.85	-1.96	3.04
DBM	-7.30	-1.79	-2.78
DPM	-5.25	0.00	0.00
TTFA	-1.58	0.00	0.00

Notes: All data were obtained in $CHCl_3$ solution, and the dissymmetry factors represent limiting values. The wavelength maxima of the 0-1 CPL bands are given in nanometers.

Table 3. Luminescence dissymmetry factors and CPL wavelength maxima obtained for the $Eu(DK)(HFBC)_2$ compounds, and their DMSO and DMF adducts

DK	$CHCl_3$	DMSO	DMF
a) $^5D_0 \rightarrow {}^7F_1$ $[g_{lum} \times 10^2]$			
BZAC	-5.92 (593)	-2.49 (593)	-3.20 (593)
DBM	3.29 (593)	1.05 (593)	1.48 (593)
DPM	-8.96 (593)	-5.23 (593)	-6.89 (593)
TTFA	-2.17 (588) -5.03 (597)	-1.33 (588) 1.45 (593)	-1.04 (588) -1.45 (597)
b) $^5D_0 \rightarrow {}^7F_2$ $[g_{lum} \times 10^3]$			
BZAC	4.91	3.75	2.93
DBM	-5.19	-3.08	-2.41
DPM	7.20	5.94	7.50
TTFA	9.20 -4.46	-2.80 4.70	2.45 -2.27

Notes: All data were obtained in $CHCl_3$ solution, and the dissymmetry factors represent limiting values. The wavelength maxima of the 0-1 CPL bands are given in nanometers.

sistent with the existence of two species in solution, each of which experienced differing perturbations upon adduct formation. Formation of the DMSO adduct led to rather dramatic changes in the CPL spectra, as has been shown in Figs. 5 and 6. Once again it was found that the process of adduct formation affected each CPL peak in a different manner: the band at lower wavelength was scarcely affected, but the peak at higher wavelength was replaced by a band of opposite sign.

The dissymmetry factors corresponding to the compounds having CDK = HFBC have been collected in Table 3.

CONCLUSIONS

That formation of adduct complexes can greatly affect the stereochemistry of Eu(III) β-diketone compounds has been amply demonstrated. In addition, it has been shown that multiple emitting species are capable of coexisting in solution under a given set of conditions. The particular distribution of these is dictated by the nature of the β-diketone ligands, and by the steric requirements of the substrates.

A determination of the wavelengths associated with the CPL maxima within the 0–1 transitions proved illuminating. For each of the $Eu(DK)_2(CDK)$ or $Eu(DK)(CDK)_2$ compounds (either the free complex or the adduct), CPL maxima were only observed at three wavelengths (as indicated in the tables). The CPL observed at each maximum could be either positive or negative in sign, depending on the particular complex and substrate in question. It was often observed that formation of the adduct complex diminished the observed optical activity of several of the Eu(III) complexes. We may interpret this result to imply that the process of adduct formation could result in the stabilization of the other epimer, and that these could coexist under those conditions. This explanation would in turn explain the variability observed in the dissymmetry factors obtained with the $Eu(DK)_2(HFBC)$ compounds, even though here the chirality of the complex was due only to the presence of a single vicinal effect. In most cases only a single conformation did predominate, but varying amounts of the other enantiomer were also present. The degree of stereoselectivity would naturally be dictated by the particular nature of the β-diketone ligand. Similar arguments could be advanced to explain the variabilities found in the chiralities of the $Eu(DK)(CDK)_2$ compounds.

It has been found that $Eu(DK)_3(S)_2$ adducts generally adopt the coordination polyhedron of a square antiprism.[15] Within this constraint, three structures are possible for the adduct complexes, and these have been illustrated elsewhere.[10] The presence of differing β-diketone ligands (most of which are not symmetrical) within these polyhedra will lead to the production of a large number of diastereomers. However, it is probably true that

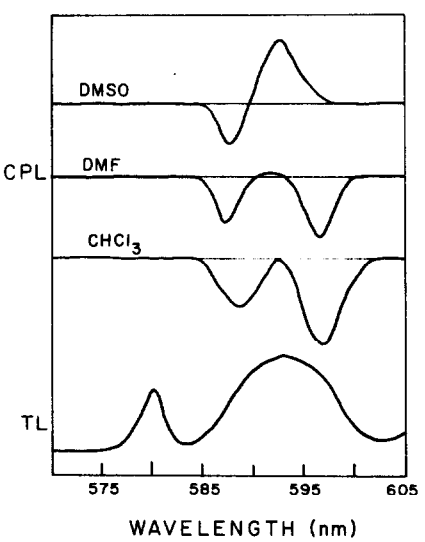


Fig. 5. Circularly polarized luminescence spectra obtained for $Eu(TTFA)(HFBC)_2$ dissolved in $CHCl_3$, and for its DMF and DMSO adducts. The data cover the $^5D_0 \rightarrow {}^7F_0$, $^7F_1$ transitions. The total luminescence lineshape of each compound is essentially the same, and is shown as the lowest trace.

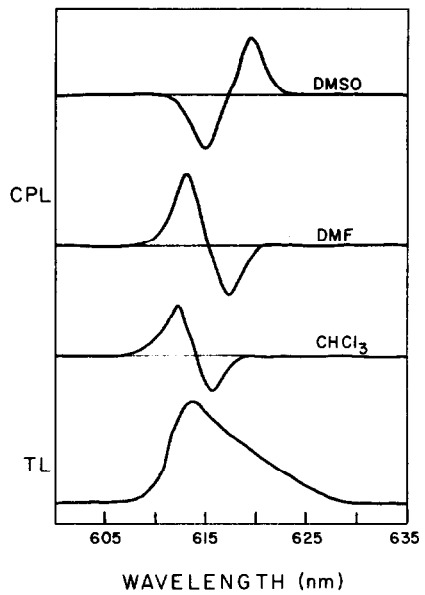


Fig. 6. Circularly polarized luminescence spectra obtained for $Eu(TTFA)(HFBC)_2$ dissolved in $CHCl_3$, and for its DMF and DMSO adducts. The data cover the $^5D_0 \rightarrow {}^7F_2$ transition. The total luminescence lineshape of each compound is essentially the same, and is shown as the lowest trace.

the chiroptical properties at the Eu(III) ion are determined primarily by the dissymmetric placement of the ligands (configurational effects). In that case, it should ultimately be possible to identify each of the three basic square antiprisms as leading to a particular CPL lineshape. Each of these conformations would in turn be capable of existing as either of its two epimers, and the stereoisomer populations consequently determine the magnitude of any observed optical activity.

It was noted in the earlier work[5,6,8,9] that stereoselective effects observed in $Eu(CDK)_3$ complexes were much greater in DMSO adducts relative to those obtained in DMF adducts. This trend has continued in the mixed-ligand complexes. In any situation where the conformational equilibria could be altered, such alterations were found to be induced by the DMSO solvent. DMF adducts generally resembled the free compounds quite closely. These trends indicate that the DMSO substrate is more sterically demanding than is the DMF substrate.

A final note concerns the degree of stereoselectivity in the mixed-ligand complexes relative to that observed in the $Eu(CDK)_3$ compounds. Extremely large stereoselective effects were observed in the DMSO and DMF adducts of the $Eu(CDK)_3$ compounds, and this effect was attributed to the existence of large steric interactions among the CDK ligands upon adduct formation. Replacement of one CDK ligand by a DK ligand greatly reduces the magnitude of these effects, and replacement of another CDK ligand by a DK ligand essentially reduces the stereoselective effects to nothing. These trends imply that the achiral DK ligands possess considerably smaller steric requirements than do the bulky CDK ligands. Consequently, the compounds containing higher amounts of DK ligands would more readily form adducts with bulky substrates than would Eu(III) compounds having higher amounts of CDK ligands.

Acknowledgement—This work was supported by the Camille and Henry Dreyfus Foundation, through a Teacher–Scholar award to HGB.

REFERENCES

1. G. R. Sullivan, *Topics in Stereochemistry* 1978, **10**, 287.
2. H. L. Goering, J. N. Eikenberry, G. S. Koermer and C. J. Lattimer, *J. Am. Chem. Soc.* 1974, **96**, 1493.
3. F. S. Richardson and J. P. Riehl, *Chem. Rev.* 1977, **77**, 773.
4. H. G. Brittain, *Coord. Chem. Rev.* 1983, **48**, 243.
5. H. G. Brittain and F. S. Richardson, *J. Am. Chem. Soc.* 1976, **98**, 5858.
6. H. G. Brittain and F. S. Richardson, *J. Am. Chem. Soc.* 1977, **99**, 65.
7. H. G. Brittain, *Inorg. Chem.* 1980, **19**, 2233.
8. H. G. Brittain, *Polyhedron* 1983, **2**, 261.
9. H. G. Brittain, *J. Chem. Soc. Dalton Trans.* 1982, 2059.
10. H. G. Brittain, *J. Chem. Soc. Dalton Trans.* 1983, 1165.
11. C. K. Chan and H. G. Brittain, *J. Inorg. Nucl. Chem.* 1981, **43**, 2399.
12. C. S. Springer, Jr., R. E. Sievers and B. Feibush, *Inorg. Chem.* 1974, **10**, 1242.
13. R. M. King and G. W. Everett, Jr., *Inorg. Chem.* 1971, **10**, 1237; 1972, **11**, 2041.
14. H. G. Brittain, *J. Am. Chem. Soc.* 1979, **101**, 1733.
15. S. P. Sinha, *Structure and Bonding* 1976, **25**, 69.

Polyhedron Vol. 4, No. 1, pp. 47–51, 1985
Printed in Great Britain.

0277–5387/85 $3.00 + .00
© 1985 Pergamon Press Ltd.

IONIC EQUILIBRIA IN FERRIC SULFATE–SULFURIC ACID SOLUTIONS

C. K. LEE and L. L. TAVLARIDES*
Department of Chemical Engineering and Materials Science, Syracuse University, Syracuse, NY 13210, U.S.A.

(*Received* 5 *January* 1984; *accepted* 2 *March* 1984)

Abstract—The ionic equilibria of ferric sulfate–sulfuric acid aqueous solution are modeled mathematically, taking into account the effect of ionic strength. Results of this analysis indicate that ion interactions can significantly change the ionic concentration of the solutions which could lead to errors in the evaluation of data on iron(III) extraction kinetics or equilibrium.

Equilibrium and kinetic studies of iron(III) extraction by organic chelating agents have been widely investigated[1–7] because of the practical importance of these reactions in the hydrometallurgical field. In the extraction of metals such as copper, uranium, cobalt, and nickel from their leach solutions, iron(III) is typically present as an impurity. Therefore, to properly analyze selective nonferrous metal extraction, it is necessary to model the iron(III) speciation in the aqueous phase. Various investigators have assumed that only the ferric ion (Fe^{3+}) is extracted during iron(III) extraction,[5,7] such as iron(III) nitrate extraction by 8-hydroxy quinoline. However, other researchers[1,4,6] suggest that both Fe^{3+} and $FeOH^{2+}$ are simultaneously extracted by the organic reagent, such as oximes and tri-*n*-butylacetohydroxamic acid. Thus, regardless of which iron species is extracted, it is necessary to have an accurate estimate of the reactive species concentration in the aqueous phase in order to develop an accurate equilibrium and/or kinetic model for the two-phase extraction system.

In a recent work, Freeman and Tavlarides[8] developed a model for estimating the equilibrated ionic species concentration in the copper sulfate–sulfuric acid system. This model considers the coupling of the copper sulfate ion-pair dissociation and the bisulfate ion dissociation in aqueous solution. The analysis includes the effects of ionic strength and temperature. These results have been successfully applied to model the chemical equilibrium of the copper(II)-sulfate/β-alkenyl-8-hydroxy quinoline extraction system.[9] For iron(III) extracted by an organic chelating agent, few published works consider the ionic equilibria in the aqueous phase. Typically, the reactant in the aqueous phase is obtained by assuming complete dissociation of the iron salt in solution. The concentration of the ferric ion is then regarded as either equal or proportional to the $[Fe]^T$. Indeed, iron(III) exists as at least seven species in the acid sulfate system. Dousma *et al.*[10] presented an equilibrium model for the iron(III) system which considered the influence of sulfate ions on the formation of iron oxides. The model, however, does not properly account for the variation of the stability constant as a function of ionic strength. The purpose of this work is to present a comprehensive model for the ferric sulfate–sulfuric acid aqueous phase ionic equilibria in which the effect of ionic strength is considered. The model employs a straightforward mathematical calculation to predict the concentrations of ionic species.

AQUEOUS IONIC EQUILIBRIA

Models for the ferric sulfate dissociation and its related ionic species equilibria can be developed from the information available in the literature. There are many ionic equilibrium relationships that may be used to depict the speciation in the iron(III) acid sulfate solution. However, the work by Dousma *et al.*[10] indicates that only some of the equilibria need to be considered. The pertinent reactions for the aqueous phase equilibria of ferric sulfate–sulfuric acid solution can be represented by the following nine equations.

*Author to whom correspondence should be addressed.

$$Fe_2(SO_4)_3 \overset{k_1}{\rightleftharpoons} 2Fe^{3+} + 3SO_4^{2-} \quad (1)$$

$$HSO_4^- \overset{k_2}{\rightleftharpoons} H^+ + SO_4^{2-} \quad (2)$$

$$Fe^{3+} + SO_4^{2-} \overset{k_3}{\rightleftharpoons} FeSO_4^+ \quad (3)$$

$$Fe^{3+} + HSO_4^- \overset{k_4}{\rightleftharpoons} FeHSO_4^{2+} \quad (4)$$

$$Fe^{3+} + 2SO_4^{2-} \overset{k_5}{\rightleftharpoons} Fe(SO_4)_2^- \quad (5)$$

$$Fe^{3+} + H_2O \overset{k_6}{\rightleftharpoons} FeOH^{2+} + H^+ \quad (6)$$

$$2FeOH^{2+} \overset{k_7}{\rightleftharpoons} Fe(OH)_2Fe^{4+} \quad (7)$$

$$Fe^{3+} + 2H_2O \overset{k_8}{\rightleftharpoons} Fe(OH)_2^+ + 2H^+ \quad (8)$$

$$H_2O \overset{k_9}{\rightleftharpoons} H^+ + OH^-. \quad (9)$$

Of these nine reactions, the first is assumed to dissociate completely into Fe^{3+} and SO_4^{2-} in the aqueous solution because of the strong electrolytic behavior of ferric sulfate. Therefore, only eight equilibrium relations need to be considered. Concentrations of the ferric ion, hydrogen ion, and other ionic species are estimated by modeling the aqueous phase mathematically. In addition to the equilibria expressed in eqns (2)–(9), the mass balances of the total sulfur and iron concentrations, and the electroneutrality of the solution are also considered. Accordingly, the following set of eleven nonlinear algebraic equations can be obtained:

HSO_4^- *dissociation*

$$k_2 = \frac{[HSO_4^-]}{[H^+][SO_4^{2-}]}. \quad (10)$$

$FeSO_4^+$ *formation*

$$k_3 = \frac{[FeSO_4^+]}{[Fe^{3+}][SO_4^{2-}]}. \quad (11)$$

$FeHSO_4^{2+}$ *formation*

$$k_4 = \frac{[FeHSO_4^{2+}]}{[Fe^{3+}][HSO_4^-]}. \quad (12)$$

$Fe(SO_4)_2^-$ *formation*

$$k_5 = \frac{[Fe(SO_4)_2^-]}{[Fe^{3+}][SO_4^{2-}]^2} \quad (13)$$

$FeOH^{2+}$ *formation*

$$k_6 = \frac{[FeOH^{2+}][H^+]}{[Fe^{3+}]}. \quad (14)$$

$Fe(OH)_2Fe^{4+}$ *formation*

$$k_7 = \frac{[Fe(OH)_2Fe^{4+}]}{[FeOH^{2+}]^2}. \quad (15)$$

$Fe(OH)_2^+$ *formation*

$$k_8 = \frac{[Fe(OH)_2^+][H^+]^2}{[Fe^{3+}]}. \quad (16)$$

H_2O *dissociation*

$$k_9 = [H^+][OH^-]. \quad (17)$$

Sulfate balance

$$[S]^T = [SO_4^{2-}] + [HSO_4^-] + [FeSO_4^+] + [FeHSO_4^{2+}] + 2[Fe(SO_4)_2^-]. \quad (18)$$

Iron balance

$$[Fe]^T = [Fe^{3+}] + [FeSO_4^+] + [FeHSO_4^{2+}] + [Fe(SO_4)_2^-] + [FeOH^{2+}] + 2[Fe(OH)_2Fe^{4+}] + [Fe(OH)_2^+]. \quad (19)$$

Electroneutrality

$$[H^+] + 3[Fe^{3+}] + [FeSO_4^+] + 2[FeHSO_4^{2+}] + 2[FeOH^{2+}] + 4[Fe(OH)_2Fe^{4+}] + [Fe(OH)_2^+] = 2[SO_4^{2-}] + [HSO_4^-] + [Fe(SO_4)_2^-] + [OH^-]. \quad (20)$$

Equations (10)–(20) can be combined with the ionic strength relationship

$$I = \frac{1}{2}\sum_{j=1}^{n} (z_j)^2 C_j \quad (21)$$

for constant values of k_i, $i = 2,9$, to obtain four nonlinear algebraic equations:

$$[Fe]^T - [S]^T - [Fe^{3+}] + [SO_4^{2-}] + k_2[H^+][SO_4^{2-}] + k_5[Fe^{3+}][SO_4^{2-}]^2 - k_6[Fe^{3+}]/[H^+] - 2k_7k_6^2[Fe^{3+}]^2/[H^+]^2 - k_8[Fe^{3+}]/[H^+]^2 = 0 \quad (22)$$

$$2[Fe]^T + [H^+] - 2[SO_4^{2-}] - k_2[H^+][SO_4^{2-}] + [Fe^{3+}] - k_3[SO_4^{2-}][Fe^{3+}] - 3k_5[Fe^{3+}][SO_4^{2-}]^2 - k_8[Fe^{3+}]/[H^+]^2 - k_9/[H^+] = 0 \quad (23)$$

$$[S]^T - [SO_4^{2-}] - k_2[H^+] - k_3[Fe^{3+}][SO_4^{2-}] - k_2k_4[H^+][SO_4^{2-}][Fe^{3+}] - 2k_5[Fe^{3+}][SO_4^{2-}]^2 = 0 \quad (24)$$

$$I - \frac{1}{2}([H^+] + 4[SO_4^{2-}] + k_2[H^+][SO_4^{2-}] + 9[Fe^{3+}] + k_3[SO_4^{2-}][Fe^{3+}] + 4k_2k_4[H^+][SO_4^{2-}][Fe^{3+}] + k_5[Fe^{3+}][SO_4^{2-}]^2 + 4k_6[SO_4^{2-}]/[H^+] + 16k_7k_6^2[SO_4^{2-}]^2/[H^+]^2 + k_8[Fe^{3+}]/[H^+] + k_9/[H^+]) = 0. \quad (25)$$

The dependence of the stability constants k_2–k_9 on ionic strength is included in this formulation. The correlations[11–18] for stability constants applied here for model computations at 25°C are

$$k_2 = (1/0.0104)\exp\{-5.29\sqrt{I}/(1 + 0.56\sqrt{I})\} \quad (26)$$

$$\log k_3 = 4.04 - 6\sqrt{I}/(1 + 1.7\sqrt{I}) + 0.233I \quad (27)$$

$$k_4 = 6 - 1.36(I - 1.2) \quad (28)$$

$$\log k_5 = \log k_3 + 1.34 - 2\sqrt{I}/(1 + 1.9\sqrt{I}) - 0.077I \quad (29)$$

$$\log(k_6/6.5 \times 10^{-3}) = -2.04\sqrt{I}/(1 + 2.5\sqrt{I}) + 0.01I \quad (30)$$

$$\log k_7 = 1.46 + 4.08\sqrt{I}/(1 + 2.1\sqrt{I}) + 0.075I \quad (31)$$

$$k_8 = 7 \times 10^{-8} + 1.4 \times 10^{-7}I \quad (32)$$

$$k_9 = 10^{-14}. \quad (33)$$

These stability constants, which are dependent on ionic strengths, are substituted into eqns (22)–(25) to solve for the independent variables $[H^+]$, $[SO_4^{2-}]$, $[Fe^{3+}]$, and the ionic strength I. The Secant method [19] is employed here. The roots of the equations must be positive and the resulting values for concentrations must be physically meaningful. Otherwise, the initial approximated values of the roots must be adjusted to obtain the proper set of roots.

RESULTS AND DISCUSSION

The results of computation presented here for ferric sulfate–sulfuric acid solutions are a general case based on assumed values for the total iron and total sulfur concentrations.

Figure 1 shows the concentration profiles of iron ionic species in the aqueous phase as a function of total sulfur concentration at a constant total iron concentration 0.003M. It can be noted here that $FeSO_4^+$ is the dominant iron species existing in the aqueous phase. The concentration of other sulfate-bearing iron species is lower than that of $FeSO_4^+$. At high total sulfur concentration ($\sim 10^{-1}$mol/dm^3), the concentration of $FeOH^{2+}$ is much lower than that of Fe^{3+}. However, at low sulfur concentration ($\sim 10^{-3}$mol/dm^3), the concentration of these two iron species are of the same magnitude. The concentration of $FeOH^{2+}$ becomes larger than that of Fe^{3+} below a certain low-level concentration of sulfur ($< 7 \times 10^{-3}$mol/dm^3). The concentrations of other hydroxy-bearing iron species, $Fe(OH)_4Fe^{4+}$, and $Fe(OH)_2^+$, are at least an order of magnitude lower than that of Fe^{3+}. These concentrations are decreased precipitously as the sulfur concentration increases. The composition of Fe^{3+} in the solution is about 2–7% of the total iron concentration. Further, the Fe^{3+} concentration is not linearly related to the total iron present in the solution.

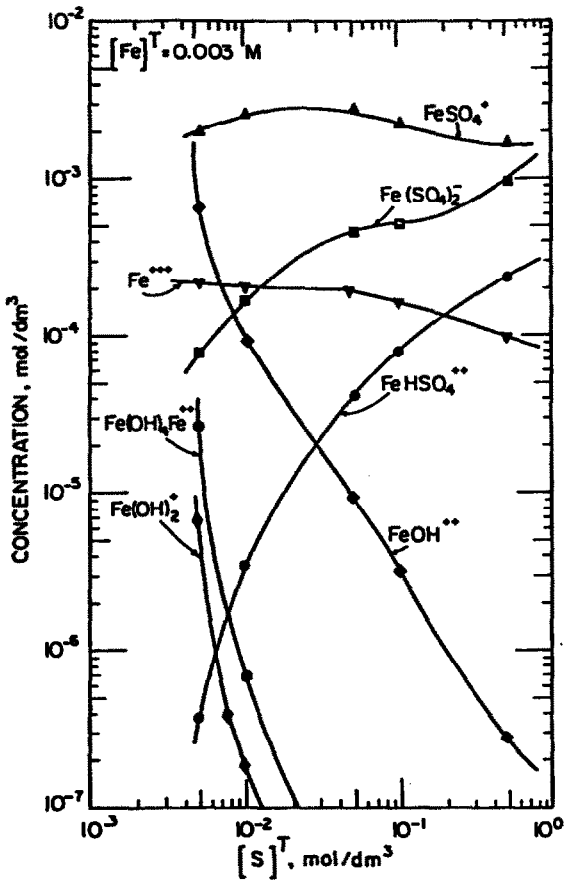


Fig. 1. Concentration profiles of various iron ionic species as a function of total sulfur concentration at a constant total iron concentration of 0.003 mol/dm^3.

Figure 2 shows the dependence of hydrogen ion on the total sulfur and total iron concentration. The H^+ concentration changes rapidly with total sulfur concentration, especially as the ratio of $[Fe]^T$ to $[S]^T$ approaches 2/3, the value of the stoichiometric coefficient of ferric sulfate compound. If the ratio of $[Fe]^T$ to $[S]^T$ equals 2/3, it indicates that there is no additional sulfuric acid added into the solution and the solution is expected to contain a low concentration of H^+. The similar phenomenon can be seen from the plot of $[H^+]$ as a function of $[Fe]^T$ in the same figure. At low iron concentration the $[H^+]$ does not change significantly. This may be because the acidity associated with iron at low iron concentrations may not change the acidity of the solution, in which the sulfur concentration (and the corresponding hydrogen ion concentration) is already high. Figure 3 shows the concentration profiles of various ionic species with total sulfur concentration at a constant total iron concentration of 0.1M. The profiles show trends similar to that in Figs. 1 and 2, although the iron concentration here is several orders of magnitude higher. Figure 4 shows the variation of Fe^{3+} and $FeOH^{2+}$

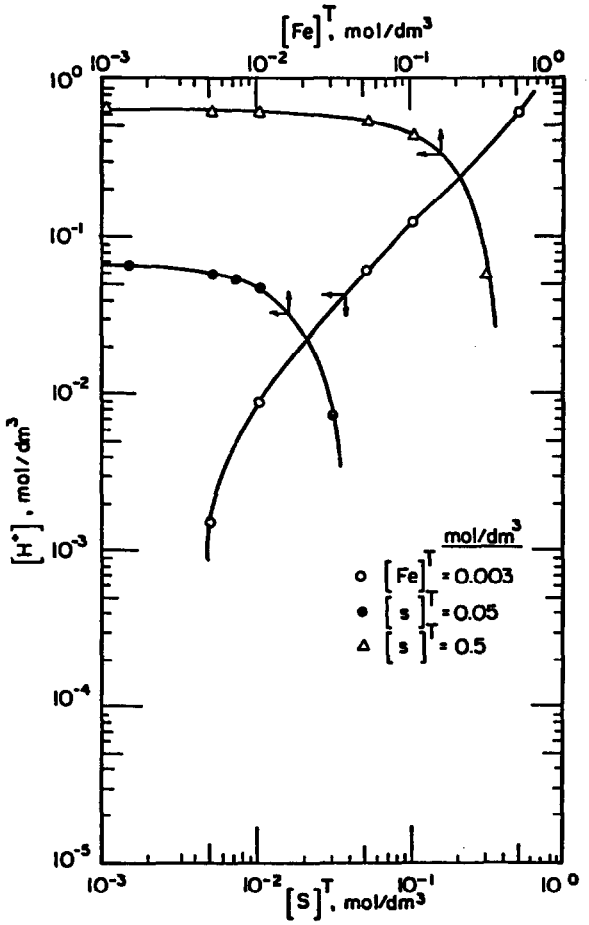


Fig. 2. Effects of total sulfur and total iron concentration on the hydrogen ion concentration profile.

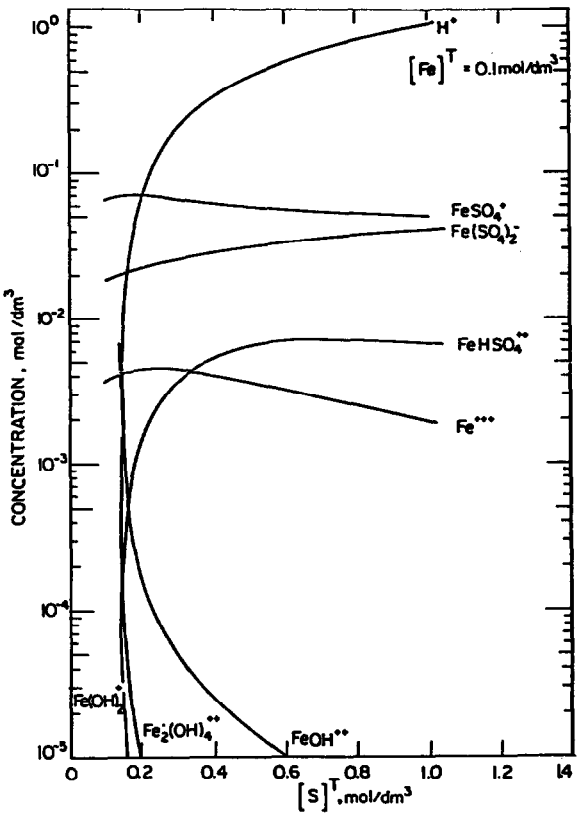


Fig. 3. Concentration profiles of various iron ionic species as a function of total sulfur concentration at a constant total iron concentration of 0.1 mol/dm³.

concentration as a function of total iron concentration at two levels of total sulfur concentration. One can see from Fig. 4 that the concentrations of both Fe^{3+} and $FeOH^{2+}$ increase rapidly with total iron content. In addition, at low iron concentration ($< 10^{-2}$mol/dm³), the concentration of Fe^{3+} is an order of magnitude higher than that of $FeOH^{2+}$.

Accordingly, these results clearly show the nonlinear dependence of Fe^{3+}, $FeOH^{2+}$, and other ionic species on the total iron concentration. Thus, to properly model metal ion extraction kinetics[20] or two-phase metal ion distribution data[21] that are based on knowing the concentration of Fe^{3+} or $FeOH^{2+}$ ions, aqueous phase equilibrium modeling as shown here is necessary for proper estimation of metal ion concentrations. One, therefore, cannot assume that concentrations of Fe^{3+} and $FeOH^{2+}$ in the aqueous phase are linearly related to total iron concentration in analysis of equilibrium or kinetic data in the liquid–liquid, two-phase extraction system.

CONCLUSION

A chemical equilibrium model is developed to predict metal speciation and concentrations in the iron(III) sulfate system. The relations are highly nonlinear and give rise to a wide range of concen-

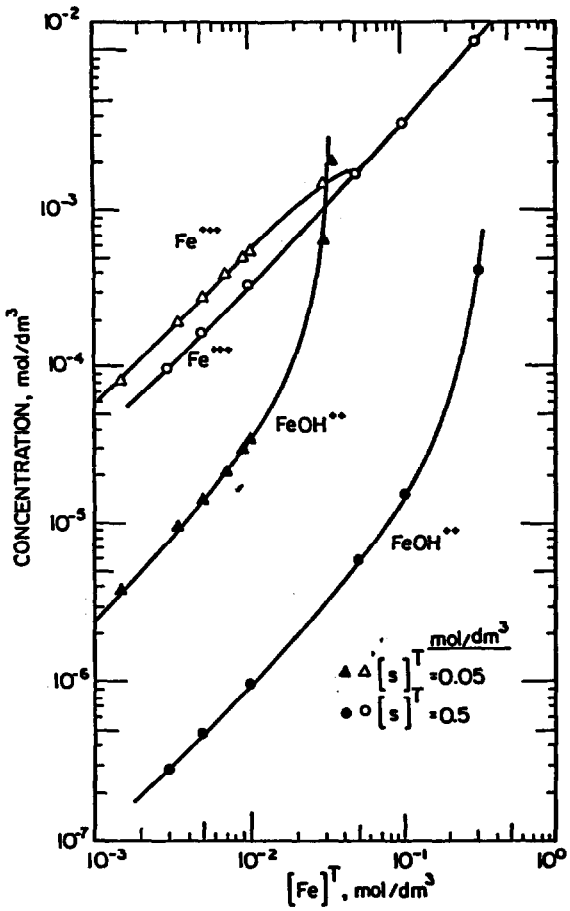


Fig. 4. Dependence of Fe^{3+} and $FeOH^{2+}$ concentrations on the total iron concentration at two levels of total sulfur concentration.

trations of the iron complexes over realistic concentration ranges.

Iron(III) extraction equilibrium and kinetics investigations in which the hydrogen ion, the ferric ion, and $FeOH^{2+}$ ion are considered important variables should include the effects of ionic interactions. Nonlinear dependence of Fe^{3+} and $FeOH^{2+}$ concentrations in the ferric sulfate–sulfuric acid solutions indicates that the consideration of ionic equilibria is necessary to obtain an accurate equilibrium model or chemical kinetic model for the two-phase extraction system.

The analysis above is readily employed to yield calculated values for the concentration of each species in ferric sulfate–sulfuric acid solution.

The temperature dependence of the ionic equilibria can be included if temperature dependence of the equilibrium constants can be obtained. This dependence can be estimated by the Van't Hoff equation if the enthalpy change for each reaction is available.

Acknowledgement—Support of this research by the Department of Energy under Contract DE–AC02–82ER13002 is gratefully acknowledged.

REFERENCES

1. J. S. Preston, *J. Inorg. Nucl. Chem.* 1975, **37**, 1235.
2. V. I. Lakshmanan, G. J. Lawson and J. L. Tomliens, *J. Inorg. Nucl. Chem.* 1975, **37**, 2181.
3. P. G. Christie, V. I. Lakshmanan and G. J. Lawson, *Hydrometallurgy* 1976, **2**, 105.
4. Y. Homatsu, H. Honda and T. Sekine, *J. Inorg. Nucl. Chem.* 1976, **38**, 1861.
5. C. A. Fleming, *Inst. of Min. and Metall. Trans. C.* 1976, **85**, 211.
6. R. Chiarizia, P. R. Danesi and S. Fornarini, *J. Inorg. Nucl. Chem.* 1979, **41**, 1465.
7. C. A. Fleming and M. J. Nico, *J. Inorg. Nucl. Chem.* 1980, **42**, 1327.
8. R. W. Freeman and L. L. Tavlarides, *J. Inorg. Nucl. Chem.* 1981, **43**, 2467.
9. C. K. Lee and L. L. Tavlarides, *Metall. Trans. B.* 1983, **14**, 153.
10. J. Dousma, D. denOttelander and P. L. deBruyn, *J. Inorg. Nucl. Chem.* 1979, **41**, 1565.
11. R. M. Smith and A. E. Martell, *Critical Stability Constant*, Vol. 4. Plenum Press, New York (1976).
12. M. W. Lister and D. E. Rivington, *Canad. J. Chem.* 1955, **33**, 1591.
13. B. N. Mattoo, *Z. Phys. Chem.* 1959, **79**, 156.
14. G. G. Davis and W. MacF. Smith, *Canad. J. Chem.* 1962, **40**, 1836.
15. J. Dousma and P. L. deBruyn, *J. Collid. and Interf. Sci.* 1976, **56**, 527.
16. R. S. Sapleszko, R. C. Patel and E. Matijević, *J. Phys. Chem.* 1977, **81**, 1061.
17. M. Magini, *J. Chem. Phys.* 1979, **70**, 317.
18. R. M. Milburn and W. C. Vosburgh, *J. Am. Chem. Soc.* 1955, **77**, 1352.
19. P. Wolfe, *Commun. ACM*, Vol. 2 (1959).
20. C. K. Lee and L. L. Tavlarides, *I&EC Fundl.*, submitted.
21. R. K. Agarwal, M.S. Thesis, Syracuse University, Syracuse, New York (1983).

Polyhedron Vol. 4, No. 1, pp. 53–58, 1985
Printed in Great Britain.

0277–5387/85 $3.00 + .00
© 1985 Pergamon Press Ltd.

SOLUBILITY EQUILIBRIA OF SOLID SOLUTIONS OF HYDROXYL- AND CHLOR-APATITE OF ARSENIC

T. S. B. NARASARAJU, P. LAHIRI,* P. R. YADAV and U. S. RAI*
Department of Chemistry, Banaras Hindu University, Varanasi-221005, India

(*Received* 30 *January* 1984; *accepted* 2 *March* 1984)

Abstract—The solubility equilibria of arsenic hydroxylapatite, $Ca_{10}(AsO_4)_6(OH)_2$, chlorapatite, $Ca_{10}(AsO_4)_6(Cl)_2$, and their nine solid solutions were investigated at 37°C in the pH range, 4.6 to 7.8, in buffered systems through microanalytical determination of calcium, arsenic and chloride in their saturated solution. Stoichiometric dissolution of the samples was proved by the constancy of the ionic products of the apatite phase in the saturated solution.

Arsenic hydroxylapatite [AsHA], $Ca_{10}(AsO_4)_6(OH)_2$, which is an isomorph of calcium hydroxylapatite, $Ca_{10}(PO_4)_6(OH)_2$, is obtained by incorporation of arsenic in the human-skeletal system through $PO_4^{3-} \rightleftharpoons AsO_4^{3-}$ exchange.[1] The presence of a large excess of chloride ions in the body fluids enables the formation of another isomorph arsenic chlorapatite [AsClA], $Ca_{10}(AsO_4)_6(Cl)_2$, at the bone/body fluid interface. While partial replacement of OH^- by Cl^- in AsHA results in the formation of a series of solid solutions of hydroxyl- and chlor-apatite of arsenic complete replacement results in the formation of arsenic chlorapatite. The formation of AsHA and AsClA at the bone/body fluid interface leads to a disturbance in the calcium and phosphorus metabolism through a shift in the calcification and resorption equilibrium. Explanation and possible elimination of such pathological conditions can be provided by investigations on the solubility of AsHA, AsClA and their solid solutions under a simulated biological condition. The present work was undertaken to investigate the dependence of the solubility product of such samples on their chloride content which is significant from the biological point of view.

EXPERIMENTAL

While AsHA was obtained by a wet method[2,3] the AsClA and its solid solutions with AsHA were prepared by an appropriate solid state reaction[4,5] using AsHA and $CaCl_2$ as starting materials. The homogeneity of the samples were confirmed through chemical, X-ray, electronmicroscopic, infrared and thermal analyses as reported earlier.[5] The solubility product of each sample was investigated at the biologically significant temperature of 37°C by analyses of its saturated solution at a few chosen pH values in the range 4.70–7.38 in buffered systems, the final pH of each system being measured using a digital pH meter (pH 5651, E CIL). The experimental details for the equilibration of the samples to prepare their saturated solutions and to separate them from the likely colloidal component were reported earlier[6–8]. Microanalytical methods were used to determine the ingredients present in the saturated solution. Calcium was determined complexometrically[9,10] while arsenic and chloride were estimated spectrophotometrically[11–13], separate aliquots being taken each time.

RESULTS AND DISCUSSION

A few representative sets of results on the determination of the solubility product of AsHA, AsClA and nine of their solid solutions are included in Table 1. The hydroxyl ion concentration of each sample at a given pH was incorporated in column (6) of the table. The experimentally determined concentrations of calcium, arsenic and chloride are given in columns (3)–(5). In order to scrutinize stoichiometric dissolution of the samples the g · atom ratios, Ca/As are reported in column (8) of the table. From the total arsenic content, given in column (7) of the table and pH of the saturated solution, concentration of H_3AsO_4, $H_2AsO_4^-$, $HAsO_4^{2-}$ and AsO_4^{3-} were evaluated using the three

*Author to whom correspondence should be addressed.

Table 1. Solubility product of arsenic hydroxylapatite, arsenic chlorapatite and their solid solutions

S.No.	Final pH	Measured conc. (g atoms/l) Ca ($\times10^3$)	As ($\times10^3$)	Cl ($\times10^3$)	Calculated conc. (g ions/l) OH^- ($\times10^7$)	AsO_4^{3-}	g atom ratio	pk_{ip}	Average pk_{ip}
				Solute $Ca_{10}(AsO_4)_6(OH)_2$					
1.	5.56	13.00	7.48	-	0.036	3.05	1.73	92.84	
2.	5.68	12.25	7.23	-	0.047	5.09	1.69	91.52	
3.	5.75	11.50	6.49	-	0.056	6.27	1.77	91.11	
4.	5.82	9.75	5.74	-	0.066	7.55	1.77	91.26	
5.	5.90	8.50	5.18	-	0.079	9.82	1.69	90.95	91.83
6.	6.13	6.00	5.49	-	0.134	1.79	1.71	90.44	
7.	6.40	2.50	1.49	-	0.251	2.41	1.67	92.93	
8.	6.68	1.50	0.874	-	0.478	4.37	1.71	92.46	
9.	7.16	0.75	0.436	-	1.440	1.20	1.71	93.04	
				Solute $Ca_{10}(AsO_4)_6(OH)_{1.8}(Cl)_{0.2}$					
1.	5.46	11.75	6.98	0.229	0.030	1.98	1.68		
2.	5.52	10.75	6.24	0.191	0.033	2.13	1.72		
3.	5.58	9.50	5.62	0.191	0.038	2.50	1.69		
4.	5.62	8.25	4.76	0.153	0.041	2.56	1.73		94.11
5.	6.28	2.00	1.25	0.038	0.190	12.23	1.60		
6.	6.70	1.10	0.65	0.023	0.501	34.95	1.69		
7.	7.08	0.65	0.374	0.015	1.200	78.79	1.73		
				Solute $Ca_{10}(AsO_4)_6(OH)_{1.6}(Cl)_{0.4}$					
1.	5.31	10.75	6.48	0.491	0.020	0.85	1.65	95.35	
2.	5.43	9.00	5.24	0.420	0.026	1.19	1.71	94.05	
3.	5.50	8.00	4.74	0.344	0.031	1.47	1.68	94.96	
4.	5.69	6.00	3.49	0.268	0.048	2.56	1.71	94.51	94.46
5.	6.06	3.25	1.89	0.114	0.114	7.17	1.71	94.03	
6.	6.72	0.85	0.499	0.038	0.524	28.97	1.70	95.85	
7.	7.15	0.60	0.374	0.023	1.41	100.56	1.76	93.02	

dissociation constants[14] of H_3AsO_4; $K_1 = 4.0 \times 10^{-3}$, $K_2 = 1.0 \times 10^{-7}$ and $K_3 = 3.2 \times 10^{-12}$ and pKw = 13.54. The concentrations of H_3AsO_4, $H_2AsO_4^-$ and $HAsO_4^{2-}$ are eliminated from the table as they are not used in the expression of the solubility product of apatitic phase. However, the concentrations of AsO_4^{3-}, needed to calculate the ionic product of the samples are reported in column (7) while the values of $pK_{ip}(-\log K_{ip})$ and their average are given in columns (9) and (10) respectively.

The buffer combination of desired pH maintained at a molarity of 0.165 with respect to sodium nitrate in order to keep the ionic strength constant was used as the medium of dissolution. To overcome the inaccuracy involved in the evaluation of the activity coefficients of the dissolved ionic species of these systems, La Mer[15] suggested that an aqueous solution of 0.165 M sodium chloride, a solvent of biological importance may be considered as a standard solvent of reference in which all the activity coefficients may be assigned the value of unity. Since the use of sodium chloride is not permissible in these systems sodium nitrate was used and the ionic product of the samples evaluated were taken as the solubility product.

The results included in the present table established that the solubilities of AsHA, AsClA and their solid solutions increased with increasing hydrogen ion concentration of the medium of dissolution. It can be attributed that a saturated aqueous solution of AsHA exhibits the following equilibrium:

$$Ca_{10}(AsO_4)_6(OH)_2 \rightleftharpoons 10Ca^{2+} + 6AsO_4^{3-} + 2OH^- . \quad (1)$$

Table 1. (*Continued*)

S.No.	Final pH	Measured conc. (g atoms/l) Ca ($\times10^3$)	As ($\times10^3$)	Cl ($\times10^3$)	Calculated conc. (g ions/l) OH^- ($\times10^7$)	AsO_4^{3-}	g atom ratio	pk_{ip}	Average pk_{ip}
				Solute $Ca_{10}(AsO_4)_6(OH)_{1.4}(Cl)_{0.6}$					
1.	5.15	10.25	5.86	0.651	0.014	0.37	1.74	96.79	
2.	5.35	8.50	5.11	0.536	0.022	0.80	1.66	95.36	
3.	5.40	7.50	4.36	0.491	0.025	0.86	1.72	95.67	
4.	5.44	7.00	4.24	0.420	0.027	1.00	1.65	95.56	95.16
5.	5.44	4.00	2.37	0.249	0.051	1.92	1.68	95.99	
6.	6.18	2.50	1.49	0.153	0.151	9.50	1.67	93.39	
7.	7.02	0.65	0.373	0.042	1.040	64.43	1.74	93.41	
				Solute $Ca_{10}(AsO_4)_6(OH)_{1.2}(Cl)_{0.8}$					
1.	5.05	10.00	5.74	0.727	0.011	0.23	1.74	97.11	
2.	5.12	9.00	5.24	0.727	0.014	0.29	1.71	96.88	
3.	5.20	8.50	4.86	0.689	0.016	0.39	1.74	96.31	
4.	5.36	6.00	3.36	0.459	0.022	0.55	1.78	96.82	96.14
5.	5.52	4.50	2.60	0.363	0.033	0.89	1.73	96.70	
6.	6.55	0.85	0.511	0.076	0.354	15.27	1.66	95.83	
7.	6.79	0.85	0.499	0.057	0.616	30.62	1.68	93.36	
				Solute $Ca_{10}(AsO_4)_6(OH)_{1.0}(Cl)_{1.0}$					
1.	4.94	9.00	5.403	0.881	0.0087	0.13	1.66	97.89	
2.	5.01	8.50	4.860	0.842	0.0102	0.16	1.74	97.53	
3.	5.05	7.55	4.36	0.766	0.0110	0.17	1.73	98.86	
4.	5.08	7.00	4.14	01612	0.0120	0.19	1.69	98.02	97.30
5.	5.28	5.25	3.12	0.517	0.0190	0.36	1.68	97.49	
6.	6.10	1.60	0.90	0.153	0.1250	4.06	1.77	96.02	
7.	6.72	0.65	0.37	0.065	0.5240	21.48	1.75	95.34	
				Solute $Ca_{10}(AsO_4)_6(OH)_{0.8}(Cl)_{1.2}$					
1.	4.91	7.55	4.49	0.925	0.008	0.09	1.68	98.47	
2.	5.01	6.50	3.86	0.766	0.010	0.13	1.68	98.29	
3.	5.12	5.25	2.99	0.612	0.013	0.16	1.75	98.07	
4.	5.20	4.25	2.37	0.517	0.015	0.18	1.78	99.07	98.57
5.	5.66	1.75	0.997	0.191	0.045	0.64	1.75	99.86	
6.	6.45	0.55	0.320	0.069	0.281	6.37	1.71	98.80	
7.	7.13	0.25	0.145	0.034	1.340	36.03	1.72	97.53	

The presence of AsO_4^{3-} ion in an aqueous media as a product of dissolution further establishes the following equilibria which are all pH dependent.

$$AsO_4^{3-} + H_3O^+ \rightleftharpoons HAsO_4^{2-} + H_2O \quad (2)$$

$$HAsO_4^{2-} + H_3O^+ \rightleftharpoons H_2AsO_4^- + H_2O \quad (3)$$

$$H_2AsO_4^- + H_3O^+ \rightleftharpoons H_3AsO_4 + H_2O \quad (4)$$

The OH^- ion of eqn (1) on the other hand participates in an additional pH dependent equilibrium characteristic of all aqueous media as shown below:

$$H_3O^+ + OH^- \rightleftharpoons 2H_2O. \quad (5)$$

A shift from left to right occurs in all the above equilibria when H_3O^+ ion concentration is increased. All these equilibria are collectively responsible for influencing equilibrium (1). But eqn (2) shows the presence of AsO_4^{3-} ion which being

Table 1. (*Continued*)

S.No.	Final pH	Measured conc. (g atoms/l) Ca ($\times10^3$)	As ($\times10^3$)	Cl ($\times10^3$)	Calculated conc. (g ions/l) OH^- ($\times10^7$)	AsO_4^{3-}	g atom ratio	pk_{ip}	Average pk_{ip}
			Solute $Ca_{10}(AsO_4)_6(OH)_{0.6}(Cl)_{1.4}$						
1.	4.70	7.25	4.28	1.03	0.005	0.03	1.69	99.64	
2.	4.82	6.56	3.99	0.929	0.007	0.05	1.62	99.12	
3.	5.01	5.75	3.41	0.766	0.010	0.11	1.68	97.84	
4.	5.12	3.50	1.99	0.536	0.013	0.11	1.75	99.11	98.83
5.	5.40	0.15	1.23	0.306	0.025	0.24	1.74	99.45	
6.	6.35	0.75	0.42	0.268	0.223	5.52	1.78	95.39	
7.	7.38	0.11	0.624	0.0151	2.39	34.53	1.76	99.26	
			Solute $Ca_{10}(AsO_4)_6(OH)_{0.4}(Cl)_{1.6}$						
1.	4.65	6.75	3.86	1.07	0.004	0.02	1.74	99.86	
2.	4.74	5.10	2.91	0.842	0.005	0.03	1.75	100.86	
3.	4.82	4.80	2.82	0.766	0.007	0.04	1.70	100.31	
4.	5.04	3.45	1.99	0.574	0.010	0.08	1.73	100.31	100.52
5.	5.68	1.15	0.624	0.172	0.047	0.44	1.84	100.88	
6.	6.45	0.30	0.165	0.057	0.281	3.29	1.81	100.88	
7.	7.10	0.17	0.099	0.027	1.25	22.40	1.71	99.66	
			Solute $Ca_{10}(AsO_4)_6(OH)_{0.2}(Cl)_{1.8}$						
1.	4.68	4.50	2.70	1.07	0.005	0.02	1.66	100.92	
2.	5.09	2.15	1.25	0.421	0.012	0.06	1.72	101.87	
3.	5.41	1.25	0.748	0.229	0.025	0.15	1.67	102.19	
4.	5.67	0.85	0.510	0.153	0.046	0.34	1.66	102.02	101.2
5.	6.13	0.50	0.282	0.848	0.134	1.45	1.77	99.14	
6.	6.39	0.30	0.162	0.054	0.245	2.51	1.85	102.03	
7.	7.21	0.13	0.075	0.023	1.620	24.37	1.73	100.24	
			Solute $Ca_{10}(AsO_4)_6(Cl)_2$						
1.	4.67	3.20	1.87	0.612	-	0.012	1.71	102.69	
2.	4.81	2.45	1.46	0.497	-	0.019	1.67	103.00	
3.	5.06	1.70	0.99	0.341	-	0.041	1.71	102.93	
4.	5.61	0.74	0.42	0.153	-	0.210	1.76	102.94	103.32
5.	6.12	0.28	0.16	0.054	-	0.800	1.72	104.66	
6.	6.77	0.13	0.075	0.027	-	5.260	1.73	103.67	
7.	7.42	0.065	0.037	0.015	-	22.820	1.73	103.35	

a direct participant is naturally more dominant in influencing the equilibrium represented by eqn (1).

An additional enhancement of the solubility of apatite could be justified on the basis of eqn (5) which accounts for the removal of OH^- ion, a product of dissolution. The marked pH dependence of the solubilities of AsHA and its solid solutions with AsClA can thus be accounted for. Analogous to the equilibria operative in the case of AsHA as mentioned above, a saturated solution of AsClA is characterized by the following equilibrium in addition to those given in eqns (2)–(4).

$$Ca_{10}(AsO_4)_6(Cl)_2 \rightleftharpoons 10Ca^{2+} + 6AsO_4^{3-} + 2Cl^-. \quad (6)$$

It is evident that the role of equilibrium (5) being absent, the equilibrium (6) is controlled by equilibria (2)–(4). The above arguments are substantiated by the observed fact that the calculated proportion of AsO_4^{3-} ions of the saturated solution

given in column (7) of the table of all samples decreased with an increase in the hydrogen ion concentration of the medium of dissolution. The marked pH dependence of the solubilities of AsHA and its solid solution with AsClA can thus be accounted for.

Another significant finding of the present investigations has been that the solubilities of the samples were found to decrease with an increase in the proportion of their Cl^- content, the experimental conditions being the same. A three-pronged explanation to account for the lower solubility of AsClA over that of AsHA and for a systematic diminution of solubilities of the solid solutions with increasing chloride content may be suggested. The first is based on the thermoanalytical approach that the free energy of dissolution of an ionic crystal is dependent on ionic replacement and the lattice energy. The thermodynamical derivation which represents the dependence of the decrease in the free energy of dissolution of a solute on the radius of the anion replaced is given below:

$$\Delta^0_{G_{soln}} = \{(164Z^2 + m)/(r_+ + 0.85) - (164Z^2 - n)/(r_- + 0.1)\} + \{332Z^2/R_0 + \left(1 - \frac{1}{n_B}\right) - 8.03(m+n)\}(\text{k cal/mole}).$$

It involves the dependence of ΔG^0 solution on the replacement of an anion of the solute by another of a different ionic radius as the cations are the same in both solutes. The average change in the solubility of an ionic component depends exclusively on the relative variation in $\Delta G^0_{hydration}$ and $\Delta G^0_{lattice}$ term as shown above by the first and second terms for sparingly soluble salts like apatites. This is justified by the fact that the alterations in hydration energies[16] for the pair of ions involved (Cl^- and OH^- ions) in the replacement investigated are of very small magnitude. It is evident from the above expression that decrease in solubility increases when the change brought about by ionic replacement is more in lattice energy than in the hydration energy. The lattice energy of AsHA is lower than the chloride substituted product could be proved by noting their decomposition temperature from thermoanalytical studies.[13] The higher stability of AsClA over AsHA can be attributed to a more compact packing of ions in the lattice of Cl^- substituted apatites than that of AsHA. This in turn, is due to the spherical symmetry of Cl^- ions unlike that of OH^-. The observed decrease in the solubility of apatites with an increase in the chloride content of samples can thus be accounted for on the basis of the accompanying increase in the lattice energies.

The second explanation for the low solubilities of AsClA and solid solutions is based on the concept of ionic equilibria prevalent in these systems and on the divergence in the extent of dissociation of water and hydrochloric acid. The extent to which the ionic equilibrium of water (eqn 5) is affected, diminished as one goes from AsHA to AsClA due to depletion in the supply of OH^- ions accompanying dissolution. The equilibrium (5) remains unaffected as Cl^- ions produced due to dissolution of AsClA forms a highly dissociated hydrochloric acid.

The third explanation which can be applied exclusively to the lower solubilities of the solid solutions over that of AsHA is based on structural consideration as was shown by Young *et al.*[17] According to them ions such as F^-, Cl^- and OH^- or a combination of them exist in apatites in columns or linear chains coincident with their six-fold screw axis. It was established[18,19] through infrared spectral studies that the OH^- and Cl^- ions constituting the lattice of a solid solution of AsHA and AsClA are mutually linked up through hydrogen bonding. The hindrance caused to the diffusion of the OH^- ions through the column mentioned above can be a factor in reducing the solubility of chloride containing solutes since the columns offer themselves as the most vulnerable points[20,21] for the diffusion of the ions located in them into the medium of dissolution. A constant value for the solubility product of apatites at a given temperature and the agreement of ratios of measured concentrations of the dissolved species with the corresponding ratios of the solute could prove that the apatites exhibit stoichiometric dissolution.

Acknowledgements—The authors thank Prof. B. M. Shukla, former Head, Department of Chemistry for encouragement and facilities and financial assistance given by B.H.U. is also gratefully acknowledged.

REFERENCES

1. A. S. Posner, cited in *Phosphorus and its Compounds*. (Edited by J. R. Van Wazer), Vol. II, pp. 1429–59. Interscience, New York (1961).
2. T. S. B. Narasaraju, K. K. Rao, U. S. Rai and B. K. Kapoor. *Indian J. Chem.* 1977, **15A**, 1014.
3. T. S. B. Narasaraju, R. P. Singh and V. L. N. Rao, *J. Inorg. Nucl. Chem.* 1972, **34**, 2072.
4. U. S. Rai, K. K. Rao and T. S. B. Narasaraju, *Indian J. Chem.* 1979, **18A**, 168.
5. T. S. B. Narasaraju, P. Lahiri, P. R. Yadav and U. S. Rai, *Curr. Sci.*, 1982, **51**, 772.
6. T. S. B. Narasaraju, K. K. Rao and U. S. Rai, *Can. J. Chem.* 1979, **57**, 1919.
7. N. S. Chickerur, R. P. Singh and T. S. B. Narasaraju, *Naturwiss.* 1969, **56**, 282.
8. T. S. B. Narasaraju, N. S. Chickerur and R. P Singh, *J. Inorg. Nucl. Chem.* 1971, **33**, 3194.

9. G. Schwarzenbach, *Complexometric Titrations*, p. 63. Interscience, New York (1960).
10. R. P. Singh, N. S. Chickerur and T. S. B. Narasaraju, *Z. Anal. Chem.* 1968, **237**, 117.
11. T. S. B. Narasaraju, R. P. Singh and V. L. N. Rao, *Z. Anal. Chem.* 1970 **251**, 300.
12. Foster Dee Snell and Cornelia T. Snell, *Colorimetric Method of Analyses*, Vol. II, p. 196. Van Nostrand, Toranto (1954).
13. T. S. B. Narasaraju, U. S. Rai and K. K. Rao, *Ind. J. Chem.* 1978, **1B**, 952.
14. T. S. Hill, *J. Am. Chem. Soc.* 1943, **65**, 1564.
15. V. K. La Mer. *J. Phys. Chem.* 1962, **66**, 973.
16. L. Benjamin and V. Gold, *Trans. Faraday Soc.* 1954, **50**, 797.
17. R. A. Young, W. Vanderlugt and T. S. Elliot. *Nature* 1969, **223**, 739.
18. R. A. Young, *J. Dent. Res.* 1974, **53**, 193.
19. E. Dykes and J. C. Elliot. *Celcif. Tissue Res.* 1971 **7**, 241.
20. G. Montel, *C.R. Acad. Sci. Paris.* 1961, **253**, 468.
21. G. Montel, *Bull. Soc. Chim. Fr.* 1968, 1693.

Polyhedron Vol. 4, No. 1, pp. 59–63, 1985
Printed in Great Britain.

0277–5387/85 $3.00 + .00
© 1985 Pergamon Press Ltd.

STUDIES ON EXTRACTION OF COPPER(II) WITH 1-PHENYL-3-METHYL-4-ACYL-5-PYRAZOLONE

Y. AKAMA,* K. SATO, M. UKAJI and T. KAWATA
Department of Chemistry, Meisei University, Hodokubo, Hino, Tokyo 191, Japan

and

M. KAJITANI
Department of Chemistry, Faculty of Science and Technology, Sophia University, Kioi-Cho, Chiyoda-ku, Tokyo 102, Japan

(*Received* 25 *January* 1984; *accepted* 2 *March* 1984)

Abstract—The extraction of Cu(II) with 1-phenyl-3-methyl-4-acyl-5-pyrazolone (HA), in different organic solvents has been studied. The extraction mechanism of Cu(II) and the composition of the extracted species has been determined. Cu(II) was extracted as CuA_2, or in the presence of TOPO, as CuA_2TOPO. The extraction constants do not change regularly with increasing the length of acyl chain in the 1-phenyl-3-methyl-4-acyl-5-pyrazolone derivatives. The effect of the temperature on the extraction of Cu(II) has also been investigated.

Metal extraction from aqueous solution with 1 - phenyl - 3 - methyl - 4 - benzoyl - 5 - pyrazolone (PMBP) has been studied extensively.[1–9] PMBP is an excellent complexing agent of metals due to the great reactivity of its –CO group and stability of its complex. The extraction of Cu(II) by PMBP from aqueous solution has also been reported in a previous paper by Mirza[10] and Zolotov *et al.*[11] Recently 1 - aryl - 3 - methyl - 4 - aroyl - 5 - pyrazolone has been introduced for extraction of La(III) and Ba(II) by Umetani *et al.*[12] Furthermore, Tochiyama *et al.*[13] developed a method for the extraction of lanthanides, using a mixture of 1 - phenyl - 3 - methyl - 4 - octanoyl - 5 - pyrazolone and TOPO. However, there has been little systematic study of the extraction of metal ions utilizing the 1 - phenyl - 3 - methyl - 4 - acyl - 5 - pyrazolone derivatives. Thus, the acyl derivatives of the type $(C_{10}H_9N_2O)$-$(C_nH_{2n+1}CO)$ (n = 2–10) were synthesized systematically by our laboratory and the solvent extraction of various metal ions by these derivatives has been investigated. Compared to other β-diketones such as TTA and AA, these derivatives have a lower pKa value. Therefore, it was hoped that these derivatives might prove to be more attractive as ligands for the extraction of metals. The present work was undertaken in order to investigate the extraction equilibria of Cu(II) at 25°C utilizing these derivatives in different organic solvents and the dependence of the extraction constants on the number of carbon atoms in the acyl chain.

Data on the extraction of metal ions with PMBP at various temperatures are very scarce. Therefore, the temperature dependence of the extraction constant was also measured in the range of 6–37°C for the extraction of Cu(II) by PMBP diluted with MIBK.

EXPERIMENTAL

Reagents. 1 - phenyl - 3 - methyl - 4 - acyl - 5 - pyrazolone was synthesized as described[14] and purified by several recrystallizations from methanol, and elemental analysis was done for these reagents as shown in Table 1. Here the reagents are represented by C_N in which N means the number of carbon atoms involved in the acyl chain. The solution of Cu was prepared by dissolution of 1.00 g Cu metal (99.99%) in nitric acid solution, and 10 ppm Cu(II) solution was used for the extraction studies. All other chemicals were of analytical grade.

*Author to whom correspondence should be addressed.

Table 1. Elemental analyses and some physical properties of 1-phenyl-3-methyl-4-acyl-5-pyrazolone and PMBP

Reagent [a]	M.p. (°C)	pKa in 10 %(v/v) dioxane, 25 °C	Analyses % [b]		
			C	H	N
C_3	61 - 62	4.1_7	68.2 (67.81)	6.2 (6.13)	11.9 (12.17)
C_4	77 - 78	4.0_6	68.6 (68.83)	6.6 (6.60)	11.5 (11.47)
C_5	60 - 61	4.0_5	69.6 (69.74)	7.2 (7.02)	11.0 (10.84)
C_6	59 - 60	4.1_5	70.9 (70.56)	7.5 (7.40)	10.5 (10.29)
C_7	77 - 78	4.1_0	71.2 (71.30)	7.7 (7.74)	9.9 (9.78)
C_8	77 - 78	4.1_0	72.9 (71.97)	8.0 (8.05)	9.4 (9.33)
C_9	29 - 30	4.1_7	72.6 (72.58)	8.3 (8.34)	9.0 (8.91)
C_{10}	43 - 44		73.7 (73.14)	8.7 (8.59)	8.6 (8.53)
C_{11}	46 - 47		73.6 (73.65)	8.6 (8.83)	8.1 (8.18)
PMBP	117 - 118	3.8_0	73.3 (73.37)	4.9 (5.07)	10.0 (10.07)

a) C_3 : $C_{13}H_{14}N_2O_2$; C_4 : $C_{14}H_{16}N_2O_2$; C_5 : $C_{15}H_{18}N_2O_2$; C_6 : $C_{16}H_{20}N_2O_2$
C_7 : $C_{17}H_{22}N_2O_2$; C_8 : $C_{18}H_{24}N_2O_2$; C_9 : $C_{19}H_{26}N_2O_2$; C_{10} : $C_{20}H_{28}N_2O_2$
C_{11} : $C_{21}H_{30}N_2O_2$; PMBP : $C_{17}H_{14}N_2O_2$

b) Calculated values are given in parentheses .

Procedure. Equal volumes (10 cm^3) of the aqueous (10 ppm Cu) and organic (0.01M PMBP or any other reagents) phases were shaken mechanically in a 50 cm^3 glass-stopped centrifuge tube for about 30 min at 25°C. The aqueous pH was controlled by the addition of perchloric acid, while the ionic strength was kept at 0.1 M with sodium perchlorate. After centrifugation, the copper in the aqueous phase was determined by atomic absorption. The amount of copper extracted into the organic phase was obtained from the difference between the aqueous copper concentration before and after the equilibration. The pH of the aqueous phase was also measured after the extraction in all experiments.

RESULTS AND DISCUSSION

The solvent extraction behaviour of Cu(II) can be understood by the variation of distribution ratio D as a function of the aqueous phase acidity and as a function of the extractant concentration. For the extraction of Cu(II), plot of log D vs log [reagent concentration] at constant ionic strength and pH are in all cases linear with slope 2 indicating that the complexes formed are CuA_2. The experimental data obtained for the extraction of Cu(II) by C_8-benzene and PMBP–MIBK solutions are given in Fig. 1. The total concentrations of the reagent are plotted instead of the equilibrium concentrations, as these magnitudes are directly proportional. The plots of log D vs pH also gave straight lines of slope near 2, indicating that 2 moles of hydrogen ions are released during the formation of the extracted species. The results of experiments are presented in Fig. 2, for 0.01M C_8 in chloroform, benzene and MIBK. These plots were in all other 4-acyl derivatives [HA] straight lines with a slope of 2. Thus, the extraction process may be represented by the equation

$$Cu^{2+} + 2HA \rightleftharpoons CuA_2 + 2H^+$$

$$K_{ex} = [CuA_2]_{org}[H^+]^2_{aq}/[Cu^{2+}]_{aq}[HA]^2_{org}$$

hence

$$\log K_{ex} = \log D - 2pH + 2\log [HA]:$$

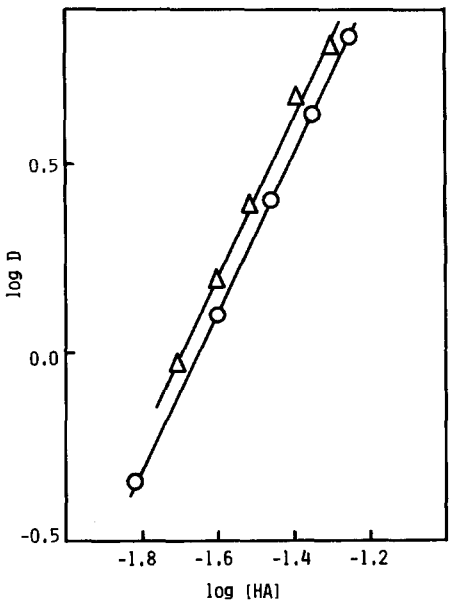


Fig. 1. Variation of distribution ratio for Cu(II) as a function of PMBP and C_8 concentration at constant pH. –△–, C_8 in benzene, pH = 1.54: –○–, PMBP in MIBK, pH = 1.07.

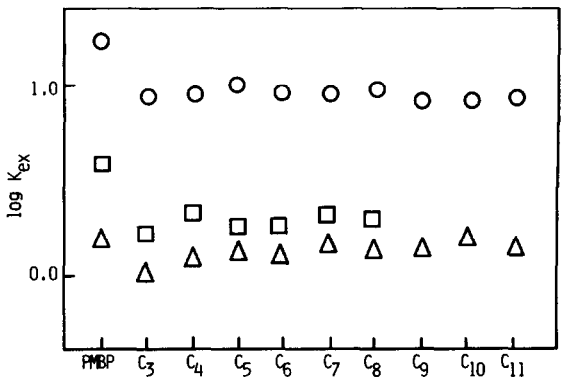


Fig. 3. Comparison of extraction constants for 1-phenyl-3-methyl-4-acyl-5-pyrazolone and PMBP complexes of Cu(II). –○–, MIBK; –□–, benzene; –△–, chloroform.

where HA represents the ligand, A its anion and K_{ex} is the extraction constant for copper complex. The index *org* and *aq* denote organic and aqueous phase respectively, and D is the distribution ratio of Cu(II).

The values of log K_{ex} have been calculated for all the systems as shown in Fig. 3. The extraction does not change regularly with increasing the length of acyl chain in the extractant. As can be seen from Fig. 3, the log K_{ex} values between C_3 and C_{11} were constant in MIBK, benzene and chloroform systems, respectively. When benzene was used as organic solvent for the extraction of Cu(II) with PMBP, the value of log K_{ex} is 0.55 and is about 0.2 for 4-acyl derivatives. On the other hand, the values[15] of log K_{ex} for $Cu(TTA)_2$ and $Cu(AA)_2$ complexes in benzene were −1.32 and −3.93 respectively. Thus, these 4-acyl derivatives and PMBP have a larger extraction constant for Cu(II) than TTA and AA. This effect is certainly due to the large acid dissociation constant of 4-acyl derivatives compared to the other β-diketones. The values of pKa for 4-acyl derivatives and PMBP were measured in 10% (v/v) dioxane–water at 25°C, which were given in Table 1. It is apparent from the results that the increase in number of methylene groups in these derivatives did not have an important influence on the acid dissociation.

A comparison of log K_{ex} value shows that Cu(II)

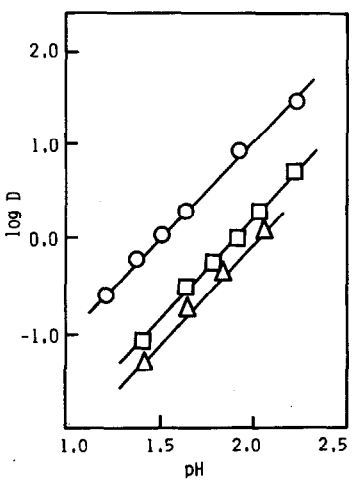


Fig. 2. Variation of distribution ratio for Cu(II) as a function of pH at constant C_8 concentration (0.01 M). –○–, MIBK; –□–, benzene; –△–, chloroform.

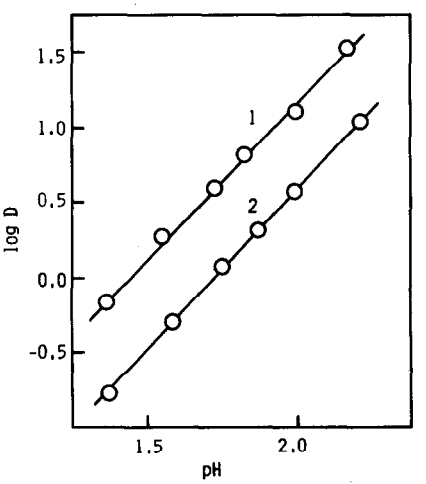


Fig. 4. Variation of distribution ratio with pH for Cu(II) with (1) 0.01 M PMBP + 0.01 M TOPO, and (2) 0.01 M PMBP, in benzene.

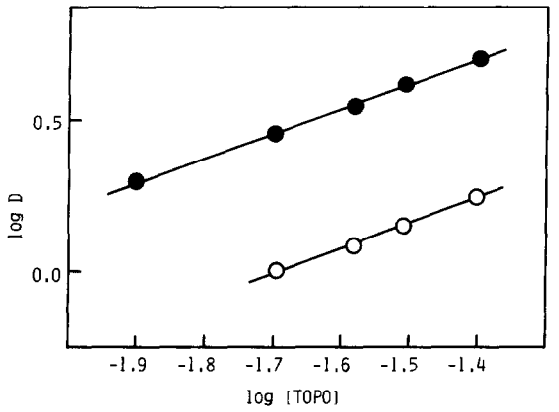


Fig. 5. Variation of distribution ratio for Cu(II) as a function of TOPO concentration (PMBP = 0.01M). —●—, pH = 1.55; —○—, pH = 1.34.

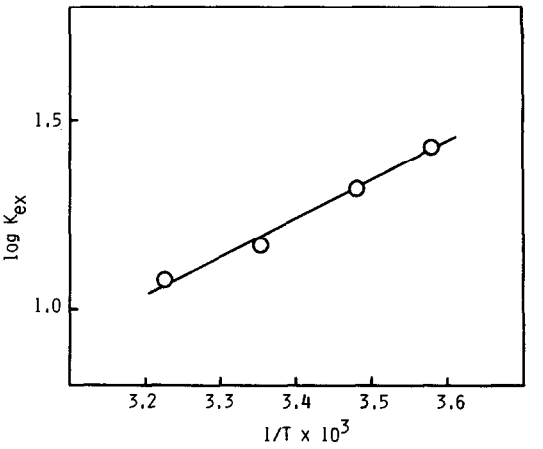


Fig. 7. Variation of extraction constant for Cu(II) as a function of temperature.

is better extracted by MIBK-4-acyl derivative systems than benzene and chloroform. However, when benzene or chloroform were used as organic solvents the value of log K_{ex}, showed no marked difference. The higher extractibility of the Cu(II) complexes in the MIBK-4-acyl derivative systems, as represented by K_{ex} values, may be due to the difference in the distribution coefficient of the Cu(II) complexes or synergistic effect by MIBK. Furthermore, the small difference of the K_{ex} values between the PMBP and other 4-acyl derivatives is certainly due to the difference in the acid dissociation constant of these extractants. It appears that PMBP is a better extractant of Cu(II) than other 4-acyl derivatives in the same experimental conditions.

The effect of the addition of trioctyl phosphine oxide (TOPO) to the organic phase has also been studied. When TOPO is added to the PMBP-benzene solution, the synergistic effect is observed, i.e. an enhancement of the distribution ratio of Cu(II). In order to find the extraction mechanism, the influence of various factors upon the distribution ratio was investigated. The plots of log D vs pH of the aqueous phase in the presence and the absence of TOPO gave straight lines with a slope of 2, respectively, as shown in Fig. 4. The slope 2 for the linear region of these curves indicates that two molecules of PMBP are involved in the extracted species of Cu(II).

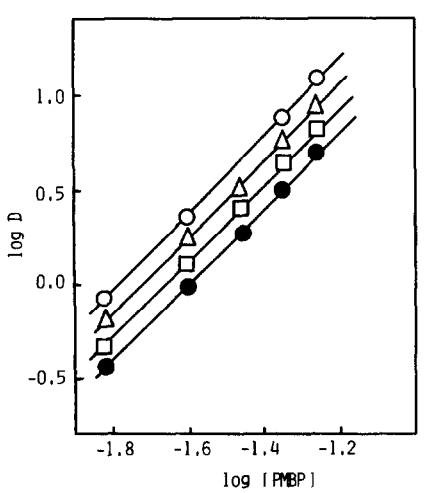


Fig. 6. Variation of distribution ratio for Cu(II) as a function of PMBP concentration in MIBK at constant temperature and pH (1.06) —○—, 6°C; —△—, 14.5°C; —□—, 25°C; —●—, 37°C.

The influence of TOPO concentration on the distribution ratio of Cu(II) at constant pH of aqueous phase and constant PMBP concentration was studied. The results obtained are presented in Fig. 5. The slope near 1 of curves indicating that only one TOPO molecule is associated with the extracted species of Cu(II). The overall reaction mechanism of the synergistic extraction can be written as follows:

$$Cu^{2+} + 2HPMBP + TOPO \rightleftharpoons [Cu(PMBP)_2TOPO] + 2H^+.$$

The extraction of Cu(II) with various concentrations of PMBP in MIBK at temperature between 6 and 37°C gave the results in Fig. 6. The values of the extraction constant increase monotonously with a decrease in the temperature. A plot of log K_{ex} against 1/T gave a straight line as shown in Fig. 7. The value of the enthalpy change, ΔH of -19.3 kJ/mol was calculated from the slope.

Acknowledgement—The present work was partially supported by a Grant-in-Aid for Scientific Research from the Ministry of Education, Science and Culture.

REFERENCES

1. Yu. A. Zolotov, M. K. Chmutova and P. N. Palei, *J. Anal. Chem. USSR* 1966, **21**, 1079.
2. Yu. A. Zolotov, N. T. Sizonenko, E. S. Zolotovtskaya and E. I. Yakovenko, *J. Anal. Chem. USSR* 1969, **24**, 15.
3. M. K. Chmutova, G. A. Pribylova and B. F. Myasoedov, *J. Anal. Chem. USSR* 1973, **28**, 2076.
4. Y. Akama, T. Nakai and F. Kawamura, *Bunseki Kagaku* 1976, **25**, 496.
5. E. Ivanova, S. Mareva and N. Jordanov, Fresenius *Z. Anal. Chem.* 1977, **288**, 62.
6. A. Roy and K. Nag, *J. Inorg. Nucl. Chem.* 1978, **40**, 331.
7. E. Uhlemann, B. Maack and M. Raab, *Anal. Chim. Acta* 1980, **116**, 153.
8. J. P. Brunette, M. Taheri, G. Goetz–Grandmont and M. J. F. Leroy, *Polyhedron* 1982, **1**, 461.
9. F. T. Coronel, St. Mareva and N. Yordanov, *Talanta* 1982, **29**, 119.
10. M. Y. Mirza, *Talanta* 1978, **25**, 685.
11. Yu. A. Zolotov and N. T. Sizonenko, *J. Anal. Chem. USSR* 1970, **25**, 40.
12. S. Umetani, M. Matsui, J. Tôei and T. Shigematsu, *Anal. Chim. Acta* 1980, **113**, 315.
13. O. Tochiyama and H. Freiser, *Anal. Chim. Acta* 1981, **131**, 233.
14. B. S. Jensen, *Acta Chem. Scand.* 1959, **13**, 1890.
15. J. Stary, *The Solvent Extraction of Metal Chelates.* Pergamon Press, Oxford (1964).

Polyhedron Vol. 4, No. 1, pp. 65–68, 1985
Printed in Great Britain.

0277-5387/85 $3.00 + .00
© 1985 Pergamon Press Ltd.

SELENIUM DIBROMIDE AND DICHLORIDE IN ACETONITRILE

JOHN MILNE
Ottawa-Carleton Institute for Research and Graduate Studies in Chemistry, University of Ottawa Campus, Ottawa, Canada, K1N 9B4

(*Received* 31 *January* 1984; *accepted* 2 *March* 1984)

Abstract—The nature of 2/1 Cl/Se and Br/Se stoichiometric mixtures in acetonitrile has been studied by UV-visible and Raman spectroscopy. For both mixtures the selenium dihalide has been shown to be the predominant species in solution, although there are other species present in equilibrium with the dihalide, according to

$$3SeCl_2 = Se_2Cl_2 + SeCl_4$$

$$2SeBr_2 = Se_2Br_2 + Br_2$$

as demonstrated by both techniques. The Raman spectra of $SeCl_2$ and $SeBr_2$ are given. Force constant calculations show that the bonds in the dihalides are the strongest SeCl and SeBr bonds known.

Diorganyl selenium compounds are well-known in the chemical literature but little work has been carried out on the dihalides, which are only known in the gas phase, or in the case of selenium bromide, in solution. Attempts to isolate the solids (or liquids) leads to disproportionation producing elemental selenium, diselenium dihalide and the tetrahalide.[1,2] In non-aqueous solutions, selenium tetrabromide yields $SeBr_2$, Br_2 and Se_2Br_2.[3,4] However, $SeCl_4$ remains intact as the monomer in solution.[5] The Raman spectrum of $SeCl_2$ has been recorded at 350°C,[6] but that of $SeBr_2$ has not yet been published. Selenium dichloride has been shown to exist in concentrated HCl[7] but its existance in non-aqueous solvents has not yet been studied. Selenium difluoride has been studied by matrix isolation[8] and force constants have been calculated. It was considered of interest to study the equilibria involving selenium dichloride and dibromide in acetonitrile by UV-visible spectrophotometry, establish their Raman spectra and determine the stretching force constants for these interesting molecules for comparison with the force constants of the related seleninyl halides.[9]

EXPERIMENTAL

Materials

Acetonitrile (MeCN) and nitromethane ($MeNO_2$) were purified by refluxing over P_2O_5 for one hour and distilling (respective B. P. 81–82°C and 100–1°C). Selenium (Baker AR) was ground before use. Bromine (Baker AR) was distilled (boiling point 59°C). Selenium tetrabromide and selenium tetrachloride were prepared according to standard methods.[10,11]

Procedures

Solutions of selenium tetrahalide, selenium dihalide and diselenium dihalide in acetonitrile were made up by weight from appropriate stoichiometric ratios of selenium and selenium tetrahalide. Spectrophotometric measurements were made with a Varian DMS 90 UV-visible spectrophotometer using 1 mm path-length quartz cells. Raman spectra were recorded using a Jobin-Yvon monochromator in conjunction with PAR photon counting. The spectra were excited with a Spectra Physics krypton ion laser operating at 647.1 nm. All spectra were recorded at 25°C.

RESULTS AND DISCUSSION

UV-visible spectrophotometry

The spectra of a 1.2×10^{-3} mol l^{-1} solution of Se_2Cl_2 and 6.2×10^{-4} mol l^{-1} solution of $SeCl_4$ in MeCN are given in Fig. 1 (traces A and B respectively). Selenium tetrachloride exhibits a shoulder at 255 nm and a peak at 225 nm while diselenium dichloride shows a shoulder at 340 nm and peaks at 295 and 245 nm. The spectrum of a solution with Se-Cl stoichiometry corresponding to that of $SeCl_2$ ($c_{Se} = 3.1 \times 10^{-3}$ mol l^{-1}) is also shown in Fig. 1 (trace D); this spectrum has bands

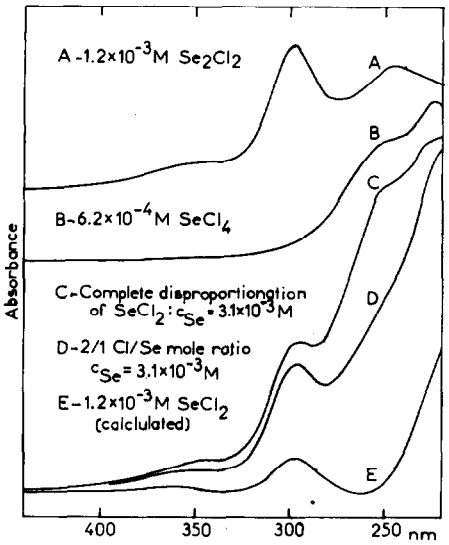


Fig. 1. UV-visible spectra of selenium chlorides in MeCN.

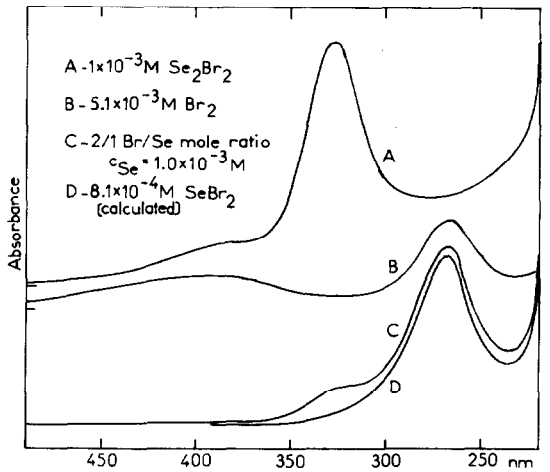


Fig. 2. UV-visible spectra of selenium bromides in MeCN.

corresponding to those of $SeCl_4$ and Se_2Cl_2 suggesting that $SeCl_2$ is completely disproportionated in MeCN according to

$$3SeCl_2 \overset{K_{disp}}{\rightleftharpoons} Se_2Cl_2 + SeCl_4. \quad (1)$$

However, calculation of the spectrum for complete disproportionation of $SeCl_2$ in this solution ($[Se_2Cl_2] = [SeCl_4] = 1.0 \times 10^{-3}$ mol l^{-1}) gives the trace designated as C in Fig. 1. Complete disproportionation does not account for the observed spectrum and some $SeCl_2$ must be present. By assuming various concentrations of Se_2Cl_2 ($[Se_2Cl_2] = [SeCl_4]$) and using the spectra of these species, the spectrum of $SeCl_2$ may be generated by difference from the observed spectrum for 2/1 mole ratio Cl/Se stoichiometry (trace D). The lowest concentration of $SeCl_2$ producing a spectrum which is positive across the measured range of wavelength (220–500 nm) is 1.2×10^{-3} mol l^{-1}; this corresponds to a disproportionation constant K_{disp} ($K_{disp} = [Se_2Cl_2][SeCl_4]/[SeCl_2]^3$) of 2.1×10^2 $mol^{-1}l$. The $SeCl_2$ spectrum generated is given in Fig. 1 (trace E). The concentration of $SeCl_2$ must however be regarded as a minimum, and K_{disp} is smaller than 2.1×10^2 $mol^{-1}l$ as is indicated by the Raman spectra discussed below. At this concentration, even with this minimum amount of $SeCl_2$ present the $SeCl_2$ represents 0.45 mole fraction of all the selenium species whereas Se_2Cl_2 and $SeCl_4$ represent 0.225 mole fraction each.

Selenium tetrabromide is known to decompose in non-aqueous solvents to $SeBr_2$, Se_2Br_2 and Br_2.[3,4] The spectrum of a solution in MeCN, corresponding to the stoichiometry for $SeBr_2$, $c_{SeBr_2} = 1 \times 10^{-3}$ mol l^{-1}, is given in Fig. 2 (trace C). The spectra of Se_2Br_2, 1.0×10^{-3} mol l^{-1} (trace A) and Br_2, 5.1×10^{-3} mol l^{-1} (trace B) are given in the same figure The spectrum corresponding to $SeBr_2$ has a shoulder at 327 nm corresponding to the principal peak in the spectrum of Se_2Br_2, but the intensity of the peak at 268 nm is far too great to be accounted for by Br_2 alone, which has a peak near this wavelength. The strong peak at 268 nm is due to $SeBr_2$; as in carbon tetrachloride,[3] $SeBr_2$ represents the major constituent in solutions of 2 : 1 Br/Se stoichiometry. Selenium dibromide absorbs weakly at 390 nm, whereas both Br_2 and Se_2Br_2 absorb strongly.[3] The absorbance at this wavelength may be used to evaluate the equilibrium constant for the reaction

$$2SeBr_2 \overset{K_d}{\rightleftharpoons} Se_2Br_2 + Br_2. \quad (2)$$

Using the extinction coefficients at 390 nm for Br_2 and Se_2Br_2 (146 and 920 $cm^{-1}mol^{-1}$ respectively), the concentrations of Br_2 and Se_2Br_2 may be evaluated ($[Br_2] = [Se_2Br_2] = 0.94 \times 10^{-4}$ mol l^{-1}); the concentration of $SeBr_2$ may be determined from the difference ($[SeBr_2] = 8.1 \times 10^{-4}$ mol l^{-1}). The equilibrium constant, K_d, for this reaction is 1.4×10^{-2}. The spectrum of $SeBr_2$ (trace D in Fig. 2) is determined by subtracting the spectra of Br_2 and Se_2Br_2 from trace C in Fig. 2. The equilibrium constant, K_d, is smaller than that observed for the same equilibrium in carbon tetrachloride, indicating a relatively greater stability for $SeBr_2$ in MeCN. This probably results from the greater basicity of MeCN relative to that of carbon tetrachloride, producing stronger solvation.

Raman spectroscopy

The Raman spectrum of Se_2Cl_2 in MeCN, listed in Table 1, is very similar to that reported by Kiefer[12] for Se_2Cl_2. The strongest band at 369 cm^{-1} in coincident with an MeCN band; for purposes of identification of Se_2Cl_2 in solution, the band at 138 cm^{-1}, which is also quite strong, can be used. The spectrum of $SeCl_4$ in MeCN exhibits an band at 258 cm^{-1} and additional stronger bands which lie under the solvent peak at 370 cm^{-1}. In nitromethane ($MeNO_2$), which has no bands in this region, $SeCl_4$ bands are observed at 357 and 392 cm^{-1}. In neither case is a band observed at 545 cm^{-1} where elemental chlorine exhibits a peak.[6] Unlike $SeBr_4$, or $SeCl_4$ in the gas phase at 350°C,[6] $SeCl_4$ is stable in these solvents. The spectrum of a solution in MeCN with a 2/1 Cl/Se stoichiometry, which is listed in Table 1, is clearly not consistent with that expected for a mixture of $SeCl_4$ and Se_2Cl_2. A strong peak is observed at 412 cm^{-1}, an additional peak at 381 cm^{-1} is partly masked by the solvent band at 370 cm^{-1} and a third band is observed at 165 cm^{-1}. The only peak observed which can be attributed to either of the disproportionation products is that at 135 cm^{-1} due to Se_2Cl_2. There must therefore also be a small contribution to the peak at 381 cm^{-1} from Se_2Cl_2 (369 cm^{-1}) as well as that from the solvent. The spectrum of $SeCl_2$ in acetonitrile agrees well with that observed by Ozin and Van der Voet for $SeCl_2$ in the gas phase at 350°C.[6] It should be noted that the predominance of $SeCl_2$ in these solutions, where concentrations are several times greater than those solutions studied by UV-visible spectrophotometry, indicates that K_d is smaller than the estimate determined above on the basis of the UV-visible spectra.

The spectra of selenium bromides in acetonitrile solutions, which are red in color, are very difficult to obtain due to absorption of the laser exciting line. No spectra could be obtained using argon ion laser excitation. However, by utilizing the krypton ion laser line at 647.1 nm and by using solutions relatively dilute for Raman spectroscopy in solution (~ 0.3 mol l^{-1}), it was possible to obtain reasonable spectra of solutions with 2/1 Br/Se stoichiometry. The spectra show no bands due to Br_2 (304 cm^{-1} for MeCN solution) or for Se_2Br_2 (strongest band at 254 cm^{-1})[12] as expected from the equilibrium constant determined above, which indicates a $SeBr_2$ concentration nearly 9 times greater than that of Se_2Br_2 ($[Se_2Br_2] = [Br_2]$). Apparently the concentration of these dissociation products is too low for observation. Polarization measurements on the spectrum of $SeBr_2$ indicates that the band at 266 cm^{-1} is the symmetric SeBr stretching mode, which lies below the antisymmetric stretching mode at 290 cm^{-1}, observed in the infrared spectrum of non-aqueous solutions of $SeBr_2$.[4]

Force constants

The three bands observed in the Raman spectra for $SeCl_2$ and $SeBr_2$ can be used to calculate force constants for these molecules with a quite reasonable degree of accuracy. The General Valence Force Field equations given by Siebert[13] may be used, assuming the stretch-bend interaction con-

Table 1. Raman spectra of selenium chlorides and bromides

Se_2Cl_2 in MeCN	$SeCl_4$ in MeCN	$SeCl_4$ in $MeNO_2$	$SeCl_2$ [b] in MeCN	$SeCl_2$ [c] vapour	$SeBr_2$ [b] in MeCN
81(1,sh)					96(2,p?)
139(3)			135(0)		
			165(1)	153	
		205(0)			
	259(1)	258(1)			266(9,p)
291(1)					290(10,dp)
369(10)[a]	360-390(10)[a]	353(10)			
		388(6)	381(8)[a]	377	
409(1)			412(10)	415	

a. Peaks coincident with solvent peak at 370 cm^{-1}

b. 2/1 Cl(Br)/Se stoichiometry

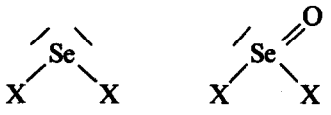
c. ref. 6

Table 2. Vibrational assignment, bond angles and force constants for selenium dihalides; SeX stretching force constants for analogous seleninyl halides

Molecule	$\angle(SeX_2)$	$\nu_1(A_1)$	$\nu_2(A_1)$	$\nu_3(B_1)$	f	f'	d	$f(SeOX_2)$[a]
			(cm^{-1})		(mdyn $Å^{-1}$)			
SeF_2 (matrix)[8]	94	700	269	672	4.24	0.21	0.34	3.81
$SeCl_2$ (vapour)[6]	96	415	153	377	2.25	0.27	0.18	1.78
$SeCl_2$ (MeCN)	96	412	165	381	2.25	0.23	0.21	1.70
$SeBr_2$ (MeCN)	100	266	96	290	1.76	0.05	0.14	1.62

a. Milne, J., Spectrochim. Acta 1982, 38A, 569

stant to be negligible. The vibrational assignment, bond angle ($\angle$(XSeX))[8,14] and calculated force constants are given in Table 2. The set of force constants for SeF_2, based upon the matrix isolation spectra of Willner,[8] assuming the stretch-bend interaction constant, g, to be zero, are also given in Table 2. The effect on the SeF stretching force constant of ignoring g is small;[8] in general, for purposes of comparing stretching force constants, the calculations are acceptable. As expected, the stretching force constants decrease with increasing halogen atomic weight, reflecting a decrease in SeX bond strength. The remarkable feature of these SeX bond stretching force constants is their magnitude. In the case of the chlorides and bromides they are the largest SeX force constants measured. In the case of SeF_2 only the equatorial SeF bonds in SeF_4 are stronger. In all cases the stretching constants are greater than those of the analogous seleninyl halides. The replacement of a non-bonded electron pair in SeX_2 molecules by a doubly-bonded oxygen



rather than strengthening the SeX bonds, as expected on the basis of the resultant electron withdrawal from selenium, in fact causes a weakening of these bonds. In the case of $SeCl_2$ and $SeOCl_2$, this weakening of the bond is also reflected in SeCl bond lengths, 2.18 and 2.20 Å respectively.[15,16] It is interesting to note in this connection that the doubly-bonded oxygen repels neighbouring SeCl bond pairs in the $SeOCl_3^-$ anion more strongly than does the non-bonded electron pair.[17]

Acknowledgements—The Natural Sciences and Engineering Research Council of Canada is thanked for financial support, and Lisa Frost and Mani Mahadevan are thanked for their contribution as summer research assistants.

REFERENCES

1. D. M. Yost and J. B. Hatchen, *J. Am. Chem. Soc.* 1931, **53**, 2549.
2. G. V. Golubkova and E. S. Petrov, *Izv. Sib. Otd. Akad. Nauk. SSSR, Ser. Khim. Nauk.* 1976, **5**, 90.
3. N. W. Tideswell and J. D. McCullough, *J. Am. Chem. Soc.* 1956, **78**, 3026.
4. N. Katsaros and J. W. George, *Inorg. Chem.* 1969, **8**, 759.
5. N. Katsaros and J. W. George, *Inorg. Chim. Acta* 1969, **3**, 165.
6. G. A. Ozin and A. Van der Voet, *J. Chem. Soc. D* 1970, 896.
7. M. Mahadevan and J. B. Milne, Inorg. Chem. 1983, **22**, 1648.
8. H. Willner, *Zeit. anorg. allg. Chem.* 1981, **481**, 117.
9. J. Milne, *Spectrochim. Acta* 1982, **38A**, 569.
10. G. Brauer, *Handbook of Preparative Inorganic Chemistry*, Vol. I, p. 427 Riley, New York (1963).
11. *Inorganic Syntheses*, Vol. 5, p. 125. McGraw-Hill, New York (1957).
12. W. Kiefer, *Spectrochim. Acta* 1971, **27A**, 1285.
13. H. Siebert, *Anwendungen der Schwingungsspektroskopie in der Anorganischen Chemie*, p. 29: Springer, Berlin (1966).
14. E. Nagy-Felsobuki and J. B. Peel, *Chem. Phys.* 1980, **45**, 189.
15. P. A. Akishin, V. P. Spiridonov and R. A. Mishulina, *Vestn. Mosk. Univ. Ser. II Khim.* 1961, **17**, 23.
16. D. Gregory, I. Hargittai and M. Kolonits *J. Mol. Struct.* 1976, **31**, 261.
17. B. Krebs, M. Hucke, M. Hein and A. Schäffer, *Zeit. anorg. allg. Chem.* 1983, **38b**, 20.

Polyhedron Vol. 4, No. 1, pp. 69–73, 1985
Printed in Great Britain.

0277–5387/85 $3.00 + .00
© 1985 Pergamon Press Ltd.

MOLYBDENUM CARBONYL COMPLEXES OF BINUCLEATING PYRIDINE-BASED LIGANDS

JOSEPH A. CONNOR,* E. JOYCE JAMES and COLIN OVERTON
Chemical Laboratory, University of Kent, Canterbury, Kent CT2 7NH, England

(*Received* 1 *February* 1984; *accepted* 2 *March* 1984)

Abstract—Reaction of $[Mo(CO)_4(diene)]$ with 4,4′-bipyridine (44′B), *trans*-1,2-bis(2-pyridyl)ethene (2-bpe) and *trans*-1,2-*bis*(4-pyridyl)-ethene (4-bpe) gives polymeric $[Mo(CO)_4(44'B)]_n$, mononuclear *cis*-$[Mo(CO)_4(2\text{-bpe})_2]$ and binuclear $[Mo(CO)_4(4\text{-bpe})]_2$ respectively. Reaction of the same ligands with $[Mo(CO)_4(bpy)]$ (bpy is 2,2′-bipyridine) produces the bridged binuclear complexes $[\{Mo(CO)_3(bpy)\}_2(44'B)]$ and $[\{Mo(CO)_3(bpy)\}_2(4\text{-bpe})]$. Products are characterised by microanalysis and spectroscopy (IR, ^1H NMR, UV/vis). Reduction of $[\{Mo(CO)_3(bpy)\}_2(44'B)]$ produces an anion in which the unpaired electron is localised on the chelating bpy ligand.

Complexes in which there is electronic interaction through a conjugated bridging ligand between two metal atoms in different formal oxidation states are the objects of attention as models for electron transfer reactions.[1] A rich variety of such models incorporating later members of the *d*-transition series iron, cobalt, ruthenium and rhodium, have been described, but relatively few compounds containing earlier members of the series have been prepared.[2] We report the results of investigations of the reaction of the molybdenum(0) complexes *cis*-$[Mo(CO)_4L_2]$ (L_2 is bicyclo-[2.2.1]-hepta-2,4-diene, or 2,2′-bipyridine) with potentially binucleating ligands 4,4′-bipyridine (44′B), *trans*-1,2-bis(2-pyridyl)ethene (2-bpe) and *trans*-1,2-bis(4-pyridyl)ethene (4-bpe). Our observations emphasize the influence of both steric constraints and chelation in defining the substitution products and suggest that the interaction between the metal atoms in these binuclear products is only weak.

RESULTS

Substitution in hexacarbonylmolybdenum. Reaction between hexacarbonylmolybdenum and 44′B in refluxing toluene produced a bright red insoluble precipitate which was shown to be the polymer $[Mo(CO)_4(44'B)]_n$ rather than the molecular binuclear complex $[Mo_2(CO)_{10}(\mu^2\text{-}44'B)]$. Attempts to prepare this molecular binuclear complex by halide substitution[3] in $[Mo(CO)_5Br]^-$ with 44′B in the presence of $AgBF_4$ were similarly unsuccessful. Reaction between equimolar quantities of $[Mo(CO)_5(THF)]$ and 44′B in dichloromethane gave an orange product characterised as $[Mo(CO)_5(44'B)]$ by microanalysis and IR spectra: reaction of this rather poorly-soluble material with further $[Mo(CO)_5(THF)]$(1 mol) produced insoluble red material which was shown to be $[Mo(CO)_4(44'B)]_n$ from analysis and IR spectra. Reaction between $Mo(CO)_6$ and 2-bpe in toluene at reflux temperature gives orange $[Mo(CO)_4(2\text{-bpe})_2]$.

Substitution in (*bicyclo*[2.2.1]-*hepta*-2,4-*diene*) *tetracarbonylmolybdenum*, [*Mo*(*CO*)$_4$(*NBD*)]. This complex is known[4] to react under mild conditions with 2,2′bipyridine (bpy) to substitute the diene and form the mononuclear complex *cis*-$[Mo(CO)_4(bpy)]$. With 44′B, the product of the substitution reaction is the red polymer $[Mo(CO)_4(44'B)]_n$. Introduction of an olefinic link in the substituting ligand as in 4-bpe leads to a dark red binuclear complex $[Mo(CO)_4(4\text{-bpe})]_2$, on reaction with $[Mo(CO)_4(NBD)]$ in THF, rather than either $[Mo(CO)_4(4\text{-bpe})_2]$ or a polymer. A simple change in ligand geometry between 4-bpe and 2-bpe results in the formation of a yellow-orange mononuclear $[Mo(CO)_4(2\text{-bpe})_2]$, in which one donor nitrogen atom on each ligand is not coordinated, rather than $[Mo(CO)_4(2\text{-bpe})]_2$.

Substitution in (2,2′-*bipyridine*)*tetracarbonyl-molybdenum*, [*Mo*(*CO*)$_4$(*bpy*)]. This complex reacts with bpy at high temperature (refluxing tetralin or 1-methylnaphthalene) to form[5] *cis*-$[Mo(CO)_2(bpy)_2]$. With 44′B as nucleophile, substitution

*Author to whom correspondence should be addressed.

proceeds under much milder conditions in refluxing acetonitrile solution to form the black, binuclear, air-stable complex [{Mo(CO)$_3$(bpy)}$_2$(44′B)]. This complex is rather poorly soluble in most solvents at room temperature. The analogous complex of 4,4′-di(*t*-butyl)-2,2′-bipyridine, L_R, namely [{Mo(CO)$_3L_R$}$_2$(44′B)] prepared from *cis*-[Mo(CO)$_4L_R$], is fairly soluble in common organic solvents and can be crystallised from chloroform. The reaction of [Mo(CO)$_4$(bpy)] with 4-bpe in refluxing acetonitrile gave the purple–black, binuclear air-stable complex [{Mo(CO)$_3$(bpy)}$_2$(4-bpe)]. Surprisingly, there was no net reaction between [Mo(CO)$_4$(bpy)] and 2-bpe under similar conditions (refluxing acetonitrile): only unchanged starting materials were recovered.

Spectroscopic measurements

IR spectra in the region 2100–1600 cm^{-1} both in the solid state and in solution are consistent with *cis*-disubstitution in [Mo(CO)$_4$(2-bpe)$_2$] and [Mo(CO)$_4$(4-bpe)]$_2$, and with *fac*-geometry in [{Mo(CO)$_3$(bpy)}$_2$L] (L = 44′B, 4-bpe) (Table 1). The presence of a second metal atom in the binuclear systems exerts no significant influence on the frequency of the ν(CO) absorptions. The position of the lowest energy MLCT band in the visible region of the electronic spectrum (Table 1) demonstrates the effect of extending the chromophore in the binuclear complexes by comparing [Mo(CO)$_4$(bpy)](431 nm) with [{Mo(CO)$_3$(bpy)}$_2$(44′B)] (489 nm) and [{Mo(CO)$_3$(bpy)}$_2$(4-bpe)] (580 nm).

In the ^{1}H NMR spectra, the coordination shifts of the binucleating ligands 44′B and 4-bpe are generally small (*ca.* 0.1 ppm) and rather insensitive to changes occurring at the metal atom (Table 2); however, there are significant shifts in the resonances of the spectator bpy ligands which, with the exception of H6, generally move to lower field.

Reduction reactions

Reduction of [{Mo(CO)$_3$(bpy)}$_2$(44′B)] with potassium amalgam in dimethoxyethane solution gives a red-purple solution. The ESR spectrum of this solution is very similar to that of the bpy radical anion with g_{av} 2.005 and a signal width of 25G. Reduction of [{Mo(CO)$_3L_R$}$_2$(44′B)] (which is more soluble in dimethoxyethane) produced a red-purple solution. The ESR spectrum of this solution is qualitatively different to the foregoing and very similar to that of the L_R radical anion with g_{av} 2.006 (28G). These spectra were quite distinct from the spectrum of the 44′B radical anion produced under similar conditions. These experiments strongly suggest that the unpaired electron density is largely localised on the bpy (or L_R) ligand rather than on the 44′B ligand in these complexes. There is no evidence for molybdenum hyperfine interaction in these spectra.

DISCUSSION

Our lack of success in preparing either [Mo(CO)$_4$(44′B)$_2$] or [Mo$_2$(CO)$_{10}$(44′B)] by apparently obvious and straightforward methods stands in contrast to the ease with which [Mo(CO)$_4$(2-bpe)$_2$] was prepared. The lability of [Mo$_2$(CO)$_{10}$(pyrazine)] in solution has been described.[6] The influence of the ethene link, both in imposing stereochemistry and restricting reactivity by steric factors is evident from a comparison of results reported here. Thus, whereas bpy provides a chelate complex *cis*-[Mo(CO)$_4$(bpy)], 2-bpe forms a di-substituted mononuclear complex *cis*-[Mo(CO)$_4$(2-bpe)$_2$], and whereas 44′B forms polymeric [Mo(CO)$_4$(44′B)]$_n$, 4-bpe will form a bi-

Table 1. IR[a] (2100–1700 cm^{-1}) and Visible[b] (25000–14000 cm^{-1}) absorption spectra

	ν(CO)/cm^{-1}				ν(MLCT)/cm^{-1}	
[Mo(CO)$_5$(44'B)]	2070m	1980w	1935s	1890s	25200	AN
cis-[Mo(CO)$_4$(bpy)]	2014m	1911vs	1882s	1830s	23200	AN
cis-[Mo(CO)$_4$(44'B)]$_n$	2016m	1886s	1862s	1814m	24000	DMSO
cis-[Mo(CO)$_4$(2-bpe)$_2$]	2005s	1895vs	1860s	1835s	23900	AN
cis-[Mo(CO)$_4$(4-bpe)]$_2$	2010s	1900vs	1860s	1819vs	18870	DMSO
fac-[{Mo(CO)$_3$(bpy)}$_2$(44'B)]		1885s	1757s		19650	DMSO
fac-[{Mo(CO)$_3$(L_R)}$_2$(44'B)]		1905s	1779s		20450	AN
fac-[{Mo(CO)$_3$(bpy)}$_2$(4-bpe)]		1895s	1760s		17240	AN

a) Nujol mull; b) dimethylsulphoxide (DMSO), acetonitrile (AN)

Table 2. Proton NMR chemical shifts, δ ppm of ligands and their complexes in solution

	2-H	3-H	4-H	5-H	6-H	α-H	solvent
2,2'-bipyridine(bpy)		8.49	7.80	7.28	8.68		a
4,4'-$(Me_3C)_2$-2,2-bipyridine(L_R)		8.40	(1.34)	7.47	8.61		d
1,2-bis(2-pyridyl)ethene(2-bpe)		7.70	7.58	7.23	8.63	7.75	b
1,2-bis(4-pyridyl)ethene(4-bpe)	8.60	7.50		7.50	8.60	7.40	c
4,4'-bipyridine(44'B)	8.74	7.83		7.83	8.74		d
cis-[$Mo(CO)_4$(bpy)]		8.16	7.95	7.39	9.12		e
cis-[$Mo(CO)_4(L_R)$]		8.62	(1.42)	7.63	8.86		d
cis-[$Mo(CO)_4$(2-bpe)$_2$]		7.80	7.55	7.00	9.10	7.60	b
		7.69		7.20	8.50		
cis-[$Mo(CO)_4$(4-bpe)]$_2$	8.69	7.65		7.65	8.69	7.53	d
fac-[{$Mo(CO)_3$(bpy)}$_2$(44'B)]	8.74	7.84		7.84	8.74		d
		8.55	8.13	7.61	8.99		
fac-[{$Mo(CO)_3(L_R)$}$_2$(44'B)]	8.76	7.73		7.73	8.76		c
		8.33	(1.49)	7.55	8.98		
fac-[{$Mo(CO)_3$(bpy)}$_2$(4-bpe)]	8.73	7.64		7.64	8.73	7.54	d
		8.54	8.12	7.58	8.94		

a) $CDCl_3$; b) d_6-acetone; c) CD_3CN; d) d_6-dmso; e) CD_2Cl_2

nuclear complex $[Mo(CO)_4(4\text{-bpe})]_2$. The contrast between the complexes $[Mo(CO)_4(2\text{-bpe})_2]$ and $[Mo(CO)_4(4\text{-bpe})]_2$ emphasizes the importance of the mutual disposition of the donor functions in these ligands which is underlined by the formation of $[\{Mo(CO)_3(bpy)\}_2(4\text{-bpe})]$ in comparison with the apparent inability of 2-bpe to form an analogous bridged binuclear complex.

NMR studies suggest that the binucleating ligands 44'B and 4-bpe do not undergo much net change when coordinated as bridging ligands, whereas the chelating bpy or L_R ligands in the same complexes do experience change as a result of the introduction of either 44'B or 4-bpe. These observations are emphasized by the results of the one-electron reduction of the complexes $[\{Mo(CO)_3(bpy)\}_2(44'B)]$ and $[\{Mo(CO)_3(L_R)\}_2(44'B)]$ in which the chelating (bpy or L_R) ligand is reduced rather than the bridging (44'B) ligand. These observations are in contrast to those[7] on the one-electron reduction of $[Mo_2(CO)_8(bpym)]$ (bpym is 2,2'-bipyrimidine) in which the binucleating, bridging ligand is reduced. Later experiments on $[Mo_2(CO)_8(bpym)]$ have shown that electrochemical reduction in THF is reversible ($E_{\frac{1}{2}} = -0.67, -1.51$ V vs S.C.E.). The one-electron reduction product ($E_{\frac{1}{2}} = -0.67$ V) shows a complex 5-line ESR signal (g_{av} 2.0022) consistent with localisation of the unpaired electron density on molybdenum. Electrochemical studies on $[\{Mo(CO)_3(bpy)\}_2(44'B)]$ in acetonitrile solution indicate that both oxidation ($E_{\frac{1}{2}} = +0.3$ V) and reduction ($E_{\frac{1}{2}} = -1.62, -1.88$) are reversible.

EXPERIMENTAL

All preparations were carried out in an atmosphere of oxygen-free dry dinitrogen. Solvents were dried, deaerated and distilled under nitrogen immediately prior to use. IR spectra were recorded in solution using 1.0 mm path length solution cells and as mulls with Nujol and hexachlorobutadiene on PE 257 or 625 spectrometers. UV and visible spectra were recorded on a Unicam SP 800 spectrometer. NMR spectra were recorded on either Brucker WP 80 or Jeol PS 100 spectrometers using Fourier transform techniques. ESR spectra were recorded on a Varian E 112 spectrometer operating at 9.238 GHz.

Microanalyses were carried out by Mr. M. Hart at Manchester and Mr. A. Fassam at Canterbury. Molybdenum hexacarbonyl was purchased from Pressure Chemical, Pittsburg, and 4,4'-bipyridyl, 2-bpe and 4-bpe were purchased from Aldrich. The complex $[Mo(CO)_4(\eta^2, \eta^2\text{-}C_7H_8)]$ was prepared,

using freshly distilled bicyclo[2.2.1]hepta-2,4-diene, according to the literature.[8]

Preparation of (4,4′-bipyridine)tetracarbonylmolybdenum polymer

Freshly sublimed hexacarbonylmolybdenum (1.00 g, 3.78 mmol) and 4,4′-bipyridine (0.29g, 1.85 mmol) were heated together in toluene at reflux for 6h under anaerobic conditions. On cooling the mixture, a bright red precipitate was isolated by filtration from the yellow mother liquor and extracted with warm petroleum ether (60–80°C boiling fraction) (5 × 50 cm^3). The red powder was dried in a vacuum to yield 0.59 g of material (43% yield based on Mo). Found: C, 45.5; H, 2.1; Mo, 27.5; N, 7.6. Calc. for $(C_{14}H_8MoN_2O_4)_n$: C, 46.1; H, 2.2; Mo, 26.4; N, 7.7%.

Preparation of (4,4-bipyridine)pentacarbonylmolybdenum

(a) A mixture of $Et_4N[Mo(CO)_5Br]$ (0.446 g, 1 mmol)[9] and 4,4′-bipyridine (0.156 g, 1 mmol) in dichloromethane (30 cm^3) was treated with $AgBF_4$ (0.19 g, 1 mmol) and stirred rapidly. Filtration after 15 minutes was followed by concentration by distillation under reduced pressure to give a red solid which did not redissolve. Found C, 45.3; H, 2.3; N, 7.4.

(b) A solution of 4,4′-bipyridine (0.31 g, 2 mmol) in dichloromethane was added to $[Mo(CO)_5(THF)]$ (*ca.* 0.6 g based on presumed quantitative conversion of 0.53 g $Mo(CO)_6$ in THF) at room temperature. An orange solid which precipitated from the mixture was isolated by filtration. This solid appears to be photosensitive and is converted by the action of direct sunlight to the red solid complex $[Mo(CO)_4(44'B)]_n$ already mentioned. The orange solid was analysed: Found: C, 45.8; H, 2.3; N, 7.0. Calc. for $C_{15}H_8MoN_2O_5$: C, 45.9; H, 2.0; N, 7.1%.

Preparation of tetracarbonyl bis(1,2-bis(2-*pyridyl*)*ethene*)*molybdenum*

Solid *cis*-$[Mo(CO)_4(\eta^2,\eta^2\text{-}C_7H_8)]$ (0.78 g, 2.6 mmol) and solid 2-bpe (0.94 g, 5.2 mmol) were placed in a Schlenk tube and tetrahydrofuran (30 cm^3) was added. The mixture was stirred for 18 hr (overnight). The orange–red reaction mixture was evaporated to dryness under reduced pressure and the residue was extracted with dichloromethane, filtered and then carefully placed beneath a layer of petroleum ether (40–60°C boiling fraction). The solution was stored at 278K and after six days the crystalline material was isolated by filtration. The orange crystals were washed with petrol. Yield 1.1 g, 75%. Found: C, 58.7; H, 3.3; N, 10.1. Calc. for $C_{28}H_{20}MoN_4O_4$: C, 58.7; H, 3.5; N, 9.8%.

Preparation of tetracarbonyl(1,2-bis(4-*pyridyl*)*ethene*)*molybdenum dimer*

Solid 4-bpe (0.81 g, 4.4 mmol) was added portionwise to a stirred solution of $[Mo(CO)_4(\eta^2,\eta^2\text{-}C_7H_8)]$ (0.67 g, 2.2 mmol) in THF (30 cm^3). The colour of the mixture turned deep red immediately. The reaction mixture was stirred at room temperature overnight, concentrated under reduced pressure. The residue was extracted with dichloromethane and the extract solution was placed beneath a layer of petroleum ether. Red-brown crystals were isolated by filtration after four days, washed with petroleum ether and dried under vacuum. Yield 0.55 g, 65%. Found: C, 48.9; H, 2.6; N, 7.3. Calc. for $C_{14}H_{10}MoN_2O_4$: C, 49.2; H, 2.5; N, 7.2%.

Preparation of μ^2-(4,4′-*bipyridine*)bis{(2,2′-*bipyridine*)*tricarbonylmolybdenum*}

Solid 4,4′-bipyridine (0.214 g, 1.37 mmol) was added to a solution of $[Mo(CO)_4(bpy)]$ (1.00 g, 2.75 mmol) in acetonitrile (30 cm^3) and the mixture was heated at reflux for 12 hr, during which time the colour changed from red to black. A black solid precipitated from the solution on cooling. The solid was isolated by filtration, washed with chloroform (5 × 15 cm^3) until the washings were no longer red, then once with petrol and then dried under vacuum. Yield: 0.828 g, 73%. Found: C, 51.8; H, 2.7; Mo, 23.7; N, 9.9. Calc. for $C_{36}H_{24}Mo_2N_6O_6$: C, 52.2; H, 2.9; Mo, 23.2; N, 10.1%. Using a similar procedure with (4,4′ - di(tert - butyl) - 2,2′ - bipyridine)tetracarbonylmolybdenum gave well-formed purple-black crystals of $[\{Mo(CO)_3L_R\}_2(44'B)]$. Yield 59%. Found: C, 58.6; H, 5.6; Mo, 18.2; N, 7.6. Calc. for $C_{52}H_{56}Mo_2N_6O_6$: C, 59.3; H, 5.3; Mo, 18.2; N, 7.6%. Using 4-bpe with $[Mo(CO)_4(bpy)]$ in a similar sequence produced $[\{Mo(CO)_3(bpy)\}_2(4abpe)]$ as a purple–black solid. Yield 82%. Found: C, 52.7; H, 3.1; N, 9.8. Calc. for $C_{38}H_{26}Mo_2N_6O_6$: C, 53.4; H, 3.1; N, 9.8%.

Acknowledgements—We thank the Science and Engineering Research Council for support through a Studentship awarded to C.O. and other support, the University of Manchester for the award of a Rona Robinson studentship to E.J.J., Dr. N. El-Murr, Institut de Recherches sur la Catalyse, Villeurbanne, France, for the electrochemical measurements, and Miss L. R. Duncan for the preparation of $[Mo(CO)_5(44'B)]$.

REFERENCES

1. R. D. Cannon, *Electron Transfer Reactions*. Butterworths, London (1980).

2. C. Creutz, *Prog. Inorg. Chem.* 1983, **30**, 1.
3. J. A. Connor, E. M. Jones and G. K. McEwen, *J. Organometallic Chem.* 1972, **43**, 357.
4. J. A. Connor and C. Overton, *J. Organometallic Chem.* 1983, **249**, 165.
5. M. H. Chisholm, J. A. Connor, J. C. Huffman, E. M. Kober and C. Overton, *Inorg. Chem.* 1984, **23**, 2298.
6. R. Ernhoffer and R. E. Shepherd, *J.C.S. Chem. Comm.* 1978, 859.
7. C. Overton and J. A. Connor, *Polyhedron* 1982, **1**, 53.
8. E. W. Abel, M. A. Bennett, R. Burton and G. Wilkinson, *J. Chem. Soc.* 1958, 4559.
9. E. W. Abel, I. S. Butler and J. G. Reid, *J. Chem. Soc.* 1963, 2068.

Polyhedron Vol. 4, No. 1, pp. 75–80, 1985
Printed in Great Britain.

0277–5387/85 $3.00 + .00
© 1985 Pergamon Press Ltd.

ON THE CHELATION OF STANNATE (IV), ANTIMONATE(V) AND TELLURATE(VI) ANIONS WITH CYCLIC AND ACYCLIC HEXOLS

JOLOCAM MBABAZI
Department of Chemistry, Makerere University, P.O. Box 7062, Kampala, Uganda

(*Received* 5 *May* 1983; *accepted after revision* 2 *March* 1984)

Abstract—Conductimetric, potentiometric and titrimetric studies of aqueous telluric acid at pH 4.8–11.0 in the presence of acyclic hexols show that whereas only 1 : 1 complexes are formed at low pH, 1 : 3 polyol-tellurates exist only in strongly alkaline media. The 1 : 2 chelates behave as transient intermediates. Cyclohexols exclusively form 1 : 1 complexes with stannate(IV), antimonate(V) and tellurate(VI) oxyanions, even at extreme pH conditions.

The stability of polyol-tellurate complexes,[1] like that of the periodate analogues,[1,2] increases with pH. As a result, apart from the expected 1 : 1 polyol-tellurates,[3,4] complexes of other stoichiometries might exist at high pH. Part of this investigation was to put this possibility to experimental test, using cyclic and acyclic hexols, and falls in line with recent studies[5–7] on related systems. The extension of this work to stannate and antimonate hexahydroxyanions was prompted by their isostructural and isoelectronic nature with telluric acid.[8–11] Although it had earlier been reported that complexes are formed between polyols and antimonic acid in aqueous solution,[12] the evidence was inconclusive about their stoichiometries, presumably due to the appreciable degree of aggregation of antimonate ions in acidic aqueous media.[13] Polyol-antimonates of known structure are however mentioned elsewhere in the literature,[14,15] but the materials and experimental conditions used are different from those employed in the present study. Electrophoretic migration of polyols in aqueous sodium stannate[16] is evidence that similar complexes are formed, but to what extent is yet to be fully established. The present work endeavours to fill portions of this gap.

EXPERIMENTAL

A Wayne–Kerr Universal bridge and a dip cell (const. = 1.37 cm^{-1}) were used for electrolytic conductance studies. The experimental techniques used were similar to those earlier described under telluric acid,[6] except for stannate and antimonate solutions to which potentiometric and indicator titrations did not apply. Studies on stannate and antimonate anions were carried out using sodium stannate, $Na_2Sn(OH)_6$, and potassium antimonate, $KSb(OH)_6 \cdot \frac{1}{2}H_2O$, respectively. Stock solutions (0.010 M) of potassium antimonate were prepared as described in Ref. 12; their pH was raised using solid potassium hydroxide, and lowered using dilute hydrochloric acid. That of stannate solutions was raised using solid sodium hydroxide, and the pH readings taken on these solutions using a glass electrode were corrected for the sodium error.

RESULTS

(1) *Telluric acid*

Addition of sufficient dulcitol, as shown by pH titration studies, increased the acidity of telluric acid. This effect, a well-known phenomenon,[3,6] is indicative of complex formation. In such titrations, it may be shown that the pH of the solution at half-neutralisation, $(pH)_{\frac{1}{2}}$, is numerically equal to the pKa value of the weak acid. A plot of $(pH)_{\frac{1}{2}}$ showed a discontinuity at a 1 : 1 dulcitol-tellurate mole ratio. The acidity of the mixtures did not appear to increase further after ~2 : 1 polyol-tellurate mole ratio. A similar investigation with other acyclic hexols mannitol, sorbitol, allitol and altritol, and their cyclic counterparts *allo*, *epi*, *cis*, *muco*, *meso* and *neo*inositol gave similar results, but the decrease in pH of telluric acid solutions caused by the presence of equimolar quantities of polyol was in the order : dulcitol > mannitol, allitol > altritol, sorbitol > cyclohexols. The acidity of telluric acid was little affected by *scyllo*inositol. Titration of telluric acid to a phenol-

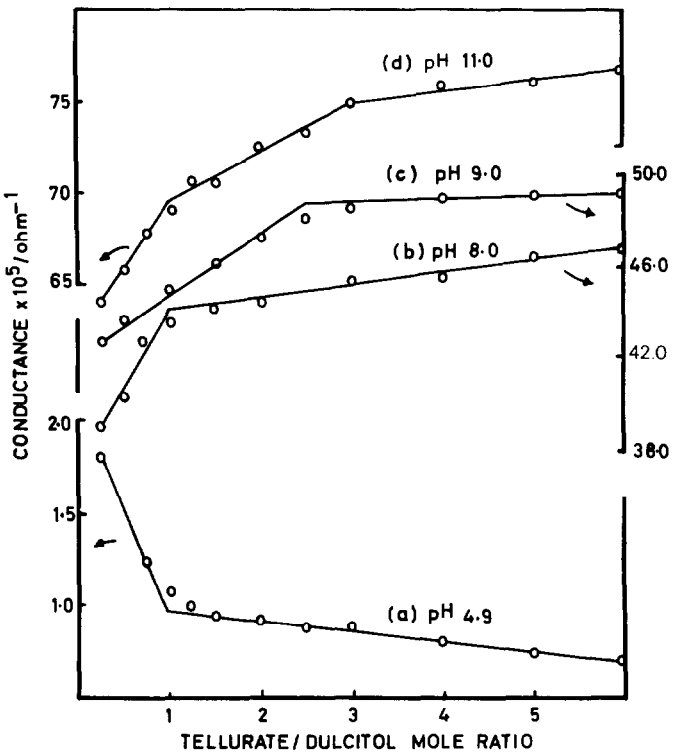


Fig. 1. Conductances of telluric acid (0.010 M) at various *initial* pH, after addition of dulcitol, at 25°C.

phthalein endpoint in the presence of the alditols showed evidence for only 1 : 1 complexes when the titres were plotted against the polyol-tellurate mole ratio. The cyclitols, however, gave poor endpoints.

When the conductance measurements at constant tellurate concentrations were plotted against the tellurate-polyol mole ratio (Fig. 1) according to the method of Yoe and Jones,[17] formation of only a 1 : 1 complex of dulcitol was indicated in the pH range 4.8–8. At pH > 10 a 1 : 3 dulcitol-tellurate complex was indicated. In the intermediate pH range the plots gave curves with discontinuities lying between tellurate-polyol mole ratios 2 and 3. The corresponding pH measurements (Fig. 2) gave

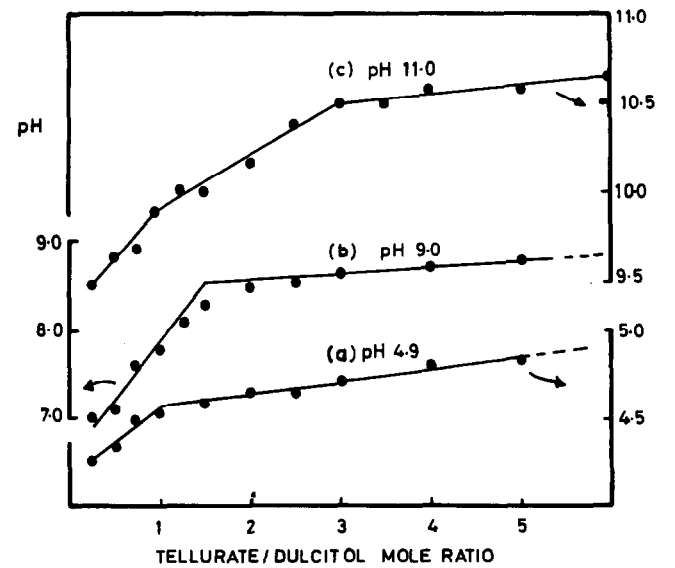


Fig. 2. Final pH values of telluric acid (0.010 M) at various *initial* pH, after addition of dulcitol, at 25°C.

consistent results at all other pH values, but indicated tellurate-polyol mole ratios between 1 and 2 in this pH range. The implication of these two seemingly different results was that a mixture of 1 : 1, 1 : 2 and 1 : 3 dulcitol-tellurate complexes were simultaneously present in the solutions. The absence of unambiguous discontinuities at the 2 : 1 tellurate-polyol mole ratio indicated that the 1 : 2 dulcitol-tellurate complex existed as a transient intermediate. The behaviour of other linear hexols was almost similar. With cyclohexols, only 1 : 1 complexes were indicated at all the pH values. Except for *scyllo*inositol for which there was hardly any pH change, corresponding pH measurements yielded consistent results.

The existence of 1 : 1 (at low pH) and 1 : 3 alditol-tellurates (at high pH) was further confirmed by Job's method of continuous variations[18] using conductance and pH measurements (Fig. 3). Regarding cyclohexol-tellurate systems, the changes in the conductance or pH of telluric acid caused by their presence were in most cases too small to give a conclusive Job's plot.

As a general rule, therefore, whereas cyclitols formed only 1 : 1 complexes, the linear hexols were able to complex, pH dependently, with up to three tellurates per molecule.

Sucrose[5] can similarly bind up to four tellurates per molecule.

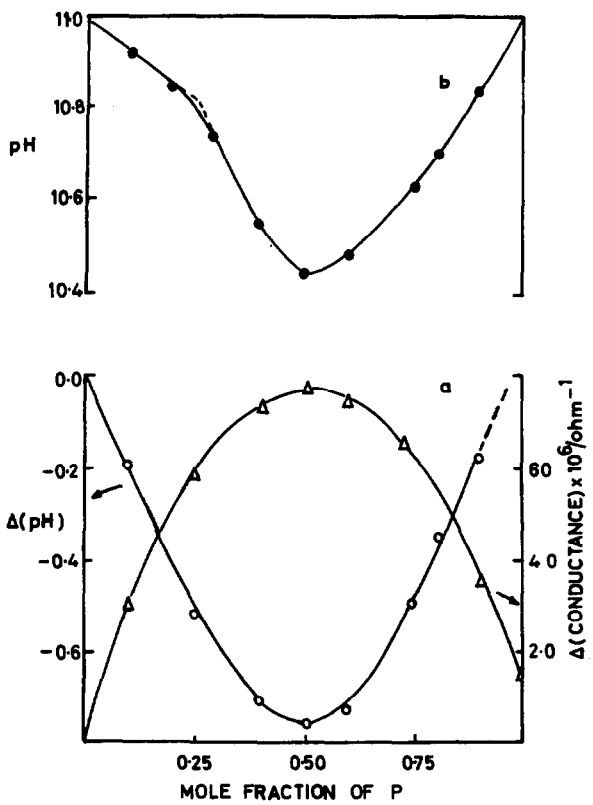


Fig. 3. Job's plot (change in conductance or pH at 25°C) for (a) dulcitol-telluric acid mixtures after 24 h or more, and (b) mannitol-telluric acid mixtures, each initially at pH 11, after 10 min or more. (P = polyol.).

(2) *Antimonate anions*

The conductance of potassium antimonate at its natural (7.45, 0.010 M) and higher pH was observed to be lowered by addition of increasing quantities of polyol. The Yoe–Jones[17] conductance plots showed evidence of only 1 : 1 complexes (Fig. 4). The presence of hexols in acidified potassium antimonate at pH 4.0 increased the conductance (Fig. 4) and lowered the pH (not shown) of the solution, with indication of only 1 : 1 polyol-antimonate complexes.

Corresponding pH measurements gave consistent results, although in the pH range 5–11 the readings did not show any significant deviation from the initial pH. A notable exception to this observation was the dulcitol-antimonate system, which showed definite and conclusive results throughout the entire pH range (4.0–12.0) investigated. The general trend at low and high pH was similar to that in Fig. 2.

Job's plots[18] (conductance and pH changes) at initial pH 4.0 showed maxima and minima, respectively, at polyol mole fraction 0.5 (see Fig. 3a), thus further confirming the existence only 1 : 1 complexes at low pH. At higher pH values, however, the changes in conductance or pH caused by the presence of these polyols were in most cases not large enough to give meaningful curves.

(3) *Stannate anions*

Solutions of sodium stannate at their natural pH (11.7, 0.010M) develop turbidity within 10–15 min, due to the formation of colloidal stannic acid;[19] however, *freshly* prepared solutions are usable. The stability of sodium stannate solutions is greatly increased by the presence of suitable polyols: equilibrated solutions containing sufficient amounts of various hexols hardly exhibit any turbidity.

Stannate-hexol systems closely resembled the antimonate analogues. When the conductance data at constant stannate concentrations was plotted against the stannate-polyol mole ratio,[17] the existence of only 1 : 1 complexes at pH 11.7–13.0 was evident (see Fig. 4d). With acyclic hexols, corresponding pH measurements gave consistent results. The pH of stannate solutions in the presence of cyclohexols did not vary significantly from the initial value. No confirmatory results were obtained using the method of continuous variations.[18]

Comparing the three aqueous polyol-oxyanion

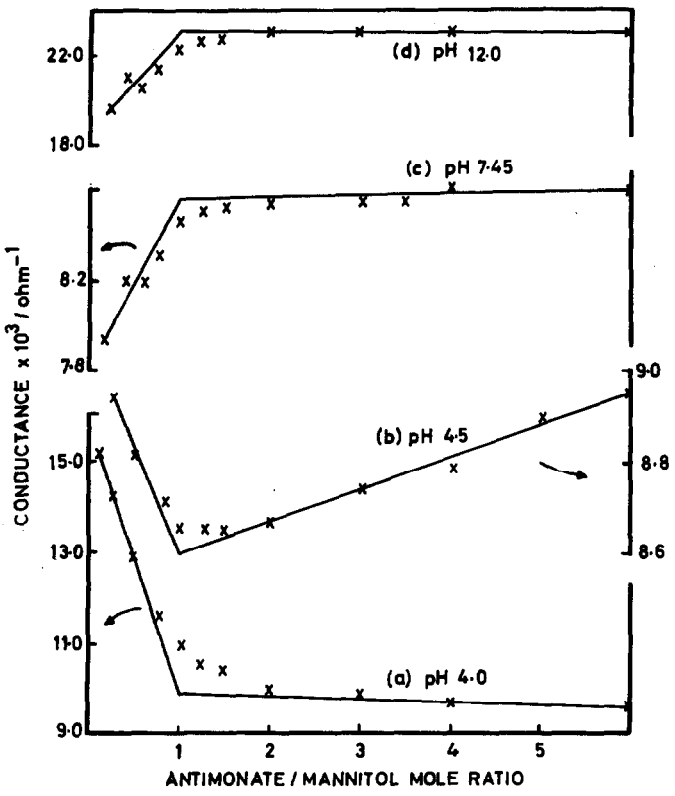


Fig. 4. Conductances of potassium antimonate (0.010 M) at various *initial* pH, after addition of mannitol, at 25°C.

systems, whereas equilibration times at 25°C progressively decreased from *ca.*24 hr for telluric acid at pH 4.8 to about 10 min at pH 11 for each polyol, with stannate- and antimonate-hexol solutions equilibration often took much longer, requiring up to 4 days with some cyclitols.

DISCUSSION

Tin, antimony and tellurium are three consecutive members of the same period along the Periodic Table. However, of the three isostructural and isoelectronic species $Sn(OH)_6^{2-}$, $Sb(OH)_6^-$ and $Te(OH)_6$, only telluric acid is able to form 1 : 3 polyol-oxyanion chelates with acyclic hexols. Calculations based on the Te–OH bond distances in $Te(OH)_6$ octahedra give an average value of 0.271 nm for the O–O distance in telluric acid in the solid state[8–11] and 0.274 nm in aqueous solution.[20] The corresponding distance in $Sb(OH)_6^-$ is quoted as 0.280 nm[21] in the solid state, and, like that in $Te(OH)_6$, is bound to be slightly longer in aqueous solution. It therefore still remains that in solution the O–O separation in the hexahydroxyantimonate anion is definitely larger than that in telluric acid. The O–O distance in $Sn(OH)_6^{2-}$ is, on the basis of periodicity, expected to be longer than that in $Sb(OH)_6^-$ by about 0.01 nm. In linear hexols, all the six carbon atoms may lie in the same plane. In this conformation, calculations (based on the mean bond lengths C–O = 0.143 nm and C–C = 0.154 nm, assuming tetrahedral angles at all the carbon atoms) show that the O–O distances in *gauche*- and *trans*-1,2-diol groups are 0.282 and 0.365 nm respectively, although in an eclipsed conformation the oxygens can approach each other to within 0.245 nm. Since complex-formation between polyols and oxyacids is thought to involve two hydroxyls from the oxyanion and two from the polyol[3], it is plausible that the $M(OH)_6$ (M = Sn, Sb, Te) species whose O–O distance is closest to that in a near-eclipsed 1,2-diol group would be able to form a relatively stable, near-planar five-membered ring without undue distortion of the two C–O bonds.

In this respect, $Te(OH)_6$ is apt to satisfy this requirement better than either $Sb(OH)_6^-$ or $Sn(OH)_6^{2-}$ ions. On the other hand, the O–O separation in *gauche*-1,2-diols is sufficiently close to that in antimonate and stannate anions for the formation of five-membered rings to be likely. Nevertheless the puckered nature of the rings so formed would render such complexes less stable than the tellurate analogues. Thus whereas the stability of the chelate formed by telluric acid with

a near-eclipsed 1,2-diol group is such that it allows the formation of three such rings on an acyclic hexol, antimonate and stannate complexes with *gauche*-1,2-diols are probably not stable enough as to allow more than one oxyanion to cling to one such molecule.

The relative (Fischer projection) configurations for five alditols studied are given in Fig. 5. Although internal rotation about the C–C bonds is possible, the configuration of each hexol is fixed by the OH groups being "locked" in position by intramolecular hydrogen bonding. It is therefore interesting to note that despite their differing configurations, acyclic hexols are each able to bind up to three tellurates per molecule. Due to the presumed stepwise nature of the complex-formation process,[6] it is reasonable to think that the initial complexation of a linear hexol with one tellurate ion reduces the H-bonding between the remaining four hydroxyls on the polyol. This effect is enhanced by the fact that intramolecular H–bonding decreases with pH. Thus at high pH the two effects permit the remaining two uncomplexed pairs of 1,2-diol groups on the alditol to rotate more freely about the C–C bonds, and consequently create a conformation that meets the specific structural features[3] required by two more tellurates. Consistent with this view is that the 1 : 3 hexol-tellurates are indeed observed only in strongly alkaline media.

Owing to the presence of six OH groups on the polyol, there are a number of ways in which hexahydroxyanions can combine with a linear hexol to form a 1 : 1 anionic complex. Nevertheless

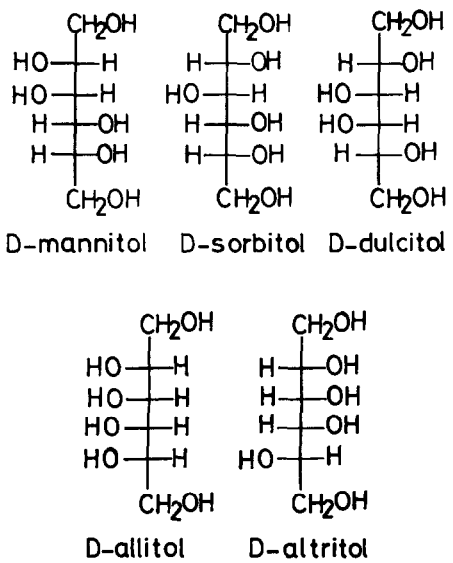


Fig. 5. Fischer projection configurations of some acyclic hexols studied.

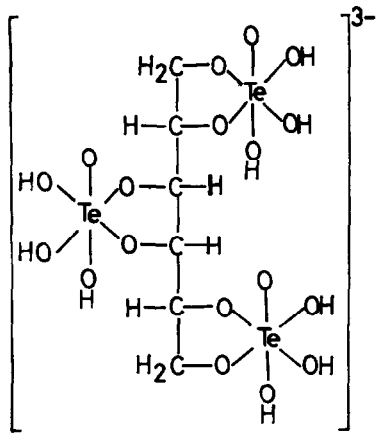


Fig. 6. Possible structure of a 1 : 3 acyclic hexol-tellurate complex.

molecular models show that formation of a 1 : 3 alditol-tellurate complex necessitates the adoption of only one possible structure (Fig. 6), that caters for minimum steric effects, ring size and stability. Any other structure may be discounted on the basis of the relatively poor complexing ability exhibited by 1,3-propanediol and its substituted derivatives, as compared to that with 1,2-propanediol or glycerol.[3] Inevitably, the hexol whose OH configuration in its normal state already meets such structural requisites should react fastest and (though not necessarily) form the most stable complexes. In conformity, it was observed that of the acyclic hexols investigated, dulcitol (Fig. 5, cf. Fig. 6) reacted fastest, and caused the largest deviations in the conductance and pH of each of the oxyacid anion solutions.

A common feature in cyclohexol-oxyanion systems encountered in this study was the exclusive formation of 1 : 1 complexes, even at high pH values. The O–O distance in the more stable chair form of *cis*- and *trans*-1,2-diol groups of cyclohexols are identical (0.282 nm). The O–O separation in $Sb(OH)_6^-$ ions in solution, as we have already seen, is very close to this value as compared to that in $Te(OH)_6$ or $Sn(OH)_6^{2-}$. Antimonate ions should therefore be able to form stronger 1 : 1 cyclitol complexes. Such complexation would to a large extent be expected to involve *cis*-1,2-diol groups, resulting in planar, or near-planar, five-membered rings. Consistent with this assertion is the observation that the cyclohexols possessing more *cis*-1,2-diol groups electrophoretically migrate faster in stannate solution.[16] The deviation of the O–O distances in $Sn(OH)_6^{2-}$ and $Te(OH)_6$ above and below that in 1,2-cyclohexol diol groups, respectively, is just about the same (~ 0.01 nm), and is certainly not so large as not to warrant

formation of fairly stable *cis*-stannate and tellurate cyclohexol complexes. Due to the presence of only one *cis*-1,2-diol group on *meso*inositol, it is not unexpected that 1 : 1 oxyanion chelates were exclusively formed with this compound. Complexation with *trans*-1,2-diol groups on the cyclohexol would result in severely puckered and correspondingly unstable chelates. For this reason, *scyllo*inositol, with all its three 1,2-diol groups *trans* to each other, is a poor complexing agent.

If this were all, a 1 : 2 polyol-oxyanion chelate would be afforded with *muco*inositol by complexation at each of the two *cis*-diol positions. Similar considerations would lead one to expect 1 : 2 cyclitol-oxyanion complexes from the *epi* and *neo*, and up to 1 : 3 such chelates with the *allo* and *cis* isomers. Molecular models, however, confirm that the exclusive formation of 1 : 1 complexes with each inositol throughout the entire pH range investigated arises from the presence of more than one hydroxyanion on a cyclohexol molecule being sterically unfavoured.

REFERENCES

1. B. M. I. Alesofie and W. J. Popiel, *Talanta* 1973, **20**, 251.
2. W. J. Popiel and M. S. Rustom, *Carbohydr. Res.* 1977, **56**, 407.
3. H. R. Ellison, J. O. Edwards and E. A. Healy, *J. Am. Chem. Soc.* 1962, **84**, 1820.
4. P. J. Antikainen and E. Huttunen, *Suomen Kem.* 1973, **B46**, 184.
5. W. J. Popiel and M. S. Rustom, *J. Inorg. Nucl. Chem.* 1978, **40**, 921.
6. J. Mbabazi and W. J. Popiel, *J. Inorg. Nucl. Chem.* 1979, **41**, 1491.
7. J. Voelkel and W. Szydlowska, *Makromol, Chem.* 1981, **182**, 255.
8. O. Lindqvist, *Acta Chem. Scand.* 1970, **24**, 3178.
9. O. Lindqvist and M. S. Lehmann, *Acta Chem. Scand.* 1973, **27**, 85.
10. L. Falck and O. Lindqvist, *Acta Crystallogr.* 1978, **B34**, 3145.
11. D. F. Mullica, J. D. Korp, W. O. Milligan, G. W. Beall and I. Bernal, *Acta Cryst.* 1980, **B36**, 2565.
12. S. H. Gate and E. Richardson, *J. Inorg. Nucl. Chem.* 1961, **23**, 257.
13. J. Lemerle, *Rev. Chim. Miner.* 1973, **10**, 529.
14. E. V. Zimakova, U. M. Kurkchi and R. K. Dzhiyanbaeva, *Sb. Nauch. Tr. Tashkent Un-t* 1976, 498, 104; *Chem. Abstracts*, 1977, 86, 182272w.
15. G. D. Burt and A. Mudrak, *Chem. Abstracts* 1980, **92**, 75844m.
16. E. M. Lees and H. Weigel, *J. Chromatog* 1964, **16**, 360.
17. J. H. Yoe and A. L. Jones, *Ind. Engng. Chem., Anal. Ed.* 1944, **16**, 111.
18. P. Job, *Ann. Chim.* 1928, **9**, 113.
19. T. J. Lewis and T. M. Walters, *J. Appl. Chem.* 1960, **10**, 403.
20. E. Andersson, O. Lindqvist and T. Yamaguchi, *Acta Chem. Scand.* 1981, **A35**, 591.
21. T. Asai, *Bull. Chem. Soc. Jpn.* 1975, **48**, 2677.

Polyhedron Vol. 4, No. 1, pp. 81–87, 1985
Printed in Great Britain.

0277-5387/85 $3.00 + .00
©1985 Pergamon Press Ltd.

DIORGANOTIN(IV) COMPLEXES OF N-ACETYLAMINO ACIDS

G. K. SANDHU,* R. GUPTA and S. S. SANDHU
Department of Chemistry, Guru Nanak Dev University, Amritsar 143 005, India

and

R. V. PARISH
Department of Chemistry, The University of Manchester Institute of Science and Technology, Manchester M60 1QD, England

(*Received* 25 *July* 1983; *accepted* 2 *March* 1984)

Abstract—Sixteen complexes of general formula R_2SnL_2 and $R_2(L)SnOSn(L)R_2$ (where L = N-acetyl-L-leucine or N-acetyl-L-phenylalanine) R = CH_3, C_2H_5, n-C_4H_9, or n-C_8H_{17}) have been prepared by interaction between the ligand and R_2SnO in 2:1 or 1:1 molar ratio. The complexes were characterized by IR, ^1H NMR and ^{119}Sn Mössbauer spectroscopy. All the 2:1 complexes are assigned six-coordinate, distorted octahedral geometry with chelating carboxylate groups, while the 1:1 complexes have oxygen-bridged binuclear five-coordinate, trigonal-bipyramidal configurations. The amido –C=O and –NH groups are hydrogen bonded in the solid state.

Considerable interest has been shown in organotin(IV) derivatives of amino and N-acetylamino acids as possible biocides.[1,2] Much of this work has concerned triorganotin derivatives,[3–6] and relatively few diorganotin compounds of this type have been characterised.[7–12] We report here the synthesis and characterisation of a series of dialkyltin(IV) derivatives of N-acetyl-L-leucine (L_1) and N-acetyl-L-phenylalanine (L_2).

EXPERIMENTAL

Chemicals. N-acetyl-L-leucine, N-acetyl-L-phenylalanine and diethyltin(IV) oxide were prepared by the reported methods.[13,14] Dimethyl-, di-*n*-butyl-, and di-*n*-octyl-tin(IV) oxides were obtained from Alfa Products, U.S.A., and used as such.

Instruments. Melting points were determined in open capillaries, and are uncorrected. Elemental analyses were carried out by the Microanalytical Service, Calcutta University. Tin was estimated gravimetrically as SnO_2. Molecular weights were determined both by cryoscopy (in benzene or nitrobenzene) and by the Rast method (in molten camphor). IR spectra were recorded on Perkin Elmer 577 and Pye Unicam P321 instruments, in KBr or chloroform. ^1H NMR spectra were recorded on Tesla BS487 (80 MHz) and Varian Analytical (60 MHz) instruments, with TMS as internal standard. ^{119}Sn Mössbauer spectra were obtained with a Harwell 6000 Series spectrometer with samples cooled by liquid nitrogen (*ca.* 80 K) and source ($BaSnO_3$) at room temperature. Isomer shifts are relative to SnO_2 at room temperature.

Preparation of complexes. Complexes were prepared by refluxing the N-acetylamino acid and the dialkyltin(IV) oxide in 1:1 or 2:1 molar ratio in a benzene–ethanol mixture (3:1 v/v) with azeotropic removal of water. The mixture was filtered and the solvent removed. The 2:1 dimethyl- and diethyltin(IV) complexes were obtained as white solids, and were recrystallised from benzene. The dibutyl and dioctylderivatives were oils which solidified after 1–2 days in vacuum; they were then recrystallised from benzene. The 1:1 complexes were oils which solidified on trituration with petroleum ether (bp 60–80°C).

RESULTS AND DISCUSSION

Dialkyltin(IV) complexes of N-acetyl-L-leucine (L_1) and N-acetyl-L-phenylalanine (L_2) in 1:1 and 1:2 ratio have been prepared and characterised by analysis, molecular weight determination, IR,

*Author to whom correspondence should be addressed.

^{1}H NMR and ^{119}Sn Mössbauer spectroscopy. The complexes are all white solids, which are monomeric in solution (Table 1). The sharp melting points suggest that this structure is retained in the solid.

IR data

IR data for the amino acids and the complexes are given in Table 2. The free ligands show broad O–H absorption at 3000–2500 cm^{-1} which is absent in the spectra of the complexes, showing the deprotonation and coordination of the carboxylate groups. The values of $\Delta\nu$ [ν_{asy}(COO) – ν_{sym}(COO)] are all about 200 cm^{-1}, indicating that the carboxyl groups are chelated.[15]

The N–H stretching frequencies of the solid complexes are higher than those of the sodium salts, suggesting that the amido nitrogen is not coordinated, which would be consistent with its low basicity.[16] For some solid samples (Nos. 5, 9–11 and 15 of Table 2) and for chloroform solutions, the bands are sharp; those of the other solids are considerably broadened, indicating intermolecular hydrogen bonding, presumably to an amido carbonyl group of an adjacent molecule.[3,4,8]

The C=O stretching frequencies for the amido groups are slightly greater for the complexes than for the free ligands, the shift being greater for those which are not hydrogen bonded. For the remainder, the solution spectra show a further increase in

Table 1. Physical and analytical data of dialkyltin(IV) complexes with N-acetyl-amino acids[a]

	Complex	Yield (%)	M.P. (°C)	Elemental Analysis Found (Calc) (%) C	H	N	Sn	Molecular Weight Cryosc.	Rast	Calc.
1.	$(L_1)_2Sn(CH_3)_2$	84	160	44.29 (43.84)	7.54 (6.90)		24.64 (24.09)	450[b]	510	492.7
2.	$(L_2)_2Sn(CH_3)_2$	73	210	50.86 (51.36)	4.66 (5.35)	5.31 (4.99)		640	580	560.7
3.	$(L_1)_2Sn(C_2H_5)_2$	75	171	47.01 (46.09)	7.94 (7.29)	6.02 (5.37)	23.58 (22.79)	524[c]	611	520.7
4.	$(L_2)_2Sn(C_2H_5)_2$	84	220	53.90 (52.99)	6.23 (5.77)	5.49 (4.75)		615[c]	525	588.7
5.	$(L_1)_2Sn(n\text{-}C_4H_9)_2$	75	185	50.62 (49.93)	8.35 (7.97)		20.53 (20.58)	598[c]	582	576.7
6.	$(L_2)_2Sn(n\text{-}C_4H_9)_2$	83	160	56.68 (55.83)	5.79 (6.51)	4.50 (4.34)	17.65 (18.41)	580[c]	670	644.7
7.	$(L_1)_2Sn(n\text{-}C_8H_{17})_2$	70	115-120	55.38 (55.75)	9.25 (9.00)		18.19 (17.25)	610[c]	629	688.7
8.	$(L_2)_2Sn(n\text{-}C_8H_{17})_2$	70	140	60.24 (60.26)	6.98 (7.66)		14.98 (15.68)	650[c]	696	756.7
9.	$[(L_1)Sn(CH_3)_2]_2O$	90	140	37.64 (36.50)	6.66 (6.08)	4.65 (4.25)	36.89 (36.11)	710[b]	615	657.4
10.	$[(L_2)Sn(CH_3)_2]_2O$	85	85-87	43.75 (43.01)	5.07 (4.86)	4.27 (3.85)	33.36 (32.72)	665[b]	690	725.4
11.	$[(L_1)Sn(C_2H_5)_2]_2O$	90	185-197	39.13 (40.37)	6.65 (6.72)	4.65 (3.92)	34.12 (33.27)	876[b]	790	713.4
12.	$[(L_2)Sn(C_2H_5)_2]_2O$	90	230	45.82 (46.07)	4.66 (5.63)	3.86 (3.58)	30.86 (30.38)	847	710	781.4
13.	$[(L_1)Sn(n\text{-}C_4H_9)_2]_2O$	87	150	46.70 (46.52)	8.23 (7.73)	4.09 (3.39)	29.56 (28.76)	855[c]	865	825.4
14.	$[(L_2)Sn(N\text{-}C_4H_9)_2]_2O$	75	195	51.64 (51.04)	7.25 (6.71)				820	893.4
15.	$[(L_1)Sn(n\text{-}C_8H_{17})_2]_2O$	60	50-53	54.09 (54.88)	8.21 (9.14)			1130[b]		1049.4
16.	$[(L_2)Sn(n\text{-}C_8H_{17})_2]_2O$	75	133-135	57.15 (57.99)	8.35 (8.23)		22.16	1085[b]		1117.4

[a] L_1 = N-acetyl-L-leucine; L_2 = N-acetyl-L-phenylalanine. [b] In bromoform. [c] In nitrobenzene.

Table 2. IR spectral data (cm^{-1}, KBr/$CHCl_3$)[a]

	Compound	ν (N-H) solid/ solution	ν (C=O)amide solid/ solution	$\nu(COO)_{asym}$	$\nu(COO)_{sym}$	$\Delta\nu$	ν(Sn-C)	ν(Sn-O)	ν(Sn-O-Sn)
1.	$H(L_1)$ [b]	3300 s,sp	1620 s,sp	1700 s,b	1250 s,b	450			
2.	$H(L_2)$ [b]	3340 s,sp	1630 s,sp	1700 s,b	1240 s,b	460			
3.	$Na(L_1)$	3300 s,b	1640 s,b	1600 s,b	1400 s,b	200			
4.	$Na(L_2)$	3200 s,b	1640 s,b	1600 s,sp	1400 m,b	200			
5.	$(L_1)_2Sn(CH_3)_2$	3360 m,sp	1650 m,b	1580 s,b	1380 m,sp	200	500 m,sp	470 m,sp	
6.	$(L_2)_2Sn(CH_3)_2$	3330 s,sp	1640 s,b	1600 s,sp	1385 s,sp	215	540 m,b	450 m,b	
7.	$(L_2)_2Sn(C_2H_5)_2$	3300 s,b	1640 s,b	1590 s,sp	1385 m,sp	205	545 m,sp	500 s,sp	
8.	$(L_2)_2Sn(C_2H_5)_2$	3320/3420 s,sp s,sp	1640/1670 s,b s,b	1580 s,b	1380 s,b	200	575 m,sp	500 s,sp	
9.	$(L_1)_2Sn(n\text{-}C_4H_9)_2$	3360 s,sp	1665 s,sp	1590 s,b	1390 s,b	200	570 s,sp	465 m,sp	
10.	$(L_2)_2Sn(n\text{-}C_4H_9)_2$	3360 s,sp	1670 s,sp	1585 s,sp	1400 m,sp	185	590 m,b	495 m,sp	
11.	$(L_2)_2Sn(n\text{-}C_8H_{17})_2$	3350 s,sp	1670 s,sp	1590 s,b	1390 s,b	200	570 s,sp	455 m,sp	

cont.....

(Table 2, cont)

	Compound	ν(N-H) solid/ solution	ν(C=O)$_{amide}$ solid/ solution	$\nu(COO)_{asym}$	$\nu(COO)_{sym}$	$\Delta\nu$	ν(Sn-C)	ν(Sn-O)	ν(Sn-O-Sn)
12.	$(L_2)_2Sn(n\text{-}C_8H_{17})_2$	3340/3400 s,sp m,sp	1640/1660 s,b s,sp	1595 s,sp	1405 m,sp	190	555 m,sp	465 w,b	
13.	$[(L_1)Sn(CH_3)_2]_2O$	3370 m,sp	1630 s,b	1590 s,sp	1385 m,sp	205	510 w,sp	480 w,b	630 s,sp
14.	$[(L_2)Sn(CH_3)_2]_2O$	3300 s,sp	1640 s,b	1590 s,sp	1390 m,sp	200			
15.	$[(L_1)Sn(C_2H_5)_2]_2O$	3350/3400 s,sp s,sp	1630/1670 s,sp s,sp	1585 s,sp	1395 m,sp	190	535 s,sp	495 m,sp	585 m,sp
16.	$[(L_2)Sn(C_2H_5)_2]_2O$	3300/3350 s,b m,sp	1650/1680 s,sp s,b	1595 s,sp	1390 m,b	205	550 s,sp	490 m,b	640 m,sp
17.	$[(L_1)Sn(n\text{-}C_4H_9)_2]_2O$	3340/3400 m,b m,sp	1625/1670 s,b s.sp	1600 s.sp	1390 m,b	210	540 s,sp	500 m,sp	640 s,sp
18.	$[(L_2)Sn(n\text{-}C_4H_9)_2]_2O$	3340/3400 m,b m,sp	1625/1670 s,b s,sp	1585 s,sp	1390 m,b	195	555	495 m,sp	610 m,b
19.	$[(L_2)Sn(n\text{-}C_8H_{17})_2]_2O$	3340/3400 m,b m,sp	1630/1660 m,b s,sp	1580 m,sp	1380 s,sp	200			

[a] s, strong; m, medium; w, weak; sp, sharp; b, broad. [b] L_1 = N-acety-L-leucine; L_2 = N-acetyl-L-phenylalanine

Table 3. ^{1}H NMR spectral data ($CDCl_3$, Scale)[a]

	Compound	δ-C_6H_5	δ-NH	δ-CH	δ $\equiv$CH	δ CH_2	δCH_3CO	Sn-R δCH_2/CH_3	δCH_3
1.	$H(L_1)$		7.93 (d,1H)	4.13 (m,1H)		1.43 (q,2H)	1.80 (s,3H)		0.90 (d,6H)
2.	$H(L_2)$	7.25 (b,5H)	7.67 (b,2H)	5.10 (m,1H)		3.24 (t,2H)	2.22 (s,3H)		
3.	$(L_2)_2Sn(C_2H_5)_2$	7.26 (b,10H)	5.90 (b,2H)	4.83 (b,2H)		3.23 (b,4H)	2.01 (s,6H)	1.31 (b,4H)	0.76 (b,6H)
4.	$(L_1)_2Sn(n\text{-}C_4H_9)_2$		6.65 (d,2H)	4.50 (bm,2H)	2.34 (bm,2H)		2.01 (s,6h)	1.88-1.10 (bm,16H)	1.10-0.50 (bm,18H)
5.	$(L_2)_2Sn(n\text{-}C_4H_9)_2$	7.30 (bm,10H)	5.90 (bm,2H)	4.93 (bm,2H)		5.9 (m,2H)	2.00 (s,6H)	1.6-1.16 (bm,12H)	1.16-0.56 (bm,6H)
6.	$(L_1)_2Sn(n\text{-}C_8H_{17})_2$		5.92 (bd,2H)	4.65 (bm,2H)	1.5 (bm,2H)	1.87-1.46 (bm,12H)	2.00 (s,6H)	1.46-1.00 (bm,20H)	1.00-0.60 (t,18H)
7.	$(L_2)_2Sn(n\text{-}C_8H_{17})_2$	7.26 (b,10H)	6.00 (b,2H)	5.00 (bm,2H)		3.26 (m,4H)	2.00 (s,6H)	1.7-1.10 (bm,28H)	1.04-0.70 (bm,6H)
8.	$[(L_1)Sn(CH_3)_2]_2O$		6.00 (bm,2H)	4.37 (b,2H)	2.34 (bm,2H)	1.55 (b,4H)	2.02 (s,6H)		1.0-0.40 (bm,24H)
9.	$[(L_2)Sn(C_2H_5)_2]_2O$	7.26 (b,10H)	6.15 (bd,2H)	4.73 (b,2H)		3.16 (b,4H)	2.00 (s,6H)	1.33 (b,8H)	0.66 (b,12H)
10.	$[(L_2)Sn(n\text{-}C_4H_9)_2]_2O$	7.23 (b,10H)	6.00 (b,2H)	5.20 (b,2H)		3.16 (b,4H)	1.96 (s,6H)	1.5-1.16 (bm,28H)	1.16-0.08 (bm,10H)
11.	$[(L_2)Sn(n\text{-}C_8H_{17})_2]_2O$	7.26 (b,10H)	5.93 (b,2H)	4.73 (b,2H)		3.16 (b,6H)	1.97 (b,6H)	1.67-1.07 (b, 56H)	1.0-0.67 (b,12H)

[a] s, singlet; d, doublet; t, triplet; q, quartet; m, multiplet; b, broad.

frequency, again consistent[4] with loss of hydrogen bonding on dissolution.

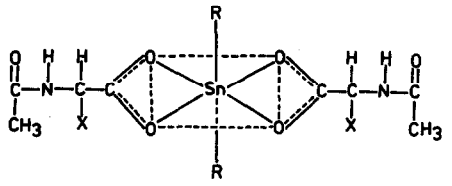
The presence of only one Sn–C band in the 590–610 cm^{-1} region indicates that the two alkyl groups are in *trans*-axial positions.[3,12,17] Bands assignable to the Sn–N stretching vibration are not observed in the spectra of the complexes, indicating that the ligand nitrogen atoms are not coordinated. For the 1:1 complexes (Nos. 13–20 of Table 2), a broad strong band at 640–610 cm^{-1} is assigned to an Sn–O–Sn stretching vibration.[18]

^{1}H NMR data

The ^{1}H NMR spectra of the ligands and the soluble complexes were recorded in DMSO, TFA and $CDCl_3$, and the data are given in Table 3. In

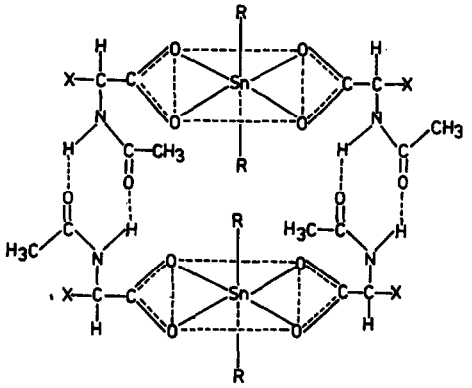
Table 4. Sn-119m Mössbauer spectral data (at 80 K; mm s^{-1})

	Complex	IS(SnO_2)	QS	Line widths
1.	$(L_1)_2Sn(CH_3)_2$	1.32	3.63	1.14, 1.32
2.	$(L_2)_2Sn(CH_3)_2$	1.26	3.44	0.93, 1.11
3.	$(L_1)_2Sn(C_2H_5)_2$	1.34	3.35	0.86, 0.90
4.	$(L_2)_2Sn(C_2H_5)_2$	1.34	3.35	0.91, 0.97
5.	$(L_1)_2Sn(C_4H_9)_2$	1.42	3.46	0.97, 0.94
6.	$(L_2)_2Sn(C_4H_9)_2$	1.33	3.38	0.93, 1.09
7.	$(L_1)_2Sn(n\text{-}C_8H_{17})_2$	1.42	3.39	0.89, 0.93
8.	$(L_2)_2Sn(n\text{-}C_8H_{17})_2$	1.44	3.60	0.93, 1.03
9.	$[(L_1)Sn(n\text{-}C_4H_9)_2]_2O$	1.30	3.17	0.91, 1.13
10.	$[(L_2)Sn(n\text{-}C_4H_9)_2]_2O$	1.28	3.10	0.86, 1.23
11.	$[(L_2)Sn(n\text{-}C_8H_{17})_2]_2O$	1.36	3.37	0.87, 1.26



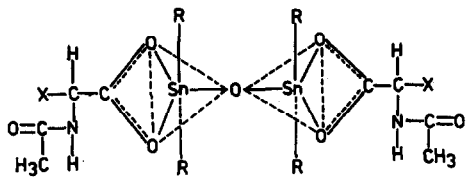
[X= $CH_2CH(CH_3)_2$, $CH_2C_6H_5$]

Fig. 1.



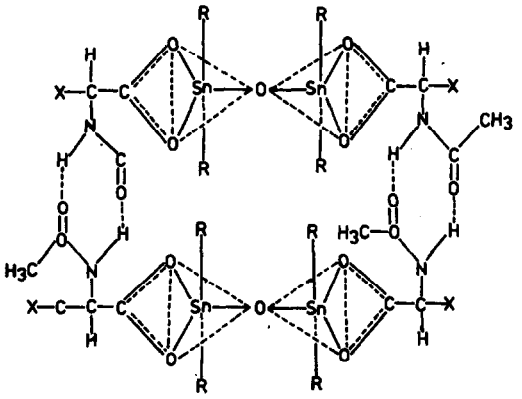
[X= $-CH_2CH(CH_3)_2$, $-CH_2C_6H_5$]

Fig. 2.



[X= $-CH_2CH(CH_3)_2$, $-CH_2C_6H_5$]

Fig. 3.



[X= $-CH_2CH(CH_3)_2$, $-CH_2C_6H_5$]

Fig. 4.

the spectra of the N-acetylamino acids themselves, the signal for the peptide group (CONH) proton is broad and appears at 7.93δ(L_1) and 7.67δ(L_2); it is shifted to higher field in the complexes (7.2–5.3δ), indicating non-coordination to tin and loss of hydrogen bonding.[4,19,20] The dimethyl- and diethyltin complexes show single resonances for the alkyl groups, indicating *trans* configurations.

^{119}*Sn Mössbauer data*

The 2:1 complexes have isomer shift (IS) values of *ca.* 1.35 mm s^{-1} and quadrupole splittings (QS) of *ca.* 3.45 mm s^{-1} (Table 4). These data cannot be directly interpreted in terms of the structure, since other diorganotin(IV) complexes with similar parameters have been assigned five-coordinate[10,21–23] or six-coordinate structures.[12,14,24,25] Indeed, when the other ligands have high electronegativity, the QS is governed mainly by the C–Sn–C bond angle;[26–28] the values observed here correspond to bond angles of 138–146°. However, in the light of the other data, the Mössbauer parameters are best interpreted in terms of distorted *trans* octahedral configurations.

The 1:1 complexes have lower QS values, corresponding to five-coordination. The calculated C–Sn–C bond angles are again 138–148°.

Structures

$R_2Sn(L)_2$ complexes (1:2). The Mössbauer, NMR and IR data suggest distorted *trans*-octahedral structures (Fig. 1) for all complexes in solution and for compounds 5, 9–11 (Table 2) in the solid state. For the other solid complexes, the IR data suggest dimeric, hydrogen-bonded structures (Fig. 2).

$R_2(L)SnOSn(L)R_2$ complexes (1:1). The 1:1 complexes are assigned five-coordinate trigonal-bipyramidal structures with Sn–O–Sn bridging and effectively linear C–Sn–C groups. In solution the complexes are monomeric (Fig. 3), as is the solid complex $[(L_1)Sn(C_2H_5)_2]_2O$. The remaining solid complexes appear from their IR spectra to have dimeric, hydrogen-bonded structures (Fig. 4).

Acknowledgement—One of us (R.G.) is grateful to CSIR, New Delhi, India for financial assistance.

REFERENCES

1. M. J. Koopmans, *Dutch Pat.* 1961, **96**, 805 [CA **55**, 27756f].
2. D. A. Kochin, S. G. Verenika and I. B. Chemareva, *Dokl. Akad Nauk SSSR* 1961, **139**, 1335.
3. B. Y. K. Ho and J. J. Zuckerman, *Inorg. Chem.* 1973, **12**, 1552.
4. G. Domazetis, R. J. Magee and B. D. James, *J. Organomet. Chem.* 1979, **173**, 357.

5. B. Y. K. Ho, J. J. Zuckerman and J. A. Zubieta, *J. Chem. Soc. Chem. Commun.* 1975, 88.
6. B. Y. K. Ho and J. J. Zuckerman, *Inorg. Nucl. Chem. Lett.* 1973, **9**, 849.
7. W. T. Hall and J. J. Zuckerman, *J. Inorg. Nucl. Chem.* 1977, **16**, 1239.
8. G. Domazetis, R. J. Magee and B. D. James, *J. Organomet. Chem.* 1978, **162**, 239.
9. G. Domazetis and M. F. Mackay, *J. Cryst. Mol. Struct.* 1979, **9**, 57.
10. L. Pellerito, M. L. Lo Giudice, G. Ruisi, N. Bertazzi, R. Barbieri and F. Huber, *Inorg. Chim. Acta* 1976, **17**, L21.
11. R. Barbieri, L. Pellerito and F. Huber, *Inorg. Chim. Acta* 1978, **30**, L321.
12. S. S. Sandhu, S. S. Sandhu (Jr), G. K. Sandhu, R. V. Parish and O. Parry, *Inorg. Chim. Acta* 1982, **58**, 251.
13. H. D. DeWitt and A. W. Ingersall, *J. Am. Chem. Soc.* 1951, **73**, 3359.
14. M. Dub (Ed.), *Organometallic Compounds*, Vol. II, p. 368. Springer-Verlag, New York (1967).
15. J. Catterick and P. Thornton, *Adv. Inorg. Chem. Radiochem.* 1977, **20**, 291.
16. H. C. Freeman, *Inorganic Biochemistry* (Edited by G. I. Eichorn), Chap. 4, p. 119. Elsevier, Amsterdam (1975).
17. R. Okawara and M. Wada, *Adv. Organomet. Chem.* 1967, **5**, 137.
18. C. S. C. Wang and J. M. Shreeve, *J. Organomet. Chem.* 1972, **46**, 271.
19. N. N. Serge and H. L. Robert, *Hydrogen Bonding*, p. 82. Van Nostrand Reinhold, New York (1977).
20. D. J. Melvin and L. J. Schaad, *Hydrogen Bonding*, p. 39. Marcel Dekker, New York (1974).
21. V. G. K. Das, N. S. Weng, P. J. Smith and R. Hill, *J. Chem. Soc. Dalton Trans.* 1981, 552.
22. L. Pellerito, G. Ruisi and R. Barbieri, *Inorg. Chim. Acta* 1979, **32**, 39.
23. W. D. Honnick and J. J. Zuckerman, *J. Organomet. Chem.* 1979, **178**, 133.
24. A. G. Maddock and R. H. Platt, *J. Chem. Soc.(A)* 1971, 1191.
25. R. Barbieri and R. Herber, *J. Organomet. Chem.* 1972, **42**, 65.
26. R. V. Parish and C. E. Johnson, *J. Chem. Soc.(A)* 1971, 1906.
27. T. K. Sham. and G. M. Bancroft, *Inorg. Chem.* 1975, **14**, 2281.
28. R. V. Parish, *Mössbauer Spectroscopy Applied to Inorganic Chemistry* (Edited by G. J. Long). Plenum Press, New York (1984).

Polyhedron Vol. 4, No. 1, pp. 89–95, 1985
Printed in Great Britain.

0277–5387/85 $3.00 + .00
© 1985 Pergamon Press Ltd.

STRUCTURAL STABILITY INDEX OF HETEROPOLY- AND ISOPOLY-ANIONS—II

KENJI NOMIYA and MAKOTO MIWA*
Department of Industrial Chemistry, Faculty of Engineering, Seikei University, Musashino, Tokyo 180, Japan

(*Received* 14 *November* 1983, *accepted* 30 *March* 1984)

Abstract—The structural stability indexes of some previously unreported heteropoly- and isopoly-compounds are discussed. Compounds studied here are mono-substituted Keggin and Dawson heteropolyanions with the general formulas $[XZ(H_2O)M_{11}O_{39}]^{n-}$ and $[X_2Z(H_2O)M_{17}O_{61}]^{n-}$ (X is a heteroatom; Z is a substituted metal ion; M is Mo, or W), two Finke-type heteropolyanions with the formulas $[P_2W_{18}Z_4(H_2O)_2O_{68}]^{10-}$ and $[P_4W_{30}Z_4(H_2O)_2O_{112}]^{16-}$ (Z = Co(II), Cu(II), Zn(II)), heteropolyvanadates containing high valence heteroatoms $[XV_{13}O_{38}]^{7-}$ (X = Mn(IV), Ni(IV)), isopolyvanadate $[V_{10}O_{28}]^{6-}$, some heteropolyvanadates with capped-Keggin structures, and $[As_4W_{40}O_{140}]^{28-}$ as an inorganic cryptate. An additional rule concerning the conversion between the heteropoly- and isopoly-anions is proposed as the fourth rule. The actual stability of heteropolyanions with the small structural index is interpreted by the presence of a significant contribution from the heteroatom or other supporting metal ions.

Pope's proposal[1] concerning the heteropoly "blue" formation, i.e. only the heteropolyanions belonging to Type I (monooxo terminal groups) and the Type III (both monooxo and *cis*-dioxo terminal groups) can be converted to the reduced blue forms, has been disproved. For example, Yamase *et al.* have recently demonstrated the one-electron reduction of $[Mo_7O_{24}]^{6-}$ anion (Type II; *cis*-dioxo terminal groups) by an illumination ($\lambda > 300$ nm), analyzed the ESR spectrum of irradiated single-crystal and determined the crystal structure of the blue compound by the X-ray diffraction.[2–4] However, taking advantage of Pope's proposal we could introduce the structural stability on the basis of closed loop into the chemistry of heteropoly- and isopoly-compounds. In the previous paper,[5] using the interpenetrating loop $-O_c-M-O_b-M-O_c-$ formed by a junction of M ion and bridging oxygens (O_b, O_c) around the heteropolyanion cage, we defined the structural stability index (η) as the number of closed loops per MO_6 octahedron and discussed the relative stability of the polyanion skeletons, the degree of condensation and the interconversion within the same family of the heteropolyanion. These have been summarized in three rules; (1) the heteropolyanions with the larger structural stability index are more stable, (2) the heteropolyanions with an identical index within the same series can be interconverted or converted from one polyanion to another, and (3) the index reveals the degree of condensation. The index has been estimated according to $\eta = (\Sigma B \cdot C)/A$, where A is the number of MO_6 octahedra constituting the polyanion cage, B the number of MO_6 constituting the closed loop and C the number of closed loop. In this paper, we wish to report the structural stability indexes of the compounds, which have not been previously discussed, and to propose an additional rule about the conversion between the heteropoly- and isopoly-anions.

RESULTS AND DISCUSSION

In our view, the structural stabilities of heteropoly- and isopoly-compounds appear, to a first approximation, to be dominated by the number of closed loop, and the structural stability index appears to be representative of a topological index for such compounds. The problem is limited to only whether the closed loop exists or not in those compounds. For example, the difference between Mo and W in the $[XM_{12}O_{40}]^{n-}$ (M = Mo, W), although their actual stabilities

*Author to whom correspondence should be addressed.

are different, cannot be taken into account. This results in each of heteropolyanions $[XMo_{12-n}W_nO_{40}]^{m-}$ and $[XMo_{12-n}V_nO_{40}]^{m-}$ having the same index ($\eta = 2$) as the Keggin-type ion. Moreover, in the mono-substituted lacunary heteropolyanions $[XZ(H_2O)M_{11}O_{39}]^{n-}$ and $[X_2Z(H_2O)M_{17}O_{61}]^{n-}$ shown in Fig. 1 (X is a hetero-atom such as Si, P, As; Z is a substituted metal ion; M is Mo, W),[6,7] there exist the "homo"-closed loop such as $-O_b-M-O_c-M-O_b-$ and the "hetero"-closed loop such as $-O_b-M-O_c-Z-O_b-M-O_c-$, but since such loops are treated without distinction, their stability indexes become the same index ($\eta = 2$) as that of parent Keggin- and Dawson-type heteropolyanions. This is also the case for the di-substituted Keggin ions such as $[Ti_2PW_{10}O_{40}]^{7-}$ and $[\{C_pFe(CO)_2Sn\}_2W_{10}PO_{38}]^{5-}$, which have been recently isolated by Knoth *et al.*[8] From this standpoint, the structural stabilities of two Finke-type polyanions, $[P_2W_{18}Z_4(H_2O)_2O_{68}]^{10-}$ and $[P_4W_{30}Z_4(H_2O)_2O_{112}]^{16-}$ (Z = Co, Cu, Zn),[9,10] can be discussed (Fig. 2). Finke *et al.* have examined the reaction of a trivacant Keggin ion β-$[PW_9O_{34}]^{9-}$ ($\eta = 0.67$) with the inorganic Z(II) ions, with the goal of preparing $[PW_9(ZO)_3O_{34}]^{9-}$, which should contain a Z_3O_3 "mini surface" closely resembling a fragment of the "polar" $(000\bar{1})$ surface of ZO, and demonstrated that the di-substituted dimers $[PW_9Z_2(H_2O)O_{34}^{5-}]_2$ are unexpectedly formed, yet exclusively. In these polyanions, two $[PW_9O_{34}]^{9-}$ units are located above and below the three parts of four edge-sharing ZO_6 octahedra so that two tri-substituted Keggin ions may interpenetrate. The other Finke-type polyanion has been obtained by the reaction of trivacant Dawson ion α-$[P_2W_{15}O_{56}]^{12-}$ ($\eta = 0.8$), which was prepared by base degradation of α-$[P_2W_{18}O_{62}]^{6-}$, with the inorganic Z(II) ions. The structures have been determined by the ^{183}W-NMR and X-ray analyses.[9,10]

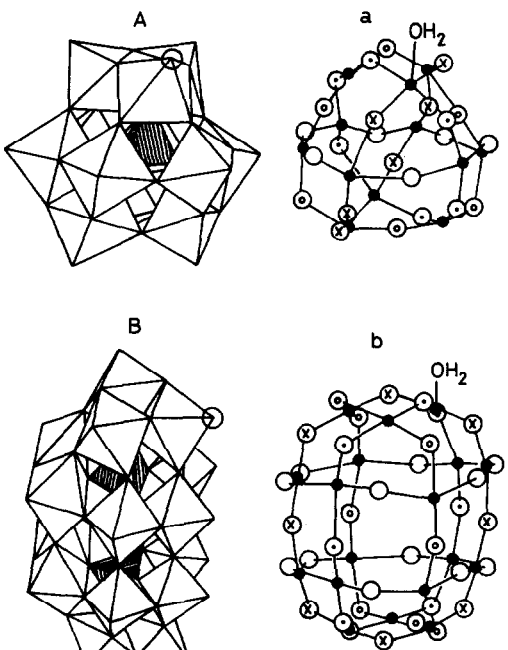


Fig. 1. Polyhedral models of the mono-substituted Keggin (*A*) and Dawson (*B*) heteropolyanions. The circles show the positions of water molecules. Framework bond models of (*A*) and (*B*) are shown in (a) and (b), respectively. Open circles are bridging oxygens and filled circles are molybdenum or tungsten atoms. Terminal oxygens and the internal heteroatoms are omitted. The uniformly marked oxygens identify one closed loop.

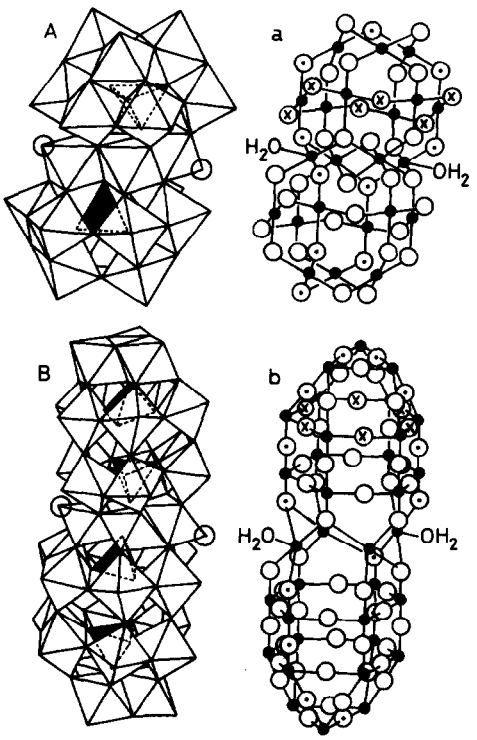


Fig. 2. Polyhedral models of Finke-type polyanions, $[P_2W_{18}Z_4(H_2O)_2O_{68}]^{10-}$ (*A*) and $[P_4W_{30}Z_4(H_2O)_2O_{112}]^{16-}$ (*B*).[9,10] The circles show the positions of water molecules. Framework bond models of (*A*) and (*B*) are shown in (a) and (b), respectively. Open circles are bridging oxygens, filled circles are tungsten atoms, and central four shaded circles are Z(Co, Cu, Zn). Terminal oxygens and the internal heteroatoms are omitted. The oxygens illustrated by cross within a circle represent one of local closed loops, and the oxygens by dot within a circle represent one of closed loops passing through two subunits.

In the first polyanion, we can find two local "homo"-closed loops and six "hetero"-closed loops, or $(B, C)_{homo} = (6, 2)$ and $(B, C)_{hetero} = [(6, 4) + (10, 2)]$, thus the stability index $\eta = (6 \times 2 + 6 \times 4 + 10 \times 2)/(18 + 4) = 2.55$ and in the second polyanion, we can find four "homo"- and six "hetero"-closed loops, or $(B, C)_{homo} =$

(6, 4) and $(B, C)_{hetero} = [(8, 4) + (14, 2)]$, thus the index $\eta = (6 \times 4 + 8 \times 4 + 14 \times 2)/(30 + 4) = 2.47$. It seems reasonable that these polyanions are obtained as main products, since the evaluated indexes are larger than those of initially desired tri-substituted Keggin- and Dawson-polyanions (both $\eta = 2$).

Some heteropolyvanadates with interesting structures have been known which have never been observed in the heteropolyanions of Mo and W. A heteropolyanion with the highest degree of condensation is the $[XV_{13}O_{38}]^{7-}$ (X = Mn(IV), Ni(IV)) compounds, which belong to Type **III** in the Pope's classification and their heteropoly "blue" compounds are also known (Fig. 3).[11] These polyanions consists of one XO_6 and 13-VO_6 octahedra always sharing edges and the structure is similar to that of $[W_{10}O_{32}]^{4-}$, but has a central heteroatom and three more VO_6 octahedra surrounding it, the crystallographic structure being shown in the reference.[12] Using a molecular model, we have estimated 4.92 as a stability index from $A = 13$ and $(B, C) = [6, 8) + (4, 4)]$. In view of the Mn(IV) and Ni(IV) octahedral complexes, these polyanions are known to be more stable than the Waugh-type ones $[XMo_9O_{32}]^{6-}$ ($\eta = 2$) both in the solid and in aqueous solution.[11] This fact is reasonable as expected from the large index viz. the first rule.

Recently Sasaki *et al.* have found that the 1 : 14 vanadophosphate polyanion exists as the only detectable heteropolyanion in a wide range of V : P ratios in the NaH_2PO_4–$NaVO_3$–H_2SO_4 aqueous system ($1/2 \leq V:P \leq 14$, $1 < pH < 6$) at room temperature using ^{31}P- and ^{51}V-NMR techniques.[13,14] In the polyanion twelve V atoms form the usual Keggin structure and the remaining two V atoms occupy the pits on the Keggin molecule, viz. "bicapped Keggin" structure is confirmed. The crystallographic structure of the stable *trans*-located bicapped Keggin ion has been shown in the reference.[14] One or more capped Keggin structures have never been observed in the heteropolyanion of Mo and W, because such species become positively charged.

Using molecular models, we counted the number of closed loops on a capped Keggin ion series of $[PV_{12+n}O_{40+n}]^{(15-3n)-}$ ($n = 1 - 4$) in Fig. 4. In the Keggin structure ion of $n = 0$, α-$[PV_{12}O_{40}]^{15-}$, there are six capping sites by trigonal bipyramidal VO_5 unit. However, since the total charges of the penta- and hexa-capped ions become zero and three positive, respectively, their structural parameters will be meaningless. In the monocapped Keggin ion of $n = 1$, there are the same number of closed loops as observed in the parent ion, because of no additional closed loop passing through the cap. Only a parameter A is varied from 12 to 13. The bicapped ion of $n = 2$ contains two types of isomer; one is the configuration that two caps are *trans*-located and the other that two caps are *cis*-located. In the "*trans*" isomer, there exists eight additional closed loops passing through six VO_6 octahedra and two *trans*-located VO_5 caps, besides the contribution

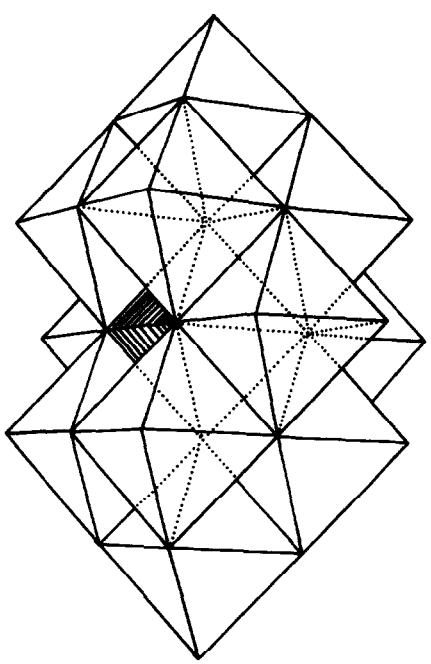


Fig. 3. Polyhedral model of the $[XV_{13}O_{38}]^{7-}$ (X = Mn(IV), Ni(IV)).[12] Shaded octahedron represents X.

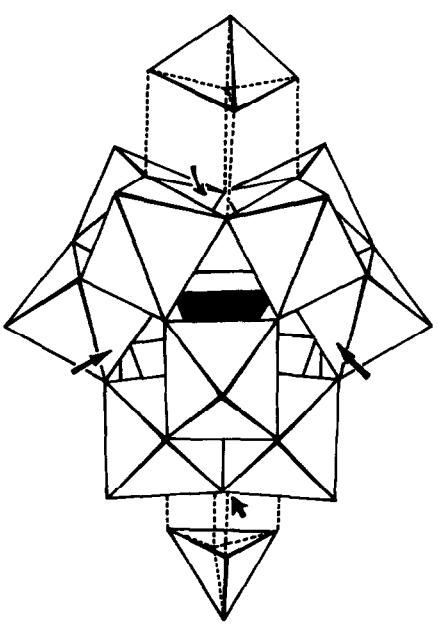


Fig. 4. Polyhedral model of the $[PV_{12+n}O_{40+n}]^{(15-3n)-}$ ($n = 1$–4).[13,14] Arrows show capping sites by trigonal bipyramidal VO_5 unit.

Table 1. Structural parameters of a capped Keggin heteropolyvanadate series $[PV_{12+n}O_{40+n}]^{(15-3n)-}$

	Formula	Structure and Configuration	A	(B, C)	η
n = 0	$PV_{12}O_{40}^{15-}$	Keggin structure	12	(6, 4)	2
n = 1	$PV_{13}O_{41}^{12-}$	monocapped Keggin structure	13	(6, 4)	1.85
n = 2	$PV_{14}O_{42}^{9-}$	bicapped Keggin structure			
		(1) "trans"-isomer	14	[(8, 8) + (6, 4)]	6.29
		(2) "cis"-isomer	14	(6, 4)	1.71
n = 3	$PV_{15}O_{43}^{6-}$	tricapped Keggin structure			
		(1) "cis-cis"-isomer	15	[(7, 3) + (6, 4)]	3
		(2) "trans-cis"-isomer	15	[(8, 8) + (6, 4)]	5.87
n = 4	$PV_{16}O_{44}^{3-}$	tetracapped Keggin structure			
		(1) "trans"-vacant isomer	16	[2(8, 8) + (8, 2) + (12, 2) + (6, 4)]	12
		(2) "cis"-vacant isomer	16	[2(7, 3) + (8, 8) + (6, 4)]	8.125

from the Keggin ion itself, or $(B, C) = (6, 4)$. On the other hand, in the "*cis*" isomer there is no additional loop passing through two *cis*-located VO_5 caps. Thus, only a parameter A is varied from 12 to 14 and the parameters (B, C) of the Keggin ion are not influenced by attaching two *cis*-caps. The tricapped Keggin ion of $n = 3$ contains also two types of isomer; one is the configuration that three caps are *cis*-located to each other, and the other that two of three caps are *trans*-located and the remaining cap is *cis*-located to them. In the former ("*cis–cis*") configuration, we can count three additional closed loops passing through four VO_6 octahedra and three VO_5 caps, besides the contribution from the Keggin ion itself. On the other hand, in the latter ("*trans-cis*") configuration, we can count eight closed loops passing through two *trans*-located caps and no closed loop through two *cis*-located caps as additional loops. The results are presented in Table 1. The structural stability indexes indicate that the capping markedly varies the structural stability of the parent Keggin ion, especially the monocapped ion and "*cis*" bicapped ion are less stabilized than the parent ion, whereas the "*trans*" bicapped ion is remarkably stabilized. The tetracapped polyanion of $n = 4$ has two types of isomer. They become substantially identical with the isomers of the bicapped ion, because the positioning way of two vacant sites in the six possible sites can be considered. As shown in Table 1, the stability indexes of them are much larger than that of "*trans*" bicapped ion. These are attributed to the presence of many closed loops passing through "*trans*"-located caps, "*cis-cis*"-located caps and four caps consisting of two sets of "*trans*"-caps, in addition to the closed loop of the parent Keggin ion. However, it has not been known whether the tetracapped polyanion is an existing material or not. When it is actually nonexistent, other factors should be taken into account for the interpretation such as the effects of the electric charge, the number and degeneracy of geometrical isomers in the polyanion, in addition to the structural stability index.

An isopolyanion with larger index than that observed in the isopolyanions of Mo and W such as $[Mo_6O_{19}]^{2-}$, $[W_6O_{19}]^{2-}$, $[W_{10}O_{32}]^{4-}$, metatungstate $[H_2W_{12}O_{40}]^{6-}$ $(\eta = 2)$ is found in the isopolyvanadate $[V_{10}O_{28}]^{6-}$. This isopolyanion contains two VO_6 octahedra with no oxo-type oxygens[15] which cannot be treated as "heteroatom" (Fig. 5). For the isopolyvanadate, we have estimated 2.8 as the stability index from $A = 10$ and $(B, C) = [(6, 2) + (4, 4)]$. This isopolyanion has been used as a starting material for the preparation of $[XV_{13}O_{38}]^{7-}$ compounds, but it has been also

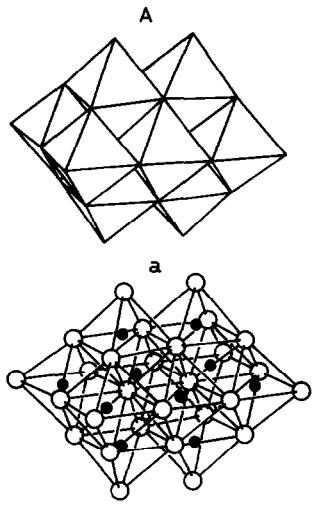


Fig. 5. Polyhedral model (A) of the $[V_{10}O_{28}]^{6-}$ and its framework bond model (a).[15] Open circles are oxygens and filled circles are vanadium atoms.

known to be recovered by a decomposition of the 1:13 heteropolyvanadate under an appropriate pH.[11] Noteworthily, it has been shown by ^{51}V-NMR that the aforementioned bicapped Keggin-ion readily decomposes to the isopolyvanadate by the raised pH of the aqueous solution.[14]

Here we wish to propose an additional rule; when a heteropolyanion decomposes, or degradates, into some isopolyanions under an appropriate condition, the isopolyanion possessing the

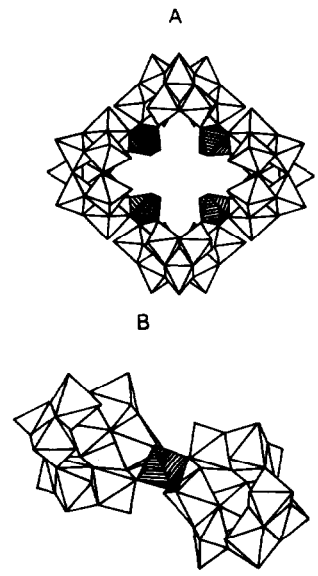


Fig. 6. Polyhedral model (A) of the $[As_4W_{40}O_{140}]^{28-}$.[23] Four $[AsW_9O_{33}]$ subunits are linked by four WO_6 octahedra indicated by shade. Arsenic atoms are omitted. Partial representation (B) of (A), polyhedral model of the two $[AsW_9O_{33}]$ units linked by a WO_6 octahedron.

Table 2. Structural parameters of some heteropoly- and isopoly- anions

Formula		A	(B, C)	η
$XZ(H_2O)M_{11}O_{39}^{n-}$	mono-substituted Keggin ion	12	$[(6, 2)_{homo} + (6, 2)_{hetero}]$	2
$X_2Z(H_2O)M_{17}O_{61}^{n-}$	mono-substituted Dawson ion	18	$\{[(6, 2) + (8, 1)]_{homo} + (8, 2)_{hetero}\}$	2
			or	
			$\{[(6, 1) + (8, 2)]_{homo} + [(6, 1) + (8, 1)]_{hetero}\}$	2
$P_2W_{18}Z_4(H_2O)_2O_{68}^{10-}$	Finke-type ion	22	$\{(6, 2)_{homo} + [(6, 4) + (10, 2)]_{hetero}\}$	2.55
$P_4W_{30}Z_4(H_2O)_2O_{112}^{16-}$	Finke-type ion	34	$\{(6, 4)_{homo} + [(8, 4) + (14, 2)]_{hetero}\}$	2.47
$XV_{13}O_{38}^{7-}$		13	[(6, 8) + (4, 4)]	4.92
$XV_{14}O_{42}^{9-}$	"trans"-isomer of bicapped Keggin ion	14	[(8, 8) + (6, 4)]	6.29
$V_{10}O_{28}^{6-}$		10	[(6, 2) + (4, 4)]	2.8
$As_4W_{40}O_{140}^{28-}$	inorganic cryptate	40	(6, 4)	0.6

largest stability index is predominantly produced. This is the case not only for the heteropolyvanadate anions, but also for the Waugh-type $[XMo_9O_{32}]^{6-}$ and the Anderson-type $[XMo_6O_{24}H_6]^{3-}$ polyanions. The starting material in the preparations of the latter compounds is the $[Mo_7O_{24}]^{6-}$ ($\eta = 1$). When these heteropoly compounds are passed through a cation-exchange resin column and are converted to the soluble forms in non-aqueous solvents, the isopolyanion $[Mo_6O_{19}]^{2-}$ ($\eta = 2$) as a decomposed product or an impurity is predominantly produced.[16,17] The proposed rule predicts that a part or all of $[W_6O_{19}]^{2-}$, $[W_{10}O_{32}]^{4-}$ and $[H_2W_{12}O_{40}]^{6-}$ isopolytungstates will be possibly produced by degradation of some heteropolytungstates. In the preparation by the Brown–Mair method of various Keggin-type $[XW_{12}O_{40}]^{n-}$ polyanions,[18,19] the actual starting material is considered to be paratungstate $[H_2W_{12}O_{42}]^{10-}$ ($\eta = 0$) produced from an acidic aqueous solution of sodium tungstate. In this preparation, metatungstic acid is produced as by-product. Purification has been performed on the basis of the difference of thermal stabilities of the desired product and the metatungstic acid. In such a purification we have experienced that the metatungstic acid is also produced by thermal degradation of once formed dodecatungstometallic acid $H_n[XW_{12}O_{40}]$. This fact is also compatible with the rule.

In spite of $\eta = 0$, the Silverton-type polyanions $[XMo_{12}O_{42}]^{8-}$ (X = Ce(IV), Th(IV), U(IV)) are very stable and their counter cations can be exchanged without any decomposition of the skeleton.[20] This stability index is smaller than that ($\eta = 1$) of its starting material $[Mo_7O_{24}]^{6-}$. In this case, the high valence heteroatom of rare earth element should contribute significantly to the actual stability. In addition, it has been known that, in the preparation of the X = Co(III) compound in Anderson-type $[XMo_6O_{24}H_6]^{3-}$ ($\eta = 1$), the Evans–Showell-type heteropolyanion $[Co_2Mo_{10}O_{38}H_4]^{6-}$ ($\eta = 0$) is produced as major byproduct and the isolated X = Co(III) compound can be almost entirely converted to the latter compound in the presence of catalyst.[21] These facts are also attributed to the specific effect of the Co(III) ion as the heteroatom, because such phenomena have been known only in the case of X = Co(III) compound. Recently an interesting heteropolyanion $[As_4W_{40}O_{140}]^{28-}$, which shows a cryptate-like function, has been reported.[22,23] This compound consists of four $[AsW_9O_{33}]$ subunits and four WO_6 octahedra linking them, the former being considered as a half-Dawson-type polyanion (Fig. 6). This macrocyclic polyanion has four local closed loops belonging to the subunits and has no closed loop passing through inter-subunits. The stability index is estimated to be 0.6 from $A = 40$ and $(B, C) = (6, 4)$, indicating that this polyanion itself is metastable. Thus, the actual stability may possibly be due to the presence of other supporting elements and cations. This may lead to the apparent crown-ether or cryptate function.

The structural parameters of the compounds studied here are summarized in Table 2.

REFERENCES

1. M. T. Pope, *Inorg. Chem.* 1972, **11**, 1973.
2. T. Yamase, R. Sasaki and T. Ikawa, *J. Chem. Soc. Dalton Trans.* 1981, 628.
3. T. Yamase, *J. Chem. Soc. Dalton Trans.* 1982, 1987.
4. Y. Ohashi, K. Yanagi, T. Sasada and T. Yamase, *Bull. Chem. Soc. Jpn.* 1982, **55**, 1254.
5. K. Nomiya and M. Miwa, *Polyhedron* 1984, **3**, 341.
6. L. C. W. Baker, V. S. Baker, K. Eriks, M. T. Pope, M. Shibata, O. W. Rollins, J. H. Fang and L. L. Koh, *J. Am. Chem. Soc.* 1966, **88**, 2329.
7. L. C. W. Baker and J. S. Figgis, *J. Am. Chem. Soc.* 1970, **92**, 3794.
8. P. J. Domaille and W. H. Knoth, *Inorg. Chem.* 1983, **22**, 818.
9. R. G. Finke, M. Droege, J. R. Hutchinson and O. Gansow, *J. Am. Chem. Soc.* 1981, **103**, 1587.
10. R. G. Finke and M. W. Droege, *Inorg. Chem.* 1983, **22**, 1006.
11. C. M. Flynn and M. T. Pope, *J. Am. Chem. Soc.* 1970, **98**, 85.
12. A. Kobayashi and Y. Sasaki, *Chem. Lett.* 1975, 1123.
13. R. Kato, A. Kobayashi and Y. Sasaki, *J. Am. Chem. Soc.* 1980, **102**, 6571.
14. R. Kato, A. Kobayashi and Y. Sasaki, *Inorg. Chem.* 1982, **21**, 240.
15. H. T. Evans, *Inorg. Chem.* 1966, **5**, 967.
16. K. Nomiya, R. Kobayashi and M. Miwa, *Bull. Chem. Soc. Jpn.* 1983, **56**, 3505.
17. K. Nomiya and M. Miwa, unpublished results.
18. D. H. Brown and J. A. Mair, *J. Chem. Soc.* 1962, 3946.
19. K. Nomiya, M. Miwa, R. Kobayashi and M. Aiso, *Bull. Chem. Soc. Jpn.* 1981, **54**, 2983.
20. L. C. W. Baker, G. A. Gallagher and T. P. McCutcheon, *J. Am. Chem. Soc.* 1953, **75**, 2493.
21. H. T. Evans and J. S. Showell, *J. Am. Chem. Soc.* 1969, **91**, 6881.
22. M. Leyrie and G. Hervé, *Nouv. J. Chim.* 1978, **2**, 233.
23. F. Robert, M. Leyrie, G. Hervé, A. Tézé and Y. Jeannin, *Inorg. Chem.* 1980, **19**, 1746.

Polyhedron Vol. 4, No. 1, pp. 97–101, 1985
Printed in Great Britain.

0277–5387/85 $3.00 + .00
© 1985 Pergamon Press Ltd.

TRANSITION METAL COMPLEXES OF THE SCHIFF BASE DERIVATIVES OF THE LIGAND 1,8-DIHYDROXY-3,6-DIMETHYL-2-ACETYLNAPHTHALENE

FRANCESC TEIXIDOR, LUIS ESCRICHE, ANTONI LLOBET and J. CASABÓ*
Departament de Quimica Inorgánica, Facultat de Ciències, Universitat Autònoma de Barcelona,
(Bellaterra) Barcelona, Spain

(*Received* 4 *October* 1983; *accepted after revision* 30 *March* 1984)

Abstract—New Schiff bases derived from 2-acetyl-1,8-dihydroxy-3,6-dimethylnaphthalene(H_2addn) and 1,2-propanediamine(pn), 2,3-butanediamine(pn) and 1,2-cyclohexyldiamine(chn) have been prepared and characterized as (H_4addn-diam). In this work is reported an improved experimental method which yields well characterized mononuclear species of H_4addn-en and H_4addn-pn with Cu(II), Ni(II) and Co(II). The Cu(II) complex has been studied by esr which unambigously shows a N_2O_2 coordination mode for the metal ion. Based on the spectral characteristics of these complexes we conclude that all metal atoms have the same coordination mode. Only one binulear complex, [$NiUO_2$(addn-en)] is reported in this work. All attempts to synthesize binuclear complexes with first transition series metal ions were unsuccessful.

Binucleating ligands and their mononuclear and binuclear metal complexes are of current interest and since the early 1970's the field has been extensively growing.[1–3] In order to synthesize and later compare this kind of metal complexes we selected as ligands Schiff bases derived from 2-acetyl-1,8-dihydroxy-3,6-dimethylnaphthalene(H_2addn) and 1,2-alkyldiamines, namely: ethylenediamine(en), 1,2-propanediamine(pn), 2,3-butanediamine(bn) and 1,2-cyclohexyldiamine(chn). Schiff bases derived from H_2addn with ethylenediamine, 1,3-propanediamine and diethylenetriamine and some mononuclear complexes of these ligands had already been reported;[2] however we observed that the chemical analyses of the complexes obtained with our ligands following the reported method were not in agreement with the expected stoichiometries. In fact, these solids were mixtures of the correct complexes and yellow impurities of unknown stoichiometries. We report on in this paper a modification of the reported method which yields uniquely the desired mononuclear complex together with a study of the complexes obtained.

Binuclear complexes. Cu/Cu, Ni/Ni, VO/VO, Ni/Cu with several Schiff bases have also been reported[2] however with the ligands employed in this communication all attempts we have made to get these using only VIIIb transition metals have been unsuccessful. In all cases we obtained not well characterized materials with slightly low metal contents. The only dinuclear complex obtained had to contain at least one cation with a strong affinity toward oxygen.

EXPERIMENTAL

Dehydroacetic acid was generously supplied by INDUKERN (Barcelona). 2-acetyl-1,8-dihidroxy-3,6-dimethylnaphthalene (H_2addn) was prepared from dehydroacetic acid by literature method.[4,5] Its purity was checked by elemental analysis, ^{1}H NMR, IR electronic and mass spectroscopy and compared to literature data.[2,4,5]

Preparation of the Schiff bases (H_4addn-diam; diam = en,, pn, bn, chn)

To a solution of H_2addn (1,2 g 0.0052 mol) in hot EtOH (80 cm^3), the corresponding diamine (0.0026 mol) dissolved in hot EtOH (10 cm^3) was added all at once. The mixture was refluxed for 2–3 hr. During this time a yellow (en, pn) or orange (chn, bn) solid was precipitated. While warm, the precipitate was filtered, washed with EtOH and dried at 70°C (Table 1). For chn, an additional

*Author to whom correspondence should be addressed.

Table 1. Analytical data for the ligands

Compound	Colour	Yield	C %		H %		N %	
			Calc.	Found	Calc.	Found	Calc.	Found
H_2addn	colorless	22.4 %	73.04	73.0	6.09	6.2	-	-
H_4addn-en	yellow	95.0 %	74.18	74.2	6.61	6.6	5.79	5.9
H_4addn-pn	yellow	80.0 %	74.70	74.3	6.83	7.1	5.62	5.6
H_4addn-chn	orange	49.0 %	75.84	75.6	7.06	7.0	5.20	5.2
H_4addn-bn	orange	56.0 %	74.97	74.8	7.08	7.2	5.46	5.3

product was obtained after setting the filtered mother liquor at r.t. for few hours. The analyses were identical to these of the first precipitate, however the m.p. was very much different.

Preparation of mononouclear complexes M(H_2-addn-diam) (M = Cu, Ni, Co, diam = *ethylenediamine, 1,2-propanediamine*)

Copper(II) *or nickel*(II) *complexes.* A stirred suspension of H_4addn-diam (diam=en, pn) (0.001 mol) in hot MeOH (300 cm^3) was brought to reflux, and copper acetate monohydrate or nickel acetate (0.001 mol) dissolved in hot MeOH (50 cm^3) was added in small portions until the metal salt addition was finished (7–8 hr). The mixture was refluxed for an additional 2 hr period. During this time a coloured solid precipitated which was filtered, washed with MeOH and dried at 70 °C (Table 2).

Cobalt(II) *complexes.* The procedure was as before but all the operation was carried out under a nitrogen atmosphere and the solvents employed had been previously degassed (Table 2).

Preparation of UO_2Ni (addn-pn)

To a refluxing solution of Ni(H_2addn-pn) (0.001 mol; CH_2Cl_2, 70 cm^3) were consecutively and slowly added methanol (75 cm^3) and LiOH (0.002 mol; methanol, 25 cm^3). After keeping the solution at the boiling temperature for a $\frac{1}{2}$ hr, $UO_2(CH_3COO)_2$ (0.001 mol; methanol, 40 cm^3) was slowly added during 1 hr and the mixture was refluxed overnight. The solvent was slowly evaporated until the first precipitate appeared. After keeping the system at r.t. for a few hours the precipitate was filtered, washed with Et_2O and dried under vacuum (Table 2).

Physical measurements

Infrared spectra were obtained in the range 4000–250 cm^{-1} using a Beckman IR-20A spectrometer. Solid state spectra were recorded as KBr pellets. UV-visible near IR spectra were obtained with a Beckman Acta III and Beckman 2000 recording spectrometer, in EtOH or CH_2Cl_2 solutions. The ^{1}H NMR spectra were recorded at 80 MHz using a Brucker WP8054 spectrometer. The mass spectra of H_2addn was obtained using a Hewlet-Packard 2985 GC/MS system spectrometer. Electron spin resonance of the copper compounds were obtained at the X band (9.4093 GH_z) using a Varian spectrometer. Elemental Analysis were carried out with a Perkin–Elmer Elemental Analyzer 240B and the metal analysis using a EDTA method[6] after destroying the complexes with $HNO_3/HClO_4$ mixture acids.

Table 2. Analytical data for the complexes

Compound	Colour	Yield	C %		H %		N %		Metal	
			Calc.	Found	Calc.	Found	Calc.	Found	Calc.	Found
Cu(H_2addn-en)	dark-green	86 %	65.99	66.5	5.50	5.6	5.13	5.1	11.64	11.6
Cu(H_2addn-pn)	black	60 %	66.47	66.6	5.76	5.8	5.00	4.9	11.34	11.1
Ni(H_2addn-en)	green	69 %	66.58	66.4	5.55	5.7	5.18	5.1	10.92	10.6
Ni(H_2addn-pn)	black	74 %	67.05	66.9	5.81	5.7	5.04	5.2	10.57	10.3
Co(H_2addn-en)	green	75 %	66.54	66.6	5.55	5.4	5.18	5.2	10.91	10.7
Co(H_2addn-pn)	dark-red	80 %	67.03	66.8	5.77	5.9	5.05	5.1	10.63	10.4
UO_2Ni(addn-pn)	red	65 %	45.22	46.0	3.65	3.7	3.40	3.5	7.31(Ni)	7.40(Ni)

RESULTS AND DISCUSSION

Ligands

All the diimines synthesized were very insoluble in almost all the common solvents and this fact seriously limited their study. The compound with ethylenediamine had been previously obtained by M. Vidali *et al.*[2] and our results were in accordance with them.

IR spectra show bands at 3400 cm^{-1} (ν(OH)), 1600 cm^{-1} (ν(CN)) and 1270–1280 cm^{-1} (ν(CO)) in agreement with the values reported in the literature.[4,7] Electronic spectra show bands at 22,500–23,000 cm^{-1} due to the azomethine group.[8]

Mononuclear complexes

By reaction of H_4addn-diam (diam=en, pn) with Cu(II), Ni(II) and Co(II) acetates six mononuclear complexes M(H_2addn-diam) were obtained. The Cu(II) and Ni(II) complexes with H_4addn-en were previously reported.[2] However we found that the metal contents of the complexes made following the reported method were low. Upon slow evaporation of a Cl_2CH_2 solution of "Cu (H_2addn-pn)" we observed that in fact these solids were composed of two materials, one amorphous and yellow and the other one crystalline and deep coloured. A pure crystalline solid was obtained by slow diffusion of ethyl acetate into a solution of "Cu(H_2addn-pn)" in pyridine. Analysis of this compound gave for the first time satisfactory elemental analysis for the stoichiometry proposed. In addition, we found that solids with satisfactory elemental analysis and good yields (Table 2) would be obtained directly from synthesis with a variation of the reported method that consists in a very slow addition of the metal acetate through a period of 7–8 hr as indicated in the experimental section.

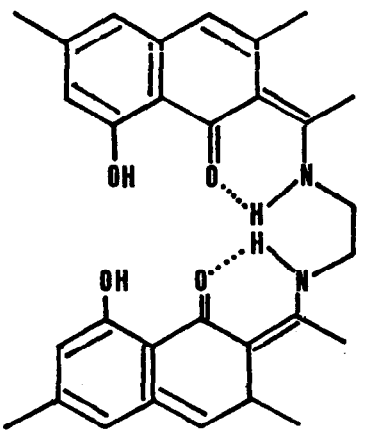


Fig. 1. H_4addn-diam.

All complexes synthesized decompose above 300°C and they are only soluble in very good solvating solvents (pyridine, dimethylsulfoxide, N,N-dimethylformamide, chloromethane...) the nickel(II) complexes are the least soluble of all of them.

IR spectra show bands at 3400 cm^{-1} ν(OH), 1630–1640 cm^{-1} (ν(CN)) and 1330–1345 cm^{-1} ($\nu(CO)$) compatible with a N_2O_2 coordination mode of the metal ion.[2,9]

The electronic spectra of the Cu(II) complexes (Table 3) show bands in the low energy region. The lowest energy bands at 14,815 cm^{-1} are assigned to a $^2E \rightarrow {}^2T_2$ d–d transition and they are in the range found for square planar N_2O_2 coordination mode as it is observed in the Cu(II) complexes derived from several salicylaldiimines[10–13] in which only the square planar N_2O_2 coordination mode can be found.

The electronic spectra of the Ni(II) complexes only show one band (at 17,544–17,241 cm^{-1}) which can be assigned to a d–d transition. Similar spectra are found in Ni(II) complexes with salicylaldiimines.[10,11] This band is assigned to the transition $^1A(F) \rightarrow {}^1B(G)$ for a d^8 ion in a C_{2v} local symmetry environment.

The electronic spectra of the Co(II) complexes (Table 3) is in general difficult to interpret due to spin-orbit and vibronic effects. Only a shoulder can be observed in the visible region for all of the complexes synthesized at 19231–18868 cm^{-1} which is assigned to d–d transitions. In the near infrared zone we found a weak band at 10,870 cm^{-1} for the complex with H_4addn-en. This spectra is compatible with a square planar N_2O_2 metal coordination mode as is observed in Co(II) complexes with salicylaldiimines.[10,14,15]

Although the spectral data strongly suggest the presence of the N_2O_2 isomer for all of the complexes synthesized, in our opinion these are not completely conclusive and, on the other hand, they do not give any information concerning purity with respect to the O_2O_2 isomers. Unfortunately no other proof has been given about it in this kind of complex, so we report on the esr spectra of the Cu(II) complexes which in our opinion, gives us definitive evidence for the N_2O_2 metal coordination mode.

EPR spectra for the Cu(II) complexes were recorded at room temperature in CH_3Cl solution. Figure 2 shows the typical first derivative of the spectra of the Cu(II) complexes.

The hyperfine structure of the spectra consists of four non symmetrical bands where the non symmetry is due to relaxation problems due to the

Table 3. Esr spectral characteristics for several Cu(II) complexes

Compounds	g	a_1/g(Gauss)	a_2/g(Gauss)	references
N,N'-Bis(acetylacetone)ethylenediimino copper(II)	2.111	88.7	-	(29)
N,N'-Bis(2-acetiminodimedone)ethylene-diimino-copper(II)	2.105	88.7	-	(29)
N,N'-Bis(salicylaldehyde)ethylene-diimino-copper(II)	2.110	90.7	-	(29)
N,N'-Bis(o-hydroxyacetophenone)-ethy-lenediimino-copper(II)	2.096	89	-	(29)
Cu(H_2addn-en)	2.10	87.2	13.1	(a)
Cu(H_2addn)pn	2.11	87.3	12.7	(a)

(a) This work.

coupling with the nuclear magnetic moment $I = 3/2$ of the ^{63}Cu atom, which is typical of almost all Cu(II) complexes. In the last two bands, at higher field, the superhyperfine structure is observable (five bands with relative intensities 1 : 2 : 3 : 2 : 1) due to the coupling with the two equivalents ^{14}N atoms ($I = 1$). The hyperfine and superhyperfine splitting constants a_1/g, a_2/g and g factor calculated from the spectra are shown in Table 7. The spectral characteristics of several Cu(II) complexes with Schiff bases[16] are also reported in Table 3. For all of them it has been established a square planar N_2O_2 metal coordination mode by X-ray diffraction studies. Due to the great similarity between them, we propose a similar structure for our two Cu(II) complexes.

Binuclear complexes Binuclear complexes with several Schiff bases, Cu/Cu, Ni/Ni, VO/VO, Ni/Cu are reported in the literature. However, we have not been successful in getting any homo- or hetero-dinuclear complexes using only VIIIb transition metals and the ligands reported in this communication.

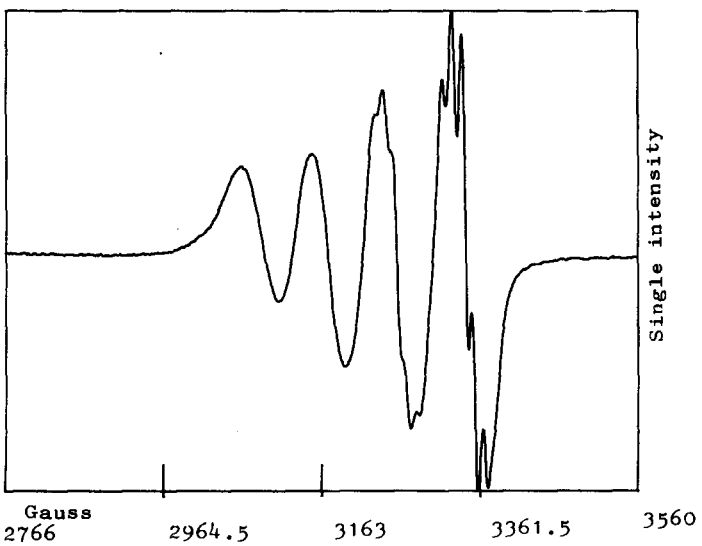


Fig. 2. First derivative esr spectra of Cu(H_2addn-en) at 298 K in CH_3Cl solution (frequency 9.4093 GH_z).

In addition to the reported method for Schiff base derivatives H_2addn we have tried many preparative routes for these homo- and heterobinuclear complexes with our ligands. In all cases, except one (UO_2Ni(addn-pn)) we have obtained black materials not well characterized with low metal contents. We think that it is due to the low reactivity of the phenolic moiety of the ligands, so only oxocations with strong oxygen affinity as UO_2^{2+} and perhaps VO^{2+} should give homo- or heteropolynuclear complexes with Schiff bases derived from 2-acetyl-1,8-dihydroxy-3,6-dimethylnaphthalene.

Acknowledgements—This work was supported in part by "Comisión Asesora de Investigatión Científica y Técnica". We are indebted to "Laboratoire de Chimie de Coordination of the CNRS" (Toulouse, France), specially Mr. A. Mari, for recording esr spectra.

REFERENCES

1. D. Fenton and U. Casellato, *Inorg. Chim. Acta* 1982, **62**, 57.
2. M. Vidali, R. Graziani, P. A. Vigato and U. Casellato, *Inorg. Chim. Acta* 1980, **38**, 85.
3. M. Melnik, *Coord. Chem. Rev.* 1982, **42**, 259.
4. Collie, *J. Chem. Soc.* 1893, **63**, 639; 1907, **91**, 787.
5. P. Bethell and R. Maitland, *J. Chem. Soc.* 1962, 3751.
6. G. Schwarzenbach, *Complexometric Titrations*. Methuen, London (1969).
7. H. Okawa and S. Kida, *Bull Chem. Soc. Jpn.* 1972, **45**, 1759.
8. B. Bosnich, *J. Amer. Chem. Soc.* 1968, **90**, 627.
9. W. E. Radzinski and T. M. Aminabhavi, *Inorg. Chim. Acta* 1983, **69**, 83.
10. K. S. Patel and J. C. Bailov, *J. Inorg. Nucl. Chem.* 1970, **35**, 1399.
11. R. Holm, *J. Amer. Chem. Soc.* 1960, **82**, 5635.
12. R. S. Downing and F. L. Urbach, *J. Am. Chem. Soc.* 1969, **91**, 5977.
13. S. M. Crawford, *Spectrochim. Acta* 1963, **19**, 255.
14. H. Nishikawa and S. Yamada, *Bull. Chem. Soc. Jpn.* 1964, **37**, 8.
15. S. Yamada, *Coord. Chem. Rev.* 1966, **1**, 415.
16. V. C. Swett and E. O. Dudek, *J. Phys. Chem.* 1968, **72**, 1244.

Polyhedron Vol. 4, No. 1, pp. 103–113, 1985
Printed in Great Britain.

0277–5387/85 $3.00 + .00
© 1985 Pergamon Press Ltd.

PREPARATIONS, STRUCTURES AND THERMAL DECOMPOSITION OF SOME BIS(PENTAFLUOROBENZOATO)DIOXOURANIUM(VI) COMPLEXES

GLEN B. DEACON* and PETER I. MACKINNON
Chemistry Department, Monash University, Clayton, Victoria, 3168, Australia

and

JOHN C. TAYLOR
Division of Energy Chemistry, C.S.I.R.O., Lucas Heights Research Laboratories, Private Mail Bag 7, Sutherland, N.S.W. 2232, Australia

(*Received* 21 *February* 1984; *accepted* 30 *March* 1984)

Abstract—Reaction of $UO_2(O_2CCH_3)_2$ with pentafluorobenzoic acid yields $UO_2(O_2CC_6F_5)_2$, which has been converted into the solvated complexes $UO_2(O_2CC_6F_5)_2L_2{\cdot}S$ [L_2 = 2,2′-bipyridyl (bpy), S = 0.33 (PhH) or 0.07 (*t*-BuOH); L = Ph_3PO, S = *t*-BuOH; L = Ph_3AsO, *S* = 0.40 (*t*-BuOH)] and the solvent free $UO_2(O_2CC_6F_5)_2L_2$ [L_2 = bpy; L = Ph_3PO]. The crystal structure of $UO_2(O_2CC_6F_5)_2$bpy (orthorhombic, space group $P2_12_12_1$; a = 18.45(2), b = 18.94(2), c = 7.069(8) Å, Z = 4] reveals distorted hexagonal bipyramidal stereochemistry with a *trans* UO_2 group, chelating pentafluorobenzoate ligands, and chelating 2,2′-bipyridyl, which is significantly displaced from the hexagonal plane. The structure of $UO_2(O_2CC_6F_5)_2(OPPh_3)_2{\cdot}t$-BuOH [rhombohedral, space group *R*3; a = 21.51(3) Å, α = 117.28(5)°, Z = 3] shows *trans* UO_2, pseudo *trans* Ph_3PO ligands, and one unidentate and one *disordered* chelating pentafluorobenzoate ligand, whilst *t*-BuOH could not be located because it is highly disordered. Relationships between $\nu(CO_2)$ frequencies and the carboxylate coordination are discussed, and $UO_2(O_2CC_6F_5)_2(OAsPh_3)_2{\cdot}0.40$ (*t*-BuOH) is considered to have stereochemistry similar to that of the phosphine oxide complex. The complexes undergo decarboxylation in dimethyl sulphoxide yielding pentafluorobenzene and carbonatodioxouranium(VI) species not $UO_2(C_6F_5)_2$ derivatives.

Although there has been some investigation of uranyl benzoates[1,2] and recent studies of uranyl *p*-aminosalicylates[3] and anthroates,[4,5] the chemistry of uranyl complexes with aromatic carboxylates has been neglected by comparison with the behaviour of uranyl alkanoates, aminopolycarboxylates, and pyridinecarboxylates.[6,7] In addition, little is known of complexes with fluorinated carboxylates. We now report a study of uranyl pentafluorobenzoate and its coordination derivatives with 2,2′-bipyridyl, triphenylphosphine oxide, and triphenylarsine oxide. Since the complexes are potential sources of uranyl pentafluorophenyl derivatives by decarboxylation reactions, a well established route to Main Group element fluorocarbon compounds[8,9] and of increasing value for transition metal analogues,[9–11] their thermal decomposition has also been studied.

*Author to whom correspondence should be addressed.

RESULTS AND DISCUSSION

Preparations of dioxobis(pentafluorobenzoato)uranium(VI) derivatives

Uranyl pentafluorobenzoate was conveniently prepared by reaction of uranyl acetate with pentafluorobenzoic acid.

$$UO_2(O_2CCH_3)_2 + 2C_6F_5CO_2H \rightarrow UO_2(O_2CC_6F_5)_2 + 2CH_3CO_2H.$$

Some difficulty was experienced in obtaining the compound analytically pure, partly owing to solvent retention.

Reaction of uranyl pentafluorobenzoate with 2,2′-bipyridyl in ethyl acetate, in diethyl ether followed by crystallization from benzene, and in *t*-butanol yielded solvent-free $UO_2(O_2CC_6F_5)_2bpy$, $UO_2(O_2CC_6F_5)_2bpy.0.33(C_6H_6)$ and $UO_2(O_2CC_6F_5)_2bpy.0.07(t\text{-BuOH})$ respectively. In the last two cases, the solvent was retained on prolonged heating under vacuum. The compositions were established by ^1H NMR measurements and were consistent with analytical data. Reactions of uranyl pentafluorobenzoate with triphenylphosphine oxide and triphenylarsine oxide in *t*-butanol yielded $UO_2(O_2CC_6F_5)_2(OPPh_3)_2.t\text{-BuOH}$ and $UO_2(O_2CC_6F_5)_2(OAsPh_3)_2.0.40(t\text{-BuOH})$ respectively. The former complex was isolated solvent-free from a similar preparation in benzene containing a trace of ethanol.

Properties of dioxobis(pentafluorobenzoato)-uranium (VI) *compounds*

Vibrational assignments for structurally significant IR and, for representative compounds, Raman frequencies are given in Table 1. For $UO_2(O_2CC_6F_5)_2bpy$ and $UO_2(O_2CC_6F_5)_2(OPPh_3)_2$ there is little difference between the values for the solvent-free complexes and various solvates (Table 1), indicating that solvation does not cause significant structural modification. The separations between the $\nu(CO_2)$ frequencies for $UO_2(O_2CC_6F_5)_2$ and the bipyridyl complex are significantly less than that for sodium pentafluorobenzoate[12] (Table 1), indicative[13] of bidentate or bridging bidentate carboxylate coordination. (For $[(C_6F_5)_2Ph_3PO]TlO_2CC_6F_5]_2$, in which the $C_6F_5CO_2$ groups are both chelating and bridging,[14] the separation[15] is 161 cm^{-1}.) By contrast, the complexes $UO_2(O_2CC_6F_5)_2L_2$ ($L = Ph_3PO$ or Ph_3AsO) show two sets of $\nu(CO_2)$ frequencies (Table 1), one with a separation much larger than ionic, indicative[13] of unidentate carboxylate coordination, and one smaller than ionic, as expected for bidentate or bridging bidentate pentafluorobenzoate. Crystallography (next section) has confirmed the presence of both unidentate and chelating carboxylate ligands in $UO_2(O_2CC_6F_5)_2(OPPh_3)_2.t\text{-BuOH}$. This coordination arrangement differs from that proposed[16] for $UO_2(O_2CCH_3)_2(OPPh_3)_2$, viz. solely bidentate carboxylate groups. The $\nu(CO_2)$ frequencies for this complex (this work) show a very low separation compared with acetate ions[13] (Table 1) consistent with chelating acetate ligands.

Table 1. Some vibrational assignments for dioxobis(pentafluorobenzoato)uranium(VI) complexes

Compound	$\nu_{as}(CO_2)^a$ (cm^{-1})	$\nu_s(CO_2)^a$ (cm^{-1})	$\Delta\nu$ (cm^{-1})	$\nu_{as}(OUO)^a$ (cm^{-1})	$\nu_s(OUO)^b$ (cm^{-1})	$\nu(E=O)^{a,c}$
$UO_2(O_2CC_6F_5)_2$	1562	1455, 1443	113	948	872	
$UO_2(O_2CC_6F_5)_2bpy$	1580, 1558	1410	159	932	853	
$UO_2(O_2CC_6F_5)_2bpy.0.33(C_6H_6)$	1582, 1560	1409	162	932	*d*	
$UO_2(O_2CC_6F_5)_2bpy.0.07(t\text{-BuOH})$	1580, 1558	1415	154	936	*d*	
$UO_2(O_2CC_6F_5)_2(OPPh_3)_2$	1665 1570	1343 1412	322 158	923	*d*	1135
$UO_2(O_2CC_6F_5)_2(OPPh_3)_2.t\text{-BuOH}$	1668 1567	1338 1411	330 156	923	844	1133
$UO_2(O_2CC_6F_5)_2(OAsPh_3)_2.0.40(t\text{-BuOH})$	1660, 1648	1340	314	910	*d*	863
	1569	1406	163			
$UO_2(O_2CCH_3)_2(OPPh_3)_2$	1557	1463	94	917, 911	*d*	1155
$C_6F_5CO_2Na^e$	1610	1400	210			
$CH_3CO_2Na^f$	1578	1414	164			

[a] I.r. data. [b] Raman data. [c] E = P or As. [d] Not determined. [e] From ref.12. [f] From ref.13.

All uranyl pentafluorobenzoates show only one ν_{as}(OUO) frequency and, where Raman data were obtained, one ν_s(OUO) frequency (Table 1), and the IR and Raman values are not coincident. This is indicative of essentially linear OUO stereochemistry. Slight deviations ($<10°$) from linear OUO observed in the crystal structures of two of the complexes may not be meaningful (see below), and in any case such deviations may be too small to give two observable bands in both IR and Raman spectra. The ν(PO) and ν(AsO) frequencies (Table 1) of the $UO_2(O_2CC_6F_5)_2L_2$ (L = Ph_3PO or Ph_3AsO) complexes show the shifts from free ligand values[17,18] expected[19-22a] on coordination.

The molar conductances of the complexes in methanol are approximately half the values expected[23] for 1:1 electrolytes in this solvent, and indicate that substantial ionization occurs, e.g.

$$UO_2(O_2CC_6F_5)_2 \rightleftharpoons UO_2(O_2CC_6F_5)^+ + C_6F_5CO_2^-.$$

The ^{19}F NMR spectra in $(CD_3)_2SO$ (Experimental Section) show some broadening, which could be due to exchange phenomena associated with partial ionization. Better resolution is observed on heating and for $UO_2(O_2CC_6F_5)_2$ in ether, in which significant ionization is not expected. Only features indicative[24a] of uranium(VI) were observed in the visible spectra (Experimental Section), hence it is unlikely that broadening arises from paramagnetic species of lower oxidation state.

Crystal and molecular structures of $UO_2(O_2CC_6F_5)_2$bpy *and* $UO_2(O_2CC_6F_5)_2(OPPh_3)_2$·*t*-BuOH

The molecular structures of the complexes of uranyl pentafluorobenzoate with 2,2′-bipyridyl and triphenylphosphine oxide were determined by X-ray crystallography. The former is monomeric and has hexagonal bipyramidal stereochemistry around the uranium(VI) ion (Fig. 1). Oxygens O(3), O(4),O(5), O(6) from the two chelating pentafluorobenzoate ligands and the nitrogen atoms of bipyridyl, N(1) and N(2) occupy equatorial coordination sites. However, the bipyridyl ligand is twisted out of the plane described by O(3), O(4), O(5), O(6) and uranium, with N(1) and N(2) being symmetrically displaced from this plane by $-0.79(5)$ and 0.74(4) Å respectively (Table 2). The plane of the bipyridyl makes a dihedral angle of *ca.* 38° with the O(3), O(4), O(5), O(6) and uranium plane. Selected bond lengths and angles are given in Table 3.

The dioxouranium angle, O(1)–U–O(2), 172(2)°

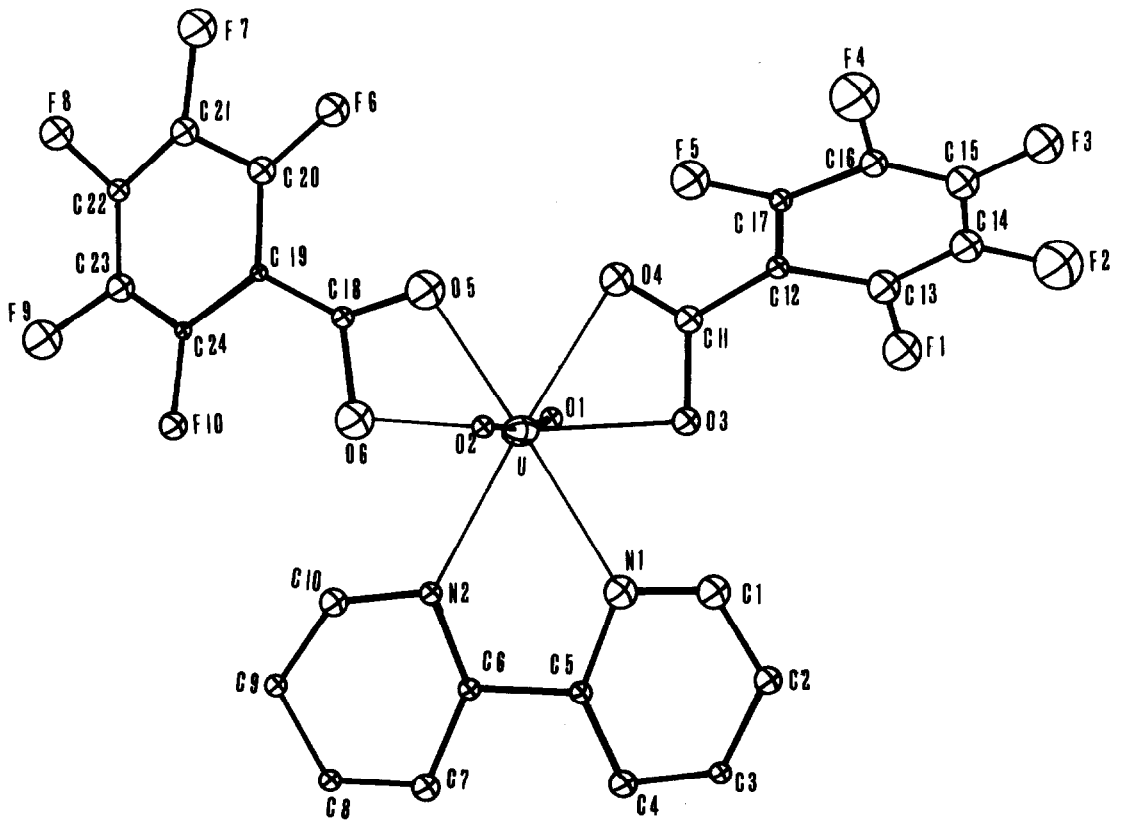


Fig. 1. Molecular structure of 2,2′-bipyridyldioxobis(pentafluorobenzoato)uranium(VI).

Table 2. Least squares planes

Atoms in the plane	Atoms not in the plane	Deviations[a] from the plane (Å)
Complex	$UO_2(O_2CC_6F_5)_2bpy$	
U		0.004(2)
O(3)		0.01(4)
O(4)		-0.02(4)
O(5)		0.02(5)
O(6)		-0.01(5)
	N(1)	-0.79(5)
	N(2)	0.74(4)
Complex	$UO_2(O_2CC_6F_5)_2(OPPh_3)_2$.t-BuOH	
U		0.000(3)
O(3)		0.12(8)
O(4)		-0.01(11)
O(5)		-0.14(10)
O(6)		0.10(8)
O(7)		-0.06(10)

[a]The planes are given by the equations (i) 0.341X - 0.573Y - 0.745Z - 0.572 = 0 for $UO_2(O_2CC_6F_5)_2$bpy and (ii) 0.255X + 0.815Y' - 0.597Z - 11.16 = 0 for $UO_2(O_2CC_6F_5)_2(OPPh_3)_2$.*t*-BuOH where X = *ax*, Y = *by*, Y' = *b*-($\frac{1}{2}$ + y) and Z = *cz*.

is seemingly distorted from the linear configuration usually found in molecular uranyl complexes.[25] Several other monomeric complexes have an apparently bent uranyl group, e.g. 176.6(6)° in $UO_2(trop)_2.EtOH$[26] (trop = tropolonate), 174.8° in $UO_2(ox)_2.(Hox)$[27] (Hox = quinolin-8-ol) and 174.2(6)° and 173.8(5)° respectively in the α and β forms of a uranyl Schiff base complex.[28] However, the difficulties associated with the accurate location of light atoms in the presence of very heavy ones in X-ray studies may serve to limit the accuracy of the determination of these angles. Nevertheless, the dioxouranium(VI) group may actually be distorted in capped polyhedra.[29]

Displacement of the 2,2′-bipyridyl ligand from the equatorial plane can be attributed to steric crowding of the uranium ion. The ionic radius of eight-coordinate uranium(VI) is only 0.86 Å.[30] Consequently, the angles O(1)–U–N(1) and O(2)–U–N(2) are both considerably contracted from the ideal value of 90° to 76(1)° and the intramolecular contracts O(1)...N(1), 2.66 Å and O(2)...N(2), 2.63 Å are somewhat shorter than the sum of the Van der Waal's radii of oxygen (1.40 Å) and nitrogen (1.50 Å).[31] This may also reflect the steric strain around uranium. The bites of the two pentafluorobenzoate ligands, 1.97 and 2.08 Å, are sufficiently small to allow hexagonal bipyramidal stereochemistry. However, the bite of the 2,2′-bipyridyl ligand is much larger, 2.62 Å, causing congestion around the uranium and consequently the twisting of this ligand from the plane. However, in view of the structure of $UO_2(O_2CC_6F_5)_2(OPPh_3)_2$.*t*-BuOH (below), it is surprising that steric strain is not relieved by adopting pentagonal bipyramidal stereochemistry with one unidentate pentafluorobenzoate.

The complex $UO_2(O_2CC_6F_5)_2(OPPh_3)_2$.*t*-BuOH is also monomeric (Fig. 2), but in this case, the stereochemistry is pentagonal bipyramidal with one unidentate and one chelating carboxylate. The pentafluorophenyl ring of the latter is disordered with occupancies of 64% in one position and 36% in the other, and the two rings are displaced up to

Table 3. Selected bond lengths (Å) and angles (°)

$UO_2(O_2CC_6F_5)_2bpy$				$UO_2(O_2CC_6F_5)_2(OPPh_3)_2.t\text{-BuOH}$			
(i) Bond Distances							
Coordination to Uranium							
U-O(1)	1.64(3)	U-O(2)	1.69(3)	U-O(1)	1.87(4)	U-O(2)	1.63(4)
U-N(1)	2.53(3)	U-N(2)	2.47(3)	U-O(3)	2.31(4)	U-O(4)	2.38(5)
U-O(3)	2.24(3)	U-O(4)	2.38(3)	U-O(5)	2.47(5)	U-O(6)	2.47(5)
U-O(5)	2.29(3)	U-O(6)	2.22(4)	U-O(7)	2.17(5)		
(ii) Angles							
Around Uranium							
O(1)-U-O(2)	172(2)	O(2)-U-O(3)	90(1)	O(1)-U-O(2)	171(2)	O(2)-U-O(3)	94(2)
O(1)-U-O(3)	93(1)	O(2)-U-O(4)	88(1)	O(1)-U-O(3)	87(2)	O(2)-U-O(4)	90(2)
O(1)-U-O(4)	88(1)	O(2)-U-O(5)	90(1)	O(1)-U-O(4)	91(2)	O(2)-U-O(5)	83(2)
O(1)-U-O(5)	87(1)	O(2)-U-O(6)	89(1)	O(1)-U-O(5)	90(2)	O(2)-U-O(6)	87(2)
O(1)-U-O(6)	86(1)	O(2)-U-N(1)	112(1)	O(1)-U-O(6)	86(2)	O(2)-U-O(7)	94(2)
O(1)-U-N(1)	76(1)	O(2)-U-N(2)	76(1)	O(1)-U-O(7)	94(2)	O(3)-U-O(4)	168(2)
O(1)-U-N(2)	110(1)						
Hexagonal ring angles, *ca.* 60°				Pentagonal ring angles, *ca.* 72°			
N(1)-U-N(2)	63(1)	N(1)-U-O(3)	67(1)	O(3)-U-O(5)	71(2)	O(5)-U-O(6)	49(2)
O(3)-U-O(4)	54(1)	O(4)-U-O(5)	69(1)	O(6)-U-O(4)	72(2)	O(4)-U-O(7)	87(2)
O(5)-U-O(6)	52(1)	O(6)-U-N(2)	69(1)	O(7)-U-O(3)	81(2)		
Dihedral angles between planes							
Hexagonal ring-bpy 37(2), 38(1)							
(iii) Intramolecular contacts (Å)							
O(1)...N(1)	2.66	O(2)...N(2)	2.63	O(1)...O(7)	2.97	O(2)...O(7)	2.81
O(3)...O(4)	1.97	O(5)...O(6)	2.08	O(3)...O(5)	2.87	O(3)...O(7)	2.93
N(1)...N(2)	2.62			O(4)...O(6)	2.85	O(4)...O(8)	3.54
				O(4)...O(7)	3.13	O(5)...O(6)	2.06

1 Å from each other. However, the unidentate carboxylate is not significantly disordered. The lattice solvent, *t*-BuOH, is also highly disordered and could not be satisfactorily located. Consequently, it was omitted from the analysis. Selected bond lengths and angles are given in Table 3.

The oxygens O(3), O(4) from the triphenylphosphine oxide molecules and O(5), O(6) and O(7) from the pentafluorobenzoate ligands occupy the equatorial positions in a *planar* arrangement (Table 2) unlike the structure of $UO_2(O_2CC_6F_5)_2bpy$. The triphenylphosphine oxide ligands are in a pseudo-*trans* configuration in keeping with their steric requirements, and are almost centrally disposed about the uranium ion which is almost on a pseudo-centre of symmetry. Consequently, the uranyl bonds, 1.63(3) and 1.87(4) Å, and angle, 171(2)°, are not considered to be significantly different from the usual values of *ca.* 1.70 Å each and 180° respectively. A similar effect occurs in the uranyl complex, $UO_2(hfa)_2NH_3$[32] (hfa = 1,1,1,5,5,5-hexafluoropentane-2,4-dionate), where the uranyl group is centric in a non-centric space group.

The five equatorial U–O distances range between 2.17(5) and 2.47(5) Å. The non-coordinated oxygen O(8) of the unidentate carboxylate is 3.93 Å from the uranium centre and hence is clearly non-bonding. In comparison with the 2,2′-bipyridyl complex in which there are short uranyl oxygen–nitrogen contacts, there are no uranyl oxygen-coordinated oxygen contacts less than twice the Van der Waal's radius of oxygen in the triphenylphosphine oxide complex.

The structures (Figs. 1 and 2) confirm conclusions as to the nature of the pentafluorobenzoate coordination derived from IR spectroscopy (above), and indicate that IR criteria developed for

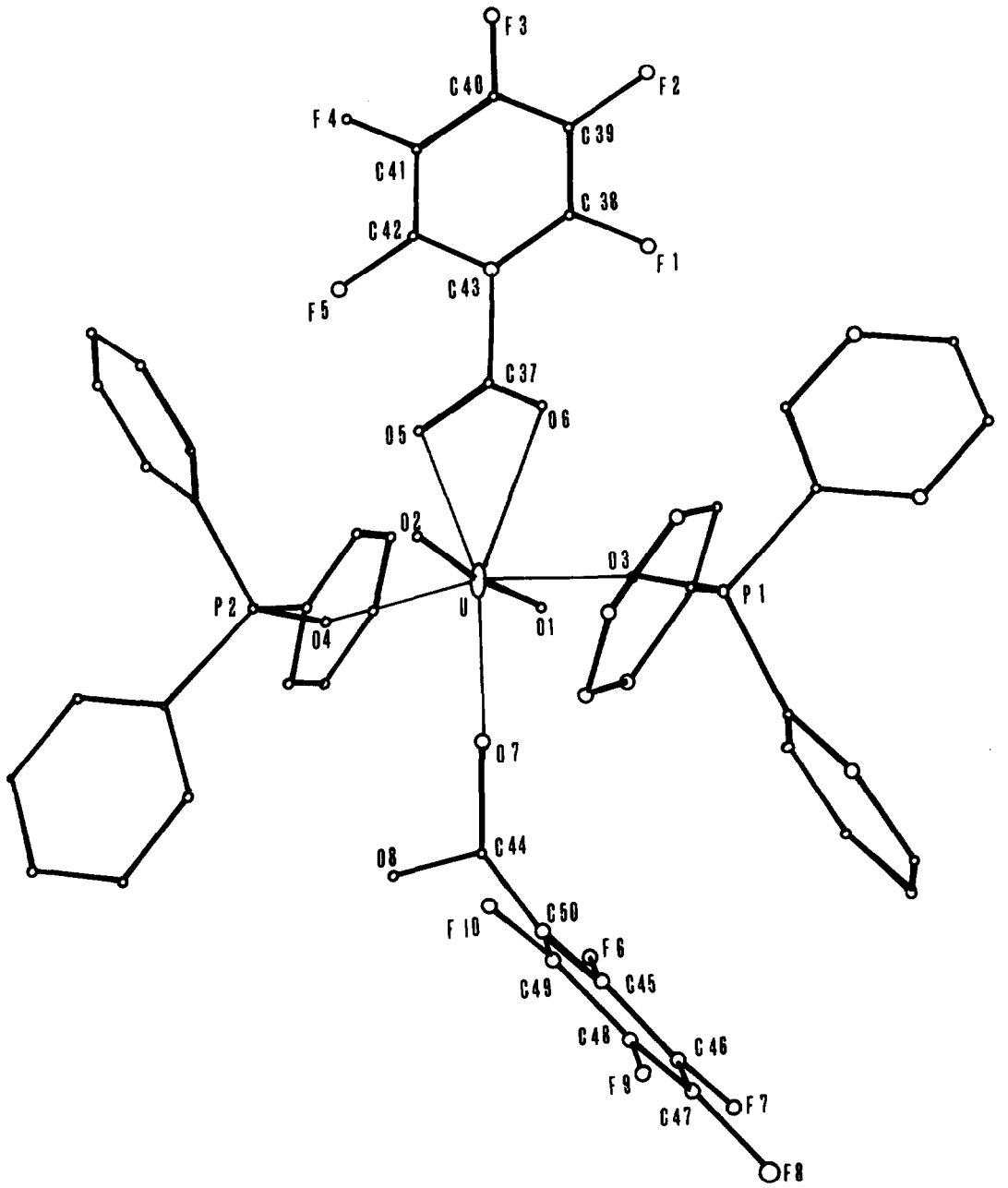


Fig. 2. Molecular structure of dioxobis(pentafluorobenzoato)-bis(triphenylphosphine oxide)uranium(VI).

acetate and trifluoroacetate coordination[13] are applicable to pentafluorobenzoate complexes. However, the inability of the IR method to distinguish chelating and bridging carboxylates is also readily apparent. For the chelating pentafluorobenzoates of the present complexes, the separations between the $\nu(CO_2)$ frequencies (*ca.* 160 cm^{-1}; Table 1) are comparable with that (161 cm^{-1})[15] for $[(C_6F_5)_2Ph_3POTlO_2CC_6F_5]_2$, in which the pentafluorobenzoate groups are both unsymmetrically bridging and chelating.[14]

The similarity between the $\nu(CO_2)$ frequencies of $UO_2(O_2CC_6F_5)_2(OPPh_3)_2.t$-BuOH and $UO_2(O_2CC_6F_5)_2(OAsPh_3)_2.0.40(t$-BuOH) makes it certain that the latter complex has pentagonal bipyramidal stereochemistry with one chelating and one unidentate carboxylate ligand. Further crystallographic study is needed to determine the structure of uranyl pentafluorobenzoate without added neutral ligands. In the light of the $\nu(CO_2)$ frequencies and a likely coordination number greater than six, the pentafluorobenzoate groups

are probably both bridging and chelating. To this stage it has not been possible to grow suitable single crystals.

Decomposition of dioxobis(pentafluorobenzoato)-uranium (VI) *complexes*

When solutions of $UO_2(O_2CC_6F_5)_2$ or $UO_2(O_2CC_6F_5)_2L_2$ (L_2 = bpy; L = Ph_3PO) in dimethyl sulphoxide [or $(CD_3)_2SO$] are allowed to stand at room temperature for an extended period or are heated, carbon dioxide is evolved and pentafluorobenzene formed. Spectroscopic data (Experimental Section) for the uranium containing products indicate the presence of uranyl groups, carbonate ligands,[22b] and O-bonded dimethyl sulphoxide[22c] [see, e.g. $UO_2F_2OS(CH_3)_2$[33]]. No bipyridyl was detected in the uranyl complex from decomposition of $UO_2(O_2CC_6F_5)_2$bpy. The products are probably dimethyl sulphoxide complexes of uranyl carbonate. Despite thorough drying of the solvent, traces of water may remain and provide the proton source for pentafluorobenzene formation,

$$\text{e.g.}\quad UO_2(O_2CC_6F_5)_2 + H_2O + n(CH_3)_2SO \rightarrow UO_2CO_3[(CH_3)_2SO]_n + CO_2 + 2C_6F_5H.$$

Since neither uranium(IV) species nor decafluorobiphenyl are formed, decarboxylation is not similar to the well-known reaction of carboxylic acids with uranyl ions.[24b] The likely path involves decarboxylation of a dissociated pentafluorobenzoate ion, protonation of the resulting carbanion giving pentafluorobenzene and base, which absorbs carbon dioxide to give carbonate.

Thermogravimetric analysis indicated that uranyl pentafluorobenzoate is stable to 250°, but decomposition of the bipyridyl and phosphine oxide complexes commences at lower temperatures. There is no evidence for formation of dioxo(pentafluorophenyl)uranium(VI) species, and the sole weight loss of particular interest is evolution of *t*-butanol from $UO_2(O_2CC_6F_5)_2$-$(Ph_3PO)_2$.*t*-BuOH prior to more extensive decomposition.

EXPERIMENTAL

(1) *General*

Microanalyses were by the Australian Microanalytical Service, Melbourne. Uranium was estimated gravimetrically as uranyl quinolin-8-olate,[34] after treatment of the compounds with dilute nitric acid. IR spectra (4000–650 or 400 cm^{-1}) were recorded as Nujol and hexachlorobutadiene mulls with Jasco IRA-1 or Perkin–Elmer 180 spectrophotometers. Identical spectra were obtained with AgCl or KBr plates, hence no carboxylate exchange reactions occur with the alkali halide plates. Bands of medium or greater intensity not listed in Table 1 are given below.† Raman spectra of crystalline solids in sealed capillary tubes were obtained on a Spex Ramalog 5 laser Raman spectrophotometer.† ^{19}F- and ^1H-NMR spectra were obtained with Bruker WH-90 or Perkin–Elmer R32 spectrometers. Proton chemical shifts are in ppm downfield from internal tetramethylsilane or sodium 3-trimethylsilypropanesulphonate and fluorine chemical shifts in ppm upfield from internal $CFCl_3$. The solvent was $(CD_3)_2SO$ or $(CD_3)_2SO/CDCl_3$. Integrations were satisfactory for the proposed compositions hence they are not listed. Conductances were measured at 20°C with a Wayne Kerr B221A bridge using a cell of standard design fitted with shiny Pt electrodes. Thermogravimetric analyses were carried out with a Mettler ME-21 microbalance with a Cahn temperature programmer. Visible and UV spectra (220–700 nm) were obtained with Pye-Unicam SP 800 or Varian Techtron 635 spectrophotometers.

(2) *Reagents and solvents*

Bis(acetato)dioxouranium(VI) dihydrate (Pronalys Grade) and 2,2′-bipyridyl were from May and Baker and pentafluorobenzoic acid was from Bristol Organics. Triphenylarsine oxide from the reported method[35] and triphenylphosphine oxide (Fluka) were recrystallized from benzene. Nitrogen was purified by BASF R3/11 oxygen removal catalyst and Union Carbide 13X molecular sieves. *t*-Butanol was degassed with purified nitrogen prior to use. Light petroleum (b.p. 40–60°) and ether were dried over sodium. Ethyl acetate was purified by the reported method.[36] Dimethyl sulphoxide was dried over potassium hydroxide and then was refluxed over and distilled from calcium hydride under nitrogen. Other solvents were not purified.

(3) *Pentafluorobenzoatouranium*(VI) *complexes*

Dioxobis(pentafluorobenzoato)uranium(VI). Pentafluorobenzoic acid (15.3 g), bis(acetato)dioxouranium(VI) dihydrate (15.4 g), and *t*-butanol (300 cm^3) were heated under reflux for 2.5 hr under nitrogen. The resulting solution was filtered through a Celite pad to remove unreacted bis(-acetato)dioxouranium(VI) and was partly evaporated under vacuum. Toluene (100 cm^3) was added.

†Full details of IR and Raman frequencies and mass spectra, which show only ligand-derived ions, are available from the Editor.

The *title compound* was isolated by evaporation to dryness under vacuum, was recrystallized three times from ethanol/toluene (1:50, v/v), and dried (60°, 10^{-3} mm, 10 hr), giving a yellow powder (43%), dec.temp., 250° (Found: C, 23.9; F, 27.1; U, 34.0%. $C_{14}F_{10}O_6U$ requires C, 24.3; F, 27.5; U, 34.4%). IR absorption (see also Table 1): 1553m, 1532s, 1483s, 1414m, 1120m, 1007m, 998s, 988m, 812m, 745m cm^{-1}. ^{19}F NMR spectrum: 141.8, br (at 60°, m, ^3J 20 Hz), F2, 6; 150.6, br (unresolved at 60°) F4; 162.2, m, F3, 5. T.G.A.: 0.01% weight loss at 25–250°. Visible spectrum (EtOH), $\lambda_{max}(\epsilon)$: 419 (27.7 mol^{-1} dm^3 cm^{-1}) nm. Mol. cond. (MeOH), 35.4 S cm^2 mol^{-1} (2.75×10^{-3} mol dm^{-3}).

2,2′-Bipyridyldioxobis(pentafluorobenzoato)uranium(VI). (i) 2,2′-bipyridyl (0.23 g) in ethyl acetate (3 cm^3) was added dropwise to a solution of dioxobis(pentafluorobenzoato)uranium(VI) (1.00 g) in boiling ethyl acetate (25 cm^3) giving a yellow precipitate of the *required compound*, which was washed with ethyl acetate and light petroleum (yield, 84%), m.p. 210–211° (dec.) (Found: C, 34.0; H, 1.1; F, 22.1%, $C_{24}H_8F_{10}N_2O_6U$ requires C, 34.0; H, 1.0; F, 22.4%). IR absorption: 1653m, 1525m, 1492s, 1432vs, 1171m, 1162m, 1005vs, 773vs cm^{-1}. ^{19}F NMR spectrum: 141.6, br (at 60°, m, ^3J 21 Hz), F2,6; 156.5, br (unresolved at 60°), F4; 162.2,m,F3,5. ^1H NMR spectrum: 7.39,m,H5,5′; 7.89,m,^3J(H4, H5), 5.9 Hz, ^3J(H4, H3), 7.9 Hz, H4,4′; 8.34, d, ^3J7.9 Hz, H3,3′; 8.63, dd, ^3J4.1 Hz, H6,6′. Visible spectrum (EtOH): $\lambda_{max}(\epsilon)$ 432 (43.5) nm. Mol. cond. (MeOH): 50.6 S cm^2 mol^{-1} (1.50×10^{-3} mol dm^{-3}). T.G.A., 47% weight loss from 221–286°.

(ii) A similar preparation in *t*-butanol gave a yellow precipitate, which was washed with light petrol and dried at 60° (10^{-3} mm, 10 hr). Further drying for longer periods and at 90° indicated constant retention of solvent (^1H NMR spectra) giving *2,2′-bipyridyldioxobis(pentafluorobenzoato)uranium(VI)-t-butanol* (14/1) (yield, 85%) m.p. 211–212°(dec.) (Found: C, 34.1; H, 1.2; F, 22.0. $C_{340}H_{122}F_{140}N_{28}O_{85}U_{14}$ requires C, 34.2; H, 1.0; F, 22.2%). IR absorption: as for the unsolvated species. ^1H NMR spectrum: as above (i), together with 1.11, s, CH_3.

(iii) A similar preparation in ether precipitated the impure title compound after several minutes (yield, 95%), dec. temp. 216–217° (Found: C, 32.9; H, 1.3%) (IR identification). Recrystallization from benzene and drying to constant composition (^1H NMR spectra) by heating under vacuum (60°/10^{-3} mm/3 hr) gave 2,2′-bipyridyldioxobis-(pentafluorobenzoato)-uranium(VI)-benzene (3/1) (Found: C, 35.8; H, 1.4; F, 23.2; N, 3.3. $C_{78}H_{30}F_{30}N_6O_{18}U_3$ requires C, 35.7; H, 1.2; F, 21.7; N, 3.2%). IR absorption: as for the unsolvated species plus 732m, 678w cm^{-1} due to benzene. ^1H NMR spectrum: 7.49, s, C_6H_6 in addition to features similar to those of the unsolvated complex.

Dioxobis(pentafluorobenzoato)bis(triphenylphosphine oxide)uranium(VI). (i) Triphenylphosphine oxide (0.81 g) in *t*-butanol (30 cm^3) was added dropwise to a solution of dioxobis(pentafluorobenzoato)uranium(VI) (1.00 g) in *t*-butanol (10 cm^3). Yellow crystals of *dioxobis(pentafluorobenzoato)bis(triphenylphosphine oxide)uranium-(VI)-t-butanol* (1/1) deposited on standing and were washed with petrol. Drying (60°, 10^{-3} mm, 4hr) did not change the composition (^1H NMR spectra) (yield, 58%), m.p. 104–110° (Found: C, 49.1; H, 3.0; F, 14.6%. $C_{54}H_{40}F_{10}O_9P_2U$ requires C, 49.0; H, 3.1; F, 14.4%). IR absorption: 1648m, 1500m, 1488m, 1438s, 1122s, 1079s, 1006m, 991s, 930m, 775m, 738m, 725vs, 693vs cm^{-1}. ^{19}F NMR spectrum: 141.6, br d, ^3J *ca.* 18 Hz, F2,6; 156.5, br, F4; 162.2, m, F3, 5. ^1H NMR spectrum: 1.14, s, CH_3; 4.20, s(br), OH; 7.54, m, aromatic. Mol. cond. (MeOH): 45.5 S cm^2 mol^{-1} (1.56×10^{-3} mol dm^{-3}). T.G.A., (under vacuum), 5.2% weight loss (28–105°) (Calc. for *t*-BuOH loss: 5.6%); 56.6% (28–420°).

(ii) Addition of petrol (b.p. 60–80°) to stoichiometric amounts of dioxobis(pentafluorobenzoato)uranium(VI) and triphenylphosphine oxide in benzene/ethanol (30:1, v/v) crystallized the unsolvated *title compound* (yield, 46%), m.p. 118–120° (Found: C, 48.6; H, 2.6; F, 15.2. $C_{50}H_{30}F_{10}O_8P_2U$ requires C, 48.1; H, 2.4; F, 15.2%). IR absorption: similar to that of the solvate, except that 1006m cm^{-1} was not observed. ^{19}F and ^1H NMR spectra: as for the solvate with omission of *t*-BuOH features. T.G.A., 55.6% weight loss (100–419°).

Dioxobis(pentafluorobenzoato)bis(triphenylarsine oxide)uranium-t-butanol (5/2). Triphenylarsine oxide (0.48 g) in *t*-butanol (3 cm^3) was added dropwise to a solution of $UO_2(O_2CC_6F_5)_2$ (0.50 g) in the same solvent (5 cm^3) at 80°. Yellow crystals of the *title compound* deposited on standing and had constant composition (^1H NMR) on drying at 60° (10^{-3} mm) (yield, 46%), m.p. 92–96° (Found: C, 45.4; H, 2.7; F, 14.0, $C_{252}H_{170}As_{10}F_{50}O_{42}U_5$ requires C, 45.4; H, 2.5; F, 13.9%). IR absorption: 1515m, 1438vs, 1275m, 1086m, 993s, 768s, 745s, 734s, 689s, cm^{-1}. ^{19}F NMR spectrum: 141.6, br, F2, 6; 155.0, br, F4; 162.2, br, F3, 5. ^1H NMR spectrum: 1.11, s, CH_3; 4.25, vbr, OH (intensity too low for integration); 7.73, m, aromatic.

Bis(acetato)dioxobis(triphenylphosphine oxide)uranium(VI). The complex was obtained by a

slight modification of the reported[16] method, m.p. 209–211°, lit.[16] m.p. 208–210°. IR absorption: 1486m, 1440vs, 1140m, 1120vs, 1090s, 1071m, 998m, 943m, 923s, 760s, 747s, 722vs, 698s, 687s, 672vs cm^{-1}.

(4) *Decomposition of dioxobis(pentafluorobenzoato)uranium(VI) complexes*

(i) Dioxobis(pentafluorobenzoato)uranium(VI) (0.92 g) was treated with dry dimethyl sulphoxide (10 ml) under purified nitrogen and the resulting solution was stirred at room temperature. A slow stream of nitrogen was passed over the reaction mixture and then through barium hydroxide solution. A slight precipitate of barium carbonate was obtained in 10 hr. On heating at 60–80° for 6 hr, precipitation of barium carbonate increased and an orange solid deposited from the dimethyl sulphoxide. The product was collected under nitrogen, washed with dry ether, dried (25°, 10^{-3} mm, 3 hr) and stored under nitrogen. IR absorption: 1460vs(br) [$\nu_{as}(CO_3)$], 1395s [$\nu_s(CO_3)$], 1018s(br) [CH_3rock], 985vs(br) [ν(SO)], 948vs [ν_{as}(OUO)], 930m, 918m, 880s cm^{-1}. Visible absorption (Nujol mull): 366, 418 nm. ^{1}H NMR spectrum (CF_3CO_2H): 3.17, s, CH_3. The product gave a positive qualitative test for carbonate and was hygroscopic.

(ii) A solution of 2,2′-bipyridyldioxobis(pentafluorobenzoato)-uranium(VI) in dry dimethyl sulphoxide was allowed to stand under nitrogen at room temperature until a precipitate formed. This was collected, washed with ether, and dried in the atmosphere. IR adsorption: 3400s(vbr) [ν(OH)], 1460vs(br) [$\nu_{as}(CO_3)$], 1410s [$\nu_s(CO_3)$], 990s [ν(SO) and CH_3 rock] cm^{-1}.

(iii) Decomposition in hexadeuterodimethyl sulphoxide. Samples of $UO_2(O_2CC_6F_5)_2$, $UO_2(O_2CC_6F_5)_2$bpy, and $UO_2(O_2CC_6F_5)_2(Ph_3PO)_2$ were dissolved in $(CD_3)_2SO$ under nitrogen and the ^{19}F NMR spectra were recorded at intervals. In all cases, only resonances attributable to the $C_6F_5CO_2$ group were observed initially, but on standing those due to pentafluorobenzene were also observed.

Extent of decomposition: $UO_2(O_2CC_6F_5)_2$: 5% and 30% C_6F_5H after 160 and 690 min. respectively at 25°; 7 and 30% C_6F_5H after 10 and 29 min at 60°. $UO_2(O_2CC_6F_5)_2$bpy: 4 and 26% C_6F_5H after 150 and 665 min at 25°; 12 and 54% C_6F_5H after 5 and 30 min at 60°. $UO_2(O_2CC_6F_5)_2(Ph_3PO)_2$: 5 and 20% C_6F_5H after 60 and 410 min at 26°. A solid isolated from the decomposition of the bipyridyl complex had IR absorption similar to that of the product from (ii) above.

(5) *Crystallography*†

Suitable crystals of $UO_2(O_2CC_6F_5)_2$bpy were obtained as yellow needles (unsolvated) upon mixing equimolar amounts of 2,2′-bipyridyl and $UO_2(O_2CC_6F_5)_2$ in acetone. Crystals of $UO_2(O_2CC_6F_5)_2(OPPh_3)_2.t$-BuOH were similarly obtained from *t*-butanol as pale yellow laths.

Crystal data. (i) $UO_2(O_2CC_6F_5)_2$bpy ≡ $C_{24}H_8F_{10}N_2O_6U$, M = 848.4, orthorhombic, space group $P2_12_12_1$; a = 18.45(2), b = 18.94(2), c = 7.069(8) Å, U = 2470 Å^3, Z = 4, D_c = 2.28 gcm^{-3}, F(000) = 1584, Mo–K_α radiation, λ = 0.7107 Å, μ_{Mo-K_α} = 65.0 cm^{-1}. (ii) $UO_2(O_2CC_6F_5)_2(OPPh_3)_2.t$-BuOH ≡ $C_{54}H_{40}F_{10}O_9P_2U$, M = 1323, rhombohedral, space group $R\bar{3}$; a = 21.51(3) Å, α = 117.28(5)°, U = 4189 Å^3, Z = 3, D_c = 1.57 g cm^{-3}, F(000) = 1782, Mo–K_α radiation, λ = 0.7107 Å, μ_{Mo-K} = 28.5 cm^{-1}.

Structure determination. (i) A single crystal of $UO_2(O_2CC_6F_5)_2$bpy was sealed in a thin walled capillary. Approximate cell dimensions and space group were determined from Weissenberg photographs. The crystal was mounted on an automatic four-circle diffractometer equipped with a Si(Li) detector and an energy discriminator. 3731 reflections were measured from $0 < 2\theta < 40°$ with a standard reflection monitored every 30 reflections. These data were corrected for absorption, Lorentz-polarization effects and averaged to give 1186 independent [F(*hkl*)] values.[37] The uranium atoms were located in a Patterson synthesis; all other atoms were located in successive difference Fourier syntheses. Hydrogen atoms were not included in the calculations. Structure factors were calculated using neutral scattering factor curves uncorrected for anomalous dispersion except for uranium.[38a,39] The structure was refined using the least-squares program LINUS[40] with unit weights and anisotropic thermal parameters for uranium and isotropic thermal parameters for all other atoms. The discrepancy indices were: $R = \Sigma(|F_o - F_c|)/\Sigma|F_o| = 0.053$ and $R' = \Sigma(|F_o|^2 - |F_c|^2)/\Sigma(|F_o|^2) = 0.104$. (ii) Similarly, a crystal of $UO_2(O_2CC_6F_5)_2(OPPh_3)_2.t$-BuOH was sealed in a capillary, 5350 *hkl* intensities were measured and indexed on a rhombohedral cell. Correction for absorption and averaging gave 1626 independent [F_o(*hkl*)] values.[37] A Patterson synthesis gave the

†Atomic coordinates, thermal parameters, and a complete set of bond lengths and angles have been deposited as Supplementary Data with the Editor, from whom copies are available on request. Atomic co-ordinates have also been deposited with the Cambridge Crystallographic Data Centre.

uranium location as $(0, \frac{1}{2}, \frac{1}{2})$ suggesting position 3(e) of space group $R3$. Refinement in this space group located the triphenylphosphine oxide groups centred about the uranium but failed to locate the pentafluorobenzoate groups satisfactorily. Refinement in $R3$ showed that the uranium was slightly, but significantly, displaced from $(0, \frac{1}{2}, \frac{1}{2})$ and consequently was strongly pseudo-centric. Refinement was completed satisfactorily in R^3 by program SHELX[41] using 1303 reflections with $F_0 > \sigma(F_0)$ and unit weights. Rigid-group refinement was employed for the phenyl rings of the triphenylphosphine oxides and the pentafluorophenyl rings of the pentafluorobenzoate ligands. Carbon–carbon bond lengths were constrained to 1.38 Å and carbon-fluorine bond lengths to 1.35 Å. One pentafluorobenzoate ligand was disordered. Site occupancy factors for the disorder were refined but were constrained to sum to one. Several weak peaks in the final difference synthesis were attributed to the lattice solvent, *t*-butanol. Attempts to refine the molecule as a rigid tetrahedron led to unreasonably large temperature factors. The solvent was then omitted from the calculations. Uranium and phosphorus were refined anisotropically whereas all other atoms were given isotropic temperature factors. Hydrogen atoms were included in the refinement in calculated positions 0.95 Å from the atoms to which they are bound, with isotropic temperature factors. Neutral scattering factor curves corrected for anomalous dispersion were employed for all atoms.[38b] The discrepancy index was $R = 0.070$.

Acknowledgement—We are grateful to the Australian Institute of Nuclear Science and Engineering for a scholarship to P.I.M., to the Australian Research Grants Scheme for support, to Dr. C. G. Barraclough, University of Melbourne for the Raman spectra, and to Dr. T. Hambley, Lucas Heights for assistance with computing.

REFERENCES

1. R. M. Rojas Lopez, J. Arenas Rosado and J. Bermudez Polonio, *An. de Quim.* 1972, **68**, 223.
2. J. Bermudez Polonio, R. M. Rojas Lopez and J. Arenas Rosado, *An. de Quim.* 1969, **65**, 545.
3. G. Bandoli and D. A. Clementi, *J. Inorg. Nucl. Chem.* 1981, **43**, 2843.
4. V. Albano, D. Braca, C. Concilio and E. N. Reri, *Cryst. Str. Comm.* 1978, **7**, 133.
5. C. Concilio and G. Porzi, *Ann. de Chimica* 1980,**70**, 309.
6. K. W. Bagnall, *MTP International Review of Science.* Inorganic Chemistry, Series 2, Vol. 7, p. 41. Butterworths, London (1975).
7. V. Casellato, P. A. Vigato and M. Vidali, *Coord. Chem. Rev.* 1978, **26**, 85.
8. G. B. Deacon, *Organomet. Chem. Rev.* (*A*) 1970, **5**, 355.
9. Yu. A. Ol'dekop and N. A. Maier, *Synthesis of Organometallic Compounds by Decarboxylation Reactions of Metal Acylates.* Science and Technology, Minsk (1976).
10. G. B. Deacon, S. J. Faulks and J. M. Miller, *Transition Met. Chem.* 1980, **5**, 305.
11. G. B. Deacon and I. L. Grayson, *Transition Met. Chem.* 1982, **7**, 97; 1983, **8**, 131.
12. J. E. Connett, A. G. Davies, G. B. Deacon and J. H. S. Green, *J. Chem. Soc.* (*C*) 1966, 106.
13. G. B. Deacon and R. J. Phillips, *Coord. Chem. Rev.* 1980, **33**, 227.
14. K. Henrick, M. McPartlin, G. B. Deacon and R. J. Phillips, *J. Organomet. Chem.* 1981, **204**, 287.
15. R. J. Phillips, Ph.D. Thesis. Monash (1980).
16. C. Pannatoni, G. Graziani, B. Zarli and G. Bombieri, *Inorg. Chem.* 1969, **8**, 320.
17. H. Halmann and S. Pinchas, *J. Chem. Soc.* 1958, 3264.
18. G. B. Deacon and J. H. S. Green, *Spectrochim. Acta* (*A*) 1969, **25**, 355.
19. F. A. Cotton, R. D. Barnes and E. J. Bannister, *J. Chem. Soc.* 1960, 2199.
20. D. M. L. Goodgame and F. A. Cotton, *J. Chem. Soc.* 1961, 2298, 3735.
21. G. A. Rodley, D. M. L. Goodgame and F. A. Cotton, *J. Chem. Soc.* 1965, 1499.
22. K. Nakamoto, *Intrared Spectra of Inorganic and Coordination Compounds*, 2nd Edn. (a) p. 209 (b) p. 169 (c) p. 210. Wiley-Interscience, New York (1970).
23. W. J. Geary, *Coord. Chem. Rev.* 1971, **7**, 81.
24. E. Rabinowitch and R. L. Belford, *Spectroscopy and Photochemistry of Uranyl Compounds*, (a) p. 91; (b) p. 257. Pergamon Press, Oxford (1964).
25. J. I. Bullock, *J. Chem. Soc.* (*A*), 1969, 781.
26. D. A. Clemente, G. Bandoli, M. Vidali, P. A. Vigato, R. Portanova and L. Magon, *J. Cryst. Mol. Struct.* 1973, **3**, 221.
27. D. Hall, A. D. Rae and T. N. Waters, *Acta Cryst.* 1967, **22**, 258.
28. A. M. Brock, D. H. Cook, D. E. Fenton, G. Bombieri, E. Forsellini and F. Benetollo, *J. Inorg. Nucl. Chem.* 1978, **40**, 1551.
29. J. C. Taylor, W. I. Stuart and I. A. Mumme, *J. Inorg. Nucl. Chem.* 1981, **43**, 2419.
30. R. D. Shannon, *Acta Cryst.* 1976, A32, 751.
31. L. Pauling, *The Nature of the Chemical Bond*, p. 260. Cornell University Press, New York (1960).
32. D. A. Johnson, J. C. Taylor and A. B. Waugh, *J. Inorg. Nucl. Chem.* 1979, **41**, 827.
33. M. C. Chakravorti and P. K. Bharadwaj, *J. Inorg. Nucl. Chem.* 1978, **40**, 1643.
34. A. I. Vogel, *A Textbook of Quantitative Inorganic Analysis*, 3rd Edn. p. 540. Longmans, London (1961).

35. L. R. Shriner and C. N. Wolf, *Org. Synth. Coll.* **4**, 1963, 910.
36. A. I. Vogel, *A Textbook of Practical Organic Chemistry*, 3rd Edn. p. 174. Longmans, London (1956).
37. M. M. Elcombe, G. W. Cox, A. W. Pryor and F. H. Moore, *AAEC/TM* 578, 1971.
38. *International Tables for X-Ray Crystallography*, (a) Vol. 3, Table 3.3.1A, (b) Vol. 4, Tables 2.2.4 and 2.3.1. Kynock Press, Birmingham (1962).
39. D. T. Cromer and D. Liberman, *J. Chem. Phys.* 1970, **53**, 1891.
40. P. Coppens and W. C. Hamilton, *Acta Cryst.* 1970, **A26**, 71.
41. G. M. Sheldrick, *SHELX*-76 *Program System.* University of Cambridge (1976).

Polyhedron Vol. 4, No. 1, pp. 115–120, 1985
Printed in Great Britain.

0277–5387/85 $3.00 + .00
© 1985 Pergamon Press Ltd.

CONDUCTOMETRIC TITRATION STUDY OF THE REACTIONS OF SOME TRIALKYLPHOSPHINES WITH BROMINE, IODINE AND IODINE BROMIDE

GORDON S. HARRIS* and J. S. McKECHNIE
Chemistry Department, University of St. Andrews, St. Andrews, Fife, Scotland

(*Received* 19 *December* 1983; *accepted* 30 *March* 1984)

Abstract—The reactions of tributyl-, trioctyl-, and tricyclohexyl-phosphine with bromine, iodine and iodine bromide have been studied by conductometric titration in acetonitrile. In general, evidence was obtained for the formation, in solution, of highly conducting 0.5 : 1, 1 : 1, and 2 : 1 adducts. The 1 : 1 and 2 : 1 adducts (R_3PX_2 and R_3PX_4) were isolated and the electrolytic conductivity of their acetonitrile solutions measured. Values of molar conductivity are reported; these point to strong electrolyte behaviour, hence the 1 : 1 and 2 : 1 adducts must be formulated as the phosphonium salts, $R_3PX^+X^-$ and $R_3PX^+X_3^-$ respectively.

It is well known that organophosphines react readily with halogens to form 1 : 1 addition compounds (i.e. triorganophosphine dihalides, R_3PX_2) some of which are molecular (e.g. Me_3PF_2[1]) whilst others are ionic (e.g. $Ph_3PI_2 \equiv Ph_3PI^+I^{-2}$). We have previously shown that the molecular adducts may undergo partial ionisation when dissolved in solvents of high dielectric constant such as acetonitrile,[3] and that the ionic adducts behave as strong 1 : 1 electrolytes in this solvent.[4] Conductometric titration studies of various R_3P–X_2 systems in acetonitrile have shown that in addition to 1 : 1 adducts, numerous 2 : 1 adducts (i.e triorganophosphine tetrahalides, R_3PX_4) are readily formed, and that these too are strong 1 : 1 electrolytes.[4,5] Our conductance studies of compounds of these types have been, in the main, confined to halogen adducts of aromatic phosphines;[4,5] in this paper we report the results of a conductometric titration investigation of the reactions of some alkylphosphines (tri-*n*-butyl-, trioctyl-, and tricyclohexyl-phosphine) with iodine, bromine, and iodine bromide. Earlier workers have reported that these phosphines form 1 : 1 adducts with halogens[6–8] and that the iodine compounds give conducting solutions in nitrobenzene.[6]

RESULTS AND DISCUSSION

Conductometric titrations

These were carried out for the nine systems R_3P–X_2 (R = *n*-butyl, octyl, cyclohexyl†; $X_2 = Br_2$, I_2, IBr) in acetonitrile. Several types of behaviour were observed and graphs representative of these are shown in Figs. 1 and 2. The systems R_3P–Br_2 and R_3P–IBr gave conductometric titration graphs of similar type, exemplified by the graph of the Oc_3P–IBr system (A, Fig. 1). Breaks in the graph occur at the 0.5 : 1, 1 : 1 and 2 : 1 ratios corresponding to the formation, consecutively, of three adducts in solution, thus,

$$R_3P \xrightarrow{\frac{1}{2}X_2} \underset{[0.5:1\ \text{adduct}]}{R_3PX} \xrightarrow{\frac{1}{2}X_2} \underset{[1:1\ \text{adduct}]}{R_3PX_2} \xrightarrow{X_2} \underset{[2:1\ \text{adduct}]}{R_3PX_4}$$

The high values of conductivity at the breaks indicate that the adducts are ionic. The observed yellow colour and the UV spectra of the solutions at the 1 : 1 and 2 : 1 breaks confirm the presence of trihalide ion at these ratios, with the exception of the 1 : 1 ratio for the Bu_3P–Br_2 system. The reaction steps may thus be more fully represented as follows, with the modification, noted below, in the

*Author to whom correspondence should be addressed.

†Hereafter, the symbols Bu, Oc and Hex, respectively, are used for these organic groups.

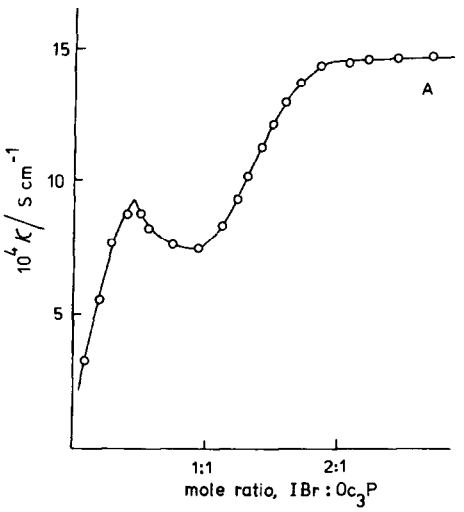


Fig. 1. Conductometric titration of trioctylphosphine with iodine bromide.

formulation of the 1 : 1 adduct in the Bu_3P–Br_2 system:

Step 1. $R_3P + \frac{1}{2}X_2 \longrightarrow \frac{1}{2}(R_3P)_2X^+X^-$ [0.5 : 1 adduct].

Step 2. $\frac{1}{2}(R_3P)_2X^+X^- + \frac{1}{2}X_2 \longrightarrow \frac{1}{2}(R_3P)_2X^+X_3^-$ [1 : 1 adduct].

Step 3. $\frac{1}{2}(R_3P)_2X^+X_3^- + X_2 \longrightarrow R_3PX^+X_3^-$ [2 : 1 adduct].

In the Bu_3P–Br_2 system the solution at the 1 : 1 mole ratio was colourless; tribromide ion was therefore not present and the 1 : 1 adduct must in this case be represented, $Bu_3PBr^+Br^-$. In the systems involving IBr, identification (by UV) of the trihalide anion as I_2Br^- confirmed that it is bromine that is bonded to phosphorus in the cation (e.g. $Oc_3PI_2Br_2 \equiv Oc_3PBr^+I_2Br^-$).

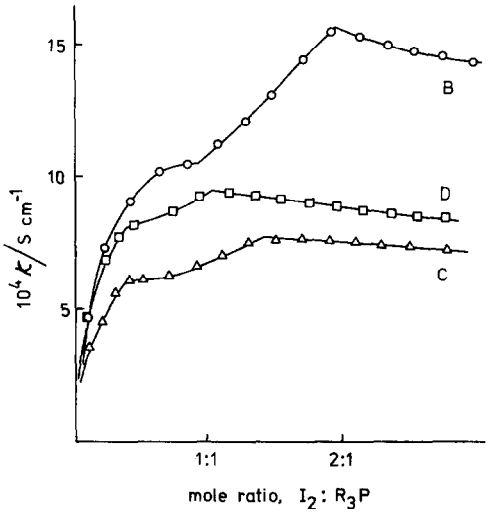


Fig. 2. Conductometric titration of R_3P with iodine. (B) Bu_3P–I_2. (C) Oc_3P–I_2. (D) Hex_3P–I_2.

The formation of a 0.5 : 1 adduct (R_3PX) in solution was of interest since an adduct of this stoicheiometry was not observed in a conductometric titration study of the systems Ph_3P–Br_2 and Ph_3P–IBr in acetonitrile;[4] however, in the systems Ph_3P–ICl in acetonitrile and Ph_3P–I_2 in nitrobenzene[10] there is evidence for the formation of highly conducting 0.5 : 1 adducts.

The three systems involving iodine gave conductometric titration graphs of shape different from the above systems, and from one another (B, C and D; Fig. 2). That of the Bu_3P–I_2 system (B, Fig. 2) had breaks at the 1 : 1 and 2 : 1 mole ratios and resembled closely the graph of the Ph_3P–I_2 system;[4] the reaction therefore occurs in two steps:

$$Bu_3P \xrightarrow{I_2} Bu_3PI_2 \xrightarrow{I_2} Bu_3PI_4.$$

Again, conductivity values at the breaks are high indicating that the adducts in solution are ionic—$Bu_3PI^+I^-$ and $Bu_3PI^+I_3^-$ respectively.

In the conductometric titration of trioctylphosphine with iodine, breaks in the graph occurred at the 0.5 : 1 and 1.5 : 1 ratios (C, Fig. 2). The first of these corresponds with the adduct Oc_3PI[$\equiv (Oc_3P)_2I^+I^-$]. The second break represents an adduct of formula Oc_3PI_3; this stoicheiometry is unexpected for a compound of phosphorus and we have not previously encountered it in any triorganylphosphine–halogen system. We propose, for this adduct, the dimeric formula $(Oc_3PI_3)_2$ which corresponds to $(Oc_3PI^+)_2I^-I_3^-$. The ionic structure accords with the high conductivity of the solution and the presence in the UV spectrum of absorption due to tri-iodide ion. Mixed-anion compounds of a similar kind are known e.g. $(Ph_3AsOH^+)_2Br^-Br_3^-$;[11,12] and, recently, we have isolated the phosphorus compound $(PhPBr_5)_2$, which also behaves as a mixed-anion compound, $(PhPBr_3^+)_2Br^-Br_3^-$.[13]

The graph of the Hex_3P–I_2 system (D, Fig. 2) had distinct breaks at the 0.5 : 1 and 1 : 1 mole ratios. Thus, conductometric titration gives evidence for Hex_3PI [$\equiv (Hex_3P)_2I^+I^-$] and Hex_3PI_2[$\equiv (Hex_3P)_2I^+I_3^-$] in acetonitrile solution, but this system and the previous one are unusual in that conductometric titration does not provide evidence for the presence of 2 : 1 adducts in solution.

Preparation of adducts

Attempts were made to prepare the adducts indicated by the conductometric titrations, from acetonitrile solutions of the components in the appropriate molar ratios. In no system however was a 0.5 : 1 adduct (R_3PX) isolated; all attempts to prepare compounds of this stoicheiometry yielded instead the 1 : 1 adduct (R_3PX_2). This suggests that the 0.5 : 1 adducts are probably not stable as solids and implies that there is some disproportionation of the 0.5 : 1 compounds in solution,

$$R_3PX \rightleftarrows \tfrac{1}{2}R_3PX_2 + \tfrac{1}{2}R_3P,$$

and presumably for solubility reasons it is the 1 : 1 adduct which crystallises from solution.

1 : 1 Adducts were readily obtained as crystalline solids from acetonitrile solutions of R_3P and halogen in the 1 : 1 molar ratio. The tri-*cyclo*hexylphosphine compounds crystallised as the monosolvates, $Hex_3PX_2 \cdot CH_3CN$.

2 : 1 Adducts were obtained for each system; those involving tri*cyclo*hexylphosphine were crystalline solids whilst those involving tributylphosphine and trioctylphosphine were oils and in one case a low melting solid. It is not unknown for phosphonium compounds to exist at room temperature as oils or semi-solids[14] and in the present case it is presumed that the long chain alkyl groups have an inhibitory effect on crystallisation of the ionic phosphonium trihalide structure.

The 1.5 : 1 adduct, Oc_3PI_3, indicated by the conductometric titration of the Oc_3P–I_2 system was obtained as a low melting solid. From the system Hex_3P–I_2, higher adducts (2 : 1, 3 : 1 and 4 : 1) were obtained as crystalline solids despite there being no conductometric titration evidence for their existence in acetonitrile solution. It must be assumed therefore that in acetonitrile at high mole ratios (greater than 1 : 1) further overlapping equilibria are involved

$$Hex_3PI_2 + I_2 \rightleftarrows Hex_3PI_4[\equiv Hex_3PI^+I_3^-]$$

$$Hex_3PI_4 + I_2 \rightleftarrows Hex_3PI_6[\equiv Hex_3PI^+I_5^-]$$

$$Hex_3PI_6 + I_2 \rightleftarrows Hex_3PI_8[\equiv Hex_3PI^+I_7^-].$$

The tendency for higher polyiodides to form in iodide-iodine systems is well known and, in particular, compounds containing the hepta- and ennea-iodide ions have been reported previously.[15]

Electrolytic conductance of the adducts

Electrolytic conductance measurements were made on acetonitrile solutions of the adducts in the concentration range 0.002–0.03 M. For each compound, points on the molar conductivity vs square root of molar concentration plot lay approximately on a straight line of negative slope. For the purpose of comparison, values of molar conductivity at concentration 0.01 M were taken from the graph and these are recorded in Table 1; the high values found indicate that all of the adducts behave as strong electrolytes in acetonitrile. Previous workers found that whereas trialkylphosphine diiodides gave strongly conducting solutions in nitrobenzene, the corresponding dibromides gave low values of conductivity suggesting non-electrolyte behaviour in this solvent.[6] Our results for acetonitrile solutions are consistent with all of these trialkylphosphine halogen adducts being formulated as ionic phosphonium halides and polyhalides as in the case of the corresponding halogen adducts with triphenylphosphine.[4,5]

EXPERIMENTAL

As most of the compounds involved in this work were extremely sensitive to moisture, all manipulations were carried out in a dry-box with a dry nitrogen atmosphere. A vacuum system was used in the purification and handling of volatile compounds. Apparatus and solvents were thoroughly dried before use.

Standard reagents and solvents were of the best grade available commercially and were purified by conventional methods. The alkyl phosphines used were purified thus: tri(*n*-butyl)phosphine—vacuum distillation; trioctylphosphine—fractional freezing; tricyclohexylphosphine—recrystallisation from acetone. Acetonitrile of a purity suitable for conductance measurements was obtained using the method described by Smith and Witten.[16] The halogen adducts of the alkyl phosphines were prepared in acetonitrile by admixture of the phosphine and halogen in the correct molar ratio; the mixture was kept overnight with shaking. Some adducts precipitated directly on mixing the components but more generally were obtained either by addition of diethyl ether to the acetonitrile solution or by freeze-drying of it. All of the adducts were extremely unstable hydrolytically and some were unstable thermally (halogen lost readily). Therefore analysis and other measurements were carried out soon after their preparation. Elemental analyses and properties of the adducts are given in the Table. Carbon, hydrogen and nitrogen were determined micro-analytically using a Perkin–Elmer model 240 Elemental Analyser; halogens were de-

Table 1. Elemental analysis (%)[a] and properties of the adducts

Adduct	Colour	M.p.[b] °C	C	H	Br	I	N	Λ[c] S cm^2 mol^{-1}
Bu_3PBr_2 [g]	white	186 - 190	40.8 (39.8)	7.9 (7.5)	43.0 (44.1)			93.3
Bu_3PI_2 [g]	white	190 - 195	31.5 (31.6)	6.0 (6.0)		56.5 (55.6)		90.0
Bu_3PIBr	pale yellow	176 - 178	34.7 (35.2)	6.5 (6.7)				103.7
Bu_3PBr_4 [e]	orange	24 - 26	28.9 (27.6)	5.5 (5.2)	57.9 (61.2)			137.4
Bu_3PI_4	red-brown	22 - 28	20.2 (20.3)	4.1 (3.8)		69.7 (71.5)		150.8
$Bu_3PI_2Br_2$	dark red	- [d]	23.1 (23.4)	4.5 (4.4)				136.4
Oc_3PBr_2	white	150 - 155	53.9 (54.3)	10.1 (9.7)	29.5 (30.1)			87.4
Oc_3PI_2	white	155 - 160	46.4 (46.1)	8.3 (8.2)		41.1 (40.7)		77.0
Oc_3PIBr	pale yellow	130 - 140	50.0 (49.9)	9.0 (8.9)	13.3 (13.8)	22.4 (22.0)		83.0
Oc_3PBr_4	orange	< 18	42.5 (41.8)	8.0 (7.5)	45.6 (46.3)			124.0

(continued)

(Table 1 continued)

Adduct	Colour	M.p.[b] °C	C	H	Br	I	N	Λ[c] S cm^2 mol^{-1}
Oc_3PI_3	dark red	*ca.* 20	38.7 (38.4)	6.8 (6.8)		49.0 (50.6)		109.5
Oc_3PI_4	dark red	-[d]	32.0 (32.8)	6.0 (5.9)		57.4 (57.8)		123.9
$Oc_3PI_2Br_2$	dark red	-[d]	36.2 (36.7)	6.8 (6.6)	20.5 (20.4)	31.7 (32.4)		120.8
$Hex_3PBr_2.CH_3CN$[f]	pale yellow	245 - 247	49.7 (49.9)	7.9 (7.5)	33.3 (33.2)		2.7 (2.9)	115.6
$Hex_3PI_2.CH_3CN$[f]	pale yellow	260 - 265	42.5 (41.8)	6.4 (6.3)		43.8 (44.1)	2.3 (2.4)	117.8
$Hex_3PIBr.CH_3CN$[f]	white	238 - 240	45.1 (45.4)	7.1 (6.9)	14.5 (15.1)	25.1 (24.0)	2.6 (2.6)	98.0
Hex_3PBr_4[g]	orange	156 - 157	35.7 (36.0)	5.6 (5.5)	53.6 (53.2)			136.3
Hex_3PI_4[g]	brown	204 - 206	27.8 (27.4)	4.4 (4.2)		64.7 (64.4)		120.1
$Hex_3PI_2Br_2$	dark orange	132 - 133	31.1 (31.2)	5.0 (4.8)	23.2 (23.0)	37.1 (36.6)		102.2
Hex_3PI_6	black	136 - 138	19.6 (20.7)	3.0 (3.2)		74.1 (73.1)		107.2
Hex_3PI_8	dark green	150 - 155	17.2 (16.7)	2.7 (2.8)		76.3 (78.3)		108.4

[a]Calculated values are given in parentheses. [b]With decomposition. [c]In 0·01 mol dm^{-3} acetonitrile solution (for Hex_3PI_6 and Hex_3PI_8, 0·005 mol dm^{-3} was used for solubility reasons). [d]Oil at room temperature. [e]Bromine lost readily at room temperature. [f]The unsolvated forms have been reported (Ref. 7). [g]Although previously reported (Refs. 6, 7, 8), these compounds are included here to record their molar conductivity.

termined potentiometrically as silver halide after hydrolysis of the adduct.

Conductance measurements were made in a sealed cell of the dipping electrode type. The electrode supports were mounted on a ground glass cone which fitted a vessel containing the solution. The latter was prepared *in situ* in the dry-box. Conductance was measured by means of a Wayne–Kerr B641 Autobalance Bridge. The apparatus for conductometric titrations was of conventional type scaled down so that the entire titration could be carried out in the dry-box. UV spectra were recorded on a Unicam SP800 UV-visible recording spectrophotometer; the solutions were contained in stoppered cells. Trihalide ions have characteristic absorption in the UV which enables their identification.[17]

REFERENCES

1. A. J. Downes and R. Schmutzler, *Spectrochim. Acta* 1967, **23A**, 681.
2. K. B. Dillon and T. C. Waddington, *Nature Phys. Sci.* 1971, **230**, 158.
3. G. S. Harris, F. Inglis, and R. Schmutzler, *J. Fluorine Chem.* 1980, **16**, 293.
4. A. D. Beveridge, G. S. Harris and F. Inglis, *J. Chem. Soc.* (*A*) 1966, 520.
5. G. S. Harris and M. F. Ali, *Inorg. Nucl. Chem. Lett.* 1968, **4**, 5.
6. K. Issleib and W. Seidel, *Z. anorg. Chem.* 1956, **288**, 201.
7. K. Issleib and A. Brack, *Z. anorg. Chem.* 1954, **277**, 258.
8. N. G. Feshchenko, T. I. Alekseeva, and A. V. Kirsanov, *Zh. Obschch. Khim.* 1968, **38**, 545.
9. M. F. Ali and G. S. Harris, *J. Chem. Soc. Dalton* 1980, 1545.
10. D. M. Beaumont and G. S. Harris, unpublished work.
11. G. S. Harris and F. Inglis, *J. Chem. Soc.* (*A*) 1967, 497.
12. M. Calleri and G. Ferguson, *Cryst. Struct. Comm.* 1972, **1**, 331.
13. H. A. Aughsteen Ph.D. Thesis, St. Andrews (1975).
14. G. M. Kosolapoff and L. Maier, *Organic Phosphorus Compounds*, Vol. II, p. 189. Wiley-Interscience, New York (1982).
15. E. H. Wiebenga, E. E. Havinga, and K. H. Boswijk, *Adv. Inog. Chem. and Radiochem.* 1961, **3**, 133.
16. J. W. Smith and L. B. Witten, *Trans. Faraday Soc.* 1951, **47**, 1304.
17. A. I. Popov and R. F. Swenson, *J. Am. Chem. Soc.* 1955, **77**, 3724.

Polyhedron Vol. 4, No. 1, pp. 121–125, 1985
Printed in Great Britain.

0277-5387/85 $3.00 + .00
© 1985 Pergamon Press Ltd.

THE PREPARATION AND X-RAY CRYSTAL AND MOLECULAR STRUCTURE OF (α,1,2-η-6-METHYLBENZYL) BIS(TRIPHENYLPHOSPHINE)RHODIUM(I)

S. DAVID CHAPPELL and DAVID J. COLE-HAMILTON*
Donnan Laboratories, University of Liverpool, PO Box 147, Liverpool L69 3BX, England

and

ANITA M. R. GALAS, MICHAEL B. HURSTHOUSE and NIGEL P. C. WALKER
Chemistry Department, Queen Mary College, Mile End Road, London E1 4NS, England

(*Received* 26 *January* 1984; *accepted* 30 *March* 1984)

Abstract—Reaction of $[RhCl(PPh_3)_3]$ with [*o*-$MeC_6H_4CH_2MgBr$] affords high yields of the non-fluxional complex, $[Rh(CH_2C_6H_4Me)(PPh_3)_2]$ which has been shown crystallographically to contain a 1-3-η-benzyl group bound through the phenyl carbon atom that is not substituted with the methyl group. Crystals of this compound are triclinic, space group $P\bar{1}$, with $a = 10.561(6)$. $b = 17.705(3)$, $c = 10.934(4)$ Å, $\alpha = 80.69(3)$, $\beta = 116.86(4)$, $\gamma = 102.30(4)°$ and $Z = 2$. The structure was solved via the heavy-atom method and refined to $R = 0.032$ using 5379 diffractometer data with $I > 1.56(I)$. Attempts to prepare π-bonded xylylene complexes from this compound by reaction with base have been unsuccessful, but protonation followed by recrystallisation from acetone gives $[Rh\{(CH_3)_2CO\}_2(PPh_3)_2]BF_4$.

In a number of recent publications[1,2] we have detailed reactions of the *o*-methylbenzyl ligand with transition metal complexes and shown that its behaviour depends very much on the nature of the metal. Thus, with platinum(II), simple σ-bonded complexes are formed although these can undergo cyclisation to give xylylidene complexes on refluxing in xylene.[1] In contrast, simple σ-bonded complexes of ruthenium(II) have not been isolated, the cyclisation being so facile that even at −30°C the only isolable products contain a coordinated η^2:η^2-*o*-xylylene unit.[2]

We now report yet another mode of coordination for the *o*-methylbenzyl group, as a π-allyl (1-3-η-benzyl) ligand to rhodium.

RESULTS AND DISCUSSION

Reaction of $[RhCl(PPh_3)_3]$ with one mole equivalent of [*o*-$CH_3C_6H_4CH_2MgBr$] in diethyl ether results in a red compound analysing as $[Rh(CH_2C_6H_4CH_3)(PPh_3)_2]$. If this compound contained a simple σ-bonded alkyl group, as is the case for $[Pt(CH_2C_6H_4CH_3)_2L_2]$ (L = PEt_3 or PPh_3)[1] and $[Ni(CH_2C_6H_4CH_3)_2(PBu_3)_2]$[3], it would be a three coordinate 14e complex of rhodium(I). X-Ray crystallographic studies, however, show that the *o*-methylbenzyl ligand is bound as a 3e donor.

This allylic binding for benzyl ligands has now been reported for a number of different metals, the first such complex, $[Mo(C_5H_5)(CH_2C_6H_5)(CO)_2]$, having been isolated[4] in 1966. In rhodium chemistry, $[RhCl_2(CH_2Ph)PPh_3 \cdot PhCH_2Cl]$ prepared[5] from $[RhCl(PPh_3)_3]$ and $[PhCH_2Cl]$, [Rh(cod)(*o*-$RCHC_6H_4X$)] (cod = cyclo-octa-1,5-diene) arising[6] from reaction of styrene (R = Me, X = H), *o*-methylstyrene (R = Me, X = Me) or β-methylstyrene (R = Et, X = H) with $[RhCl(cod)]_2$ and [^{i}PrMgBr], $[Rh(CH_2C_6Me_5)\{P(O^iPr)_3\}_2]$ obtained[7] by deprotonation of $[Rh(C_6Me_6)\{P(O^iPr)_3\}_2]BF_4$ and $[Rh(C_5H_5)(PMe_3)(CH_3CHC_6H_5)]PF_6$ formed[8] on protonation of $[Rh(C_5H_5)(PMe_3)(C_2H_3C_6H_5)]$ are all believed to contain 1–3-η bound benzyl groups.

*Author to whom correspondence should be addressed.

X-RAY STRUCTURE OF $[Rh(\alpha,1,2\text{-}\eta\text{-}6\text{-}CH_2C_6H_4CH_3)(PPh_3)_2]$

A diagram of the molecule appears in Fig. 1 and selected bond lengths and angles in Tables 1 and 2.

The complex exhibits distorted square planar geometry with the *o*-methylbenzyl group bound in an allylic fashion, via C(1), C(2) and C(3). There is no evidence to suggest that the alternative isomer (that in which C(7), the methyl substituted carbon atom of the phenyl ring is involved in bonding to the metal) is present in the solid state. As expected,[9] on account of the greater negative charge that resides on the α-carbon atom (C(1)) than on C(3), the rhodium atom is significantly closer to the exocyclic carbon atom (Rh–C(1) = 2.140 Å, Rh–C(3) = 2.286 Å). The difference (0.146 Å) is somewhat smaller than that observed in $[Co(CH_2C_6H_5)\{P(OMe)_3\}_3]$ (0.372 Å),[9] $[Mo(CH_2C_6H_4CH_3)(C_5H_5)(CO)_2]$ (0.21 Å)[10] and $[Rh(CH_2C_6Me_5)\{P(O^iPr)_3\}_2]$ (0.352 Å),[7] although similar to that found for [Rh(cod) (*o*-$CH_3CHC_6H_4CH_3$)] (0.153 Å).[6] Presumably the presence of a methyl group in the unbound *ortho* position causes a lengthening of the Rh–C(1) bond on account of steric interaction with the other ligands in the molecule.

As observed[7] for $[Rh(CH_2C_6Me_5)\{P(O^iPr)_3\}_2]$ the Rh–P bond *trans* to the methylene group is significantly longer than the other.

Table 1. Selected bond lengths (Å) for $[Rh(CH_2C_6H_5Me)(PPh_3)_2]$

Rh-P(1)	2.276(3)	C(3)-C(4)	1.407(7)
Rh-P(2)	2.223 (3)	C(4)-C(5)	1.408(8)
Rh-C(1)	2.140(8)	C(5)-C(6)	1.362(9)
Rh-C(2)	2.212(6)	C(6)-C(7)	1.309 (8)
Rh-C(3)	2.286(5)	C(7)-C(8)	1.517 (9)
C(1)-C(2)	1.406(6)	C(2)-C(7)	1.451 (7)
C(2)-C(3)	1.410(6)		

Although C(1), C(3), P(1), P(2), and Rh are all in the same plane the small bite size of the allyl group makes the C(1)–Rh–C(3) only 65.7°. This is compensated for by opening of all the other angles around rhodium, particularly P(1)–Rh–P(2) (101.6°) and C(3)–Rh–P(1) (98.1°). Furthermore, the effect of coordination of rhodium on the angles at C(2) is to decrease C(1)–C(2)–C(3) to 117.2°, a figure comparable with those found[11] in $[M(\alpha,1,2\text{-}CPh_3)(acac)]$, (M = Pd(116.1°) or Pt(114.6°), acac = 1,3-pentanedionate). The other external angle, C(1)-C(2)-C(7), opens slightly (122.4°).

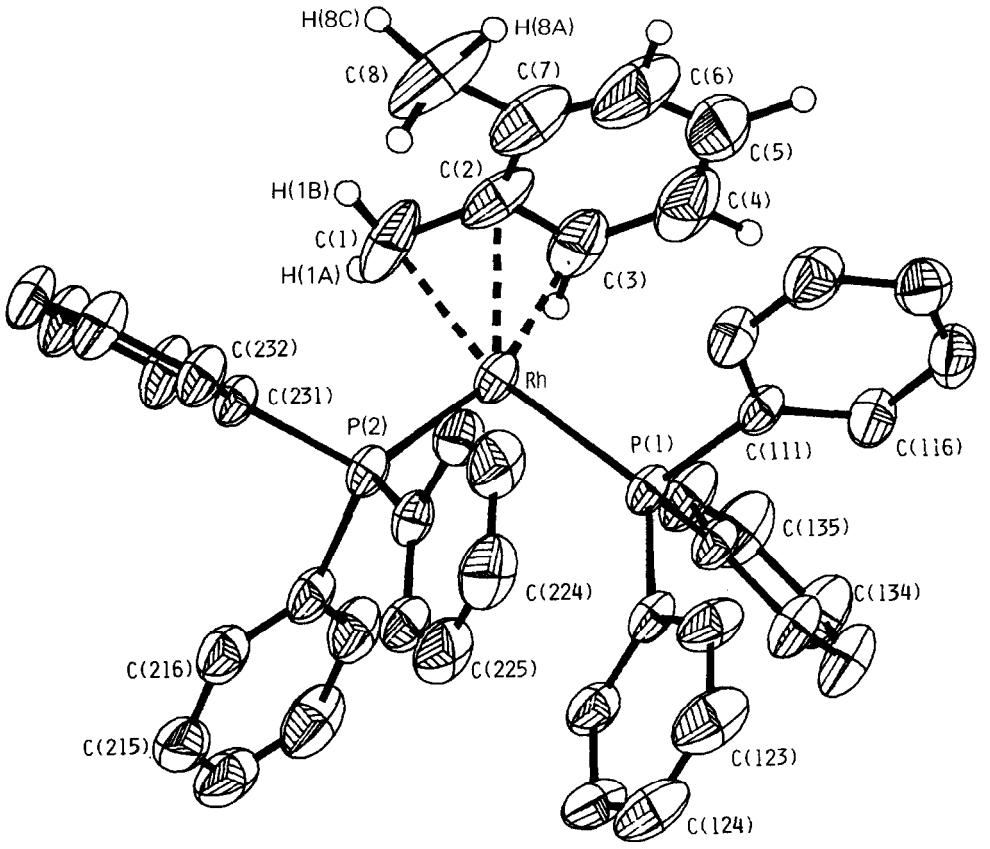


Fig. 1. Solid state structure and numbering scheme for $[Rh(CH_2C_6H_4Me)(PPh_3)_2]$.

Table 2. Selected bond angles (°) for $[Rh(CH_2C_6H_5Me)(PPh_3)_2]$

P(1)-Rh-P(2)	101.6(0)	C(3)-C(4)-C(5)	121.3(5)
P(1)-Rh-C(3)	96.1(2)	C(4)-C(5)-C(6)	116.8(5)
P(2)-Rh-C(1)	94.7(2)	C(5)-C(6)-C(7)	127.9(6)
C(1)-Rh-C(3)	65.7(3)	C(6)-C(7)-C(8)	126.2(5)
Rh-C(1)-C(2)	73.9(4)	C(2)-C(7)-C(6)	116.6(5)
Rh-C(3)-C(2)	68.9(3)	C(1)-C(2)-C(7)	122.4(4)
C(1)-C(2)-C(3)	117.2(4)	C(3)-C(2)-C(7)	119.7(5)
C(2)-C(3)-C(4)	118.1(5)	C(2)-C(7)-C(8)	117.0(5)

The co-ordination also affects the bonding of the hydrogen atoms to C(1) and C(3). Thus C(1) is significantly pyramidalised (Σ angles = 348°) with H(1A), particularly bent out of the main ligand plane (δ = 0.29 Å), whilst H(3), attached to C(3) is also displaced in a similar direction (δ = 0.18 Å).

In all 1-3-η-benzyl complexes that have previously been structurally characterised,[6,7,9-13] dimensions of the uncoordinated fragment of the phenyl ring resemble those of a *cis* 1–3-butadiene group. Uniquely, however, $[Rh(CH_2C_6H_4Me)(PPh_3)_2]$ displays apparent allylic character in the ring with the adjacent bond lengths, C(7)–C(6)(1.309 Å) and C(6)–C(5)(1.362 Å) being the shortest. This is somewhat surprising, particularly as the closely related [Rh(cod)(6,7-dimethylbenzyl)] exhibits[6] the more usual *cis*-1,3-butadiene type alternation of bond lengths.

SPECTROSCOPIC PROPERTIES

The ^{1}HYNMR spectrum of $[Rh(CH_2C_6H_4CH_3)(PPh_3)_2]$, apart from phenyl resonances, resembles that of $[Rh(cod)(o\text{-}CH_3CHC_6H_4CH_3)]$ showing a broad singlet at δ2.23 (CH_3) and multiplets at δ2.35*dd* (*syn* CH_2), 2.52*dt*(*anti*-CH_2), 5.5*bd* (C(3)*H*) and 6.6 m (C(4)*H* and C(6)*H*). The resonance from C(5)H is evidently obscured by the other phenyl resonances. Unlike the spectra of most 1-3-η-benzyl complexes, this spectrum is temperature invariant suggesting that a process such as that shown in Fig. 2 does not occur. This process, which is facile for symmetrically substituted benzyl groups does not occur in other *o*-methyl substituted 1-3-η-benzyl groups.[8] This is presumably because steric interactions of the methyl group with the rest of the molecule render form **II** a high energy species. The ^{31}PYNMR spectrum of $[Rh(CH_2C_6H_4Me)(PPh_3)_2]$ (see experimental) is temperature invariant and shows non-equivalent phosphorus atoms, suggesting that the solid state structure is preserved in solution.

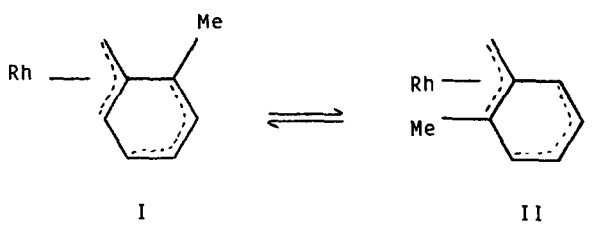


Fig. 2. Possible isomers for 1-3-η-*o*-methylbenzyl complexes.

REACTION CHEMISTRY

Protonation of $[Rh(CH_2C_6H_4Me)(PPh_3)_2]$ with fluoroboric acid leads to a red compound which gives $[Rh\{OC(CH_3)_2\}_2(PPh_3)_2][BF_4]$ on recrystallisation from acetone-diethylether, we presume that this reaction proceeds by protonation of the *o*-methylbenzyl ligand to give *o*-xylene although this has not been identified.

Attempts to prepare *o*-xylylene complexes by removal of a proton[14] have been unsuccessful. Although reactions occur, the products are too insoluble (reaction of [KOBu^t]) for characterisation.

EXPERIMENTAL

Microanalyses were by Elemental Microanalysis Ltd., and nuclear magnetic resonance spectra were recorded on Perkin–Elmer R12B (^{1}H) and Bruker WM250 (^{31}P) NMR spectrometers, the latter operating in the Fourier Transform mode with noise proton decoupling. All solvents were thoroughly dried by distillation from sodium diphenylketyl (tetrahydrofuran, diethylether, toluene and light petroleum (boiling range 40–60°C)) or calcium hydride (CH_2Cl_2) and degassed before use. All manipulations were carried out under dry oxygen free nitrogen using standard Schlenk line and catheter tubing techniques. Melting points were measured on an electrothermal melting point apparatus in sealed capillaries under nitrogen and are uncorrected.

$[RhCl(PPh_3)_3]$,[15] $[o\text{-}MeC_6H_4CH_2MgBr]$[2] were prepared by standard literature methods.

(1) *(α,1,2-η-6-methylbenzyl)bis(triphenylphosphine) rhodium*(I)

A suspension of $[RhCl(PPh_3)_3]$ (1.0 g) in diethylether (40 cm^3) was stirred with $[o\text{-}MeC_6H_4CH_2MgBr]$ (1.2 cm^3, 1.0M) for 16h. The orange solid remaining after filtration was extracted with toluene (10 cm^3) and the filtered toluene extract treated with petroleum (10 cm^3). The solution was filtered (several times) to remove precipitated $[MgCl_2]$, $[MgBr_2]$ and excess Grignard re-

agent. On cooling to −30°C, red crystals of the complex separated. These were collected and dried *in vacuo*. M.p. 162–165°C. Found: C, 72.23; H, 5.37; P, 7.91. Calc. C, 72.13; H, 5.33,; P 8.47%. NMR (C_6D_6)† δ 2.23s (CH_3); 2.35 *dd*, $J_{syn\text{-}anti\text{-}CH_2}$ = 5 Hz, J_{PH} = 10 Hz (*syn*-CH_2); 2.52*dt*, $J_{P(1)H}$ = $J_{P(2)H}$ = 5 Hz (*anti*-CH_2); 5.6 bd $J_{C(3)H-C(4)H}$ = 4Hz (C(3)*H*); 6.6 m (C(4)*H* and C(6)*H*). ^{13}C: δ19.61s (CH_3), δ42.85dd, J_{PC} = 10 Hz, J_{RhC} = 32 Hz (CH_2), 90.0d, J_{PC} = 14.6 Hz (C(3).). ^{31}P: δ39.85dd, J_{RhP} = 260 Hz, J_{PP} = 24 Hz; δ46.98dd, J_{Rh-P} = 342 Hz.

(2) *Bis(propan-2-one)bis(triphenylphosphine)rhodium(I) tetrafluoroborate*

The complex [$Rh(CH_2C_6H_4CH_3)(PPh_3)_2$] (0.5 g) was stirred with [HBF_4] (2 cm^3, 40%) in diethylether (40 cm^3) for 16 hr. The resulting red solid was collected by filtration and recrystallised from acetone-diethylether as brick-red crystals of the complex. Found: C, 61.14; H, 5.03; P, 8.20; Calc. C, 60.72; H, 5.06; P, 8.20%. NMR ($(CD_3)_2CO$)†, ^1H δ7.85*s* (CH_3). ^{31}P δ 50.55*d*, J_{RhP} = 202 Hz. IR max cm^{-1} 1656vs, 1664ssh (ν C = 0).

(3) *Reaction of* [$Rh(CH_2C_6H_4CH_3)(PPh_3)_2$] *with* [*KOBu^t*]

The complex [$Rh(CH_2C_6H_4CH_3)(PPh_3)_2$] (0.5 g) was stirred with [KOBu^t] in (0.2 g) in diethylether (40 cm^3) for 16 hr. The resulting orange-pink solid was insoluble in all common solvents and was not further characterised.

CRYSTALLOGRAPHIC STUDIES

Crystal data

$C_{44}H_{39}P_2Rh$, M = 731.9, triclinic, a = 10.561(6), b = 17.705(3), c = 10.934(4), Å, α = 80.69(3), β = 116.86(4), γ = 102.30(4)°, U = 1777.0 Å^3, space group $P\bar{1}$, Z = 2, D_c = 1.37 gm cm^{-3}, F(000) = 756, λ = 0.71069 Å, μ = (Mo-K_α) = 5.28 cm^{-1}.

DATA COLLECTIONS

Unit cell parameters were determined and intensity data collected at room temperature on an ENRAF–NONIUS CAD4 diffractometer using graphite-monochromated Mo-K_α radiation and an ω-2θ scan procedure.[16] 6231 data were measured of which 5382 were considered observed ($I \geq \sigma$ 1.56(I)). A semi-empirical absorption correction[17] using normalised and averaged ψ scan measurements from five reflections was applied to the data; the maximum and minimum transmission was 99.8 and 95.2% respectively.

STRUCTURE SOLUTION AND REFINEMENT

The structure was solved and developed by use of the heavy atom method. After isotropic refinement of all the non-hydrogen atoms, the DIFABS method of absorption correction[18] was further applied to the data. Refinement using anisotropic thermal parameters for all atoms revealed the location of all hydrogen atoms; however, bond length constraints were required for the refinement of the hydrogen atoms on the *o*-methylbenzyl ligand. In the final refinement, three strong low angle reflections were omitted and the blocked full-matrix least-squares was carried out with $\omega = 1/\sigma^2(F_0)^2 + 0.00015F_0^2$ weighting; the final R factors were:

$$R = \Sigma|\Delta F|/\Sigma|Fo| = 0.032 \text{ and}$$

$$R\omega = [\Sigma\omega\,|\,\Delta F\,|^2/\Sigma\omega\,|\,Fo\,|^2]^{1/2} = 0.033.$$

All computations were made using the SHELX–76[19] program on a Digital VAX–11/750 computer. Final atomic fractional coordinates, thermal parameters, complete lists of bond lengths and angles and structure-factor tables have been deposited as supplementary data with the Editor, from whom copies are available on request. Atomic co-ordinates have also been deposited with the Cambridge Crystallographic Data Centre.

Acknowledgements—We thank the SERC for a fellowship (A.M.R.G.) a studentship (S.D.C.) and support in purchasing the diffractometer, VAX computer and the multi-nuclear NMR machine. We are also grateful to Johnson Matthey Ltd., for loans of rhodium trichloride.

REFERENCES

1. S. D. Chappell and D. J. Cole-Hamilton, *J. Chem. Soc. Dalton Trans.* 1983, 1051.
2. S. D. Chappell, D. J. Cole-Hamilton, A. M. R. Galas, and M. B. Hursthouse, *J. Chem. Soc. Dalton Trans.* 1982, 1867.
3. K. Jacob, K-H. Thiele, C. H. Keilberg and R. Niebuhr, *Z. Anorg. Allg. Chem.* 1975, **415**, 109.
4. R. B. King and A. Fronzaglia, *J. Am. Chem. Soc.* 1966, **88**, 709.
5. C. O'Connor, *J. Inorg. Nucl. Chem.* 1970, **32**, 2299.
6. H. O. Stuhler and J. Pickardt, *Z. Naturforsch* 1981, **36b**, 315.
7. R. R. Burch, E. L. Muetterties and V. W. Day, *Organometallics* 1982, **1**, 188.
8. H. Werner and R. Feiser, *J. Organometal Chem.* 1982, **232**, 351.

†Phosphine phenyl resonances not analysed, ^1H and ^{13}C chemical shifts in ppm downfield of tetramethylsilane, ^{31}P chemical shifts in ppm to lowfield of 85% H_3PO_4.

9. J. R. Bleeke, R. R. Burch, C. L. Coulman and B. C. Schardt, *Inorg. Chem.* 1981, **20**, 1316.
10. F. A. Cotton and M. D. LaPrade, *J. Am. Chem. Soc.* 1968, **90**, 5418.
11. A. Sonada, P. M. Bailey and P. M. Maitlis, *J. Chem. Soc. Dalton Trans.* 1979, 346.
12. U. Behrens and E. Weiss, *J. Organometal Chem.* 1975, **96**, 399.
13. U. Behrens and E. Weiss, *J. Organometal Chem.* 1975, **96**, 435.
14. M. A. Bennett, I. J. McMahon and T. W. Turney, *Angew. Chem. Int. Edn. Engl.* 1982, **21**, 379.
15. J. A. Osborn and G. Wilkinson, *Inorg. Synth.* 1967, **X**, 68.
16. M. B. Hursthouse, R. A. Jones, K. M. A. Malik and G. Wilkinson, *J. Am. Chem. Soc.* 1979, **101**, 4128.
17. A. C. T. North, D. C. Phillips and F. S. Mathers, *Acta Crystallogr., Sect A* 1968, **24**, 351.
18. N. Walker and D. Stuart, *Acta Crystallogr., Sect A* 1983, **39**, 158.
19. G. M. Sheldrick, *SHELX* 76. *A Program for Crystal Structure Determination.* University of Cambridge, England (1976).

Polyhedron Vol. 4, No. 1, pp. 127–131, 1985
Printed in Great Britain.

0277–5387/85 $3.00 + .00
© 1985 Pergamon Press Ltd.

SYNTHESIS OF 1,2-ETHANEDIYLBIS(DIPHENYLPHOSPHONIUM)-PH,P'H' HEXACHLOROMOLYBDATE(III) I AND NONACHLORODIMOLYBDATE(III) II. THE CRYSTAL STRUCTURE OF $(dppeH_2)_3[MoCl_6]_2 \cdot 12H_2O$

ANTONI HERBOWSKI*
Department of Inorganic and Radiation Chemistry, Institute of Chemistry, Silesian University, 9 Szkolna Str., 40–006 Katowice, Poland

TADEUSZ LIS
Institute of Chemistry, University of Wrocław, 14 F. Joliot-Curie Str., 50-383 Wrocław, Poland

(*Received* 20 *January* 1984; *accepted* 30 *March* 1984)

Abstract—Two compounds of the formulae $(dppeH_2)_3[MoCl_6]_2 \cdot 12H_2O$ **I** and $(dppeH_2)_3[Mo_2Cl_9]_2$ **II** are described. For compound **I**, which proved to be active in olefin epoxidation, the crystal structure was determined. The rose-pink crystals are triclinic, space group $P\bar{1}$ with $a = 13.715(9)$, $b_3 = 14.686(7)$, $c = 12.512(7)$ Å, $\alpha = 109.56(4)$, $\beta = 97{,}98(4)$ and $\gamma = 91.27(5)°$, $V = 2345$ Å, $D_m = 1.42$ and $D_c = 1.44\ gcm^{-3}$, $Z = 1$. Block-diagonal least squares refinement of the structure has led to a final value of the conventional R factor of 0.049 for the 3914 independent reflections with $I > 3\sigma(I)$. Bond distances are in the range: Mo–Cl 2.439(2)–2.469(2) Å, and P–C 1.771(9)–1.806(8) Å.

Investigations of the monomeric and dimeric molybdenum(III) complexes with chlorine of the formulae $MoCl_6^{3-}$ and $Mo_2Cl_9^{3-}$ are described in detail in the monograph of Stiefel[1] and particularly in the many papers of Wentworth[2] and Smith.[3] Recently a number of other papers dealing further with the above mentioned molybdenum(III) complexes have also been published.[4] Looking for new efficient catalysts for the epoxidation of olefins, two phosphonium salts of the following formulae: $(dppeH_2)_3[MoCl_6]_2 \cdot 12H_2O$ **I** and $(dppeH_2)_3[Mo_2Cl_9]_2$ **II** were obtained (where $dppeH_2^{2+} \equiv$ 1,2-ethanediylbis(diphenylphosphonium)–PH,P'H' cation).

EXPERIMENTAL

Preparation of the complexes

1. $(dppeH_2)_3[Mo_2Cl_9]_2$ **II.** The green Mo(III) acidic–water solution was prepared by reduction of ammonium paramolybdate with zinc amalgam in the presence of HCl.[5] The dppe solution in conc. HCl (0.022M) was added dropwise to the constantly stirred above Mo(III) solution until the precipitation was completed. The green colour changed to pinkish–red. Then, the pink precipitate was separated, washed with conc. HCl and then dry methanol, and finally dried under vacuum. Found: C, 42.1; H, 3.6; Cl, 28.4; Mo, 17.0. Calc for $C_{39}H_{39}Cl_9Mo_2P_3$: C, 42.1; H, 3.2; Cl 28.7; Mo, 17.3%.

2. $(dppeH_2)_3[MoCl_6]_2 \cdot 12H_2O$ **I.** To the red solution from 1, an additional 40 cm^3 of the dppe solution in conc. HCl were added, and then the whole mixture was saturated with argon and left in the cold under argon for several days. The pinkish–rose crystal which appeared were washed with dry methanol and finally dried. Found C, 46.8; H, 4.8; Cl, 21.3; Mo, 9.7. Calc for $C_{39}H_{51}Cl_6MoO_6P_3$: C, 46.0, H, 4.7; Cl, 20.7; Mo, 9.4%.

$(dppeH_2)_3[MoCl_6]_2 \cdot 12H_2O$ *for the X-ray diffraction*

The $Cs_3Mo_2Cl_9$[3a] was dissolved in 12N HCl solution of dppe (0.025 M) and heated to 70°C until a saturated solution was obtained. This solution was filtered and saturated with gaseous HCl for 1 hr and finally left for 3 days without any

*Author to whom correspondence should be addressed.

Table 1. Selected distances (Å) and angles (°) for $(dppeH_2)_3(MoCl_6)_2 \cdot 12H_2O$

(a) Bond lengths			
Mo - Cl(1)	2.451(3)	Mo - Cl(4)	2.469(2)
Mo - Cl(2)	2.465(3)	Mo - Cl(5)	2.444(2)
Mo - Cl(3)	2.439(2)	Mo - Cl(6)	2.443(3)
P(1) - C(11)	1.801(9)	P(1) - C(A1)	1.771(9)
P(2) - C(21)	1.777(9)	P(2) - C(B1)	1.786(9)
P(3) - C(31)	1.796(7)	P(3) - C(C1)	1.775(9)
P(1) - C(1)	1.801(9)	P(2) - C(2)	1.780(10)
P(3) - C(3)	1.806(8)		
(b) Interbond Angles			
Cl(1) - Mo - Cl(2)	89.3(1)	Cl(1) - Mo - Cl(3)	177.7(1)
Cl(1) - Mo - Cl(4)	92.6(1)	Cl(1) - Mo - Cl(5)	90.1(1)
Cl(1) - Mo - Cl(6)	90.5(1)	Cl(2) - Mo - Cl(3)	88.4(1)
Cl(2) - Mo - Cl(4)	90.4(1)	Cl(2) - Mo - Cl(5)	91.8(1)
Cl(2) - Mo - Cl(6)	179.6(1)	Cl(3) - Mo - Cl(4)	87.8(1)
Cl(3) - Mo - Cl(5)	89.5(1)	Cl(3) - Mo - Cl(6)	91.8(1)
Cl(4) - Mo - Cl(5)	176.6(1)	Cl(4) - Mo - Cl(6)	89.3(1)
Cl(5) - Mo - Cl(6)	88.6(1)	C(1) - P(1) - C(11)	109.3(5)
C(1) - P(1) - C(A1)	108.8(5)	C(11) - P(1) - C(A1)	113.2(5)
C(2) - P(2) - C(21)	108.1(5)	C(2) - P(2) - C(B1)	108.6(5)
C(21) - P(2) - C(B1)	114.7(5)	C(3) - P(3) - C(31)	111.8(4)
C(3) - P(3) - C(C1)	111.0(4)	C(31) - P(3) - C(C1)	111.9(4)

contact with air. The above procedure resulted in the deposition of pinkish–rose crystals.

The electronic spectra of the compounds were recorded in MgO and KBr with the Beckmann 5420 type Spectrophotometer. The IR spectra in KBr and Nujol were measured with the Perkin–Elmer 180 type spectrophotometer.

The crystal structure of **I** was determined by X-ray analysis. Direct methods with MULTAN programs were used to locate the Mo, Cl and P atoms, while difference-Fourier syntheses yielded the C and O atoms. The C and P bonded hydrogen atoms were placed in geometrically calculated positions at a distance 1.0 Å for C–H and 1.4 Å for P–H.[6a] Refinement gave R = 0.049 and $R_w = 0.059$.† A difference synthesis computed towards the end of the refinement process was featureless and water hydrogen atoms were not localized. All calculations were performed with the Syntex XTL/XTLE programs.[18] Table 1 summarizes principal interatomic distances and angles. Figures 1 and 2 show the crystal structure of $[HP(C_6H_5)_2(CH_2)_2(C_6H_5)_2PH]_3[MoCl_6]_2 \cdot 12H_2O$.

†Atomic co-ordinates, thermal parameters and lists of F_o/F_c values have been deposited as supplementary data with the Editor, from whom copies are available on request. Atomic co-ordinates have also been deposited with the Cambridge Crystallographic Data Centre.

RESULTS

The particular form of the Mo(III) complexes with chlorine in aqueous HCl solutions depends strongly on both the concentration of the acid and of molybdenum.[3a] In the highly acidic solutions containing small amounts of molybdenum(III), $MoCl_6^{3-}$ predominates. With the increasing concentration of molybdenum, the monomeric anion turns partly into $Mo_2Cl_9^{3-}$. In other words, at high concentrations of both, the equilibrium can be written formally as:

$$Mo_2Cl_9^{3-} + 3Cl^- \rightleftharpoons 2MoCl_6^{3-}.$$

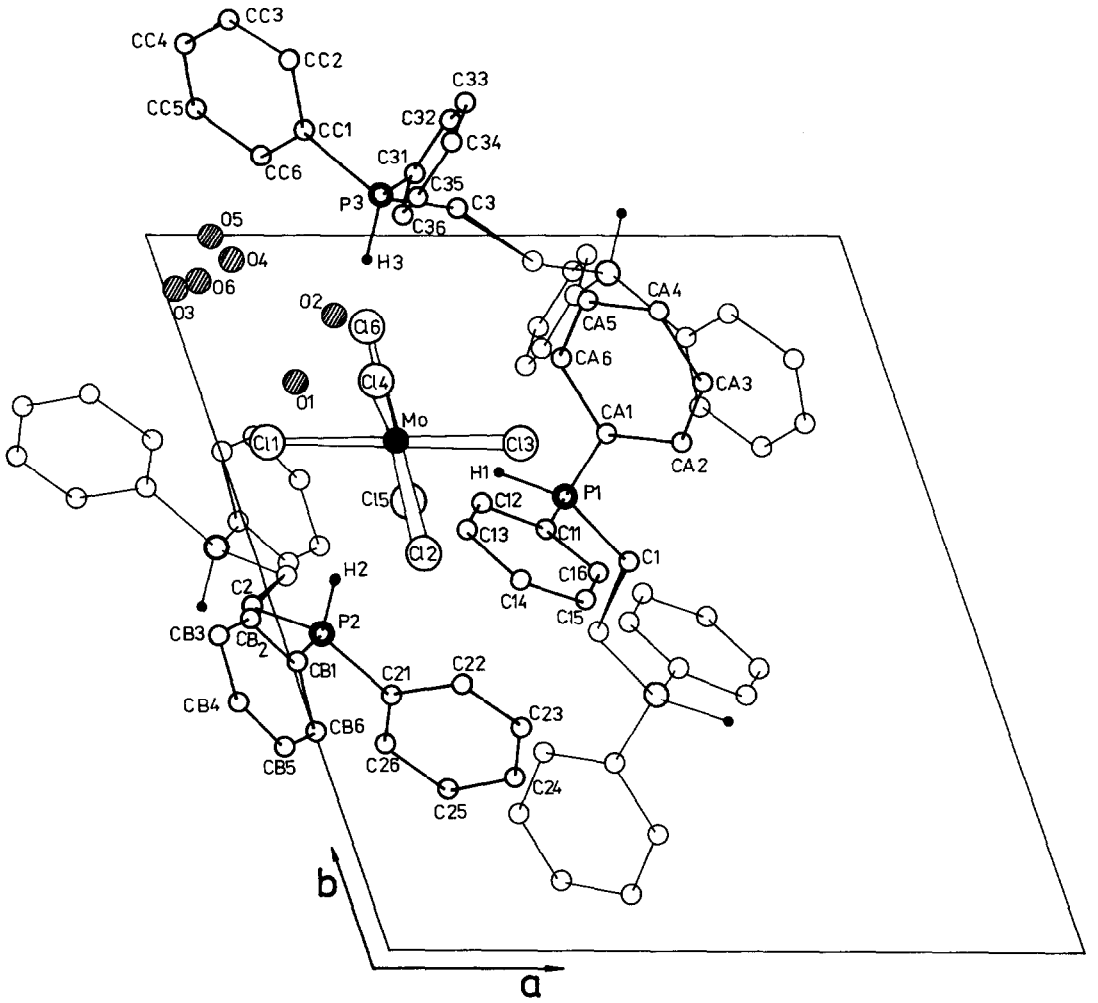


Fig. 1. The crystal structure viewed down *c* showing atom numbering.

Due to the reaction of the dppe solution in HCl with Mo(III) dissolved in the HCl–H_2O system, the pink amorphous deposit of $(dppeH_2)_3[Mo_2Cl_9]_2$ was formed. On the other hand, the monomeric complex did not precipitate from this solution. The $(dppeH_2)_3[MoCl_6]_2 \cdot 12H_2O$ crystals resulting from the red solution left after separation of the compound **II**, was additionally saturated with dry HCl. This effect is most probably due to the low concentration of the $MoCl_6^{3-}$ anion which does not suffice for the precipitation of the monomer. The dppe in the HCl solution is also insufficient for the precipitation of the monomeric phosphonium compound from the dilute K_3MoCl_6 solution in 12N HCl.

One should pay attention to the fact that the freshly precipitated $(dppeH_2)_3[Mo_2Cl_9]_2$ dissolves partially in concentrated HCl due to monomerisation of **II** according to the previously quoted equilibrium equation (which contributes to some loss of $(dppeH_2)_3[Mo_2Cl_9]_2$ in the course of the synthesis).

The precipitated **I** and **II** do not dissolve any more neither in HCl, nor in the majority of other solvents. They are relatively stable under air but under influence of humidity, they oxidize slowly towards some unidentified products.

The IR spectra of **I** and **II** are almost identical. They both lack the $\nu Mo = O$ vibration band at *ca.* 950 cm^{-1}.[7] Nevertheless, the absorption bands at 330, 285, 280 and 268 cm^{-1} for **I**, and at 290 and 226 cm^{-1} for **II** correspond with different vibrational modes of Mo–Cl and Mo–Cl–Mo. The exact interpretation and differentiation of those modes in respect to the monomeric and dimeric compounds is not quite clear in the literature. The 305 and 280 cm^{-1} bands are attributed by some authors[8] to the vibrations of the Mo–Cl–Mo bridges, while others[4a,9] ascribed them to the terminal Mo–Cl vibrations. The "ragged" band at *ca.* 900 cm^{-1} and another one at 2400 cm^{-1} are affected by the phosphonium fragment of the $dppeH_2^{2+}$ cation as has been proved for dppe · 2HCl.[10] In the free phosphine those two bands do not appear. The 2400 cm^{-1} band is

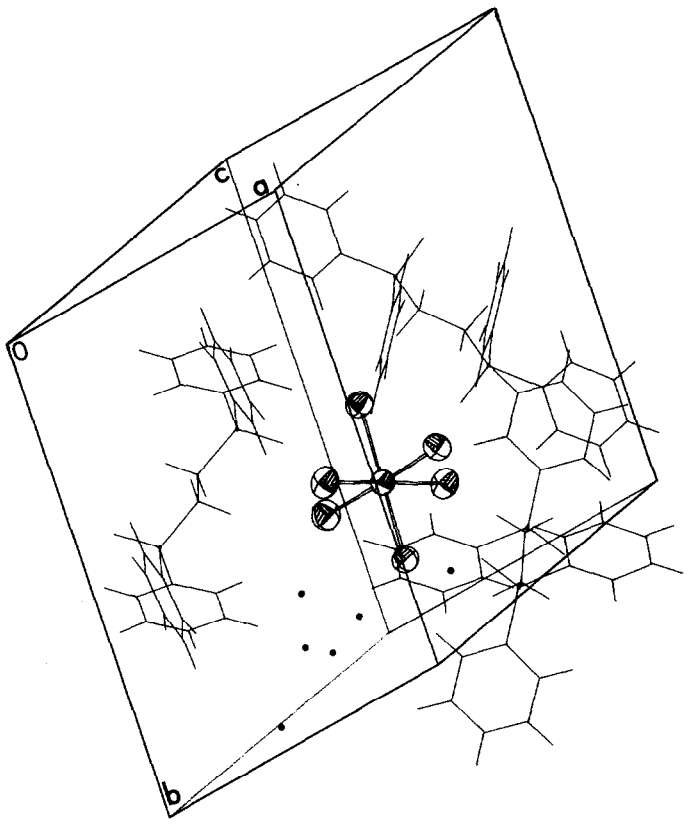


Fig. 2. The packing of the crystal.

caused by νP–H vibrations.[11] The band at 3500 cm^{-1} in the IR spectrum of $(dppeH_2)_3[MoCl_6]_2 \cdot 12H_2O$ gives evidence of the presence of water which was also confirmed by X-ray analysis. This water contributes most probably to the low stability of the respective crystals which gradually turn into the amorphous pink powder. The vacuum drying of crystals results in the total "liberation" of water. This is the reason why there is a poorer (although still satisfactory) agreement between the results of elementary analysis and the calculated composition of the monomeric compound than in the case of the dimeric one. Due to the extremely low solubility of **I** and **II**, their electronic spectra could be recorded only in the solid state. Those spectra resemble, both in respect of the band positions and shape, the reflexion spectra of K_3MoCl_6, $Cs_3Mo_2Cl_9$ and a whole series of the similar compounds.[3c] The observed electronic transitions for $(dppeH_2)_3[MoCl_6]_2 \cdot 12H_2O$ are typical of the numerous Mo–d^3 compounds and they can be described as similar to these, characterising the rigorously regular octahedron.[12] The electronic transitions in $(dppeH_2)_3[Mo_3Cl_9]_2$ (Table 2) should be discussed in the light of the recent results of Trogler[4c] who attributed the three d–d bands (ν_1, ν_2, ν_3) to $e' \rightarrow e'(^1E)$, $a_1' \rightarrow e'(^1E)$ and $a_1' \rightarrow a_2''$ transitions (D_{3h}).

The $MoCl_6^{3-}$ ion has (taking into account the measurement error) the structure of a regular octahedron similar to that found in K_3MoCl_6.[13] The average Mo–Cl bond length is equal to 2.45(1) Å. In the crystals of **I** there are three crystallographically independent $\{HP(C_6H_5)_2$

Table 2. Visible absorption spectra λ_{max} cm^{-1} of compounds **I** and **II**

Compounds	ν_4	ν_3	ν_2	ν_1
I	23 810	ca. 19 000	14 925	
II	23 530	19 230	15 150	13 160

$(CH_2)_2(C_6H_5)_2PH\}^{2+}$ cations with their own symmetry centres. The $P–C_{bridge}$ and $P–C_{Ph}$ average bond lengths are equal to 1.795(9) and 1.784(9) Å, respectively, and are slightly smaller than the corresponding bond lengths of 1.838(8) and 1.815(8) Å, respectively, in a dppe coordinated to a metal ion[14] (C_{bridge} = methylene carbon atom, C_{Ph} = phenyl carbon atom). There are also differences in the $C_{Ph1}–P–C_{bridge}$, $C_{Ph_2}–P–C_{bridge}$ and $C_{Ph1}–P–C_{Ph2}$ bond angles which in the phosphonium ion equal 109.7(5)°, 109.5(5)° and 113.2(5)°, respectively, while in the coordinated phosphine, the angles of $C_{Ph}–P–C_{bridge}$ and $C_{Ph}–P–C_{Ph}$ are 104.4° and 104.6°, respectively.

Although the data for the phosphonium cation of R_3PH^+ type are not available to us, in general, the P–C bond lengths in phosphonium groups are shorter by about 0.02–0.04 Å than those in phosphines free or coordinated to a metal ion.[15] Consequently, the P–C bond becomes shorter and C–P–C angle increases because of stronger repulsions between the carbon atoms.[16]

From the examined compounds there is only $(dppeH_2)_3[MoCl_6]_2 \cdot 12H_2O$, which proves to be an active catalyst in the process of olefin epoxidation, while both substances are inactive in the decomposition reactions of the organic hydroperoxides.[17]

REFERENCES

1. E. I. Stiefel, *Prog. Inorg. Chem.* 1977, **22**, 1.
2. (a) J. L. Hayden and R. A. D. Wentworth, *J. Am. Chem. Soc.*, 1968, **90**, 529. (b) R. Saillant and R. A. D. Wentworth, *Inorg. Chem.* 1968, **7**, 1606. (c) R. Saillant, R. A. D. Wentworth, *Ibid*, 1969, **8**, 1226. (d) R. Saillant, R. B. Jackson, W. E. Streib, K. Folting and R. A. D. Wentworth, *Inorg. Chem.* 1971, **10**, 1435. (e) W. H. Delphin and R. A. D. Wentworth, *Inorg. Chem.* 1973, **12**, 1914. (f) W. H. Delphin and R. A. D. Wentworth, *Ibid.* 1974, **13**, 2037. (g) W. H. Delphin and R. A. D. Wentworth, *J. Am. Chem. Soc.* 1973, **95**, 7920. (h) M. S. Matson and R. A. D. Wentworth, *J. Am. Chem. Soc.* 1974, **96**, 7837.
3. (a) J. Lewis, R. S. Nyholm and P. W. Smith, *J. Chem. Soc(A)* 1969, 57. (b) P. Boyd, P. W. Smith and A. G. Wedd, *Austr. J. Chem.* 1969, **22**, 653. (c) P. W. Smith and A. G. Wedd, *J. Chem. Soc. (A)* 1970, 2447. (d) T. E. Grey and P. W. Smith, *Austr. J. Chem.* 1969, **22**, 121; 1627. (e) T. E. Grey and P. W. Smith, *Ibid.* 1971, **24**, 73.
4. (a) J. A. Creighton and T. J. Sinclair, *Spectrochim. Acta, Part A* 1977, **35**, 507. (b) L. Natkaniec, *Bull. Acad. Pol. Ser. Sci. Chim.* 1978, **26**, 625. (c) R. H. Summerville and R. Hoffmann, *J. Am. Chem. Soc.* 1979, **101**, 3821. (d) A. P. Ginsberg, *J. Am. Chem. Soc.* 1980, **102**, 111. (e) W. C. Trogler, *Inorg. Chem.* 1980, **19**, 697.
5. W. G. Palmer, *Experimental Inorganic Chemistry*, p. 419. University Press Cambridge (1959).
6. (a) D. E. C. Corbridge, *The Structural Chemistry of Phosphorus* Chap. 10. Amsterdam (1974). (b) D. E. C. Corbridge, *Phosphorus, Studies in Inorganic Chemistry*, Chap. 11. Elsevier, Amsterdam (1980).
7. D. A. Edwards, *J. Inorg. Nucl. Chem.* 1965, **27**, 303.
8. F. A. Cotton and B. F. G. Johnson, *Inorg. Chem.* 1964, **3**, 1609.
9. W. H. Delphin, R. A. D. Wentworth and M. S. Matson, *Inorg. Chem.* 1974, **13**, 2552.
10. dppe · 2HCl was precipitated from the dppe-solution in *n*-hexane using gaseous HCl.
11. M. Van der Akker and F. Jellinek, *Rec. Trav. Chim.* 1967, **86**, 275.
12. A. B. P. Lever, *Inorganic Electronic Spectroscopy*. Elsevier, New York (1970).
13. Z. Amilius, B. Van Laar and H. M. Rietveld, *Acta Cryst. Sect. B* 1969, **25**, 400.
14. (a) M. R. Churchill and F. J. Rotella, *Inorg. Chem.* 1978, **17**, 668. (b) G. J. Palenik, M. Mathew, W. L. Steffen and G. Beran, *J. Am. Chem. Soc.* 1975, **97**. 1059. (c) K. Libson, B. L. Barnett, E. Deutsch, *Inorg. Chem.* 1983, **22**, 1695.
15. (a) B. E. Boland-Lussier, M. R. Churchill, R. P. Hughes and L. Reingold, *Organometallics* 1982, **1**, 628. (b) A. C. Skapski and F. A. Stephens, *J. Cryst. Mol. Struct.* 1974, **4**, 77.
16. C. A. Tolman, *Chem. Rev.* 1977, **77**, 313.
17. unpublished results.
18. Syntex (1976). XTL/XTLE Structure Determination System. Syntex Analytical Instruments, Cupertino, California.

Polyhedron Vol. 4, No. 1, pp. 133–141, 1985
Printed in Great Britain.

0277–5387/85 $3.00 + .00
© 1985 Pergamon Press Ltd.

MODEL SELECTION FOR COMPLEX SYSTEMS INVOLVING POLYNUCLEAR SPECIES

MYLES L. LAMSON,* JEFFREY L. FOX and WILLIAM I. HIGUCHI
Department of Pharmaceutics, College of Pharmacy, University of Utah,
Salt Lake City, UT 84112, U.S.A.

(*Received* 7 *February* 1984; *accepted* 30 *March* 1984)

Abstract—1-hydroxyethylidene-1,1-bisphosphonic acid (HEDP) is a phosphonate chelate with several diagnostic and therapeutic applications. Previous studies have indicated that calcium complex aggregation occurs in the basic range of pH; results from this study indicate that complex aggregation occurs throughout the physiological range of pH as well. Calcium complex formation data were used for PQ analyses and plots of the derivative of Z with respect to total diphosphonate at constant free calcium ion concentration were shown to provide valuable information with regard to model selection. A link-addition stepwise complex formation model was shown to be most appropriate; a robust feature of all aggregate formation models examined is a strong pH dependence of polynuclear complex formation in the pH range 5.5–7.0.

Much of the currently available literature on the formation of polynuclear complexes is attributable to, or derived from, work done in European laboratories in the 1940s, 50s and 60s. L. G. Sillén was directly or indirectly responsible for most of that work and has published extensively on analytical and graphical techniques for identifying such solution systems (e.g. Refs. 1–4). When computers became available in the late 1950s and 60s for routine data analysis, Sillén was among the first to develop expertise in computer modeling of complex solution equilibria using non-linear least squares techniques.[5–7] As the number of parameters in a system becomes larger statistical measures such as error square sums and correlations, and formation curve data, become less sensitive to differences between models. With current levels of computing power and the refinement of simulation techniques and computer graphics it is now recognized that visual comparisons are equally as important as statistical measures in determining the suitability of a particular model for a complex solution system.[8,9]

Aqueous solutions of calcium and 1-hydroxyethylidene - 1, 1 - bisphosphonic acid (HEDP) provide an example of a system in which individual species, hence a particular model, are difficult to identify.[10–14] Several conjectures have been made regarding solution composition and stability constants involved in this system, the most recent studies involving macromolecular techniques and sophisticated non-linear least squares approaches which indicate that polynuclear aggregation is likely to occur. Analysis of pH titration data is entirely inadequate in this situation and formation curve data by itself may not be sufficient to allow discrimination of various types of stepwise polynuclear complex formation. This work involves a computer graphics based simulation technique which allows a sensitive visual comparison of formation data derived from various polynuclear complex formation models and experimental data; it is based on a derivation by Sillén describing average numbers of ligand molecules and central atoms per complex.

EXPERIMENTAL

All solutions were prepared using reagent grade deionized water produced by a four cartridge Millipore water purification unit, and having typical measured resistance of 18 MΩ and organic impurities on the order of ppb. Calcium standard solutions were 0.100 M Radiometer standards, stored in plastic containers enclosed in evacuated metal cans. Ionic strength in all experiments was maintained at 0.10 M with Baker reagent grade tetramethylammonium chloride (TMACl), and base titrations were done with tetram-

*Author to whom correspondence should be addressed.

ethylammonium hydroxide (TMAOH), supplied as Eastman 10% aqueous reagent grade.

HEDP used in all experiments was supplied as a disodium salt by Proctor and Gamble. The salt was converted to the pure acid form by passing through a Dowex cation exchanger prepared by eluting with 1 M HCl followed by pure water until pH reached approx. 5. The HEDP solutions were then standardized by titrating with TMAOH. Yield from the cation exchange column was found to be 97%, and solutions were checked for metal complex impurities by UV-visible spectroscopy.

Precautions were taken throughout the preparation of solutions and the execution of experiments to exclude atmospheric CO_2 by bubbling with pre-purified N_2 gas which had been passed through a series of gas washing bottles containing concentrated NaOH and pure deionized water. This provided N_2 gas free of any trace of CO_2 and saturated with water vapor. The gas was then directed to a 9 l. Pyrex storage container with an Ascarite vent, to recently prepared solutions, or to the reaction vessel. Bubbling with the water saturated gas avoided any loss of volume from the reaction vessel and proved effective in maintaining CO_2-free solutions. CO_2 is eliminated from pure water by bubbling for approx. 30 mins.

All experiments were done in a water-jacketed 250 cm^3 beaker, closed at the top and with inlet ports for a mechanical stirrer, Radiometer calcium and reference electrodes, a Radiometer combined pH electrode, a line supplying CO_2-free nitrogen gas, and titrant delivery tips for either or both of $CaCl_2$ and TMAOH. Calcium electrode performance was rapid and reproducible for all but the very lowest of free calcium ion concentrations; a slight hysteresis effect was noted in electrode response when titrating a solution of constant calcium ion concentration with a base followed by an acid. In order to avoid any inconsistancy due to this effect, standards and samples were titrated in exactly the same manner with the initial approach to the desired pH from the same direction, etc. Standard curves were obtained before and after each run by titrating a 0.100 M solution of TMACl with 0.100 M $CaCl_2$ calcium standard. Standard curves were generally within 1–2 tenths of a millivolt down to the μM level and were averaged by the computer program which processed the raw data. Radiometer equipment was used for all experiments, including two PHM-84 research meters, two ABU12 autoburets, a TTT80 titrator, and strip chart recorder.

RESULTS

Preprocessed but unsmoothed data from pH titration experiments done at 1 : 1 and 2 : 1 ratios of total calcium to total diphosphonate are shown in Figs. 1 and 2, respectively. Careful examination of these plots of unsmoothed data reveals a slight kink in each of the titration curves near the beginning of the plateau region just after the second equivalence point. This characteristic of the curves represents the onset of significant amounts of polynuclear complex formation, as discussed later. At the lowest levels of total calcium and total HEDP, where little complexation of any kind is occurring, the third equivalence point begins to

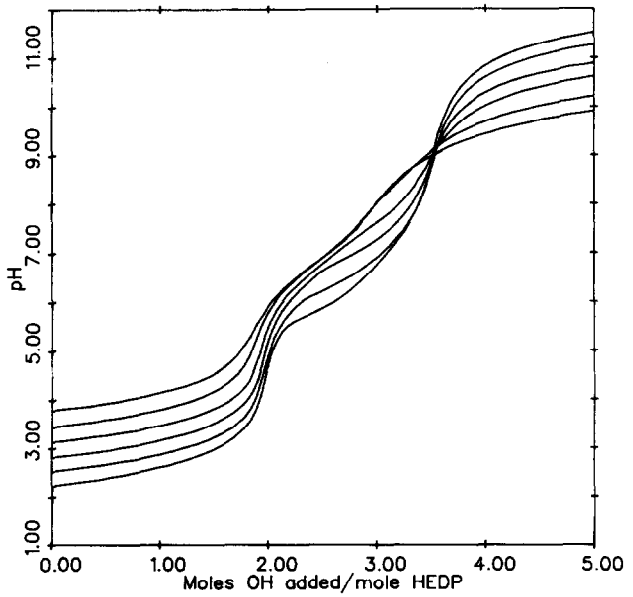


Fig. 1. Experimental pH titration data at 1 : 1 ratios of total calcium to total HEDP. Total diphosphonate concentrations are 0.100, 0.220, 0.480, 1.100 and 2.300 mM.

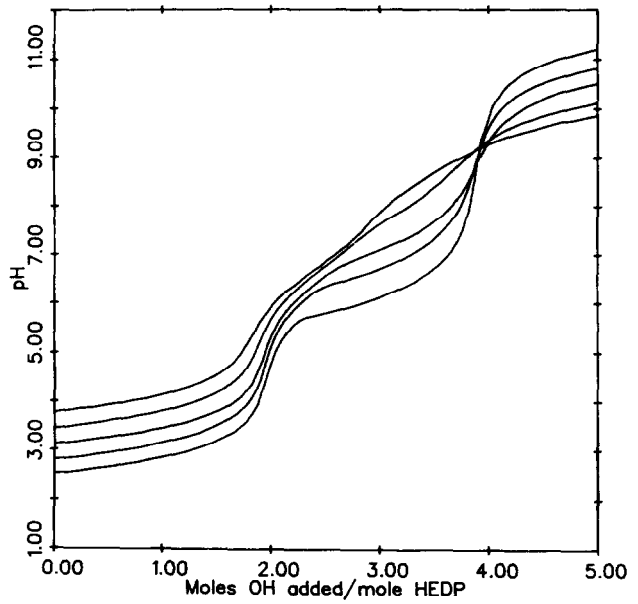


Fig. 2. Experimental pH titration data at 2 : 1 ratios of total calcium to total HEDP. Concentrations of total diphosphonate are 0.100, 0.220, 0.480, 1.100 and 2.300 mM.

appear. In comparing Figs. 1 and 2 it is noted that titration curves for 2 : 1 ratios of CATOT to DPTOT are shifted downward considerably in the neutral range of pH relative to 1 : 1 titrations, representing a higher degree of complexation.

Calcium ion titrations done at constant pH 8.0 are plotted as formation number ((CATOT–Ca^{2+})/DPTOT) vs free calcium ion concentration in Fig. 3. Formation number in these experiments is noted to be a function of total diphosphonate as well as calcium ion concentration, indicating the presence of polynuclear species.[15] In modeling to be discussed later, only data from approximately the lower two-thirds of these formation curves were used since it has been previously shown that solutions with a Ca/DP ratio greater than 2 : 1 eventually precipitate.[16] Data with ratios less than 2 : 1 are used in parameter fitting since the solution reactions may safely be assumed to be at a stable equilibrium.

MODELING OF TITRATION DATA

Some previous workers[12,14] had not considered the formation of polynuclear complexes in modeling the Ca-HEDP system; others had formulated a polynuclear model[11,13,16] involving specific large

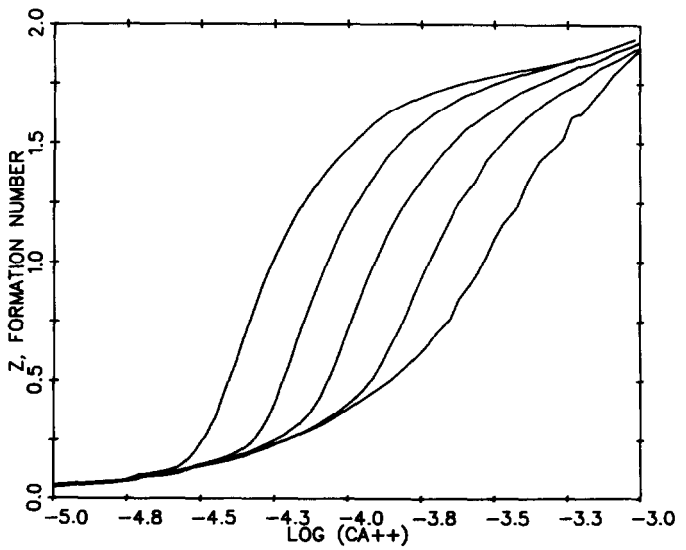


Fig. 3. Experimental calcium complex formation curves at a constant pH 8.0. Total diphosphonate concentrations are 0.100, 0.219, 0.478, 1.030 and 2.300 mM.

aggregate species which fit the data well but required an unnecessarily large number of physical parameters and seemed to lack specific evidence for the species chosen. The approach taken here is to develop a simpler model (i.e. fewest parameters) which is consistent with formation curve data that implies the existence of stepwise polynuclear species. Sillén described three such models of stepwise polynuclear complex formation where the overall complex formation constant varies as a function of aggregate size.[2] In these "core-links" models only two additional parameters are necessary to describe the formation of a whole series of polynuclear aggregates. Instead of specifying the largest complex in the model this formulation is represented by an infinite series and the experimental data determine the importance of the larger aggregates, as well as allowing one to calculate the concentration distribution of the aggregates, average species size, etc. Although the particular models Sillén had applied to other systems do not adequately describe the HEDP equilibria, another type of stepwise polynuclear model has been derived which goes a long way toward the stated objective of having the fewest number of parameters while doing a better job of fitting experimental data over a broad range of conditions.

The application of a stepwise complex formation model to these data has been justified by *PQ* analysis, a model-independent approach to determining the average numbers of metal ions and ligand molecules per aggregate over the range of the formation data.[4] The expressions used to determine $\bar{P}$ and $\bar{Q}$ from the Ca–HEDP formation data are:

$$\bar{P} = \frac{Z}{R - \alpha_0} = \text{average Ca per complex} \quad (1)$$

$$\bar{Q} = \frac{1 - \alpha_0}{R - \alpha_0} = \text{average DP per complex} \quad (2)$$

where

$$R = \text{const} - \int \left(\frac{\partial Z}{\partial \log \text{DPTOT}}\right)_{Ca^{2+}} d(\log \text{Ca}) \quad (3)$$

$$\log \alpha_0 = \text{const} + R - \int Z_{\text{DPTOT}}\, d(\log \text{Ca}) \quad (4)$$

$$Z = \frac{\text{CATOT} - [Ca^{2+}]}{\text{DPTOT}}. \quad (5)$$

At the lowest levels of free calcium ion concentration complex formation is negligible ($Z \approx 0$), free diphosphonate is approximately equal to DPTOT and thus the constants above are equal to 1.0 and -1.0, respectively. Plots of $\bar{P}$ vs $\bar{Q}$ show whether certain complexes are preferred (clustering of points) or whether stepwise complexation is occurring (a straight line with a slope equal to the combining ratio).

To evaluate R in eqn (3), 25 least squares splines were computed for values of Z vs log(DPTOT) at 25 levels of constant free calcium ion concentration. Derivatives of these splines were calculated at each value of log [DPTOT] for each of the values of log $[Ca^{2+}]$, another spline was computed for the derivatives vs log $[Ca^{2+}]$ and these curves at constant DPTOT were integrated starting at $Z \approx 0$. This provided values of R at 25 levels of free calcium ion concentration for each of the formation curves. Formation curves were then integrated from the region of negligible complex formation up to the 25 successive levels of log $[Ca^{2+}]$ and the fraction of uncomplexed diphosphonate, α_0, was calculated from the values of R and the formation curve integral at each free calcium ion level. These values were used in turn to calculate $\bar{P}$ and $\bar{Q}$ and plots of P vs Q demonstrated a uniform and linear relationship, supporting the occurrence of stepwise polynuclear complex formation. Furthermore, as discussed in the results section to follow, an intermediate calculation in this *PQ* analysis, namely the determination of $[\partial Z/\partial(\log \text{DPTOT})]_{Ca^{2+}}$ vs log $[Ca^{2+}]$, proved to be extremely useful in discriminating between various stepwise models.

Model calculations of formation curves or pH titration curves were done by finding the roots of the non-linear equations describing the mass balances of calcium ion, protons and diphosphonate.[17] The mass balances included the simpler species as listed in Table 1, as well as stepwise species described below, and a root-finding technique described by Powell[18] was used to solve the system.

Stepwise aggregate species were included in the mass balance expressions in the following manner. For simplification in the following discussion $A = \text{CaDP}$, $B = \text{Ca}_2\text{DP}$; total calcium in the polynuclear species then equals ATOT plus 2*BTOT while total diphosphonate equals ATOT + BTOT. The three Sillen stepwise formation models each involve two constants: k_0, a constant affecting horizontal displacement of the formation curves, and k, which affects separation. The overall formation constant for a particular stepwise aggregate, k_n, is a function of k and k_0. The difference in the three Sillen models has to do with the way k_n varies with respect to aggregate size, for example:

$$k_n = k_0 k^n,$$

Table 1. Parameters used in or estimated from model 7

Formation Constant	log K or pK_a
K_1	1.7
K_2	2.59
K_3	7.02
K_4	10.78
$K_{Ca \cdot OH}$	1.4
$K_{Ca \cdot OH \cdot OH}$	3.8
$K_{Ca \cdot DP}$	5.51*
$K_{Ca \cdot Ca \cdot DP}$	7.52*
$K_{Ca \cdot H \cdot DP}$	14.49*
K_0	-7.02*
K_{step}	0.0253*

*Fitted parameters noted by asterisk

or

$$k_n = k_0 n k^n,$$

or

$$k_n = k_0 k^n / n.$$

For the relation $k_n = k_0 k^n$ (model 1), the equilibrium expressions for the series of aggregate species are:

$$A + B \leftrightarrow AB \qquad AB = k_1[A][B] = k_0 k[A][B]$$

$$A + 2B \leftrightarrow AB_2 \qquad AB_2 = k_2[A][B]^2 = k_0 k^2[A][B]^2$$

$$A + 3B \leftrightarrow AB_3 \qquad AB_3 = k_3[A][B]^3 = k_0 k^3[A][B]^3$$

$$A + nB \leftrightarrow AB_n \qquad AB_n = k_n[A][B]^n = k_0 k^n[A][B]^n.$$

The total quantity of A (i.e. CaDP) in the series of aggregates is calculated from:

$$\text{ATOT} = A + AB + AB_2 + AB_3 + \ldots + AB_\infty.$$

Substituting in the previous relations and expressing as a summation:

$$\text{ATOT} = [A] + k_0[A] \sum_{n=1}^{\infty} (k[B])^n.$$

This geometric series can be shown to converge for $|k[B]| < 1.0$ and has the closed form expression

$$\text{ATOT} = [A] + \frac{k_0 k[A][B]}{1 - k[B]}.$$

The series describing BTOT involves the square of the geometric series and can be reduced to the closed form expression

$$\text{BTOT} = [B] + \frac{k_0 k[A][B]}{(1 - k[B])^2}.$$

Likewise, similar closed form expressions can be derived for the other two Sillen overall stepwise formation models. These expressions, as well as three other models employing k_n as an overall formation constant, are presented as models 1–6 in Table 2.

Additionally, models 1–3 in Table 2 were implemented assuming that the formation constants, k_n, represented not overall formation constants, but rather equilibrium constants for addition of a subsequent link (Ca_2DP) to the aggregate. In model 7, for example, where $k_n = k_0 k^n$, the algebra is the following:

$$A + B \leftrightarrow AB \qquad AB = k_0 k[A][B]$$

$$AB + B \leftrightarrow AB_2 \qquad AB_2 = k_0^2 k^3[A][B]^2$$

$$AB_2 + B \leftrightarrow AB_3 \qquad AB_3 = k_0^3 k^6[A][B]^3$$

$$AB_3 + B \leftrightarrow AB_4 \qquad AB_4 = k_0^4 k^{10}[A][B]^4$$

$$AB_{n-1} + B \leftrightarrow AB_n \qquad AB_n = k_0^n k^{n(n+1)/2}[A][B]^n$$

then

$$\text{ATOT} = [A] + [A] \sum_{n=1}^{\infty} (k^{n(n+1)/2} k_0^n [B]^n).$$

This expression is not reducible to a closed from but does converge provided that $|k| < 1.0$. The series must be evaluated term by term with an appropriate criterion for termination. Similar expressions may be derived for models 7–9 in Table 2.

RESULTS

The various stepwise formation models presented in Table 2 were evaluated initially by running a simulation graphics program[8] at a Tektronix graphics terminal, and manually altering the formation constants. The set of five formation curves, along with the experimental data, would be

Table 2. Summary of core-link models

Model	k_n	ATOT	BTOT
1	k_0k^n	$A + \frac{k_0kAB}{1-kB}$	$B + \frac{k_0kAB}{(1-kB)^2}$
2	k_0nk^n	$A + \frac{k_0kAB}{(1-kB)^2}$	$B + \frac{k_0kAB(1+kB)}{(1-kB)^3}$
3	k_0k^n/n	$A-k_0A\cdot\ln(1-kB)$	$B + \frac{k_0kAB}{1-kB}$
4	k_0e^{nk}	$A + \frac{k_0ABe^k}{1-Be^k}$	$B + \frac{k_0kA^kBe}{(1-Be^k)^2}$
5	k_0-nk	$A + (\frac{AB}{1-B})(k_0 \frac{K}{1-B})$	$B + (\frac{AB}{(1-B)^2})(k_0 - \frac{k(1+B)}{1-B})$
6	$k_0(1-k^n)$	$A + k_0AB(\frac{1}{1-B} - \frac{k}{1-kB})$	$B + k_0AB(\frac{1}{(1-B)^2} - \frac{k}{(1-kB)^2})$
7	k_0k^n	$A + A\sum_{n=1}^{\infty}(k \frac{n(n-1)}{2} k_0^nB^n)$	$B + A\sum_{n=1}^{\infty}(nk \frac{n(n+1)}{2} k_0^nB^n)$
8	k_0nk^n	$A + A\sum_{n=1}^{\infty}(n!k \frac{n(n+1)}{2} k_0^nB^n)$	$B + A\sum_{n=1}^{\infty}(nn!k \frac{n(n+1)}{2} k_0^nB^n)$
9	k_0k^n/n	$A + A\sum_{n=1}^{\infty}(\frac{k \frac{n(n+1)}{2} k_0^nB^n}{n!})$	$B + A\sum_{n=1}^{\infty}(\frac{nk \frac{n(n+1)}{2} k_0^nB^n}{n!})$

notes: k_n for models 1-6 represent overall formation constants; k_n for models 7-9 represent link-addition constants.

displayed immediately after entering trial values for constants, allowing determination of good initial estimates prior to least squares minimization. Little or no difference was observed in models 1–3 except in regard to magnitude of the constants required; shapes and separations of the curves in the best cases were virtually identical and it was not possible in any case to produce a crossover point, i.e. that point on the formation curves where Z is independent of total diphosphonate, greater than $Z = 1.5$. This value for the crossover point may be explained in the following way: best observed values of k were in the range 0.01–0.2 and $[Ca_2DP] \approx 0.1$ mM, yielding a product $kB \approx 10^{-5}$. If it is assumed that nearly all DP is present as either stepwise cores (CaDP) or links (Ca_2DP) at the crossover point then, for model 1:

$$Z = \frac{\text{complexed Ca}}{\text{total HEDP}} = \frac{\text{ATOT} + 2^*\text{BTOT}}{\text{ATOT} + \text{BTOT}}$$

where

$$\text{ATOT} = \text{total CaDP} = A + \frac{k_0kAB}{1-kB}$$

$$\text{BTOT} = \text{total } Ca_2DP = B + \frac{k_0kAB}{(1-kB)^2}.$$

Since $kB << 1.0$,

$$\text{ATOT} = A + k_0kAB, \quad \text{BTOT} = B + k_0kAB$$

and if most of the CaDP and Ca_2DP is incorporated in polynuclear aggregates at the higher formation numbers then $k_0kAB \gg A,B$ and ATOT $\approx$ BTOT. Therefore, $Z = 3^*\text{ATOT}/2^*\text{ATOT} = 1.5$. The situation is similar for all of models 1–6, implying that models which employ k_n as an overall formation constant are inappropriate.

Strong evidence for the interpretation of the

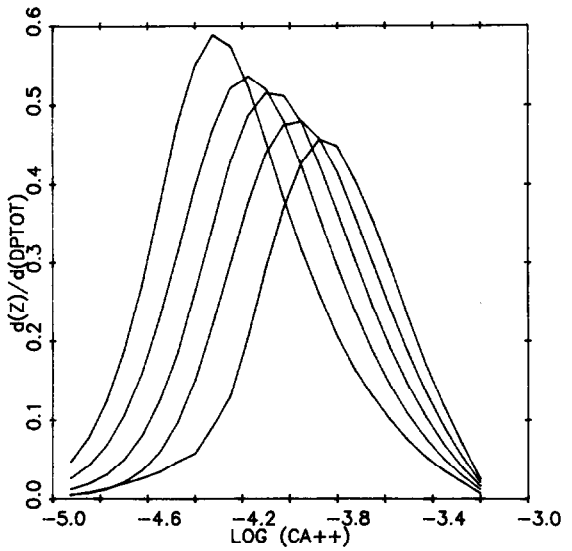


Fig. 4. Intermediate output from *PQ* analysis. Partial derivatives of Z with respect to DPTOT at constant $[Ca^{2+}]$ for model 1 simulated at pH 8.0.

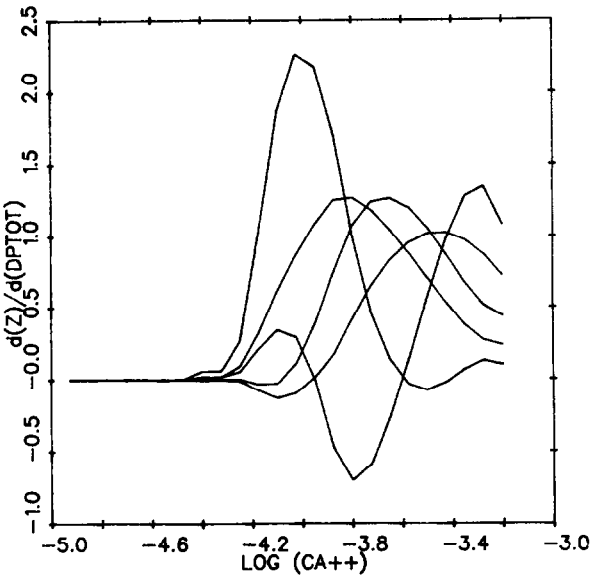


Fig. 6. Intermediate output from *PQ* analysis. Partial derivatives of Z with respect to DPTOT at constant $[Ca^{2+}]$ for Grabenstetter model simulated data at pH 8.0.

stepwise k_n as link-addition association constants is presented by plots of intermediate results in the *PQ* analysis. Several formation curve data sets were generated from the various stepwise models, incorporating about the same amount of random error as was observed in the actual experimental data. These data sets were then processed by a program designed to do a *PQ* analysis, i.e. a strictly model independent determination of average numbers of calcium ions and diphosphonate molecules per complex. When the intermediate results of this calculation were plotted it was noticed that there were striking differences between the various data sets, differences much greater than might be noticed among the original formation curves from which they were produced. The plots of $[\partial Z/\partial(\log \mathrm{DPTOT})]_{Ca^{2+}}$ vs $\log Ca^{2+}$ are shown in Figs. 4–7. These derivative plots are a sort of qualitative fingerprint for the various types of polynuclear complex formation, showing dramatic differences in form compared to the subtle

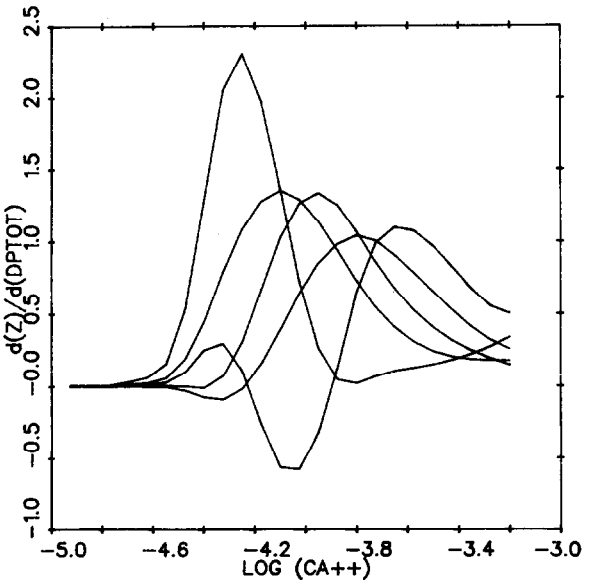


Fig. 5. Intermediate output from *PQ* analysis. Partial derivatives of Z with respect to DPTOT at constant $[Ca^{2+}]$ for model 7 simulated data at pH 8.0.

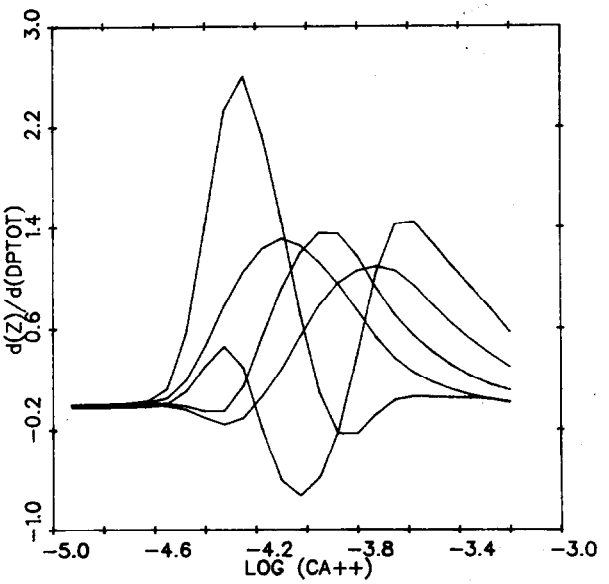


Fig. 7. Intermediate output from *PQ* analysis. Partial derivatives of Z with respect to DPTOT at constant $[Ca^{2+}]$ for actual experimental data at pH 8.0.

differences in spacing of curves in the original plots of formation number vs free calcium ion. It is evident in Figs. 4–7 that model 1 data produces entirely different derivative curves than either model 7 or the actual experimental data. Another model suggested by Grabenstetter,[11] which is not a stepwise model but does include C3D2 and C7D4 complexes, produces derivative curves which are similar to curves produced by the experimental data but no so close a match as with derivative curves produced from model 7 data. The similarity of the Grabenstetter model with model 7 is due to the correspondence and importance of two aggregates common to both models, C3D2 and C7D4. Based on these observations it was decided to do final parameter estimation using stepwise complex formation model 7, the link addition model corresponding to Sillén model 1.

Final parameter estimates are shown in Table 1 for model 7; experimental data and model generated curves using these constants are shown in Fig. 8. It was noted that best fits were obtained when species having 10–15 or more Ca_2DP links were present in small but significant concentrations. These aggregates have a marked pH dependence in the region pH 5–7, increasing in concentration by several orders of magnitude for a relatively small change in pH. In the basic range of pH the concentration of aggregate species is relatively constant.

DISCUSSION

The use of interactive graphics for visual observation of changes in formation curves and plots of the derivative of Z with respect to DPTOT is a powerful technique for discriminating between various complex formation models and for establishing good initial estimates for least squares minimization. Derivative curves decisively ruled out the interpretation of k_n as an overall stepwise formation constant, as opposed to constants for addition of subsequent links to an aggregate.

Formation curve data is considerably more sensitive to changes in solution conditions than pH titration data, and is thus more useful in determining metal complex formation constants. pH titration data exhibits relatively small changes, even in simple mono-nuclear systems, for given changes in conditions. Formation curves on the other hand may shift back and forth as a function of pH, up and down as a function of metal ion concentration and in polynuclear systems may also be a function of ligand concentration. Therefore in this type of complex forming solution system much more useful information is gained by titrating with the metal ion at constant pH than by titrating with a base at constant MTOT.

With regard to this particular system it is concluded that aggregate species of calcium and HEDP are important in the physiological range of pH and exhibit dramatic pH dependence in the range 5–7. The CaHDP complex has a well-determined constant and is important in the neutral region. Previously reported values of K_{Ca_2DP} in the range of 10^{10}–10^{12} are grossly high and probably represent an apparent formation constant for aggregate species.

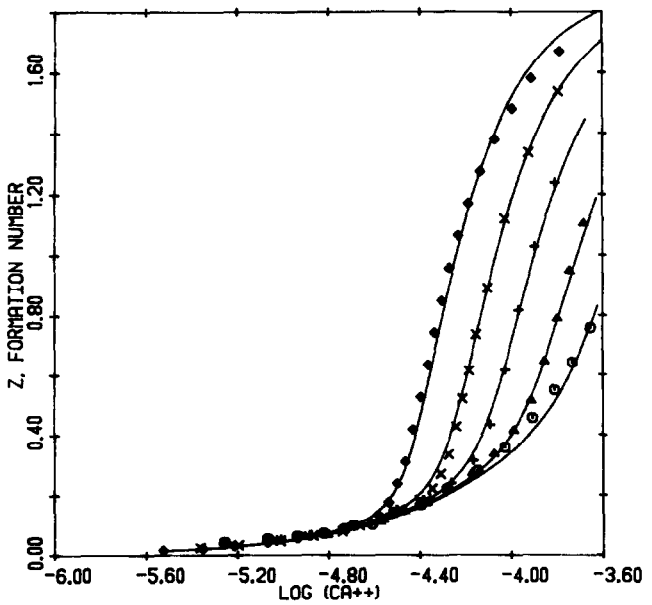


Fig. 8. Best fitting formation curves at pH 8.0. Least squares fit to mononuclear equilibria and stepwise polynuclear model 7.

REFERENCES

1. L. G. Sillén, *Acta Chem. Scand.* 1954, **8**, 299.
2. L. G. Sillén, *Acta Chem. Scand*, 1954, **8**, 318.
3. L. G. Sillén and G. Biedermann, *Acta Chem. Scand.* 1956, **10**, 1011.
4. L. G. Sillén, *Acta Chem. Scand.* 1961, **15**, 1981.
5. L. G. Sillén, D. Dyrssen and N. Ingri, *Acta Chem. Scand.* 1961, **15**, 694.
6. L. G. Sillén, *Acta Chem. Scand.* 1962, **6**, 159.
7. L. G. Sillén, *Acta Chem. Scand.* 1964, **18**, 1085.
8. J. L. Fox, M. L. Lamson and W. I. Higuchi, *Abstracts of Papers Presented Before the* APhA *Academy of Pharmaceutical Sciences*, p. 129, Vol. 8 (1978).
9. M. L. Lamson, J. L. Fox and W. I. Higuchi, *Proc. 2nd Int. Symp. on Radiopharmaceuticals*, pp. 615–525. Society of Nuclear Medicine, New York (1979).
10. P. Deitsch, T. Günther and M. Röhnelt, *Naturforsch.* 1976, **31**, 661.
11. R. J. Grabenstetter and W. A. Cilley, *J. Phys. Chem.* 1971, **75**, 676.
12. H. Wada and Q. Fernando, *Anal. Chem.* 1972, **44**, 1640.
13. B. H. Wiers, *J. Phys. Chem.* 1971, **75**, 682.
14. M. I. Kabachnik, R. P. Latovski and T. Y. Medved, *Dokl Acad. Nauk. USSR* 1967, **177**, 582.
15. E. Hogfeldt, *Treatise of Analytical Chemistry* (Edited by Kolthoff and Elving), 2nd Ed. Chap 16, Part I, Vol. 2, pp. 63–127. Wiley-Intersience, New York (1979).
16. B. H. Wiers, *Inorg. Chem.* 1971, **10**, 2581.
17. M. L. Lamson, Ph.D. dissertation. University of Michigan (1982).
18. M. J. D. Powell, *In Numerical Methods for Non-Linear Algebraic Equations* (Edited by P. Rabinowitz, Chap. 7, pp. 115–161. Gordon & Breach, New York (1970).

Polyhedron Vol. 4, No. 1, pp. 143–148, 1985
Printed in Great Britain.

0277–5387/85 $3.00 + .00
© 1985 Pergamon Press Ltd.

SYNTHESIS OF TWO COMPLEXES OF CADMIUM(II) IODIDE WITH BENZENECARBOTHIOAMIDE (BCTA): CRYSTAL AND MOLECULAR STRUCTURE OF $[Cd(BCTA)_2I_2]$

A. CASTIÑEIRAS*, A. ARQUERO and J. R. MASAGUER
Departamento de Química Inorgánica, Facultad de Ciencias Universidad Autónoma, Canto Blanco, Madrid-34, Spain

A. RUIZ-AMIL
Instituto de Química Inorgánica "Elhuyar", Serrano 113, Madrid-6, Spain

and

S. MARTINEZ-CARRERA and S. GARCIA-BLANCO
Departamento de Rayos X, Instituto "Rocasolano", Serrano 119, Madrid-6, Spain

(*Received* 18 *November* 1983; *accepted* 16 *April* 1984)

Abstract—The reaction between CdI_2 and benzenecarbothioamide (BCTA) in ethanol produces crystalline $[Cd(BCTA)_2I_2]$ but in 1,2-dichloroethane it yields $[Cd(BCTA)I_2]$ in powder form. $[Cd(BCTA)_2I_2]$ has been characterized by X-ray crystallography, and both complexes have also been identified by infrared spectra in the solid phase, ^1H NMR, and electrical conductivity studies in solution. The crystals of $[Cd(BCTA)_2I_2]$ are monoclinic, space group $P2_1/c$, with $a = 747.6(1)$ pm, $b = 1958.7(13)$ pm, $c = 1363.6(6)$ pm, $\beta = 110.307(3)°$ and $Z = 4$. Least-squares refinement of the structure based on 4260 observations led to final discrepancy indices of $R = 0.043$ and $R_w = 0.054$. The geometry around the cadmium atom is slightly distorted from the tetrahedral. The BCTA is coordinated through the sulphur atom: Cd–I(1) = 277.2(1) pm, Cd–I(2) = 272.6(1) pm, Cd–S(1) = 256.7(3) pm, Cd–S(2) = 257.5(2) pm. The electrical conductivity studies and NMR and IR spectra are consistent with the structure found for $[Cd(BCTA)_2I_2]$ and suggest a dimeric *trans* symmetric tetrahedral structure with halogen bridging (C_{2h}) for $[Cd(BCTA)I_2]$.

Although usually lacking structural X-ray diffraction data, there have been numerous studies published concerning complexes of the halides of group IIB metals with a variety of thioamide compounds.[1,2] In the particular case of complexes of benzenecarbothioamide, however, little work has been done.[3,4] It is known that, with some exceptions,[5] benzenecarbothioamides have a strong tendency to coordinate with metals via the sulphur atom of the thioarbonyl group,[6,7] thus behaving as weak bases according to Pearson's HSAB theory.[8] Since the halides of group IIB metals are soft Lewis acids,[9] stable complexes may be expected to be formed between these two groups of compounds. Although the halides of group IIB metals generally form tetrahedral monomeric complexes, tetrahedrally coordinated dimer monoadducts with halogen bridging and both tetrahedral and octahedral polymers are also common.[10,11]

Part of a comprehensive investigation into the compounds formed by the halides of group IIB metals interacting with a variety of benzenecarbothioamides, the present article reports a structural study of the compounds resulting from the reaction between cadmium(II) iodide and benzenecarbothioamide (BCTA).

*Author to whom correspondence should be addressed. Permanent address: Departamento de Química Inorgánica, Facultad de Farmacia, Universidad de Santiago de Compostela, Spain.

RESULTS AND DISCUSSION

Neither adduct is sensitive to moisture. They are both soluble in methanol, ethanol, DMSO and acetonitrile, and insoluble in chloroform and carbon tetrachloride. The milimolar conductivities in acetonitrile of $Cd(BCTA)_2I_2$ ($17\,\Omega^{-1}cm^2mol^{-1}$) and of $Cd(BCTA)I_2$ ($26\,\Omega^{-1}cm^2mol^{-1}$) are lower than the values reported for 1:1 electrolytes.[12]

The structure of $Cd(BCTA)_2I_2$. In the $Cd(BCTA)_2I_2$ molecule (Fig. 1), the cadmium atom is surrounded by two atoms of iodine and two sulphur atoms belonging to the two molecules of BCTA.† On the basis of the bond angles measured at the central atom (Table 1) the complex may be described as having distorted tetrahedral coordination. The Cd–I distances are in the range previously reported for Cd–I bonds.[13] The Cd–S distances lie between the 245 pm found in dichlorobisthioureacadmium(II),[14] in which there is also distorted tetrahedral geometry about the metal atom, and the 260 pm of bisethylenethioureacadmium(II) thiocyanate.[15]

The two molecules of BCTA coordinated to the cadmium atom are crystallographically independent and differ somewhat one from another. Table 2 lists a number of significant data which we interpret as follows. Molecule I seems to be bent between the phenyl ring and the thioamide group with a torsion angle (ϕ) of 5.5°. In molecule II, on the contrary, this torsion angle is 34°. A similar situation has been found in $Cu(BCTA)_3Cl$, in which one of the ligand molecules has a small torsion angle (16.8°) compared with the other two (30.9° and 39.5°).[7] In $Hg(BCTA)I_2$, which is a dimer, the ligand molecule has a torsion angle of 25.3°.[16]

The lengths of the C–S and C–N bonds in the two ligand molecules are within the expected range of values for molecules with a thioamide group.[17]

†Atomic positional and thermal parameters, complete tables of bond distances and bond angles, planes, torsion angles, interatomic contacts greater than 3.0 and less than 3.5 Å and a list of F_0/F_c values have been deposited as supplementary material with the Editor, from whom copies are available on request. Atomic coordinates have also been deposited with the Cambridge Crystallographic Data Centre.

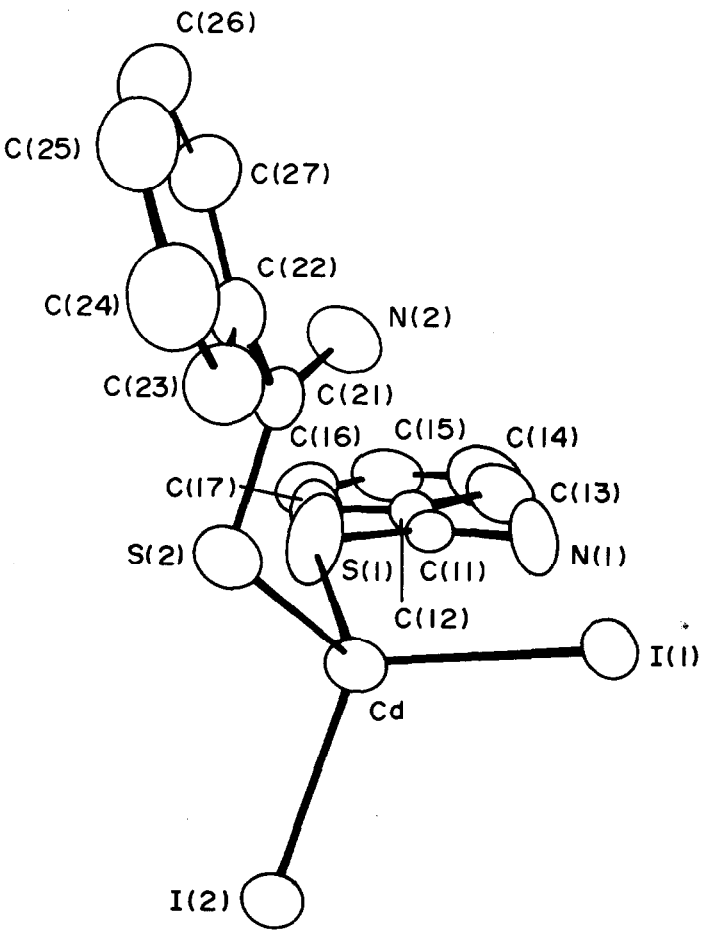


Fig. 1. Molecular geometry and atom-labelling scheme for molecule $Cd(BCTA)_2I_2$.

Table 1. Important bond distances (pm) and bond angles (deg) in $Cd(BCTA)_2I_2$. ESD's in brackets

Distances:					
Cd - I(1)	277.2(1)	S(1) - C(11)	169.2(7)	S(2) - C(21)	169.0(5)
Cd - I(2)	272.6(1)	N(1) - C(11)	130.5(9)	N(2) - C(21)	129.9(7)
Cd - S(1)	256.7(3)	C(11) - C(12)	148.9(9)	C(21) - C(22)	147.7(8)
Cd - S(2)	257.5(2)	C(12) - C(13)	138.9(9)	C(22) - C(23)	140.9(9)
		C(13) - C(14)	138.3(11)	C(23) - C(24)	139.3(10)
		C(14) - C(15)	136.1(14)	C(24) - C(25)	135.8(14)
		C(15) - C(16)	137.7(12)	C(25) - C(26)	138.9(12)
		C(16) - C(17)	138.4(11)	C(26) - C(27)	140.1(12)
		C(12) - C(17)	137.4(10)	C(22) - C(27)	138.3(10)
Angles:					
S(1)-Cd-S(2)	105.3(2)	S(1)-C(11)-N(1)	121.3(7)	S(2)-C(21)-N(2)	123.2(7)
I(2)-Cd-S(2)	105.3(2)	N(1)-C(11)-C(12)	118.7(7)	N(2)-C(21)-C(22)	118.7(8)
I(2)-Cd-S(1)	115.1(2)	S(1)-C(11)-C(12)	119.9(6)	S(2)-C(21)-C(22)	118.0(6)
I(1)-Cd-S(2)	104.9(2)	C(11)-C(12)-C(17)	120.8(7)	C(21)-C(22)-C(27)	121.1(8)
I(1)-Cd-S(1)	112.2(2)	C(11)-C(12)-C(13)	120.6(7)	C(21)-C(22)-C(23)	119.7(8)
I(1)-Cd-I(2)	112.8(2)	C(12)-C(13)-C(14)	119.6(8)	C(22)-C(23)-C(24)	118.9(8)
Cd-S(1)-C(11)	111.4(4)	C(13)-C(14)-C(15)	121.3(9)	C(23)-C(24)-C(25)	121.6(8)
Cd-S(2)-C(21)	110.9(4)	C(14)-C(15)-C(16)	119.7(9)	C(24)-C(25)-C(26)	120.1(9)
		C(15)-C(16)-C(17)	119.4(8)	C(25)-C(26)-C(27)	119.3(9)
		C(12)-C(17)-C(16)	121.4(8)	C(22)-C(27)-C(26)	120.7(9)

In both ligand molecules the length of the C–C bond joining the phenyl ring and the thioamide group is rather greater than the 146.6 pm normal in $C(sp^2)$—$C(sp^2)$ bonds.[18] This implies less conjugation than normal.

The bond lengths and bond angles in the phenyl rings of the two ligand molecules are as expected for an aromatic ring and agree well with those found for N,N-dimethylbenzenecarbothioamide[19] and in the copper and mercury complex referred to above.[7,16]

Table 2. Significant torsion angles (deg) in $Cd(BCTA)_2I_2$

Molecule I:	
S(1)-C(11)-C(12)-C(17)	-6.01
S(1)-C(11)-C(12)-C(13)	173.12
N(1)-C(11)-C(12)-C(13)	-4.95
N(1)-C(11)-C(12)-C(17)	175.92
Molecule II:	
S(2)-C(21)-C(22)-C(23)	34.36
S(2)-C(21)-C(22)-C(27)	-143.37
N(2)-C(21)-C(22)-C(27)	34.20
N(2)-C(21)-C(22)-C(23)	-148.07

IR spectra. The most significant bands of the IR spectra of BCTA[5] and the two adducts are shown in Table 3. In both adducts the NH_2 vibrations in the plane with the exception of $\rho(NH_2)$, are considerably stronger due to a conjugation effect resulting from the mesomeric delocalization mentioned above. $\rho(NH_2)$ may contain a signifiant contribution from ν(CS), which would explain its appearing in the adducts at lower frequencies than in the free ligand. The out-of-plane NH_2 deformation vibrations are weak, and they seem not to have undergone any significant modifications.

The ν(CN) mode of the BCTA–NCS group at 1400 cm^{-1} appears at higher frequencies in the adducts, whereas the ν(CS) vibration at 880 cm^{-1} in the free ligand shifts lower in both complexes and is split in $Cd(BCTA)_2I_2$. Both these shifts are to be expected when there is coordination with the metal via the sulphur atom, for the CN bond is thereby strengthened, and the CS bond weakened, by the mesomeric effect mentioned above. The presence of two different conformations of BCTA may explain the splitting of the ν(CS) peak and of

Table 3. IR frequencies (cm^{-1}) for ligand and adducts*

BCTA	$Cd(BCTA)_2I_2$	$Cd(BCTA)I_2$	Assignments
3362vs	3400vs	3380vs	$\nu_{as}(NH_2)$
3190vs	3190vs	3200vs	$\nu_s(NH_2)$
1623vs	1640vs	1630vs	$\delta(NH_2)$
1284m	1265m	1270m	$\rho(NH_2)$
725w			$\omega(NH_2)$
615w	615w	610w	$\tau(NH_2)$
1400s	1450s	1440s	ν(CN)
880vs	870s 855s	873s	ν(CS)
1135w	1115vw	1130w	ν(CC)
529w	530m	521m	δ(NCS)
382vw	375w	374w	ρ(NCS)
572m,br	582m,br	580s,br	π(NCS)
	334w-320sh	342w	ν(CdS)
	164s-138m	133s,br	$\nu(CdI)_t$
		108s	$\nu(CdI)_b$

*Abbreviations: m, medium; s, strong; w, weak; sh, shoulder; br, broad; v, very; t, terminal; b, bridging.

other unassigned peaks observed in $Cd(BCTA)_2I_2$ but not in the monoadduct. The flattening of the ν(CC) mode in the complexes may be due to coupling with ν(CS), which is common in thioamides.

Table 3 also includes the far-infrared band observed in the spectra of the solid adducts, together with the proposed assignments. Two bands at 334 and 320 cm^{-1} in $Cd(BCTA)_2I_2$ and a band at 342 cm^{-1} in $Cd(BCTA)I_2$ may be attributed to ν(CdS).[2,20] Cd–I vibrations often lie below 200 cm^{-1},[21] and in the spectrum of $Cd(BCTA)_2I_2$ two moderate-to-strong bands at 164 and 138 cm^{-1} may be assigned to the symmetric and antisymmetric Cd–I modes. The existence of these two bands, together with the two assigned to ν(CdS), is a strong indication of C_{2v} symmetry in the adduct,[22] with tetrahedral geometry about the metal atom. The spectrum of $Cd(BCTA)I_2$ is rather different in this region, one of the bands lying at much lower frequency than in $Cd(BCTA)_2I_2$. This behaviour can only be explained on the assumption that the monoadduct has a dimer structure with iodine bridging between the cadmium atoms. If so, the strong band at the higher frequency must correspond to the terminal Cd–I stretching mode (ν_t) and the 108 cm^{-1} band to Cd–I bridge stretching (ν_b).[13,23] This assignment implies a ν_t/ν_b ratio of 0.81, which falls within the range 0.63–0.85 for binuclear complexes.[24] The presence of a single ν(CdS) band, one terminal Cd–I stretching mode and another bridging mode, all of them IR-active, therefore suggests that the monoadduct $Cd(BCTA)I_2$ has a *trans* symmetric tetrahedral dimer structure (C_{2h}).[25]

NMR spectra. The ^1H NMR spectrum of free BCTA shows two separate broad singlets at 9.75 and 9.40 ppm which are due to two different kinds of proton (*cis* and *trans* to the thiocarbonyl sulphur) and reflect the restricted rotation about the carbon–nitrogen bond, which has partial double bond character.

In $Cd(BCTA)_2I_2$ the NMR spectrum shows a single peak for each amide proton which has been shifted to low field (9.80 and 9.48 ppm). The retention of the separate signals for the amide protons, together with the shift to low fields, is interpreted as showing the preservation of the

partial double-bond character of the carbon–nitrogen bond and indicates coordination through the sulphur atom of the ligands.[26]

The NMR spectrum of $Cd(BCTA)I_2$ shows two broad singlets at 9.68 and 9.35 ppm which are due to the amide protons. The presence of the two amide proton signals also supports coordination through the sulphur atom in the monoadduct. The fact that, unlike the case of $Cd(BCTA)_2I_2$, the two signals observed in the NMR spectrum lie at higher field than in free BCTA does not rule out coordination via the sulphur atom, since this behaviour has also been observed in other cadmium monoadducts.[27]

EXPERIMENTAL

Preparation of $Cd(BCTA)_2I_2$. CdI_2 (4 mmol) was dissolved in dry cold ethanol and added to a solution of 8 mmol of BCTA in the same solvent. The resulting mixture was stirred for 24 hr, and after addition of carbon tetrachloride and prolonged cooling, bright yellow crystals formed which were separated by decanting off excess solvent, washed with carbon tetrachloride and dried *in vacuo*. (R = 97%), m.p. 132°C. Found: Cd, 17.03; C, 26.11; H, 2.18; N, 4.37. Calc. for $C_{14}CdH_{14}I_2N_2S_2$: Cd, 17.55; C, 26.25; H, 2.20; N, 4.37%.

Preparation of $Cd(BCTA)I_2$. A solution of BCTA in dry 1,2-dichloroethane was gradually stirred into a suspension of 4 mmol of CdI_2 in the same solvent. The resulting suspension was stirred for 24 hr and the supernatant filtered off. The white solid remaining was washed with carbon tetrachloride and dried *in vacuo*. ($R = 93\%$), m.p. 155°C. Found: Cd, 22.90; C, 15.87; H, 1.31; N, 2.69. Calc. for $C_7CdH_7I_2NS$: Cd, 22.23, C, 16.70; H, 1.40; N, 2.78%.

Analytical methods. After digestion with HNO_3/H_2O_2 and adjustment to pH 6 with hexamethylenetetramine, the cadmium was titrated with standard EDTA solution and xylenol orange.[28] C, H and N were analyzed in a Perkin–Elmer 240 microanalyzer.

Other determinations. The IR spectra were recorded using a Perkin–Elmer 180 spectrophotometer with a far-IR accessory. The samples were run as KBr discs and as Nujol and Fluorolube mulls between CsI pellets in the 4000–250 cm^{-1} region and also as Nujol mulls between polyethylene windows in the 400–50 cm^{-1} region. The conductivity measurements were carried out with a WTW LF-3 type conductivity bridge and LT A type electrode using 10^{-3} M solutions in acetonitrile. ^1H NMR spectra were obtained in DMSO solvent with tetramethylsilane as the internal standard using a Hitachi–Perkin–Elmer R 24-A apparatus.

Structure analysis. A crystal of $Co(BCTA)_2I_2$ of $0.3 \times 0.3 \times 0.2$ mm was selected to collect intensities on a Phillips PW 1100 four-circle automatic diffractometer at room temperature using graphite-monochromated MoK_α radiation ($\lambda = 0.71070$ Å) and employing ω-2θ scan technique. 5434 independent reflections were collected and of these 4260 for which $I > 2\sigma(I)$ were used in the structure determination and refinement. Lp corrections were applied to the data as were empirical absorption corrections.

The structure was solved and developed by the heavy-atom method. The hydrogen atom positions on the benzenecarbothioamide ligand were calculated geometrically and included with fixed isotropic thermal parameters set equal to those of the atoms to which they are bonded. Full-matrix least-squares refinement with anisotropic temperature factors for the remaining atoms converged at $R = 0.043$ and $R_w = 0.054$. The weighting scheme used in the last cycle was $w = k/\sigma^2$, $\sigma = A + BF_0$[29] where A and B are 4.0875, −0.6059 ($0.3 < F_0 < 3.2$); 2.6376, 0.0101 ($3.2 < F_0 < 7.2$); 4.0000, −0.1390 ($7.2 < F_0 < 20.0$); 1.4679, 0.0000 ($20.0 < F_0 < 50.6$); −0.6209, 0.0373 ($50.6 < F_0 < 410.7$) and $k = 0.4954$. The scattering factors were taken from International Tables.[30] Final difference Fourier maps showed no distinguishing features. All refinements were done with the X-ray System.[31]

Crystal Data. $C_{14}H_{14}CdI_2N_2S_2$, M = 640.61, monoclinic, space group $P2_1/c$ (C_{2h}^5 No. 14), $a = 7.476(1)$, $b = 19.587(13)$, $c = 13.633(6)$ Å, $\beta = 110.307(3)°$, $V = 1872$ Å^3, $Z = 4$, $D_c = 2.272$ g cm^{-3}, $F(000) = 1192$, $\mu = 46.35$ cm^{-1}.

Acknowledgements—The authors are grateful to the Departamento de Química Inorgánica, Facultad de Química, Santiago de Compostela, for the facilities offered for certain experimental measurements, and to the Centro de Proceso de Datos del M.E.C. for the use of the Univac 1108 computer.

REFERENCES

1. C. D. Flint and M. Goodgame, *J. Chem. Soc.* (*A*) 1968, 750; A. Ray and D. N. Sathyanarayana, *Bull. Chem. Soc. Jpn.* 1972, **45**, 2712; D. Negoiu, V. Meresan and C. Fulea, *An. Univ. Bucaresti Chim.* 1973, **22**, 39; A. J. Aarts, H. O. Desseyn and M. A. Herman, *Bull. Soc. Chim. Belg.* 1977, **86**, 581.
2. A. J. Aarts, H. O. Desseyn and M. A. Herman, *Bull. Soc. Chim. Belg.* 1977, **86**, 345.
3. S. Iskikara, *Chem. Zent.* 1928, **98**, 1765; F. Karparek and J. Mollin, *J. Chem. Soc. Chem. Commun.* 1960,

25, 2919; D. P. N. Satchell and T. V. Weill, *J. Chem. Soc. Perkin II* 1977, 592.
4. J. A. Aarts, H. O. Desseyn, B. J. van der Vecken and M. A. Herman, *Can. J. Spect.* 1979, **24,** 29.
5. F. Cornea, F. Zalam, E. Turcu and C. Gheorghim, *Rev. Roumanie Chim.* 1979, **24,** 987; A. Castiñeiras and J. R. Masaguer, *An. Quím.* 1982, **78B,** 42.
6. A. J. Aarts, H. O. Desseyn and M. A. Herman, *Transition Met. Chem.* 1979, **4,** 46; K. Banergee and S. Raychaudhury, *Bull. Chem. Soc. Jpn.* 1982, **55,** 3621.
7. A. T. H. Lenstra, S. Travernier and W. Versichell, *Bull. Soc. Chim. Belg.* 1977, **86,** 419.
8. R. G. Pearson (Editor) *Hard and Soft Acids and Bases.* Dowden, Hutchinson and Ross, Stroudsburg (1973).
9. P. P. Singh, S. K. Srivastava and A. K. Srivastava, *J. Inorg. Nucl. Chem.* 1980, **42,** 521.
10. R. G. Goel and W. O. Ogini, *Inorg. Chem.* 1977, **16,** 1968; R. Battistuzzi and G. Peyronel, *Spectrochim. Acta Part. A* 1980, **36A,** 113; O. A. De Oliveira, A. P. Chagas and C. Airoldi, *Inorg. Chem.* 1983, **22,** 136.
11. G. Schmauss and H. Specker, *Z. Anorg. Allg. Chemie* 1968, **363,** 133.
12. W. J. Geary, *Coord. Chem. Rev.* 1971, **7,** 81.
13. Ch. W. G. Ansell, M. McPartlin, P. A. Tasker and A. Thambythurai, *Polyhedron* 1983, **2,** 83.
14. M. Nardelli, L. Cavalca and A. Bracibanti, *Gazz. Chim. Ital.* 1957, **87,** 137.
15. L. Cavalca, M. Nardelli and G. Fava, *Acta Cryst.* 1960, **13,** 125.
16. A. Castiñeiras, W. Hiller, J. Strähle, A. Arquero and J. R. Masaguer, submitted for publication in *Z. Naturforsch.*
17. A. Christensen, H. J. Geise and B. J. van der Vecken, *Bull. Soc. Chim. Belg.* 1975, **84,** 1173.
18. M. G. Brown, *Trans. Farad. Soc.* 1959, **55,** 694.
19. W. Walter S. Harto and J. Voss, *Acta Cryst.* 1976, **B32,** 2876.
20. A. C. Fabretti, G. C. Pellacani and G. Peyronel, *J. Inorg. Nucl. Chem.* 1974, **36,** 1751; G. Marcotrigiano, *Z. Anorg. Allg. Chemie* 1976, **422,** 80.
21. G. Marcotrigiano and R. Battistuzzi, *J. Inorg. Nucl. Chem.* 1974, **36,** 3719; A. Devillanova and G. Verani, *Transition Met. Chem.* 1977, **2,** 9.
22. R. J. Clark and C. S. Williams, *Inorg. Chem.* 1965, **4,** 350.
23. C. E. Coates and D. Ridley, *J. Chem. Soc.* 1964, 166; K. Getharani and D. N. Sathyanarayana, *Inorg. Nucl. Chem. Lett.* 1977, **13,** 247.
24. J. R. Ferraro, *Low-Frequency Vibrations of Inorganic and Coordination Compounds.* Plenum Press, New York (1971).
25. G. B. Deacon, J. H. S. Green and D. J. Harrison, *Spectrochim. Acta* 1968, **24A,** 1921.
26. D. R. Eaton and K. Zaw, *J. Inorg. Nucl. Chem.* 1976, **38,** 1007.
27. A. Arquero, A. Castiñeiras and J. R. Masaguer, *Presented in part at the 4th Annual Meeting of the Portuguese Chemical Society,* Lisbon, Portugal (1981).
28. E. Merck, *Komplexometrische Bestimmungsmethoden mit Titriplex.* Darmstadt, 1969.
29. M. Martinez-Ripoll and F. H. Cano, PESOS program. Instituto "Rocasolano", C.S.I.C., Serrano 119, Madrid-6, Spain, 1975.
30. *International Tables for X-Ray Crystallography,* Vol. IV. Kynoch Press, Birmingham (1974).
31. K. M. Stewart, G. L. Kruger, H. L. Ammon, C. Dickinson and S. R. Hall, "The XRAY System-version of June 1972" Tech. Rep. TR-192. Computer Science Center, Univ. of Maryland, College Park, Maryland (1972).

Polyhedron Vol. 4, No. 1, pp. 149–153, 1985
Printed in Great Britain.

0277–5387/85 $3.00 + .00
© 1985 Pergamon Press Ltd.

HETEROPOLY COMPOUNDS AS OCTAHEDRAL HIGH VALENCE COMPLEX. SPECTROCHEMICAL PROPERTIES OF WAUGH-STRUCTURE ENNEAMOLYBDONICKELATE(IV) AND ENNEAMOLYBDOMANGANATE(IV) IONS

KENJI NOMIYA, RYOICHI KOBAYASHI and MAKOTO MIWA*
Department of Industrial Chemistry, Faculty of Engineering, Seikei University, Musashino, Tokyo 180, Japan

(*Received* 6 *December* 1983; *accepted after revision* 16 *April* 1984)

Abstract—Electronic absorption and magnetic circular dichroism (MCD) spectra in UV-vis region of Waugh-structure $[XMo_9O_{32}]^{6-}$ (X = Ni(IV), Mn(IV)) ion in aqueous solution and solid IR spectra have been measured. The Ni(IV) ion in the polyanion has a low-spin d^6 electronic configuration and the Mn(IV) ion has a d^3 configuration. Visible absorption spectrum of the nickelate(IV) polyanion is interpreted to be mainly governed by charge-transfer transitions of the "ligand", Mo_9O_{32}, to Ni(IV) ion, rather than d–d transitions, while visible absorption of the manganate(IV) polyanion is governed, to a great extent, by d–d transitions. It is indicated by the MCD spectrum that the splitting of the first d–d absorption in the manganate(IV) polyanion is due to a contribution of the spin-forbiden transition, rather than from a trigonal splitting of the spin-allowed transition. Absorption and MCD spectra in UV region are due to charge-transfer transition within a common "ligand", which are less influenced by the kind of heteroatom, Ni(IV) or Mn(IV). The MCD pattern by the intra-ligand charge-transfer is especially characteristic of the Waugh-structure polyanions.

INTRODUCTION

Enneamolybdo polyanions with the formula $[XMo_9O_{32}]^{6-}$, the so-called Waugh-type heteropolyanion, have been known for only two cases, viz. in which a heteroatom is such as Mn(IV) and Ni(IV) of unusually high oxidation states. The polyanion is constituted of the "ligand", Mo_9O_{32}, formed by edge-sharing condensation of nine octahedral oxomolybdates and the heteroatom located in an octahedron of bridged oxygens. Two compounds have been prepared first by Hall.[1] Crystal and molecular structures of $[MnMo_9O_{32}]^{6-}$ ion are established; the MnO_6 octahedron has D_3 symmetry.[2,3] Visible absorption spectrum has been assigned on the basis of d^3 ion.[4,5] Hyperfine structure of its single-crystal ESR spectrum has been well-analyzed.[6,7] Recently, the chirality of one of the enantiomers was demonstrated by observing a Pfeiffer effect.[8] The $[NiMo_9O_{32}]^{6-}$ anion, an isomorph of the manganate(IV) polyanion, is diamagnetic and the central Ni(IV) ion is a low-spin d^6 ion.[9] Absorption spectrum of the nickelate(IV) polyanion has been measured by several workers, but discussion is lacking.[4,10,11]

In this paper, absorption and magnetic circular dichroism (MCD) spectra in the UV-vis region of two polyanions in aqueous solution and solid IR spectra are presented. Visible absorption of the nickelate(IV) polyanion is interpreted to be mainly governed by charge-transfer transition of the "ligand" to Ni(IV) ion, rather than by d–d transitions, while that of the manganate(IV) polyanion is governed by d–d transitions to a great extent. Absorption and MCD spectra in the UV region are due to an intra-ligand charge-transfer, which is less influenced by the kind of heteroatom. The MCD pattern is especially characteristic of the Waugh-structure of polyanions and it may be usable as a tool for structural classification of other polyanions.

EXPERIMENTAL

Electronic absorption spectra were measured by a Hitachi 340–spectrophotometer with an attached computer-key board. The intensity is ex-

*Author to whom correspondence should be addressed.

pressed in terms of the molar absorptivity ϵ which has the units of $mol^{-1}dm^3cm^{-1}$. MCD spectra were recorded by a JASCO J-40AS spectropolarimeter mounted with 10.0 kG electromagnet. The MCD intensity is expressed in terms of $\Delta\epsilon = \epsilon_l - \epsilon_r$, which has the units of $mol^{-1}dm^3m^{-1}G^{-1}$. IR spectra were recorded with a JASCO IR-G spectrophotometer. Measurements were made at room temperature.

The enneamolybdo-manganate(IV) and -nickelate(IV) compounds were prepared by the method of Baker and Weakley.[4] The orange–red (Mn) and red–black (Ni) crystals were recrystallized three times from hot water at pH 3–4. These compounds were soluble only in water. Found: H, 2.11; N, 5.05. Calc. for $(NH_4)_6[MnMo_9O_{32}]\cdot 6H_2O$: H, 2.20; N, 5.10%. Found: H, 2.05; N, 4.90. Calc. for $(NH_4)_6[NiMo_9O_{32}]\cdot 6H_2O$: H, 2.20; N, 5.09%. Green–blue hexamolybdocobaltate(III) compound, one of the Anderson-structure heteropolyanions, was prepared according to the Hall's method,[1] in order to compare with a spectrum of the enneamolybdonickelate(IV) polyanion. Found: H, 2.23; N, 3.35. Calc. for $(NH_4)_3[CoMo_6O_{24}H_6]\cdot 7H_2O$: H, 2.68; N, 3.49%.

RESULTS AND DISCUSSION

Visible absorption and MCD spectra. The spectra of $[NiMo_9O_{32}]^{6-}$ ion, measured in aqueous solution, are shown in Fig. 1. There are three precedents for electronic absorption of this anion, but an assignment of bands and an origin of transitions have not been discussed.[4,10,11] The absorption spectrum shows two broad bands at 17.7×10^3 cm^{-1} (ϵ 762) and 25–27 $\times 10^3$ cm^{-1} (ϵ 2300–2600) and the MCD spectrum shows apparent A-term shapes near the absorption positions. The Ni(IV) ion in the polyanion has a low-spin d^6 electronic configuration, but the spectral features are remarkably different from those of usual d^6 Co(III) complexes such as $[Co(en)_3]^{3+}$ and $[Co(NH_3)_6]^{3+}$ ions.[12] As an appropriate reference to an octahedral d^6 ion under similar oxomolybdate environments, the absorption and MCD spectra of $[Co^{III}Mo_6O_{24}H_6]^{3-}$ ion were also measured in aqueous solution (Fig. 2). This anion has the so-called Anderson structure; the Co(III) as a heteroatom is located in an octahedral cavity of a crown of six MoO_6 octahedra formed by edge-sharing and the "ligand" Mo_6O_{24} is protonated. Two absorption bands at 16.56×10^3 cm^{-1} (ϵ 18.0) and 24.21×10^3 cm^{-1} (ϵ 18.0) are due to the first and the second spin-allowed d–d transitions of a low-spin d^6 ion, respectively, and both MCD bands at 16.39×10^3 cm^{-1} ($\Delta\epsilon = -1.74 \times 10^{-3}$) and 23.26×10^3 cm^{-1} ($\Delta\epsilon = -1.89 \times 10^{-3}$) are observed as B-term shape. These spectra are a typical feature of many low-spin Co(III) complexes. The $|\Delta\epsilon_{max}|/\epsilon_{max}$ values for the two transitions are both 1×10^{-4}.

The $[NiMo_9O_{32}]^{6-}$ ion is isomorphous with $[MnMo_9O_{32}]^{6-}$, the site symmetry of a MnO_6 octahedron being confirmed as D_3.[2] The symmetry of a NiO_6 octahedron is probably lower than that of CoO_6 moiety in the hexamolybdopolyanion (D_{3d}).[13,14] This may lead to, more or less, the increasing absorbances of the nickelate(IV) poly-

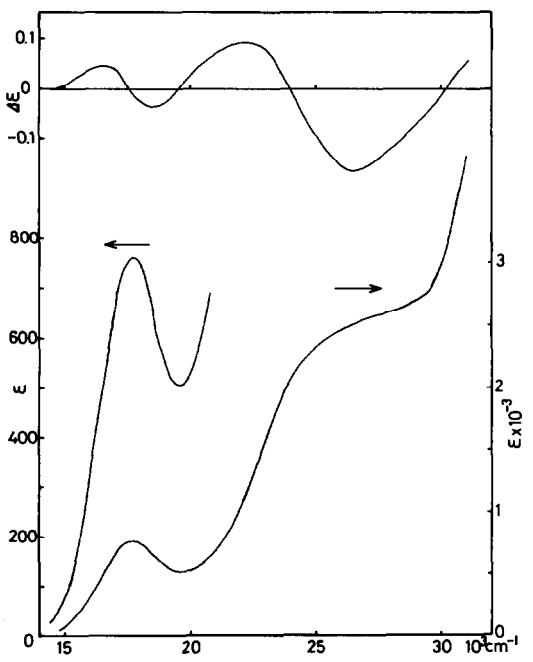


Fig. 1. Electronic absorption and MCD spectra in vis region of $(NH_4)_6[NiMo_9O_{32}]\cdot 6H_2O$ in aqueous solution.

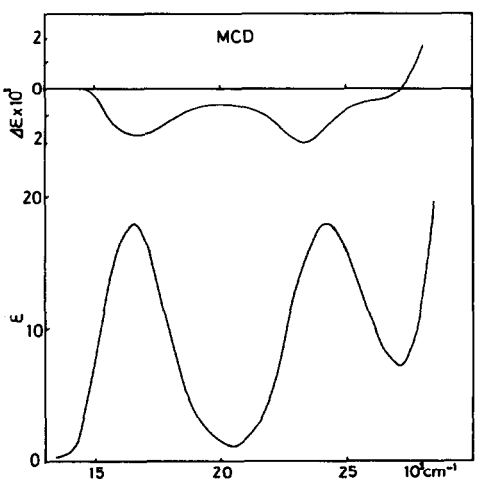


Fig. 2. Electronic absorption and MCD spectra in vis region of $(NH_4)_3[CoMo_6O_{24}H_6]\cdot 7H_2O$ in aqueous solution.

anion. Nevertheless, the $|\Delta\epsilon_{max}|/\epsilon_{max}$ values for observed A-term shapes have the values with the same order ($\sim 10^{-4}$) as those of the Co(III) hexamolybdopolyanion. This is caused by the fact that the MCD intensity also increases correspondingly with the increased absorption. Moreover, the MCD band observed in the first *d–d* transition band region of many low-spin Co(III) complexes is generally B-term with a negative sign, in which the A-term is swamped, although an A-term shape in the second *d–d* band region is sometimes observed in the Co(III) oxalato complexes.[15] Thus, it is conclusively suggested that the intense absorption and the observed A-term shape MCD of the nickelate(IV) are governed by some transitions other than *d–d* transitions.

In the nickelate(IV), in order to stabilize the unusual oxidation state of central Ni(IV) ion with the "ligand", the strong interaction between Ni(IV) ion and the ligand should be taken into account. Thus, the charge-transfer transitions of the Mo_9O_{32} to Ni(IV) may be plausibly assigned to the observed bands. This type of transition (ligand to heteroatom) has been observed in other polyanions; at 27×10^3 cm^{-1} ($\epsilon \sim 1000$) in $[Co^{III}{}_2Mo_{10}O_{38}H_4]^{6-}$ anion[16] and at 25×10^3 cm^{-1} (ϵ 1180) in $[Co^{III}W_{12}O_{40}]^{5-}$ anion,[17] in which those MCD appear as B-term shapes with positive sign. For octahedral Ni(IV) complexes with N-coordinating ligand, it has been well-established that two intense absorption bands in the visible region can be assigned as ligand-to-metal charge-transfer transitions.[18,19]

The lower frequency absorption band in the visible region implies, to a small extent, the *d–d* transition character. The higher frequency absorption band may be superimposed by the tail of the intra-ligand charge-transfer, which is observed in the UV region.

The spectral form of the $[MnMo_9O_{32}]^{6-}$ ion in aqueous solution has been known to depend markedly on the pH.[4] The absorption and MCD spectra of the polyanion, measured in the aqueous solution of pH 4.3, are shown in Fig. 3. The Mn(IV) ion is isoelectronic with Cr(III) ion of d^3. The spin-forbidden transitions ($^2E, {}^2T_{1g} \leftarrow {}^4A_{2g}$) at 14.4×10^3 cm^{-1} (ϵ 3) and near 15×10^3 cm^{-1}, and the first spin-allowed transition ($^4T_{2g} \leftarrow {}^4A_{2g}$) near 20×10^3 cm^{-1} are seen. Schatz *et al.* have suggested that the MCD can greatly aid in the detection of assignment of spin-forbidden Cr(III) transition.[12] This is also the case for the spin-forbidden transitions of the manganate(IV) polyanion. In fact, the MCD in the region of ca 15×10^3 cm^{-1} is relatively large in comparison with the intensity of absorption, i.e.

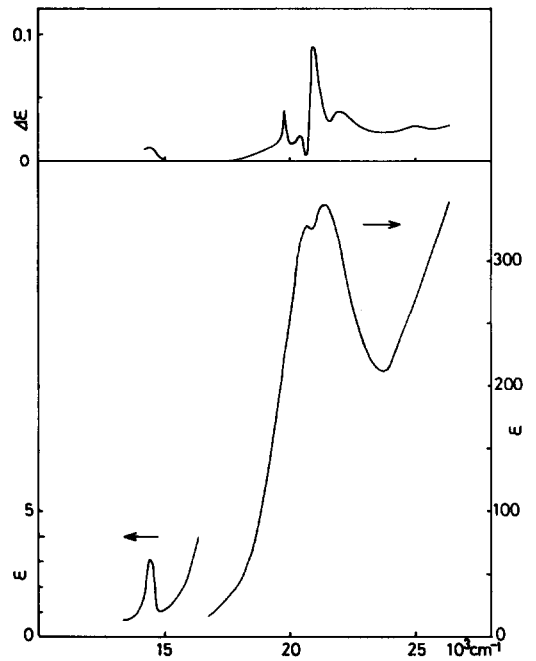


Fig. 3. Electronic absorption and MCD spectra in vis region of $(NH_4)_6[MnMo_9O_{32}] \cdot 6H_2O$ in aqueous solution.

$|\Delta\epsilon_{max}|/\epsilon_{max} = 4 \times 10^{-3}$. The absorbance of the first spin-allowed transition is more intense than those of common Cr(III) complexes,[12] and therefore possibly contain, to some extent, the charge-transfer transition of the ligand to Mn(IV) ion. The second spin-allowed transition ($^4T_{1g}(F) \leftarrow {}^4A_{2g}$) near 25×10^3 cm^{-1} is masked by the steeply-increasing absorbance in the UV region. However, this band is explicitly shown by a small and broad band with positive sign in the MCD spectrum.

A splitting of the first transition (20.7×10^3 and 21.4×10^3 cm^{-1}, ϵ 329 and 346, respectively) has been due to a trigonal distortion of the MnO_6 octahedron, that is, due to a splitting of $^4T_{2g}$ term in D_3 symmetry.[4,5] However, another possibility can be also considered. For example, Pope *et al.* have suggested that one of the components of the split band may be due the superposition of a spin-forbidden band ($^2T_{2g}$) on the main absorption.[20] Two possible assignments are distinguishable by the MCD spectrum. In the trigonal complexes such as $[Cr(ox)_3]^{3-}$ and $[Cr(en)_3]^{3+}$, an apparent A-term shape of MCD in the first transition region has been usually observed. It has been attributed to a superposition of B-terms of opposite sign, belonging to $^4E_a \leftarrow {}^4A_2$ and $^4A_1 \leftarrow {}^4A_2$.[12] However, in this manganate(IV) polyanion, the MCD in the first transition region shows many components with positive sign. Furthermore, a sharp and unique MCD band is observed at 19.8×10^3 cm^{-1}, which may be due to the spin-forbidden transition ($^2T_{2g} \leftarrow {}^4A_{2g}$).

Such a transition in the first *d–d* transition region has been also suggested by Jørgensen.[21] These suggest that the observed splitting arises from a contribution of the $^2T_{2g}$ state, rather than from a trigonal splitting of the $^4T_{2g}$ state.

UV absorption and MCD spectra. The UV absorption and MCD spectra of two polyanions are shown in Fig. 4. Absorptions at 41.7×10^3 cm^{-1} (ϵ 44500) in the nickelate(IV) and at $41.7 \times 10^3\,cm^{-1}$ (ϵ 45700) in the manganate(IV), are due to the charge-transfer within the common ligand. These bands are more shifted to high frequency region in comparison with those of Co(III) hexamolybdopolyanion ($31–32.5 \times 10^3$ cm^{-1} shoulder) and of Keggin structure polyanions (X = P, 32.6×10^3 cm^{-1}, ϵ 23900; X = Si, 33.3×10^3 cm^{-1}, ϵ 21000; for the tetrabutylammonium salts in acetonitrile).

The MCD of the intra-ligand charge-transfer is less influenced by the heteroatom. It should be noted that the MCD spectral pattern is characteristic of the Waugh-structure of polyanions and can be distinguished from those of other types of polyanions such as Keggin- and Anderson-types. The MCD in the UV region of Anderson-structure Co(III) polyanion is shown in Fig. 5 and those of Keggin-structure dodecatungsto- and dodecamolybdo-polyanions have been previously reported.[22] In the chemistry of polyanions, the MCD of intra-ligand charge-transfer may be usable as a powerful tool for structural classification.

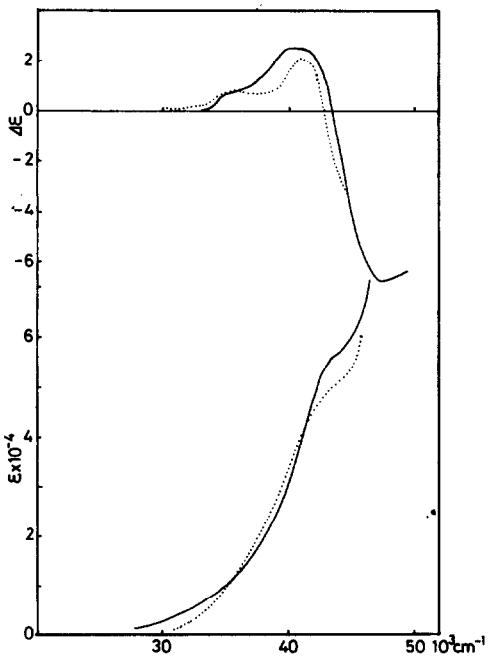


Fig. 4. Electronic absorption and MCD spectra in UV region of $(NH_4)_6[XMo_9O_{32}] \cdot 6H_2O$ in aqueous solution; X = Mn (—) and Ni(. . . .).

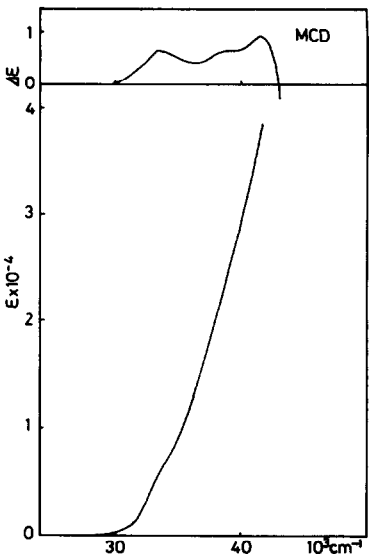


Fig. 5. Electronic absorption and MCD spectra in UV region of $(NH_4)_3[CoMo_6O_{24}H_6] \cdot 7H_2O$ in aqueous solution.

IR spectra. The IR spectra of two enneamolybdopolyanions, measured in KBr disk, are shown in Fig. 6. They are very similar to each other. Characteristic bands of the Waugh-structure unit are presented in the range of 1000–400 cm^{-1}. The spectrum consists of two prominent groups of bands; one at higher frequency region (930–830 cm^{-1}) and the other at lower one (720–490 cm^{-1}). Detailed analysis of vibration of these ions has not been performed yet.

Each MoO_6 octahedron in the Mo_9O_{32} unit has two terminal oxygens in the *cis* position and four edge-sharing oxygens, two oxygens of the latter

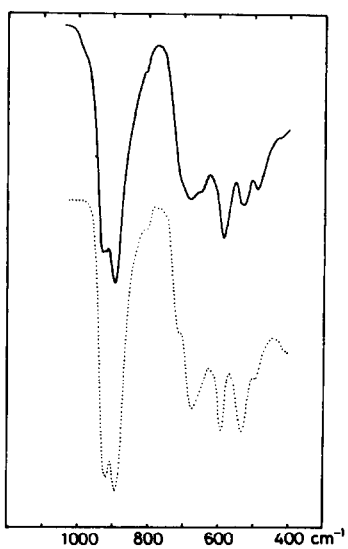


Fig. 6. IR spectra measured in KBr disk of $(NH_4)_6[XMo_9O_{32}] \cdot 6H_2O$; X = Mn (—) and Ni (· · · ·).

being coordinated to the heteroatom. Generally, the Mo-terminal oxygen bond has a double-bond character and its force constant is larger than those of the Mo-bridged oxygen bonds.[23] Moreover, it has been known that the stretchings between Mo atom and terminal oxygen atoms appear at the highest frequency region among all the vibrations of the intra-MoO_6 and the inter-MoO_6.[24] If this is the case, the band group of 930–830 cm^{-1} may be tentatively assigned as Mo-terminal oxygen stretchings.

REFERENCES

1. R. D. Hall, *J. Am. Chem. Soc.* 1907, **29**, 692.
2. J. L. T. Waugh, D. P. Shoemaker and L. Pauling, *Acta Cryst.* 1954, **7**, 438.
3. R. Allman and H. D'Amour, *Z. Krist.* 1975, **141**, 342.
4. L. C. W. Baker and T. J. R. Weakley, *J. Inorg. Nucl. Chem.* 1966, **28**, 447.
5. A. G. Paulusz and H. L. Burrus, *Chem. Phys. Lett.* 1972, **17**, 527.
6. P. G. Rasmussen, K. M. Beem and E. J. Hornyak, *J. Chem. Phys.* 1969, **50**, 3647.
7. C. R. Byfleet, W-C. Lin and C. A. McDowell, *Mol. Phys.* 1970, **18**, 363.
8. K. Nomiya, R. Kobayashi and M. Miwa, *Bull. Chem. Soc. Jpn.* 1983, **56**, 3505.
9. P. Ray, A. Bhaduri and B. Sarma, *J. Ind. Chem. Soc.* 1948, **25**, 51.
10. R. Schaal and P. Souchay, *Anal. Chim. Acta* 1949, **3**, 1.
11. Y. Shimura, H. Itoh and R. Tsuchida, *Nippon Kagaku Zasshi*, 1954, **75**, 560.
12. A. J. McCaffery, P. J. Stephens and P. N. Schatz, *Inorg. Chem.* 1967, **6**, 1614.
13. H. Evans Jr, *Acta Cryst. Sect. B* 1974, **30**, 2095.
14. A. Perloff, *Inorg. Chem.* 1970, **9**, 2228.
15. M. Matsuoka and Y. Shimura, *Bull. Chem. Soc. Jpn.* 1976, **49**, 2118.
16. Y. Sasaki and K. Matsumoto, *Kagaku no Ryoiki* 1975, **29**, 853.
17. K. Nomiya, R. Kobayashi and M. Miwa, *Bull. Chem. Soc. Jpn.* 1983, **56**, 2272.
18. E. I. Baucom and R. S. Drago, *J. Am. Chem. Soc.* 1971, **93**, 6469.
19. A. G. Lappin, M. C. M. Laranjeira and R. D. Peacock, *Inorg. Chem.* 1983, **22**, 786.
20. B. W. Dale, J. M. Buckley and M. T. Pope, *J. Chem. Soc. A* 1969, 301.
21. C. K. Jørgensen, *Acta Chem. Scand.* 1958, **12**, 1539.
22. K. Nomiya and M. Miwa, *Polyhedron* 1983, **2**, 955.
23. C. Rocchiccioli-Deltcheff, R. Thouvenot and M. Fouassier, *Inorg. Chem.* 1982, **21**, 30.
24. C. Rocchiccioli-Deltcheff, R. Thouvenot and R. Franck, *Spectrochim. Acta* 1976, **32A**, 587.

Polyhedron Vol. 4, No. 1, pp. 155–158, 1985
Printed in Great Britain.

0277-5387/85 $3.00 + .00
© 1985 Pergamon Press Ltd.

METAL COMPLEXES OF SOME ASYMMETRIC DIAMINODIAMIDE LIGANDS—III[1,2]

RATES OF CONVERSION FROM OCTAHEDRAL TO SQUARE PLANAR COMPLEXES OF Ni(II)

MARIEL M. MUIR,* JOSE A. DIAZ,[3] LOURDES M. TORRES, and PORFIRIO NAZARIO
Department of Chemistry, University of Puerto Rico, Rio Piedras, Puerto Rico 00931

(*Received* 17 *January* 1984; *accepted* 16 *April* 1984)

Abstract—Dissociation of the two amide protons from complexes of asymmetric diaminodiamides with Ni(II) in aqueous solution occurs under moderately basic conditions. The loss of the protons is accompanied by a conversion of the complex from octahedral to square planar. The rates of conversion for complexes NiL^{2+} were measured spectrophotometrically and were found to depend linearly on $[OH^-]$. The diaminodiamide ligands used were S, R, S- and S, S, S-N, N′-dialanylpropylenediamine (DAPN), S, S-N, N′-dialanylethylenediamine (DAEN), R-N, N′-diglycylpropylenediamine (DGPN), and N, N′-diglycylethylenediamine (DGEN). The rates varied in the order SS-DAEN > DGEN > SRS-DAPN > R-DGPN ≈ SSS-DAPN.

The dissociation of amide protons at acidic or neutral pH in metal complexes of peptides or other amides is well known.[2,4–13] The previous paper in this series[1] reported the equilibria in aqueous solution between Ni(II) and a series of asymmetric diaminodiamides of general formula H_2N–C*HR–CO–NH–C*HR′–CH_2–NH–CO–C*HR–NH_2. The ligands used were: *S*, *R*, *S*- and *S*, *S*, *S*-*N*, *N*′-dialanylpropylenediamine (DAPN, R = R′ = CH_3), *S*, *S*-dialanylethylenediamine (DAEN), R = CH_3, R′ = H), *R*-N, N′-diglycylpropylenediamine (DGPN, R = H, R′ = CH_3), and N, N′-diglycylethylenediamine (DGEN, R = R′ = H). The absolute configuration at each asymmetric carbon is indicated by *S* or *R*. DAPN has three asymmetric carbon atoms, each marked in the general formula. In DAEN only the outer two and in DGPN the centre one of the marked carbon atoms are asymmetric. The N, N′ indicates bonding of the two alanyl or glycyl groups to different nitrogen atoms of the central diamine moiety.) The equilibrium constants were determined for the formation of the octahedral complexes NiL^{2+} and NiL_2^{2+} and for deprotonation and conversion to the square planar $NiH_{-2}L$.[1,13]

$$Ni^{2+} + L \overset{K_1}{\rightleftharpoons} NiL^{2+} \quad (1)$$

$$NiL^{2+} + L \overset{K_2}{\rightleftharpoons} NiL_2^{2+} \quad (2)$$

$$NiL^{2+} \overset{K_{1AB}}{\rightleftharpoons} NiH_{-2}L + 2H^+. \quad (3)$$

The values of the equilibrium constants showed a significant degree of stereoselectivity for these complexes, especially for the processes corresponding to K_2 and K_{1AB}.[1] This was attributed to steric effects, which seemed greatest for K_{1AB}, the constant for the amide deprotonation and octahedral – square planar conversion. To further analyze these steric effects and to try to determine the probable structure for the octahedral complex NiL^{2+}, it was of interest to study the rates of the conversion for the same series of ligands used for the equilibrium studies.[1] The rates for the system DGEN – Ni(II) have been reported.[14] The conversion was slow and dependent on the pH.

RESULTS AND DISCUSSION

The kinetic studies were carried out at constant pH values greater than 8.5 in order to force the reactions to completion. First, the aquonickel(II) complex and the ligand hydrochloride were mixed

*Author to whom correspondence should be addressed.

and the protons on the ligand partly neutralized. Upon adjustment of the pH to a basic value, the formation of the octahedral complex NiL^{2+} was assumed to be very fast compared to the subsequent conversion to the square planar complex. This was consistent with observations of the short time required by the system to reach equilibrium at lower pH values, where the predominant species formed is NiL^{2+}. In general, the rates of formation of octahedral Ni(II) complexes are very fast compared to the slow rates observed in this work.[15]

The reactions were followed at several pH values above 8.5. Linear first-order plots of log $(A - A_\infty)$ as a function of the time were obtained over several half-lives, which also suggests that the above assumption is valid. The value of k_{obs} was a linear function of $[OH^-]$, which is similar to the result reported[14] for the DGEN system. In that study it was suggested that the removal of the first peptide hydrogen is the rate-determining step and that the second peptide hydrogen was released more rapidly.

The intermediate species $NiH_{-1}L^+$ could not be detected in solution and the equilibrium studies[1] confirm that no appreciable concentration of $NiH_{-1}L^+$ builds up during the reaction. Thus, the reaction sequence can be written as:

$$Ni^{2+}(aq) + L \xrightarrow{\text{fast}} NiL^{2+} \quad (4)$$

$$NiL^{2+} + OH^- \xrightarrow{k_2} NiH_{-1}L^+ + H_2O \quad (5)$$

$$NiH_{-1}L^+ + OH^- \xrightarrow{\text{fast}} NiH_{-2}L + H_2O \quad (6)$$

and the rate expression as:

$$\frac{d[NiH_{-2}L]}{dt} = -\frac{d[NiL^{2+}]}{dt} = k_{obs}[NiL^{2+}] = k_2[NiL^{2+}][OH^-] \quad (7)$$

Some average values for k_{obs} are listed in Table 1 and the values of k_2 in Table 2. All rate constants were calculated by a linear least squares routine and the standard deviations reported are the standard deviations in the slopes of the lines. The intercepts of the plots of k_{obs} as a function of $[OH^-]$ were all zero within experimental error, so no hydroxide-free term is included in the rate expression. Data for several runs obtained with a pH-stat are included in Table 1. These agreed well with the data obtained spectrophotometrically using buffers for pH control.

The relative rates are in the order:

SS-DAEN > DGEN > SRS-DAPN > R-DGPN ≈ SSS-DAPN.

For the DGEN system, when the ligand to metal ratio exceeded 1:1, a second term in the rate law was observed and interpreted as due to reaction of the bis complex, NiL_2^{2+}.[14] This could not be observed for the systems with SS-DAEN, SRS-DAPN, or SSS-DAPN, which is consistent with

Table 1. Pseudo first order rate constants for the reaction of NiL^{2+} to give $NiH_{-2}L$ at 25.0°C

L	pH	$10^2 k_{obs}$ s^{-1} [a]	L	pH	$10^2 k_{obs}$ s^{-1}
DGEN	8.50	0.42 (2)	SS-DAEN	8.88	2.04(9)
	8.75	0.64 (8)		9.16	4.2 (3)
	8.88	0.84 (3)		9.47	8.7 (7)
	9.00	0.89 (8)			
	9.09	1.9 (2)			
	9.18	2.5 (3)	SRS-DAPN	9.04	1.02(8)
	9.25	2.2 (3)		9.05	1.12(9)
	9.41	3.3 (2)		9.15	1.21(9)
				9.16	1.3 (2)
R-DGPN	8.50	0.099(6)			
	8.75	0.27 (3)			
	8.88	0.28 (2)	SSS-DAPN	8.88	0.24(2)
	9.00	0.25 (1)		9.16	0.33(2)
	9.08	0.29 (1)		9.47	0.56(4)
	9.15	0.37 (4)			
	9.23	0.39 (3)			
	9.34	0.48 (2)			
	9.41	0.58 (3)			
	9.42	0.59			

a) Values for k_{obs} are average values from two to five different runs. The average deviation is given in parentheses.

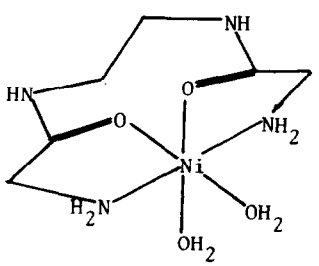
Table 2. Second order rate constants for the reaction of NiL^{2+} to give $NiH_{-2}L$ at 25°C

L	$10^{-2}k_2$ $mol^{-1}L\ s^{-1}$
DGEN	8.2 (7)
DGEN [a]	6.2 (7)
R-DGPN	1.08(8)
SS-DAEN	18.8 (2)
SRS-DAPN	4.1 (4)
SSS-DAPN	0.91(9)

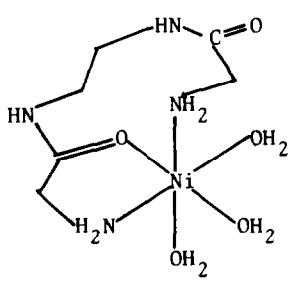
a) Calculated from values of k_{obs} in Table II, Ref. 14. The value for k_2 in the text of that paper does not correspond to either the table of Fig. 2 of the reference.

the lower stability observed for the NiL_2^{2+} complex for those ligands compared to DGEN.[1]

The observed order of reactivity permits an assignment of the probable structure for the octahedral complex NiL^{2+}, which was not possible with only the equilibrium data.[1] Two possible structures have been suggested[14] for the 1:1 octahedral complex, as shown in structures **I** and **II**. The structure



I



II

assignment depends on the choice of the rate-determining step. There are two possibilities for this. One is that the rearrangement of the monoprotonated intermediate to the square planar form is the slow step. This is not consistent, however, with similar conversions for the Ni(II): trien system,[16] which are very fast, nor with the slow rate of formation of $CuH_{-2}L$ for these ligands.[17,18] The more likely possibility, which fits well with the data from this work, is that the slow step is not the conversion of the octahedral to the square planar form but rather the change from carbonyl to amido nitrogen coordination when the proton from the amide bond is lost.

For the terdentate structure **II**, the monoprotonated intermediate from the octahedral complex in the SRS–DAPN:Ni(II) system can have all methyls nearly equatorial, but for the SSS–DAPN:Ni(II) at least one axial methyl group is obtained. Then if deprotonation and change of coordination from oxygen to nitrogen (effectively a substitution reaction) is the slow step, the SSS–DAPN complex would react more slowly than the SRS–DAPN complex, as observed. However, if rearrangement of the octahedral to the square planar form were the rate-determining step, then the rate for the SSS–DAPN complex should be faster, not slower, than the rate for the SRS-complex. Thus, the most reasonable assumption about the mechanism is consistent with the relative rates if the octahedral complex has the terdentate structure **II**. All the ligands in this study had the same skeletal structure, so no variation in ring sizes was observed. Such a variation might be helpful in confirming this assignment.

EXPERIMENTAL SECTION

Materials

The syntheses and characterization of the ligands have been reported,[19] as have the methods[2] for standardization of aqueous solutions of the ligand dihydrochloride salts and of $NiCl_2$.

Analytical grade boric acid and sodium borate decahydrate were used without further purification. Morpholine was distilled with a long fractionating column. Morpholinium chloride was prepared by two methods.

(a) To 43.5 cm^3 of morpholine in a 200 cm^3 round bottom flask in an ice bath was slowly added with stirring 42 cm^3 of 12 M HCl. The mixture was allowed to stand several days in the refrigerator. The product precipitated as long needles.

(b) Dry HCl gas was bubbled through freshly distilled morpholine. A bulky precipitate formed. This was dissolved in a minimal volume of boiling isopropyl alcohol to which a few drops of water were added. On cooling, the product precipitated as long needles. After a second recrystallization, the product was filtered under N_2, washed with diethyl ether, and dried in a vacuum desiccator over P_2O_5.

Trimethylamine hydrochloride was recrystallized by dissolving in boiling ethanol, cooling, adding ether, and cooling in the refrigerator overnight. The precipitate was filtered, washed with ether and dried in a vacuum desiccator over P_2O_5 for several days.

Buffer solutions

Three different types of buffers were used: morpholine–morpholinium chloride, borate–boric acid, and trimethylamine. A typical preparation for each type is given below.

Borate—boric acid buffer. In a 250 cm^3 volumetric flask were placed 0.309 g (0.00500 mol) of boric acid, 4.10 g (0.0489 mol) of sodium borate, and 16.5 g KCl. Water was added to the mark. The final pH was 8.88.

Morpholine—morpholinium chloride buffer. Morpholine (2.17 g, 0.00249 mol) was mixed with 0.59 g (0.00469 mol) of morpholinium chloride and 18.2 g of KCl in a 50 cm^3 volumetric flask. Water was added to the mark. The final pH was 9.05.

Trimethylamine buffer. Trimethylammonium chloride (2.285 g, 0.0239 mol) was partly neutralized by adding 0.1 g (0.0025 mol) of NaOH. To this were added 2.372 g KCl and the volume adjusted to 50 × cm^3 with water. The pH was 9.25.

Kinetic studies

A stock solution of complex was prepared by adding 3.00 cm^3 of an approx. 0.02 M aqueous solution of the ligand dihydrochloride $[H_2L]Cl_2$ to 3.00 cm^3 of 0.0195 M $NiCl_2$ solution, 0.1 M in KCl. The ionic strength of the ligand solution was adjusted with KCl so that the final ionic strength of the reaction mixture of buffer and complex would be 1.0 M. Standard NaOH was added to give a ratio a of base to ligand of nearly 2. The solution was kept in a constant temperature bath at 25.0°C.

A buffer solution (2.70 cm^3) was placed in a quartz 1.00 cm spectrophotometer cell. This was placed in the thermostatted cell compartment of a Hitachi-Perkin Elmer 139 spectrophotometer. The wavelength of the spectrophotometer was set to 415 nm, which is the wavelength of maximum absorbance for the planar complex, the final product, and the spectrophotometer was adjusted for 100% T with buffer solution in the reference cell. When both solutions had reached thermal equilibrium, 0.30 cm^3 of the stock solution of complex was injected with a syringe into the buffer solution in the sample cell. The absorbance was recorded as a function of time until no further change in absorbance could be observed. The pH of the reaction mixture was measured. The change in pH from the initial value for the buffer solution was not more than 0.03 pH units.

REFERENCES

1. Part II: M. M. Muir, J. A. Diaz and L. Oyola, *Polyhedron* 1984, **3**, 551.
2. Part I. M. M. Muir and P. R. Rechani, *Inorg. Chim. Acta* 1974, **11**, 137.
3. Taken from the thesis presented by J. A. D. to the University of Puerto Rico in partial fulfillment of the requirements for the degree Ph.D., 1977.
4. S. Lindskog, *Struct. Bonding* 1970, **8**, 153.
5. M. Llinas, *Struct. Bonding* 1974, **17**, 135.
6. A. S. Mildvan and C. M. Grisham, *Struct. Bonding* 1975, **20**, 1.
7. J. A. Fee, *Struct. Bonding* 1975, **23**, 1.
8. M. F. Dunn, *Struct. Bonding* 1975, **23**, 61.
9. F. P. Bossu, K. L. Chellappa and D. W. Margerum, *J. Am. Chem. Soc.* 1977, **99**, 2195.
10. J. C. Cooper, L. F. Wong and D. W. Margerum, *Inorg. Chem.* 1978, **17**, 261.
11. Y. Sugiera and Y. Mino, *Inorg. Chem.* 1979, **18**, 1336.
12. G. D. Owens, K. L. Chellappa and D. W. Margerum, *Inorg. Chem.* 1979, **18**, 960.
13. K. S. Bai and A. E. Martell, *J. Am. Chem. Soc.* 1969, **91**, 4412.
14. K. S. Bai and A. E. Martell, *Inorg. Chem.* 1970, **9**, 1126.
15. M. Eigen and R. G. Wilkins, *Adv. in Chem. Series* 1965, **49**, 55.
16. R. Wilkins, R. Jelin, D. Margerum, and D. Weatherburn, *J. Am. Chem. Soc.* 1969, **91**, 4326.
17. T. Kaden, *Helv. Chim. Acta* 1971, **54**, 625.
18. D. Wagnerova, T. Kaden and A. Zuberbuhler, *Helv. Chim. Acta* 1969, **52**, 1776.
19. M. M. Muir, P. R. Rechani and J. A. Diaz, *Synth. React. Inorg. Met. -Org. Chem.* 1981, **11**, 381.

Polyhedron Vol. 4, No. 1, pp. 159–162, 1985
Printed in Great Britain.

0277–5387/85 $3.00 + .00
© 1985 Pergamon Press Ltd.

INHIBITORIAL EFFECT OF THE Cu(II) AND Ni(II) COMPLEXES WITH POLYAMINES AND IMIDAZOLE DERIVATIVES ON THE Ca, Mg-DEPENDENT ATP-ase SUBSTRATE

L. V. TATJANENKO and YU. SH. MOSHKOVSKY
Research Institute for Biological Tests of Chemical Compounds, Kupavna, Moscow, U.S.S.R.

I. A. ZAKHAROVA
S. N. Kurnakov Institute of General and Inorganic Chemistry, Academy of Science, Leninsky Prospect 31, Moscow, U.S.S.R.

and

G. PONTICELLI*, M. MASSACESI
Istituto di Chimica Generale ed Inorganica, Via Ospedale 72, Cagliari, Italy

and

G. DEVOTO
Cattedra di Chimica A, Istituto di Medicina del Lavoro, Via S. Giorgio 12, Cagliari, Italy

(*Received* 4 *October* 1983, *accepted* 16 *April* 1984)

Abstract—The investigation of the inhibitory activity on the Ca,Mg-dependent ATP-ase substrate of some Cu(II) and Ni(II) complexes with polyamines and imidazole derivatives is reported. These results show that the Cu(II) complexes have high inhibitorial effect with the exception of the following very stable compounds: square planar $[Cu(N\text{-}PropIm)_2(NCS)_2]$, distorted octahedral $[Cu(bipy)_2(NCS)_2]$ and five coordinate $[Cu(Me_6tren)(NCS)]$ (SCN). The Ni(II) derivatives present a medium inhibitorial activity except to the stable tetrahedral $[Ni(N\text{-}PropIm)_2(NCS)_2]$, hexacoordinate [Ni(dpt)(tn)(NCS)] (SCN) and fivecoordinate $[Ni(dpt)(tn)]Br_2$ and $[Ni(Me_6tren)(NCS)]$ (SCN). An explanation of these conclusions is reported.

The adenosine triphosphatase (ATP-ase) is an enzyme very significant for the organism. This enzyme is, membrane bonded with outer cell position a convenient model to study different types of complexes, since chloride and other anion concentrations in the intercellular medium are high enough to exclude the hydrolysis of the complexes. The ATPase is extracted from rabbit muscles.[1]

In particular Ca, Mg-dependent ATP-ase has been selected to investigate the factors influencing the biological activity of the coordination compounds, the donor capability and the different hindrance of the coordinated ligand (polyamines and imidazole derivatives) and the structure of the complexes.

Copper (II) and Ni(II) complexes give the possibility of studying the above stereochemical factor.

The inhibitorial effect of the Cu(II) and Ni(II) compounds with polyamines and imidazole derivatives on the Ca, Mg-dependent ATP-ase mash has now been studied to verify the above cited chemical behaviour.

EXPERIMENTAL

All the investigated complexes were prepared and characterized according to the previous papers.[2–8]

*Author to whom correspondence should be addressed.

The extraction method of the sarcoplasmatic reticulum (SR) containing ATP-ase is obtained by the skeletal muscles of a particular type of rabbits selected as a certain line. The inhibitorial activity of the ligands and the complexes with aqueous solution ATP-ase is determinated by the amperometric titration.[9] All the ligands have no inhibitorial activity.

RESULTS AND DISCUSSION

Copper (II) complexes. The thiocyanate compounds $[Cu(den)(NCS)_2]$ and $[Cu(dpt)(NCS)_2]$, $[Cu(Me_6tren)(NCS)](SCN)$, $[Cu(en)_2(SCN)_2]$, $[Cu(bipy)_2(NCS)_2]$, $[Cu(N\text{-}PropIm)_4]Cl_2$, $[Cu(N\text{-}PropIm)_2Cl_2]$, $[Cu(N\text{-}PropIm)_4]Br_2$, $[Cu(N\text{-}PropIm)_2Br_2]$ and $[Cu(N\text{-}PropIm)_2(NCS)_2]$ (where den = diethylentriamine, dpt = 3, 3′-diaminodipropylamine, Me_6tren = tris(2-dimethylaminoethyl)amine, en = ethylenediamine, bipy = α, α'-bipyridine and N-PropIm = N-propylimidazole) have been previously prepared.[2-7] They are generally characterized by magnetic moments, infrared spectra, electronic spectroscopy in solid and in the solution state and molar conductivity values. The polyamine ligands bind through all the nitrogen atoms of the amino groups. The N-PropIm behaves as an monodentate N-bonded ligand. From these experimental data we were able to find the stereochemistry in the solid state of these compounds which are: square pyramidal, trigonal bipyramidal, tetragonally distorted hexacoordinate and tetrahedral.

In Table 1 are reported the complexes, their inhibitorial activity with respect to Ca, Mg-dependent ATP-ase mash and the stereochemistry of the solid compounds.

The stereochemistry of these solid complexes is preserved also in methanol or in aqueous solution as confirmed by the same shape of the reflectance and the absorption spectra and by the conductivity values with the exception of the $[Cu(den)(NCS)_2]$ and $[Cu(dpt)(NCS)_2]$ derivatives. The last complexes, distorted square pyramidal in the solid state, in solution lose one of the two thiocyanate groups in the coordination sphere changing their structure in square planar species.[2]

The high inhibitorial effect of the $[Cu(den)(NCS)_2]$ and $[Cu(dpt)(NCS)_2]$ on the enzyme, 72 and 77% respectively, is due to the introduction in the Cu(II) coordination sphere of two $-S^-$ anions in the apical positions so that the stereochemistry is modified to tetragonally distorted hexacoordinate.

The $[Cu(Me_6tren)(NCS)]$ SCN and $[Cu(bipy)_2(NCS)_2]$, trigonal bipyramidal and tetragonally distorted octahedral respectively in the solid state have low inhibitorial effect, 25–26%, because these structures are particularly stable in solution: this fact is due to a partial substitution of the $-S^-$ anions of the ferment without modification of the stereochemistry.

In the $[Cu(en)_2(SCN)_2]$, tetragonally distorted hexacoordinate, the inhibitorial activity is 83% because the two slightly bonded thiocyanate groups are easily substituted by the donor atoms of the enzyme. In this case the stereochemistry is preserved also in ATP-ase mash.

The inhibitorial effect between 75 and 95% of the complexes $[M(L)_2X_2]$ and $[M(L)_4]X_2$, where L = N-PropIm, X = Cl, Br, tetrahedral in the solid state, can be so explained. The $[Cu(L)_2X_2]$ derivatives replace the halides in the coordination sphere with thiol groups and the structure is rearranged in solution to tetragonally distorted octahedral with other two $-S^-$ anions that are bonded in the apical positions of the complexes. The $[Cu(L)_4X_2]$ compounds are rearranged in ATPase mash and bind two thiol groups in axial positions instead of the halides that before were out of the inner sphere. The stereochemistry, in both case, is modified to tetragonally distorted octahedral. Only in the $[Cu(N\text{-}PropIm)_2(NCS)_2]$, *trans*-square planar in solid state, have we observed that the inhibitorial activity drops to 0%, probably because of the high stability of this compound.

Nickel(II) complexes. We have now extended this study to the Ni(II) complexes $[Ni(dpt)(tn)]Br_2$, $[Ni(dpt)(tn)(NCS)]$ (SCN), $[Ni(Me_6tren)(NCS)]$ (SCN), $[Ni(trien)(en)]Cl_2$, $[Ni(tn)_3](ClO_4)_2$, $[Ni(NEtIm)_6]Cl_2$, $[Ni(N\text{-}PropIm)_6]Cl_2$ and $[Ni(N\text{-}PropIm)_2(NCS)_2]$ (where dpt = 3, 3′-diaminodipropylamine, tn = 1, 3-diaminopropane, Me_6tren = tris(2-dimethylaminoethyl)amine, trien = triethylenetetramine, N-EtIm = N-ethylimidazole and N-PropIm = N-propylimidazole).[6-8]

These derivatives have been previously prepared and characterized by magnetic moments, infrared spectra, electronic spectroscopy in solid and in solution state and molar conductivity values. The polyamine ligands bind through all the nitrogen atoms of the amino groups; the N-EtIm and N-PropIm behave as monodentate N-bonded.

In the Table are reported the complexes, their inhibitorial activity in the ATP-ase mash and their solid stereochemistry.

The structure of these solid complexes is preserved both in methanol and in ATP-ase aqueous solution as confirmed by the same shape of the electronic and absorption spectra and by the conductivity data.

In the solid hexacoordinate $[Ni(dpt)(tn)(NCS)]$ (SCN) the inhibitorial effect is 15% because the

Table 1. Inhibitory activity of the Cu(II) and the Ni(II) complexes

Complex	Inhibitory activity %(±2) $c = 10^{-4}$M	Stereochemistry in the solid state
$[Cu(den)(NCS)_2]$	72	distorted square pyramidal
$[Cu(dpt)(NCS)_2]$	77	distorted square pyramidal
$[Cu(Me_6tren)(NCS)](SCN)$	25	trigonal bipyramidal
$[Cu(en)_2(SCN)_2]$	83	tetragonal distorted octahedral
$[Cu(bipy)_2(SCN)_2]$	26	tetragonal distorted octahedral
$[Cu(N\text{-}PropIm)_4]Cl_2$	75	tetrahedral
$[Cu(N\text{-}PropIm)_2Cl_2]$	87	distorted tetrahedral
$[Cu(N\text{-}PropIm)_4]Br_2$	83	tetrahedral
$[Cu(N\text{-}PropIm)_2Br_2]$	95	distorted tetrahedral
$[Cu(N\text{-}PropIm)_2(NCS)_2]$	0	trans square planar
$[Ni(dpt)(tn)(NCS)](SCN)$	15	distorted octahedral
$[Ni(dpt)(tn)]Br_2$	0	square pyramidal
$[Ni(N\text{-}PropIm)_2(NCS)_2]$	0	distorted tetrahedral
$[Ni(N\text{-}PropIm)_6]Cl_2$	29	octahedral
$[Ni(N\text{-}EtIm)_6]Cl_2$	43	octahedral
$[Ni(trien)(en)]Cl_2$	51	octahedral
$[Ni(tn)_3](ClO_4)_2$	25	octahedral
$[Ni(Me_6tren)(NCS)](SCN)$	25	trigonal bipyramidal

NCS group, weaker than a nitrogen atom of the polyamine, is partially displaced by the $-S^-$ anion of the enzyme.

The [Ni(dpt)(tn)] Br_2, square pyramidal in solid state, has no inhibitorial effect: this fact is due to the bonds being very strong and shorter than those of the preceding hexacoordinate derivative and so it is difficult to substitute the positions of the chelating polyamines with thiol groups of the enzyme.

For the solid octahedral complexes $[Ni(L)_6]$ Cl_2, where L = N-PropIm and N-EtIm, the inhibitorial activity is 29% and 43% respectively because the N-PropIm is more basic than the N-EtIm and N-PropIm can be more difficultly substituted by the $-S^-$ anions of the ATP-ase.

The increase of the inhibitorial effect of these complexes with respect to the nickel polyamine derivatives is due to a lower coordinating strength of the alkyl-imidazole in comparison with the chelating ligands.

In the solid octahedral [Ni(trien)(en)] Cl_2 the high value of 51% is due to the easy substitution on the inner sphere by thiol groups of the enzyme with respect to the pentacoordinate [Ni(dpt)(tn)] Br_2.

The solid octahedral $[Ni(tn)_3]$ $(ClO_4)_2$ has an inhibitorial effect of 25% in ATP-ase mash, a value higher than that of [Ni(dpt)(tn)(NCS)] (SCN) because the $-S^-$ anions of the enzyme can be easily substituted in the perchlorate derivative: the chelate effect of the dpt is stronger than the tn ligand.

The [Ni(Me_6tren)(NCS)] (SCN) presents a value of 25% as the [Cu(Me_6tren)(NCS)] (SCN) because in these very stable trigonal bipyramidal deriva-

tives only a partial substitution of the coordinated thiocyanate occurs with the thiol group of the ATP-ase.

Finally in the tetrahedral $[Ni(N\text{-}PropIm)_2(NCS)_2]$ the inhibitorial activity is 0%, as the analogous square planar Cu(II) derivative, because of the high strength of the bonds in these complexes.

It is important to note that in all the Ni(II) derivatives the stereochemistry did not change from the solid state to the ATP-ase mash.

CONCLUSIONS

As far as the inhibitory mechanism the interaction of the complexes in aqueous solution ATP-ase occurs with the sulphur anion(s) of the thiolate groups of the enzyme.

In the $M(L)_nX_2$ (where M = Pd(II), Pt(II), L = isoxazole, benzoxazole and imidazole derivatives; $n = 2$–4; X = Cl, Br, I)[10] and $Pd(ox)(L)_n$ (where ox = oxalate; L = precedent heterocyclic ligands; n = 1,2)[11] the replacement of the $-S^-$ anions of the ATP-ase produces square planar species without modification of the solid stereochemistry.

In the Cu(II) complexes the stereochemistry is generally modified from the solid state to the ATP-ase mash because the $-S^-$ anions replace the counteranions and/or another possible coordination site, while in the nickel derivatives the solid structure is preserved also in the solution ferment.

We can conclude that the inhibitorial activity depends for the Cu(II) and Ni(II) complexes very strongly on the stereochemical factor resulting from the type and the steric hindrance of the coordinate ligands.

REFERENCES

1. I. A. Zakharova, L. V. Tatjanenko, Yu. Sh. Moshkovsky, L. M. Raykhman and T. A. Kondratjeva, *Biofisica* 1979, **XXII**, 418.
2. A. Cristini and G. Ponticelli, *J. Inorg. Nucl. Chem.* 1973, **35**, 2691.
3. M. Ciampolini and N. Nardi, *Inorg. Chem.* 1966, **5**, 41.
4. B. A. Sastry, M. N. Chary, M. Massacesi and G. Ponticelli, *J. Mol. Struct.* 1982, **78**, 289.
5. M. Massacesi and G. Ponticelli, *J. Inorg. Nucl. Chem.* 1974, **36**, 2209.
6. G. Ponticelli and C. Preti, *J. Chem. Soc. Dalton Trans*, 1972, 708.
7. R. P. Taylor, D. H. Templeton, A. Zalkin and W. Dew Harrocks, *Inorg. Chem.* 1968, **7**, 2629.
8. E. Cara, A. Cristini, A. Diaz and G. Ponticelli, *J. Chem. Soc. Dalton Trans.* 1972, 527.
9. E. Benesch, H. A. Lardy and R. Benesch, *J. Biol. Chem.* 1965, **216**, 663.
10. I. A. Zakharova, Ja. V. Salin, L. V. Tatjanenko, Yu. Sh. Moshkovsky and G. Ponticelli, *J. Inorg. Biochem.* 1981, **15**, 89; M. Massacesi, R. Pinna, M. Biddau, G. Ponticelli and I. A. Zakharova, *Inorg. Chim. Acta, Bioinorg. Sect.* 1983, **80**, 151; M. Biddau, G. Devoto, M. Massacesi, R. Pinna, G. Ponticelli and I. A. Zakharova, *Polyhedron*, 1983, **2**, 1261.
11. G. Devoto, M. Biddau, M. Massacesi, R. Pinna, G. Ponticelli, L. V. Tatjanenko and I. A. Zakharova, *J. Inorg. Biochem.* 1983, **19**, 311.

Polyhedron Vol. 4, No. 1, pp. 163–168, 1985
Printed in Great Britain.

0277–5387/85 $3.00 + .00
© 1985 Pergamon Press Ltd.

STEREOCHEMICAL VERSATILITY OF Cu(II): Cu(II) COMPLEXES OF BENZYL METHYL KETONE SEMICARBAZONE

ANIL JAGGI, SULEKH CHANDRA and K. K. SHARMA*
Department of Chemistry, Zakir Husain College, Ajmeri Gate, Delhi 110006, India

(*Received* 4 *January* 1984; *accepted* 16 *April* 1984)

Abstract—Copper(II) complexes of the general composition Cu(ligand)$_2$X$_2$ (where X = Cl, Br, NO_3, ClO_4 and $\frac{1}{2}SO_4$) and Cu(ligand)$(CH_3COO)_2$ have been synthesised with benzymethylketonesemicarbazone. All the complexes prepared have been characterised by elemental analysis, magnetic moment, conductance, IR, electronic and electron spin resonance spectral studies. The complexes Cu(ligand)$_2$X$_2$ (X = Cl, Br, NO_3) and Cu(ligand)$(CH_3COO)_2$ may have tetragonal symmetry while the Cu(ligand)$_2$X$_2$ (ClO_4 and $\frac{1}{2}SO_4$) may be five-coordinate trigonal bipyramidal in structure.

Cambell *et al.*[1,2] have reported the electronic spectra and the esr spectra of Cu(II) complexes of the type Cu(ligand)$_2$X$_2$ where X = Cl, Br and the ligands are the semicarbazones of cyclopentanone methylisopropylketone and diacetylketone. Their results show that the stereochemistry of these complexes changes from six-coordinate tetragonal to five coordinate trigonal bipyramidal, as the alkyl group on the ketone becomes bulky. In the present studies we report the synthesis and stereochemistry of Cu(II) complexes of benzylmethyl ketonesemicarbazone. Our results show that the stereochemistry of these complexes also depends on the coordinated anions, i.e. with chloride, bromide, nitrate and acetate, the complexes have six-coordinate tetragonal geometry but perchlorate and sulphate impart pentacoordinate geometry.

EXPERIMENTAL

(a) *Preparation of semicarbazone*

The semicarbazone of the ketone was prepared as described in the literature.[2,3]

(b) *Preparation of complexes*

The complexes were prepared by mixing the hot aqueous solution of the hydrated Cu(II) salts and the benzylmethyl ketonesemicarbazone in the molar ratio 1:2. On cooling the solution a crystalline complex precipitated out in each case. In all the cases good analytical results were obtained for CuL_2X_2 (X = Cl, Br, NO_3, ClO_4 and $\frac{1}{2}SO_4$) and $CuL(CH_3COO)_2$ see Table 1. The chloro, bromo and nitrate complexes are soluble in water, ethanol and methanol, while the acetate, sulphate and perchlorate complexes are poorly soluble in water as well as common organic solvents.

Physical measurements

The magnetic susceptibilities were measured (at 298 K) on a Gouy balance, using Hg[Co(CNS)$_4$] as the calibrating agent. Infrared spectra of the complexes were recorded on Perkin–Elmer 621 automatic recording spectrophotometer, the KBr medium. Electronic spectra of the complexes were recorded on DMR-21 automatic recording spectrophotometer in Nujol mull. The esr spectra of the polycrystalline samples of the complexes were recorded on a Varian E4–ESR spectrometer operating at ~9.4 GHz and 100 KHz with field modulation and phase-sensitive detection.

Carbon and hydrogen analyses were performed in the microanalytical laboratory. The nitrogen contents of the complexes were determined using Kjeldahl's method. The copper in the complexes was estimated gravimetrically by precipitation as CuCNS.

RESULTS AND DISCUSSION

The composition of the complexes are given in Table 1. With the exception of Cu(ligand)-$(CH_3COO)_2$ all the other complexes have the gen-

*Author to whom correspondence should be addressed.

eral composition $Cu(ligand)_2X_2$ where X = Cl, Br, NO_3, ClO_4 and $\frac{1}{2}SO_4$. Similarly all the complexes exhibit normal magnetic moments corresponding to one unpaired electron (1.88–2.0 BM) the only exception being $Cu(ligand)(CH_3COO)_2$ which shows a subnormal magnetic moment (1.54 BM). The low solubility value and low magnetic moment of $Cu(ligand)(CH_3COO)_2$ indicate a polymeric structure for the complex.

The infrared bands for the ligand and complexes and their possible assignments are presented in Table 2. The IR spectrum of the ligand exhibits characteristic bands for νC–H, νN–H, νC=O and δNH and νC=N. A broad band at 3580 cm^{-1} in the ligand may be assigned to non-bonded νN–H and a series of bands in the range 3000–3400 cm^{-1} may be assigned to bonded νN–H and νC–H modes. A band at 1740 cm^{-1} is characteristic of carbonyl group absorption whereas the bands at 1580 and 1470 cm^{-1} are assignable to νC=N and amide I coupled with each other. A strong band at 1430 cm^{-1} is mainly due to (νC–N + δNH) and is known as amide II band due to secondary amine. Fraser and Price[6] suggested that this may be due to out-of-phase combination of O–C–N and N–H vibrational modes. However, the corresponding in-phase mode primarily due to C–N stretching is the strong band at 1295 cm^{-1} and is so called amide III which in fact is a combination of (νC–N + δNH_2). Thus in the region ranging from 1150–100 cm^{-1}, there are three bands at 1130 and 1000 cm^{-1} assignable to δNH_2. A strong band at 920 cm^{-1} is due to δ(O=C–N) and a group of bands at 775 and 690 cm^{-1} are assigned to π(O=C–N_2) as suggested by Campbell *et al.*[7] The spectra of the complexes reported here contain most of these bands and also the band corresponding to the anions. The characteristic band in the ligand, at 1740 cm^{-1} due to νC=O group is shifted towards lower frequency by ~ 40 cm^{-1}. The amide II band which appears at 1430 cm^{-1} in the ligand, is also shifted towards lower frequency in the complexes. These observations suggest a possibility of coordination through C=O oxygen. A strong band at 1580 cm^{-1} in the ligand apparently has a large contribution from νC=N. Further a coordination[8] through O increases the double bond character of the CN bond. It has been observed that this band is shifted towards higher frequency side in the complexes. On the basis of above observations we propose that the ligand behaves as bidentate coordinated through oxygen of the carbonyl group and nitrogen of the hydrazinic residue.

$Cu(ligand)_2X_2$ (X = Cl, Br, NO_3)

The $Cu(ligand)_2X_2$ (X = Cl, Br, NO_3) complexes may be considered to have a tetragonal structure, with planar arrangement of the ligand molecule around the Cu(II), and the anions occupying the axial position.

The electronic spectra of six-coordinate Cu(II)

Table 1. Colour and composition of complexes

Complex	Colour	Elemental Analyses %, Found (Calcd)			
		Cu	C	H	N
$Cu(L)_2Cl_2$	Blue	12.24 (12.29)	46.50 (46.46)	5.03 (5.02)	16.26 (16.20)
$Cu(L)_2Br_2$	Greenish blue	10.50 (10.51)	39.75 (39.73)	4.02 (4.30)	13.95 (13.90)
$Cu(L)_2(NO_3)_2$	Green	11.05 (11.15)	42.01 (42.14)	4.60 (4.56)	19.70 (19.67)
$Cu(L)_2SO_4$	Blue	11.78 (11.73)	44.30 (44.32)	4.78 (4.80)	15.50 (15.51)
$Cu(L)_2(ClO_4)_2$	Bluish	9.68 (9.70)	36.60 (36.67)	3.90 (3.97)	12.78 (12.83)
$CuL(CH_3COO)_2$	green	17.08 (17.04)	45.02 (45.14)	5.08 (5.10)	11.30 (11.27)

Table 2. IR spectral bands (cm^{-1}) and their tentative assignments

Compound*	Assignments						
	$\nu_{CH} + \nu_{NH}$	ν_{C-O}	$\nu_{C=N}$ and amide I	Mainly $\nu_{C-N} + \delta_{NH_2}$ $\nu_{C-N} + \delta_{NH_2}$ amide II	δNH_2	$\delta O-C-N$	$\delta O-C-N_2$
L	3400(w) 3300(w) 3000(w)	1740(s)	1580(s) 1470(m)	1430(m) 1295(m)	1130(m) 1080(m)	920(w)	790(w) 690(w)
$Cu(L)_2Cl_2$	3390(w) 3300(w) 3000(w)	1700(s)	1600(s) 1470(m)	1410(m) 1270(m)	1140(m) 1050(m)	-	730(w)
$Cu(L)_2Br_2$	3400(w) 3300(w) 3000(w)	1705(s)	1605(s) 1470(m)	1415(m) 1275(m)	1150(m) 1050(m)	-	730(w)
$Cu(L)_2(NO_3)_2$	3390(w) 3300(w) 2990(w)	1700(s)	1600(s) 1472)m)	1410(m) 1270(m)	1160(m) 1050(m)	910(w)	730(w)
$Cu(L)(CH_3COO)_2$	3380(w) 3260(w) 2990(w)	1705(s)	1600(m) 1475(m)	1400(m) 1270(m)	1140(m) 1035(m)	910(w)	780(w)
$Cu(L)_2SO_4$	3390(w) 3300(w) 2995(w)	1710(s)	1605(s) 1470(m)	1405(m) 1275(m)	1140(m) 1050(m)	910(w)	750(w)
$Cu(L)_2(ClO_4)_2$	3400(w) 3300(w) 3000(w)	1710(s)	1600(s) 1470(m)	1405(m) 1270(m)	1140(m) 1050(m)	910(w)	740(w)

w = weak, s = strong, m = medium; * L = Benzylmethylketonesemicarbazone

complexes have either D_{4h} or C_{4v} symmetry, and the E_g and T_{2g} levels of the ^2D free-ion term will split into B_{1g}, A_{1g} and B_{2g}, E_g levels respectively. Thus three spin allowed transitions are expected in the visible and near-IR region, but only a few complexes are known, in which such bands are resolved either by Gaussian analysis or single crystal polarization studies.[9] These bands have been assigned due to the $^2B_{1g} \rightarrow {}^2A_{1g}$ $(d_{x^2-y^2} \rightarrow d_{z^2})$, $^2B_{1g} \rightarrow {}^2B_{2g}$ $(d_{x^2-y^2} \rightarrow d_{xy})$ and $^2B_{1g} \rightarrow {}^2E_g$ $(d_{x^2-y^2} \rightarrow d_{xz}, d_{yz})$ transitions in order of increasing energy. The energy level sequence will depend on the amount of tetragonal distortion due to the ligand field and the Jahn–Teller effect.[10] The electronic spectra of the complexes reported here show only a broad absorption ranging 13,800–14,800 cm^{-1} and a well defined shoulder at 16,300–16,600 cm^{-1} (Table 3). This may be assigned to the $^2B_{1g} \rightarrow {}^2A_{1g}$ and $^2B_{1g} \rightarrow {}^2B_{2g}$ is usually not observed as a separate band in tetragonal field.[11] The splitting of the ^2E_g state is a measure of the in-plane and the axial field. Since the in-plane field is approximately constant in the present complexes, the change of the position of the bands would be mainly due to the axial field. In the complexes reported here the $^2B_{1g} \rightarrow {}^2A_{1g}$ transition is shifted to higher energy, the order being Cl < Br < NO_3.

All the complexes show isotropic esr spectra characteristic of tetragonal Cu(II) complexes. g_0-values are given in Table 4. The anisotropic g-values have been calculated using the following expressions,[13-15]

$$g_{\parallel} = 2 - \frac{8\lambda}{\Delta E_2}, \quad \text{and} \quad g_{\perp} = 2 - \frac{2\lambda}{\Delta E_3}$$

where

$$\lambda = 823\ cm^{-1} \quad \text{and} \quad \Delta E_2 = {}^2B_{1g} \rightarrow {}^2B_{2g},$$

and

$\Delta E_3 = {}^2B_{1g} \rightarrow {}^2E_g$ excitation energies respectively.

The stronger interaction along the z axis is to be accompanied by an increase in the value of $g_{\parallel}$. The stronger axial bonding however, leads to an increase in the length of bond in the xy plane, which results in a decrease of both in-plane covalency and the energy of $d_{x^2-y^2} \rightarrow d_{xy}$ transition.[16] Both these factors tend to increase the value of $g_{\parallel}$. The $g_{\parallel}$-values for the complexes studied follow the order, $Cu(ligand)_2(NO_3)_2 > Cu(ligand)_2Cl_2 > Cu(ligand)_2Br_2$. This appears to be the order of the

Table 3. The magnetic moment (B.M.) and the electronic spectral bands of the complexes

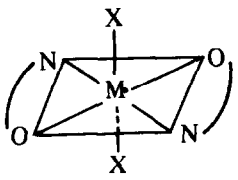
Complex	μ_{eff}	$\lambda_{max}(cm^{-1})$ Assignments	
		$^2B_{1g} \rightarrow {}^2A_{1g}$	$^2B_{1g} \rightarrow {}^2E_g$
$Cu(L)_2Cl_2$	1.96	13800	16300
$Cu(L)_2Br_2$	1.90	14290	16400
$Cu(L)_2(NO_3)_2$	1.88	14800	16400
$Cu(L)(CH_3COO)_2$	1.54	14800	16600
		$^2A_1 \rightarrow {}^2E''$	
$Cu(L)_2SO_4$	2.0	11900	
$Cu(L)_2(ClO_4)_2$	1.98	12000	

strength of metal–anion interactions for nitrate, chloride and bromide. Our results are in agreement with the respective position of the anions as given in the spectrochemical series.[11]

In axial symmetry the g-values are related by the expression,[10] $G = (g_\parallel - 2)/(g_\perp - 2)$, which measures the exchange interaction between copper centres in the polycrystalline solid. According to Hathaway,[17–20] if the value of G is greater than four, the exchange interaction is negligible, whereas when the value of G is less than four, a considerable exchange interaction is indicated in the solid complex. The calculated G values are given in Table 4. The G values in these complexes are greater than four suggesting that there are no interactions between the copper centres in solid. The following structure may be suggested for the complexes.

Table 4. ESR spectral data for the complexes

Complex	$g_\parallel$	$g_\perp$	g_e	G	R
$Cu(L)_2Cl_2$	2.247	2.043	2.111	5.80	-
$Cu(L)_2Br_2$	2.234	2.052	2.114	4.03	-
$Cu(L)_2(NO_3)_2$	2.270	2.058	2.128	4.65	-
$Cu(L)(CH_3COO)_2$	2.316	2.187	2.230	1.689	-
	g_1	g_2	g_3		
$Cu(L)_2SO_4$	2.137	2.343	2.461	-	1.746
$Cu(L)_2(ClO_4)_2$	2.140	2.375	2.461	-	1.569



X=Cl, Br, NO_3

Fig. 1.

Cu(ligand) $(CH_3COO)_2$

As discussed earlier this complex is insoluble in water as well as in common organic solvents and shows a subnormal magnetic moment (1.54 BM). These observations suggest a polymeric structure for this complex. The $\nu_a(COO^-)$ and $\nu_s(COO^-)$ of acetate ion[16] are observed at 1560 and 1416 cm^{-1} respectively. The separation between the two ν(C–O) is much larger in unidentate complexes than in the free ion.[16] In the case of bidentate complexes, the separation between the two frequencies is smaller than in the free ion values and in the bridging complex. In this complex, the $\nu_a(COO^-)$ and $\nu_s(COO^-)$ are obtained at 1555 and 1420 cm^{-1}, respectively.

The electronic spectrum of this complex see Table 2, exhibits bands corresponding to the tetragonal geometry. The esr spectrum of this complex is much different than for the chloro bromo an nitrate complexes. $g_\parallel$ and $g\perp$ values for the complex are much greater than for the chloro, bromo and nitrate complexes. This difference may be attributed to the polymeric nature of the complex. g-values of the same order have already been reported for dimeric Cu(II) acetate.[20b] The G value has been found in the complex to be less than four (1.797) which suggests exchange interaction between the copper centres in the solid state.

Cu(ligand)$_2$$(ClO_4)_2$ and Cu(ligand)$_2$$(SO_4)$

The infrared spectra of these complexes exhibit bands corresponding to the unidentate behaviour of the perchlorate and sulphate group[21] and a five-coordinated structure can be suggested for these complexes. There are two basic configurations[22] that can be adopted—trigonal bipyramidal (TBP) and square pyramidal (SP). In practice, there appears to be very little difference in energy,[23] between the two configurations.

The two configurations SP and TBP are characterized by the ground state $d_{x^2-y^2}$ and d_z^2 respectively.[24,25] The esr spectra of Cu(II) complexes provide a very good basis for distinguishing between these two ground states. For systems with $g_3 > g_2 > g_1$ the ratio[26] of $(g_2 - g_1)/(g_3 - g_2)$ (hereafter called parameter R) is a very useful parameter for this purpose. If the ground state is predominantly d_z^2 the value of R is greater than one. On the other hand for the ground state predominantly $d_{x^2-y^2}$ the value of R is less than one. The complexes under study show the value of R is greater than one (Table 4) indicating d_z^2 as the ground state. Thus these complexes may be five-coordinate trigonal bipyramidal.

The electronic spectra of these complexes exhibit a single absorption band at 12,000 cm^{-1} (see Table 3) which may be assigned to $^2A_1 \rightarrow {}^2E''$ transition. These are similar to earlier reported trigonal bipyramidal Cu(II) complexes.[4]

REFERENCES

1. M. J. M. Campbell and R. Grzeskowiak, *Inorg. Nucl. Chem. Lett.* 1969, **5**, 27.
2. M. J. M. Campbell and R. Grzeskowiak, *Inorg. Nucl. Chem. Lett.* 1974, **10**, 473.
3. A. I. Vogel, *A Text Book of Practical Organic Chemistry*, p. 344. Longmans, London (1973).
4. S. Chandra, S. P. Dubey, K. B. Pandeya and R. P. Singh, *Acta Chim. Acad. Sci. Hung.* 1982, **109**, 165.
5. W. H. T. Davison and P. E. Chiristie, *Chem. Abs.* 1955, 3389.
6. R. D. B. Fresher and W. C. Price, *Proc. Roy. Soc.* 1953, **66**, 1410.
7. M. J. M. Campbell and R. Greskowiak, *J. Inorg. Nucl. Chem.* 1968, **30**, 1865.
8. H. Sterk and E. Ziegler, *Moasth Chem.* 1966, **97**, 1131.
9. A. Eranshaw, L. F. Larkworthy and K. C. Patel, *J. Chem. Soc. A* 1969, 1339; A. B. P. Lever and E. Mantovani, *Inorg. Chem.* 1971, **10**, 817; B. J. Hathaway, *Struct. Bonding* 1973, **14**, 49. Y. Nishida and S. Kida, *Coord. Chem. Rev.* 1979, **27**, 275.
10. I. M. Procter, B. J. Hathaway and P. Nicholls, *J. Chem. Soc.* A 1968, 1678; A. A. G. Tomlinson, B. J. Hathaway, D. E. Billig and P. Nicholls, *J. Chem. Soc. A* 1969, 65: *J. Inorg. Nucl. Chem.* 1977, **39**, 417.
11. A. B. P. Lever, *Inorganic Electronic Spectroscopy*. Elsevier, Amsterdam (1968).
12. F. K. Kneubuhl, *J. Chem. Phys.* 1960, **33**, 1074.
13. A. Abragam and M. H. L. Pryce, *Proc. Roy. Soc.* 1951, **A206**, 164.
14. *Idem, Ibid.* 1951, **205**, 135.
15. D. Poddar, *Physica* 1942, **9**, 709.
16. D. W. Smith, *J. Chem. Soc. A* 1970, 3108.
17. B. J. Hathaway and D. E. Billig, *Coord. Chem. Rev.* 1970, **5**, 143.
18. B. J. Hathaway, *Essay in Chemistry* (Edited by J. N. Bradley and R. D. Gillard), p. 61. Academic Press, New York (1971).
19. B. J. Hathaway, R. J. Dudley and P. Nicholls, *J. Chem. Soc. A* 1968, 1845.
20. (a) R. J. Dudley and B. J. Hathaway, *J. Chem. Soc.*

A 1970, 1725. (b) B. Bleaney and K. D. Bowers, *Proc. Roy. Soc.* (*London*) 1952, **A214**, 451.
21. K. Nakamoto, *Infrared and Raman Spectra of Inorganic and Coordination Compounds*, 2nd Edn. Wiley-Interscience, New York (1978).
22. L. Sacconi, *Transition Metal Chemistry* (Edited by R. L. Carlin), p. 221. Marcel Decker, New York (1968).
23. C. J. Ballhausen and C. J. Jorgenson, *Kgl. Donske Vindenskab Selskab. Met. Esy. Medd.* 1955, **29**, 14.
24. R. Barbucci and A. Bencini and D. Gatteschi, *Inorg. Chem.* 1977, **16**, 2117.
25. A. Bencini and D. Gatteschi, *Inorg. Chem.* 1977, **16**, 1994.
26. M. F. El-Shazly, A. El-Dissowky, T. Salem and M. Osman, *Inorg. Chem. Acta* 1980, **40**, 1.

Polyhedron Vol. 4, No. 1, pp. 169–172, 1985
Printed in Great Britain.

0277–5387/85 $3.00 + .00
© 1985 Pergamon Press Ltd.

MAGNETIC PROPERTIES AND OPTICAL SPECTRA OF CINCHONINIUM TETRACHLOROCOBALTATE(II)

K. DYREK* and M. DYREK
Faculty of Chemistry, Jagiellonian University, Karasia 3, 30–060 Cracow, Poland

and

A. WESEŁUCHA-BIRCZYŃSKA
Regional Laboratory of Physicochemical Analyses and Structural Investigations, Karasia 3, 30–060 Cracow, Poland

(*Received* 5 *September* 1983; *accepted after revision* 16 *April* 1984)

Abstract—Distorted tetrahedral symmetry of cobalt in cinchoninium tetrachlorocobaltate(II) ($C_{19}H_{24}ON_2[CoCl_4].2H_2O$) has been postulated on the basis of reflectance spectra, magnetic moment measurements and ESR spectra. The covalent character of the metal–ligand bonds was inferred from the reflectance spectra. The presence of magnetic dipolar interactions was inferred from the ESR spectra.

The cinchonine dihydrochloride ($C_{19}H_{22}ON_2.2HCl$) forms crystalline compounds with tetrachloro-complexes of Co(II), Cu(II), Zn(II), Cd(II) and Hg(II) of the general formula: $C_{19}H_{24}ON_2[MCl_4].2H_2O$ (where M—metal ion).[1] The IR spectra have shown the existence of interactions between the central ion and the two atoms of cinchonine molecule: oxygen atom in the hydroxyl group at the carbon atom joining the quinoline ring to quinuclidine one and nitrogen atom in the quinuclidine group.[1]

The crystallographic investigations pointed out that the complexes of Co(II), Zn(II), Cd(II) and Hg(II) are isomorphous.[2] The crystal structure of the complex of cadmium was solved by Oleksyn *et al.*[3] According to these authors the orthorhombic unit cell contains tetrachlorocadmate anion, cinchoninium cation and two water molecules. The authors observed some deviations from the ideal tetrahedral coordination at the central atom connected with the fact that two of the four chloride ions are involved in hydrogen bonds.

The aim of the present work was to obtain more precise information concerning distortion of the coordination tetrahedron and the type of interactions between ligands and central ion. From isomorphous series of the complexes the cinchoninium tetrachlorocobaltate(II) was chosen as an object of magnetic and optical investigations.

*Author to whom correspondence should be addressed.

EXPERIMENTAL

The polycrystalline cinchoninium tetrachlorocobaltate(II) was prepared as described in Ref. 1. The Co(II)-complex diluted with isostructural Zn-complex was obtained by evaporation of the water solution of both complexes mixed in the appropriate ratio.

Reflectance spectra were recorded with a Beckman DK 2A spectrophotometer in the range of 200–2500 nm with $BaSO_4$ as a standard. Magnetic susceptibility measurements were performed in the temperature range 4–350 K using a Faraday balance. ESR spectra were recorded at 4 K and at 77 K using an ESR spectrometer (constructed at the Technical University, Wrocław, Poland) operating in X-band with modulation frequency 100 kHz.

RESULTS AND DISCUSSION

In the reflectance spectrum of the cinchoninium tetrachlorocobaltate(II) the bands appear at 5410 cm^{-1} (ν_2) and at 15015 cm^{-1} (ν_3) (taken at the centre of the bands) (Fig. 1)—assigned to the transitions: $^4A_2 \rightarrow {}^4T_1(F)$ and $^4A_2 \rightarrow {}^4T_1(P)$, respectively—which indicates the tetrahedral coordination of Co(II).[4] The values of crystal field parameter $\Delta_{tetra} = \nu_1[^4A_2 \rightarrow {}^4T_2(F)]$ and Racah parameter B′ were estimated using the relations derived by Cotton and Goodgame.[5] The value of crystal field splitting Δ_{tetra} is equal to 3090 cm^{-1}. The Racah parameter B′ has a value of about

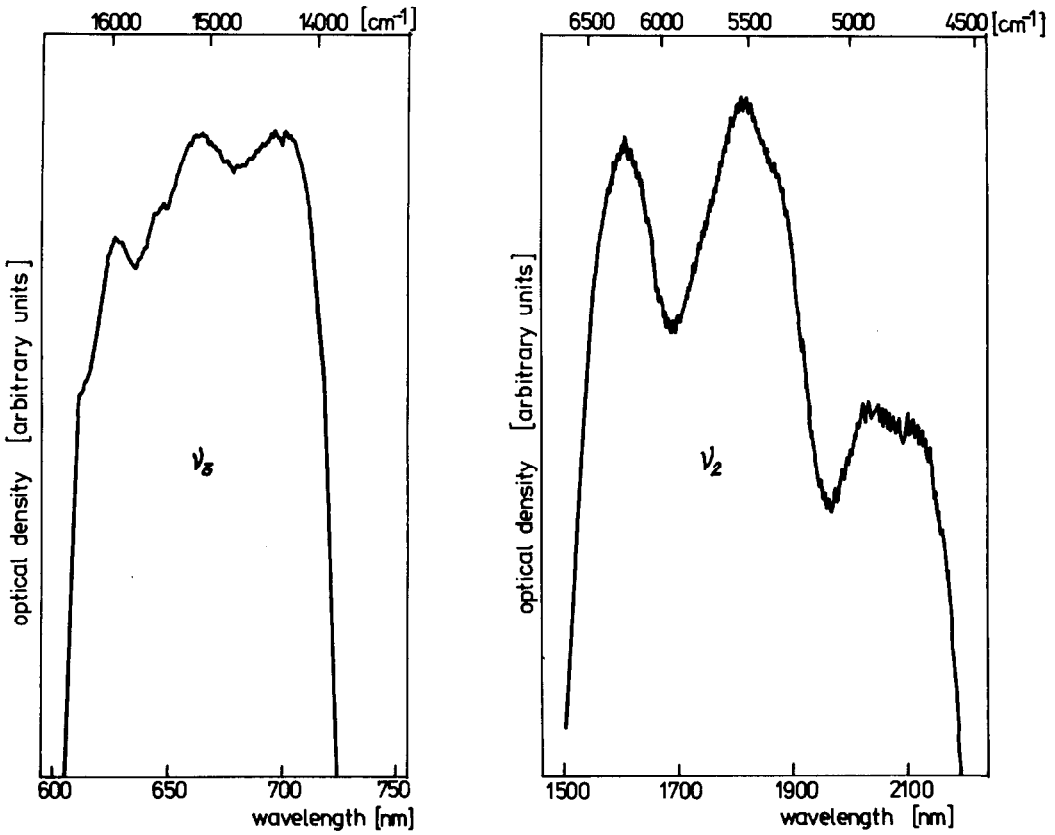


Fig. 1. Reflectance spectrum of cinchoninium tetrachlorocobaltate(II) in the range of transitions: $\nu_2[^4A_2 \rightarrow {}^4T_1(F)]$ and ν_3 $[^4A_2 \rightarrow {}^4T_1(P)]$.

745 cm^{-1} which represents an appreciable reduction from the free-ion value[6] B = 980 cm^{-1} and indicates significant covalent character of the metal-ligand bonds. This conclusion corroborates the suggestion of Oleksyn *et al.*[4] concerning formation of hydrogen bonds between chloride ions present in the first coordination sphere of Co^{2+} and protons from cinchoninium cation and water molecules. Indeed, the bonding of protons to chloride ions results in lowering of their electronegativity and in consequence changes the character of metal–ligand bonds into more covalent.

The absorption band ν_2 reveals a structure which may be due to the spin-orbit coupling and/or to the lowering of the site symmery of Co^{2+} ion. As shown by Ferguson[7] two limiting cases may be considered: 1st, the spin-orbit splitting is dominating over the splitting by the low symmetry crystal field; 2nd, the low symmetry crystal field splitting is large as compared with the spin-orbit splitting. In the first case the combined effect of the tetrahedral crystal field and the spin-orbit coupling results in splitting of the $^4T_1(F)$ term into four states. In the second case three components are obtained from the $^4T_1(F)$ term due to the strong interaction with low symmetry crystal field. Each of these components is then split into two levels by the spin-orbit coupling.

The absorption band ν_2 is split into three components and corresponds to the case for which low symmetry crystal field splitting is greater than spin-orbit splitting. The low energy component of the ν_2 band reveals an additional splitting, most probably related to the spin-orbit coupling. The absorption band ν_3 is more complicated, due to the contribution of the transitions between quartet ground state and the levels originating from the doublet terms of higher energy.

Further information concerning symmetry of the environment of the central Co(II) ion can be obtained from measurements of magnetic susceptibility. The plot of reciprocals of magnetic susceptibility corrected for diamagnetism ($\chi_{dia} = -335 \times 10^{-6}$ c.g.s.u.)[8] and for temperature independent paramagnetism ($\chi_{t.i.p.} = 8N\mu_\beta^2/\Delta_{tetra} = 675 \times 10^{-6}$ c.g.s.u.,[9] where N = Avogadro's number, μ_β = Bohr magneton, $\Delta_{tetra} = 3090$ cm^{-1}—crystal field splitting calculated from reflectance spectra) vs absolute temperature is a straight line with θ value close to zero. The μ_{eff} value, equal to 4.59 μ_β, confirms tetrahedral coordination of Co^{2+}.[10]

In the ESR spectrum of the Co(II)-complex taken at 4 K an asymmetric signal appears with g-factors: 5.610 ± 0.005 and 2.138 ± 0.005 for the low field and high field component, respectively (Fig. 2, solid line). At 77 K the signal is strongly broadened. Narrowing of the signal and good resolution of its components may be achieved by dilution of the cinchoninium tetrachlorocobaltate(II) with an isostructural Zn-complex. The dashed line in Fig. 2 represents the signal of such complex (Co:Zn ratio 1:2) recorded at 4 K. All three features of the highly aniso-

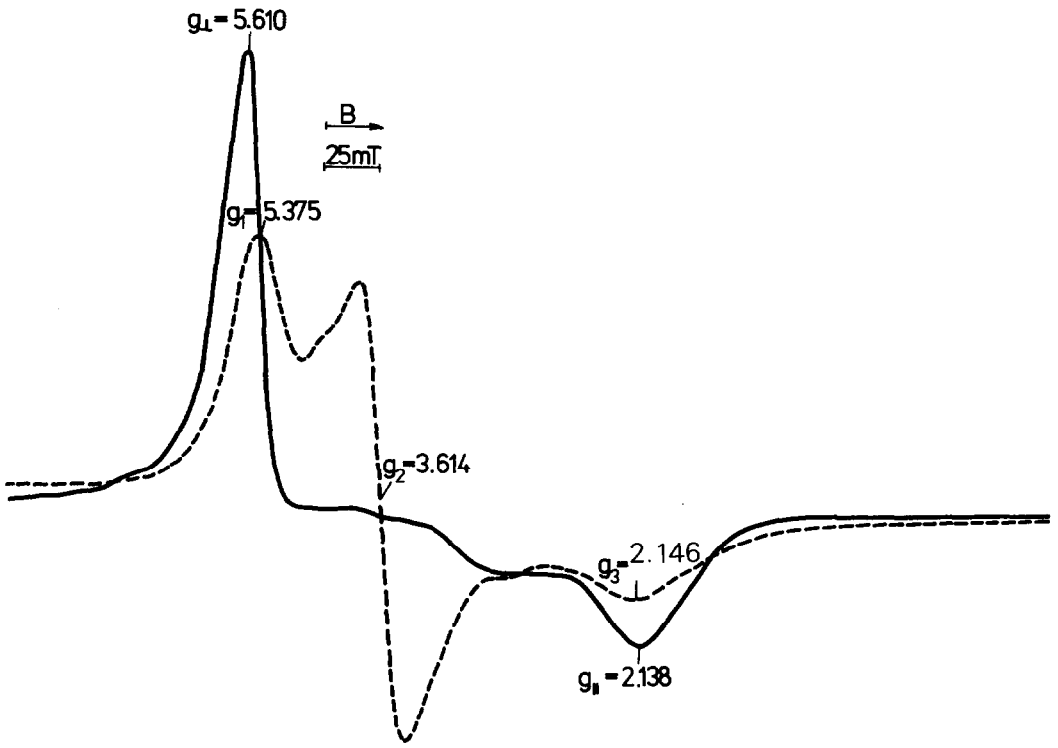


Fig. 2. ESR spectra of cinchoninium tetrachlorocobaltate(II) pure (—) and diluted with isostructural Zn(II) complex (----) in the molar ratio 1:2. Spectra taken at 4 K.

tropic ESR signal are well resolved with $g_1 = 5.375 \pm 0.005$, $g_2 = 3.614 \pm 0.005$, $g_3 = 2.146 \pm 0.005$, whereas in the pure Co(II)-complex the g_2 component is only slightly marked. Such changes in the shape and width of the ESR signal occurring upon dilution with the diamagnetic Zn-complex may be caused by weakening of the dipolar interactions between Co^{2+} ions.

The g-tensor values and the relaxation characteristics of the ESR signal of cinchoninium tetrachlorocobaltate(II) are very similar to those reported by Bencini *et al.*[11] for pseudotetrahedral high-spin complexes of Co(II) containing halides and phenylphosphine oxide or quinoline as ligands. The interpretation of single crystal data performed by these authors, based on the angular overlap model, allows us to assign the ESR spectra of Co(II)-complex to a $M_S = -1/2 \rightarrow +1/2$ transition of Co^{2+} in pseudotetrahedral environment, assuming nonparallel g- and D-tensors and large absolute value of the zero-field splitting.

The distortion of the $CoCl_4^{2-}$ tetrahedron, indicated by anisotropy of the ESR signal as well as by splitting of the ν_2 band in reflectance spectra may be related to the presence of cinchonine in the outer sphere of the complex. The interaction of cinchonine with Co^{2+} ion was shown by one of us previously[1] on the basis of IR spectra. This conclusion is in agreement with the model proposed by Oleksyn *et al.*[3]

Acknowledgements—The authors are greatly indebted to Professor M. Che, University Paris VI, France, for allowing measurements of reflectance spectra and to Mrs M. Chatry for taking the spectra. We wish to thank Professor P. Hagenmuller and Professor M. Pouchard, University of Bordeaux I, France, for allowing measurements of magnetic susceptibility and Dr. J-C. Grenier for the help in performing the measurements. We thank also Dr. H. Drulis, Institute for Low Temperature and Structure Research, Wrocław, Poland, for taking the ESR spectra at liquid helium temperature.

REFERENCES

1. M. Dyrek, *Rocz. Chem.* 1976, **50**, 2027.
2. (a) J. Chojnacki, B. Oleksyn and S. Hodorowicz, *Rocz. Chem.* 1975, **49**, 429. (b) B. Oleksyn, K. Stadnicka and S. Hodorowicz, *Rocz. Chem.* 1976, **50**, 1645.
3. B. Oleksyn, K. Stadnicka and S. Hodorowicz, *Acta Cryst.* 1978, **34B**, 811.
4. F. A. Cotton and G. Wilkinson, *Advanced Inorganic Chemistry*. p. 871, Interscience, New York (1967).
5. F. A. Cotton and M. Goodgame, *J. Am. Chem. Soc.* 1961, **83**, 1777.
6. A. Gołębiewski, Chemia kwantowa związków nieorganicznych (Quantum chemistry of inorganic compounds) p. 411. PWN, Warszawa, Poland (1969).
7. J. Ferguson, *J. Chem. Phys.* 1963, **39**, 116.

8. (a) W. Klemm, *Z. Anorg. Allg. Chem.* 1940, **244**, 377; 1941, **246**, 347. (b) *Landolt–Börnstein (Neue Serie)*, Gruppe 2, Bd. 2, Edit. Springer Verlag, Berlin (1966).
9. A. Earnshaw, *Introduction to Magnetochemistry*, p. 67. Academic Press, New York (1968).
10. A. Weiss and H. Witte, *Magnetochemie*, p. 178, Edit. Chemie, Weiheim, Germany (1973).
11. (a) A. Bencini and D. Gatteschi, *Inorg. Chem.* 1977, **16**, 2141. (b)A. Bencini, C. Benelli, D. Gatteschi and C. Zanchini, *Inorg. Chem.* 1979, **18**, 2137.

Polyhedron Vol. 4, No. 1, pp. 173–176, 1985
Printed in Great Britain.

0277–5387/85 $3.00 + .00
© 1985 Pergamon Press Ltd.

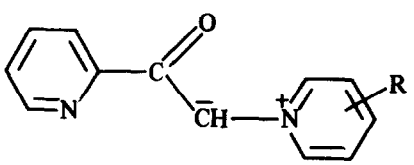
ELECTROCHEMICAL REDUCTIONS OF SUBSTITUTED PYRIDINIUM 2-PYRIDYLCARBONYLMETHYLIDES, THEIR Pt(II) COMPLEXES, AND SUBSTITUTED N-(2-PYRIDYLCARBONYL)METHYLPYRIDINIUM PERCHLORATES

GEN-ETSU MATSUBAYASHI* and KOSUKE UEYAMA
Department of Applied Chemistry, Faculty of Engineering, Osaka University, Yamada-oka, Suita, Osaka 565, Japan

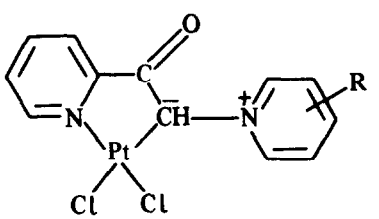
(*Received* 3 *January* 1984; *accepted* 16 *April* 1984)

Abstract—The title pyridinium salts and pyridinium ylide-platinum(II) complexes have been reduced through a one-electron process at more positive potentials by 0.3 ~ 0.6 V than the corresponding ylides. Both the reduced pyridinium salts and Pt(II)-ylide complexes reacted with dioxygen, followed by elimination of the *N*-methylene and ylide protons to form pyridinium ylides and Pt(II)-pyridinium ylide complexes containing the three-coordinate ylide carbon atom, respectively.

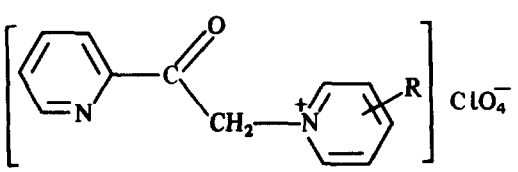
Reduction of pyridinium salts is of chemical as well as biological interest in relation to the behaviour of co-enzymes, NAD^+ and $NADP^+$. Although reductions of *N*-alkyl pyridinium salts have been widely investigated,[1] no attention has been paid to reductive behaviours of pyridinium compounds having an *N*-ylide bond and of related compounds. In the course of studies of pyridinium ylide-metal complexes[2–4] we have investigated the electrochemical reductions of substituted pyridinium 2-pyridylcarbonylmethylides (**I**), their dichloroplatinum(II) complexes (**II**), and substituted *N*-(2-pyridylcarbonyl)methylpyridinium perchlorates (**III**), together with substituted *N*-benzylpyridinium perchlorates (**IV**).



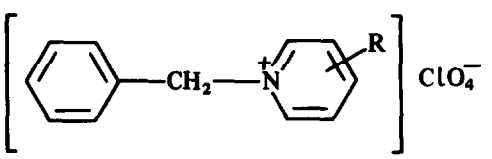
I



II



III



IV

*Author to whom correspondence should be addressed.

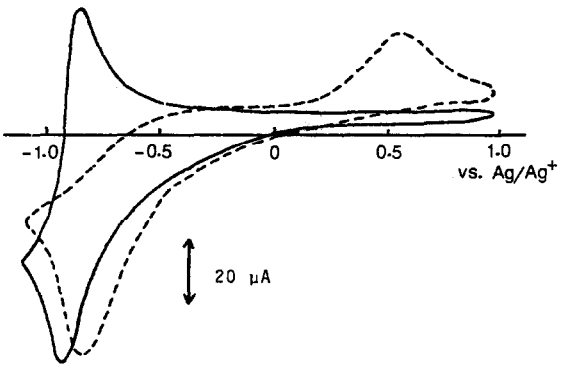


Fig. 1. Cyclic voltammetric scans of $Y_{CN}H$ under the nitrogen atmosphere (———) (a) and in the presence of dioxygen (------) (b) in acetonitrile (0.1 M[NBu^n_4]ClO_4); scan rate 0.5 V s^{-1}.

R	I	II	III	IV
4–CN	Y_{CN}	$Y_{CN}Pt$	$Y_{CN}H$	B_{CN}
4–C(O)Me	Y_{CM}	$Y_{CM}Pt$	$Y_{CM}H$	B_{CM}
4–C(O)OMe	Y_{AC}	$Y_{AC}Pt$	$Y_{AC}H$	B_{AC}
4–Me	Y_{ME}	$Y_{ME}Pt$	$Y_{ME}H$	B_{ME}
3,5–Me_2	Y_{LU}	$Y_{LU}Pt$	$Y_{LU}H$	

Figure 1(a) shows a cyclic voltammetric scan of $Y_{CN}H$ in acetonitrile under the nitrogen atmosphere. A reversible cathodic peak appears at −0.94 V vs Ag/Ag^+. The coulometry at this potential indicated that the wave corresponds to a one-electron reduction process. A cyclic voltammetric scan of B_{CN} also exhibited a reversible one-electron reduction wave at nearly the same potential (see Table 1). Thus, the reduction seems to be active in the pyridinium rings. Although $Y_{CM}H$ and $Y_{AC}H$ as well as B_{CM} and B_{AC} also gave essentially reversible redox waves, $Y_{ME}H$, $Y_{LU}H$, and B_{ME} exhibited irreversible reduction waves. On the other hand, all the ylides exhibited irreversible reduction peaks at more negative potentials because of electron-rich carbanion groups bound with the pyridinium nitrogen atom.

In the presence of dioxygen (O_2) the cyclic voltammetry of $Y_{CN}H$ gave an irreversible reduction peak at −0.85 V and the appearance on the return sweep of an anodic peak at +0.58 V (Fig. 1b). This anodic peak potential was identical with the peak potential for an oxidation of Y_{CN}. Moreover, the electronic absorption spectrum measured under the controlled potential electrolysis at −0.95 V for $Y_{CN}H$ displayed a new band at 494 nm whose intensity increased with performing the electrolysis. This band is identical with that of Y_{CN}. The reduced pyridinium salt is reasonably considered to react with O_2 immediately to form O_2^- and the pyridinium salt, as was seen in reactions of N,N' - dimethyl - 4,4' - bipyridinium radical with O_2.[5] Thus, the basic O^{2-} may eliminate the N-methylene proton of $Y_{CN}H$ to yield Y_{CN} (Scheme).

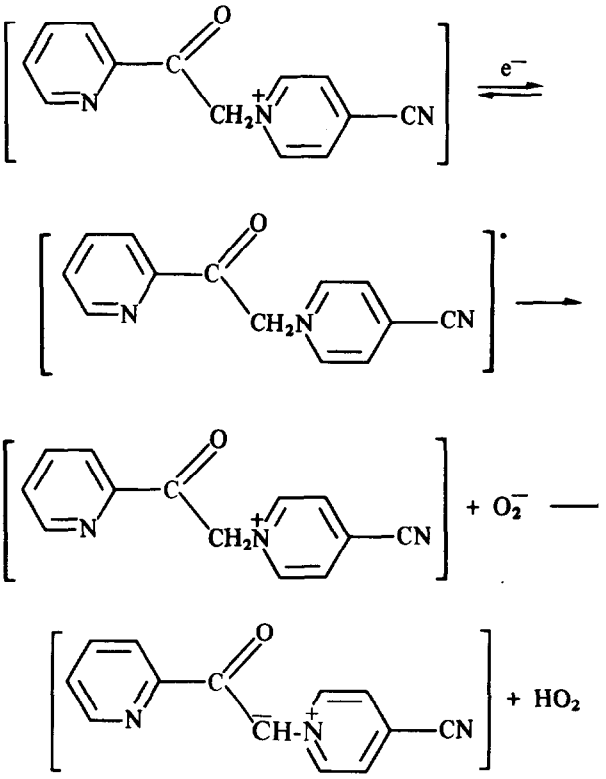


Table 1. Cathodic peak potentials of cyclic voltammetry[a] and peak separations in parentheses[b]

R	CN	CM	AC	ME	LU
Y_R	-1.50(-)	-1.44(-)	-1.61(-)	-2.02(-)	
Y_RPt	-1.14(60)	-1.17(70)	-1.26(60)	-1.50(-)	
Y_RH	-0.94(60)	-1.00(110)	-1.07(70)	-1.60(-)	-1.70(-)
B_R	-0.93(60)	-1.00(60)	-1.06(60)	-1.70(-)	

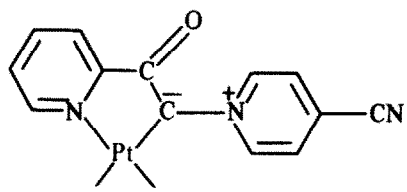
a) V vs. Ag/Ag^+ in acetonitrile. b) mV and (-) indicates irreversible reduction waves.

Table 2. IR carbonyl stretching frequencies of substituted pyridinium 2-pyridylcarbonyl-methylides and related compounds in Nujol mulls (cm^{-1})

R	CN	CM	AC	ME	LU
Y_R	1531	1510	1500	1529	1530
Y_RPt	1685	1695	1690	1694	1696
Y_RH	1705	1705	1715	1701	1721

An acetonitrile solution of $Y_{LU}H$ giving an irreversible cathodic peak at -1.70 V was electrolyzed at -1.30 V in the presence of O_2 to exhibit an absorption band at 450 nm ascribable to Y_{LU}. This finding suggests that O_2^- eliminates the N-methylene proton of $Y_{LU}H$ to yield Y_{LU}, since O_2 is reduced to O_2^- at -1.30 V in acetonitrile.[6] Moreover, an acetonitrile solution containing both $Y_{LU}H$ and B_{CN} was electrolyzed at the controlled reduction potential B_{CN} (-1.00 v) in the presence of O_2 to given the absorption band due to Y_{LU}, which also indicates the same proton-elimination by O_2^- formed by the reaction of the reduced B_{CN} with O_2.

The Pt(II)-ylide complexes (II) showed the IR ν(C=O) bands at $160 \sim 190\ cm^{-1}$ higher frequencies than the free ylides, indicating the ylide carbon-to-platinum bonding of II (Table 2).[2,3] The electronic configuration of the ylide carbon atom in Y_RPt seems to be close to that in the corresponding Y_RH, since the latter compounds are regarded as ones where the ylide carbon atom of a corresponding ylide is linked with proton instead of the metal ion. In fact, cyclic voltammograms of Y_RPt under nitrogen atmosphere exhibited quite a similar reduction behaviour to that of Y_RH. However, cathodic peak potentials of Y_RPt (R = CN, CM, and AC) are somewhat more negative than those of the corresponding Y_RH. This seems to be due to weaker electron-withdrawing effect of the Pt(II) ion than proton, which is noticed also in lower ν(C=O) frequencies of Y_RPt than those of Y_RH (Table 2). Although a cyclic voltammogram of $Y_{CN}Pt$ in acetonitrile showed a cathodic peak at -1.14 V owing to the reversible one-electron reduction, in the presence of O_2 the reversible reduction wave was changed to an irreversible one, followed by the occurrence of an anodic peak at -0.26 V. The visible absorption spectrum observed for $Y_{CN}Pt$ under the controlled potential electrolysis at -1.14 V showed a new band at 669 nm. This finding resembles that observed for the electrically reduced $Y_{CN}H$. Assuming that the one-electron reduced $Y_{CN}Pt$ complex also is oxidized by O_2 and that the ylide proton is eliminated by O_2^-, the band at 669 nm may be ascribed to the new Pt(II)-ylide complex (V) having the three-coordinate ylide carbon. The ylide proton of $Y_{CN}Pt$



V

can be expected to be eliminated by bases. In fact, we have confirmed that addition of an excess of triethylamine or ethylenediamine to Y_{CN} in acetonitrile showed an absorption band at the same wavelength as the above-mentioned electrolysis of the complex in the presence of O_2. Moreover, the three-coordinate (sp^2) geometry of the ylide carbon ligating platinum has been confirmed by the X-ray analysis of $[(C_5H_4NC(O)CNC_5H_3Me_2\text{-}3,5)(NH_2CH_2CH_2NH_2)Pt(II)]^+ClO_4^- \cdot 2H_2O$ which was prepared by the reaction of $Y_{LU}Pt$ with ethylenediamine.[7] This complex showed an absorption band at 572 nm in acetonitrile which was the same as the band maximum observed under the controlled potential electrolysis of $Y_{LU}Pt$ at -1.70 V in acetonitrile in the presence of O_2.

EXPERIMENTAL

Materials

Substituted pyridinium 2-pyridylcarbonylmethylides (I) were prepared according to the literature methods.[3] Substituted N-(2-pyridylcarbonyl)methylpyridinium perchlorates (III) were prepared by reactions of 2-(bromoacetyl)pyridinium bromide[9] with corresponding substituted pyridines in benzene, followed by exchange of the bromide ion with the perchlorate ion and recrystallized from water. Substituted N-benzylpyridinium perchlorates (IV) were prepared by reactions of benzylbromide with substituted pyridines in benzene, followed by the procedures described for compounds (III).

Preparation of dichloro(substituted pyridinium 2-pyridylcarbonylmethylide)Pt(II) (II)

A dichloromethane (30 cm^3) solution of dichlorobis(dimethylsulphide)Pt(II)[10] (0.18 g, 50 mmol) was added dropwise to Y_{CN} (0.11 g, 50 mmol) in the same solvent (30 cm^3) and the solution was stirred for 2 hr. A yellow precipitate of $Y_{CN}Pt$ was collected by filtration, washed with dichloromethane, and dried *in vacuo* (0.19 g, 74% yield); m.p. 273°C (dec.). Found: C, 31.37; H, 1.70; N, 8.47%. Calc. for $C_{13}H_9N_3OCl_2Pt$: C, 31.88; H, 1.85; N, 8.58%. The salts, $Y_{AC}Pt$ and $Y_{CM}Pt$, were also prepared in the same way. $Y_{AC}Pt$, m.p. 266°C (dec.). Found: C, 32.54; H, 2.52; N, 5.52%. Calc. for $C_{14}H_{12}N_2O_2Cl_2Pt$: C, 33.18; H, 2.39; N, 5.53%. $Y_{CM}Pt$, m.p. 229°C (dec.). Found: C, 31.34; H, 2.18; N, 5.09%. Calc. for $C_{14}H_{12}N_2O_3Cl_2Pt$: C, 32.17; H, 2.31; N, 5.36%.

$Y_{ME}Pt$ and $Y_{LU}Pt$ were prepared according to the literature.[3]

Physical measurements

Cyclic voltammetric scans were performed using a Nikkokeisoku NPS-2 potentiosweeper, a Hokuto-denko HA-104 potentiostat, and a Riken-denshi F-3DP *xy* recorder. A Beckman-type platinum working electrode was used. An acetonitrile solution of 0.01 M $AgNO_3$ equipped with a Ag wire was the reference electrode and a platinum plate (2 × 2 cm^2) was the counter electrode. All cycles were recorded on 1×10^{-3} M compounds in acetonitrile solutions containing 0.1 or 0.05 M $[NBu^n_4][ClO_4]$ as a supporting electrolyte. Electronic and IR absorption spectra were recorded on Union-giken 401 and Hitachi 215 spectrophotometers, respectively.

REFERENCES

1. *Free Radicals in Biology*, (Edited by W. A. Pryor), Vol. II, p. Academic Press, New York (1976).
2. H. Koezuka, G. Matsubayashi, and T. Tanaka, *Inorg. Chem.* 1976, **15**, 417.
3. G. Matsubayashi and Y. Kondo, *J. Organomet. Chem.* 1981, **219**, 269.
4. I. Kawafune and G. Matsubayashi, *Inorg. Chim. Acta* 1983, **70**, 1.
5. C. L. Bird and A. T. Kuhn, *Chem. Soc. Rev.* 1981, 49.
6. D. T. Sawyer and J. S. Valentine, *Acc. Chem. Res.* 1981, **14**, 393.
7. G. Matsubayashi, K. Ueyama, and K. Nakatsu, *J. Organomet. Chem.* 1982, **240**, 103.
8. G. Matsubayashi, *Bull. Chem. Soc. Jpn.* 1981, **54**, 915.
9. G. R. Clemo, W. McG. Morgan, and R. Rapper, *J. Chem. Soc.* 1937, 965.
10. E. G. Cox, H. Saenger, and W. Wardlaw, *J. Chem. Soc.* 1934, 182.

Polyhedron Vol. 4, No. 2, pp. 177–200, 1985
Printed in Great Britain

0277–5387/85 $3.00 + .00
© 1985 Pergamon Press Ltd.

POLYHEDRON REPORT NUMBER 10

CARBON–HYDROGEN BOND ACTIVATION IN EARLY TRANSITION METAL SYSTEMS

IAN P. ROTHWELL
Department of Chemistry, Purdue University, West Lafayette, IN 47907, U.S.A.

CONTENTS

I. INTRODUCTION. 179

II. CH BOND ACTIVATION IN ALKYL GROUPS. 180
1. α-Hydride abstraction. 180
2. β-Hydride abstraction and benzyne formation. 181
3. γ-Hydrogen abstraction. 182
4. Activation of other CH bonds in alkyl groups. 182

III. CYCLOMETALLATION OF HETERO-ATOM DONOR LIGANDS..... 182
1. Activation of β-CH bonds in amido ligands. 182
2. γ-CH bond activation in dialkylamido and alkoxide ligands. 183
3. Distal CH bond activation in aryloxide ligands. 184

IV. MECHANISTIC ASPECTS OF INTRAMOLECULAR CH BOND ACTIVATION AT d^0-METAL CENTERS 188
1. Homolytic pathway. 188
2. Multicenter pathway. 191
(i) Ligand geometry. 193
(ii) Leaving group. 194
(iii) The metal. 195

V. INTERMOLECULAR CH BOND ACTIVATION 196
1. Mechanistic considerations. 196
2. Activation of aromatic CH bonds by benzyne intermediates. 197
3. Hydrocarbon activation by $C\overset{*}{p}_2Th(CH_2CMe_2CH_2)$. 200
4. Hydrocarbon activation by $C\overset{*}{p}_2LuR$(R=H, Me). 200

VI. CONCLUDING REMARKS. 200

I. INTRODUCTION

The search for mild, homogeneous ways of activating hydrocarbon CH bonds is one of the most challenging and intellectually stimulating problems facing organo-transition metal chemists today. Many reactions in which simple CH bonds are activated by interaction with soluble transition metal complexes have been reported in the last 20 years.[1–3] Some systems have been developed that can carry out the relatively mild functionalization (metallation) of even the most difficult hydrocarbon CH bond, i.e. that found in methane. However, most successes have been with the intermolecular activation of aromatic CH bonds and the intramolecular activation of a range of CH bond types in coordinated ligands.[4–6] These latter reactions, initially termed ortho-metallations but now generally referred to as cyclometallations, have allowed a great deal of controlled mechanistic studies to be carried out giving insight into how transition metals can activate such normally inert groups.

A mechanistic similarity exists for nearly all of the early systems that were developed.[1-6] In the case of cyclometallation reactions an oxidative–addition pathway involves the CH bond being added to the metal center to generate a hydride and chelated alkyl (aryl) function. In the case of metal centers such as Rh(I), Ir(I) and Pt(II) the addition occurs to a d^8 metal center to give a d^6, oxidized configuration which is then either stable or else undergoes reductive loss of the hydride with a leaving group. In other systems either reductive loss of ligands or a dissociation step (either thermally or photochemically induced) precedes the oxidative addition of the CH bond. The most extensively studied species capable of intermolecularly activating CH bonds in simple hydrocarbons are the transition metal polyhydrides and the Pt(II)/acid systems. In the platinum systems developed by a number of workers, activation of aromatic, benzylic and even aliphatic CH bonds takes place in complex, acidic mixtures as detected by catalyzed H/D exchange reactions.[7-9] The activation step involves oxidative-addition to a Pt(II) center; Pt metal and Pt(IV) salts being inactive under the reaction conditions. The polyhydride complexes, typified by Cp_2MH_3(M=Nb, Ta), involve initial reductive elimination of H_2 to generate the unsaturated, active species.[10] Compounds of this type can cause extensive H/D exchange in aromatic rings. Special mention must be made of some recently developed systems. Tungstenocene, generated either photochemically or thermally, has been shown to be active towards both aliphatic and aromatic CH bonds,[11] while the unsaturated iridium cyclopentadienyl intermediates developed by Bergman[12] and Graham[13] are very good at oxidatively adding hydrocarbons. The coupling of iridium complexes with readily hydrogenated olefins has allowed Crabtree to be able to mildly dehydrogenate saturated alkanes.[14] Again in these cases the act of CH bond activation involves an oxidative-addition pathway.

It must be pointed out that although the cyclometallation reaction is believed to proceed by an oxidative-addition pathway for Pt(II), the extensive and well studied cyclopalladation reaction almost certainly is electrophilic in nature.[15] Similarly the large number of oxidations and coupling reactions of aromatic compounds catalyzed by Pd^{2+} occurs via a predominantly electrophilic mechanism.[16]

Over the past 5 years a body of literature has developed in which a new type of hydrocarbon activation can be observed. Typically this involves early *d*-block, lanthanide or actinide elements in their highest formed oxidation states. For *d*-block elements the d^0-metal configuration precludes the oxidative-addition pathway characteristic of the vast majority of CH bond activations, either by the systems mentioned or by metal surfaces. Very recent and exciting work by Watson and Marks has shown that such systems are capable of activating even methane itself. Hence, it appears that a new and potentially very important type of hydrocarbon activation is emerging. This paper reviews the present literature on this subject, dealing both with the intramolecular metallation of ligands as well as the activation of "free" hydrocarbons themselves.

II. CH BOND ACTIVATION IN ALKYL GROUPS

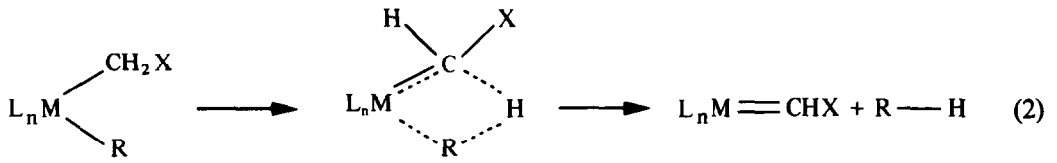
1. *α-Hydride abstraction*[17]

It might at first sight appear strange to find this important reaction included in a review of CH bond activation. However, from the purist's point of view it involves a cyclometallation reaction at a d^0-metal center to generate a two membered ring! The reaction has a number of characteistics found in more distal CH bond activations, except that the new metal–carbon bond that is formed is a π-bond. The classical (if one can consider a reaction only nine years old as classical) example of α-hydride abstraction is the initial reaction discovered by Schrock (1).[18]

$$Cl_2Ta(CH_2CMe_3)_3 + 2LiCH_2CMe_3 \rightarrow Ta(=CHCMe_3)(CH_2CMe_3)_3 + 2LiCl + Me_4C \qquad (1)$$

During the course of the reaction the α-CH bond is activated by the Ta(V) center and the hydrogen atom is lost from the complex with a leaving group, either Cl or R, to generate the alkylidene function. If one counts the alkylidene ligand as CR_2^{2-} then the tantalum maintains its highest oxidation state. It is not the purpose of this paper to review the extensive literature on α-hydride abstraction processes, a number of excellent reviews by Schrock being already available.[17] However, it is important to mention that theoretical studies by Hoffman *et al.*[19] have indicated that the course of the reaction proceeds through a concerted pathway in which the α-hydrogen is transferred to the leaving group with no net change in metal oxidation state throughout the course of the reaction.

A four-center transition state can be postulated in which metal–carbon and carbon–hydrogen bonds are being both broken and formed (2).



(2)

This proposed pathway is of direct relevance to the mechanisms of both more distal and intermolecular CH bond activations.

Recently a number of photochemically induced α-hydride abstractions on d^0-metal centers have been reported, e.g. (3),[20] (4)[21]

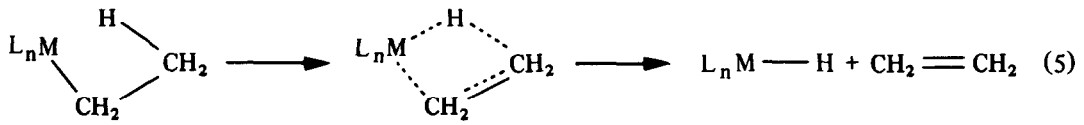
$$(OAr')_2Ta(CH_3)_3 \rightarrow (OAr')_2Ta(=CH_2)(CH_3) + CH_4 \quad (3)$$
$$(OAr' = 2,6\text{-di-}tert\text{-butylphenoxide})$$

$$(Bu^tN)_2Re(CH_2SiMe_3)_3 \rightarrow (Bu^tN)_2Re(=CHSiMe_3)(CH_2SiMe_3) + Me_4Si. \quad (4)$$

It is yet to be determined whether the thermal and photochemical activation of α-CH bonds are mechanistically related.

2. *β-Hydrogen abstraction and benzyne formation*

The abstraction of β-hydrogens from metal alkyl groups is a common decomposition pathway and can readily occur at d^0-metal centers.[22] However, the formation of an intermediate hydrido-olefin (which may or may not dissociate the olefin) must be considered a special case of CH bond activation as the alkyl group itself is acting as a unique type of leaving group (5).



(5)

Again a four-center transition state is the expected pathway for the reaction.

In contrast to this behavior the activation of β-(ortho) CH bonds of aryl groups has characteristics similar to more distal CH bond activations. Here the hydrogen does not remain on the metal but is lost with a suitable leaving group. A number of important examples of this reaction are known (6),[23] (7),[24] (8).[25]

$$Cp^*TaMe_3Ph \longrightarrow Cp^*Ta(C_6H_4)Me_2 + MeH$$



(6)

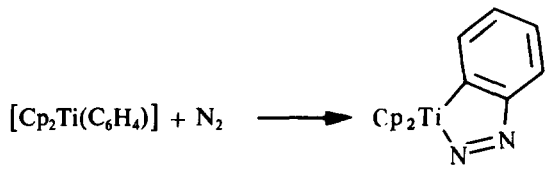
In the case of the tantalum complex the resulting benzyne (*o*-phenylene) group is sufficiently stable to be structurally characterized. The structural data is supportive of the idea that the ligand is best considered as $C_6H_4^{2-}$, i.e. the metal maintains a d^0-configuration.[23]

Two other examples involve the thermal generation of intermediate benzyne complexes from the bis-phenyl compounds $Cp_2M(C_6H_5)_2$ (M=Ti, Zr)(7) and $Cp^*_2U(C_6H_5)_2$ (8)

$$Cp_2Zr(C_6H_5)_2 \rightarrow [Cp_2Zr(C_6H_4)] + C_6H_6 \quad (7)$$

$$Cp^*_2U(C_6H_5)_2 \rightarrow [Cp^*_2U(C_6H_4)] + C_6H_6 \quad (8)$$

In both these cases the benzyne complex is too reactive to isolate, even reacting in the case of M=Ti with dinitrogen (9).[26]



(9)

The overall sequence of events can hence be considered the activation of the *ortho*-CH bonds and their eventual functionalization.

3. *γ-Hydrogen abstraction*

Unlike α- and β-hydrogen abstraction, the activation of γ-CH bonds in alkyl groups is generally recognized as being an example of *distal*-CH bond activation. The rationale for this thinking is that the metal is having minimal influence through the carbon chain on the CH bond being activated. Unfortunately, the effect that metal substituents have on γ-CH bonds, for instance, in neopentyl (CH_2CMe_3) or trimethylsilyl (CH_2SiMe_3) groups is not known. It is hence not possible to say whether metals such as Ta(V), Th(IV) or Pt(II) are electronically activating (or deactivating) these CH bonds. Metallation of these types of ligands at the γ-position has been observed both at dinuclear centers[27] and also in mononuclear complexes.[28] For the case of cyclometallation at Pt(II) (10) Whitsides *et al.* have carried out a thorough kinetic and mechanistic study.[29]

$$cis\text{-}Pt(PR_3)_2(CH_2CMe_3)_2 \rightarrow \overline{Pt(CH_2CMe_2CH_2)}(PR_3)_2 + CMe_4. \quad (10)$$

Only one example of the cyclometallation of these groups at d^0-metal centers has been reported. The complexes $C\overset{*}{p}_2ThR_2$(R=CH_2SiMe_3, CH_2CMe_3) undergo the smooth loss of one equivalent of Me_4X(X=C or Si) to generate a four-membered metallocycle (11.)[30]

$$C\overset{*}{p}_2Th(CH_2XMe_3)_2 \rightarrow C\overset{*}{p}_2\overline{Th(CH_2XMe_2CH_2)} + XMe_4 \quad (11)$$

In the case of X = Si the product was characterized by X-ray diffraction techniques. Kinetic data for the reactions showed they are unimolecular, and labelling studies showed that the γ-CH bonds are activated directly.[30]

4. *Activation of other* CH *bonds in alkyl groups*

The γ-CH bond represents the most distal part of alkyl ligands that have been activated intramolecularly. This is not surprising due to the tight restrictions that are placed on the structure of the ligand by the presence of other more facile reactions such as α- and β-hydrogen abstraction. There are numerous reactions reported in which the sp^2CH bonds of Cp co-ligands are activated to cleavage.[31] Use of the $C\overset{*}{p}(C_5Me_5)$ ligand normally reduces this type of reaction. However, in the case of the thermolysis of $C\overset{*}{p}_2TiMe_2$ Bercaw has shown that the product is obtained via initial α-hydrogen abstraction to generate a methylidene function which then activates and adds a CH bond of one of the $C\overset{*}{p}$-methyl groups.[32] Labelling studies clearly show that the generated methane does not contain hydrogen atoms from the $C\overset{*}{p}$-methyl groups (12).

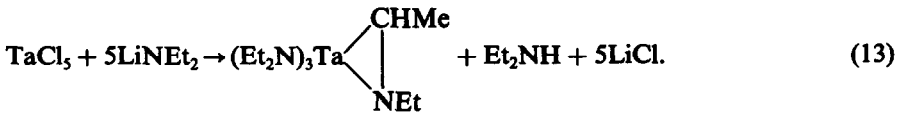
$$(C_5Me_5)_2Ti(CD_3)_2 \rightarrow [(C_5Me_5)_2Ti(=CD_2)] + CD_4 \rightarrow (C_5Me_5)(\eta^6\text{-}C_5Me_4CH_2)Ti\text{–}CD_2H \quad (12)$$

III. CYCLOMETALLATION OF HETERO-ATOM DONOR LIGANDS

1. *Activation of β-CH bonds in amido ligands*

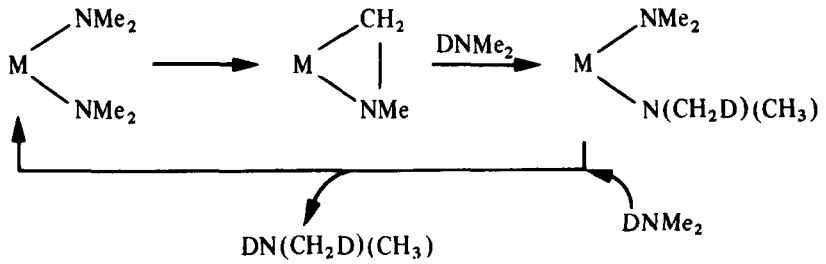
The dialkylamido ligand is an important group in early transition metal chemsitry. Its use as an ancillary ligand has made significant contributions to the isolation of metal complexes with low coordination numbers and complexes containing metal–metal bonds.[33,34] Unlike the extensive cyclometallation chemistry associated with amine complexes of the Gp VIII metals,[4-6] analogous reactions with early transition metals are less extensive. One of the first reactions reported in which

the β-CH bonds of dialkylamido groups is cleaved at a d^0-metal center involved in the treatment of $TaCl_5$ with $LiNEt_2$ (13).[35]



$$TaCl_5 + 5LiNEt_2 \rightarrow (Et_2N)_3Ta(CHMe)(NEt) + Et_2NH + 5LiCl. \quad (13)$$

Due to the large steric pressure around the metal atom, generation of amine occurs with metallation of the β-CH bond. More recent work by Nugent *et al.* has demonstrated that this type of reaction is in fact common for a number of d^0-metal dimethylamido complexes.[36] However, the generation of the iminomethyl group had to be inferred from its reactions. Hence, he has shown that $(CH_3)_2ND$ in the presence of $M(NMe_2)_x$ (M=Zr, x = 4; Nb, Ta, x = 5 and W, x = 6) undergoes catalytic scrambling of deuterium into the methyl groups This result can be explained if one proposes a reversible metallation of the dimethylamido group along with facile exchange of dimethylamine with coordinated dimethylamido groups (14).



$$M(NMe_2)_2 \rightarrow M(CH_2)(NMe) \xrightarrow{DNMe_2} M(NMe_2)(N(CH_2D)(CH_3)) \quad (14)$$

$$M(NMe_2)(N(CH_2D)(CH_3)) \rightarrow M(NMe_2)_2 + DN(CH_2D)(CH_3)$$

Furthermore, it was demonstrated that once formed the azametallocyclo-propane underwent facile insertion of olefins, allowing aminomethylation of olefins to be catalyzed by complexes of this type (15).

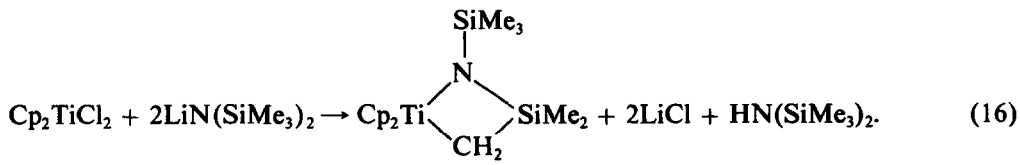
$$Me_2NH + CH_2{=}CHC_3H_7 \rightarrow MeNHCH_2C(Me)HC_3H_7. \quad (15)$$

Addition of $LiNMe_2$ to the complex $C\overset{*}{p}TaMe_3Cl$ initially generates the substitution product $C\overset{*}{p}Ta(NMe_2)Me_3$.[36b] However, at ambient temperatures this decomposes by loss of methane to generate the cyclometallated, imine complex (15a). A kinetic study showed a first order dependence with a kinetic isotope effect (k_H/k_D) of 9.7 at 34°C.[36b] when using $N(CD_3)_2$.

$$C\overset{*}{p}_2Ta(NMe_2)Me_3 \rightarrow C\overset{*}{p}Ta(NMeCH_2)Me_2 + MeH. \quad (15a)$$

2. γ-CH *bond activation in dialkylamido and alkoxide ligands*

The sterically very demanding ligand bis-(trimethylsilyl)amide, $N(SiMe_3)_2$, has received considerable attention due to its ability to impose low coordination numbers on a variety of transition metals.[33] It was demonstrated as early as 1974 by Bradley *et al.* that it was possible to activate the γ-CH bonds in this ligand leading to a cyclometallated product containing a four-membered ring (16). In this case the four-membered ring contains four different elements.[36c]



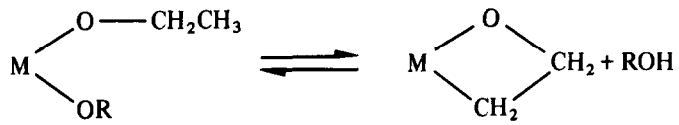
$$Cp_2TiCl_2 + 2LiN(SiMe_3)_2 \rightarrow Cp_2Ti(N(SiMe_3))(SiMe_2)(CH_2) + 2LiCl + HN(SiMe_3)_2. \quad (16)$$

Later work by Andersen has shown that both Zr(IV) and the actinide metal centers Th(IV) and U(IV) can similarly activate and metallate this bond. A reinvestigation of reaction (16) by this group has shown that the cyclometallation step probably occurs from a monosubstituted product $Cp_2TiCl[N(SiMe_3)_2]$ by loss of HCl.[36d] The zirconium analogue was prepared by addition of

$LiN(SiMe_3)_2$ to $Cp_2Zr(H)Cl$ to give the metallacycle directly. Presumably the leaving group in this case is the hydride ligand.[36d] In the case of the actinide systems,[37] it was shown possible to catalytically deuterate the $SiMe_3$ groups using D_2 (Scheme I). The catalytic cycle makes use of a hydride ligand as a leaving group for the metallation reaction coupled with the reverse hydrogenolysis of the metal–carbon bond so formed (Scheme I).

Thermal elimination of alkane from the complexes $R_2M(N(SiMe_3)_2]_2$ was shown to proceed with the loss of two hydrogens from the γ-carbon,[38] leading to a bridging alkylidene as shown (Scheme II). Presumably initial γ-CH bond activation is followed by α-hydride abstraction from the generated metallacycle. When equimolar mixtures of $Me_2Zr[N(SiMe_3)_2]_2$ and $Et_2Hf[N(SiMe_3)_2]_2$ were mixed and thermolyzed, a 1 : 2 : 1 mixture of dinuclear complexes containing Zr_2, ZrHf and Hf_2, respectively, was isolated.[39] Due to the dimeric nature of these products, confirmed by X-ray crystallography,[38] whether one or both of the hydrogen abstraction steps occurs intermolecularly is uncertain. On treatment with dmpe, the dimers both cleave and undergo a rearrangement to bis-cyclometallated complexes (Scheme II).[39] During the course of this reaction, the initially unmetallated amide ligand has transferred a γ-hydrogen to the initially bridging alkylidene group. The fact that the analogous titanium complex does not undergo the same thermal reactions is good support for the idea that the reaction does not involve a radical pathway (*vide infra*).

Early transition metal ethoxides have been shown to be active catalysts for H/D exchange in CH_3CH_2OD.[36] Deuterium is incorporated exclusively into the methyl group. The reversible formation of a four membered metallocycle was proposed (17), with a reverse alcoholysis of the metal–carbon bond formed. An intriguing observation was that multiple exchange occurred,[36] implying that α-hydride abstraction from the metallocycle was somehow taking place.



(17)

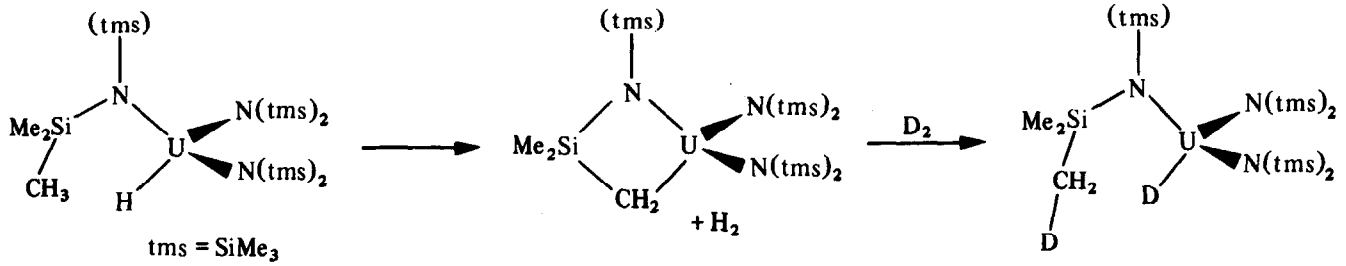
3. *Distal* CH *bond activation in aryloxide ligands*

The ligand 2,6-di-*tert*-butylphenoxide (OAr′) has been shown to undergo cyclometallation at a number of early transition metal centers. In the case of tantalum, introduction of the ligand onto the metal by way of its lithium salt yields the tri-chloro compound shown by X-ray diffraction to be mononuclear.[40] Treatment of this compound with methyl lithium gives the expected substitution product $Ta(OAr')_2Me_3$ (Fig. 1) (18).[41]

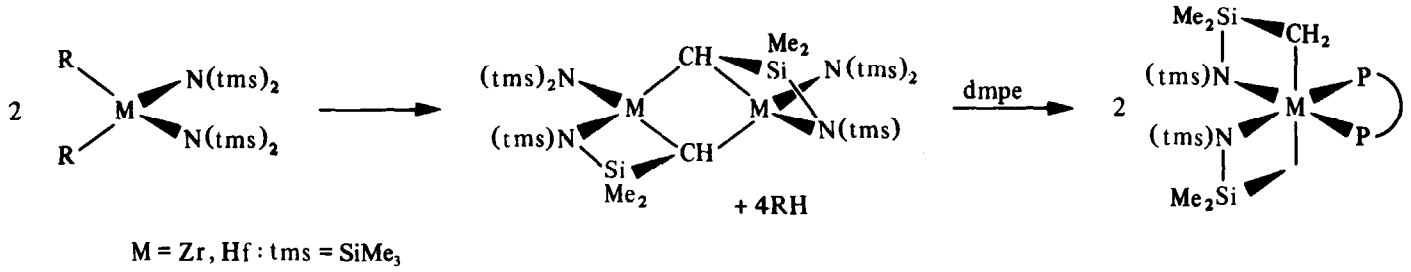
$$TaCl_5 \xrightarrow{2LiOAr'} Ta(OAr')_2Cl_3 \xrightarrow{3LiMe} Ta(OAr')_2Me_3. \qquad (18)$$

On thermolysis this complex undergoes the smooth loss of first one and then a second equivalent of methane to generate the mono-cyclometallated and bis-cyclometallated compounds (Scheme III).[42] The cyclometallation involves the activation and cleavage of an α-CH bond to generate a six-membered metallocycle. Labelling studies using $Ta(OAr')_2(CD_3)_3$ show that the methane comes from direct loss of the leaving group with the activated hydrogen, giving CD_3H.[43] Kinetic data show that both steps of the reaction are unimolecular.[44] In contrast to these thermal reactions, the photolysis of the tri-methyl complex leads to the rapid and efficient formation of a methylidene complex with loss of one equivalent of methane (3). At 25°C over a period of a few hours this complex "isomerizes" to the mono-cyclometallated species.[20] This step is intriguing as it demonstrates that alkylidene groups, apart from their known importance in olefin metathesis[45] and implied involvement in olefin polymerization,[46] can be active functional groups for aliphatic CH bond activation. The CH bond is "added" to the tantalum–carbon double bond, and in some respects represents the reverse of an α-hydride abstraction.[17] Labelling studies clearly differentiate the thermal and photochemical routes to the mono-metallated complex (Scheme IV).

Addition of $LiCH_2SiMe_3$ to $Ta(OAr')_2Cl_3$ leads directly to an alkylidene complex (Fig. 2).[41,43] On thermolysis this complex again undergoes cyclometallation of the aryloxide groups, although in this case no intermediate mono-metallated complex could be isolated.[43] Hence, three possible pathways for the reaction exist (Scheme V). However, irrespective of which pathway is operative one of the steps must again involve addition of the aliphatic CH bond to an alkylidene group.



Scheme I. Reversible cyclometallation of the ligand $N(SiMe_3)_2$ on uranium allowing deuteration of the CH_3 groups (from Ref. 37).



M = Zr, Hf : tms = $SiMe_3$

Scheme II. Thermal metallation behavior of the complexes $R_2M[N(SiMe_3)_2]_2$ (M = Zr, Hf) (from Refs. 38 and 39).

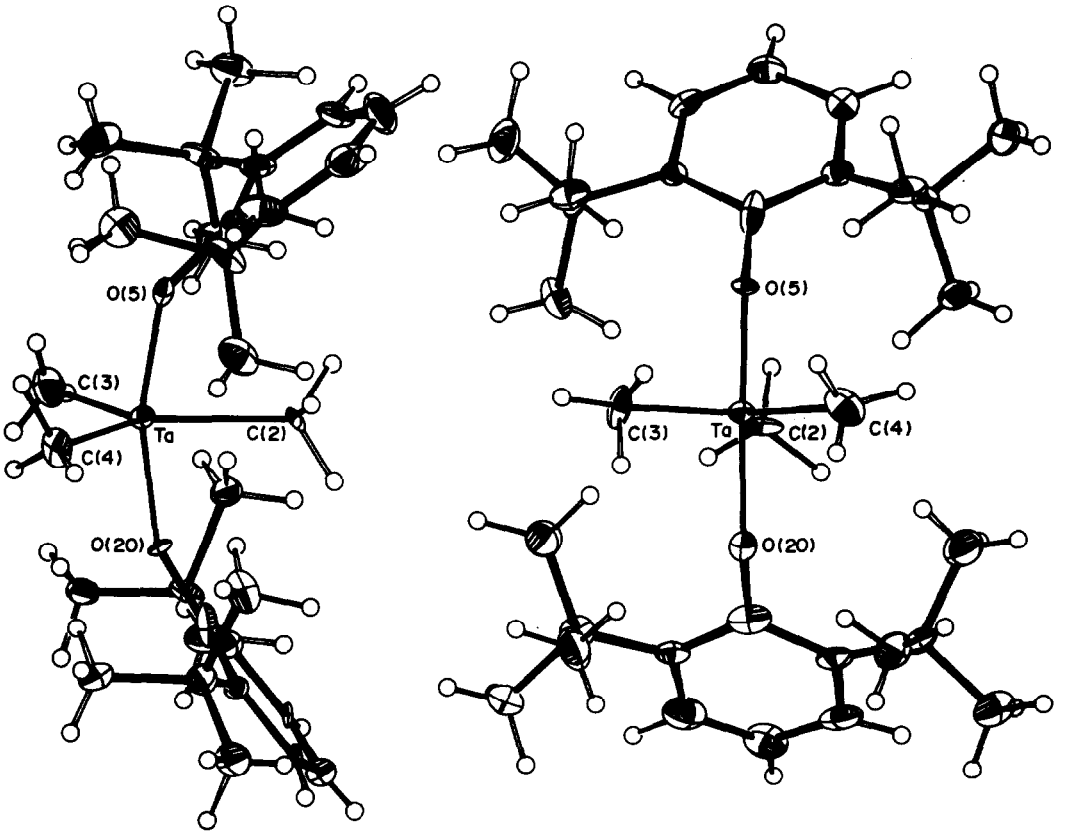
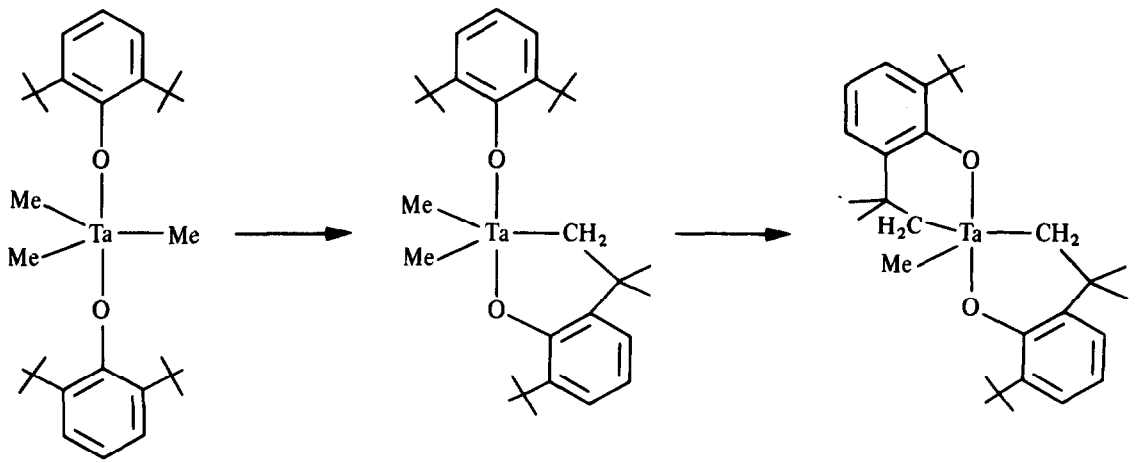
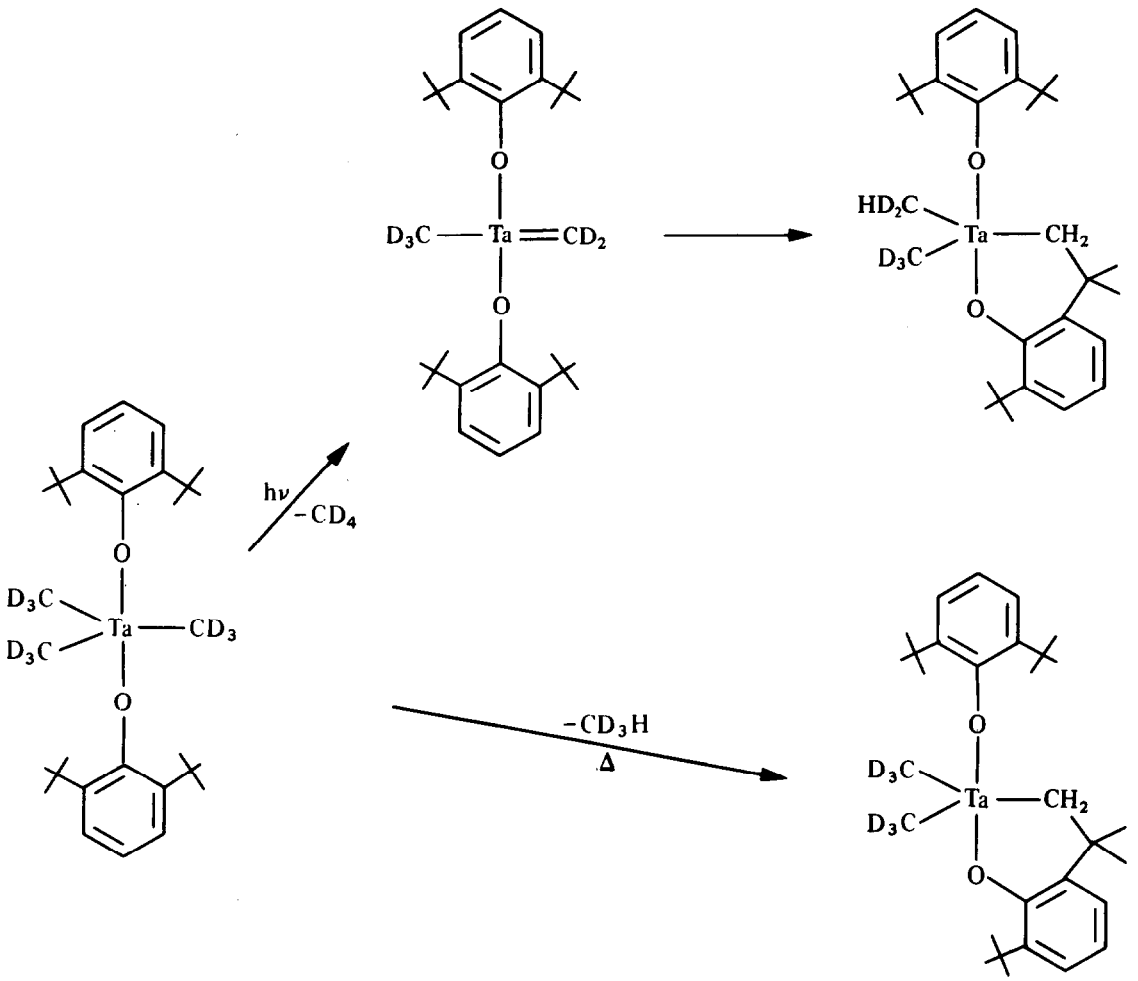


Fig. 1. Two ORTEP views of the molecule $Ta(OAr')_2Me_3$ showing the distorted tbp geometry and relatively close approach of ϵ-CH bonds. Some pertinent bond distances (Å) and angles (°) are: Ta–O = 1.94(av), Ta–C(3) = 2.136(10), Ta–C(4) = 2.138(10), Ta–C(2) = 2.248(10), O–Ta–O = 164.1(2), C(3)–Ta–C(4) = 104.7(4).

The treatment of $Ta(OAr')_2Cl_3$ with phenyl-lithium leads directly to a mono-metallated complex which has been structurally characterized (Fig. 3).[43] Presumably this facile metallation occurs from a tri-phenyl complex, although it is possible that loss of HCl or benzene occurs from an intermediate compound $Ta(OAr')_2(Ph)_2Cl$. On thermolysis the mono-metallated compound undergoes loss of one equivalent of benzene and formation of a bis-metallated species. The structure of this complex can be readily deduced from its ^1H NMR spectrum (Fig. 4).[47]



Scheme III. Thermal activation of the ϵ-CH bonds in $Ta(OAr')_2Me_3$, OAr' = 2,6-di-*tert*-butylphenoxide (from Ref. 42).



Scheme IV. Comparison of the thermal and photochemical reactivity of $Ta(OAr')_2Me_3$, OAr' = 2,6-di-*tert*-butylphenoxide (from Ref. 20).

If *o*-tolyllithium is used in the reaction then the initial product is $Ta(OCH_2)(OAr')(o\text{-tol})_2$ (OCH_2 = cyclometallated OAr'). However, on thermolysis the bis-metallated product contains a mixture of *meta*- and *para*-tolyl groups, the aryl ligand having undergone isomerization.[47] The obvious explanation for this result is the intermediacy of a benzyne complex which rapidly undergoes insertion of the aliphatic CH bond. This idea breaks down when one realizes that it is impossible for an *o*-tolyl group to isomerize to a *p*-tolyl through only one intermediate, it needs two benzyne complexes to be formed successively. Furthermore, the aryl group was shown to undergo isomerization in the bis-cyclometallated product itself, a 50/50 mixture of *p*- and *m*-tolyl groups being given irrespective of the isomer initially used.[47] These results can be explained if the bis-cyclometallated complex is in equilibrium with a mono-metallated benzyne complex at high temperature (Scheme VI). Use of LiC_6D_5 conclusively shows that the benzyne complex is only formed once bis-metallation has taken place. At high temperatures the deuterium label is scrambled statistically over all aliphatic and Ta–Ph positions as a result of the equilibrium in Scheme VI.[47] Although attainable only at high temperature, the equilibrium demonstrates in the ring closure that activation of aliphatic CH bonds is possible by insertion into one of the metal–carbon bonds of a benzyne (*o*-phenylene) ligand.

Thermolysis of the complexes $M(OAr')_2(CH_2Ph)_2$(M=Ti, Zr) (Fig. 5) leads to the loss of one equivalent of toluene and formation of a mononuclear, monometallated compound (Scheme VII).[48] This behavior contrasts with the case of the γ-CH activation of the $N(SiMe_3)_2$ ligands which led to dinuclear complexes with loss of two equivalents of alkane (Scheme II). If the tetraalkyl $M(CH_2SiMe_3)_4$(M = Ti, Zr) is heated with excess Ar'OH, the mono-metallated, bis-aryloxide

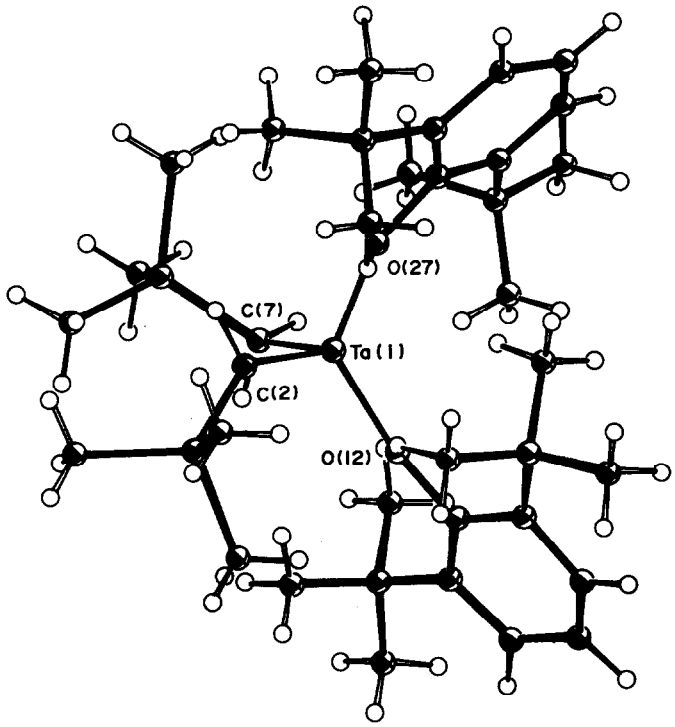


Fig. 2. An ORTEP view of $Ta(OAr')_2(=CHSiMe_3)(CH_2SiMe_3)$ showing the pseudo-tetrahedral environment and almost linear Ta–O–C angles. Some pertinent bond distances (Å) and angles (°): Ta–O = 1.86(av), Ta–C(2) = 1.888(29), Ta–C(7) = 2.165(24), Ta–O–C = 170(av).

complex $\overline{M(O–CH_2)}(OAr')_2$ is generated (Scheme VII). The stage at which alkane loss and cyclometallation occurs is unknown. However, the fact that the previous complex reacts with Ar'OH to give an identical product indicates the intermediacy of $M(OAr')_2(CH_2SiMe_3)_2$.[48] If only two equivalents of HOAr' is heated with $Ti(CH_2SiMe_3)_4$ a complex mixture is given. From this mixture a series of complexes $\overline{Ti(O–CH_2)}(OAr')(CH_2SiMe_3)(L)$ (L = neutral donor ligand) can be precipitated by addition of excess L in hexane. For L = pyridine an X-ray diffraction study clearly shows the presence of the cyclometallated chelate (Fig. 6). Although the complex $\overline{Zr(O–CH_2)}(OAr')_2$ reacts with HCl to give the mono-halide $Zr(OAr')_3Cl$ all attempts to reverse this reaction, (19), i.e. cyclometallation with loss of HCl, have failed.

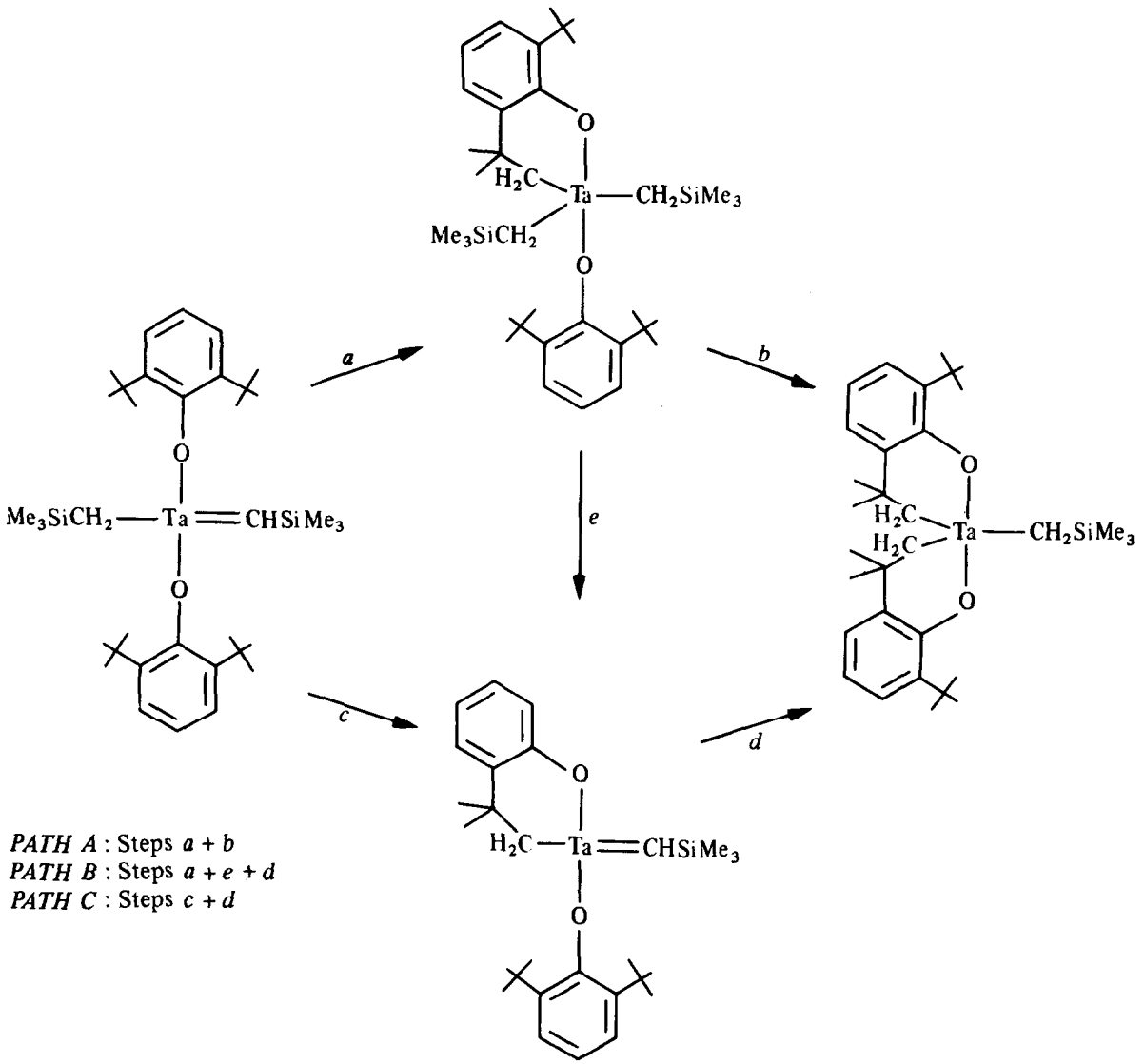
$$\overline{Zr(OC_6H_3Bu^tCMe_2CH_2)}(OAr')_2 + HCl \rightarrow Zr(OAr')_3Cl. \quad (19)$$

IV. MECHANISTIC ASPECTS OF INTRAMOLECULAR CH BOND ACTIVATION AT d^0-METAL CENTERS

The elucidation of the mechanism of these cyclometallations is essential to our understanding of the intermolecular activation of hydrocarbons by similar metal centers. Two pathways are generally considered, one being a homolytic initiation involving free radicals while the other contains a multicenter transition state. It is difficult to see how a radical pathway could be extrapolated to intermolecular activations with ease, however, the multicenter pathway can be generalized for both inter- and intra-molecular activations. Although it is now generally accepted that the activation occurs via a four-center transition state it is important to review the data which argues against the homolytic pathway.

1. *Homolytic pathway*

This mechanism probably gains consideration due to the fact that the majority of cyclometallation reactions at these d^0-metal centers involve alkyl leaving groups. The facile (sometimes explosive) thermal decomposition of a large number of early transition metal per-alkyl



Scheme V. Possible pathways for the observed thermal reactivity of $Ta(OAr')_2(=CHSiMe_3)(CH_2SiMe_3)$, OAr' = 2,6-di-*tert*-butylphenoxide (from Ref. 43).

complexes is thought in part to be due to initial homolysis of the metal alkyl bond leading to a radical chain process.[49,50] Hence the impression that metal–alkyl bonds are thermally unstable on these metals. Strong support from a mixture of general chemical considerations and labelling studies is available to show that radicals are not generated during the above cyclometallations.

For example, the thermolysis of $Ta(OAr')_2(CH_3)_3$ in C_6D_6 or $C_6D_5CD_3$ does not result in the formation of any CH_3D, only CH_4 being generated (Scheme IV).[43] Similarly homolytic bond scission during the γ-CH bond activation of $Cp^*_2Th(CH_2SiMe_3)_2$ is ruled out by the observations that no deuterium incorporation into the Me_4Si group occurs when the reaction is carried out in cyclohexane-d_{12}.[30] Strong support against homolytic initiation is also obtained by studying the thermal stability of electronically identical complexes, only some of which do undergo cyclometallation. Hence, although the complexes $R_2M[N(SiMe_3)_2]_2$(M=Zr, Hf) readily lose alkane at 160°C *in vacuo* to form the dimeric, γ-metallated complex (Scheme II),[38] the titanium analogue is thermally stable at 190°C for extended periods.[38] The lack of metallation in this complex will be discussed later. However, the important point is that the metal–carbon bond in these systems does not undergo homolysis under conditions where cyclometallation does not occur. In fact it is generally accepted that the Ti–R bond is significantly weaker than the alkyl bond to its 2nd and

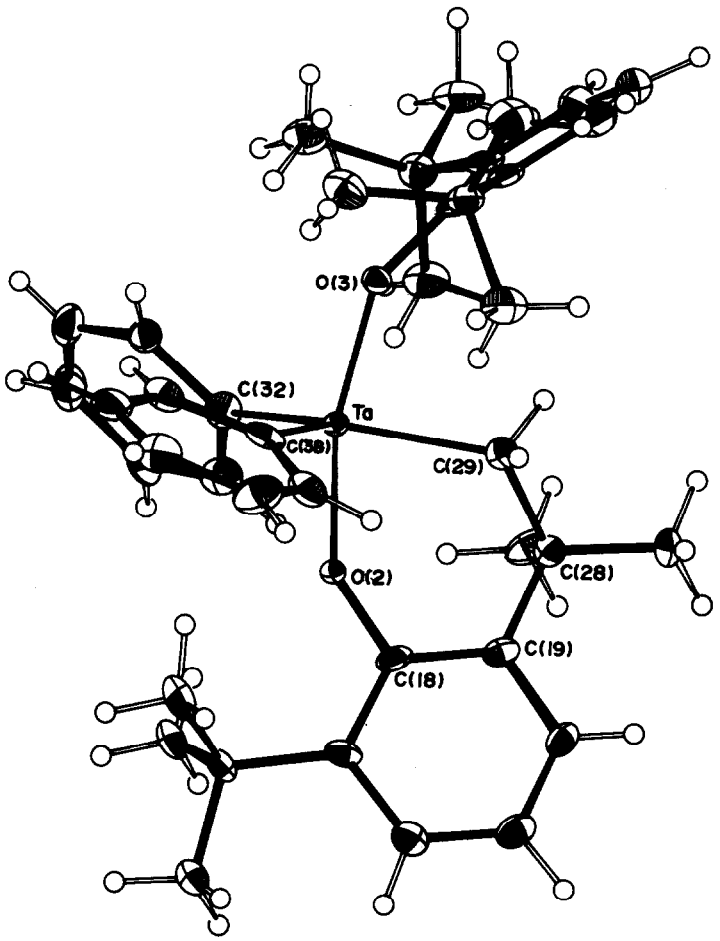


Fig. 3. An ORTEP view of the monocyclometallated complex $\overline{Ta(OC_6H_3Bu^tCMe_2CH_2)}(OAr')(Ph)_2$ emphasizing the six-membered chelate ring generated on metallation of the OAr' ligand.

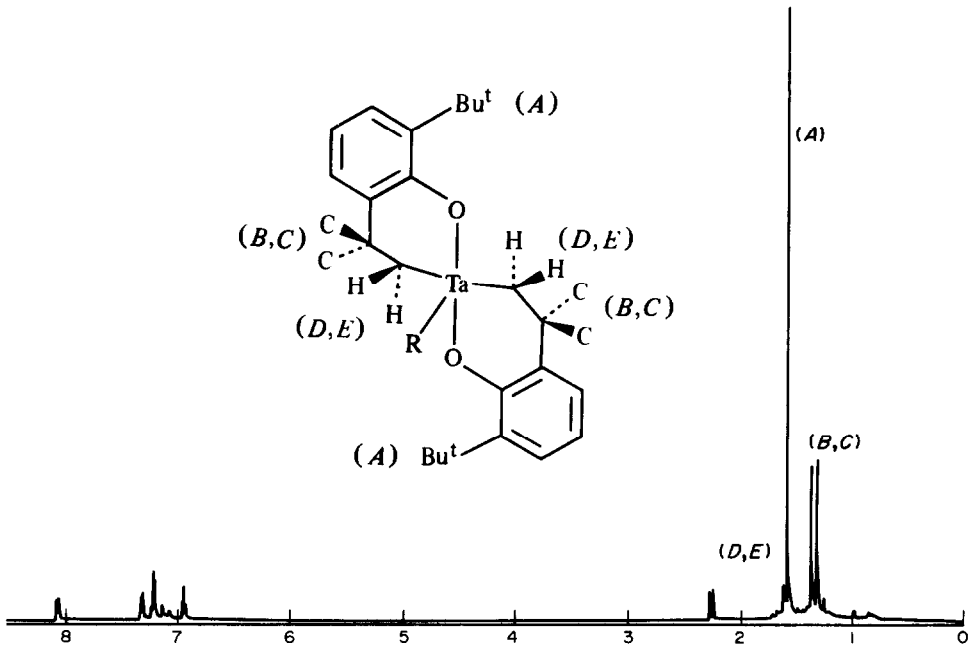
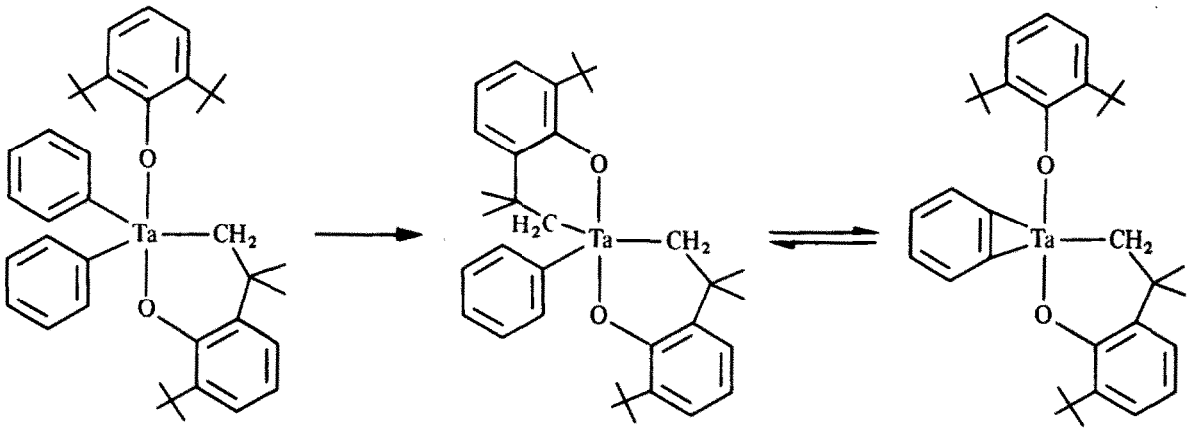


Fig. 4. Expected structure and the ^1H NMR spectrum of the bis-cyclometallated complex $\overline{Ta(OC_6H_3Bu^tCMe_2CH_2)_2}(Ph)$. Due to the molecular symmetry the metallated methylene protons appear as AB patterns while the CMe_2CH_2 methyl groups in the chelate ring are non-equivalent.



Scheme VI. The thermal reactivity of the complex $Ta(OC_6H_3Bu^tCMe_2CH_2)(OAr')(Ph)_2$ showing high temperature equilibrium with a benzyne (*o*-phenylene) complex (from Ref. 47).

3rd row congeners.[51] Again although the complex $Ta(OAr')_2(CH_3)_3$ undergoes thermal metallation, the complexes $Ta(OAr^*)_2Me_3$(OAr^* = 2,6-di-isopropylphenoxide; 2,6-dimethylphenoxide) are thermally stable for large periods of time, no CH_3D being given in deuterated solvents.[52] Hence the Ta–CH_3 bond in a mononuclear TaO_2C_3 environment is not inherently unstable and is only lost when groups that can be cyclometallated are present.

2. *Multicenter pathway*

It is now generally accepted that both α- and β-hydrogen abstraction in metal alkyl complexes occurs via a four-center transition state. This type of pathway for more distal CH bond activations

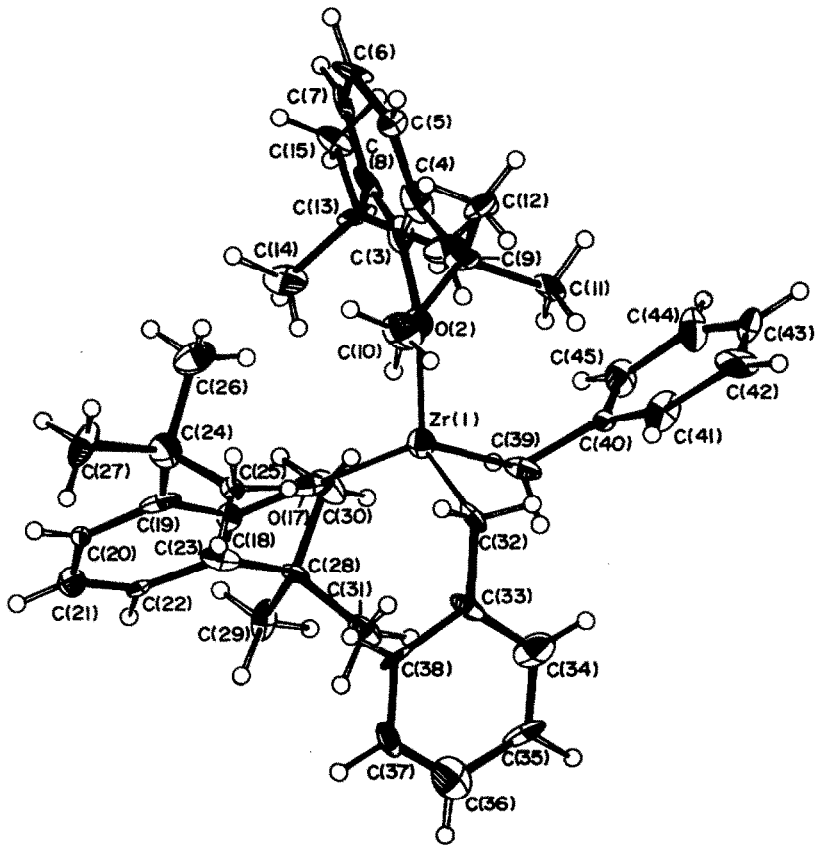
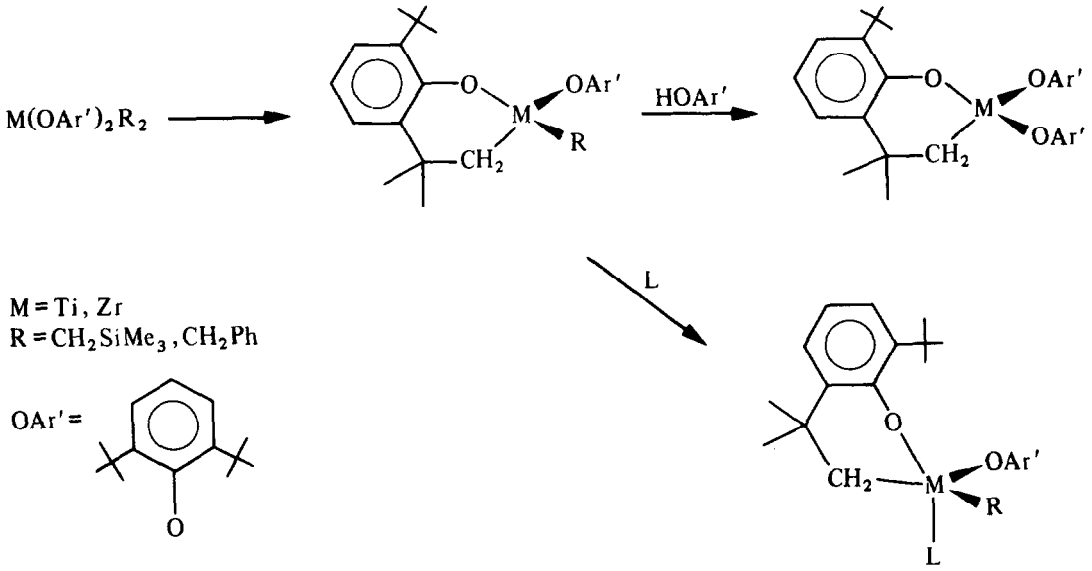


Fig. 5. An ORTEP view of the molecule $Zr(OAr')_2(CH_2Ph)_2$. Some pertinent bond distances (Å) and angles (°) are: Zr–O = 1.93(av), Zr–C = 2.25(av), Zr–O–C = 172(av).



Scheme VII. Reactivity of the complexes $R_2M(OAr')_2$(M = Ti, Zr; R = CH_2Ph, CH_2SiMe_3; OAr' = 2,6-di-*tert*-butylphenoxide).

at d^0-metal configurations is not preferred just by default, evidence being against the homolytic path. On the contrary, there is now kinetic data and other evidence in direct support of this pathway.

Marks *et al.* have reported a kinetic study of the γ-CH bond activation during the thermolysis of complexes $C\overset{*}{p}_2Th(CH_2XMe_3)_2$(X = C, Si) (Reaction 11).[30] Quantitatively monitoring the reaction by ^1H NMR showed first-order kinetics, the neopentyl group ring closing faster than the silicon analogue. Activation parameters are collected in Table 1. Similar measurements by our group at Purdue on the cylometallation of 2,6-di-*tert*-butylphenoxide have been carried out on reactions at Ta, Ti and Zr metal centers (Table 1).[42,52] On tantalum we have compared the kinetics of the first and second ring closure reactions (Scheme III). A series of kinetic runs on the two complexes $M(OAr')_2(CH_2Ph)_2$ have also been made (Scheme VII). An example of a first-order plot for the titanium complex and also a plot of ln (k/T) vs $T^{-1}(K^{-1})$ are given in Figs. 7 and 8. Activation parameters using either Arrhenius or Activated Complex Theory are collected in Table 1.

One characteristic of all four reactions is the presence of a negative value for the entropy of activation. In the case of the four-coordinate complexes this value is both large and negative. These entropy changes suggest the presence of a highly ordered transition state and can be compared with the large, positive values found for the cyclometallation of neopentyl groups on Pt(II).[29] Here,

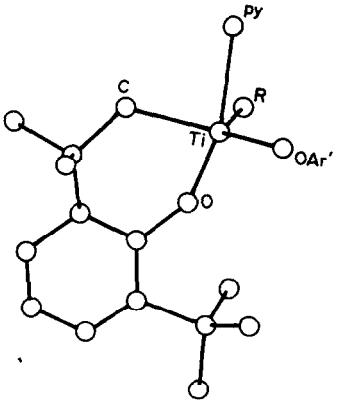


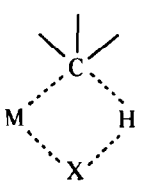
Fig. 6. A representation of the geometry found in the solid state for the complex $Ti(OC_6H_3Bu^tCMe_2CH_2)(OAr')(CH_2SiMe_3)(py)$ showing only the chelate ring and donor atoms of the other ligands. Some pertinent bond distances (Å) are: Ti–O (chelate) = 1.810(4), Ti–OAr' = 1.850(4), Ti–C (chelate) = 2.095(6), Ti–CH_2SiMe_3 = 2.131(6), Ti–N(py) = 2.293(5).

Table 1. Activation parameters for a number of d^0-cyclometallation reactions[a]

Reaction	Ea	Log A	$\Delta H\ddagger$	$\Delta S\ddagger$
b	23.6 ± 0.7	10 ± 1	23.0 ± 0.7	-13 ± 2
c	22.4 ± 1.0	9 ± 1	21.6 ± 1.0	-19 ± 3
d	21.3 ± 0.6	9 ± 1	20.6 ± 0.6	-17 ± 2
e	25.9 ± 0.9	11 ± 1	25.2 ± 0.9	-9 ± 1
f	27.2 ± 1.0	11 ± 1	26.4 ± 1.0	-7 ± 1
g	30.8 ± 1.0	12 ± 1	29.5 ± 1.0	-6 ± 1

a. Ea and $\Delta H\ddagger$ in kcal mol^{-1}; $\Delta S\ddagger$ in e.u.
b. Thermolysis of $Ti(OAr')_2(CH_2Ph)_2$ (Scheme VII).
c. Thermolysis of $Zr(OAr')_2(CH_2Ph)_2$ (Scheme VII).
d. Reaction (*11*), X = C.
e. Reaction (*11*), X = Si.
f. First ring closure of $Ta(OAr')_2Me_3$ (Scheme III).
g. Second ring closure of Scheme III.

Whitesides has interpreted the data as indicative of a rate-determining reductive elimination of alkane from the Pt(IV) hydridoalkyl formed by oxidative-addition of the γ-CH bond.[29] These entropy changes (Table 1) are hence further evidence against a dissociative or homolytic pathway, the transition state clearly could not represent a process *decreasing* the coordination environment of the metal. A multicenter pathway is hence implicated. In the example shown (20)



(20)

the four-center transition state involves four-electrons, two each from the CH bond to be broken and the M–X bond of the leaving group. Evidence that the CH bond is being broken in the transition state comes from the observation of large kinetic isotope effects, e.g. a k_H/k_D of 9.7 for reaction 15a. Consideration of this type of transition state allows one to make certain assumptions concerning the nature of complexes that will undergo such cyclometallations.

(i) *Ligand geometry*. Clearly this mechanistic pathway requires the CH bond that is to be activated to come into close proximity of the metal and the eventual leaving group. This requires not only the correct geometry for the ligand, but also in order to force the CH bond onto the metal one requires steric bulk. This necessity for steric bulk in the metal coordination sphere can be seen by considering the distal cyclometallation reactions outlined above. The recognition that steric pressure is essential for mild cyclometallation was recognized early by Cope *et al.* and later successfully exploited by Shaw and others in order to design, with some rationality, ligands that would more readily cyclometallate.[54]

The rationale for this steric dependence has been argued to be entropic. As early as 1915 it was recognized that ring closure reactions for organic molecules were enhanced by the presence of substituents on the carbon skeleton.[55] This phenomenon is referred to as the "gem-dimethyl" or "Thorpe–Ingold" effect.[55,56] In the case of cyclometallation reactions it can be argued that the attainment of the highly restrictive transition state in which the ligand geometry is effectively "trapped" represents a severe loss of entropy over the ground state in which the ligand is free to move. Restricting the movement of the ligand in the ground state by introducing considerable bulk both on the ligand and in the coordination sphere will hence reduce this entropic loss. The faster rate of cyclometallation of the complex $Ti(OAr')_2(CH_2Ph)_2$ over its zirconium analogue can be seen from Table 1 to be entropic in nature. This can be rationalized if one considers the coordination sphere about each metal. Although the four ligands are identical, Ti–X bonds are consistently

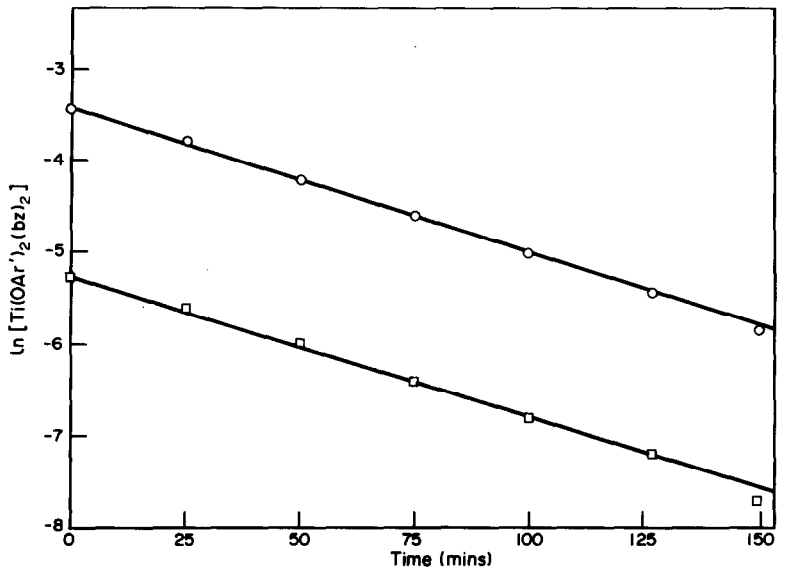


Fig. 7. First-order plot for the disappearance of $Ti(OAr')_2(CH_2Ph)_2$ at 95°C to generate the mono-cyclometallated complex (Scheme VII). Initial concentrations are 0.032M(2) and 0.005(1).

0.1–0.2A shorter than Zr–X bonds. Hence, the coordination sphere is contracted in the titanium complex. This will have the effect of not only "pulling in" the CH bond to be metallated, but also making ring closure easier.

However, the presence of too much bulk in the coordination sphere, or bulk of the wrong type, can be a hindrance and not a help in some situations. In the complexes $R_2M[N(SiMe_3)_2]_2$ (M=Ti, Zr, Hf) only the 2nd and 3rd row elements undergo thermal metallation.[38] It can be argued that the more compact coordination sphere of the titanium complex "cuts off" the γ-CH bond from the metal, not allowing it access to the metal center for activation. The possibility that these reactions may occur inter-molecularly due to the dimeric nature of the products is an uncertainty in considering the mechanism.

(ii) *Leaving group.* If one carries out a rough thermodynamic assessment of the transition state one can see that one is forming a new M–C bond along with an H–X bond. This is occurring at

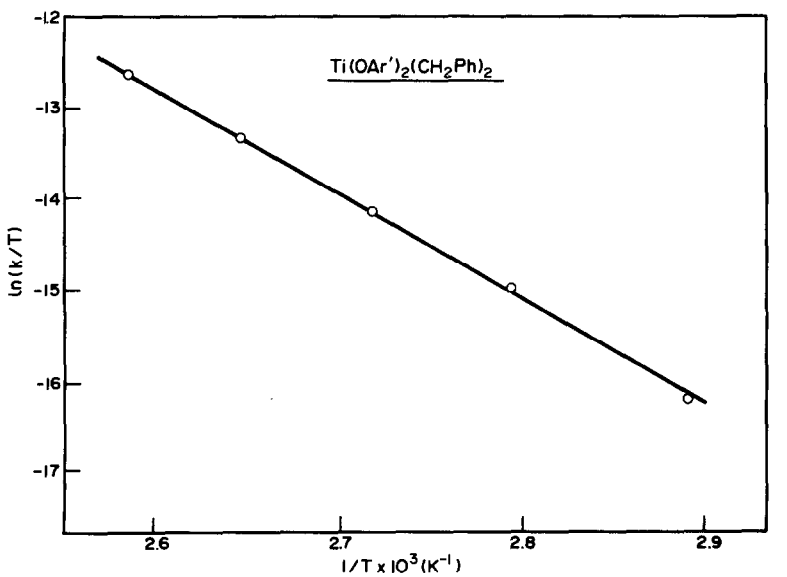
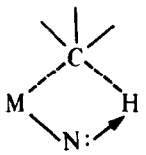


Fig. 8. Plot of $ln\ (k/T)$ vs $T^{-1}(K^{-1})$ for the cyclometallation of OAr' in $Ti(OAr')_2(CH_2Ph)_2$ (see Table 1).

the expense of the C–H and M–X bonds. If one considers alkyl leaving groups, i.e. X=R, then the equation appears pretty well balanced. From the data in Table 1, it can be seen for the complexes $M(OAr')_2(CH_2Ph)_2$(M=Ti, Zr) that there is little enthalpic difference to the reaction, despite the fact that Zr–CH_2Ph bonds are known to be at least 10 kcal mol^{-1} stronger than the Ti–CH_2Ph bond.[51] This is entirely consistent with the four-center transition state, as one is both making and breaking M–C bonds. Hence, as for a given alkyl the bond strengths run approximately parallel down a triad, it is not surprising to find little difference in $\Delta H\ddagger$ for these two reactions.

This thermodynamic consideration may also explain why, unlike GpVIII cyclometallation reactions, halide ligands do not appear to be good leaving groups for this type of reaction. Even accounting for back reactions between the cyclometallated product and the generated HX(X=Cl, Br), early transition metal halides do not readily undergo cyclometallation reactions. For example, thermolysis of the compounds $Ta(OAr')_2Cl_3$, $Ti(OAr')_2Cl_2$ and $M(OAr')_3Cl$ (M=Ti, Zr, Hf) under vacuum at temperatures of 170–200°C causes no reaction except sublimation.[52] One explanation is that the halide group is sterically very small. However, the complexes $M(OAr')_3Cl$ are extremely crowded and for M=Ti, Zr the metallated complexes $M(O\text{-}CH_2)(OAr')_2$ can be independently synthesized (19). This lack of metallations involving halide groups can be explained by the high strength of the M–Cl bond for early transition metals. This bond has a dissociation energy of 100–120 kcal mol^{-1} compared to 45–60 kcal mol^{-1} for alkyl groups bound to the same metal. The reaction appears, therefore, to be enthalpically inhibited.

A similar rationale can be applied to the use of alkoxide or dialkylamide leaving groups, but a complexity is present for these hetero-atom donor leaving groups. The four center transition state indicated (20) does not have any net charge. However, the charge distribution *within* the trapezoid is not indicated. Clearly this will depend on the electronegativity of the elements involved. For X=C one imagines a rather uniform distribution of charge. In the case of OR and NR_2 leaving groups, the availability of lone-pairs on the donor atom is an added complexity. This is illustrated (21).

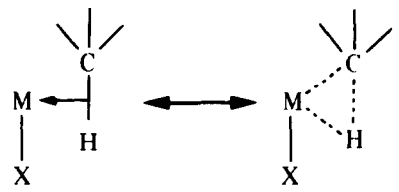


(21)

In effect the pathway, although still multicenter, is now appearing to be highly electrophilic in character in which the metal activated CH bond is protonating the lone pair of the leaving group (base). One is then left with a coordinated alcohol or amine after the ring closure is complete. This pathway is the reverse of the alcoholysis or aminolysis of metal–carbon bonds.[57] Enthalpically the situation is now difficult to assess, because the bond to the leaving group has not been completely broken. However, structural data clearly show that on d^0-metal centers bond lengths to coordinated alcohols and amines are much longer than to alkoxides and amides[58] so that the bond has been considerably weakened by its protonation.

Analysis of the postulated transition state also helps understand the high activity of alkylidene groups for intramolecular CH bond activation (Scheme IV). Although entropic factors will be similar, the new metal–carbon bond will be formed only at the expense of the π-component of the M=C bond. Hence enthalpically the situation appears more favourable than simple alkane for alkyl exchange.

(iii) *The metal.* Clearly the metal center must have available to it empty orbitals of the correct symmetry with which to interact with the CH bond in the transition state. This is not a problem with most early transition metal d^0-compounds. There is a large body of evidence, both structural and spectroscopic, that it is possible for CH bonds to act as two-electron donating groups to electron deficient metal centers.[59,60] This typically is found where the metal would be two electrons short of attaining a stable, 18-electron count. More recently work by Green has shown that such interactions are possible in the ground state to d^0-metal centers such as Ti(IV).[61,62] In particular, strong interaction to the α- and β-CH bonds was structurally characterized. It is hence reasonable to assume that this may be the initial type of interaction between the electron deficient metal and the CH bond to be activated (22).



(22)

This three-center, two-electron bond then weakens the CH bond and leads into the four-center transition state in which the hydrogen atom is transferred to the leaving group.

The solid state structure of the complex $Yb[N(SiMe_3)_2]_2$ (dmpe) has been found to contain an interaction between one of the methyl groups and the metal in the ground state.[63] The hydrogen atoms on this group were refined and shown to be pointing *away from* the metal center in contrast to situations with *d*-block metals where M . . . HC type interactions are prevalent. The structure was interpreted in terms of the CH_3 group bridging between the Yb metal atom and Si atom, there being considerable lengthening of the Si–CH_3 bond (Fig. 9). The implications of this observed ground state structure on the known γ-CH bond activation in this ligand is that one would expect the Yb–CH_3 interactions to increase the acidity of the γ-hydrogens. This would allow the reaction to proceed in a transfer of the acidic hydrogen to the leaving group. All evidence so far available does not point to a process in which the leaving hydrogen is lost *exo* to the complex, i.e. to an external base similar to an S_E2 process.

In the solid state structure of complexes containing the 2,6-di-*tert*-butylphenoxide (OAr′) ligand, it is typically found that one of the CH bonds of the *tert*-butyl groups is pointing almost directly at the metal center. In the case of the complex $Ta(OAr')_2Me_3$ distances range from 2.8 to 3.0A while in the chloride $Ta(OAr')_2Cl_3$ (Fig. 10) one of the CH bonds seems to "occupy" the position *trans* to the axial chloride in a square based pyramidal structure. The Ta–H distance was refined to 2.67A. Although it is very doubtful that any significant ground state interaction is taking place in these complexes, the attainment of a multicenter transition state between the metal and these CH bonds is clearly very feasible.

Another factor to consider is the influence that the ancillary ligands have on both the energy and availability of metal orbitals with which the CH bond can interact. This is a difficult effect to evaluate even qualitatively. However, one would predict that ligands that reduce the electron deficiency of the metal center, e.g. strong π-donor ligands such as NR_2, will tend to inhibit interactions to CH bonds.

IV. INTERMOLECULAR CH BOND ACTIVATION

1. *Mechanistic considerations*

Unlike in the previous sections where mechanism was considered last, it is useful to reverse the situation for intermolecular hydrocarbon activation just so that one can see what one is up

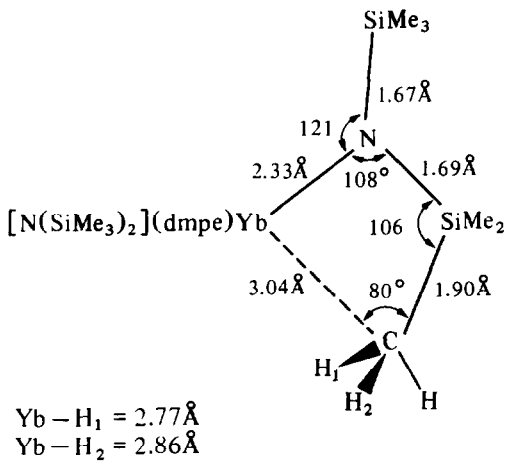


Fig. 9. Representation of the Yb–CH_3 ground state interaction found in the solid state structure $Yb[N(SiMe_3)_2]_2$ (dmpe) (dmpe = $Me_2PCH_2CH_2PMe_2$) (from Ref. 63).

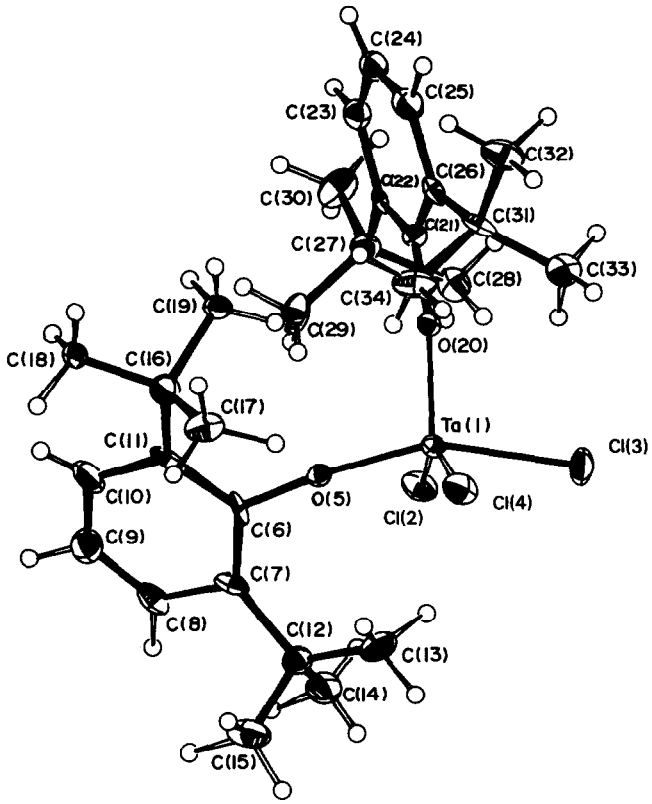
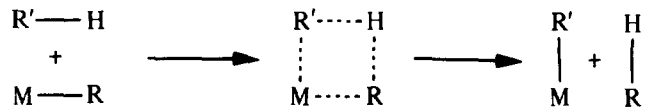


Fig. 10. An ORTEP view of the molecule $Ta(OAr')_2Cl_3$ showing the close approach of an ϵ-CH bond to the axial position of a square-pyramidal geometry.

against. Extrapolating from the results for cyclometallation reactions it is possible to envisage how a d°-metal center might activate a CH bond in a normally inert hydrocarbon. Initially, the CH bond must enter the coordination sphere of the metal, interact with one of the metal orbitals and then progress through a transition state in which the new metal–carbon bond is formed and the hydrogen atom is lost with the leaving group (23).



(23)

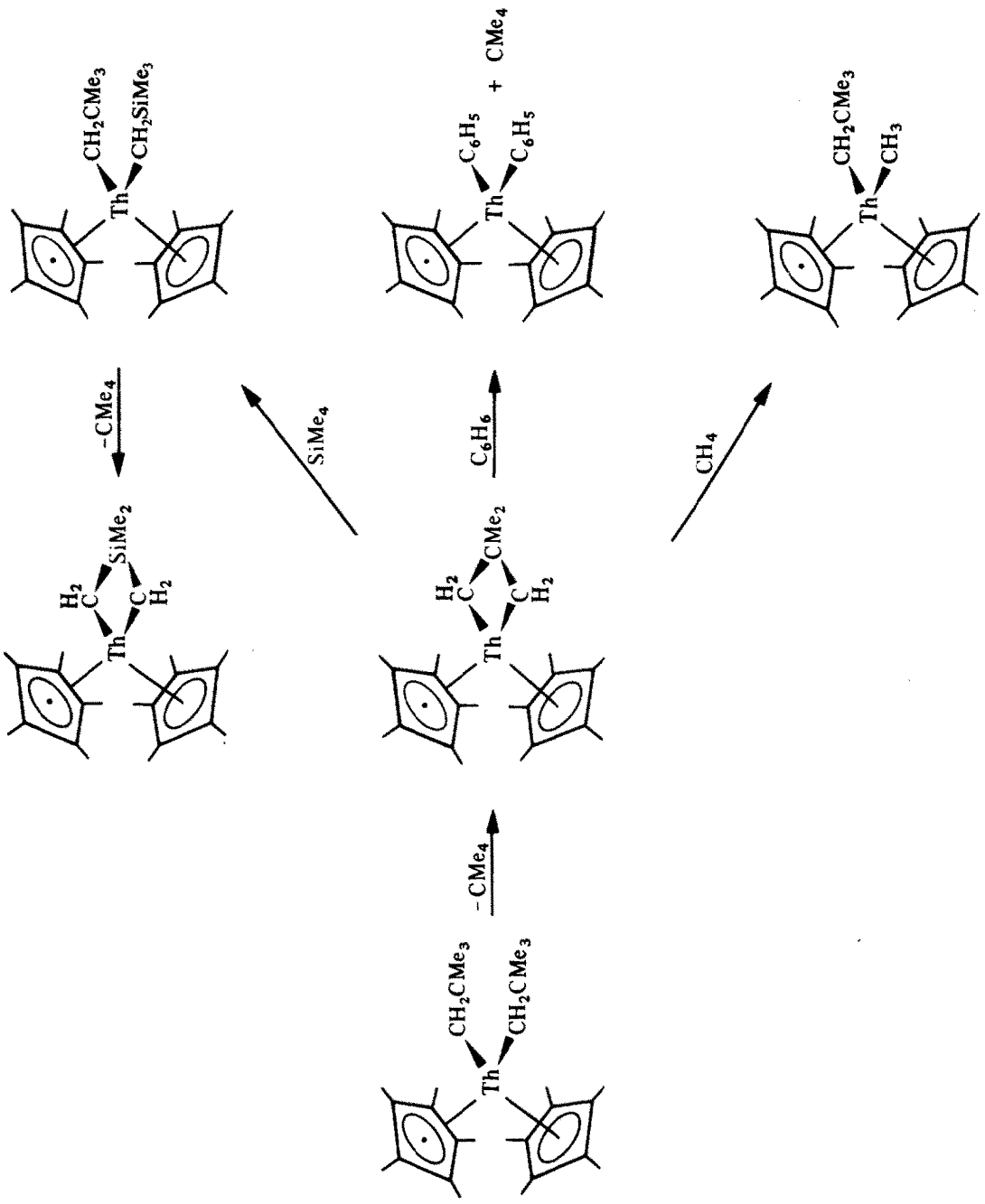
From the previous discussions one would clearly choose an alkyl leaving group on enthalpic grounds, and the overall reaction would hence represent an alkyl exchange. Clearly what is against the intermolecular reaction is its bi-molecular nature and the strongly negative values of $\Delta S\ddagger$ one might expect in order to achieve the transition state.

An intermolecular reaction which is of direct relevance to this problem is the hydrogenolysis of d°-metal alkyl complexes.[64] This is now a common reaction and one of excellent synthetic utility.[65,66] The mechanism of this reaction has been discussed and proposed to be via a four-center transition state.[67,68] The more extensively documented reactivity of H_2 with d°-metal alkyls over alkyl exchange reactions may be a reflection of the steric differences between H_2 and alkane CH bonds. In terms of electron donating ability one predicts that CH bonds would be superior to H_2 due to the latter's higher ionization potential.[69]

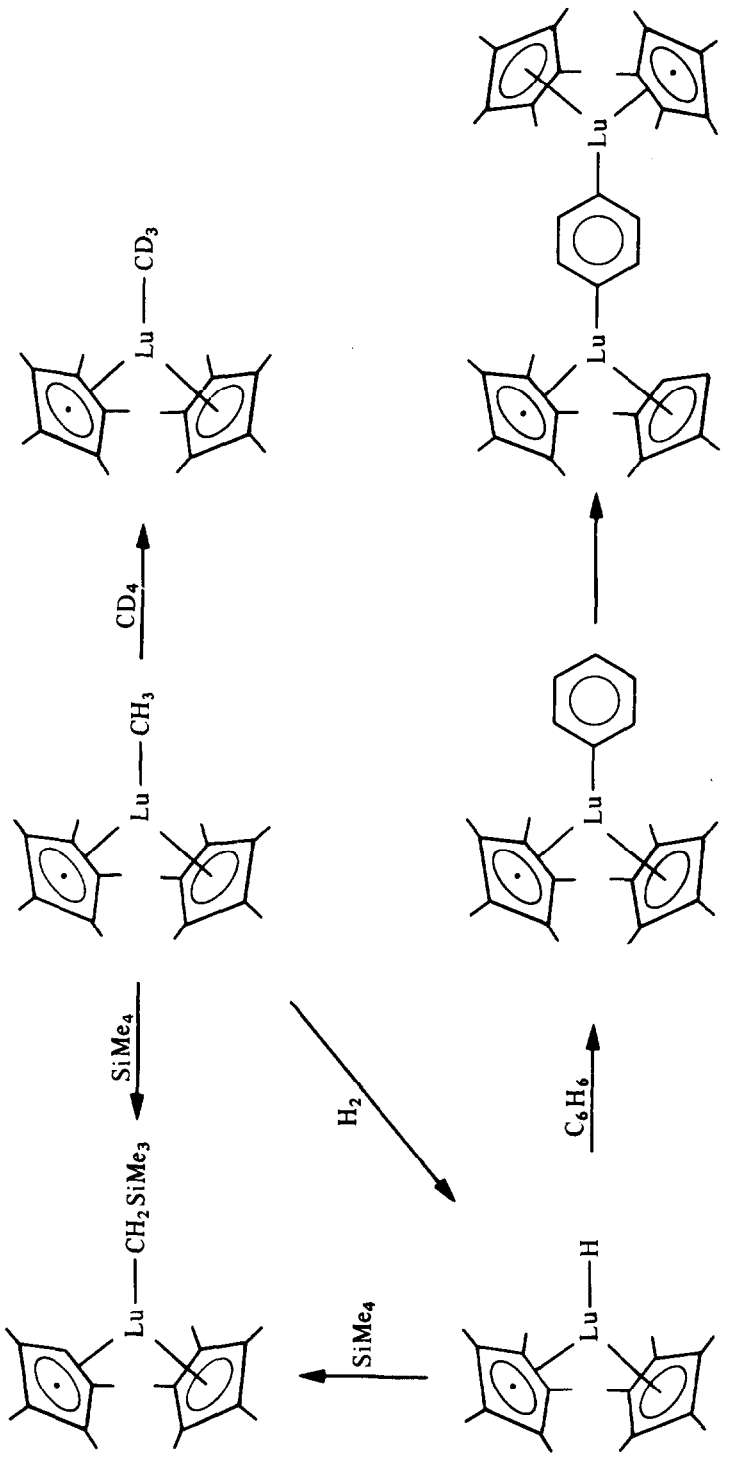
The systems that successfully activate hydrocarbons are small and can be discussed individually.

2. *Activation of aromatic* CH *bonds by benzyne intermediates*

Any reaction in which aromatic CH bonds are activated represents a somewhat special case due to the presence of the aromatic π-bonds with which the molecule can initially bond to the d°-metal allowing the CH bonds to come into close proximity with the metal for activation.



Scheme VIII. Activation of sp^2- and sp^3-CH bonds by Cp^*_2Th derivatives (from Refs. 30 and 72).



Scheme IX. Activation of hydrocarbons by derivatives of Cp^*_2Lu (from Refs. 73–75).

Erker has demonstrated that the thermal formation of benzyne groups from the complexes Cp_2MAr_2 (Reaction 7) (M=Ti, Zr) is reversible. Hence the thermolysis of bis-tolyl derivatives in benzene results in the formation of mixed phenyl, tolyl derivatives. Direct exchange of aromatics can be ruled out. The final products were analyzed by photolysis and characterization of the generated biphenyl molecules.[70]

Marks has demonstrated similar reactivity for the uranium complex $C\overset{*}{p}_2U(C_6H_5)_2$. Thermolysis in C_6D_6 generates the complex $C\overset{*}{p}_2U(C_6H_4D)(C_6D_5)$, the deuterium being incorporated into the ortho-position. Under identical conditions the uranium complex undergoes benzene exchange approximately 10^2 times faster than $Cp_2Zr(C_6H_5)_2$.[71] In both of these reactions the CH bond is inserting into the highly strained metal–carbon bond of a metallocyclopropane ring.

Although a benzyne complex has been shown to be able to reversibly activate aliphatic CH bonds intramolecularly (Scheme VI),[47] the intermolecular generation of an alkyl, aryl complex by reaction of a benzyne complex with an alkane has yet to be documented.

3. *Hydrocarbon activation by* $C\overset{*}{p}_2\overline{Th(CH_2CMe_2CH_2)}$

As mentioned previously, Marks *et al.* have demonstrated that complexes containing thoracyclobutane rings can be prepared by thermolysis of the complexes $C\overset{*}{p}_2Th(CH_2XMe_3)_2$ (X=C, Si) (Reaction 11).[30] The neopentyl derivative $C\overset{*}{p}_2\overline{Th(CH_2CMe_2CH_2)}$ undergoes a number of intermolecular reactions with hydrocarbons (Scheme VIII).[72] Benzene reacts to yield the di-phenyl compound with overall loss of neopentane. The first step of the reaction represents a ring opening reaction, in which the aromatic CH bond is activated. The second step may involve direct aryl for alkyl exchange, or else proceed via a benzyne intermediate. The use of toluene yields a 75/25 mixture of aromatic and benzylic products.[30]

The thoracyclobutane ring can also activate Me_4Si and even methane itself.[72] The products are initially the mixed alkyl, neopentyl derivatives but in the case of Me_4Si a further ring closure occurs to generate the metallo-silacyclobutane ring (Scheme VIII). This silicon analogue does not undergo any of these ring opening reactions. The rationale for this is the decrease in ring strain due to the longer C–Si bonds. Accurate thermochemical measurements[72] indicate a difference in ring strain of 10 kcal mol^{-1} for these metallocycles giving much more driving force for the hydrocarbon activation by $C\overset{*}{p}_2\overline{Th(CH_2CMe_2CH_2)}$.

4. *Hydrocarbon activation by* $C\overset{*}{p}_2LuR$(R=H, Me)

In a series of papers[73–75] Watson has reported the remarkable organometallic chemistry of complexes containing the $C\overset{*}{p}_2Lu$ unit. Both inter- and intra-molecular activation of sp^2 and sp^3 CH bonds can take place (Scheme IX).[74] Perhaps the most remarkable reactivity involves the observation of methane exchange on the complex $C\overset{*}{p}_2LuMe$.[75] This reaction occurs readily at 70°C in cyclohexane-d_{12} and can be followed by ^1H and ^{13}C NMR using labelled methane ($^{13}CH_3$). A similar reactivity was noted for the yttrium analogue. Kinetic studies showed the reaction to be first-order in methane and a four-center transition state was proposed.

Both the complexes $C\overset{*}{p}_2M(CH_3)$(M=Lu, Y) exist as assymetric dimers in the solid state containing one bridging methyl group. The Lu–Me–Lu angle was determined to be almost linear by X-ray diffraction and can be pictured as an Lu–CH_3 group acting as a two electron donor to the other metal through one of the CH bonds. One can imagine this interaction to be a model of the initial methane–Lu interaction that eventually leads to alkane exchange.

VI. CONCLUDING REMARKS

The ability of d^0-metal centers to activate, cleave and in some cases functionalize normally inert CH bonds has clearly been demonstrated. All present mechanistic data can be accommodated into a multicenter transition state in which the new metal carbon bond is formed at the direct expense of a metal–ligand (leaving group) bond. The future for hydrocarbon activation at d^0-metal centers appears bright, especially in view of the recently demonstrated mild activation of even methane itself.

Acknowledgements—I should like to thank the National Science Foundation, the donors of the Petroleum Research Fund administered by the American Chemical Society, and the Research Corporation for financial support of various aspects of my research.

REFERENCES

1. G. W. Parshall, *Catalysis* 1977, **1**, 335.
2. D. E. Webster, *Adv. Organomet. Chem.* 1977, **15**, 147.
3. A. E. Shilov and A. A. Shteinman, *Coord. Chem. Rev.* 1977, **24**, 97.
4. M. I. Bruce, *Angew. Chem. Intl. Ed.* 1977, **16**, 73.
5. J. Dehand and M. Pfeffer, *Coord. Chem. Rev.* 1976, **18**, 327.
6. G. W. Parshall, *Acc. Chem. Res.* 1975, **8**, 113 and *Ibid.* 1970, **3**, 139.
7. J. L. Garnett and R. L. Hodges, *J. Am. Chem. Soc.* 1967, **87**, 4546.
8. J. L. Garnett and R. S. Kenyon, *Austral. J. Chem.* 1974, **27**, 1023.
9. J. L. Garnett and R. S. Kenyon, *Austral. J. Chem.* 1974, **27**, 1033.
10. E. K. Barefield, G. W. Parshall and F. N. Tebbe, *J. Am. Chem. Soc.* 1970, **92**, 5234.
11. M. Berry, K. Elmitt and M. L. H. Green, *J. Chem. Soc., Dalton Trans.* 1979, 1950.
12. A. H. Janowicz and R. G. Bergman, *J. Am. Chem. Soc.* 1982, **104**, 352.
13. J. K. Hoyano and W. A. G. Graham, *J. Am. Chem. Soc.* 1982, **104**, 3723.
14. R. H. Crabtree, *CHEMTECH* 1982, **12**, 506.
15. A. J. Deeming and I. P. Rothwell, *Pure Appl. Chem.* 1980, **52**, 649 and references therein.
16. G. W. Parshall, *Homogeneous Catalysis*. Wiley, New York (1980).
17. (a) R. R. Schrock, *Acc. Chem. Res.* 1979, **12**, 98; (b) R. R. Schrock, In *Reactions of Coordinated Ligands* (Edited by P. S. Bratermann). Plenum Press, New York (1982); (c) R. H. Grubbs, *Prog. Inorg. Chem.* 1978, **24**, 1.
18. R. R. Schrock, *J. Am. Chem. Soc.* 1976, **98**, 5399.
19. R. J. Goddard, R. Hoffmann and D. J. Eluvanthingal, *J. Am. Chem. Soc.* 1980, **102**, 7667.
20. L. R. Chamberlain, A. P. Rothwell and I. P. Rothwell, *J. Am. Chem. Soc.* 1984, **106**, 1847.
21. D. S. Edwards, L. V. Bland, J. W. Ziller, M. R. Churchill and R. R. Schrock, *Organometallics* 1983, **2**, 1505.
22. F. A. Cotton and G. Wilkinson, *Advanced Inorganic Chemistry*. Wiley, New York (1981).
23. S. J. McLain, R. R. Schrock, P. R. Sharp, M. R. Churchill and W. J. Youngs, *J. Am. Chem. Soc.* 1979, **101**, 263.
24. (a) G. Erker, *J. Organomet. Chem.* 1977, **134**, 189; (b) K. Kropp and G. Erker, *Organometallics* 1982, **1**, 1246.
25. P. J. Fagan, J. M. Marinquez, E. A. Maatta, A. M. Seyam amd T. J. Marks, *J. Am. Chem. Soc.* 1981, **103**, 6650.
26. P. C. Wailes, R. S. P. Coutts and H. Weingold, *Organometallic Chemistry of Titanium, Zirconium and Hafnium*. Academic Press, New York (1974).
27. R. A. Andersen, R. A. Jones and G. Wilkinson, *J. Chem. Soc. Dalton* 1978, 446.
28. T. H. Tulip and D. L. Thorn, *J. Am. Chem. Soc.* 1981, **103**, 2448.
29. R. DiCosimo, S. S. Moore, A. F. Sowinski and G. M. Whitesides, *J. Am. Chem. Soc.* 1982, **104**, 124.
30. J. W. Bruno, T. J. Marks and V. W. Day, *J. Am. Chem. Soc.* 1982, **104**, 7357.
31. J. P. Collman and L. S. Hegedus, *Principles and Applications of Organotransition Metal Chemistry*. University Science Books, Mill Valley, California (1980).
32. C. McDade, J. C. Green and J. E. Bercaw, *Organometallics* 1982, **1**, 1629.
33. D. C. Bradley and M. H. Chisholm, *Acc. Chem. Res.* 1976, **9**, 273.
34. M. H. Chisholm and F. A. Cotton, *Acc. Chem. Res.* 1978, **11**, 356.
35. (a) M. F. Lappert, P. P. Power, A. R. Sanger and R. C. Srivastara, *Metal and Metalloid Amides*. Wiley, New York (1980); (b) C. Airoldi, D. C. Bradley and G. Vuru, *Trans. Met. Chem.* 1979, **4**, 64.
36. (a) W. A. Nugent, D. W. Overall and S. J. Holmes, *Organometallics* 1983, **2**, 161; (b) J. M. Mayer, C. J. Curtis and J. E. Bercaw, *J. Am. Chem. Soc.* 1983, **105**, 2651; (c) C. R. Bennett and D. C. Bradley, *J. Chem. Soc., Chem. Comm.* 1974, 29; (*d*) S. J. Simpson and R. A. Andersen, *Inorg. Chem.* 1981, **20**, 3627.
37. S. J. Simpson, H. W. Turner and R. A. Andersen, *Inorg. Chem.* 1981, **20**, 2991.
38. R. P. Planalp, R. A. Andersen and A. Zalkin, *Organometallics* 1983, **2**, 16.
39. R. P. Planalp and R. A. Andersen, *Organometallics* 1983, **2**, 1675.
40. L. Chamberlain, I. P. Rothwell and J. C. Huffman, *Inorg. Chem.* 1984, **23**, 2575.
41. L. Chamberlain, J. Keddington and I. P. Rothwell, *Organometallics* 1982, **1**, 1098.
42. L. Chamberlain, J. Keddington, I. P. Rothwell and J. C. Huffman, *Organometallics* 1982, **1**, 1538.
43. L. Chamberlain, I. P. Rothwell and J. C. Huffman, *J. Am. Chem. Soc.* 1982, **104**, 7338.
44. L. Chamberlain and I. P. Rothwell, unpublished results.
45. Ref. 17(a) and references therein.
46. (a) K. J. Ivin, J. J. Rooney, D. Stewart, M. L. H. Green and R. J. Mahtab, *J. Chem. Soc. Chem. Comm.* 1978, 604; (b) H. W. Turner and R. R. Schrock, *J. Am. Chem. Soc.* 1982, **104**, 2331.
47. L. Chamberlain and I. P. Rothwell, *J. Am. Chem. Soc.* 1983, **105**, 1665.

48. S. Latesky, A. K. McMullen and I. P. Rothwell, unpublished results.
49. R. P. Schrock and G. W. Parshall, *Chem. Rev.* 1976, **76**, 243.
50. P. J. Davidson, M. F. Lappert and R. Pearce, *Chem. Rev.* 1976, **76**, 219.
51. J. A. Connor, *Topics Curr. Chem.* 1977, **71**, 71.
52. L. Chamberlain, A. K. McMullen, S. L. Latesky and I. P. Rothwell, unpublished results.
53. A. C. Cope and E. C. Friedrich, *J. Am. Chem. Soc.* 1968, **90**, 909.
54. B. L. Shaw, *J. Am. Chem. Soc.* 1975, **97**, 3856.
55. G. S. Hammond, *Steric Effects of Organic Chemistry*. Wiley, New York (1956).
56. (a) R. M. Beesley, C. K. Ingold and J. F., Thorpe, *J. Chem. Soc.* 1915, **107**, 1080; (b) C. K. Ingold, *J. Chem. Soc.* 1921, **119**, 305.
57. Thermochemical measurements typically use alcoholysis of metal–alkyl bonds.
58. In the d^0-complex $TaCl_3(NMe_2)_2$ the Ta–NMe_2 distances, 1.96 Å(av.) are considerably shorter than the Ta–$NHMe_2$ distance of 2.37 Å. See M. H. Chisholm, J. C. Huffman and L. S. Tan, *Inorg. Chem.* 1981, **20**, 1859.
59. (a) R. B. Colvert and J. R. Shapley, *J. Am. Chem. Soc.* 1978, **100**, 7726; (b) J. M. Williams, R. K. Brown, A. J. Schultz, G. D. Stucky and S. D. Ittel, *J. Am. Chem. Soc.* 1978, **100**, 7407; (c) M. A. Beno, J. M. Williams, M. Tachikawa and E. L. Muetterties, *J. Am. Chem. Soc.* 1980, **102**, 4918; (d) M. Pasquali, C. Floriani, A. Gaetani-Manfredotti and A. Chiesi-Villa, *J. Am. Chem. Soc.* 1978, **100**, 4918; (e) M. Brookhart, W. Lamanna and M. B. Humphrey, *J. Am. Chem. Soc.* 1982, **104**, 2117; (f) S. Trifimenko, *J. Am. Chem. Soc.* 1968, **90**, 4754; *Inorg. Chem.* 1970, **9**, 2483; (g) F. A. Cotton and A. G. Stanislowski, *J. Am. Chem. Soc.* 1974, **96**, 5074.
60. M. Brookhart and M. L. H. Green, *J. Organomet. Chem.* 1983, **250**, 395.
61. Z. Dawood, M. L. H. Green, V. S. B. Mtetwa and K. Prout, *J. Chem. Soc. Chem. Comm.* 1982, 802.
62. Z. Dawood, M. L. H. Green, V. S. B. Mtetwa and K. Prout, *J. Chem. Soc., Chem. Comm.* 1982, 1410.
63. T. D. Tilley, R. A. Andersen and A. Zalkin, *J. Am. Chem. Soc.* 1982, **104**, 3725.
64. J. M. Mayer and J. E. Bercaw, *J. Am. Chem. Soc.* 1982, **104**, 2154.
65. S. J. Holmes and R. R. Schrock, *Organometallics* 1983, **2**, 1463.
66. W. J. Evans, J. H. Meadows, A. L. Wayda, W. E. Hunter and J. L. Atwood, *J. Am. Chem. Soc.* 1982, **104**, 2008.
67. K. W. Chiu, R. A. Jones, G. Wilkinson, A. M. R. Galas, M. B. Hursthouse and K. M. Abdul-Malik, *J. Chem. Soc. Dalton* 1981, 1204.
68. K. I. Gell, B. Posin, J. Schwartz and G. M. Williams, *J. Am. Chem. Soc.* 1982, **104**, 1846.
69. *JANEF Thermochemical Tables* (1971). Natl. Stand. Ref. Data. Ser., Natl., Bur. Stand., NSRDS-NBS 37, 2nd Edn. U.S. Govt Printing Office, Washington, D.C.
70. G. J. Erker, *J. Organomet, Chem.* 1977, **134**, 189.
71. T. J. Marks, *Science* 1982, **217**, 989.
72. J. W. Bruno, T. J. Marks and L. R. Morss, *J. Am. Chem. Soc.* 1983, **105**, 6824.
73. P. L. Watson, *J. Am. Chem. Soc.* 1983, **105**, 6491.
74. P. L. Watson, *J. Chem. Soc., Chem. Comm.* 1983, 276.
75. P. L. Watson, *J. Am. Chem. Soc.* 1982, **104**, 337.

Polyhedron Vol. 4, No. 2, pp. 201–206, 1985
Printed in Great Britain.

0277–5387/85 $3.00 + .00
© 1985 Pergamon Press Ltd.

POLAROGRAPHIC STUDY OF Eu(III)-SUCCINATE-ETHYLENEDIAMINE AND Eu(III)-MALONATE-ETHYLENEDIAMINE MIXED SYSTEMS

MADHU SHIVHARE and MUKHTAR SINGH*
Chemistry Department, Agra College, Agra 282002, India

(*Received* 1 *November* 1983, *accepted after revision* 16 *April* 1984)

Abstract—The mixed complexes of Eu(III) with succinate ($succ^{2-}$) and malonate (mal^{2-}) and ethylenediamine (en) have been studied polarographically at 25°C and at constant ionic strength, μ = 0.1 ($NaNO_3$) and pH 6. The reduction of the complexes in each case is quasi-reversible and diffusion-controlled. In each system three mixed complexes are formed, viz. $[Eu(succ)(en)]^+$, $[Eu(succ)(en)_2]^+$ and $[Eu(succ)_2(en)]^-$ with stability constants $\log \beta_{11}$ = 9.2, $\log \beta_{12}$ = 17.5 and $\log \beta_{21}$ = 11.7; and $[Eu(mal)(en)]^+$, $[Eu(mal)_2(en)_2]^-$ and $[Eu(mal)_3(en)]^{3-}$ with stability constants $\log \beta_{11}$ = 11.4, $\log \beta_{22}$ = 19.08 and $\log \beta_{31}$ = 13.5 respectively.

Macero *et al.*[1,2] studied polarographically the formate and acetate complexes of Eu(III). Zutshi[3] reported results on Eu(III)-benzoate and salicylate complexes in formamide water mixtures. Holleck[4] reported complexation of Eu(III) with citrate, tartrate, salicylate and lactate ions. Onstott[5] studied the polarographic behaviour of Eu(III) in the presence of ethylenediamine tetraacetic acid (EDTA) and concluded that the formation of different complex species is pH dependent. Tananaeva and Kostromina[6] also studied polarographically the complexing of Eu(III) with EDTA at different pH values. Lal[7–9] has studied polarographically the complexation of Eu(III) with some amino acids viz. L-proline, DL-tryptophan and L-histidine. In all these systems the reduction of Eu(III) is quasi-reversible and diffusion-controlled. Eu(III) forms two successive complexes with L-proline, while a single complex is formed each with DL-tryptophan and L-histidine. A critical examination of the work of Lal, however, shows that while computing the values of stability constants the total (analytical) concentration has been considered instead of the free ligand concentration which ought to have been calculated from the pH of the solution and pK_a of each amino acid. Very recently, Rao and Singh[10] have reported that for the system Eu(III)-crotonic/acrylic acid while the reduction of Eu(III) is quasi-reversible in 1.0 M $NaClO_4$, the Eu(III) complexes with these acids are reduced reversibly at d.m.e. Bhansali and Nemade[11] have reported a polarographic study of Eu(III)-hydroxamic acid complexes. In both hydroxamic acids—phenyl acetohydroxamic acid (PAHA) and acetohydroxamic acid (AHA)—the polarographic reduction of Eu(III) has been found to be quasi-reversible and diffusion-controlled.

From the foregoing survey of the literature it is evident that the mixed complexes of Eu(III) with carboxylate ions and ethylenediamine have not been studied polarographically so far. The present paper therefore reports our results of polarographic study on Eu(III)-succinate-ethylenediamine and Eu(III)-malonate-ethylenediamine mixed systems.

EXPERIMENTAL

All the chemicals used were of A.R. grade. Ethylenediamine was A.R., BDH product and its stock solution was prepared in doubly distilled water. Stock solution (0.025 M) of Eu_2O_3 (Sigma, U.S.A.) was prepared by dissolving the oxide in the minimum amount of perchloric acid and diluting it with doubly distilled water. The concentration of Eu_2O_3 was kept constant at 0.5×10^{-3} M in each case. Potassium salts of succinic and malonic acids were used as the source of $succ^{2-}$ and mal^{2-} ions. The ionic strength was maintained constant at $\mu = 0.10$ ($NaNO_3$). Polarograms were obtained by means of a manual polarograph (Toshniwal CL 02) in conjunction with Toshniwal polyflex galvanometer (PL 50). Throughout the measurements

*Author to whom correspondence should be addressed.

the current at the end of the drop (i.e. the maximum current) was recorded. Purified nitrogen was used for removing the dissolved oxygen. All the measurements were made at 25 ± 0.1°C. Saturated calomel electrode (S.C.E.) was used as reference electrode. The d.m.e. had the following characteristics (0.1 M $NaNO_3$, open circuit): m = 3.98 mg/sec, t = 2.2 sec, $m^{2/3}\ t^{1/6}$ = 2.90 $mg^{2/3}\ sec^{-1/2}$, h_{corr} = 55 cms.

RESULTS AND DISCUSSION

The reduction of Eu(III) in succinate, malonate and ethylenediamine media separately, was found to be quasi-reversible and diffusion-controlled. The same was true in the case of the mixed systems. The wave heights are diffusion-controlled as the plots of i_d vs $h_{corr}^{1/2}$ are linear and pass through the origin. The stability constants of simple complexes of Eu(III) with succinate, malonate and ethylenediamine were determined separately prior to the study of the mixed ligand systems. Identical conditions were maintained in both the simple and mixed systems. Millicoulometric[12] studies indicate that one electron is involved in the reduction process in each case.

NATURE OF THE REDUCTION

The slopes of linear plots of $\log i/i_d - i$ vs $E_{d.e.}$ are of the order of 90 mV. The value is appreciably greater than the theoretical value of 59 mV expected for a one-electron reversible reduction process. The fact that α is greater than 0.5 at different concentrations of the ligands shows that reduction of Eu(III) is not totally[13] irreversible. The standard rate constant ($k_{s,h}$) of the electrode reaction of Eu(III) in the presence of increasing concentrations of the ligands is of the order of 1×10^{-3} cm/sec. This clearly[14] shows that the reduction of Eu(III) is quasi-reversible in the presence of increasing concentrations of the ligands. The reversible half-wave potential ($E'_{1/2}$) was determined by Gellings method.[15]

The pK_1 and pK_2 values of ethylenediamine at 25 ± 0.1°C and at $\mu = 0.1$ ($NaNO_3$) were determined by the titration method[16] using a glass electrode. These worked out to be: $pK_1 = 7.18$ and $pK_2 = 9.96$. The free ligand concentration, [en], was calculated from the pH value of the solution and pK values of the ligand.

(i) E(III)-*succinate and* Eu(III)-*malonate system*

Plots of $E'_{1/2}$ vs log [$succ^{2-}$], and vs log [mal^{2-}] are smooth curves thereby showing the formation of successive complexes. DeFord and Hume's[17] method has been applied to determine the stability constants of successive complexes. The polarographic characteristics and F_j [X] functions of Eu(III)-succinate and Eu(III)-malonate systems, respectively, are listed in Tables 1 and 2. With $succ^{2-}$, Eu(III) forms three successive complexes, viz $[Eu(succ)]^+$, $[Eu(succ)_2]^-$ and $[Eu(succ)_3]^{3-}$ with stability constants, log $\beta_1 = 2.9$, log $\beta_2 = 4.5$ and log $\beta_3 = 5.9$ respectively. With mal^{2-} Eu(III) forms four successive complexes, viz., $[Eu(mal)]^+$, $[Eu(mal)_2]^-$, $[Eu(mal)_3]^{3-}$ and $[Eu(mal)_4]^{5-}$ with stability constants log $\beta_1 = 4.1$, log $\beta_2 = 5.6$, log $\beta_3 = 6.6$ and log $\beta_4 = 8.5$ respectively.

(ii) Eu(III)-*ethylenediamine system*

Plot of $E'_{1/2}$ vs log [en] is a straight line thereby showing the formation of single complex species. The composition and stability constant of this species have been determined by Lingane's[18] method. The composition of the complex works

Table 1. Eu(III)-succinate system. $[Eu^{3+}] = 0.5 \times 10^{-3}$ M; $\mu = 0.1$ ($NaNO_3$); pH 6; temp. = 25 ± 0.1°C

$[Succ^{2-}]$ M	i_d μA	$-E_{1/2}$ V (S.C.E.)	$-E^r_{1/2}$ V (S.C.E.)	Slope mV	F_0 [X]	F_1 [X] x10^{-2}	F_2 [X] x10^{-3}	F_3 [X] x10^{-5}
0.00	2.76	0.700	0.690	75	–	–	–	–
0.005	2.58	0.721	0.710	78	2.30	–	–	–
0.01	2.55	0.749	0.740	80	7.50	6.50	–	–
0.02	2.51	0.792	0.780	82	42.67	20.83	64.15	–
0.04	2.51	0.822	0.814	85	137.33	34.07	65.17	8.77
0.06	2.44	0.845	0.837	88	345.90	57.49	82.48	8.74
0.08	2.38	0.863	0.855	90	717.49	89.50	101.98	8.99
0.10	2.31	0.875	0.869	90	1275.26	127.42	119.42	8.94

Table 2. Eu(III)-malonate system. $[Eu^{3+}] = 0.5 \times 10^{-3}$ M; $\mu = 0.1$ ($NaNO_3$); pH 6; temp. 25 ± 0.1°C

$[Mal^{2-}]$ M	i_d μA	$-E_{1/2}$ V (S.C.E.)	$-E^r_{1/2}$ V (S.C.E.)	Slope mV	F_0 [X]	F_1 [X] $\times 10^{-3}$	F_2 [X] $\times 10^{-5}$	F_3 [X] $\times 10^{-6}$	F_4 [X] $\times 10^{-8}$
0.00	2.76	0.700	0.690	75	-	-	-	-	-
0.005	2.58	0.800	0.790	80	52.48	10.29	-	-	-
0.01	2.55	0.833	0.825	80	207.96	20.69	-	-	-
0.02	2.41	0.851	0.844	83	460.87	22.99	5.49	7.45	3.22
0.04	2.38	0.890	0.882	85	2055.13	51.35	9.83	14.57	3.39
0.06	2.24	0.918	0.910	90	6493.81	108.21	16.03	20.05	3.17
0.08	2.17	0.940	0.935	90	17745.98	221.81	26.22	27.75	3.34
0.10	2.07	0.960	0.954	90	39064.29	390.63	37.86	33.86	3.28

out to be $[Eu(en)_2]^{3+}$ with stability constant log $\beta_2 = 14.4$.

(iii) Eu(III)-*succinate-ethylenediamine mixed system*

The concentration of succinate was varied from 0 to 0.1 M keeping [en] constant at 0.72×10^{-7} M. The $E_{1/2}$ values were more negative than those obtained in the absence of en (Table 4) thereby showing the formation of mixed complexes. The system was repeated at another concentration of en (1.47×10^{-7} M). The method of Schaap and McMasters[19] was used to determine the composition and stability constants of the mixed complexes. The polarographic characteristics and F_{ij} [X, Y] functions (X = $succ^{2-}$, Y = en) of this system have been presented in Table 5. From the plots of F_{ij} [X, Y] data vs [$succ^{2-}$] the following intercept values for constants A, B, C and D are obtained.

For series 1: log A = 0.30, log B = 3.20, log C = 4.84 and log D = 6.11.

For series 2: log A = 0.90, log B = 3.57, log C = 5.0 and log D = 6.21.

The stability constants have been calculated from these constants. Three mixed complexes, as noted below are formed:

$[Eu(succ)(en)]^+$; $\log \beta_{11} = 9.2$
$[Eu(succ)(en)_2]^+$; $\log \beta_{12} = 17.5$
$[Eu(succ)_2(en)]^-$; $\log \beta_{21} = 11.7$.

Table 3. Eu(III)-ethylenediamine system. $[Eu^{3+}] = 0.5 \times 10^{-3}$ M; $\mu = 0.1$ ($NaNO_3$); pH 6; temp. = 25 ± 0.1°C

$[en]_t$ M	$[en]_f$ $\times 10^7$ M	i_d μA	$-E_{1/2}$ V (S.C.E.)	$-E^r_{1/2}$ V (S.C.E.)	Slope mV
0.00	0.00	2.76	0.700	0.690	75
0.01	0.720	2.58	0.820	0.810	78
0.02	1.47	2.51	0.848	0.840	80
0.04	2.95	2.48	0.857	0.850	85
0.06	4.36	2.44	0.882	0.875	85
0.08	5.88	2.41	0.918	0.900	90
0.10	2.38	2.33	0.925	0.910	90

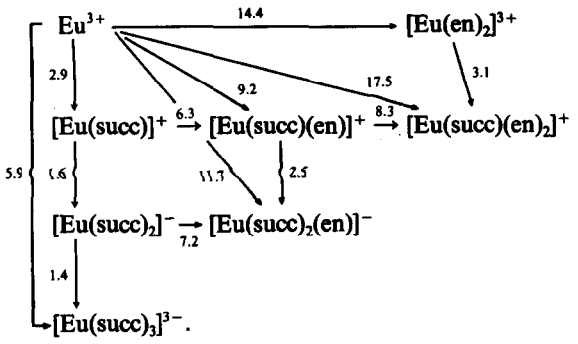
Table 4. Eu(III)-succinate-ethylenediamine system. $[Eu^{3+}] = 0.5 \times 10^{-3}$ M; $\mu = 0.1$ ($NaNO_3$); pH 6; temp. = 25 ± 0.1°C $(E_{1/2})_s = -0.70$ V (S.C.E.) $(E'_{1/2})_s = -0.69$ v (S.C.E.)

$[Succ^{2-}]$ M	i_d μA	$-E_{1/2}$ V (S.C.E.)	$-E^r_{1/2}$ (S.C.E.)	Slope mV	$F_{00}[X,Y]$	$F_{10}[X,Y]$ x10^{-2}	$F_{20}[X,Y]$ x10^{-4}	$F_{30}[X,Y]$ x10^{-5}
		Series 1 : [en] = 0.72x10^{-7} M						
0.01	2.58	0.765	0.755	75	13.42	11.42	-	-
0.02	2.51	0.808	0.799	78	76.55	37.27	10.63	-
0.04	2.48	0.838	0.829	80	249.79	61.94	11.48	-
0.06	2.41	0.860	0.852	82	629.41	104.56	14.76	12.90
0.08	2.34	0.875	0.869	85	1256.55	156.81	17.60	13.25
0.10	2.34	0.888	0.993	85	2168.00	216.60	20.06	13.06
		Series 2 : [en] = 1.47x10^{-7} M						
0.01	2.58	0.776	0.766	75	20.60	12.60	-	-
0.02	2.51	0.820	0.810	80	117.51	54.75	8.37	-
0.04	2.48	0.848	0.840	85	383.44	93.86	13.96	-
0.06	2.44	0.870	0.863	90	952.70	157.45	19.90	16.50
0.08	2.34	0.884	0.878	90	1784.26	222.03	23.00	16.25
0.10	2.27	0.896	0.891	90	3050.84	304.28	26.62	16.62

Table 5. Eu(III)-malonate-ethylenediamine system. $[Eu^{3+}] = 0.5 \times 10^{-3}$ M; $\mu = 0.1$ ($NaNO_3$); pH 6; temp. = 25 ± 0.1°C $(E_{1/2})_s = -0.70$ V (S.C.E.), $(E'_{1/2})_s = -0.69$ V (S.C.E.)

$[Mal^{2-}]$ M	i_d μA	$-E_{1/2}$ V (S.C.E.)	$-E^r_{1/2}$ V (S.C.E.)	Slope mV	$F_{00}[X,Y]$	$F_{10}[X,Y]$ x10^{-3}	$F_{20}[X,Y]$ x10^{-5}	$F_{30}[X,Y]$ x10^{-6}	$F_{40}[X,Y]$ x10^{-8}
		Series 1 : [en] = 0.7x10^{-7} M							
0.01	2.58	0.840	0.830	75	252.69	25.06	-	-	-
0.02	2.51	0.869	0.859	78	891.12	44.45	8.22	-	-
0.04	2.48	0.907	0.898	80	3673.32	91.78	15.94	24.85	4.71
0.06	2.44	0.934	0.926	85	11089.70	184.79	26.13	33.55	4.59
0.08	2.41	0.958	0.950	85	28648.37	358.07	41.25	44.06	4.75
0.10	2.33	0.975	0.969	85	60936.85	609.34	58.13	52.13	4.61
		Series 2 : [en] = 1.47x10^{-7} M							
0.01	2.58	0.855	0.845	75	447.30	43.93	-	-	-
0.02	2.51	0.885	0.877	78	1598.60	79.53	19.76	28.80	-
0.04	2.48	0.920	0.913	80	6589.61	164.54	31.13	42.82	8.20
0.06	2.44	0.949	0.941	82	19893.90	331.43	48.57	57.61	7.93
0.08	2.41	0.970	0.965	85	51392.53	642.30	75.28	76.60	8.32
0.10	2.33	0.990	0.984	85	109315.06	1093.07	105.30	91.30	8.13

The results of the present study are summarised in the following diagram where the numerical values shown are the equilibrium constants for the reactions indicated:



The mixing constant (K_m) for the reaction

$$1/2[Eu(succ)_2]^- + 1/2[Eu(en)_2]^{3+} \rightleftharpoons [Eu(succ)(en)]^+$$

is given by the relation

$$\log K_m = \log \beta_{11} - 1/2(\log \beta_{20} + \log \beta_{02}).$$

This works out to be +0.5. The positive value of log K_m indicates that the mixed complex $[Eu(succ)(en)]^+$ is more stable than the parent binary complexes, $[Eu(succ)_2]^-$ and $[Eu(en)_2]^{3+}$.

The equilibrium constants for the following disproportionation reactions

$$2[Eu(succ)(en)]^+ \rightleftharpoons [Eu(succ)_2]^- + [Eu(en)_2]^{3+} \quad (1)$$

$$2[Eu(succ)_2(en)]^- \rightleftharpoons [Eu(succ)_3]^{3-} + [Eu(en)_2]^{3+} + succ^{2-} \quad (2)$$

work out to be −0.5 and 3.1 respectively. The negative log value of equilibrium constant for the reaction (1) shows that the formation of mixed species, $[Eu(succ)(en)]^+$ is favoured over the binary complexes. This is in agreement with the conclusion arrived at on the basis of log K_m value. The positive log value for the reaction (2), however, shows that the mixed complex $[Eu(succ)_2(en)]^-$ is not favoured over the binary complexes.

The stability of the three mixed complexes follows the order:

$$[Eu(succ)(en)_2]^+ > [Eu(succ)_2(en)]^- > [Eu(succ)(en)]^+.$$

(iv) Eu(III)-*malonate-ethylenediamine system*

The concentration of malonate, was varied from 0 to 0.1 M keeping [en] (the free ligand concentration) constant at 0.72×10^{-7} M. The $E_{1/2}$ values were more negative than those obtained in the absence of en (Tables 2 and 5) thereby showing the formation of mixed complexes. The system was repeated at another concentration of en (1.47×10^{-7} M). The method of Schaap and McMasters was used to determine the composition and stability constants of the mixed complexes. The polarographic characteristics and F_{ij} [X, Y] functions [X = mal^{2-}, Y = en) of this system have been presented in Table 5. From the plots of F_{ij} [X, Y] data vs $[mal^{2-}]$ the following intercept values for constants A, B, C, D and E are obtained.

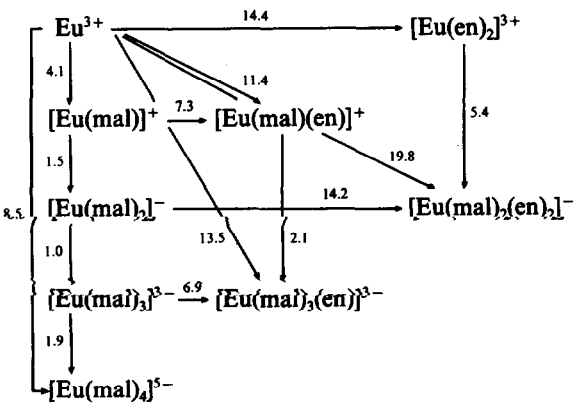
For series 1: log A = 0.30, log B = 4.44, log C = 5.77, log D = 6.77 and log E = 8.60.

For series 2: log A = 0.90, log B = 4.60, log C = 6.14, log D = 7.0 and log E = 8.90.

The stability constants have been calculated from these constants. Three mixed complexes, as noted below, are formed:

$[Eu(mal)(en)]^+$; $\log \beta_{11} = 11.4$
$[Eu(mal)_2(en)_2]^-$; $\log \beta_{22} = 19.8$
$[Eu(mal)_3(en)]^{3-}$; $\log \beta_{31} = 13.5$.

The results of the present study are summarised in the following diagram where the numerical values shown are the logarithms of the equilibrium constants for the reactions indicated:



The mixing constant (K_m) for the reaction

$$1/2[Eu(mal)_2]^- + 1/2[eu(en)_2]^{3+} \rightleftharpoons [Eu(mal)(en)]^+$$

is given by the relation

$$\log K_m = \log \beta_{11} - 1/2(\log \beta_{20} + \log \beta_{02}).$$

This works out to be −1.4. A negative value of log K_m indicates that the mixed complex, [Eu-

$(mal)(en)]^+$ is less stable than the parent binary complexes, $[Eu(mal)_2]^-$ and $[Eu(en)_2]^{3+}$.

The equilibrium constants for the following disproportionation reactions

$$2[Eu(mal)(en)]^+ \rightleftharpoons [Eu(mal)_2]^- + [Eu(en)_2]^{3+} \quad (1)$$

$$2[Eu(mal)_2(en)]^{3-} \rightleftharpoons [Eu(mal)_4]^{5-} + [Eu(en)_2]^{3+} + 2mal^{2-} \quad (2)$$

work out to be +2.8 and +6.0 respectively. The large positive values of equilibrium constant for the reactions (1) and (2) show that the formation of the mixed species $[Eu(mal)(en)]^+$ and $[Eu(mal)_3(en)]^{3-}$ is not favoured over the binary complexes.

The stability of the mixed complexes follows the order:

$$[Eu(mal)_2(en)_2]^- > [Eu(mal)_3(en)]^{3-} > [Eu(mal)(en)]^+.$$

REFERENCES

1. D. J. Macero, L. B. Anderson and P. Malachesky, *J. Electroanal. Chem.* 1965, **10**, 76.
2. D. J. Macero, H. B. Herman and A. J. Dukat, *Analyt. Chem.* 1965, **37**, 675.
3. K. Zutshi, *Rev. Polarogr. Jpn* 1967, **14**, 294.
4. L. Holleck, *Z. Naturforsch* 1947, **26**, 81.
5. E. I. Onstott, *J. Am. Chem. Soc.* 1952, **74**, 3773.
6. N. N. Tananaeva and N. A. Kostromina, *Zh. Neor. Khim.* 1969, **14**, 1205.
7. S. Lal, *Aust, J. Chem.* 1947, **26**, 81.
8. S. Lal, *Bull. Chem. Soc., Jpn.* 1973, **46**, 2232.
9. S. Lal, *Monatsh. Chem.* 1974, **105**, 974.
10. A. J. Rao and Mkhan Singh, *Indian J. Chem.* 1979, **18A**, 86.
11. P. K. Bhansali and B. I. Nemade, *Proc. Indian Acad. Sci. (Chem. Sci.)* 1982, **91**, 409.
12. T. DeVries and L. Kroon, *J. Am. Chem. Soc.* 1953, **85**, 2489.
13. R. Goto and I. Tachi, *Proc. Intern. Polarogr. Congr.* 1951, **1**, 69.
14. P. Delahay, *J. Am. Chem. Soc.* 1953, **75**, 1430.
15. P. J. Gellings, *Z. Electrochem.* 1962, **66**, 477, 48, 799; 1963, **67**, 167.
16. S. Chaberek and A. E. Martell, *J. Am. Chem. Soc.* 1953, **75**, 1430.
17. D. D. DeFord and D. N. Hume, *J. Am. Chem. Soc.* 1951, **73**, 5321.
18. J. J. Lingane, *Chem. Rev.* 1941, **29**, 1.
19. W. B. Schaap and D. L. McMasters, *J. Am. Chem. Soc.* 1961, **83**, 4699.

Polyhedron Vol. 4, No. 2, pp. 207–213, 1985
Printed in Great Britain.

0277–5387/85 $3.00 + .00
© 1984 Pergamon Press Ltd.

POLAROGRAPHIC STUDY OF MIXED LIGAND COMPLEXES OF Pb(II) WITH CARBOXYLATE IONS AND IMIDAZOLE

MADHU SHIVHARE and MUKHTAR SINGH*
Chemistry Department, Agra College, Agra 282002, India

(*Received* 21 *November* 1983; *accepted* 16 *April* 1984)

Abstract—Mixed complexes of Pb(II) with some carboxylate ions, viz. tartrate ($tart^{2-}$), malonate (mal^{2-}) and citrate ($citr^{3-}$); and imidazole (im) have been studied polarographically at 25°C and at constant ionic strength μ = 2.0 ($NaNO_3$) and at pH 6. The polarographic reduction of the complexes in each case is reversible and diffusion-controlled. Pb(II) forms a single mixed complex with tartrate and imidazole, viz [Pb(tart)(im)] with stability constant $\log \beta_{11} = 4.19$; with mal^{2-} and im, three mixed complexes, [Pb(mal)(im)], [Pb(mal)$(im)_2$] and [$Pb(mal)_2(im)]^{2-}$ with stability constants $\log \beta_{11} = 4.3$, $\log \beta_{12} = 7.3$ and $\log \beta_{21} = 5.5$ respectively are formed. With $citr^{3-}$ and im a single mixed species, $[Pb(citr)(im)]^-$ with stability constant $\log \beta_{11} = 8.0$ is formed. Various equilibria involved in the mixed systems have been discussed.

Although the polarographic method has been widely used in single[1] ligand systems, no general discussion of the application of the method to the study of mixed-ligand complexes was published until 1961 when Schaap and McMasters[2] extended DeFord and Hume's[3] polarographic method for studying single ligand complexes. This extension of the polarographic method of DeFord and Hume by Schaap and McMasters to the study of mixed ligand complexes has opened new vistas in the field of coordination chemistry. Since then many mixed-ligand systems[4] have been studied polarographically. A survey of the literature reveals that single ligand complexes of Pb(II) with various carboxylate ions have been studied polarographically by several workers.[5–12] These carboxylate ions include acetate, formate, oxalate, tartrate, citrate, malonate, succinate, glutamate, adipate and phthalate. With most of the carboxylate ions Pb(II) forms successive complexes. The composition and stability constants of these complexes have been determined by DeFord and Hume's method. However, simple complexes of Pb(II) with imidazole have not been studied polarographically so far. Li *et al.*[13] and Tanford and Wagner[14] have studied the complexes of Cd(II) with imidazole and it has been stressed that imidazole acts as a monodentate ligand. Kim *et al.*[15] have studied the mixed complexes of Pb(II) with histidine and hydroxide ion in the pH range 9–13 and determined the composition of the complexes by applying Schaap and McMasters method. Gaur and Bahgel[16] have reported that Pb(II) forms only one mixed complex with formate and maleate ions.

In earlier publications[17–19] we have reported polarographic studies on the composition and stability constants of mixed ligand complexes of Cd(II) with imidazole and various carboxylate ions. However no polarographic studies on the mixed complexes of Pb(II) with imidazole and carboxylate ions have been attempted so far. The present paper reports the results of a polarographic study on the composition and stability constants of mixed complexes of Pb(II) with imidazole and some carboxylate ions, i.e. tartrate, citrate and malonate.

EXPERIMENTAL

All the chemicals used were of analytical reagent grade and their solutions were prepared in double-distilled water. The ionic strength was maintained constant at $\mu = 2.0$ ($NaNO_3$). Imidazole and potassium salts of tartaric, malonic and citric acids were used as ligands. The concentration of Pb(II) was kept at 1×10^{-3} M. Polarograms were obtained by means of a manual polarograph (Toshniwal CL 02) in conjunction with Toshniwal polyflex galvanometer (PL 50). Throughout the measurements the current at the end of the drop (i.e. the max-

*Author to whom correspondence should be addressed.

imum current) was recorded. Purified nitrogen was used for removing the dissolved oxygen. All the measurements were made at 25 ± 0.1°C. Saturated calomel electrode (S.C.E.) was used as a reference electrode. The d.m.e. had the following characteristics (2.0 M $NaNO_3$, open circuit): m = 1.52 mg/sec; t = 3.04 sec; $m^{2/3}t^{1/6}$ = 1.59 $mg^{2/3}$ $sec^{-1/2}$, h_{corr} = 51 cm.

RESULTS AND DISCUSSION

The polarographic reduction of Pb(II) in the presence of $tart^{2-}$, mal^{2-}, $citr^{3-}$ and im separately, was found to be reversible and diffusion-controlled. The same was true in the case of the mixed systems as the slopes of $E_{d.e.}$ vs log $i/i_d - i$ plots were of the order of 31 ± mV and the plots of i_d vs $h_{corr}^{1/2}$ were linear and passed through the origin.

The pK_a value of im at 25 ± 0.1°C and at $\mu = 2.0$ ($NaNO_3$) has been determined by titration method[20] using a glass electrode. This worked out to be 7.09. The free ligand concentration, [im], was calculated from the pH value of the solution and pK_a value of the ligand.

(i) Pb(II)-$tart^{2-}$, Pb(II)-mal^{2-} *and* Pb(II)-$citr^{3-}$ *systems*

The stability constants of simple complexes of Pb(II) with carboxylate ions and imidazole were determined separately prior to the study of mixed ligand systems. Identical conditions were maintained in both the simple and mixed systems.

Plots of $E_{1/2}$ vs log[$tart^{2-}$] and log[mal^{2-}] are smooth curves thereby indicating the formation of successive complexes. DeFord and Hume's method has been applied to determine the stability constants of successive complexes. The polarographic characteristics and $F_j[X]$ functions of Pb(II)-$tart^{2-}$ and Pb(II)-mal^{2-} systems, respectively, are listed in Tables 1 and 2. With $tart^{2-}$, two successive complexes, viz., [Pb(tart)] and $[Pb(tart)_2]^{2-}$ with stability constants $\log \beta_1 = 1.30$ and $\log \beta_2 = 2.90$ respectively are formed. With mal^{2-} three successive complexes, viz. [Pb(mal)], $[Pb(mal)_2]^{2-}$ and $[Pb(mal)_3]^{4-}$ with stability constants $\log \beta_1 = 2.6$, $\log \beta_2 = 3.3$ and $\log \beta_3 = 4.5$ are formed respectively. The values of $\log \beta_1$, $\log \beta_2$ and $\log \beta_3$ for Pb(II)-mal^{2-} system obtained by Gaur and Palrecha[12] at $\mu = 2.0$ and 30°C are respectively 2.6, 3.6 and 4.3. A comparison of these values with those obtained in the present study shows that there is a difference of ±0.3 and ±0.2 log unit in the values of $\log \beta_2$ and $\log \beta_3$ respectively. This may be attributed partly to a difference in the temperature in the two cases and partly to the experimental error involved in the reproducibility of $E_{1/2}$ values. The plot of $E_{1/2}$ vs log[$citr^{3-}$] is a straight line which shows the formation of a single complex. The composition and stability constant are determined by Lingane's[1] method. The composition of the complex works out to be $[Pb(citr)]^-$ with stability constant $\log \beta_1 = 3.4$.

(ii) Pb(II)-im *system*

Plot of $E_{1/2}$ vs log[im] is a smooth curve thereby showing the formation of successive complexes. The composition and stability constants of the

Table 1. Polarographic characteristics and $F_j[X]$ functions for Pb(II)-tartrate system: [Triton X-100] = 2×10^{-3}%. $[Pb^{2+}] = 1 \times 10^{-3}$ M; $\mu = 2.0$ ($NaNO_3$); pH 6; temp. = 25 ± 0.1°C

$[tart^{2-}]$	i_d μA	$-E_{1/2}$ V (S.C.E.)	Slope mV	$F_0[X]$	$F_1[X]$	$F_2[X]$ x10^{-2}
0.00	7.26	0.400	30	–	–	–
0.10	6.60	0.426	30	8.34	73.44	–
0.20	6.46	0.444	31	34.63	168.25	7.41
0.30	6.40	0.455	31	82.48	271.60	8.38
0.40	6.33	0.462	32	143.81	357.03	8.42
0.50	6.33	0.467	32	212.34	422.69	8.05
0.60	6.20	0.472	33	320.00	531.97	8.53

Table 2. Polarographic characteristics and $F_j[X]$ functions for Pb(II)-malonate system: [Triton X-100] = 2×10^{-3}%. $[Pb^{2+}] = 1 \times 10^{-3}$ M; $\mu = 2.0$ ($NaNO_3$); pH 6; temp. = 25 ± 0.1°C

$[Mal^{2-}]$ M	i_d μA	$-E_{1/2}$ V (S.C.E.)	Slope mV	$F_0[X]$	$F_1[X]$ $\times 10^{-2}$	$F_2[X]$ $\times 10^{-3}$	$F_3[X]$ $\times 10^{-4}$
0.00	7.26	0.400	30	-	-	-	-
0.10	6.53	0.459	30	110.36	10.93	6.93	-
0.20	6.46	0.474	31	358.92	17.89	6.94	-
0.30	6.40	0.490	31	1262.11	42.03	12.67	3.53
0.40	6.33	0.500	32	2780.35	69.48	16.37	3.57
0.50	6.27	0.508	33	5240.82	104.77	20.15	3.71
0.60	6.20	0.515	33	9140.08	164.66	24.71	3.78

complexes have been determined by DeFord and Hume's method. An analysis of $F_j[X]$ functions (Table 4) reveals the formation of three successive complexes, viz $[Pb(im)]^{2+}$, $[Pb(im)_2]^{2+}$ and $[Pb(im)_3]^{2+}$ with stability constants, $\log \beta_1 = 2.9$, $\log \beta_2 = 4.3$ and $\log \beta_3 = 6.3$.

(iii) Pb(II)-$tart^{2-}$-im *system*

[$tart^{2-}$] was varied from 0 to 0.6 M keeping [im] constant at 0.0064 M. The $E_{1/2}$ values were more negative than those obtained in the absence of im (Tables 1 and 5) thereby showing the formation of mixed complexes. The composition and stability constants of the mixed complexes have been determined by Schaap and McMasters method.[2] The polarographic characteristics and $F_{ij}[X, Y]$ functions [X = $tart^{2-}$, Y = im) of this system at fixed concentration (free) of im (0.0064 M) are presented in Table 5. From the plots of $F_{ij}[X, Y]$ data vs [$tart^{2-}$] the following intercept values for constants A, B and C are obtained.

$\log A = 1.30$, $\log B = 2.07$ and $\log C = 3.17$. An

Table 3. Polarographic characteristics of Pb(II)-citrate system: [Triton X-100] = 2×10^{-3}%. $[Pb^{2+}] = 1 \times 10^{-3}$ M; $\mu = 2.0$ ($NaNO_3$); pH 6; temp. = 25 ± 0.1°C

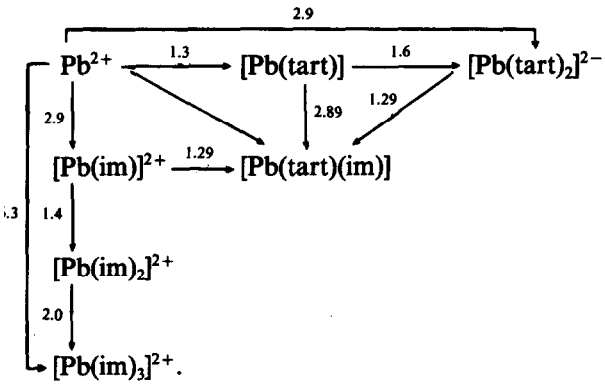
$[Citr^{3-}]$ M	i_d μA	$-E_{1/2}$ V (S.C.E.)	Slope mV
0.00	7.26	0.400	30
0.05	6.60	0.436	30
0.10	6.46	0.450	31
0.15	6.40	0.460	32
0.20	6.27	0.467	33
0.25	6.13	0.470	33
0.30	6.0	0.474	33

Table 4. Polarographic characteristics and $F_j[X]$ functions for Pb(II)-imidazole system: [Triton X-100] = 2×10^{-3}%. $[Pb^{2+}] = 1 \times 10^{-3}$ M; $\mu = 2.0$ ($NaNO_3$); pH 6; temp. = 25 ± 0.1°C

$[Im]_{total}$ M	$[Im]_{free}$	i_d μA	$-E_{1/2}$ V (S.C.E.)	Slope, mV	F_0 [X]	F_1 [X] $\times 10^{-2}$	F_2 [X] $\times 10^{-4}$	F_3 [X] $\times 10^{-6}$
0.00	0.00	6.60	0.400	30	-	-	-	-
0.20	0.0016	5.94	0.411	30	2.61	-	-	-
0.04	0.0032	5.67	0.416	31	4.04	9.50	4.68	-
0.06	0.0047	5.61	0.423	32	7.06	12.89	10.40	-
0.08	0.0064	5.61	0.430	32	12.02	17.50	14.84	2.00
0.10	0.0079	5.47	0.436	33	19.93	23.96	20.20	2.33
0.15	0.0072	5.41	0.448	33	51.41	42.00	28.33	2.19
0.20	0.0162	5.34	0.458	33	113.40	69.38	37.08	2.21

analysis of these constants shows the formation of only one mixed complex, [Pb(tart)(im)] with stability constant $\log \beta_{11} = 4.19$.

The results of the present study are summarised in the following diagram where the numerical values shown are the logarithms of the equilibrium constants for the reactions indicated:



The mixing constant (K_m) for the reaction

$$\tfrac{1}{2}[Pb(tart)_2]^{2-} + \tfrac{1}{2}[Pb(im)_2]^{2+} \rightleftharpoons [Pb(tart)(im)]$$

is given by the relation

$$\log K_m = \log \beta_{11} - \tfrac{1}{2}(\log \beta_{20} + \log \beta_{02}).$$

This works out to be +0.59. The positive value of log K_m indicates that the mixed complex [Pb(tart)(im)] is more stable than the parent binary complexes, $[Pb(tart)_2]^{2-}$ and $[Pb(im)_2]^{2+}$.

The equilibrium constant (log value) for the following disproportionation reaction

$$2[Pb(tart)(im)] \rightleftharpoons [Pb(tart)_2]^{2-} + [Pb(im)_2]^{2+}$$

works out to be −1.8. The negative log value shows that the formation of mixed species [Pb(tart)(im)] is favoured over the simple binary complexes. This is in agreement with the conclusion arrived at on the basis of log K_m value.

(iv) Pb(II)-*malonate-imidazole system*:

$[mal^{2-}]$ was varied from 0 to 0.6 M keeping [im] constant at 0.0032 M. The composition and stability constants were determined by Schaap and McMasters method. The system was repeated at another concentration (free) of im (0.0064 M). The polarographic characteristics and $F_{ij}[X, Y]$ functions ($X = mal^{2-}$, $Y = im$) of this system at fixed [im] are presented in Table 6. From the plots of $F_{ij}[X, Y]$ data vs. $[mal^{2-}]$; the following intercept values for the constants A, B, C and D are obtained.

For series 1: log A = 0.69, log B = 3.14, log C = 3.47 and log D = 4.64.
For series 2: log A = 1.30, log B = 3.47, log C = 3.60 and log D = 4.77.

Table 5. Polarographic characteristics and $F_{ij}[X, Y]$ functions for Pb(II)-tartrate-imidazole system; [Triton X-100] = 2×10^{-3}%. $[Pb^{2+}] = 1 \times 10^{-3}$ M; μ = 2.0 ($NaNO_3$); pH 6; temp. = 25 + 0.1°C ($E_{1/2}$), = −0.40 V (S.C.E.)

$[Tart^{2-}]$ M	i_d μA	$-E_{1/2}$ V (S.C.E.)	Slope mV	$F_{00}[X,Y]$	$F_{10}[X,Y]$ $\times 10^{-1}$	$F_{20}[X,Y]$ $\times 10^{-3}$
0.10	6.53	0.450	31	54.72	34.72	-
0.20	6.53	0.458	31	102.09	41.04	1.45
0.30	6.46	0.466	32	192.39	57.46	1.51
0.40	6.40	0.473	32	335.46	78.86	1.67
0.50	6.33	0.478	33	500.49	96.09	1.68
0.60	6.27	0.481	33	638.92	103.15	1.51

Table 6. Polarographic characteristics and $F_{ij}[X, Y]$ functions for Pb(II)-malonate-imidazole system: [Triton X-100] = 2×10^{-3}%. $[Pb^{2+}] = 1 \times 10^{-3}$ M; μ = 2.0 ($NaNO_3$); pH 6; temp. = 25 ± 0.1°C ($E_{1/2}$), = −0.40 V (S.C.E.)

$[Mal^{2-}]$ M	i_d μA	$-E_{1/2}$ V (S.C.E.)	Slope mV	$F_{00}[X,Y]$	$F_{10}[X,Y]$ $\times 10^{-2}$	$F_{20}[X,Y]$ $\times 10^{-3}$	$F_{30}[X,Y]$ $\times 10^{-4}$
Series 1 : $[Im]_{free}$ = 0.0032 M							
0.05	6.46	0.460	30	120.53	-	-	-
0.10	6.46	0.468	31	224.85	21.98	7.98	4.07
0.20	6.40	0.483	31	731.39	36.31	11.15	3.54
0.30	6.33	0.494	32	1741.80	57.89	14.63	4.42
0.40	6.20	0.504	32	3877.93	96.82	20.70	4.42
0.50	6.13	0.611	33	6764.72	135.19	24.23	4.24
0.60	6.07	0.618	33	11800.40	196.59	30.43	4.57
Series 2 : $[Im]_{free}$ = 0.0064 M							
0.05	6.40	0.465	31	179.82	31.96	-	-
0.10	6.40	0.476	31	423.83	40.38	10.38	6.38
0.20	6.33	0.488	32	1091.18	53.55	11.77	8.88
0.30	6.27	0.499	32	2598.66	85.65	18.16	4.88
0.40	6.20	0.509	33	5727.98	142.64	28.16	6.04
0.50	6.13	0.516	33	9988.49	199.36	33.87	5.94
0.60	6.07	0.523	33	17424.00	290.06	43.34	6.55

Table 7. Polarographic characteristics and $F_{ij}[X, Y]$ functions for Pb(II)-Citrate-imidazole system: [Triton X-100] = 2×10^{-3}%. $[Pb^{2+}] = 1 \times 10^{-3}$ M; μ = 2.0 ($NaNO_3$); pH 6; temp. = 25 ± 0.1°C $(E_{1/2})_s$ = −0.40 V (S.C.E.)

$[Citr^{3-}]$ M	i_d μA	$-E_{1/2}$ V (S.C.E.)	Slope mV	$F_{00}[X,Y]$	$F_{10}[X,Y]$ $\times 10^{-2}$	$F_{20}[X,Y]$ $\times 10^{-2}$	$F_{30}[X,Y]$ $\times 10^{-3}$
Series 1 : $[Im]_{free}$ = 0.0032 M							
0.05	6.53	0.440	30	25.62	4.32	38.48	-
0.10	6.33	0.454	31	77.09	7.30	49.09	-
0.15	6.20	0.464	31	171.63	11.17	58.50	9.60
0.20	6.07	0.474	31	302.65	14.93	62.66	9.33
0.25	5.94	0.477	32	493.79	19.59	68.76	9.90
0.30	5.94	0.482	32	729.12	24.17	72.56	9.50
Series 2 : $[Im]_{free}$ = 0.0064 M							
0.05	6.33	0.444	31	35.35	-	-	-
0.10	6.33	0.458	31	105.29	8.92	49.20	-
0.15	6.07	0.467	32	221.38	13.69	64.61	20.40
0.20	6.07	0.475	33	412.99	19.84	79.20	22.60
0.25	5.94	0.481	33	674.45	26.33	89.32	22.12
0.30	5.94	0.487	33	1076.58	35.21	104.00	23.33

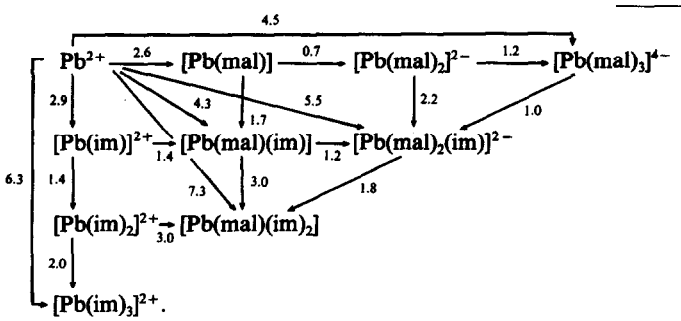
The stability constants of the mixed complexes have been calculated from the values of these constants. Three mixed complexes as noted below are formed:

$$[Pb(mal)(im)]; \quad \log \beta_{11} = 4.3$$

$$[Pb(mal)(im)_2]; \quad \log \beta_{12} = 7.3$$

$$[Pb(mal)_2(im)]^{2-}; \quad \log \beta_{21} = 5.5.$$

The results of the present study are summarised in the following diagram where the numerical values shown are the logarithms of the equilibrium constants for the reactions indicated:



The mixing constant (K_m) for the reaction

$$\tfrac{1}{2}[Pb(mal)_2]^{2-} + \tfrac{1}{2}[Pb(im)_2]^{2+} \rightleftharpoons [Pb(mal)(im)]$$

is given by the relation

$$\log K_m = \log \beta_{11} - \tfrac{1}{2}(\log \beta_{20} + \log \beta_{02}).$$

This works out to be + 0.5. The positive log value shows that the mixed complex, [Pb(mal)(im)] is more stable than the parent binary complexes, $[Pb(mal)_2]^{2-}$ and $[Pb(im)]^{2+}$.

The equilibrium constants for the following disproportionation reactions

$$2[Pb(mal)(im)_2] \rightleftharpoons [Pb(mal)_2]^{2-} + [Pb(im)_2]^{2+} \quad (1)$$

$$2[Pb(mal)(im)_2] \rightleftharpoons [Pb(mal)_2]^{2-} + [Pb(im)_3]^{2+} + im \quad (2)$$

$$2[Pb(mal)_2(im)]^{2-} \rightleftharpoons [Pb(mal)_3]^{4-} + [Pb(im)_2]^{2+} + mal^{2-} \quad (3)$$

work out to be -2.0, -5.0 and -2.20 respectively. The large negative log values show that the formation of mixed complexes, $[Pb(mal)(im)]$, $[Pb(mal)(im)_2]$ and $[Pb(mal)_2(im)]^{2-}$ is favoured over the simple ones.

The stability of these mixed complexes follows the order:

$$[Pb(mal)(im)_2] > [Pb(mal)_2(im)]^{2-} > [Pb(mal)(im)].$$

(v) Pb(II)-*citrate-imidazole system*:

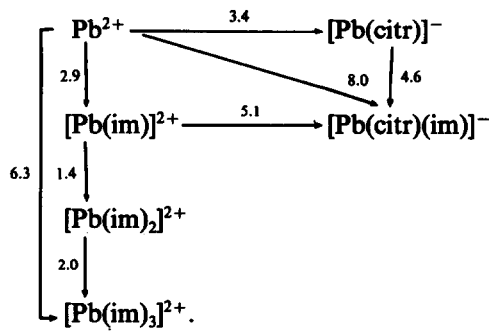
$[citr^{3-}]$ was varied from 0 to 0.3 M keeping [im] constant at 0.0032 M. The system was repeated at another concentration (free) of im(0.0064 M). The composition and stability constants were determined by Schaap and McMasters method. The polarographic characteristics and $F_{ij}[X, Y]$ functions ($X = citr^{3-}$, $Y = im$) are presented in Table 7. From the plots of $F_{ij}[X, Y]$ data vs. $[citr^{3-}]$, the following intercept values for constants A, B, C and D are obtained.

For series 1: log A = 0.60, log B = 2.38, log C = 3.64 and log D = 3.97.

For series 2: log A = 1.20, log B = 2.60, log C = 3.66 and log D = 4.20.

An analysis of these constants shows the formation of only one mixed species, $[Pb(citr)(im)]^-$ with $\log \beta_{11} = 8.0$. A negative value of $\log \beta_{12}$ precludes the formation of the species, $[Pb(citr)(im)_2]^-$.

The results of the present study are summarised in the following diagram where the numerical values shown are the logarithms of the equilibrium constants for the reactions indicated:



Acknowledgement—One of the authors (Km. M. Shivhare) is grateful to CSIR, New Delhi for the award of a Senior Research Fellowship.

REFERENCES

1. J. J. Lingane, *Chem. Rev.* 1941, **29**, 1.
2. W. B. Schaap and D. L. McMasters, *J. Am. Chem. Soc.* 1961, **83**, 4699.
3. D. D. DeFord and D. N. Hume, *J. Am. Chem. Soc.* 1951, **75**, 5321.
4. P. N. Gupta and S. A. Bhatt, *J. Electrochem. Soc. India* 1982, **13**, 171.
5. E. A. Burns and D. N. Hume, *J. Am. Chem. Soc.* 1956, **78**, 3958.
6. H. M. Hershenson, R. T. Brooks and M. E. Murphy, *J.Am.Chem.Soc.* 1957, **79**, 2046.
7. D. S. Jain and J. N. Gaur, *J. Indian Chem. Soc.* 1966, **43**, 425.
8. T. Meites and L. Meites, *J. Am. Chem. Soc.* 1949, **71**, 3269; 1950, **72**, 180; 1950, **72**, 184; 1951, **73**, 1161.
9. L. Meites, *J. Am. Chem. Soc.* 1951, **73**, 3727.
10. T. Nozak, M. Kodowak, D. Sagawa and K. Orita, *Chem. Abstr.* 1970, **72**, 106577.
11. J. K. Gupta and C. M. Gupta, *J. Prakt Chem.* 1969, **39**, 685.
12. J. N. Gaur and M. M. Palrecha, *Talanta* 1967, **15**, 583.
13. N. C. Li, J. M. White and E. Doody, *J. Am. Chem. Soc.* 1954, **76**, 6219.
14. C. Tanford and M. L. Wagner, *J. Am. Chem. Soc.* 1953, **75**, 434.
15. K. Kim, Y. K. Park, J. D. Suh and C. H. Lee, *Chem. Abstr.* 1974, **80**, 3173q.
16. J. N. Gaur and S. C. Baghel, *Proc. 14th Semin, Electrochem.* 1973. Centre for Electrochemical Research, Institute of Karaikudi, India.
17. M. Shivhare and M. Singh, *J. Inorg Nucl. Chem.* 1981, **43**, 1599.
18. M. Shivhare, Krishna and M. Singh, *J. Inorg. Nucl. Chem.* 1981, **43**, 2885.
19. M. Shivhare and M. Singh, *J. Electrochem. Soc., India* 1981, **30**, 277.
20. S. Chaberek and A. E. Martell, *J. Am. Chem. Soc.* 1953, **75**, 1430.

Polyhedron Vol. 4, No. 2, pp. 215–219, 1985
Printed in Great Britain

0277–5387/85 $3.00 + .00
© 1985 Pergamon Press Ltd.

TRANSITION METAL COMPLEXES WITH 1,3-BIS-(2-HYDROXYPHENYL)-1,3-PROPANEDIONE—I

MONONUCLEAR COMPLEXES

F. TEIXIDOR, A. LLOBET, L. ESCRICHE and J. CASABÓ*
Departament de Química Inorgànica, Universitat Autònoma de Barcelona, (Bellaterra), Barcelona, Spain

(*Received* 17 *November* 1983; *accepted* 16 *April* 1984)

Abstract—Reaction of 1,3-(2-hydroxyphenyl)-1,3-propanedione ($BhPPH_3$), a ligand with three possible sites of coordination acting as a chelating agent, with metal acetates results in the formation of mononuclear species $M(BhPPH_2)_2S,S'$ (M=Mn, Fe, Co, Ni, Zn; S,S'=CH_3OH, C_2H_5OH or H_2O); $M'(BhPPH_2)_2$ (M'=Cu, Pd), and $M''(BhPPH_2)_3S,S'$ (M''=Fe, Al). The complexes have been studied by ^{1}H-NMR when possible, and IR spectra. The position of the methine proton (=CH−) at 6.88 ppm in $Zn(BhPPH_2)_2S,S'$ indicates that $BhPPH_3$ behaves in mononuclear complexes as a common β-diketone. Most of the complexes lose S,S' molecules on heating but a crystal structure of $Zn(BhPPH_2)_2 \cdot 2C_2H_5OH$ indicates that the C_2H_5OH molecules are oxygen bonded to the metal centre.

The chemistry of β-diketones has received considerable interest through the years.[1–3] They appear to have been investigated with virtually every metal and metalloid[4] in the periodic table, mainly due to the interest in the structure and reactivity of these compounds.[5] On the other hand, in the last decade a growing interest in physico-chemical studies, homogeneous catalysts and the design of compounds with unusual properties[6] has stimulated the development of discrete di- and tri-nuclear complexes. Ligands such as β-triketones and the analogous β-ketophenols,[6,7] diamine Schiff base derivatives of 1,3,5-triketones, keto-acids and ketophenols[8] have been shown to form homo- and heterodi-nuclear complexes. To our knowledge a very limited literature about tri-nucleating ligands exists.[9,10] It has been proven that the heterodinuclear complexes may be obtained more easily when the ligand contain two sites with different ligand field strengths, e.g. O_2O_2 and N_2O_2. However, concern is increasing to obtain stable mononuclear complexes of these polychelating ligands since they, may be transformed by heating into homodinuclear complexes,[6] e.g. the mononuclear Cu(II) chelate of 2-acetoacetylphenol which is obtained at 15°C. rearranges to the binuclear chelate on heating.[11] With the aim of obtaining a ligand that (a) has three possible compartments, with one of these compartments more reactive and clearly different from the other two, and (b) the synthesis of homotri-, and heterotrinuclear complexes, we have tested for the first time as a complexing agent the compound 1,3-bis-(2-hydroxyphenyl)-1,3-propanedione. ($BhPPH_3$)

As may be seen in Fig. 1 there are three possible sites of coordination, two of them equivalent (ketophenol) and the β-diketone. In this paper we have reacted $BhPPH_3$ with stoichiometric amounts of metal salts and have obtained pure mononuclear complexes with the metal chelated, in all cases, by the β-diketone group. An overnight refluxing of some of these complexes yielded again the starting mononuclear material. Forthcoming papers will deal with the synthesis and physical properties of di and trinuclear complexes.

EXPERIMENTAL

General

IR spectra were obtained on a Beckman IR-20A as KBr pellets. The ^{1}H NMR and ^{13}C-NMR were recorded on a Bruker WP8OSY. The mass spectrum was recorded in a HP5985 GC/MS system. The TLC were done using DC-Alufolien Kieselgel

*Author to whom correspondence should be addressed.

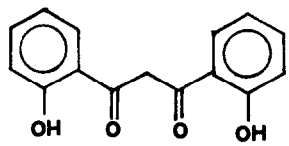


Fig. 1.

60 F_{254}(Merck). All reagents were analytical grade and were used as received. The complexes were analysed in our laboratories as follows: The transition metal ions by titration with EDTA and C,H on a Perkin–Elmer 240B. All yields are quoted relative to $BhPPH_3$.

Synthesis of 1,3-*bis*-(2-*hydroxyphenyl*)-1,3-*propanedione* ($BhPPH_3$)

The synthesis was performed as previously reported[12] however it afforded much better yield when dilute hydrochloric acid ($\simeq 5\%$) was used instead of acetic acid.[13]

Synthesis of complexes of general formula $M(BhPPH_2)_2 \cdot S,S'$

In Table 1 the meaning of M,S and S', the colour, the yields and the observed and calculated analyses for the different complexes are indicated.

Synthesis of $Zn(BhPPH_2)_2 \cdot CH_3OH \cdot H_2O$

This preparation describes a typical procedure. Subsequent descriptions include only the essential differences. To 25 cm^3 of warm methanol in a 100 cm^3 beaker was added 512 mg (2 mmol) of $BhPPH_3$. After complete dissolution hydrated zinc acetate 220 mg (1 mmol) in 15 cm^3 of warm methanol was added. Almost instantly, a pale yellow crystalline solid begins to separate. The contents of the beaker was stirred and kept warm for an additional five minute period. After cooling the mixture to 25°C the solid was separated by filtration and washed with methanol and ether. The pale yellow solid was dried under vacuum.

Crystals suitable for an X-ray analysis were obtained in the following way. The crude compound was dissolved in the minimum amount of tetrahydrofuran (THF) and ethanol was added (approximately four times the volume of THF). Upon the slow evaporation of the mixture large pale yellow crystals with general formula $Zn(BhPPH_2)_2 \cdot 2EtOH$ were obtained.

The syntheses concerning Mn, Co, Ni, Cu and Fe have been done in a similar way. However, the $Fe(BhPPH_2)_2 \cdot CH_3OH \cdot H_2O$ complex was obtained using Mohr's salt in water solution.

Synthesis of $Pd(BhPPH_2)_2$

Under N_2, to 25 cm^3 of warm methanol in a 100 cm^3 three necked flask were added 512 mg (2 mmol) of $BhPPH_3$. After this dissolved, lithium methanolate (2 mmol)[14] and $PdCl_4Na_2$ (1 mmol) were subsequently added in this order. On cooling the resulting reddish solution a dark yellow solid separated which was filtrated and washed with

Table 1. Color, yield and analytical data for $M(BhPPH_2)_2S,S'$ and $M(BhPPH_2)_3S,S'$ complexes

Complex	Color	Yield	Analyses Calc.			Analyses Found		
			C	H	M	C	H	M
$Mn(BhPPH_2)_2 \cdot CH_3OH \cdot H_2O$	orange	66	60.49	4.58	8.92	59.77	4.40	8.76
$Mn(BhPPH_2)_2$	orange		63.73	3.92	9.72	63.60	3.81	9.67
$Fe(BhPPH_2)_2 \cdot CH_3OH \cdot H_2O$	dark red	84	60.35	4.54	9.06	60.43	4.51	8.98
$Co(BhPPH_2)_2 \cdot 2CH_3OH$	orange	79	60.65	4.77	9.30	60.04	4.52	9.18
$Co(BhPPH_2)_2$	orange		63.28	3.89	10.35	63.14	3.61	10.21
$Ni(BhPPH_2)_2 \cdot 2H_2O$	green	99	59.48	4.30	9.70	59.76	4.40	9.56
$Ni(BhPPH_2)_2$	green		63.30	3.90	10.31	63.44	3.81	10.32
$Cu(BhPPH_2)_2$	yellow	90	62.77	3.86	11.07	62.69	3.80	11.10
$Zn(BhPPH_2)_2 \cdot CH_3OH \cdot H_2O$	pale yellow	93	59.48	4.51	10.44	59.38	4.40	10.49
$Zn(BhPPH_2)_2$	pale yellow		62.57	3.85	11.35	62.44	3.78	11.34
$Zn(BhPPH_2) \cdot 2CH_3CH_2OH$	orange		61.13	5.13	9.80	61.15	5.14	9.91
$Pd(BhPPH_2)_2$	dark yellow	81	58.41	3.60	17.25	58.48	3.54	17.15
$Al(BhPPH_2)_3$	pale yellow	49	68.20	4.17		68.14	4.04	
$Fe(BhPPH_2)_3 \cdot 2H_2O$	dark violet	40	63.02	4.31		63.20	4.25	

water, methanol and ether. The solid was dried under vacuum.

Synthesis of $Al(BhPPH_2)_3$.

To 50 cm^3 of warm absolute ethanol in a 100 cm^3 beaker was added 512 mg of $BhPPH_3$. After complete dissolution, 250 mg (0.67 mmols) of $Al(NO_3)_3 \cdot 9H_2O$ in 20 cm^3 of warm absolute ethanol was added. After a few minutes a yellowish solid separated which was filtered and washed with ethanol. Yield 250 mg, 49% (Analyses as indicated in Table 1). The pH of the resulting mother liquor was acidic and upon a very slow addition of concentrated aqueous NH_3 till pH 5[15] more solid was collected. Yield 150 mg, 28%. However, the analysis of this second fraction was not completely satisfactory. A TLC of this last solid in a mixture of chloroform–methylene chloride (1/2, v/v) displayed three spots with Rf = 0.045; 0.22 and 0.34; the color intensity of the latter corresponding to pure $Al(BhPPH_2)_3$ being much stronger than the other two.

Synthesis of $Fe(BhPPH_2)_3$

The synthesis was run as for $Al(BhPPH_2)_3$. Yield, 40%. No attempt was made to get a better yield by increasing the pH of the solution.

Solvent or water molecules elimination

In all cases, except for $Fe(BhPPH_2)_2 \cdot CH_3OH \cdot H_2O$, the S,S′ molecules have been eliminated by heating the crude solid in an oven at 110–120°C for 5–10 hr. Analyses of the resulting solids have been performed indicating the stoichiometries $M(BhPPH_2)_2$.

RESULTS

Synthetic studies

The complexes $M(BhPPH_2)_2S,S'$ (M=Mn, Fe, Co, Ni, Zn; S,S′ = CH_3OH or H_2O) (see Table 1) and $M'(BhPPH_2)_2$ (M′ = Cu, Pd) were prepared by treating the corresponding hydrated metal acetate with $BhPPH_3$ in methanol.

$$M(CH_3COO)_2 \cdot xH_2O + 2BhPPH_3 \xrightarrow{MeOH} M(BhPPH_2)_2 \cdot yMeOH \cdot zH_2O + 2CH_3COOH + (x-z)H_2O \quad (y,z = 0 \text{ or } 1)$$

In a similar way, the aluminium and Fe(III) complexes were prepared from the metal nitrates and $BhPPH_3$ in methanol. In these cases the yields found were low because of the increasing acidity of the medium.

$$M(NO_3)_3 \cdot xH_2O + 3BhPPH_3 \xrightarrow{MeOH} M(BhPPH_2)_3 + 3NO_3^- + 3H^+.$$

A better yield was obtained by addition of aqueous NH_3, but, care must be taken not to exceed pH = 5.[15] Even at this pH two additional products, not yet identified and in low yield have been found in addition to $Al(BhPPH_2)_3$.

The S,S′ molecules were easily removed on heating at 110–120°C for a few hours yielding complexes of stoichiometry $M(BhPPH_2)_2$. The only case where those molecules have not been removed at these temperatures is the $Fe(BhPPH_2)_2 \cdot CH_3OH \cdot H_2O$ complex. In addition, these S,S′ molecules are easily replaceable, e.g. the dissolving of $Zn(BhPPH_2)_2 \cdot CH_3OH \cdot H_2O$ in a mixture containing tetrahydrofuran:ethanol (1/4, v/v) afforded the complex $Zn(BhPPH_2)_2 \cdot C_2H_5OH$. Efforts are now underway to correlate this exchange with the geometry and bulkiness of the alcohol.

Spectral studies

The IR spectra of the M(II) complexes exhibit very characteristic absorptions at 1620(s), 1590(s), 1520(vs), 1480(m) cm^{-1}, common in all of them Figure 2 shows the 1700–1400 cm^{-1} range for $Cu(BhPPH_2)_2$. Based on the work of Pinchas and coworkers[16] the absorptions at 1590 and 1520 cm^{-1} are tentatively assigned to C⁻⁻O and C⁻⁻C stretching modes, respectively. Absorptions at ≃3440 cm^{-1} in the complexes with solvent molecules are indicative, and consistent with the analytical data for OH groups in the molecule. The IR spectra of the non-solvated complexes display an almost identical pattern in the 1700–1400 cm^{-1} area, however in certain compounds a few differ-

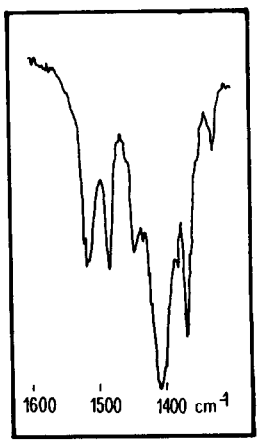


Fig. 2. IR spectrum of the complexes with general formula $M(BhPPH_2)_2 \cdot S,S'$ in the 1700–1400 cm^{-1} spectral range.

ences are observed in the 1250–1400 cm^{-1} region of the spectrum, basically two bands at 1350 and 1330 cm^{-1} in the solvated complex coalesce into one at 1330 cm^{-1}. The absence of the band at ≃3400 cm^{-1} is, however, the best indication for a non-solvated complex. In general, the IR spectra of the M(III) complexes do not differ qualitatively from those of the M(II) complexes.

The ^{1}H NMR spectra of $Zn(BhPPH_2)_2S,S'$ and $Al(BhPPH_2)_3$ are almost identical in the aromatic region. (See Fig. 3). Mainly, three groups of signals may be considered in this region (6.5–.8.5 ppm) at ≃8, 7.3 and 6.9 ppm with integrations 2:2:5, respectively. The feature of intensity 5, which is in fact a group of three signals is assigned to two protons of each benzene group of the $BhPPH_2$ moiety and to the methine (=CH–) proton. On comparison with the ^{1}H-NMR of non-coordinated $BhPPH_3$ the methine signal has been tentatively assigned at 6.85 ppm on the $Zn(BhPPH_2)_2 \cdot CH_3OH \cdot H_2O$ complex. No assignment of this (=CH–) proton signal in the $Al(BhPPH_2)_3$ complex has been made because of additional splitting of the group at 6.9 ppm. The phenolic proton resonance is observed at 10.8 ppm in $Al(BhPPH_2)_3(d\text{-}HCCl_3)$ and 11.1 ppm in $Zn(BhPPH_2)_2 \cdot CH_3OH \cdot H_2O$ (d_6-DMSO). The S,S' (methanol, ethanol, water) ^{1}H-NMR resonances occur in the region 1–5 ppm depending on the alcohol. Two groups of signals at 4.1 ppm (triplet) and 3.2 ppm (doublet) (relative intensities 1:3) are observed in $Zn(BhPPH_2)_2 \cdot CH_3OH \cdot H_2O$. In $Zn(BhPPH_2)_2 \cdot C_2H_5OH$ (See Fig. 3) three groups of signals at 4.4 ppm (triplet), 3.6 ppm (quadruplet of doublets) and 2.1 ppm (triplet) with relative intensities of 1:2:3 are observed. No significant differences were observed in the ^{1}H-NMR spectrum of $Zn(BhPPH_2)_2$, except for the absence of the S,S' signals, with respect to the solvated $Zn(BhPPH_2)_2$: S,S' complexes.

DISCUSSION

The ligand $BhPPH_3$ ≡ 1,3-bis-(2-hydroxyphenyl)-1,3-propanedione presents (Fig. 1) three possible sites of coordination acting as a chelating agent; two of them equivalent, and one, the β-diketone moiety, different and the most reactive. As a consequence it was expected that molenuclear complexes similar to these obtained with common β-diketones would be obtained. The shift of the enolic proton from 4.8 ppm in free $BhPPH_3$ to ≃7 ppm (methine protons) in complexed $BhPPH_2$ supports this expectation. The existence of S,S' molecules with –OH groups suggested to us that the Zn atom is in an octahedral arrangement of oxygens, four from the β-diketone moiety and two from the solvent or water molecules. (see Fig. 4). This geometry was further corroborated by an X-ray diffraction study[17] of $Zn(BhPPH_2)_2 \cdot 2EtOH$, the observed Zn–O distances being 2.02 Å for the equatorial Zn–O bonds and 2.17 Å (ethanol) for the axial bonds. These values compare well with others reported in the literature, e.g. in Zinc bis (benzoylacetonate)-monoethanolate, $Zn(bzac)_2 \cdot EtOH$[18] having a pseudo-square pyramidal geometry the Zn–O bond distances to the benzoylacetonate groups are approximately 1.99 Å and that to the ethanol molecule is 2.06 Å. The slightly longer distances observed in $Zn(BhPPH_2) \cdot 2EtOH$ may be due to the higher coordination of the Zn atom in this complex.

The similárity of all the IR spectra for the M(II) complexes is a good indication for a structure common in all of them and resembling that of the $Zn(BhPPH_2)_2 \cdot 2EtOH$ complex.

Few differences are believed to happen in the coordination of the central metal by the $BhPPH_3$ ligand in the non solvated complexes. The 1700–1400 cm^{-1} IR region of these complexes indicates they are oxygen-bonded β-diketonato complexes as are the solvated complexes. However, there is not enough data, at the present moment,

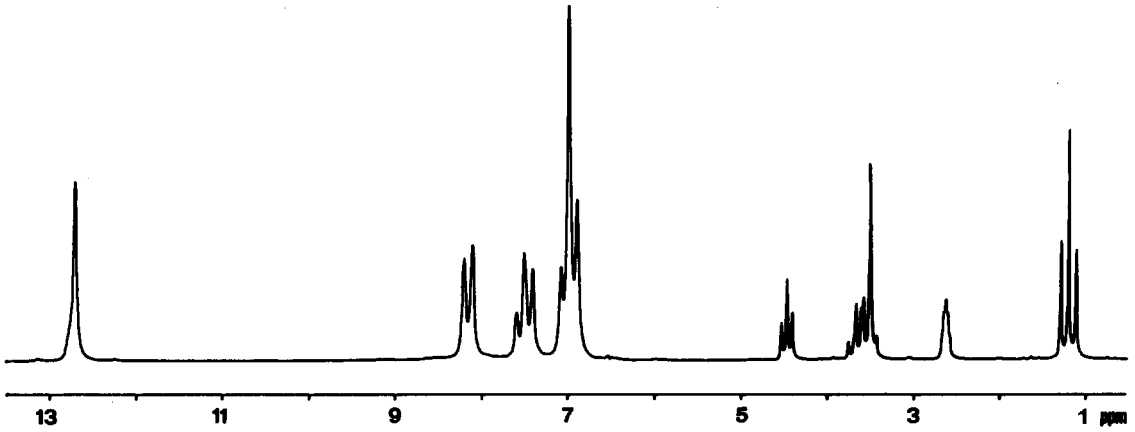


Fig. 3. ^{1}H-NMR spectrum of the complex $Zn(BhPPH_2)_2 \cdot 2CH_3CH_2OH$ in d_6-dmso.

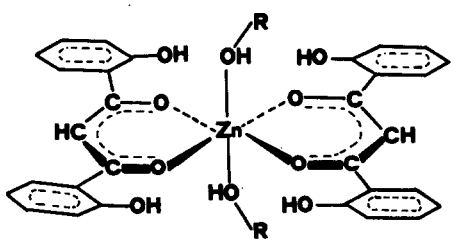


Fig. 4. Proposed structure for the complexes $Zn(BhPPH_2)_2 \cdot 2ROH$. Phenylic protons have been omitted for clarity.

to speculate on the total coordination about the central metal. Even though the solvating molecules are removed, a hexacoordination with all oxygens is possible via the phenolic oxygens.

REFERENCES

1. D. P. Gradden, *Coord. Chem. Rev.* 1969, **4**, 1.
2. D. Gibson, *Coord. Chem. Rev.* 1969, **4**, 225.
3. J. J. Fortman and R. E. Sievers, *Coord. Chem. Rev.* 1971, **6**, 331.
4. R. M. Pike, *Coord. Chem. Rev.* 1967, **2**, 163.
5. R. C. Mehrotra, R. Bohra and D. P. Gaur, *Metal β-diketonates and Allied Derivatives*. Academic Press, London (1978).
6. U, Casellato, S. Tamburini, P. A. Vigato, A. de Stefani, M. Vidali and D. E. Fenton, *Inorg. Chim. Acta* 1983, **69**, 45.
7. P. A. Vigato, U. Casellato, S. Tamburini, F. Milani and M. M. Musiani, *Inorg. Chim. Acta* 1982, **61**, 89.
8. U. Casellato, P. A. Vigato, D. E. Fenton and M. Vidali, *Chem. Soc. Rev.* 1979, **8**, 199.
9. B. Andrelczyk and R. L. Lintvedt, *J. Am. Chem. Soc.* 1972, **94**, 8633.
10. M. D. Glick and R. L. Lintvedt, *Prog. Inorg. Chem.* 1976, **21**, 233.
11. Y. Taguchi, F. Sagara, H. Kobayashi and K. Veno, *Bull. Chem. Soc. Japan* 1970, **43**, 2470.
12. F. Eiden and H. D. Schweiger, *Synthesis* 1974, 511.
13. F. Eiden, Personal communication.
14. It was prepared by dissolving, under N_2, Lithium metal in reactive grade methanol.
15. Universal pH indicator paper (Merck).
16. S. Pinchas, B. L. Silver and I. Laulicht, *J. Chem. Phys.* 1967, **46**, 1506.
17. X. Solans, M. Font-Altaba, J. L. Briansó, A. Llobet, F. Teixidor and J. Casabó, *Acta Cryst.* 1983, **C39**, 1512.
18. R. L. Belford, N. D. Chasteen, M. A. Hitchman, P. K. Hon, C. E. Pfluger and I. C. Pual, *Inorg. Chem.* 1969, **8**, 1313.

Polyhedron Vol. 4, No. 2, pp. 221–226, 1985
Printed in Great Britain.

0277–5387/85 $3.00 + .00
© 1985 Pergamon Press Ltd.

A POLAROGRAPHIC STUDY OF THE MIXED COMPLEXES OF Pb(II) WITH OXALATE AND MALONATE IONS

G. RUIZ-CABRERA, J. C. RODRÍGUEZ-PLACERES, F. RAMOS-STEFFENS and A. ARÉVALO*
Department of Physical Chemistry, University of La Laguna, Teneriffe, Canary Islands, Spain

(*Received* 17 *January* 1984; *accepted* 16 *April* 1984)

Abstract—The coordinated mixed Pb(II)-oxalate–malonate system has been polarographically studied in aqueous medium. The ionic strength has been maintained constant at $\mu = 1.0$ by using $NaClO_4$. Application of the Schaap and McMasters method detected only the existence of the $[Pb–ox–mal]^{2-}$ complex, the overall stability constant of which was $\beta_{11} = 4.1 \times 10^5$.

The various coordination equilibria are discussed on the basis of statistical aspects.

Systematic studies have been carried out in this Department for several years on mixed coordination equilibria in aqueous and aqueous-organic media.[1–6] Analysis of mixed coordinated systems by using bidentate ligands has proved useful in establishing structural aspects[5] and particular characteristics of metal ion coordination chemistry.[4] In this paper we report the analysis of the Pb(II)–oxalate–malonate coordinated system in aqueous medium.

EXPERIMENTAL

Each of the $i - E$ curves was plotted with a Metrohm E506 polarograph with an E505 polarographic stand. Two Ag/AgCl/NaCl sat. Metrohm EA427 electrodes were used as counter and reference electrodes and the working electrode was of mercury drops. The temperature in the cell was 25 ± 0.05°C and the Pb(II) concentration was 0.099 mM. Ionic strength was adjusted in all cases to $\mu = 1.0$ M with $NaClO_4$. Measurements of pH were carried out with a pHM84 digital potentiometer with a GK 2401C Radiometer combined electrode. With the exception of the soln. of Pb(II) in the absence of ligand, which was polarographed at pH 5, all the rest were polarographed at a pH of 7.5 in order to ensure that the concentration of both the oxalate and malonate ions was not below 99% of the total concentrations of their respective salts.[7,8] The concentration of metal ion was constant at 0.099 mM in all recordings. Drop-time was controlled at 3.0 s.

The sodium perchlorate and sodium oxalate were Merck products of p.a. quality, the malonic acid from Carlo Erba R.P.E. and the sodium hydroxide used in the preparation of the sodium malonate and for adjusting the pH was also of p.a. quality from May and Baker.

RESULTS AND DISCUSSION

The plots of $\log[(\bar{i}_d - \bar{i})/\bar{i}]$ vs E show that the discharges occurred by a reversible bielectronic process. The values for the reversible half-wave potentials were directly obtained from these plots. The application of the Schaap and McMasters method[9] to determine mixed complexes requires prior knowledge of the constants of simple complexes, so we have previously studied the simple Pb(II)–oxalate and Pb(II)–malonate systems at a constant ionic strength $\mu = 1.0$ adjusted with $NaClO_4$,[10] using the De Ford and Hume method[11] to demonstrate stabilization of the complexes with 1 and 2 oxalate ligands and with 1, 2 and 3 malonate ligands, respectively. The corresponding formation constants are shown in Table 1.

It seems logical from the above to accept that the F_{00} function of Schaap and McMasters presents at the most the following expression:

$$F_{00} = \{1 + \beta_{01}[mal] + \beta_{02}[mal]^2 + \beta_{03}[mal]^3\} + \{\beta_{10} + \beta_{11}[mal] + \beta_{12}[mal]^2\}[ox] + \{\beta_{20} + \beta_{21}[mal]\}[ox]^2. \quad (1)$$

*Author to whom correspondence should be addressed.

Table 1. Stability constants of the simple systems of Pb(II) with oxalate and malonate ligands

System	Coordinated species	Stability constants
Pb^{2+} - oxalate	Pbox	1.10^4
	$[Pb(ox)_2]^{2-}$	$1,9.10^6$
Pb^{2+} - malonate	Pb(mal)	$8,0.10^2$
	$[Pb(mal)_2]^{2-}$	$1,04.10^4$
	$[Pb(mal)_3]^{4-}$	$3,8\ .10^4$

Table 2. Analysis of the Pb(II)–$Na_2C_2O_4$–$Na_2H_2C_3O_4$–$NaClO_4$ system in aqueous medium and $[H_2C_3O_4^{2-}] = 0.20$ M. Schaap and McMasters method. Characteristics of the reduction of Pb^{2+} in $NaClO_4$ 1 M: $-E_{1/2}^r = 346.8$ mV; $\bar{i}_d = 145.9$ mm. Other characteristics: $m = 1{,}627$ mg/sec; sens. $= 4.10^{-9}$ A/mm

$[C_2O_4^{2-}]$/M	$\bar{i}_d$/mm	$-E_{\frac{1}{2}}^r$ /mV.	F_{00}	F_{10}
0,01	119,9	441,3	1905,8	102580
0,015	120,3	445,6	2654,6	118307
		445,8	2696,2	121080
0,02	120,4	449,0	3456,1	128805
		449,5	3593,2	135660
0,025	121,1	451,4	4141,9	130476
		452,1	4373,9	139756
0,03	121,5	454,6	5296,1	147203
		454,7	5337,5	148583
0,04	120,0	462,5	9739,6	177192
		462,6	9815,8	178716
0,06	122,0	465,7	12515	193917
		465,8	12613	195550
0,07	122,0	468,6	15685	211500
		469,0	16181	218586
0,09	123,0	473,6	22960	245333
		474,2	24058	257533
0,10	122(*)	476,0	27904	270240
		475,9	27687	268070
0,11	122,0	477,6	31605	279318
		477,2	30636	270509
0,12	121,8	479,6	36990	300913
		480,2	38758	315650

(*): interpolated value

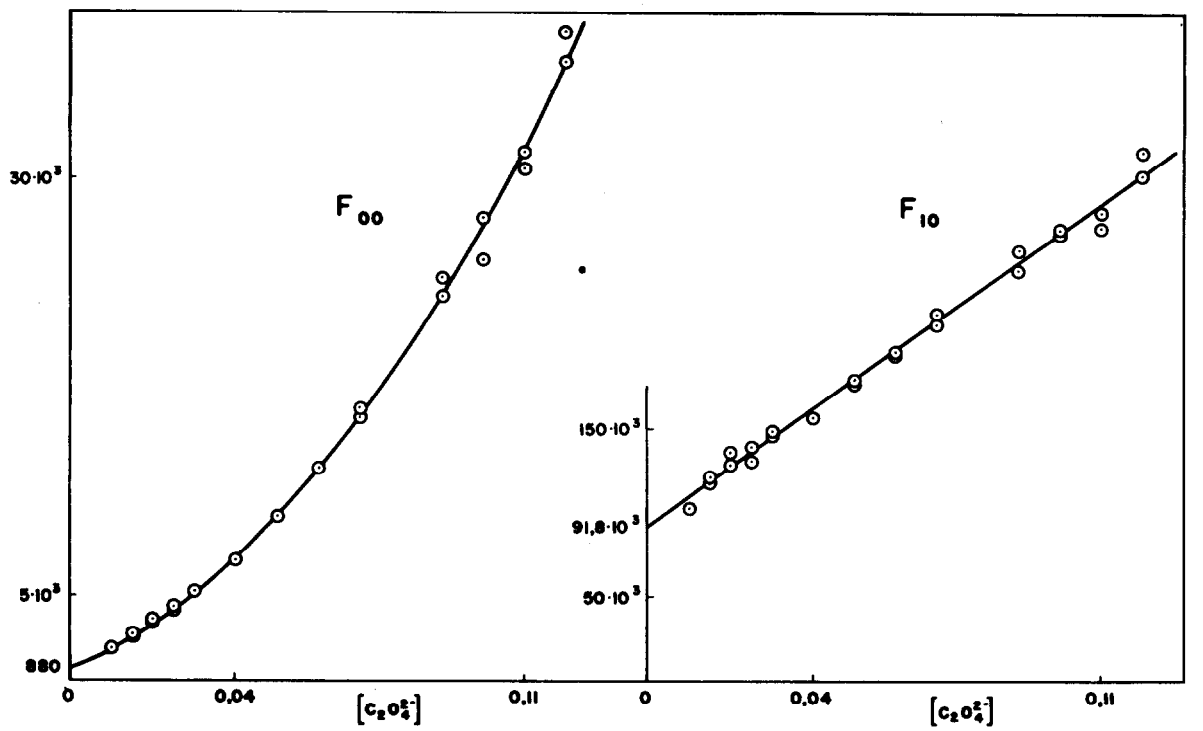


Fig. 1. Plot of the functions F_{00} and F_{10} vs $[ox^{2-}]$. Study with $[mal^{2-}] = 0.2$ M.

If the concentration of malonate is maintained constant while that of oxalate is varied, the F_{00} function becomes:

$$F_{00} = A + B[ox] + C[ox]^2 \qquad (2)$$

where A, B and C represent the arrangements expressed in (1). These coefficients may be calculated by a Leden-type treatment.

Six experimental studies were carried out in all. Table 2 gives the reversible half-wave potentials together with the limiting diffusion currents and the values of the F_{00} and F_{10} functions for the study carried out at a constant concentration of malonate of 0.2 M. The plot of the successive F_{i0} functions, Fig. 1, confirms the expected linear dependence of the F_{10} function vs [ox].

In every case it was observed that the value of A calculated from expression (1) agreed satisfactorily with that determined experimentally. The values of A, B and C obtained from the six studies carried out are given in Table 3.

The data of B, notably greater than $\beta_{10} = 10^{4}$,[10] reveal the presence of mixed complexes with an oxalate ion.

Figure 2 shows a good linear dependence of the

Table 3. Pb(II)–Na_2ox–Na_2mal–$NaClO_4$ system $\mu = 1.0$

$[mal^{2-}]$/M	A	B.10^{-3}	C.10^{-6}
0,02	20	17,7	1,5
0,05	70	32	1,6
0,08	150	45,8	1,5
0,10	220	48,8	2
0,12	310	58,9	1,8
0,20	880	91,8	1,8

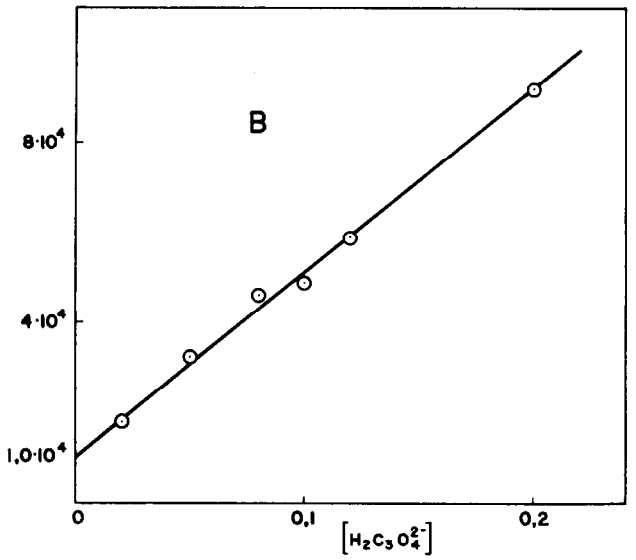


Fig. 2. Plot of coefficient B vs [mal^{2-}].

values of B vs [malonate] allowing β_{10} to be obtained from the intercept at [malonate] = 0 and β_{11} from the slope. Adjusting by square minima method gives $\beta_{10} = 1.1 \times 10^4$ and $\beta_{11} = 4.0 \times 10^5$. The value of β_{10}, in good agreement with that obtained from the study of the simple Pb(II)–malonate system: $\beta_{10} = 1.0 \times 10^4$,[10] provides further evidence for the validity of the results.

The values of C: (a) are relatively close to the stability constant of the complex

$$[Pb(C_2O_4)_2]^{2-}: \beta_{20} = 1.9 \times 10^6$$

and (b) do not show any regularity which would allow us to assume the stabilisation of the complex

$$[Pb(C_2O_4)_2(H_2C_3O_4)]^{4-}.$$

This result is similar to that observed in the study of the Cu(II)–oxalate–malonate system[5] and it suggests the impossibility of the malonate ligand to be coordinated to Pb^{2+} by the extreme positions of the probable octahedral structure of this ion.

Watters' formulae

The constant obtained from the mixed complex can be compared with that statistically predictable which was evaluated according to the formulae proposed by Watters[12]:

$$\beta_{11} = 2\beta_{20}^{1/2}\beta_{02}^{1/2} = 2,8.10^5$$

it is in good agreement with the value obtained experimentally:

$$\beta_{11} = 4,0.10^5.$$

ANALYSIS OF THE COORDINATION EQUILIBRIA

All the results corresponding to the coordination equilibria of the Pb(II) ion with oxalate and malonate ligands are shown in the scheme in Fig. 3. The stepwise constants are logarithmically expressed.

Let us first consider the equilibria of the Pb(II) with only one ligand. Table 4 gives the values of K_i/K_{i+1} for the Pb(II)–malonate system, and they are compared with those obtained for the oxalate and succinate[13] and those expected, taking into account only statistical factors and octahedral coordination.[14]

The formation of the 1:1 complex is greatly favoured by entropic factors while, due to steric effects, the formation of complexes with a greater number of ligands will be progressively hindered, particularly as the length of the chain is increased.

These predictions agree qualitatively with the tendency observed in Table 4 for K_1/K_2, although it is impossible to evaluate their influence quantitatively in order to compare if the one consideration alone interprets the results obtained. The relative proximity between the values calculated for K_1/K_2 in both cases, and the fact that it diminishes with the ion size increase would be justified by the similar influence of the entropic effects and the greater steric hindrance as the length of the chain is increased.

The high values of K_1/K_2 and the relatively low values of K_2/K_3 seem to point to the low relative stability of the complexes with two malonate and/or succinate ligands.

The tendency of the complexes $Pb(H_2C_3O_4)$ and PbC_2O_4 to take a malonate ion as second ligand is

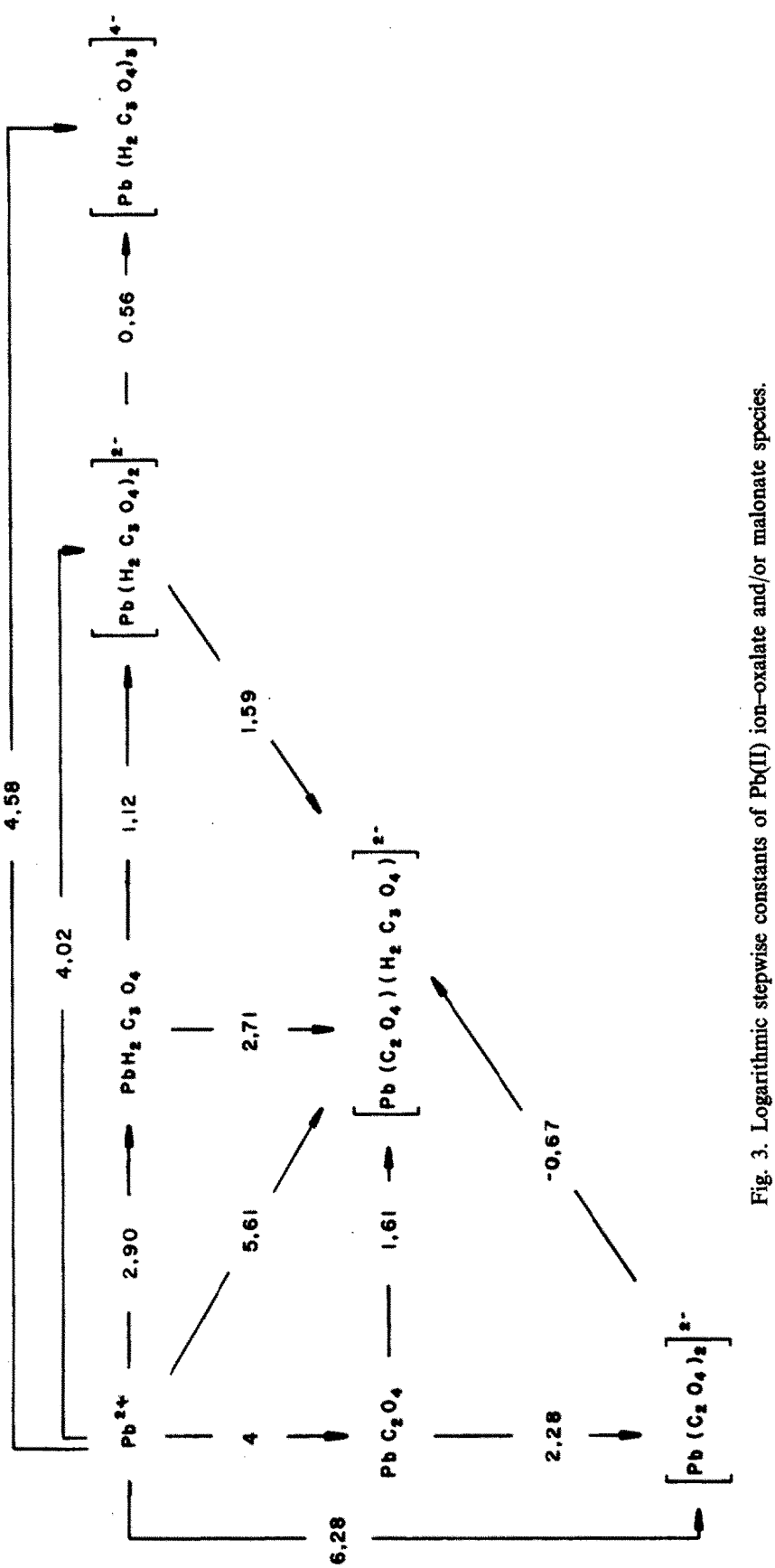


Fig. 3. Logarithmic stepwise constants of Pb(II) ion–oxalate and/or malonate species.

Table 4.

K_i/K_{i+1}	Statistic	Pb(II)-oxal.	Pb(II)-mal.	Pb(II)-succ.
K_1/K_2	0,96	52,6	61,5	79
K_2/K_3	9,75	-	3,56	1,24

seen as follows:

$$PbH_2C_3O_4 + H_2C_3O_4^{2-} \rightleftharpoons [Pb(H_2C_3O_4)_2]^{2-}$$
$$\log K_{(1)} = 1.12 \quad (1)$$

$$PbC_2O_4 + H_2C_3O_4^{2-} \rightleftharpoons [Pb(C_2O_4)(H_2C_3O_4)]^{2-}$$
$$\log K_{(2)} = 1.61. \quad (2)$$

Theoretically, taking into account statistical factors alone, it would be expected that the equilibrium (2) were the more stable, its constant being greater than that of (1) by the statistical factor of 2, ($\log K = 0.301$). The difference found, $\log K = 0.49$, is slightly greater than that expected.

The tendency of the same complexes to coordinate an oxalate ion as second ligand should also be observed:

$$PbH_2C_3O_4 + C_2O_4^{2-} \rightleftharpoons [Pb(C_2O_4)(H_2C_3O_4)]^{2-}$$
$$\log K_{(3)} = 2.71$$

$$PbC_2O_4 + C_2O_4^{2-} \rightleftharpoons [Pb(C_2O_4)_2]^{2-}$$
$$\log K_{(4)} = 2.28.$$

Considerations analogous to those above are valid in this case in which the difference found, $\log K = 0.43$, is also slightly greater than expected.

Both results indicate a greater relative stability of the mixed complex than could be expected on the basis of the constants of the simple complexes $[Pb(H_2C_3O_4)_2]^{2-}$ and $[Pb(C_2O_4)_2]^{2-}$.

This greater stability is also reflected in the value calculated by means of the equation proposed by Watters: $(\beta_{11})_w = 2.8 \times 10^5$, lower by 30% than that obtained experimentally, which is a shift similar to that found in the analysis of the equilibria discussed earlier in this work.

REFERENCES

1. A. Arévalo, J. C. Rodríguez-Placeres, T. Moreno and J. Segura, *J. Electroanal. Chem.* 1978, **92**, 55.
2. J. C. Rodríguez-Placeres, J. J. Arias, T. Borges and F. García-Montelongo, *Anal. Quím.* 1980, **76**, 397.
3. M. Barrera, J. C. Rodríguez-Placeres, J. E. García and A. Arévalo, *Anal. Quím.* 1981, **77**, 194.
4. J. C. Rodríguez-Placeres, M. Barrera, C. Carreño and A. Arévalo, *Anal. Quím.* 1981, **77**, 199.
5. J. C. Rodríguez-Placeres, J. J. Arias, J. P. Pérez-Trujillo and F. García-Montelongo, *J. Inorg. Nucl. Chem.* 1981, **43**, 1681.
6. J. C. Rodríguez-Placeres, M. Barrera, T. Moreno and A. Arévalo, *Anal. Quím.* 1983, **79**, 316.
7. E. Bottari and L. Ciavatta, *Gazzeta* 1965, **95**, 908.
8. H. J. Bruin, D. Kaitis and R. B. Temple, *Austral. J. Chem.* 1962, **15**, 457.
9. W. Schaap and D. L. McMasters, *J. Am. Chem. Soc.* 1961, **83**, 4699.
10. M. Pérez-Sánchez, G. Ruiz-Cabrera, J. C. Rodríguez-Placeres and A. Arévalo, *Anal. Quím.* 1984, **3**, 50.
11. D. D. De Ford and D. N. Hume, *J. Am. Chem. Soc.* 1951, **73**, 5321.
12. J. I. Watters and R. Dewitt, *J. Am. Chem. Soc.* 1960, **82**, 1333.
13. G. Ruiz-Cabrera, M. Pérez-Sánchez, J. C. Rodríguez-Placeres and A. Arévalo, *Anal. Quím.* 1984, **80**, 54.
14. M. T. Beck, *Chemistry of Metal Equilibria.* Van Nostrand, Amsterdam (1970).

Polyhedron Vol. 4, No. 2, pp. 227–231, 1985
Printed in Great Britain.

0277-5387/85 $3.00 + .00
© 1985 Pergamon Press Ltd.

SYNTHESIS AND SPECTRAL PROPERTIES OF A NEW BINUCLEAR IRON COMPLEX: THE ION TETRACYANO(4-CYANOPYRIDINE)FERRATE(II)-μ-CYANO-PENTACYANOFERRATE(II)†

AÍDA BEN ALTABEF, SILVIA A. BRANDÁN and NÉSTOR E. KATZ*
Cátedra de Fisicoquímica III, Facultad de Bioquímica, Química y Farmacia, Universidad Nacional de Tucumán, Ayacucho 491, 4000 S. M. de Tucumán, Argentina

(*Received* 20 *February* 1984; *accepted* 16 *April* 1984)

Abstract—A new cyano-bridged binuclear complex of Fe(II) can be prepared by mixing pentacyano(ammine)ferrate(II) with 4-cyanopyridine at a mole ratio 2:1. IR and UV-VIS spectra, together with kinetic data on ligand substitution, point to the following structure: $(NC)_5Fe–NC–Fe(CN)_4(N⬡–CN)^{6-}$, both in solid state and in aqueous solution, thus demonstrating that cyanide forms a bridge between two iron atoms which is much more stable than that formed by 4-cyanopyridine.

The interest in ligand-bridged complexes stems from their importance as intermediates in electron- or energy-transfer reactions.[1,2] Binuclear complexes are also important for structural, redox and substitution studies of bidentate ligands.[3] On the other hand, cyanoferrate complexes may be used as simple models for biological systems such as cytochromes or haemoglobin.[4]

In this work, we report the preparation and spectral and kinetic properties of the new binuclear iron complex obtained from $[Fe(CN)_5(NH_3)]^{3-}$ and N⬡–CN (4-cypy) mixed at a mole ratio 2:1. Both cyanide and 4-cypy are ambidentate ligands, so that two different bridged complexes may be synthesized. In a recent paper,[5] we attributed the visible spectra of a stoichiometric mixture in aqueous solution of $[Fe(CN)_5(NH_3)]^{3-}$ and $[Fe(CN)_5(4\text{-cypy})]^{3-}$ to a binuclear complex bridged by 4-cypy. This conclusion must now be corrected in view of the present investigation. Information about the degree of metal–metal interaction in the new species will also be disclosed.

EXPERIMENTAL

Sodium pentacyano(ammine)ferrate(II) trihydrate was obtained following Kenney *et al.*[6] 4-cypy was of analytical reagent grade. Deionized water was used throughout.

In order to verify the formation of a binuclear complex when $[Fe(CN)_5(NH_3)]^{3-}$ and 4-cypy were mixed in aqueous solution at a mole ratio 2:1 we resorted to the well-known continuous variations and mole ratio methods.[7] In the first case, 9 aqueous solutions of $[Fe(CN)_5(NH_3)]^{3-}$ and 4-cypy were mixed in variable proportions (0.1–0.9), the total concentration being constant and equal to 8×10^{-4} M. After 4 hr, the absorbance (A) of the solutions was measured at $\lambda = 400$ nm and at room temperature. In the second case, A was measured in similar conditions, but now maintaining [4-cypy] $= 2 \times 10^{-4}$ M and varying the metal concentration from 0 to 4.5×10^{-4} M. In both cases, duplicate runs were made using a Metrolab RC 325 spectrophotometer.

The preparation of the solid binuclear complex was carried out by reacting 0.8 mmol of 4-cypy and 1.6 mmol of $[Fe(CN)_5(NH_3)]^{3-}$ in 10 cm^3 of water. After 1 hr in the dark at room temperature, the mixture was cooled at 0 °C for 30 min. The precipitate obtained was filtered at 0 °C and kept in a desiccator over P_4O_{10}.

Iron and sodium analyses were made by atomic absorption spectroscopy. A Varian Techtron AA5 spectrometer was used for this purpose, and $Na_2[Fe(CN)_5NO].2H_2O$ was the chosen standard.

UV-VIS spectra of the sample were made in aqueous solution (immediately after dissolution) at a $C = 2.4 \times 10^{-4}$ M in the range 200–600 nm on a Perkin–Elmer Coleman 124 spectrophotometer.

†Presented at the "3er. Congreso Argentino de Fisicoquímica", La Plata, Argentina, September 1983.

Author to whom correspondence should be addressed. Member of the "Carrera del Investigador Científico", CONICET.

IR spectra were obtained as KBr pellets, using a Perkin–Elmer 580B spectrophotometer.

Ligand substitution kinetic experiments were accomplished at pseudo-first-order conditions: [complex] = 8×10^{-5} M; [py] = 0.1 M. The absorbance changes corresponding to the reaction:

$$Fe_2(CN)_{10}(4\text{-cypy})^{6-} + 2\,py \rightarrow 2\,Fe(CN)_5(py)^{3-} + 4\text{-cypy} \quad (1)$$

were measured on a Metrolab RC 325 visible spectrophotometer at $\lambda = 365\,nm$ (maximum of the final product) and $T = (25.0 \pm 0.2)$ °C.

RESULTS

Figure 1 shows the results obtained by applying the method of continuous variations. Y is defined as the difference between A of the mixture and A of the initial complex, $[Fe(CN)_5(NH_3)]^{3-}$. x is the

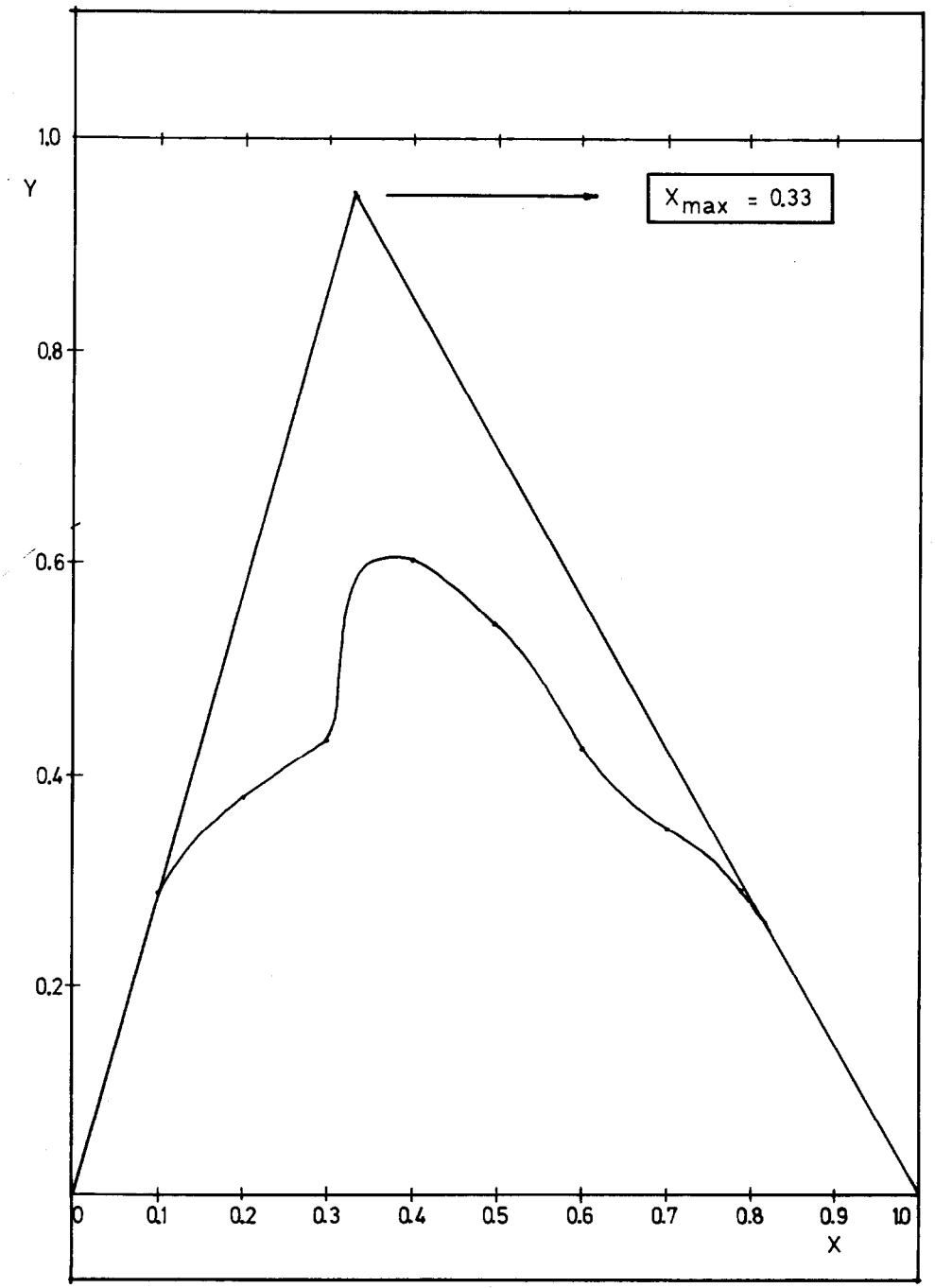


Fig. 1. Job's analysis at 400 nm for the reaction between $[Fe(CN)_5(NH_3)]^{3-}$ and 4-cypy in aqueous solution. Total concentration – 8×10^{-4} M.

proportion of 4-cypy to $[Fe(CN)_5(NH_3)]^{3-}$ ($x < 1$). From the intersection of the tangents to the curve at $x = 0$ and at $x = 1$, a value of $x_{max} = 0.33$ results, and from the equation:

$$m/n = (1 - x_{max})/x_{max} \quad (2)$$

where m/n is the stoichiometric ratio iron:4-cypy,[7] m/n equals 2. The different curvatures for $x \rightarrow 0$ and for $x \rightarrow 1$ indicates formation of more than one complex between $[(Fe(CN)_5(NH_3)]^{3-}$ and 4-cypy.[8,9]

The mole ratio method gives the results shown in Fig. 2. Y is defined as above, while $[Me]/[L] = [Fe(CN)_5(NH_3)^{3-}]/[4\text{-cypy}]$. Two sharp discontinuities at $[Me]/[L] = 1$ and 2 indicate formation of a monomeric complex[9] and a binuclear one, respectively.

Experimental iron and sodium contents of the

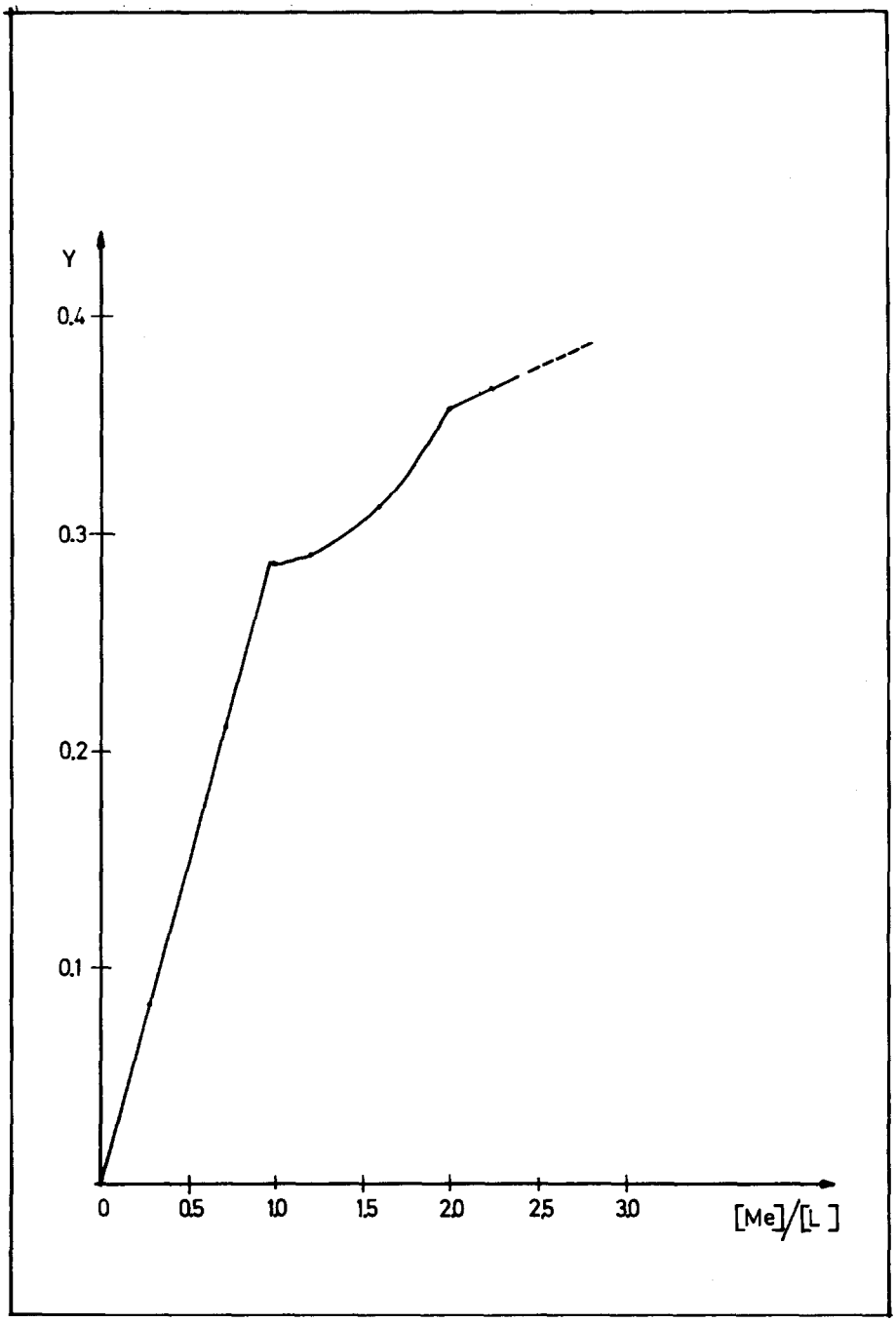


Fig. 2. Mole ratio analysis at 400 nm for the reaction between $[Fe(CN)_5(NH_3)]^{3-}$ and 4-cypy in aqueous solution. [L] = [4-cypy] = 2×10^{-4} M.

solid sample were 16.7 and 21.3% respectively, while corresponding theoretical values (calculated for $Na_6[Fe_2(CN)_{10}(4\text{-cypy})].3H_2O$) were 16.8 and 20.7%.

The UV-VIS spectrum showed bands at λ = 470, 400 and 268 nm (error = $\pm$2 nm), with ϵ = 3.7, 2.0 and 3.8 $\times$ 10^3 M^{-1} cm^{-1} (error $\simeq$ $\pm$5%) respectively.

IR bands appeared at 3470, 2245, 2115, 2055, 1655, 1620, 1488, 1412, 1215, 1018, 835, 825, 570, 560, 535, 495 and 415 cm^{-1} (error $\cong$ 0.5%).

In order to obtain the pseudo-first-order rate constant k_{-1} for process (1), values of ln $(A_\infty - A_t)$ were represented vs time t. Plots were linear up to three half-lives and from their slopes, a value of $k_{-1} = (1.3 \pm 0.1) \times 10^{-3}\, s^{-1}$ was determined.

DISCUSSION

When $[Fe(CN)_5(NH_3)]^{3-}$ is dissolved in water, the ion $[Fe(CN)_5(H_2O)]^{3-}$ is rapidly generated.[10] With ligand L in excess, monomeric species of the type $[Fe(II)(CN)_5L]^{n-}$ can be obtained in good yields. However, if the ratio $[Fe(CN)_5(H_2O)^{3-}]$/[L] is 2:1, dimeric complexes can be synthesized.[11] In this work, when L = 4-cypy, a new ion of formula $[Fe_2(CN)_{10}$ (4-cypy)$]^{6-}$ appeared in aqueous solution, as verified from the continuous variations and the mole ratio methods. Figures 1 and 2 show, in effect, complex formation at the stoichiometric ratio iron:4-cypy = 2:1. Moreover, the solid sodium salt prepared at 0°C has the formula $Na_6[Fe_2(CN)_{10}(4\text{-cypy})].3H_2O$, as deduced from iron and sodium analyses.

With the empirical formula of the new species known, we proceed to investigate its structure. The visible band at 470 nm (ϵ = 3.7 $\times$ 10^3 M^{-1} cm^{-1}) can be assigned to a charge transition $d_\pi(Fe) \rightarrow \pi^*$ (4-cypy), by comparison with data for the monomeric complex $[Fe(CN)_5(4\text{-cypy})]^{3-}$ (λ_{max} = 476 nm, ϵ_{max} = 5.5 $\times$ 10^3 M^{-1} cm^{-1}).[9] If we consider the structure Fe(II)–NC–⟨⬡⟩N–Fe(II), this band must be shifted to higher λ values (with an increase in ϵ) when compared to the mononuclear compound. This occurs in the case of binuclear Fe(II) complexes bridged by aromatic heterocyclic ligands,[11] as shown in Table 1. In the present complex, the observed shift is opposite (i.e. to lower λ and ϵ values) and similar to that produced when a coordinated cyanide is protonated at low values of pH.[9,10] On the other hand, the band at 400 nm corresponds to analogous bands belonging to cyanide-bridged complexes (see Table 1). Although the charge transfer $d_\pi(Fe) \rightarrow \pi^*$ (nitrile end of 4-cypy) is expected to fall at a similar value of λ (405 nm), the experimental value of ϵ (2.0 $\times$ 10^3 M^{-1} cm^{-1}) is much lower than the expected one (7.4 $\times$ 10^3 M^{-1} cm^{-1}). Therefore, from UV-VIS studies, the formation of an Fe(II)–NC–Fe(II) bridge is deduced, and the previous assignment[5] must be corrected.

IR data confirm the above conclusion, Indeed, when a nitrile group is bonded to strong π donors such as $[Ru(NH_3)_5]^{2+}$ or $[Fe(CN)_5]^{3-}$, $\nu_{CN(nitrile)}$ must be shifted *ca.* 60 cm^{-1} below the value for the free ligand (2242 cm^{-1}).[16] The observed value for the complex studied here (2245 cm^{-1}) is clear evidence that 4-cypy is not coordinated through the

Table 1. Comparison of charge transfer spectra in monuclear and binuclear complexes of the type $[Fe(II)(CN)_5L]^{n-}$

Ligand L	λ_{max}(nm)	10^{-3} ϵ_{max}($M^{-1}cm^{-1}$)	Reference
N⟨⬡⟩N	450	5.0	10
N⟨⬡⟩N–Fe(CN)$_5^{3-}$	508	13	11
N⟨⬡⟩CN	476	5.5	9, 12
NC⟨⬡⟩N	405	7.4	12
Fe(CN)$_5$ N⟨⬡⟩CN^{3-}	470 400	3.7 2.0	this work
NC–Fe(CN)$_4$(H$_2$O)$^{3-}$	390	0.7	13
NC–Fe(CN)$_5^{4-}$	390	0.8	14
CN–Co(en)$_2$SO$_3$	398	0.8	15

nitrile group to a $[Fe(CN)_5]^{3-}$ moiety. Moreover, in the cyanide stretching region, two bands are observed at 2115 and 2055 cm^{-1} (with an approximate intensity ratio of 1;9) which must be due to bridging and terminal cyanides respectively; it is well accepted that bridge formation causes a positive shift in $\nu_{CN(cyanide)}$.[15,17,18] A small blue shift of the 4-cypy characteristic frequencies (when compared to the $[Fe(CN)_5(4\text{-cypy})]^{3-}$ complex[9]) and new bands at 835 and 535 cm^{-1} can also be attributed to the $[(NC)_5Fe\text{–}NC\text{–}Fe(CN)_4(4\text{-cypy})]^{6-}$ structure.

The value obtained for k_{-1} ($1.3 \times 10^{-3}\ s^{-1}$) is slightly higher than that corresponding to 4-cypy dissociation from its monomeric complex with $Fe(CN)_5^{3-}$ ($1.02 \times 10^{-3}\ s^{-1}$).[12] This fact agrees with the shift to lower values of λ_{max} and both phenomena may be accounted for by the decrease of π backbonding Fe→4-cypy caused by the inductive effect of a second $[Fe(CN)_5]^{3-}$ group coordinated *trans*- to 4-cypy. The rate constant for bridge rupture is nearly 10 times more rapid than that of 4-cypy dissociation;[13] the observed rate constant thus corresponds to the latter process.

In conclusion, the new complex must be formulated as sodium tetracyano (4-cyanopyridine)ferrate(II)-μ-cyano-pentacyanoferrate(II) trihydrate: $Na_6[(NC)_5Fe\text{–}NC\text{–}Fe(CN)_4(N\text{⬡}\text{–}CN)].3H_2O$. Its spectral and kinetic properties are not very different from those of the monomeric complex $[(NC)_5Fe\text{–}N\text{⬡}\text{–}CN]^{3-}$, pointing to a small interaction between the metallic centres. The mixed-valence complex (II–III) must present an electron delocalization of *ca.* 1%.[11] The greater stability of an Fe(II)-NC-Fe(II) bridge compared to that of an Fe(II)–NC-⬡N–Fe(II) bridge may be explained by considering that while the formation rate constants must be of the same order of magnitude,[10] the dissociation rate is nearly 5 times greater for the Fe(II)–NC-⬡N bond[12] than for the Fe(II)–NC bond.[13]

Acknowledgements—We thank CONICET, SUBCYT and UNT for financial support, Dr. G. Bossi for AA measurements, Lic. M. E. García Posse for running IR spectra and Dra. D. A. de Iglesias for permission given to use the UV-vis spectrophotometer.

REFERENCES

1. F. Basolo and R. G. Pearson, *Mechanisms of Inorganic Reactions*, p. 454. Wiley, New York (1968).
2. J. A. Gelroth, J. E. Figard and J. D. Petersen, *J. Am. Chem. Soc.* 1979, **101**, 3649.
3. R. A. De Castelló, C. P. Mac-Coll, N. B. Egen and A. Haim, *Inorg. Chem.* 1966, **8**, 699.
4. R. E. Shepherd, *J. Am. Chem. Soc.* 1976, **98**, 3329.
5. M. del V. Hidalgo and N. E. Katz, *J. Mol. Struct.* 1981, **75**, 209.
6. D. J. Kenney, T. P. Flynn and J. B. Gallini, *J. Inorg. Nucl. Chem.* 1961, **20**, 75.
7. M. T. Beck, *Chemistry of Complex Equilibria*, p. 86. Van Nostrand, New York (1970).
8. R. K. Hessley, S. Waykole and R. L. Sublett, *Can. J. Chem.* 1979, **57**, 2292.
9. N. G. del V. Moreno, N. E. Katz, J. A. Olabe and P. J. Aymonino, *Inorg. Chim. Acta* 1979, **35**, 183.
10. H. E. Toma and J. M. Malin, *Inorg. Chem.* 1973, **12**, 1039.
11. F. Felix and A. Ludi, *Inorg. Chem.* 1978, **17**, 1782.
12. A. P. Szecsy, S. S. Miller and A. Haim, *Inorg. Chim. Acta* 1978, **28**, 189.
13. E. B. Borghi, M. A. Blesa, P. J. Aymonino and J. A. Olabe, *J. Inorg. Nucl. Chem.* 1981, **43**, 1849.
14. A. D. James and R. S. Murray, *J. Chem. Soc. Dalton Trans.* 1976, 1182.
15. K. L. Scott, R. S. Murray, W. C. E. Higginson and S-W. Foong, *J. Chem. Soc. Dalton Trans.*, 1973, 2335.
16. R. E. Clarke and P. C. Ford, *Inorg. Chem.* 1970, **9**, 495.
17. K. Nakamoto, *Infrared Spectra of Inorganic and Coordination Compounds*, 3rd Edn, p. 266. Wiley, New York (1978).
18. R. A. De Castelló, C. P. Mac-Coll and A. Haim, *Inorg. Chem.* 1971, **10**, 203.

Polyhedron Vol. 4, No. 2, pp. 233–242, 1985
Printed in Great Britain.

0277–5387/85 $3.00 + .00
© 1985 Pergamon Press Ltd.

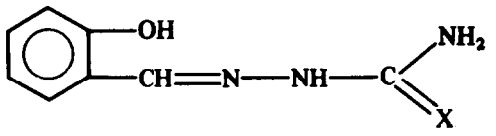
SYNTHESIS, PHYSICOCHEMICAL PROPERTIES AND VOLTAMMETRIC CHARACTERIZATION OF SOME NEW Fe(III) COMPLEXES WITH SEMICARBAZONE-BASED LIGANDS

VUKADIN M. LEOVAC,* LUKA BJELICA and LJILJANA JOVANOVIĆ
Institute of Chemistry, Faculty of Sciences, V. Vlahovića 2, 21000 Novi Sad, Yugoslavia

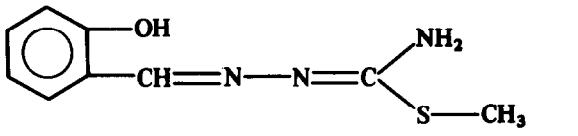
(*Received* 10 *February* 1984; *accepted* 16 *April* 1984)

Abstract—Several bis(ligand) octahedral complexes of iron(III) with salicylaldehyde semi-, thiosemi-, and S-methylthiosemi- carbazones have been synthesized and characterized by elemental analysis, conductivity and magnetic measurements, electronic and IR spectra, as well as by linear sweep and cyclic voltammetry. General procedures for the syntheses of all types of complexes have been established, giving better defined reaction conditions. Physicochemical properties of the novel complexes have been related to those of the already known compounds of the same type.

It has been established[1–4] that salicylaldehyde semicarbazone (H_2L^1), thiosemicarbazone (H_2L^2), and S-methylthiosemicarbazone (H_2L^3):



($X{=}O \sim H_2L^1$; $X{=}S \sim H_2L^2$)



(H_2L^3)

use in coordination with Fe(III) the following sets of donor atoms: ONO, ONS and ONN, respectively. Depending on pH of the reacting medium, these ligands can take part in coordination either as mono- (HL^-) or di-anion (L^{2-}). The syntheses of the following types of octahedral bis(ligand) chelate complexes of Fe(III): $[Fe(HL)_2]X$ (X = Cl, etc., HL = HL^1, HL^3)[1,4]; Fe(HL)L (HL = HL^3, L = L^3)[4]; and $M[FeL_2]$ (M = Li, NH_4, etc. L = L^1, L^2)[1,3] have been reported in addition to the mono(ligand) complexes $Fe(HL)Cl_2$ (HL = HL^1, HL^2, HL^3).[1,2,4]

Not all types of Fe(III) bis(ligand) complexes have been prepared with each of the above ligands so, we have investigated the preparation of the missing complexes (i.e. $Fe(HL^1)L^1$, $Li[FeL_2^1]$, $[Fe(HL^2)_2]Cl$, $Fe(HL^2)L^2$, and $Li[FeL_2^3]$). The novel complexes have been characterized both crystalline and in solution, and their physicochemical properties have been related to those of the already known compounds.

EXPERIMENTAL

Chemicals and methods

The ligands employed in syntheses were prepared according to procedures described earlier.[5,6] For all syntheses only the Merck $FeCl_3{\cdot}6H_2O$ reagent grade was used. Other chemicals for syntheses were also of p.a. quality of different make.

The voltammetric, conductometric and spectrophotometric measurements were carried out in spectroscopic and freshly distilled p.a. solvents, respectively. The salts serving as supporting electrolytes (tetrabutylammonium perchlorate, TBAP, lithium perchlorate and lithium chloride) were used after recrystallization.

The C,H,N analysis procedure and magnetic susceptibility measurements have been described earlier.[7]

Chlorine was determined by combustion after Schöniger followed by titration with silver nitrate.

For all measurements the air-dry complexes were used except for voltammetric investigations, where drying at 110°C was applied.

Conductivity measurements were carried out using a conductivity meter Radiometer CDM3.

*Author to whom correspondence should be addressed.

IR spectra were recorded in KBr, employing a Perkin–Elmer 457 instrument.

Electronic spectra within the range of 37,000–12,500 cm^{-1} were recorded for the solutions of complexes in N,N-dimethylformamide (DMF) on a Cary 219 spectrophotometer.

Voltammetric experiments were carried out in the thoroughly deaerated (with purged nitrogen) 1 mM solutions of complexes in DMF, containing 0.1 M supporting electrolyte. An AMEL three-electrode set-up was used together with a Hewlett Packard 7044A x–y recorder, or a Hewlett Packard 1741A storage oscilloscope for recording the voltammograms. As the working electrode a glassy carbon disc (geometric surface area: 7 mm^2) was used with a Pt ring counter electrode. An aqueous saturated calomel electrode (Ingold) served as reference and all potentials are reported with respect to this electrode. The experiments were carried out at room temperature, and IR drop corrections were made, when necessary.

Preparation of complexes

For a comparative study of the novel and the already synthesized complexes we prepared all of them according to our own procedures. Since some significant alterations were made in the already known procedures, we have included them here, along with the original ones.

$[Fe(HL^1)_2]Cl{\cdot}H_2O$. The mixture of 1.0 g of $FeCl_3{\cdot}6H_2O$ and 1.2 g of H_2L^1 was dissolved by heating in 15 cm^3 of EtOH (pH 0.4). By adding aqueous ammonia the pH was adjusted to 1.0. This was accompanied by a change of colour of the solution from yellow–brown to deep-purple. The solution was left at room temperature for 24 hr. The black crystals obtained were filtered off and washed with EtOH and Et_2O. Yield: 0.8 g.

$[Fe(HL^2)_2]Cl$. 0.6 g of $FeCl_3{\cdot}6H_2O$ was dissolved by heating in 15 cm^3 of EtOH and mixed with 0.5 g of $NaOAc{\cdot}3H_2O$. After addition of the acetate pH changed from the initial 1.5 to 2.0. The precipitated NaCl was, after solution cooling to room temperature, filtered off and 0.95 g of H_2L^2 was added to the solution. The mixture was heated gently for 5 min with constant stirring. The ligand dissolution was accompanied by precipitation of black crystals, which, after keeping the reacting mixture at room temperature for 1 hr, were filtered off and washed with EtOH and Et_2O. Yield: 0.9 g.

$Fe(HL^1)L^1{\cdot}H_2O$. 0.50 g of $[Fe(HL^1)_2]Cl{\cdot}H_2O$ was dissolved by heating in 30 cm^3 of MeOH. The warm mixture was filtered, then 0.1 g of $LiOAc{\cdot}2H_2O$ added to the solution and the reacting mixture heated for about 10 min. A colour change from deep-purple to brown was noticeable. The reacting mixture was left at room temperature for 5 hr. The black crystals were washed with MeOH and Et_2O. Yield: 0.35 g.

$Fe(HL^2)L^2$ was prepared in a way analogous to the preceeding one. In contrast to the former one, this complex was also obtained by a direct synthesis, as follows:

The mixture of 0.6 g of $FeCl_3{\cdot}6H_2O$ and 1.0 g of $NaOAc{\cdot}3H_2O$ was dissolved by heating in 15 cm^3 of EtOH. The NaCl was filtered off, and to the solution (pH 6) a portion of 0.8 g of H_2L^2 was added. The mixture was heated gently to the complete ligand dissolution (about 10 min). The obtained microcrystalline black precipitate was filtered off and washed with EtOH and Et_2O. Yield: 0.70 g.

$Li[FeL_2^1]{\cdot}3H_2O$. The mixture containing 0.70 g of $[Fe(HL^1)_2]Cl{\cdot}H_2O$ and 0.080 g of $LiOH{\cdot}H_2O$ in 10 cm^3 of EtOH was heated gently† for 5 min and the solution after filtration left at room temperature for 24 hr. The microcrystalline black crystals were washed with the EtOH–Et_2O (1:1) mixture, and finally with Et_2O. Yield: 0.35 g.

$Li[FeL_2^2]{\cdot}H_2O$. The mixture of 0.45 g of $Fe(HL^2)L^2$ and 0.080 g of $LiOH{\cdot}H_2O$ in 7 cm^3 of MeOH was heated for 5 min. Dissolution of the starting complex was accompanied by formation of the needle-like black–green crystals, which, after solution cooling to room temperature, were filtered off and washed with MeOH and Et_2O. Yield: 0.35 g.

$Li[FeL_2^3]{\cdot}H_2O$. 0.94 g of $Fe(HL^3)L^3$ was added into 20 cm^3 of MeOH and all heated gently. Afterwards, to it was added 0.125 g of $LiOH{\cdot}H_2O$ dissolved in 5 cm^3 of MeOH, and the reacting mixture heated gently to complete dissolution of the complex. After warm filtration, 10 cm^3 of Et_2O were added and the solution left in a closed vessel at room temperature for 15 hr. The black cubic crystals obtained (which if powdered are of dark-green colour) were filtered off and washed with MeOH and Et_2O. Yield: 0.60 g.

If the solution after filtration was transferred to an evaporating dish and left to concentrate at room temperature to one third of the starting volume, greenish flaky crystals were formed. The crystals were washed with 10 cm^3 of MeOH–Et_2O (1:1) mixture, and finally with Et_2O. Yield: 0.60 g. (This, easier soluble, modification was chemically identical to the former one.)

†Overheating of the mixture resulted in complex degradation and precipitation of the ligand.

$Fe(HL^1)Cl_2 \cdot 2H_2O$. The mixture of 0.45 g of H_2L^1 and 1.5 g of $FeCl_3 \cdot 6H_2O$ was dissolved by heating in 5 cm^3 of acetone. The green solution after filtration was left in an open Erlenmeyer flask for about 3 days. The black crystals were filtered off and washed with EtOH and Et_2O. Yield: 0.20 g.

$Fe(HL^2)Cl_2 \cdot H_2O$. 0.80 g of $FeCl_3 \cdot 6H_2O$ and 0.50 g of H_2L^2 were dissolved by heating in 7 cm^3 of EtOH and left at room temperature for 24 h. The black crystals were filtered off and washed with EtOH, then with 20 cm^3 of the EtOH–Et_2O (1:1) mixture and finally wiht Et_2O. Yield: 0.35 g.

Complexes $[Fe(HL^3)_2]Cl$, $Fe(HL^3)L^3$ and $Fe(HL^3)Cl_2$ were prepared following strictly the procedures described earlier.[4]

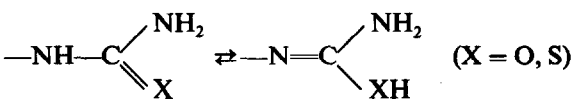
RESULTS AND DISCUSSION

Syntheses and general characteristics of complexes

The results of elemental analysis of the complexes obtained by the above procedures have been presented in Table 1.

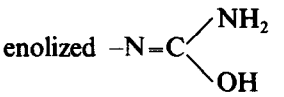
Formation of different types of complexes is made possible by coordination of the ligand either as a mono- or di-anion. The mono-anion, HL^-, results from deprotonation of the phenolic OH group, leading to formation of the cationic complex, $[Fe(HL)_2]^+$†. For an efficient crystallization of this complex, the ethanolic solution of the Fe(III) salt ought to have pH 1–2. This can be adjusted by adding the necessary amount of either aqueous ammonia, or ethanolic solution of $NaOAc \cdot 3H_2O$.

Complexes of the non-electrolyte type, Fe(HL)L, to which in a DMF solution (as it will be discussed later on) corresponds, most probably, a dimeric formula $[Fe(HL)_2][FeL_2]$, are formed as the result of a further deprotonation of the ligand, leading to its di-anionic form, L^{2-}. This deprotonation is made possible in the case of semi- and thiosemi- carbazones by a tautomeric equilibrium:



taking place at the chalcogen atom. In contrast to this, the di-anion form in the case of S-methylthiosemicarbazone is formed by deprotonation (apart from phenolic group) of the coordinated NH_2 group.[4]

Syntheses of the crystalline complexes of the non-electrolyte type with all three ligands were accomplished in two different ways, i.e. by direct and indirect synthesis. The first method involved reacting the ethanolic solution of Fe(III) hydroxo-acetate (obtained in the reaction of $FeCl_3 \cdot 6H_2O$ and $NaOAc \cdot 3H_2O$, after removal of NaCl) and a stoichiometric amount of the ligand. The indirect synthesis can be realized either by reacting the methanolic solution of the cationic complex and an excess of $LiOAc \cdot 2H_2O$, or, by mixing the methanolic solutions of the corresponding cationic and anionic complex in a stoichiometric ratio. In all three cases the complexes of a satisfactory purity are formed. This holds for H_2L^2 and H_2L^3 complexes, while the direct synthesis in the case of H_2L^1 resulted in $[Fe(HL^1)_2]OAc \cdot H_2O$. This indicates a hindered deprotonation of the OH group from the



The anionic type of complexes, i.e. the corresponding lithium salts, $Li[FeL_2] \cdot xH_2O$, were obtained in the reaction of alcoholic solutions of either cationic, or, non-electrolyte complexes and a smaller excess of $LiOH \cdot H_2O$.

In contrast to the above group, the mono-(ligand) complexes can be obtained from concentrated solutions of $FeCl_3 \cdot 6H_2O$ and the corresponding ligand in EtOH and Me_2CO, respectively, in the presence of an excess of the Fe(III) salt.

All described complexes are black crystals, while in powdered state they are brown. The exception is $Li[FeL_2^3] \cdot H_2O$ which is green. The complexes are mostly soluble in MeOH, EtOH and DMF; the solubility of the anionic and mono(ligand) complexes being generally the highest and that of the non-electrolyte type the lowest. The former two types of complexes are moderately soluble in water, the others being practically insoluble. Dissolution in water is often accompanied by the complex decomposition. All the complexes are insoluble in Et_2O.

On the basis of the data presented in Table 2, it can be concluded that mono(ligand) and cationic complexes are thermally less stable than other types of complexes. The common characteristic of the non-electrolyte complexes is that they are susceptible to certain changes at higher temperatures, which are not easily observable due to

†Isolation of the crystalline $[Fe(HL^1)_2]Cl.H_2O$, described earlier,[1] was not possible with the $FeCl_3.6H_2O$ at our disposal without a pH adjustment; the later fact was not mentioned in the original work.

Table 1. Analytical data for Fe(III) complexes

Complex	C(%)		H(%)		N(%)		Cl(%)		H_2O(%)	
	a	b	a	b	a	b	a	b	a	b
$Fe(HL^1)Cl_2 \cdot 2H_2O$	28.99	28.18	4.26	3.55	12.94	12.32	20.24	20.79	10.91	10.57
$[Fe(HL^1)_2]Cl \cdot H_2O$	41.43	41.27	4.08	3.90	18.48	18.04	7.54	7.61	3.33	3.87
$Fe(HL^1)L^1 \cdot H_2O$	45.41	44.78	4.43	3.99	19.61	19.57				
$Li[FeL^1_2] \cdot 3H_2O$	40.08	40.79	4.32	4.28	17.25	17.83			10.53	11.47
$Fe(HL^2)Cl_2 \cdot H_2O$[c]	29.16	28.35	3.03	2.97	12.45	12.39	20.80	20.92	4.70	5.31
$[Fe(HL^2)_2]Cl$	40.22	40.06	3.56	3.36	17.38	17.55	7.24	7.38		
$Fe(HL^2)L^2$	43.54	43.35	3.50	3.41	19.21	18.95				
$Li[FeL^2_2] \cdot H_2O$[d]	40.78	41.13	3.59	3.45	18.13	17.98				
$Li[FeL^3_2] \cdot 2H_2O$	42.19	42.12	4.37	4.32	16.28	16.36			7.50	7.02

[a]Found. [b]Calculated. [c]$Fe(HL^2)Cl_2 \cdot 2.5\ H_2O$ reported in ref. 2. [d]$Li[FeL^2_2] \cdot 2H_2O$ reported in ref. 3.

their dark colour. After these changes, on elevation of temperature, the substance decomposes with evolution of gaseous products. Thus, no melting occurs. Some other complexes behave similarly.

Molar conductivity

The results of molar conductivity measurements have been presented in Table 2. Although the selected solvents, MeOH and DMF, are not the best for conductivity measurements, due to their possible interactions with the dissolved complexes,[8] they were chosen to support the suggested formulae, for the reason of a relatively good solubility of the studied complexes. In general, the conductivities of all types of complexes are lower in DMF than usually expected for 1:1 electrolytes (65–90) while the values measured in MeOH fall mostly within the range for 1:1 electrolytes (80–115).[8]

The lower conductivity of cationic complexes in DMF can be explained by possible interaction of the complexed Fe(III) species with almost unsolvated Cl^- (the donor/acceptor properties of

Table 2. Physical properties of investigated Fe(III) complexes

Complex	Conductivity, Λ_M[a]		M_p, °C	μ_{eff}(solid)[b], BM
	MeOH	DMF		
$Fe(HL^1)Cl_2 \cdot 2H_2O$	110.4	54.9[c]	260[d]	5.22
$[Fe(HL^1)_2]Cl \cdot H_2O$	78.7	36.1	238	5.86
$Fe(HL^1)L^1 \cdot H_2O$	e	7.8[c]	>400[d]	5.84
$Li[FeL^1_2] \cdot 3H_2O$	43.2	51.5	295	6.03
$Fe(HL^2)Cl_2 \cdot H_2O$	81.8	49.9[c]	200	5.99
$[Fe(HL^2)_2]Cl$	84.3	19.1	228	5.87
$Fe(HL^2)L^2$	e	91.2[c]	258[d]	5.85
$Li[FeL^2_2] \cdot H_2O$	77.2	48.6	>340[d]	2.73
$Fe(HL^3)Cl_2$	82.1	45.6[c]	235	5.75
$[Fe(HL^3)_2]Cl$	87.4	27.1	219	5.86
$Fe(HL^3)L^3$	14.2[c]	6.4[c]	>380[d]	5.89
$Li[FeL^3_2] \cdot 2H_2O$	76.5	29.7	260	5.95

[a]In S mol^{-1} cm^2; 1 mM at 23°C. [b]Measured at 298 K. [c]Calculated for dimer. [d]Temperature at which change occurs, decomposition without melting. [e]Sparingly soluble.

DMF and Cl^- are about the same),[9] resulting thus in the ion-pair formation. The same holds for anionic complexes where Li^+ solvation by DMF must be taken into account. In addition, although it is not obvious from the first sight, the non-electrolyte complexes in DMF may be still present in the dimeric form, i.e. $[Fe(HL)_2][FeL_2]$, as it was confirmed by voltammetric study (see later). The extremely low conductivity of these complexes (with the exception of the thiosemicarbazone one) can be explained also by interactions of the weakly solvated constituent cation and anion. In contrast to this, the suggested dimeric structure for non-electrolyte complexes could not be confirmed in MeOH, because of low solubility of the two complexes and the inconvenience of MeOH as solvent in voltammetric measurements. Finally, the supposed dimeric formula of the mono(ligand) complexes in DMF, i.e. $[Fe(HL)_2][FeCl_4]$, is suggested (apart from the voltammetric experiments) by the data characteristic for 1:1 electrolytes.

Magnetic susceptibilities

As can be seen from Table 2, all of the complexes, with the exception of $Li[FeL_2^2]\cdot H_2O$, have at room temperature the values for effective magnetic moments characteristic for the high-spin octahedral Fe(III) complexes (term $^6A_1$). This means that neither a change in charge of the complex/ligand, nor even a change of the set of coordinated atoms from N_2O_4 (in H_2L^1) via $N_2O_2S_2$ (in H_2L^2) to N_4O_2 (in H_2L^3), have enough influence on the strength of the ligand field sufficient to change the spin state of the central Fe(III) ion. The only exception is, as stated above, $Li[FeL_2^2]\cdot H_2O$, which as well as the earlier described di-hydrate $Li[FeL_2^2]\cdot 2H_2O$ (μ_{eff} (300) = 2.19 B.M.),[3] has the effective magnetic moment characteristic for a low-spin Fe(III) state (term $^2T_2$).

Such low μ_{eff} values for the obtained complex, as well as for the already reported di-hydrate, is not, undoubtedly, a consequence of the change of charge on the ligand, but is due to the strong polarizing effect of the Li^+ ion.[3]

IR spectra

As has been already mentioned,[1-3] each of the ligands under consideration use three donor atoms† in coordination. Two donor atoms are common for all three ligands, namely: oxygen from the phenolic hydroxyl and nitrogen from the azomethine group. The third donor atom in H_2L^1 is oxygen of the C=O group,[1] the sulphur of the analogous C=S group[2] in H_2L^2 and the nitrogen from the NH_2 group[3] in H_2L^3.

The IR spectra of the ligands and complexes described here, indicate that the above donor atoms are engaged in coordination. The strong band appearing at 1270 cm^{-1} in the IR spectra of all three ligands, assigned to valence vibration of the phenolic C–O group,[12] is shifted in the complexes toward higher energies ($1290 \pm 10\ cm^{-1}$), indicating that the oxygen takes part in coordination.

The very strong and sharp band for the azomethine group, ν(C=N), which in the spectra for free ligands H_2L^2 and H_2L^3 is at $1600 \pm 10\ cm^{-1}$, is shifted for complexes by about $10\ cm^{-1}$ to lower energies,[13,14] while in the case of H_2L^1 complexes it is shifted by the same amount in the opposite direction.[10]

The very strong band ν(C=O)(H_2L^1), appearing at $1690\ cm^{-1}$ in the ligand spectrum is also shifted due to coordination towards lower frequencies ($\Delta\nu = 45\ cm^{-1}$).

An indication that the sulphur atom in H_2L^2 (as the third donor atom) is coordinated, is the absence of the bands at 1070 and 1370 cm^{-1}, corresponding to ν_s and ν_{as}(C=S) in the free ligand spectrum.[15]

Coordination of nitrogen from the NH_2 group of H_2L^3 can be substantiated by its deprotonation leading to a di-anionic form of the ligand, and by a shift of the strong and sharp $\delta(NH_2)$ band from 1635 to $1600\ cm^{-1}$. It should be mentioned that this band in the spectra for other two ligands is not well separated from the main ν(C=N) band. Therefore, it appears as a shoulder at $1615\ cm^{-1}$, remaining in complexes, practically, at the same position.

Electronic spectra

The corresponding electronic spectral data for all types of complexes in DMF are given in Table 3. It is common for all complexes that only a few well developed absorption maxima ($\epsilon < 7{,}000$) are formed in the visible region, the other appearing as broad absorption bands or shoulders. Thus, the main spectral characteristics of a particular type of complexes arise in UV region, where they are influenced by the structure of the ligand involved in coordination. Generally, the UV spectra of cationic and mono(ligand) species resemble the

†In Refs. 10 and 11 the examples have been reported for a bidentate coordination of salicylaldehyde semicarbazone.

Table 3. Electronic spectral data for Fe(III) complexes in DMF

Complex	$\lambda^{a}_{max}(\varepsilon^{b})$
$Fe(HL^1)Cl_2 \cdot 2H_2O$[c]	18,250(0.31), 31,450(2.56), 36,230(4.53)
$[Fe(HL^1)_2]Cl \cdot H_2O$	18,800(0.30), 22,320(sh)[d], 31,250(sh), 32,680(sh), 36,100(3.80)
$Fe(HL^1)L^1 \cdot H_2O$[c]	22,830(0.86), 28,730(3.54), 33,110(sh), 35,710(6.24)
$Li[FeL^1_2] \cdot 3H_2O$	~17,600(b.p.)[e], 20,490(sh), 23,360(0.42), 28,410(2.98), 34,960(2.17)
$Fe(HL^2)Cl_2 \cdot H_2O$[c]	~19,000(sh), 28,650(sh), 29,940(4.85), 30,960(4.63 sh), 32,570(4.56), 33.670(4.48 sh)
$[Fe(HL^2)_2]Cl$	~19,100(sh), ~23,200(sh), 28,650(sh), 30,030(4.10), 31,150(sh), 32,470(3.50), 33.560(sh)
$Fe(HL^2)L^2$[c]	20,160(sh), 30,030(sh), 31,050(5.56 sh) 34,500(6.0 b.p.)
$Li[FeL^2_2] \cdot H_2O$	16,500(0.19), 27,100(1.88 sh), 31,250(2.10), 36,360(2.60)
$Fe(HL^3)Cl_2$[c]	22,520(0.43), 28,570(sh), 30,030(3.64), 31,150(sh), 32,900(sh), 34,130(4.25)
$[Fe(HL^3)_2]Cl$	22,520(0.31), 28,570(sh), 29,850(3.16), 32,890(3.0 sh), 34,250(3.34)
$Fe(HL^3)L^3$[c]	21,270(1.22), 28,820(4.92), 31,350(4.84), 35,090(6.26)
$Li[FeL^3_2] \cdot 2H_2O$	~16,700(0.15), 21,190(0.74), 31,250(2.72), 36,360(2.09)

[a] In cm^{-1}. [b] In $dm^3\ mol^{-1}\ cm^{-1} \times 10^{-4}$. [c] Taken as dimer. [d] Shoulder. [e] Broad peak.

spectra of ligand alone, with usually two well separated absorption bands. For thiosemi- and S-methylthiosemi- carbazone complexes the main absorption occurs at $\sim 30{,}000\ cm^{-1}$ ($\epsilon > 30{,}000$) and in the range of 32,000–34,000 cm^{-1} (ϵ30,000–40,000) where two insufficiently separated absorption maxima are observed. The exceptions are the semicarbazone complexes of the same type, where one of two main peaks appearing in the spectrum of the ligand alone at 31,000 cm^{-1} in the complexes disappears. The other significant maximum in these spectra at $\sim 36{,}000\ cm^{-1}$ ($\epsilon > 30{,}000$) is also present in the spectrum of the ligand itself.

The spectra for all three anionic complexes differ from each other and from those for corresponding ligands. The common characteristic of $Li[FeL^2_2]$ and $Li[FeL^3_2]$ is the appearance of a band at $\sim 36{,}000\ cm^{-1}$ ($\epsilon > 20{,}000$) which does not exist in the corresponding ligand spectrum. This reflects the structural/electronic differences of the ligand in H_2L and L^{2-} form.

Electronic spectra of non-electrolyte type of complexes resemble the superimposed spectra of the corresponding cationic and anionic species. It also may be a confirmation of the supposed dimeric structure of the non-electrolyte complexes in DMF solutions.

Finally, it is well known that the electronic spectra of iron(III) complexes contain only exceptionally *d–d* transitions; the bands being sometimes overlapped by the strong charge transfer absorptions.[16] Hence, it might be expected that all absorptions in the studied complexes occuring below $29{,}000\ cm^{-1}$ belong to $d - \pi^*$ interactions. The absorptions at >29,000 cm^{-1}, since they are in

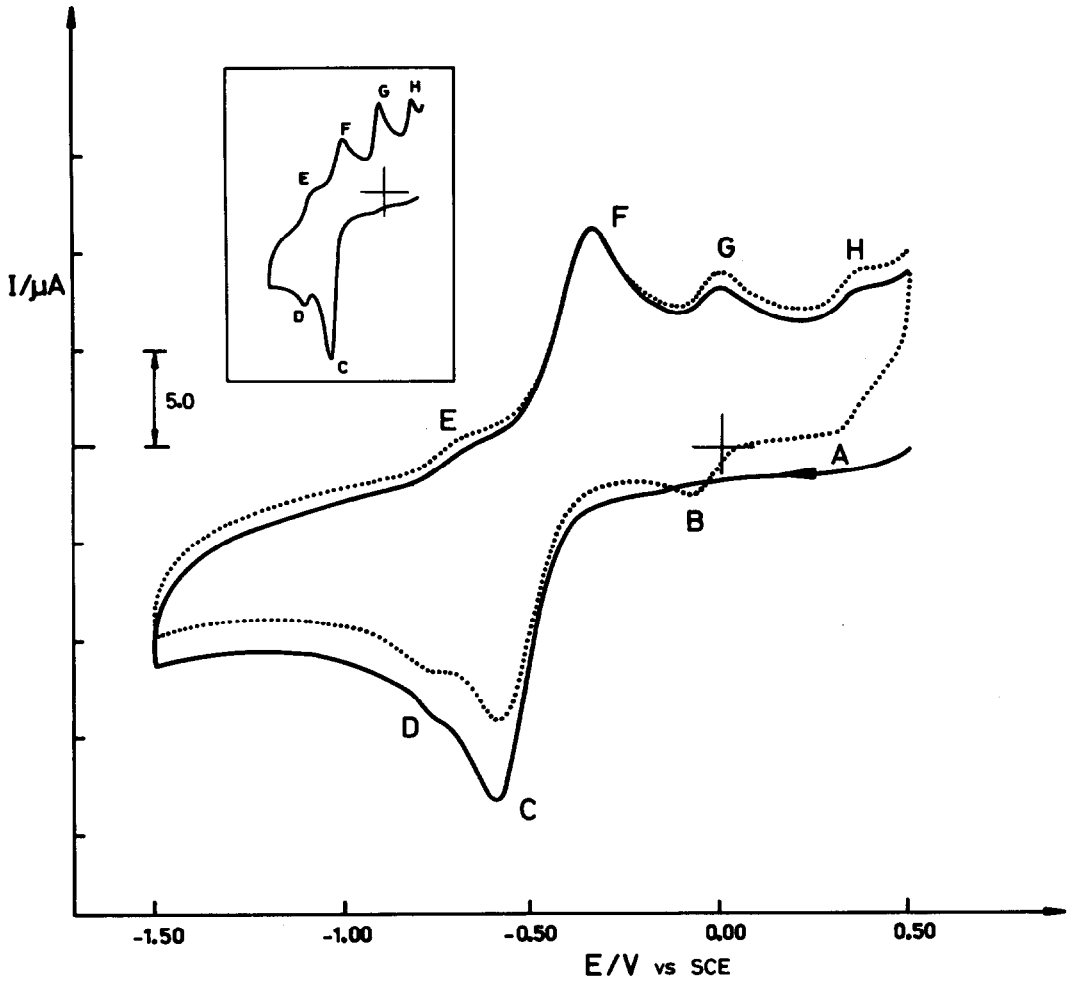


Fig. 1. Cyclic voltammograms for $[Fe(HL^2)_2]Cl$ and $[Fe(HL^3)_2]Cl$ (inset); 1 mM DMF solutions, 0.1 M LiCl. ———, 1st cycle; . . . . . , 2nd cycle. Sweep rate: 0.200 V s^{-1}.

some way present in the ligand spectrum, may be attributed to the ligand π–π^* transitions.

Voltammetric studies

It has been found that shapes of cyclic voltammograms for some complexes are greatly affected by the nature of the supporting electrolyte present in the solution. In the presence of an "inert" electrolyte, such as TBAP, the voltammetric curves, with exception of those for the anionic complexes, are ill-defined and difficult to interpret. The addition of LiCl to the solutions of H_2L^2 and H_2L^3 complexes resulted in much better defined voltammograms. This favourable effect can be ascribed both to the ability of Fe(III) to form relatively stable complexes with chloride, and to the ion-pairing effect of the lithium ion. Hence, all the voltammograms presented were recorded for the complex solutions containing 0.1 M lithium chloride. On the other hand, it appeared that the electrode reactions in the presence of this electrolyte are coupled to a number of chemical reactions†.

We have presented here the voltammetric characteristics for the novel complexes in comparison to those of the already known compounds. To facilitate discussion, all the reduction-oxidation peaks have been identified and denoted by capital letters.

Cyclic voltammogram for the newly synthesized cationic complex $[Fe(HL^2)_2]Cl$ (Fig. 1) is quite similar to that (shown in the inset) for the analogous compound in the H_2L^3 series.[18] Thus, similarity of the cyclic voltammograms is another confirmation of the supposed complex type. From the difference between the first and the second scan it can be concluded that only the main reduction

†A detailed electrochemical study of the full range of Fe(III) complexes with all three ligands, including the possible reaction schemes, will be described elsewhere.[17]

peak (denoted as C) and its oxidation counterpart (F) are directly related to the species present in the bulk; the other peaks being the consequences of coupled chemical reactions. The detailed studies showed that the species corresponding to peak C is not a bis(ligand) complex cation $[Fe(HL^2)_2]^+$, but a mono(ligand) one, $[Fe(HL^2)Cl_x]^{2-x}$, where x is most likely equal to 3. The C–F separation is, within the range of scan rates employed, characteristic for an apparent quasi-reversible one-electron process, involving chemical complications. The reduction peak D (oxidation counterpart: E), which in this case is much less separated from peak C if compared to the picture shown in the inset, obtained at the same sweep rate, can be assigned to the reduction of the anionic species $[FeL_2^2]^-$, formed by a chemical reaction following the electronation at C. After an oxidation at potential E, this species undergoes a further oxidation at peak H (reduction counterpart: A), after which follows another chemical reaction. Peak G (counterpart: B) represents the oxidation of $FeCl_2$, resulting from another chemical reaction i.e. the ligand releasing process occuring after the reduction at peak C.

The cyclic voltammograms presented for $Li[FeL_2^3]$ (Fig. 2) were recorded within two complementary potential amplitudes. The reason was the inability of the voltammetric equipment employed to complete a full cycle when an asymmetric potential signal was applied. It is evident that voltammetric behaviour of complexes of this type is much simpler than of the former ones. The

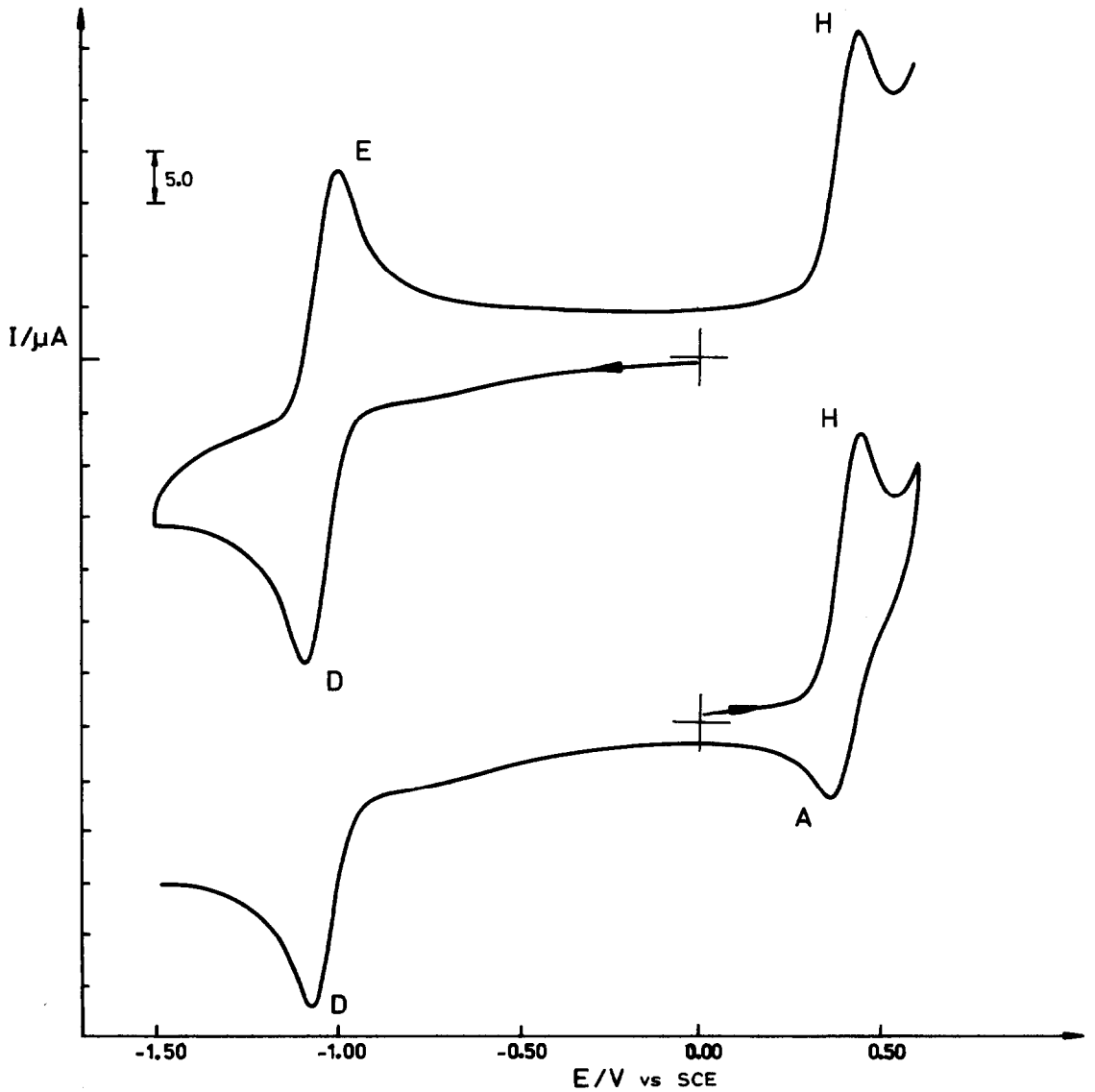


Fig. 2. Cyclic voltammograms for $Li[FeL_2^3]$; 1 mM DMF solution, 0.1 M LiCl. Sweep rate: 0.200 V s^{-1}.

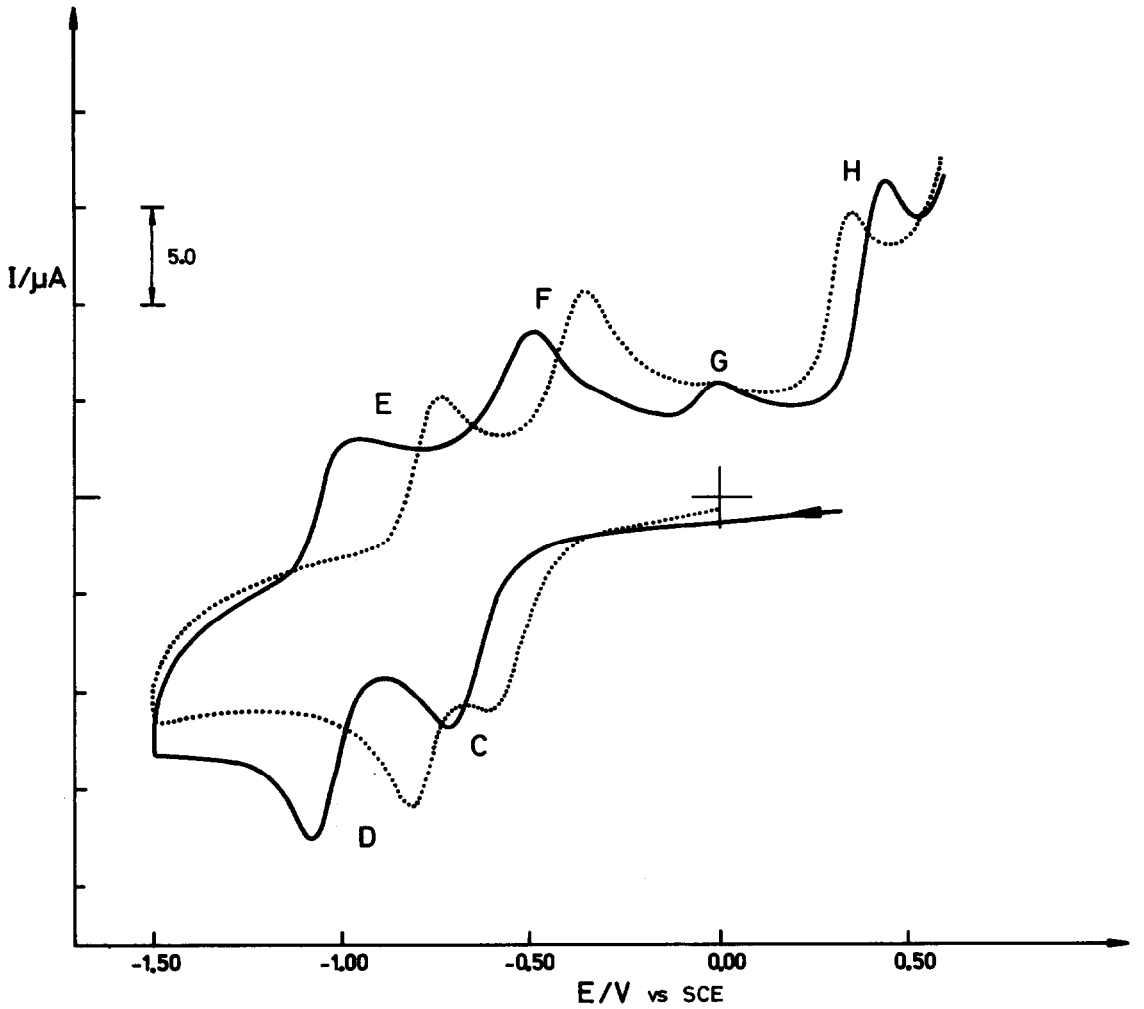


Fig. 3. Cyclic voltammograms for 0.5 mM DMF solutions of non-electrolyte complexes, 0.1 M LiCl. ....., $Fe(HL^2)L^2$; ———,$Fe(HL^3)L^3$. Sweep rate: 0.200 V s^{-1}.

complex is reduced in a one-electron quasi-reversible process (peak D; counterpart: E) and oxidized in a similar process (peak H; counterpart: A). The peak assignation was accomplished on the basis of the voltammograms for $[Fe(HL^3)_2]Cl$ and $Fe(HL^3)L^3$, as well as for $Li[FeL_2^2]$.[19]

Since for the anionic complex solutions containing TBAP or $LiClO_4$ the cyclic voltammograms obtained were generally of the same shape as the above ones, it can be concluded that Cl^- ion has no effect on the primary reactants, nor on the electrode reaction products. The difference in D/E peak potentials for the voltammograms recorded in the presence of TBAP and Li salts, respectively, consists in their anodic shifting with increasing Li^+ concentration, due to the ion-pair formation of Li^+ with both the reduced dianionic $[FeL_2]^{2-}$ and (to some extent) the original $[FeL_2]^-$ species.

Cyclic voltammograms for the non-electrolyte type of complexes, $Fe(HL^2)L^2$ and $Fe(HL^3)L^3$ (Fig. 3) do not reflect properties of the one unique species, but, as it can be concluded from the voltammograms shown in Figs. 1 and 2, they are composed of the parts characteristic for the corresponding cationic and anionic complex. This gives strong support to the idea that a more appropriate coordination formula for these complexes in DMF solutions should be $[Fe(HL)_2][FeL_2]$‡. As it has been already mentioned, this was also confirmed in the complex synthesis by mixing solutions of the corresponding constituent complexes. It should be mentioned that a similar conclusion on a dimeric nature is also valid for $Fe(HL)Cl_2$ complexes, whose more correct coordination formula, as stated above, should be $[Fe(HL)_2][FeCl_4]$.

Some cyclic voltammetry data on the non-electrolyte complexes obtained at glassy carbon

‡Another piece of evidence suggesting the same could be gained from the rotating disc experiments, resulting in two well defined waves, characteristic for pure cationic and anionic complexes, respectively.

Table 4. Cyclic voltammetry data for non-electrolyte type complexes on glassy carbon electrode[a]

Complex	v[b]	$E^{c}_{p(C)}$	$E_{p(F)}$	$E_{p(D)}$	$E_{p(E)}$	$E_{p(H)}$	$E_{p(A)}$	$\frac{I^{d}_{p(C)}}{c\,v^{1/2}}$	$\frac{I_{p(D)}}{c\,v^{1/2}}$	$\frac{I_{p(H)}}{c\,v^{1/2}}$
$Fe(HL^1)L^1 \cdot H_2O$	0.02	i.d.[e]	i.d.	-1.01	i.d.	+0.69	f	i.d.	41.4	i.d.
	0.20	-0.74	-0.43	-1.03	i.d.	+0.72	f	i.d.	43.1	i.d.
	2.00	-0.79	-0.37	-1.09	i.d.	i.d.	f	i.d.	42.1	i.d.
$Fe(HL^2)L^2$	0.02	-0.53	-0.40	-0.81	-0.74	+0.34	g	52.2	52.2	58.8
	0.20	-0.60	-0.35	-0.81	-0.73	+0.36	+0.28	49.1	49.1	55.7
	2.00	-0.66	-0.32	-0.83	-0.73	+0.37	+0.27	i.d.	i.d.	55.8
$Fe(HL^3)L^3$	0.02	-0.64	i.d.	-1.05	i.d.	+0.42	g	48.9	62.7	55.8
	0.20	-0.70	-0.51	-1.07	-0.97	+0.44	+0.37	55.2	59.5	53.3
	2.00	-0.76	-0.46	-1.10	-0.97	+0.45	+0.36	53.7	59.0	53.9

[a]In DMF solution, complex 0.5 mM(taken as dimer), 0.1 M LiCl supporting electrolyte. [b]Sweep rate, in V s^{-1}. [c]Electrode potentials in V vs. SCE. Letters in parentheses denote the corresponding peak. [d]In μA mM^{-1} $V^{-1/2}$ $s^{1/2}$. [e]Ill-defined peak. [f]Irreversible oxidation at H, no reduction peak A at the subsequent scan. [g]Due to the coupled chemical reaction, no peak A appear at this sweep rate.

electrode have been given in Table 4. Comparing the peak potentials for C/F, D/E and A/H couples for these complexes, it can be concluded that the thiosemicarbazone complexes are more easily reduced/oxidized than those of the other two classes of complexes. The effect is most pronounced in the case of D/E couple corresponding to bis(ligand) anionic species, where two sulphur atoms involved in coordination can facilitate stabilization of the product formed by the electron transfer.

The $\Delta E_p/\Delta \log v$ analysis gave a slope of about 60 mV per tenfold increase in sweep rate for peaks C/F, but less than 30 mV for all other peak couples. This indicates the possible kinetic complications, described above.

The voltammograms for the H_2L^1 complexes were not well defined (especially at higher sweep rates) in all supporting electrolytes used. Hence, they were less suitable for analysis. The exception was the anionic complex which behaves similarly to the analogous compounds described above.

Acknowledgement—The authors thank the Scientific Fund of SAP Vojvodina for financial support of the present work.

REFERENCES

1. N. M. Samus and V. G. Chebanu, *Zhur. Neorg. Khim.* 1969, **14**, 2089.
2. A. V. Ablov and N. V. Gerbeleu, *Zhur. Neorg. Khim.* 1965, **10**, 61.
3. V. V. Zelentsov, A. V. Ablov, K. I. Turte, R. A. Stukan, N. V. Gerbeleu, E. V. Ivanov, A. P. Bogdanov, N. A. Barba and V. G. Bodyu, *Zhur. Neorg. Khim.* 1972, **17**, 1929.
4. N. V. Gerbeleu, K. I. Turte, V. D. Canić, V. M. Leovac and V. B. Arion, *Koordinatsionnaya Khimiya* 1980, **6**, 446.
5. A. I. Vogel, *A Text-book of Practical Organic Chemistry, p.* 344. Longman, London (1972).
6. Gy. Argay, A. Kálmán, B. Ribár, V. M. Leovac and A. F. Petrović, *Monatsh. Chem.* 1983, **114**, 1205.
7. V. M. Leovac, V. Divjaković, D. Petrović, Gy. Argay and A. Kálmán, *Polyhedron* 1983, **2**, 1307.
8. W. J. Geary, *Coord. Chem. Rev.* 1971, **7**, 81.
9. V. Gutman, *Khimiya koordinatsionnykh soedinenii v nevodnykh rastvorakh*, trans. from English, p. 217. Mir, Moscow (1971).
10. R. N. Ray and B. K. Mohapatra, *Indian J. Chem.* 1980, **19A**, 590.
11. P. L. Maurya, B. V. Agarwala and A. K. Deu, *Indian J. Chem.* 1980, **19A**, 807.
12. L. J. Bellamy, *The Infrared Spectra of Complex Molecules*, p. 108 Methuen, London (1959).
13. D. M. Wiles and T. Supruchuk, *Canad. J. Chem.* 1969, **47**, 1097.
14. M. S. Patil and J. R. Shah, *J. Indian Chem. Soc.* 1981, **58**, 944.
15. N. V. Gerbeleu, *Zhur. Neorg. Khim.* 1968, **13**, 2467.
16. F. A. Cotton and G. Wilkinson, *Advanced Inorganic Chemistry*, p. 761. Wiley-Interscience, New York (1980).
17. L. Bjelica, Lj. Jovanović and V. M. Leovac, to be published.
18. L. Bjelica, Lj. Jovanović, V. Leovac and F. Gaál, *7th Yugoslav Symposium on Electrochemistry*, pp. 163–167. Ohrid (1981).
19. Lj. Jovanović, L. Bjelica and V. Leovac, *8th Yugoslav Symposium on Electrochemistry*, pp. 30–34, Dubrovnik (1983).

Polyhedron Vol. 4, No. 2, pp. 243–249, 1985
Printed in Great Britain.

0277–5387/85 $3.00 + .00
© 1985 Pergamon Press Ltd.

THE EFFECT OF THE C-METHYL SUBSTITUTION ON THE MOLECULAR GEOMETRY OF THE SILATRANE SKELETON: THE CRYSTAL STRUCTURES OF 1-(4′-TOLYL)-SILATRANE AND 1-(4′-TOLYL)-3,7,10-TRIMETHYLSILATRANE

L. PÁRKÁNYI*
Central Research Institute of Chemistry of the Hungarian Academy of Sciences, H-1525-Budapest, P.O. Box 17, Hungary

P. HENCSEI, L. BIHÁTSI and I. KOVÁCS
Institute for Inorganic Chemistry, Technical University of Budapest, H-1521-Budapest, Hungary

and

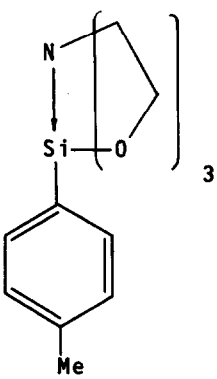
Á. SZÖLLŐSY
Institute for General and Analytical Chemistry, Technical University of Budapest, Hungary

(*Received* 10 *February* 1984; *accepted* 16 *April* 1984)

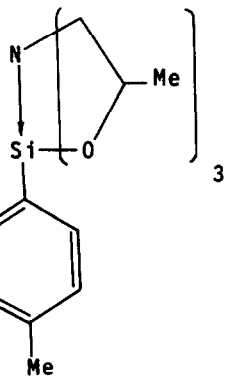
Abstract—Unsubstituted (**1**) and 3,7,10-trimethyl substituted (**2**) 1-(4′-tolyl)-silatranes were synthesized. ^{1}H, ^{13}C, ^{15}N and ^{29}Si NMR spectra were recorded and assigned. The conformation of the **2** stereoisomers in solution were characterized by the NMR spectra. **1** is monoclinic, $P2_1/c$, with $a = 13.454(2)$, $b = 13.888(2)$, $c = 14.345(2)$ Å, $\beta = 99.10(2)°$. The major stereoisomer fraction of **2** is orthorhombic, *Pbca*, with $a = 12.168(2)$, $b = 13.754(4)$, $c = 20.260(3)$ Å. The structures were solved by direct methods and were refined by least squares to R values of 0.039 and 0.066 for 3523 and 2158 reflexions. The N→Si distances are **1**: 2.169(2) (mean) and **2**: 2.236(3) Å. The solid state conformation of the **2** major stereoisomer fraction is different from that in solution and this is the first example of a silatrane crystal structure where the silatrane moiety lacks C_3 symmetry.

The crystal structures of 1-hydrogen-3,7,10-trimethylsilatrane[1] and 1-chloromethyl-3,7-dimethylsilatrane[2] of the C-methyl substituted silatrane series have been determined and the X-ray structure determination of 1-chloromethyl-3,7,10-trimethylsilatrane is also referenced in the literature[3] though no atomic coordinates or molecular geometry have yet been published.

To elucidate the effect of the C-methyl substitution on the molecular geometry (particularly on the length of the N→Si approach) we synthesized 1-(4′-tolyl)-silatrane (**1**) [1-(4′-tolyl)-2,8,9-trioxa-5-aza-silatricyclo[3.3.3.$0^{1,5}$]-undecane] and 1-(4′-tolyl)-3,7,10-trimethylsilatrane (**2**) [1-(4′-tolyl)-2,8,9-trioxa-3,7,10-trimethyl-5-aza-silatricyclo[3.3.3.$0^{1,5}$]-undecane) and their conformation was studied by NMR and X-ray crystal structure analysis.



1



2

*Author to whom correspondence should be addressed.

EXPERIMENTAL

(1) *Synthesis*

1-(4′-tolyl)-silatrane (**1**) was prepared according to Frye *et al.*[4] The crude product was recrystallized from petroleum ether. M.p. 196–198°C (Lit.: 195–195.5°C[5]). 1-p-tolyl-3,7,10-trimethylsilatrane (**2**): p-$CH_3C_6H_4Si(OCH_3)_3$ (17.0 g, 80 mmol) and $N[CH_2CH(OH)CH_3]_3$ (15.3 g, 80 mmol) was reacted in 50 cm^3 xylene at 110–112°C for 2 hr in the presence of KOH catalyst (0.2 g). The methanol by-product (7.5 cm^3) was distilled from the system. The crude product was precipitated by adding 20 cm^3 petroleum ether to the solution. The compound was recrystallized from benzene. Yield: 19.3 g (78%), m.p.: 147–148°C. [Found: C, 61.1 (62.5); H, 8.03 (8.20); N, 4.17 (4.55); Si, 9.23 (9.13)%]. IR (cm^{-1}): 263m, 330s, 431m, 514s, 546s, 626vs, 667w, 703w, 770vs, 810m, 885s, 975vs, 982vs, 1060s, 1070s, 1092m, 1105vs, 1150vs, 1180m, 1268w, 1330w, 1375m, 1460w, 1500w, 1596w, 2890m, 2975s, 3070w.
MS (*m/e*): 307(16%) (M^+), 216 (100%)($M-R^+$).

(2) *The separation of the stereoisomers of 2*

The synthesis of **2** leads to a mixture of diastereomers. The theoretical isomer ratio is 1 : 3. Their separation was performed by HPLC using a HPLC-DUPONT 830 chromatograph, normal phase Chromsil column, dichloromethane : hexane = 1 : 4 eluent, UV detector (254 nm). The minor stereoisomer had shorter retention time. Crystals for single crystal X-ray analysis were prepared from the fraction of the major stereoisomer.

(3) *NMR studies*

The ^{15}N and ^{29}Si-NMR spectra were recorded at 2.35T on a JEOL FX-100 spectrometer. ^{13}C and ^1H-NMR spectra were recorded at 4.7 and 7.0T on Bruker spectrometers WP200 SY and WH300, respectively. Samples were taken in $CDCl_3$ solutions and TMS was used as internal reference standard for the ^1H, ^{13}C and ^{29}Si spectra. The ^{15}N-NMR chemical shifts were determined relative to external aqueous $K^{15}NO_3$ then were converted to external nitromethane ($\delta_{CH_3NO_2} = 0.0$ ppm). Shifts upfield from the reference have negative values.

(4) *Crystallographic studies*

Unit cell determinations and intensity data collections were performed on an Enraf–Nonius CAD4 diffractometer. Unit cell parameters were obtained by least squares refinement of the setting angles of 25 carefully centered high-angle reflexions.

Crystal data. Compound **1**: $C_{13}H_{19}NO_3Si$, F.wt. = 265.4 a.m.u., monoclinic, a = 13.454(2), b = 13.888(2), c = 14.345(2)Å, β = 99.10(2)°, V = 2646.6(1.9) Å^3, space group $P2_1/c$, Z = 8, D_c = 1.332 gcm^{-3}, $F(000)$ = 1136, $\mu(Mo\text{–}K_\alpha$–, λ = 0.7107 Å) = 1.7 cm^{-1}. Compound **2**: $C_{16}H_{25}NO_3Si$, F.wt. = 307.5 a.m.u., orthorhombic, a = 12.168(2), b = 13.754(4), c = 20.260(3) Å, V = 3390.7 (2.0) Å^3, space group *Pbca*, D_c = 1.205 gcm^{-3}, μ ($Mo\text{–}K_\alpha$–) = 1.4 cm^{-1}.

Data collection

CAD4 diffractometer, graphite monochromated $Mo\text{–}K_\alpha$ radiation, 2θ–ω scan.

Compound **1**: $1.5 \leq \theta \leq 25°$, 4134 non-zero unique intensities collected, 3523 observed [$F^2 \geq 2\sigma(F^2)$].

Compound **2**: $1.5 \leqq \theta \leqq 30°$, 3282 non-zero unique intensities, 2158 observed [$F^2 \geqq 2\sigma(F^2)$].

The solution and refinement of the structures

Both structures were solved by direct methods and subsequent Fourier syntheses. Hydrogen atomic positions were generated from assumed geometries. No absorption correction was applied.

Compound **1**: Difference maps clearly showed partial disorder in molecule B of the asymmetric unit. Multiplicities of disordered atoms were refined in isotropic least squares and were kept fixed during full-matrix anisotropic refinement. No hydrogen atomic parameters were refined. The final R-values were: $R = \Sigma|\Delta F|/\Sigma|F_0| = 0.039$, $R_w = [\Sigma|w\Delta F^2|/\Sigma wF_0^2]^{1/2} = 0.054$ with $w = [\sigma^2(F) + 0.25(pF_0)^2]^{-1}$, $p = 0.01$.

Compound **2**: The structure was refined by full-matrix anisotropic least-squares. Hydrogen atomic coordinates with isotropic temperature factors were also refined in two final cycles. $R = 0.066$, $R_w = 0.067$, w as in compound **1**.

Final atomic coordinates, thermal parameters and lists of F_0/F_c values have been deposited with the Editor as supplementary data.† Programs, computer and sources of scattering factors are given in Ref. 6.

DISCUSSION

NMR results

Due to the incomplete chromatographic separation of the **2** diastereomers the NMR spectra of the pure minor stereoisomer could only be recorded. The fraction of the major component always contained some of the minor stereoisomer as was observed in the spectra.

The chemical shifts (ppm) of **1** and **2** are listed

†Atomic coordinates have also been deposited with the Cambridge Crystallographic Data Centre for inclusion in their Data Base. Copies are also available, on request, from the Editor at Queen Mary College.

Table 1. NMR data of compounds **1** and **2**

	1	2 major	2 minor
$\delta^{29}Si$	- 80.6	- 80.6	- 83.1
$\delta^{15}N$		-344.3	-342.7
$\delta^{13}C$ $ArCH_3$	21.10	21.05	
C-1	138.85	138.66	139.07
C-2,6	132.92	134.54	
C-3,5	127.49	127.79	
C-4	136.41	136.91	136.75
N-C	50.44	65.21(2C) 58.98	61.29
O-C	57.31	66.86 65.14 65.06	63.46
CH_3		22.90 20.23 20.11	20.45
$\delta^{1}H$ ArH	7.0-7.1 m (2) 7.5-7.6 m (2)	6.9 -7.0 m (2) 7.45-7.60 m (2)	
$ArCH_3$	2.28 s (3)	2.30 s (3)	
NCH_2	2.78 t (6)	2.43 2.20 */-13.3 Hz /-13.3 Hz* *6.0 Hz/ 6.6 Hz/* 2.27 1.81 */-12.1 Hz /-12.1 Hz* *4.1 Hz/ 11.1 Hz/* 2.20 1.97 */-12.4 Hz /-12.4 Hz* *4.1 Hz/ 11.1 Hz/*	2.47 1.91 */-12.3 Hz /-12.3 Hz* *4.1 Hz/ 11.1 Hz/*
OCH_2 (OCH)	3.81 t (6)	3.7-3.95 m	4.06m
CH_3		1.21 d 1.16 d 1.15 d	1.17 d

in Table 1. The silatrane skeleton consists of three fused five-membered rings (Si–O–C–C–N). ^{1}H-NMR data indicate a homogeneous conformational state of the rings in the minor component of **2** with quasi-equatorial methyl groups in the dominant conformation as shown by the ^{3}J coupling constants. One of the methyl groups adopts a quasi-axial position, however, in the major stereoisomer component (^{3}J = 6.0 and 6.6 Hz). This result is further supported by the ^{13}C-NMR spectrum since the chemical shift increase caused by an axial methyl group in β position is smaller than that induced by an equatorial one,[7] facilitating also the assignment of the NCH_2 signals. The change in J_{gem} accounts for small deformations in the ring bearing the axial methyl group. This arrangement enhances the conformational stability of the silatrane moiety as was shown by temperature-dependent NMR measurements.[8]

The crystal structures

The two molecules of the asymmetric unit of **1** are depicted in Fig. 1 and the molecules of **2** in Fig. 2. Bond distances and angles observed in the silatrane moieties are given in Tables 2 and 3.

The single crystal of **2** subjected to X-ray struc-

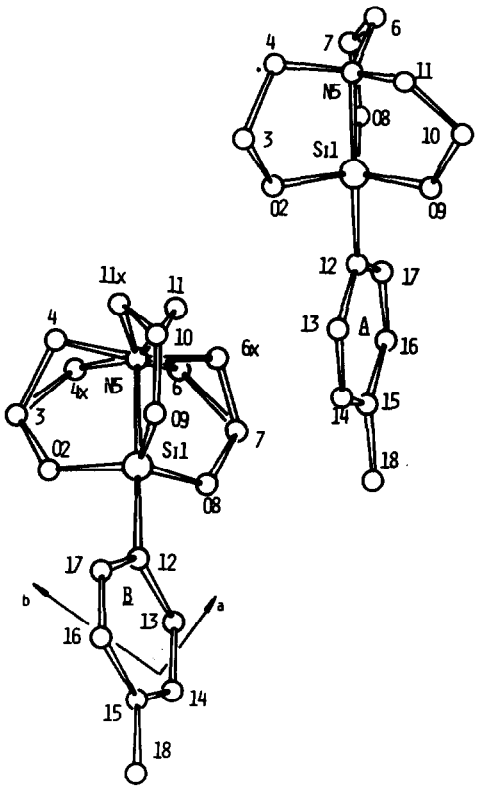


Fig. 1. The two molecules of the asymmetric unit of compound **1**. Numbers are for carbon atoms unless indicated otherwise. Hydrogen atoms are omitted for clarity. Site occupancy factors of the disordered carbon atoms in molecule B are 0.85 (C(6), C(4), C(11)) and 0.15 (C(4)x, C(6)x, C(11)x).

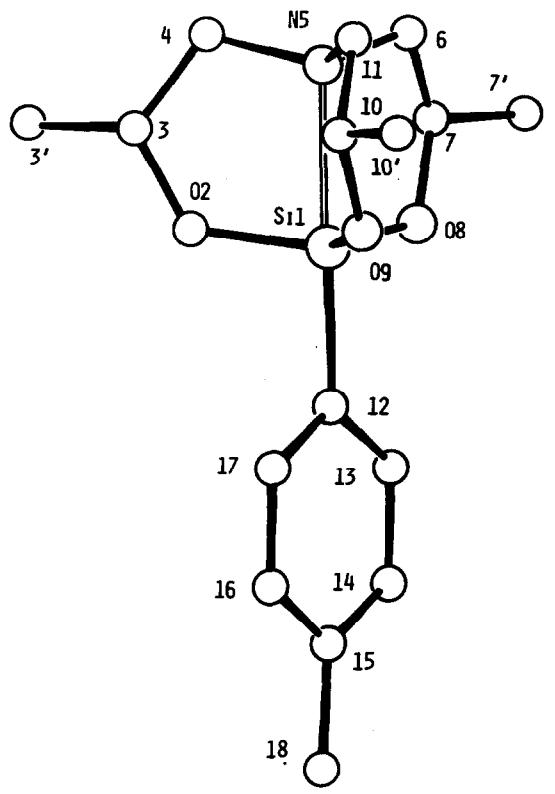


Fig. 2. The molecular diagram of compound **2**.

ture analysis contains molecules of the major stereoisomer component (see Fig. 3).

The length of the N→Si dative bond (*d*) is longer by 0.067 Å in **2** than in **1**. This result is contradictory to the findings of Demidov *et al.*[3,9] who reported the same *d* distances (2.12 Å) for the unsubstituted, 3,7-dimethyl- and 3,7,10-trimethyl-substituted chloromethyl derivatives, stating that the N→Si interaction is unaffected by methyl substitution in the silatrane skeleton.

The most important factor in the formation of the peculiar N→Si interaction is the electron withdrawing property of the apical substituent on silicon. The correlation utilizing the inductive Taft constant[10] of the *p*-tolyl group results in a calculated *d*-value of 2.172 Å, while the correlation of the group electronegativity with *d*[11] predicts a 2.163 Å long dative bond. The two methods give rather good approximations of the bond length observed in **1** and the significant deviation in **2** may be attributable to the methyl substitution.

The methyl substituents may have electronic effects besides causing conformational changes in the silatrane skeleton. As electron-releasing groups they may reduce the electron-withdrawing effect of the oxygen atoms attached to silicon. The less-positive silicon atom forms a weaker interaction with the lone pair from nitrogen.

Considerable changes also take place in the silatrane moiety on methyl substitution. The silatrane skeleton is formed by three five-membered rings of envelope-like conformation. In derivatives, unsubstituted in the silatrane skeleton, carbon atoms in α-position to nitrogen sit on the flaps of the envelopes. The remaining atoms [Si, O, C(β), N] form a quasi-planar moiety. The mean deviation of these atoms from their weighted least squares planes in **1** (averaged over the six rings in the asymmetric unit omitting disordered carbon atoms with the lower site-occupancy) is 0.035 Å and the normal distance of the flap carbon atoms from this plane is 0.455 Å.

Contrary to **1**, the methyl substituted carbon atoms (in β-position to nitrogen) in **2** are out of the quasi-planar moiety formed by the Si, O, C(α), N atoms (Fig. 3). The mean distance of the plane-forming atoms from their weighted least squares planes is 0.014 Å, while the average distance of the C(β) atoms from this plane is 0.325 Å. All methyl substituents are in quasi-equatorial position (the mean deviation of the methyl carbon atoms from the plane is 0.117Å). The average O–C–C–N

Table 2. Bond lengths (Å) and angles (°) in the silatrane moiety of compound **1**. Bonds and angles involving atoms of the lower site occupancy are omitted

Bond lengths:

	A	B		A	B		A	B
Si(1)-O(2)	1.659(1)	1.658(1)	O(2)-C(3)	1.409(3)	1.414(3)	C(6) -C(7)	1.484(4)	1.522(4)
Si(1)-N(5)	2.171(1)	2.167(1)	C(3)-C(4)	1.498(4)	1.517(4)	C(7) -O(8)	1.415(3)	1.409(3)
Si(1)-O(8)	1.655(1)	1.660(1)	C(4)-N(5)	1.471(3)	1.472(3)	O(9) -C(10)	1.416(3)	1.408(3)
Si(1)-O(9)	1.655(1)	1.653(1)	N(5)-C(6)	1.469(3)	1.436(3)	C(10)-C(11)	1.489(4)	1.484(4)
Si(1)-C(12)	1.887(1)	1.892(2)	N(5)-C(11)	1.457(3)	1.482(3)			

Bond angles:

	A	B		A	B
O(2)-Si(1)-N(5)	82.7(1)	83.2(1)	Si(1)-N(5) -C(4)	104.5(2)	103.9(2)
O(2)-Si(1)-O(8)	119.0(1)	118.1(1)	Si(1)-N(5) -C(6)	104.4(2)	105.9(2)
O(2)-Si(1)-O(9)	118.3(1)	117.9(1)	Si(1)-N(5) -C(11)	104.5(2)	103.9(2)
O(2)-Si(1)-C(12)	96.5(1)	97.0(2)	C(4) -N(5) -C(6)	113.0(3)	116.1(3)
N(5)-Si(1)-O(8)	82.9(1)	82.7(1)	C(4) -N(5) -C(11)	115.3(3)	112.2(3)
N(5)-Si(1)-O(9)	83.0(1)	83.0(1)	C(6) -N(5) -C(11)	113.7(3)	113.3(3)
N(5)-Si(1)-C(12)	178.8(1)	179.7(1)	N(5) -C(6) -C(7)	106.8(3)	106.9(3)
O(8)-Si(1)-O(9)	118.2(1)	119.6(1)	C(6) -C(7) -O(8)	109.6(4)	109.9(4)
O(8)-Si(1)-C(12)	98.3(1)	97.1(2)	Si(1)-O(8) -C(7)	122.6(2)	123.5(2)
O(9)-Si(1)-C(12)	96.6(1)	96.9(2)	Si(1)-O(9) -C(10)	123.3(2)	123.6(2)
Si(1)-O(2)-C(3)	123.0(2)	123.0(2)	O(9) -C(10)-C(11)	109.5(4)	110.4(4)
O(2) -C(3)-C(4)	109.4(4)	109.1(4)	N(5) -C(11)-C(10)	108.1(3)	106.8(3)
C(3) -C(4)-N(5)	106.0(3)	105.6(3)			

Table 3. Bond lengths (Å) and angles (°) in the silatrane moiety of compound **2**

Bond lengths:

Si(1)-O(2)	1.655(2)	C(3)-C(3')	1.459(6)	C(7) -C(7')	1.477(6)
Si(1)-N(5)	2.236(3)	C(3)-C(4)	1.450(5)	C(7) -O(8)	1.395(5)
Si(1)-O(8)	1.646(3)	C(4)-N(5)	1.463(5)	O(9) -C(10)	1.411(5)
Si(1)-O(9)	1.652(2)	N(5)-C(6)	1.461(5)	C(10)-C(10')	1.487(6)
Si(1)-C(12)	1.889(4)	N(5)-C(11)	1.453(5)	C(10)-C(11)	1.450(6)
O(2) -C(3)	1.399(5)	C(6)-C(7)	1.408(5)		

Bond angles:

O(2) -Si(1)-N(5)	82.0(2)	Si(1) -N(5) -C(6)	103.4(3)
O(2) -Si(1)-O(8)	117.4(2)	Si(1) -N(5) -C(11)	104.5(3)
O(2) -Si(1)-O(9)	116.1(2)	C(4) -N(5) -C(6)	114.5(5)
O(2) -Si(1)-C(12)	98.9(2)	C(4) -N(5) -C(11)	114.7(5)
N(5) -Si(1)-O(8)	81.6(2)	C(6) -N(5) -C(11)	113.5(5)
N(5) -Si(1)-O(9)	81.7(2)	N(5) -C(6) -C(7)	110.8(6)
N(5) -Si(1)-C(12)	179.0(2)	C(6) -C(7) -C(7')	122.0(6)
O(8) -Si(1)-O(9)	120.5(2)	C(6) -C(7) -O(8)	113.7(6)
O(8) -Si(1)-C(12)	97.5(2)	C(7') -C(7) -O(8)	113.8(6)
O(9) -Si(1)-C(12)	98.2(2)	Si(1) -O(8) -C(7)	123.2(4)
Si(1)-O(2) -C(3)	123.5(4)	Si(1) -O(9) -C(10)	122.3(4)
O(2) -C(3) -C(3')	113.2(6)	O(9) -C(10)-C(10')	112.0(6)
O(2) -C(3) -C(4)	113.9(6)	O(9) -C(10)-C(11)	112.0(6)
C(3')-C(3) -C(4)	116.9(7)	C(10') -C(10)-C(11)	117.7(7)
C(3) -C(4) -N(5)	110.1(6)	N(5) -C(11)-C(10)	110.3(6)
Si(1)-N(5) -C(4)	104.6(3)		

torsion angle is less by 10° in **2** [29(1)°] than in **1** [39(2)°]. Thus the solid state conformation of the **2** major stereoisomer fraction is different from that in solution as indicated by the NMR data. Axial methyl groups present in solution may result from ring inversion.

Though collective conformational transitions are assumed for the silatrane moiety with the retention of the C_3 symmetry,[8,9] the crystal structure of **2** is the first example of a silatrane skeleton without C_3 symmetry (Fig. 3). While C(3) and C(7) atoms lie on the same side of the least squares

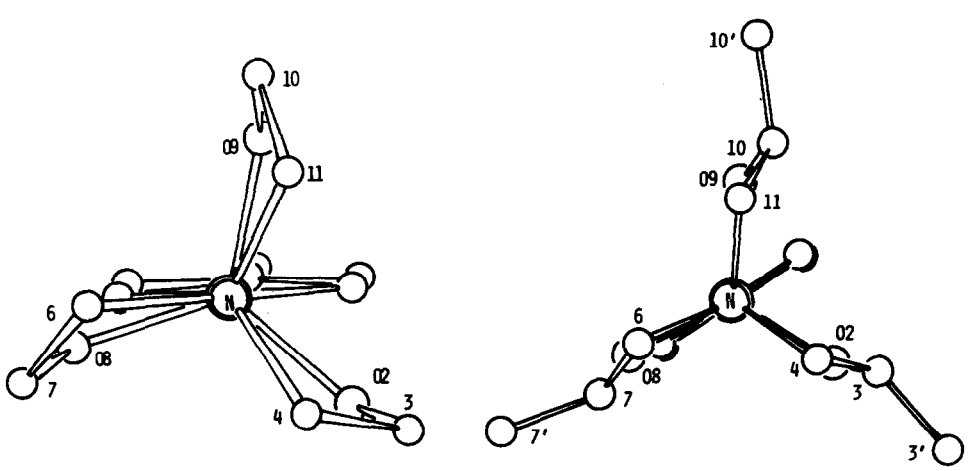


Fig. 3. Compounds **1** (molecule A) and **2** as viewed down the N→Si bond axis.

planes defined by the other four atoms of their five-membered rings, C(10) is on the opposite side. Thus "flap-atoms" C(3) and C(10) face each-other and the C(3′) and C(10′) methyl groups point to opposite directions.

The configurations around the silicon and nitrogen atoms are in good correlation with d in both compounds. The distance of silicon from the plane formed by the equatorial oxygen atoms (ΔSi) and the distance of nitrogen from the plane of its substituent carbon atoms (ΔN) were shown to be in linear correlation with d.[11] Strong N→Si interaction leads to the formation of a more regular trigonal bipyramid around silicon which lies closer to the equatorial plane. The flattened tetrahedron around the nitrogen atom changes inversely with d: a weaker interaction (longer d) results in a more flattened tetrahedron. The observed and calculated ($\Delta\text{Si} = 0.488d - 0.863$; $\Delta\text{N} = -0.391d + 1.214$ Å) values are as follows: Compound **1** observed [calculated]: ΔSi = 0.204(2) [0.195], ΔN = 0.3663(2) [0.3659], compound **2**: ΔSi = 0.2360(9) [0.2282], ΔN = 0.357(3) [0.340] Å.

Acknowledgement—We thank Prof. G. Fritz (Karlsruhe, F. R. G.), Drs L. Szilágyi (Debrecen, Hungary) and E. Kocsi (Budapest, Hungary) for their valuable contribution in the NMR measurements and the chromatographic work.

REFERENCES

1. M. P. Demidov, G. G. Aleksandrov, Yu. T. Struchkov, V. P. Baryshok, V. M. Dyakov, Yu. L. Frolov and M. G. Voronkov, *Koord. Khim.* 1981, **7**, 1262.
2. M. G. Voronkov, M. P. Demidov, V. E. Shklover, V. P. Baryshok, V. M. Dyakov and Yu. L. Frolov, *Zh. Strukt. Khim.* 1980, **21**(2), 100.
3. M. P. Demidov, V. E. Shklover, V. P. Baryshok, V. M. Dyakov, Yu. L. Frolov and M. G. Voronkov, II. *Vses. Sov. Organ. Kristallokhim.*, Zvenigorod, 1978. Tezisy dokl., p. 76. Chernogolovka (1978).
4. C. L. Frye, G. E. Vogel and J. A. Hall, *J. Am. Chem. Soc.* 1961, **83**, 996.
5. A. Daneshrad, C. Eaborn, R. Eidenschink and D. R. M. Walton, *J. Organomet. Chem.* 1975, **90**, 139.
6. L. Párkányi, P. Hencsei and L. Bihátsi, *J. Organomet. Chem.* 1982, **232**, 315.
7. E. Pretsch, T. Clerc, J. Seibl and W. Simon, *Tabellen zur Strukturaufklärung organischer Verbindungen mit spektroskopischen Methoden*, p. C55. Springer Verlag, Berlin (1981).
8. S. N. Tandura, V. A. Pestunovich, M. G. Voronkov, G. I. Zelchan, V. P. Baryshok and Yu. A. Lukina, *Dokl. Akad. Nauk SSSR*, 1977, **235**, 406.
9. M. G. Voronkov, V. M. Dyakov and S. V. Kirpichenko, *J. Organomet. Chem.* 1982, **233**, 1.
10. A. A. Kemme, Ya. Ya. Bleidelis, V. A. Pestunovich, V. P. Baryshok and M. G. Voronkov, *Dokl. Akad. Nauk SSSR*, 1978, **243**, 688.
11. L. Párkányi, P. Hencsei, L. Bihátsi and T. Müller, *J. Organomet. Chem.* 1984, **269**, 1.

Polyhedron Vol. 4, No. 2, pp. 251–258, 1985
Printed in Great Britain.

0277–5387/85 $3.00 + .00
© 1985 Pergamon Press Ltd.

SYNTHESIS AND SOME REACTIONS OF TRIS (PENTAFLUOROPHENYL) ANTIMONY COMPOUNDS

PREM RAJ*, A. K. SAXENA, KIRAN SINGHAL and ASHOK RANJAN
Department of Chemistry, Lucknow University, Lucknow 226 007, India

(*Received* 1 *March* 1984; *accepted* 16 *April* 1984)

Abstract—$(C_6F_5)_3Sb$ has been found to react with interhalogens and halo-pseudohalogens, IX(X = Cl, Br, N_3 and NCO), pseudohalogen $(SCN)_2$ and elemental sulphur to give oxidative addition products (**I–VI**). $(C_6F_5)_3SbS$(**VI**) may also be prepared by the reaction of $(C_6F_5)_3SbCl_2$ with H_2S. Metathetical reactions of $(C_6F_5)_3SbCl_2$ with appropriate metallic salts yield covalent pentacoordinate disubstituted products (**V, VII–XII**) of the general formula, $(C_6F_5)_3SbY_2$ (Y = NCS, NCO, –ONCMe$_2$, –ONCMePh –$\overline{NCO(CH_2)_2CO}$ and *p*–$NO_2C_6H_4OCO$). Treatment of $(C_6F_5)_3SbCl_2$ with aqueous NaN_3 gives the binuclear oxo-bridge compound, $[(C_6F_5)_3Sb—O—Sb(C_6F_5)_3](N_3)_2$ · (**III**) and (**IV**) are also accessible by displacement reaction of (**I**) or (**II**) with the corresponding metallic salt. Molecular weight, conductance measurements, and IR spectra on the new organoantimony(V) derivatives have been obtained.

Reductive cleavage reactions of $(C_6F_5)_3SbS$ with hexaaryldileads, Ar_6Pb_2(Ar = Phenyl, *p*-tolyl) produce $(C_6F_5)_3Sb$ and the corresponding bis(triaryllead) sulphide but treatment of $(C_6F_5)_3SbX_2$(X = NCO, Cl) with Ar_6Pb_2 gave Ar_4Pb and Ar_2PbX_2 together with $(C_6F_5)_3Sb$.

$(C_6F_5)_3SbCl_2$ and bis(triorganotin)sulphides undergo exchange of anionic groups.

Despite a considerable interest in the chemistry of hydrocarbon derivatives of antimony(III) and antimony(V), very few studies have been devoted to the corresponding fluorocarbon analogues.[1–3] Although the synthesis of tris(pentafluorophenyl) antimony[4] was reported as early as 1964, studies on vibrational spectra together with the preparation of dihalides, $(C_6F_5)_3SbX_2$ were only made after a decade.[5] Since then a single reference[6] describing the chemical behaviour of $(C_6F_5)_3Sb$ and the isolation of a few tris(pentafluorophenyl) antimony oxy has appeared.

As a part of our research programme on organoantimony(V) compounds[7] coupled with the limited published data on such compounds further investigation on pentafluorophenyl antimony(III) and antimony(V) has been undertaken.

It may be noted that organometallic compounds based on fluorocarbons have been reported not only to possess interesting properties but also provide instructive comparison with compounds based on hydrocarbon ligands.[8] In the present communication we wish to report: (i) oxidative addition reactions of $(C_6F_5)_3Sb$ with interhalogens, halo-pseudohalogens, pseudohalogen and elemental sulphur; (ii) metathetical reactions of $(C_6F_5)_3SbCl_2$ and $(C_6F_5)_3SbIX$(X = Cl, Br) with metallic salts to give disubstituted pseudohalide, oximate, amide and carboxylate and halo-pseudohalo derivatives, respectively; (iii) reductive cleavage of $(C_6F_5)_3SbS$ and $(C_6F_5)_3SbX_2$(X = NCO, Cl) with hexaaryldilead compounds, and (iv) action of $(C_6F_5)_3SbCl_2$ on bis(triorganotin) sulphides.

*Author to whom correspondence should be addressed.

EXPERIMENTAL

Tris(pentafluorophenyl)antimony[4] was prepared from pentafluorophenyl magnesium bromide, C_6F_5Br(Imperial Smelting Company, Bristol) and antimony trichloride(Fluka) and was converted to the corresponding dichloride in the reported manner.[5] Hexaaryldileads[9] and bis(triorganotin) sulphides[10] were synthesised by the reported methods.

Iodine monochloride (Fluka) was distilled before use. Iodine monobromide was prepared and purified by the published method.[11]

Fresh iodine isocyanate[12], iodine-azide[13] and thiocyanogen[9] in approximately known concentrations were generated in an appropriate solvent

by standard methods. Freshly prepared metallic salts except NaN_3, were dried *in vacuo* before use.

All solvents were purified and dried by standard procedures and reactions were carried out under anhydrous conditions.

IR spectra were recorded in the range 4000–200 cm^{-1} by using KBr/CsI pellets on a Perkin–Elmer 577 spectro-photometer. The molar conductance of 10^{-3} M solutions was determined at 25°C with a Phillips Conductivity assembly PR–9500. Molecular weight was determined cryoscopically in benzene using a Beckmann thermometer of accuracy of ±0.01°C.

Typical experimental details of the reactions are described below. Relevant IR assignments, analytical data and molar conductance values are listed in Tables 1–2.

Oxidative addition reactions

Reaction of $(C_6F_5)_3Sb$ *with* ICl *and* IBr, **(I, II)**. A solution of iodine monochloride (0.325 g · 2 mmol) in acetonitrile (40 cm^3) was added dropwise to a stirred solution of tris(pentafluorophenyl)antimony (1.246 · 2 mmol) in the same solvent (50 cm^3) at −5°C during 1 hr. The reactants were allowed to attain room temperature and stirred further for 30 min to ensure complete reaction. Concentration of the solution followed by the addition of petroleum–ether (bp. 60–80°C) afforded off white crystalline solid, tris(pentafluorophenyl) antimony (V) chloride iodide, m.p. 165–66°C.

Similarly, 1:1 molar reaction of tris(pentafluorophenyl) antimony (1.246 g, 2 mmol) and iodine monobromide (0.414 g, 2 mmol) yielded tris(pentafluorophenyl) antimony(V) bromide iodide, m.p. 126°C.

Reaction of $(C_6F_5)_3Sb$ *with* IN_3 *and* INCO, **(III, IV)**. A freshly generated solution of iodine azide (0.338 g, 2 mmol) in acetonitrile (50 cm^3) at −10°C was added to a precooled (−10°C) vigorously stirred solution of tris(pentafluorophenyl) antimony (1.246 g, 2 mmol) in the same solvent (50 cm^3) during 15 min under nitrogen atmosphere. The reactants were stirred for 1 hr at initial temperature and then allowed to come at room temperature. The solution was evaporated under reduced pressure and cooled overnight, after adding petroleum–ether (bp. 40–60°C) (10 cm^3). A pale yellow crystalline solid thus obtained was characterised as tris(pentafluorophenyl)antimony azide iodide **(III)**, m.p. 260°C.

$(C_6F_5)_3SbINCO$ **(IV)** was obtained as a white crystalline solid by the method described above by

Table 1. Analytical data of tris(pentafluorophenyl)antimony(V) derivatives

S.No.	Compound	Colour	m.p. (°C)	Yield (%)	Λ_M (Ohm^{-1} cm^2 $mole^{-1}$) for 10^{-3}M solution in acetonitrile	Analysis found (Calcd) C	H	N	Sb
I	$(C_6F_5)_3SbICl$	Brown	165–66	62	34.80	27.33 (27.53)	–	–	15.42 (15.50)
II	$(C_6F_5)_3SbIBr$	Brown	126	70	32.37	26.00 (26.05)	–	–	14.58 (14.67)
III	$(C_6F_5)_3SbIN_3$	Pale yellow	260 (d)	58	34.80	27.22 (27.30)	–	5.16 (5.30)	
IV	$(C_6F_5)_3SbINCO$	white	82	62	28.21	27.11 (27.30)	–	1.72 (1.76)	
V	$(C_6F_5)_3Sb(NCS)_2$	brownish yellow	205 (d)	74	16.42	32.41 (32.50)	–	3.60 (3.79)	16.38 (16.47)
VI	$(C_6F_5)_3SbS$	Off white	122	80	–	32.96 (33.00)	–	–	18.50 (18.58)
VII	$[\{(C_6F_5)_3Sb\}_2O](N_3)_2$	white	280 (d)	65	13.02	32.01 (32.12)	–	5.83 (6.24)	
VIII	$(C_6F_5)_3Sb(NCO)_2$	white	250 (d)	70	16.00	33.80 (33.98)	–	3.82 (3.96)	
IX	$(C_6F_5)_3Sb(\overline{NCO(CH_2)_2CO})_2$	white	245	68	18.42	38.06 (38.12)	0.92 (0.98)	3.38 (3.42)	14.80 (14.86)
X	$(C_6F_5)_3Sb(OOCC_6H_4NO_2\text{-}\underline{p})_2$	white	210	70	20.20	40.01 (40.23)	0.62 (0.84)	2.62 (2.93)	11.42 (11.69)
XI	$(C_6F_5)_3Sb(ON{=}CMe_2)_2$	white	198	60	18.92	37.49 (37.57)	1.29 (1.57)	3.36 (3.65)	15.69 (15.87)
XII	$(C_6F_5)_3Sb(ON{=}CMePh)_2$	white	55	55	19.40	45.62 (45.82)	1.46 (1.81)	3.01 (3.14)	13.26 (13.67)

Table 2. Relevant IR absortions of the anions in tris(pentafluorophenyl)antimony(V) compounds (cm^{-1})

III	IV	V	VII	VIII	IX	X	XI	XII	ASSIGNMENTS
2150m	2150m	2055mbr	2180m	2160mbr	-	-	-	-	ν_{asy} (NCX)
1275m	1230w	760 840vw	1290w	C	-	-	-	-	ν_{sy} (C-X)
665w	608m	475m	625w	625w	-	-	-	-	δ (N_3/NCX)
-	-	-	-	-	1700s	1685m 1682m[b]	-	-	ν_{asy} (CO/OCO)
-	-	-	-	-	1235m	1310m 1310m[b]	-	-	ν_{sy} (CO/OCO)
-	-	-	-	-	-	-	1632m[a]	1635m[a]	ν (C=N)
-	-	-	-	-	-	-	915m	925m	ν (N-O)
-	-	-	-	-	-	505w	485w	480w	ν (Sb-O)
-	372sh 368m[a]	-	365m[a]	-	415w	-	-	-	ν (Sb-N)
-	-	-	-	-	-	2920m	2920m	2925m	ν (C-H)

a = Overlapped by C_6F_5 absorptions; b = In $CHCl_3$ solution; c = Absent

w = weak, m= Medium, br = Broad, s = Strong, Sh = shoulder, vw = very weak

employing an equimolar ratio of the corresponding reactants, m.p. 82°C.

Reaction of $(C_6F_5)_3Sb$ *with* $(SCN)_2$, **(V)**. A freshly prepared solution of thiocyanogen (0.25 g, 2 mmol) in CCl_4(30 cm^3) was added to a stirred tris(pentafluorophenyl) antimony (1.246 g, 2 mmol) solution in CCl_4(50 cm^3) at −5°C during 15 min. The reaction mixture was subsequently stirred for 1 hr and warmed to room temperature. The removal of the volatiles under reduced pressure afforded a pale yellow solid. After recrystallisation from ethanol it was characterised as tris(pentafluorophenyl)antimony diisothiocyanate **(V)**, m.p. 205°C (d).

Reaction of $(C_6F_5)_3Sb$ *with sulphur*, **(VI)**. A solution of tris(pentafluorophenyl)antimony (1.246 g, 2 mmol) in acetonitrile (50 cm^3) was refluxed with elemental sulphur (0.064 g, 2 mmol) for 1 hr under nitrogen atmosphere. The solution was concentrated and cooled overnight to afford off-white crystalline solid. It was characterised as tris(pentafluorophenyl)antimonysulphide **(VI)**, m.p. 122°C.

The same product **(VI)** was obtained when the reaction was repeated in benzene as solvent.

(ii) *Metathetical reactions*

Reaction of $(C_6F_5)_3SbCl_2$ *with* AgSCN *and* KNCO, (V and **VIII**). Tris(pentafluorophenyl)antimony dichloride (1.3888 g, 2 mmol), and silver thiocyanate (0.464 g, 4 mmol) were stirred together in benzene (100 cm^3) at room temperature for 3 hr and then refluxed for 1 hr to ensure completion of the reaction. Silver chloride was filtered off and concentration of the solution under reduced pressure followed by the addition of petroleum–ether (bp. 40–60°C) yielded off-white crystalline tris(pentafluorophenyl) antimony diisothiocyanate (V), m.p. 205°C.

Similarly, 1 : 2 molar reaction of tris(pentafluorophenyl)antimony(V) dichloride (1.388 g, 2 mmol) and potassium cyanate (0.324 g, 4 mmol) was found to give tris(pentafluorophenyl)antimony(V) diisocyanate, m.p. 250°C (d).

Reaction of $(C_6F_5)_3SbCl_2$ *with* NaN_3, **(VII)**. An aqueous solution of sodium azide (0.264 g, 4 mmol) was added to an ethereal solution of tris(pentafluorophenyl)antimony dichloride (1.388g, 2 mmol) and the mixture was stirred for 3 hr at room temperature. The ether layer was separated and dried over sodium sulphate. It was then evaporated and cooled to yield off-white crystalline solid which was characterised as oxybis(tris(pentafluorophenyl)antimony)diazide **(VII)**, m.p. 280°C.

Reaction of $(C_6F_5)_3SbICl$ *with* KNCO, **(IV)**. A suspension of potassium cyanate (1 g, 1.24 mmol) in acetonitrile was added to a solution of tris(pentafluorophenyl)antimony chloride iodide (0.785 g, 1 mmol) in the same solvent (60 cm^3) and refluxed for 3–4 hr. The mixture was then filtered

to remove potassium chloride and unreacted potassium cyanate. The filtrate was concentrated under vacuum to afford white solid, which was recrystallised from petroleum–ether (bp. 40–60°C) and characterised as tris(pentafluorophenyl)antimony(V) iodide isocyanate, m.p. 82°C.

The similar procedure as described above was adopted to obtain tris(pentafluorophenyl)antimony(V) iodide azide from tris(pentafluorophenyl)antimony chloride iodide (0.785 g, 1 mmol) and sodium azide (0.08 g, 1.23 mmol). Compounds **(III)** and **(IV)** may also be prepared by the reaction of tris(pentafluorophenyl)antimony bromide iodide with the corresponding metallic salt.

Preparation of tris(pentafluorophenyl)antimony disubstituted amide, -oximate and carboxylate derivatives **(IX, X–XII).** In a typical experiment tris(pentafluorophenyl)antimony dichloride (0.694 g, 1 mmol) and sodium succinimide (0.238 g, 2 mmol) in benzene (60 cm^3) was stirred at room temperature for 3 hr. Sodium chloride was filtered off and the filtrate was concentrated under vacuum followed by the addition of *n*-hexane (10 cm^3) and on scratching yielded a white solid. It was recrystallised from petroleum–ether (bp. 40–60°C) and characterised as tris(pentafluorophenyl)antimony disuccinimide **(IX)** m.p. 245°C.

Compounds **(X)–(XII)** were synthesised from tris(pentafluorophenyl)antimony dichloride and the corresponding sodium salt of oxime or carboxylate in 1 : 2 molar ratio, respectively under conditions similar to those described for the disuccinimide.

(iii) *Reductive cleavage reactions*

Reaction of $(C_6F_5)_3SbS$ *with* Ar_6Pb_2(1 : 1). To an acetonitrile solution (50 cm^3) of tris(pentafluorophenyl)antimony sulphide (0.652 g, 1 mmol) hexaphenyldilead (0.876 g, 1 mmol) in the same solvent (30 cm^3) was added and stirred for 3 hr at room temperature. The solution was concentrated and petroleum–ether (bp. 60–80°C) was added to precipitate a white crystalline solid characterised as bis(triphenyllead) sulphide, m.p. 140–141°C (lit,[14] m.p. 139–143°C). After filtering the precipitate, the filtrate was concentrated and cooled to yield off-white crystals of tris(pentafluorophenyl)antimony m.p. 74°C (lit.,[4] m.p. 74°C).

Similarly, reaction of tris(pentafluorophenyl) antimony sulphide with hexa-*p*-tolyl dilead produced bis(tri-*p*-tolyllead) sulphide m.p. 143–144°C (lit.,[14] m.p. 144°C) and tris(pentafluorophenyl)-antimony, m.p. 74°C (lit.,[4] m.p. 74°C).

Reaction of $(C_6F_5)_3Sb(NCO)_2$ *with* Ph_6Pb_2 (1 : 1). To a refluxing solution of hexaphenyl dilead (0.876 g; 1 mmol in chloroform (50 cm^3) was added dropwise a chloroform solution of tris(pentafluorophenyl)antimony diisocyanate (0.707 g, 1 mmol). The reactants were refluxed for 5 hr and then cooled at ice temperature. The solid thus separated was filtered off and identified as diphenyllead diisocyanate m.p. 230–235°C (d). (Found: C, 38.98; H, 2.29; N, 6.29; Calc. for $C_{14}H_{10}N_2O_2Pb$; C, 39.17; H, 2.348; N, 6.52; IR ν_{asy}(NCO2180 cm^{-1}). The filtrate was concentrated to dryness under vacuum and then treated with *n*-hexane/benzene mixture (1 : 1, 10 cm^3) to afford insoluble tetraphenyl lead, m.p. 227–238°C (lit.,[11] m.p. 228°C). The filtrate on concentration and cooling gave tris(pentafluorophenyl)antimony, m.p. 74°C (lit.,[4] m.p. 74°C).

Similarly, reaction of tris(pentafluorophenyl)-antimony dichloride (0.694 g, 1 mmol) and hexaphenyl dilead (0.876 g, 1 mmol) afforded diphenyllead dichloride m.p. 285°C (lit.,[11] m.p. 284–286°C), tetraphenyllead m.p. 226–227°C (lit.,[11] m.p. 228°C) and tris(pentafluorophenyl)antimony, m.p. 73°C (lit.[4] m.p. 74°C).

(iv) *Action of* $(C_6F_5)_3SbCl_2$ *on bis(triorganotin)-sulphides*

Reaction of $(C_6F_5)_3SbCl_2$ *with* $(Bu_3Sn)_2S$. To a well stirred ice cold solution of tris(pentafluorophenyl)antimony dichloride (0.614 g, 1 mmol) in chloroform (50 cm^3) bis(tributyltin)sulphide (0.616 g; 1 mmol) in the same solvent (40 cm^3) was added drop-wise during half an hour. The reactants were further stirred for 3 hr and simultaneously allowed to attain room temperature. The solution was concentrated to dryness and the residue was dissolved in hot petroleum-ether (bp 60–80°C). The solution was cooled and filtered, the solid was identified as tris(pentafluorophenyl)antimony sulphide m.p. 122°C. The filtrate was concentrated at reduced pressure to yield tributyltin chloride, characterised as tributyltin fluoride m.p. 242°C (lit.,[11] m.p. 244°C).

Under similar conditions tris(pentafluorophenyl)antimony dichloride (0.694 g; 1 mmol) afforded tris(pentafluorophenyl)antimony sulphide m.p. 122°C and triphenyltin chloride m.p. 105°C, (lit.,[11] m.p. 105–107°C).

RESULTS AND DISCUSSION

(i) *Oxidative addition reactions*

Freshly generated solutions of thiocyanogen $(SCN)_2$ and iodine-azide and -isocyanate in acetonitrile were found to react separately with tris(pentafluorophenyl)antimony at − 10°C to give high yields of respective oxidative addition product in which antimony is in the pentavalent state.

Reaction with $(SCN)_2$ was performed in the dark to retard its polymerization.

$$(C_6F_5)_3Sb + (SCN)_2 \rightarrow (C_6F_5)_3Sb(NCS)_2 \quad (1)$$

$$(C_6F_5)_3Sb + IX \rightarrow (C_6F_5)_3SbIX \quad (2)$$

$$(X = N_3, NCO).$$

Whereas reactions of $(SCN)_2$ have earlier been demonstrated to cleave metal–carbon bonds (M = Sn, Pb)[9] those of IN_3 and INCO are being reported for the first time with an organometallic compound. However, reactions involving regio and stereospecific additions of IN_3 and INCO to olefins and other systems in synthetic organic chemistry are well known.[12,13]

Parallel reactions of interhalogens, viz. ICl and IBr with $(C_6F_5)_3Sb$ under identical conditions as described above were found to produce mixed halo derivatives (**I & II** Table 1).

$$(C_6F_5)_3Sb + IX \rightarrow (C_6F_5)_3SbIX, \quad (3)$$

$$X = Cl, Br.$$

It may be added that ICl, IBr and $(SCN)_2$ behave as electrophilic reagents towards symmetrical tetraorganometallic derivatives of group IVB(M = Ge, Sn, Pb)[9,11] and cleave the metal-carbon bond(s) to different extents depending upon the relative strength of electrophile used. However, no traces of any pentafluorophenyl-thiocyanate or -halide or of corresponding bis(pentafluorophenyl) derivative, $(C_6F_5)_3SbX$(X = NCS, N_3, NCO, Cl, Br), the products normally expected from the possibility of metal-carbon bond cleavage were observed in the above described reactions.

Elemental sulphur was also found to add oxidatively to $(C_6F_5)_3Sb$ in refluxing benzene or acetone solution in a dry nitrogen atmosphere to give tris(pentafluorophenyl)antimony sulphide (**VI**). Similar observations have been made for triarylantimony (III) compounds.[1]

$$(C_6F_5)_3Sb + S \rightarrow (C_6F_5)_3SbS \quad (4)$$

$(C_6F_5)_3SbS$ can also be obtained by passing H_2S gas in alcoholic–ammonia solution of $(C_6F_5)_3SbCl_2$. The molecular weight of sulphide derivative determined cryoscopically in benzene indicates that it exists as a monomer. It may be mentioned that tris(perfluoroalkyl)antimony has been reported not to react with sulphur.[15]

(ii) *Metathetical reactions*

$(C_6F_5)_3SbCl_2$ is an important source for obtaining various disubstituted tris(pentafluorophenyl)-antimony(V) derivatives (**V, VIII–XII**, Table 1). Thus the treatment with the corresponding sodium or silver salts in benzene under mild conditions leads to the replacement of both the chloride atoms. The metallic chlorides separate immediately in each case after mixing the reactants.

$$(C_6F_5)_3SbCl_2 + 2MY \rightarrow (C_6F_5)_3SbY_2 + 2MCl \quad (5)$$

M = Ag; Y = NCO, NCS

M = Na; Y = $ONCMe_2$; ONCMePh, $\overline{NCO(CH_2)_2CO}$, and $OOCC_6H_4NO_2 - p$.

In sharp contrast, $(C_6F_5)_3AsCl_2$ has been reported to give monosubstituted products.[16] This difference in behaviour can be attributed to the greater tendency of antimony to expand its coordination sphere, and to the lower element–chlorine bond energy.

Formation of oxo-bridge compound (**VII**). Reaction of aqueous NaN_3 with $(C_6F_5)_3SbCl_2$ in ether solution, however, yielded binuclear oxo-bridge compound (**VIII**, Table 1) instead of $(C_6F_5)_3Sb(N_3)_2$.

$$(C_6F_5)_3SbCl_2 + 2NaN_3 \rightarrow [(C_6F_5)_3Sb{-}O{-}Sb(C_6F_5)_3](N_3)_2 + 2NaCl. \quad (6)$$

Formation of such a binuclear derivative is not surprising since Goel *et al.* have reported that $R_3Sb(N_3)_2$(R = Me, Ph) could only be prepared and isolated in the presence of hydrazoic acid in benzene. One of the most usually employed methods for the preparation of organometallic azides involving a water/ether system as described above resulted in the formation of oxo-bridge compound $[R_3Sb{-}O{-}SbR_3](N_3)_2$.[17]

Selective replacement reactions. Equimolar reactions involving mixed halogen compounds $(C_6F_5)_3SbIX$(X = Cl, Br) and metallic salts in benzene produced mixed iodo-pseudohalo derivatives, through selective replacement of chloride or bromide group by a pseudohalo group. The iodide invariably remains bonded to the antimony irrespective of the nature of the metallic salt used.

$$(C_6F_5)_3SbICl + NaN_3 \rightarrow (C_6F_5)_3SbI(N_3) + NaCl \quad (7)$$

$$(C_6F_5)_3SbIBr + MNCO \rightarrow (C_6F_5)_3SbI(NCO) + MBr \quad (8)$$

$$(M = K, Ag).$$

This behaviour of tris(pentafluorophenyl)antimony mixed halides is somewhat different from those observed for similar reactions of mixed halides of diaryl-lead(IV) and -tin(IV), where both the different halo groups are replaced by the anionic groups.[18,19] It may be added that in case of group IVB metals identically placed iodide is more readily replaced by silver salts and the chloride and bromide are replaced by the anions attached to the alkali metals.[10] Selective replacement of halo groups (Cl, Br) have earlier been reported in case of mixed tetrahalocyclopentane tellurates(IV).[20]

The products (**III** and **IV** obtained through exclusive replacement of halo group are similar to those obtained by the oxidative addition method (eqn 2) mentioned above and had similar m.p. and superimposable IR spectra.

(III) *Reductive cleavage reactions*

(a) *Reaction of* $(C_6F_5)_3SbX_2$(X = NCO, Cl) *with* Ar_6Pb_2. Exploratory work reveals that higher valent metallic halides, viz. Cu(II), Hg(II) and Fe(III) cleave the Pb–Pb bond in hexaorganodilead compounds while themselves getting reduced to the lower oxidation state.[21,22] It was therefore, considered worthwhile to study the reactions of tris(pentafluorophenyl)antimony dichloride and diisocyanate against Pb–Pb bond. The former are readily reduced to $(C_6F_5)_3Sb$ in the sense of equation shown below

$$Ar_6Pb_2 + (C_6F_5)_3SbX_2 \rightarrow Ar_4Pb + Ar_2PbX_2 + (C_6F_5)_3Sb \quad (9)$$

Ar = Phenyl, *p*-tolyl

X = Cl, NCO.

The reaction appears to involve the cleavage of Pb–Pb bond and Pb–C bond in hexaaryldilead yielding stable Ar_4Pb and unstable Ar_2 Pb (eqn 10) which further reduces the perfluorophenyl antimony(V) to perfluorophenyl antimony(III) (eqn 11).

$$Ar_3Pb—PbAr_3 \rightleftharpoons Ar_4Pb + Ar_2Pb \quad (10)$$

$$Ar_2Pb + X_2Sn(C_6F_5)_3 \rightarrow (C_6F_5)_3Sb + Ar_2PbX_2 \quad (11)$$

(b) *Reaction of* $(C_6F_5)_3SbS$ with Ar_6Pb_2. It has been reported by Okawara *et al.* that the Sb–S bond in triorganoantimony sulphides is semipolar in nature, which facilitates the resonance hybrid of sulphides in the ground state due to which triorganoantimony(V) sulphides are more reactive.[23,24]

$$R_3Sb^+–S^- \rightleftharpoons R_3Sb = S.$$

It is therefore not surprising that on reaction of $(C_6F_5)_3SbS$ with hexaaryldileads insertion of sulphur into Pb–Pb bond takes place.

$$(C_6F_5)_3SbS + Ar_3Pb—PbAr_3 \rightarrow Ar_3Pb–S–PbAr_3 + (C_6F_5)_3Sb \quad (12)$$

The reaction seems to proceed through initial rupture of Pb–Pb bond followed by the insertion of sulphur which may be attributed to the enhanced semipolar nature of Sb–S bond in tris(pentafluorophenyl)antimony sulphides, which facilitates the homolytic fission of Pb–Pb bond coupled with the remarkable reactivity of Pb–Pb bond.[25] In the process tris(pentafluorophenyl)antimony(V) is reduced to tris(pentafluorophenyl)antimony (III). Similar results have been observed for the reactions of triorganoantimony sulphides with hexaarylditins.

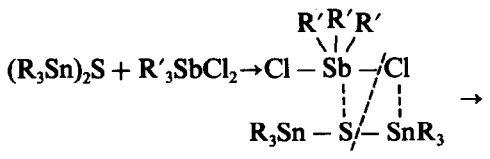
It can be thus concluded that the reactions of hexaaryldileads with tris(pentafluorophenyl)antimony(V) derivatives proceed via two different pathways depending upon the nature of the anion attached to antimony atom. In the case of sulphide derivative (eqn 12) cleavage of the Pb–Pb bond is favoured while in the other cases (X = NCO, Cl dissociation of hexaaryldileads to Ar_4Pb and Ar_2Pb occurred (eqn 9). Both these reactions thus lend support to an earlier held view that the reactions of hexaorganodileads with different reagents differed mechanistically.[25]

(iv) *Action of* $(C_6F_5)_3SbCl_2$ *on bis(triorganotin)-sulphide*

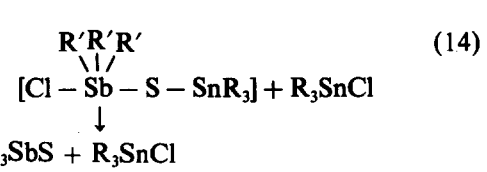
Bis(triorganotin)sulphides were found to react with tris(pentafluorophenyl)antimony dichloride in 1 : 1 molar ratio resulting in the complete exchange of anionic groups.

$$(R_3Sn)_2S + (C_6F_5)_3SbCl_2 \rightarrow 2R_3SnCl + (C_6F_5)_3SbS. \quad (13)$$

The separation of the products does not pose much difficulty due to the difference of the solubilities in organic solvents. The reaction seems to proceed via a four- centred cyclic transition state involving sulhpur atom as represented below



$$(R_3Sn)_2S + R'_3SbCl_2 \rightarrow Cl-Sb(R'R'R')-Cl \rightarrow R_3Sn-S-SnR_3$$



$$[Cl-Sb(R'R'R')-S-SnR_3] + R_3SnCl \rightarrow R'_3SbS + R_3SnCl \quad (14)$$

(where R′ = C_6F_5; R = C_4H_9, C_6H_5).

An analogous mechanism has been proposed for the reaction of $[Ph_3Sn]_2O$ and $HgCl_2$.[26]

The molar conductance values of 10^{-3} M solution in acetonitrile of the newly synthesised tris(pentafluorophenyl)antimony(V) compounds range between 13–35 mol^{-1} cm^2, which indicate their non-conducting nature.[27] The values for compounds (I–IV) containing a halide atom are almost of the same order and higher than the rest of the compounds but do not suggest conducting behaviour.

The observed molecular weight data of the compounds in freezing benzene were found comparable with those of theoretical values which suggests that these compounds exist as monomers.

The newly isolated compounds are stable at room temperature and soluble in organic solvents, viz. chloroform, acetonitrile, benzene etc. Compounds (II), (IV) and (VIII), however decompose on storage. Isocyanate derivatives were also found to be moisture sensitive.

IR SPECTROSCOPY

All the isolated compounds (I–XII; Table 1) exhibit IR absorptions characteristic of C_6F_5 group and are in conformity with those reported earlier for tris(pentafluorophenyl)antimony and its dihalides.[5,28] The IR frequencies due to fundamental modes of vibrations of the anionic groups are listed in Table 2.

Absorptions associated with the various modes of vibrations of the pseudohalide groups have been identified and indicate the nature of bonding to the antimony atom. The chalcogenate group, NCX(X = S or O) gives rise to three fundamental modes of vibrations due to the $\nu(C\equiv N)$, $\nu(C-X)$ and $\delta(NCX)$. The observed frequencies for these modes of vibrations are listed in Table 2, and are fully consistent with a N-bonded NCX group, in consonance with the usual iso-structure of the hydrocarbon counter parts of the antimony(V).[29] The vibrations associated with the N_3 stretchings and bending modes (**III** and **VII**, Table 2) suggest the presence of a covalently bonded linear N = N = N group. The asymmetric N = N = N stretching is fairly shifted to higher frequency as compared to $Ph_3Sb(N_3)_2$[17,28] or $Ph_3SnI(N_3)$[30] but other modes of vibrations are not significantly changed. Compound (**VII**), however, exhibits an additional strong band at 705 cm^{-1}, which can be safely assigned to the ν(Sb–O–Sb)[29,6] vibration, indicating the formation of an oxo-bridge binuclear derivative.

Tris(pentafluorophenyl)antimony disuccinimide (**IX**) displays a strong band at 1700 cm^{-1} assignable to "ester-like" CO group. The symmetric stretching mode appears at 1235 cm^{-1}. Pattern and position of the bands are comparable with those of reported triarylantimony diamides.[7]

The separation (375 cm^{-1}) between the asymmetric and symmetric (O = C = O) stretching frequencies for tris(pentafluorophenyl)antimony di(*p*-nitrobenzoate), which occur at 1685 cm^{-1} and 1310 cm^{-1}, respectively, in the solid state suggest the presence of a monodentate "ester-like" carboxylate group with a penta-coordinate structure about the antimony atom. In chloroform solution the 1685 cm^{-1} band is shifted to 1682 cm^{-1} but the symmetric (O – C–O) stretching frequency remains unchanged and thus carboxylate group retains its unidentate character in solution as well.[29,31] The non-conducting and monomeric nature and the absence of carboxylate ion in the IR spectra further rules out the possibility of an ionic structure.

The IR spectra of O-tris(pentafluorophenyl)antimony dioximates (**XI** and **XII**) do not exhibit any band in the region 3000–3380 cm^{-1}, assignable to the intramolecularly hydrogen bonded OH in free oximes.[32] The C = N vibrations *ca.* 1630 ± 5 cm^{-1} appear as medium bands and are lowered by *ca.* 40 cm^{-1} as compared to the free oximes (~ 1668 cm^{-1}). The lowering of the νC = N vibration may be attributed to the stabilization of the C = N bond by resonance with the non-bonding electron pair on oxygen atom of the amino group. However, this type of lowering may also be related to the mass effect as has been observed earlier, in case of group IVB elements.[33]

The appearance of a medium band in the region 915–925 cm^{-1} can be attributed to a N–O stretching vibration[34] while the Sb–O stretching is tentatively assigned at 480 ± 5 cm^{-1} on the basis of reported Sb–O frequencies in the corresponding organoantimony oxinate derivatives.[35]

A noticeable feature of the IR spectra of all the isolated disubstituted compounds is the absence of the ν_{sym} (Sb–C) absorption corresponding to the *t*-mode which should be located in the region 250–300 cm^{-1} as reported by earlier workers.[5,6]

Thus on the basis of IR evidences coupled with their monomeric and non-conducting nature and in accordance with the structures of other organoantimony(V) compounds,[6,7,17,29] the newly synthesised disubstituted derivatives (except for (VII)) can reasonably be assigned a trigonal bipyramidal structure with the anionic groups at the axial positions and C_6F_5 groups occupying the equatorial positions. A trigonal bipyramidal structure containing an oxygen bridge (Sb–O–Sb) can be proposed for compound (VII).

Acknowledgement—The authors are thankful to the Head of the Chemistry Department, Lucknow University for providing the necessary Laboratory Facilities, the Director RSIC, Lucknow for obtaining IR spectra and Council of Scientific and Industrial Research, New Delhi for financial assistance (KS & AR).

REFERENCES

1. G. O. Doak and L. D. Freedman, *Organometallic Compounds of Arsenic, Antimony and Bismuth.* Wiley-interscience, New York, (1970).
2. A. T. Rake and J. M. Miller, *J. Chem. Soc. A* 1970, 1881.
3. J. P. Crow and W. R. Cullen, Organic compounds of arsenic antimony and bismuth. In *Inorganic Chemistry, Series One, M.T.P. International Review of Science* (Edited by H. J. Emeléus and B. J. Aylett) Vol. 4, p. 383. Butterworths, London (1972).
4. M. Fild, O. Glemser and G. Christoph, *Angew. Chem.* 1964, **76**, 953.
5. B. A. Nevett and A. Perry, *Spectrochim. Acta* 1975, **A31**, 101.
6. A. Otero and P. Royo, *J. Organometal. Chem.* 1978, **154**, 13.
7. Prem Raj, Ashok Ranjan and A. K. Saxena, *Ind. J. Chem.* 1983, **22A**, 120; Prem Raj, Ashok Ranjan, Kiran Singhal and Rajiv Rastogi, *Synth. React. Inorg. Metal-Org. Chem.* 1984, **14**(2), 269.
8. R. D. Chambers and T. Chivers, *Organometal Chem. Rev.* 1966, **1**, 279.
9. S. N. Bhattacharya, Prem Raj and R. C. Srivastava, *J. Organometal. Chem*, 1975, **87**, 279.
10. R. C. Poller, *The Chemistry of Organotin Compounds*, p. 131. Logos Press, London (1970).
11. S. N. Bhattacharya, Prem Raj and R. C. Srivastava, *J. Organometal. Chem.* 1976, **105**, 45.
12. L. F. Fieser and M. Fieser, *Reagents for Organic Synthesis*, p. 500. Wiley, New York, (1968).
13. S. N. Moorthy and D. Devaprabhakara, *Chem. Ind.* 1975, 217.
14 R. W. Leeper, L. Summers and H. Gilman, *Chem. Rev.* 1954, **54**, 101.
15. R. E. Banks and R. N. Haszeldine, Polyfluoroalkyl derivatives of metalloids and non-metals. In *Advances in Inorganic Chemistry and Radiochemistry* (Edited by H. J. Emeléus and A. G. Sharpe), Vol. 3, p. 367. Academic Press, New York (1961)
16. A. Otero and P. Royo, *J. Organometal. Chem.* 1978, **149**, 315.
17. R. G. Goel and D. R. Ridley, *Inorg. Chem.* 1974, **13**, 1253.
18. S. N. Bhattacharya and Prem Raj, *J. Inorg. Nucl. Chem.* 1978, **40**, 1699; Prem Raj, *Ind. J. Chem.* 1979, **17B**, 616.
19. S. N. Bhattacharya and Prem Raj, *Int. Conf. on Coordination Chemistry of Ge, Sn, Pb.* Nottingham, England (1977).
20. T. N. Srivastava, R. C. Srivastava and Mala Singh, *J. Organometal Chem.* 1978, **157**, 405.
21. D. P. Arnold and P. R. Wells, *J. Organometal. Chem.* 1976, **113**, 311.
22. D. P. Arnold and P. R. Wells. *J. Organometal Chem.* 1975, **111**, 1285.
23. M. Shindo, Y. Matsumura and R. Okawara, *J. Organometal. Chem.* 1968, **11**, 299.
24. J. Otera and R. Okawara; *J. Organometal. Chem.* 1969, **16**, 335.
25. H. Shapiro and F. W. Frey, *The Organic compounds of Lead*, p. 166. Wiley, N.Y. (1968).
26. D. Datta, B. Majee and A. K. Ghosh, *J. Organometal Chem.* 1971, **29**, 251.
27. W. J. Geary; *Coord. Chem. Rev.* 1971, **7**, 81.
28. D. A. Long and D. Steele, *Spectrochim. Acta* 1963, **19**, 1955; I. J. Hyams, E. P. Lippincott and R. T. Bailey, *Spectrochim. Acta* 1966, **22**, 695.
29. E. Maslowsky, *J. Organometal. Chem.* 1974, **70**, 153.
30. Prem Raj, Ashok Ranjan, Kiran Singhal and A. K. Saxena, *Acta. Chem. Scand*, submitted.
31. H. Schmidbaur and H. Stüehler, *Angew Chem. Int. Ed.* 1972, **11**, 145.
32. R. E. Rundle and M. Parsole, *J. Chem. Phys.* 1952, **20**, 1487.
33. P. G. Harrison and J. J. Zuckermann, *Inorg. Chem.* 1970, **9**, 175.
34. S. Califanio and W. Luttke. *Z. Phys. Chem.* 1956, **6**, 83; J. Fabian, M. Legrand and P. Poirlier, *Bull. Soc. Chim. Fr.* 1956, 1499.
35. H. A. Meinema and J. G. Noltes, *J. Organometal. Chem.* 1969, **16**, 257.

Polyhedron Vol. 4, No. 2, pp. 259–268, 1985
Printed in Great Britain.

0277–5387/85 $3.00 + .00
© 1985 Pergamon Press Ltd.

PROTONATION EQUILIBRIA AND COMPLEX FORMATION ABILITY OF 2-AMINO-3-AMINOMETHYL-4,6-DISUBSTITUTED PYRIDINES

Z. CIMERMAN and Z. ŠTEFANAC*
Laboratory of Analytical Chemistry, Faculty of Science, University of Zagreb, Strossmayerov trg 14, 41000 Zagreb, Yugoslavia

(*Received* 18 *January* 1984; *accepted* 16 *April* 1984)

Abstract—The protonation equilibria of 2-amino-3-aminomethyl-4,6-disubstituted pyridines were studied by potentiometric titrations and by UV and ^{13}C NMR spectrometry. Protonation constants $\log K_1$ and $\log K_2$ potentiometrically determined for 4-methoxymethyl-6-methyl (8.959 and 5.778), 6-methoxymethyl-4-methyl (8.964 and 5.407), and 4,6-dimethyl derivative (9.141 and 6.604), were compared with the values obtained by the spectrometric methods. Complex formation of these compounds with Cu(II), Ni(II), Zn(II) and Co(II) was investigated in solution whereby the outstanding effect of the pH value was established and the presence of the species with 1 : 1 and 2 : 1 ligand to metal ratios confirmed. Stability constants obtained by potentiometric titrations show a decrease of the complex stability in the order Cu > Ni > Zn with respective $\log \beta_1$ values of 5.85, 3.56 and 2.93. Series of complexes isolated in the crude state were characterized by elemental analyses and spectrometric data, the latter serving also as the basis for making an attempt at the discernment of the coordination mode and sites.

Manifold approaches pursued in the studies of aminopyridines comprise also the correlations of structure and ionization.[1] The complex formation ability of a number of these heteroaromatic ligands presents another interesting topic.[2–7] In both cases additional substituents have been shown to play a decisive role depending on the species and position of substituents. Therefore with available newly synthesised 2-amino-3-aminomethylpyridines bearing two more substituents we performed concurrently the determination of protonation constants and the investigation of complexation ability. The series comprised 4-methoxymethyl-6-methyl (ligand **I**), 6-methoxymethyl-4-methyl (ligand **II**) and 4,6-dimethyl (ligand **III**) derivative.

The behaviour of the complexes formed with transition metals in solution and the characteristics of isolated crude species are discussed.

EXPERIMENTAL

Apparatus

The IR spectra were recorded in KBr or CsBr pellets with Perkin–Elmer spectrophotometers Models 457 and 580B. The mass spectra were taken on a Varian MAT CH7 or a CEC 21-110C instrument. Electronic absorption spectra were obtained using a Perkin–Elmer spectrophotometer Model 200. ^{13}C NMR spectra were recorded on a Jeol JNM–FX–100FT spectrometer in D_2O with tetramethylammonium chloride as internal standard at room temperature.

The pH was measured at (25.0 ± 0.2)°C with a Radiometer PHM-64 pH/mV meter providing a reading accuracy to within ± 0.002 pH units. Radiometer glass electrode G202 B and saturated calomel electrode K-401 were used. Before each measurement the assembly was standardized with two buffer solutions: 0.05 mol dm^{-3} potassium hydrogenphthalate ($pH_{25°C}$ = 4.008) and 0.01 mol dm^{-3} sodium tetraborate ($pH_{25°C}$ = 9.180).

Materials

Deuterium oxide, 99.5 atom. % D and dideutero-sulphuric acid, 99.5 atom. % D, 96–98% in D_2O were purchased from E. Merck, Darmstadt. Sodium deuteroxide was prepared by dissolving sodium in D_2O. Tetramethylammonium chloride, for synthesis, E. Merck, Darmstadt was recrystallized from the ethanol/petroleum ether system. All other chemicals and solvents were of analytical purity grade, Kemika, Zagreb. The quartz doubly distilled water was used throughout.

*Author to whom correspondence should be addressed.

Procedures

Preparation of ligands. 2-amino-3-aminomethyl-4-methoxymethyl-6-methylpyridine (ligand **I**), 2-amino-3-aminomethyl-6-methoxymethyl-4-methylpyridine (ligand **II**) and 2-amino-3-aminomethyl-4,6-dimethylpyridine (ligand **III**) were obtained as dihydrochlorides by courtesy of Dr. D. Korunčev, Pliva, Pharmaceutical and Chemical Works, Zagreb. Free amines were prepared and purified to analytical grade according to the procedure described in Ref. 8. The pure products were checked by elemental analyses, IR and ^{1}H NMR spectrometric data.

Preparation of metal complexes. For all complexes 0.1 mol dm^{-3} solutions of ligands and metal salts were used. The complexes Cu(ligand **I**)$_2$ $SO_4 \cdot 2H_2O$ and Cu(ligand **III**)$_2SO_4 \cdot 2H_2O$ crystallized after mixing a methanolic solution of the corresponding ligand with an aqueous solution of cupric sulphate in the 3:1 molar proportion.

Zn(ligand **I**)$_2SO_4$ precipitated readily from a methanolic solution containing zinc sulphate and a threefold excess of ligand **I**.

Cu(ligand **I**)$SO_4 \cdot 3H_2O$ was prepared by mixing equimolar amounts of ligand **I** and cupric sulphate dissolved in minimum quantities of methanol and water, respectively. The complex crystallized from this solution after it had been evaporated to half of the volume and kept at 0°C for several days.

Cu(ligand **I**)$_2(ClO_4)_2$ crystallized by the addition of a saturated aqueous solution of sodium perchlorate to the aqueous solution containing ligand **I** and cupric sulphate in the 3:1 molar proportion.

Zn(ligand **I**) $[B(C_6H_5)_4]_2$ and Ni(ligand **I**)$_2$ $[B(C_6H_5)_4]_2$ precipitated from an aqueous solution containing equimolar amounts of metal(II) salt and ligand **I** in the presence of sodium tetraphenylborate.

Characterization of isolated complexes

Cu(ligand **I**)$_2SO_4 \cdot 2H_2O$, $C_{18}H_{34}N_6O_8SCu$, violet crystals, m.p. 197°C (decomp.). Found (calc.): C 39.58 (38.74); H 6.46 (6.14); N 15.07 (15.06); S 5.37 (5.74); Cu 11.16 (11.38)%.

IR spectrum, $\tilde{\nu}$ cm^{-1} rel. intensity: 3420 b, 3250 b, 3120 b, 2930 m, 1640 sh, 1620 s, 1592 m, 1570 sh, 1470 m, 1450 m, 1395 m, 1325 w, 1190 m, 1170–1070 vs, vb, 975 m, 865 vw, 800 w, 690 w, 613 s, 550 w, 420 vw.

Cu(ligand **III**)$_2SO_4 \cdot 2H_2O$, $C_{16}H_{30}N_6O_6SCu$, violet crystals, m.p. 215°C (decomp.). Found (calc.): C 38.87 (38.58); H 6.02 (6.07); N 17.01 (16.87); Cu 12.76 (12.26)%.

IR spectrum, $\tilde{\nu}$ cm^{-1} intensity: 3420 b, 3260 b, 3140 b, 2960 w, 2920 w, 1640 s, 1620 s, 1595 s, 1570 sh, 1505 m, 1475 m, 1450 m, 1390 m, 1330 w, 1215 w, 1010–1170 vs,vb, 975 m, 855 vw, 800 m, 700 vw, 612 s, 550 vw, 535 w, 410 w.

Zn(ligand **I**)$_2SO_4$, $C_{18}H_{30}N_6O_6SZn$, white powder, m.p. 257 °C (decomp.). Found (calc.): C 41.09 (41.27); H 5.96 (5.77); N 16.28 (16.04)%.

IR spectrum, $\tilde{\nu}$ cm^{-1} rel. intensity: 3420 b, 3320 s, 3240 sh, 3190 s, 2930 m, 1650 s, 1600 s, 1595 sh, 1575 s, 1470 m, 1450 s, 1420 m, 1400 m, 1330 w, 1200 s, 1165 sh, 1145 sh, 1110 vs, 1070 s, 1055 s, 975 s, 825 m, 810 m, 675 m, 650 s, 613 s, 590 m, 550 vw, 490 vw, 290 vw.

Cu(ligand **I**)$SO_4 \cdot 3H_2O$, $C_9H_{21}N_3O_8SCu$, green crystals. Found (calc.): C 27.43 (27.37); H 5.91 (5.36); Cu 16.28 (16.09)%.

IR spectrum, $\tilde{\nu}$ cm^{-1} rel. intensity: 3380 sh, 3260 b, 3100 sh, 1640 s, 1620 sh, 1590 sh, 1550 w, 1480 m, 1390 w, 1310 w, 1110 vs, 1040 vs, 960 s, 790 m, 630 m, 604 s.

Cu(ligand **I**)$_2(ClO_4)_2$, $C_{18}H_{30}N_6O_{10}Cl_2Cu$, brown needles, m.p. 185°C (decomp.). Found (calc.): C 34.86 (34.60); H 4.91 (4.84); N 13.57 (13.45)%.

IR spectrum, $\tilde{\nu}$ cm^{-1} rel. intensity: 3470 m, 3410 m, 3300 m, 3200 m, 2930 w, 1620 s, 1600 sh, 1560 w, 1540 w, 1470 m, 1435 w, 1390 w, 1145 vs, 1115 vs, 1090 vs, 960 w, 870 w, 830 w, 795 w, 690 w, 628 s.

Zn(ligand **I**)$[B(C_6H_5)_4]_2$, $C_{57}H_{55}N_3OB_2Zn$, white powder, m.p. 82 °C (decomp.). Found (calc.): C 77.21 (77.35); H 6.50 (6.26); N 4.85 (4.74)%.

IR spectrum, $\tilde{\nu}$ cm^{-1} rel. intensity: 3420 m, 3350 m, 3210 m, 3180 sh, 3060 s, 3000 m, 1960 w, 1890 w, 1825 w, 1640 s, 1625 sh, 1605 m, 1575 m, 1480 s, 1425 s, 1410 w, 1395 sh, 1335 w, 1265 m, 1180 w, 1150 w, 1120 w, 1090 w, 1070 w, 1030 w, 850 m, 735 vs, 710 vs, 625 w, 615 m, 605 m, 585 vw, 465 vw.

Ni(ligand **I**)$_2[B(C_6H_5)_4]_2$, $C_{66}H_{70}N_6O_2B_2Ni$, pink powder, m.p. 112 °C (decomp.). Found (calc.): C 74.50 (74.81); H 6.49 (6.66); N 7.88 (7.93); Ni 5.21 (5.54)%.

IR spectrum, $\tilde{\nu}$ cm^{-1} rel. intensity: 3400 sh, 3300 m, 3210 m, 3060 s, 3005 m, 2930 w, 1950 w, 1830 w, 1640 m, 1610 s, 1580 m, 1480 s, 1428 m, 1400 w, 1300 vw, 1265 w, 1180 m, 1150 m, 1110 m, 1030 w, 850 m, 736 vs, 710 vs, 625 w, 615 m, 605 m, 482 vw, 462 vw, 420 vw.

IR spectra of ligands for comparison, $\tilde{\nu}$ cm^{-1} rel. intensity: (ligand **I**) 3345 s, 3300 sh, 3180 s, 3005 w, 2925 m, 2885 m, 1660 s, 1592 s, 1570 s, 1460 s, 1430 s, 1398 s, 1325 m, 1280 m, 1190 m, 1150 m, 1090 s, 1080 sh, 980 m, 955 s, 940 s, 865 m, 815 s, 806 m, 695 w, 650 w, 610 m, 580 m, 550 w, 520 w, 420 w, 355 m; (ligand **III**) 3360 s, 3300 s, 3180 s, 3010 w, 2975 m, 2910 m, 1665 s, 1655 sh, 1592 s, 1570 sh, 1480 s, 1455 s, 1415 m, 1325 m, 1272 m,

1210 s, 1190 w, 1140 w, 975 w, 955 m, 920 s, 860 m, 815 s, 790 s, 690 m, 640 m, 610 m, 550 w, 540 w, 505 w, 410 w, 362 w.

Determination of the protonation constants of ligand I by ^{13}C nuclear magnetic resonance. Samples were obtained in the following way: a 0.447 mol dm^{-3} solution of ligand I was prepared by dissolving a weighed amount of compound in D_2O and dividing it into a series of aliquots. The pD of each aliquot was adjusted with a concentrated solution of NaOD or D_2SO_4 in D_2O, and the ionic strength of 2.0 (NaCl) was maintained. From the measured pH the pD of the samples was calculated from: pD = pH + 0.4.[9] The values for ^{13}C chemical shifts δ(ppm) obtained with tetramethylammonium chloride as internal standard were converted to the TMS scale by adding 56.5 ppm to each value.

Determination of stability and protonation constants by potentiometric titrations. A vessel with a capacity of 50 cm^3, thermostatted at (25.0 ± 0.2)°C was used for the potentiometric titrations. The vessel's cap was equipped with inlets for the two electrodes, the burette and the nitrogen flow. Titrant (0.2 mol dm^{-3} NaOH) was added from a 2.5 cm^3 automatic burette with an accuracy of volume addition of ± 0.003 cm^3. The solution was stirred during the titration with a magnetic stirrer in addition to being blown through by the nitrogen stream.

The ligands, converted into the protonated form by adding a standard HNO_3 solution in excess, were titrated in the absence (protonation constants) and in the presence (stability constants) of metals. The concentrations of metals in titration samples varied (ligand to metal ratios were 1:2, 1:4, 1:6, 1:8, 1:10 and 1:20). A constant ionic strength of 0.35 (KNO_3) was maintained during the measurements.

The measured pH values were converted into the hydrogen ion concentrations according to Irving *et al.*[10]

The protonation and stability concentration constants were calculated on a Univac 1110 computer at the Zagreb University Computing Centre using the Miniquad programme.[11]

UV/VIS spectrophotometric measurements. The UV spectra of aqueous ligand solutions were taken at various pH values. Bathochromic shifts were observed with decreasing pH of the solutions (Fig. 3). The UV/VIS spectra of ligands and complexes taken in the methanolic medium are summarized in Table 1.

The modified continuous variation method of Job[12] and the molar ratio method of Yoe and Jones,[13] were both pursued throughout in determining the ligand to metal ratio.

The apparent stability constants were calculated from the data obtained by the continuous variation method using the programme of Likussar[14] and the PDP-8/E (058/10-Syst.) DEC computer.

RESULTS AND DISCUSSION

Protonation equilibria of ligands

Three well separated inflections in potentiometric titration curves of ligands **I**, **II** and **III** (Fig. 1) prove that all ligands have three protonation steps. However, it was possible to calculate with sufficient precision only the first two

Table 1. UV/VIS spectrophotometric data for ligands **I**, **II** and **III** and a series of metal complexes in the methanolic medium

Compound	λ_{max}/nm (ε_{max})	
Ligand I		305($5.8\cdot10^3$); 240($8.6\cdot10^3$); 207($1.2\cdot10^4$)
Cu(II)-complex	660(42) ;	341($4.5\cdot10^3$); 258($7.2\cdot10^3$); 217($4.4\cdot10^3$)
Co(II)-complex	520(sh.) ;	350($1.0\cdot10^4$); 260($1.6\cdot10^4$); 218($1.8\cdot10^4$)
Ni(II)-complex	590(7.2) ;	348($1.1\cdot10^2$); 262($2.5\cdot10^2$)
Zn(II)-complex		330($7.1\cdot10^2$); 271($6.0\cdot10^2$); 258($5.3\cdot10^2$)
Ligand II		299($4.6\cdot10^3$); 240($6.6\cdot10^3$); 207($1.3\cdot10^4$)
Cu(II)-complex	660(35) ;	331($3.3\cdot10^3$); 258($6.0\cdot10^3$); 218($4.6\cdot10^3$)
Ligand III		297($5.7\cdot10^3$); 240($7.6\cdot10^3$); 207($1.3\cdot10^4$)
Cu(II)-complex	660(53) ;	330($5.6\cdot10^3$); 258($8.0\cdot10^3$); 214($6.2\cdot10^3$)
Co(II)-complex	510(sh) ;	346($1.3\cdot10^4$); 260($1.8\cdot10^4$); 215($2.3\cdot10^4$)
Zn(II)-complex		324($1.1\cdot10^3$); 258($1.4\cdot10^3$)

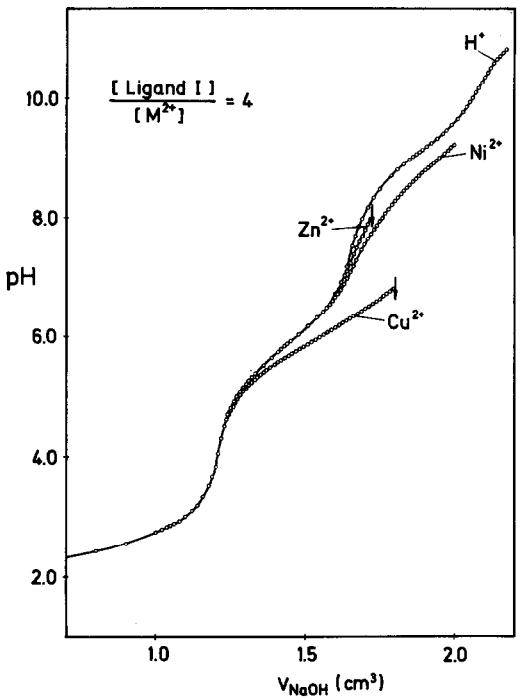


Fig. 1. Potentiometric titration curves of a 5.00 × 10^{-3} mol dm^{-3} solution of ligand I alone and in the presence of metals. Each curve represents the mean value of 2–4 consecutive titrations.

protonation constants (Table 2). The values of the third constant were too low to achieve the reliability range with the concentrations (5 × 10^{-3} mol dm^{-3} solutions) applied. According to the literature data for amino- and aminomethyl-pyridines[1] the first constant was tentatively assigned to the protonation of the 3-aminomethyl group and the second constant to the protonation of the ring nitrogen. As experimental evidence for presumed protonation equilibria of ligands, the protonation constants of particular functional groups of ligand **I** were determined by ^{13}C nuclear magnetic resonance spectrometry.

Assignment of aliphatic carbon atoms and the C-5 aromatic carbon atom was performed on the basis of the one-bond carbon-proton couplings observed in the undecoupled spectra. The remaining four aromatic carbon atoms were preliminarily assigned using the literature data for chemical shifts of structurally resembling monosubstituted pyridines.[15–17] A significant effect of substituents in positions 3, 4 and 6 of the pyridine ring was not expected, since in all cases aliphatic groups are bound straight to the ring. Carbon-proton couplings through two and/or three bonds to 5-H as well as to protons of aliphatic groups confirmed the assignment of aromatic carbon atoms. The chemical shifts, splitting patterns, coupling constants and assignment of the ^{13}C NMR resonances of ligand **I** at pD 11.5 are summarized in Table 3.

The pD dependence of the chemical shifts is shown in Fig. 2. A decrease in pD from 11 to 8 is accompanied by upfield shifts of C-3 and 3-CH_2 resonances, indicating protonation of the 3-aminomethyl group.[18] As the pD decreases further, the resonance pattern of all ring carbon atoms significantly changes. Signs and $\Delta\delta$ amounts roughly correspond to those noted for the protonation of the pyridine, except in the case of C-5 where a small upfield shift is observed.[19] The differences in the range $1 < \Delta\delta < 5$ ppm can be explained if the number, the nature and arrangement of substituents are considered. Thus, changes in the spectra of ligand I in the pD range from 8 to 4 can be reasonably ascribed to the protonation of the ring nitrogen. Further decreasing of pD down to 0.1 changes insignificantly the ^{13}C NMR spectra. It is obvious that extremely acidic conditions are necessary for the protonation of the 2-amino group of ligand **I**. This is in accordance with very weak basicity of the amino group observed for 2- and 4-monoaminopyridines, as well as with the resonance equilibria presumed by Albert for monocations.[1] Charge delocalization over both nitrogens, in the manner of an amidinium cation, effectively prevents addition of the second proton.

Logarithmic values of protonation constants K_1 and K_2 determined graphically from the plot δ vs pD are 6.3 and 9.4, respectively.

Table 2. Protonation constants of the ligands determined by potentiometric titration in aqueous solution at (25.0 ± 0.2)°C, I = 0.35 (KNO_3)

Ligand	log K_1 ± S.D.	log K_2 ± S.D.	log β_2 ± S.D.
I	8.959±0.002	5.778±0.004	14.737±0.003
II	8.964±0.002	5.407±0.004	14.371±0.003
III	9.141±0.001	6.604±0.002	15.745±0.002

Table 3. Chemical shifts, splitting patterns and coupling constants in the ^{13}C NMR spectrum of ligand I by pD 11.5

Chemical shifts, δ_{TMS} (ppm)	Splitting pattern (coupling constant J, Hz)			Assignment
23.66	quartet (127.0)	doublet (~2)		6-CH_3
37.00	triplet (136.7)			3-CH_2
59.13	quartet (142.8)	triplet (~4)		4-CH_3
72.28	triplet (144.0)	quartet (~5)	doublet (~5)	4-CH_2
115.56	doublet (163.6)	quartet (~4)	triplet (~4)	C-5
117.66		triplet (~5)	doublet (~5)	triplet (~5) C-3
147.73		triplet (~4)	triplet (~4)	C-4
156.40		quartet (~6)	doublet (~2)	C-6
157.91		triplet (~4)		C-2

The digital resolution of 1.2 Hz makes unobtainable distinct multiplets in cases of small coupling constants.

The potentiometrically determined values for the protonation constants of ligand I (Table 2) differ from the values obtained by ^{13}C NMR by 0.5 logarithmic units in the case of K_1 and by 0.4 logarithmic units in the case of K_2. These deviations may be expected, since the potentiometric titrations were done in H_2O, and the NMR measurements in D_2O.[9] Additional reasons for the disagreement of the corresponding results are different ionic strength, concentrations and temperatures of solutions measured by both methods. As the thermodynamic corrections were not accomplished it has to be called to mind that the potentiometric concentration constants are compared with spectrometric mixed constants.

The correlation of protonation constants of ligands I, II and II (Table 2) shows differences in basicity between the ligands, being more explicit in the case of the second constant related to the protonation of the heterocyclic nitrogen. The basicity of ligands decreases in the order ligand III > ligand I > ligand II.

The influence of the 4- and 6-substituted groups on the basicity of the ring nitrogen is also evidenced from the UV spectra. Decreasing pH in the range of the protonation of the ring nitrogen causes bathochromic shifts of the lower energy transition maxima by all ligands according to the behaviour of 2-aminopyridines.[20] The plot of λ_{max} vs pH (Fig. 3) shows the same sequence of the ligands' basicity decrease as the potentiometrically determined constants.

The log K_1 values obtained are merely comparable with the one cited for the primary amino group of 3-aminomethylpyridine as pK_a 8.04 being very likely only an approximate value.[1] The explanation for the differences of log K_1 within the series of ligands I, II and III has to be ascribed to the nature and arrangement of additional substituents on the pyridine ring. Their base-strengthening or base-

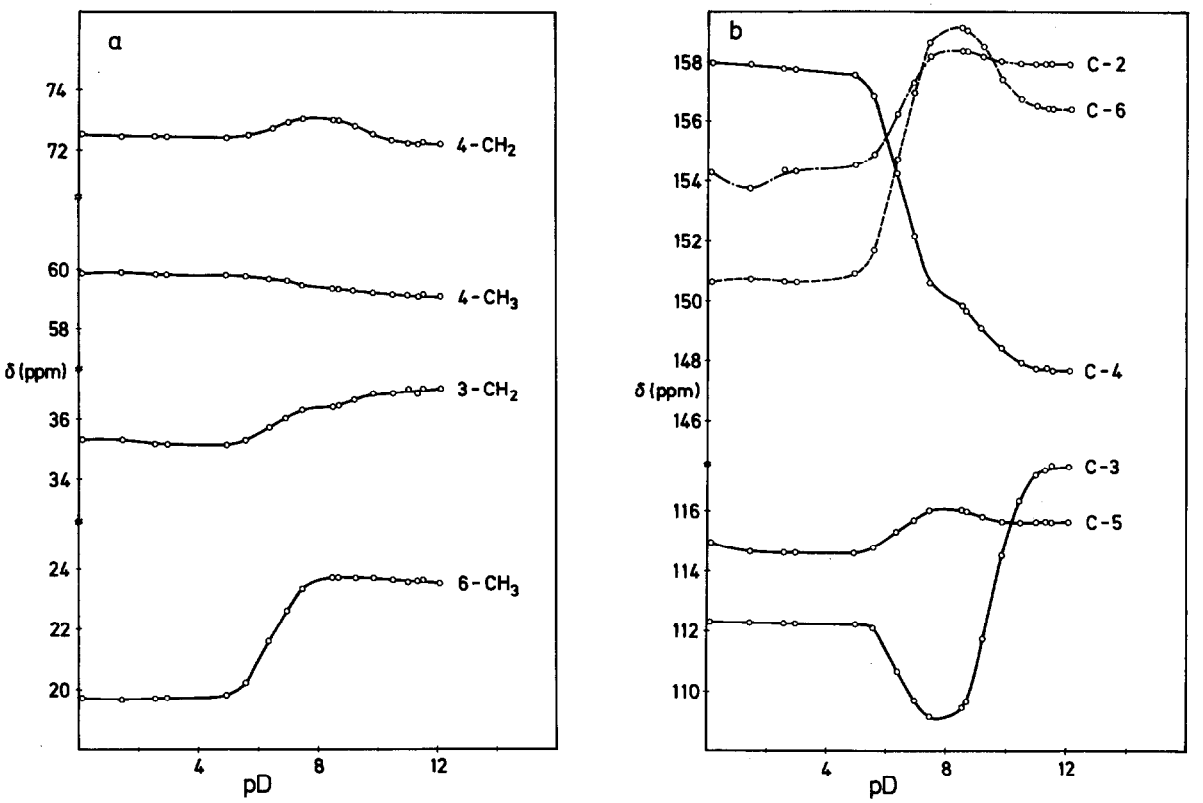


Fig. 2. pD dependence of the ^{13}C chemical shifts of ligand I: (a) resonances of aliphatic carbon atoms; (b) resonances of aromatic carbon atoms.

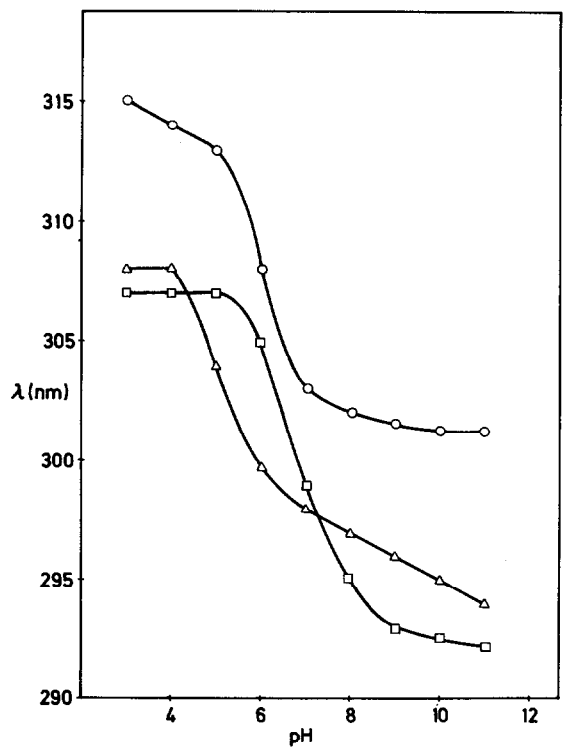


Fig. 3. pH dependence of UV absorption maxima of ligands: I (○), II (△) and III (□).

weakening effects are more evidently reflected by the differences in $\log K_2$ values related to the proton uptake by pyridine nitrogen. The specification of the net result and the symbol of the mesomeric and inductive effects of the methyl, aminomethyl and methoxymethyl substituents with regard to their positions as well as a potentially evoked steric hindrance of the latter in the 6-position is inaccessible. Therefore the $\log K_2$ values of the studied ligands cannot be meaningfully correlated either with one another or with the data from the literature for the pyridine bearing the very same remaining two substituents, i.e. amino and methyl group.

Complexes with Cu(II), Ni(II), Zn(II) *and* Co(II)

In solution complexes of ligands **I**, **II** and **III** with Cu(II), Ni(II) and Zn(II) are formed immediately. The formation of complexes with Co(II) is very slow at room temperature. The complex formation is affected by the pH of the solution (Fig. 4). A significant increase of ligands' complexation ability is observed by increasing pH in the range $5 < pH < 7$ with optimal conditions for complex formation about $pH \geq 8$. The conditions mentioned before are valid for aqueous and methanolic media.

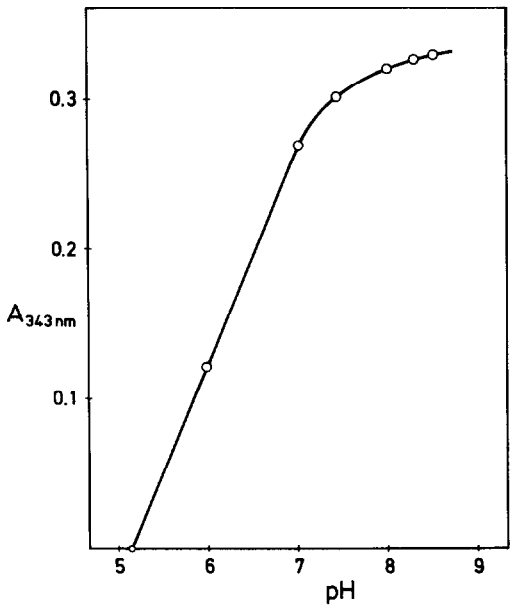


Fig. 4. Effect of pH on complex formation of ligand I with Cu(II). [Cu(II)] = 4×10^{-4} mol dm^{-3}; [ligand I] = 1.2×10^{-3} mol dm^{-3}.

In distinction from 2-picolylamine which forms 1:1, 2:1 and 3:1 complexes[2,3,6] with ligands **I**, **II** and **III** only the presence of 1:1 and 2:1 species was evidenced in solution. The ligands bearing the methyl (**I** and **III**) or methoxymethyl group (**II**) in the 6-position conform in this respect understandably to 6-methyl-2-picolylamine which forms unstable strongly dissociated 3:1 complexes.[4] The spectrophotometrically determined ligand to metal ratio of the species formed in the methanolic solution is 2:1 for the complexes of Zn(II), Ni(II) and Co(II) (Table 4). In the case of the complex of ligand **I** with Zn(II) simultaneous presence of the 1:1 species is observed. The equilibrium of 1:1 and 2:1 species is most probably the reason for high relative errors obtained for apparent stability constants of Cu(II) complexes.

Judging from apparent constants determined by UV spectrophotometry (Table 4), the stability of 2:1 complexes decreases in the order Co > Ni > Zn.

Potentiometric stability constants (Table 5) for all studied complexes could not be determined because of a very low formation rate of Co(II) complexes. In some systems precipitation took place during titration. Since the data could only be taken before the start of precipitation, the number of data was sometimes insufficient to attain good precision [in the case of ligand **I** and Zn(II)]. Table 5 illustrates that the stability of the complexes decreases following the sequence Cu > Ni > Zn. It is the usual stability sequence proposed for the complexes of transition metals.[21] The inversion of this stability sequence observed by comparing apparent constants for Co(II) and Ni(II) complexes (Co > Ni) is characteristic of the complexes of pyridines, having substituents in α-position to the heterocyclic nitrogen.[22]

Considering the ligands, the complex stability decreases in the order ligand **III** > ligand **I** ≥ ligand **II**. This order indicates a low influence of ligands' total basic strength on the complex stability more effected by the steric hindrance of the bulky methoxymethyl group positioned in the neighbourhood of the coordination sites.

Preparation of the crude complexes was not always successful, although the conditions were

Table 4. Ligand to metal ratios and apparent stability constants determined by UV spectrophotometry in methanolic solutions

Complex	λ_{max} (nm)	[Ligand]+[Me(II)] (mol dm^{-3})	[Ligand]/[Me(II)]	log K'	Rel. error (%)
Ligand I-Cu(II)	341	$2 \cdot 10^{-4}$	1:1	4.64	9.06
Ligand I-Co(II)	350	$2 \cdot 10^{-4}$	2:1	8.42	5.82
Ligand I-Ni(II)	348	$1 \cdot 10^{-2}$	2:1	5.73	5.94
Ligand I-Zn(II)	330 271	$3 \cdot 10^{-3}$	2:1 1:1	5.50 3.60	4.17 4.41
Ligand II-Cu(II)	331	$4 \cdot 10^{-4}$	1:1	4.50	16.16
Ligand III-Cu(II)	330	$2 \cdot 10^{-4}$	1:1	4.83	12.98
Ligand III-Co(II)	346	$2 \cdot 10^{-4}$	2:1	9.59	7.19
Ligand III-Zn(II)	324	$2 \cdot 10^{-3}$	2:1	6.65	4.21

Table 5. Stability constants determined by potentiometric titration in aqueous solution at (25.0 ± 0.2)°C, I = 0.35 (KNO_3)

Ligand	Metal ion	$\log\beta_1$ ± S.D.	$\log\beta_2$ ± S.D.
I	Cu^{2+}	5.853±0.008	10.18±0.01
I	Ni^{2+}	3.56±0.01	5.85±0.03
I	Zn^{2+}	2.93±0.09	5.7±0.4 *
II	Cu^{2+}	5.78±0.02	10.10±0.03
III	Cu^{2+}	6.52±0.01	11.42±0.02

* The limited number of obtainable experimental data due to precipitation in the system worsened the precision.

carefully checked. Due to easy decomposition of most often very unstable complexes recrystallization had to be avoided and it was not always possible to obtain pure compounds.

Characterization of the prepared complexes by elemental analyses indicated 2:1 and 1:1 ligand to metal ratios, corresponding to the results of the measurements in solution. The results of elemental analyses were confirmed to a certain extent by fast atom bombardment mass spectrometry (FAB) with glycerol used as dispersant.[23] In the mass spectra obtained for positive ions, the characteristic distribution of ^{63}Cu and ^{65}Cu isotopes with the relative abundances of 100 and 44.7% respectively served well to distinguish not only the molecular ions but also a number of copper containing fragment ions. The molecular formulae corresponding to the 2:1 ligand to metal ratio were found for copper complexes of ligands I and III with sulphate anion as well as of ligand I with perchlorate anion.

$$425 \xrightarrow[*]{-17} 408 \xrightarrow[*]{-17} 391$$

Cu(ligand I)$_2$

$$244 \xrightarrow{-17} 227$$

Cu(ligand I)

$$365 \xrightarrow[*]{-17} 348 \xrightarrow[*]{-15} 333$$

Cu(ligand III)$_2$

$$214 \xrightarrow{-17} 197$$

Cu(ligand III)

The established partial fragmentation pathways were based in addition to the expected isotope peaks pattern also on the presence of several metastables denoted with asterisks in the schemes given above. The mass spectra of nickel and zinc complexes taken under analogous conditions were not amenable to a detailed interpretation.

The attempt to elucidate the coordination mode in complexes of the 2:1 ligand to metal ratio is based merely on the IR spectra taken in the 200–4000 cm^{-1} region.

For interpretative comparison the well documented data on the corresponding complexes of 2-aminomethylpyridine[6] and 6-methyl-2-aminomethylpyridine[5] have been taken. These compounds behave as bidentate ligands even in the case of the 6-methyl derivative with evidenced influence of a remarkable steric interference. The sterically hindered 2-aminopyridine was also shown to appear as bidentate in nickel complexes containing two molecules of the ligand.[7]

Presuming that because of the steric arrangement the studied ligands behave as bidentate too, alternative sets of two coordination sites have to be considered: nitrogen atoms of the 2-amino and 3-aminomethyl groups as well as those belonging to the pyridine ring and the 2-amino group.

More exaggerated changes in the regions of 3000–3500 and 1600–1700 cm^{-1} of the IR spectra of the amino group bearing ligands are caused by association than by coordination. Therefore lower N–H stretching accompanied by higher in-plane

bending frequencies than expected for free groups, observed consistently for all investigated complexes has only a limited reliability as an evidence for coordination of nitrogen atoms of both amino groups. On the basis of changes in the 800–200 cm^{-1} region a far more reliable conclusion could be arrived at supposing that carefully checked assignments of the characteristic bands are submitted. From the isotopic labelling it was possible only to assign by deuteration the band of ligand **I** at 650 cm^{-1} (N,N-d_2 at 450 cm^{-1}) as belonging to 3-aminomethyl group out-of-plane bending vibration. In Cu(II) and Zn(II) complexes this band of a characteristic broadened shape is shifted to 690 and 675 cm^{-1}, respectively. In the nickel complex the region is overlapped with one of strong tetraphenylborate absorption bands which are the only bands to be found below 800 cm^{-1} in this spectrum. The band at 520 cm^{-1} in the spectrum of ligand **I**, (505 cm^{-1} of ligand **III**) ascribed to CCN skeletal bending vibrations is, as presumed, shifted to 550 cm^{-1} in copper and zinc complexes.

The remaining bands characteristic of the ligand are too vague even for hypothetical consideration. Thus the bands at 610 and 420 cm^{-1} in the case of ligand **I** or at 610 and 410 cm^{-1} for ligand **III** assigned to pyridine in-plane and out-of-plane ring deformation are not well defined in the spectra of complexes. Namely, the first band is hidden by absorption of sulphate or perchlorate while the second one appears simply as a weak, broadened deviation of the spectrum curve. It ought to be mentioned however, that no shifts of these bands to higher frequencies have been observed either.

As the assignments of bands characteristic of metal–ligand bonds are lacking, the proposal for nitrogen atoms of both amino groups to act as coordination sites appears artificial indeed. But further investigations indispensable as the complement of the insufficient evidence are not feasible with regard to the means at disposal.

The absorption bands concerned show the well-known characteristic differences noted for coordinated as compared to free anions.

A very wide band with broad maxima at 1145, 1115 and 1090 cm^{-1} dominates in the spectrum of Cu(ligand **I**)$_2$$(ClO_4)_2$ complex. The emphasized intensity and manifold splitting even if the absorption of the ligands' ether groups is considered could be interpreted by means of coordinated perchlorate.[24] However, the absence of the band at 930 cm^{-1} as well as the fact that a single sharp band is present at 628 cm^{-1} unambiguously point at the free anion,[25] and therefore a four-coordination of copper in the [Cu(ligand **I**)$_2$]$(ClO_4)_2$ complex species.

The absorption corresponding to the C–O–C asymmetric stretching of ligands **I** and **III** is overlaid by a very strong and very broad band at 1170–1070 cm^{-1} in the spectra of Cu(ligand **I**)$_2$ and Cu(ligand **III**)$_2$ complexes with sulphate. The accompaniment by a strong sharp band at 613 cm^{-1} complements the pattern characteristic of the free sulphate. Considering as more plausible the analogy rather with potentially π-bonding than with σ-bonding ligands, e.g. 1,3-propylenediamine, the four-coordination of copper has been assumed.[26]

Therefore the corresponding complexes have been formulated as dihydrates [Cu(ligand **I**)$_2$-$SO_4 \cdot 2H_2O$ and [Cu(ligand **III**)$_2$]$SO_4 \cdot 2H_2O$. Shoulders at 1165 and 1145 cm^{-1} on the very strong, broad absorption band centered at 1110 cm^{-1} in part appertaining to the ligands' ether groups as well as the bands of 1070 and 1055 cm^{-1} joined to the fact that the band at 613 cm^{-1} is accompanied by an additional one at 650 cm^{-1} have been taken as evidence for the sulphato complex [Zn(ligand **I**)$_2$$SO_4$].

The positions of bands characteristic of tetraphenylborate in the spectrum of the nickel complex although corresponding to those of the free anion have not been taken as a proof. The presumption of the species [Ni(ligand **I**)$_2$][$(BPh_4)_2$] is based on the light pink colouration congruent with yellow complexes of the four-coordinated nickel with diamines[27] and substituted pyridines.[24,28] The congruence is extended further to the complexes of the higher coordinated nickel present in solution only. Thus the dissolving of the crude pink complex afforded a light blue acetone and a greenish blue methyl isobutylketone solution. Besides, a solution identical with the latter has been obtained by extraction of a mixture set up for the preparation of the nickel complex with perchlorate as anion. The greenish blue colouration of the extract changed to pink after three days.

In addition, the feature of absorption bands due to NH stretching and in-plane bending vibrations of both amino groups resembles the 3100–3500 and 1600–1650 cm^{-1} regions of the complex Cu(ligand **I**)$_2$$(ClO_4)_2$ with presumably four-coordination of the metal.

Acknowledgements—The authors are indebted to Professor J. Seibl, ETH Zentrum Zürich, for taking the mass spectra and helping with interpretation and to Dr. Z. Meić, Institute R. Bošković, Zagreb, who kindly made recording of the ^{13}C NMR spectra possible. Special thanks are due to members of Institute for Medical Research and Occupational Health, Zagreb, Professor Vl. Simeon for useful suggestions concerning the determination of the potentiometric constants and to Z. Kralj for immediate help with computation.

REFERENCES

1. A. Albert, Ionization constants. In *Physical Methods in Heterocyclic Chemistry* (Edited by A. R. Katritzky), Vol I, pp. 1–108. Academic Press, New York (1963).
2. A. R. Nicholson and G. J. Sutton, *Austral. J. Chem.* 1969, **22**, 59; *Idem, Ibid.* 1969, **22**, 373.
3. S. Utsuno and K. Sone, *Bull. Chem. Soc. Jpn.* 1964, **37**, 1028.
4. S. Utsuno and K. Sone, *Bull. Chem. Soc. Jpn.* 1967, **40**, 105.
5. S. Utsuno and K. Sone, *J. Inorg. Nucl. Chem.* 1966, **28**, 2647. S. Utsuno, *Ibid.* 1970, **32**, 1631.
6. M. L. Niven, G. C. Percy and D. A. Thornton, *J. Mol. Struct.* 1980, **68**, 73.
7. M. Jamnicky and E. Jona, *Proc. Conf. Coord. Chem.* 1978, **7**, 77.
8. D. Korunčev, A. Deljac and D. Cvek, Yugoslav Pat. No. 35 242 (Appl. 27.3.1973.)
9. P. K. Glasoe and F. A. Long, *J. Chem. Phys.* 1960, **64**, 188.
10. H. M. N. Irving, M. G. Miles and L. D. Pettit, *Anal. Chim. Acta* 1967, **38**, 475.
11. P. Gans, A. Vacca and A. Sabatini, *Inorg. Chim. Acta* 1976, **18**, 237.
12. W. C. Vosburgh and G. R. Cooper, *J. Am. Chem. Soc.* 1941, **63**, 437.
13. J. H. Yoe and A. L. Jones, *Ind. Eng. Chem. Anal. Edn.* 1944, **16**, 111.
14. W. Likussar, *Anal. Chem.* 1973, **45**, 1926.
15. A. Marker, A. J. Canty and R. T. C. Brownlee, *Austral. J. Chem.* 1978, **31**, 1255.
16. L. Stefaniak, *Org. Magn. Res.* 1979, **12**, 379.
17. H. L. Retcofsky and R. A. Friedel, *J. Phys. Chem.* 1968, **72**, 2619.
18. J. E. Sarneski and C. N. Reilley, The determination of proton binding sites by NMR titrations. In *Essays on Analytical Chemistry, A. Ringbom's Memorial Volume* (Edited by E. Vanninen), pp. 35–49. Pergamon Press, Oxford (1977).
19. E. Pretsch, T. Clerc, J. Seibl and W. Simon, *Tabellen zur Strukturaufklärung organischer Verbindungen mit spektroskopischen Methoden*, 2nd Edn, pp. C-155. Springer Verlag, Berlin (1981).
20. S. F. Mason, The electronic absorption spectra of heterocyclic compounds. In *Physical Methods in Heterocyclic Chemistry* (Edited by A. R. Katritzky), Vol. II, pp. 46. Academic Press, New York (1963).
21. D. P. Mellor and L. Malley, *Nature (London)* 1947, **159**, 380. *Idem, Ibid.* 1948, **161**, 436.
22. J. L. Walter and S. M. Rosalie, *J. Inorg. Nucl. Chem.* 1966, **28**, 2969.
23. K. L. Rinehart, Jr., *Science* 1982, **218**, 254.
24. S. Buffagni, L. M. Vallarino and J. V. Quagliano, *Inorg. Chem.* 1964, **3**, 671.
25. B. J. Hathaway and A. E. Underhill, *J. Chem. Soc.* 1961, 3091.
26. B. J. Hathaway and D. E. Billing, *Coord. Chem. Rev.* 1970, **5**, 143.
27. J. L. Burmeister, T. P. O'Sullivan and K. A. Johnson, *Inorg. Chem.* 1971, **10**, 1803.
28. W. E. Bull and L. E. Moore, *J. Inorg. Nucl. Chem.* 1965, **27**, 1341.

Polyhedron Vol. 4, No. 2, pp. 269–277, 1985
Printed in Great Britain.

0277–5387/85 $3.00 + .00
© 1985 Pergamon Press Ltd.

THE HYDROPHILIC LIPOPHILIC BALANCE OF HYDROXYOXIMES AND THE MECHANISM OF COPPER EXTRACTION

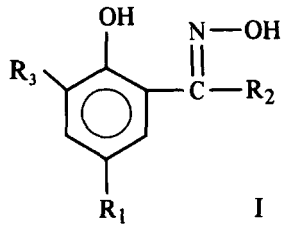
J. SZYMANOWSKI
Politechnika Poznanska, Pl.Sklodowskiej-Curie 2, Poznan, Poland

(*Received* 3 *January* 1984; *accepted* 16 *April* 1984)

Abstract—The polarity of some model hydroxyoximes is discussed and their *HLB* coefficients are estimated. It is shown that the rate of copper extraction by the hydroxyoximes can be related to the oxime hydrophilic lipophilic balance. The extraction mechanism is discussed for hydroxyoximes exhibiting different hydrophobicity. It is shown that the contribution of the volume reaction is less than 10% and higher than 90% for oximes which contain not less than 11 and not more than 3 carbon atoms in the alkyls, respectively.

In recent years the mechanism of copper extraction by hydroxyoxime extractants has been the subject of many investigations and discussions. Taking into account the low solubility of the hydroxyoximes in the aqueous phase and their tendency to be adsorbed at the interface of organic hydrophobic diluent–water systems, it was elucidated that the reaction between copper and the commercial hydroxyoxime extractants proceeds in the interphase. Appropriate extraction data supporting this mechanism have been described in several independent papers.[1–7]

The oxime molecule may be adsorbed at the interface due to the presence of the polar phenolic and oximino groups and appropriate long alkyl, preferably located at position 5 directly opposite to the phenolic group.



I

The penetration range of the oxime molecules into the aqueous phase depends upon the length of the alkyl groups and must increase as the molecular mass of the oxime decreases, i.e. as the length of the alkyl radicals decreases. The oxime molecule then becomes more hydrophilic, i.e. less hydrophobic, and the solubility of the oxime in the aqueous phase is increased. Thus, as the length of the alkyl radicals decreases the reaction mechanism may change, and depending upon the oxime hydrophobicity the reaction may proceed either at the interface, in the bulk of the aqueous phase or simultaneously in both.[8–12]

In surfactant chemistry surface active agents are characterized by the hydrophilic lipophilic balance, abbreviated as *HLB*.[13–14] This parameter determines the hydrophilicity of surfactants and is directly connected to the surfactant properties and adsorption abilities at the interface. However, surfactant properties are also influenced by other parameters and therefore the relations between surfactant properties and their *HLB* values are usually different although analogous for different homologous series.[15,16] Therefore the discussion in this work will be limited only to oximes of formula I, where R_1 and R_2 represent alkyls and R_3 represents hydrogen. The relationship between *HLB* and the mechanism of copper extraction will be discussed. We have recently given a short description of the *HLB* system.[11]

EXPERIMENTAL

Extraction data was determined for some pure hydroxyoximes of formula I, where R_1 represents a longer alkyl (C_1–C_{12}) and R_2 represents a shorter alkyl (C_1–C_3). The results published by Preston and Luklinska[17] were also considered. The experimental conditions were as follows: rising drop method, $T = 30°C$, 0.02 M oxime in toluene, 0.02 M $Cu(ClO_4)_2$ in $HClO_4$ solution at pH 0.9.

HLB^G coefficients were determined according to the relation:

$$HLB^G = 20\,\frac{M_H^{eff}}{M} \qquad (1)$$

where M_H^{eff} is the effective molecular mass of the hydrophilic groups in the oxime molecules, M is the molecular mass of the hydroxyoxime and HLB^D coefficients were calculated using increment numbers as determined by Davies[18], using the following relationship:

$$HLB^D = 7 + \Sigma\Delta HLB_i^D \qquad (2)$$

where ΔHLB_i^D are the increment numbers determined by Davies.

The effective molecular mass of the phenolic group was assumed to be 17 and the effective molecular mass of the oximino group was calculated from polarity data determined for model hydroxyoximes by means of gas chromatography, according to the method previously used for non-ionic surfactants.[19-24] The increment number for the oximino group was also determined from our gas chromatographic data. The influence of the chromatographic parameters and of the oxime structure upon different polarity parameters will be discussed separately.[24]

RESULTS

The hydrophilic lipophilic balance of hydroxyoximes

The influence of the percentage by weight of phenolic and oximino groups upon the polarity index of hydroxyoximes (PI), where: PI = 100 log $(C - 4.7) + 60$, and the carbon number C corresponds to the location of the methanol peak on the hydrocarbon scale, is shown in Fig. 1. The experimental points are fairly linear and the influence of the hydrophilic groups upon the oxime polarity may be qualitatively estimated from the gradients. They characterize the increase of the polarity index per 1% wt content of the hydrophilic groups and show the much higher influence of the phenolic group in comparison to the oximino group. The slopes equal 13.16 and 6.76 for the phenolic and oximino groups, respectively. Thus, under our experimental conditions the phenolic group shows a polarity twice that of the oximino group. The effective molecular mass of the oximino group is thus: $M_{NOH}^{eff} = M_{OH}\ 6.76/13.16 = 8.7$, and the group number is then: $\Delta HLB_{NOH}^D = \Delta HLB_{OH}^D\ 6.76/13.16 = 1.0$.

The relation between HLB coefficients on the Griffin and Davies scales estimated for hydroxyoximes of formula I, where the sum of carbon atoms in R_1 and R_2 can be varied from 1 to 15, is shown in Fig. 2. The non-linearity arises because the HLB^G coefficient is proportional to the percentage by weight of the hydrophilic groups, while the HLB^D coefficient is an additive function of the hydroxyoxime structure. Both functions are monotonous, and HLB^G and HLB^D decrease as the length of the alkyl groups increases. For the hydroxyoximes considered HLB^G and HLB^D are related to the number of carbon atoms in both

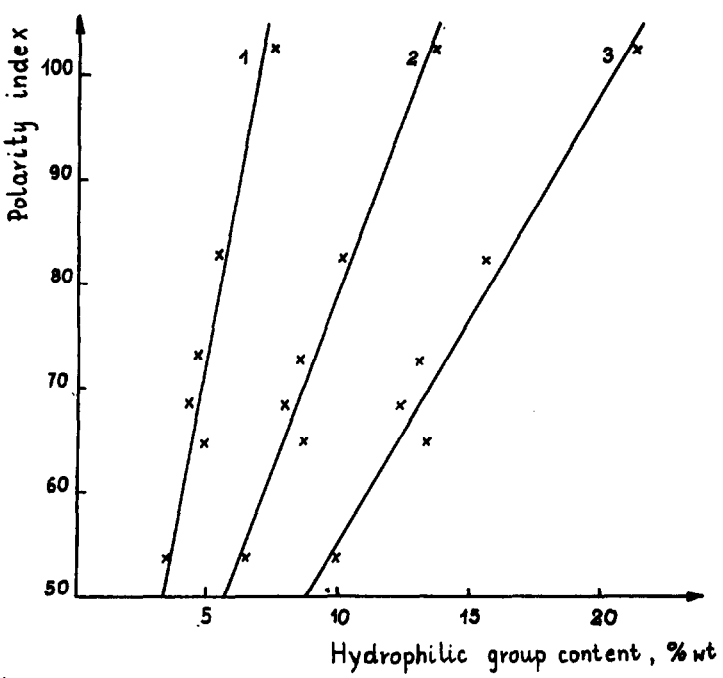


Fig. 1. The influence of the content of hydrophilic groups in hydroxyoximes upon the polarity index (1—OH, 2—NOH, 3—OH + NOH).

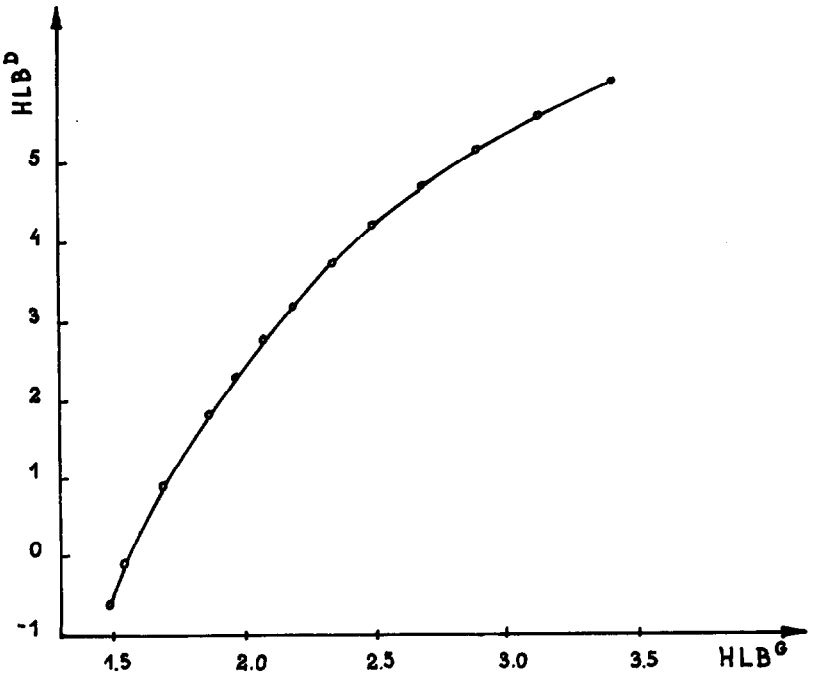


Fig. 2. The relation between HLB coefficients of hydroxyoximes.

alkyls according to the following relations:

$$HLB^G = \frac{514}{137 + 14n} \quad (3)$$

$$HLB^D = 9.9 - 0.475(7 + n) \quad (4)$$

where n denotes the sum of the carbon atoms in both the alkyls. Thus, the relation between the considered *HLB* coefficients is as follows:

$$HLB^G = \frac{514}{331 - 29.5HLB^D} \quad (5)$$

For the hydroxyoximes considered HLB^G values vary in the range 1.5–3.5, and the HLB^D values vary from -1 to 6. These low *HLB* values are in agreement with the very low solubility of the hydroxyoximes in aqueous solutions. The hydroxyoximes polarity can be compared, for example to the polarity of adducts of ethylene oxide and commercial nonylphenol, containing from 0 to 1 oxyethylene units in the molecule, i.e. to mixtures of nonylphenol and 2-hydroxyethyl-nonylphenyl ether obtained when the mole ratio of the ethylene oxide to nonylphenol does not exceed 1.

Hydrophilic lipophilic balance and the regions of copper extraction by the hydroxyoximes

Such high hydrophobicity of hydroxyoximes supports the interfacial mechanism for the oxime reaction with copper. The largest part of the hydroxyoxime molecule should be within the organic region of the interphase as the weakly hydrophilic groups cannot penetrate deeply into the aqueous phase. However, due to the very low hydrophilicity of hydroxyoximes having a large alkyl group, the decrease in the length of the hydrocarbon chain causes a sharp increase in the polarity, although the hydrophobic part of the molecule always dominates the hydrophilic groups. However, the oxime molecule may penetrate more deeply into the aqueous layer in the direct neighbourhood of the interface, and eventually a change in the extraction mechanism occurs. In the homogeneous phase the reaction proceeds more quickly than in a heterogeneous system with a small interfacial area.[25] The relations between the logarithm of the relative extraction rates and the estimated values of the *HLB* coefficients are shown in Figs. 3 and 4. Due to the non-linear relation between the HLB^G and HLB^D coefficients relations which were different but similarly shaped were obtained. In the region of low *HLB* values (below $HLB^G = 2.2$ and $HLB^D = 3$) the extraction rate depends strongly upon the oxime structure, e.g. a long alkyl group in position 3 sharply decreases the extraction rate, whilst a long alkyl in position 5 when R_2 is short increases the extraction rate (points on Figs. 3 and 4 at $HLB^G = 2$ and $HLB^D = 2.3$). The influence of oxime structure upon extraction rate is observed in the region where extraction proceeds at the interface, or the interfacial reaction definitely dominates the vol-

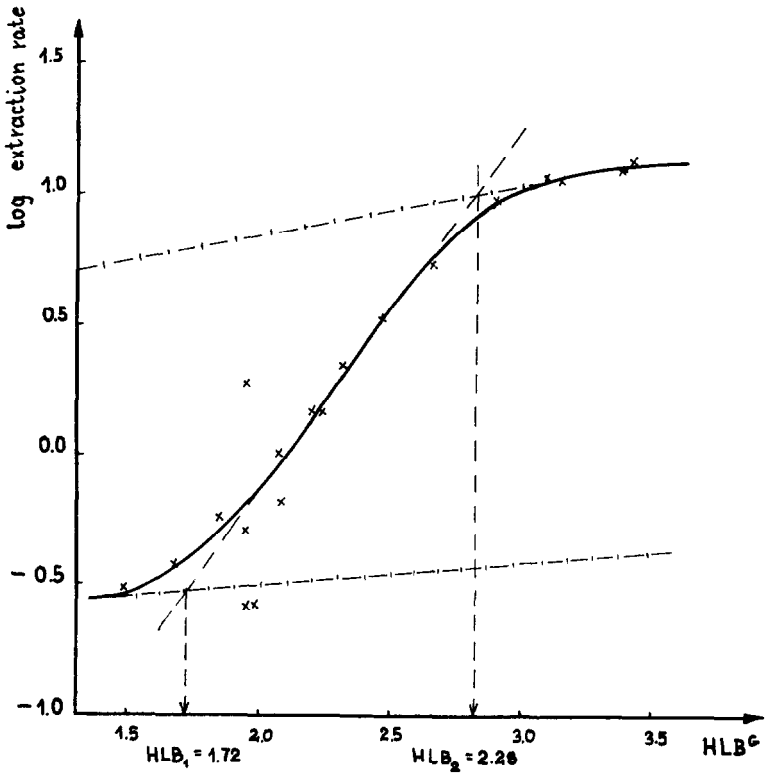


Fig. 3. The influence of the hydrophilic lipophilic balance upon copper extraction by hydroxyoximes.

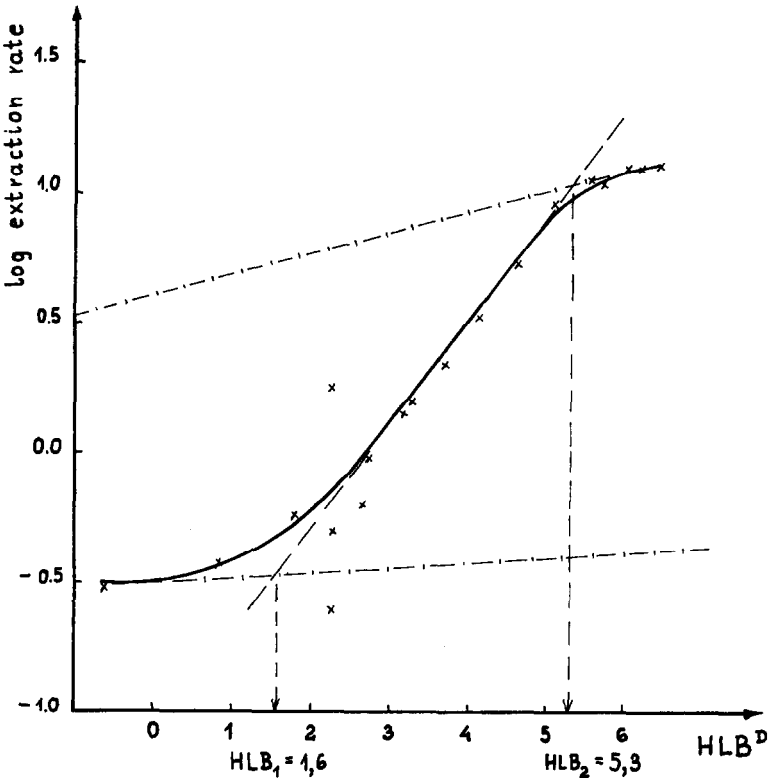


Fig. 4. The influence of the hydrophilic lipophilic balance upon copper extraction by hydroxyoximes.

ume reaction in the aqueous phase. In surfactant chemistry it is well known that adsorption properties of surface active agents depend upon the structure of the hydrophobic part of the molecule and therefore in the region of low *HLB* values the discussion should be limited to the homologous series of hydroxyoximes where the length of the R_2 group is fixed but the length of the R_1 group may differ. The structure of the R_1 group should be similar in all the compounds investigated; a straight chain R_1 group is preferred.

From the data presented in Figs. 3 and 4 the regions of bulk reaction, interfacial reaction and of the mixed mechanism were obtained when appropriate asymptotes to the curves were drawn and the points of intersection determined. The obtained values of critical *HLB* coefficients and equivalent numbers of carbon atoms in both alkyls are given in Table 1. Reasonable agreement was observed between the critical numbers of carbon atoms calculated from HLB^G and HLB^D coefficients.

The results obtained show that under our experimental conditions the extraction of copper by hydroxyoximes proceeds at the interface or in the bulk of the aqueous phase when the number of carbon atoms in both alkyls is not less than 11 or not greater than 3, respectively. For oximes having a total of from 3 to 11 carbon atoms in both alkyls the extraction occurs at the interface as well as in the bulk of the aqueous phase.

The critical length of the alkyl groups can change slightly depending upon the experimental conditions and upon the method used for the extraction rate determination. This is due to different hydrodynamic conditions and different physico chemical parameters describing the extraction system; in particular the influence of the diluent type should be quite substantial.

Mechanism of copper extraction

For hydroxyoximes of formula **I**, where the number of carbon atoms in both alkyls is not greater than 3 the reaction with copper proceeds in the homogeneous aqueous phase. When diffusion does not influence the process, the reaction can be described according to Pratt and Tiley[25] by the following steps:

$$Cu^{2+} + RH = CuR^+ + H^+ \quad (6)$$

$$CuR^+ + RH = CuR_2 + H^+ \quad (7)$$

$$\overline{CuR_2} = CuR_2 \quad (8)$$

where the bar determines the organic phase.

The slowest step is the formation of the intermediate 1 : 1 complex, and if only the forward reaction is considered the following kinetic equation is obtained:

$$v = k[RH][Cu^{2+}]. \quad (9)$$

When kinetic studies are carried out at relatively low oxime concentrations (below 0.1 M)[7,17,26] then the concentration of oxime in the aqueous phase is proportional to that in the organic phase. At concentrations higher than 0.1 M the concentration of oxime in the aqueous phase is approximately constant and does not depend upon concentration of oxime in the organic phase. In the case discussed here, because of the low oxime concentration and the use of toluene as a diluent, oxime association in the organic phase can be neglected.[4,17,27,28] Thus,

$$v = k'[\overline{RH}][Cu^{2+}]. \quad (10)$$

However, when kinetic experiments are carried out at higher oxime concentrations (above 0.1 M or above 0.01 M when an aliphatic hydrocarbon is used as the diluent) oxime association should be considered.[4,6,27–29]

For hydroxyoximes having a total of not less than 11 carbon atoms in both alkyl groups the reaction proceeds in the interphase. Thus, the generally accepted mechanism[1,30] with some modifications[4,7] can be considered:

$$Cu^{2+}_{int} + RH_{ad} = CuR^+_{int} + H^+_{int} \quad (11)$$

$$CuR^+_{int} + RH_{int} = CuR_{2int} + H^+_{int} \quad (12)$$

$$\overline{CuR_2} = CuR_{2\,int} \quad (13)$$

Table 1. Critical HLB values and equivalent length of the alkyl groups

Critical parameter	HLB^G	n^G	HLB^D	n^D
HLB_1	1.72	11.6	1.6	10.5
HLB_2	2.82	3.2	5.3	2.6

where the subscripts "ad" and "int" denote molecules adsorbed at the interface and present in the interfacial layers, respectively (Fig. 5). The formation of the complex 2 : 1 is the slowest step.

However, in this case further data and explanation is needed to support this mechanism. The surface activity of hydroxyoximes and their adsorption at the interface of an organic-aqueous surface is apparent[31–34] and the assumption that the adsorbed molecule of the oxime reacts with copper in the first step (reaction 11) is justifiable. However, the resulting charged complex, probably hydrated, must show a higher hydrophilicity than the oxime molecule and therefore it will penetrate more deeply into the aqueous layers in the neighbourhood of the interface. Thus, it is very improbable that such a strongly orientated complex will react with a second adsorbed oxime molecule. It is more probable that it will react with an oxime molecule in the interfacial aqueous layer or after its very slow reorientation with an oxime molecule in the interfacial organic layer. It seems that the reorientation of the oxime molecules can proceed more easily and more quickly than the reorientation of the charged hydrated complex. If the formation of complex 2 : 1 is the slowest step, then the intermediate complex 1 : 1 has to accumulate in the interphase and must exist in rather high concentrations. Its existence within the interphase is more probable.[35] Thus, blocking of the interface by the copper complex is possible. This may result in the formation of an interfacial film.[2,36,37]

If we assume reaction (12) is the slowest step and consider only forward reaction then the following relationship is obtained:

$$v = \frac{k[Cu^{2+}_{int}][RH_{ad}][RH_{int}]}{[H^{+}_{int}]}. \qquad (14)$$

Under perfect hydrodynamic conditions:

$$[Cu^{2+}_{int}] = [Cu^{2+}] \quad \text{and} \quad [H^{+}_{int}] = [H^{+}] \qquad (15)$$

and depending upon the location of the oxime molecule taking part in the slowest step:

$$[RH_{int}] = [RH] \quad \text{or} \quad [RH_{int}] = [\overline{RH}]. \qquad (16)$$

When the concentration of oxime in the organic phase is sufficiently low, as was described previously, then the concentration of oxime in the aqueous phase becomes proportional to that in the organic phase and oxime association in the organic phase can be neglected. Thus, in both cases considered

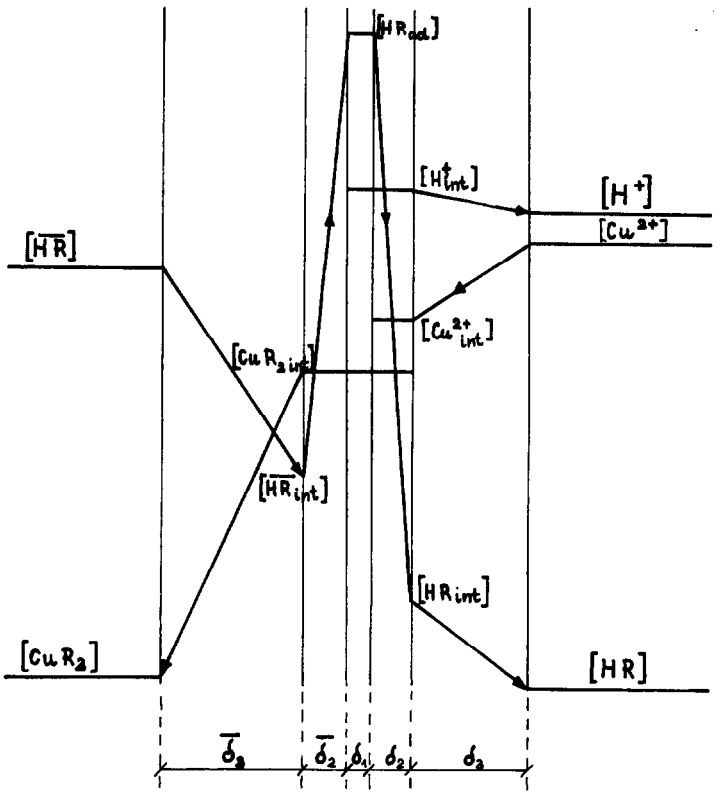


Fig. 5. Reagent concentrations in the interfacial region (δ_1—adsorption layer, $\delta_2\delta_2^1$—interfacial layers, δ_3, δ_3^1—diffusion layers).

similar expression for the extraction rate is obtained:

$$v = \frac{k[Cu^{2+}][\overline{RH}][RH_{ad}]}{[H^+]}. \quad (17)$$

The concentration of adsorbed oxime molecules is equivalent to the surface excess. A general relationship between the surface excess and the bulk oxime concentration is given by:

$$\Gamma = a[\overline{RH}]^b \quad (18)$$

where a and b are empirical coefficients.

For very low oxime concentrations it may be assumed that $b = 1$. Thus, $[RH_{ad}] = a[\overline{RH}]$ and the relationship described by Freiser[38,39] is obtained:

$$v = \frac{k[Cu^{2+}][\overline{RH}]^2}{[H^+]}. \quad (19)$$

For concentrations of oxime greater than 10^{-3} M in an aliphatic diluent or greater than 4×10^{-2} M in toluene the coefficient b can be assumed to be 0.[4,26] Thus,

$$v = \frac{k[Cu^{2+}][\overline{RH}]}{[H^+]}. \quad (20)$$

A similar kinetic equation has been reported previously.[7,30,40] However, in most cases the experimentally determined reaction order towards oxime varied between the border values 2 and 1, and sometimes even became zero.[2,4,5,17,37] This is due to diffusion processes which occur under experimental conditions[41] and sometimes also to incorrectly selected oxime concentration at which the above simplifications do not apply.

It is also improbable that under experimental conditions in which a large interface is formed an equilibrium concentration of adsorbed molecules is obtained.[2,31,42] Probably, the concentration of oxime at the interface is lower than that predicted by the interfacial tension isotherm, and moreover, it can change during the experiment. In considering this problem it is necessary to obtain data by means of real dynamic methods, e.g. the method of oscillating jets or drops.

For oximes containing a total of from 3 to 11 carbon atoms in the alkyl groups both the bulk and interfacial reactions must be considered. Thus, the reaction rate is equal to:

$$v = v_v + v_s = k_v[Cu^{2+}][\overline{RH}] + \frac{k_s[Cu^{2+}][\overline{RH}]^n}{[H^+]} \quad (21)$$

where v_v, v_s are the extraction rates for volume and interfacial processes, respectively, k_v, k_s are the specific rates constants for volume and interfacial processes, respectively n is the empirical coefficient characteristic of the experimental conditions being used.

The kinetic parameters required to solve eqn (22) cannot be obtained from our data. However, we can estimate the contribution of the volume reaction to the overall extraction rate for oximes having different numbers of carbon atoms in the alkyl groups. The contribution (β) of the volume reaction to the measured reaction rate (v) can be expressed by the following equation:

$$v = v_v\beta + v_s(1 - \beta). \quad (22)$$

Thus,

$$\beta = \frac{v - v_s}{v_v - v_s} \cdot 100\%. \quad (23)$$

The estimated values are presented in Fig. 6. The lower limit of the shaded area was calculated by assuming that the rates of the interfacial and volume reactions are constant and independent of the length of the alkyl groups. The upper limit was calculated by considering linearly extrapolated values of the interfacial and volume reaction rates.

The results obtained show that for oximes having a total of not less than 11 carbon atoms in the alkyl groups the contribution of the volume reaction is less than 10%, while for oximes having a total of not more than 3 carbon atoms the contribution is above 90%. A contribution of 50% is obtained for oximes containing 6–7 carbon atoms in the alkyl groups.

Some predictions can also be made for the commercial hydroxyoximes having a branched nonyl group (P 50, SME 529 and Lix 65N). The extra aromatic ring in Lix 65N is equivalent only to a little more than 3 carbon atoms in the aliphatic chain. In surfactant chemistry such an assumption is usually made when the polarity, the hydrophilic lipophilic balance and/or critical micelle concentrations are discussed. Thus, the minimum contribution of the volume reaction can be estimated as follows: P 50—about 20%, SME 529—about 15% and Lix 65N—about 15%. However, these contributions can be sharply increased when the commercial extractants are contaminated with oximes of lower molecular mass obtained as by-products in the acylation of nonylphenol with benzoyl chloride, benzotrichloride or acetyl anhydrate in the presence of aluminum chloride, i.e. during the manufacture of SME 529 and Lix 65N.

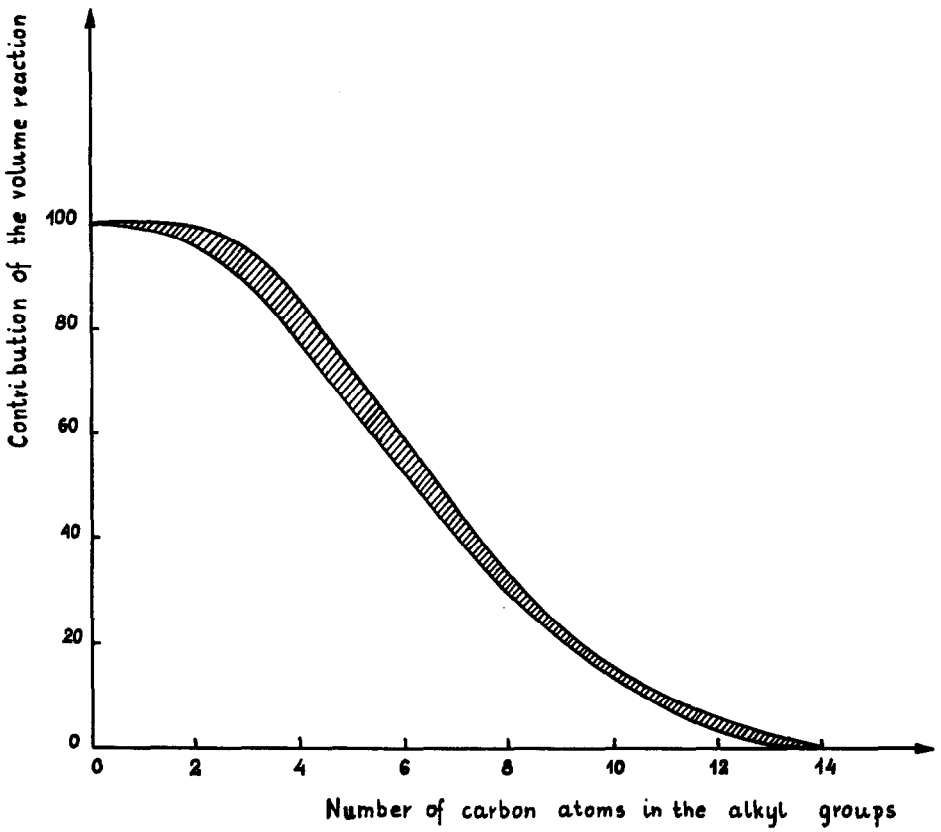


Fig. 6. The influence of the number of carbon atoms in the alkyl groups upon the contribution of the volume reaction.

Comments upon the mechanism of copper extraction by commercial extractants

Most of the authors who have investigated the kinetics of copper extraction used commercial reagents, either directly or after some kind of purification. We believe that such a kinetic and interfacial data can be misinterpreted, and that commercial extractants, even after "purification", are not the most suitable reagents for mechanistic studies. The following points should be stressed here.

1. Commercial nonylphenol is formed from an identified propylene trimer which is a mixture of several components, not only the isomers of nonene. We have observed about 30 components in a commercial nonylphenol; the main component comprising only about 25%.

2. Commercial nonylphenol contains only about 90% 4-alkylphenol. It also contains about 10% 2-alkylphenol and less than 2% alkylphenyl ether. Small amounts of other impurities can be also present. The presence of these by-products and derivatives formed during the oxime manufacture has not been discussed in the literature. The removal of the above by-products either from raw nonylphenol or from the extractant manufacturing process is very difficult.

3. It is probable that commercial reagents also contain small amounts of ketones or aldehydes which did not react completely in the oximation step.

4. Lesser or greater amounts of the dealkylated oximes are present in commercial extractants. They influence the extraction mechanism and enhance the contribution of the volume reaction. Thus, parallel complexation of copper by alkylated and dealkylated oximes should be considered. Additional equilibria should be also discussed:

$$R'_2Cu = R'R''Cu = R''_2Cu \qquad (24)$$

where R'H and R''H denote alkylated and dealkyalted oximes, respectively.

5. Taking into account oxime isomerisation the use of P 50 or SME 529 rather than Lix 65N should be preferred. In most of the published papers the structure of the separated E-Lix 65N isomer was not proved, and the given statements can not be accepted in the meaning of the organic chemistry.

6. As complete analysis of commercial extractants is not possible the impurity content can not be determined and the quality of the separated fraction can not be proved. Moreover, the separation of pure oximes having the high purity necessary for kinetic and mechanistic studies is very difficult.

7. When the raw material or the separated fractions are stored it is possible that some components may precipitate and the isomerisation of oximes may occur.

8. Those reagents are rendered unsuitable for kinetic, mechanistic or interfacial studies, especially when an interfacial mechanism is been deduced.

CONCLUSIONS

The rate of copper extraction by hydroxyoximes can be related to the oxime hydrophilic lipophilic balance.

Depending upon the oxime hydrophilicity either the interfacial reaction, the volume reaction or both of these must be considered.

The contribution of the volume reaction is less than 10% and higher than 90% for oximes which contain a total of not less than 11 and not more than 3 carbon atoms in the alkyl groups, respectively.

The minimum contribution of the volume reaction for commercial extractants can be estimated as follows: Lix 65N—5%, SME 529—15% and P 50—20%.

Commercial oxime extractants are not the most suitable reagents for the kinetic and mechanistic studies of copper extraction as their use can cause misleading results.

Acknowledgement—I wish to thank the British Council for the financial assistance.

REFERENCES

1. D. S. Flett, *Acc. Chem. Res.* 1977, **10**, 99.
2. G. A. Yagodin, S. Yu. Ivakhno and V. V. Tarasov, *Proc. ISEC'80 Liege 1980*, Vol. 3 (15B), paper 80-140 (1980).
3. L. Hummelstedt, E. Paatero, T. Nyberg and L. Rosenback, *Ibid.* Vol. 2 (10A), paper 80-73 (1980).
4. M. Cox, C. G. Hirons and D. S. Flett, *Ibid.* Vol. 1, paper 80-118 (1980).
5. C. A. Fleming, M. J. Nicol, R. D. Hancock and N. P. Finkelstein, *J. Appl. Chem. Biotechnol.* 1978, **28**, 443.
6. C. Hanson, M. A. Hughes and R. J. Whewell, *J. Appl. Chem. Biotechnol.* 1978, **28**, 426.
7. I. Komasawa, T. Otake and T. Muraoka, *J. Chem. Eng. Japan* 1980, **13**, 204.
8. Y. Miyake, Y. Takenoshita and M. Teramoto, *Proc. ISEC'83, Denver 1983*, 301.
9. V. V. Tarasov, G. Yagodin, A. Pichugin and S. Ivakhno, *Ibid.* 299.
10. G. Yagodin, V. V. Tarasov and A. Pichugin, *Ibid.* 20.
11. J. Szymanowski, M. Cox and C. G. Hirons, *J. Chem. Techn. Biotechnol.*, 1984, **34A**, 218.
12. D. Stepniak-Biniakiewicz, J. Szymanowski and V. V. Tarasov, *J. Chem. Techn. Biotechnol.* Submitted for publication.
13. W. C. Griffin, *J. Soc. Cosmet. Chem.* 1949 **1**, 311.
14. W. C. Griffin, *Ibid.* 1954, **5**, 249.
15. J. Broniarz, J. Szymanowski and M. Wisniewski, *Tluszcze Srodki Piorace Kosmetyki* 1973, **17**, 73.
16. J. Broniarz, J. Szymanowski and M. Wisniewski, *Ibid.* 1973, **17**, 131.
17. J. S. Preston and Z. B. Luklinska, *J. Inorg. Nucl. Chem.* 1980, **42**, 431.
18. J. T. Davies, *Proc. Int. Cong. Surface Activity*, Vol. 1, p. 426. London (1957).
19. J. Broniarz, M. Wisniewski and J. Szymanowski, *Tenside* 1973, **10**, 75.
20. J. Broniarz, M. Wisniewski and J. Szymanowski, *Tenside* 1974, **11**, 27.
21. J. Szymanowski, A. Voelkel, J. Beger and C. Poschmann, *Tenside*, 1983, **20**, 173.
22. J. Szymanowski and A. Voelkel, *Tenside*, 1983, **20**, 231.
23. J. Szymanowski and A. Voelkel, *Tenside*, 1983, **20**, 237.
24. J. Szymanowski, A. Voelkel, J. Beger and H. J. Binte, *J. Prakt. Chemie*, in press.
25. J. M. Pratt and R. I. Tilley, *Hydrometallurgy* 1979, **5**, 29.
26. T. Komasawa, T. Otake and A. Yamada, *J. Chem. Eng. Japan* 1980, **13**, 130.
27. L. Hummelstedt, E. Paatero, T. Nyberg and L. Rosenback, *Proc. ISEC'80, Liege 1980*, Vol. 2 (10A), paper 80-73 (1980)
28. A. J. van der Zeeuw and R. Kok, *Proc. ISEC'77, Montreal 1977, CIM Special Volume*, Vol. 21, p. 210 (1979).
29. R. J. Whewell, M. A. Hughes and C. Hanson, *Proc. ISEC'77, Montreal 1977, CIM Special Volume*, Vol. 21, p. 185 (1979).
30. D. S. Flett, D. N. Okuhara and D. R. Spink, *J. Inorg. Nucl. Chem.* 1973, **35**, 2471.
31. J. Szymanowski, unpublished data.
32. M. Cox and D. S. Flett, *Proc. ISEC'77, Montreal 1977, CIM Special Volume*, Vol. 21, p. 63 (1979).
33. M. H. Hughes, E. Mistry and R. J. Whewell, *J. Inorg. Nucl. Chem.* 1978, **40**, 1694.
34. T. A. B. Al-Diwan, M. A. Hughes and R. J. Whewell, *J. Inorg. Nucl. Chem.* 1977, **39**, 1419.
35. W. J. Albery, P. R. Fisk. *Proc. Soc. Chem. Ind. Symp. Hydrometallurgy'81, Manchester* F.6. (1981).

36. J. Szymanowski, I.Wolniewicz and V. V. Tarasov, *Chem. Stos.* submitted for publication.
37. C. A. Fleming, *NIM Report* 1793, S. Africa 1976.
38. H. Freiser, *Proc. ISEC'80, Liege 1980,* Vol. 1, paper 80-II (1980).
39. P. Carter and H. Freiser, *Anal. Chem.* 1980, **52**, 511.
40. D. R. Spink and D. N. Okuhara, *Met. Trans. AIME* 1974, **5**, 1935.
41. E. S. Perez de Ortiz, M. Cox and D. S. Flett, *Proc. ISEC'77, Montreal 1977, CIM Special Volume,* Vol. 21, p. 203 (1977).
42. J. M. R. de Carvalho and M. J. Slater, *Proc. ISEC'83, Denver 1983,* 297 (1983).

Polyhedron Vol. 4, No. 2, pp. 279–283, 1985
Printed in Great Britain.

0277–5387/85 $3.00 + .00
© 1985 Pergamon Press Ltd.

COMPARATIVE STUDY OF HYDROXO-FLUORO AND HYDROXO-SULPHIDO MIXED LIGAND COMPLEXES OF ALUMINIUM(III) AND GALLIUM(III)

IMRE TÓTH*, LÁSZLÓ ZÉKÁNY and ERNŐ BRÜCHER
Department of Inorganic and Analytical Chemistry, Lajos Kossuth University, H-4010 Debrecen, Hungary

(*Received* 26 *October* 1983; *accepted after revision* 16 *April* 1984)

Abstract—The mixed ligand complex formation had been studied in the aluminate–fluoride, gallate–fluoride, aluminate–sulphide and gallate–sulphide systems by spectrophotometric as well as potentiometric methods using glass and sulphide selective electrodes. The formation of the species $Al(OH)_3F^-$ and $Ga(OH)_2S^-$ has been demonstrated and the equilibrium constants have been determined. Similar interaction could not be detected in the aluminate–sulphide and gallate–fluoride systems.

The differences in behaviour of the metal ions to the characteristically hard fluoride and soft sulphide ligands can be interpreted in that the Ga^{3+} ion may form complexes with charged soft ligands too, its behaviour then differing from that of the typically hard Al^{3+} ion.

The development in the semiconductor industry has led to a considerable increase in the demand for high-purity gallium and its compounds.[1] Virtually the only raw material source for gallium production is the aluminate liquor in the Bayer alumina production cycle; the essence of the various procedures is always the selective separation of gallium from a large excess of aluminium. Liquid-liquid extraction methods of separation are currently finding increasing application.[2] Accordingly, there may well be practical importance to a study of the differences in coordination chemical properties of aluminium(III) and gallium(III), which are well known to behave very similarly.

The stability constants of the Al^{3+}-fluoro complexes are higher than those of the corresponding Ga^{3+} complexes; in aqueous solution the species AlF_6^{3-} has been identified, whereas the coordination of more than three F^- ions to Ga^{3+} in solution has not been described.[3]

Data on the hydroxo complexes are much more contradictory; their study, particularly at moderate pH values, is greatly hampered by the formation of very complex polynuclear species.[4] This is probably the reason why the stability data on the hydroxo-fluoro mixed ligand complexes are unknown, even though the reaction between $Al(OH)_3$ and F^- is a familiar one in classical analysis, and the reaction between aluminate and F^- ions is utilized for quantitative analytical purposes.[5]

It is also well known that the addition of $(NH_4)_2S$ to a solution of Al^{3+} ions results in the precipitation of $Al(OH)_3$ and the behaviour of Ga^{3+} is similar. However, in the presence of Zn(II), Pb(II) or As(III) gallium(III) mixed-sulphides can be precipitated and the various ZnS minerals always contain traces of gallium too, in the absence of aluminium. In the study of the Ga^{3+}–OH^-–S^{2-}–Zn^{2+} system the formation of species $Ga(OH)_2S^-$ has been assumed but the stability constant was not determined.[6]

The presence of polynuclear hydroxo complexes need not be considered at pH > 10, where the metal ions are present only as $M(OH)_4^-$ (M = Al or Ga)[4], and our investigations were therefore carried out in this pH range.

EXPERIMENTAL

Chemicals and analytical methods

Gallium nitrate and aluminium nitrate stock solutions were prepared by dissolving 5N gallium (Timföldgyár és Aluminiumkohó, Ajka) and aluminium (p.a., Reanal) in nitric acid. The concen-

*Author to whom correspondence should be addressed.

trations of the metal ions in the solutions were determined complexometrically.

The KOH solution used for the pH-potentiometric titrations was stored in an argon atmosphere. Its concentration was measured pH-potentiometrically with potassium hydrogen phthalate (Merck).

The Na_2S stock solution was prepared by dissolution of $Na_2S \cdot 9H_2O$ (p.a., Merck) in boiled-out bidistilled water; it was stored in an argon atmosphere. Its concentration was determined by oxidation with KIO_3 in basic medium to sulphate,[7] or in acidic medium to sulphur,[8] with back-titration of the excess KIO_3. The agreement of the results of the determinations within 1% showed that all of the sulphur in the Na_2S solution was in the oxidation state -2.

The aluminate and gallate solutions were obtained from the $M(NO_3)_3$ solutions by the addition of excess KOH solution to yield $K[M(OH)_4]$ solutions. The passage of CO_2 led to the separation of precipitates of $M(OH)_3$, which can be centrifuged. The precipitates were redissolved to remove nitrate, and again precipitated with CO_2. The metal contents of the resulting $K[M(OH)_4]$ solutions were determined complexometrically.

The NaF solution was prepared from NaF (p.a., Reanal) by direct weighting.

Procedures

Spectrophotometric measurements were made at 25 ± 0.2°C with a Beckmann Acta M IV instrument.

Potentiometric experiments were performed at 25 ± 0.2°C and constant ionic strength: 0.5 mol dm^{-3} KNO_3. OP-208 and OP-208/1 Radelkis pH-meters, a Radiometer GK2401B combined electrode, a Radelkis OP-S 07110 sulphide-selective electrode, and an OP 8202 Ag/AgCl reference electrode incorporated with a ceramic-filter KNO_3 salt bridge were used. The pH-meter was calibrated with freshly-prepared saturated $Ca(OH)_2$ solution (Reanal, pH = 12.454) and 0.01 mol dm^{-3} $Na_2B_4O_7 \cdot 10H_2O$ (Reanal, pH = 9.18). The stoichiometric equilibrium constants were calculated from the measured pH values with the method of Irving *et al.*[9] In 0.5 mol dm^{-3} KNO_3 solution the stoichiometric ionic product of water was determined to be $pK_w = 13.83 \pm 0.01$.

During titrations, the absence of CO_2 and O_2 was ensured by passage over the solutions of argon freed from oxygen with alkaline pyrogallol solution. A magnetic stirrer was used for mixing.

Sulphide ion concentration was determined via calibration curves. At 25°C and constant ionic strength the electrode potential (E) is as follows:[10]

$$E = \text{const.} - 0.0296 \log [S^{2-}]. \quad (1)$$

The constants describing the protonation equilibria of the S^{2-} ion are $K_1^H = [HS^-]/[S^{2-}][H^+]$ and $K_2^H = [H_2S]/[HS^-][H^+]$; these can be used to express the S^{2-} ion concentration:

$$[S^{2-}] = \frac{T_S}{1 + K_1^H[H^+] + K_1^H K_2^H [H^+]^2} \quad (2)$$

where $T_S = [S^{2-}] + [HS^-] + [H_2S]$. Since log $K_2^H = 7.0$ and log $K^H = 13.9$[11], if pH > 9.0 we have $K_1^H K_2^H [H^+]^2 \ll K_1^H [H^+]$ and $K_1^H [H^+] \gg 1$, so that eqns (1) and (2) give

$$E = \text{const.} - 0.0296 \log \frac{T_S}{K_1^H [H^+]}. \quad (3)$$

In analytical chemistry the pH-dependence of the electrode potential as in eqn (3) is generally taken into account with the use of buffers; this is usually not possible in coordination chemical equilibrium investigations. The pH-dependence can be taken into account through the simultaneous measurement of the H^+ ion concentration, but even then the S^{2-} ion concentration can be calculated only if K_1^H is known[11]; this can cause problems, because of the uncertainty in the protonation constant.

If the values of K_1^H and K_2^H are considered, it holds in the interval $9 < pH < 11.5$ that $T_S = [HS^-]$, and thus eqn (3) can be written as

$$E = \text{const.}' - 0.0296(pH - p[HS^-]). \quad (4)$$

Calibration curves plotted on the basis of eqn (4) are to be seen in Fig. 3. The very good linearity demonstrates the applicability of the method. For calibration plots recorded at five different times the slope is almost the theoretical one: -28.81 ± 0.05; the intercept too is very reproducible, with a mean value of -502.5 ± 0.3 mV. The concentration range is $pT_S = 2$–4.5, with pH = 9.0–11.5.

RESULTS AND DISCUSSION

(a) *Aluminate–fluoride and gallate–fluoride systems*

The interactions between aluminate or gallate and fluoride ions were studied pH-potentiometrically at constant total metal ion concentration (0.01 moldm^{-3}) and at variable total fluoride ion concentration. The results are presented in Fig. 1.

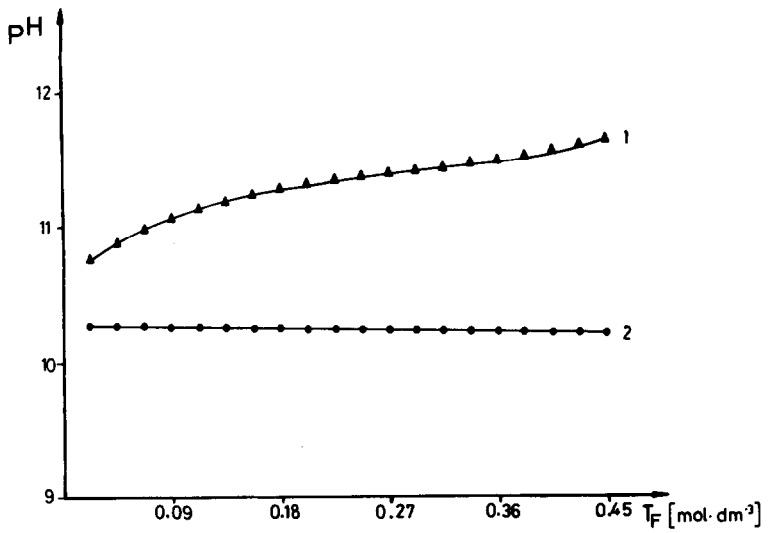


Fig. 1. Variation of pH as a function of the total fluoride concentration in the aluminate–fluoride and gallate–fluoride systems. $T_M = 0.01$ mol dm^{-3}; $C_{KNO_3} = 0.5 - T_F$ mol dm^{-3}. Al^{3+}(1), Ga^{3+}(2).

It may be seen from Fig. 1 that the addition of F^- leads to a pH increase in the aluminate solution, whereas the pH in the gallate solution is unchanged. The pH change in the aluminate–fluoride system was interpreted by the assumption of the following simple equilibrium:

$$Al(OH)_4^- + F^- \rightleftharpoons Al(OH)_3F^- + OH^- \quad (5)$$

$$K_m = \frac{[Al(OH)_3F^-][OH^-]}{[Al(OH)_4^-][F^-]}. \quad (6)$$

The equilibrium constant K_m can be calculated for each experimental point via the following equations: $T_{Al} = [Al(OH)_4^-] + [Al(OH)_3F^-]$; $T_F = F^- + [Al(OH)_3F^-]$ and $T_{OH^-} = [OH^-]_{T_F=0} + [Al(OH)_3F^-]$.

In the concentration interval $T_F = 0-0.36$ mol dm^{-3}, log $K_m = -2.20 \pm 0.13$. The constants calculated at higher T_F values exhibited a slight shift; this indicates that, although the average ligand number at the highest T_F value too is only $\bar{n} = 0.55$, a small degree of formation of the species $Al(OH)_2F_2^-$ may be assumed. In connection with the parent fluoro complexes, it is known that the difference between the stepwise stability constants is only -1.1 log unit;[13] on this basis it may be assumed that the difference between the stepwise constants is likewise not large when the mixed ligand complexes are formed. However, the equilibrium constant describing formation of the complex $Al(OH)_2F_2^-$ cannot be determined under the concentration conditions we employed.

The data in Fig. 1 indicate that Ga^{3+} does not form a mixed ligand complex under these conditions. This is probably the consequence of the relatively stronger Ga–OH bonds which result in the higher stability of the complex $Ga(OH)_4^-$.

Under conditions similar to those above, we were unable to detect the formation of mixed hydroxo–halo complexes in the gallate–chloride, gallate–bromide and gallate–iodide systems either.

(b) *Aluminate–sulphide and gallate–sulphide systems*

The interaction between the gallate and sulphide ions was studied via the HS^- absorption band with maximum at 230 nm.[11] The spectra of solutions with a constant total sulphide concentration and various concentrations of $K[Ga(OH_4)]$, but free from foreign ions, were compared with the spectra of solutions of identical composition, but not containing sulphide. The resulting spectra may be seen in Fig. 2(a). Before the spectra in Fig. 2(b) were recorded, the increase in the pH of the solutions, due to the base excess in the gallate solution, was compensated by the addition of perchloric acid.

The changes visible in Figs. 2(a) and (b) point to the interaction of the gallate and sulphide ions, the extent of which increases as the gallate concentration rises, while it decreases with increase of the OH^- ion concentration. Similar studies were made on the aluminate–sulphide system, but a change indicative of an interaction was not observed.

In the potentiometric investigations, gallate and aluminate solutions with concentrations of 1.0×10^{-3}, 3×10^{-3}, 5×10^{-3} and 1.0×10^{-2} mol dm^{-3} were titrated with 5.0×10^{-2} mol dm^{-3} Na_2S solution, with simultaneous measurement of the pH and the potential of the sulphide-selective electrode. Fig. 3 depicts the experimental results, together

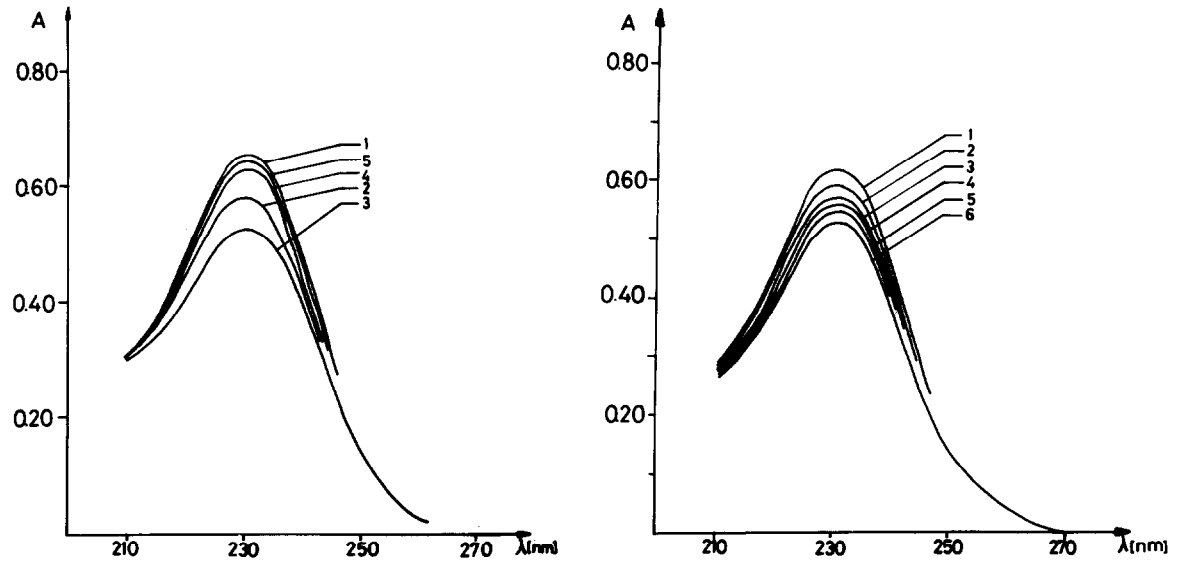


Fig. 2. Spectra of sulphide solutions at various total gallium concentrations. d = 10 mm; $T_S = 8.4 \times 10^{-5}$ mol dm^{-3}; (a) T_{Ga}(mol dm^{-3}) and pH: 0 and 11.0 (1), 1.0×10^{-4} and 10.8 (2), 1.0×10^{-3} and 11.2 (3), 3.0×10^{-3} and 11.8 (4), 7.0×10^{-3} and 12.8 (5). (b) pH = 10.1; T_{Ga}(mol dm^{-3}): 0.0 (1), 1.0×10^{-4} (2), 1.0×10^{-3} (3), 5×10^{-3} (4), 7.0×10^{-3} (5), 1.0×10^{-2} (6).

with the calibration plot recorded in the absence of the metal ions.

The findings of an interaction between gallate and sulphide ions (Fig. 2), and of a lower sulphide ion concentration in the presence of gallate ion (Fig. 3), may be interpreted by assumption of the following equilibrium:

$$Ga(OH)_4^- + HS^- \rightleftharpoons Ga(OH)_2S^- + OH^- + H_2O \quad (7)$$

$$K'_m = \frac{[Ga(OH)_2S^-][OH^-]}{[Ga(OH)_4^-][HS^-]}. \quad (8)$$

Of the equilibrium concentrations necessary for calculation of K'_m, $[OH^-]$ and $[HS^-]$ are direct experimental data, while $[Ga(OH)_2S^-]$ and $[Ga(OH)_4^-]$ can be calculated via the following material balances: $T_S = [HS^-] + [Ga(OH)_2S^-]$ and $T_{Ga} = [Ga(OH)_4^-] + [Ga(OH)_2S^-]$.

The value of the equilibrium constant calculated for the experimental points is log $K'_m = -1.72 \pm 0.08$. The mixed ligand complex $Ga(OH)_2S^-$ predominates at pH values around 9 but its concentration decreases with increasing pH and at pH > 12 is negligible.

Naturally, the equilibrium in eqn (7) cannot be

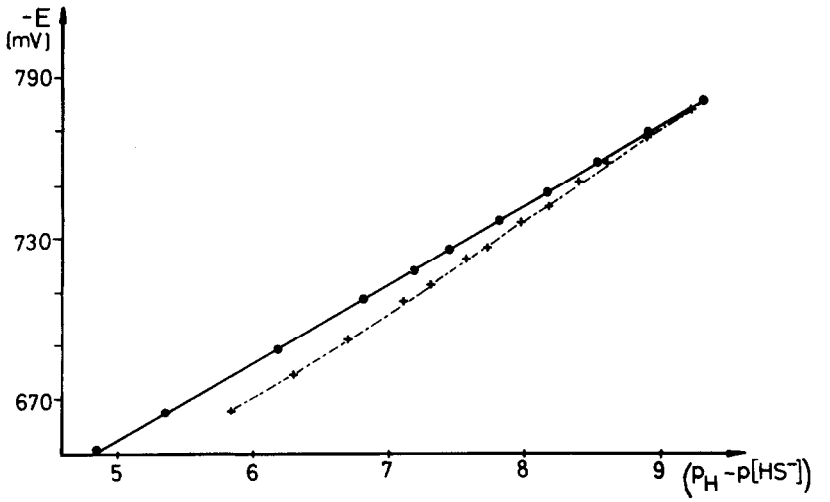


Fig. 3. Variation of the potential of the sulphide-selective electrode as a function of (pH − p[HS$^-$]): T_{Ga} = 5.0×10^{-3} mol dm^{-3}, I = 0.5 mol dm^{-3} KNO_3 (—×—); I = 0.5 mol dm^{-3} KNO_3 (-●-).

differentiated with a potentiometric method from an equilibrium in which an HS^- ligand replaces an OH^- ion and a species $Ga(OH)_3SH^-$ is formed. The numerical value of $K''_m = [Ga(OH)_3SH^-][OH^-]/[Ga(OH)_4^-][HS^-]$ is the same as that of the constant in eqn (8). Although a number of examples are known where HS^- behaves as a ligand[13,14] the simultaneous coordination of OH^- and HS^+ ions has been assumed only in the formation of Zn(OH)(SH), and even here merely as a possible alternative to the species $ZnS \cdot H_2O$.[15]

In aqueous solution, Al^{3+} and Ga^{3+} are generally considered to behave very similarly. Nevertheless, aluminate and gallate ions display opposite behaviour with fluoride and sulphide ligands. Although it is true that the interactions between aluminate and fluoride, and between gallate and sulphide, are not very strong, and can be observed only at a comparatively low OH^- ion excess, these findings do suggest a definite difference in the complex-forming tendencies of the Al^{3+} and Ga^{3+} ions.

The sulphide ion is a soft ligand, though because of its high basicity it also forms very stable, poorly soluble compounds with several not typically soft metal ions.[16]

Since the Al^{3+} ion forms stronger electrostatic bonds than the Ga^{3+} ion, the fact that there is no interaction between Al^{3+} and S^{2-}, whereas there is such an interaction between Ga^{3+} and S^{2-}, can only be explained by the participation of the Ga^{3+} 3*d* electrons in the bonding formed. The charge density of those of the Ga^{3+} d^{10} electrons with the appropriate direction may be shifted slightly towards the empty *d* orbitals of the sulphide ion; accordingly, besides the electrostatic interaction, a weak covalent bond may also develop. The formation of such a weak $d\pi$–$d\pi$ bond is given as the explanation of the stability of the complexes of In^{3+} (which has similar properties to those of Ga^{3+}) with various substituted carboxylic acids.[17] A metal→ligand electron shift is similarly assumed from an IR and ^{1}H-NMR spectroscopic study of complexes of Ga^{3+} and In^{3+} with various ligands containing the mercapto group.[18] It has been concluded from thermodynamic data that Ga^{3+} does not behave as typically hard in the formation of the Ga(III)-azide complexes; a part is also played in this by the properties of the ligand.[19] Thus, in agreement with these literature data,[17–19] our experimental results show that the Ga^{3+} ion may also form complexes with charged soft ligands; its behaviour then differs from that of the typically hard Al^{3+} ion, and to a certain extent is reminiscent of that of the similarly d^{10} Zn^{2+} ion.

REFERENCES

1. I. G. Lossmann and H. F. Repko, *Metall* 1978, **38**, 713.
2. C. M. Wang. L. Q. Zhang, J. G. Yu, J. H. Li, S. Q. Sun and J. Z. He, *Abst. Paper Am. Chem. Soc.* 1981, **182**, 148.
3. R. E. Smith and A. E. Martell, *Critical Stability Constants*, Vol. 4. p. 101. Plenum Press, New York (1976).
4. C. F. Baes and R. E. Mesmer, *The Hydrolysis of Cations*. Wiley, New York (1976).
5. M. T. Beck, *Magy. Kém. Folyóirat* 1950, **56**, 367.
6. I. Sz. Csausz and I. A. Seka, (a) *Zh. Neorg. Khim.* 1962, **7**, 2162. (b) 1963, **8**, 490.
7. P. O. Bethge, *Anal. Chim. Acta* 1954, **10**, 310.
8. E. Schulek and Z. L. Szabó, A kvantitativ analitika elvi alapjai és módszerei. *Tankönyvkiadó, Budapest* 1973. p. 224–235.
9. H. M. N. Irving, M. G. Miles and L. P. Pettit, *Anal. Chim. Acta* 1967, **38**, 475.
10. T. M. Hseu and G. A. Rechnitz, *Anal. Chem.* 1968, **40**, 1054.
11. A. J. Ellis and R. M. Golding, *J. Chem. Soc.* 1959, 127.
12. R. E. Mesmer and C. F. Baes, *Inorg. Chem.* 1969, **8**, 618.
13. J. Ste-Marie, A. E. Torma and S. O. Gübeli, *Can. J. Chem.* 1964, **42**, 662.
14. G. Schwarzenbach and M. Widmer, *Helv. Chim. Acta* 1966, **49**, 111.
15. A. E. Gubeli and J. Ste-Marie, *Can. J. Chem.* 1967, **45**, 2101.
16. S. Ahrland, *Structure and Bonding*, Vol. 5. p. 118. Springer-Verlag, Berlin (1968).
17. R. Sarin and K. N. Munshi, *J. Inorg. Nucl. Chem.* 1973, **35**, 201.
18. N. Kojima, Y. Sugiura and H. Tanaka, (a) *Bull. Chem. Soc. Jpn.* 1976, **49**, 3023. (b) *Chem. Pharm. Bull.* 1978, **26**, 440. (c) *Chem. Pharm. Bull.* 1978, **26**, 579.
19. E. Avsa, *Acta Chem. Scand. A.* 1982, **36**, 627.

Polyhedron Vol. No. 2, pp. 285–297, 1985
Printed in Great Britain.

0277–5387/85 $3.00 + .00
© 1985 Pergamon Press Ltd.

ORGANO-IMIDO ALKOXIDES OF TUNGSTEN(VI). THE CRYSTAL AND MOLECULAR STRUCTURES OF $[W(NPh)(\mu\text{-}OMe)(OMe)_3]_2$ AND $[W(NPh)(OCMe_3)_3Cl(NH_2CMe_3)]$

ALASTAIR J. NIELSON* and JOYCE M. WATERS
Department of Chemistry, University of Auckland, Private Bag, Auckland, New Zealand

and

DONALD C. BRADLEY*
Department of Chemistry, Queen Mary College, Mile End Road, London, El 4NS, England

(*Received* 7 *March* 1984; *accepted* 17 *April* 1984)

Abstract—Reaction of phenylimido tungsten tetrachloride with MeOH and *t*-butylamine gave the dimeric complexes $[W(NPh)(\mu\text{-}OMe)(OMe)_3]_2$ and $[W(NPh)(\mu\text{-}OMe)(OMe)_2Cl]_2$. With ethanol $[W(NPh)(\mu\text{-}OEt)(OEt)_2Cl]_2$ was formed whereas *iso*propyl and *neo*pentyl alcohols gave the monomeric complexes $[W(NPh)(OR)_4(NH_2CMe_3)]$ (R = $CHMe_2$, CH_2CMe_3); *t*-butanol gave $[W(NPh)(OCMe_3)_3Cl(NH_2CMe_3)]$ which could not be converted to $[W(NPh)(OCMe_3)_4]$. Further reaction of $[W(NPh)(\mu\text{-}OMe)(OMe)_3]_2$ with $o\text{-}HOC_6H_4CH = NC_6H_3Me_2$(salim-H) gave the salicylaldimine complex $[W(NPh)(OMe)_3(salim)]$. The products were characterised by analytical data, IR, ^1H NMR, ^{13}C NMR and mass spectroscopy. The crystal and molecular structures of the title complexes have been determined from single crystal X-ray diffractometer data. Crystals of $[W(NPh)(\mu\text{-}OMe)(OMe)_3]_2$ are triclinic with $a = 8.473(7)$, $b = 10.776(5)$, $c = 7.683(3)$ Å, $\alpha = 102.26(3)$, $\beta = 102.68(4)$, $\gamma = 71.13(6)°$, space group $P\bar{1}$ Crystals of $[W(NPh)(OCMe_3)_3Cl(NH_2CMe_3)]$ are monoclinic with $a = 9.341(2)$, $b = 29.608(7)$, $c = 10.257(2)$ Å, $\beta = 106.28(2)°$, space group, $P2_1/c$. Both structures were solved by Patterson and Fourier methods and refined to $R = 0.075$ for the 1022 observed data of $[W(NPh)(\mu\text{-}OMe)(OMe)_3]_2$ and to $R = 0.074$. For the 2033 observed data of $[W(NPh)(OCMe_3)_3Cl(NH_2CMe_3)]$. The former molecule is shown to be a dimer, the two halves of the molecule being related by a centre of symmetry. Both W atoms adopt a distorted octahedral coordination geometry and they are linked by two methoxy bridges. *Trans* to one of the bridging donors is the phenyl imido group with a W–N bond length of 1.61(4) Å; the remaining coordination sites are filled with methoxy groups. The structure of $W(NPh)(OCMe_3)_3Cl(NH_2CMe_3)$ is monomeric with the phenylimido group *trans* to the NH_2CMe_3 ligand in a distorted octahedral coordination geometry. Remaining sites are filled with the chloride and 3 $OCMe_3$ ligands. The W–N (imido) bond length is 1.71(2) Å, whilst W–N(amine) is 2.40(2) Å

Although many examples of early transition metal alkoxides are known, a few complexes only have been prepared which additionally contain the multiply-bonded organo-imido function, W=NR.[1] Those reported to date include the silyloxy complexes $(Me_3SiO)_3V(NSiMe_3)$,[2] $(Me_3SiO)_3V(N\text{-}t\text{-}Bu)$ and $(Me_3SiO)_2M(N\text{-}t\text{-}Bu)_2$(M = Cr, Mo)[3] prepared from the metal oxychloride and HMDS or *t*-BuNHSiMe$_3$, the tungsten complexes $WO(NR)(OEt)_2$[4] and $(t\text{-}BuO)_2W(N\text{-}t\text{-}Bu)_2$[5] which result from alcohol exchange of halide or amido ligands of complexes already containing the imido moiety, and the rhenium complexes $(Me_3SiO)Re(N\text{-}t\text{-}Bu)_3$ and $Re_3(N\text{-}t\text{-}Bu)_4O_4(OSiMe_3)_3$.[6] We report here the synthesis and characterisation of organo-imido alkoxides of tungsten(VI) which are readily prepared from a variety of alcohols under mild conditions. A

*Authors to whom correspondence should be addressed.

preliminary account of this work has already appeared.[7]

RESULTS AND DISCUSSION

Preparation of complexes. In benzene solution phenylimido tungsten tetrachloride reacts with four equivalents of MeOH in the presence of excess ammonia to give, on recrystallisation, yellow, air and moisture sensitive crystals of $[W(NPh)(\mu\text{-}OMe)(OMe)_3]_2$ (**1**) Triethylamine may also be used as base but the best yields and cleanest product were obtained by addition of 5 equivalents of *t*-butylamine to $[W(NPh)Cl_4]_n$ in petroleum ether, followed by 4 equivalents of MeOH. Addition of the MeOH/*t*-butylamine mixture to $[W(NPh)Cl_4)]_n$ resulted in several petroleum ether soluble products of which the major component was (**1**) but considerable insoluble material also formed. Extraction of this residue with toluene and cooling the solution yielded a crystalline product analysing as $[W(NPh)(OMe)_3Cl]_n$ (**3**) where it is proposed n = 2. Methylimido tungsten tetrachloride reacted with $MeOH/Me_3CNH_2$ to give $[W(NMe)(\mu\text{-}OMe)(OMe)_3]_2$ (**2**) in approximately 50% yield but the petroleum ether insoluble material did not yield a single crystalline product on extraction with toluene.

The X-ray crystal structure analysis of (**1**) shows the molecule to be a dimer with the two halves centrosymmetrically related. Each tungsten adopts a distorted octahedral coordination geometry with oxygen donors of 2 methoxy groups forming bridges between them. The phenylimido group is *trans* to one of these bridges. A view of the molecule is shown in Fig. 1. Bond distance and angle data are given in Tables 1 and 2.

The phenylimido group is essentially linear with a W–N̂–C(1) angle of 174(2)°. The short W–N bond distance of 1.61(4)° indicates considerable multiple bond character for this bond and the value is in accord with that predicted (1.71 Å) by Nugent and Haymore for a W–N triple bond.[1] It also lies within the range of values found (1.61–1.77 Å) in other tungsten imido complexes.[8,9] A slight *trans* lengthening of the W–O(1′) bond (2.16 Å) is noted resulting in an asymmetric bridging arrangement. The three terminal methoxy ligands approach more closely to the tungsten atom than do their bridging counterparts with observed W–O distances of 1.92(3), 1.92(2) and 1.89(3) Å. These bond lengths are comparable with those observed in other alkoxide complexes.[10] The slightly longer distances of 2.05(2) and 2.16(2) Å for W–O(1) and W-O(1′) respectively are also in accord with those found in comparable bridging alkoxy groups.

The octahedral coordination geometry is distorted away from an ideal arrangement with the atoms O(1), O(2), O(3), and O(4) being displaced away from the imido nitrogen towards the *trans* donor (the average angle subtended by N and each of the above four O donors at W is 99°). Such a distortion has been observed in other complexes involving the phenylimido and related, nitrido, ligands where a relatively short M–N distance is found.[11]

Reaction of EtOH with phenylimido tungsten tetrachloride gave a toluene soluble product analysing as $W(NPh)(OEt)_3Cl$ (**4**) for which pre-

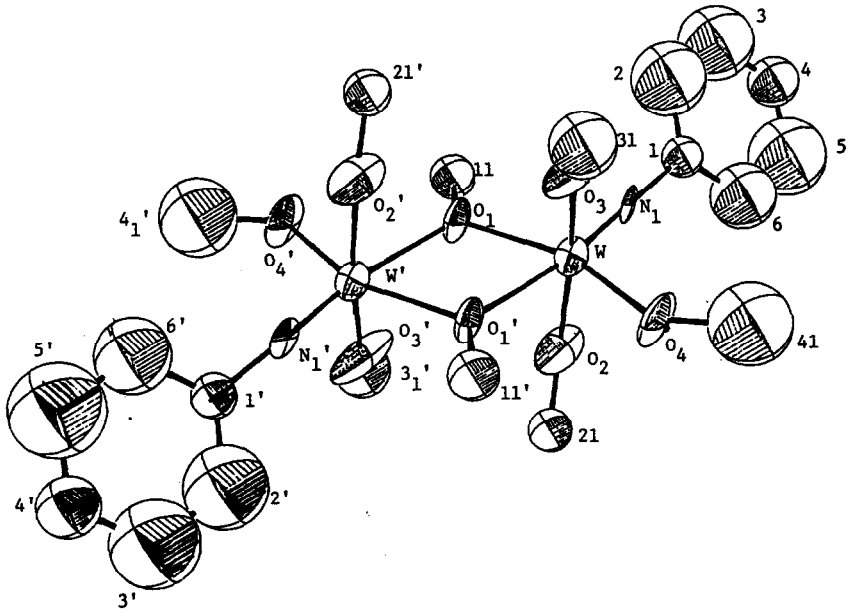
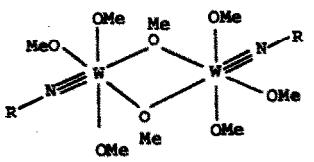
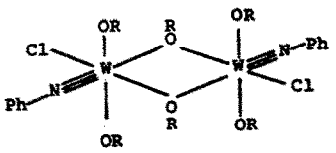


Fig. 1. The $[W(NPh)(\mu\text{-}OMe)(OMe)_3]_2$ molecule. Thermal ellipsoids have been drawn at the 50% probability level. Hydrogen atoms have been omitted for clarity.



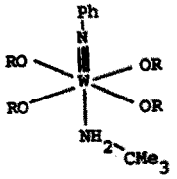
(1) R = Ph

(2) R = Me



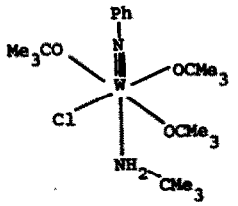
(3) R = Me

(4) R = Et

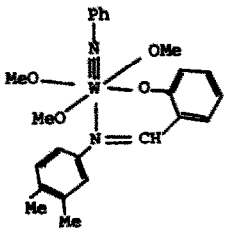


(5) R = $CHMe_2$

(6) R = CH_2CMe_3



(7)



(8)

Table 1. Bond distances (in Å) for $[W(NPh)(\mu\text{-}OMe)(OMe)_3]_2$. Standard deviations are in parentheses

W - N	1.61(4)	W ..W	3.467(4)
W - O(1)	2.05(2)	N - C(1)	1.48(4)
W - O(1′)	2.16(2)	O(1)- C(11)	1.46(5)
W - O(2)	1.92(3)	O(2)- C(21)	1.38(5)
W - O(3)	1.89(3)	O(3)- C(31)	1.27(7)
W - O(4)	1.92(2)	O(4)- C(41)	1.43(9)

liminary X-ray crystallographic results show a bridging ethoxide. *iso* Propyl and *neo*pentyl alcohols reacted to give yellow crystalline complexes $[W(NPh)(OR)_4(NH_2CMe_3)]$ [R = $CHMe_2$ (**5**), R = CH_2CMe_3 (**6**)] with little apparent formation of petroleum ether insoluble material. Replacement of Me_3CNH_2 by PMe_3 occurred for (**5**) but the product $[W(NPh)(OCHMe_2)_4(PMe_3)]$ (**9**) could only be obtained as an oil and was characterised by IR and proton NMR spectroscopy.

t-Butanol reacted with $W(NPh)Cl_4$ and *t*-butylamine to give the complex $W(NPh)(OCMe_3)_3Cl(NH_2CMe_3)$ (**7**), this being the only product even with excess alcohol and extended reaction periods. This complex failed to give clean reaction products on further reaction with $LiOCMe_3$ or *t*-butanol in the presence of ammonia gas. However, reaction of phenylimido tungsten tetrachloride with four equivalents of $LiOCMe_3$ in diethyl ether gave $W(NPh)(OCMe_3)_4$ which was recently reported by Schrock.[12] Phenylimido tungsten tetrachloride when reacted with *t*-butanol/NH_3 failed to give a characterisable product.

The X-ray crystal structure analysis of (**7**) shows this molecule to be monomeric with the expected distorted octahedral coordination geometry. There are no unusual intermolecular contacts. Bond length and angle data are listed in Tables 3 and 4. Figure 2 gives a view of the molecule and shows the phenylimido and amino ligands occupying *trans* coordination sites. The geometry of the former group conforms to the expected as outlined for (**1**) with an approximately linear bridging mode (W–N(1)–C(1) 171(1)°) and a short W–N(1) bond distance of 1.71(2) Å indicating essentially triple bond character. The increase in the average N(1)–W-donor angle to 98.2° is also expected and has been commented on previously for (**1**). The *trans* influence of the phenylimido group is apparent from the long W–N(3) bond distance of 2.40(2) Å, a value which is longer than in comparable complexes.[13] It reflects the purely σ-nature of the W–N (amino) bond. The two *trans* tertiary butoxide groups have W–O distances {W–O(2) 1.86(1) and W–O(4) 1.91(2) Å} which are indistinguishable from one another and from their *cis* counterpart [W–O(5) 1.85(1)]. The three are consistent with a measure of π-donation from the oxygen donors. The W–Cl bond distance of 2.500(4) is long and has a value lying at the upper limit of the range for this ligand.[14]

Results of preliminary work show that $[W(NPh)(\mu\text{-}OMe)(OMe)_3]_2$ (**1**) is a convenient starting material for the synthesis of other W(VI) imido complexes. Thus reaction with *o*-$HOC_6H_4CH{=}NC_6H_3Me_2$ (salim-H) gave the salicylaldiminato complex $[W(NPh)(OMe)_3(salim)]$ for which we propose structure (**8**) based on the preference, determined crystallographically in (**1**)

Table 2. Bond angles (in deg.) for $[W(NPh)(\mu\text{-}OMe)(OMe)_3]_2$. Standard deviations are in parentheses

N - W - O(1)	100(1)	O(2) - W - O(3)	167(2)
N - W - O(1′)	168(1)	O(2) - W - O(4)	88(1)
N - W - O(2)	98(2)	O(3) - W - O(4)	87(1)
N - W - O(3)	95(2)	W - N - C(1)	174(2)
N - W - O(4)	103(1)	W - O(1)- W′	112(1)
O(1)- W - O(1′)	68(1)	W - O(1)- C(11)	121(2)
O(1)- W - O(2)	88(1)	W′ - O(1)- C(11)	128(2)
O(1)- W - O(3)	92(1)	W - O(2)- C(21)	134(3)
O(1)- W - O(4)	157(1)	W - O(3)- C(31)	151(5)
O(1′)- W - O(2)	81(1)	W - O(4)- C(41)	131(4)
O(1′)- W - O(3)	86(1)	N - C(1)- C(2)	118(2)
O(1′)- W - O(4)	88(1)	N - C(1)- C(6)	122(2)

Table 3. Selected bond distances (Å) for $[W(NPh)(OCMe_3)_3Cl(NH_2CMe_3)]$. Standard deviations are in parentheses

W - Cl	2.500(6)	N(1) - C(1)	1.41(2)
W - N(1)	1.71(2)	O(2) - C(21)	1.44(3)
W - O(2)	1.86(1)	N(3) - C(31)	1.44(3)
W - N(3)	2.40(2)	O(4) - C(41)	1.44(3)
W - O(4)	1.91(2)	O(5) - C(51)	1.43(3)
W - O(5)	1.85(1)		

Table 4. Selected bond angles (°) for $[W(NPh)(OCMe_3)_3Cl(NH_2CMe_3)]$. Standard deviations are in parentheses

W - N(1) - C(1)	171(1)	N(1) - W - O(2)	101.2(7)
W - O(2) - C(21)	153(1)	N(1) - W - N(3)	168.4(7)
W - N(3) - C(31)	130(2)	N(1) - W - O(4)	98.6(7)
W - O(4) - C(41)	147(1)	N(1) - W - O(5)	102.7(7)
W - O(5) - C(51)	143(1)	O(2) - W - N(3)	79.4(7)
Cl - W - N(1)	90.3(5)	O(2) - W - O(4)	158.2(6)
Cl - W - O(2)	87.0(4)	O(2) - W - O(5)	91.8(6)
Cl - W - N(3)	78.1(5)	N(3) - W - O(4)	79.3(7)
Cl - W - O(4)	84.0(5)	N(3) - W - O(5)	99.0(6)
Cl - W - O(5)	166.9(5)	O(4) - W - O(5)	92.5(6)

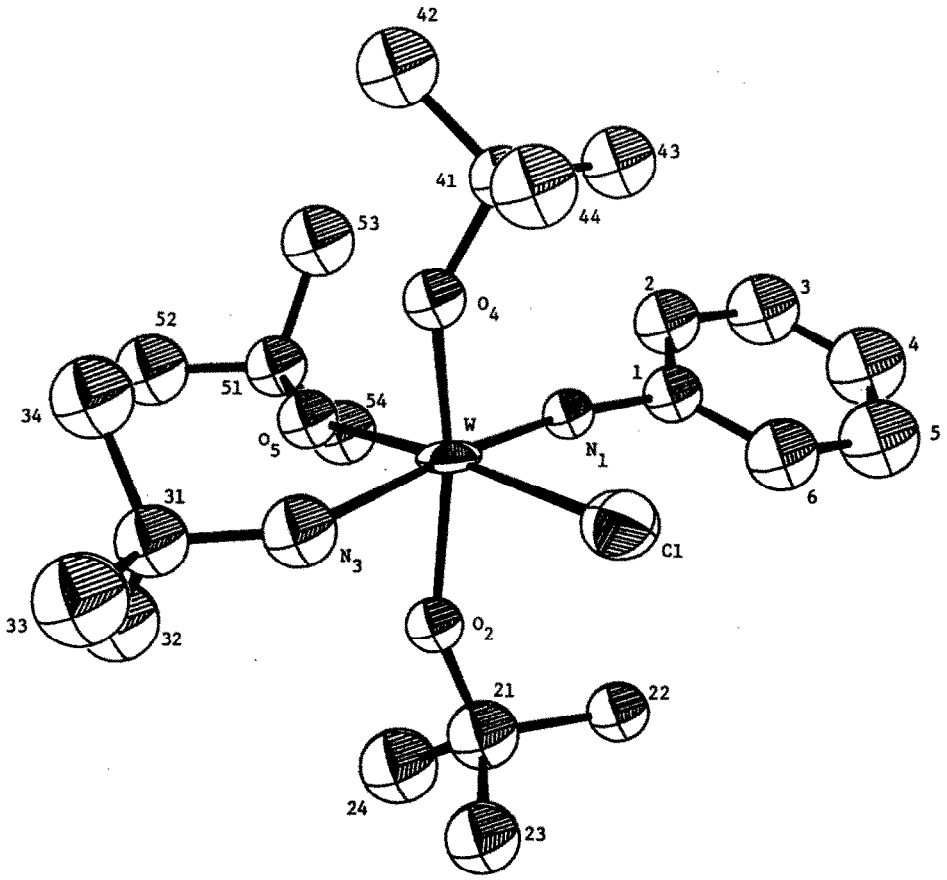


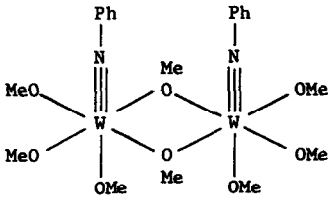
Fig. 2. The $[W(NPh)(OCMe_3)_3Cl(NH_2CMe_3)]$ molecule. Thermal ellipsoids have been drawn at the 50% probability level. Hydrogen atoms have been omitted for clarity.

and (7), for the neutral ligand to coordinate *trans* to the imido function.

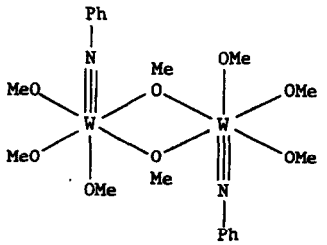
IR spectra. Characteristic ν(C–O) and ν(M–O) IR absorptions are shown in Table 5. Bridging and terminal modes were assigned for (4) by comparison with the complexes $[M(OEt)_5]_2$ (M = Nb, Ta[15]) but as the other proposed dimers do not react with bridge splitting ligands L(L = Py, PPh_3, PMe_3, etc.) the specific absorptions attributable to bridging alkoxide cannot be ascertained by comparison with a monomeric species. However, the complexes are most likely alkoxy bridged as in (1), with ν(M–Cl) falling in the vicinity of 320 cm^{-1}. In addition to absorptions found for *iso* propoxides, the spectrum of complex (5) contains a strong doublet at 1365 and 1350 cm^{-1} characteristic of *gem*-dimethyl groups.[16] The *neo*-pentoxy complex (6) shows only two ν(C–O) absorptions at similar frequency to the free ligand. In the ν(M–O) region of the *t*-butoxy complex (7), containing mutually *trans* alkoxides and a *trans* chloro alkoxide, three strong absorptions occurred.

We have been unable to assign ν(WN) for the complexes since the 1100–1300 cm^{-1} metal imido region contains several ligand vibrations. In the case of the dimers (1)–(4), this region is free of absorptions. However we note a strong band near 1380 cm^{-1} in the phenyl imido complexes, which shifts to 1310 cm^{-1} in the methylimido complex (2), and which, although outside the recognised range,[1] may represent this vibration.

NMR spectra. Well-resolved singlets at δ 4.34 and 4.59 ppm (1 : 3 ratio) were observed for bridging and terminal methoxy groups in the hydrogen-1 NMR spectrum of complex (1) indicating little intermolecular exchange at 32 °C. Another isomer (bridging and terminal methoxide singlets at 4.42 and 4.63 ppm respectively,—ratio 1 : 3) was found consistently at 20% of the total after repeated recrystallisations of samples obtained from NH_3, Et_3N or Me_3CNH_2 base reactions. At lower temperatures, peak broadening obscured the minor component resonances so that dynamic processes could not be studied. However since the X-ray cyrstallographic structure of (1) showed bridging methoxide *trans* to the phenylimido moiety, structures (1a) and (1b) are not preferred and a species of higher association may be present.



(1a)



(1b)

Several methoxide resonances were observed for the proposed dimer $[W(NPh)(OMe)_3Cl]_2$ but precipitation occurred before frozen-out spectra could be obtained at lower temperatures. Similarly, a complex set of quartets arose for the methylene quartet of the ethoxy group in $[W(NPh)(OEt)_3Cl]_2$ with little apparent freezing out at low temperatures before solubility problems were encountered.

For the *iso*propoxy complex (5), the CH septet appeared at δ 4.98 ppm, occurring 0.4 and 0.6 ppm downfield from the α-CH proton resonances of the terminal methoxy and *neo*pentoxy groups respectively in (1) and (6). Although not structurally characterised in these complexes we believe the *t*-butylamine nitrogen to lie *trans* to the phenylimido group, as found for the *t*-butoxy complex (7). Molecular models indicate less steric crowding for four equatorial *iso*propoxides in which the α-CH protons are directed above the plane, orientated so that they would experience anisotropy effects associated with the W≡NPh function. While it is apparent that the influence should reduce on increasing the C–O–W bond angle, the CH septet does not shift when the bulky Me_3CNH_2 ligand is replaced by PMe_3. Protons attached to the α-carbon of the *neo*pentoxy ligands are directed away from the influence of anisotropy which is reflected in the higher field shift. The lone doublet observed for the methyl groups of (5) and the methylene singlet of (6) suggest lack of the asymmetry, in accord with the structures proposed.

In the aromatic region, the *ortho* protons appear to be influenced by anisotropy effects generated at the imido linkage, as well as by alkoxide proximity. The aromatic protons in (1) compose a roughly symmetrical sextet, the lower field triplet comprising of 2 protons. For *iso*propoxy complex (5) the *ortho* protons shift further downfield while the *neo*pentoxy complex(6) produces a two proton lower-field triplet and a one proton triplet at higher field. Although the aromatic region shows apparent deceptive simplicity it is interesting to note that with small cross-ring couplings, the latter triplet approximates to the A part of an AB_2 system.

Methoxide resonances in a ratio of 2 : 1 observed

Table 5. Physical data for organo-imido alkoxide complexes of tungsten (VI)

Complex	m.pt. (°C)	Analyses[a] (%) C	H	N	I.r. spectra (cm^{-1}) ν(C-O[h])	ν(W-O)	^{1}H n.m.r. spectra[b,c] (δ) alkoxide[h]	others
(1) [W(NPh)(μ-OMe)(OMe)$_3$]$_2$[e]	106-108	30.1 (30.1)	4.3 (4.3)	3.5 (3.5)	1100,1060(*t*) 1010(*b*)	525,502	4.34 (s,3H,Me*b*) 4.59 (s, H,Me*t*)	6.52 (m,5H,aromat.)
(2) [W(NMe)(μ-OMe)(OMe)$_3$]$_2$	90-92	18.0 (17.8)	4.9 (4.5)	4.2 (4.2)	1100,1065(*t*) 1010(*b*)	510	4.18 (s,3H,Me*b*) 4.37 (s,6H,Me*t*)	4.86 (s[f],3H,NMe)
(3) [W(NPh)(μ-OMe)(OMe)$_2$Cl]$_2$[d]	120-122	26.6 (26.8)	3.5 (3.5)	3.4 (3.5)			4.43 (s,3H.Me*t* 4.40,4.65,4.79 4.87,5.0,5.08 (5s[6:1.5:8:1:2:5], 9H,Me)	7.1 (m,5H,aromat)
(4) [W(NPh)(μ-OEt)(OEt)$_2$Cl]$_2$[d]	164-166	32.5 (32.3)	4.6 (4.5)	3.1 (3.1)	1142,1090,920(*t*) 1030,882(*t*)	528,480	1.34 (m,9H,Me) 5.0-5.8 (m,6H,CH_2)	7.1-7.8 (m,5H,aromat)
(5) W(NPh)(OCHMe$_2$)$_4$(NH_2CMe_3)		44.4 (45.2)	8.1 (7.6)	4.5 (4.8)	1165,1105,974	600	1.20 (d[g],24H,Me) 4.92 (sep[g],4H,CH)	1.26 (s,9H,CMe_3) 2.52 (b,2H,NH_2) 7.15 (m,5H,aromat)
(6) W(NPh)(OCH_2CMe_3)$_4$(NH_2CMe_3)	138-140	51.3 (51.7)	9.0 (8.7)	4.0 (4.0)	1076,1018	642	0.94 (s,36H,CMe_3) 4.22 (s,8H,OCH_2)	1.29 (s,9H,CMe_3) 2.68 (b,2H, NH_2 7.0 (m,5H,aromat)
(7) W(NPh)($OCMe_3$)$_3$Cl(NH_2CMe_3)[e]	125-128	43.3 (43.8)	6.9 (7.2)	4.8 (4.6)	955	576,552, 538	1.32[i] (s,27H,CMe_3)	1.32[i] (s,9H,CMe_3) 2.57 (b,2H,NH_2) 6.66 & 6.92 (m,5H,aromat)
(8) W(NPh)(OMe)$_3$(salim)	102-104	48.7 (48.7)	5.1 (4.8)	4.7 (4.7)	1143,1050	560,530, 500	4.32 (s,6H,Me) 4.80 (s,3H,Me)	1.87 & 2.02 (s,6H,Me) 6.02-7.2 (m,12H,aromat) 7.65 (s,1H,CH)

[a]Calculated figures are given in parentheses. [b]Data for $CDCl_3$ solutions. [c]Assignment given in parentheses, s=singlet, d=doublet, m=multiplet, t=triplet, sep=septet, b=broad. [d]Structures proposed as alkoxy bridged dimers. [e]Characterised by X-ray crystallography. [f]183-W sidebands at 4.80 and 4.92 ppm. [g]J = 6 Hz. [h]*b* = bridging alkoxide, *t* = terminal alkoxide. [i]Resonance overlap.

for salicylaldiminato complex (**8**) are tentatively ascribed to two mutually *trans* methoxides and methoxide *trans* to the phenoxy ligand respectively. The upfield shift of 0.72 ppm for the methine proton compared with the free ligand confirmed coordination of the salim.

Carbon-13 spectra of the complexes (Table 6) show deshielding of the alkoxy α-carbon on coordination and little change for the remainder. The methoxy dimer (**1**) exhibits three α-carbon resonances in approximate ratio of 1 : 2 : 1 of which the lower field resonance is tentatively assigned to bridging methoxide and the remaining 2 : 1 resonances to *trans* terminal and *trans* bridging methoxide respectively. Both the *iso*propoxy and *neo*pentoxy complexes show only one α-carbon resonance being consistent with the four meridional alkoxides proposed. The *t*-butoxy complex (**7**) exhibits two α-carbons in an approximate 2 : 1 ratio, the former assigned to two mutually *trans*-*t*-butoxides and the latter to *t*-butoxide *trans* to chloride.

Strong deshielding of the *ipso* aromatic carbons occurs in the complexes similar to nitro benzene[17] where electron withdrawal from the ring is found. Table 7 shows increased *ipso*-carbon deshielding with increase in + I effect of the alkoxy *R* group but steric effects may also be involved. However C-*para* shows increasing shielding with increasing *R* group + I effect, where steric considerations are not important. The inconsistent *t*-butoxy complex probably involves deshielding contributions from chlorine which are manifest in the complex [W(NPh)Cl_4(NCEt)]. Bond order and excitation energy would vary little in the PhNW system of complexes (**5**), (**6**) and (**7**), correlation of electron density with chemical shift may be apparent, making C-*para* sensitive to electron donation from the alkoxy ligands. If oxygen and imido nitrogen share tungsten π-orbitals of similar energy a mechanism for this essentially *cis* effect would exist.

Mass spectra. Parent molecular ions were not observed for any of the complexes and only for the larger alkoxides were low abundant species (0.1–0.5%) observed with the correct isotope pattern. For [W(NPh)$(OCHMe_2)_4(NH_2CMe_3)$] (**5**) the species $W(NPh)(OCHMe_2)_n^+$ were observed for $n = 1$, 3 and 4 but not for $n = 2$. Data for lower mass components showed that considerable synthetic chemistry had occurred in the mass spectrometer with the low abundant molecular ions $WO(OCHMe_2)_n^+$ ($n = 3$, 2), $W(NPh)O(H)_2^+$, $W(NPh)OH^+$, $W(NPh)O^+$ and even $CpWH_2^+$. The *neo*pentoxy complex (**6**) exhibited W(NPh)$(OCH_2CMe_3)_3(OCCMe)^+$ as the only imido species present but mass data for $WO(OCH_2CMe_3)_4^+$ and other species related to this by methyl group loss were identified. Isotope patterns consistent with fragment $W(OCH_2CMe_3)_3(OCH_2CMe_2)^+$, $W(OCH_2CMe_3)_3(OCH_2CMe_2CH_2)^+$ and $W(OCH_2CMe_3)_3(OCHCMe_2)^+$ were also observed.

Several fragments were observed for W(NPh)$(OCMe_3)_3Cl(NH_2CMe_3)$ (**7**) but the profusion of peaks at lower mass number did not allow a reliable determination of metastable peaks. The mass spectrum showed the most abundant species were derived from the loss of $OCMe_3$ groups with the fragments $W(NPh)(OCMe_3)_nCl^+$ ($n = 3$, 2, 1), $W(NPh)(OCMe_3)_n^+$ ($n = 3$, 2) and similar species $W(OCMe_3)_nCl^+$ ($n = 3$, 2), resulting from loss of the imido function.

EXPERIMENTAL

$WOCl_4$ was prepared by reaction of WO_3 with thionyl chloride;[18] $[PhNWCl_4]_n$ by reaction of $WOCl_4$ with phenylisocyanate.[19] Trimethylphosphine was prepared by a literature method.[20] Alcohols were distilled from the magnesium alkoxide under nitrogen prior to use and *neo*pentyl alcohol was used as supplied. *t*-Butylamine was distilled from calcium hydride and stored in a Schlenk flask under N_2. Petroleum ether and toluene were distilled from sodium wire under N_2. All manipulations were carried out under streams of nitrogen using normal air-sensitive techniques. IR spectra were recorded on a Perkin–Elmer 597 spectrometer, ^1H NMR on a Varian T60 Model spectrometer and ^{13}C NMR spectra on a Jeol FX60 spectrometer. Mass spectra were obtained on an AEI MS 902 instrument at Queen Mary College, with direct insertion using probe temperatures ranging from 50–65° at 70 eK and accelerating voltages of 4, 6 or 8 kV. Data were based on ^{182}W and ^{35}Cl. Analytical data were obtained by Professor A.D. Campbell and associates, University of Otago, New Zealand. Melting points were determined in sealed tubes under nitrogen on an electrothermal melting point apparatus and are uncorrected.

Di-μ-methoxyhexakismethoxybis(phenylimido) ditungsten(VI) (**1**). *t*-Butylamine (2.53 cm^3, 24 mmol) was added to a well stirred suspension of finely ground phenylimido tungsten tetrachloride (2.0 g, 4.8 mmol) in petroleum ether (150 cm^3). Methanol (1.0 cm^3, 25 mmol) in petroleum ether (50 cm^3) was immediately added and the mixture stirred for 6 hours. The yellow solution was filtered, the precipitate washed with petroleum ether (50 cm^3) and the combined filtrates reduced to *ca.* 30 cm^3 *in vacuo*. On cooling in dry ice–acetone the complex separated as yellow microcrystals which were filtered off and washed with cold (*ca.* −40 °C)

Table 6. ^{13}C NMR data for phenylimido tungsten alkoxide complexes (ppm from tms) in $CDCl_3$

Complex	Alkoxide		Amine		Aromatics[b,c]
	α-carbon[a]	β-carbon	α-carbon	β-carbon	
$[W(NPh)(\mu\text{-}OMe)(OMe)_3]_2$ (1)	62.79, 10.29	-	-	-	126.71 (*p*)
	63.14, 10.64				127.85 (*o,m*)
	64.96, 12.46				151.35 (*i*)
$W(NPh)(OCHMe_2)_4(NH_2CMe_3)$ (5)	75.61, 8.71	25.81	50.13	30.71	124.73 (*p*)
					126.75 (*m*)
					127.59 (*o*)
					152.91 (*i*)
$W(NPh)(OCH_2CMe_3)_4(NH_2CMe_3)$ (6)[b]	84.80, 8.7	33.50	49.97	29.80	126.52 (*o,m,p*)
					152.48 (*i*)
$W(NPh)(OCMe_3)_3Cl(NH_2CMe_3)$ (7)	81.00, 9.1	31.36	50.58	30.68	125.67 (*m,p*)
	83.14, 11.24				127.42 (*o*)
					153.62 (*i*)
$W(NPh)(OCMe_3)_4$	81.42, 9.52	31.36	-	-	125.25 (*p*)
					127.00 (*m*)
					127.75 (*o*)
					153.88 (*i*)

[a] Downfield shifts on coordination of alcohol are italicised. [b] Assignment given in parentheses, *o* = *ortho*, *m* = *meta*, *p* = *para*, *i* = *ipso*, *p*-carbon assigned from peak height, *m,o*-carbons tentatively assigned (*o*-carbon downfield in (1) and (7).
[d] γ-Carbon of OCH_2CMe_3 29.80.

Table 7. Carbon 13 data for the aromatic resonances in relation to benzene[a]

Complex	*ipso*	*ortho*	*meta*	*para*
$[W(NPh)(\mu\text{-}OMe)(OMe)_3]_2$	+22.85	-0.65	-0.65	-1.79
$W(NPh)(OCH_2CMe_3)_4(NH_2CMe_3)$	+23.98	-1.98	-1.98	-1.98
$W(NPh)(OCHMe_2)_4(NH_2CMe_3)$	+24.36	-0.91	-1.75	-3.77
$W(NPh)(OCMe_3)_3Cl(NH_2CMe_3)$	+25.12	-1.08	-2.83	-2.83
$W(NPh)(OCMe_3)_4$	+25.38	-0.75	-1.50	-3.25
$W(NPh)Cl_4(NCEt)$[b]	+20.48	+3.23	+3.08	+6.00
$PhNO_2$[c]	+20.0	-4.8	+0.9	+5.8

[a]Benzene 128.5 ppm, relative to TMS. Positive values indicate deshielding, negative values indicate shielding.

[b]Values taken from ref.8. [c]Values taken from ref. 17. *para*-Carbon assigned from relative peak height, *ortho*- and *meta*-carbons tentative assignment.

petroleum ether (20 cm^3). Reduction in volume of the mother liquors and cooling to −78 °C gave a further crop of crystalline material. Yield: 1.2 g (63%).

IR (Nujol) bands at 1578 w (aromatic C=C), 1380s, 1170m, 1152m, 1100s, 1060s and 1010 (ν(C–O)), 868s, 860s and 790 (monosubstituted benzene), 570w, 525s (ν(M–O) terminal), 502s (ν(M–O) bridge), 390w, 328w, 289w cm^{-1}.

Dichloro-di-μ-methoxytetramethoxybis(phenylimido)ditungsten(VI) (**3**). Methanol (0.47 cm^3, 11.5 mmol) and *t*-butylamine (1.52 cm^3, 14.4 mmol) in petroleum ether (50 cm^3) were added to phenylimido tungsten tetrachloride (1.2 g, 2.9 mmol) suspended in petroleum ether (80 cm^3) and the mixture stirred for 6 hours and filtered. The residue was extracted with toluene (2 × 50 cm^3), the solution filtered and the combined extracts reduced in volume to *ca.* 15 cm^3. On standing at −20 °C the solution deposited the complex as a microcrystalline solid. Yield: 0.58 g (51%), similar IR spectrum to (**1**).

Dichloro-di-μ-ethoxytetraethoxybis(phenylimido)ditungsten(VI) (**4**). Ethanol (0.67 cm^3, 11.5 mmol) and *t*-butylamine (1.1 cm^3, 14.7 mmol) in petroleum ether (50 cm^3) were added to phenylimido tungsten tetrachloride (1.2 g, 2.9 mmol) suspended in petroleum ether (60 cm^3) and the mixture stirred for 4 hr. The solvent was filtered off and discarded. The yellow residue was extracted with warm toluene (2 × 30 cm^3) and the combined extracts filtered. Reduction of the volume to *ca.* 10 cm^3 and standing the solution at −20 °C gave the complex as yellow crystals. Yield: 0.82 g (64%).

IR (Nujol) bands at 1580w (C=C, aromatic), 1430s, 1355s, 1272m and 1090s (ν(C–O) terminal), 1030s (ν(C–O) bridge), 920s (ν(C–O) terminal), 882s (ν(C–O) bridge), 805w, 760s and 688s (monosubstituted benzene), 640s, 600m, 555s, 528s, (ν(W–O) terminal), 480s, (ν(W–O) bridge), 382m, 326m, 320m, 284m cm^{-1} (ν(W–Cl) terminal).

*t-Butylaminotetra*isopropoxy*(phenylimido)tungsten*(VI) (**5**). *t*-Butylamine (1.26 cm^3, 12 mmol) was added to phenylimido tungsten tetrachloride (1.0 g, 2.4 mmol) suspended in petroleum ether (100 cm^3). *iso*Propanol (0.75 cm^3, 9.9 mmol) in petroleum ether (50 cm^3) was added immediately and the mixture stirred for 6 hr. The yellow solution was filtered and the solvent volume reduced to *ca.* 5 cm^3 whereupon the complex precipitated as yellow crystals. Cooling the solution to −76 °C gave further crystalline material which was filtered, washed with cold petroleum ether (10 cm^3 at *ca.* −76 °C) and dried *in vacuo*. Yield: 1.0 g (71%).

IR (Nujol) bands at 1600m and 1580s (NH), 1480s, 1355s, 1320s, 1272s, 1215m, 1160s and 1105s, (ν(C–O) terminal), 1025m, 1005m, 974s, (ν(C–O) terminal), 922m, 910m, 840s, 785m, 758s and 688s (mono substituted benzene), 580s (ν(W–O) terminal), 535s, 450s, 420m, 320m, 290m cm^{-1}. *m/e* 509.1 $[W(NPh)(OCHMe_2)_4^+]$, 450.2 $[W(NPh)(OCHMe_2)_3^+]$, 375.0 $[WO(OCHMe_2)_3^+]$, 332.8 $[W(NPh)(OCHMe_2)^+]$, 291 $[W(NPh)(O)H_2]$, 290 [W(NPh)(O)H], 289.8 [W(NPh)(O)], 248.9 $[WCpH_2]$.

*t-Butylaminotetra*neopentoxy*(phenylimido)tungsten*(VI) (**6**). *neo*Pentanol (1.0 g, 11.5 mmol), phenylimido tungsten tetrachloride (1.2 g, 2.9 mmol) and *t*-butylamine were reacted together and the product isolated as for complex (**5**). Yield: 1.25 g (63%).

IR (Nujol) bands at 1600m (NH), 1470s, 1358s, 1272m, 1288m, 1258m, 1056s and 1018s (ν(C–O) terminal), 933m, 840m, 785m, 755m, and 682 (mono substituted benzene), 645s (ν(W–O)), 450m, 400w, 342w cm^{-1}. *m/e* 588.9 $[W(NPh)(OCH_2CMe_3)_3(OC_2{=}CMe)^+]$, 528.6 $W[OCH_2CMe_3)_3(OCH_2CMe_2CH_2)^+]$, 515.5 $[W(OCH_2CMe_3)_3(OCH_2CMe_2)^+]$, 514.6 $[W(OCH_2CMe_3)_3(OCHCMe_2)^+]$.

tris(t-butoxy)t-butylaminochloro(phenylimido)tungsten(VI). (**7**). *t*-Butanol (1.45 cm^3, 15.5 mmol) in petroleum ether (30 cm^3) was added to phenylimido tungsten tetrachloride (1.3 g, 31.0 mmol) in petroleum ether (60 cm^3) containing *t*-butylamine (1.64 cm^3 15.5 mmol) as for (**5**). After stirring for 4 hr the solution was filtered, the solvent removed, and the residue held *in vacuo* to remove excess *t*-butanol. The remaining solid was dissolved in petroleum ether (30 cm^3), the solution concentrated to *ca.* 10 cm^3 and left to stand at −20°C giving the complex as large yellow crystals. Yield: 1.32 g (70%).

IR (Nujol) bands at 1600w (C=C, aromatic), 1580, 1564w (NH), 1480s, 1358s, 1260w, 1225m, 1164s, 1130w, 1120w, 1024m, 955s, (ν(C–O) terminal), 780s, 758s and 590m (mono substituted benzene), 575m, 550m and 538m (ν(W–O)), 464m, 380w, 370w, 350w, 280w $(\nu(W\text{–}Cl)^{cm^{-1}}$.

Tetra-t-butoxy(phenylimido)tungsten(VI). The complex was prepared by adding $LiOCMe_3$ (1 g, 12 mmol) in diethyl ether (20 cm^3) to $[W(NPh)Cl_4]_n$ (1.3 g, 3 mmol) dissolved in diethyl ether (30 cm^3) and stirring the solution for 12 hr. After filtering, the solvent was removed and the residue recrystallised from petroleum ether. The properties of the complex were recently described.[12]

Tetrachloro(methylimido)tungsten(VI). Tungsten oxytetrachloride (5.5 g, 16.1 mmol) and methylisocyanate (0.95 cm^3, 16.1 mmol) were refluxed in benzene (75 cm^3) for 12 hr. The solution was

filtered while hot and the volume reduced to *ca.* 30 cm^3 whereupon orange crystals of the product were deposited. Yield: 2.3 g (40%). Reduction of the solvent volume gave further product which was contaminated with $WOCl_4$. (Found: C, 3.9; H, 1.0; N, 3.6. CH_3Cl_4NW requires C, 3.4; H, 0.9; N, 3.9%.) The complex (0.1 g) was dissolved in propionitrile and the solvent removed to give a yellow solid soluble in chloroform. ^1H NMR $\delta(CDCl_3)$ 2.44 (t, 3H, Me), 2.65 (q, 3H, CH_2), 6.83 (s, 3H, NMe), ^{183}W sidebands at 6.74 and 6.92 ppm.

Di-μ-methoxyhexakismethoxybis(methylimido) ditungsten(VI) (**2**). Methanol (4.1 cm^3, 10.2 mmol) in petroleum ether (50 cm^3) was reacted with a mixture of methylimido tungsten tetrachloride (0.9 g, 2.56 mmol) and *t*-butylamine (1.34 cm^3, 12.7 mmol) as for the preparation of $[W(NPh)(\mu\text{-}OMe)(OMe)_3]_2$ (**1**). The resulting colourless solution was filtered and the solvent removed to give a white solid shown to be the pure complex by ^1H NMR. Yield: 0.48 g (57%). Recrystallisation from petroleum ether/CCl_4 (1 : 1) gave the complex as large colourless prisms.

IR (Nujol) bands at 1458s, 1304s, 1280m, 1158s, 1100s and 1070s and 1020s (ν(C–O)), 800m, 720w, 575s, 510s (ν(W–O)), 420m, 330m, 295m cm^{-1}.

N(Phenyl-3,4-dimethyl)salicyldiminato(phenylimido)trismethoxytungsten(VI) (**8**). To a solution of di-μ-methoxyhexakismethoxybis(phenylimido)-ditungsten(VI) (1.2 g, 3.0 mmol) in benzene 30 cm^3) was added N(phenyl-3,4-dimethyl)-salicylaldimine (0.68 g, 3.0 mmole) in benzene (20 cm^3) and the solution stirred for 3 hr. The solvent was removed *in vacuo* and the resulting oil washed with petroleum ether (50 cm^3) followed by diethyl ether (2 × 50 cm^3 portions) to give the complex as a yellow solid. Yield: 1.77 g (99%).

IR (Nujol) band at 1595s, 1536m, 1455s, 1358m, 1332m, 1300s, 1192m, 1143s, and 1050s (ν(C–O) terminal), 990w, 948w, 918w, 885w, 840m, 760s, 750s, 685m, 668m, 560s and 530s and 500s (ν(W–O)), 420w, 400m, 318m, 280w cm^{-1}.

Tetra-iso-*propoxy(phenylimido)trimethylphosphinetungsten*(VI) (**9**). Trimethylphosphine (0.15 cm^3, 1.36 mmol) was added to *t*-butylamino-tetra-*iso*-propoxyphenylimidotungsten(VI) (**5**) (0.5 g, 0.85 mmol) dissolved in petroleum ether (30 cm^3) and the mixture stirred for 3 hr. The solution was filtered and the solvent removed to give a yellow-brown gum which failed to solidify on standing or by attempted crystallisation from petroleum ether or CCl_4. Yield: 0.5 g (100%).

IR (Nujol) bands at 1600m (C=C, aromatic), 1580m (PMe_3), 1480s, 1360s, 1320s, 1275s, 1215m, 1160s, and 1120s (ν(C–O) terminal), 1064m, 1022m, 970s,b (PMe_3 and (C–O) terminal), 900m, 840s, 790s, 760s and 590s (monosubstituted benzene), 600s (ν(W–O)), 525m, 450m, 423m, 380w, 300w cm^{-1}. ^1H NMR $\delta(CDCl_3)$ 1.2 (*d*(J = 6 Hz), 24H, Me), 1.24 (*d*(J = 3 Hz), 9H, PMe_3), 4.87 (septet 4H, methylenes), 6.84 (m, 5H, aromatic Hs).

X-ray data collection and structure solution Crystals of both $[W(NPh)(\mu\text{-}OMe)(OMe_3)]_2$ and $W(NPh)(OCMe_3)_3Cl(NH_2CMe_3)$ were sealed under nitrogen in capillaries and mounted on an Enraf–Nonius CAD4 diffractometer. For each crystal cell constants were determined from a least-squares refinement of the setting angles of 23 reflections.

Crystal data for $[W(NPh)(\mu\text{-}OMe)(OMe)_3]_2$: $C_{20}H_{34}N_2O_8W_2$, M = 399.1 triclinic, space group $P\bar{1}$, $a = 8.473(7)$ $b = 10.776(5)$, $c = 7.683(3)$ Å, $\alpha = 102.26(3)$, $\beta = 102.68(4)$, $\gamma = 71.13(6)°$, $U = 640(1)$ Å^3, $z = 1$, d(calc.) = 2.071 g cm^{-3}, $\mu(MoK_\alpha)$ = 86.4 cm^{-1}. A total of 1752 independent data was collected ($\theta_{max} = 21°$) with MoK_α radiation using the $\omega/2\theta$ scan mode.

A variable ω scan width of $(0.9 + 0.347 \tan\theta)°$ was calculated for each reflection as well as a variable horizontal aperture width of $(1.9 + 1.2 \tan\theta)$ mm. A maximum scan time of 80 sec was set for each reflection where $\theta < 17°$ but this was raised to 90 sec for reflections with $\theta > 17°$ but $< 21°$. A marked drop in intensity of the 3 standards monitored was noted during data collection (final intensities had fallen to 80% of their starting values) and the data were scaled to take account of this (even during the crystal alignment process the peaks were broad and some showed signs of splitting). An empirical absorption correction[21] was applied with maximum and minimum transmission factors of 0.999 and 0.439 respectively being determined. The structure was solved by Patterson and Fourier methods and refined by a full-matrix least squares method. The final cycle converged to an R of 0.075 for the 84 variables and 1022 data for which $F^2 > 3\sigma(F^2)$. In the refinement the atoms of the phenyl ring were treated as a rigid group (C–C, 1.395; C–H, 1.08 Å). Anisotropic thermal motion was assumed for the W, N and O atoms; for all other atoms isotropic thermal motion was assumed. The atomic scattering factors were taken from the tabulations of Cromer and Waber,[22] anomalous dispersion corrections were by Cromer.[23] The function minimized during refinement was $\Sigma w(|F_o| - |F_c|)^2$; unit weights were used.

Crystal data for $W(NPh)(OCMe_3)_3Cl(NH_2CMe_3)$: $C_{22}H_{52}N_2O_4W_1Cl_1$, M = 628.0, monoclinic, space group $P2_1/c$, $a = 9.341(2)$, $b = 29.608(7)$, $c = 10.257(2)$ Å, $\beta = 106.28(2)$, $U = 2723(2)$ Å^3, $z = 4$, d(calc.) = 1.532 g cm^{-3}, μ =

($Cu\text{-}K_\alpha$) = 91.7 cm^{-1}. A total of 3145 independent data was collected (θ_{max} = 58°) with CuK_α radiation using the $\omega/2\theta$ scan mode. A variable ω scan width of (0.8 + 0.142 tanθ) was calculated for each reflection as well as a variable horizontal aperture width of (2.0 + 1.1 tanθ) mm. A maximum scan time of 99 sec was set for each reflection where $\theta < 30°$ but this was raised to 120 sec for the remainder of the data. A significant drop in intensity of the 3 standards monitored (final intensities fell to ~90% of their starting values) and the data were scaled to take account of this. An empirical absorption correction was applied[21] with maximum and minimum transmission factors of 0.999 and 0.527 respectively. The structure was solved by Patterson and electron density methods and the final least squares cycle converged to values of R and R_w of 0.074 and 0.077 respectively for the 290 variables and 2023 data for which $F^2 > 3\sigma(F^2)$. For this compound, only the W and Cl atoms were refined anisotropically. The atomic scattering factors were taken from the tabulations of Cromer and Waber,[22] anomalous dispersion corrections were by Cromer.[23] In the refinement, the atoms of the phenyl ring were treated as a rigid group (C–C, 1.395; C–H, 1.08 Å). The function minimised was $\Sigma w(|F_o| - |F_c|)^2$; a weight of $1.066/(\sigma^2(F) + 0.008269F^2)$ was calculated for each reflection. The nitrogen atom of the Me_3CNH_2 group was identified on the basis of its different geometry in comparison with the oxygen atoms of the three $OCMe_3$ groups. Hydrogen sites, however, could not be unequivocally assigned to peaks on a final difference map. Initially no distinction was made between N and O atoms and the values of the thermal parameters determined were in support of the assignment made. The positions of the methyl hydrogen atoms were idealized at a C–H distance of 1.08 Å. Final atomic coordinates with isotropic thermal parameters for both compounds tables of anisotropic thermal parameters, tables of calculated hydrogen sites and lists of $F_o|F_c$ have been deposited with the Editor as supplementary material.†

Acknowldegements—We thank S.E.R.C. for initial support for this research (A. J. N. and D. C. B.).

†Atomic co-ordinates for these structures have also been deposited with the Cambridge Crystallographic Data Centre for inclusion in their Data Base. Copies are also available on request from the Editor at Queen Mary College.

REFERENCES

1. W. A. Nugent and B. L. Haymore, *Coord. Chem. Rev.* 1980, **31**, 123.
2. A. F. Shihada, *Z. Anorg. Allg. Chem.* 1974, **408**, 9.
3. W. A. Nugent and R. L. Harlow, *J. C. S. Chem. Commun.* 1979, 342.
4. A. A. Kuznetsova, Yu. G. Podzolko and Yu. A. Buslaev, *Russ. J. Inorg. Chem.* 1969, **14**, 393.
5. W. A. Nugent, *Inorg. Chem.* 1983, **22**, 965.
6. W. A. Nugent and R. L. Harlow, *J. C. S. Chem. Commun.* 1979, 1105.
7. A. J. Nielson and J. M. Waters, *Polyhedron* 1982, **1**, 561.
8. A. J. Nielson and J. M. Waters, *Aust. J. Chem.* 1983, **36**, 243; D. C. Bradley, M. B. Hursthouse, K. M. A. Malik and A. J. Nielson, *J. C. S. Chem. Commun.* 1981, 103.
9. M. G. B. Drew, K. C. Moss and N. Rolfe, *Inorg. Nucl. Chem. Lett.* 1971, **7**, 1219; M. G. B. Drew, G. W. A. Fowles, D. A. Rice and N. Rolfe, *J. C. S. Chem. Commun.* 1971, 231.
10. F. A. Cotton, T. R. Felthouse and D. G. Lay, *Inorg. Chem.* 1981, **20**, 2219; M. Chisholm, J. C. Huffman and J. Leonelli, *J. C. S. Chem. Commun.* 1981, 270.
11. D. Bright and J. A. Ibers, *Inorg. Chem.* 1969, **16**, 703; 709.
12. S. F. Pedersen and R. R. Schrock, *J. Am. Chem. Soc.* 1982, **104**, 7483.
13. D. C. Bradley, M. H. Chisholm, G. E. Heath and M. B. Hursthouse, *J. C. S. Chem. Commun.* 1969, 1261.
14. V. W. Eichler and H. J. Seifert, *Z. Anorg. Allg. Chem.* 1977, **431**, 123; M. G. B. Drew, G. W. A. Fowles, E. M. Page and D. A. Rice, J. C. S. Dalton, 1981, 2409; *J. Am. Chem. Soc.* 1979, **101**, 5827.
15. D. C. Bradley, R. C. Mehrotra and D. P. Gaur, *Metal Alkoxides*, p. 119. Academic Press, New York (1978).
16. C. G. Barraclough, D. C. Bradley, J. Lewis and I. M. Thomas, *J. Chem. Soc.* 1961, 2601.
17. G. C. Levey, R. L. Lichter and G. L. Nelson, *Carbon-13 Nuclear Magnetic Resonance Spectroscopy* 2nd Edn, p. 111. Wiley, New York (1980).
18. R. Colton and I. B. Tonkins, *Aust. J. Chem.* 1965, **18**, 447.
19. D. C. Bradley, M. B. Hursthouse, K. M. A. Malik, A. J. Nielson and R. L. Short, *J. C. S. Dalton*, 1983, 2651.
20. W. Wolfsberger and H. Schmidbaur, *Synth. React. Inorg. Metal-Org. Chem.* 1974, **4**, 149.
21. A. C. T. North, D. C. Philips and F. S. Mathews, *Acta Cryst., Sect. A.* 1968, **24**, 351.
22. D. T. Cromer and J. T. Waber, *International Tables for X-Ray Crystallography*, Vol 4, Table 2.2B. Kynoch Press, Birmingham (1974).
23. D. T. Cromer, *International Tables for X-Ray Crystallography*, Vol 4, Table 2, 3.1 Kynoch Press, Birmingham (1974)

Polyhedron Vol. 4, No. 2, pp. 299–301, 1985
Printed in Great Britain.

0277–5387/85 $3.00 + .00
© 1985 Pergamon Press Ltd.

MIXED LIGAND Cu(II) AMINO ACID COMPLEXES CONTAINING 2,2′-BIPYRIDYL. CYCLIC VOLTAMMETRIC STUDIES OF THE REDUCTION IN AQUEOUS MEDIA

GEORGE THOMAS and P. S. ZACHARIAS*
School of Chemistry, University of Hyderabad, Hyderabad 500134, India

(*Received* 8 *February* 1984; *accepted* 17 *April* 1984)

Abstract—The reduction of the title ternary complexes was studied by cyclic voltammetry in aqueous media. Reversible one-electron reduction was involved generating an intermediate Cu(I) species which subsequently dissociated to Cu^0 at the mercury electrode. The intermediate ternary Cu(I) amino acid complexes were found to be less unstable than the corresponding Cu(I) binary complexes. The pH-dependence of these ternary complexes was also studied.

Ternary complexes of Cu(II) containing a bidentate aromatic nitrogen base such as 2,2′-bipyridyl (BPY) and a bidentate oxygen donor ligand, have been shown to possess unusual stabilization.[1] When the bidentate oxygen donor ligand is replaced by a ligand such as glycine containing O and N donor atoms, the stability of the resultant ternary complexes is reduced but it is still higher than that for CuN_4 chromophore.[2] Ternary complexes containing an amino acid as a second ligand are of considerable significance as they are potential models for enzyme-metal ion-substrate complexes and have close similarity to biologically important Cu(II) mixed amino acid complexes, containing L-histidine and L-threonine.[3] Ternary complexes of the type Cu(BPY)(AA), where AA is the amino acid, are studied extensively by different workers.[4] But its redox behaviour has not yet been studied in detail except for a brief polarographic study of its reduction.[5] This report deals with the result of an extensive study of the reduction of Cu(II)(BPY)(AA)† complexes using cyclic voltammetry.

EXPERIMENTAL

The complexes discussed here, were prepared using a reported method[5] and purified by using prep. tlc on silica gel with *n*-butanol–water–methanol (20 + 40 + 40) solvent system. Cyclic voltammograms were recorded using a PAR model 370 electrochemistry system which includes the 174A polarographic analyzer, 175 universal programmer, RE 0074 X–Y recorder, and a 377 A cell system. The electrochemical measurements were done using hanging mercury drop electrode (HMDE), a platinum-wire auxiliary electrode, and a saturated calomel electrode (SCE).

RESULTS AND DISCUSSION

Cyclic voltammograms (CV) were recorded from aqueous solutions of the samples at mercury electrode in the range +0.1 to −0.6 V vs SCE. Cyclic voltammetric behaviour of the Cu(II) complexes are similar and a representative voltammogram is shown in Fig. 1(a). The relevant CV data for all complexes are given in Table 1. Each complex displays one reduction peak C at ~ -0.23 V and on reverse scan an anodic peak D appears at ~ -0.15 V. At slow scan rates ($\nu < 0.01\ Vs^{-1}$) an additional anodic peak B appears at $\sim +0.02$ V and in such cases, a new cathodic peak A, at ~ -0.03 V appears from second and subsequent scans. This behaviour is shown in Fig. 1(b), and is very similar to that of binary Cu(II) complexes of amino acids.[6] In these binary complexes peaks C and D are established as due to a one-electron redox process of the $Cu(II)(AA)_2$ complex. In an analogous manner

*Author to whom correspondence should be addressed.

†AA = Gly, Ala, Ile, Val and Ser

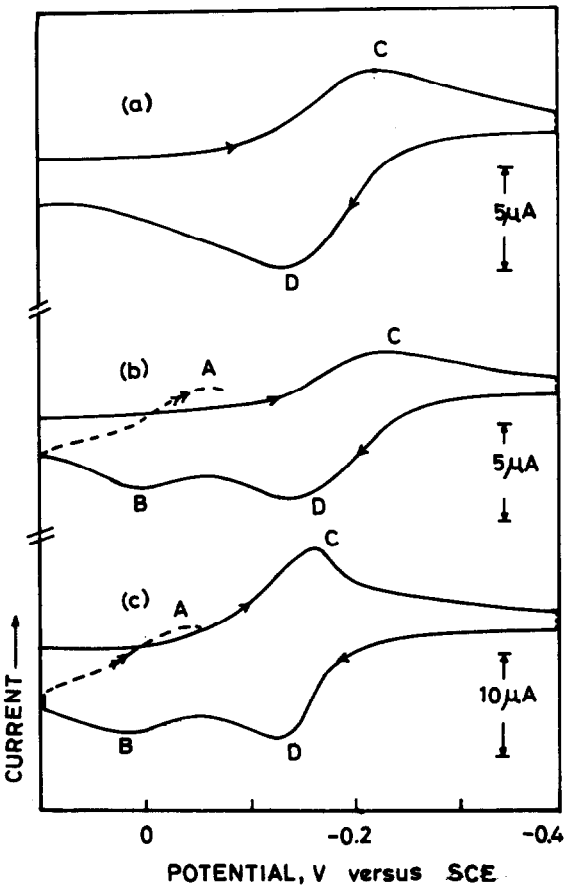


Fig. 1. Cyclic voltammograms recorded at HMDE, at 25°C. (a) Cu(BPY)(Ala) at 20 mV/s; (b) Cu(BPY)(Ala) at 10 mV/s; (c) $Cu(BPY)_2$ at 20 mV/s.

peak C of the ternary bipyridyl complexes results from a one-electron reduction and peak D from the re-oxidation of the reduced species. This can be represented by eqn (1).

$$Cu(II)(BPY)(AA) \overset{1e}{\rightleftharpoons} [Cu(I)(BPY)(AA)]. \quad (1)$$

The electrogenerated Cu(I) amino acid complexes are unstable in aqueous media and can dissociate or disproportionate to give Cu(O) at the electrode.[6-8] The peaks B and A at slow scan rates result from the redox process represented in eqn (2).

$$Cu^0(Hg) \overset{2e}{\rightleftharpoons} Cu^{2+}(aq). \quad (2)$$

In Cu(II)(BPY)(AA) complexes, peaks B and A develop only at slow scan rates ($\sim 0.01\ Vs^{-1}$), whereas in binary Cu(II) amino acid complexes these peaks are observable even at scan rates as high as $0.1\ Vs^{-1}$. This suggests that the intermediate Cu(I)(BPY)(AA) has a longer life-time than the corresponding Cu(I) binary amino acid complexes.

The binary Cu(II) bipyridyl complex, $Cu(BPY)_2$ gives a CV profile similar to that of binary Cu(II) amino acid complexes,[6] $Cu(AA)_2$, and is shown in Fig. 1(c). It also displays peaks corresponding to the C–D and A–B couples. From a comparison of this behaviour with that of binary Cu(II) amino acid and dipeptide[8] complexes, the peaks C and D are attributed to a one-electron redox process similar to that in eqn (1) and the peaks A and B to the process similar to that in eqn (2). This CV profile (appearance of peaks A and B at normal scan rates) indicates that the $Cu(I)(BPY)_2$ intermediate has a shorter life-time than that of Cu(I)(BPY)(AA) complexes mentioned earlier. The ternary bipyridyl Cu(II) complexes, Cu(II)(BPY)(L), where L has both O and N donor atoms (CuN_3O chromophore) is known to be more stable than the binary bipyridyl [$Cu(II)(BPY)_2$] complexes.[1,2] The observed stability of the intermediate Cu(I) species [Cu(I)(BPY)(AA)] over the Cu(I) bipyridyl species [Cu(I)(BPY)] can also be of similar origin.

Table 1. Cyclic voltammetric data on the reduction of Cu(II)(BPY)(AA) complexes[a]

Complex	E_p,C	E_p,D	ΔE_p,C-D	$E^{o'}$,C-D
(1) Cu(BPY)(Gly)	-0.220	-0.145	0.075	-0.183
(2) Cu(BPY)(Ala)	-0.215	-0.135	0.080	-0.175
(3) Cu(BPY)(Ile)	-0.240	-0.150	0.090	-0.195
(4) Cu(BPY)(Val)	-0.255	-0.160	0.095	-0.208
(5) Cu(BPY)(Ser)	-0.225	-0.135	0.090	-0.180

[a]All results were obtained in aqueous solution (0.6–0.8 mol dm^{-3}) of the complexes at pH about 7.5. Scan rate: $0.02\ Vs^{-1}$. Potentials are expressed in volts verses SCE.

Protonation. It is known that the structure of Cu(II) amino acid complexes is dependent on the pH conditions and the metal-to-ligand ratio. Hence the pH-dependence of the CV pattern of these ternary complexes were studied in the acid-pH range (the pH was decreased gradually by the stepwise addition of $HClO_4$). All ternary complexes show a similar behaviour on protonation. As the pH decreases the peaks C and D decrease in height and finally disappear. At the same time a new set of cathodic (C′) and anodic peaks (D′) appear at ~ -0.11 and ~ -0.05 V respectively and finally at low pH values (~ 3.2) they become the only set of peaks (Fig. 2). This new pair of peaks corresponds to a one-electron reversible redox process ($\Delta E_p \simeq 60$ mV; $i_pa/i_pc \simeq 1$). The decrease in height and the final disappearance of peaks C and D are due to the continuous depletion of the starting complex, Cu(BPY)(AA) due to protonation.

In the case of the protonation of binary[6] $[Cu(AA)_2]$ and ternary[7] [Cu(II)(A)(B)] Cu(II) amino acid complexes they completely dissociate to free Cu(II) ions at pH about 3.2. This was demonstrated by the appearance of the characteristic redox peaks of free Cu(II) ions (shown in Fig. 2 for comparison). But, for the bipyridyl ternary systems the peaks C′ and D′ do not correspond to free Cu(II) ions. The binary Cu(II) bipyridyl complex, $Cu(II)(BPY)_2$, also show a behaviour similar to that of ternary Cu(II)(BPY)(AA) complexes on protonation (Fig. 2). These observations show that the end product of the protonation of the ternary [Cu(II)(BPY)(AA)] and binary $[Cu(II)(BPY)_2]$ bipyridyl Cu(II) complexes is the same. The monobipyridyl Cu(II) complex,[4] $Cu(BPY)(H_2O)_2$, which is stable even at very low pH values can be a definite possibility as the end product of the protonation of the above complexes.

Acknowledgements—We thank the Department of Science and Technology, New Delhi, for financial support.

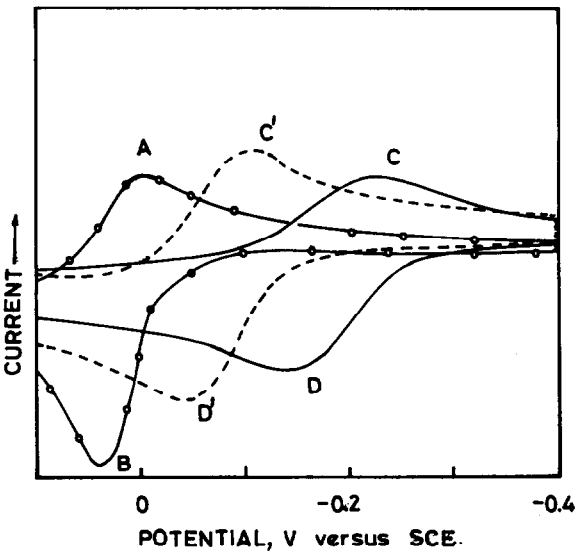


Fig. 2. Cyclic voltammograms of (——) Cu(BPY)(Ser) at pH = 7.5 (5 μA/in.); (---) Cu(BPY)(Ser) at pH = 3.12 (5 μA/in.); (–O–O–) $Cu(ClO_4)_2$ in aqueous solution (10 μA/in.).

REFERENCES

1. H. Sigel, P. R. Huber, R. Griesser and B. Prijs, *Inorg. Chem.* 1973, **12**, 1198.
2. H. Sigel and R. Griesser, *Helv. Chim. Acta* 1967, **50**, 1842.
3. B. Sarkar and T. P. A. Kruck, *Biochemistry of Copper* (Edited by J. Peisach, P. Aisen and W. E. Blumberg), p. 183. Academic Press, New York (1966).
4. F. Debreczeni and I. Nagypal, *Inorg. Chim. Acta* 1982, **57**, 135 and refs. therein.
5. W. L. Kwik, K. P. Ang and G. Chen, *J. Inorg. Nucl. Chem.* 1980, **42**, 303.
6. George Thomas and P. S. Zacharias, *Polyhedron*, in press.
7. George Thomas and P. S. Zacharias, *Indian J. Chem.*, in press.
8. George Thomas and P. S. Zacharias, *Polyhedron*, 1984, **3**, 861.

Polyhedron Vol. 4, No. 2, pp. 303–306, 1985
Printed in Great Britain.

0277–5387/85 $3.00 + .00
© 1985 Pergamon Press Ltd.

REACTIONS OF BIS-μ-IODO-BIS(DINITROSYLIRON) WITH HALIDE IONS AND WITH THIOLS: AN ELECTRON PARAMAGNETIC RESONANCE STUDY

ANTHONY R. BUTLER, CHRISTOPHER GLIDEWELL,* ANDREW R. HYDE and JOHN C. WALTON
Chemistry Department, University of St. Andrews, St. Andrews, Fife KY16 9ST, Scotland

(*Received* 29 *November* 1983; *accepted* 17 *April* 1984)

Abstract—Solutions of $Fe_2(NO)_4I_2$ in DMF exhibit EPR spectra characteristic of $[Fe(NO)_2]^+$ at concentrations of 2×10^{-4} mol dm^{-3}, and of an equilibrium mixture of $[Fe(NO)_2]^+$, $Fe(NO)_2I$, and $[Fe(NO)_2I_2]^-$ at higher concentrations: in THF solutions only $Fe(NO)_2I$ is observed, regardless of concentration. Addition of excess halide ions X^- (X=Cl, Br, I) to the DMF solution yields $[Fe(NO)_2X_2]^-$, but addition of excess I^- or Br^- to the THF solution yields $[Fe(NO)_2I_2]^-$ or $Fe_2(NO)_4Br_2$ respectively. In mixed THF/Et_3N solutions, mixtures of $[Fe(NO)_2]^+$, $Fe(NO)_2I$, and $[Fe(NO)_2I_2]^-$ are again formed, and subsequent addition of a thiol RSH causes formation of $[Fe(NO)_2(SR)_2]^-$, a precursor of $Fe_2(NO)_4(SR)_2$. A scheme is suggested to describe the steps in the preparatively useful conversion of $Fe_2(NO)_4I_2$ into $Fe_2(NO)_4(SR)_2$.

The μ_2-diiodo complex $Fe_2(NO)_4I_2$ reacts[1] with thiols in the presence of a base, in THF solution, to yield the Roussin esters $Fe_2(NO)_4(SR)_2$, in a preparatively useful procedure (eqn 1),

$$Fe_2(NO)_4I_2 + 2RSH + 2B \xrightarrow{THF} Fe_2(NO)_4I_2 + 2BH^+I^-. \quad (1)$$

It has been reported[2] that according to conductance measurements in dilute solutions (5×10^{-5} to 10^{-3} mol dm^{-3}) of $Fe_2(NO)_4I_2$ in DMF, complete dissociation occurs (eqn 2),

$$Fe_2(NO)_4I_2 \rightarrow 2[Fe(NO)_2]^+ + 2I^-. \quad (2)$$

It was suggested from Λ_i values, that the $Fe(NO)_2^+$ ion is essentially unsolvated in DMF. We have observed[3] in DMF solution the formation of mononuclear iron species such as $[Fe(NO)_2(SR)_2]^-$ $Fe(NO)_2(SR)(DMF)$ and $[Fe(NO)_2(DMF)_2]^+$, characterized by EPR spectroscopy, and we report here the results of an EPR study of the dissociation of $Fe_2(NO)_4I_2$ and of its reactions with halide ions and with thiols.

Because the conversion of $Fe_2(NO)_4I_2$ to $Fe_2(NO)_4(SR)_2$ is, for experimental convenience, carried out in THF, while the conductance measurements were performed[2] in DMF solutions, we have studied the EPR spectra of $Fe_2(NO)_4I_2$ in both these solvents.

RESULTS AND DISCUSSION

A dilute solution of $Fe_2(NO)_4I_2$ in DMF (2×10^{-4} mol dm^{-3}) shows a five-line EPR spectrum assignable to $Fe(^{14}NO)_2^+$ (see Table 1). No coupling assignable either to ^{127}I or to the hydrogens of coordinated solvent molecules was observed. This observation is consistent both with the complete ionisation of $Fe_2(NO)_4I_2$, according to eqn (1), as found[2] by conductance at this concentration, and also with the unsolvated nature of the cation, deduced[2] from the application, to the molar conductivities of the ions, of Walden's rule in the form $\Lambda_i \times r_i$ = constant for a medium of fixed viscosity. The failure to observe hyperfine coupling other than to ^{14}N in this cation is surprising since reaction of $Fe_2(NO)_4(SMe)_2$ with DMF yields[3] the complexes $[Fe(NO)_2(SMe)(DMF)]$ and $[Fe(NO)_2(DMF)_2]^+$, in both of which coupling to the unique hydrogen of coordinated DMF is clearly resolved. The question of the solvation of $[Fe(NO)_2]^+$ and of the other mononuclear iron complexes described in this work, is perhaps best left open.

More concentrated solutions in the same solvent (10^{-1} mol dm^{-3}) exhibit more complex spectra com-

*Author to whom correspondence should be addressed.

Table 1. EPR parameters for dissociation products of $Fe_2(NO)_4X_2$

	Species	g	$A(^{14}N)$/G	A(X)†/G
(i) In DMF				
	$Fe(NO)_2^+$	2.032	2.3	—
	$Fe(NO)_2Cl_2^-$	2.036	‡	4.7
	$Fe(NO)_2br$	2.037	‡	19.2
	$Fe(NO)_2Br_2^-$	2.049	2.3	19.4
	$Fe(NO)_2I$	2.053	‡	19.2
	$Fe(NO)_2I_2^-$	2.079	‡	20.6
(ii) In THF				
	$Fe(NO)_2I$	2.060	‡	16.6
	$Fe(NO)_2I_2^-$	2.080	‡	20.5
(iii) In H_2O§				
	$Fe(NO)_2^+$	2.033	‡	—
	$Fe(NO)_2Cl_2^-$	2.034	‡	5.3
	$Fe(NO)_2Br$	2.039	‡	19.5
	$Fe(NO)_2Br_2^-$	2.045	‡	19.5
	$Fe(NO)_2I$	2.055	‡	20.2
	$Fe(NO)_2I_2^-$	2.070	‡	20.2

†X = $^{35,37}Cl(I = 3/2)$; $^{79,81}Br(I = 3/2)$; $^{127}I(I = 5/2)$: hyperfine couplings due to individual isotopes of chlorine or bromine were not resolved.
‡Not resolved.
§Data in H_2O from Ref. 4.

prising, in addition to the five line spectrum of $[Fe(NO)_2]^+$, a six-line spectrum assignable to $Fe(NO)_2I$ and an eleven-line spectrum assignable to $[Fe(NO)_2I_2]^-$. The assignments follow straightforwardly from the multiplicites ($I(^{127}I) = 5/2$) and from the previous observation[4,5] of these and similar species in aqueous or ethanolic solutions, where they were generated by the action of NO gas on mixtures of Fe(II) and halide ions: in addition, the ion $Fe(NO)_2I_2^-$ has been isolated[6] in analytically pure form as its $(Ph_3P)_2N^+$ salt. The large line-widths of $Fe(NO)_2I$ and $Fe(NO)_2I_2^-$ in DMF solution prevented resolution of the coupling to ^{14}N. This was, in general, not resolved[4,5] in either aqueous or ethanolic solutions.

These observations are consistent with the occurrence of the following independent equilibria (eqn 3), characterised by the equilibrium constants K_1 – K_3:

$$2[Fe(NO)_2]^+ + 2I^- \overset{K_1}{\rightleftharpoons} 2Fe(NO)_2I \overset{K_2}{\rightleftharpoons} Fe_2(NO)_4I_2 \overset{K_3}{\rightleftharpoons} [Fe(NO)_2]^+ + [Fe(NO)_2I_2]^- \quad (3)$$

Measurements of the absolute concentrations of the paramagnetic ions by EPR spectroscopy yielded values for these constants at 240 K, in DMF:

$\log_{10}K_1$, 2.58 ± 0.09; $\log_{10}K_2$, 2.71 ± 0.36; $\log_{10}K_3$, − 2.78 ± 0.57.

For the dependent equilibria (eqns 4–6),

$$Fe(NO)_2^+ + 2I^- \overset{K_4}{\rightleftharpoons} [Fe(NO)_2I_2]^- \quad (4)$$

$$Fe_2(NO)_4I_2 \overset{K_5}{\rightleftharpoons} 2[Fe(NO)_2]^+ + 2I^- \quad (5)$$

$$2Fe(NO)_2I \overset{K_6}{\rightleftharpoons} [Fe(NO)_2]^+ + [Fe(NO)_2I_2]^- \quad (6)$$

the values (240 K) are: $\log_{10}K_4$, 5.10 ± 0.38; $\log_{10}K_5$, − 7.88 ± 0.30; $\log_{10}K_6$, − 0.07 ± 0.22; where $K_4 = K_1^2K_2K_3$, $K_5 = (K_1^2K_2)^{-1}$, and $K_6 = K_2K_3$.

The precision of the values is necessarily low, as not all the independent species are observable by EPR spectroscopy. The concentration of I^- was determined from the charge balance, after measurement of the concentrations of $[Fe(NO)_2]^+$ and $[Fe(NO)_2I_2]^-$: the concentration of undissociated $Fe_2(NO)_4I_2$ was determined from the mass balance after measurement of the concentration of all the mono-iron complexes, and deduction of the I^- concentration.

Addition of excess of potassium iodide to a DMF solution of $Fe_2(NO)_4I_2$ (10^{-2} mol dm^{-3}) gave, as expected, $[Fe(NO)_2I_2]^-$ as the sole paramagnetic species detected. Similarly, addition of excess of KBr or KCl to such a solution yielded $[Fe(NO)_2Br_2]^-$ and $[Fe(NO)_2Cl_2]^-$ respectively. The only other paramagnetic species detected was $Fe(NO)_2Br$: $Fe(NO)_2Cl$ was not observed under these conditions. The chloro- and bromo-complexes were identified by comparison of their EPR spectra with those recorded[4,5] earlier in ethanol/water mixtures. Their ready formation is further evidence of the lability of halide ions in these species, (see eqn 3). In $Fe(NO)_2Br$ alone we were able to resolve the ^{14}N hyperfine coupling (see Table 1).

In contrast to the behaviour of $Fe_2(NO)_4I_2$ in DMF, solutions in THF over a similar range of concentration (10^{-1}–10^{-4} mol dm^{-3}) showed only a single paramagnetic species, $Fe(NO)_2I$. Neither $[Fe(NO)_2]^+$ nor $[Fe(NO)_2I_2]^-$ was detected at any concentration, while no paramagnetic species at all were detected in chloroform solution. Upon addition of an excess of iodide ions to the THF solutions, the spectrum of $Fe(NO)_2I$ was replaced by that of $[Fe(NO)_2I_2]^-$ but upon addition of an excess of bromide ions, the EPR spectrum disappeared. We conclude that, in THF, halide exchange to yield $Fe(NO)_2Br$ is followed by complete dimerisation to yield the diamagnetic $Fe_2(NO)_4Br_2$. In support of this interpretation, it was found that a solution of preformed $Fe_2(NO)_4Br_2$ in THF gave no detectable EPR spectrum.

The position of the equilibrium (eqn 7)

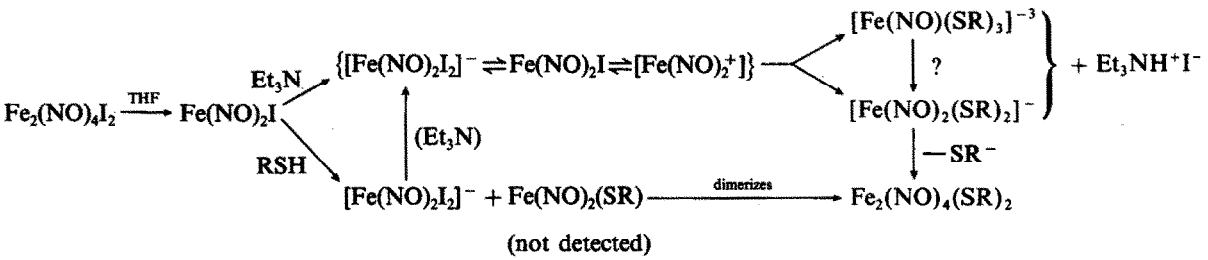
$$Fe_2(NO)_4X_2 \rightleftharpoons 2Fe(NO)_2X \qquad (7)$$

depends upon both the solvent, and the nature of X. That it lies further to the right, in any given solvent, when X = I than when X = Br or SR is consistent with the magnitude of the Fe–Fe interaction in these species. In $Fe_2(NO)_4I_2$, the Fe–Fe distance is[7] 3.05 Å, while in $Fe_2(NO)_4(SEt)_2$ it is[8] only 2.72 Å. The bond angles in the Fe_2X_2 rings in these two compounds are virtually identical, and using these angles, and a reasonable estimate, 2.38 Å, of the Fe–Br bridging distance, an estimate of *ca.* 2.8 Å is obtained for the Fe–Fe distance in $Fe_2(NO)_4Br_2$. The diamagnetism of these systems suggests that the Fe–Fe interaction is bonding, and hence it is deduced that this interaction contributes least to the stability of the dimer when X = I and most when X = SR.

Although only $Fe(NO)_2I$ was formed in solutions of $Fe_2(NO)_4I_2$ in THF, addition of triethylamine to such a solution yielded a mixture of $[Fe(NO)_2]^+$ $Fe(NO)_2I$, and $[Fe(NO)_2I_2]^-$: using pure triethylamine as the solvent, the only paramagnetic species detected was the solvo-cation $[Fe(NO)_2(NEt_3)_2]^+$, in which hyperfine coupling to the ^{14}N of two coordinated solvent molecules was detected, with $A(^{14}NEt_3)$ of 4.8 G.

Upon addition of a thiol (chosen throughout as *i*-PrSH, for convenience in spectral assignment, since this thiol has only a single α-hydrogen) to a solution of $Fe_2(NO)_4I_2$ in THF/Et_3N, the spectrum characteristic of $[Fe(NO)_2]^+$, $Fe(NO)_2I$, and $[Fe(NO)_2I_2]^-$ was replaced by a spectrum characteristic of two paramagnetic species (**1**) [$g = 2.029$; $A(2^{14}N) = 2.6$G; $A(2^1H) = 1.3$G] and (**2**) [$g = 2.040$; $A(1^{14}N) = 13.5$G]. Species (**1**) was readily identified[3] as the anion $[Fe(NO)_2(SPr^i)_2]^-$, and we have shown previously[3] that anions of the general type $[Fe(NO)_2(SR)_2]^-$ can readily lose RS^- to yield $Fe_2(NO)_4(SR)_2$. The identification of species (**2**) poses more of a problem: it is a mono-nitrosyl species, but no coupling to hydrogen is resolvable. Another mono-nitrosyl species having a similar large A value is formed from $Fe_4S_4(NO)_4$ and SH^-, but this latter, upon oxidation by air is replaced by a species having $A(^{14}N)$ of 5.0 G, typical of $[Fe(NO)(SR)_3]^-$ species.[9] Hence we tentatively identify the 13 G species as a reduced anion $[Fe(NO)(SR)_3]^{-x}$ ($x > 1$): if $[Fe(NO)(SR)_3]^{-x}$ is formed from $Fe_2(NO)_4I_2$ or any of its dissociation products by substitution, without change of the formal oxidation state of the iron, then $x = 3$. The fate of this 13 G species has not been established, but conversion of similar mono-nitrosyl iron complexes to di-nitrosyl species under mild conditions is well established. For example, reaction of either $Fe(NO)(S_2CNMe_2)_2$ or $Fe_4S_4(NO)_4$ with MeS^- yields[9] $[Fe(NO)_2(SMe)_2]^-$; reduction of $Fe_4S_4(NO)_4$ yields[10] $[Fe_4S_3(NO)_7]^-$; while $[Fe(CO)_3NO]^-$ yields $[Fe(NO)_2X_2]^-$ (X = Cl, Br, I) with haloalkanes,[6] and $[Fe(NO)_2(SR)_2]^-$ with alkanethiols.[9] Hence it is possible that the 13 G mono-nitrosyl species could be converted firstly to a di-nitrosyl, and thence to $Fe_2(NO)_4(SR)_2$.

When the thiol was added to the THF solution of $Fe_2(NO)_4I_2$ prior to the addition of any Et_3N, the resulting EPR spectrum was quite different from that obtained in the presence of the amine. Upon addition of the thiol, the spectrum of $Fe(NO)_2I$ was replaced by that of $[Fe(NO)_2I_2]^-$, but no other paramagnetic species were detected. We interpret this as arising from displacement of iodide by SR to yield $Fe(NO)_2SR$ which immediately dimerises to yield the isolable product $Fe_2(NO)_4(SR)_2$; the displaced iodide ion then coordinates to a further $Fe(NO)_2I$ to yield



Scheme 1. Steps in the conversion of $Fe_2(NO)_4I_2$ to $Fe_2(NO)_4(SR)_2$.

$[Fe(NO)_2I_2]^-$, (eqns 8–10):

$$Fe(NO)_2I + RSH \rightarrow Fe(NO)_2SR + H^+ + I^- \quad (8)$$

$$2Fe(NO)_2SR \rightarrow Fe_2(NO)_4(SR)_2 \quad (9)$$

$$Fe(NO)_2I + I^- \rightarrow [Fe(NO)_2I_2]^-. \quad (10)$$

In contrast to the ready dissociation of $Fe_2(NO)_4I_2$, the esters $Fe_2(NO)_4(SR)_2$ undergo very little dissociation, even in highly polar solvents, as discussed above. In support of eqns (8) and (9), it was found that reaction of $Fe_2(NO)_4I_2$ with a 100-fold excess of *i*-PrSH in THF, even in the absence of any amine, leads to formation of $Fe_2(NO)_4(S\text{-}i\text{-}Pr)_2$ in 93% isolated yield.

We can accordingly suggest the sequence of reactions involved in the conversion of $Fe_2(NO)_4I_2$ to $Fe_2(NO)_4(SR)_2$ in THF solutions (see Scheme 1): with the exception of $Fe(NO)_2SR$ all the paramagnetic species in this Scheme have been detected by EPR spectroscopy. Triethylammonium iodide is insoluble in THF, and it is the precipitation of this salt from the solution which drives the equilibria towards the formation of $Fe_2(NO)_4(SR)_2$ in preparatively useful yields when stoichiometric quantities of $Fe_2(NO)_4I_2$ and RSH are employed.

The sequence of reactions leading from $Fe_2(NO)_4I_2$ to $Fe_2(NO)_4(SR)_2$ is at last partially reversible, in DMF. Addition of excess potassium iodide to a DMF solution of $Fe_2(NO)_4(SMe)_2$ gave $[Fe(NO)_2I_2]^-$ as the sole paramagnetic species detectable: likewise, addition of potassium bromide gave $[Fe(NO)_2Br_2]^-$. However, no paramagnetic halogeno complexes were observed upon addition of either KF or KCl to $Fe_2(NO)_4(SMe)_2$: the observed EPR spectrum in each case indicated a mixture of $Fe(NO)_2(SMe)(DMF)$ and $[Fe(NO)_2(DMF)_2]^+$.

EXPERIMENTAL

Literature methods[11–13] were used for the preparation of $Fe_2(NO)_4Br_2$, $Fe_2(NO)_4I_2$ and $Fe_2(NO)_4(SR)_2$. Solutions for EPR examinations were prepared using dry, redistilled solvents, deoxygenated with a stirring nitrogen stream: all manipulations of solutions were made under dry nitrogen.

EPR spectra were measured in 1 mm quartz capillaries using a Bruker ER 200D Spectrometer. Di-*t*-butyl nitroxide was used as the standard in the measurement of line positions; diphenyl picryl hydrazyl was used as the standard in the measurement of intensities.

Acknowledgement—We thank the S.E.R.C. and the Cancer Research Campaign for financial support.

REFERENCES

1. T. B. Rauchfuss and T. D. Weatherill, *Inorg. Chem.* 1982, **21**, 827.
2. G. Piazza and G. Innorta, *J. Organometallic Chem.* 1982, **240**, 257.
3. A. R. Butler, C. Glidewell, A. R. Hyde, J. C. Walton and Wang Guang-hui, unpublished observations.
4. L. Burlamacchi, G. Martini and E. Tiezzi, *Inorg. Chem.* 1969, **8**, 2021.
5. G. Martini and E. Tiezzi, *Trans. Faraday Soc.* 1971, **67**, 2538.
6. N. G. Connelly and C. Gardner, *J. Chem. Soc. Dalton Trans.*, 1976, 1525.
7. L. F. Dahl, E. R. de Gil and R. D. Feltham, *J. Am. Chem. Soc.* 1969, **91**, 1653.
8. J. T. Thomas, J. H. Robertson and E. G. Cox, *Acta Cryst.* 1958, **11**, 599.
9. C. Glidewell, A. R. Hyde and J. C. Walton, unpublished observations.
10. C. T.-W. Chu and L. F. Dahl, *Inorg. Chem.* 1977, **16**, 3245.
11. H. Soling and R. W. Asmussen, *Acta Chem. Scand.* 1957, **11**, 1534.
12. B. Haymore and R. D. Feltham, *Inorg. Synth.* 1973, **14**, 81.
13. A. R. Butler, C. Glidewell, A. R. Hyde, J. McGinnis and J. E. Seymour, *Polyhedron*, 1983, **2**, 1045.

Polyhedron Vol. 4, No. 2, pp. 307–310, 1985
Printed in Great Britain.

0277–5387/85 $3.00 + .00
© 1985 Pergamon Press Ltd.

SYNTHESIS AND CHARACTERISATION OF PENTACOORDINATED RUTHENIUM(II) HYDRAZONE DERIVATIVES†

S. A. PARDHY, K. JOSEPH, SARADA GOPINATHAN and C. GOPINATHAN*

Inorganic Chemistry Division, National Chemical Laboratory, Poona 411 008, India

(*Received* 11 *November* 1983; *accepted after revision* 17 *April* 1984)

Abstract—Several new pentacoordinated ruthenium(II) compounds, $Ru(PPh_3)_2L$, of Schiff bases LH_2 are reported. The Schiff bases used have been derived from isonicotinoyl hydrazone and β-diketones or salicylaldehyde, or azines and mixed azines obtained from salicylaldehyde, benzoylacetone or 2-hydroxyacetophenone. These new compounds are highly coloured crystalline solids, stable and monomeric in toluene. They readily absorb carbon monoxide gas to give a carbonyl derivative of the type $Ru(PPh_3)_2CO(L)$ in quantitative yields.

Wilkinson *et al.*[1] reported the preparation and characterisation of several ruthenium(II) bis-triphenylphosphine-Schiff base complexes having an octahedral geometry. The Schiff bases used for this study were derived from aliphatic diamines and β-diketones or aromatic aldehydes. A *trans* structure for the phosphine groups was ascertained for all these complexes.

Little is mentioned in the literature about pentacoordinated ruthenium(II) phosphine complexes of tridentate hydrazones and azines. Dibasic tridentate chelating ligands are reported to form unstable ruthenium(II) complexes probably because of the formation of coordinately unsaturated ruthenium.[1] It is probable that stable complexes of pentacoordinated ruthenium(II) may be formed from hydrazones and azines. Several hydrazones of isonicotinoyl hydrazide (a) and azines (b) of salicylaldehyde

(a)

$R = H, CH_3, CF_3$
$R' = C_4H_3SCOCH_2, CH_3COCH_2$
$C_6H_5COCH_2, C_6H_4OH$

(b)

$R,R' = H$ or CH_3

and hydroxyacetophenone, listed below, have been used for our study:

1. Acetylacetone-isonicotinoyl hydrazone [acac-inh]H_2.[2,3]
2. Trifluoroacetylacetone-isonicotinoyl hydrazone [tfacac-inh]H_2.[2]
3. Thenoylacetone-isonicotinoyl hydrazone [ta-inh]H_2.[2]
4. Trifluorothenoylacetone-isonicotinoyl hydrazone [tfta-inh]H_2.[2]
5. Benzoylacetone-isonicotinoyl hydrazone [ba-inh]H_2.[2]
6. Salicylaldehyde-isonicotinoyl hydrazone [sa-inh]H_2.[4]
7. Salicylaldehyde azine [sa-a]H_2.[5]
8. Salicylaldehyde-benzoylacetone azine [saba-a]H_2.[6]
9. 2-Hydroxyacetophenone azine [ha-a]H_2.[7]
10. Salicylaldehyde-2-hydroxyacetophenone azine [Saha-a]H_2.[6]

EXPERIMENTAL

Reactions were carried out under dry, oxygen-free nitrogen using dry, degassed solvents. Acetylacetone-isonicotinoyl hydrazone was prepared as reported earlier.[3]

Salicylaldehyde-2-hydroxyacetophenone azine [saha-a]H_2. This was obtained from 2-hydroxyacetophenone hydrazone (1.50 g; 0.01 mol) and salicylaldehyde (1.22 g; 0.01 mmol) by refluxing them (2 hr) in methanol (30 cm^3). The crystals obtained on cooling the contents were recrystallised from benzene. M.p. 163°. Found: C, 70.72; H, 5.47;

*Author to whom correspondence should be addressed.

†NCL Communication No. 3400.

Calc. for $C_{15}H_{14}O_2N_2$: C, 70.86; H, 5.51%. Mol.wt by mass spectrum, 254.

Ru(PPh$_3$)$_2$(acac-inh). The disodio derivative of the ligand [acac-inh]H_2 was prepared from oil-free sodium hydride (0.057 g; 20% excess of 0.002 mol), ligand (0.219 g; 0.001 mol) and ether (30 cm^3). The dry sodio derivative was suspended in benzene (30 cm^3) and $Ru(PPh_3)_3Cl_2$ (0.96 g; 0.01 mol) was added to it and the mixture refluxed overnight. The contents were then centrifuged to remove the precipitated sodium chloride. The benzene extract was concentrated to get brown crystals of the product. Yield 0.5 g (60%).

Ru(PPh$_3$)$_2$(saha-a). This compound was obtained from the reaction between the disodio derivative of the ligand [saha-a]H_2 (prepared from 0.057 g of sodium hydride and 0.304 g of the ligand) and $Ru(PPh_3)_3Cl_2$ (0.96 g; 0.001 mol) similar to the previous preparation. The dark coloured crystals weighed 0.57 g (65%).

Ru(PPh$_3$)$_2$(CO)(saha-a). $Ru(PPh_3)_2$(saha-a) (0.10 g) was dissolved in benzene (10 cm^3), warmed upto boiling and pure carbon monoxide bubbled through it for 30 min. The solution was evaporated *in vacuo* and washed with hexane to get a yellow solid. The yield was quantitative. Found: C, 68.63; H, 4.54; P, 6.34. Calc. for $Ru(P_2C_{36}H_{30})(CO)(C_{15}H_{12}O_2N_2)$: C, 68.95; H, 4.64; P, 6.85%.

Other ligands and ruthenium compounds were prepared similarly (Table 1).

RESULTS AND DISCUSSION

Isonicotinoyl hydrazone derivatives of β-diketones or salicylaldehyde reacted with $Ru(PPh_3)_3Cl_2$ in the presence of sodium hydride to give chlorine-free pentacoordinated ruthenium(II) complexes. Salicylaldehyde azine, 2-hydroxyacetophenone azine and the other two mixed azines also gave similar products. These compounds were found to be monomeric in toluene (vapour pressure osmometry). Unlike the light coloured hexacoordinated ruthenium(II) complexes, these new products were highly coloured crystalline compounds (Table 1).

Infrared spectra (ν in cm^{-1}) of isonicotinoyl hydrazone derivatives show ν N–H ~ 3200 cm^{-1} and characteristic amide I band ν C=O ~ 1665 cm^{-1}.[3] Complete absence of these bands in all the ruthenium(II) compounds suggests the loss of N–H proton through enolisation of carbonyl group during the complex formation. The high frequency shift of enolic/phenolic νC–O is consistent with oxygen coordination to ruthenium. The νN–N[8] occurring in the ligands in the range of 1010–1030 cm^{-1} undergoes a slight positive shift in their complexes indicating the coordination of one of the azomethine nitrogens to ruthenium. Further, the deformation mode of the pyridine ring of the free hydrazone at about 620 cm^{-1} shows no shift in the complexes indicating the non-coordination of the ring nitrogen.

Similarly azine derivatives also have given chlorine-free ruthenium(II) complexes. The tridentate nature of the azine ligand is confirmed from the splitting of νC=N [1600, 1590 cm^{-1}] and νN–N (940, 910 cm^{-1}].[9] Similar features are observed by us in the tin(IV) and titanium(IV) complexes of these ligands.[5,10]

^{31}P NMR spectra of azine complexes have been obtained using 85% phosphoric acid as external standard. The proton decoupled spectra of the complexes furnish only a singlet in the region

Table 1. Bis-triphenylphosphine ruthenium(II) complexes of hydrazones, $Ru(PPh_3)_2L$

No.	Product *	Colour, m.p. (°C)	% Analysis Found (calc.) C	H	N	P
1.	Ru(PPh$_3$)$_2$ (acac-inh)	Brown	66.70(66.91)	5.01(4.86	4.77(4.98)	7.36(7.35)
2.	Ru(PPh$_3$)$_2$(tfacac-inh)	Brown 105	64.00(63.94)	4.45(4.30)	4.62(4.76)	7.10(7.03)
3.	Ru(PPh$_3$)$_2$(ta-inh)	Brown 95	66.01(65.93)	4.45(4.50)	4.44(4.60)	6.71(6.81)
4.	Ru(PPh$_3$)$_2$(tfta-inh)	Brown 65	62.35(62.24)	4.00(3.94)	4.22(4.35)	6.40(6.43)
5.	Ru(PPh$_3$)$_2$(ba-inh)	Brown 145	68.96(69.02)	4.86(4.75)	4.52(4.64)	6.80(6.85)
6.	Ru(PPh$_3$)$_2$(sa-inh)	Brown 75	68.00(68.06)	4.51(4.51)	4.71(4.86)	7.08(7.17)
7.	Ru(PPh$_3$)$_2$(sa-a)	Green 120	69.64(69.52)	4.76(4.63)	3.17(3.24)	7.09(7.18)
8.	Ru(PPh$_3$)$_2$(saba-a)	Green 130	70.59(70.43)	4.99(4.87)	3.02(3.10)	6.71(6.86)
9.	Ru(PPh$_3$)$_2$(ha-a)	Green 105	70.15(70.03)	5.01(4.93)	3.10(3.14)	7.02(6.95)
10.	Ru(PPh$_3$)$_2$(saha-a)	Green 100	69.69(69.78)	4.73(4.78)	3.01(3.19)	7.00(7.07)

* Abbreviations same as in the text in both the tables.

+29 ppm (positive value, lower field relative to phosphoric acid). Octahedral ruthenium(II) complexes with *trans* phosphine groups also have given a singlet for ^{31}P NMR spectra. Hence these azine compounds can presumably possess a trigonal bipyramidal geometry around ruthenium having *trans* phosphorus atoms as shown below:

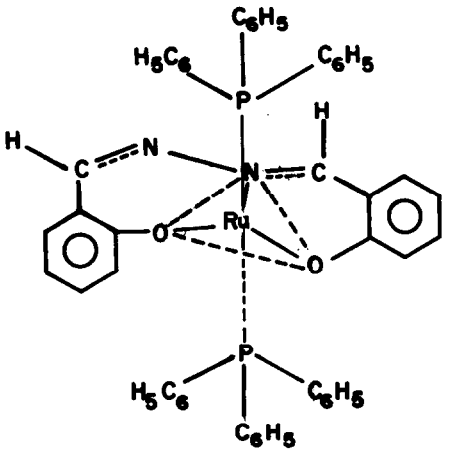


Fig. 1.

In benzene these ruthenium complexes reacted with carbon monoxide under refluxing conditions (30 min) giving $Ru(PPh_3)_2(CO)L$ in quantitative yields. The appearance of a single $\nu C{\equiv}O \sim 1940\ cm^{-1}$ confirms the formation of mono-carbonyl complexes. The pale yellow colour of the carbonyl complexes indicates them to be coordinately saturated species probably having octahedral geometry.

The electronic spectra of the ligands and their ruthenium compounds were obtained in chloroform solutions in the concentration range of 10^{-3}–10^{-5} molar at ambient temperature. The spectra of the ligands have shown absorption bands in the region ~260–280 nm which can be considered to be a $\pi \rightarrow \pi^*$ benzenoid band. The most intense band in the long wave length region ~330–360 nm for azines and thenoyl isonicotinoyl hydrazone might be considered to be caused by the lengthening of the π system due to the interaction of aromatic ring. The complexes derived from isonicotinoyl hydrazone exhibit an intense additional band ~440 nm (Table 2). Relatively higher intensities ($\epsilon = 10{,}000$) suggest that most probably

Table 2. Electronic spectra of hydrazone ligands and their bis-triphenylphosphine ruthenium(II) complexes in chloroform at ambient temperatures

No.	Ligand/Complex	λmax (in nm) (ϵ =)
1.	[acac-inh]H_2	260 (11000)
2.	Ru(PPh_3)$_2$(acac-inh)	420(1370), 270(14800), 262(16900), 258(16200), 242(12600)
3.	[tfacac-inh]H_2	264(12000)
4.	Ru(PPh_3)$_2$(tfacac-inh)	444(3850), 270(36200), 264(41500), 256(44200), 242(54200)
5.	[ta-inh]H_2	330(26000), 260(97000), 242(100000)
6.	Ru(PPh_3)$_2$(ta-inh)	440(10700), 292(56200), 264(40000), 256(43000), 242(45800)
7.	[tfta-inh]H_2	352(16600), 344(17000), 320(18900), 272(12400)
8.	Ru(PPh_3)$_2$(tfta-inh)	406(6100), 324(37300), 270(36900), 262(38500), 240(43100)
9.	[ba-inh]H_2	282(9300)
10.	Ru(PPh_3)$_2$(ba-inh)	450(8500), 270(31500), 264(34600), 240(45400)
11.	[sa-inh]H_2	332(9300), 286(13000), 240(8700)
12.	Ru(PPh_3)$_2$(sa-inh)	442(7100), 270(39200), 264(41500), 256(41500), 240(42300)
13.	[sa-a]H_2	356(29000), 292(32000), 240(14400)
14.	Ru(PPh_3)$_2$(sa-a)	330(8300), 270(15400), 264(23900), 256(23900), 242(25200)
15.	[saba-a]H_2	395(60000), 284(19000), 242(40000)
16.	Ru(PPh_3)$_2$(saba-a)	556-596(1015), 400(6000), 380(6800), 270(15700) 264(17900), 258(18800), 242(21200)
17.	[ha-a]H_2	362(22000), 292(25800), 240(17600)
18.	Ru(PPh_3)$_2$(ha-a)	348(10400), 270(15400), 264(22000), 256(23100), 242(25500)
19.	[saha-a]H_2	360(28400), 292(30400), 242(11600)
20.	Ru(PPh_3)$_2$(saha-a)	358(11700), 270(20900), 264(21400), 256(21200), 242(24800)
21.	Ru(PPh_3)$_2Cl_2$	270(17000), 262(19100), 256(19000), 242(19700)

these are ligand-to-metal charge-transfer transitions. A hypsochromic shift for the long wave length band of azine is observed in the spectra of azine derivatives of ruthenium. This may probably be due to the formation of two dissimilar rings when the metal complex is formed thereby distorting the planarity of the azine ligand.

All these azine and hydrazone derivatives have retained the absorption characteristics of $Ru(PPh_3)_3Cl_2$. We could not confidently assign the *d–d* transition bands in these complexes as the spectra did not give distinct absorption bands in the visible range 450–700 nm within the solution concentrations used by us.

REFERENCES

1. J. R. Thornback and G. Wilkinson, *J. Chem. Soc. Dalton Trans.* 1978, 110.
2. *Chem. Abstr.* 1970, **73**, 123454, 123455.
3. K. Joseph, S. A. Pardhy, S. Gopinathan and C. Gopinathan, *Ind. J. Chem.* 1982, **21A**, 1137.
4. P. P. T. Sah and S. A. Peoples, *J. Am. Pharm. Assoc., Sci. Ed.* 1954, **43**, 513.
5. H. A. Patwardhan, S. Gopinathan and C. Gopinathan, *Ind. J. Chem.* 1978, **16A**, 224.
6. S. A. Pardhy, S. Gopinathan and C. Gopinathan, *Ind. J. Chem.* 1983, **22A**, 73.
7. L. Gunther and S. Kurt, *Chem. Ber.* 1944, **77B**, 293.
8. V. B. Rana, J. N. Gurtu and M. P. Teotia, *J. Inorg. Nucl. Chem.* 1980, **42**, 331.
9. S. Satpathy and B. Sahoo, *J. Inorg. Nucl. Chem.* 1970, **32**, 2223.
10 S. A. Pardhy, S. Gopinathan and C. Gopinathan, *Ind. J. Chem.* 1983, **22A**, 73.

Polyhedron Vol. 4, No. 2, pp. 311–316, 1985
Printed in Great Britain.

0277–5387/85 $3.00 + .00
© 1985 Pergamon Press Ltd.

CALCULATION OF THE ^{13}C MAGNETIC SHIELDING IN CYCLOPENTADIENYL COMPLEXES BY ELIMINATING EFFECTS DUE TO CHARGE

NATALIYA A. OGORODNIKOVA* and DMITRII N. KRAVTSOV
A. N. Nesmeyanov Institute of Organo-Element Compounds, Academy of Sciences, Vavilov Street 28, Moscow, U.S.S.R.

(*Received* 2 *February* 1984; *accepted* 17 *April* 1984)

Abstract—A method for estimating the contributions of different factors to the ^{13}C NMR chemical shifts of a ligand has been proposed which is based on elimination of the charge effect and a determination of the combined effect of the remaining factors (the coordination effect). This enabled the authors to establish a relationship between the ^{13}C NMR data and the chemical properties of cyclopentadienyl metal compounds.

As regards the ^{13}C NMR spectroscopy of organometallic compounds of transition metals, no general satisfactory theoretical or empirical relationships to estimate the contributions of different factors to chemical shifts have yet been established.[1-3]

An attempt has been made[4] to estimate the net charges in the cyclopentadienyl rings of nonparamagnetic pentahapto-cyclopentadienyl complexes with transition or non-transition metals on the basis of the ^{19}F NMR data for their *p*-fluorophenyl derivatives according to Taft's approach.

The aim of this work was to estimate the combined effect of the factors arising from coordination, on the ^{13}C chemical shifts of the cyclopentadienyl ligand by using the proportionality factor for ^{13}C NMR chemical shifts 128.5 ppm per unit of charge[5] and the data on electron density in cyclopentadienyl ring for a number of complexes.[4]

RESULTS AND DISCUSSION

Our approach will be illustrated by the example of ferrocene. The net charge f in the cyclopentadienyl ring of the ferrocene molecule is 0.26 e (Table 1), the net charge decrease on each carbon atom with respect to the cyclopentadienyl anion is (1.0–0.26): 5 = 0.15 e (Table 2, Column 2), which must result in some de-shielding of carbon atoms by 0.15 × 128.5 = 19.3 ppm (Column 3) as compared with the cyclopentadienyl anion (δ 102.8 ppm, two first lines of Table 2). Then the chemical shift of the carbon atoms of a planar cyclopentadienyl ring having the same charge as it has in ferrocene $\delta\ Cp^{-0.26}$, must be 102.8 + 19.3 = 122.1 ppm (Column 4). In reality it is 67.9 ppm in ferrocene (Column 5). Hence the combined effect of factors not involving the charge is 67.9 − 122.1 = − 54.2 ppm (Column 6). These values are graphically represented in Fig. 1.

Table 2 (Column 6) lists the calculated coordination effect (this will be our short notation for the combined effect of factors not involving the charge and arising from coordination, on chemical shifts of the ring carbon nuclei) for all the investigated cyclopentadienyl compounds of transition and non-transition metals. The resulting picture is much clearer than that which can be derived directly from the ^{13}C chemical shifts.

Indeed, the change of shielding of the carbon atoms of a cyclopentadienyl ligand produced by coordination with metal may be both larger and smaller than it is in the cyclopentadienyl anion (Fig. 2). The information that can be derived from chemical shifts is not characteristic of the metal nature, since the shielding of carbon atoms of the cyclopentadienyl ring for non-transition metal compounds lies within the range of shielding of transition metal compounds (Fig. 2).

At the same time, the coordination effect in all the investigated cyclopentadienyl compounds of both transition and non-transition metals is a shielding one, being markedly higher for transition than for non-transition metals. The coordination effect (Table 3) is at a maximum in iron-subgroup metallocenes, nearly the same in cyclopentadienyl-

*Author to whom correspondence should be addressed.

Table 1. The net charges (f) in the cyclopentadienyl ring[4] and the ^{13}C chemical shifts of the cyclopentadienyl ligand in cyclopentadienyl metal compounds

Compound	f (a.u.)	$\delta^{13}C$ (ppm)	Reference
$Cp^-(S)Na^+$ [a]	-I.0	I02.7 [b]	5
$Cp^-(S)Li^+$ [a]	-I.0	I02.9 [b]	5
KCp	-0.72	I03.I [c]	8
NaCp	-0.69	I02.7 [c]	5
LiCp	-0.64	I03.2 [c]	5
TlCp	-0.44	I07.5 [d]	9
$CuCp(PEt_2Ph)$	-0.45	94.7 [c]	
$PdCp(C_3H_5)$	-0.29	94.3 [e]	I0
$FeCp_2$	-0.26	67.9 [f]	I0
$RuCp_2$	-0.25	70.6 [e]	I0
$OsCp_2$	-0.25	63.9 [e]	I0
Rh(NBD)Cp	-0.23	84.8	II
Rh(COD)Cp	-0.I9	86.5	II
$MnCp(CO)_3$	-0.05	83.I [f]	I0
$ReCp(CO)_3$	-0.02	84.5 [e]	I0
$[FeCp_2]H]^+$	-0.03	78.0 [g]	I2
$MoCp_2(NO)I$	+0.04	III.6 [h]	I3

[a] Solvent-separated ion pairs [4–7]; [b] HMPTA; [c] THF; [d] $C_6D_6/(CD_3)_2SO$ I:3; [e] C_6D_6; [f] $CDCl_3$; [g] $BF_3 \cdot H_2O$; [h] CH_2Cl_2.

manganese- and -rheniumtricarbonyl, still rather high in diene complexes of rhodium, much smaller in Pd, Cu and Mo compounds, and quite small in Tl and alkali metal compounds. It can easily be seen that this series correlates fairly well with the metal-ring bond strength.

It is most convenient to illustrate this relationship on the example of the preparation of some cyclopentadienyl metal compounds from others. Indeed, the reaction of cyclopentadienyl compounds of non-transition metals Li, Na, K, Tl with halogenides, carbonyl, nitrosyl, phosphine halogenides and other complex halogenides of metals is the most general method for preparing mono-, bis-, and poly-cyclopentadienyl metal compounds. Reactions of copper cyclopentadienyltriethylphosphine or palladium allylcyclopentadienyl (representatives of the group of transition metal complexes where the coordination effect is relatively small) with iron chloride yield ferrocene.[17,18]

These are followed by compounds with a much stronger metal-ring bond. In most reactions of (diene)cyclopentadienyl complexes of rhodium the Rh–Cp fragment remains unaffected. Then, cyclopentadienylmanganese- and -rheniumtricarbonyl are very stable, and ferrocene, ruthenocene, and osmocene are extremely stable compounds.

We will now give a more detailed characterisation of these groups of compounds.

In cyclopentadienyl compounds of alkali metals the position of the ^{13}C chemical shift is practically independent of the nature either of metal or solvent and is about the same as the ^{13}C chemical shift for the "free" cyclopentadienyl anion (Table 4). The obvious reason is that the de-shielding effect of charge decrease in the cyclopentadienyl rings in alkali metal compounds is not high with respect to the cyclopentadienyl anion (Table 2, Column 3) and is normally offset by the combined shielding effect of other factors (Column 6). When, under the influence of solvent, the metal atom moves farther away from the cyclopentadienyl ring, the shielding effect of coordination decreases, but the negative charge in the ring, and therefore the shielding effect

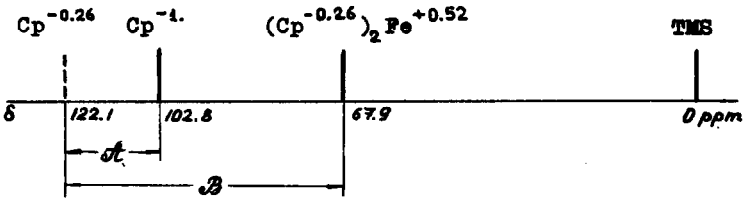
Table 2. The change in shielding of ^{13}C nuclei of the cyclopentadienyl ligand upon coordination with metal

Compound	Δf_c	Ring charge decrease effect (ppm)	δCp^f (ppm)	^{13}C chemical shift (ppm) [i]	Coordination effect (ppm)
I	2	3 (A,Fig.I)	4	5	6 (B,Fig.I)
$Cp^-(S)Na^+$ [a]	0			I02.7 [b]	
$Cp^-(S)Li^+$ [a]	0			I02.9 [b]	
KCp	0.06	7.7	II0.5	I03.I [c]	-7.4
NaCp	0.06	7.7	II0.5	I02.7 [c]	-7.8
LiCp	0.07	9.0	III.8	I03.2 [c]	-8.6
TlCp	0.II	I4.I	II6.9	I07.5 [d]	-9.4
$CuCp(PEt_2Ph)$	0.II	I4.I	II6.9	94.7 [c]	-22.2
$PdCp(C_3H_5)$	0.I4	I8.0	I20.8	94.3 [e]	-26.5
$FeCp_2$	0.I5	I9.3	I22.I	67.9 [f]	-54.2
$RuCp_2$	0.I5	I9.3	I22.I	70.6 [e]	-5I.5
$OsCp_2$	0.I5	I9.3	I22.I	63.9 [e]	-58.2
Rh(NBD)Cp	0.I5	I9.3	I22.I	84.8	-37.3
Rh(COD)Cp	0.I6	20.6	I23.4	86.5	-36.9
$MnCp(CO)_3$	0.I9	24.4	I27.2	83.I [f]	-44.I
$ReCp(CO)_3$	0.20	25.7	I28.5	84.5 [e]	-44.0
$FeCp_2]H\}^+$	0.I9	24.4	I27.2	78.0 [g]	-49.2
$MoCp_2(NO)I$	0.2I	27.0	I29.8	III.6 [h]	-I8.2

[a] Solvent-separated ion pairs [4–7]; S - solvent; [b] HMPTA; [c] THF; [d] $C_6D_6/(CD_3)_2SO$ I:3; [e] C_6D_6; [f] $CDCl_3$; [g] $BF_3 \cdot H_2O$; [h] CH_2Cl_2; [i] Cf.refs. in Table I.

of the charge, increases and the two effects compensate each other. For this reason, the ^{13}C NMR data for cyclopentadienyl compounds of alkali metals are insufficient for deciding in what particular form the corresponding compound is present in solution. The degree to which the state of cyclopentadienyl ring approaches that of anion may be determined from the ^7Li NMR shifts of cyclopentadienyl lithium in different solvents,[7] the ^{19}F NMR shifts of *p*-fluorophenylcyclopentadienyl compounds of alkali metals[6] (Table 4), as well as from the spin–spin coupling constants $^1J(^{13}C, ^1H)$ of cyclopentadienyl compounds of alkali metals[5,9] (Table 4).

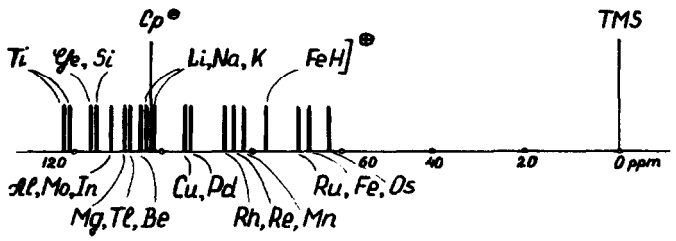
Cyclopentadienylthallium merits special attention. As regards the polarity of the metal-ring bond this complex is not different from the copper derivative (Table 1), but the coordination effect with thallium is not high and, according to this characteristic, it falls into the category of non-



A - the de-shielding effect of ring charge decrease in ferrocene with respect to the cyclopentadienyl anion.

B - effect of coordination with iron atom in ferrocene molecule.

Fig. 1. The relative contributions to the shielding of the ^{13}C nuclei of the cyclopentadienyl ligand in ferrocene molecule.



δ (ppm)	Compound	Reference
123.1	$TiCpCl_3$	10
121.3	$TiCp_2Cl_2$	14
116.8	$TiCp_2Ph_2$	14
116.7	$GeCpMe_3$	15
115.8	$SiCpMe_3$	15
111.6	$MoCp_2(NO)I$	13
111.6	$AlCpMe_2$	9
111.5	$InCpEt_2$	9
108.6	$MgCp_2$	16
107.5	TlCp	9
104.7	BeCp(σ-Ph)	9
~103	LiCp, NaCp, KCp	cf. Table 4
94.7	$CuCp(PEt_2Ph)$	
94.3	$PdCp(C_3H_5)$	10
86.5	Rh(COD)Cp	11
84.8	Rh(NBD)Cp	11
84.5	$ReCp(CO)_3$	10
83.1	$MnCp(CO)_3$	10
78.0	$\{FeCp_2]H\}^+$	12
70.6	$RuCp_2$	10
67.9	$FeCp_2$	10
63.9	$OsCp_2$	10

Fig. 2. The ^{13}C chemical shifts of the cyclopentadienyl ligand. Corresponding metal compounds are given in the list.

transition metals (Table 3) which is quite consistent with its actual chemical properties.

The next group includes compounds of palladium, copper and molybdenum, the metals of Groups VIII, I and VI of the Periodic Table, respectively. $PdCp(C_3H_5)$, $CuCp(PEt_2Ph)$ and $MoCp_2(NO)I$ are compounds of quite different types. Their respective electron densities in the cyclopentadienyl ring are also different (Table 1). However their coordination effects are close (Table 3) and they exhibit similar chemical behaviour, namely the tendency for the σ, π-rearrangement of the cyclopentadienyl group.

The hypothesis that the lability of the π-cyclopentadienyl group in allylcyclopentadienylpalladium is due to its possible rearrangement into that of σ-bonded type during the reaction was first advanced by Nesmeyanov and Rubezhov as early as in 1964[18] and was later used by Werner[21] to explain the reactions between allylcyclopentadienyl compounds of palladium and a number of Lewis bases. In 1980 he published a paper in which the σ, π-rearrangement of the cyclopentadienyl group in allylcyclopentadienyl compounds of palladium was demonstrated experimentally.[22] If the tert-butyl group is in position 2 of the allyl ligand, then, on addition of a phosphine molecule, the π-cyclopentadienyl group is transformed into that of the σ-bonded type. If it is the methyl group which is located in position 2 of the allyl ligand, the complex resulting from reaction with phosphine exists in solution as a mixture of two isomers, π-cyclopentadienyl-σ-allyl and π-allyl-σ-cyclopentadienyl, in comparable concentrations. The σ, π-rearrangement of the cyclopentadienyl group in allylcyclopentadienylpalladium is initiated by introduction of additional phosphine ligand.

It has been supposed that the oxidative addition of monohapto-cyclopentadienyl compound of copper at the carbon–halogen bond may be the first

Table 3. Effect of coordination with metal (ppm)

$OsCp_2$	-58.2
$FeCp_2$	-54.2
$RuCp_2$	-51.5
$FeCp_2]H\}^+$	-49.2
$MnCp(CO)_3$	-44.1
$ReCp(CO)_3$	-44.0
Rh(NBD)Cp	-37.3
Rh(COD)Cp	-36.9
$PdCp(C_3H_5)$	-26.5
$CuCp(PEt_2Ph)$	-22.2
$MoCp_2(NO)I$	-18.2
TlCp	-9.4
LiCp	-8.6
NaCp	-7.8
KCp	-7.4

step of reactions between pentahapto-cyclopentadienylphosphine complexes of copper and different organic halides.[23] Actually, the proton spectrum of cyclopentadienyltriethylphosphinecopper in liquid sulphur dioxide at $-70°C$ contains three lines with area ratio 2 : 2 : 1. Such a spectrum indicates that the solution contains the σ-cyclopentadienyl compound.[24] The SO_2 molecule, being a Lewis base, may play the same role in the solution of copper compound as the phosphine molecule in allylcyclopentadienylpalladium, provoking the σ, π-rearrangement of the cyclopentadienyl group.

In reactions of the copper and palladium compounds in question the σ, π-rearrangement may be promoted by the approaching reactant molecules as well.

The σ, π-rearrangement of the cyclopentadienyl ligand may be assumed to occur as well in bis-(cyclopentadienyl)nitrosyl complexes of molybdenum $MoCp_2(NO)X$ where X is a one-electron ligand.

X-ray examination of these complexes has shown that their two cyclopentadienyl rings are structurally identical but exhibit asymmetric bonding to the metal atom with two relatively short, one intermediate, and two long Mo–C bond dis-

Table 4. The ^{13}C chemical shifts of the cyclopentadienyl ring in alkali metal compounds

Compound	Solvent	$\delta^{13}C$ (ppm)	$^1J(^{13}C,^1H)$ (Hz)	Ref.	$\delta^{19}F$ [b] (ppm)
$Cp^-(S)Li^+$ [a]	HMPTA	102.9	153.7	5	17.9
$Cp^-(S)Na^+$ [a]	HMPTA	102.7	153.7	5	17.8
LiCp	THF	103.2	159.6	5	11.1
LiCp	THF	103.5		19	
LiCp	diglym	103.3		19	
LiCp	$(CD_3)_2SO$	103.7		19	
LiCp	DME/C_6D_6 3:1	103.6	159.4	9	
NaCp	THF	102.7	157.4	5	12.3
NaCp	DME/C_6D_6 3:1	103.4	156.5	9	
KCp	THF	103.1		8	13.2
KCp	DME/C_6D_6 3:1	104.8	155.9	9	
MCp [c]	THF	103.1		20	

[a] Solvent-separated ion pairs [4–7].

[b] Measured for ~0.1 M solutions of $MC_5H_4C_6H_4F$-p, M=Li,Na,K [6] in ppm relative to C_6H_5F; the positive sign indicates the shift to strong field.

[c] The alkali metal unspecified.

tances.[25,26] These complexes may be considered as twenty-electron ones. Several ideas have been advanced to obviate this quite unusual situation and to explain the equivalence of the protons and carbon atoms of the rings in the NMR spectra of these complexes at normal temperature.

King proposed that they contain one trihapto- and one pentahapto-cyclopentadienyl rings, with the trihapto-ring rapidly rotating about the metal-ring axis and fast exchange taking place between the rings.[27] Cotton considered the equivalent rings as donors of four electrons[28] and believed that such a peculiar type of the ring-metal bonding was merely a transient situation in the rapid exchange of the pentahapto- and monohapto-cyclopentadienyl rings.[29] According to McCleverty, the apparent equivalence of the cyclopentadienyl groups could arise via electronic interchange of the two rings through η^5-, η^4-, η^3-, η^2- and η^1-bonding modes. Consequently, the compounds must react in solution in a way typical of species containing M–C σ bonds.[30] In fact, he showed that reactions between bis(cyclopentadienyl)nitrosyliodide of molybdenum and different acids such as HI, RCO_2H, or $RCOCH_2OCR$ involved cleavage of cyclopentadiene and formation of the corresponding iodide, carboxylate, or β-diketonate.[31] Furthermore, reactions with dienophiles yielded Diels–Adler adducts.[32]

From the above data one may draw the conclusion that the complexes characterized by an intermediate coordination effect show a tendency for σ, π-rearrangement of the cyclopentadienyl ligands. Complexes having a high effect of coordination with the metal do not show such a tendency.

Hence, the proposed method of estimation of the contributions of different factors to the ^{13}C NMR chemical shifts of the ligand consisting in elimination of the effect of charge and determination of the combined effect of the remaining factors (the coordination effect) permits us to establish the relationship between the ^{13}C NMR data and the chemical properties of cyclopentadienyl compounds of a large variety of metals.

Acknowledgement—The authors are very grateful to Nina P. Gambaryan for helpful discussion.

REFERENCES

1. B. E. Mann and B. F. Taylor, ^{13}C *NMR Data for Organometallic Compounds*. Academic Press, New York (1981).
2. G. L. Nelson and E. A. Williams, *Progress in Physical Organic Chemistry* (Edited by R. W. Taft), Vol. 12, p. 229 (1976).
3. B. E. Mann, *Advances in Organometallic Chemistry* (Edited by F. G. A. Stone and R. West), Vol. 12, p. 135 (1974).
4. N. A. Ogorodnikova and A. A. Koridze, *Polyhedron* 1983, **2**, 941.
5. N. A. Ogorodnikova, A. A. Koridze, E. I. Fedin and P. V. Petrovsky, *Izv. AN SSSR. Ser. Khim.* 1983, 2047.
6. N. A. Ogorodnikova, A. A. Koridze and S. P. Gubin, *J. Organometal. Chem.* 1981, **215**, 293.
7. R. H. Cox and W. H. Terry, *J. Mag. Reson.* 1974, **14**, 317.
8. D. H. O'Brien, A. J. Hart and C. R. Russel, *J. Am. Chem. Soc.* 1975, **97**, 4410.
9. P. Fischer, J. Stadelhofer and J. Weidlein, *J. Organometal. Chem.* 1976, **116**, 65.
10. A. N. Nesmeyanov, E. I. Fedin, L. A. Fedorov and P. V. Petrovsky, *Zh. Strukt. Khimii* 1972, **13**, 1033.
11. G. M. Bodner, B. N. Storhoff, D. Doddrell and I. J. Todd, *J. Chem. Soc. Chem. Commun.* 1970, 1530.
12. A. A. Koridze, P. V. Petrovsky, S. P. Gubin and E. I. Fedin, *J. Organometal. Chem.* 1975, **93**, C26.
13. A. A. Koridze, private communication.
14. L. F. Farnell, E. W. Randall and E. Rosenberg, *J. Chem. Soc., Chem. Commun.* 1971, 1078.
15. Yu. K. Grishin, N. M. Sergeyev and Yu. A. Ustynyuk, *Org. Mag. Reson.* 1972, **4**, 377.
16. P. C. Lauterbur and R. B. King, *J. Am. Chem. Soc.* 1965, **87**, 3266.
17. G. Wilkinson and T. S. Piper, *J. Inorg. Nucl. Chem.* 1956, **2**, 32.
18. S. P. Gubin, A. Z. Rubezhov, B. L. Winch and A. N. Nesmeyanov, *Tetrahedron Lett.* 1964, 2881.
19. U. Edlund, *Org. Mag. Reson.* 1977, **9**, 593.
20. H. Spiesecke and W. G. Schneider, *Tetrahedron Lett.* 1961, 468.
21. H. Werner, *Angew. Chem., Int. Ed. Engl.* 1977, **16**, 1; H. Werner and A. Kühn, *Angew. Chem., Int. Ed. Engl.* 1977, **16**, 412.
22. H. Werner, A. Kühn and C. Burschka, *Chem. Ber.* 1980, **113**, 2291.
23. O. Wennerström and J. Raston, *Acta Chem. Scand.* 1978, **B32**, 463; J.-E. Månsson and O. Wennerström, *Acta Chem. Scand.* 1978, **B32**, 515.
24. G. M. Whitesides and J. S. Fleming, *J. Am. Chem. Soc.* 1967, **89**, 2855.
25. F. A. Cotton and G. A. Rusholme, *J. Am. Chem. Soc.* 1972, **94**, 402.
26. J. L. Calderon, F. A. Cotton and P. Legzdins, *J. Am. Chem. Soc.* 1969, **91**, 2528.
27. R. B. King, *Inorg. Chem.* 1968, **7**, 90.
28. J. L. Calderon, F. A. Cotton, B. G. de Boer and J. Takats, *J. Am. Chem. Soc.* 1971, **93**, 3592.
29. F. A. Cotton, In *Dynamic Nuclear Magnetic Resonance Spectroscopy* (Edited by F. A. Cotton and L. M. Jackman). Academic Press, New York (1975).
30. M. M. Hunt, W. G. Kita, B. E. Mann and J. A. McCleverty, *J. Chem. Soc., Dalton Trans.* 1978, 467; J. A. McCleverty and A. G. Murray, *J. Chem. Soc., Dalton Trans.* 1979, 1424.
31. M. M. Hunt, W. G. Kita and J. A. McCleverty, *J. Chem. Soc., Dalton Trans.* 1978, 474.
32. M. M. Hunt and J. A. McCleverty, *J. Chem. Soc., Dalton Trans.* 1978, 480.

Polyhedron Vol. 4, No. 2, pp. 317–320, 1985
Printed in Great Britain.

0277–5387/85 $3.00 + .00
© 1985 Pergamon Press Ltd.

KINETICS OF THE REACTION OF DI-μ-ACETATODI-μ-OXALATODIAQUODIRUTHENIUM(II,III) ANION WITH N-(2-HYDROXYETHYL)-ETHYLENEDIAMINE-TRIACETATOAQUOTITANIUM(III)

YOICHI SASAKI,† MARIA A. EVERHART and JOSEPH E. EARLEY*
Department of Chemistry, Georgetown University, Washington, D.C. 20057 U.S.A.

(*Received* 13 *March* 1984; *accepted* 14 *April* 1984)

Abstract—Reduction of $[Ru_2(CH_3COO)_2(C_2O_4)_2(H_2O)_2]^-$ by N-(2-hydroxyethyl)–ethylenediaminetriacetatoaquotitanium(III) [Ti(HEDTA)] involves several distinct stages. The first stage has a half-time of less than 1 ms, and is interpreted as a substitution reaction leading to a multinuclear intermediate. The second stage has a second-order rate constant of $5 \times 10^3\ M^{-1}s^{-1}$ [25°C, $\mu = 0.1$ m ($LiCF_3SO_3$)]. The rate-limiting process for the second stage is electron transfer within the assembled multinuclear complex. Subsequent slower stages correspond to breakup of the multinuclear Ru(II)$_2$–Ti(IV) complex formed by electron transfer. The overall rate of reduction of this oxidant by Ti(HEDTA) is less than the corresponding rate for the reaction in which Ti^{3+} acts as reductant, mainly because the stability of the binuclear complex is reduced by the presence of the aminoacid ligand. The data are consistent with the conclusion that the ligand increases the rate of intramolecular ET, probably by reducing geometric change associated with oxidation of Ti(III) to Ti(IV).

In previous papers,[1] we have shown that electron-transfer (hereafter, ET) reactions having Ru(III) complexes as oxidants and Ti(III) species as reductants involve a variety of mechanisms. In the absence of suitable bridging groups, outer-sphere ET occurs if an electron-delocalizing ligand is present on either redox partner. If a ligand that has an open coordination-position and also a pi-electron system that facilitates overlap between electron–donor and electron–acceptor orbitals, is present on the oxidant, then an inner-sphere mechanism prevails. In most cases of this type, formation of a multinuclear complex determines the overall redox rate, since the rate of intramolecular ET is faster than the substitution reaction. However, there is evidence for rate-limiting ET if 3-formylpentane-2,4-dione is the bridging ligand. Carboxylate ligands are efficient bridges, and generally give rise to substitution-limited reactions. However, when $Ru_2(CH_3COO)_2(C_2O_4)_2(H_2O)_2^-$ is the oxidant, ET from Ti^{3+} (through the remote carboxyl group of a μ-oxalato ligand bridging two ruthenium atoms) is slower than the corresponding reaction of monomeric carboxylato-Ru(III) oxidants.

Aminoacid ligands on one of the redox partners can alter the kinetics of oxidation-reduction reactions in at least two ways. On the one hand, differences in substitution-rate[2] can cause differences in rates of formation (or decomposition) of the multinuclear intermediates of inner-sphere reactions; on the other hand, variation of ligands in the first coordination-spheres of oxidant and reductant metal-ions can give rise to substantial differences in the free energy change for intramolecular ET step. Such differences can alter the rate of intramolecular ET within a bridged complex.[3] This latter effect is parallel to the influence of free-energy changes on the rates of ET in the encounter-complexes of reactions involving outer-sphere mechanisms. We now report the effect of an aminoacid ligand on the rate of a Ru (III)–Ti(III) reaction that, in the absence of the ligand, is rate-limited by ET through the bridging ligand.

†On temporary leave from the Faculty of Science, Tohoku University, Sendai, Japan.

*Author to whom correspondence should be addressed.

EXPERIMENTAL

Bis μ-oxalato-μ-diacetatodiaquodiruthenium (II,III) anion

$Ru_2(CH_3COO)_4Cl$ (0.2 g) was added to a solution made by dissolving 0.15 g of oxalic acid in 200 cm^3 of water. The solution was allowed to stand at room temperature until no further change in absorption spectrum occurred (4 *d*). The dark product passed directly through Sephadex G–10 and Dowex 50 columns (though the starting complex was retained) but was retained on Sephadex G–15. The product moved as a single band when eluted from Sephadex G–15 with acidified 0.2% LiCl. Solutions for kinetic runs were prepared by dilution of chromatographic-column effluents, without intermediate preparation of solid. The spectrum of the solutions was reproducible and was the same whether Sephadex or Dowex 50 was used to remove unreacted $Ru_2(CH_3COO)_4Cl$. The peak at 475 nm which is characteristic of $Ru_2(CH_3COO)_2(C_2O_4)_2(H_2O)_2^-$ was both sharper and up to 50% more intense in these solutions than in solutions of the same ruthenium concentration prepared from the solid identified as $[HRu_2(CH_3COO)_2(C_2O_4)_2(H_2O)_2 \cdot 2H_2O]$.[2d]

N-(2-hydroxyethyl)-ethylenediaminetriacetatoaquotitanium(III) (hereafter designated as Ti (HEDTA)) was prepared by reacting Ti^{3+} with a $HEDTA^-$ solution that had a concentration that was 30–50% larger than neccessary for stoichiometric formation of the Ti(HEDTA) complex. Procedures and reagents used for kinetic studies were generally as previously described.[1] A microcomputer-linked Durrum stopped-flow spectrophotometer was used. About 1000 points were taken during each kinetic run.

When Ti(HEDTA) was added to solutions containing $[Ru_2(CH_3COO)_2(C_2O_4)_2(H_2O)_2]^-$, absorbance between 375 and 550 nm decreased by 25% during the time of mixing (1 ms). This was followed by a biphasic absorbance increase, which preceeded slower absorbance-decrease. Absorbance decrease in this case was sufficiently slow as to be neglected for the purpose of fitting the biphasic increase, and was not studied further. In the case of the reaction of the same oxidant with Ti^{3+}, initial absorbance-decrease was not observed, absorbance–increase was monophasic, and the eventual absorbance–decrease was faster than when Ti(HEDTA) was reductant. In the case of the reaction of the same oxidant with Ti^{3+}, spectrophotometric titration showed that one mole of $[Ru_2(CH_3COO)_2(C_2O_4)_2(H_2O)_2]^-$ was consumed for each mole of Ti(III) added.

Kinetic data for the absorbance–increase observed when Ti(HEDTA) was reductant were fitted in terms of a double exponential, yielding two rate constants. The rate constant for the faster change (which accounted for 80% of the absorbance–increase) was designated k_f, that for the slower change was designated k_s. A linear-least-squares program was used to estimate a trial value of k_s from kinetic data taken near the absorbance maximum. Using this value, a second linear-least-squares treatment was applied to data taken during the main absorbance increase to estimate a trial value for k_f. Alternatively, the limiting absorbance-value corresponding to the faster relaxation was estimated and used in the linear-least-squares treatment of the initial data. All the data was then displayed on a CRT and compared with simulation, using the parameters derived by the double-least-squares program. Parameters were adjusted, taking account of instrumental factors, until the simulation agreed with the data within experimental scatter. Reproducibility of k_f was ± 10%.

As before,[2d] kinetic data for Ti^{3+}-reductions were fitted to a double exponential, yielding a rate constant, k_f, corresponding to the absorbance–increase and another, k_s, corresponding to the eventual absorbance–decrease. Kinetic data for both reductions are given in Table 1.

In the case of the Ti(HEDTA) reaction, the value of k_f is linearly dependent on reductant concentration, with a second-order rate constant $k_{2f} = 5 \pm 10^3\ M^{-1}s^{-1}$, but is nearly independent of ionic strength and acidity. The slower reaction measured by k_s and the ultimate absorbance–decrease were not systematically investigated. Results obtained in the case of the reduction of the oxidant by Ti^{3+} are qualitatively similar to those observed earlier,[1d] again showing less than first-order dependence on [Ti(III)] and evidence of approach to a high-[Ti(III)]-low-acid limiting rate. The data listed in Table 1 are consistent with a high-[Ti(III)]-low-acid limiting rate constant of about $10^2\ sec^{-1}$.

DISCUSSION

As in the case of previous Ru(III)–Ti(III) reactions we have studied, the main chemical change in the process of current interest is oxidation of Ti(III)–Ti(IV), with concomitant reduction of Ru(III)–Ru(II). Rates of outersphere Ru(III)–Ti(III) reactions depend on the thermodynamic driving-force in a straightforward way. The rate of the absorbance increase that we observe is more than an order of magnitude faster than the outer-sphere ET rate that is predicted on the basis of the

Table 1. Rate of reaction of Ti^{3+} and Ti(HEDTA) with $[Ru_2(CH_3COO)_2(C_2O_4)_2(H_2O)_2]^-$, 25.0°, $\mu = 0.1M$ ($LiCF_3SO_3$)

[Ti]/mM	[H] /mM	k_f/s^{-1}	$k_{2f}/mM^{-1}s^{-1}$	k_s/s^{-1}
1.7	24	8.4	4.9	0.02[c]
1.7	39	6.3	3.7	0.01[c]
1.7	55	5.5	3.2	0.01[c]
3.0[a]	50	20.4	6.8	
1.7	100	6.1	3.6	
2.1	100	13.6	6.3	
2.9	100	16.4	5.6	0.03[c]
3.0[a]	100	10.0	3.3	
3.0[a]	100	8.2	2.7	
3.0[a]	100	11.5	3.3	
6.0[a]	100	23.0	3.8	
4.7	100	18.7	4.0	
4.7	100	26.6	5.6	
4.7	100	23.5	5.0	
4.8	100	30.2	6.3	
9.0[b]	100	35.8		
3.0[b]	200	24.5		
1.7[b]	100	36		0.17[d]
3.4[b]	100	60		0.13[d]
4.3[b]	100	78		0.14[d]
4.7[b]	100	73		0.14[d]
.86[b]	100	15		0.08[d]
9.0[b]	100	70		0.15[d]
4.5[b]	100	67		
6.7[b]	100	89		0.14[d]
1.7[b]	184	70		0.15[d]

a) μ = 1M ($LiCF_3SO_3$)

b) No HEDTA present, in other runs total ligand concentration was 130% to 150% of the Ti(III) concentration.

c) Rate constant for secondary increase in absorbance.

d) Estimate of rate constant for eventual decrease, treated as a psuedo-first order process.

redox potentials of the two couples involved.[1] We conclude that the reaction of present interest proceeds by means of a mechanism that is faster than outer-sphere ET, namely inner-sphere ET involving a multinuclear intermediate.

Ti(HEDTA) reduces $Ru(NH_3)_5NCS^{2+}$ with a (substitution-limited) second-order rate constant of $3 \times 10^4\ M^{-1}s^{-1}$, which value is higher than the corresponding value for the reaction involving Ti^{3+} and the same oxidant. This indicates that the ligand increases the lability of the water molecule coordinated to Ti(III). Rates of substitution-limited redox reactions of Ti^{3+} depend on the charge type of the redox partners. On the basis of this information, one would expect that the rate of formation of the multinuclear intermediate in reaction of $[Ru_2(CH_3COO)_2(C_2O_4)_2(H_2O)_2]^-$ with Ti(HEDTA) would be greater than $5 \times 10^5\ M^{-1}s^{-1}$. The initial rapid (1 ms) bleaching that we observe can be taken to correspond to formation of an intermediate in which Ti(III) is joined to the diruthenium moiety by an oxalato ligand. In the case of the corresponding reduction involving the Ti(III) aquoion, the intermediate has a formation constant of 300/M: the stability of the intermediate in the reaction of present interest should be somewhat less. On this basis, the absorbance–increase measured by k_f would be due to ET within that intermediate. If the formation of the intermediate is a rapid prior equilibrium, and the formation constant for that intermediate is not large, one would expect that

$$k_f = k_{ET}K[\text{Ti(HEDTA)}]$$

The rate constant k_f, for reaction of $[Ru_2(CH_3COO)_2(C_2O_4)_2(H_2O)_2]^-$ with Ti(HEDTA), is linearly dependent on reductant concentration yielding a second order rate constant (k_{2f}) of $5 \times 10^3\ M^{-1}s^{-1}$. Variation in ionic strength, or in acidity, has little effect on this rate constant. Since Ti(HEDTA) is uncharged, the effect of ionic strength on K should be small. Since the formation of Ti(HEDTA) is complete, no serious acid-dependence of the prior equilibrium is expected. In order to obtain k_{ET} for the Ti(HEDTA) reaction from k_f, an estimate of K is needed. On the basis of comparable reactions, a value of $10\ M^{-1}$ seems reasonable, as an upper limit. Thus the lower limit for k_{ET} is $5 \times 10^2\ s^{-1}$.

The second-order kinetics observed in the reaction of $[Ru_2(CH_3COO)_2(C_2O_4)_2(H_2O)_2]^-$ with Ti(HEDTA) contrasts sharply with previously reported kinetics for reaction of Ti^{3+} with the same oxidant. Our present data on this reaction confirm the prior report that, at high $[Ti^{3+}]$ and low $[H^+]$ a limiting rate is reached. Although the qualitative features of the earlier work have been reproduced, the limiting rate now reported has a somewhat higher value than that reported earlier. This divergence may mainly reflect an ionic strength influence on the formation constant of the multinuclear complex, and/or on the intramolecular redistribution of charge, however the possibility that the divergence arises in the preparation of the oxidant solutions has not been ruled out. (Precipitation may cause rearrangement of $[Ru_2(CH_3COO)_2(C_2O_4)_2(H_2O)_2]^-$.)

The presence of the aminoacid ligand causes a gross change in kinetic behavior. Difference in extinction coefficients brings into prominence the initial intermediate-formation reaction which is not directly (or at least not easily) observable in the absence of the ligand. The presence of the aminoacid changes the formation constant of the intermediate. In the case of Ti^{3+}, the intermediate has a stability constant of $2 \times 10^2\ M^{-1}$. The more negative charge of the complex reductant would be expected to give rise to a less-stable intermediate, and this in turn accounts for the difference in dependence of rate on [Ti(III)] that is observed.

In the presence of the aminoacid ligand there in no acidic proton on the reductant. Base catalysis that is a general feature of Ti(III) redox reactions is not present in this case. Even without formation of a conjugate base, the rate of intramolecular ET seems faster (by about two orders of magnitude) when the ligand is present than when it is absent. Presence of HEDTA would be expected to reduce geometric differences between Ti(III) and Ti(IV) that retard oxidation of Ti(III)–Ti(IV), and hence to increase the rate of the ET reaction. The effectiveness of proton dissociation in fostering intramolecular ET is presumably connected with reducing the same barrier. The presence of the ligand decreases stability of the intermediate and hence reduces overall redox rate.

Acknowledgement—A travel grant from the Yoshida Foundation to Y.S. is gratefully acknowledged. $LiCF_3SO_3$ and CF_3SO_3H solution were kindly supplied by Dr. Patrizia Barone.

REFERENCES

1. (a) J. E. Earley, R. N. Bose and B. B. Berrie, *Inorg. Chem.* 1983, **22**, 1836. (b) R. A. Lee and J. E. Earley, *Inorg. Chem.* 1981, **20**, 1739. (c) R. N. Bose and J. E. Earley, *J. Chem. Soc.* (*Chem. Commun.*) 1983, 59. (d) R. N. Bose, P. A. Wagner and J. E. Earley, *Inorg. Chem.*, in press. (e) B. H. Berrie and J. E. Earley, *Inorg. Chem.* in press.
2. H. Ogino, T. Watanabe and N. Tanaka, *Inorg. Chem.* 1975, **14**, 2093.
3. K. M. Davies and J. E. Earley, *Inorg. Chem.* 1976, **15**, 1074.

Polyhedron Vol. 4, No. 2, pp. 321–324, 1985
Printed in Great Britain.

0277-5387/85 $3.00 + .00
© 1985 Pergamon Press Ltd.

THE REACTION OF PENTABORANE(9) WITH SODIUM CYANIDE AND SODIUM CYANOTRIHYDROBORATE

J. G. TAYLOR and M. G. H. WALLBRIDGE*
Department of Chemistry, University of Warwick Coventry CV4 7AL, England

(*Received* 9 *April* 1984; *accepted* 14 *April* 1984)

Abstract—The reaction of pentaborane(9) with NaCN occurs in a 1:1 molar ratio at temperatures between −30° and +10°C to yield the complex $Na[B_5H_9CN]$, which can be isolated in the form of a dioxanate. When excess pentaborane(9) is used the reaction is relatively clean and yields predominantly the $[B_9H_{14}]^-$ ion. With $NaBH_3CN$ no intermediates of the type $Na[B_5H_9CN]$ are detected, and the major product is the $[B_9H_{14}]^-$ ion, but no hydrogen is evolved in the reaction. Structures for the intermediate anions are suggested. No monocarbon carbaboranes were detected in any of the reactions.

The boron hydrides are usually described as being electron deficient, and not unexpectedly therefore they react with a range of nucleophiles. Interactions with the cyanide ion in particular are varied and lead to bridging,[1] cleavage,[1] and adduct[2] type products, depending on the borane used, as shown in eqns (1)–(3).

$$B_2H_6 + CN^- \rightarrow [H_3BCNBH_3]^- \quad (1)$$

$$B_4H_{10} + 2CN^- \rightarrow [BH_3CN]^- + [B_3H_7CN]^- \quad (2)$$

$$B_{10}H_{14} + 2CN^- \rightarrow [B_{10}H_{13}CN]^{2-} + HCN \quad (3)$$

The adduct type reaction, (3), was of interest to us since the $[B_{10}H_{13}CN]^{2-}$ anion can be protonated to give $B_{10}H_{12}CNH_3$, which is a useful precursor to CB_{10} and CB_9 carbaborane frameworks, where the carbon atom has become incorporated into a cage system.[3] We were encouraged to investigate the reaction with pentaborane(9), B_5H_9, (**1**), for two reasons. Firstly, a preliminary investigation had reported the formation of a simple 1:1 salt, $Na[B_5H_9CN]$, but the product had not been further characterised.[1] Secondly, we had shown in related studies that (**1**), on reaction with the hydride ion as a nucleophile, underwent a rearrangement reaction with the evolution of hydrogen to yield the $B_9H_{14}^-$ ion.[4]

Here we describe the results of investigations of the action of both NaCN and $NaBH_3CN$ on (**1**), at low and ambient temperatures.

EXPERIMENTAL

The reactions were performed using standard vacuum line techniques. In order to facilitate the recording of the ^{11}B NMR spectra, the 100 cm³ round-bottomed reaction flask was fitted with a side-arm incorporating a 5 mm diameter NMR tube that could be flame-sealed. The ^{11}B NMR spectra were recorded at a frequency of 128.4 MHz on a Bruker WH400 spectrometer. No deuterated lock solvents were used, and peaks in the spectra were externally referenced to BF_3.etherate (0 ppm). The IR spectra were recorded on a Perkin–Elmer 580 spectrometer by means of KBr disks. Carbon and hydrogen analyses were performed by Elemental Micro-Analysis Ltd., Devon. Reagent grade pentaborane(9), sodium cyanide, sodium cyanotrihydroborate, 1, 2-dimethoxyethane and 1, 4-dioxan were used, the solvents being dried over lithium aluminum hydride prior to vacuum-line transfer.

Reaction of pentaborane(9) *with* NaCN *and* $NaBH_3CN$

Dry finely ground sodium cyanide (0.31 g, 6.3 mmol) and degassed 1, 2-dimethoxyethane (10 cm³) were placed in a 100 cm³ round-bottomed flask fitted with a side-arm which contained a small sintered disc, and a sealed-on 5 mm NMR tube

*Author to whom correspondence should be addressed.

which had a constriction where it could be sealed-off. Pentaborane(9) (0.40 g, 6.3 mmol) was then condensed into the flask under vacuum at − 196°C. In the low-temperature experiments the reaction temperature was allowed to rise slowly over 30 min, and was then maintained at −25°C by means of a slush-bath (CCl_4) for 2 hr. The temperature was then allowed to rise to +10°C over 4 hr. The reaction mixture was stirred magnetically at the different temperatures, and the sodium cyanide dissolved slowly over the 6 hr period affording a colourless solution. Checks made at various times confirmed that no hydrogen was evolved during the reaction. An aliquot of the clear solution was filtered into the NMR tube through a small sintered glass disc, and the tube was then sealed-off and stored at −196°C. The remaining solution was evaporated to give a clear oil which turned pale-yellow after 3–4 hr at room temperature. Addition of dry 1, 4-dioxan (20 cm^3) to the original cold reaction mixture followed by removal of the solvent under vacuum yielded a slightly oily white solid. Washing with aliquots (10 cm^3) of 1, 4-dioxan followed by pumping yielded a dry white solid (1.50 g). Found: C, 34.9; H, 7.76, B, 21.6. Calc. for $NaB_5H_9CN.1.5C_4H_8O_2$: C, 34.4; H, 8.61, B, 22.1%. The IR spectrum of the solid showed bands at 2500(s), 2460(s) and 2380(s) cm^{-1} from ν(B–H), and 2250(s), 2210(sh) and 2200(sh) cm^{-1} from ν(C–N), where s = strong and sh = shoulder.

The reactions of (**1**) with both NaCN and $Na[BH_3CN]$ at room temperature were performed in a similar manner, except that the mixture was allowed to warm to room temperature immediately after the transfer of (**1**). The reactions appeared to be complete after 3–4 hr as judged by the disappearance of (**1**) from the ^{11}B NMR spectra, and the dissolution of the sodium cyanide.

RESULTS AND DISCUSSION

Sodium cyanide and (**1**) react in dimethoxyethane in a 1:1 molar ratio over the temperature range −30° to +10°C. The reaction is slow in that the solid cyanide dissolves over about 6 hr, but the initial reaction products definitely arise from a 1:1 molar reaction, since when excess cyanide is used only 1 mole dissolves per mole of

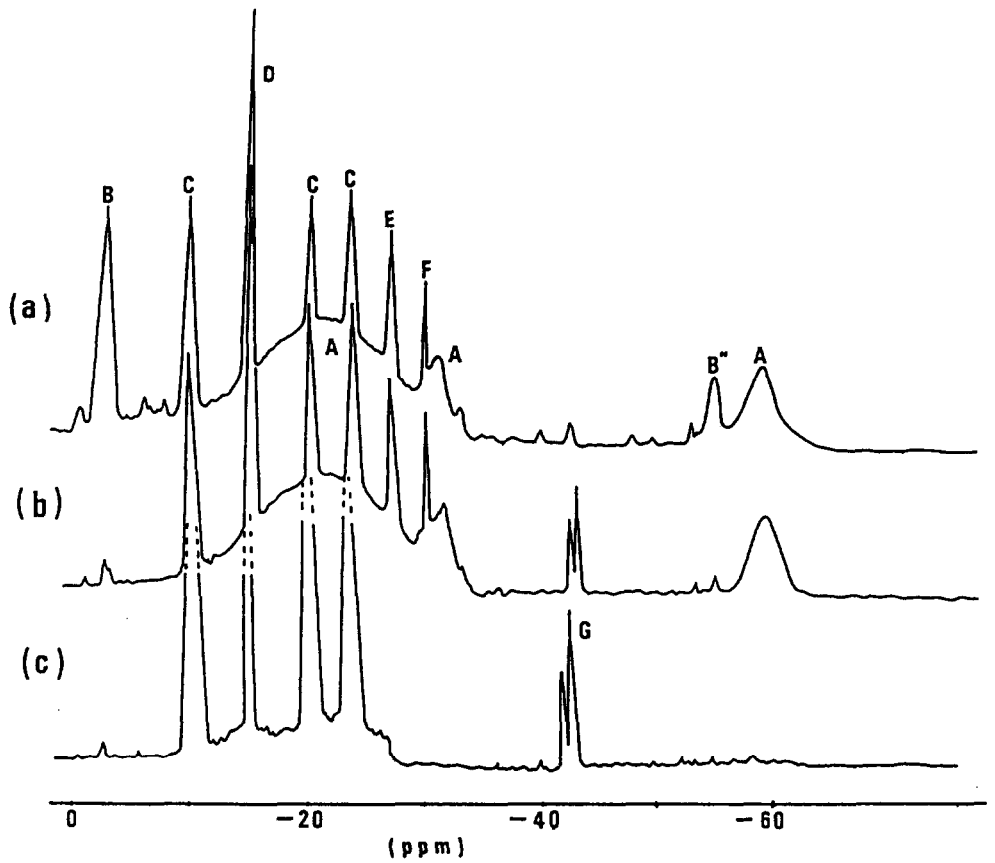


Fig. 1. (a) $^{11}B\{^1H\}$ NMR spectrum at +10°C of B_5H_9/NaCN (1:1 molar ratio) in 1, 2-dimethoxyethane. (b) A similar mixture allowed to react at +25°C. (c) A mixture of B_5H_9/NaCN (2:1 molar ratio) allowed to react at +25°C.

(1). However, in contrast the 1 : 1 molar mixture will react further with an exess of (1) as described below. A notable feature is that only minute traces of hydrogen were detected over the course of the reaction. This is in contrast to the reaction involving the hydride ion where, in addition to the 1 mole of hydrogen expected, further hydrogen is evolved as the reaction proceeds.[4]

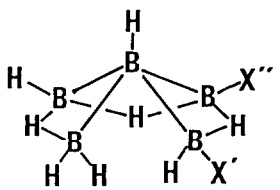
The reaction may be followed conveniently by changes in the $^{11}B\{^1H\}$ NMR spectrum recorded at 10°C. A typical spectrum, as shown in Fig. 1(a), is obtained from a reaction mixture (1:1 molar ratio) which had been allowed to warm from −30° to +10°C over 6 hr, when all the solid sodium cyanide had dissolved. The major part of the reaction products (for a mass balance of the different products see details of the 1:1 molar reaction run at room temperature given below) consists of three very broad resonances (labelled A in Fig. 1a) with relative intensities of 3:1:1.

The peaks narrow slightly on cooling to −60°C, but do not show any ^{11}B–^1H coupling at either temperature. The broadness of the peaks, and the lack of any ^{11}B–^1H coupling, is reminiscent of the spectra of other substituted pentaborane compounds including the unsymmetrical adducts $B_5H_9.2L$ (L = NMe_3 or PMe_3).[4-6] These resonances would appear therefore to be best assigned to an open-cage species, *arachno*-$[B_5H_9CN]^-$, (2), in which the cyanide group is attached to the B(2) or B(3) positions. Such a species is iso-electronic and -structural with *arachno*-B_5H_{11}. The resonance of intensity 3 then arises from the three unsubstituted basal boron atoms, which are either equivalent due to a fluxional process, or not resolved within the very broad peak. The high-field resonance is assigned to the apical boron atom B(1), and the remaining resonance to the B–CN group.

peratures. The low-field resonance, B (intensity 4), exhibits a ^{11}B–^1H coupling of 94 Hz which is intermediate between the values normally associated with B–H (terminal) (*ca.* 140 Hz) and B–H (bridging) (*ca.* 40 Hz).[7] However, the high-field signal, B′, (intensity 1) does not show any ^{11}B–^1H coupling, and presumably arises from a B–CN group. It would appear therefore as though the initial attack of the cyanide ion occurs at the apical boron atom, yielding an ion as in (2), or possibly occupies a bridging position between the apical site and one of the basal atoms causing asymmetry in the field around the apical boron, and a broadening of the resonance. Although nucleophilic substitution in (1) is usually found to occur at the basal borons, it is known that such substitution can also occur at the apical position as in $B_5H_9 \cdot 2L$ [L = PMe_3,[8] $Ph_2P(CH_2)PPh_2$[5]]. Also since the room temperature product appears to be basal substituted, it is relevant that a rapid isomerisation process is known to occur in alkyl- and halopentaboranes, when the group is transferred at ambient temperatures or above from the apical to basal positions.[6]

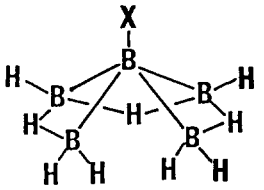
Species C (Fig. 1a) arises from the *arachno*-$[B_9H_{14}]^-$ ion, as shown by a comparison of ^{11}B NMR chemical shifts and coupling constants,[9] and becomes a major product if the reaction is run at room temperature as outlined below. The species D and E were not unambiguously identified, but it is likely that D is an end product of B–H condensation reactions [i.e. $(B_nH_n)^{2-}$], in view of the presence of $[B_9H_{14}]^-$, and small amounts of the $[B_3H_8]^-$ ion (F) also observed. The chemical shift and ^{11}B–^1H coupling constant of D do in fact compare well with those of the $[B_{12}H_{12}]^{2-}$ ion.[10]

A solid product can be isolated from the reaction mixture by the addition of 1, 4-dioxan. After washing and pumping dry the IR spectrum shows evidence for the existence of B–H (*ca.* 2500 cm^{-1}), C ≡ N (*ca.* 2200 cm^{-1}) and co-ordinated dioxan. The solvated species appears to have a composition best represented by $Na[B_5H_9CN] \cdot 1.5C_4H_8O_2$.



(1)

(X'=CN, X''=H; X'=H, X''=CN)



(2)

(X = CN)

The two resonances B, B′ in Fig. 1(a) arise from a reactive low-temperature intermediate, since they disappear at the same rate over a few hours when the NMR sample is warmed to room temperature, and do not appear at all in reaction mixtures which have been held throughout at ambient tem-

When the reaction (1:1 molar ratio) was carried out at 25°C over 4 hr, the ^{11}B NMR spectrum of the clear solution (Fig. 1b) was similar to that discussed above, but no signals due to the species B were observed. The overall mass balance (based on the ratios of integrated intensities in the ^{11}B NMR spectrum) for the different products was approximately $[B_5H_9CN]^-$ (55%), $[B_9H_{14}]^-$ (20%), species D, $[B_{12}H_{12}]^{2-}$? (20%), and $[B_3H_8]^-$ (5%). The other unknown minor species E in the low-temperature spectrum also disappears on warming, but does so at a different rate to B, and we assume therefore that these two species are not related.

Significant changes did occur in the final spectrum when 2 moles of (**1**) was allowed to react with 1 mole of cyanide at 25°C for 4 hr. In this case no resonances due to either species A or B were observed, and the spectrum contained essentially only resonances arising from the $[B_9H_{14}]^-$ ion, (Fig. 1c) species D again presumably $[B_{12}H_{12}]^{2-}$, and also $[BH_3CN]^-$, (G), which was only formed in any significant quantity when excess of (**1**) was present. The relative proportions of these three products from the integrated ratios were 80, 10 and 5% respectively, with other minor resonances making up the remaining 5% of the products. The reactions involving an excess of (**1**) were always the cleanest, giving the minimum number of products, and again a noteworthy feature of the reaction is the absence of any hydrogen being evolved over the 4 hr reaction time.

Only a few reactions between (**1**) and $Na[BH_3CN]$ were investigated. The 1:1 molar reaction carried out at room temperature showed no broad signals (A or B) assigned to $[B_5H_9CN]^-$ as above. Instead the major products were again the $[B_9H_{14}]^-$ anion, and the species, $[B_{12}H_{12}]^{2-}$?, together with smaller quantities of F, $[B_3H_8]^-$ and traces of unreacted $[BH_3CN]^-$, and $[BH_3CNBH_3]^-$.

All of the reactions described were carried out many times with very little variation in the results. Possibly the most interesting point is the fate of the cyanide ion, in that the only obvious product which incorporates it is the $[B_5H_9CN]^-$ ion, but in many of the reactions it would appear to act as an intermediate in the conversion of (**1**) to higher borane anions. We have not detected any incorporation of the cyanide ion into the borane fragment, to form a monocarbon carbaborane as found with $B_{10}H_{14}$; instead it acts as a simple substituent as in the $[B_5H_9CN]^-$ ion. We have not detected any HCN in the reactions, and in view of these results it is tempting to speculate that the conversion of (**1**) to higher anions may be generally catalysed by anions, and of the three investigated in any detail (H^-, BH_4^- and CN^-) it is not surprising that hydrogen evolution occurs with the hydridic ions. We are currently investigating further whether other non-hydridic anions are also capable of achieving similar transformations.

Acknowledgement—We thank Dr. R. E. Williams for a gift of pentaborane(9), and the S.E.R.C. for support of this work.

REFERENCES

1. V. D. Aftandilian, H. C. Miller and E. L. Muetterties, *J. Am. Chem. Soc.* 1961. **83**, 2471.
2. W. H. Knoth and E. L. Muetterties, *J. Inorg. Nucl. Chem.* 1961, **20**, 66.
3. W. H. Knoth, *J. Am. Chem. Soc.* 1967, **89**, 1274.
4. C. G. Savory and M. G. H. Wallbridge, *J.C.S. Dalton Trans.* 1973, 179.
5. N. W. Alcock, H. M. Colquhoun, G. Haran, J. F. Sawyer and M. G. H. Wallbridge, *J.C.S. Dalton Trans.* 1982, 2243.
6. D. F. Gaines, *Acc. Chem. Res.* 1973, **6**, 416, and references therein.
7. H. Nöth and B. Wrackmeyer, *NMR of Boron Compounds.* Springer–Verlag, Berlin (1978).
8. A. V. Fratini, G. W. Sullivan, M. L. Denniston, R. K. Hertz and S. G. Shore, *J. Am. Chem. Soc.* 1974, **96**, 3013.
9. N. N. Greenwood, H. J., Gysling, J. A. McGinnety and J. D. Owen, *J.C.S. Chem. Comm.* 1970, 505.
10. V. D. Aftandilian, H. C. Miller, G. W. Parshall and E. L. Muetterties, *Inorg. Chem.* 1962, **1**, 734.

Polyhedron Vol. 4, No. 2, pp. 325–331, 1985
Printed in Great Britain.

0277–5387/85 $3.00 + .00
© 1985 Pergamon Press Ltd.

DICARBOXYLATE RHODIUM COMPLEXES WITH DIOLEFINS AND CARBON MONOXIDE

L. A. ORO,* M. T. PINILLOS and M. P. JARAUTA
Departamento de Química Inorgánica, Universidad de Zaragoza, Zaragoza, Spain

(*Received* 2 *March* 1984; *accepted* 14 *April* 1984)

Abstract—Dinuclear rhodium complexes of the type $[Rh_2(C_2O_4)(diolefin)_2]$ (diolefin = 1,5-cyclooctadiene,2,5-norbornadiene and tetrafluorobenzobarrelene) with bridging oxalate ligands have been obtained by reaction of [Rh(acac)(diolefin)] with oxalic acid (2 : 1 mol ratio). The use of a 1 : 1 molar ratio affords $[Rh(HC_2O_4)(COD)]$, that reacts with [Ir(acac)(COD)] yielding the heterodinuclear [(COD)Rh(C_2O_4)Ir(COD)] complex. Treatment of $[Rh_2(C_2O_4)(diolefin)_2]$ complexes with phenanthroline type ligands leads to ionic complexes of formula [Rh(diolefin)(phen)][Rh(C_2O_4)(diolefin)]. Bubbling of carbon monoxide through solutions of the diolefin complexes leads to the formation of carbonylrhodium species of formula $[Rh_2(C_2O_4)(CO)_2L_2]$ (L = CO, PPh_3, *t*-BuNC) or $[Rh(CO)_2(phen)]$ – $[Rh(C_2O_4)(CO)_2]$. Other related malonate complexes are also described.

A number of organorhodium(I) compounds containing bidentate oxygen anions have been reported.[1] In particular the β-diketonate anions form a variety of complexes which have six-membered rings. Concerning rhodium(I) complexes which have five-membered rings, some tropolonate derivatives have been recently reported.[2] We describe in this paper some organorhodium complexes with the oxalate group. This dicarboxylate anion forms well-defined complexes which have five-membered rings, and it is able to function as a bidentate ligand to two metals simultaneously. In contrast, monocarboxylate anions in rhodium(I) chemistry are usually bound in a symmetrical *syn–syn* bridging.[3]

RESULTS AND DISCUSSION

Oxalate diolefin complexes

The reaction of [Rh(acac)(COD)] with a stoichiometric amount of oxalic acid leads to the formation of the yellow microcrystalline compound $[Rh(HC_2O_4)(COD)]$ (**I**). The experimental molecular weight measurements suggest a self-association by hydrogen bonding (Scheme 1). The acidic hydrogen atom in complex **I** can be removed with ease; thus, addition of [M(acac)(diolefin)] derivatives gives dinuclear complexes of formula [(COD)Rh(C_2O_4)Rh(diolefin)] (diolefin = 1,5-cyclooctadiene, COD (**II**) or tetrafluorobenzobarrelene, TFB (**III**)) or the heterodinuclear compound [(COD)Rh(C_2O_4)Ir(COD)] (**IV**).

A direct method of preparing homodinuclear complexes involves the reaction of two moles of [Rh(acac)(diolefin)] with one mole of oxalic acid, according to eqn (1):

$$2[Rh(acac)(diolefin)] + H_2C_2O_4 \cdot 2H_2O \rightarrow [Rh_2(C_2O_4)(diolefin)_2] + 2\,Hacac + 2\,H_2O \quad (1)$$

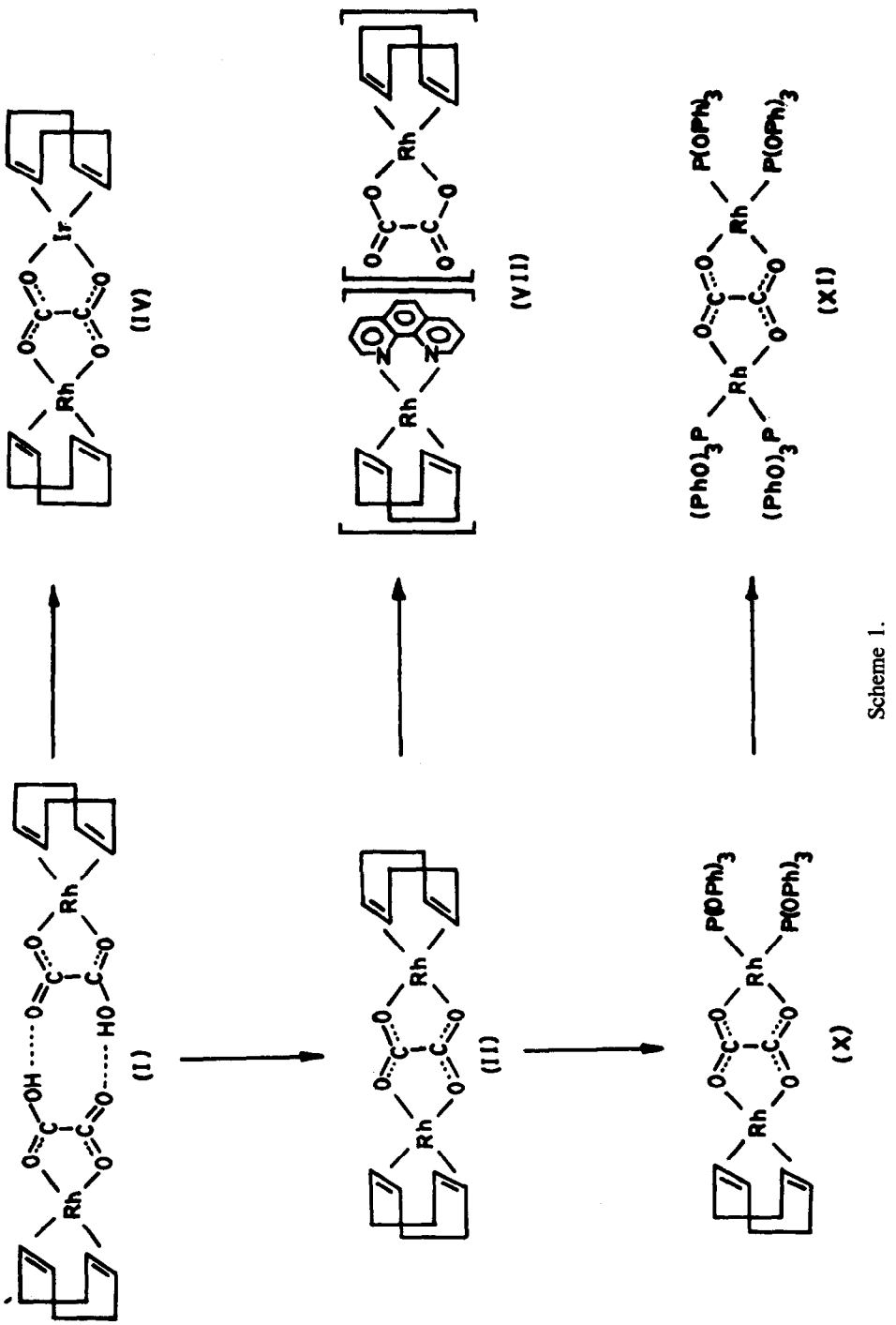
[diolefin = COD(**II**), TFB(**V**), NBD(**VI**)].

Molecular weight measurements confirm the dinuclear formulation. Scheme 1 shows the suggested structures (five-membered chelate rings).

The $[Rh_2(C_2O_4)(diolefin)_2]$ complexes usually react readily with different ligands. Thus, addition of the bidentate nitrogen donor ligand 1,10-phenanthroline leads to the formation of ionic derivatives of formula [Rh(diolefin)(phen)] – [Rh(C_2O_4)(diolefin)] (diolefin = COD(**VII**) or TFB(**VIII**)). Similarly, complex **V** reacts with 2,2′-bipyridine to give the analogous [Rh(TFB)(bipy)] [Rh(C_2O_4)(TFB)] derivative (**IX**). The electrical conductivities of complexes **VIII**–**IX** show them to be 1/1 electrolytes. In particular the constituent cations of these complexes are reported species[4,5] of high stability.

The stepwise addition of triphenylphosphite to $[Rh_2(C_2O_4)(COD)_2]$ affords the dinuclear derivatives [(COD)Rh(C_2O_4)Rh$\{P(OPh)_3\}_2$] (**X**) and $Rh_2(C_2O_4)\{P(OPh)_3\}_4$] (**XI**), but no further reaction

*Author to whom correspondence should be addressed.



Scheme 1.

was observed by adding excess of triphenylphosphite at room temperature. A similar reaction has been previously reported by Haines[6] by stepwise addition of triphenylphosphite to the compound $[Rh_2Cl_2(COD)_2]$, but the chloride bridges of the $[Rh_2Cl_2\{P(OPh)_3\}_4]$ complex can be cleaved with formation of $[RhCl\{P(OPh)_3\}_3]$. On the other hand, the related complex $[Rh_2(C_2O_4)(PPh_3)_4]$ (**XII**) can be prepared by adding four moles of triphenylphosphine to one mole of complex **II**.

Table 1 lists the analytical data for the isolated complexes.

Oxalate carbonyl complexes

Bubbling carbon monoxide through a dichloromethane solution of complex **II** leads to the displacement of the coordinated diolefin, causing an instantaneous change in colour from yellow to violet, which is followed by the precipitation of violet microcrystals, which were identified as the complex $[Rh_2(C_2O_4)(CO)_4]_x$ (**XIII**). The usual planarity of the oxalate group[7] probably favours the presence of an intermolecular rhodium–rhodium interaction[2a,8] in complex **XIII** as is suggested by the dark colour and dichroism of the compound, along with a complex IR spectrum in nujol mull (2100–1990 cm^{-1} region). Unfortunately, the low solubility of this complex prevents us from molecular weight measurements, but a tetranuclear formulation cannot be completely excluded. Thus, the related dinuclear $[Rh_2(Biim)(COD)_2]$ complex[9] containing the planar biimidazolate dianion forming five-membered rings reacts with carbon monoxide with formation of the tetranuclear red compound $[Rh_4(Biim)_2(CO)_8]$.[9] Furthermore, we have observed that a dinuclear complex of formula $[Rh_2(Biim)(CO)_2(PPh_3)_2]$ is obtained by addition of triphenylphosphine to $[Rh_4(Biim)_2(CO)_8](PPh_3/Rh: 1/1)$.

Addition of triphenylphosphine to solutions of the carbonyl derivative **XIII** leads to the formation of $[Rh_2(C_2O_4)(CO)_2(PPh_3)_2]$ (**XIV**). This product has an IR spectrum exhibiting only one terminal metal carbonyl stretching frequency (1987 cm^{-1}, CH_2Cl_2) suggesting a *trans*-configuration as observed for *trans*-$[Rh_2Cl_2(CO)_2(PPh_3)_2]$.[10] No further reaction was observed by adding excess of triphenylphosphine, although complex **XII** can be obtained by reaction of complex **II** with triphenylphosphine.

The reaction of complex **X** with carbon monoxide leads to the displacement of the coordinated diolefin, yielding to complex $[Rh_2(C_2O_4)(CO)_2\{P(OPh)_3\}_2]$ which was not isolated as a solid, but the presence of one ν(CO) band (2005 cm^{-1}, CH_2Cl_2) suggests a *trans*-configuration as observed for complex **XIV**.

The reaction of one mole of complex **XIII** with two moles of tert-butylisocyanide leads to the formation of *trans*-$[Rh_2(C_2O_4)(CO)_2(t\text{-}BuNC)_2]$ (**XV**) ($\nu C{\equiv}O$: 2010 cm^{-1}, CH_2Cl_2) but an ionic compound analyzing as $[Rh(CO)(t\text{-}BuNC)_3] - [Rh(C_2O_4)(CO)(t\text{-}BuNC)]$ (**XVI**) was obtained when four moles of tert.-butylisocyanide were used.

The [Rh(diolefin)(L–L)][$Rh(C_2O_4)$(diolefin)] complexes (L–L = phen or bipy) react with carbon monoxide with formation of complexes of the type $[Rh(CO)_2(L\text{–}L)][Rh(C_2O_4)(CO)_2]$ (L–L = phen (**XVII**) or bipy (**XVIII**). The complex IR spectra in the carbonyl-stretching frequency region, along with the dichroism and intense colour of the complexes when solids, indicate an ionic chain-like structure involving metal–metal interactions, as reported for related $[Rh(CO)_2(L\text{–}L)][RhCl_2(CO)_2]$ complexes.[8,11] In fact the observed IR absorptions are the result of the superimposed individual *cis*-dicarbonyl bands of $[Rh(CO)_2(L\text{–}L)]^+$ and $[Rh(CO)_2Cl_2]^-$.

The above mentioned ionic derivatives behave as 1 : 1 electrolytes in solution. In general low values of the molar conductivities are found (Table 1), probably due to the low mobility of the relatively bulky ions.

Finally, some oxidative addition reactions have been studied. Thus, complex **XIV** undergoes reactions with iodine or methyl iodide leading to formation of complexes of the type $[Rh_2(C_2O_4)I_2Z_2(CO)_2(Phh_3)_2]$ (Z = I (**XIX**) or Me (**XX**)). The presence of only one terminal ν(CO) band in the dinuclear rhodium(III) complexes at 2095 and 2053 cm^{-1} (CH_2Cl_2) respectively, suggests that a single symmetrical derivative was formed. As expected the ν(CO) vibration of the oxidation products is shifted towards higher energies relative to the parent compound (65–110 cm^{-1}). Table 1 lists some relevant data for the carbonyl derivatives. In general, only a ν(COO) band from the coordinated oxalate anion, in the range 1610–1670 cm^{-1} was unequivocally assigned, due to the presence of several absorptions in the 1300–1350 cm^{-1} range, masking the expected ν(COO) bands.

Malonate complexes

Some dinuclear complexes with the related malonate group have been prepared according to eqn (1), when malonic acid is added to acetone solutions of Rh(acac)(diolefin) complexes. These compounds of formula $[Rh_2\{CH_2(CO_2)_2\}(diolefin)_2]$ (diolefin = COD (**XXI**), TFB (**XXII**), NBD (**XXIII**)) react with carbon monoxide with formation of $[Rh_2\{CH_2(CO_2)_2\}(CO)_4]_x$ (**XXIV**). The latter complex reacts with a stoichiometric amount of

Table 1. Analytical and other data for the compounds

Complex	Found(calcd.)% C	H	N	Colour	Yield	Mol.wt. ($CHCl_3$) (found(calcd.))	Λ_M $ohm^{-1}cm^2mol^{-1}$
$Rh(HC_2O_4)(COD)$ (I)	40.0 (39.6)	4.4 (4.3)	-	yellow	62%	300 (643)	---
$Rh_2(C_2O_4)(COD)_2$ (II)	42.4 (42.7)	4.7 (4.8)	-	yellow	85%	510 (548)	---
$(COD)Rh(C_2O_4)Rh(TFB)$ (III)	42.1 (42.0)	2.9 (2.8)	-	yellow	72%	628 (711)	---
$(COD)Rh(C_2O_4)Ir(COD)$ (IV)	36.1 (37.1)	4.0 (4.2)	-	yellow	65%	599 (601)	---
$Rh_2(C_2O_4)(TFB)_2$ (V)	41.9 (41.8)	1.6 (1.7)	-	yellow	82%	746 (758)	---
$Rh_2(C_2O_4)(NBD)_2$ (VI)	40.1 (41.0)	3.4 (3.2)	-	yellow	64%	478 (466)	---
$\|Rh(COD)(phen)\|\|Rh(C_2O_4)(COD)\|\cdot H_2O$ (VII)	50.8 (50.9)	4.8 (5.1)	3.9 (3.9)	red	74%	-	91[a]
$\|Rh(TFB)(phen)\|\|Rh(C_2O_4)(TFB)\|$ (VIII)	49.3 (49.2)	2.2 (2.3)	3.0 (3.0)	orange	89%	-	15[b]
$\|Rh(TFB)(bipy)\|\|Rh(C_2O_4)(TFB)\|$ (IX)	47.9 (46.1)	2.2 (2.4)	3.1 (3.8)	orange	88%	-	79[a]
$(COD)Rh(C_2O_4)Rh\{P(OPh)_3\}_2$ (X)	54.0 (54.1)	4.1 (4.6)	-	pale-yellow	71%	1022 (917)	---
$Rh_2(C_2O_4)\{P(OPh)_3\}_4$ (XI)	57.9 (57.7)	3.9 (4.0)	-	pale-yellow	70%	1535 (1466)	---
$Rh_2(C_2O_4)(PPh_3)_4$ (XII)	66.3 (65.1)	4.5 (5.0)	-	yellow	72%	--	---

$Rh_2(C_2O_4)(CO)_4$ (XIII)	17.77 (17.9)	-	-	violet	82%	--	---
$Rh_2(C_2O_4)(CO)_2(PPh_3)_2$ (XIV)	54.9 (55.0)	3.3 (3.7)	-	yellow	83%	874 (797)	---
$Rh_2(C_2O_4)(CO)_2(t\text{-BuNC})_2$ (XV)	32.6 (31.8)	3.5 (3.6)	5.4 (5.6)	green	83%	516 (554)	---
$\|Rh(CO)(t\text{-BuNC})_3\|\|Rh(C_2O_4)(CO)(t\text{-BuNC})\|$ (XVI)	42.2 (43.0)	5.3 (5.9)	8.2 (8.6)	brown	87%	--	60[a]
$\|Rh(CO)_2(phen)\|\|Rh(C_2O_4)(CO)_2\|$ (XVII)	36.9 (36.6)	1.4 (1.5)	4.8 (4.6)	dark-blue	80%	--	26[c]
$\|Rh(CO)_2(bipy)\|\|Rh(C_2O_4)(CO)_2\|\cdot H_2O$ (XVIII)	33.1 (33.0)	1.7 (1.7)	4.8 (4.5)	black	80%	--	22[c]
$Rh_2(C_2O_4)I_4(CO)_2(PPh_3)_2$ (XIX)	34.8 (35.2)	2.2 (2.6)	-	brown	79%	1382 (1330)	---
$Rh_2(C_2O_4)I_2Me_2(CO)_2(PPh_3)_2$ (XX)	43.5 (43.7)	3.1 (3.7)	-	yellow	96%	1158 (1163)	---
$Rh_2\{CH_2\text{-}(CO_2)_2\}(COD)_2$ (XXI)	43.5 (43.1)	5.0 (4.9)	-	yellow	55%	--	---
$Rh_2\{CH_2\text{-}(CO_2)_2\}(TFB)_2$ (XXII)	42.6 (41.9)	1.8 (1.9)	-	orange	60%	--	---
$Rh_2\{CH_2\text{-}(CO_2)_2\}(NBD)_2$ (XXIII)	41.5 (41.2)	3.7 (3.7)	-	red	82%	--	---
$Rh_2\{CH_2\text{-}(CO_2)_2\}(CO)_4$ (XXIV)	20.0 (20.9)	0.5 (0.8)	-	yellow	73%	--	---
$Rh_2\{CH_2\text{-}(CO_2)_2\}(CO)_2(PPh_3)_2$ (XXV)	55.7 (56.7)	3.6 (3.9)	-	orange	85%	884 (908)	---

[a]Acetone. [b]Nitrobenzene. [c]Methanol.

triphenylphosphine yielding *trans*-$[Rh_2\{CH_2(CO_2)_2\}(CO)_2(PPh_3)_2]$ (ν(CO): 1970 cm^{-1}, CH_2Cl_2). In the above mentioned complexes, the malonate group is probably acting as bidentate to two rhodium atoms through symmetrical chelate carboxylate bonding (four-membered rings).

EXPERIMENTAL

C, H and N analyses were carried out with a Perkin–Elmer 240-B microanalyzer. IR spectra were recorded on a Perkin–Elmer 599 spectrophotometer over the range 4000–200 cm^{-1}, using Nujol mulls between polyethylene sheets or in dichloromethane solutions between sodium chloride windows, and calibrated with polystyrene. Molecular weights were measured with a Perkin–Elmer 115 osmometer. Conductivity measurements were carried out, with a Philips 9509 conductimeter.

$[RhCl(COD)]_2$, $[RhCl(NBD)]_2$, $[RhCl(TFB)]_2$, $(IrCl(COD)]_2$, Rh(acac)(COD), [Rh(acac)(TFB)], [Rh(acac)(NBD)], [Ir(acac)(COD)], were prepared by published methods.[12–17] Other chemicals were grade reagents and were used without purification.

Preparation of $[Rh(HC_2O_4)(COD)]$ **(I)**

$H_2C_2O_4 \cdot 2H_2O$ (81.24 mg, 0.644 mmol) was added to a solution of Rh(acac)(COD) (200 mg, 0.644 mmol) in dichloromethane (30 cm^3). The suspension was stirred for 30 min and filtered off. The yellow filtrate was vacuum-concentrated to *ca.* 2 cm^3 and addition of ether gave rise to the formation of a yellow solid, which was filtered off, washed with ether and vacuum-dried. Yield: 120.1 mg (62%).

Preparation of $[(COD)Rh(C_2O_4)Rh(TFB)]$. *General method for the synthesis of* **(III)** *and* **(IV)**

[Rh(acac)(TFB)] (75.453 mg, 0.176 mmol) was added to a solution of $[Rh(HC_2O_4)(COD)]$ (52.9 mg, 0.176 mmol) in dichloromethane (20 cm^3). This solution was stirred for 3 hr. Vacuum-concentration and addition of hexane led to the precipitation of the pale yellow complex which was filtered off washed with hexane and vacuum-dried. Yield: 80 mg (72%).

Complex **(IV)** was obtained in a similar way by adding a calculated amount of [Ir(acac)(COD)] (39.9 mg, 0.099 mmol) to a solution of $[Rh(HC_2O_4)(COD)]$ in dichloromethane (30 mg, 0.099 mmol) under nitrogen. Ether was used for the precipitation of this complex.

Preparation of $[Rh_2(C_2O_4)(COD)_2]$. *General method for the synthesis of* **(II)**, **(V)** *and* **(VI)**

To a solution of [Rh(acac)(COD)] (100 mg, 0.322 mmol) in acetone (20 cm^3), was added the stoichiometric amount of $H_2C_2O_4 \cdot 2H_2O$ (20.3 mg, 0.161 mmol). A yellow precipitate was formed immediately. After stirring for 2 hr, it was filtered off, washed with acetone and vacuum-dried. Yield: 70 mg (85%).

Complexes **(V)** and **(VI)** were similarly prepared by the route described above, starting from a calculated amount of [Rh(acac)(TFB)] or [Rh(acac)(NBD)]. The reaction to obtain complex **(VI)** was carried out under nitrogen with deoxygenated solvent.

Preparation of $[Rh(COD)(phen)][Rh(C_2O_4)(COD)] \cdot H_2O$. *General method for the synthesis of* **(VII–IX)**

Addition of 1,10-phenanthroline (7.7 mg, 0.039 mmol) to a solution of $[Rh_2(C_2O_4)(COD)_2]$ (20 mg, 0.039 mmol) in 20 cm^3 of dichloromethane caused a colour change from yellow to red. The solution was stirred for 30 min under nitrogen atmosphere, then the solvent was evaporated off under reduced presure, and addition of ether led to the complete precipitation of a red solid. This was filtered off, washed with ether and vacuum-dried. Yield: 20 mg (74%).

This way, 1,10-phenanthroline and 2,2′-bipyridine reacted with $[Rh_2(C_2O_4)(TFB)_2]$ to give the complexes **(VIII)** and **(IX)**.

Preparation of $[(COD)Rh(C_2O_4)Rh\{P(OPh)_3\}_2]$ **(X)**

$P(OPh)_3$ (41.2 μl, 0.156 mmol) was added to a solution of $[Rh_2(C_2O_4)(COD)_2]$ (40 mg, 0.78 mmol) in dichloromethane (30 cm^3); the colour of the solution changed from yellow to pale yellow. After stirring for 2 hr under nitrogen atmosphere, the solvent was evaporated off under reduced pressure and ether was added to give a pale yellow solid. This was filtered off, washed with ether and vacuum-dried. Yield: 56.4 mg (71%).

Preparation of $[Rh_2(C_2O_4)\{P(OPh)_3\}_4]$. *General method for the synthesis of* **(XI)** *and* **(XII)**

To a stirred suspension of $[Rh_2(C_2O_4)(COD)_2]$ (30 mg, 0.058 mmol) in deoxygenated ether (20 cm^3) was added $P(OPh)_3$ (61.85 μl, 0.235 mmol). The suspension immediately turned into a yellow solution, then a pale-yellow solid was observed. This was filtered off, washed with ether and vacuum-dried. Yield: 60 mg (70%).

Preparation of $[Rh_2(C_2O_4)(CO)_4]_x$. *General method for the synthesis of* **(XIII)**, **(XVII–XVIII)** *and* **(XXIV)**

Bubbling of carbon monoxide through a solution of $[Rh_2(C_2O_4)(COD)_2]$ (55.4 mg, 0.108 mmol) in 20 cm^3 of dichloromethane, for 30 min gave a violet solid. The suspension was vacuum-concentrated to

ca. 4 cm^3 and ether was added. The complex was filtered off, washed with ether and vacuum-dried. Yield: 50 mg (82%).

Methanol was used to precipitate complex (**XXIV**).

Preparation of $[Rh_2(C_2O_4)(CO)_2(PPh_3)_2]$. *General method for synthesis of* (**XIV–XV**) *and* (**XXV**)

A stoichiometric amount of PPh_3 (63.7 mg, 0.242 mmol) was added to a suspension of $[Rh_2(C_2O_4)(CO)_4]$ (49.3 mg, 0.121 mmol) in dichloromethane, and the resulting yellow solution was stirred for 2 hr. Addition of hexane to the concentrated solution (3 cm^3) gave a yellow solid, which was filtered off, washed with hexane and vacuum-dried. Yield: 88 mg (83%).

Complex (**XV**) was prepared under nitrogen atmosphere.

Reaction of (**XIII**) *with* t-*butylisocyanide*

To a suspension of $[Rh_2(C_2O_4)(CO)_4]$ (35.6 mg, 0.087 mmol) in 20 cm^3 of deoxygenated dichloromethane was added *t*-BuNC (38.58 μl, 0.350 mmol) under nitrogen atmosphere. The suspension was stirred for 5 hr giving a yellow solution.

The solvent was evaporated off to 2 cm^3 under reduced pressure, and then ether was added to give a brown solid which was filtered off, washed with ether, and vacuum-dried. This complex analyzed as $[Rh(CO)(t\text{-BuNC})_3][Rh(C_2O_4)(CO)(t\text{-BuNC})]$.

Preparation of $[Rh_2(C_2O_4)I_4(CO)_2(PPh_3)_2]$ (**XIX**)

To a solution of $[Rh_2(C_2O_4)(CO)_2(PPh_3)_2]$ (30 mg, 0.034 mmol) in 30 cm^3 of dichloromethane was added the stoichiometric amount of iodine (17.25 mg, 0.068 mmol); the colour of the solution changed from yellow to brown. The progress of the reaction was followed by IR spectra. After 90 min stirring the solvent was evaporated off to 3 cm^3 and hexane was added to give a dark brown solid. This was filtered off, washed with hexane and vacuum-dried. Yield: 37 mg (79%).

Preparation of $[Rh_2(C_2O_4)I_2Me_2(CO)_2(PPh_3)_2]$ (**XX**)

A suspension of $[Rh_2(C_2O_4)(CO)_2(PPh_3)_2]$ (22 mg, 0.025 mmol) in 30 cm^3 of methyl iodide was stirred. After 5 min, the suspension turned into a yellow solution, then the complex precipitated as a yellow solid. This suspension was stirred for 2 hr, after which time the solvent was evaporated to small volume and the product was filtered off, washed with hexane and vacuum-dried. Yield: 28 mg (96%).

Preparation of $[Rh_2\{CH_2\text{–}(CO_2)_2\}(COD)]$. *General method for the synthesis of* (**XXI–XXIII**)

A stoichiometric amount of $CH_2\text{–}(CO_2H)_2$ (11.7 mg, 0.112 mmol) was added to a solution of [Rh(acac)(COD)] (70 mg, 0.225 mmol) in 20 cm^3 of acetone. The mixture was stirred for 2 hr, during which time the product precipitated as a yellow solid. This was filtered off, washed with acetone and vaccum-dried. Yield: 32 5 mg (55%).

Complex (**XXIII**) is air-sensitive, so it was prepared under nitrogen atmosphere and ether was used as solvent.

Note added in proof: We have been informed about an independent preparation of $[Rh_2(C_2O_4)(CO)_4]$ by P. B. Hitchcock, S. Morton and J. F. Nixon (Paper D26, 2nd International Conference on the Chemistry of the Platinum Group Metals, Edinburgh, July 1984). We thank Dr. J. F. Nixon for useful discussion.

REFERENCES

1. R. P. Hughes, In Comprehensive Organometallic Chemistry (Edited by G. Wilkinson, F. G. A. Stone and E. W. Abel), Vol. 5, p. 278. Pergamon Press, Oxford (1982).
2. (a) M. Valderrama and L. A. Oro, *J. Organometal. Chem.* 1981, **218**, 241. (b) M. Valderrama, H. Rafart and L. A. Oro, *Transition Met. Chem.* 1981 **6**, 221. (c) I. G. Leipoldt, L. D. Bok, S. S. Basson and H. Meyer, *Inorg. Chim. Acta* 1980, **42**, 105.
3. A. Dobson and S. D. Robinson, *Platinum Met. Rev.* 1976, **20**, 56.
4. C. Cocevar, G. Mestroni and A. Camus, *J. Organometal. Chem.* 1971, **16**, 863.
5. R. Usón, L. A. Oro, R. Sariego, M. Valderrama and C. Rebullida, *J. Organometal. Chem.* 1980, **197**, 87.
6. L. M. Haines, *Inorg. Chem.* 1970, **9**, 1517.
7. P. T. Cheng, B. R. Loescher and S. C. Nyburg, *Inorg. Chem.* 1971, **10**, 1275.
8. F. Pruchnik and K. Wajda, *J. Organometal. Chem.* 1979, **164**, 71.
9. S. W. Kaiser, R. B. Saillant, W. M. Butler and P. G. Rasmussen, *Inorg. Chem.* 1976, **15**, 2681; 2688.
10. D. F. Steele and T. A. Stephenson, *J. Chem. Soc., Dalton Trans.* 1972, 2161.
11. R. D. Gillard, K. Harrison and I. H. Mather, *J. Chem. Soc., Dalton Trans.* 1975, 133.
12. G. Giordano and R. H. Crabtree, *Inorg. Synth.* 1979, **19**, 218.
13. E. W. Abel, M. A. Bennett and G. Wilkinson, *J. Chem. Soc.* 1959, 3178.
14. D. M. Roe and A. G. Massey, *J. Organometal. Chem.* 1971, **28**, 273.
15. R. H. Crabtree and G. E. Morris, *J. Organometal. Chem.* 1977, **135**, 395.
16. F. Bonati and G. Wilkinson, *J. Chem. Soc.* 1964, 3156.
17. S. D. Robinson and B. L. Shaw, *J. Chem. Soc.* 1965, 4997.

Polyhedron Vol. 4, No. 2, pp. 333–342, 1985
Printed in Great Britain.

0277–5387/85 $3.00 + .00
© 1985 Pergamon Press Ltd.

MIXED-LIGAND LANTHANIDE COMPLEXES—II

COMPLEXES OF β-DIKETONE AND HETEROCYCLIC AMINE. SYNTHESIS AND SPECTROSCOPIC STUDIES

K. IFTIKHAR*† and N. AHMAD
Chemistry Department, Aligarh Muslim University, Aligarh 202001 (U.P.), India

(*Received* 12 *October* 1983; *accepted after revision,* 14 *April* 1984)

Abstract—The imidazole adducts of tris(heptafluorooctanedionato)lanthanide(III), [Ln(fod)$_3$ · im] have been synthesized and characterized. The electronic spectra in the visible region have been analysed and spectral parameters ($\bar{\beta}$, $b^{1/2}$, δ and T_λ) and oscillator strengths calculated and discussed. These complexes are more covalent than the analogous [Ln(fod)$_3$ · pz] complexes, pz = pyrazole. The covalency is more in solution than in the solid state. The experimental and the calculated oscillator strengths are in good agreement. The band shape for the hypersensitive transition in the solid and solution spectra is compared with the other known systems and discussed. The difference in the band shape of the hypersensitive transition in the solid and in solution is indicative of solvent molecule coordination. The Mössbauer spectrum of [Eu(fod)$_3$ · im] is reported. The dipolar shift produced in the NMR spectrum of [Eu(fod)$_3$ · im] is upfield in comparison to the signal of the organic moiety itself as well as in its diamagnetic analogues. The coordinated base does not dissociate even in DMSO solution. Due to their poor solubility these compounds are not suitable for use as induced NMR shift reagents.

In the last several years there has been considerable interest in the lanthanide complexes especially concerning specific $f-f$ features of Ln^{3+} spectra in solution to give information regarding structure and composition of the complexes.[1–5] The lanthanide tris β-diketoenolates are being used as induced NMR shift reagents.[6] In the earlier reports we investigated some mixed-ligand lanthanide complexes with β-diketone and nitrogen containing ligands, their electronic spectral features and possible use as pseudo-contact NMR shift reagents.[7–10]†† In this study we report mixed-ligand complexes of most of the lanthanides (except Ce and Pm), yttrium and lanthanum with 1,1,1,2,2,3,3 - heptafluoro–7,7–dimethyl–4,6–octanedione(Hfod) and imidazole(im). Our interest in these newly synthesized adducts is to check their ability as potential shift reagents (the analogous adducts of Ln(fod)$_3$ with pyrazole, (pz), were found to produce larger dipolar shifts in the NMR spectrum of organic moieties,[9] to investigate their electronic spectra for ascertaining the dependence of the hypersensitive bands on the environment about the lanthanide ions and to study the Mössbauer effect in the [Eu(fod)$_3$ · im].

EXPERIMENTAL SECTION

Materials. Lanthanide oxides (Leico Chemicals, U.S.A.) were converted to the corresponding chlorides. Hfod (PCR Chemicals, U.S.A.), imidazole (Fluka, Switzerland) and xylenol–orange (BDH, England) were used in this study. Imidazole was crystallized from chloroform before use. DMSO–d_6 (99.9% d atom) was purchased from Aldrich Chemicals, U.S.A. Spectroscopic grade ethanol (E. Merck) was used for obtaining optical spectra.

Synthesis. The Ln(fod)$_3$ chelates were synthesized by the method of Springer *et al.*[11] The adducts were synthesized by mixing Ln(fod)$_3$ and imidazole (1 : 1 ratio) in ethanol on a hot plate. The products, thus, formed were washed several times with chloroform and hexane and dried *in vacuo* over phosphorus pentoxide.

*Author to whom correspondence should be addressed.

†Present address: Department of Chemistry South Gujarat University SURAT - 395 007.

††Part I of this series is Ref. 8.

Methods. The complexes were subjected to microanalyses for carbon, hydrogen and nitrogen, while the metals were estimated by complexometric titrations with EDTA using xylenol–orange as the indicator. The IR spectra were recorded both in Nujol and KBr on a 621-Perkin-Elmer IR Spectrometer. The magnetic susceptibility was measured by the NMR method using methanol as the solvent at the probe temperature. The NMR spectra of the complexes were recorded on a Varian A-60 machine.

Beckman DU-2 and Cary-17 D spectrophotometers were used, for obtaining optical spectra in solution and in the solid state. The solvent used for the solution spectra was ethanol and the concentration range was between 10^{-2} and 10^{-3}M.

For the measurements of the Mössbauer effect a 10 mCi source of Sm-151 in the form of Sm_2O_3 was used. This source had near natural line-width and an appreciable recoilless fraction (0.38) at room temperature. The absorbers were prepared in the form of pressed disc, the concentration of natural europium being maintained at 100 mg/cm^2 for comparison purposes. Spectra were run at room temperature. The data was computer fitted on a DECK-10 using a non-linear least square curve fitting programme.

Method of calculation is similar to those reported earlier.[8,9]

RESULTS AND DISCUSSION

The $Ln(fod)_3$ complexes are soluble in all common organic solvents but imidazole as well as the adducts of $Ln(fod)_3$ with imidazole are only soluble in polar solvents. This suggests that imidazole coordinates to $Ln(fod)_3$ and maintains its integrity in the adducts. All of the adducts synthesized are new. However, it should be pointed out that analogous mixed-ligand complexes $[Ln(dpm)_3 \cdot im]$ (dpm = dipivaloylmethane) have previously been reported.[7] The complexes, under study, are well defined solids with sharp melting points. The melting points are higher than those of 2,2′-bipyridyl[8](bpy), 1,10–phenanthroline[8](phen) and pyrazole[9] (pz) adducts of $Ln(fod)_3$ but lower than those of $[Ln(dpm)_3 \cdot im]$. These are quite stable and can be handled without any effect of air or moisture, in contrast to the behaviour of $Ln(fod)_3$ and $[Ln(fod)_3 \cdot pz]$ complexes which were found to be very sensitive to moisture. All the adducts behave as non-electrolytes as revealed by their molar conductance in methanol.[12]

The partial decomposition of these complexes starts after melting in the temperature range 220–240°C (Table 2). The total weight loss (5.5–6.5%) in this temperature range is consistent with the loss for imidazole (the theoretical weight loss for imidazole is 6.1–6.3%). One sharp DTA peak is identified in all cases in this temperature range. This indicates the coordinated nature of imidazole. The remaining proportion of the TGA curves, show the same behaviour as reported for the chelates[11] which is quite understandable since the material left after elimination of the imidazole is $Ln(fod)_3$.

The IR spectra of the adducts show presence of coordinated imidazole. The N–H frequency appearing in solid imidazole as a very broad band (2100–3300 cm^{-1})[13] because of intermolecular hydrogen bonding, appears as a comparatively sharp band (3120–3185 cm^{-1}) in the adducts. The observed shift and sharpness in the N–H band suggests a decrease in hydrogen bonding and interaction of ring nitrogen with lanthanide atom. The metal–nitrogen frequency in the analogous pyrazole adducts[9] was observed in the range 290–305 cm^{-1}. The band occurring between 280–290 cm^{-1} in the present complexes, which does not have its equal in the chelate and/or ligand can be assigned to metal–nitrogen frequency.[14] Most of the absorptions of imidazole do not appear, probably these are obscured by chelate absorptions. The absorption peaks occurring in the chelates are also present in the adducts with their positions slightly shifted (Table 3). The metal-oxygen frequencies are lower in the adducts than those of the $Ln(fod)_3$ complexes.

Thus, the adducts on the basis of their elemental analyses molar conductance, magnetic moments (Table 1), thermal analyses (Table 2) and IR spectral studies (Table 3) have been assigned to the general formula, $[Ln(fod)_3 \cdot im]$ where Ln stands for the trivalent lanthanides (except Ce and Pm) yttrium and lanthanum.

Mössbauer effect

The isomer shift is given by the following equation,

$$\text{I.S.} = 4/5\pi \; Ze^2R^2(\delta R/R)[|\psi(0)|^2_{\text{abs.}} - |\psi(0)|^2_{\text{source}}] \quad (1)$$

where all the notations have their usual connotations.[15] The Mössbauer spectra of Eu_2O_3 and $[Eu(Fod)_3 \cdot im]$ are shown in Figs. 1 and 2. The spectrum of $[Eu(Fod)_3 \cdot im]$ shows a definite negative isomer shift (-0.50 mm/sec) relative to Eu_2O_3, since for 21.7 KeV transition in Eu-151, δR (eqn 1) is positive.[16] Any deviation of the shift from zero indicates covalent bonding between the metal and the ligand. The negative isomer shift proves that the *s*-electron density (in europium nucleus) in the complex is lower than the corresponding *s*-electron density in Eu_2O_3. This decrease may be due to transfer of electrons from ligands to unfilled 4*f*

Table 1. Some characterizing data for [Ln(fod)$_3$ · im] complexes

Complexes	mp, °C	% Metal[a]	% C[a]	% H[a]	% N[a]	Colour	Λ_M Ohm^{-1} cm^2 mole^{-1}	μ_{eff} (BM)
[Y(fod)$_3$. im]	178	8.48 (8.54)	38.29 (38.00)	3.26 (3.26)	2.67 (2.68)	White	10.9	Diamag
[La(fod)$_3$. im]	208	12.78 (12.73)	36.02 (36.26)	3.31 (3.12)	2.50 (2.57)	White	-	Diamag
[Pr(fod)$_3$. im]	187	12.79 (12.89)	36.90 (36.20)	3.18 (3.11)	2.49 (2.56)	Green	10.6	3.52
[Nd(fod)$_3$. im]	187-88	13.08 (13.13)	36.25 (36.10)	2.99 (3.10)	2.62 (2.55)	Violet	-	3.82
[Sm(fod)$_3$. im]	185	13.83 (13.63)	35.91 (35.90)	3.15 (3.08)	2.52 (2.54)	White	-	2.22
[Eu(fod)$_3$. im]	185-86	13.68 (13.76)	35.78 (35.84)	3.03 (3.08)	2.57 (2.53)	White	13.2	3.68
[Gd(fod)$_3$. im]	185-86	14.15 (14.16)	35.52 (35.68)	3.08 (3.06)	2.54 (2.52)	White	-	7.80
[Tb(fod)$_3$. im]	158-59	14.32 (14.30)	35.66 (35.61)	3.10 (3.06)	2.49 (2.52)	White	-	9.69
[Dy(fod)$_3$. im]	186	14.50 (14.56	35.24 (35.50)	2.89 (3.04)	2.50 (2.51)	White	11.8	10.35
[Ho(fod)$_3$. im]	186	14.80 (14.76)	35.46 (35.42)	2.92 (3.04)	2.44 (2.50)	Light yellow	-	10.45
[Er(fod)$_3$. im]	168-70	15.01 (14.91)	35.30 (35.36)	3.08 (3.03)	2.57 (2.50)	Pink	-	9.39
[Tm(fod)$_3$. im]	161	15.02 (15.06)	35.80 (35.30)	3.06 (3.03)	2.61 (2.50)	White	14.1	7.41
[Yb(fod)$_3$. im]	153	15.37 (15.36)	34.99 (35.18)	3.15 (3.02)	2.42 (2.49)	White	-	4.66
[Lu(fod)3 . im]	132	15.50 (15.51)	35.36 (35.12)	3.06 (3.01)	2.50 (2.48)	White	11.3	Diamag

Calculated values are in parentheses.

Table 2. TGA data for some of the complexes

Complexes	mp, °C	temp, °C	% wt loss for imidazole	
			theor	exptl
[La(fod)$_3$.im]	208	220	6.22	6.50
[Gd(fod)$_3$.im]	185-86	240	6.12	5.50
[Tb(fod)$_3$.im]	158-59	246	6.06	6.00
[Dy(fod)$_3$.im]	186	225	6.10	6.00

Table 3. IR frequencies (cm^{-1}) in [Ln(fod)$_3$ · im] complexes

Complexes	ν N-H	ν C = C	ν C = O	ν M-O	ν M - N
[Y(fod)$_3$.im]	3200 s	1626 s	1582 w	398 b	290 vw
[La(fod)$_3$.im]	3130 s	1616 s	1584 w	376 b	290 vw
[Pr(fod)$_3$.im]	3185 s	1648 s	1580 w	390 b	287 vw
[Nd(fod)$_3$.im]	3170 s	1640 s	1584 w	377 b	285 vw
[Sm(fod)$_3$.im]	3145 s	1624 s	1580 w	390 b	288 vw
[Eu(fod)$_3$.im]	3120 s	1621 s	1588 w	366 b	280 vw
[Gd(fod)$_3$.im]	3158 s	1630 s	1589 w	375 b	283 vw
[Tb(fod)$_3$.im]	3158 s	1626 s	1583 w	382 b	284 vw
[Dy(fod)$_3$.im]	3142 s	1630 s	1588 w	374 b	284 vw
[Ho(fod)$_3$.im]	3122 s	1630 s	1585 w	377 b	284 vw
[Er(fod)$_3$.im]	3140 s	1626 s	1580 w	385 b	282 vw
[Tm(fod)$_3$.im]	3130 s	1625 s	1580 w	395 b	280 vw
[Yb(fod)$_3$.im]	3140 s	1624 s	1584 w	376 b	289 vw

s = strong; w = weak ; b = broad & vw = very weak.

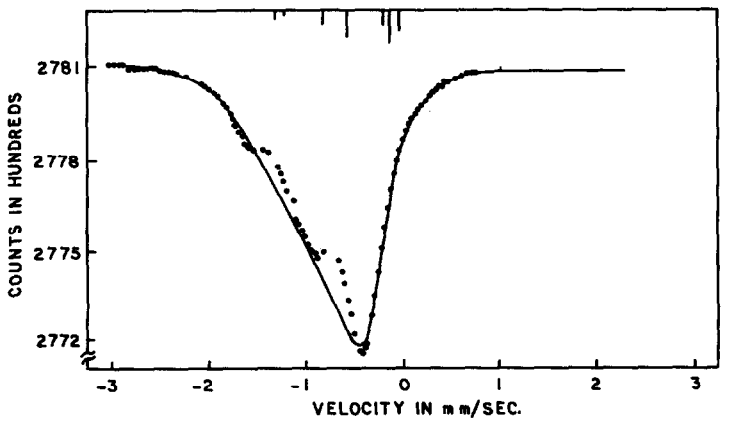


Fig. 2. Mössbauer spectrum of [Eu(fod)$_3$ · im].

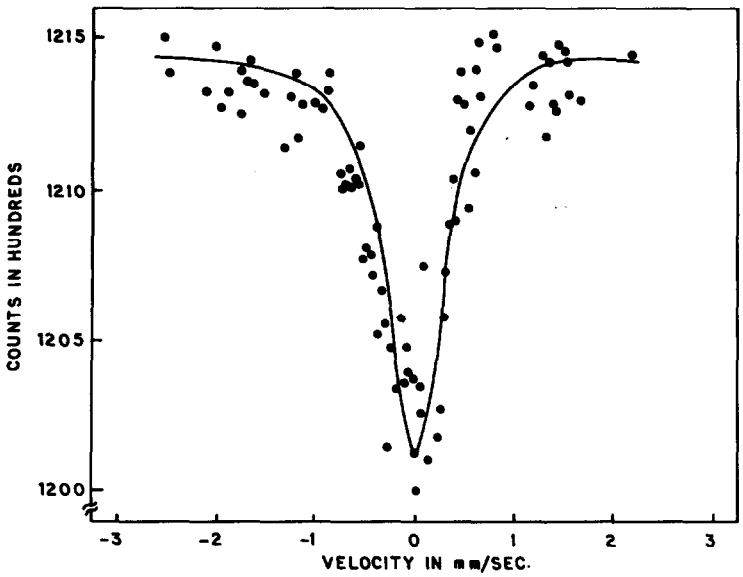


Fig. 1. Mössbauer spectrum of Eu_2O_3.

shell and this will involve a change in the configuration from $4f^6 5s^2 5p^6$ (Eu_2O_3) to $4f^{6+x}5s^2 5p^6$ (complex) where $0 < X < 1$. Since this increases the screening of the 5*s* electrons by the 4*f* shell it results in a net decrease in *s*-electron density at the nucleus (*x* will be zero for a purely ionic compound).

Electronic spectra

The electronic spectra of the complexes are recorded in ethanol and in the solid state. The spectra of the complexes show a shift of spectral bands towards lower energy as compared to those of the respective aquoions[17] which is known as nephelauxetic effect. The nephelauxetic parameter ($\bar{\beta}$),[18] the bonding parameter ($b^{1/2}$)[19] and Sinha's covalency parameter (δ)[20] for the complexes of Pr^{3+}, Nd^{3+}, Ho^{3+} and Er^{3+} are presented in Table 4. The nephelauxetic parameter is less than one and $b^{1/2}$ and δ are positive for these complexes which show covalent bonding between the metal and the ligand. The $b^{1/2}$ and δ in these adducts are in the order Pr > Nd > Ho > Er which reveals that for the same ligand covalency decreases as the atomic

Table 4. Covalency parameters

Complexes	$\bar{\beta}$	$b^{\frac{1}{2}}$	δ
$[Pr(fod)_3.im]$	0.9796	0.1010	2.0825
$[Pr(fod)_3.pz]$[a]	0.9828	0.0926	1.7460
$[Nd(fod)_3.im]$	0.9823	0.0941	1.8009
	(0.9948)[b]	(0.0510)[b]	(0.5227)[b]
$[Nd(fod)_3.pz]$[a]	0.9960	0.0448	0.4036
$[Ho(fod)_3.im]$	0.9874	0.0795	1.2792
	(0.9985)[b]	(0.0274)[b]	(0.1502)[b]
$[Er(fod)_3.im]$	0.9908	0.0678	0.9285
	(0.9990)[b]	(0.0224)[b]	(0.1001)[b]
$[Er(fod)_3.pz]$[a]	0.9923	0.0623	0.7811

[a] ref. 9 ; [b] the values given in parentheses are those calculated from solid state spectra.

number of the lanthanide increases. A comparison of the covalency parameters ($\bar{\beta}$, $b^{1/2}$ and δ) calculated from the solid state spectra with those of values obtained from ethanolic spectra reveals that covalency is more in solution (Table 4). The magnitude of $\bar{\beta}$ is similar to that obtained for the analogous pyrazole adducts,[9] it is perhaps instructive to compare the nephelauxetic effect of the two complexes, for any given metal ion. It is obvious from the Table 4 that, although we are looking for a very small effect, imidazole is a stronger ligand than pyrazole in a nephelauxetic sense and the covalency is higher in the former complexes.

The intensity of the *f–f* transitions of the complexes present interesting features. The experimental and the calculated oscillator strengths are listed in Table 5. The intensity of normal *f-f*-transitions do not show much change whereas hypersensitive transitions (which are very sensitive to the environment) display large changes in the intensity as compared to the corresponding aquo-ions.[17] The oscillator strength of the hypersensitive transitions in Nd^{3+}, Ho^{3+} and Er^{3+} is six, ten and eleven respectively, times higher than the corresponding aquo-ions. It is important to note that the oscillator strength of the hypersensitive transition of imidazole complexes for any given metal ion is higher as compared with those of pyrazole complexes.[9] Imidazole being more basic

Table 5. Oscillator strength

Complexes	[S' L' J']	Energy cm^{-1}	$10^6 P_{exptl}$	$10^6 P_{calcd}$
$[Pr(fod)_3.im]$	$^3P_2$	22321	18.13	18.13
	$^3P_1$	21276	4.40	3.09
	$^3P_0$	20202	5.13	7.32
	$^1D_2$	16077	5.45	5.45
$[Nd(fod)_3.im]$	$^2P_{1/2}$	22222	0.60	0.60
	$^2K_{15/2}$	20833	0.53	0.53
	$^4(G_{9/2}, G_{7/2})$	18867	8.44	6.97
	$[^4G_{5/2}, ^2G_{7/2}]$	17241	61.27	59.48
$[Ho(fod)_3.im]$	$(^5G, ^3G)_5$	23529	1.69	1.59
	$[^5G_6]$	22026	66.38	65.63
	$^5(S_2, F_4, F_3)$	18181	7.74	7.74
$[Er(fod)_3.im]$	$^4G_{11/2}$	26315	19.82	31.85
	$^4F_{5/2}$	21739	4.30	4.31
	$^4F_{7/2}$	20345	2.09	7.00
	$[^2H_{11/2}]$	18867	26.36	17.74
	$^4S_{3/2}$	18181	2.68	3.93
	$^4F_{9/2}$	15151	6.91	4.05

Hypersensitive transitions are enclosed in square brackets.

(pka = 7.1) than pyrazole (pka = 2.52) leads to a greater deal of covalency in its bonding which results in higher oscillator strength.[1,4]

Both changes in line shape and intensity of the hypersensitive transitions can be used as qualitative indication of symmetry.[21] Figures 3–5 show the shape of the hypersensitive bands of Nd^{3+}, Ho^{3+} and Er^{3+} complexes in ethanol solution and solid state. The complexes show remarkable spectral changes on passing from solid to solution states which demonstrate a change in the environment about the lanthanide ion in the two states, thus, indicating that expansion of coordination occurs. However, the band shape of ethanolic spectra of these complexes are quite similar to the band shapes of the eight-coordinate complexes in non-polar solvents or seven-coordinate complexes in polar solvents.[10,21,22] Occurrence of similar spectra is indicative of similar symmetries (i.e. similar coordination number).[23] Thus these complexes which are seven-coordinate take one solvent molecule and behave like eight-coordinate in solution.[10] The reflectance spectra of [Nd(fod)$_3$ · im] and [Nd(fod)$_3$ · pz] do not resemble one another but both acquire the same shape on passing from solid to solution (Fig. 3), thus indicating similar geometrical arrangement in solution but different in the solid states.

The oscillator strength due to the hypersensitive transition of the neodymium complex is higher than the oscillator strengths of other β-diketonate complexes in polar and non-polar solvents.[8,22,23] [Nd(fod)$_3$ · im] have a lower molecular symmetry than the other complexes and low molecular symmetry is usually responsible for higher oscillator strength.[22]

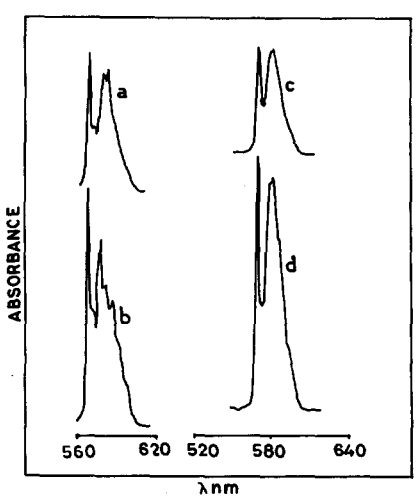


Fig. 3. Spectra of Nd^{3+} $^4I_{9/2} \rightarrow {}^4G_{5/2}$, $^2G_{7/2}$ Transition: (a) [Nd(fod)$_3$ · im] solid; (b) [Nd(fod)$_3$ · pz] solid; (c) [Nd(fod)$_3$ · im] in ethanol; (d) [Nd(fod)$_3$ · pz] in ethanol.

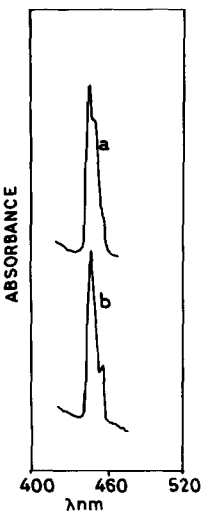


Fig. 4. Spectra of Ho^{3+} $^5I_8 \rightarrow {}^5G_6$ transition: (a) [Ho(fod)$_3$ · im] solid; (b) [Ho(fod)$_3$ · im] in ethanol.

The oscillator strength of the hypersensitive transition in the holmium complex is lower than those of eight- and ten-coordinate complexes.[10] It may be noted that the gradation of hypersensitivity is [Ho(fod)$_3$ · bpy · 2H$_2$O] > [Ho(fod)$_3$ · phen] > [Ho(fod)$_3$ · im]. This trend is in agreement with the conclusion of Henrie *et al.* that hypersensitivity depends upon the number of coordinated ligands.[1] The small difference in the oscillator strength of [Ho(fod)$_3$ · im] as compared to other seven-coordinate complexes reported in the literature[10,21] is due to the change in the nature of ligands present.

The oscillator strength of the hypersensitive transition in the erbium complex is the same as reported for Er(fod)$_3$ in ethanol (in solution Er(fod)$_3$ takes two solvent molecules and becomes eight-coordinate).[22] However, the magnitude is higher than [Er(fod)$_3$ · phen]. The lower value in phen complexes is due to splitting of the hypersensitive band into three.[8] It is instructive to note that the

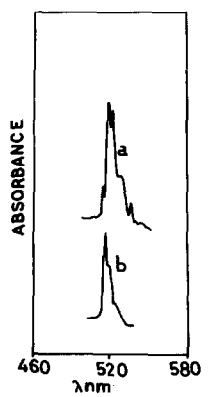


Fig. 5. Spectra of Er^{3+} $^4I_{15/2} \rightarrow {}^2H_{11/2}$ transition (a) [Er(fod)$_3$ · im] solid; (b) [Er(fod)$_3$ · im] in ethanol.

oscillator strength is much lower than some six-coordinate Er^{3+} complexes.[24] The lower value is consistent with a less asymmetric field around the erbium ion, accepting the premise that hypersensitivity depends on the asymmetry of the field on the ion.[23,25]

By the substitution of P_{exptl} and published values of matrix elements[26] in the Judd–Ofelt[27] equation, a set of three parameters (T_2, T_4 and T_6) are obtained. The T_λ parameters along with T_λ parameters of some analogous *fod* complexes[8–10] are collected in Table 6. The change in T_λ parameters show that T_2 is the most sensitive to the change in environment (i.e. change in the ligand). However, it is not true for the Nd^{3+} complexes where there is no trend. Also T_4 is negative in $[Nd(fod)_3 \cdot pz]$ and $[Nd(fod)_3 \cdot bpy \cdot 2H_2O]$ which is meaningless. This is really surprising in view of the fact that the Judd–Ofelt theory accounts reasonably for the other complexes and hence calls for further investigations.

NMR Spectra

The complexes of the diamagnetic trivalent ions La^{3+}, Y^{3+} and Lu^{3+} form a convenient series where ionic radius decrease (1.06, 0.88 and 0.85°A, respectively), while there are no paramagnetic effects to mask the relatively small shifts caused by coordination alone. The NMR spectra of the complexes have been recorded in DMSO-d_6 and spectral data are summarized in Table 7. The NMR signals of the *fod* moiety of the adducts appear at 0.98–1.07 ppm and 5.56–5.76 ppm for the *t*-butyl and the methine protons, respectively, as relatively sharp singlets. These signals of *t*-butyl and methine protons are shifted to high fields in the mixed-ligand complexes as compared to those of their respective chelates.[11] The reason for the high field shift would be the same as given for the analogous complexes.[8,9] Other signals can be assigned to those of the imidazole coordinated to the chelate. The signals of imidazole, in the complex, were found to shift remarkably to lower fields as compared to free imidazole. This deshielding effect of imidazole protons obviously suggests the coordinated nature of heterocyclic amine even in DMSO-d_6 solution. The shift is larger for H-2 (0.59–0.47 ppm) than for H-4 and H-5 (0.19–0.12 ppm). It is interesting to note that the signal for the N–H proton (H-3) is not seen in the spectra of the complex, although an N-H signal is observed in IR spectra.

The NMR spectra of the DMSO-d_6 solution of

Table 6. T_λ Parameters of some of the complexes ($T_\lambda \times 10^9$)

Complexes	T_2	T_4	T_6
$[Pr(fod)_3 . im]$[a, e]	64.745	2.551	28.416
$[Pr(fod)_3 pz]$[b, e]	235.337	1.152	13.146
$[Pr(fod)_3 . phen]$[c, f]	247.279	5.305	11.867
$[Pr(fod)_3 . bpy . 2H_2O]$[c, f]	35.848	5.848	17.925
$[Nd(fod)_3 . im]$[a, e]	19.654	6.681	26.195
$[Nd(fod)_3 . pz]$[b, e]	754.028	-1953.991	2809.555
$[Nd(fod)_3 . phen]$[c, f]	234.772	23.108	86.119
$[Nd(fod)_3 . bpy . 2H_2O]$[c, f]	1883.170	-818.700	1183.570
$[Ho(fod)_3 . im]$[a, e]	14.387	1.621	3.912
$[Ho(fod)_3 . phen]$[d, f]	24.645	5.842	4.377
$[Ho(fod)_3 . bpy . 2H_2O]$[d, f]	30,343	3.035	2.377
$[Er(fod)_3 . im]$[a, e]	24,338	1.372	4.856
$[Er(fod)_3 . pz]$[b, e]	20.149	3.083	0.399
$[Er(fod)_3 . phen]$[c, f]	19.930	0.152	1.596
$[Er(fod)_3 . bpy . 2H_2O]$[c, f]	47.800	2.430	1.962

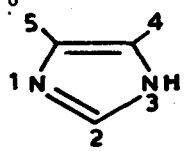
[a] this work; [b] ref. 9; [c] ref. 8; [d] ref. 10; [e] spectra observed in ethanol; [f] spectra observed in hexane.

Table 7. NMR spectral data[a]

Complexes	Signals due to imidazole			Signals due to β-keto enolate	
	H-3	H-2	H-4 & H-5	CH	Bu^t
Imidazole [b]	12.53	7.78	7.18	-	-
$[La(fod)_3 \cdot im]$ [c]	d	8.35	7.30	5.76	1.07
$[Y(fod)_3 \cdot im]$ [c]	d	8.25	7.30	5.70	1.03
$[Lu(fod)_3 \cdot im]$ [c]	d	8.37	7.37	5.65	0.98
$[Eu(fod)_3 \cdot im]$ [c]	7.67	3.50	2.63	1.12	0.58

[a] Chemical shifts in ppm downfield with respect to internal Me_4Si.

[b] in $CDCl_3$; [c] in DMSO-d_6; [d] not observed.



the complexes show no resonance for free imidazole or free β-diketone; no change in signal line width or position is observed even on keeping the solutions for a few hours. This clearly proves that the imidazole as well as the diketone remain coordinated in solution and there is no dissociation even of heterocyclic amine.

The NMR spectrum of $[Eu(fod)_3 \cdot im]$ shows the expected narrow signals. Europium complexes are well known for producing downfield shifts but there are reports in which the $Eu(dpm)_3$ complex was used where upfield shifts were also observed in the substrates.[28,29] It is noteworthy that all of the signals in $[Eu(fod)_3 \cdot im]$ are shifted to upfield with respect to the signal of the organic moiety itself as well as its diamagnetic analogues.

One of the intentions of this study was to examine $[Ln(fod)_3 \cdot im]$ complexes as potential shift reagents. The complexes of praseodymium and europium added to a CCl_4 solution of t-butanol do not show any significant change in the spectrum of 1-butanol. Thus these adducts are not suitable for use as NMR shift reagents in contrast to the analogous pyrazole complexes which produce large dipolar shifts in the NMR spectra of organic moieties.[9]

Acknowledgements—We express our thanks to Dr. A. U. Malik for criticism and valuable suggestions. The research associateship to KI, from CSIR is gratefully acknowledged. We thank the referees for constructive criticism.

REFERENCES

1. D. E. Henrie, R. L. Fellows and G. R. Choppin, *Coord. Chem. Rev.* 1976, **18**, 199.
2. K. B. Yatsimirskii and N. N. Davidenko, *Coord. Chem. Rev.* 1979, **27**, 223.
3. S. F. Manson, *Structure and Bonding* 1980, **39**, 43.
4. R. D. Peacock, *Structure and Bonding* 1975, **22**, 83.
5. A. F. Kirby and R. A. Palmer, *Inorg. Chem.* 1981, **20**, 1030, 4219.
6. *Nuclear Magnetic Resonance Shift Reagents* (Edited by R. E. Sievers). Academic Press, New York (1973).
7. M. Sayeed and N. Ahmad, *J. Inorg. Nucl. Chem.* 1981, **43**, 3197.
8. K. Iftikhar, M. Sayeed and N. Ahmad, *Inorg. Chem.* 1982, **21**, 80.
9. K. Iftikhar, M. Sayeed and N. Ahmad, *Bull. Chem. Soc. Jpn.* 1982, **55**, 2258.
10. K. Iftikhar and N. Ahmad, *Aust. J. Chem.* 1983, **36**, 699.
11. C. S. Springer, Jr., D. W. Meek and R. E. Sievers, *Inorg. Chem.* 1967, **6**, 1105.
12. W. J. Geary, *Coord. Chem. Rev.* 1971, **7**, 81.
13. W. J. Devis and J. Smith, *J.Chem. Soc(A)* 1971, 317.
14. H. Branic, R. S. T. L. Bruce, H. L. Freeman, N. J. Hair and J. James, *Inorg. Chem.* 1976, **15**, 2226.
15. D. Shirley, M. Kaplan, R. W. Grant and D. A. Keller, *Phys. Rev.* 1962, **127**, 2097.
16. P. Kienle, G. M. Kalvius and S. L. Ruby, In

Hyperfine Structure and Nuclear Radiations (Edited by E. Mathias and D. A. Shirley). North-Holland, Amsterdam (1968).
17. W. T. Carnall, P. R. Fields and K. Rajnak, *J. Chem. Phys.* 1968, **49**, 4412.
18. C. K. Jorgensen, *Prog. Inorg. Chem.* 1962, **4**, 73.
19. D. E. Henrie and G. R. Choppin, *J. Chem. Phys.* 1968, **49**, 477.
20. S. P. Sinha, *Spectro. Chim. Acta.* 1966, **22**, 57.
21. D. G. Karraker, *Inorg. Chem.* 1967, **6**, 1863.
22. D. G. Karraker, *J. Inorg. Nucl. Chem.* 1971, **33**, 3713.
23. B. R. Judd, *J. Chem. Phys.* 1966, **44**, 839.
24. T. Isobe and S. Misumi, *Bull. Chem. Soc. Jpn.* 1974, **47**, 281.
25. C. K. Jorgensen and B. R. Judd, *Mol. Phys.* 1964, **8**, 281.
26. W. T. Carnall, P. R. Fields and K. Rajnak, *J. Chem. Phys.* 1968, **49**, 4424.
27. W. T. Carnall, P. R. Fields and B. J. Wybourne, *J. Chem. Phys.* 1965, **42**, 3797.
28. T. H. Siddal, III, *J. Chem. Soc. Chem. Commun.* 1971, 452.
29. D. E. U. Ekong, J. I. Okogun and M. E. Obasi, *J. Chem. Soc. Perkin I* 1972, 1943.

Polyhedron Vol. 4, No. 2, pp. 343–348, 1985
Printed in Great Britain.

0277–5387/85 $3.00 + .00
© 1985 Pergamon Press Ltd.

PREPARATION AND CHARACTERIZATION OF HETEROBIMETALLIC TETRAXANTHATES AND THEIR COMPLEXES WITH LEWIS BASES

R. C. AGGARWAL*, NANHAI SINGH and SUNITA SINGH
Department of Chemistry, Banaras Hindu University, Varanasi 221 005, India

(*Received* 13 *February* 1984; *accepted* 25 *April* 1984)

Abstract—Some new heterobimetallic tetraxanthates of the type $M[Ag(Etxant)_2]_2$ [M = Co(II) or Ni(II), Etxant = ethylxanthate] and their complexes of general formula $M[Ag(Etxant)_2]_2.xL$ [$x = 2$ when L = dimethylsulphoxide (DMSO), triphenylphosphine (PPh_3), pyridine(py) or 2-aminopyridine (2-ampy); $x = 3$ when L = 2,2′-bipyridine (bipy)] have been prepared and characterized by elemental analysis, molar conductance, magnetic susceptibility, infrared and electronic spectral studies. Magnetic and electronic spectral studies indicate square planar geometry around Ni(II) and Co(II) in heterobimetallic tetraxanthates and $Ni[Ag(Etxant)_2]_2.2PPh_3$ and octahedral geometry around the above metal ions in the remaining complexes.

In previous papers[1,2] we reported the synthesis and characterization of heterobimetallic tetraxanthates of the type $MM'(Etxant)_4$ and their complexes with Lewis bases. This work has now been extended to the hitherto uninvestigated heterobimetallic xanthates and their complexes with Lewis bases such as DMSO, PPh_3, py, 2-ampy or bipy in which one of the metal ions is Ag^+ and the other is Ni^{2+} or Co^{2+}. A further point of interest in these studies was to examine whether the Lewis bases bond to Ag(I), Co(II)/Ni(II) or both with or without disrupting the structure of the parent Lewis acids. The synthesis and structural studies of $Co[Ag(Etxant)_2]_2$ and $Ni[Ag(Etxant)_2]_2$ and their complexes with DMSO, py, 2-ampy, bipy and PPh_3 were therefore undertaken and results of these studies are embodied in the present paper.

EXPERIMENTAL

Material and methods. Metal salts and potassium ethylxanthate used in the preparative work were BDH or RIEDEL(LR) grade. The 2-ampy, bipy and PPh_3 were used as such while py, DMSO, and solvents were freshly distilled and dried before use.

Preparation of $M[Ag(Etxant)_2]_2$ *and their complexes with Lewis bases*

$K[Ag(Etxant)_2]$ was prepared in situ by adding with constant stirring, silver nitrate (1 m mole) dissolved in 50 cm^3 water to a 150 cm^3 solution in 80:20 DMF water (v/v) containing potassium ethylxanthate (2 m mole). To the above solution cobalt or nickel nitrate (0.5 m mole) dissolved in 25 cm^3 water, was added gradually with vigorous stirring. The amorphous heterobimetallic tetraxanthates thus precipitated were filtered, washed with ether and dried *in vacuo*.

The complexes $M[Ag(Etxant)_2]_2.xL$ were prepared by mixing together 25 cm^3 dichloromethane suspension containing heterobimetallic xanthates (1 m mole) and 30 cm^3 ethanolic solution of the appropriate Lewis bases (4 m mole). The complexes which precipitated after prolonged stirring and keeping the reaction mixture for several hours were filtered, washed with ethanol and then with ether and dried *in vacuo*.

$Ni[Ag(Etxant)_2]_2\ 2PPh_3$ was prepared by adding $NiCl_2.2PPh_3$[3] (1 m mole) dissolved in 50 cm^3 acetone to a 200 cm^3 solution of $K[Ag(Etxant)_2]$ (2 m mole) in 80:20 DMF-water (v/v). The light orange complex precipitated on stirring the reaction mixture was filtered, washed with acetone followed by ether and dried *in vacuo*. Our attempts to synthesize the analogous Co(II) compound was not successful.

*Author to whom correspondence should be addressed.

Table 1. Analytical data of heterobimetallic xanthates and their complexes with Lewis bases

Complex	Colour	Decomposition temp. (°C)	Found (Calcd)%				μ_{eff} (B.M.)	Λ_M mhos cm^2 mol^{-1}
			Ni/Co	Ag	S	N		
$Ni[Ag(Etxant)_2]_2$	Light brown	179	7.71(7.74)	28.00(28.43)	33.62(33.76)	-	dia	-
$Ni[Ag(Etxant)_2]_2.2PPh_3$	Light orange	128	4.45(4.54)	16.25(16.81)	19.80(19.95)	-	dia	2.70
$Ni[Ag(Etxant)_2]_2.2DMSO$	Green	118	6.35(6.42)	23.02(23.58)	27.80(28.00)	-	3.05	-
$Ni[Ag(Etxant)_2]_2.2py$	Green	110	6.29(6.40)	22.95(23.53)	27.80(27.94)	3.00(3.05)	3.25	4.82
$Ni[Ag(Etxant)_2]_2.2(2ampy)$	Bluish green	250	6.10(6.20)	22.52(22.78)	26.90(27.05)	5.82(5.91)	3.10	5.24
$Ni[Ag(Etxant)_2]_2.3$ bipy	Yellowish orange	250	4.72(4.78)	17.20(17.58)	20.72(20.88)	6.78(6.85)	3.22	28.41
$Co[Ag(Etxant)_2]_2$	Olive green	250	7.62(7.76)	27.92(28.42)	33.62(33.76)	-	2162	-
$Co[Ag(Etxant)_2]_2.2$ DMSO	Light pink	120	6.34(6.44)	23.46(23.58)	27.82(28.00)	-	5.10	-
$Co[Ag(Etxant)_2]_2.2$ py	Pink	115	6.38(6.42)	23.20(23.52)	27.82(27.95)	2.98(3.05)	4.48	-
$Co[Ag(Etxant)_2]_2.2(2$ ampy)	Pink	250	6.10(6.22)	22.50(22.78)	26.90(27.04)	5.80(5.91)	5.15	10.25
$Co[Ag(Etxant)_2]_2.3$ bipy	Dark brown	250	4.62(4.65)	17.27(17.57)	20.67(20.89)	6.78(6.85)	5.17	34.50

Table 2. Electronic spectral bands and their assignments in heterobimetallic xanthates and their Lewis base complexes

Complex	Bands (cm^{-1})	Assignment
Ni[Ag(Etxant)$_2$]$_2$	15500, 20600, 23800	$^1A_{1g} \rightarrow {}^1B_{1g}$, $^1A_{1g} \rightarrow {}^1A_{2g}$
Ni[Ag(Etxant)$_2$]$_2$.2PPh$_3$	16000, 20600, 23800	$^1A_{1g} \rightarrow {}^1B_{1g}$, $^1A_{1g} \rightarrow {}^1A_{2g}$
Ni[Ag(Etxant)$_2$]$_2$.2DMSO	10500, 15400, 21000	$^3A_{2g} \rightarrow {}^3T_{2g}(\nu_1)$ $^3A_{2g} \rightarrow {}^3T_{1g}(F)(\nu_2)$ $^3A_{2g} \rightarrow {}^3T_{1g}(P)(\nu_3)$
Ni[Ag(Etxant)$_2$]$_2$.2py	10500, 15900, 23500	$^3A_{2g} \rightarrow {}^3T_{2g}(\nu_1)$ $^3A_{2g} \rightarrow {}^3T_{1g}(F)(\nu_2)$ $^3A_{2g} \rightarrow {}^3T_{1g}(P)(\nu_3)$
Ni[Ag(Etxant)$_2$]$_2$.2(2ampy)	10600, 16000, 25000	$^3A_{2g} \rightarrow {}^3T_{2g}(\nu_1)$, $^3A_{2g} \rightarrow {}^3T_{1g}(F)(\nu_2)$ $^3A_{2g} \rightarrow {}^3T_{1g}(P)(\nu_3)$
Ni[Ag(Etxant)$_2$]$_2$.3bipy	19200, 12500 } split 10500 }	$^3A_{2g} \rightarrow {}^3T_{1g}(\nu_2)$, $^3A_{2g} \rightarrow {}^3T_{2g}(\nu_1)$
Co[Ag(Etxant)$_2$]$_2$	16600, 8060, 10520	$^2A_{1g} \rightarrow {}^2E_{2g}$, $^2A_{1g} \rightarrow {}^2E'_g$
Co[Ag(Etxant)$_2$]$_2$.2DMSO	10500, 15400, 20800	$^4T_{1g} \rightarrow {}^4T_{2g}$, $^4T_{1g} \rightarrow {}^4A_{2g}$, $^4T_{1g} \rightarrow {}^4T_{1g}(P)$
Co[Ag(Etxant)$_2$]$_2$.2py	10500, 16100, 20850	$^4T_{1g} \rightarrow {}^4T_{2g}$, $^4T_{1g} \rightarrow {}^4A_{2g}$, $^4T_{1g} \rightarrow {}^4T_{1g}(P)$
Co[Ag(Etxant)$_2$]$_2$.2(2ampy)	10250, 14800, 20000	$^4T_{1g} \rightarrow {}^4T_{2g}$, $^4T_{1g} \rightarrow {}^4A_{2g}$, $^4T_{1g} \rightarrow {}^4T_{1g}(P)$
Co[Ag(Etxant)$_2$]$_2$.3bipy	17050, 10250	$^4T_{1g} \rightarrow {}^4T_{2g}$, $^4T_{1g} \rightarrow {}^4T_{1g}(P)$

Table 3. Selected IR bands (cm^{-1}) of $M[Ag(Etxant)_2]_2$ and their Lewis base complexes

Complex	ν (C—O)	ν (C...S)
$Ni[Ag(Etxant)_2]_2$	1260 (s)	1005 (s)
$Ni[Ag(Etxant)_2]_2.2PPh_3$	1165 (m)	1010 (m)
$Ni[Ag(Etxant)_2]_2.2DMSO$	1200 (s)	1020 (s)
$Ni[Ag(Etxant)_2]_2.2py$	1205 (m)	1000 (m)
$Ni[Ag(Etxant)_2]_2.2(2ampy)$	1150 (m)	1005 (m)
$Ni[Ag(Etxant)_2]_2.3bipy$	1180 (s)	990, 1005 split
$Co[Ag(Etxant)_2]_2$	1250 (m)	1010 (s)
$Co[Ag(Etxant)_2]_2.2DMSO$	1185 (m)	1010 (m)
$Co[Ag(Etxant)_2]_2.2py$	1200 (m)	1015 (m)
$Co[Ag(Etxant)_2]_2.2(2ampy)$	1190 (s)	1000 (m)
$Co[Ag(Etxant)_2]_2.3bipy$	1190 (s)	995, 1010 split

s = strong, m = medium

Analysis and physical measurements. The complexes were analyzed for their metal contents applying standard literature procedures.[4] Nitrogen was estimated microanalytically. Sulphur was estimated as $BaSO_4$. The experimental details pertaining to the determination of molar conductance and recording of magnetic susceptibility, x-ray diffraction, IR and electronic spectra were the same as described in our previous paper.[1] The relevant analytical and physico-chemical data are given in Tables 1–4.

RESULTS AND DISCUSSION

The analytical data show the formation of heterobimetallic tetraxanthates $M[Ag(Etxant)_2]_2$ and their complexes $M[Ag(Etxant)_2]_2.xL$ with Lewis bases. All the heterobimetallic xanthates and their Lewis base complexes do not melt but decompose in specific temperature ranges. The two Lewis acids and their complexes are insoluble in water and common organic solvents but slightly soluble in nitrobenzene and dimethylformamide. Very low values of molar conductance of bimetallic xanthates in 10^{-3}M nitrobenzene solution indicate their nonionic[5] nature. However, the molar conductance values for tris-bipy complexes (28.4–34.5 mhos cm^2 mol^{-1}) in the same solvent suggest their 1:1 electrolytic behaviour.

Table 4. *d*-spacings (Å) of some strong lines from X-ray powder diffraction on heterobimetallic xanthates

$Ni[Ag(Etxant)_2]_2$	$Co[Ag(Etxant)_2]_2$
9.33	9.20
8.89	-
8.50	7.49
6.91	-
6.32	5.90
4.73	4.83
4.62	4.54
4.29	3.96
4.18	3.80
4.11	-
3.86	3.44
3.69	3.18
3.28	2.90
2.94	2.35

Magnetic and electronic spectral studies. The magnetic moment data given in Table 1 are consistent with square planar geometry around Ni(II)[6] in $Ni[Ag(Etxant)_2]_2$, $Ni[Ag(Etxant)_2]_2.2PPh_3$ and around Co(II)[7] in $Co[Ag(Etxant)_2]_2$ and spin free octahedral geometry[8-11] around Ni(II) and Co(II) in the remaining complexes.

The visible region spectra of $Ni[Ag(Etxant)_2]_2$ and $Ni[Ag(Etxant)_2]_2.2PPh_3$ give three absorption bands which are similar in positions to the bands reported for square planar $Ni(Etxant)_2$ and $NiZn(Etxant)_4$ suggesting square planar[12] geometry around Ni(II) with D_{4h} symmetry. The very similar values 15500 and 16000 cm^{-1} of ν_1 band in $Ni[Ag(Etxant)_2]_2$ and its PPh_3 complex, therefore support the view that the two triphenylphosphine molecules must be bonded to Ag(I) rather than Ni(II). Bonding of the soft PPh_3 molecules to Ag(I) rather than to the borderline Ni(II) is expected on the basis of the HSAB principle.

Py, 2-ampy and DMSO complexes of Ni $Ag(Etxant)_2$ show three d-d transitions which are similar to the ν_1, ν_2 and ν_3 bands reported for a number of octahedral Ni(II) complexes.[10,13] $Ni[Ag(Etxant)_2]_2.3bipy$ exhibits two split bands at 10500 and 125000 cm^{-1} and a shoulder at 19200cm^{-1}. The spectral features suggest distorted octahedral[9,14] environment around Ni(II), in the above complex.

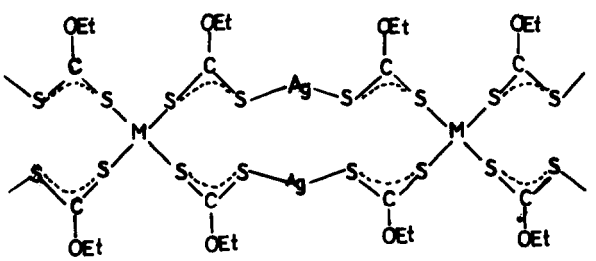
The positions of the *d–d* transitions observed in the electronic spectra of $Co[Ag(Etxant)_2]_2$ and its DMSO, py, 2-ampy and bipy complexes are consistent with square planar geometry around Co(II)[15-17] in the former case and octahedral geometry[13,14] around the above metal ion in the latter complexes. The value of (B = 700 cm^{-1}) for $Co[Ag(Etxant)_2]_2$ has been calculated from the most characteristic band for square planar geometry around Co(II) at 10520 cm^{-1} as suggested by Kida.[17]

IR spectra. The bands observed in the IR spectra of heterobimetallic xanthates in 1250–1260 and 1005–1010 cm^{-1} and in their complexes with Lewis bases in 1150–1205 and 990–1020 cm^{-1} regions are assigned to ν(C–O) and ν(C=S) modes respectively.[1,8,9,18,19] The presence of a single ν(C=S) band in the above complexes and a doublet at 995 and 1000 cm^{-1} due to the above mode in the IR spectra of $M[Ag(Etxant)_2]_2.3bipy$, suggests uninegative bidentate[1,18] behaviour of the xanthate group in the former complexes and its uninegative monodentate[9] behaviour in the latter complexes.

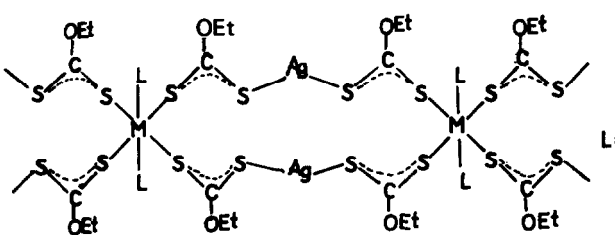
The IR spectra of the heterobimetallic tetraxanthate complexes exhibit bands characteristic of coordinated Lewis bases.[20-23] The coordinated nature of the Lewis bases in the above complexes is further evident from a marked negative shift[24] of about 50–110 cm^{-1} in ν(C–O) frequency.

X-Ray powder diffraction pattern. The $Co[Ag(Etxant)_2]_2$ and $Ni[Ag(Etxant)_2]_2$ have identical X-ray diffraction patterns and also their *d*-spacings are comparable (Table 4) suggesting them to be isostructural.

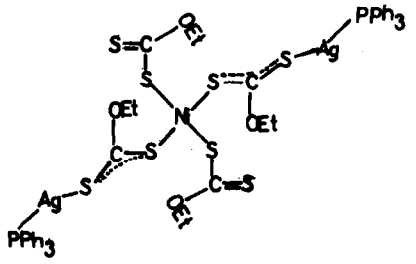
From the composition and physicochemical studies described above structures **I, II, III** and **IV** are proposed for heterobimetallic tetraxanthates and their complexes with Lewis bases. The disposition of the xanthate groups around Ag(I) is probably non-linear as is common with two coordinated complexes of Ag(I) with sulphur donor ligands.[25,26]



I



II



III

$$Ni\left[Ag(Etxant)_2\right]_2 2PPh_3$$

$$\left[M(bipy)_3\right]^{2+}\left[Ag(Etxant)_2\right]_2^{2-} \quad IV$$

REFERENCES

1. R. C. Aggarwal, Nanhai Singh and Sunita Singh, *Ind. J. Chem.* 1982, **21A**, 268.
2. R. C. Aggarwal, Nanhai Singh and Sunita Singh, *Ind. J. Chem.* 1983 **22A**, 161.
3. F. A. Cotton, O. D. Faut and D. M. L. Goodgame, *J. Am. Chem. Soc.* 1961, **83**, 344.
4. A. I. Vogel, *A Text Book of Quantitative Inorganic Analysis*. Longmans, London (1961).
5. W. J. Geary, *Coord. Chem. Rev.* 1971, **7**, 81.
6. M. Frazini, *Z Krist.* 1963, **118**, 393.
7. R. L. Carlin, *Trans Met Chem.* 1965, **1**, 28.
8. D. Coucouvanis and J. P. Fackler, *Inorg. Chem.* 1967, **6**, 2047.
9. D. C. Holah and C. N. Murphy, *Inorg. Nucl. Chem. Lett.* 1972, **8**, 1069.
10. A. G. Kruger and G. Winter, *Aust. J. Chem.* 1971, **24**, 161.
11. B. N. Figgis and J. Lewis, *Prog. Inorg. Chem.* 1964, **6**, 192.
12. C. K. Jorgensen, *J. Inorg. Nucl. Chem.* 1962, **24**, 1571.
13. A. B. P. Lever, *Inorganic Electronic Spectroscopy*, p. 320. Elsevier, New York (1968).
14. D. C. Holah and C. N. Murphy, *Can. J. Chem.* 1971, **49**, 2726.
15. Y. Nishida and S. Kida, *Inorg. Nucl. Chem. Lett.* 1971, **7**, 325.
16. Y. Nishida and S. Kida, *Coord. Chem. Rev.* 1979, **27**, 275.
17. Y. Nishida, K. Hayashida and S. Kida, *Inorg. Chim. Acta* 1978, **31**, 19.
18. D. C. Bradley and M. H. Gitlitz, *J. Chem. Soc.(A)* 1969, 1152.
19. D. Concouvanis, *Prog. Inorg. Chem.* 1970, **11**, 233; 1979, **26**, 301.
20. W. L. Reynolds, *Prog. Inorg. Chem.* 1970, **12**, 69.
21. G. B. Deacon and J. H. S. Green, *Chem. Ind.* 1965, 1031.
22. R. J. H. Clark and C. S. Williams, *Inorg. Chem.* 1965, **4**, 350.
23. B. Hutchison, J. Takemoto and K. Nakamoto, *J. Am. Chem. Soc.* 1970, **92**, 3335.
24. M. R. Hunt, A. G. Kruger, L. Smith and G. Winter, *Aust. J. Chem.* 1971, **24**, 53.
25. I. Lindquist, *Acta Cryst.* 1957, **10**, 29.
26. D. Harker, *J. Chem. Phys.* 1936, **4**, 381.

Polyhedron Vol. 4, No. 2, pp. 349–356, 1985
Printed in Great Britain.

0277–5387/85 $3.00 + .00
© 1985 Pergamon Press Ltd.

BEHAVIOUR OF α-FUNCTIONAL ORGANOTRANSITION METALS.[1] SYNTHESIS, CHARACTERISATION AND SOME REACTIONS OF 1-ACETOXYALKYL DERIVATIVES OF IRON(II) AND MOLYBDENUM(II)

SUSANNA E. HIMMEL, G. BRENT YOUNG*,
DAWNING C. M. FUNG and CHRISTINE HOLLINSHEAD
Chemistry Department, Imperial College, London SW7 2AY, England

(*Received* 2 *March* 1984; *accepted* 4 *May* 1984)

Abstract—Acetoxyalkyl metal derivatives $M(C_5H_5)(CO)_n[CHROC(O)Me]$[M = Fe, n = 2; M = Mo, n = 3; R = H, Me] are readily prepared by reaction of bromoalkylacetates with the appropriate cyclopentadienylcarbonylmetallate anion. The complexes are characterised by their NMR (^1H and ^{13}C) and IR parameters and by mass spectrometry. The acetoxyethyl species are thermally labile via β-hydrogen transfer. Treatment of acetoxymethyl complexes with protic acids leads to carbon-oxygen cleavage and release of acetic acid; HCl affords chloromethyl complexes, carboxylic acids yield new carboxylatomethyl derivatives, HBF_4 leads to decomposition. The metalloesters are resistant to hydrolysis, transesterification and carboxylate displacement by nucleophiles (HO^-, MeO^-, H_2N^- Et_2N^-). Migratory insertion of CO could not be induced.

There has been considerable interest recently in α-functional organotransition metals, stemming from their implication in a variety of metal-mediated processes. Notable among these derivatives are 1-hydroxyalkyls, which feature as intermediates in the palladium-catalysed oxidative hydrolysis of alkenes (Wacker process)[2] and in the Fischer–Tropsch and related reductions of carbon monoxide catalysed by a variety of metals.[3] Several hydroxymethylmetal complexes have been successfully isolated in investigations aimed at modelling the latter process.[4–6] A variety of ingenious routes have been employed. Acetoxyalkyl ligands seemed attractive as precursors to an assortment of α-functional alkylmetals including hydroxyalkyls, as well as offering a relatively unexplored class of α-functional organometal. An acetoxymethyliron derivative has been described previously, prepared by a less direct route,[4] and has lately found synthetic application.[7] We now report a general, direct synthesis of 1-acetoxyalkyl derivatives of iron and molybdenum, as well as some of their reactivity. A brief report has appeared very recently of analogous ruthenium complexes prepared by this method.[6]

*Author to whom correspondence should be addressed.

EXPERIMENTAL

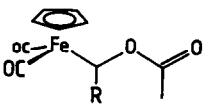
General. NMR measurements were performed on Bruker WM250 (^1H, ^{13}C, ^{31}P; FT mode), JEOL FX90Q (^1H, ^{13}C; FT mode) and Perkin–Elmer R32 (^1H; CW mode) instruments. IR data were obtained on a Perkin–Elmer 683 spectrophotometer. Mass spectra were recorded on a VG7070E instrument. All chemical manipulations were carried out in dried, degassed solvents under an atmosphere of purified argon. Diethyl ether and tetrahydrofuran (thf) were distilled under nitrogen from sodium benzophenone anion as were toluene and petroleum ether (40–60° fraction). Dicyclopentadienyltetracarbonyldiiron and dicyclopentadienylhexacarbonyl-dimolybdenum were purchased from Strem Chemicals and were recrystallised prior to use. H.P.L.C. analyses were carried out using an automated Spectra-Physics SP8100 system equipped with SP8440 uv/visible detector and an SP4200 computing integrator. Reaction products were separated on a 25 cm column of ODS bonded on 5μ silica, eluting with methanol and monitoring at 215 nm. Elemental analyses were by Pascher, Bonn.

Preparation of bromomethylacetate.[8]

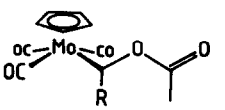
Paraformaldehyde (12 g, 0.4 mol) was mixed with acetyl bromide (30 cm^3, 0.4 mol) under dry nitrogen. A catalytic amount of $ZnCl_2$ (0.2 g

1.5 mmol) was added. When the considerably exothermic reaction had subsided, the reaction was stirred for a further 3 hr at 90–95°C. Pure bromomethylacetate was recovered from the reaction mixture by distillation (b.p. 132–138°C, 760 Torr). ^{1}H NMR (chloroform-*d*): 5.76 (s, 2H), 2.11 (s, 3H).

1



2



(a) R = H
(b) R = Me

Preparation of 1-*bromoethylacetate*

This was achieved by a modification of the method in Ref. 8; no zinc catalyst was employed. A 25% excess of acetaldehyde (36 cm^3, 35.2 g 0.8 mol) was slowly added to stirred acetyl bromide (38 cm^3 73.8 g 0.6 mol) at 40°C and with exclusion of light. The mixture was stirred for a further 2 hr at 40°C, and the product was purified by distillation at reduced pressure (30°C at 6 Torr). ^{1}H NMR (chloroform-*d*): 6.67 (q, 1H), 2.1 (s, 3H), 2.00 (d, 3H).

Preparation of acetoxymethyl cyclopentadienyl dicarbonyl iron(II)

To a stirred 0.4% sodium amalgam [prepared from 23 cm^3 mercury and 0.96 g (43 mg-atom) sodium] was added a solution of $[Fe(C_5H_5)(CO)_2]_2$ (6.4 g 20 mmol) in thf (80 cm^3). The mixture was stirred for 24 hr. The yellow ethereal solution of $Na[Fe(C_5H_5)(CO)_2]$ was filtered off and to it was slowly added at ambient temperature, bromomethylacetate (5.4 cm^3, 8.82 g, 57.8 mmol). These reagents were stirred for a further 24 hr. The solvent was removed at reduced pressure and the residue extracted with petroleum ether. The supernatant was filtered off and the solvent once more evaporated leaving a red oil, which, from its ^{1}H NMR spectrum, was predominantly the desired product. Purification was achieved by liquid chromatography at 0°C on grade A activated alumina.

Two yellow by-products were eluted first, using petroleum ether and $Fe(C_5H_5)(CO)_2[CH_2OC(O)Me]$ was eluted as a third fraction using 1:1 petroleum ether/diethyl ether. The compound is an orange-red oil at ambient temperature but is crystalline at −20°C. (Yield 7.6g, 76% prior to chromatography.) Found; C, 47.91; H, 4.03; Calc. for $C_{10}H_{10}O_4Fe$: C, 48.04; H, 4.04%.

Preparation of 1-*acetoxyethylcyclopentadienyldicarbonyliron(II)*

A solution of $Na[Fe(C_5H_5)(CO)_2]$ (40 mmol) in thf (100 cm^3) prepared as above was very slowly added to a vigorously stirred sample of 1-bromoethylacetate (6 cm^3, 40 mmol) at −78°C. The mixture was stirred for 4 hours at this temperature, and then allowed to reach ambient. The solvent was evaporated at reduced pressure leaving an oily residue. This was extracted with petroleum, filtered and concentrated under vacuum to a dark red gum. Purification by chromatography at 0°C on alumina as described above afforded a dark red oil. The thermal lability of this compound at ambient temperatures precluded elemental analysis and its identity was established by its spectroscopic characteristics (see Tables 1 and 2).

Table 1. NMR characteristics for acetoxyalkylmetals and derivatives

Complex	δ^1H[a]				$\delta^{13}C$[a]					
	CHR	CH_3	C_5H_5	CH_3'	CHR	CH_3	C_5H_5	CH_3'	C=O	C=O
$CpFe(CO)_2CH_2OAc$[b]	4.88	1.76	4.01	-	53.72	21.2	85.34	-	216.05	170.44
$CpFe(CO)_2CMeHOAc$[b]	5.31q[c]	1.74	4.24	1.29d[c]	68.08d	21.37	85.57	31.76	216.48	169.05
$CpMo(CO)_3CH_2OAc$[b]	5.40	1.73	4.59	-	50.97	20.93	92.61	-	239.40[d] 226.90[e]	170.58
$CpMo(CO)_3CMeHOAc$[b]	7.06q[f]	1.69	4.68	1.83d[f]	64.34	21.28	92.90	30.23	240.03[d] 227.05[e]	169.35
$CpFe(CO)_2CH_2C\ell$[g]	4.20	-	5.02	-			h			
$CpMo(CO)_3CH_2C\ell$[g]	4.00	-	4.56				h			

a in ppm relative to Me_4Si. b in benzene-d_6. *c* $^3J(H–H)$ = 6 *Hz*. d *trans* to CHROAc. e *cis* to CHROAc. f $^3J(H–H)$ = 7 Hz. g in acetone-d_6. h not measured.

Table 2. IR characteristics for acetoxyalkylmetals and derivatives

Complex	Infrared Absorption (cm^{-1})										
$CpFe(CO)_2CH_2OAc$[a]	3950w	3110w	2980sh	2930m	2860vs	2010vs	1950vs	1780s	1730s	1435m	1420m
	1370s	1270s	1137s	1110vs	1013s	944s	843m	833m	750vs		
$CpFe(CO)_2CMeHOAc$[a]	3940w	3110w	2980w	2940m	2850br	1990vs	1925vs	1905sh	1890s	1765s	1445w
	1430w	1415m	1367m	1345w	1325w	1240w	1180m	1100m	1080m	1060m	1035s
	1020sh	1000m	975m	945w	925m	850m	830m	750w	645m	600s	
$CpMo(CO)_3CH_2OAc$[b]	3940w	3120w	2010vs	1945vs	1725s	1250m	1165m	1095s	1045m	995m	950m
	935m	855w	830m	820m	810m	705w	630w				
$CpMo(CO)_3CMeHOAc$[a]	3940w	3120w	2950w	2920w	2870w	2020vs	1995s	1940vs	1885w	1850vs	1720s
	1425m	1370m	1240s	1190m	1100m	1075m	1010m	930m		815s	775m
$CpFe(CO)_2CH_2Cl$[b]	3960w	3120w	2060s	2025vs	1955vs	1945sh	1465m	1435m	1420m	1350vs	1340w
	1150m	1100m	1060vs	1040m	1000m	840s	835m	750m			
$CpMo(CO)_3CH_2Cl$[b]	2040vs	1965vs	1950vs	1840vs	820m	722m					

a thin film, KBr plates. b Nujol mull, KBr plates.

Preparation of acetoxymethylcyclopentadienyldicarbonylmolybdenum(II)

To $Na[Mo(C_5H_5)(CO)_3]$, in thf (70 cm^3), prepared from $[Mo(C_5H_5)(CO)_3]_2$ (2.0 g 4 mmol) and a 0.2% sodium amalgam (8 cm^3) was slowly added bromomethylacetate (1.2 cm^3, 8 mmol). The mixture was stirred for 24 hr before the solvent was evaporated at reduced pressure. The brown residue was extracted with 40–60 petroleum ether (40 cm^3) the supernatant filtered off and evaporated to dryness, leaving a dun oil, which crystallised on cooling. Recrystallisation from 1 : 1 ether/petroleum ether yielded dark yellow crystals of $Mo(C_5H_5)(CO)_3[CH_2OC(O)Me]$ (yield 2.3 g 91.2%). Found: C, 41.42; H, 3.20. Calc. for $C_{10}H_{10}O_5Mo$: C, 41.53; H, 3.17%.

Preparation of 1-acetoxyethylcyclopentadienyldicarbonylmolybdenum(II)

$Mo(C_5H_5)(CO)_3[CHMeOC(O)Me]$ was prepared by the same procedure as $Mo(C_5H_5)(CO)_3CH_2OC(O)Me$ except that the petroleum extract was purified by chromatography at 0°C on grade A activated alumina. The first (unidentified) product was eluted with 40–60 petroleum ether; the second, and desired, product with 1:1 ether/petroleum ether. This was recovered as red/brown oil (yield 0.4 g, 16%). The high thermal lability even at ambient temperature precluded elemental analyses. Spectroscopic characteristics appear in Tables 1 and 2.

Reaction of $Fe(C_5H_5)(CO)_2[CH_2OC(O)Me]$ *with hydrogen chloride*

Dry, gaseous HCl was passed into a solution of $Fe(C_5H_5)(CO)_2[CH_2OC(O)Me]$ (0.20 g 0.8 mmol) in 40–60 petroleum ether (40 cm^3) for 15 min. The solvent was evaporated at reduced pressure, yielding an orange oil. Orange crystals of $Fe(C_5H_5)(CO)_2CH_2Cl$, identified by its NMR and IR characteristics,[4] were obtained from 40–60° petroleum (yield 0.15 g, 83%).

Reaction of $Mo(C_5H_5)(CO)_3[CH_2OC(O)Me]$ *with hydrogen chloride*

Dry, gaseous HCl was bubbled into a solution of $Mo(C_5H_5)(CO)_3[CH_2OC(O)Me]$ (0.13 g, 0.4 mmol) in 40–60 petroleum ether (30 cm^3) for 20 min. The supernatant was filtered from a small amount of fine brown precipitate. The solvent was evaporated to give $Mo(C_5H_5)(CO)_3CH_2Cl$, pure by NMR (yield, 0.11 g, 93%).

Reaction $Mo(C_5H_5)(CO)_3[CH_2OC(0)Me]$ *with* HBF_4

To a stirred solution of $Mo(C_5H_5)(CO)_3[CH_2OC(O)Me]$ (0.085 g, 0.3 mmol) in diethyl ether (40 cm^3) at ambient temperature was dropwise added an ethereal solution of HBF_4 (1 cm^3 of 0.4 M solution, 0.4 mmol). The mixture was stirred for 30 min and the solvent reduced in volume and cooled. Red crystals of $[Mo(C_5H_5)(CO)_3]BF_4$ were identified from their published characteristics.[9]

(yield 0.076 g, 76%). A violet precipitate, identified as $[Mo(C_5H_5)(CO)_3]_2$ may also be produced on longer stirring. Acetic acid was the major organic byproduct of the reaction, characterised by HPLC analysis of the reaction mixture and by its ^1H NMR spectrum.

Reaction of $Fe(C_5H_5)(CO)_2[CH_2OC(O)Me]$ *with* HBF_4

To a stirred solution of $Fe(C_5H_5)(CO)_2[CH_2OC(O)Me]$ (0.100 g, 0.4 mmol) in diethyl ether (10 cm^3) was slowly added, at ambient temperature, a solution of HBF_4 in the same solvent (3 cm^3 of 0.28 M, 0.84 mmol). A red oil separated immediately. The supernatant was removed by cannula, and the red oil concentrated *in vacuo*. The characteristics of the resulting crystalline material agreed closely with those reported for $[Fe(C_5H_5)(CO)_3]BF_4$.[10] Acetic acid was identified by HPLC and ^1H NMR as the predominant organic by-product.

Carboxylate exchange on $Fe(C_5H_5)(CO)_2[CH_2OC(O)Me]$ *and* $Mo(C_5H_5)(CO)_3[CH_2OC(O)Me]$

These reactions were monitored by ^1H NMR in an appropriate solvent (benzene-d_6) to which the carboxylic acid was added, or in acetic acid-d_4. The appearance of the characteristic signal for the methyl substituent of CH_3CO_2H (2.08 ppm in acetic acid-d_4) was used to monitor the rate and extent of exchange. In addition, the spectroscopic characteristics of the organometallic product were verified.

Carbonyl insertion studies. Two approaches were used (i) The acetoxymethylmetal (*ca.* 3 mmol) was dissolved in acetone (10 cm^3) and maintained at 23°C in a sealed reactor under an atmosphere of CO (120 atm). The mixture was stirred overnight. There was no reduction in gas pressure. The solution was recovered, the solvent removed and the residual material characterised by NMR and IR spectra. (ii) The metalloester (*ca.* 1 mmol) was dissolved in acetone or nonane and a 5-fold excess of tertiary phosphine introduced. The mixture was heated to 50 or 90°C overnight. The solvent was evaporated and the residual material was spectroscopically analysed.

RESULTS AND DISCUSSION

Syntheses

Bromomethylacetate reacts smoothly with sodium cyclopentadienylcarbonylmetallates in tetrahydrofuran (thf) to afford, in good yield, acetoxymethylmetal species via nucleophilic displacement of bromide. The iron(II) complex, **1a,** is a moderately air-sensitive red oil at ambient temperature,[4] but which affords orange-red crystals at −20°C, while the corresponding molybdenum(II) derivative, **2a,** forms dark yellow, air-sensitive crystals. Both compounds are stable indefinitely at −20°C under inert atmospheres. Their identities were established by ^1H and ^{13}C NMR and IR measurements, by mass spectrometry and by elemental analyses.

Reaction of the same organometallic anions with 1-bromoethylacetate proceeds more slowly and in poorer yields. This may in part reflect the sensitivity of a concerted halide displacement to increasing steric obstruction, but it must also derive largely from the high thermal lability of these complexes. Both are prone to decomposition even below 0°C. This feature has made purification (by chromatography) the more difficult, has severely limited the range of reactivity studies and has excluded elemental analysis. Nevertheless, both species have been identified by their characteristic spectra. The 1-acetoxyethyliron(II) complex **1b** is a brown–yellow oil at ambient temperatures; its molybdenum analogue, **2b,** also an oil, is orange–red. Both are extremely air-sensitive.

Spectroscopy

(i) *NMR.* Spectroscopic data for the acetoxyalkylmetals (and some of their reaction products) are presented in Table 1. All four complexes display at least three characteristic resonances in their respective ^1H NMR spectra. One, a singlet, at higher field, derives from the hydrogens of the acetoxyl group; the position of this signal varies little, irrespective of the central metal or the substituents on the α-carbon of the acetoxyalkyl ligand. A second singlet characterises the hydrogens of the η^5-cyclopentadienyl moiety. The chemical shifts are somewhat more sensitive to the metal than to the substitution pattern; C_5H_5 bound to Mo resonates 0.4–0.6 ppm to lower field than in its iron congeners. The same influence by the metal is evident for the α-hydrogen(s) of the acetoxyalkyl group, whose resonance is of particular diagnostic value in these systems. As would be expected, the presence of an α-methyl substituent in **1b** and **2b** induces a downfield shift in the α-H signal, relative to the acetoxymethyl homologues **1a** and **2a** respectively. The other consequence of the α-methyl group is the appearance of the α-hydrogen resonance as a characteristic 1:3:3:1 quartet. The β-hydrogens themselves give rise to a 1:1 doublet at higher field and here again, there is a significant downfield shift for the molybdenum complex relative to iron.

These trends in chemical shifts for hydrogens close to the metal centre, as the metal is varied, must derive in part from the inductive effects of the $M(C_5H_5)(CO)_n$ fragment and also from contributions to shielding by the nonbonding metal *d*-electrons. Although the $Mo(CO)_3$ and $Fe(CO)_2$ moieties are isolobal, without detailed calculations it is not clear to what extent the differing spatial extensions of 3*d* and 4*d* orbitals will be offset by the disparities in metal–ligand bond lengths. The simple view is that the Mo(II) centre is a d^4-species with three powerfully π-acidic carbonyl groups and is likely to be relatively deshielding—either by induction or by more contracted *d*-orbitals—than the corresponding d^6 Fe(II) system with but two carbonyl ligands.

The ^{13}C chemical shifts appear generally less sensitive to the nature of the metal centre; the shifts for the carbon σ-bound to Mo(II) are, in fact, very slightly shielded relative to their iron-bonded counterparts. There is the expected downfield shift of this signal in both of the 1-acetoxyethyl complexes. The resonances ascribed to the CO ligands, on the other hand show no dependence on the alkyl ligand, but occur at significantly lower field in the molybdenum(II) species. Similar downfield shifts have been reported for related compounds and were interpreted as an indication of increasing retrodative M–L π-bonding,[11] consistent with the ^1H NMR shift trends.

(ii) *IR*. A full compilation of characteristic stretching frequencies for complexes 1 and 2 appears in Table 2. Of particular note are the ligand vibrations assigned to ν(C≡O) and ν(C=O). In acetoxymethyl derivatives **1a** and **2a**, the absorption patterns are remarkably similar, given the differing geometries and apparently different extents of M–C π-bonding (*vide supra*). Very strong bands occur at 2010 and 1950 cm^{-1} in the spectrum of **1a** while for **2a**, the corresponding ν(C≡O) appear at 2010 and 1945 cm^{-1}. The strong ester carbonyl absorbtions for **1a** and **2a** are found at 1730 and 1725 cm^{-1} respectively.

The spectra of acetoxyethyl complexes **1b** and **2b**

Table 3. Mass spectroscopic data for acetoxymethylmetal complexes

$Fe(C_5H_5)[(CO)_2CH_2OC(O)CH_3]$

m/e	rel. int.(%)	fragment
250	2	$Fe(C_5H_5)(CO)_2(CH_2OAc)^+$
222	18	$Fe(C_5H_5)(CO)(CH_2OAc)^+$
194	92	$Fe(C_5H_5)(CH_2OAc)^+$
151	23	$Fe(C_5H_5)CH_2O^+$
133	85	$Fe(C_5H_5)CH_2^+$
121	100	$Fe(C_5H_5)^+$
56	49	Fe^+

$Mo(C_5H_5(CO)_3CH_2OC(O)CH_3$

m/e	rel. int.(%)	fragment
318	1	$Mo(C_5H_5)(CO)_3(CH_2OAc)^+$
290	9	$Mo(C_5H_5)(CO)_2(CH_2OAc)^+$
262	18	$Mo(C_5H_5)(CO)(CH_2OAc)^+$
234	60	$Mo(C_5H_5)(CH_2OAc)^+$
191	100	$Mo(C_5H_5)CH_2O^+$
175	25	$Mo(C_5H_5)CH_2^+$
161	68	$Mo(C_5H_5)^+$
96	20	Mo^+

are more complex in the $\nu(C{\equiv}O)$ region. Three bands, at 1990, 1925 and 1980 cm^{-1} arise from **1b**, while five maxima, at 2020, 1995, 1940, 1885 and 1850 cm^{-1} are observed for **2b**.

Mass spectrometry

Only the complexes **1a** and **2a** displayed sufficient thermal stability to allow characterisation by mass spectrometry. The salient features of their very similar fragmentation patterns appear in Table 3. Both species give rise to very weak molecular ions. Stepwise loss of carbonyl ligands occurs readily for both metals and some or all of these fragmentations give rise to metastable peaks. Scission of both of the C–O bonds in the ligand, generating $[(C_5H_5)MCH_2O]^+$ and $[(C_5H_5)MCH_2]^+$ is observed in each case; the former is more apparent for Mo, the latter for Fe. Both systems produce strong ion currents for $[M(C_5H_5)]^+$.

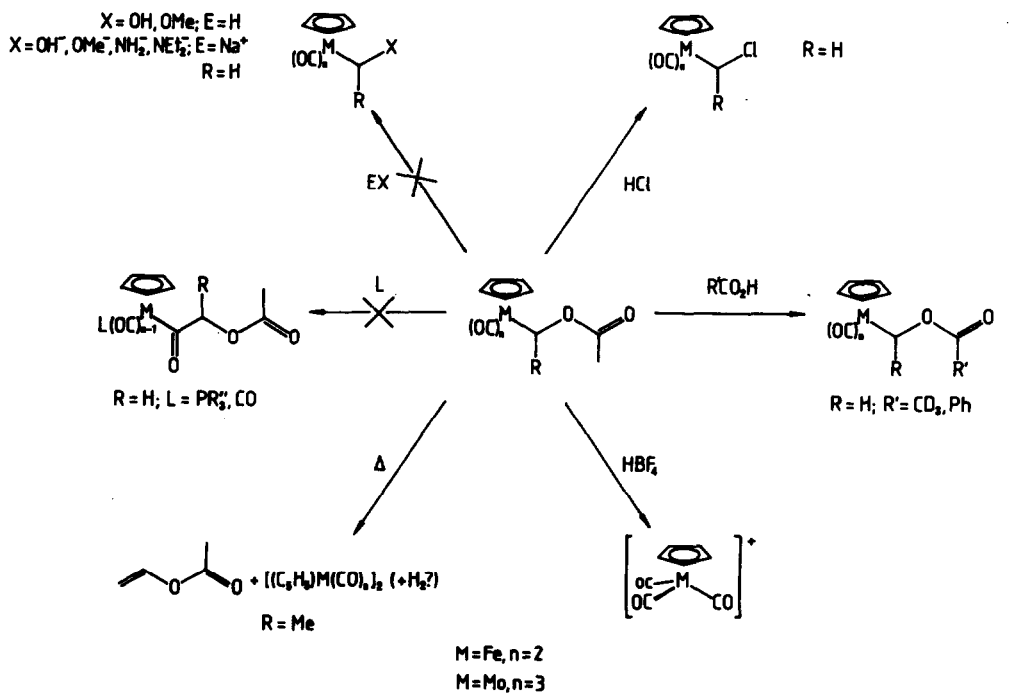
Reactivity (see Scheme 1)

(*i*) *Protic acids.* The thermal lability of **1b** and **2b** (and their organometallic reaction products) precluded satisfactory reaction studies. The ultimate products of reaction of **1a** and **2a** with protic acids are determined by the capacity of the counter "anion" (in HX) to form a covalent bond with the α-carbon. Thus, both complexes react smoothly under mild conditions with dry HCl to yield the chloromethylmetal derivatives.[4] A twofold excess of benzoic acid added to solutions of **1a** and **2a** yields $[Mo(C_5H_5)(CO)_3CH_2OC(O)Ph]$ and $[Fe(C_5H_5)(CO)_2CH_2OC(O)Ph]$ respectively.[12] Acetate metathesis is somewhat faster for molybdenum. Both reactions proceed to the extent of *ca.* 80% conversion over several days at ambient temperature. Acetate *exchange* in the presence of acetic acid-d_4 is immeasurably slow under the same conditions. When, however, **1a** or **2a** are dissolved in acetic acid-d_4 and heated to 60°C, acetic acid-d_1 is slowly liberated to a final extent of 80–90%. The NMR characteristics of the other hydrogens of **1a** or **1b** remain unaffected by the process. Such redistribution reactions are unusual in purely organic esters, but may occur when the carbenium ion of the migrating alkyl moiety forms particularly readily, usually in the presence of a strong acid catalyst.[3] Indeed, when a catalytic amount of HBF_4 is added to a solution of **2a** in acetic acid-d_4, the transcarboxylation reaction proceeds (more rapidly) to completion in less than 24 hr at ambient temperature.

When **1a** or **2a** react with HBF_4 alone, acetic acid is once more the preponderant organic product. NMR analyses revealed complex mixtures of organometallic products from which $[M(C_5H_5)(CO)_3]BF_4$ were the only isolable, identifiable products.[9,10]

There was some indication from NMR observations that excess *p*-toluenesulphonic acid reacts with **1a** and **2a** to give the respective tosylate esters, but attempts to isolate these on a larger scale led only to decomposition.

The acetoxymethyl complexes are similar to



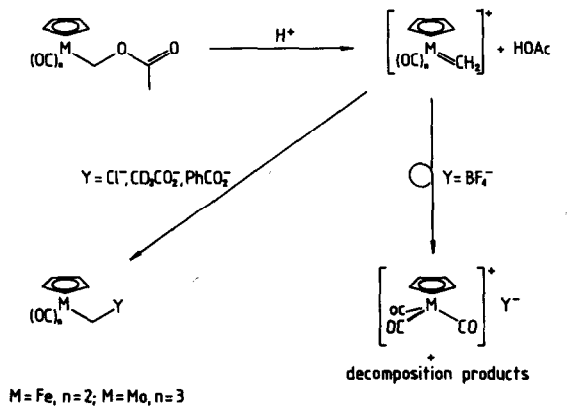
their alkoxymethyl analogues inasmuch as it is the C–O rather than the C–M bond which is the more susceptible to protolytic cleavage.[4] The trans-carboxylation reaction with carboxylic acids is parallelled in aliphatic ester chemistry by the acid catalysed reaction of *tert*-butylacetate, in which the ready formation of the *tert*-butyl carbenium ion is proposed to be crucial.[13] This analogy lends weight to the suggestion[4] that the behaviour of the metalloesters **1** and **2** reflects access to carbenemetal cations of the type $[M(C_5H_5)(CO)_nCH_2]^+$. Thus all the protolytic reactions are envisaged to proceed (Scheme 2) via electrophilic attack on the ester oxygen, causing C–O scission to yield acetic acid. In the presence of a compatible nucleophile (Cl^-, RCO_2^-) the electrophilic carbenemetal species is scavenged. Otherwise (as with BF_4^-), decomposition ensues, via disproportionation and/or oligomerisation. We were not able to detect the carbene intermediate either directly or by its reaction in the presence of cyclohexene.[4] On the other hand, we observed no trace in NMR or IR spectra, of $[M(C_5H_5)(CO)_n(\eta^2\text{-cyclohexene})]^+$[14] which might arise via protolytic M–C cleavage under these conditions.

In contrast with conventional esters, we were unable to achieve either hydrolysis of **1a** and **2a**, to give the hydroxymethyl derivatives nor trans-esterification with methanol to give the known methoxymethylmetals either in the presence or absence of catalytic amounts of acid (HBF_4). In view of the reported ease of related reverse reactions,[4,6] this may indicate a thermodynamic rather than a kinetic impediment.

(*ii*) *Other nucleophiles.* Hydroxymethyl complexes were inaccessible by treatment of **1a** or **2a** in acetone with KOH. Even in presence of 18-crown-6-ether and excess of KOH, the acetoxymethyl complexes were recovered unchanged after 3 days at ambient temperature. **1a** and **2a** were similarly unreactive with NaOMe, $NaNH_2$ and $NaNEt_2$ at temperatures below their own thermolytic limits (Scheme 1).

(*iii*) *Carbonyl insertion.* We were interested to compare the reactivity, in particular of the C—O bond, in **1a** and **2a**, with that in the corresponding acetoxyacetyl derivatives. Hydroxymethyl species have only rarely been sufficiently robust to survive the conditions required to induce migratory insertion of CO to form hydroxyacetylmetals (which is one of the proposed steps in Fischer–Tropsch-type reductive oligomerisation of CO).[5,6] When **1a** and **2a** in acetone were treated with CO (120 atm) at 25°C, no reaction (other than some thermal decomposition) was observed over 16 hr. Addition of Ph_3P or Me_3P also failed to induce insertion at temperatures up to 90°C.

Thermal decomposition. Under dark, anaerobic conditions, the 1-acetoxyethyl complexes **1b** and **2b** decomposed cleanly at ambient temperatures to give vinyl acetate and $[M(C_5H_5)(CO)_n]_2$ in 1:2 ratio. We presume, but did not monitor, concomitant evolution of dihydrogen. Thus, β-hydrogen migration is facile for these systems, and the dimeric products can be ascribed to binuclear elimination of dihydrogen from the intermediate hydridometal complexes. Thermolysis of **1a** and **2a** required much higher temperatures and led to a complex array of organic products, including small amounts of acetic acid. Methyl acetate was not formed. The indications are that, as in the protolysis reactions, the C–O bond is thermally more susceptible than the C–M bond.



Acknowledgement—We are grateful to the University of London for the award of an Overseas Research Student grant (to S.E.H.). We also thank the S.E.R.C. and the Royal Society for funding our H.P.L.C. facility.

REFERENCES

1. Part 1, Z. Y. Yang and G. B. Young, *J. Chem. Soc. Dalton Trans.* 1984, 2019.
2. P. M. Henry, *Palladium-Catalysed Oxidation of Hydrocarbons*, Reidel, Dordrecht (1980). P. M. Henry, *Adv. Organomet. Chem.* 1975, **13**, 363. J.-E. Bäckvall, B. Åkermark and S. O. Ljunggren, *J. Am. Chem. Soc.* 1979, **101**, 2411. J.-E. Bäckvall, *Acc. Chem. Res.* 1983, **16**, 335.
3. C. Masters, *Adv. Organomet. Chem.* 1979, **17**, 61. E. L. Muetterties, *Catal. Rev.* 1981, **23**, 69. D. L. King, J. A. Cusumano and R. L. Garten, *Catal. Rev.* 1981, **23**, 233. I. Wender, *Catal Rev.* 1976, **14**, 97. E. L. Muetterties and J. Stein, *Chem. Rev.* 1979, **79**, 479. J. Evans, *Chem. Soc. Rev.* 1981, **10**, 159. C. P. Casey, S. M. Neumann, M. A. Andrews and D. R. McAlister, *Pure Appl. Chem.* 1980, **52**, 625.

4. M. L. H. Green, M. Ishaq and R. N. Whitely, *J. Chem. Soc* (A) 1967, 1508.
5. J. R. Sweet and W. A. G. Graham. *J. Am. Chem. Soc.* 1982, **104**, 2811. *Idem. Ibid., J. Organomet Chem.* 1979, **173**, C9. C. J. May and W. A. G. Graham, *Ibid.* 1982, **234**, C49. C. P. Casey, M. A. Andrews, D. R. McAlister, W. D. Jones and S. G. Harsey, *J. Mol. Catal.* 1981, **13**, 43. C. P. Casey, M. A. Andrews, D. R. McAlister and J. E. Rinz, *J. Am. Chem. Soc.* 1980, **102**, 1927. C. P. Casey, M. A. Andrews and D. R. McAlister, *Ibid.* 1979, **101**, 3371. C. P. Casey, M. A. Andrews and J. E. Rinz, *Ibid.* 1979, **101**, 741. G. R. Clark, C. E. L. Headford, K. Marsden and W. R. Roper, *J. Organomet. Chem.* 1982, **231**, 335. C. E. L. Headford and W. R. Roper, *Ibid.* 1980, **198**, C7. K. L. Brown, G. R. Clark, C. E. L. Headford, K. Marsden and W. R. Roper, *J. Am. Chem. Soc.* 1979, **101**, 503. C. Lapinte and D. Astruc, *J. Chem. Soc. Chem. Commun.* 1983, 430. B. B. Wayland, B. A. Woods and V. A. Minda, *Ibid.* 1982, 634. D. L. Thorn, *Organometallics* 1982, **1**, 197. D. L. Thorn and T. H. Tulip, *Ibid.* 1982, **1**, 1580. Y. C. Lin, D. Milstein and S. S. Wreford, *Ibid.* 1983, **2**, 1461. G. D. Vaughn and J. A. Gladysz, *J. Am. Chem. Soc.* 1981, **103**, 5608. H. Berke, G. Huttner, G. Weiler and L. Zsolnai, *J. Organomet. Chem.* 1981, **219**, 353.
6. G. O. Nelson, *Organometallics* 1983, **2**, 1474.
7. C. P. Casey, P. J. Fagan and W. H. Niles, *J. Am. Chem. Soc.* 1982, **104**, 1134.
8. L. H. Ulich and R. Adams, *J. Am. Chem. Soc.* 1921, **43**, 660.
9. W. Beck and K. Schloter, *Z. Naturforschung* 1978, **33B**, 1214.
10. A. Davison, M. L. H. Green and G. Wilkinson, *J. Chem. Soc.* 1961, 3172. R. B. King, *Inorg. Chem.* 1962, **1**, 964.
11. L. J. Todd, J. R. Wilkinson, J. P. Hickey, D. L. Bleach and K. W. Barnett, *J. Organomet. Chem.* 1978, **154**, 151 and references cited therein.
12. ^{1}H NMR data (benzene-d_6) for: $Fe(C_5H_5)(CO)_2$-$CH_2OC(O)Ph$: 8.15 dd (2H, aromatic) 7.31–7.03 m (3H, aromatic), 5.48s (2H, CH_2), 4.21 (5H, C_5H_5); $Mo(C_5H_5)(CO)_2CH_2OC(O)Ph$; 8.105 dd (2H, aromatic) 7.16–6.88 m (3H, aromatic) 5.39s (2H, CH_2), 4.62s (5H, C_5H_5); free acetic acid appears at 1.57 ppm.
13. E. Taschner, C. Wasielewski and J. F. Biemat, *Ann.* 1961, **646**, 119. E. Taschner, A. Chimiak, B. Bator and T. Sokolowsha, *Ibid* 1961, **646**, 134.
14. E. O. Fischer and K. Fichtel, *Chem. Ber.* 1962, **95**, 2063. W. P. Giering, M. Rosenblum and J. Tancrede, *J. Am. Chem. Soc.* 1972, **94**, 7170.

Polyhedron Vol. 4, No. 2, pp. 357–364, 1985
Printed in Great Britain.

0277–5387/85 $3.00 + .00
© 1985 Pergamon Press Ltd.

RHODIUM AND IRIDIUM COMPLEXES CONTAINING THE ANION OF 1-PHENYL-3-METHYL-4-BENZOYL-PYRAZOLONE-5, A SOPHISTICATED ANALOGUE OF β-DIKETONES

FLAVIO BONATI
Dipartimento di Scienze Chimiche dell'Università, 62032 Camerino, Italy

and

LUIS A. ORO* and M. TERESA PINILLOS
Departamento de Química Inorgánica, Universidad de Zaragoza, Zaragoza, Spain

(*Received* 3 *February* 1984; *accepted* 6 *May* 1984)

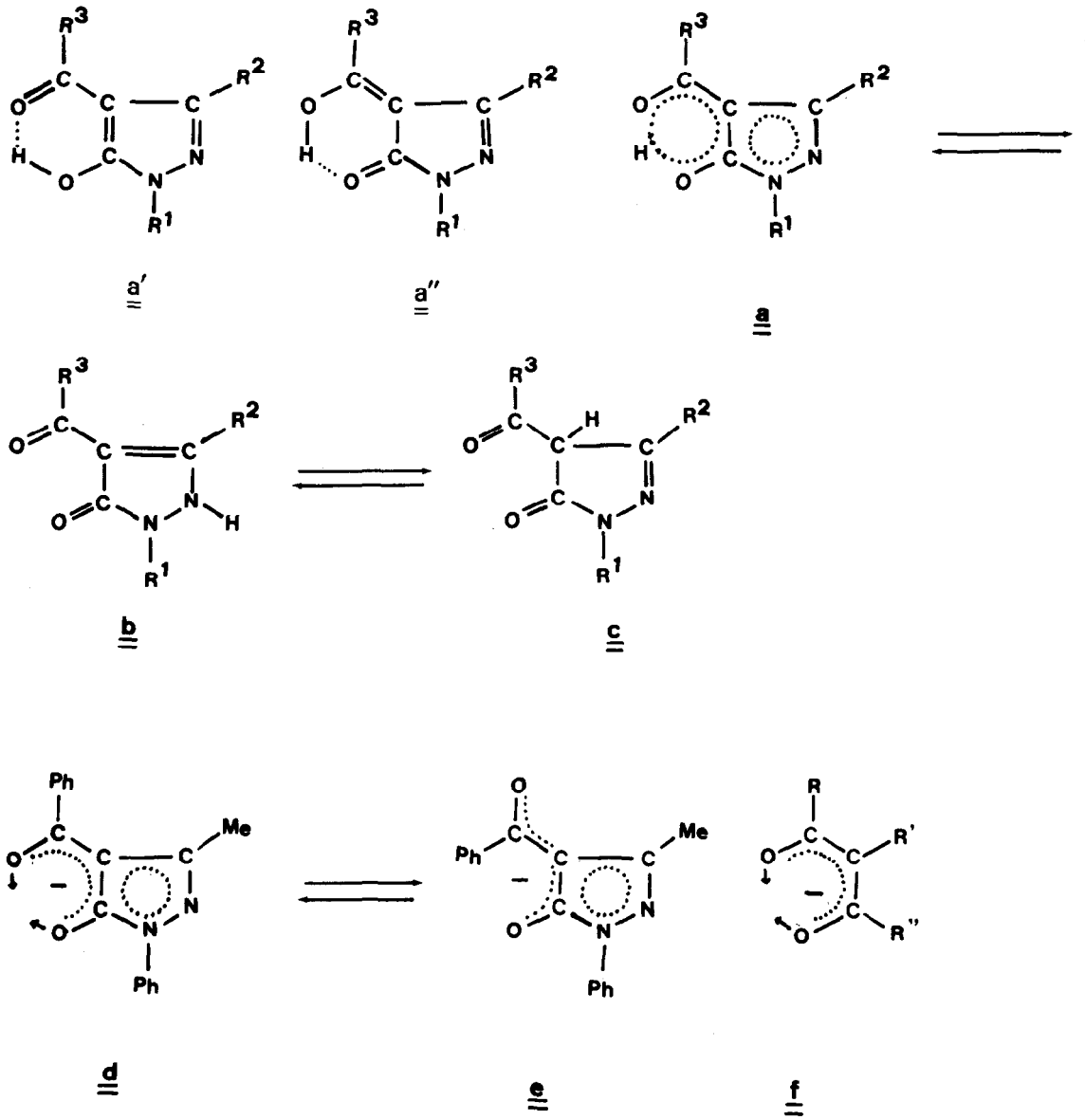
Abstract—Several (diolefin)M(A) complexes (M = Rh, Ir) were prepared, where AH is 1-phenyl-3-methyl-4-benzoylpyrazolone-5, a very stable asymmetric analogue of acetylacetone. In these complexes the diolefin could be replaced by one mole of $(Ph_2PCH_2CH_2)_2$, two of CO or of PPh_3, or three of $CNBu^t$, while 1,10-phenanthroline displaced the chelating ligand to yield $[(cyclooctadiene)Rh(phen)]^+ (A)^-$. Some compounds X–Y (X–Y = iodine or MeI) added oxidatively yielding the corresponding trivalent species. Using ^{31}P NMR spectra the presence of the expected steric isomers was detected in $(Ph_3P)(CO)Rh(A)$ and in $(Ph_3P)(CO)Rh(A)(X)(Y)$.

4-Acyl-pyrazolones-5, AH, are a class of potentially bidentate ligands which were originally investigated by Jensen[1] as reagents for radiochemical separations. These molecules are comparable to β-diketones because in both the classes keto-enol tautomerism is possible, the enolic hydrogen may be replaced by a metal ion, and a considerable number of various substituents can be placed on the ligand. In the acylpyrazolones structures such as **a**, **b** or **c** must be considered as possible tautomers, and **a** results from a proton shift between the two oxygen atoms, **a′** and **a″** being the two limiting cases. Structures like **b** are not likely to be important since when $R^1 = R^3 = Ph$ and $R^2 = Me$ protonation takes place at the nitrogen atom only at pH equal or lower than 0.5.[2] In addition, enolic structures should be considered having intermolecular, rather than intra-molecular, hydrogen bonds.

In the case of the molecule AH investigated here ($R^1 = R^3 = Ph$, $R^2 = Me$) two crystalline tautomers can be isolated[1b, 3a, 4a] for which different structural assignments are available. Whichever of these is accepted, the ligand is obtained upon deprotonation, so that -in any case- the deprotonated species, A^-, (**d** or **e**) may be a bidentate, uninegative ligand to be compared with an asymmetric β-diketonate, **f**. The advantage of A^- over the latter will be due to more extended delocalization of the change, so that, even if one or both the phenyl substituents are not involved in it, quite stable compounds are to be expected.

With 1 - phenyl - 3 - methyl - 4 - benzoyl - pyrazolone - 5 several metal derivatives were described including mono- and divalent cations[4b, 3c] or lanthanides;[4c, 4d] its use for the spectrophotometric determination of trace elements[3b] was also reported, but no organometallic derivatives had been investigated before our paper. Therefore, following up our interest in the field of rhodium and iridium compounds we decided to investigate their derivatives containing the A^- ligand; suitable derivatives[5,6] are available for comparison and include also X-ray crystal structures of symmetric or of asymmetric β-diketonates, such as dicarbonyl(acetylacetonato)rhodium(1)[5] or carbonyl(triphenylphosphino)-(thenoyltrifluoroacetato)rhodium(1).[6a]

*Author to whom correspondence should be addressed.



RESULTS AND DISCUSSION

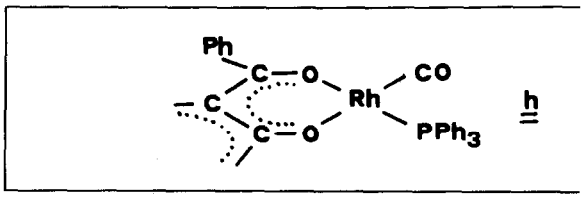
The ligand 1 - phenyl - 3 - methyl - 4 - benzoyl - pyrazolone - 5, AH, reacts with dinuclear rhodium(I) complexes of the type $[RhCl(diolefin)]_2$[7-9] or $[RhCl(monoolefin)_2]_2$,[10,11] in the presence of triethylamine, yielding mononuclear complexes of formula Rh(A)(diolefin)† (diolefin = 1,5 - cyclooctadiene (COD) (I), 2,5 - norbornadiene (NBD) (II), tetrafluorobenzobarrelene (TFB) (III)) or Rh(A)(monoolefin)$_2$ (ethylene (IV), cyclooctene (COE)(V)) Alternatively Rh(A)(diolefin) compounds can be obtained by reacting $[RhCl(diolefin)]_2$ complexes with TlA (VI) (prepared by addition of AH to Tl (acac)). The ethylene ligands can be displaced from complex (IV) by chelating diolefins such as 1,5-cyclooctadiene. In this manner complex (IV) reacts with benzoquinone (BQ) with formation of Rh(A) (BQ) (VII). On the other hand, the polymeric cyclooctatetraene complex $[Rh_2Cl_2(COT)]_n$[13] reacts with AH and NEt_3 yielding the dinuclear $Rh_2(A)_2(COT)$ (VIII) derivative. Similarly the $[RhCl(C_3H_5)_2]_2$ complex[14] affords the Rh(A) $(C_3H_5)_2$ (IX) derivative (Table 1).

The above mentioned complexes have been identified by elemental analyses, IR spectroscopy, molecular weight measurements and in some cases by proton or by $^{31}P\{^1H\}$-NMR spectroscopy. In particular the ^1H-NMR spectrum of Rh(A) (COD) shows resonances at 1.80–1.85 and 2.47–2.52 ppm

†The related Ir(A)(COD) complex (X) was similarly prepared from $[IrCl(COD)]_2$.[12]

($\diagdown$CH$_2$), 4.15 and 4.30 ppm (–CH = CH–) (COD ligand) and 1.70 (Me) and 7–8 ppm (Ph) (A ligand). The inequivalence of the olefinic protons is also observed for the dinuclear $Rh_2(A)_2(COT)$ compound [4.76 and 4.92 ppm (COT); 1.64 (Me) and 7–8 ppm (Ph) (A ligand)]. However in the Rh(A)(BQ) complex only one type of olefinic proton at 5.20 ppm is observed, along with the expected resonances of the A ligand [1.76 (Me); 7–8 ppm (Ph)]. These value are different from those published for the ligand (2.07 and 7.20–8.0 ppm,[4a] or 2.10 and 7.20–8.07[4d]), but are comparable with those of some metal complexes in the same solvent. In these the aryl signal is a multiplet between 7 and 8 ppm, while the methyl singlet is displaced to higher field than in the ligand: namely to 1.73 in $Zn(A)_2 \cdot EtOH$, 2.00 in $Be(A)_2$,[4b] or 2.05 in $Zr(A)_4$[3a].

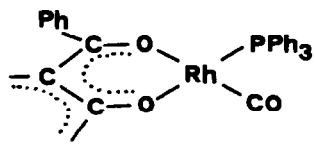
Attempts to react the free nitrogen atom of the ligand A [complex (I)] with $[Au(PPh_3)S]^+$ (prepared from $AuCl(PPh_3)/AgClO_4$) or $AgClO_4$ were unsuccessful, in accord with the low basicity[2] of the nitrogen atom of ligand A.



h

Complex (I) reacts with two moles of triphenylphosphine or one mole of bis(1,4)-diphenylphosphino)butane (dppb) or excess of *tert*-butyl-isocyanide, with displacement of the cyclooctadiene ligand and formation of Rh(A)$(PPh_3)_2$ (XI), Rh(A)(dppb) (XII) or $Rh(A)(CNBu^t)_3$ (XIII). Since both (XII) and (XIII) were found to be monomers in chloroform solution, in the former the diphosphine must be chelating, rather than bridging, and the rhodium atom is four-coordinated while in the latter it is five-coordinated. Remarkably, the ionic [Rh(COD)-(phen)]A (XIV) complex is obtained by reaction with 1,10-phenanthroline, thus showing that the existence of the A^- anion is possible even though compounds of alkali or of alkaline earth metals, e.g. $Na(A) \cdot 2H_2O$ or $Ba(A)_2 \cdot 2H_2O$,[4b] were reported to have negligible electrical conductance values and, presumably, to be nonionic. Addition of iodine to complexes (I) and (X) produces the rhodium(III)-complex $Rh(A)(I)_2(COD)$ (XV) and the iridium(III) analogue $Ir(A)(I)_2(COD)$ (XVI).

The addition of AH to the solution obtained by refluxing $RhCl_3 \cdot XH_2O$ in dimethylformamide results in the formation of $Rh(A)(CO)_2$ (XVII). The latter complex can also be obtained by carbonylation of Rh(A)(COD), and in the solid state, it exhibits two strong ν(CO) bands (2015 and 2085 cm^{-1}) as expected for *cis*-dicarbonyl derivatives, in contrast with other $Rh(X)(CO)_2$ complexes (HX = acetylacetone, tropolone, Schiff base from salicylaldehyde and an amine): in some of these the complex ν(CO) absorptions observed in the solid state are due to metal–metal interactions.[15,16] These are not possible here if at least one of the phenyl groups does not lie in the plane of the ligand. The position of the two carbonyl stretching frequencies is similar to those of other square planar Rh(I) derivatives such as $(OC)_2Rh$(acetylacetonato) (2083 and 2015 cm^{-1} in petroleum ether)[17] or $(OC)_2Rh(\mu$-pyrazolato-*N*,*N*')BH_2 (2082 and 2013 cm^{-1} in cyclohexane):[18] it is, then, evident that the asymmetric A^- ligand has the same net effect on the groups *trans* to itself as other symmetric O,O'- or *N*,*N*'-chelating ligands.



k

As with the corresponding β-diketonates, triphenylphosphine reacts with the complex (XVII) with displacement of only one CO group and formation of $Rh(A)(CO)(PPh_3)$ (XVIII): this shows only one intense and broad CO stretching vibration in Nujol mull (1985 cm^{-1}) and in dichloromethane solution (1985 cm^{-1}). For the compound (XVIII) two isomers, **h** and **k**, are possible which are likely to show overlapping ν(CO). However their presence can be detected through ^{13}C- or ^{31}P-NMR spectroscopy. Indeed, in the latter case in the $^{31}P\{^1H\}$-NMR spectrum (see Table 2), a stronger and a weaker signal is present, each signal is coupled with ^{103}Rh, and the two ^1J (^{103}Rh–^{31}P) coupling constants are nearly the same. This similarity suggests, in turn, a very similar *trans*-influence of each oxygen donor atom so that the reaction of (XVII) with PPh_3 affords an appreciable quantity of each isomer. On the other side with asymmetric β-diketonates or with other asymmetric ligands (e.g. 8-hydroxyquinolinato) the isolation of a single isomer is reported to be due to a different *trans*-influence of the donor atoms.[6]

The complex (XVIII) undergoes oxidative addition with methyl iodide or with iodine affording (XIX) or (XX), respectively. Since the starting

Table 1. Analytical and other data for the compounds

Complex	Found(calcd.)(%)			Colour	Yield	Mol.wt.($CHCl_3$) (found(calcd.))
	C	H	N			
Rh(A)(COD) (I)	61.05 (61.48)	5.39 (5.16)	5.19 (5.74)	yellow	81	520 (488)
Rh(A)(NBD) (II)	60.69 (61.03)	4.48 (4.48)	5.43 (5.93)	yellow	90	--
Rh(A)(TFB) (III)	57.23 (57.44)	3.54 (3.16)	4.27 (4.62)	yellow	95	650 (606)
Rh(A)$(C_2H_4)_2$ (IV)	56.83 (57.81)	4.77 (4.82)	6.18 (6.42)	yellow	60	--
Rh(A)$(COE)_2$ (V)	65.75 (65.99)	6.88 (6.88)	4.49 (4.66)	yellow	90	--
Tl(A) (VI)	42.16 (42.39)	2.89 (2.72)	5.55 (5.82)	white	80	--
Rh(A)(BQ) (VII)	56.66 (56.57)	3.54 (3.51)	5.60 (5.77)	red	90	500 (488)
$Rh_2(A)_2$(COT) (VIII)	57.81 (58.35)	3.75 (3.96)	6.01 (6.48)	yellow	70	901 (864)
Rh(A)$(C_3H_5)_2$ (IX)	59.24 (59.75)	4.92 (5.01)	6.01 (6.05)	yellow	85	470 (462)
Ir(A)(COD) (X)	51.77 (51.98)	4.75 (4.36)	4.56 (4.85)	yellow	71	--

TABLE 1 (contin.)

$Rh(A)(PPh_3)_2$ (XI)	69.65 (70.35)	5.27 (4.79)	2.80 (3.10)	orange	65	--
Rh(A)(dppb) (XII)	66.80 (67.00)	5.20 (5.12)	3.01 (3.47)	yellow	90	824 (806)
$Rh(A)(CNBu^t)_3$ (XIII)	61.38 (61.05)	6.46 (6.40)	11.19 (11.12)	yellow	70	698 (629)
$\|Rh(COD)(phen)\|A^a$ (XIV)	66.06 (66.47)	5.05 (5.94)	8.52 (8.37)	orange	75	--
$Rh(A)(I)_2(COD)$ (XV)	39.55 (40.46)	4.22 (3.40)	3.25 (3.77)	violet	60	--
$Ir(A)(I)_2(COD)$ (XVI)	35.85 (36.11)	2.98 (3.03)	3.35 (3.37)	brown	65	--
$Rh(A)(CO)_2$ (XVII)	52.18 (52.31)	2.95 (3.00)	5.92 (6.42)	yellow	70	454 (436)
$Rh(A)(CO)(PPh_3)$ (XVIII)	63.93 (64.49)	4.34 (4.21)	4.00 (4.18)	yellow	80	--
$Rh(A)(Me)(I)(CO)(PPh_3)$ (XIX)	54.10 (54.70)	4.03 (3.85)	3.10 (3.45)	yellow-brown	80	--
$Rh(A)(I)_2(CO)(PPh_3)$ (XX)	47.72 (46.78)	3.12 (3.05)	2.91 (3.03)	brown	85	947 (924)

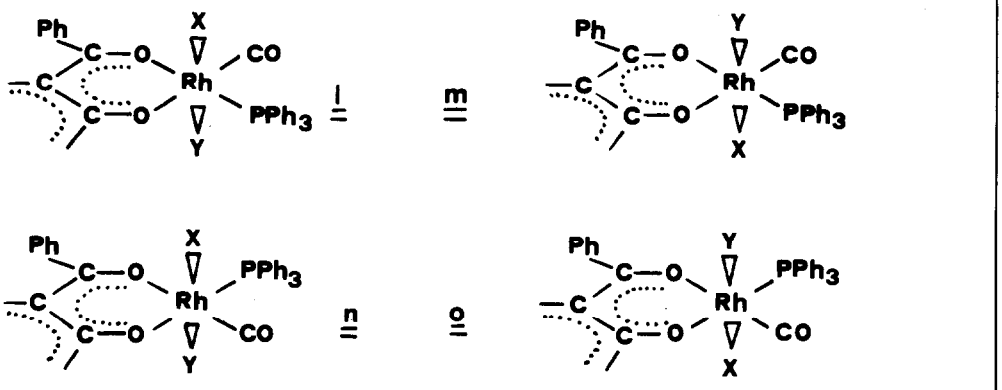
[a] Λ_M = 86 $ohm^{-1}cm^2mol^{-1}$ ($5x10^{-4}$ M acetone solution).

Table 2. ^{31}P-NMR spectra

Compound	δ_P(ppm)	^1J(Rh-P) (Hz)
Rh(A)(CO)(PPh_3)	45.8[b]	179.9
(XVIII)	49.8	177.0
Rh(A)$(I)_2$(CO)(PPh_3)	24.3[b]	107.3
(XX)	25.9	106.5
Rh(A)(Me)(I)(CO)(PPh_3)	28.0[b,c]	135,140
(XIX)	28.3[c]	108[d]

[a]$CDCl_3$ solution at room temperature. All signals are doublets and lie downfield from reference, external 85% phosphoric acid. [b]more intense signal. [c]this doublet is formed by two overlapping doublets. [d]the difference between the two coupling constants is less than 5 Hz.

material contains the two isomers, addition of X–Y to **h** will give isomers **l** and **m**, while addition to **k** will give **n** and **o**:



Correspondingly the phosphorus NMR spectrum of (**XIX**) (Table 2) contains two pairs of nearly overlapping doublets each being due to two of the four isomers described above with one more abundant than the other (*ca.* 1 : 3), in agreement with the different relative abundance of the isomers **h** and **k** in the starting compound (**XVIII**).

In the special case where X = Y = iodine, then **l** = **m** and **n** = **o**. Correspondingly the spectrum of (**XX**) contains only two doublets, with different relative intensity (*ca.* 1 : 2) as required by the presence of only two isomers with different relative abundance.

Both phosphorus chemical shifts and coupling constants for this type of octahedral isomers are likely to be rather similar, as shown e.g. by the ^1J(Rh–P) values for the P atom *trans* to chlorine in *mer*- or in *fac*-$(Et_3P)_3RhCl_3$: 114 and 112 Hz, respectively.[19] Therefore, while the similarity of the values recorded for our species must correspond to closely related isomers and does not suggest a rearrangement of the ligands during oxidative addition, assignment of each doublet to each isomer is not possible.

Independent confirmation of the presence of the four isomers of (**XIX**) or of the two isomers of (**XX**) might come from their ^{13}C- or ^{1}H-NMR spectra: different chemical shifts or different coupling constants with ^{103}Rh should be observed for the methylrhodium moiety of (**XIX**). Infrared spectral evidence is not conclusive since the carbonyl stretching vibration is likely to be found in the same range as that of the other isomers. Nevertheless, the infrared spectrum of (**XX**) does show two equally intense ν(CO) in Nujol mull: these are

due to solid state splitting since they are not present when the measurement is carried out in dichloromethane solution.

EXPERIMENTAL

The C, H and N analyses were made with a Perkin–Elmer 240-B microanalyzer, the IR spectra were recorded on a Perkin–Elmer 599 spectrophotometer (over the range 4000–200 cm^{-1}) using Nujol mulls between polyethylene sheets or in dichloromethane solutions. Molecular weights were measured with a Perkin–Elmer 115 osmometer. Conductivity was measured in 5×10^{-4}M acetone solutions, with a Philips 9509 conductimeter. The ^{1}H-NMR spectra were recorded on a Varian XL-200 instrument.

The ligand 1 - phenyl - 3 - methyl - 4 - benzoyl - pyrazolone - 5 (m.p. 91°C) was prepared according to the published method.[1b]

Preparation of Rh(A)(COD) **(I)** *and related complexes* **[(II)–(V), (VIII)–(X)]**

(i) $[RhCl(COD)]_2$[7] (246.5 mg, 0.5 mmol) was added with stirring to a solution of the ligand AH (278.3 mg, 1 mmol) and NEt_3 (139.1 μl, 1 mmol) in methanol (25 cm^3). The precipitate formed was stirred for 2 hr and then filtrated off and washed with methanol.

(ii) TlA (240.84 mg, 0.5 mmol) was added to a solution of $[RhCl(COD)]_2$ (123.3 mg, 0.25 mmol) in dichloromethane (25 cm^3). The formed TlCl was filtered off, and the complex was precipitated by the addition of methanol.

The complexes **(II)–(V)** and **(VIII)–(X)** were similarly prepared by the two routes described above, starting from 0.5 mmol of the corresponding dimers $[RhCl(diolefin)]_2$,[8,9] $[RhCl(monoolefin)_2]_2$,[10,11] $[RhCl(C_3H_5)_2]_2$,[14] $(IrCl(COD)]_2$[12] and $[Rh_2Cl_2(COT)]_n$.[13] (Methanol/water (1/1) was used for the precipitation of complex **(IX)**).

Preparation of TlA (VI)

Tl(acac) (151.7 mg, 0.5 mmol) was added with stirring to a solution of AH (139.1 mg, 0.5 mmol) in dichloromethane (25 cm^3). The precipitate formed was filtered off and washed with dichloromethane.

Preparation of Rh(A)(BQ) (VII) *and related complexes* **[(XI)–(XIV)]**

To a solution of $Rh(A)(C_2H_4)_2$ **(IV)** (109.1 mg; 0.25 mmol) in diethyl ether (50 cm^3) under nitrogen, was addeed the stoichiometric amount of benzoquinone (BQ) (27.1 mg, 0.25 mmol). A precipitate formed immediately; which was filtered off, and washed with diethyl ether.

The complexes **(XI)–(XIV)** were obtained in a similar way by adding a calculated amount of the corresponding ligand to a solution of Rh(A)(COD) **(I)** (122.1 mg, 0.25 mmol) in diethyl ether (50 cm^3) under nitrogen. The ionic [Rh(COD)(phen)]A was obtained when 1,10-phenantroline was used.

Preparation of $Rh(A)(CO)_2$ **(XVII)**

(i) Carbon monoxide was bubbled through a solution of Rh(A)(COD) (122.1 mg, 0.25 mmol) in dichloromethane (25 cm^3) for 30 min. The complex was obtained by addition of hexane.

(ii) A mixture of $RhCl_3 \cdot xH_2O$ (100 mg) and an excess of ligand AH (90 mg) in dimethylformamide (10 cm^3) were refluxed for 1 hr. The complex was precipitated by the addition of water and recrystallized from dichloromethane–hexane.

Preparation of $Rh(A)(CO)(PPh_3)$ **(XVIII)**

PPh_3 (65.6 mg, 0.25 mmol) was added to a solution of $Rh(A)(CO)_2$ (109.1 mg, 0.25 mmol) **(XVII)** in dichloromethane (25 cm^3). The complex was separated by the addition of hexane.

Preparation of $M(A)(I)_2(COD)$ M = Rh**(XV)**, Ir**(XVI)**

To a stirred solution of M(A)(COD) (M = Rh(I) (122.1 mg, 0.25 mmol), Ir(X) (144.4 mg, 0.25 mmol) in diethyl ether (50 cm^3) was added dropwise a solution of the stoichiometric amount of iodine in ether (5 cm^3). The resulting precipitate was filtered off, and washed with diethyl ether.

Preparation of $Rh(A)(Me)(I)(CO)(PPh_3)$ **(XIX)**

A solution of $Rh(A)(CO)(PPh_3)$ **(XVIII)** (335.3 mg, 0.5 mmol) in methyl iodide (50 cm^3) was stirred for 1 hr and then, evaporated *in vacuo*. Crystallization was induced by the addition of diethyl ether.

Preparation of $Rh(A)(I)_2(CO)(PPh_e)$ **(XX)**

A solution of $Rh(A)(CO)(PPh_3)$ **(XVIII)** (335.3 mg, 0.5 mmol) in dichloromethane (50 cm^3) was treated with a stoichiometric amount of iodine (126.9 mg, 1 mmol). After stirring for 1 hr the solution was concentrated *in vacuo;* slow addition of ether gave the compound.

Acknowledgements—The authors thank Ms. Maria Bonfà (University of Milan) for the recording of ^{31}P-NMR spectra, and Consiglio Nazionale delle Ricerche (Rome) and C.A.I.C.Y.T. (Spain) for financial support.

REFERENCES

1. (a) B. S. Jensen, *Acta Chem. Scand.* 1959, **13**, 1347. (b) *Idem., Ibid.* 1668. (c) *Idem., Ibid.* 1890. (d) Yu.

A. Zolotov and N. M. Kuz'min, *Extraktsia Metallov Atsilpirazolonami*. Nauka, Moscow (1977) (*Chem. Abs.* 1978, **89**, 81023x). (e) *Primenenie Proizvodnykh Pyrazolona y Analiticheskoi Khimii* (Edited by F. R. Verzhbitskii). Permskii University, Perm, 1977 (*Chem. Abs.* 1979, **91**, 116842j).

2. Yu. A. Zolotov and V. G. Lambrev, *Nauk SSSR, Inst. Geokhim. i Analit. Khim.* 1966 65 (*Chem. Abs.* 1966, **65** 9808).
3. (a) M. Y. Mirza and F. I. Nwabue, *J. Inorg. Nucl. Chem.* 1981, **43**, 1817. (b) M. Y. Mirza and F. I. Nwabue, *Talanta* 1981, **28**, 49. (c) M. Y. Mirza and R. T. Bailey, *J. Inorg. Nucl. Chem.* 1979, **41**, 772.
4. (a) E. C. Okafor, *Z. Naturforsch.* 1980, **35b**, 1019. (b) *Idem. Spectrochim. Acta*, 1981, **37A**, 945. (c) *Idem., Z. Naturforsch.* 1980, **35b**, 715. (d) *Idem., J. Inorg. Nucl. Chem.* 1980, **42**, 1155.
5. F. Huq and A. C. Skapski, *J. Cryst. Mol. Struct.* 1974, **4**, 411.
6. (a) J. G. Leipoldt, L. D. C. Bok, J. S. Van Vollenhoven and A. I. Pieterse, *J. Inorg. Nucl. Chem.* 1978, **40**, 61. (b) J. G. Leipoldt, S. S. Basson, L. D. C. Bok and T. I. A. Gerber, *Inorg. Chim. Acta* 1978, **26**, L35. (c) J. G. Leipoldt, L. D. C. Bok, S. S. Basson and T. I. A. Gerber, *Inorg. Chim. Acta* 1979, **34**, L293. (d) J. G. Leipoldt and E. C. Grobler, *Inorg. Chim. Acta* 1983, **72**, 17.
7. G. Giordano and R. H. Crabtree, *Inorg. Synth.* 1979, **19**, 218.
8. E. W. Abel, M. A. Bennett and G. Wilkinson, *J. Chem. Soc.* 1959, 3178.
9. D. M. Roe and A. G. Massey, *J. Organometal. Chem.* 1971, **28**, 273.
10. R. Cramer, *Inorg. Chem.* 1962, **1**, 722.
11. L. Porri, A. Lionetti, G. Allegra and A. Immirzi, *J. Chem. Soc. Chem. Commun.* 1965, 336.
12. L. J. Herde, J. C. Lambert and C. V. Senoff, *Inorg. Synth.* 1979, **15**, 8.
13. M. A. Bennett and J. D. Saxby, *Inorg. Chem.* 1968, **7**, 321.
14. J. Powell and B. L. Shaw, *J. Chem. Soc. (A)* 1968, 583.
15. R. Ugo, G. La Monica, S. Cenini and F. Bonati, *J. Organometal. Chem.* 1968, **11**, 159 and references therein.
16. M. Valderrama and L. A. Oro, *J. Organometal. Chem.* 1981, **218**, 241.
17. F. Bonati and G. Wilkinson, *J. Chem. Soc.* 1964, 3156.
18. F. Bonati, G. Minghetti and G. Banditelli, *J. Organometal. Chem.* 1975, **87**, 365.
19. P. S. Pregosin, R. W. Kunz, *^{31}P and ^{13}C-NMR of Transition Metal Phosphine Complexes*. Tables 16, 20, pp. 110–114 and 122–123. Springer-Verlag, Berlin (1979).

Polyhedron Vol. 4, No. 3, pp. 365–368, 1985
Printed in Great Britain

0277–5387/85 $3.00 + .00
© 1985 Pergamon Press Ltd

SYNTHESIS, VIBRATIONAL SPECTRA AND STEREOCHEMISTRY OF LANTHANIDE TRIS(CHLOROSULPHATES), $Ln(SO_3Cl)_3$ (Ln = La, Ce, Pr, Nd, Sm, Gd, Tb, Dy, Ho AND Er)

S. A. A. ZAIDI,* S. REHAN A. ZAIDI, MOHD. SHAKIR and MOHAMMAD ASLAM

Division of Inorganic Chemistry, Department of Chemistry, Aligarh Muslim University, Aligarh—202001, U.P. (India)

and

Z. A. SIDDIQI

Institut für Anorganische-Chemie, Göttingen, F.R.G.

(*Received* 3 *January* 1984; *accepted* 23 *June* 1984)

Abstract—Lanthanide(III) chlorosulphates, $Ln(SO_3Cl)_3$ (Ln = La, Ce, Pr, Nd, Sm, Gd, Tb, Dy, Ho and Er) have been synthesized by solvolytic reaction of chlorosulphuric acid on the corresponding benzoates. The low conductivity values and the IR spectra of these compounds suggest a cation–anion interaction leading to covalent bonding. The bands observed in the reflectance spectra and the values of magnetic moments may indicate a coordination number of 6 for these metals, with bidentate chlorosulphate groups.

Edwards *et al.*[1] indicated a quantitative comparison of transition metal fluoro- and chlorosulphates obtained by the reaction of halosulphuric acid on corresponding halides with interhalogen or alkali interhalogens. They have shown that the transition metal fluoro- and chlorosulphates are prepared more conveniently by displacement reactions of halosulphuric acid. Later Robinson and Ciruna[2] prepared alkali and alkaline earth metal chlorosulphates with excess of chlorosulphuric acid serving as chlorosulphonating agent as well as the medium of reaction. Recently, there have been several reports of the synthesis of covalent metal chlorosulphates[3–5] and oxychlorosulphates.[6–8] Here we report the synthesis and characterization of lanthanide(III) chlorosulphates.

EXPERIMENTAL

Pure chlorosulphuric acid (Riedel), cerium oxide (BDH), neodymium oxide, gadolinium oxide, samarium oxide, dysprosium oxide, proseodynium oxide, lanthanum oxide (all Indian Rare Earth Ltd) holmium oxide, erbium oxide and terbium oxide (Koch–Light) were used as received.

N,*N*′-dimethyl formamide (E. Merck) was used after drying over KOH followed by distillation. Thionyl chloride (E. Merck) was used after distillation. Sodium benzoate (E. Merck) was used as received.

Preparation of lanthanide benzoate[9]

The metal oxide (2 g) was made into a paste by adding 5 cm^3 water and mixing. The paste was dissolved in 6 cm^3 6.0 *M* HCl. The solution was neutralized to incipient precipitation with 1 *N* NH_4OH adjusted to pH 2 with 1 *M* HCl. The solution was diluted to 200 cm^3, warmed up to near boiling and then treated with 40 cm^3 1 *M* sodium benzoate over a period of 1 h. The mixture was digested for about 4 h, cooled and filtered, washed free from chloride ions and vacuum dried. The product was dehydrated at 85°C.

* Author to whom correspondence should be addressed.

Table 1. Analytical data, colour and molar conductivity value of the metal tris(chlorosulphates)

Compound	Molar conductance ($ohm^{-1} cm^2 mol^{-1}$)	% of S found (calc.)	% of Cl found (calc.)	% of M found (calc.)	Colour
$La(SO_3Cl)_3$	39	18.80 (19.80)	21.96 (21.93)	27.20 (28.60)	White
$Ce(SO_3Cl)_3$	45	21.20 (19.75)	22.50 (20.88)	26.35 (28.78)	White
$Pr(SO_3Cl)_3$	60	20.63 (19.72)	20.90 (21.84)	26.76 (28.89)	Green
$Nd(SO_3Cl)_3$	35	19.58 (19.59)	22.25 (21.70)	26.79 (29.38)	Reddish violet
$Sm(SO_3Cl)_3$	55	19.28 (19.35)	20.12 (21.43)	28.95 (30.25)	White
$Gd(SO_3Cl)_3$	59	20.06 (19.08)	22.50 (21.07)	30.23 (31.20)	White
$Tb(SO_3Cl)_3$	42	20.93 (19.02)	20.86 (21.06)	30.69 (31.43)	White
$Dy(SO_3Cl)_3$	65	17.77 (18.88)	22.53 (20.92)	30.93 (31.91)	Grey
$Ho(SO_3Cl)_3$	40	19.59 (18.80)	19.86 (20.82)	30.45 (32.24)	White
$Er(SO_3Cl)_3$	36	17.08 (18.71)	19.92 (20.72)	29.98 (32.54)	White

Table 2. IR frequencies (cm^{-1}) of the lanthanide tris(chlorosulphates) and their possible assignments*

Compound	ν_6(E) S–Cl wag	ν_2(A) S–Cl stretch	ν_3(A) Symmetric SO_3 deformation	ν_5(E) Asymmetric SO_3 deformation	ν_1(A) Symmetric SO_3 stretch	ν_4(E) Asymmetric SO_3 stretch
$La(SO_3Cl)_3$	300 m 320 m	440 m	560 s	640 s 690 m	1070 s	1140 s 1190 s
$Ce(SO_3Cl)_3$	320 m 330 m	445 m	570 s	650 s 670 s	1090 s	1150 s 1170 s
$Pr(SO_3Cl)_3$	310 m 330 m	450 m	590 s	640 m 680 m	1070 m	1140 m 1160 m
$Nd(SO_3Cl)_3$	330 m 340 m	440 m	590 s	660 sh 680 s	1060 m	1160 bm 1210 s
$Sm(SO_3Cl)_3$	300 m 320 m	430 m	590 s	630 s 660 m	1090 m	1140 s 1190 m
$Gd(SO_3Cl)_3$	320 m 330 m	430 m	590 s	630 m 650 m	1080 s	1140 m 1155 m
$Tb(SO_3Cl)_3$	310 m 320 m	400 m	580 s	640 s 670 s	1080 s	1150 m 1180 m
$Dy(SO_3Cl)_3$	320 m 330 m	420 m	560 s	630 s 680 m	1070 s	1160 m 1220 m
$Ho(SO_3Cl)_3$	300 m 310 m	445 m	560 s	660 s 690 s	1080 m	1150 m 1200 m
$Er(SO_3Cl)_3$	300 m 320 m	435 m	580 s	650 s 680 s	1070 m	1140 m 1190 m

* s, strong; m, medium; sh, shoulder; b, broad.

Table 3. Magnetic moments and electronic spectral data with possible assignments

Compound	μ_{eff} B.M.	Energy (kK)	Assignment
$La(SO_3Cl)_3$	Diamagnetic	15.62	—
		10.50	
$Ce(SO_3Cl)_3$	2.85	22.78	
		19.23	—
		16.67	
$Pr(SO_3Cl)_3$)	3.90	22.73	$^3P_2 \leftarrow {}^3H_4$
		20.83	$^3P_0 \leftarrow {}^3H_4$
		16.67	$^1D_2 \leftarrow {}^3H_4$
$Nd(SO_3Cl)_3$	3.75	20.20	$^4G_{9/2} \leftarrow {}^4I_{9/2}$
		18.87	$^4G_{7/2} \leftarrow {}^4I_{9/2}$
		14.33	$^4F_{9/2} \leftarrow {}^4I_{9/2}$
		12.50	$^4F_{7/2} \leftarrow {}^4I_{9/2}$
		11.38	$^4F_{5/2}, {}^2H_{9/2} \leftarrow {}^4I_{9/2}$
$Sm(SO_3Cl)_3$	—	24.71	$^3P_{3/2} \leftarrow {}^6H_{5/2}$
		22.22	$^6P_{3/2} \leftarrow {}^6H_{5/2}$
		20.68	$^4I_{9/2} \leftarrow {}^6H_{5/2}$
		17.78	$^4G_{5/2} \leftarrow {}^6H_{5/2}$
$Gd(SO_3Cl)_3$	8.30	22.73	
		20.83	
		19.23	—
		17.24	
		13.81	
		12.50	
$Dy(SO_3Cl)_3$	10.41	20.83	$^5D_2 \leftarrow {}^6H_{15/2}$
		19.23	$^5D_1 \leftarrow {}^6H_{15/2}$
		17.24	$^5D_2 \leftarrow {}^6H_{15/2}$
$Ho(SO_3Cl)_3$	10.20	—	—
$Er(SO_3Cl)_3$	—	24.28	$^2H_{9/2} \leftarrow {}^4I_{15/2}$
		23.26	$^4F_{7/2} \leftarrow {}^4I_{15/2}$
		17.86	$^4S_{3/2} \leftarrow {}^4I_{15/2}$
		14.29	$^4F_{9/2} \leftarrow {}^4I_{15/2}$

Synthesis of rare earth metal tris(chlorosulphates) $Ln(SO_3Cl)_3$ (Ln = La, Ce, Pr, Nd, Sm, Gd, Tb, Dy, Ho *and* Er)

The dehydrated metal benzoates (~ 5 g) were added in portions to excess chlorosulphuric acid (~30 cm^3) kept in a closed reaction vessel and the temperature of the reaction mixture was not allowed to rise above 40°C. The reaction which was very vigorous was allowed to subside, after which the solution was magnetically stirred for about 6 h. The solid compounds formed were vacuum-filtered, washed several times with chlorosulphuric acid and lastly with thionyl chloride and dried under vacuum at 60–80°C to a constant weight.

The elements chlorine and sulphur were estimated according to usual gravimetric methods,[10] while metals were estimated by EDTA titration using bromopyrogallol red and Eriochrome Black T as indicators.[11]

The IR spectra were recorded on a Perkin–Elmer 621 spectrophotometer as Nujol mulls, contained in envelope cells of thin polyethylene film sealed from all sides.

Diffuse reflectance spectra were taken on a Carl–Zeiss VSU-2P spectrophotometer using MgO as the reflectance standard.

The electrical conductivities of 1 m*M* solutions of the metal chlorosulphate dissolved in DMF were obtained using a Systronic type 302 conductivity bridge thermostatted at 25 ± 0.05°C. The magnetic susceptibility measurements were carried out by using a Model 155 vibrating sample magnetometer at 23°C. All manipulations were done in a dry-box under dry nitrogen.

RESULTS AND DISCUSSION

The results of elemental analyses (Table 1) are in agreement with the proposed composition,

$Ln(SO_3Cl)_3$ (Ln = La, Ce, Pr, Nd, Sm, Gd, Tb, Dy, Ho and Er).

The probable structure of and mode of bonding in the present metal chlorosulphates have been proposed after carefully examining the observed frequencies characteristic of the chlorosulphate group in the IR spectra.

The IR spectra (Table 2) show a lowering of the C_{3v} symmetry of the free chlorosulphate ion. This would be sufficient to produce nine normal modes of vibration for SO_3Cl^- irrespective of the mode of coordination of the anion (except Cl coordination).

The observed magnetic moments for a few metal tris(chlorosulphates) at room temperature are comparable with the distorted octahedral rare earth compounds. The results of the magnetic susceptibility measurement and spectral studies indicate a distorted octahedral geometry for those compounds having a coordination number of 6 for the metal, which is unlike that reported[12] for the corresponding fluorosulphates.

Acknowledgement—Three of us (M.S., M.A. and S.R.A.Z.) are thankful to the CSIR, New Delhi, India for financial assistance.

REFERENCES

1. D. A. Edwards, M. J. Stiff and A. A. Woolf, *Inorg. Nucl. Chem. Lett.* 1967, 427.
2. E. A. Robinson and J. A. Ciruna, *Can. J. Chem.* 1968, **46**, 1715.
3. Z. A. Siddiqi, M. Aslam, N. A. Ansari, M. Shakir and S. A. A. Zaidi, *Synth. React. Inorg. Met.–Org. Chem.* 1981, **11**, 475.
4. Z. A. Siddiqi, M. Shakir, M. Aslam, T. A. Khan and S. A. A. Zaidi, *Synth. React. Inorg. Met–Org. Chem.* 1983, **4**, 397.
5. Z. A. Siddiqi, M. Shakir, M. Aslam, S. R. A. Zaidi and S. A. A. Zaidi, *Indian J. Chem.* 1983, **22A**, 1078.
6. Z. A. Siddiqi, Lutfullah, S. A. A. Zaidi and K. S. Siddiqi, *Bull. Soc. Chim. Fr.* 1980, **5–6**, 228.
7. Z. A. Siddiqi, Lutfullah and S. A. A. Zaidi, *Bull. Soc. Chim. Fr.* 1980, **11–12**, 466.
8. Z. A. Siddiqi, Lutfullah, N. A. Ansari and S. A. A. Zaidi, *J. Inorg. Nucl. Chem.* 1981, **43**, 397.
9. M. D. Taylor, C. P. Carter and C. I. Wynter, *J. Inorg. Nucl. Chem.* 1968, **30**, 1503.
10. I. Vogel, *A Text Book of Quantitative Inorganic Analysis*, Vol. 1, p. 399. Longmans Green (1958).
11. F. J. Welcher, *The Analytical Uses of Ethylenediamine Tetraacetic Acid*, p. 181. D. Van Nostrand, Princeton, NJ (1958).
12. W. M. Johnson and J. W. Macklin, *Inorg. Chem.* 1976, **15**, 1216.

Polyhedron Vol. 4, No. 3, pp. 369–378, 1985
Printed in Great Britain

0277–5387/85 $3.00 + .00
© 1985 Pergamon Press Ltd

STUDIES OF METAL CHELATES WITH THE NOVEL LIGAND 2,2,7-TRIMETHYL-3,5-OCTANEDIONE

THOMAS J. WENZEL,*† ERIC J. WILLIAMS, R. CURTIS HALTIWANGER‡ and ROBERT E. SIEVERS*

Department of Chemistry and Cooperative Institute for Research in Environmental Sciences, University of Colorado, Boulder, CO 80309, U.S.A.

(*Received* 4 *February* 1984; *accepted* 25 *July* 1984)

Abstract—The synthesis of the novel ligand 2,2,7-trimethyl-3,5-octanedione, H(tod), is described, as well as the preparation of some of the transition metal and lanthanide complexes containing the anion of this unsymmetrical beta-diketone ligand. The structure of $Cu(tod)_2$ has been determined by X-ray crystallography to be square-planar with the isobutyl groups *cis* to each other. Thermogravimetric analyses indicate that several of these metal complexes are volatile and thermally stable compounds. Metal complexes containing this ligand also show unusually high solubilities in non-polar solvents such as *n*-hexane. The properties of these compounds indicate that they may be useful for vapour-plating of metals, as fuel additives, and in other applications.

Metal chelate complexes with beta-diketone ligands have been employed for a variety of interesting applications including gas chromatography and trace analysis of metals,[1–13] solvent extraction of metals,[14–18] vapor-plating of metals,[19,20] and fuel additives.[21–25] Metal chelates of the novel ligand 2,2,7-trimethyl-3,5-octanedione, H(tod), have a number of properties that make them ideal candidates for some of the above applications. Several of the metal complexes of this ligand are volatile and thermally stable. These metal chelates are highly soluble in non-polar solvents, even more so than complexes of the isomeric ligand, 2,2,6,6-tetramethyl-3,5-heptanedione, H(thd). In addition, rare earth chelates of H(tod) exhibit antiknock activity and may catalytically eliminate some undesirable combustion products of fuels.[26,27] One final important property of the H(tod) ligand is that the starting materials for its synthesis, neopentanoic acid and methylisobutyl ketone, are much less expensive than those of H(thd) and fluorinated beta-diketones.

In this paper we describe the synthesis of H(tod) and the preparation of the Cr(III), Mn(III), Fe(III), Co(III), Ni(II), Cu(II), Pd(II), La(III) and Ce(IV) complexes with this ligand. The volatility and thermal stability of these chelates have been examined. The molecular structure of $Cu(tod)_2$ is shown, and the solubilities of $Cu(tod)_2$ in a variety of solvents, as well as the partition coefficient between octanol and water, are presented. Finally, an evaluation of some of these chelates for use in fields such as extraction of metal ores, vapour deposition of metals, and fuel combustion modification is discussed.

EXPERIMENTAL

Equipment

Mass spectra were measured with a Varian MAT CH5 single focussing spectrometer. Elemental analyses were performed by Huffman Laboratories (Wheatridge, CO). Reflection information for the crystal structure determination was collected by a Nicolet P1 autodiffractometer using Mo-K_α radiation. The thermogravimetric analyses were performed on a Perkin–Elmer TGS-2 Thermogravimetric Analysis (TGA) System. The sample was kept under a 60 cm^3 min^{-1} flow of dry helium and heated at 10° min^{-1}. Spectrophotometric analyses were performed on a Cary 219 UV-VIS Spectrophotometer or on a Perkin–Elmer Model 360 Atomic Absorption Spectro-

* Present address: Chemistry Department, Bates College, Lewiston, ME 04240, U.S.A.

† Author to whom correspondence should be addressed.

‡ Present address: Chemistry Department, Campus Box 215, University of Colorado, Boulder, CO 80309, U.S.A.

meter. pH values were measured by a Broadley-James pH electrode connected to a Model NX pH meter (Sargent–Welch).

Reagents

All reagents were used as received without further purification. Neopentanoic acid was a gift from Exxon Chemicals (Houston, TX). Sodium hydride and $PdCl_2$ were obtained from Alfa Div., Ventron (Danvers, MA). Methylisobutyl ketone, 1-octanol, hexanes, molecular sieves (3 and 4 Å), the transition metal salts and lanthanum(III) oxide came from Fisher Scientific (Fair Lawn, NJ). Molecular sieves (13X) were obtained from Linde Div. (South Plainfield, NJ). The rare earth chloride mixture was a gift from Molycorp (White Plains, NY). Cerium(III) nitrate hexahydrate, was obtained from Matheson, Coleman, and Bell (Cincinnati, OH). The chloride of La(III) was synthesized by dissolving the metal oxide (La_2O_3) in concentrated hydrochloric acid and evaporating to dryness.

Synthetic procedures

Preparation of 2,2,7-trimethyl-3,5-octanedione, H(tod). Two procedures were used for the synthesis of the ligand. Procedure 1 was used initially in order to obtain the highest purity of H(tod) for further synthetic work. Later, it was determined that procedure 2 would yield product of suitable purity for most purposes but with less time and effort expended. Both procedures are reported here.

Procedure 1

To a 2 l three necked round bottom flask was added a magnetic stirring bar, 67 g of sodium hydride (50% dispersion in mineral oil) and 350 cm^3 of dried (4 Å molecular sieves) toluene. The flask was immersed in a hot water bath atop a stirrer-hot plate and then fitted with a reflux condenser, a pressure-equalizing dropping funnel of at least 100 cm^3 capacity, and a glass inlet for a nitrogen purge gas system (dried by 13X molecular sieves). Ethyl pivalate* (107 cm^3) was added to the flask via one of the necks and methyl isobutyl ketone (88 cm^3) was added to the dropping funnel. Heat was applied to the water bath, stirring was begun and the purge gas was passed through the flask at a low flow rate. When the water bath boiled, the ketone was added at a rate of between 0.5 and 1.0 $cm^3\ min^{-1}$, such that the entire volume was dispensed over the course of about three hours. When the addition was complete, the green–yellow mixture was heated an additional 30 min and then allowed to stir overnight without heat but with the purge gas flowing.

The next day the flask was packed in an ice bath, and, while stirred vigorously with the purge gas flowing, 300 cm^3 of an 18% (6 *M*) aqueous hydrochloric acid solution was *slowly* added (caution: hydrogen evolution). When the neutralization was complete, the mixture was filtered to remove the suspended solids, which were discarded. The mixture was transferred to a separatory funnel, the organic layer was isolated and the solvent was removed by rotary evaporation.

The crude H(tod) was purified first by vacuum distillation (1 torr, 50–80°C) to separate the ligand from high-boiling but organic-soluble impurities. Next, the copper complex was synthesized, as described below, to isolate the beta-diketone from any by-products that are formed by self-condensation of the ketone. Crude $Cu(tod)_2$ (20 g) was placed in a 250 cm^3 separatory funnel with 30 cm^3 of hexane and 150 cm^3 of 10% (1 *M*) aqueous sulphuric acid, and the mixture was shaken until no blue colour remained in the organic phase. The organic solution was isolated and the solvent was removed by rotary evaporation, which left H(tod) of about 97–99% purity.

Procedure 2

To a 1 l round bottom flask to which was fitted a Claisen adaptor containing a reflux condenser and a pressure-equalizing dropping funnel, was added 67 g of sodium hydride, 350 cm^3 of freshly distilled ethyl pivalate, and a Teflon-covered magnetic stirring bar. The flask was fitted with a heating mantle and positioned above a magnetic stirring device. Methyl isobutyl ketone (88 cm^3) was added to the dropping funnel. A ground-glass adaptor, which served as the inlet for a dry helium purge gas system, was fitted to the dropping funnel and a low flow of helium gas (approximately 30 $cm^3\ min^{-1}$) was used to continuously purge the system of air and water vapour. Stirring was begun and heat was applied until the ester came to a low reflux. The ketone was dispensed at a rate such that the entire volume was added over the course of 4–5 h. Heating was continued for an additional 1 h, after which time the green–yellow mixture was left stirring under helium overnight at room temperature.

The next day the flask was packed in an ice bath and 120 cm^3 of absolute ethanol was added via the dropping funnel (caution: hydrogen is evolved and foaming occurs). Following the ethanol, 300 cm^3 of

*Synthesized by the acid-catalyzed condensation of ethanol and neopentanoic acid. Stored over anhydrous magnesium sulfate and distilled prior to use.

an 18% (6 *M*) aqueous hydrochloric acid solution was slowly added. During the neutralization the helium flow was continued and the mixture was stirred as vigorously as possible. When the neutralization was complete, the mixture was filtered through a coarse-pore sintered-glass funnel, the organic layer was isolated, and the bulk of the ester and alcohol was removed by rotary evaporation. The excess unreacted ester, which served as a solvent as well as a reactant, can be recycled in subsequent syntheses. The residue then was vacuum distilled and the fraction coming over at 53–55°C (1 torr) was collected. This pale yellow liquid consists of 90–95% H(tod). Yield: 82 g (61%).

The identity of the ligand was verified by gas chromatographic–mass spectrometric and proton nuclear magnetic resonance analyses. The IR spectrum of a neat sample between NaCl plates showed strong absorbances at 2900, 1600, 1450, 1350, 1300, 1220, 1130 and 950 cm^{-1}.

Preparation of tris(2,2,7-trimethyl-3,5-octanedionato)chromium(III), $Cr(tod)_3$. The $Cr(tod)_3$ complex was prepared by an earlier reported procedure.[28] To a mixture consisting of 67 cm^3 of distilled water and 173 cm^3 of ethanol was added 8 g of $CrCl_3 \cdot 6H_2O$, 15.4 g of H(tod), and 53.3 g of urea. The mixture was stirred and heated under reflux for 20 h. When the mixture had cooled to room temperature 200 cm^3 of distilled water was added, and a dark purple oil formed, which was extracted into hexane. This solution was filtered and the solvent removed by rotary evaporation. Sublimation of the oil gave a solid material that was re-sublimed to yield $Cr(tod)_3$. M.p.: 122–123°C. Found: C, 65.88; H, 9.82. Calc. for $Cr(C_{11}H_{19}O_2)_3$: C, 65.86; H, 9.55%. A molecular ion corresponding to $Cr(tod)_3^+$ is observed in the mass spectrum of this product.

Preparation of tris(2,2,7-trimethyl-3,5-octanedionato(manganese(III), $Mn(tod)_3$. To 100 cm^3 of methanol in an open beaker exposed to oxygen in the air was added 7.7 g of manganese(II) acetate tetrahydrate with stirring. After the solution turned from light pink to brown (about 15 min), 18.4 g of H(tod) was added at once with stirring. The solution was stirred for about 30 min, during which time the pH was brought up to a value of 8 by dropwise addition of 4 *M* aqueous NaOH (about 25 cm^3). After 30 additional minutes the precipitate that had formed was collected by suction filtration, dissolved in hexanes and filtered through a medium porosity sintered glass funnel. The solvent was removed by rotary evaporation and the resulting dark oil solidified on standing overnight. Recrystallization from hot methanol resulted in brown flakes that were collected by filtration. M.p.: 88–90°C. Found: C, 64.89; H, 9.42. Calc. for $Mn(C_{11}H_{19}O_2)_3$: C, 65.54; H, 9.50%. The mass spectrum of this compound shows a molecular ion corresponding to $Mn(tod)_3^+$.

Preparation of tris(2,2,7-trimethyl-3,5-octanedionato)iron(III), $Fe(tod)_3$. To 1 g of $FeCl_3 \cdot 6H_2O$ in 3 cm^3 of distilled water was added 50 cm^3 of a saturated aqueous sodium acetate solution. To this solution was added a mixture of 2 g of H(tod) in 15 cm^3 of ethanol and, the solution was stirred overnight. The bright red solid that resulted was collected by suction filtration and dissolved in hexanes. This solution was filtered and the solvent removed by rotary evaporation. Sublimation gave the bright red $Fe(tod)_3$. M.p.: 78–80°C. Found: C, 65.55; H, 9.64. Calc. for $Fe(C_{11}H_{19}O_2)_3$: C, 65.44; H, 9.49%. The mass spectrum of this product exhibits a molecular ion corresponding to $Fe(tod)_3^+$.

Preparation of tris(2,2,7-trimethyl-3,5-octanedionato)cobalt(III), $Co(tod)_3$. Cobalt(II) nitrate hexahydrate (5.8 g) was dissolved in 60 cm^3 of 50% aqueous ethanol in an open beaker and a solution of 11.0 g of H(tod) in 30 cm^3 of ethanol was stirred in. A solution of 2.6 g of NaOH dissolved in 50 cm^3 of aqueous ethanol was stirred into the above solution, and the combined solution turned bright pink. This solution was warmed to *ca* 50–60°C and stirred for 2 h, over which time the solution turned dark green. After 2 h the solution was filtered through a medium porosity sintered-glass funnel and the filtrate extracted with hexanes. Removal of the solvent by rotary evaporation left a dark green oil which solidified in a vacuum oven (1 torr, 90°C) after 3 h. This solid was dissolved in hexanes, filtered through a medium pore glass funnel and the solvent allowed to evaporate overnight in a hood to dryness. The product, $Co(tod)_3$, was a dark green powder. M.p.: 152–157°C. Found: C, 64.83; H. 9.48. Calc. for $Co(C_{11}H_{19}O_2)_3$: C, 65.11; H, 9.44%. The mass spectrum of this compound shows a molecular ion at *m/z* 608, which corresponds to $Co(tod)_3^+$.

Preparation of bis(2,2,7-trimethyl-3,5-octanedionato)nickel(II), $Ni(tod)_2$. To a solution of 5.0 g of nickel(II) acetate tetrahydrate in 50 cm^3 of hot water was added a solution of 12.0 g of H(tod) in 40 cm^3 of methanol. The pH was adjusted to about 8 by adding concentrated ammonium hydroxide. The solution was stirred for 30 min, then decanted, leaving in the beaker a thick turquoise-coloured oil. This oil was dissolved in 50 cm^3 of hexanes and filtered through a medium porosity sintered glass funnel. Removal of the solvent produced bright green crystals, which were recrystallized from hot methanol. Vacuum sublimation and subsequent drying *in vacuo* at 110°C over P_4O_{10} produced a bright green product. M.p.: 146–148°C. Found: C, 62.12; H, 9.09. Calc. for $Ni(C_{11}H_{19}O_2)_2$: C, 62.14; H,

9.01%. The mass spectrum shows a molecular ion that is characteristic of $Ni(tod)_2^+$, with the isotope pattern expected for ions containing nickel.

Preparation of bis(2,2,7-trimethyl-3,5-octanedionato)copper(II), $Cu(tod)_2$. The $Cu(tod)_2$ complex was synthesized by a previously described procedure for preparing Cu(II) beta-diketonates.[29] To 100 cm^3 of the vacuum-distilled organic residue obtained from the synthesis of the ligand was added 300 cm^3 of methanol. Cupric acetate hydrate (40 g) was added to 500 cm^3 of distilled water and heated to just below the boiling point. The hot solution was filtered directly into the stirred H(tod) solution. The resulting mixture was allowed to stand for 4 h, and the solid that formed was collected by suction filtration and washed with cold methanol. Recrystallization from hexanes gave a purple powder. M.p.: 116–117°C. Found: Cu, 14.47; C, 61.48; H, 8.89. Calc. for $Cu(C_{11}H_{19}O_2)_2$: Cu, 14.77; C, 61.44; H, 8.91%.

Preparation of bis(2,2,7-trimethyl-3,5-octanedionato)palladium(II), $Pd(tod)_2$. $Pd(tod)_2$ was prepared by a modification of a reported procedure.[30] To a suspension of 0.9 g of $PdCl_2$ in a mixture of 25 cm^3 of methanol and 25 cm^3 of distilled water was added a solution of 2.3 g of H(tod) in 10 cm^3 of methanol. After the mixture was stirred for one hour, the solid material which had formed was recovered by suction filtration and dissolved in hexanes. The hexane solution was filtered and the solvent removed by rotary evaporation to yield bright orange–yellow crystals. Sublimation *in vacuo* gave the desired product, $Pd(tod)_2$. M.p.: 152–156°C. Found: C, 56.32; H, 8.74. Calc. for $Pd(C_{11}H_{19}O_2)_2$: C, 55.87; H, 8.10%. The mass spectrum of this product exhibits a molecular ion corresponding to $Pd(tod)_2^+$ with the isotope pattern characteristic of Pd-containing ions. The asymmetry of the ligand causes both *cis* and *trans* isomers of the complex to be formed. The proton NMR spectrum of $Pd(tod)_2$ exhibits distinctive resonances for both isomers, with one of the isomers predominating.

Preparation of tris(2,2,7-trimethyl-3,5-octanedionato)lanthanum(III) dihydrate, $La(tod)_3 \cdot 2H_2O$. The synthesis of this compound was accomplished by a ligand exchange between $LaCl_3 \cdot 7H_2O$ and $Ba(tod)_2$. The $Ba(tod)_2$ was prepared by adding 5.9 g of $Ba(OH)_2$ to 27 cm^3 of water and heating the solution to boiling. The hot solution was filtered directly into a solution of 10 g H(tod) in 10 cm^3 of methanol. After the mixture was stirred overnight, the white $Ba(tod)_2$ that had formed was collected, dried *in vacuo* over P_4O_{10}, and used directly in the ligand interexchange synthesis.

The $La(tod)_3 \cdot 2H_2O$ was prepared by adding a warm solution of 0.5 g $LaCl_3 \cdot 7H_2O$ in 20 cm^3 of ethanol to a warm solution of 1 g $Ba(tod)_2$ in 60 cm^3 of ethanol. A fine precipitate, presumably $BaCl_2$, formed immediately, and the mixture was heated and stirred for 90 min. The solution was filtered through a 5-micron Millipore filter to remove the $BaCl_2$. The ethanol was removed to leave a thick yellow oil that gradually solidified on standing. Recrystallization from hexanes gave an off-white solid. M.p.: 95–97°C. Found: C, 54.01; H, 7.92. Calc. for $La(C_{11}H_{19}O_2)_3 \cdot 2H_2O$: C, 54.69; H, 8.48%. The mass spectrum of this product shows a molecular ion corresponding to anhydrous $La(tod)_3$.

Preparation of tetrakis(2,2,7-trimethyl-3,5-octanedionato)cerium(IV), $Ce(tod)_4$. Ten grams of $Ce(NO_3)_3 \cdot 6H_2O$ was dissolved in 30 cm^3 of methanol. To this solution was added a solution of 17 g of H(tod) in 50 cm^3 of methanol. The solution was stirred and 4 *M* aqueous NaOH was slowly added until pH was approximately 7. During the addition of base, the solution gradually turned a dark red colour and precipitate started to settle out at about pH 6.4. The entire mixture was then added to a separatory funnel: distilled water (100 cm^3) and hexanes (75 cm^3) were added, and the $Ce(tod)_4$ was extracted into the organic phase. This layer was collected, filtered through a medium porosity sintered glass funnel, and the solvent in the filtrate was removed by rotary evaporation. Dark red crystals of $Ce(tod)_4$ (m.p.: 134–136°C) were collected.

When crude H(tod) was used without purification [via $Cu(tod)_2$], a dark red oil was obtained rather than crystals. In this case crystallization was achieved by dissolving the oil in about 100 cm^3 of hexanes and adding this solution to 400 cm^3 of 95% ethanol. Upon standing overnight crystals of $Ce(tod)_4$ formed and were collected by suction filtration. These were dissolved in hexanes and filtered through a medium porosity sintered-glass funnel. The solvent was removed by rotary evaporation, leaving dark red crystals of $Ce(tod)_4$. Found: C, 60.05; H, 8.66. Calc. for $Ce(C_{11}H_{19}O_2)_4$: C, 60.51; H, 8.77%. The mass spectrum of this compound shows a peak at *m/z* 872, corresponding to the molecular ion, $Ce(tod)_4^+$.

Preparation of mixed rare earth chelates of H(tod), $RE(tod)_x$. A mixture of all the hydrated rare earth chlorides was employed. The percent of each metal was governed by the amount occurring in the oxide extract of the ore. In samples of roasted leachates from bastansite ore from the Molycorp (Union Oil Co.) mine at Mountain Pass, CA, the basic composition was found to be 50% cerium, which forms the $Ce(tod)_4$ chelate, and 50% other lanthanides, principally La(III), Nd(III), and Pr(III), which may consist of chelates of the formula $RE(tod)_3$ and $RE(tod)_2(OH)$. One mole of the rare

earth chloride mixture (approximate molecular weight of the hydrated chloride is 356 g mol^{-1}) was mixed with 3.5 moles of H(tod).

To 162 g of the powdered rare earth chloride mixture dissolved in 100 cm^3 of absolute methanol was added 304 g of H(tod) which previously had been dissolved in 300 cm^3 of absolute methanol. The mixture was stirred with an overhead stirring apparatus while 4 *M* aqueous NaOH was slowly added to bring the pH up to 8. As the pH increased, a thick, dark red oil formed and settled to the bottom of the beaker. The methanol–water layer was decanted and the red oil was dissolved in hexanes. This solution was filtered through a medium porosity glass funnel and the solvent was removed by rotary evaporation. Crystallization of the $RE(tod)_x$ mixture, which appeared in the form of a dark red oil, was achieved by dissolving approximately 100 g of the oil in 300 cm^3 of hexanes and adding this solution to 1000 cm^3 of 95% ethanol. This solution was allowed to stand overnight, during which time plate-like crystals and a solid glassy material formed on the bottom of the beaker. The crystals, collected by suction filtration, were dark red in colour while the glassy material was a much lighter rust colour. Both solids were recrystallized from hexanes, and when analyzed for metal content by X-ray fluorescence showed different ratios of lanthanides.[27] The $RE(tod)_x$ mixture exhibits a mass spectrum that is characteristic of a composite of the various metal : tod complexes.

Structure determination

The structure was determined by direct methods. Single crystals in the form of blue plates were prepared by recrystallization of purified $Cu(tod)_2$ from absolute methanol. The unit cell was found to be monoclinic (space group : $P2_1/n$) with dimensions $a = 20.369(4)$ Å, $b = 10.371(2)$ Å, $c = 11.526(2)$ Å, $\beta = 90.04(1)°$, and volume of 2435(1) $Å^3$. The density of $Cu(tod)_2$ was determined in aqueous $ZnBr_2$ solution and was found to be 1.15 g cm^{-3}. Using the value 430.1 g $mole^{-1}$ for the molecular weight, the calculated density for four molecules in the unit cell is 1.17 g cm^{-3}. The least squares refinement yielded $R = 0.065$ and $R_w = 0.080$. Atomic coordinates and thermal parameters and a list of F_o/F_c values has been deposited as supplementary material with the Editor.*

Solubility determinations

The solubilities of $Cu(tod)_2$ and $Cu(thd)_2$ were determined at room temperature and the method used depended on the concentration of the complex at equilibrium. When possible, measured filtered aliquots of a saturated solvent : chelate solution were subjected to gentle heat until the solvent had been removed, as evidenced by constant weight. A spectrophotometric method also was used in which 1 cm^3 filtered aliquots of the equilibrated solution were diluted to 10 cm^3 with hexanes and the visible absorption spectrum obtained over the range 450–900 nm. Standard solutions were made up in an identical fashion and the analytical wavelength used was the absorption maximum at 650 nm. A third method, which was used to evaluate aqueous samples, employed atomic absorption spectroscopy of acidified samples for Cu(II) using standard flame techniques. An extra step in determining the partition coefficient involved centrifuging the aqueous layer to remove any remaining octanol. The extraction isotherm was evaluated at room temperature using distilled water and kerosene.

RESULTS AND DISCUSSION

H(tod) at room temperature is a colourless liquid that shows high solubility in organic solvents, but not in water. The proton NMR spectrum of H(tod) in chloroform shows a doublet (0.90 ppm) and a complex multiplet (2.20 ppm), corresponding to the isobutyl protons, and singlets (1.17, 5.63 and 16.00 ppm), which correspond to tert-butyl protons, a methine proton, and an enol proton, respectively. The enol form of H(tod) is favoured over the keto form in deuterated chloroform by a factor of *ca* 6 to 1. The IR spectrum of H(tod) exhibits absorbances in the region 3000–700 cm^{-1} that are characteristic of the O—H, C—H, C=O and C—O groups, and the mass spectrum is consistent with expected fragmentations.

The metal chelates listed in the experimental section are generally highly coloured, powdery or crystalline materials, and are stable when exposed to air at room temperature. These complexes are highly soluble in organic solvents, but only very sparingly soluble in water. The IR spectra of the compounds are very similar and show broad absorptions with little fine structure.

The mass spectra of these complexes are also quite similar. Table 1 shows the most abundant fragments for all the metal chelates, and it can readily be seen that a number of fragments are common among the mass spectra. For example, all of the compounds show a molecular ion peak. Most of the chelates [except Ni(II)] show a fragment which corresponds to the loss of one ligand; the tris-chelates [except La(III)] exhibit loss of two ligands, as does the tetrakis-chelate of Ce(IV). Also, all of the complexes

* Atomic coordinates have also been submitted to the Cambridge Crystallographic Data Centre.

Table 1. Results from mass spectral analyses of metal : tod chelates*

Compound	Mass (*m/z*)	Assignment	Compound	Mass (*m/z*)	Assignment
Cu(II)	429, 431	$[M]^+$	Mn(III)	604	$[M]^+$
	372, 374	$[M-C_4H_9]^+$		421	$[M-L]^+$
	315, 317	$[M-2C_4H_9]^+$		364	$[M-L-C_4H_9]^+$
	246, 248	$[M-L]^+$		238	$[M-2L]^+$
	189, 191	$[M-L-C_4H_9]^+$		183	$[HL-H]^+$
	127	$[HL-C_4H_9]^+$		127	$[HL-C_4H_9]^+$
	85	$[C_5H_9O]^+$		57	$[C_4H_9]^+$
Ni(II)	424, 426, 427, 428	$[M]^+$	Cr(III)	599, 601, 602, 603	$[M]^+$
	367, 369, 370, 371	$[M-C_4H_9]^+$		416, 418, 419, 420	$[M-L]^+$
	213, 215, 216	$[M-L-28]^+$		233, 235, 236, 237	$[M-2L]^+$
	183	$[HL-H]^+$		85	$[C_4H_9O]^+$
	127	$[HL-C_4H_9]^+$		57	$[C_4H_9]^+$
	85	$[C_4H_9O]^+$	Fe(III)	603, 605, 606	$[M]^+$
	57	$[C_4H_9]^+$		548, 549	$[M-C_4H_9]^+$
Pd(II)	470, 471, 472, 474, 476	$[M]^+$		420, 422, 423	$[M-L]^+$
	287, 288, 289, 291, 293	$[M-L]^+$		363, 365, 366	$[M-L-C_4H_9]^+$
	258, 259, 260, 262, 264	$[M-C_5H_9O-28]^+$		237, 239, 240	$[M-2L]^+$
	230, 231, 232, 234, 236	$[M-L-C_4H_9]^+$		127	$[L-C_4H_9]^+$
	201, 202, 203, 204, 206, 208	$[M-L-C_5H_9O]^+$		57	$[C_4H_9]^+$
	85	$[C_5H_9O]^+$	La(III)	688	$[M]^+$
	57	$[C_4H_9]^+$		637	$[M-C_4H_9]^+$
Co(III)	608	$[M]^+$		505	$[M-L]^+$
	425	$[M-L]^+$		183	$[HL-H]^+$
	368	$[M-L-C_4H_9]^+$		127	$[HL-C_4H_9]^+$
	242	$[M-2L]^+$	Ce(IV)	872	$[M]^+$
	127	$[L-C_4H_9]^+$		689	691
	57	$[C_4H_9]^+$		506, 508	$[M-2L]^+$
				183	$[HL-H]^+$
				127	$[HL-C_4H_9]^+$
				85	$[C_5H_9O]^+$
				57	$[C_4H_9]^+$

* M = intact molecule: L = ligand.

show fragments that are indicative of the tod ligand, such as *m/z* 127, 85 and 57. Another interesting feature of the mass spectra of these complexes is that the solid probe temperature required to volatilize these compounds into the source of the mass spectrometer was always quite low, of the order of 200°C or less. Thus no special provision for vaporization or ionization, such as fast atom bombardment, is needed to acquire these mass spectra, which makes these chelates quite attractive for such analytical techniques as metal isotope ratio measurements or isotope dilution–mass spectrometry in metal determinations.

Crystal and molecular structure of $Cu(tod)_2$

The structure of $Cu(tod)_2$, shown in Fig. 1 along with the atomic numbering scheme, is similar to that of the isomeric chelate $Cu(thd)_2$, the structure of which had been determined previously.[31] $Cu(tod)_2$ crystallizes in the *cis*-configuration and is monomeric and approximately square planar. There was no evidence of the presence of any *trans* isomer in any of the crystalline samples, but the *trans* isomer may exist in solution and be interconverted as the *cis* isomer .crystallizes. Selected bond angles and distances are given in Table 2.

It is apparent from the edge-on view of the molecule in Fig. 1 that the molecule contains no inversion centre since the two chelate rings are not exactly planar. This geometry is different from that reported for $Cu(thd)_2$[31] and $Ni(thd)_2$,[32] which contain centres of inversion. This difference is likely due to packing stresses induced in the molecule when an isobutyl moiety is substituted for a tert-butyl group in the ligands with subsequent loss of symmetry.

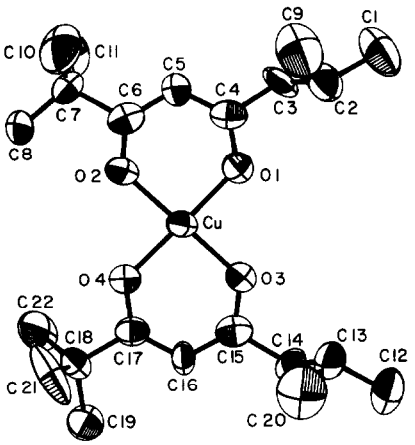


Fig. 1. Molecular structure of $Cu(tod)_2$.

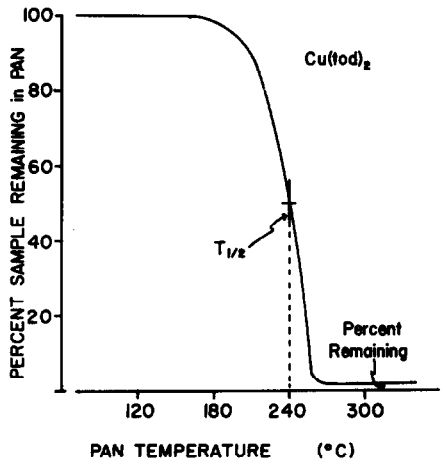


Fig. 2. Thermogram of $Cu(tod)_2$.

Thermogravimetric analyses

In the thermogravimetric analyses the sample was continuously weighed under a flow of helium, while the temperature was increased at 10°C min^{-1}. The important information gained from the analysis includes an estimate of the volatility and the gross thermal stability of the complex. If thermal decomposition is negligible under the conditions required for vaporization, one rapid way to compare volatilities of complexes is to measure the temperatures at which half the sample weight is lost and the amount and appearance of any residue remaining in the pan at the end of the heating (see Fig. 2). The former is a measure of the volatility of a compound and the latter is a measure of the thermal stability.

The results of the thermogravimetric analysis of metal chelates of tod are shown in Table 3. Most of the complexes are reasonably volatile and thermally stable. Some, such as the chelates of Mn(III), Ce(IV) and La(III), show appreciable residue under these heating conditions, though even these samples are partially vaporized without decomposition.

Table 2. Selected bond distances and angles for $Cu(tod)_2$

Bond	Distance (Å)	Bond	Angle (°)
Cu—O1	1.889(7)	O1—Cu—O2	92.7(3)
Cu—O2	1.874(7)	O3—Cu—O4	92.9(3)
Cu—O3	1.876(7)	Cu—O1—C4	126.3(7)
Cu—O4	1.895(7)	Cu—O2—C6	127.2(7)
O1—C4	1.309(12)	Cu—O3—C15	125.6(7)
O2—C6	1.285(11)	Cu—O4—C17	127.2(7)
O3—C15	1.316(13)	O1—C4—C5	124.9(11)
O4—C17	1.277(11)	O2—C6—C5	125.4(11)
C4—C5	1.373(14)	O3—C15—C16	125.4(11)
C5—C6	1.381(15)	O4—C17—C16	124.8(11)
C15—C16	1.362(15)	C4—C5—C6	123.0(11)
C16—C17	1.362(14)	C15—C16—C17	124.2(11)
C3—C4	1.486(15)	C3—C4—C5	120.7(11)
C6—C7	1.564(15)	C5—C6—C7	120.8(11)
C14—C15	1.542(15)	C14—C15—C16	121.4(11)
C17—C18	1.541(15)	C16—C17—C18	122.8(11)

Table 3. Results from thermogravimetric analysis of metal : tod chelates*

Compound	$T_{1/2}$† (°C)	% remaining‡
$Cu(tod)_2$	240	ND§
$Ni(tod)_2$	247	ND
$Co(tod)_3$	244	ND
$Mn(tod)_3$	232	10
$Ce(tod)_4$	275	15

* Samples were heated from 25 to 500°C at 10°C/min under helium flow (60 cm^3 min^{-1}).

† Temperature at which one-half of the original sample weight remains in the pan.

‡ Percent of the original sample weight that remains at the end of the experiment.

§ No detectable residue (visibly) remained in the pan at the end of the experiment.

Table 4. Solubility of Cu(II) chelates*

Solvent	$Cu(tod)_2$	$Cu(thd)_2$
n-Hexane	1.58×10^{-1}	5.32×10^{-2}†
Methanol	3.39×10^{-2}	4.00×10^{-3}
1-Octanol	5.16×10^{-2}‡	9.99×10^{-3}
	5.55×10^{-2}§	
Water	5.98×10^{-4}	1.43×10^{-4}‖

* All values in g cm^{-3} at 30°C.
† Lit. value: 4.47×10^{-2} g cm^{-3} at 20°C.[43]
‡ Gravimetric analysis.
§ Spectrophotometric analysis.
‖ From Ref. 43.

Solubility and extraction studies

The solubilities of $Cu(tod)_2$ and the isomeric chelate, $Cu(thd)_2$, in various solvents are shown in Table 4. It can be seen from these data that $Cu(tod)_2$ is at least twice as soluble in these solvents as $Cu(thd)_2$.

The partition coefficient of $Cu(tod)_2$ distributed between 1-octanol and water was also determined. This value (normally reported[33] as log P_{oct}), is 3.64 $\pm$0.20; high values such as this have often previously been taken as an indication a compound is likely to be highly soluble in lipids.[33] A qualitative test showed that $Cu(tod)_2$ formed a deep blue clear solution when dissolved in melted bacon fat. While bioavailability of metal ions depends on complex factors, $Cu(tod)_2$ might be useful as a source of Cu(II) for individuals who suffer from copper deficiency diseases, such as Menkes syndrome.[34] Until toxicity data are available care should be taken in handling these compounds in the laboratory. Accidental exposure of $Cu(tod)_2$ under a fingernail resulted in blue staining that did not disappear for several days.

The high solubility of $Cu(tod)_2$ further indicated that this ligand is of potential use in the solvent extraction of metals, such as in the recovery of metals from leached ores. In order to evaluate this potential, an extraction isotherm was determined and is shown in Fig. 3. The isotherm indicates that H(tod) in kerosene will efficiently extract copper from an aqueous solution at pH values greater than 5. Another experiment was conducted to determine the effectiveness of H(tod) in extracting aqueous solutions of high copper concentrations, such as those typically found in ore leachate solutions.[18] A 50% by volume solution of H(tod) in kerosene (100 cm^3 total solution) was used to extract successive 100 cm^3 aliquots of an aqueous ammoniacal solution containing approximately 15 g Cu l^{-1} at pH 11. After five extractions the concentration of copper in the organic phase was 59 g Cu l^{-1}. Assuming stoichiometry of two ligands per metal ion, the theoretical maximum is 77 g Cu l^{-1} and the extraction efficiency is 77%. These experiments indicate that H(tod) is an effective and inexpensive extraction agent.

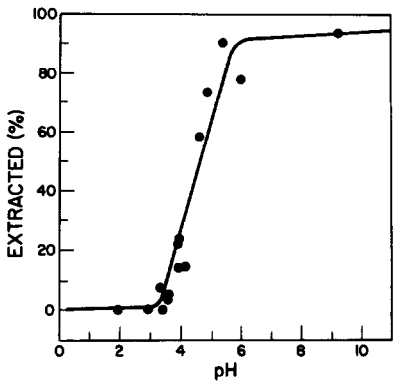


Fig. 3. Extraction isotherm for water: kerosene system using aqueous Cu(II) and H(tod) in kerosene.

Vapour deposition

In vapour deposition experiments the metal chelate was heated under a flow of a gas until it was vaporized and was transported to a target heated at substantially higher temperatures. When the vapours contacted the hot target, a layer of the metal was deposited and the organic by-products swept away by the gas flow. This technique has previously been tested with other metal chelates[19,20] with varying degrees of success. In favourable cases the plated surface has been found to be conducting and of high purity. The process allows good control of the uniformity and thickness of the film, and the metal can be deposited in intricate patterns determined by selective heating. In some of the more successful previous studies, complexes with ligands containing fluorinated substituents, primarily 1,1,1-trifluoro-2,4-pentanedione and 1,1,1,5,5,5-hexafluoro-2,4-pentanedione, were employed. Although the complexes are more volatile, these ligands are relatively expensive while the complexes synthesized from H(tod) offer a much less expensive alternative.

The $Cu(tod)_2$ complex was tested for its utility in vapour-plating. Passage of the vaporized complex in a flow of nitrogen through a glass tube maintained at about 350°C in an oven resulted in a copper deposit on the walls of the tube. In previous studies[19,20] hydrogen was usually used as the carrier gas as well as the metal reducing agent. In those experiments the effluent material was trapped in a cold trap and found to consist of some of the original metal complex and some ligand. In our experiments, since nitrogen is not capable of acting as a reductant, the metal plating is a result of thermal decomposition of

the chelate. The organic products of the thermal decomposition were trapped in a liquid nitrogen cold trap and analyzed by gas chromatography–mass spectrometry. The only peak observed in the chromatogram corresponded to H(tod) ligand. The regeneration of H(tod), which can be used to synthesize more $Cu(tod)_2$, is particularly fortunate because it offers the possibility of cyclic transport and deposition processes. Other decomposition products may not have been readily detectable by gas chromatography–mass spectrometry. In previous studies of the thermal decomposition of metal chelates of 2,4-pentanedione, compounds such as CO_2, methane, acetone and the ligand were observed.[35,36] Our procedure would not detect CO_2 or methane, but ketones, such as methylisobutyl ketone and pinacolone, were not observed.

This technique should be applicable for a wide range of metal complexes of tod, especially those that were shown by thermogravimetric analysis to be volatile and reasonably thermally stable.

Fuel additive studies

In previous studies by Sievers and coworkers[21–24] and Hartle,[25] certain rare earth beta-diketonate complexes were found to possess antiknock activity. The lanthanides are considerably less toxic than presently used lead additives[37] and are less likely to foul noble metal catalysts, a problem associated with lead and manganese fuel additives.

The β-diketonate compounds most studied for their antiknock ability are the rare earth chelates of 2,2,6,6-tetramethyl-3,5-heptanedione. In the earlier studies the Ce(IV) complex was found to be superior to any of the other individual lanthanides, but a mixture of all the rare earth : thd complexes can be used without significant sacrifice in effectiveness. Rare earth ores from the Molycorp mine (the largest supplier of rare earths in the U.S.) yield concentrates in which Ce constitutes about 50% of the metal content. 50% in cerium.

Another potential benefit of using rare earth chelate fuel additives is that their utilization may catalytically eliminate some undesirable combustion products of fuels.[38–40] Rare earth oxides are formed during the combusion of the chelates and, in previous studies, these have been found to catalyze the low-temperature oxidation of organic compounds[41–44] and the decomposition of nitrogen oxides.[45,46] The particles of the rare earth oxides are very finely divided and most are exhausted with the gases : however, some oxides form a coat on the walls of the combustion chamber and exhaust system and may function as surface catalysts.

As most internal combustion engines age, carbonaceous deposits gradually form on the interior engine surfaces. These deposits increase the fuel octane requirement [termed octane requirement increase (ORI)] needed by the engine to maintain a suitable performance level. Such deposits can also lead to "Dieseling" or run-on after turning off the ignition. The rare earth chelates have been shown to catalyze the elimination of these carbon deposits.[45] The elimination of these deposits should enhance the performance of the engine by reducing ORI as well as "Dieseling".

CONCLUSIONS

The beta-diketone, 2,2,7-trimethyl-3,5-octanedione [H(tod)], has been synthesized, and some transition metal and lanthanide complexes with this ligand prepared. H(tod) can be synthesized from methylisobutyl ketone and an ester of neopentanoic acid and is an effective complexing agent for extraction of Cu(II) from aqueous solution into an organic phase. Metal chelates of the beta-diketone exhibit high solubility in non-polar organic solvents and show moderate thermal stability and volatility. The structure of crystalline $Cu(tod)_2$ is *cis*, monomeric and approximately square planar. The properties of these metal chelates make them valuable for applications such as metal ore extraction, vapour-plating of metals and fuel additives.

REFERENCES

1. R. W. Moshier and R. E. Sievers, *Gas Chromatography of Metal Chelates*. Pergamon Press, Oxford (1965).
2. P. C. Uden and D. E. Henderson, *Analyst (London)* 1977, **102**, 889.
3. W. J. Biermann and H. Gesser, *Anal. Chem.* 1960, **32**, 1525.
4. W. D. Ross, *Anal. Chem.* 1963, **35**, 1596.
5. H. Kawaguchi, T. Sakamoto and A. Mizuike, *Talanta* 1973, **20**, 321.
6. R. M. Dagnall, T. S. West and P. Whitehead, *Analyst (London)* 1973, **98**, 647.
7. T. Sakamoto, H. Kawaguchi and A. Mixuike, *J. Chromatogr.* 1976, **121**, 383.
8. M. S. Black and R. E. Sievers, *Anal. Chem.* 1976, **48**, 1872.
9. G. P. Morie and T. R. Sweet, *Anal. Chim. Acta* 1966, **34**, 314.
10. R. W. Moshier and J. E. Schwarberg, *Talanta* 1966, **13**, 445.
11. R. E. Sievers and W. D. Ross, *Talanta* 1968, **15**, 87.
12. J. Savory, P. Mushak, F. W. Sundermann, R. M. Estes and N. O. Rozel, *Anal. Chem.* 1970, **42**, 294.
13. C. Genty, C. Houin, P. Malherbe and R. Schott, *Anal. Chem.* 1971, **43**, 235.

14. W. G. Schribner and Antoinette M. Kotecki, *Anal. Chem.* 1965, **37(11)**, 1304.
15. W. G. Schribner, W. J. Treat, J. D. Weis and R. W. Moshier, *Anal. Chem.* 1965, **37(9)**, 1136.
16. H. Koshimura and T. Okubo, *Anal. Chim. Acta* 1970, **49**, 67.
17. H. Koshimura, *J. Inorg. Nucl. Chem.* 1976, **38**, 1705.
18. Preliminary Report: Lix©54, a new reagent for metal extractions from ammoniacal solutions, available from Henkel Corp.
19. R. L. Van Hemert, L. B. Spendlove and R. E. Sievers, *J. Electrochem. Soc.* 1965, **112**, 1123.
20. R. W. Moshier, R. E. Sievers and L. B. Spendlove, U.S. Patent 3,356,527 (1967).
21. K. J. Eisentraut, R. L. Tischer and R. E. Sievers, U.S. Patent 3,794,473 (1974).
22. R. L. Tischer, K. J. Eisentraut, K. Scheller, R. E. Sievers, R. C. Bausman and P. R. Blum, paper presented at the American Chemical Society meeting, San Francisco, August 1976.
23. R. L. Tischer, K. J. Eisentraut, K. Scheller, R. E. Sievers, R. C. Bausman and P. R. Blum, U.S. NTIS AD Rep. AD/A-006151 (1974).
24. R. E. Sievers and J. E. Sadlowski, *Science* 1978, **201**, 217.
25. R. J. Hartle, U.S. Patent 4,036,605 (1977).
26. R. E. Sievers and T. J. Wenzel, U.S. Patent 4,251,233 (1981).
27. T. J. Wenzel, Ph.D. thesis, University of Colorado (1981).
28. G. S. Hammond, D. C. Nonhebel and C. H. S. Wu, *Inorg. Chem.* 1963, **2**, 73.
29. J. T. Adams and C. R. Hauser, *J. Am. Chem. Soc.* 1944, **66**, 1220.
30. I. Yoshida, H. Kobayashi and K. Ueno, *J. Inorg. Nucl. Chem.* 1973, **35**, 4061.
31. N. I. Kirillova, *Beta-diketonaty Met.* (*Mater. Vses. Semin. "Str., Svoistva Primen, Beta-Diketonatov Met."*), 2nd, 1976, 41–45.
32. F. A. Cotton and J. J. Wise, *Inorg. Chem.* 1966, **5**, 1200.
33. A. Leo, C. Hansch and D. Elkins, *Chem. Rev.* 1971, **71**, 525.
34. E. J. Underwood, *Trace Elements in Human and Animal Nutrition*, 3rd edn. Academic Press, New York (1971).
35. R. G. Charles and M. A. Pawlikowski, *J. Phys. Chem.* 1958, **62**, 440.
36. J. Von Hoene, R. G. Charles and W. M. Hickam, *J. Phys. Chem.* 1958, **62**, 1098.
37. D. Arevela, "Toxicity of rare earths", *Prog. Pharmacol.* 1979, **2**, 69.
38. W. E. Lyons and L. J. McKone, U.S. Patent 2,086,775 (1937).
39. F. J. Sergey, J. M. Masellei and M. V. Ernest, U.S. Patent 3,903,020 (1974).
40. S. G. Hinden, U.S. Patent 3,870,455 (1973).
41. W. F. Libby, *Science* 1971, **171**, 499.
42. L. A. Pedersen and W. F. Libby, *Science* 1972, **176**, 1355.
43. R. C. Vickery, *Science* 1971, **172**, 86.
44. R. J. H. Voorhoeve, J. P. Remeika, P. E. Freeland and B. Matthias, *Science* 1972, **177**, 353.
45. M. I. Seegall, J. C. Napier and W. A. Compton, Environ. Prot. Agency (U.S.) Rep. EPA-EHS:70-114 (PB204011) (1971), p. 52.
46. M. S. Peters and J. L. Wu, *Atmos. Environ.* 1977, **11**, 459.

Polyhedron Vol. 4, No. 3, pp. 379–382, 1985
Printed in Great Britain

0277–5387/85 $3.00 + .00
Pergamon Press Ltd

THE PREPARATION AND X-RAY CRYSTAL STRUCTURE OF $W_3(\mu CN)_3(NO)_3(CO)_9$

HELEN M. DAWES and MICHAEL B. HURSTHOUSE*
Chemistry Department, Queen Mary College, Mile End Road, London E1 4NS, U.K.

ALAN A. DEL PAGGIO and EARL L. MUETTERTIES†
Chemistry Department, University of California, Berkeley, CA 94720, U.S.A.

and

ADRIAN W. PARKINS*
Chemistry Department, Queen Elizabeth College, Campden Hill Road, London W8 7AH, U.K.

(*Received* 14 *June* 1984; *accepted* 13 *July* 1984)

Abstract—The nitrosation of $Na[W(CO)_5CN]$ using amyl nitrite and sulphuric acid in a two phase water–diethyl ether system gives the trinuclear compound $W_3(\mu CN)_3(NO)_3(CO)_9$. A single crystal X-ray diffraction study showed that the compound contains a nine-membered ring of three tungsten atoms and three bridging cyanide groups. The terminal carbonyl and nitrosyl ligands were not distinguishable.

The three groups CO, CN^- and NO^+ are isoelectronic and so might be expected to have similar bonding properties. However, detailed calculations have revealed[1,2] considerable differences in the electronic requirements of each group when coordinated to a transition metal. It is, therefore, not surprising that few complexes have been prepared which contain all three groups. That the electronic requirements are not completely incompatible is established by the isolation of $K_2[Co(NO)CO(CN)_2]$[3] and $[CpM(CO)(NO)CN]^-$ (M = Cr, Mo, W).[4] In an attempt to prepare a neutral cyanonitrosyl carbonyl we investigated the reaction of $Na[W(CO)_5CN]$ with nitrosating agents.

RESULTS AND DISCUSSION

Preliminary studies showed that $Na[W(CO)_5CN]$ in water reacts vigorously with $NO[PF_6]$ but the reaction proceeded with extensive decomposition. However, by using a two phase water–diethyl ether system an orange yellow product can be obtained from the ether layer. The nitrosation can also be carried out using sodium or amyl nitrite and sulphuric acid. Amyl nitrite and sulphuric acid is the preferred reagent.

The IR spectrum of the product, **I**, shows a strong band at 1713 cm^{-1} indicating that it contains a nitrosyl group. The elemental analysis of the product corresponds to the empirical formula $W(CO)_3(NO)(CN)$. The compound does not sublime *in vacuo*, but was volatile enough to give a mass spectrum which suggested a trimeric structure $[W(CO)_3(NO)(CN)]_3$. The trimeric structure was subsequently confirmed by X-ray crystallography. The formation of the trimer is a consequence of the high lability of carbonyl groups in the presumed intermediate $ONW(CO)_4CN$ [eqn (1)].

$$3[W(CO)_5CN]^- \xrightarrow{NO^+} 3[ONW(CO)_4CN] \xrightarrow{\text{spontaneously}} W_3(\mu CN)_3(NO)_3(CO)_9 + 3CO. \quad (1)$$

*Authors to whom correspondence should be addressed.

†Deceased 12 January 1984.

Table 1. IR spectrum of $W_3(\mu CN)_3(NO)_3(CO)_9$ in CCl_4

Frequency (cm^{-1})	Intensity
1713	Strong
1996	Strong
2016	Strong
2036	Very strong
2099	Weak
~ 2150	Very weak

Legzdins[5] and coworkers have previously commented on the high lability of carbonyl groups in transition metal carbonyl nitrosyl halides.

The IR spectrum of I in CCl_4 solution in the 2200–1600 cm^{-1} region is given in Table 1.

A detailed examination of the IR spectrum gave very little additional structural information. This was because we could not confidently distinguish the bands due to CN from those due to CO and lack of good precedents in the literature. IR data have been reported[6,7] for the $[W(CO)_5CN]^-$ ion, but the frequencies vary considerably with the counter ion. A value of 2121 cm^{-1} has been reported[7] for the stretching frequency for the bridging cyanide in $PPN[(CO)_5W—C{\equiv}N—W(CO)_5]$. The value is so close to some absorptions in $[W(CO)_5CN]^-$ that there is no reliable guide to enable us to confirm or disprove the presence of bridging cyanide. We therefore decided to undertake an X-ray structural investigation of I.

The task of growing crystals of I suitable for X-ray diffraction was extremely difficult. Although the compound can be recrystallised from ethyl acetate the resulting crystals were crinkled and unsuitable for X-ray diffraction. Using acetone as solvent eventually proved to be satisfactory, but the preparation was repeated over 50 times before a suitable crystal was obtained, and, even then, the crystals were extremely fine, short needles. The structure found is shown in Fig. 1, whilst bond lengths and angles are given in Table 2.

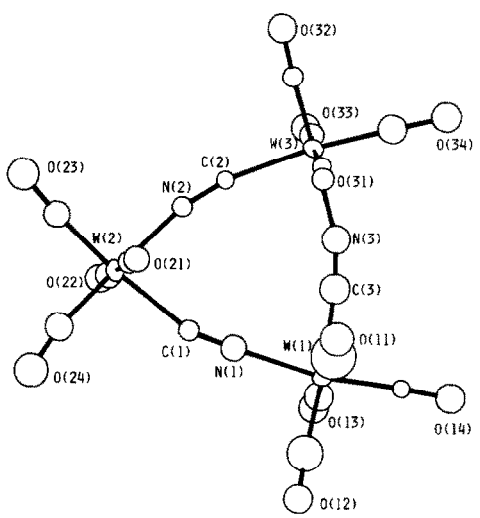


Fig. 1. The molecular structure of $W_3(\mu CN)_3(NO)_3(CO)_9$. For clarity, only the terminal oxygen atoms of the CO/NO groups are labelled.

The compound exists as a trimer with the three tungsten atoms forming an approximate equilateral triangle (W ... W 5.41, 5.34, 5.42 Å) and bridged by cyano groups, thus forming a nine-membered ring. The metal coordination geometry is distorted octahedral, being completed by bonds to a nitrosyl and three carbonyl groups, which were not distinguishable in the structure analysis.

The W—C≡N—W links are bowed outwards from the W—W vector (see Table 2) and the $(WCN)_3$ group is slightly saucer-shaped with all but one atom of the three CN groups lying out of and on the same side of the W_3 plane (Table 3). Analogous features were found in the structure of the $(PdCN)_3$ unit in the complex $[Pd(dppe)CN]_3^{3+}(ClO_4)_3$.[8]

Although, as previously mentioned, the CO and NO groups could not be distinguished, this does not preclude the possibility that there may be some ordering, at least perhaps with regard to equatorial and axial sites. However, we presume that the apparently significant difference between M—X axial and equatorial bonds is more a reflection of a difference in *trans* influences in the two directions rather than an indication of any chemical ordering.

EXPERIMENTAL

All preparative work was carried out in a nitrogen atmosphere using nitrogen saturated solvents and the usual Schlenk procedures. $Na[W(CO)_5CN]$ was made by the method of King[5] using a 1:1 ratio of $W(CO)_6$ and $Na[N(SiMe_3)_2]$ in toluene at room temperature for 40 h.

Synthesis of $W_3(\mu CN)_3(NO)_3(CO)_9$

$Na[W(CO)_5CN]$ (1 g, 2.68 mmol) was introduced into a Schlenk tube with water (25 cm^3) and diethyl ether (50 cm^3). Amyl nitrite (2 cm^3, 1.75 g, 15 mmol) followed by aqueous sulphuric acid (10 cm^3 of 1 m dm^{-3}, 20 mmol of H^+) were added and the mixture stirred with a magnetic stirrer for 20 min at room temperature. The colour quickly changed through green and golden yellow to a dark orange solution in the ether layer. The aqueous layer was removed by pipette, and replaced by water to wash the ether layer. The water was removed by pipette, and the ether layer then dried over anhydrous $MgSO_4$, filtered through silica and concentrated to a small

Table 2. Bond lengths and angles for $W_3(\mu CN)_3(NO)_3(CO)_9$*

Bond length (Å)			
N(1)—W(1)	2.17(5)	C(3)—W(1)	2.16(8)
N(2)—W(2)	2.15(4)	C(1)—W(2)	2.20(6)
N(3)—W(3)	2.22(6)	C(2)—W(3)	2.16(5)
C(1)—N(1)	1.12(6)	C(2)—N(2)	1.18(6)
C(3)—N(3)	1.16(7)	X(11)—W(1)	1.91(7)
X(12)—W(1)	1.90(6)	X(13)—W(1)	2.08(7)
X(14)—W(1)	1.85(4)	X(21)—W(2)	2.00(5)
X(22)—W(2)	2.14(6)	X(23)—W(2)	1.87(6)
X(24)—W(2)	1.86(7)	X(31)—W(3)	2.00(5)
X(32)—W(3)	1.78(5)	X(33)—W(3)	1.89(6)
X(34)—W(3)	1.90(7)	O(11)—X(11)	1.27(8)
O(12)—X(12)	1.18(6)	O(13)—X(13)	1.12(7)
O(14)—X(14)	1.19(5)	O(21)—X(21)	1.22(5)
O(22)—X(22)	1.14(6)	O(23)—X(23)	1.21(6)
O(24)—X(24)	1.20(7)	O(31)—X(31)	1.22(5)
O(32)—X(32)	1.20(5)	O(33)—X(33)	1.23(6)
O(34)—X(34)	1.29(7)		
Bond angle (°)			
C(3)—W(1)—N(1)	79.9(23)	X(11)—W(1)—N(1)	93.3(26)
X(11)—W(1)—C(3)	90.3(30)	X(12)—W(1)—N(1)	95.1(21)
X(12)—W(1)—C(3)	175.0(25)	X(12)—W(1)—X(11)	89.6(28)
X(13)—W(1)—N(1)	91.0(23)	X(13)—W(1)—C(3)	87.3(27)
X(13)—W(1)—X(11)	174.6(27)	X(13)—W(1)—X(12)	93.3(25)
X(14)—W(1)—N(1)	170.0(18)	X(14)—W(1)—C(3)	90.1(23)
X(14)—W(1)—X(11)	87.6(25)	X(14)—W(1)—X(12)	94.9(22)
X(14)—W(1)—X(13)	87.6(22)	C(1)—W(2)—N(2)	83.5(16)
X(21)—W(2)—N(2)	83.2(19)	X(21)—W(2)—C(1)	86.1(20)
X(22)—W(2)—N(2)	91.0(20)	X(22)—W(2)—C(1)	91.9(21)
X(22)—W(2)—X(21)	174.0(20)	X(23)—W(2)—N(2)	92.1(21)
X(23)—W(2)—C(1)	175.6(22)	X(23)—W(2)—X(21)	93.7(24)
X(23)—W(2)—X(22)	88.0(24)	X(24)—W(2)—N(2)	177.2(22)
X(24)—W(2)—C(1)	94.6(23)	X(24)—W(2)—X(21)	94.7(24)
X(24)—W(2)—X(22)	91.1(25)	X(24)—W(2)—X(23)	89.8(24)
C(2)—W(3)—N(3)	83.8(29)	X(31)—W(3)—N(3)	86.7(20)
X(31)—W(3)—C(2)	92.2(19)	X(32)—W(3)—N(3)	176.0(21)
X(32)—W(3)—C(2)	94.6(20)	X(32)—W(3)—X(31)	89.6(21)
X(33)—W(3)—N(3)	88.9(23)	X(33)—W(3)—C(2)	91.0(22)
X(33)—W(3)—X(31)	174.3(22)	X(33)—W(3)—X(32)	94.9(24)
X(34)—W(3)—N(3)	90.3(24)	X(34)—W(3)—C(2)	172.9(22)
X(34)—W(3)—X(31)	83.6(23)	X(34)—W(3)—X(32)	91.0(25)
X(34)—W(3)—X(33)	92.8(25)	C(1)—N(1)—W(1)	171.8(48)
C(2)—N(2)—W(2)	168.0(38)	C(3)—N(3)—W(3)	163.6(59)
N(3)—C(3)—W(1)	159.6(66)	N(1)—C(1)—W(2)	160.3(48)
N(2)—C(2)—W(3)	166.7(40)	O(11)—X(11)—W(1)	174.4(64)
O(12)—X(12)—W(1)	171.2(51)	O(13)—X(13)—W(1)	176.0(60)
O(14)—X(14)—W(1)	169.1(38)	O(21)—X(21)—W(2)	177.6(46)
O(22)—X(22)—W(2)	172.8(50)	O(23)—X(23)—W(2)	173.8(52)
O(24)—X(24)—W(2)	168.5(54)	O(31)—X(31)—W(3)	175.6(39)
O(32)—X(32)—W(3)	175.3(44)	O(33)—X(33)—W(3)	174.3(50)
O(34)—X(34)—W(3)	169.5(51)		

* The carbon and nitrogen atoms of the terminal ligands are all labelled as X.

Table 3. Ring atom deviations from the W_3-plane

Equation of W_3 plane (referred to crystallographic axes):
$6.205x + 0.072y + 77.676z = 3.086$

Deviation (Å): N(1) −0.07, N(2) −0.06, N(3) −0.43, C(1) 0.04, C(2) −0.12, C(3) −0.53

volume *in vacuo*. The residue consisted of a yellow powder and amyl alcohol. Petroleum ether (BP40–60) was added, and the mixture swirled to wash the solid. The liquid was then removed by pipette to give the crude product as an orange yellow powder (~ 230 mg, 26%) which was dried *in vacuo*.

Recrystallisation from ethyl acetate gave yellow orange crystals. Found: C, 15.1; H, 0.1; N, 8.6; O, 19.9; W, 56.2%. $C_{12}N_6O_{12}W_3$ requires C, 14.8; H, 0.0; N, 8.6; O, 19.8; W, 56.8%.

The crystals for the X-ray structure determination were obtained by recrystallising 3 times from acetone, the third recrystallisation being carried out at *ca* 0°C.

X-ray crystallography

The crystal used for data collection had dimensions of $0.15 \times 0.07 \times 0.02$ mm and was carefully mounted inside a Lindemann capillary. All crystallographic measurements were made using a CAD4 diffractometer, operated as described previously.[9] Owing to the weakly diffracting nature of the crystal, the data collection prescan acceptance parameter, $\sigma(I)/I$, normally 0.5–0.667, was set to 1.0.

Crystal data. $C_{12}N_6O_{12}W_3$: $M = 971.88$, monoclinic, $a = 6.753(3)$, $b = 16.305(2)$, $c = 20.590(6)$ Å, $\beta = 91.34(3)°$, $U = 2266.3$ Å^3, $Z = 4$, $D_c = 2.85$ g cm^{-3}, $F(000) = 1728$, space group $P2_1/c$, Mo-K_α radiation, $\lambda = 0.71069$ Å, μ(Mo-K_α) = 146.4 cm^{-1}. Total unique data measured = 2106 ($1.5 < \theta < 20.0°$) of which only 1061 were deemed observed [$I > 1.5\sigma(I)$].

STRUCTURE ANALYSIS AND REFINEMENT

The positions of the three independent tungsten atoms were obtained by manual interpretation of the Patterson map. The rest of the structure was developed, with great difficulty, via repeated least-squares refinements and difference syntheses. In the intermediate stages, all atoms bonded to the tungstens were treated as carbons. Eventually, some indications were given that the bridging C≡N groups were ordered and it was possible to assign one atom on each of two groups as nitrogens, by virtue of their isotropic thermal parameters. The atoms of the third bridging group were not distinguishable, and were assigned on the basis of cyclic repetition. At no stage was it possible to distinguish the nitrosyl groups from the carbonyls. Accordingly the atoms of the terminal groups bonded to the metals were assigned scattering factors for (0.75C + 0.25N)[10] corresponding to complete scrambling of the groups.

In the final stages of the refinement, the metal atoms were assigned anisotropic thermal parameters. The remainder were refined isotropically. An absorption correction was applied at the stage of fully isotropic refinement using the DIFABS procedure.[11] All computations were performed on a DEC VAX 11/750 computer, using standard programs.[12] The final R-value was 0.054 (unit weights). Atomic co-ordinates and thermal parameters and a list of F_o/F_c values have been deposited as supplementary material with the Editor, from whom copies are obtainable on request.*

Acknowledgement—We thank the SERC for the award of a Senior Visiting Fellowship (to AWP) and for financial support of the X-ray work.

REFERENCES

1. R. Hoffmann, M. M-L. Chen and D. L. Thorn, *Inorg. Chem.* 1977, **16**, 503.
2. R. L. DeKoch, A. C. Sarapu and R. F. Fenske, *Inorg. Chem.* 1971, **10**, 38; R. F. Fenske and R. L. DeKoch, *Inorg. Chem.* 1972, **11**, 437.
3. H. Behrens, E. Lindner and H. Schindler, *Chem. Ber.* 1966, **99**, 2399.
4. H. Brunner, *Chem. Ber.* 1969, **102**, 305.
5. B. W. S. Kolthammer, P. Legzdins and J. T. Malito, *Inorg. Chem.* 1977, **16**, 3173.
6. R. B. King, *Inorg. Chem.* 1967, **6**, 25.
7. J. K. Ruff, *Inorg. Chem.* 1969, **8**, 86.
8. J. A. Davies, F. R. Hartley, S. G. Murray and M. A. Pierce-Butler, *J. Chem. Soc., Dalton Trans.* 1983, 1305.
9. M. B. Hursthouse, R. A. Jones, K. M. A. Malik and G. Wilkinson, *J. Am. Chem. Soc.* 1979, **101**, 4128.
10. K. D. Sales, Private communication.
11. N. Walker and D. Stuart, *Acta Cryst. Sect. A* 1983, **39**, 158.
12. G. M. Sheldrick, SHELX program for crystal structure determination. University of Cambridge (1976).

*Atomic co-ordinates and thermal parameters have also been deposited with the Inorganic Data Base at the University of Bonn.

Polyhedron Vol. 4, No. 3, pp. 383–390, 1985
Printed in Great Britain

0277–5387/85 $3.00 + .00
© 1985 Pergamon Press Ltd

TRIPLE BONDS BETWEEN MOLYBDENUM AND TUNGSTEN ATOMS SUPPORTED BY THIOLATE LIGANDS: $(RS)_3M{\equiv}M(SR)_3$

MALCOLM H. CHISHOLM,* JAMES F. CORNING, KIRSTEN FOLTING and JOHN C. HUFFMAN

Department of Chemistry and the Molecular Structure Center, Indiana University, Bloomington, IN 47405, U.S.A.

(*Received* 25 *June* 1984; *accepted* 13 *July* 1984)

Abstract—Toluene solutions of $M_2(NMe_2)_6$ and mesitylene thiol react at 80°C to yield $M_2(S\text{-mes})_6$ compounds (M = Mo and W) with the liberation of $HNMe_2$. Similarly $M_2(OBu^t)_6$ in toluene reacts with mesitylene thiol under reflux to yield $M_2(S\text{-mes})_6$ compounds. In all cases the reactions also yield some decomposition products. The compounds $M_2(SBu^t)_2(NMe_2)_4$ react with mesitylene thiol in hexane at room temperature to give $M_2(S\text{-mes})_6$ compounds without significant side reactions. The $M_2(S\text{-mes})_6$ compounds are the first examples of compounds containing triple bonds between molybdenum and tungsten atoms supported exclusively by thiolate ligands. Pertinent bond distances (Å) and angles (°) are: M—M = 2.228(1) (Mo), 2.312(2) (W); M—S = 2.325(2) (Mo), 2.32(1) (W); M—M—S = 96.6(1) (Mo), 97.2(6) (W). The preparations of the new compounds $W_2(SBu^t)_2(NMe_2)_4$ and $W_2(OBu^t)_2(S\text{-mes})_4$ are reported.

Homoleptic compounds of formula $X_3M{\equiv}MX_3$ are known for X = bulky β-elimination stabilized alkyls[1,2] (e.g. CH_2CMe_3 and CH_2SiMe_3), NMe_2[3,4] and OR,[5,6] where R = a bulky alkyl or trialkylsilyl group (e.g. *t*-Bu, *i*-Pr, CH_2-*t*-Bu, $SiMe_3$ and $SiEt_3$). We have wondered for some time whether this series could be extended to include thiolato (mercaptide), SR, ligands and phosphido, PR_2, ligands. Though there was no reason to believe that such ligands could not exist our initial attempts to prepare $(RS)_3Mo{\equiv}Mo(SR)_3$ compounds were thwarted by problems arising from molybdenum's high affinity for sulphur, facile C—S bond cleavages, polymerizations by μ-SR formation and oxidation of the Mo_2^{6+} unit.[7] We were able, however, to attach two SR ligands to the $(Mo{\equiv}Mo)^{6+}$ unit in the preparation of the compounds 1,2-$Mo_2(SR)_2(NMe_2)_4$ [eqn (1)]:[8]

$$1,2\text{-}Mo_2Cl_2(NMe_2)_4 + 2LiSR \rightarrow 1,2\text{-}Mo_2(SR)_2(NMe_2)_4 + 2LiCl \quad (1)$$

where R = Me and Bu^t.

Subsequently, by the use of the bulky aromatic thiol mesitylene thiol we were able to prepare compounds of formula $Mo_2X_2(S\text{-mes})_4$ (mes = mesitylene, 2,4,6-trimethylphenyl) according to eqn (2):[9]

$$Mo_2X_6 + 6HS\text{-mes} \rightarrow 1,2\text{-}Mo_2X_2(S\text{-mes})_4 + 4XH \quad (2)$$

where X = NMe_2, OBu^t, OPr^i and OCH_2Bu^t.

Here the use of an aromatic thiol suppresses the facile C—S bond cleavage reaction and the 2,6-dimethyl substituents on the aromatic ring suppress oligomerization reactions by μ-SR formation. The use of only one methyl substituent in the 2-position (*ortho*) led to polymeric materials, but the use of two methyl groups, one in each of the *ortho* positions in the mesitylene group, led to only partial substitution. It was not clear why only partial substitution occurred in eqn (2). Steric or electronic factors, or both, could be involved. However, we were encouraged in our quest for a successful synthesis of $M_2(SR)_6$ compounds since it seemed that by relatively subtle changes in the steric properties of the aromatic thiol or the leaving group [X in eqn (2)] we could achieve a synthesis of the target compounds. We describe here the fulfillment of this goal.[10]

* Author to whom correspondence should be addressed.

RESULTS AND DISCUSSION

Syntheses

Previously we had found that the $Mo_2(SR)_2(NMe_2)_4$ compounds, where R = Me and Bu^t, reacted with alcohols (Bu^{t}OH and Pr^{i}OH) in hydrocarbon solvents to give dimolybdenum hexaalkoxides[8] and that these do not react with bulky alkyl thiols such as Bu^{t}SH. However, from eqn (2) it was clear that aromatic thiols would replace alkoxide ligands but it was not clear why the reaction stopped with only partial substitution. Are the M_2X_2(S-mes)$_4$ compounds kinetically or thermodynamically favoured in reaction (2)? If one considers that either an equilibrium $MoOR + R'SH \rightleftharpoons MoSR' + ROH$, or a higher activation energy for the last replacements of the two OR groups on the Mo_2^{6+} centre is at fault then merely increasing the temperature of the reaction and, if necessary, the selective removal of the alcohol by azeotrope distillation, would drive the reaction to the desired $Mo_2(SR')_6$ compounds. Indeed we find that in refluxing toluene, M_2X_2(S-mes)$_4$ compounds do react further with excess mesitylene thiol to give M_2(S-mes)$_6$ compounds. However, under these more forcing conditions some thermal decomposition occurs. Little can be said concerning these decomposition products, though based on a crystallographic study[11] a very minor product, *ca* 2–5% of the sample, obtained in the reaction between $W_2(NMe_2)_6$ and mesitylene thiol, is formulated as the salt $[Me_2\overline{NCH_2CH_2CH_2C}HS\text{-mes}]^+ [WO(S\text{-mes})_4]^-$. Crystallographically there can be little if any doubt concerning the authenticity of the oxo tungsten tetrakismesitylenethiolato moiety and the origin of the oxo group must be questioned. A plausible source is from THF and the cation $[Me_2\overline{NCH_2CH_2CH_2C}HS\text{-mes}]^+$ would appear to also involve the C_4-fragment of THF coupled with the S-mes and Me_2N units.

A cleaner route, one involving milder conditions, involves the reaction shown in eqn (3). The aliphatic thiolate ligands are readily

$$M_2(SBu^t)_2(NMe_2)_4 + 6mesSH \rightarrow M_2(S\text{-mes})_6 + 4HNMe_2 + 2Bu^tSH \quad (3)$$

replaced, along with the NMe_2 groups, by the arylthiolato ligands.

Physicochemical properties

The new M_2(S-mes)$_6$ compounds are orange-red crystalline compounds that are soluble in aromatic hydrocarbon solvents. The compounds are air sensitive and thermally unstable above 80°C. They cannot be purified by sublimation. They are diamagnetic and show ^{1}H NMR data consistent with the observed $X_3M{\equiv}MX_3$ structure. Analytical, IR and ^{1}H NMR data are given in Experimental.

Solid state and molecular structures

The sample of Mo_2(S-mes)$_6$ that was examined was crystallized from toluene/hexane solutions and, in the space group $R\bar{3}$, hexane molecules are contained in the unit cell. The dimolybdenum compound has crystallographically imposed S_6 symmetry. An ORTEP view of the molecule giving the atom number scheme used in the tables is shown in Fig. 1 and a view down the Mo—Mo bond is given in Fig. 2.

The ditungsten compound crystallized from toluene/hexane in the space group $P\bar{1}$. Molecules of W_2(S-mes)$_6$ have a crystallographically imposed centre of inversion. A view of the W_2(S-mes)$_6$ molecule showing the atom number scheme is given in Fig. 3.

As would be expected the Mo_2 and W_2 containing compounds are very similar and this is shown by a comparison of selected pertinent structural parameters in Table 1. A comparison of the structural parameters associated with the central $X_3M{\equiv}MX_3$ units in structurally characterized homoleptic alkyls, amides, alkoxides and thiolates is given in Table 2. The following points are worthy of note.

(1) For related pairs of molecules the W—W distance is longer by 0.08 or 0.09 Å than the Mo—Mo distance.

(2) The M—X distance is, within the 3σ criteria, the same for Mo—X and W—X.

(3) The M—M—X angles span a small range, 96.6–103.7°. The smaller angles seen here for the thiolates are easy to understand in terms of the arrangement of all six mesityl groups which are distal with respect to the central $(M{\equiv}M)^{6+}$ core. In the alkoxide molecule $Mo_2(OCH_2Bu^t)_6$ we see four distal and two proximal arrangements of the $-CH_2Bu^t$ groups leading, respectively, to larger and smaller M—M—O angles.

(4) The M—S distances are essentially the same as were found[9] in the structure of $Mo_2(OPr^i)_2$(S-mes)$_4$. From the arguments previously presented, we conclude that they are shorter by *ca* 0.10–0.15 Å than those expected for a pure MoS σ-bond and this shortening is due to S to M π-bonding.

Concluding remarks

The use of bulky arylthiolato ligands has recently been shown to lead to unusual monomeric compounds. For example, Koch and co-workers[12]

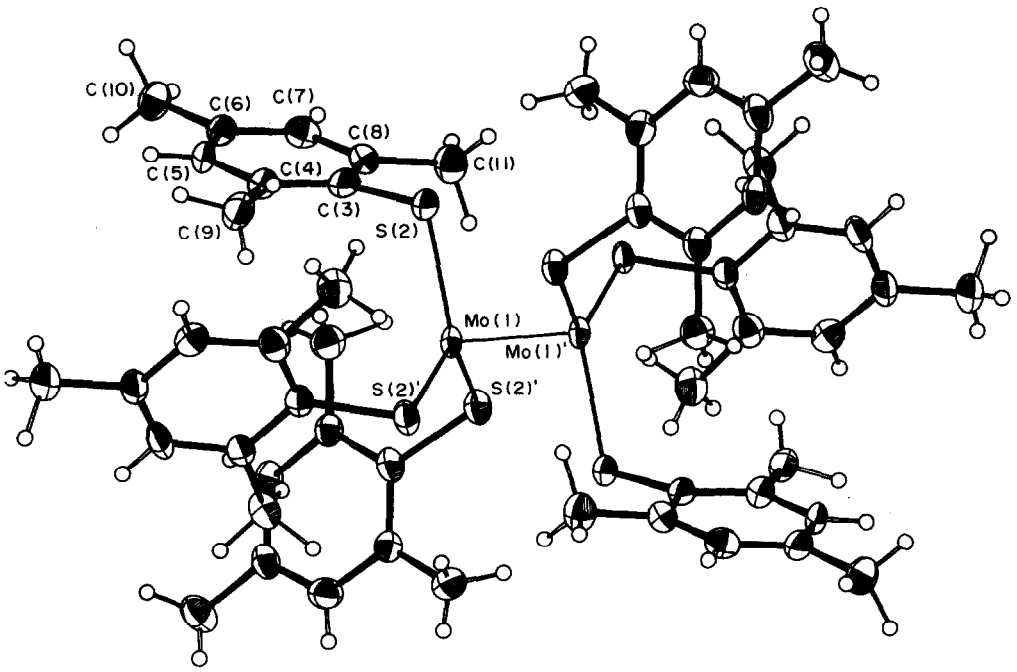


Fig. 1. An ORTEP view of the $Mo_2(S\text{-}mes)_6$ molecule giving the atom number scheme used in the tables.

were able to prepare the first example of a stable Fe(III) tetrathiolate using the metathetic exchange reaction:

$$FeCl_3 + 4LiSC_{10}H_{13} + Et_4NBr \rightarrow [Et_4N][Fe(SC_{10}H_{13})_4] + 3LiCl + LiBr,$$

where $SC_{10}H_{13}$ is the anion derived from 2,3,5,6-tetramethylphenylthiol. Attempts to extend this to Ru and Os gave rise to the first examples of the five-coordinate ruthenium state:

$$M(SC_{10}H_{13})_4(CH_3CN).^{13}$$

Dilworth and co-workers[14] have used the 2,4,6-triisopropylphenylthiolate ligand to obtain some novel carbonyl and nitrosyl mononuclear anionic

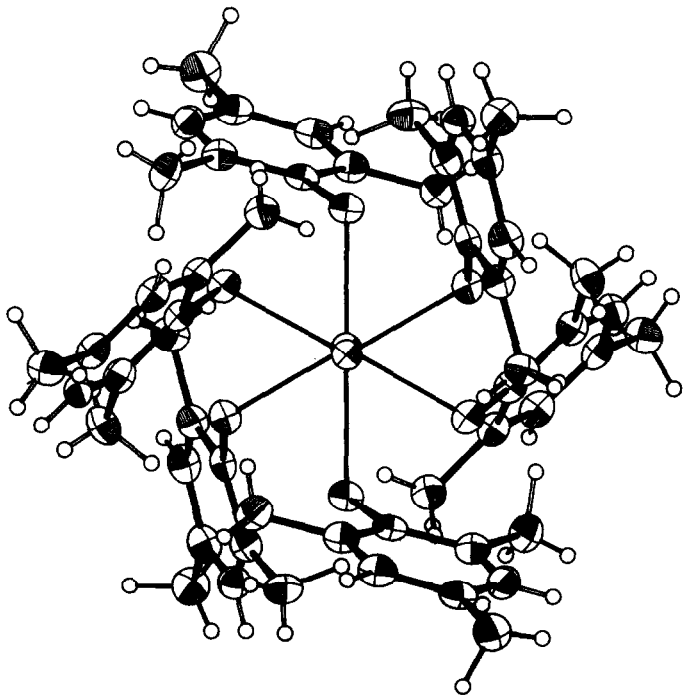


Fig. 2. An ORTEP view of the $Mo_2(S\text{-}mes)_6$ molecule looking down the Mo—Mo bond.

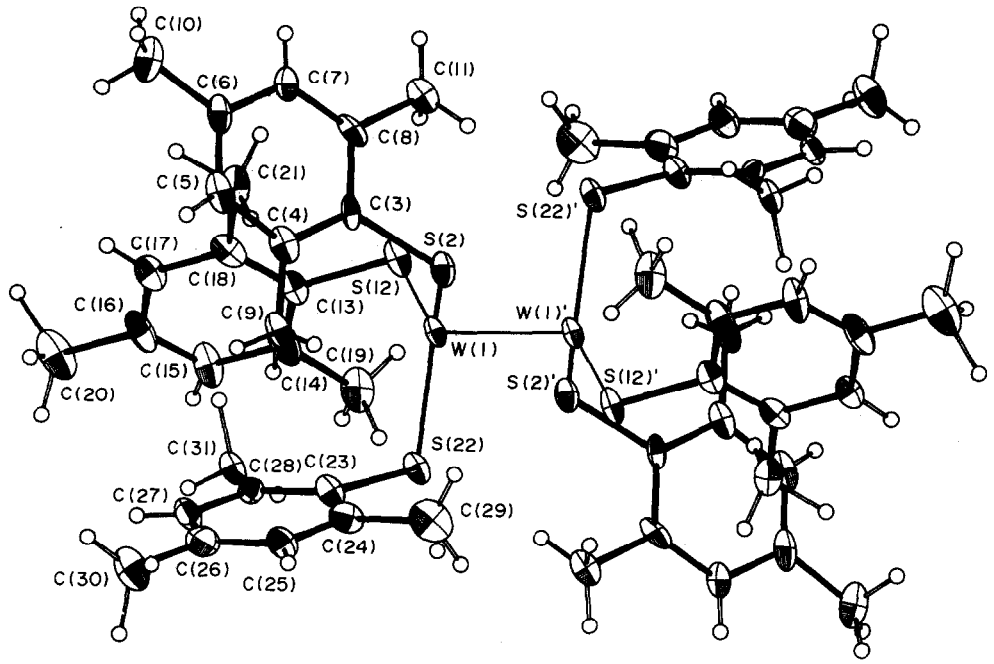


Fig. 3. An ORTEP view of the $W_2(S\text{-mes})_6$ molecule giving the atom number scheme used in the tables.

Table 1. Selected bond distances (Å) and angles (°) for the $M_2(SC_6H_2Me_3)_6$ molecules

		Distance	
A	B	Mo	W
M(1)	M(1)′	2.228(1)	2.313(2)
M(1)	S(2)	2.325(2)	2.311(4)
M(1)	S(12)		2.321(4)
M(1)	S(22)		2.303(4)
S(2)	C(3)	1.792(5)	1.79(1)
S(12)	C(13)		1.81(1)
S(22)	C(23)		1.78(1)
C	C(aromatic)*	1.38	1.39
C	C(methyl)*	1.50	1.50

			Angle	
A	B	C	Mo	W
M(1)′	M(1)	S(2)	96.6(2)	96.5(1)
M(1)′	M(1)	S(12)		97.8(1)
M(1)′	M(1)	S(22)		97.2(1)
S(2)	M(1)	S(12)	118.7(1)	119.7(1)
S(2)	M(1)	S(22)		117.0(1)
S(12)	M(1)	S(22)		118.7(1)
M(1)	S(2)	C(3)	110.1(2)	107.4(4)
M(1)	S(12)	C(13)		108.9(4)
M(1)	S(22)	C(23)		108.6(5)

* Averaged distance.

complexes of molybdenum(II), e.g.

$$[Mo(CO)_2(SC_6H_2Pr^i_3)_3]^-.$$

We have shown here that by an appropriate synthetic strategy compounds of formula $(RS)_3M{\equiv}M(SR)_3$ can be prepared for molybdenum and tungsten. There exists now the opportunity to compare the chemistry of the $(M{\equiv}M)^{6+}$ unit supported by the closely related alkoxide[15] and thiolate ligands.

Further studies are in progress.

EXPERIMENTAL

General procedures, including the preparations of $M_2(NMe_2)_6$ compounds, where M = Mo and W, $W_2(O\text{-}t\text{-}Bu)_6$ and $Mo_2(S\text{-}t\text{-}Bu)_2(NMe_2)_4$ have been described previously.[9] Mesitylene thiol was prepared from the reaction of mesitylene Grignard reagent and elemental sulphur as described below.

^1H NMR data were obtained from toluene-d_8 solutions using a Nicolet 360 spectrometer. IR spectra were recorded as Nujol mulls using a Perkin–Elmer 283 spectrophotometer. Elemental analyses were obtained from Alfred Bernhard Microanalytical Laboratories (Elbach, F.R.G.).

Preparations

Mesitylene thiol. To a solution of mesitylene magnesium bromide (135 cm^3 of a 1 *M* solution in

Table 2. Comparison of selected structural parameters for homoleptic compounds having a central $X_3M{\equiv}MX_3$ unit where M = Mo, W and X = C, N, O or S

Compound	M—M (Å)	M—X av. (Å)	M—M—X (°)	Reference
$Mo_2(CH_2SiMe_3)_6$	2.167(3)	2.13	100.6	1
$W_2(CH_2SiMe_3)_6$	2.255(2)	2.14	101.7	2
$Mo_2(NMe_2)_6$	2.214(3)	1.98	103.7	3
$W_2(NMe_2)_6$	2.294(2)	1.97	103.3	4
$Mo_2(OCH_2CMe_3)_6$	2.222(2)	1.88	103.0	5
$Mo_2(SC_6H_2Me_3)_6$	2.228(1)	2.325	96.6	This work
$W_2(SC_6H_2Me_3)_6$	2.312(2)	2.32	97.1	This work

THF), elemental sulfur (4.32 g, 0.35 g atoms) was added over a period of 20 min. The solution was hydrolyzed by the addition of H_2O (20 cm^3) followed by the slow addition of 6 *N* HCl (30 cm^3). The THF layer which separated was collected and dried over $MgSO_4$ (12 h). Upon removing the THF at reduced pressure a clear yellow oil remained which was distilled at 50°C, 30 torr yielding 2,4,6-trimethylphenyl thiol (mesitylene thiol) 16.74 g (81% yield). This was then dissolved in THF (15 cm^3) to give a 7.33 *M* solution which was stored over molecular sieves and under an atmosphere of N_2.

$W_2(NMe_2)_2(S\text{-}mes)_4$. $W_2(NMe_2)_6$ (0.46 g, 0.73 mmol) was dissolved in hexane (20 cm^3) to give a clear yellow solution. Mesitylene thiol (0.7 cm^3 of a 7.3 *M* solution in THF, 7 equiv) was added via syringe. The solution was allowed to stir at room temperature for 12 h. A gradual darkening of the solution occurred and a microcrystalline yellow-orange precipitate formed which was collected and dried *in vacuo*: $W_2(NMe_2)_2$ (S-mes)$_4$ (0.71 g, 0.67 mmol, 92% yield). Found: C, 45.01; H, 5.27; N, 2.81; S, 11.98%. Calc. for $W_2(NMe_2)_2(SC_6H_2Me_3)_4$: C, 45.28; H, 5.28; N, 2.67; S, 12.07%.

IR data: 1595 (m), 1290 (m), 1250 (ms), 1170 (m), 1140 (m), 1050 (s), 1025 (s), 935 (s), 885 (m), 840 (s), 800 (m), 730 (ms), 710 (m), 690 (m), 600 (m), 570 (wm), 550 (wm) cm^{-1}.

$W_2(O\text{-}t\text{-}Bu)_2(S\text{-}mes)_4$. $W_2(O\text{-}t\text{-}Bu)_6$ (0.3 g, 0.372 mmol) was dissolved in hexane (15 cm^3). Mesitylene thiol (1.1 cm^3 of a 7.3 *M* solution in THF) was added via syringe at room temperature. The solution was stirred for 24 h. Little colour change was detectable but a reddish precipitate formed which was collected by filtration and dried *in vacuo*. The solids were redissolved in toluene (5 cm^3) warmed to *ca* 50°C. Red-orange crystals were obtained upon cooling to −15°C: $W_2(O\text{-}t\text{-}Bu)_2(S\text{-}mes)_4$ (0.34 g, 82% yield based on W). Found: C, 47.23; H, 5.55; S, 11.45%. Calc. for $W_2(O\text{-}t\text{-}Bu)_2(SC_6H_2Me_3)_4$: C, 47.35; H, 5.72; S, 11.24%.

IR data: 1595 (ms), 1290 (m), 1260 (m), 1235 (m), 1160 (s), 1025 (ms), 965 (vs), 870 (w), 840 (s), 790 (w), 605 (wm), 550 (m), 470 (w), 420 (wm) cm^{-1}.

^1H NMR data at +21°C: O-*t*-Bu, δ = 1.90 (9H); $C_6H_2Me_3$, δ(*p*-methyl) = 2.05 (6H), δ(*o*-methyl) = 2.15 (12H), *meta*-H, δ = 6.4 (δ in ppm relative to Me_4Si).

$W_2(S\text{-}t\text{-}Bu)_2(NMe_2)_4$. $W_2Cl_2(NMe_2)_4$ (0.35 g, 0.57 mmol) was dissolved in toluene (25 cm^3). LiS-*t*-Bu (0.112 g, 1.2 mmol) was added and the reaction mixture was left to stir at room temperature for 48 h. The colour darkened from a yellow-orange to an orange-brown. The solution was evaporated to dryness *in vacuo* and hexane was added. Solids (LiCl and other insoluble materials) were removed by filtration and the hexane soluble filtrate was collected. Cooling to −15°C gave a yellow-green finely divided microcrystalline precipitate: $W_2(S\text{-}t\text{-}Bu)_2(NMe_2)_4$ (0.28 g, 68% yield based on W). Found: C, 26.41; H, 5.79; N, 7.81; S, 8.78%. Calc. for $W_2(S\text{-}t\text{-}Bu)_2(NMe_2)_4$: C, 26.59; H, 5.82; N, 7.65; S, 8.86%. $W_2(S\text{-}t\text{-}Bu)_2(NMe_2)_4$ sublimes with considerable decomposition (80°C, 10^{-2} torr) but does yield a molecular ion in the mass spectrometer: M^+ = 722 based on ^{184}W.

IR data: 1260 (wm), 1245 (ms), 1145 (s), 1039 (m), 1032 (m), 952 (s), 938 (vs), 800 (m), 565 (ms), 535 (m), 340 (wm).

^1H NMR data, 34°C in benzene-d_6: S-*t*-Bu, δ = 1.40 (9H); NMe_2, δ = 3.35 (12H) (δ in ppm relative to Me_4Si).

$M_2(S\text{-}mes)_6$ *compounds.* As noted previously the reaction between $M_2(NMe_2)_6$ compounds, where M = Mo and W, and mesitylene thiol yields $M_2(NMe_2)_2(S\text{-}mes)_4$ compounds when the reaction is carried out in hexane at room temperature. The latter compounds are virtually insoluble in hexane.

However, a similar result is obtained when the reaction is carried out in toluene, for which the M_2(S-mes)$_4$(NMe$_2$)$_2$ compounds are appreciably soluble but when the solution is refluxed for 6–8 h a further reaction with mesitylene thiol occurrs. M_2(S-mes)$_6$ compounds are formed and can be obtained as red crystals by careful recrystallation from toluene. However, the bulk material is contaminated with other products giving poor analytical data which is indicative of the presence of nitrogen containing materials. A better preparative route involves the use of the M_2(S-*t*-Bu)$_2$(NMe$_2$)$_4$ compounds and is given below.

Mo_2(S-*t*-Bu)$_2$(NMe$_2$)$_4$ (0.316 g, 0.58 mmol) was dissolved in hexane (15 cm^3). An excess of mesitylene thiol (2 cm^3 of a 7.33 *M* solution in THF) was added via syringe at room temperature. The solution was stirred for *ca* 10 h during which time some tan-coloured solids precipitated. These were removed by filtration and discarded. The orange-red filtrate was collected and reduced in volume *in vacuo*. The solution was slowly cooled to −5°C yielding a pale-red powder and some larger red crystals: Mo_2(S-mes)$_6$ (0.272 g, 43% yield based on Mo). Found: C, 59.21; H, 5.89; S, 17.61%. Calc. for $Mo_2(SC_6H_2Me_3)_6$: C, 59.01; H, 6.01; S, 17.48%.

IR data: 1598 (m), 1300 (mw), 1260 (ms), 1100 (w, br), 1030 (m, br), 845 (s), 795 (w, br), 610 (w), 550 (m), 415 (wm) cm^{-1}.

^{1}H NMR data, +34°C, benzene-d_6 solvent: *ortho*-methyls, $\delta = 2.15$; *para*-methyl, $\delta = 2.09$; *meta*-H, $\delta = 6.50$ (δ in ppm relative to Me$_4$Si).

W_2(S-mes)$_6$ was prepared in a similar manner, but employing W_2(S-*t*-Bu)$_2$(NMe$_2$)$_4$, and was obtained as a red powder or red crystals from toluene solutions in 35–40% yield based on W. Found: C, 50.53; H, 5.28; S, 15.22%. Calc. for $W_2(S_2C_6H_2Me_3)_6$: C, 50.86; H, 5.18; S, 15.07%.

IR data: 1600 (m), 1300 (m), 1260 (ms), 1180 (wm), 1100 (w, br), 1030 (s), 890 (m), 850 (s), 730 (ms), 610 (w), 555 (m), 470 (mw), 420 (m) cm^{-1}.

^{1}H NMR data, 35°C in benzene-d_6 solvent: *ortho*-methyls, $\delta = 2.18$; *para*-methyls, $\delta = 2.00$; *meta*-H, $\delta = 6.55$ (δ in ppm relative to Me$_4$Si).

Crystallographic studies

General operating procedures and listings of programs have been previously given.[16] Crystal data for the M_2(S-mes)$_6$ compounds are summarized in Table 3.

Mo_2(S-mes)$_6$. A suitable nearly equidimensional fragment was cleaved from a larger cubic shaped crystal which exhibited severe faulting on the faces. Examination of the chosen sample indicated it was crystallographically satisfactory. The sample was transferred to the goniostat using standard inert atmosphere handling techniques and cooled to −162°C for characterization and data collection.

An examination of reciprocal space revealed a trigonal lattice with rhombohedral centring. Subsequent solution and refinement confirmed the space group $R\bar{3}$. The structure was solved by "inspection", in that with $Z = 3$ (yielding a reasonable density), the only permissible location of the molecule was at a 3 site in the lattice. Assuming a Mo–Mo separation of 2.3 Å, a trial Mo was placed along the three-fold axis and a Fourier located the remaining non-hydrogens in the molecule. A difference map phased on the isotropic coordinates of the 11 unique atoms revealed three peaks of intensity 1.6–3.5 e Å^{-3} with all remaining peaks below 0.8 e Å^{-3}. The three larger peaks are apparently due to a disordered hexane solvent along the three-fold axis. When three partial occupancy carbon atoms were placed in these positions, the residual (*R*) dropped from 0.065 to 0.043.

A final difference Fourier after the full-matrix refinement was featureless, the largest peak being 0.4 e Å^{-3}. There was no evidence of hydrogens associated with the hexane. It should be noted that the solvent is poorly defined and the bond distances and angles are quite poor.*

W_2(S-mes)$_6$. A suitable crystal was cleaved to form a nearly equidimensional fragment which was transferred to the goniostat using standard inert atmosphere handling techniques. A systematic search of a limited hemisphere of reciprocal space revealed no systematic absences or symmetry, leading to the assignment of a triclinic space group. Subsequent solution and refinement of the structure (as well as statistical tests) confirmed the centrosymmetric space group $P\bar{1}$.

The location of the unique tungsten atom was achieved by direct methods and all remaining non-hydrogen atoms were located in a difference Fourier phased on the metal parameters. Hydrogen atoms were visible in a difference map phased on the non-hydrogens, and were included in the final stages of refinement (anisotropic thermal parameters for W, S, C; isotropic parameters for H).

* Final atomic positional and thermal parameters and F_o/F_c values have been deposited as supplementary material with the Editor, from whom copies are available on request. Atomic coordinates have also been submitted to the Cambridge Crystallographic Data Centre. The complete structural reports for Mo_2(S-mes)$_6$ and W_2(S-mes)$_6$, MSC Report Nos. 83046 and 84011, are available in microfiche form only from the Indiana University Library at a cost of $2.50 per report.

Table 3. Summary of crystal data

	I	II
Empirical formula	$Mo_2S_6C_{54}H_{66}\cdot xC_6H_{14}$	$W_2S_6C_{54}H_{66}$
Colour of crystal	Red	Red
Crystal dimensions (mm)	0.25 × 0.24 × 0.22	0.05 × 0.04 × 0.04
Space group	$R\bar{3}$	$P\bar{1}$
Cell dimensions		
Temperature (°C)	−162	−156
a (Å)	15.361(10)	11.019(9)
b (Å)	15.361(10)	11.692(10)
c (Å)	20.929(13)	11.559(10)
α (°)		62.63(4)
β (°)		97.03(4)
γ (°)	120	85.32(5)
Z (molecules/cell)	3	1
Volume (Å^3)	4276.79	1296.39
Calculated density (g cm^{-3})	1.381	1.633
Wavelength (Å)	0.71069	0.71069
Molecular weight	1185.53	1275.18
Linear absorption coefficient (cm^{-1})	6.762	47.950
Detector-to-sample distance (cm)	22.5	22.5
Sample-to-source distance (cm)	23.5	23.5
Average omega scan width at half-height	0.25	0.25
Scan speed (° min^{-1})	4.0	4.0
Scan width (° + dispersion)	2.0	2.0
Individual background (s)	10	10
Aperture size (mm)	3.0 × 4.0	3.0 × 4.0
2θ range (°)	6–45	6–50
Total number of reflections collected	3769	4693
Number of unique intensities	1259	4219
Number with $F > 0.0$	1195	
Number with $F > \sigma(F)$	1136	
Number with $F > 2.33\sigma(F)$	1083	
Number with $F > 3.00\sigma(F)$		3795
$R(F)$	0.0346	0.0620
$R_w(F)$	0.0295	0.0594
Goodness of fit for the last cycle	2.023	1.109
Maximum δ/σ for the last cycle	0.05	0.05

A final difference Fourier was featureless, the largest peak being 0.58 e Å^{-3}. Psi scans were essentially flat, so no absorption correction was performed.

Acknowledgements—We thank the National Science Foundation and the Wrubel Computing Center for support.

REFERENCES

1. F. Huq, W. Mowat, A. Shortland, A. C. Skapski and G. Wilkinson, *J. Chem. Soc., Chem. Commun.* 1971, 1079.
2. M. H. Chisholm, F. A. Cotton, M. W. Extine and B. R. Stults, *Inorg. Chem.* 1976, **15**, 2252.
3. M. H. Chisholm, F. A. Cotton, B. A. Frenz, W. W. Reichert, L. W. Shive and B. R. Stults, *J. Am. Chem. Soc.* 1976, **98**, 4469.
4. M. H. Chisholm, F. A. Cotton, M. W. Extine and B. R. Stults, *J. Am. Chem. Soc.* 1976, **98**, 4477.
5. M. H. Chisholm, F. A. Cotton, C. A. Murillo and W. W. Reichert, *Inorg. Chem.* 1977, **16**, 1801.
6. M. Akiyama, M. H. Chisholm, F. A. Cotton, M. W. Extine, D. A. Haitko, D. Little and P. E. Fanwick, *Inorg. Chem.* 1979, **18**, 2266.
7. M. H. Chisholm, J. F. Corning and J. C. Huffman, *Inorg. Chem.* 1982, **21**, 286.
8. M. H. Chisholm, J. F. Corning and J. C. Huffman, *Inorg. Chem.* 1983, **22**, 38.
9. M. H. Chisholm, J. F. Corning and J. C. Huffman, *Inorg. Chem.* 1984, **23**, 754.
10. A preliminary report noting the formation of $Mo_2(S\text{-}mes)_6$ has been published: M. H. Chisholm, J. F.

Corning and J. C. Huffman, *J. Am. Chem. Soc.* 1983, **104**, 5924.
11. MSC Report No. 84006. Available upon request in microfiche form from the Indiana University Library at $2.50 per copy.
12. S. A. Koch, R. Fikar, M. Millar and J. F. Lee, *Inorg. Chem.* 1982, **21**, 4105.
13. S. A. Koch and M. Millar, *J. Am. Chem. Soc.* 1983, **105**, 3362.
14. J. R. Dilworth, J. Hutchinson and J. A. Zubieta, *J. Chem. Soc., Chem. Commun.* 1983, 1034.
15. M. H. Chisholm, *Polyhedron* 1983, **2**, 681.
16. M. H. Chisholm, K. Folting, J. C. Huffman and C. C. Kirkpatrick, *Inorg. Chem.* 1984, **23**, 1037.

Polyhedron Vol. 4, No. 3, pp. 391–394, 1985
Printed in Great Britain

0277–5387/85 $3.00 + .00
© 1985 Pergamon Press Ltd

EVIDENCE FOR THE PREDOMINANCE OF TRIGONAL PYRAMIDAL ENVIRONMENTS IN TIN(II) CHEMISTRY: THE CRYSTAL STRUCTURE OF POTASSIUM (HYDROGEN(BISMALEATO))STANNATE(II)

JOHN D. DONALDSON, SUSAN M. GRIMES* and ANNA NICOLAIDES
Department of Chemistry, The City University, Northampton Square, London EC1V 0HB, U.K.

and

PETER J. SMITH
International Tin Research Institute, Fraser Road, Greenford, Middlesex, U.K.

(*Received* 3 *January* 1984; *accepted* 16 *July* 1984)

Abstract—The crystal structure of potassium (hydrogen(bismaleato))stannate(II) is reported. It has unit cell data $a = 7.361(12)$, $b = 12.305(3)$, $c = 7.246(8)$ Å, $\alpha = 97.02(6)°$, $\beta = 109.83(28)°$, $\gamma = 87.48(7)°$, $U = 612.77$ Å^3, $Z = 2$, $D_c = 2.096$ g cm^{-3}, $D_m = 2.093$ g cm^{-3} and triclinic space group $P\bar{1}$. The structure consists of layers of discrete $[Sn(CHCO_2:CHCO_2)(CHCO_2:CHCO_2H)]_2^{2-}$ moieties with potassium ions located in holes between the layers. In the discrete unit are two different maleate groups, an anisobidentate maleate ligand and a terminal unidentate monoprotomaleate ligand. The tin atom lies in a trigonal pyramidal environment with three Sn—O distances, to the maleate and monoprotomaleate ligands, of 2.199 and 2.212 Å respectively. These bonds lengths are consistent with the ^{119}Sn Mössbauer data. The preference for tin to exist in a trigonal pyramidal environment, even in the presence of potential chelating ligands is clearly shown in the structure of this complex tin(II) malcate.

Over the past few years the crystal structures of a number of tin(II) derivatives of dicarboxylic acids have been determined. Tin(II) oxalate,[1] tin(II) maleate monohydrate[2] and tin(II) malonate[3] contain tin atoms in distorted four pyramidal environments with two short and two long bonds. This is the expected environment[4] if the dicarboxylate groups are chelating.

Formation of dicarboxylatostannate(II) complexes would be expected to result in a shortening of the average Sn—O bond from those of the parent tin(II) dicarboxylates while retaining the distorted four pyramidal environment. This is certainly the case in the oxalate derivatives, $Na_2[Sn(C_2O_4)_2]$[5] and $K_2Sn(C_2O_4)_2 \cdot H_2O$[6], where the bond lengths are 2.25, 2.25, 2.36, 2.36 and 2.14, 2.20, 2.36, 2.30 Å respectively, in comparison with the bond lengths in tin(II) oxalate of 2.23, 2.23, 2.39 and 2.39 Å.

We have recently shown[7] that in the formation of dipotassium trismalonatodistannate(II) monohydrate from tin(II) malonate, the distorted four pyramidal environment for tin in the parent compound is replaced by a trigonal pyramidal arrangement of nearest neighbour atoms. Unlike the oxalate ions which chelate tin(II) to give the metal distorted four pyramidal environments, the malonate groups, although bidentate, form bridges between different tin atoms. This gives rise to an extended polymeric anionic system $Sn_2[(CH_2C_2O_4)_3]_n^{2n-}$, and not to discrete $Sn(RC_2O_4)_2^{2-}$ ions as found in $Na_2[Sn(C_2O_4)_2]$.

We now report on the crystal structure of a different type of dicarboxylatostannate(II) complex, potassium (hydrogen(bismaleato))stannate-(II), in which one of the ligand maleato groups is monoprotonated.

* Author to whom correspondence should be addressed.

EXPERIMENTAL

Preparation

Blue-black stannous oxide (0.02 mol, 2.7 g) was refluxed for 1.25 h under an oxygen-free nitrogen atmosphere in a 20% (w/v) aqueous maleic acid solution (50 cm^3) to obtain a clear solution. Potassium carbonate (0.02 mol, 2.7 g) was then added and the mixture refluxed for a further 30 min. The resulting solution was filtered hot and cooled to crystallise out the white product. The crystals were washed with petroleum ether (b.p. 40–60°C) and dried *in vacuo* over pellets of potassium hydroxide. Found: Sn, 31.0; C, 24.8; H, 1.30%. $C_8H_5O_8KSn$ requires: Sn, 30.68; C, 24.84; H, 1.30%.

X-ray crystal structure

Crystal data. $C_8H_5O_8KSn$, $M = 386.9$, space group $P\bar{1}$, $a = 7.361(12)$, $b = 12.305(3)$, $c = 7.246(8)$ Å, $\alpha = 97.02(6)°$, $\beta = 109.83(28)°$, $\gamma = 87.48(7)°$, $U = 612.77$ Å^3, $Z = 2$, $D_c = 2.096$ g cm^{-3}, $D_m = 2.093$ g cm^{-3}, $F(000) = 372$. μ(Mo-K_α) = 22.63 cm^{-1}, $\lambda = 0.70926$ Å, $R = 0.022$, $R_w = 0.024$ for 2051 unique intensity data.

The X-ray data were collected at Queen Mary College, London, as previously described.[7] The position of the tin atom was determined from a Patterson Synthesis and refined by full-matrix least squares. With phasing based on this Sn position, the positions of the K, O, and C atoms were obtained from Fourier syntheses. Anisotropic thermal parameters were assigned to all non-hydrogen atoms. The hydrogen atoms were located but their positions were not refined. All crystallographic calculations were performed using SHELX-76[8] and the diagrams were drawn by CELLPLOT,[9] on a CDC 7600 computer. Final atomic coordinates, bond lengths and angles, together with tables of F_o/F_c have been deposited as supplementary material with the Editor, from whom copies are available on request.

^{119}Sn *Mössbauer spectra*

The Mössbauer spectrum of the material was recorded at liquid nitrogen temperature using a $BaSnO_3$ source by methods described previously.[10]

RESULTS AND DISCUSSION

The structure of potassium (hydrogen-(bismaleato))stannate(II) consists of layers of discrete

$$[Sn(CHCO_2:CHCO_2)(CHCO_2:CHCO_2H)]_2^{2-}$$

moieties with potassium ions located in holes between the layers (Fig. 1).

Each tin atom is bonded to two different types of maleate group, one of which is a bridging bidentate ligand and the other a unidentate monoprotomaleato group. Both maleate groups bridge the two tin atoms in the cell forming a 14-membered ring system with two tin-to-maleate oxygen bonds at each Sn (Fig. 2). A trigonal pyramidal coordination about each Sn is completed by tin-to-monoprotomaleate oxygen atoms. The Sn—O distances to the maleate and monoprotomaleate

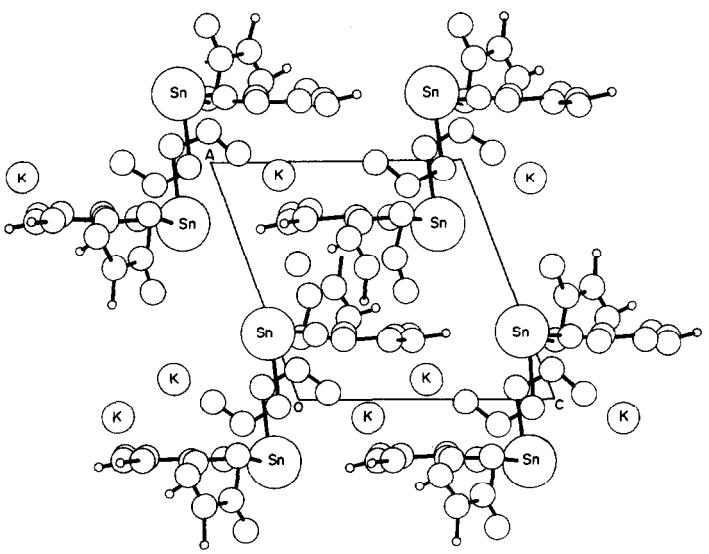


Fig. 1. Projection of the unit cell along the *y* axis.

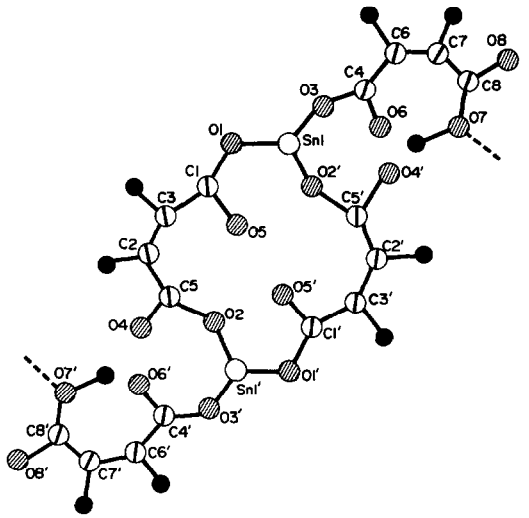


Fig. 2. Diagram showing the 14-membered ring system in $KSn(CHCO_2:CHCO_2)(CHCO_2:CHCO_2H)$.

ligands are 2.199 and 2.212 Å respectively. Three longer contacts to ligand oxygen atoms at 2.642, 2.866 and 2.931 Å complete a distorted octahedral arrangement around the tin atoms (Table 1).

The potassium atom is surrounded by six oxygen atoms with K—O distances of 2.644, 2.728, 2.752, 2.799, 2.932 and 3.052 Å.

Both the protonated and non-protonated maleate groups are structurally very similar. The bond distances and angles are consistent with a regular array of sp^2 hybridised C atoms. The existence of both inter- and intra-molecular hydrogen bonding creates an apparent polymeric chain through the lattice, with discrete anionic

$$[Sn(CHCO_2:CHCO_2)(CHCO_2:CHCO_2H)]_2^{2-}$$

unit being hydrogen-bonded to the next through the H atoms of the terminal maleate groups.

Dipotassium trismalonatodistannate(II) monohydrate was the first example of a complex dicarboxylatostannate(II) derivative shown[7] to have tin in a trigonal pyramidal coordination, in spite of its parent compound, $Sn(CH_2C_2O_4)$, having tin in a four pyramidal environment. This trigonal pyramidal arrangement about the tin in $K_2Sn_2(CH_2C_2O_4)_3 \cdot H_2O$ arises because all three malonate groups must act as bridging bidentate ligands, since the Sn : ligand ratio is 2 : 3.

The tin(II) maleate complex described here also has a trigonal pyramidal arrangement of nearest-neighbour oxygens about the tin atom, although in its parent compound, $Sn(C_4H_2O_4) \cdot H_2O$, the tin atoms lie in four pyramidal sites. In potassium [hydrogen(bismaleato)]stannate(II), however, the trigonal pyramidal arrangement about each tin atom arises, not because of a low tin : dicarboxylate ligand ratio, but, because of the presence of two anisobidentate maleate moieties and one monodentate hydrogen maleate group.

Table 1. Bond lengths (Å) and angles (°) (ESDs in parentheses)

Bond length		Bond angle	
		Tin coordination	
Sn—O(1)	2.199(2)	O(1)—Sn—O(2)	79.9(1)
Sn—O(2)	2.199(2)	O(1)—Sn—O(3)	79.9(1)
Sn—O(3)	2.212(2)	O(2)—Sn—O(3)	80.9(1)
Sn—O(4)	2.866		
Sn—O(5)	2.642		
Sn—O(6)	2.931		
		Potassium coordination	
K—O(1)	3.052		
K—O(2)	2.752		
K—O(3)	2.932		
K—O(4)	2.799		
K—O(5)	2.644		
K—O(6)	2.728		
K...H(1)	3.574		
K...H(2)	3.829		
		Maleate coordination ($CHCO_2:CHCO_2$)	
C(1)—O(1)	1.292(3)	C(1)—O(1)—Sn	102.8(1)
C(1)—O(5)	1.246(3)	C(5)—O(2)—Sn	108.3(1)
C(5)—O(4)	1.236(3)	O(1)—C(1)—O(5)	120.6(2)
C(5)—O(2)	1.284(3)	O(2)—C(1)—O(4)	123.5(2)
		Maleate coordination ($CHCO_2:CHCO_2H$)	
C(4)—O(3)	1.268(3)	Sn—O(2)—O(4)	112.0(2)
C(4)—O(6)	1.240(4)	O(3)—C(4)—O(6)	122.0(2)

It is well known[4] that the most common tin(II) environment is that of a trigonal pyramid in which the tin atom is surrounded closely by three near neighbour ligand atoms, forming three essentially covalent Sn—L bonds. Three more distant ligand atoms with Sn—L bond lengths approaching the sum of the Sn—L van der Waal's radii, complete a distorted octahedral coordination about the tin. This preference for tin to exist in the trigonal pyramidal environment is clearly demonstrated in the structures of the dipotassium trismalonatodistannate(II) monohydrate and potassium (hydrogen(bismaleato))stannate(II) complexes.

The ^{119}Sn Mössbauer parameters for the complex tin(II) maleate ($\delta = 3.22$ mm s^{-1}, $\Delta = 1.65$ mm s^{-1}) show a decrease in chemical isomer shift in going from its parent tin(II) maleate monohydrate ($\delta = 3.31$ mm s^{-1}, $\Delta = 1.76$ mm s^{-1}) to the complex,

Table 2. ^{119}Sn Mössbauer data

Compound	Average Sn—L bond length (Å)	δ* (mm s^{-1})
$Ca[Sn(CH_3CO_2)_3]_2$	2.14	2.90
$KSn(CH_2ClCO_2)_3$	2.16	2.96
$KSn(HCO_2)_3$	2.16	3.08
$K_2Sn_2(CH_2C_2O_4)_3 \cdot H_2O$	2.19	3.15
$KSn(CHCO_2 : CHCO_2)$-$(CHCO_2 : CHCO_2H)$	2.20	3.22
$SnSO_4$	2.26	3.95

* Chemical shift relative to $BaSnO_3$.

which is the expected result for the formation of ligand stannates(II). The data are also consistent with the relationship between chemical shift and tin-to-ligand bond lengths (Table 2), in that the increase in shift from 3.15 to 3.22 mm s^{-1} for $K_2Sn_2(CH_2C_2O_4)_3 \cdot H_2O$ and $KSn(CHCO_2 : CHCO_2)(CHCO_2 : CHCO_2H)$ respectively, parallels the increase in average Sn—O bond length from 2.19 Å for the malonate complex to 2.20 Å for the maleate derivative.

Acknowledgements—We thank the S.E.R.C. and the International Tin Research Institute for a CASE studentship (to A.N.).

REFERENCES

1. A. D. Christie, R. A. Howie and W. Moser, *Inorg. Chim. Acta* 1979, **36**, L447; A. Gleiges and J. Galy, *J. Solid State Chem.* 1979, **30**, 23.
2. J. C. Dewan, J. Silver, R. H. Andrews, J. D. Donaldson and D. R. Laughlin, *J. Chem. Soc., Dalton Trans.* 1977, 368.
3. Z. Arifin, J. D. Donaldson, S. M. Grimes and A. Nicolaides, to be published.
4. J. D. Donaldson and S. M. Grimes, *Rev. Silicon, Germanium, Tin Lead Compd.*, in press.
5. J. D. Donaldson, M. T. Donoghue and C. H. Smith, *Acta Cryst.* 1976, **B32**, 2098.
6. R. M. A. Grimsey, Ph.D. Thesis, London (1980); A. D. Christie, R. A. Howie and W. Moser, *Inorg. Chim. Acta* 1979, **36**, L447.
7. Z. Arifin, E. Filmore, J. D. Donaldson and S. M. Grimes, *J. Chem. Soc., Dalton Trans.* 1984, 965.
8. G. M. Sheldrick, *Program for Crystal Structure Determination.* University of Cambridge (1975).
9. D. C. Puxley and J. D. Donaldson, *Acta Cryst.* 1973, **A29**, 91.
10. J. D. Donaldson and B. J. Senior, *J. Chem. Soc.* (*A*). 1966, 1769.

Polyhedron Vol. 4, No. 3, pp. 395–399, 1985
Printed in Great Britain

0277–5387/85 $3.00 + .00
Pergamon Press Ltd

FORMATION OF Cu(II)–DICYANDIAMIDE COMPLEXES IN NEUTRAL AND ACIDIC AQUEOUS SOLUTIONS

URSZULA KOŁODZIEJ* and JAN PRZYŁUSKI

Department of Solid State Technology, Chemical Faculty, Technical University of Warsaw, 00-664 Warszawa, ul. Noakowskiego 3, Poland

(*Received* 9 *March* 1984; *accepted* 16 *July* 1984)

Abstract—This work presents spectroscopic studies and electrochemical characterization of Cu(II)–dicyandiamide (DCDA) complex formation. The range of conditions leading to the precipitation of the complex is significantly larger than that presented in the literature. In all cases the stoichiometry of the compound is: $[Cu(DCDA)_2(SO_4)(H_2O)_5]$. The spectroscopic data suggest that DCDA is a monodentate ligand forming a bond with Cu^{2+} via the nitryl nitrogen. Electroreduction of this complex is a two-step process occurring through a Cu(I)–DCDA intermediate.

The formation of cupric complexes of dicyandiamide (DCDA) was first reported in 1906 and its stoichiometry was established as: $[CuSO_4(DCDA)_2(H_2O)_4]$.[1] In subsequent years a significant revival of interest in the chemistry of these complexes took place due to their catalytic role in the reaction of alcohol addition to the nitryl group of DCDA.[2,3]

The complex studied previously was precipitated from the saturated aqueous solution of $CuSO_4 \cdot 5H_2O$ and DCDA at 273 K and exhibited the formula: $[Cu(DCDA)_2SO_4]$ as determined by elemental analysis. Its structure and bonding were not studied and the only structural information presented was limited to the observation of a 2222 cm^{-1} $\nu(C^1{\equiv}N^3)$ doublet in the IR spectra of the compound. Since this transition is characteristic of DCDA it was concluded that the nitryl group of dicyandiamide does not participate in the complex formation and does not undergo hydrolysis under given conditions.

Cu(II), Ni(II) and Zn(II) complexes of DCDA were prepared in ethanol solutions and have a general formula: $MX_2(DCDA)_2$ or $MX_2(DCDA)_4$, (where X = Cl, Br, NO_3, NCS).[4] In the case of X = ClO_4 the formula $[Cu(DCDA)_4(ClO_4)_2]$ was proposed with ClO_4 as an outershell anion. As determined by IR spectroscopy the 3350–3000 cm^{-1} $\nu(N^{5,6}{-}H)$ bond remains unchanged upon complex formation, but $\gamma(C^1{\equiv}N^3)$ and $\nu(C^1{-}N^4)$ are shifted towards higher and lower wavenumbers respectively. Based on the results presented above it was concluded that the complex is formed via the N^4 nitrogen of the guanidine group, i.e. DCDA is a monodentate ligand. This conclusion can be additionally supported by the existence of the higher local dipole moment at this nitrogen atom,[5] i.e. the guanidine nitrogen should be the most susceptible to form bonds with the cupric ion.

In general in cupric complexes DCDA can act as a ligand in the presence of other ligands of various types. The following complexes have been reported:[6,7] 1-(2-aminoethyl)biguanide(dicyandiamide)Cu(II) sulphate monohydrate:

$$[Cu(C_4H_{12}N_6)(C_2H_4N_4)]SO_4 \cdot H_2O$$

and dichlorodiaquobis(dicyandiamide)Cu(II):

$$[Cu(H_2O)_2(C_2H_4N_4)_2Cl_2].$$

Structural studies of the above complexes showed octahedral coordination of the cupric ion in both complexes. In the former both nitryl nitrogen and the guanidine nitrogen are coordinated to the copper. In the latter case DCDA is a monodentate ligand forming a coordination bond with Cu^{2+} via the N^3 nitrogen of the nitryl group. Our studies of Cu^{2+} electroreduction in the presence of selected derivatives of guanidine led us to study Cu(II)–DCDA complex formation. To date no systematic spectroscopic studies and no electrochemical characterization of these compounds have been presented in the literature.

* Author to whom correspondence should be addressed.

Table 1. Elemental analysis of $[Cu(DCDA)_2(SO_4)(H_2O)_5]$ complex

	Cu	H	C	N	S	SO_4
Calc.	15.2	4.35	11.49	26.82	7.67	22.98
Exp.	15.2	4.28	11.51	25.41	7.97	24.5

EXPERIMENTAL AND RESULTS

Preparation of complex

Cupric complexes of DCDA were precipitated at room temperature by mixing saturated aqueous solutions of $CuSO_4 \cdot 5H_2O$ and DCDA. In some cases the complexes were precipitated from 0.4 *M* H_2SO_4 or 0.4 *M* K_2SO_4 aqueous solution. The light blue precipitates obtained were repeatedly washed with water and then dried at 323 K in the air. In all experiments reagents of analytical purity and redistilled water were used.

Elemental analysis

C, H, N were determined by combustion analysis using a Perkin–Elmer Microanalyser Model 240. Cupric and additionally cuprous ions were analysed by spectrophotometry. Classical gravimetric analysis was used for sulphate determination. In no samples were cuprous ions detected. In Table 1 results of elemental analysis are presented. The following stoichiometry of the complex was assumed for the calculations: $[Cu(DCDA)_2(SO_4)(H_2O)_5]$.

UV spectroscopy studies

UV spectroscopic studies were carried out for the neutral aqueous and acidic aqueous solutions of Cu–DCDA complexes. A UV–VIS (Karl-Zeiss Jena) spectrometer was used in all experiments. The solutions were loaded into rectangular quartz cuvette of the inner thickness of 1 cm. The results are summarised in Table 2 and Figs. 1–3.

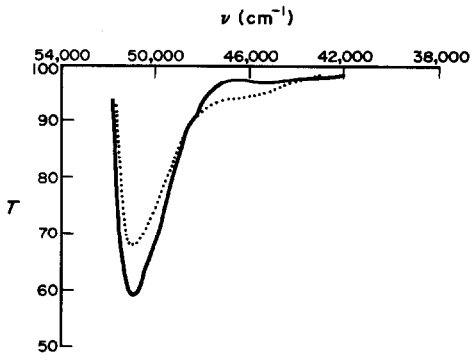


Fig. 1. UV spectrum of DCDA (2×10^{-5} *M* in 0.4 *M* H_2SO_4——) and Cu–DCDA complex precipitated from 0.4 *M* H_2SO_4 (1×10^{-5} *M* in 0.4 *M* H_2SO_4···).

Since guanylurea is the product of DCDA hydrolysis its spectrum was studied for comparison

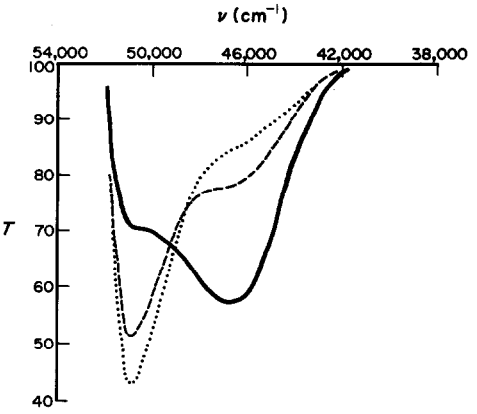


Fig. 2. UV spectrum of Cu–DCDA complex precipitated from 0.4 *M* H_2SO_4 (1×10^5 *M* in 0.4 *M* H_2SO_4——), the same solution after 7 days (– – –), after 12 days (···).

Table 2. UV optical parameters of pure and complexed DCDA

Substance	Medium	λ_{max} (nm)	log ε_{max}	Reference
DCDA	Aqueous solution	216		8
		215		9
		215	4.13	
		192	3.90	10
		215.5	4.1	This work
		191	3.8	
	0.4 *M* H_2SO_4	215*	4.1	This work
Cu–DCDA complex	Aqueous solution	216	4.4	This work
(from aqueous solution)	0.4 *M* H_2SO_4	216	4.4	This work
Guanylurea	0.4 *M* H_2SO_4	197	4.4	This work

* Maximum too broad to be determined precisely.

Table 3. IR spectroscopic parameters of DCDA and Cu–DCDA systems

Substance	$H_2N^{5,6}$	$N^3{\equiv}C^1{-}N^4{=}$	$N^{5,6}{-}C^2{=}N^4$	Other
DCDA (solid film[11])	3350, 3320	2200, 2160	1590	3400, 2880
	3170, 3140	1250	1500	2470, 2270
	1660, 1640	528	930	2110, 1570
	1080		720	
DCDA (KBr)	3380, 3330	2210, 2160	1570	3420, 2880
This work	3180, 3140	1255	1505	2740, 2105
	1660, 1640	555	930	670, 470
	1090		720	
Cu–DCDA	3420, 3320	2250, 2210	1570, 1560	975, 675
(from aqueous	3220, 3160	1300	1540	610, 470
solution)	1670, 1650	550	930	1110, 1040
Cu–DCDA	3420, 3330	2260, 2210	1570, 1560	1720, 1710
(from 0.4 *M* H_2SO_4)	3220, 3160	1300	1535	1350, 980
	1675, 1650	550	930	675, 620, 450
				1110, 1040
Cu–DCDA	3420, 3320	2250, 2210	1570, 1560	975, 675
(from 0.4 *M* K_2SO_4)	3320, 3160	1300	1530	610
	1670, 1650	550	930	1110, 1050

in order to exclude its presence in the reaction products. The appearance of a maximum at $\lambda =$ 197 nm was taken as a criterion for the hydrolysis reaction occurrence simultaneously with the complex formation reaction.

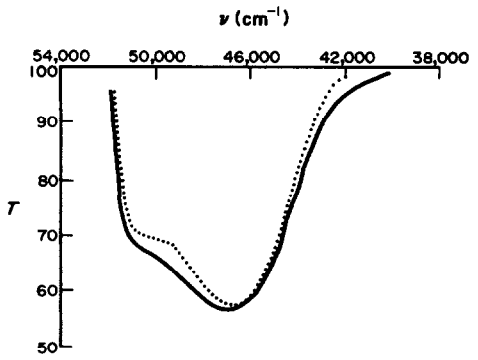


Fig. 3. UV spectrum of guanylurea (1×10^{-5} *M* in 0.4 *M* H_2SO_4——) and DCDA solution (1×10^{-5} *M* in 0.4 *M* H_2SO_4···) after 10 days.

IR spectroscopy studies

A Perkin–Elmer IR Spectrometer was used to examine IR spectra of pure DCDA and Cu–DCDA complexes. KBr pressed pellets method was applied in all cases. Typical spectra, obtained from the acidic solution, are depicted in Fig. 4. All results of IR studies are summarised in Table 3.

Conductivity studies

Specific conductivities of 0.01 *M* aqueous solutions of Cu–DCDA complexes were measured at 291 K using O.K. 102/1 Conductivity Meter (Radelkis). As the reference, conductivities of identical $CuSO_4 \cdot 5H_2O$ and pure DCDA solutions were measured. The results are listed in Table 4.

Polarographic studies

Square-wave Polarograph type OH104 (Radelkis) in two electrode configuration with mercury

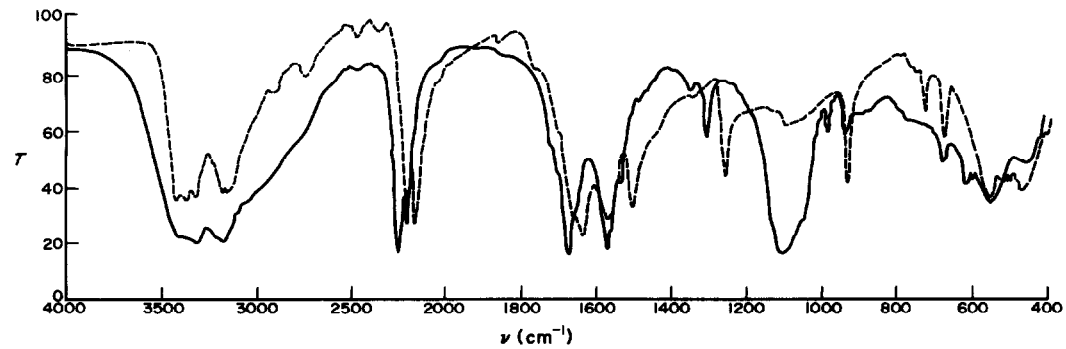


Fig. 4. IR spectrum of DCDA (– – –) and Cu–DCDA complex precipitated from 0.4 *M* H_2SO_4 (——).

Table 4. Results of specific conductivity measurements of DCDA, $CuSO_4 \cdot 5H_2O$ and cupric complex of DCDA

Solution	Specific conductivity ($10^3\ \Omega^{-1}\ cm^{-1}$)
Cu–DCDA (from aqueous solution)	1.33
Cu–DCDA (from 0.4 *M* H_2SO_4)	1.47
Cu–DCDA (from 0.4 *M* K_2SO_4)	1.22
DCDA	4.0×10^{-3}
$CuSO_4 \cdot 5H_2O$	1.16

dropping electrode and mercury pool as reference electrode was applied to study polarographic behaviour of Cu–DCDA complex. Constant concentration of cupric ions equal to 10^{-5} *M* and varying concentrations of DCDA were employed in the polarographic investigations. 0.4 *M* H_2SO_4 was used as supporting electrolyte. All measurements were performed at 293 K. The list of potentials, at which reduction peaks of the complexed copper ions appear, is presented in Table 5.

DISCUSSION AND CONCLUSIONS

DCDA can form cupric complexes in neutral as well as in acidic aqueous solutions. In both cases identical blue powder of the same stoichiometry are obtained: $[Cu(DCDA)_2(SO_4)(H_2O)_5]$ as shown by elemental analysis. It can be concluded therefore that the range of conditions leading to the precipitation of the complex is significantly larger than that presented previously.[2] This conclusion is highly consistent with the spectroscopic data showing that:

(1) Spectra of the complexes prepared under varying conditions are identical.

(2) Extinction coefficient ratio for "free" and "complexed" DCDA indicates the existence of two DCDA molecules per cupric cation in the complex.

(3) The main changes occurring in the IR spectrum upon coordination can be characterized as follows: the band characteristic of $N^4—C^1{\equiv}N^3$ skeleton observed at 1255 cm^{-1} in "free" DCDA is shifted to 1300 cm^{-1}. On the other hand the band characteristic of $N^{5,6}—C^2{=}N^4$ skeleton is shifted from 1570 cm^{-1} to 1530 cm^{-1}. Additionally the change in the positions of the doublet associated with $C^1{\equiv}N^3$ from 2210, 2160 to 2250, 2210 cm^{-1} can be observed. Finally significant broadening of the bands ascribed to ammine groups is clearly seen. From the above observations it is concluded that DCDA is a monodentate ligand being coordinated to copper via the N^4 nitrogen. This conclusion is consistent with the experimental facts presented before.[5]

The magnitude and direction of the shifts observed in the positions of selected IR bands are in good agreement with the values previously reported.[4] The position of the doublet characteristic of the nitryl group[2] is very similar to the one measured in this work (Fig. 4).

However the conclusions drawn in both papers[2,4] do not necessarily need to be correct especially in view of the fact that the vibrations of $C^1{\equiv}N^3$ group are shifted towards higher wavelength. If a metal acts as a Lewis acid and the coordination of DCDA via the lone pair of the N^3 nitrogen will result in an increase in the frequency of the corresponding IR band.[12] It is therefore probable that DCDA forms a covalent bond with Cu(II) via the N^3 nitrogen.

(4) In UV maxima of the absorption peaks in the "free' and "complexed" DCDA are identical.

(5) The shift of the absorption peak from 216 to 197 nm can be treated as a qualitative test of the hydrolysis leading to the formation of gunylurea.

(6) Existence of the 1740 cm^{-1} vibration mode (Fig. 4) in the IR spectrum additionally confirms the possibility of the hydrolysis of DCDA in acidic solutions. The above-mentioned absorption is characteristic of the carbonyl group of guanylurea.

(7) Polarographic studies of the Cu–DCDA complex led to the determination of its stoichiometry and the mechanism of the reaction occurring at the electrode. In a wide range of DCDA concentrations two one-electron peaks of the reduction could be

Table 5. Polarographic analysis data of Cu–DCDA complex

$\log c_{DCDA}$	−4.0	−3.301	−3.0	−2.301	−2.0	−1.301
E_pI (V)	−0.273	−0.225	−0.207	−0.110	−0.075	+0.030
E_pII (V)	−0.403	−0.409	−0.500	−0.567	−0.577	−0.609

$E_p(c_{DCDA} = 0) = -0.345$ V.
Potential sweep rate 2 mV/s.
Amplitude of alternating voltage 20 mV.
Life-time of a drop 2.5 s.

observed. The potentials at which the above peaks occurred depended linearly on the ligand concentration. The first peak is associated with the Cu(II) + e → Cu(I) reduction process. Its shape and measured half-width seem to suggest that the reduction process is irreversible. Its potential moves towards more positive values if the concentration of the ligand increases. The behaviour of the second peak, corresponding to the second stage of reduction, Cu(I) + e → Cu, is different, its potential moves towards more negative values upon the increase of the ligand concentration. The process is quasi-reversible.

The above collected results seem to indicate that the reduction of Cu(II) in the presence of DCDA can be characterized by the following stages:

(a) Chemical stage—the dissociation of the complex:

$$Cu(DCDA)_2^{2+} \rightarrow Cu^{2+} + 2DCDA.$$

Since in 0.4 *M* H_2SO_4 solution the Cu(II) and DCDA coexist in a form of a well-defined complex and in the polarographic process the simple Cu(II) ion is being reduced, the dissociation of the complex must precede the electrochemical process.

(b) Stage of charge-transfer E1:

$$Cu^{2+} + e \rightarrow Cu^{+}.$$

(c) Stage of the formation of $Cu(DCDA)_2^+$ complex:

$$Cu^{+} + 2DCDA \rightarrow Cu(DCDA)_2^{+}.$$

Since in the second stage of the electroreduction process the cuprous ion, not in the simple but in the complex form, is being reduced, the formation of this complex must follow the stage E1. It is reasonable to believe that this formation occurs at the electrode surface and the adsorbed DCDA molecules participate in this process.

(d) Stage of charge-transfer E2:

$$Cu(DCDA)_2^{+} + e \rightarrow Cu(Hg) + 2DCDA.$$

The stoichiometry of the Cu(I)–DCDA complex and its stability constant $\ln \beta_{CuI} = 6.9 \pm 0.3$ were derived from the relationships described in the literature.[13] In the calculations the experimental values of the potential shifts were assumed to be equivalent to the values of the reversible potentials of the half-wave in accordance with the arguments presented elsewhere.[14]

Acknowledgement—This work was financially supported by the MRI-11 grant of the Ministry of Science, Higher Education and Technology.

REFERENCES

1. H. Grossman and B. Shück, *Ber.* 1906, **39**, 3591.
2. W. A. Baker, Jr and M. Daniels, *J. Inorg. Nucl. Chem.* 1963, **25**, 1194.
3. K. Kawano and K. Odo, *Chem. Abstr.* 1963, **58**, 12150c.
4. P. K. Pando, B. S. Miskra and B. K. Moapatra, *J. Inorg. Nucl. Chem.* 1980, **42**, 497.
5. F. L. Hirshfeld and H. Hope, *Acta Cryst.* 1980, **B36**, 406.
6. L. Coghi, A. Mangia, M. Nardelli, G. Pelizzi and L. Sozzi, *J. Chem. Soc., Chem. Commun.* 1968, 1475.
7. V. Chiesi, L. Coghi, A. Mangia, M. Nardelli and G. Pelizzi, *Acta Cryst.* 1971, **B27**, 192.
8. I. Szilagyi, T. Valayi-Nagy and T. Keresztes, *Nature (London)* 1962, **196**, 376.
9. A. Pawlik, *Naturwissenschaften* 1959, **46**, 203.
10. A. I. Finkelstein, B. I. Sukhorukov and Yu. I. Mushkin, *Zh. Fiz. Khim.* 1963, **37**, 290.
11. W. J. Jones and W. J. Orville-Thomas, *Trans. Faraday Soc.* 1959, **55**, 193.
12. R. S. Drago, *Physical Methods in Chemistry*, p. 176. W. B. Saunders, Philadelphia (1977).
13. M. von Stackelberg and M. von Freyhold, *Z. Elektrochem.* 1940, **46**, 120.
14. A. M. Bond, *J. Electroanal. Chem.* 1970, **28**, 433.

Polyhedron Vol. 4, No. 3, pp. 401–407, 1985
Printed in Great Britain

0277-5387/85 $3.00 + .00
© 1985 Pergamon Press Ltd

MAGNETIC AND SPECTRAL STUDIES ON *N*-(THIOPHENE-2-CARBOXAMIDO)SALICYLALDIMINE COMPLEXES OF SOME BIVALENT 3*d* METAL IONS

B. SINGH, * R. N. SINGH and R. C. AGGARWAL
Department of Chemistry, Banaras Hindu University, Varanasi 221 005, India

(*Received* 16 *February* 1984; *accepted after revision* 16 *July* 1984)

Abstract—Metal(II) complexes of *N*-(thiophene-2-carboxamido)salicylaldimine (H_2TCS) of types $M(H_2TCS)_2Cl_2$ [M = Ni, Cu and Zn], M(HTCS)Cl [M = Co, Ni and Cu], $M(HTCS)_2$ [M = Mn, Fe, Co, Ni, Cu and Zn], $M(TCS)\cdot xH_2O$ [M = Mn, Co and Ni, $x = 2$; M = Cu, $x = 0$], $Ni(TCS)py_2$ and Cu(TCS)py have been prepared. Elemental analyses, molar conductance, magnetic moment, electronic, IR and ESR spectral studies have been used to characterize these complexes. The different modes of chelation of the ligand and the stereochemistry of the complexes are discussed.

It was previously reported that studies on coordination properties of aroyl hydrazines and their aromatic Schiff bases, specially those derived from salicylaldehyde may provide a reasonable model for the mechanism of amine oxidase inhibition by many hydrazine derivatives.[1] Recently a number of papers have been appeared on 3*d* metal complexes of *N*-salicylidene acyl hydrazines from our laboratory[2–4] and elsewhere.[5,6] This work has been extended to the hitherto uninvestigated *N*-(thiophene-2-carboxamido)salicylaldimine complexes of 3*d* metal ions because there are as many as five potential donor sites and a possibility of keto–enol tautomerism which may be expected to lead to varied bonding and stereochemical behaviour in the complexes. The results of our investigations on the synthesis and structural studies of Mn(II), Fe(II), Co(II), Ni(II), Cu(II) and Zn(II) complexes with the title ligand are reported in the present paper.

EXPERIMENTAL

All the chemicals used in the present study were of BDH LR grade or of equivalent quality. H_2TCS was prepared as described by Thyssen,[7] m.p. 178–179°C (Lit.[6] 176°C). Found: C, 58.52; H, 4.04; N, 11.42%. $C_{12}H_{10}O_2N_2S$ requires: C, 58.53; H, 4.06; N, 11.38%.

* Author to whom correspondence should be addressed.

Preparation and analysis of complexes

Dichlorobis-[*N*-(thiophene-2-carboxamido)salicylaldimine]metal(II) complexes, $M(H_2TCS)_2Cl_2$ [M = Ni, Cu and Zn], were prepared by adding ethanolic solution of appropriate metal chloride (1 mmol in 10 cm^3) containing few drops of HCl to the methanolic solution of the ligand (2 mmol in 30 cm^3) at ice-cold temperature. Copper(II) complex precipitated immediately by shaking the reaction mixture while precipitation of the remaining two complexes were effected by adding ether to the reaction mixture.

Monochloro[*N*-(thiophene-2-carboxamido)salicylaldiminato]metal(II) complexes, M(HTCS)Cl [M = Co, Ni and Cu]. The addition of methanolic solution of the ligand (1 mmol in 20 cm^3) to the ethanolic solution of appropriate metal chloride (1 mmol in 10 cm^3) with constant stirring results in the precipitation of the corresponding complexes.

Bis-[*N*-(thiophene-2-carboxamido)salicylaldiminato]metal(II) complexes, $M(HTCS)_2$ [M = Mn, Fe, Co, Ni, Cu and Zn]. These complexes were precipitated by adding boiling aqueous–ethanolic solution of the appropriate metal acetate (1 mmol in 40 cm^3) to methanolic solution of the ligand (2 mmol in 20 cm^3) slowly with constant stirring. The iron(II) complex was prepared by reaction of an aqueous solution of ferrous ammonium sulphate and methanolic solution of the ligand under nitrogen to avoid oxidation.

Diaquo[*N*-(thiophene-2-carboxamido)salicylal-

diminato]metal(II) complexes, $M(TCS)(H_2O)_2$ [M = Mn, Co and Ni] and [*N*-thiophene-2-carboxamido)salicylaldiminato]copper(II), Cu(TCS). An aqueous–ethanolic solution of appropriate metal acetate (1 mmol in 30 cm^3) was added to the methanolic solution of the ligand (1 mmol in 20 cm^3) and the pH of the reaction mixture was raised to ~7 by aqueous NaOH solution. The resulting complexes were digested on a water bath for ~2 h.

Dipyridine[*N*-(thiophene-2-carboxamido)salicylaldiminato]nickel(II), $Ni(TCS)(py)_2$ and monopyridine[*N*-(thiophene-2-carboxamido)salicylaldiminato]copper(II), Cu(TCS)py, were obtained by dissolving the corresponding parent compounds in excess of pyridine and concentrating the solution to incipient crystallization.

All the complexes prepared as above were filtered and repeatedly washed with 50% ethanol, methanol and finally with ether and dried *in vacuo*.

The complexes were analysed for their metal content employing standard literature procedures[8] after decomposing the organic matter at first with a mixture of conc. nitric and hydrochloric acids and then with conc. sulphuric acid. Chloride was estimated as AgCl and nitrogen was determined microanalytically. Hydrazine was estimated volumetrically using KIO_3 after subjecting the complexes to acid hydrolysis for ~ 3 h.

Physical measurements

Molar conductance was measured on a WTW conductivity meter in DMF at 10^{-3} *M* dilution. The magnetic susceptibility of the complexes was determined at room temperature by the Faraday method using $Co[Hg(SCN)_4]$ as calibrant and experimental magnetic susceptibilities were corrected for diamagnetism.[9] The molar conductance and magnetic moment of the complexes are included in Table 1.

The electronic spectra of the complexes were recorded on a Cary 14 spectrophotometer in Nujol. ESR spectra of copper(II) complexes in DMF solution were obtained at 77 K on a Varian E-line X-band ESR spectrometer using TCNE as a *g* marker. The ESR parameters $g_{\|}$, $g_{\perp}$, g_{iso}, $g_{half\,field}$, $A_{\|}$, $A_{\perp}$ and A_{iso} deduced[10] from the analysis of the spectra are given in Table 2. The IR spectra of the complexes and the ligand were recorded on a Perkin–Elmer spectrophotometer Model 621 in Nujol while IR spectrum of the ligand in MeCN was also obtained on Perkin–Elmer Model 257. The important IR bands and assignment thereof are given in Table 3.

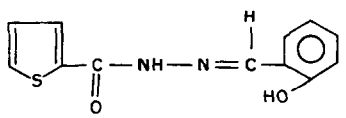


Fig. 1.

RESULTS AND DISCUSSION

The reaction of H_2TCS (Fig. 1) with metal(II) salts yields complexes of different compositions depending on the mode of preparation and metal ions. The complexes are insoluble in water and common organic solvents such as chloroform, ethanol, acetone, benzene and nitrobenzene. With the exceptions of $M(HTCS)_2$ [M = Mn, Co], $M(TCS)(H_2O)_2$ [M = Co, Ni] and $Ni(TCS)(py)_2$, all the complexes are soluble in DMF and DMSO. $Zn(H_2TCS)_2Cl_2$ melts at 190°C. While some of the complexes decompose between 210 and 280°C, the other complexes do not melt or decompose up to 340°C. The hydrated complexes lose water molecules in 130–170°C temperature range yielding anhydrous complexes. The loss of water molecules at higher temperature,[11] the presence of a band in 750–820 cm^{-1} region characteristic[12] of the coordinated water and absence of this band in the corresponding anhydrous complexes show that water molecules are coordinated to the metal ions. The soluble complexes have been found to be non-electrolytes[13] in DMF solution. The insufficient solubility of the complexes in suitable solvents precluded the molecular weight determination and growing of single crystal for X-ray crystallographic studies.

$M(H_2TCS)_2Cl_2$ [M = Ni, Cu *and* Zn] *chelates*

The magnetic moment and electronic spectral studies indicate octahedral geometry[14,15] for nickel(II) complexes. The bands observed at 11,905, 15,385 and 23,000 cm^{-1} in its electronic spectrum are assigned to $^3A_{2g}(F) \rightarrow {}^3T_{2g}(F)(\nu_1)$, $^3A_{2g}(F) \rightarrow 3T_{1g}(F)$ (ν_2) and $^3A_{2g}(F) \rightarrow {}^3T_{1g}(P)$ (ν_3) transitions respectively on the basis of idealized octahedral geometry.[15] Although the μ_{eff} value of the Cu(II) complex is normal as expected for one unpaired electron, a band at 25,000 cm^{-1} in the electronic spectrum and ESR studies suggest it to be a dimer.[16,17] The ESR spectrum gives a band at 1470 G due to the $\Delta M_s = 2$ transition indicating weak intramolecular magnetic exchange interaction[18] in a dimer. Two sets of signals appear in 2680–2980 and 2600–2900 G regions due to zero-field splitting giving an average separation of 60 G ($A_{\|}$), which is half the value expected for a monomer and confirms the dimeric nature of the complex. The Nujol mull IR spectrum of H_2TCS gives bands at 3360, 3200, 1640, 1590, 1530, 1260 and 1025 cm^{-1} which are attributed to ν(OH), ν(NH),

Table 1. Analytical data, colour, melting point, molar conductance and magnetic moment of H_2TCS complexes

Complex	Colour	M.p. (°C)	Found (calc.) (%) Metal	N_2H_4	N	Cl	Water loss	Molar conductance (Ω^{-1} M cm^2 mol^{-1} at 10^{-3} M in DMF)	Magnetic moment μ_{eff} (B.M.)
$Mn(TCS)(H_2O)_2$	Light yellow	270[d]	16.52 (16.40)	9.54 (9.55)	8.40 (8.35)	—	10.65 (10.74)	3.3	5.88
$Mn(HTCS)_2$	Yellow/ brown	> 320	10.12 (10.08)	11.64 (11.74)	10.34 (10.27)	—	—	—	5.58
$Fe(HTCS)_2$	Green	> 320	10.73 (10.23)	11.61 (11.72)	10.34 (10.25)	—	—	7.7	4.70
Co(HTCS)Cl	Orange	> 315	17.48 (17.36)	9.53 (9.42)	8.50 (8.24)	10.20 (10.45)	—	6.6	3.60
$Co(HTCS)_2$	Orange/ red	> 300	10.56 (10.73)	11.50 (11.65)	10.30 (10.20)	—	—	—	4.38
$Co(TCS)(H_2O)_2$	Orange	280[d]	17.40 (17.38)	9.54 (9.44)	8.30 (8.26)	—	10.88 (10.62)	—	3.34
$Ni(H_2TCS)_2Cl_2$	Green/ yellow	> 330	9.04 (9.44)	10.25 (10.29)	8.98 (9.00)	11.09 (11.42)	—	6.6	2.96
Ni(HTCS)Cl	Yellow/ green	> 315	17.20 (17.30)	9.50 (9.43)	8.30 (8.25)	10.80 (10.46)		3.3	2.29
$Ni(HTCS)_2$	Dark yellow	> 340	10.56 (10.69)	11.22 (11.66)	10.12 (10.20)	—	—	7.6	3.03
$Ni(TCS)(H_2O)_2$	Yellow	270[d]	17.50 (17.33)	9.42 (9.44)	8.20 (8.26)	—	10.54 (10.62)	—	3.06
$Ni(TCS)(py)_2$	Dark yellow	260[d]	12.75 (12.74)	7.02 (6.94)	12.22 (12.15)	—	—	—	2.96
$Cu(H_2TCS)_2Cl_2$	Green	> 320	10.20 (10.14)	—	8.97 (8.93)	10.90 (11.33)	—	6.2	2.20
Cu(HTCS)Cl	Brown	245–250	18.32 (18.46)	—	8.30 (8.13)	10.60 (10.31)	—	6.7	1.61
$Cu(HTCS)_2$	Green	240[d]	11.50 (11.47)	—	9.98 (10.11)	—	—	3.3	1.68
Cu(TCS)	Green	270[d]	20.56 (20.66)	—	9.32 (9.10)	—	—	3.3	1.23
Cu(TCS)py	Dark green	220[d]	16.52 (16.43)	—	10.85 (10.86)	—	—	6.9	1.32
$Zn(H_2TCS)_2Cl_2$	Yellow	190	10.32 (10.40)	10.00 (10.18)	8.85 (8.91)	11.52 (11.29)	—	7.6	Diamagnetic
$Zn(HTCS)_2$	Yellow	250[d]	11.50 (11.77)	11.62 (11.52)	10.11 (10.08)	—	—	3.3	Diamagnetic

Table 2. ESR magnetic parameters for Cu(II) complexes of H_2TCS

Complex	$g_{\parallel}$	$g_{\perp}$	g_{iso}	$A_{\parallel}$ (G)	$A_{\perp}$ (G)	A_{iso} (G)	$g_{half\ field}$
$Cu(H_2TCS)_2Cl_2$	2.3240	2.0262	2.1254	60.00	31.67	41.11	4.4108
Cu(HTCS)Cl	2.3219	2.0262	2.1247	63.33	30.00	41.11	4.3810
$Cu(HTCS)_2$	2.2494	2.0270	2.1011	173.33	30.83	78.33	4.3516
Cu(TCS)	2.2805	2.0167	2.1046	71.66	21.66	38.33	4.2723
Cu(TCS)py	2.2156	2.0152	2.0820	190.83	26.66	81.38	4.1860

Table 3. Important IR bands and their assignment in H_2TCS and its complexes

Compound	ν(OH)	ν(NH)	Amide I ν(C=O)	ν(C=N)	Amide II	Amide III	ν_{sym} (C—O)	ν_{asym} (C—O—M)	ν(N—N)	ν(M—O)	ν(M—N)	ν(M—Cl)
H_2TCS	3360mb	3200s	1640s	1590s	1530s	1295s	1260s	—	1025s	—	—	—
H_2TCS(MeCN)	3610m	3270m	1650s	1610s	1520s	1310s	1270s		1040s	—	—	—
	3530sb	3170m										
$Ni(H_2TCS)_2Cl_2$	3405mb	3270mb	1630m	1580s	1505s	1330m	1270w	—	1065w	385m	340m	295s
$Cu(H_2TCS)_2Cl_2$	3465	3185m	1610m	1580s	1505s	1325s	1275w		1065s	425s	335m	290s
	3305mb											
$Zn(H_2TCS)_2Cl_2$	3440mb	3270mb	1615m	1580s	1505s	1330m	1260w	—	1065w	360m	335m	295s
Co(HTCS)Cl	—	3210mb	1610s	1560s	1510s	1330s	1300m	1530s	1095m	405m	345m	305s
Ni(HTCS)Cl	—	3265mb	1635m	1600s	1520m	1315s	1285s	1545s	1055m	415s	360m	320s
Cu(HTCS)Cl	—	3270mb	1630m	1580s	1520s	1330m	1305m	1545s	1055m	430m	340m	—
$Mn(HTCS)_2$	—	3200mb	1595s	1575s	1505s	1330m	1280m	1530s	1085m	355m	290m	—
$Fe(HTCS)_2$	—	3200mb	1600s	1580m	1510m	1325m	1280m	1540s	1075m	—	—	—
$Co(HTCS)_2$	—	3260mb	1600s	1560s	1505s	1325s	1295s	1535s	1090w	400m	335m	—
$Ni(HTCS)_2$	—	3265mb	1625m	1580s	1505s	1325m	1300m	1535s	1055w	380m	335m	—
$Cu(HTCS)_2$	—	3270mb	1600s	1580s	1510s	1330s	1300m	1535s	1090w	425s	380s	—
$Zn(HTCS)_2$	—	3200mb	1610s	1570s	1510s	1330s	1275m	1534s	1095w	335m	290m	—
			ν(NCO^-)									
$Mn(TCS)(H_2O)_2$	3400mb	—	1570s	1590s	—	—	1290s	1545m	1085m	335m	305m	—
$Co(TCS)(H_2O)_2$	3400mb	—	1595s	1590s	—	—	1290s	1540m	1085m	335m	305m	—
$Ni(TCS)(H_2O)_2$	3400mb	—	1565s	1565s	—	—	1295s	1540m	1075w	335m	305m	—
$Ni(TCS)(py)_2$	—	—	1550s	1550s			1290s	1535m	1090s	335m	305m	—
Cu(TCS)	—	—	1570s	1590s	—	—	1305m	1540m	1080m	335m	295m	—
Cu(TCS)py	—	—	1575s	1575s	—	—	1300m	1535m	1050m	335m	300m	—

amide I, ν(C=N), amide II, ν_{sym}(C—O) of phenolic group and ν(N—N) modes respectively. The respective bands are observed at 3610, 3270, 1650, 1610, 1520, 1270 and 1040 cm^{-1} in the acetonitrile solution spectrum of the ligand showing thereby that there is intramolecular hydrogen bonding in the solid state. In the spectra of the complexes, amide I, amide II and ν(C=N) suffer a negative shift while ν(N—N) undergoes a positive shift suggesting that carbonyl oxygen and azomethine nitrogen are coordinated to the metal ions. The position of ν(OH) and ν(NH) remains unaltered in the spectrum of complexes indicating their non-involvement in bonding.

M(HTCS)Cl [M = Co, Ni *and* Cu] *chelates*

The anomalous magnetic moment of Cu(II)[19,20] and Ni(II) complexes[21–23] is attributed to metal–metal interaction and/or super-exchange phenomenon while that of Co(II) complex arises presumably due to contribution from high as well as low-spin state of the metal ion.[24] Ni(II) complex shows bands at 11,110, 17,860 and 22,730 cm^{-1} which are assigned to ν_1, ν_2 and ν_3 transitions respectively assuming pseudo octahedral geometry.[15] Three bands observed at 9305, 15,875, and 21,275 cm^{-1} in the electronic spectrum of Co(II) complex are assigned to $^4T_{1g}(F) \rightarrow {}^4T_{2g}(F)$ (ν_1) $^4T_{1g}(F) \rightarrow {}^4A_{2g}(F)$ (ν_2) and $^4T_{1g}(F) \rightarrow {}^4T_{1g}(P)$ (ν_3) transitions respectively assuming octahedral coordination around the metal ion.[15] A band at 12,500 cm^{-1} is attributed to $^2E_g \rightarrow {}^2T_{2g}(D)$ transition suggesting a distorted octahedral[15] geometry for copper(II) complex. IR spectra of the complexes indicate disappearance of ν(OH) and appearance of new bands due to ν_{asym}(C—O) in conjunction with a positive shift in ν_{sym}(C—O) which indicate bonding through phenolic oxygen[25] via deprotonation. A bathochromic shift in amide I, amide II and ν(C=N) together with a hypsochromic shift in ν(N—N) indicates coordination of ligand to the metal ions through carbonyl oxygen and azomethine nitrogen. The ESR spectrum of copper(II) complex yields a band at 1480 G and two sets of bands in 2595–2975 and 2610–2990 G ranges arising from zero-field splitting with an average separation of 63.33 G ($A_{\|}$). The value of $A_{\|}$ being half of the expected value for monomer copper(II) complexes further confirms dimeric[18]/polymeric nature of the complex.

$M(HTCS)_2$ [M = Mn, Fe, Co, Ni, Cu *and* Zn] *chelates*

The pseudo octahedral[15] configuration around the Fe, Co and Ni has been inferred from μ_{eff} values and electronic spectral studies. The lower magnetic moment[19,20] of the copper(II) complex is indicative of metal–metal interaction or super-exchange phenomenon. The manganese(II) complex shows a band at 16,670 cm^{-1} with a split band at 17,390 cm^{-1} and a strong band at 21,050 cm^{-1} which may be due to $^6A_{1g} \rightarrow 4T_{1g}(G)$ and $^6A_{1g} \rightarrow {}^4T_{2g}(G)$ transitions respectively in an idealized octahedral configuration around the metal ion. A band at 9760 cm^{-1} is assigned to $^5T_{2g} \rightarrow {}^5E_g(D)$ on the basis of the idealized octahedral geometry[15] around Fe(II). The Co(II) complex yields two bands at 9300 and 19,050 cm^{-1} assignable to ν_1 and ν_3 transitions respectively while Ni(II) complex gives three bands at 10,810, 17,390 and 22,730 cm^{-1} attributable to ν_1, ν_2 and ν_3 transitions respectively on the basis of pseudo octahedral[15] geometry around these metal ions. The copper(II) complex shows three bands at 14,815, 16,665 and 25,000 cm^{-1}. The first two bands are attributable to *d*—*d* transitions while the third band is due to dimeric/polymeric nature.[16,17] The dimeric[18] nature of the copper(II) complex is further confirmed from signal observed at 1490 G in ESR spectrum, which yields a *g* value of 4.3516. IR spectra of these complexes are similar to those of M(HTCS)Cl type of complexes and show characteristic of coordination through phenolic oxygen via deprotonation, carbonyl oxygen and azomethine nitrogen of the ligand. The magnetic moment[26,27] of Mn(II) complex in conjunction with IR and electronic spectral studies are indicative of octahedral coordination around the metal ion. The high melting or decomposition temperatures and insolubility in common organic solvents suggest a polymeric nature for the $M(HTCS)_2$ complexes.

$M(TCS)\cdot xH_2O$ [M = Mn, Co, x = 2; M = Cu, x = 0] *chelates*

The Ni(II) complex has a normal magnetic moment indicating octahedral geometry[14,15] while that of the Mn(II) complex is indicative of five unpaired spins. A strong band at 23,255 cm^{-1} in the visible spectrum of Mn(II) complex is attributed to $^6A_{1g} \rightarrow {}^4T_{1g}(G)$ transition in an idealized octahedral arrangement of the ligand around the metal ion. The electronic spectrum of Ni(II) complex yields bands at 10,810, 18,180 and 21,050 cm^{-1} assignable to ν_1, ν_2 and ν_3 transitions respectively on the basis of idealized octahedral[15] geometry. The anomalous magnetic moment of Cu(II) complex[19,20] can be explained on the basis of metal–metal interaction and/or superexchange phenomenon while that of Co(II) complex is presumably due to contribution from low- as well as high-spin states of Co(II)[24] in a dimeric structure. Three bands at 9090, 15,750 and

19,050 cm^{-1} observed in the electronic spectrum of Co(II) complex are assigned to ν_1, ν_2 and ν_3 transitions respectively assuming octahedral geometry[12] for the complex. In the spectrum of Cu(II) complex bands at 14,490 and 16,665 cm^{-1} are attributed to *d—d* transitions and a band at 25,640 cm^{-1} is attributed to dimeric[16,17] nature of the complex. A signal at 1520 G in ESR spectrum due to $\Delta M_s = 2$ transition indicates dimeric nature of the complex and thus indicating intramolecular magnetic exchange interaction. It gives two sets of bands in 2620–3050 and 2637.5–3077.5 G regions which can be explained on the basis of zero-field splitting energy. The observed $A_{\|}$ (71.66 G) value is half of the expected value for copper(II) monomers suggesting thereby that the complex is dimer.[18]

The disappearance of ν(OH) and ν(NH) and appearance of ν_{asym}(CO) and ν(NCO) indicate the bonding of carbonyl oxygen and phenolic oxygen via deprotonation. The negative shift in ν(C=N) and positive shift in ν(N—N) is characteristic of coordination through azomethine nitrogen.

Ni(TCS)(py)$_2$ *and* Cu(TCS)py

Magnetic moment and electronic spectral studies of Ni(II) complex are indicative of octahedral[15] geometry suggesting thereby that water molecules are replaced by pyridine molecules without any change in the stereochemistry of the complex. The copper(II) complex is believed to have a 5-coordinate square pyramidal geometry without any change in the dimer entity because Cu(TCS)py has an anomalous magnetic[17,20] moment similar to its parent compound Cu(TCS). The ESR spectrum of Cu(TCS)py gives a half-field signal at 1550 G due to the $\Delta M_s = 2$ transition characteristic of magnetic exchange interaction in dimeric[18] species. Of three bands at 14,715, 16,950 and 25,000 cm^{-1} in the electronic spectrum, the first two bands are attributed to *d–d* transitions and the third band at 25,000 cm^{-1} is due to dimeric nature of the complex. IR spectra have the characteristics of the bonding through carbonyl oxygen and phenolic oxygen in the deprotonated form and azomethine nitrogen similar to their parent compounds.

CONCLUSIONS

The ESR studies indicate that all of the Cu(II) complexes have axial symmetry with the unpaired electron in the $d_{x^2-y^2}$ orbital. The dimeric/polymeric nature of the complexes adduced from electronic spectral studies are supported by the ESR studies.

The IR spectral studies indicate that H_2TCS behaves: (i) as neutral bidentate ligand in $M(H_2TCS)_2Cl_2$ bonding sites being carbonyl oxygen and azomethine nitrogen; (ii) as a mononegative tridentate ligand in $M(HTCS)_2$ and M(HTCS)Cl coordination sites being deprotonated phenolic oxygen, carbonyl oxygen and azomethine nitrogen; and (iii) as a dinegative tridentate ligand bonding through phenolic oxygen, enolic oxygen, and azomethine nitrogen.

The non-ligand bands observed in the 430–335, 380–290 and 320–290 cm^{-1} ranges are tentatively assigned to ν(MO), ν(MN) and ν(MCl) modes respectively.

In all the complexes coordination of the thiophene sulphur to the metal ions is excluded as the ring stretching ($\sim$ 1430 cm^{-1}) CH bending ($\sim$ 1225 cm^{-1}) and C-ring—C-exo ($\sim$ 955) stretching mode of thiophene remain practically unchanged. The poor coordination ability of the thiophene ring sulphur has been attributed to the involvement of the lone pair electrons on sulphur in the aromatic sextet and less capacity of π-orbitals to accept electron pair from the metal.

Acknowledgements—One of us (R.N.S.) is thankful to the UGC, New Delhi, for the award of a Teacher Research Fellowship under the Faculty Improvement Programme. Sincere thanks are also due to RSIC, IIT, Bombay, for providing the ESR spectra of the complexes.

REFERENCES

1. M. F. Iskander, S. E. Zayan, M. A. Khalifa and L. El-Sayed, *J. Inorg. Nucl. Chem.* 1974, **36**, 556.
2. R. C. Aggarwal and D. S. S. Vara Prasad Rao, *Indian J. Chem.* 1981, **20A**, 855.
3. R. C. Aggarwal, N. K. Singh and R. P. Singh, *Inorg. Chem.* 1981, **20**, 2794.
4. B. Singh, R. N. Singh and R. C. Aggarwal, (i) *Synth. React. Inorg. Met.-Org. Chem.* 1984, **14**, 815; (ii) *Indian J. Chem.* 1984, **23A**, 480.
5. M. F. Iskander, L. El-Sayed, A. F. M. Hefny and S. E. Zayan, *J. Inorg. Nucl. Chem.* 1976, **38**, 2209.
6. R. L. Dutta and A. K. Sarkar, *J. Inorg. Nucl. Chem.* 1981, **20**, 2299.
7. C. Thyssen, Beilsteins, *Hand Book of Organic Chemistry*, Band XVIII, p. 291 (1934).
8. A. I. Vogel, *A Text Book of Quantitative Inorganic Analysis*. ELBS and Longmans (1973).
9. B. N. Figgis and J. Lewis, in *Modern Coordination Chemistry* (Edited by J. Lewis and R. G. Wilkins), p. 403. Interscience, New York (1960).
10. M. Symons, *Chemical and Biochemical Aspects of Electron Spin Resonance Spectroscopy*. Van Nostrand Reinhold, Scarborough, CA (1978).
11. A. C. Fabretti, G. Franchinic, C. P. Pretti and G. Tosi, *Can. J. Chem.* 1977, **55**, 344.

12. A. R. Micholson and G. J. Suttan, *Aust. J. Chem.* 1969, **22**, 373.
13. W. J. Geary, *Coord. Chem. Rev.* 1971, **7**, 81.
14. B. N. Figgis and J. Lewis, *Prog. Inorg. Chem.* 1964, **6**, 197.
15. A. B. P. Lever, *Inorganic Electronic Spectroscopy.* Elsevier, Amsterdam (1968).
16. J. Lewis, Y. C. Lin, R. K. Royston and R. C. Thompson, *J. Chem. Soc.* 1965, 6464.
17. I. G. Ross, M. L. Tonnet and S. Yamada, *Trans. Faraday Soc.* 1964, **60**, 840.
18. E. F. Hasty, L. J. Wilson and D. N. Hendrickson, *Inorg. Chem.* 1978, **17**, 1834.
19. P. W. Anderson, *Phys. Rev.* 1950, **79**, 350.
20. A. P. Ginberg, *Inorg. Chim. Acta Rev.* 1971, **5**, 45.
21. K. Barefield, D. H. Bush and S. M. Nelson, *Q. Rev.* 1968, **22(4)**, 457.
22. A. P. Ginsberg, E. Koubex and H. H. Williams, *Inorg. Chem.* 1966, **5**, 1956.
23. G. O. Carlisle and D. A. Crutchfield, *Inorg. Nucl. Chem. Lett.* 1972, **8**, 443.
24. D. L. Williums, D. W. Smith and R. C. Stoufer, *Inorg. Chem.* 1967, **6**, 590.
25. E. Sinn and C. M. Harris, *Coord. Chem. Rev.* 1969, **4**, 391.
26. J. Lewis, F. E. Mabbs and H. Weigold, *J. Chem. Soc.* 1968, 1699.
27. D. J. Hewkin and W. P. Griffith, *J. Chem. Soc. (A)* 1966, 472.

Polyhedron Vol. 4, No. 3, pp. 409–414, 1985
Printed in Great Britain

0277-5387/85 $3.00 + .00
©1985 Pergamon Press Ltd

X-RAY PHOTOELECTRON SPECTRA OF METAL COMPLEXES OF SUBSTITUTED 2,4-PENTANEDIONES*

S. SRIVASTAVA and S. BADRINARAYANAN
National Chemical Laboratory, Poona 411008, India

and

A. J. MUKHEDKAR†
University Department of Chemistry, Ganeshkhind, Poona 411007, India

(*Received* 26 *April* 1982; *accepted after revision* 25 *July* 1984)

Abstract—The X-ray photoelectron spectra of 14 complexes of Al^{3+}, Cr^{3+}, Fe^{3+}, Co^{3+} and Cu^{2+} with 3-X-2,4-pentanedione (X = H, Cl, Br) were determined to analyse the nature of metal–ligand bonding in these complexes. The trend in the position of *np* photoelectron lines of X-group with a change of metal ion was decided by the relative contribution of metal-to-ligand and ligand-to-metal charge transfer. The analysis of the satellites in the $M(2p_{3/2})$ and $M(2p_{1/2})$ spectra suggested that the metal–ligand bond in the chromium(III) complex had higher covalent character than that in the iron(III) complex. The satellite separations in the O(1*s*) spectra of $M(3\text{-Xptdn})_3$ were in the range 4.0–4.8 eV: these satellites were assigned to a shake-up transition of $L\pi \rightarrow L\pi^*$ character. The O(1*s*) spectra of $Fe(3\text{-Xptdn})_3$ and $Al(3\text{-Xptdn})_3$ displayed an additional strong peak to higher energy than that of the main peak (ΔE = 2.1–3.1 eV) when the samples of complexes were bombarded with argon ions for a longer time.

The metal 2,4-pentanedionates, $M(ptdn)_n$, form an interesting class of compounds which display the characteristic electrophilic reactions[1] of aromatic compounds. The pseudo-aromacity of the chelating ligand and the role of the coordinated metal ion in the ring current are the theme of many papers.[2] The theoretical analysis of the nature of chemical bond in $M(ptdn)_n$ suggests the participation of the metal orbitals in the metal–ligand bonding.[3] The absorption band associated with the charge transfer ($d_\varepsilon \rightarrow \pi_4$) transition in $M(3\text{-Xptdn})_n$ follows the trend of the optical electronegativity of the metal atom.[4] Recently it has been shown from the Szilard–Chalmers reactions of $M(3\text{-Xptdn})_n$ (X = Br, I) that an increasing trend of percentage retention of labelled X follows a decreasing trend of optical electronegativity.[5,6] The former trend obviously depends on the charge at the 3-carbon. The ^1H and ^{13}C NMR spectra of $Co(3\text{-Xptdn})_3$ display the following trend[7] of the coupling constant, $J_{^{13}C-^1H_3}$: $Co(3\text{-Clptdn})_3 > Co(3\text{-Brptdn})_3 > Co(3\text{-Iptdn})_3 > Co(ptdn)_3$. This study suggests the dependence of polarisation of coordinated ligands on the substituent at the 3-carbon. This paper reports the results of such a study of the X-ray photoelectron spectra of complexes with 3-substituted 2,4-pentanedionates.

EXPERIMENTAL

The complexes $M(3\text{-Xptdn})_n$ with X = H, Cl, Br were synthesised and purified by using the established methods.[8–10] The samples were dried in vacuum and were stored under dry nitrogen.

The X-ray photoelectron spectra were recorded on a V.G. Scientific ESCA-3 MK-II electron spectrometer. The Mg-K_α X-ray line (1253.6 eV) was used for photoelectron excitation.

The $Cu(2p_{3/2})$ (E_b 932.8 ± 0.2) and $Au(4f_{7/2})$ (E_b 83.8 ± 0.1) lines were used to calibrate the instrument and $Ag(3d_{5/2})$ (E_b 368.2) was used for cross-checking.[11]

* NCL Communication No. 3568.
† Author to whom correspondence should be addressed.

All the spectra were recorded using the same spectrometer parameters of 50 eV pass energy and 4 mm slit width. The reduced full width at half-maximum (FWHM) for Au($4f_{7/2}$) (E_b 83.8 eV) level under these conditions was 1.2 eV.

The powdered sample was mixed with high purity silver powder to reduce the charging effect. A thin layer of such a sample was pressed on a gold metal gauze which was welded to a nickel sample holder. The Ag($3d_{5/2}$) level (E_b 368.2 eV) obtained from this sample was sharp and did not show any observable shift. Thus the charging of the samples[12] if at all present was negligible.

The samples were cleaned using 10 kV positive argon ion[13] at current of 20 μA cm^{-2} for 3–4 s prior to recording to the PE spectra. The spectra were recorded in triplicate in the regions of interest. In most cases the binding energies were reproducible within $\pm$0.1 eV. The usual least-squares fitting procedure of determining peak positions, line-widths and areas was used.

RESULTS AND DISCUSSION

In the structurally related compounds, M(3-Xptdn)$_n$, the binding energies of X, O and M were expected to be related to the different details of metal–ligand bonding in these complexes. It was therefore possible to correlate these binding energies with the physical properties which were sensitive to the electron density on the respective groups.

Since there was more than one type of carbon in 2,4-pentanedionates, the signals due to C($1s_{1/2}$) were overlapped and one broad signal was obtained. The data of C($1s_{1/2}$) could not be therefore utilised for the structural analysis.

The binding energies of Br in M(3-Brptdn)$_n$ varied considerably and indicated a definite dependence on the central metal atom (Table 1). The following increasing trend for Br($3p_{3/2}$) and Br($3p_{1/2}$) was obtained for the octahedral complexes.

$$Cr < Co < Al < Fe. \quad (1)$$

The observed order of binding energy could be correlated with the polarisation of ligand by the metal ion. 2,4-Pentanedione being a pseudo-aromatic system, the inductive and conjugative effects of 3-Br would be transferred through the metallo-heterocyclic ring. The electronic spectra of these type of complexes in solution[3,14] showed both the ligand-to-metal and metal-to-ligand charge transfer bands. Since the binding energies of Br($3p_{3/2}$) and Br($3p_{1/2}$) in iron(III) complex were the highest, the bromine in this complex was more deshielded suggesting a favourable conjugative effect. Since the binding energies of Br($3p_{3/2}$) and Br($3p_{1/2}$) in chromium(III) complex were the least, the electron density on the bromine in this complex was much higher than that in iron(III) complex. The charge-transfer processes would be of negligible importance in the non-transition metal complexes. Thus the binding energies of Br($3p_{3/2}$) and Br($3p_{1/2}$) for aluminum(III) complex were considered as a reference to analyse the results presented by eqn (1). Since the binding energies of Br($3p_{3/2}$) and Br($3p_{1/2}$) for aluminum(III) complex were definitely less than that for iron(III) complex, the ligand-to-metal charge transfer process seemed to be more important in iron(III) complex. The binding energies of Br($3p_{3/2}$) and Br($3p_{1/2}$) for chromium(III) and cobalt(III) complexes were lower than that for aluminum complex. Thus the metal-to-ligand charge transfer superseded the polarisation effect due to the ligand-to-metal charge transfer in these complexes.

A similar comparison of Cl($2p_{3/2}$) and Cl($2p_{1/2}$) binding energy data for M(3-Clptdn)$_3$ showed the following decreasing order (Table 1):

$$Cr > Co > Fe. \quad (2)$$

This trend was the reverse of that found for Br($3p_{1/2}$) and Br($3p_{3/2}$) binding energies for M(3-Brptdn)$_3$. A reproducible value for the Cl($2p$) binding energy for Al(3-Clptdn)$_3$ could not be obtained and an analysis of these data [eqn (2)] could not be done. One could say with caution that the ligand-to-metal charge-

Table 1. Binding energies (eV) of X in M(3-Xptdn)$_n$*

X	M				
	Al^{3+}	Cr^{3+}	Fe^{3+}	Co^{3+}	Cu^{2+}
Br($3p_{3/2}$)	184.3 (3.2)	183.4 (3.3)	186.8 (3.8)	184.0 (3.8)	185.5 (3.6)
Br($3p_{1/2}$)	190.8 (3.2)	190.0 (3.5)	193.3 (4.0)	190.7 (4.0)	192.2 (3.8)
Cl($2p_{3/2}$)	—	202.0	199.6	201.2	201.6
Cl($2p_{1/2}$)	—	203.8	201.4	203.0	203.4

* Full width at half-maximum (FWHM) of the peak is given in parentheses.

Table 2. Binding energies (eV) of metal $2p$ in M(3-Xptdn)$_n$ complexes*

	M					
	Cr^{3+}		Fe^{3+}		Co^{3+}	
X	$2p_{3/2}$	$2p_{1/2}$	$2p_{3/2}$	$2p_{1/2}$	$2p_{3/2}$	$2p_{1/2}$
H	577.8 (3.6)	589.4 (3.6)	712.4 (3.6)	726.4 (3.6)	781.4 (2.0)	798.4 (1.8)
Cl	577.8 (3.6)	589.4 (3.6)	712.2 (3.6)	726.2 (3.6)	781.8 (1.2)	799.0 (2.4)
Br	577.8 (2.4)	589.3 (4.8)	712.4 (4.8)	726.4 (4.8)	781.4 (1.8)	798.5 (1.2)

* Full width at half-maximum (FWHM) of the peak is given in parentheses.

transfer process was more important in these complexes; the extent of charge-transfer in Fe(3-Clptdn)$_3$ was the least.

The observed dependence of binding energy of p-electrons in Br and Cl (eqns (1) and (2)] would be reflected in the binding energies of electrons on oxygen and metal in these complexes.

Unlike the binding energies of np electrons in X, the binding energies of M($2p_{1/2}$) and M($2p_{3/2}$) electrons did not show any significant change with the change of X (Table 2). Thus, the metal–ligand bonding seemed to involve, in effect, a synergistic phenomenon.

The complexes [except Cu(3-Xptdn)$_2$] studied in the present work were of the same symmetry, and the nature of the ligands was closely related. It was therefore envisaged that the metal $2p$ satellite structure would be similar[15] for these complexes.

The present work indicated that the satellite structure in the structurally related complexes did depend on the central metal atom (Fig. 1). The paramagnetic complex Cr(3-Xptdn)$_3$ displayed two (shake-up) satellites in both the M($2p_{3/2}$) and M($2p_{1/2}$) spectra at higher energy separated by about 4.5 and 7.1 eV from the main line. Another paramagnetic complex Fe(3-Xptdn)$_3$ displayed one satellite in both the M($2p_{3/2}$) and M($2p_{1/2}$) spectra at higher energy separated by about 3.9 eV from the main line (Table 3). The satellites in the $2p$ spectra of the diamagnetic complex Co(3-Xptdn)$_3$ were so weak that the analysis could not be done with confidence.

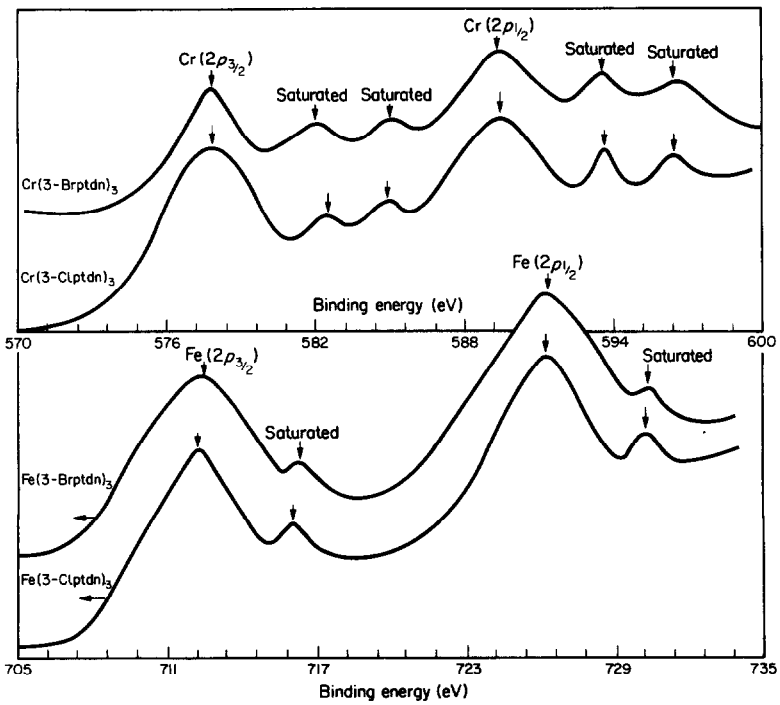


Fig. 1. $2p_{3/2}$ and $2p_{1/2}$ binding energies (eV) and satellites in M(3-Xptdn)$_3$ (M = Cr or Fe, X = Cl or Br).

Table 3. Satellite separation (ΔE) and relative intensity (I) in the metal 2*p* spectra of M(3-Xptdn)$_n$ complexes

Complex	$\Delta E2p_{3/2}$	I	$\Delta E2p_{1/2}$	I
Cr(3-Hptdn)$_3$	4.8	0.50	4.4	0.17
	7.2	0.62	7.0	0.12
Cr(3-Clptdn)$_3$	4.6	0.33	4.2	0.50
	7.0	0.33	7.0	0.39
Cr(3-Brptdn)$_3$	4.2	0.55	4.2	0.57
	7.2	0.50	7.1	0.48
Fe(3-Hptdn)$_3$	3.8	0.33	3.8	0.25
Fe(3-Clptdn)$_3$	3.8	0.37	4.0	0.37
Fe(3-Brptdn)$_3$	3.9	0.33	3.9	0.37

It was earlier reported that the diamagnetic solid compounds[16,17] did not show the shake-up satellites. The relative intensity of the M($2p_{3/2}$) satellite for diamagnetic complex Ni(ptdn)$_2$ in the vapour state was much lower than that for paramagnetic complex Ni(ptdn)$_2$ in the solid state.[18] There was an interesting report that the 2*p* spectra of the diamagnetic solid complex $K_3Co(C_2O_4)_3$ displayed strong satellites.[19]

The 2*p* satellite spectrum of the first transition metal compounds was interpreted as due to one of the following two types of transitions concurrently associated with the emitted photoelectron: (i) the excitation of a metal 3*d* electron into an unoccupied metal orbital[20] (predominantly 4*s*), and (ii) the ligand-to-metal ($L \rightarrow M$) or metal-to-ligand ($M \rightarrow L$) charge transfer.[21] According to the selection rules the 3*d*–4*s* transition was allowed for the paramagnetic compounds, and was forbidden for the diamagnetic compounds.[22] As regards the second interpretation, an intensity of a satellite associated with a charge transfer ($L \rightarrow M$ or $M \rightarrow L$) would depend on the amount of the total charge transferred through the orbitals of correct symmetry. It would also depend on the magnitude of the central ion component of the ligand orbital before ionization.[19] The analysis of the electronic spectra of Co(ptdn)$_3$ using Hückel LCAO–MO calculations suggested that the metal–ligand bond had a large component.[3] Thus the central metal atom in Co(ptdn)$_3$ was envisaged to have a large ligand orbital component. The nature of the metal–ligand bond in Co(3-Xptdn)$_3$ was expected to be similar to that in Co(ptdn)$_3$. The satellites in the M(2*p*) spectra of Co(3-Xptdn) would be therefore weak. The observed M(2*p*) spectra of Co(3-Xptdn) were in accordance with this prediction.

From the study of the structurally related nickel(II) complexes it was reported that the more covalent the bonding, the larger the satellite separation.[17] The nephelauxetic series of the ligands was correlated with the satellite separations. The present work dealt with the complexes containing similar ligands attached to the different metal ions. The separation between the first shake-up satellite and the main line for chromium(III) complexes was definitely larger than that for the iron(III) complexes. This observation suggested that the metal–ligand bond in chromium(III) complex had a higher covalent character than that in iron(III) complex.

The O(1*s*) binding energies in the complexes studied in the present work showed a small variation with metal (Table 4). The trends observed for O(1*s*) binding energies in M(ptdn)$_3$ and M(3-Clptdn)$_3$ were different from that in M(3-Brptdn)$_3$:

$$\text{M(ptdn)}_3: \text{Al} \leqslant \text{Fe} < \text{Co} < \text{Cr}, \quad (3)$$

$$\text{M(3-Clptdn)}_3: \text{Fe} < \text{Co} < \text{Cr}, \quad (4)$$

$$\text{M(3-Brptdn)}_3: \text{Fe} > \text{Al} > \text{Co} \geqslant \text{Cr}. \quad (5)$$

Table 4. Binding energies (eV) of O(1*s*) and satellite separations [ΔE (eV)] in M(3-Xptdn)$_n$

	X					
	H		Cl		Br	
M	O(1*s*)(FWHM)*	$\Delta E_{O(1s)}$ (I)†	O(1*s*)(FWHM)	$\Delta E_{O(1s)}$ (I)	O(1*s*)(FWHM)	$\Delta E_{O(1s)}$ (I)
Al	531.7 (2.6)	4.1 (0.02)	—	—	532.1 (2.6)	4.0 (0.01)
	533.8 (2.4)	4.8 (0.02)	—	—	534.7 (2.4)	4.7 (0.01)
Cr	531.9 (2.6)	4.6 (0.02)	531.7 (2.4)	4.4 (0.02)	531.9 (2.4)	4.3 (0.01)
Fe	531.7 (2.4)	4.3 (0.02)	531.4 (2.8)	4.2 (0.02)	532.2 (2.8)	4.2 (0.02)
	534.8 (2.6)	4.8 (0.02)	534.4 (2.8)	4.7 (0.01)	535.2 (2.8)	4.6 (0.02)
Co	531.8 (2.4)	4.6 (0.02)	531.6 (2.4)	4.4 (0.02)	531.9 (2.6)	4.2 (0.01)
Cu	532.8 (2.4)	—	532.7 (2.2)	—	532.6 (2.4)	—

* Full width at half-maximum (FWHM) of peak is given in parentheses.

† Relative intensity of satellite peak is given in parentheses.

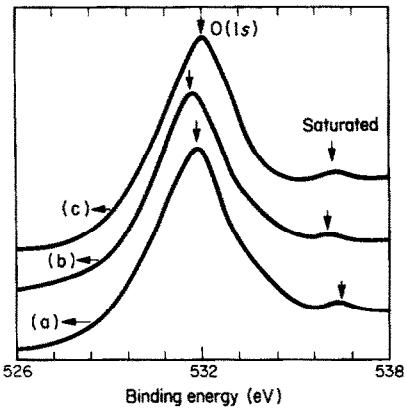


Fig. 2. O(1*s*) binding energies (eV) and satellites in $Co(3\text{-}Xptdn)_3$ [X = H (a), Cl (b) and Br (c)].

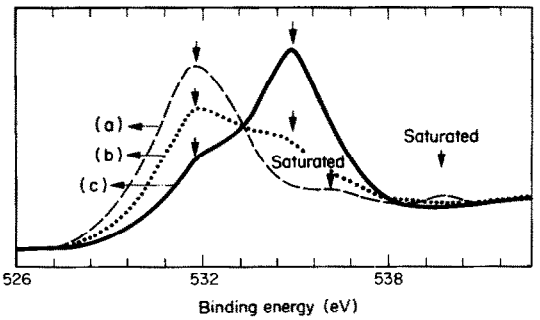


Fig. 3. O(1*s*) spectra of the $Fe(3\text{-}Hptdn)_3$ complex after argon ion bombardment for 3 (a), 10 (b) and 30 sec (c).

These trends were similar to those observed for $X(np_{3/2})$ and $X(np_{1/2})$ binding energies [eqn (1), $n = 3$; eqn (2), $n = 2$]. Thus, the polarization contributions which controlled the bindings energies of $X(np_{3/2})$ and $X(np_{1/2})$ also controlled the O(1*s*) binding energies. This observation was in conformity with the pseudo-aromatic behaviour of the coordinated ligands in these complexes.

The O(1*s*) spectra of all the complexes except that of copper(II) studied in the present work displayed a weak, but definite, satellite at binding energies higher than the main peak (Fig. 2). It was reported that $Cu(ptdn)_2$ vapour also showed a O(1*s*) satellite structure.[18] The observed satellite separations in the O(1*s*) spectra of complexes were in the range 4.0–4.8 eV (Table 4) and were higher than that reported for free 2,4-pentanedione (3.6 eV).[23] This range was equivalent to 32,263–38,716 cm^{-1}.

The analysis of electronic spectra of $M(ptdn)_3$ using the Hückel LCAO–MO calculations suggested that the bands observed in the region 32,400–44,400 cm^{-1} were associated with the $L\pi \rightarrow L\pi^*$ transition.[3] A comparison of the electronic spectra with the satellite separations in the O(1*s*) spectra of $M(ptdn)_3$ would have to be done with caution since the relative energy levels of molecular orbitals could change considerably on core level ionization. The observed satellite separation in the O(1*s*) spectra of $M(ptdn)_3$ was higher than that observed for Hptdn. Due to the polarizing effect of Xptdn it was envisaged that the separation between π and π^* molecular orbitals would be smaller for $M(3\text{-}Xptdn)_3$ as compared to that for $M(ptdn)_3$. It was observed that the satellite separations in the O(1*s*) spectra of $M(3\text{-}Xptdn)_3$ was smaller than that of $M(ptdn)_3$. These observations tempted us to assign the O(1*s*) satellite to a shake-up transition of $L\pi \rightarrow L\pi^*$ character.

As was shown in Experimental the surface of the sample was cleaned by argon ion bombardment. When the samples of $Al(3\text{-}Xptdn)_3$ and $Fe(3\text{-}Xptdn)_3$ were bombarded with argon ions for about 5 s an additional peak was observed in the O(1*s*) spectra. The intensity of this peak was stronger than the main peak when the argon ion bombardment was carried out for about 30 s (Fig. 3). The additional O(1*s*) signal was also associated with a weak satellite at binding energies higher than the additional peak.

The O(1*s*) spectra of other complexes studied in the present work did not show such an additional peak. It has been recognised that many compounds undergo surface decomposition in the X-ray flux of the spectrometer. No compound studied in the present work showed any detectable surface decomposition by X-rays even after exposure over the extended periods. The argon-ion bombardment might also cause structural changes or decomposition of the sample. Recently it was observed that the oxidation state of rhenium[24] in $(ReCl_3)_3$ was changed on the argon ion bombardment from rhenium(III) to rhenium(0). Since the position of the additional peak observed for $Al(3\text{-}Xptdn)_3$ and $Fe(3\text{-}Xptdn)_3$ was to the higher energy than that of main peak, we were tempted to assign it to the keto form of Xptdn (Fig. 4). We were, however, unable to take the reflectance IR spectrum of the irradiated samples to substantiate our prediction. It might be noted here that the stable complexes containing keto form of β-diketone were reported.[25] The forma-

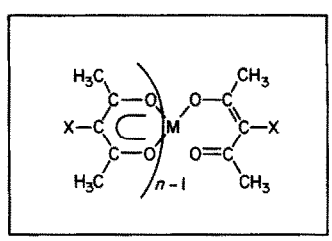


Fig. 4.

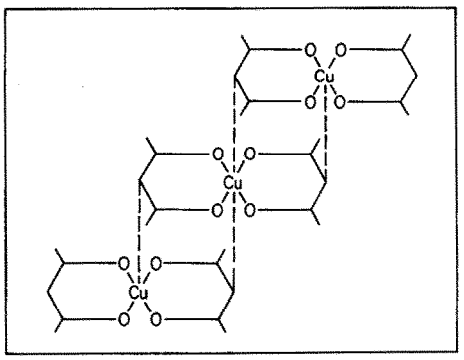


Fig. 5.

tion of such species as intermediates was also suggested from the study of mass spectra[26] of fluorine-substituted-acetylacetonates and (n, γ) reactions[5] of 3-bromo 2,4-pentanedionate of iron(III). Since the additional O(1s) signal was observed for Al(3-Xptdn)$_3$ and Fe(3-Xptdn)$_3$ and not for Cr(3-Xptdn)$_3$, Co(3-Xptdn)$_3$ and Cu(3-Xptdn)$_2$ studied in the present work, the presence of the additional O(1s) signal could be related with the nature of metal–ligand bond. Probably the M—O bond in Al(3-Xptdn)$_3$ and Fe(3-Xptdn)$_3$ had higher ionic character than that in other complexes.

The XPS of copper(II) complexes studied in the present work showed a different behaviour. The positions of the signal due to O($1s_{1/2}$) ionization indicated that the coordinated oxygen had a definite negative charge; but it was much less than that in other transition metal complexes. However, 3p photoelectron line of 3-Br for Cu(3-Brptdn)$_2$ was at a higher energy as compared to that for Cr(3-Brptdn)$_3$. The X-ray diffraction studies of Cu(ptdn)$_2$ showed[27] that the chelates were so packed that there was an interaction of the copper atom of one molecule with the 3-carbon atoms of the chelate ring of the neighbouring molecules (Fig. 5). Such interactions would explain the observed different behaviour of the XPS of copper(II) complexes.

Acknowledgement—One of us (SS) is thankful to CSIR, New Delhi for award of fellowship. Our thanks are due to Dr A. P. B. Sinha, Head, Physical Chemistry Division, NCL, Poona-8, India, for the facilities given during this work. Our thanks are also due to the referees for useful suggestions for the revision of the manuscript.

REFERENCES

1. J. P. Collman, *Adv. Chem. Ser.* 1963, **37**, 78; Q. Fernando, *Adv. Inorg. Radiochem.* 1965, **7**, 185.
2. D. W. Thompson, *Structure and Bonding* 1971, **9**, 27; J. P. Fackler, Jr., *Prog. Inorg. Chem.* 1966, **7**, 361.
3. D. W. Barnum, *J. Inorg. Nucl. Chem.* 1961, **22**, 183; C. K. Jorgensen, *Acta Chim. Scand.* 1962, **16**, 2406.
4. B. J. Kavathekar, J. N. Khanivilkar, M. P. Sahakari and A. J. Mukhedkar, *Radiochim. Acta* 1976, **23**, 88.
5. A. T. M. Sharifullah and A. J. Mukhedkar, *Radiochim. Acta* 1980, **27**, 131.
6. J. N. Khanivilkar, A. T. M. Sharifullah and A. J. Mukhedkar, *Radiochim. Acta* 1981, **28**, 69.
7. J. C. Hammel, J. A. S. Smith and E. J. Wilkins, *J. Chem. Soc. (A)* 1969, 1461.
8. R. W. Kluiber, *J. Am. Chem. Soc.* 1960, **82**, 4839.
9. P. R. Singh and R. Sahai, *Aust. J. Chem.* 1967, **20**, 639.
10. J. B. Ellern and R. O. Ragsdale, *Inorg. Synth.* 1968, **11**, 82.
11. S. Evans, *Handbook of X-ray and Ultraviolet Photoelectron Spectroscopy* (Edited by D. Briggs), p. 128. Hyden (1975).
12. W. Jolly, *Coord. Chem. Rev.* 1974, **13**, 47.
13. S. O. Grim, L. J. Matienzo and W. E. Swartz, Jr., *Inorg. Chem.* 1974, **13**, 447.
14. D. W. Barnum, *J. Inorg. Nucl. Chem.* 1961, **22**, 221.
15. M. A. Brisk and A. B. Baker, *J. Electron Spectrosc. Relat. Phenom.* 1975, **7**, 197.
16. D. C. Frost, A. Ishitani and C. A. McDowell, *Mol. Phys.* 1972, **24**, 861.
17. L. J. Matienzo, L. I. Yin, S. O. Grim and W. E. Swartz, Jr., *Inorg. Chem.* 1973, **12**, 2762.
18. J. S. H. Q. Perera, D. C. Frost and C. A. McDowell, *J. Chem. Phys.* 1980, **72**, 5151.
19. T. A. Carlson, J. C. Carver, L. J. Saethre, F. G. Santibanez and G. A. Vernon, *J. Electron Spectrosc. Relat. Phenom.* 1974, **5**, 247.
20. T. Novakov, *Phys. Rev. B* 1971, **3**, 2693; A. Rosencwaig, G. K. Wertheim and H. J. Guggenheim, *Phys. Rev. Lett.* 1971, **27**, 479.
21. K. S. Kim, *J. Electron Spectrosc. Relat. Phenom.* 1974, **3**, 217; S. Larsson, *J. Electron Spectrosc. Relat. Phenom.* 1976, **8**, 171.
22. M. O. Krause, T. A. Carlson and R. D. Dismukes, *Phys. Rev.* 1968, **37**, 170.
23. R. S. Brown, *J. Am. Chem. Soc.* 1977, **99**, 5497.
24. A. Katrib, R. M. Yousef and N. J. Fitzpatrick, *Inorg. Chem.* 1982, **21**, 1523.
25. J. V. Seyerl, D. Neugebauer and G. Huttner, *Angew. Chem. Int. Ed. Engl.* 1977, **16**, 858.
26. J. P. Westmore, *Chem. Rev.* 1976, **76**, 2622.
27. D. P. Graddon, *Coord. Chem. Rev.* 1969, **4**, 1.

Polyhedron Vol. 4, No. 3, pp. 415–417, 1985
Printed in Great Britain

0277–5387/85 $3.00 + .00
© 1985 Pergamon Press Ltd

BINUCLEAR SCHIFF-BASE COMPLEXES OF COPPER(II) LINKED BY PHTHALOYL AS A BRIDGING GROUP

K. KASUGA,* T. NAGAHARA and Y. YAMAMOTO
Department of Chemistry, Faculty of Science, Shimane University, Matsue 690, Japan

(*Received* 25 *June* 1984; *accepted* 25 *July* 1984)

Abstract—Binuclear Schiff-base complexes were prepared by bridging an unsymmetrical tetradentate Schiff-base complex of copper(II) with *m*- or *p*-phthaloyl. The complexes were characterized by means of elemental analyses, molecular weights, UV, IR and ^{1}H NMR (for metal-free ligands) spectra. ESR and magnetic susceptibility measurements show that the copper(II)–copper(II) interaction is negligibly small.

There has been considerable interest in the magnetic and spectroscopic properties of binuclear copper(II) complexes.[1] Recently, they have also received attention due to their resemblance to type-III copper proteins.[2] In this paper, we report the new type binuclear copper(II) complexes linked by *m*- or *p*-phthaloyl as shown in Fig. 1.

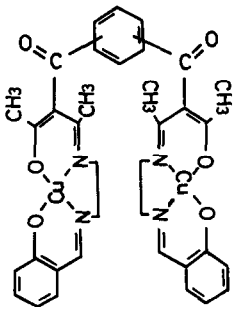


Fig. 1. The abbreviations of the binuclear Schiff-base complexes of copper(II) linked by phthaloyl.

EXPERIMENTAL

Syntheses

[*N*-(1-methyl-3-oxobutylidene)-*N'*-salicylideneethylenediaminato]copper(II), Cu(L—H), was prepared by the method described before.[3]

Preparation of a mononuclear 2-substituted copper(II) *complex.* 4-Nitrobenzoyl chloride (0.40 g, 2.2 mmol) was added to 100 cm^3 of the dichloromethane solution of 0.60 g (2.0 mmol) Cu(L—H), and was refluxed for 1 h. After concentration, the solution was chromatographed on silica gel. The parent complex, Cu(L—H), was first eluted with dichloromethane–acetone [95:5 (v/v)], followed by {*N*-[1-methyl-2-(4-nitrobenzoyl) - 3 - oxobutylidene] - *N'* - salicylideneethylenediaminato}copper(II), Cu(L—$COC_6H_4NO_2$), with dichloromethane–acetone (9:1). Upon recrystallization from acetone, the complex was obtained as bright brown needles (yield 22%). Found: C, 54.93; H, 3.99; N, 9.18%. Calc. for $C_{21}H_{19}N_3O_5Cu$: C, 55.19; H, 4.20; N, 9.19%.

Preparation of the binuclear copper(II) *complexes.* *m*-Phthaloyl dichloride (0.40 g, 2.0 mmol) was added to 100 cm^3 of dichloromethane solution of 1.20 g (4.0 mmol) Cu(L—H). After the solution was refluxed for 3 h, it was concentrated to *ca* 20 cm^3, and then was chromatographed on silica gel. The parent complex, Cu(L—H), was first eluted with dichloromethane–acetone (9:1), followed by the binuclear copper(II) complex, [(CuL)$_2$pht(*m*)], with dichloromethane–acetone (1:1). After concentration of the eluent, the pale brown precipitates of the binuclear complex were obtained by the addition of adequate amounts of hexane (yields 15%). Found: C, 55.78; H, 4.63; N, 6.62%. Calc. for $C_{36}H_{34}N_4O_6Cu_2 \cdot 0.5CH_2Cl_2$: C, 55.61; H, 4.48; N, 7.10%. The binuclear copper(II) complex, [(CuL)$_2$pht(*p*)], was prepared from *p*-phthaloyl dichloride by a similar method to that

* Author to whom correspondence should be addressed.

Table 1. Electronic, IR and molecular weight data of the copper(II) complexes

Complex	Electronic spectra λ_{max} (nm) (log ε)			IR spectra νCO (cm^{-1})	Molecular weight
$Cu(L—COC_6H_4NO_2)$	323 (4.13)	380 (3.86)	552 (2.64)	1630	
$[(CuL)_2pht(m)]$	326 (4.36)	368[sh]* (4.01)	552 (2.72)	1630	778 (746.5)†
$[(CuL)_2pht(p)]$	326 (4.36)	372[sh] (4.15)	552 (2.82)	1630	783 (746.5)†

* sh, shoulder.
† Calculated value.

described above (yields 10%). Found: C, 55.43; H, 4.10; N, 6.83%. Calc. for $C_{36}H_{34}N_4O_6Cu_2 \cdot 0.5CH_2Cl_2$: C, 55.61; H, 4.48; N, 7.10%.

Measurements

The electronic spectra were measured on a Hitachi 215 spectrophotometer. A Hitachi 115 Vapor Pressure osmometer was used for the determination of molecular weights using dichloromethane as a solvent. ^1H NMR spectra were recorded with a JEOL-MH 100 spectrophotometer at a frequency of 100 MHz. The chemical shifts were determined in ppm, using TMS as the internal standard. A PA 115 Vibrating Sample Magnetometer, operated at 10 kG, was used to measure magnetic susceptibility of the complexes. The ESR spectra (X-band) were measured with a JEOL-1X spectrophotometer.

RESULTS AND DISCUSSION

The results of electronic and IR spectra, and molecular weights are listed in Table 1.

The molecular weight measurements show the formation of the binuclear copper(II) complexes, with the results of elemental analyses. The binuclear complexes exhibit the new IR absorption at 1630 cm^{-1} assignable to νCO of the bridging groups, which also indicates the formation of the binuclear copper(II) complexes. The *d–d* absorption bands (552 nm) for the mononuclear 4-nitrobenzoyl substituted complex and the binuclear complexes are slightly shifted to the shorter wavelengths than that (556 nm) for the parent complex.

Although metal-free bridged ligands, $[(H_2L)_2pht(m)]$ and $[(H_2L)_2pht(p)]$, were not prepared from the direct reaction of *N* - (1 - methyl - 3 - oxobutylidene) - *N'* - salicylideneethylenediamine, $H_2(L—H)$, with *m*- or *p*-phthaloyl dichloride, they were obtained by elimination of copper(II) ion from the binuclear copper(II) complexes by passing gaseous hydrogen sulphide. The results of ^1H NMR spectra for the metal-free ligands are listed in Table 2.

The ^1H NMR signals of the methine proton of the parent ligand, $H_2(L—H)$, disappear in the free bridged ligands, indicating the replacement of the methine proton with the bridging groups. In addition, new ^1H NMR signals appear in the region of aromatic protons, being an indicative of introduction of the bridging groups. The methyl signals of the bridged ligands are somewhat shifted to the higher magnetic fields than that of the parent ligand, probably due to the magnetic anisotropic effect of a carbonyl group and/or benzene ring of the bridging group.

Magnetic properties

The ESR spectra of the binuclear copper(II) complexes were obtained at 77 K in the dichloromethane frozen solutions. The spectra showed axial patterns with $A \simeq 190$ G, which resembles that of the mononuclear copper(II) complex. This suggests that the copper(II)–

Table 2. ^1H NMR data of the metal-free ligands in dimethyl sulphoxide-d_6 (ppm)*

Compound	δCH_3	δCH_2CH_2	δCH	$\delta_{aromatic}$	$\delta_{azomethine}$
$H_2(L—H)$	2.05 (3H, *s*) 2.18 (3H, *s*)	3.96–4.29 (4H, *m*)	5.54 (H, *s*)	7.69–7.89 (2H, *m*) 8.25–8.45 (2H, *m*)	9.67 (H, *s*)
$[(H_2L)_2pht(m)]$	1.88 (6H, *s*) 2.05 (6H, *s*)	3.96–4.29 (8H, *m*)		7.49–7.69 (2H, *m*) 8.02–8.35 (6H, *m*)	9.54 (2H, *s*)
$[(H_2L)_2pht(p)]$	1.87 (6H, *s*) 1.96 (6H, *s*)	3.98–4.30 (8H, *m*)		7.39–7.65 (2H, *m*) 8.01–8.36 (6H, *m*)	9.53 (2H, *s*)

* *s*, singlet; *m*, multiplet.

copper(II) interaction is negligibly weak in the complexes. Magnetic susceptibilities of the binuclear copper(II) complexes were measured on solid samples in the temperature range from liquid nitrogen to room temperature.

The χ_A vs T^{-1} plots for these complexes obey the Curie law. The effective magnetic moments at room temperature and near liquid nitrogen temperature are as follows: 2.21 BM at 293 K and 2.23 BM at 80 K for [$(CuL)_2$pht(*m*)]; 2.15 BM at 293 K and 2.19 BM at 80 K for [$(CuL)_2$pht(*p*)]. The magnetic moments are almost independent of temperature. These results also suggest that the copper(II)–copper(II) interaction of the complexes is very weak.

Furthermore, the catalytic actions of the binuclear copper(II) complexes on a chemiluminescence of luminol and an oxidation of tetramethylphenylenediamine were attempted, but they did not exhibit the activities such as reported by Nishida *et al.*[2]

Acknowledgement—We wish to express our thanks to Dr M. Watanabe for his measurements of magnetic susceptibilities.

REFERENCES

1. (a) J. A. Fee, *Struct. Bonding* 1975, **23**, 1; (b) S. K. Mandel and K. Nag., *J. Chem. Soc., Dalton Trans.* 1983, 2429; (c) B. C. Whitmore and R. Eisenberg, *Inorg. Chem.* 1983, **22**, 1; (d) T. Izumitani, M. Nakamura, H. Ōkawa and S. Kida, *Bull. Chem. Soc. Jpn* 1982, **55**, 2122.
2. (a) Y. Nishida, N. Oishi and S. Kida, *Inorg. Chim. Acta* 1980, **46**, L69; (b) N. Oishi, Y. Nishida, K. Ida and S. Kida, *Bull. Chem. Soc. Jpn* 1980, **53**, 2847; (c) N. Oishi, Y. Nishida and S. Kida, *Chem. Lett.* 1981, 1031; (d) Y. Nishida, M. Takeuchi, N. Oishi and S. Kida, *Inorg. Chim. Acta* 1983, **75**, 169.
3. H. A. Kusuka, M. F. Farona, P. Paparo and S. Potterson, *J. Coord. Chem.* 1971, **1**, 259.

Polyhedron Vol. 4, No. 3, pp. 419–424, 1985
Printed in Great Britain

0277–5387/85 $3.00 + .00
© 1985 Pergamon Press Ltd

SPECTROSCOPIC STUDIES OF 4-SUBSTITUTED PYRIDINIUM 2-PYRIDYLCARBONYLMETHYLIDE–RHODIUM(I) COMPLEXES AND X-RAY MOLECULAR STRUCTURE OF (1,5-CYCLOOCTADIENE) (4-METHYLPYRIDINIUM 2-PYRIDYLCARBONYLMETHYLIDE)RHODIUM(I) PERCHLORATE

GEN-ETSU MATSUBAYASHI† and SEIGO AKAZAWA
Department of Applied Chemistry, Faculty of Engineering, Osaka University, Yamada-oka, Suita, Osaka 565, Japan

(*Received* 14 *June* 1984; *accepted* 25 *July* 1984)

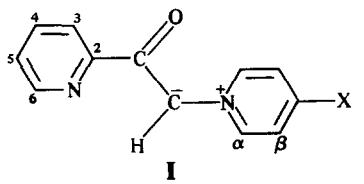
Abstract—(1,5-Cyclooctadiene) (4-substituted pyridinium 2-pyridylcarbonylmethylide)-rhodium(I) perchlorates, $[Rh(COD)(C_5H_4NC(O)\bar{C}H\overset{+}{N}C_5H_4X\text{-}4)]ClO_4$ [COD = 1,5-cyclooctadiene; X = $CH_3C(O)$, $CH_3OC(O)$, C_6H_5, CH_3, and H], have been prepared. They are shown to have the geometry with coordination by the pyridyl nitrogen and carbonyl oxygen atoms of the ylide ligands and to exhibit intramolecular rearrangement of co-ordinated COD in chloroform, methanol, and dimethyl sulphoxide based on IR and ^1H NMR spectroscopies. Although the ylides have exhibited fluorescence bands due to an intramolecular charge-transfer transition and phosphorescence bands due to a carbonyl $^3(n\text{–}\pi^*)$ transition, the complexes have given emission bands due to the metal-to-ylide ligand charge-transfer transition. A single crystal X-ray crystal structure has been determined for $[Rh(COD)(C_5H_4NC(O)\bar{C}H\overset{+}{N}C_5H_4CH_3\text{-}4)]ClO_4$. The crystals are monoclinic, space group $P2_1/n$ with cell dimensions $a = 14.887(3)$, $b = 20.274(4)$, $c = 6.966(1)$ Å, $\beta = 96.13(1)°$, and $Z = 4$. The structure has been refined by a block-diagonal least-squares method to final $R = 0.060$ for 2997 independent reflections with $|F_o| > 3\sigma(F)$. The ylide carbon–pyridinium nitrogen bond distance is 1.420(10) Å. The bonded distances from rhodium to the midpoints of the double bonds of COD are 1.982(11) and 2.014(12) Å.

Although reactivities of photo-excited states of organometallic compounds have recently attracted much interest,[1] luminescent properties of ylides and their metal complexes have been little investigated.[2,3] Pyridinium ylides are unique because the carbanion can be stabilized by a vacant π^* orbital of the pyridinium ring.[2] They show an intense absorption band due to the ylide carbon-to-pyridinium nitrogen charge-transfer (CT) transition. We have undertaken to investigate luminescent properties of several pyridinium ylides stabilized by the 2-pyridylcarbonyl group (**I**) and their rhodium(I) complexes as well as configurations of the complexes. Ylides (**I**) are able to interact with platinum(II) and palladium(II) ions through the ylide carbon atom[4,5] and with tungsten(0) and tin(IV) moieties through the carbonyl oxygen atom.[3,6] Thus, the bonding scheme of pyridinium ylides with the rhodium(I) ion is also of interest.

This paper reports luminescent properties of the ylides (**I**) and their rhodium(I) complexes,

$$[Rh(COD)(C_5H_4NC(O)\bar{C}H\overset{+}{N}C_5H_4X\text{-}4)]ClO_4$$

[X = $CH_3C(O)$, $CH_3OC(O)$, C_6H_5, CH_3, and H], and discusses their configurations based on IR and ^1H NMR spectroscopies. The X-ray molecular structure of (1,5-cyclooctadiene) (4-methylpyridinium 2-pyridylcarbonylmethylide)rhodium(I) perchlorate is also described.



I

X = $CH_3C(O)$, $CH_3OC(O)$, C_6H_5, CH_3, and H

† Author to whom correspondence should be addressed.

EXPERIMENTAL

Preparation of 4-substituted pyridinium 2-pyridylcarbonylmethylides

A benzene (120 cm^3) solution containing 2-(bromoacetyl)pyridine (1.3 g, 6.5 mmol)[7] and pyridine (0.53 g, 6.7 mmol) was refluxed for 4 h to give a white precipitate of *N*-(2-pyridylcarbonylmethyl) pyridinium bromide (1.2 g). To its aqueous (20 cm^3) solution an aqueous (10 cm^3) solution of K_2CO_3 (1.3 g, 9.4 mmol) was added with stirring to afford red solids of crude pyridinium 2-pyridylcarbonylmethylide (Y_H), which were recrystallized from a mixture of dichloromethane and petroleum ether (b.p. 40–60°C) to give red needles of Y_H (0.66 g, 39% yield), m.p. 247°C (dec.). Found: C, 72.58; H, 4.83; N, 14.02. Calc. for $C_{12}H_{10}N_2O$: C, 72.71; H, 5.09; N, 14.13%. 4-Carbomethoxypyridinium (Y_{CM}), 4-acetylpyridinium (Y_{AC}), and 4-phenylpyridinium 2-pyridylcarbonylmethylide (Y_{PH}) were also prepared by the similar procedure. Y_{CM} (63% yield), m.p. 180°C (dec.). Found: C, 65.53; H, 4.71; N, 10.92. Calc. for $C_{14}H_{12}N_2O_2$: C, 66.40; H, 4.78; N, 11.06%. Y_{AC} (39% yield), m.p. 166°C (dec.). Found: C, 68.93; H, 4.79; N, 11.52. Calc. for $C_{14}H_{12}N_2O_3$: C, 69.99; H, 5.03; N, 11.65%. Y_{PH} (55% yield), m.p. 267°C (dec.). Found: C, 40.50; H, 2.15; N, 4.55. Calc. for $C_{18}H_{14}N_2O$: C, 40.39; H, 2.26; N, 4.49%. 4-Methylpyridinium 2-pyridylcarbonylmethylide (Y_{ME}) was prepared as described elsewhere.[5]

Preparation of (1,5-cyclooctadiene) (4-substituted pyridinium 2-pyridylcarbonylmethylide)rhodium(I) perchlorate

To a methanol (20 cm^3) suspension of bis(1,5-cyclooctadiene)dichlorodirhodium(I)[8] (0.125 g, 0.25 mmol) was added a methanol (15 cm^3) solution of Y_H (0.10 g, 0.50 mmol) and the solution was stirred for 10 min at room temperature. To the brown solution was added an aqueous (10 cm^3) solution of $NaClO_4 \cdot H_2O$ (0.056 g, 0.4 mmol) to separate out brown solids. Recrystallization from methanol gave orange needles of $[Rh(COD)Y_H]ClO_4$ (**1**) (0.13 g). The Y_{ME} analogue (**2**) was prepared by the same way and recrystallized from methanol. The Y_{PH}, Y_{CM} and Y_{AC} analogues (**3**–**5**) also were prepared by the same procedure and recrystallized from acetonitrile. Analyses and preparation yields for the ylide–rhodium(I) complexes are summarized in Table 1.

Table 1. Analysis and preparation yields of $[Rh(COD)Y]ClO_4$

No.	Y	Found (Calcd) (%) C	H	N	Yield (%)
1	Y_H	46.95 (47.22)	4.52 (4.36)	5.41 (5.51)	50
2	Y_{ME}	47.81 (48.25)	4.77 (4.63)	5.29 (5.36)	62
3	Y_{PH}	52.90 (53.39)	4.50 (4.48)	4.81 (4.79)	46
4	Y_{CM}	46.56 (46.62)	4.39 (4.27)	4.97 (4.94)	55
5	Y_{AC}	48.07 (47.99)	4.56 (4.37)	5.21 (5.09)	55

Spectral measurements

^1H NMR spectra were measured using a JEOL PS-100 spectrometer equipped with a variable temperature accessory. IR and electronic absorption spectra were recorded on a Hitachi 124 and a Union 401 spectrophotometer, respectively. Total emission spectra were measured on a Hitachi MPF-3 spectrofluorimeter. Spectra of the millisecond component of the emission were obtained on the same fluorimeter using a phosphorescence accessory. Fluorescence lifetimes were determined from decay curves of fluorescence excited by irradiation on N_2 laser pulse (337 nm, $\lesssim$ 5 ns).[9] All the emission measurements were carried out in a degassed methanol/ethanol [1:4 (v/v)] solvent at 77 K.

X-ray crystal analysis

Orange needles of **2** were obtained by recrystallization from methanol. The space group and initial cell parameters were determined from oscillation and Weissenberg photographs. Accurate cell parameters were obtained from the least-squares fit of the angular coordinates of 45 reflections with 2θ values from 25 to 33° which were measured on a computer-controlled Rigaku four-circle diffractometer with Mo-K_α (λ = 0.71069 Å) radiation.

Crystal data

$C_{21}H_{24}N_2O_5ClRh$. M = 522.79. Monoclinic, space group $P2_1/n$, a = 14.887(3), b = 20.274(4), c = 6.966(1) Å, β = 96.13(1)°, V = 2090.2(7) $Å^3$, Z = 4, D_c = 1.6613(6) g cm^{-3}, $F(000)$ = 1064, μ(Mo-K_α) = 9.7 cm^{-1}.

A specimen, approximately 0.12 × 0.12 × 0.25 mm, was used for the data collection on the diffractometer. Intensity data were measured by using graphite-monochromatized Mo-K_α radiation and a ω–2θ scan technique at 2θ scan rate of 2° min^{-1}. They were corrected for Lorentz and polarization effects, but not for absorption. Of the 4789 independent reflections in the range of $2\theta < 55°$,

2997 had structure amplitudes larger than three times their standard deviations. The structure was solved by the conventional heavy-atom technique and the atomic parameters were refined by block-diagonal least-squares method. Anisotropic temperature factors were assigned to all non-hydrogen atoms and isotropic factors to hydrogen. The refinement converged at $R = \Sigma||F_o|-|F_c||/\Sigma|F_o| = 0.066$ and $R_w = [\Sigma w(|F_o|-|F_c|)^2/\Sigma w|F_o|^2]^{1/2} = 0.062$ with the weighting scheme, $1/w = \sigma^2(F_o)+0.0005F_o^2$. The final difference-Fourier map had no positive maxima > 1 e Å^{-3} except in the vicinities of positions of the metal and chlorine atoms. The atomic scattering factors were taken from the usual tabulation.[10] The final atomic coordinates and anisotropic temperature factors together with observed and calculated structure factors have been deposited with the Editor as supplementary materials. Atomic coordinates have also been deposited with the Cambridge Crystallographic Data Centre.

Crystallographic calculations were performed on an ACOS 900S computer at the Crystallographic Research Centre, Institute for Protein Research, Osaka University. Figure 1 was drawn with a local version of ORTEP-II.[11]

RESULTS AND DISCUSSION

Description of the molecular structure of [Rh(COD)($C_5H_4NC(O)\bar{C}H\overset{+}{N}C_5H_4CH_3$-4)]$ClO_4$ (2)

Figure 1 shows the molecular structure of 2 with the atom-labelling scheme. In the crystal structure no unusual intermolecular contacts were found. Pyridyl nitrogen and carbonyl oxygen atoms as well as two olefin carbon–carbon bonds are coordinated to rhodium, forming a square-planar geometry around the metal atom. The perchlorate anion does not participate in the coordination to the rhodium atom. Bond distances and angles with estimated standard deviations are given in Table 2. The Rh—N distance [2.068(6) Å] is very close to that of carbonyl(8-hydroxyquinolinato)(triphenylphosphine)rhodium(I) [2.098(9) Å].[12] The Rh—O distance [2.049(5) Å] is also quite similar to that of this compound [2.042(5) Å] and to that of benzoyl-1,1,1-trifluoroacetonato(1,5 - cyclooctadiene)rhodium(I) [2.050(4), 2.066(5) Å].[13] The COD ligand is coordinated to the metal atom with its customary "tub" conformation, the olefin bonds being orientated approximately perpendicular to the coordination plane. The distances between rhodium and the double bond centres of COD [1.982(11), 2.014(12) Å] are on the short end of the range 2.00–2.16 Å found in heavy-metal complexes with COD.[14] These short distances may result from the *trans* influence of nitrogen and oxygen atoms. On the other hand, the distances of coordinated double bonds, C(14)—C(15) and C(18)—C(19) [1.395(11) and 1.350(12) Å, respectively] are slightly longer than the uncoordinated olefinic C=C distance of 1.34 Å.[15]

All the non-hydrogen atoms of the ylide ligand as well as rhodium are approximately co-planar (±0.08 Å). The C(7)—N(2) bond [1.422(10) Å] is apparently longer than partial double bonds, N(1)—C(1), N(1)—C(5), N(2)—C(8), and N(2)—C(12) (1.346–1.390 Å) and is rather close to the C—N single bond adjacent to the N=C double bond, as was reported for *n*-butyltrichloro(*N'*-phenylpyridine-2-calbaldimine-*N*,*N'*)tin(IV) [1.441(5) Å].[16] This finding may suggest little double-bond character in this

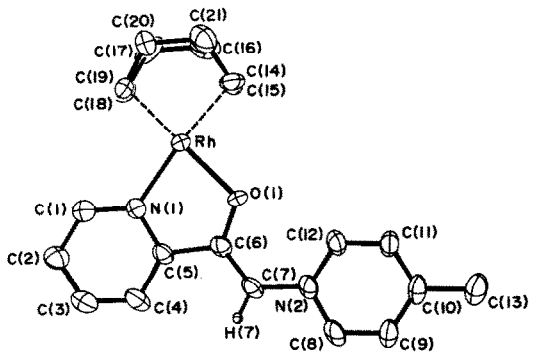
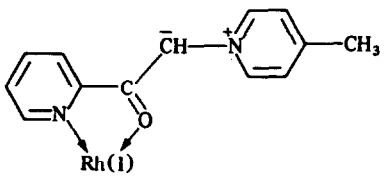


Fig. 1. View of the molecular structure of the cation moiety of [Rh(COD)Y_{ME}]ClO_4 (2) with the atom-labelling scheme. Hydrogen atoms except for H(7) are not illustrated. Thermal ellipsoids are drawn at the 30% probability level.

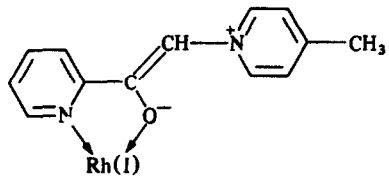
Table 2. Intramolecular bond distances and angles for [Rh(COD)Y_{ME}]ClO_4

Distances (Å)			
Rh-O(1)	2.050(5)	Rh-N	2.069(6)
Rh-C(14)	2.093(8)	Rh-C(15)	2.104(7)
Rh-C(18)	2.122(8)	Rh-C(19)	2.122(7)
O(1)-C(6)	1.304(10)	N(1)-C(1)	1.346(10)
N(1)-C(5)	1.347(10)	N(2)-C(7)	1.420(10)
N(2)-C(8)	1.390(10)	N(2)-C(12)	1.357(10)
C(1)-C(2)	1.392(12)	C(2)-C(3)	1.357(14)
C(3)-C(4)	1.355(13)	C(4)-C(5)	1.372(11)
C(5)-C(6)	1.498(11)	C(6)-C(7)	1.357(11)
C(8)-C(9)	1.371(12)	C(9)-C(10)	1.357(12)
C(10)-C(11)	1.388(11)	C(11)-C(12)	1.365(11)
C(10)-C(13)	1.505(13)	C(14)-C(15)	1.394(11)
C(15)-C(16)	1.524(13)	C(16)-C(17)	1.482(13)
C(17)-C(18)	1.536(13)	C(18)-C(19)	1.346(11)
C(19)-C(20)	1.502(12)	C(20)-C(21)	1.452(15)
Selected bond angles (°)			
N(1)-Rh-O(1)	78.6(2)	C(14)-Rh-C(15)	38.8(3)
C(14)-Rh-C(19)	82.1(3)	C(15)-Rh-C(18)	82.3(3)
C(18)-Rh-C(19)	37.1(3)	Rh-O(1)-C(6)	116.2(5)
Rh-N(1)-C(5)	115.5(5)	N(1)-C(5)-C(6)	113.1(6)
C(1)-N(1)-C(5)	117.8(6)	C(5)-C(6)-O(1)	116.3(6)
C(5)-C(6)-C(7)	119.4(6)	N(1)-C(1)-C(2)	122.7(8)
C(1)-C(2)-C(3)	117.8(8)	C(2)-C(3)-C(4)	120.2(9)
C(3)-C(4)-C(5)	120.1(8)	C(4)-C(5)-N(1)	121.4(7)
C(6)-C(7)-N(2)	125.1(7)	C(6)-C(7)-H(7)	116.9(38)
C(7)-N(2)-C(8)	117.6(6)	C(8)-N(2)-C(12)	123.5(6)
N(2)-C(8)-C(9)	119.9(7)	C(8)-C(9)-C(10)	122.1(8)
C(9)-C(10)-C(11)	116.8(8)	C(10)-C(11)-C(12)	122.1(8)
C(11)-C(12)-N(2)	120.1(7)	C(14)-C(15)-C(16)	123.5(7)
C(15)-C(16)-C(17)	116.5(8)	C(16)-C(17)-C(18)	114.1(8)
C(17)-C(18)-C(19)	124.8(8)	C(18)-C(19)-C(20)	123.0(8)
C(19)-C(20)-C(21)	116.0(7)	C(14)-C(21)-C(20)	116.5(8)

bond, which is in contrast to the appreciable partial double-bond character of the ylide carbon–nitrogen bond of 4-cyanopyridinium 2-pyridylcarbonylmethylide which was deduced on the basis of ^{1}H NMR spectra.[17] The C(6)—C(7) distance [1.356(11) Å] is significantly short compared with C(5)—C(6) [1.499(11) Å]. Moreover, the ylide carbonyl distance [C(6)—O(1), 1.304(8) Å] is markedly lengthened compared with the C=O distance predicted based on double-bond radii of carbon and oxygen atoms (1.20 Å),[18] and is somewhat longer than the C=O distance of tetracarbonyl(dimethylsulphonium 2-pyridylcarbonylmethylide)tungsten(0) [1.277(9) Å].[19] These findings are explained by assuming the resonance hybrid of canonical structures, **II** and **III**, in the present ylide ligand.



II



III

The IR carbonyl stretching band of **2** is observed at a lower frequency than that of free ligand (Table 3), indicating the contribution of the canonical structure **II**. This is also the same in the other ylide complexes **1**, **3**–**5**. The coordination through the carbonyl oxygen atom in these complexes offers a striking contrast with the ylide carbon–metal bonding in the palladium(II) and platinum(II) complexes with these ylides.[4,5]

Table 3. IR carbonyl stretching frequencies (cm^{-1}) and ^{1}H NMR chemical shifts (δ) for [Rh(COD)Y]ClO$_4$

Y	ν(C=O)[a]	δ H$_6$[b]	δ H$_\alpha$[b]
Y_H	1490 (43)	8.05 (0.45)	9.60 (0.30)
Y_{ME}	1501 (28)	8.12 (0.36)	9.39 (0.45)
Y_{PH}	1480 (35)	c	9.48 (0.51)
Y_{CM}	1501 (26)	8.37 (0.30)	9.59 (0.36)
Y_{AC}	1499 (15)	8.07 (0.48)	9.60 (0.15)

[a] Measured in Nujol mulls. $\nu_{free}-\nu_{complexed}$ in parentheses.

[b] Measured in DMSO-d_6. $\delta_{free}-\delta_{complexed}$ in parentheses.

[c] Not determined precisely owing to complexity of the signals.

* The temperature-dependent ^{1}H NMR spectra were measured for this complex in methanol-d_4 and in chloroform-d, since the solubility of [Rh(COD)Y$_H$]ClO$_4$ was not enough for the measurement. The spectra of both the complexes in these solvents were essentially identical at room temperature.

^{1}H *NMR spectra*

These complexes have shown the ^{1}H NMR signals of protons (H_6) attached to carbons adjacent to the pyridyl nitrogen atoms at considerably higher fields than the free ylides in DMSO-d_6 (Table 3). Generally, these signals are likely to occur at lower fields upon complexation through the pyridyl nitrogen atom with metal ions owing to their inductive effects.[5,6] Signals of *ortho* protons (H_α) of the pyridinium rings of the complexes are also observed at higher fields than those of the free ligands, although the chemical shifts of other protons are not precisely determined owing to their complicated signal occurrences. These unusual upfield shifts of the present complexes may be due to a significant metal-to-ylide ligand CT contribution, as will be described later. The spectra of the complexes in DMSO-d_6 have shown a signal due to the olefinic protons of the ligated COD at room temperature, although these protons are expected to be non-equivalent based on the geometry of these complexes. This indicates some positional rearrangement of ligands around the rhodium atom. The spectra of [Rh(COD)Y$_H$]Cl* in methanol-d_4 and in chloroform-d have shown also a signal due to the non-equivalent olefinic protons of the COD ligand at room temperature. On the other hand, two signals of these protons are observed at lower temperatures (Fig. 2). Both additions of free COD and Y_H to a chloroform-d solution of [Rh(COD)Y$_H$]Cl have not varied the spectrum of the complex. Thus, these findings seem to indicate an intramolecular rearrangement without dissociation of the ligands. The Gibbs free energies of activation of the rearrangement at coalescence temperatures have been estimated 11.8 ± 0.1 kcal mol^{-1} (at -27 ± 2°C) in chloroform-d and 10.6 ± 0.1 kcal mol^{-1} (at -51 ± 2°C) in methanol-d_4, using the approximate equation.[20]

Electronic absorption and emission spectra

Figure 3 shows the absorption spectra of Y_{ME} and the Y_{ME}–Rh(I) complex (**2**) in methanol/ethanol

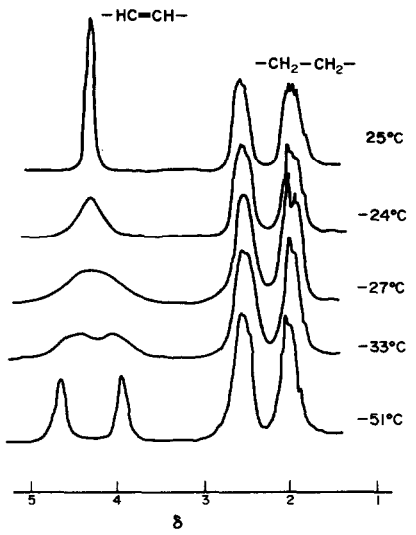


Fig. 2. Temperature-dependent ^1H NMR signals of the COD ligand of $[Rh(COD)Y_H]Cl$ in chloroform-*d*.

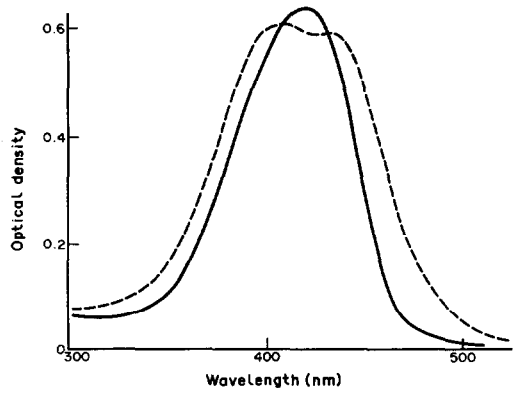


Fig. 3. Electronic absorption spectra of Y_{ME} (6.0×10^{-4} mol dm^{-3}) (——) and $[Rh(COD)Y_{ME}]ClO_4$ (**2**) (2.4×10^{-4} mol dm^{-3}) (– – –) in methanol/ethanol [1:4 (v/v)] at 298 K (1-mm cell).

[1:4(v/v)] at room temperature. The intense band of Y_{ME} at 423 nm is reasonably assigned to an intramolecular CT transition from carbanion to a pyridinium π^* orbital. Generally, pyridinium ylides are known to be stabilized by the carbanion participation in the resonance of the pyridinium ring,[2] which is in contrast with the stabilization by the carbanion delocalization to *d*-orbitals of sulphur and phosphorus atoms in sulphur and phosphorus ylides.[21,22] It is noteworthy that Y_{ME} as well as other pyridinium ylides exhibits the CT band at a longer wavelength than the corresponding triphenylphosphonium- and dimethylsulphonium ylides.[23] An electron-withdrawing substituent of the pyridinium ring would more contribute to this stabilization; the intramolecular CT absorption band of an ylide with a more electron-withdrawing substituent appears at a longer wavelength (Table 4).

Complex **2** shows broad bands at somewhat shorter wavelengths than free Y_{ME}, of which the band at a shorter wavelength is assignable to the intraligand CT transition and the other tentatively to metal-to-ligand CT one, as was observed for $W(CO)_4Y_{ME}$.[3] Coordination to the metal through the carbonyl oxygen atom decreases the intraligand CT contribution of the ylide carbon-to-pyridinium ring, causing to elevate the energy due to the CT transition. The other ylide–Rh(I) complexes have exhibited the same spectral feature (Table 5).

As is summarized in Table 4, the ylides exhibit weak fluorescences with lifetimes of $\lesssim 5$ ns and weak phosphorescences with lifetimes of 200–500 ms in methanol/ethanol [1:4 (v/v)] at 77 K. The excitation spectra which maximize the intensities of fluorescence bands correspond to intramolecular CT absorption bands. On the other hand, the excitation bands of the phosphorescence bands appear at 270–290 nm. On the basis of their lifetimes these emissions are considered to be due to the carbonyl $^3(n\text{–}\pi^*)$ transition. This finding is in contrast with the phosphorescences due to the $^3(\pi\text{–}\pi^*)$

Table 4. Absorption (at 298 K) and emission band maxima (at 77 K) (nm) for 4-substituted pyridinium 2-pyridylcarbonylmethylides in methanol/ethanol [1:4 (v/v)]

Ylide	Absorption[a]	Emission	
		Fluorescence[b]	Phosphorescence[c]
Y_H	426 (4.17)	456	460 (400)
Y_{ME}	423 (4.03)	458	460 (550)
Y_{PH}	459 (4.43)	481	521 (500)
Y_{CM}	483 (4.80)	512	500 (400)
Y_{AC}	490 (4.22)	524	532 (350)

[a] log [ε (mol^{-1} cm^{-1} dm^3)] in parentheses.
[b] Lifetimes were determined to be < 5 ns.
[c] Lifetimes (ms) in parentheses.

Table 5. Absorption (at 298 K) and emission (at 77 K) maxima (nm) for the rhodium(I)–ylide complexes, $[Rh(COD)Y]ClO_4$, in methanol/ethanol [1:4 (v/v)]

Y	Absorption*		Emission
Y_H	406 (4.3)	430 (4.3)	640
Y_{ME}	408 (4.4)	433 (4.4)	650
Y_{PH}	443 (4.4)	460 (4.3)	730
Y_{CM}	437 (4.3)	467 (4.4)	730
Y_{AC}	422 (4.2)	468 (4.2)	640

* log [ε (mol^{-1} cm^{-1} dm^3)] in parentheses.

transition observed for several *N*-benzyl-4-substituted pyridinium perchlorates which have 1–3 s as the lifetime.[6]

Figure 4 shows the emission spectrum of **2** in methanol/ethanol [1:4 (v/v)] at 77 K. The complex has shown no phosphorescence with a lifetime in the millisecond range, which is also the same as the other ylide–Rh(I) complexes. Furthermore, no flouresence due to the intraligand CT transition of the ylide has been observed. **2** shows an emission band at a longer wavelength. The excitation band which maximizes the intensity of this band also is close to its absorption band at 430 nm. Thus, the emission is tentatively ascribed to the metal-to-ligand CT transition. The lifetime of this emission has not been determined in the ns and ms regions, but has been estimated to be in the μs region. The other complexes have exhibited an emission band similar to this complex (Table 5). The Stokes shifts of the metal-to-ligand CT emissions are large, indicating markedly prolonged metal-to-ligand bond distances at excited states, as was reported for 1,2-bis(diphenylphosphinoethane)– and *cis*-1,2-bis(diphenylphosphino)-ethylene–Rh(I) complexes.[24]

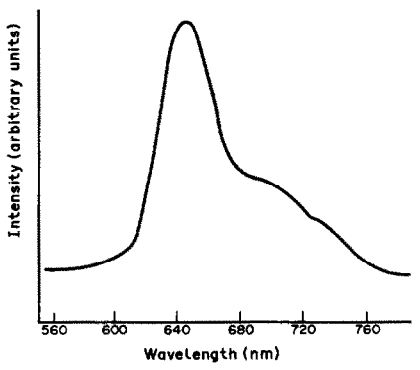


Fig. 4. Emission spectrum of $[Rh(COD)Y_{ME}]ClO_4$ (**2**) in methanol/ethanol [1:4 (v/v)] at 77 K.

Acknowledgements—We wish to express hearty thanks to Professor Toshio Tanaka of Osaka University for his continuous encouragement throughout this study. We thank Professor Kazumi Nakatsu of Kwansei Gakuin University, Nishinomiya, Hyogo, for the use of the X-ray diffractometer and the programs for the structure solution and refinement. We thank Dr Masaaki Yokoyama of Osaka University for the measurement of the fluorescence lifetimes of the ylides.

REFERENCES

1. G. L. Geoffroy and M. S. Wrighton, *Organometallic Photochemistry*. Academic Press, New York (1979).
2. I. Zugravescu and M. Pelrovanu, *N-Ylide Chemistry*. McGraw-Hill, New York (1978).
3. I. Kawafune and G. Matsubayashi, *Inorg. Chim. Acta* 1983, **70**, 1.
4. H. Koezuka, G. Matsubayashi and T. Tanaka, *Inorg. Chem.* 1976, **15**, 417.
5. G. Matsubayashi and Y. Kondo, *J. Organomet. Chem.* 1981, **219**, 269.
6. G. Matsubayashi *et al.*, to be published.
7. G. R. Clemo, W. McG. Morgan and R. Rapper, *J. Chem. Soc.* 1937, 965.
8. R. B. King, *Organometallic Synthesis*, Vol. 1, p. 132. Academic Press, New York (1965).
9. M. Yokoyama, unpublished.
10. *International Tables for X-Ray Crystallography*, Vol. 4. Kynoch Press, Birmingham (1974).
11. C. K. Johnson, ORTEP-II, Report ORNL 5138, Oak Ridge National Laboratory, Tennessee (1976).
12. J. G. Leipoldt, S. S. Basson and C. R. Dennis, *Inorg. Chim. Acta* 1981, **50**, 121.
13. J. G. Leipoldt, S. S. Basson, G. L. Lamprecht, L. D. C. Bok and J. J. J. Schlebusch, *Inorg. Chim. Acta* 1980, **40**, 43.
14. M. P. Anderson and L. H. Pignolet, *Inorg. Chem.* 1981, **20**, 4101 and references therein.
15. M. R. Churchill and S. A. Bezman, *Inorg. Chem.* 1973, **12**, 531.
16. G. Matsubayashi, T. Tanaka, S. Nishigaki and K. Nakatsu, *J. Chem. Soc., Dalton Trans.* 1979, 501.
17. G. Matsubayashi, *Bull. Chem. Soc. Jpn* 1981, **54**, 915.
18. L. Pauling, *The Nature of the Chemical Bond*, 3rd edn., p. 228. Cornell University Press, Ithaca, New York (1960).
19. G. Matsubayashi, I. Kawafune, T. Tanaka, S. Nishigaki and K. Nakatsu, *J. Organomet. Chem.* 1980, **187**, 113.
20. J. A. Pople, W. G. Schneider and H. J. Bernstein, *High Resolution Nuclear Magnetic Resonance*, p. 233. McGraw-Hill, New York (1959).
21. A. W. Johnson, *Ylide Chemistry*. Academic Press, New York, 1966.
22. B. M. Trost and L. S. Melvin, Jr, *Sulfur Ylides*. Academic Press, New York (1975).
23. K. Ueyama *et al.*, to be published.
24. G. L. Geoffroy, M. S. Wrighton, G. S. Hammond and H. B. Gray, *J. Am. Chem. Soc.* 1974, **96**, 3105.

Polyhedron Vol. 4, No. 3, pp. 425–428, 1985
Printed in Great Britain

0277–5387/85 $3.00 + .00
© 1985 Pergamon Press Ltd

A NEW COPPER(I) THIOCYANATO THIOCYANOGEN COMPLEX

S. K. TOBIA,* E. R. SOUAYA and W. G. HANNA
Chemistry Department, Faculty of Science, Ain Shams University, Abbassia, Cairo, Egypt

(*Received* 5 *March* 1984; *accepted after revision* 25 *July* 1984)

Abstract—The reaction between Cu^{2+} and SCN^-, in glacial acetic acid at a Cu/SCN ratio, of 1:4, gave a dark red solution that exhibited an absorption band at 496 nm. The colour of the freshly prepared solution was bleached by water with concomitant production of SO_4^{2-} ion. On standing, the stability of the colour towards water is increased and the position of the absorption band shifts to a higher wavelength. It is inferred that the thiocyanogen produced on oxidation of SCN^- by Cu^{2+} is stable in the non-aqueous medium and is coordinated together with SCN^- in a Cu(I) complex. The bleaching action of water is attributed to the hydrolysis of thiocyanogen, mainly to SO_4^{2-}. The presence of thiocyanogen enhanced polymerization and subsequent deposition of an orange-brown solid complex. On the basis of chemical, spectral, and thermal analyses the formula $K[Cu(SCN)_2(NCS—SCN)]$, is assigned to the new compound.

Copper(I) forms an insoluble cyanide as well as a number of soluble cyano-complexes. It also forms an insoluble thiocyanate, but no thiocyanato Cu(I) complexes have been reported previously. On the other hand, copper(II) forms homogeneous thiocyanato complexes as well as mixed ligand complexes. For example, in the presence of organic nitrogen bases, it yields with thiocyanate coloured complexes that have some analytical applications. Other coloured complexes were also obtained by oxidation of colourless redox indicators by Cu(II) in the presence of CN^- or SCN^-. Gregorowicz and Buhl[1] oxidized variamine blue with Cu(II) in the presence of SCN^-. The coloured complex was not characterized but it may be a Cu(I) complex containing SCN^- and the oxidized form of variamine blue.

The SCN^- can also be oxidized to thiocyanogen, but the presence of the latter could only be detected in non-aqueous media because of its ease of hydrolysis. In molten thiocyanate for example, the reduction of Cu(II) to Cu(I) and the oxidation of SCN^- to parathiocyanogen (polymerized thiocyanogen) or to sulphur and cyanogen has been confirmed by a number of investigators:[2]

$$2Cu(II) + 2SCN^- = (NCS—SCN) + 2Cu(I).$$

Thiocyanogen may however, be decomposed to sulphur and cyanogen:

$$(NCS—SCN) = 2S + (CN)_2.$$

Although, these reactions involve Cu(I), SCN^- and (NCS—SCN), the possibility of formation of a complex containing both thiocyanate and thiocyanogen has not been investigated before.

The formation of a complex containing both the pseudohalogen and its oxidation product has been demonstrated before in the Cu^{2+}–CN^- system.[3] Furthermore, a new Fe(II) thiocyanate thiocyanogen complex has been prepared by the reaction of Fe(III) and SCN^- in glacial acetic acid.[4] The present investigation has been undertaken to study the possibility of formation of the corresponding Cu(I) complex when Cu(II) reacts with SCN^- in a non-aqueous medium. Since thiocyanogen is known to be most stable in glacial acetic acid, the latter was used as a reaction medium in this study.

EXPERIMENTAL

Solutions

Stock solutions of Cu(II) and thiocyanate were prepared by saturating a certain volume of glacial acetic acid (AR 99.7) with anhydrous Cu(II) acetate or potassium thiocyanate at 25°C. The concentra-

* Author to whom correspondence should be addressed.

tions of these solutions were approximately 0.08 and 3.0 *M* with respect to Cu(II) and SCN^- ions respectively.

Dilute thiocyanate solutions were prepared by diluting the stock solution with glacial acetic acid, but the copper solution was used without dilution.

Thiocyanogen solution, about 0.1 *M*, was prepared by the action of bromine on silver thiocyanate, in an acetic acid medium as was described by Vanderzee and Quist.[5] The pale yellow solution obtained is known to contain the monomer and was found stable below 15°C.

Preparation of the complexes

The copper solution was run from a burette into the thiocyanate solution contained in a 50-cm^3 conical flask mounted on a magnetic stirrer, and cooled by an ice bath. The compound studied was that obtained at Cu/SCN^- ratio of 1:4. When the dark red solution obtained at this ratio was left overnight, an orange-brown solid was obtained. The latter was separated by filtration, washed with acetic acid, and dried over P_2O_5.

Analytical

The Cu(II) solution was standardized by complexometric titration using EDTA and murexide indicator. The thiocyanate solutions were standardized, after dilution with water, by the Volhard's method.

The solid complex was analyzed as follows.

Since the solid complex is suspected to contain thiocyanate and thiocyanogen, the analytical procedure used allowed for the separate determination of these two species. The procedure adopted involved treatment of the solid with 0.1 *M* NaOH which gave a precipitate containing parathiocyanogen and hydrous copper oxide. The precipitate was separated by filtration, and the filtrate was kept for the determination of SCN^- and K^+. Treatment of the precipitate with dilute HCl dissolved the copper leaving an orange residue of parathiocyanogen which was washed, dried and weighed.

The thiocyanate in the alkaline filtrate was determined by a thiocyanate-sensitive ion-selective electrode. Copper was determined either by iodometric titration or complexometrically using EDTA and murexide. Potassium was determined gravimetrically as cobaltinitrite.

An alternate method for K^+ and Cu^{2+} involved treatment of the solid with concentrated nitric acid and heating to dryness. The residue was taken up by HCl and the resulting solution was used for the determination of those ions.

The percentage of thiocyanogen was also confirmed by subtracting the thiocyanate sulphur from the total sulphur. The latter was determined by a sodium carbonate–potassium nitrate fusion method using a gravimetric finish for the determination of the sulphate formed.

Tests for thiocyanogen in the complex solution and in the solid complex were carried out as described before.[4]

The TG, DTG and DTA graphs were recorded using a Paulik–Paulik–Erdey MOM Derivatograph. Other physical measurements were essentially as described before.[4]

RESULTS AND DISCUSSION

Preliminary experiments indicated that when the thiocyanate solution was added to the copper solution, a dark brown precipitate was obtained when the SCN/Cu ratio reached 2. Chemical analysis of the precipitate showed that it was Cu(II) thiocyanate, $Cu(SCN)_2$. It decomposed on standing into CuSCN and parathiocyanogen. The compound was also insoluble in excess of thiocyanate, and therefore, the investigation of other possible complexes was impossible. For this reason, the copper solution was added to the thiocyanate solution to produce mixtures of any SCN/Cu ratio. In this investigation only the species produced at an SCN/Cu ratio of 4 was studied.

The dark red solution obtained at the above ratio exhibited an absorption band at 495 nm, and was obtained only in the non-aqueous medium. Under these conditions it is possible that the thiocyanogen formed by the oxidation of thiocyanate by copper(II) would be stable and the red colour may be attributed to a thiocyanato thiocyanogen complex of copper(I). The red colour of the freshly prepared solution is almost completely bleached by water with production of sulphate ion, as tested for by Ba^{2+}. This is explained as being due to the hydrolysis of the coordinated thiocyanogen. On standing, however, the red solution was found to gain increasing stability towards water. This suggests that, in the aged solution, the coordinated thiocyanogen must have been protected from hydrolysis, probably by acting as a bridging ligand between the metal ions rather than as a terminal one. This view is supported by a shift in the absorption band from 495 nm in the fresh solution to 500 nm in the aged solution.

The orange brown precipitate obtained when the red solution was left overnight was subjected to chemical and physical tests as described below.

Magnetic measurements showed that the solid is diamagnetic, suggesting the presence of Cu(I) in the complex.

The solid is insoluble in water and most organic solvents. Treatment with NaOH decomposed the solid into a precipitate containing hydrous copper oxide and parathiocyanogen, and alkaline solution containing K^+ and SCN^- ions. The separation of parathiocyanogen is not in itself indicative of the existence of a thiocyanato thiocyanogen complex. The solid may be a mixture of parathiocyanogen and CuSCN, or may contain $Cu(SCN)_2$ which decomposes to CuSCN and parathiocyanogen. However, the following observations provide evidence indicating that the solid is a thiocyanogen Cu(I) complex.

Chemical analysis

The results of chemical analysis are shown in Table 1. For every mole of Cu, there are two moles of SCN^- ion and one mole of NCS—SCN. If these were coordinated to Cu(I), the percent of the potassium counter ion would be 11.67 which is in good agreement with the observed value.

The thiocyanogen produced by Cu(II) would be insufficient for the above stoichiometry, but the extra may be formed by aerial oxidation of the solution standing overnight. The first yield of compound was only about 60% of that expected, but further yields were obtained when the filtrates collected were left exposed to air, until a total of about 85% yield was obtained.

The composition and stoichiometry of the solid compound was further confirmed by chemical synthesis. The same solid was obtained on treatment of a mixture containing equimolar amounts of KSCN and CuSCN, in glacial acetic acid, by a solution of thiocyanogen. A yield, better than 95% was obtained when the number of moles of thiocyanogen was equal to that of copper.

X-ray analysis

The X-ray diffraction pattern was found different from that of CuSCN or $Cu(SCN)_2$. The principal lines are found at 5.7 (100%), 3.69 (55%), 3.09 (80%), 2.95 (60%) and 2.35 (100%).

Table 1.

Component Sought	Observed	Calculated from: K $Cu(SCN)_2$(NCS-SCN)
C	13.70	14.35
N	16.50	16.74
S (total)	38.15	38.27
SCN^-	35.29	34.68
(NCS-SCN)	33.86	34.68
Cu	19.00	18.98
K	10.95	11.67

Effect of dry heating

Gentle heating of the solid in a micro test tube gave a sublimate of sulphur and cyanogen gas as indicated by a positive oxine-cyanide test.[6] Parathiocyanogen does not respond to this test.

Thermal analysis

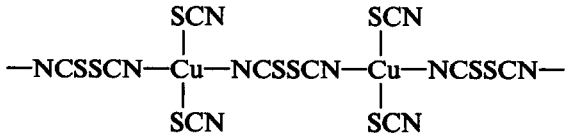
The TGA showed a weight loss occurring in two distinct stages, one between 165 and 371°C, and the other between 371 and 572°C. Each stage corresponded to about 32% loss and was accompanied by an exothermic peak in the DTA graph. The first was strong and sharp centred at 300°C, while the other was broad and complex, probably representing three or more overlapping bands. The two-stage weight loss implies the presence of two different oxidizable ligands that are differently bonded to the metal ion. The theoretical loss in each stage, as calculated from the formula $K[Cu(SCN)_2(NCSSCN)]$ is 34.68%. The difference is due to the retention of some sulphur in the residue which contained potassium sulphate, and a mixture of copper oxide and sulphide. The formation of this product was accompanied by about 6% increase in weight and took place between 572 and 667°C.

IR spectra

In addition to the band at 2080 cm^{-1} assigned to the —C≡N— asymmetric stretching on the SCN^- group, there is a stronger and sharper band at 2160 cm^{-1} assigned to the —C≡N— asymmetric stretching of thiocyanogen. This band exists at 2171 cm^{-1} in free thiocyanogen,[5] and the observed decrease may be attributed to bonding to two copper ions. On heating the solid up to 350°C, the intensity of the thiocyanogen band was decreased by about 50%, while the thiocyanate band was not changed, but it disappeared at a higher temperature. These observations are consistent with those indicated by the thermal analysis.

In the lower frequency range, the C—S stretching is represented by two bands, one at 670 cm^{-1} for thiocyanogen[5] and the other at 745 cm^{-1} for thiocyanate. The effect of thermal treatment on these bands is similar to that observed for the —C≡N— asymmetric stretching, mentioned above. The band at 610 cm^{-1} is assigned to Cu—S stretching. Not only was it maintained on heating up to 500°C, but also became sharper and stronger.

One of the possible structures which may account for all the above observations may be represented as:



in which the copper is bonded to two terminal thiocyanate groups and thiocyanogen acting as a bridging ligand to form an infinite chain polymer. Since —C—S— stretching of the thiocyanate is relatively low, it is possible that the copper is bonded through the thiocyanate sulphur.

REFERENCES

1. Z. Gregorowicz and F. Bouhl, *Z. Anal. Chem.* 1962, **187**, 1; *Acta Chim. Acad. Sci. Hung.* 1962, **32**, 145.
2. (a) G. Metzger, Rapp. CEA-T 2566 Comissarial a l'Energie Atomique, Centre d'Etudes Nucleaires, Saclay, France (1964); (b) A. Eluard and B. Tremillon, *J. Electroanal. Chem.* 1967, **13**, 208; (c) D. H. Kerridge and M. Mosely, *J. Chem. Soc.* (*A*) 1969, 2211.
3. S. K. Tobia and M. F. El-Shahat, *J. Chem. Soc.* (*A*) 1968, 2444.
4. S. K. Tobia and W. G. Hanna, *Polyhedron* 1984, **3**, 997.
5. C. E. Vanderzee and A. S. Quist, *Inorg. Chem.* 1966, **5**, 1238.
6. A. S. Kamarowsky and N. S. Polueklow, *Z. Anal. Chem.* 1934, **96**, 23.

Polyhedron Vol. 4, No. 3, pp. 429–436, 1985
Printed in Great Britain

0277–5387/85 $3.00 + .00
© 1985 Pergamon Press Ltd

EQUILIBRIUM AND KINETIC STUDIES OF THE Fe(III) COMPLEX FORMATION WITH GLYCINEHYDROXAMIC ACID

MOHAMED S. EL-EZABY* and MANSOUR M. HASSAN
Chemistry Department, Kuwait University, Faculty of Science, P.O. Box 5969, Kuwait

(*Received* 8 *May* 1984; *accepted* 25 *July* 1984)

Abstract—Spectrophotometric methods were utilized for stability constant determinations of the Fe(III) interaction with glycinehydroxamic acid (GX) at $I = 0.15$ *M* NaCl and $T = 25°C$. Program SQUAD II was used to assess the absorbance data in the wavelength range 300–520 nm. Four constants were determined for 1:1:1, 1:1:0, 2:1:1 or 3:1:3 and 2:1:0 complex species in the pH range 1.0–7.5. The kinetics of the interactions of Fe(III) with GX were also studied in the pH range 1.0–3.0 by the stopped flow method. The observed rate constant at a given pH was $k_{obs} = A + BT_{GX}$. The parameters A and B are functions of pH in the range 1.7–3.0 and only A is a function of pH in the range 1.0–1.7. The mechanism of complex formation was discussed in the light of the experimental results and the equilibrium study. It has been concluded that $FeOH^{2+}$ is the reactive species in the complex formation of $FeGXH^{3+}$ species while $Fe(OH)_2^+$ is the reactive species in the complex formation of $FeGX^{2+}$ species.

Considerable work has been done in the last decade on hydroxamate chemistry. Aside from their analytical and industrial applications, they serve as metal chelators which may function as growth factors, antibiotics, antibiotic antagonists, tumour inhibitors, antifungal agents and cell division factors.[1–11] The recent interest in hydroxamates lies in the fact that some siderochromes containing hydroxamate groups, such as peptide ferrochrome, form stable complexes with Fe(III).[12] Their specific function is to solubilize iron acting as a mediator for transporting iron from the environment to the cell. Although many hydroxamate complexes of Fe(III) have been reported quite recently,[13–15] few studies have dealt with the kinetics and mechanism of their binary complex formation.[16,17] In addition, ternary complex formation involving hydroxamates as one of the ligands were scarcely investigated.

In an attempt to study kinetically the ternary reaction of Fe(III)-pyridoxol (vitamin B_6 compound) with glycinehydroxamate, prior investigation of the binary system involving Fe(III) and glycinehydroxamate is essential. It has been reported that glycinehydroxamate forms stable monomeric complexes with Fe(III) over quite a wide pH range.[15] The study was carried out by analytical potentiometry. In this work the interaction of Fe(III) with glycinehydroxamate was followed spectrophotometrically in order to define their equilibrium reactions and their reaction kinetics. This kind of work was inevitable to account for iron exchange between its low molecular weight complexes and *apo*transferrin (iron-transport protein), and for the ability of the ligand to extract iron from ferritin (iron storage protein).

EXPERIMENTAL

Solutions of acidic iron(III) chloride (E. Merck) and glycinehydroxamic acid (GX) (E. A. Thomas, > 98%) were obtained by subdilution processes from stock solutions. The concentration of the iron(III) chloride stock solution (~ 0.1 *M* in 0.1 *M* HCl (May & Baker)) was checked by EDTA titration using salicylate indicator, at pH ≈ 1.5.[18] The stock solution of 0.1 *M* GX was prepared by accurate weighing of the required amount (used as provided) and dissolving the respective solid in 0.1 *M* HCl.

Measurements of pH were conducted using Radiometer pH-meter type 63 equipped with Radiometer combined glass electrode type GK 2311C. The pH-meter was calibrated by the two buffers method of known pHs (2 and 4 or 4 and 7) in

* Author to whom correspondence should be addressed.

the pH range used (1–7.5). Spectral measurements were made using Pye–Unicam model 8-100 as well as Schimadzu model 240 spectrophotometers in the wavelength range 250–650 nm. Kinetic measurements were done using a Durrum stopped-flow spectrophotometer D-110. The optical path length was 20.0 mm. The mixing syringes and cuvette were thermostatted at 25°C. The wavelength used was 470 nm.

In the equilibrium studies the ranges of the ligand and metal ion concentrations were $(2.0–4.0) \times 10^{-3}$ M and $(2.0–6.0) \times 10^{-4}$ M, respectively. The pH range was 1.0–7.5. In the kinetic study the ranges of the ligand and metal ion concentrations were $(4.00–40.0) \times 10^{-3}$ M and $(1.0–4.0) \times 10^{-4}$ M, respectively. The pH range was 1.0–3.0. The ionic strength was kept constant in the whole work at 0.15 M NaCl. The temperature was kept constant in the equilibrium study at (25 ± 1)°C. Hydrogen ion concentration was taken to be 10^{-pH}.

The test of the number of absorbing species was carried out using program TRIANG.[19] The computation of the equilibrium constants was made utilizing program SQUAD II.[20]

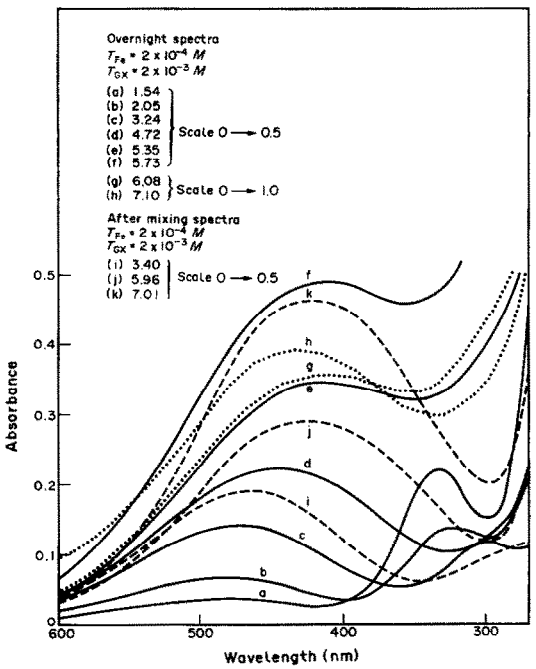


Fig. 1. Typical spectra of Fe(III)–GX system as function of pH (for freshly prepared and overnight solutions).

RESULTS AND DISCUSSION

The spectra of Fe(III)–GX system ($T_{GX} = 10T_{Fe} = 2.0 \times 10^{-3}$ M) were recorded directly after mixing the reactants at various pHs and in another they were recorded after being left overnight. The spectra in both cases were identical only in the pH range 1.0–2.5 but not at other pHs greater than 2.5 where slow spectral changes were observed by time for those taken at time of mixing. These findings were not reported in a previous work.[14] Typical spectra for fresh and overnight solution of Fe(III)–GX at different pHs are shown in Fig. 1, in the wavelength range of 600–270 nm. Although GX has no characteristic spectra in wide wavelength range (600–210 nm) in the pH range ~ 1.0–7.5, iron(III) chloride solution showed some spectral changes under identical experimental conditions. Two major absorption peaks were observed in acidic medium (1.0 M HCl), one at 335 nm and the other at 225 nm. They were appreciably affected by change in pH where both bands lost their identities. This finding was reported previously for iron(III) perchlorate solutions.[21] However, in the presence of GX a major change in the Fe(III) spectra occurred. A new band of probably charge-transfer type centred at ~ 470 nm appeared which showed a hypsochromic shift as well as hyperchromism as the pH was increased from 1.0 to 7.5. The Fe(III) band at 330 nm decreased in absorbance while that at 225 nm increased considerably as the pH was increased from 1.0 to 7.5 relative to those of free Fe(III) spectra. The band at 330 nm vanished at pHs $\geqslant$ 5.0. One should expect that spectral variations with pH serve as good indication of the presence of more than one absorbing species in the wavelength and pH ranges considered. The test for the number of absorbing species[19] indicated the presence of four species if error matrices in the absorbance values were taken in the range of 0.003–0.008 absorbance units. The number of species did not reflect the actual number of species if protonated and nonprotonated species are considered different.

Equilibrium studies

Program SQUAD II[20] has been used to determine the stability constants of various Fe(III)–GX species. The strategy which has been adopted was to separate the data into two sets, one in the pH range 1.0–3.0 and the other in the pH range 3.0–7.5. In both cases the protonation constants of the ligands as well as the hydrolysis constants of Fe(III) were kept constant while varying that of metal ions with ligand. The values of stability constants calculated from the first set were also used as constants in the second set. The constants obtained were invoked in one and the same model for further refinement. Two equilibrium models were obtained which were not easily differentiated. The final log β_{pqr} are listed in Table 1.

The presence of unprotonated species in quite acidic pH range may indicate the involvement of the amino group in complexation of Fe(III). In such a

Table 1. Summary of the formation constants ($M_pL_qH_r$) of Fe(III)–glycinehydroxamate system at $I = 0.15$ and 25°C [M = Fe(III), L = GX]

Model	Stoichiometric coefficients q	p	r	$\log \beta_{pqr}$ ($\pm\sigma$)	Reported values of $\log \beta$*	Wavelength range, No. of wavelengths, No. of solutions, pH range
	0	1	1	9.549 (0.004)‡	9.184	400–540, 15, 15
	0	1	2	17.147 (0.004)‡	16.702	1.0–7.5
	1	0	−1	−3.05§		
	1	0	−2	−6.31§		
First†	1	1	1	17.36 (0.03)	16.450	
	1	1	0	14.14 (0.09)	13.388	
	2	1	1	28.94 (0.06)	27.558	
	2	1	0	22.72 (0.09)	21.868	
Second†	1	1	1	17.36 (0.03)		
	1	1	0	13.14 (0.09)		
	2	1	0	22.62 (0.08)		
	3	1	3	48.28 (0.06)		

* M.S. El-Ezaby and S. Fareed, results to be published.

† The SD in absorbance data did not exceed 5.8×10^{-3} absorbance units in the first set and 6.2×10^{-3} in the second set.

‡ Ref. 21.

§ Ref. 14.

case the ligand acts as a tridentate species (the octahedral configuration is satisfied in the 2:1:0 complex species). However, a pentacoordinated species may also exist in solution, represented by 2:1:1 complex species. The presence of 3:1:3 species possibly indicates the bidentate nature of the ligand where the amino group or the carbonyl oxygen is not involved in the metal ion complexation (also the octahedral configuration is achieved).

The distribution diagram for the different Fe(III) complexes with GX is shown in Fig. 2. It is clear from this diagram that only two complex species (1:1:1 and 1:1:0 species) together with free Fe(III), $Fe(OH)^{2+}$ and $Fe(OH)_2^+$ coexist in the pH range 1.0–3.0, and actually complex formation occurred at pHs as low as 1.0. However, this conclusion is dependent on the relative concentration of GX to Fe(III).

The log β_{pqr} values obtained in this work are different from those reported previously, using potentiometric methods.[14] This discrepancy may be interpreted on the basis that in this work the equilibrium constants were obtained for solutions which have been kept overnight while those obtained previously were not taken under this condition, specially for pHs greater than 2.5.

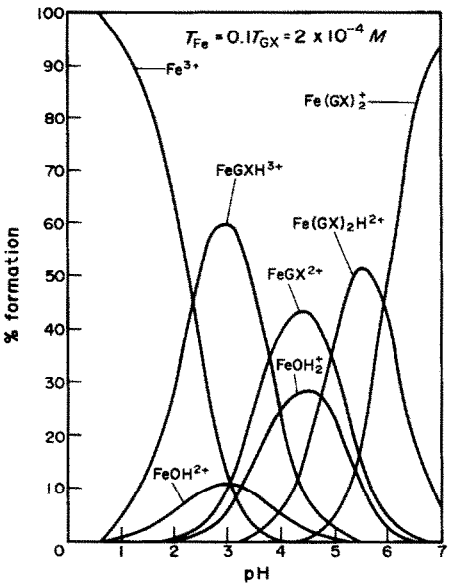


Fig. 2. Distribution diagram of Fe(III)–GX system complex species as function of pH.

Kinetic study

Two rate steps were observed in the kinetic study of Fe(III) reaction with GX in the pH range 1.0–2.5. Both steps are dependent on pH and the initial concentration of the glycinehydroxamate. The slow step was in the hour range while the fast step was in the millisecond range. The fast kinetic step is only considered in this work. It may indicate the involvement of ligand deprotonation step with subsequent formation of a chelated complex of

possibly the following structures:

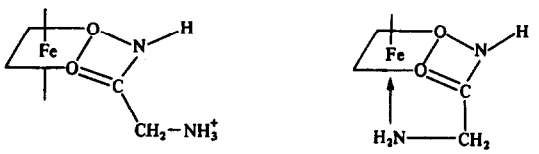


Figure 3 shows the dependence of observed pseudo-first order rate constant, k_{obs}, of the fast step on both pH and total ligand concentration of GX, T_{GX}, when the $T_{GX} > T_{Fe}$. The rate constant was first decreased as pH increased from 1.0 to 1.6, and then increased as pH increased from 1.6 to 3.0. At a given pH the rate constant is a linear function of T_{GX} [Fig. 4(a) and (b)]. Actually, two sets of curves were observed. The first set of curves below pH 1.7 were approximately parallel and of identical slopes but different intercepts [Fig. 4(a)]. The second set of curves above pH 1.6 showed quite significant slopes with small variation in the intercepts [Fig. 4(b)]. The kinetic data represented in Fig. 4(a) and (b) can be empirically expressed as follows:

$$k_{obs} = A + BT_{GX}, \qquad (1)$$

where A and B are the intercepts and slopes of the linear curves shown in Fig. 4(a) and (b), and Table 2. Both A and B are pH dependent at pHs greater than 1.7 and only A at pHs lower than 1.7.

In the pH range used (1.0–3.0) the solution of glycinehydroxamate exhibits only one species, the diprotonated species, GXH_2^+ (Table 1), while that of iron(III) exhibits several chloro complexes of iron(III)

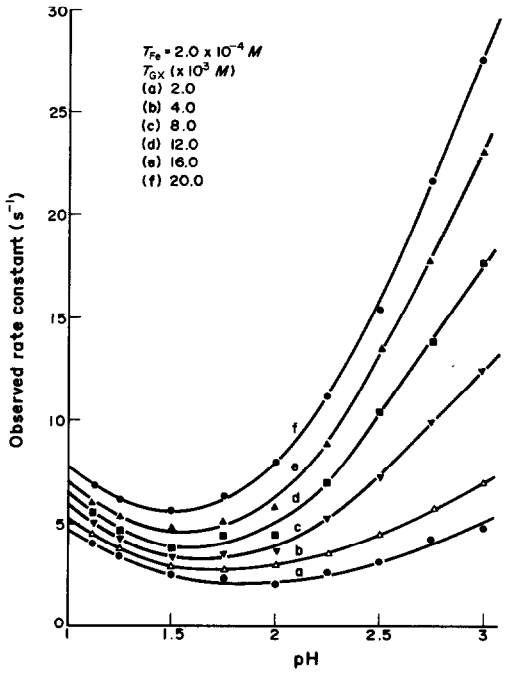


Fig. 3. Observed pseudo first order rate constants as function of pH and T_{GX}.

in addition to the aquated form and hydroxo species (Table 1). The dimeric species of Fe(III) was excluded due to the presence of high relative concentration of chloride ion ($T_{Cl} \gg T_{Fe}$). Besides, it has not been reported that chloride ion bridges two Fe(III) species. The mechanism of Fe(III) interaction with

Table 2. Summary of the values of A and B at different extrapolated pHs used in the determination of k_i and k_{-i}

pH	A	$B \times 10^{-2}$	$\frac{A([H^+]+K_{KC}) \times 10^{-2}}{K_{HC}}$	$BQ_1Q_3 \times 10^{-2}$
1.00	4.60	1.50	7.71	1.514
1.05	4.18	1.50	6.24	1.515
1.10	3.90	1.50	5.18	1.516
1.25	3.22	1.50	3.03	1.524
1.35	2.80	1.50	2.13	1.530
1.50	2.33	1.50	1.26	1.542
1.70	1.59	2.20	0.545	2.301
1.90	1.65	2.60	0.375	2.792
2.00	1.75	3.10	0.310	3.394
2.15	1.55	3.85	0.197	4.377
2.25	1.70	4.55	0.176	5.351
2.40	1.63	6.05	0.124	7.605
2.50	1.83	7.15	0.115	9.531
2.65	1.90	8.65	0.089	12.975
2.80	2.10	10.45	0.076	18.455
3.00	2.50	12.60	0.067	30.114

GX is summarized in the following scheme:

$$Fe^{3+} + GXH_2^+ \rightleftharpoons FeGXH^{3+} + H^+; \qquad k_1, k_{-1} \quad \text{(a)}$$

$$K_{1OH} \downarrow\uparrow$$

$$Fe(OH)^{2+} + GXH_2^+ \rightleftharpoons FeGXH^{3+} + H_2O; \qquad k_2, k_{-2} \quad \text{(b)}$$

$$K_{2OH} \downarrow\uparrow$$

$$Fe(OH)_2^+ + GXH_2^+ \rightleftharpoons FeGXH^{3+} + H_2O + OH^-; \qquad k_3, k_{-3} \quad \text{(c)}$$

$$K_{HC} \downarrow\uparrow$$

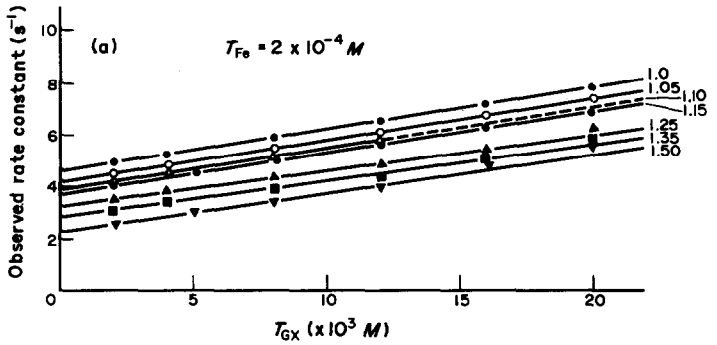
$$Fe^{3+} + GXH_2^+ \rightleftharpoons FeGX^{2+} + 2H^+; \qquad k_4, k_{-4} \quad \text{(d)}$$

$$Fe(OH)^{2+} + GXH_2^+ \rightleftharpoons FeGX^{2+} + H_2O + H^+; \qquad k_5, k_{-5} \quad \text{(e)}$$

$$Fe(OH)_2^+ + GXH_2^+ \rightleftharpoons FeGX^{2+} + 2H_2O; \qquad k_6, k_{-6} \quad \text{(f)}$$

Scheme 1.*

* For simplicity $Fe(OH)_l Cl_n(H_2O)_{6-n-l}$ species will be represented as Fe^{3+} species or $Fe(OH)_l$ (if $l > 0$).



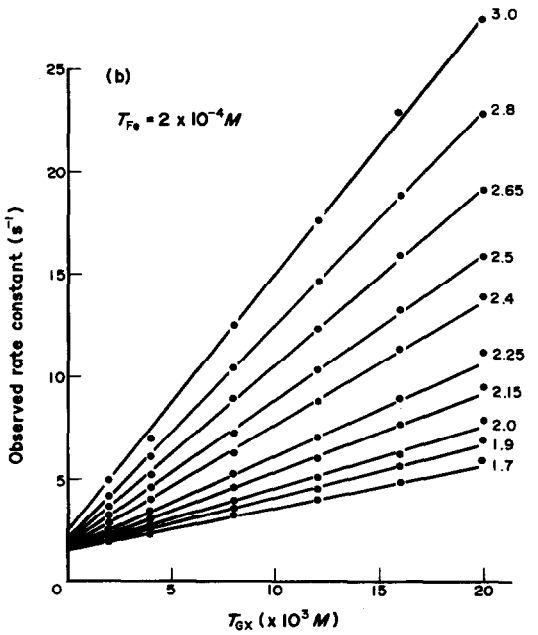


Fig. 4. (a) Observed rate constants as function of T_{GX} at various interpolated pH values in the pH range 1.0–1.50. (b) Observed rate constants as function of T_{GX} at various interpolated pH values in the pH range 1.50–3.00.

where k_i and k_{-i} are the rate constants of forward and backward reactions and K_{1OH},* K_{2OH}* and K_{HC}† are the first and second hydrolysis constants of Fe^{3+}, and the deprotonation constant of FeGXH. At constant pH (when $T_{GX} \gg T_{Fe}$) the rate equation is:

$$Q_2 \frac{d(FeGX)}{dt} = \left[\frac{T_{Fe}-(FeGX)Q_2}{Q_3}\right]\frac{T_{GX}}{Q_1}Q_4 - (FeGX)Q_5, \quad (2)$$

where

$$Q_1 = 1 + K_{1h}/[H^+] + K_{1h}K_{2h}/[H^+]^2$$

(K_{1h} and K_{2h} are the deprotonation constants of GX),

$$Q_2 = ([H^+]/K_{HC}) + 1$$

(K_{HC} is the deprotonation constant of FeGXH),

$$Q_3 = 1 + K_{1OH}/[H^+] + K_{1OH}K_{2OH}/[H^+]^2$$

(K_{1OH} and K_{2OH} are the hydrolysis constants of Fe^{3+}),

$$Q_4 = k_1 + k_2K_{1OH}/[H^+] + k_3K_{1OH}K_{2OH}/[H^+]^2 + k_4 + k_5K_{1OH}/[H^+] + k_6K_{1OH}K_{2OH}/[H^+]^2$$

and

$$Q_5 = [(k_{-3}K_W/K_{HC}) + k_{-6}] + [(k_{-2}/K_{HC}) + k_{-5}][H^+] + [(k_{-1}/K_{HC}) + k_{-4}][H^+]^2.$$

The integrated form of eqn (2) is as follows:

$$\ln \frac{(FeGX)_\infty}{(FeGX)_\infty - (FeGX)_t} = k_{obs}t, \quad (3)$$

where $(FeGX)_\infty$ ($\propto$ absorbance) is the concentration of species at infinite time (t_∞) and $(FeGX)_t$ is at time t and k_{obs} is:

$$k_{obs} = Q_5/Q_2 + Q_4T_{GX}/Q_3Q_1. \quad (4)$$

There is a correspondence between eqns (4) and (1), where

$$A = Q_5/Q_2 = \{k_{-3}K_W/K_{HC} + k_{-6} + [(k_{-2}/K_{HC}) + k_{-5}][H^+] + [(k_{-1}/K_{HC}) + k_{-4}][H^+]^2\}[(H^+)/K_{HC}) + 1]^{-1} \quad (5)$$

and

$$B = Q_4/Q_3Q_1 = (k_1 + k_2K_{1OH}/[H^+] + k_3K_{1OH}K_{2OH}/[H^+]^2 + k_4 + k_5K_{1OH}/[H^+] + k_6K_{1OH}K_{2OH}/[H^+]^2)\{(1 + K_{1OH}/[H^+] + K_{1OH}K_{2OH}/[H^+]^2)(1 + K_{1h}/[H^+] + K_{1h}K_{2h}/[H^+]^2)\}^{-1}. \quad (6)$$

Upon rearrangement of eqns (5) and (6):

$$A\left(\frac{[H^+]}{K_{HC}} + 1\right) = [(k_{-3}K_W/K_{HC}) + k_{-6}] + [(k_{-2}/K_{HC}) + k_{-5}][H^+] + [(k_{-1}/K_{HC}) + k_{-4}][H^+]^2, \quad (7)$$

$$BQ_3Q_1 = (k_1 + k_4) + \frac{K_{1OH}}{[H^+]}(k_2 + k_5) + \frac{K_{1OH}K_{2OH}}{[H^+]^2}(k_3 + k_6). \quad (8)$$

Plotting $A(1 + [H^+]/K_{HC})$ vs $[H^+]$ produced a quadratic relationship [Fig. 5(a)]. The coefficients of eqn (7) have the following values:

$$(K_W/K_{HC})k_{-3} + k_{-6} = 2.84 \pm 2.0, \quad (9a)$$

$$(k_{-2}/K_{HC}) + k_{-5} = (2.13 \pm 0.15) \times 10^3, \quad (9b)$$

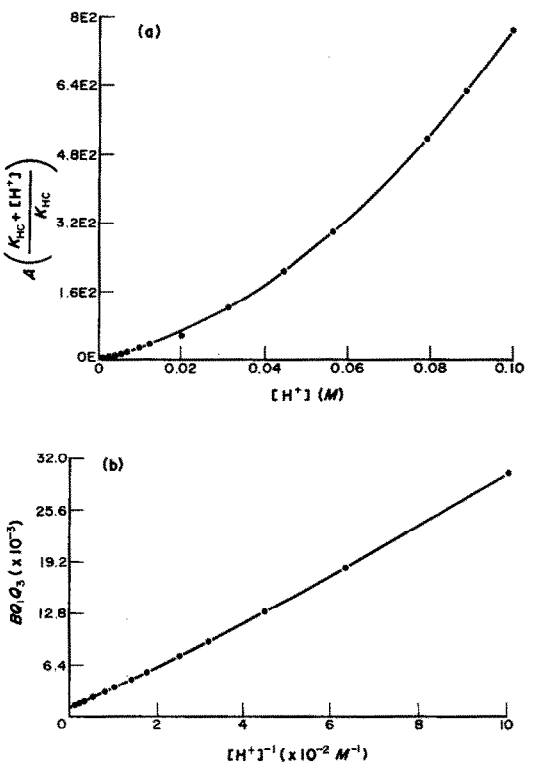


Fig. 5. (a) Plot of $A\{([H^+] + K_{HC})/K_{HC}\}$ vs $[H^+]$. (b) Plot of BQ_1Q_3 vs $[H^+]^{-1}$.

* $K_{1OH} = 9 \times 10^{-4}$ for $Fe^{3+} + H_2O \rightleftharpoons Fe(OH)^{2+} + H^+$; $K_{1OH}K_{2OH} = 4.9 \times 10^{-7}$ for $Fe^{3+} + 2H_2O \rightleftharpoons Fe(OH)_2^+ + 2H^+$.

† K_{HC} for $FeGXH \rightleftharpoons FeGX + H^+$ can be obtained from the equilibrium study.

and

$$(k_{-1}/K_{HC})+k_{-4} = (5.51 \pm 0.16) \times 10^4 \quad (9c)$$

On the other hand, the plot of BQ_3Q_1 vs $[H^+]^{-1}$ is shown in Fig. 5(b). The coefficients of eqn (8) are as follows:

$$k_1 + k_4 = (1.05 \pm 0.08) \times 10^3 \quad (10a)$$

$$(k_2 + k_5)K_{1OH} = (24.14 \pm 0.89), \quad (10b)$$

(or $k_2 + k_5 = 2.7 \times 10^4$)

and

$$(k_3 + k_6)K_{1OH}K_{2OH} = (0.563 \pm 1.50) \times 10^{-3} \quad (10c)$$

(or $k_3 + k_6 = 1.15 \times 10^4$).

In order to determine the values of the different microrate constants, it may be reasonable to assume that at lower pHs (in the pH range 1.0–1.7) the reaction leading to the formation of $FeGX^{2+}$ is much less significant than that leading to the formation of $FeGXH^{3+}$. Moreover, iron present is mainly in the form of free aquated Fe^{3+} species and aquated chloro complexes of iron(III). In other words, the reaction (a) in Scheme 1 is significant in the formation of $FeGXH^{3+}$. This is well confirmed by the pH-independence of the parameter B (or BQ_1Q_3) (Table 2) in the pH range 1.00–1.50. In such a case, eqn (8) is reduced to $BQ_1Q_3 \simeq B \simeq k_1$ which was found equal to 1.50×10^2. From the knowledge of the formation constant of $FeGXH^{3+}$ (Table 1) the backward rate constant can be estimated ($k_{-1} = 1.05 \times 10^2$). In turn, k_{-4} can be calculated from eqn 9(c) ($= 5.51 \times 10^4$) and k_4 from eqn 10(a) (0.9×10^3). The equilibrium constant of the reaction (d) in Scheme 1 is now equal to 1.63×10^{-2}. If $k_{-6} \gg k_{-3}(K_W/K_{HC})$ and $k_6 \gg k_3$ then the equilibrium constant (k_6/k_{-6}) of reaction (f) in Scheme 1 is 4.05×10^3. This will lead to a calculated equilibrium constant (in the log form) for the species 1 : 1 : 0 equal to 14.44 which differs by an amount of 0.30 from that listed in Table 1. This finding showed that the above approximation is twice as much greater than the actual value which indicates that k_3 and $k_{-3}K_W/K_{HC}$ contributes to an extent to the value of the ratio $(k_3 + k_6)/[(k_{-3}K_W/K_{HC}) + k_{-6}]$. However, there is no simple way to separate the involved microrate constants. Besides, the same argument can be employed in the case of the ratio $(k_2 + k_5)/[(k_{-2}/K_{HC}) + k_{-5}]$ ($= 0.13 \times 10^2$). If it is assumed that $k_2 \gg k_5$ and $k_{-2}/K_{HC} \gg k_{-5}$, then $k_2/k_{-2} = 1.86 \times 10^4$ which leads to a calculated equilibrium constant (in the log form) for the 1 : 1 : 1 species equal to 18.37 which is greater by approximately one log unit from the value listed in Table 1. This means that k_2/k_{-2} should be 10 times less than 1.88×10^4. If, on the contrary, $k_5 \gg k_2$ and $k_{-5} \gg k_{-2}/K_{HC}$ then $k_5/k_{-5} = 0.13 \times 10^2$. The calculated equilibrium constant (in the log form) is equal to 15.8 which is still greater by one log unit than that listed in Table 1. This result implies that both reactions (b) and (e) in Scheme 1 may be equally contributing to the formation of $FeGXH^{3+}$ and $FeGX^{2+}$, which indicates an important role played by $FeOH^{2+}$ in the complex formation of iron(III) with GX, a conclusion which was arrived at in a previous report.[17] Furthermore, the discrepancy which was observed between the equilibrium constants obtained from the equilibrium study and the kinetic study may be attributed to the fact that the effect of chloro complexes of iron(III) has been ignored.

CONCLUSION

It has been concluded that reactions (a), (b) and (f) are the most important reactions describing the interaction of iron(III) with glycinehydroxamate, which indicates that $FeOH^{2+}$ is mostly the reactive iron(III) species in the formation of $FeGXH^{3+}$ species and $Fe(OH)_2^+$ is the reactive species in the formation of $FeGX^{2+}$. This finding is interesting since it may be for the first time that $Fe(OH)_2^+$, and not only $FeOH^{2+}$,[17] is also one of the reactive species in the Fe(III) complex formation reaction. This conclusion suggests that the establishment of the first bond (by the loss of first H_2O molecule) initiates rapid ring closure of the bidentate ligand with the metal centre with the loss of a second H_2O molecule in the case of $FeGXH^{3+}$. The further rapid loss of a third H_2O molecule occurs at pHs greater than 1.7 to form $FeGX^{2+}$.

Acknowledgements—We would like to thank Mr H. Abu Soud for his assistance in the experimental work of kinetics and the University of Kuwait for the provision of Research Grant SC021.

REFERENCES

1. J. B. Neilands, in *Inorganic Biochemistry* (Edited by G. Eichhorn), Chap. 5. American Elsevier, New York (1973).
2. J. B. Neilands (ed.), *Microbial Iron Metabolism.* Academic Press, New York (1974).
3. T. Emery, in *Metal Ions in Biological Systems* (Edited by H. Sigel), Vol. 7, p. 77. Marcel Dekker, New York (1978).
4. J. B. Neilands, *Adv. Chem. Ser.* 1977, **162**, 3.
5. K. N. Raymond, *Adv. Chem. Ser.* 1977, **162**, 33.
6. D. A. Brown and M. V. Chidambaram, in *Metal Ion in Biological Systems* (Edited by H. Sigel), Vol. 14, p. 125. Marcel Dekker, New York (1982).

7. H. Maehr, *Pure Appl. Chem.* 1971, **28**, 603.
8. J. B. Neilands, *Science* 1967, **156**, 1443.
9. O. Mikes and T. Turkova, *Chem. Listy* 1964, **58**, 65.
10. R. T. Coutts, *Can. J. Pharm. Sci.* 1967, **2**, 27.
11. J. H. Weisburger and E. K. Weisburger, *Pharm. Rev.* 1973, **25**, 1.
12. D. E. Metzler, *Biochemistry*. Academic Press, New York (1977).
13. B. Chatterjee, *Coord. Chem. Rev.* 1978, **26**, 281.
14. D. A. Brown, M. V. Chidambaram and J. D. Glennon, *Inorg. Chem.* 1980, **19**, 3260.
15. D. A. Brown, W. K. Glass and S. J. C. McGardle, *Inorg. Chim. Acta* 1980, **80**, 13.
16. B. Monzyk and A. L. Crumbliss, *J. Am. Chem. Soc.* 1979, **101**, 6203.
17. N. Kujundzic and M. Pribanic, *J. Inorg. Nucl. Chem.* 1978, **40**, 729.
18. G. Schwarzenbach and H. Flaschka, *Complexometric Titrations* (Translated by H. M. N. H. Irving). Methuen, London (1969).
19. F. R. Hartley, C. Burgess and R. Alcock, *Solution Equilibria*. Ellis Horwood, Chichester (1980).
20. D. J. Leggett and W. A. E. McBryde, *Anal. Chem.* 1975, **47**, 1065.
21. L. N. Mulay and P. W. Selwood, *J. Am. Chem. Soc.* 1954, **77**, 2693.

Polyhedron Vol. 4, No. 3, pp. 437–440, 1985
Printed in Great Britain

0277-5387/85 $3.00 + .00
© 1985 Pergamon Press Ltd

SPECTROPHOTOMETRIC INVESTIGATION OF MONOBROMO AND DIBROMO COMPLEXES OF COPPER(II) IN METHANOLIC MEDIUM

P. G. DAVID
Departamento de Quimica, Universidade de Brasilia, Brasilia, Brazil

(*Received* 18 *June* 1984; *accepted* 16 *July* 1984)

Abstract—Complex formation between copper(II) and bromide in anhydrous methanol was investigated spectrophotometrically. At a constant copper(II) concentration of 3.0×10^{-4} *M*, Cu^{2+} and $CuBr^{+}$ are at equilibrium for $[Br^{-}] < 1.0 \times 10^{-3}$ *M* while $CuBr^{+}$ and $CuBr_2$ exist at equilibrium in the range of $[Br^{-}]$ 2.0×10^{-3}–40×10^{-3} *M*. An isosbestic point at 235 nm indicated the equilibrium of Cu^{2+} and $CuBr^{+}$ while a second isosbestic point at 290 nm showed the equilibrium of $CuBr^{+}$ and $CuBr_2$. Stability constants for the formation of $CuBr^{+}$ and $CuBr_2$ (K_1 and K_2, respectively) were determined as a function of ionic strength in the range 0.01–0.10. Log K_1 and log K_2 values at zero ionic strength were obtained by extrapolation of the plot of log *K* vs ionic strength, the values being 3.97 ± 0.01 and 2.31 ± 0.01.

Colour and spectral changes observed when copper(II) salts are treated with varying concentrations of alkali bromides have been investigated by a number of researchers.[1–8] Kosower *et al.*[2] observed a substantial increase in the formation of copper(II) bromide complexes in alcoholic medium in comparison with aqueous medium, while Barnes and Hume[7] encountered no substantial increase in stability in changing aqueous to alcoholic medium. The former authors have interpreted the spectral changes observed in alcoholic copper(II) perchlorate solution on addition of lithium bromide in terms of successive formation of $[CuBr]^{+}$, $[CuBr_2]$, $[CuBr_3]^{-}$, $[CuBr_4]^{2-}$, $[CuBr_5]^{3-}$ and $[CuBr_6]^{4-}$. However other investigators have interpreted their results in terms of $[CuBr_4]^{2-}$ being the highest copper(II) bromide complex. Determination of the formation constant for $CuBr^{+}$ in aqueous medium and 90% ethanol indicated a low stability in these media.[1,3–7] Matsuo[5,6] determined the formation constants in aqueous media for the succeeding complexes which also showed to have correspondingly lower stabilities. The present work deals with the investigation of the complex formation between copper(II) and bromide ion in anhydrous methanolic medium under conditions at which only $CuBr^{+}$ and $CuBr_2$ are formed: the results indicate an enhancement of the stabilities in this medium in comparison to those in water.

EXPERIMENTAL

Copper(II) perchlorate, lithium perchlorate and lithium bromide were analytical reagent grade chemicals and were dried in vacuum at 100°C for several hours before use. Methanol was distilled over magnesium methoxide; only the middle 50% of the distillate was used. Manipulations of methanolic solutions were carried out in a dry-box in a dry nitrogen atmosphere.

The electronic absorption spectra and absorbance measurements were obtained on a Cary Model 219 recording spectrophotometer. Teflon-stoppered quartz cells were employed. The cells were thermostatted at 25 ± 0.1°C by circulating water through the cell-holders from a constant-temperature water-bath. The absorbance at any wavelength was read directly from the digital display of the spectrophotometer and was reliable within ± 0.0005 units.

The procedure used in preparing solutions for recording the spectra or obtaining absorbance reading at any desired wavelength was as follows. A solution of copper(II) perchlorate [~ 0.0015 *M* (solution A)] was prepared by accurate dilution of a stock solution (~ 0.015 *M*) and was standardized spectrophotometrically as $[Cu(dmp)_2]^{2+}$ (dmp = 2,9-dimethyl-1,10-phenanthroline) following the literature procedure.[9] Also a stock solution of lithium bromide (0.2 *M*) was prepared and was

standardized by the Volhards method.[10] Solutions of lithium bromide [0.05 *M* (solution B) and 0.002 *M* (solution C)] were prepared by accurate dilution of this stock solution. Predetermined volumes of solution A (2.0 cm^3) and 0–5 cm^3 of solution B or C were mixed in a series of 10 cm^3 volumetric flasks followed by a calculated volume of 0.05 or 0.5 *M* methanolic lithium perchlorate solution to adjust the total ionic strength to the desired value within the range 0.01–0.1 and diluted to the mark with anhydrous methanol. The absorbance at the desired wavelength or the absorption curve over the range 200–500 nm was recorded (using a cell of 1-cm path-length) after 3 h within which the solutions were found to reach equilibrium. During this time the solutions were maintained at 25 ± 0.1°C.

RESULTS AND DISCUSSION

When the total concentration of copper(II) in the solution was maintained at 3.0×10^{-4} *M*, a gradual increase in the LiBr concentration from zero to 1.2×10^{-3} *M* exhibited a general increase in the absorption for $\lambda > 235$ nm with a characteristic broad peak centered around 300 nm and a decrease in absorption in the region 235–220 nm. An isosbestic point was observed at 235 nm. Further increase in the concentration of LiBr up to 2.0×10^{-3} *M* showed a general increase in the absorption in the 400–220 nm region without any isosbestic point. When the LiBr concentration was increased further (2.0×10^{-3}–40×10^{-3} *M*) a decrease in the absorption in the region 400–290 nm and an increase for $\lambda > 290$ nm was observed with the existence of an isosbestic point at 290 nm and a characteristic broad peak centred around 245 nm. An increase in the ionic strength of the medium pushed up the lower limit of LiBr concentration at which this isosbestic point at 290 nm was observed. Under the conditions of our investigation this isosbestic point was not observed for ionic strength greater than 0.1. The spectra were constant in the LiBr concentration range 0.04–0.1 *M*.*

Literature data show that a copper(II)–bromo complex occurring at low bromide concentration and exhibiting absorption maximum at around 300 nm has been assigned to[1,2,7] $CuBr^+$. Kosower *et al.*[2] has assigned an absorption maximum at 238 nm in methanolic medium to the $CuBr_2$ complex. However there has been no quantitative investigation hitherto on the successive formation of these two complexes in any medium. Our observation of the existence of an isosbestic point at 235 nm for $[LiBr] \leqslant 1.0 \times 10^{-3}$ indicates that $CuBr^+$ and Cu^{2+} are in equilibrium. We interpret the existence of a second isosbestic point at 290 nm in the LiBr concentration range 2.0×10^{-3}–40×10^{-3} *M* on the assumption that $CuBr^+$ and $CuBr_2$ are at equilibrium. The three species (Cu^{2+}, $CuBr^+$ and $CuBr_2$) are at equilibrium when the concentration of LiBr is in the range 1.0×10^{-3}–2.0×10^{-3} *M*.† The constancy of the spectra at [LiBr] 0.04–0.1 *M* clearly shows that the higher complexes may be ignored in our investigation.

From the constancy of the spectra in the LiBr concentration range 0.04–0.1 *M* we assume that only $CuBr_2$ exists in solution and, hence, it is easy to calculate the molar absorptivity values (ε_2) for this complex at any desired wavelength‡ and to determine the spectra (Fig. 1). The molar absorptivities (ε_1) and the spectra for $CuBr^+$ were determined as follows. Existence of the isosbestic point at 290 nm shows that $\varepsilon_1 = \varepsilon_2$ at this wavelength. This value can be used to calculate the concentration of $CuBr^+$ at equilibrium with Cu^{2+} from any one of the spectra obtained at $[LiBr] \leqslant 1.0 \times 10^{-3}$ *M*, at which only Cu^{2+} and $CuBr^+$ are the copper-containing species.§ Since ε_0, molar absorptivity of Cu^{2+} in methanol at any wavelength is known‖ the same spectrum may be used in calculating ε_1 at any desired wavelength (Fig. 1).‡§

The stability constants

The equilibrium constants for the formation of the complexes may be given by the following equations:

$$K_1 = \frac{[CuBr^+]}{[Cu^{2+}][Br^-]}, \qquad (1)$$

$$K_2 = \frac{[CuBr_2]}{[CuBr^+][Br^-]}. \qquad (2)$$

* The upper limit of LiBr concentration employed in the present investigation was 0.1 *M*.

† The species present are solvated. They probably are $[Cu(CH_3OH)_6]^{2+}$, $[Cu(CH_3OH)_5Br]^+$ and $[Cu(CH_3OH)_4Br_2]$.

‡ The values of ε_0, ε_1 and ε_2 at some selected wavelengths are: 300 nm (first λ_{max} for $CuBr^+$): 489, 1925, 1354; 290 nm (isosbestic point): 592, 1665, 1665; 270 nm: 858, 1299, 2114; 245 nm (λ_{max} for $CuBr_2$): 1655, 1851, 2563; 240 nm (second λ_{max} for $CuBr^+$): 1785, 1932, 2507; 235 nm (isosbestic point): 1854, 1854, 2387 l mol^{-1} cm^{-1}.

§ The equation $A = \varepsilon_0[Cu^{2+}] + \varepsilon_1[CuBr^+] = \varepsilon_0([Cu]_t - [CuBr^+]) + \varepsilon_1[CuBr^+]$ was used in calculating the concentration of $CuBr^+$ or ε_1, the other values being known.

‖ ε_0 values were calculated from the spectrum of $Cu(ClO_4)_2$ in anhydrous methanol.

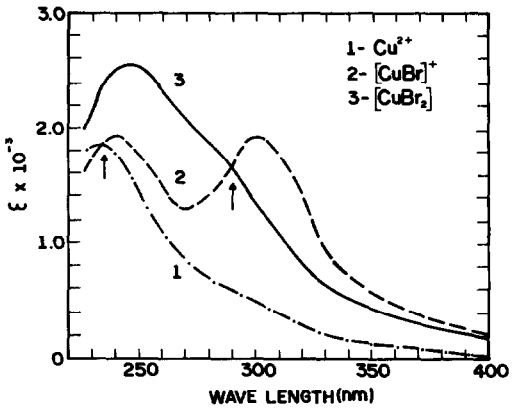


Fig. 1. Electronic absorption spectra of Cu^{2+}, $CuBr^+$ and $CuBr_2$ in methanolic medium. The arrows indicate the isosbestic points.

Since only $CuBr^+$ and Cu^{2+} are at equilibrium at LiBr concentrations 1.0×10^{-3} M and below, and only $CuBr_2$ and $CuBr^+$ at LiBr concentrations 2.0×10^{-3}–40×10^{-3} M, eqns (1) and (2) may be treated independently to determine K_1 and K_2.

If Cu^{2+} and $CuBr^+$ are at equilibrium, the absorbance, A, at any desired wavelength is

$$A=\varepsilon_0[Cu^{2+}]+\varepsilon_1[CuBr^+]. \quad (3)$$

The total analytical concentrations of copper(II) and bromide in solution are

$$[Cu]_t=[Cu^{2+}]+[CuBr^+], \quad (4)$$

$$[Br^-]_t=[Br^-]+[CuBr^+]. \quad (5)$$

Equations (1)–(5) may be solved to arrive at the equation:

$$\frac{(A-\varepsilon_0[Cu]_t)}{(A-\varepsilon_1[Cu]_t)}=-K_1\left\{[Br^-]_t-\left(\frac{A-\varepsilon_0[Cu]_t}{\varepsilon_1-\varepsilon_2}\right)\right\}. \quad (6)$$

In order to determine K_1, the absorbances at 300 nm (wavelength maximum characteristic of $CuBr^+$) were determined at constant $[Cu]_t$ and varying $[Br^-]_t$. Ionic strength was maintained constant for each run. K_1 is determined as the slope by the least square analysis of the data obtained according to the eqn (6). The fit was very good, the correlation coefficient being 0.998 ± 0.001.

If conditions are such that only $CuBr^+$ and $CuBr_2$ are at equilibrium, the absorbance and the total concentrations of copper(II) and bromide may be given by the following equations:

$$A=\varepsilon_1[CuBr^+]+\varepsilon_2[CuBr_2], \quad (7)$$

$$[Cu]_t=[CuBr^+]+[CuBr_2], \quad (8)$$

$$[Br^-]_t=[Br^-]+[CuBr^-]+2[CuBr_2]. \quad (9)$$

From eqns (1), (2) and (7)–(9) we may derive the following equation:

$$\frac{(A-\varepsilon_1[Cu]_t)}{(A-\varepsilon_2[Cu]_t)}=$$

$$-K_2\left\{[Br^-]_t-2[Cu]_t+\left(\frac{A-\varepsilon_2[Cu]_t}{\varepsilon_1-\varepsilon_2}\right)\right\}. \quad (10)$$

The absorbances at three different wavelengths (300, 270 and 245 nm) obtained at constant $[Cu]_t$, ionic strength and varying $[Br^-]_t$ were treated by eqn (10) and the least square analysis provided the K_2 values (Table 1). The fit was very good (correlation coefficient 0.998 ± 0.001) and the K_2 values at the three wavelengths are constant within the experimental error.*

The formation constant K_1 decreases considerably with increase in ionic strength while K_2 is very little influenced (Table 1). A plot of log K vs ionic strength was linear and the Y-intercept provided log K values at zero ionic strength (Fig. 2 and Table 1). The drastic decrease of K_1 values with increase in ionic strength may explain the reason for the absence of an equilibrium involving only $CuBr^+$ and $CuBr_2$ evidenced by the lack of isosbestic point at 290 nm at ionic strengths higher than 0.1. At high ionic strengths the formation of $CuBr_2$ occurs before all Cu^{2+} has been transformed to $CuBr^+$ and, consequently, the three species (Cu^{2+}, $CuBr^+$ and $CuBr_2$) are at equilibrium. The reason for the drastic decrease in K_1 values with increase in ionic strength is not well understood. It is quite probable, being a positively charged species, considerable ion-pair

Table 1. Stability constants for monobromo and dibromo complexes of copper(II) in methanolic medium

Ionic Strength	log K_1 [a]	log K_2 [a] 300 nm	270 nm	245 nm	Average
0	3.97 [b]	....	....	....	2.31 [b]
0.010	3.92	2.29	2.32	2.30	2.30
0.025	3.65	2.25	2.27	2.26	2.26
0.050	3.35	2.23	2.22	2.24	2.23
0.075	3.10	....	2.20	2.22	2.21
0.100	2.88	....	2.19	2.17	2.18

[a] The precision of the log K values, based on run-to-run variability, is ±0.01.

[b] Obtained as the Y-intercept (by the least-square analysis) of the plot of log K vs ionic strength (Fig. 2): correlation coefficient was -0.998 ± 0.001.

* The three wavelengths chosen correspond to the absorption maxima of $CuBr^+$ and $CuBr_2$ (300 and 245 nm, respectively), and the wavelength minimum of the absorption well of $CuBr^+$ (270 nm).

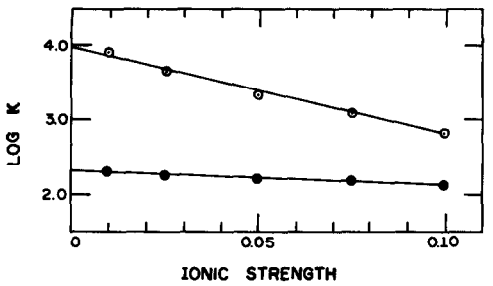


Fig. 2. Plot of log K vs ionic strength. The lower line (●) represents log K_1 and the upper one (⊙) log K_2.

formation occurs and this may influence the formation constants.

There is a lack of literature values for K_1 and K_2 in non-aqueous solvents that could be compared with our results. Barnes and Hume,[7] working with 90% ethanol, obtained low K_1 values comparable with those in aqueous medium.[1,5] However, since the 10% water can have considerable influence on K_1, their values are of little use for comparison. Also the fact that literature values are obtained at unit ionic strength makes the comparison difficult. However, our results show that the stabilities of $CuBr^+$ and $CuBr_2$ increase in methanol in comparison to aqueous medium, in agreement with the qualitative observations of Kosower *et al.*[2]

REFERENCES

1. P. S. Farrington, *J. Am. Chem. Soc.* 1952, **74**, 1966.
2. E. M. Kosower, R. L. Martin and V. W. Meloche, *J. Am. Chem. Soc.* 1957, **79**, 1509.
3. M. W. Lister and P. Rosenblum, *Can. J. Chem.* 1960, **80**, 1827.
4. D. A. L. Hope, R. J. Otter and J. E. Prue, *J. Chem. Soc.* 1960, 5226.
5. S. Matsuo, *Nippon Kagaku Zasshi* 1961, **82**, 32, 1330, 1334; *Chem. Abstr.* 1962, **56**, 61, 12304.
6. S, Matsuo, *Nippon Kagaku Zasshi* 1962, **83**, 1229; *Chem. Abstr.* 1963, **59**, 12313.
7. J. C. Barnes and D. N. Hume, *J. Phys. Chem.* 1963, **67**, 526.
8. J. C. Barnes and D. N. Hume, *Inorg. Chem.* 1963, **2**, 444.
9. J. Fries, *Análisis de Trazas*, p. 74. E. Merck, Darmstadt (1971).
10. J. R. Caldwell and H. V. Moyer, *Ind. Eng. Chem., Anal. Ed.* 1935, **7**, 38.

Polyhedron Vol. 4, No. 3, pp. 441–445, 1985
Printed in Great Britain

0277–5387/85 $3.00 + .00
© 1985 Pergamon Press Ltd

THALLIUM-205 NMR STUDY OF Tl(I) MACROCYCLIC COMPLEXES IN NONAQUEOUS SOLVENTS

YANG-CHIH LEE, JOHN ALLISON and ALEXANDER I. POPOV*
Department of Chemistry, Michigan State University, East Lansing, MI 48824, U.S.A.

(*Received* 10 *April* 1984; *accepted* 21 *August* 1984)

Abstract—Thallium-205 and carbon-13 NMR measurements were used to determine, in nonaqueous solvents, the stabilities of thallium(I) complexes with macrocyclic ligands of different structures but very nearly the same cavity sizes. In a given solvent the complexing abilities of the ligand vary in the order DA18C6 > 18C6 > DC18C6 > DB18C6 > DT18C6. In all cases the stabilities of the complexes varied inversely with the Gutmann donicities of the solvents.

It is well known that the stability of a macrocyclic complex depends on a number of factors. The most emphasized factor is usually the consonance between the cavity size of the ligand and the cationic diameter although its importance has been questioned recently.[1] Other important variables are the number and the nature of heteroatoms in the ring, the flexibility of the ligand, the properties of the anion, the number and the nature of substituent groups on the macrocycle, and physicochemical properties of the solvent such as the solvating ability, the dipole moment and the dielectric constant.

Precise information on the size relationships of the macrocyclic cavities and ions is not available. The former have been estimated from molecular models;[2] Pauling's ionic radii are nearly universally accepted, but it should be noted that his values for the alkali ions have been disputed.[3]

It was of interest to us to investigate the stabilities of Tl^+ complexes with a series of cylic ligands where the cavity size remained very nearly the same. Several such ligands, all with 18-atom cavities, but with different structures, have been described. For this investigation we selected 18-crown-6 (18C6), dibenzo-18-crown-6 (DB18C6), *cis–syn–cis*-dicyclohexano-18-crown-6 (DC18C6), 1,10-diaza-18-crown-6 (DA18C6) and 1,10-dithia-18-crown-6 (DT18C6). As in our previous studies,[4] the formation constants were determined from the variation of ^{205}Tl chemical shift with the [ligand]/[Tl^+] mole ratio. In one case (see below) ^{13}C NMR was used and the chemical shifts of the ligand carbons was followed as the function of the [Tl^+]/[ligand] mole ratio.

The solvents were selected so as to represent as wide a variety of donicities as conveniently possible. However, except for nitromethane, thallium(I) salts and/or thallium(I) complexes were insoluble or very sparingly soluble in solvents of low solvating abilities, and we were unable to make meaningful NMR measurements in these media.

Macrocyclic complexes of the thallium(I) ion are interesting from the point of view of coordination chemistry of this ion; in addition, since the size and the properties of Tl^+ and K^+ ions are very similar, the Tl^+ ion can be used as a probe for the behaviour of the K^+ ion in cases where direct measurements on the latter ion are difficult. This factor is especially important in studies of biological systems[5,6] and, in particular, of ion transport across biological membranes.

Macrocyclic complexes of the Tl^+ ion in nonaqueous solvents, except for methanol, have not been studied very intensively. Formation constants of several complexes in methanol have been determined by various techniques. Those involving 18C6 and its analogues are given together with our results in Table 1. In addition, Srivanavil *et al.*[7] measured *relative* formation constants, $K_{(ML)}/K_{(TIL)}$, of 15C5, 18C6, DB18C6 and DC18C6 complexes: M stands for an alkali ion, ammonium ion and silver(I)

* Author to whom correspondence should be addressed.

Table 1. Stability constants of some thallium(I)–crown ether complexes in various solvents at 25°C

			Log K_f				
			Ligands				
Solvent	D*	DN†	18C6	DB18C6	DC18C6‡	DA18C6	DT18C6
$MeNO_2$	35.9	2.7	> 5§	> 5	> 5	> 5	> 5
MeCN	38.0	14.1	> 5§	> 5	> 5	> 5	4.16 ± 0.06
Me_2CO	20.7	17.0	> 5	3.39 ± 0.02 (1:1) 1.36 ± 0.22 (2:1)	> 5	> 5	3.12 ± 0.04
Sulfolane	42.0	14.8	4.23 ± 0.04	4.04 ± 0.06	4.10 ± 0.07	> 5	2.66 ± 0.03
DMF	3.61	26.6	3.43 ± 0.08‖	2.13 ± 0.03	2.78 ± 0.06	3.55 ± 0.03	1.19 ± 0.06
H_2O	78.5	33.0	2.27 ± 0.04¶	1.50 ± 0.02**	2.49 ± 0.04¶	0.96 ± 0.01	0.93 ± 0.14§
DMSO	45.0	29.8	1.92 ± 0.01§	~ 0	1.26 ± 0.04	2.39 ± 0.02	~ 0
HMPA	30.0	38.2	1.35 ± 0.02	~ 0	—	—	~ 0

* Dielectric constant.
† Gutmann donor number.[17]
‡ DC18C6 in the *cis–syn–cis* isomer.
§ Ref. 15.
‖ Studied by ^{13}C NMR.
¶ Ref. 16.
** Ref. 17.

ion. These measurements were made in methanol, dimethylformamide and dimethyl sulfoxide solutions.

EXPERIMENTAL

Salt and ligand purification

Thallium salts were of reagent grade quality. Thallium(I) nitrate (Alfa) and perchlorate (K & K) were purified by recrystallization from deionized distilled water and then dried at 120°C for 2 days.

The crown ether 18C6 (Parish) was purified by the usual technique of converting it to the acetonitrile complex, filtering and driving off acetonitrile under vacuum at 40°C;[8] DB18C6 (Parish) and DA18C6 (Merck) were recrystallized from benzene and heptane respectively, and dried under vacuum; DT18C6 (Parish) was used as received except for vacuum drying at 50°C.

The mixture of DC18C6 isomers (Parish) was separated by the method described by Izatt *et al.*[9] except that the hydrogen sulfide was obtained by a dropwise addition of a 30% phosphoric acid solution to a concentrated aqueous solution of sodium sulfide. Using this method 31% of *cis–anti–cis* and 26% of *cis–syn–cis* isomers were separated. The melting points of the two isomers were identical with the literature values. An attempt was made to separate the two isomers on an alumina column[10] but the method was more tedious and the yields of each isomer were much lower.

Solvents

Nitromethane (NM), (Aldrich), dimethylformamide (DMF) (Mallinckrodt) and dimethylsulfoxide (DMSO) (Fisher), were refluxed over calcium hydride under reduced pressure for 1–3 days. Hexamethylphosphoramide (HMPA) (Aldrich) was refluxed over calcium oxide under reduced pressure for 24 h. Acetone (AC) (Mallinckrodt), acetonitrile (AN) (Mallinckrodt) and tetrahydrofuran (THF) (Baker) were refluxed over calcium hydride. Methanol (Mallinckrodt) was refluxed over magnesium turnings and iodine for 12–24 h. After the above described treatment, the solvents were fractionally distilled, transferred in a dry box under a nitrogen atmosphere and further dried for 4–20 h over freshly activated 3 or 4 Å molecular sieves.

The water content of purified solvents was determined using a Varian Aerograph Model 920 gas chromatograph and was found to be always below 100 ppm. The purity of these solvents was also checked by ^{13}C NMR. No detectable impurities were observed.

The deuterated solvents, chloroform-*d* (Aldrich Gold Label), acetonitrile-d_3, D_2O and methanol-d_4, all from Stohler Isotope Chemicals, were used as received.

NMR measurements

All ^{205}Tl NMR measurements were carried out at 14.09 kG and at 34.61 MHz in F.T. mode, on a highly modified Varian DA-60 spectrometer equipped with a wideband probe capable of multinuclear operation.[11] The external reference was a 1.5 *M* aqueous solution of thallium acetate. The chemical shifts obtained were then related to an infinitely dilute aqueous solution of the Tl^+ ion. A variable temperature probe was used for measurements between room temperature and 95°C.

Carbon-13 NMR measurements were made on a Bruker WM-250 spectrometer at 58.75 KG and 62.89 MHz. The methyl carbon of acetonitrile-d_3 (used as the lock) was used as the external reference.

Both the ^{205}Tl and ^{13}C resonances were corrected for the differences in the bulk diamagnetic susceptibility differences between the aqueous reference and the nonaqueous solvents. Since dilute solutions ($\sim$ 0.01–0.02 *M*) were used in this investigation, no correction was made for the solutes, such correction would have been much smaller than the experimental error. Chemical shifts downfield from the reference are indicated as *positive*.

A series of solutions was prepared for each solvent in an inert atmosphere glove-box. The concentration of the thallium(I) salt was kept constant ($\sim$ 0.02–0.005 *M*, depending on the solvent) while the concentration of the macrocyclic ligand was varied. Thallium-205 chemical shifts were determined for each solution. In all cases the exchange was fast and only one population-averaged signal was obtained. The variation of the chemical shift with the [ligand]/[Tl^+] mole ratio was used to calculate the complexity constant and the chemical shift of the complexed cation. We have shown previously[12] that in the case of fast exchange and a 1 : 1 complex formation the observed chemical shift is given by the equation:

$$\delta_{obs} = [(KC_m^t - KC_l^t - 1) \pm (K^2C_l^{t^2} + K^2C_m^{t^2} - 2K^2C_l^tC_m^t + 2KC_l^t + 2KC_m^t + 1)^{1/2}]\left(\frac{\delta_f - \delta_c}{2KC_m^t}\right) + \delta_c$$

where K is the stability constant, C_l^t and C_m^t represent the stoichiometric concentrations of the ligand and of the metal ion respectively and δ_f and δ_c are the chemical shifts of the free and complexed metal ion respectively.

For most complexes the value of δ_c cannot be obtained directly. Our procedure is to introduce the values of the experimental parameters δ_{obs}, δ_f, C_l^t and C_m^t and to vary K and δ_c until the calculated chemical shifts correspond, within experimental errors, to the experimental values. A nonlinear least squares curve-fitting program KINFIT[13] was used in the calculations. In general, this technique is not applicable if the complexation constants are greater than 10^5 and it can be somewhat marginal if the K_f values are between 10^4 and 10^5.

It is interesting to note that in some solvents, when the [ligand]/[Tl^+] mole ratio is between 0 and 1, the resonance lines are extremely broad due to the exchange between the free and the complexed Tl^+ ion. For example, for the DB18C6–Tl^+ system in HMPA, $W_{1/2}$ (width at half weight) was 1100 Hz at [L]/[M^+] mole ratio of 0.61, and 1760 Hz for the dicyclohexano complex in sulfolane at a mole ratio of 0.55. In NM solutions the ^{205}Tl resonance lines were too broad to be observed when [DB18C6]/[Tl^+] mole ratio was below 0.9. In all of the above cases chemical shifts either could not be measured with good precision, or could not be measured at all. Thus the range of mole ratios at which chemical shifts could be measured was decreased (often substantially), with a resulting decrease in the accuracy of the K_f measurement.

In the case of ^{13}C NMR, the concentration of the crown ether was kept constant at 0.01 *M*, while the concentration of the Tl^+ ion was varied. In this case, of course, the range of chemical shifts was only $\sim$ 1 ppm, but since these could be measured with a precision of $\pm$0.01 ppm, the variation in ^{13}C chemical shifts with the mole ratio was adequate for calculations of K_f values.

RESULTS AND DISCUSSION

Variations in the ^{205}Tl chemical shifts with the ligand/thallium ion mole ratio for the macrocyclic 18C6, DB18C6, DC18C6 in various solvents are illustrated in Figs. 1–3. Very similar behaviour was observed with DA18C6 and DT18C6. It is evident that, in general, the plots can be divided into three groups: (i) plots with a slight (or zero) slope and without any indication of an abrupt change in slope at any given mole ratio; (ii) plots with a pronounced change in curvature at the 1 : 1 mole ratio; (iii) plots formed by two straight lines intersecting at a mole ratio of 1 : 1; beyond this mole ratio the chemical shift remains essentially constant. Qualitatively, these data indicate: (i) very little or no complexation, (ii) significant complexation, (iii) the formation of a stable complex with $K_f > 10^5$, respectively.

These plots clearly illustrate the sensitivity of the ^{205}Tl resonance frequency towards even minor changes in the immediate vicinity of the Tl^+ ion. For example, the difference between the chemical shifts of the free Tl^+ ion in nitromethane and in hexamethylphosphoramide is $\sim$ 900 ppm.

Table 1 summarizes complexation constants

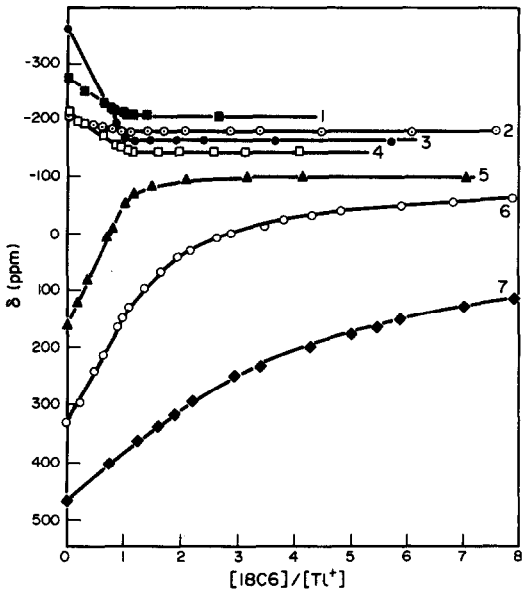


Fig. 1. Thallium-205 chemical shifts as a function of [18C6]/[Tl^+] mole ratio in different solvents. 1, Sulfolane; 2, AC; 3, NM; 4, AN; 5, DMF; 6, DMSO; 7, HMPA.

obtained in neat solvents. Some values obtained in previous investigations are also given for comparison. It is easily seen that the stability of Tl^+–macrocycle complexes are very strongly influenced by the nature of the solvents. Since these complexes

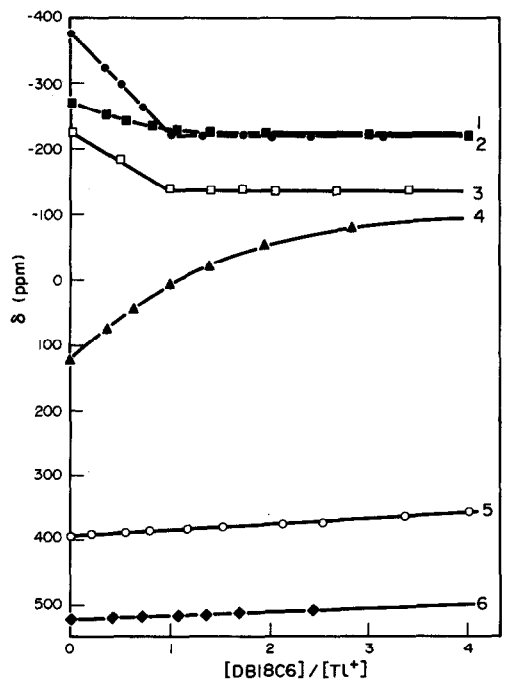


Fig. 2. Thallium-205 chemical shifts as a function of [DB18C6]/[Tl^+] mole ratio in different solvents. 1, Sulfolane; 2, NM; 3, AN; 4, DMF; 5, DMSO; 6, HMPA.

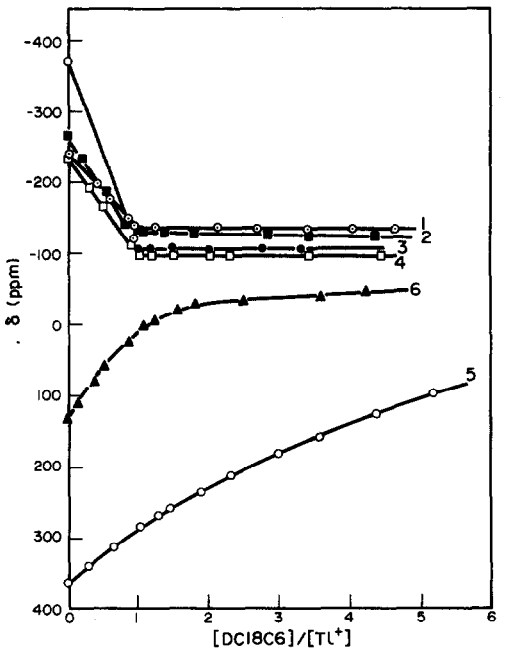


Fig. 3. Thallium-205 chemical shifts as a function of [*cis–syn–cis*-DC18C6]/[Tl^+] mole ratio in different solvents. 1, AC; 2, sulfolane; 3, NM; 4, AN; 5, DMF; 6, DMSO.

are formed by an ion–molecule interaction, and the ionic strength was < 0.02 *M*, the effect of the dielectric constant of the medium is minimal.[14]

On the other hand, there should be an inverse correlation between the solvating ability of a solvent and the stability of the complex. Unfortunately, at this time, there is no unambiguous way to define and measure this solvent property. A number of empirical classifications have been proposed and a comprehensive review of these systems is given by Griffiths and Pugh.[18] One of the most convenient empirical scales is that proposed by Gutmann[19] which is based on the enthalpy of the reaction between the given solvent and antimony(V) chloride in 1,2-dichloroethane. Gutmann solvent donicities for our solvents are shown in Table 1. It is evident that, in general, the complexes are quite stable in solvents of low donicities and the stability decreases with increasing solvating ability of the solvent. Thus for a given complex the stability decreases in the order NM > AN > AC > sulfolane > DMF > water > DMSO > HMPA.

It should be noted that since the dielectric constants of the solvents are quite elevated, and dilute solutions were used, it seems unlikely that the complex formation had a significant competition from ion pair formation. While measurements of ion pair formation constants for thallium(I) salts in nonaqueous solvents have been rather sparse, Yeager and Kratochvil studied electrical conductance of thallium(I)/perchlorate in AN solutions[20]

and calculate ion pair formation constant value of 32, while similar measurements by Prue and Sherrington in DMF solutions showed the salt to be completely dissociated.[21]

It is seen that in solvents with high donor ability such as DMSO and HMPA, the formation constants are either small or, in the case of DB18C6 and DT18C6 have a value of zero. A seeming discrepancy is observed in aqueous solutions where, despite the high donicity of the solvent, fairly stable complexes are formed. Here the soft–hard interaction plays an important role. Water being a "hard" base will solvate the soft Tl^+ ion less effectively than DMSO or HMPA, and, therefore, will interfere less with the complexation reaction. We observed previously that in pyridine solutions Li^+[22] and Cs^+[23] macrocyclic complexes are more stable than in methanol although the former has a higher donor number, 33 vs 26. Pyridine being a softer base than methanol has a weaker interaction with a hard acid, Li^+ ion than methanol.

In a given solvent, the complexing ability of the ligands vary in the order DA18C6 > 18C6 > *cis–syn–cis*-DC18C6 > DB18C6 > DT18C6. It has been shown previously by Frensdorff[23] that the substitution of two ether oxygens of 18C6 by two >NH groups decreases the stabilities of the alkali and alkaline earth complexes but enhances significantly the stability of the Ag^+ complex. Presumably in our case, since the Tl^+ ion is "softer" than an alkali or an alkaline earth cation,[24] it will interact more strongly with a softer base (NH) than the latter ions. In the case of the DT18C6, although sulphur is a softer base than either oxygen or nitrogen, it is considerably larger and, therefore, the cavity size is probably much smaller than in the oxa- or aza-18C6 macrocycles. In addition, it seems likely that the DT18C6·Tl^+ complex has the same configuration as the DT18C6·$PdCl_2$ complex where the metal ion is coordinated only to the two sulphur atoms and is outside the macrocyclic cavity.[26]

The DB18C6 and DC18C6 complexes are somewhat less stable than those with the unsubstituted ligand. The cyclohexyl and the benzene groups increase the rigidity of the ligand and, in the latter case, decrease somewhat the cavity size.

It is interesting to note that in acetone solutions the chemical shift goes downfield as the ligand is added, passes through a minimum and then shifts upfield. This behaviour is analogous to the one we previously observed for the Cs^+–cryptand 222 system in pyridine and several other solvents[27] and which is indicative of a step-wise formation of ML and ML_2 complexes. The values of K_1 and K_2 are given in Table 1.

Acknowledgement—We gratefully acknowledge the support of this study by a National Science Foundation research grant CHE-8010808.

REFERENCES

1. G. W. Gokel, D. M. Goli, C. Minganti and L. Echegoyen, *J. Am. Chem. Soc.* 1983, **105**, 6786.
2. C. J. Pedersen, *J. Am. Chem. Soc.* 1970, **92**, 386.
3. D. F. C. Morris, *Struct. Bonding (Berlin)* 1968, **4**, 63.
4. S. Khazaeli, A. I. Popov and J. L. Dye, *J. Phys. Chem.* 1982, **86**, 5018; S. Khazaeli, J. L. Dye and A. I. Popov, *J. Phys. Chem.* 1983, **87**, 1830, and references listed therein.
5. C. Moore and B. C. Pressman, *Biochem. Biophys. Res. Commun.* 1964, **15**, 562.
6. G. Cornelius, W. Gartner and D. M. Hayhes, *Biochem.* 1974, **13**, 3052.
7. C. Sriranavit, J. I. Zink and J. J. Dechter, *J. Am. Chem. Soc.* 1977, **99**, 5876.
8. G. W. Gokel and D. J. Cram, *J. Org. Chem.* 1974, **39**, 6.
9. R. M. Izatt, B. L. Haymore, J. S. Bradshaw and J. J. Christensen, *Inorg. Chem.* 1975, **14**, 3132.
10. R. M. Izatt, D. P. Nelson, J. H. Rytting and B. L. Haymore, *J. Am. Chem. Soc.* 1971, **93**, 1619.
11. D. D. Traficante, J. A. Simms and M. Mulcay, *J. Mag. Res.* 1984, **15**, 484.
12. E. T. Roach, P. R. Handy and A. I. Popov, *Inorg. Nucl. Chem. Lett.* 1973, **9**, 359.
13. V. A. Nicely and J. L. Dye, *J. Chem. Educ.* 1971, **48**, 443.
14. A. J. Smetana and A. I. Popov, *J. Chem. Thermod.* 1979, **11**, 1145.
15. G. Rounaghi and A. I. Popov, *J. Inorg. Nucl. Chem.* 1981, **43**, 911.
16. R. M. Izatt, R. E. Terry, B. L. Haymore, L. D. Hansen, N. K. Dalley, A. G. Avondet and J. J. Christensen, *J. Am. Chem. Soc.* 1976, **98**, 7620.
17. E. Shchori, N. Nae and J. Jagur-Grodzinski, *J. Chem. Soc., Dalton Trans.* 1975, 2381.
18. T. R. Griffiths and D. C. Pugh, *Coord. Chem. Rev.* 1979, **29**, 129.
19. V. Gutmann and E. Wychem, *Inorg. Nucl. Chem. Lett.* 1966, 257.
20. H. L. Yeager and B. Kratochvil, *J. Phys. Chem.* 1970, **74**, 963.
21. J. E. Prue and P. J. Sherrington, *Trans. Faraday Soc.* 1961, **57**, 1795.
22. A. J. Smetana and A. I. Popov, *J. Solution Chem.* 1980, **9**, 183.
23. M. Shamsipur and A. I. Popov, *J. Am. Chem. Soc.* 1979, **101**, 4051.
24. H. K. Frensdorff, *J. Am. Chem. Soc.* 1971, **93**, 600.
25. R. G. Pearson, *J. Am. Chem. Soc.* 1963, **85**, 3533.
26. B. Metz, D. Moras and R. Weiss, *J. Inorg. Nucl. Chem.* 1975, **36**, 785.
27. E. Mei, J. L. Dye and A. I. Popov, *J. Am. Chem. Soc.* 1977, **99**, 5308.

Polyhedron Vol. 4, No. 3, pp. 447–450, 1985
Printed in Great Britain

0277–5387/85 $3.00 + .00
© 1985 Pergamon Press Ltd

IR, PMR AND MÖSSBAUER STUDIES ON THE COMPLEXES OF TRIPHENYLTIN CHLORIDE AND TRIPHENYLTIN ISOTHIOCYANATE WITH A SERIES OF *N*-ALKYLSALICYLIDENEIMINES

LIAN E. KHOO
School of Chemical Sciences, Universiti Sains Malaysia, Penang, Malaysia

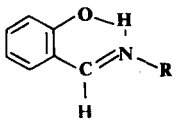
and

FRANK E. SMITH*
Chemistry Department, Laurentian University, Sudbury, Ontario, Canada P3E 2C6

(*Received* 13 *July* 1984; *accepted* 21 *August* 1984)

Abstract—Eleven new complexes of the type Ph_3SnX: *o*-$HOC_6H_4CH{=}NR$ (X = Cl, NCS; R = CH_3, *t*-Bu, $PhCH_2$, *n*-C_6H_{13}, *c*-C_6H_{11}, $HOCH_2CH_2$) have been synthesized by the reactions of triphenyltin chloride or isothiocyanate with the *N*-alkylsalicylideneimines. The complexes are non-electrolytes in nitrobenzene. IR, PMR and Mössbauer spectroscopic studies indicate that the ligands are behaving as monodentates via the phenolic oxygen atoms, and that the complexes all have trigonal bipyramidal geometry with the phenyl groups occupying the equatorial positions.

Several reports concerning the Schiff-base complexes of mono- and diorganotin compounds have appeared recently.[1–6] We now wish to report the results of our investigations on the Schiff-base complexes of triorganotin compounds. We have synthesised and characterised a series of new complexes between Ph_3SnX (X = Cl, NCS) and the Schiff bases:



where R = CH_3, *t*-Bu, $PhCH_2$, *n*-C_6H_{13}, *c*-C_6H_{11}, $OHCH_2CH_2$.

EXPERIMENTAL

Triphenyltin chloride was purchased from Alfa Inorganics and used without further purification. Triphenyltin isothiocyanate (m.p. 168–170°C) was prepared from triphenyltin chloride and potassium thiocyanate by the literature method,[7] and recrystallised from benzene before use.

The *N*-alkylsalicylideneimines were synthesised by the condensation of salicylaldehyde with the appropriate primary amine in refluxing benzene, the water formed being removed azeotropically. The Schiff bases were purified by fractional distillation.

The complexes were prepared by refluxing the calculated amounts of ligand and triphenyltin chloride or isothiocyanate in 95% ethanol for 1–2 h. The complexes crystallised out when the solutions were cooled in a refrigerator overnight. They were filtered off and recrystallised from ethanol. Melting points for the complexes are given in Table 1.

Conductance measurements in nitrobenzene were made at room temperature using a Phillips PW 9501 conductivity bridge with a cell constant of 0.71 cm^{-1}. Molar conductances of the complexes are recorded in Table 1.

The IR spectra of the ligands and complexes were recorded in the region 4000–600 cm^{-1} with a Beckmann Acculab '4' instrument either as neat liquid film or Nujol mulls between NaCl plates. For the 600–200 cm^{-1} region, the Beckmann IR4250 spectrophotometer was used and the spectra were recorded as neat liquid or Nujol mulls, CsI discs, or between polythene plates.

PMR spectra were obtained with a Varian CFT-20 spectrometer with deuterochloroform as solvent.

Mössbauer spectra were recorded at the International Tin Research Institute, Greenford, England.

* Author to whom correspondence should be addressed.

Table 1. Analytical, melting point and conductivity data for the complexes

Complex $Ph_3SnX:o\text{-}HOC_6H_4CH{=}NR$		Elemental analysis (%) Found (calc.)				m.p. (°C)	Molar conductance (ohm^{-1} cm^2 mol^{-1})
X	R	C	H	N	Sn		
Cl	CH_3	60.00 (59.98)	4.79 (4.66)	2.68 (2.69)	23.15 (22.80)	106–108	1.60
NCS	CH_3	59.98 (59.68)	4.61 (4.46)	5.10 (5.16)	22.89 (21.85)	136–138	2.29
Cl	*t*-Bu	61.70 (61.87)	5.55 (5.38)	2.49 (2.49)	21.63 (21.08)	136–138	1.51
NCS	*t*-Bu	61.03 (61.55)	5.23 (5.18)	5.06 (4.79)	20.28 (20.51)	177–180	3.02
Cl	$PhCH_2$	64.04 (64.40)	4.85 (4.75)	2.33 (2.35)	20.54 (19.89)	110–111	1.51
NCS	$PhCH_2$	64.40 (63.99)	4.78 (4.57)	4.93 (4.52)	19.34 (19.16)	160–161	2.13
Cl	$HOCH_2CH_2$	58.10 (58.89)	4.78 (4.77)	2.81 (2.55)	21.91 (21.55)	111–112	1.51
NCS	$HOCH_2CH_2$	58.42 (58.65)	4.78 (4.58)	4.89 (4.89)	21.45 (20.70)	128–130	2.66
Cl	*c*-C_6H_{11}	62.95 (63.02)	5.79 (5.49)	2.14 (2.38)	20.21 (20.16)	130–132	1.42
NCS	*c*-C_6H_{11}	62.61 (62.86)	5.48 (5.29)	4.64 (4.58)	17.23 (19.41)	173–175	2.57
Cl	*n*-C_6H_{13}	62.74 (63.02)	6.13 (5.81)	2.37 (2.37)	19.69 (20.09)	66–67	1.42

Tin was estimated as SnO_2. Microanalyses were carried out by the Chemistry Department, National University of Singapore, Singapore.

RESULTS AND DISCUSSION

Regardless of the proportions of ligand and triphenyltin compound used, the complexes all crystallised with 1:1 stoichiometry. They were all yellow in colour, thermally stable with sharply-defined melting points and were found to be soluble in the common organic solvents. Microanalytical and conductance data for the complexes are presented in Table 1. The observed molar conductances in nitrobenzene were in the range 1.4–3.0 ohm^{-1} cm^2 mol^{-1}, indicating that the compounds were non-electrolytes and that in each instance, the chloride or isothiocyanate group is bound to the tin atom. (Molar conductances expected for 1:1 and 1:2 electrolytes in nitrobenzene are 25–35 and 44–60 ohm^{-1} cm^2 mol^{-1}, respectively.[8]

Some data from the PMR spectra of the complexes are listed in Table 2. Comparison of the integrated intensities of the ligand and organotin protons confirms the 1:1 stoichiometry of the complexes. The sharp singlet assigned to the azomethine proton[9] of the ligands ($\delta \sim 8.2$ ppm) was found to be unchanged on coordination, indicating that the N-atom is not coordinated to the metal. On the other hand, the peak due to the phenolic proton for each ligand molecule ($\delta \sim 13$ ppm) was significantly broadened on complex formation. As the ring formed by the intramolecular hydrogen bond of the Schiff-base ligand is retained, but distorted in the complexes,[1,3] coordination through oxygen will result in a weakening of the O—H bond, and a strengthening of the C=N···H hydrogen bond, which in turn leads to the observed broadening of the peak due to the phenolic proton. Similar observations have been reported for the dialkyltin chloride complexes of N-arylsalicylideneimines,[4] and of *N,N'*-bis(salicylaldehyde) ethylenediimine.[10]

Table 2. PMR data for the complexes

Complex $Ph_3SnX:o\text{-}HOC_6H_4CH{=}NR$		Azomethine proton CH=NR (ppm)	Phenolic OH δ (ppm)
X	R		
Cl	CH_3	8.17	13.20
NCS	CH_3	8.10	13.10
Cl	$PhCH_2$	8.23	13.18
NCS	$PhCH_2$	8.28	13.18
Cl	*t*-Bu	8.25	13.08
NCS	*t*-Bu	8.13	13.00
Cl	*c*-C_6H_{11}	8.27	13.0
NCS	*c*-C_6H_{11}	8.25	12.9
Cl	$HOCH_2CH_2$	8.28	*
NCS	$HOCH_2CH_2$	8.10	*
Cl	*n*-C_6H_{13}	8.24	13.05

* Not detected.

The IR evidence (Table 3) also suggests that the ligands are behaving as monodentates via the oxygen atoms. A strong band assigned to the C=N stretching vibration[9–11] is observed at 1633–1645 cm^{-1} for the ligands. However, in the complexes, this band shifts slightly towards higher frequency (1645–1660 cm^{-1}). Similar shifts in C=N stretching frequency for ligands of this type have been found to indicate coordination to the tin atom by oxygen.[1–5,10] This has been confirmed by the X-ray

Table 3. IR data for the complexes

Complex $Ph_3SnX:o\text{-}HOC_6H_4CH{=}NR$			ν (Sn—Ph)			
X	R	ν (CN)* (cm^{-1})	(cm^{-1})	(cm^{-1})	ν (CN)† (cm^{-1})	ν (Sn—Cl) (cm^{-1})
Cl	CH_3	1660	275	230	—	235
NCS	CH_3	1660	275	230	2050	—
Cl	*t*-Bu	1653	280	230	—	240
NCS	*t*-Bu	1650	275	230	2060	—
Cl	$PhCH_2$	1650	270	225	—	235
NCS	$PhCH_2$	1655	275	235	2070	—
Cl	$HOCH_2CH_2$	1645	275	220	—	225
NCS	$HOCH_2CH_2$	1655	275	230	2060	—
Cl	*c*-C_6H_{11}	1645	270	225	—	235
NCS	*c*-C_6H_{11}	1650	275	230	2060	—
Cl	*n*-C_6H_{13}	1655	275	220	—	235

* ν (CN) for ligand.
† ν (CN) for NCS group.

structural analysis of the complex of dimethyltin dichloride with *N,N*-ethylenebis(salicylideneimine).[12]

Due to the strong intramolecular hydrogen bonding present, the stretching vibration of the phenolic O—H is lowered and broadened[13] and the weak, broad bands observed in the spectra of the ligands in the 2600–3000 cm^{-1} range are attributed to these restricted vibrations. For the complexes, these bands are shifted towards higher energies by about 200 cm^{-1}, which is further evidence that the ring formed by the intramolecular hydrogen bond of the ligand although distorted, is still present after complex formation has occurred.[10]

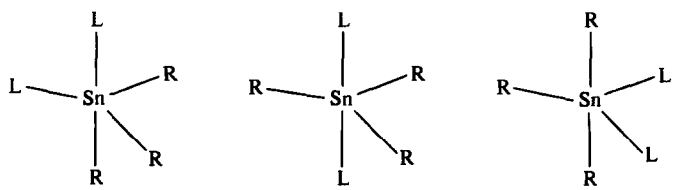
In the case of the ligand

$$o\text{-}HOC_6H_4CH{=}NCH_2CH_2OH,$$

a band at 3350 cm^{-1} is assigned to the alcoholic O—H stretching absorption. This band does not change on complex formation, indicating that the free alcohol group present in this molecule plays no part in the coordination of the ligand to the metal.

In the low frequency IR region, bands observed at ~ 220 and ~ 280 cm^{-1} in all the complexes are assigned to tin–phenyl stretching vibrations. The frequencies of these vibrations are largely unaffected by changes in the coordination number of the tin atom, and occur at almost the same frequencies as in the parent triphenyltin chloride and isothiocyanate.[14] Each of the triphenyltin chloride complexes displayed a band in the region 225–240 cm^{-1}. These are assigned to the Sn—Cl stretching mode, which is sensitive to an increase in coordination round the tin atom, and in each case is shifted downfield by some 100 cm^{-1} from its value in triphenyltin chloride.[14] The strong absorption observed at ~ 2060 cm^{-1} for all the isothiocyanate complexes suggests that the thiocyanate groups are *N*-bonded in each case.[15]

The results so far discussed, including the analytical, PMR, conductivity and IR data, strongly support the assignment of a five-coordinate structure to the complexes. The three possible isomers for trigonal bipyramidal complexes of this type are shown in Fig. 1. It has been shown,[16,17] that each of these three possible isomers would be expected to show a different quadrupole splitting (ΔE_Q) value in the Mössbauer spectrum. For isomers



I II III

Fig. 1. Possible isomers of trigonal bipyramidyl R_3SnL_2.

Table 4. Mössbauer data for the complexes*

Complex	Isomer shift† δ (mm s^{-1})	Quadrupole splitting (ΔE_Q) (mm s^{-1})
o-$HOC_6H_4CH{=}NCH_3$: Ph_3SnCl	1.24	3.10
o-$HOC_6H_4CH{=}NCH_3$: Ph_3SnNCS	1.20	3.22
o-$HOC_6H_4CH{=}NCH_2CH_2OH$: Ph_3SnCl	1.26	3.23
o-$HOC_6H_4CH{=}NCH_2CH_2OH$: Ph_3SnNCS	1.21	3.42

* The accuracy for all these parameters is ± 0.05 mm s^{-1}.
† Relative to $BaSnO_3$.

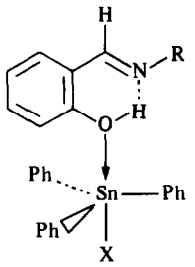


Fig. 2. Proposed structures of the complexes.

of type **I**, the range of ΔE_Q is 1.7–2.3 mm s^{-1}, for **II**, 3–3.9 mm s^{-1} and for **III**, 3.5–4.1 mm s^{-1}. The ΔE_Q values (Table 4) obtained for the complexes described herein fall in the range 3.10–3.42 mm s^{-1}, and thus clearly belong to category **II**.

We believe that the complexes of the *N*-alkylsalicylideneimines with triphenyltin chloride and isothiocyanate have five-coordinate, trigonal bipyramidal structures, with the phenyl groups occupying the equatorial positions and the ligands behaving as monodentates through the phenolic oxygen atoms, as shown in Fig. 2. The assignment of such structures is entirely consistent with the stereochemistry of other triorganotin complexes.[18]

Acknowledgements—We thank Dr P. J. Smith for the Mössbauer spectra, Mr C. L. Yee for technical assistance and Universiti Sains Malaysia and NSERC (Canada) for financial support.

REFERENCES

1. B. S. Saraswat, G. Srivatava and R. C. Mehrotra, *J. Organomet. Chem.* 1979, **164**, 153.
2. B. S. Saraswat, G. Srivastava, R. C. Mehrotra, G. Sawhney and J. S. Baijal, *J. Inorg. Nucl. Chem.* 1980, **42**, 805.
3. B. S. Saraswat, G. Srivastava and R. C. Mehrotra, *Inorg. Chim. Acta* 1979, **36**, 289.
4. L. E. Khoo and F. E. Smith, *Polyhedron* 1982, **1**, 213.
5. T. N. Srivastava and A. K. S. Chuhan, *J. Inorg. Nucl. Chem.* 1977, **39**, 371.
6. T. N. Srivastava, A. K. S. Chuhan and M. Agarwal, *J. Inorg. Nucl. Chem.* 1979, **41**, 896.
7. K. C. Panda, *J. Organomet. Chem.* 1968, **13**, 187.
8. J. A. Walmsley and S. Y. Tyree, *Inorg. Chem.* 1963, **2**, 312.
9. G. C. Percy and D. A. Thornton, *J. Inorg. Nucl. Chem.* 1972, **34**, 3369.
10. K. Kawakami, M. Miya-uchi and T. Tanaka, *J. Inorg. Nucl. Chem.* 1971, **33**, 3773.
11. L. E. Clougherty, J. A. Sousa and G. M. Wyman, *J. Org. Chem.* 1957, **22**, 462.
12. L. Randaccio, *J. Organomet. Chem.* 1973, **55**, C58.
13. H. H. Freedman, *J. Am. Chem. Soc.* 1961, **83**, 2900.
14. R. C. Poller, *The Chemistry of Organotin Compounds*, p. 227. Logos Press (1970).
15. R. A. Bailey, S. L. Kozak, T. W. Michelsen and W. N. Mills, *Coord. Chem. Rev.* 1971, **6**, 407.
16. G. M. Bancroft, V. G. Kumar Das and T. K. Sham, *J. Chem. Soc., Chem. Commun.* 1974, 236.
17. G. M. Bancroft, V. G. Kumar Das, T. K. Sham and M. G. Clark, *J. Chem. Soc., Dalton Trans.* 1976, 643.
18. P. G. Harrison, K. Lambert, T. J. King and B. Majee, *J. Chem. Soc., Dalton Trans.* 1983, 363.

Polyhedron Vol. 4, No. 3, pp. 451–455, 1985
Printed in Great Britain

0277–5387/85 $3.00 + .00
Pergamon Press Ltd

METAL–(PHENYLTHIO)ACETIC ACID INTERACTIONS—IV. THE CRYSTAL STRUCTURE OF TETRA-μ-[(2,4-DICHLORO-5-METHYLPHENYLTHIO)ACETATO-*O,O'*]-BIS[ACETONECOPPER(II)], A DIMERIC COMPLEX HAVING COORDINATED ACETONE MOLECULES*

GRAHAM SMITH and ERIC J. O'REILLY
Department of Chemistry, Queensland Institute of Technology, Brisbane 4000, Australia,

COLIN H. L. KENNARD†
Department of Chemistry, University of Queensland, Brisbane 4067, Australia

and

THOMAS C. W. MAK and WAI-HING YIP
Department of Chemistry, The Chinese University of Hong Kong, Shatin, New Territories, Hong Kong

(*Received* 22 *March* 1984; *accepted* 4 *May* 1984)

Abstract—The crystal structure of the acetone adduct of copper(II) (2,4-dichloro-5-methylphenylthio)acetate has been determined by single crystal X-ray diffraction and refined by least squares to 0.051 for 3701 "observed" reflections. Crystals of the compound are triclinic, space group $P\bar{1}$ with one dimer in a cell with $a = 8.357(1), b = 12.502(2), c = 13.721(2)$ Å, $\alpha = 107.20(1)$, $\beta = 96.09(1)$, $\gamma = 104.94(1)°$. The complex is a tetracarboxylate bridged dimer of the copper acetate hydrate type, with a Cu—Cu separation of 2.646(1) Å and a mean Cu—O (equatorial) distance of 1.961(4) Å, while the axial positions of the dimer are occupied by coordinated acetone molecules [Cu—O, 2.206(3) Å]. X-ray crystal data and the results of chemical analyses are also presented, indicating that a second chemical polymorph has both acetone and water molecules, with a similar dimeric structure but having solvated acetone.

The structural systematics of the tetracarboxylate bridged dimeric copper(II) complexes have been of interest to inorganic chemists since 1953 when the crystal structure of copper acetate monohydrate was reported.[2] To date more than 50 of these dimer structures have been determined by X-ray diffraction.[3–7] In $[Cu_2(R \cdot CO_2)_4(L)_2]$ the nature of R varies but the equatorial CuO_4 moieties change little within the series, the largest variation existing in the Cu—L axial distances. So far, the longest Cu—L distances are found for the anhydrous analogues, copper(II) propionate,[8] copper(II) butyrate[9] and copper(II) (2-chlorophenoxy)acetate,[7] in which the axial positions are occupied by oxygens from adjacent carboxylate groups, extending the structures into polymer chains. Other oxygen donor groups found are water [as in the copper(II) acetate monohydrate structure], methanol, ethanol, dimethylsulfoxide, urea, acetic acid, dimethylformamide and 1,4-dioxane while nitrogen base donors include pyridine and substituted pyridines, quinoline, 2-aminopyrimidine, 4-diazobicyclo-[2.2.2]octane and thiocyanate ion. In the present work, compounds prepared from (2.4-dichloro-5-methylphenylthio)acetic acid (DCMPTAH) were found from elemental analyses to have acetone in a formula consistent with dimeric species, $Cu_2(R \cdot CO_2)_4(acetone)_2$ (**1**) and $Cu_2(R \cdot CO_2)_4(acetone)_2(H_2O)_2$ (**2**). Although other molecules analogous to acetone [DMSO and urea] have been found in the axial positions in this

* For Part III see Ref. 1.

† Author to whom correspondence should be addressed.

dimer series no examples involving acetone are known. Furthermore, the occurrence of acetone as a ligand is to date unknown in copper(II) chemistry, although it is commonly found as a molecule of solvation in complexes. The only examples of co-ordinated acetone *per se* among general complexes is in oxochlorobis-[1,2-bis(diphenylphosphino)-ethane]molybdenum(IV) acetonetrichlorozincate(II) acetone (1/1).[10] The present crystal structure of **1** confirms the presence of acetone in the axial position of a stable coordinated copper(II) dimer.

EXPERIMENTAL

Preparation of complexes **1** *and* **2**

$CuCO_3 \cdot Cu(OH)_2$ [0.9 g (4.0 mmol)] was added to a solution of (2,4-dichloro-5-methylphenylthio)-acetic acid (DCMPTAH) [0.5 g (2.0 mmol)] in 70% ethanol/water and the resulting mixture was digested at 50–55°C for *ca* 5 h with continuous stirring. The unreacted carbonate was then removed by filtration and the filtrate allowed to evaporate slowly at room temperature. After several days, a greyish-blue microcrystalline solid was deposited which was subsequently redissolved in acetone. Two different chemical polymorphs were then re-deposited. The first (**1**) forming as dark green prisms in very low yield, was found to have a molecular weight equivalent to $Cu(DCMPTA)_2$(acetone) (precise X-ray cell parameters and measured density). The major product (**2**) formed late in crystallization as light green flat needles for which elemental analysis (C, 38.4; H, 3.47%), X-ray cell parameters and density determination indicated the formula $Cu(DCMPTA)_2(acetone)(H_2O)$. (Calc. for $C_{21}H_{22}Cl_4CuO_6S_2$; C, 39.8; H, 3.46%.)

Crystallography for **1** *and* **2**

Crystal data. (**1**) $C_{42}H_{40}Cl_8Cu_2O_{10}S_4$, M_r = 1243.7, a = 8.357(1), b = 12.502(2), c = 13.721(2) Å, α = 107.20(1), β = 96.09(1), γ = 104.94(1)°, U = 1297.1(3) Å^3, D_f = 1.59, D_c = 1.592 g cm^{-3}, Z = 1 (dimer), Mo-K_α radiation, λ = 0.71069 Å, μ(Mo-K_α) = 14.7 cm^{-1}, $F(000)$ = 630, space group $P\bar{1}$.

(**2**) $C_{42}H_{44}Cl_8Cu_2O_{12}S_4$, M_r = 1279.8, a = 8.140(3), b = 9.501(5), c = 18.58(1) Å, α = 90.73(5), β = 99.56(5), γ = 108.72(4)°, U = 1338.6(13) Å^3, D_f = 1.60, D_c = 1.587 g cm^{-3}, Z = 1 (dimer), Mo-K_α radiation, λ = 0.71069 Å, μ(Mo-K_α) = 14.3 cm^{-1}, $F(000)$ = 650, space group $P\bar{1}$ (assumed).

Data collection, structure solution and refinement. For **1**, 4995 reflections were collected from one crystal (0.36 × 0.28 × 0.12 mm) on a Nicolet R3m four-circle diffractometer [graphite crystal monochromatized Mo-K_α radiation, λ = 0.71069 Å; ω–2θ scans at 2.02–8.38 deg min^{-1}; $2\theta_{max}$ = 52°]. Of these, 3701 reflections with $I > 2.5\sigma(I)$ were considered observed and used in structure analysis, after correcting for absorption. The automatic centrosymmetric Σ_2 sign expansion direct methods of SHELX 76[11] failed to locate the Cu atom. It was subsequently located by shifting the Cu atomic co-ordinates found from the first E-map so as to place the inversion centre of the assumed dimer at a crystallographic origin. The structure was then solved by heavy atom and Fourier methods, and refined by blocked-matrix least-squares with anisotropic thermal parameters for all non-hydrogen atoms. Hydrogen atoms were located in a difference-Fourier synthesis and were included in the refinement at fixed positions with their isotropic U values set invariant at 0.05 Å^2. Final residuals were R [$= \Sigma \|F_o - F_c\| / \Sigma |F_o|$] 0.051 and Rw [$= \Sigma w(\|F_o - F_c\|^2 / \Sigma w|F_o|^2)^{1/2}$] 0.058 with $w = 2.64/(\sigma^2 F_o + 5.3 \times 10^{-4} F_o^2)$ found to be suitable. An analysis of the data indicated that 10 intense low-angle reflections were affected by extinction and were removed before the final cycle of refinement. The maximum peak in the last difference-Fourier was equivalent to 0.18 e Å^{-3}. Neutral atom scattering factors were used,[12] while Cu, Cl and S were corrected for the effects of anomalous dispersion.[12]

Atomic coordinates, thermal parameters, observed and calculated structure factors and intra-ligand bond distances and angles have been deposited with the Editor as supplementary material; copies are available on request from the Editors or the authors. Atomic coordinates have also been deposited with the Cambridge Crystallographic Data Centre. Bond distances and angles about the coordination polyhedron are given in Table 1.

DISCUSSION

Complex **1** forms centrosymmetric tetracarboxylate bridged dimers of the copper(II) acetate monohydrate type[2] (Fig. 1), The four Cu—O (equatorial) distances in the square pyramidal CuO_4L "ends" of the dimer are similar [range 1.958–1.964 Å; mean 1.961(4) Å]. These results emphasize the consistency of this distance among the entire dimer series (1.96 Å mean[3]). The Cu—Cu separation [2.646(1) Å] falls within the quite large range of distances found for the series (2.563–2.886 Å[7]). The value, however, correlates with the out-of-plane distance for the Cu atom, indicating that variation in the Cu—Cu separation is accommodated by a

Table 1. Bond distances (Å) and angles (°) about the coordination sphere for $[Cu_2(DCMPTA)_4(acetone)_2]$ but including the bonded acetone*

a. Distances

Cu-O(10)A	1.958(4)	Cu-Cu'	2.646(1)
Cu-O(10)B	1.959(3)	C(1)Ac-C(2)Ac	1.504(8)
Cu-O(11)A'	1.964(4)	C(2)Ac-C(3)Ac	1.488(11)
Cu-O(11)B'	1.962(3)	C(2)Ac-O(2)Ac	1.209(5)
Cu-O(2)Ac	2.206(3)		

b. Angles

O(2)Ac-Cu-O(10)A	95.6(1)	O(11)A'-Cu-O(11)B'	88.4(2)
O(2)Ac-Cu-O(10)B	93.7(1)	C(9)A-O(10)A-Cu	125.2(3)
O(2)Ac-Cu-O(11)A'	96.5(1)	C(9)B-O(10)B-Cu	125.9(2)
O(2)Ac-Cu-O(11)B'	93.7(1)	C(9)A'-O(11)A'-Cu	120.7(3)
O(10)A-Cu-O(10)B	88.0(2)	C(9)B'-O(11)B'-Cu	120.3(3)
O(10)A-Cu-O(11)A'	167.9(1)	C(2)Ac-O(2)Ac-Cu	132.9(4)
O(10)A-Cu-O(11)B'	89.3(2)	C(1)Ac-C(2)Ac-C(3)Ac	115.9(3)
O(10)B-Cu-O(11)A'	91.8(2)	C(1)Ac-C(2)Ac-O(2)Ac	121.8(6)
O(10)B-Cu-O(11)B'	167.8(1)	C(3)Ac-C(2)Ac-O(2)Ac	122.3(5)

* Distances and angles for the (phenylthio)acetate ligands are available from the editor. Primed atoms are generated by an inversion operation.

movement of the Cu atom in and out of the square plane. In this compound, the role of the acetone molecules is of interest since they are coordinated in the axial positions of the dimer [Cu—O, 2.206(3) Å]. The acetones are asymmetrically oriented with the Cu—O—C angle 132.9(4)° roughly consistent with the angle of approach of a lone pair of electrons on the keto oxygen. This is similar to the disposition of the acetone in the tetrahedral (acetone trichlorozincate) ion in $[MoCl\{Ph_2P(CH_2)_2PPh_2\}_2]^+[ZnCl_3(CH_3)_2CO]^- \cdot (CH_3)_2CO$.[10] The Br—O—C angle (125°) in the hydrogen bonded acetone/molecular bromine (1 : 1) adduct shows analogous directional properties in the hydrogen bonding interactions.[13]

The coordinated acetone molecule has seldom been observed in crystalline solids, so that the present example represents a good system for structural observation since it is relatively unperturbed in its mode of attachment and is quite stable under the conditions of the determination. It has both chemical and thermal stability with all atoms of the acetone molecule having normal thermal parameters. This contrasts with the molybdenum zincate complex[10] where the structure analysis was completed at −70°C. The bond distances for the acetone molecule, C=O [1.209(5)

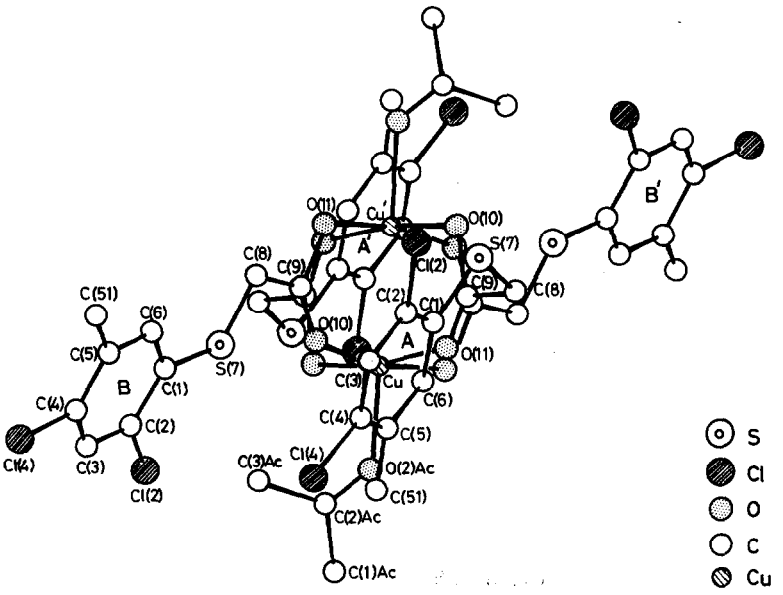


Fig. 1. Molecular stereochemistry and atom naming scheme for $[Cu_2(DCMPTA)_4(acetone)_2]$.

Å] and C—C [1.488(11), 1.504(8) Å] are compared with those for an acetone solvate molecule in the structure of a complex of comparable precision, $[Ba(C_{12}H_8N_2)_2(C_6H_2N_3O_7]\cdot(CH_3)_2CO$, [1.220(5), 1.478(6), 1.499(7) Å].[14] The bond angles C—C—O and C—C—C for (**1**) [121.3(5), 121.8(6)° and 115.9(3)°] are also comparable [120.8(4), 122.8(4)° and 116.4(4)°] indicating distortion away from the repulsive influence of the oxygen lone pairs. The planar nature of the acetone molecule is preserved (intra-angle sum = 360.0°). It would therefore appear that the molecule is not affected significantly on being complexed.

Although it is not altogether surprising to find acetone as a coordinated molecule, or more specifically as an axial ligand in a copper dimer system (considering the number of urea and alcohol examples), the low incidence of examples is probably attributable to steric constraints. In examples where the acid residue is not too bulky, the acetone molecules are able to displace water from the axial sites and coordinate. This process is achieved readily by dissolution of the complex in acetone. In a number of the copper(II) dimers, because of a lack of solubility in this solvent, formation of the acetone adduct is not obtained. In the case of the analogous green phenoxyalkanoic acid complex dimer, $[Cu_2(2,4\text{-}D)_4(H_2O)_2]\cdot 2H_2O$ is readily formed from the monomeric blue complex $[Cu(2,4\text{-}D)_2(H_2O)_4]$ by dissolution in a non-aqueous solvent.[15] The use of acetone results in the deposition of a dark green complex (assumed to be an acetone adduct) but this rapidly reverts in air to the original pale blue form. The probable reason for the forming of stable **1** and not a Cu(2,4-D)-acetone adduct could be due to the greater steric freedom allowed by the longer C—S—C compared to C—O—C chain. This places the bulk of the substituted phenyl ring systems at a more favourable distance from the dimer unit. Therefore, other examples of acetone adducted copper(II) dimers will be found where suitable steric conditions are met to allow this penetration of acetone. Although the structure of compound **2**, $[Cu_2(DCMPTA)_4(acetone)_2]\cdot 2H_2O$ was not determined, analytical evidence indicates that it is a chemical polymorph of **1** differing only in the presence of additional water molecules probably coordinated with lattice acetones.

The substituted (phenylthio)acetate ligands in complex **1** are considerably different conformationally. Whereas ligand B is extended and assumes a relatively planar disposition, the second ligand (A) is convoluted. This is in evidence in the torsion angles for the thioacetate side-chains [C(6)—C(1)—S(7)—C(8), C(1)—S(7)—C(8)—C(9) and S(7)—C(8)—C(9)—O(10)] which are +6.4, −77.4, +109.7 and +5.8, +69.8 and +10.1° for the A and B residues respectively. This difference in conformation is common in other examples of phenoxyalkanoic acid dimers[7,15] and for the (phenylthio)acetic acid (PTAH) dimer, $[Cu_2(PTA)_4(py)_2]$.[16] It is presumably an artifact of the packing efficiency involving dimers which are considerably extended in the peripheral areas because of the acid residues.

Compared to the free (unsubstituted) acid,

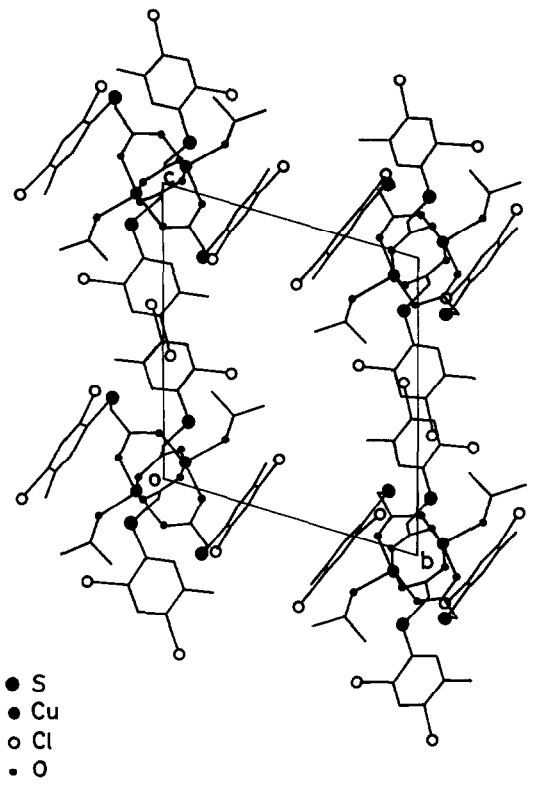


Fig. 2. Molecular packing in the unit cell viewed down *a*.

(phenylthio)acetic acid,[17] and the known complexes of this acid, $[Zn(PTA)_2(H_2O)_2]$,[17] $[Cd(PTA)_2(H_2O)]_n$,[17] $[Cu_2(PTA)_4(py)_2]$.[16] $[Ba(PTA)_2]_n$,[1] $[K(PTA)(PTAH)]_n$,[1] the thioacetate side-chains are also changed conformationally. In **1**, the thioether (S) to carboxyl (O) interactive distances for the individual ligands [3.25 Å (A) and 2.99 Å (B)] are markedly different and different to 2.85 Å for PTAH, 3.03 Å (Zn), 3.01, 3.06 Å (Cd), 3.07, 3.25 Å (Cu), 2.79 Å (Ba) and 2.84, 2.88 Å (K). This inconsistency contrasts with the relatively small spread of values for the O(ether)—O(carboxyl) interactive distances in the phenoxyalkanoic acids,[18] or the metal complexes of these acids,[19] irrespective of side-chain conformation. The reason is probably found in the relatively weaker S—O, cf. O—O interaction for the phenylthio vs the phenoxy acids.

The packing of molecules of **1** in the unit cell (Fig. 2) involves discrete non-interactive dimers. This is the common packing type for such dimers because of the usual non-associative nature of the groups defining the extremeties of the molecules. Exceptions are, of course, those dimers which are sub-units of polymer systems. These form through the axial ligand, either by bi-functional donor molecules (e.g. 1,4-dioxane or pyrimidine) or by the carboxyl oxygens of adjacent dimers (e.g. anhydrous complexes).

Acknowledgements—We thank the University of Queensland and the Queensland Institute of Technology for financial support and for data preparation services and the Chinese University of Hong Kong for provision of data collection facilities.

REFERENCES

1. T. C. W. Mak, W.-H. Yip, G. Smith, E. J. O'Reilly and C. H. L. Kennard, *Inorg. Chim. Acta* 1984, **88**, 35.
2. J. N. van Niekerk and F. R. L. Schoening, *Acta Cryst.* 1953, **6**, 227.
3. M. Melnik, *Coord. Chem. Rev.* 1982, **42**, 259.
4. G. Smith, E. J. O'Reilly and C. H. L. Kennard, *Inorg. Chim. Acta* 1981, **49**, 53.
5. M. Bukowska-Strzyzenoska, J. Skeweranda, E. Huyduk and J. Mrozinski, *Inorg. Chim. Acta* 1983, **73**, 207.
6. V. M. Rao, D. H. Sathyanarayana and H. Manohar, *J. Chem. Soc., Dalton Trans.* 1983, 2167.
7. G. Smith, E. J. O'Reilly, C. H. L. Kennard and A. H. White, *J. Chem. Soc., Dalton Trans.* (in press).
8. Yu. A. Simonov and T. I. Malinovskii, *Sov. Phys. Cryst.* 1970, **15**, 310.
9. M. J. Bird and T. R. Lomer, *Acta Cryst.* 1972, **B28**, 242.
10. V. C. Adam, U. A. Gregory and B. T. Kilbourn, *J. Chem. Soc., Chem. Commun.* 1970, 1401.
11. G. M. Sheldrick, SHELX 76, *Program for Crystal Structure Determination.* University of Cambridge, England (1976).
12. *International Tables for X-ray Crystallography*, Vol. IV. Kynoch Press, Birmingham (1974).
13. O. Hassel and N. O. Stromme, *Acta Chem. Scand.* 1959, **13**, 275.
14. R. Postina, J. A. Kanters, A. J. M. Duisenberg, K. Venkatasubramanian and N. S. Poonia, *Acta Cryst.* 1983, **C39**, 1221.
15. G. Smith, E. J. O'Reilly and C. H. L. Kennard, *Inorg. Chim. Acta* 1981, **49**, 54.
16. E. J. O'Reilly, G. Smith, C. H. L. Kennard, T. C. W. Mak and W.-H. Yip, *Inorg. Chim. Acta* 1984, **83**, L63.
17. T. C. W. Mak, W.-H. Yip, G. Smith, E. J. O'Reilly and C. H. L. Kennard, *Inorg. Chim. Acta* 1984, **84**, 57.
18. C. H. L. Kennard, G. Smith and A. H. White, *Acta Cryst.* 1982, **B38**, 868.
19. G. Smith, E. J. O'Reilly, C. H. L. Kennard, K. Stadnika and B. Oleksyn, *Inorg. Chim. Acta* 1981, **47**, 111.

Polyhedron Vol. 4, No. 3, pp. 457–461, 1985
Printed in Great Britain

0277–5387/85 $3.00 + .00
Pergamon Press Ltd

RAMAN STUDY OF HALOGEN EXCHANGE EQUILIBRIA IN LOW MELTING MIXTURES CONSISTING OF SODIUM TETRACHLOROALUMINATE AND TETRABROMOALUMINATE

R. W. BERG,* E. KEMNITZ,† H. A. HJULER, R. FEHRMANN and N. J. BJERRUM

Chemistry Department A, The Technical University of Denmark, Building 207, DK-2800 Lyngby, Denmark

(*Received* 5 *December* 1983; *accepted* 9 *May* 1984)

Abstract—The halogen-redistribution reactions between $[AlCl_4]^-$ and $[AlBr_4]^-$ in molten mixtures of $NaAlCl_4$ and $NaAlBr_4$ with widely varying mole ratios have been studied by Raman spectroscopy at 160–300°C and the melting points have been measured. By monitoring the intensities of the totally symmetric stretching a_1-modes of both the parent tetrahalides as well as those of the mixed halides $[AlCl_3Br]^-$, $[AlCl_2Br]^-$ and $[AlClBr_3]^-$ it is concluded that the mixtures equilibrate very fast and consist of an almost random distribution of the five species. $NaAlCl_4$ and $NaAlBr_4$ form an eutectic mixture with a molar ratio near to 4:1, with a melting point of *ca* 142°C.

In the search for low-melting molten salt electrolytes for use in batteries it was deemed of interest to investigate the mixed tetrachloroaluminate–tetrabromoaluminate system. This system is of special interest because of its Lewis-acid neutrality.

This paper is concerned with the equilibrium between sodium melts of $[AlCl_4]^-$ and $[AlBr_4]^-$ and the mixed halides $[AlCl_3Br]^-$, $[AlCl_2Br_2]^-$, and $[AlClBr_3]^-$ which probably are formed rapidly at 200°C, judging from previous studies on mixed solutions in dichloromethane and other solvents at room temperature.[1–3]

The object was to study the halogen-exchange distribution of the species *by means of* their *Raman spectra* as a function of temperature and composition, and to confirm that the redistribution is random and that there is no preference of any of the species. Finally, the melting points of the mixtures were recorded to see if any low-melting eutectic exists in this system.

EXPERIMENTAL

Preparation of samples

Because of the sensitivity to water of the reagents, drybox and vacuum-line techniques were employed. $AlCl_3$ or $AlBr_3$ of highest attainable purities[4] were mixed with an equimolar amount of NaCl or NaBr, respectively, in evacuated Pyrex cells. The sodium halides have previously been purified by recrystallization after flushing with dry hydrogen halide gas. Each of these mixtures was equilibrated in rocking furnaces and recrystallized as described elsewhere.[4] The melting point of the pure $NaAlCl_4$ and $NaAlBr_4$ was 156.7 and 201.5°C, respectively.

Mixtures of various Cl:Br molar ratios were obtained by mixing different weighed proportions of the pure $NaAlCl_4$ and $NaAlBr_4$ compounds in sealed Pyrex tubes. The compositions of the prepared mixtures are given in Table 1.

The Raman spectra were measured as previously,[5] using 488.0 and 514.5 nm argon-ion laser radiation and a JEOL-JRS-400D spectrometer equipped with a four-window accurately regulated furnace. Detection of signals was done with a cooled extended S-20 PM-tube and a photon counting system. The first Raman spectrum of each sample was obtained at 160°C within 5 min after melting the solid mixture by gentle heating in a soft flame and inserting into the preheated furnace.

The melting points of the mixtures were determined visually by slowly heating the Raman cells immersed in a well-stirred oil bath. The temperature accuracy is *ca* 1°C; the small amount of sample did not allow a higher precision. For the neat compounds, an accuracy better than 0.1°C was obtained as described previously.[6]

* Author to whom correspondence should be addressed.
† On leave from Sektion Chemie der Humboldt-Universität zu Berlin, Hessische Str. 1-2, 1040 Berlin, German Democratic Republic.

Table 1. Compositions and melting points of the samples

Sample weight (g)	X_{NaAlCl_4}* (accuracy ±0.0001)	T_m† (°C)
1.30	1.0000	156.6
1.40	0.8750	143
1.38	0.7496	142.5
1.33	0.6674	144.5–146.5
1.05	0.5797	151–153
2.01	0.5000	158.5
1.62	0.4199	166.0
2.19	0.3334	169.0
2.41	0.2499	174.5
2.94	0.1250	186.5
2.10	0.0000	201.5

*Formal mole fraction calculated from the starting materials: $X_{NaAlCl_4} = \frac{n_{NaAlCl_4}}{n_{NaAlCl_4} + n_{NaAlBr_4}}$, where n denotes number of moles.

† T_m is the melting point or melting interval.

RESULTS AND DISCUSSION

Raman spectra

Selected Raman spectra of various molten mixtures of $NaAlCl_4$ and $NaAlBr_4$ at 210°C are given in Fig. 1. Similar spectra were obtained at 160 and 300°C using green or blue laser light with no significant change in band positions or relative intensities, and no time dependence. The Raman spectra of the ions $[AlCl_4]^-$ and $[AlBr_4]^-$ are well known, and dominated by a strongly polarized totally symmetric stretching band, the a_1-mode, occurring at *ca* 350 and 210 cm^{-1}, respectively.[2,3,5,7,8] For the mixed species $[AlCl_nBr_{4-n}]^-$ ($n = 1$, 2 or 3) the Raman spectra are equally characterised by a strong polarized a_1-mode attributed to the totally symmetric stretching vibration of the halogen atoms; moving to progressively lower frequencies as bromide replaces chloride in the mixed aluminium tetrahalides.[2,3] The individual a_1-bands due to all five possible mixed tetrahalides can readily be identified in our spectra (Fig. 1) on the basis of their intensity variation with changing chloride content. The positions of the a_1-bands found in this work are shown in Table 2, and as it is seen, in perfect agreement with previous results obtained on solid mixed tetramethylammonium tetrahalide aluminates at room temperature.[2,3]

Halogen-redistribution equilibria

The spectra obtained as soon as possible after melting did not deviate from later spectra. This proves that equilibrium is reached at least within a few minutes at 160°C. This is in accordance with the observation[3] that less than 2 s are needed to obtain equilibrium when organic solutions of $[AlCl_4]^-$ and $[AlBr_4]^-$ are mixed at room temperature, according to ^{27}Al NMR spectra.

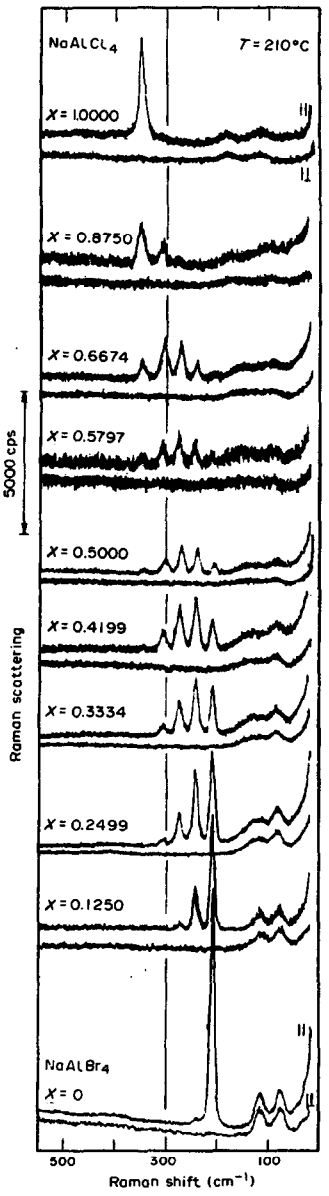


Fig. 1. Raman spectra of mixtures of $NaAlCl_4$ and $NaAlBr_4$ at 210°C as a function of X_{NaAlCl_4}. Excitation 488.0 nm at 300 mW. Resolution 4 cm^{-1}. Scan rate 25 cm^{-1} min^{-1}. || and |⊥ denote polarized and depolarized spectra.[5]

The halogen redistribution among the five possible tetrahaloaluminate ions occur according to the three reactions

$$2[AlCl_nBr_{4-n}]^- \rightleftharpoons [AlCl_{n+1}Br_{3-n}]^- + [AlCl_{n-1}Br_{5-n}]^- \quad (1)$$

Table 2. Raman bands arising from the totally symmetric a_1-vibration of halogen atoms in molten $Na[AlCl_nBr_{4-n}]$ mixtures, $n = 0$–4: band positions* are given in cm^{-1}

X_{NaAlCl_4}†	$AlCl_4^-$	$AlCl_3Br^-$	$AlCl_2Br_2^-$	$AlClBr_3^-$	$AlBr_4^-$
1.00	350	—	—	—	—
0.75	349	305	274	243	—
0.50	350	305	273	242	211
0.25	—	304	273	242	209
0.00	—	—	—	—	211
Literature‡	352	308	278	247	214
Intensity§	1	0.7	1.0	1.8	2.25

* Obtained by calibration of the spectra using emission lines of a Neon lamp.
† See Table 1.
‡ Solid tetramethylammonium tetrahalide aluminates[2,3] at room temperature.
§ Relative scattering powers calculated as described in the text.

with $n = 1$, 2 or 3. The equilibrium constants are given by

$$K_n = \frac{(x_{AlCl_{n+1}Br_{3-n}^-}) \cdot (x_{AlCl_{n-1}Br_{5-n}^-})}{(x_{AlCl_nBr_{4-n}^-})^2} \qquad (2)$$

where x denotes concentration or mole fraction.

Similar redistribution reactions have previously been analysed in general,[9] and it has been shown that, for the case of complete randomization, the equilibrium constants take the values $K_1 = K_3 = 3/8$ and $K_2 = 4/9$ and the mole fraction of the individual ions follows a binomial distribution: if X is the formal mole fraction of $[MZ_4]$, the mole fractions of the general species $[MZ_nY_{4-n}]$ are given by X^4, $4X^3(1-X)$, $6X^2(1-X)^2$, $4X(1-X)^3$ and $(1-X)^4$ for $n = 4$, 3, 2, 1 and 0, respectively.

According to this distribution,[9] (i) all five species should occur in appreciable mole fractions (>0.01) when $0.3 < X < 0.7$, (ii) 4 species should occur in appreciable amounts near $X = 0.2$ and $X = 0.8$, (iii) the $[MZ_3Y]$, $[MZ_2Y_2]$ and $[MZY_3]$ species have their maximal mole fractions at $X = 0.75$, 0.50, and 0.25, and (iv) $[MZ_4]$ and $[MY_4]$ have mole fractions of 1/16 at $X = 0.5$.

Qualitatively, these features are nearly what is observed in the spectra (Fig. 1), and hence the distribution of $[AlCl_nBr_{4-n}]^-$ ions are nearly random. This was also found at room temperature in organic solutions.[1–3] The situation is not unique, but has, e.g. also been found in $TiCl_4$–$TiBr_4$ mixtures.[10]

To study the phenomenon quantitatively, Raman a_1-bands of all samples were recorded under as near as possible identical conditions. The stability of the instrumental set-up (of the order $\pm 10\%$) was repeatedly checked by recording of the neat spectra. In this way a set of comparable spectra was obtained from which the relative scattering intensities of the a_1-bands as a function of X_{NaAlCl_4} could be measured. The data are given in Table 3 in arbitrary units (mm on our chart paper), and a graphical representation is shown in Fig. 2. Here, each curve represents the equilibrium mole fraction of the particular

Table 3. Relative Raman scattering intensities of the a_1-bands of $Na[AlCl_nBr_{4-n}]$ melts at 210°C (488.0 nm excitation, arbitrary units, estimated accuracy $\pm 10\%$)

X_{NaAlCl_4}	$AlCl_4^-$	$AlCl_3Br^-$	$AlCl_2Br_2^-$	$AlClBr_3^-$	$AlBr_4^-$
1.0000	106	—	—	—	—
0.8750	42	31	11	2	—
0.6674	17	31	28	14	3
0.5797	11	28	36	27	9
0.5000	7	19	32	27	10
0.4199	5	16	40	40	27
0.3334	2	15	33	55	53
0.2499	—	8	26	69	94
0.1250	—	2	13	49	117
0.0000	—	—	—	—	238

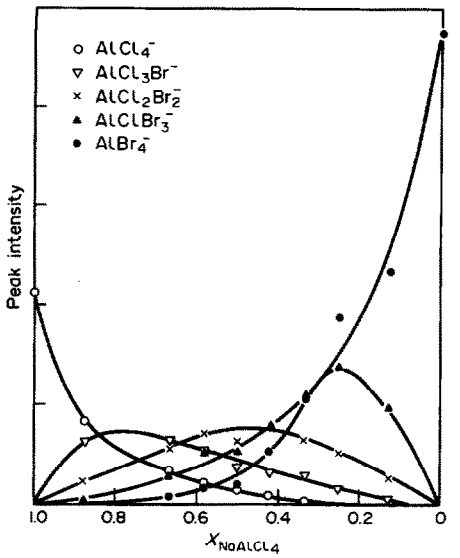


Fig. 2. Raman scattering intensity curves for the individual $[AlCl_nBr_{4-n}]^-$ ions as a function of X_{NaAlCl_4}. Each curve has a different mole fraction scale, depending on the a_1-band scattering power of the particular ion.

$[AlCl_nBr_{4-n}]^-$ ion, but on different scales due to the different scattering power of each ion (the Raman signal is proportional to the concentration*).

The scale of the curves for the ions $[AlCl_4]^-$ and $[AlBr_4]^-$ can easily be obtained, knowing the scattering power of the neat systems. Using the fact that the mole fraction sum must be unity in all mixtures, the scale of the three other curves can be calculated. (We used a graphical technique to avoid the numerical problems due to the scattering of the points. The three curves in Fig. 2 were read off at $X = 0.2$, 0.4, 0.6 and 0.8 to obtain four linear equations in the three scaling parameters. The first and last equation was added to obtain three equations, which were solved.)

From the scaling parameters, the relative scattering powers of the ions shown in the bottom of Table 2 were obtained. The corresponding scaled mole fractions are shown in Table 4 and Fig. 3(A). From the mole fractions in Table 4, the equilibrium constants K_n [equation (2)] were calculated to be $K_1 = 1.0$, $K_2 = 0.4$, and $K_3 = 0.21$ and their uncertainties were estimated to be ~ 0.4, ~ 0.1, and ~ 0.02, respectively.

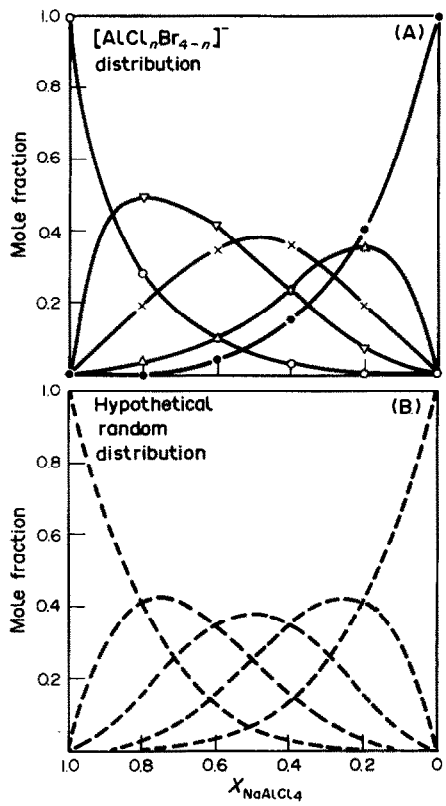


Fig. 3. Distribution curves for the individual $[AlCl_nBr_{4-n}]^-$ ions as a function of X_{NaAlCl_4}. (A) Experimental curves brought to same scale by normalization of the mole fraction sum. (B) The hypothetical, completely random distribution.

The completely random distribution[9] is given in Fig. 3(B) for comparison. It is evident that the $[AlCl_nBr_{n-4}]^-$ distribution is nearly but not totally random, maybe due to steric factors. For example, the formation of $[AlCl_3Br]^-$ seems to be slightly favoured, which is reflected in the small value of K_3, whereas $[AlClBr_3]^-$ doesn't entirely reach the

*The concentration is to a good approximation proportional to the mole fraction since the molar volumes of $NaAlCl_4$ and $NaAlBr_4$ melts at 210°C are *ca* 115 and 136 cm^3 mol^{-1}, respectively, according to available density expressions.[11,12]

Table 4. Calculated mole fractions, x, of the mixed tetrahalide ions in a mixture of $NaAlCl_4$ and $NaAlBr_4$ at 210°C

X_{NaAlCl_4}	$x_{AlCl_4^-}$	$x_{AlCl_3Br^-}$	$x_{AlCl_2Br_2^-}$	$x_{AlClBr_3^-}$	$x_{AlBr_4^-}$	Sum of x
0.2	0.28	0.49	0.19	0.03	~ 0.00	0.99
0.4	0.10	0.41	0.34	0.10	0.04	0.99
0.6	0.03	0.23	0.36	0.23	0.15	1.00
0.8	~ 0.00	0.07	0.19	0.35	0.40	1.01

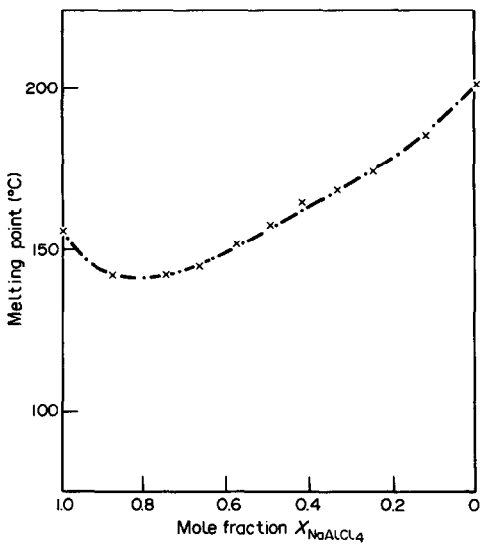


Fig. 4. Phase diagram of the binary $Na[AlCl_4]$–$Na[AlBr_4]$ system.

statistically predicted mole fraction and K_1 is therefore slightly increased relative to the random value.

The same trend in K_1 and K_3 (0.425 and 0.35) was found by Jones,[3] who however had a higher K_2 value (0.8) for the tetramethylammonium $[AlCl_nBr_{4-n}]^-$ system dissolved in acetonitrile at room temperature.

Melting points

The experimentally determined melting points are given in Table 1. The phase diagram of the binary $NaAlCl_4$–$NaAlBr_4$ system is depicted in Fig. 4. This diagram has not previously been reported. The melting points of $NaAlCl_4$[6] and $NaAlBr_4$[13] are known from the NaX–AlX_3 (X = Cl or Br) phase diagrams to be 156.7 and 201°C, respectively, in good agreement with the results obtained here. Also, the phase diagram of the KCl—$AlBr_3$ system has been studied.[14] At the composition $KAlClBr_3$, a melting point of 171°C was observed. This is 3.5°C lower than our value for $NaAlClBr_3$, which seems reasonable, noting that $KAlBr_4$ melts at 192°C,[13] i.e. 9°C lower than $NaAlBr_4$.

In conclusion, it is seen from Fig. 4 that a soft eutectic exists around 142°C at X_{NaAlCl_4} = ca 0.80. For purposes where one needs a low-melting Lewis-neutral solvent, it is of importance to know that it is possible to lower the melting point from the 156.7°C of an equimolar NaCl–$AlCl_3$ melt[6] down to *ca* 142°C by substituting 20% of the chloride by bromide. Probably, a further reduction in the melting point is possible by substituting some of the sodium by, for example, potassium; it is known that the pure chloride system has an eutectic at *ca* 125°C at a Na/K ratio of *ca* 1/3.[15]

Acknowledgements—R. W. Berg and H. A. Hjuler are grateful for support from the Danish Technical Science Research Foundation. E. Kemnitz is grateful for the fellowship from the Danish–GDR cultural exchange program. The Danish Natural Science Foundation is acknowledged for a new Argon laser tube.

REFERENCES

1. R. G. Kidd and D. R. Truax, *J. Am. Chem. Soc.* 1968, **90**, 6867.
2. R. H. Bradley, P. N. Brier and D. E. H. Jones, *J. Chem. Soc. A* 1971, 1397.
3. D. E. H. Jones, *J. Chem. Soc., Dalton Trans.* 1972, 567.
4. R. W. Berg, H. A. Hjuler, R. Fehrmann and N. J. Bjerrum (in preparation).
5. R. W. Berg, S. von Winbush and N. J. Bjerrum, *Inorg. Chem.* 1980, **19**, 2688.
6. R. W. Berg, H. A. Hjuler and N. J. Bjerrum, *Inorg. Chem.* 1984, **23**, 557.
7. D. H. Brown and D. T. Stewart, *Spectrochim. Acta* 1970, **26A**, 1344.
8. G. M. Begun, C. R. Boston, G. Torsi and G. Mamantov, *Inorg. Chem.* 1971, **10**, 886.
9. G. Calingaert and H. A. Beatty, *J. Am. Chem. Soc.* 1939, **61**, 2748.
10. R. J. H. Clark and C. J. Willis, *Inorg. Chem.* 1971, **10**, 1118.
11. R. W. Berg, H. A. Hjuler and N. J. Bjerrum, *J. Chem. Eng. Data* 1983, **28**, 251 (and references therein).
12. C. R. Boston and W. M. Ewing, *J. Chem. Eng. Data* 1971, **16**, 65.
13. J. Kendall, E. D. Crittenden and H. K. Miller, *J. Am. Chem. Soc.* 1923, **45**, 963. The high precision of this old work has been repeatedly checked, e.g. see C. T. H. M. Cronenberg and J. W. van Spronsen, *Z. Anorg. Allg. Chem.* 1967, **354**, 103.
14. V. A. Plotnikov and V. I. Shvarzman, *Zap. Inst. Khim., Akad. Nauk, U.S.S.R.* 1937, **4**, 137; *Zhur. Fiz. Khim.* 1938, **12**, 120.
15. W. Fischer and A. L. Simon, *Z. Anorg. Allg. Chem.* 1960, **306**, 1.

Polyhedron Vol. 4, No. 3, pp. 463–466, 1985
Printed in Great Britain

0277–5387/85 $3.00 + .00
Pergamon Press Ltd

KINETICS AND MECHANISM OF THE INTERACTION OF HEXAAQUOCHROMIUM(III) WITH OCTACYANOMOLYBDATE(IV) IONS

S. I. ALI* and ZAKIR MURTAZA
Department of Chemistry, Jamia Millia Islamia, Jamia Nagar, New Delhi-110 025, India

(*Received* 6 *February* 1984; *accepted* 9 *May* 1984)

Abstract—The kinetics of the interaction of hexaaquochromium(III) ion with potassium octacyanomolybdate(IV) have been studied using conductance and spectrophotometric data. The mechanism of the reaction is discussed and the effect of H^+ ion and the ionic strength on the rate of the reaction determined. The reaction is found to be pseudo-first order with respect to potassium octacyanomolybdate(IV) and inverse first order with $[H_3O^+]$. The rate of the reaction increases with increase in ionic strength and temperature. Activation parameters have been calculated using the Arrhenius equation and have the values $\Delta E^* = 1.3 \times 10^2$ kJ mol^{-1}, $\Delta H^* = 129$ kJ mol^{-1}, $\Delta S^* = -315$ e.u., $\Delta F^* = 2.3 \times 10^2$ kJ and $A = 1.5 \times 10^{-3}$. The mechanism proposed is based on ion-pair formation and the rate equation obtained is given by:

$$k_{obs} = \frac{[kK_E[H_3O^+] + k'K'_Ek_h][Mo(CN)_8^{4-}]}{[H_3O^+] + k_h + [K_E[H_3O^+] + K'_Ek_h][Mo(CN)_8^{4-}]}.$$

The kinetics of the substitution of aquo ligands in hexaaquochromium(III) ion by different ligands has been studied by several workers.[1–6] The ligands which substitute the aquo ligands are oxalate, malonate, citrate and acetate and these reactions follow the S_N1 mechanism. The reaction rates are independent of anion concentration and inversely proportional to hydrogen ion concentration over a particular pH range. Further it has also been found that all the six aquo ligands are not totally substituted but only four are substituted easily to form a complex the diaquo-bis-oxalato chromium(III) and subsequent chelation occurs only when the anion is added in excess to the thoroughly aged corresponding dichelated chromium(III) ion. Similar reactions were studied by others[7–12] using oxalate, malonate, glycinate, 1,10-phenanthroline, 2,2′-dipyridyl and other multidentate ligands. In the study involving substitution by oxalate ion, it has been shown that the substitution proceeds through the mechanism of ion-pair association with the formation of mono-oxalato complex as also in the case of malonate. The reactions in both the cases are found to be first order with respect to chromium(III) and pseudo-first order rate constant increases linearly with increase in anion concentration and the reaction rates are inversely proportional to hydrogen ion concentration. The substitution of aquo ligands by 2,2′-dipyridyl in water–ethanol mixture proceeds through the S_N2 mechanism. Thus, the ligand substitution reactions in the case of chromium(III) do not follow any single mechanism and the reaction path depends on the nature of the incoming ligand and the experimental conditions. In this paper the investigations on the kinetics of the interaction of chromium(III) with octacyanomolybdate(IV) ions have been reported and a mechanism of the reactions has been proposed from which the rate equation has been derived.

MATERIALS AND METHODS

Potassium octacyanomolybdate(IV) was prepared by the methods of Leipoldt *et al.*[13] It was crystallized four to five times from ethanol–water mixture and dried in a desiccator over calcium chloride. Its solution was prepared in distilled water and strength determined by titrating it potentiometrically against ceric sulphate. The solution of chromium(III) nitrate was prepared by dissolving its

* Author to whom correspondence should be addressed.

A.R. crystals in water and strength determined gravimetrically by precipitating it as barium chromate.[14]

Kinetic runs of temperature equilibrated solutions of chromium(III) nitrate and potassium octacyanomolybdate(IV) of desired concentrations mixed in the reaction vessels and kept in a thermostat controlled at the selected temperature within ± 0.1°C were carried out. The course of the reaction was followed by measuring optical density at 380 nm, the wavelength of the maximum absorption of the complex formed by pipetting aliquots of the reaction mixture at definite time intervals and cooled in an ice bath to quench the reaction. The pseudo-first order rate constants for the reaction were obtained by plotting $\ln(O.D._\infty - O.D._0)/(O.D._\infty - O.D._t)$ against time. The pH of the solutions were adjusted with buffer of CH_3COONa–CH_3COOH mixtures, HNO_3 or HCl solutions and ionic strength with KNO_3 solutions.

Optical density measurements were carried out with Spectromom 361 Spectrophotometer using 1 cm cell and pH measurements were made on Elico pH meter model L1-10 using glass electrode EM 60. The conductance measurements were carried out on Toshniwal's digital conductivity meter (S.No. 052, type CL 01/10) with a dip cell (cell constant = 0.981).

RESULTS AND DISCUSSION

The stoichiometry of the reaction between chromium(III) and potassium octacyanomolybdate(IV) was determined[15,16] by the method of continuous variation and was found to be 1 : 1. The same results were obtained by the mole ratio method.[17] No evidence was found for the stoichiometry of 1 : 2 or 2 : 1 in solution. Depending upon the H^+ ion concentration, the reaction can be represented by the following equations:

$$Cr(H_2O)_6^{3+} + Mo(CN)_8^{4-} \rightarrow [Cr(H_2O)_5Mo(CN)_8]^- + H_2O, \quad (1)$$

$$Cr(H_2O)_5OH^{2+} + Mo(CN)_8^{4-} \rightarrow [Cr(H_2O)_4OHMo(CN)_8]^{2-} + H_2O. \quad (2)$$

In the first set of kinetic experiments, the concentration of octacyanomolybdate(IV) ion was varied (3.5–7.5×10^{-2} M) and that of hexaaquochromium(III) ion fixed (5.0×10^{-3} M). In these experiments the ionic strength (1.0 M) and pH (3.42) of the solutions were kept constant. The observed rate constant values at 40°C are 0.37, 2.30, 3.03, 3.22, 3.38, 3.84, 4.25 and 4.76×10^{-4} s^{-1} at 3.5, 5.0, 5.5, 6.0, 6.25, 6.5, 7.0 and 7.5×10^{-2} M concentrations of complex respectively. The rate of the reaction obtained is pseudo-first order with respect to the octacyanomolybdate(IV) ion.

The rate of the reaction is found to increase with decrease in H^+ ion concentration at fixed octacyanomolybdate (5.0×10^{-2} M), hexaaquochromium (5.0×10^{-3} M) and ionic strength (1.0 M). Acetate buffer, nitric acid or hydrochloric acid solutions were used for adjusting the pH of the solution. The rate constant values were found to be the same whether the pH was adjusted with HCl, HNO_3 or acetate buffer solutions. No catalytic effect by NO_3^- ions or coordination by the acetate buffer was observed in the reaction. The plot of $\log k$ vs $\log[H^+]$ is linear with a slope of -1.0 at the lower values of the latter indicating that the reaction has inverse first order dependence on $[H^+]$.

The effect of varying ionic strength on the reaction rate was studied by adding different amounts of KNO_3 at constant hydrated cation and complex anion concentrations. It was observed that increase in ionic strength (0.85–2.0 M) increases the rate of the reaction indicating the easy removal of coordinated water molecules from the ion pair. A plot of $\log k/k_0$ vs $\sqrt{\mu}$ gives a linear curve. The rate of the reaction was studied at six different temperatures (30–50°C) keeping the concentrations of hexaaquochromium(III) (5.0×10^{-3} M) and octacyanomolybdate(IV) (5.0×10^{-2} M) ions constant and maintaining fixed ionic strength (1.0 M) and pH (3.42). It was found that the rate of the reaction increases with increase in temperature. The activation parameters were calculated using the Arrhenius equation, the values are $\Delta E^* = 1.3 \times 10^2$ kJ mol^{-1}, $\Delta H^* = 129$ kJ mol^{-1}, $\Delta S^* = -315$ e.u., $\Delta F^* = 2.3 \times 10^2$ kJ and $A = 1.5 \times 10^{-3}$.

For the system $Cr(H_2O)_6^{3+}$–$Mo(CN)_8^{4-}$, the variation of conductance with concentration was compared with the limiting Onsager equation. A plot of equivalent conductance versus square root of concentration gives a slope which is considerably lower than the theoretical Onsager slope furnishing evidence for the ion-pair formation between hexaaquochromium(III) and octacyanomolybdate(IV) ions. The ion-pair formation between the two reacting species is followed by associative interchange in which bond making plays a significant role. On adding excess nitrate, the water molecules which are coordinated in the ion-pair reorient considerably around nitrate ions through hydrogen bonding. As a result, nitrate ions facilitate the removal of coordinated water molecules from the ion-pair and these water molecules are then engaged in the solvation of nitrate ions. A similar effect of ionic strength was observed by Hamm and coworkers.[6] The two species existing in the hydrogen ion concentration range studied are $Cr(H_2O)_6^{3+}$ and

$[Cr(H_2O)_5OH]^{2+}$, both of which interact and form ion-pairs with $Mo(CN)_8^{4-}$. No evidence has been obtained for the existence of the dimeric species $Cr_2(H_2O)_8(OH)_2^{4+}$ in this system which will require a stoichiometry of 2 : 1 for the reaction instead of 1 : 1. This has not been observed even at high temperatures. The possibility of the formation of protonated species of $Mo(CN)_8^{4-}$ in solution specially at the low pH range was investigated. At the concentration ranges studied, no evidence was found for it. The rate constant values at low pH do not show a marked change. It is inferred from these results that very weak hydrogen bonding between the proton and the nitrogen of CN may exist.

The influence of chromic ions on potassium hexacyanoferrate(II) has been investigated in detail. It has been found that chromic ions catalyse the decomposition of potassium hexacyanoferrate(II) to potassium aquopentacyanoferrate(II):[18]

$$Fe(CN)_6^{4-} + H_2O \xrightarrow{Cr^{3+}} Fe(CN)_5H_2O^{3-} + CN^-.$$

In the case of potassium octacyanomolybdate(IV), no evidence has been found for its catalytic decomposition into potassium aquoheptacyanomolybdate(IV) by chromium(III) ions. As there is no release of CN^- ions in this case, so there is also no possibility for the existence of cyanochromium(III), $CrCN^{2+}$, which has been shown to be formed when an inert cobalt(III) cyano complex oxidizes the labile chromium(II) aqua ion giving an isocyanochromium(III) complex[19,20] which isomerises to the carbon bonded species. Careful measurement of conductance during the progress of the reaction rules out such possibilities.

The dependence of k_{obs} on octacyanomolybdate(IV) and hydrogen ion is consistent with an ion-pair mechanism. The mechanism may be represented considering that both $Cr(H_2O)_6^{3+}$ and $Cr(H_2O)_5OH^{2+}$ (obtained by the ionization of $Cr(H_2O)_6^{3+}$) react with octacyanomolybdate(IV) ions to form the respective complexes. Anation, water exchange and ion-pair[21] formation has also been observed for aquopentaaminechromium(III) ions in acidic aqueous solutions containing chloride or thiocyanate ions and for the systems[22] $Coen_2(H_2O)_2^{3+}$–$C_2O_4^{2-}$ equilibria. Ion-pair formation has also been observed in the case of the interaction of hexaaquochromium(III) with acetate ions[23] when the ion-pairs formed are $Cr(H_2O)_6^{3+}$, $^-OOCCH_3$ and $[Cr(H_2O)_5OH]^{2+}$, $^-OOCCH_3$ which undergo anation reaction, giving out an H_2O molecule and forming the complex.

On the basis of the above results the following ion-pair mechanism has been proposed for the interaction of hexaaquochromium(III) with octacyanomolybdate(IV) ions:

$$Cr(H_2O)_6^{3+} + H_2O \overset{k_h}{\rightleftharpoons} Cr(H_2O)_5OH^{2+} + H_3O^+ \quad (3)$$

$$Cr(H_2O)_6^{3+} + Mo(CN)_8^{4-} \overset{K_E}{\rightleftharpoons} Cr(H_2O)_6^{3+}, Mo(CN)_8^{4-} \quad (4)$$

$$Cr(H_2O)_6^{3+}, Mo(CN)_8^{4-} \overset{k}{\rightarrow} [Cr(H_2O)_5Mo(CN)_8]^- + H_2O \quad (5)$$

$$Cr(H_2O)_5OH^{2+} + Mo(CN)_8^{4-} \overset{K_E}{\rightleftharpoons} Cr(H_2O)_5OH^{2+}, Mo(CN)_8^{4-} \quad (6)$$

$$Cr(H_2O)_5OH^{2+}, Mo(CN)_8^{4-} \overset{k'}{\rightarrow} [Cr(H_2O)_4OHMo(CN)_8]^{2-} + H_2O \quad (7)$$

$$Cr(H_2O)_4OHMo(CN)_8^{2-} + H_3O^+ \xrightarrow{\text{fast}} [Cr(H_2O)_5Mo(CN)_8]^- + H_2O. \quad (8)$$

From the above mechanism the following rate equation is derived:

$$k_{obs} = \frac{[kK_E[H_3O^+] + k'K'_Ek_h][Mo(CN)_8^{4-}]}{[H_3O^+] + k_h + [K_E[H_3O^+] + K'_Ek_h][Mo(CN)_8^{4-}]} \quad (9)$$

or

$$\frac{1}{k_{obs}} = \frac{[H_3O^+] + k_h}{[kK_E[H_3O^+] + k'K'_Ek_h][Mo(CN)_8^{4-}]} + \frac{K_E[H_3O^+] + K'_Ek_h}{kK_E[H_3O^+] + k'K'_Ek_h}. \quad (10)$$

From (10) the plot of $1/k_{obs}$ vs $1/Mo(CN)_8^{4-}$ (Fig. 1) should be linear with an intercept, $K_E[H_3O^+] + K'_Ek_h/kK_E[H_3O^+] + k'K'_Ek_h$ and slope $[H_3O^+] + k_h/kK_E[H_3O^+] + k'K'_Ek_h$. The values of the intercept and the slope are dependent on the hydrogen ion concentration. The mechanism confirms the result of variation of k_{obs} with $[H_3O^+]$ and also the ionic strength. It is based on an eigen mechanism, the rate determining step being the loss of water molecules from the primary coordination sphere. The reaction is associative interchange (I_a) type for the reaction of $Cr(H_2O)_6^{3+}$ and $Mo(CN)_8^{4-}$ and dissociative interchange (I_d) type for $[Cr(H_2O)_5OH]^{2+}$ and $Mo(CN)_8^{4-}$. The final product of the reaction was isolated in the solid state and its composition

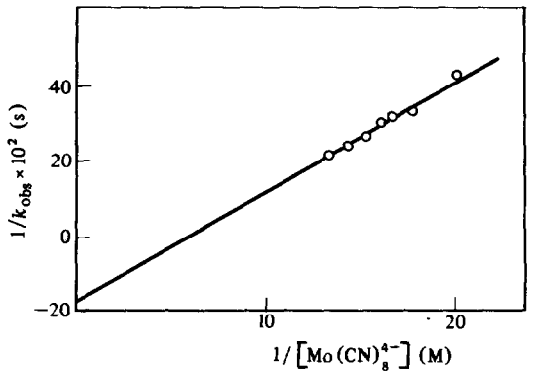


Fig. 1. Plot of $1/k_{obs}$ vs $1/[Mo(CN)_8^{4-}]$.

and structure were determined[17] with the help of elemental and IR analysis. According to the elemental analysis the final product was $KCrMo(CN)_8 \cdot 2H_2O$.

Acknowledgements—The financial support of the research project from the U.G.C., New Delhi and a senior research fellowship from C.S.I.R., New Delhi (to Z.M.) are thankfully acknowledged.

REFERENCES

1. J. N. Mandal and G. S. De, *Indian J. Chem.* 1980, **19A**, 25.
2. B. N. Niogy and G. S. De, *Proc. Indian Acad. Sci. (Chem. Sci.)* 1983, **92**, 153.
3. R. E. Hamm and R. E. Davis, *J. Am. Chem. Soc.* 1953, **75**, 3085.
4. R. E. Hamm, *J. Am. Chem. Soc.* 1953, **75**, 5670.
5. R. E. Hamm and R. H. Perkins, *J. Am. Chem. Soc.* 1955, **77**, 2083.
6. R. E. Hamm, R. L. Johnson, R. H. Perkins and R. E. Davis, *J. Am. Chem. Soc.* 1958, **80**, 4469.
7. D. Banerjee and S. Duttachaudhuri, *J. Inorg. Nucl. Chem.* 1968, **30**, 871.
8. D. Banerjee and C. Chatterjee, *J. Inorg. Nucl. Chem.* 1969, **31**, 3845.
9. D. Banerjee and S. Duttachaudhuri, *J. Inorg. Nucl. Chem.* 1970, **32**, 1617.
10. D. Banerjee and P. Chaudhuri, *J. Inorg. Nucl. Chem.* 1970, **32**, 2697.
11. D. Banerjee and J. Roy, *Z. Anorg. Allg. Chem.* 1973, **399**, 115.
12. J. N. Mandal and G. S. De, *Indian J. Chem.* 1978, **16A**, 580.
13. J. G. Leipoldt, L. D. C. Bok and P. J. Colliers, *Z. Anorg. Allg. Chem.* 1974, **409**, 343.
14. A. I. Vogel, *A Text Book of Quantitative Inorganic Analysis*, 4th edition, p. 459. Longman, London (1978).
15. W. U. Malik and S. I. Ali, *Naturwissenschaften* 1959, **20**, 579.
16. W. U. Malik and S. I. Ali, *J. Inorg. Nucl. Chem.* 1961, **20**, 155.
17. S. I. Ali and Zakir Murtaza, *Indian J. Chem.* 1984, **23A**, 258.
18. W. U. Malik, *J. Sci. Ind. Res.* 1959, **188**, 463.
19. J. H. Espenson and J. P. Birk, *J. Am. Chem. Soc.* 1965, **87**, 3280.
20. J. P. Birk and J. H. Espenson, *J. Am. Chem. Soc.* 1968, **90**, 2266.
21. N. V. Duffy and J. F. Earley, *J. Am. Chem. Soc.* 1968, **89**, 272.
22. P. M. Brown and G. H. Harris, *Inorg. Chem.* 1968, **7**, 1872.
23. S. C. Tyagi and A. A. Khan, *J. Inorg. Nucl. Chem.* 1979, **41**, 1447.

Polyhedron Vol. 4, No. 3, pp. 467–470, 1985
Printed in Great Britain

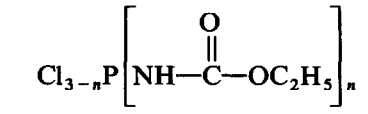
0277–5387/85 $3.00 + .00
© 1985 Pergamon Press Ltd

REACTIONS OF PHOSPHORUS HALIDES WITH URETHANE

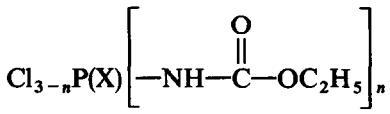
R. P. NARAIN* and MAHTAB Z. SIDDIQUI
Department of Chemistry, University of Gorakhpur, Gorakhpur—273001, India

(*Received* 20 *March* 1984; *accepted* 9 *May* 1984)

Abstract—By the reaction of phosphorus trichloride, thiophosphoryl chloride, phosphorus oxychloride and phosphorus pentachloride with urethane in stoichiometric ratio 1 : 1 or 1 : 2 in benzene, compounds of the type



and

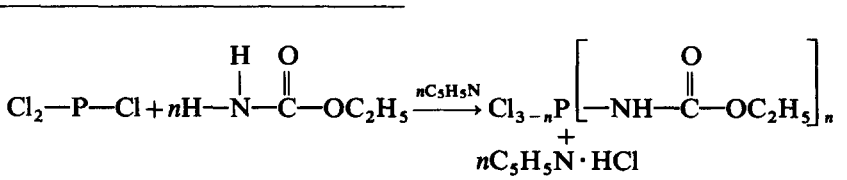


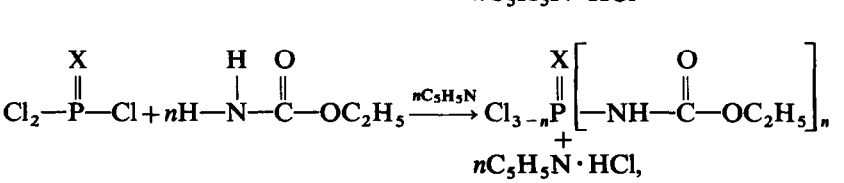
(X = S, O or Cl; n = 1 or 2) have been synthesized. A probable mechanism for their formation has also been suggested.

The reaction between phosphorous acid and alkylurethanes was attempted by Derkach *et al.*[1] in attempts to prepare some insecticidal organophosphorus compounds. The reaction of amido esters of urethanephosphorus acid with acid chlorides in the presence of a base as an acid acceptor has been carried out by Antokhina *et al.*[2] Triaryl phosphine urethane has been synthesized by Gerber *et al.*[3] Semashko has recently reported the herbicidal activity of compounds containing phosphorus-nitrogen linkage and containing phosphorus in trivalent state.[4]

In the present communication we report the facile formation of the compounds having phosphorus–nitrogen linkages, formed by the reaction of phosphorus halides with urethane.

Phosphorus trichloride, thiophosphoryl chloride, phosphorus oxychloride and phosphorus pentachloride were reacted with urethane in molar ratios 1:1 and 1:2 in the medium of benzene containing pyridine. The reactions may be represented by the equations:





where X = S, O or Cl; n = 1 or 2.

It was found that the compound obtained from PCl_3 and urethane in molar ratio 1 : 1 was orange in colour and in molar ratio 1 : 2 it was yellowish

* Author to whom correspondence should be addressed.

whereas the rest of the compounds were light brownish/white coloured crystalline solids. All of them were soluble in alcohol, carbon tetrachloride, chloroform, acetone and acetophenone. They appeared to decompose in their melting point determination.

EXPERIMENTAL

All glass apparatus with interchangeable joints was used throughout and special precautions were taken to exclude moisture.

Benzene, pyridine, ether, acetone and acetophenone were purified by standard procedures.

The phosphorus halides employed were of BDH grade and distilled twice before use.

Urethane (Loba Chemie) was recrystallized before use.

Silica gel G (BDH) was used for TLC and spots were detected by UV lamp, iodine chamber and heating the plates in an oven after spraying with 10% H_2SO_4.

ANALYSIS

Phosphorus was estimated gravimetrically as ammonium phosphomolybdate. Sulphur and chlorine were estimated gravimetrically as barium sulphate and silver chloride.[5]

IR spectra (ν_{max} in cm^{-1}) of compounds were recorded on Perkin–Elmer spectrophotometer model 577 in Nujol and NMR [chemical shifts in τ (ppm)] were recorded on a Perkin–Elmer R-32 instrument (90 Mc) in $CDCl_3$ with TMS as internal standard, both working at the Chemical Laboratories of Central Drug Research Institute, Lucknow, India. The values obtained were interpreted by comparing the absorption bands and τ values with those reported in the literature[6,7] (Table 1).

Molecular weights were determined cryoscopically using acetophenone as a solvent.

Methods of preparation being the same for all the reactions, only one method has been described in detail while a summary of all is given in Table 1.

REACTION OF PHOSPHORUS TRICHLORIDE WITH URETHANE MOLAR RATIO 1:1

To a solution of phosphorus trichloride (4.25 g) taken in benzene (20.00 g) was added urethane (2.75 g) dissolved in pyridine. The reaction was exothermic. The contents of the flask were cooled and stirred during the addition of the reactants. After addition, the contents were subjected to refluxing for 7 h. Benzene was distilled off and the residue was washed several times with dry pyridine to remove the pyridine hydrochloride. Final traces of pyridine hydrochloride were removed by sublimation under reduced pressure. The solid obtained was washed with ether, dried in vacuum and recrystallized from dry acetone. The purity of the compound was checked by thin layer chromatography.

THIN LAYER CHROMATOGRAPHY

The chromatoplate was prepared by applying a uniform layer of silica gel in water, drying first at room temperature for 8 h and then at 100°C for 30 min. A 10% solution of the compound in dry acetone was applied over the plate which was then dried at room temperature for 2 h and at 100°C for 10 min.

The plate was then put in the eluant containing ethyl acetate–benzene mixture 1:2 by volume.

Finally the spots were located in UV light under a UV lamp, as well as in an iodine chamber. A single spot was obtained.

Found: P, 16.24; Cl, 37.28%. $C_3H_6O_2NPCl_2$ requires: P, 16.31; Cl, 37.36%.

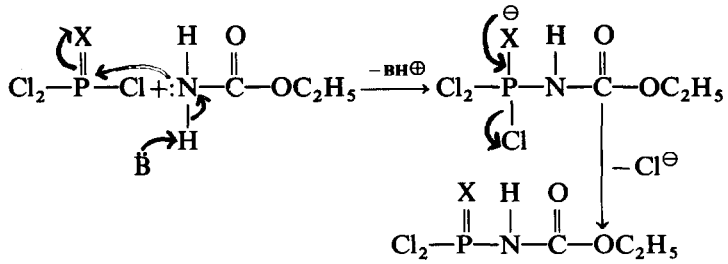
RESULTS AND DISCUSSION

Since the urethane molecule has two reacting sites, ethoxy and amino, reactions of urethane with phosphorus halides are therefore possible from both ends. There is also the possibility of removal of both the amino protons with the Cl atoms of phosphorus halides. Since the IR spectra of the compounds showed a peak in the region 820–850 cm^{-1}, characteristic of P—N linkage, the reaction appears to have taken place from the amino end. Further, the presence of a sharp proton as singlet (τ value 2.48) in NMR spectra, could be attributed to —NH group of urethane molecule. This confirms the removal of a hydrogen by a Cl atom of the phosphorus halide, even when the phosphorus halide urethane molar ratio is 1:2.

The reaction is slow due to the $-I$ effect of the keto group and pyridine is needed for the completion of the reaction. The formation of pyridine hydrochloride further confirms that the reaction has taken place from the amino end of the urethane molecule.

The reaction appears to be initiated by the nucleophilic attack of nitrogen of urethane over the phosphorus atom of the halide with the liberation of a proton. This attack is then either followed or accompanied by the elimination of a halide ion.[8] The

entire mechanism may be depicted as follows:



$$BH^{\oplus} + Cl^{\ominus} \longrightarrow BHCl.$$

Table 1. Urethane derivatives of phosphorus halides and their characterization data

S.N.	Reactants (g)		Molecular formula (% yield)	% Phosphorus		% Chlorine		% Sulphur		Molecular weight	
				Calc.	Found	Calc.	Found	Calc.	Found	Calc.	Found
1.	PCl_3 (4.25)	+urethane (2.75)	$C_3H_6O_2NPCl_2$ (55)	16.31	16.24	37.36	37.28	—	—	190.0	195.17
2.*	PCl_3 (5.08)	+urethane 6.58)	$C_6H_{12}O_4N_2PCl$ (55)	12.78	12.63	14.63	14.59	—	—	242.5	238.48
3.	$P(S)Cl_3$ (3.00)	+urethane (1.57)	$C_3H_6O_2NPCl_2S$ (58)	13.96	13.97	31.98	32.02	14.41	14.33	222.0	214.15
4.*	$P(S)Cl_3$ (3.12)	+urethane (3.28)	$C_6H_{12}O_4N_2PClS$ (52)	11.29	11.22	12.93	12.88	11.65	11.60	274.5	277.16
5.	$P(O)Cl_3$ (4.20)	+urethane (2.44)	$C_3H_6O_3NPCl_2$ (58)	15.04	15.07	34.46	34.15	—	—	206.0	211.48
6.*	$P(O)Cl_3$ (1.81)	+urethane (2.10)	$C_6H_{12}O_5N_2PCl$ (58)	11.99	11.87	13.73	13.74	—	—	258.5	259.45
7.	PCl_5 (2.10)	+urethane (0.89)	$C_3H_6O_2NPCl_4$ (52)	11.87	11.73	54.40	54.45	—	—	261.0	259.94
8.*	PCl_5 (1.58)	+urethane (1.35)	$C_6H_{12}O_4N_2PCl_3$ (50)	9.88	9.73	33.97	33.74	—	—	313.5	318.35

Significant bands (ν cm^{-1}) in IR absorption spectra (Nujol)

Bond	$C_3H_6O_2NPCl_2$	$C_6H_{12}O_4N_2PClS$
P—N	820	850
P=S	—	730
P—Cl	500	490
C=O	1670	1670

Characteristic τ values in NMR spectra ($CDCl_3$) $C_3H_6O_2NPCl_2$

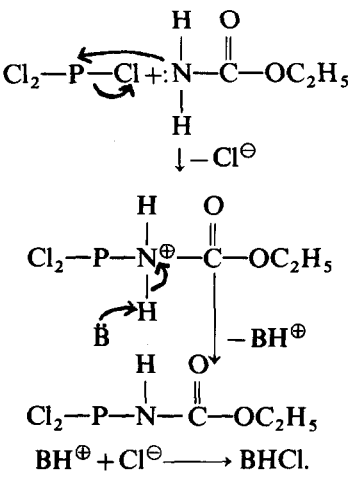
τ Value	Number of protons	Assignment†
2.48	1	NH(s)
5.50	2	CH_2(m)
8.73	3	CH_3(t)

* Molar ratio 1 : 2.

† s, singlet; m, multiplet; t, triplet.

The catalyst (B) would finally combine with halide ion to give base hydrochloride.

However, in phosphorus trichloride the above mode of attack may be ruled out because of the absence of a double bond attached to the phosphorus atom. Here the nucleophilic attack of the nitrogen of urethane over the phosphorus atom is facilitated by the vacant 3*d*-orbitals and this attack is either followed or accompanied by the elimination of a proton and a halide ion.[9] The entire mechanism may be depicted as:



The reaction provides a convenient route for the establishment of P—N bond.

Acknowledgements—We express our gratitude to Professor R. P. Rastogi, Head, Department of Chemistry, University of Gorakhpur, Gorakhpur for providing necessary laboratory facilities. One of us (M.Z.S.) is thankful to the State Council of Science and Technology, Lucknow, for providing a Junior Research Fellowship.

REFERENCES

1. G. I. Derkach, V. S. Odinisov and V. S. Petrenko (Inst. Org. Khim., Kiev, USSR), *Popov. Akad. Nauk Ukr. RSR, Ser. B* 1969, **31**, 261; *Chem. Abs.* 1961, **71**, 29543.
2. L. A. Antokhina and P. I. Alimov (Inst. Org. Fiz. Khim. im. Arbuzova, Kazan, USSR), *Izv. Akad. Nauk SSSR, Ser. Khim.* 1974, **2**, 401; *Chem. Abs.* 1974, **81**, 24958.
3. H. Gerber, M. Halmann and D. Vofsi (Weizmann Inst. Sci., Rehovot, Israel), *Phosphorus* 1976, **6**, 111 (*Eng.*); *Chem. Abs.* 1976, **85**, 108725.
4. Z. T. Semashko, *Inst. Org. Khim., Kiev, USSR. Sint. Issled. Biot. Soedin. Tezisy dokl. Konf. Molodykh. Uch. 6th* 1978, 10 (*Russ.*) (Edited by Yu. P. Romadan). Zinatne, Righa, U.S.S.R; *Chem. Abs.* 1980, **93**, 25822.
5. J. R. Walter, I. Smith and R. L. Shriner, *The Examination of New Organic Compounds.* Wiley, New York (1956).
6. *Handbook of Chem. & Physics,* 59th edition 1978–79. CRC Press, West Palm Beach, FL. F-269, F-259.
7. J. R. Dyer, *Applications of Absorption Spectroscopy of Organic Compounds.* Offset Press, New Delhi (1974).
8. A. J. Kirby and S. G. Warren, *The Organic Chemistry of Phosphorus,* Monograph 5, p. 236. Elsevier, Amsterdam (1967).
9. As above but p. 278.

Polyhedron Vol. 4, No. 3, pp. 471–474, 1985
Printed in Great Britain

0277-5387/85 $3.00 + .00
© 1985 Pergamon Press Ltd

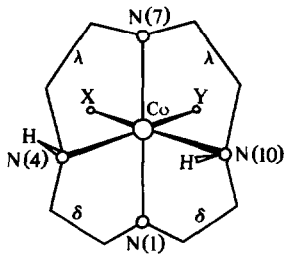
(1,4,7,10-TETRAAZACYCLODODECANE) (DIAMINE OR ALANINE)–COBALT(III) COMPLEXES

MATSUO NONOYAMA* and TAKAKO KURIMOTO
Department of Chemistry, Faculty of Science, Nagoya University,
Chikusa, Nagoya, 464 Japan

(*Received* 27 *March* 1984; *accepted* 9 *May* 1984)

Abstract—(1,4,7,10-Tetraazacyclododecane) [diamine or (*S*)-alanine]–cobalt(III) complexes [diamine = ethylenediamine, 2-(aminomethyl)pyridine, (*R*)-1,2-propanediamine, (*R,R*)-1,2-diaminocyclohexane, trimethylenediamine and 2-methyl-1,3-diaminopropane] are prepared and characterized spectroscopically. The ligand field transitions occur at lower energies than those of the corresponding tetraamine analogues. Severe distortions caused by the too small size of the cyclic ligand are one of the origins. The distortions also exert influence upon circular dichroism spectra.

Contrary to a majority of cyclic tetramines which are coordinated in a planar structure[1] the cavity formed by 1,4,7,10-tetraazacyclododecane (cyclen) is too small to accommodate a transition metal ion in the plane of the N_4 donor atoms and then cyclen is, usually, coordinated in a folded *cis*-arrangement (structure **I**). Even in a folded arrangement there



I

are still significant distortions from a regular octahedron as have been revealed for $[Co(cyclen)(NO_2)_2]^+$ and $[Co(cyclen)(acac)]^{2+}$ (acac = acetylacetonate ion). The apical donors, N(1) and N(7), are remarkably deviated from the ideal positions and the angles of N(1)—Co—N(7) are 164.4(2)° for the former and 166.1(3)° for the latter.[2,3] The distortions should be reflected in properties of complexes of cyclen but little is known of cobalt(III) complexes of cyclen.[2–5] To see the effect of the distortions we have studied spectroscopically some new cobalt(III) derivatives of cyclen, $[Co(cyclen)(diamine)]^{3+}$ and $[Co(cyclen)(ala)]^{2+}$. The abbreviations used are given in the footnote of Table 1.

RESULTS AND DISCUSSIONS

The mixed complexes $[CoL(diamine)]^{3+}$ [Table 1 (L represents cyclen)] were easily obtained by the reaction of $[CoLCl_2]Cl \cdot 1.5\text{-}H_2O$ with a diamine in dimethylsulphoxide. These complexes are red despite a "CoN_6" chromophore, for which are usually observed a yellow or an orange colour like the colours of $[Co(en)_3]^{3+}$ and $[Co(NH_3)_6]^{3+}$. The red amino acid complex $[CoL(ala)](ClO_4)_2 \cdot 0.5H_2O$ was similarly prepared. For the complexes of ala and the unsymmetrical diamines two isomers are possible, since the different orientations of the hydrogen atoms on N(4) and N(10) (structure **I**: determined by X-ray analysis for X = Y = NO_2 and X – Y = acac)[2,3] make the two sites of coordination, X and Y, inequivalent.† Attempts to separate the isomers are so far unsuccessful. The ^1H NMR spectra of the complexes (X – Y = pn and ala) show a single methyl doublet at 1.47 ppm(pn) and 1.54(ala), and give no indication of the presence of isomers. This suggests either an accidental coincidence of the methyl chemical shifts between the two isomers or the presence of only one isomer. Attempts to resolve

* Author to whom correspondence should be addressed.

† The ^{13}C NMR spectrum of $[CoL(en)]^{3+}$ shows that cyclen adopts the configuration of structure **I**: the signals of cyclen are at 59.1, 56.1, 51.6 and 47.3 ppm, and those of en at 46.2 and 45.5 ppm.

Table 1. Analytical results of the complexes

Complex	Analysis, found (calc.) (%) C	H	N
$[CoL(en)]Cl_3 \cdot 1.25H_2O$	28.60 (28.58)	7.75 (7.32)	20.05 (20.00)
$[CoL(pic)]Cl_3 \cdot 1.5H_2O$	35.40 (35.57)	6.60 (6.61)	17.67 (17.78)
$[CoL(pn)]Br_3 \cdot 4H_2O$	21.21 (21.41)	5.96 (6.21)	13.52 (13.62)
$[CoL(chxn)]Br_3 \cdot 3.5H_2O$	25.81 (25.94)	6.29 (6.38)	12.93 (12.97)
$[CoL(tn)]Cl_3 \cdot 3H_2O$	28.54 (28.37)	8.27 (7.79)	17.85 (18.04)
$[CoL(bn)]Cl_3$	33.72 (33.86)	7.52 (7.58)	19.39 (19.74)
$[CoL(ala)](ClO_4)_2 \cdot 0.5H_2O$	24.70 (25.06)	4.99 (5.16)	13.27 (13.28)

Abbreviations: L, 1,4,7,10-tetraazacyclododecane; en, ethylenediamine; pic, 2-(aminomethyl)pyridine; pn, (*R*)-1,2-propanediamine; chxn, (*R,R*)-1,2-diaminocyclohexane; tn, trimethylenediamine; bn, 2-methyl-1,3-diaminopropane; ala, (*S*)-α-alanine.

chiral $[CoL(bn)]^{3+}$ by column chromatography[6] are also wasteful so far.

The absorption spectral data are given in Table 2 and Figs 1–3. Comparison of the data with those of other "CoN_6" type complexes reveals that remarkable red shifts and enhanced intensities of the ligand field transitions are characteristic for the cyclen complexes [cf. $\nu_1(^1A_{1g} \rightarrow {}^1T_{1g}) = 21.30 \times 10^3$ cm^{-1} ($\log \varepsilon = 1.94$) and $\nu_2(\rightarrow {}^1T_{2g}) = 29.40$ (1.90) for $[Co(en)_3]^{3+}$, and 20.96 (1.68) and 29.40 (1.60) for $[Co(NH_3)_6]^{3+}$]. Chelate effect produced by an ethylene chain (a five-membered chelate ring) is completely cancelled out and the transition peaks are at even lower energies than those of $[Co(NH_3)_6]^{3+}$. The apparent weakening of the ligand field strength of cyclen is considered to be due to severe distortions around a cobalt atom caused by an unsuitable size of the cyclic ligand. The

Table 2. Absorption spectra of the complexes in aqueous solutions

Complex	Absorption maxima, ν_{max} [10^3 cm^{-1} ($\log \varepsilon$)]			
$[CoL(en)]Cl_3 \cdot 1.25H_2O$	20.5 (2.30)	29.3 (2.20)	44.0 (4.32)	
$[CoL(pic)]Cl_3 \cdot 1.5H_2O$	20.5 (2.31)	29.0 (2.25)	43.7 (4.28)	47.9 (4.32)
$[CoL(pn)]Br_3 \cdot 4H_2O$	20.5 (2.32)	29.3 (2.20)	44.0 (4.29)	
$[CoL(chxn)]Br_3 \cdot 3.5H_2O$	20.4 (2.30)	29.2 (2.20)	43.0 (4.32)	
$[CoL(tn)]Cl_3 \cdot 3H_2O$	20.0 (2.26)	29.2 (2.15)	42.8 (4.30)	
$[CoL(bn)]Cl_3$	20.0 (2.24)	29.3 (2.15)	43.0 (4.30)	
$[CoL(ala)(ClO_4)_2 \cdot 0.5H_2O$	19.8 (2.37)	28.4 (2.28)	43.8 (4.26)	
$[Co(NH_3)_4(pn)]^{3+}$	21.5 (1.81)*			
$[Co(NH_3)_4(chxn)]^{3+}$	21.3 (1.85)†			
$[CoL(acac)](ClO_4)_2$	18.7 (2.50)	26.5sh	30.3 (3.52)	36.5sh
			42.0 (4.36)	43.9 (4.35)‡

* Reference 12.
† Reference 8.
‡ This work.

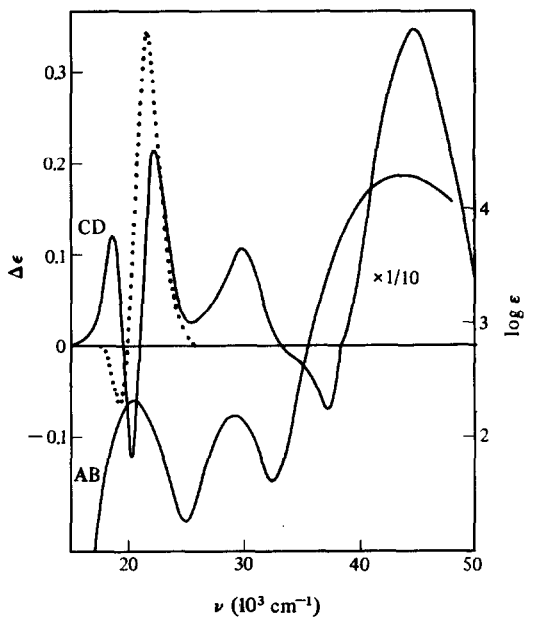


Fig. 1. Absorption and CD spectra of [CoL(pn)] $Br_3 \cdot 4H_2O$ (——) and $[Co(NH_3)_4(pn)]^{3+}$ (····).[8]

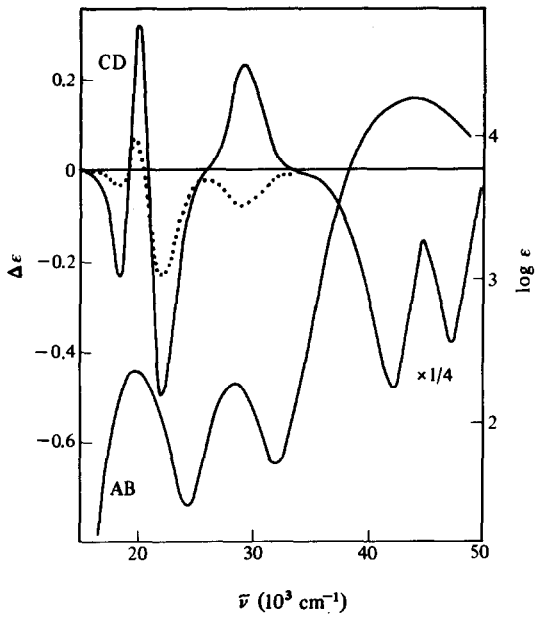


Fig. 3. Absorption and CD spectra of [CoL(ala)] $(ClO_4)_2 \cdot 0.5H_2O$ (——) and $[Co(NH_3)_4(ala)]^{2+}$ (····).[9]

distortions, simultaneously lowering the symmetry of the ligand field, enhance the intensities of the transitions.[7]

Circular dichroism (CD) spectra are a better reflection of fine properties of complexes. The CD spectra of optically active complexes are shown in Figs 1–3, where they are compared with those of the corresponding tetraamine complexes in the $\nu_1(^1A_{1g} \rightarrow {}^1T_{1g})$ region. The CD spectra of $[Co(NH_3)_4(XY)]^{n+}$ (XY = pn, chxn and ala) are induced solely by the vicinal effects of the chiral ligands.[8,9] In the ν_1 region the CD patterns of pn and chxn complexes are significantly varied when $(NH_3)_4$ are replaced by cyclen, while in the case of ala the pattern modification is relatively small and intensities of extremes are altered. The part of cyclen shown in structure I has a plane of symmetry [N(4), N(10), Co, X and Y] but is prochiral. The change of the CD patterns may, on the one hand, be caused by the chiralty induced by the presence of the chiral pn and chxn ligands. Another origin should also be considered. An apparent CD pattern is usually a sum of each component of the split transitions due to a lower symmetry ligand field than an O_h one and the relative energy levels of each split state are disturbed by the severe distortions in the cyclen complexes compared with those of $(NH_3)_4$ complexes.[7] The disturbed energy levels should result in a different CD pattern.

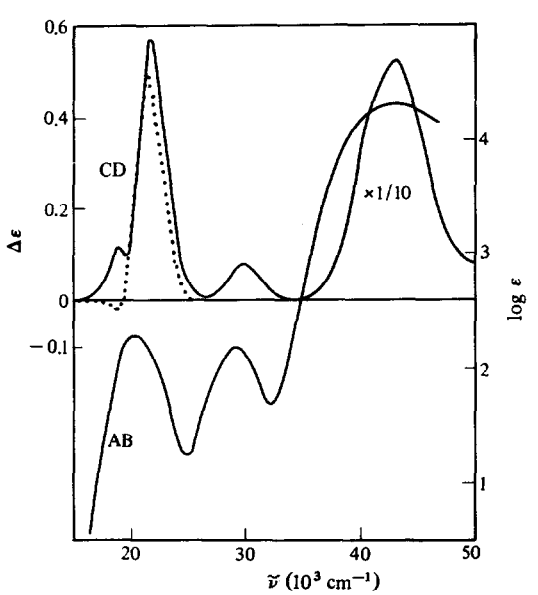


Fig. 2. Absorption and CD spectra of [CoL(chxn)] $Br_3 \cdot 3.5H_2O$ (——) and $[Co(NH_3)_4(chxn)]^{3+}$ (····).[8]

The apparently enhanced CD intensity of $[CoL(ala)]^{2+}$ is not extraordinary if the molar extinction coefficient of the ν_1 band ($\varepsilon = 232$) is taken into consideration (cf. $\nu_1 = 20.3 \times 10^3\ cm^{-1}$ ($\varepsilon = 78$) for $[Co(NH_3)_4(ala)]^{2+}$). The intrinsically low symmetry of the ala complex probably results in the relatively small modification of the CD pattern upon replacement of $(NH_3)_4$ with cyclen.

The above data reveal that the absorption maxima (ν_1) of $[CoL(XY)]^{n+}$ are at an even lower energy than those of the corresponding $[Co(NH_3)_4(XY)]^{n+}$, so there arises a doubt about the absorption maximum reported for $[CoL(acac)]^{2+}$ [$\nu_1 = 2.0 \times 10^4\ cm^{-1}$

($\varepsilon = 200$)],[3] since it is comparable in energy to that for $[Co(en)_2(acac)]^{2+}$ [19.8×10^3 cm^{-1} ($\varepsilon = 159$)].[13] The remeasurement of the spectrum of $[CoL(acac)]^{2+}$ gave the value $\nu_1 = 18.7 \times 10^3$ cm^{-1} ($\varepsilon = 318$). This is consistent with the above results.

EXPERIMENTAL

Measurements

Measurements were carried out by the methods reported previously.[10] ^{13}C NMR spectra were recorded on a JEOL FX-60 spectrometer. The analytical results are given in Table 1.

Synthesis

The ligand cyclen was prepared by the procedure of Richmann and Atkins[11] from diethylenetriamine and diethanolamine. $[CoLCl_2]Cl \cdot 1.5H_2O$ was synthesized by the known method.[5]* $[CoL(diamine)]X_3 \cdot nH_2O$ (X = Cl, Br) (Table 1).

A mixture of 1 mmol of $[CoLCl_2]Cl \cdot 1.5H_2O$ and 1 mmol of a diamine in 50 cm^3 of dimethylsulphoxide was stirred at *ca* 50°C for 1 h and the reaction mixture was diluted with water. The solution acidified with hydrochloric acid was absorbed on a short column of SP Sephadex C-25 and washed with 0.02 N aqueous hydrochloric acid to remove byproducts and the starting material. The main pink band was eluted with 2 N hydrochloric acid and the eluent was evaporated to a small volume under reduced pressure. Upon addition of sufficient ethanol to the concentrated solution the chloride precipitated in a yield of 50–70%. The chloride was recrystallized from aqueous ethanol and dried in air. The bromide was isolated similarly by using hydrobromic acid instead of hydrochloric acid.

* For the preparation of $[CoL(NO_2)_2]Cl$ $NaNO_2$ was used at twice the amount indicated in Ref. 5.

$[CoL(ala)](ClO_4)_2 \cdot 0.5H_2O$

To a solution of 1 mmol of alanine and 1 mmol of 1,8-diazabicyclo(5.4.0)-7-undecene in 30 cm^3 of dimethylsulphoxide was added 1 mmol of $[CoLCl_2]Cl \cdot 1.5H_2O$ and the mixture was stirred at room temperature for one day. The mixture was diluted with water, acidified with hydrochloric acid, and absorbed on a column (3 cm ∅ × 150 cm) of SP Sephadex C-25. The column was eluted with 0.2 M aqueous sodium sulphate and a main red band was collected. The complex was isolated as the perchlorate in the usual manner[6] in a yield of 158 mg.

Acknowledgement—We thank Dr Y. Yoshikawa for measurements of ^{13}C NMR spectra.

REFERENCES

1. *Coordination Chemistry of Macrocyclic Compounds* (Edited by G. A. Melson). Plenum Press, New York (1979).
2. Y. Iitaka, M. Shina and E. Kimura, *Inorg. Chem.* 1974, **13**, 2886.
3. N. Matsumoto, A. Hirano, T. Hara and A. Ohyoshi, *J. Chem. Soc., Dalton Trans.* 1983, 2405.
4. J. H. Loehlin and E. B. Fleicher, *Acta Cryst.* 1976, **B32**, 3063.
5. J. P. Collman and P. W. Schneider, *Inorg. Chem.* 1966, **5**, 1380.
6. Y. Yoshikawa and K. Yamasaki, *Coord. Chem. Rev.* 1979, **28**, 205.
7. A. B. P. Lever, *Inorganic Electronic Spectroscopy.* Elsevier, Amsterdam (1968).
8. M. Kunimatsu, H. Kanno, M. Kojima and J. Fujita, *Bull. Chem. Soc. Jpn* 1980, **53**, 1571.
9. J. Fujita, T. Yasui and Y. Shimura, *Bull. Chem. Soc. Jpn* 1965, **38**, 654.
10. M. Nonoyama and K. Sakai, *Inorg. Chim. Acta* 1983, **72**, 57.
11. J. E. Richmann and T. J. Atkins, *J. Am. Chem. Soc.* 1974, **96**, 2268.
12. C. J. Hawkins, E. Larsen and I. Olsen, *Acta Chem. Scand.* 1965, **19**, 1915.
13. A. J. McCaffery, S. F. Mason and B. J. Norman, *J. Chem. Soc.* 1965, 5094.

Polyhedron Vol. 4, No. 3, pp. 475–479, 1985
Printed in Great Britain

0277-5387/85 $3.00 + .00
Pergamon Press Ltd

SYNTHESIS AND CHARACTERIZATION OF MIXED LIGAND COMPLEXES OF COPPER(II), NICKEL(II), COBALT(II) AND ZINC(II) WITH GLYCINE AND URACIL OR 2-THIOURACIL

MADHU GUPTA and M. N. SRIVASTAVA*
Chemical Laboratories, University of Allahabad, Allahabad, India

(*Received* 15 *November* 1983; *accepted after revision* 22 *May* 1984)

Abstract—Mixed ligand complexes of Cu(II), Ni(II), Co(II) and Zn(II) formed with glycine and uracil or 2-thiouracil have been synthesized and characterized by elemental analysis, conductance, spectral (IR and electronic spectra) and magnetochemical measurements. Results show that glycine is bidentate in all cases; uracil behaves as a bidentate ligand in Cu(II) complex, coordinating through its one carbonyl oxygen and nitrogen, whereas in other cases it is only monodentate, coordinating only through nitrogen. With thiouracil, coordination occurs from carbonyl oxygen and one nitrogen in Cu(II) and Ni(II) complexes, but in the Co(II) complex coordination occurs from thionyl sulphur and nitrogen. In the Zn(II) complex it shows tridentate behaviour, coordinating through oxygen, sulphur and one nitrogen. Mixed Cu(II), Co(II) and Zn(II) complexes of uracil and of Ni(II) and Zn(II) with thiouracil are octahedral, whereas the mixed Ni(II) complex with uracil shows distorted tetrahedral geometry, and the mixed Co(II)–thiouracil complex is square planar. The mixed Cu(II)–thiouracil complex has a binuclear structure, with square planar arrangement around each copper atom.

Mixed ligand complexes are well known to play an important role in biological systems[1] and are being much investigated in solution. Recently Srivastava *et al.*[2] studied potentiometrically the formation of some mixed ligand transition metal complexes in solution, formed with aspartic/glutamic acid and uracil or thymine. The present paper describes the preparation and characterization of some mixed ligand Cu(II), Ni(II), Co(II) and Zn(II) complexes formed with glycine and uracil or 2-thiouracil and their structural studies by spectral (IR and electronic spectra) and magnetochemical measurements.

EXPERIMENTAL

Materials

Glycine (B.D.H.), uracil (Fluka), 2-thiouracil (B.D.H.), cupric chloride (B.D.H., AR) nickel chloride (B.D.H., AR) cobalt chloride (Chemapol) zinc chloride (Merck) and sodium hydroxide (Merck).

Solutions of uracil and 2-thiouracil were prepared by dissolving them in one equivalent of alkali.

Preparation

The metal ion and the two ligand solutions (glycine and uracil/2-thiouracil) were mixed in a molar ratio of 1:1:1, in the order of uracil/2-thiouracil followed by glycine and the pH of the mixture solutions was adjusted to 6–7 by further adding alkali, where necessary. On first adding uracil or 2-thiouracil, precipitates appeared [Cu(II): green; Ni(II): light green; Co(II): pink-violet; Zn(II): colourless] which dissolved on adding glycine to yield clear solutions. The products were obtained by concentration and adding alcohol. They were washed first with 50% alcohol–water mixture, then with absolute alcohol a number of times and finally with ether and dried in an air oven at 50°C. The complexes were also heated in an air oven

*Author to whom all correspondence should be addressed.

successively at 100 and 150°C for about 2 h each time to note any loss of water on heating. It is observed that on heating at 100°C the mixed complexes of Cu(II) and Ni(II) with uracil and of Co(II) with 2-thiouracil lose one water molecule, whilst Co(II) with uracil and of Cu(II) with 2-thiouracil lose two molecules; on the Zn(II) complex with 2-thiouracil there was practically no effect. The mixed Zn(II) complex with uracil loses one water molecule at 100°C and one more on further heating at 150°C. In the mixed Ni(II) thiouracil complex, the loss of water begins from 100°C and is completed by 150°C, the total loss corresponding to one water molecule.

The IR spectra were recorded on a Perkin–Elmer spectrophotometer model 177 covering the range 4000–650 cm^{-1} in KBr discs. The absorption spectra were recorded in aqueous solutions in the range 330–900 nm on a Beckman spectrophotometer model 26. The reflectance spectra of insoluble complexes were recorded in MgO on a spectrophotometer VSU-2P in the range 220–1000 nm.

RESULTS AND DISCUSSION

Given formulae (Table 1) conform to analytical data. Conductance measurements show that the mixed complexes of Ni(II) and Co(II) with uracil are 1:1 electrolytes, whereas the corresponding complexes of Cu(II) and Zn(II) are 1:2 electrolytes. The mixed 2-thiouracil complexes are insoluble in water, as well as in common organic solvents.

IR studies

Some principal IR frequencies of the ligands and their mixed metal complexes are given in Table 2. Results show that the νNH_3^+ of glycine[3,4] (3150 cm^{-1}) disappears on coordination, and instead νNH frequencies appear in the 3400–3200 cm^{-1} region in the metal complexes. $\nu_{as}COO^-$ and ν_sCOO^- frequencies of course appear in their usual region around 1600 and 1400 cm^{-1} respectively. The $\nu C{=}O$ bands of uracil (1712 and 1655 cm^{-1}) are in general little affected in the metal complexes, but in the Cu(II) complex the 1712 cm^{-1} band is considerably lowered in its position to 1670 cm^{-1}. Its $\nu NH + \nu CH$ bands (3130 and 3070 cm^{-1}) appear around 3060 cm^{-1} in the metal complexes.

In 2-thiouracil complexes its secondary amide I band $\nu C{=}O$ (1685 cm^{-1}) is considerably lowered to 1650–1640 cm^{-1} in Cu(II) and Zn(II) complexes, and to 1670 cm^{-1} in the Ni(II) complex, whereas in the Co(II) complex there is little effect. The $\nu NH + \nu CH$ bands (3125 and 3075–3030 cm^{-1}) appear in the 3160–3000 cm^{-1} region in the metal complexes. The thioamide(III) band[5,6] (1150 cm^{-1}) is raised to 1180–1170 cm^{-1} [in the Co(II) complex it is unaffected] whereas the thioamide(IV) band[7] (840 cm^{-1}) (possibly having a major contribution from $\nu C{=}S$)[8,9] is lowered to 830–825 cm^{-1} in Co(II) and Zn(II) complexes, but in Cu(II) and Ni(II) complexes its position remains unchanged.

In addition the metal complexes also show

Table 1. Analytical data of complexes and some physical properties*

Complex	Colour	Found (calc.) (%) M	C	H	N	S	% Loss in weight (H_2O) 100°C	150°C	Λ_M (ohm^{-1} cm^2 mol^{-1})
$Na_2[Cu(gly)(Ur)(OH)_2]\cdot H_2O$	Blue	18.5 (18.3)	20.7 (20.8)	3.22 (3.17)	12.4 (12.1)	—	4.4	—	220.0
$Na[Ni(gly)(Ur)(OH)]\cdot H_2O$	Green	19.2 (19.4)	23.7 (23.8)	3.26 (3.31)	13.8 (13.9)	—	5.7	—	142.3
$Na[Co(gly)_2(Ur)_2]\cdot 2H_2O$	Pink	11.8 (12.1)	29.8 (29.5)	3.81 (3.89)	17.3 (17.2)	—	6.8	—	83.8
$Na_2[Zn(gly)(Ur)(OH)_2(H_2O)]\cdot H_2O$	Colourless	17.7 (17.8)	19.8 (19.6)	3.06 (3.00)	11.4 (11.4)	—	4.4	5.2	252.0
$[Cu_2(OH)_2(gly)(Tur)]\cdot 2H_2O$	Green	32.0 (31.9)	18.0 (18.0)	3.20 (3.26)	10.5 (10.5)	8.0 (8.0)	9.0	0.6	—
$[Ni(gly)(Tur)(H_2O)_2]\cdot H_2O$	Yellowish-green	18.6 (18.7)	22.8 (22.9)	4.20 (4.14)	13.5 (13.3)	10.1 (10.2)	2.6	2.1	—
$[Co(gly)(Tur)]\cdot H_2O$	Grey	21.3 (21.2)	25.7 (25.9)	3.28 (2.23)	15.2 (15.1)	11.6 (11.5)	6.3	—	—
$[Zn(gly)(Tur)(H_2O)]$	Colourless	23.1 (22.9)	25.4 (25.3)	3.12 (3.16)	14.7 (14.7)	11.4 (11.3)	—	—	—

* All the complexes did not melt up to 300°C. Ur, uracil; Tur, 2-thiouracil; gly, glycine.

Table 2. Important IR bands and their assignments

Compound	IR bands (cm^{-1})							
	νNH_3^+	νNH_2	$\nu_{as}COO^-$	$\nu_s COO^-$	$\nu NH + \nu CH$	$\nu C{=}O$	Thioamide(III) band	Thioamide(IV) band
Glycine	3150	—	1590	1410	—	—	—	—
Uracil	—	—	—	—	3130	1712	—	—
					3070	1655		
$Na_2[Cu(gly)(Ur)(OH)_2]\cdot H_2O$	—	3360	1610	1410	3050	1670	—	—
		3250			3000	1650		
$Na[Ni(gly)(Ur)(OH)]\cdot H_2O$	—	3380	1640	1418	3060	1714	—	—
						1660		
$Na[Co(gly)_2(Ur)_2]\cdot 2H_2O$	—	3420	1620	1420	3070	1718	—	—
		3200				1665		
$Na_2[Zn(gly)(Ur)(OH)_2(H_2O)]\cdot H_2O$	—	3270	1600	1412	3070	1718	—	—
						1660		
2-Thiouracil	—	—	—	—	3125	1685	1150	840
					(3075–3030)			
$[Cu_2(OH)_2(gly)(Tur)]\cdot 2H_2O$	—	3300, 3260	1600	1400	3140, 3110	1640	1170	840
		3200			2995			
$[Ni(gly)(Tur)(H_2O)_2]\cdot H_2O$	—	(3400–3200)	1595	1390	3160	1670	1172	840
					(3080–3040)			
$[Co(gly)(Tur)]\cdot H_2O$	—	3350	1620	1412	3140	1680	1152	830
					3020			
$[Zn(gly)(Tur)(H_2O)]$	—	3240	1600	1378	3080	1650	1180	825

Table 3. Magnetic moments and electronic spectral data

Complex	μ_{eff} B.M. (at 306 K)	Band position (10^3 cm^{-1})
$Na_2[Cu(gly)(Ur)(OH)_2]\cdot H_2O$	1.90	14.08, 29.41
$[Cu_2(OH)_2(gly)(Tur)]\cdot 2H_2O$	Diamagnetic	15.15, 24.39, 27.78, 33.48
$Na[Ni(gly)(Ur)(OH)]\cdot H_2O$	3.03	13.89, 28.57(sh), 33.48
$[Ni(gly)(Tur)(H_2O)_2]\cdot H_2O$	2.92	17.09, 28.57
$Na[Co(gly)_2(Ur)_2]\cdot 2H_2O$	4.10	13.71(sh), 19.76, 26.67
$[Co(gly)(Tur)]\cdot H_2O$	2.49	19.53, 28.57

broad bands in the 3700–3450 cm^{-1} region, attributed to νOH of water or OH^- groups.[10]

It may be thus concluded that glycine is bidentate in all cases, coordinating through $-NH_2$ and COO^- groups. In the Cu(II) complex, uracil acts as a bidentate ligand by coordinating through its one carbonyl oxygen and nitrogen, whereas in the other cases it is only monodentate coordinating through only one nitrogen. It may be however noted that since the Co(II) complex is a 1:1 electrolyte, in it deprotonation from only one uracil occurs, the other one being simply coordinated to the metal ion. With 2-thiouracil, in Cu(II) and Ni(II) complexes coordination occurs from the carbonyl oxygen (C=O) and nitrogen, in the Co(II) complex it is from thiocarbonyl sulphur (C=S) and nitrogen, whereas in Zn(II) complex thiouracil is possibly tridentate, coordinating through carbonyl oxygen, thiocarbonyl sulphur and nitrogen.

Magnetic moments and electronic spectra

The magnetic moment of the Cu(II)–glycine–uracil complex is 1.90 B.M. corresponding to one unpaired electron. Its electronic spectrum shows a charge-transfer band at 29,410 cm^{-1} and one broad asymmetric band with λ_{max} at 710 nm (14,085 cm^{-1}). It thus suggests its distorted octahedral structure. But the corresponding Cu(II)–thiouracil–glycine complex is diamagnetic, suggesting its dimetic nature,[12] which is also supported by spectral evidence. Its electronic spectrum shows three charge-transfer bands at 33,480, 27,780 and 24, 390 cm^{-1}, out of which the band observed at 27,780 cm^{-1} is characteristic of dimeric copper(II) complexes.[13] The main *d–d* absorption band is observed at 15,150 cm^{-1} with a shoulder at 12,500 cm^{-1}. The complex is thus dimeric possibly with a square planar arrangement around each copper atom.

The magnetic moments of nickel(II) complexes are Ni(II)–glycine–uracil (μ_{eff} = 3.03 B.M.) and Ni(II)–glycine–2-thiouracil (μ_{eff} = 2.92 B.M.) suggesting that they have octahedral or distorted tetrahedral geometry.[14] The electronic spectrum of the nickel(II)–glycine–thiouracil complex shows two bands at 17,095 and 28,570 cm^{-1} assigned as ν_2 and ν_3 transitions[11] respectively. Its ν_1 transition, however could not be observed, as it is likely to appear beyond 900 nm. It thus supports its octahedral geometry. But the electronic spectrum of the nickel(II)–glycine–uracil complex shows only one *d–d* absorption band at 13,890 cm^{-1}, and two charge-transfer bands at 28,570(sh) and 33,480 cm^{-1}. It thus suggests a tetrahedral geometry, and the 13,890 cm^{-1} band may be assigned as ν_3 transition.[11] The other two ν_1 and ν_2 transitions would of course appear at much lower frequencies beyond 1000 nm, and hence could not be observed.

The magnetic moment of the Co(II)–glycine–uracil complex is 4.10 B.M. Its electronic spectrum shows a charge transfer band at 26,670 cm^{-1}, the ν_3 transition[11] at 19,765 cm^{-1} and a weak shoulder at 13,715 cm^{-1}, thus suggesting an octahedral geometry. The other two ν_1 and ν_2 transitions are not observed because the ν_2 transition in Co(II) complexes is normally very weak and may or may not be observed, whereas the ν_1 transition is likely to appear at much lower frequencies beyond 1000 nm. The magnetic moment of the Co(II)–glycine–thiouracil complex (μ_{eff} = 2.49 B.M.) suggests it to be a low spin square planar[14] complex. The electronic spectrum shows a charge-transfer band at 28,570 cm^{-1}. The visible *d–d* band[11] is observed at 19,530 cm^{-1}, which may be assigned as a transition from the lower filled orbitals to the empty $d_{x^2-y^2}$ orbital.

REFERENCES

1. H. Sigel, *Metal Ions in Biological Systems; Vol. 2, Mixed Ligand Complexes.* Marcel Dekker, New York (1973).
2. N. B. Nigam, P. C. Sinha and M. N. Srivastava, *Proc. Symp. Coordination Chemistry*, Indian Council of Chemists, Agra (1981); *Indian J. Chem.* 1983, **22A**, 818.
3. L. J. Bellamy, *The Infrared Spectra of Complex*

Molecules, Vol. I, 3rd edition. Chapman & Hall, London (1975).
4. C. N. R. Rao, *Chemical Applications of Infrared Spectroscopy*. Academic Press, New York (1963).
5. E. Spinner, *J. Chem. Soc.* 1960, 1237.
6. C. N. R. Rao and R. Venkatraghvan, *Spectrochim. Acta* 1962, **18**, 541.
7. I. Suzuki, *Bull. Chem. Soc. Jpn* 1962, **35**, 1286, 1449, 1456.
8. R. K. Gosavi, U. Agarwala and C. N. R. Rao, *J. Am. Chem. Soc.* 1967, **89**, 235.
9. U. Agarwala, Lakshmi and P. Bhaskara Rao, *Inorg. Chim. Acta* 1968, **2**, 337.
10. K. Nakamoto, *Infrared Spectra of Inorganic and Coordination Compounds*, 2nd edition. Wiley–Interscience, New York (1970).
11. A. B. P. Lever, *Inorganic Electronic Spectroscopy*. Elsevier, Amsterdam (1968).
12. M. Kato, H. B. Jonassen and J. C. Fanning, *Chem. Rev.* 1964, **64**, 99.
13. R. Tsuchida and S. Yamada, *Nature* (*London*) 1955, **176**, 1171.
14. F. A. Cotton and G. Wilkinson, *Advanced Inorganic Chemistry*, 3rd edition. Wiley Eastern, New Delhi (1979).

Polyhedron Vol. 4, No. 3, pp. 481–484, 1985
Printed in Great Britain

0277–5387/85 $3.00 + .00
Pergamon Press Ltd

SOLVENT COMPLEXES OF THE TYPE $[Fe^{III}(CN)_5L]^{n-}$

GRAŻYNA STOCHEL and ZOFIA STASICKA*
Department of Inorganic Chemistry, Jagiellonian University, 30-060 Kraków, Poland

(*Received* 11 *November* 1983; *accepted* 22 *May* 1984)

Abstract—The title complexes have been prepared *in situ* by photolyzing the $[Fe(CN)_5NO]^{2-}$ ion in some aliphatic alcohols, formamide and its derivatives, pyridine, acetonitrile and dimethylsulphoxide. Characterization of the complexes was made on the basis of three pieces of evidence: (i) the spectral properties, (ii) the presence of the titratable hydrogen in the complexes with protogenic solvents, and (iii) the anation reaction with the N_3^- and NCS^- ions.

The pentacyano(ligand)ferrate(III) complexes have been intensively studied for a long time.[1–12] Nevertheless, we have recently identified some new $[Fe^{III}(CN)_5L]^{n-}$ complexes, where L = solvent or deprotonated solvent molecule.

Moreover, a new way of generation of the iron(III) complexes in photochemical reaction of nitrosylpentacyanoferrate(II) is proposed.

RESULTS AND DISCUSSION

Electronic spectra of the $[Fe^{III}(CN)_5L]^{n-}$ complexes are characterized among others by two intense bands at 23–25 and 28–30 $\times 10^3$ cm^{-1} that are relatively independent of the identity of the ligand L.[2–12] These bands were assigned to the $CN \rightarrow Fe$ LMCT and LF transitions, respectively.[2–7] When ligand L contains acidic proton, i.e. L = L'H, in the spectrum of the deprotonated form, $[Fe^{III}(CN)_5L']^{(n+1)-}$, only one intensive band, relatively independent of the ligand L', is observed[3,8,13] at 22–23 $\times 10^3$ cm^{-1}.

The spectral features characteristic of the $[Fe^{III}(CN)_5 L]^{2-}$ complexes has been revealed by irradiated ($\bar{\nu} > 21 \times 10^3$ cm^{-1}) solutions of $[Fe(CN)_5NO]^{2-}$ in several solvents such as: water, methanol, ethanol, ethylene glycol, formamide, *N*-methylformamide, *N*,*N*-dimethylformamide, pyridine, acetonitrile and dimethylsulphoxide (Table 1). When the exposure was performed in protogenic solvents in the presence of alkalis, the spectra characteristic of the $[Fe^{III}(CN)_5L']^{3-}$ complexes were observed (Table 1).

Photochemical production of the $[Fe(CN)_5H_2O]^{2-}$ and $[Fe(CN)_5OH]^{3-}$ complexes in the aqueous system was substantiated earlier,[9,10,13,14] and the spectrum of the photoproduct generated in pyridine solution is consistent with that of the $[Fe(CN)_5py]^{2-}$ complex obtained by oxidation of the $[Fe(CN)_5py]^{3-}$ one.[4,5] This leads to the conclusion that also in the other cases (Table 1, Nos 2–7, 9, 10, 12–15) the $[Fe^{III}(CN)_5L]^{n-}$ complexes were generated. Among the complexes listed in Table 1 only those with L = H_2O, OH^- and py were recognized earlier,[4,5,9,10,12] whereas those with L = DMSO or CH_3OH were postulated to be generated.[9,13,15,16] The remaining complexes are here reported for the first time. The photochemical method of their generation is expected to operate also in the case of other pentacyano(ligand)ferrate(III) complexes.

The $[Fe^{III}(CN)_5L'H]^{2-}$ complexes, where L'H = MeOH, EtOH, ethylene glycol or formamide, were found to be transformed into the $[Fe^{III}(CN)_5L']^{3-}$ ones by addition of solid or concentrated aqueous alkalis (Fig. 1). The change was reversed by addition of CH_3COOH to the former solution.

The equilibrium constant for the reaction:

$$[Fe(CN)_5CH_3OH]^{2-} + OH^- \overset{K_1}{\rightleftharpoons} [Fe(CN)_5OCH_3]^{3-} + H_2O \quad (1)$$

was evaluated roughly by a spectrophotometric titration of the methanolic complex with OH^- in

* Author to whom correspondence should be addressed.

Table 1. Electronic spectra of the $[F^{III}(CN)_5L]^{n-}$ complexes generated photochemically

	$[Fe(CN)_5L]^{2-}$					$[Fe(CN)_5L']^{3-}$		
		$\bar{\nu}_{max}$ (10^3 cm^{-1}) [ε (M^{-1} cm^{-1})]						$\bar{\nu}_{max}$ (10^3 cm^{-1}) [ε (M^{-1} cm^{-1})]
No.	L	$\bar{\nu}_1$		$\bar{\nu}_2$		No.	L	
1	H_2O*	25.5	(800)	29.4	(800)	11	OH^-*	25.5 (1800)
2	CH_3OH†	24.7	(1020)	29.1	(940)	12	CH_3O^-†	22.5 (2340)
3	C_2H_5OH†	24.7		29.1		13	$C_2H_5O^-$†	21.4
4	$HOCH_2CH_2OH$†	24.5	(~800)	28.9	(~790)	14	$HOCH_2CH_2O^-$†	22.3 (900–1400)
5	$HCONH_2$†	24.5		28.0		15	$HCONH^-$†	21.4
6	$HCONHCH_3$†	24.3		28.3				
7	$HCON(CH_3)_2$†	24.2		28.5				
8	C_5H_5N†‡	24.2		27.2				
9	CH_3CN†	24.2		29.9				
10	CH_3SOCH_3†	23.2	(1020)	28.5	(1200)			

* References 10 and 12.
† This work.
‡ See also Ref. 5.

aqueous methanol using the relation:

$$\log\left(\frac{A}{A_\infty - A}\right) = \log [OH^-] + \log\left(\frac{K_1}{[H_2O]}\right) \quad (2)$$

as described in Experimental. Plots of log $[A/(A_\infty - A)]$ vs log $[OH^-]$ were found to be linear within the OH^- concentration not higher than 10^{-2}. Above this value the reaction between nitrosylpentacyanoferrate(II) and the OH^- ions[14,17] started to interfere. The average value of K_1 is $(5.1 \pm 2.9) \times 10^1$ at 295 K and $\mu = 0.1$.

The solvent complexes were found to undergo substitution of the solvent molecule by water, N_3^-, SCN^- ions and, in the case of aprotic systems, by OH^- ions. The equilibrium constant for the anation reaction:

$$[Fe(CN)_5CH_3OH]^{2-} + NCS^- \overset{K_3}{\rightleftharpoons} [Fe(CN)_5SCN]^{3-} + CH_3OH \quad (3)$$

was evaluated from plotting the data as suggested by an equation similar to that of (2). The average value of K_3 is $(2.7 \pm 0.9) \times 10^1$ M^{-1} at 295 K and $\mu = 0.1$.

This value was used to assess the affinity of the

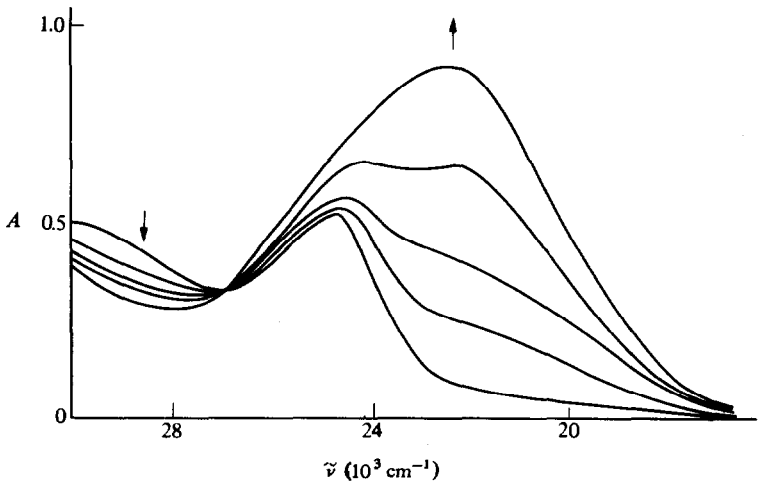


Fig. 1. Spectrophotometric titration of $[Fe(CN)_5CH_3OH]^{2-}$ with NaOH; initial concentration of the complex, $c = 0.927 \times 10^{-4}$ M, $\mu = 0.1$ ($NaClO_4$), $T = 295$ K; arrows show order of spectra with successive increase in the OH^- concentration: $\leq 3.84 \times 10^{-5}$, 3.67×10^{-4}, 7.34×10^{-4}, 1.48×10^{-3} and 3.84×10^{-2} M.

CH_3OH ligand for $[Fe(CN)_5]^{2-}$ relative to displacement of water:

$$[Fe(CN)_5H_2O]^{2-} + CH_3OH \overset{K_4}{\rightleftharpoons} [Fe(CN)_5CH_3OH]^{2-} + H_2O \quad (4)$$

since $K_4 = K_5/K_3$, where K_5 is the equilibrium constant for the reaction:

$$[Fe(CN)_5H_2O]^{2-} + NCS^- \overset{K_5}{\rightleftharpoons} [Fe(CN)_5SCN]^{3-} + H_2O \quad (5)$$

taken from the literature data.[12] The average value of $K_4 = (2.5 \pm 0.9) \times 10^1$ is in unexpected agreement with the value of 4.3×10^1 calculated from the empiric correlation between the association constant of L for $[Fe(CN)_5]^{2-}$, K_f, and pK_a of the ligand (for methanol $pK_a = -2.079$[18]):

$$\log K_f = (0.36 \pm 0.07)pK_a + (2.38 \pm 0.60) \quad (6)$$

formulated by Shepherd *et al.*[3]

EXPERIMENTAL

Reagents

Anhydrous sodium nitrosylpentacyanoferrate(II), $Na_2[Fe(CN)_5NO]$, was prepared by a repeated recrystallization of a commercial dihydrate from aqueous solution and drying of a pulverized sample at 440 K up to the constant weight. Organic solvents were purified by fractional distillation and dried when it was necessary. Alkalis were purified from carbonates, other chemicals were best available commercial reagents used without further purification.

Preparation of complexes

Complexes of the type $[Fe(CN)_5L]^{2-}$ [where $L = CH_3OH$, C_2H_5OH, $HOCH_2CH_2OH$, $HCONH_2$, $HCONHCH_3$, $HCON(CH_3)_2$, C_5H_5N, CH_3CN or $(CH_3)_2SO$] were prepared *in situ* by irradiation of 1×10^{-3} M solutions of anhydrous $Na_2[Fe(CN)_5NO]$ in a proper solvent. Irradiations were carried out using a high-pressure mercury lamp (HBO 200, Narva, D.D.R.), at 295 ± 1 K. Exposure was limited to less than 10% conversion to avoid secondary thermal reactions.[19] Thus the solution studied contained only the $[Fe(CN)_5L]^{2-}$ complex and parent $[Fe(CN)_5NO]^{2-}$, that fortunately did not affect considerably the results. The same method was used to prepare the deprotonated complexes, $[Fe(CN)_5L']^{3-}$ (where $L' = CH_3O^-$, $C_2H_5O^-$, $HOCH_2CH_2O^-$ or $HCONH^-$) except that irradiated solutions contained additionally 1×10^{-2} M NaOH.

Spectrophotometric titrations

Volumetric flasks containing equal amounts of the $[Fe(CN)_5CH_3OH]^{3-}$ complex in methanolic solution (containing 0.1% H_2O) and various amounts of NaOH or KSCN were suspended in temperature bath controlled to ± 1 K for 0.5 h. Ionic strength was maintained at $\mu = 0.1$ using $NaClO_4$ in the former, and $NaNO_3$ in the latter case. The solution spectra were recorded to determine the equilibrium amounts of $[Fe(CN)_5CH_3OH]^{2-}$ and $[Fe(CN)_5OCH_3]^{3-}$ or $[Fe(CN)_5SCN]^{3-}$. Plots of $\log [A/(A_\infty - A)]$ vs $\log [OH^-]$ were made, where A is the absorbance at 20 or 21×10^3 cm^{-1} of the $[Fe(CN)_5OCH_3]^{3-}$ species ($\varepsilon_{20} = 1300$, $\varepsilon_{21} = 1850$) corrected to the minor contributions of the $[Fe(CN)_5NO]^{2-}$ ($\varepsilon_{20} = 9$, $\varepsilon_{21} = 10$) and $[Fe(CN)_5CH_3OH]^{2-}$ ($\varepsilon_{20} = 68$, $\varepsilon_{21} = 100$) complexes at these wave numbers. A_∞ is the value for total conversion of the methanol complex into the methoxo one. In the case of KSCN titrant, the data were analysed at 17.0×10^3 cm^{-1}, where absorbance from the $[Fe(CN)_5SCN]^{3-}$ complex ($\varepsilon = 2680$[11]) exceeded considerably those of $[Fe(CN)_5CH_3OH]^{2-}$ ($\varepsilon = 40$) and $[Fe(CN)_5NO]^{2-}$ ($\varepsilon = 5$).

The electronic spectra were measured using a Specord UV-VIS or VSU 2P spectrophotometer [both C. Zeiss (Jena, D.D.R.)]. All operations were performed in the dark.

Acknowledgement—We thank the Polish Academy of Sciences for support.

REFERENCES

1. A. G. Sharpe, *The Chemistry of Cyano Complexes of the Transition Metals*. Academic Press, London (1976).
2. W. Haberditzl, K. Schleinitz and H. G. Bartel, *Z. Naturforsch.* 1968, **23b**, 1397.
3. C. R. Johnson, R. E. Shepherd, B. Marr, S. O'Donnell and W. Dressick, *J. Am. Chem. Soc.* 1980, **102**, 6227 (and references cited therein).
4. N. V. Hrepic and J. M. Malin, *Inorg. Chem.* 1979, **18**, 409 (and references cited therein).
5. H. E. Toma and J. M. Malin, *J. Am. Chem. Soc.* 1975, **97**, 288.
6. G. Calzaferi and F. Felix, *Helv. Chim. Acta* 1977, **60**, 730.
7. C. D. Della Vedova, S. Del, V. Alonso, D. J. Roncoglia and P. J. Aymonino, *Inorg. Chim. Acta* 1983, **73**, 221.

8. G. Stochel and Z. Stasicka, *Proc. 3rd Symposium on Photochemical and Thermal Reactions of Coordination Compounds*, p. 107, Mogilany-Kraków, Poland (1980).
9. S. K. Wolfe and J. A. Swinehart, *Inorg. Chem.* 1975, **14**, 1049.
10. T. Jarzynowski, T. Senkowski and Z. Stasicka, *Pol. J. Chem.* 1981, **55**, 3 (and references cited therein).
11. B. Jaselskis, *J. Am. Chem. Soc.* 1961, **83**, 1082.
12. J. H. Espenson and G. Wolenuk, *Inorg. Chem.* 1972, **11**, 2034.
13. A. B. Nikolski and A. M. Popov, *Dokl. Akad. Nauk SSSR* 1980, **250**, 902.
14. T. Jarzynowski, T. Senkowski and Z. Stasicka, *Rocz. Chemii* 1977, **51**, 2298.
15. H. Toma and C. Creutz, *Inorg. Chem.* 1977, **16**, 545.
16. H. Symons, D. West and J. Wilkinson, *J. Chem. Soc., Chem. Commun.* 1973, 917.
17. J. A. McCleverty, *Chem. Rev.* 1979, **79**, 53.
18. C. E. Newall and A. M. Eastham, *Can. J. Chem.* 1961, **39**, 1752.
19. G. Stochel and Z. Stasicka (to be published).

Polyhedron Vol. 4, No. 3, pp. 485–487, 1985
Printed in Great Britain

0277–5387/85 $3.00 + .00
© 1985 Pergamon Press Ltd

COMPLEXES OF *N*-METHYL-4-MERCAPTOPIPERIDINE WITH SOME METAL IONS

W. GAETE* and J. ROS
Departament de Química Inorgànica, Facultat de Ciències, Universitat Autònoma de Barcelona (Bellaterra), Barcelona, Spain

(*Received* 1 *December* 1983; *accepted* 22 *May* 1984)

Abstract—Complexes of *N*-methyl-4-mercaptopiperidine in its zwitterionic form with Co(II) and Zn(II) salts, and in anionic form with Cu(I) and Ag(I) salts have been prepared. Stoichiometry of the complexes, $Co(HRS)_2CoX_4$ (X = Cl and Br), $Co(HRS)_2X_2$ (X = ClO_4, NO_3), $Co(HRS)_3X_3$ (X = NO_3, ClO_4), $Zn(HRS)_2ZnX_4$ (X = Cl and Br), $Zn(HRS)_2(NO_3)_2$, Ag(RS) and Cu(RS), have been established by chemical analysis. The solid complexes have been further characterized by IR and electronic spectra measurements.

As part of our work on the coordination of mercaptoamines to metal ions we have reported the synthesis, properties and structures of some complexes formed by *N*-methyl-4-mercaptopiperidine.[1–5] The observed molecular structures with the ligand in its zwitterionic form $\overset{(+)}{N}H(CH_3)C_5H_9S^-$ (hereafter HRS) are discrete molecules[3] in $Hg(HRS)_2$, dimeric molecules[2,5] in $Zn_2(HRS)_2X_4$ (X = Cl, Br and I) and one-dimensional polymeric chains[1] in $Cd(HRS)_2(ClO_4)_2$. When the ligand is in the anionic form $N(CH_3)C_5H_9S^-$ (RS^-), cyclic tetrameric molecules are formed in[4] $Ni_4(RS)_8$. In all the cases the ligand coordinates only by the sulphur atom.

In continuation of our studies on this type of metal complexes we now report on the synthesis and spectral properties of some metal complexes with the ligand both in its zwitterionic and anionic form.

EXPERIMENTAL

Preparation of the ligand

HRS was synthesized following a previously reported method.[6]

Preparation of the complexes

$Co(HRS)X_2 \cdot \frac{1}{2}H_2O$ (X = Cl *and* Br). In order to prevent oxidation, all reactions and operations were carried under moisture free nitrogen. The complexes were prepared by the addition of a solution of HRS in absolute ethanol to a solution containing the equivalent amount of the cobalt salt in absolute ethanol. The products were separated by filtration, washed with cold absolute ethanol, then dry diethylether and finally vacuum dried at room temperature.

$Zn(HRS)X_2 \cdot H_2O$ (X = Cl *and* Br) *and* $Zn(HRS)_2(NO_3)_2$. Zinc complexes were prepared as described above but without the nitrogen atmosphere. In the $Zn(HRS)Br_2$ preparation the solvent used was methanol. Preparation of $Zn(HRS)_2(NO_3)_2$ involved the addition of a solution of zinc nitrate in ethanol to an ethanolic solution of HRS.

$Co(HRS)_3X_3$ (X = NO_3 *and* ClO_4). Complexes of Co(III) were prepared by the addition of a solution of HRS in water to an aqueous solution of the Co(II) salt. A stream of air was bubbled through the solution during 2 or 3 h. By cooling at 4–5°C the solid compounds precipitated.

Ag(RS) *and* Cu(RS). These complexes were prepared by the addition of a solution of HRS in water containing some drops of methanol to a solution containing the equivalent amount of $AgNO_3$ or $Cu(NO_3)_2 \cdot 6H_2O$ and NH_3 in water. The products which formed after the reactants had been heated for several minutes, were cooled to room temperature, collected by filtration and washed with ethanol and ether.

Physical measurements

IR spectra (4000–250 cm^{-1}) of complexes were recorded on a Beckman IR-20A spectrophotometer. The samples were either pressed in a potassium

* Author to whom correspondence should be addressed.

halide pellet or run as Nujol mulls between polyethylene plates. Electronic diffuse reflectance spectra at room temperature were recorded on a Beckman ACTA III (800–190 nm) and on a Beckman ACTA VII B spectrophotometer.

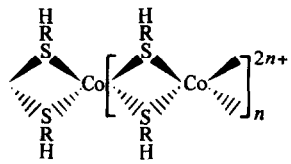
RESULTS AND DISCUSSION

The complexes are listed in Table 1 with their elemental analysis. In the hydrated complexes absorptions due to the stretching $\nu_{(O-H)}$ and bending $\delta_{(HOH)}$ vibrations indicate that the water molecules are not coordinated. In the zwitterionic complexes, absorptions due to $\nu_{(N-H)}$ stretching vibrations appear between 2680 and 2710 cm^{-1} indicating hydrogen bond formation.

Complexes with the ligand in zwitterionic form

Co(II) *complexes.* The green complexes are insoluble in common organic solvents. In water and polar solvents they decompose. The solid electronic spectra of the complexes show a strong absorption in the 600–800 nm spectral range assignable to the $^4A_2 \rightarrow {}^4T_1(P)$ transition [7] (ν_3). The shape and bandwidth of these bands are wider than those reported for the $(HRS)_2(CoX_4)$ salts.[8] In the near-IR region, two broad absorptions are observed (1250 and 1660 nm for $Co(HRS)Cl_2 \cdot \frac{1}{2}H_2O$, and 1300 and 1670 nm for $Co(HRS)Br_2 \cdot \frac{1}{2}H_2O$) assignable to the $^4A_2 \rightarrow {}^4T_1(F)$ (ν_2) transition. These facts suggest the existence of two kinds of tetrahedral Co(II) atoms. When the electronic spectra of the $(HRS)_2CoX_4$ compounds and those of the corresponding $Co(HRS)_2X_2$ salts are added, the resulting spectra agree well with those observed, giving support to our assumption.

Based on these observations, a polymeric tetrahedral cation with sulphur-bridging atoms neutralized by CoX_4^{2-} anions is postulated for these Co(II) complexes:



Co(III) *complexes.* The dark brown complexes are insoluble in H_2O and in most organic solvents.

The IR spectrum of the nitrate compound exhibits the characteristically intense ν_3 (1360 cm^{-1}) and moderately strong ν_2 (835 cm^{-1}) bands of ionic nitrate.[9] The presence of the ν_3 (1140–1070 cm^{-1})

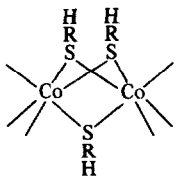
Table 1. Analytical data of complexes

Compound		% C	% H	% N	% S	% M*	% Cl
$Co(HRS)Cl_2 \cdot \frac{1}{2}H_2O$	Calc.	26.7	4.18	5.18	11.9	21.8	26.3
	Found	26.6	5.26	5.14	12.1	21.8	26.4
$Co(HRS)Br_2 \cdot \frac{1}{2}H_2O$	Calc.	20.1	3.90	3.90	8.93	16.4	
	Found	19.9	3.95	3.85	9.04	15.9	
$Zn(HRS)Cl_2 \cdot H_2O$	Calc.	25.2	5.23	4.90	11.2	22.9	24.8
	Found	25.7	5.23	5.06	11.8	22.9	25.0
$Zn(HRS)Br_2 \cdot \frac{1}{2}H_2O$	Calc.	19.7	3.56	3.83	8.78	17.9	
	Found	19.6	3.42	3.90	9.03	17.8	
$Zn(HRS)_2(NO_3)_2 \cdot H_2O$	Calc.	30.1	5.96	11.9	13.6	13.9	
	Found	30.0	6.17	11.7	13.6	13.9	
$Co(HRS)_3(NO_3)_3 \cdot H_2O$	Calc.	32.9	6.25	19.2	14.6	8.98	
	Found	32.9	6.20	19.9	14.6	9.11	
$Co(HRS)_2(ClO_4)_3 \cdot H_2O$	Calc.	28.1	5.33	5.46	12.5	7.67	
	Found	27.6	4.85	5.55	12.5	7.66	
Ag(RS)	Calc.	30.3	5.04	5.88	13.5	45.3	
	Found	30.1	5.13	5.97	13.7	45.5	
Cu(RS)	Calc.	37.2	6.20	7.23	16.5	32.8	
	Found	37.1	6.30	7.10	16.2	32.5	

* Metal.

and ν_4 (625 cm^{-1}) bands in the IR spectrum of the perchlorate complex suggests this group is not coordinated.[9] The electronic spectra of the two complexes are similar. They show strong absorption at 445 and 580 nm with a broad tail extending up to 800 nm due to $^1A_{1g} \rightarrow {}^1T_{2g}$ (ν_2) and $^1A_{1g} \rightarrow {}^1T_{1g}$ (ν_1) transitions, as expected for spin paired trivalent cobalt complexes in octahedral environment. The calculated ligand field parameters are: $10Dq$ = 18,060 and B = 366 cm^{-1} (β = 0.34). The calculated absorptions for the spin forbidden transitions $^1A_{1g} \rightarrow 3T_{2g}$ (ν_3) and $^1A_{1g} \rightarrow 3T_{1g}$ (ν_4) are 600 and 710 nm. The fourth-derivative curves with the spectrum manually digitized from chart paper[10] reveal that two additional bands are resolved at 600 and 690 nm, in good agreement with the calculated values.

The complexes are probably polymeric octahedrally coordinated cations with sulphur-bridging atoms neutralized by nitrate or perchlorate anions:



Zn(II) *complexes.* In the reaction of HRS with Zn(II) salts two kinds of complexes are obtained depending on the solvent used. When the solvent is water, dimeric molecules of $Zn_2(HRS)_2X_4$ are obtained,[2] but if ethanol or methanol are used, the amorphous complexes $Zn(HRS)X_2$ (X = Cl and Br) and $Zn(HRS)_2(NO_3)_2$ here reported are formed.

The $\nu_{(Zn-S)}$ stretching vibrations are assigned to the absorptions at 290 and 277 cm^{-1} in the bromide compound and at 282 and 277 cm^{-1} in the nitrate complex and are not observed in the chlorocomplex because they are masked by the strong and broad absorption at 282 cm^{-1}, assignable to the $\nu_{(Zn-Cl)}$ stretching vibration. The proposed structures for these complexes consist of polymeric tetrahedral cations with sulphur-bridging atoms as in the $Cd(HRS)_2(ClO_4)_2 \cdot 2H_2O$ complex[1] neutralized by tetrahalozincate and nitrate anions respectively. When the tetrahalozincates are dissolved in water they decompose, finally becoming the known dimeric complexes $Zn_2(HRS)_2X_4$.

Complexes with the ligand in anionic form

Ag(I) *and* Cu(I) *complexes.* The reactions of formation of these complexes may be written:

$$Ag^+ + HRS + NH_4OH \rightarrow AgRS + NH_4^+ + H_2O$$

and

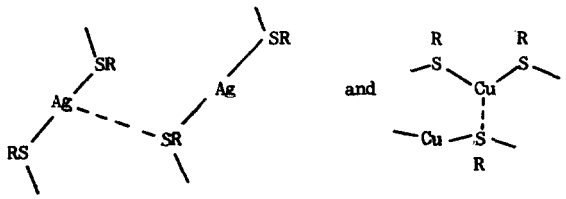
$$2Cu^{2+} + 4HRS + 4NH_4OH \rightarrow 2CuRS + RS{-}SR + 4NH_4^+ + 4H_2O,$$

where RS—SR is the correspondent disulphide.

The IR spectra of these complexes in the 4000–400 cm^{-1} range are identical with those of the free HRS ligand and of the $Ni_4(RS)_8$ complex whose structure has been well established.[4] The absorptions observed in the 400–250 cm^{-1} range may be assigned to metal–sulphur stretching vibrations. The high number of absorptions may indicate the presence of different kinds of coordination around the metal atoms.

The crystal structure for the silver cyclohexanethiolate has been described[11] as being a one-dimensionally non-molecular solid with some silver atoms approximately linear and others possessing severely distorted trigonal planar stereochemistry. Otherwise several Cu(I) thiolate show polymeric pseudotrigonal structures.[12]

The insolubility in the common organic solvents of the AgRS and CuRS complexes support the hypothesis that they are polymeric in the solid state, with structural fragments such as:



REFERENCES

1. J. C. Bayón, M. C. Briansó, J. L. Briansó and P. González Duarte, *Inorg. Chem.* 1979, **18**, 3478.
2. M. C. Briansó, J. L. Briansó, W. Gaete, J. Ros and C. Suñer, *J. Chem. Soc., Dalton Trans.* 1981, 852.
3. H. Barrera, J. C. Bayón, P. González Duarte, J. Sola, J. M. Viñas, M. C. Briansó, J. L. Briansó and X. Solans, *Polyhedron* 1982, **1**, 647.
4. W. Gaete, J. Ros, X. Solans, M. Font-Altaba and J. L. Briansó, *Inorg. Chem.* 1984, **23**, 39.
5. J. C. Bayón, I. Casals, W. Gaete, P. González Duarte and J. Ros, *Polyhedron* 1982, **1**, 157.
6. H. Barrera and R. E. Lyle, *J. Org. Chem.* 1962, **27**, 64.
7. A. B. P. Lever, *Inorganic Electronic Spectroscopy.* Elsevier, New York (1968).
8. H. Barrera, W. Gaete, M. Izquierdo, J. Ros and A. Soriano (submitted for publication).
9. K. Nakamoto, *Infrared Spectra of Inorganic and Coordination Compounds.* Wiley–Interscience, New York (1970).
10. J. R. Dickinson, T. R. Griffiths and P. J. Potts, *J. Inorg. Nucl. Chem.* 1975, **37**, 511.
11. I. G. Dance, *Inorg. Chim. Acta* 1977, **25**, L17.
12. I. G. Dance and J. C. Calabresse, *Inorg. Chim. Acta* 1976, **19**, L41.

Polyhedron Vol. 4, No. 3, pp. 489–490, 1985
Printed in Great Britain

0277–5387/85 $3.00 + .00
Pergamon Press Ltd

LATTICE ENERGIES OF THE ALKALI METAL BIFLUORIDES, $U(MHF_2)$

JOHN EMSLEY
Department of Chemistry, King's College, Strand, London WC2R 2LS, U.K.

(*Received* 11 *April* 1984; *accepted* 22 *May* 1984)

Abstract—The experimental determination of the hydrogen bond energy of the bifluoride ion makes possible accurate lattice energies of the alkali metal bifluorides, $U(MHF_2)$; see Table 1. From these it is possible to estimate those of NH_4HF_2 and the alkaline earth bifluorides.

From the time when it was discovered that the bifluoride ion harboured a unique hydrogen bond[1] there have been many attempts to evaluate its energy. During the past 25 years over 15 communications have been published offering values ranging from 125 to 262 kJ mol^{-1}.[2] Some were based on the Born–Haber cycle shown below in which $\Delta H_1^{\ominus}$ defined the hydrogen bond energy and $\Delta H_2^{\ominus}$ can be obtained from eqn (1):

$$\begin{array}{ccccc} M^+(g) + F^-(g) + HF(g) & \xrightarrow{\Delta H_1^{\ominus}} & M^+(g) + HF_2^-(g) \\ \uparrow U(MF) & & \uparrow U(MHF_2) \\ MF(s) + HF(g) & \xrightarrow{\Delta H_2^{\ominus}} & MHF_2(s) \end{array}$$

$$\Delta H_2^{\ominus} = \Delta H_f^{\ominus}(MHF_2)(s) - \Delta H_f^{\ominus}(MF)(s) - \Delta H_f^{\ominus}(HF)(g). \quad (1)$$

The weak link in this cycle is $U(MHF_2)$ and attempts have been made to calculate the lattice energies of the alkali metal bifluoride in order to obtain $\Delta H_1^{\ominus}$.[3–5] The best of these efforts led to a $\Delta H_1^{\ominus}$ value of 176 kJ mol^{-1}.[5]

An alternative approach[6] to the problem was to choose a fluoride with a large cation, viz. Me_4NF, and to assume that $U(Me_4NHF_2) = U(Me_4NF)$ so that $\Delta H_1^{\ominus} = \Delta H_2^{\ominus}$. This produced a value of 155 kJ mol^{-1}. Seemingly more realistic was the suggestion[5] that there would be a difference of 30 kJ mol^{-1} between these lattice energies in which case $\Delta H_1^{\ominus}$ would be 185 kJ mol^{-1}.

The recent measurement[7] of $\Delta H_1^{\ominus}$ directly, by ion cyclotron resonance, has settled the issue; $\Delta H_1^{\ominus}$ is 163 $\pm$4 kJ mol^{-1}. This value is supported by *ab initio* calculations employing the largest basis set[2] which gave a value of 169 kJ mol^{-1}.

Using the experimental value for $\Delta H_1^{\ominus}$ it is now possible to return to the Born–Haber cycle and use the bond energy of the bifluoride hydrogen bond to obtain the actual bifluoride lattice energies. These are given in the Table 1. In all cases they are significantly higher by 5–10% than those calculated.[3–5] [The error in $U(MHF_2)$ could not be estimated since some of the published $\Delta H_f^{\ominus}$ data for the fluorides and bifluorides did not include error limits. However the error in $U(MHF_2)$ is probably *ca* $\pm$10 kJ mol^{-1}.]

With reliable $U(MHF_2)$ values for the alkali metals the Kapustinskii equation (2)

$$U \text{ kJ mol}^{-1} = 107{,}900\nu Z_+ Z_-/(r_+ + r_-) \quad (2)$$

can be used to obtain a so-called thermochemical radius for the bifluoride ion,[11] thus $r_-(HF_2^-)$ = 165 pm (using Li^+ = 74 pm); 165 (Na^+ = 102); 160 (K^+ = 138); 163 (Rb^+ = 149) and 167 (Cs^+ = 170).[12] The average radius is 164 pm.* Armed with this it is then possible to compute the lattice energies of the following bifluorides: NH_4HF_2 = 606 kJ mol^{-1} ($r_+NH_4^+$ = 146)[12] which compares fairly well with the reported value of 733 kJ mol^{-1};[14] $Mg(HF_2)_2$ = 2743 kJ mol^{-1} [cf. $U(MgF_2)$ =

* The R(F . . . F) internuclear distance is 226 pm[13] to which the ionic radius of the end fluorine atoms adds *ca* 2 × 133 pm making an overall longitudinal length of 492 pm and a radius of 246 pm. The average of this and the latitudinal radius (133 pm) gives 189 pm. A relationship to the thermochemical radius is not obvious.

Table 1. Lattice energies of the alkali metal bifluorides, $U(MHF_2)$*[a] (all energies in kJ mol^{-1}; 298.15 K)

	Li	Na	K	Rb	Cs
$-\Delta H_f^{\ominus}(MHF_2)(s)$[9]	923.9	906.2	920.4	909.2	904.2
$-\Delta H_f^{\ominus}(MF)(s)$[9]	611.7	569.0	562.8	551.5	545.2
$U(MF)$[10]	1025	903.7	801.2	768.1	715.5
$U(MHF_2)$	903	807	725	692	640
ΔU†	122	97	76	76	75

* $U(MHF_2) = -\Delta H_f^{\ominus}(MHF_2)(s) + \Delta H_f^{\ominus}(MF)(s) - \Delta H_f^{\ominus}(HF)(g) + U(MF) - \Delta H_1^{\ominus}$, where $\Delta H_f^{\ominus}(HF)(g) = 271.1 \pm 2.1$ kJ $mole^{-1}$,[8] and $\Delta H_1^{\ominus} = 163 \pm 4$ kJ mol^{-1}.[7]

† $\Delta U = U(MF) - U(MHF_2)$.

2922 kJ mol^{-1}];[11] $Ca(HF_2)_2 = 2452$ kJ mol^{-1} [cf. $U(CaF_2) = 2597$ kJ mol^{-1}];[11] $Sr(HF_2)_2 = 2312$ kJ mol^{-1} and $Ba(HF_2)_2 = 2158$ kJ mol^{-1}.

Table 1 also spotlights another misconception—that as the cation gets larger the difference between the fluoride and bifluoride lattice energies would decrease. Rather it appears to level off at *ca* 75 kJ mol^{-1}. Yet if $\Delta H_2^{\ominus}$ for Me_4NHF_2 were really 155 kJ mol^{-1} as reported,[6] and $\Delta H_1^{\ominus}$ is 163 kJ mol^{-1}, then $U(Me_4NF) - U(Me_4NHF_2)$ is only 8 kJ mol^{-1}. Perhaps the much larger radius of Me_4N^+ makes this likely but others have argued that, even for this cation, lattice expansion to accommodate the bifluoride ion must occur and that this will be significant.[15]

An alternative explanation would seem to be that this value of $\Delta H_2^{\ominus}$, determined experimentally, is incorrect. Good grounds for suspecting this to be the case lies with the Me_4NF itself. Despite many attempts, this salt has never been obtained anhydrous and recent work has shown that removal of water results in decomposition.[16] This being so, then whatever reaction the original workers[6] thought they were following it almost certainly was not $Me_4NF + HF \rightarrow Me_4NHF_2$. It was merely fortuitous that the value they reported for $\Delta H_2^{\ominus}$ of 155 kJ mol^{-1}, and the assumption made about $U(Me_4NF) - U(Me_4NHF_2)$ being zero was an example of two wrongs almost cancelling each other out.

REFERENCES

1. R. M. Bozorth, *J. Am. Chem. Soc.* 1923, **45**, 2128.
2. These are summarized in Table 1 of J. Emsley, R. J. Parker and R. E. Overill, *J. Chem. Soc., Faraday Trans. 2* 1983, **79**, 1347.
3. T. C. Waddington, *Trans. Faraday Soc.* 1958, **54**, 25.
4. H. P. Dixon, H. D. B. Jenkins and T. C. Waddington, *J. Chem. Phys.* 1972, **57**, 4388.
5. H. D. B. Jenkins and K. F. Pratt, *J. Chem. Soc., Faraday Trans. 2* 1977, **73**, 812.
6. S. A. Harrell and D. H. McDaniel, *J. Am. Chem. Soc.* 1964, **86**, 4497.
7. J. W. Larson and T. B. McMahon, *J. Am. Chem. Soc.* 1982, **104**, 5848.
8. D. D. Wagman, W. H. Evans, I. Halow, V. B. Parker, S. M. Bailey and R. H. Schumm, *Selected Values of Chemical Thermodynamic Properties.* Technical Note 270-3, Nat. Bur. Stand., Washington, D.C. (1971).
9. F. D. Rossini *et al.*, Nat. Bur. Stand. (U.S.) Circ. No. 500 (1952); Suppl. (1954). Data reproduced in Ref. 4 [$\Delta H_f^{\ominus}(MHF_2)(s)$] and in D. F. C. Morris, *Struct. Bonding (Berlin)* 1968, **4**, 63 [$\Delta H_f^{\ominus}(MF_2)(s)$].
10. *Comprehensive Inorganic Chemistry* (Edited by J. C. Bailar, H. J. Emeléus, R. Nyholm and A. F. Trotman-Dickenson), Vol. i, pp. 346 and 411. Pergamon Press, Oxford (1973).
11. D. A. Johnson, *Some Thermodynamic Aspects of Inorganic Chemistry*, 2nd edition. Cambridge University Press, Cambridge (1982).
12. R. D. Shannon and C. T. Previtt, *Acta Cryst. (B)* 1969, **25**, 925; 1970, **26**, 1046.
13. B. L. McGraw and J. A. Ibers, *J. Chem. Phys.* 1963, **39**, 2677.
14. T. C. Waddington, *Adv. Inorg. Chem. Radiochem.* 1959, **1**, 190.
15. K. M. Harmon and R. R. Lovelace, *J. Phys. Chem.* 1982, **86**, 900.
16. R. K. Sharma and J. L. Fry, *J. Org. Chem.* 1983, **48**, 2112.

Polyhedron Vol. 4, No. 3, pp. 491–496, 1985
Printed in Great Britain

0277-5387/85 $3.00 + .00
© 1985 Pergamon Press Ltd

DIMERIZATION OF COPPER(II) DECANOATE IN 1,4-DIOXANE–WATER MIXED SOLVENTS

YUKIO FUJII,* KAZUSHI JIMBO, HIROMICH YAMADA and MASATERU MIZUTA
Faculty of Engineering, Gifu University, 1-1 Yanagido, Gifu 501-11, Japan

(*Received* 13 *April* 1984; *accepted* 22 *May* 1984)

Abstract—Complex formation of copper(II) with decanoic acid (HA) has been studied by potentiometric measurement in 1,4-dioxane–water mixtures at a constant ionic concentration of 0.1 mol dm^{-3} (Na, H)ClO_4 and at 25°C. The experimental data can be interpreted with the formation of CuA^+, CuA_2 and Cu_2A_4. The dimerization constant formulated as:

$$2CuA_2 \overset{K_{dim}}{\rightleftharpoons} Cu_2A_4$$

was found to be log K_{dim} = 3.75, 4.02 and 4.26 for 0.3, 0.4 and 0.5 mole fractions of dioxane, respectively. Absorbances at 373 and 670 nm are interpreted with the aid of the formation constants determined by potentiometry. Solvent effect on the dimerization of the monomeric copper(II) decanoate is discussed on the basis of selective solvation of CuA_2 and Cu_2A_4 with water molecules.

The cupric alkanoates are well-known to be binuclear in the crystalline and in nonpolar organic solvents.[1] The binuclear (dimeric) structures also persist in solutions such as acetic acid,[2] chloroform[3] and 1,4-dioxane.[4]

Recently, Yamada and others[5,6] have reported on the solvent extraction of copper(II) with decanoic acid into some alkanols. According to their results, the extracted species of copper(II) were not only the dimeric decanoates, Cu_2A_4 and $Cu_2A_4(HA)_2$, but also the monomeric ones, CuA_2 and CuA_2HA. The dimerization constant defined by $K_{dim} = [Cu_2A_4]/[CuA_2]^2$ decreased with increasing water concentration in the organic phase.

More studies are necessary for a full understanding of the formation of both the monomeric and dimeric species in the solvents whose coordinating ability is greater than that of 1,4-dioxane or alkanols but less than that of water.

In the present work we chose binary mixtures of 1,4-dioxane and water. The formation and dimerization of copper(II) decanoates were investigated by potentiometry and spectrophotometry.

EXPERIMENTAL

Reagents

Sodium perchlorate. After the precipitation of heavy metal impurities as hydroxides, the sodium perchlorate was recrystallized from distilled water.

1,4-*Dioxane.* For the preparation of acetal- and peroxide-free 1,4-dioxane, anhydrous tin(II) chloride was added to 1,4-dioxane (R.G.). It was boiled under reflux for 8 h with 5% of its volume of 1 mol dm^{-3} hydrochloric acid. The distillate was stirred with pellets of sodium hydroxide and the aqueous phase was removed. The organic phase was stored over sodium and distilled only when needed.

Copper(II) perchlorate. Copper(II) perchlorate was prepared by dissolving copper metal (99.99%) in hot aqueous perchloric acid solution. The copper(II) perchlorate hydrates crystallized from the solution were dissolved in the mixture of 1,4-dioxane and water. The concentration of copper(II) was determined by complexiometry when necessary.

Sodium hydroxide solution. Carbonate-free sodium hydroxide solution was prepared by electrolysis of 1 mol dm^{-3} aqueous sodium perchlorate solution at a current density about 5 mA

* Author to whom correspondence should be addressed.

cm^{-2} with a couple of platinum electrodes and a salt bridge fitted with a frittered glass membrane to an edge. The alkaline solution was titrated with a standard solution of potassium hydrogen phthalate.

Decanoic acid. Decanoic acid (C.P.) was purified twice by distillation. The middle fraction distilling at 269–271°C was collected. The purity of the purified decanoic acid was 99.5±0.5%, as determined by titration with the standard alkaline solution.

Apparatus

The e.m.f. measurements of the cells were carried out using an Orion research microprocessor ionalyzer Model 901 with a reading accuracy of ±0.1 mV. Orion cupric ion electrode (No. 94-24) and glass electrode (No. 91-01) were used for measurements of cupric and hydrogen ion concentrations, respectively. Spectrophotometric measurements were performed on a Shimadzu double-beam spectrophotometer Model UV 210A using fused silica cells (pass length 10 mm).

Measurements

All titrations were performed at 25.0±0.1°C in a bath which was placed in a room thermostatted at 25 ±1°C. The ionic concentration in the 1,4-dioxane–water mixtures was kept constant at 0.1 mol dm^{-3} (Na, H)ClO_4. The mixtures which contain a definite amount of copper(II) perchlorate and/or decanoic acid were titrated with the sodium hydroxide solution.

We have chosen the Ag–AgCl reference electrode of the Wilhelm type[7] for studies in the 1,4-dioxane–water mixtures. The chemical cell used is depicted by the following scheme:

Ag–AgCl|0.1 mol dm^{-3} NaCl D–W soln (satd AgCl)||0.1 mol dm^{-3} $NaClO_4$ D–W soln|
test soln (0.1 mol dm^{-3} (Na, H)ClO_4 D–W soln)|cupric ion electrode or glass electrode

where D–W denotes the mixture of 1,4-dioxane and water. The e.m.f. of the cells in mV unit gives rise to the following Nernstian responses:

$$E_H = E_H^{\circ\prime} + 59.1 \log [H^+]$$
$$([H^+] \leqslant 10^{-2.5} \text{ mol dm}^{-3})$$

and

$$E_{Cu} = E_{Cu}^{\circ\prime} + 29.4 \log [Cu^{2+}]$$
$$([Cu^{2+}]: 10^{-2.5}\text{–}10^{-5.5} \text{ mol dm}^{-3}),$$

where E_H and E_{Cu} refer to the e.m.f. of the respective electrodes against the Ag–AgCl electrode. The conditional standard potentials, $E_H^{\circ\prime}$ and $E_{Cu}^{\circ\prime}$, were kept constant throughout a series of titrations in a given mixed solvent. The values were $E_H^{\circ\prime} = 449.4$ mV and $E_{Cu}^{\circ\prime} = 362.0$ mV in the mixture of 0.5 mole fraction dioxane–water.

All potentiometric experiments were carried out under an atmosphere of nitrogen gas. A calibrated micropipette equipped with a micrometer (0–0.2 cm^3, 2.5×10^{-4} cm^3/div.) was used for the titration with the alkaline solution. By the titrations, the uncertainty of the total ionic concentration did not exceed 2% as compared with that of original medium, i.e. 0.1 mol dm^{-3}.

RESULTS AND DISCUSSION

Determination of acid dissociation constant of decanoic acid

The acid dissociation equilibrium for decanoic acid is described as:

$$HA \overset{K_a}{\rightleftharpoons} H^+ + A^-,$$
$$K_a = [H^+][A^-]/[HA], \quad (1)$$

where HA and A^- denote decanoic acid and its anion, respectively. The constant K_a was evaluated by potentiometric titration of the acid with standard alkaline solution. The concentration of unionized carboxylic acid in the mixed solvent [HA] is given by:

$$[HA] = C_{HA} - C_{OH}, \quad (2)$$

where C_{HA} and C_{OH} denote the total concentration of the acid and alkali added for the titration, respectively. Assuming that the acid anion does not associate with HA, the concentration of A^- can be equal to C_{OH}. Then eqns (1) and (2) lead to:

$$\log [H^+] = \log K_a - \log C_{OH}/(C_{HA} - C_{OH}). \quad (3)$$

Equation (3) shows that the plot of log $[H^+]$ vs log $C_{OH}/(C_{HA} - C_{OH})$ will give a linear relation with a slope of −1. The plot is shown in Fig. 1. The intercept of the plot (at abscissa = 0) gives the value of log K_a. The numerical pK_a values of the acid in 1,4-dioxane–water mixtures are listed in Table 1.

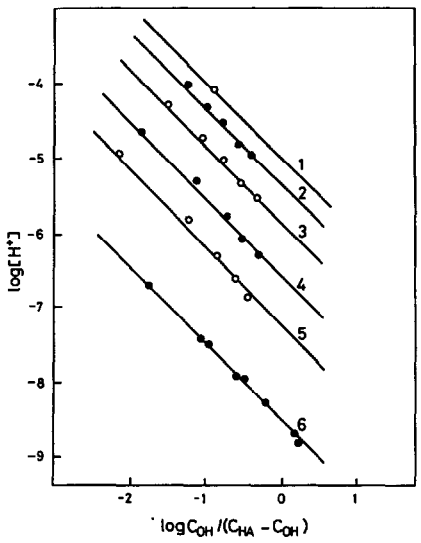


Fig. 1. $\log [H^+]$ against $\log C_{OH}/(C_{HA}-C_{OH})$ for determination of the acid dissociation constant of decanoic acid. The total ionic concentration is 0.1 mol dm^{-3} (Na, H)(ClO_4, A). The numbers refer to solvents listed in Table 1. The slope of the straight line is -1.

The value of K_a decreases with increasing the content of dioxane. This shows that dioxane is a weaker base with regard to decanoic acid than water. It may also be interpreted in terms of dielectric constant of the mixed solvent and hydration of the acid in the mixed solvent.[8,9]

Evaluation of the composition and the stability constant of copper(II) *decanoate*

The chemical species of copper(II) decanoate formed in the mixed solvents being denoted as $CuA_a^{(2-a)+}$ and $Cu_2A_4^{(4-b)+}$, the formation equilibria are written as:

$$Cu^{2+} + aA^- \overset{\beta_{1a}}{\rightleftharpoons} CuA_a^{(2-a)+},$$
$$\beta_{1a} = [CuA_a^{(2-a)+}]/[Cu^{2+}][A^-]^a, \quad (4)$$

$$2Cu^{2+} + bA^- \overset{\beta_{2b}}{\rightleftharpoons} Cu_2A_b^{(4-b)+},$$
$$\beta_{2b} = [Cu_2A_b^{(4-b)+}]/[Cu^{2+}]^2[A^-]^b. \quad (5)$$

Assuming that the perchlorate ion and the acid HA do not associate with any species, the material balance of copper(II) can be written as:

$$C_{Cu} = [Cu^{2+}] + \Sigma[CuA_a^{(2-a)+}] + 2\Sigma[Cu_2A_b^{(4-b)+}]. \quad (6)$$

Substituting eqns (1), (4) and (5) into eqn (6), we obtain the relationship:

$$(C_{Cu} - [Cu^{2+}])/[Cu^{2+}] = \Sigma\beta_{1a}[A^-]^a + 2\Sigma\beta_{2b}[A^-]^b[Cu^{2+}]. \quad (7)$$

The plot of the left-hand side of eqn (7) against $[Cu^{2+}]$ should be linear with an intercept $I = \Sigma\beta_{1a}[A^-]^a$ and a slope $S = 2\Sigma\beta_{2b}[A^-]^b$. Figure 2 shows the relation of $\log [Cu^{2+}]$ to $\log [A^-]$ in 0.5 mole fraction 1,4-dioxane–water mixture (83 w%

Table 1. Acid dissociation constant of decanoic acid in 1,4-dioxane–water mixed solvent

No.	solvent[a] mf	solvent[a] w%	dielectric constant[b] (20°C)	pK_a[c]
1	0.0	0	80.4	4.97
2	0.1	35	48.3	5.30
3	0.2	55	30.7	5.82
4	0.3	68	19.5	6.54
5	0.4	76	14.0	7.25
6	0.5	83	9.5	8.48

[a] Mole fraction (mf) and weight percent (w%) of 1,4-dioxane.

[b] G. Åkerlöf, *J. Am. Chem. Soc.* 1932, **54**, 4125.

[c] pK_a is given in molarity.

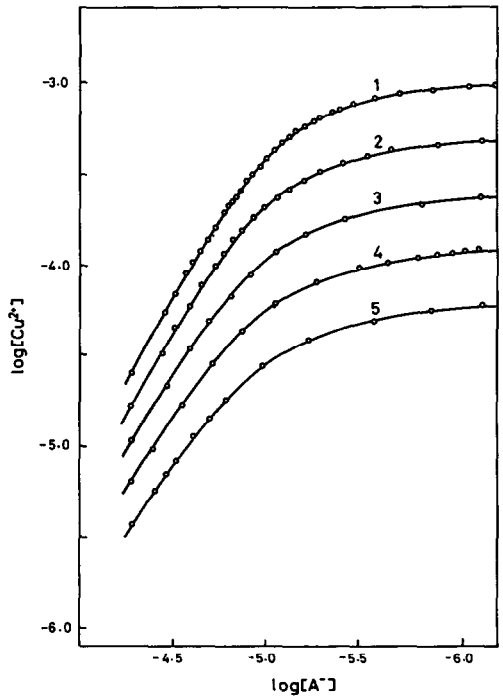


Fig. 2. $\log [Cu^{2+}]$ as a function of $\log [A^-]$. Solvent: 0.5 mole fraction 1,4-dioxane–water mixture. C_{HA} (mol dm^{-3}): 0.050. C_{Cu} (mol dm^{-3}): No. 1, 1.00×10^{-3}; No. 2, 500×10^{-4}; No. 3, 2.50×10^{-4}; No. 4, 1.25×10^{-4}; No. 5, 6.25×10^{-5}. The solid curves are the best fit ones calculated with the equilibrium constants in Table 2.

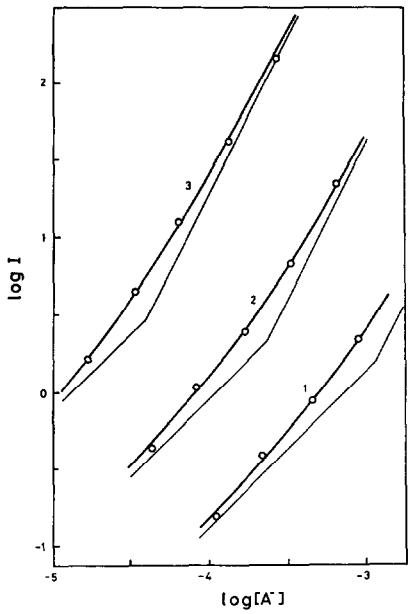


Fig. 3. Relationship between log I and log [A^-]. Solvents (mole fraction of dioxane): No. 1, 0.3; No. 2, 0.4; No. 3, 0.5. The solid curves are normalized ones, i.e. $Y = \log(x + px^2)$ vs $X = \log x$. The straight lines are the asymptotes of the normalized curves.

dioxane). The data was calculated according to eqn (7) and the values of log I and log S were plotted against the value of log [A^-]. In Fig. 3 the plot of log I against log [A^-] is given; the slope of the plot is close to 2 and tends to decrease to unity with decreasing [A^-], i.e. $a = 1$ and 2. The monomeric copper(II) species are therefore CuA^+ and CuA_2, as well as Cu^{2+}.

Figure 4 shows the plot of log S against log [A^-]. The plot lies along a straight line with a slope of 4, i.e.

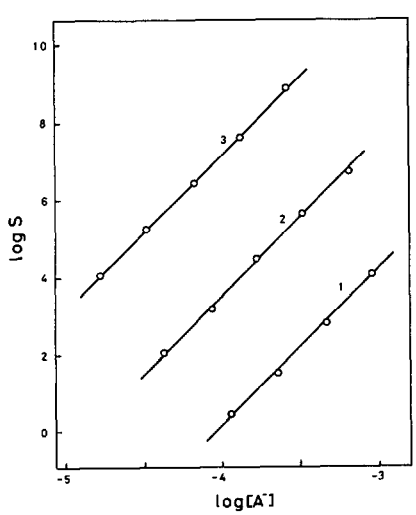


Fig. 4. Relationship between log S and log [A^-]. The numbers correspond to those in Fig. 3. The slope of the straight lines is 4.0.

Table 2. Formation constant of copper(II) decanoates

solvent (dioxane, mf)	log β_{11}	log β_{12}	log β_{24}
0.3	3.11	6.04	15.83
0.4	3.95	7.55	19.12
0.5	4.86	9.28	22.82

$b = 4$, when Cu_2A_4 is the sole dimeric species of copper(II) decanoate. The same species was also found in acetic acid by Cheng and Howald,[2] and Sawada *et al.*[10]

The values of log I and log S were independent of the total concentration of decanoic acid ranging from 0.025 to 0.200 mol dm^{-3}. As can be seen from eqn (7), this evidence strongly suggests that the formation of copper(II) decanoate complexes solvated with the free acid HA can be negligible in these mixed solvents.

The following equilibria are relevant to the formation of copper(II) decanoates:

$$Cu^{2+} + A^- \overset{\beta_{11}}{\rightleftharpoons} CuA^+,$$

$$Cu^{2+} + 2A^- \overset{\beta_{12}}{\rightleftharpoons} CuA_2,$$

$$2Cu^{2+} + 4A^- \overset{\beta_{24}}{\rightleftharpoons} Cu_2A_4.$$

The formation constants evaluated by the curve fitting method for these equilibria are collected in Table 2. The values in Table 2 show that the higher the water concentration in the solvent, the lower the formation constants.

Absorption spectra in the UV and visible regions

The UV and visible spectra of a large number of copper(II) alkanoates and their derivatives have been measured in organic solvents and on single crystals.[1,11] According to the results, these complexes have three bands at about 300, 375 (shoulder) and 700 nm. At about 375 nm, the band which is characteristic of the dimeric copper(II) alkanoates appears both in solution and in crystal. Originally, Tuchida and Yamada[12,13] suggested that the band was a diagnostic property of copper–copper linkage.

Now suppose that the dimeric copper(II) decanoate is responsible for the band at 373, the absorbance (abbreviated as A) can be written as:

$$A_{373} = \varepsilon_{24}[Cu_2A_4] \qquad (8)$$

where ε_{24} denotes the molar extinction coefficient of the dimeric species at a maximum absorbance (373 nm). From eqns (1), (5) and (8) the following

expression is derived:

$$\log A_{373} = \log \beta_{24}\varepsilon_{24}K_a^4 + 4 \log [HA] + 2(\log [Cu^{2+}] - 2 \log [H^+]). \quad (9)$$

As seen from Fig. 5, a plot of $\log A_{373}$ against $\log [Cu^{2+}] - 2 \log [H^+]$ leads to a linear relation with a slope of 2 at a constant [HA]. This fact confirms that the sole species absorbing at this region is the dimeric copper decanoate denoted as Cu_2A_4.

The band at about 700 nm is to be assigned to the normal metal–ligand interaction. The absorbing species and its molar extinction coefficient were evaluated as follows. With the aid of potentiometric results described above, the apparent molar extinction coefficient at 670 nm can be expressed as:

$$\bar{\varepsilon} = \frac{A_{670}}{C_{Cu} - [Cu^{2+}]} = \frac{\varepsilon_{11}[CuA^+] + \varepsilon_{12}[CuA_2] + \varepsilon_{24}[Cu_2A_4]}{[CuA^+] + [CuA_2] + 2[Cu_2A_4]} = \frac{\varepsilon_{11}\beta_{11} + \varepsilon_{12}\beta_{12}[A^-] + \varepsilon_{24}\beta_{24}[A^-]^3[Cu^{2+}]}{\beta_{11} + \beta_{12}[A^-] + 2\beta_{24}[A^-]^3[Cu^{2+}]}, \quad (10)$$

where ε_{11}, ε_{12} and ε_{24} are molar extinction coefficients of the species CuA^+, CuA_2 and Cu_2A_4, respectively, and A_{670} is the absorbance at 670 nm.

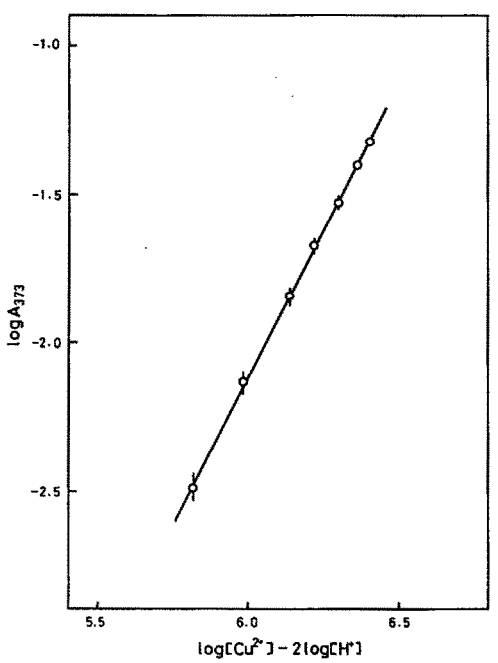


Fig. 5. Correlation between $\log A_{373}$ and $\log [Cu^{2+}] - 2 \log [H^+]$. Solvent: 0.5 mole fraction 1,4-dioxane–water mixture. Total ionic concentration: 0.1 mol dm^{-3} (Na, H)ClO_4. C_{Cu} (mol dm^{-3}), 1.00×10^{-3}; C_{HA} (mol dm^{-3}), 0.050. The solid line is the straight line with a slope of 2.0.

Table 3. Absorbing species and their molar extinction coefficients

acid (HA)	species	solvent	λ_{max}	ε	ref.
acetic	Cu_2A_4	1,4-dioxane	375 670	132 460	a
acetic	$Cu_2A_4(HA)_2$	acetic acid	375 670	106 410	b
acetic	Cu_2A_4	1,4-dioxane	373 662	102 440	c
propionic	$Cu_2A_4(HA)_2$	chloroform	375 670	120 410	d
octanoic	$Cu_2A_4(HA)_2$	heptane	375 680	120 400	e
decanoic	Cu_2A_4 + $Cu_2A_4(HA)_2$	1-octanol	368 690	132 410	f
decanoic	Cu_2A_4	1,4-dioxane-water	373 670	130±10* 403±15*	g

[a] Reference 11.
[b] Reference 10.
[c] K. Hasegawa, N. Nakasuka and M. Tanaka, *Bull. Chem. Soc. Jpn* 1981, **54**, 1731.
[d] D. P. Graddon, *Nature* 1960, **186**, 715.
[e] M. Jaycock, A. D. Jones and C. Robinson, *J. Inorg. Nucl. Chem.* 1974, **36**, 887.
[f] Reference 5.
[g] This work.
* Calculated from eqn (10); $\varepsilon_{11} < 10$, $\varepsilon_{12} = 195 \pm 10$.

Successive approximations are repeated until the error square sum U, defined as $U = (\bar{\varepsilon} - \bar{\varepsilon}_{cal})^2$, reaches a minimum and the final set of values ε_{11}, ε_{12} and ε_{24} is determined (Table 3). As the dimerization reaction proceeds, the wavelengths of maximal absorption were seen to be shifted from *ca* 740 to 670 nm. This phenomenon can be interpreted by eqn (10). A similar phenomenon was also observed in other systems, such as copper(II) decanoate in 1-octanol[5] and copper(II) acetate in acetic acid.[2,10] Table 3 shows that all these solutions absorb light at about 375 nm (ε = 100–130/two atoms of copper) and 670 nm (ε = 400–460/two atoms of copper).

Solvent effect on the dimerization of copper(II) decanoate

There have been some studies in the monomer–dimer equilibrium of copper(II) alkanoates in donating solvents.[2,5,6,10,14–16] The apparent dimerization constant K_{dim} is given by:

$$2CuA_2 \overset{K_{dim}}{\rightleftharpoons} Cu_2A_4, \quad K_{dim} = [Cu_2A_4]/[CuA_2]^2. \quad (11)$$

The value of K_{dim} may be evaluated by the equation:

$$K_{dim} = \beta_{24}/\beta_{12}^2. \quad (12)$$

Table 4. Dimerization constant of the monomeric copper(II) decanoate in 1,4-dioxane–water mixed solvents

solvent (dioxane, mf)	log[H_2O]	log[dioxane]	log K_{dim}
0.3	1.25	0.88	3.75
0.4	1.11	0.94	4.02
0.5	0.97	0.97	4.26

The values of K_{dim} thus obtained are summarized in Table 4. It is obvious from the table that the dimerization constant decreases with increasing water concentration in the mixed solvent.

The solvent effect on the dimerization equilibrium is considered by:

$$2CuA_2S_2 \overset{K^\circ_{dim}}{\rightleftharpoons} Cu_2A_4S_2 + 2S, \quad (S = \text{solvent molecule}) \qquad (13)$$

$$K^\circ_{dim} = [Cu_2A_4S_2][S]^2/[CuA_2S_2]^2.$$

Then the constant K°_{dim} is related to the apparent constant K_{dim}:

$$K_{dim} = K^\circ_{dim}[S]^{-2}. \qquad (14)$$

With the assumption that the term $[S]^2$ is equal to $[H_2O]^x x[\text{dioxane}]^y$, where $x+y=2$, the following relation is derived:[17]

$$\log K_{dim} = \log K^\circ_{dim} - x \log [H_2O] - y \log [\text{dioxane}]. \qquad (15)$$

Our data fitted with $x = 1.8$, $y \simeq 0$ and $\log K^\circ_{dim} = 6.0$. This finding which was obtained from this rough estimation suggests that the solvent molecules liberated are not dioxane but water at least in the range of the solvent studied. Then we conclude that the reaction is expressed as:

$$2CuA_2(H_2O)_2 \rightleftharpoons Cu_2A_4(H_2O)_2 + 2H_2O.$$

The specific hydration of copper(II) decanoates is attributable to the stronger basicity of water than that of 1,4-dioxane; the latter has lower donor number (DN = 14.8) than that of the former (DN = 18.0).[18]

According to the solvent extraction studies, copper(II) alkanoates have the molecular formula of $Cu_2A_4(HA)_2$ in non-polar organic solvents such as hexane, benzene and carbon tetrachloride, and have those of CuA_2, CuA_2HA, Cu_2A_4 and $Cu_2A_4(HA)_2$ in donating solvents: alkanols and ketones. In the present system, the following species solvated with the free acid were not found: CuA_2HA and $Cu_2A_4(HA)_2$. This shows that the reaction of $Cu_2A_4(HA)_2$ with water results in the species CuA_2 and/or Cu_2A_4.

Acknowledgement—We are grateful to Professor Motoharu Tanaka of Nagoya University for his valuable discussion.

REFERENCES

1. M. Kato, H. E. Jonassen and J. C. Fanning, *Chem. Rev.* 1964, **64**, 99 (and earlier references cited therein).
2. A. T. A. Cheng and R. A. Howald, *Inorg. Chem.* 1968, **7**, 2100.
3. D. P. Graddon, *J. Inorg. Nucl. Chem.* 1961, **17**, 222.
4. R. L. Martin and A. Whitley, *J. Chem. Soc.* 1958, 1934.
5. H. Yamada, S. Suzuki and M. Tanaka, *J. Inorg. Nucl. Chem.* 1981, **43**, 1873.
6. H. Yamada, R. Kitazaki and I. Kakimi, *Bull. Chem. Soc. Jpn* 1983, **56**, 3302.
7. W. Forsling, S. Hietanen and L. G. Sillen, *Acta Chem. Scand.* 1952, **6**, 901.
8. R. P. Bell and R. P. Robinson, *Trans. Faraday Soc.* 1961, **57**, 965.
9. M. Yasuda, *Bull. Chem. Soc. Jpn* 1959, **32**, 429.
10. K. Sawada, H. Ohtaki and M. Tanaka, *J. Inorg. Nucl. Chem.* 1972, **34**, 625.
11. L. Dubicki and R. L. Martin, *Inorg. Chem.* 1966, **5**, 2203.
12. R. Tuchida and S. Yamada, *Nature* 1955, **176**, 1171.
13. S. Yamada, H. Nakamura and R. Tuchida, *Bull. Chem. Soc. Jpn* 1957, **30**, 953.
14. P. Gerding, *Acta Chem. Scand.* 1960, **20**, 2624.
15. H. Grasdalen and I. Svare, *Acta Chem. Scand.* 1971, **25**, 1089.
16. R. D. Cannon, *Inorg. Chem.* 1981, **20**, 2341.
17. D. J. Glover, *J. Am. Chem. Soc.* 1965, **87**, 5275, 5279.
18. V. Gutmann, *Coordination Chemistry in Non-Aqueous Solvents*. Springer, Wien (1968).

Polyhedron Vol. 4, No. 3, pp. 497–503, 1985
Printed in Great Britain

0277–5387/85 $3.00 + .00
© 1985 Pergamon Press Ltd

3,6-BIS(2′-PYRIDYL)PYRIDAZINE DINUCLEAR COMPLEXES: PALLADIUM(II), PLATINUM(II) AND FIRST ROW TRANSITION METAL(II) MIXED COMPLEXES

MAURO GHEDINI* and FRANCESCO NEVE
Dipartimento di Chimica, Università della Calabria, I 87030 Arcavacata (CS), Italy

FRANCA MORAZZONI
Dipartimento di Chimica Inorganica e Metallorganica, Università di Milano, Via Venezian, 21—I 20133 Milano, Italy

and

CESARE OLIVA
Dipartimento di Chimica Fisica ed Elettrochimica, Università di Milano, Via Golgi, 19—I 20133 Milano, Italy

(*Received* 4 *April* 1984; *accepted* 22 *May* 1984)

Abstract—New Pd(II) and Pt(II) 3,6-bis(2′-pyridyl)pyridazine (dppn) mononuclear complexes of the type $M(dppn)Cl_2$ were prepared and characterized. From $M(dppn)Cl_2$, the bimetallic homonuclear complexes $M(dppn)MCl_4$ were prepared by reaction with $Pd(PhCN)_2Cl_2$ or K_2PtCl_4. Bimetallic heteronuclear species of the type $M(dppn)M'Cl_4$ were prepared reacting the mononuclear complexes with the stoichiometric amount of $M'Cl_2$ (M′ = Cu, Co, Ni). All the described reaction give product in high yield. The isolated compounds, almost completely insoluble in most organic solvents, were characterized by elemental analysis, IR, ESR, reflectance spectra, and magnetic moment measurements. On the basis of these data the geometries around the metals are discussed.

Coordination compounds containing two different metal centers are receiving a great deal of interest both as homogeneous catalysts capable of carrying out multistep reactions and as models for surface catalysis.[1–4]

Approaching the synthesis of binuclear complexes by means of ligands capable of binding metals in a nearby and fixed position, the tetranitrogenated compound 3,6-bis(2′-pyridyl)pyridazine (dppn) seems to be a good candidate. Nevertheless, only few examples of binuclear complexes of this ligand with first row transition metals are reported in the literature[5–7] and even less is known on its bimetallic derivatives with second and third row transition metals.[8] The present investigation aims to acknowledge the reactivity of dppn toward Pd(II) and Pt(II), and its ability in mixed complex formation.

* Author to whom all correspondence should be addressed.

RESULTS AND DISCUSSION

In order to obtain bimetallic compounds from dppn, two step synthesis was carried out: preparation of a mononuclear dppn species, followed by reaction with a second metal ion.

Mononuclear complexes

Dppn (1) and $Pd(PhCN)_2Cl_2$, or K_2PtCl_4 (1 : 1 molar ratio), when dissolved in appropriate solvents give in good yields yellow and brown, respectively, diamagnetic solid products whose elemental analyses are in agreement with mononuclear species of formula $M(dppn)Cl_2$ (2: M = Pd; 3 : M = Pt).

IR spectra, in the region characteristic of pyridazine[9] and pyridine[10] ring vibrations (Table 1), show that dppn behaves as a monochelating ligand. The two absorptions in the M—Cl stretching region (Table 1) are consistent with a MCl_2 frame in a

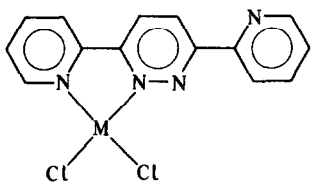
Table 1. Selected IR absorption bands* of mononuclear complexes in the regions: (a) 1610–1540, (b) 1050–970 and (c) 400–200 cm^{-1}

No.	Compound	a	b	c
1	dppn	1580(m); 1563(m)	991(m)	
2	$Pd(dppn)Cl_2$	1608(m); 1587(m) 1565(m); 1548(m)	1047(w); 1037(m) 991(w)	347(m) 342(m)
3	$Pt(dppn)Cl_2 \cdot 2H_2O$	1606(m); 1587(m) 1568(m); 1548(m)	1035(w) 987(w)	339(2) 312sh(m)
4	$Pd(dppn)Br_2$	1601(m); 1585(m) 1568(m); 1544(m)	1041(w); 1037(m) 989(w)	229(m)
5	$Pd(dppn)I_2$	1600(m); 1587(m) 1568(m); 1545(m)	1037(w); 1024(m) 988(w)	

* As KBr pellets or Nujol mulls.

cis arrangement, in agreement with what observed by Durig[11] and Walton[12] in $M(bipy)Cl_2$ (M = Pd and Pt).

On the basis of these results and in analogy with the molecular structure of $Mn(dppn)_2(NO_3)_2$[13] and $[Cu(dppn)_2Cl]Cl \cdot 5H_2O$,[14] the following coordination scheme can be suggested for complexes **2** and **3** in the solid state (Scheme 1):



Scheme 1.

Compound **2** metathesizes with LiX giving the corresponding products **4** and **5** (Table 1) and, when suspended in dichloromethane, quickly reacts with triphenylphosphine giving $Pd(Ph_3P)_2Cl_2$ and dppn in quantitative yields.

Bimetallic homonuclear complexes

When complexes **2** and **3** are reacted in a 1:1 molar ratio with $Pd(PhCN)_2Cl_2$ or K_2PtCl_4 orange, respectively brown, diamagnetic products analyzing for the dinuclear compounds $Pd(dppn)PdCl_4$, **6**, and $Pt(dppn)PtCl_4$, **7**, are obtained.

The reduced number of bands observed above 1000 cm^{-1} in the IR spectra of **6** and **7**, with respect to the parent compounds **2** and **3**, accounts for the change of coordinated nitrogens from two to four (Table 2).

Compound **6** reacts with triphenylphosphine (1:4 ratio) giving two equivalents of $Pd(Ph_3P)_2Cl_2$ and dppn in quantitative yields. This result supports the hypothesis of a structure with two metals coordinated through the four nitrogen atoms, and a *cis* configuration of the dppn ligand. Since a square

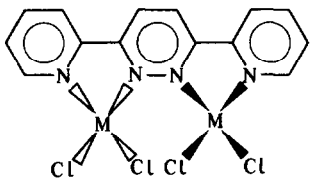
Table 2. Selected IR absorption bands* of bimetallic homonuclear complexes in the regions: (a) 1610–1540, (b) 1050–970 and (c) 400–200 cm^{-1}

No	Compound	a	b	c
6	$Pd(dppn)PdCl_4$	1600(m)	1046(w); 1037(m)	371(s) 345(s); 320(s)
7	$Pt(dppn)PtCl_4 \cdot 0.1dppn$	1601(m)	1045(w); 1040(m)	364sh(m) 340(s); 310sh(m) 291(m)
8	$Pd(dppn)PdCl_2Br_2$	1598(m)	1038(w); 1030(m)	360(m) 341(s); 310(m) 229(m)
9	$Pd(dppn)PdCl_2I_2$	1592(m)	1028(m); 1011(w)	360(m) 342(s); 324sh(s)

* As KBr pellets or Nujol mulls.

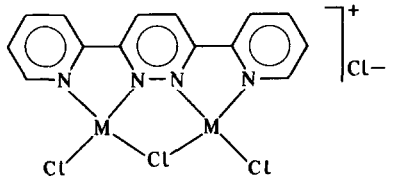
planar environment would be expected for the two palladium(II) or platinum(II) centers, whilst an overall planar configuration should be improbable, owing to the steric hindrance between the two internal chlorine atoms, different geometries will be considered. Recently Newkome *et al.*[15] reported for palladium(II) complexes, with either 6,6'-disubstituted bipyridine or 6-monosubstituted bipyridine, a drastic deviation from a wholly planar configuration.

By analogy, the MCl_2 moieties in **6** and **7** could be shifted above and below the dppn plane (Scheme 2):



Scheme 2.

An alternative way of removing the steric hindrance between the chlorine atoms might be the formation of a chlorine bridged binuclear derivative, as formulated by Denti *et al.*[16] for $CuCl_2(\mu\text{-dppn})(\mu\text{-Cl})CuCl(H_2O)$, with an uncoordinated chloride ion (Scheme 3):



Scheme 3.

The assignment of the metal–halide vibrations in compound **6** (Table 2) is in agreement with a terminal Pd—Cl stretching frequency (371 cm^{-1}) and, tentatively, with bridged Pd—Cl—Pd (345 and 320 cm^{-1}).[17] The IR spectra of compounds deriving from the reaction of $Pd(dppn)X_2$ with $Pd(PhCN)_2Cl_2$ show four bands, 360, 341, 310 and 229 cm^{-1} for **8** (X = Br), while three bands are observed for **9** (X = I), 360, 342 and 324 cm^{-1}.

On the basis of the present data the assignment of the actual structure to compounds **6–9** is uncertain, although the presence of bands in the 340–310 cm^{-1} region, tentatively attributed to Pd—Cl—Pd stretching frequencies, seems to suggest a structure as depicted in Scheme 3.

Bimetallic heteronuclear complexes

Synthesis and characterization. The mononuclear compound $Pt(dppn)Cl_2$ (**3**) and a stoichiometric amount of $Pd(PhCN)_2Cl_2$ react to give the brown diamagnetic product **10**, whose analytical data are in agreement with platinum, palladium and dppn in 1:1:1 ratios. The IR spectrum in the regions characteristic of the polydentate ligand (Table 3) is consistent with a twice chelating dppn.

Although elemental analyses do not exclude the possibility that product **10** is a 1:1 mixture of the homonuclear complexes **6** and **7**, its far IR spectrum shows four strong absorptions, none of these overlapping with bands of complexes **6** or **7** (Tables 2 and 3): complex **10** can then be regarded as

Table 3. Selected IR absorption bands* of bimetallic heteronuclear complexes in the regions: (a) 1610–1540, (b) 1050–970 and (c) 400–200 cm^{-1}

No.	Compound	a	b	c
10	$Pd(dppn)PtCl_4$	1601(m)	1046(w); 1035(m)	369(s); 348(s) 338sh(s); 280(s)
11	$Pd(dppn)CuCl_4$	1600(m)	1040(w); 1030(m)	364(s); 350sh(m) 313(s); 285(s); 268(s)
12	$Pt(dppn)CuCl_4$	1598(m)	1038(m); 1022(m) 1010(w)	362(s); 344sh(s) 304(s); 270(s); 210(s)
13	$Pd(dppn)CoCl_4$	1608(m)	1041(m); 1028(m) 1017(w)	366(s); 349sh(m) 295(br); 276sh(br) 243(m); 232(m); 206(m)
14	$Pt(dppn)CoCl_4 \cdot 0.5CH_3CN$	1593(m)	1042(m); 1018(m) 1011(w)	359(s); 346sh(s); 298(s) 278sh(s); 237(m)
15	$Pd(dppn)NiCl_4 \cdot 2H_2O$	1603(m)	1042(m); 1028(m) 1019(w)	361(s); 350sh(s); 308(m) 287(br); 239(m); 209(m)
16	$Pt(dppn)NiCl_4 \cdot H_2O$	1598(m)	1042(m); 1025(w) 1015(m)	353(s); 348sh(s) 310sh(m); 294(s)

* As KBr pellets or Nujol mulls.

Table 4. ESR parameters and magnetic susceptibility data

No.	Compound	$g_{\parallel}$	$g_{\perp}$	$K_{\parallel}$	$K_{\perp}$	μ_{RT} (B.M.)
11	$Pd(dppn)CuCl_4$	2.263	2.120	0.70	0.70	1.83
12	$Pt(dppn)CuCl_4$	2.332	2.130	0.76	0.68	1.74
13	$Pd(dppn)CoCl_4$	*	*			5.04
14	$Pt(dppn)CoCl_4 \cdot 0.5CH_3CN$	*	*			3.7†
15	$Pd(dppn)NiCl_4 \cdot 2H_2O$	*	*			3.45
16	$Pt(dppn)NiCl_4 \cdot H_2O$	*	*			2.53†
17	$[IrCl(PPh_3)_2(\mu\text{-dppn})(\mu\text{-NO})CuCl][PF_6]_2$	2.296	2.053	0.56	0.69	1.96

* Description in the text.

† Values lower than spin only value could be due to the presence of a variable quantity of a clatrated molecule in the paramagnetic unities.

a bimetallic heteronuclear species having a probable coordination scheme like 3.

Complexes **2** and **3** react with a number of metal(II) chlorides (1:1 ratio) in the appropriate solvents to give compound **11–16** for which the analytical data (see Experimental) are in agreement with the proposed stoichiometry or their solvated forms. IR absorptions in the 1610–1540, 1050–970 and 400–200 cm^{-1} regions (Table 3) are consistent with bimetallic heteronuclear complexes.

Electronic and magnetic properties. Bimetallic heteronuclear complexes, beside to play an important role as models of heterogeneous metal catalysts, may be an elucidative test of the structure of the reported compounds. Actually some of coordination centers like Cu(II), Co(II), Ni(II) are spectroscopic and magnetic active centres and can be useful structural probes when they substitute Pt(II) and Pd(II) in bimetallic compounds.

Pd/Cu *and* Pt/Cu *compounds* (**11**, **12**) contain Cu(II) as paramagnetic center (magnetic moment values in Table 4). The values of g components $g_{\parallel} > g_{\perp} > 2$ (Table 4) account for the well known d^9 configuration with the unpaired electron mainly in the $d_{x^2-y^2}$ orbital. Axial symmetry of the g tensor is in agreement with this ground state configuration. No hyperfine coupling with Cu(II) nucleus was observed.

By using the Figgis equations[18]

$$g_{\parallel} = 2.00 + \frac{8k_{\parallel}^2\lambda_0}{\Delta_1} \qquad \Delta_1 = E_{x^2-y^2} - E_{xy}$$

$$g_{\perp} = 2.00 + \frac{2k_{\perp}\lambda_0}{\Delta_2} \qquad \Delta_2 = E_{x^2-y^2} - E_{xz,yz}$$

$$\lambda_0 = 828 \text{ cm}^{-1}$$

and assuming for Δ_1 and Δ_2 values the energies of the *d–d* transitions observed in the diffuse reflectance spectra (Table 5), the best fit was obtained for the higher energy absorption corresponding to the Δ_1 energy difference. The results of such a calculation are reported in Table 4.

The ESR spectra of **11** and **12** account either for a tetragonal elongated octahedral geometry or for a compressed tetrahedral geometry, both consistent with the tetracoordinated paramagnetic centres present in these complexes. Actually the energy of the observed *d–d* transition is more consistent with the compressed tetrahedral geometry.

Table 5. Electronic diffuse reflectance data*

No.	Compound	ν_1	ν_2	ν_1'	ν_2'	ν_3'	ν_1''	ν_2''	ν_3''
11	$Pd(dppn)CuCl_4$	7143	12,200						
12	$Pt(dppn)CuCl_4$	5882	11,500						
13	$Pd(dppn)CoCl_4$						7407	11,100	16,660
14	$Pt(dppn)CoCl_4 \cdot 0.5CH_3CN$						7400	11,100	16,660
15	$Pd(dppn)NiCl_4 \cdot 2H_2O$			8690	14,280	21,740			
16	$Pt(dppn)NiCl_4 \cdot H_2O$			8330	12,500				
17	$[IrCl(PPh_3)_2(\mu\text{-dppn})(\mu\text{-NO})CuCl][PF_6]_2$	14,800	7143						

* Symbols are in agreement with O_h symmetry: ν_1' ($^3A_{2g} \rightarrow {}^3T_{2g}$), ν_2' [$^3A_{2g} \rightarrow {}^3T_{1g}(F)$], ν_3' [$^3A_{2g} \rightarrow {}^3T_{1g}(P)$], ν_1'' ($^4T_{1g} \rightarrow {}^4T_{2g}$), ν_2'' ($^4T_{1g} \rightarrow {}^4A_{2g}$), ν_3'' [$^4T_{1g} \rightarrow {}^4T_{1g}(P)$].

In order to obtain additional data to support one of the two possible symmetries, we have investigated the heterobimetallic compound $[Ir(PPh_3)_2Cl(\mu\text{-dppn})(\mu\text{-NO})CuCl][PF_6]_2$,[17] which is related to **11** and **12** for what concerns dppn coordination and whose crystal structure shows an overall planar coordination around the copper atom.[8] The best fit between the g values of **17** and the experimental energies of the observed d–d transitions (Tables 4 and 5) was obtained for the higher energy absorption corresponding to Δ_2. Moreover the parallel component of the hyperfine coupling with the Cu nucleus was observed ($A_{\parallel} = 150\ cm^{-1}$ 10^4).

The higher value of Δ_2 exhibited by compound **17** with respect to **11** and **12** is probably attributable to an enhanced back-donation from the $d_{xz,yz}$ Cu(II) orbitals toward dppn and NO π^* orbitals, due to the overall planar geometry of the $[IrCl(\mu\text{-dppn})(\mu\text{-NO})CuCl]^{2+}$ moiety. Where the bridged NO group is not present (**11** and **12**), the energy trend which fits the magnetic parameters changes from $\Delta_2 > \Delta_1$ to $\Delta_1 > \Delta_2$. This leads us to suggest for complexes **11** and **12** a field geometry around the Cu(II) centres quite different from that present in **17** and assignable more to a compressed tetrahedral symmetry than to an elongated octahedral one.

Pd(Pt)/Co(Ni) *compounds* (13–16)

Co(II) and Ni(II) are well known to be very sensitive probes for assigning the planar ligand field since they change their spin state even by small displacement of the metal from the ligand plane.

Pd/Co and Pt/Co compounds (**13**, **14**) are both high spin complexes, with ESR spectra interpretable in terms of $S' = 1/2$ fictitious spin state. Though the resonance lines of the polycrystalline sample show broad shape, even at 4.2 K, differences of symmetry between the Pd/Co derivative and the Pt one can be observed. The Pd derivative shows rhombic symmetry ($g_1 = 4.32, g_2 = 2.45, g_3 = 1.85$) whilst an axial symmetry is displayed by the Pt derivative ($g_1 = 3.70, g_2 = 1.62$).

Electronic diffuse reflectance spectra of Pd/Co and Pt/Co are very similar and both spectral patterns are characteristic of a distorted octahedral symmetry (Table 5). Such a distortion is not enough to change the spin state of Co(II) and even if definitive conclusions about the molecular structure are difficult to be drawn, we can assume that the cobalt ion cannot lie in the plane of the surrounding groups. Pd/Ni and Pt/Ni compounds (**15**, **16**) are paramagnetic high spin complexes. ESR spectra of the polycrystalline sample at −160°C are peculiar to the $S = 1$ spin state: the strong resonance lines at 1500 G are assignable to the $\Delta M_s = \pm 2$ transition; the lines of $\Delta M_s = \pm 1$ transition, centred at 3000 G, are broad and unresolved.

Electronic diffuse reflectance spectra are characteristic of a distorted octahedral geometry.

The magnetic behaviour of Ni(II) compounds excludes an overall planar geometry around the d^8 coordination centre.

In view of the results reported for Co(II) and Ni(II) heterobimetallic compounds, as well as from the comparison with the Ir/Cu derivative, it seems definitively confirmed that in Cu(II) compounds **11** and **12**, the copper atom and the ligands are not coplanar.

Concluding remarks

The satisfactory yields obtained and the very mild conditions used in the reported syntheses confirm that dppn is a good assembler for mixed complexes when the mononuclear compounds $Pd(dppn)Cl_2$ or $Pt(dppn)Cl_2$ are used as starting materials.

However the steric requirements of the dppn ligand are not always strong enough to fix both metal centers in the same coordination geometry. While in bimetallic Pt/Pt, Pd/Pd and Pd/Pt complexes both metal centres show the same coordination symmetry, in the other reported bimetallic compounds each centre seems to display an independent coordination geometry. Indeed the Cu centre has the same planar field geometry as the Ir centre in the Ir nitrosyl compound **17**, but an overall planar geometry cannot be proposed in the Pd(Pt)/Cu complexes **11** and **12**, which do not contain the additional steric requirements of the NO bridging ligand. In the same way Co and Ni centres show coordination geometry quite different from that of the other centre (Pd or Pt) present in the same molecule. Although the geometrical properties of the two metal centres in most mixed compounds are independent, magnetic properties indicate that a sort of influence of one centre on the other is present. Indeed the magnetic moment values of the paramagnetic Pt containing derivatives are all lower than those of the corresponding Pd ones. This aspect has a different meaning depending on the partner of Pt and Pd. For Cu compounds the variation of the magnetic moment value should correspond to an increased distortion of the tetrahedral symmetry on switching from Pd to Pt. This is consistent with the increase of the difference between the covalence of the "in plane" and "out of plane" ligands ($\Delta K = |K_{\parallel} - K_{\perp}|$) on going from Pd to Pt; it seems that Pt induces higher compression of the tetrahedral symmetry of the Cu centre than Pd does. The

highest ΔK value was observed in the wholly planar Ir/Cu compound.

For Ni compounds the distortion from the octahedral symmetry decreases on switching from Pd to Pt: for Co compounds it increases.

Therefore for Ni and Cu compounds Pt is likely to display a higher ability than Pd to force the metal partner into a planar geometry.

EXPERIMENTAL

IR spectra were recorded with a Perkin–Elmer 180 (4000–200 cm^{-1}) spectrometer. The solid samples were run as KBr pellets or Nujol mulls. ESR spectra were recorded on a Varian E.109 spectrometer, operating at the X-band frequency, equipped with a Varian temperature control and an Oxford liquid helium cryostat.

Electronic diffuse reflectance spectra were recorded on a Beckman K-2A spectrophotometer. Elemental analyses were performed by the microanalysis Laboratory of the Istituto di Farmacia dell'Università di Pisa, Italy.

The ligand 3,6-bis(2'-pyridyl)pyridazine (dppn) and the starting complex $Pd(PhCN)_2Cl_2$ or K_2PtCl_4 were prepared as described in the literature.[19–21]

Preparation of $Pd(dppn)Cl_2$ (**2**)

To a solution of 0.23 mmol of dppn (25 cm^3) in acetonitrile, was added a solution (25 cm^3) containing 0.23 mmol of $Pd(PhCN)_2Cl_2$ in acetonitrile. The mixture was stirred at room temperature for 12 h. The yellow precipitate was filtered, washed with dichloromethane, ethanol, diethyl ether and dried under vacuum: yield 98%. Found: C, 41.50; H, 2.33; N, 13.23%. Calc. for **2** ($C_{14}H_{10}Cl_2N_4Pd$): C, 40.85; H, 2.45; N, 13.61%.

Preparation of $Pt(dppn)Cl_2$ (**3**)

To a solution of 0.25 mmol of K_2PtCl_4 in 10^{-1} N hydrochloric acid (200 cm^3) was added 0.25 mmol of dppn. The mixture was stirred under reflux for 30 min. After cooling the brown precipitate was filtered, washed with water, ethanol, diethyl ether and dried under vacuum: yield 95%. Found: C, 31.38; H, 2.07; N, 10.33%. Calc. for **3** ($C_{14}H_{20}Cl_2N_4Pt \cdot 2H_2O$): C, 31.35; H, 2.63; N, 10.45%.

Preparation of $Pd(dppn)X_2$ [X = Br (**4**); X = I (**5**)]

To a suspension of 0.2 mmol of **2** in acetonitrile (15 cm^3) was added 5 mmol of appropriate LiX. The mixture was stirred at room temperature for 10 days. The orange or deep red precipitate was filtered, washed with water, ethanol, diethyl ether and dried under vacuum: yield 97% (**4**), 88% (**5**). Found: C, 33.90; H, 1.95; N, 10.80%. Calc. for **4** ($C_{14}H_{10}Br_2N_4Pd$): C, 33.60; H, 2.01; N, 11.19%. Found: C, 28.46; H, 1.64; N, 9.42%. Calc. for **5** ($C_{14}H_{10}I_2N_4Pd$): C, 28.29; H, 1.69; N, 9.42%.

Reaction of **2** *with triphenylphosphine*

To a suspension of 0.17 mmol of **2** in dichloromethane (10 cm^3), a solution (10 cm^3) containing 0.40 mmol of triphenylphosphine in dichloromethane was added. The mixture was stirred at room temperature for 1 h. The yellow precipitate was filtered, washed with a few millilitres of diethyl ether and dried under vacuum. $Pd(PPh_3)_2Cl_2$ was recovered in quantitative yield. From the mother liquor free dppn was detected by TLC.

Preparation of $Pd(dppn)PdCl_2X_2$ [X = Cl (**6**); X = Br (**8**); X = I (**9**)]

In a typical preparation to a suspension of 0.1 mmol of the appropriate species (**2**, **4** or **5**) in 10 cm^3 of dichloromethane an acetonitrile solution (10 cm^3) containing 0.1 mmol of $Pd(PhCN)_2Cl_2$ was added. The mixture was stirred at room temperature for 4 h (**6**) or 18 h (**8** and **9**). The yellow (**6**) or orange (**8**) or brown (**9**) precipitate was filtered, washed with ethanol, diethyl ether and dried under vacuum: yield 95% (**6**), 96% (**8**), 95% (**9**). Found: C, 28.84; H, 1.64; N, 9.49%. Calc. for **6** ($C_{14}H_{10}Cl_4N_4Pd_2$): C, 28.55; H, 1.71; N, 9.51%. Found: C, 25.59; H, 1.54; N, 8.30%. Calc. for **8** ($C_{14}H_{10}Br_2Cl_2N_4Pd_2$): C, 24.81; H, 1.64; N, 8.39%. Found: C, 21.61; H, 1.26; N, 6.74%. Calc. for **9** ($C_{14}H_{10}Cl_2I_2N_4Pd_2$): C, 21.79; H, 1.31; N, 7.26%.

Preparation of $Pt(dppn)PtCl_4$ (**7**)

In a typical preparation to a suspension of 0.2 mmol of **3** in 10^{-1} N hydrochloric acid (200 cm^3), 0.20 mmol of K_2PtCl_4 were added. The mixture was stirred under reflux for 1 h. After cooling the brown precipitate was filtered, washed with water, ethanol, dichloromethane and dried under vacuum yield 95%. Sometime this compound retains small amounts of free dppn. The best analytical data were obtained after washing it many times with dichloromethane. Found: C, 23.48; H, 1.50; N, 7.97%. Calc. for **7** ($C_{14}H_{10}Cl_4N_4Pt_2 \cdot 0.1$dppn): C, 23.42; H, 1.40; N, 7.80%.

Reaction of **6** *with triphenylphosphine*

To a suspension of 0.19 mmol of **6** in dichloromethane (10 cm^3), a dichloromethane solution (10 cm^3) containing 0.97 mmol of triphenylphosphine was added. The mixture was stirred at room temperature for 5 h. The yellow precipitate was filtered, washed with a few millilitres of diethyl ether and dried under vacuum. The precipitate, identified as $Pd(PPh_3)_2Cl_2$ by comparison with an authentic sample, was recovered in quantitative yield. From the mother liquor free dppn was detected by TLC.

Preparation of $Pt(dppn)PdCl_4$ (**10**)

To a suspension of 0.2 mmol of **3** in 15 cm^3 of dichloromethane an acetonitrile solution (15 cm^3) containing 0.2 mmol of $Pd(PhCN)_2Cl_2$ was added. The mixture was stirred at room temperature for 48 h. The brown precipitate was filtered, washed with ethanol, diethyl ether and dried under vacuum: yield 96%. Found: C, 23.82; H, 1.40; N, 7.90%. Calc. for **10** ($C_{14}H_{10}Cl_4N_4PdPt$): C, 24.82; H, 1.49; N, 8.27%.

Preparation of $M(dppn)M'Cl_4$ (**11**: M = Pd, M' = Cu; **12**: M = Pt, M' = Cu; **13**: M = Pd, M' = Co; **14**: M = Pt, M' = Co; **15**: M = Pd, M' = Ni; **16**: M = Pt, M' = Ni)

In a typical preparation to a suspension of 0.3 mmol of **2** or **3** in acetonitrile (10 cm^3) an ethanolic solution (10 cm^3) containing 0.3 mmol of the appropriate MCl_2 (M = Cu, Co, Ni) was added. The mixture was stirred at room temperature for 24 h. The precipitate was filtered, washed with ethanol, diethyl ether and dried under vacuum. **11**: brown, yield 98%. Found: C, 30.90; H, 1.80; N, 10.27%. Calc. for $C_{14}H_{10}Cl_4CuN_4Pd$: C, 30.80; H, 1.84; N, 10.26%. **12**: brown yellow, yield 94%. Found: C, 26.84; H, 1.63; N, 8.73%. Calc. for $C_{14}H_{10}Cl_4CuN_4Pt$: C, 26.49; H, 1.59; N, 8.83%. **13**: green, yield 95%. Found: C, 31.05; H, 2.01; N, 10.73%. Calc. for $C_{14}H_{10}Cl_4CoN_4Pd$: C, 31.06; H, 1.86; N, 10.35%. **14**: greenish, yield 76%. Found: C, 28.84; H, 1.69; N, 9.66%. Calc. for $C_{14}H_{10}Cl_4CoN_4Pt \cdot 0.5CH_3CN$: C, 27.69; H, 1.78; N, 9.68%. **15**: pale yellow, yield 85%. Found: C, 29.09; H, 2.01; N, 10.42%. Calc. for $C_{14}H_{10}Cl_4N_4NiPd \cdot 2H_2O$: C, 29.13; H, 2.45; N, 9.71%. **16**: yellow-green, yield 93%. Found: C, 26.30; H, 1.85; N, 8.64%. Calc. for $C_{14}H_{10}Cl_4N_4NiPt \cdot H_2O$: C, 25.96; H, 1.87; N, 8.65%.

Acknowledgements—We thank the Italian M.P.I. for financial support for this research. Thanks are due to Italian C.N.R. for the use of the apparatus.

REFERENCES

1. H. Beinert, *Coord. Chem. Rev.* 1980, **33**, 55.
2. R. Eisenberg and D. E. Hendriksen, *Adv. Catal.* 1979, **28**, 119; R. Colton and M. J. Cormick, *Coord. Chem. Rev.* 1980, **31**, 1.
3. S. Gambarotta, F. Arena, C. Floriani and P. F. Zanazzi, *J. Am. Chem. Soc.* 1982, **104**, 5082.
4. J. P. Colman, R. K. Rothrock, R. G. Finke, E. J. Moore and F. Rose-Munch, *Inorg. Chem.* 1982, **21**, 146 (and references cited therein).
5. P. W. Ball and A. B. Blake, *J. Chem. Soc. (A)* 1969, 1415.
6. A. Dei, *Congr. Naz. Chim. Inorg. (Atti)* 1977, 10th, H12.
7. M. Ghedini, G. De Munno, G. Denti, A. M. Manotti Lanfredi and A. Tiripicchio, *Inorg. Chim. Acta* 1982, **57**, 87.
8. A. Tiripicchio, A. M. Manotti Lanfredi, M. Ghedini and F. Neve, *J. Chem. Soc. Chem. Commun.* 1983, 97; M. Ghedini and F. Neve, *J. Chem. Soc., Dalton Trans.* (in press).
9. H. D. Stidham and J. V. Tucci, *Spectrochim. Acta (A)* 1967, **23**, 2233.
10. A. R. Katritzky and A. R. Hands, *J. Chem. Soc.* 1958, 2202.
11. J. R. Durig, B. R. Mitchell, D. W. Sink, J. N. Willis, Jr. and A. S. Wilson, *Spectrochim. Acta (A)* 1967, **23**, 1121.
12. R. A. Walton, *Spectrochim. Acta* 1965, **21**, 1975.
13. J. E. Andrew, A. B. Blake and L. R. Fraser, *J. Chem. Soc., Dalton Trans.* 1975, 800.
14. A. M. Manotti Lanfredi, A. Tripicchio, M. Ghedini and G. De Munno, *Acta Cryst.* 1982, **B38**, 1165.
15. G. R. Newkome, F. R. Franczek, V. K. Gupta, W. E. Puckett, A. C. Pantaleo and G. E. Kiefer, *J. Am. Chem. Soc.* 1982, **104**, 1782.
16. G. De Munno, G. Denti and P. Dapporto, *Inorg. Chim. Acta* 1983, **74**, 199.
17. B. Crociani, T. Boschi, R. Pietropaolo and U. Belluco, *J. Chem. Soc. (A)* 1970, 531.
18. B. N. Figgis, *Introduction to Ligand Field*, p. 295. Interscience, New York (1966).
19. W. Butte and F. H. Case, *J. Org. Chem.* 1961, **26**, 4690.
20. M. S. Karash, R. C. Seyler and F. R. Mayo, *J. Am. Chem. Soc.* 1938, **60**, 882.
21. G. B. Kauffman and D. O. Cowan, *Inorg. Synth.* 1963, **7**, 240.

Polyhedron Vol. 4, No. 3, pp. 505–511, 1985
Printed in Great Britain

0277–5387/85 $3.00 + .00
Pergamon Press Ltd

PREPARATION, CRYSTAL AND MOLECULAR STRUCTURE OF, AND NMR PARAMETERS FOR, THE EXOPOLYHEDRAL HETEROCYCLIC PLATINAUNDECABORANE [μ-2,7-(SCSNEt$_2$)-7-(PMe$_2$Ph)-*NIDO*-7-PtB$_{10}$H$_{11}$]

MICHAEL A. BECKETT, NORMAN N. GREENWOOD,* JOHN D. KENNEDY and MARK THORNTON-PETT

Department of Inorganic and Structural Chemistry, University of Leeds, Leeds LS2 9JT, U.K.

(*Received* 1 *May* 1984; *accepted* 22 *May* 1984)

Abstract—The compound [μ-2,7-(SCSNEt$_2$)-7-(PMe$_2$Ph)-*nido*-7-PtB$_{10}$H$_{11}$] has been obtained in a yield of 52% from the reaction of [7,7-(PMe$_2$Ph)-*nido*-7-PtB$_{10}$H$_{12}$] and [AuBr$_2$(S$_2$CNEt$_2$)], and identified by single crystal X-ray diffraction analysis and multi-element single and double resonance NMR spectroscopy. The yellow-orange compound crystallizes in the monoclinic space group $P2_1/n$ with a = 1179.2(2), b = 1244.9(5), c = 1641.4(2) pm, β = 95.45(1)°, Z = 4, and the structure (R = 0.0209, R_w = 0.0211 for 3719 observed reflections) is that of a *nido*-7-platinaundecaborane with an exopolyhedral *N*,*N*-diethyldithiocarbamate ligand bridging the Pt(7) and B(2) positions to give a Pt–B–S–C–S five-membered ring. The *tetrahapto* platinum-to-borane bonding has a considerable twist distortion relative to other *nido*-7-platinaundecaboranes which do not possess this cyclic feature. The NMR parameters exhibit no anomalies and are consistent with the crystal molecular structure. A plot of $\delta(^{11}B)$ vs $\delta(^1H)$ for directly bound *exo*-terminal hydrogen atoms shows good correlation with the slope 16:1.

We have become interested in the incidence of cyclic exopolyhedral metal-to-cluster linkages in polyhedral metalloborane compounds, and have reported the synthesis of both five-membered and six-membered rings during the course of our recent work on metallaboranes of the heavier transition metals.[1–6]

Currently the best represented of these exopolyhedral cyclisation processes is that of *ortho*-cycloboronation; this occurs with P-phenyl ligands on the metal centres and leads to five-membered M–P–C–C–B rings.[1–3,6] Known incidences include six-vertex *closo* clusters,[1] and ten-vertex *nido*,[3,6] *isonido*,[2] *isocloso*,[3] and *arachno*[7] clusters (see Fig. 1). In most of these the *ortho*-cycloboronation usually occurs at reasonably low temperatures and is generally concerted with other processes. Recently, however, it has been reported that it can be induced to occur independently of these processes, although high temperatures of 220–250°C are then required.[7]

The other examples of exopolyhedral linkages include an acetate linkage on a *closo* ten-vertex system, which gives a five-membered Ir–O–C–O–C ring to the carbon atom of an iridacarborane cage; this is obtained in low yield in an obscure reaction process.[4] By contrast, an *ortho*-oxyphenylene linkage on a *nido* eleven-vertex system, which results in a six-membered Pt–P–C–C–O–B ring, can be obtained in a quantitative yield in a designed synthesis.[5]

Here we now report a further type of exopolyhedral cyclisation process resulting in a five-membered Pt–S–C–S–B ring on an eleven-vertex *nido*-platinaundecaborane cluster [Fig. 1(a)]; this presumably occurs *via* a ligand-exchange-type process from the reaction of [7,7-(PMe$_2$Ph)$_2$-*nido*-7-PtB$_{10}$H$_{12}$] with [AuBr$_2$(SCSNEt$_2$)] prior to the formation of a boron–sulphur bond.

An ORTEP drawing of the molecular structure of the exopolyhedral heterocyclic platinaundecaborane [μ-2,7-(SCSNEt$_2$)-7-(PMe$_2$Ph)-*nido*-7-Pt$_{10}$H$_{11}$] is shown in Fig. 2. Selected interatomic distances and selected angles between interatomic vectors are given in Tables 1 and 2 respectively. The gross heavy-atom structure of the cluster can be seen

* Author to whom correspondence should be addressed.

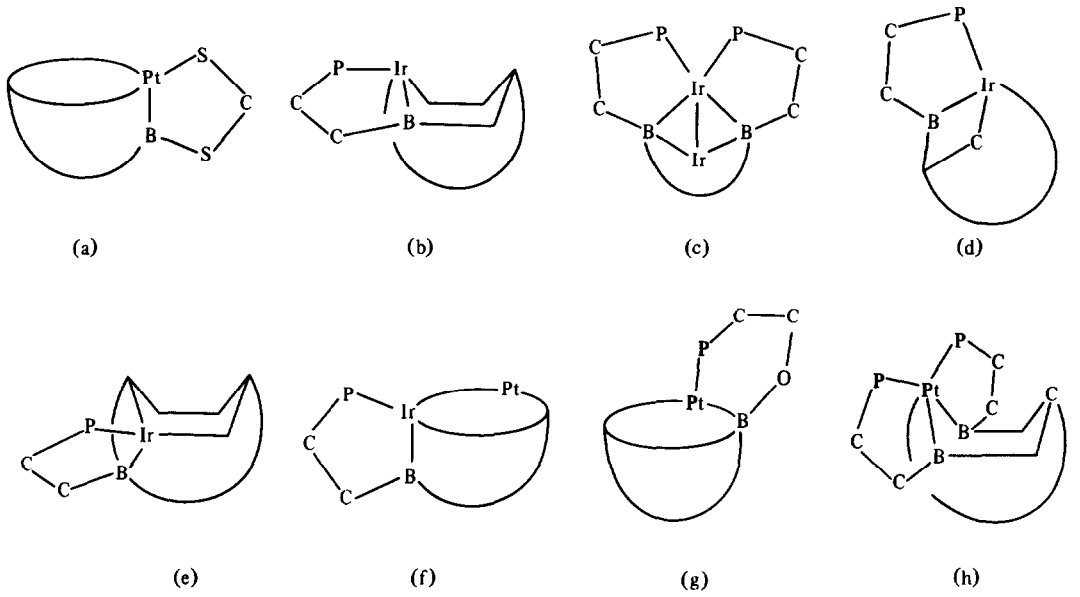


Fig. 1. Examples of exopolyhedral heterocycles involving metalloboranes.

(a) $[(SCSNEt_2)(PMe_2Ph)PtB_{10}H_{11}]$ (this work), (b) $[(PPh_3)(Ph_2PC_6H_4)HIrB_9H_{12}]$,[3]
(c) $[(CO)_3(PPh_3)(Ph_2PC_6H_4)_2Ir_2B_4H_2]$,[1] (d) $[(PPh_3)(Ph_2PC_6H_4)IrB_8H_6(OMe)C(OH)]$,[2]
(e) $[(PPh_3)(Ph_2PC_6H_4)HIrB_9H_{12}]$,[3] (f) $[(PMe_3)Pt(PPh_3)(Ph_2PC_6H_4)HIrB_9H_{10}]$,[6]
(g) $[(PPh_3)(Ph_2PC_6H_4O)PtB_{10}H_{11}]$,[5] (h) $[(Ph_2PC_6H_4)_2PtB_8H_8CH_2]$.[7]

to be that of an open-faced eleven-vertex cluster based on an icosahedron with one vertex removed and is thus similar to related species such as $[B_{11}H_{13}]^{2-}$,[8] and $[Me_2TlB_{10}H_{12}]^-$.[9] The title compound was prepared from $[7,7\text{-}(PMe_2Ph)_2\text{-}nido\text{-}7\text{-}PtB_{10}H_{12}]$ and comparable boron–boron and boron–hydrogen bond lengths[10] and associated interatomic angles for the two related compounds are, within experimental error, in close agreement. The Pt(7)–P(1) bond length of 234.6(3) pm is directly comparable to other known Pt–P bond lengths in platinaborane clusters.[11] The Pt(7)–S(2) bond length

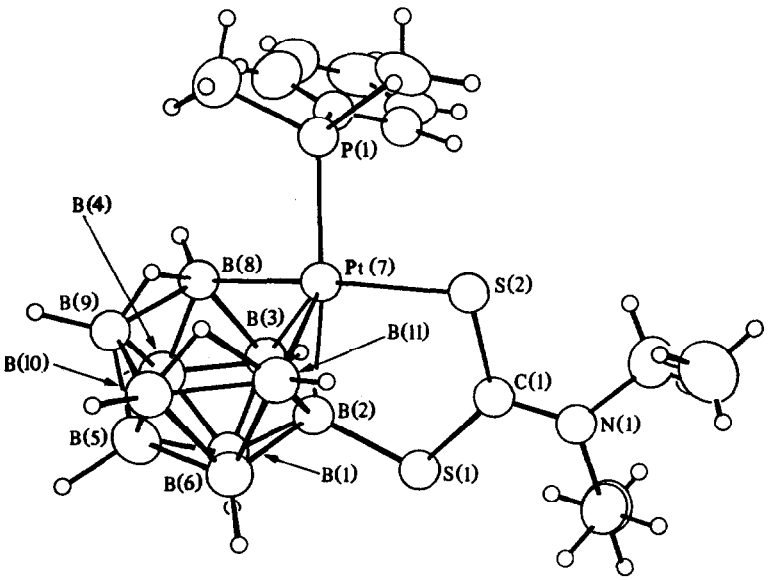


Fig. 2. ORTEP drawing of $[\mu\text{-}2,7\text{-}(SCSNEt_2)\text{-}7\text{-}(PMe_2Ph)\text{-}nido\text{-}7\text{-}PtB_{10}H_{11}]$ showing numbering scheme.

Table 1. Selected interatomic distances (pm) for [μ-2,7-(SCSNEt$_2$)-7-(PMe$_2$Ph)-7-PtB$_{10}$H$_{11}$] with estimated standard deviations in parentheses*

(a) From the platinum atom			
Pt(7)–S(2)	235.6(3)	Pt(7)–P(1)	234.6(3)
Pt(7)–B(2)	216.9(6)	Pt(7)–B(3)	218.2(6)
Pt(7)–B(11)	226.8(7)	Pt(7)–B(8)	223.5(6)
(b) Boron–boron			
B(1)–B(2)	176.1(8)	B(1)–B(3)	178.3(9)
B(1)–B(4)	180.3(9)	B(1)–B(6)	178.2(9)
B(1)–B(5)	177.5(9)		
B(2)–B(3)	183.1(8)		
B(2)–B(6)	177.5(8)	B(3)–B(4)	176.9(9)
B(2)–B(11)	180.4(8)	B(3)–B(8)	181.2(8)
B(4)–B(5)	179.2(9)	B(6)–B(5)	177.6(9)
B(4)–B(8)	179.3(9)	B(6)–B(11)	176.0(8)
B(4)–B(9)	179.1(9)	B(6)–B(10)	180.0(8)
B(5)–B(9)	174.8(9)	B(5)–B(10)	176.3(9)
B(8)–B(9)	187.7(9)	B(10)–B(11)	183.5(8)
B(9)–B(10)	193.8(9)		
(c) Boron–hydrogen			
B(1)–H(1)	121.3(41)		
B(3)–H(3)	109.3(10)		
B(4)–H(4)	108.5(42)	B(6)–H(6)	109.1(45)
B(5)–H(5)	108.5(10)		
B(8)–H(8)	107.2(41)	B(11)–H(11)	111.0(35)
B(9)–H(9)	123.1(54)	B(10)–H(10)	112.2(42)
B(8)–H(8, 9)	130.9(43)	B(11)–H(10, 11)	132.7(41)
B(9)–H(8, 9)	111.1(47)	B(10)–H(10, 11)	121.4(42)
(d) Other			
S(1)–B(2)	189.7(6)		
C(1)–S(1)	175.6(6)	C(1)–S(2)	173.3(6)
C(1)–N(1)	132.1(6)		
N(1)–C(2)	149.3(6)	N(1)–C(4)	148.7(6)
P(1)–C(131)	182.2(4)		
P(1)–C(11)	182.6(6)	P(1)–C(12)	181.9(6)

* The two columns in (a), (b) and (c) compare pairs of distances that would be identical if the molecule had C_s symmetry about the Pt(7)–B(1)–B(5) plane.

is very similar to the Pt(7)–P(1) bond length at 235.6(3) pm, and the angle S(2)–Pt(7)–P(1) of 95.7° is again very similar to the P–Pt–P angle of 95.4° in the related compound [7,7-(PMe$_2$Ph)$_2$-*nido*-7-PtB$_{10}$H$_{12}$]. A view of the platinum bonding environment looking down the plane containing S(2), Pt(7) and P(1) towards the four boron atoms to which the platinum atom is directly bonded is shown in Fig. 3. Here it can be seen that the platinum tetragonal bonding plane, as defined by the S(2), Pt(7) and P(1) plane, is set at an angle of *ca* 36° to that expected for an undistorted dsp^2 hybridization involving two-electron three-centre Pt(7)–B(2)–B(11) and Pt(7)–B(3)–B(8) bonds. Indeed, the observed geometry is with P(1) approximately *trans* to B(2) {P(1)–Pt(7)–B(2) angle 174.2(1)°} and S(2) approximately *trans* to B(8) {S(2)–Pt(7)–B(8) angle 174.9(11)°} indicating a "quasi conical" three-orbital four electron contribution rather than a square-planar two-orbital two-electron contribution of the Pt to the cluster bonding. The angle of twist (36°) is greater than that in the related [7,7-(PMe$_2$Ph)-*nido*-7-PtB$_{10}$H$_{12}$] cluster compound (21°) and this can be partly attributed to the constraints placed upon the metal centre by the exopolyhedral Pt–B–S–C–S five-membered ring. The platinum–boron bond lengths of the title compound of 216.9(6) B(2), 226.8(7) B(11), 218.2(6) B(3) and 223.5(6) B(8) are significantly shorter than the corresponding platinum–boron distances in the related compound [7,7-(PMe$_2$Ph)$_2$-*nido*-7-PtB$_{10}$H$_{12}$] of 223.1(10) B(2), 232.5(11) B(11), 223.5(9) B(3), and

Table 2. Selected angles (°) between interatomic vectors for [μ-2,7-(SCSNEt$_2$)-7-(PMe$_2$Ph)-7-PtB$_{10}$H$_{11}$] with estimated standard deviations in parentheses

At the platinum atom			
P(1)–Pt(7)–S(2)	95.70(5)		
P(1)–Pt(7)–B(2)	174.2(1)	S(2)–Pt(7)–B(3)	126.6(2)
P(1)–Pt(7)–B(3)	126.0(2)	S(2)–Pt(7)–B(2)	90.1(2)
P(1)–Pt(7)–B(8)	88.0(2)	S(2)–Pt(7)–B(11)	89.5(2)
P(1)–Pt(7)–B(11)	131.2(1)	S(2)–Pt(7)–B(8)	174.9(1)
N,*N*-diethyldithiocarbamate ligand and exopolyhedral ring			
Pt(7)–S(2)–C(1)	104.0(2)	B(2)–S(1)–C(1)	104.3(3)
S(1)–C(1)–S(2)	123.3(3)		
S(2)–C(1)–N(1)	120.0(4)	S(1)–C(1)–N(1)	116.8(4)
S(2)–Pt(7)–B(2)	90.1(2)	S(1)–B(2)–Pt(7)	112.3(3)
Boron–platinum–boron			
B(8)–Pt(7)–B(3)	48.4(2)	B(11)–Pt(7)–B(2)	47.9(2)
B(8)–Pt(7)–B(2)	86.3(3)	B(11)–Pt(7)–B(3)	85.9(3)
B(8)–Pt(7)–B(11)	90.7(3)		
B(3)–Pt(7)–B(2)	49.8(2)		

232.3(11) B(8), and this may also be due to the bond distances and angles of the five-membered exocyclic ring; a further factor may be the effective electronegativity differences between the S and P ligands on platinum and between S and H on boron. The boron–sulphur bond length B(2)–S(1) of 189.7(6) pm indicates a bond order of one between the two atoms and is consistent with the bond length of other sulphur–boron single bonds such as in the *arachno*-[6,9-(Me$_2$S)$_2$B$_{10}$H$_{12}$] cluster compound (192 ± 1 and 193 ± 1 pm)[12] and the *arachno*-[4-(Me$_2$S)-7-MeOB$_9$H$_{12}$] cluster (194 pm).[13] The interatomic distances and angles together with the conformation of the *N*,*N*-diethyldithiocarbamate ligand are all essentially identical with those reported[14,15] for the polyhedral [(SCSNEt$_2$)AuC$_2$B$_9$H$_{11}$] and [(SCSNEt$_2$)$_2$Au$_2$B$_8$H$_{10}$] cluster compounds.

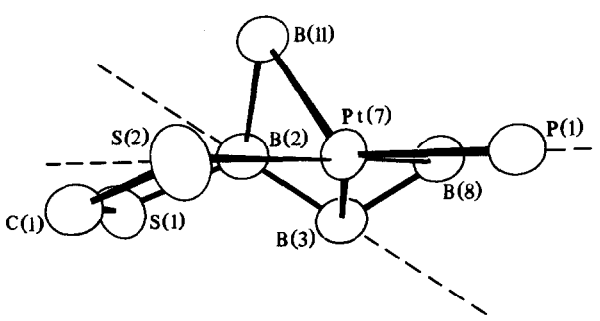


Fig. 3. View of the Pt(7)–P(1)–S(2) plane of the platinum and circumjacent atoms of [μ-2,7-(SCSNEt$_2$)-7-(PMe$_2$Ph)-7-PtB$_{10}$H$_{11}$]. The twist angle θ (between the hatched lines as defined in Ref. 10) is *ca* 36°. The dihedral angle between the Pt(7)–P(1)–S(2) and B(2)–B(3)–B(8)–B(11) planes is 72.8°, and the five-membered Pt(7)–S(2)–C(1)–S(1)–B(2) ring has the "opened envelope" configuration with the angle between the S(2)–C(1)–S(1)–B(2) and S(2)–Pt(7)–B(2) planes being 22.1°.

The NMR properties that we have been able to measure are summarized in Table 3, and are consistent with the structure, confirming that the crystal used for X-ray diffraction is representative of the bulk sample. The boron-11 NMR spectrum is similar to those obtained in these laboratories for a variety of substituted *nido*-7-platinaundecaboranes.[5,16–18] Satellites arising from coupling $^1J(^{195}\text{Pt}–^{11}\text{B})$ were not resolved under the conditions used, and so specific peak assignments are hindered. The substituted site B(2) is readily identified, however, and the highest field resonances will be due to B(4) and B(6). There seem to be no large anomalous cluster-nucleus-shielding effects associated with the large (36°) twist of the formal platinum bonding axes as discussed above, which implies that the twist does not perturb the intracluster bonding to any great extent which would be consistent with a "quasi-conical" contribution of three platinum bonding orbitals to the cluster bonding scheme.[19] The phosphorus parameters $\delta(^{31}\text{P})$ and $^1J(^{195}\text{Pt}–^{31}\text{P})$ are also in normal ranges for the {Pt(PMe$_2$Ph)$_2$} unit in polyhedral platinaboranes.[5,11,20–23]

The proton chemical shifts also show no abnormalities. There is a good general linear relation

Table 3. Selected NMR parameters for [μ-2,7-(SCSNEt$_2$)-7-(PMe$_2$Ph)-7-PtB$_{10}$H$_{11}$] in $CDCl_3$ solution at +21°C[a]

		$\delta(^{11}B)$ (ppm)[b]	$\delta(^1H)$ (ppm)[c]
Borane cluster		+27.8	+4.87[d]
		+15.6	+3.67
		+14.3	+3.84
		+9.1[e]	—[e]
		+0.3	+2.45
		−0.5	+2.75
		−6.2	+2.03
		−9.1	+2.65
		−22.9[f]	+1.25[f]
		−28.3[f]	+1.57[f]
	Bridge hydrogen atoms		−0.97[g]
			−2.35[h]
Other ligands		$SCSNC\mathit{H}_2CH_3$	*ca* +3.9[i]
		$SCSNCH_2C\mathit{H}_3$	+1.30,[j] +1.38[j]
		$P(C\mathit{H}_3)_2Ph$	+1.96,[k] +1.98[l]
		$PMe_2C_6\mathit{H}_5$	*ca* +7.8[m]

[a] $\delta(^{31}P)$ +7.4 ppm (rel. 85% H_3PO_4), $^1J(^{195}Pt–^{31}P)$ 2928±8 Hz ($CDCl_3$ solution at −50°C).

[b] $\delta(^{11}B)$±0.5 ppm relative to [$BF_3(OEt_2)$] (15% in $CDCl_3$).

[c] $\delta(^1H)$±0.05 ppm relative to [$Si(CH_3)_4$]; terminal ^1H resonances assigned to corresponding ^{11}B resonances by selective ^1H–{^{11}B} experiments.

[d] $^nJ(^{195}Pt–^1H)$ *ca* 57 Hz.

[e] No ^1H resonance associated with this boron position; this is therefore assigned to the S-substituted B(2) atom.

[f] (4, 6) positions.

[g] $^2J(^{195}Pt–^1H)$ *ca* 39 Hz.

[h] $^2J(^{195}Pt–^1H)$ *ca* 45 Hz.

[i] Complex multiplet arising from four independent dithiocarbamate methylene protons, of which the two resonances in each will have mutually geminal couplings $^2J(^1H–^1H)$, and of which all have vicinal couplings $^3J(^1H–C–C–^1H)$ *ca* 6 Hz (see footnote j).

[j] Triplet: $^3J(^1H–C–C–^1H)$ *ca* 6 Hz.

[k] $^2J(^{31}P–^1H)$ *ca* 9.1 Hz; $^3J(^{195}Pt–^1H)$ 28.3±0.5 Hz.

[l] $^2J(^{31}P–^1H)$ *ca* 8.8 Hz; $^3J(^{195}Pt–^1H)$ 29.0±0.5 Hz.

[m] Two resonance bands at 100 MHz with δ_{max} *ca* 7.45 and 7.51 ppm.

between the shieldings of the terminal protons and the shielding of the nuclei of the boron atoms to which they are directly bonded, with a slope of $\delta(^{11}B):\delta(^1H)$ of *ca* 16:1 (Fig. 4) as observed for a variety of other platinaboranes and related species.[16–18,23] The difference in shielding between the two bridge protons is perhaps somewhat larger than expected, and may arise from aromatic anisotropic shielding contributions which could occur in the liquid state from a platinum–phosphorus bond rotamer which has the phenyl group above the open face. Of some interest is that, because of the fixed Pt–S–C–S–B ring, each of the two protons in each of the two ethyl *N*,*N*-diethyldithiocarbamate methylene groups is chemically distinct and therefore together these afford a

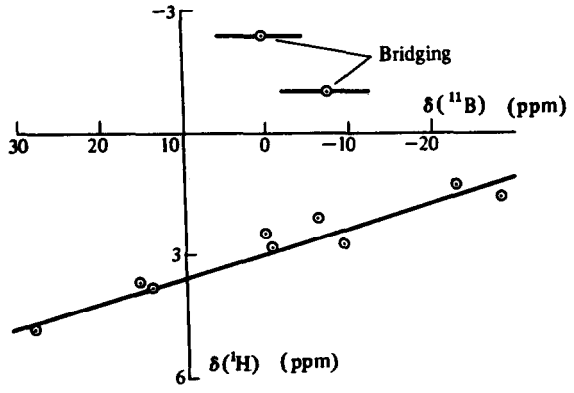


Fig. 4. Proton vs boron-11 nuclear shielding correlation plot for [μ-2,7(SCSNEt$_2$)-7-(PMe$_2$Ph)-7-PtB$_{10}$H$_{11}$]. The line drawn has slope $\delta(^{11}B):\delta(^1H)$ 16:1.

complex spectrum which consists of the AB parts of two overlapping ABX_3 systems (at δ *ca* +3.9).

EXPERIMENTAL

General

The *nido*-platinaundecaborane cluster compound $[(PMe_2Ph)_2PtB_{10}H_{12}]$ and the gold(III) complex $[AuBr_2(SCSNEt_2)]$ were prepared according to published methods.[10,24] CH_2Cl_2 was refluxed over and distilled from CaH_2 before use, and AnalaR benzene and 60°–80° light petroleum were used as supplied without further purification. Nitrogen gas was dried by passing through conc. H_2SO_4 and then over KOH pellets. Preparative thin layer chromatographic techniques have been described elsewhere.[10]

Preparation of $[SCSNEt_2)(PMe_2Ph)PtB_{10}H_{11}]$

To a solution of $[(PhMe_2P)_2PtB_{10}H_{12}]$ (0.2 mmol, 0.120 g) in dry CH_2Cl_2 (25 cm^3) under an atmosphere of dry N_2 was added via a tipper tube solid $[AuBr_2(SCSNEt_2)]$ (0.2 mmol, 0.120 g). The reaction mixture was stirred under a N_2 atmosphere at room temperature (20°C) for 2 days and then the solvent was removed under reduced pressure (water pump/25°C). Subsequent manipulations were carried out in air. The solid residue was chromatographed on silica preparative TLC plates with 100% CH_2Cl_2 as the eluant. An orange-yellow band at R_f 0.8 (the title compound) was removed from the silica and purified further by preparative TLC using 50/50 CH_2Cl_2/60°–80° light petroleum (R_f 0.5) and then 100% benzene (R_f 0.5) as the eluants. The compound was obtained as yellow-orange crystals, by evaporation of a solution in CH_2Cl_2/60°–80° light petroleum, in *ca* 52% yield (0.060 g). A single crystal suitable for an X-ray diffraction analysis was grown by diffusion of solvents (CH_2Cl_2/60°–80° light petroleum) at 4°C.

Crystallographic studies

All crystallographic measurements were made on a Syntex $P2_1$ diffractometer operating in the ω–2θ scan mode using graphite monochromatised Mo-K_α radiation (λ = 71.069 pm) following a standard procedure described in detail elsewhere.[25] The data set was corrected for absorption empirically.[26]

Crystal data. $C_{13}H_{32}B_{10}NPPtS_2$, M = 600.69, monoclinic, a = 1179.2(2), b = 1244.9(5), c = 1641.4(2) pm, β = 95.45(1)°, U = 2.400(1) nm^3, space group $P2_1/n$ (= $P2_1/c$, No. 14), Z = 4, D_c = 1.66 g cm^{-3}, μ(Mo-K_α) = 58.38 cm^{-1}, $F(000)$ = 1172, T = 290 K. 4727 data were collected, 3719 were considered observed [$I > 2\sigma(I)$]. Scans from 1° below $K_{\alpha 1}$ to 1° above $K_{\alpha 2}$, scan speeds = 2.0–29.3° min^{-1}, $4.0 < 2\theta < 50.0°$.

Structure determination and refinement. The structure was determined by standard heavy atom procedures and refined by full-matrix least squares using the SHELX program system.[27] All non-hydrogen atoms were assigned anisotropic thermal parameters with the phenyl rings refined as rigid bodies with hexagonal geometry (C–C = 139.5 pm). All of the hydrogen atoms were located experimentally and refined freely with individual isotropic thermal parameters. A weighting scheme of $\omega = 1/[\sigma^2(F_o) + 0.0001(F_o)^2]$ was used at the end of refinement to give a flat analysis of variance with increasing sin θ and $[F/F_{max}]^{1/2}$. Final R values were R = 0.0209 and R_w = 0.0211.*

NMR spectroscopy

100-MHz ^1H, ^1H-{^{11}B} and ^1H-{^{31}P}, 32 MHz ^{11}B and ^{11}B-{^1H}, and 40-MHz ^{31}P-{^1H} NMR experiments were carried out on a JEOL FX-100 pulse (F.t.) NMR spectrometer. High field (128 MHz) ^{11}B and ^{11}B-{^1H} NMR experiments were performed as part of the SERC service at Sheffield on a Bruker WH-400 pulse (F.t.) NMR spectrometer. Solutions and conditions are specified in Table 1. Chemical shifts are given in ppm to high frequency (low field) of $[SiMe_4]$ for ^1H, in ppm to high frequency (low field) of $[BF_3 \cdot OEt_2]$ in $CDCl_3$ [Ξ 32,083,971 Hz][23] for ^{11}B, and in ppm to high frequency (low field) of 85% H_3PO_4 [Ξ 40,480,730 Hz] for ^{31}P.

Acknowledgements—We thank the SERC for financial support, and Johnson Matthey Ltd for the loan of precious metals.

REFERENCES

1. J. E. Crook, N. N. Greenwood, J. D. Kennedy and W. S. McDonald, *J. Chem. Soc., Chem. Commun.* 1982, 383.
2. J. E. Crook, N. N. Greenwood, J. D. Kennedy and W. S. McDonald, *J. Chem. Soc., Chem. Commun.* 1981, 933.
3. J. Bould, N. N. Greenwood, J. D. Kennedy and W. S. McDonald, *J. Chem. Soc., Chem. Commun.* 1982, 465.
4. J. E. Crook, N. N. Greenwood, J. D. Kennedy and W. S. McDonald, *J. Chem. Soc., Chem. Commun.* 1983, 83.
5. J. E. Crook, N. N. Greenwood and J. D. Kennedy,

*Atomic coordinates have been deposited with the Editor and with the Cambridge Crystallographic Data Centre.

Paper in preparation on the synthesis and structure of organyloxy substituted platinaundecaboranes; see also J. E. Crook, PhD Thesis, University of Leeds (1982); and N. N. Greenwood and J. D. Kennedy, *Metal Interactions with Boron Clusters* (Edited by R. N. Grimes), pp. 109–110. Plenum, New York (1982).
6. J. Bould, J. E. Crook, N. N. Greenwood and J. D. Kennedy, *J. Chem. Soc., Chem. Commun.* 1983, 949.
7. K. Baše, B. Štíbr, G. A. Kukina and I. A. Zakharova, *Proc. Conf. Coord. Chem. (8th)*, 1980, pp. 17–19 (*Chem. Abs.* 1981, **95**, 23933g); G. A. Kukina, S. V. Sergienko, M. A. Porai-Koshits, K. Baše and I. A. Zakharova, *Izv. Akad. Nauk SSSR Ser. Khim.* 1981, **12**, 2838 (*Chem. Abs.* 1982, **96**, 85632n).
8. C. J. Frische, *Inorg. Chem.* 1967, **6**, 1199.
9. N. N. Greenwood and J. A. Howard, *J. Chem. Soc., Dalton Trans.* 1976, 177.
10. S. K. Boocock, N. N. Greenwood, J. D. Kennedy and W. S. McDonald, *J. Chem. Soc., Dalton Trans.* 1981, 2573.
11. S. K. Boocock, N. N. Greenwood, M. J. Hails, J. D. Kennedy and W. S. McDonald, *J. Chem. Soc., Dalton Trans.* 1981, 1415.
12. D. E. Sands and A. Zalkin, *Acta Cryst.* 1962, **15**, 410.
13. J. Plešek, S. Heřmánek and B. Štíbr, *Coll. Czech. Chem. Commun.* 1970, **35**, 344.
14. M. A. Beckett, J. E. Crook, N. N. Greenwood and J. D. Kennedy, *J. Chem. Soc., Dalton Trans.* 1984, 1427.
15. H. M. Colquhoun, T. J. Greenhough and M. G. H. Wallbridge, *J. Chem. Soc., Dalton Trans.* 1978, 303.
16. J. E. Crook, N. N. Greenwood, J. D. Kennedy and W. S. McDonald, *J. Chem. Soc., Dalton Trans.* 1984, 2487.
17. R. Ahmad, N. N. Greenwood, J. D. Kennedy, work in preparation for publication in *J. Chem. Soc., Dalton Trans.*, on the preparation and properties of substituted *nido*-7-platinaundecaboranes.
18. R. Ahmad, PhD Thesis, University of Leeds (1982).
19. M. A. Beckett and J. D. Kennedy, Work presented at the NATO Advanced Study Institute on NMR Spectroscopy, Stirling, Scotland, September 1982. *J. Chem. Soc., Dalton Trans.* (in preparation).
20. N. N. Greenwood, M. J. Hails, J. D. Kennedy and W. S. McDonald, *J. Chem. Soc., Dalton Trans.* (in press, DAL/4988).
21. M. A. Beckett, J. E. Crook, N. N. Greenwood and J. D. Kennedy, *J. Chem. Soc., Dalton Trans.* (in preparation).
22. Y. M. Cheek, N. N. Greenwood, M. J. Hails and J. D. Kennedy (in preparation).
23. J. D. Kennedy, in *NMR in Inorganic and Organometallic Chemistry* (Edited by J. Mason), Chapter 9. Plenum, New York (1985) (in press).
24. H. A. J. Blaauw, R. J. F. Nivard and F. J. M. Van der Kerk, *J. Organomet. Chem.* 1964, **2**, 236.
25. A. Modinos and P. Woodward, *J. Chem. Soc., Dalton Trans.* 1974, 2065.
26. N. Walker and D. Stuart, *Acta Cryst.* 1983, **A39**, 158.
27. G. M. Sheldrick, *SHELX 76, Program System for X-ray Structure Determination.* University of Cambridge (1976).

Polyhedron Vol. 4, No. 3, pp. 513–516, 1985
Printed in Great Britain

0277–5387/85 $3.00 + .00
Pergamon Press Ltd

HYDRATES OF SODIUM THIOSULPHATE

D. A. EDWARDS* and A. A. WOOLF
School of Chemistry, University of Bath, Bath BA2 7AY, U.K.

(*Received* 22 *March* 1984; *accepted* 9 *May* 1984)

Abstract—Dehydration of sodium thiosulphate pentahydrate with organic solvents produces mixtures of the anhydrous salt and dihydrate for compositions up to $2H_2O$ and of di- and pentahydrates above this composition, with occasional traces of monohydrate present. This confirms the stable compounds in the Na_2S_2O–H_2O system. The constituents in mixtures were identified qualitatively and semi-quantitatively by Raman spectroscopy. X-ray powder diffractometry is much inferior for identification purposes. Correlations between vibrational frequencies and structure are suggested.

The $Na_2S_2O_3$–H_2O system is difficult to study experimentally because of marked supercooling and superheating phenomena. The two most detailed studies differ considerably. Burke and Young[1] isolated various hydrates after heat treatment of solutions and determined their solubilities over a temperature range. Intersections of solubility curves were identified with transitions between hydrates. In this way twelve hydrates were classified into five systems. Picon[2] after heat treating his solutions observed the temperatures at which all crystalline material had dissolved and plotted liquidus curves intersecting at transition points. He claimed only eight distinct hydrates, two of which had not been obtained by Burke and Young, a primary set of 10, 5, 2, and 1 hydrates and a secondary set of 12, 6, 5 and 1 hydrates. Members of the secondary series could be converted by seeding into members of the primary series but not vice versa. The various hydrates were identified by their crystalline appearance and by thiosulphate analysis. These analyses, apart from that for the pentahydrate, only approximated the suggested compositions because of the difficulty in freeing the crystals from the adherent viscous mother liquors.

Recently the dehydration of the solid pentahydrate and thiosulphate solutions with organic solvents has been examined in order to prepare anhydrous thiosulphate for use as a primary volumetric standard.[3] Any composition between 0 and $5H_2O$ can be obtained under appropriate conditions and hence alternative preparations of some of the above hydrates in a pure form seemed possible. Raman spectroscopy was explored as the main method for identifying the solid phases produced.

EXPERIMENTAL

Aqueous thiosulphate solutions can be partially dehydrated and precipitated by shaking with MeOH or CH_2OHCH_2OMe at room temperature whereas EtOH, Me_2CHOH, Me_2CO and MeCN reprecipitate the pentahydrate from solution. The crystalline pentahydrate is completely dehydrated in refluxing MeOH, $Me_2C(OMe)_2$ or CH_2OHCH_2OMe and partly dehydrated with Me_2CO, EtOH, MeCN or $O(CH_2CH_2OMe)_2$. Methanol, ethanol and acetone, or their mixtures, were chosen as the most suitable solvents because of their ease of removal from any solid phase. A number of different techniques were investigated to produce compositions between 0 and $5H_2O$. These compositions were measured from the water loss at 130°C after at least a 12 h heating.

Method 1. $Na_2S_2O_3 \cdot 5H_2O$ (5g) were heated under reflux for 2.5 h with various volumes of acetone. Compositions were generally reproducible to ± 0.1 H_2O. Some results are collected in Fig. 1. The Me_2CO/H_2O ratios are based on the total water present in the original pentahydrate and solvent, and not on the final solution composition.

Method 2. $Na_2S_2O_3$ (3.5 g) was equilibrated with methanol–water mixtures (50 cm^3) for 2 days. The solid compositions with mole ratios $MeOH/H_2O$ of 2/1, 3/1 and 6/1 were 3.86, 1.85 and $0.09H_2O$. Another set of results using $Na_2S_2O_3$ (5.0 g) with

* Author to whom correspondence should be addressed.

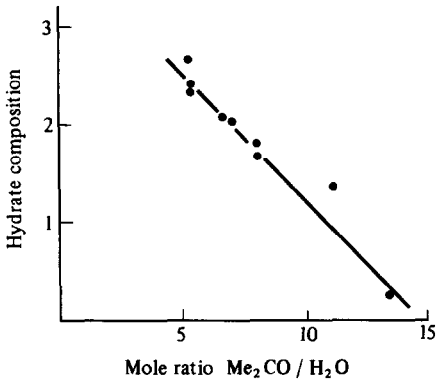


Fig. 1. Dehydration of $Na_2S_2O_3 \cdot 5H_2O$ with acetone–water mixtures.

MeOH–H_2O mixtures (50 cm^3) and shaking for 7 h gave compositions 4.31, 1.59 and 0.36H_2O at mole ratios of 2/1, 3/1 and 5/1 respectively.

Method 3. 5 cm^3 aliquots of a 5.92 molal $Na_2S_2O_3 \cdot 5H_2O$ aqueous solution were injected into 50 cm^3 of MeOH–EtOH mixtures. The compositions 2.13, 2.18, 2.91 and 4.25H_2O were precipitated from 100%, 80%, 60% and 50% MeOH mixtures.

Method 4. 10 cm^3 aliquots of a 6.00 molal $Na_2S_2O_3 \cdot 5H_2O$ aqueous solution were mixed with different volumes of MeOH at 22°C. At mole ratios MeOH/H_2O of 8.26, 4.13 and 2.07 the hydrated compositions were 1.12, 1.48 and 4.61H_2O respectively. The effect of raising the temperature (20–50°C range) at a fixed MeOH/H_2O ratio was to decrease the water of hydration. The composition was also variable to a small extent with the method of mixing and the geometry of the container. Hence to obtain reproducible compositions the exact experimental conditions need to be specified as illustrated for the dihydrate.

Preparation of the dihydrate

$Na_2S_2O_3 \cdot 5H_2O$ (8.00 g) were shaken with 50 cm^3 of MeOH in a boiling tube (20 cm × 2.54 cm diam.) held horizontally for 6 h at room temperature (24–25°C). The filtered solid was held over H_2SO_4 aq. (density 1.402) in a desiccator overnight and checked for weight constancy over a longer period.

The composition reached was $Na_2S_2O_3 \cdot 1.994H_2O$. Another experiment using 7.50 g of pentahydrate with 50 cm^3 of MeOH gave $Na_2S_2O_3 \cdot 1.999H_2O$. With 6.00 g the composition had dropped to 0.641H_2O.

Examination of hydrates

X-ray powder diffractometry. X-ray films taken on conventional cameras (Straumanis and Guinier–De Wolff mountings) were difficult to measure because of the complexity of the patterns and large number of weak lines. A graphical output (1° of θ = 2 cm) from a Philips goniometer diffractometer (PW 1050) linked to an Xe proportional counter (PW 1965) and single channel analyser (PW 4620) enabled mixed powder patterns to be separated. Specimens were contained in planchettes covered with adhesive tape and since they were not rotated the relative intensity values of peaks were not on an absolute scale. The patterns for the 0 and 5 hydrates have been tabulated previously.[4]

The d spacings observed from the dihydrate over a θ range 4.5–32° using Cu-K_α radiation were

9.678, 9.732, 5.695, 5.588, 5.412, 4.832, 4.695, 4.448, 4.396, 4.222, 4.084, 3.802, 3.693, 3.576, 3.507, 3.440, 3.414, 3.305, 3.255, 3.193, 3.079, 2.944, 2.881, 2.831, 2.792, 2.747, 2.739, 2.705, 2.683, 2.655, 2.629, 2.613, 2.543, 2.492, 2.456, 2.424, 2.356, 2.313, 2.279, 2.260, 2.249, 2.227, 2.214, 2.115, 2.049, 2.015, 1.999, 1.965, 1.933, 1.909, 1.863, 1.689, 1.590, 1.523, 1.495, 1.445.

The better defined thirty reflections were used to obtain a unit cell by means of a systematic computer fitting.[5] The best cell was monoclinic with a = 11.431, b = 4.452, c = 20.368 AU, β = 93.79° and cell volume 1034.4 AU^3. A value of Z = 6 was calculated from a measured density of 1.88 g cm^{-3}.

The powder patterns of the hydrates prepared from organic solvents were then examined. Only the lines of the 0, 2 and 5 hydrates were observed. Compositions with less than 2H_2O were mixtures of the 0 and 2 hydrates, and compositions above 2H_2O consisted of mixtures of 2 and 5 hydrates.

However in two instances a few additional weak lines were observed which were identified as belonging to the monohydrate. An impure specimen of this hydrate (composition 1.50H_2O) was made by Picon's method.[2] Anhydrous thiosulphate was added to water to give the composition $Na_2S_2O_3 \cdot 4.10H_2O$. After dissolution above 80°C the solution was held at 58–59°C for two days and the liquid decanted from the crystals after cooling to 35°C. The crystals were mixtures of the mono- and dihydrates.

An insufficiency of suitable lines prevented a unit cell being obtained for the monohydrate.

Heat of solution of hydrates. It was hoped to detect hydrates by breaks or non-linearities in the heat-composition curve. Samples (0.1–0.2 g) were injected into 50–100 cm^3 water in a conventional isoperibol calorimeter and the heat change measured. The results are summarized in Fig. 2.

Raman spectra. These were obtained on solid samples in "Pyrex" capillary tubes using the 514.5

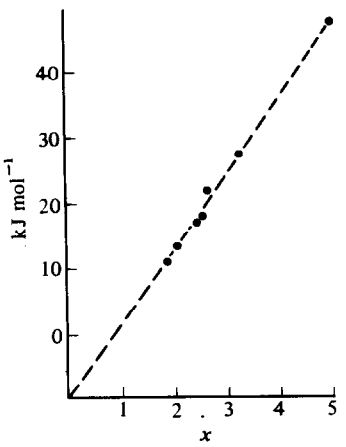


Fig. 2. Heats of solution of $Na_2S_2O_3 \cdot xH_2O$ compositions.

and 488 nm lines from an Ar^+ laser. The scattered radiation was resolved on a double monochromator (Spex 1401). Relative intensities were not corrected for frequency variation of the monochromator–photomultiplier detector response. Band frequencies, apart from those of the broadest peaks, were accurate to within ± 2 cm^{-1}. The Raman spectra characterized the individual compounds $Na_2S_2O_3 \cdot xH_2O$ ($x = 0, 1, 2, 5$) and enabled mixtures to be rapidly identified. By using the relative peak heights of the symmetric ν(SO) bands it was possible to calculate a mixture composition in close agreement with the gravimetric composition.

DISCUSSION

Dehydration of sodium thiosulphate pentahydrate, or hydration of the anhydrous salt, with organic solvents produce only the stable species in the $Na_2S_2O_3$–H_2O system, i.e. 0, 1, 2 and 5 hydrates or mixtures thereof. Picon[2] by careful heat treatment obtained the 1 and 2 hydrates from pentahydrate solutions but noted that if the dehydrations were rapid or brusque then only the dihydrate resulted. He obtained the same dihydrate, admixed with the anhydrous salt, from vacuum or desiccant dehydration. Recent Russian work using DTA and DSC techniques confirms the latter observation and an X-ray powder identification of the dihydrate was given without any analytical composition.[6] We were able to prepare the pure dihydrate for the first time, without adherent solution or enclosed anhydrous material, by simply shaking the pentahydrate with methanol at the correct $MeOH/H_2O$ ratio. The main evidence that it was a distinct species, rather than an accidental mixture of the correct composition, was provided by the Raman spectra. All the solid thiosulphates give more than the expected six Raman active bands ($3A_1 + 3E$) of the $S_2O_3^{2-}$ ion because of lattice splittings of the E modes (Table 1). The S—S stretch is the most intense for all compounds but cannot be used alone for identification because only the pentahydrate's frequency is different from the rest. However the other A_1 fundamentals (the S—O stretches and bends) are diagnostic. A 1–2% impurity in the dihydrate could be detected.

It is difficult to rationalize changes in Raman bands as the anhydrous salt becomes hydrated, no doubt because of irregularities in the sequence of structures. Only full structures of $Na_2S_2O_3 \cdot 5H_2O$ and $Na_2S_2O_3$ are available. For example one would

Table 1. Solid state Raman spectra (Δ cm^{-1})

Vibrational mode*	$S_2O_3^{2-}$ ion[11]	$Na_2S_2O_3 \cdot 5H_2O$†	$Na_2S_2O_3 \cdot 2H_2O$	$Na_2S_2O_3 \cdot 1H_2O$	$Na_2S_2O_3$
$\nu_1(A_1)$	1002	1016 (18)	996 sh	1037 (20)	1002 (21)
ν_s(SO)			992 (21)		
$\nu_2(A_1)$,	451	433 (100)	453 (100)	453 (100)	452 (100)
ν(SS)					
$\nu_3(A_1)$,	672	669 (10)	656 (18)	702 (23)	672 (26)
δ_s(SO)		629 br (4)			
$\nu_4(E)$,	1125	1161 (7)	1155 (12)	1153 (5)	1157 (9)
ν_a(SO)		1110 (5)	1121 br (4)	1140 (8)	1136 (5)
$\nu_5(E)$,	541	543 br (8)	549 br (2)	546 (5)	558 (4)
δ_a(SO)			524 (2)	532 sh (3)	535 (3)
$\nu_6(E)$,	339	341 (7)	359 br (8)	360 sh (2)	362 (4)
$\rho_r(SO_3)$		320 (9)	342 br (11)	337 br (3)	325 (7)
ν(OH)		3442 br (18)	3422 br (2)	3370 br (5)	
		3411 br (22)	3367 br (9)		

* Relative intensities are given in parentheses and vibrational modes are given for the free ion of C_{3v} symmetry.
† These results agree with those in Ref. 12.

Table 2. Crystallographic data

Compound	Unit cell volume (AU^3)	X-ray density ($g\ cm^3$)	Molecular volume (cm^3)
$Na_2S_2O_3$	448.0[9]	2.344	67.4(5)
	442.8[10]	2.372	66.6(5)
	441.8[4]	2.376	66.5(4)
$Na_2S_2O_3 \cdot 2H_2O$	1034.4	1.870	103.8(0)
$Na_2S_2O_3 \cdot 5H_2O$	941.5[7]	1.751	141.7(5)
	936.1[8]	1.761	140.9(4)
	936.0[4]	1.753	141.5(3)

have expected the ν(S—O) stretch to weaken as hydration and hence hydrogen bonding increased rather than the irregular sequence found, $1H_2O > 5H_2O > 0H_2O > 2H_2O$. However the difference in the ν(S—S) stretches between the pentahydrate and the other solids may simply reflect differences in hydrogen bonding to sulphur. In the solid pentahydrate the water molecules are non-equivalent.[7,8]

The ten OH groups form hydrogen bonds, two to adjacent water molecules, four to oxygens on thiosulphate ions and four to sulphurs on thiosulphate ions. It is the latter set which would weaken the ν(S—S) stretch. In the other compounds either no hydrogen bonding occurs, or only OH...O interactions are present and hence ν(S—S) would remain invariant.

The crystallographic data (Table 2) confirm the irregularity in the structural sequence. All unit cells were monoclinic but the dihydrate with the peculiar number of six molecules per cell must have units in special positions. (A search for alternative hexagonal or trigonal cells failed.) A comparison of molecular volumes shows that the pentahydrate contracts by about 10% compared with the sum of anhydrous salt plus water volumes whereas the dihydrate molecular volume is about 1% greater than the molecular volume sum. This is compatible with the ν(S—O) sequence found in the Raman spectra (i.e. $5H_2O > 0H_2O > 2H_2O$). Thermal data also indicate a weakening of hydrogen bonding in the dihydrate compared with the pentahydrate. In Fig. 3 heats of solution are given with respect to (a) the infinitely dilute solution, and (b) the previously reported heats of fusion or melting with respect to the molten state.[13] If one assumes the differences in disruption heats of the hydrated lattices are mainly due to differences in hydrogen bonding then on a purely statistical basis the expected dihydrate levels should be at 4/10 of the pentahydrate levels as indicated by the dotted lines. In each case the dihydrate is destabilized with respect to these hypothetical levels.

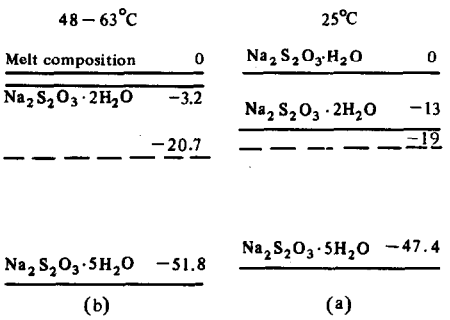


Fig. 3. Heats of melting and heats of solution (kJ mol^{-1}).

Although we were unable to isolate metastable phases by treatment with organic solvents we have established that Raman spectroscopy would be the most favourable technique to follow the *in situ* equilibration of phases from the metastable part of the $Na_2S_2O_3$–H_2O system.

REFERENCES

1. S. W. Young and W. E. Burke, *J. Am. Chem. Soc.* 1906, **28**, 315.
2. M. Picon, *Bull. Soc. Chim. France* 1924, **35**, 1093.
3. A. A. Woolf, *Anal. Chem.* 1982, **54**, 2134.
4. Joint Committee on Powder Diffraction Standards 1975, 25-860 and 1981, 31-1325A.
5. D. Taupin, *J. Appl. Cryst.* 1968, **1**, 178 and 1973, **6**, 380. (Programme implemented at S. W. Region Univ. Computer Centre, Bath. Information manual E6301/1B1 by M. Cartwright, Nov. 1976.)
6. B. M. Nirsha, G. M. Serebrennikova, Yu. V. Oboznenko, B. V. Zhadanov, V. I. Safanova and V. A. Olikova, *Zhur. Neorg. Khim.* 1982, **27**, 3035.
7. G. C. Lisensky and H. A. Levy, *Acta. Cryst.* 1978, **B34**, 1975.
8. A. A. Uraz and N. Armagan, *Acta. Cryst.* 1977, **B33**, 1396.
9. E. Sandor and L. Csordas, *Acta. Cryst.* 1961, **14**, 237.
10. H. von Benda and K. von Benda, *Z. Naturforsch.* 1979, **34B**, 957.
11. B. Meyer, M. Ospina and L. B. Peter, *Analyt. Chim. Acta* 1980, **117**, 301.
12. W. Mikenada and H. Steidl, *Spectrochim. Acta* 1982, **38A**, 1059.
13. F. Gronvold and K. K. Meisingset, *J. Chem. Thermodynamics* 1982, **14**, 1083.

Polyhedron Vol. 4, No. 3, pp. 517–520, 1985
Printed in Great Britain

0277–5387/85 $3.00 + .00
Pergamon Press Ltd

PREPARATION AND CRYSTALLOGRAPHIC INVESTIGATION OF THE SPINEL SERIES: $Mn_{1+2s}Cr_{2-3s}Sb_sO_4$ ($0.05 \leqslant s \leqslant 0.30$)

P. GARCÍA CASADO
Facultad de Farmacia, Universidad de Navarra, 31008 Pamplona, Spain

and

I. RASINES*
Instituto Elhúyar, Serrano 113, 28006 Madrid, Spain

(*Received* 3 *January* 1984; *accepted* 14 *April* 1984)

Abstract—$Mn_{1+2s}Cr_{2-3s}Sb_sO_4$, a new series of spinels, have been prepared and studied using X-ray powder data. For s going from 0.05 to 0.30, a gradually increases from 8.441(1) to 8.472(1) Å, and u slightly decreases, from 0.262 to 0.258. Interatomic distances are given. The $Mn_{1+2s}Cr_{2-3s}Sb_sO_4$ ($0.05 < s < 0.30$) series may be conceived as the result of partial substitution of Cr^{3+} by $2/3Mn^{2+} + 1/3Sb^{5+}$ in the normal spinel, $MnCr_2O_4$.

The spinels are usually formulated as AB_2X_4, A and B being metals and X oxygen or chalcogen. AB_2O_4 is the composition of the most abundant group of spinels, i.e. those constituted by metals in oxidation states II–III or II–IV. Other stoichiometries such as $Co_{7/3}Sb_{2/3}O_4$, $Li_{4/3}Ti_{5/3}O_4$, $Cu_{1/2}Fe_{5/2}O_4$ and $CrMnNiO_4$, are also known. All of these non-deficient compounds could be formulated as M_3X_4. For two metals, M and M′, in oxidation states m and m' respectively, the following compounds are possible: $M_bM'_cX_4$, where $b = (3m' - 8)/(m' - m)$ and $c = (8 - 3m)/(m' - m)$. For three metals, M, M′ and M″, and oxidation states m, m' *and* m'', the series $M_sM'_dM''_eX_4$, where $d = (8 - 3m'' - ms + m''s)/(m' - m'')$ and $e = (3m' - 8 + ms - m's)/(m' - m'')$ could exist when s, d and e are positive.

In attempts to study new mixed oxides of antimony, we have prepared 12 samples of the series $Mn_{1+2s}Cr_{2-3s}Sb_sO_4$ ($0.05 \leqslant s \leqslant 0.60$). For $s >$ 0.30, a mixture of phases was obtained; for $0.05 \leqslant s \leqslant 0.30$, six polycrystalline spinels resulted, in which a gradual variation of a, the unit-cell parameter, was observed. The aim of this paper is to report how the mentioned series was prepared and to establish the cell dimension, a, the positional parameter, u, for oxygen atoms, and the distribution of cations for six samples ($0.05 \leqslant s \leqslant 0.30$) of the series.

EXPERIMENTAL

The samples were prepared from mixtures of analytical grade Mn metal, Cr_2O_3 and Sb_2O_3, molar ratios $Mn:Cr:Sb = (1+2s):(2-3s):s$ ($s = 0.05$, 0.10, ... 0.30), which were heated in air at 1073, 1273, 1473, 1573 and 1623 K during 1 day. After each thermal treatment the materials were quenched and ground. Additional experimental details were as indicated elsewhere.[1] The unit-cell parameters were refined from the 2θ values of the last eight reflections; the arbitrarily chosen Debye–Waller factors, B_j, for the calculation of the intensities were 0.30 and 0.80 Å^2 for Sb and O atoms respectively; the values 0.62 and 0.63 for Mn and Cr were obtained from these two by interpolation of the respective atomic masses between those of O and Sb. Intensities were calculated for u, the oxygen positional parameter, equal to 0.255, 0.256, . . . 0.269, and assuming $Mn_{1.00}$ at tetrahedral (a) sites.

RESULTS AND DISCUSSION

The six $Mn_{1+2s}Cr_{2-3s}Sb_sO_4$ ($0.05 \leqslant s \leqslant 0.30$) samples were obtained as polycrystalline powders, coloured from medium brown to black, which gave

* Author to whom correspondence should be addressed.

Table 1. X-ray diffraction data for the $Mn_{1+2s}Cr_{2-3s}Sb_sO_4$ series of spinels

	$Mn_{1.10}Cr_{1.85}Sb_{0.05}O_4$				$Mn_{1.20}Cr_{1.70}Sb_{0.10}O_4$				$Mn_{1.30}Cr_{1.55}Sb_{0.15}O_4$			
hkl	d_o	d_c	I_o	I_c	d_o	d_c	I_o	I_c	d_o	d_c	I_o	I_c
111	4.879	4.873	108	139	4.89	4.88	143	144	4.885	4.890	140	157
220	2.9848	2.9843	290	303	2.988	2.987	254	288	2.991	2.988	316	277
311	2.5453	2.5451	860	1000	2.548	2.547	849	1000	2.550	2.548	904	1000
222	2.4364	2.4367	50	81	2.439	2.438	63	89	2.441	2.440	61	98
400	2.1109	2.1103	199	218	2.113	2.112	190	224	2.1126	2.1130	226	230
331	—	1.9365	—	2	—	1.9379	—	3	—	1.9390	—	5
422	1.7233	1.7230	89	91	1.7239	1.7242	81	88	1.7249	1.7253	81	85
511-333	1.6249	1.6245	391	344	1.6261	1.6256	340	338	1.6265	1.6266	359	339
440	1.4928	1.4922	426	415	1.4933	1.4932	396	416	1.4945	1.4941	395	417
531	1.4273	1.4268	12	14	1.4280	1.4278	16	16	1.4286	1.4286	15	18
620	1.3349	1.3346	31	30	1.3354	1.3356	30	30	1.3362	1.3364	29	29
533	1.2874	1.2872	81	85	1.2883	1.2882	107	85	1.2888	1.2889	80	86
622	1.2727	1.2725	42	41	1.2735	1.2734	41	44	1.2739	1.2742	44	48
444	1.2187	1.2184	25	26	1.2193	1.2192	30	28	1.2198	1.2199	34	29
711-551	1.1820	1.1820	9	9	1.1830	1.1828	10	10	1.1831	1.1835	9	11
642	1.1280	1.1280	52	40	1.1287	1.1288	55	38	1.1294	1.1294	39	36
731-553	1.0991	1.0989	140	128	1.0996	1.0997	153	131	1.1003	1.1004	140	133
800	1.0550	1.0551	49	50	1.0558	1.0559	60	51	1.0564	1.0565	63	51
733	—	—	—	—	—	—	—	—	—	—	—	—
822-660	0.9949	0.9948	22	22	0.9955	0.9955	21	20	0.9963	0.9961	22	19
751-555	0.9747	0.9747	94	87	0.9754	0.9754	105	87	0.9760	0.9760	105	89
662	0.9682	0.9682	25	23	0.9690	0.9689	29	24	0.9694	0.9695	18	26
840	0.9437	0.9437	37	33	0.9444	0.9444	39	36	0.9450	0.9450	31	39
911-753	0.9265	0.9265	5	5	—	0.9272	—	6	0.9278	0.9277	5	7
664	0.8997	0.8998	8	9	0.9005	0.9005	9	9	0.9010	0.9010	7	8
931	0.8848	0.8849	107	87	0.8855	0.8855	100	86	0.8860	0.8860	108	87
844	0.8615	0.8615	218	163	0.8621	0.8621	224	167	0.8626	0.8626	197	169
933-771-755	—	0.8484	—	4	—	0.8490	—	5	—	0.8495	—	6
10.20-862	0.8278	0.8277	46	43	0.8283	0.8283	54	40	0.8288	0.8288	41	39
951-773	0.8160	0.8160	219	163	0.8166	0.8166	232	162	0.8171	0.8171	209	164
10.22-666	0.8122	0.8120	60	48	0.8128	0.8128	70	50	0.8133	0.8133	63	54
953	0.7871	0.7871	18	16	0.7877	0.7877	17	17	0.7882	0.7882	23	19

good X-ray diffraction patterns. The a values showed a gradual slight variation, confirming the existence of the series. The observed, d_o, and calculated, d_c, interplanar spacings are included in Table 1. Thus, $Mn_{1+2s}Cr_{2-3s}Sb_sO_4$ $(0.05 \leqslant s \leqslant 0.30)$ is a series of cubic spinels, space group $Fd3m$ (No. 227), $Z = 8$, and the a, U and D_c values shown in Table 2.

The observed, I_o, and calculated, I_c, intensities which gave the best discrepancy factors,

$$R = (\sum |I_o^{1/2} - I_c^{1/2}|)/\sum I_o^{1/2},$$

are also included in Table 1. Those calculated were obtained for the distribution of cations and u values—origin at centre $(\bar{3}m)$—of Table 2, where the resulting R factors are also shown. The observed a and u values are comparable to those established by Raccah *et al.*[2] for $MnCr_2O_4$ $(s = 0)$: $a = 8.43$ Å, $u = 0.264$.

The observed M—O and O—O distances and the average M—O distances calculated from Shannon[3] ionic radii are included in Table 3. The observed and calculated octahedral M—O distances are practically identical, but the observed tetrahedral M—O distances are slightly shorter than those calculated.

The observed M—O distances of Table 3 have been determined as functions of the experimental a and u values, $M—O = a(3u^2 - 2u + 3/8)^{1/2}$ at octahedral sites, and $M—O = a3^{1/2}(u - 1/8)$ in the tetrahedral sublattice. For u values typical of spinels, $0.241 \leqslant u \leqslant 0.269$, if a is increased, both distances increase; and when u is reduced, the octahedral distance is enlarged where the tetrahedral one diminishes.

Trends in a, u and M—O distances of Tables 2 and

Table 1—*continued*

	$Mn_{1.40}Cr_{1.40}Sb_{0.20}O_4$				$Mn_{1.50}Cr_{1.25}Sb_{0.25}O_4$				$Mn_{1.60}Cr_{1.10}Sb_{0.30}O_4$			
hkl	d_o	d_c	I_o	I_c	d_o	d_c	I_o	I_c	d_o	d_c	I_o	I_c
111	4.886	4.883	155	171	4.885	4.887	160	166	4.8912	4.8913	170	171
220	2.990	2.990	306	267	2.992	2.993	319	251	2.9950	2.9953	291	240
311	2.549	2.550	957	1000	2.5527	2.5523	973	1000	2.5537	2.5544	1023	1000
222	2.4409	2.4416	67	106	2.4441	2.4436	65	112	2.4450	2.4457	78	120
400	2.1137	2.1145	172	235	2.1158	2.1163	176	241	2.1178	2.1180	207	246
331	—	1.9404	—	6	—	1.9420	—	10	—	1.9436	—	14
422	1.7268	1.7265	92	82	1.7276	1.7279	83	79	1.7296	1.7293	86	77
511-333	1.6282	1.6277	344	340	1.6287	1.6291	362	330	1.6308	1.6304	336	326
440	1.4957	1.4952	403	417	1.4967	1.4964	414	419	1.4984	1.4977	394	420
531	1.4299	1.4297	16	21	1.4308	1.4308	17	22	1.4325	1.4320	13	23
620	1.3375	1.3373	26	28	1.3387	1.3384	32	27	1.3396	1.3395	31	27
533	1.2895	1.2898	93	87	1.2911	1.2909	96	87	1.2921	1.2920	102	88
622	1.2756	1.2751	50	52	1.2765	1.2761	49	53	1.2775	1.2772	48	56
444	1.2207	1.2208	33	30	1.2218	1.2218	28	32	1.2225	1.2228	27	34
711-551	1.1842	1.1844	8	12	1.1853	1.1853	12	12	1.1859	1.1863	9	13
642	1.1301	1.1302	42	35	1.1312	1.1312	43	33	1.1320	1.1321	49	31
731-553	1.1011	1.1011	131	135	1.1020	1.1020	137	137	1.1028	1.1030	157	140
800	1.0572	1.0573	46	52	1.0580	1.0581	50	53	1.0589	1.0590	51	53
733	—	—	—	—	—	1.0333	—	1	—	1.0350	—	1
822-660	0.9967	0.9968	26	19	0.9977	0.9976	19	17	0.9983	0.9984	18	16
751-555	0.9767	0.9766	108	90	0.9775	0.9775	85	90	0.9782	0.9783	98	90
662	0.9702	0.9702	27	28	0.9710	0.9710	32	29	0.9717	0.9718	24	30
840	0.9457	0.9456	34	41	0.9464	0.9464	31	45	0.9471	0.9472	30	48
911-753	—	0.8771	—	8	0.9290	0.9292	6	9	—	0.9299	—	9
664	0.9016	0.9016	10	8	0.9020	0.9024	8	8	0.9031	0.9031	10	8
931	0.8867	0.8866	104	87	0.8872	0.8874	90	85	0.8880	0.8881	108	84
844	0.8633	0.8632	228	171	0.8639	0.8640	199	175	0.8647	0.8647	175	178
933-771-755	—	0.8501	—	7	—	0.8508	—	8	—	0.8515	—	9
10.20-862	0.8294	0.8294	33	37	0.8300	0.8301	46	35	0.8308	0.8307	34	34
951-773	0.8177	0.8177	190	165	0.8183	0.8183	191	161	0.8190	0.8190	150	159
10.22-666	0.8139	0.8139	72	58	0.8145	0.8145	50	58	0.8152	0.8152	51	60
953	0.7887	0.7887	22	21	0.7894	0.7894	14	21	0.7900	0.7900	24	22

3 are clear if the $Mn_{1+2s}Cr_{2-3s}Sb_sO_4$ series is thought as derived from the normal spinel $MnCr_2O_4$ by partial replacement of Cr^{3+} at octahedral positions by the more voluminous $2/3Mn^{2+} + 1/3Sb^{5+}$ *cation*. As the substitution goes along, a increases and u is lowered: both contribute to the enlargement of the octahedral distances; and the diminishing effect of u on the tetrahedral distances is

Table 2. Structural data for six samples of the series $Mn_{1+2s}Cr_{2-3s}Sb_sO_4$ ($0.05 \leqslant s \leqslant 0.30$)

s	a (Å)	U (Å^3)	D_c (g cm^{-3})	Distribution of cations*	u	R
0.05	8.444(1)	601.4	5.01	$Mn(Mn_{0.10}Cr_{1.85}Sb_{0.05})$	0.262	0.065
0.10	8.447(1)	602.7	5.08	$Mn(Mn_{0.20}Cr_{1.70}Sb_{0.10})$	0.261	0.079
0.15	8.452(1)	603.8	5.15	$Mn(Mn_{0.30}Cr_{1.55}Sb_{0.15})$	0.261	0.066
0.20	8.458(1)	605.1	5.23	$Mn(Mn_{0.40}Cr_{1.40}Sb_{0.20})$	0.261	0.068
0.25	8.465(1)	606.6	5.30	$Mn(Mn_{0.50}Cr_{1.25}Sb_{0.25})$	0.259	0.068
0.30	8.472(1)	608.1	5.37	$Mn(Mn_{0.60}Cr_{1.10}Sb_{0.30})$	0.258	0.068

* Octahedral (d) cations are in parentheses.

Table 3. Observed (o) and calculated (c) distances (Å) for $MnCr_2O_4$* and six samples of the series $Mn_{1+2s}Cr_{2-3s}Sb_sO_4$ ($0.05 \leqslant s \leqslant 0.30$)

	Tetrahedral (a) sites			Octahedral (d) sites			
s	M—O_o	M—O_c	O—O_o	M—O_o	M—O_c	O—O_o	O—O'_o
0.00*	2.03	2.04	3.32	2.00	2.00	2.65	2.99
0.05	2.00	2.04	3.27	2.01	2.01	2.70	2.99
0.10	1.99	2.04	3.25	2.02	2.02	2.72	2.99
0.15	1.99	2.04	3.25	2.02	2.03	2.73	2.99
0.20	1.99	2.04	3.25	2.03	2.04	2.73	3.00
0.25	1.97	2.04	3.21	2.04	2.05	2.78	3.00
0.30	1.95	2.04	3.19	2.05	2.06	2.80	3.00

* Calculated from a and u values of Raccah *et al.*[2]

somewhat more pronounced than that produced by raising a.

Acknowledgements—We express our gratitude to Miss B. Galar for technical assistance. One of us, I.R., acknowledges the financial aid of the Comisión Asesora de Investigación Científica y Técnica.

REFERENCES

1. P. García Casado and I. Rasines, *Z. Krist.* 1982, **160**, 34.
2. P. M. Raccah, R. J. Bouchard and A. Wold, *J. Appl. Phys.* 1966, **37**, 1436.
3. R. D. Shannon, *Acta Cryst. A* 1976, **32**, 751.

Polyhedron Vol. 4, No. 3, pp. 521–522, 1985
Printed in Great Britain

0277–5387/85 $3.00 + .00
© 1985 Pergamon Press Ltd

COMMUNICATION

ON A CONVENIENT SYNTHESIS OF $WOCl_4$ AND THE QUESTION OF THE EXISTENCE OF Cp_2WOCl_2

ROBERT H. CRABTREE* and GREGORY G. HLATKY

Sterling Chemistry Laboratory, 225 Prospect Street, New Haven, Connecticut, U.S.A.

(*Received* 10 *April* 1984; *accepted* 5 *July* 1984)

Abstract—$WOCl_4$ is synthesised from tungstic acid in refluxing $SOCl_2$. The literature report of the synthesis of Cp_2WOCl_2 from $WOCl_4$ and cyclopentadiene could not be confirmed.

We were attracted to the report of Multani *et al.*[1] on a synthesis of a material described as Cp_2WOCl_2 by simple reflux of $WOCl_4$ with cyclopentadiene in benzene. This seemed an unexpectedly simple entry into the "Cp_2W" series. Although the product is a 20-electron molecule as written, ways exist to reduce the electron count, e.g. $(\eta^3\text{-Cp})(\eta^5\text{-Cp})WOCl_2$ or $[(\eta^5\text{-Cp})_2WO]Cl_2$.

The reported synthesis appears to be quite general, a whole range of unprecedented organometallic compounds being formed, e.g. $(C_7H_7)MOCl_2$[2] from $MOCl_4$ and cycloheptatriene (M = Mo or W) and $(C_8H_7)_2MoOCl_2$[3] from $MoOCl_4$ and cyclooctatetraene. Related Ti, Zr and Hf complexes are also reported.

We were unable to repeat the synthesis of Cp_2WOCl_2 and the recent report by Deacon *et al.*[4] on their failure to confirm other work by Multani *et al.*[1] prompts us to report our results. The reported synthesis of Cp_2WOCl_2 requires $WOCl_4$ and in the course of this work, we discovered a new and much more convenient synthesis of this compound, which we report here.

$WOCl_4$ has been synthesised by several methods, all of which require relatively forcing conditions. The best ones previously available were chlorination of WO_3 with $SOCl_2$ for 6–12 h at 200°C,[5] with Cl_2–CCl_4 for 3 h at 200°C,[6] or with C_5Cl_8 for 10 min at 290°C.[7] In contrast, the corresponding molybdenum complex, $MoOCl_4$, can be readily prepared from MoO_3 in refluxing $SOCl_2$[8] (79°C). WO_3 does not react at all under these conditions. The closely related hydrated oxide, tungstic acid,[9] $WO_3 \cdot xH_2O$ does react, when freshly prepared, and 65% yields of $WOCl_4$ can be isolated by sublimation. These are the mildest conditions yet reported for the synthesis of this compound.

On refluxing the $WOCl_4$ so obtained with dry cyclopentadiene by the method of Multani *et al.*[1] we obtained a tan solid that seemed to be a mixture of oxyhalides but did not appear to contain any organic material (^1H NMR) and could not be recrystallised. We could not obtain any characterisable organometallic product *via* the alternative route described by Multani *et al.*[1] from NaC_5H_5 and $MoOCl_4$.[1,10] Since the IR spectra and physical properties of our materials were quite different from those reported for Cp_2WOCl_2, we clearly did not obtain the previously reported material. We cannot, of course, exclude the possibility that some subtle but important differences in experimental technique are responsible for our failure to obtain Cp_2WOCl_2.

We also tried to repeat the synthesis of $(C_7H_7)MoOCl_2$[2] and $(C_7H_7)_2ZrCl_2$[3] by refluxing cycloheptatriene with $MoOCl_4$ and $ZrCl_4$, again without success.

EXPERIMENTAL

Solvents and reagents (Aldrich Chemical Co.) were distilled before use. Metal halides were purchased (Alfa) except for $WOCl_4$, which was synthesised. Reactions were carried out under dry

* Author to whom correspondence should be addressed.

N_2. IR spectra were recorded on a Nicolet 7000 FT-IR.

Tungsten oxytetrachloride

Tungstic acid (1 g, obtained by Morley's[9] method A from ammonium or sodium tungstate and 1 N HCl) was placed in a widemouth Schlenk tube fitted with a reflux condenser. $SOCl_2$ (20 cm^3) was added and the mixture refluxed for 6 h under dry air or nitrogen. The Schlenk tube was cooled, and the volatiles removed *in vacuo* (care should be taken to prevent damage to the vacuum pump by the HCl present in the flask, by interposing an NaOH acid-trap after the cold trap). Pure $WOCl_4$ was then sublimed *in vacuo* as glistening red needles on to a cold finger inserted into the Schlenk tube. Yield: 0.65 g (65%) of a red product, m.p. 208°C (lit.:[7] 210°C). Found: Cl, 41.28%. Calc. for Cl_4OW: Cl, 41.5%. It was instantly decomposed by water and slowly decomposed by atmospheric moisture.

REFERENCES

1. S. P. Anand, R. K. Multani and B. D. Jain, *Curr. Sci.* 1968, 487.
2. K. M. Sharma, S. K. Anand, R. K. Multani and B. D. Jain, *J. Organomet. Chem.* 1970, **23**, 173.
3. K. M. Sharma, S. K. Anand, R. K. Multani and B. D. Jain, *J. Organomet. Chem.* 1970, **22**, 685.
4. G. B. Deacon, T. D. Tuong and D. G. Vince, *Polyhedron* 1983, **2**, 969.
5. H. Hecht, G. Jander and H. Schlapmann, *Z. Anorg. Allg. Chem.* 1947, **254**, 261.
6. A. Michael and A. Murphy, *Am. Chem. J.* 1910, **44**, 382.
7. S. E. Feil, S. Y. Tyree, F. N. Collier, R. E. McCarley and P. B. Fleming, *Inorg. Synth.* 1967, **9**, 123.
8. R. Colton, I. B. Tompkins and P. W. Wilson, *Aust. J. Chem.* 1964, **17**, 496.
9. (a) A. M. Morley, *J. Chem. Soc.* 1930, 1987; (b) The product should not be heated prior to reaction with the $SOCl_2$,
10. S. P. Anand, R. K. Multani and B. D. Jain, *J. Organomet. Chem.* 1969, **17**, 423.

Polyhedron Vol. 4, No. 3, p. 523, 1985
Pergamon Press Ltd. Printed in Great Britain

BOOK REVIEW

Gmelin Handbook of Inorganic Chemistry. Ti—Organotitanium Compounds. Part 4: Mononuclear Compounds 4, Cumulative Index for Parts 1 to 4. Published by Gmelin Institute for Inorganic Chemistry of the Max Planck Society for the Advancement of Science, Springer, Berlin, 8th edition, 1984, 17 illustrations, ix + 242 pp., DM851, approx. $330.20.

The growth of organotitanium chemistry over the past decade is appropriately recognised in the publication of this, the fourth in a series of volumes concerned with organotitanium chemistry. It covers the literature in detail up to the end of 1979, a few later references also being included. The volume continues the treatment of titanium compounds with two ^{5}L-groups (^{5}L being the symbolism used to represent a ligand bound to titanium by five carbon atoms), and concludes with a discussion of complexes containing ^{n}L-ligands where $n > 5$. Some examples of compounds treated in this volume are $(\pi\text{-}C_5H_5)_2Ti(CO)_2$, the titanacyclic compounds $(\pi\text{-}C_5H_5)_2Ti([CH_2]_4)$, $(\pi\text{-}C_5H_5)_2Ti([CH_2]_5)$ and $(\pi\text{-}C_5H_5)_2Ti(C_6H_5C{=}C_6H_5]_2)$, the π-allyl complex $(\pi\text{-}C_5H_5)_2TiC_3H_5\text{-}\pi$, compounds with arene ligands such as $(\pi\text{-}C_6H_6)_2Ti$ and $\pi\text{-}C_6H_6Ti(Cl_2AlCl_2)_2$, as well as the compounds $\pi\text{-}C_7H_7TiC_5H_5\text{-}\pi$, $\pi\text{-}C_8H_8TiC_5H_5\text{-}\pi$ and $(\pi\text{-}C_5H_4(CH_2)_2C_5H_4\text{-}\pi)TiCl_2$ which contain ^{7}L-, ^{8}L- and ^{10}L-ligands, respectively. The volume is authoritative and beautifully produced, and many data are contained in well-arranged tables. There is also an empirical formula index and a very large (85 pp.) ligand formula index which should assist readers greatly. The cost is, of course, immense and one only hopes that libraries can continue to afford to buy quality productions such as this undoubtedly is.

R. J. H. CLARK

Department of Chemistry
University College
20 Gordon St.
London WC1H 0AJ
U.K.

Polyhedron Vol. 4, No. 3, p. 525, 1985
Pergamon Press Ltd. Printed in Great Britain

ERRATUM

R. K. Iyer, S. G. Deshpande and V. Amirthalingam, Preparation, properties and molecular structure of monohydrogen diethylenetriaminepentaacetatostannate(IV) trihydrate—an eight coordinated 1 : 1 tin(IV) chelate. *Polyhedron* 1984, **3**, 1099–1104.

The authors regret that Fig. 3 (p. 1103) of the above article is incorrect. The correct figure is published below.

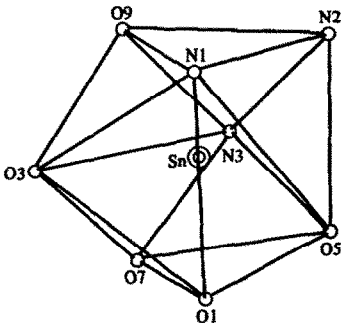


Fig. 3. The coordination polyhedra around Sn^{4+}—a distorted dodecahedron [the two interlocking trapezia are formed by the nearly planar groups: (1) $O_5N_2O_9O_3$ and (2) $O_1N_1N_3O_7$].

Polyhedron Vol. 4, No. 4, pp. 527–531, 1985
Printed in Great Britain

0277–5387/85 $3.00 + .00
© 1985 Pergamon Press Ltd

FAR-IR SPECTRA OF CHARGE-TRANSFER COMPLEXES BETWEEN IX (X = Cl, Br OR I) AND *TRANS*-1,2-BIS(4-PYRIDYL)ETHYLENE, 1,2-BIS(4-PYRIDYL)ETHANE AND 4,4′-BIPYRIDYL

KOYO AIDA, KANJI YOSHIDA* and KEIKO KATO†
Department of Engineering Science, Faculty of Engineering, Tohoku University, Sendai, Japan

(*Received* 6 *April* 1984: *accepted* 9 *July* 1984)

Abstract—Far-IR spectra of charge-transfer complexes of *trans*-1,2-bis(4-pyridyl)ethylene (Bpe), 1,2-bis(4-pyridyl)ethane (Bpa) and 4,4′-bipyridyl (4,4′-Bpy) with IX (X = Cl, Br or I) have been measured as solids. Assignments for the modified IX stretching and the intermolecular NI stretching vibrations are proposed. The force constants for these vibrations have been calculated assuming a linear triatomic model, putting a donor molecule as a point mass. It is concluded that the donor tendency towards the halogens is in the order Bpe > Bpa > 4,4′-Bpy.

Numerous studies have been reported on the vibrational spectra of charge-transfer (CT) complexes between halogens or interhalogens and pyridine (Py) or substituted Pys.[1–9] With regard to 4,4′-bipyridyl (4,4′-Bpy) as a donor, Yagi *et al.*[2] have reported far-IR frequencies of its ICl and IBr complexes. 4,4′-Bpy is a weak base consisting of two Py rings joined together at the 4-position on each ring. *trans*-1,2-Bis(4-pyridyl)ethylene (Bpe) and 1,2-bis(4-pyridyl)ethane (Bpa) are analogous compounds in which two Py rings are separated by C=C and C—C bonds, respectively. It is of interest to measure the far-IR spectra of their IX (X = Cl, Br or I) complexes and to investigate their donor ability towards halogens in comparison with that of 4,4′-Bpy.

EXPERIMENTAL

Bpe and Bpa from Aldrich Chemical Co. were purified by recrystallization from benzene and a benzene–cyclohexane (1 : 3) mixed solvent, respectively. Bpe: m.p. 152°C (lit.,[10] 151–152°C). Bpa: m.p. 110°C (lit.,[10] 110–111°C). 4,4′-Bpy from Wako Chemical Co. was used without further purification, m.p. 112.5°C (lit.,[11] 111.8–120°C). I_2 was purified by sublimation under vacuum. ICl and IBr from Nakarai Chemical Co. were used without further purification. CCl_4 was dried with $CaCl_2$ and then distilled twice.

Complexes were prepared by slowly mixing CCl_4 solutions (~0.05 *M*) of the two components. Complexes were obtained in the form of fine needles with light yellow (ICl complexes), yellow (IBr complexes) and dark orange (I_2 complexes), except for the I_2 complex of Bpa, which was obtained in the form of red brown plates. The products were filtered, washed with CCl_4 and dried in *vacuo*. Analytical results are given in Table 1 and are in good agreement with those values calculated for 1 : 2 complexes. Decomposition points for these complexes are also included in the table.

Far-IR spectra (400–50 cm^{-1}) were recorded on a Hitachi FIS-III spectrophotometer which was evacuated to remove atmospheric water vapor. Samples were measured in Nujol mulls spread on polyethylene plates.

RESULTS AND DISCUSSION

Hassel and Rømming[12] have reported an X-ray study on the structure of the Py·ICl complex and have shown that the ring nitrogen atom forms a donor–acceptor bond with the iodine atom, resulting in a linear N—I—Cl arrangement. It seems quite reasonable to assume the same arrangement for each nitrogen atom with IX in the present complexes. Then, we can expect three vibrational

* Present address: Suntory Ltd, Osaka, Japan.
† Author to whom correspondence should be addressed.

Table 1. Analytical results for halogen complexes

			C (%)	H (%)	N (%)	Halogen (%)	Decomposition point (°C)
Bpe	2ICl	Found	29.74	1.92	5.13	63.56	154
		Calc.	28.40	1.97	5.57	64.06	
	2IBr	Found	24.83	1.45	4.42	70.20	150
		Calc.	24.17	1.68	4.73	69.42	
	$2I_2$	Found	20.87	1.34	3.78	74.02	144
		Calc.	20.87	1.45	4.09	73.59	
Bpa	2ICl	Found	29.43	2.31	5.44	63.55	148
		Calc.	28.29	2.36	5.55	63.80	
	2IBr	Found	24.59	1.85	4.41	68.67	145
		Calc.	24.09	2.01	4.72	69.18	
	$2I_2$	Found	21.32	1.56	3.83	72.86	126
		Calc.	20.81	1.73	4.08	73.38	
4,4′-Bpy	2ICl	Found	25.55	1.53	5.51	67.80	145
		Calc.	24.95	1.66	5.86	67.52	
	2IBr	Found	21.84	1.42	4.81	72.00	140
		Calc.	21.06	1.40	4.95	72.59	
	$2I_2$	Found	18.66	1.18	4.03	76.00	136
		Calc.	18.08	1.21	4.25	76.46	

modes for this portion, the modified interhalogen IX stretching, the intermolecular NI stretching and the NIX bending vibrations. These vibrations are expected to appear in the far-IR region. The far-IR spectra for these CT complexes are shown in Fig. 1, together with those for free donor molecules.

It is well established that the IX stetching vibration decreases in frequency and increases in intensity upon complex formation. For instance, Yarwood[6] has reported the ICl stretching frequency in the Py·ICl complex to be near 270 cm^{-1}, which is lower than that of "free" ICl at 384 cm^{-1}.[13] He has also assigned absorptions near 175 and 80 cm^{-1} to the intermolecular NI stretching and the NICl bending vibrations, respectively.

As Fig. 1 shows, two new bands appear upon complex formation in each case. Taking their positions into consideration, these absorptions can

Table 2. Far-IR frequencies (cm^{-1}) for halogen complexes

	2ICl		2IBr		$2I_2$	
	ν_{ICl}	ν_{NI}	ν_{IBr}	ν_{NI}	ν_{II}	ν_{NI}
Bpe	262	151	184	138	155	110
Bpa	266	150	187.5	138	157.5	108.5
4,4′-Bpy	276	155	198 189	139	158	114
4,4′-Bpy*	274	154.5	194.5 187	138	—	—
2,2′-Bpy*	284.5 268	151 130.5	211 203	135	—	—
Py*	274 266	178 169.5	199 190	158.5	—	—

* Ref. 2.

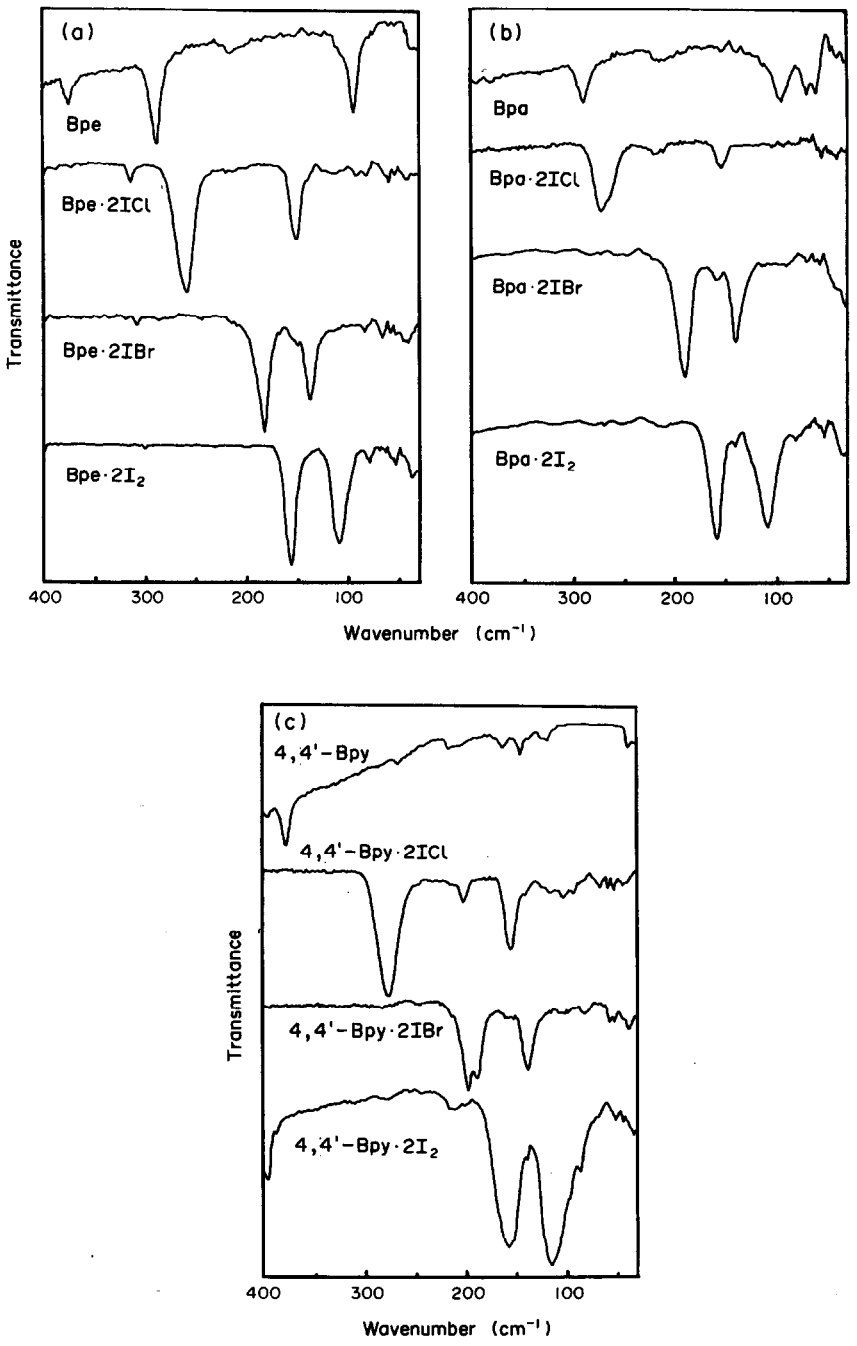


Fig. 1. Far-IR spectra of: (a) Bpe and its halogen complexes, (b) Bpa and its halogen complexes, and (c) 4,4'-Bpy and its halogen complexes.

be assigned to the modified IX stretching and the intermolecular NI stretching vibrations, respectively. A possible NIX bending vibration could not be clearly identified in each case. They are probably too weak to be observed. The fact that only one absorption appears for each stretching vibration suggests that the vibrational coupling between two NIX groups must be very small.

The proposed assignments are summarized in Table 2, together with those for 4,4'-Bpy, 2,2'-Bpy and Py reported by Yagi *et al.*[2] The splitting of the IBr stretching frequency in the 4,4'-Bpy·2IBr complex has already been discussed by Yagi *et al.*[2] and the present results are in good agreement with theirs.

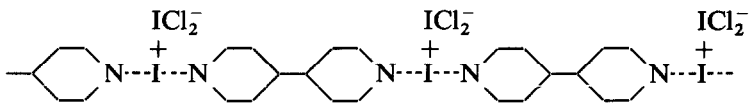
The results for 4,4'-Bpy·2ICl are of some interest in view of its structure. Popov *et al.*[11] have proposed the following polymeric structure for this complex

because of its high decomposition point starting at 230°C, higher than usual for a monomeric CT complex such as 2,2′-Bpy·2ICl, which has a decomposition point starting at 140°C.[11] However, the present ICl complex of 4,4′-Bpy has a decomposition point starting at 145°C, almost the same decomposition point as those of the other complexes, as Table 1 shows. Moreover, if the ICl complex has the above polymeric structure, then we can expect a strong absorption near 230 cm^{-1}, which is assigned to the ν_3-vibration of the ICl_2^- ion. However, there is no absorption near 230 cm^{-1} in the far-IR spectrum of 4,4′-Bpy·2ICl, as Fig. 1 shows. These facts suggest that the present ICl complex of 4,4′-Bpy is not the same complex as that of Popov *et al.*[11] Considering the spectra shown in Fig. 1 and the decomposition points listed in Table 1, it is most likely that these CT complexes, including 4,4′-Bpy·2ICl, have a monomeric structure with the usual donor–acceptor bonds.

As halogens are sacrificial acceptors, increasing electron transfer is accompanied by a progressive weakening of the interhalogen bond. Thus, the relative change in the interhalogen stretching force constant can be used to measure the extent of donor–acceptor interaction. Several attempts have been made to calculate the force constants for the halogen complexes with nitrogen donors under the assumption of a linear triatomic model, putting a donor molecule as a point mass.[2,4] It is not certain whether the same assumption holds in the present complexes, as there are two NIX groups in each of the present complexes. However, as was pointed out before, the vibrational coupling between these two NIX groups seems to be very small. In the case of *p*-dithian·2IX (X = Br or I), the calculation has been made under the assumption of a linear triatomic model, with no vibrational coupling between two SIX groups, and the results were found to be reasonable. Therefore, it is worthwhile to make the same calculation under this simple assumption.

An additional assumption is necessary about the interaction constant, k_{12}, because there are three force constants for two observable stretching frequencies. So far, $k_{12} = 0.40$ N cm^{-1} has been widely used by previous authors for many halogen complexes of nitrogen donors.[2,4,6] Adopting the same value for k_{12}, the force constants were calculated with a linear D—I—X model, where D represents the whole donor molecule. The results are given in Table 3.

In order to verify the aforementioned treatment,



the force constant for the "pure" dative structure, $D^+—I^-$, k^o_{DI}, has been calculated. Yarwood[14] has shown that k^o_{DI} is about 2.5 N cm^{-1} for halogen complexes of Py. From Table 3, it is seen that this value is nearly 2.5 N cm^{-1} for each complex and this probably suggests that the treatment is reasonable.

Table 3 shows that the relative change in the interhalogen stretching force constant, W, defined by $(k^o_{IX} - k_{IX})/k^o_{IX}$, where k^o_{IX} denotes the force constant calculated from the gas-phase frequency, increases in the order I_2, IBr and ICl for each donor molecule. Also, the intermolecular stretching force constant, k_{DI}, which directly reflects the strength of the donor–acceptor bond, increases in the same order. This is in agreement with what might be expected from the strength of acidity of halogens.

For the same acceptor molecule, W increases in the order 4,4′-Bpy, Bpa and Bpe. With regard to 4,4′-Bpy and Bpe, this is in agreement with their pK_a value. The pK_a value for Bpa is not known, but from Table 3 it is expected to be close to that of Bpe, i.e. somewhere around 5.5. In conclusion, the donor tendency towards the halogens is in the order 4,4′-Bpy < Bpa < Bpe.

Table 3. Force constants (N cm^{-1}) calculated with $k_{12} = 0.40$ N cm^{-1}

	pK_a*		k_{IX}	k_{DI}	W†	k^o_{DI}
Bpe	5.9	2ICl	1.23	1.18	0.48	2.46
		2IBr	1.12	1.09	0.45	2.42
		$2I_2$	1.11	0.76	0.35	2.17
Bpa	—	2ICl	1.26	1.18	0.47	2.51
		2IBr	1.16	1.09	0.43	2.53
		$2I_2$	1.14	0.75	0.33	2.27
4,4′-Bpy	4.9	2ICl	1.35	1.15	0.43	2.67
		2IBr	1.24	1.02	0.39	2.62
		$2I_2$	1.14	0.75	0.33	2.27

* D. K. Lavallee and E. B. Fleisher, *J. Am. Chem. Soc.* 1972, **94**, 2538.

† $W = (k^o_{DI} - k_{DI})/k^o_{DI}$, where $k^o_{ICl} = 2.38$ N cm^{-1}, $k^o_{IBr} = 2.05$ N cm^{-1} and $k^o_{II} = 1.71$ N cm^{-1}.

REFERENCES

1. S. G. W. Ginn and J. L. Wood, *Trans. Faraday Soc.* 1966, **62**, 777.
2. Y. Yagi, A. I. Popov and W. B. Person, *J. Phys. Chem.* 1967, **71**, 2439.
3. R. F. Lake and H. W. Thompson, *Proc. R. Soc.* 1967, **A297**, 440; *Spectrochim. Acta* 1968, **24A**, 1321.
4. J. Yarwood and W. B. Person, *J. Am. Chem. Soc.* 1968, **90**, 594, 3930.
5. S. G. W. Ginn, I. Haque and J. L. Wood, *Spectrochim. Acta* 1968, **24A**, 1531.
6. J. Yarwood, *Spectrochim. Acta* 1970 **26A**, 2079.
7. K. Sasaki and K. Aida, *J. Inorg. Nucl. Chem.* 1980, **42**, 13.
8. K. Kato, K. Sasaki and K. Aida, *Spectrochim. Acta* 1982, **38A**, 1011.
9. K. Kato, N. Yoshio and K. Aida, *Spectrochim. Acta*, 1984, **40A**, 373.
10. H. I. Thayer and B. B. Corson, *J. Am. Chem. Soc.* 1948, **70**, 2330.
11. A. I. Popov, J. C. Marshall, F. B. Stute and W. B. Person, *J. Am. Chem. Soc.* 1961, **83**, 3586.
12. O. Hassel and C. Rømming, *Acta Chem. Scand.* 1956, **10**, 696.
13. K. Sasaki, I. Kuwano and K. Aida, *J. Inorg. Nucl. Chem.* 1981, **43**, 485.
14. J. Yarwood (Ed.), *Spectroscopy and Structure of Molecular Complexes.* Plenum, New York (1973).

Polyhedron Vol. 4, No. 4, pp. 533–538, 1985.
Printed in Great Britain

0277–5387/85 $3.00 + .00
© 1985 Pergamon Press Ltd

CATALYTIC ISOMERISATION OF ALKENES BY $Fe(CO)_4$

V. V. KANE, J. R. C. LIGHT* and M. C. WHITING
Dyson Perrins Laboratory, Oxford, U.K.; and Chemistry Department, The University, Bristol BS8 1TS, U.K.

(*Received* 17 *May* 1984; *accepted* 27 *July* 1984)

Abstract—Photolysis of alkene solutions of iron dodecacarbonyl at wavelengths greater than 500 nm causes dissociation into $Fe(CO)_4$. With ethylene and propene the latter forms (alkene)$Fe(CO)_4$ complexes. With higher alkenes it promotes isomerisation of terminal to internal alkenes. This isomerisation is non-sequential.

Preliminary observations on the isomerisation of *n*-octenes by photolysed $Fe_3(CO)_{12}$ have been published,[1] and the full details of this are presented here, together with evidence that $Fe(CO)_4$ is the catalytic agent. The participation of $Fe(CO)_4$ has been suggested in other reactions,[2] produced from $Fe_3(CO)_{12}$ thermally or by IR irradiation of $Fe(CO)_5$, and the existence of discrete $Fe(CO)_4$ has been demonstrated in frozen gas matrices[3] and in a polymer matrix.[4]

RESULTS AND DISCUSSION

Formation of $Fe(CO)_4$

The electronic spectrum of iron dodecacarbonyl has a maximum at 450 nm overlapping the tail of strong absorption in the UV region. There is a more pronounced maximum at 605 nm, and the radiation used was filtered to ensure absorption in this region only. At 373 K the thermal decomposition of $Fe_3(CO)_{12}$ to $Fe(CO)_5$ in hexane solution is appreciable but at 293 K formation of $Fe(CO)_5$ was immeasurable in the dark.

Irradiation of solutions of $Fe_3(CO)_{12}$ at 293 K under nitrogen produces $Fe(CO)_5$ in 96% yield according to the equation

$$5Fe_3(CO)_{12} \rightarrow 12Fe(CO)_5 + 3(Fe),$$

where (Fe) represents iron bound in the uncharacterised precipitate. Similar results were obtained under argon and hydrogen atmospheres. Replacement of the nitrogen by carbon monoxide, however, led to all the iron being converted to $Fe(CO)_5$:

$$Fe_3(CO)_{12} + 3CO \rightarrow 3Fe(CO)_5$$

and no initial precipitate was formed, although of course $Fe(CO)_5$ itself decomposes slowly giving a brown precipitate.

These results suggested that the photodissociation was simply

$$Fe_3(CO)_{12} \rightarrow 3Fe(CO)_4.$$

Reaction with ethylene

Irradiation of iron dodecacarbonyl solutions in the presence of ethylene gave a solution having a complex IR spectrum in the metal–carbonyl stretching region (Table 1). Bands due to $Fe(CO)_5$ and $(C_2H_4)Fe(CO)_4$ were detected, and the PMR spectrum[5] confirmed the presence of $(C_2H_4)Fe(CO)_4$. The presence of other species was suspected because of variations in relative peak heights and half-widths, and of small shifts in the position of maxima in IR spectra obtained from different experiments. These variations did not appear to be produced by differences in concentration, temperature or length of irradiation. Small differences resulted from the use of non-purified hydrocarbon solvents, and large ones from the use of halogenated solvents, or unfiltered radiation.

The solutions were stable at 195 K in the dark, but decomposed to $Fe_3(CO)_{12}$ in sunlight. They were moderately sensitive to oxygen, but not at all to hydrogen, carbon monoxide, propene or propyne. Addition of cyclopentadiene appeared to displace some ethylene.

* Author to whom correspondence should be addressed at: Chemistry Department, Queen Mary College, London E1 4NS, U.K.

Table 1. IR spectra in the metal–carbonyl region (in *n*-heptane, except where stated)

Species	Maxima (cm^{-1})						
$Fe_3(CO)_{12}$		2046(s)	2024(s)				
$Fe(CO)_5$			2024(s)		2001(s)		1964(vw)
$Fe(CO)_5$ in CCl_4			2028(s)		1999(s)		
$(C_2H_4)Fe(CO)_4$[16]	2088(s)		2013(sh)	2007(s)		1986(s)	
$C_2H_4 + Fe_3(CO)_{12} + h\nu$	2086(w)		2023(s)	2008(s)	2001(s)	1984(s)	
$C_3H_6 + Fe_3(CO)_{12} + h\nu$	2083(vw)		2024(s)		2001(s)	1982(s)	
$C_5H_6 + Fe_3(CO)_{12} + h\nu$	2089(w)	2047(s)	2024(s)		2001(s)	1982(s)	1974(s)

Reaction with propene

Solutions similar to, but much less stable than, those obtained with ethylene were obtained with propene.

The PMR spectrum of $C_3H_6Fe(CO)_4$ was obtained in $CFCl_3$ at 203 K and at temperatures up to 243 K showed no appreciable change, but thereafter the rate of decomposition of the complex increased and was rapid at 273 K.

The measured parameters of the spectrum are compared with literature values[6] for propene itself in Table 2. The value of zero given to J_{23}, J_{24} and J_{34} is only approximate, there being considerable peak broadening in the spectrum, probably due to suspended particles of iron produced by decomposition of the complex. However, double irradiation experiments confirmed the values obtained, and showed no signs of J_{23}, J_{24} or J_{34} coupling.

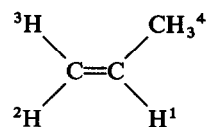
As expected the chemical shifts of protons attached to carbon atoms interacting directly with the metal are shifted to higher field. The methylene protons have a similar chemical shift to those in the ethylene complex, but the relative values of the shifts of the protons *cis* and *trans* to the lone proton are reversed with respect to the free propene, assuming that the protons have been correctly assigned (on the basis of the *trans* coupling being greater than the *cis*). The chemical shift of the methyl protons remains effectively the same.

A discussion of the significance of the value of J_{23} in terms of the bonding in the complex would not be helpful in view of the uncertainty in the value of J_{23}, and the doubts which have been expressed about the validity of correlations between coupling constants and bond angles. The reduction of coupling constants in going from the free propene to the complex is paralleled in other π-alkene complexes of iron tetracarbonyl such as $(H_2C{=}CHCOOCH_3)Fe(CO)_4$.[7]

Isomerisation of alkenes

The preceding experiments demonstrate that $Fe(CO)_4$ is formed by dissociation of $Fe_3(CO)_{12}$ resulting from absorption of light at 605 nm, and that it forms complexes with ethylene and propene. It seemed likely that it might catalyse the isomerisation of alkenes, as has since been reported to occur when alkenes were treated with various iron carbonyl species.[8] This photochemical route seemed to be a particularly clean way of preparing (alkene)$Fe(CO)_4$ species, since they would not absorb light of such wavelengths. Using hex-1-ene under the conditions

Table 2. Chemical shifts and coupling constants for propene and propeneiron tetracarbonyl



Proton	Chemical shift (δ value) Propene[6]	Complex
1	5.767	3.35
2	4.883	2.65
3	4.968	2.41
4	1.713	1.73
	Coupling constants (Hz)	
J_{12}	10.02	7.5
J_{13}	16.81	12.5
J_{14}	6.40	6.0
J_{23}	2.08	0.0
J_{24}	−1.33	0.0
J_{34}	−1.75	0.0

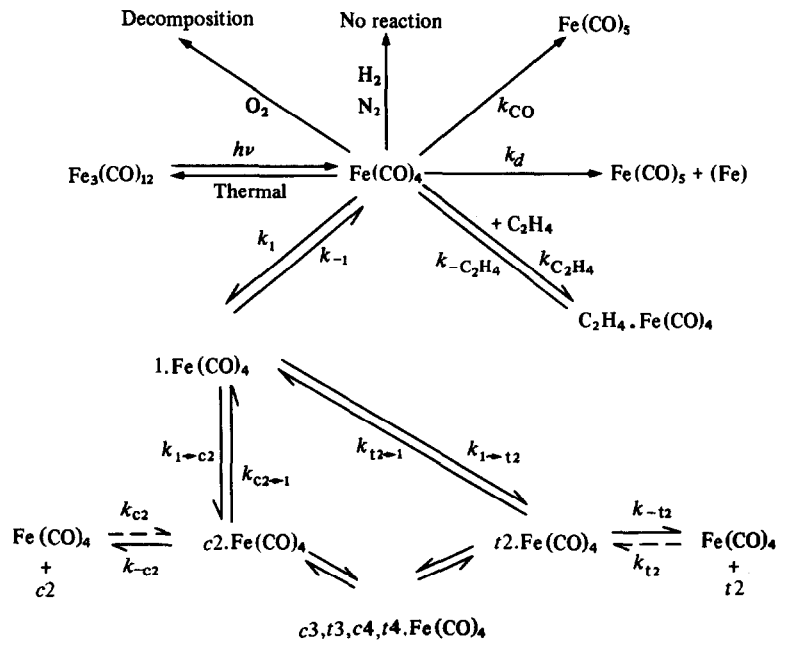
Table 3. Isomerisation of oct-1-ene in light petroleum at 293 K; product ratios, relative to *trans*-oct-3-ene = 100

Time (s)	*trans*-4 (*t*4)	*cis*-4 (*c*4)	*trans*-3 (*t*3)	*cis*-3 (*c*3)	*trans*-2 (*t*2)	*cis*-2 (*c*2)	% isomerisation
90	58.3	7.8	100	19.5	93.7	23.7	4.1
180	56.2	8.2	100	16.4	103.0	21.7	10.4
270	61.7	7.2	100	16.7	102.9	23.5	10.3
360	60.9	5.1	100	15.9	98.8	22.5	15.9
450	61.1	6.4	100	14.1	98.2	22.2	19.2
540	59.3	7.2	100	15.1	95.4	24.9	22.4
630	59.7	6.2	100	13.3	94.2	21.8	28.4
720	58.0	10.1	100	14.7	99.9	24.6	27.7
(Dequil.)[1]	82	15	100	17	104	27	—
(Dcalc.)*	59	7	100	19	97	23	—

* By least-square extrapolation.

described above it was shown that extensive isomerisation occurred, giving up to 96% of internal hexenes; that the presence of alkene inhibited the disproprotionation reaction (no immediate precipitate); that carbon monoxide inhibited the isomerisation; and that no reaction takes place in the absence of light. Using oct-1-ene it was found that no reduction to octane occurred.[9] When the mixtures obtained after varying degrees of reaction were analysed ("method B")[10] and the ratios of the products to *trans*-oct-3-ene (chosen arbitrarily) were extrapolated to zero conversion,[22] the initial product-mixture from oct-1-ene was shown already to contain substantial amounts of the oct-3-enes and oct-4-enes. Indeed, its composition did not differ greatly from that of an equilibrium mixture of the *n*-octenes.[12]

It is quite possible that the equilibrium coefficients for the six internal octenes as $Fe(CO)_4$ complexes are very similar to those for the octenes themselves, and



(1 = oct-1-ene etc.)

$k_{CO} > k_{C_2H_4} > k_1 > k_d > k_{t2}, k_{c2}, k_{H_2}\ k_{N_2}$

$k_{1\rightarrow c2}$ etc. $> k_{-c2}$ etc.

Scheme 1.

that (oct-1-ene)$Fe(CO)_4$ rapidly converts to this equilibrium mixture, before the much slower equilibration between these alkenes and their complexes makes significant progress. Alternatively, the rate of dissociation of the complexes may be slower than that of the isomerisation processes but not much slower than the slowest of these, perhaps $k_{t3\rightarrow c4}$. In that case the kinetic product mixture will be distorted from the hypothetical equilibrium mixture. The marked delay in the precipitation of iron (or iron sub-carbonyl species) when hex-1-ene is present suggests that the complexing rate of a terminal alkene, k_1, compares favourably with that of disproportionation, k_d, and this was confirmed when oct-1-ene and $Fe_3(CO)_{12}$ were irradiated in a *ca* 700 : 1 molar ratio, when at least 270 mol of oct-1-ene were isomerised per mol of $Fe_3(CO)_{12}$. However, the similar isomerisation of *cis*- and *trans*-oct-4-enes could not be examined in detail, because the disproportionation process in this case proved to be relatively too fast. Evidently complexing rates for disubstituted alkenes are much lower than for terminal alkenes and the $Fe(CO)_4$ complexes much less stable.

We may summarise the behaviour of $Fe(CO)_4$ in the scheme shown; its properties are reminiscent of those of a reactive intermediate of moderate stability, like CCl_2, and could in principle be explored quantitatively, using visible-light photolysis of $Fe_3(CO)_{12}$ as a cleaner source of this species than, e.g. thermolysis of $Fe_2(CO)_9$. This would require more rigorous exclusion of unwanted reactants (oxygen, impurities in solvents etc.) than was attempted here. Our work has no bearing on the mechanism of the isomerisation reaction. It has been suggested[13] that it occurs via an intermediate of the type $(CO)_3Fe(alkene)_2$ and our results are consistent with this view, providing the intermediate can be generated by some such process as the following:

$$(CO)_4Fe(alkene) + Fe(CO)_4 \rightleftharpoons (alkene)Fe(CO)_3 + Fe(CO)_5,$$

$$(alkene)Fe(CO)_3 + alkene \rightleftharpoons (alkene)_2Fe(CO)_3.$$

EXPERIMENTAL

In pilot experiments using commercial solvents unexpected peaks were obtained in the metal–carbonyl stretching region of the IR spectra. These were due to alkene impurities in the hydrocarbons (*n*-heptane, iso-octane, methylcyclohexane and cyclopentane) compexing the $Fe(CO)_4$ formed during irradiation. They were eliminated by carefully purifying the solvents (stirring for 1 week with acid potassium permanganate solution, separating, drying and filtering through two silica gel columns).

Iron dodecarbonyl was prepared both from iron pentacarbonyl[14] and di-iron nonacarbonyl.[15]

General procedure

Solutions of iron dodecacarbonyl were prepared by stirring the solid in the solvent and filtering under nitrogen and with as much protection from daylight as possible. The concentration of the solutions was calculated from the absorbance of the 605 nm absorption in the VIS (using a Unicam SP800 spectrophotometer; molar absorption coefficient of $Fe_3(CO)_{12} = 2505\ m^2\ mol^{-1}$). 25–50 cm^3 portions of the solutions in glass tubes fitted with gas inlet and outlet were immersed in a cooling bath maintained at 283–293 K by circulating the coolant through ice. The coolant contained sodium dichromate (4 g dm^{-3}), a 1 cm thickness of which was sufficient to absorb all radiation of shorter wavelength than 500 nm. Light was provided by a 2 kW xenon arc lamp. The products were examined by IR spectroscopy in 1 mm solution cells (NaCl) on a Perkin–Elmer 257 over the range 4000–650 cm^{-1}. Concentrations of $Fe(CO)_5$ were determined from the optical densities of the two major peaks by comparison with a calibration graph. Vapour phase chromatograms were run on a Perkin–Elmer F11 using a 2 m long $\frac{1}{8}''$ diameter stainless steel column packed with 25% M. & B. Embaphase silicone oil on 60–80 mesh Diatoport-S at 298 K using a flame ionisation detector, except for the analysis of octene mixtures, where method B of ref. 10 was used.

Thermal stability of $Fe_3(CO)_{12}$

A solution of $Fe_3(CO)_{12}$ in *n*-heptane was protected from the light and heated to 373 K in a stream of nitrogen. The issuing gas was passed through a trap at 195 K. Several samples were collected in succession and all contained $Fe(CO)_5$ (IR).

In a related experiment at 293 K a little $Fe(CO)_5$ was obtained initially (presumably from prior decomposition) but, thereafter, none. Thus decomposition of $Fe_3(CO)_{12}$ is appreciable at 373 K but not at 293 K.

Photolysis of $Fe_3(CO)_{12}$ *under nitrogen*

A solution of $Fe_3(CO)_{12}$ (5.67×10^{-5} mol) in *n*-heptane was irradiated at 293 K for 75 min in a slow stream of N_2. The amount of $Fe(CO)_5$ carried forward in the gas stream (8.20×10^{-8} mol) was

negligible compared to that remaining in solution (1.30×10^{-4} mol). The intense green of the $Fe_3(CO)_{12}$ had given way to the pale straw-colour of $Fe(CO)_5$, and a black precipitate had formed (5.1 mg). On the basis of carbonyl groups the yield of $Fe(CO)_5$ was 96%. The precipitate had a broad absorption at 2000 cm^{-1} and contained 57% iron (determined by dissolution in conc. HCl, reduction with $SnCl_2$, and titration against standard potassium dichromate). Qualitatively similar results were obtained under argon and hydrogen.

Photolysis of $Fe_3(CO)_{12}$ *under carbon monoxide*

A solution of $Fe_3(CO)_{12}$ (2.20×10^{-5} mol) in *n*-heptane was irradiated for 30 min in a slow stream of CO. A clear pale-yellow solution of $Fe(CO)_5$ was obtained (6.44×10^{-5} mol; 98% of the iron used) but no precipitate.

Photolysis of $Fe_3(CO)_{12}$ *under ethylene*

Passage of a slow stream of C_2H_4 through a solution of $Fe_3(CO)_{12}$ in *n*-heptane during irradiation gave a pale yellow solution, and no precipitate. The solution appeared to contain $(C_2H_4)Fe(CO)_4$ (IR, Table 1). It slowly decomposed, depositing a brown precipitate, but in sunlight some $Fe_3(CO)_{12}$ (IR, UV–VIS) was reformed. At low temperature in the dark the solution was stable for at least 2–3 weeks.

PMR spectrum of $(C_2H_4)Fe(CO)_4$

The IR spectra of solutions obtained from the irradiation of $Fe_3(CO)_{12}$ with C_2H_4 in *n*-heptane and in $CFCl_3$ were different. However, when the two solutions were diluted each with an equal volume of the other solvent (i.e. *n*-heptane with $CFCl_3$; $CFCl_3$ with *n*-heptane) the resulting solutions had identical spectra. This suggests that the differences in the spectra are a solvent effect and that the species present are in fact the same. Solutions in CCl_4 paralleled the behaviour of those in $CFCl_3$. The slow decomposition of the complex, on the other hand, is probably different in the two types of solvents, since in hydrocarbons a brown precipitate is formed, whereas in the chlorinated solvents it is white.

$Fe_3(CO)_{12}$ (0.379 g) was stirred with $CFCl_3$ in a current of C_2H_4 and irradiated for 80 min. The solution was concentrated by vacuum evaporation of the solvent at 195 K and separated from solid matter by allowing it to evaporate in vacuum at 293 K and condensing the evaporate. The PMR spectrum (100 M.c. Varian HA100 NMR spectrometer) of the solution was compared with one of C_2H_4 in $CFCl_3$. There was an additional sharp singlet at δ 2.31 (relative to TMS), attributed to the complex.[5]

Reactions of $(C_2H_4)Fe(CO)_4$

A solution of the complex in *n*-heptane was prepared as before. After bubbling H_2, CO, propene and propyne through separate portions of the solution no change was found in the IR spectrum of the metal–carbonyl region. Bubbling oxygen through reduced the intensity of the spectrum.

Reactions of $Fe(CO)_4$ *with cyclopentadiene*

A solution of $Fe_3(CO)_{12}$ in *n*-heptane was irradiated for 5 min in the presence of C_5H_6. The solution became colourless and had a characteristic spectrum (Table 1). After 24 h a brown precipitate had formed.

Reaction of $(C_2H_4)Fe(CO)_4$ *with cyclopentadiene*

A solution of the ethylene complex was prepared in the usual way. C_5H_6 was added. The IR spectrum of the solution (2087, 2047, 2007, 2001, 1982, 1975 cm^{-1}) had the appearance of a mixture of the ethylene and cyclopentadiene complexes. After 24 h a brown coating had appeared on the tube, and after 48 h the IR spectrum of the solution had reverted almost completely to that of the ethylene complex, but was less intense.

Photolysis of $Fe_3(CO)_{12}$ *under propene*

This was effected in the same way as for ethylene. A mixture of $Fe(CO)_5$ with the $(CH_3CHCH_2)Fe(CO)_4$ complex was obtained, and the propene complex identified by its PMR spectrum as described above. The propene complex was much less stable than the ethylene analogue, but could be kept satisfactorily at 195 K in the dark. It did not react with H_2.

Isomerisation of 1*-hexene*

A solution of $Fe_3(CO)_{12}$ (7.97×10^{-5} mol), 1-hexene (1 cm^3) and *n*-octane (1 cm^3) in *n*-heptane (50 cm^3) was irradiated for 35 min. A heavy precipitate was produced and the solution was pale yellow.

The trap contained $Fe(CO)_5$ (2.55×10^{-7} mol). After standing, the characteristic green of $Fe_3(CO)_{12}$ returned (VIS showed 6.79×10^{-6} mol), and the solution also contained $Fe(CO)_5$ (1.97×10^{-4} mol). After 16 h the concentration of $Fe_3(CO)_{12}$ had increased to 1.06×10^{-5} mol. The ratio of internal

hexenes to 1-hexene was 41:1 (VPC). The IR spectrum indicated a trace of some compound other than $Fe(CO)_5$, presumably a hexene complex.

A solution of $Fe_3(CO)_{12}$ was divided into three 25 cm^3 portions (3.89×10^{-5} mol in each) and 1 cm^3 1-hexene was added to each. The first was kept dark, and no reaction occurred. The second was irradiated under N_2 and gave $Fe(CO)_5$ (1.06×10^{-4} mol; IR peak ratios and the presence of an additional small peak indicated some undecomposed hexene complex). The ratio of internal hexenes to 1-hexene was 1.44 to 1. The third solution was irradiated under CO. No isomerisation occurred, but a little alkene complex appeared to be present in the $Fe(CO)_5$ (1.15×10^{-4} mol).

Isomerisation of oct-1-ene

The $Fe(CO)_4$ was produced in these experiments by light from a tungsten–iodine lamp (3400 K) filtered through a Kodak No. 8 yellow filter, and the solvent was light petroleum. 25 cm^3 of $Fe_3(CO)_{12}$ solution (2 mg dm^{-3}) and 80 mg of oct-1-ene were irradiated. 30 mg of octene isomerised, i.e. 274 mol of oct-1-ene per mol $Fe_3(CO)_{12}$. In a similar experiment, the product ratios of the internal octenes were measured by VPC at 90 s intervals throughout the irradiation (Table 3). In further experiments, *cis*-oct-4-ene isomerised less than 1% after 24 min and *trans*-oct-4-ene about 2% in 23 min.

Acknowledgements—We thank the SERC for a postdoctoral fellowship to one of us (J.R.C.L.) in 1968–9, and B.P. plc for a fellowship to V.V.K. in 1963–1964. Preliminary observations were made by Dr M. D. Carr, who also devised the extrapolation procedure for the estimation of initial product distribution.

REFERENCES

1. M. D. Carr, V. V. Kane and M. C. Whiting, *Proc. Chem. Soc.* 1964, 408.
2. J. C. Hileman, *Prep. Inorg. React.* 1964, **1**, 77.
3. M. Poliakoff and J. J. Turner, *J. Chem. Soc., Dalton Trans.* 1973, 1351; and 1974, 2276.
4. M. A. De Paoli and S. M. de Oliveira, *J. Chem. Phys.* 1984, **80**, 730.
5. M. I. Davis and C. S. Speed, *J. Organomet. Chem.* 1970, **21**, 401.
6. A. B. Bothner-By and C. Naar-Colin, *J. Am. Chem. Soc.* 1961, **83**, 231.
7. E. Weiss, K. Stark, J. E. Lancaster and H. D. Murdoch, *Helv. Chim. Acta* 1963, **46**, 288.
8. E. A. Koerner von Gustorf and F.-W. Grevels, *Forsch.* 1969, **13**, 366.
9. M. D. Carr and M. C. Whiting, unpublished observations.
10. N. C. G. Campbell, J. R. P. Clarke, R. R. Hill, P. Oberhansli, J. H. Parish, R. M. Southam and M. C. Whiting, *J. Chem. Soc. (B)* 1968, 349.
11. M. Monitz and M. C. Whiting, *J. Chem. Soc., Perkin II* 1982, 613.
12. M. D. Carr, J. R. P. Clarke and M. C. Whiting, *Proc. Chem. Soc.* 1963, 333.
13. R. L. Whetten, Ke-Jian Fu and E. R. Grant, *J. Am. Chem. Soc.* 1982, **104**, 4270; and references therein.
14. W. McFarlane and G. Wilkinson, *Inorg. Synth.* 1966, **8**, 181.
15. J. Dewar and H. O. Jones, *Proc. R. Soc.* 1906, **A79**, 66.
16. H. D. Murdoch and E. Weiss, *Helv. Chim. Acta* 1963, **46**, 1588.

Polyhedron Vol. 4, No. 4, pp. 539–543, 1985
Printed in Great Britain

0277–5387/85 $3.00 + .00
Pergamon Press Ltd

SYNTHESIS, PROPERTIES AND CRYSTAL STRUCTURE OF AN *N*-CYANO-*N'*-METHYL-*N''*-[2-{(5-METHYL-1*H*-IMIDAZOL-4-YL)-METHYLTHIO}ETHYL]GUANIDINE Cu(II) PERCHLORATE COMPLEX

A. SANCHO, J. BORRAS* and L. SOTO-TUERO
Departamento de Química Inorgánica, Facultad de Farmacia, Universidad de Valencia, Valencia, Spain

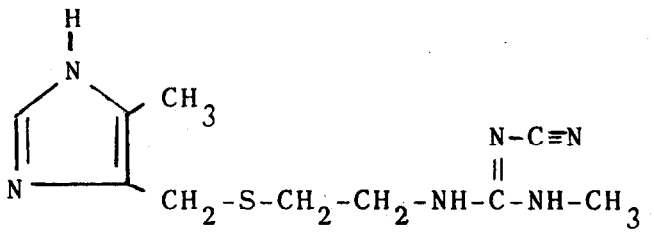
and

C. ESTEBAN-CALDERON, M. MARTINEZ-RIPOLL and S. GARCIA-BLANCO
Departamento de Rayos X, Instituto Rocasolano CSIC, Serrano 119, Madrid-6, Spain

(*Received* 4 *January* 1984; *accepted* 9 *May* 1984)

Abstract—A Cu(II) complex has been prepared with *N*-cyano-*N'*-methyl-*N''*-[2-{(5-methyl-1*H*-imidazol-4-yl)-methylthio}ethyl]guanidine, cimetidine (CM), at 1 : 3 metal to ligand ratio with the formula $Cu(CM)_2(ClO_4)_2$. Magnetic moment, IR, diffuse reflectance and EPR spectra of this compound have been recorded and discussed. The structure of $Cu(CM)_2(ClO_4)_2$ has been determined by X-ray crystallography and refined to $R = 0.042$ for 1265 observed reflexions. Cimetidine acts as a bidentate ligand through N(2) and S atoms. Cu^{2+} ions are six coordinated with a distorted octahedral environment. The cation and the perchlorate ions are linked by N—H . . . O, hydrogen bonds.

Cimetidine (CM) which has been widely studied as histamine H_2-receptor antagonist[1,2] has the structure:



and may be regarded as being composed of three main structural moieties: 4,5-disubstituted imidazole, cysteamine and the *N*-cyanoazomethine derivative. Cimetidine can act either as a bidentate ligand by formation of a 5-membered ring through N (imidazole) and S or as a tridentate ligand by coordination through N (imidazole), S and the N atom from the nitrile group.

An extensive literature exists on the metal complexes of imidazole.[3,4] mercapto-[5] and cyano[6,7]-type ligands. The study of these compounds is rapidly expanding owing to the fact that the interaction between such ligands and metal ions plays an important role in a variety of biological systems.[8]

Patel *et al.*[9] and Güven *et al.*[10] have carried out a colorimetric determination of cimetidine based on complex formation with Cu(II) acetate; however, no characterization of this complex has been reported.

It should be emphasized that complex formation between metal ions and active drugs could modify the therapeutic action of the latter.

* Author to whom correspondence should be addressed.

Our work reports the preparation, spectral and crystal structure determination of the copper(II) complex of cimetidine.

EXPERIMENTAL

Preparation of the complex

A methanolic solution of cimetidine (7.5 mmol in 50 cm^3) was slowly added to a stirred clean methanolic solution of $Cu(ClO_4)_2$ (3 mmol in 20 cm^3). A green solution was obtained; on keeping this solution open to the atmosphere at room temperature, green crystals separated within 24 h. The crystals were washed with methanol and stored under vacuum. A yield of 95% of green crystals that melt at 203°C was recovered.

Single crystals suitable for X-ray diffraction were grown in gel media by the standard technique.[11]

Analyses

The composition of the compounds was determined as follows: copper volumetrically by the iodide–thiosulphate method and C, H, N, and Cl were carried out by an elemental analyzer M.O.V. Carlo Erba.

Found: C, 31.80; H, 4.36; N, 21.93; Cu, 8.21; Cl, 9.27%. Calc. for $Cu(C_{10}H_{16}SN_6)_2(ClO_4)_2$: C, 31.29; H, 4.17; N, 21.91; Cu, 8.28; Cl, 9.24%.

Molar conductances in aqueous solution were measured using a Radiometer CDC 304 electrode (cell constant 1.0 cm) in conjunction with a radiometer CDM 83 conductivity bridge.

Spectroscopic measurements

IR spectra were taken on a Perkin–Elmer model 577 spectrophotometer as Nujol mulls (below 400 cm^{-1}) and KBr discs.

X-band EPR spectra of powder samples were recorded at room temperature on a JEOL MES-3X spectrometer. The microwave frequency was determined using DPPH as a reference and the magnetic field calibrated with a Newport Instruments NMR magnetometer.

Solid reflectance spectra were made with a Perkin–Elmer Hitachi 200 spectrophotometer, with reflectance attachment fitted.

Magnetic susceptibility measurements were made by the Gouy method with $[Ni(en)_3]S_2O_3$ as calibrant.[12]

Diamagnetic corrections were estimated from the Pascal constants.[13]

X-ray analysis

Crystal data are: $Cu(C_{10}H_{16}N_6S)_2(ClO_4)_2$, $M_r = 767.12$, $D_x = 1.51$ g cm^{-3}, monoclinic, $P2_1/c$, $a = 12.306(3)$, $b = 8.576(3)$, $c = 15.995(4)$ Å, $\beta = 94.48(2)°$, $V = 1683(1)$ $Å^3$, $Z = 2$, $\lambda(\text{Mo-}K_\alpha) = 0.71069$ Å, $\mu(\text{Mo-}K_\alpha) = 9.9$ cm^{-1}. Four-circle diffractometer, graphite monochromator, $\omega/2\theta$ scan, $\theta_{max} = 30°$, 4838 independent reflexions, 1265 observed with $I > 3\sigma(I)$, no crystal decomposition, no absorption corrections. Scattering factors[14] for neutral atoms and anomalous dispersion corrections for Cl, S and Cu. Structure solution with MULTAN,[15] anisotropic refinement[16] with full-matrix least-squares, unit weights, H-atoms found on a difference map and included in the refinement as isotropic fixed contribution. Final disagreement indices are $R = 0.042$ and $wR = 0.046$.

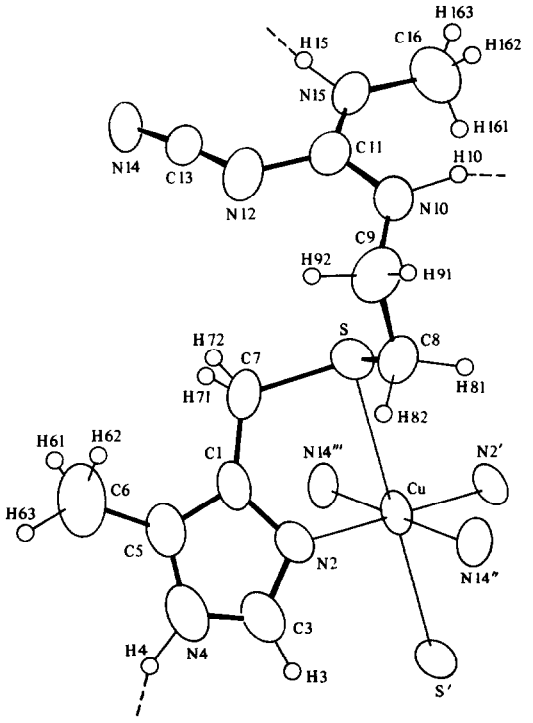


Fig. 1. Perspective drawing[17] of the cimetidine molecule together with the Cu^{2+} environment. The metal atom lies on a symmetry centre. For symmetry codes, see Table 2. Thermal ellipsoids at the 50% level. Dashed lines represent the hydrogen bonds with the perchlorate group.

* Atomic coordinates, thermal parameters, full lists of bond lengths and angles, and F_o/F_c values have been deposited as supplementary material with the Editor, from whom copies are available on request. Atomic coordinates have also been deposited with the Cambridge Crystallographic Data Centre.

Table 1. Bond lengths (Å) and bond angles (°) (ESDs in parentheses): for symmetry codes see Table 2

C(1)—N(2)	1.40(1)	C(11)—N(12)	1.35(1)
C(1)—C(5)	1.35(1)	C(11)—N(15)	1.33(1)
C(1)—C(7)	1.49(1)	N(12)—C(13)	1.30(1)
N(2)—C(3)	1.33(1)	C(13)—N(14)	1.15(1)
C(3)—N(4)	1.33(1)	N(15)—C(16)	1.47(1)
N(4)—C(5)	1.37(1)	Cl—O(1)	1.423(6)
C(5)—C(6)	1.50(1)	Cl—O(2)	1.428(7)
S—C(7)	1.813(8)	Cl—O(3)	1.412(9)
S—C(8)	1.809(9)	Cl—O(4)	1.427(8)
C(8)—C(9)	1.53(1)	Cu—S	2.790(2)
C(9)—N(10)	1.46(1)	Cu—N(2)	1.980(6)
N(10)—C(11)	1.34(1)	Cu—N(14)^{II}	2.042(7)
N(2)—C(1)—C(5)	108.8(7)	N(10)—C(11)—N(15)	119.6(8)
N(2)—C(1)—C(7)	122.0(7)	N(12)—C(11)—N(15)	122.9(8)
C(5)—C(1)—C(7)	129.1(8)	C(11)—N(12)—C(13)	119.4(7)
C(1)—N(2)—C(3)	105.9(6)	N(12)—C(13)—N(14)	172.3(8)
N(2)—C(3)—N(4)	110.7(7)	C(11)—N(15)—C(16)	125.9(8)
C(3)—N(4)—C(5)	108.5(7)	O(1)—Cl—O(2)	109.8(4)
N(4)—C(5)—C(6)	122.1(8)	O(1)—Cl—O(3)	108.9(5)
C(1)—C(5)—N(4)	106.2(8)	O(1)—Cl—O(4)	108.7(4)
C(1)—C(5)—C(6)	131.7(9)	O(2)—Cl—O(3)	109.9(5)
C(1)—C(7)—S	115.1(6)	O(2)—Cl—O(4)	108.9(5)
C(7)—S—C(8)	102.1(4)	O(3)—Cl—O(4)	110.6(5)
S—C(8)—C(9)	114.5(6)	N(2)—Cu—N(14)^{III}	88.6(3)
C(8)—C(9)—N(10)	112.2(7)	N(2)—Cu—S	78.9(2)
C(9)—N(10)—C(11)	122.4(7)	S—Cu—N(14)^{III}	86.5(2)
N(10)—C(11)—N(12)	117.5(8)		

RESULTS

X-ray analysis

Figure 1 shows a perspective drawing of the molecular structure. The perchlorate group is not shown. The distribution of bond lengths and bond angles (Table 1) indicate some degree of electronic delocalization (Fig. 2) around Cu(II) and within the pentagonal ring, which does not deviate significantly from planarity.

The Cu^{2+} ions, which lie on centres of symmetry, are six coordinated from two chelating (S and imidazole N) and two cyanonitrogen atoms from neighbouring molecules. The geometrical features around Cu^{2+} are in Table 1.

The cimetidine molecules are connected to the perchlorate groups by N—H ... O (ClO_4) hydrogen bonds (Table 2). One of the oxygen atoms of the ClO_4^- group, O(3), is not involved in the hydrogen bonds and shows the smallest distance Cl—O = 1.412(9) Å.

Molar conductance in 10^{-3} M aqueous solution at 25°C is 191 ohm^{-1} mol^{-1} cm^2. This value is slightly below the range expected for 1:2 electrolytes,[19] probably due to H-bond formation

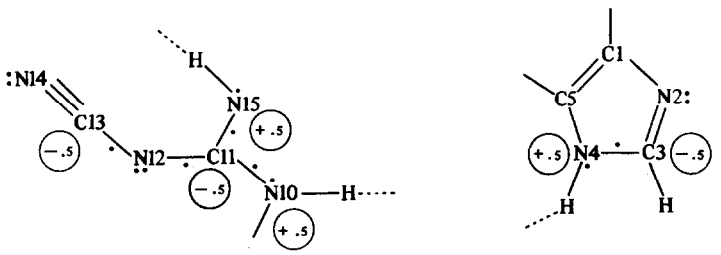


Fig. 2. Major electronic distribution according to Linnett's[18] model in two parts of the cimetidine molecule.

Table 2. Hydrogen bonds: ESDs in parentheses

X—H...Y	X...Y (Å)	X—H (Å)	H...Y (Å)	< X—H...Y (°)
N(4)—H(4)...O(2)^{IV}	2.92(1)	1.01	1.93	164
N(10)—H(10)...O(4)^{V}	2.98(1)	1.02	2.13	140
N(15)—H(15)...O(1)^{VI}	2.95(1)	1.02	2.06	145

Symmetry code

I	$-x, -y, -z$	IV	$-x, -0.5+y, 0.5-z$
II	$x, -1+y, z$	V	$1-x, -0.5+y, 0.5-z$
III	$-x, 1-y, -z$	VI	$1-x, 0.5+y, 0.5-z$

between ClO_4^- and cimetidine, as shown by X-ray data.

IR spectra

A comparison of the IR spectrum of the ligand with those of the complex reveals the following important features. The IR spectrum of the complex shows three well-characterized bands located at 3360, 3280 and 3160 cm^{-1} assigned to the stretching vibrations of the N—H group. In the ligand, however, only two bands appeared at 3220 and 3140 cm^{-1}, which might be due to the presence of hydrogen bonds in the complex.[20] This is consistent with the proposed structure for X-ray. The —C≡N stretching band in the complex is found at 2200 cm^{-1}, this band appears slightly shifted compared to the corresponding vibration in free ligand. This is in agreement with the coordination of this group.[21] The peaks at 1582 and 1451 cm^{-1} of imidazole group assigned to the antisymmetric and symmetric C=N—C=C stretching vibration respectively are shifted to 1605 and 1440 cm^{-1} in the complex which indicates the involvement of this group in the coordination.[22] The complex shows two bands at 1095 and 630 cm^{-1} which supports a T_d symmetry for ClO_4^- groups.[23] The C—S stretching vibration which in the free ligand appears at 680 cm^{-1} is shifted to 710 cm^{-1}.

The broad band at 300 cm^{-1} may be assigned to M—S[5] and M—N[24] (nitrile) stretching vibration. The band at 260 cm^{-1} can be assigned to νM—N (imidazole).[25]

The EPR spectrum obtained from a solid sample shows the parallel component (at about 2.20) overlapping the perpendicular one ($g_\perp = 2.08$). The fact that this value is greater than 2.04 are in good agreement with the values expected for copper in an elongated tetragonal octahedral environment.[26]

The electronic spectrum of the compound in the visible region shows a band at 16,000 cm^{-1} with a shoulder at about 12,000 cm^{-1} and a band at 27,030 cm^{-1}. The first band and shoulder may be assigned to *d–d* transitions of Cu(II) ions. The last band is a charge transfer transition.

The magnetic behaviour was studied at room temperature. The μ_{eff} value is 2.11 B.M.

The *d–d* spectrum[27] and the magnetic moment confirms a pseudooctahedral stereochemistry around Cu(II).

REFERENCES

1. C. Wastell and P. Caece, *Cimetidine*. Churchill Livingstone, London (1978).
2. R. W. Brimblecombe, W. A. M. Duncan, G. J. Durant, C. Emmett, C. R. Ganellin, G. B. Leslie and M. E. Parsons, *Gastroenterology* 1978, **74**, 339.
3. B. Cornilsen and K. Nakamoto, *J. Inorg. Nucl. Chem.* 1974, **36**, 2467.
4. M. E. Bridson and W. R. Walker, *Aust. J. Chem* 1970, **23**, 1973.
5. M. Akbar Ali and S. E. Livingstone, *Coord. Chem. Rev.* 1974, **13**, 101.
6. K. B. Yatsimirskii and V. P. Vasilev, *Instability Constants*. Pergamon Press, London (1960).
7. P. Rigo and A. Turco, *Coord. Chem. Rev.* 1974, **13**, 133.
8. E. T. Adman, R. E. Stenkamp, L. C. Sieker and L. H. Jensen, *J. Mol. Biol.* 1978, **123**, 35.
9. R. B. Patel, T. P. Gandhi, G. F. Shah, P. R. Patel, M. R. Patel, V. C. Patel and R. N. Gilbert, *Indian Drugs* 1981, **18**, 177.
10. K. C. Güven, G. Güvener, G. Sunam and O. Ozdemir, *Eczacilik Bul.* 1982, **24**, 30.
11. D. H. Busch, *Inorganic Syntheses*, Vol. 20. John Wiley, New York (1980).
12. N. F. Curtis, *J. Chem. Soc.* 1961, 3147.
13. A. Earnshaw, *Introduction to Magnetochemistry*. Academic Press, London (1968).
14. *International Tables for X-ray Crystallography*, Vol. IV. Kynoch Press, Birmingham (1974).
15. P. Main, S. J. Fiske, S. E. Hull, L. Lessinger, G.

Germain, J. P. Declerq and M. M. Woolfson, *MULTAN80. A System of Computer Programs, for the Automatic Solution of Crystal Structures from X-ray Diffraction Data.* University of York, England, and University of Louvain, Belgium (1980).
16. J. M. Stewart *et al.*, *The XRAY76 System.* Computer Science Center, University of Maryland, College Park, Maryland (1976).
17. C. K. Johnson, *ORTEP. Report ORNL-3794.* Oak Ridge National Laboratory, Tennessee (1965).
18. J. W. Linnett, *The Electron Structures of Molecules. A New Approach.* Methuen, London (1966).
19. R. J. Angelici, *Synthesis and Technique in Inorganic Chemistry*, 2nd edition. Saunders, Philadelphia (1977).
20. L. J. Bellamy, *Infrared Spectra of Complex Molecules*, Vol. 1. Chapman & Hall, London (1975).
21. B. J. Hathaway, D. G. Holah and J. D. Postlethwaite, *J. Chem. Soc.* 1961, 3215.
22. T. J. Lane, I. Nakagawa, J. L. Walter and A. J. Kandathil, *Inorg. Chem.* 1962, **1**, 267.
23. B. J. Hathaway and A. E. Underhill, *J. Chem. Soc.* 1961, 3091.
24. T. R. Ferraro, *Low Frequency Vibrations of Inorganic and Coordination Compounds.* Plenum Press, New York (1971).
25. B. C. Cornielsen and K. Nakamoto, *J. Inorg. Nucl. Chem.* 1974, **36**, 2467.
26. B. J. Hathaway and D. E. Billings, *Coord. Chem. Rev.* 1970, **5**, 143.
27. A. B. P. Lever, *Inorganic Electronic Spectroscopy.* Elsevier, Amsterdam (1968).

Polyhedron Vol. 4, No. 4, pp. 545–550, 1985
Printed in Great Britain

0277–5387/85 $3.00 + .00
© 1985 Pergamon Press Ltd

THE EXTRACTION OF MOLYBDENUM(VI) FROM PERCHLORIC ACID SOLUTION BY TRI-*n*-BUTYL PHOSPHATE

J. J. CRUYWAGEN* and T. RYPSTRA
Department of Chemistry, University of Stellenbosch, Stellenbosch 7600, Republic of South Africa

(*Received* 13 *March* 1984; *accepted* 9 *May* 1984)

Abstract—The extraction of molybdenum(VI) by tri-*n*-butyl phosphate (TBP) from 1 M $NaClO_4$ medium has been investigated as a function of molybdenum concentration (10^{-4}–10^{-2} M) in the pH_c range 0.7–3.2. At molybdenum(VI) concentration $\gtrsim 5 \times 10^{-4}$ M a polynuclear species, which has been identified as the $Mo_6O_{19}^{2-}$ ion, predominates in the TBP phase. At very low molybdenum(VI) concentration ($< 10^{-4}$ M) mononuclear species predominate. A conditional formation constant for the hexanuclear species in the organic phase (0.15 M $HClO_4$) has been determined, i.e. $K = (1.3 \pm 0.4) \times 10^{20}$.

Depending on the conditions, molybdenum(VI) is extracted quite effectively by tributyl phosphate (TBP) from aqueous acid solutions.[1–7] At relatively high hydrogen ion concentrations cationic species of molybdenum(VI) occur which can form extractable complexes with suitable ligands. For example, large distribution ratios are observed when molybdenum(VI) is extracted from $\gtrsim 3$ M hydrochloric acid solution and it has been shown that the major species in the TBP phase is the solvated chloro-complex $MoO_2Cl_2 \cdot 2TBP$.[1–3] At pH ~ 1.5 conditions are again relatively favourable for the extraction of molybdenum(VI) provided its concentration is not too low.[2,5,7] The extraction behaviour of molybdenum(VI) at this pH, however, is very complex, because various mono- and polynuclear species, cationic as well as anionic, can exist in simultaneous overlapping equilibria. At very high dilution (~ 5×10^{-5} M) monomeric molybdic acid, $Mo(OH)_6$, is the predominant species, in equilibrium with the ions $HMoO_4^-$ and $Mo(OH)_5(H_2O)^+$.[8] The polynuclear species which occur at higher molybdenum(VI) concentrations in the pH range 1–3 are still incompletely characterised. Interpretation of the distribution data is therefore very difficult and the extraction system not well understood. Although it has been concluded[3,7,9] that polymeric species are extracted into TBP, virtually nothing is known about the nature of these species. The situation for other solvents is much the same as that for TBP.[10]

In this study the distribution of molybdenum(VI) between TBP and perchloric acid has been determined as a function of both pH and molybdenum(VI) concentration. The UV spectra of equilibrated TBP phases at various acid and molybdenum concentrations have also been measured. The objective was to obtain data that could lead, firstly, to a better understanding of the extraction system and, secondly, to the identification of molybdenum(VI) species in the TBP phase.

EXPERIMENTAL

All reagents were of analytical grade (Merck p.a.) and solutions were prepared with de-ionised distilled water. Sodium molybdate, $Na_2MoO_4 \cdot 2H_2O$, was purified and recrystallised as described by Sasaki and Sillén.[11] The stock solution, standardised gravimetrically by precipitation of molybdate as $PbMoO_4$,[12] was kept in a polythene bottle. Sodium perchlorate solution was prepared from recrystallised $NaClO_4$ and standardised by drying samples to constant weight at 130°C. Perchloric acid was standardised indirectly against potassium hydrogen phthalate by titration with sodium hydroxide. The TBP used was purified as described elsewhere.[13]

Equilibrations were carried out by shaking equal volumes (usually 10 cm^3) of "wet" TBP and aqueous solution in a centrifuge tube for 18 h in a constant temperature room at 25 ± 1°C. The time needed for equilibration depended on both molybdenum and acid concentration. Preliminary experiments

* Author to whom correspondence should be addressed.

showed that under certain conditions at least 6 h were needed to establish equilibrium. The molybdenum concentration in each phase was determined by atomic absorption[14] using a Varian Techtron Model AA-120 instrument in conjunction with a Vitatron UR400 recorder. An air–acetylene flame was used. The lamp current was set at 5 mA and absorbances were measured at 313.3 nm. A series of standard solutions were prepared for each phase. The molybdenum concentrations of the standard solutions were checked colorimetrically by the Tiron method.[15]

The equilibrium concentration of perchlorate ions in the aqueous phase was kept constant at 1.0 M, using sodium perchlorate. Since the extraction of perchloric acid and sodium perchlorate is interdependent and a function of the concentration of their ions in solution the initial perchlorate ion concentration had to be varied with variation in pH to maintain a constant perchlorate ion concentration in the aqueous phase. The hydrogen ion concentration of the aqueous phase was measured to within 0.01 pH units with a Metrohm E300 pH meter using a glass and calomel combination electrode. The potassium chloride solution of the electrode was replaced by a saturated sodium chloride solution to prevent precipitation of potassium perchlorate. Solutions with the compositions (0.10 M $HClO_4$ + 0.90 M $NaClO_4$), (0.01 M $HClO_4$ + 0.99 M $NaClO_4$) and (0.001 M $HClO_4$ + 0.999 M $NaClO_4$) were used as standards for $-\log[H^+]$ 1.0, 2.0 and 3.0 respectively. For brevity $-\log[H^+]$ will be represented by pH_c.

Absorption spectra of TBP phases were measured with a Zeiss Model PMQII spectrophotometer, using calibrated quartz cuvettes of suitable pathlengths ranging from 0.01 to 2.00 cm. The cuvette compartment was kept at 25°C by circulating water from a thermostat bath.

RESULTS AND DISCUSSION

Distribution behaviour of molybdenum(VI)

The results of the extraction of molybdenum(VI) by TBP from 1 M perchlorate solution in the pH_c range 0.7–3.7 are shown in Fig. 1. The initial molybdenum(VI) concentration in the aqueous phase was varied from 10^{-4} to 10^{-2} M. At the lowest molybdenum concentration, 1×10^{-4} M, where polynuclear species are present only in very small amounts,[9] the extraction is rather poor. With increase in concentration, condensation of molybdenum(VI) becomes significant and the extraction at $pH_c < 3$ improves. This shows that one or more

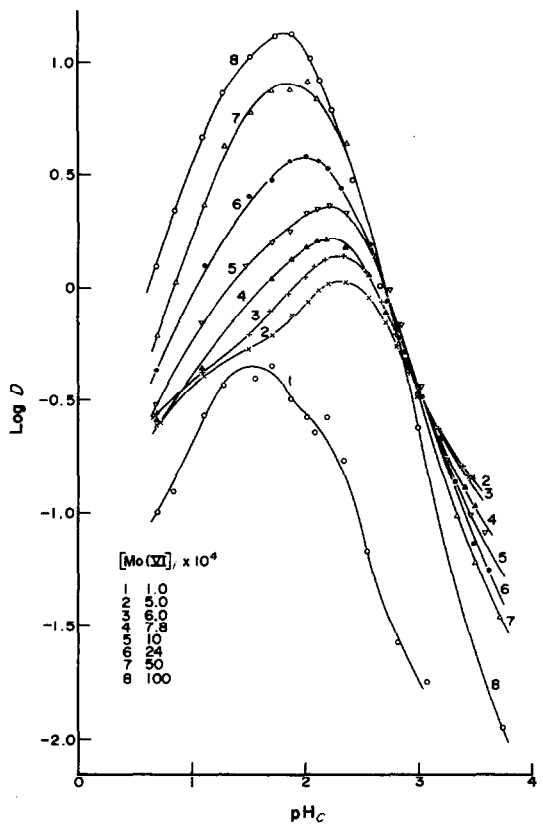


Fig. 1. The distribution of molybdenum(VI) between TBP and aqueous perchloric acid as a function of pH_c at various initial molybdenum(VI) concentrations.

polynuclear species are extracted into the TBP phase. Further, from the increase in the distribution ratio, D, with increase in molybdenum(VI) concentration at $pH_c \lesssim 3$ it may be concluded that the weight average degree of condensation is greater in the TBP phase than in the aqueous phase.[16] At $pH_c \gtrsim 3$ just the opposite applies; D decreases with increasing molybdenum(VI) concentration. In this pH_c region the major condensed species are the hepta- and octamolybdate ions[17] $Mo_7O_{24}^{6-}$, $HMo_7O_{24}^{5-}$, $H_2Mo_7O_{24}^{6-}$ and $Mo_8O_{26}^{4-}$, which apparently do not extract. As the molybdenum(VI) concentration increases, the relative concentrations of these species increase, thereby causing a decrease in extraction.

It is seen that all the distribution curves show a maximum. The pH_c at which maximum extraction occurs, depends on the molybdenum(VI) concentration, a feature which again illustrates the complexity of the extraction system. At molybdenum(VI) concentrations above $\sim 5 \times 10^{-4}$ M the TBP phase showed a distinct yellow colour which happened to be most intense at the pH_c values where maximum extraction takes place. This pointed to the presence of a species predominating in the

TBP phase but which does not occur in significant concentrations in the aqueous phase.

Species in the TBP phase

The yellow species in the organic phase could be identified from its UV spectrum. The spectrum of the yellow molybdenum containing TBP phase (Fig. 2) showed three prominent absorption bands at wavelengths 222, 257 and 325 nm which is characteristic of the hexamolybdate ion $Mo_6O_{19}^{2-}$. Although this polyion does not appear to exist in significant concentrations in aqueous solution it can be prepared[18] by precipitation from aqueous solution as the yellow compound $[(C_4H_9)_4N]_2Mo_6O_{19}$. This compound, however, was found to be insoluble in TBP but its UV spectrum can be measured by dissolving it in acetonitrile.[19] The molar absorptivities measured at wavelengths 222, 257 and 325 nm for the hexameric ion in acetonitrile namely 23.1×10^3, 13.9×10^3 and 6.8×10^3 agreed satisfactorily (within 5%) with those obtained for the yellow molybdenum(VI) species extracted by TBP. The possibility of course still exists that on dissolution in acetonitrile a conversion of the hexameric ion to some other polyanion might occur and that the observed peaks belong to this polyanion. This was ruled out by measuring the spectrum of a very thin compressed transparent disk of the solid $[(C_4H_9)_4N]_2Mo_6O_{19}$ mixed with potassium chloride. The spectrum of the solid was practically identical to that of the hexameric ion in solution.

A systematic survey of the spectra of TBP extracts in the pH_c range 0.7–3.7 at various molybdenum(VI) concentrations indicated (Figs 2 and 3) that no other polynuclear species were present in significant amounts. If such ions do extract they are converted to the more stable (in TBP) hexanuclear species. At very low molybdenum(VI) concentrations ($< 1 \times 10^{-4}$ M) the absorption bands at wavelengths 222, 257 and 325 are practically absent and the spectrum (Fig. 2) resemble that of the mononuclear species $[Mo(OH)_5(H_2O)]^+$ in aqueous solutions.[8]

Only when molybdenum(VI) is extracted from an aqueous phase of pH_c lower than ~ 0.7 did the spectra of the TBP phase clearly indicate the presence of another polynuclear species. For example when the pH_c of the aqueous phase is 0.53 (total acid concentration in the organic phase 0.56 M) and the molybdenum(VI) concentration in the TBP phase relatively low, i.e. $\sim 1.5 \times 10^{-3}$ M, a shoulder in the spectrum is observed at ~ 246 nm. Since in aqueous solution, dimeric cationic species show a strong absorption band at this wavelength,[20] it may be concluded that a dimeric cation, most likely the singly charged ion $HMo_2O_6^+$, is extracted as an ion pair $HMo_2O_6^+ClO_4^-$(org), at low pH_c. In fact when a TBP solution, containing the yellow hexanuclear species, is mixed with another strongly acidified TBP solution (0.7 M in $HClO_4$) the yellow colour completely disappears after some time and the spectrum of this solution then showed only the strong absorption band at 246 nm characteristic of the dinuclear cations.

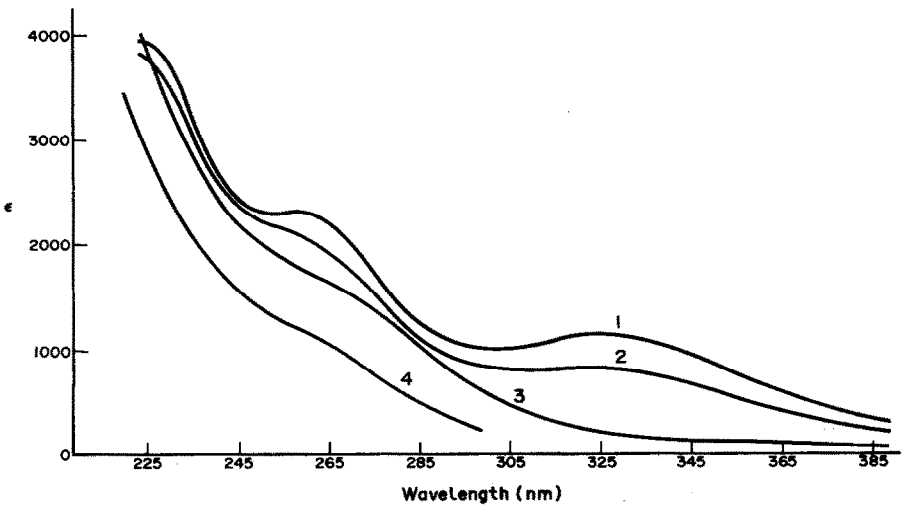


Fig. 2. UV absorption spectra of TBP extracts of molybdenum(VI) at $pH_c = 2.0$: 1, $[Mo(VI)]_{org} = 1.98 \times 10^{-3}$ M; 2, $[Mo(VI)]_{org} = 2.48 \times 10^{-4}$ M; 3, $[Mo(VI)]_{org} = 5.7 \times 10^{-5}$ M; 4, spectrum of $[Mo(OH)_5(H_2O)]^+$ in aqueous solution.[8]

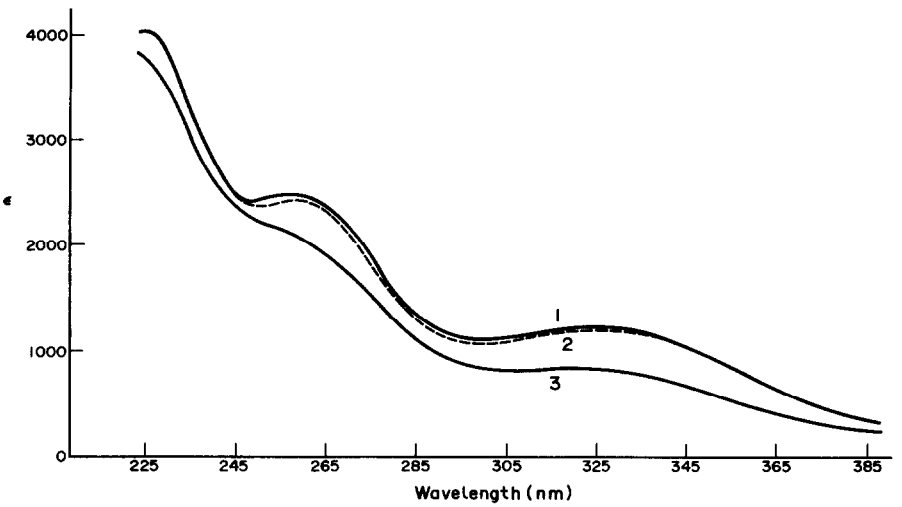


Fig. 3. UV absorption spectra of TBP extracts of molybdenum(VI) at different pH_c values: 1, $[Mo(VI)]_{org} = 4.61 \times 10^{-2}$ M; $pH_c = 1.2$; 2, $[Mo(VI)]_{org} = 4.27 \times 10^{-3}$ M; $pH_c = 2.65$; 3, $[Mo(VI)]_{org} = 2.48 \times 10^{-4}$ M; $pH_c = 2.00$.

Equilibria in the TBP phase

From the results discussed earlier it is evident that the distribution behaviour of molybdenum(VI), in the pH_c range 0.7–3.2 at concentrations above $\sim 10^{-4}$ M, is to a large extent governed by the stability of the $Mo_6O_{19}^{2-}$ ion in the TBP phase. The slight shoulder at $pH_c \sim 2$, shown by the distribution curve for molybdenum(VI) concentration 1×10^{-4} M (Fig. 1) suggests that hexamolybdate ions already start to form at extremely low concentration in the TBP phase. To obtain a quantitative measure of the thermodynamic stability of the hexanuclear species in the TBP phase a conditional equilibrium constant for its formation at perchloric acid concentration 0.15 M was determined spectrophotometrically. A concentration of 0.15 M in perchloric acid is obtained in the TBP phase when the aqueous phase has a pH_c of 2.0 and a perchlorate ion concentration of 1.0 M after equilibration. The conditional equilibrium constant, K, is defined as follows:

$$K = C_h/C_m^6, \qquad (1)$$

where C_h and C_m denote the concentrations of the hexanuclear and mononuclear species respectively in the TBP phase. It seems reasonable to assume that the hexamolybdate is present as an ion pair in the organic phase, tentatively formulated as the complex $[H^+_{(org)}]_2[Mo_6O^{2-}_{19(org)}]$. At relatively high and constant perchloric acid concentration the possible ionisation of the complex can be ignored. Very little is known about the nature of the monomeric molybdenum(VI) species in TBP, but the spectrum of an extremely dilute (5×10^{-5} M) solution at perchloric acid concentration 0.15 M is very similar to that of $[Mo(OH)_5(H_2O)]^+$ in aqueous solution (Fig. 2). Presumably this species is extracted as the ion pair $[Mo(OH)^+_{5(org)}][ClO^-_{4(org)}]$.

The molar absorptivity, ε, of a solution containing the above-mentioned species is given by:

$$\varepsilon = \frac{A}{Bd} = \frac{\varepsilon_m + \varepsilon_h K C_m^5}{1 + 6KC_m^5}, \qquad (2)$$

where A is the absorbance measured in a cuvette of pathlength d cm; B is the total molybdenum(VI) concentration: ε_m and ε_h are the molar absorptivities of the monomeric and hexanuclear species respectively.

The molybdenum(VI) concentration was varied over the range 2×10^{-2}–1×10^{-4} M by appropriate dilution of a TBP extract obtained at $pH_c = 2.0$. The perchloric acid concentration of the TBP used for dilution was 0.15 M. The absorbance of the various solutions was measured at wavelength 325 nm and used to solve eqn (2) employing a package computer programme BMDX85.[21] Provision was made in a subroutine for an iterative computation of C_m from the total molybdenum(VI) concentration, B, for each data point using the equation:

$$B = C_m + 6KC_m^6. \qquad (3)$$

The values for the parameters thus computed were:

$$K = (1.3 \pm 0.4) \times 10^{20}, \quad \varepsilon_m = 0,$$

$$\varepsilon_h = (7.3 \pm 0.1) \times 10^3.$$

The value of zero for ε_m is in agreement with the

practically negligible absorption of the monomeric species in aqueous solution[8] at 325 nm. The large value of K makes it impossible in practice to measure the absorbance of a TBP solution containing practically exclusively monomeric species. For example, using K, it can be calculated that, at a concentration as low as 5×10^{-5} M, approximately 10% of the molybdenum(VI) is already in the hexanuclear state.

The remarkable stability of the $Mo_6O_{19}^{2-}$ in TBP, in contrast with its practical absence in aqueous solution can be ascribed to its very compact structure and low charge density. The structure[22] can be visualised as comprising of six MoO_6 octahedra arranged in such a way that they all share a common vertex, resulting in an octahedral array of molybdenum atoms.

The compactness of the hexamolybdate ion's structure is most probably also the reason for its exceptional kinetic stability in TBP. For example, on dilution depolymerization of the hexamer takes place very slowly and equilibrium is established only after about 10 h. Even if the TBP phase is equilibrated with strongly alkaline solution, it can take up to 6 h before the hexamer is completely converted to MoO_4^{2-}. Its formation is also rather slow. Only under conditions where the hexamolybdate did not occur in the TBP phase had extraction equilibrium been established within a few minutes.

CONCLUSION

The distribution behaviour of molybdenum(VI) between TBP and aqueous perchlorate solution in the pH_c range 0.7–3.0 is essentially determined by the remarkable thermodynamic and kinetic stability in the TBP phase of a polynuclear ion which has been identified as the hexamolybdate ion, $Mo_6O_{19}^{2-}$. These findings provide a much better understanding not only of this particular extraction system but also of various other molybdenum(VI) extraction systems previously investigated.[3,5,7,10]

For example, when 1×10^{-3} M molybdenum(VI) in perchloric acid solution is equilibrated with propylene carbonate,[23] the shape of the extraction curve obtained is similar to that of curve 5 in Fig. 1. The spectrum reported for the propylene carbonate phase showed three absorption maxima at the wavelengths now known to be characteristic of the $Mo_6O_{19}^{2-}$ species. However, an incorrect assumption about the equilibria in the aqueous phase led to the conclusion that the condensed species in the organic phase consisted of 13 molybdenum atoms. In view of the results of the present investigation the possibility of studying by solvent extraction the hitherto incompletely characterized molybdenum(VI) equilibria in aqueous solution in the pH_c range 1–3 now appears to be very promising. Such an investigation is currently being conducted in this laboratory.

Finally, considering the kinetic stability of $Mo_6O_{19}^{2-}$ in TBP, an interesting possibility for the separation of molybdenum(VI) from other elements by solvent extraction presents itself. Molybdenum(VI) can be extracted by TBP from an aqueous mixture at $pH_c \sim 2$. Other species that co-extract can be separated by rapid back-extraction at a suitable pH, leaving behind in the TBP phase most of the molybdenum(VI) as the stable hexamolybdate. The molybdenum(VI) can then be recovered completely as MoO_4^{2-} by equilibrating the TBP phase for some time with an alkaline solution.

Acknowledgement—Financial support by the South African Council for Scientific and Industrial Research is gratefully acknowledged.

REFERENCES

1. I. Nelidow and R. M. Diamond, *J. Phys. Chem.* 1955, **59**, 710.
2. I. Gerlit, *International Conference on the Peaceful Uses of Atomic Energy, Geneva*, 1955, Vol. 7, p. 145, United Nations, New York (1956).
3. Von K.-H. Arend and H. Specker, *Z. Anorg. Allg. Chem.* 1964, **333**, 18.
4. B. Jezowska-Trzebiatowska, S. Kopacz and A. Bartecki, *Russ. J. Inorg. Chem.* 1968, **13**, 989.
5. I. L. Jenkins and A. G. Wain, *J. Appl. Chem.* 1963, **13**, 561.
6. J. D. Cocker and V. M. Sinclair, *U.K. Atomic Energy Authority Rep.*, 1959, IG. Memo 466 (D).
7. S. Kopacs, *Russ. J. Inorg. Chem.* 1973, **18**, 1172.
8. J. J. Cruywagen, J. B. B. Heyns and E. F. C. H. Rohwer, *J. Inorg. Nucl. Chem.* 1976, **38**, 2033.
9. J. J. Cruywagen and H. A. C. McKay, *J. Inorg. Nucl. Chem.* 1970, **32**, 255.
10. T. Sekine and Y. Hasegawa, *Solvent Extraction Chemistry, Fundamentals and Applications*, pp. 573–576. Marcel Dekker, New York (1977).
11. Y. Sasaki and L. G. Sillén, *Ark. Kemi* 1968, **29**, 253.
12. A. I. Vogel, *A Textbook of Quantitative Inorganic Analysis*, 3rd edition, p. 506. Longmans, Green, New York (1961).
13. K. Alcock, S. S. Grimley, T. V. Healy, J. Kennedy and H. A. C. McKay, *Trans. Faraday Soc.* 1956, **52**, 39.
14. W. J. Price, *Analytical Atomic Absorption Spectrometry*, p. 202. Heydon, London (1972).
15. F. Will and J. H. Yoe, *Anal. Chim. Acta* 1953, **8**, 546.
16. F. Rossotti and H. Rossotti, *The Determination of Stability Constants*, p. 386. McGraw-Hill, New York (1961).
17. J. J. Cruywagen, *Inorg. Chem.* 1980, **19**, 552 and references cited therein.

18. J. Fuchs and K. F. Jahr, *Z. Naturforsch.* 1968, **B23**, 1380.
19. H. So and M. T. Pope, *Inorg. Chem.* 1972, **11**, 1441 and private communication.
20. J. J. Cruywagen, J. B. B. Heyns and E. F. C. H. Rohwer, *J. Inorg. Nucl. Chem.* 1978, **40**, 53.
21. *Biomedical Computer Programs, X-Series Supplement* (Edited by W. J. Dixon). University Press, California (1972).
22. H. R. Alcock, E. C. Bissell and E. T. Shawl, *J. Am. Chem. Soc.* 1972, **94**, 1063.
23. K. Murata and S. Ikeda, *J. Inorg. Nucl. Chem.* 1970, **32**, 267.

Polyhedron Vol. 4, No. 4, pp. 551–561, 1985
Printed in Great Britain

0277-5387/85 $3.00 + .00
Pergamon Press Ltd

SYNTHESIS AND CHARACTERIZATION OF NEUTRAL LIGAND-BRIDGED BINUCLEAR DIALKYLCOBALT(III) COMPLEXES

ALBERT W. HERLINGER* and K. RAMAKRISHNA
Department of Chemistry, Loyola University of Chicago, Chicago, IL 60626, U.S.A.

(*Received* 22 *July* 1983; *accepted in revised form* 22 *May* 1984)

Abstract—A series of neutral ligand-bridged binuclear dialkylcobalt(III) chelates has been prepared. Chelate systems based on monoanions of dimethylglyoxime (dmgH) and cyclohexanedionedioxime (chdH) and dianions of bis(acetylacetone)ethylenediimine (BAE) and bis(salicydaldehyde)ethylenediimine (SALEN) are employed. Symmetric complexes RCo(chel)LCo(chel)R, where R = CH_3 or CH_2Cl and chel = dmgH, chdH, BAE or SALEN, were obtained by addition of a bidentate ligand L to a solution of the anhydrous RCo(chel) complex. The bridging ligands were pyrazine (pyz), 4,4′-bipyridine (bpy), 4,4′-trimethylenebipyridine (tbpy), *p*-dithiane (dth) and 1,2-bis(diphenylphosphino)ethane (diphos). A single step direct synthesis of the dialkyl complexes was also achieved by reacting a cobalt(I) chelate, prepared *in situ*, with the appropriate alkyl halide in the presence of the bridging ligand. The isolated products were characterized by elemental analysis, magnetic susceptibility, ^1H NMR, and UV–visible spectroscopy. The water molecule *trans* to the alkyl group in RCo(chel)OH_2 complexes may be displaced by bidentate ligands. Depending upon reaction stoichiometry, mononuclear RCo(chel)L or binuclear RCo(chel)LCo(chel)R compounds are obtained. The mononuclear complexes function as ligands and provide a convenient synthetic route to unsymmetric bridged complexes RCo(chel)LCo(chel′)R. Reaction of bis(acetylacetonato)cobalt(II) with $CH_3Co(dmgH)_2$tbpy yields the ligand-bridged compound $CH_3Co(dmgH)_2$tbpy$Co(acac)_2$. Magnetic susceptibility measurements establish the paramagnetic character of this mixed-valent complex. The effective magnetic moment is 4.84 B.M. at 19.2°C.

The study of cobalt chelates as models for vitamin B_{12} and B_{12} coenzyme is well documented.[1–3] Special aspects of the chemistry of these compounds such as unusually stable cobalt–carbon bonds and remarkable rapid ligand substitution reactions make them interesting in their own right. Ligand-bridged complexes are of particular interest in view of the role they play as reaction intermediates in inner-sphere electron transfer processes.[4] Reports of cyano- and azido-bridged anionic organocobaloximes,†[5] neutral cyano-, thiocyanato- and selenocyanato-bridged dicobaloximes,[6] and doubly alkylated binuclear cobalt complexes with bridging carbonyls[7] have appeared. To our knowledge, however, no such compounds containing long chain non-linear bridging ligands have been prepared.

We wish to report here the synthesis and characterization of neutral ligand-bridged binuclear dialkylcobalt(III) compounds containing pyrazine (pyz), 4,4′-bipyridine (bpy), 4,4′-trimethylenebipyridine (tbpy), *p*-dithiane (dth) or 1,2-bis(diphenylphosphino)ethane (diphos) as the bridging ligand L. The bridging groups were chosen so as to include a variety of ligand types, i.e. nitrogen heterocycles with extended π-electron systems, a nitrogen heterocycle with conjugated π-systems separated by a saturated alkyl chain, a saturated sulfur heterocycle, and a bulky phosphine. Except for diphos, the ligands which have two donor sites are restricted by their geometry to function either as a monodentate or a bridging ligand. Both symmetric RCo(chel)LCo(chel)R and unsymmetric RCo(chel)LCo(chel′)R complexes (where R = CH_3 or CH_2Cl and chel = dmgH, chdH, BAE or SALEN) have been prepared. The methods used to prepare the ligand-bridged complexes appear quite general and

* Author to whom correspondence should be addressed.

† Cobaloxime is the trivial name for complexes with the bis(dimethylglyoximato)cobalt unit, $Co(dmgH)_2$.

provide synthetic routes to a series of complexes in which portions of the complex may be systematically varied. Such a series is amenable to a study of structure–reactivity relationships and some of our preliminary findings have been reported.[8]

EXPERIMENTAL

Spectral studies

Electronic spectra of the complexes were recorded in the 200–550 nm region using a Perkin–Elmer Coleman 575 spectrometer. The spectra were obtained from dry CH_2Cl_2 solutions that were approximately 5×10^{-5} M in complex.

^{1}H NMR spectra were recorded on a Varian A-60A spectrometer operating at 36°C or a Varian EM-360 spectrometer operating at 28°C. The spectra of the diamagnetic complexes were obtained from d_1-chloroform solutions. In one case, d_6-DMSO was added to increase the solubility of the SALEN complex which is only slightly soluble in $CDCl_3$. All spectra were referenced to TMS as internal standard.

Magnetic susceptibility measurements

Magnetic susceptibility measurements for paramagnetic compounds were obtained at room temperature by the Gouy method using mercury tetrathiocyanocobaltate(II) as calibrant.[9] The apparatus employed a Sartorius 2442 electrobalance and an Alfa model 7500 electromagnet operating at 10,000 G. Molar susceptibilities were corrected for diamagnetic contributions of all atoms with Pascal's constants and converted to values expressed in Bohr magnetons using the standard equation:

$$\mu_{eff} = 2.84(\chi_m T)^{1/2} \text{ B.M.},$$

where T is the absolute temperature.[9]

Elemental analysis

Satisfactory elemental analyses were obtained for all compounds. Analysis for carbon, hydrogen and nitrogen were performed by Micro-Tech Laboratories, Inc. (Skokie, IL).

Preparation of complexes

All reagents were purchased from Aldrich Chemical Co. and used without further purification. The Schiff bases BAE and SALEN were prepared by literature methods.[10] Solutions containing alkylcobalt compounds were protected from direct exposure to light. Solvents were refluxed over P_2O_5 and distilled under dry N_2 prior to use.

The complexes

$$CH_3Co(dmgH)_2OH_2,^{11}$$

$$CH_2ClCo(dmgH)_2OH_2,^{11}$$

$$CH_3Co(SALEN)OH_2^{12}$$

and

$$CH_3Co(BAE)OH_2^{13}$$

were also prepared by methods reported in the literature. These complexes were dehydrated by heating *"in vacuo"*. The BAE and SALEN aquo complexes yield monomeric five coordinate complexes when heated at ~80°C for 12 h. By contrast, the dmgH complexes require heating to ~110°C and yield six coordinate dimeric compounds.[14]

The syntheses for

$$CH_3Co(dmgH)_2L,$$

$$CH_3Co(BAE)L,$$

$$CH_3Co(SALEN)L$$

for L = py, bpy and tbpy were by procedures published for analogous compounds.[9] This involves displacement of the axial water molecule from the corresponding aquo complex by stoichiometric quantities of the base L.

$RCo(dmgH)_2LCo(dmgH)_2R$

Complexes of this formulation were prepared by mixing equimolar amounts of the bridging ligand L and the $[RCo(dmgH)_2]_2$ dimer in dichloromethane solutions for R = CH_3 or CH_2Cl and L = dth, pyz, bpy, tbpy or diphos. In a typical synthesis 0.26 g (0.42 mmol) of $[CH_3Co(dmgH)_2]_2$ and 0.051 g (0.42 mmol) of *p*-dithiane were placed in a dry Schlenk reaction vessel and 50 cm^3 of freshly distilled CH_2Cl_2 was added under a purge of dry dinitrogen. The reaction mixture was stirred at room temperature until all of the reactants dissolved. Addition of 40 cm^3 of anhydrous ether caused the yellow complex to precipitate from solution. The product was collected by filtration, washed with anhydrous ether, and dried *in vacuo* at room temperature. The yield was approximately 90%.

The diphos bridged complexes were prepared by this procedure except that product isolation was affected by evaporation of the reaction mixture to dryness. Satisfactory elemental analyses were obtained for all reported compounds. These results are reported in Table 1.

Table 1. Analytical data

Complex	% C (calc.)	% H (calc.)	% N (calc.)
$CH_3Co(dmgH)_2dthCo(dmgH)_2CH_3$	36.20 (36.27)	5.71 (5.77)	15.44 (15.38)
$CH_3Co(dmgH)_2pyzCo(dmgH)_2CH_3$	38.68 (38.35)	5.71 (5.52)	22.73 (22.35)
$CH_2ClCo(dmgH)_2diphosCo(dmgH)_2CH_3$	48.80 (49.12)	5.15 (5.21)	10.52 (10.42)
$CH_3Co(dmgH)_2bpyCo(dmgH)_2CH_3$	43.79 (43.98)	5.05 (5.49)	18.31 (18.32)
$CH_2ClCo(dmgH)_2bpyCo(dmgH)_2CH_2Cl$	40.35 (40.34)	4.64 (4.80)	16.85 (16.81)
$CH_3Co(BAE)bpyCo(BAE)CH_3$	57.63 (57.76)	6.63 (6.68)	11.19 (11.23)
$CH_3Co(SALEN)bpyCo(SALEN)CH_3$	63.12 (63.16)	4.96 (5.02)	10.03 (10.04)
$CH_3Co(dmgH)_2tbpyCo(dmgH)_2CH_3$	46.20 (46.16)	5.90 (5.95)	17.28 (17.37)
$CH_2ClCo(dmgH)_2tbpyCo(dmgH)_2CH_2Cl$	41.97 (42.52)	5.33 (5.25)	15.87 (16.00)
$CH_3Co(chdH)_2tbpyCo(chdH)_2CH_3$	51.01 (51.43)	6.20 (6.15)	15.24 (15.38)
$CH_3Co(dmgH)_2tbpyCo(BAE)CH_3$	52.63 (52.49)	6.56 (6.51)	14.03 (14.05)
$CH_3Co(dmgH)_2tbpyCo(acac)_2$	50.38 (50.60)	5.72 (5.92)	11.07 (11.06)

$CH_3Co(BAE)bpyCo(BAE)CH_3$

The synthesis of the compound was carried out in a darkened room under dry conditions using a Schlenk reaction vessel under a purge of N_2. Typically 0.31 g (1.04 mmol) of $CH_3Co(BAE)$ and 0.10 g (0.52 mmol) of 4,4′-bipyridine were dissolved in 30 cm^3 of freshly distilled CH_2Cl_2 with stirring. After several minutes the solution was evaporated to dryness and a dark brown solid isolated. The solid was suspended in 50 cm^3 of anhydrous ether, collected by filtration, washed with anhydrous ether and air dried.

$CH_3Co(SALEN)bpyCo(SALEN)CH_3$

In a typical synthesis, 0.50 g (1.47 mmol) of anhydrous $CH_3Co(SALEN)$ and 0.142 g (0.735 mmol) of 4,4′-bipyridine were dissolved in 30 cm^3 of freshly distilled CH_2Cl_2 under a dry N_2 purge. After stirring for several minutes, the resulting dark red solution was evaporated to dryness. The red powder was suspended in absolute ethanol and collected by filtration. The isolated product was washed with anhydrous ether and dried *in vacuo* at room temperature.

$CH_3Co(chdH)_2tbpyCo(chdH)_2CH_3$

This procedure closely follows that reported for the synthesis of [RCo(BAE)],[2] [RCo(SALEN)][3] and [$RCo(dmgH)_2L$] complexes.[1,11] The method permits the direct preparation of symmetric ligand-bridged binuclear dialkylcobalt(III) complexes. All [$RCo(dmgH)_2LCo(dmgH)_2R$] compounds reported in Table 1 were also obtained by this route. The method is particularly useful for the preparation of complexes for which the aquo complex required in the previously described syntheses is unobtainable. Our attempts to prepare the aquo isopropyl complex $C_3H_7Co(dmgH)_2OH_2$, for example, were unsuccessful. The ligand-bridged isopropyl complex $(C_3H_7)Co(dmgH)_2bpyCo(dmgH)_2(C_3H_7)$, however, can be readily obtained by this procedure.

In a typical synthesis, 0.50 g (3.5 mmol) of 1,2-cyclohexanedionedioxime and 0.42 g (1.8 mmol) of $CoCl_2 \cdot 6H_2O$ were placed in a Schlenk reaction vessel and 50 cm^3 of methanol was added under a N_2 purge. The mixture was stirred until the cobalt salt dissolved. An aqueous solution of 0.14 g (3.4 mmol) of NaOH and an ethanolic solution of 0.17 g (0.88 mmol) of 4,4′-trimethylenebipyridine were added to the reaction mixture. The mixture was cooled to −20°C and aqueous solutions containing 0.14 g (3.4 mmol) of NaOH and 0.03 g (0.8 mmol) of $NaBH_4$ were added while the stirring continued. Subsequently, 1.0 g (7.0 mmol) of CH_3I was added and the reaction mixture slowly returned to room temperature. The mixture was filtered, and upon addition of 200 cm^3 of H_2O to the filtrate orange-red crystals separate from solution upon standing. These were collected by filtration, washed with anhydrous ether, and dried *in vacuo* at room temperature. The yields based on $CoCl_2$ were generally 30–40%.

$CH_3Co(dmgH)_2tbpyCo(acac)_2$

For the preparation of this mixed-valent complex, 0.650 g (1.07 mmol) of $[CH_3Co(dmgH)_2]_2$ and 0.420 g (2.14 mmol) of 4,4′-trimethylenebipyridine were dissolved in 30 cm^3 of dry freshly distilled CH_2Cl_2 in a Schlenk reaction vessel under a purge of dry N_2. To this solution, 0.550 g (2.14 mmol) of anhydrous bis(acetylacetonato)cobalt(II), dissolved in 25 cm^3 of freshly distilled CH_2Cl_2 were added with stirring at room temperature. The solution was concentrated by means of a rotary evaporator and precipitation occurred. The yellow product was collected by filtration, washed with anhydrous

ether, and dried *in vacuo* at room temperature. The compound is air stable in the solid state, but slowly undergoes oxidation in solution.

$CH_3Co(dmgH)_2tbpyCo(BAE)CH_3$

This compound was prepared by essentially the method described above for the mixed-valent complex. $CH_3Co(dmgH)_2tbpy$ was prepared from the corresponding aquo complex by reaction with tbpy. A mixture of 0.60 g (1.2 mmol) of $CH_3Co(dmgH)_2tbpy$ and 0.35 g (1.2 mmol) of $CH_3Co(BAE)$ was placed in a Schlenk reaction vessel and 30 cm^3 of freshly distilled CH_2Cl_2 was added under a purge of N_2. The reaction mixture was stirred until all reagents dissolved. The solution was concentrated under reduced pressure and anhydrous ether added to induce precipitation. The yellow product was collected by filtration, washed with anhydrous ether, and dried *in vacuo* at room temperature.

RESULTS AND DISCUSSION

Syntheses

The syntheses of the ligand-bridged binuclear dialkylcobalt(III) compounds RCo(chel)LCo(chel)R for various combinations of akyl groups, equatorial chelate systems, and bridging ligands are described in the Experimental Section. One general method of preparation involves the addition of stoichiometric quantities of a suitable bidentate ligand to an anhydrous RCo(chel) complex. Alternatively, the bridged complex may be prepared from the aquo complex by ligand displacement with the bridging ligand. The dialkyl ligand-bridged compounds may also be obtained directly by reacting a cobalt(I) chelate, prepared *in situ*, with alkyl halides in the presence of the bridging ligand. All compounds are light sensitive, particularly in solution.

Alkyl groups are known to exert large *trans* effects in metal complexes.[15] This has been demonstrated in vitamin B_{12} derivatives[16] and cobaloxime analogues.[17] *Trans*-labilization by the alkyl group makes dehydration of $RCo(chel)OH_2$ complexes relatively facile and stable "ligand free" anhydrous $[RCo(dmgH)_2]_2$, RCo(BAE) and RCo(SALEN) compounds readily form. The dmgH complexes are dimeric and hexacoordinate in solution[14] while the BAE[2] and SALEN[3] complexes are monomeric and pentacoordinate. These "ligand free" materials provide a convenient synthetic route to hexacoordinate alkylcobalt(III) compounds since they exhibit Lewis acidity towards many ligands. Depending upon reaction stoichiometry, addition of bidentate ligands to the anhydrous complexes yields mononuclear RCo(chel)L or binuclear ligand-bridged compounds. The reactions proceed according to eqns (1) and (2):

$$RCo(chel) + L \rightarrow RCo(chel)L. \quad (1)$$

$$2RCo(chel) + L \rightarrow RCo(chel)LCo(chel)R. \quad (2)$$

The isolated mononuclear complexes have one donor site of a coordinated ligand which is not bound. Thus, mononuclear complexes may function as Lewis bases and provide a synthetic route to mixed-valent complexes and unsymmetric ligand-bridged complexes [RCo(chel)LCo(chel')R]. To illustrate the utility of the mononuclear complexes, the mixed-valent complex

$$[CH_3Co(III)(dmgH)_2(tbpy)Co(II)(acac)_2]$$

and the bridged complex

$$[CH_3Co(dmgH)_2(tbpy)Co(BAE)CH_3]$$

were prepared. The reaction scheme has the advantage of offering a common route to a variety of products using a common intermediate.

The axial position *trans* to the alkyl group in

$$[RCo(dmgH)_2X], \quad [RCo(BAE)X]$$

and

$$[RCo(SALEN)X]$$

complexes is labile to ligand substitution.[18] Simple ligand displacement reactions are restricted to this site since the equatorial ligand and the alkyl group are substitution inert under mild conditions. The property of having a single labile coordination site introduces an element of synthetic control in the reaction of $[RCo(chel)(H_2O)]$ complexes with potentially chelating ligands. The axial water molecule of these aquo complexes is easily displaced by bidentate ligands; and depending upon reaction stoichiometry, either mononuclear [RCo(chel)L] or ligand-bridged binuclear [RCo(chel)LCo(chel)R] complexes are obtained.

The final method of preparation of ligand-bridged dialkylcobalt complexes utilizes a strongly nucleophilic Co(I) species generated by pre-reduction of the Co(II) chelate with $NaBH_4$. The procedure is similar to that used to prepare $[RCo(dmgH)_2X]$,[1,11] [RCo(BAE)][2] and [RCo(SALEN)][3] complexes. The nucleophilicity of Co(I) in cobaloximes has been discussed, and it is generally assumed that the high energy $(e_g)^2$ electrons outside a $(t_{2g})^5$ core of the metal ion attack the electrophilic carbon of the alkyl halide.[19] The reaction is essentially oxidative-

addition of an alkyl halide to a d^7 metal complex. This method is particularly useful for the synthesis of [RCo(chel)LCo(chel)R] compounds for which the [RCo(chel)(H_2O)] precursor required in the ligand displacement route is difficult to prepare.

Characterization

The isolated products were characterized by elemental analysis, magnetic susceptibility, ^1H NMR and UV–visible spectroscopy. Analytical results for the compounds reported here are consistent with the indicated stoichiometries. The electronic spectra of the ligand-bridged binuclear dialkylcobalt(III) complexes and some related mononuclear complexes are reported in Table 2. The ^1H NMR spectral data reported in Table 3 indicate that, for the bidentate ligands used in this study, the [$RCo(dmgH)_2LCo(dmgH)_2R$] complexes are undissociated in chloroform solution. The measured magnetic susceptibility of the mixed-valent complex [$CH_3Co(dmgH)_2tbpyCo(acac)_2$] yields an effective magnetic moment of 4.82 B.M. at 19.2°C. The oxygen atoms of the acac ligands and a nitrogen atom from tbpy provide a square-pyramidal crystal field environment for the metal ion. Cobalt(II), in this configuration, should be in a high spin state. Magnetic moments for similar complexes have been observed in the 4.1–4.7 B.M.[20–22] range and that for $Co(acac)_2$ is 4.93 B.M.

Electronic spectra

The electronic spectra of all complexes are quite similar. The similarity is most evident between mononuclear and bridged complexes containing the same equatorial chelates and bidentate ligand L, but it also extends to complexes having different in-plane ligands. The spectra generally consist of a distinct intense band at *ca* 240 nm, several ill-resolved bands in the 250–400 nm region, and a weak low energy absorption in the visible region between 400 and 500 nm. These general spectral characteristics resemble those of the closely related cyano-bridged dicobaloximes.[6]

If there are no interactions between metal centers, a symmetrical ligand-bridged complex may be viewed as two RCo(chel)X units. With tbpy as the bridging ligand, the conjugated π-electron systems of the pyridine rings are separated by a saturated alkyl chain. Metal–metal interactions are not expected to be transmitted across such a ligand bridge. Thus, the electronic spectra of the pyridine complex

$$[CH_3Co(dmgH)_2(py)]$$

and

$$[CH_3Co(dmgH)_2(tbpy)Co(dmgH)_2CH_3]$$

should be quite similar. Consistent with this expectation, a comparison of the spectral data in

Table 2. Electronic spectra

Complex	λ_{max} [nm ($\varepsilon \times 10^{-3}$)]*
$CH_3Co(dmgH)_2dthCo(dmgH)_2CH_3$	240 (59.8); 291 (30.9); $383_{(sh)}$ (4.8); 441 (2.6)
$CH_2ClCo(dmgH)_2dthCo(dmgH)_2CH_2Cl$	244 (37.9); 303 (16.9); $390_{(sh)}$ (2.4); 438 (1.2)
$CH_2ClCo(dmgH)_2pyzCo(dmgH)_2CH_2Cl$	242 (60.0); 300 (21.6); 355 (12.0); 415 (3.0)
$CH_3Co(dmgH)_2diphosCo(dmgH)_2CH_3$	243 (50.4); 310 (21.9)
$CH_2ClCo(dmgH)_2diphosCo(dmgH)_2CH_2Cl$	245 (44.3); 312 (27.0); 425 (1.0)
$CH_3Co(dmgH)_2bpyCo(dmgH)_2CH_3$	240 (54.6); $285_{(sh)}$; $299_{(sh)}$; 331 (15.3); 416 (3.0)
$CH_2ClCo(dmgH)_2bpyCo(dmgH)_2CH_2Cl$	244 (44.0); $285_{(sh)}$ (18.0); 310 (15.6); 418 (1.2)
$CH_3Co(BAE)bpyCo(BAE)CH_3$	235 (42.0); 270 (27.6); 315 (15.0); 345 (10.8); 390 (4.8); 430 (2.4)
$CH_3Co(SALEN)bpyCo(SALEN)CH_3$	238 (82.8); $250_{(sh)}$; 342 (25.2); 390 (12.0); 460 (6.0)
$CH_3Co(dmgH)_2tbpyCo(dmgH)_2CH_3$	238 (52.8); 282 (22.8); 375 (5.4); 420 (3.0)
$CH_2ClCo(dmgH)_2tbpyCo(dmgH)_2CH_2Cl$	243 (55.6); 300 (18.6); 360 (5.4); 415 (1.8)
$CH_3Co(chdH)_2tbpyCo(chdH)_2CH_3$	238 (47.5); 295 (19.0); 380 (4.8); 425 (3.0)
$CH_3Co(dmgH)_2tbpyCo(BAE)CH_3$	239 (55.2); 265 (33); 300 (20.4); 350 (8.4); 420 (2.4)
$CH_3Co(dmgH)_2tbpyCo(acac)_2$	235 (35.4); $262_{(sh)}$; 282 (25.2); 370 (2.4); 420 (1.2)
$CH_3Co(dmgH)_2py$†	242 (17.8); $288_{(sh)}$ (9.81); 375 (3.13); $425_{(sh)}$ (1.43)
$CH_3Co(BAE)$‡	216; 275; $309_{(sh)}$; $342_{(sh)}$; $392_{(sh)}$; $439_{(sh)}$; 671
$CH_3Co(SALEN)py$§	352; 394; $440_{(sh)}$; 490

* (sh), shoulder.
† Reference 6.
‡ Reference 2.
§ Reference 25.

Table 3. Proton magnetic resonance spectra

Complex	Chemical shift (τ)*†		
	R—Co	Chel	L
$CH_3Co(dmgH)_2dthCo(dmgH)_2CH_3$	8.89 (s, 3)	7.79 (s, 12)	7.45 (s, 4)
$CH_2ClCo(dmgH)_2dthCo(dmgH)_2CH_2Cl$	6.14 (s, 1)	7.72 (s, 6)	7.45 (s, 2)
$CH_2ClCo(dmgH)_2pyzCo(dmgH)_2CH_2Cl$	6.10 (s, 1)	7.74 (s, 6)	1.44 (s, 1)
$CH_3Co(dmgH)_2diphosCo(dmgH)_2CH_3$	8.94 (d, 3) $J = 4$ Hz	8.22 (d, 14)‡ $J = 3$ Hz	2.40–3.14 (n, 10) ~ 8.1 (t)‡
$CH_2ClCo(dmgH)_2diphosCo(dmgH)_2CH_2Cl$	6.30 (s, 2)	8.18 (d, 14)‡ $J = 3$ Hz	2.35–3.07 (n, 10) ~ 8.1 (t)‡
$CH_3Co(dmgH)_2bpyCo(dmgH)_2CH_3$	9.15 (s, 3)	7.84 (s, 12)	2.40 (d, 2) 1.18 (d, 2) $J = 6$ Hz
$CH_2ClCo(dmgH)_2bpyCo(dmgH)_2CH_2Cl$	6.17 (s, 1)	7.80 (s, 6)	2.38 (d, 1) 1.18 (d, 1) $J = 6$ Hz
$(CH_3)_2CHCo(dmgH)_2bpyCo(dmgH)_2CH(CH_3)_2$	9.54 (d, 3)§ $J = 7$ Hz	7.87 (s, 6)	2.45 (d, 1) 1.20 (d, 1) $J = 5$ Hz
$CH_3Co(BAE)bpyCo(BAE)CH_3$	7.50 (s, 3)	8.00 (s, 12) 6.78 (s, 4) 4.97 (s, 2)	2.30 (d, 2) 0.88 (b, d, 2) $J = 5$ Hz
$CH_3Co(SALEN)bpyCo(SALEN)CH_3$	7.44 (s, 3)	6.47 (s, 4) 3.77–2.67 (m, 8) 2.11 (s, 2)	2.40 (d, 2) 1.26 (d, 2) $J = 5$ Hz
$CH_3Co(dmgH)_2tbpyCo(dmgH)_2CH_3$	9.19 (s, 3)	7.88 (s, 14)§	~ 8.10‡ 7.30 (t, 2); $J = 8$ Hz 2.82 (d, 2); $J = 6$ Hz 1.43 (d, 2); $J = 6$ Hz
$CH_2ClCo(dmgH)_2tbpyCo(dmgH)_2CH_2Cl$	6.23 (s, 1)	7.83 (s, 7)‡	~ 8.12 (m)‡ 7.30 (t, 1); $J = 8$ Hz 2.82 (d, 1); $J = 6$ Hz 1.48 (d, 1); $J = 6$ Hz
$CH_3Co(dmgH)_2tbpyCo(BAE)CH_3$	9.20 (s, 3) 7.60 (s, 3)	7.85 (s, 12) 8.00 (s, 14)‡ 6.80 (s, 4) 5.01 (s, 2)	~ 8.24‡ 7.32 (t, 4); $J = 8$ Hz 2.83 (d, 4); $J = 5$ Hz 1.49 (d, 2); $J = 6$ Hz 1.32 (b, m, 2)
$CH_3Co(chdH)_2tbpyCo(chdH)_2CH_3$	9.14 (s, 3)	8.37 (b, m, 9)‖ 7.30 (b, m, 10)‖	2.84 (d, 2); $J = 6$ Hz 1.50 (d, 2); $J = 6$ Hz

* Reported relative to TMS as an internal standard.

† The numbers in parentheses refer to integrated intensities. The meaning of the symbols is as follows: s, singlet; d, doublet; t, triplet; n, complex doublet; m, multiplet; b, broad.

‡ Resonances overlap and integrate together.

§ Septet of isopropyl group not observed.

‖ Overlaps methylene proton resonance of tbpy.

Table 2 for these two compounds shows that their electronic spectra are virtually identical.

The most intense and highest energy absorption band in the electronic spectrum of the binuclear complexes is relatively insensitive to the nature of the bridging ligand. In all cases, this band appears at *ca* 240 nm. In the absorption spectrum of related mononuclear complexes, a band in this region has been assigned on the basis of molecular orbital calculations[23,24] to a $\pi \rightarrow \pi^*$ transition of the equatorial ligand. By analogy, then, the 240 nm band is empirically ascribed to an inter-π-electron transition of the equatorial chelate ligand system.

The overlapping of absorption bands in the 260–400 nm region makes assigning these bands difficult. Further, both the bridging ligands and the cobalt chromophore absorb in this spectral region. Specific assignment of these bands was not attempted.

The lowest energy band is sensitive to both axial and equatorial ligands. In the spectra of related mononuclear[24] and dinuclear[7] complexes, a band in the 400–500 nm region with extinction coefficient of *ca* 10^3 has been assigned on the basis of a molecular orbital calculation as a Co—C charge transfer transition. This band has been used as a diagnostic tool to indicate a covalently bonded alkyl group.[24] Tetragonal cobalt(III) complexes are also expected to exhibit *d–d* transitions in this spectral region.[25,26] Electronic bands in the spectra of *trans*-diacidotetraaminecobalt(III) complexes[27] and *trans*-diacidobis(diamine)cobalt(III) complexes[25] for example have assigned as ligand field transitions consistent with a D_{4h} symmetry model. The *d–d* transitions observed for these classical complexes are, however, generally of lower intensity ($\varepsilon < 50$) than the charge transfer band observed in the alkylcobalt complexes.[6,24] Except for the

$$[CH_3Co(dmgH)_2diphosCo(dmgH)_2CH_3]$$

complex, a band ($\varepsilon \sim 10^3$) in this spectral region is observed for all bridged complexes. In view of the intensity of this band and the fact that it is not observed in the spectrum of

$$[Co(dmgH)_2(py)_2](ClO_4),^6$$

it is assigned by analogy to a Co—C charge transfer transition. In the spectrum of the diphos complex, a very broad band at 310 nm obscures this region. It is evident, however, from the ^{1}H NMR spectrum of the diphos complex (*vide infra*) that the cobalt bonded methyl group is present.

The spectra of

$$[CH_3Co(dmgH)_2tbpyCo(BAE)CH_3]$$

and

$$[CH_3Co(dmgH)_2tbpyCo(acac)_2]$$

appear to be a simple superposition of the spectra of the two complexes which formally form these binuclear compounds. The conjugated π-electron systems of tbpy are separated by a saturated alkyl chain and metal–metal interactions are not expected to be transmitted via this ligand. The spectra are compatible with an interpretation involving two separate isolated metal centers and assignments are on this basis. In the spectrum of

$$[CH_3Co(dmgH)_2tbpyCo(BAE)CH_3],$$

the absorption band at 239 nm is the π–π^* transition of the equatorial ligands and the weak band at 420 nm is assigned as the Co—C charge transfer transition. Two poorly resolved bands at 205 and 300 nm and a weak band at 350 nm are attributed to metal *d–d* and/or bridging ligand transitions. Bands appearing close to these wavelengths in the electronic spectrum of the mixed-valent tbpy bridged complex are assigned similarly. The 282 nm band, however, is undoubtedly of complex origin since both $Co(acac)_2$ and

$$[CH_3Co(dmgH)_2tbpyCo(dmgH)_2CH_3]$$

absorb strongly at this wavelength. For $Co(acac)_2$ a band at 283 nm is assigned to a π–π^* transition of the acac ligand, while in the symmetric tbpy bridged complex a band at this wavelength is associated with either metal *d–d* and/or bridging ligand transitions.

Proton NMR spectra

^{1}H NMR data for the ligand-bridged dialkylcobalt complexes are reported in Table 3. An examination of the data reveals that the spectra have the following features in common: (1) a high field resonance due to a cobalt-bound alkyl group, (2) bridging ligand resonances, and (3) signals associated with the equatorial chelate system. The dmgH and chdH complexes exhibit an additional very low field resonance characteristic of the strongly hydrogen bonded protons remaining on the oxime oxygens of these ligands.[18,28] This signal, which is not reported in Table 3, generally appears in the $\tau - 8.4$ to -8.8 ppm range.

The ^{1}H NMR spectral data indicates that both donor atoms of L are coordinated and the complexes are best formulated as two RCo(chel) units symmetrically bridged by a bidentate ligand located *trans* to the alkyl groups. Evidence for this comes by comparison of the spectra of binuclear complexes with those of the mononuclear compounds and signal intensity ratios. Small differences in the chemical shifts of protons located close to the donor atoms of L are expected if only one end of the bidentate ligand is coordinated. While these

differences are observed for the mononuclear complexes, no such splittings are apparent in the spectra of symmetric binuclear complexes. In every case, a single resonance was observed for each type of proton of the bridging ligand. A comparison of signal intensities also confirms the presence of the bridged complexes in solution. The intensity ratios of signals arising from the chelate ligand system (chel) or the axial alkyl group to signals associated with L in the bridged complexes are twice these ratios in the corresponding mononuclear compounds.

The association of alkylcobaloximes in solution is readily disrupted by many coordinating ligands to form stable six-coordinate complexes as illustrated in eqn (3):

$$[CH_3Co(dmgH)_2]_2 + 2L \rightleftarrows 2[CH_3Co(dmgH)_2L]. \quad (3)$$

In nearly all cases the equilibrium favoring formation of the adduct is essentially complete and only the mononuclear complex is observed.[18] For the bidentate ligands used in this investigation, no signals attributable to free ligand, mononuclear complex, or "ligand free' RCo(chel) species were observed in the ^1H nuclear magnetic resonance spectra of the bridged compounds. The $[RCo(dmgH)_2LCo(dmgH)_2R]$ complexes are essentially undissociated in chloroform solution. However, equilibria involving appreciable concentrations of all these species are possible for weakly coordinating and/or severely sterically hindered ligands.*

The situation is different for SALEN[2] and BAE[3] complexes where the equilibrium involving adduct formation may be incomplete and exchange is rapid on the NMR time scale. $CH_3Co(BAE)$ and $CH_3Co(SALEN)$, for example, do not bind a sixth ligand as strongly as "ligand free" $[CH_3Co(dmgH)_2]_2$,[30,31] and $[CH_3Co(BAE)py]$ does not exhibit slow exchange in solutions containing excess ligand at $-90°C$.[18] The ^1H NMR spectrum of

$$[CH_3Co(SALEN)tbpyCo(SALEN)CH_3]$$

recorded in $CDCl_3$ with d_6-DMSO added to increase its solubility is substantially different from that of the

$$[CH_3Co(SALEN)DMSO]$$

complex.[32] Thus the tbpy bridged complex must be more stable than the DMSO adduct. No quantitative studies of chemical shift as a function of ligand concentration were conducted so the quantitative extent of adduct formation is not known. However, based on our observations with the DMSO complexes and a comparison of base strengths, it appears that the stability of the tbpy bridged $CH_3Co(BAE)$ and $CH_3Co(SALEN)$ complexes are comparable to the corresponding pyridine complexes.[32]

The NMR spectrum of

$$[CH_3Co(dmgH)_2dthCo(dmgH)_2CH_3],$$

shown in Fig. 1, is representative of that observed for the binuclear complexes. Assignments were made by comparison with the spectra of related mononuclear complexes, characteristic group chemical shifts, and signal intensities.[14,18] The highest field resonance in the spectrum occurs at τ 8.89 ppm relative to TMS and is assigned to the cobalt bonded methyl group. The intense singlet at τ 7.79 ppm is within the range of chemical shifts expected for the dmgH—CH_3 resonance in alkylcobaloximes[18] and it is assigned accordingly. The remaining signal at τ 7.45 ppm is 0.30 ppm upfield from the resonance for the methylene protons in uncomplexed *p*-dithiane. This upfield shift of the protons adjacent to the donor sulfur atom which occurs upon complexation is somewhat greater than that observed in the related thioxane mononuclear complex ($\Delta\tau$ = 0.22 ppm).[18] A single observed resonance for the bridging ligand indicates both donor atoms are coordinated. The intensities of the signals shown in the figure are in the ratio expected for a symmetrically bridged dithiane complex, i.e. 3:12:4. An additional signal arising from the oxime oxygen protons of the dmgH ligands not shown in Fig. 1 appears at $\tau - 8.6$ ppm.

The spectral changes which occur upon varying the axial alkyl group from —CH_3 to —CH_2Cl are exemplified by the dithiane and pyrazine bridged chloromethyl-compounds. In the spectra of $[CH_2ClCo(dmgH)_2LCo(dmgH)_2CH_2Cl]$ complexes, the signal associated with the alkyl group shifts to substantially lower fields and the intensity reflects the decreased number of protons. The chemical shift of the —CH_2Cl group in the dithiane complex is τ 6.14 ppm and it is found at τ 5.10 ppm in the pyrazine complex. The intensity ratios for the signals are as expected. The aromatic protons of pyrazine are shifted *ca* 0.42 ppm from the free ligand value and appear at τ 1.44 ppm as a singlet as expected for a symmetrical bridged binuclear compound. The chemical shift of the dithiane protons appears at identical positions in the methyl- and chloromethyl-complexes.

* The formation constant for the equilibrium involving the formation of the binuclear complex $CH_3Co(dmgH)_2LCo(dmgH)_2CH_3$, where L = triethylenediamine, is sufficiently small that both "ligand free" and bridged complexes are observed.[29]

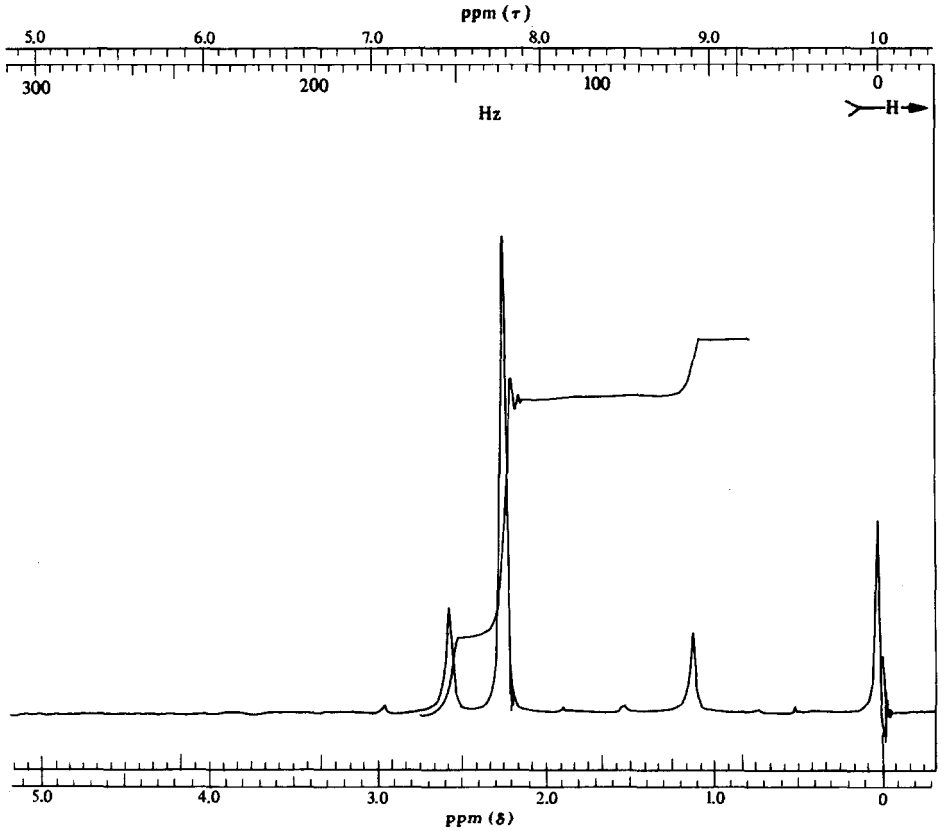


Fig. 1. The ^{1}H NMR spectrum of $[CH_3Co(dmgH)_2dthCo(dmgH)_2CH_3]$.

The dmgH—CH_3 resonance in the binuclear dimethylglyoximato-complexes is sensitive to the nature of the axial alkyl group. This resonance shifts to slightly higher fields as the alkyl group becomes more electron donating. The order which is most clearly seen in the bipyridine bridged complexes listed in Table 3 is chloromethyl < methyl < isopropyl. This can be interpreted simply in terms of increased electron density on cobalt being transmitted to the methyl hydrogens thereby causing a greater shielding. These results are qualitatively in agreement with previous NMR work on the *cis*-effect in cobaloximes. A correlation between the proton resonances of the in-plane hydrogens and the Hammett σ para-function of the axial ligand has been demonstrated.[32,33]

The bridged alkylcobaloximes typically exhibit a singlet in the τ 7.72–8.22 ppm range due to the dmgH–CH_3 protons and another singlet due to protons of the cobalt bound alkyl group. In methyl-complexes the alkyl resonance is found in the τ 8.89–9.15 ppm range. With diphos as the bridging ligand these resonances are expected to split into doublets in the region of slow exchange through a spin interaction with ^{31}P. Whereas in the fast exchange region, rapid ligand dissociation would cause the doublets to collapse to singlets. Doublets with scalar coupling constants of 3 Hz are observed in ^{1}H NMR spectra of both diphos bridged complexes in the dmgH—CH_3 resonance region. In the methyl-complex, the ^{1}H–^{31}P coupling to the axial alkyl group is sufficient to give rise to a doublet (J = 4 Hz), but the splitting is not apparent in the chloromethyl-complex. These observations are similar to those for related mononuclear complexes containing phosphorus ligands. It has been reported that the scalar interactions of protons of axial haloalkyl groups with ^{31}P is considerably smaller than that of axial alkyl groups and in some cases may not be observed.[34]

The aromatic protons of the bridging diphos ligand appear as a complex doublet centered at *ca* τ 2.76 ppm. This chemical shift is close to the value observed for this resonance in the free ligand. The ethylene protons which appear as a triplet (J = 5 Hz) at τ 7.90 ppm in diphos are shifted slightly upfield in the bridged complexes. The center of the triplet lies under the dmgH—CH_3 resonance and appears as a shoulder at *ca* τ 8.1 ppm on this latter signal.

The ^{1}H NMR spectra of the 4,4′-bipyridine complexes, $[CH_3Co(chel)bpyCo(chel)CH_3]$, as expected are quite similar to analogous $[CH_3Co(chel)py]$ complexes.[34,35] The conjugation in these systems can be disrupted by a twisting of the

aromatic rings with respect to each other. The rings generally are not coplanar and conjugation does not extend between ring systems. The bridging bpy ligand shows a characteristic "para" pattern when the nitrogens are equivalent. For the free ligand, the $AA'XX'$ spin system produces two sets of doublets (J = 6 Hz) centered at τ 2.49 and 1.29 ppm. Each peak shows an additional splitting of 1 Hz arising from magnetic non-equivalence of the hydrogens. The bridged complexes show a similar pattern of doublets at chemical shifts close to free ligand values. The lowest field aromatic resonance which shows the greatest shift upon complexation is ascribed to the bpy protons adjacent to the nitrogens. Splitting arising from magnetic non-equivalence which is evident in the spectra of dmgH complexes is not as apparent for the BAE and SALEN complexes. The lowest field aromatic resonance in the spectrum of the BAE complex, for example, is substantially broadened and shows no splitting.

The axial methyl resonance in

$$[CH_3Co(BAE)bpyCo(BAE)CH_3]$$

occurs 0.24 ppm to lower fields than in the base free $CH_3Co(BAE)$ complex. At 60 MHz, the —CH, $—CH_2$, and $—CH_3$ proton resonances of the BAE ligand in the bpy bridged complex appear as singlets at τ 4.97, 6.78 and 8.00 ppm, respectively. The shifts of these resonances upon addition of a sixth ligand to the base free $CH_3Co(BAE)$ complex is analogous to that which is observed for the pyridine complex.[35] However, the non-equivalence of the BAE methyl groups and the splittings of the methylene proton resonance which are apparent at 100 MHz[32,35] were not observed.

The spectrum of

$$[CH_3Co(SALEN)bpyCo(SALEN)CH_3]$$

is complicated somewhat by the presence of d_6-dimethylsulfoxide which was added to increase the solubility of this complex in chloroform. The coordinating properties of DMSO make displacement of the bridging bpy ligand possible; but the observed chemical shifts are substantially different from values for the DMSO complex.[32] We have not attempted to analyse the spectra of the SALEN aromatic hydrogens which is a broad multiplet τ (3.77–2.67 ppm), but singlets at τ 2.11 and 6.47 ppm are due to the methine and methylene protons, respectively. The non-equivalence of the methylene hydrogens previously observed at 100 MHz[32] was not apparent under the spectral conditions used here.

The chemical shift of the axial methyl group in $[CH_3Co(chel)L]$ complexes depends upon electronic effects of both axial and equatorial ligand systems.[18,32] Similar effects are observed for the bridged complexes. The axial methyl resonance, for example, occurs at lower fields when the bridging ligand contains sulfur or phosphorus donor atoms as compared to oxygen or nitrogen atoms. The equatorial ligand also has a substantial effect on this resonance. A comparison of the bipyridine complexes shows this nicely. In the dmgH complex this resonance appears at τ 9.15 ppm, whereas it shifts to lower fields in the BAE and SALEN complexes, i.e. τ 7.50 and 7.44 ppm, respectively. The results are comparable to those observed in the pyridine complexes,[35] but not as large as those reported in methylatocobalt(aeitoporphyrin).[36] In the latter complex a substantial shielding from the porphyrin ring current is expected and the axial methyl resonance occurs at τ 15.15 ppm. The down-field shift in the BAE and SALEN complexes compared to the dmgH complex (in which there is no ring current) may also be due to an equatorial ring current.[35] In the present situation however, the ring current would have a deshielding effect on the axial methyl group since it is now situated at the edge of the ring rather than in the center.

The spectra of the 4,4′-trimethylenebipyridine bridged complexes are very similar to the bpy bridged complexes; i.e. the resonances due to the axial alkyl groups and equatorial chelate systems appear at nearly identical chemical shifts. There is no conjugation between the aromatic rings which are separated by a saturated alkyl chain. The tbpy ligand also shows a characteristic "para" pattern when the nitrogens are equivalent. The aromatic hydrogens produce two sets of doublets (J = 6 Hz) centered at τ 2.73 and 1.42 ppm which show additional splitting of *ca* 1 Hz from magnetic non-equivalence. Again, this splitting is much less evident in the bridged complexes. The trimethylene chain gives rise to a complex triplet (J = 8 Hz) centered at τ 7.30 ppm and a quintet at τ 7.90 ppm. This latter resonance is partially obscured by a signal arising from the equatorial ligand systems in the complexes and these lie too close together to integrate as separate peaks.

Except in the aromatic region, the ^1H NMR spectrum of $[CH_3Co(dmgH)_2tbpyCo(BAE)CH_3]$ appears to be a composite of the spectra of two $CH_3Co(chel)X$ units which form this unsymmetric complex. Singlets at τ 9.20 and 7.60 ppm arise from protons of the axial methyl groups of $[CH_3Co(dmgH)_2X]$ and $[CH_3Co(BAE)X]$, respectively. The methyl resonance of BAE in the bridged complex appears as a singlet at 8.00 ppm. The dmgH—CH_3 singlet is at τ 7.85 ppm. The BAE methine and methylene proton resonances are at chemical shifts close to their values in $[CH_3Co(BAE)bpyCo(BAE)CH_3]$. The spectrum

in the aromatic region is more like that observed for the mononuclear $[CH_3Co(dmgH)_2tbpy]$ complex. This is not unexpected since in both cases the nitrogen atoms of tbpy are not equivalent. The highest field aromatic signal, a doublet at τ 2.83 ppm of intensity four, arises from tbpy ring protons farthest from nitrogen. The ring protons adjacent to the coordinated nitrogens give rise to two signals of equal intensity (2), i.e. a doublet and a broad absorption band at slightly lower fields. By comparison with the spectra of symmetric complexes, the signals are empirically assigned to protons closest to the $CH_3Co(dmgH)_2$ and $CH_3Co(BAE)$ bound nitrogens, respectively.

In the spectrum of

$$[CH_3Co(chdH)_2tbpyCo(chdH)_2CH_3],$$

the aromatic resonances of tbpy appear as described for the other symmetrically bridged tbpy complexes. The methylene proton resonances lie under the very broad complex absorbance envelope of the 1,2-cyclohexanedionedioxime equatorial ligand. The saturated cyclohexane ring hydrogens give rise to two broad, poorly resolved bands at τ 8.37 and 7.30 ppm. The protons farthest from the oxime nitrogen atoms overlap the proton resonance of the central methylene group of tbpy. Similarly, the lower field resonance which is associated with the protons adjacent to the oxime nitrogens overlaps the resonance signal of the methylene groups attached to the pyridine rings.

REFERENCES

1. G. N. Schrauzer, *Acc. Chem. Res.* 1968, **1**, 97.
2. G. Costa, G. Mestroni, G. Tauzher and L. Stefani, *J. Organomet. Chem.* 1966, **6**, 181; G. Costa and G. Mestroni, *J. Organomet. Chem.* 1968, **11**, 325.
3. G. Costa, G. Mestroni and L. Stefani, *J. Organomet. Chem.* 1967, **7**, 493; G. Costa, G. Mestroni and G. Pellizer, *J. Organomet. Chem.* 1968, **11**, 333.
4. A. Haim, *Acc. Chem. Res.* 1975, **8**, 264.
5. D. Dodd and M. D. Johnson, *J. Chem. Soc., Dalton Trans.* 1973, 1218.
6. P. L. Gaus and A. L. Crumbliss, *Inorg. Chem.* 1976, **15**, 2080; J. M. Ciskowski and A. L. Crumbliss, *Inorg. Chem.* 1979, **18**, 638.
7. N. E. Schore, C. Ilenda and R. G. Bergman, *J. Am. Chem. Soc.* 1976, **98**, 7436.
8. K. Ramakrishna and A. W. Herlinger, Abstract of Papers, Eleventh Great Lakes Regional Meeting of the American Chemical Society, Steven's Point, Wisconsin, 1977, No. 138.
9. B. Figgis and J. Lewis, *Techniques of Inorganic Chemistry* (Edited by H. Jonassen and A. Weissberger), Vol. IV, p. 137. Interscience, New York (1965); B. N. Figgis and R. S. Nyholm, *J. Chem. Soc.* 1958, 4190.
10. A. E. Martell, R. L. Belford and M. Calvin, *J. Inorg. Nucl. Chem.* 1958, **5**, 170.
11. G. N. Schrauzer, *Inorg. Synth.* 1969, **11**, 69.
12. V. L. Goedken, S. Peng and Y. Park, *J. Am. Chem. Soc.* 1974, **96**, 284.
13. G. N. Schrauzer, J. W. Siebert and R. J. Windgassen, *J. Am. Chem. Soc.* 1968, **90**, 6681.
14. A. W. Herlinger and T. L. Brown, *J. Am. Chem. Soc.* 1972, **94**, 388; L. M. Ludwick and T. L. Brown, *J. Am. Chem. Soc.* 1969, **91**, 5188.
15. F. Basolo and R. G. Pearson, *Prog. Inorg. Chem.* 1962, **4**, 381.
16. D. G. Brown, *Prog. Inorg. Chem.* 1973, **18**, 177.
17. L. Siebles and E. Deutsch, *Inorg. Chem.* 1977, **16**, 2273.
18. T. L. Brown, L. M. Ludwick and R. S. Steward, *J. Am. Chem. Soc.* 1972, **94**, 384; R. J. Guschl, R. S. Steward and T. L. Brown, *Inorg. Chem.* 1974, **13**, 417; and R. J. Guschl and T. L. Brown, *Inorg. Chem.* 1974, **13**, 959.
19. G. N. Schrauzer, E. Deutsch and R. J. Windgassen, *J. Am. Chem. Soc.* 1968, **90**, 2441.
20. L. Sacconi, *J. Chem. Soc., A* 1970, 248.
21. M. Ciampolini, *Struct. Bonding (Berlin)* 1969, **6**, 52.
22. L. Sacconi, M. Ciampolini and G. P. Speroni, *Inorg. Chem.* 1965, **4**, 116.
23. G. DeAlti, V. Galasso, A. Bigotto and G. Costa, *Inorg. Chim. Acta* 1969, **3**, 533.
24. G. N. Schrauzer, L. P. Lee and J. W. Sibert, *J. Am. Chem. Soc.* 1970, **92**, 2997.
25. J. H. Dunlop and R. D. Gillard, *Mol. Phys.* 1963, **7**, 493; *J. Chem. Soc.* 1964, 2822.
26. E. Ochiai, K. M. Long, C. R. Sperati and D. H. Busch, *J. Am. Chem. Soc.* 1969, **91**, 3201.
27. A. D. Wentworth and T. S. Piper, *Inorg. Chem.* 1965, **4**, 709.
28. R. D. Gillard and G. Wilkinson, *J. Chem. Soc.* 1963, 6041.
29. T. L. Brown, Department of Chemistry, University of Illinois, Urbana, IL, private communication.
30. S. Bruckner, M. Calligaris, G. Nardin and L. Randaccio, *Inorg. Chim. Acta* 1969, **3**, 308.
31. H. A. O. Hill, J. M. Pratt and R. J. P. Williams, *Discuss. Faraday Soc., No. 47* 1969, **47**, 165.
32. H. A. O. Hill, K. G. Morallee, G. Pellizer, G. Mestroni and G. Costa, *J. Organomet. Chem.* 1968, **11**, 167.
33. H. A. O. Hill and K. G. Morallee, *J. Chem. Soc., Chem. Commun.* 1967, 888.
34. R. S. Steward, Ph.D. Thesis, University of Illinois, Urbana, IL (1971).
35. D. Dodd and M. D. Johnson, *J. Organomet. Chem.* 1973, **52**, 1.
36. D. A. Clarke, R. Grigg and A. W. Johnson, *J. Chem. Soc., Chem. Commun.* 1966, 208.

Polyhedron Vol. 4, No. 4, pp. 563–565, 1985
Printed in Great Britain

0277–5387/85 $3.00 + .00
© 1985 Pergamon Press Ltd

CATIONIC DI-IRON COMPLEXES $\{[\eta\text{-}C_5H_5Fe(CO)_2]_2[\mu\text{-}(C_nH_{2n-1})]\}^+$

J. W. JOHNSON
Exxon Research and Engineering, Annandale, NJ 07036, U.S.A.

and

J. R. MOSS*
Department of Chemistry, University of Cape Town, Rondesbosch 7700, South Africa

(*Received* 9 *April* 1984; *accepted* 22 *May* 1984)

Abstract—The reactions of the complexes $[CpFe(CO)_2]_2[\mu\text{-}(CH_2)_n]$ with Ph_3CPF_6 yield cationic di-iron complexes of the type $\{[CpFe(CO)_2]_2[\mu\text{-}(C_nH_{2n-1})]\}^+$ (n = 3–6). The ^1H NMR spectra for the cationic complexes where n = 4–6 and the variable temperature spectra for the cation where n = 3 are reported and discussed.

The reaction of $[CpFe(CO)_2]_2[\mu\text{-}(CH_2)_3]$ with Ph_3CPF_6 is known to give the cationic complex $\{[CpFe(CO)_2]_2[\mu\text{-}C_3H_5]\}^+PF_6^-$ (I).[1] The structure and low temperature ^1H NMR spectrum of this cationic complex have been reported[2] as well as a detailed discussion of the energies involved in the fluxional processes occurring in solutions of $\{[CpFe(CO)_2]_2[\mu\text{-}(C_3H_5)]\}^+PF_6^-$.[3]

We now find that reactions of the complexes $[CpFe(CO)_2]_2[\mu\text{-}(CH_2)_n]$ (where n = 4–6) with Ph_3CPF_6 in dichloromethane give yellow crystalline complexes

$$\{[CpFe(CO)_2]_2[\mu\text{-}(C_nH_{2n-1})]\}^+PF_6^-.$$

These cationic complexes show four strong ν(CO) bands in their IR spectra and two singlet resonances for the cyclopentadienyl protons in their ^1H NMR spectra. These data are consistent with structures for these complexes where one iron atom is π-bonded and the other σ-bonded to the alkenyl chain, e.g. for n = 4:



Fp = $CpFe(CO)_2$

I

These cationic complexes are formed as a result of hydride abstraction from the β-carbon atom of $[CpFe(CO)_2]_2[\mu\text{-}(CH_2)_n]$. An alternative route to the BF_4^- salt of the cation where n = 5 has been reported by the reaction of

$$[CpFe(CO)_2(CH_2{=}CH_2)]^+$$

with

$$CpFe(CO)_2(CH_2CH{=}CH_2)$$

and some related cations have also been prepared by this method.[4]

In the ^1H NMR spectrum of I at room temperature we observe a singlet at δ 5.50 ppm for the 10 cyclopentadienyl protons and a low field quintet at δ 6.80 ppm due to the CH proton (H_X); the CH_2 protons (H_A and H_B) (see Fig. 1) are coalesced into the base line at this temperature. On cooling to below −10°C the spectrum sharpens and four resonances are observed: the cyclopentadienyl protons remain unchanged as a singlet at δ 5.50 ppm, the H_X proton is observed as a triplet of triplets at δ 6.80 ppm, $^3J(H_AH_X)$ 14.0, $^3J(H_BH_X)$ 6.0 Hz and H_A and H_B

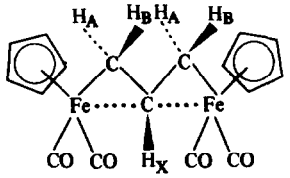


Fig. 1.

* Author to whom correspondence should be addressed.

protons as two doublets of doublets at δ 2.92 ppm, $^3J(H_BH_X)$ 6.0, $^2J(H_AH_B)$ 2.8 and δ 2.35 ppm, $^3J(H_AH_X)$ 14.0, $^2J(H_AH_B)$ 2.8 Hz. The ^{1}H NMR spectrum of I did not change further on cooling to -70°C. This low temperature limiting spectrum is consistent with an A_2B_2X spin system of a rigid η^3-allyl group.[5] On heating the solution of I, the low field triplet of triplets (assigned to H_X) broadened and became a binomial quintet at δ 6.80 ppm, which became sharp above 25°C. The two doublets of doublets (assigned to H_A and H_B) coalesced at 37 $\pm$2°C and then sharpened to a doublet at δ 2.65 ppm, $^3J(H_{A,B}H_X)$ 10 Hz.

Similar changes in the ^{1}H NMR spectrum of the BF_4^- salt of I and some related compounds have been reported although these authors interpreted their results in terms of unsymmetrical hybrid structures.[6] We interpret our ^{1}H NMR results as follows: at low temperature, a symmetrical carbonium ion static structure for I is present, as is found in the solid state.[2] On heating the solution, rotation about the CH_2—CH bonds of the allyl group in I occurs thus equilibrating protons A and B of the A_2B_2X spin system to give an A_4X system.

EXPERIMENTAL

The compounds $[CpFe(CO)_2]_2[\mu\text{-}(CH_2)_n]$ (n = 3, 4, 5 or 6)[7] and

$$\{[CpFe(CO)_2]_2[\mu\text{-}(C_3H_5)]\}^+PF_6^-$$ [1]

were prepared by literature methods. IR spectra were recorded on a Perkin–Elmer 180 spectrophotometer, ^{1}H NMR spectra at 60 MHz were recorded on a Perkin–Elmer R12 spectrometer and the variable temperature ^{1}H NMR spectra of $\{[CpFe(CO)_2]_2[\mu\text{-}(C_3H_5)]^+\}^+PF_6^-$ were obtained using a Bruker WH-270 spectrometer operating in FT mode. All NMR spectra were recorded on d_6-acetone solutions with internal tetramethylsilane as reference standard. Conductivity measurements were made on approximately 10^{-3} M solutions in nitrobenzene. Melting points were determined on a Kofler hot-stage microscope and are uncorrected. Solvents were dried and saturated with nitrogen before use and all reactions were carried out under an atmosphere of nitrogen.

Preparation of $\{[CpFe(CO)_2]_2[\mu\text{-}(C_4H_7)]\}^+PF_6^-$

A solution of $[CpFe(CO)_2]_2[\mu\text{-}(CH_2)_4]$ (0.45 g, 1.10 mmol) in dichloromethane (5 cm^3) was added to a solution of Ph_3CPF_6 (0.48 g, 1.24 mmol) in dichloromethane (10 cm^3) and the reaction mixture allowed to stand for 17 h. The solution was filtered and diethyl ether added to precipitate the product as yellow microcrystals (0.20 g 33%), decomp. without melting > 115°C. Found: C, 38.76; H, 3.13; F, 18.65%. $C_{18}H_{17}F_6Fe_2O_4P$ requires: C, 39.03; H, 3.09; F, 20.58%. IR (CH_2Cl_2) $\nu_{(CO)}$ 2073s, 2036s, 2007s, 1950s cm^{-1}; molar conductance 30.9 ohm^{-1} cm^2 mol^{-1}; ^{1}H NMR δ 5.89 ppm (5H, s, C_5H_5) 5.36 ppm (1H, broad, m, =CH), 5.03 ppm (5H, s, C_5H_5), 3.96 ppm (1H, d, $=CH_2$, J = 8.2 Hz), 3.53 ppm (1H, d, $=CH_2$, J = 14.3 Hz), 1.64 ppm (2H, m, CH_2), 1.24 ppm (2H, m, CH_2Fe).

Preparation of $\{[CpFe(CO)_2]_2[\mu\text{-}(C_5H_9)]\}^+PF_6^-$

This was prepared similarly from $[CpFe(CO)_2]_2[\mu\text{-}(CH_2)_5]$ (0.50 g, 1.19 mmol), Ph_3CPF_6 (0.46 g, 1.18 mmol) and dichloromethane (16 cm^3). The product was obtained as yellow microcrystals (0.33 g, 49%), decomp. without melting 115–128°C. Found: C, 39.62; H, 3.37; F, 20.16%. $C_{19}H_{19}F_6Fe_2O_4P$ requires: C, 40.18; H, 3.37; F, 20.07%. IR (CH_2Cl_2) $\nu_{(CO)}$ 2075s, 2038s, 2004s, 1945s cm^{-1}; molar conductance 33.2 ohm^{-1} cm^2 mol^{-1}; ^{1}H NMR δ 5.83 ppm (5H, s, C_5H_5), 4.94 ppm (5H, s, C_5H_5), 4.00 ppm (1H, broad, d, $=CH_2$, $J \sim 7$ Hz), 3.54 ppm (1H, broad, d, $=CH_2$, $J \sim 13$ Hz), 1.51 ppm (4H, broad, m, CH_2), 1.10 ppm (2H, broad, m, CH_2Fe) (the resonance due to =CH was not resolved).

Preparation of $\{[CpFe(CO)_2]_2[\mu\text{-}(C_6H_{11})]\}^+PF_6^-$

This was prepared similarly from $[CpFe(CO)_2]_2[\mu\text{-}(CH_2)_6]$ (0.53 g, 1.22 mmol), Ph_3CPF_6 (0.48 g, 1.23 mmol) and dichloromethane (16 cm^3). The product was obtained as yellow microcrystals (0.24 g, 34%), m.p. 108–119°C decomp. Found: C, 40.67; H, 3.72; F, 20.02%. $C_{20}H_{21}F_6Fe_2O_4P$ requires: C, 41.27; H, 3.64; F, 19.58%. IR (CH_2Cl_2) $\nu_{(CO)}$ 2076s, 2038s, 2003s, 1941s cm^{-1}; molar conductance 32.5 ohm^{-1} cm^2 mol^{-1}; ^{1}H NMR δ 5.89 ppm (5H, s, C_5H_5), 4.92 ppm (5H, s, C_5H_5), 4.05 ppm (1H, d, $=CH_2$, J = 7.8 Hz), δ 3.62 ppm (1H, d, $=CH_2$, J = 14.4 Hz), δ 1.52 ppm (6H, broad, m, CH_2), δ 0.95 (2H, broad, m, CH_2Fe) (the resonance due to =CH was not resolved).

Acknowledgements—We thank the University of Cape Town and the C.S.I.R. for financial support. High field NMR spectra were recorded at the University of Wisconsin–Madison.

REFERENCES

1. R. B. King and M. B. Bisnette, *J. Organomet. Chem.* 1967, 7, 311.
2. M. Laing, J. R. Moss and J. Johnston, *J. Chem. Soc., Chem. Commun.* 1977, 656.

3. G. E. Jackson, J. R. Moss and L. G. Scott, *S. Afr. J. Chem.* 1983, **36**, 69.
4. P. J. Lennon, A. Rosan, M. Rosenblum, J. Tancrede and P. Waterman, *J. Am. Chem. Soc.* 1980, **102**, 7033; T. C. T. Chang, B. M. Foxman, M. Rosenblum and C. Stockman, *J. Am. Chem. Soc.* 1981, **103**, 7361.
5. W. R. McClellan, H. H. Hoehn, H. N. Gripps, E. L. Muetterties and B. W. Howk, *J. Am. Chem. Soc.* 1961, **83**, 1601; F. A. Cotton, J. W. Faller and A. Musco, *Inorg. Chem.* 1967, **6**, 181.
6. R. C. Kerber, W. P. Giering, T. Bauch, P. Waterman and E.-H. Chou, *J. Organomet. Chem.* 1976, **120**, C31.
7. R. B. King, *Inorg. Chem.* 1963, **2**, 531.

Polyhedron Vol. 4, No. 4, pp. 567–575, 1985
Printed in Great Britain

0277–5387/85 $3.00 + .00
Pergamon Press Ltd

THE ISOLATION AND X-RAY STRUCTURE OF A COMPLEX BETWEEN LITHIUM PICRATE AND DIBENZO-36-CROWN-12

SIMON M. DOUGHTY and J. FRASER STODDART*
Department of Chemistry, The University, Sheffield S3 7HF, U.K.

HOWARD M. COLQUHOUN
New Science Group, Imperial Chemical Industries PLC, The Heath, Runcorn WA7 4QE, U.K.

and

ALEXANDRA M. Z. SLAWIN and DAVID J. WILLIAMS
Chemical Crystallography Laboratory, Department of Chemistry, Imperial College, London SW7 2AY, U.K.

(*Received* 13 *April* 1984; *accepted* 22 *May* 1984)

Abstract—The crystal structure of 2Li picrate.dibenzo-36-crown-12.2H_2O was determined by X-ray diffraction methods. The 2:1 (metal:ligand) complex crystallises in the monoclinic system, space group $P2_1/c$ with $a = 9.748(2)$, $b = 22.559(4)$, $c = 12.474(2)$ Å, and $\beta = 107.05(1)°$. The Li^+ ions are 5-coordinated within a distorted trigonal bipyramidal geometry to *one* water molecule, *two* crown ether oxygen atoms, and the *phenoxide* and *nitro* group oxygen atoms of a picrate counterion. The picrate ions are nearly parallel to the benzo rings in the host with a minimum inter-group separation of 3.37 Å. However, ^1H NMR spectroscopy of a range of DB3*n*C*n* (n = 9–12) hosts in CD_2Cl_2 reveals little if any interaction between picrate and benzo-rings in solution.

Dibenzo-crown ethers of the general type DB3*n*C*n* (n = 6–12) form[1,2] stable adducts in solution with $[Pt(bipy)(NH_3)_2][PF_6]_2$, not only by virtue of the expected electrostatic interaction and [N—H---O] hydrogen bonding, but also as a result of charge transfer between the bipyridyl (bipy) ligand (π-acceptor) in the complex and the benzo-rings (π-donors) of the host. Stability constant measurements indicated[2] optimum binding (free energy of complexation of 7.2 kcal mol^{-1} in MeCN) when n = 10, and X-ray crystal structures of the 1:1 adducts where n = 8 and 10 confirmed that, when n = 10, the macrocycle is sufficiently large and flexible to allow both benzo-rings to enter into stabilising charge transfer interactions with the bipyridyl ligand such that the platinum complex is completely encapsulated by DB30C10 in a U-shaped cavity. Subsequently, an X-ray crystallographic investigation of the 1:1 complex formed between $[Diquat][PF_6]_2$ and DB30C10 revealed[3,4] very similar gross structural features for this complex. Intermolecular charge transfer interactions combine with Coulombic (ion-dipole) forces and weak [C—H---O] hydrogen bonding to stabilise the complex. Stability constant measurements once again indicated[3,4] optimum binding (free energy of complexation of 5.8 kcal mol^{-1} in Me_2CO) when n = 10 in the range (n = 9–12) of DB3*n*C*n* hosts examined. These observations are summarised (cf. ref. 4) diagrammatically in Fig. 1. They led us to speculate that it might even be possible to stabilise, by a similar charge transfer interaction, organic anions, such as picrate, which carry several electron withdrawing groups. The idea we set out to test is presented diagrammatically in Fig. 2. We were encouraged to carry out some experiments in the knowledge that, although the crystal structures of some metal picrate (pic) complexes (e.g.

$[K(pic).(B15C5)_2]$,[5] $[Na(pic).B15C5]$[6]

and

$[TlMe_2(pic).DB18C6]$[7])

* Author to whom correspondence should be addressed.

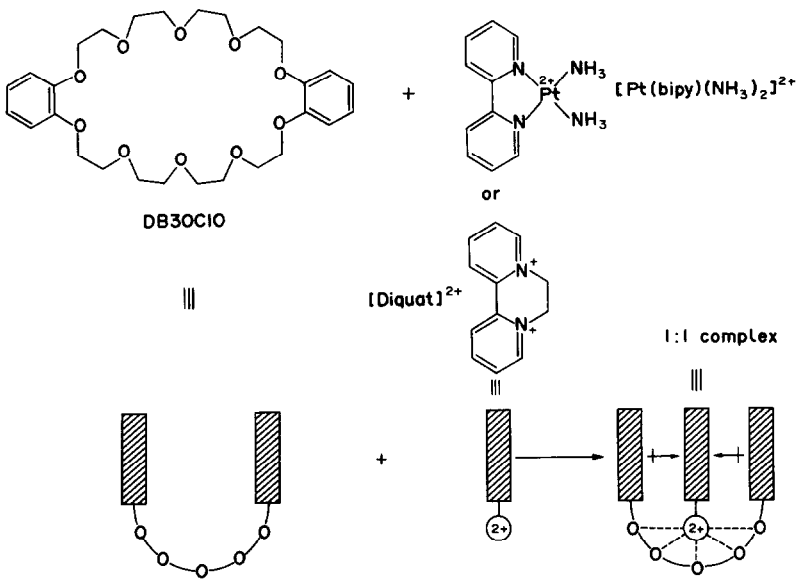


Fig. 1. The formation of 1:1 complexes between DB30C10 and either $[Pt(bipy)(NH_3)_2]^{2+}$ or $[Diquat]^{2+}$ dications. The schematic representation shows the pole–dipole (----) and charge transfer (↔) interactions.

with benzo- and dibenzo-crown ethers show no near approaches between the picrate and the catechol rings of the hosts, others (e.g.

$$[Ba(pic)_2.DB24C8.2H_2O],^{8}$$

$$[Ca(pic)_2.B15C5.3H_2O]^{9}$$

and

$$[Li(pic).B15C5.2H_2O]^{10})$$

reveal the stacking of the picrate rings alongside the catechol rings. 3,5-Dinitrobenzoate (dnb) rings have also been found (e.g. in $[Ca(dnb)_2.(B15C5)_2.3H_2O]$)[11] lying parallel to catechol rings in solid state structures of crown ether complexes.

The main reasons for choosing lithium picrate as the guest salt in our investigations were the following: (i) being a monocation, lithium only associates with one picrate anion; (ii) being a hard cation, lithium is strongly anionophilic; and (iii) the tendency of lithium ions to coordinate to water molecules (see later) renders it highly flexible in its adaptation to a crown ether cavity.

This paper describes the isolation of

$$3Li(pic).2DB30C10.5H_2O$$

and

$$2Li(pic).DB36C12.2H_2O$$

and an X-ray structural investigation of

$$2Li(pic).DB36C12.2H_2O.$$

Comparisons are drawn between the conformation of DB36C12 in this 2:1 complex and the host conformations in $2NaPF_6.DB36C12$[12] and

$$2[Rh(cod)(NH_3)_2PF_6].DB36C12.$$[13]

The nature of the first coordination sphere of the lithium ion is compared with that in complexes involving other crown ethers and synthetic ionophores. Finally, ^1H NMR spectroscopic data for some 1:1 complexes between Li(pic) and

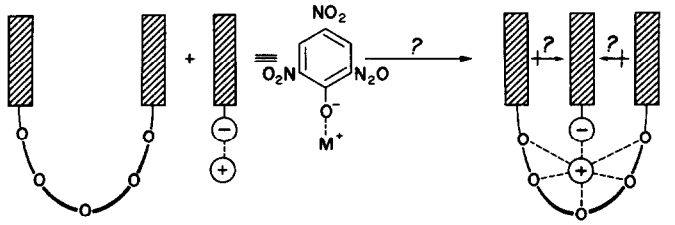


Fig. 2. A schematic representation of the proposed 1:1 complex formation between DB30C10 and alkali metal picrates.

DB3*n*C*n* ($n = 9$–12) ethers are interpreted with reference to previous investigations of the analogous 1:1 complexes involving $[Pt(bipy)(NH_3)_2][PF_6]_2$ and $[Diquat][PF_6]_2$ as guests.

EXPERIMENTAL

The crown ethers 18C6 and DB24C8 were obtained from Aldrich. The stepwise syntheses of DB27C9, DB30C10, DB33C11 and DB36C12 have been described briefly elsewhere.[1] A full account of their synthesis will be published shortly.[4] ^{1}H NMR spectra (tetramethylsilane as lock and internal standard) were recorded on a Perkin–Elmer R34 (220 MHz) spectrometer.

Isolation of 3Li picrate.2DB30C10.5H_2O

Lithium picrate monohydrate (25.3 mg, 0.1 mmol) and DB30 C10 (53.6 mg, 0.1 mmol) were dissolved in acetonitrile (3 cm^3). This solution was layered firstly with ether and then with light petroleum (b.p. 60–80°C). After 48 h, the mixture contained a fibrous micro-crystalline material, m.p. 73–76°C, which was isolated by filtration. ^{1}H NMR spectroscopy (CD_2Cl_2) revealed (cf. Table 4) the presence of the following signals: δ 2.92 (6H, s, $2CH_3CN$), 3.50–3.80 (19H, m, γ- and δ-OCH_2 protons and H_2O), 3.87 (8H, m, β-OCH_2 protons), 4.10 (8H, m, α-OCH_2 protons), 6.80 (8H, m, catechol ring protons) and 8.81 (3H, s, picrate protons). This spectrum is, therefore, consistent with a stoichiometry of 3:2:3 for Li picrate:DB30C10:H_2O. The sample was dried under high vacuum. Yield 49 mg, 80%; IR data (Nujol): 3570 m, 3490 m (ν_{OH}), 1560s, 1330s (ν_{NO_2}), 1125s (ν_{CO}) cm^{-1}.

Found: C, 47.1; H, 5.3; N, 6.6%. $C_{74}H_{98}O_{48}N_9Li_3$ (i.e. 3Li picrate.2DB30C10.5H_2O) requires: C, 46.7; H, 5.2; N, 6.6%.

Isolation and X-ray structural analysis of 2Li picrate.DB36C12.2H_2O

On standing overnight, the CD_2Cl_2 solution of DB36C12 containing 1.0 equivalent of lithium picrate, which had been used to record ^{1}H NMR spectra, deposited a small crop of pale yellow needles. IR data (Nujol): 3560 m, 3440 m (ν_{OH}), 1365 s, 1325 s (ν_{NO_2}) cm^{-1}. From these, a single crystal was chosen for X-ray study.

Crystal data. $C_{32}H_{48}O_{12}.Li_2C_{12}H_4O_{14}N_6.2H_2O$, monoclinic, $a = 9.748(2)$, $b = 22.559(4)$, $c = 12.474(2)$ Å, $\beta = 107.05(1)°$, $U = 2622$ Å^3, space group $P2_1/c$, $Z = 2$, $M = 1129.9$, $D_c = 1.44$ g cm^{-3}, μCu-K_α 10 cm^{-1}.

Measurements. Refined unit cell parameters were obtained by centering 18 reflections on a Nicolet R3m diffractometer. 3624 Independent reflections ($\theta < 55°$) were measured with Cu-K_α radiation (graphite monochromator) using the omega scan measuring routine. Of these, 3280 were unique, and 2995 had $|F_o| > 3\sigma(|F_o|)$ and were considered observed. Lorentz and polarisation corrections were applied. No absorption correction was applied.

Structure analysis. The structure was solved by direct methods. An *E* map computed with 418 *Es* > 1.62 for the phase solution with the highest "figure of merit" gave the positions of all non-hydrogen atoms. A ΔF map revealed disorder to be present in the macrocycle associated with O(4), C(5) and C(8) [and, of course, with the symmetry related O(4′), C(5′) and C(8′)]. These atoms were assigned two alternative sites in each case, with occupation factors of 0.65 and 0.35. All the ordered non-hydrogen atoms and the major (0.65) sites associated with the disorder were refined anisotropically. The minor site atoms were refined isotropically. The hydrogen atoms were placed at idealised positions (C—H = 0.96 Å), assigned isotropic thermal parameters, $U(H) = 1.2U_{eq}(C)$, and allowed to ride on their parent carbon atoms. The hydrogens belonging to the minor (0.35) fraction of the disorder were disregarded. Refinement was by block cascade full matrix least squares to $R = 0.055$, $R_w = 0.068$ [$w^{-1} = \sigma 2(F) + 0.006F^2$]. Computations were carried out on an Eclipse S140 computer using the SHELTXL program system.[14] Scattering factors were taken from the *International Tables for X-Ray Crystallography*.[15]

Final atomic coordinates, including those of the hydrogen atoms, and thermal parameters have been deposited with the Editor as supplementary data.*

RESULTS AND DISCUSSION

Tables 1 and 2 record the bond lengths and bond angles respectively for 2Li(pic).DB36C12.2H_2O. Torsional angles for the C—C and C—O bonds on the macrocyclic ring are listed in Table 3 together with those for $2NaPF_6$.DB36C12[12] and 2[Rh(cod)$(NH_3)_2PF_6$].DB36C12[13]. In common with both the sodium and rhodium complexes, the macrocycle (Figs 3 and 4) possesses a crystallographic centre of symmetry and binds the guest species in a displaced manner to opposite faces of the host. There is disorder associated with O(4), C(5) and O(8)—and of course, with the symmetry related O(4′), C(5′) and O(8′)—in the polyether chain. Not surprisingly, in such a large and flexible macrocycle,

* Atomic coordinates have also been deposited with the Cambridge Crystallographic Data Centre.

Table 1. Bond lengths (Å)

Li^+—O(7)	2.234(5)	Li^+—O(10)	1.983(5)
Li^+—O(23)	1.936(5)	Li^+—O(22)	2.067(6)
Li^+—O(24)	1.962(6)	O(1)—C(2)	1.423(5)
O(1)—C(22′)	1.359(3)	C(2)—C(3)	1.405(7)
C(3)—O(4)	1.386(5)	C(3)—O(4*)	1.465(9)
O(4)—C(5)	1.493(7)	O(4*)—C(5*)	1.489(13)
C(5)—C(6)	1.315(7)	C(5*)—C(6)	1.494(11)
C(6)—O(7)	1.389(5)	O(7)—C(8)	1.323(6)
O(7)—C(8*)	1.379(10)	C(8)—C(9)	1.437(8)
C(8*)—C(9)	1.398(11)	C(9)—O(10)	1.391(4)
O(10)—C(11)	1.437(4)	C(11)—C(12)	1.472(5)
C(12)—O(13)	1.429(4)	O(13)—C(14)	1.404(3)
C(14)—C(15)	1.492(4)	C(15)—O(16)	1.419(4)
O(16)—C(17)	1.370(3)	C(17)—C(18)	1.358(4)
C(17)—C(22)	1.406(4)	C(18)—C(19)	1.378(5)
C(19)—C(20)	1.343(7)	C(20)—C(21)	1.388(5)
C(21)—C(22)	1.361(5)	C(22)—O(1′)	1.359(3)
C(23)—O(23)	1.237(3)	C(23)—C(24)	1.439(3)
C(23)—C(28)	1.442(4)	C(24)—N(1)	1.465(4)
C(24)—C(25)	1.359(3)	N(1)—O(17)	1.216(3)
N(1)—O(18)	1.215(4)	C(25)—C(26)	1.387(4)
C(26)—N(2)	1.456(3)	C(26)—C(27)	1.359(3)
N(2)—O(19)	1.212(4)	N(2)—O(20)	1.221(4)
C(27)—C(28)	1.387(3)	C(28)—N(3)	1.434(3)
N(3)—O(21)	1.224(4)	N(3)—O(22)	1.219(3)

* Refers to atoms with partial occupancy, 0.35.

there are significant differences in the conformations of the polyether chains in the three different complexes. However, in the region of the macrocycle between O(16′) and C(11) via C(6) there are, with two exceptions—O(1)C(2)C(3)O(4) in $2NaPF_6$.DB36C12 and O(7)C(8)C(9)O(10) in $2[Rh(cod)(NH_3)_2PF_6]$.DB36C12—gross similarities between the torsional angles in the polyether chains of the three complexes.

The five-fold coordination geometry of the Li^+ ion is that of a distorted trigonal bipyramid with the [Li^+---O] bonds to the ether oxygen O(7) [2.234(5)] and the phenoxide oxygen O(23) [1.936(5)] forming the apices, and those to the ether oxygen O(10) [1.983(5)], the *ortho*-nitro group oxygen O(22) [2.067(6)] and the oxygen of the water molecule O(24) [1.962(6)] Å the equatorial components. The angles at the Li^+ ion to the equatorial ligands are 129.0(3), 120.2(3) and 109.7(2)° respectively with the lithium atom being slightly displaced (0.12 Å) from the plane of O(10), O(22) and O(24) towards O(23). This coordination has also been found[16] in the crystal structure of the 1:2 complex of an 18,18′-spirobi-(19-crown-6) derivative with lithium iodide dihydrate. Square pyramidal geometry has been observed more frequently in crystalline complexes between crown ethers and lithium ions (e.g. in

[LiSCN.12C4],[17] [LiSCN.12C4],[18]

[LiSCN.DB14C4],[19] [LiSCN.B13C4][20]

and

[$LiN(SiMe_3)_2$.12C4][21]).

In the complexes involving the thiocyanate counterion, the nitrogen atom of the anion provides the fifth coordination site for the cation. In some cases, namely with [$LiNO_3$.B14C4][22] and with an analogous complex[23] involving a chiral dimethyl derivative of benzo-14-crown-4, although the cation is hexacoordinated, the geometry of the coordi-

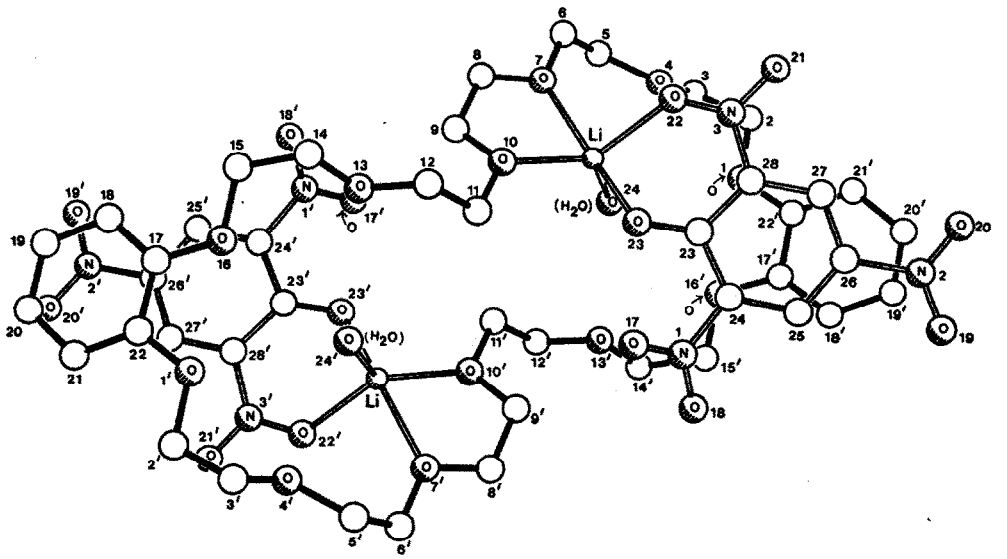


Fig. 3. Crystal structure of 2Li(pic).DB36C12.2H_2O showing the atomic numbering scheme.

Table 2. Bond angles (°)

O(7)—Li^+—O(10)	77.8(2)	O(7)—Li^+—O(23)	170.3(3)
O(10)—Li^+—O(23)	98.1(2)	O(7)—Li^+—O(22)	92.7(2)
O(10)—Li^+—O(22)	129.0(3)	O(23)—Li^+—O(22)	83.0(2)
O(7)—Li^+—O(24)	90.6(2)	O(10)—Li^+—O(24)	120.2(3)
O(23)—Li^+—O(24)	99.1(2)	O(22)—Li^+—O(24)	109.7(2)
C(2)—O(1)—C(22')	118.0(3)	O(1)—C(2)—C(3)	109.9(4)
C(2)—C(3)—O(4)	107.2(4)	C(2)—C(3)—O(4*)	128.8(4)
C(3)—O(4)—C(5)	113.8(4)	C(3)—O(4*)—C(5*)	100.9(7)
O(4)—C(5)—C(6)	116.9(5)	O(4*)—C(5*)—C(6)	105.3(8)
C(5)—C(6)—O(7)	117.3(4)	C(5*)—C(6)—O(7)	119.0(5)
Li^+—O(7)—C(6)	133.7(3)	Li^+—O(7)—C(8)	110.3(3)
C(6)—O(7)—C(8)	115.6(3)	Li^+—O(7)—C(8*)	96.8(4)
C(6)—O(7)—C(8*)	124.0(5)	O(7)—C(8)—C(9)	115.7(4)
O(7)—C(8*)—C(9)	114.7(7)	C(8)—C(9)—O(10)	114.5(3)
C(8*)—C(9)—O(10)	110.3(4)	Li^+—O(10)—C(9)	114.9(3)
Li^+—O(10)—C(11)	125.5(2)	C(9)—O(10)—C(11)	117.1(3)
O(10)—C(11)—C(12)	116.2(3)	C(11)—C(12)—O(13)	109.3(3)
C(12)—O(13)—C(14)	111.0(3)	O(13)—C(14)—C(15)	108.3(3)
C(14)—C(15)—O(16)	107.7(2)	C(15)—O(16)—C(17)	116.7(2)
O(16)—C(17)—C(18)	125.3(3)	O(16)—C(17)—C(22)	115.6(2)
C(18)—C(17)—C(22)	119.1(3)	C(17)—C(18)—C(19)	120.6(3)
C(18)—C(19)—C(20)	120.3(3)	C(19)—C(20)—C(21)	120.6(4)
C(20)—C(21)—C(22)	119.6(4)	C(17)—C(22)—C(21)	119.9(3)
C(17)—C(22)—O(1')	115.1(3)	C(21)—C(22)—O(1')	125.0(3)
O(23)—C(23)—C(24)	122.7(2)	O(23)—C(23)—C(28)	125.8(2)
C(24)—C(23)—C(28)	111.5(2)	Li^+—O(23)—C(23)	126.9(2)
C(23)—C(24)—N(1)	118.1(2)	C(23)—C(24)—C(25)	125.7(2)
N(1)—C(24)—C(25)	116.3(2)	C(24)—N(1)—O(17)	117.5(3)
C(24)—N(1)—O(18)	118.8(2)	O(17)—N(1)—O(18)	123.7(3)
C(24)—C(25)—C(26)	118.3(2)	C(25)—C(26)—N(2)	119.5(2)
C(25)—C(26)—C(27)	121.2(2)	N(2)—C(26)—C(27)	119.2(2)
C(26)—N(2)—O(19)	117.8(3)	C(26)—N(2)—O(20)	118.1(2)
O(19)—N(2)—O(20)	124.1(2)	C(26)—C(27)—C(28)	120.0(2)
C(23)—C(28)—C(27)	123.3(2)	C(23)—C(28)—N(3)	119.9(2)
C(27)—C(28)—N(3)	116.7(2)	C(28)—N(3)—O(21)	118.3(2)
C(28)—N(3)—O(22)	121.3(2)	O(21)—N(3)—O(22)	120.4(2)
Li^+—O(22)—N(3)	130.4(2)		

* Refers to atoms with partial occupancy, 0.35.

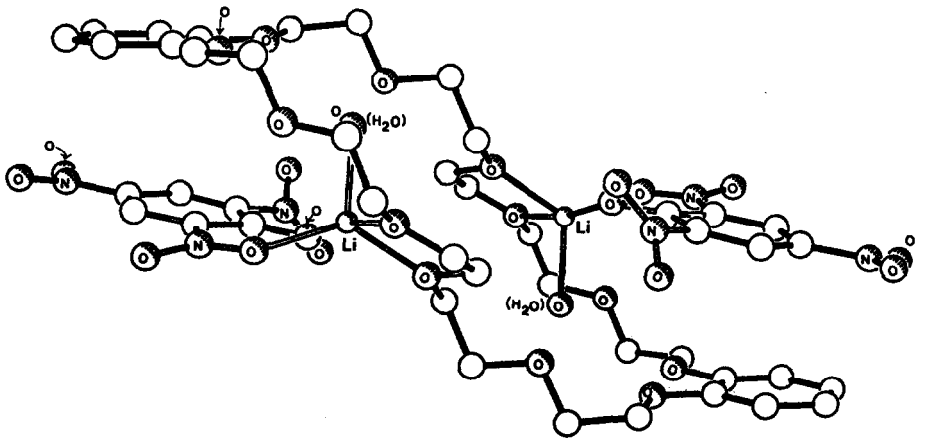


Fig. 4. Side-on view of the crystal structure. Note the stacking of the picrate and catechol rings.

Table 3. A comparison of the torsional angles (°) in DB36C12 in the three different crystalline complexes

Torsional angle	2Li(picrate). DB36C12.2H_2O	2$NaPF_6$. DB36C12	2[Rh(cod)$(NH_3)_2PF_6$]. DB36C12
C(17′)—C(22′)—O(1)—C(2)	−175	179	176
C(22′)—O(1)—C(2)—C(3)	178	172	−174
O(1)—C(2)—C(3)—O(4)	70*	178	71
C(2)—C(3)—O(4)—C(5)	−179*	179	171
C(3)—O(4)—C(5)—C(6)	−173*	−172	−68
O(4)—C(5)—C(6)—O(7)	−61*	−64	−68
C(5)—C(6)—O(7)—C(8)	−137*	180	159
C(6)—O(7)—C(8)—C(9)	173*	−175	−175
O(7)—C(8)—C(9)—O(10)	28*	65	−15
C(8)—C(9)—O(10)—C(11)	168	−179	−166
C(9)—O(10)—C(11)—C(12)	−59	84	−105
O(10)—C(11)—C(12)—O(13)	89	56	−58
C(11)—C(12)—O(13)—C(14)	−172	−177	−62
C(12)—O(13)—C(14)—C(15)	−175	155	−130
O(13)—C(14)—C(15)—O(16)	69	−43	82
C(14)—C(15)—O(16)—C(17)	173	−118	83
C(15)—O(16)—C(17)—C(22)	−174	−73	168
O(16)—C(17)—C(22)—O(1′)	−1	−4	−3

* Associated with regions of disorder.

nation is better perceived as being square pyramidal. In other cases, namely with

[Li(pic).B15C5.2H_2O],[10] [$LiClO_4$.18C6.2H_2O][24]

and

[LiSCN.18C6.2H_2O],[24]

four-fold coordination with tetrahedral geometry is displayed; recently, the previously unknown coordination number of 8 was found[25] in the X-ray structures of

[Li(PPh_2).$(12C4)_2$]

and

[Li($AsPh_2$).$(12C4)_2$].

Although in

[Li(pic).B15C5.2H_2O][10]

and

[Ca$(pic)_2$.B15C5.3H_2O],[9]

the cation is coordinated exclusively within the anionic and solvent environments, in the present structure, crown ether oxygen atoms as well as solvent (H_2O) and anion (pic) play a role, cf. the crystal structures of

[LiI.18,18′-spirobi-19C6.2H_2O][16]

and

[LiSCN.18C6.2H_2O].[24]

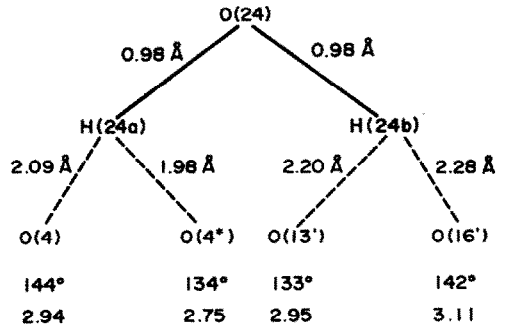


Fig. 5. The parameters associated with the H_2O molecule coordinated to the Li^+ ion and hydrogen bonded to the crown ether.

Table 4. ^{1}H NMR chemical shifts* (δ, CD_2Cl_2) for 18C6, DB27C9, DB30C10, DB33C11 and DB36C12 as well as for the 1 : 1 complexes of these crown ethers with lithium picrate [Li(pic)]

Crown ether or complex	Picrate H	C_6H_4	OCH_2^{α}	$OCH_2^{\alpha'}$	OCH_2^{β}	$OCH_2^{\beta'}$	OCH_2^{γ}	$OCH_2^{\gamma'}$	OCH_2^{δ}	$OCH_2^{\delta'}$	OCH_2^{ε}
18C6	—	—	3.58(s)	—	—	—	—	—	—	—	—
Li(pic).18C6†	8.86(s)	—	3.68(s)	—	—	—	—	—	—	—	—
	—	—	*(+0.10)*	—	—	—	—	—	—	—	—
DB27C9	—	6.89(s)	4.14(m)	4.14(m)	3.87(m)	3.87(m)	3.77(s)	3.73(m)	—	3.67(m)	—
Li(pic).DB27C9†	8.80(s)	6.87(m)	4.13(m)	4.13(m)	3.85(m)	3.85(m)	3.77(s)	3.72(m)	—	3.71(m)	—
	(−0.06)	*(−0.02)*	*(−0.01)*	*(−0.01)*	*(−0.02)*	*(−0.02)*	*(0.00)*	*(−0.01)*	—	*(+0.04)*	—
DB30C10	—	6.88(s)	4.11(m)	—	3.83(m)	—	3.70(m)	—	3.64(m)	—	—
Li(pic).DB30C10†	8.82(s)	6.80(m)	4.08(m)	—	3.88(m)	—	3.73(m)	—	3.73(m)	—	—
	(−0.04)	*(−0.08)*	*(−0.03)*	—	*(+0.05)*	—	*(+0.03)*	—	*(+0.09)*	—	—
DB33C11	—	6.88(s)	4.12(m)	4.12(m)	3.83(m)	3.83(m)	3.70(m)	3.70(m)	3.62(m)	3.62(m)	3.60(s)
Li(pic).DB33C11	8.77(s)	6.86(s)	4.12(m)	4.12(m)	3.86(m)	3.86(m)	3.72(m)	3.72(m)	3.67(m)	3.67(m)	3.65(s)
	(−0.09)	*(−0.02)*	*(0.00)*	*(0.00)*	*(+0.03)*	*(+0.03)*	*(+0.02)*	*(+0.02)*	*(+0.05)*	*(+0.05)*	*(+0.05)*
DB36C12	—	6.88(s)	4.12(m)	—	3.83(m)	—	3.68(m)	—	3.63(m)	—	3.60(s)
Li(pic).DB36C12†	8.78	6.86(s)	4.12(m)	—	3.83(m)	—	3.69(m)	—	3.65(m)	—	3.65(s)
	(−0.08)	*(−0.02)*	*(0.00)*	—	*(0.00)*	—	*(+0.01)*	—	*(+0.02)*	—	*(+0.05)*

* The values in italics in parentheses indicate how strongly the respective signals are shifted relative to either Li(pic).18C6 in the case of the picrate protons, or the free crowns in the case of the C_6H_4 and OCH_2 protons. The OCH_2 protons are labelled α, β, γ etc. in the shorter polyether chain, and α', β', γ' etc. in the longer polyether chain, both starting from the benzo-rings.

† No attempt was made to dry the solvent (CD_2Cl_2) or the salt [Li(pic)]. Significantly, therefore, broad signals, which were assigned to H_2O, were observed at δ 4.20, 3.60, 3.62, 3.53 and 3.26 for the complexes involving 18C6, DB27C9, DB30C10, DB33C11 and DB36C12, respectively.

The water molecule is involved in intracomplex hydrogen bonding with the disordered O(4) and forms a bifurcated hydrogen bond to O(13′) and O(16′). This situation is portrayed graphically in Fig. 5. All three nitro groups are rotated out of the plane of the picrate ring. The rotations are 45.2, 5.7 and 12.5°, for the groups associated with N(1), N(2) and N(3), respectively.

In view of the observation of a near-parallel (9.9° between the mean planes) overlap and close approach [3.37 Å between C(19′) and the C(26)—N(2) bond] of the picrate and catechol rings, it was decided to find out if there was any evidence for this stacking phenomenon in solution. In the crystal structures of

$$[Pt(bipy)(NH_3)_2(PF_6)_2.DB30C10.0.6H_2O]^{1,2}$$

and

$$[Diquat.(PF_6)_2.DB30C10],^{3,4}$$

the near parallel guest and host aromatic rings were separated by *ca* 3.5 and 3.4 Å, respectively. Evidence was obtained[1–4] for charge transfer stabilisation of both these supramolecular structures in solution by spectroscopic (^{1}H NMR and UV) methods. In the event, it was only just possible to dissolve 1.0 molar equivalent of lithium picrate in CD_2Cl_2 solutions containing the DB3*n*C*n* (*n* = 9–12) ethers. In Table 4, the chemical shifts of guest and host protons are compared with those for [Li(pic).18C6] and the free host, respectively. The changes (0.01–0.09 ppm) in chemical shifts were extremely small compared with those observed previously[1–4] for the dicationic complexes. It was, therefore, concluded that, even in the most favoured situation (DB30C10), any charge transfer stabilisation of the picrate anion by benzo-rings in DB3*n*C*n* ethers is very small in solution if indeed it exists at all. It has to be remembered that in the one case (DB36C12), where we have unequivocal structural information, it is for 2:1 stoichiometry in the solid state. Also, all the solution work has been carried out—and had to be—with a 1:1 stoichiometry. The possibility exists that, even in the solid state, the stacking of host and guest aromatic rings does not arise because of charge transfer. Moreover, there is no evidence in the appropriate region (300–400 nm) of the UV spectra of 1:1 complexes of DB30C10 and DB36C12 with lithium picrate in acetonitrile of a charge transfer band. Thus, we believe it is more likely that, although ion pairing does occur between the picrate anion and the lithium cation in CD_2Cl_2 solution, this electrostatic interaction, together with three electron withdrawing nitro groups, is not sufficient to annul the effect of the negative charge on the anion and render this aromatic ring system a π-acceptor towards the electron rich π-donating catechol units. In summary, although lithium picrate complexes with DB3*n*C*n* ethers in solution, it appears to do so without any appreciable ordering of guest and host aromatic ring systems.

Acknowledgements—We thank Imperial Chemical Industries PLC, the Science and Engineering Research Council, and the Agricultural and Food Research Council for support.

REFERENCES

1. H. M. Colquhoun, J. F. Stoddart, D. J. Williams, J. B. Wolstenholme and R. Zarzycki, *Angew. Chem. Int. Ed. Engl.* 1981, **20**, 1051.
2. H. M. Colquhoun, S. M. Doughty, J. M. Maud, J. F. Stoddart, D. J. Williams and J. B. Wolstenholme, *Israel J. Chem.* (in press).
3. H. M. Colquhoun, E. P. Goodings, J. M. Maud, J. F. Stoddart, D. J. Williams and J. B. Wolstenholme, *J. Chem. Soc., Chem. Commun.* 1983, 1140.
4. H. M. Colquhoun, E. P. Goodings, J. M. Maud, J. F. Stoddart, J. B. Wolstenholme and D. J. Williams, *J. Chem. Soc., Perkin Trans.* 2, in press.
5. V. W. Bagwat, H. Manohar and N. S. Poonia, *Inorg. Nucl. Chem. Lett.* 1981, **17**, 207.
6. D. L. Ward, A. I. Popov and N. S. Poonia, *Acta Cryst.* 1984, **C40**, 238.
7. J. Crowder, K. Henrick, R. W. Matthews and B. Podejma, *J. Chem. Res. (S)* 1983, 82.
8. D. L. Hughes and J. N. Wingfield, *J. Chem. Soc., Chem. Commun.* 1977, 804.
9. V. W. Bhagwat, H. Manohar and N. S. Poonia, *Inorg. Nucl. Chem. Lett.* 1980, **16**, 289.
10. V. W. Bhagwat, H. Manohar and N. S. Poonia, *Inorg. Nucl. Chem. Lett.* 1980, **16**, 373.
11. P. D. Cradwick and N. S. Poonia, *Acta Cryst.* 1977, **B33**, 197.
12. J. M. Maud, J. F. Stoddart, H. M. Colquhoun and D. J. Williams, *Polyhedron* 1984, **3**, 675.
13. H. M. Colquhoun, S. M. Doughty, J. F. Stoddart and D. J. Williams, *Angew. Chem. Int. Ed. Engl.* (in press).
14. G. M. Sheldrick, *SHELXTL, An Integrated System for Solving, Refining, and Displaying Crystal Structures from Diffraction Data.* University of Göttingen, F.R.G. (1978).
15. *International Tables for X-Ray Crystallography*, Vol. 4, pp. 99 and 149. Kynoch Press, Birmingham, U.K. (1974).
16. M. Czugler and E. Weber, *J. Chem. Soc., Chem. Commun.* 1981, 472.
17. P. Groth, *Acta Chem. Scand.* 1981, **A35**, 463; F. A. L. Anet, J. Krane, J. Dale, K. Daasvatan and P. O. Kristiansen, *Acta Chem. Scand.* 1973, **27**, 3395; A. Pullman, C. Giessner-Prettre and Y. V. Kruglyak, *Chem. Phys. Lett.* 1975, **35**, 156.
18. P. Groth, *Acta Chem. Scand.* 1981, **A35**, 460; J. Dale and J. Krane, *J. Chem. Soc., Chem. Commun.* 1972, 1012.

19. G. Shoham, W. N. Lipscomb and U. Olsher, *J. Chem. Soc., Chem. Commun.* 1983, 208; U. Olsher, *J. Am. Chem. Soc.* 1982, **104**, 4006.
20. G. Shoham, W. N. Lipscomb and U. Olsher, *J. Am. Chem. Soc.* 1983, **105**, 1247; *J. Chem. Soc., Dalton Trans.* 1981, 501.
21. P. P. Power and X. Xiaojie, *J. Chem. Soc., Chem. Commun.* 1984, 358.
22. E. M. Holt, G. D. Malpass, Jr., R. G. Ghirardelli, R. A. Palmer and B. Bubin, *Acta Cryst.* 1984, **C40**, 394.
23. E. M. Holt, G. D. Malpass, Jr., R. G. Ghirardelli, R. A. Palmer and B. Bubin, *Acta Cryst.* 1984, **C40**, 396.
24. P. Groth, *Acta Chem. Scand.* 1982, **A36**, 109.
25. H. Hope, M. M. Olmstead, P. P. Power and X. Xu, *J. Am. Chem. Soc.* 1984, **106**, 819.

Polyhedron Vol. 4, No. 4, pp. 577–582, 1985
Printed in Great Britain

0277–5387/85 $3.00 + .00
Pergamon Press Ltd

EFFECT OF INORGANIC AQUEOUS ANIONS ON THE SYNERGIC EXTRACTION OF CADMIUM AND ZINC WITH 1-PHENYL-3-METHYL-4-BENZOYL-PYRAZOL-5-ONE (HPMBP) AND LIPOPHILIC AMMONIUM SALTS

J. P. BRUNETTE,* Z. LAKKIS, M. LAKKIS and M. J. F. LEROY
Laboratoire de Chimie Minérale E.N.S.C.S., Associé au C.N.R.S. (E.R.A. 468), 1, rue Blaise Pascal, 67008 Strasbourg Cedex, France

(*Received* 9 *March* 1984; *accepted* 9 *May* 1984)

Abstract—As a part of a systematic study of the synergic extractions of metals with mixtures of acidic chelating extractants and lipophilic anion-exchangers (B, X with X^- = inorganic anion), the extractions of M = Cd and Zn from perchlorate, nitrate and sulphate media with 1-phenyl-3-methyl-4-benzoyl-pyrazol-5-one (HL) and tri-*n*-octylammonium salts (TOAH.X) or aliquat 336 (TOMA.X) in toluene have been investigated. Three key equilibria describe the extractions:

(a) $$M^{2+} + 2\overline{HL} \rightleftharpoons \overline{ML_2} + 2H^+.$$

(b) $$\overline{B.X} + \overline{HL} \rightleftharpoons \overline{B.L} + H^+ + X^-$$

with B efficiency TOMA < TOAH and X efficiency $ClO_4 < NO_3 < SO_4$.

(c) $$\overline{ML_2} + \overline{B.L} \rightleftharpoons \overline{B.ML_3}$$

with B efficiency TOMA > TOAH and Ni ~ Co > Cd > Zn.

As a consequence of the conflicting orders of efficiencies of TOMA and TOAH in equilibria b and c, TOAH.X is a better synergic extractant from perchlorate medium than TOMA.X whereas the inverse is observed from nitrate and sulphate media. Equilibrium c is independent of the inorganic anions. Constants of equilibria a, b and c are given. $B.ML_3$ species are not extracted in 1-octanol.

Metal cations M^{m+} with a usual coordination number $N_c > 2m$, are extracted in a water-immiscible organic solvent containing a chelating acidic extractant HL as hydrated complexes following:

$$M(H_2O)_x^{m+} + m\overline{HL} \rightleftharpoons \overline{ML_m(H_2O)_y} + mH^+.$$

If HL is associated with a solvating extractant S, the coordinated water molecules in the extracted species may be substituted by S, forming more lipophilic complexes and, then, a synergic extraction is observed following:

$$M(H_2O)_x^{m+} + m\overline{HL} + y\overline{S} \rightleftharpoons \overline{ML_mS_y} + mH^+.$$

Another fact which may limit the extraction efficiency is the formation of $ML_{(m+1)}^-$ inextractable anions.[1] This difficulty, together with the substitution of water molecules in the extracted species, may be solved by using lipophilic ammonium salts (B.X) as co-extractants. Then, the extraction is partly described by the following equilibrium

$$ML_{(m+1)}^- + \overline{B.X} \rightleftharpoons \overline{B.ML_{m+1}} + X^-$$

(X^- = inorganic anion). A great number of papers are now available that describe synergic metal extractions with combinations of acidic chelating extractants and lipophilic anion-exchangers.[1–7] However, if the stoichiometry of the extracted species is generally well-known the role of the inorganic anions has been poorly investigated.[3,4,6] This paper tries to elucidate this aspect in relation to the extraction of divalent cations (Zn, Cd in comparison with Ni, Co) with mixtures of HPMBP (noted HL) and lipophilic ammonium salts (B.X) (with $B^+ = TOAH^+$ = tri-*n*-octylammonium or

* Author to whom correspondence should be addressed.

B^+ = $TOMA^+$ = methyl-tri-*n*-alkyl ammonium = aliquat 336 cation) from perchlorate, nitrate and sulphate aqueous media.

EXPERIMENTAL

Reagents and solutions

HPMBP was prepared as described previously[8] and purified by several recrystallizations in a 1:10 toluene–ethanol mixture. Fluka chemicals (aliquat 336; tri-*n*-octylamine = TOA) were used to prepare the extractant solutions: for solutions containing HL + TOMA.X, the Cl^- anions of the commercial aliquat 336 were eliminated by several washings with a 1 M solution of the appropriate inorganic acid (0.33 M for H_2SO_4) until traces of Cl^- were no longer detected by $AgNO_3$ tests on the washing solutions. A similar treatment was used for HL + TOA solutions with a view to protonating TOA and to form the appropriate tertiary ammonium salt. The ammonium salts initial concentrations in toluene or 1-octanol were varied from 0 to 0.1 M (0 to 0.05 for HPMBP). Organic solutions were systematically pre-equilibrated against an aqueous solution, free of extractable metal, of the same composition as the one that is used in the corresponding metal extraction procedure. The total aqueous inorganic anion concentrations were kept equal to 1 M (ClO_4^-, NO_3^-) or 0.33 M (SO_4^{2-}). The initial total metal concentrations were $1–2 \times 10^{-3}$. pH was adjusted by 0.1 M NaOH solutions of suitable compositions.

Extraction and analytical procedures

The distribution measurements were performed in a thermostatted vessel (25.0 ± 0.2°C) using a batch technique. Equal volumes of the organic and aqueous phases were shaken for at least 10 minutes, which was generally sufficient to reach equilibria, and then separated by gravity. For each experimental point, aliquots of each phase were withdrawn and analysed by atomic absorption using a IL 453 spectrometer.

RESULTS AND DISCUSSION

Extractions with HPMBP alone

The extractions of divalent transition metals, M, with HPMBP (noted HL) have been accurately described by Zolotov,[12–14] Navratil[9,10] or Lambrev[11] and their collaborators. Nevertheless, new experiments were needed because of the different experimental conditions of the present paper i.e. metal concentration, nature of diluents (toluene, octanol) and inorganic anions (perchlorate, nitrate, sulphate) and ionic strength (1 M).

In all cases, plots of log D_M *vs* pH ($D_M = [\overline{M}][M]^{-1}$) (at constant $[\overline{HL}]$) and log D_M *vs* log $[\overline{HL}]$ (at constant pH) are straight lines of slope 2 showing that the extractions are well described by equilibrium (1) where the solvating molecules (H_2O, 1-octanol) have been omitted (overlined symbols refer to the organic phase):

$$M^{2+} + 2\overline{HL} \overset{K_1}{\rightleftharpoons} \overline{ML_2} + 2H^+. \qquad (1)$$

The corresponding equilibrium constants K_1 are given in Table 1.

If toluene is the diluent, divalent metals are extracted following Cu > Zn > Ni ~ Co > Cd; this order agrees with the usual order of distribution constants of the hydrated metal chelates.[16,17]

If 1-octanol is the diluent, a synergic effect is observed. It is due to the substitution of water solvating molecules by 1-octanol in the extracted species. Then, a new selectivity order is observed: Cu > Ni ~ Co > Zn > Cd that is the order usually followed by the formation constants of the corresponding β-diketonates.[15,16]

Extractions of Cd *and* Zn *with mixtures of* HPMBP *and* TOAH.X *or* TOMA.X *in 1-octanol*

As previously observed for Co and Ni,[3] no synergic effect on the extractions of Cd and Zn is observed by addition of amines or ammonium salts to HPMBP in 1-octanol. On the contrary,

Table 1. log K_1 (± ~ 0.10)

Diluent	Toluene			1-Octanol		
X	ClO_4*	NO_3	SO_4†	ClO_4	NO_3	SO_4
Zn	−4.85	−5.35	−6.20	−2.35	−2.45	−3.35
Cd	−8.15	−8.65	−9.50	−3.55	−3.95	−4.95
Co[3]	−7.25	—	−7.80	−2.00	—	−2.85

* −6.70 and 0.95 for Ni and Cu respectively.
† 0.00 for Cu.

Table 2. Liquid–liquid behaviour of HPMBP + B.X

Equilibria				Constant
(2)	$\overline{TOA} + H^+ + X^-$	$\overset{K_2}{\rightleftharpoons}$	$\overline{TOAH.X}$	$K_2(X)$
(3)	$\overline{TOA} + \overline{HL}$	$\overset{K_3}{\rightleftharpoons}$	$\overline{TOAH.L}$	$\log K_3 = 2.45$*
(4)	$\overline{B.X} + \overline{HL}$	$\overset{K_4}{\rightleftharpoons}$	$\overline{B.L} + H^+ + X^-$	$K_4(X, B)$

X	Cl	NO_3	ClO_4
$\log K_2(X)$	3.55*	5.05	6.40
$\log K_4(X, TOAH)$	−1.10	−2.60	−3.95
$\log K_4(X, TOMA)$	−2.70	−4.20	−7.00

*From Ref. 3—other constants obtained by pH measurements on the two phases systems—$[Cl^-]$ determined by potentiometric measurements ($\log K_i$: ±0.05–0.10).

antagonistic effects occur for TOA and $X = SO_4$ due to "$\overline{TOA} + \overline{HL} \overset{k}{\rightleftharpoons} \overline{TOAH.L}$" that decreases $[\overline{HL}]$ by formation of $\overline{TOAH.L}$ ($\log k = 2.15$).[3]

Behaviour of mixtures of HPMBP *and* TOAH.X *or* TOMA.X *in liquid–liquid systems (diluent = toluene)*

With a view to understanding the extractions of metals from various aqueous media with mixtures of HPMBP and amines or ammonium salts, a preliminary work has been performed to point out the equilibria that occur if the liquid–liquid system is free of extractable metals. They are summarized in Table 2.

It shows that the anionic exchanges between ammonium salts ($\overline{TOAH.X}$, $\overline{TOMA.X}$) and $\overline{HPMBP}$ follow the orders $ClO_4^- < NO_3^- < Cl^-$, order of the hydratation heats of the anions in water (inverse order of their extractabilities by amines[18]) and TOAH > TOMA.

The formation of the ammonium pyrazolonate compound is most probably favoured with tertiary ammoniums because of intramolecular hydrogen bonds.

If inorganic anions in the aqueous phase are sulphate ones, under the herein experimental conditions ($[SO_4] = 0.33$ M; pH > 3), $\overline{TOAH.L}$ and $\overline{TOMA.L}$ are approximately the only ammonium species in the organic phases.

Synergic extractions from perchlorate medium (organic: toluene + HPMBP + ammonium salts)

As previously observed for Co and Ni[3], the addition of TOA enhances the extraction of Cd with HPMBP (Fig. 1). The slopes of the experimental curves $\log D_{Cd}$ vs pH ($[\overline{HL}]_i$ and $[\overline{TOA}]_i$ constant, (i denoting initial concentrations) increase from 2 ($[\overline{TOA}]_i = 0$) to 2.5 approximately. By comparison to the extractions of Co and Ni in the same experimental conditions,[3] equilibrium (5) is assumed to describe the synergic extraction of Cd.

$$M^{2+} + 3\overline{HL} + \overline{B.ClO_4} \overset{K_5}{\rightleftharpoons} \overline{B.ML_3} + 3H^+ + ClO_4^- . \quad (5)$$

Taking into account the ratios of reagents involved in the organic metal species and equilibrium (4), the experimental curves can be corrected. According to equilibrium (5), after suitable corrections, curves $\log D_{Cd}$ vs pH or $\log [\overline{HL}]$ become straight lines of slope 3 whereas $\log D_{Cd}$ vs $\log [\overline{TOAH.ClO_4}]$ have a slope of 1 which is in good agreement with equilibrium (5). Assuming arbitrarily that the ammonium salts are

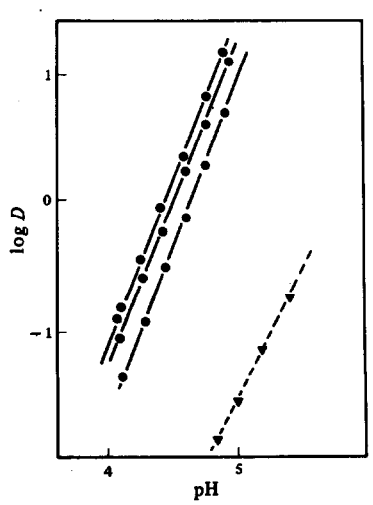


Fig. 1. Extraction of Cd from ClO_4^- medium $[ClO_4^-] = 1$ M; $[\overline{HPMBP}]_i = 0.02$ M; from the right to the left $[\overline{TOA}]_i = 0, 0.0066, 0.04, 0.1$ M; diluent: toluene.

Table 3. Synergic extraction constants from perchlorate medium log K_5 (± 0.05)

B\M	Ni	Co	Zn	Cd
TOAH	−4.25*	−4.90*	−5.20	−6.60
TOMA	−4.85	−5.10	−5.70	−7.00

* From Ref. 3.

monomers and taking log $[ClO_4^-] = 0$, constants of equilibria (5) K_5 have been calculated (Table 3).

As it is shown on Fig. 2, the synergic effect is less important for Zn than for Cd under the same experimental conditions. Slopes of experimental plots log D_{Zn} vs pH remain lower than 2.3 with increasing $[\overline{TOA}]_i$ which shows that $\overline{TOAH.ZnL_3}$ and $\overline{ZnL_2}$ are co-extracted. An iterative calculation using log $K_1(Zn, ClO_4) = -4.85$ (Table 1) fits with log $K_5 = -5.2 \pm 0.1$.

The synergic extractions of Cd, Zn, Co and Ni with HPMBP and TOMA.ClO_4 in toluene have been also performed. The results are not very different from the ones with TOAH.ClO_4. A like analysis of the experiments has been realized. The corresponding extraction constants are given in Table 3.

The synergic extractions follow the order Ni > Co > Zn > Cd that is the one observed for extractions with HPMBP alone in *n*-octanol. Similar conclusions can be drawn out, i.e. the ML_3^- formation constants are here determinative.

Though the opposite is generally observed, the extractions are more effective with the tertiary ammonium salt ($\overline{TOAH.ClO_4}$) than with the quaternary one ($\overline{TOMA.ClO_4}$). In fact, equilibrium (5) may be considered as the summation of equilibrium (1) (extraction of M with $\overline{HL}$ alone), (4) (anionic exchange between $\overline{B.X}$ and $\overline{HL}$) and (6):

$$\overline{ML_2 aq.} + \overline{B.L} \overset{K_6}{\rightleftharpoons} \overline{B.ML_3} \qquad (6)$$

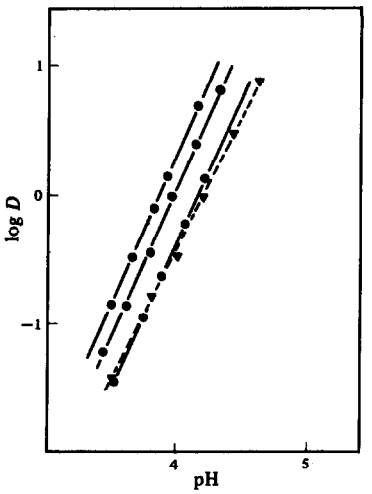


Fig. 2. Extraction of Zn from ClO_4^- medium $[ClO_4^-] = 1$ M; $[\overline{HPMBP}]_i = 0.02$ M; from the right to the left $[\overline{TOA}]_i = 0, 0.0066, 0.04, 0.1$ M; diluent: toluene.

K_6 are given in Table 4. The formation of $\overline{B.ML_3}$ is favoured with quaternary ammonium salts (log K_6(TOMA) − log K_6(TOAH) ~ 2.6) whereas the $\overline{B.L}$ formation by anionic exchange [equation (4)] is favoured with tertiary ammonium salts (log K_4(TOAH) − log K_4(TOMA) ~ 3).

Synergic extractions from sulphate medium (organic: toluene + HPMBP + ammonium salts)

Typical experimental extraction curves log D_M vs pH at constant $[\overline{HL}]_i$, $[\overline{TOA}]_i$ or $[\overline{TOMA.L}]_i$ (*i* denotes initial concentrations) are shown in Figs. 3 and 4 (Cd and Zn extractions, respectively).

The addition of TOMA.L to HL in toluene enhances greatly the extractions of Cd and Zn from sulphate medium. After suitable corrections that take into account the quantities of extractants involved in the organic metal species, log–log plots

Table 4. log K_6 (± 0.2) ($\overline{ML_2} + \overline{B.L} \rightleftharpoons \overline{B.ML_3}$)

B	TOAH			TOMA		
X	ClO_4	NO_3	SO_4	ClO_4	NO_3	SO_4
Cd	5.50	5.55	5.50	8.15	8.20	8.20
Zn	3.60	4.05	3.90	6.15	6.60	6.00
Co	6.30*	—	6.10*	9.15	—	—
Ni	6.40*	—	—	8.85	—	—

* From Ref. 3.

show that the extractions are well described by equilibrium (7).

$$M^{2+} + 2\overline{HL} + \overline{B.L} \overset{K_7}{\rightleftharpoons} \overline{B.ML_3} + 2H^+ \qquad (7)$$

(M = Cd, Zn; B = TOMA).

The difference between equilibria (7) and (1) gives the synergic equilibrium (6) with $\log K_6 = 8.2 \pm 0.2$ and 6.0 ± 0.2 respectively for M = Cd and Zn. These values are closed to the ones determined from perchlorate medium (Table 4) showing that equilibrium (6) does not depend on the nature of the inorganic anions.

A smaller synergic effect is observed with TOA (Fig. 3 and 4). It is maximum for the ratio $[\overline{HL}]_i : [\overline{TOA}]_i = 3$ which corresponds to the stoichiometry of the extracted species $\overline{TOAH.M(PMBP)_3}$. With an excess of TOA, an antagonistic effect may be observed that is due to an excessive formation of $\overline{TOAH.PMBP}$ and a simultaneous missing of $\overline{HPMBP}$ following equilibrium (3) (Zn extraction, Fig. 4). Equilibrium (3) has to be considered for a quantitative explanation of the experimental curves, particularly at high pH. For each experimental point, K_6 can be determined by using the equations:

$$K_1 = [\overline{ML_2}][H^+]^2[M^{2+}]^{-1}[\overline{HL}]^{-2}$$

$$K_3 = [\overline{TOAH.L}][\overline{TOA}]^{-1}[\overline{HL}]^{-1}$$

$$[\overline{TOA}]_i = [\overline{TOA}] + [\overline{TOAH.L}] + [\overline{TOAH.ML_3}]$$

$$[\overline{HL}]_i = [\overline{HL}] + [\overline{TOAH.L}] + 3[\overline{TOAH.ML_3}] + 2[\overline{ML_2}]$$

$$[\overline{M}] = [\overline{ML_2}] + [\overline{TOAH.ML_3}]$$

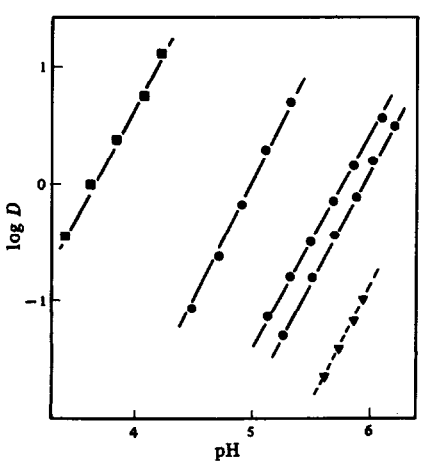


Fig. 3. Extraction of Cd from SO_4^{2-} medium; $[SO_4^{2-}] = 0.33$ M; $[\overline{HPMBP}]_i = 0.02$ M; dashed line: HPMBP alone; continuous lines: from the left to the right $[\overline{TOMA}]_i = 0.0066$ M, $[\overline{TOA}]_i = 0.0066$, 0.04, 0.1 M; toluene.

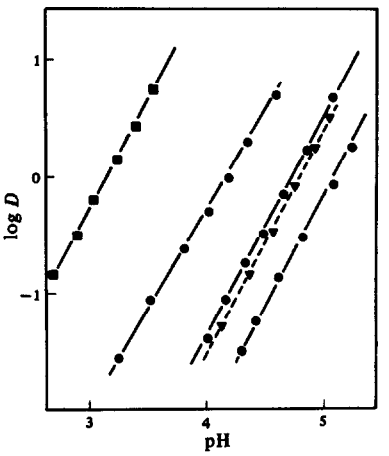


Fig. 4. Extraction of Zn from SO_4^{2-} medium; $[SO_4^{2-}] = 0.33$ M; $[\overline{HPMBP}]_i = 0.02$ M; dashed line: HPMBP alone; continuous lines: from the left to the right $[\overline{TOMA}]_i = 0.0066$ M, $[\overline{TOA}]_i = 0.0066$, 0.04, 0.1 M; toluene.

and

$$K_6 = [\overline{TOAH.ML_3}][\overline{ML_2}]^{-1}[\overline{TOAH.L}]^{-1}.$$

Calculations give $\log K_6 = 5.50 \pm 0.2$ and 3.90 ± 0.2 for Cd and Zn respectively which is in good agreement with calculated values from perchlorate medium (Table 4).

Synergic extractions from nitrate medium (organic: toluene + HPMBP + ammonium salts) and conclusions

The quantitative study of the synergic extractions of Cd and Zn from perchlorate and sulphate media has shown that the magnitude of the synergism is mainly dependent on the nature of inorganic anions because of equilibrium (4) which determines the formation of the synergic agent $\overline{B.L}$. Equilibrium (4) constants for $X = NO_3$ (Table 2) are intermediate between the ones for $X = ClO_4$ or SO_4. Then, an intermediate synergic effect is expected. Consequently, synergic extractions of Cd and Zn by mixtures of $\overline{HPMBP}$ and $\overline{TOAH.X}$ or $\overline{TOMA.X}$ from nitrate medium have been performed with a view to checking the thermodynamic pattern obtained from the other media. Using the constants of equilibria, 1, 2, 3 and 4 determined for a nitrate aqueous medium (Table 2) and mass-balance equations, $\log K_6$ has been determined for each experimental point. The results are given on Table 4 by comparison to the other aqueous media. The good fit of the results, particularly for the cadmium synergic extractions, strongly supports the conclusions drawn from the results in perchlorate and sulphate media:

The magnitude of the synergisms mainly results from two equilibria—the anionic exchange equilibrium (4) that determines the concentration of the real synergic agent $\overline{B.L}$ (ammonium acylpyrazolonate) with the orders of efficiencies TOAH > TOMA and $SO_4 > NO_3 > ClO_4$, and the synergic equilibrium (6) that determines the formation of the extracted synergic species $\overline{B.ML_3}$ with TOMA ≫ TOAH. As a consequence of these conflicting orders, the tertiary amines are better (or equivalent) synergic agents than quaternary ammonium salts for extractions performed from perchlorate medium whereas the inverse is observed for the extraction performed from nitrate and sulphate media (with a maximum of divergence for the latter).

Acknowledgements—American Institute of Chemical Engineers is acknowledged for the organization of ISEC'83 Conference in Denver where some conclusions of this paper was originally presented (Aug. 30th, 1983). We wish to thank C.N.R.S. of Lebanon for a grant offered to Z. Lakkis and C.N.R.S. of France for its financial support. Y. Wahl-Hiss is acknowledged for technical assistance in metal determinations.

REFERENCES

1. W. Bacher and C. Keller, *J. Inorg. Nucl. Chem.* 1973, **35**, 2945.
2. G. Duyckaerts and J. F. Desreux, *Proc. Int. Solv. Ext. Conf. ISEC'77*, CIM Special Volume **21**, 1977, 73 and included references.
3. J. P. Brunette, M. Lakkis, G. Goetz-Grandmont and M. J. F. Leroy, *Polyhedron* 1982, **1**, 461, and included references.
4. J. P. Brunette, M. Taheri, G. Goetz-Grandmont and M. J. F. Leroy, *Polyhedron* 1982, **1**, 457.
5. Y. Sasaki and H. Freiser, *Inorg. Chem.* 1983, **22**, 2289.
6. Y. Inoue, O. Tochiyama and T. Takahashi, *J. Inorg. Nucl. Chem.* 1979, **41**, 1375.
7. Y. Inoue, O. Tochiyama and I. Oda, *J. Inorg. Nucl. Chem.* 1981, **43**, 2529.
8. B. S. Jensen, *Acta Chem. Scand.* 1959, **13**, 1668.
9. O. Navratil, *Chem. Listy.* 1974, **68**, 470.
10. O. Navratil and J. Smola, *Coll. Czech. Chem. Com.* 1971, **36**, 3549.
11. V. G. Lambrev and V. S. Vlasov, *Zh. Anal. Khim.* 1970, **25**, 1638.
12. Yu. A. Zolotov and N. T. Sizonenko, *Zh. Anal. Khim.* 1970, **25**, 54.
13. Yu. A. Zolotov, O. M. Petrukhin and L. G. Gavrilova, *J. Inorg. Nucl. Chem.* 1970, **32**, 1679.
14. Yu. A. Zolotov and L. G. Gavrilova, *Zh. Anal. Khim.* 1970, **25**, 813.
15. R. C. Mehrotra, R. Bohra and D. P. Gaur, *Metal β-diketonates and Allied Derivatives*, p. 71. Academic Press, New York (1978).
16. T. Sekine, R. Murai, M. Niitsu and N. Ihara, *J. Inorg. Nucl. Chem.* 1974, **36**, 2569.
17. T. Sekine and Y. Hasegawa, *Solvent Extraction Chemistry*, pp. 176–177. Marcel Dekker, New York (1977).
18. J. F. Desreux, *Ind. Chim. Belg.* 1972, **37**, 637.

Polyhedron Vol. 4, No. 4, pp. 583–586, 1985
Printed in Great Britain

0277–5387/85 $3.00 + .00
Pergamon Press Ltd

REDUCTIVE NITROSYLATION OF TETRAOXOMETALLATES—XI. MOLYBDATE HYDROXYLAMINE REACTION IN THE PRESENCE OF CYANIDE: SYNTHESIS OF MONO- AND DINITROSYL CYANOMOLYBDATES AND THEIR 2,2′-BIPYRIDINE AND 1,10-PHENANTHROLINE DERIVATIVES DIRECTLY FROM MOLYBDATE

RAMGOPAL BHATTACHARYYA,* GOBINDA PRASHAD BHATTACHARJEE and ALOK MOHAN SAHA

Department of Chemistry, Jadavpur University, Calcutta 700 032, India

(*Received* 17 *November* 1983; *accepted* 9 *May* 1984)

Abstract—The new molybdenum cyanonitrosyl complexes, $R_2[Mo(NO)(CN)_5]\cdot 2H_2O$ (R = Ph_4P and Bu_4N) and $[Mo(NO)(CN)_3(L\text{–}L)]\cdot H_2O$ [L–L = 2,2′-bipyridine (bipy) or 1,10-phenanthroline (phen)] were synthesized directly from $[MoO_4]^{2-}$ in aqueous-alkaline (pH ~ 8) and aerobic media, either by using the counter ions (R) or L–L ligands. However, the same reaction if conducted at a lower pH (~ 5) in the presence of a further excess of $NH_2OH\cdot HCl$, dinitrosylation occurs and hitherto unknown

$(Ph_4P)_2[Mo(NO)_2(CN)_4]\cdot 2H_2O$ and $[Mo(NO)_2(CN)_2(phen)]\cdot 2H_2O$

complexes were obtained. The mononitrosyl series show a single ν_{NO} vibrational mode in their IR spectra at 1650–1700 cm^{-1} region whilst the *cis*-dinitrosyl species show two such bands one around 1650 and the other around 1780 cm^{-1}. The presence of lattice-water molecules in the complexes have been corroborated from thermoanalytical studies. The anionic complexes show 2:1 electrolytic behaviour and the neutral species are non-electrolyte and monomeric. The diamagnetic complexes grossly show a single MLCT ($d \rightarrow \pi^*NO$) transition.

Reductive nitrosylation of $[MoO_4]^{2-}$ using NH_2OH and CN^- in an alkaline medium and generation of $\{Mo(NO)\}^{+}$ moiety as $[Mo(NO)(CN)_5]^{4-}$ has been known for many years,[2,3] but until our recent preliminary communication,[4] such a reaction converting $[MoO_4]^{2-}$ to $\{Mo(NO)_2\}^{2+}$ was unknown. Also, though, the paramagnetic $[Mo(NO)(CN)_5]^{3-}$ anion containing $\{Mo(NO)\}^{2+}$ moiety has been recently characterized,[5] the corresponding dianion, $[Mo(NO)(CN)_5]^{2-}$ is still unknown. The present paper describes for the first time a direct conversion of $[MoO_4]^{2-}$ to $\{Mo(NO)\}^{3+}$ moiety representing a missing link in the series of isostructural anions, $[Mo(NO)(CN)_5]^{n-}$ ($n = 4$–2) using KCN and NH_2OH in an alkaline medium as evidenced by synthesizing the hitherto unknown $R_2[Mo(NO)(CN)_5]^{2-}$ species (while writing out the manuscript we noticed that the phosphonium salt has been recently reported by Wieghardt *et al.*[6]) and its 2,2′-bipyridine (bipy, L–L) and 1,10-phenanthroline (phen, L–L) derivatives of the types $[Mo(NO)(CN)_3(L\text{–}L)]$ in an aerobic condition. We also describe here, a further reductive conversion of MoO_4^{2-} to the $\{Mo(NO)_2\}^{2+}$ stage, and the synthesis of so far unknown products[4] $[Mo(NO)_2(CN)_4]^{2-}$ and $[Mo(NO)_2(CN)_2(phen)]$.

EXPERIMENTAL

Materials and methods

All reagents were of reagent grade and used without further purification. For physicochemical

* Author to whom correspondence should be addressed.

measurements, the solvents were further purified using literature methods.[7] IR spectra were recorded as KBr discs in a Perkin–Elmer 597 spectrophotometer calibrated with polystyrene. Solution conductances were measured with a Wayne–Kerr Autobalance Precision Bridge B 331 and the electronic spectra (800–200 nm) were taken using a Pye Unicam SP8–150 UV–VIS spectrophotometer. Magnetic susceptibilities were measured with a Gouy balance using $Hg[Co(NCS)_4]$ as a calibrant. T.G.A. curves were recorded in a Shimadzu (Japan) DT-30 Thermoanalyser. A Knauer vapour pressure osmometer was used for the molecular weight determination. The elements C, H and N were analysed microanalytically and Mo and P by standard methods.[8]

Preparation of the complexes (for complexes **1–4**)

A mixture of $Na_2MoO_4 \cdot 2H_2O$ (0.5 g; 2.0 mmol) and KCN (2.0 g; 30 mmol) in water (25 cm^3) was stirred at 60–70°C for 5 min. To the resulting solution, $NH_2OH \cdot HCl$ (2.2 g; 32 mmol) was added with constant stirring at 60–70°C when a red solution was obtained. Stirring and heating was continued for another 30 min and the clear solution (pH ~ 11) was cooled to room temperature and the pH of the solution was reduced to 8 with 6 M HCl (*solution A*).

Tetraphenylphosphonium pentacyanomononitrosyl molybdate(II) *dihydrate*

$\{(Ph_4P)_2[Mo(NO)(CN)_5] \cdot 2H_2O\}$ (**1**).

An aqueous (40 cm^3) solution of Ph_4PBr (1.4 g; 5.7 mmol) was added to the solution A with stirring at 40–50°C when the solution became turbid. The turbid solution was cooled to 0°C and the yellow solid obtained was filtered off, washed with H_2O, EtOH, Et_2O and dried over fused $CaCl_2$ at a reduced pressure. The compound was crystallised from CH_3CN–Et_2O mixture as yellow microcrystals. Yield: 1.39 g; 65%. Found: C, 66.0; H, 4.3; N, 8.5; P, 6.1; Mo, 10.3; H_2O, 3.4%: $C_{53}H_{44}N_6P_2O_3Mo$ requires: C, 65.6; H, 4.5; N, 8.7; P, 6.4; Mo, 9.9 and H_2O, 3.7%. IR: ν_{CN} 2160(s), 2120(sh); ν_{NO} 1650(s); ν_{MoN} (NO) 610(w); ν_{MoC} 350 (w) cm^{-1}. UV–VIS: ν_{max} (cm^{-1}) 23,260 (90). Λ_M = 235 ohm^{-1} cm^2 mol^{-1} (in CH_3CN).

Tetrabutylammonium pentacyanomononitrosyl molybdate(II) *dihydrate*

$\{(Bu_4N)_2[Mo(NO)(CN)_5] \cdot 2H_2O\}$ (**2**).

The same procedure as described under complex **1** was followed using tetrabutylammonium chloride as the precipitating agent instead of Ph_4PBr. Yield, 0.96 g; 63%. Found: C, 57.6; H, 9.6; N, 14.0; Mo, 12.7; H_2O, 4.3%: $C_{37}H_{76}N_8O_3Mo$ requires: C, 57.2; H, 9.8; N, 14.4; Mo, 12.4; H_2O, 4.6%. IR: ν_{CN} 2160(s), 2120(sh); ν_{NO} 1680(s); ν_{MoN}(NO) 620 (w); ν_{MoC} 355(w) cm^{-1}. UV–VIS: ν_{max} (cm^{-1}) 27,780(100). $\Lambda_M(CH_3CN)$ = 242 ohm^{-1} cm^2 mol^{-1}.

Tricyano - unis{2,2′ - *bipyridine*}*mononitrosyl molybdenum*(II) *monohydrate*

$\{[Mo(NO)(CN)_3(bipy)] \cdot H_2O\}$ (**3**).

Solution A was added to a hot aqueous solution (25 cm^3) of bipy (0.5 g; 3.2 mmol) with stirring at the room temperature and the pH of the solution was adjusted to 3.5–4. The separated yellow solid was filtered off, washed with H_2O, EtOH, Et_2O and dried over fused $CaCl_2$ at a reduced pressure. The compound was crystallised from DMF–Et_2O mixture as a bright yellow solid. Yield, 0.54 g; 69%. Found: C, 41.7; H, 2.2; N, 21.9; Mo, 25.8; H_2O, 4.6%; mol. wt (DMF, osmometric) 347: $C_{13}H_{10}N_6O_2Mo$ requires: C, 41.3; H, 2.6; N, 22.2; Mo, 25.4; H_2O, 4.8%. Mol. wt 378. IR: ν_{CN} 2160(s), 2130(sh); ν_{NO} 1690(s); ν_{MoN} (NO) 615(w); ν_{MoN}(L–L) 390(w); ν_{MoC} 355(w) cm^{-1}. UV–VIS: ν_{max} (cm^{-1}) 26,600 (80).

Tricyano - unis{1,10 - *phenanthroline*}*mononitrosyl molybdenum*(II) *monohydrate*

$\{[Mo(NO)(CN)_3(phen)] \cdot H_2O\}$ (**4**).

The same procedure was followed as described under complex **3** using phen instead of bipy to get a yellow compound. Yield, 0.5 g; 60%. Found: C, 45.1; H, 2.4; N, 20.5; Mo, 24.6; H_2O, 4.4%; mol. wt (DMF, osmometric) 388: $C_{15}H_{10}N_6O_2Mo$ requires: C, 44.8; H, 2.5; N, 20.9; Mo, 23.9; H_2O, 4.5%. Mol. wt 402. IR: ν_{CN} 2160(s), 2130(sh); ν_{NO} 1700(s); ν_{MoN} 610(w); ν_{MoN} (L–L) 400(w); ν_{MoC} 360(w) cm^{-1}. UV–VIS: ν_{max} (cm^{-1}) 26,320(75).

Complexes **5** *and* **6**

A mixture of $Na_2MoO_4 \cdot 2H_2O$ (0.5 g; 2.0 mmol) and NaOH (0.5 g; 12.5 mmol) in water (25 cm^3) was stirred at 80°C for 10 min. To the resulting solution, first KCN (2.4 g; 37 mmol) and then $NH_2OH \cdot HCl$ (3.8 g; 55 mmol) were added with stirring at 80°C when an orange red solution was obtained. To this solution, 5–6 drops of 12 M HCl were added and stirred for 5 min when the colour of the solution became red. The solution was stirred for another 5 min and then cooled (pH ~ 7.5). The pH of the solution was then reduced to 5.5 with 6 M HCl (*solution B*).

Tetraphenylphosphonium tetracyanodinitrosyl molybdate(0) *dihydrate*

$\{(Ph_4P)_2[Mo(NO)_2(CN)_4] \cdot 2H_2O\}$ (**5**).

The same procedure as described under complex **1** was followed using the solution B when a greenish yellow solid was separated out and recrystallised as described under complex **1**. Yield, 1.0 g; 50%. Found: C, 63.8; H, 4.0; N, 8.4; P, 6.1; Mo, 10.0; H_2O, 3.9%: $C_{52}H_{44}N_6O_4P_2Mo$ requires: C, 64.1; H, 4.5; N, 8.6; P, 6.4; Mo, 9.8 and H_2O, 3.7%. IR: ν_{CN} 2140(sh), 2110(s); ν_{NO} 1792(s), 1658(s); $\nu_{MoN}(NO)$ 610(w); ν_{MoC} 345(w) cm^{-1}. UV–VIS: ν_{max} (cm^{-1}) 22,800(945). $\Lambda_M(CH_3CN) = 232$ ohm^{-1} cm^2 mol^{-1}.

Dicyano - unis{1,10 - phenanthroline}dinitrosyl molybdenum (0) *dihydrate*

$$\{[Mo(NO)_2(CN)_2(phen)]\cdot 2H_2O\} \quad (6).$$

A hot aqueous solution (40 cm^3) of phen (0.7 g; 3.5 mmol) was added to solution B with stirring at 50°C. The separated yellow solid was filtered off, washed with H_2O, EtOH, Et_2O and dried at a reduced pressure over fused $CaCl_2$. The compound was crystallised from CH_3CN–Et_2O mixture as golden yellow needles. Yield, 0.35 g; 40%. Found: C, 39.5; H, 2.7; N, 19.5; Mo, 22.4; H_2O, 9.0%; mol. wt (CH_3CN, osmometric) 400. $C_{14}H_{12}N_6O_4Mo$ requires: C, 39.6; H, 2.8; N, 19.8; Mo, 22.6; H_2O, 8.5%. Mol. wt 424. IR: ν_{CN} 2150(s), 2130(s); ν_{NO} 1780(s), 1665(s); ν_{MoN} 620(w); ν_{MoN}(L–L) 400 (w); ν_{MoC} 350(w) cm^{-1}. UV–VIS: ν_{max} 23,000 (2960) cm^{-1}.

The anionic complexes are soluble in acetone, acetonitrile and nitromethane but insoluble in methanol, ethanol, benzene and ether. Also, whilst compound **3** is soluble only in DMF or DMSO (and moderately in acetonitrile), **6** is also soluble in acetone, acetonitrile or nitromethane.

RESULTS AND DISCUSSIONS

It is quite interesting to note that, in the presence of an excess of $NH_2OH\cdot HCl$ (as the source of NO group) and CN^-, it is the actual pH of the finally prepared solution (A or B) which decides whether the reaction will be stopped at $\{Mo(NO)\}^{3+}$ stage or can progress further furnishing $\{Mo(NO)_2\}^{2+}$ moiety. While the facile conversion to the former proceeds at a relatively higher pH ($\sim$ 8), the latter requires a slightly acidic medium (pH $\sim$ 5). Interestingly, in a drastically alkaline condition and in the presence of a limited amount of NH_2OH and an excess of CN^-, such a reaction produces $\{Mo(NO)\}^+$ system (see Ref. 2). It may, however be recalled here, that the pH sensitivity of the analogous nitrosylation reaction using NCS^- is extremely acute.[9] In this connection mention may be made that the complex $[Mo(NO)_2(CN)_4]^{2-}$ was alleged to be obtained by the treatment of $[MoCl_2(NO)_2(py)_2]$ with KCN/MeOH, but no details regarding the preparation and characterization were reported.[10]

The IR data (see Experimental) indicate that irrespective of the nature of the complexes, ν_{CN} band is always split and centred around the same region. Of course, as usual,[9] the mononitrosyl species show a single ν_{NO} band and the dinitrosyl species, having *cis*-configuration with respect to each other, show two bands.

Considering the NO^+ formalism[11] the mononitrosyl complexes possessing $\{Mo(NO)\}^{3+}$, $[\{Mo(NO)\}^4]$ moiety should have the central metal ion in the +2 oxidation state and in the dinitrosyl species $[\{Mo(NO)_2\}^{2+}$, i.e. $\{Mo(NO)_2\}^6]$, the same is in the zero valent state, which are further confirmed by the observed diamagnetism of all the isolated complexes. Assuming that, apart from the complexes **1** and **2**, the L–L derivatives, viz. **3** and **4** may also be described by a similar MO picture to that applicable to[11] C_{4v} cases, the single electronic absorption band obtained in these cases may be designated as $e \rightarrow b_2$[11] transition. Another possible transition $e \rightarrow e$, otherwise observable in the thiocyanato complexes[9] around 30 kK, is not observed here due possibly to its occurrence at a still higher energy where it is masked by intense intraligand transition bands. If the symmetry species of the dinitrosyl complexes are approximated as C_{2v} then their MO configuration may be $(a_2)^2$ $(a_1)^2$ $(b_2)^2$ (see ref. 11) and accordingly three electronic transitions ($b_2 \rightarrow a_1$, $b_2 \rightarrow b_1$ and $b_2 \rightarrow b_2$) should be observed.[11] However, only a very intense band (possibly due to $b_2 \rightarrow b_1$ transition, $b_2 \rightarrow a_1$ is expected[11] at a lower energy) is observed in both the cases. Others are either unobserved or concealed by the absorption due to the organic moieties. It is noteworthy that the dinitrosyl complexes of the present cyano series absorb more intensely than their mononitrosyl analogues, as was also observed in the cases of the thiocyanato complexes.[9]

The neutral complexes are non-electrolytes and the anionic ones are 2:1 electrolytes[12] in CH_3CN. The lattice held water molecules in the mononitrosyl complexes can be removed at a lower temperature than the dinitrosyl complexes where the two water molecules are rather strongly held as evidenced from their TGA and DTA curves. This fact indicates that in the dinitrosyl complexes, the water molecules are possibly more strongly hydrogen bonded to the NO^+ and CN^- ligands, as structurally characterized in the cases of some other cyanonitrosyl species.[13,14]

Acknowledgements—The work is financed by the U.G.C., New Delhi and A.M.S. thanks the commission for a fellowship. Donation of the IR spectrophotometer, used in this work from the Alexander Von Humboldt Foundation is gratefully acknowledged.

REFERENCES

1. R. G. Bhattacharyya and P. S. Roy, *Trans. Met. Chem.* (in press).
2. W. Hieber, R. Nast and G. Gehring, *Z. Anorg. Allg. Chem.* 1948, **256**, 169.
3. K. G. Caulton, *Coord. Chem. Rev.* 1975, **14**, 317.
4. R. G. Bhattacharyya, G. P. Bhattacharjee and A. M. Saha, *Trans. Met. Chem.* 1983, **8**, 255.
5. S. Sarkar and A. Müller, *Z. Naturforsch*, 1978, **33B**, 1053.
6. K. Wieghardt, G. B. Dahman, W. Swiridoft and J. Weiss, *Inorg. Chem.* 1983, **22**, 1221.
7. D. D. Perrin, W. L. F. Armarego and D. R. Perrin, *Purification of Laboratory Chemicals.* Pergamon Press, New York (1966).
8. A. I. Vogel, *A Text Book of Quantitative Inorganic Analysis.* The English Language Book Society and Longmans, London (1968).
9. R. G. Bhattacharyya and G. P. Bhattacharjee, *J. Chem. Soc., Dalton Trans.* 1983, 1593.
10. S. Sarkar and P. Subramaniam, *J. Inorg. Nucl. Chem.* 1981, **43**, 202.
11. J. H. Enemark and R. D. Feltham, *Coord. Chem. Rev.* 1974, **13**, 339.
12. W. J. Geary, *Coord. Chem. Rev.* 1971, **7**, 81.
13. A. Tullberg and N. Vannerberg, *Acta Chem. Scand.* 1967, **21**, 1462.
14. S. Jagner and N. Vannerberg, *Acta Chem. Scand.* 1968, **22**, 3330.

Polyhedron Vol. 4, No. 4, pp. 587–590, 1985
Printed in Great Britain

0277–5387/85 $3.00 + .00
Pergamon Press Ltd

THE THERMAL DECOMPOSITION, IR SPECTRUM AND CRYSTAL STRUCTURE OF AMMONIUM MANGANESE(II) TRIS(HYDROGENSELENITE), $NH_4Mn(HSeO_3)_3$

JUSSI VALKONEN* and SIRPA JALKANEN
University of Jyväskylä, Department of Chemistry, 40100 Jyväskylä 10, Finland

(*Received* 24 *February* 1984; *accepted* 9 *May* 1984)

Abstract—The compound $NH_4Mn(HSeO_3)_3$ has been prepared and its IR spectrum and thermal behaviour have been investigated. It crystallizes in the monoclinic space group with cell dimensions $a = 13.716(5)$ Å, $b = 7.678(2)$ Å, $c = 9.416(3)$ Å and $\beta = 98.51(2)°$. The space group is $P2_1/c$. The structure is a three-dimensional network. The manganese atom is six coordinated by oxygen atoms, which form bridges between selenium and manganese atoms.

Manganese forms several compounds with the selenium(IV) anions: selenite, SeO_3^{2-}, hydrogenselenite, $HSeO_3^-$, and diselenite, $Se_2O_5^{2-}$. The hydrogenselenite has been reported only for manganese(III).[1,2,14] The known manganese(II) selenites are $MnSeO_3$, $MnSeO_3H_2O$, $MnSeO_3D_2O$, $MnSeO_32H_2O$ and $MnSe_2O_5$,[3–7] and the double selenites

$$Na_2Mn(SeO_3)_22H_2O, \quad K_2Mn_2(Se_2O_5)_33H_2O$$

and

$$(NH_4)_2Mn(SeO_3)_2.$$[8,9]

The structures of the double selenites are unknown and the aim of this investigation was to investigate the structure of ammonium manganese(II) selenite.

EXPERIMENTAL

Synthesis

The compound was synthesized as described for $(NH_4)_2Mn(SeO_3)_2$,[9] but it can also be crystallized from an aqueous solution containing manganese selenite and ammonium selenite in molar ratio 1 : 15. Crystals are well-formed, light-coloured prisms. Manganese and selenium were analyzed with a Perkin–Elmer 5000 AAS-spectrophotometer and ammonium was analyzed by distillation and titration. The results of analyses are NH_4: 3.7% (3.9), Mn: 12.1% (12.0) and Se: 52.9% (51.8), calculated values for $NH_4Mn(HSeO_3)_3$ in parentheses.

Thermal analysis

The thermoanalytical investigation was carried out with a Perkin–Elmer Thermogravimetric System TGS-2. The sample size was about 10 mg, the heating rate 4° min^{-1} and the atmosphere was air with a flow of 50 cm^3 min^{-1}.

IR spectrum

The IR spectrum was recorded with a Perkin–Elmer 283 IR spectrophotometer. Scan range was from 4000 to 200 cm^{-1}, scan time 12 min and the method KBr pellet technique.

Data collection

Conditions for unit cell determination and data collection are given in Tables 1 and 2. Semi-empirical absorption corrections were made on the bais of a ϕ-scan with five different 2θ values. The largest measured relative reduction in intensity was from 1.00 to 0.51.

The structure was solved by direct methods using the program package Multan.[10] The refinement was carried out with the program XRAY,[11] using the scattering factors of Cromer and Mann[12] for neutral atoms. The picture was drawn with the program ORTEP, which is a part of the XRAY system.

* Author to whom correspondence should be addressed.

Table 1. Conditions of data collection

Diffractometer:	Syntex $P2_1$
Radiation:	Mo-K_α
Monochromator:	Graphite crystal
Collection method:	$\theta/2\theta$
Scan speed:	3° min^{-1}
2Θ range:	4–60°
Number of independent reflections collected:	3079
Number of independent reflections refined:	1637 [$I > 4\sigma(I)$]
R (isotropic):	5.5%
R (anisotropic):	4.1%
Refinement type:	Full matrix

Table 2. Crystal data

Formula: $NH_4Mn(HSeO_3)_3$
Formula weight: 456.87
Crystal system: Monoclinic
Space group: $P2_1/c$ (No. 14)
$a = 13.716(5)$ Å
$b = 7.678(2)$ Å
$c = 9.416(3)$ Å
$\beta = 98.51(2)°$
$V = 980.7(5)$ Å^3
$Z = 4$
$D_x = 3.09$ g cm^{-3}
$D_m = 3.1$ g cm^{-3}
μ(Mo-K_α) = 123.30 cm^{-1}

Refinement was based on structure factors and unit weights.

RESULTS AND DISCUSSION

Thermal analysis

The thermal behaviour of $NH_4Mn(HSeO_3)_3$ is shown in Fig. 1 and Table 3.

The first stage is the liberation of selenium dioxide.

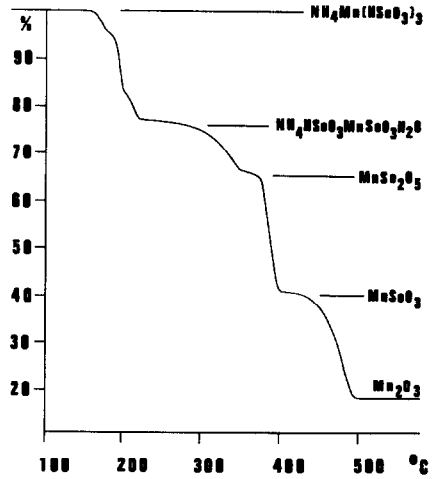


Fig. 1. The thermal decomposition of $NH_4Mn(HSeO_3)_3$.

The composition of the reaction product is not clear: it is either a mixture of ammonium hydrogen selenite and manganese selenite or a double salt. The next stage is the formation of manganese diselenite. In the third stage selenium dioxide is again liberated, this time with the formation of manganese selenite. In the fourth stage, manganese selenite decomposes to manganese(III) oxide, which converts to Mn_3O_4 at high temperature. The decomposition of the hydrogenselenite to diselenite and normal selenite is in good agreement with the literature.[13]

IR spectrum

The IR spectrum is shown in Fig. 2 and Table 4. The IR spectra of the selenite and hydrogenselenite are quite similar. The main differences between the spectra of the selenite and hydrogenselenite ions are the peaks at 2405 and 1237 cm^{-1} for hydrogenselenite.

The ammonium ion causes a strong peak at wavenumber 1425 cm^{-1} as well as at wavenumbers above 2900 cm^{-1}, where also the peaks of hydrogen bonds of OH group are situated. The results agree

Table 3. The thermal behaviour of $NH_4Mn(HSeO_3)_3$

	Reaction	Weight left (%) obs.	Weight left (%) calc.	Temperature range (°C)
1	$NH_4Mn(HSeO_3)_3 \rightarrow NH_4HSeO_3MnSeO_3H_2O + SeO_2\uparrow$	76.0	75.71	140–210
2	$NH_4HSeO_3MnSeO_3H_2O \rightarrow MnSe_2O_5 + NH_3\uparrow + 2H_2O\uparrow$	65.0	64.10	270–330
3	$MnSe_2O_5 \rightarrow MnSeO_3 + SeO_2\uparrow$	40.5	39.81	350–380
4	$MnSeO_3 \xrightarrow{+O_2} \frac{1}{2}Mn_2O_3 + SeO_2\uparrow$	18.0	17.28	420–480
5	$Mn_2O_3 \xrightarrow{-O_2} \frac{2}{3}Mn_3O_4$	17.1	16.69	910–940

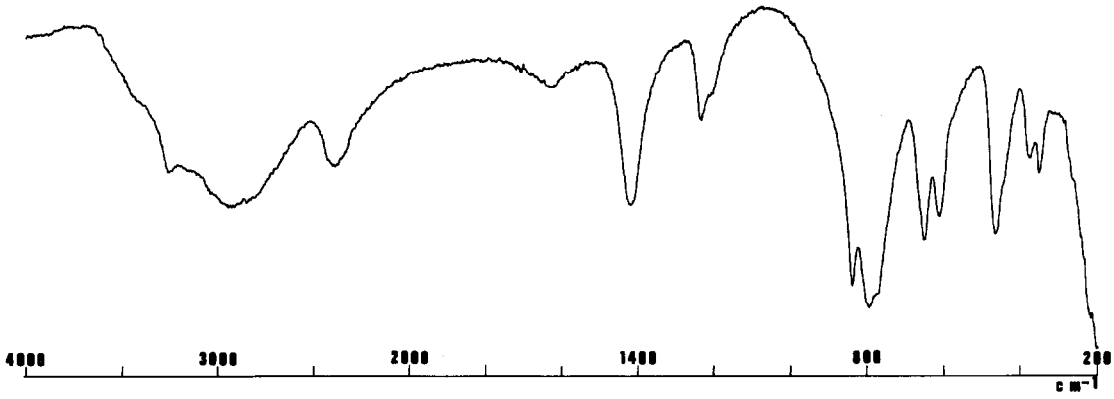


Fig. 2. The IR spectrum of $NH_4Mn(HSeO_3)_3$.

Table 4. Assignments of the IR spectrum of $NH_4Mn(HSeO_3)_3$

Wavenumber (cm^{-1})	Assignment	Wavenumber (cm^{-1})	Assignment
3428, 3254, 2924	ν(OH, NH_4)	841	ν_s(SeO)
2405	ν(OH)	800, 775	ν_{as}(SeO)
1425	$\nu_4(NH_4)$	658, 615	ν(SeOH)
1237, 1210	δ(OH)	469	$\delta(SeO_2)$
		383	δ_{as}(OSeOH)
		354	δ_s(OSeOH)

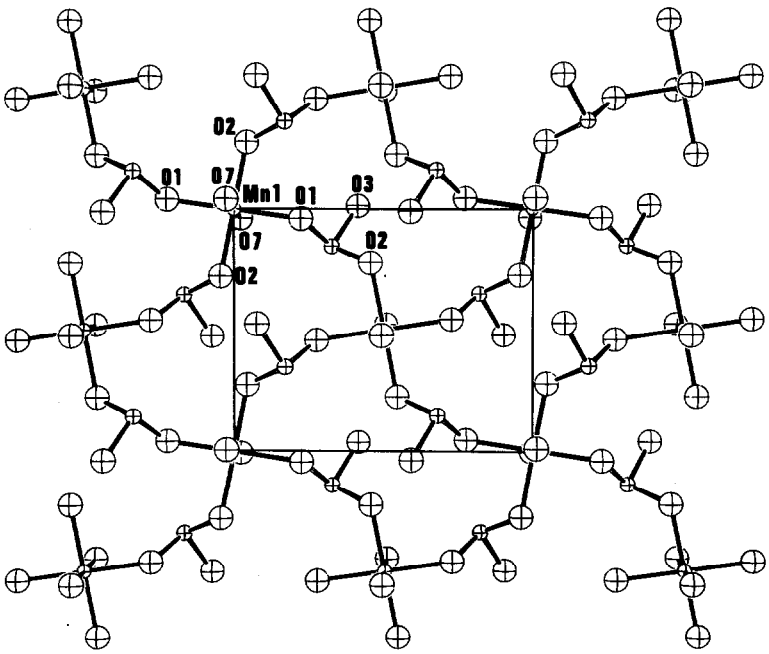


Fig. 3. The structure of $NH_4Mn(HSeO_3)_3$ along the *a*-axis. The value of the *x*-coordinate is approximately 0.

Table 5. Bond distances (Å) for $NH_4Mn(HSeO_3)_3$

Mn(1)—O(1) (*2)	2.157(6)	Mn(2)—O(4) (*2)	2.189(7)
Mn(1)—O(2) (*2)	2.167(7)	Mn(2)—O(5) (*2)	2.175(6)
Mn(1)—O(7) (*2)	2.217(6)	Mn(2)—O(8) (*2)	2.204(6)
Se(1)—O(1)	1.685(6)	Se(2)—O(4)	1.673(6)
Se(1)—O(2)	1.656(7)	Se(2)—O(5)	1.651(7)
Se(1)—O(3)	1.776(7)	Se(2)—O(6)	1.738(7)
Se(3)—O(7)	1.643(7)	N(1)—O(3)	3.054(2)
Se(3)—O(8)	1.641(7)	N(1)—O(5)	2.851(10)
Se(3)—O(9)	1.770(6)	N(1)—O(6)	3.089(12)
Mn(1)—Se(1)	3.288(1)	N(1)—O(7)	3.034(12)
Mn(1)—Se(3)	3.467(1)	N(1)—O(8)	2.879(12)
Mn(2)—Se(2)	3.336(1)	N(1)—O(9)	2.861(12)
Mn(2)—Se(3)	3.581(1)		

with those for manganese(III) selenito complexes of the type $MMn(SeO_3)_2nH_2O$, where M = H, NH_4, K and Rb,[14] $Sr(HSeO_3)_2$,[15] and $Ca(HSeO_3)_2H_2O$.[13] The weak peak at wavenumber 1635 cm^{-1} is caused by moisture or ammonium ion.

Crystal structure

The crystal data are given in Table 2, interatomic distances in Table 5 and the picture of the structure in Fig. 3.*

The structure of ammonium manganese tris(hydrogenselenite) forms a three-dimensional network, which can be thought to consist of two very similar layers oriented in the *yz*-plane. The first layer consists of Mn(1), Se(1), O(1), O(2) and O(3) atoms and the *x*-coordinate has value close to 0. The second layer consists of Mn(2), Se(2), O(4), O(5) and O(6) atoms and the *x*-coordinate is about 0.5. Layers are connected together through the selenite group containing the selenium atom Se(3), which is located between the layers.

The manganese atoms lie in special positions with fixed coordinates, each surrounded by six oxygen atoms forming an elongated octahedron. The oxygen–manganese–oxygen angles are 180° or vary between 86.4 and 93.6°.

Selenite groups form trigonal pyramids with selenium atoms at the apex. One selenium–oxygen distance is elongated in each selenite group, which is characteristic of the hydrogenselenite. This elongation is caused by hydrogen atoms, which draw oxygen atoms toward themselves. All manganese–oxygen and selenium–oxygen distances are in good agreement with other manganese selenites.[2,5–7]

Nitrogen atoms of the ammonium group are located in holes between the layers. The hydrogen atoms could not be found, but possible hydrogen bond distances less than 3.2 Å are listed in Table 5.

* Atomic coordinates have also been deposited with the Institut für Anorganische Chemie, Bonn, F.R.G. for inclusion in their Data Base.

REFERENCES

1. B. L. Khandelwal and S. P. Mallela, *Thermochim. Acta* 1979, **33**, 355.
2. M. Koskenlinna and J. Valkonen, *Acta Chem. Scand.* 1977, **A31**, 638.
3. K. Kohn, K. Inoue, O. Horie and S. Akimoto, *J. Solid State Chem.* 1976, **18**, 27.
4. M. Nilson, *Bull. Soc. Chim. France* 1875, **23**, 353.
5. M. Koskenlinna and J. Valkonen, *Acta Chem. Scand.* 1977, **A31**, 752.
6. M. Koskenlinna, L. Niinistö and J. Valkonen, *Cryst. Struct. Commun.* 1976, **5**, 663.
7. M. Koskenlinna, L. Niinistö and J. Valkonen, *Acta Chem. Scand.* 1976, **A30**, 836.
8. S. P. Malela and B. L. Khandelwal, *Russ. J. Inorg. Chem.* 1980, **25**, 1659.
9. F. L. Hahn, *Z. Anorg. Allg. Chem.* 1926, **150**, 126.
10. P. Main, *MULTAN 80*, University of York, York, England (1980).
11. J. M. Stewart, *XRAY1976*, Technical Report TR-446, University of Maryland, Maryland, U.S.A. (1976).
12. D. Cromer and J. Mann, *Acta Cryst.* 1968, **A24**, 321.
13. M. Ebert and D. Havlicek, *Coll. Czech. Chem. Commun.* 1981, **46**, 1740.
14. B. L. Khandelwal and S. P. Mallela, *Transition Met. Chem.* 1980, **5**, 235.
15. M. Ebert and D. Havlicek, *Coll. Czech. Chem. Commun.* 1982, **47**, 1923.

Polyhedron Vol. 4, No. 4, pp. 591–593, 1985
Printed in Great Britain

0277–5387/85 $3.00 + .00
Pergamon Press Ltd

FORMATION AND TRANSFORMATION OF Pb_2SiO_4

OSAMU YAMAGUCHI,* HIROSHI OKA and KIYOSHI SHIMIZU
Department of Applied Chemistry, Faculty of Engineering, Doshisha University, Kyoto 602, Japan

(*Received* 12 *December* 1983; *accepted* 11 *May* 1984)

Abstract—A new modification of Pb_2SiO_4 was formed by the simultaneous hydrolysis of lead and silicon alkoxides, followed by washing and drying. It has a hexagonal unit cell with $a = 9.928$ Å and $c = 7.184$ Å. The IR spectra indicate that this modification contains $[SiO_4]^{4-}$ and $[Si_2O_7]^{6-}$ groups in the structure. The transformation process is examined by high-temperature X-ray diffraction.

Lead orthosilicate, Pb_2SiO_4, exists in at least three polymorphic modifications: L(low)-, M(medium)- and H(high)-forms. The system PbO—SiO_2 has a wide glass-forming range extending beyond the orthosilicate composition; therefore, almost all studies on the formation and transformation of Pb_2SiO_4 have been carried out by the crystallization from the glass.[1–7] However, there has been conflicting information in the literature concerning the identities and names of the modifications.

In the present study, a new modification of Pb_2SiO_4 was formed by the simultaneous hydrolysis of lead and silicon alkoxides, followed by washing and drying. On the basis of this result, the characterization and transformation of alkoxy-derived Pb_2SiO_4 were examined by differential thermal analysis, high-temperature X-ray diffraction, and infrared spectrum analysis.

EXPERIMENTAL

Silicon ethoxide, $Si(OC_2H_5)_4$, was a pure grade. Lead amyloxide, $Pb(OC_5H_{11})_2$, was synthesized by the reaction of anhydrous lead acetate with sodium amyloxide in the presence of an excess amount of isoamyl alcohol.[8,9] The mixed alkoxides prepared in the mole ratio $Pb^{2+}:Si^{4+} = 2:1$ were refluxed for 10 h at 131°C and then hydrolyzed by adding distilled water at 25°C. The hydrolysis product was separated from the suspension by filtration, washed repeatedly with hot water, and dried at 80°C under

* Author to whom correspondence should be addressed.

Table 1. X-ray diffraction data of the starting powder

$d_{obs.}$	$d_{cal.}$	I/I_0	hkl
8.59	8.60	10	100
4.96	4.96	10	110
4.29	4.30	55	200
4.08	4.08	30	111
3.59	3.59	2	002
3.31	3.31	15	102
3.25	3.25	65	210
2.961	2.961	85	211
2.910	2.910	55	112
2.866	2.866	100	300
2.482	2.482	5	220
2.384	2.385	5	310
2.240	2.240	2	302
2.149	2.149	10	400
2.041	2.042	20	222
1.987	1.987	10	312
1.972	1.972	10	320
1.928	1.928	5	213
1.902	1.902	20	321
1.876	1.876	20	410
1.844	1.844	15	402
1.663	1.663	2	412
1.624	1.625	5	420
1.612	1.612	5	331
1.572	1.572	2	214
1.550	1.551	5	502
1.522	1.522	5	304,323
1.510	1.510	5	511

reduced pressure. The average particle size of the resulting starting powder, determined by electron microscopy, was *ca* 450 Å.

Differential thermal analysis (DTA) was conducted in air at a rate of 10°C min^{-1}; α-alumina was used as a standard material. The starting powder was examined by X-ray diffraction using nickel-filtered Cu–K_α radiation. The goniometer scanning speed of 1/4° min^{-1} was selected so as to achieve accurate *d* spacings. The diffractometer was calibrated with high purity silicon. The specimens obtained in the heating and cooling processes at a rate of 10°C min^{-1} were identified by high-temperature X-ray diffraction. Infrared spectroscopy (IR) was performed on a dispersion in potassium bromide, using the pressed disk technique.

RESULTS AND DISCUSSION

The identities and names of the modifications of Pb_2SiO_4 were inconsistent due to contradictory results. Because the present results were in general agreement with those of Furukawa *et al.*,[7] their nomenclature was used in the description of the present results.

Table 1 shows the X-ray diffraction data of the starting powder; these diffraction data are different from those of the modifications of Pb_2SiO_4 reported previously. Many compounds have been reported in the system PbO—SiO_2. As will be described, lead silicates other than Pb_2SiO_4 and free species were not observed throughout the heating process. Therefore, the starting powder can be considered to be a compound corresponding to Pb_2SiO_4. The diffraction pattern was indexed as a hexagonal unit cell with $a = 9.928$ Å and $c = 7.184$ Å.

A DTA curve in the heating process revealed small and sharp endothermic peaks at 570–625°C and 720–760°C, respectively. High-temperature X-ray diffraction analysis confirmed that the first endothermic peak (at 570–625°C) is due to the transformation of the hexagonal phase (starting powder) into H—Pb_2SiO_4, and the second endothermic peak (at 720–760°C) to the melting of H—Pb_2SiO_4. The melting temperature (at 744°C) was in agreement with the reported one.[10] In the cooling process from H—Pb_2SiO_4 (at 625–720°C), a small exothermic peak was observed at 490–530°C, corresponding to the transformation of H— into M—Pb_2SiO_4; however, H—Pb_2SiO_4 transformed sluggishly into M—Pb_2SiO_4. Thus, pure M—Pb_2SiO_4 was difficult to obtain under the present conditions; the X-ray diffraction pattern of the mixture of M— and H—Pb_2SiO_4 (M ≫ H) was

Table 2. IR spectrum data of the starting powder, M—Pb_2SiO_4 and H—Pb_2SiO_4 (cm^{-1})

Starting powder		M-Pb_2SiO_4		H-Pb_2SiO_4	
1056	w	1085	s	1091	m
928	m	1043	s	1051	m
881	s	1000*	w	1003	m
844	m	937	s	942	s
652	w	896	s	899	s
519	m	885*	sh	882	m
474	m	848*	w	845	m
		654	s	644	w
		618	w	617	sh
		505	s	493	s
		462	s	452	sh
		419	m	438	s
		383	w		

The characters of the bands are: s, strong; m, medium; w, weak; sh, shoulder.
* Absorption bands resulting from H—Pb_2SiO_4.

observed at room temperature. This result is in agreement with that reported by Furukawa *et al.*[7] On the other hand, pure H—Pb_2SiO_4 was easily obtained at room temperature by rapid quenching from the temperature between 625 and 720°C. No L—Pb_2SiO_4 phase, being always the first product crystallized from the $2PbO \cdot SiO_2$ glass, could be recognized in the present study.

Table 2 shows the IR data of the starting powder, M—Pb_2SiO_4, and H—Pb_2SiO_4. Goetz *et al.*[5,6] showed that H—Pb_2SiO_4 ("M" in their nomenclature) is constructed from $[Si_4O_{12}]^{8-}$ rings, that M—Pb_2SiO_4 ("H" in their nomenclature) is a polysilicate chain structure, and that L—Pb_2SiO_4 is a pyrosilicate with $[Si_2O_7]^{6-}$ units; these results suggesting that all modifications of Pb_2SiO_4 contain the oxygens which are not bonded to silicons. Furukawa *et al.*[7] supported the silicate structures proposed by Goetz *et al.*[5,6] The IR data of M— and H—Pb_2SiO_4 in the present study were consistent with their data.[5–7] On the other hand, the spectrum data of the starting powder are in good agreement with those of phase X crystallized from $5PbO \cdot 3SiO_2$ and $3PbO \cdot 2SiO_2$ glasses.[7] According to the data for phase X, there are two types of silicon in the structure, $[SiO_4]^{4-}$ and $[Si_2O_7]^{6-}$ groups. It is evident therefore that the starting powder contains both silicate anions, so that the crystal-chemical formula is represented by $Pb_6O(SiO_4)(Si_2O_7)$.

REFERENCES

1. H. W. Billhardt, *Glastech. Ber.* 1969, **42**, 498.
2. W. R. Ott and M. G. McLaren, *J. Am. Ceram. Soc.* 1970, **53**, 374.
3. R. M. Smart and F. P. Glasser, *J. Am. Ceram. Soc.* 1974, **57**, 378.
4. J. Goetz, D. Hoebbel and W. Wieker, *Z. Anorg. Allg. Chem.* 1975, **416**, 163.
5. J. Goetz, D. Hoebbel and W. Wieker, *Z. Anorg. Allg. Chem.* 1975, **418**, 29.
6. J. Goetz, D. Hoebbel and W. Wieker, *J. Non-cryst. Solids* 1976, **20**, 413.
7. T. Furukawa, S. A. Brawer and W. B. White, *J. Am. Ceram. Soc.* 1979, **62**, 351.
8. L. M. Brown and K. S. Mazdiyasni, *J. Am. Ceram. Soc.* 1972, **55**, 541.
9. O. Yamaguchi, M. Yamadera and K. Shimizu, *Bull. Chem. Soc. Jpn* 1977, **50**, 2805.
10. R. F. Geller, A. S. Creamer and E. N. Bunting, *J. Res. Nat. Bur. Stand.* 1934, **13**, 237.

Polyhedron Vol. 4, No. 4, pp. 595–598, 1985
Printed in Great Britain

0277-5387/85 $3.00 + .00
Pergamon Press Ltd

BI- AND TRIHETERONUCLEAR COMPLEXES OF URANIUM AND GROUP VI TRANSITION METALS

ALAIN DORMOND* and CLAUDE MOISE
Laboratoire de Synthèse et d'Electrosynthèse Organométalliques Associé au CNRS (LA 33), Faculté des Sciences, 6 Bd Gabriel 21100 Dijon, France

(*Received* 27 *March* 1984; *accepted* 19 *May* 1984)

Abstract—The new heterobimetallic compounds $Cp_3U[OCM(CO)_2Cp']$ containing uranium and group VI transition metals are synthesized from Cp_3UCl and $Na[M(CO)_3Cp']$ or from Cp_3UCH_3 and $H[M(CO)_3Cp']$ (M = Mo, W; Cp = C_5H_5; Cp' = C_5H_5 or C_5Me_5). In a same manner, the trimetallic $Cp_2U[OCMo(CO)_2Cp]_2$ is obtained starting from $Cp_2U(NEt_2)_2$ and $H[Mo(CO)_3Cp]$. All these complexes exhibit low CO stretching frequencies characteristic of isocarbonyl linkages between uranium and Mo or W atoms.

There is now a great interest in heterobimetallic complexes incorporating both early and late transition metals; this increase of interest is due to their potential importance in catalysis[1,2] and organic synthesis.[3] Among heterobinuclear complexes reported to date are compounds containing both group IV (Ti, Zr) and group VI (Mo, W) metals. In these compounds, the two metal atoms are not directly bonded but are linked by a bridging carbonyl ligand.[4–8]

In cyclopentadienyllanthanide series, the reaction with some group VI metallate anions has been described,[9] but, at this time, there is no report on analogous investigations in actinide series. In an effort to develop the chemistry of cyclopentadienyluranium compounds, we have studied the condensation reactions of metallate anions $[M(CO)_3Cp']^-$ (M = Mo, W; Cp' = C_5H_5 or C_5Me_5) with Cp_3UCl and the elimination reactions between the hydrides $H[M(CO)_3Cp']$ and Cp_3UCH_3, Cp_3UNEt_2 and $Cp_2U(NEt_2)_2$. We report in this paper the synthesis and characterization of new bi- and triheteronuclear systems incorporating both uranium and group VI transition metal atoms.

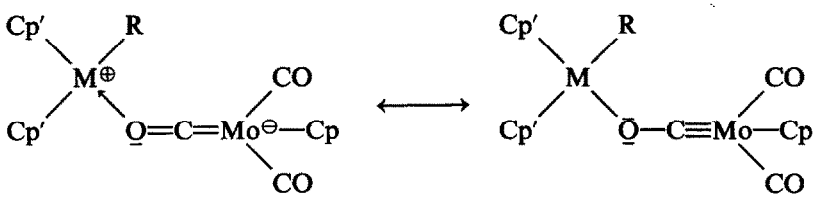
RESULTS AND DISCUSSION

In THF solution at −50°C, Cp_3UCl reacts readily with $Na[Mo(CO)_3Cp]$ in the molar ratio 1:1. The solution turns deep red and NaCl deposits. After removal of the solvent, **1** can be isolated in quantitative yield as a reddish brown compound but always containing small amounts of NaCl [equation (1)]

$$Cp_3UCl + Na[Mo(CO)_3Cp] \xrightarrow[-NaCl]{THF} Cp_3U[OCMo(CO)_2Cp]. \quad (1)$$

1

If pentane is added to the THF solution, **1** deposits immediately as a brown microcrystalline compound. Moreover, **1** is quantitatively obtained by a methane elimination reaction[10] from Cp_3UCH_3 and $H[Mo(CO)_3Cp]$ in heptane or toluene solutions at −50°C. In a similar manner, the bimetallic



M = Ti, Zr; Cp = C_5H_5; Cp' = C_5H_5 or C_5Me_5

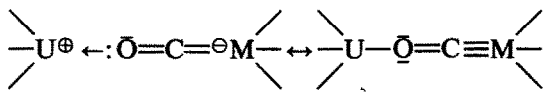
* Author to whom correspondence should be addressed.

complexes **2** and **3** are obtained with high yields [equation (2)].

$$Cp_3UCH_3 + H[M(CO)_3Cp'] \xrightarrow{-CH_4} Cp_3U[OCM(CO)_2Cp'] \quad (2)$$

1: M = Mo; Cp′ = Cp
2: M = Mo; Cp′ = C_5Me_5
3: M = W; Cp′ = Cp

The IR solid spectra of these compounds exhibit a very low carbonyl stretching frequency at *ca.* 1640 cm^{-1} indicative of an isocarbonyl linkage between U and Mo (or W) atoms.[4,5,7–10,11]



These complexes may be considered formally to consist of the acid–base adducts of the Lewis acid Cp_3U^+ and the metallate anions $[M(CO)_3Cp']^-$. The formation of an isocarbonyl bridge preferentially to a direct metal–metal bond may be rationalized in terms of the preference of the "hard" uranium centre to form a bond with the "hard" oxygen site rather than the "soft" molybdenum or tungsten centres. This trend reflects the well known oxophilic character of actinides (or early transition metals) in relatively high oxidation state.[12]

Compounds **1**, **2** and **3** are poorly soluble in non coordinating solvents such as toluene or hydrocarbons: all attempts at recrystallization lead to the formation of the hydrides $H[M(CO)_3Cp']$ and of unidentified uranium byproducts. A similar hydride formation has been observed with analogous titanium (or vanadium) heterobimetallic systems.[11] All these complexes are highly soluble in THF; the NMR spectra of the deep red solutions show a sharp C_5H_5 singlet at *ca* −3.2 ppm (C_5H_5 resonance of Cp_3UCl in THF occurs at −3.4 ppm); the IR spectra exhibit strong CO stretching peaks which are quite identical to those of the free carbonyl anions $[M(CO)_3Cp']^-$, thereby suggesting a substantial dissociation corresponding to an ionic structure: the companion cation is presumably $[Cp_3U(THF)]^+$ [equation (3)].

$$Cp_3U[OCM(CO)_2Cp'] \xrightarrow{THF} [Cp_3U(THF)]^+ + [M(CO)_3Cp']^- \quad (3)$$

These complexes react with anhydrous HCl or CCl_4 affording in a quantitative yield Cp_3UCl and respectively $H[M(CO)_3Cp']$ and $Cl[M(CO)_3Cp']$ (identified by NMR and IR spectroscopy). Such cleavage reactions cannot thus be used as a diagnostic tool of metal–metal bonds in heterobimetallic complexes as it has been previously claimed[6,13] but seems to be a general feature of "early–late" transition metal binuclear compounds.[5,8,11]

The bisdialkylamido derivative $Cp_2U(NEt_2)_2$ reacts quantitatively in heptane solution at −70°C when mixed with $H[Mo(CO)_3Cp]$ in a 1:2 ratio. A red powder deposits and no remaining hydride or Cp_2UNEt_2 are present in the colourless supernatant heptane. This red powder is very thermally unstable and decomposes readily at room temperature affording $H[Mo(CO)_3Cp]$ and intractable uranium products. This instability precludes recrystallization and elemental analysis. Its IR spectrum shows only three intense CO absorptions at 1900, 1740 and 1640 cm^{-1}.

The stoichiometry of the reaction and the IR data are in agreement with the trimetallic structure **4** [equation (4)].

$$Cp_2U(NEt_2)_2 + 2H[Mo(CO)_3Cp] \rightarrow Cp_2U(O{-}C{\equiv}Mo(CO)_2Cp)_2 \quad (4)$$

4

If dissolved in THF, even at low temperature, **4** evolves immediately with formation of $H[Mo(CO)_3Cp]$ and of the compound **1** identified by IR and NMR spectroscopy.

1 can be also obtained from Cp_3UNEt_2 in toluene or THF [equation (5)] and from the biscyclopentadienyl Cp_2UNEt_2 when performed in THF medium [equation (6)]

$$Cp_3UNEt_2 + H[Mo(CO)_3Cp] \xrightarrow[\text{or toluene}]{THF} \mathbf{1} + HNEt_2 \quad (5)$$

$$Cp_2U(NEt_2)_2 + \tfrac{2}{3}H[Mo(CO)_3Cp] \xrightarrow{THF} 1 + HNEt_2 + ? \quad (6)$$

This ligand redistribution is indicative of the greater stability of a triscyclopentadienyl versus a biscyclopentadienyl uranium moiety. This is a general trend in actinide series which reflects the tendency of the cyclopentadienyl ligands to saturate the actinide coordination sphere.[14,15]

These studies provide further examples which illustrate the similar properties of actinides and IVA transition metal cyclopentadienyl derivatives. Both series give closely related bimetallic systems which exhibit an isocarbonyl linkage. Nevertheless, it has been recently related a series of Zr–Fe and Zr–Ru complexes[16] which adopt metal–metal bonded

Table 1. Analytical and IR data

	Compound	Found (required) % C	H	M	U	νC≡O (cm^{-1}) Nujol mulls (THF solution)		
1	$Cp_3U[OCMo(CO)_2Cp]$	39.99 (40.70)	3.06 (2.95)	13.93 (14.16)	35.35 (35.10)	1900 (1899	1740 1794	1634 1744)
2	$Cp_3U[OCMo(CO)_2(C_5Me_5)]$	43.93 (44.92)	3.86 (4.02)	12.30 (12.82)	32.90 (31.81)	1902 (1888	1737 1785	1645 1731)
3	$Cp_3U[OCW(CO)_2Cp]$	34.94 (36.03)	2.60 (2.61)	22.92 (24.02)	32.30 (31.07)	1898 (1895	1735 1795	1635 1743)
4	$Cp_2U[OCMo(CO)_2Cp]_2$	—	—	—	—	1900	1740	1640

structures; it seems therefore to be of interest to examine if similar attachment mode is possible in the actinide series and further work in this field is in progress.

EXPERIMENTAL

Microanalysis were by Service Central d'Analyse, CNRS (Lyon). Spectrometers: IR Perkin–Elmer 580B; spectra in nujol mulls or in THF solutions (NaCl cells), NMR Hitachi Perkin–Elmer R24 (protonated solvents) or Jeol FX100. ^1H data references to Me_4Si. All operations were performed under argon and all solvents were distilled from sodium/benzophenone under argon immediately before use.

The following complexes: Cp_3UCl,[17] Cp_3UCH_3,[18] Cp_3UNEt_2,[19] $NaM(CO)_3Cp'$,[20] $HM(CO)_3Cp'$[20] were prepared according to literature methods.

Analytical and IR data were collected in Table 1.

Preparation of $Cp_3U[OCMo(CO)_2Cp]$

Method A: to a stirred solution of Cp_3UCl (1.56 g) in THF (40 cm^3) at −50°C was added dropwise a solution of $Na[Mo(CO)_3Cp]$ (0.89 g) in THF (20 cm^3), the reaction mixture develops immediately a deep red colour and white NaCl deposits. The solution was allowed to rise to room temperature, filtered, concentrated to *ca* 10 cm^3 and pentane (30 cm^3) was added. The reddish-brown powder was collected, washed with pentane and dried. Yield 2.15 g (96%).

Method B: to a stirred solution of Cp_3UCH_3 (1.12 g) in toluene (20 cm^3) at −50°C, was added a solution of $H[Mo(CO)_3Cp]$ (0.615 g) in heptane (20 cm^3). The mixture was allowed at −25°C and brown crystals deposit within *ca* 1 h. Yield 1.64 g (97%). Compounds (2) $\{Cp_3U[OCMo(CO)_2(C_5Me_5)]\}$ and (3) $\{Cp_3U[OCW(CO)_2Cp]\}$ were obtained in an identical manner.

Method C: to a stirred solution of Cp_3UNEt_2 (1.1 g) in toluene (20 cm^3) at −50°C was added $H[Mo(CO)_3Cp]$ (0.57 g) in heptane (10 cm^3) and the mixture was allowed to rise to room temperature. **1** crystallises readily. Yield 1.1 g (81%).

If the reaction was performed in THF, the IR spectrum of the solution showed two strong peaks at 1898 and 1787 (very broad) cm^{-1}. The same spectrum was recorded when a small amount of $HNEt_2$ was added to a THF solution of **1**.

Cleavage of $Cp_3U[OCMo(CO)_3Cp]$

HCl: To a suspension of **1** (0.5 g) in toluene (10 cm^3) at −70° was added slowly a dilute solution of HCl in toluene (10 cm^3). After 1 h, the brown solution was allowed to room temperature, evaporated to dryness and $H[Mo(CO)_3Cp]$ was extracted by sublimation. The brown residue was Cp_3UCl and a very small amount of $Cl[Mo(CO)_3Cp]$.

CCl_4: In the same manner, after similar treatment, the residue contains a mixture of Cp_3UCl and of $Cl[Mo(CO)_3Cp]$ in equimolecular amounts.

Preparation of $Cp_2U[OCMo(CO)_2Cp]_2$ (4)

To a stirred solution of $Cp_2U(NEt_2)_2$ (1.02 g) in heptane (20 cm^3) at −70° was added $H[Mo(CO)_3Cp]$ (0.95 g) in heptane (20 cm^3). A red powder deposits readily. Yield 1.1 g (91%). **4** may be stored 24 h at −70°C without noticeable decomposition. At room temperature under argon it decomposes within *ca* 10 minutes affording quantitatively $HMoCO_3Cp$ and an unidentified black powder.

Reaction of $Cp_2U(NEt_2)_2$ *with* $H[Mo(CO)_3Cp]$ *in* THF

To a solution of $Cp_2U(NEt_2)_2$ (1.02 g), 2×10^{-3} mol in THF (10 cm^3) at room temperature, was

added dropwise a 10^{-3} mol solution of $H[Mo(CO)_3Cp]$ in THF; the consumption of the hydride solution (1.4 cm^3) was monitored by IR. After filtration, concentration and addition of pentane (30 cm^3) moderately pure **1** was isolated. Yield 0.5 g (56%).

Acknowledgement—We thank Mr D. Arnoult for his technical assistance.

REFERENCES

1. C. Masters, *Adv. Organomet. Chem.* 1979, **17**, 61.
2. K. S. Wong and J. A. Labinger, *J. Am. Chem. Soc.* 1980, **102**, 3652.
3. J. Schwartz, M. J. Loots and M. Kosugi, *J. Am. Chem. Soc.* 1980, **102**, 1333.
4. A. M. Hamilton Jr., W. S. Willis and G. D. Stucky, *J. Am. Chem. Soc.* 1981, **103**, 4255.
5. J. S. Merola, R. A. Gentile, G. B. Ansell, M. A. Modrick and S. Zentz, *Organometallics* 1982, **1**, 1731.
6. P. Renaut, G. Tainturier and B. Gautheron, *J. Organomet. Chem.* 1978, **150**, C9.
7. J. C. Huffman, J. A. Marsella and K. G. Caulton, *J. Am. Chem. Soc.* 1981, **103**, 209.
8. J. A. Marsella, J. C. Huffman, K. G. Caulton, B. Longato and J. A. Norton, *J. Am. Chem. Soc.* 1982, **104**, 6360.
9. A. E. Crease and P. Legzdins, *J. Chem. Soc., Dalton Trans.* 1973, 501.
10. J. R. Norton, *Acc. Chem. Res.* 1979, **12**, 139.
11. C. Moise and P. Braunstein (to be published).
12. J. M. Manriquez, P. J. Fagan, T. J. Marks, C. Secaur Day and V. W. Day, *J. Am. Chem. Soc.* 1978, **100**, 7112 (and references therein).
13. J. Abys and W. M. Risen Jr., *J. Organomet. Chem.* 1981, **204**, C5.
14. R. D. Ernst, N. J. Kennelly, C. Secaur Day, V. W. Day and T. J. Marks, *J. Am. Chem. Soc.* 1979, **107**, 2656.
15. A. Dormond, *J. Organomet. Chem.* 1983, **256**, 47.
16. C. P. Casey, R. F. Jordan and A. L. Rheingold, *J. Am. Chem. Soc.* 1983, **105**, 665.
17. T. J. Marks, A. M. Seyam and W. A. Watcher, *Inorg. Synth.* 1976, **16**, 147.
18. T. J. Marks, A. M. Seyam and J. R. Kolb, *J. Am. Chem. Soc.* 1973, **95**, 5529.
19. A. L. Arduini, N. M. Edelstein, J. D. Jamerson, J. G. Reynolds, K. Schmid and J. Takats, *Inorg. Chem.* 1981, **20**, 2470.
20. P. Braustein and J. Dehand, *Bull. Soc. Chim. Fr.* 1975, 1997 (and references therein).

Polyhedron Vol. 4, No. 4, pp. 599–601, 1985
Printed in Great Britain

0277–5387/85 $3.00 + .00
Pergamon Press Ltd

SYNTHESIS AND BASE HYDROLYSIS OF CHLORO(N-(2-PYRIDINYLMETHYLENE)-N′-[3-[(2-PYRIDINYLMETHYLENE)AMINO]-PROPYL]-1,3-PROPANEDIAMINE)COBALT(III) PERCHLORATE

GEOFFREY A. LAWRANCE
Department of Chemistry, The University of Newcastle, N.S.W. 2308, Australia

(*Received* 10 *April* 1984; *accepted* 22 *May* 1984)

Abstract—Synthesis of $[Co(pyDPT)Cl](ClO_4)_2$ from pentadentate ligand and cobalt(II) yields one *cis* isomer. Hydrolysis in base is extremely rapid (k_{OH} 1.8×10^6 M^{-1} s^{-1} at 25°C) in this complex, where the geometry and ligand character fix the single site for conjugate base formation as *cis* to the leaving group.

Studies of the base hydrolysis of haloamine complexes have been extensive in recent years.[1–4] At least for cobalt(III), the dissociative conjugate base (S_N1cb) mechanism appears to operate

$$Co(ligNH)X_n^{m+} + OH^- \rightleftharpoons Co(ligN^-)X_n^{(m-1)+} + H_2O$$
$$\downarrow$$
$$Co(ligNH)X_{(n-1)}(OH)^{m+} \xleftarrow[\text{fast}]{OH_2} Co(ligN^-)X_{(n-1)}^{m+} + X^-$$

where ligNH represents an N-donor ligand with at least one available site for deprotonation.

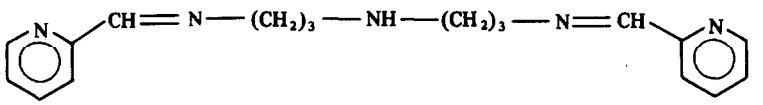
With certain unsaturated multidentate ligands such as N-(2-pyridinylmethylene)-N′-[3-[(2-pyridinylmethylene)amino]-propyl]-1,3-propanediamine (pyDPT, **I**)[5] the available sites for conjugate base formation when complexed is limited to one.

Provided the coordinated geometry of the ligand is established, the disposition of the site of deprotonation to the leaving group is firmly established. In general, such pentadentate ligands can form a number of geometrical isomers (**II–V**), although all need not occur. In this paper the synthesis, characterization and base hydrolysis of one isomer of the chlorocobalt(III) complex of **I** is reported.

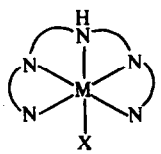
EXPERIMENTAL

Synthesis of $[Co(pyDPT)Cl](ClO_4)_2$

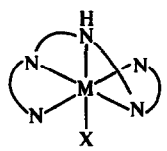
A solution of 1,7-diamino-4-azaheptane (5.2 g, 0.05 mol) in methanol (200 cm^3) was reacted with



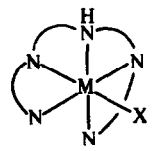
I



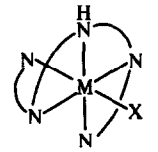
II



III



IV



V

pyridine-2-aldehyde (10.7 g, 0.1 mol) essentially as previously described.[5] A solution of $CoCl_2 \cdot 6H_2O$ (11.9 g, 0.05 mol) in methanol (100 cm^3) was added, and air bubbled through the solution for 1 h. Concentrated HCl (40 cm^3) was added to the dark brown solution, producing an immediate deep red colour. Solid $LiClO_4$ was added with stirring until precipitation commenced. After cooling in an icebath, the purple precipitate was collected on a frit and dried at the pump. The crude material was dissolved in a minimum volume of warm aqueous HCl (1 M, ~60°C), filtered, and solid $NaClO_4$ added with stirring until precipitation commenced. After ice cooling, the purple product was collected, washed with ethanol and ether, and dried in a vacuum desiccator. (Yield 7.3 g.) Found: C, 36.1; H, 3.8; N, 11.5. Calc. for $C_{18}H_{23}N_5Cl_3CoO_8$: C, 35.87; H, 3.85; N, 11.62%. Visible absorption maxima (λ, nm (ε, M^{-1} cm^{-1}) in 1 *M* HCl: 539 (78), 453 (51).

Hydrolysis kinetics. The kinetics of base hydrolysis were followed at 325 nm using a Varian 635 spectrophotometer and a thermostatted (±0.1°C) cell holder. Succinate buffers (pH 4.5–6.0) were employed, with ionic strength (0.1 M) controlled with $NaClO_4$. Complex concentrations of $2 \rightarrow 5 \times 10^{-4}$ M were employed. Rate constants were determined by standard Guggenheim methods, with first order behaviour observed for at least three half-lives.

Physical methods. IR spectra were recorded as KBr discs on a Perkin–Elmer 300 spectrometer, while visible absorption spectra were recorded with a Varian 635 spectrophotometer. ^1H and ^{13}C NMR spectra were recorded using Varian HA-100 and Jeol FX-60 spectrometers respectively, with NaTPS and dioxan as internal references respectively.

RESULTS AND DISCUSSION

The synthesis described yields predominantly one isomer, since the recrystallized product behaves as a single species when it is chromatographed on various cation exchange resins. That the condensation has proceeded as expected is clear from the ^1H NMR and IR spectra. The IR shows an NH stretch at 3210 cm^{-1}, a C=N stretch at 1628 cm^{-1} and pyridine ring vibrations at 1600, 1570, 1480 and 1445 cm^{-1}, analogous to positions observed in the cobalt(II) complex of **I**.[5] Integration of the ^1H NMR spectrum indicates the presence of two imine protons, eight pyridine ring protons and a single amine proton (Fig. 1), in addition to methylene resonances. The ^1H NMR is not consistent with a symmetrical *trans* stereochemisty; rather, an unsymmetrical *cis* stereochemistry exists. This was confirmed by ^{13}C NMR, where resonances assignable to six methylene carbons (14.8, 21.9, 30.1, 34.1, 41.5, 42.8 ppm *vs* dioxan) were observed in addition to multiple resonances in the pyridine ring region (87.0, 84.8, 76.1, 64.5, 63.9 ppm) which are split slightly under higher resolution. Further, two imine carbon resonances at 110.9 and 108.8 ppm were observed, and support the assignment of resonances at 9.28 and 9.44 ppm in the ^1H NMR spectrum to nonequivalent imine protons.

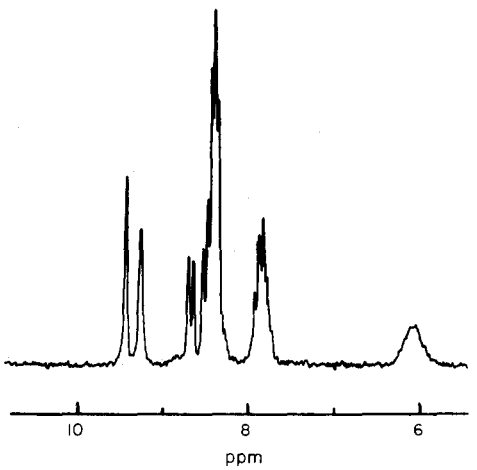


Fig. 1. Section of the ^1H NMR spectrum of $[Co(pyDPT)Cl](ClO_4)_2$ in DCl, showing the nonequivalent imine proton resonances (left of figure), pyridine ring proton resonances, and the single amine proton resonance (right of figure).

The NMR spectroscopy shows that *trans* isomers **II** and **III** are not the product. A *cis* isomer **IV** or **V** is the isolated species, and Dreiding models indicate that isomer **V** with the central saturated tridentate amine component in the *mer* geometry is less strained, and this is the proposed structure for the isolated complex.

Hydrolysis in base is extremely rapid. To determine the kinetics of hydrolysis, it was necessary to employ succinate buffers where the pH is below 6. The observed rate constants displayed a first order dependence with respect to hydroxide ion concentration over the range studied (Table 1), with the second order rate constant at 25°C 1.8×10^6 M^{-1} s^{-1}. Activation parameters for the process are $\Delta H^{\neq}$ 58 kJ mol^{-1} and $\Delta S^{\neq}$ +70 J K^{-1} mol^{-1}. From the rapid disappearance of the amine proton signal in the ^1H NMR spectrum of the complex in acid buffers in D_2O, the proton exchange rate was estimated to be of the order of 10^8 M^{-1} s^{-1}. Although limited solubility did not permit an accurate rate constant to be determined, clearly base abstraction is not rate determining in this system.

Table 1. Rate constants for hydrolysis of $[Co(pyDPT)Cl](ClO_4)_2$ in aqueous succinate buffers*

Temperature (°C)	pH	$10^9 \cdot [OH^-]$†	$10^3 \cdot k_{obs}$‡ (s^{-1})	$10^{-6} \cdot k_{OH}$§ ($M^{-1}\,s^{-1}$)
25.1	4.49	0.403	0.725	1.794
25.1	4.76	0.751	1.38	1.837
9.0	5.15	0.699	0.292	0.418
16.9	5.11	0.891	0.777	0.872
25.1	5.07	1.534	2.80	1.827
33.2	5.06_5	2.795	9.33	3.340
39.6	5.08_5	4.536	23.7	5.229
25.1	5.38	3.133	5.56 (5.61)‖	1.775
25.1	5.62	5.444	9.85	1.810
25.1	5.94	11.375	19.7	1.732

* $I = 0.1$ M ($NaClO_4$); $I_{buffer} = 0.01$ M.

† Calculated from standard values of $\gamma_{\pm}$, pK_w at each temperature.

‡ Average of three independent runs; average error < 5% in each case.

§ k_{OH}(average) $= 1.80(\pm 0.03) \times 10^6\ M^{-1}\,s^{-1}$ at 25.1°C; $\Delta H^{\neq} = 58(\pm 1)$ kJ mol^{-1}; $\Delta S^{\neq} = +70$ J K^{-1} mol^{-1}.

‖ $I_{buffer} = 0.05$ M.

The observed second order rate constant for hydrolysis is much larger than those usually observed for ammine and saturated amine complexes, but is of the same order of magnitude as rate constants reported for unsaturated and multidentate amine ligand complexes, including macromonocyclic ligand complexes.[1] The activation entropy is consistent with a conjugate base mechanism, where a large positive contribution due to the preequilibrium deprotonation applies. The single site available for the deprotonation fixes the geometry of the leaving group as *cis* to the conjugate base in this case, and it is apparent that this arrangement is appropriate for the S_N1cb mechanism to operate. Experiments investigating the site of deprotonation have inferred that sites both *cis* and *trans* to the leaving group may be effective in the S_N1cb mechanism.[6–9] With appropriate ligand design and favourable geometrical isomer formation, N-donor complexes with a single fixed deprotonation site can be prepared. Isolation of a complex with a single *trans* site to complement this study will be pursued.

REFERENCES

1. *Spec. Period. Rep.: Inorg. React. Mech.*, 1971–80, **1–7**.
2. J. O. Edwards, F. Monacelli and G. Ortaggi, *Inorg. Chim. Acta* 1974, **11**, 47.
3. M. L. Tobe, *Acc. Chem. Res.* 1970, **3**, 377.
4. R. G. Wilkins, *The Study of Kinetics and Mechanisms of Reactions of Transition Metal Complexes*. Allyn & Bacon, Boston (1974).
5. C. T. Spencer and L. T. Taylor, *Inorg. Chem.* 1973, **12**, 644.
6. D. A. Buckingham, P. A. Marzilli and A. M. Sargeson, *Inorg. Chem.* 1968, **8**, 1595.
7. D. A. Buckingham, P. J. Creswell and A. M. Sargeson, *Inorg. Chem.* 1975, **14**, 1485.
8. V. Sakaguchi, K. Maeda and H. Yoneda, *Bull. Chem. Soc. Jpn.* 1976, **49**, 397.
9. D. Fenemor and D. A. House, *J. Inorg. Nucl. Chem.* 1976, **38**, 1559.

Polyhedron Vol. 4, No. 4, pp. 603–614, 1985
Printed in Great Britain

0277–5387/85 $3.00 + .00
Pergamon Press Ltd

BIS(DIMETHYLPHOSPHINO)METHANE COMPLEXES OF IRON AND RUTHENIUM

WAI KWOK WONG, KWOK W. CHIU and GEOFFREY WILKINSON*
Chemistry Department, Imperial College, London SW7 2AY, U.K.

and

ANDREW J. HOWES, MAJID MOTEVALLI and MICHAEL B. HURSTHOUSE*
Queen Mary College, Mile End Road, London E1 4NS, U.K.

(*Received* 30 *May* 1984; *accepted* 7 *June* 1984)

Abstract—The interaction of iron(II) acetate in presence of bis(dimethylphosphino)methane (dmpm) with dimethyl- and diethylmagnesium leads to *cis*-$FeMe_2(dmpm)_2$ and $(\eta^2$-$C_2H_4)Fe(dmpm)_2$, respectively; $(PhCH_2)_2Mg$ gives the *trans*-dibenzyl while *o*-$C_6H_4(CH_2MgCl)_2$ gives $C_6H_4(CH_2)_2Fe(dmpm)_2$. On the basis of NMR spectra the latter is best formulated as an "olefin" complex with both uni- and bidentate dmpm ligands. Also described are $[M(dmpm)_3]X_2$, M = Fe, Ru, X = Cl, PF_6; $Fe(dmpm)_3$, which has one unidentate ligand; *cis*-$Fe(CO)_2(dmpm)_2$; $Fe(CO)(dmpm)_2$; $[RuH(dmpm)_3]PF_6$ and $[FeH(dmpm)_3]BF_4$. The X-ray crystal structures of $Fe(\eta^1$-dmpm)$(dmpm)_2$ and the *trans*-$[RuH(\eta^1$-dmpm)$(dmpm)_2]^+$ ion as its PF_6^- salt have been determined. Both complexes contain one unidentate and two bidentate dmpm ligands. The iron complex has square pyramidal geometry with the two chelating dmpm ligands spanning basal edges [Fe—P = 2.161(3) Å] and the unidentate ligand bonding at the axial site [Fe—P = 2.165(3) Å]. The ruthenium complex has an analogous arrangement of dmpm ligands: [Ru—P(chel) = 2.318–2.338(4) Å, Ru—P(uni) = 2.348(4) Å], with the Ru—H bond [1.68(5) Å] *trans* to the Ru—P(unidentate) bond. Crystals of *cis*-$FeMe_2(dmpm)_2$ have also been examined, but severe rotational disorder has precluded the determination of any meaningful geometrical data.

Although many transition metal complexes of bis(diphenylphosphino)methane (dppm) acting as a uni or bidentate ligand or as a bridging group are well known,[1] relatively few studies have been made using the methyl analogue, bis(dimethylphosphino)methane (dmpm),[2] probably because this ligand is more difficult to make.

We now describe some complexes of iron and ruthenium with uni- and bidentate dmpm ligands. ^1H and ^{31}P—$\{^1H\}$ nuclear magnetic resonance data are collected in Table 1. The X-ray crystal structures of $Fe(dmpm)_2(\eta^1$-dmpm), and *trans*-$[RuH(\eta^1$-dmpm$)(dmpm)_2]PF_6$ have been determined.

RESULTS AND DISCUSSION

Alkylation of iron(II) acetate

Me_2Mg. Treatment of $Fe(O_2CMe)_2$ with Me_2Mg in the presence of dmpm in thf led to an air-sensitive orange crystalline compound $FeMe_2(dmpm)_2$ which is readily soluble in hydrocarbons. The compound was also isolated but in lower yield in the reaction of $[Fe(dmpm)_3]Cl_2$ (see later) with methyllithium.

The ^1H NMR spectrum shows a multiplet for the Fe-methyl groups at −0.03 ppm. The ^{31}P–$\{^1H\}$ NMR spectrum shows a complex 12-line pattern centred at 13.6 ppm from the dmpm ligands as expected for a *cis*-configuration for the compound.

An attempt to confirm this assignment via an X-ray structure determination has not been completely successful. The compound crystallises in the cubic system with extensive orientational disorder of the molecule (see Experimental) and we have not been able to extract from the structure analysis any meaningful geometrical parameters.

Et_2Mg. When $Fe(O_2CMe)_2$ was treated with Et_2Mg in the presence of dmpm in thf a golden yellow crystalline compound of stoichiometry $(C_2H_4)Fe(dmpm)_2$ was isolated. The compound is air- and moisture-sensitive and is very soluble in hexane. No metal-hydride stretch was observed in

*Authors to whom correspondence should be addressed.

Table 1. ^{1}H and $^{31}P-\{^{1}H\}$ NMR data

	^{1}H*	Assignment	$^{31}P-\{^{1}H\}$†	Assignment
$(\eta^2\text{-}C_2H_4)Fe(dmpm)_2$	2.84m(4)	PCH_2P	1.24s	Me_2P
	1.54quin(4)	$(\eta^2\text{-}C_2H_4)$; $J = 9$ Hz		
	1.29brs(12)	Me_2P		
	0.96brs(12)	Me_2P		
cis-$Me_2Fe(dmpm)_2$	3.02brm(2)	PCH_2P	AA'BB' 12-line	
	2.57brm(2)	PCH_2P	pattern centered	
	1.30d(6)	Me_2P; $J = 4.4$ Hz	at 13.63 ppm, with	
	1.11m(12)	Me_2P	separation between the	
	0.96br.s(6)	Me_2P	two outer most peaks	
	−0.03m(6)	$FeCH_3$	263.6 Hz	
trans-$(PhCH_2)_2Fe(dmpm)_2$	7.46m(10)	$PhCH_2Fe$	1.67s	Me_2P
	2.46brm(4)	PCH_2P		
	0.70–1.36brm(24)	Me_2P		
	0.12brm(4)	$PhCH_2Fe$		
$(CH_2C_6H_4CH_2)Fe(dmpm)_2$	7.1–7.5m(4)	C_6H_4	41.9brs(1)	Unidentate $Me_2PCH_2PMe_2$
	1.85d(6)	Unidentate Me_2P; $J = 6.0$ Hz	−11.5d(2)	Bidentate $Me_2PCH_2PMe_2$
	0.89d(3)	Uncoordinated Me_2P; $J = 7.11$ Hz	−60.5brs(1); $J = 11.1$ Hz	Uncoordinated $Me_2PCH_2PMe_2$
	0.85d(3)	Uncoordinated Me_2P; $J = 7.1$ Hz		
	2.20m(2)	Bidentate PCH_2P		
	1.15m(12)	Bidentate Me_2P		
	1.62m(2)	Unidentate PCH_2P		
	−1.6brd(4)	$FeCH_2$; $J = 12.6$ Hz		

cis-$Fe(CO)_2(dmpm)_2$	2.71t(1)	Bidentate $Me_2PCH_2PMe_2$; J = 10.4 Hz	46.4m(1)	Unidentate $Me_2PCH_2PMe_2$
			−6.3d(2)	Bidentate $Me_2PCH_2PMe_2$ J = 17.7 Hz
	2.69t(1)	Bidentate $Me_2PCH_2PMe_2$; J = 10.4 Hz		
			−58.7br.s(1)	Uncoordinated $Me_2PCH_2PMe_2$
	1.77brd(2)	Unidentate $Me_2PCH_2PMe_2$; J = 7.7 Hz		
	1.42d(6)	Unidentate $Me_2PCH_2PMe_2$; J = 8.2 Hz		
	1.28d(6)	Bidentate $Me_2PCH_2PMe_2$; J = 4.4 Hz		
	1.22d(6)	Bidentate $Me_2PCH_2PMe_2$; J = 4.9 Hz		
	0.92s(6)	Uncoordinated $Me_2PCH_2PMe_2$		
$[Fe(dmpm)_3]Cl_2$‡	3.6m(6)	$Me_2PCH_2PMe_2$	−2.9s	$Me_2PCH_2PMe_2$
	1.78d(36)	$Me_2PCH_2PMe_2$; J = 14.8 Hz		
$[Fe(dmpm)_3]I_2$‡	3.6m(6)	$Me_2PCH_2PMe_2$	−3.2s	$Me_2PCH_2PMe_2$
	1.80d(36)	$Me_2PCH_2PMe_2$; J = 14.8 Hz		
$Fe(dmpm)_3$	3.14m(4)	Bidentate $Me_2PCH_2PMe_2$	18.4quin(1)	Unidentate $Me_2PCH_2PMe_2$; J = 26.6, 6.5 Hz
	1.98t(2)	Unidentate $Me_2PCH_2PMe_2$; J = 3.4 Hz		
	1.71d(6)	Unidentate $Me_2PCH_2PMe_2$; J = 3.8 Hz	−12.2d(4)	Bidentate $Me_2PCH_2PMe_2$; J = 6.5 Hz
	1.52brs(12)	Bidentate $Me_2PCH_2PMe_2$		
	1.28brs(12)	Bidentate $Me_2PCH_2PMe_2$	−61.0d(1)	Uncoordinated $Me_2PCH_2PMe_2$; J = 26.6 Hz
	1.06d(6)	Uncoordinated $Me_2PCH_2PMe_2$; J = 3.8 Hz		

(*Continued overleaf*)

Table 1 (*cont.*). ^1H and ^{31}P–$\{^1H\}$ NMR data

	^1H*	Assignment	^{31}P—$\{^1H\}$†	Assignment
$[FeH(dmpm)_3]BF_4$§	3.28m(4)	Bidentate $Me_2PCH_2PMe_2$	28.7m(1)	Unidentate $Me_2PCH_2PMe_2$
	2.13t(2)	Unidentate $Me_2PCH_2PMe_2$; J = 3.8 Hz	7.0d(4)	Bidentate $Me_2PCH_2PMe_2$; J = 35.4 Hz
	1.79d(6)	Unidentate $Me_2PCH_2PMe_2$; J = 6.0 Hz		
	1.73brs(12)	Bidentate $Me_2PCH_2PMe_2$	−53.1m(1)	Uncoordinated $Me_2PCH_2PMe_2$
	1.48brs(12)	Bidentate $Me_2PCH_2PMe_2$		
	1.18brs(6)	Uncoordinated $Me_2PCH_2PMe_2$		
	−9.18quin.d(1)	Fe—H; J = 48.9, 10.3 Hz		
$[Ru(dmpm)_3]Cl_2$‡	3.69m(6)	$Me_2PCH_2PMe_2$	−31.4s	$Me_2PCH_2PMe_2$
	1.78d(36)	$Me_2PCH_2PMe_2$; J = 6.6 Hz		
$[RuH(dmpm)_3]PF_6$§	3.42m(4)	Bidentate $Me_2PCH_2PMe_2$	2.12quind(1)	Unidentate $Me_2PCH_2PMe_2$; J = 26.6 Hz; J = 22.2 Hz
	2.01m(2)	Unidentate $Me_2PCH_2PMe_2$		
	1.72br.s(6)	Unidentate $Me_2PCH_2PMe_2$		
	1.67d(12)	Bidentate $Me_2PCH_2PMe_2$; J = 2.2 Hz	−25.3d(4)	Bidentate $Me_2PCH_2PMe_2$; J = 26.6 Hz
	1.49m(12)	Bidentate $Me_2PCH_2PMe_2$		
	1.12d(6)	Uncoordinated $Me_2PCH_2PMe_2$; J = 3.6 Hz	−54.6d(1)	Uncoordinated $Me_2PCH_2PMe_2$; J = 22.2 Hz
	−7.64dp(1)	Fe—H; J = 48.9, 10.3 Hz		

* In C_6D_6 referenced to Me_4Si (δ0.0).
† In C_6D_6 referenced to external 85% H_3PO_4 (δ0.0) negative for upfield shift.
‡ In d_4-methanol.
§ In d_6-acetone.

the IR spectrum. In the ^1H NMR spectrum, other than the resonance due to dmpm, there is a quintet [J(P—CH_2) = 9.0 Hz] centred at 1.84 ppm for the protons of bound ethylene indicating that the C_2H_4 group protons are equivalent and are coupled to four equivalent P atoms. The ^{31}P—$\{^1H\}$ spectrum shows only a singlet at 1.24 ppm for the dmpm ligands. The spectroscopic data is thus consistent with a square pyramidal geometry (**I**) earlier, where the η^2-ethylene occupies the axial site.

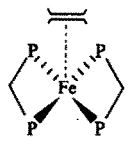
The ethylene complex is doubtless formed via the diethyl intermediate, *cis*-$Et_2Fe(dmpm)_2$, which undergoes β-hydride transfer with elimination of ethane. A similar mechanism has been invoked for the formation of $(\eta^2\text{-}C_2H_4)Ru(PMe_3)_4$.[3]

$(PhCH_2)_2Mg$. Alkylation of the acetate leads to a dark red compound which is slightly soluble in saturated hydrocarbons but very soluble in toluene. The ^1H NMR spectrum shows a broad multiplet at 0.12 ppm for the benzyl methylene protons while the ^{31}P—$\{^1H\}$ spectrum shows a singlet at 1.67 ppm for dmpm. Spectroscopic and analytical data confirm the formulation *trans*-$(PhCH_2)_2Fe(dmpm)_2$.

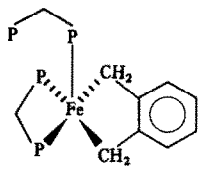
o-$C_6H_4(CH_2MgCl)_2$. In this case alkylation leads to a dark red hexane soluble compound, $C_6H_4(CH_2)_2Fe(dmpm)_2$. The ^1H NMR spectrum shows a broad singlet at 2.31 ppm and a broad doublet (J = 12.6 Hz) at −1.60 ppm for the methylene protons of the *o*-xylidene moiety. The ^{31}P–$\{^1H\}$ spectrum shows a broad singlet, a doublet (J = 11.1 Hz), and a broad singlet (relative intensities 1:2:1) at 41.9, −11.5 and −60.5 ppm, respectively. This indicates the presence of both uni- and bidentate dmpm. The resonances at 41.9 and −60.5 ppm can be assigned respectively to the coordinated and the uncoordinated phosphorus atoms of the unidentate ligand.

There are two possible structures for the compound having either a σ-bonded or a π-bonded *o*-xylidene (**IIa** and **IIb**). For σ-bonded *o*-xylidenes the ^1H chemical shifts of the methylene protons are at 1.91 and 1.66 ppm for $Fe(CH_2C_6H_4CH_2)(dmpe)_2$[4] and at 3.28 ppm for $Pt(CH_2C_6H_4CH_2)(COD)$, whereas for π-bonded *o*-xylidenes they are at 2.49 and −0.39 ppm for $W(CH_2C_6H_4CH_2)_3$[6] and at 1.89 and −0.13 ppm for $Ru(CH_2C_6H_4CH_2)L_3$,[7] (L = PMe_3, PEt_3, PMe_2Ph). The high chemical shift of the methylene protons at −1.60 ppm in the present compound is consistent with a π-bonded *o*-xylidene group. Further, the presence of a unidentate dmpm with an uncoordinated phosphorus atom is in accord with an 18-e species (**IIb**) rather than a 16-e species (**IIa**). Unfortunately single crystals suitable for X-ray work were not obtained.

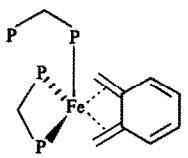
* Now formulated in H. H. Karsch, *Chem. Ber.* 1984, 117, 3123.



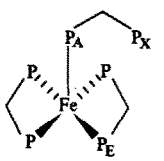
I



IIa



IIb



III

Synthesis and reactions of [M(dmpm)$_3$]X_2; M = Fe, Ru, X = Cl, PF_6

Iron. Treatment of $FeCl_2$ with excess dmpm in refluxing ethanol produces high yields of a pale yellow compound of stoichiometry $Fe(dmpm)_3Cl_2$ which is a 1:2 electrolyte in methanol. The ^1H NMR spectrum shows a multiplet and a doublet (J = 14.8 Hz) of relative intensity 1:6 at 3.6 and 1.78 ppm for the methylene protons and the methyl protons of the dmpm moiety, respectively. The ^{31}P–$\{^1H\}$ spectrum shows a singlet at −2.9 ppm. The compound is thus $[Fe(dmpm)_3]Cl_2$, with octahedral Fe^{II}.

Reduction of $[Fe(dmpm)_3]Cl_2$ with excess sodium amalgam in thf gave an extremely air-sensitive, dark red crystalline compound of stoichiometry $Fe(dmpm)_3$ which is monomeric in benzene. This complex has been mentioned also in a recent paper.[2b] The ^{31}P–$\{^1H\}$ NMR spectrum shows a doublet of quintets (J = 26.6 Hz, 6.5 Hz), a doublet (J = 6.5 Hz), and a doublet (J = 26.6 Hz) of relative intensities 1:4:1 at 18.4, −12.2 and −61.0 ppm. The resonances at 18.4 and −61.0 ppm correspond respectively to the coordinated and uncoordinated phosphorus of unidentate dmpm. The data are consistent with a square pyramidal geometry (**III**) where the unidentate dmpm occupies the axial site and there is free rotation about the Fe—P bond of this ligand in solution at room temperature.

Thus in solution, the equatorial phosphorus P_E should be dynamically equivalent, and the ^{31}P–$\{^1H\}$ NMR spectrum for **III** should exhibit a

doublet of quintets for P_A (coupled to P_X and four P_E, a doublet for P_E (coupled to P_A), and a doublet for P_X (coupled to P_A) of relative intensities 1:4:1, respectively. Based on the coupling pattern and intensity ratio, the resonances at 18.4, −12.2, and −61.0 ppm can be assigned to P_A, P_E and P_X respectively.

The square pyramidal geometry is confirmed by a single crystal X-ray diffraction study. A diagram of the molecular structure is given in Fig. 1, whilst selected bond lengths and angles are given in Table 2. The molecule lies on a crystallographic mirror plane which bisects the two bidentate dmpm ligands which form the base of the square pyramidal co-ordination geometry. However, the unidentate dmpm ligand is disordered and adopts two mirror symmetry related conformations; this places the uncoordinated phosphorus and the bridge methylene carbon slightly off the plane, with a concommitant orientational disorder of the two methyl carbons. The "free" end of this unidentate ligand is oriented so that the Fe—P(3) and C(3)—P(4) bonds have a mutually *trans* configuration. Perhaps the most significant feature of the structure is that the axial and based Fe—P bonds are equal within the limits of experimental error.

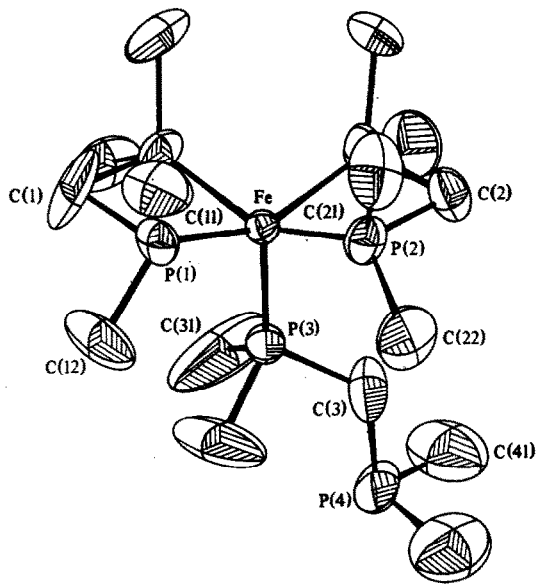


Fig. 1. The structure of $Fe(\eta^1\text{-dmpm})(dmpm)_2$.

The interaction of $[Fe(dmpm)_3]Cl_2$ with excess Na/Hg under CO pressure in thf gave *cis*-$Fe(CO)_2(dmpm)_2$ and $Fe(CO)(dmpm)_2$ (see below).

Ruthenium. Treatment of $RuCl_2(PPh_3)_3$ with excess dmpm in refluxing ethanol gave a white crystalline compound, $[Ru(dmpm)_3]Cl_2$, which is a

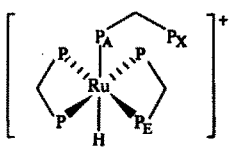
Table 2. Selected bond lengths and angles for $Fe(dmpm)_3$

	Bond lengths (Å)		
P(1)—Fe	2.167(4)	P(2)—Fe	2.158(4)
P(3)—Fe	2.166(5)	C(1)—P(1)	1.849(11)
C(11)—P(1)	1.830(10)	C(12)—P(1)	1.849(9)
P(1)—P(1a)	2.599(6)	C(2)—P(2)	1.843(10)
C(21)—P(2)	1.850(9)	C(22)—P(2)	1.835(9)
P(2)—P(2a)	2.569(6)	C(3)—P(3)	1.800(14)
C(31)—P(3)	1.796(11)	C(3)—P(4)	1.856(14)
C(41)—P(4)	1.768(12)		
	Bond angles (°)		
P(2)—Fe—P(1)	97.8(2)	P(3)—Fe—P(1)	107.1(2)
P(3)—Fe—P(2)	104.8(2)	C(1)—P(1)—Fe	97.7(4)
C(11)—P(1)—Fe	123.9(4)	C(11)—P(1)—C(1)	105.3(6)
C(12)—P(1)—Fe	127.6(4)	C(12)—P(1)—C(1)	100.5(7)
C(12)—P(1)—C(11)	97.6(5)	P(1)—Fe—P(1)(a)	73.7(2)
P(1)—C(1)—P(1)(a)	89.3(7)	C(2)—P(2)—Fe	97.0(3)
C(21)—P(2)—Fe	122.9(4)	C(21)—P(2)—C(2)	102.7(5)
C(22)—P(2)—Fe	128.2(4)	C(22)—P(2)—C(2)	106.0(5)
C(22)—P(2)—C(21)	96.6(5)	P(2)—Fe—P(2)(a)	73.1(2)
P(2)—C(2)—P(2)(a)	88.4(6)	C(3)—P(3)—Fe	119.3(5)
C(31)—P(3)—Fe	121.1(4)	C(31)—P(3)—C(3)	97.2(6)
C(41)—P(4)—C(3)	99.6(5)	P(4)—C(3)—P(3)	122.3(7)
C(41)—P(4)—C(41)	98.0(9)	C(31)—P(3)—C(31)	95.1(10)

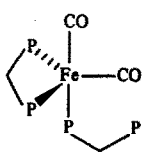
Key to symmetry operations relating designated atoms to reference atoms at (*x*, *y*, *z*): (a) 1.0-*x*, *y*, *z*.

1 : 2 electrolyte in methanol. It is the analogue of the above iron compound and the NMR spectra (Table 1) are similar. The PF_6^- salt can be prepared quantitatively by metathesis of the chloride with excess NH_4PF_6 in methanol.

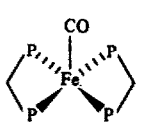
Interaction of $[Ru(dmpm)_3](PF_6)_2$ with excess Na/Hg in thf gave a white crystalline compound of stoichiometry $[RuH(dmpm)_3]PF_6$. The compound is insoluble in hexane, toluene and Et_2O, but readily soluble in acetone and thf; it decomposes slowly in air. The IR spectrum shows a metal-hydride stretch at 1828 cm^{-1} and the ^1H NMR spectrum a complex pattern for the dmpm ligands plus a metal-hydride resonance at −7.64 ppm as a doublet of quintets (J = 62.7 Hz, 23.0 Hz). The $^{31}P-\{^1H\}$ spectrum shows a quintet of doublets (J = 26.6, 22.2 Hz), a doublet (J = 26.6 Hz), and a doublet (J = 22.2 Hz) of relative intensities 1 : 4 : 1 centred at 2.1, −25.3, and 54.6 ppm. The spectroscopic data are consistent with an



IV



V



VI

octahedral geometry (IV) where a unidentate dmpm ligand and the hydride are *trans* and there is free rotation about the Ru—P bond of the unidentate ligand in solution at room temperature.

In solution, the equatorial phosphorus atoms P_E should be dynamically equivalent; the ^1H NMR spectrum should exhibit a doublet of quintets for the hydride (coupled to P_A and four P_E). The $^{31}P-\{^1H\}$ spectrum should exhibit a quintet of doublets for P_A (coupled to four P_E and P_X), a doublet for P_E (coupled to P_A), and a doublet for P_X (coupled to P_X) of relative intensities 1 : 4 : 1, respectively. Thus the resonances at 2.1, −25.3, and −54.6 ppm can be assigned to P_A, P_E and P_X respectively.

The structure of the cation is shown in Fig. 2; selected bond lengths and angles are given in Table 3. The metal has essentially octahedral geometry with the Ru—H bond *trans* to the phosphorus of the unidentate dmpm. The arrangement of the dmpm ligands in this complex is different from that found in the iron complex described above. Although the two bidentate dmpm ligands have, themselves, a pseudo mirror-like arrangement, the "chain" of the unidentate ligand does not lie even approximately along this direction but is oriented close to the direction of the Ru—P(4) bond. Steric pressure arising from this feature may well account for the length of the Ru—P(4) bond, which is the longest of the four, quite variable, "equatorial" Ru—P bonds which could be expected to have very similar lengths. The "axial" Ru—P bond, *trans* to the Ru—H bond, is longest and indicates a small *trans* influence for the H ligand.

Reactions of $Fe(dmpe)_3$

Carbon monoxide. When $Fe(dmpm)_3$ was treated with CO (60 psi), yellow (major product) and orange (minor product) compounds were isolated. The yellow compound, which is readily soluble in hydrocarbons, is $Fe(CO)_2(dmpm)_2$. Both compounds were identical to those obtained from $[Fe(dmpm)_3]Cl_2$ as above. The $^{31}P-\{^1H\}$ NMR spectrum of the yellow complex shows a multiplet, a doublet (J = 17.7 Hz) and a broad singlet of relative intensities 1 : 2 : 1 at 46.4, −6.3 and −58.7 ppm, which can be respectively assigned to the P atoms of the coordinated unidentate ligand, the bidentate ligand and the uncoordinated P atom of the unidentate ligand. The IR spectrum in hexane shows two terminal CO stretches at 1902 and 1848 cm^{-1} indicating a *cis*-dicarbonyl configuration. Thus, the yellow compound is trigonal bypyramidal *cis*-$Fe(CO)_2(\eta^2$-dmpm$)(\eta^1$-dmpm) (V).

The orange compound has a terminal CO stretch at 1887 cm^{-1} and the $^{31}P-\{^1H\}$ NMR shows a singlet at 47.3 ppm; the compound is evidently $Fe(CO)(dmpm)_2$ with a square pyramidal structure (VI).

Methyl iodide. When $Fe(dmpm)_3$ was treated with excess methyl iodide, a pale yellow crystalline compound of stoichiometry $[Fe(dmpm)_3]I_2$ was isolated. The compound is insoluble in hydrocarbons and thf but readily soluble in alcohols and in methanol is a 1 : 2 electrolyte. The ^1H and ^{31}P NMR spectra are similar to those of the chloride.

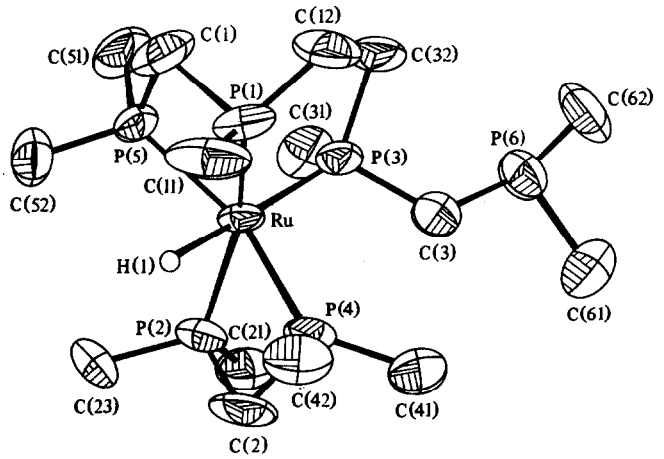


Fig. 2. The structure of the cation *trans*-$[RuH(\eta^1\text{-dmpm})(dmpm)_2]^+$.

Fluoroboric acid. When $Fe(dmpm)_3$ was treated with one equivalent of HBF_4 in diethyl ether at $-78°C$, a yellow crystalline compound of stoichiometry $[FeH(dmpm)_3]BF_4$ was isolated. The compound is insoluble in hydrocarbons, toluene and thf. The IR spectrum shows a metal-hydride stretch at 1823 cm^{-1}. The ^1H NMR spectrum shows a complex pattern for the dmpm ligands, and a metal-hydride resonance as doublet of quintet at -9.18 ppm ($J = 48.9$ and 10.3 Hz). The $^{31}P\text{-}\{^1H\}$ spectrum shows a multiplet, a doublet ($J = 35.4$ Hz) and a multiplet of relative intensities 1:4:1 at 28.7, 7.0 and -53.1 ppm can be assigned to P_A, P_B and P_X, respectively. The structure is thus the same as the ruthenium analogue (IV).

EXPERIMENTAL

Microanalyses were by Pascher (Bonn). IR spectra were obtained on a Perkin–Elmer 683 spectrometer; data given in cm^{-1} for Nujol mulls unless otherwise specified. NMR spectra were recorded on a JEOL FX90Q; data in δ ppm referenced to $Me_4Si(^1H)$ and 85% $H_3PO_4(^{31}P)$. Conductivities were measured using a Data Scientific PT1-18 conductivity meter. Molecular weights were determined cryoscopically in benzene.

All operations were carried out under argon or *in vacuo*. All chemicals used were of reagent grade. Solvents were dried by standard procedures, distilled, and deaerated prior to use. Melting points were taken in sealed capillaries and are uncorrected. $RuCl_2(PPh_3)_3$[8] and $Fe(O_2CMe)_2$[9] were made by standard methods. Bis(dimethylphosphino) methane was prepared by first, synthesis of $Cl_2AlCH_2AlCl_2$ from Al and CH_2Cl_2, reaction of this with PCl_3 to give $Cl_2PCH_2PCl_2$ and finally methylation of the latter with MeMgCl.[10]

cis-*Dimethylbis*[*bis*(*dimethylphosphino*)*methane*]*iron*(II)

Dmpm (0.35 cm^3, 2.3 mmol) and Me_2Mg (3.8 cm^3 of 0.56 *M* solution in Et_2O, 2.1 mmol) were added to a suspension of $Fe(O_2CMe)_2$ (0.33 g, 1.9 mmol) in thf (40 cm^3) at $-78°C$ and the mixture allowed to warm slowly to room temperature and stirred for additional 12 h. The dark red solution was evaporated under vacuum and the residue extracted with hexane (2×30 cm^3). The solution was filtered, concentrated to *ca* 10 cm^3, and cooled to $-20°C$ to give red-orange crystals. Yield: 0.5 g, 73%; m.p. 108°C (decomp. with gas evolution). [Found (required): C, 40.6 (40.2); H, 9.5 (9.5); P, 35.0 (34.6)%.] IR. 1422m, 1410m, 1354w, 1284m, 1269s, 1172w, 1146m, 1058s, 942s, 924vs, 912vs, 856s, 829m, 716s, 687s, 671m, 643m, 456w, 416s.

η^2-*Ethylene bis*[*bis*(*dimethylphosphino*)*methane*]*iron*(0)

Dmpm (0.8 cm^3, 5.3 mmol), Et_2Mg (3.5 cm^3 of 0.61 *M* solution in Et_2O, 2.1 mmol) and $Fe(O_2CMe)_2$ (0.36 g, 2 mmol) in thf (50 cm^3) were warmed from $-78°$ to room temperature and stirred for 12 h. The solvent was removed under vacuum and the residue extracted with hexane; the solution was filtered, concentrated to *ca.* 5 cm^3 and cooled to $-78°C$ to give yellow microcrystals. Yield 0.23 g, 30%; m.p. 120°C (decomp. with gas evolution). [Found (required): C, 41.0 (40.4); H, 9.1 (9.0); P, 34.4 (34.8)%.] IR 1420m, 1416m, 1407m, 1279m, 1267s,

Table 3. Selected bond lengths and angles for $[HRu(dmpm)_3]PF_6$

	Bond lengths (Å)		
P(1)—Ru	2.323(4)	P(2)—Ru	2.314(4)
P(3)—Ru	2.348(4)	P(4)—Ru	2.338(4)
P(5)—Ru	2.318(4)	H(1)—Ru	1.684(52)
C(1)—P(1)	1.859(15)	C(11)—P(1)	1.816(9)
C(12)—P(1)	1.820(10)	C(2)—P(2)	1.841(9)
C(22)—P(2)	1.811(9)	C(23)—P(2)	1.824(9)
C(3)—P(3)	1.829(9)	C(31)—P(3)	1.834(9)
C(32)—P(3)	1.811(9)	C(2)—P(4)	1.849(10)
C(41)—P(4)	1.820(9)	C(42)—P(4)	1.806(8)
C(1)—P(5)	1.840(14)	C(51)—P(5)	1.843(9)
C(52)—P(5)	1.820(10)	C(3)—P(6)	1.853(9)
C(61)—P(6)	1.854(11)	C(62)—P(6)	1.839(11)
F(1)—P(7)	1.582(6)	F(2)—P(7)	1.591(7)
F(3)—P(7)	1.592(7)	F(4)—P(7)	1.547(6)
F(5)—P(7)	1.566(7)	F(6)—P(7)	1.565(7)
	Bond angles (°)		
P(2)—Ru—P(1)	160.3(1)	P(3)—Ru—P(1)	99.9(2)
P(3)—Ru—P(2)	99.8(2)	P(4)—Ru—P(1)	103.6(2)
P(4)—Ru—P(2)	71.8(2)	P(4)—Ru—P(3)	104.2(2)
P(5)—Ru—P(1)	72.1(2)	P(5)—Ru—P(2)	104.9(2)
P(5)—Ru—P(3)	97.2(2)	P(5)—Ru—P(4)	158.6(1)
H(1)—Ru—P(1)	81.5(18)	H(1)—Ru—P(2)	78.8(18)
H(1)—Ru—P(3)	178.5(17)	H(1)—Ru—P(4)	75.9(18)
H(1)—Ru—P(5)	82.7(18)	C(1)—P(1)—Ru	95.9(5)
C(11)—P(1)—Ru	117.3(4)	C(11)—P(1)—C(1)	106.6(7)
C(12)—P(1)—Ru	129.6(4)	C(12)—P(1)—C(1)	103.7(7)
C(12)—P(1)—C(11)	100.9(5)	C(2)—P(2)—Ru	94.8(4)
C(22)—P(2)—Ru	127.6(4)	C(22)—P(2)—C(2)	104.0(5)
C(23)—P(2)—Ru	121.7(4)	C(23)—P(2)—C(2)	105.9(5)
C(23)—P(2)—C(22)	99.4(5)	C(3)—P(3)—Ru	115.1(3)
C(31)—P(3)—Ru	115.2(4)	C(31)—P(3)—C(3)	101.8(5)
C(32)—P(3)—Ru	120.3(4)	C(32)—P(3)—C(3)	102.1(5)
C(32)—P(3)—C(31)	99.5(5)	C(2)—P(4)—Ru	93.8(3)
C(41)—P(4)—Ru	130.5(2)	C(41)—P(4)—C(2)	103.7(5)
C(42)—P(4)—Ru	120.2(4)	C(42)—P(4)—C(2)	106.3(5)
C(42)—P(4)—C(41)	98.8(5)	C(1)—P(5)—Ru	96.5(5)
C(51)—P(5)—Ru	128.8(4)	C(51)—P(5)—C(1)	103.9(7)
C(52)—P(5)—Ru	117.8(4)	C(52)—P(5)—C(1)	106.1(7)
C(52)—P(5)—C(51)	101.0(5)	C(61)—P(6)—C(3)	97.7(5)
C(62)—P(6)—C(3)	100.6(5)	C(62)—P(6)—C(61)	99.1(6)
P(5)—C(1)—P(1)	95.1(6)	P(4)—C(2)—P(2)	95.4(4)
P(6)—C(3)—P(3)	120.2(5)		
F(2)—P(7)—F(1)	88.7(4)	F(3)—P(7)—F(1)	89.8(4)
F(3)—P(7)—F(2)	87.1(4)	F(4)—P(7)—F(1)	179.4(4)
F(4)—P(7)—F(2)	90.7(4)	F(4)—P(7)—F(3)	90.4(4)
F(5)—P(7)—F(1)	89.2(4)	F(5)—P(7)—F(2)	90.5(5)
F(5)—P(7)—F(3)	177.4(4)	F(5)—P(7)—F(4)	90.7(4)
F(6)—P(7)—F(1)	89.0(4)	F(6)—P(7)—F(2)	177.0(4)
F(6)—P(7)—F(3)	91.0(5)	F(6)—P(7)—F(4)	91.6(4)
F(6)—P(7)—F(5)	91.4(4)		

1124m, 1115m, 1058s, 941m, 921vs, 908vs, 880m, 850m, 830m, 800w, 716s, 686s, 663m, 645s, 520w, 479w, 438m.

trans-*Bis(benzyl)bis[bis(dimethylphosphino)-methane]iron*(II)

As earlier but using dmpm (1.8 cm^3, 12 mmol), $(PhCH_2)_2Mg$ (16.5 cm^3 of 0.38 *M* solution in Et_2O, 6.3 mmol) and $Fe(O_2CMe)_2$ (1 g, 5.7 mmol) in thf (100 cm^3). The hexane extract was concentrated to *ca.* 10 cm^3 and cooled to −20°C to give dark-red crystals. Yield: 0.29 g, 10%; m.p. 92°C decomp. [Found (required): C, 57.0 (56.5); H, 8.3 (8.2), P, 23.9 (24.3)%.] I.R. 3072w, 3055w, 1590s, 1496w, 1482s, 1428m, 1419w, 1410m, 1302w, 1292m, 1284m, 1272m, 1200m, 1174w, 1150w, 1082m, 1073m, 1027m, 989m, 943vs, 924s, 863m, 834m, 794m, 747s, 723s, 696s, 670w, 652m, 553s, 530m.

Benzo(6) buten-1,4-diylbis[bis(dimethylphosphino)-methane]iron(II)

As earlier but from dmpm (1 cm^3, 6.6 mmol), *o*-$C_6H_4(CH_2MgCl)_2$ (90 cm^3 of 0.073 *M* solution in thf; 6.6 mmol) and $Fe(O_2CMe)_2$ (0.57 g, 3.3 mmol) in thf (50 cm^3). The hexane extract was concentrated to *ca* 30 cm^3, and cooled to −20°C to give dark red crystals. Yield: 1.0 g, 75% m.p. 78–79°C. [Found (required): C, 49.8 (50.0); H, 8.3 (8.3); P, 28.5 (28.7)%. *M*, 460 (432).] IR 3040w, 3020w, 3002w, 1430m, 1420m, 1341m, 1285m, 1271m, 1150w, 1130w, 1072m, 1065m, 1021w, 980w, 940vs, 925vs, 890s, 860m, 830s, 811w, 770w, 748s, 720s, 700s, 685s, 665m, 655m, 630w, 590m, 490w, 460w, 423m.

Tris[bis(dimethylphosphino)methane]iron(II) *dichloride*

Dmpm (5.5 cm^3, 36.3 mmol) and $FeCl_2$ (1.4 g, 11.2 mmol) in ethanol (100 cm^3) were refluxed for 14 h. The pale yellow solid precipitated on cooling to 20°C was collected, washed with diethyl ether (2 × 50 cm^3) and crystallized from methanol to give white microcrystals. Yield: 5.7 g; 95%; m.p. 264°C. [Found (required): C, 33.8 (33.6); H, 8.1 (7.9); P, 34.2 (34.7); Cl, 13.0 (13.3)%.] Conductivity: Λ_M = 130 ohm^{-1} cm^2 mol^{-1} (10^{-3} M in MeOH). IR 1430m, 1420m, 1405m, 1355w, 1300m, 1288m, 1280m, 1090m, 920vs, 875w, 850w, 842w, 833w, 735s, 720m, 692w, 660w, 409m.

Tris[bis(dimethylphosphino)methane]iron(0)

A suspension of $[Fe(dmpm)_3]Cl_2$ (3.0 g, 5.6 mmol) in tetrahydrofuran (150 cm^3) was transferred to a flask containing sodium amalgam (0.5 g, 21.7 mmol Na in 15 cm^3 Hg) and the mixture was stirred for 7 d. The dark red solution was filtered, evaporated and the residue extracted into hexane (3 × 40 cm^3). The filtered solution was concentrated to *ca* 30 cm^3 and cooled to −20°C to give red crystals. Yield: 1.9 g, 75%, m.p. 76°C. [Found (required): C, 38.9 (38.8); H, 9.2 (9.1); P, 40.3 (40.1)%. *M*, 440 (464)] IR 1425m, 1405w, 1350w, 1275m, 1260m, 1054m, 920vs, 905vs, 882s, 843m, 831m, 809w, 760w, 720m, 681s, 645s, 458m, 430m.

Dicarbonylbis[bis(dimethylphosphino)methane]-iron(0)

Method A. A suspension of $[Fe(dmpm)_3]Cl_2$ (0.8 g; 1.5 mmol) in thf (70 cm^3) with sodium amalgam (0.3 g, 13 mmol of Na in 10 cm^3 Hg) was pressurized with CO (60 psi) in a pressure bottle. The mixture was heated at 70°C with stirring for 3 d. The orange solution was filtered, evaporated and the residue extracted with hexane (2 × 40 cm^3). The filtered extract was concentrated to *ca* 25 cm^3 and cooled to −20°C to give pale yellow crystals and a small amount of orange crystals which can be easily separated by hand. For the yellow compound: yield, 0.4 g, 70%; m.p. 69°C. [Found (required): C, 37.6 (37.5); H, 7.3 (7.3); P, 32.0 (32.3); O, 8.3 (8.3)%. *M*, 370 (384).] IR (hexane) 1902s, 1848s. For the orange crystals: IR (hexane) 1887s.

Method B. A solution of $Fe(dmpm)_3$ (0.23 g, 0.5 mmol) in hexane (50 cm^3) was pressurized with CO (60 psi) in a pressure bottle. After 2 d at 20°C the orange solution was filtered, evaporated under vacuum and the residue extracted with hexane (2 × 30 cm^3). The filtered solution was concentrated to *ca* 10 cm^3 and cooled to −20°C to give yellow crystals together with a trace amount of orange crystals identical with those obtained in method A.

Tris-[bis(dimethylphosphino)methane]iron(II) *diiodide*

To a solution of $Fe(dmpm)_3$ (0.39 g, 0.84 mmol) in hexane (50 cm^3) was added methyl iodide (1.0 cm^3, 1.8 M in ethyl ether), when a white solid formed immediately. The mixture was stirred for 16 h, the solid filtered, washed with diethyl ether (2 × 40 cm^3) and recrystallized from methanol to give pale yellow micro-crystals. Yield: 0.5 g, 85%; m.p. 315–318°C (decomp.). [Found (required): C, 25.0 (25.1); H, 5.9 (5.9); P, 25.8 (25.9); I, 35.2 (35.4)%.] Conductivity: Λ_M = 140 ohm^{-1} cm^2 mol^{-1}, (10^{-3} *M* in MeOH). IR 1420m, 1405m, 1307m, 1290m, 1285m, 1019w, 921vs, 875m, 845m, 740s, 721m, 670m, 405m.

Hydridotris[bis(dimethylphosphino)methane]-iron(II) tetrafluoroborate

To a solution of $Fe(dmpm)_3$ (0.23 g, 0.5 mmol) in Et_2O (50 cm^3) at −78°C was added dropwise 0.5 cm^3 of aqueous HBF_4 (65%) *ca.* 6 mmol cm^{-3} to give a yellow precipitate. After stirring at −78°C for 1 h the solid was collected and dissolved in thf. The solution was evaporated under vacuum and the residue extracted into CH_2Cl_2 which was concentrated to *ca* 2 cm^3. On addition of Et_2O (*ca* 2 cm^3) until yellow crystals began to precipitate and cooling to −20°C yellow crystals were obtained. Yield: 0.19 g, 70%; m.p. 198°C decomp. [Found (required): C, 32.3 (32.7); H, 7.7 (7.8); P, 33.3 (33.8); F, 13.4 (13.8)%.] IR 1823m, 1422m, 1292m, 1279m, 1136w, 1084s, 1048vs, 1030s, 922vs, 893m, 872m, 854w, 843m, 816w, 762w, 728m, 716m, 705m, 684w, 687w, 428m, 412m.

Tris[bis(dimethylphosphino)methane]-ruthenium(II) hexafluorophosphate

A solution of dmpm (0.7 cm^3, 4.7 mmol) and $RuCl_2(PPh_3)_3$ (1.3 g, 1.4 mmol) in EtOH (50 cm^3) was refluxed for 12 h. After cooling to room temperature, a solution of NH_4PF_6 10.7 g, 4.3 mmol) in H_2O (30 cm^3) was added and the solution concentrated until crystals started to deposit when it was cooled at 0°C to give white crystals. Yield: 1 g, 90%; m.p. 320°C. [Found (required): C, 22.7 (22.5); H, 5.4 (5.3); P, 30.6 (31.0); Cl, 0.5 (0)%.] Conductivity: Λ_M = 140 ohm^{-1} cm^2 mol^{-1} (10^{-3} M in MeOH). IR 1428m, 1307s, 1293m, 1120m, 936vs, 885s, 850vs.br, 756m, 739m, 710w, 685w, 568s.

Hydridotris[bis(dimethylphosphino)methane]-ruthenium(II) hexafluorophosphate

A suspension of $Ru(dmpm)_3(PF_6)_2$ (0.8 g; 1 mmol) and Na/Hg (0.1 g, Na in 10 cm^3 Hg) in thf (50 cm^3) was stirred at room temperature for 2 d. The pale yellow solution was filtered and evaporated under vacuum. The residue was washed with petroleum (2 × 30 cm^3), toluene (2 × 30 cm^3) and diethylether (2 × 30 cm^3) then extracted into thf (2 × 30 cm^3). The filtered thf solution was concentrated to *ca* 5 cm^3 and cooled to −20°C to give white crystals. Yield: 0.5 g, 76%; m.p. 216–220°C. [Found (required): C, 27.7 (27.5); H, 6.6 (6.6); P, 32.6 (33.1)%.] IR 1828m, 1428m, 1296w, 1100m, 928s, 898s, 878m, 856m, 836vs, 768w, 732m, 721m, 708w, 686w, 660w, 569s.

Crystallographic studies

Crystals of the three compounds examined were sealed under argon in glass capillaries for the X-ray work. Following initial, photographic, crystal quality checks, all subsequent X-ray measurements were made using a CAD4 diffractometer and graphite monochromated Mo-K_α radiation (λ = 0.71069 Å). Cell dimensions were determined, and intensities measured using standard procedures.[11]

The structures of the $Fe(dmpm)_3$ and $[RuH(dmpm)_3]PF_6$ complexes were determined and refined routinely, although in the case of the iron complex some problems arose due to disorder. Whilst a structure in which the molecule conformed exactly to the space-group requirements of mirror symmetry refined to an R value of 0.046, some of the atoms of the unidentate dmpm ligand showed very high anisotropic "thermal motion". Attempts were made to model this, in terms of 50/50 disorder of two mirror related conformations of the ligand, in which the bridging methylene carbon and the non-coordinated phosphorus atom lay just off the crystallographic mirror plane, and the pairs of methyl groups on each phosphorus had lost their mutual mirror relationship by virtue of torsions in the Fe—P, P—C and C—P bonds away from values which would give the ideal geometry. However, following refinement using this model, some of the resulting geometry parameters were quite unacceptable. Accordingly we have used the simpler model and assume that the high apparent thermal motion is either real, or represents a continuous disorder between the two "off-mirror" conformations.

For both structures, all heavy atoms were refined with anisotropic thermal parameters. Hydrogen atoms were included in idealised positions and assigned an overall isotropic thermal parameter for each group.

Crystal data, details of the intensity measurements and refinements are given in Table 4. Atomic co-ordinates, thermal parameters, complete lists of bond-lengths and angles and tables of F_o/F_c values have been deposited as supplementary material with the Editor, from whom copies are available on request.*

Crystals of the complex *cis*-$FeMe_2(dmpm)_2$ were also examined, but were found to belong to a cubic space group, probably I432, with orientational disorder of the molecule such that the Fe–ligand bonds lay along the crystallographic axes. Although attempts are being made to arrive at a model for this structure, the results, which will be reported elsewhere, are not likely to be very significant, geometrically. Accordingly only details of the crystal

* Atomic co-ordinates have also been deposited with the Cambridge Crystallographic Data Centre.

Table 4. Details of crystal data, intensity data collection and refinement

	$Fe(dmpm)_3$	$[RuH(dmpm)_3]PF_6$	*cis*-$FeMe_2(dmpm)_2$
Crystal data			
Formula	$C_{15}H_{42}P_6Fe$	$C_{15}H_{43}F_6P_7Ru$	$C_{12}H_{34}P_4Fe$
Formula weight	464.17	655.43	358.13
Crystal system	Orthorhombic	Monoclinic	Cubic
a (Å)	15.334(2)	16.258(6)	10.771(3)
b (Å)	13.419(4)	11.627(3)	10.771(3)
c (Å)	12.410(4)	16.355(3)	10.771(3)
β (°)	—	109.69(2)	—
V (Å^3)	2553.67	2910.84	1228.83
Space group	$Cmc2_1$	$P2_{1/n}$	[*I*432]
Z	4	4	2
D_c (g cm^{-3})	1.207	1.495	0.97
$F(000)$	992	1344	544
μ (cm^{-1})	8.98	8.66	9.35
Data collection*			
θ_{min}, θ_{max}	1.5, 25.0	1.5, 25.0	1.5, 25.0
Total data	1344	5813	1239
Total unique	1225	5120	363
Total observed	993	3331	186
Significance test	$F_o > 3\sigma(F_o)$	$F_o > 4\sigma(F_o)$	$F_o > 3\sigma(F_o)$
Refinement			
No. of parameters	141	332	—
Weighting scheme	0.0001	0.0005	—
Parameter g in $\omega = 1/[\sigma^2(F_o)+gF_o^2]$			
$R = \Sigma\Delta F_o/\Sigma F_o$	0.0384	0.048	
$R = \Sigma\omega+\Delta F_o/\Sigma\omega+F_o$	0.0342	0.050	

* All sets of intensity data were corrected for absorption empirically (A.C.T. North, D.C. Phillips and F. S. Matthews, *Acta Cryst.* 1966, **A24**, 351. N. Walker and D. Stuart, *Acta Cryst.* 1983, **A39**, 158.)

data and data collection are reported here. These are included in Table 4.

Acknowledgements—We thank the S.E.R.C. for support and Johnson Matthey PLC for loan of ruthenium.

REFERENCES

1. R. J. Puddephat, *Chem. Soc. Revs.* 1983, **12**, 99; A. T. Hutton, B. Shebanzadeh and B. L. Shaw, *J. Chem. Soc., Chem. Commun.* 1984, 549.
2. See H. H. Karsch: (a) *Angew. Chem. Int. Ed. Engl.* 1982, **21**, 311; (b) *Chem. Ber.* 1983, **116**, 1643 (and references therein); M. L. Kulberg and C. P. Kublak, *Organometallics* 1984, **4**, 632.
3. W. K. Wong, K. W. Chiu, J. A. Statler, G. Wilkinson, M. Motevalli and M. B. Hursthouse, *Polyhedron* 1984, **3**, 1255.
4. G. S. Girolami, R. Tooze, G. Wilkinson and M. B. Hursthouse (unpublished work).
5. (a) M. F. Lappert, T. R. Martin, C. L. Raston, B. W. Skelton and A. H. White, *J. Chem. Soc., Dalton Trans.* 1982, 1959. (b) S. D. Chappell and D. J. Cole-Hamilton, *J. Chem. Soc., Dalton Trans.* 1983, 1051.
6. M. F. Lappert, C. L. Raston, B. W. Skelton and A. H. White, *J. Chem. Soc., Chem. Commun.* 1981, 485.
7. S. D. Chappell, D. J. Cole-Hamilton, A. M. R. Galas and M. B. Hursthouse, *J. Chem. Soc., Dalton. Trans.* 1982, 186.
8. P. S. Hallman, T. A. Stephenson and G. Wilkinson, *Inorg. Synth.* 1970, **12**, 238.
9. J. Catterick, P. Thornton and B. W. Fitzsimmons, *J. Chem. Soc., Dalton Trans.* 1977, 1420.
10. H. Lehmkuhl and R. Schäfer, *Tetrahedron Lett.* 1966, **21**, 2315; M. R. Ort and E. M. Mottus, *J. Organomet. Chem.* 1973, **50**, 47; cf. also, S. Hietkamp, H. Sommer and O. Stelzer, *Angew. Chem. Int. Ed. Eng.* 1982, **21**, 376.
11. R. A. Jones, K. M. A. Malik, M. B. Hursthouse and G. Wilkinson, *J. Am. Chem. Soc.* 1979, **101**, 4128.

Polyhedron Vol. 4, No. 4, pp. 615–620, 1985
Printed in Great Britain

0277–5387/85 $3.00 + .00
Pergamon Press Ltd

THE CRYSTAL AND MOLECULAR STRUCTURE OF DINITRATOBIS(2-METHYLMERCAPTOANILINE)Cd(II) MONOHYDRATE: A TRIGONAL BIPYRAMIDAL $CdSN_2O_2$ POLYHEDRON WITH AN ADDITIONAL WEAKLY BOUND SULFUR

E. A. H. GRIFFITH, N. G. CHARLES, P. F. RODESILER and E. L. AMMA*
Department of Chemistry, University of South Carolina, Columbia, SC 29208, U.S.A.

(*Received* 11 *October* 1983: *accepted after revision* 7 *June* 1984)

Abstract—The single crystal X-ray structure determination of dinitratobis-(2-methylmercaptoaniline) has been carried out. The structure consists of neutral molecules separated by ordinary van der Waals distances with the water molecules of hydration simply filling holes. The geometry about Cd^{2+} may be best described as trigonal bipyramidal $CdSN_2O_2$ with an additional weakly bound sulfur. The two oxygen ligands are from different nitrate groups and one of the 2-methylmercaptoaniline ligands contributes a nitrogen and a sulfur to the coordination polyhedron while the other contributes only an aniline nitrogen, i.e. one of the normally chelating ligands is nitrogen bonded to the metal with only weakly bound sulfur. The bonded distances are: Cd—S, 2.715(3), Cd—N, 2.369(8), 2.33(1); Cd—O, 2.3887(9), 2.353(9) Å and a long Cd—S of 3.118(3) Å. Diffraction data: monoclinic, $P2_1/n$; $a = 12.268(2)$ Å, $b = 7.909(1)$ Å, $c = 24.631(4)$ Å, $\beta = 103.4(2)°$, $D_M = 1.54(2)$ g cm^{-3}, $D_C = 1.52$ g cm^{-3}; $Z = 4$, $\lambda = 0.71073$ Å. The structure was refined by full matrix least squares including anisotropic temperature factors, absorption corrections and anomalous dispersion corrections to a final conventional R of 0.057.

The binding of sulfur, nitrogen and oxygen to metal is of considerable importance in a number of biological processes of metalloenzymes. This is particularly true for the case of Zn metalloenzymes.[1] For example, the structural site of horse liver alcohol dehydrogenase (LADH) is accepted as a more or less tetrahedral ZnS_4 site.[2] The catalytic site of this enzyme is a ZnS_2NO location.[3,4] Enzymatic sites in some other metalloenzymes are: carboxypeptidase, ZnO_2N_2;[5] carbonic anhydrase, ZnN_3O;[6] alkaline phosphatase, ZnN_3O;[7] superoxide dismutase ZnN_3O;[8] and metallothionein Zn_xS_y(clusters).[9] In a number of these enzymes the replacement of Zn^{2+} by Cd^{2+} decreases, but does not destroy, enzymatic activity,[1,10] and this coupled with the recent developments in ^{113}Cd NMR spectroscopy has led to the observation and interpretation of ^{113}Cd NMR of these and other Cd substituted enzymes.[11–35]

We have been actively synthesizing model compounds for these and other Cd substituted enzymes, determining crystal structures and measuring solution and solid state cross polarization magic angle spinning (CP/MAS) ^{113}Cd NMR[36–45] in an attempt to correlate structure, metal stereochemistry and metal coordination with ^{113}Cd NMR chemical shifts. Clearly, one is interested in synthesizing $CdS_xN_yO_z$ type systems observing their solution and solid state (CP/MAS) ^{113}Cd NMR and correlating the solid state structure and solid state and solution NMR. A relatively straightforward synthesis problem along these lines is offered by the ligand 2-methylmercaptoaniline which should bind to Cd^{2+} via S and N to form cadmium-(2-methylmercaptoaniline)$_2^{2+}$ a $CdS_2N_2^{2+}$ system. Although Cd^{2+} binds two ligands, one binds via S and N as expected, but the other binds only via the nitrogen atom and Cd prefers to bind to oxygen of nitrate rather than a sulfur atom. Unfortunately, the ^{113}Cd NMR in this case is beset by technical problems; nevertheless, the stereochemistry and coordination polyhedron of the metal is interesting and unusual and we report the structure at this time and shall report the ^{113}Cd NMR solid and solution results at a later time.

* Author to whom correspondence should be addressed.

EXPERIMENTAL

A methanol solution (50 cm^3) of 2-methylmercaptoaniline [Aldrich] (2.78 g, 0.02 mol) was added to a solution of 3.08 g, 0.01 mol of $Cd(NO_3)_2 \cdot 4\ H_2O$ [Mallinckrodt] in 100 cm^3 of methanol/water (1/1) with stirring and gentle heating (40°C). After approximately 15 min the solution was allowed to evaporate slowly at ambient temperature. Diffraction quality crystals appeared in 4–5 days.

X-RAY DATA AND STRUCTURE ANALYSIS

The crystals were found to be air and light sensitive and were sealed into thin walled glass capillaries. Data collection and refinement parameters are enumerated in Table 1. The structure was solved by standard heavy atom methods. The atom parameters, B_{eq}, anisotropic temperature factors and F_o, F_c tables have been deposited. The interatomic distances, angles and least squares planes are found in Table 2.

DESCRIPTION OF STRUCTURE AND DISCUSSION

The structure may be described as isolated uncharged molecules of dinitratobis(2-methylmercaptoaniline) Cd(II) (Fig. 1), separated by ordinary van der Waals distances between molecules. The water molecules of hydration seem only to fill interstices. The shortest oxygen of water of hydration O(7)–O, distance is greater than 4 Å. The

Table 1. $C_{14}H_{20}CdS_2O_7N_4$: cell data, data collection and refinement parameters

Diffractometer: Enraf–Nonius CAD-4 interfaced to PDP 11/60
$a = 12.268(2)$ Å; $b = 7.909(1)$Å; $c = 24.631(4)$ Å;
$\beta = 103.40(1)°$; $D_m = 1.54(2)$ g cm^{-3}; $D_c = 1.82$ g cm^{-3};
$Z = 4$; wavelength, Mo-K_α 0.71073 Å;
Graphite monochromator used, $\theta = 6.1°$;
Formula weight = 532.7; space group $P2_1/n$, $\mu = 11.5$ cm^{-1};
Size of crystal $0.22 \times 0.27 \times 0.75$ mm;
Faces: {001}, {100}, {010};
Absorption corrections made; max, min transmission factors 0.807 and 0.732 (Frenz, 1980);[55]

$$P \text{ factor} = 0.030 \quad \text{in} \quad \sigma(F_0^2) = [\sigma(I_{raw})^2 + (P \times I_{raw}{}^2]^{1/2}/Lp \quad \text{and} \quad w = \frac{1}{\sigma(F_0)^2}.$$

Data considered non-zero if $F^2 > 4\sigma(F^2)$;
3952 independent *hkl*s measured in $\omega - 2\theta$ mode to $2\theta_{max} = 60°$, *hkl* range = 0–17, 0–11, 34–33; 2249 reflections used to solve and refine structure, $F_{unobserved} = 106 > F_{min} = 12.0$;
Variable scan speed with preliminary scan speed of 4° min^{-1} 2θ;
Three standard reflections monitored every 100 reflections, decay less than 2% I;
Room temperature ~ 18°C;
Structure refined by full-matrix least squares, including anisotropic temperature factors and anomalous dispersion corrections with weights based upon intensity statistics (Frenz, 1980);[55]
Function minimized here and below

$$\sum_i w_i[|F_o|_i - |F_c|_i]^2.$$

Final least squares performed on Amdahl V6 (Stewart, 1979)[56] with f, Δf, and $\Delta f'$ from *International Tables*, Vol. 4;[57]
Largest shift at end of refinement = 0.03σ, av < 0.01σ,
No. of variables = 253; final $R = 0.057$, weighted $R = 0.077$;
Error of obs of unit weight = 5.03; $F(000) = 1072$;
Final difference Fourier qualitatively featureless;
All computer programs used were either those in the Enraf–Nonius SDP package[55] on the PDP 11/60 or the X-ray 79 system[56] on the Amdahl V-6;
ORTEP[58] was calculated on the Amdahl V-6.

Table 2. $C_{14}H_{20}CdS_2O_7N_4$: bonded distances (Å) and angles (°) with ESDs in parentheses

Cd—S(1)	2.715(3)	O(1)—N(3)	1.14(1)	C(2)—C(3)	1.37(1)
Cd—O(1)	2.387(9)	O(2)—N(3)	1.24(1)	C(3)—C(4)	1.33(2)
Cd—O(3)	2.517(9)	O(3)—N(3)	1.28(2)	C(4)—C(5)	1.36(3)
Cd—O(4)	2.71(1)	O(4)—N(4)	1.32(1)	C(5)—C(6)	1.35(3)
Cd—O(6)	2.353(9)	O(5)—N(4)	1.22(1)	C(8)—C(9)	1.37(2)
Cd—N(1)	2.369(8)	O(6)—N(4)	1.16(1)	C(8)—C(13)	1.40(2)
Cd—N(2)	2.33(1)	N(1)—C(1)	1.40(1)	C(9)—C(10)	1.37(1)
S(1)—C(2)	1.76(1)	N(2)—C(8)	1.47(1)	C(10)—C(11)	1.38(2)
S(1)—C(7)	1.82(1)	C(1)—C(2)	1.39(2)	C(11)—C(12)	1.41(3)
S(2)—C(9)	1.76(1)	C(1)—C(6)	1.46(2)	C(12)—C(13)	1.40(2)
S(2)—C(14)	1.81(1)				

S(1)—Cd—O(1)	103.9(2)	Cd—N(1)—C(1)	112.0(6)
S(1)—Cd—O(3)	139.3(3)	Cd—N(2)—C(8)	113.6(7)
S(1)—Cd—O(4)	76.8(2)	O(1)—N(3)—O(2)	122(1)
S(1)—Cd—O(6)	93.8(3)	O(1)—N(3)—O(3)	120(1)
S(1)—Cd—N(1)	72.7(2)	O(2)—N(3)—O(3)	118(1)
S(1)—Cd—N(2)	141.0(2)	O(4)—N(4)—O(5)	122(1)
O(1)—Cd—O(3)	50.4(3)	O(4)—N(4)—O(6)	115(1)
O(1)—Cd—O(4)	77.0(3)	O(5)—N(4)—O(6)	122(1)
O(1)—Cd—O(6)	116.3(3)	N(1)—C(1)—C(2)	122.8(9)
O(1)—Cd—N(1)	80.2(3)	N(1)—C(1)—C(6)	121(1)
O(1)—Cd—N(2)	108.4(3)	C(2)—C(1)—C(6)	116(1)
O(3)—Cd—O(4)	68.1(3)	S(1)—C(2)—C(1)	119.0(7)
O(3)—Cd—O(6)	77.2(4)	S(1)—C(2)—C(3)	119.7(9)
O(3)—Cd—N(1)	121.3(3)	C(1)—C(2)—C(3)	121(1)
O(3)—Cd—N(2)	78.8(3)	C(2)—C(3)—C(4)	120(1)
O(4)—Cd—O(6)	48.2(3)	C(3)—C(4)—C(5)	123(1)
O(4)—Cd—N(1)	135.9(3)	C(4)—C(5)—C(6)	118(1)
O(4)—Cd—N(2)	131.2(3)	C(1)—C(6)—C(5)	121(2)
O(6)—Cd—N(1)	161.4(4)	N(2)—C(8)—C(9)	119(1)
O(6)—Cd—N(2)	91.0(4)	N(2)—C(8)—C(13)	118(1)
N(1)—Cd—N(2)	91.8(3)	C(9)—C(8)—C(13)	122(1)
Cd—S(1)—C(2)	95.2(4)	S(2)—C(9)—C(8)	116.7(8)
Cd—S(1)—C(7)	102.1(5)	S(2)—C(9)—C(10)	122.9(9)
C(2)—S(1)—C(7)	104.4(6)	C(8)—C(9)—C(10)	120(1)
C(9)—S(2)—C(14)	104.5(6)	C(9)—C(10)—C(11)	121(1)
Cd—O(1)—N(3)	100.2(8)	C(10)—C(11)—C(12)	118(1)
Cd—O(3)—N(3)	89.7(7)	C(11)—C(12)—C(13)	122(1)
Cd—O(4)—N(4)	86.3(7)	C(8)—C(13)—C(12)	116(1)
Cd—O(6)—N(4)	108.4(7)		

Least squares planes and lines

	Plane or line	Maximum deviation (Å)	Out of plane (Å)
I	N(2), S(1), O(1), Cd	0.26(1)	
II	N(1), N(2), S(1), O(6)	0.26(1)	Cd 0.57(2)
III	C(2), S(1), C(7)		
IV	Cd—S(1)		
V	C(9), S(2), C(14)		
VI	Cd—S(2)		

Angle between normals to planes and lines (°).

III, IV	14.8(3)
V, VI	41.1(3)

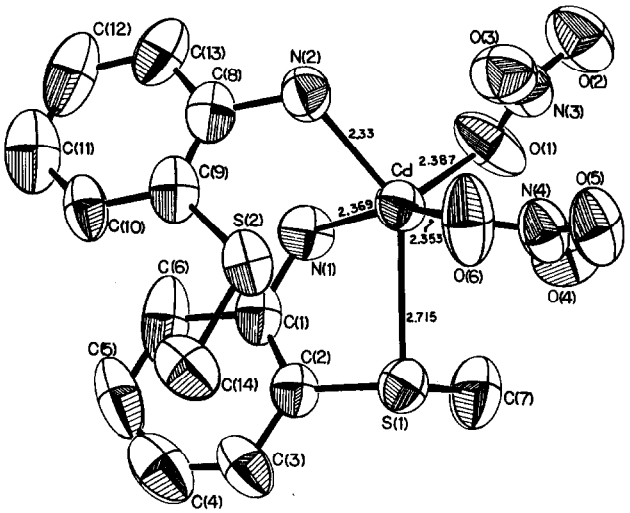


Fig. 1. An ORTEP[58] view of an isolated molecule of dinitratobis(methylmercaptoaniline)Cd(II). The bonded distances to Cd are shown, but the others are deleted for simplicity. The notation is consistent with the tables. The ellipsoids are drawn at the 50% probability level.

environment about the Cd atom may be described as distorted trigonal bipyramidal, with N(1) and O(6) being the axial ligands, or as a distorted square pyramid with O(1) as the apical atoms. In either description there seems to exist a weak Cd—S(2) interaction at 3.118(3) Å. The relative merits of these two descriptions may be seen from the sum of the angles around Cd. In what would be the equatorial plane in the TBP description, the sum is 353° (Table 2) and the analysis of the least squares plane of the equatorial plane atoms shows that (Table 2) Cd is displaced toward O(6) by 0.26 Å whereas the other three atoms are ~0.1 Å toward N(1). The N(1)—Cd—O(6) angle is 161.4(4)° rather than the ideal value of 180°. In the square pyramid description, N(2) and S(1) are ~ 0.2 Å on one side of the best least squares plane of N(1), N(2), S(1) and N(1) and O(6) are ~ 0.2Å on the other side with Cd 0.57 Å from the plane on the same side as N(1) and O(6). There is some preference for the trigonal bipyramidal description of the Cd environment. Trigonal bipyramidal Cd(II) has also been previously observed[46–49,52] and tetragonal pyramidal Cd(II) has also been observed.[50,51]

The most surprising feature of the structure is the fact that S(2) at 3.118(3) Å is only weakly bonded to Cd! The orientation of the mercapto group supports this view of little Cd—S covalent bonding. Considering cadmium's preference for sulfur coordination, this is most unusual. However, two other cases of non-sulfur bonding[53,54] have been reported but these involve carboxylate groups which are much better complexing agents than the nitrate ion. The shortest Cd—O(NO_3) distances of 2.387(9) and 2.353(9) Å are somewhat longer than those observed in tetrahedral dinitratobis(tetramethylthiourea)Cd(II)[41] at 2.290(4), 2.299(4) Å but shorter than the 2.42(1) Å average in dinitratobis(α,α'-dipyridyl)Cd(II).[39] The next closest set of Cd—O distances are Cd—O(3) 2.517(9) and Cd—O(4) 2.71(1) Å. The latter must have very little covalent bonding associated with it and arises primarily from the orientational packing properties of that nitrate group. On the other hand, considering the Cd—O(3) distance of 2.517(9) Å, although longer by 0.13 Å than the longest of the Cd—O "bonded" distances in this structure, its exclusion from the coordination sphere is somewhat arbitrary. However, it no doubt contributes to the distortion of the N(1)—Cd—O(6) angle from the ideal value of 180°. It is to be noted that the next longest Cd—O distances in dinitratobis(tetramethylthiourea) are at 2.68 (1) Å.[41]

The angle between the normal to the C(2), S(1), C(7) plane and Cd—S(1) of 14.8(3)° is close to the 19° expected for the utilization of a pure sulfur sp^3 lone pair in forming the Cd—S bond. In fact, one would expect this angle to be somewhat less than 19° due to repulsions between lone pair electrons. The analogous angle for the C(9)—S(2)—C(14) normal and the Cd—S(2) line is 41.1(3)°.

Unfortunately, although we originally made the compound to study ^{113}Cd NMR of sulfur nitrogen coordinated Cd complexes, the solution NMR spectra is difficult to observe due to exchange processes. The CP/MAS ^{113}Cd NMR is complex and beset with technical problems at this time.

Nevertheless, the structure is of some interest, particularly since in this case Cd prefers coordination to oxygen of nitrate rather than to the sulfur atom.

Acknowledgements—We wish to thank the PHS for research support with Grant GM-27721 and the NSF-supported regional NMR center at the University of South Carolina (CHE 78-18723) and Colorado State University (CHE 78-18581) for their help, discussions and assistance with the ^{113}Cd NMR data.

REFERENCES

1. F. Chlebowski and J. E. Coleman, *Metal Ions in Biological Chemistry* (Edited by H. Sigel), **6**, 1–140 (1976).
2. T. Boiwe and C. Brandon, *Eur. J. Biochem.* 1977, **77**, 173.
3. H. Eklund, B. Nordström, E. Zeppezauer, G. Söderlund, I. Ohlsson, T. Boiwe, B. O. Söderberg, O. Tapia and C. I. Branden, *J. Mol. Biol.* 1976, **102**, 27.
4. (a) D. E. Drum, J. H. Harrison, T. K. Li, J. L. Bethune and B. L. Vallee, *Proc. Nat. Acad. Sci. USA* 1967, **57**, 1434. (b) D. E. Drum, T. K. Li and B. L. Vallee, *Biochemistry* 1969, **8**, 3792. (c) D. E. Drum and B. L. Vallee, *Biochemistry* 1970, **9**, 4078.
5. A. Quiocho and W. N. Lipscomb, *Adv. Protein Chem.* 1971, **25**, 1.
6. K. Kannan, B. Nostrand, K. Fridborg, S. Lövgren, A. Ohlsson and M. Petef, *Proc. Nat. Acad. Sci. USA* 1975, **72**, 51.
7. (a) J. R. Knox and H. W. Wycoff, *J. Mol. Biol.* 1973, **74**, 533. (b) J. M. Sowadski, B. A. Foster and H. W. Wycoff, *J. Mol. Biol.* 1981, **150**, 245.
8. J. S. Richardson, K. A. Thomas, B. H. Rubin and D. C. Richardson, *Proc. Nat. Acad. Sci. USA* 1975, **72**, 1349.
9. Y. Boulanger, C. M. Goodman, C. P. Forte, S. W. Fesik and I. M. Armitage, *Proc. Nat. Acad. Sci. USA* 1983, **80**, 1501.
10. J. McD. Armstrong, D. V. Meyer, J. A. Verpoorte and J. T. Edsall, *J. Biol. Chem.* 1966, **241**, 5137.
11. I. M. Armitage, R. T. Pajer, A. J. M. Schoot Uiterkamp, J. F. Chlebowski and J. E. Coleman, *J. Am. Chem. Soc.* 1976, **98**, 5710.
12. J. F. Chlebowski, I. M. Armitage and J. E. Coleman, *J. Biol. Chem.* 1977, **252**, 7053.
13. J. L. Sudmeier and S. J. Bell, *J. Am. Chem. Soc.* 1977, **99**, 4499.
14. I. M. Armitage, A. J. M. Schoot Uiterkamp, J. F. Chlebowski and J. E. Coleman, *J. Magn. Reson.* 1978, **29**, 375.
15. T. Drakenberg, B. Lindman, A. Cave and J. Parello, *FEBS Lett.* 1978, **92**, 346.
16. D. B. Bailey, P. D. Ellis, A. D. Cardin and W. D. Behnke, *J. Am. Chem. Soc.* 1978, **100**, 5236.
17. P. J. Sadler, A. Bakka and P. J. Beynon, *FEBS Lett.* 1878, **94**, 315.
18. A. Cave, J. Parello, T. Drakenberg, E. Thulin and B. Lindman, *FEBS Lett.* 1979, **100**, 148.
19. J. D. Otvos and I. M. Armitage, *J. Am. Chem. Soc.* 1979, **101**, 7734.
20. S. Forsen, E. Thulin and H. Lilja, *FEBS Lett.* 1979, **104**, 123.
21. B. R. Bobsein and R. J. Myers, *J. Am. Chem. Soc.* 1980, **102**, 2454.
22. D. B. Bailey, P. D. Ellis and J. A. Fee, *Biochem.* 1980, **19**, 591.
23. N. B. H. Jonsson, L. A. Tibell, J. L. Evelhoch, S. J. Bell and J. L. Sudmeier, *Proc. Nat. Acad. Sci. USA* 1980, **77**, 3269.
24. J. D. Otvos and I. M. Armitage, *Biochemistry* 1980, **19**, 4031.
25. A. J. M. Schoot Uiterkamp, I. M. Armitage and J. E. Coleman, *J. Biol. Chem.* 1980, **255**, 3911.
26. S. Forsen, E. Thulin, T. Drakenberg, J. Krebs and K. Seamon, *FEBS Lett.* 1980, **117**, 189.
27. J. P. Otvos and I. M. Armitage, *Proc. Nat. Acad. Sci. USA* 1980, **77**, 7094.
28. J. L. Evelhoch, D. F. Bocian and J. L. Sudmeier, *Biochemistry* 1981, **20**, 4951.
29. B. R. Bobsein and R. J. Myers, *J. Biol. Chem.* 1981, **256**, 5313.
30. P. Linse, H. Gustavsson, B. Lindman and T. Drakenberg, *J. Magn. Reson.* 1981, **45**, 133.
31. T. Andersson, T. Drakenberg, S. Forsen and E. Thulin, *Eur. J. Biochem.* 1982, **126**, 501.
32. Y. Boulanger and I. M. Armitage, *J. Inorg. Biochem.* 1982, **17**, 147.
33. Y. Boulanger, I. M. Armitage, K. Miklossy and D. R. Winge, *J. Biol. Chem.* 1982, **257**, 13717.
34. E. O. Martins and T. Drakenberg, *Inorg. Chim. Acta* 1982, **67**, 71.
35. J. L. Sudmeier, S. J. Bell, M. C. Storm and M. F. Dunn, *Science* 1981, **212**, 560.
36. E. A. H. Griffith and E. L. Amma, *J. Chem. Soc., Chem. Commun.* 1979, 1013.
37. P. F. Rodesiler, E. A. H. Griffith, P. D. Ellis and E. L. Amma, *J. Chem. Soc. Chem. Commun.* 1980, 492.
38. P. F. Rodesiler and E. L. Amma, *J. Chem. Soc., Chem. Commun.* 1982, 182.
39. R. W. Turner, P. F. Rodesiler and E. L. Amma, *Inorg. Chim. Acta* 1982, **66**, L12.
40. P. F. Rodesiler, R. W. Turner, N. G. Charles, E. A. H. Griffith and E. L. Amma, *Inorg. Chem.* 1984, **23**, 999.
41. E. A. H. Griffith, N. G. Charles, P. F. Rodesiler and E. L. Amma, *Acta Cryst.* 1983. **C39**, 331.
42. E. A. H. Griffith, N. G. Charles and E. L. Ammma, *Acta Cryst*, 1982, **B38**, 202.
43. R. W. Turner, N. G. Charles and E. L. Amma, *Cryst. Struct. Comm.* 1982, **11**, 241.
44. N. G. Charles, E. A. H. Griffth, P. F. Rodesiler and E. L. Amma, *Inorg. Chem.* 1983, **22**, 2717.
45. P. F. Rodesiler, E. A. H. Griffith, N. G. Charles and E. L. Amma, *Acta Cryst* (in press).
46. P. L. Orioli and M. Ciampolini, *J. Chem. Soc., Chem. Commun.* 1972, 1280.
47. W. Clegg and P. J. Wheatley, *J. Chem. Soc., Dalton Trans.* 1973, 90.

48. G. R. Clark and J. D. Orbell, *J. Chem. Soc., Chem. Commun.* 1975, 697.
49. H. B. Burgi, H. Gehrer, P. Strickler and F. K. Winkler, *Helv. Chim. Acta* 1976, **59**, 2558.
50. M. Cannas, G. Carta, A. Cristini and G. Marongiu, *J. Chem. Soc., Dalton Trans.* 1976, 210.
51. G. R. Clark and J. D. Orbell, *Acta Cryst.* 1978, **B34**, 1815.
52. M. G. B. Drew and S. Hollis, *Acta Cryst.* 1978, **B34**, 2853.
53. P. DeMeester and D. J. Hodgson, *J. Am. Chem. Soc.* 1978, **100**, 6884.
54. R. J. Flook, H. C. Freeman, C. J. Moore and M. L. Scudder, *J. Chem. Soc., Chem. Commun.* 1973, 753.
55. B. A. Frenz, *Enraf–Nonius Structure Determination Package*, 1980, Version 17, with local modifications.
56. J. M. Stewart, *The X-ray System*, 1979, Tech. Rep. TR-445 Computer Science Center, University of Maryland, College Park, Maryland.
57. *International Tables for X-ray Crystallography* (Edited by C. H. MacGillavry and G. D. Rieck), Vol. 3, pp. 201–244 Kynock Press, Birmingham, U.K.
58. C. K. Johnson, *ORTEP II*, 1970. Report ORNL-3794. Oak Ridge National Laboratory, Tennessee.

Polyhedron Vol. 4, No. 4, pp. 621–622, 1985
Printed in Great Britain

0277–5387/85 $3.00 + .00
Pergamon Press Ltd

ALKALI-METAL TETRAFLUOROMANGANATE(III) MONOHYDRATES, $AMnF_4 \cdot H_2O$ (A = Rb OR Cs)

M. N. BHATTACHARJEE, M. K. CHAUDHURI,* H. S. DASGUPTA and A. KATHIPRI

Department of Chemistry, North-Eastern Hill University, Shillong 793 003, India

(*Received* 4 *August* 1983; *accepted after revision* 7 *June* 1984)

Abstract—Deep brown crystalline $AMnF_4 \cdot H_2O$ have been synthesized from the reactions of $KMnO_4$ with AHF_2 (A = Rb or Cs) and 40% HF at *ca* 100°C, and also from the reaction of MnO(OH) with AHF_2 and 40% HF. Characterisation and assessment of molecular structure of the compounds were made.

We have reported recently[1,2] the synthesis and structural assessment of A_2MnF_5 (A = NH_4, Na, K or Cs) compounds. In this paper we report the synthesis of $AMnF_4 \cdot H_2O$ (A = Rb or Cs) achieved from the reaction of MnO_4^- or MnO(OH) with AHF_2 and 40% HF, at relatively higher temperatures, without making use of any reducing agent or MnF_3.

EXPERIMENTAL

All chemicals were of reagent grade. MnO(OH)[3] and AHF_2[4] were prepared by the literature methods.

Magnetic susceptibility, IR and reflectance spectral measurements were made by the methods described in one of our previous papers.[5]

Synthesis

Since the two methods developed for the synthesis of the title compounds are general, only two typical procedures are described.

Method 1. Finely powdered $KMnO_4$ (6.3 m mol) and AHF_2 (12.6 m mol) were separately dissolved in 40% HF (total 400–500 m mol) by slightly warming over a steam-bath, and then mixed together. The resulting dark pink solution was heated on a steam-bath first until crystals began to appear, and then for an additional 2 h. The reaction container was cooled in a freezer for *ca.* 7 h. The deep brown crystallized $AMnF_4 \cdot H_2O$ was separated by decanting and dried by placing between folds of a filter paper, and then stored in a sealed polythene capsule. The yield of $RbMnF_4 \cdot H_2O$ was 88% and that of $CsMnF_4 \cdot H_2O$ was 79%.

Method 2. This method of synthesis was similar to that of the method 1 except that freshly prepared MnO(OH) was used instead of $KMnO_4$. The yields of $RbMnF_4 \cdot H_2O$ and $CsMnF_4 \cdot H_2O$ obtained by this method were 82% and 81% respectively.

Found: Rb, 36.51; Mn, 23.57; F, 32.53%. $RbMnF_4 \cdot H_2O$ requires: Rb, 36.46; Mn, 23.44; F, 32.42%. IR (cm^{-1}): ν_{Mn-F}, 600 m; ν_{Mn-F}, 530 s; ν_{O-H}, 3465 s; δ_{H-O-H}, 1640 m. Reflectance spectral data (cm^{-1}): $^5B_{1g} \rightarrow {}^5A_{1g}$, 12,100; $^5B_{1g} \rightarrow {}^5B_{2g}$, 18, 400; $^5B_{1g} \rightarrow {}^5E_g$, 21,700. μ (299 K), 4.9 BM.

Found: Cs, 47.29; Mn, 19.54; F, 26.85%. $CsMnF_4 \cdot H_2O$ requires: Cs, 46.15; Mn, 19.49; F, 26.96%. IR (cm^{-1}): ν_{Mn-F}, 600 m; ν_{Mn-F}, 535 s; ν_{O-H}, 3460 m; δ_{H-O-H}, 1642 m. Reflectance spectral data (cm^{-1}): $^5B_{1g} \rightarrow {}^5A_{1g}$, 12,000; $^5B_{1g} \rightarrow {}^5B_{2g}$, 18,850; $^5B_{1g} \rightarrow {}^5E_g$, 22,800. μ(299 K), 5.1 BM.

Elemental analyses and chemical determination of oxidation state of manganese were accomplished by standard methods.[5]

RESULTS AND DISCUSSION

In the course of our previous studies,[1,2] we observed that the heating of 40% HF solutions of A_2MnF_5 (A = NH_4, Na, K or Cs) at *ca.* 100°C, in order to concentrate, reproduced the crystalline A_2MnF_5 compounds only when the cation A^+ was NH_4^+, Na^+ or K^+ but not Cs^+. Instead the Cs^+ salt gave a deep brown crystalline compound with the atomic ratio Mn : F as 1 : 4. Accordingly, the reaction of $KMnO_4$ or MnO(OH) with AHF_2

* Author to whom correspondence should be addressed.

(A = Cs or Rb) and 40% HF at *ca.* 100°C produced deep brown crystalline compounds of the type $AMnF_4 \cdot H_2O$.

The compounds can be stored undecomposed in sealed polyethylene capsules. The chemically estimated oxidation states of manganese lie between 2.9 and 3.1, and the room temperature magnetic moments of $RbMnF_4 \cdot H_2O$ and $CsMnF_4 \cdot H_2O$ were found to be 4.9 and 5.1 B.M. respectively in conformity with those reported for the salts of the alleged tetrafluoromanganate(III) ion.[6,7] The IR spectra of the two salts resemble each other very closely with their most prominent feature being the absorptions at 600 and $\sim 530\,cm^{-1}$ which have been assigned to manganese–fluorine vibrations.[8–10] The typical pattern implies the presence of an octahedral or a distorted octahedral environment around manganese(III) in the complex ion (cf. the analysis of ν_{M-F} in MF_6^{n-} complexes).[1,2,8] The two extra vibrations at *ca.* 1640 and *ca.* 3460 cm^{-1} resemble in their shapes and positions those observed for the $K_2MnF_5 \cdot H_2O$[11] enabling us to infer that each of the newly synthesized compounds contains one molecule of uncoordinated water. The reflectance spectra of the compounds exhibit bands at $\sim$ 12,000, $\sim$ 18,500 and $\sim$ 22,000 cm^{-1} which have been assigned to the transitions $^5B_{1g} \rightarrow {}^5A_{1g}$, $^5B_{1g} \rightarrow {}^5B_{2g}$ and $^5B_{1g} \rightarrow {}^5E_g$ respectively[12] owing to the appreciably large splitting of ^5E_g ground state of Mn^{3+} in the complex ion as a consequence of Jahn–Teller effect. Thus it is evident that the effective field around manganese(III) in the complex ion is most probably D_{4h} which it attained through a polymeric structure involving *trans*-linked —F—Mn—F— chains.

Acknowledgement—We gratefully acknowledge the award of a UGC fellowship by the University to M.N.B.

REFERENCES

1. M. N. Bhattacharjee, M. K. Chaudhuri, H. S. Dasgupta and D. T. Khathing, *J. Chem. Soc., Dalton Trans.* 1981, 2587.
2. M. N. Bhattacharjee, M. K. Chaudhuri, H. S. Dasgupta, A. Kathipri and D. T. Khathing, *Synth. React. Inorg. Met.-Org. Chem.* 1982, **12**, 485.
3. G. Brauer (Ed.), *Handbook of Preparative Inorganic Chemistry*, Vol. 2, p. 1457. Academic Press, London (1965).
4. M. K. Chaudhuri and P. K. Choudhury, *Chem. Ind. (London)* 1978, 88.
5. M. N. Bhattacharjee and M. K. Chaudhuri, *Polyhedron* 1984, **3**, 599.
6. R. Hoppe, W. Daehne and W. Klemm, *Ann. Chim.* 1962, **658**, 1.
7. R. Hoppe, W. Liebe and W. Daehne, *Z. Anorg. Allg. Chem.* 1961, **307**, 276.
8. R. D. Peacock and D. W. A. Sharp, *J. Chem. Soc.* 1962, 2762.
9. A. Sebatine and L. Sacconi, *J. Am. Chem. Soc.* 1964, **86**, 17.
10. J. R. Allan, R. H. Nuttal and D. W.A. Sharp, *J. Inorg. Nucl. Chem.* 1965, **27**, 1305.
11. A. J. Edwards, *J. Chem. Soc. A* 1971, 2653.
12. T. S. Davis, J. P. Fackler, Jr. and T. J. Weeks, *Inorg. Chem.* 1968, **7**, 1994.

Polyhedron Vol. 4, No. 4, pp. 623–627, 1985
Printed in Great Britain

0277-5387/85 $3.00 + .00
© 1985 Pergamon Press Ltd

SPECIFIC EFFECTS OF SIMPLE ORGANIC SULPHONATE ANIONS ON THE MERCURY ION-ASSISTED AQUATION OF CHLOROCOBALT(III) COMPLEXES: DEVIATIONS FROM THE PRIMARY SALT EFFECT

MASAYASU IIDA*
Department of Chemistry, Faculty of Science, Nara Women's University, Nara 630, Japan

and

HIDEO YAMATERA
Department of Chemistry, Faculty of Science, Nagoya University, Nagoya 464, Japan

(*Received* 4 *October* 1983; *accepted after revision* 7 *June* 1984)

Abstract—Kinetic effects of various 1–1 electrolytes on the $CoClL_n^{2+} + Hg^{2+}$ reaction (L_n: neutral ligands) were studied with varying concentrations of the added electrolytes (0.025–1.0 mol dm^{-3}). Unusual deviations from the expected primary salt-effects have been observed in the reactions of the complexes containing bipyridine or phenanthroline in the presence of simple organic sulphonate ions. The results were interpreted in terms of the Guggenheim equation for the activity coefficients of the reactants and the activated complexes, and the specific effects were attributed to the hydrophobic interactions between the complex cations and the sulphonate anions.

The rate of a second-order reaction between two cations or two anions generally increases with increasing ionic strength according to the primary salt effect.[1] In the presence of long-chained alkane sulphonates and polyalkanesulphonates, the Hg^{2+}-assisted aquation of $[CoCl(NH_3)_5]^{2+}$ is drastically accelerated and this extreme case in the salt effects can be attributed to the large negative potentials on the polyanions.[2,3] On the other hand, the polysulphonate anions are much less effective on the electron-transfer reaction between $[Co(phen)_3]^{2+}$ and $[Co(phen)_3]^{3+}$.[4] This unusual effect was attributed to the hydrophobic interaction between the phenanthroline complexes and the polyanions.

No studies have been reported, however, for the effects of simple organic electrolytes on the reactions between cations. The present paper reports the study of the specific effects of simple organic sulphonate ions on the Hg^{2+}-assisted aquation of *cis*-$[CoCl(OH_2)(bpy)_2]^{2+}$ and of *cis*-$[CoCl(OH_2)(phen)_2]^{2+}$, comparing them with the effects of these anions on similar reactions of $[CoCl(NH_3)_5]^{2+}$, *cis*-$[CoCl(NH_3)(en)_2]^{2+}$, and *cis*-$[CoCl(py)(en)_2]^{2+}$. The specific effects of the added anions will reveal the specific interactions between the complex cations and the added anions during the reaction.

EXPERIMENTAL

Cobalt(III) complexes

The complexes, $[CoCl(NH_3)_5](ClO_4)_2$, *cis*-$[CoCl(NH_3)(en)_2](ClO_4)_2$, *cis*-$[CoCl(py)(en)_2](ClO_4)_2$, and *cis*-$[CoCl(OH_2)(phen)_2](ClO_4)_2$ were prepared by the published methods.[5–8] The complex *cis*-$[CoCl(OH_2)(bpy)_2](ClO_4)_2$ was obtained from *cis*-$[CoCl_2(bpy)_2]Cl \cdot 2H_2O$ in a manner similar to that for the preparation of the corresponding phenanthroline complex.

A preparation of *cis*-$[CoCl(NH_3)(bpy)_2](ClO_4)_2$ was made as follows. To a solution of *cis*-$[CoCl_2(bpy)_2]Cl$ (1 g) in methanol (50 cm^3) was added dropwise a concentrated aqueous ammonia (2–3 cm^3) at −20°C until the colour of the solution changed from purple to red. Perchloric acid (*ca* 10 mol dm^{-3}) was added (2–3 cm^3) to control the pH value to 1–2. When the solution was left at room temperature, a fine crystalline precipitate separated out which was assigned to $[CoCl(NH_3)(bpy)_2](ClO_4)_2 \cdot 2H_2O$ by elemental analysis. Found: C,

* Author to whom correspondence should be addressed.

36.21; H, 3.39; N, 10.29%. Calc: C, 36.4; H, 3.49; N, 10.6%. Absorption maximum, 522 nm ($\log \varepsilon = 1.75$).

Chemicals

Sodium methanesulphonate was prepared by neutralizing methanesulphonic acid with a sodium carbonate solution. The crystalline product was then obtained in a rotating evaporator. Found: C, 10.41; H, 2.54%. Calc. for CH_3SO_3Na: C, 10.17; H, 2.56%. Sodium benzenesulphonate, an extra pure reagent of Nakarai Chemicals Ltd., was recrystallized from water–methanol solution and dried at 80°C. Methanol was dried through a column of Molecular Sieve Type 3A and then distilled. Sodium perchlorate was prepared by neutralizing perchloric acid with a sodium hydroxide solution.

Kinetic runs

Each kinetic run was carried out under a pseudo-first-order condition with a solution containing 1.13×10^{-2} mol dm^{-3} $Hg(ClO_4)_2$ and 1.0×10^{-3} mol dm^{-3} of a cobalt(III) complex.[9]* The kinetic measurements were made at 25 ± 0.1°C with a Shimadzu UV-210A spectrophotometer. The pH values of the reaction solutions were controlled to 2.0 ± 0.2. (The pH values were slightly changed with the addition of the salts.) The reaction showed no pH dependency in this region.

The spectra of the final reaction solutions agreed with those of the aquated complexes (with aqua substituted for chloro ligand), and no by-products were detected by SP-Sephadex column chromatography. The decrease in the concentration of the chloro cobalt(III) complex was followed at 270 nm for $[CoCl(NH_3)_5]^{2+}$, at 290 nm for *cis*-$[CoCl(NH_3)(en)_2]^{2+}$, at 310 nm for *cis*-$[CoCl(py)(en)_2]^{2+}$, at 550 nm for *cis*-$[CoCl(OH_2)(bpy)_2]^{2+}$, and at 410 nm for *cis*-$[CoCl(OH_2)(phen)_2]^{2+}$.

RESULTS AND DISCUSSION

Fundamental kinetic studies have already been reported[9–11] for the reactions studied here except for those of *cis*-$[CoCl(OH_2)(bpy)_2]^{2+}$, *cis*-$[CoCl(OH_2)(phen)_2]^{2+}$, and *cis*-$[CoCl(NH_3)(bpy)_2]^{2+}$. The reactions, *cis*-$[CoCl(OH_2)(bpy)_2]^{2+} + Hg^{2+}$ and *cis*-$[CoCl(OH_2)(phen)_2]^{2+} + Hg^{2+}$, go to completion in about 3 h when $[Hg^{2+}] = 10^{-2}$ mol dm^{-3}, and the spectrum changes with isosbestic points at 502 and 428 nm for the former reaction and at 513 and 445 nm for the latter. All the reactions studied here can then be expressed as follows.

$$CoClL_n^{2+} + Hg^{2+} \xrightarrow[H_2O]{k} CoOH_2L_n^{3+} + HgCl^+$$

$$-\frac{d[CoClL_n^{2+}]}{dt} = k[CoClL_n^{2+}][Hg^{2+}] \quad (1)$$

$$k_{obs} = k[Hg^{2+}] \quad (2)$$

where L_n is the neutral ligands.

The *cis*-$[CoCl(NH_3)(bpy)_2]^{2+} + Hg^{2+}$ reaction proceeds very slowly and the spectrum of the reaction solution showed no detectable change in several days even when $[Hg^{2+}] = 0.1$ mol dm^{-3}.† Therefore, kinetic salt effect could not be studied for this reaction.

Figures 1–3 show the effects of the various reagents on the reactions. In explaining the results, we notice the following facts. Firstly both the methanesulphonic acid and the benzenesulphonic acid are strong acids and their salts are completely dissociated into ions in the present pH regions. Secondly no cobalt(III) complexes with the methanesulphonate or benzenesulphonate ligand were detected throughout the reactions. Then, these sodium sulphonates can be considered to be simple and inert 1–1 electrolytes. According to the Debye–Brønsted equation, simple 1–1 electrolytes largely accelerate 2+–2+ reactions and the pseudo-first-order rate constant (k_{obs}) can be expressed as a

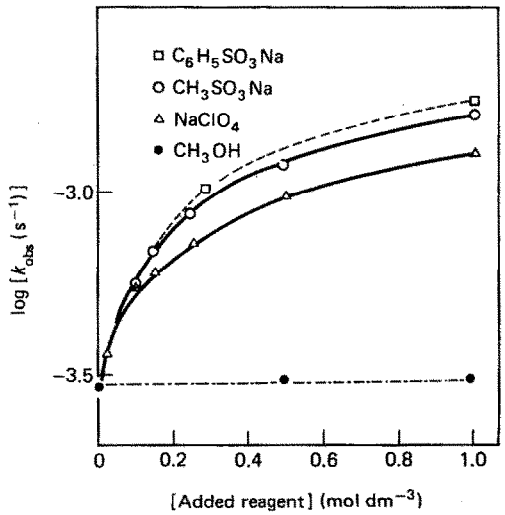


Fig. 1. Effects of the added salts (and methanol) on the $[CoCl(NH_3)_5]^{2+} + Hg^{2+}$ reaction.

* As the solubility of the phenanthroline complex is less than 1.0×10^{-3} mol dm^{-3} when $NaClO_4$ is present in more than 0.5 mol dm^{-3}, the concentration of the complex was around 5×10^{-4} mol dm^{-3} in such cases.

† The complex rapidly hydrolysed in an ammoniacal solution (pH 9) and the final reaction solution contained free chloride ions equimolar with the cobalt(III).

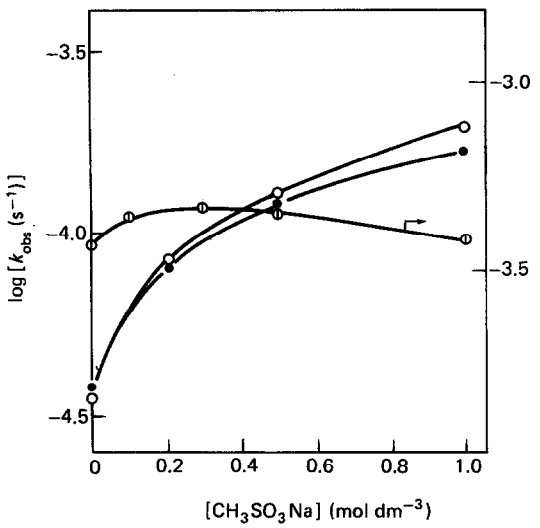


Fig. 2. Effects of CH_3SO_3Na on the *cis*-$[CoCl(NH_3)(en)_2]^{2+}+Hg^{2+}$ (○), the *cis*-$[CoCl(py)(en)_2]^{2+}+Hg^{2+}$ (●), and the *cis*-$[CoCl(OH_2)(bpy)_2]^{2+}+Hg^{2+}$ (◑) reactions.

function of the concentration (c) of the added salts, i.e.

$$\log k_{obs} = \log k_0 + 8A\frac{\sqrt{c}}{1+\sqrt{c}} \quad (3)$$

where k_0 is the rate constant at infinite dilution and A is the Debye–Hückel parameter (0.521 at 25°C, in water). The effects of 1–1 electrolytes qualitatively followed equation (3); the effects of the sulphonate anions on the *cis*-$[CoCl(OH_2)(bpy)_2]^{2+}+Hg^{2+}$ and *cis*-$[CoCl(OH_2)(phen)_2]^{2+}+Hg^{2+}$ reactions are exceptions. The anomalous effect of the sulphonates may be attributed to hydrophobic interaction between the organic sulphonate ions and the coordinated bpy or phen. However, the fact that methanol had no substantial effect on the reactions shows that the effect of the sulphonate ions cannot be attributed to a simple hydrophobic interaction, but can be understood to arise from cooperative hydrophobic and electrostatic interactions.

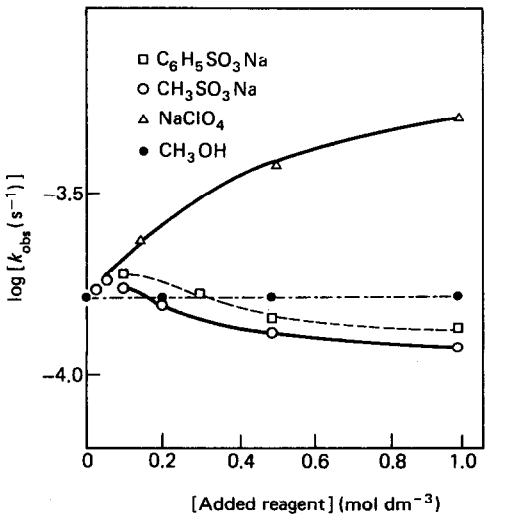


Fig. 3. Effects of the added reagents on the *cis*-$[CoCl(OH_2)(phen)_2]^{2+}+Hg^{2+}$ reaction.

In order to numerically express the specific effects of the anions we use the Guggenheim equation for the activity coefficients (y_i):

$$\log y_i = -Az_i^2\frac{\sqrt{c_j}}{1+\sqrt{c_j}} + \sum_j B_{ij}c_j \quad (4)$$

where z_i is the charge number of the ith ion and B_{ij} is the coefficient of specific interaction between the ith and jth ions.

As the sizes of the complex cations used here are widely ranged and the contribution of the reactants to the ionic strength cannot be neglected, the following equation will be appropriate in the place of equation (4),

$$\log y_i = -Az_i^2\frac{\sqrt{c_j+0.037}}{1+Ba\sqrt{c_j+0.037}} + \sum_j \beta_{ij}c_j \quad (5)$$

where a is the closest distance of approach of the complex cation with the added anion, B is the Debye–Hückel B parameter, and β_{ij} is the refined coefficient of specific interaction between the i and j ions. The rate constants of the reaction between M cations and N cations can be expressed as:

$$\log k_{obs} = \log k_0 + \frac{8A\sqrt{c_A+0.037}}{1+Ba\sqrt{c_A+0.037}} + (\beta_{MA}+\beta_{NA}-\beta_{XA})c_A \quad (6)$$

where β_{MA}, β_{NA}, and β_{XA} are the specific interaction coefficients of the M cation, the N cation, and the activated complex with the supporting A anion, respectively. In the present case, the M cation denotes the cobalt(III) complex and the N cation the mercury ion, respectively. We can assume that β_{NA} is nearly zero and that the value of β_{XA} can be approximated as a function of only β_{MA}, because it seems no remarkable specific interaction between Hg^{2+} and the anions used here. Then, β_{XA} is taken as $\lambda\beta_{MA}$ where λ is a constant.

Equation (6) is reduced to equation (7)

$$\log k' = \log k_{obs} - \frac{4.17\sqrt{c_A+0.037}}{1+0.329\mathring{a}\sqrt{c_A+0.037}} = \log k_0 + (1-\lambda)\beta_{MA}c_A \quad (7)$$

where $\mathring{a}$ is defined as $a/10^{-10}$ m.

The value of $\mathring{a}$ in equation (7) can be estimated

Table 1. Specific interaction coefficients, $(1-\lambda)\beta_{MA}$, between the cobalt(III) complexes (M^{2+}) and the anions (A^-)

Complex cation	A^-		
	ClO_4^-	$CH_3SO_3^-$	$C_6H_5SO_3^-$
$[CoCl(NH_3)_5]^{2+}$	−0.12	0.04	0.06
cis-$[CoCl(NH_3)(en)_2]^{2+}$		−0.04	
cis-$[CoCl(py)(en)_2]^{2+}$		−0.07	−0.23
cis-$[CoCl(OH_2)(bpy)_2]^{2+}$		−0.7±0.1	
cis-$[CoCl(OH_2)(phen)_2]^{2+}$	−0.02±0.1	−1.6±0.2	−1.4±0.2

from the ionic radii of the metal complexes and that of Hg^{2+}. It seems reasonable to take $\mathring{a} = 6$ for $[CoCl(NH_3)_5]^{2+}+Hg^{2+}$, *cis*-$[CoCl(NH_3)(en)_2]^{2+}+Hg^{2+}$, and *cis*-$[CoCl(py)(en)_2]^{2+}+Hg^{2+}$ systems, and $\mathring{a} = 7$–9 for *cis*-$[CoCl(OH_2)(bpy)_2]^{2+}+Hg^{2+}$ and *cis*-$[CoCl(OH_2)(phen)_2]^{2+}+Hg^{2+}$ systems. The values of the left-hand side of equation (7) are plotted against c_A as in Figs 4–6 and so the slope of the linear part of the plot gives $(1-\lambda)\beta_{MA}$. The results are listed in Table 1. As all the reaction systems are of the same type, including a dipositive complex ion, a uninegative anion, and an Hg^{2+} ion, the value of $\lambda\beta_{MA}$ reflects the specific interaction between the anion and the complex ion. Large negative values of $-\lambda\beta_{MA}$ seem to indicate that the hydrophobic interaction between the metal complexes and the added anions will prevent the metal complexes from contacting with the mercury ions.

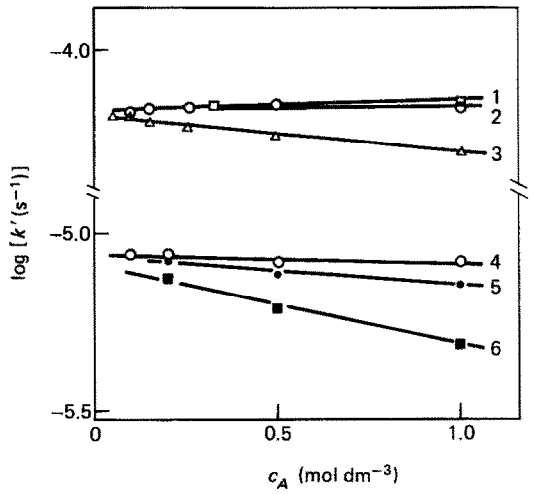


Fig. 4. Determination of $(1-\lambda)\beta_{MA}$ from log k' vs c_A plots. (I) $[CoCl(NH_3)_5]^{2+}+Hg^{2+}$ in the presence of $C_6H_5SO_3Na$ (1), CH_3SO_3Na (2), and of $NaClO_4$ (3); $[CoCl(NH_3)(en)_2]^{2+}+Hg^{2+}$ in the presence of CH_3SO_3Na (4); *cis*-$[CoCl(py)(en)_2]^{2+}+Hg^{2+}$ in the presence of CH_3SO_3Na (5), and of $C_6H_5SO_3Na$ (6).

In order to clarify the specific role of the sulphonate ions we have determined the activation parameters of the *cis*-$[CoCl(OH_2)(phen)_2]^{2+}+Hg^{2+}$ reaction in the presence of $CH_3SO_3^-$ or ClO_4^- by changing temperatures, 25–45°C. Table 2 shows the results. Addition of sodium perchlorate greatly decreases both the activation enthalpy and the activation entropy. It can be explained as is the case for the anion effects on the $[CoF(NH_3)_5]^{2+}+Al^{3+}$ reaction.[12] That is, the presence of ClO_4^- is electrostatically advantageous to the approach of the two reactant cations to each other and so the

Table 2. Salt effects on the activation parameters for the *cis*-$[CoCl(OH_2)(phen)_2]^{2+}+Hg^{2+}$ reaction

	$\Delta H^{\ddagger}$ (kJ mol^{-1})	$\Delta S^{\ddagger}$ (J K^{-1} mol^{-1})
No salt added (I = 0.04 mol dm^{-3})	107±5	41±10
1 mol dm^{-3} $NaClO_4$	55±3	−122±15
1 mol dm^{-3} CH_3SO_3Na	99±4	10±18

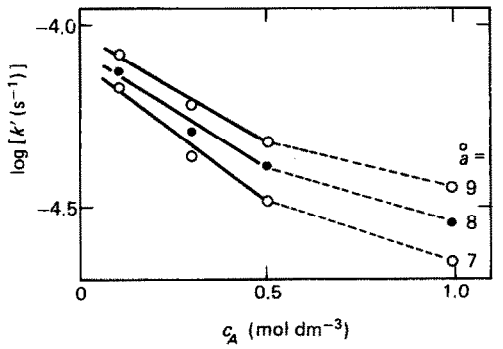


Fig. 5. Determination of $(1-\lambda)\beta_{MA}$ from log k' vs c_A plots. (II) *cis*-$[CoCl(OH_2)(bpy)_2]^{2+}+Hg^{2+}$ in the presence of CH_3SO_3Na.

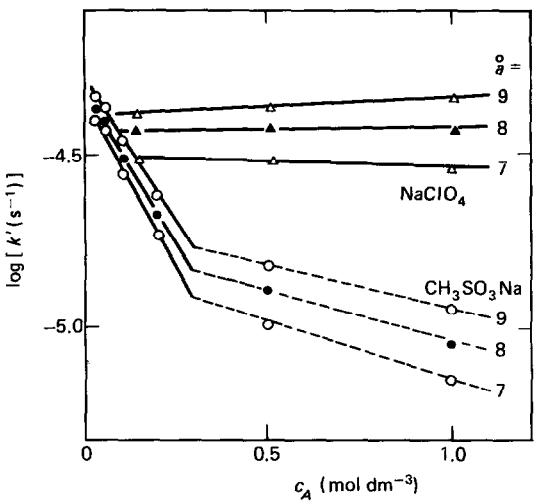


Fig. 6. Determination of $(1-\lambda)\beta_{MA}$ from log k' vs c_A plots. (III) *cis*-$[CoCl(OH_2)(phen)_2]^{2+} + Hg^{2+}$ in the presence of $NaClO_4$ and of CH_3SO_3Na.

activation enthalpy is depressed, while the activation entropy is decreased as a result of ClO_4^- sterically hindering the reactant cations from contacting each other.

When $CH_3SO_3^-$ is present, the effect on the activation parameters becomes appreciably smaller. The activation entropy shows that the probability to form the activated complex containing $CH_3SO_3^-$ is higher than in the case of ClO_4^-. On the other hand, the larger value of the activation enthalpy in the former case reveals that the activated complex containing the anion is more unstable than in the latter case. This tendency gives the following information on the structure of the activated complex with considering the hydrophobic interaction between the metal complexes and $CH_3SO_3^-$ (Fig. 7): $CH_3SO_3^-$ will predominantly be present in the part of the phenanthroline ligand of the cobalt(III) complex by the hydrophobic interaction and will not so largely prevent Hg^{2+} from approaching to the chloride ligand in the cobalt(III) complex as is the case of ClO_4^-. This entropic effect will result in making the two reactant cations approach more closely, and therefore, the electrostatic repulsion between the two cations makes the activated complex more unstable. This enthalpic disadvantage overcomes the entropic advantage and then the reaction rate becomes significantly smaller than the case where ClO_4^- is added.

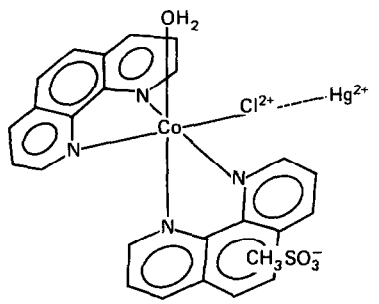


Fig. 7. A proposed structure of the activated complex for the *cis*-$[CoCl(OH_2)(phen)_2]^{2+} + Hg^{2+}$ reaction in the presence of $CH_3SO_3^-$.

In conclusion, we revealed that even the simple organic sulphonate ions such as $CH_3SO_3^-$ and $C_6H_5SO_3^-$ specifically affect the reaction containing the bipyridine or the phenanthroline complex as a reactant and it can be attributed to the hydrophobic interaction between the added anions and the metal complexes.

REFERENCES

1. A. A. Frost and R. G. Pearson, *Kinetics and Mechanism*, p. 150. Wiley, New York (1961).
2. H. Morawetz and B. Vogel, *J. Am. Chem. Soc.* 1969, **91**, 563.
3. J.-R. Cho and H. Morawetz, *J. Am. Chem. Soc.* 1972, **94**, 375.
4. S. Brückner, C. Crescenzi and F. Quadrifoglio, *J. Chem. Soc.* (*A*) 1970, 1168.
5. W. A. Hynes, L. K. Yanowski and M. Shiller, *J. Am. Chem. Soc.* 1938, **60**, 3053.
6. S. M. Jørgensen, *J. Prak. Chem.* 1890, **41**, 454.
7. J. C. Bailar, Jr. and L. B. Clapp, *J. Am. Chem. Soc.* 1945, **67**, 171.
8. M. P. Hancock, J. Josephensen and C. E. Schäffer, *Acta Chem. Scand.* 1976, **A30**, 79.
9. D. A. Buckingham, I. I. Olsen and A. M. Sargeson, *Aust. J. Chem.* 1967, **20**, 597.
10. C. Bifano and R. G. Link, *Inorg. Chem.* 1968, **7**, 908.
11. S. W. Foong, B. Kipling and A. G. Sykes, *J. Chem. Soc.* (*A*) 1971, 118.
12. M. Iida, M. Ando and H. Yamatera, *Bull. Chem. Soc. Jpn* 1982, **55**, 1446.

Polyhedron Vol. 4, No. 4, pp. 629–632, 1985
Printed in Great Britain

0277–5387/85 $3.00 + .00
Pergamon Press Ltd

STUDIES ON IRON(III) COMPLEX WITH 5,6-DIAMINO-1,3-DIMETHYLURACIL

YOSHIHISA OKAMOTO,* HIROKO AMEMIYA and TOSHIO KINOSHITA
School of Pharmaceutical Sciences, Kitasato University, 5-9-1, Shirokane, Minato-ku, Tokyo 108, Japan

and

MICHIKO SHIRAI and YOSHIO MATSUMOTO
Department of Chemistry, Faculty of Hygienic Sciences, Kitasato University, 1-15-1, Kitasato, Sagamihara City, Kanagawa Prefecture 228, Japan

(*Received* 27 *February* 1984; *accepted* 7 *June* 1984)

Abstract—Reaction of 5,6-diamino-1,3-dimethyluracil (DDU) with iron(III) ion gave a fine blue colouration due to the formation of $Fe[(DDU—H)_3]\cdot 2HClO_4$. An oxidation product (7), $C_{12}H_{12}N_6O_4$, was also isolated from the reaction mixture.

Since von Euler and Martius[1] reported a strong reducing agent named reductone in 1933, many reducing agents have been reported as this kind of von Euler's reductone. The structure of the reductone is characterized as enediol conjugated with carbonyl group (Scheme 1). Some of enediamines, enedithiols, enaminols, and enaminothiols have also been reported to be reducing agents like enediols.[2] One of features of the reductone is a fine blue colouration which is unstable and brought about by iron(III) ions.[3] However, there is no report of such a blue colouration on enediamine reductones. In the course of synthesizing purine analogues from uracil derivatives,[4] we found that DDU as enediamine reductone reacted with iron(III) ions to bring about a fine blue colouration accompanied by oxidation. Although the blue substance in the colouration is very unstable in the solutions like that of enediol reductone, we were able to isolate the blue substance as a powder.

EXPERIMENTAL

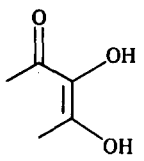
All organic chemicals except **4** were synthesized. Elementary analyses (C, H, N) were carried out on a Perkin–Elmer 240B instrument. The X-ray fluorescence analyses (Cl, Fe) were performed on a Rigaku Geiger Flex 3063P instrument by the method of Kawashima and Matsumoto.[5]† Iron and nitrogen were also determined on a Shimadzu Atomic Absorption/Flame Emission Spectrophotometer (AA-630-02), and by the method of Kjeldahl, respectively. The IR spectra were run on a Shimadzu IR-G spectrophotometer.

Synthesis of the blue complex: tris(5,6-diamino-1,3-dimethyl-1,2,3,4-tetrahydropyrimidin-2,4-dionato) iron(III) *diperchlorate* (**6**)

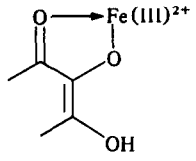
A solution of $Fe(ClO_4)_3\cdot 6H_2O$ (0.8 g, 1.7 mmol) in 10 cm^3 of ethanol was added to a solution of DDU monohydrate (0.3 g, 1.6 mmol) in 50 cm^3 of ethanol with stirring at room temperature. After 8 min, a blue powder precipitated was collected by filtration, washed with small volume of ethanol, and dried in a vacuum desiccator. Yield 60 mg (14.7%), mp > 300°C. The above filtrate was allowed to stand for 3 days to precipitate crystals of compound **7** in 37% yield (90 mg). [The blue complex **6** was also obtained in similar yield when the reduced amount of $Fe(ClO_4)_3\cdot 6H_2O$ (0.1 g, 0.2 mmol) was employed in the above experiment.] Found: C, 28.18; H, 3.57; N, 21.81%. Calc. for $C_{18}H_{29}Cl_2Fe_1N_{12}O_{14}$: C, 28.29; H, 3.82; N, 22.0%. The blue complex **6** (about 20 mg)

* Author to whom correspondence should be addressed.

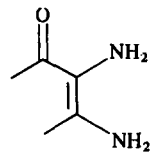
† The sample solution (20 μl) was spotted on a cellophane film and after drying it on air, the X-ray fluorescence analyses were carried out.



Reductone



Iron (III) complex (blue)



Enediamine reductone

Scheme 1.

was dissolved in 5 cm^3 of both water and 0.1 N HCl solution in order to determine the elemental ratio between Cl and Fe, and between Fe and N, respectively, using the analytical methods described above. Fe: Cl: N = 1.00: 2.06: 11.9.

RESULTS AND DISCUSSION

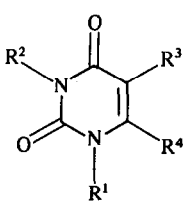
Colouration

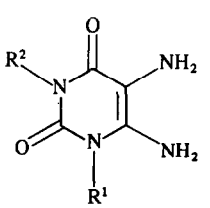
When a solution of DDU in water was treated with iron(III) chloride, a fine blue (λ_{max} 656 nm) appeared simultaneously, and the colour disappeared gradually. This blue colouration was independent of counter anions of the iron(III) salts. The blue colouration was not observed in the solution of DDU both above pH 8 and below pH 3. In general, the blue complex is somewhat more stable in organic solvents such as alcohols, acetonitrile, and tetrahydrofuran than in water, and the decolourizing rate in water is dependent on pH values of the solutions, the higher, the faster. Namely, the blue complex becomes somewhat stable in an acidic solution which is adjusted below pH 3 after the colouration. Iron(II) salts such as chloride, sulphate and perchlorate gave no colouration with DDU. When excess of hydrogen peroxide was added to the mixed solution of DDU and iron(II) salts, the blue colour developed immediately: addition of 1 drop of hydrogen peroxide (30%) to a mixed solution of DDU (0.01 g) and iron(II) sulphate (0.01 g) in 2 cm^3 of water brought about a fine blue colouration. When iron(III) salts were added to a solution of DDU in the presence of excess amount of ascorbic acid in water, the blue colouration did not occur. These results indicate that iron(III) ions are essential for the blue colouration with DDU.

In order to study the relation between structure and colouration, several uracil derivatives were reacted with iron(III) ions (Scheme 2). 5-Amino-1,3,6-trimethyluracil (**1**), 6-amino-1,3-dimethyluracil (**2**) and 6-amino-5-*N*-(2′,2′-dicyanovinyl)amino-1,3-dimethyluracil (**3**) did not show any colouration with iron(III) ions, however, 5,6-diamino-3-methyluracil (**5**) reacted with iron(III) ions to give a blue colouration. Hydrochloride salts of DDU and **5** did not afford the blue colouration but a red colouration in water. Similarly, when hemisulphate of 5,6-diaminouracil (**4**) reacted with iron(III) ions in water, a red colour gradually developed. These results indicate that free enediamine in DDU is essential for the blue colouration with iron(III) ions. This strongly corresponds to the fact that enediols conjugated with carbonyl group mostly show a blue colouration with iron(III) ions.[3]

Composition of the blue substance

Although the blue colouration is very unstable in its various solutions, we found that when DDU reacted with iron(III) perchlorate in ethanol, a small amount of blue powder was immediately precipitated from the blue coloured solution. The precipitates were collected, washed with a small volume of ethanol, and dried in a vacuum desiccator. Hereupon, it is worth noting that 1,3,6,8-tetramethyl - 2,4,5,7(1*H*,3*H*,6*H*,8*H*)pyrimido[5,4 - g]pteridine-

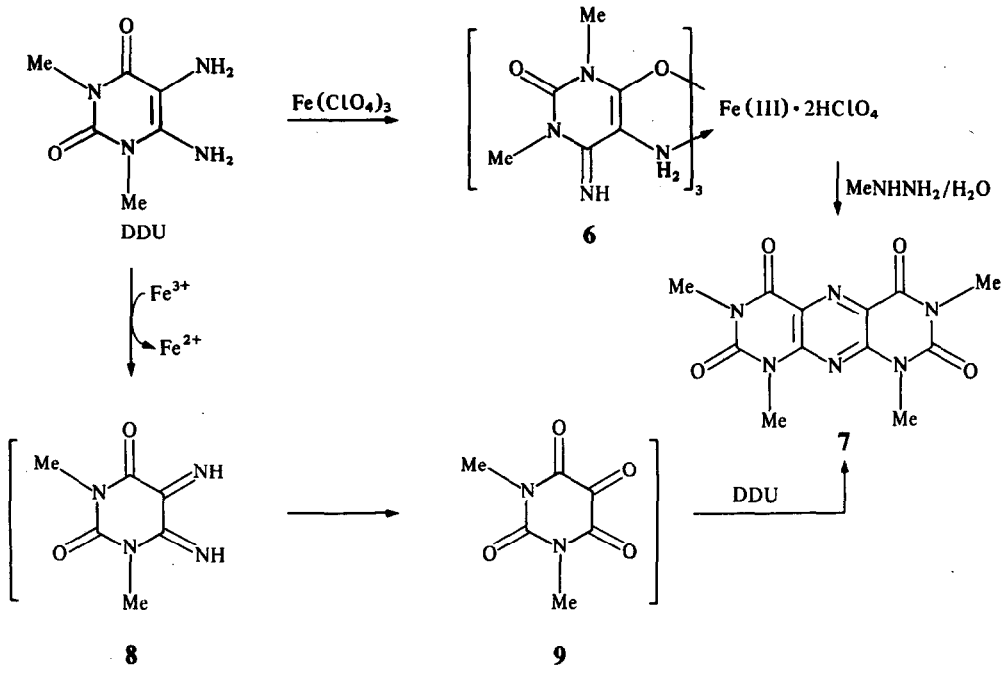




1 $R^1 = R^2 = R^4 = CH_3$, $R^3 = NH_2$
2 $R^1 = R^2 = CH_3$, $R^3 = H$, $R^4 = NH_2$
3 $R^1 = R^2 = CH_3$, $R^3 = -CH = C(CN)_2$, $R^4 = NH_2$

(DDU) $R^1 = R^2 = CH_3$
4 $R^1 = R^2 = H$
5 $R^1 = H$, $R^2 = CH_3$

Scheme 2.



Scheme 3.

tetrone (7) was only precipitated as crystals from the filtrate after a few days (Scheme 3). Compound 7 was identified by comparison with the authentic sample prepared by the method of Yoneda and Nishigaki.[6] The molecular formula of the blue substance was determined as $C_{18}H_{29}Cl_2Fe_1N_{12}O_{14}$ on the basis of the results of elementary analyses which were performed by the methods described in Experimental. It should be noted that the blue substance is very hygroscopic. The mass spectrum could not be obtained because of its non-volatility. The ^1H NMR spectrum showed signals at 3.33 and 3.43 ppm which might be attributed to methyl protons, although the resolution was very poor because of the iron(III) ion's paramagnetism.* The IR spectrum is shown in Fig. 1, where characteristic

*The spectra were run on a Varian T-60 (60 MHz) spectrometer with $(CD_3)_2SO$ as the solvent and $(CH_3)_4Si$ as the internal standard.

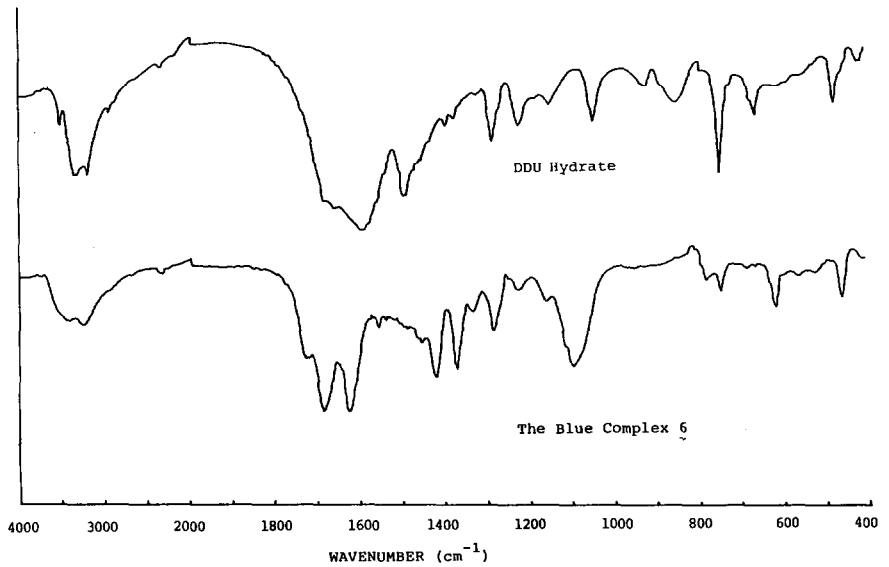


Fig. 1. The IR spectra of the blue complex (6) and DDU hydrate (in KBr pellet).

absorption bands for carboxamide amidine moiety [—C(=O)NMe— and —C(=NH_2^+)NMe—] were observed at 1685 and 1625 cm^{-1}.* The absorption bands of ferric perchlorate [$Fe(ClO_4)_3 \cdot 6H_2O$] at 1142 (strong), 1115 (s), 1090 (s), 638 (medium) and 628 (m) cm^{-1} may be due to the hydrogen bonded O—Cl bond whose absorption bands were observed at 1115 (s), 1099 (s) and 1070 (s) as a broad line, and 630 (weak) and 619 (m) cm^{-1} in the case of the blue substance. The shift to the lower wavelength of these absorption bands of the blue substance might be due to the hydrogen bonded O—Cl bond such as Cl—O···H—N. In addition to the above analytical results, the blue substance was hydrolyzed to determine its ligand. The blue substance was treated with methylhydrazine at room temperature to give **7** which did not afford any colouration with iron(III) ions. Since DDU itself is able to be converted to **7** by its self-condensation,[8] we propose DDU as the ligand of the blue complex, and determined it as $Fe[(DDU—H)_3] \cdot 2HClO_4$ (**6**).

Conclusion

As an enediamine reductone, DDU reacted with iron(III) ions like enediol reductones to give the blue complex **6** and compound **7**. The molar ratio of iron(III) ion to the ligand in **6** is 1 to 3. This is an interesting result since the blue colouration by the reaction of iron(III) ions with enediol reductone is due to the formation of a complex of which the molar ratio of iron(III) ion to the ligand is reported as 1 to 1.[2,3] The formation of **7** may be rationalized as shown in Scheme 3. DDU is oxidized with iron(III) ion to **8** which is further hydrolyzed to **9**. DDU, then, reacts with **8** and/or **9** to give **7** by loss of ammonia and/or water, respectively.

* A number of carboxamide–alkylamidine derivatives, R-$CONH(CH_2)_n$-$C(=NH_2^+)NH_2 \cdot Cl^-$ ($n = 1, 2$), were synthesized and their IR spectra were measured.

REFERENCES

1. H. von Euler and C. Martius, *Lieb. Ann.* 1933, **505**, 73.
2. H. von Euler and H. Hasselquist, *Reduktone*. T. Enke, Stuttgart (1950); D. Nomura, S. Adachi, K. Yamafuji and H. von Euler, *Chemie und Biochemie der Reduktone und Reduktonate und Biochemische Ergebniss an Ascorbinsaure*. Uchida Rokakuho, Tokyo, Japan (1960) (Japanese).
3. F. Arndt, L. Loewe and E. Ayca, *Chem. Ber.* 1952, **85**, 1150; A. E. Harvey, Jr. and D. L. Manning, *J. Am. Chem. Soc.* 1950, **72**, 4488; G. Schwarzenbach and A. Willi, *Helv. Chim. Acta* 1951, **34**, 528.
4. Y. Okamoto and T. Ueda, *Chem. Pharm. Bull.* 1976, **24**, 547.
5. T. Kawashima and Y. Matsumoto, unpublished results.
6. F. Yoneda and S. Nishigaki, *Chem. Pharm. Bull.* 1971, **19**, 1060.
7. T. Ueda, Y. Okamoto, T. Tsuji and M. Muraoka, *Chem. Pharm. Bull.* 1968, **16**, 2355.
8. W. Pfleiderer, *Angew. Chem.* 1956, **68**, 386.

Polyhedron Vol. 4, No. 4, pp. 633–641, 1985
Printed in Great Britain

0277-5387/85 $3.00 + .00
Pergamon Press Ltd

EPR AND ELECTRONIC ABSORPTION STUDIES OF Mn^{2+} ION IN $3CdSO_4 \cdot 8H_2O$ SINGLE CRYSTALS

N. SATYANARAYANA
Department of Physics, Indian Institute of Technology, Madras 600 036, India

(*Received* 27 *February* 1984; *accepted* 7 *June* 1984)

Abstract—EPR and electronic absorption spectra of the Mn^{2+} ion in $3CdSO_4 \cdot 8H_2O$ crystals have been studied at 300 K and 80 K. The EPR spectra have been analysed using the spin Hamiltonian for rhombic symmetry. The spin Hamiltonian g, A, B_2^0, B_4^0 and B_4^2 parameters were evaluated from the EPR analysis. The site symmetry of the Mn^{2+} ion in the lattice was also suggested for the two observed magnetic complexes. The characteristic features of the absorption spectrum showed splitting and better resolution of the absorption bands at 80 K than 300 K. By solving energy matrices corresponding to octahedral symmetry, band positions have been calculated. A good fit was obtained between the observed and calculated band positions for $Dq = 700\ cm^{-1}$, $B = 835\ cm^{-1}$, $C = 2982\ cm^{-1}$ and $\alpha = 76\ cm^{-1}$ values. By evaluating the above parameters, crystal field transitions were also assigned.

The EPR and electronic absorption spectra of the Mn^{2+} ion introduced into various crystalline materials have been the subject of a number of recent studies. Mn^{2+} (high spin system) is one of the most studied transition metal ions because of many interesting reasons.[1–5] The advantage of studying this ion is that it can easily exist in any of several symmetries and ligand environments. The EPR and electronic absorption spectra of Mn^{2+} ion can be observed at room temperature, because of large spin–lattice relaxation time. Since the Mn^{2+} ion has electron spin of 5/2, one would observe the zero field splitting. The zero field splitting parameter is highly sensitive to the local symmetry and ligand field environment. Using the Mn^{2+} ion as a probe and EPR as the experimental tool, one can study fairly accurately the symmetry of host lattices.[6–9]

In the high spin case, the ground state of Mn^{2+} will become $t_{2g}^3 e_g^2 ({}^6S)$ level. In the free ion state, the d^5 ion gives rise to a number of quartet and doublet excited levels and the transitions between these levels are spin forbidden. In octahedral symmetry one can get all the transitions from the sextet level to quartet and doublet levels. Generally, spin forbidden bands are weak in intensity and hence, the electronic absorption studies become interesting.[10,11] We have, therefore, attempted to study the EPR and electronic absorption of Mn^{2+} ion in the $3CdSO_4 \cdot 8H_2O$ lattice.

EXPERIMENTAL

Good quality single crystals of pure and Mn^{2+} ion doped $3CdSO_4 \cdot 8H_2O$ with well-defined morphology were grown by the slow evaporation method from the saturated aqueous solution. In order to get the impurity doped crystals a small amount (0.2 mol. to 4 mol. wt %) of $MnSO_4 \cdot H_2O$ (AR grade BDH company) powder was added to the saturated aqueous solutions. All Mn^{2+} doped crystals were pale pink in colour. Morphology of the host lattice did not change on increasing the concentration of the dopant. Single crystals of $3CdSO_4 \cdot 8H_2O$ were verified by X-ray diffractometer. The crystallographic $\bar{a}$, $\bar{b}$ and $\bar{c}$ axes were identified by taking oscillation photographs.

The $3CdSO_4 \cdot 8H_2O$ crystals belong to monoclinic system with space group $C_{2/c}$.[12] There are two chemically distinguishable Cd(Cd_I and Cd_{II}) atoms per unit cell and its unit cell dimensions are $a = 9.44$ Å, $b = 11.87$ Å, $c = 16.49$ Å and $\beta = 117°2'$. According to crystal structure, Cd_I (two) sites are at the special positions (1/4, μ, 0) while the Cd_{II} (four) atoms are at the general positions in the lattice; x, y, z; $x + 1/2, \bar{y}, z$; $x, y + 1/2, \bar{z}$; $\bar{x}, \bar{y}, z$. The Cd_I atoms at the special positions are completely equivalent, whereas the other Cd_{II} atoms at the general positions are inequivalent, thus, showing two magnetically inequivalent Cd_{II} atoms present in the lattice. In

the $3CdSO_4 \cdot 8H_2O$ lattice, Cd_I is surrounded by six oxygen ligands (two from the two water molecules and four from the four sulphate molecules) forming an approximately octahedral symmetry. Cd_{II} is also surrounded by six oxygen ligands but the symmetry is highly distorted octahedron.

EPR MEASUREMENTS

The EPR spectra were recorded at ambient temperature (300 K) on a VarianE-4 Spectrometer operating at X-band frequencies at about 9.45 GHz with a 100 kHz field modulation. The crystals were mounted at the end of the single circular goniometer which can fit onto the EPR rectangular cavity operating in TE_{102} mode. The EPR spectra were recorded about the three orthogonal $\bar{a}$, $\bar{b}$ and $\bar{c}^*$ axes in turn with an accuracy of $\pm 2°$ and spectra were recorded at every 10° for rotation about the three axes. Very little quantity of DPPH powder was used as a g-marker.

Electronic absorption spectra were recorded on a Cary-14 spectrophotometer. A cold finger type cryostat was used for recording the absorption spectra at low temperature (80 K). Complete calculations were made using the IBM 370/155 computer for the analysis of EPR and electronic absorption spectra.

EPR THEORY

The different crystal field effects on Mn^{2+} ion can be expressed in terms of different spin Hamiltonians.[13] In the present case, the symmetry of the spin Hamiltonian has been assumed to be rhombic. The spin Hamiltonian for rhombic symmetry is of the form;

$$\mathcal{H} = g\beta\bar{H}\cdot\bar{S} + B_2^0O_2^0 + B_2^2O_2^2 + B_4^0O_4^0 + B_4^2O_4^2 + A.\bar{I}.\bar{S} \quad (1)$$

where, B_n^m ($n = 0, 2, 4$ and $m = 0, 2, 4$ for d-orbitals) forms a set of empirical coefficients which can be calculated from the experimentally observed results. The crystalline electric field can be expressed as a series of terms of the spin operators (O_n^m) as described by Stevens.[14,15] In equation (1), the last term describes the hyperfine interaction and the first term gives the Zeeman energy of the Hamiltonian. When the molecular z-axis coincides with the external magnetic field, the off-diagonal terms in the energy matrix are small. Hence, we get the symmetric EPR spectrum about the $1/2 \rightarrow -1/2$ transitions as described by the first three terms in the spin Hamiltonian equation (1). However, when the magnetic field is along the molecular X and Y directions, the EPR spectrum will not be symmetric about $1/2 \rightarrow -1/2$ transitions. In these directions, the off-diagonal terms cannot be neglected as compared to the Zeeman splittings.[16] The energy level expressions have been derived using the second order perturbation theory for the allowed $M = \pm 1$ transitions.[17] The transition fields due to the hyperfine corrections are[18]

$$H_{Mm} = H_M - \frac{A_m}{g\beta} - \frac{A^2}{4g\beta} \times \left[\frac{F(M)f(-m)}{E_M - E_{M-1}} + \frac{F(-M)-f(m)}{E_M - E_{M+1}} - \frac{F(M-1)f(-m)}{E_{M-1} - E_{M-2}} - \frac{F(M+1)f(m)}{E_{M-1} - E_M}\right] \quad (2)$$

where E_m denotes energy level of M and

$$F(M) = (S+M)(S-M+1);$$

$$f(M) = (I+M)(I-M+1).$$

EPR STUDIES

Results

The EPR spectra of Mn^{2+} ion in $3CdSO_4 \cdot 8H_2O$ crystals at room temperature (300 K) have been recorded at regular intervals of 10° rotation about the three crystallographic orthogonal $\bar{a}$, $\bar{b}$ and $\bar{c}^*$ axes with an accuracy of $\pm 2°$. Figures 1–3 show the EPR spectra of Mn^{2+} ion recorded when the magnetic field ($\bar{H}$) is parallel to molecular Z-, Y- and X-axes respectively. These axes were found by searching directions corresponding to the maxima in the spread of the spectra in the three $\bar{a}\bar{b}$-, $\bar{b}\bar{c}^*$- and $\bar{c}\bar{a}^*$-planes. The direction in which the fine structure of five sextet lines has maximum separation is denoted as Z-axis spectrum. Similarly, the next consecutive maxima in the spectra were assigned to Y- and X-axes, spread in the X-axis spectrum found to be minimum and was approximately half of the spread of the Z-axis spectrum, which is perpendicular to ZY-plane. The Y-axis is perpendicular to ZX-plane and the spread of the spectrum was found to be three fourths of the spread of the Z-axis spectrum.

The observed angular variation spectra showed the existence of two different types of Mn^{2+} sites in the lattice with different intensity ratio (20:1). The lines with higher intensity correspond to site 1 and those with low intensity correspond to site 2. Site 2 could not be analysed because of the weak intensity of the lines. Complete analysis has been done only for the high intensity lines (site 1). Site 1 did not split but showed single site in all three planes.

Figure 4 shows the angular variation plot for the extreme sets of observed hyperfine lines (i.e. $M_s =$

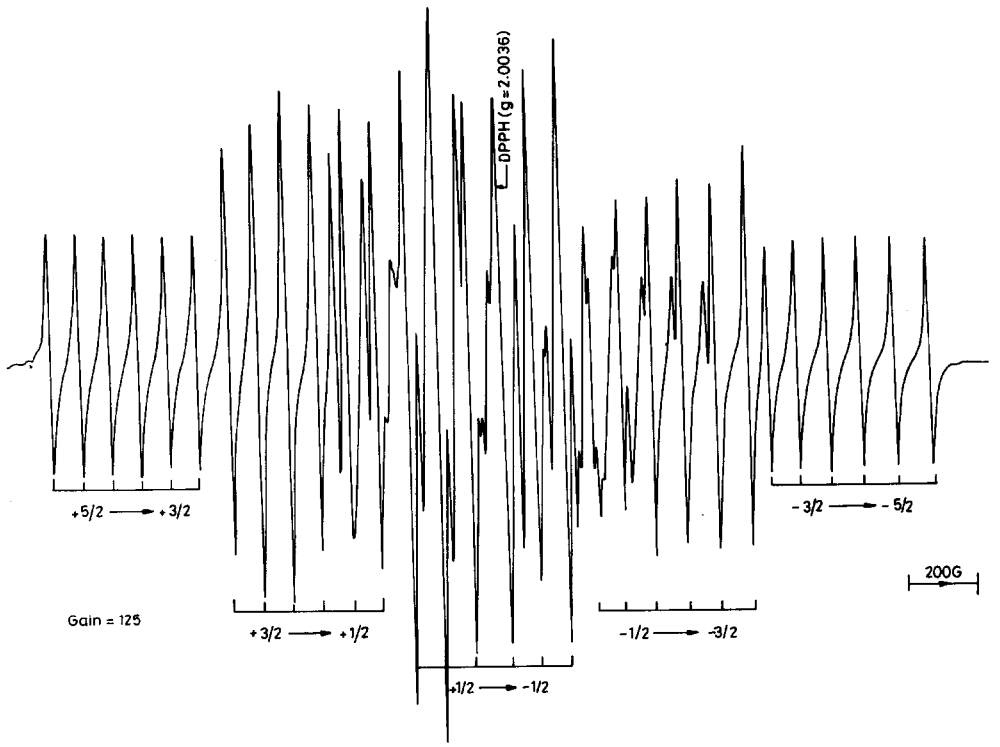


Fig. 1. EPR spectrum of $3CdSO_4 \cdot 8H_2O : Mn^{2+}$ crystal recorded at 300 K, where $\bar{H}$ is parallel to Z-axis in the ac^*-plane.

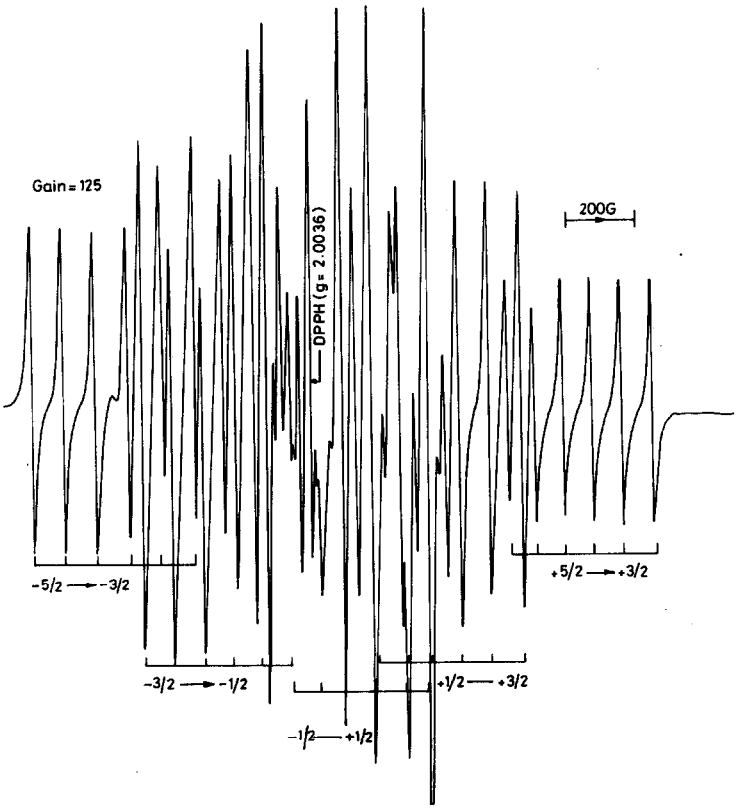


Fig. 2. EPR spectrum of Mn^{2+} doped $3CdSO_4 \cdot 8H_2O$ crystal recorded when $\bar{H}$ is parallel to Y-axis in the ab-plane.

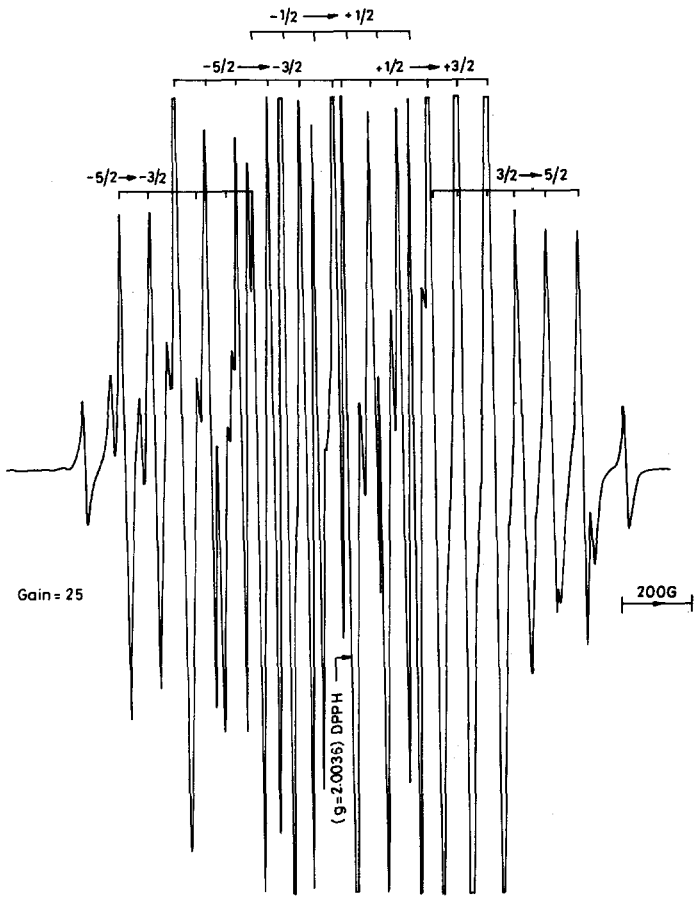


Fig. 3. EPR spectrum of Mn^{2+} ion in $3CdSO_4 \cdot 8H_2O$ crystal recorded when $\bar{H}$ is parallel to X-axis in the ac^*-plane.

$\pm 5/2 \rightarrow \pm 3/2$) in the ZX-plane of Mn^{2+} ion for site 1 in $3CdSO_4 \cdot 8H_2O$ lattice. The angular variation of the high field side resonance lines correspond to $M_s = -5/2 \rightarrow -3/2$, $M_I = 5/2, 3/2, 1/2, -1/2, -3/2$ and $-5/2$ transitions while the angular variation of low field side lines correspond to $M_s = +5/2 \rightarrow 3/2$, $M_I = 5/2, 3/2, 1/2, -1/2, -3/2$ and $-5/2$. The two extreme sets of six hyperfine lines are found to cross each other at about 54° and at 90° (along x-axis), the two transitions are completely reversed, i.e. low field set reached the high field side and the high field side hyperfine set reached the low field side. Again after 90°, the above two sets of six hyperfine lines were merged at 126°. Finally, at 180°, the two sets appear as observed at 0°. A similar behaviour of angular variation seen in the case of fine structure transitions (i.e. $M_s = 5/2 \rightarrow 3/2$, $3/2 \rightarrow 1/2$, $1/2 \rightarrow -1/2$, $-1/2 \rightarrow 3/2$ and $-3/2 \rightarrow -5/2$) and are shown in Fig. 5.

CALCULATION OF SPIN HAMILTONIAN PARAMETERS

Since the total spread of the EPR spectrum of Mn^{2+} is different in three directions, the observed angular variation spectra were analysed using rhombic spin Hamiltonian of the form given in equation (1) which is expressed in terms of Stevens operators. In order to evaluate the spin Hamiltonian parameters from the EPR spectra, the following iterative procedure has been used.

The fine structure positions from each set of six hyperfine lines are found, by taking the mean of the extreme hyperfine lines. The centre field (H_0) position of the spectrum has been calculated from the five fine structure field positions. The centre field has been eliminated by taking the pair of equations involving $\pm M_s$ transitions of each group. So, we get two equations which were in terms of B_2^0 and B_2^2 parameters. By solving the two equations, the values of B_2^0 and B_2^2 were obtained. Similarly, we can get other parameters B_4^0 and B_4^2 by substituting the B_2^0 and B_2^2 values in Y- and X-axes spectra respectively. By substituting the B_2^0, B_2^2, B_4^0 and B_4^2 values in the second order energy expressions, magnetic field positions were generated for all resonance lines. If the calculated magnetic fields do not coincide with the observed spectrum, another set of calculated field

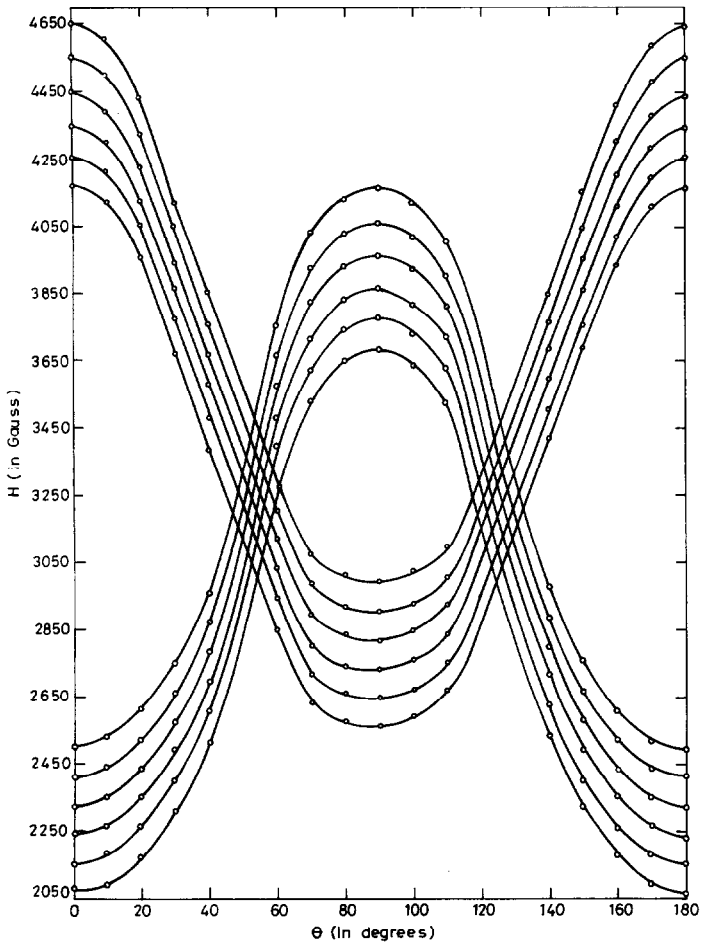


Fig. 4. An angular variation of the lowest and highest field hyperfine corresponding to the transitions ($M_s = \pm 5/2 \rightarrow \pm 3/2$) for Mn^{2+} ion in $3CdSO_4 \cdot 8H_2O$ crystal recorded when the magnetic field is varied in the ZX-plane.

positions are generated by taking the new set of B_2^0, B_2^2, B_4^0 and B_4^2 values. This procedure was repeated until a best fit between the observed and calculated resonance field positions is obtained. The best fit for the spin Hamiltonian parameters are given in Table 1. The principal g_{xx}, g_{yy}, g_{zz}, A_{xx}, A_{yy} and A_{zz} parameters have been obtained directly from the EPR spectra recorded along the three principal X-, Y- and Z-axes. The above measured parameters are found to be almost isotropic and are given in Table 1. Table 2, gives the observed and calculated resonance

Table 1. Spin-Hamiltonian parameters obtained from the EPR spectra of Mn^{2+} ion in $3CdSO_4 \cdot 8H_2O$ lattice

		$B_2^0 = 89.06$ G
$g_{zz} = 2.0095$	$A_{zz} = 90$ G	
		$B_2^2 = 24.66$ G
$g_{yy} = 2.0004$	$A_{yy} = 89.8$ G	$B_4^0 = -0.024$ G
$g_{xx} = 2.0065$	$A_{xx} = 90$ G	$B_4^2 = -0.185$ G

line positions for all the transitions, i.e. $M_s = \pm 5/2$, $\pm 3/2$ and $\pm 1/2$ along the Z-axis. Similarly, we have also calculated the resonance field positions for all transitions along the X- and Y-axes.

DISCUSSION

Since the Mn^{2+} ion has 5/2 spin, the five electrons will give rise to fine structure EPR lines and these arise because of the transition between the spin levels. The interest in the EPR spectra of Mn^{2+} is due to the spin transitions which are highly angular dependent and the angular variation follows the $(3\cos^2\theta - 1)$ rule. In Fig. 5, the five fine structure transitions become a single transition when the magnetic field is making an angle 54° to the Z-axis, i.e. at 54°56′ the $(3\cos\theta^2 - 1)$ term becomes zero. Hence, we get an almost merged single spectrum of six lines at 54°56′ which is shown in Fig. 4. At this angle all the spin or dipolar contributions along the

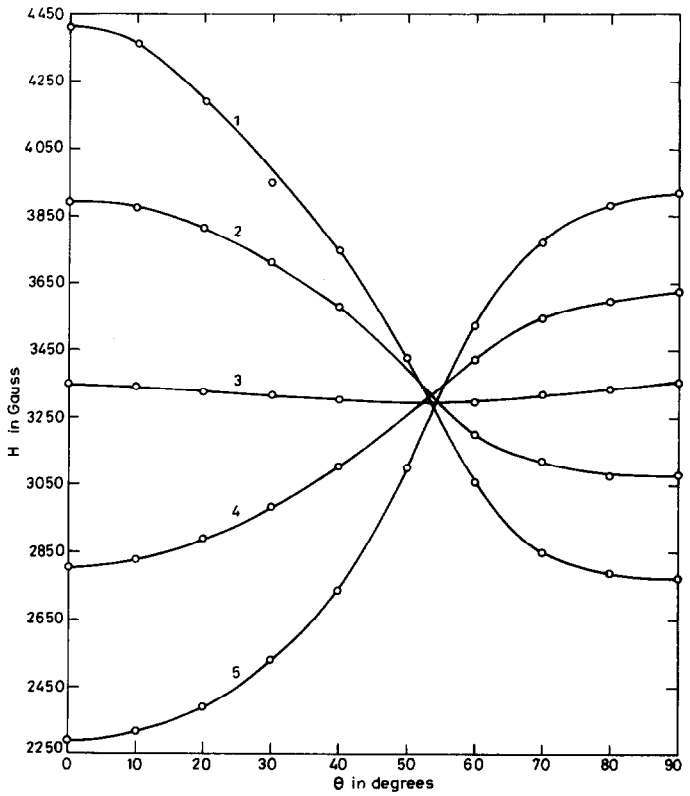


Fig. 5. Angular variation of the fine structure of the allowed quintet transitions of Mn^{2+} ion in $3CdSO_4 \cdot 8H_2O$ crystal, recorded when the magnetic field is varied in the ZX-plane.

Table 2. Observed and calculated transitions of magnetic field positions of Mn^{2+} ion in $3CdSO_4 \cdot 8H_2O$ lattice

Transition $M_s = \pm 1$	Observed (G)	Calculated (G)	Transition $M_s = \pm 1$	Observed (G)	Calculated (G)
	2070	2076		3120	3120
	2155	2161		3200	3200
$5/2 \rightarrow 3/2$	2240	2246	$+1/2 \rightarrow -1/2$	3291	3291
	2324	2331		3380	3380
	2410	2414		3476	3476
	2500	2497		3570	3563
	2591	2593		3659	3657
	2680	2681		3745	3743
$3/2 \rightarrow 1/2$	2764	2768	$-1/2 \rightarrow -3/2$	3832	3831
	2850	2854		3925	3922
	2930	2939		4020	4020
	3024	3023		4119	4112
	4172	4171			
	4260	4258			
$-3/2 \rightarrow -5/2$	4350	4358			
	4449	4443			
	4548	4540			
	4650	4642			

magnetic field are zero. The angular variation of five fine structure lines is shown in Fig. 5, which also behaved in a similar way as discussed. The observed EPR spectra can be interpreted on the basis of crystal structure of the host lattice. In the lattice, there are two chemically inequivalent cadmium atoms. If the Mn^{2+} ion enters the Cd_1 site, the EPR spectra should show single site in all orientations, whereas if it enters in Cd_2 site, the EPR spectra should show two sites, in general orientations and single site along the three crystallographic axes. Suppose, Mn^{2+} ion enters both the sites with equal population, then it will be highly complicated EPR spectrum as it has been observed in the case of VO^{2+} ion (high concentration) doped $3CdSO_4 \cdot 8H_2O$ lattice. In the present case, the site I did not show any splittings in any orientations and hence, the observed site is due to the replacement of Cd_1 site by Mn^{2+} ion in the lattice as observed in the case of VO^{2+} ion (low concentration) in $3CdSO_4 \cdot 8H_2O$ crystals.[18] Site 2 which appear in Z-axis spectrum, could be due to the substitution of Cd_2 site, because in other orientation, the above site was splitting, thus showing very small intensity of lines. Hence, site 2 could not be examined.

RELATIVE SIGNS OF A AND B_2^0

The relative signs of A and B_2^0 can be derived by correlating the observed hyperfine coupling separation in the high and low field sides. In the present case, the separation of the hyperfine coupling constant was found to be larger at high field (95.6 G) than that at low field side (85.2 G). Assuming A to be $-$ve, and B_2^0 to be $+$ve and vice versa, the resonance field positions have been calculated from the resonance field expressions given by Low[2] and compared with the observed field positions. In the present lattice, the observed spacing between the hyperfine lines coincide well with the calculated ones for $-$ve A and $+$ve B_2^0 values. Hence, the signs of A and B_2^0 are taken to be $-$ve and $+$ve respectively.

COVALENCY OF THE METAL–LIGAND BOND

The nature of bonding between the Mn^{2+} ion and its surroundings can be found by calculating the hyperfine coupling from the EPR spectrum. It has been reported that the hyperfine coupling constant decreases with increase in the degree of covalency.[19] In the present case, the average hyperfine coupling constant was found to be 90.5 G. The average covalency per bond for the complex has been estimated from the curve given by Simanek and Muller[20] and was found to be $\approx 7\%$ for the $Mn—O_w$ bond.

ELECTRONIC ABSORPTION STUDIES

The Mn^{2+} ion (d^5) has five unpaired electrons in the valency shell distributed in the t_{2g} and e_g orbitals in O_h symmetry. In the free ion state, it will give rise to a number of free ion terms with the increasing order of energy $^6S, {}^4G, {}^4P, {}^4D, {}^2I, {}^2G, {}^2H, {}^4F, {}^2D, {}^2F, {}^2F, {}^2S, {}^2D, {}^2G, {}^2P$ and ^2D. These levels can split further when the d^5 ion is placed into different crystal field environments.

The electronic absorption spectrum of the Mn^{2+} ion in $3CdSO_4 \cdot 8H_2O$ crystal has been studied at room temperature (300 K) and liquid nitrogen temperature 80 K in the region 6000–2500 Å which is shown in Fig. 6. The above figure has the characteristic features of Mn^{2+} ion in octahedral symmetry and showed eight absorption bands. On cooling down to liquid nitrogen temperature, the above spectrum was resolved and showed twelve absorption bands at 19,231, 23,255, 24,752, 24875, 27,472, 27,932, 28,169, 29,585, 32,467, 38,095, 38,855 and 43,478 cm^{-1} and almost all the bands showed small blue shifts. The above weak intensity bands are spin forbidden. In the present case, in octahedral symmetry all the optical transitions occur from sextet $^6A_{1g}$ ground state to all quartet and doublet levels. The observed spectrum was analysed assuming octahedral site symmetry. The energy matrices for octahedral symmetry were given by Orgel and Tanabe and Sugano.[21,22] These matrices involved the crystal field parameter Dq and the interelectronic repulsion parameters B and C. As can be seen in Fig. 6, some of the bands at 24,752, 24,875 and 29,585 cm^{-1} are sharp in intensity. The above sharp intensity bands are observed due to $^4A_{1g}(G)$, $^4E_g(D)$ and $^4E_g(G)$ energy level transitions respectively, because of their energy expressions are independent of Dq parameter. These transitions are useful to calculate the interelectronic repulsion B and C parameters.

In order to evaluate the crystal field parameter (Dq) and interelectronic repulsion parameters (B and C) diagonalisation method has been used to solve the energy matrices. To get the best fit, between experimentally observed and calculated energy positions a new parameter (α) has been introduced into the energy matrices as an element and called Trees correction.[24] The complete energy matrices inclusive of Trees correction have been given by Mehra.[25] First B and C parameters were calculated from the energy matrix corresponding $^4E_g(G, D)$ levels. The solved expressions for B and C from the

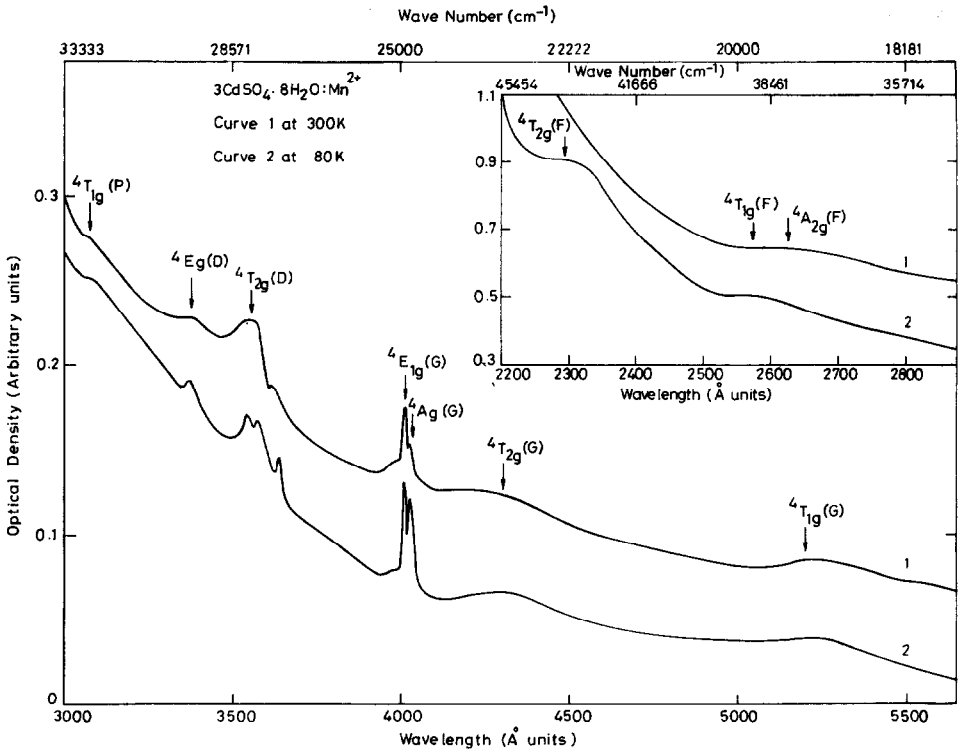


Fig. 6. The electronic absorption spectrum of Mn^{2+} ion in $3CdSO_4 \cdot 8H_2O$ crystal recorded in the visible and UV regions. Curve 1 recorded at 300 K: Curve 2 recorded at 80 K.

above levels are as follows:

$$B = \frac{94 \pm \sqrt{49(E_1 - E_2)^2 - 76S\alpha^2}}{49},$$

$$C = (E_1 + E_2 - 278 - 26)/10,$$

Table 3. Band positions and their assignments of transitions of Mn^{2+} ion in $3CdSO_4 \cdot 8H_2O$ lattice: $Dq = 700\ cm^{-1}$, $B = 835\ cm^{-1}$, $C = 2982\ cm^{-1}$ and $\alpha = 76\ cm^{-1}$

S. No.	Band position (cm^{-1}) Observed at 80 K	Calculated	Assignment of transition
1.	19,231	19,201	$^6A_{1g} \rightarrow {}^4T_{1g}(G)$
2.	23,255	23.124	$\rightarrow {}^4T_{2g}(G)$
3.	24,752	24,753	$\rightarrow {}^4A_{1g}(G)$
4.	24,878		$\rightarrow {}^4E_g(G)$
	27,472		
5.	27,932	28,049	$\rightarrow {}^4T_{2g}(D)$
	28,169		
6.	29,585	29,587	$\rightarrow {}^4E_g(D)$
7.	32,256	32,058	$\rightarrow {}^4T_{1g}(P)$
8.	38.095	38,226	$\rightarrow {}^4A_{1g}(E)$
9.	39,215	40,891	$\rightarrow {}^4T_{1g}(F)$
10.	43,478	43,323	$\rightarrow {}^4T_{2g}(F)$

where E_1 and E_2 are the respective transition energies of $^4E_g(D)$ and $^4E_g(G)$ levels. Using the experimentally observed energy values E_1 and E_2, B and C parameters have been evaluated to be 835 and 2982 cm^{-1} respectively. Using the B, C and α (for a free ion $\alpha = 76\ cm^{-1}$) values in the energy matrices, the band positions were calculated by diagonalisation method for different Dq values. Exact Dq value has been fixed from the good fit of the experimentally obtained band positions with the calculated ones and Dq value was found to be 700 cm^{-1}. Exact crystal field transitions were also assigned for all the observed bands. Table 3, gives the observed and calculated band positions along with their crystal field transitions.

The energy difference between the split components (27,472, 27,932 and 28,169 cm^{-1}) of the band at 28,049 cm^{-1} is compared with the calculated spin–orbit couplings for different transitions. The experimentally observed band splittings agree well with the calculated ones for $^2T_{2g}(D)$ level. Hence, the resolved fine structure is attributed to the spin–orbit splittings of the $^2T_{2g}(D)$ level at 80 K. The observed spin–orbit splittings are shown in a schematic energy level diagram (Fig. 7).

EPR results proved that the Mn^{2+} ion has substituted the Cd_1 site in the $3CdSO_4 \cdot 8H_2O$ lattice. In this case, the site symmetry of the ion

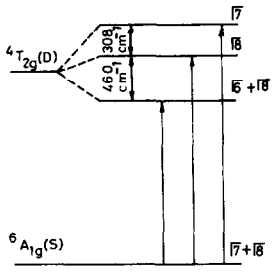


Fig. 7. The observed spin–orbit splittings of $^6A_{1g}(S) \rightarrow {}^4T_{2g}(D)$ band.

is expected to be approximately octahedral, but, although the observed electronic absorption spectrum could be fitted to octahedral, the electronic absorption bands could not be resolved further. This is purely because of weak intensity nature of the bands, which are all due to spin forbidden transitions. Hence, the electronic absorption results also suggest that the Mn^{2+} ion has entered the Cd_I site in the $3CdSO_4 \cdot 8H_2O$ lattice.

Acknowledgements—Thanks are due to Prof. S. Radhakrishna, Dr K. Harinaran and Dr Shakuntala Sastry for their helpful discussions and interest in this work.

REFERENCES

1. B. Bleaney and D. J. E. Ingram, *Proc. R. Soc.* 1965, **A205**, 336.
2. W. Low, *Paramagnetic Resonance in Solids*; Suppl. 2, pp. 57, 60 Academic Press, New York (1960).
3. H. A. Kuska and M. J. Rogers, *Radical Ions*. Interscience, New York (1968).
4. D. J. E. Ingram, *Proc. Phys.* 1953, **A66**, 412.
5. W. Low, *Phys. Rev.* 1957, **105**, 793.
6. A. K. Jain, *J. Phys. Chem. Solids* 1983, **44**, 535.
7. J. M. Baker, B. Bleaney and W. Hayes, *Proc. R. Soc.* 1958, **A247**, 141.
8. L. M. Matarese and C. Kikuchi, *J. Phys. Chem. Solids* 1956, **1**, 117.
9. G. D. Wakins, *Bull. Am. Phys. Soc.* 1957, **2**, 345.
10. A. B. P. Lever, *Inorganic Electronic Spectroscopy*. Elsevier, Amsterdam (1968).
11. J. S. Griffith, *The Theory of Transition Metal Ions*. Cambridge University Press, Cambridge, England (1961).
12. Babu Verghese and S. Srinivasan, *XIII National Conference on Crystallography*, March (1982).
13. K. W. H. Stevens, *Proc. Phys. Soc.* 1952, **A65**, 209.
14. B. Bleaney and K. W. H. Stevens, *Ret. Prog. Phys.* 1953, **160**, 108.
15. P. G. Nair, K. V. Lingam and R. Venkataraman, *J. Phys. Chem. Solids* 1968, **29**, 2183.
16. D. A. Jones, J. M. Baker and D. F. D. Popes, *Proc. Phys. Soc.* 1959, **74**, 249.
17. R. Lacriox, *Helv. Phys. Acta* 1957, **30**, 374.
18. N. Satyanarayana, *Ph.D. Thesis*, Indian Institute of Technology, Madras (1983).
19. J. S. Van Wieringen, *Disc. Faraday Soc.* 1955, **19**, 118,
20. E. Simanek and K. A. Muller, *J. Phys. Chem. Solids* 1969, **31**, 1027.
21. L. E. Orgel, *J. Chem. Phys.* 1955, **23**, 1004.
22. Y. Tanabe and S. Sugano, *J. Phys.* 1954, **9**, 53.
23. C. J. Ballhausen, *Introduction to Ligand Field Theory*. McGraw-Hill, New York (1962).
24. R. E. Trees, *Phys. Rev.* 1953, **83**, 756.
25. K. A. Mehra, *J. Chem. Phys.* 1968, **48**, 4384.

Polyhedron Vol. 4, No. 4, pp. 643–647, 1985
Printed in Great Britain

0277–5387/85 $3.00 + .00
© 1985 Pergamon Press Ltd

AN NMR STUDY OF THE COMPLEXES OF Zn(II) AND Cd(II) IONS WITH TRIS(DIMETHYLAMINO)PHOSPHINE SULPHIDE: LIGAND EXCHANGE KINETICS

K. ALOUANI and M. R. KHADDAR
Laboratoire de Chimie de Coordination en Solution, Département de Chimie, Faculté des Sciences de Tunis, Tunis, Tunisie

and

L. RODEHÜSER, P. R. RUBINI and J.-J. DELPUECH*
L.E.S.O.C., UA CNRS 406, Faculté des Sciences, Université de Nancy I, B.P. No. 239, 54506 Vandoeuvre-les-Nancy Cedex, France

(*Received* 17 *July* 1984; *accepted* 21 *August* 1984)

Abstract—The preparation of the complex species $[Cd(TDPS)_4](ClO_4)_2$ and $[Zn(TDPS)_4](ClO_4)_2$ (TDPS = tris(dimethylamino)phosphine sulphide) is described; their solutions in CD_2Cl_2 have been examined by ^{31}P and ^{35}Cl NMR. The ligand exchange mechanism for both complexes was found to be of the interchange type and the corresponding values for the rate constant and the activation parameters are $k(25°C) = (1.36 \pm 0.34) \times 10^5$ and $(1.35 \pm 0.35) \times 10^4$ s^{-1}; $\Delta H^{\neq} = (36.4 \pm 1.3)$ and $(40.9 \pm 2.5$ (kJ mol^{-1}; $\Delta S^{\neq} = (-24.6 \pm 5.8)$ and (-28.8 ± 10.3) J mol^{-1} K^{-1}; for the Cd and Zn complex respectively.

Information about the ligand substitution on Zn^{2+} and Cd^{2+} ions is relatively rare as a consequence of the great lability of their complexes in solution.[1] These ions however, particularly Zn^{2+}, are of great importance biologically. In their complexes Zn^{2+} and Cd^{2+} are commonly characterized by coordination numbers of 4, 5 and 6.[2] In the classification of Lewis acids,[3] Cd^{2+} is considered as soft and Zn^{2+} as "borderline". The Zn^{2+} ion therefore forms kinetically stable complexes with the hard Lewis bases hexamethylphosphoramide (HMPA),[4] nonamethylimidodiphosphoramide (NIPA)[5] and octamethylpyrophosphoramide (OMPA),[6] all containing the P=O group, as well as with soft bases like thiourea.[7] Ligand exchange kinetics could also be studied in the case of Cd^{2+} with the ligands NIPA[5] and OMPA.[6] It seemed interesting to compare the behaviour of the complexes of Zn^{2+} and Cd^{2+} with HMPA to those with thio-HMPA, tris(dimethylamino) phosphine sulphide (TDPS), in order to evaluate the influence of the substitution of the "hard" O-atom by the "soft" sulphur.

In this paper we describe the preparation of the complexes $ZnL_4(ClO_4)_2$ and $CdL_4(ClO_4)_2$ (L = TDPS) and the kinetics of the ligand exchange reactions in solution. Only a few complexes of TDPS are reported in the literature,[8] especially of Co(II), Ni(II), and Cu(I) perchlorates showing equally tetracoordination. Zirconium(IV) and tin(IV) chlorides form adducts with the ligand.[9]

EXPERIMENTAL

Materials

Tris(dimethylamino)phosphine sulphide (TDPS) was prepared by refluxing tris(dimethylamino) phosphine with a stoichiometric amount of sulphur in benzene.[10] The purity of the product was controlled by ^1H and ^{31}P NMR. The solvents used in the experiments are Fluka "puriss" grade nitromethane, Prolabo "normapur grade" dichloromethane, C.E.A. (Service des molécules marquées) deuterated CD_2Cl_2 and CD_3NO_2. The complexes were synthesized starting from $Cd(ClO_4)_2$, $6H_2O$ and $Zn(ClO_4)_2$, $6H_2O$ (Alfa Ventron) according to a

* Author to whom correspondence should be addressed.

method described by Van Leeuwen *et al.*[11] The precipitation of the complex $Cd(TDPS)_4(ClO_4)_2$ takes place immediately. The preparation of the $Zn(TDPS)_4(ClO_4)_2$ complex provides in a first step an oil which is washed several times with anhydrous ether until the precipitation of a solid occurs. These products should be handled with utmost care! During the manipulation of the very dry Zn-complex a violent explosion happened. Therefore all further attempts to synthesize this salt were abandoned. Found: C, 26.4; H, 6.71; P, 11.12; S, 11.68; Cd, 10.35%. Calc. for $Cd(TDPS)_4(ClO_4)_2$: C, 26.4; H, 6.6; P, 11.36; S, 11.7; Cd, 10.3%. Found: C, 27.48; H, 7.09; P, 11.68; S, 12.02; Zn, 6.48%. Calc. for $Zn(TDPS)_4(ClO_4)_2$: C, 27.5; H, 6.9; P, 11.9; S, 12.25; Zn, 6.25%.

All solutions were prepared by weight; all manipulations were carried out under purified argon in a glove box.

NMR spectroscopy

NMR spectra were taken on Bruker WP 80 and WH 90 spectrometers and on a 250 MHz Cameca apparatus. ^{31}P NMR was performed at 32.44 MHz (100–800 scans of 4K/8K points over a frequency range of 2 kHz) with 85% H_3PO_4 in H_2O as an external reference and CD_2Cl_2 as an internal lock substance. All ^{31}P spectra are broad band decoupled from proton.

Line-shape measurements

Theoretical line shapes are computed using a matrix formalism due to Anderson,[12] Kubo[13] and Sack[14] and the program ECHGN.[15]

In the case of the Zn complex the site exchange occurs between two singlets. The population vector **P** and the exchange matrix are therefore

$$\mathbf{P} = r, 1$$

and

$$\mathbf{E} = \begin{vmatrix} -1 & 1 \\ r & -r \end{vmatrix} \times k\left(r = \frac{[TDPS]_{bound}}{[TDPS]_{free}}\right).$$

The ^{31}P NMR spectrum of the ligand molecules bound to Cd^{2+} consists of three signals of relative intensities 12.5, 75 and 12.5 (see below) leading to $\mathbf{P} = 0.125r, 0.75r, 0.125r, 1$ and

$$\mathbf{E} = \begin{vmatrix} -1 & 0 & 0 & 1 \\ 0 & -1 & 0 & 1 \\ 0 & 0 & -1 & 1 \\ 0.125r & 0.75r & 0.125r & -r \end{vmatrix} \times k.$$

All calculations were performed on a Texas Instruments 980A mini-computer equipped with a Hewlett–Packard 7280 Å digital plotter.

RESULTS AND DISCUSSION

Stoichiometry of the complexes in solution

The solid complexes $Cd(TDPS)_4(ClO_4)_2$ and $Zn(TDPS)_4(ClO_4)_2$ retain their stoichiometry on dissolution in an inert solvent. This was proven by comparing the areas of the ^{31}P NMR signals of free and bound TDPS stemming from a solution of known quantities of complex and added free TDPS in CH_2Cl_2 at low temperature (−90°C). The calculated ratio r was confirmed experimentally in both cases.

Generally, ion pair formation is favoured in solvents of low dielectric constant[16] such as dichloromethane ($\varepsilon_{20} = 9.08$).

Therefore the dissociation of the salts is incomplete in this solvent. A ^{35}Cl NMR study of the Cd^{2+}-complex at 30°C shows clearly the presence of ion pairs. In the liquid state the predominant mechanism for the relaxation of the ^{35}Cl nucleus is quadrupolar relaxation and its rate therefore depends on the intensity of the electric field gradient at the nucleus.

The relaxation time T_2 is related to the width of the NMR line at its half-height, $\Delta\nu_{1/2}$, by $\Delta\nu_{1/2} = 1/\pi T_2$.

When the solvation shell of the perchlorate ion is highly symmetrical the field gradient at the chlorine nucleus is zero. $Cd(ClO_4)_2$ in D_2O, e.g. yields a ^{35}Cl NMR signal of a width of 6.5 Hz proving a very symmetrical arrangement of the solvent molecules around the anion.

For ClO_4^- in contact with a counterion however the field gradient is large and the resulting NMR signal very broad. In fact the observed line is always an averaged signal due to a rapid exchange of the ClO_4^- ion between the bound site and a "free" site in the bulk of the solution.

Therefore, in our case, the observed linewidth indicates that a fraction of the anions is associated with the complex ion $Cd(TDPS)_4^{2+}$.

A solution of the complex CdL_4^{2+}, $2ClO_4^-$ alone gives rise to a ^{35}Cl NMR signal of 155 Hz line-width. Upon addition of excess TDPS the width reduces to 85 Hz ($C_{complex} = 0.1$ M, $C_{free} = 0.256$ M). Further addition of ligand lowers the signal width to 64 Hz. Addition of nitromethane, a solvent of a much higher dielectric constant ($\varepsilon_{20} = 38.6$) than dichloromethane, to the initial solution produces the same effect.

The results corroborate the hypothesis of ion-pair formation in the system studied. It is however impossible to decide whether the perchlorate anion

forms a contact ion-pair with the cation or an outer-sphere complex, $[CdL_4, ClO_4]^+$.

NMR parameters

The ^1H signals corresponding to the methyl groups of the ligands in both the cadmium and zinc complexes appear at lower field than those of the non-bonded molecules. The effect is more important for the zinc complex ($\Delta\delta = 0.18$ ppm) than for the Cd^{2+}-complex ($\Delta\delta = 0.11$ ppm). These observations suggest a predominant deshielding effect of the electrical field created by the cation.[17,18] It may also be noticed that the coupling constant $^3J_{P-H}$ increases from 10.5 to 11.5 Hz when TDPS is coordinated. Complexation of TDPS shifts the $^{31}P\{^1H\}$ signals to higher fields for the two complexes: $\Delta\delta = -7.25$ ppm for CdL_4^{2+} and -3.97 ppm for ZnL_4^{2+}. For the complex $Zn(HMPA)_4(ClO_4)_2$ Lincoln and Tkaczuk[4] found a low field shift ($\Delta\delta \simeq 2.5$ ppm). This example shows once more that the sign and the amplitude of the difference between the ^{31}P chemical shifts of free and bound organophosphorus ligands cannot be explained in a simple manner as it had been noticed before in reports[5,6,19] on the coordination of these molecules.

The ^{31}P signal of the cadmium complex consists of one main line (75% of the total intensity), accompanied by two satellites of equal intensities ($\sim$ 12.5% each). Cadmium has two magnetically active isotopes, ^{111}Cd and ^{113}Cd, of closely similar abundance (12.75 and 12.26%), both with spin $I = 1/2$. As their gyromagnetic ratios are identical within 4%, only one coupling constant is observed, $^2J_{^{31}P-Cd} = 30.75$ Hz.

Kinetic measurements

When excess TDPS is added to a solution of the complex ML_4^{2+}, two ^{31}P NMR signals are observed at low temperature (-94°C for M = Cd, -70°C for M = Zn) as mentioned above.

On increasing the temperature, coalescence of the lines occurs (Fig. 1). A complete line-shape analysis of the spectra of six solutions for the Cd complex and two solutions for the Zn compound yields the rate constants $k_{NMR} = \tau_c^{-1}$, where τ_c represents the mean lifetime of TDPS coordinated to the cation,

$$TDPS_{bound} \overset{k_{NMR}}{\rightleftharpoons} TDPS_{free}.$$

Enthalpies and entropies of activation are calculated from a set of k_{NMR} values determined at different temperatures. The variation of k_{NMR} with the concentration of free TDPS allows us to draw some

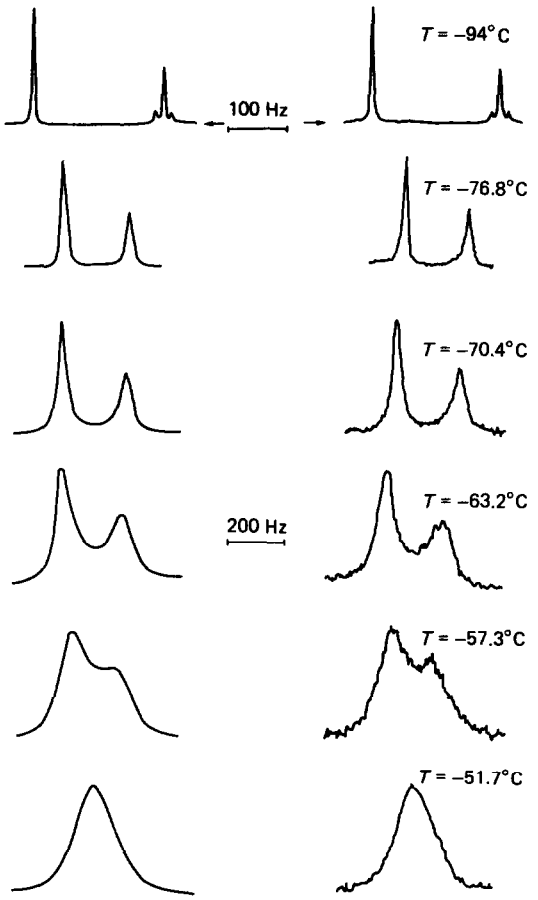


Fig. 1. Calculated (left) and experimental (right) $^{31}P\{^1H\}$ NMR spectra at different temperatures for the system $Cd(TDPS)_4^{2+}/TDPS/CD_2Cl_2$. $[TDPS]_{bound} = 0.275$ and $[TDPS]_{free} = 0.33$ mol l^{-1}.

conclusions concerning the mechanism of the exchange process. The results are summarized in Tables 1 and 2.

A better precision could have been obtained for the system Zn—TDPS by increasing the number of solutions differing in concentration of free ligand but all further experiments have been abandoned when the hazards of explosion of this product became evident (see Experimental).

As it can be seen from Table 1, the values of k_{NMR} at -73°C and of k_{NMR} at 25°C are not rigorously constant for different concentrations of free ligand but do not depend either in a simple manner on this parameter. The relative dispersal of the k_{NMR} values cannot be explained in terms of the ion-pair formation mentioned before and is attributed to experimental errors. We conclude that the rate constants are independent of free ligand for the exchange on the CdL_4^{2+} complex. The same conclusion holds for the Zn complex (Table 2).

The mean values for the exchange parameters

Table 1. Solution compositions and kinetic parameters for TDPS exchange on the $Cd(TDPS)_4^{2+}$ complex ion in CD_2Cl_2

$[TDPS]_{bound}$* (mol l^{-1})	$[TDPS]_{free}$† (mol l^{-1})	k_{NMR} (25°C) (s^{-1})	k_{NMR} (−73°C)§ (s^{-1})	ΔH^* (kJ mol^{-1})	ΔS^* (J mol^{-1} K^{-1})
0.275	0.33	1.5×10^5	85.0	36.1	−24.2
0.275	0.175	1.9×10^5	72.4	37.9	−16.5
0.545	0.625	1.4×10^5	51.1	37.9	−19.4
0.205	0.45	1.1×10^5	55.2	36.4	−25.9
0.41	0.256	0.9×10^5	58.7	35.3	−31.3
0.10	0.20	1.4×10^5	95.2	34.7	−30.0

* Concentration of TDPS bound to the cation.
† Concentration of free TDPS added to the solution.
§ Values interpolated from the linear regression line.

are $k(25°C) = (1.36 \pm 0.34) \times 10^5$ s^{-1}; $\Delta H^* = (36.4 \pm 1.3)$ kJ mol^{-1}; $\Delta S^* = (-24.6 \pm 5.8)$ J mol^{-1} K^{-1} for $Cd(TDPS)_4^{2+}$ and $k(25°C) = (1.35 \pm 0.35) \times 10^4$ s^{-1}; $\Delta H^* = (40.9 \pm 2.5)$ kJ mol^{-1}; $\Delta S^* = (-28.8 \pm 10.3)$ J mol^{-1} K^{-1} for $Zn(TDPS)_4^{2+}$.

The mechanism of a ligand exchange reaction independent of the free ligand concentration can be of the dissociative (D) or interchange (I) type.[20] In the first case it is assumed that the intermediate ML_3^{2+} (M = Zn or Cd) is formed in the initial step. This mechanism should be characterized by a high activation enthalpy and a strongly positive value of the activation entropy. This is obviously not the situation encountered here. An interchange mechanism implies the formation of an outer-sphere complex (OSC)

$$ML_4^{2+} + L^* \overset{K_{OSC}}{\rightleftharpoons} (ML_4 \ldots L^*)^{2+},$$

$$(ML_4 \ldots L^*)^{2+} \overset{k_I}{\rightleftharpoons} (ML_3L^* \ldots L)^{2+} \rightarrow ML_3L^{*2+} + L.$$

The observed rate constant k_{NMR} in this case is

$$k_{NMR} = \frac{k_I K[L]}{1 + K[L]}.$$

For high values of K ($K[L] \gg 1$) k_{NMR} becomes equal to k_I and is therefore independent of the concentration of free ligand.

This mechanism is compatible with the values of the observed ΔH^*, intermediate between those obtained for a purely associative (A) mechanism (e.g. exchange on $Zn(HMPA)_4^{2+}$)[4] and a pure D mechanism (e.g. exchange on $Zn(S{=}C[NMe_2]_2)_4^{2+}$][7] by Lincoln and co-workers and those of ΔS^* which are only slightly negative.

For all these reasons the interchange mechanism appears more likely than a pure dissociative pathway.

The activation parameters for the exchange on Zn and Cd complexes are comparable; the exchange rate is lower for the zinc compound than for CdL_4^{2+} as expected on the base of the ionic radii of the two metals (0.74 Å for Zn^{2+} and 0.97 Å for Cd^{2+}).[21] Electrostatic interactions between the ligand and the cation are certainly prevailing since there is no ligand field stabilization effect for these ions because of their complete *d*-shells. Although determined under quite different conditions, the substitution of water is reported to be equally about ten times faster on Cd^{2+} than on Zn^{2+}.[1] Steric reasons are to be considered too. The large sulphur atom produces more crowding

Table 2. Solution compositions and kinetic parameters for TDPS exchange on the $Zn(TDPS)_4^{2+}$ complex ion in CD_2Cl_2

$[TDPS]_{bound}$* (mol l^{-1})	$[TDPS]_{free}$† (mol l^{-1})	k_{NMR} (25°C) (s^{-1})	k_{NMR} (−29°C)§ (s^{-1})	ΔH^* (kJ mol^{-1})	ΔS^* (J mol^{-1} K^{-1})
0.285	0.295	1.1×10^4	275.2	39.1	−36.1
0.560	0.625	1.6×10^4	283.1	42.6	−21.5

* Concentration of TDPS bound to the cation.
† Concentration of free TDPS added to the solution.
§ Values interpolated from the linear regression line.

in the neighbourhood of the Zn^{2+} ion than of Cd^{2+}, leading to a relative destabilization of the OSC in the former case compared to the latter.

CONCLUSION

For the first time to our knowledge a complete study of the kinetics and mechanism on a cadmium complex with a neutral unidentate ligand has been realized in the work described here. Only a value of a rate constant, $k(25°C) = 1.6 \times 10^8\ s^{-1}$, had been reported for the exchange of water.[22]

Publications of zinc-complexes with this kind of ligands are equally rather rare; only two papers[4,7] report a complete study of the kinetics and mechanism of exchange reactions on this cation of biological interest. In one case, with the ligand HMPA, a purely associative mechanism was found, in the other, with tetramethylthiourea, a purely dissociative one. Our study gives evidence for the existence of a third possible exchange pathway for tetracoordinated zinc-complexes, an interchange mechanism. The greater bulkiness of thio-HMPA as compared to HMPA probably prohibits the formation of a five-coordinate intermediate necessary for an associative mechanism.

Other studies of metal perchlorates with this promising organophosphorus ligand had been planned; the hazards of explosion however, inherent in the combination of perchlorate and P=S groups suggests the choice of another anion to continue this work.

Acknowledgements—This work has been possible due to a cooperation between the Centre National de la Recherche Scientifique (France) and the Direction de la Recherche Scientifique et Technique (Tunisia). The authors are indebted to these organizations for financial support.

REFERENCES

1. M. Eigen, *Pure Appl. Chem.* 1963, **6**, 97.
2. F. A. Cotton and G. Wilkinson, *Advanced Inorganic Chemistry*. Wiley, New York (1980).
3. R. G. Pearson, *J. Chem. Educ.* 1968, **45**, 581.
4. M. N. Tkaczuk and S. F. Lincoln, *Aust. J. Chem.* 1980, **33**, 2621.
5. P. R. Rubini, L. Rodehüser and J.-J. Delpuech, *Inorg. Chem.* 1979, **18**, 2962.
6. G. Doucet Ladevèze, L. Rodehüser, P. R. Rubini and J.-J. Delpuech, *Nouv. J. Chim.* 1984, **8**, 93.
7. M. N. Tkaczuk and S. F. Lincoln, *Aust. J. Chem.* 1979, **32**, 1915.
8. W. E. Slinkard and D. W. Meek, *Inorg. Chem.* 1969, **8**, 1811.
9. E. Le Coz and J. E. Guerchais, *Bull. Soc. Chim. France* 1971, **74**, 80.
10. H. J. Vetter and H. Noth, *Chem. Ber.* 1963, **96**, 1308.
11. P. W. N. M. Van Leeuwen and W. L. Groeneveld, *Inorg. Nucl. Chem. Lett.* 1967, **3**, 145.
12. P. W. Anderson, *J. Phys. Soc. Jpn* 1954, **9**, 316.
13. R. Kubo, *J. Phys. Soc. Jpn* 1954, **9**, 935.
14. R. A. Sack, *Mol. Phys.* 1958, **1**, 163.
15. M. L. Martin, J.-J. Delpuech and G. J. Martin, *Practical NMR Spectroscopy*. Heyden, London (1979).
16. H. A. Berman, H. J. C. Yeh and T. R. Stengle, *J. Phys. Chem.* 1975, **79**, 2551.
17. J.-J. Delpuech, A. Péguy and M. R. Khaddar, *J. Magn. Reson.* 1972, **6**, 325.
18. A. M. Buckingham, *Can. J. Chem.* 1960, **38**, 300.
19. L. Rodehüser, P. Rubini and J.-J. Delpuech, *Inorg. Chem.* 1977, **16**, 2837.
20. C. H. Langford and H. B. Gray, *Ligand Substitution Processes*. Benjamin, New York (1965).
21. *The Handbook of Chemistry and Physics*, 55th edition, E-69. Chemical Rubber Publishing, Cleveland, OH (1975).
22. J. Burgess, *Metal Ions in Solution*. Ellis Horwood, Chichester (1978) (and references cited therein).

Polyhedron Vol. 4, No. 4, pp. 649–651, 1985
Printed in Great Britain

0277–5387/85 $3.00 + .00
© 1985 Pergamon Press Ltd

PREPARATION, CHARACTERIZATION AND CYCLIC VOLTAMMETRIC BEHAVIOUR OF DIMERIC SULPHIDOMOLYBDENUM(V) DITHIOCARBAMATE COMPLEXES

K. S. NAGARAJA and M. R. UDUPA*
Department of Chemistry, Indian Institute of Technology, Madras-600 036, India

(*Received* 2 *March* 1984; *accepted* 17 *August* 1984)

Abstract—$Mo_2S_4(R_2dtc)_2$ (R = methyl, ethyl or benzyl; R_2 = pyrrolidinyl, piperidinyl or 4-morpholinyl) have been prepared starting from ammonium tetrathiomolybdate. The IR spectra of the complexes suggested the bidentate nature of the dithiocarbamate with the disulphido bridged structure. The dimeric structure of the complexes is further confirmed by the mass spectral data. The cyclic voltammetric peak potentials for the select complexes are observed at −1.00 and −1.27 V vs SCE.

The genetic, enzymological and biophysical experiments on molybdo-enzymes show[1] that they contain two Mo atoms per molecule. Further, the recognition[2] of the importance of sulphido ligation in the molybdo-enzymes has led to study[3] of dimeric sulphidomolybdenum(V) dithiocarbamates. The electrochemical investigations of $Mo_2S_4(Et_2dtc)_2$ and $Mo_2S_4(n\text{-}Bu_2dtc)_2$ were reported[4–6] in the literature. In the present paper, we report the characterization and cyclic voltammetric studies of $Mo_2S_4(R_2dtc)_2$ (R = methyl, ethyl or benzyl; R_2 = pyrrolidinyl, piperidinyl or 4-morpholinyl) complexes, which have been prepared by following an elegant method.

EXPERIMENTAL

Materials

Laboratory grade chemicals were used as supplied. Ammonium tetrathiomolybdate and the ligands were prepared[7] using the procedure reported elsewhere. General method of preparation of di-μ-sulphidobis[sulphido(dithiocarbamato)molybdenum (V)], $Mo_2S_4(dtc)_2$. Ammonium tetrathiomolybdate (10 mmol) in water (40 cm^3) and sodium dithiocarbamate (40 mmol) in water (100 cm^3) were mixed and stirred for 0.5 h. The precipitated dark red complex was filtered, washed with water and finally with methanol and dried. Yield 70%. The elemental analyses of the complexes are given in Table 1. The complexes are found to be insoluble in water and common organic solvents, but are soluble in dimethylsulphoxide or dimethylformamide. The IR, UV–visible and mass spectra were recorded on Perkin–Elmer 257, Carl Zeiss DMR-21 and VG micro-mass 70-70 FF spectrometers respectively. The voltammetric measurements were made with a three electrode McKee–Pedersen potentiostatic circuit constructed from operational amplifiers. The working electrode was a Pt foil. A Pt wire sealed in the glass tube served as auxiliary electrode and SCE was used as the reference electrode. The reference electrode was separated from the experimental solution by means of a non-aqueous salt bridge. Sweep rates varied between 0.01–0.3 V s^{-1}. Deaeration of the solution was performed by passing purified nitrogen. All the potentials are reported w.r.t. SCE.

RESULTS AND DISCUSSION

Hitherto reported procedures[4–6] to synthesise complexes with the $Mo_2S_4^{2+}$ core described various starting compounds which were prepared with relatively great difficulty. We have employed ammonium tetrathiomolybdate which was obtained by passing hydrogen sulphide gas through an ammoniacal solution of ammonium molybdate. The complete substitution of the oxo groups in MoO_4^{2-} ion was monitored by the characteristic UV–visible spectra.

* Author to whom correspondence should be addressed.

Table 1. Analytical data for $Mo_2S_4(R_2dtc)_2$ complexes

Complex	Found (calc.) (%)				
	C	H	N	S	Mo
$Mo_2S_4(Me_2dtc)_2$	13.0 (12.8)	2.3 (2.1)	4.8 (5.0)	45.4 (45.7)	34.0 (34.2)
$Mo_2S_4(Et_2dtc)_2$	19.4 (19.5)	3.3 (3.3)	4.4 (4.5)	41.7 (41.6)	31.1 (31.2)
$Mo_2S_4(pyrroldtc)_2$	19.5 (19.6)	2.6 (2.6)	4.6 (4.6)	41.8 (41.9)	31.3 (31.3)
$Mo_2S_4(pipdtc)_2$	22.3 (22.5)	2.8 (3.1)	4.4 (4.4)	39.9 (40.0)	30.1 (29.9)
$Mo_2S_4(4\text{-morphdtc})_2$	18.5 (18.6)	2.5 (2.5)	4.4 (4.3)	39.7 (39.8)	29.8 (29.8)
$Mo_2S_4(dibenzdtc)_2$	41.9 (41.7)	3.5 (3.3)	3.2 (3.2)	29.6 (29.7)	22.2 (22.1)

The complexes are found to be diamagnetic. Mo(V) has d^1 electronic configuration and is expected to be paramagnetic. However in dimeric complexes of this type $Mo_2S_4^{2+}$, the d_{xy} orbitals of the two Mo atoms are oriented to allow direct overlap across MoS_2Mo bridge and as such the bonding level of this interaction accommodates the two electrons in accordance with the diamagnetism observed. The electronic spectra of the complexes (Table 2) exhibited λ_{max} around 470 and 320 nm, which are attributed[3] to $S_t \rightarrow Mo$ charge-transfer and internal ligand $\pi \rightarrow \pi^*$ transitions respectively.

The IR spectra of the complexes showed absorptions (Table 2) around 1500 and 960 cm^{-1}, which are characteristic[8] of bidentate dithiocarbamate ligand. The higher value of $\nu_{(CN)}$ for $Mo_2S_4(Me_2dtc)_2$ is explained due to the electron releasing methyl groups attached to the nitrogen atom exerting hyperconjugation effect. The decrease in $\nu_{(CN)}$ value of $Mo_2S_4(dibenzdtc)_2$ when compared to $Mo_2S_4(Me_2dtc)_2$ is attributed to the presence of electron withdrawing phenyl rings attached to methylene groups. The bands (Table 2) observed around 540 and 525 cm^{-1} are assigned[4] to $\nu_{(Mo=S)}$ (terminal). The observation of two bands indicate that the complexes are of *syn* form, that is two terminal sulphido groups are *cis* to each other. The bands at 475 and 340 cm^{-1} are due to asymmetric and symmetric stretching vibrations of a sulphur bridged[4] MoS_2Mo group. The absorption observed in the spectra of the complexes at 380 cm^{-1} is attributed[7] to $\nu_{(Mo-S)_{dtc}}$. The 15 line mass spectrum

Table 2. UV–visible* and IR†‡ spectral data

Complex	λ_{max} (nm)	$\nu_{(CN)}$	$\nu_{(CS)}$	$\nu_{(Mo=S_t)}$	ν_{MoS_bMo}	$\nu_{Mo-S_{dtc}}$
$Mo_2S_4(Me_2dtc)_2$	470	1550s	960s	540m	475m	375s
	320			520m	340m	
$Mo_2S_4(Et_2dtc)_2$	475	1520s	960s	545m	470m	380s
	325			520m	350m	
$Mo_2S_4(pyrroldtc)_2$	475	1520s	960s	545m	470m	375s
	320			525m	345m	
$Mo_2S_4(pipdtc)_2$	470	1515s	960s	545m	470m	375s
	325			525m	340m	
$Mo_2S_4(4\text{-morphdtc})_2$	470	1500s	950s	550m	470m	380s
	310			570m	355m	
$Mo_2S_4(dibenzdtc)_2$	465	1515s	965s	550m	465m	385s
	330			520m	340m	

* Recorded in Nujol mull.

† KBr pellet.

‡ Frequencies (cm^{-1}).

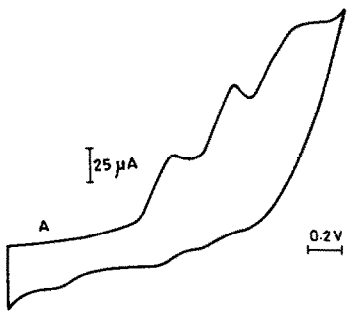


Fig. 1. Cyclic voltammogram of $Mo_2S_4(Et_2dtc)_2$ (2 mmol) in DMSO, sweep rate 0.2 V s^{-1}.

over 592–576 m/z (parent-32) units, of $Mo_2S_4(Et_2dtc)_2$ confirms[9] the dimeric nature.

The cyclic voltammograms of Mo_2S_4(4-morphdtc)$_2$ were recorded in dimethylsulphoxide using tetramethyl ammonium perchlorate as the supporting electrolyte. Two reversible cathodic peaks are observed at potentials −0.97, −1.27; −1.05, −1.27 and −1.07, −1.28 V vs SCE for $Mo_2S_4(Et_2dtc)_2$, Mo_2S_4(pyrroldtc)$_2$ and Mo_2S_4(4-morphdtc)$_2$ respectively with the sweep rate of 0.1 V s^{-1}. The cyclic voltammogram of $Mo_2S_4(Et_2dtc)_2$ (Fig. 1) is comparable to that reported by Schultz *et al.*[4] The cathodic peak potentials around −1.00 and −1.2 V are attributed to the successive one electron reduction. The peak current for the second wave varies with the sweep rate, which may suggest that the reduction is preceded by a chemical decomposition step. The first cathodic peak potential seems to be susceptible to the electronic effects of the coligand which is present along with Mo_2S_4 core.

Acknowledgements—We thank Drs R. Narayan and C. Nanjundiah for help and encouragement. We are further grateful to CSIR, India for financial support.

REFERENCES

1. E. I. Stiefel, *Prog. Inorg. Chem.* 1977, **22**, 1.
2. J. T. Spence, *Coord. Chem. Rev.* 1969, **4**, 475.
3. A. Muller, R. G. Bhattacharya, N. Mohan and B. Pfefferkorn, *Z. Anorg. Allg. Chem.* 1979, **454**, 118.
4. F. A. Schultz, V. R. Ott, D. S. Rollison, D. C. Bravard, J. W. McDonald and W. E. Newton, *Inorg. Chem.* 1978, **17**, 1758.
5. H. D. Faulkner, *J. Electrochem. Soc.* 1978, **125**, 287C.
6. K. F. Miller, A. E. Bruce, J. L. Corbin, S. Wherland and E. I. Stiefel, *J. Am. Chem. Soc.* 1980, **102**, 5102.
7. F. W. Moore and M. L. Larson, *Inorg. Chem.* 1967, **6**, 998.
8. D. Coucouvanis, *Prog. Inorg. Chem.* 1969, **11**, 235.
9. M. R. Udupa and K. S. Nagaraja, *Thermochim. Acta* 1982, **56**, 241.

Polyhedron Vol. 4, No. 4, pp. 653–656, 1985
Printed in Great Britain

0277–5387/85 $3.00 + .00
© 1985 Pergamon Press Ltd

PREPARATION OF MIXED ISOPROPYL/TRIMETHYLSILYL DERIVATIVES OF BORIC ACID, $(Me_3SiO)_nB(O^iPr)_{3-n}$ ($n = 1$–3), AND THEIR GC–MS SPECTRA

HIROAKI WADA, SHUNJI ARAKI, KAZUYUKI KURODA and CHUZO KATO*
Department of Applied Chemistry, Waseda University, Shinjuku-ku, Tokyo 160, Japan

(*Received* 28 *November* 1983; *accepted in revised form* 17 *August* 1984)

Abstract—Boric acid was trimethylsilylated with $Me_3SiCl/(Me_3Si)_2O$ in the presence of 2-propanol. The resulting mixture was analysed by using a combined gas chromatograph–mass spectrometer. The compounds $(Me_3SiO)_nB(O^iPr)_{3-n}$ ($n = 0$–3) were detected as products.

We have already reported[1] that by the reaction of silicate minerals such as hemimorphite with trimethylsilylating reagent containing ethylene glycol, a viscous "silicate–organic copolymer" was formed as a result of the partial esterification of unsilylated silanol groups. Therefore, it was interesting to study the possibility of preparing partially esterified trimethylsilyl derivatives of boric acid. Though there have been many reports on the preparation and properties of fully trimethylsilylated boric acid,[2–4] no investigations on the preparation of partially trimethylsilylated alkyl derivatives of boric acid have been reported.

The purpose of this study is to report the preparation and GC–MS analysis of the partially trimethylsilylated isopropyl derivatives of boric acid.

EXPERIMENTAL

Materials

Boric acid and 2-propanol were reagent grade and were used without purification.

Trimethylchlorosilane (Shin-etsu Chemicals) was washed with hydrochloric acid and was distilled before use.

Hexamethyldisiloxane was obtained by the hydrolysis of trimethylchlorosilane and was distilled once.

Preparation

5 cm^3 of trimethylchlorosilane, 5 cm^3 of hexamethyldisiloxane and 0.2 cm^3 of 2-propanol were put in a 50-cm^3 flask. The solution was stirred for 30 min. Then 0.2 g of boric acid was added to the solution. After stirring for 3 h, the solution was filtered in order to remove unreacted boric acid and concentrated by use of an aspirator.

The product obtained was a colourless liquid containing hexamethyldisiloxane.

Analysis

The mass spectra were obtained using a gas chromatograph–mass spectrometer GCMS-QP1000 (Shimadzu Seisakusho Ltd). The electron energy was 70 eV. The ion source temperature was maintained at 250°C and separator at 270°C. The GC column (length 1.5 m and inside diameter 3 mm) was packed with 5 wt.% of OV-17 on 80/100 mesh Chromosorb W.

RESULTS AND DISCUSSION

Figure 1 shows chromatographic separation of the product. Four peaks were found in TII (total ion intensity) chromatogram (upper part of the figure), though peaks c and d were not well separated. Changes of the intensity of several masses characteristic of each peak with time are shown in Fig. 1 (mass chromatogram; lower part of the figure).

The mass spectra of peaks a–d in the TII chromatogram are shown in Fig. 2(a–d). Under the present experimental conditions, boric acid would not polymerise in this low pH,[5] therefore, trialkyl borate (a), di- and monoalkyl substituted trimethylsilyl derivatives of boric acid, b and c respectively, were expected to be formed in addition to the fully silylated derivative (d).

Though no molecular ion M^+ was observed in all

* Author to whom correspondence should be addressed.

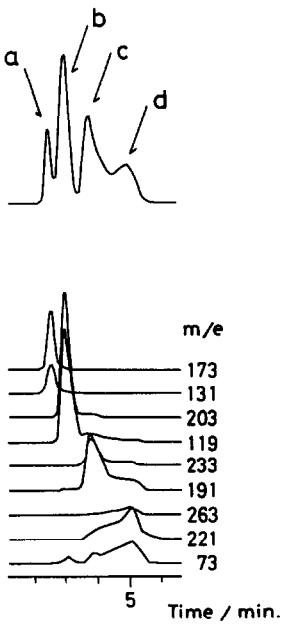
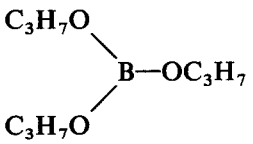
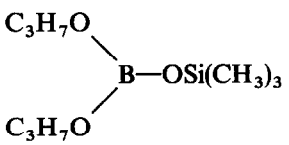


Fig. 1. TII and mass chromatograms.

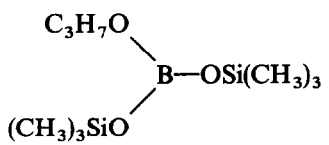
spectra, the peaks [exactly corresponding to $(M-15)^+$ (loss of a methyl group) respectively] were detected in each spectrum. The observed and calculated abundance of $(A-1)^+$, A^+ and $(A+1)^+$ ions were summarised in Table 1 by the consideration of isotopes of boron, carbon and silicon ["A" represents $(M-15)^+$ ion]. In view of these data, it could be concluded that the compounds formed were **1–4**.



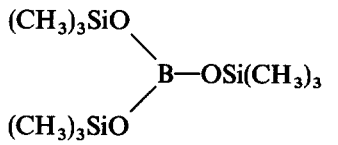
1



2



3



4

In the spectra of the compounds containing trimethylsilyl group (Fig. 2b–d), the peak at *m/e* 73 (known as $(CH_3)_3Si$ group) increased with the increase in the number of the trimethylsilyl group compared to the $(M-15)^+$ ion.

In the spectrum of tris(trimethylsilyl)borate (Fig. 2d), *m/e* 221 was observed. Butts and Rainey[6] proposed that the loss of 42 mass units (263 → 221) was due to the loss of CH_3BO neutral fragment by considering the following points.

(1) A peak at *m/e* 220 was not observed. This fact clearly indicated that the ion at *m/e* 221 did not contain a boron atom.

(2) In the case of other trimethylsilylated anions such as sulphate, carbonate and oxalate, they found that, in general, the central hetero-atom is lost early in the fragmentation pattern with the rearrangement of the silyl groups.

According to our results, the peak ratio (*m/e* 221 : *m/e* 222 : *m/e* 223) was 8.6 : 1.9 : 1.0, which was in fair agreement with the calculated ratio 8.1 : 1.9 : 1.0 assuming that CH_3BO was lost from the $(M-15)^+$ ion. Moreover, in mass spectra of other trimethylsilyl derivatives, an intense peak at *m/e* 221 was frequently observed in addition to *m/e* 73 and 147.[7–9] In conclusion, *m/e* 221 could be assigned to be due to the rearrangement of trimethylsilyl groups.

Although the shift of 42 mass units was also observed in Fig. 2a (173 → 131), in Fig. 2b (203 → 161), and in Fig. 2c (233 → 191), it was not possible

Table 1. Abundance of $(A-1)^+$, A^+ and $(A+1)^+$

compound	A^+ m/e	relative ratio $(A-1)^+$	A^+	$(A+1)^+$	
1	173	2.7	11	1	calc.*
		2.5	12	1	obs.
2	203	1.6	6.9	1	calc.
		1.4	7.2	1	obs.
3	233	1.2	4.9	1	calc.
		1.0	5.0	1	obs.
4	263	0.9	3.9	1	calc.
		0.9	4.0	1	obs.

*Calculated on the basis of natural abundance: ^{10}B (19.7%), ^{11}B (80.3%); ^{12}C (98.892%), ^{13}C (1.108%); ^{28}Si (92.18%), ^{29}Si (4.71%), ^{30}Si (3.12%).

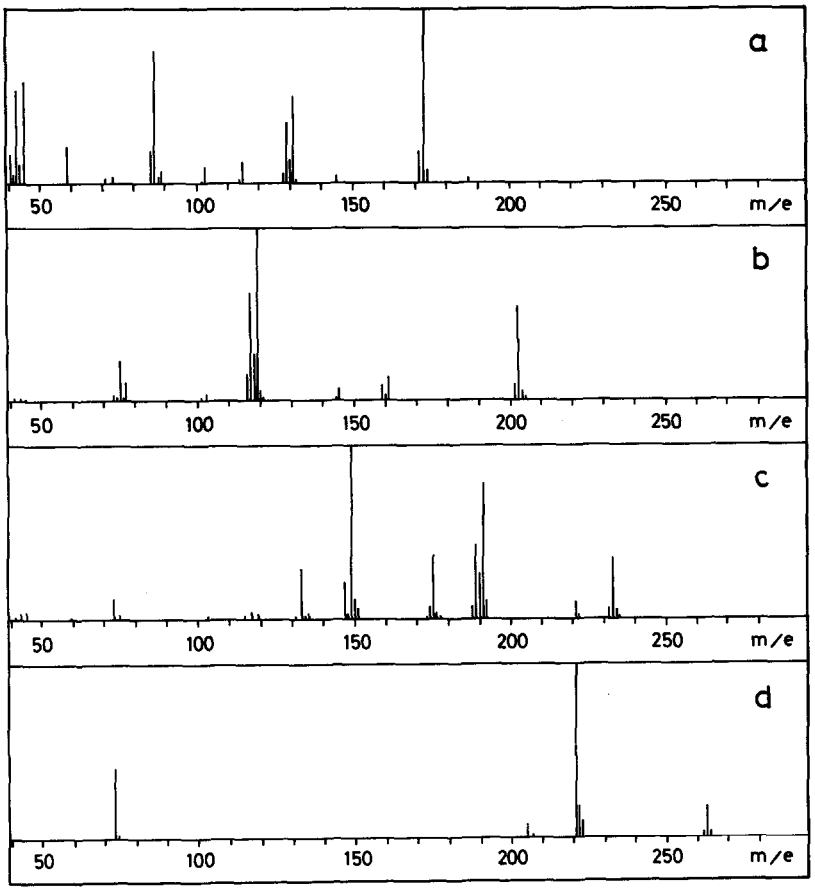


Fig. 2. Mass spectra of the compounds: (a) **1**, (b) **2**, (c) **3** and (d) **4**.

to conclude that it was actually due to the loss of CH_3BO. Namely, it could not be understood whether the peaks at *m/e* 130, 160, and 190 in Fig. 2a–c were the isotopic peaks of *m/e* 131, 161 and 191 ions and/or those of *m/e* 129, 159 and 189 ions respectively. Loss of 42 mass units from $(M-15)^+$ ion was reported by Calhoun and Masson,[10] who studied the 2-propanol/calcium silicate system. They tentatively proposed that it was due to $(M-15)^+-C_3H_6$. According to our calculation of the relative intensities of the peak at *m/e* 191, 192 and 193 in Fig. 2c, it seemed likely that the loss of 42 mass units was due to the loss of C_3H_6 rather than that of CH_3BO.

Furthermore, Calhoun and Masson[10] observed peaks corresponding to $(M-15)^+-44$, which were also shown in our spectra (*m/e* 129 in Fig. 2a, 159 in Fig. 2b, and 189 in Fig. 2c), and proposed that it was due to $(M-15)^+-C_3H_8$. However, taking into account the fragmentation patterns of other alkyl borates,[11] these peaks could also be ascribable to $(M-59)^+$ (loss of an isopropoxy group from M^+). On the basis of above data, it was unable to identify each peak of the spectra because of the complex overlapping of the peaks.

A strong peak at *m/e* 87 in Fig. 2a was ascribed to $C_3H_7OBOH^+$[11] or $O_2BOCHCH_3^+$ by the comparison of the calculated ratio (1:4.1) with the observed ratio (1:4.2) of *m/e* 86 and 87.

In Fig. 2c, peaks at *m/e* 147, 133, 131, 119, 117, 73, 45 and 43 were observed. These peaks are also found in the mass spectrum of hexamethyldisiloxane (HMD). Since HMD (b.p. *ca* 100°C) was eluted much earlier than the compound **1** on chromatogram, it was thought that these peaks were due to the formation of $(CH_3)_2Si{=}O^+{-}Si(CH_3)_3$ (*m/e* 147)[12] by the rearrangement of two trimethylsilyl groups of the compound **3**. These peaks could not be observed in Fig. 2d (spectrum of compound **4**; fully trimethylsilylated derivative). In the mass spectrum of the compound **4** reported by Butts and Rainey,[6] a very small peak at *m/e* 147 was detected. The absence of this peak in our spectrum is probably due to its much lower relative intensity than the "base peak" (*m/e* 221). Peaks other than *m/e* 147 were in good agreement with those obtained by them.

Although the difference of the reactivity of trimethylsilyl group and alkyl group was not well known, we have already reported that the compounds containing both isopropyl and trimethylsilyl groups were formed in the case of silicates.

Mono-, di- and tri-isopropyl-substituted trimethylsilyl derivatives of monomeric and dimeric silicates were formed by trimethylsilylation of olivine[13] and hemimorphite[14] respectively. It was thought that the same types of reaction occurred in boric acid and 2-propanol system, though we were not able to determine one of the reactions (trimethylsilylation and esterification) occurred first or the two processes proceeded simultaneously.

The yield of the product was so small that the amount of each compound was insufficient to be analysed by spectroscopic methods. However, it can be thought that trimethylsilylation is a promising technique for the investigation and the syntheses of organic–inorganic copolymers containing not only silicon but also boron.

REFERENCES

1. K. Kuroda and C. Kato, *Makromol. Chem.* 1978, **179**, 2793.
2. H. Steinberg, *Organoboron Chemistry, Vol.* 1 : *Boron–Oxygen and Boron–Sulphur Compounds.* Interscience, New York (1964).
3. S. K. Mehrotra, G. Srivastava and R. C. Mehrotra, *Indian J. Chem.* 1976, **14A**, 137.
4. E. W. Abel and A. Singh, *J. Chem. Soc.* 1959, 690.
5. J. L. Anderson, E. M. Eyring and M. P. Whittaker, *J. Phys. Chem.* 1964, **68**, 1128.
6. W. C. Butts and W. T. Rainey, Jr, *Anal. Chem.* 1971, **43**, 538.
7. C. R. Masson, W. D. Jamieson and F. G. Mason, in *Physical Chemistry of Process Metallurgy, The Richardson Conference* (Edited by J. H. E. Jeffes and R. J. Tait), p. 223. Institute of Mining and Metallurgy, London (1974).
8. H. P. Calhoun and C. R. Masson, *J. Chem. Soc., Dalton Trans.* 1978, 1342.
9. H. P. Calhoun, W. D. Jamieson and C. R. Masson, *J. Chem. Soc., Dalton Trans.* 1979, 454.
10. H. P. Calhoun and C. R. Masson, *J. Chem. Soc., Dalton Trans.* 1980, 1282.
11. R. H. Cragg and A. F. Weston, *J. Organomet. Chem.* 1974, **67**, 161.
12. J. A. McCloskey, R. N. Stillwell and A. M. Lawson, *Anal. Chem.* 1968, **40**, 233.
13. K. Kuroda, T. Koike and C. Kato, *J. Chem. Soc., Dalton Trans.* 1981, 1957.
14. K. Kuroda and C. Kato, *J. Inorg. Nucl. Chem.* 1979, **41**, 947.

Polyhedron Vol. 4, No. 4, pp. 657–661, 1985
Printed in Great Britain

0277-5387/85 $3.00 + .00
© 1985 Pergamon Press Ltd

SPECTROSCOPIC STUDIES OF MIXED HALOGENOTETRAPHOSPHAZENES

T. TUNDE BAMGBOYE
Department of Chemistry, University of Ilorin, Ilorin, Nigeria

(*Received* 5 *October* 1983; *accepted in revised form* 17 *August* 1984)

Abstract—Cyclotetraphosphazenes substituted non-geminally by fluorine and either chlorine or bromine have been prepared. The compounds with the general formula $P_4N_4F_{8-n}X_n$, where X = Cl or Br and $n = 2$ and 4, result from the reactions under pressure between either hydrogen chloride or bromide and dimethylaminofluorocyclotetraphosphazenes. In most cases mixture of isomers are obtained. The main structural evidence is obtained by ^{19}F NMR assisted by GLC and IR spectroscopy.

The fluorination of $P_4N_4Cl_8$ or $P_4N_4Br_8$ with potassium fluorosulphite is a stepwise process leading exclusively to geminal isomers. The alternative isomers in which the different halogen atoms occupy non-geminal positions must therefore be obtained by an indirect method as summarised by the equations:

$$P_4N_4Cl_8 + 2nHNMe_2 \rightarrow P_4N_4Cl_{8-n}(NMe_2)_n + nNMe_2H, HCl, \quad (1)$$

$$P_4N_4Cl_{8-n}(NMe_2)_n + SbF_3 \rightarrow P_4N_4F_{8-n}(NMe_2)_n + SbCl_3, \quad (2)$$

$$P_4N_4F_{8-n}(NMe_2)_n + 2nHX \rightarrow P_4N_4F_{8-n}X_n + nNMe_2H_2X. \quad (3)$$

Equation (1) is the aminolysis of $P_4N_4Cl_8$ to give the non-geminal substituted isomers, which can be fluorinated using antimony trifluoride [eqn (2)], then the resulting dimethylaminofluorotetraphosphazenes are finally treated with either HCl or HBr to give the non-geminal bromo- or cloro-fluorotetraphosphazenes [eqn (3)].

Both non-geminally[1] and geminally[2] substituted mixed halides of the trimer are well established, but only the geminally substituted chloro-fluorotetraphosphazenes have been reported.[2] We expect that the method used for non-geminally substituted trimer might give these compounds.

Attempts to prepare the non-geminal isomers of $P_4N_4F_4Cl_4$ (**VII** and **VIII**), $P_4N_4F_4Br_4$ (**VII** and **VIII**), $P_4N_4F_6Cl_2$ (**XI** and **XII**) and $P_4N_4F_6Br_2$ (**XIII** and **XIV**) (see Fig. 1) are presented.

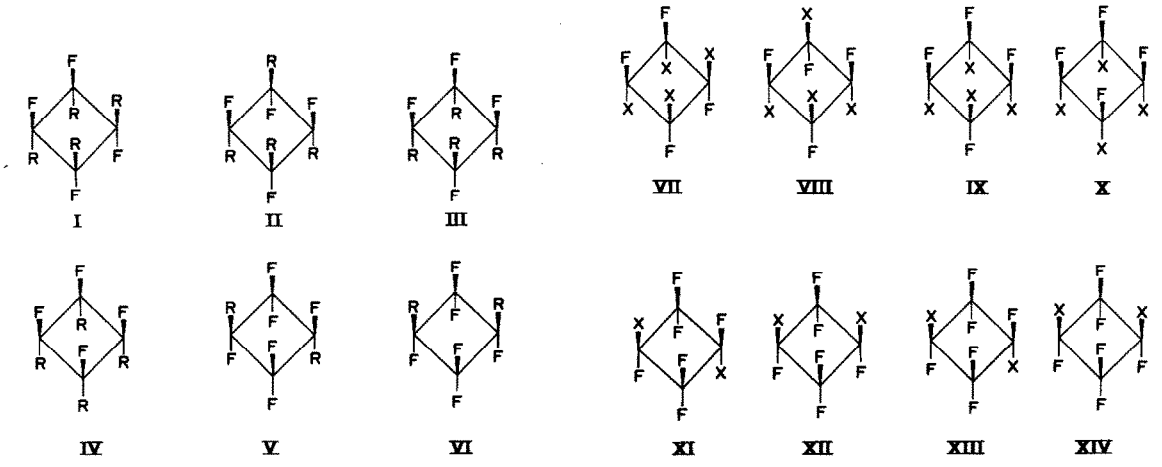


Fig. 1. R or X = NMe_2, Cl or Br in all structures.

EXPERIMENTAL

Reactions of the starting materials with either hydrogen chloride or hydrogen bromide followed the same pattern and details for one reaction with hydrogen chloride are given below. Other reactions are summarized in Table 1. All reactions were monitored by GLC. Mass spectra confirmed the stoichiometry of the compounds.

Reaction of $P_4N_4F_4(NMe_2)_4$ **(I** *and* **II)** *with hydrogen chloride*

The reaction was carried out in a Carius tube fitted with a Rotaflo Tf6/24 valve and a standard taper joint for attachment to a vacuum line. The phosphazene (0.8 g, 0.002 mol) was added to the Carius tube and degassed, after which hydrogen chloride (2.48 g, 0.069 mol) was condensed into the sample by cooling the tube in liquid nitrogen. The "Rotaflo" valve was closed and the tube surrounded by a protective wire gauze. After about 30 days the tube was cooled at −196°C and the excess hydrogen chloride removed at −45°C on a vacuum line at 0.01 mm pressure.

The remaining solid was extracted with boiling petrol (60–80°C) to separate the mixed halide from dimethylaminohydrochloride. After the removal of the solvent the product was a colourless liquid.

Examination of the material by GLC (5 ft × $\frac{3}{8}$ in. stainless steel column packed with 10% silicone gum rubber on Chromosorb W at 60°C) showed a broad asymmetric peak characteristic of two components with very similar retention times, the ratio of these was estimated as 1 : 1.2. Because of the closeness of the retention times, separation to give pure isomers by preparative GLC was not feasible.

Mass spectrometry confirmed the presence of $P_4N_4F_4^{35}Cl_4$ by the observation of a parent ion at m/z 396 with the correct isotopic distribution pattern for four chlorine atoms; completion of the reaction was also confirmed by the absence of peaks associated with amine containing mixed halides.

Instruments

A Varian-Aerograph 90 P-3 preparative gas–liquid chromatograph was used with helium carrier gas. NMR spectra were obtained with a Varian HA100 spectrometer. Fluorine resonances were obtained on 10% (w/v) solutions in carbon tetrachloride with trichlorofluoromethane as internal standard. IR spectra were obtained for either liquid film samples or solutions in carbon tetrachloride on a Perkin–Elmer 457 spectrometer. Mass spectra were obtained on an AEI MS902 double-focusing mass spectrometer. Introduction of liquid samples was through the all glass heated inlet system while for solids the direct insertion leak was used.

RESULTS AND DISCUSSION

Preparation

In the trimer, the mixed halide reactions had to be carried out at elevated temperatures;[1] but it is interesting to note here that in the tetramer series, the reactions were performed at room temperatures. This is a consequence of the known greater reactivity of the tetrameric compounds.[3]

The rate of deaminolysis was faster with hydrogen bromide than with hydrogen chloride, probably as a

Table 1. Reaction with HCl and HBr

Reactant	Product	Relative area under peak	Retention time (min)	Analytical data N (%) Found	Calc.	Reaction conditions t (°C)	Time (h)
$P_4N_4F_4(NMe_2)_4$ (I and II)	$P_4N_4F_4Cl_4$ (VII)	1.0	3.4				
	$P_4N_4F_4Cl_4$ (VIII)	1.2	3.6	13.7	14.1	60	720
$P_4N_4F_6(NMe_2)_2$ (V and VI)	$P_4N_4F_6Cl_2$ (XIV)	1.0	2.7				
	$P_4N_4F_6Cl_2$(XIII)	1.8	5.0	14.7	15.4	50	240
$P_4N_4F_4(NMe_2)_4$ (I and II)	$P_4N_4F_4Br_4$ (VII)	1.0	38.5	9.8	9.7	100	432
	$P_4N_4F_4Br_4$ (VIII)	1.1	40.2				
$P_4N_4F_6(NMe_2)_2$ (V and VI)	$P_4N_4F_6Br_2$ (XI)	1.0	31.0				
	$P_4N_4F_6Br_2$ (XII)	1.5	35.0	12.3	12.3	90	120

result of hydrogen bromide being a stronger nucleophile than hydrogen chloride.[4]

The deaminolysis of $P_4N_4F_{8-n}(NMe_2)_n$ ($n = 2$ and 4) with hydrogen halide[5] probably involved a preliminary coordination to the basic ring nitrogen atom (i.e. the nitrogen atom flanked by two amine groups).

Vibrational spectra

The IR data for the compounds are collected in Tables 2 and 3. For purposes of comparison, the vibrational spectra of the four compounds are discussed together. The vibrational spectra of $P_4N_4F_6Br_2$ and $P_4N_4F_6Cl_2$ are, as expected, very similar with major differences occurring in the 530–580 cm^{-1} region which contains bands ascribed to the PBr and PCl stretching vibrations respectively. The strongest band in the spectra of these compounds is a ring stretching mode occurring at 1360–1400 cm^{-1}. Two effects to consider here are namely (a) the fact that this mode moves to higher energy with increasing fluorine content and (b) this is a degenerate mode in $P_4N_4Cl_8$ (the chloro precursor) and with decreasing symmetries would expect (in $P_4N_4F_4X_4$, $P_4N_4F_6X_2$; X = Cl, Br compounds) the degeneracy to be raised. Other ring modes can be assigned to bands occurring at *ca* 1040, 810, 665, 425 and 415 cm^{-1}.

The remaining bands are thus due to PF_2 asymmetric in-phase and out-of-phase stretches, PF_2 symmetric in-phase and out-of-phase stretches,

Table 2. IR spectra* of compounds $P_4N_4F_4Br_4$ (VII) and $P_4N_4F_4Cl_4$ (VIII)

VII	VIII	Assignment
1360 vs	1370 vs	Ring
1038 s	1040 s	
945 vs	945 vs	νPF
905 w	908 m	
785 vs	800 vs	Ring
695 m	718 vs	Ring
665 m	688 m	
	565 vs	νPCl
530 vs		νPBr
418 m	423 m	Ring

* Obtained as liquid film.

Table 3. IR spectra* of compounds $P_4N_4F_6Cl_2$ (XI) and $P_4N_4F_6Br_2$ (XIII)

XI	XIII	Assignment
1380 vs	1400 vs	Ring
1060 vs	1060 vs	
960 vs	965 vs	$\nu_a PF_2$ (i.p) + PF
908 m	908 m	$\nu_a PF_2$ (o.p)
810 vs	812 vs	Ring
745 vs	750 vs	$\nu_s PF_2$ (i.p)
718 m	718 m	$\nu_s PF_2$ (o.p)
650 s	670 vs	Ring
	580 s	νPCl
530 vs		νPBr
485 m	492 m	νPF_2
415 w	425 m	Ring

* Obtained as liquid film.

PF_2 deformation and PF stretching vibrations. The bands at *ca* 965, 960 and 908 cm^{-1} can be associated with PF_2 asymmetric (in-phase and out-of-phase) vibrations. The band at *ca* 956 cm^{-1} is also due to PF stretching vibrations. The PF_2 deformations occur at *ca* 492 and 485 cm^{-1}.

Apart from differences in the region associated with PBr and PCl stretching vibrations, the IR spectra of compounds $P_4N_4F_4Br_4$ and $P_4N_4F_4Cl_4$ are indeed very similar. The bands at *ca* 565 cm^{-1} in $P_4N_4F_4Cl_4$ and at *ca* 530 cm^{-1} in $P_4N_4F_4Br_4$ are assigned to the phosphorus–halogen stretching modes.

^{19}F NMR spectra

Elemental analysis and mass spectrometry were used to confirm the stoichiometry of the compounds summarised in Fig. 1.

The complete ^{19}F NMR data for the compounds are collected in Table 4. Figure 2 shows the spectrum of compound $P_4N_4F_4Cl_4$. This consists of two doublets most probably arising from the two isomers shown to be present by GLC. Figure 1 shows the four possible non-geminal isomers for a compound with stoichiometry $P_4N_4F_4X_4$ (X = Cl, Br). For the compound $P_4N_4F_4X_4$ (X = Cl), compounds **VII**, **VIII** and **X** are likely isomers but **IX** can be eliminated as its spectrum would give three doublets.

Compounds **I** and **II** (see Fig. 1) for which X-ray structures are available[6,7] are the amino-fluoride precursors of the isomers of compound $P_4N_4F_4Cl_4$ and on this basis compounds **VII** and **VIII** are the most likely structures.

Invoking a "*cis*-effect"[8] pragmatically, chemical

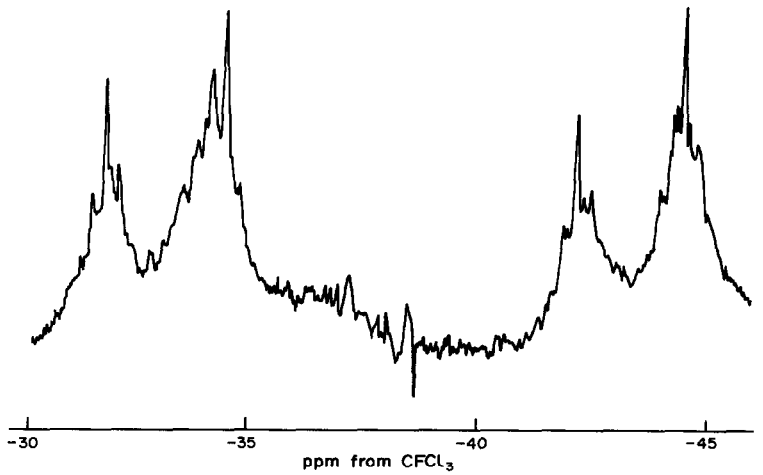


Fig. 2. ^{19}F NMR spectrum of $P_4N_4F_4Cl_4$ (VII and VIII).

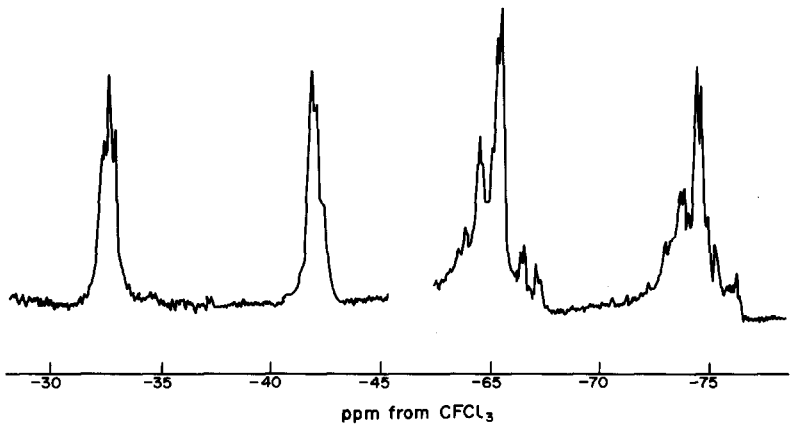


Fig. 3. ^{19}F NMR spectrum of $P_4N_4F_6Cl_2$ (XI).

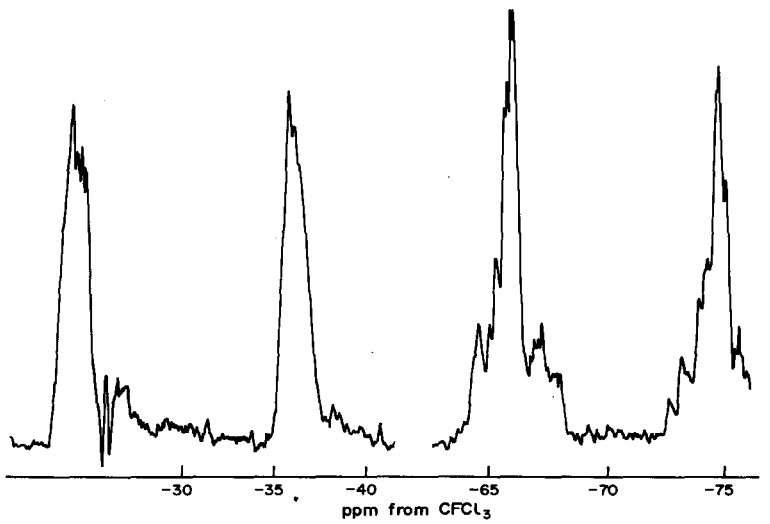


Fig. 4. ^{19}F NMR spectrum of $P_4N_4F_6Br_2$ (XIII).

Table 4. ^{19}F NMR data of compounds $P_4N_4F_6Cl_2$ (XI), $P_4N_4F_6Br_2$ (XIII), $P_4N_4F_4Cl_4$ (VII), $P_4N_4F_4Cl_4$ (VIII) and $P_4N_4F_4Br_4$

Compound	δ†(PF_2)	δ(PFCl)	δ(PFBr)	J*(PF)PFCl (Hz)	J*(PF)PF_2 (Hz)	J*(PF)PFBr (Hz)
XI	−70.8	−38.5		957	910	
XIII	−71.2		−30.8		955.6	986.5
VII		−39.09		935		
VIII		−37.18		963		
$P_4N_4F_4Br_4$	−70.86		−28.88			1010
			−31.56		927	960
			−34.38			996

† δ (ppm) relative to $CFCl_3$.

shifts of two compounds could be related to their structures. In compound **VII** the two fluorine nuclei are *cis* to each other and this will show higher field shift to compound **VIII**. On this basis, compound **VII** with a shift of *ca* −39 ppm is assigned a *cis–cis–trans*-configuration while compound **VIII** with a shift of −37 ppm is assigned a *cis–trans–cis–trans*-configuration. This is also confirmed by GLC evidence which showed shorter retention time for the *cis*-isomer in contrast to the aminochlorides and aminofluorides (an observation noted by Green and Sowerby).[9]

In the ^{19}F NMR data for the compound $P_4N_4F_4Br_4$ the sigmal at −70 ppm indicates an isomer with a geminal PF_2 group. Alternatively, the compound of composition $P_4N_4F_5Br_3$ may also be present but mass spectral data did not confirm this. Therefore assignment of this structure is not unambiguous in contrast to the chloride analogue.

For the compounds $P_4N_4F_6X_2$ (X = Cl, Br), the ^{19}F NMR spectra consists basically of two doublets in the intensity ratio of 2 : 1 (see Figs 3 and 4). The two doublets indicate two types of fluorine environments namely (PF_2) and (PFCl) groupings for compound (X = Cl) and (PF_2) and (PFBr) groupings for compound (X = Br).

The possible structures compatible with the observed ^{19}F NMR spectra are explicable by a consideration of the isomers of compounds **V** and **VI** (see Fig. 1) which are starting materials to compounds $P_4N_4F_6X_2$ (X = Cl, Br). This starting material—$P_4N_4F_6(NMe_2)_2$—consisted of approximately equal amounts of two isomers thought to be 1,*trans*-5-$P_4N_4F_6(NMe_2)_2$ (**V**) and 1,*cis*-5-$P_4N_4F_6(NMe_2)_2$ (**VI**) as discussed in Ref. 10. In view of this, it is most likely that these dibromo- and chloro-compounds also have these structures.

Evidence from GLC analyses showed the presence of two isomers in each of the compounds. On this basis, the isomers with the shorter retention times could be assigned the *cis*-isomer.[10] Hence compounds **XI** with X = Cl and compound **XIII** with X = Br are assigned a 1,*trans*-5-configuration and compound **XII** with X = Cl and compound **XIV** with X = Br the 1,*cis*-5-configuration.

Acknowledgement—Thanks to Dr D. B. Sowerby of Nottingham University, for his help in going through the manuscript and most particularly for the critical discussion of the ideas expressed in certain phases of evaluation.

REFERENCES

1. P. Clare, B. Green and D. B. Sowerby, *J. Chem. Soc., Dalton Trans.* 1972, 2374.
2. J. Emsley and N. Paddock, *J. Chem. Soc.* (*A*) 1968, 2590.
3. D. Millington and D. B. Sowerby, *J. Chem. Soc., Dalton Trans.* 1972, 2035.
4. T. T. Bamgboye, Ph.D. Thesis, University of Nottingham (1976).
5. D. Feakins, W. A. Last, S. N. Nabi and R. A. Shaw, *J. Chem. Soc.* (*A*) 1968, 1831.
6. M. J. Begley, D. Millington, T. J. King and D. B. Sowerby, *J. Chem. Soc., Dalton Trans.* 1974, 1162.
7. D. Millington, T. J. King and D. B. Sowerby, *J. Chem. Soc., Dalton Trans.* 1973, 396.
8. B. Green and D. B. Sowerby, *J. Chem. Soc.* (*A*) 1970, 987.
9. B. Green, D. B. Sowerby and P. Clare, *J. Chem. Soc.* (*A*) 1971, 3487.
10. D. Millington and D. B. Sowerby, *Phosphorus* 1974, **51**, 51.

Polyhedron Vol. 4, No. 4, pp. 663–668, 1985
Printed in Great Britain

0277–5387/85 $3.00 + .00
© 1985 Pergamon Press Ltd

REACTIONS OF COORDINATED MERCAPTIDE GROUP—III. REACTIONS OF ACYL CHLORIDES ON BIS(THIOSEMICARBAZONATO) CHELATES OF NICKEL(II)

SULEKH CHANDRA
Department of Chemistry, Zakir Husain College, Ajmeri Gate, Delhi-110006, India

(*Received* 20 *March* 1984; *accepted* 17 *August* 1984)

Abstract—Reactions of acetyl chloride and benzoyl chloride have been carried out on bis(thiosemicarbazonato)nickel(II) complexes of acetone and ethylmethyl ketone thiosemicarbazones. The reactions are taking place at the coordinated mercaptide group forming thioester *in situ*. The products which are obtained during reactions are characterised by elemental analyses, magnetic, moments, IR and electronic spectral studies.

Studies on the reactions of coordinated ligands are important in view of the fact that the coordinated metal ions, influence to a very great extent, the course of many complicated reactions, occurring during the metabolic activities,[1–3] in living organisms. Reactivity of the coordinated sulphur atom towards nucleophiles is of particular significance, in this context.

Amongst the most powerful nucleophiles, the mercaptide ion is of great significance in organic chemistry[4] and its nucleophilic property is not deterred even when this mercaptide group is bound to a metal ion as is the case in the formation of coordinated thioesters by the reactions of coordinated mercaptide group with alkyl halides.[5–7]

In this paper the reactions of acyl chlorides are reported on bis(thiosemicarbazonato)nickel(II) complexes. The reactions take place on the coordinated mercaptide group forming thioester *in situ*.

EXPERIMENTAL

All chemicals used were of AnalaR grade. The reactions were carried out in pyrex glass apparatus with interchangeable joints. Extreme precautions were taken to exclude moisture throughout the experiment. The solvents were dried before use. Pyridine (Fluka) was dried over KOH followed by distillation (b.p. 115–116°C). Dimethylformamide (Fluka) was dried over anhydrous K_2CO_3 followed by distillation (b.p. 153–154°C). Acetyl chloride and benzoyl chloride were dried by simple distillation (b.p. 51–52 and 197–198°C) respectively.

Preparation of bis(thiosemicarbazonato)nickel(II) complexes

These complexes were prepared by the method reported earlier.[8]

Reactions of acyl chlorides on acetone/ethylmethyl ketone bis(thiosemicarbazonato)nickel(II)

The reactions were carried out in two ways.

Reactions on dry chelates. Dry powdered bis chelates (0.05 mol) were taken in a 100 cm^3 round bottom flask and to it CH_3COCl/C_6H_5COCl (0.1 mol) was slowly added with constant stirring. On refluxing the contents on a water bath a green compound separated out. This was filtered under reduced pressure, washed with dry ether and dried under vacuum. The compound so obtained give analyses for $NiL_2 \cdot 2RCOCl$ (Table 1).

Reactions in DMF/Py medium. Dry powdered bis chelates (0.05 mol) were suspended in 100 cm^3 of dimethylformamide or pyridine in a 250 cm^3 round bottom flask and to it CH_3COCl/C_6H_5COCl (0.1 mol) was added dropwise with constant stirring. An exothermic reaction occurs and a dirty green to green solution is obtained. On adding *n*-hexane to this solution a yellowish green compound is obtained. Extra solvent is removed by decantation. The compound is dried under vacuum. These compounds give analysis corresponding to $NiL_2 \cdot 2RCOCl \cdot 2DMF/Py$ (Table 1).

Physical measurements

Magnetic susceptibility measurements were carried out on Gouy balance using $Hg[Co(CNS)_4]$

Table 1. Colour and composition of reaction products

Serial No.	Complex reaction products*	Colour	Elemental analysis [% found(calc.)]			
			Ni	C	H	N
	I					
1	$R_1 = R_2 = CH_3$	Greenish	18.71 (18.65)	30.55 (30.50)	5.75 (5.72)	26.72 (26.69)
2	$R_1 = CH_3, R_2 = C_2H_5$	Greenish	17.01 (16.93)	34.65 (34.61)	6.35 (6.24)	24.25 (24.23)
	II					
3	$R = R_1 = R_2 = CH_3$	Green	12.20 (12.17)	30.25 (30.33)	4.68 (4.63)	17.70 (17.69)
4	$R = R_1 = CH_3, R_2 = C_2H_5$	Green	10.65 (10.64)	39.25 (39.15)	4.75 (4.71)	15.25 (15.22)
5	$R = C_6H_5, R_1 = R_2 = CH_3$	Green	9.90 (9.65)	44.00 (44.09)	4.35 (4.34)	14.10 (14.02)
6	$R = C_6H_5, R_1 = CH_3, R_2 = C_2H_5$	Green	9.38 (9.35)	46.00 (45.80)	4.75 (4.78)	13.42 (13.38)
	IIa (DMF)					
7	$R = R_1 = R_2 = CH_3$	Green	9.50 (9.31)	34.82 (34.79)	5.85 (5.80)	18.12 (18.03)
8	$R = R_1 = CH_3, R_2 = C_2H_5$	Green	8.88 (8.91)	35.51 (33.45)	6.20 (6.16)	17.36 (17.26)
9	$R = C_6H_5, R_1 = R_2 = CH_3$	Green	7.68 (7.76)	45.25 (45.11)	5.42 (5.37)	15.20 (15.03)
10	$R = C_6H_5, R_1 = CH_3, R_2 = C_2H_5$	Green	7.51 (7.48)	46.60 (46.56)	5.75 (5.69)	14.52 (14.49)
	Py					
11	$R = R_1 = R_2 = CH_3$	Green	9.25 (9.13)	41.75 (41.72)	5.00 (5.06)	17.71 (17.69)
12	$R = R_1 = CH_3, R_2 = C_2H_5$	Green	8.88 (8.75)	43.60 (43.58)	5.51 (5.45)	16.90 (16.94)
13	$R = C_6H_5, R_1 = R_2 = CH_3$	Green	7.68 (7.64)	50.78 (50.74)	4.80 (4.76)	14.74 (14.80)
14	$R = C_6H_5, R_1 = CH_3, R_2 = C_2H_5$	Green	7.41 (7.36)	52.02 (51.99)	5.20 (5.10)	14.30 (14.27)
	III					
15	$R_1 = R_2 = CH_3$	Green	13.75 (13.72)	22.45 (22.44)	5.15 (5.14)	19.75 (19.64)
16	$R_1 = CH_3, R_2 = C_2H_5$	Green	12.90 (12.86)	26.40 (26.33)	5.90 (5.70)	18.45 (18.43)
	IIIa (DMF)					
17	$R_1 = R_2 = CH_3$	Green	11.55 (11.52)	33.00 (32.96)	6.30 (6.28)	16.50 (16.48)
18	$R_1 = CH_3, R_2 = C_2H_5$	Green	10.80 (10.79)	35.37 (35.31)	6.65 (6.62)	25.78 (25.75)
	Py					
19	$R_1 = R_2 = CH_3$	Green	11.30 (11.25)	41.50 (41.40)	5.40 (5.36)	16.20 (16.10)
20	$R_1 = CH_3, R_2 = C_2H_5$	Green	10.25 (10.20)	41.70 (41.68)	5.25 (5.21)	19.55 (19.45)

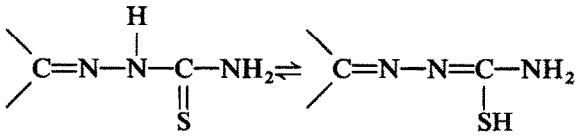
* Figure 1.

as calibrating agent ($\chi_g = 16.44 \times 10^{-6}$ cgs units at 20°C). IR spectra of the ligand and complexes were recorded on a Perkin–Elmer 621 automatic recording spectrophotometer. Electronic spectra were recorded on a Backman DK-2 automatic recording spectrophotometer.

Analysis for carbon and hydrogen were carried out in microanalytical laboratory of Chemistry Department of Delhi University. Nitrogen in the complexes was determined by Kjeldahl's method. Nickel was determined gravimetrically as nickel dimethylglyoxime.

RESULTS AND DISCUSSION

Thiosemicarbazones, like thiosemicarbazide, exist predominantly in their enolic form (**b**) in alkaline solution:[9]



a **b**

In this form they react with bivalent nickel to form neutral bis chelates, NiL_2. These complexes were diamagnetic and square planar.[9] From the structure of the complex NiL_2 [Fig. 1 (**I**)] it is apparent that there are two possible sites for acylation and aroylation,

(i) the coordinated mercaptide group,
(ii) the free $-NH_2$ group.

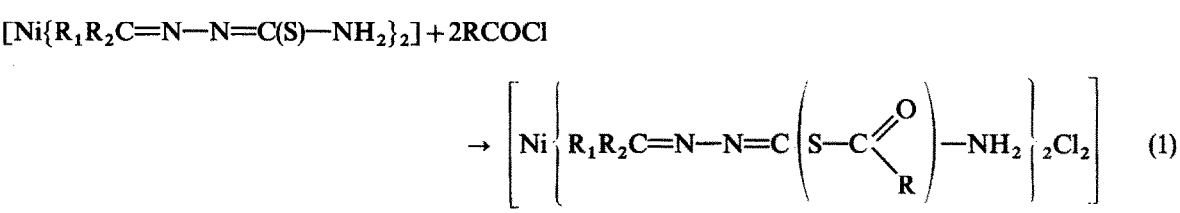
IR spectra of these complexes excludes the possibility of acylation and aroylation at the free-NH_2 group. IR spectra of the parent complex NiL_2 [Fig. 1 (**I**)] and the complexes [Fig. 1 (**II** and **IIa**)] display sharp bands of medium intensity at 3350 and 3300 cm^{-1} which are characteristics of ν_{NH_2} stretching frequencies.[10] A third band of a comparable intensity occurs at 1610 cm^{-1} which can be attributed to the δ_{NH_2} deformation mode.[10] The appearance of these bands confirms the presence of primary amine. In contrast, a secondary amine usually exhibits a strong characteristic band in the deformation region at rather lower frequency and a single ν_{NH} stretching frequency.[11]

On the basis of these spectral observations, the electrophilic nature of the attacking acyl chlorides and the usual inability of amide nitrogen to undergo chemical reaction, it would appear that acylation and aroylation take place at the coordinated mercaptide group.

Reaction on dry bis-chelates

Dry powdered samples of ketone bis-(thiosemicarbazonato)nickel(II) dissolve with change in colour in acetyl chloride or benzoyl chloride on gentle warming. The endothermic reaction (1) takes place at the coordinated mercaptide group producing thioester *in situ*.

The axial position of the complexes are occupied by chloride ions to give six-coordinated tetragonal structure [Fig. 1 (**II**)]. These complexes show magnetic moments corresponding to two unpaired electrons (Table 2). Electronic spectra of these complexes have been recorded in Nujol mull. All these complexes display electronic spectral bands at 9000–9100, 16,000–16,400 and 23,500–24,000 cm^{-1} which may be assigned to ν_1 ($^3A_{2g} \rightarrow {}^3T_{2g}$), ν_2 [$^3A_{2g}$



$R_1 = CH_3, R_2 = CH_3$ or C_2H_5 and $R = CH_3$ or C_6H_5

$\rightarrow {}^3T_{1g}(F)$] and ν_3 [$^3A_{2g} \rightarrow {}^3T_{1g}(P)$] transitions respectively for tetragonal nickel(II) complexes.[12,13] When reactions are carried out in the presence of coordinating solvent, viz. dimethylformamide and pyridine, axial positions in the resulting complexes are occupied by the solvent molecules [reaction (2)] [Fig. 1 (**IIa**)].

These reaction products also show magnetic moments corresponding to two unpaired spins (Table 2) and exhibit electronic spectral bands at 10,000, ν_1($^3A_{2g} \rightarrow {}^3T_{2g}$), 17,000, ν_2($^3A_{2g} \rightarrow {}^3T_{1g}$) and 24,500 cm^{-1} ν_3[$^3A_{2g} \rightarrow {}^3T_{1g}(P)$] corresponding to tetragonal geometry. The transition energy of the complexes obtained in reaction (2) is higher than the complexes of reaction (1). This may be attributed to the higher ligand field of the solvent (DMF/Py) molecules than the chloro group.

$$[Ni\{R_1R_2C{=}N{-}N{=}C(S){-}NH_2\}_2] + 2RCOCl$$

$$\xrightarrow{DMF/Py} \left[Ni\left\{ R_1R_2C{=}N{-}N{=}C\left(S{-}C\begin{matrix} \overset{O}{\parallel} \\ R \end{matrix} \right){-}NH_2 \right\}(DMF/Py)_2 \right] Cl_2 \qquad (2)$$

$$R_1 = CH_3, R_2 = CH_3 \text{ or } C_2H_5 \text{ and } R = CH_3 \text{ or } C_6H_5$$

It is interesting to note that reaction (1) without solvent is endothermic while reaction (2) in coordinated solvents like dimethylformamide and pyridine is exothermic. This may be explained on the following lines. In the course of reaction (2), the solvent molecules first occupy axial positions to form a neutral pseudo-octahedral complex as shown below:

$$[Ni\{R_1R_2C{=}N{-}N{=}C(S){-}NH_2\}_2(solvent)_2]$$

These mercaptide groups in the intermediate complex would become more reactive compared to those in the parent compound, as the equatorial metal sulphur link is weakened because of axial coordination.

All these reactions products are highly sensitive to moisture. The coordinated thioester group undergoes hydrolysis [reactions (3) and (4)] to yield the corresponding acid and the coordinated thioketo group.

The reaction products are also paramagnetic and exhibit magnetic moments in the range 2.98–3.02 BM (Table 2). Electronic spectra of these complexes exhibit bands at 9600–10,000, 16,800–17,000 and 24,200–24,600 cm^{-1} (Table 2) corresponding to pseudo-octahedral geometry.

Acids which are obtained during hydrolysis reactions have been characterised by their IR and spectral studies.

$$\left[Ni\left\{ R_1R_2C{=}N{-}N{=}C\left(S{-}C\begin{matrix} \overset{O}{\parallel} \\ R \end{matrix} \right){-}NH_2 \right\}_2 Cl_2 \right] + 4H_2O$$

$$\rightarrow [Ni\{R_1R_2C{=}N{-}NH{-}C(S){-}NH_2\}_2(H_2O)_2]Cl_2 + 2RCOOH \qquad (3)$$

$$\left[Ni\left\{ R_1R_2C{=}N{-}N{=}C\left(S{-}C\begin{matrix} \overset{O}{\parallel} \\ R \end{matrix} \right){-}NH_2 \right\}_2(Py/DMF)_2 \right] Cl_2 + 2H_2O$$

$$\rightarrow [Ni\{R_1R_2C{=}N{-}NHC(S){-}NH_2\}_2(Py/DMF)_2]Cl_2 + 2RCOOH \qquad (4)$$

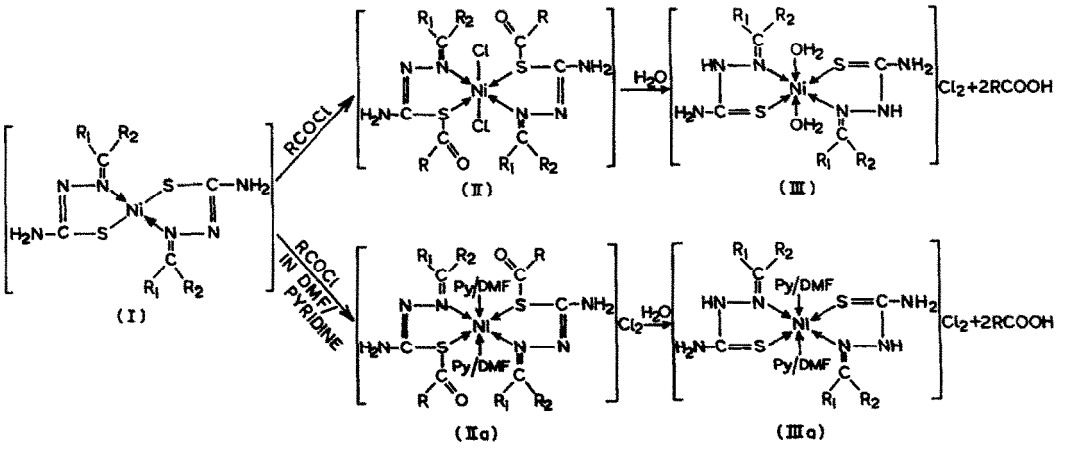
$$R_1 = CH_3, R_2 = CH_3 \text{ or } C_2H_5 \text{ and } R = CH_3 \text{ or } C_6H_5$$

Table 2. Magnetic moment (BM), electronic spectral bands (cm^{-1}) and their tentative assignments

Complex	μ_{eff} (BM)	λ_{max}	Assignment
1	Diamagnetic	17,500	$^1A_{1g} \rightarrow {}^1A_{2g}$
		22,000	$^1A_{1g} \rightarrow {}^1B_{1g}$
2	Diamagnetic	17,500	$^1A_{1g} \rightarrow {}^1A_{2g}$
		22,000	$^1A_{1g} \rightarrow {}^1B_{1g}$
3	3.02	9000	$^3A_{2g} \rightarrow {}^3T_{2g}$
		16,000	$^3A_{2g} \rightarrow {}^3T_{1g}(F)$
		23,500	$^3A_{2g} \rightarrow {}^3T_{1g}(P)$
4	3.12	9000	$^3A_{2g} \rightarrow {}^3T_{2g}$
		16,000	$^3A_{2g} \rightarrow {}^3T_{1g}(F)$
		23,500	$^3A_{2g} \rightarrow {}^3T_{1g}(P)$
5	2.98	9100	$^3A_{2g} \rightarrow {}^3T_{2g}$
		16,400	$^3A_{2g} \rightarrow {}^3T_{1g}(F)$
		24,000	$^3A_{2g} \rightarrow {}^3T_{1g}(P)$
6	3.10	9100	$^3A_{2g} \rightarrow {}^3T_{2g}$
		16,400	$^3A_{2g} \rightarrow {}^3T_{1g}(F)$
		24,000	$^3A_{2g} \rightarrow {}^3T_{1g}(P)$
7	3.01	10,000	$^3A_{2g} \rightarrow {}^3T_{2g}$
		17,000	$^3A_{2g} \rightarrow {}^3T_{1g}(F)$
		24,500	$^3A_{2g} \rightarrow {}^3T_{1g}(P)$
8	3.00	10,000	$^3A_{2g} \rightarrow {}^3T_{2g}$
		17,000	$^3A_{2g} \rightarrow {}^3T_{1g}(F)$
		24,500	$^3A_{2g} \rightarrow {}^3T_{1g}(P)$
9	2.98	10,000	$^3A_{2g} \rightarrow {}^3T_{2g}$
		17,000	$^3A_{2g} \rightarrow {}^3T_{1g}(F)$
		24,500	$^3A_{2g} \rightarrow {}^3T_{1g}(P)$
10	3.02	10,000	$^3A_{2g} \rightarrow {}^3T_{2g}$
		17,000	$^3A_{2g} \rightarrow {}^3T_{1g}(F)$
		24,500	$^3A_{2g} \rightarrow {}^3T_{1g}(P)$

Table 2—*continued*

Complex	μ_{eff} (BM)	λ_{max}	Assignment
11	3.01	10,200	$^3A_{2g} \rightarrow {}^3T_{2g}$
		17,000	$^3A_{2g} \rightarrow {}^3T_{1g}(F)$
		24,500	$^3A_{2g} \rightarrow {}^3T_{1g}(P)$
12	3.05	10,200	$^3A_{2g} \rightarrow {}^3T_{2g}$
		17,000	$^3A_{2g} \rightarrow {}^3T_{1g}(F)$
		24,500	$^3A_{2g} \rightarrow {}^3T_{1g}(P)$
13	3.00	10,200	$^3A_{2g} \rightarrow {}^3T_{2g}$
		17,000	$^3A_{2g} \rightarrow {}^3T_{1g}(F)$
		24,500	$^3A_{2g} \rightarrow {}^3T_{1g}(P)$
14	2.98	10,200	$^3A_{2g} \rightarrow {}^3T_{2g}$
		17,000	$^3A_{2g} \rightarrow {}^3T_{1g}(F)$
		24,500	$^3A_{2g} \rightarrow {}^3T_{1g}(P)$
15	3.02	9600	$^3A_{2g} \rightarrow {}^3T_{2g}$
		16,000	$^3A_{2g} \rightarrow {}^3T_{1g}(F)$
		23,600	$^3A_{2g} \rightarrow {}^3T_{1g}(P)$
16	3.01	9600	$^3A_{2g} \rightarrow {}^3T_{2g}$
		16,000	$^3A_{2g} \rightarrow {}^3T_{1g}(F)$
		23,600	$^3A_{2g} \rightarrow {}^3T_{1g}(P)$
17	3.02	9900	$^3A_{2g} \rightarrow {}^3T_{2g}$
		17,000	$^3A_{2g} \rightarrow {}^3T_{1g}(F)$
		24,000	$^3A_{2g} \rightarrow {}^3T_{1g}(P)$
18	3.02	9900	$^3A_{2g} \rightarrow {}^3T_{2g}$
		17,000	$^3A_{2g} \rightarrow {}^3T_{1g}(F)$
		24,000	$^3A_{2g} \rightarrow {}^3T_{1g}(P)$
19	3.01	10,000	$^3A_{2g} \rightarrow {}^3T_{2g}$
		17,000	$^3A_{2g} \rightarrow {}^3T_{1g}(F)$
		24,000	$^3A_{2g} \rightarrow {}^3T_{1g}(P)$
20	2.99	10,000	$^3A_{2g} \rightarrow {}^3T_{2g}$
		17,000	$^3A_{2g} \rightarrow {}^3T_{1g}(F)$
		24,000	$^3A_{2g} \rightarrow {}^3T_{1g}(P)$



R = CH_3/C_6H_5 ; $R_1 = R_2 = CH_3$ or $R_1 = CH_3$ and $R_2 = C_2H_5$

Fig. 1.

REFERENCES

1. G. L. Eichhorn, *Advances in Chemistry*, Series No. 37, p. 37. American Chemical Society, Washington, D.C. (1963).
2. D. H. Busch, *Advances in Chemistry*, Series No. 37, p. 1. American Chemical Society, Washington, D.C. (1963).
3. H. L. Bender, *Advances in Chemistry*, Series No. 37, p. 19. American Chemical Society, Washington, D.C. (1963).
4. F. E. Ray, *Organic Chemistry*. J. B. Lippincott, Philadelphia, PA (1947); E. S. Gould, *Mechanism and Structure in Organic Chemistry*. Holt, Rinehart & Winston, New York (1964).
5. C. W. Blomstrand, *Z. Prakt. Chem.* 1888, **38**, 329.
6. C. W. Blomstrand, *Z. Prakt. Chem.* 1883, **27**, 196.
7. S. Chandra, K. B. Pandeya and R. P. Singh, *Synth. React. Inorg. Met.-Org. Chem.* 1980, **9**, 53.
8. S. Chandra, K. B. Pandeya and R. P. Singh, *Nat. Acad. Sci. Lett.* 1978, **2**, 89.
9. S. Chandra, K. B. Pandeya and R. P. Singh, *Ind. J. Chem.* 1979, **18A**, 476.
10. M. L. Morris and D. H. Busch, *J. Am. Chem. Soc.* 1960, **82**, 1521.
11. L. J. Bellamy, *Infrared Spectra of Complex Molecules*. Wiley, New York (1954).
12. L. Sacconi, *Transition Metal Chemistry* (Edited by R. L. Carlin), Vol. 4, p. 344. Marcel Dekker, New York (1968).
13. A. B. P. Lever, *Inorganic Electronic Spectroscopy*. Elsevier, Amsterdam (1968).

Polyhedron Vol. 4, No. 4, pp. 669–674, 1985
Printed in Great Britain

0277-5387/85 $3.00 + .00
© 1985 Pergamon Press Ltd

CONVERSION OF DEXTROSE INTO HYDROGEN USING AQUEOUS TRIS(2,2'-BIPYRIDINE)RHODIUM(III) COMPLEX AS A PHOTOCATALYST AND ENHANCED BY EFFICIENT HETEROGENEOUS REDOX CATALYSTS

BRUNO HUBESCH* and BERNARD MAHIEU
Université de Louvain, Laboratoire de Chimie Inorganique et Nucléaire, Chemin du Cyclotron, 2, B-1348 Louvain-la-Neuve, Belgium

(*Received* 9 *January* 1984; *accepted* 17 *August* 1984)

Abstract—Photoreduction of water is achieved with the system tris(2,2'-bipyridine)rhodium(III)/dextrose under UV illumination. A strong pH effect is exhibited with a maximum at pH = 1.30. Explanations are given both in terms of thermodynamics and kinetics of the involved reaction. Heterogeneous redox catalysts are tested, with best efficiency for TiO_2 supported Pt(0).

The conversion and storage of solar energy in the form of a chemical potential has aroused considerable interest, from the point of view of fundamental knowledge, and for its application in the near future. The production of clean fuels, such as hydrogen, has recently been extensively studied in systems using either homogeneous (dyes, metal complexes) or heterogeneous (semiconductor material) photosensitizers.[1,17,18]

When decomposition of water aims only at the production of hydrogen, various organic electrodonors such as substituted tertiary amines are used as reducing agents. The latter are stoichiometrically oxidized with respect to the hydrogen evolution.

The use of raw material or biological wastes like carbohydrates as a donor material, though requiring more energetic photons, should render the energy conversion aspect more promising because of a valuable recovery of otherwise worthless biochemicals.

As a continuation of earlier work on the photogeneration of hydrogen with the CdS/tertiary amines or carbohydrates systems,[2] this report describes results obtained with the tris(2,2'-bipyridine)rhodium(III)/dextrose/redox catalyst system. Dextrose (D) is chosen to represent heavier oligo- and polysaccharides and the rhodium complex is a good homogeneous UV-photosensitizer.

The effect of pH in hydrogen productivity efficiency and the action of heterogeneous redox catalysts, i.e. platinum deposited on finely dispersed supports, are particularly studied. These two factors markedly affect the overall efficiency of the process.

EXPERIMENTAL

Chemicals

The following reagents were used without further purification (unless otherwise stated) and obtained from commercial sources as indicated hereafter: $RhCl_3 \cdot 3H_2O$ (for synthesis, Merck); $CoCl_2 \cdot 6H_2O$ (pur, Merck); 2,2'-bipyridine, TiO_2, Nb_2O_5 and Al–Ni 50/50 alloy (A.R. quality grade, U.C.B.); $SrTiO_3$ (purity > 99.5%, Alfa Ventron); H_2PtCl_6 10% solution (A.R. Merck); *N*-ethylmorpholine (for synthesis, Merck); Al_2O_3–Pt 10% (purissimum, Fluka); charcoal–Pt 10% (catalyst grade, Koch–Light Laboratories); Ru sponge (spectrographic standard substance, Johnson Matthey & Co.).

Monodistilled water was used to make up the aqueous solutions (resistivity > 10^6 Ω. cm).

Procedure for the preparation of the catalysts

Catalysts 1–4: Ni–Al alloy, $H_2PtCl_{6\,aq}$, platinum on charcoal or on activated Al_2O_3 were used from commercial sources without any further preparation.

Catalyst 5: an aqueous solution (50 μl) of H_2PtCl_6 0.20 M was added to a suspension of TiO_2 (1.0 g in 5 cm^3 H_2O). The mixture was stirred in air for 24 h at

* Author to whom correspondence should be addressed.

room temperature and evaporated to dryness on the sandbath. This last operation was repeated after addition of 5 cm^3 water and mixing. The solid obtained was ground in an agate mortar and put for 24 h in an oven at 120°C. This impregnated powder was reduced for 2 h under a flow of H_2 at 200°C, allowed to cool down to 25°C for another 2 h and to stand 2 h under H_2.

Catalyst 6: same procedure as for catalyst 5 using a suspension of Nb_2O_5 (0.5 g in 2.5 cm^3 H_2O) and $SrTiO_3$ (0.5 g in 2.5 cm^3 H_2O).

Catalyst 7: same procedure as for catalyst 5 using 500 μl of aqueous H_2PtCl_6.

Catalyst 8: metallic Ru sponge was heated at 960°C in air for 42 h (conditions previously established by thermogravimetric analysis).

Catalyst 9: $SrTiO_3/RhO_x$ was prepared according to reference 5.

The percentage of metal loading for these catalysts is indicated in Table 2.

Procedure for hydrogen generation experiments

As a function of pH. Illumination experiments were conducted on a 30 cm^3 aliquot of an aqueous solution containing 25 mg tris(2,2'-bipyridine)Rh(III)chloride tetrahydrate, 270 mg dextrose (5×10^{-2} M) at adjusted pH (pH 0.00: H_2SO_4 1 M; pH 0.61: H_2SO_4 0.25 M; pH 0.77: $KHSO_4$ 2 M; pH 1.30: $KHSO_4$ 0.5 M/K_2SO_4 0.5 M; pH 2.00: $KHSO_4$ 0.24 M/K_2SO_4 0.24 M; pH 2.73: H_3PO_4 0.2 M/NaH_2PO_4 0.6 M; pH 4.36: NH_4Cl 0.5 M/NaH_2PO_4 0.5 M; pH 7.00: NaH_2PO_4 0.5 M/Na_2HPO_4 0.5 M; pH 9.23: H_3BO_3 0.2 M/KOH 0.1 M; pH 14.0 NaOH 1 M).

The round bottomed 100 cm^3 Pyrex bulb was dipped to half its height in a thermostatted water bath held at 30 ± 1°C. The solution was thoroughly stirred (750 rpm) and the upper part of the vessel illuminated as close as possible by three 125 W high pressure Hg-lamps (Philips). The solution was degassed under vacuum before irradiation so that the internal pressure reached about 20 mmHg (2.7 kPa). At the end of an experiment, the internal pressure was brought to atmospheric pressure by admission of water through a side arm fitted with a Teflon plug.

As a function of the catalysts. The redox catalysts were all tested in identical experimental conditions, i.e. 25 mg $Rh(bipy)_3Cl_3 \cdot 4H_2O$/48.5 mg 2,2'-bipyridine (1.1×10^{-2} M)/2.700 g dextrose (0.5 M)/30 cm^3 $KHSO_4$ 0.2 M (pH 1.30)/redox catalyst as stated in the Table 2.

A 100 cm^3 quartz bulb was used and its bottom thermostatted at 21 ± 1°C. The light source was provided by a 1000 W ultrahigh pressure Xe–Hg lamp (Müller Electronik-Optik, $\lambda > 260$ nm) fitted with an IR water filter (spectral transmission 200–900 nm); the light beam was focused on the solution by means of appropriate lenses.

Analysis of the gas

The residual gas contained in the flask after equilibration of pressure was collected through a septum valve and quickly injected as previously described[2] into the gas chromatograph (Porapak column at 50°C, N_2 as carrier). The VPC detector was a catharometer calibrated by means of a 99.98% pure H_2 standard. Analysis showed that the gas is mainly H_2 with some residual air and water vapour. Known volumes of gas were analyzed and total volume measured in a reversed burette in a water bath or with an appropriate syringe.

Preparation of the tris(2,2'-bipyridine)rhodium(III) trichloride complex $Rh(bipy)_3Cl_3 \cdot 4H_2O$ was made according to the reference 3. The yield was 96.5%. The water content was measured by thermogravimetric analysis.

The electronic spectrum showed maxima at 305 nm and 319 nm with absorption coefficients (ε) amounting to 45,000 and 43,500 l $mole^{-1}$ cm^{-1} respectively [lit.[4] for $Rh(bipy)_3(ClO_4)_3$ λ max (ε): 305(33,800), 318(31,600)] [lit.[3] for $Rh(bipy_3)(SO_4)_{1.5}$ λ max (ε): 305(43,800), 318(46,700)]. pH measurements were made by means of a calibrated (±0.01) pH meter fitted with a glass–calomel combined electrode (Radiometer Copenhague). Spectrofluorimetric experiments were performed with a Perkin–Elmer MPF-3 spectrofluorimeter.

RESULTS AND DISCUSSION

The proposed reaction scheme is shown in the equation sequence (1)–(4) where D stands for dextrose and bipy for 2,2'-bipyridine. It should be pointed out that the photoreaction proceeds without any relay species.

$$Rh(bipy)_3^{3+} \underset{\text{radiationless decay}}{\overset{h\nu}{\rightleftharpoons}} {}^*Rh(bipy)_3^{3+} \quad \text{(counterion: } Cl^-\text{)}, \quad (1)$$

$${}^*Rh(bipy)_3^{3+} \xrightarrow{D} \text{reduced rhodium(II) complex} + D^+, \quad (2)$$

$$\xrightarrow{D^+} Rh(bipy)_2^+ + bipy + D^{2+},$$

$$Rh(bipy)_2^+ + 2H_3O^+ \xrightarrow{bipy} Rh(bipy)_3^{3+} + 2H_2O + H_2\nearrow, \quad (3)$$

$$D^{2+} \xrightarrow{H_2O} \text{aldonic acids}. \quad (4)$$

Table 1. Photogenerated H_2 evolution rates as a function of pH in the $Rh(bipy)_3^{3+}$/dextrose/buffer systems (see Experimental for reaction conditions)

pH	Irradiation time (h)	Volume of H_2 produced (ml)	Average H_2 evolution rate ($\mu l\ h^{-1}$)*
14.0	24.5	0	0
9.27	24	0.13	5.4±0.3
7.00	24	0.17	7.0±0.1
4.36	22	2.02	91.8±3.7
2.73	18.5	0.925	50.0±2.8
1.30	22.5	73.06	3247±116
0.77	22	44.93	2042±254
0.61	17	37.14	2185±120
0.00	17	0.80	47.3±1.6

*The quoted errors on average evolution rates are calculated as standard deviation for 10 samples at least and include the error on calibration.

and the overall reaction may be written

$$\text{Dextrose} + H_2O \xrightarrow{h\nu} \text{aldonic acid} + H_2. \quad (5)$$

Table 1 and Fig. 1 show a strong pH effect on the H_2 evolution. This may arise from several factors:

(1) A thermodynamic reason is invoked (redox potential of some occurring species of the type $Rh(bipy)_{3-n}^{x+}$ are represented in Fig. 3). The driving force of reaction (3) is modulated by the H_3O^+ concentration as E_0 $[Rh(bipy)_3^{3+}/Rh(bipy)_2^{+}]$ = −0.67 V (NHE at pH = 7)[3] and E_0 $[H_3O^+/H_2]$ = 0.00–0.059 pH) V. This explains the noncapability of reaction (3) to occur in alkaline media. Indeed, from pH = 9.23 and above a dark red-violet colour develops slowly and accumulates in solution as the reaction proceeds; at pH = 14.0 this colour is obtained within a minute; admission of air consumes this coloured species which is again formed after an air-free illumination and the cycle can be repeated several times. This air sensitive reduced complex has the spectrophotometric characteristics of $Rh(bipy)_2^{+}$ (λ max = 520 nm) and has been reported as such in voltametric experiments.[24]

(2) A kinetic hindrance for H_2 evolution caused by overvoltage (no specific redox catalyst being added because of voluntary limitation of experimental parameters in the reaction) adds to the thermodynamic conditions. This is invoked for the non-evolution of H_2 in neutral and the low level evolution in weakly acidic media.

(3) Maximum H_2 evolution occurs around pH = 1.30 and stronger acidic media (i.e. pH = 0.0) nearly make it stop. Chemical stability of the tris(2,2′-bipyridine)rhodium(III) photosensitizer may be affected by protonation of the ligand [equation (6)] and subsequent loss of the photophysical characteristics.

$$Rh(bipy)_3^{3+} \overset{H^+}{\rightleftharpoons} Rh(bipy)_3H^{4+} \overset{H^+}{\rightleftharpoons} Rh(bipy)_2^{3+} + (\text{bipy } H_2)^{2+} \overset{H^+}{\rightleftharpoons} \cdots \quad (6)$$

The unsaturated $Rh(bipy)_x^{3+}$ species then undergoes rapid aquation or addition of the chloride counterion.

In this context, the $Rh(bipy)_3^{3+}$ complex displays a similar mechanistic behaviour as during its relay role in the $Ru(bipy)_3^{2+}/Rh(bipy)_3^{3+}$/tertiary amine/bipy/redox catalyst system,[19] although UV excitation and quenching by dextrose does occur. UV sensitization has been chosen to permit difficult (i.e. endoergic) reaction to take place efficiently. This disadvantage of using UV can be lowered, if one bears in mind that the absorption bands of the rhodium complex are shifted towards visible light[21] because of modification of the ligand[3] (phenanthroline, dimethylbipyridine, ...) or change of the metal cation (iridium and osmium complexes behave similarly).[6,20]

Extensive photophysical studies of rhodium (III) complexes with polyheterocyclic nitrogen ligands[7–11] show that luminescence takes place mostly at visible wavelengths (450 nm, 485 nm, 580 nm, i.e. 2–3 eV). Thus, a shift of the absorption bands towards the visible should not considerably affect the emission energies and hence the thermodynamic and redox properties. However, preliminary spectrofluorimetric experiments with $Rh(bipy)_3Cl_3$ and dextrose rather emphasize a radiationless decay

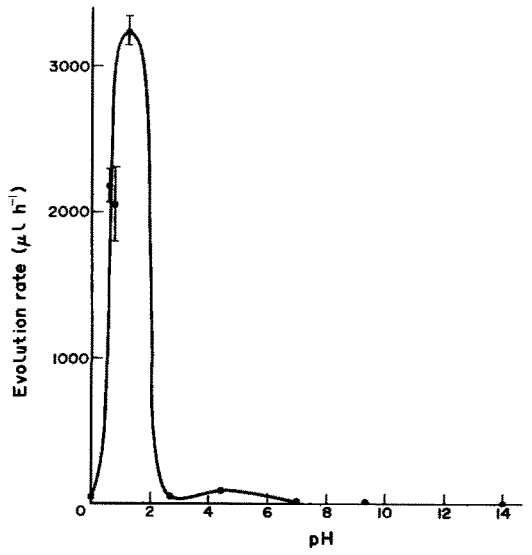


Fig. 1.

Table 2. Photogenerated H_2 evolution rates as a function of the catalyst in the $Rh(bipy)_3^{3+}$/dextrose/bipy/buffer 1.30/catalyst system (see Experimental for reaction conditions)

Catalyst number	Nature of the catalyst (weight)	Metal loading (weight %)	Metal content concentration in the irradiated mixture (mol per noble metal per litre of solution)	Surface area of the support ($m^2\ g^{-1}$)	Granulometry [mean particle size (μm)]
0	No catalyst added	—	—	—	—
1	Ni–Al alloy (30 mg)	50/50	$8.4\times10^{-3}/1.8\times10^{-2}$	—	10 μ
2	H_2PtCl_6 (aqueous, 50 μl, 0.2 M)	3.9	3.4×10^{-4}	Colloid	Colloid
3	Charcoal/Pt (10 mg)	10	1.7×10^{-4}	—	2.8 ± 0.5
4	Al_2O_3/Pt (10 mg)	10	1.7×10^{-4}	—	2.4 ± 0.3
5	TiO_2/Pt (10 mg)	0.2	3.4×10^{-6}	5.83	3.2 ± 0.4
6	Nb_2O_5–$SrTiO_3$/Pt (10 mg)	0.2	3.4×10^{-6}	1.69–3.87	3.5 ± 0.3–2.9 ± 0.4
7	TiO_2/Pt (10 mg)	2	3.4×10^{-5}	5.83	2.9 ± 0.2
7+8	TiO_2/Pt (10 mg)	2	3.4×10^{-5}	5.83	2.9 ± 0.2
	$+RuO_2$ (10 mg)	76.5	2.5×10^{-3}	—	$\geqslant 10\ \mu$
9	$SrTiO_3/RhO_x$ (10 mg)	0.2	5.3×10^{-6}	3.87	2.9 ± 0.2
6	TiO_2/Pt (10 mg) $+Cobipy_3Cl_2$ (25 mg)	2	3.4×10^{-5}	5.83	2.9 ± 0.4

Catalyst number	Volume of H_2 evolved (ml)	Average evolution rate ($\mu l\ h^{-1}$)	Irradiation time (h)	Turnover number (mol $\frac{1}{2}H_2$/mol metal catalyst)	Turnover rate (turnover number/time unit) (h^{-1})	Relative efficiency (H_2 rate with catalysis/H_2 rate not catalysed)
0	0.01	0.3 ± 0.02	24	—	—	1
1	1.04	44.9 ± 7.1	23.15	1	—	150
2	1.21	73.5 ± 5.0	16.5	10	0.6	245
3	1.69	74.2 ± 5.6	22.75	30	1.2	247
4	1.55	112.0 ± 9.2	13.83	28	2	373
5	2.84	162.5 ± 8.1	17.5	2476	142	541
6	3.02	172.0 ± 12.4	17.6	2644	150	573
7	2.40	183.1 ± 16.3	13.13	210	16	610
7+8	3.30	200.2 ± 7.5	16.5	292	18	667
9	2.18	106.5 ± 4.8	20.5	1234	60	355
6	2.59	156.7 ± 9.6	16.5	226	14	522

mode (see also reference 23). The type of excitation is also important: a metal to ligand charge transfer (MLCT) promotes an effective electron transfer from a donor to an excited state.

In the present case, $Rh(phen)_3^{3+}$, which is closely related to $Rh(bipy)_3^{3+}$ from a structural point of view, exhibits dual luminescence emission, showing both a metal-centred (^{3}MC) excited state at 298 K and a ligand centred excited state (^{3}LC) in a rigid matrix at 77 K. The temperature plays a major role and its variations should yield information about the transition from one excitation mode to another, which may pass by MLCT.

Further work is required to elucidate this question. On the other hand, the use of dextrose, or its heavier derivatives, as an electron-donor is also favoured by the application potentialities of its oxidation products, aldonic acids.

Table 2 and Fig. 2 display the catalytic capability of some platinum carrying substrates for enhancing the H_2 evolution.

Some of these catalysts were highly efficient compared with an experiment where no catalyst was added.

The most active ones are the semiconductors supporting platinum metal (TiO_2, Nb_2O_5, $SrTiO_3/Pt^0$) which are known for their small overpotential for H_2 evolution in water electrolysis.[12,13] Many factors contribute to the catalytic efficiency: degree of dispersion and area of the support, electrical properties of the powder (conducting as charcoal, insulating as Al_2O_3 or semi-

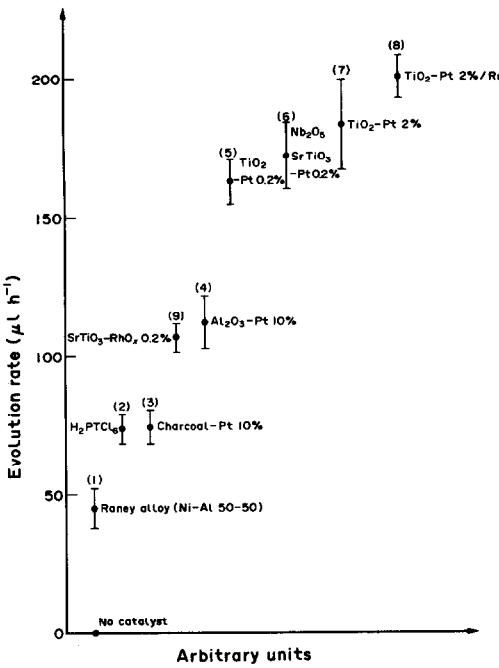


Fig. 2.

conducting) and optical properties. This latter behaviour is thought to explain the higher capability of semiconductors: these may act in a photoactive step of the reduction process by involving both band-gap excitation (i.e. generation of a chemically reactive hole–electron pair) and electron injection in the conduction band (E_0 [$Rh(bipy)_3^{3+}/Rh(bipy)_2^{+}$] $= -0.67$ V $< E_0$ (e_{CB}^- $SrTiO_3$ and Nb_2O_5) $= -0.60$ V, $< E_0$ (e_{CB}^- in TiO_2) $= -0.25$ V).[14,16] Since E (H_3O^+/H_2) $= -0.077$ V at pH = 1.30, heterogeneous efficient H_2 evolution may occur. On the other hand, surface states of the catalysts may act in a favourable way and strong metal–support interaction of low temperature reduced noble metals on TiO_2[15] is responsible for a long-term chemical stability of the deposits. Addition of RuO_2 slightly enhanced the overall efficiency, probably by oxidation catalysis. H_2PtCl_6 has a homogeneous catalytic role, as no visible colloid was detected by laser light scattering after irradiation. Ni^0–Al^0 alloys must not be considered as good catalysts: 82.5% of the Ni content was recovered in solution (as determined by dimethylglyoxime gravimetry) $Co(bipy)_3Cl_2$, tested as a potential relay, decreases the efficiency. $SrTiO_3$ loaded with rhodium oxide RhO_x showed a good activity as previously observed in water photolysis experiments.[5]

Further investigation is in progress using gamma-radiation induced preparations of finely dispersed noble metal catalyst aggregates. Catalysis experiments were conducted in the presence of free bipyridine (10^{-2} M) ($pK_A = 4.30$)[22] to avoid kinetic limitation in reaction (3), as this compound is known to have a catalytic role in the regeneration of $Rh(bipy)_3^{3+}$ from $Rh(bipy)_2^{+}$ when used as a relay.[3]

Differences in efficiency between pH and catalysis experiments result from changes of the experimental conditions [addition of bipyridine (i.e. change of pH), temperature, presence of potassium sulphate, type of vessels and lamps, etc.]. Nevertheless each type of experiment has been achieved in carefully controlled identical conditions.

The considerations in the present work permit optimistic views as to the double purpose of producing hydrogen from photoreduction of water while revalidating worthless biochemicals.

Acknowledgements—We express our appreciation to Professor D. Apers and Professor C. Ronneau for stimulating discussions. B. Hubesch is indebted to Professor J. M. Lehn (Strasbourg, France) for scientific contacts.

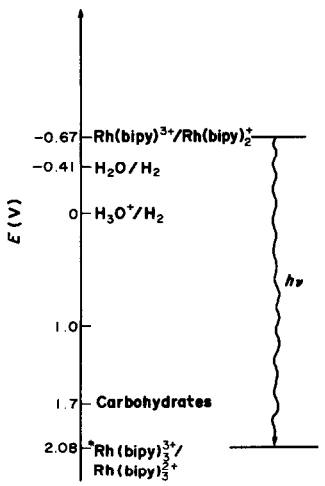


Fig. 3. Redox potentials of rhodium complexes.

REFERENCES

1. *Photogeneration of Hydrogen* (Edited by A. Harriman and M. A. West). Academic Press, London (1983) (and references therein).
2. B. Hubesch and B. Mahieu, *Inorg. Chim. Acta* 1982, **65**, L65–L67.
3. M. Kirch, J. M. Lehn and J. P. Sauvage, *Helv. Chim. Acta* 1979, **62**, 1345.
4. B. Martin and G. M. Waind, *J. Chem. Soc.* 1958, 4284.
5. J. M. Lehn, J. P. Sauvage, R. Ziessel and L. Hilaire, *Isr. J. Chem.* 1982, **22**, 168.
6. V. Balzani, F. Bolleta, M. T. Gandolfi and M. Maestri, *Top. Curr. Chem.* 1978, **75**, 1.

7. F. Bolleta, A. Rossi, F. Barigelletti, S. Dellonte and V. Balzani, *Gazz. Chim. Ital.* 1981, **111**, 155.
8. R. J. Watts and J. Van Houten, *J. Am. Chem. Soc.* 1978, **100**, 1718.
9. D. H. W. Carstens and G. A. Crosby, *J. Mol. Spectrosc.* 1970, **34**, 113.
10. G. A. Crosby and W. H. Elfring Jr., *J. Phys. Chem.* 1976, **80**, 2206.
11. R. Ballardini, G. Varani and V. Balzani, *J. Am. Chem. Soc.* 1980, **102**, 1719.
12. M. H. Miles and M. A. Thomason, *J. Electrochem. Soc.* 1976, **123**, 1459.
13. S. Srinivasan and F. J. Salzano, *Int. J. Hydrogen Energy* 1977, **2**, 53.
14. H. Gerischer, *Pure Appl. Chem.* 1980, **52**, 2649 (see also reference 16).
15. S. J. Tauster, S. C. Fung and R. L. Garten, *J. Am. Chem. Soc.* 1978, **100**, 170.
16. D. Duonghong, J. Ramsden and M. Grätzel, *J. Am. Chem. Soc.* 1982, **104**, 2977.
17. *Fourth International Conference on Photochemical Conversion and Storage of Solar Energy*, Jerusalem (1983) Book of Abstracts.
18. *Research on Photosynthesis and Photoconversion of Solar Energy*, Report of Special Research, Ministry of Education, Science and Culture, Japan (1982).
19. (a) K. Kalyanasundaram, *Nouv. J. Chim.* 1979, **3**, 511; (b) Q. G. Mulazzani, M. Ventrun and M. Z. Hoffman, *J. Phys. Chem.* 1982, **86**, 242; (c) Q. G. Mulazzani, S. Emmi, M. Z. Hoffman and M. Venturi, *J. Am. Chem. Soc.* 1981, **103**, 3362; (d) S. F. Chan, Mei Chou, C. Creutz, T. Matsubara and M. Sutin, *J. Am. Chem. Soc.* 1981, **103**, 369.
20. J. V. Caspar, B. Pat. Sullivan and T. J. Meyer, *Organometallics* 1983, **2**, 551.
21. (a) K. R. Mann, N. S. Lewis, V. M. Miskowski, D. K. Erwin, G. S. Hammond and H. B. Gray, *J. Am. Chem. Soc.* 1977, **99**, 5525; (b) W. R. Tikkanen, E. Binamira-Soriaga, W. C. Kaska and P. C. Ford, *Inorg. Chem.* 1983, **22**, 1147.
22. *Stability Constants*, Special Publication No. 17 (1964) and No. 25. The Chemical Society, London (1971).
23. (a) R. Ballardini, G. Varani, M. T. Indelli, F. Scandola and V. Balzani, *J. Am. Chem. Soc.* 1978, **100**, 7219; (b) V. Balzani, F. Scandola, G. Orlandi, N. Sabbatini and M. T. Indelli, *J. Am. Chem. Soc.* 1981, **103**, 3370.
24. G. Kev, K. De Armond and K. Hanck, *J. Phys. Chem.* 1974, **78**, 727.

Polyhedron Vol. 4, No. 4, pp. 675–679, 1985
Printed in Great Britain

0277-5387/85 $3.00 + .00
© 1985 Pergamon Press Ltd

STRUCTURAL STABILITY INDEX OF HETEROPOLY- AND ISOPOLY-ANIONS—III. APPLICATION TO SITE-VACANT FRAGMENTS OF KEGGIN AND DAWSON POLYANIONS α-$[PW_{12}O_{40}]^{3-}$ AND α-$[P_2W_{18}O_{62}]^{6-}$

KENJI NOMIYA and MAKOTO MIWA*
Department of Industrial Chemistry, Faculty of Engineering, Seikei University, Musashino, Tokyo 180, Japan

(*Received* 20 *March* 1984; *accepted* 17 *August* 1984)

Abstract—For some site-vacant species of Keggin and Dawson polyanions α-$[PW_{12}O_{40}]^{3-}$ and α-$[P_2W_{18}O_{62}]^{6-}$ containing hypothetical species, the structural stability indexes have been estimated. For the hypothetical species, the effect of negative charge should be also taken into account as a main factor. The electric condition has been proposed as a criterion for the existing polyanions. The site-vacant species of Keggin and Dawson polyanions, which have not been found yet, have been discussed using a combination of the structural stability and the electric condition.

In our previous papers,[1,2] the structural stabilities of a number of heteropoly- and isopoly-anions have been discussed in terms of the stability index η. The index has been estimated according to $\eta = (\Sigma B \cdot C)/A$, where A is the number of octahedral MO_6 units constituting the polyanion cage, B the number of MO_6 units constituting the closed loop and C the number of closed loops. The closed loop consists of the interpenetrating loop $-O_c-M-O_b-M-O_c-$ formed by a junction of M ion and bridging oxygens (O_b, O_c) around the polyanion cage. Site-vacant polyanions, formed by removal of some MO_6 octahedra from Keggin- and Dawson-structure polyanions $[XM_{12}O_{40}]^{n-}$ and $[X_2M_{18}O_{62}]^{n-}$ (M = Mo, W), have been used as starting materials for the preparation of other interesting heteropolyanions.[3–13] In this paper, we discuss the structural stabilities of some site-vacant Keggin and Dawson polyanions containing hypothetical species and also show that the electric charge is another important factor.

RESULTS AND DISCUSSION

The site-vacant polyanions derived from the Keggin-structure α-$[PW_{12}O_{40}]^{3-}$ ion have some isomers, which correspond to the geometrical isomers of α-$[PZ_xW_{12-x}O_{40}]^{n-}$ arising from partial substitution of a metal ion Z. They have been previously counted by Pope and Scully.[14] Using the molecular models, we have counted the number of closed loops and estimated the stability index. The formulae and structural parameters of the species with non-zero η are listed in Table 1. The numbering of the vacant sites is performed according to the method of Pope and Scully (Fig. 1).[14] The total isomers in di- and tri-vacant Keggin ions are 5 and 13, respectively. It can be readily verified that unlisted isomers such as the 1,4-vacant $[PW_{10}O_{38}]^{11-}$ ion, the 1,2,4- and 1,4,12-vacant $[PW_9O_{36}]^{13-}$ ions, the 1,2,6- and 1,3,4-vacant $[PW_9O_{35}]^{11-}$ ions, the 1,4,9-, 1,4,10- and 1,5,10-vacant $[PW_9O_{37}]^{15-}$ ions have no closed loop, or $\eta = 0$. The isolated polyanions are only monovacant $[PW_{11}O_{39}]^{7-}$ and trivacant $[PW_9O_{34}]^{9-}$ ions[15–23] and the others are unknown, or hypothetical. The 1,2,3- and 1,6,7-isomers of the trivacant $[PW_9O_{34}]^{9-}$ ion are usually designated B-α and A-α, respectively.[16] The latter is also called a half-Dawson structure polyanion.[1,2] The crystal and molecular structures of the trivacant species, $[PMo_9O_{34}H_3]^{6-}$ and $[PMo_9O_{34}H_6]^{3-}$, which are protonated forms of the 1,6,7-trivacant $[PMo_9O_{34}]^{9-}$ ion, have been determined by D'Amour and Allmann,[21] Strandberg,[22] and D'Amour.[23] Recently, the mono- and trivacant species have also been found in the aqueous solutions by base degradations of $[SiW_{12}O_{40}]^{4-}$ and $[PW_{12}O_{40}]^{3-}$ polyanions.[24,25]

* Author to whom correspondence should be addressed.

Table 1. Structural parameters of site-vacant species derived from Keggin-type heteropolyanion α-$PW_{12}O_{40}^{3-}$ by removal of some WO_6 octahedra

Formula	Vacant site (equivalent isomers)	A	(B, C)	η
Parent ion				
$PW_{12}O_{40}^{3-}$		12	(6, 4)	2
Monovacant ion				
$PW_{11}O_{39}^{7-}$	1-	11	(6, 2)	1.09
Divacant ion				
$PW_{10}O_{37}^{9-}$	1,2- (1,3-) 1,6- (1,7-)	10	(6, 1)	0.6
$PW_{10}O_{38}^{11-}$	1,5- (1,10-; 1,8-; 1,12-)	10	(6, 1)	0.6
	1,11-	10	(6, 2)	1.2
Trivacant ion				
$PW_9O_{34}^{9-}$	1,2,3- 1,6,7-			
$PW_9O_{36}^{13-}$*	1,2,5- (1,3,11-; 1,10,11-; 1,3,8-; 1,2,11-; 1,11,12-) 1,3,5- (1,2,8-; 1,10,12-) 1,5,8- (1,7,10-; 1,6,12-) 1,5,11- (1,7,11-; 1,6,10-; 1,8,11-; 1,7,12-; 1,6,11-)	9	(6, 1)	0.67
Tetravacant ion				
$PW_8O_{33}^{13-}$*	1,2,3,5- (1,2,3,8-; 1,2,3,11-; 1,10,11,12-) 1,6,7,11- (1,5,8,11-; 1,6,7,12-; 1,6,7,10-)			
$PW_8O_{34}^{15-}$*	1,2,5,8- (1,3,5,11-; 1,7,10,11-; 1,6,10,12-; 1,3,5,8-; 1,2,8,11-; 1,7,10,12-; 1,6,11,12-) 1,2,5,11- (1,3,8,11-; 1,7,11,12-; 1,6,10,11-)	8	(6, 1)	0.75
Pentavacant ion				
$PW_7O_{31}^{15-}$*	1,2,3,5,11- (1,2,3,5,8-; 1,2,3,8,11-; 1,7,10,11,12-; 1,6,10,11,12-) 1,2,5,8,11- (1,3,5,8,11-; 1,6,7,10,11-; 1,6,7,11,12-; 1,6,7,10,12-)	7	(6, 1)	0.86
Hexavacant ion				
$PW_6O_{28}^{15-}$*	1,2,3,5,8,11- (1,6,7,10,11,12-)	6	(6, 1)	1

* Species that conflict with the electric condition (1) in the text.

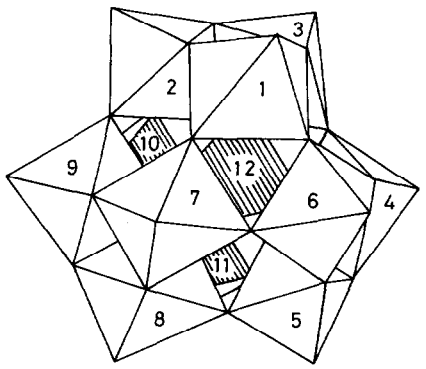


Fig. 1. Idealized α-Keggin structure polyanion and the numbering of vacant site according to Pope and Scully.[14] Tetrahedral part of the central heteroatom is omitted for clarity.

The index of structural stability has been conveniently applied only to isolated, or existing polyanions, but not to hypothetical ones. Whether such polyanions exist or not should be due to many factors other than the structural stability. The most important factor will be the effect of the negative charge of the polyanion. We therefore explored the heteropoly- and isopoly-anions of more than 250 examples which have been shown to be isolated or existing compounds, including a number of combinations of X, Z and M in the substituted polyanions $[XZ(H_2O)M_{11}O_{39}]^{n-}$ and $[X_2Z(H_2O)M_{17}O_{61}]^{n-}$ (X is a heteroatom, Z is a substituted metal ion and M is Mo or W). The following relation about the negative charge could

be deduced:

$$-4/3 \leqslant p \leqslant -1/6. \quad (1)$$

In this relation, p is $-n/A$, $-n$ is a charge of polyanion and A is the number of octahedral MO_6 units constituting the skeleton of polyanion to whom the number of $ZO_5(H_2O)$ unit in the substituted polyanions is also included. The total charge $-n$ involves the contribution from the heteroatom. The p is representative of mean electric charge per MO_6 unit. The lower limit of p is observed in the polyanions such as $[M_6O_{19}]^{8-}$ (M = Nb, Ta)[26] and $[XW_6O_{24}]^{8-}$ (X = Ni(IV), Mn(IV)),[27,28] and the upper limit in the $[PRe(VII)W_{11}O_{40}]^{2-}$ polyanion.[29] The relation (1) results in an electric condition for the isolated or existing polyanions, independently of the magnitude of the structural stability index. If the condition (1) can be applied to the polyanions in the Table 1, the following species are excluded; $[PW_9O_{36}]^{13-}$ in the trivacant ions and all of the tetravacant ($[PW_8O_{33}]^{13-}$, $[PW_8O_{34}]^{15-}$), the pentavacant ($[PW_7O_{31}]^{15-}$) and the hexavacant ($[PW_6O_{28}]^{15-}$) ions. These are asterisked in Table 1. In the remainder, the divacant ions $[PW_{10}O_{37}]^{9-}$ and $[PW_{10}O_{38}]^{11-}$ containing two geometrical isomers with non-zero η have been unknown. Even though they exist, three polyanions except the 1,11-vacant $[PW_{10}O_{38}]^{11-}$ ion are predicted to be unstable or metastable from the magnitude of the index.[1,2]

Here it should be noted that the asterisked species in Table 1 may possibly exist in the protonated forms or the modified forms by some attaching groups, whenever the electric condition is attained. The $[CH_3AsMo_6O_{21}(H_2O)_6]^{2-}$ anion previously reported by Matsumoto is an assemblage of six MoO_6 octahedra and a tetrahedral CH_3AsO_3 group, the former constituting a ring with alternate edge- and corner-sharing and the latter locating in the centre of ring.[30,31] Thus, this polyanion can be considered to be the derivative of the 1,2,3,5,8,11-hexavacant Keggin ion, or the compound possessing the similar skeleton. However, the electric condition (1) is kept, since each molybdenum atom has two terminal oxygens in the *cis* position and is coordinated by one water molecule. The structural stability is based on one closed loop passing through six MoO_6 octahedra ($\eta = 1$).

The site-vacant polyanions studied here lead to the substituted Keggin ions by filling the sites with other metal ions. Since the stability indexes of the substituted polyanions are the same as that of the Keggin ion ($\eta = 2$),[2] the structural stabilities of the site-vacant polyanions become to be more increased by filling the lacunary sites. Even though some site-vacant polyanions as precursors of substituted ions are unstable, the idea of structural stability does not preclude the presence of polyanions substituted in such lacunary sites. For instance, 1,4-substituted Keggin ions $[Ti_2W_{10}PO_{40}]^{7-}$ and $[\{CpFe(CO)_2Sn\}_2W_{10}PO_{38}]^{5-}$ have been recently prepared by Knoth and Domaille.[32] Although the 1,4-vacant polyanion $[PW_{10}O_{38}]^{11-}$ is considered to be a precursor of them, it is predicted to be unstable from the stability index ($\eta = 0$). In fact, such di-substituted polyanions have been prepared not from an isolated $[PW_{10}O_{38}]^{11-}$ compound, but from the "template" reactions of $TiCl_4$ and $CpFe(CO)_2SnCl_3$ with aqueous solutions of sodium tungstate and sodium dihydrogen phosphate under rather basic conditions.[32]

In the Dawson-structure α-$[P_2W_{18}O_{62}]^{6-}$ polyanion, many site-vacant species and their geometrical isomers can also be considered. The combination of the electric condition and the structural stability index with $\eta > 0.6$ allows the existence of limited species of them. They are listed in Table 2 together with the structural parameters. The numbering of the vacant sites is performed according to the method of Contant and Ciabrini (Fig. 2).[33] The stability index of more than 0.6 may be a criterion for many isolated polyanions.[1,2]

Only a few examples have been isolated.[33–36] Two monovacant polyanions, the so-called α_1- and α_2-forms of $[P_2W_{17}O_{61}]^{10-}$, have been well-known.[33,36] The stability index is estimated to be 1.29 for α_1-(4-vacant) form and 1.18 for α_2-(1-vacant) one. These indexes indicate both isomers will be formed in nearly equal probability or in the rather inclination to α_1-form, if the main factor that governs the metal departure from 1- and 4-positions of α-$[P_2W_{18}O_{62}]^{6-}$ is regarded as quite equivalent. However, it has been known that the partial degradation of the parent ion gives α_2-form only, and the α_1-form is produced by acidifying of the further alkaline-degraded solution of α_2-form, and then the α_1-form slowly isomerises into the α_2-form.[34] These should be attributed to the essential natures of the metals of 1- and 4-positions, but not to the structural stabilities, and should also depend strongly upon the experimental conditions.

Only one of many possible trivacant polyanions has been prepared, the vacant sites of which are suggested to be 1,2,3-positions.[4,33,34] Of the polyanions listed in Table 2, the hexavacant $[H_2P_2W_{12}O_{48}]^{12-}$ ion, which is a protonated form of the $[P_2W_{12}O_{48}]^{14-}$ ion, has been known.[33,34] The vacant sites are probably 1,4,9,10,15,16-positions. Only from the electric condition ($p = -1.5$), other unlisted hexavacant species, for instance, 1,2,3,16,17,18-vacant $[P_2W_{12}O_{50}]^{18-}$ ion is excluded, although its stability index is adequately

Table 2. Structural parameters of site-vacant species derived from Dawson-type heteropolyanion α-$P_2W_{18}O_{62}^{6-}$ by removal of some WO_6 octahedra*

Formula	Vacant site (equivalent isomers)	A	(B, C)	η
Parent ion				
$P_2W_{18}O_{62}^{6-}$		18	[(6, 2)+(8, 3)]	2
Monovacant ion				
$P_2W_{17}O_{61}^{10-}$	1- (α_2-isomer)†	17	[(6, 2)+(8, 1)]	1.18
	4- (α_1-isomer)†	17	[(6, 1)+(8, 2)]	1.29
Divacant ion				
$P_2W_{16}O_{59}^{12-}$	1,2- (1,3-)	16	(6, 2)	0.75
	4,10-	16	(8, 2)	1
	1,4- (1,9-)			
	4,5-	16	[(6, 1)+(8, 1)]	0.88
	4,9-			
$P_2W_{16}O_{60}^{14-}$	1,17- (1,18-)	16	(6, 2)	0.75
	4,13-	16	(8, 2)	1
	1,6- (1,7-; 4,3-)			
	1,10- (1,15-; 4,16-)			
	1,12- (1,13-; 4,18-)	16	[(6, 1)+(8, 1)]	0.88
	4,6-			
	4,8-			
	1,16-	16	[(6, 2)+(8, 1)]	1.25
	4,7-	16	[(6, 1)+(8, 2)]	1.38
Trivacant ion				
$P_2W_{15}O_{56}^{12-}$	1,2,3-	15	(6, 2)	0.8
	1,4,9-	15	[(6, 1)+(8, 1)]	0.93
$P_2W_{15}O_{58}^{16-}$	1,17,18- (1,2,18-; 1,3,17-)	15	(6, 2)	0.8
	1,16,17- (1,16,18-; 1,2,16-; 1,3,16-; 1,3,18-; 1,2,17-)	15	(6, 2)	0.8
	4,7,10- (4,10,13-; 4,7,13-)	15	(8, 2)	1.07
	1,4,6- (1,7,9-)			
	1,4,7- (1,6,9-)			
	1,6,7-			
	1,10,15-	15	[(6, 1)+(8, 1)]	0.93
	1,12,13-			
	1,10,16- (1,15,16-; 1,9,16-; 1,4,16-)			
	4,5,7- (4,5,8-; 4,6,7-)			
	4,6,9- (4,7,8-; 4,7,9-)			
$P_2W_{15}O_{59}^{18-}$	1,10,12- (1,13,15-)			
	1,10,13- (1,12,15-)	15	[(6, 1)+(8, 1)]	0.93
	1,6,16- (1,7,16-; 1,13,16-; 1,12,16-)			
Tetravacant ion				
$P_2W_{14}O_{55}^{16-}$	1,2,3,16- (1,2,3,17-; 1,2,3,18-)	14	(6, 2)	0.86
	1,4,6,9- (1,4,7,9-)	14	[(6, 1)+(8, 1)]	1
	1,4,9,16-			
$P_2W_{14}O_{56}^{18-}$	4,7,10,13-	14	(8, 2)	1.14
	1,4,6,7- (1,6,7,9-)	14	[(6, 1)+(8, 1)]	1
	4,5,7,8- (4,6,7,9-)			
Pentavacant ion				
$P_2W_{13}O_{51}^{14-}$	1,4,9,10,15-	13	(8, 1)	0.62
$P_2W_{13}O_{52}^{16-}$	1,4,9,10,16- (1,4,10,15,16-)	13	(8, 1)	0.62
Hexavacant ion				
$P_2W_{12}O_{48}^{14-}$	1,4,9,10,15,16-	12	(8, 1)	0.67

* Species allowed from both the electric condition (1) and the structural stability with $\eta > 0.6$.
† Refs 33 and 36.

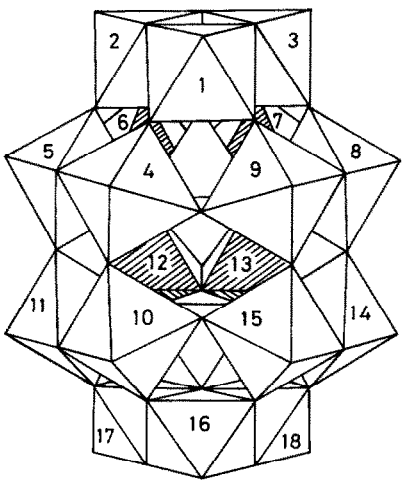


Fig. 2. Idealized α-Dawson structure polyanion and the numbering of vacant site according to Contant and Ciabrini.[33]

large, or $\eta = 1$ ($A = 12$ and $(B, C) = (6, 2)$). If the 1,2,3,16,17,18-isomer is readily protonated or modified with some attaching groups and the electric restriction is relaxed, such a form can possibly exist and may be more stable than the 1,4,9,10,15,16-isomer. Although many possible di-, tetra- and pentavacant species are listed in Table 2, none of them have been prepared.

Our approach rules out the possibility of the species with more than heptavacant species, except the half-unit of the Dawson-structure which corresponds to the enneavacant Dawson polyanion and also to the 1,6,7-isomer of the trivacant Keggin ion. This prediction may be justified from the polarographic experiments of the alkaline degradation of $[P_2W_{18}O_{62}]^{6-}$ in solution by Contant and Ciabrini.[34]

REFERENCES

1. K. Nomiya and M. Miwa, *Polyhedron* 1984, **3**, 341.
2. K. Nomiya and M. Miwa, *Polyhedron* 1984, **3**, 1161.
3. R. G. Finke, M. Droege, J. R. Hutchinson and O. Gansow, *J. Am. Chem. Soc.* 1981, **103**, 1587.
4. R. G. Finke and M. W. Droege, *Inorg. Chem.* 1983, **22**, 1006.
5. W. H. Knoth, *J. Am. Chem. Soc.* 1979, **101**, 759.
6. W. H. Knoth, *J. Am. Chem. Soc.* 1979, **101**, 2211.
7. F. Zonnevijlle and M. T. Pope, *J. Am. Chem. Soc.* 1979, **101**, 2731.
8. R. K. C. Ho and W. G. Klemperer, *J. Am. Chem. Soc.* 1978, **100**, 6772.
9. W. H. Knoth, P. J. Domaille and D. C. Roe, *Inorg. Chem.* 1983, **22**, 198.
10. F. Zonnevijlle, C. M. Tourné and G. F. Tourné, *Inorg. Chem.* 1982, **21**, 2742.
11. F. Zonnevijlle, C. M. Tourné and G. F. Tourné, *Inorg. Chem.* 1982, **21**, 2751.
12. M. M. Mossoba, C. J. O'Connor, M. T. Pope, E. Sinn, G. Hervé and A. Tézé, *J. Am. Chem. Soc.* 1980, **102**, 6864.
13. S. P. Harmalker, M. A. Leparulo and M. T. Pope, *J. Am. Chem. Soc.* 1983, **105**, 4286.
14. M. T. Pope and T. F. Scully, *Inorg. Chem.* 1975, **14**, 953.
15. C. M. Tourné, G. F. Tourné, S. A. Malik and T. J. R. Weakley, *J. Inorg. Nucl. Chem.* 1970, **32**, 3875.
16. R. Massart, R. Contant, J.-M. Fruchart, J.-P. Ciabrini and M. Fournier, *Inorg. Chem.* 1977, **16**, 2916.
17. R. Contant, J.-M. Fruchart, G. Hervé and A. Tézé, *C. R. Acad. Sci.* 1974, **278C**, 199.
18. G. Hervé and A. Tézé, *Inorg. Chem.* 1977, **16**, 2115.
19. A. Tézé and G. Hervé, *J. Inorg. Nucl. Chem.* 1977, **39**, 999.
20. K. Y. Matsumoto and Y. Sasaki, *Bull. Chem. Soc. Jpn* 1976, **49**, 156.
21. H. D'Amour and R. Allmann, *Naturwiss.* 1974, **61**, 31.
22. R. Strandberg, *Acta Chem. Scand.* 1974, **28A**, 217.
23. H. D'Amour, *Acta Cryst.* 1976, **B32**, 729.
24. D. L. Kepert and J. H. Kyle, *J. Chem. Soc., Dalton Trans.* 1978, 137.
25. J. H. Kyle, *J. Chem. Soc., Dalton Trans.* 1983, 2609.
26. R. Mattes, H. Bierbuesse and J. Fuchs, *Z. Anorg. Allg. Chem.* 1971, **385**, 230.
27. V. S. Sergienko, *Koord. Khim.* 1979, 936.
28. F. A. Cotton and G. Wilkinson, *Advanced Inorganic Chemistry*, 4th edition, p. 857. Wiley, New York (1980).
29. P. T. Meiklejohn, M. T. Pope and R. A. Prados, *J. Am. Chem. Soc.* 1974, **96**, 6779.
30. K. Y. Matsumoto, *Bull. Chem. Soc. Jpn* 1979, **52**, 3284.
31. H. Takahama, A. Yagasaki and Y. Sasaki, *Chem. Lett.* 1982, 1953.
32. P. J. Domaille and W. H. Knoth, *Inorg. Chem.* 1983, **22**, 818.
33. R. Contant and J.-P. Ciabrini, *J. Inorg. Nucl. Chem.* 1981, **43**, 1525.
34. R. Contant and J.-P. Ciabrini, *J. Chem. Res.* (M) 1977, 2601; (S) 1977, 222.
35. C. M. Tourné and G. F. Tourné, *Bull. Soc. Chim. Fr.* 1969, 1124.
36. R. Acerete, S. Harmalker, C. F. Hammer, M. T. Pope and L. C. W. Baker, *J. Chem. Soc., Chem. Commun.* 1979, 777.

Polyhedron Vol. 4, No. 4, pp. 681–685, 1985
Printed in Great Britain

0277–5387/85 $3.00 + .00
© 1985 Pergamon Press Ltd

METAL COMPLEXES OF ANTI-INFLAMMATORY DRUGS—I. COMPLEXES OF IRON(III), COBALT(II), NICKEL(II), COPPER(II) AND ZINC(II) WITH 4-HYDROXY-3-(5-METHYL-3-ISOXAZOLOCARBAMYL)-2-METHYL-2*H*-1,2-BENZOTHIAZINE-1,1-DIOXIDE (ISOXICAM)

D. O. HARRISON, R. THOMAS and A. E. UNDERHILL*
School of Physical and Molecular Sciences, University College of North Wales, Bangor, Gwynedd, U.K.

and

J. K. FLETCHER, P. S. GOMM and F. HALLWAY
Department of Chemistry, Rugby School, Rugby, Warwickshire, U.K.

(*Received* 1 *September* 1983; *accepted after revision* 17 *August* 1984)

Abstract—The preparation, spectroscopic and magnetic properties are reported for complexes of iron(III), cobalt(II), nickel(II), copper(II) and zinc(II) with the anti-inflammatory drug 4-hydroxy-3-(5-methyl-3-isoxazolocarbamyl)-2-methyl-2*H*-1,2-benzothiazine-1,1-dioxide (isoxicam). In all the complexes studied the isoxicam acts as a chelate monoanionic ligand with coordination involving the enolate oxygen atom and the carbonyl oxygen atom of the amide group. The copper(II) complex appears to be square planar whereas the hydrated cobalt(II), nickel(II) and, by inference, zinc(II) complexes possess an octahedral stereochemistry involving two coordinate drug molecules. The iron(III) complex contains three coordinated chelate isoxicam ligands.

The current therapeutic approach to treating musculoskeletal diseases, such as rheumatoid arthritis, relies heavily on non-steroidal anti-inflammatory agents.[1,2] However, these drugs may cause adverse reactions such as peptic ulceration and gastrointestinal bleeding. Recently increasing interest has been shown in the therapeutic use of metallic compounds in treating connective tissue disease.[3] Copper[4,5] and gold[6,7] preparations specifically have been shown to exhibit anti-inflammatory effects. Copper complexes of a number of non-steroidal anti-inflammatory drugs have been reported to be more potent anti-inflammatory agents and less ulcerogenic than the parent anti-inflammatory drug.[8]

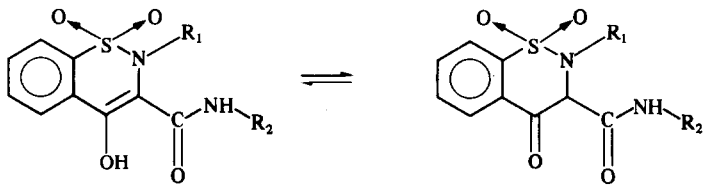
The work reported here is part of a comprehensive study aimed at isolating and characterising coordination compounds formed between non-steroidal anti-inflammatory drugs and transition metal ions. Non-steroidal anti-inflammatory agents may be characterised chemically as lipophilic, moderately strong organic acids. Although many such agents are arylalkanoic acids[2] current interest has focussed on a series of enolizable amides.[9] Three *N*-heterocyclic 3-carboxamides of 4-hydroxy-2-methyl-2*H*-1,2-benzothiazine-1,1-dioxide, namely sudoxicam ($R_1 = CH_3$; R_2 = 2-thiazole), piroxicam ($R_1 = CH_3$; R_2 = 2-pyridyl) and isoxicam ($R_1 = CH_3$; R_2 = 5-methyl-3-isoxazolyl) (see Fig. 1), have attracted particular attention as anti-arthritis drugs.[10,11]

This paper presents the results of an investigation of the complexes formed by isoxicam with some first row transition metal ions.

EXPERIMENTAL

Isoxicam was supplied by Warner–Lambert/Parke–Davis and was used without further purification. All metal salts used, with the exception of iron(III) chloride hexahydrate (B.D.H.), were of Analar reagent grade.

* Author to whom correspondence should be addressed.



Enol form Keto form

R_1 = H or alkyl group
R_2 = aryl or heterocyclic group

Fig. 1.

Preparation of complexes

Isoxicam (1.5 g; 1 mole equiv) was dissolved in 0.1 M sodium hydroxide (50 cm^3) by slow addition of the alkali with constant agitation and warming to $\leqslant$ 60°C. The volume of alkali was deliberately kept to a minimum to exclude excess hydroxide ions. The resulting pale yellow solution was filtered to remove excess undissolved ligand and the filtrate was added slowly with stirring to a cold solution of the metal chloride (0.5 mole equiv) in 35 cm^3 of ethanol [for Fe(III), Co(II), Ni(II) or Cu(II)) or water (Zn(II)]. The resulting precipitate of the metal complex was filtered off under vacuum, washed with cold ethanol, followed by cold ethoxyethane and dried at 80°C. All the metal complexes were obtained in high yield (> 90%) as microcrystalline powders.

Physical measurements

Carbon, hydrogen and nitrogen analyses were performed in the microanalytical laboratory of the University College of North Wales, Bangor. The diffuse reflectance spectra were determined on a Beckmann DK-2A spectrophotometer fitted with a standard reflectance accessory. IR spectra (4000–650 cm^{-1}) were recorded on a Perkin–Elmer 197 spectrophotometer in sodium dry Nujol mull using KBr plates. Room temperature magnetic measurements on powdered samples were made on a Newport Instruments Gouy balance using gouy tubes calibrated with $HgCo(CNS)_4$.

RESULTS AND DISCUSSION

The complexes were all obtained from solutions of the sodium salt of isoxicam and were precipitated with isoxicam present as a mono-anionic ligand (see Table 1). The Co(II), Ni(II), Fe(II) and Zn(II) complexes were all hydrated but the Cu(II) complex was obtained in an anhydrous state.

IR spectra

A partial assignment of the absorption bands observed for isoxicam and the metal complexes is given in Table 1. The IR spectra of the complexes are

Table 1. IR absorption bands (cm^{-1})

	—O—H	N—H str	—HN—C=O str	—C=N— str	SO_2 asy str	SO_2 sym str
Isox	3290* s	3165 w	1633	1550	1350 s	1190 s
$Fe(isox)_3 \cdot 3H_2O$	3000–3500 b	— —	1620 s	1550	1350 s	1190
$Co(isox)_2 \cdot 4H_2O$	3000–3500 b	—	1620 b	1550	1335 s	1185
$Ni(isox)_2 \cdot 5H_2O$	3000–3500 b	—	1625 b	1550	1330 s	1185
$Cu(isox)_2$	—	3150 w	1620 b	1550	1340 s	1190
$Zn(isox)_2 \cdot 4H_2O$	3000–3500 b	—	1620 b	1550	1330	1180

* Enol —OH.

Table 2. Analysis of isoxicam complexes

	Found (%)			Required (%)		
	C	H	N	C	H	N
$Fe(isox)_3 \cdot 3H_2O$	45.62	3.35	11.44	45.45	3.79	11.36
$Co(isox)_2 \cdot 4H_2O$	41.88	3.92	10.22	42.06	4.01	10.52
$Ni(isox)_2 \cdot 5H_2O$	41.23	3.81	10.20	41.14	4.16	10.29
$Cu(isox)_2$	45.41	3.67	10.92	45.93	3.28	11.48
$Zn(isox)_2 \cdot 4H_2O$	41.54	3.16	10.38	41.72	3.97	10.43

very similar to one another and to that of isoxicam itself. The ligand shows a sharp absorption band at 3290 cm^{-1} characteristic of a free O—H group. The absence of this absorption band in the anhydrous $Cu(isox)_2$ complex indicates that the isoxicam is attached to the metal as an anionic ligand via the oxygen atom of the tautomeric enol form. The intensity and broadness of the 3000–3500 cm^{-1} absorption in the remaining hydrated complexes suggests the presence of hydrogen bonded water molecules. The intensity and broadness of the bands in this region for the hydrated complexes (Table 2) is partially reduced on heating the complexes to 200°C, indicating that partial dehydration can occur at elevated temperatures.

The sharp band observed at 1633 cm^{-1} in the free ligand is assigned to the carbonyl stretch of the secondary amide group —CO—NHR_2. This is lowered to 1620 cm^{-1} in all the complexes. The N—H stretch observed in the ligand at 3165 cm^{-1} as a weak absorption is only seen in the anhydrous $Cu(isox)_2$ complex. In the hydrated complexes this vibration is obscured by the broad bands due to hydrogen bonding. The band at 1550 cm^{-1} assigned to the C=N stretching vibration and the two very strong bonds at 1350 and 1190 cm^{-1} and assigned to the asymmetric and symmetric stretching vibrations of the SO_2 group in the free ligand, appear at very similar frequencies in the complexes.

From a consideration of the IR spectra it is clear that in these complexes isoxicam acts as a mono-anionic ligand species through the enolate oxygen atom. It is probable that a second metal ligand bond is formed through the carbonyl oxygen atom of the amide group forming a six-membered chelate ring. It is also possible that the amide nitrogen atom may be involved in some of the complexes.

Diffuse-reflectance spectra (see Table 3)

Isoxicam and all the complexes exhibit an intense charge transfer band above 24,000 cm^{-1}. The reflectance spectra of $Zn(isox)_2 \cdot 4H_2O$ (d^{10}) complex and of isoxicam itself in the region 4000–24,000 cm^{-1} are quite similar, and show only a number of low intensity bands that may be considered to be IR overtones of the ligand. The reflectance spectrum of the zinc(II) complex has therefore been used as reference spectrum for the other complexes as the absorption bands due to isoxicam are slightly more intense in the zinc complex than in the free ligand.

For octahedral cobalt(II) complexes three bands are expected corresponding to the three spin-allowed transitions: $^4T_{1g}(F) \rightarrow {}^4T_{2g}(F)$ (ν_1); $^4T_{1g}(F)$

Table 3. Diffuse reflectance spectra and room-temperature magnetic moments*

	μ_{eff} (BM)	Absorption bands (cm^{-1})	D_q (cm^{-1})
$Fe(isox)_3 \cdot 3H_2O$	5.40	20,000 (str, 1.35)	—
$Co(isox)_2 \cdot 4H_2O$	5.25	$\nu_1[^4T_{1g}(F) \rightarrow {}^4T_{2g}(F)]$† 8850 (0.29)	1110
$Ni(isox)_2 \cdot 5H_2O$	3.40	$\nu_1[^3A_{2g}(F) \rightarrow {}^3T_{2g}(F)]$† 10,500 (0.19); $\nu_2[^3A_{2g}(F) \rightarrow {}^3T_{1g}(F)]$† 16,700 (0.25)	1050
$Cu(isox)_2$	1.82	16,700 (sh, 0.40)	1670

* Figures in parentheses represent intensity of the band on the arbitrary Beckmann scale.
† For convenience pseudo-octahedral symmetry is assumed in assigning these bands.

$\rightarrow {}^4A_{2g}$ (ν_2) and ${}^4T_{1g}(F) \rightarrow {}^4T_{1g}(P)$ (ν_3). However, it has been pointed out[12] that the transition ${}^4T_{1g}(F) \rightarrow {}^4A_{2g}$ corresponds to a two-electron jump and as such will have a much lower oscillator strength than the other two bands and will be much weaker. The reflectance spectrum of $Co(isox)_2 \cdot 4H_2O$ is similar to that formed by complexes in which Co(II) is surrounded by six O donor ligands. Since all the ligands are not identical the complex will not possess O_h symmetry, nevertheless, the departure from O_h seems small and for convenience assignments will be based on pseudo-octahedral symmetry. The single band at 8850 cm^{-1} has therefore been assigned to the ν_1 transition with the ν_2 and ν_3 bands considered to be obscured by the charge transfer edge. The reflectance spectra clearly show the complex to be octahedral and this is supported by the magnetic moment (5.25 BM) which lies in the range normally observed for a high spin cobalt(II) octahedral complex.[13]

The magnetic moment of the $Ni(isox)_2 \cdot 5H_2O$ complex, $\mu_{eff} = 3.4$ BM, does not distinguish clearly between spin-free hexacoordinate nickel(II) and tetrahedral nickel(II) in which there are low-symmetry components of the ligand field. The intensity and position of the reflectance spectra, however, suggests pseudo-octahedral symmetry for the nickel(II) ions. Magnetic moments as high as 3.41 BM are common for tetragonal octahedral complexes.[14] Three bands are expected for octahedral Ni(II) complexes and are assigned, assuming pseudo-O_h symmetry, in increasing order of energy, as the ${}^3A_{2g}(F) \rightarrow {}^3T_{2g}(F)$ (ν_1); ${}^3A_{2g}(F) \rightarrow {}^3T_{1g}(F)$ (ν_2) and ${}^3A_{2g}(F) \rightarrow {}^3T_{1g}(P)$ (ν_3). The bands observed at 10,500 and 16,667 cm^{-1} are therefore assigned to the ν_1 and ν_2 transitions respectively with the ν_3 band obscured by the charge transfer edge. The absence of clear splitting of these bands indicates that the extent of departure from O_h symmetry is small.

The microanalysis and IR spectrum indicate that the $Cu(isox)_2$ complex is anhydrous. The copper(II) ion complex may therefore be a four coordinate monomeric complex or a tetragonally distorted polymeric six coordinate complex.* In that latter case the amido nitrogen atoms would be involved. The reflectance spectrum is similar to those reported[15] for copper compounds in which the copper ion is in either an essentially square coplanar environment or in an octahedral environment with a very large tetragonal distortion.

The reflectance spectrum of $Fe(isox)_3 \cdot 3H_2O$ is quite featureless except for a pronounced shoulder at 20,000 cm^{-1} on the edge of the charge transfer band. All *d–d* transitions are spin forbidden and therefore any absorption bands will be extremely weak for an octahedral d^5 ion. The magnetic moment of 5.4 BM is consistent with a high spin complex, being close to the expected spin-only value of 5.9 BM.

GENERAL DISCUSSION

The reflectance spectra and magnetic moments indicate a pseudo-octahedral structure for the $Co(isox)_2 \cdot 4H_2O$, $Ni(isox)_2 \cdot 5H_2O$ and $Fe(isox)_3 \cdot 3H_2O$ complexes (Table 3).

In the $M(isox)_2 \cdot nH_2O$ complexes, the divalent metal ion is coordinated by two chelate isoxicam mono-anionic ligands with two water molecules completing a pseudo-octahedral structure. The complexes are neutral but it is not possible to tell whether the compounds are obtained in the *cis-* or *trans*-form. The $Fe(isox)_3 \cdot 3H_2O$ complex contains three chelate mono-anionic isoxicam ligands giving pseudo-octahedral environment around the iron(III) ion.

The loss of the protonic hydrogen atom from the enol form of the drug produces the anionic ligand which completes bidentate metal attachment by utilising the carbonyl oxygen of the secondary amide group. This can be seen from the disappearance of the O—H absorption band in the complexes and the shift in the position of the C=O absorption band. The bonding of the isoxicam to the metal ion in this way results in six-membered chelate rings and the formation of compounds that resemble β-diketonate complexes.

Acknowledgements—We would like to thank Warner–Lambert/Park–Davis for the supply of isoxicam, Dr P. J. Sadler (Birkbeck College, London) for infrared studies, and The Royal Society for a research in schools award (to P.S.G.). One of us (P.S.G.) would like to thank Mr B. Rees (Headmaster), Dr P. J. Cheshire (Head of Science), the Governors of Rugby School, for the provision of research facilities, and the Rokeby Trust (Rugby School) for further financial assistance.

REFERENCES

1. S. Wong, *Annu. Rep. Med. Chem.* 1975, **10**, 172.
2. J. G. Lombardino, *Annu. Rep. Med. Chem.* 1978, **13**, 167.
3. B. M. Sutton, *Annu. Rep. Med. Chem.* 1979, **14**, 321.
4. J. R. J. Sorenson, *Prog. Med. Chem.* 1978, **15**, 211.
5. J. R. J. Sorenson, *J. Med. Chem.* 1976, **19**, 135.
6. Empire Rheumatism Council, *Ann. Rheum. Dis.* 1961, **20**, 15.
7. A. A. Isab and P. J. Sadler, *J. Chem. Soc., Dalton Trans.* 1982, 135.

* We acknowledge the referee's suggestion on this compound.

8. D. H. Brown, W. E. Smith, J. W. Teape and A. J. Lewis, *J. Med. Chem.* 1980, **23**, 729.
9. J. G. Lombardino, E. H. Wiseman and W. M. McLamore, *J. Med. Chem.* 1971, **14**, 1171.
10. J. G. Lombardino and E. H. Wiseman, *J. Med. Chem.* 1972, **15**, 848; J. G. Lombardino, E. H. Wiseman and J. Chiaini, *J. Med. Chem.* 1973, **16**, 493; J. G. Lombardino, *J. Med. Chem.* 1981, **24**, 39.
11. H. Zinnes *et al.*, *J. Med. Chem.* 1982, **25**, 12.
12. S. Koide, *Philos. Mag.* 1959, **4**, 243.
13. B. N. Figgis and J. Lewis, *Prog. Inorg. Chem.* 1964, **6**, 37.
14. A. B. P. Lever, *Inorg. Chem.* 1965, **4**, 763.
15. D. E. Billing and A. E. Underhill, *J. Inorg. Nucl. Chem.* 1968, **30**, 2147.

Polyhedron Vol. 4, No. 4, pp. 687–695, 1985
Printed in Great Britain

0277–5387/85 $3.00 + .00
© 1985 Pergamon Press Ltd

PROTONATION OF CLUSTER MOLECULES: BRIDGING HYDROGEN SITES IN TETRAHEDRAL, OCTAHEDRAL AND CAPPED SQUARE PYRAMIDAL CLUSTERS: Be_4H_8, B_4H_8, $B_6H_7^-$ AND B_6H_8 AS MAIN GROUP MODELS FOR TRANSITION METAL CLUSTER SYSTEMS

M. A. CAVANAUGH, T. P. FEHLNER* and R. STRAMEL
Department of Chemistry, University of Notre Dame, Notre Dame, IN 46556, U.S.A.

and

M. E. O'NEILL and K. WADE*
Department of Chemistry, Durham University, Durham DH1 3LE, U.K.

(*Received* 14 *February* 1984; *accepted* 17 *August* 1984)

Abstract—Main group structural models for tetrahedral and octahedral transition metal clusters containing bridging hydrogens are developed using the MNDO quantum chemical technique. The bridging hydrogens in (hypothetical) Be_4H_8 and B_4H_8 tetrahedral systems (μ_3- and μ_2-respectively) are shown to mimic the bridging proton locations in the $H_4Re_4(CO)_{12}$ and $H_4Ru_4(CO)_{12}$ clusters in agreement with simple localized bond models. The perturbation of octahedral cluster bonding by bridging hydrogens is examined via the series $B_6H_6^{2-}$, $B_6H_7^-$ and B_6H_8 which demonstrates increasing preference for capped square pyramidal cluster geometry relative to octahedral with increasing protonation. Localized bond models suggest that frameworks which derive stability from localized bond resonance will be destabilized with increasing protonation relative to more classical forms. Framework protonation fixes 3-centre bond location and reduces the number of resonance structures. Alternatively, an analysis of Mulliken populations suggests that cluster frameworks in which charge asymmetry is significantly increased by protonation are disfavoured over those in which the asymmetry is decreased or maintained on protonation.

Cluster shapes are known to be related to the numbers of electrons that can be thought to hold the skeletal atoms together.[1–8] While specific relationships are well established for main group clusters, the situation for transition metal systems is much less rigorously defined.[9] Still, the detailed comparison of related main group and transition metal clusters provides a systematic way of exploring the latter for evidence of unique behaviour. Thus, we have previously demonstrated for some capped trimetal compounds that the main group analogues adequately explain not only subtle geometrical features but also important characteristics of the electronic structures of the metal compounds.[10] Having demonstrated in at least one system that the main group analogues of transition metal clusters can be used as more than formal models, we now use the same approach to explore the effects of ligand hydrogen atoms on cluster structure.

Recognition of the fact that the type, number and arrangement of hydrogen ligands affects cluster structure is nothing new. The influence of hydrogen atoms on cluster shapes and the site preferences they show are subjects of continuing interest to many researchers including ourselves.[10–15] For example, certain isoelectronic clusters exhibit shapes that differ with the number of hydrogen ligands, e.g. for tetranuclear clusters formally held together by seven skeletal bond pairs, the butterfly shape of tetraborane(10), B_4H_{10}, may be contrasted with the square planar shape of the cyclobutadiene dianion $C_4H_4^{2-}$. Both of these are *arachno* species formally related to the octahedron as the parent polyhedron (the former with a *cis*, the latter with a *trans*

* Author to whom correspondence should be addressed.

arrangement of vacant sites), the difference being dictated by the bonding requirements of the extra six hydrogen atoms of B_4H_{10}. The difference between η^3-allyl-metal complexes (which contain a butterfly-shaped C_3M unit) on the one hand and η^2-carboxylate–metal complexes (which contain planar CO_2M units) on the other hand again reflects the bonding requirements of the extra hydrogen atoms of the former.

The positions preferred by ligands like hydrogen atoms or carbonyl groups tend to reflect the electron distribution in clusters, and vice versa. Hydrogen ligands tend to occupy sites in which they can acquire the most negative (or least positive) charge.[15] Metal carbonyl clusters bearing a relatively high negative charge tend to have more bridging (i.e. electron-withdrawing) carbonyl groups than analogous neutral clusters.[16] For carbonyl but not hydrogen ligands, there is the added complication of the relative capacities for π-bonding of different potential sites.

Addition of protons to anionic clusters to generate hydride clusters is a process that may be accompanied by structural changes that sometimes appear puzzling. For example, whereas $Os_6(CO)_{18}^{2-}$ and $HOs_6(CO)_{18}^{-}$ have octahedral arrangements of their metal atoms, the neutral cluster $H_2Os_6(CO)_{18}$ has a capped square pyramidal arrangement of its metal atoms.[11] Two questions arise: what causes the cluster structure to change on protonation, and is this behaviour peculiar to transition metal systems? This work seeks to answer these questions by exploring the effects of protonation on selected main group cluster systems.

Our approach is to use available quantum chemical techniques to explore aspects of the geometrical structures of main group analogues of specific transition metal cluster systems.[10,17] The calculational technique used is chosen to fit the problem. Here we concern ourselves with the site preferences shown by hydrogen ligands and the structural effects of these ligands when attached to two types of cluster compounds:

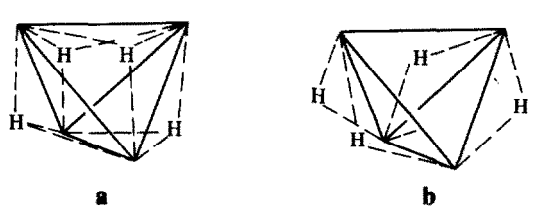
(1) Tetrahedral tetranuclear clusters held together by four or six skeletal bond pairs, exemplified by the species Be_4H_8 and B_4H_8 respectively. [The former represents a hypothetical molecular form of beryllium hydride, which is known only as the polymeric solid $(BeH_2)_n$;[18] the latter is a frequently invoked intermediate in the chemistry of B_4H_{10} and other boranes,[19] though too short-lived to have been isolated and/or structurally characterized.]

(2) Octahedral or capped square pyramidal hexanuclear clusters held together by seven skeletal bond pairs, exemplified by the hypothetical species $B_6H_7^-$ and B_6H_8.

TETRAHEDRAL TETRANUCLEAR CLUSTERS

Tetrahedral clusters of four tervalent units may be held together by four skeletal bond pairs (in four 3-centre face bonds, as in the case of B_4Cl_4[20] or six skeletal bond pairs (in six 2-centre edge bonds, as in tetrahedrane, C_4H_4, or derivatives thereof). In molecular orbital terms, in the former, the a_1 and t_2 skeletal bonding MOs are filled. In the latter, the e symmetry bonding MOs also are occupied.

The influence of electron numbers and electron distribution on ligand hydrogen sites is illustrated by the metal carbonyl hydride clusters $(Re_4(CO)_{12}H_4$ (**1**)[21] and $Ru_4(CO)_{12}H_4$ (**2**).[22] The former, with four skeletal bond pairs and μ_3-hydrogen atoms bridging the four triangular faces of the Re_4 tetrahedron (Scheme 1a), has an eclipsed configuration of its four $Re(CO)_3$ units with respect to the Re_4 tetrahedron edges. The latter, with six metal–metal bond pairs, has a staggered arrangement of its $Ru(CO)_3$ units, and the hydrogen ligands bridge four of the six Ru_4 tetrahedral edges (Scheme 1b). These differences, and the hydrogen site preferences in related tetranuclear clusters containing 3, 4 or 6 hydride ligands, have been discussed in detail by Hoffmann *et al.*,[23] who pointed out that the bridging hydrogen atoms occupy the sites that are closest to the regions of maximum metal–metal bonding electron density, as if the hydrides were formed from the parent anions $[M_4(CO)_{12}]^{4-}$ by protonation of the 3-centre face bonds in $[Re_4(CO)_{12}]^{4-}$ or by protonation of four of the 2-centre edge bonds in $[Ru_4(CO)_{12}]^{4-}$. Extended Hückel MO calculations on the species $Fe_4(CO)_{12}H_4^{4+}$ and $Fe_4(CO)_{12}H_4$ as models for **1** and **2** respectively, however, though favouring an eclipsed orientation of the carbonyl ligands in the former and a staggered orientation in the latter, indicated that face-bridging μ_3-sites would be preferred for the hydrogen atoms in both cases, although the energy difference between edge and face sites was small in the case of $Fe_4(CO)_{12}H_4$. These calculations therefore left unresolved the question of whether the hydrogen atoms in **2** occupy μ_2-edge-bridging sites because these are intrinsically preferred for bonding purposes, in spite of the indication to the contrary given by the calculations,



Scheme 1.

or whether these sites are occupied by the hydrogen atoms because the staggered $Ru(CO)_3$ orientation forces them there.

In order to obtain further information about such systems, and in the hope of clarifying the problem, we have carried out MNDO calculations[24]* on two key systems that may be regarded as the main group element "parent" systems for the above transition metal clusters, *viz.* Be_4H_8 as the parent species for $Re_4(CO)_{12}H_4$ (BeH and $Re(CO)_3$ units are isolobal[25] sources of one electron and three AOs for cluster bonding), and B_4H_8 as the parent species for $Ru_4(CO)_{12}H_4$ (BH and $Ru(CO)_3$ units are isolobal sources of two electrons and three AOs for cluster bonding). Possible structures for B_4H_8 have been discussed by Pepperberg, Halgren and Lipscomb[26] who calculated that a relatively open structure, of topology 2112C, in which one boron atom used only three of its four valence-shell AOs, was more likely than compact effectively *closo* structures based on roughly tetrahedral arrangements of the four boron atoms. In our own MNDO calculations on Be_4H_8 and B_4H_8, we therefore imposed a tetrahedral arrangement of the skeletal atoms, albeit capable of distortion from T_d to D_{2d} symmetry if edge-bridging sites were preferred by the extra four hydrogen atoms. Optimized geometries and heats of formation were calculated for both Be_4H_8 and B_4H_8 with (a) μ_3 face-bridging endo hydrogen atoms and (b) μ_2 edge-bridging endo hydrogen atoms in a D_{2d} array.

Be_4H_8: (a) $Be_4(H_{exo})_4(\mu_3\text{-}H_{endo})_4$. Calculation of the heat of formation of Be_4H_8 with bond distances assumed to be as follows: d(Be–H_{exo}), 1.16 Å; d(Be–H_{endo}), 1.30 Å; d(Be–Be), 1.80 Å; angle H_{exo}–Be–Be, 144.5°, gave a value of ΔH_f° of 614 kJ mol^{-1}. After total optimization, it was found that the tetrahedral symmetry and triply-bridging state of coordination of the endo hydrogen atoms were retained. The optimized structure was an expanded version of the original [Fig. 1(a)], placing the metal and endo hydrogen atoms at the vertices of an almost perfect cube, with d(Be–H_{exo}) 1.29 Å, d(Be–H_{endo}) 1.64 Å; d(Be–Be) 2.32Å, angle H_{exo}–Be–Be, 145.2°; and ΔH_f° −727 kJ mol^{-1}.

(b) $Be_4(H_{exo})_4(\mu_2\text{-}H_{endo})_4$. Calculation of the heat of formation of Be_4H_8 assuming d(Be–H_{exo}) = 1.19 Å; d(Be–H_{endo}) 1.32 Å; d(Be–Be) 1.81 Å (whether bridged by μ_2 hydrogen atoms or not) and bond angles H_{exo}–Be–Be, 144.5° and H_{exo}–Be–H_{endo}, 97.5°, gave a value for ΔH_f° of +546 kJ mol^{-1}. When totally optimized, the structure changed from the edge-bridged to the face-bridged structure $Be_4(H_{exo})_4(\mu_3\text{-}H_{endo})_4$ [Fig. 1(a)]. When the structure was allowed to refine while restricted to the edge-bridged geometry [Fig. 1(b)], the heat of formation ΔH_f° fell to −479 kJ mol^{-1}, still some 248 kJ mol^{-1} less stable than the optimized face-bridged form $Be_4(H_{exo})_4(\mu_3\text{-}H_{endo})_4$.

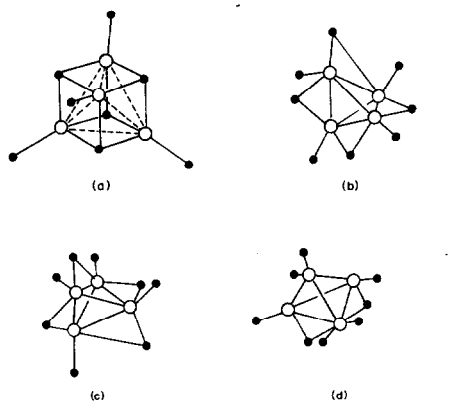


Fig. 1. Representations of the MNDO structures for: (a) Be_4H_8 fully optimized while retaining tetrahedral beryllium core; (b) Be_4H_8 edge-bridged; (c) B_4H_8 fully optimized while retaining cluster geometry; (d) B_4H_8 optimized beginning with face-bridging hydrogens. The open circles are Be or B while the closed circles are H.

B_4H_8: $B_4(H_{exo})_4(\mu_2\text{-}H_{endo})_4$. Calculation of the heat of formation of B_4H_8 assuming d(B–H_{exo}) 1.19 Å, d(B–H_{endo}) 1.32 Å, d(B–B) 1.81 Å (whether bridged or not), angles H_{exo}–B–B 144.5° and H_{exo}–B–H_{endo} 97.5°, gave a value of ΔH_f° = 297 kJ mol^{-1}. When totally optimized, the structure [Fig. 1(c)] retained the edge-bridging hydrogen characteristic, though the B_4 symmetry changed from T_d to D_{2d} as the bridged edges lengthened and the unbridged edges shortened. The optimized structure, with ΔH_f° 185 kJ mol^{-1}, has d(B–B) 1.66 Å (unbridged), 1.96 Å (bridged) d(B–H_{endo}) 1.37 Å, d(B–H_{exo}) 1.16 Å, angles H_{exo}–B–H_{endo} 102.5°, H_{exo}–B–B 138–172°.

(b) $B_4(H_{exo})_4(\mu_3\text{-}H_{endo})_4$. Calculation of the heat of formation of B_4H_8, assuming d(B–H_{exo}) 1.16 Å, d(B–H_{endo}) 1.30 Å, d(B–B) 1.80 Å and angle H–B–B 144.5°, gave a value of ΔH_f° = 1746 kJ mol^{-1}. Total optimization of this structure caused loss of the face-bridged feature, generating a structure in which two of the endo hydrogen atoms were edge-bridging, the other two becoming extra terminal hydrogen atoms. This structure [Fig. 1(d)] was calculated to have ΔH_f° = 95 kJ mol^{-1}. Optimization of the bond lengths while retaining the face-bridging $H_4B_4(\mu_3\text{-}H)_4$ structure gave a value of ΔH_f° of 1208 kJ mol^{-1}, some 1023 kJ mol^{-1} less stable than the edge-bridged structure.

The structural and thermodynamic data for these

* Note that we are not concerned with absolute values of energies but with trends in related compounds. In this way artifacts of the method cancel out.

Table 1. Bond distances and angles in the totally optimized structures of $H_4Be_4(\mu_3\text{-}H)_4$ and $H_4B_4(\mu_2\text{-}H)_4$

	Bond distance (Å)			Bond angle (°)	
Compound	M–M	$M–H_{exo}$	$M–H_\mu$	$H_{exo}–M–H_\mu$	$H_{exo}–M–M$
$H_4Be_4(\mu_3\text{-}H)_4$	2.32*	1.29	1.64	145	145
$H_4B_4(\mu_2\text{-}H)_4$	1.96*	1.16	1.37	103	138–172

* Bridged skeletal distances; the unbridged B–B distance in $H_4B_4(\mu_2\text{-}H)_4$ is 1.66 Å.

Table 2. Enthalpies of formation and charges on bridging hydrogen atoms of edge- and face-bridged $H_4Be_4(\mu\text{-}H)_4$ and $H_4B_4(\mu\text{-}H)_4$ with MNDO-optimized structures

	ΔH_f° (kJ mol^{-1})		Atomic charges	
Compound	μ_2-H	μ_3-H	μ_2-H	μ_3-H
$H_4Be_4(\mu\text{-}H)_4$	−479	−727	−0.02	−0.14
$H_4B_4(\mu\text{-}H)_4$	+185	+1208	+0.02	+0.38

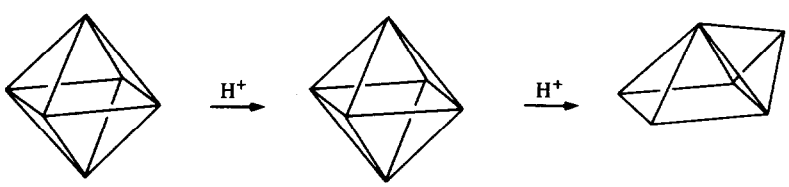
species are summarized in Tables 1 and 2. From these, it is clearly apparent that the face-bridged T_d structure $(H_{exo})_4Be_4(\mu_3\text{-}H_{endo})_4$ [Fig. 1(a)] is preferred to the edge-bridged structure for Be_4H_8, whereas for the boron compound B_4H_8, the reverse is true, the edge-bridged D_{2d} structure $(H_{exo})_4B_4(\mu_2\text{-}H_{endo})_4$ [Fig. 1(c)] being preferred. Moreover, neither of the alternative structures considered, viz. $H_4Be_4(\mu_2\text{-}H)_4$ for Be_4H_8 or $H_4B_4(\mu_3\text{-}H)_4$ for B_4H_8, was found to be in a potential energy well. The former reverted to the preferred $H_4Be_4(\mu_3\text{-}H)_4$ on optimization. The latter rearranged to $(H_{exo})_4(H_{endo})_2B_4(\mu_2\text{-}H)_2$ as an alternative preferred structure. For these admittedly simple systems, the findings support the intuitive picture that the endo hydrogen atoms occupy sites that represent regions of greatest skeletal bonding electron density.

HEXANUCLEAR CLUSTERS

In the previous section we found the location of the hydrogen ligands on the main group clusters considered mimicked quite well the analogous transition metal systems. The formation of these tetrahedral clusters might have been considered to take place via the sequential protonation of the anions $Be_4H_4^{4-}$ and $B_4H_4^{4-}$. Protonation/deprotonation of clusters is a real process in both main group as well as transition metal chemistry. Hence, another aspect of hydrogen ligand effects that may be informatively approached via main group analogues is the tendency for changes in cluster structure to occur with extent of protonation. As mentioned above there are known systems where cluster structure changes with protonation. A well established example chosen for discussion here is shown in Scheme 2 below.[11,27]

The dianion, $Os_6(CO)_{18}^{2-}$ formally contains 7 skeletal electron pairs and, in accord with the predictions of the electron counting rules, exhibits an octahedral (*closo*) core of metal atoms. On the other hand, protonation to $H_2Os_6(CO)_{18}$ causes cluster rearrangement and a capped square pyramidal structure is found, a cluster structure not observed in main group systems even though examples of mixed main group-transition metal clusters of this type are known.[8,28] This structural change, which is not predicted by skeletal electron counting rules, has been attributed to lowest coordination site preference of the bridging hydrogens[11] such as is generally observed in the boron hydrides.[29]

Aspects of the problem presented by this structural change have already been considered by Evans in work in which the extended Hückel method was applied to an energy analysis of idealized structures for $B_6H_6^{2-}$, $B_6H_7^-$ and B_6H_8.[30] Thus, he



$Os_6(CO)_{18}^{2-}$ $HOs_6(CO)_{18}^-$ $H_2Os_6(CO)_{18}$

Scheme 2.

found an octahedral structure for $B_6H_6^{2-}$, an edge-bridged octahedral structure for $B_6H_7^-$, and an octahedral structure with hydrogens on opposite edges for B_6H_8 to have the lowest energies. His calculations also showed that as protons were added to $B_6H_6^{2-}$, the trigonal prismatic and capped square pyramidal structures were stabilized relative to the octahedral arrangement and that while site preference for bridging hydrogens was not significant in fully triangulated polyhedra, there was preference for tetragonal faces over trigonal faces when both kinds of sites were available in the structure.

Brint, Spalding and co-workers have explored the lowest energy structures for $B_6H_6^{2-}$, $B_6H_7^-$ and B_6H_8 using MNDO and *ab initio* techniques in which the boron cluster core was not constrained in any fashion.[31] This work demonstrated that the boron core is disrupted by protonation to such an extent that a definable cluster structure is lost.

The work reported here supplements these earlier studies in that we approach the problem from another point of view and try to provide a simple rationale for the effects of protonation which has some predictive value. Our approach is to use the MNDO technique[24] to explore the protonation of octahedral and square-pyramidal $B_6H_6^{2-}$ while requiring the systems to retain these two core symmetries. Attention is focused on (a) the lowest energy site of protonation and (b) the relative energy of the two structures as a function of protonation, note being taken of changes in molecular orbital properties as a function of protonation. We also consider whether the changes that occur on protonation of $B_6H_6^{2-}$ can be used to explain the structural change observed when $Os_6(CO)_{18}^{2-}$ is protonated. Although the quantitative results of the calculations are reported, only the relative changes are considered significant.

Proton location. The optimized structures for $B_6H_7^-$ and B_6H_8 restricted to octahedral and square-pyramidal core geometries are shown schematically in Fig. 2. Complete optimization of $B_6H_6^{2-}$ resulted in a perfectly octahedral structure [Fig. 2(a)] with a ΔH_f° of 138 kJ mol^{-1}. This result is in agreement (both in energy and bond lengths) with that reported by Brint *et al.*[31] Complete optimization of $B_6H_7^-$ results in collapse of the octahedral arrangement whether the additional proton is placed on an edge or face, or is terminal. The resulting structure here also compares to that reported previously[31] with a ΔH_f° of -92 kJ mol^{-1} being obtained. In order to maintain an octahedral structure, the optimization was then limited to proton location, and the B_6 octahedron was held fixed. Starting conditions for the additional proton on typical terminal, edge, or face hydrogen sites were tried and Fig. 2(b) shows the resulting, lowest energy, structure with ΔH_f° of -24 kJ mol^{-1}.

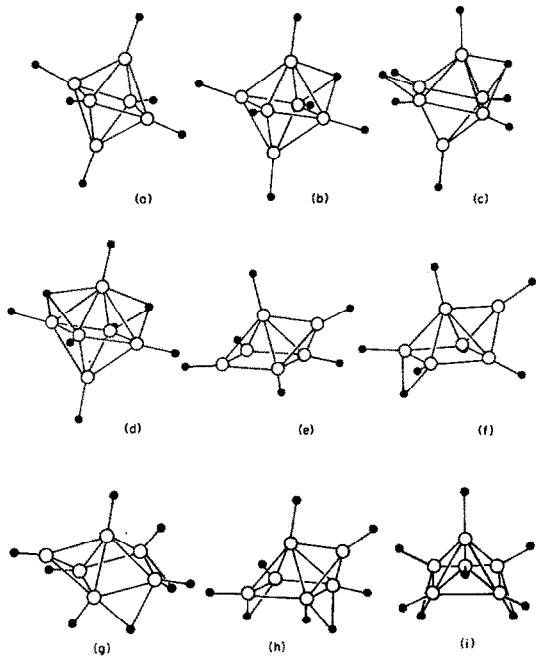


Fig. 2. Representations of the MNDO structures for: (a) $B_6H_6^{2-}$ fully optimized; (b) $B_6H_7^-$ optimized while retaining cluster geometry; (c) B_6H_8 optimized beginning with *trans* face-bridging hydrogens; (d) B_6H_8 optimized beginning with *cis* face-bridging hydrogens; (e) $B_6H_6^{2-}$ optimized while retaining capped square-pyramidal cluster geometry; (f) $B_6H_7^-$ optimized while retaining capped square-pyramidal geometry; (g), (h) and (i) B_6H_8 optimized while retaining capped square-pyramidal geometry. The open circles are B while the closed circles are H.

Calculation of the heat of formation of B_6H_8 also required constraint of the boron structure to an octahedral arrangement. The structure with all protons optimized is shown in Fig. 2(c). This result was obtained from starting conditions of two protons in *trans* faces of the octahedron. However, if one proton is understood to have remained in the starting face, the second proton has moved on to one of the edges of the face it originally capped. The ΔH_f° of this structure is 362 kJ mol^{-1}. Comparison of this energy with that derived from a "*cis*"-face starting condition with a ΔH_f° of 367 kJ mol^{-1} [Fig. 2(d)] shows only a slight preference for the former structure.

For the capped square pyramidal cases, the MNDO method was used to determine the optimized position of the capping boron for a square based pyramid having the same parameters as the octahedral structure used above. After the boron position had been established, the B_6 structure was

held in place while the H's were allowed to optimize to low energy positions [Fig. 2(e)]. Four starting positions for the additional proton of $B_6H_7^-$ were used: central in the bottom square face; back edge, opposite the capping boron atom; front edge, under the capping boron; and back face, opposite the capping boron. With the exception of the "front edge" starting position, which sought a high energy structure of 201 kJ mol^{-1}, the other three starting conditions resulted in a common structure shown in Fig. 2(f) ($\Delta H_f^\circ = 101$ kJ mol^{-1}). The additional proton is centered in an imaginary face trans to the boron cap.

In the case of B_6H_8, complete optimization of the protons gave three structures of similar energy [Fig. 2(g), 392 kJ mol^{-1}; 2(h), 415 kJ mol^{-1}; and 2(i), 420 kJ mol^{-1}]. In all three cases the protons are located approximately 1 Å below the basal plane occupying adjacent edges in the first instance and opposite edges in the second and third cases.

As with the tetrahedral clusters, we first sought a rationalization of the calculated stable proton locations using localized 2- and 3-centre bond descriptions of cluster bonding. For the two systems of interest, these have already been derived by Lipscomb and co-workers[32,33] and the rules for treating systems of this complexity are adequately described elsewhere.[34] Briefly, the two principal skeletal bond arrangements for the octahedral $B_6H_6^{2-}$ are shown in Fig. 3(a) where the number of resonance forms is also indicated. For each, half of the faces are occupied by a 3-centre bond while only one quarter of the edges accommodate 2-centre bonds. Therefore, in agreement with the lowest energy MNDO structure found, face protonation should be preferred if the incoming proton is thought to seek out the site of maximum available electron density. Once face protonated, susceptibility of the product $B_6H_7^-$ to further protonation will be different from that of $B_6H_6^{2-}$. The attachment of the first proton to $B_6H_6^{2-}$ creates a localized 4-centre B_3H bond in a face and, if one assumes this bond is fixed, then the disposition of the other 2- and 3-centre bonds can be easily determined. Considering only edges for the second protonation and again assuming maximum bond density is the controlling factor, the overall probabilities for the three types of edges *a*, *b*, *c* [Fig. 3(b)] are 0, 0.31, 0.38 respectively (MNDO point calculations for these idealized structures yield $\Delta H_f^\circ = 565{,}435$ and 414 kJ mol^{-1} respectively). Thus, the edge preferred on the basis of the MNDO technique is also the one marginally preferred by these localized bonding arguments. As is illustrated in Fig. 2, there is little difference between the MNDO energies for two locations for the second proton and this structural imprecision is reproduced, albeit in a different form, in the localized bond picture.

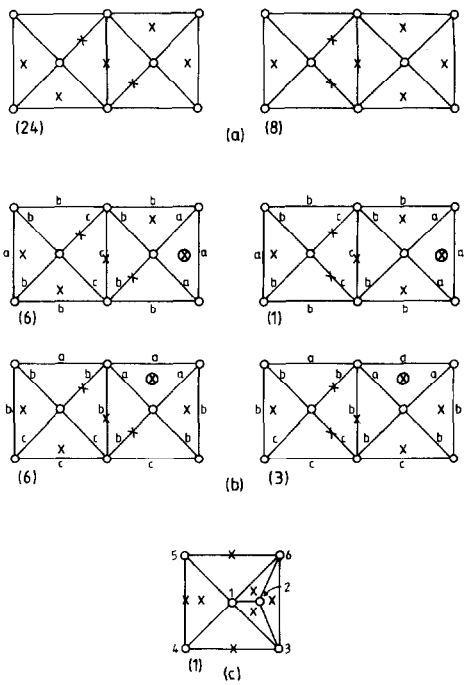


Fig. 3. (a) Localized bond networks for octahedral $B_6H_6^{2-}$. (The octahedron is shown cut open to yield two edge-fused square pyramids. Note that three edges are therefore shown twice.) The × 's indicate the "locations" of the seven cluster pairs. (b) Four possible localized bond networks for octahedral $B_6H_7^-$ where the ringed × indicates the location of the first proton on $B_6H_6^{2-}$. (c) Localized bond network for capped square-pyramidal $B_6H_6^{2-}$. Figures in parentheses show the numbers of equivalent resonance forms for each bond network.

For the capped square-pyramidal $B_6H_6^{2-}$-structure, the only localized bond scheme possible is shown in Fig. 3(c). It has the unsatisfactory feature of a 2-centre and 3-centre bond adjacent in one face.[33] With excessive electronic charge in the region of atoms 4 and 5, it is not surprizing that the preferred site for protonation [MNDO results (Fig. 2)] is the 4–5 edge. By converting the 2-centre B–B bond on that edge into a 3-centre BHB bond, protonation effectively moves this electron pair from too close proximity to the 3-centre bond in the adjacent face. The preferred site of the second proton is not obvious from this simple bonding picture and, indeed, the MNDO results give three possibilities of similar energy (Fig. 2).

Two ideas are suggested by this analysis: (a) in accord with the results on the tetrahedral clusters, proton location can be correlated with bond density in the original anion and (b) protonation effectively reduces the number of canonical forms in the valence

bond description. The latter idea provides a way of rationalizing the relative energies of possible cluster structures.

Cluster energetics on protonation. In Fig. 4 the energy difference between octahedral and square pyramidal structures is shown as a function of protonation (see also Table 3). Two sets of calculations are shown: one with fixed, reasonable BB distances and one in which the boron framework was allowed to partially relax to accommodate the spatial requirements of the added proton. The calculated heats of formation are given in Table 3. In both cases the same, relative, trend was observed, namely, a large decrease in energy difference as protons are added to the cluster. Indeed, when the cage is allowed to distort, the more stable diprotonated form is the square pyramid. Using the MNDO-optimized framework structures, Gaussian-70 and extended Hückel calculations were performed and yielded the same trend in stabilities. Hence, the energetics are consistent with Evans' findings[30] and also correlate with the observed behavior of $Os_6(CO)_{18}^{2-}$ on protonation.[11,27] Consistent with the main group model, the preference for capped square pyramidal structure in the transition metal system must be small as $Ru_6(CO)_{18}^{2-}$ retains an octahedral cluster geometry even on diprotonation.

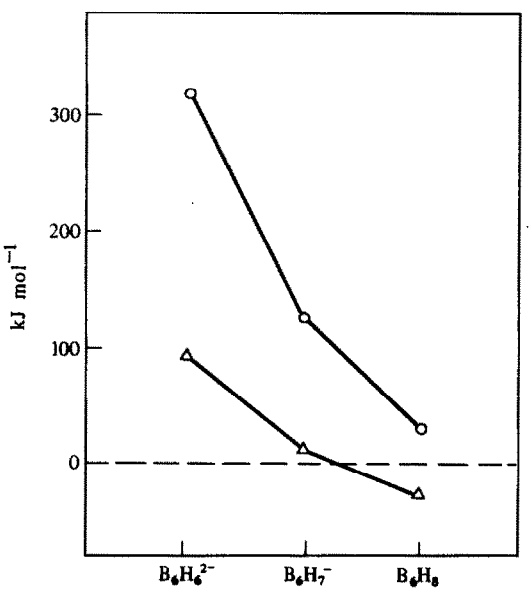


Fig. 4. Difference in enthalpies of formation of the capped square-pyramidal and octahedral cluster geometries for $B_6H_6^{2-}$ as a function of protonation. Open circles are frozen core geometries with total proton optimization while triangles are for partially relaxed core geometries (see text) with total proton optimization.

It is of interest to seek an explanation of this trend in energetics in the localized bond model as this approach was useful in rationalizing proton location. The pertinent localized bond descriptions of the two dianion structures are given in Fig. 3. The octahedral structure, and most stable form, has 32 resonance forms while the more classical capped square pyramidal structure has only one bond description. As was pointed out in the last section, the addition of a proton can be viewed as generating a localized 3-centre-2 electron bond thereby reducing by a factor of 2 the number of resonance forms available to the octahedral cluster structure. Further protonation again reduces the number of resonance forms. Hence, if one postulates that the octahedral form derives a significant portion of its stability from resonance stabilization, its stability should decrease on protonation relative to the square pyramidal form which has no apparent resonance stabilization. Indeed, the latter benefits from protonation and becomes favored as the extent of protonation increases. For the octahedral structure this conclusion is also reflected in the loss of a symmetrical charge distribution over the skeleton upon protonation (Table 4) whereas the square pyramidal structure, already having an asymmetric charge distribution, is much less affected.

CONCLUSIONS

For the main group model cluster systems studied, we have found that bridging protons tend to be located at sites which in the unprotonated cluster exhibit maximum available charge. Localized 2- and

Table 3. Enthalpies of formation (kJ mol^{-1}) for MNDO-optimized structures

	Cage fixed			Cage relaxation allowed		
Species	Octahedral	Capped square pyramid	Difference	Octahedral	Capped square pyramid	Difference
$B_6H_6^{2-}$	138	453	315	138	229	91
$B_6H_7^-$	−24	101	125	−65	−54	11
B_6H_8	362	392	30	320	293	−27

Table 4. Standard deviations in the net charges calculated (extended Hückel–Mulliken populations) for B and H atoms in the fully optimized fixed cage structures in the $B_6H_6^{2-}$ series

		Octahedral	Capped square pyramid	Difference
$B_6H_6^{2-}$	Bs	0.00	0.17	0.17
	Hs	0.00	0.01	0.01
	Total	0.00	0.18	0.18
$B_6H_7^-$	Bs	0.17	0.16	−0.01
	Hs	0.07	0.04	−0.03
	Total	0.24	0.20	−0.04
B_6H_8	Bs	0.16	0.16*	−0.00
	Hs	0.08	0.05*	−0.03
	Total	0.24	0.21*	−0.03

* Standard deviation of charges calculated for structures shown in Fig. 2(g) and (h).

3-centre bond treatments provide guides to the likely protonation sites of tetrahedral $Be_4H_4^{4-}$ or $B_4H_4^{4-}$, and of octahedral or capped square pyramidal $B_6H_6^{2-}$. Protonation creates fixed localized 3-centre 2-electron B_2H bonds or 4-centre 2-electron B_3H or Be_3H bonds and 2- or 3-centre skeletal bonds, so restricting the scope for resonance stabilization of the skeletal bonding. Forms that depend on such resonance stabilization (such as octahedral $B_6H_6^{2-}$) are therefore destabilized on protonation relative to forms (such as capped square pyramidal $B_6H_6^{2-}$) that offer little or no scope for resonance.

Protonation introduces significant cluster charge redistribution, and cluster forms in which charge asymmetry is significantly increased by protonation are disfavoured. Thus, even though protonation leaves the cluster electron count unaffected, it can constitute a perturbation large enough to cause structural rearrangement.

Our findings on this series of real and hypothetical tetranuclear and hexanuclear main group cluster systems reinforce our view that such systems serve as useful models for transition metal clusters, delineating the essential features of metal carbonyl cluster systems (notably various tetrahedral clusters $M_4H_4(CO)_{12}$, and capped square pyramidal species such as $H_2Os_6(CO)_{18}$) that superficially appear to pose problems that have no parallel in main group cluster chemistry.

Acknowledgements—The support of a joint NATO grant is gratefully acknowledged. M.A.C., T.P.F. and R.S. thank the National Science Foundation for support and the University of Notre Dame Computing Center for computing time. M.E.O'N. and K.W. thank the Science and Engineering Research Council for support.

REFERENCES

1. R. E. Williams, *Inorg. Chem.* 1971, **10**, 210.
2. K. Wade, *J. Chem Soc. D.* 1971, 792.
3. R. W. Rudolph and W. R. Pretzer, *Inorg. Chem.* 1972, **11**, 1974.
4. D. M. P. Mingos, *Nature Phys. Sci.* 1972, **236**, 99.
5. R. N. Grimes, *Ann. N.Y. Acad. Sci.* 1974, **239**, 180.
6. R. W. Rudolph, *Acc. Chem. Res.* 1976, **9**, 446.
7. K. Wade, *Adv. Inorg. Chem. Radiochem.* 1976, **18**, 1.
8. R. N. Grimes (ed.), *Metal Interactions with Boron Clusters.* Plenum, New York (1982).
9. B. F. G. Johnson (ed.), *Transition Metal Clusters.* John Wiley, New York (1980).
10. K. S. Wong, K. J. Haller, T. K. Dutta, D. M. Chipman and T. P. Fehlner, *Inorg. Chem.* 1982, **21**, 3197; R. L. DeKock, K. S. Wong and T. P. Fehlner, *Inorg. Chem.* 1982, **21**, 3203.
11. M. McPartlin, C. R. Eady, B. F. G. Johnson and J. Lewis, *J. Chem. Soc., Chem. Commun.* 1976, 883; C. R. Eady, P. F. Jackson, B. F. G. Johnson, J. Lewis, M. C. Malatesta, M. McPartlin and W. J. H. Nelson, *J. Chem. Soc., Dalton Trans.* 1980, 383.
12. B. F. G. Johnson and J. Lewis, *Adv. Inorg. Chem. Radiochem.* 1981, **24**, 225.
13. R. Bau, R. G. Teller, S. W. Kirtley and R. F. Koetzle, *Acc. Chem. Res.* 1979, **12**, 176.
14. A. P. Humphries and H. D. Kaesz, *Prog. Inorg. Chem.* 1979, **25**, 145.
15. R. L. DeKock and C. P. Jasperse, *Inorg. Chem.* 1983, **22**, 3839, 3843.
16. P. Chini, G. Longoni and V. G. Albano, *Adv. Organomet. Chem.* 1976, **14**, 285; P. Chini and B. T. Heaton, *Top. Curr. Chem.* 1977, **71**, 1.
17. R. L. DeKock, T. P. Fehlner, C. E. Housecroft, T. V. Lubben and K. Wade, *Inorg. Chem.* 1982, **21**, 25.
18. D. A. Everest, *Comp. Inorg. Chem.* 1973, **1**, 544.
19. L. H. Long, *J. Inorg. Nucl. Chem.* 1970, **32**, 1097; N. N. Greenwood, *Comp. Inorg. Chem.* 1973, **1**, 769.
20. M. Atoji and W. N. Lipscomb, *Acta Crystallogr.* 1953, **6**, 547; *J. Chem. Phys.* 1953, **21**, 172.
21. R. Saillant, G. Barcelo and H. D. Kaesz, *J. Am. Chem. Soc.* 1970, **92**, 5739.
22. R. D. Wilson, S. M. Wu, M. R. Churchill and A. Lashewycz, *J. Am. Chem. Soc.* 1977, **99**, 7384.
23. R. Hoffmann, B. E. R. Schilling, R. Bau, H. D. Kaesz and D. M. P. Mingos, *J. Am. Chem. Soc.* 1978, **100**, 6088.
24. M. J. S. Dewar and W. Thiel, *J. Am. Chem. Soc.* 1977, **99**, 4899; W. Thiel, *QCPE* 1978, **11**, 353. The problems of MNDO with cluster systems are pointed out (see also Ref. 15).
25. M. Elian and R. Hoffmann, *Inorg. Chem.* 1975, **14**, 1058.
26. I. M. Pepperberg, T. A. Halgren and W. N. Lipscomb, *Inorg. Chem.* 1977, **16**, 363.
27. J. Lewis and B. F. G. Johnson, *Pure Appl. Chem.* 1982, **54**, 97 and references therein.
28. C. E. Housecroft and T. P. Fehlner, *Adv. Organomet. Chem.* 1982, **21**, 57.

29. R. E. Williams, *Adv. Inorg. Chem. Radiochem.* 1976, **18**, 67.
30. J. Evans, *J. Chem. Soc., Dalton Trans.* 1978, 25.
31. P. Brint, E. F. Healy, T. R. Spalding and T. Whelan, *J. Chem. Soc., Dalton Trans.* 1981, 2515.
32. W. N. Lipscomb, *Boron Hydrides.* W. A. Benjamin, New York (1963).
33. I. R. Epstein and W. N. Lipscomb, *Inorg. Chem.* 1971, **10**, 1921.
34. M. E. O'Neill and K. Wade, *Polyhedron* 1984, **3**, 199.

Polyhedron Vol. 4, No. 4, pp. 697–705, 1985
Printed in Great Britain

0277-5387/85 $3.00 + .00
© 1985 Pergamon Press Ltd

METAL–PHENOXYALKANOIC ACID INTERACTIONS—XVI.* MOLECULAR STRUCTURES OF THE DIVALENT COBALT, COPPER, MANGANESE, NICKEL AND ZINC COMPLEXES WITH (2-NITROPHENOXY)ETHANOIC ACID: THE CRYSTAL STRUCTURES OF (2-NITROPHENOXY)ETHANOIC ACID, CATENA-{DIAQUABIS[(2-NITROPHENOXY)ETHANOATO-*O*]-MANGANESE(II)}, TETRAAQUABIS[(2-NITROPHENOXY)ETHANOATO]COPPER(II) DIHYDRATE AND BIS(2-AMINOPYRIMIDINE)AQUABIS-[(2-NITROPHENOXY)ETHANOATO]COPPER(II)

COLIN H. L. KENNARD† and STEPHEN W. STEWART
Department of Chemistry, University of Queensland, Brisbane 4067, Australia

ERIC J. O'REILLY and GRAHAM SMITH
Department of Chemistry, Queensland Institute of Technology, Brisbane 4000, Australia

and

ALLAN H. WHITE
Department of Physical and Inorganic Chemistry, University of Western Australia, Nedlands, 6009, Australia

(*Received* 22 *June* 1984; *accepted* 21 *August* 1984)

Abstract—The crystal structures of 2-nitrophenoxyethanoic acid (2-NPAH), *catena*-[diaquabis(2-nitrophenoxyethanoato)manganese(II)] (**1**), tetraaquabis(2-nitrophenoxyethanoato)copper(II) dihydrate (**2**) and aquabis(2-aminopyrimidine)bis(2-nitrophenoxyethanoato)copper(II) (**3**) have been determined by X-ray diffraction. The planar 2-NPAH molecule undergoes conformational change upon coordination in complexes **1** and **2** but remains unchanged in **3**. Complex **1** is a distorted octahedral [Mn–O, 2.156–2.213(3) Å] with *trans*-related waters and unidentate bridging carboxyls giving a polymer structure. In contrast **2** is a discrete centrosymmetric monomer with two unidentate acid ligands [Cu–O 1.943(5) Å] and four waters [Cu–O 1.954(5), 2.578(7) Å] giving a tetragonally distorted octahedral coordination. **3** is five-coordinate square pyramidal with two unidentate carboxyls [Cu–O, 1.947(5) Å], two hetero-nitrogens from 2-aminopyrimidine ligands [Cu–N, 2.078(5) Å] and a single water [Cu–O, 2.211(7) Å] on a two-fold rotation axis. Single crystal X-ray data are also presented which confirms that the Zn(II) analogue of 2-NPAH is isomorphous with **1** and that the Co(II) and Ni(II) complexes are isomorphous with **2**.

Previous articles in this series[2,3] reported the unusual complex chemistry of (2-chlorophenoxy)ethanoic acid (2-CPAH). The pyridine adduct of nickel(II) (2-chlorophenoxy)ethanoate $[Ni_2(2\text{-}CPA)_4(py)_4(H_2O)]\cdot H_2O$ was found to be a bis-carboxylate-mono-aqua bridged dimer, involving facially linked octahedra.[2] The copper(II) complexes are similarly unconventional. Anhydrous copper(II) (2-chlorophenoxy)ethanoate, $[Cu_2(2\text{-}CPA)_4]_n$ and its 2-aminopyrimidine adduct $[Cu_2(2\text{-}CPA)_4(2\text{-aminopyrimidine})_2]_n$ are tetracarboxylate bridged dimer polymers.[3] In the anhydrous complex, the step-polymer forms through the axial positions of the dimers which are occupied by the oxygens from

* Part XV[1]. The Cd and Pb^{II} complexes of phenoxyethanoic acid, $[Cd(PA)_2(H_2O)_2]$ and $[Pb_2(PA)_4(H_2O)]_n$.

† Author to whom correspondence should be addressed.

adjacent carboxyl groups, similar to anhydrous copper(II) propanoate[4] and copper(II) butanoate.[5] The pyrimidine adduct is a zig-zag chain polymer, the off-sets provided through the meta-related nitrogens of the pyrimidine molecules in the axial dimer positions. In contrast, a third complex,[3] $[CaCu(2\text{-}CPA)_4(H_2O)_5]$, although a tetracarboxylate bridged dimer, has one "half" of the dimer comprising a conventional $Cu(O)_4(OH_2)$ moiety, the other "half" an eight-coordinate $Ca(O)_4(OH_2)_4$ unit.

In order to provide some clarification of this unusual phenomenon among the 2-chloro-substituted phenoxyalkanoates, a systematic investigation of the divalent metal complexes of other 2-substituted acids was initiated. The first of these, (2-nitrophenoxy)ethanoic acid (2-NPAH), provided a number of crystalline complexes suitable for X-ray examination, including some which showed polymorphic relationships. The crystal structures of $[Mn(2\text{-}NPA)_2(H_2O)_2]_n$ (**1**), $[Cu(2\text{-}NPA)_2(H_2O)_4]\cdot 2H_2O$ (**2**) and $[Cu(2\text{-}NPA)_2(2\text{-aminopyrimidine})_2(H_2O)]$ (**3**) are reported, together with X-ray data confirming the isomorphism between **1** and the Zn(II) analogue, and between **2** and both the Co(II) and Ni(II) analogues. The crystal structure of the parent acid (2-NPAH) also allows comparison of the structural features of complexed and uncomplexed acid.

EXPERIMENTAL

Preparation of complexes

All complexes were prepared by mixing together hot aqueous solutions containing 2 : 1 molar ratios of the ammonium salt of 2-NPAH and the appropriate metal acetate. Crystals were allowed to grow from these solutions after partial room temperature evaporation over a period of several weeks. Complex **2** $[Cu(2\text{-}NPA)_2(H_2O)_4]\cdot 2H_2O$ was found to acquire opacity and lose crystallinity presumably due to loss of water, even when stored in a closed sample vial. To prevent this the crystal used for X-ray data collection was coated with epoxy resin. Loss of crystallinity was not found to be a serious problem with the other complexes [Co(II) and Ni(II)], but stored samples underwent some efflorescent decomposition with formation of a red solution on the crystals. The supernantant liquors from the preparations of all three complexes also reverted to this red colour, presumably a breakdown product from the (nitrophenoxy)ethanoic acid.

Adduct **3** $[Cu(2\text{-}NPA)_2(2\text{-aminopyrimidine})_2(H_2O)]$ was prepared by digesting a 50% aqueous ethanolic suspension of **2** with a slight excess of 2-aminopyrimidine. Evaporation at room temperature gave blue crystals of the complex.

*Analyses**

(i) $[Mn(2\text{-}NPA)_2(H_2O)_2]_n$ (**1**). Found: C, 39.8; H, 3.36; N, 5.72%. Calc. for $C_{16}H_{16}MnN_2O_{12}$: C, 39.8; H, 3.34; N, 5.80%.

(ii) $[Zn(2\text{-}NPA)_2(H_2O)_2]_n$ (**1a**). Found: C, 39.0; H, 3.33; N, 5.70%. Calc. for $C_{16}H_{16}N_2O_{12}Zn$: C, 38.9; H, 3.27; N, 5.67%.

(iii) $[Cu(2\text{-}NPA)_2(H_2O)_4]\cdot 2H_2O$ (**2**). Found:† C, 39.1; H, 3.37; N, 5.67%. Calc. for $C_{16}H_{24}CuN_2O_{16}$: C, 34.1; H, 4.29; N, 4.97%.

(iv) $[Co(2\text{-}NPA)_2(H_2O)_4]\cdot 2H_2O$ (**2a**). Found: C, 34.8; H, 4.40; N, 5.06%. Calc. for $C_{16}H_{24}CoN_2O_{16}$: C, 34.4; 4.33; N, 5.01%.

(v) $[Ni(2\text{-}NPA)_2(H_2O)_4]\cdot 2H_2O$ (**2b**). Found: C, 34.5; H, 4.40; N, 5.01%. Calc. for $C_{16}H_{24}N_2NiO_{16}$: C, 34.4; H, 4.33; N, 5.01%.

Crystallography

Crystal data and details of structure solution and refinement for [2-NPAH], **1**, **2** and **3** are contained in Table 1. Single crystal X-ray photographic data for the Zn(II), Co(II) and Ni(II) complexes were obtained using an Enraf–Nonius Weissenberg goniometer and are as follows:

(**1a**) $[Zn(2\text{-}NPA)_2(H_2O)_2]_n$, $C_{16}H_{16}N_2O_{12}Zn$, $Mr = 493.7$, $a = 14.3(1)$, $b = 7.9(1)$, $c = 4.5(1)$, $\alpha = 114(1)$, $\beta = 90(1)$, $\gamma = 90(1)°$; $V = 464$ Å^3, $Z = 1$, $\rho_c = 1.76$ g cm^{-3}, $\rho_f = 1.77$ g cm^{-3}, $F(000) = 252$, space group $P\bar{1}$.

(**2a**) $[Co(2\text{-}NPA)_2(H_2O)_4]\cdot 2H_2O$, $C_{16}H_{24}CoN_2O_{16}$, $Mr = 559.3$, $a = 6.4(1)$, $b = 5.1(1)$, $c = 36.6(1)$Å, $\beta = 100(1)°$, $V = 1176$ Å^3, $Z = 2$, $\rho_c = 1.58$ g cm^{-3}, $\rho_f = 1.59$ g cm^{-3}, $F(000) = 578$, space group $P2_1/c$.

(**2b**) $[Ni(2\text{-}NPA)_2(H_2O)_4]\cdot 2H_2O$, $C_{16}H_{24}N_2NiO_{16}$, $Mr = 559.1$, $a = 6.4(1)$, $b = 5.1(1)$, $c = 36.6(1)$ Å, $\beta = 100(1)°$, $V = 1176$ Å^3, $Z = 2$, $\rho_c = 1.58$ g cm^{-3}, $\rho_f = 1.58$ g cm^{-3}, $F(000) = 580$, space group $P2_1/c$.

* No analysis was possible on the complex $[Cu(2\text{-}NPA)_2(2\text{-aminopyrimidine})_2(H_2O)]$ (**3**) because of the small amount of available sample.

† $[Cu(2\text{-}NPA)_2(H_2O)_4]\cdot 2H_2O$ (**2**) was found to effloresce rapidly at room temperature so that the results obtained represent something less than the six-hydrate of the X-ray determination. The Co(II) and Ni(II) complexes were more stable.

Table 1. Crystal data for [2-NPAH], $[Mn(2\text{-NPA})_2(H_2O)_2]_n$ (1), $[Cu(2\text{-NPA})_2(H_2O)_4]\cdot 2H_2O$ (2) and $[Cu(2\text{-NPA})_2(2\text{-aminopyrimidine})_2(H_2O)]$, (3)

	2-NPAH	1	2	3
Formula	$C_8H_7NO_5$	$C_{16}H_{16}MnN_2O_{12}$	$C_{16}H_{24}CuN_2O_{16}$	$C_{24}H_{24}CuN_8O_{11}$
Mr	197.1	483.2	563.9	664.0
a (Å)	11.496(2)	14.319(6)	6.349(2)	25.418(9)
b (Å)	7.783(1)	7.912(5)	5.117(2)	5.718(1)
c (Å)	19.577(3)	4.558(2)	35.820(14)	18.785(3)
α (°)		114.69(4)		
β (°)	98.35(1)	90.47(4)	99.04(3)	99.73(2)
γ (°)		90.36(4)		
V (Å^3)	1733	469	1149	2690
Z	8	1	2	4
ρ_c (g cm^{-3})	1.510	1.710	1.629	1.638
ρ_f (g cm^{-3})	1.50	1.69	1.64	1.68
Space group	$C2/c$	$P\bar{1}$	$P2_1/c$	$C2/c$
$F(000)$	816	247	582	1364
μ(Mo-K_α) (cm^{-1})	1.39	8.2	10.8	9.3
R	0.085	0.049	0.062	0.049
$R\omega$*	0.088	0.052	0.064	0.051
A*	1.00	3.06	3.30	2.13
B*	1.87×10^{-3}	3.53×10^{-4}	4.1×10^{-4}	6.4×10^{-4}
Crystal size (mm)	$0.24\times0.22\times0.20$	$0.55\times0.23\times0.09$	$0.35\times0.30\times0.10$	$0.25\times0.17\times0.08$
Data collected	1329	1741	1382	1542
Data used	774	1430	927	997
Discrimination	$I > 1.5\sigma(I)$	$I > 2.5\sigma(I)$	$I > 2.5\sigma(I)$	$I > 2.5\sigma(I)$

* $\omega = A/(\sigma^2 F_o + BF_o^2)$.

Data for 1 and 2 were collected on a Syntex $P2_1$ diffractometer, and solved by the heavy atom method and refined using SHELX-76.[6] Data for 2-NPAH and 3 were obtained on a Nicolet $R3m$ diffractometer and the structures solved and refined using the Nicolet SHELXTL[7] structure solution package. 2-NPAH was solved using direct methods while for 3 the heavy atom method was used. Anisotropic thermal parameters were used for all heavy atoms except those of the nitro groups which were apparently disordered (complexes 1 and 2). In these cases, allowance was made for the disorder by incorporating all the atoms in the refinement with their site occupancies fixed at values obtained from least-squares refinement. Hydrogens were located from difference-Fourier syntheses and included in the refinement at fixed positions with their isotropic U values set invariant at 0.05 Å^2. Neutral atom scattering factors were used,[8] while the heavy atoms were corrected for the effects of anomalous dispersion.[8] Final residuals R and Rw are defined as follows:

$$R = [\sum||F_o|-|F_c||/\sum|F_o|],$$

$$Rw = [(\sum w(||F_o|-|F_c||^2/\sum w|F_o|^2)^{1/2}].$$

Atomic coordinates, thermal parameters and observed and calculated structure factors have been deposited with the Editor as supplementary material; copies are available on request. Atomic coordinates have also been deposited with the Cambridge Crystallographic Data Centre. Bond distances and angles are given in Table 2.

DISCUSSION

2-*NPAH*

Molecules of 2-NPAH form centrosymmetric, hydrogen bonded cyclic dimers [O...O, 2.606(8) Å] similar to all known examples of phenoxyalkanoic acids.[9] This distance lies within the range for members of this series [2.654 Å mean for 16 examples].[9] The molecules are essentially planar (Fig. 1) with the oxoethanoic acid side chain torsion angles, C(2)–C(1)–O(7)–C(8), C(1)–O(7)–C(8)–C(9) and O(7)–C(8)–C(9)–O(11) being −178.8, +177.5, and −171.8° respectively. However, the oxygens of the nitro group are canted at an angle to the plane of the benzene ring [torsion angle C(1)–C(2)–N(2)–O(22), +144.9°]. The angle may be dependent upon the attainment of a discrete O(7) (ether) . . . O(21)(nitro) interactive distance (in this case, 2.650

Table 2. Comparative bond distances (Å) and angles (°) for 2-NPAH, $[Mn(2\text{-NPA})_2(H_2O)_2]_n$ (1), $[Cu(2\text{-NPA})_2(H_2O)_4]\cdot 2H_2O$ (2) and $[Cu(2\text{-NPA})_2(2\text{-aminopyrimidine})_2(H_2O)]$ (3)

Coordination sphere					
1		2		3	
Distance					
Mn–O(11)	2.172(2)	Cu–O(11)	1.943(5)	Cu–O(11)	1.947(5)
Mn–O(10)′	2.156(3)	Cu–Ow(2)	2.578(7)	Cu–N(1)p	2.078(5)
Mn–Ow(1)	2.213(3)	Cu–Ow(3)	1.954(5)	Cu–Ow(1)	2.211(7)
Angle					
O(10)′–Mn–O(11)	93.5(1)	O(11)–Cu–Ow(2)	100.0(2)	O(11)–Cu–N(1)p	90.8(2)
O(11)–Mn–Ow(1)	89.5(1)	O(11)–Cu–Ow(3)	90.9(2)	O(11)–Cu–Ow(1)	89.0(2)
Ow(1)–Mn–O(10)′	87.1(1)	Ow(2)–Cu–Ow(3)	90.0(2)	O(11)–Cu–N(1)p′	89.5(2)
Mn–O(11)–C(9)	126.2(2)	Cu–O(11)–C(9)	123.9(5)	O(11)–Cu–O(11)′	178.0(3)
Mn–O(10)–C(9)	125.4(2)			N(1)p–Cu–Ow(1)	98.3(1)
				N(1)p–Cu–N(1)p′	163.5(3)
				Cu–O(11)–C(9)	122.6(5)
				Cu–N(1)p–C(2)p	125.1(4)
				Cu–N(1)p–C(6)p	118.1(4)

Intraligand					
2-NPAH	1	2	3	Aminopyrimidine ligand of 3	
Distance					
C(1)–C(2)	1.405(9)	1.405(6)	1.399(12)	1.394(11)	N(1)p–C(2)p	1.377(9)
C(1)–C(6)	1.381(9)	1.376(5)	1.393(12)	1.383(11)	N(1)p–C(6)p	1.332(9)
C(1)–O(7)	1.363(7)	1.359(5)	1.346(9)	1.345(12)	C(2)p–N(21)p	1.345(12)
C(2)–C(3)	1.380(8)	1.399(7)	1.394(12)	1.351(15)	C(2)p–N(3)p	1.367(8)

C(2)–N(2)	1.458(8)	1.449(5)	1.468(11)	1.492(12)	N(3)p–C(4)p	1.310(10)
C(3)–C(4)	1.370(9)	1.358(8)	1.353(16)	1.376(13)	C(4)p–C(5)p	1.383(11)
C(4)–C(5)	1.374(11)	1.384(9)	1.368(16)	1.380(15)	C(5)p–C(6)p	1.376(9)
C(5)–C(6)	1.377(9)	1.390(8)	1.399(13)	1.378(14)		
O(7)–C(8)	1.418(8)	1.432(6)	1.449(10)	1.427(9)		
C(8)–C(9)	1.503(9)	1.524(4)	1.523(11)	1.510(13)		
C(9)–O(10)	1.258(8)	1.257(4)	1.218(12)	1.222(9)		
C(9)–O(11)	1.262(9)	1.244(4)	1.275(11)	1.280(9)		
N(2)–O(21)	1.212(8)	1.232(7)	1.204(9)	1.151(15)		
N(2)–O(22)	1.196(9)	1.249(7)	1.225(13)	1.175(13)		

Angle

C(6)–C(1)–C(2)	117.4(5)	118.5(4)	116.8(9)	116.3(9)	C(2)p–N(1)p–C(6)p	116.4(5)
C(6)–C(1)–O(7)	124.9(6)	122.6(4)	123.9(7)	123.8(7)	N(1)p–C(2)p–N(3)p	122.3(6)
C(2)–C(1)–O(7)	117.8(5)	118.8(3)	119.3(7)	119.8(7)	N(1)p–C(2)p–N(21)p	120.8(5)
C(1)–C(2)–C(3)	121.3(5)	120.8(4)	122.8(8)	123.5(8)	N(3)p–C(2)p–N(21)p	116.9(6)
C(1)–C(2)–N(2)	121.1(5)	122.8(4)	120.9(7)	119.6(9)	C(2)p–N(3)p–C(4)p	117.9(6)
C(3)–C(2)–N(2)	117.6(6)	116.3(4)	116.3(8)	116.8(7)	N(3)p–C(4)p–C(5)p	123.2(6)
C(2)–C(3)–C(4)	119.4(6)	119.9(5)	120.0(9)	118.8(8)	C(4)p–C(5)p–C(6)p	115.8(7)
C(3)–C(4)–C(5)	120.7(6)	119.5(6)	118.0(9)	120.1(10)	C(5)p–C(6)p–N(1)p	119.9(9)
C(4)–C(5)–C(6)	119.7(6)	121.5(5)	123.9(9)	119.9(9)		
C(5)–C(6)–C(1)	121.6(6)	119.7(5)	118.5(8)	121.4(8)		
C(1)–O(7)–C(8)	116.6(4)	118.7(3)	117.8(6)	119.2(6)		
O(7)–C(8)–C(9)	109.1(5)	113.8(6)	112.7(7)	108.8(6)		
C(8)–C(9)–O(10)	120.7(6)	118.4(4)	121.5(8)	120.3(7)		
C(8)–C(9)–O(11)	114.3(5)	115.3(4)	112.6(8)	113.5(6)		
O(10)–C(9)–O(11)	124.9(6)	126.3(4)	125.9(8)	126.2(8)		
C(2)–N(2)–O(21)	118.3(5)	120.2(4)	119.8(7)	120.3(9)		
C(2)–N(2)–O(22)	119.3(6)	121.1(4)	118.6(7)	119.4(9)		
O(21)–N(2)–O(22)	122.4(6)	115.4(4)	121.0(9)	120.3(10)		

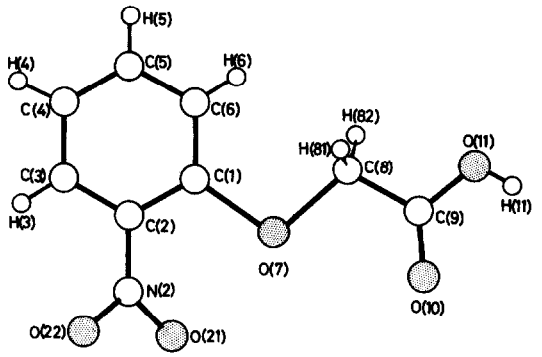


Fig. 1. Molecular conformation and atom numbering scheme for (2-nitrophenoxy)ethanoic acid (2-NPAH).

Å), which becomes too short in the planar conformation (*ca* 2.42 Å). However, there are no inter-dimer interactions involving the nitro groups, the regularly separated layers stacking down the approximate *c* direction of the cell.

Disorder of the nitro oxygens, evident in this structure as high atomic thermal parameters, also occurs in the complexed ligands in complexes **1–3**. This effect occurs to varying extent in these complexes, presumably due to steric effects imposed by the different modes of complexation found. It is considered feasible that this disorder in the nitro group is directly responsible for the difficulties encountered in the preparation of crystals of these complexes and their subsequent stability.

$[Mn(2\text{-}NPA)_2(H_2O)_2]_n$ (1)

The manganese(II) complex of 2-NPA (**1**) is centrosymmetric six-coordinate (Fig. 2) with the slightly distorted MO_6 octahedron occupied by two waters [Mn–O, 2.213(3) Å] and two carboxylate oxygens from unidentate 2-NPA ligands [Mn–O, 2.172(2) Å]. The remaining two coordination positions are filled by the second oxygens from the carboxyl groups of the adjacent complex units [Mn–O, 2.156(3) Å]. This results in infinite two-dimensional polymer chains which extend down the *c* crystallographic axis, with the Mn centres separated by the *c* cell parameter [4.558(2) Å]. In this respect, the complex is similar to *catena*-diaquabis(phenoxyethanoato-*O*)manganese(II) and its isomorphous and isostructural analogues of the type $[M(phenoxy)_2(H_2O)_2]_n$, where M = Co, Mg, Mn and phenoxy = phenoxyethanoato, (4-chlorophenoxy)ethanoato and (4-fluorophenoxy) ethanoato.[10,11] With the 2-NPA series, isomorphism has also been proved but between **1** and the zinc(II) complex, whereas in the general phenoxy series previously mentioned, the Zn(II) complexes are different but isomorphous with the Cd(II) complexes.[1,12]

The side-chain conformation of the 2-NPA ligands in **1** changes relative to the free acid, the torsion angles being −169.2, +160.0 and +144.9° respectively. Despite these changes, the O(7)...O(10) interactive distance [2.702(4) Å] is not significantly changed compared to 2-NPAH [2.628(8) Å]. Polymerization, with its more rigid stereochemical requirements is probably the primary interactive force in formation of these complexes, with the secondary packing effects, including the disordered nitro groups resulting in the conformational changes. The O(7)(ether)...O(21)A(nitro) distance is 2.577(4) Å while the only intermolecular association

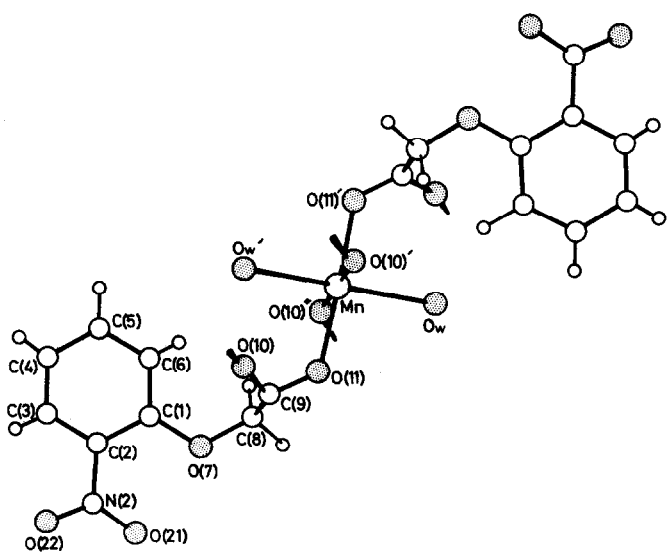


Fig. 2. Molecular configuration for $[Mn(2\text{-}NPA)_2(H_2O)_2]_n$ (**1**).

of note is between the coordinated water (Ow) and the nitro oxygen [O(21)] (2.884 Å).

$[Cu(2\text{-}NPA)_2(H_2O)_4]\cdot 2H_2O$ (2)

The complex **2** has a centrosymmetric, tetragonally distorted octahedral coordination about copper (Fig. 3). The CuO_6 coordination polyhedron consists of two oxygens from unidentate 2-NPA carboxylate groups [Cu–O, 1.943(5) Å] and two waters [Cu–Ow(3), 1.954(5) Å] in the square plane, while another two waters [Cu–O, 2.578(7) Å] occupy the elongated axial positions. Although the O–Cu–O angles within the square plane are quite regular, one of the angles to the axial oxygen [O(11)–Cu–Ow(2), 100.0(2)°] is distorted, indicating possible repulsion away from the influence of the substituted phenoxy ring system. In common with the manganese complex **1**, the conformation of the oxoethanoate side-chain is considerably different compared to 2-NPAH. The equivalent torsion angles are +176.6, +79.8 and −173.4° respectively. The oxygens of the nitro group also adopt positions out of the plane of the benzene ring placing O(21) 2.572(9) Å from O(7) [the torsion angle C(1)–C(2)–N(2)–O(22) Å is −148.5°]. The water of solvation [Ow(1)] is associated with a coordinated water [Ow(3)] by relatively strong hydrogen bonds (2.66 Å) although this bond appears to be the one dissociated first, giving water loss followed by decomposition and loss of crystallinity in the solid state. The presence of the water then provides a route for further decomposition processes involving the nitro groups, a phenomenon observed also for the Ni(II) and Co(II) analogues. Such lability is, however, not reflected in any abnormal thermal parameter found for Ow(1) in the crystallographic analysis. This stability may arise because of hydrogen bonding associations with Ow(1) [to O(21), 2.872 (intramolecular); to O(10), 2.770 (inter); to Ow(2), 2.661 (inter)]. The molecules of **2** pack in the unit cell as discrete monomeric units with the only other intermolecular contacts involving the coordinated waters [Ow(3)] and the coordinated carboxyl oxygens [O(11)] [2.731 and 2.891 Å].

Data obtained from single crystal diffractometry and from elemental analyses confirm that the Co^{II} and Ni^{II} complexes of 2-NPA, $[Co(2\text{-}NPA)_2(H_2O)_4]\cdot 2H_2O$ (**2a**) and $[Ni(2\text{-}NPA)_2(H_2O)_4]\cdot 2H_2O$ (**2b**) are isomorphous and isostructural with (**2**).

$[Cu(2\text{-}NPA)_2(2\text{-}aminopyrimidine)_2(H_2O)]$ (3)

Complex **3** is five-coordinate, square pyramidal with molecular two-fold rotational symmetry coincident with crystallographic symmetry (Fig. 4). The MO_3N_2 coordination sphere consists of a single water [Cu–Ow, 2.211(7) Å], lying on the two-fold axis, two oxygens from unidentate carboxylate groups of the 2-NPA ligands [Cu–O, 1.947(5) Å], and two hetero-nitrogens from the 2-amino-pyrimidine molecules [Cu–N, 2.078(5) Å]. This stereochemistry is known among nitrogen base adducts of copper(II) phenoxyalkanoates, where two complexes, aquabis[(phenoxy)ethanoato]bis-(pyridine)copper(II)[13] and aquabis[(4-chloro-2-methylphenoxy)ethanoato]bis(pyridine)copper(II)[14] have the same five-coordination with crystallographically imposed two-fold symmetry. Some distortion of the ideal 90° angles about Cu, apparently arising from the interactive influence of the 2-amino group of the pyrimidine ligand [N(21)p . . . Ow, 3.094 Å] results in an N(1)p–Cu–N(1)p′ angle of 163.5(3)°. The effect may also be influenced

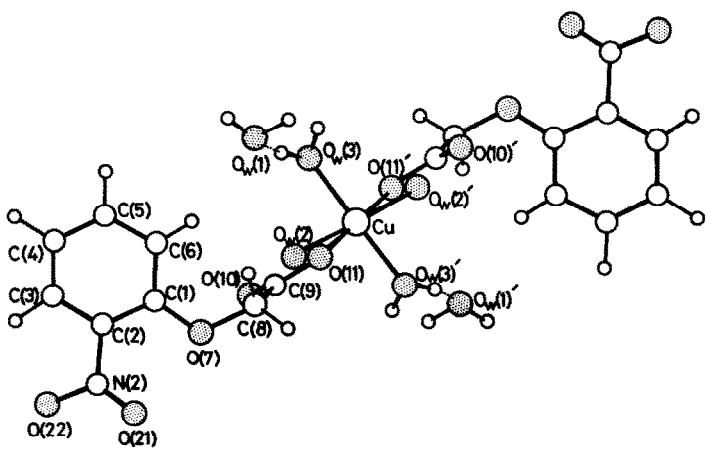


Fig. 3. Molecular configuration for $[Cu(2\text{-}NPA)_2(H_2O)_4]\cdot 2H_2O$ (**2**). Primed atoms are generated by the inversion operation.

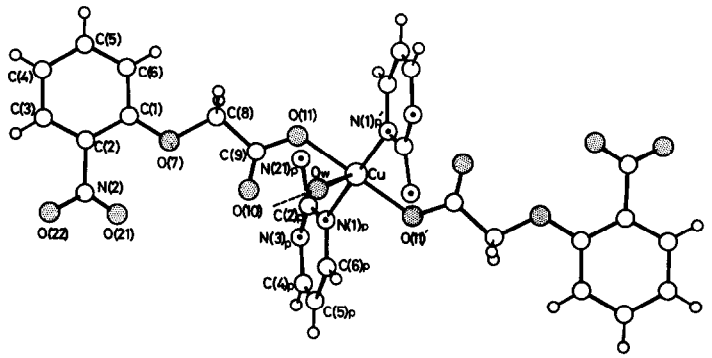


Fig. 4. Molecular configuration for [Cu(2-NPA)$_2$(2-aminopyrimidine)$_2$(H_2O)] (**3**). Primed atoms are generated by two-fold rotation.

by the relatively close approach of the second carboxyl oxygen [O(10)] to the Cu [2.685(5) Å], which stabilizes the structure. In addition, the water molecule is hydrogen bonded to the "free" carboxyl oxygen of an adjacent complex unit down the *b* axis of the cell in a manner similar to both the above pyridine adducts.[13,14]

The reason for the relatively greater stability of this structure compared to **1** and **2** appears to lie in the reversion to five-coordination and is furthermore reflected in the retention of the planar conformation of the free acid [comparative torsion angles, −174.8, −174.6 and −164.2° respectively]. The 2-aminopyrimidine group also exerts its influence on the complex stabilization as shown in the adducts with copper(II) (2-chlorophenoxy)ethanoate[3] [a tetracarboxylate bridged dimer polymer with the pyrimidine ring acting as an axial bridging ligand via the 1 and 3 hetero nitrogens] and copper(II) (4-fluorophenoxy)ethanoate[15] [a discrete tetracarboxylate bridged dimer with the 2-aminopyrimidines occupying the axial positions]. The structural features of the 2-aminopyrimidine molecule[15] undergo no significant change upon complexation. The same nitro group disorder exists with a closely similar O(7) . . . O(22) interactive distance [2.555(10)Å] while the C(1)–C(2)–N(2)–O(22) torsion angle is +161°.

SUMMARY CONCLUSIONS

The substituent group in the ortho-position in 2-substituted phenoxyalkanoic acids plays a steric role in determining the final sterochemistry of the metal complex formed. With complexes of 2-NPAH, there are large conformational changes which prevent one of the oxygens of the bulky nitro group approaching too closely the ether oxygen of the oxoethanoate side chain. In some cases, the oxygens of the nitro groups are rotationally disordered and this is considered to be the reason for difficulties in the preparation of stable crystals of these compounds.

Acknowledgements—We thank Professor B. R. Penfold of the Chemistry Department, University of Canterbury, Christchurch, New Zealand, for the use of facilities in relation to 2-NPAH and compound **3**, and Dr Vicki McKee for helpful advice. Also thanked are the University of Western Australia, The University of Queensland and the Queensland Institute of Technology Research and Development Committee for financial support in this project.

REFERENCES

1. C. H. L. Kennard, G. Smith, E. J. O'Reilly, T. C. W. Mak and W.-H. Yip, *Inorg. Chim. Acta.* (manuscript submitted).
2. C. H. L. Kennard, E. J. O'Reilly and G. Smith, *Polyhedron* 1984, **3**, 689.
3. G. Smith, E. J. O'Reilly, C. H. L. Kennard and A. H. White, *J. Chem. Soc., Dalton Trans.* 1985 (in press).
4. A. V. Ablov, Yu. A. Simenov and T. I. Malinovskii, *Sov. Phys.–Dokl.* 1967, **11**, 1029.
5. M. J. Bird and T. R. Lomer, *Acta Crystallogr. Sect. B* 1972, **28**, 242.
6. G. M. Sheldrick, SHELX-76, *Program for Crystal Structure Determination.* Cambridge University, England (1976).
7. G. M. Sheldrick, *SHELXTL User Manual, Revision* 3, 1981. Nicolet XRD Corporation, Cupertino, California.
8. *International Tables for X-ray Crystallography*, Vol. 4. Kynoch Press, Birmingham (1974).
9. C. H. L. Kennard, G. Smith and A. H. White, *Acta Cryst. Sect. B* 1982, **36**, 868.
10. G. Smith, E. J. O'Reilly and C. H. L. Kennard, *J. Chem. Soc., Dalton Trans.* 1980, 2462.
11. E. J. O'Reilly, G. Smith and C. H. L. Kennard, *Inorg. Chim. Acta* 1984, **90**, 63.

12. G. Smith, E. J. O'Reilly, C. H. L. Kennard, K. Stadnicka and B. Oleksyn, *Inorg. Chim. Acta* 1981, **47**, 111.
13. C. K. Prout, M. J. Barrow and F. J. C. Rossotti, *J. Chem. Soc. A.* 1971, 3326.
14. G. Smith, E. J. O'Reilly, C. H. L. Kennard and T. C. W. Mak, *Inorg. Chim. Acta* 1982, **65**, L219.
15. J. Scheinbein and E. Schempp, *Acta Cryst. Sect. B* 1976, **32**, 607.

Polyhedron Vol. 4, No. 4, pp. 707–712, 1985
Printed in Great Britain

0277-5387/85 $3.00 + .00
© 1985 Pergamon Press Ltd

SPECTROSCOPIC STUDIES ON COPPER(II)–TRIPHENYLARSINE OXIDE SQUARE PLANAR COMPLEXES

OTACIRO RANGEL NASCIMENTO
Instituto de Física e Química de São Carlos, USP, Caixa Postal 369, 13.560—São Carlos—SP, Brazil

and

ANTONIO CARLOS MASSABNI*
Instituto de Química de Araraquara, UNESP, Caixa Postal 174, 14.800—Araraquara—SP, Brazil

(*Received* 10 *May* 1984; *accepted* 4 *September* 1984)

Abstract—Electronic and ESR spectra of the complexes $[Cu(II)(tpa_so)_4][Cu(I)Cl_2]_2$, $[Cu(tpa_so)_4](NO_3)_2$ and $[Cu(tpa_so)_4](ClO_4)_2$ are discussed. Results showed the three complexes are square planar. X-ray powder diagrams show the complexes are not isomorphous, but the ESR spectra are very similar to each other, suggesting the same local square planar symmetry. For $[Cu(II)(tpa_so)_4]$ $[Cu(I)Cl_2]_2$ $g_{\|} = 2.324$; $g_{\perp} = 2.062$, $A_{\|} = 163.0$ and $A_{\perp} = 24.0$ gauss. For a single crystal of this complex three bands assigned to *d–d* transitions were observed at 13,000, 15,300 and 18,500 cm^{-1}.

Triphenylarsine oxide (tpa_so) forms solid complexes with several transition metal ions, including copper(II)[1,2] and the complexes are in general similar to the analogous complexes with triphenylphosphine oxide.[1]

Copper(II) complexes are difficult to characterize by considering only electronic spectra and magnetic susceptibility data. With $CuCl_2$ and $CuBr_2$, according to Goodgame and Cotton,[1] the tpa_so complexes have the formula $[CuX_2(tpa_so)_2]$. The chlorocomplex was yellow-brown and the bromocomplex was purple when freshly prepared but changed to olive-green when the complex was dried. On the basis of electronic spectra and magnetic susceptiblity measurements the authors could not characterize the two complexes. Later, by comparing the electronic spectra of the chlorocomplex with those of $[Cu(tpa_so)_4](ClO_4)_2$ previously described,[3] Rodley, Goodgame and Cotton[2] suggested the formula $[Cu(tpa_so)_4][CuCl_4]$ but the presence of the $[CuCl_4]^{2-}$ anion was not confirmed by the electronic spectra. $[Cu(tpa_so)_4](ClO_4)_2$ was considered by the last named authors as square planar. Electronic and vibrational spectra indicated the existence of the cation $[Cu(tpa_so)_4]^{2+}$ in both complexes.

The formula and structure of the olive-green bromocomplex remained uncertain. According to the same authors the formulation $[Cu(tpa_so)_4][CuBr_4]$ was improbable and the presence of the cation $[Cu(tpa_so)_4]^{2+}$ could not be confirmed by the electronic spectra.

The reaction between $CuCl_2$ and diphenylmethylarsine oxide gave two products: one blue and one brown. Nyholm[4] had already obtained these two products starting with $CuCl_2$ and diphenylmethylarsine. He suggested the formula $[Cu(II)(dpma_so)_4][Cu(I)Cl_2]_2$ for the blue product and the brown compound had the same composition as the blue but with 5–10% of $CuCl_2$, probably as the polymer ion $CuCl_3^-$.

The other complex considered in this paper is $[Cu(tpa_so)_4](NO_3)_2$ which was previously reported by Phillips and Tyree.[5] This complex is interesting because several other transition metal complexes contain the NO_3^- group coordinated to the metal ion. With triphenylphosphine oxide (tppo), for example, the complex is $[Cu(NO_3)_2(tppo)_2]$.[6]

* Author to whom correspondence should be addressed.

Coordination of a fifth arsineoxide or phosphine oxide ligand, or even a ClO_4^- anion, was shown by Hunter *et al.*[7] These authors studied complexes of the type $[ML_5]^{2+}$ and $[M(ClO_4)L_4]^{2+}$ where M = Mn(II), Fe(II), Co(II), Ni(II) and Cu(II), L = tmpo (trimethylphosphine oxide) or tma_so (trimethylarsine oxide). They observed a weak copper(II)–ligand interaction with tmpo and tma_so on the basis of the results from IR spectra. The same conclusion was applied for tppo and tpa_so complexes, for which the same pentacoordinated structure was suggested.

In an attempt to prepare the complex of $CuCl_2$ with tpa_so, following Goodgame and Cotton's procedure a brown complex of formula $2CuCl_2 \cdot 3(tpa_so)$ was obtained. Recrystallization in acetone yielded good blue crystals of the complex $[Cu(II)(tpa_so)_4][Cu(I)Cl_2]_2$ whose structure we previously described.[8] This complex contains the square planar $[Cu(II)(tpa_so)_4]^{2+}$ cation and the linear $[Cu(I)Cl_2]^-$ anion.

The main goal of this paper is to describe electronic and ESR spectra of the Cu(II)–Cu(I) complex and to compare the spectroscopic data with those of the complexes $[Cu(tpa_so)_4](NO_3)_2$ and $[Cu(tpa_so)_4](ClO_4)_2$. The results showed that the three complexes contain the square planar $[Cu(tpa_so)_4]^{2+}$ species.

EXPERIMENTAL

Synthesis of the complexes

$[Cu(tpa_so)_4](ClO_4)_2$ and $[Cu(tpa_so)_4](NO_3)_2$ were easily obtained according to the procedure described in the literature.[3] Addition of tpa_so to $Cu(ClO_4)_2$ or $Cu(NO_3)_2$ dissolved in hot anhydrous ethanol precipitated the solid complexes immediately. Both complexes are insoluble in all solvents used and it was impossible to recrystallize them to obtain good crystals for X-ray diffraction measurements.

$[Cu(II)(tpa_so)_4][Cu(I)Cl_2]_2$—the brown complex $2(CuCl_2) \cdot 3(tpa_so)$ was dissolved in hot acetone and on cooling a blue solid precipitated. A few days after filtration good blue crystals were formed in the filtrate at room temperature.

ANALYSIS

The complexes were analysed for carbon, hydrogen (microanalysis) and copper(II) in the case of the chlorocomplex. Copper(II) was determined with edta.

Found: C, 53.7; H, 3.90%. Calc. for $[Cu(tpa_so)_4](ClO_4)_2$: C, 55.72; H, 3.87%.

Found: C, 57.9; H, 4.14%. Calc. for $[Cu(tpa_so)_4](NO_3)_2$: C, 58.55; H, 4.06%.

Found: C, 53.3; H, 3.66; Cu, 11.86%. Calc. for $[Cu(II)(tpa_so)_4][Cu(I)Cl_2]_2$: C, 53.32; H, 3.70; Cu, 11.75%. (m.p. 243–244°C).

PHYSICAL MEASUREMENTS

Electronic spectra of the solid complexes were obtained at room temperature over a 2000–300 nm range on Cary Model 17 and Beckman DK-2 spectrophotometers using fluorolube mulls or a crystal in the case of $[Cu(II)(tpa_so)_4][Cu(I)Cl_2]_2$ and quartz cells.

IR spectra of CsI pellets (4000–200 cm^{-1}) were recorded on a Perkin–Elmer 567 spectrophotometer.

ESR spectra were recorded on a Varian Model E-109 system spectrometer. Quartz sample tubes were employed for polycrystalline samples. Spectra were calibrated with diphenylpicrylhydrazyl (dpph, $g = 2.0036$) as a field marker.

X-ray powder diagrams were measured using a Phillips X-ray unit (model 1130/00) with horizontal goniometer (PW 1380/01) and a graph detection system mounted in our laboratory.

RESULTS AND DISCUSSION

X-ray powder diagrams of the nitrate and perchlorate complexes showed they are isomorphous. However, the powder diagram of $[Cu(II)(tpa_so)_4][Cu(I)Cl_2]_2$ is quite different from those of the other two complexes. The differences are in the position and the number of lines. This result permits us to conclude the complex is not isomorphous with the nitrate and perchlorate complexes. This is probably due to the presence of the $[Cu(I)Cl_2]^-$ anion, which alters symmetry of the crystal structure.[8] This change does not occur with NO_3^- and ClO_4^- anions.

In spite of the fact that the three complexes are not isomorphous they show powder ESR spectra very

Table 1. The EPR parameters of the three copper complexes: $[Cu(II)(tpa_so)_4][Cu(I)Cl_2]_2$, $[Cu(tpa_so)_4](NO_3)_2$ and $[Cu(tpa_so)_4](ClO_4)_2$

Complex	$g_\parallel$ (0.003)	$g_\perp$ (0.003)	$A_\parallel$ (G)	$A_\perp$ (G)
$Cu(I)Cl_2^-$*	2.324	2.062	163±2	24±2
NO_3^-†	2.303	2.064	161±3	33±5
ClO_4^-†	2.310	2.067	159±3	31±5

* Single crystal sample.
† Powder samples.

similar to each other in type of lines and on values of parameters. Such ESR parameters are presented in Table 1. The similarity of ESR data suggests the same square planar local symmetry for the three complexes.

Figures 1 and 2 show the angular variation of the ESR spectrum of a crystal of the complex $[Cu(II)(tpa_so)_4][Cu(I)Cl_2]_2$; *a* and *b* are the crystal axes and c^* is the third triorthogonal axis. It is clear from Fig. 2 the hyperfine interaction lines with copper nuclear spin and the existence of two copper(II) ions magnetically inequivalent per unit cell in close agreement with X-ray data.

ESR parameters of $[Cu(II)(tpa_so)_4][Cu(I)Cl_2]_2$ compared well with the ones extracted from the literature for $CaCuSi_4O_{10}$[9,10] which is square planar. The values obtained from ESR spectra confirm the axial symmetry of the square planar structures. The fitting was done by using the spin Hamiltonian with hyperfine interaction given by

$$\mathcal{H} = \mu_B \mathbf{H}\cdot\tilde{g}\cdot\mathbf{s}+\mathbf{I}\cdot\tilde{A}\cdot\mathbf{S}. \quad (1)$$

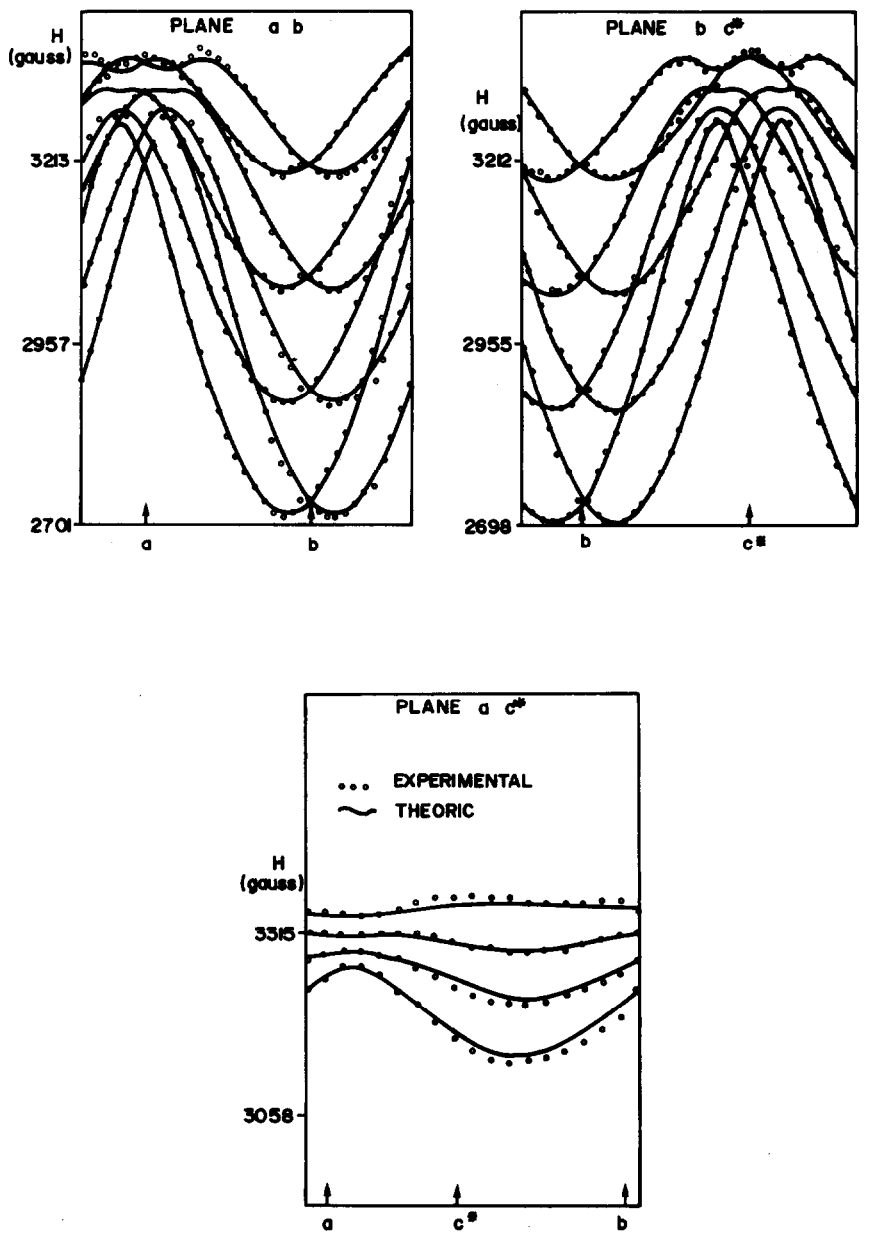


Fig. 1. The angular variation of the EPR spectra for the single crystal of the $[Cu(II)(tpa_so)_4][Cu(I)Cl_2]_2$ complex. The *a* and *b* directions are the crystalline axes and c^* is the third three orthogonal axes.

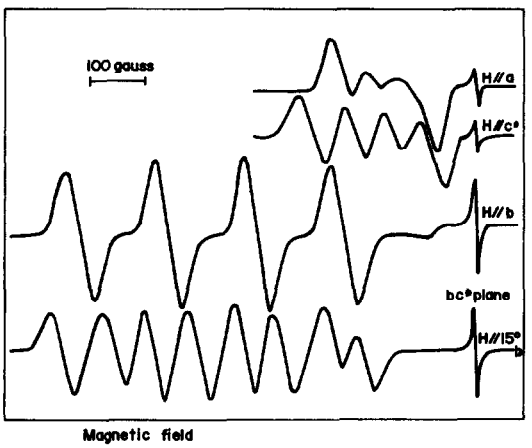


Fig. 2. The EPR spectra, with the hyperfine splitting of the Cu(II) ion in the $[Cu(II)(tpa_so)_4][Cu(I)Cl_2]_2$ single crystal complex in four directions of the magnetic field H. The lowest spectrum shows the two magnetically inequivalent Cu(II) ions in the bc^* plane.

calculated to the second order[11] where the resonant magnetic field H is given by

$$H = \frac{h\nu}{g\mu_B} - \frac{A}{g\mu_B} M_I - \frac{A_\perp^2(A_\parallel^2 + A^2)}{4h\nu g\mu_B A^2}[(I+1)I - M_I^2] - \frac{(A_\parallel^2 - A_\perp^2)g_\parallel^2 g_\perp^2 \sin^2\theta\cos^2\theta}{2h\nu g^5 \mu_B A^2} M_I^2 \quad (2)$$

with

$$A^2 = \frac{1}{g^2}(g_\parallel^2 A_\parallel^2 \sin^2\theta + g_\perp^2 A_\perp^2 \cos^2\theta)$$

and

$$g^2 = (g_\parallel^2 \sin^2\theta + g_\perp^2 \cos^2\theta),$$

where ν is the microwave frequency; μ_B is a Bohr magneton; $g_\parallel$, $A_\parallel$ are the axial components and $g_\perp$, $A_\perp$ the perpendicular components of the gyromagnetic and hyperfine tensors; I and M_I are the copper nuclear spin and magnetic quantum number respectively. The fitting shows that some rhombic distortion exists, as suggested by X-ray data, but the distortion is very small. The system used for crystal orientation is shown in Fig. 3 in a schematical way, as well as the axial direction with respective angles.

Electronic spectra of the $[Cu(tpa_so)_4](NO_3)_2$ and $[Cu(tpa_so)_4](ClO_4)_2$ complexes are shown in Fig. 4. Both spectra are very similar to each other in type and position of bands. The following assignments were done: (a) d–d transitions for NO_3^- and ClO_4^- complexes: 14,900 cm^{-1}; 13,150 cm^{-1} (shoulder); 17,500 cm^{-1} and 18,500 cm^{-1}; (b) the band at 21,700 cm^{-1} which appears for both complexes is a charge-transfer band.

In the electronic spectrum of the $[Cu(II)(tpa_so)_4][Cu(I)Cl_2]_2$ complex, also shown in Fig. 4, three bands are observed in the 10,000–22,500 cm^{-1} region. The three bands at 13,000, 15,300 and 18,500 cm^{-1} were assigned to d–d transitions. Measurements in the crystal were carried out at room temperature and at N_2 liquid temperature. There are some shifts and changes in relative intensities of the bands when we compare the spectra at these two temperatures. Crystal features (size and shape) did not permit us to obtain better details of the electronic spectra in the near infrared region with polarized light.

Spectroscopic and X-ray data for $[Cu(II)(tpa_so)_4][Cu(I)Cl_2]_2$ compared well with those of the compound $CaCuSi_4O_{10}$[10] concerning the local symmetries.

By considering the same energy level diagram (Fig. 5) for d orbitals we can calculate $r_\parallel$, $r_\perp$, α and β parameters using ESR and electronic spectra data

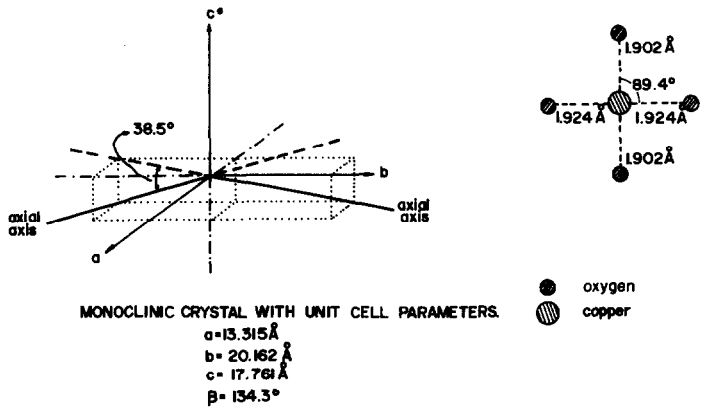


Fig. 3. Schematic diagram of the axial directions of the two Cu(II) complexes per unit cell and the square planar symmetry with the distances from the Cu(II) and oxygen atoms.

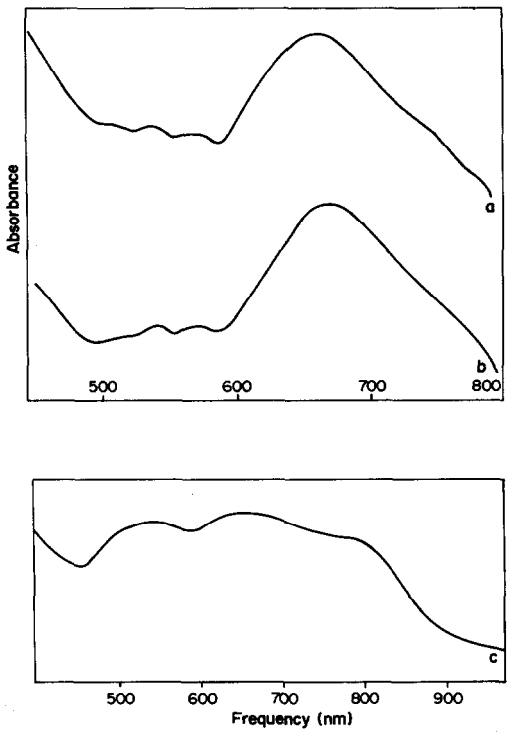


Fig. 4. Electronic spectra of the complexes (fluorolube mulls): (a) $[Cu(tpa_so)](NO_3)_2$, (b) $[Cu(tpa_so)_4](ClO_4)_2$ and (c) $[Cu(II)(tpa_so)_4][Cu(I)Cl_2]_2$.

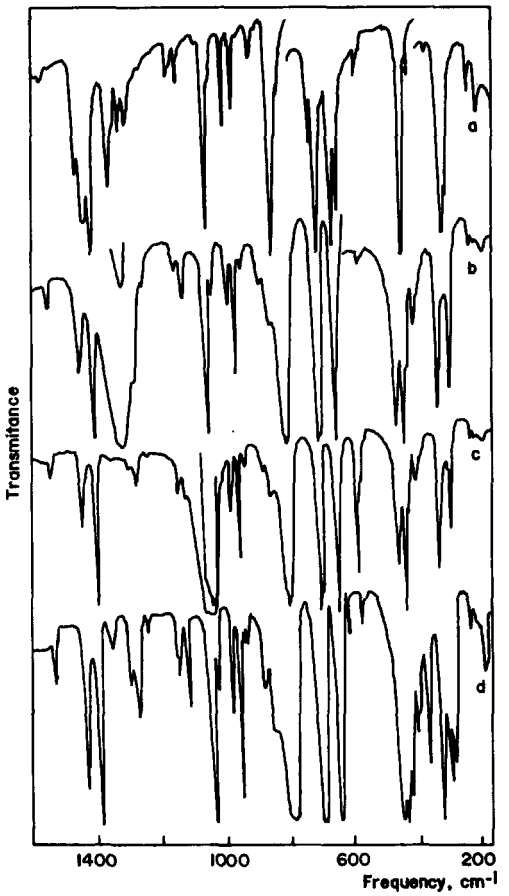


Fig. 6. IR spectra (CsI pellets): (a) tpa_so, (b) $[Cu(tpa_so)_4](NO_3)_2$, (c) $[Cu(tpa_so)_4](ClO_4)_2$, (d) $[Cu(II)(tpa_so)_4][Cu(I)Cl_2]_2$.

(see Table 2). The results obtained for these parameters are in good agreement with each other; α and β values show the degree of participation of d orbitals on the metal–ligand bond.[12]

Figure 6 shows the IR spectra of free tpa_so and of the three $[Cu(tpa_so)_4]^{2+}$ complexes. The (As–O) stretching frequency for $[Cu(II)(tpa_so)_4][Cu(I)Cl_2]_2$ is at 838 cm^{-1} and for the free ligand at 880 cm^{-1}. For nitrate and perchlorate complexes $\nu_{(As-O)}$ occurs at 840–860 cm^{-1}. Bands typical of ionic NO_3^- and ClO_4^- groups are also observed. We found $\nu_{(Cu-O)}$ at 448 cm^{-1} for both NO_3^- and ClO_4^- complexes and at 470 and 418 cm^{-1} for $[Cu(II)(tpa_so)_4][Cu(I)Cl_2]_2$.[3,7] For the anion we found $\nu[Cu(I)Cl]$ at 235 cm^{-1}. The tpa_so bands of the cation $[Cu(tpa_so)_4]^{2+}$ present in the three complexes are very similar in the IR spectra.

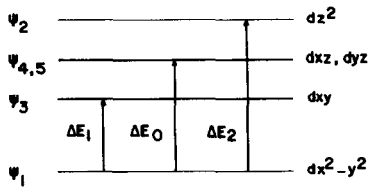


Fig. 5. Energy levels diagram showing the electronic transitions for $[Cu(II)(tpa_so)_4][Cu(I)Cl_2]_2$.

In conclusion, as discussed above, it is assigned that these three copper(II) complexes are in the same

Table 2. The spectroscopic parameters, calculated reduction factor $r_\parallel$ and $r_\perp$ and the d-wave functions covalence degrees α and β for the complexes $[Cu(II)(tpa_so)_4][Cu(I)Cl_2]_2$ and $CaCuSi_4O_{10}$ (Refs 10 and 12) and the assumed energy levels

Complex	ΔE_0*	ΔE_1*	ΔE_2*	$g_\parallel$	$g_\perp$	$r_\parallel$	$r_\perp$	α	β
$CaCuSi_4O_{10}$	15.8	12.9	18.8	2.326	2.054	0.80	0.72	0.80	0.90
$[Cu(II)(tpa_so)_4]^{2+}$	15.3	13.0	18.5	2.324	2.062	0.80	0.76	0.80	0.95

* The energy transitions are given in 10^3 cm^{-1}.

square planar symmetry shown by the spectroscopic data and by the crystallographic structure of $[Cu(II)(tpa_so)_4][Cu(I)Cl_2]_2$.

Acknowledgements—This work was sponsored with grants from FINEP and CNPq.

REFERENCES

1. D. M. L. Goodgame and F. A. Cotton, *J. Chem. Soc.* 1961, 2298.
2. G. A. Rodley, D. M. L. Goodgame and F. A. Cotton, *J. Chem. Soc.* 1965, 1499.
3. E. Bannister and F. A. Cotton, *J. Chem. Soc.* 1960, 1878.
4. R. S. Nyholm, *J. Chem. Soc.* 1951, 1767.
5. D. J. Phillips and S. Y. Tyree Jr., *J. Chem. Soc.* 1961, 1806.
6. E. Bannister and F. A. Cotton, *J. Chem. Soc.* 1960, 2276.
7. S. H. Hunter, R. S. Nyholm and G. A. Rodley, *Inorg. Chim. Acta* 1969, **3**, 631.
8. R. H. P. Francisco, R. H. Almeda Santos, J. R. Lechat and A. C. Massabni, *Acta Cryst.* 1981. **B37**, 232.
9. A. Parst, *Acta Cryst.* 1959, **12**, 733.
10. M. G. Clark and R. G. Burns, *J. Chem. Soc.* (*A*) 1967, 1034.
11. A. Abragam and B. Bleaney, *Electron Paramagnetic Resonance of Ions.* Clarendon Press, Oxford (1970).
12. B. J. Hathaway and D. E. Billing, *Coord. Chem. Rev.* 1970, **5**, 143.

Polyhedron Vol. 4, No. 4, pp. 713–716, 1985
Printed in Great Britain

0277–5387/85 $3.00 + .00
© 1985 Pergamon Press Ltd

SPECIATION OF STRONTIUM IN HUMAN AND BOVINE MILK

GILLIAN L. SMITH, SIÂN B. REES and DAVID R. WILLIAMS*
Department of Applied Chemistry, UWIST, PO Box 13, Cardiff CF1 3XF, U.K.

(*Received* 14 *May* 1984; *accepted* 4 *September* 1984)

Abstract—The speciation of strontium in human and bovine milk has been computed using a chemical equilibrium model and the ECCLES program. The calculations show that the low-molecular-mass distribution of Sr(II) ions parallel that of Ca(II) ions. The analytical techniques used to remove strontium from milk include liquid–liquid extraction using dicyclohexyl-18-crown-6. This method relies on the selective complexation of Sr(II) ions by this ligand. The ability of dicyclohexyl-18-crown-6 to chelate both Sr(II) and Ca(II) ions in milk was investigated using the computer model.

The role of strontium in biological systems received but scant attention until the late 1940s, mainly because there were no reasons to suspect that the element was present in man and also, as with many ultra-trace elements, analytical methods were not available for detecting and measuring strontium. It is now known that strontium in mammals is inextricably linked with the biochemistry of calcium and that milk, being our principal source of calcium, also carries our main strontium-90 threat. This is not surprising since milk and dairy products are vitally important components of our diet, accounting for up to 90% of calcium intake.[1] Strontium, from group IIA of the Periodic Table, occurs with calcium and barium and has biological and physical properties similar to those for these elements.

Strontium presents a threat to man because of its radioactive isotopes. Strontium-90 is widely used in medical and research establishments and produced as a by-product of nuclear fission, 2 to 5 atoms of strontium-90 being produced for every 100 nuclei undergoing fission. Of the six strontium isotopes produced by nuclear fission, strontium-90 is the most important and the most prevalent. It is also the most persistent source of strontium radiation to man, since it has a half-life of 28 years.[2]

Inside the body, strontium-90 enters the blood by absorption from the gastrointestinal tract, from where it is continuously removed by incorporation into new bone or is lost from the blood by urinary and faecal excretion.[1,3] The distribution of strontium in the body parallels that of calcium, high levels being found in teeth, bones and other calcified tissues. Strontium's tendency to occur with calcium is also apparent in foodstuffs—those high in calcium also accumulating strontium. This was clearly demonstrated in the Windscale fire of 1957 in which iodine-131 and strontium-90 scattered over surrounding farmland resulted in the contamination of milk and dairy products. Strontium-90 reaches the milk within a few hours of ingestion by the cow, the maximum activity (which may be up to 4% of the total imbibed) occurring after about 2 days.

The majority of strontium in milk is bound to the protein casein. However, the smaller ultrafilterable portion is of nutritional importance, since the chemical speciation of strontium-90 in this fraction will dictate its bioavailability.

Although the total amount of strontium present in a given milk sample can now be accurately analysed (usually from analysis of the radioactive decay product, yttrium-90), its chemical speciation in such a biofluid is still beyond the reach of the most sophisticated analytical techniques. However, we have for many years used computer simulation models to evaluate the low-molecular-mass (LMM) metal-ion distributions in biofluids such as blood plasma. The approach relies on the assumption that many biological fluids approximate to a steady-state or equilibrium situation. It is thus possible to use thermodynamic chemical equilibrium models to compute the metal–ligand speciation of the biofluid based on analyses of total ligand and total metal ion concentration data and the relevant formation constants.

The ECCLES program has been used to establish

* Author to whom correspondence should be addressed.

simulation models for blood plasma, milk and other biofluids.[4,5] The milk model has now been extended to encompass the pollutant strontium. The total ligand concentrations in human[6–12] and bovine[6–13] milk are listed in Tables 1 and 2, respectively. Values for the total and free concentrations of the biologically essential metal ions are given in Tables 3 and 4.[3,13–15] Formation constants for these metal ions with the former ligands were as previously used in the blood plasma model.[4] The additional formation constants for the strontium system were extracted from literature compilations and corrected to blood plasma conditions of 37°C, I = 150 mmol dm^{-3} NaCl. Milk has an ionic strength of approximately 80 mmol dm^{-3} and the constants are not expected to differ much from those of blood plasma. The total ligand, free metal ion concentrations and formation constant data were used to compute the LMM metal-ion distribution of strontium in human and bovine milk at a pH of 6.8.

Table 1. Total ligand concentrations in human milk

Ligand	Concentration (mol dm^{-3})	Reference
Alanate	1.46×10^{-4}	6–8
Aminobutyrate	1.46×10^{-5}	6, 7
Arginate	1.01×10^{-5}	6–8
Aspartate	3.80×10^{-5}	6–8
Citrullinate	1.10×10^{-5}	6, 8
Cystinate	2.51×10^{-5}	6, 8
Glutaminate	1.72×10^{-4}	6–8
Glutamate	9.25×10^{-4}	6–8
Glycinate	8.09×10^{-5}	6–8
Histidinate	2.42×10^{-5}	6–8
Hydroxyprolinate	5.34×10^{-6}	6
Isoleucinate	1.04×10^{-5}	6–8
Leucinate	2.49×10^{-5}	6–8
Lysinate	2.45×10^{-5}	6–8
Methionate	4.37×10^{-6}	6–8
Ornithinate	3.18×10^{-5}	6–8
Phenylalanate	1.04×10^{-5}	6–8
Prolinate	5.04×10^{-5}	6–8
Serinate	8.07×10^{-5}	6–8
Taurinate	3.54×10^{-4}	6–8
Threoninate	6.67×10^{-5}	6–8
Tryptophanate	1.00×10^{-6}	9, 8
Tyrosinate	1.25×10^{-5}	6–8
Valinate	5.16×10^{-5}	6–8
Carbonate	4.00×10^{-3}	9
Phosphate	1.60×10^{-3}	9–11
Sulphate	4.37×10^{-4}	9, 11
Ammonia	1.17×10^{-4}	9
Citrate	1.00×10^{-3}	12
Lactate	6.30×10^{-4}	10
Pyruvate	5.60×10^{-5}	10
Histamine	3.60×10^{-6}	10
Thiocyanate	1.40×10^{-5}	*
Silicate	1.38×10^{-4}	*
Malate	3.50×10^{-5}	*
Oxalate	3.20×10^{-6}	*
Salicylate	5.00×10^{-6}	*
Succinate	4.20×10^{-5}	*
Ascorbate	4.30×10^{-5}	*

* Estimate based on concentrations in blood plasma (Ref. 4).

Table 2. Total ligand concentrations in bovine milk

Ligand	Concentration (mol dm^{-3})	Reference
Alanate	2.13×10^{-5}	6–8
Aminobutyrate	1.76×10^{-6}	6–8
Arginate	1.20×10^{-5}	6, 7
Aspartate	6.27×10^{-5}	6–8
Citrullinate	1.70×10^{-6}	8
Cystinate	9.24×10^{-6}	6–8
Glutaminate	8.93×10^{-5}	6–8
Glutamate	2.16×10^{-5}	6–8
Glycinate	1.44×10^{-4}	6–8
Histidinate	4.70×10^{-6}	6, 8
Hydroxyprolinate	1.27×10^{-6}	7, 8
Isoleucinate	4.03×10^{-6}	6–8
Leucinate	4.55×10^{-6}	6–8
Lysinate	2.67×10^{-5}	6–8
Methionate	9.00×10^{-7}	7
Ornithinate	1.04×10^{-5}	6–8
Phenylalanate	8.73×10^{-6}	6–8
Prolinate	3.05×10^{-5}	7, 8
Serinate	1.59×10^{-5}	6–8
Taurinate	6.23×10^{-5}	6–8
Threoninate	1.06×10^{-5}	6–8
Tryptophanate	1.00×10^{-6}	8
Tyrosinate	1.06×10^{-6}	6–8
Valinate	1.10×10^{-5}	6–8
Carbonate	4.40×10^{-4}	13
Phosphate	1.10×10^{-2}	10, 13
Sulphate	1.08×10^{-3}	10, 13
Ammonia	4.80×10^{-4}	10
Citrate	1.70×10^{-3}	12
Lactate	6.30×10^{-4}	10
Pyruvate	1.20×10^{-4}	10
Histamine	2.70×10^{-7}	10
Thiocyanate	1.70×10^{-4}	*
Silicate	1.30×10^{-4}	*
Malate	3.00×10^{-5}	*
Oxalate	1.00×10^{-5}	*
Salicylate	5.00×10^{-6}	*
Succinate	4.00×10^{-5}	*
Ascorbate	1.10×10^{-4}	*

* Estimate based on concentrations in blood plasma (Ref. 4).

Table 3. Metal ion concentrations in human milk

Metal ion	Free concentration (mol dm^{-3})	Total concentration (mol dm^{-3})	Reference
Ca(II)	2.52×10^{-3}	3.45×10^{-3}	14
Mg(II)	6.00×10^{-4}	9.28×10^{-4}	14
Cu(II)	1.00×10^{-14}	5.72×10^{-10}	15*
Zn(II)	2.00×10^{-10}	5.00×10^{-6}	15*
Fe(III)	1.00×10^{-20}	1.10×10^{-11}	15*
Sr(II)	1.01×10^{-6}	1.14×10^{-6}	3*

* Concentration in LMM fraction estimated from total concentration.

RESULTS AND DISCUSSION

The distribution of LMM strontium and calcium complexes in human milk are shown in Table 5. Those for bovine milk are given in Table 6. The similarities between the LMM distributions of calcium and strontium are clear. In human and bovine milk both of the metals are present mainly as the free metal ions, the major complexes present being citrate and phosphate species. Bovine milk has higher citrate and phosphate concentrations and this is reflected in the increased percentage of both calcium and strontium present complexed to these ligands. It is interesting to note that the strontium citrate complex is charged, whereas the strontium hydrogen phosphate species formed is neutral and thus more likely to cross cellular membranes and thus more bioavailable.

As a consequence of the chemical similarities between strontium and calcium, it is likely that analytical techniques used to remove Sr from milk will also deplete the biofluid of calcium. Analytical techniques have been developed which selectively remove strontium using ion exchange or nitrate

Table 4. Metal ion concentrations in bovine milk

Metal ion	Free concentration (mol dm^{-3})	Total concentration (mol dm^{-3})	Reference
Ca(II)	2.00×10^{-3}	3.76×10^{-3}	13
Mg(II)	8.10×10^{-4}	1.66×10^{-3}	13
Cu(II)	1.00×10^{-15}	5.72×10^{-10}	15*
Zn(II)	1.00×10^{-8}	1.55×10^{-4}	15*
Fe(III)	1.00×10^{-8}	1.00×10^{-15}	15*
Sr(II)	1.01×10^{-6}	1.34×10^{-6}	3*

* Concentration in LMM fraction estimated from total concentration.

Table 5. Predominating low-molecular-mass Sr(II) and Ca(II) complexes in human milk

Metal ion	Species formed*	log β	% metal in LMM fraction
Sr(II)	Sr^{2+}		87.8
	$Sr(CTA)^-$	2.8	8.0
	$Sr(PO_4)H^0$	12.71	1.8
	$Sr(LTA)^+$	0.90	0.4
	$Sr(SO_4)^0$	1.00	0.4
	$Sr(PO_4)H_2^+$	18.48	0.2
	$Sr(GLU)H^+$	9.50	0.1
	$Sr(MLA)^0$	1.60	0.1
Ca(II)	Ca^{2+}		73.0
	$Ca(CTA)^-$	3.26	19.0
	$Ca(PO_4)^-$	6.05	2.1
	$Ca(PO_4)H^0$	12.70	1.5
	$Ca(CO_3)H^+$	10.90	1.0
	$Ca(GLU)H^+$	10.40	0.9
	$Ca(LTA)^+$	1.30	0.9
	$Ca(SO_4)^0$	1.20	0.5
	$Ca(PO_4)H_2^+$	18.60	0.2

* Abbreviations used in Tables 5–8: CTA, citrate; PO_4, phosphate; LTA, lactate; CO_3, carbonate; GLU, glutamate; SO_4, sulphate; MLA, malate; CRE, dicyclohexyl-18-crown-6.

Table 6. Predominating low-molecular-mass Sr(II) and Ca(II) complexes in bovine milk

Metal ion	Species formed	log β	% metal in LMM fraction
Sr(II)	Sr^{2+}		74.7
	$Sr(CTA)^-$	2.80	12.3
	$Sr(PO_4)H^0$	12.71	10.2
	$Sr(PO_4)H_2^+$	18.48	1.0
	$Sr(LTA)^+$	0.90	0.4
	$Sr(PO_4)^-$	4.00	0.1
	$Sr(MLA)^0$	1.60	0.1
	$Sr(SO_4)^0$	1.00	0.1
Ca(II)	Ca^{2+}		53.2
	$Ca(CTA)^-$	3.26	25.0
	$Ca(PO_4)^-$	6.05	10.0
	$Ca(PO_4)H^0$	12.70	7.1
	$Ca(PO_4)_2H_3^-$	32.30	1.2
	$Ca(PO_4)H_2^+$	18.60	0.9
	$Ca(PO_4)_2H_2^{2-}$	25.30	0.7
	$Ca(LTA)^+$	1.30	0.6

Table 7. Predominating low-molecular-mass Sr(II) and Ca(II) complexes in human milk in the presence of 10^{-4} mol dm^{-3} dicyclohexyl-18-crown-6

Metal ion	Species formed	log β	% metal in LMM fraction
Sr(II)	$Sr(CRE)^{2+}$	5.0	82.2
	Sr^{2+}	—	15.8
	$Sr(CTA)^{-}$	2.8	1.4
Ca(II)	Ca^{2+}	—	72.2
	$Ca(CTA)^{-}$	3.26	18.8
	$CaPO_4^{-}$	6.05	2.0
	$CaHPO_4^{0}$	12.70	1.4
	$Ca(CRE)^{2+}$	2.51	1.2

Table 8. Predominating low-molecular-mass Sr(II) and Ca(II) complexes in bovine milk in the presence of 10^{-4} mol dm^{-3} dicyclohexyl-18-crown-6

Metal ion	Species formed	log β	% metal in LMM fraction
Sr(II)	$Sr(CRE)^{2+}$	5.00	84.5
	Sr^{2+}	—	11.7
	$Sr(CTA)^{-}$	2.80	1.9
	$SrHPO_4^{0}$	12.71	1.6
Ca(II)	Ca^{2+}	—	53.0
	$Ca(CTA)^{-}$	3.26	24.9
	$CaPO_4^{-}$	6.05	9.9
	$CaHPO_4^{0}$	12.70	7.0

precipitation. Kimura has developed a method of selectively removing strontium from milk involving liquid–liquid extraction using the macrocyclic ether dicyclohexyl-18-crown-6.[16] This method relies on the ability of the ligand to complex strontium more strongly than calcium. This was evaluated using the ECCLES program using formation constants for dicyclohexyl-18-crown-6 reported in the literature.[17] Tables 7 and 8 show the effect on the LMM distribution of Sr(II) and Ca(II) ions in human and bovine milk of the presence of 10^{-4} mol dm^{-3} of dicyclohexyl-18-crown-6. Clearly, the crown ether is selective for strontium ions mobilising some 80% of the strontium whilst the calcium distribution is virtually unaffected. This selectivity for Sr(II) ions is undoubtedly due to the difference in ionic radii between the Ca^{2+} and Sr^{2+} ions, Sr^{2+} being of optimum size to sit in the hole of the crown ether molecule. Hence, such liquid–liquid extraction techniques may successfully be used to selectively remove strontium from milk for analysis purposes.

REFERENCES

1. R. S. Russell, *Radioactivity and Human Diet.* Pergamon Press, Oxford (1966).
2. F. A. Fry, N. J. Dodd, N. Green, R. O. Major and B. T. Wilkins, NRPB-R134 (1981).
3. F. W. Lengemann, R. A. Wentworth and C. L. Comar, *Lactation. Vol.* 3. *Nutrition and Biochemistry of Milk/Maintenance* (Edited by B. L. Larson and V. R. Smith), p. 159. Academic Press, London (1974).
4. P. M. May, P. W. Linder and D. R. Williams, *J. Chem. Soc., Dalton Trans.* 1977, 588.
5. P. M. May, G. L. Smith and D. R. Williams, *J. Nutr.* 1982, **112**, 1990.
6. D. K. Rassin, J. A. Sturman and G. E. Gaull, *Early Hum. Dev.* 1978, **2/1**, 1.
7. M. D. Armstrong and K. N. Yates, *Proc. Soc. Exp. Biol. Med.* 1963, **113**, 680.
8. H. Ghadimi and P. Pecora, *Am. J. Clin. Nutr.* 1963, **13**, 75.
9. B. Blanc, *World Rev. Nutr. Diet.* 1981, **36**, 1.
10. R. Jenness, *Lactation. Vol.* 3. *Nutrition and Biochemistry of Milk/Maintenance* (Edited by B. L. Larson and V. R. Smith), p. 1. Academic Press, London (1974).
11. J. A. Lemons, L. Moye, D. Hall and M. Simmons, *Pediatr. Res.* 1982, **16**, 113.
12. B. Lönnerdal, A. G. Stanislowski and L. S. Hurley, *J. Inorg. Biochem.* 1980, **12**, 71.
13. C. Holt, D. G. Dalgleish and R. Jenness, *Anal. Biochem.* 1981, **113**, 154.
14. C. Holt, *J. Nutr.* 1981, **111**, 2240.
15. B. Lönnerdal, C. L. Keen and L. S. Hurley, *Annu. Rev. Nutr.* 1981, **1**, 149.
16. T. Kimura, K. Iwashima, T. Ishimori and T. Hamada, *Anal. Chem.* 1979, **51**, 1113.
17. R. M. Izatt, R. E. Terry, D. P. Nelson, Y. Chan, D. J. Eatough, J. S. Bradshaw, L. D. Hansen and J. J. Christensen, *J. Am. Chem. Soc.* 1976, **98**, 7626.

Polyhedron Vol. 4, No. 4, pp. 717–721, 1985
Printed in Great Britain

0277–5387/85 $3.00 + .00
© 1985 Pergamon Press Ltd

CHEMISTRY OF IRON COMPLEXES—IV. SPECTROSCOPIC, MAGNETIC AND OTHER PROPERTIES OF COMPLEXES OF IRON(II) IODIDE AND IRON(II) TETRACARBONYL IODIDE WITH BIS(TERTIARYPHOSPHINE/ARSINE OXIDES)

T. S. LOBANA,* H. S. CHEEMA and S. S. SANDHU
Department of Chemistry, Guru Nanak Dev University, Amritsar-143005, India

(*Received* 30 *April* 1984; *accepted* 4 *September* 1984)

Abstract—Bis(tertiaryphosphine/arsine oxides), $Ph_2E(O)(CH_2)_nE(O)Ph_2$ react with iron(II) iodide and iron(II) tetracarbonyliodide forming complexes of the type: (i) $[Fe(L–L)_3]I_2mH_2O$(L–L, *n*, E, *m*; mdpo, 1, P, 2; tmdpo, 4, P, 1); (ii) $[Fe(L–L)_2I_2]\cdot mH_2O$(L–L, *n*, E, *m*: edpo, 2, P, 1; tmdao, 4, As, 0); (iii) $[Fe(L–L)_2][FeI_4]\cdot 2H_2O$(L–L, *n*, E: edao, 2, As) and (iv) $[Fe(L–L)(CO)_2I]I\cdot H_2O$[L–L = mdpo, edpo, edao, tmdpo, tmdao and (for *n* = 6, E = P) hmdpo]. All the complexes have been characterized through elemental analysis, IR, far-IR and UV–visible spectra, molar conductance, magnetic moments and t.g.a. studies. Iron(II) iodide complexes are high-spin with μ_{eff} values of 4.94–5.24 B.M., whereas the iron(II) tetracarbonyl iodide complexes show intermediate magnetic moment values (3.85–3.98 B.M.). The water is present as lattice water.

Although numerous complexes of bis (tertiaryphosphine/arsine oxides) with a number of metal ions are known, yet there are a few complexes reported with iron(III) and none with iron(II).[1–3] The coordination chemistry of iron is important from biological and industrial aspects. In order to understand in detail how the bidentate bis(tertiaryphosphine/arsine oxides) behave in case of iron systems, we undertook the detailed study of iron(II) and iron(III) complexes. Consequently, a number of new iron(II) and iron(III) complexes have been synthesised and characterized with various techniques including ESR, Mössbauer, etc. It was also intended: (i) to correlate the number of CH_2 groups connecting (PO) or (AsO) groups with the stoichiometry of the complexes; (ii) to compare the Lewis acidity of iron(II) with that of iron(III); and (iii) to compare the Lewis basicity of the (AsO) group with that of the (PO) group. In one of the papers[4] we have reported the complexes of iron(III) chloride and nitrate with bis(tertiaryphosphine oxides) with structures: *trans*-$[Fe(L–L)_2Cl_2][FeCl_4]$(L–L = mdpo, edpo, tmdpo, hmdpo); $[Fe(ONO_2)_3(L–L)]$ (L–L = tmdpo, hmdpo); $[Fe_2(L–L)_3(ONO_2)_4](NO_3)_2$ (L–L = mdpo) and $[Fe(L–L)_2(ONO_2)_2](NO_3)$ (L–L = edpo). In this paper, we are reporting the complexes of iron(II) with ditertiaryphosphine/arsine dioxides (I and II)

$$Ph_2P(O)(CH_2)_nP(O)Ph_2$$

I

$$Ph_2As(O)(CH_2)_nAs(O)Ph_2$$

II

where $n = 1$; mdpo-methylene bis(diphenylphosphine oxide); $n = 2$, edpo or edao-1,2-ethylene bis(diphenylphosphine or arsine oxide); $n = 4$, tmpdo or tmdao-1,4-tetramethylene bis(diphenylphosphine or arsine oxide); $n = 6$, hmdpo-1,6-hexamethylene bis(diphenylphosphine oxide).

EXPERIMENTAL

Ligands

The ligands were obtained by the oxidation of corresponding phosphines/arsines by 30% H_2O_2 in acetone or benzene.[1]

Preparation of the complexes

Iron(II) iodide complexes were obtained by adding the solution of a ligand in chloroform to iron(II) iodide solution in a 5:1 acetone:benzene

* Author to whom correspondence should be addressed.

mixture (1 : 1 molar solutions were reacted), followed by refluxing for half an hour. The complexes separated out as viscous liquids either after concentrating or on the addition of petroleum–ether (40–60°C). They were solidified on further treatment with petroleum–ether after removing the mother liquor. The solid complexes were filtered, dried and recrystallised from the mixture of solvents used for the preparation of the complexes.

The mixed ligand complexes with iron(II) tetracarbonyl iodide were obtained by adding the solution of a ligand in chloroform to iron(II) carbonyl iodide solution in a 5 : 1 acetone : benzene mixture (for tmdpo ligand, carbonyl iodide solution was in chloroform). The reaction was allowed to take place in a dark room at about 25°C. The complex separated out as a dark brown viscous liquid as such or after the addition of petroleum-ether (40–60°C) and solidified on further treatment with petroleum-ether. The solid thus obtained was filtered, washed several times with the solvents used in the preparation of the complexes and finally dried *in vacuo*.

The analytical data and the techniques used for characterization

The elemental analyses for carbon and hydrogen were carried out at the University College of Sciences, Calcutta (India). Iron was estimated by the phenanthroline method spectrophotometrically.[5] The molar conductances of millimolar solutions of complexes in nitrobenzene were measured with Toshniwal conductivity Bridge type CLOI/O2A. The IR spectra in the range 4000–650 cm^{-1} (in nujol) were recorded on spectromom 2000. The far-IR spectra in the range 650–200 cm^{-1} were recorded at the University of Surrey (U.K.). The reflectance spectra in the range 350–1000 nm were recorded with spectrophotometer VSU-2P type. The magnetic susceptibility measurements (solid samples) were carried out using Gouy's method. The apparatus was calibrated with $HgCo(NCS)_4$ and the diamagnetic corrections were applied employing Pascal's constants.[6] The X-ray diffraction patterns (powder) of iron(II) iodide complexes were taken by using Debye–Scherrer camera of radius 57.3 mm mounted

Table 1. The analytical data and some physical properties

S. No.	Complex	Analytical data			M.p. (°C)	Λ_m (ohm^{-1} cm^2 mol^{-1})
		% C	% H	% Fe		
1	$[Fe(mdpo)_3]I_2 \cdot 2H_2O$	55.62 (56.46)	4.45 (4.39)	3.84 (3.51)	258	55
2	$[Fe(edpo)_2I_2] \cdot H_2O$	53.06 (52.52)	4.30 (4.94)	5.31 (4.71)	218	3
3	$[Fe(tmdpo)_3]I_2 \cdot H_2O$	59.79 (59.21)	5.51 (5.05)	3.28 (3.10)	248	50
4	$[Fe(edao)_2][FeI_4] \cdot 2H_2O$	37.08 (36.11)	3.20 (3.24)	6.52 (6.48)	216	30
5	$[Fe(tmdao)_2I_2]$	47.57 (47.93)	3.79 (3.99)	3.94 (3.99)	194	*
6	$[Fe(CO)_2(mdpo)I]I \cdot H_2O$	39.86 (40.50)	2.61 (3.00)	6.60 (7.00)	—	20
7	$[Fe(CO)_2(edpo)I]I \cdot H_2O$	40.24 (41.25)	2.47 (3.18)	6.45 (6.87)	—	22
8	$[Fe(CO)_2(tmdpo)I]I \cdot H_2O$	43.40 (42.75)	3.63 (3.56)	6.18 (6.47)	—	29
9	$[Fe(CO)_2(hmdpo)I]I \cdot H_2O$	45.04 (44.13)	3.36 (3.75)	6.07 (6.47)	—	33
10	$[Fe(CO)_2(edao)I]I \cdot H_2O$	36.74 (37.25)	3.91 (2.88)	5.78 (6.28)	—	31
11	$[Fe(CO)_2(tmdao)I]I \cdot H_2O$	37.30 (37.97)	2.69 (3.38)	5.62 (5.90)	—	34

* Sparingly soluble in nitrobenzene.

on Phillips generator of the type PW-1720. The t.g.a. off iron(II) iodide complexes was carried out with a manually operated instrument supplied by FCI unit, Sindri (India).

RESULTS AND DISCUSSION

Iron(II) iodide complexes

The elemental analyses reveal the compositions: $FeI_2(L\text{–}L)_3 \cdot mH_2O$ (L–L, m; mdpo, 2; tmdpo, 1); $FeI_2(L\text{–}L)_2 \cdot mH_2O$ (L–L, *m*: edpo, 1; tmdao, 0) and $FeI_2(L\text{–}L)H_2O$ (L–L = edao). The complexes are turmeric in colour and the melting points of the complexes usually lie in the range of those of the ligands (Table 1). The molar conductance values (in nitrobenzene) for the complexes of mdpo and tmdpo lie in the range 50–55 $ohm^{-1}\ cm^2\ mole^{-1}$) and support the formulation: $[Fe(L\text{–}L)_3]I_2 \cdot mH_2O$. The complex of edao has a molar conductance of ~ 15 $ohm^{-1}\ cm^2\ mole^{-1}$ and is lower than expected for a 1:1 electrolyte (20–30 $ohm^{-1}\ cm^2\ mole^{-1}$). Nevertheless, in the literature, a number of iron(III) complexes have been reported to show low conductance values and still formulated as 1:1 electrolytes.[3,4] On the same basis, the complex of edao has been formulated as $[Fe(edao)_2][FeI_4] \cdot 2H_2O$. The complexes, $[Fe(L\text{–}L)_2I_2] \cdot mH_2O$ (L–L = edpo, tmdao) are nonelectrolytes.

In the IR spectra, the $\nu_{(PO)}$ and $\nu_{(AsO)}$ show usual downward shifts and appear as either single or double peaks (Table 2).[1,4,7,8] The decrease in $\nu_{(PO)}$ and $\nu_{(AsO)}$ is less than that found in iron(III) complexes.[3,4] This demonstrates that iron(II) iodide has poor Lewis acidity as compared to that of iron(III) halides. Thus a hard "O" will bind more strongly to iron(III) than to iron(II) which has been made considerably softer by iodide group. There is no change in $\nu_{(P\text{–}C)_{aromatic}}$ as compared to that of free ligand and this is unlike the behaviour of iron(III) complexes which have been observed to show a decrease of up to 30 cm^{-1}.[4,7] In the far-IR spectra, the assignments to $\nu_{(Fe\text{–}O)}$ have been made in the ranges 385–390 cm^{-1} and 360–365 cm^{-1} for the respective phosphine oxide and arsine oxide complexes.[1,8–12]

The water present in the samples is not coordinated as there are no peaks in the region 785–805 cm^{-1} attributable to rocking and wagging modes of coordinated water.[13] The content of the

Table 2. The IR spectra, reflectance spectra and magnetic moments of the complexes

S. No.	Complex	μ_{eff} (B.M.)	$\nu_{(PO)}$/ (AsO) (cm^{-1})	$\nu_{(CO)}$ (cm^{-1})	*d–d* bands (cm^{-1})	Charge transfer bands (cm^{-1})
1	$[Fe(mdpo)_3]I_2 \cdot 2H_2O$	5.22	1160s, b	—	10,800w 10,000w	24,100sb
2	$[Fe(edpo)_2I_2] \cdot H_2O$	5.02	1175s, b	—	10,530w	26,000s, sp
3	$[Fe(tmdpo)_3]I_2 \cdot H_2O$	5.24	1180s, sp 1160s, sp	—	10,530w	26,000s, b
4	$[Fe(edao)_2][FeI_4] \cdot 2H_2O$	5.04	850s, b	—	—	25,640s, sp
5	$[Fe(tmdao)_2I_2]$	4.94	860s, b	—	10,700w	26,310s, sp
6	$[Fe(CO)_2(mdpo)I]I \cdot H_2O$	3.88	1165s, b	2080m, sp 2025m, sp	—	—
7	$[Fe(CO)_2(edpo)I]I \cdot H_2O$	3.87	1180s, b	2080m, sp 2030m, sp	—	—
8	$[Fe(CO)_2(tmdpo)I]I \cdot H_2O$	3.98	1180s, sp 1160s, sp	2080m, sp 2030m, sp	—	—
9	$[Fe(CO)_2(hmdpo)I]I \cdot H_2O$	3.86	1160s, b	2065m, sp 2010m, sp	—	—
10	$[Fe(CO)_2(edao)I]I \cdot H_2O$	3.85	850s, b	2060m, sp 2010m, sp	—	—
11	$[Fe(CO)_2(tmdao)I]I \cdot H_2O$	3.90	840s, b	2080m, sp 2030m, sp	—	—

* $\nu_{(H_2O)}$ and $\delta_{(HOH)}$ lie in the range 3200–3300 and 1620–1645 cm^{-1} respectively.
† The IR spectrum of *cis*-$[Fe(CO)_4I_2]$ shows two medium bands at 2135 and 2090 cm^{-1}.

water remains constant even if a sample is exposed for a prolonged period thereby confirming that the complexes are stoichiometrically hydrated. In the thermogravimetric analysis, the water is lost below 120°C in the complexes **1**, **2**, **3** and **4** and the loss in weight corresponds to $2H_2O$, $1H_2O$, $1H_2O$ and $2H_2O$ in the respective complexes.

In the ligand field of O_h-symmetry, the ground ^5D of the free iron(II) ion splits into $^5T_{2g}$ and ^5E_g states, whereas in a T_d symmetry, the order of splitting is the inverse. The reflectance spectra of the complexes of mdpo, edpo, tmdpo and tmdao show weak bands in the range 10,000–10,800 cm^{-1} attributed to $^5T_{2g} \rightarrow {}^5E_g$ transition (Table 2). The other weak bands, lie in the range 18,520–21,740 cm^{-1}. These assignments are in agreement with those reported for octahedral iron(II) systems.[11,12,14,15] The charge-transfer bands in the range 24,100–26,310 cm^{-1} have been detected in all the complexes.[16]

The magnetic moment values of the complexes lie in the range 4.94–5.24 B.M. (Table 2).[17–19] Somewhat low values for the complexes of edpo, edao and tmdpo may be due to orbital quenching on account of lower symmetry in the complexes. The X-ray-powder photographs of the complexes show that the complexes are crystalline, but efforts to grow a single crystal resulted in failure precluding detailed X-ray structure determination.

Substitution reactions in cis-$Fe(CO)_4I_2$

The substitution reactions of *cis*-$Fe(CO)_4I_2$ with the ligands under consideration yield mixed ligand complexes having 1:1 metal to ligand ratio. These are light-sensitive and not very stable. The molar conductance of the complexes in the range 20–34 ohm^{-1} cm^2 $mole^{-1}$ support the formulation: $[Fe(CO)_2(L\text{–}L)I]I \cdot H_2O$ (Table 1). All these complexes are paramagnetic with μ_{eff} values of 3.85–3.98 B.M., conforming to a triplet ground state and correspond to the moment expected for two unpaired electrons with an additional contribution of about 1.00 B.M. from the second-order Zeeman effect.[20] In the present case, low-lying excited levels of multiplicities 5 and 1 will be present and therefore, an increased contribution from the second order Zeeman effect may not be unexpected. Konig and Madeja[21] have reported μ_{eff} values of ~ 3.9 B.M. for a number of iron(II) complexes with N-donors. It would be relevant to point out here that *cis*-$Fe(CO)_4I_2$ is diamagnetic, its derivatives $[Fe(CO)_2(L\text{–}L)I]I \cdot H_2O$ paramagnetic with intermediate values and complexes of iron(II) iodide (as seen in the previous section) with ditertiaryphosphine/arsine dioxides are paramagnetic having μ_{eff} values corresponding to 4 unpaired electrons. Since the ligands under consideration are weak-field ligands, the replacement of two CO groups by one bidentate L–L, leads to paramagnetism and further loss of CO groups (observed under UV photolysis) leads to the complexes having normal μ_{eff} values. Thus it is apparent that intermediate values are on account of changing ligand field from strong field CO groups to weak field phosphine/arsine oxide ligands. Thus the species $[Fe(CO)_2(L\text{–}L)I]^+$ possessing two CO groups, one bidentate oxygen donor L–L, and iodide group generate a situation in which magnetic moment values become intermediate.

In the IR spectra, each complex shows two $\nu_{(CO)}$ peaks one each in the regions 2060–2080 cm^{-1} and 2010–2030 cm^{-1} respectively (Table 2). In *cis*-$Fe(CO)_4I_2$, one peak at 2135 cm^{-1} decreases to low energy by 55–75 cm^{-1} while the other peak at 2090 cm^{-1} by 60–80 cm^{-1}. The appearance of two peaks in the substituted derivatives show that the carbonyl groups are in the *cis*-position.[22,23] Thus the cations, $[Fe(L\text{–}L)(CO)_2I]^+$ may be assigned *cis*-trigonal bipyramidal structure with CO groups either in the equatorial plane or one in the axial and the other in the equatorial plane. The absorption due to $\nu_{(P\text{–}C)_{Ar}}$, $\nu_{(P\text{–}O)}$ and $\nu_{(As=O)}$ show the usual trends on complexation. The water is present as lattice water as shown by IR spectroscopy due to the absence of rocking and wagging modes in the region 785–805 cm^{-1}.[13] The t.g.a. of the light-sensitive iron carbonyl derivatives was not possible due to low-thermal stability. It may be added here that the water is present as stoichiometric water and its content does not change on exposure as was seen by the reproducible magnetic moments and other data. It may be worth remarking that the carbonyl complexes are probably the first examples among metal carbonyl chemistry (*d*-block) exhibiting intermediate μ_{eff} values.

At the end, it may be appropriate to add that the iron(II) iodide complexes did not show Mössbauer absorption (probably due to heavy atom absorption) and ESR spectra (due to large zero-field splitting) at room temperature.

CONCLUSIONS

The carbonyl complexes have all 1:1 metal to ligand ratio, i.e. the increase in number of CH_2 groups appears to have no effect on the stoichiometry and probably they have similar structure. The similar behaviour has been noted earlier in case of complexes of ditertiaryphosphine oxides with iron(III) halides.[4,7] The behaviour of complexes of iron(II) iodide is variable; mdpo and tmdpo forming 1:3 complexes, edpo and tmdao forming 1:2 complexes whereas edao forms a 1:1

complex. Further iron(II) iodide acts as a poor Lewis acid as compared to iron(III) halides with respect to phosphine oxide ligands. However, there is no difference in behaviour with respect to arsine oxide ligands. It is also inferred from here that arsine oxide ligands are better donors relatively speaking as compared to phosphine oxides with respect to iron(II) iodide.

Acknowledgements—One of us (HSC) is thankful to the UGC for financial support and to the Guru Nanak Dev University, Amritsar for providing research facilities.

REFERENCES

1. T. S. Lobana and S. S. Sandhu, *J. Chem. Sci. (Guru Nanak Dev University)* 1979, **5**, 102.
2. T. S. Lobana, S. S. Sandhu and H. S. Cheema, *J. Chem. Sci. (Guru Nanak Dev University)* 1981, **7**, 58.
3. S. A. Cotton, *Coord. Chem. Rev.* 1972, **8**, 185.
4. T. S. Lobana, H. S. Cheema and S. S. Sandhu, *J. Chem. Soc., Dalton Trans.* 1983, 2039.
5. A. I. Vogel, *A Text Book of Quantitative Inorganic Analysis*, p. 787. ELBS and Longman (1973).
6. A. Earnshaw, *Introduction to Magnetochemistry*, p. 5. Academic Press, London (1968).
7. H. S. Cheema, Ph.D. Thesis submitted to Guru Nanak Dev University, Amritsar, India (1983).
8. K. P. Nakamoto, *Infrared Spectra of Inorganic and Coordination Compounds*, p. 150. Wiley–Interscience, New York (1970).
9. D. M. Adams, *Metal–Ligand and Related Vibrations*, p. 85. E. Arnold, London (1966).
10. A. Reckziegel and M. Bigorgne, *J. Organomet. Chem.* 1965, **3**, 341.
11. A. M. Brodie, J. E. Douglas and C. J. Wilkins, *J. Chem. Soc. (A)* 1969, 1931.
12. (a) D. Forster and D. M. L. Goodgame, *J. Chem. Soc.* 1965, 454; (b) D. M. L. Goodgame, M. Goodgame, M. A. Hitchman and M. J. Weaks, *Inorg. Chem.* 1965, **5**, 635; (c) D. M. Adams, *Metal–Ligand and Related Vibrations*, p. 238. E. Arnold, London (1966).
13. (a) H. Meider and P. Bronzan, *Polyhedron* 1983, **2**, 69; (b) T. S. Lobana, H. S. Cheema and S. S. Sandhu, *Polyhedron* 1984, **3**, 911.
14. C. K. Jörgenson, *Acta Chem. Scand.* 1954, **8**, 1502.
15. C. J. Ballhausen, *Introduction to Ligand Field Theory*, p. 252. McGraw-Hill, New York (1962).
16. K. Madeja and E. König, *J. Inorg. Nucl. Chem.* 1963, **25**, 377.
17. B. N. Figgis, *Introduction to Ligand Fields*, p. 240. Wiley–Interscience, New York (1966).
18. R. J. H. Clark, R. S. Nyholm and F. B. Taylor, *J. Chem. Soc. (A)* 1967, 1802.
19. B. N. Figgis, J. Lewis, G. A. Webb and F. E. Mabbs, *J. Chem. Soc. (A)* 1966, 1411.
20. C. J. Ballhausen and R. W. Asmussen, *Acta Chem. Scand.* 1957, **11**, 479.
21. E. König and K. Madeja, *Inorg. Chem.* 1968, 7, 1848.
22. L. E. Orgel, *Inorg. Chem.* 1962, **1**, 25.
23. T. A. Manual, *Inorg. Chem.* 1963, **2**, 854.

Polyhedron Vol. 4, No. 4, pp. 723–729, 1985
Printed in Great Britain

0277–5387/85 $3.00 + .00
© 1985 Pergamon Press Ltd

EXTRACTION OF COPPER(II) AND NICKEL(II) BY LONG-CHAIN ALIPHATIC DIOXIMES

L. R. M. PAPING, C. P. J. RUMMENS, P. H. A. VRIENS, J. H. M. C. VAN WOLPUT and T. P. M. BEELEN*

Laboratory of Inorganic Chemistry, Eindhoven University of Technology, P.O. Box 513, 5600 MB Eindhoven, The Netherlands

(*Received* 18 *June* 1984; *accepted* 4 *September* 1984)

Abstract—In the search for a selective nickel extractant symmetric dialkyl dioximes have been studied in the extraction of copper and nickel ions from ammoniacal and acidic solutions. Extraction from ammoniacal solutions showed great differences between copper and nickel. Because of slow kinetics for nickel, much more copper than nickel was extracted at short contact times, but since nickel forms more stable chelates, more nickel than copper was extracted after long contact times. Because of steric hindrance and solubility the extraction was also dependent on the length of the alkyl chains of the aliphatic dioximes. Two different chelates, CuL_2 and $Cu_4L_3(OH)_2$, were involved in the extraction of copper from acidic solutions. Kinetic measurements of the extraction of nickel from acidic solutions showed a first order dependence in ligand and nickel concentrations and almost zero order in H^+ concentration, demonstrating that the reaction of Ni^{2+} with the first non-ionized dioxime molecule is rate determining.

From analytical chemistry it is well-known that nickel ions react with dimethylglyoxime to form quantitatively the red bis(dimethylglyoximato) nickel(II) chelate. The relatively low solubility of dimethylglyoxime in organic solvents makes this compound unattractive for extraction. Burkin and Preston[1] investigated some aliphatic *vic.*-dioximes with alkyl groups ranging from C5 to C7 and found extremely low extraction rates for nickel, especially with compounds containing secondary alkyl groups. From previous work[2,3] it became clear that the use of *vic*-bicyclic dioximes increases enormously the extraction rate for nickel. Unfortunately, however, in contrast with monocyclic *vic*-dioximes, their $pH_{1/2}$ values for copper are smaller than those for nickel. Navtanovich and co-workers[4] discovered that the extraction of Cu(II) and Ni(II) from ammoniacal solutions is dependent on the total number of carbon atoms. Equilibrium was not established in the extraction and re-extraction of nickel. The extraction of copper(II) and nickel(II) from ammoniacal solutions is not identical in character with the pH dependent extraction from acidic solutions.[2,3] Although, because of the ammonia, the pH is greater than 7, no precipitation of metal hydroxides occurs because metal ammine complexes are formed in the water layer. The expected extraction equation is

$$M(NH_3)_n^{2+} + 2H_2A \rightleftharpoons M(HA)_2 \cdot xNH_3 + 2NH_4^+ + (n-x-2)NH_3.$$

If copper forms a much stronger ammine complex than nickel, it is perhaps possible that under special conditions Ni^{2+} is extracted, but Cu^{2+} is held in the water layer.

In this study the extraction properties of dialkyldioximes of the type C_nH_{2n+1}–C(NOH)–C(NOH)–C_nH_{2n+1} are described. The ammoniacal extraction is compared with the pH dependent extraction from acidic solutions.

EXPERIMENTAL

UV–visible spectra were obtained on a Unicam Sp.800D, while ESR measurements were done at room temperature with a Varian E15 spectrometer.

The extraction experiments were carried out in a three-necked flask with a stirring device and continuous pH measurements. The starting volumes of water and organic solvent were both 250 cm^3.

* Author to whom correspondence should be addressed.

Stirring was stopped when no further change of the pH was noticed, indicating that equilibrium was reached. For analysis equal small volumes of water layer and organic layer were withdrawn from the system. To measure the distribution coefficient as a function of pH thereafter a small quantity of 4N acid or base was added, and the process of stirring until equilibrium and withdrawal of small portions of the aqueous and organic solutions was repeated at a different pH. Care was taken to keep the volumes of the aqueous and organic solutions equal. Although in this procedure the electrolyte concentration does not stay constant, we preferred this model because it is convenient to execute and because in a separate experiment it was shown that in the applied concentration range the influence of the electrolyte concentration is negligible.

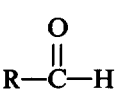
Organic solvents used were methylisobutylketone (MIBK) and chloroform and as inorganic salt metal nitrate was used. NaOH was used as base and HNO_3 as acid.

Kinetic measurements were carried out in a flask provided with a magnetic stirrer. The water layer containing the nickel nitrate was acidifed with 4N HNO_3 till the desired pH and then an equal volume (50 cm^3) of organic phase, in which the ligand was dissolved, was added. Under stirring 10 cm^3 of the mixture was withdrawn after 5, 10, 20 and 30 min. The two layers of these withdrawals separated immediately and it appeared that the volumes of both separated layers were equal (5 cm^3). UV spectroscopy applied to the organic phase gave the absorption at 30,500 cm^{-1}. Since the solvent and the ligand have no absorption below 35,000 cm^{-1} the absorption can be ascribed to the chelate formed during the extraction. According to the Lambert–Beer's law this absorption is proportional to the chelate concentration. When plotting the absorption against the contact time a straight line was obtained for the first 20 min and only a small deviation of the straight line was visible after longer reaction times. This straight line indicated that the initial reaction rate is not, or hardly, inhibited after 20 min, so the initial rate could easily be determined from this straight line.

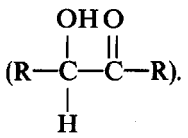
SYNTHESIS OF DIALKYLDIOXIMES

All dioximes were prepared as described in the following general procedure.

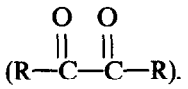
Under nitrogen 0.39 mol freshly distilled alkylaldehyde



was dissolved in 120 cm^3 ethanol. 0.02 mol 3-benzyl-5-(2-hydroxyl-ethyl)-4-methyl-1,3-thiazolium chloride was added and subsequently 0.12 mol triethyl amine was added dropwise under vigorous stirring (Stetter synthesis).[5,6] After refluxing for two hours the reaction mixture was poured out into ice, filtered, washed with water and extracted with chloroform. The organic layer was washed with aqueous $NaHCO_3$, dried with Na_2SO_4 and distilled to give the dialkylhydroxy ketone



This dialkylhydroxy ketone was dissolved in 100 cm^3 2-ethoxyethanol with 30 cm^3 glacial acetic acid. To this solution, heated at 80°C, 0.044 mol Bi_2O_3 was added fast. After that the reaction mixture was heated for one and a half hours at 105°C, filtered and the residue was extracted with chloroform. The organic layer was washed with water till free from acid, dried and distilled to give the dialkyldiketone



0.4 mol $NH_2OH \cdot HCl$ and 0.32 mol NaOAc were dissolved in 25 cm^3 water and 50 cm^3 ethanol. To this 0.135 mol dialkyldiketone was added. The reaction mixture was refluxed for half-an-hour, cooled, and the residue filtered and washed with hot water. Recrystallization from diluted alcohol gave the pure dialkyldioxime (R–C(NOH)–C(NOH)–R) in an overall yield of about 25%. The results of elemental analyses are presented in Table 1.

RESULTS

In Fig. 1 the results are shown for the extraction of Cu(II) and Ni(II) from ammoniacal solutions by solutions of dialkyl dioximes in methylisobutylketone (MIBK) as a function of the number of alkyl carbon atoms at two different extraction times. Equilibrium was not yet reached after 240 min in the extraction of Ni(II) by dioximes with 5, 7 and 11 carbon atoms in the alkyl groups, but was reached after 48 h. By contrast, the equilibrium at about 80% extraction was reached within 10 min in the extraction of Cu(II) by dialkyldioximes with 3 and more carbon atoms in the alkyl groups.

The dependencies of the extractions of Cu(II) and Ni(II) by dipentyldioxime (dodecane-6,7-dione dioxime) on the NH_3 and NH_4^+ concentration are presented in Figs. 2 and 3.

Table 1. Synthesized dialkyl dioximes with analytical results

Compound	Found			Calc.		
	%C	%H	%N	%C	%H	%N
C_3H_7–C(NOH)C(NOH)–C_3H_7	55.6	9.3	16.1	55.8	9.4	16.3
C_5H_{11}–C(NOH)C(NOH)–C_5H_{11}	63.1	10.7	12.4	63.1	10.6	12.3
C_7H_{15}–C(NOH)C(NOH)–C_7H_{15}	67.5	11.2	9.9	67.6	11.1	9.8
C_9H_{19}–C(NOH)C(NOH)–C_9H_{19}	70.9	12.1	7.9	70.5	11.8	8.2
$C_{11}H_{23}$–C(NOH)C(NOH)–$C_{11}H_{23}$	73.7	12.5	6.9	72.7	12.2	7.1

The pH dependent extraction of Cu(II) from nitrate solutions by a solution of dipentyldioxime in chloroform is shown in Fig. 4.

It is clear that at pH > 5 more than 50% (which is the theoretical limit if a CuL_2 chelate is formed) is extracted. The shape of the UV spectrum also changed at pH > 5. Thus it is clear that two different chelates are involved: chelate A at low pH and chelate B at pH > 5. When using an excess of Cu(II) compared to dioxime, the UV spectrum indicated that the extraction at pH = 4.3 resulted in chelate A with only a slight fraction of chelate B. Evaporation of the organic phase and recrystallization with ethanol and water gave a brown solid which was filtered and dried at 60°C. Elemental analysis of this compound gave: Cu, 13.8; N, 10.5; C, 55.2; H, 8.7%. After isolation the compound was only slightly soluble in chloroform, in contrast with the extracted chelate B. Further it was found that the extracted chelate A was unstable when the organic layer was dried with Na_2SO_4.

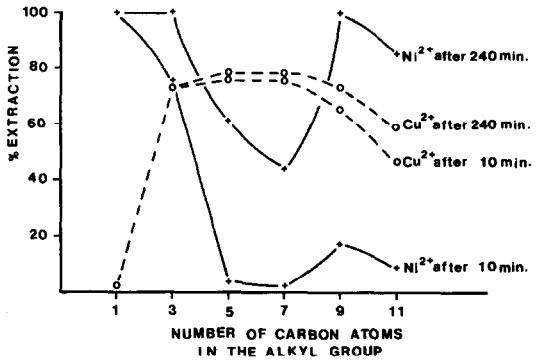


Fig. 1. Extraction of Cu(II) and Ni(II) by dialkyldioximes R–C(NOH)–C(NOH)–R as a function of the number of carbon atoms in the alkyl group R. Initial aqueous metal nitrate concentration 0.05 M. Initial dioxime concentration in methylisobutylketone (MIBK) 0.3 M. Initial NH_3 concentration 1.33 M. Initial NH_4NO_3 concentration 0.33 M.

The ESR spectrum of the chelate A in chloroform is depicted in Fig. 5.

The extraction of excess Cu(II) at pH = 8.4 resulted, according to the UV spectrum, in an organic solution containing nearly pure chelate B. Evaporation of the organic phase and recrystallization with dioxane and water gave a green solid that was dried at 60°C. Elemental analysis of this compound gave Cu, 23.5; N, 8.0; C, 46.8; H, 7.5%. After redissolving the compound in chloroform the UV spectrum deviated somewhat from that of the extracted chelate A. No ESR spectrum could be observed for this compound in solution at room temperature.

Kinetic measurements were done on the extraction of Ni(II) from a nitrate solution by dipentyldioxime to obtain some information why this reaction is so slow (no equilibrium within days).

If Figs. 6, 7 and 8 the initial extraction rate is presented as a function of initial H_2A, Ni^{2+} and H^+ concentrations. The order in dipentyldioxime concentration is calculated from the slope in Fig. 6 as 0.90. The order in Ni^{2+} concentration calculated from the slope of the line in Fig. 7 is 0.91. Because only

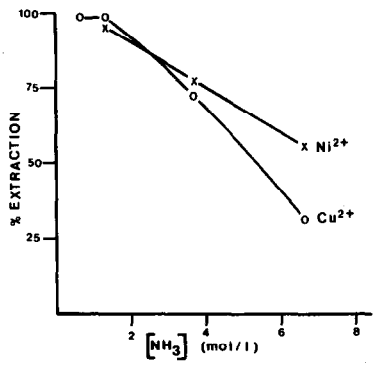


Fig. 2. Extraction of Cu(II) and Ni(II) by dipentyldioxime as a function of the initial NH_3 concentration after a contact time of 240 min. Initial dioxime concentration in MIBK is 0.55 M. Initial NH_4NO_3 concentration 0.33 M.

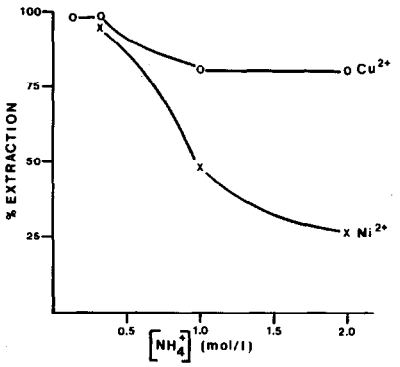


Fig. 3. Extraction of Cu(II) and Ni(II) by dipentyldioxime as a function of the initial NH_4NO_3 concentration after a contact time of 240 min. Initial dioxime concentration in MIBK is 0.55 M. Initial NH_3 concentration 1.33 M.

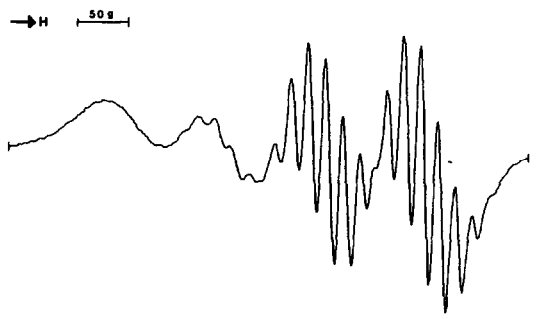


Fig. 5. ESR spectrum of the copper(II)–dipentyldioxime chelate (chelate A) in chloroform at room temperature.

two measurements were done for the hydrogen ion dependence, the order of -0.16 in H^+ should be regarded as an order of magnitude estimate.

DISCUSSION

Extraction of Cu(II) *and* Ni(II) *from ammoniacal solutions by aliphatic dioximes*

From Fig. 1 it can be seen that the only dialkyldioxime which is really selective for nickel above copper in the extraction from ammoniacal solutions is dimethylglyoxime. However, the extracted bis(dimethylglyoximato)nickel(II) chelate precipitates in the organic layer, and the back-extraction is blocked. Caton[7] explains this poor solubility by nickel–nickel interactions which prevent solvation. This interaction is possible because of the close packing of molecules in the crystal, a packing that cannot occur with larger alkyl groups according to Sharpe and Wakefield.[8] Dyrssen[9] stated that the bisdimethylglyoxymato)copper(II) chelate possesses two additional water molecules and that this chelate is soluble in water. The low percentage extraction of Cu(II) by dimethylglyoxime can be explained by the formation of such a hydrophilic aqua chelate. When larger alkyl groups are introduced in the dioxime the bulky hydrophobic substituents cause a change in the distribution coefficient of the copper chelate to the advantage of the organic layer. But also a destabilization of the two water molecules in the octahedral copper chelate is to be expected. In Fig. 1 it is clearly seen that from dipropyl to diheptyl dioxime these two effects keep each other in balance, but for longer alkyl groups the destabilization effect is stronger. Furthermore a small negative kinetic effect caused by steric hindrance can be seen for long alkyl groups.

In contrast with copper, nickel does not form octahedral chelates, but forms square planar chelates with dioximes. From the fact that after a contact time of 48 h the Ni extraction was almost complete, it can be concluded that the lower nickel

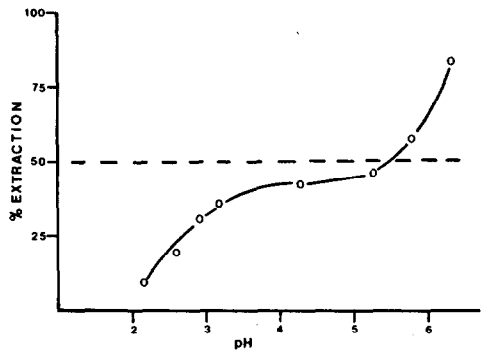


Fig. 4. Extraction of Cu(II) by dipentyldioxime as a function of the equilibrium pH. Initial aqueous copper nitrate concentration and the initial dipentyldioxime concentration in chloroform both are 0.001 M.

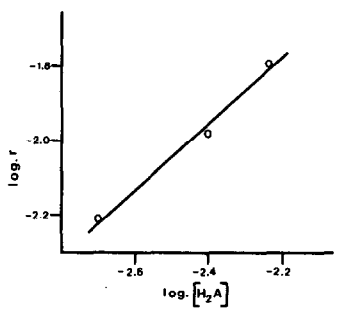


Fig. 6. Dependence of the initial rate of extraction of nickel by dipentyldioxime on the concentration of dipentyldioxime in chloroform. Initial pH is 3.52. Initial aqueous nickel nitrate concentration 0.00397 M.

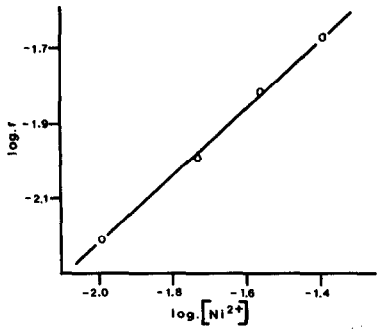


Fig. 7. Dependence of the initial rate of extraction of nickel(II) by dipentyldioxime on the concentration of Ni^{2+} in the aqueous phase. Initial dipentyldioxime concentration in chloroform is 0.00612 M. Initial pH is 3.65.

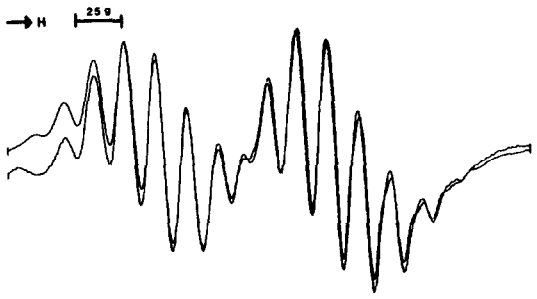


Fig. 9. The two high field copper bands from the ESR spectrum of Fig. 5 together with the computer simulation for a CuN_4 chromophore. The input values for the simulation are $A_{Cu} = 92$ G; $A_N = 16.2$ G; linewidth = 10.5/8.5 G; modulation 5 G; lineform Lorentz; ^{63}Cu = 70% and ^{65}Cu = 30%.

extraction observed for dioxime with pentyl, heptyl and undecyl groups after four hours is not caused by a difference in thermodynamic stability of the chelate formed, but is caused by a difference in extraction rate. This difference in extraction rate can be caused by steric hindrance. The steric hindrance from alkyl groups with 5 to 7 carbon atoms is most effective, according to Fig. 1. The reason why longer chains do not produce such a great hindrance is probably that longer chains are causing a greater insolubility of the dioxime in water, which means that the reaction takes place in the interface with the two long carbon chains pointed into the organic phase.

Comparing the extraction behaviour of Cu with that of Ni it can be noticed that after a contact time of 10 min, more Cu than Ni was extracted, because of favourable kinetics for Cu. On the other hand, after a long contact time more Ni than Cu was extracted, because Ni forms more stable chelates.

Figure 2 shows that the extraction of copper and nickel is dependent on the ammonia concentration. The dependence of copper is stronger which can be explained by the fact that copper forms more stable complexes with ammonia than nickel. Figure 3 shows that the extraction of copper and nickel also depends on the NH_4^+ concentration. The expected reaction equation for the extraction is:

$$M(NH_3)_n^{2+} + 2H_2A \leftrightharpoons M(HA)_2 + 2NH_4^+ + (n-2)NH_3.$$

The extracted copper chelate will probably have two water or ammonia molecules in the axial position.

A useful selectivity for nickel above copper is not found in the extraction by dialkyldioximes from ammoniacal solutions. At high ammonia concentrations and low NH_4^+ concentrations nickel is favoured but no good separation can be obtained.

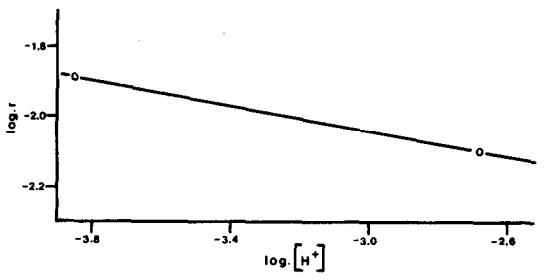


Fig. 8. Dependence of the initial rate of extraction of nickel(II) by dipentyldioxime on the concentration of hydrogen ions in the aqueous phase. Initial dipentyldioxime concentration in chloroform is 0.00415 M. Initial aqueous nickel nitrate concentration is 0.003 M.

The pH dependent extraction of Cu(II) *by dipentyldioxime*

The extraction (Fig. 4) and UV spectroscopic results demonstrate that two different kinds of chelate are involved in the extraction of Cu(II) by dipentyldioxime. Elemental analysis of chelate A formed at low pH values indicates that a CuL_2 chelate is formed. Found: Cu, 13.8; H, 8.7; N, 10.5; C, 55.2%. Calculated for $Cu(C_{12}H_{22}N_2O_2)_2$: Cu, 12.3; H, 8.5; N, 10.9; C, 55.9%. The percentage of copper observed is somewhat high, probably because of the presence of a small amount of chelate B, which has a higher percentage of copper (23.5%). No additional water molecules were found, but it is not excluded that these molecules were present in the extracted chelate and disappeared during heating at 60°C. The presence of water molecules also explains

the instability in solution with Na_2SO_4, a water absorber, and the change in solubility properties after drying at 60°C. If Na_2SO_4 absorbs the two axial water molecules, this means that these are fairly weakly coordinated and so it is not surprising that they dissociate at 60°C.

Cu^{2+} is a d^9 system with one unpaired electron, which means that four main lines can be expected in the ESR spectrum, because $I = 3/2$ both for ^{63}Cu and ^{65}Cu. The normal way of coordination for unstrained dioximes is the N,N-configuration. Because $I = 1$ for nitrogen, nine equidistant lines are to be expected on each copper line with intensity ratio of 1:4:10:16:19:16:10:4:1. Furthermore, we must take into account that copper consists of 59.1% of ^{63}Cu and for 30.9% of ^{65}Cu with a slight difference in magnetic moment (0.70904×10^{-4} vs 0.75958×10^{-4} rad. s^{-1} G^{-1}).

A computer simulation of the spectrum is shown in Fig. 9 together with the experimental spectrum and an excellent fit is noticeable.

The left part of the simulation is somewhat raised compared to the observed spectrum because the overlap with the third copper band could not be taken in account with our program. This simulation proves that indeed chelate A has N,N-coordination.

Chelate B is formed at high pH values (pH > 5) with an excess of copper. This phenomenon is also seen in the extraction of copper by δ-H_2CQD (see Ref. 2) and in the extraction of copper by α-benzildioxime (Einaga and Ishii).[10]

The elemental analysis of chelate B can be explained by assuming a $Cu_4(C_{12}H_{22}N_2O_2)_3(OH)_2C_4H_8O_2$ chelate. The expected elemental analysis for this chelate—Cu, 24.1; N, 8.0; C, 45.5; H, 7.2%—is in reasonable agreement with the observed values: Cu, 23.5; N, 8.0; C, 46.8; H, 7.5%. The dioxane molecule would then be introduced during the recrystallization. This would also explain why the UV spectrum changed after isolation. These results are insufficient to determine the structure of chelate B directly after extraction. The absence of an ESR spectrum points to the formation of a chelate with a strong copper–copper coupling, as was also found for the Cu:H_2CQD = 2:3 chelate.[2] A composition of $Cu_4(C_{12}H_{22}N_2O_2)_3(OH)_2 \cdot xH_2O$ is possible for the extracted chelate but other compositions cannot be excluded. The high copper extraction as observed in Fig. 4 can readily be explained by such a chelate. The significance of this chelate B for the extraction of copper is very small, because when dipentyldioxime is used in practical processes excess ligand will be used and the pH will be kept low (to prevent copper hydroxide precipitation) and under these circumstances no chelate B will be formed.

Kinetic measurements and pH dependency of the nickel extraction by dipentyldioxime

To find the rate-determining step kinetic measurements were performed on the extraction of nickel(II) by dipentyldioxime. From Fig. 6 the order in dipentyldioxime is calculated to be 0.90, which approximates 1 and not 2 as was found by Navtanovich and co-workers for the extraction from ammoniacal solutions. The order in Ni^{2+} is 0.91 (Fig. 7) in good agreement with the expected order of 1. The order in H^+ is 0.16 (Fig. 8) which is not far from zero. These orders can be explained when we assume the following reaction scheme:

$$\overline{H_2A} \underset{k_{-1}}{\overset{k_1}{\rightleftharpoons}} H_2A^*, \tag{1}$$

$$Ni^{2+} + H_2A^* \overset{k_2}{\rightleftharpoons} Ni(HA)^{+}{}^* + H^+, \tag{2}$$

$$Ni(HA)^{+}{}^* + H_2A \overset{k_3}{\rightleftharpoons} Ni(HA)_2^* + H^+, \tag{3}$$

$$Ni(HA)_2^* \overset{k_4}{\rightleftharpoons} \overline{Ni(HA)_2}. \tag{4}$$

Compounds marked with an asterisk are supposed to be in the interface or in the water layer and compounds marked with bars in the organic layer.

If reaction (2) is the rate-determining step, the initial extraction rate will be given by

$$r = k_2[H_2A^*][Ni^{2+}] = k_2 \cdot K_1[\overline{H_2A}][Ni^{2+}] \tag{5}$$

with

$$K_1 = \frac{k_1}{k_{-1}} = \frac{[H_2A^*]}{[\overline{H_2A}]}.$$

This would explain the first order in H_2A and in Ni^{2+} and the zero order in H^+.

Because of the low pH value it is unlikely that the dipentyldioxime dissolves in the water layer. The reaction, therefore, presumably takes place in the interface. The acidic water layer does not make it very attractive for the dioxime part of ligand (which is acidic too) to appear at the interface. Because of this low interfacial dioxime concentration equation (2) will be the rate-determining step. In ammoniacal solutions Navtanovich and co-workers[4] found a second-order rate dependence in H_2A, which means that in their case the reaction of Ni^{2+} with the second H_2A molecule was rate-determining. The ammonia causes a high pH value and it is reasonable to assume that the dioxime part of the ligand is pulled to the interface and is ionized. This causes a high interfacial dioxime concentration and as a result the normally expected second order in H_2A is found.

The overall extraction equation for Ni at low pH

$$Ni^{2+} + 2H_2A \rightleftharpoons Ni(HA)_2 + 2H^+$$

is completely different from the equation for the extraction from ammoniacal solutions. It is therefore not surprising that different orders are found.

REFERENCES

1. A. R. Burkin and J. S. Preston, *J. Inorg. Nucl. Chem.* 1975, **37**, 2187.
2. L. R. M. Paping, T. P. M. Beelen, C. P. J. Rummens and R. Prins, *Polyhedron* 1982, **1**, 6, 503.
3. L. R. M. Paping, T. P. M. Beelen, M. Mols and R. Prins, Accepted for publication in *Polyhedron*.
4. M. L. Navtanovich, L. S. Lutova and V. L. Kheifets, *Russ. J. Inorg. Chem.* 1979, **24**, 243.
5. H. Stetter, R. Y. Ramsch and H. Kuhlmann, *Synthesis* 1976, **11**, 733.
6. H. Stetter and G. Dämbkes, *Synthesis* 1977, **6**, 403.
7. J. E. Caton and C. V. Banks, *Talanta* 1966, **13**, 967.
8. A. G. Sharpe and D. B. Wakefield, *J. Chem. Soc.* 1957, 281.
9. D. Dyrssen, *Trans. R. Inst. Technol. Stockholm* 1964, **220**, 14.
10. H. Einaga and H. Ishii, *Bull. Chem. Soc. Jpn* 1970, **43**, 2970.

Polyhedron Vol. 4, No. 4, pp. 731–737, 1985
Printed in Great Britain

0277–5387/85 $3.00 + .00
© 1985 Pergamon Press Ltd

^{1}H NMR STUDIES OF U(IV)–1,2-CYCLOHEXANE(DINITRILO)-*N,N,N',N'*-TETRAACETIC ACID COMPLEXES

LECHOSŁAW LATOS-GRAŻYŃSKI

Institute of Chemistry, Wrocław University, 50 383 Wrocław, 14 F. Joliot-Curie, Poland

(*Received* 30 *April* 1984; *accepted* 4 *September* 1984)

Abstract—^{1}H NMR spectrum of a U(IV)–*trans*-1,2-cyclohexane(dinitrilo)-*N,N,N',N'*-tetraacetic acid (CyDTA) complex (prepared by dissolving U(IV)(CyDTA)$(H_2O)_3$ in aqueous Na_2SO_4 solution) has been studied as a function of pH and temperature. The magnetic moment of the complex is 2.96 μ_B (pH = 2.7). The isotropic shift is mainly due to pseudocontact contribution. Three species for the U(IV)–CyDTA system in the presence of SO_4^{2-} are postulated in the pH range 5.5–8.0. The characteristic ^{1}H NMR spectrum of U(IV)–CyDTA in the absence of SO_4^{2-} has been observed (pH = 10). Eight, widely spread, acetate methylene resonances are present. Possible structures for all the observed species are discussed. The formation of dimers has been considered to account for the lowering of magnetic moments for high pH species. The assignment of resonances has been confirmed by selective deuteration of the acetate methylenes.

Polyaminepolyacetic acids can be treated as potential sequestering agents for the actinides.[1]

Ligands with a large number of donor sites (equal or larger than the coordination number of the actinide ion, e.g. diethylenetriaminepentaacetic or triethylenetetraaminehexaacetic acids, should be useful for such purposes. Hence, the study of the actinide–complexone systems in aqueous solutions are being pursued.

^{1}H NMR spectroscopy allows detailed studies of paramagnetic metal ion–complexone systems[2] to be carried out.

The formation of different ionic forms, dimerization and molecular rearrangement have pronounced influences on the ^{1}H NMR spectra.

Trans - 1,2 - cyclohexane(dinitrilo) - *N,N,N',N'* - tetraacetic acid (CyDTA) has been chosen for these studies as the flexibility of this ligand is restricted by its own molecular structure. This property differentiates essentially the studied system from those reported earlier in the literature, i.e. U(IV)–aminoacids,[3,4] U(IV)–EDTA.[5]

Previous potentiometric work on U(IV)–CyDTA and similar systems[6,7] indicated that a stable form of the 1:1 complex is U(IV)CyDTA$(H_2O)_2$ between pH 1 and 3.5. At high pH values the complex apparently loses a proton to form U(IV)CyDTA $(H_2O)(OH)$ which undergoes an olation reaction:

$$2[\text{U(IV)CyDTA}(H_2O)(OH)] \rightleftharpoons [\text{U(IV)CyDTA(OH)}]_2 + 2H_2O$$

to form dimeric hydroxo-bridged species.[6]

The influence of the pH, temperature and the addition of monodentate ligands on equilibria taking place in aqueous solutions has been analyzed in this paper by means of ^{1}H NMR spectroscopy.

Particularly, the solution structures of complexes have been a matter of interest.

EXPERIMENTAL

Reagents and solutions

Cs_2UCl_6 prepared by a literature method has been used as a convenient source of U(IV).[8]

U(IV)CyDTA$(H_2O)_3$ was prepared by adding 1 equiv. of CyDTA · H_2O (Merck) to an acidic solution of 1 equiv. of Cs_2UCl_6 and adjusting pH to 1.0 with aqueous NH_3. The greyish-green precipitate was filtered when the solution was hot and washed twice with water and once with acetone.

The resulting complex was analyzed for C, N, H. Found: N, 4.61; C, 26.22; H, 3.95%. Calc. for $UC_{14}H_{24}O_{11}N_2$: N, 4.41; C, 26.48; H, 3.81%.

The presence of three water molecules was confirmed thermogravimetrically. Aqueous solutions of 0.1–0.2 M UCyDTA in 1 M Na_2SO_4 or sarcosine (saturated solution) were prepared by adding the U(IV)CyDTA$(H_2O)_3$ complex to the hot solution of 1 M Na_2SO_4 (sarcosine) in D_2O (99.8% IBJ) with stirring until the solid dissolved. The resulting solutions were cooled and the pH adjusted with DCl (IBJ) or aqueous NH_3.

A D_2O solution of 0.2 M UCyDTA containing no Na_2SO_4 was prepared by adding D_2O to the U(IV)CyDTA$(H_2O)_3$ powder and stirring. Aqueous NH_3 was added until all solid dissolved (pH = 6).

Solutions containing 0.1 M UCyDTA for magnetic susceptibility measurements were prepared in a similar manner.

The complex of formula U(IV)(d_8-CyDTA)$(H_2O)_3$ (deuterated on acetate methylene groups of CyDTA) has been synthesized to achieve full resonance assignments. The Ni(CyDTA) complex was deuterated as described previously[9] (pH = 13.4, 95°C, 3 h heating).

The resulting solution was acidified to pH = 0 (RT), then the pH was adjusted to 3 with KOH and evaporated to dryness.

The dry residue was dissolved in D_2O and the deuteration was repeated under the same conditions as in the first stage. In this step an exchange of in-plane (deuterated) and out-of-equatorial Ni(CyDTA) plane acetate groups takes place.[9]

The procedure was repeated three times. 95% deuteration of the acetate methylene groups was achieved as shown by the ^1H NMR spectrum of the reaction mixture with added potassium cyanide. Diamagnetic $Ni(CN)_4^{2-}$ which formed did not interfere in the NMR spectrum of released d_8-CyDTA.

The final reaction mixture was acidified to give 6 M solution with respect to HCl and concentrated. KCl which precipitated during the concentration was filtered.

The residual solution contained: d_8-CyDTA (cationic form), uncoordinated Ni(II) and KCl.

Cs_2UCl_6 was added in the amount equimolar to CyDTA taken for the deuteration.

The pH was adjusted to 1 with aqueous NH_3. The greyish-green precipitate containing only U(IV)(d_8-CyDTA)$(H_2O)_3$ was filtered.

The process was feasible because of a larger stability constant for U(IV)–CyDTA[6] than for Ni(II)–CyDTA.[10]

Equipment

^1H NMR spectra were recorded with a JEOL PS 100 spectrometer operating in the CW or pulse mode depending on the sample concentration. The sample temperature was calibrated by measuring the peak separation of ethylene glycol or methanol.[11]

Chemical shifts were measured with respect to 2,2-dimethyl-2-silylpentane-5-sulphonate (Merck).

The magnetic susceptibilities of the U(IV)–CyDTA system were determined by Evans' technique[12,13] at 30°C.

Adjustments of pH were made with the Mera-Elmat 512 pH-meter. All reported values refer to the pH-meter readings for the solutions at room temperature. No correction was made for the large abundance of D_2O in the aqueous solutions.

RESULTS

The ^1H NMR spectrum of the U(CyDTA) complex at pH = 2.97 in 1 M Na_2SO_4 is shown in Fig. 1. The identical spectrum pattern was observed at the same pH in the presence of sarcosine. The

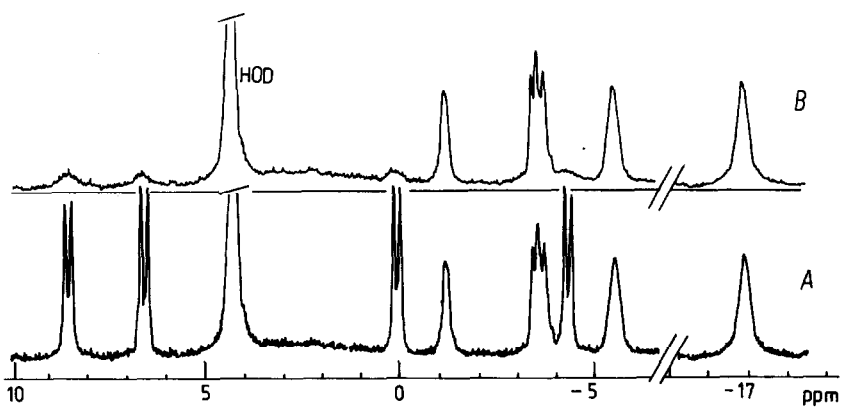


Fig. 1. ^1H NMR spectra of (A) 0.2 M U(IV)CyDTA and (B) 0.2 M U(IV)(d_8-CyDTA) in 1 M Na_2SO_4 (D_2O, 90°C, pH = 2.97).

synthesis of the selectively deuterated U(d_8-CyDTA) complex has allowed an unambiguous assignment of acetate methylene resonances of all species studied in this work in a similar manner as presented in Figs 1 and 2.

Two AX systems correspond to acetate methylene protons. The coupling constant between A and X is 16 Hz. This value agrees with coupling constants measured for other metal–CyDTA complexes.[14]

The remaining, paramagnetically shifted resonances have been assigned to the cyclohexane part of the ligand.

The Curie plot of U(CyDTA) (pH = 2.7, saturated solution of sarcosine) is presented in Fig. 2. The extrapolated chemical shift values ($T^{-1} \rightarrow 0$) are similar to those observed for diamagnetic CyDTA complexes.[14]

The characteristic deviation from linearity for only two acetate resonances probably results from the acetate chelate ring conformation changes. As these resonances participate in the same process they should belong to one set of acetate groups.

The Curie plot of U(CyDTA) in the presence of SO_4^{2-} (pH = 2.7, 1 M Na_2SO_4) demonstrated very similar features to those found for U(CyDTA)(sar). However, the curvature was well defined for all resonances.

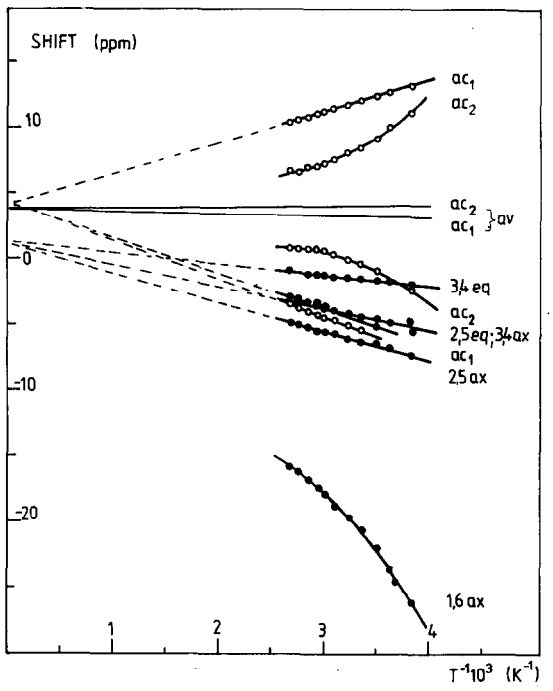


Fig. 2. Temperature dependence of the chemical shift of U(CyDTA) in the solution of sarcosine. Circles, acetate methylene protons; filled circles, cyclohexane protons; eq, equatorial; ax, axial; ac_i, acetate methylene equivalent by symmetry; ac_1, methylene carbon is in the antiperiplanar position to the 1, 6 ax proton; ac_2, methylene carbon is in the synclinical position to the 1, 6 ax proton; ac av, average shift of two methylene protons.

At pH below 1 the decomposition of U(CyDTA) unit was observed.

Above pH 3 the U(CyDTA) resonances become broader. In the pH range 3.5–6.5 (1 M Na_2SO_4, 30°C) the observed spectra are composed of two sets of resonances: one characteristic of the low pH form and the second one belonging to the form prevailing in the solution at pH 6.

Successive pH increase caused the appearance of two new sets of resonances dominating at pH 6.5–7 and 7.2–8.0 respectively (Figs 3 and 4).

Hence, the existence of three different species has to be considered to account for the observed NMR spectra for pH above 5.5 in the presence of SO_4^{2-}. The considerable resonance broadening and overlap made it difficult to carry out full assignments. However, the acetate methylene resonances could be distinguished (Figs. 3 and 4). The dependence of the chemical shifts on pH (1 M Na_2SO_4, 95°C) has been measured.

Contrary to the corresponding low temperature experiment no separate spectra for different ionic species could be seen above pH 5.5. Due to the fast exchange, the averaged shifts have been measured. The pH titration caused the smooth changes of resonances positions from those observed for pH 1–3 to those for pH 5–7.

Some small changes were observed as the pH was increased from 6.5 to 7.5 suggesting the presence of other forms in solution, the subsequent pH increase resulted in precipitation of U(CyDTA) hydroxo complexes.

The NMR spectra of U(CyDTA) solutions which do not contain Na_2SO_4 are essentially different from these discussed above (Fig. 5).

The spectrum of U(CyDTA) (pH = 10.0, 30°C, no Na_2SO_4 added) consists of eight acetate methylene resonances spreading from 10 to 100 ppm (85.4, 74.6, 66.7, 66.2, 30.5, 26.8, 11.2 and 10.4 ppm) and of the group of resonances assigned to the cyclohexane part of the ligand (12.0, 9.6, −7.2 and 13.3 ppm).

At 95°C the spectrum simplified and only four acetate methylene resonances were observed due to exchange processes averaging the peak positions for each acetate group independently.

The dependencies of chemical shifts on T^{-1} demonstrated large deviations from the regular Curie behaviour. The extrapolated chemical shift values ($T^{-1} \rightarrow 0$) fell in a region completely different than found for diamagnetic CyDTA complexes.

The lowering of pH from 10 to 6 resulted in a spectrum similar to that observed in 1 M Na_2SO_4 (Fig. 3).

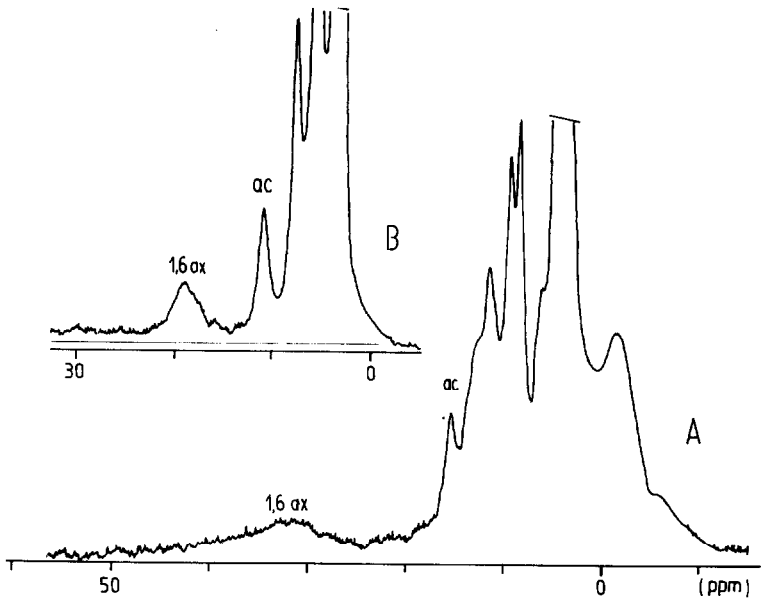


Fig. 3. ^{1}H NMR spectra of U(IV)–CyDTA in 1 M Na_2SO_4: (A) 30°C; (B) 95°C (pH = 5.7 at 30°C).

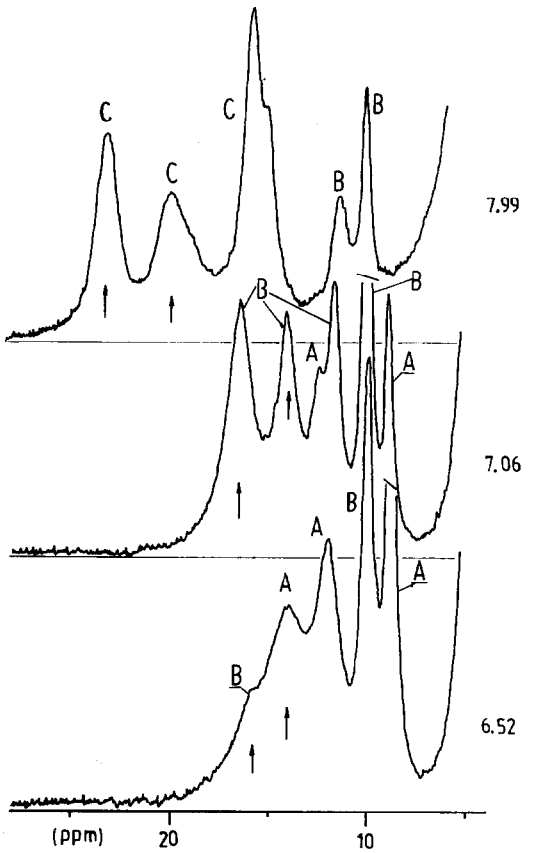


Fig. 4. ^{1}H NMR spectra of U(IV)–CyDTA in 1 M Na_2SO_4 (30°C, respective pH values marked in the figure). A, B, C correspond to species subsequently formed as pH increased. Arrows indicate the resonances of acetate methylene protons. Very broad resonance (32 ppm at 30°C, pH = 6.52) not shown.

Molar susceptibilities have been measured by the NMR procedure[12,13] as a function of pH. The measured values corrected for diamagnetic contributions are collected in Table 1.

Smooth changes of the susceptiblity and magnetic moment have been observed in the pH region where equilibria between several species have been postulated.

DISCUSSION

U(*CyDTA*)–SO_4^{2-} *system*

The U(IV)CyDTA$(H_2O)_3$ complex has limited solubility in water. The presence of additional ligands in the coordination sphere is necessary to increase the solubility in the pH range 1–3.

A complex of formula U(CyDTA)$(H_2O)SO_4$, analogous to the previously studied U(EDTA)$(H_2O)SO_4$,[5] accounts for the observed NMR spectra. The magnetic moment is 2.96 μ_B which may indicate the presence of two unpaired electrons in a cubic or slightly perturbed cubic symmetry for the U(IV) ion.[5] As the acetate methylene resonances are shifted downfield and upfield with respect to their diamagnetic positions a pseudocontact mechanism should dominate these paramagnetic shifts.

The respective geometric factors have been calculated assuming cubic symmetry (a square antiprism gave similar results).

The effective axial symmetry approach, frequently used for f^n ion complexes,[5,16,17] has been applied

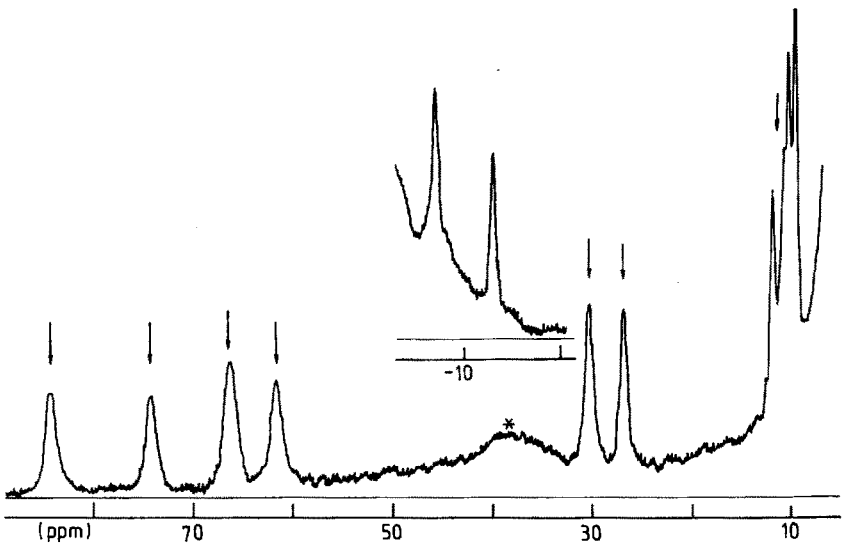


Fig. 5. ^{1}H NMR spectrum of the U(IV)CyDTA complex at pH = 10.0 (30°C). Arrows indicate the resonances of acetate methylene protons. Resonances overlapped with solvent signal not shown. *, resonance not identified.

with the main magnetic axis connecting the U(IV) with a centre of the C_1–C_6 ethylenic bond of the CyDTA ligand.

The chair conformation of cyclohexane ring and the puckered conformation of acetate chelate rings (the U–N–C_α and N–C_α–H dihedral angle equals 60–90°) have been considered.

The U–N and U–O bond lengths have been taken as 2.5 Å similar to those $Zr(NTA)_2$.[15]

A linear dependence of paramagnetic shifts on calculated geometric factors has been found (Fig. 6).

The resonance assignments have been confirmed by the analysis of the spin–spin couplings resolved in the cyclohexane part of the spectrum at 95°C (Table 2).

The observed linear correlation confirms the validity of the assumption stated above. Particularly, the term $\chi_{xx}-\chi_{yy}$ has to be relatively small allowing for the axial symmetry approximation.

The H_2O and SO_4^{2-} ligand occupying two of the eight available coordination places of U(IV) are required to be in fast exchange to achieve effective axial symmetry.

Lowering the temperature to 2°C increased the acetate methylene linewidths and the spin coupling was no longer observed.

This is in agreement with the mechanism mentioned above. As compared to $U(EDTA)(H_2O)SO_4$ the rigid structure of the CyDTA ligand prevents a

Table 1.

Proposed formula	pH	Magnetic moment (μ_B)
$U(CyDTA)(H_2O)SO_4$	1.0–3.0	2.96
$[U(CyDTA)(OH)SO_4]_2$	5.0–6.0	2.2
$[U(CyDTA)(OH)SO_4]_n$	6.5–7.9	1.9*
$[U(CyDTA)(OH)]_2$	10.0	2.18

* Precipitation might take place.

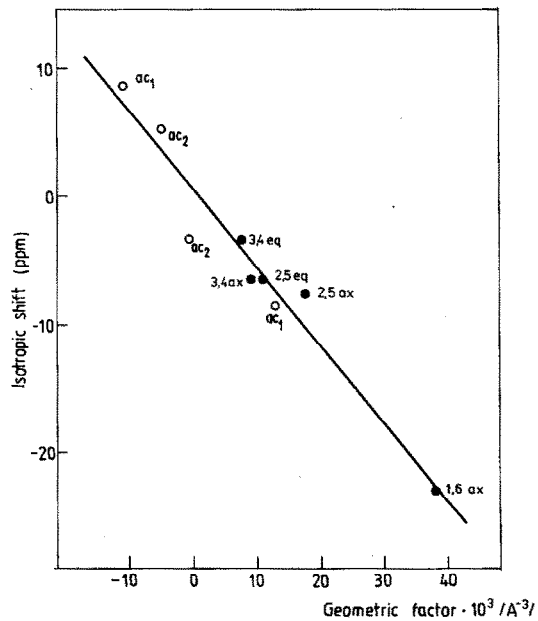


Fig. 6. $U(CyDTA)(H_2O)SO_4$, the plot of the shift vs geometric factors. (ZnCyDTA used as a diamagnetic reference).[14] Denotation as in Fig. 2.

Table 2. ^1H NMR chemical shifts for U(CyDTA)$(H_2O)SO_4$ (30°C, ppm vs TMS*)

Assignment	Shift
1, 6 ax	−28.26
2, 5 ax	−8.89
2, 5 eq	−5.87
3, 4 ax	−5.87
ac_1	−8.89
	13.78
ac_2	−1.89
	7.76

metal centred rearrangement which preserves the U(CyDTA)$(H_2O)SO_4$ structure up to 100°C.

Observation of AX patterns for the U(CyDTA) complex is caused by non-equivalency of the methylenic protons due to non-labile bonding between the metal ion and the two nitrogen donor groups of the CyDTA ligand.[14] However, some changes of conformation of the acetate chelate rings were noticed as deviation from Curie behaviour was observed for the acetate methylene resonances (Fig. 2).

Above pH 3 a variety of new U(CyDTA) forms has been found. The magnetic moment was noticeably smaller as compared to U(CyDTA)$(H_2O)SO_4$ (Table 1). This suggests considerable spin pairing through μ-oxo or μ-hydroxo bridges.[5] Hence, the formation of dimeric (polymeric) species is consistent with the magnetic susceptibility data.

The following equilibria were considered:

$$\begin{array}{c} \qquad\qquad\qquad\

contributions. However, there are no structural data available to distinguish between these two possibilities.

Acknowledgement—This work was supported by the Polish Academy of Sciences.

REFERENCES

1. K. N. Raymond and W. L. Smith, *Struct. Bonding (Berlin)* 1981, **43**, 159; (a) V. Castellato, P. A. Vigato and M. Vidali, *Coord. Chem. Rev.* 1978, **26**, 85.
2. L. Latos-Grażyński and B. Jeżowska-Trzebiatowska, *J. Coord. Chem.* 1980, **10**, 159 and references cited therein.
3. C. Miyake and S. Imoto, *Chem. Phys. Lett.* 1974, **24**, 606.
4. C. Neveu, G. Folcher and A. M. Laurent, *J. Inorg. Nucl. Chem.* 1976, **38**, 1223.
5. D. L. Ehman and D. T. Sawyer, *Inorg. Chem.* 1970, **9**, 205.
6. G. H. Carey and A. E. Martell, *J. Am. Chem. Soc.* 1968, **90**, 32.
7. N. P. Ermolaev and N. N. Krot, *Zh. Neorg. Khim.* 1963, **8**, 2447.
8. G. Hitchison and G. Candela, *J. Chem. Phys.* 1957, **27**, 707; (b) G. Giolitti and G. Bucci, *Gazz. Chim. Ital.* 1905, **35**, 162; (c) C. K. Janczak, Ph.D. Thesis, Institute of Low Temperature, Wrocław (1978).
9. L. Erickson, D. C. Young, G. F.L-. Ho, S. R. Watkins, J. B. Terrill and C. N. Reilley, *Inorg. Chem.* 1971, **10**, 441.
10. A. E. Martell and R. M. Smith, *Critical Stability Constants*. Plenum Press, New York (1974).
11. A. L. Van Geet, *Anal. Chem.* 1968, **40**, 2227; 1972, **42**, 679.
12. D. F. Evans and T. A. James, *J. Chem. Soc., Dalton Trans.* 1979. 724.
13. D. F. Evans, *J. Chem. Soc.* 1959, 2003.
14. R. J. Day and C. N. Reilley, *Anal. Chem.* 1965, **37**, 1326.
15. J. L. Hoard, E. Willstadter and J. V. Sivelrton, *J. Am. Chem. Soc.* 1968, **87**, 1610.
16. C. N. Reilley, B. W. Good and R. D. Allendoerfer, *Anal. Chem.* 1976, **48**, 1446.
17. L. Kulberg and G. R. Chopin, *Inorg. Chem.* 1977, **16**, 2926.
18. G. Johansson, *Acta. Chem. Scand.* 1968, **22**, 389.
19. J. Granot and D. Fiat, *J. Magn. Reson.* 1975, **19**, 372.
20. W. B. Lewis, J. A. Jackson, J. F. Lemons and H. Taube, *J. Chem. Phys.* 1962, **36**, 694; (a) R. G. Shulman and V. Jaccarino, *Phys. Rev.* 1958, **109**, 1084; (b) R. E. Watson and A. J. Freeman, *Phys. Rev. Lett.* 1961, **6**, 277.
21. G. A. Elgavish and J. Reuben, *J. Am. Chem. Soc.* 1977, **99**, 5590.

Polyhedron Vol. 4, No. 4, pp. 739–745, 1985
Printed in Great Britain

0277–5387/85 $3.00 + .00
© 1985 Pergamon Press Ltd

PRESSURE DEPENDENCE OF ^{35}Cl NQR IN HEXACHLORO- ($N_3P_3Cl_6$) AND OCTACHLORO- ($N_4P_4Cl_8$) CYCLOPHOSPHAZENES

V. KRISHNAN, K. R. SRIDHARAN and J. RAMAKRISHNA*
Department of Physics, Indian Institute of Science, Bangalore 560012, India

(*Received* 19 *June* 1984; *accepted* 4 *September* 1984)

Abstract—High pressure studies of ^{35}Cl NQR in the hexachlorocyclophosphazene $N_3P_3Cl_6$ and in the *K*- and *T*-forms of octachlorocyclophosphazene have been carried out at room temperature. For $N_3P_3Cl_6$, the pressure dependence of all the four lines is linear up to a pressure of about 3500 kg cm^{-2} when a significant change in the slope is observed for all the lines, due to a possible phase transition. In contrast, the pressure dependence of the two lines in the *K*-form (metastable) and the four lines in the *T*-form of the tetramer($N_4P_4Cl_8$), is observed to be non-linear. The results are discussed on the basis of competing dynamic and static effects.

Cyclophosphazenes belong to a family of inorganic ring polymers. There has been considerable interest in these compounds, due largely to their applications in diverse fields. The temperature dependence of ^{35}Cl NQR in a number of chlorocyclophosphazenes including $N_3P_3Cl_6$ and $N_4P_4Cl_8$ has already been reported.[1] Lucken[2] has found the asymmetry parameter in $N_3P_3Cl_6$ to be very small. Dalgleish *et al.*[3,4] have reported measurement of ^{35}Cl NQR in $N_3P_3Cl_6$ and in other exocyclic substituents in a small pressure range of 0–1000 kg cm^2. The maximum shift in the NQR frequency with pressure was found to be about 80 kHz kbar^{-1} in these compounds, which reveals appreciable volume effects even at a relatively small compression.

Since the $N_3P_3Cl_6$ molecule in the solid state is known to have a mirror plane, and the phosphazene ring deviates slightly from the planar structure (so that it has a tendency to have a chair conformation), it was thought worthwhile to investigate the effect of pressure. Similarly, the high pressure experiments on the two forms of $N_4P_4Cl_8$ the results of which are reported in this paper for the first time, were planned to study the effect of pressure on the two isomeric structures.

EXPERIMENTAL

A home-made super-regenerative spectrometer that could operate in the frequency range 20–40 MHz was used to record the ^{35}Cl NQR spectra, with lock-in detection. High pressures were generated using a locknut type high pressure cell[5] made of alloy steel. Liquid paraffin was used as the pressure transmitting medium.

The compounds $N_3P_3Cl_6$ and $N_4P_4Cl_8$ were recrystallized by slow evaporation from petroleum ether. The *T*-form of $N_4P_4Cl_8$ was obtained from the *K*-form by heating the sample to 75°C in a precision temperature controlled oven. The *K*-form (metastable) is known to pass irreversibly into the *T*-form at a temperature of about 65°C.[6]

RESULTS

$N_3P_3Cl_6$

The relative intensity of the 4 lines, which is 2:1:1:2 at atmospheric pressure, is retained at higher pressures as well. This indicates that these molecules continue to possess the mirror symmetry at higher pressures also. The pressure vs NQR frequency plots (Figs 1 and 2) for $N_3P_3Cl_6$ show a linear variation with an appreciable fall in the slope around a pressure of 3500 kg cm^{-2}. Changes in the slope of the pressure vs NQR frequency graph in compounds similar to $N_3P_3Cl_6$ have been reported[4] and these are attributed to minor changes in the packing of the molecules in the solid at high pressure.

The values of the derivatives $(\delta\nu/\delta P)_T$ of the NQR frequency obtained through least square fit of our data (up to a maximum pressure of 3250 kg cm^{-2} is given in Table 1. The corresponding values of Dalgleish *et al.*[3] are also given in the table for

* Author to whom correspondence should be addressed.

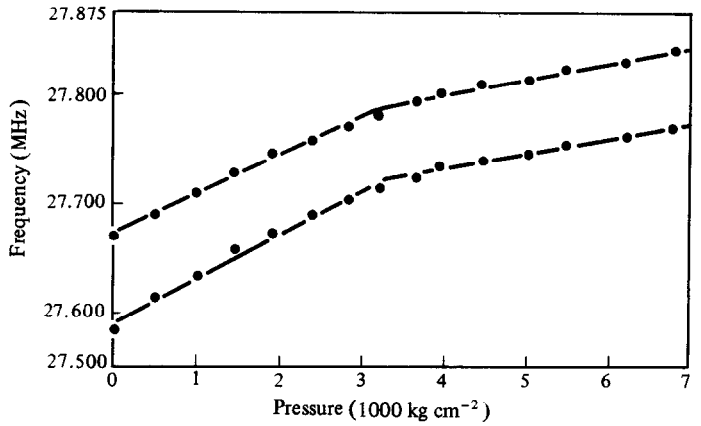


Fig. 1. Pressure dependence of ^{35}Cl NQR in $N_3P_3Cl_6$ (lines I and II) at room temperature (297 K).

comparison. The small differences between these two sets, could arise from a fall in the compressibility of $N_3P_3Cl_6$ at higher pressures (> 1000 kg cm^{-2}).

$N_4P_4Cl_8$—K-*form*

The ^{35}Cl NQR spectrum of this compound has two lines of almost equal intensity in conformity with its $\bar{4}$ site symmetry.[6] The frequency separation between the two lines is only about 130 kHz at room temperature. This separation reduces progressively with pressure becoming 15 kHz at a pressure of 7200 kg cm^{-2}. Such behaviour is consistent with the idea that the frequency separation is caused by thermal motion, i.e. the two sites are otherwise chemically equivalent.

The changes brought about by the pressure on the relative intensity of the two lines is yet another interesting observation. The intensity undergoes a perceptible change around a pressure of 2500 kg cm^{-2}, the higher frequency line becoming much stronger than the other line. Such an increase in relative intensity continues up to the maximum pressure investigated, at which the relative intensity is almost 4:1. Throughout this process, the linewidth of the two lines remain essentially unaffected, i.e. there are no observable line-broadening effects to account for the change in the intensities. Such a change in relative intensity with pressure therefore may be due to relaxation effects.

The pressure dependence of the NQR frequency in the *K*-form of $N_4P_4Cl_8$ is shown in Figs 3 and 4. The

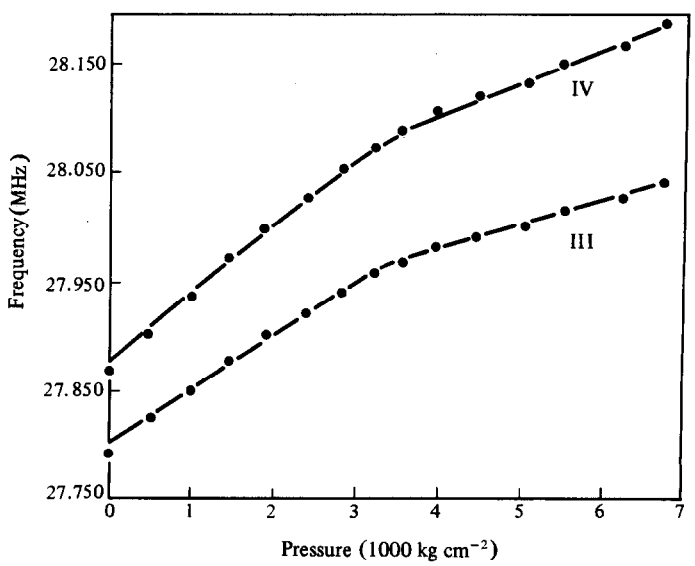


Fig. 2. Pressure dependence of ^{35}Cl NQR in $N_3P_3Cl_6$ (lines IV and III) at room temperature (297 K).

Table 1. Pressure and temperature derivatives of ^{35}Cl NQR frequency in $N_3P_3Cl_6$

Resonance	ν_0* (MHz)	$\left(\frac{\partial \nu}{\partial P}\right)_T$ (Hz kg cm^{-2})	$\left(\frac{\partial \nu}{\partial T}\right)_P$† (Hz K^{-1})	$\left(\frac{\partial \nu}{\partial T}\right)_V$ (Hz K^{-1})	$\left(\frac{\partial \nu}{\partial P}\right)_T$† (Hz kg cm^{-2})
I	28.4807	+36.9	−3565	−2711	+47.3
II	28.4410	+33.3	+3120	−2354	+37.6
III	28.7860	+49.6	−3819	−2678	+60.6
IV	28.8470	+64.5	−3877	−2393	+78.0

* ^{35}Cl NQR frequency obtained by extrapolation to 0 K.[1]
† Data from Dalgleish *et al.*[4]

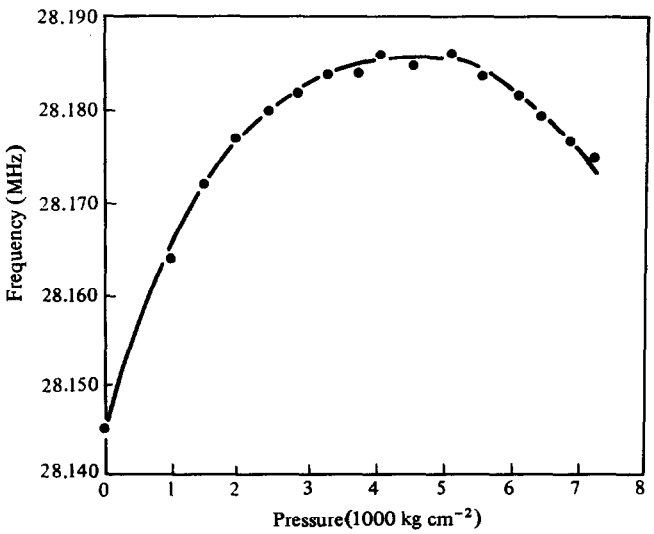


Fig. 3. Pressure dependence of ^{35}Cl NQR in $N_4P_4Cl_8$ (line I) at room temperature (297 K).

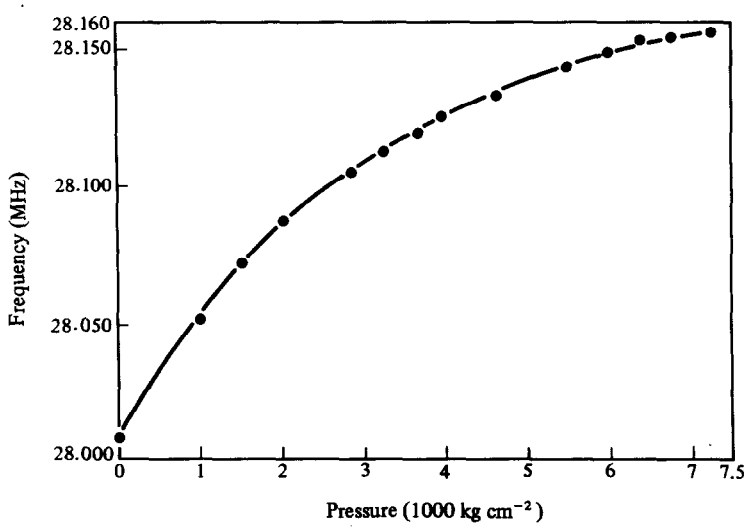


Fig. 4. Pressure dependence of ^{35}Cl NQR in $N_4P_4Cl_8$ (*K*-form) (line II) at room temperature (297 K).

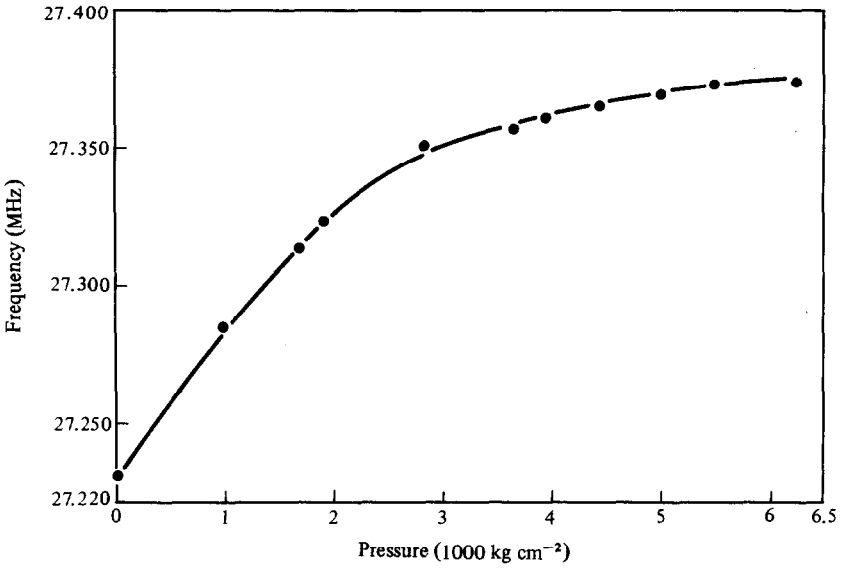


Fig. 5. Pressure dependence of ^{35}Cl NQR in $N_4P_4Cl_8$ (*T*-form) (line I) at room temperature (297 K).

pressure dependence is non-linear in direct contrast to the case with the trimer $N_3P_3Cl_6$. The pressure coefficient even becomes negative for the higher frequency line beyond a pressure of 5000 kg cm^{-2}.

$N_4P_4Cl_8$—T-*form*

$N_4P_4Cl_8$ *T*-form with a $\bar{1}$ site symmetry gives four ^{35}Cl NQR lines with relative intensities 2:3:2:3. The maximum frequency separation between the lines (I and IV) is about 1.350 MHz at room temperature. The doublet at the centre (lines II and III) has a frequency separation of about 55 kHz at room temperature.

The pressure dependence for the four ^{35}Cl NQR lines is shown in Figs. 5–7. The pressure dependence is non-linear, with the highest frequency line having the minimum pressure coefficient (at atmospheric pressure) and showing a decrease in the frequency with pressure beyond a pressure of 4000 kg cm^{-2}. These are similar to the observation made with the *K*-form. There were however no intensity anomalies

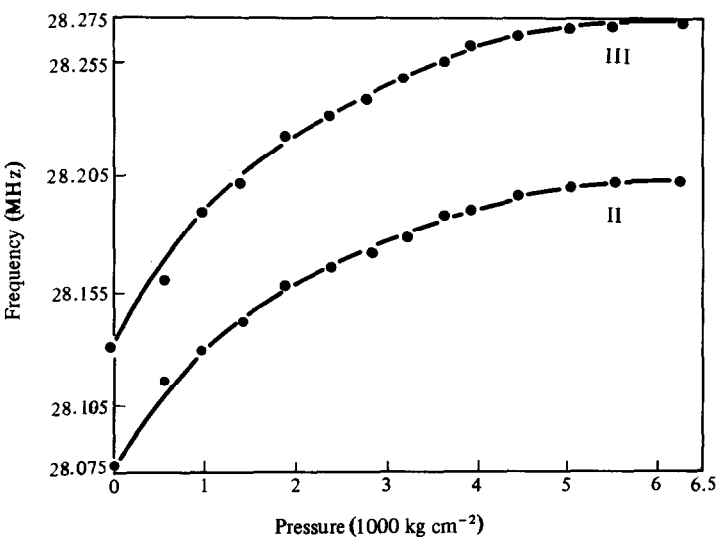


Fig. 6 Pressure dependence of ^{35}Cl NQR in $N_4P_4Cl_8$ (*T*-form) (lines III and II) at room temperature (297 K).

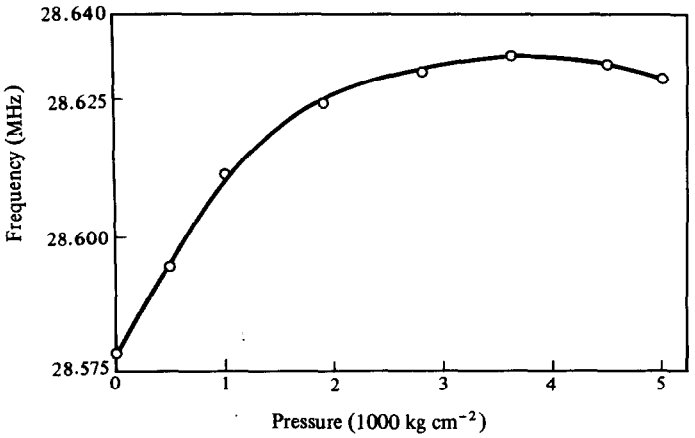


Fig. 7. Pressure dependence of ^{35}Cl NQR in $N_4P_4Cl_8$ (*T*-form) (line IV).

in the present case, throughout the range of pressure investigated. Also the absolute values of the pressure coefficients for the *T*-form are much higher than those for the *K*-form. Another contrasting feature concerns the frequency separation between the two lines at the centre (lines II and III) at higher pressures. While the separation narrows progressively with pressure in the *K*-form, it marginally increases in the *T*-form. This reveals the absence of any tendency for the molecule to acquire a two-fold axis of symmetry[6] at high pressure. (Addition of such a two-fold axis would lead to the merger of the two lines.)

PRESSURE DEPENDENCE OF NQR

The effect of torsional motions on the average value of the EFG can be expressed as

$$q = q_0(1 - 3/2\langle\theta^2\rangle) \qquad (1)$$

where $\langle\theta^2\rangle$ is the effective mean square amplitude of the torsional oscillations about the principal axes of the EFG tensor. q_0 is the EFG in the absence of all lattice vibrations. The variations of the first term on the r.h.s. with pressure, represents the effect of compression on the state lattice. Similarly the pressure dependence of the second term represents the damping of the torsional oscillations with pressure. Thus the second term leads to a positive pressure coefficient of NQR frequency. At high enough pressures, when the motions are effectively damped, the effects of compression of the static lattice, will become important. Negative pressure coefficients have also been reported in some molecular solids,[9] which have been explained as due to anisotropic polarisation of chlorine $3p_\pi$ orbitals of appropriate symmetry. (Static effects dominating over the dynamic effects.)

THERMODYNAMICAL ANALYSIS OF THE DATA

Using the thermodynamical relation[7]

$$\left(\frac{\partial v}{\partial T}\right)_P = \left(\frac{\partial v}{\partial T}\right)_V - \frac{\alpha}{\beta}\left(\frac{\partial v}{\partial P}\right)_T \qquad (2)$$

the partial derivative $(\partial v/\partial T)_V$ (Bayer term) that represents changes in the NQR frequency due to explicit temperature effects can be obtained from the observed values of $(\partial v/\partial T)_P$ and $(\partial v/\partial P)_T$. Very little data concerning the thermal expansion coefficient (α) and the isothermal compressibility (β) of covalent bonded phosphorus compounds are available. Dalgleish *et al.*[3] have obtained an approximate estimate for the ratio α/β, for similar compounds. The same is used in the present work. The $(\partial v/\partial T)_V$ so obtained are given in Table 2 for $N_3P_3Cl_6$; in Table 3 for $N_4P_4Cl_8$ *K*-form and in Table 4 for $N_4P_4Cl_8$ *T*-form. Whereas for $N_3P_3Cl_6$ a rigid vibrational motion of the whole molecule at a frequency 23 cm^{-1}, is also a localized PCl_2 bending mode at 55–60 cm^{-1}, is consistent with the observed value for $(\partial v/\partial T)_V$, a rigid vibrational mode around 20 cm^{-1} is consistent with our observation for $N_4P_4Cl_8$ *K*-form. The latter figure also compares very well with a reported[1] mean value of 19.4 cm^{-1} for this compound.

In the case of $N_4P_4Cl_8$ *T*-form, however, there seems to be some discrepancy between two sets of values for $(\partial v/\partial T)_V$. Part of this might be traced to the approximate value chosen for the ratio α/β in equation (2). It must however be pointed out that the same value used in the analysis of the data for *K*-form provides a satisfactory fit. In order to clarify this, the frequency of the vibrational mode, f_t, that could give a reasonable fit to the data was estimated using α/β as a variable parameter (Table 4). It appears from these

Table 2. Coefficients of rate of change of NQR frequency with temperature for each resonance in $N_3P_3Cl_6$

	Resonances			
	Line I	Line II	Line III	Line IV
Experimental $(\partial\nu/\partial T)_V$ values (Hz K^{-1})	−2711	−2354	−2678	−2393
Calculated $(\partial\nu/\partial T)_V$*				
(i) 23 cm^{-1} vibrational mode of the whole molecule	−2371	−2365	−2393	−2403
(ii) 55 cm^{-1} PCl_2 bending mode	−2439	−2433	−2461	−2472

* Dalgleish *et al.*[4]

Table 3. Temperature and pressure derivatives of the ^{35}Cl NQR frequency in $N_4P_4Cl_8$ (*K*-form)

Resonance	ν_0* (MHz)	$\left(\frac{\partial\nu}{\partial T}\right)_P$† (Hz K^{-1})	$\left(\frac{\partial\nu}{\partial P}\right)_T$ (Hz kg cm^{-2})	$\left(\frac{\partial\nu}{\partial T}\right)_V$ (experimental) (Hz K^{-1})	$\left(\frac{\partial\nu}{\partial T}\right)_V$ (calc.) (Hz K^{-1})
I	28.733	−2641.3	+41.3	−1691.4	−1619.2
II	28.740	−2053.0	+18.1	−1636.7	−1619.2

* NQR frequency extrapolated to 0 K.
† Kaplanky *et al.*[1]

Table 4. Temperature and pressure derivatives of ^{35}Cl NQR in $N_4P_4Cl_8$ (*T*-form)

Resonance	NQR frequency at $T \simeq 297$ K (MHz)	$\left(\frac{\partial\nu}{\partial T}\right)_P$* (Hz K^{-1})	$\left(\frac{\partial\nu}{\partial P}\right)_T$ (Hz kg cm^{-2})	$\left(\frac{\partial\nu}{\partial T}\right)_V$ Observed (Hz K^{-1})	$\left(\frac{\partial\nu}{\partial T}\right)_V$ Estimated (Hz K^{-1})
Line I	27.232	−2434	+58.5	−1089	−1707
Line II	28.079	−2447	+46.0	−1389	−1874
Line III	28.134	−2328	+50.1	−1176	−1530
Line IV	28.578	−2043	+33.0	−1285	−1345

* Kaplanski *et al.*[1]

calculations that a lower value of about 15 for α/β (rather than 23 assumed earlier) provides a good agreement between the observed and estimated values for $(\partial\nu/\partial T)_V$. It is therefore quite probable (in the absence of precise data) that the ratio of α/β is appreciably small for the *T*-form compared to the *K*-form. One indication of such a possibility could be obtained from a comparison of the pressure coefficients for the two compounds near atmospheric pressure. The *T*- form has relatively higher coefficients which could result from relatively higher compressibility for this compound.

DISCUSSION

The trimeric ($N_3P_3Cl_6$) compound shows a linear variation for NQR frequency with pressure (up to about 3500 kg cm^{-2}) while both forms of the tetramer ($N_4P_4Cl_8$) reveal a non-linear pressure dependence. Non-linear pressure dependence of

Table 5. Frequency of the torsional modes in $N_4P_4Cl_8$-(*T*-form) as estimated from pressure dependence of NQR frequency

	Line I		Line II		Line III		Line IV	
α/β*	f_t (cm^{-1})	f_t† (cm^{-1})	f_t (cm^{-1})	f_t† (cm^{-1})	f_t (cm^{-1})	f_t† (cm^{-1})	f_t (cm^{-1})	f_t† (cm^{-1})
15	19.07		18.22		20.29		20.29	
20	22.85		19.55		22.2		21.8	
		19.2		18.6		20.6		22.1
25	25.44		21.23		24.5		23.22	
30	30.42		23.38		28.05		24.98	

* α = coefficient of thermal expansion (K^{-1}). β = isothermal compressibility (kg^{-1} cm^2).
† Kaplansky *et al.*[1]

NQR has been reported in a number of molecular solids.[8–10] The observed pressure dependence is the net result of the dynamic (resulting from a reduction in the torsional amplitudes) and static (resulting from an increase in intermolecular interaction, and bond polarisation effects) contributions to the volume effects. At higher pressures (> 5000 kg cm^{-2} in the present investigations) the static effects dominate over the dynamic effects. Negative pressure coefficients in 1,3,5-trichlorobenzene have been interpreted by Jones *et al.*[9] on the basis of anisotropic polarisation effects involving the lone pair electrons in the chlorine atoms. The anisotropic polarisation is assumed to result from the distortion of the $3p_\pi$ orbitals due to an admixture with $3d_\pi$ orbitals at higher pressures. Such an admixture increases in effect the size of the $3p_\pi$ orbital, thereby reducing the quadrupole coupling constant.

Dixon *et al.*[6] have invoked the presence of appreciable π-character for the P–Cl bonds in the *T*-form of the *tetramer*-$N_4P_4Cl_8$ to account for the large frequency separation (about 1.4 MHz) between the NQR lines. According to such a scheme, the lowest NQR frequency has been assigned to the chlorine atom that has the maximum π-character. The highest frequency line (line IV) is expected to have the lowest π-character; consequently the anisotropic polarisation effects of the $3p_\pi$ orbitals should be comparatively smaller for this line. Our results show that the highest frequency line, having maximum NQR frequency apart from having the lowest pressure coefficient exhibits fall in the NQR frequency at higher pressures. Anisotropic polarisation effects therefore seem to be inadequate to account for the observed pressure dependence in the compound. Other intermolecular effects that become significant in these non-planar molecules under high pressure conditions may have to be considered.

Acknowledgements—V.K. thanks UGC for a Teacher fellowship. J.R. thanks CSIR for financial assistance in the form of a research grant.

REFERENCES

1. M. A. Kaplansky and M. A. Whitehead, *Can. J. Chem.* 1967, **45**, 1670.
2. E. A. C. Lucken, *Proc. Coll. Ampere* 1962.
3. W. H. Dalgleish and A. L. Porte, *J. Mag. Reson.* 1975, **20**, 359.
4. W. H. Dalgleish, R. Keat, A. L. Porte and R. A. Shaw, *J. Mag. Reson.* 1975, **20**, 351.
5. K. V. Ramanathan and R. Srinivasan, *J. Phys.* 1978, **11**, 480.
6. M. Dixon, D. B. Jenkins, J. A. S. Smith and D. A. Tong, *Trans. Faraday Soc.* 1967, **63**, 2852.
7. J. Kushida, G. B. Benedek and R. Bloembergen, *Phys. Rev.* 1956, **104**, 1364.
8. R. J. C. Brown, D. C. Woodland and R. deBoer, *J. Chem. Soc., Faraday Trans.* 2, 1979, **75**, 7050.
9. L. V. Jones, M. Sabir and J. A. S. Smith, *J. Chem. Soc., Faraday Trans.* 2, 1978, **74**, 1723.
10. G. A. Matzkamin, T. N. O'Neal, T. A. Scott and P. J. Haigh, *J. Chem. Phys.* 1966, **44**, 4171.

Polyhedron Vol. 4, No. 4, pp. 747–756, 1985
Printed in Great Britain

0277–5387/85 $3.00 + .00
© 1985 Pergamon Press Ltd

^{119}Sn MÖSSBAUER, IR, ^{1}H NMR SPECTROSCOPIC AND THERMAL DECOMPOSITION STUDIES ON ORGANOTIN(IV) ADDUCTS WITH GLYCYLGLYCINE

LORENZO PELLERITO and M. TERESA LO GIUDICE
Istituto di Chimica Generale, University of Palermo, Italy

G. C. STOCCO
Istituto di Farmacologia e Farmacognosia, University of Palermo, Italy

JOHN D. DONALDSON and SUSAN M. GRIMES*
Department of Chemistry, The City University, Northampton Square, London EC1V 0HB, U.K.

and

PETER J. SMITH
International Tin Research Institute, Fraser Road, Greenford, Middlesex UB6 7AQ, U.K.

(*Received* 13 *August* 1984; *accepted* 4 *September* 1984)

Abstract—The complexes $R_2SnCl_2 \cdot (H_2glygly)$, ($H_2glygly$ = glycylglycine) (R = Me, Bu^n, Oct^n, Ph) and $RSnCl_3 \cdot (H_2glygly)$ (R = Bu^n, Oct^n, Ph) have been prepared and characterised by chemical analysis, thermal properties and IR and Mössbauer spectroscopy. The IR data are consistent with the glycylglycine ligand acting as a monodentate ligand through the amino-nitrogen. The Mössbauer isomer shift data suggest the bonding in the diorganotin complexes is relatively weak between the tin(IV) moiety and the ligand. ^{1}H NMR spectroscopy was used to probe the nature in solution of the $Me_2SnCl_2 \cdot (H_2glygly)$ adduct.

The preparation and characterisation by infrared and ^{119}Sn Mössbauer spectroscopy of some organotin(IV) derivatives with biological molecules have been reported.[1–5] On the other hand there are only a few examples of adducts of glycylglycine acting as neutral ligand.[6,7] Owing to the increasing interest in glycylglycine derivatives, new compounds $R_nSnCl_{4-n} \cdot (H_2glygly)$ have been prepared for $n = 2$ with R = Me, Bu^n, Oct^n and Ph and for $n = 1$ with R = Bu^n, Oct^n and Ph and characterised by chemical analysis, their thermal behaviour and by infrared and ^{119}Sn Mössbauer spectroscopy in the solid state. ^{1}H NMR was used to assess the behaviour of $Me_2SnCl_2 \cdot (H_2glygly)$ adduct, as representative of the series, in D_2O solution. There have been no reports in the literature giving details of any thermal study on complexes related to those prepared in this work and one of the aims of the present study is to identify and assign the stages involved in the decomposition processes of the adducts. Two different types of glycylglycine adduct are examined, viz. monoorganotin(IV) derivatives whose parent organotin(IV) chlorides are liquids and diorganotin(IV) derivatives that have solid parent organotin(IV) chlorides.

EXPERIMENTAL

The organotin(IV) chlorides were a gift from Schering AG (Bergkamen). The organotin(IV) chloride glycylglycine adducts were prepared by refluxing 1:1 molar quantities of the appropriate organotin(IV) chloride and glycylglycine in dry methanol until the reaction mixture became clear. The products obtained on cooling the solution were washed with dry methanol and dried under vacuum.

* Author to whom correspondence should be addressed.

All operations were carried out under N_2 atmosphere.

The compounds were analysed for tin gravimetrically as SnO_2[8] and for chlorine by titration with mercuric perchlorate following the destruction of organic matter by the oxygen flask method. C, H and N were determined at the Laboratorio di Chimica Organica (Milano). Analytical data for the glycylglycine complexes are reported in Table 1.

The thermal behaviour of the adducts was studied on a Stanton Redcroft STA 780 simultaneous thermal analyser. Infrared spectra were obtained using a Perkin–Elmer 580 spectrophotometer as split mulls (CsI windows) for the solid adducts. The spectrum in D_2O solution for the $Me_2SnCl_2 \cdot (H_2glygly)$ adduct was measured with CaF_2 liquid cells (0.05 mm pathlength) using a compensation technique.

Mössbauer spectra were determined using apparatus and techniques previously described,[5,9] with a $Ca^{119}SnO_3$ source [10 mCi (Radiochemical Centre, Amersham)] at room temperature with constant acceleration and a triangular wave-form. The experimental spectra are computer fitted to Lorentzian shapes.

^1H NMR spectra were recorded with a Bruker WP 80 SY spectrometer operating at 80 MHz in the FT mode; the temperature of the probe was *ca.* 31°C.

RESULTS AND DISCUSSION

Thermal properties

In view of the difference in the nature of the mono- and di-organotin compounds, their thermal decomposition processes are discussed separately. To help assign the stages involved in the decomposition of these materials, the thermal analysis was also carried out on the individual parent materials and on an intimately ground 1:1 mixture of glycylglycine with the organotin halides.

R_2SnCl_2–glycylglycine systems

There appears to be no general pattern of decomposition of the complexes of the type $R_2SnCl_2 \cdot (H_2glygly)$ (where R = Me, Bu^n, Oct^n or Ph). The thermal decompositions are different and characteristic of the specific adducts. All of the parent diorganotin(IV) dichloride salts melt without decomposition and volatilise off at higher temperatures. Glycylglycine itself decomposes in three stages, losing 18% of its weight at 215°C, about 30% of its weight at 243°C and the remainder at temperatures above 300°C. The weight losses are assigned to loss of NH_3, loss of CO_2, and final volatilisation of the residue respectively. The data for the decomposition stages of the adducts, the mixtures and the organotin(IV) parent compounds are in Table 2.

The differential weight loss (DTG) curve for the volatilisation of the diphenyltin(IV)dichloride suggests that a two-stage process is involved. Such a process would be consistent with the known rearrangement of Ph_2SnCl_2 to give $SnCl_4$ and Ph_3SnCl whose decomposition temperatures are 114 and 240°C respectively. There is no evidence in the DTG curves, in the region of vaporisation, of the other diorganotin(IV)dichlorides for similar rearrangements.

Table 1. Analytical data of $H_2glygly$ adducts with R_nSnCl_{4-n} (%: calc. in parentheses)

	C	H	N	Cl	Sn
$Me_2SnCl_2 \cdot H_2glygly$	21.6	4.08	7.59	20.0	33.5
	(20.48)	(4.01)	(7.96)	(20.16)	(33.74)
$Bu^n_2SnCl_2 \cdot H_2glygly$	33.8	6.13	7.33	16.3	27.3
	(33.05)	(6.01)	(6.43)	(16.26)	(27.23)
$Oct^n_2SnCl_2 \cdot H_2glygly$	43.1	7.61	5.70	13.0	21.8
	(43.82)	(7.72)	(5.12)	(12.94)	(21.65)
$Ph_2SnCl_2 \cdot H_2glygly$	39.8	4.04	5.98	15.2	25.3
	(40.38)	(3.81)	(5.89)	(14.90)	(24.94)
$Bu^nSnCl_3 \cdot H_2glygly$	23.4	4.28	6.71	25.3	29.0
	(23.19)	(4.14)	(6.76)	(25.67)	(28.65)
$Oct^nSnCl_3 \cdot H_2glygly$	30.3	5.53	5.74	22.1	25.5
	(30.63)	(5.36)	(5.95)	(22.61)	(25.23)
$PhSnCl_3 \cdot H_2glygly$	27.9	2.81	6.57	24.7	27.6
	(27.66)	(3.02)	(6.45)	(24.49)	(27.33)

There is some similarity in the thermal decompositions of the mixture of R_2SnCl_2 with glycylglycine where R = Bu^n, Oct^n or Ph. In each, the diorganotin(IV)dichloride melts and the glycylglycine dissolves in the molten phase. Except for the case of the dioctyltin(IV)dichloride mixture, the melts decompose by volatilisation of most of the diorganotin(IV)dihalide leaving impure glycylglycine to decompose at a higher temperature. For the dioctyltin(IV)dichloride mixture, the weight loss due to the volatilisation of $Oct^n_2SnCl_2$ overlaps the weight loss due to the decomposition of glycylglycine. The dimethyltin(IV)dichloride–glycylglycine mixture loses 42% weight at 50°C before melting at 107°C and subsequently losing the organotin(IV)halide and glycylglycine residues by volatilisation at 133 and 248°C. These results can be explained if part of the dimethyltin(IV)dichloride undergoes rearrangement to give $Sn(CH_3)_4$ and $SnCl_4$ (boiling points 78 and 114°C respectively). A broad DTG feature is found over this temperature range and is more consistent with loss of two volatile

Table 2. Thermal analytical data for R_nSnCl_{4-n} adducts with H_2glygly

System	Temperature (°C)	Weight loss (%)	Assignment
R = Me; $n = 2$			
(a) Me_2SnCl_2	107	0	Melting
	145	100	Volatilisation
(b) $Me_2SnCl_2 + H_2$glygly	50	42	
	107	0	Melting
	133	28	
	248	30	
(c) $Me_2SnCl_2 \cdot H_2$glygly	51	5	Elimination of HCl
	107	5	
	157	62	
	260	30	
R = Bu; $n = 2$			
(a) $Bu^n_2SnCl_2$	45	0	Melting
	80	100	Volatilisation
(b) $Bu^n_2SnCl_2 + H_2$glygly	49	0	Melting
	80	75	Volatilisation of Bu_2SnCl_2
	204	6	Decomposition of impure
	270	8	glycylglycine
(c) $Bu^n_2SnCl_2 \cdot H_2$glygly	39	0	Melting
	80	70	
	175	10	
	243	12	
R = Oct; $n = 2$			
(a) $Oct^n_2SnCl_2$	45	0	Melting
	107	100	Volatilisation
(b) $Oct^n_2SnCl_2 + H_2$glygly	51	0	Melting; dissolution of
	120	100	glygly; volatilisation
(c) $Oct^n_2SnCl_2 \cdot H_2$glygly	91	0	Melting
	220	83	
	336	5	
R = Ph; $n = 2$			
(a) Ph_2SnCl_2	44	0	Melting
	114	100	Volatilisation
(b) $Ph_2SnCl_2 + H_2$glygly	42	0	Melting
	80	70	
	260	12	
(c) $Ph_2SnCl_2 \cdot H_2$glygly	50	10	
	200	40	
	300	20	

Table 2—*continued.*

System	Temperature (°C)	Weight loss (%)	Assignment
R = Bu; $n = 1$			
(a) Bu^nSnCl_3	44	100	Volatilisation
(b) $Bu^nSnCl_3 + H_2glygly$	20	8	Elimination of HCl
	120	10	
	180	40	
	237	10	
	250	12	
(c) $Bu^nSnCl_3 \cdot H_2glygly$	20	5	
	170	50	
	250	25	
R = Oct; $n = 1$			
(a) Oct^nSnCl_3	87	100	Volatilisation
(b) $Oct^nSnCl_3 + H_2glygly$	66	8	Elimination of HCl
	170	57	
	360	12	
(c) $Oct^nSnCl_3 \cdot H_2glygly$	27	11	Elimination of HCl
	192	62	
	360	12	
R = Ph; $n = 1$			
(a) $PhSnCl_3$	66	100	Volatilisation
(b) $PhSnCl_3 + H_2glygly$	66	50	Rearrangement of $PhSnCl_3$ to form Ph_4Sn and $SnCl_4$
	170	15	
	221	8	
	270	10	
(c) $PhSnCl_3 \cdot H_2glygly$	66	43	
	258	18	
	310	20	

components than with a one-stage decomposition. During the evaporation of $SnCl_4$ there is evidence for a melting endotherm on the DTA trace that would be consistent with the melting and volatilisation of undecomposed Me_2SnCl_2.

The fact that the organotin(IV)dihalides volatilise off from molten mixtures at temperatures similar to their boiling points suggests that there is no strong interaction between the organotin moiety and the glycylglycine ligand in the adducts.

The thermal decomposition of the adducts fall into two classes, following one of two distinct mechanisms: viz. (1) in which the decomposition of the adduct follows a process similar to that of the mixture, and (2) in which the decomposition involves a reaction within the lattice which does not occur in the mixture.

Both the dioctyl- and dibutyltin(IV)dichloride derivatives of glycylglycine decompose following mechanism (1). Figure 1 shows the TG, DTG and DTA traces for the decomposition of: (A) $Oct_2^nSnCl_2$, (B) $Oct_2^nSnCl_2 + H_2glygly$ and (C) $Oct_2^nSnCl_2 \cdot (H_2glygly)$. The difference between the decomposition of the adduct, $Oct_2^nSnCl_2 \cdot (H_2glygly)$ and the mixture $Oct_2^nSnCl_2 + (H_2glygly)$ is that melting occurs at a lower temperature in the mixture allowing glycylglycine to dissolve in the melt but the adduct is stable to a higher temperature. The mixture containing dibutyltin(IV)dichloride and the adduct $Bu_2^nSnCl_2 \cdot (H_2glygly)$ both melt at approximately the same temperature and decompose in a similar manner, indicating that the bonding in the dibutyl adduct is weak.

Thermal decomposition of those adducts involving some reaction in the lattice which is absent in the decomposition of the mixtures, is evident in the dimethyltin(IV) and diphenyltin(IV) systems. The mechanism of decomposition of these complexes involves the elimination of HCl from the lattice to give a glycylglycinate which subsequently decomposes in a different manner to those of the mixtures. Figure 2 shows the TG, DTG, and DTA traces for the decomposition of: (A) Me_2SnCl_2, (B) $Me_2SnCl_2 + H_2glygly$ and (C) $Me_2SnCl_2 \cdot (H_2glygly)$.

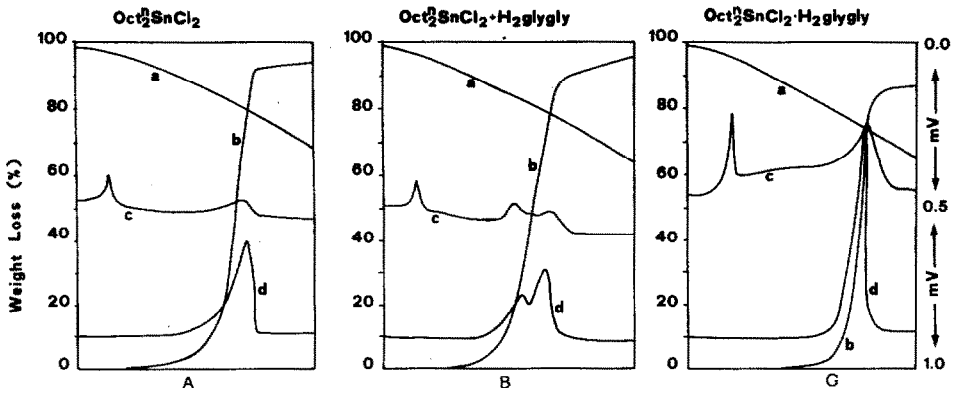


Fig. 1. TG, DTG and DTA traces of the decomposition of $Oct_2^nSnCl_2$(A); of equimolar mixture of $Oct_2^nSnCl_2$ and H_2glygly (B); and of the adduct $Oct_2^nSnCl_2(H_2glygly)$ (C). (a = temperature curve; b = TG curve; c = DTA curve; d = DTG curve.)

$RSnCl_3$–glycylglycine systems

All of the parent organotin trihalides, on reaching their boiling points, volatilise off losing 100% weight in one step. There is no evidence from differential weight losses to indicate decomposition occurring in more than one stage.

Both the octyl- and butyltin(IV)trichloride adducts with glycylglycine decompose at temperatures lower than the boiling points of their parent organotin compounds but in a similar manner to the mixtures $RSnCl_3$–glycylglycine (R = Bu^n, Oct^n). The two adducts appear to undergo a three-stage weight loss, although the unusually broad DTG peaks suggest that the decompositions are more complex. The three stages of weight losses are assigned to the initial elimination of HCl forming monoorganotin(IV)trichloride glycylglycinates followed by loss of organotin(IV)chlorides and finally by the break-down of the glycylglycine moiety. The mixture of octyltin(IV)trichloride and glycylglycine decomposes in a similar manner but the solid phase decomposes at a lower temperature. Although the decomposition of the mixture of Bu^nSnCl_3 and glycylglycine appears to be a multi-stage process, combination of certain weight losses gives a trace similar to that obtained for the adduct. Figure 3 shows the TG, DTG and DTA traces for: (A) Oct^nSnCl_3, (B) $Oct^nSnCl_3 + H_2$glygly and (C) $Oct^nSnCl_3 \cdot (H_2glygly)$. Both the adduct, $PhSnCl_3 \cdot (H_2glygly)$, and the mixture of $PhSnCl_3$ and glycylglycine begin to lose weight at 66°C which is the boiling point of $PhSnCl_3$. The complexity of the corresponding DTG peaks strongly suggests that the decompositions of the adduct and the mixture of the starting materials are not simple. The initial weight losses indicate it is possible to consider the rearrangements of $PhSnCl_3$ to form tetraphenyltin and $SnCl_4$, followed by the loss of the latter.

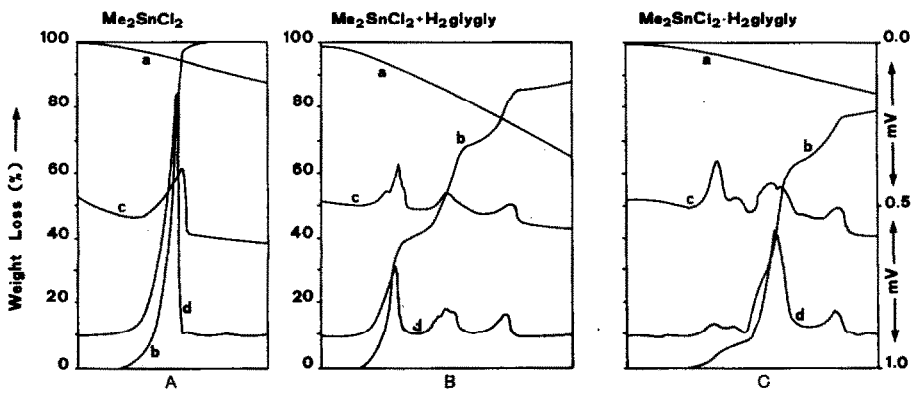


Fig. 2. TG, DTG and DTA traces of the decomposition of Me_2SnCl_2(A); of equimolar mixture of Me_2SnCl_2 and H_2glygly (B); and of the adduct $Me_2SnCl_2 \cdot (H_2glygly)$ (C). (a = temperature curve; b = TG curve; c = DTA curve; d = DTG curve.)

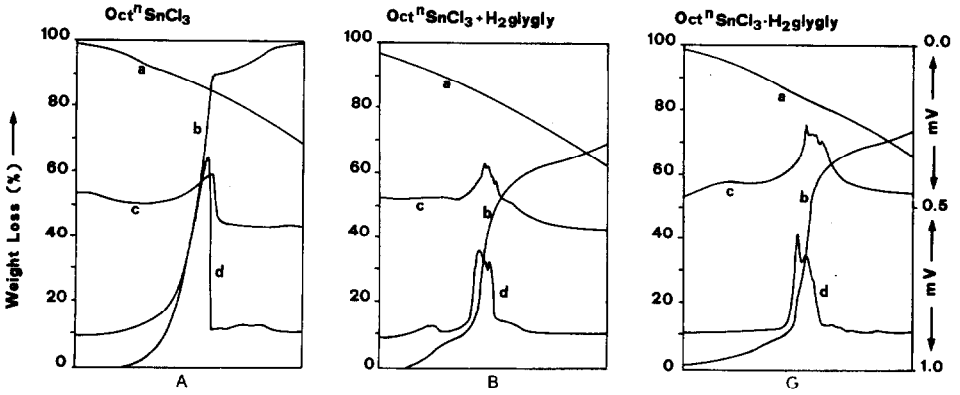


Fig. 3. TG, DTG and DTA traces of the decomposition of Oct^{n}SnCl$_3$ (A); of equimolar mixture of Oct^{n}SnCl$_3$ and H$_2$glygly (B); and of the adduct Oct^{n}SnCl$_3$·(H$_2$glygly) (C). (a = temperature curve; b = TG curve; c = DTA curve; d = DTG curve.)

IR spectra

Coordination by the amino group of aminoacids and simple dipeptides to (organo)metallic ions is reported to give rise to substantial shifts of the NH_2 stretching frequencies.[10] As pointed out, direct comparison should be made not with the zwitterion but with matrix-isolated species (where the NH_2 group in place of NH_3^+ is present) but this possibility is lacking for H_2glygly.

Therefore, the frequencies of the glycylglycine adducts are compared to a copper complex,[11] whose structure is chelated through the amino group as is that of trimethyltin(IV)glycylglycinate.[10]

Hardly any significant shift is observed for the 3300 cm^{-1} band in the spectra of all adducts. The broad absorptions which are observed, however, offer a striking contrast with the same vibration in the free ligand, where it is present as a relatively narrow peak. This suggests, although this is not a unique case,[12] that hydrogen bonding is prominent in these organotin(IV) derivatives, such as might be expected if the ligand, binding through the amino end, adopts a conformation which enables it to form inter- and/or intra-molecular hydrogen bonds via the COOH group. For some derivatives (Bu^{n}SnCl$_3$, Oct^{n}SnCl$_3$) the occurrence of more bands than expected symmetric and asymmetric stretching vibrations, is likely to be due to crystal effects.[10] In D_2O solution, a single broad band is observed at *ca* 3400 cm^{-1}.

The lower frequency broad bands (3230–3110 cm^{-1}) are probably due to a superimposition of $\nu_{s(NH_2)}$ and $\nu_{(N-H)(amide)}$.

The most relevant feature in the IR spectra of all solids is the appearance of the intense band at *ca* 1730 cm^{-1} (see Table 3) which is assigned to the un-ionised COOH group of the ligand. The same absorption, albeit reduced in intensity, is present in the D_2O solution spectrum which is somewhat shifted to lower wavelength in going from solid state to solution (Me_2SnCl_2 adduct). This frequency closely agrees with the solution spectra of both the ligand and metal.[13] The adduct of SiF_4 with glycine, binding with the amino nitrogen has been proposed.

Vibrations at 1678 and 1575 cm^{-1} are present in the adducts. The former is assigned to the amide I mode (mainly C=O stretching) of the peptide group[13] and appears virtually unshifted in D_2O solution (1675 cm^{-1}). The absence of absorptions in the region 1650–1600 cm^{-1} in the solid, rules out coordination of the peptide carbonyl oxygen to the organotin moiety. Indeed the shift of the 1678 cm^{-1} amide I vibration to lower wavelength (*ca* 1630) has been associated with binding to the peptide group through oxygen, both in the solid state and solution in a series of metal complexes.[11,13] Noticeably this frequency shift has been used[10] as a diagnostic tool in elucidating the different binding of Hglygly$^-$ in triorganotins. The amide carbonyl frequency in Me_3Sn(Hglygly) is observed at 1683 cm^{-1} and a five-coordinated, presumably trigonal–bipyramidal structure with carboxylic oxygen and amino nitrogen occupying axial positions has been proposed, while in (Cyh)$_3$Sn(Hglygly) (Cyh = cyclohexyl) the lowering of this frequency value to 1658 cm^{-1} has been taken as an indication of both the amide carbonyl oxygen and terminal amino group nitrogen atoms of the Hglygly$^-$ ligand being involved in coordination to tin to create a hexa-coordinated arrangement. Since all the obtained H_2glygly adducts exhibit the unshifted 1678 cm^{-1} $\nu_{(C=O)(amide\ I)}$ band, in addition to the un-ionised $\nu_{(COOH)}$ vibration, this suggests that only the amino

Table 3. IR data for R_nSnCl_{4-n} adducts of H_2glygly*

Me_2SnCl_2	$Bu^n_2SnCl_2$	$Oct^n_2SnCl_2$	Ph_2SnCl_2	Bu^nSnCl_3	Oct^nSnCl_3	$PhSnCl_3$	Assignment
3275m, bd	3340m, bd	3335m, bd	3340m, bd	3340m, bd	3320m, bd	3360m, bd	
3165m, bd	3230m, bd	3210m, bd	3230m, bd	3200m, bd	3180m, bd	3180m, bd	(NH)
				3130m, bd	3110m, bd		
1745s (1730m)	1740s	1720s	1740s	1738s	1732s	1730s	(C = O) carboxylic
1678s (1675s)	1678s	1678s	1678s	1678s	1678s	1678s	(C = O) amide I
1575m, bd (1595m, bd)	1550m		1565m, bd	1575m, bd	1565m, bd	1565m, bd	$as^{(COO^-)}$† amide II
1397w							$s^{(COO^-)}$†
1215m, bd	1195m	1215m, bd	1230m, bd†	1205w	1200w	1250s†	(C = O) + (OH) and/or Ph vibration
	605s	605s					$s^+ as^{(SnC_2)II}$
560							$as^{(SnC_2)}$
	525s	525s					$s^+ as^{(SnC_2)I}$
525m							$s^{(SnC_2)}$
				475m			(SnC)
			440m			442s	*y*-Mode Ph
360m							
345m	305m, sh		340m, bd			360vs	(Sn–Cl) + ligand
265m	285s, bd	280s, bd		270s	270s	275s	(Sn–Cl) + ligand

* Nujol or hexachlorobutadiene mulls: s = strong, m = medium, w = weak, sh = shoulder, bd = broad, v = very. Values in parentheses refer to D_2O solution spectrum.
† See text for discussion of the assignment.

group is coordinated. Moreover, in D_2O solution the Me_2SnCl_2 adduct shows vibrations at 1595, 1483, 1443 and 1397 cm^{-1}. The 1595 and 1397 cm^{-1} absorptions are identical to those reported[13] for the Cu(II) complex at $2 < pH < 4.2$ which are assigned to the asymmetric and symmetric COO^- stretching vibrations respectively. Therefore, in solution, the adduct is likely to undergo a partial dissociation and/or ionisation of the COOH group. The main difference in the solution spectrum of the Me_2SnCl_2 adduct relative to those of the Cu complex in this pH region is the absence of the 1630 cm^{-1} vibration indicating the absence of peptide oxygen binding.

Vibrations in the 1575–1550 cm^{-1} range have been assigned[11] to the amide II mode [$\nu_{(CN)} + \delta_{(NH)}$] and to the NH_2 scissoring mode for solid complexes, while the former vibration is found at 1487 cm^{-1} in D_2O solution, which is shifted to 1508 cm^{-1} if peptide oxygen is coordinated.[13] In the solid adducts presented in this work, broad bands at *ca* 1570 cm^{-1} are observed (with the exception of the $Oct_2^nSnCl_2$ derivative) and are tentatively assigned to the amide II mode, although superimposition with the NH_2 scissoring cannot be excluded.

The absorption which is observed in the 1250–1200 cm^{-1} range is more intense in the dialkyltin(IV) adducts and, while some authors[14] have assigned it to a un-ionised COOH group vibration [$\nu_{C=O} + \delta_{(OH)}$] in glycinium fluoride and glycinium hexafluorosilicate and adducts of SiF_4 and glycine, an unambiguous assignment is difficult since CH_3, CH_2 and NH_2 vibrational modes are expected in this range. In the complex Me_2Sn(glygly-O,N)[15] this region of the spectrum is free from absorptions of comparable intensity, which might support the previous assignment. The bands at 1250 and 1230 cm^{-1} in the $PhSnCl_3$ and Ph_2SnCl_2 adducts respectively, suffer from the same ambiguity, since they are present also in the parent compounds.[16]

Skeletal vibrations of the organometallic moieties may in principle provide structural information, although the symmetry of the adducts is expected to be generally low, even in the most favourable case (Me_2SnCl_2L). In this instance both ν_{as} and $\nu_{s(SnC_2)}$ could be assigned (560 and 525 cm^{-1} respectively) which rules out a D_{2h} symmetry for the adduct such as might be envisaged in the rather unlikely case of an all-*trans* $Me_2SnCl_2L_2$ unit,[17] spanned by bridging H_2glygly units which are coordinated only with amino nitrogen and/or peptide oxygen alternately in a linear polymeric structure.

In the low frequency region under the heading Sn–Cl + ligand vibrations (Table 3), are listed all frequencies observed in the 400–200 cm^{-1} region, with the exception of a weak band at 390 cm^{-1} (Me_2SnCl_2 and Bu^nSnCl_3 adducts) and at 380 cm^{-1} ($Bu_2^nSnCl_2$ adduct).

The ligand itself shows absorptions in this range (400, 310, 235 cm^{-1}) and while some authors report[18] a shift to lower wavelength of the $\nu_{(Sn-Cl)}$ vibrations in a series of Me_2SnCl_2 adducts with *N*,*N*-dimethylnicotinamide-isonicotinamide and their thio-derivatives, there seems to be no general trend in the observed frequencies with respect to those of the organotin(IV) halides;[19,21] the frequencies found in the Me_2SnCl_2 adduct are virtually unchanged or shifted to higher wavelengths. Little change, if any, is observed for the Ph_2SnCl_2 and the previous examples, the Sn–Cl stretching modes are either absent or shifted to lower frequency.

^{119}Sn *Mössbauer spectra*

The ^{119}Sn Mössbauer parameters for the organotin(IV) chloride adducts are given in Table 4. The isomer shift values, δ, show the expected trends for adduct formation in that they are all lower than those of their parent organotin(IV) chlorides.[22] The isomer shifts, δ, for the monoalkyltin(IV) derivatives are lower than for the corresponding dialkytin(IV) adducts as would be expected owing to the increase in covalent bonding on replacement of a second chlorine with an alkyl group. Replacement of alkyl groups by phenyl groups is known to result in lower isomer shift values in organotin(IV) compounds and the parameters found for the phenyltin(IV) adducts in this work are consistent with previous data.[23]

Evidence of solid state intermolecular chemical interactions is afforded by a preliminary variable temperature ^{119}Sn Mössbauer study. ^{119}Sn Mössbauer resonance areas have been collected for

Table 4. Mössbauer parameters for R_nSnCl_{4-n} adducts with H_2glygly

Compound*	δ†	Δ‡
$Me_2SnCl_2 \cdot H_2$glygly	1.36	3.58
$Bu_2SnCl_2 \cdot H_2$glygly	1.40	3.71
$Oct_2SnCl_2 \cdot H_2$glygly	1.48	3.82
$Ph_2SnCl_2 \cdot H_2$glygly	0.76	1.80
$BuSnCl_3 \cdot H_2$glygly	1.04	2.06
$OctSnCl_3 \cdot H_2$glygly	1.09	2.01
$PhSnCl_3 \cdot H_2$glygly	1.02	2.18

* Absorber thicknesses (mg ^{119}Sn cm^{-2}) were $\sim$ 0.5.

† Isomer shift with respect to room temperature $CaSnO_3$.

‡ Nuclear quadrupole splitting at liquid N_2 temperature.

$77 < T < 127$ K. The plot of ln vs $A(T)$ is linear and the slope d ln $A/dT = -1.41 \times 10^{-2}$ K^{-1} has been calculated, for a series of eight points, which is lower than the slope (-1.8×10^{-2} K^{-1}) found for compounds of known structure consisting of non interacting monomeric molecules.[24,25]

^{1}H NMR

The solution properties of the $Me_2SnCl_2 \cdot (H_2glygly)$ specimen in D_2O have been investigated both by IR and ^{1}H NMR spectroscopy. In view of the physiological activity of many organotin derivatives, knowledge of specific binding sites and stability of complexes in aqueous solution may be of some interest.

The binding of metal ions by aminoacids and peptides as models for their interaction with proteins, has attracted considerable interest.[26] The complexes have been mostly detected and characterised by the pH titration method and complexation at the amino group of the *N*-terminal aminoacid has been evidenced. On the basis of NMR data[27,28] however, initial binding to the *C*-terminal end has been proposed. First of all the solution of the complex was compared with an equimolar mixture of Me_2SnCl_2 and $H_2glygly$. The pH value of a 0.2 M solution of the former is 4.08, while it is 2.87 for the latter. In three days there was no significant change in the pH's of the equimolar mixtures and the adduct. This is consistent with stability of the adduct in solution and the lack of conversion to a chelate complex, such as that observed[27] in the reaction of glycine with *cis*-$(NH_3)_2Pt(H_2O)_2^{2+}$ in water, in which glycine coordinates through oxygen only and slowly converts into the chelate $(NH_3)_2Pt(gly\text{-}O,N)^+$. In this work, the reverse process, is being observed namely the solution behaviour of the preformed adduct, which has been obtained under different conditions.

On the assumption that at pH 2.87, little, if any, coordination of $H_2glygly$ to the organometallic moiety has taken place in the equimolar mixture, the spectrum of the adduct could be interpreted in terms of a dissociation equilibrium which gives rise to free $H_2glygly$ along with the coordinated species (Table 5) as previously shown by the infrared spectra. The peaks at δ: 0.73 and 0.81 ppm are therefore assigned to the β- and α-methylene protons of the free ligand respectively.[25]

However, at pH 4 the possibility of carboxylate coordinated species cannot be discounted. The doublet pattern of the α-methylene resonances is absent, indicating fast exchange of the peptide proton with solvent and/or rapid exchange of $H_2glygly$ between the free and complexed forms.[25]

Table 5. ^{1}H NMR data*

Compound	δ_{CH_2}	$\delta_{CH_3(Sn)}$	^2J (^{119}Sn–^{1}H)† (Hz)
(A) Me_2SnCl_2 + $H_2glygly$‡	0.73 0.82	3.80	102.6
(B) $Me_2SnCl_2 \cdot H_2glygly$	0.61 0.73 0.80 0.81 0.94	3.72	100.2

* Chemical shifts (δ) in ppm relative to the DOH resonance. Positive shifts are upfield from DOH signal. This peak is reported (M. K. Kine and A. E. Martell, *J. Am. Chem. Soc.* 1969, **91**, 872) to vary in position depending on the concentration of solute and acidity of solution. Since pH only varies by *ca* 1 unit in going from solution A to B, reference to DOH is not expected to alter significantly the δ values of the resonances of identical species.

† $^2J(^{117}Sn–^1H)$ values are *ca* 4 Hz less than $^2J(^{119}Sn–^1H)$ values.

‡ Equimolar mixture, $C = 0.2$ M, to that of the adduct.

The resonances for the α-methylene protons of unionised $H_2glygly$, coordinated at the amino end in the adduct, are expected to follow the same trend as in the protonation, namely a down-field shift, while the methylene protons adjacent to the coordinated amino group are expected to show an up-field shift. Hence resonances at δ 0.61 and 0.94 ppm are assigned to the α- and β-methylene groups of the parent adduct. The resonance at δ 0.80 ppm might be accounted for by the rapid formation of a small amount of $Me_2Sn(glygly\text{-}O,N)^+$ complex, undetected in the infrared spectra, in which both the carboxylate and the amino end are coordinated, presumably to different organometallic moieties, since a seven-membered chelate ring is not normally stable. The complex might be expected to exhibit resonance at *ca* δ 0.80 ppm and δ 1.02 ppm on the basis of the data reported by Rabenstein *et al.*[25] for complexes of divalent metal ions (Cd^{2+} and Zn^{2+}) with simple peptides. Only one resonance due to the organometallic moiety is observed, flanked by satellites due to $^2J(^{119/117}Sn–^1H)$ coupling, indicating rapid exchange between aquated and complexed forms. The observed $^2J(^{119}Sn–^1H)$ value is indeed somewhat less than the value for the parent Me_2SnCl_2 in D_2O(106.8 Hz) and consistent with a hexa-coordinated species. The spectrum in DMSO-d_6 was also examined, although it bears little significance as to the nature of D_2O solutions. Since

the peptide hydrogen resonances are present at δ (from TMS) 8–9 ppm, this rules out any involvement in bonding of a negative peptide group.

Acknowledgements—The financial support from NATO (Grant No. 1762), from Consiglio Nazionale delle Ricerche (Rome), from Ministero della Pubblica Istruzione (Rome) and from S.E.R.C. and the International Tin Research Institute (for a studentship to S.M.G.) is gratefully acknowledged.

REFERENCES

1. L. Pellerito, G. Ruisi, N. Bertazzi, M. T. Lo Giudice and R. Barbieri, *Inorg. Chim. Acta* 1976, **17**, L9.
2. L. Pellerito, M. T. Lo Giudice, G. Ruisi, N. Bertazzi, R. Barbieri and F. Huber, *Inorg. Chim. Acta* 1976, **17**, L21.
3. L. Pellerito, G. Ruisi, R. Barbieri and M. T. Lo Giudice, *Inorg. Chim. Acta* 1977, **22**, L33.
4. R. Barbieri, L. Pellerito and F. Huber, *Inorg. Chim. Acta* 1978, **30**, 321.
5. G. C. Stocco, L. Pellerito, M. A. Girasolo and A. G. Osborne, *Inorg. Chim. Acta* 1984 (in press).
6. M. F. Mogilevkina, N. A. Volkova and I. M. Ceremisina, *Koord. Khim.* 1976, **2**, 1403.
7. L. Pellerito, G. Ruisi, M. T. Lo Giudice, R. Cefalu, J. D. Donaldson and S. M. Grimes, *Inorg. Chim. Acta* 1982, **62**, 149.
8. W. P. Neumann, *Die Organische Chemie des Zinns*. F. E. Verlag, Stuttgart (1976) (and references therein).
9. R. Barbieri, G. Alonzo, A. Silvestri, N. Burriesci, N. Bertazzi, G. C. Stocco and L. Pellerito, *Gazz. Chim. Ital.* 1974, **104**, 885.
10. B. Y. K. Ho and J. J. Zuckerman, *Inorg. Chem.* 1973, **12**, 1552.
11. J. B. Hodgson, G. C. Percy and D. A. Thornton, *Spectrosc. Lett.* 1979, **12**, 297 (and references therein).
12. G. Roge, F. Huber, H. Preut, A. Silvestri and R. Barbieri, *J. Chem. Soc., Dalton Trans.* 1983, 595.
13. M. Tasumi, S. Takahashi, T. Nakata and T. Miyazawa, in *Infrared and Raman Spectroscopy of Biological Molecules* (Edited by T. M. Theophanides), p. 225. D. Reidel, Dordrecht (1979).
14. A. A. Ennan, L. A. Gavrilova, A. N. Chebotarev and N. V. Andreeva, *Russ. J. Inorg. Chem.* 1981, **20**, 26.
15. R. Barbieri *et al.*, Private communication.
16. R. C. Poller, *J. Inorg. Nucl. Chem.* 1962, **24**, 593.
17. I. R. Beattie and G. P. McQuillan, *J. Chem. Soc.* 1963, 1519.
18. G. Matsubayashi, M. Hiroshima and T. Tanaka, *J. Inorg. Chem.* 1971, **33**, 378.
19. H. Geissler and H. Kriegsmann, *J. Organomet. Chem.* 1968, **11**, 85.
20. F. K. Butcher, W. Gerrard, E. F. Mooney, R. G. Rees, H. A. Willis, A. Anderson and H. A. Gebbie, *J. Organomet. Chem.* 1964, **1**, 431.
21. R. C. Poller, *Spectrochim. Acta* 1966, **22**, 935.
22. R. V. Parish, *Prog. Inorg. Chem.* 1972, **15**, 101 (and references therein).
23. R. V. Parish and R. H. Platt, *Inorg. Chim. Acta* 1970, **4**, 65.
24. K. C. Molloy, J. J. Zuckerman, H. Schumann and G. Rodewald, *Inorg. Chem.* 1980, **19**, 1089.
25. R. Barbieri, A. Silvestri, F. Huber and C. D. Hager, *Inorg. Chim. Acta* 1981, **55**, L13.
26. H. Siegel and R. B. Martin, *Chem. Rev.* 1982, **82**, 385.
27. D. L. Rabenstein and S. Libich, *Inorg. Chem.* 1972, **11**, 2960.
28. T. G. Appleton and J. R. Hall, *J. Chem. Soc., Chem. Commun.* 1983, 911.

Polyhedron Vol. 4, No. 4, pp. 757–760, 1985
Printed in Great Britain

0277–5387/85 $3.00 + .00
© 1985 Pergamon Press Ltd

COMPLEXES OF 4-METHOXY-2-(5-METHOXY-3-METHYL-PYRAZOL-1-YL)-6-METHYLPYRIMIDINE, AN ANTI-INFLAMMATORY AGENT—I. COPPER(II) PERCHLORATE COMPLEXES

J. GARCIA, M. MOLLA and J. BORRAS*
Departamento de Química Inorgánica, Facultad de Farmacia, Universidad de Valencia, Valencia, Spain

(*Received* 13 *February* 1984; *accepted* 9 *May* 1984)

Abstract—The preparation and properties of copper(II) complexes of 4-methoxy-2-(4-methoxy-3-methyl-pyrazol-1-yl)-6-methylpyrimidine, are reported. Complexes of formulae $[Cu(L)_2](ClO_4)_2$, $[Cu(L)_2(H_2O)](ClO_4)_2$ and $[Cu(L)(OH)]ClO_4$ were synthesized. The ESR spectrum of $[Cu(L)_2](ClO_4)_2$ indicates that the complex has a tetragonal symmetry, with the unpaired electron in the $d_{x^2-y^2}$ orbital. The *d–d* electron spectrum suggests that $[Cu(L)_2(H_2O)](ClO_4)_2$ has a bipyramidal trigonal geometry around the copper(II) ion.

In the present paper we initiate the study of interaction between metal ions and a biologically active pyrimidyl-pyrazole ligand, used as an anti-inflammatory agent:[1,2] 4-methoxy-2-(5-methoxy-3-methyl-pyrazol-1-yl)-6-methylpyrimidine (mepirizol, hereinafter L). We report for the first time the preparation and characterization of some copper perchlorates of L, as an integral part of our studies. The structure of the ligand is shown in Fig. 1.

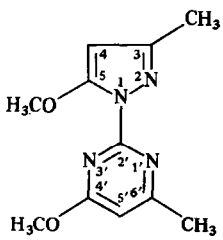


Fig. 1.

EXPERIMENTAL

The ligand kindly provided by "Laboratorios Robert" was purified by recrystallization from methanol. It melted at 92°C.[3]

Found: C, 56.2; H, 6.0; N, 23.8%. Calc. for $C_{11}H_{14}N_4O_2$: C, 56.4; H, 6.0; N, 23.9%.

Copper(II) was determined by iodometric titration, after prior decomposition by heating in sulphuric acid. Carbon, hydrogen and nitrogen were determined by elemental analysis.

Physical measurements

Molar conductances of the complexes were measured in methanol using a Radiometer CDC 304 electrode (cell constant 1.0 cm) in conjunction with a Radiometer CDM 83 conductivity bridge.

Magnetic susceptibility measurements were carried out in the solid state at room temperature (20°C) using a Gouy Balance with $[Ni(en)_3]S_2O_3$ as calibrant.

Electronic spectra were measured on a Perkin–Elmer Hitachi 200 spectrophotometer with reflectance attachment fitted.

IR spectra were obtained using a Perkin–Elmer 577 instrument, using Nujol mulls supported between CsI windows for the range 4000–200 cm^{-1}.

Thermal (TGA–DTG–DTA) analyses were performed using a Settaram simultaneous thermobalance.

X-band ESR spectra of powder samples were recorded at room temperature on a JEOL MES-3X spectrometer. The microwave frequency was determined using DPPH as a reference and the magnetic field calibrated with a Newport Instruments NMR magnetometer.

Preparation of the metal complexes

$[Cu(L)_2(H_2O)](ClO_4)_2$ (*compound* I). This was prepared by addition of 40 cm^3 of an aqueous solution

* Author to whom correspondence should be addressed.

of the ligand (2.5×10^{-2} M) to 200 cm^3 of aqueous solution of the copper(II) perchlorate (2×10^{-2} M) (acidified with 1 M $HClO_4$ to pH = 3). The compound separated immediately at room temperature, and was filtered, washed with cold water and dried over silica gel.

$[Cu(L)_2](ClO_4)_2$ (*compound* **II**). This compound was prepared by addition of 25 cm^3 of an ethanolic solution of copper(II) perchlorate (0.2 M) at pH = 3, to 500 cm^3 of an ethanolic solution of the ligand (3×10^{-2} M). The resulting solution was warmed in a water bath for 15 min and then cooled to room temperature. The product, which crystallized in a few hours, was collected by filtration, washed with ethanol and dried over silica gel.

$[Cu(L)(OH)](ClO_4)$ (*compound* **III**). 40 cm^3 of an aqueous solution of ligand (2.5×10^{-2} M) was added to 200 cm^3 of an aqueous solution of copper(II) perchlorate (2×10^{-2} M) at pH = 5. The compound precipitated immediately at room temperature. The compound was isolated following the same procedure as in the first case.

RESULTS AND DISCUSSION

Table 1 shows analytical data, colour and molar conductivity values of the complexes. The Λ values fall in the range expected for 1:2 electrolytes in compounds **I** and **II**, and 1:1 for compound **III**.[4]

The thermal study on the compound **I** shows a weight loss between 50 and 140°C. The DTA curve indicates that the weight loss up to 140°C is associated with two endothermic processes, one due to loss of a water molecule and the other due to a rearrangement of compound **I** to give compound **II** as indicated by the fact that the brown solid obtained after dehydration has an X-ray powder pattern identical to compound **II**.

Thermal study of $[Cu(L)_2](ClO_4)_2$ shows stability up to 201°C, at which temperature decomposition takes place through an exothermic process. Thermal study of $[Cu(L)(OH)](ClO_4)$ shows that this complex is stable up to 199°C.

Table 1.

Compound	Colour	Cu (%)		C (%)		N (%)		Cl (%)		Λ_M (Ω^{-1} cm^{-1})*
		Found	Calc.	Found	Calc.	Found	Calc.	Found	Calc.	
I $[Cu(L)_2](ClO_4)_2 \cdot H_2O$	Green	8.3	8.5	35.2	35.3	14.8	14.9	9.2	9.5	192.7
II $[Cu(L)_2](ClO_4)_2$	Brown	8.6	8.7	36.1	36.1	15.4	15.3	9.8	9.7	186.9
III $[Cu(L)(OH)](ClO_4)$	Blue	15.4	15.3	31.6	31.9	13.2	13.5	8.0	8.4	104.7

* 10^{-3} M solution in methanol.

IR spectra

The IR spectra of ligand and compounds show a very large number of bands, in the range studied. Meaningful correlations between spectra and structure are difficult.

The band centred at *ca* 1600 cm^{-1} assigned to C–N vibrations is shifted in IR complexes to a high energy (15 cm^{-1}), indicating nitrogen atom participation in the coordination.

The presence of a strong band at *ca* 1090–1110

Table 2.

Compound	μ_{eff} (MB) (20°C)	Electronic spectra (kK)	ESR parameters $\langle g_0 \rangle$	$g_{\parallel}$	$g_{\perp}$	$A_{\parallel}$ (cm^{-1})
$[Cu(L)_2](ClO_4)_2 \cdot H_2O$	2.02	11.8, 25.0	2.166			
$[Cu(L)_2](ClO_4)_2$	1.91	13.9, 20.8	2.141*	2.294	2.065	163
$[Cu(L)(OH)](ClO_4)$	1.60	14.3, 27.0				
$[Cu(L)_2]^{2+}$ Water		12.8, 27.8				
Nitromethane		13.9, 23.0				

* From $\langle g_0 \rangle = (g_{\parallel} + 2g_{\perp})/3$.

cm^{-1} and a sharp one at *ca* 625 cm^{-1} in all complexes suggests that the perchlorate groups are ionic with T_d symmetry,[5] except perhaps for a weak interaction, since ionic and weakly coordinated monodentate perchlorate groups usually have very similar spectra.[6–8]

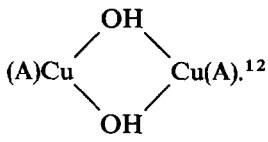
All IR complexes show two bands at 300 and 270 cm^{-1}, assigned to Cu–N vibrations (Cu–N pyrazole and pyrimidine rings respectively).[9,10]

The broad band at 3380 cm^{-1} shown by complex **I** is assigned to ν_{O-H} of water. The IR spectrum of complex **III** shows a sharp peak at 3560 cm^{-1} assigned to ν_{O-H} of the OH group and a peak at 500 cm^{-1} assigned to Cu–OH bridging vibration.[10,11]

Electronic properties

In Table 2 are listed the magnetic moment values, polycrystalline ESR parameters and spectral data for the complexes.

The μ_{eff} values for compounds **I** and **II** are well above the spin-only magnetic moment and are of little use as structural probes. The obtained value of μ_{eff} for complex **III** is lower then $\mu_{s.o.}$ and suggests the existence of an antiferromagnetic interaction between copper(II) ions. A similar behaviour has been observed in several other complexes of the type $[Cu(A)(OH)]_2X_2$ (where A is a bidentate ligand) containing the dimeric structural unit



[12]

The electronic spectrum of complex **I** contains a single broad band at 12 kK (Fig. 2). The spectrum is similar to those shown by complexes of the type $[Cu(A)_2(X)]Y$ for which a trigonal bipyramidal coordination environment for copper(II) is generally accepted.[13–16] Accordingly we propose here the same stoichiometry for $[Cu(L)_2(H_2O)](ClO_4)_2$. This interpretation is in agreement with the existence of $[Cu(L)_2(H_2O)]^{2+}$ in compound **I**.

The diffuse reflectance spectrum of $[Cu(L)_2](ClO_4)_2$ shows two broad bands at 13.9 and 20.8 kK. The band at 13.9 kK is consistent with a compressed tetrahedral stereochemistry for the copper(II) ion which results from coordination of copper(II) to four nitrogen atoms of the ligands. For steric reasons both ligands are rotated toward a tetrahedral geometry as is usually the case in similar complexes.[17,18]

The band at 20.8 kK is assigned to a metal–ligand ($t_{2g} \rightarrow \pi^*$) charge transfer.[19,20] The presence of a CT

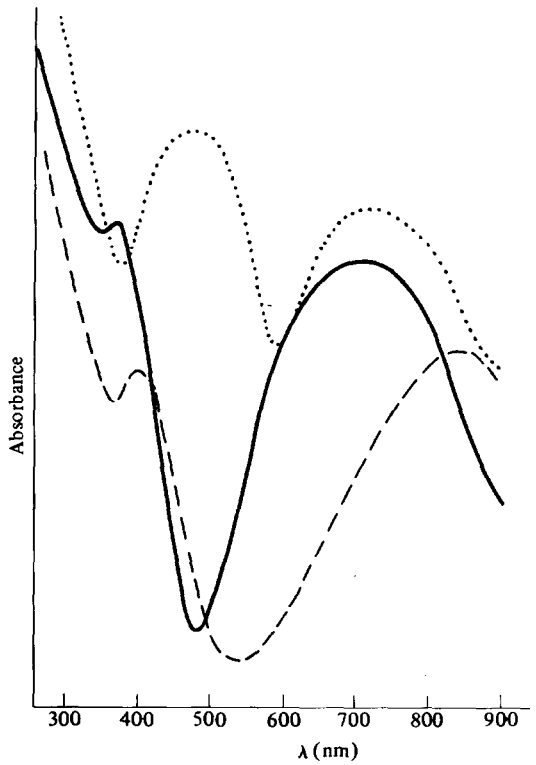


Fig. 2. Electronic reflectance spectra of $[Cu(L)_2(H_2O)](ClO_4)_2$ (– – –), $[Cu(L)_2](ClO_4)_2$ (···) and $[Cu(L)(OH)](ClO_4)$ (——).

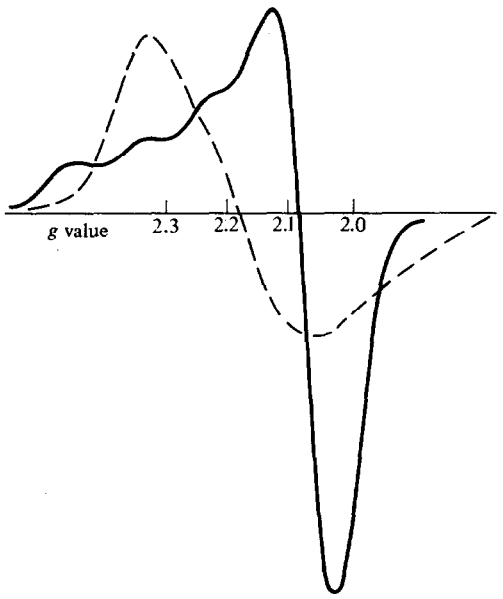


Fig. 3. Polycrystalline ESR spectra of $[Cu(L)_2](ClO_4)_2$ (——) and $[Cu(L)_2(H_2O)](ClO_4)_2$ (– – –).

band in the visible region has been previously reported for several systems where steric hindrance occurs.[21]

The electronic spectrum of $[Cu(L)(OH)](ClO_4)$ presents a broad band at 14.3 kK consistent with a tetrahedral compressed environment for the copper(II) ion.[22]

The polycrystalline ESR spectra of compounds **I** and **II** are shown in Fig. 3.

The spectrum of compound **III** is of poor resolution and contains a single peak at above 3100 G. Observation of ESR spectra of this type is relatively common in doubly bridged dimers such as $[Cu(A)(OH)]_2^{2+}$[23] and originates either from simple paramagnetic impurities or from a $\Delta m_s = \pm 2$ transition.[24,25]

The ESR powder spectrum of compound **II** is typical of a copper(II) ion in axial surroundings with a distorted tetrahedral environment. The nuclear hyperfine splitting of $g_{\|}$ is observed with three of the four components clearly resolved, the other one being obscured by the $g_{\perp}$ component. Measured g ($g_{\|} \gg g_{\perp} > 2$) and $A_{\|}$ values are indicative of $d_{x^2-y^2}$ (or d_{xy} ground state).[26,27]

The ESR powder spectrum of compound **I** is broad and nearly isotropic. This behaviour is common to other complexes with trigonal bipyramidal geometry such as $[Cu(bipy)_2(CN)](NO_3)\cdot 2H_2O$.[15]

REFERENCES

1. E. Takabatake, R. Kodama, Y. Tanaka, R. Dohmori, H. Tachizawa and P. Naito, *Chem. Pharm. Bull.* 1970, **18**, 1900.
2. Y. Oshima, T. Akimoto, W. Tsukada, T. Yamasaki, K. Yamaguchi and H. Kojima, *Chem. Pharm. Bull.* 1969, **17**, 1492.
3. Laboratorios Roberts, Barcelona, Spain (private communications).
4. W. J. Geary, *Coord. Chem. Rev.* 1971, **7**, 81.
5. B. Hathaway and A. E. Underhill, *J. Chem. Soc.* 1961, 3091.
6. M. R. Litzow, L. F. Power and A. M. Tait, *J. Chem. Soc. (A)* 1970, 3226.
7. H. Nakai, *Bull. Chem. Soc. Jpn* 1971, **44**, 2412.
8. P. Balaiah, B. A. Sastry, M. N. Chary, G. Ponticelli and M. Massacesi, *J. Mol. Struct.* 1982, **78**, 289.
9. N. Saha and S. K. Kar, *J. Inorg. Nucl. Chem.* 1977, **39**, 1238.
10. B. J. Hathaway and A. A. G. Tomlinson, *Coord. Chem. Rev.* 1970, **5**, 1.
11. J. R. Ferraro, *Low Frequency Vibrations of Inorganic and Coordination Compounds.* Plenum Press, New York (1971).
12. D. L. Lewis, W. E. Hatfield and D. J. Hodgson, *Inorg. Chem.* 1974, **13**, 147.
13. R. C. Slade, A. A. G. Tomlinson, B. J. Hathaway and D. E. Billing, *J. Chem. Soc. (A)* 1968, 61.
14. B. J. Hathaway, I. M. Procter, R. C. Slade and A. A. G. Tomlinson, *J. Chem. Soc. (A)* 1969, 2219.
15. S. Tyagi and B. J. Hathaway, *J. Chem. Soc., Dalton Trans.* 1983, 199.
16. H. Nakai and Y. Debuchi, *Bull. Chem. Soc. Jpn* 1975, **48**, 2557.
17. B. J. Hathaway, *J. Chem. Soc., Dalton Trans.* 1972, 1196.
18. N. Ray, S. Tyagi and B. J. Hathaway, *J. Chem. Soc., Dalton Trans.* 1982, 143.
19. A. B. P. Lever, *J. Chem. Ed.* 1974, **51**, 612.
20. J. E. Fergusson and C. A. Ramsay, *J. Chem. Soc.* 1965, 5222.
21. W. Geary, *J. Chem. Soc. (A)* 1969, 71.
22. F. A. Walker , H. Sigel and D. B. McCormick, *Inorg. Chem.* 1972, **11**, 2756.
23. D. L. Lewis, K. T. McGregor, W. E. Hatfield and D. J. Hodgson, *Inorg. Chem.* 1974, **13**, 1013 (and references therein).
24. J. F. Boas, R. H. Dunhill, J. R. Pilbrow, R. C. Srivastava and T. D. Smith, *J. Chem. Soc. (A)* 1969, 94.
25. J. R. Pilbrow, A. D. Toy and T. D. Smith, *J. Chem. Soc. (A)* 1969, 1029.
26. B. J. Hathaway and D. E. Billing, *Coord. Chem. Rev.* 1970, **5**, 143.
27. M. Massacesi, G. Ponticelli and W. G. Krishnan, *J. Mol. Struct.* 1980, **69**, 165.

Polyhedron Vol. 4, No. 4, pp. 761–764, 1985
Printed in Great Britain

0277-5387/85 $3.00 + .00
Pergamon Press Ltd

ELECTRON SPIN RESONANCE AND OPTICAL ABSORPTION STUDIES OF COPPER–OXIME CHELATES IN DIMETHYL FORMAMIDE AND PYRIDINE

C. KESAVULU, R. SESHADRI NAIDU and R. RAGHAVA NAIDU*
Department of Chemistry, Sri Venkateswara University, Tirupati-517 502 (A.P.), India

(*Received* 30 *January* 1984; *accepted* 22 *May* 1984)

Abstract—ESR and optical absorption studies on Cu(II) chelates of 2-hydroxyacetophenone-, resacetophenone-, peonol- and 2-hydroxy-1-naphthaldoximes have been made in dimethyl formamide and pyridine. The studies show that both these solvents interact with copper in the axial plane and the interaction is greater with pyridine. The magnetic moment data indicate that all the chelates exist as monomers in both the solvents.

Oximes have been found to possess various insecticidal, miticidal and nematocidal activities.[1] They were employed as antidotes against organophosphorus poisons.[2] The oximes have good chelating properties and they were exploited as analytical reagents for the separation and determination of many metal ions. Considering the potential role of copper in biological systems and the growing importance of oximes as chelating agents it was considered desirable to investigate the nature of bonding in the chelates. Among the several *o*-hydroxyaromaticoximes, 2-hydroxyacetophenone-, resacetophenone-, peonol-(4-methoxy-2-hydroxyacetophenone) and 2-hydroxy-1-naphthaldoximes were used in the present investigation to prepare copper(II) chelates. The optical absorption and ESR spectral studies in dimethyl formamide and pyridine were carried out to study the solute–solvent interaction and to determine the covalency of metal–ligand bond.

EXPERIMENTAL

The copper complexes of 2-hydroxyacetophenone-, resacetophenone-, peonol- and 2-hydroxy-1-naphthaldoximes were prepared according to the procedures described in the literature.[3–6]

A Shimadzu-UV-180 Spectrophotometer was used to record electronic spectra. The solutions studied were dimethyl formamide and pyridine and the data were obtained at room temperature.

ESR spectra were recorded with a varian E-4 X-band Spectrometer employing 4–8 G modulation amplitude and operating at a frequency of 9.5 GHz. The spectra were recorded at room temperature (300 K) in dimethyl formamide and pyridine.

RESULTS AND DISCUSSION

Cu–2-hydroxyacetophenoneoxime, Cu–resacetophenoneoxime, Cu–peonoloxime and Cu–2-hydroxy-1-naphthaldoxime chelates are powders which are insoluble in water and soluble in dimethyl formamide and pyridine. They were found to be stable in air and non-hygroscopic. The results of elemental analysis gave 1:2 metal–ligand stoichiometry. Square planar structures have been assigned to these chelates by the earlier workers.[6,7]

The electronic spectra of all these chelates in dimethyl formamide and pyridine consist of very intense absorption bands in the 300–400 nm region. These are ascribed to charge-transfer and free ligand absorption. The absorption bands were also observed in the 500–600 nm region. These are weak and broad and are assigned to *d–d* transitions of copper(II) in tetragonal field.[8] The similarity of the spectra suggests identical coordination environments in these chelates.[9]

Belford and co-workers[10] have studied the spectra of copper acetylacetone in a variety of solvents which can coordinate along the *Z*-axis. The solvent molecules exert a *Z* component field proportional to their position in the spectrochemical series. Some solvents exert little or no effect since the basicity is extremely low whereas solvents with more basicity coordinate more strongly. Repelling the advance of solvent molecules are two electrons in the d_{z^2} orbital so only the most basic species can force their way in

* Author to whom correspondence should be addressed.

to form strong bonds. There are three *d–d* electronic transitions possible in a tetragonal complex, viz.:

$$d_{xz}, d_{yz} \rightarrow d_{x^2-y^2} \quad (\nu_1),$$
$$d_{xy} \rightarrow d_{x^2-y^2} \quad (\nu_2),$$
$$d_{z^2} \rightarrow d_{x^2-y^2} \quad (\nu_3).$$

The frequency of these transitions will be strongly dependent upon the field experienced by the various *d* orbitals. Frequency ν_2 should remain constant at $10\,Dq_{oh}$ since neither the d_{xy} nor $d_{x^2-y^2}$ orbital has a Z component. They should thus be completely unaffected by any incoming ligands on the Z-axis and the separation corresponds to the splitting $10\,Dq_{oh}$ in a hypothetical purely octahedral complex having six identical ligands. As the tetragonal field approaches the octahedral configuration as the Z field strength approaches that of x and y, ν_1 should diminish and approach ν_2. The third transition ν_3 should also decrease as Z ligand basicity increases eventually disappearing in the octahedral limit as x^2-y^2 and z^2 collapses to form the degenerate e_g orbitals.

The absorption band near 18,000 cm^{-1} for the chelates in dimethyl formamide suggests strong distortion from octahedral stereochemistry.[11] In the spectra of pyridine solutions of these oximates this band is lowered to 16,000 cm^{-1} region. A comparison of the absorption maxima values in both the solvents suggests that the distortion is less in pyridine solution than in dimethyl formamide. Suresh Babu *et al.*[7] determined the electronic spectra of these chelates in nujol mull and reported the absorption maxima in the region 18,690–19,280 cm^{-1}. They have assigned this band to a $^2B_{1g} \rightarrow {}^2E_g$ transition. In the present investigations this band is lowered and appeared in the 18,000 and 16,000 cm^{-1} regions in dimethyl formamide and pyridine respectively. This lowering can be attributed to the interaction of solvent molecules with copper along the Z-axis. The extent of lowering of this transition may be taken as a measure of the donor strength of the solvent. It is evident from the data (Table 1) that the interaction of pyridine with copper is more than with DMF which is also supported by the increased solubility of the oximates in pyridine through weak complex formation. The interaction of both the solvents leads to tetragonal distortion. However, the extent of distortion is less with pyridine suggesting that its coordinating ability is more compared to DMF. This is in good agreement with Belford and others.[10]

The room temperature ESR spectra of Cu–2-hydroxyacetophenoneoxime, Cu–resacetophenoneoxime, Cu–peonoloxime and Cu–2-hydroxy-1-naphthaldoxime in DMF and pyridine exhibit several interesting phenomena. Except for Cu–2-hydroxy-1-naphthaldoxime, curves of all the other three chelates consist of four apparently equally spaced absorption lines. These four lines in the multiplet correspond to the $(2I+1 = 4)$ spin orientations of the copper nuclei with $I = \frac{3}{2}$. The hyperfine structure in these solutions is resolvable at room temperature which is of some interest since Bagguely and Griffiths[12] found it impossible to resolve the hyperfine structure in dilute copper Tutton salts at room temperature due to a short spin–lattice relaxation time of about 2×10^{-9} s. Measurements on the resonance of $[Cu(NH_3)_4]^{2+}$ and $[Cu(H_2O)_6]^{2+}$ ions in water solution have also shown no hyperfine structure. Apparently the spin–lattice relaxation times in the present copper–oxime chelates are greater than in the ionic Tutton salts. This may be caused by much stronger bonds between the copper and its neighbours (O and N atoms of oxime) with the result that the oscillational frequencies are much higher giving a smaller Fourier component in the region of the resonance frequency. In the spectra of all the chelates the expected nuclear interaction between the unpaired electron and each copper

Table 1. Analytical and optical absorption spectral data of the chelates

Chelate	Colour	Metal (%)	Carbon (%)	Hydrogen (%)	Nitrogen (%)	Absorption maxima (cm^{-1}) DMF	Pyridine
Cu–2-hydroxyaceto-phenoneoxime	Brown	17.31 (17.48)	52.90 (52.80)	4.39 (4.40)	7.71 (7.70)	18,180	16,130
Cu–resacetophenoneoxime	Brown	16.10 (16.07)	48.85 (48.85)	4.11 (4.05)	7.14 (7.08)	19,040	16,940
Cu–peonoloxime	Light brown	15.00 (15.00)	51.00 (51.00)	5.10 (4.80)	6.70 (6.60)	18,180	16,920
Cu–2-hydroxy-1-naphthaldoxime	Light brown	14.42 (14.57)	60.80 (60.60)	3.70 (3.70)	6.37 (6.40)	18,520	15,880

Table 2. ESR, bonding and magnetic parameters of the chelates in DMF

Chelate	$\langle g \rangle$	$\langle A \rangle$ ($\times 10^4$ cm^{-1})	K	χ_m ($\times 10^6$ CGS)	μ_{eff} (B.M.)
Cu–2-hydroxyacetophenoneoxime	2.052	73.36	0.254	1315	1.777
Cu–resacetophenoneoxime	2.084	77.82	0.298	1363	1.805
Cu–peonoloxime	2.062	74.01	0.265	1329	1.785
Cu–2-hydroxy-1-naphthaldoxime	2.076	—	—	1348	1.798

isotope is not detected. It may be due to the fact that at room temperature the ESR signal of the less abundant copper isotope is obscured by the random motion of the paramagnetic centres.[13]

The Cu–2-hydroxy-1-naphthaldoxime chelate did not give a four line spectrum either in DMF or pyridine but showed only one line. However a normal spectrum was obtained when the chelate was diluted with a diamagnetic zinc complex of this oxime. It would therefore appear that the anisotropic molecular reorientation of the chelate in solution is responsible for this. Unusual spectra of this type have been noted earlier for complexes bearing large organic ligand substituents.[14–16]

The ESR spectra of most copper(II) complexes in solution at room temperature normally exhibit four hyperfine lines with spin dependent line widths due to the tumbling motion of the microcrystalline units.[17] This tumbling motion will average the anisotropic g and A values observed in solids. The ESR spectra of copper(II) complexes in glassy state give the principal g and A values.[18–21] If the solvent is non-interacting, the g and A values correspond to the molecular g and A values of the complex in the solid state. On the other hand if the electron donor solvents like pyridine interact with the complex weak complexes will be formed and the g and A values will also be different.

The values of $\langle g \rangle$ for Cu–2-hydroxyacetophenoneoxime, Cu–resacetophenoneoxime, Cu–peonoloxime and Cu–2-hydroxy-1-naphthaldoxime chelates are given in Tables 2 and 3. The values are greater in pyridine than in DMF suggesting that pyridine interacts to a greater extent compared to DMF. The greater interaction is also evidenced from the shift of the optical absorption peak to lower wave number region. It is known that square planar complexes of copper(II) usually form five coordinate square pyramidal complexes on adduct formation with amines or pyridine.[22–25] It is therefore very probable that the present copper oximates also form mono adducts with square pyramidal geometry. This causes the copper atom to move out of the plane as the fifth ligand is added causing a decrease in the in-plane binding and thereby also the covalency. The result would be a positive shift of the $\langle g \rangle$ values in pyridine.[26]

The hyperfine structure due to the anisotropic terms are averaged out in solution so that the observed splitting is due only to the isotropic term which according to Abragam and Pryce[27] is proportional to the square of the electron's wave function at the nucleus. The copper–oxime chelates under investigation showed lower values of $\langle A \rangle$ in pyridine than in DMF. The variation of the splitting with solvent thus indicates that the stronger the solvated complex the smaller the value of the unpaired electron's wave function at the nucleus. Apparently the bonding solvent pulls the electron away from copper.

The values for paramagnetic susceptibility (χ_m), magnetic moment (μ_{eff}) and the Fermi contact term are calculated using the following expressions:

$$\chi_m = N\beta^2\langle g \rangle^2 S(S+1)/3KT,$$

$$\mu_{eff} = \langle g \rangle \sqrt{S(S+1)},$$

$$K = \frac{\langle A \rangle}{P} + \langle g \rangle - 2.0023.$$

Table 3. ESR, bonding and magnetic parameters of the chelates in pyridine

Chelate	$\langle g \rangle$	$\langle A \rangle$ ($\times 10^4$ cm^{-1})	K	χ_m ($\times 10^6$ CGS)	μ_{eff} (B.M.)
Cu–2-hydroxyacetophenoneoxime	2.100	66.94	0.268	1378	1.819
Cu–resacetophenoneoxime	2.112	70.26	0.305	1394	1.829
Cu–peonoloxime	2.082	68.03	0.270	1355	1.803
Cu–2-hydroxy-1-naphthaldoxime	2.110	—	—	1392	1.827

The magnetic moment values of the chelates lie above the spin only value of 1.73 B.M. and occur in the range 1.8–2.0 B.M. normally found for Cu(II) complexes in the absence of any antiferromagnetic coupling. The values are consistent with an orbital non-degenerate ground state for the Cu(II) ion.[28] The slight increase above the spin-only value arises probably from the mixing in of orbitally degenerate excited state into the ground state via spin orbit coupling. The values further suggest that the copper oximates are mononuclear in both the solvents.

Acknowledgements—We are grateful to Dr J. L. Rao, Reader in Physics for his valuable suggestions. One of the authors (C.K.) is thankful to the Government of Andhra Pradesh for the financial assistance.

REFERENCES

1. D'Silva, D. J. Themistocles (Union Carbide Corp.), June 1977, US 4,029,688 (Cr 260, 465, 4; Co7C 121/00); June 1974, Appl. 483,882.
2. E. S. Rachaman, Y. Ashani, H. Leader, I. Granoth, H. Edery and G. Porath, *Arzneim-Forsch.* 1979, **29**, 875.
3. N. A. Raju and K. Neelakantam, *Curr. Sci.* 1950, **19**, 383.
4. G. Raja Reddy, Ph.D. thesis, Sri Venkateswara University, Tirupati, India (1970).
5. S. N. Podder, *Z. Anal. Chem.* 1957, **154**, 254.
6. R. Seshadri Naidu, A. Ramesh and R. Raghava Naidu, *Proc. Indian Acad. Sci (Chem. Sci.)* 1980, **89**, 417.
7. V. Suresh Babu, A. Ramesh, P. Raghuram and R. Raghava Naidu, *Polyhedron* 1982, **1**, 607.
8. T. N. Waters and D. Hall, *J. Chem. Soc.* 1959, 1200.
9. A. Graham, T. Bowmaker, N. Waters and P. E. Wright, *J. Chem. Soc.* 1975, 867.
10. R. L. Belford, M. Calvin and G. Belford, *J. Chem. Phys.* 1957, **26**, 1165.
11. K. C. Patel and D. E. Goldberg, *J. Inorg. Nucl. Chem.* 1973, **35**, 4041.
12. D. M. S. Bagguley and J. H. E. Griffiths, *Proc. Phys. Soc., London* 1952, **A65**, 594.
13. J. M. Assour, *J. Chem. Phys.* 1965, **43**, 2477.
14. H. J. Stoklosa, H. L. Huffman and J. R. Wasson, *J. Inorg. Nucl. Chem.* 1973, **35**, 2584.
15. H. J. Stoklosa, G. L. Seebach and J. R. Wasson, *J. Phys. Chem.* 1974, **78**, 962.
16. D. K. Johnson, H. J. Stoklosa, J. R. Wasson and G. L. Seebach, *J. Inorg. Nucl. Chem.* 1975, **37**, 1397.
17. H. M. McConnel, *J. Chem. Phys.* 1956, **25**, 709.
18. R. H. Sands, *Phys. Rev.* 1955, **99**, 1222.
19. D. E. O'Reilley, *J. Chem. Phys.* 1958, **29**, 1188.
20. G. Malmstrom and T. Vanngard, *J. Mol. Biol.* 1960, **2**, 118.
21. F. M. Roberts and W. S. Koski, *J. Am. Chem. Soc.* 1980, **82**, 3006.
22. K. E. Falk, E. Ivanova, B. Ross and T. Vanngard, *Inorg. Chem.* 1970, **9**, 556.
23. D. Dyrssen and M. Hennichs, *Acta Chem. Scand.* 1961, **15**, 47.
24. D. P. Graddon and R. A. Schulz, *Aust. J. Chem.* 1965, **18**, 1731.
25. D. P. Graddon and G. M. Mockler, *Aust. J. Chem.* 1968, **21**, 617.
26. B. R. McGarvey, *J. Phys. Chem.* 1956, **60**, 71.
27. A. Abragam and M. H. L. Pryce, *Proc. Phys. Soc., London* 1951, **206**, 164.
28. B. N. Figgis and J. Lewis, *Prog. Inorg. Chem.* 1964, **6**, 37.

Polyhedron Vol. 4, No. 4, pp. 765–768, 1985
Printed in Great Britain

0277–5387/85 $3.00 + .00
Pergamon Press Ltd

RUTHENIUM(II) COMPLEXES OF 2-(*p*-TOLUIDINO)PYRIDINE AND RHODIUM(III) COMPLEXES OF *N,N'*-DI(2-PYRIDYL)-1,3-DIAMINO-5-CHLOROBENZENE

MATSUO NONOYAMA
Department of Chemistry, Faculty of Science, Nagoya University, Chikusa, Nagoya, 464 Japan

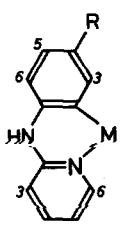
(*Received* 14 *February* 1984; *accepted* 7 *June* 1984)

Abstract—An attempted cyclometallation of 2-(*p*-toluidino)pyridine by dichlorotricarbonylruthenium(II) in refluxing 2-(methoxy)ethanol gave [$RuCl(CO)_2$(tpf)] containing the *N*-(*p*-tolyl)-*N*-(2-pyridyl)-formamide ligand coordinated to the ruthenium atom through the pyridine-N and amide carbonyl-C atoms. On the other hand *N,N'*-di(2-pyridyl)-1,3-diamino-5-chlorobenzene is, as expected, cyclometallated by hexachlorotetrakis(tri-*n*-butylphosphine)dirhodium(III) in refluxing xylene to give [$RhCl_2$(dcb)(PBu_3)], where the dcb is coordinated to the rhodium atom through the two pyridine-N and phenyl-2C atoms forming a fused six-membered metallaheterocycle. Cyclorhodation to form a six-membered metallaheterocycle is a rare example. The ligand H(dcb) is also easily cyclometallated with hexabromotetrakis(tri-*n*-butylphosphine)dirhodium(III) and lithium tetrachloropalladate(II). The adducts of pyridine and tri-*n*-butylphosphine are also prepared and characterized.

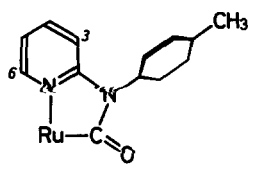
In a previous paper[1] 2-anilinopyridine derivatives

(p-R-C_6H_4–NH–C_5H_4N-2: R = H, CH_3, Cl)

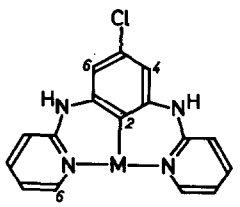
have been reported to be easily cyclopalladated with tetrachloropalladate ion and to form six-membered pallada-heterocycles (partial structure I, M = Pd). Six-membered pallada-heterocycles are not so popular as the corresponding five-membered ones.[2] Therefore, it is interesting to investigate possibility of other metals and other ligands to form similar six-membered metalla-heterocycles. In this paper ruthenium(II) complexes of 2-(*p*-toluidino)pyridine, and rhodium(III) and palladium(II) complexes of *N,N'*-di(2-pyridyl)-1,3-diamino-5-chlorobenzene* have been studied as an extention of the previous study.[1]



I



II



III

RESULTS AND DISCUSSION

The reaction of 2-(*p*-toluidino)pyridine with dichlorotricarbonylruthenium(II) in boiling 2-(methoxy)ethanol gave [$RuCl(CO)_2$(tpf)] (**1**) (data in Table 1). 2-Anilinopyridine gave a similar complex (**4**). The IR spectrum (Nujol mull) of **1** shows no $\nu_{(N-H)}$ band. The spectrum shows $\pi_{(C-H)}$ of a phenyl ring at 809 cm^{-1} (the band is at 811 cm^{-1} for free 2-(*p*-toluidino)pyridine) and lacks the characteristic bands of a 1,2,4-trisubstituted benzene ring which

* H(tpf) = *N*-(*p*-tolyl)-*N*-(2-pyridyl)formamide. H(dcb) = *N,N'*-di(2-pyridyl)-1,3-diamino-5-chlorobenzene.

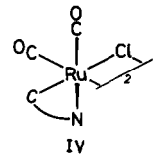
Table 1. Melting points, yields and analytical results for the complexes*

No.	Complex	M.P. (°C)	Yield (%)	Analysis, found(calc.) % C	H	N
1	$[RuCl(CO)_2(tpf)]$	255(dec)	25	44.52 (44.62)	2.64 (2.75)	6.95 (6.94)
2	$[RuCl(CO)_2(tpf)(py)]$	ca. 150	81	49.92 (49.75)	3.58 (3.34)	8.61 (8.70)
3	$[RuCl(CO)_2(tpf)(PBu_3)]$	192-194	64	53.47 (53.51)	6.32 (6.32)	4.87 (4.67)
4	$[RuCl(CO)_2(ppf)]$	256(dec)	ca. 5	43.42 (43.14)	2.32 (2.33)	7.24 (7.19)
5	[PdCl(dcb)]	285(dec)	89	43.75 (43.92)	2.61 (2.76)	12.61 (12.80)
6	$[RhCl_2(dcb)(PBu_3)]$	295(dec)	40	50.17 (50.05)	5.80 (5.85)	8.42 (8.34)
7	$[RhBr_2(dcb)(PBu_3)]$	290(dec)	50	44.21 (44.21)	5.24 (5.17)	7.29 (7.36)
8	$[RhCl(dcb)(PBu_3)(py)]Cl$	290(dec)	74	52.72 (52.78)	5.77 (5.91)	9.37 (9.33)
9	$[RhCl(dcb)(PBu_3)_2]Cl$	265(dec)	43	54.74 (54.96)	7.61 (7.61)	6.43 (6.41)

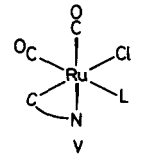
* Abbreviations: H(tpf), *N*-(*p*-tolyl)-*N*-(2-pyridyl)formamide; H(ppf), *N*-phenyl-*N*-(2-pyridyl)formamide; H(dcb), *N*,*N*'-di(2-pyridyl)-1,3-diamino-5-chlorobenzene; PBu_3, tri-*n*-butylphosphine; py, pyridine; dec, decomposition.

are at 814 and 877 cm^{-1} for the cyclopalladated 2-(*p*-toluidino)pyridine complex [PdCl(map)][1] (cf. partial structure I, R = CH_3). The most remarkable band is a very strong absorption at 1663 cm^{-1} and should indicate the presence of an organic carbonyl group (C=O).[3] A strong band at 1024 cm^{-1} also stands out. In the metal–carbonyl region, $\nu_{(C\equiv O)}$, two strong bands at 2066 and 1997 cm^{-1} are observed and coordination of Cl is suggested by two strong bands at 285 and 225 cm^{-1}.

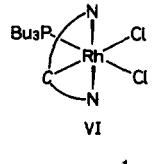
Complex **1** was not soluble in common solvents without donor property but dissolved in dimethylsulphoxide (dmso). The ^1H NMR spectrum of the dmso-d_6 solution (60 MHz vs TMS) shows the signals of phenyl ring protons at δ = 7.13 *d* and 7.45 *d* ppm (the sum of the intensities amounts to 4 H) but it shows no signal due to an N–H group. The spectral pattern is very different from that of [PdCl(map)] (cf. partial structure I) which shows phenyl protons at 6.85 *s* ppm (an intensity of 2 H) and 7.46 *s* (1 H). Thus the possibility of cyclometallation is eliminated and the carbonylation of the amino group to produce an amide group (partial structure II) is suggested. For **1** is proposed structure **IV** (C–N represents the chelate ring of partial structure II). A doublet at 6.53 ppm (1 H) is remarkable and is assigned to 3-H of the pyridine ring because the 3-H is situated nearly above the benzene ring on the amide-nitrogen atom and should be shielded by the ring current. The low



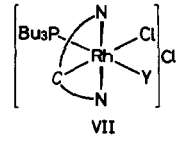
IV



V



VI



VII

frequency $\nu_{(Ru-Cl)}$ bands are consistent with structure **IV**, where the Cl donor is coordinated *trans* to a σ-carbon donor with a strong *trans* influence.[4]

The reaction of **1** with pyridine (py) gave the adduct $[RuCl(CO)_2(tpf)(py)]$ (**2**) (Table 1). The IR

spectrum (CH_2Cl_2 solution) shows two $\nu_{(C\equiv O)}$ bands at 2068 and 1998 cm^{-1} to reveal *cis*-coordination of the two CO groups. The IR and ^1H NMR spectra are essentially similar to those of **1**, except for the signals and bands due to the added pyridine ligand. The coordination mode of partial structure **II** is held and structure **V** (I = py) is proposed for **2**. The tri-*n*-butylphosphine (PBu_3) adduct [RuCl(CO)$_2$(tpf)(PBu_3)] (**3**) (Table 1) shows a very broad $\nu_{(C\equiv O)}$ band at *ca* 1960 cm^{-1}. Distinction between *cis*- and *trans*-coordination of the two CO groups is impossible from the IR spectrum (CH_2Cl_2 solution). The ^{13}C NMR spectrum ($CDCl_3$ vs TMS) gave two signals at 202.5 and 208.6 ppm due to carbonyl groups, although the S/N ratio was not good (the former signal seems to be a doublet (J = *ca* 18 Hz) and the latter a broad singlet). The *cis*-coordination of the two CO groups is suggested [structure **V** (L = PBu_3)]. Low frequency $\nu_{(Ru-Cl)}$ bands at 272 (**2**) and 279 (**3**) cm^{-1} are consistent with structure **V**, where Cl is coordinated *trans* to a σ-carbon donor with a strong *trans* influence.[4]

N,*N*′-di(2-pyridyl)-1,3-diamino-5-chlorobenzene was easily cyclopalladated with lithium tetrachloropalladate to give the complex [PdCl(dcb)] (**5**) (Table 1). The IR spectrum (Nujol mull) shows $\nu_{(NH)}$ at 3343 and 3310 cm^{-1} and $\nu_{(Pd-Cl)}$ at 258 cm^{-1}. The ^1H NMR spectrum (dmso-d_6 vs DSS) shows a singlet of metallated phenyl ring 4,6-protons at 6.89 ppm (an intensity of 2 H) and a signal of amino protons at 10.11 ppm (2 H). In the spectrum, the triplet of the phenyl ring 2-H of free H(dcb) at 7.92 ppm (J = 1.8 Hz) disappeared. Partial structure **III** is proposed for **5** (in **5** the fourth site of coordination of partial structure **III** is occupied by Cl). The doublet of pyridine ring 6-H at 8.32 ppm of free H(dcb) is deshielded in **5** and appears at 9.10 ppm.

The ligand H(dcb) was also cyclometallated with hexachlorotetrakis(tri - *n* - butylphosphine) - dirhodium(III) in refluxing xylene to give [$RhCl_2$(dcb)(PBu_3)] (**6**) (Table 1). The IR spectrum (nujol mull) shows $\nu_{(NH)}$ as a complex pattern in the region 3100–3300 cm^{-1} and two strong bands at 233 and 200 cm^{-1} are assigned to $\nu_{(Rh-Cl)}$. The low frequency bands disappear in the spectrum of [$RhBr_2$(dcb)(PBu_3)] (**7**). The ^1H NMR spectrum (dmso-d_6 vs DSS) is broad and complicated, and difficult to be interpreted. Addition of pyridine to the dmso-d_6 solution simplifies the complex spectral pattern.

The ^1H NMR spectra of dmso-d_6 solutions of **6** and **7** in the presence of excess pyridine-d_5 show a signal of the amino group at 10.72 (**6**) or 10.38 ppm (**7**), a singlet of metallated phenyl ring 4,6-protons at 7.13 (**6**) or 7.12 (**7**), and a doublet (J = 6.4 Hz) of pyridine ring 6-protons at 9.15 (**6**) or 9.25 (**7**). Like **5**, **6** and **7** lack the signal of the phenyl ring 2-proton in the spectra. Structure **VI** for **6** and **7** is proposed (where N–C–N represents the chelate ring corresponding to partial structure **III**: for **7** Cl is replaced with Br).

The isolated complex [RhCl(dcb)(PBu_3)(py)]Cl (**8**) (Table 1) shows a similar IR spectrum to that of **6** with additional bands of the pyridine ligand, but one $\nu_{(Rh-Cl)}$ band is observed at 209 cm^{-1}. This may have structure **VII** (Y = py). A similar tri-*n*-butylphosphine complex [RhCl(dcb)(PBu_3)$_2$]Cl (**9**) gives $\nu_{(Rh-Cl)}$ at 202 cm^{-1} and the ^1H NMR spectrum ($CDCl_3$ vs TMS) is similar to that of the pyridine-d_5 adduct of **6**. A signal of NH is observed at 10.48 ppm, a singlet of phenyl 4,6-protons at 7.32, and a doublet (J = 6.4 Hz) of pyridine ring 6-protons at 9.50 ppm. Structure **VII** (Y = PBu_3) is assumed for **9**.

EXPERIMENTAL

Measurements

The measurements were carried out by the methods reported previously.[5]

Synthesis of the ligands

The method of preparation of 2-(*p*-toluidino)-pyridine was reported previously.[1] *N*,*N*′-di(2-pyridyl)-1,3-diamino-5-chlorobenzene was obtained similarly from 1,3-diamino-5-chlorobenzene and 2-chloropyridine at a yield of 53%. M.p. 159–161°C. Found: C, 64.62; H, 4.34; N, 18.85%. Calc. for $C_{16}H_{13}N_4Cl$: C, 64.76; H, 4.42; N, 18.88%. ^1H NMR (dmso-d_6 vs DSS) δ = 6.73–7.15 ppm (m; py 3,5-H), 7.60 (d, J = 1.8 Hz; Ph 4,6-H), 7.70 (t, 6.4 Hz; py 4-H), 7.92 (*t*, 1.8 Hz; Ph 2-H), 8.32 (d, 4.8 Hz; py 6-H), 9.25 (s; NH). IR (Nujol mull), 3230 and 3175, $\nu_{(NH)}$; other characteristic bands, 1614, 1578, 1290 and 761 cm^{-1}.

Synthesis of the complexes

Melting points, yields and analytical results of the complexes prepared are given in Table 1.

[RuCl(CO)$_2$(tpf)] (**1**). A mixture of 1 mmol of dichlorotricarbonylruthenium(II) and 1 mmol of 2-(*p*-toluidino)pyridine in 30 cm^3 of 2-(methoxy)ethanol was refluxed for 3.5 h. White precipitates formed were collected, washed with ethanol, and dried in air. [RhCl(CO)$_2$(ppf)] (**4**) was similarly prepared from 2-anilinopyridine but only in a low yield. The IR spectral data suggest that this has the structure corresponding to partial structure **II**. IR (Nujol mull) 2060 and 1990, $\nu_{(C\equiv O)}$; 1669, amide $\nu_{(C=O)}$; 285 and 218 cm^{-1}, $\nu_{(Ru-Cl)}$.

[PdCl(dcb)] (**5**). To a solution of lithium tetrachloropalladate, prepared *in situ* from 1 mmol of palladium(II) chloride and 2 mmol of lithium chloride in 30 cm^3 of methanol, was added 1 mmol of *N,N'*-di(2-pyridyl)-1,3-diamino-5-chlorobenzene and the mixture was stirred for 1 h at room temperature. Off-white precipitates were collected, washed with methanol, and dried in air. An attempt to prepare the bromo analogue in the presence of five-fold excess of lithium bromide (that is, lithium tetrabromopalladate was prepared *in situ* from 1 mmol of palladium(II) chloride and 5mmol of lithium bromide in 30 cm^3 of methanol) only resulted in formation of the compound of composition $[PdCl_{0.5}Br_{0.5}(dcb)]$ at a yield of 89%. M.p. 285°C (dec.). Found: C, 41.61; H, 2.50; N, 12.18%. Calc. for $C_{16}H_{12}N_4PdCl_{1.5}Br_{0.5}$: C, 41.79; H, 2.63; N, 12.18%. The spectroscopic properties of $[PdCl_{0.5}Br_{0.5}(dcb)]$ are very similar to those of **5**.

$[RhCl_2(dcb)(PBu_3)]$ (**6**). A mixture of 1/2 mmol of hexachlorotetrakis(tri - *n* - butylphosphine) - dirhodium(III)[6] and 1 mmol of *N,N'*-di(2-pyridyl)-1,3-diamino-5-chlorobenzene in 20 cm^3 of xylene was refluxed for 8 h with stirring to precipitate yellow powder. The product was collected, washed with xylene and *n*-hexane, and dried in air. The yellow bromo analogue (**7**) was prepared similarly by using hexabromotetrakis(tri-*n*-butylphosphine)-dirhodium(III) instead of hexachlorotetrakis(tri-*n*-butylphosphine)dirhodium(III) and the product was recrystallized from acetone.

*Pyridine and tri-*n*-butylphosphine adducts.* Addition of pyridine (excess) or tri-*n*-butylphosphine (a stoichiometric amount) to a dichloromethane suspension of the complexes prepared above gave a clear solution which was then treated with florisil. To the filtrate was added an equivolume of *n*-hexane and the mixture was concentrated to a small volume to crystallize the adduct.

Acknowledgement—I wish to thank Dr Y. Yoshikawa for the measurements of ^{13}C NMR spectra.

REFERENCES

1. M. Nonoyama, *Transition Met. Chem.* 1982, **7**, 281.
2. (a) I. Omae, *Chem. Rev.* 1979, **79**, 287; (b) J. A. Clark and M. Kilner, *J. Chem. Soc., Dalton Trans.* 1983, 2613; (c) G. R. Newkome, W. E. Puckett, V. K. Gupta and F. R. Fronczek, *Organometallics* 1983, **2**, 1247 (and references cited therein).
3. L. J. Bellamy, *The Infrared Spectra of Complex Molecules*, 3rd Edn., p. 241. Chapman and Hall, London (1975).
4. T. G. Appleton, H. C. Clark and L. M. Manzer, *Coord. Chem. Rev.* 1973, **10**, 335.
5. M. Nonoyama, *J. Organomet. Chem.* 1984, **262**, 407.
6. J. Chatt, N. P. Johnson and B. L. Shaw, *J. Chem. Soc.* 1964, 2508.

Polyhedron Vol. 4, No. 4, pp. 769–771, 1985
Printed in Great Britain

0277–5387/85 $3.00 + .00
Pergamon Press Ltd

DIAMINE PLATINUM(II) COMPLEXES OF 2,2′-DIAMINOBIPHENYL

CECILIA RADLOWSKI and CHUI FAN LIU*
Department of Chemistry, University of Illinois at Chicago, Chicago, IL 60680, U.S.A.

and

CHANG HWAN KIM, SUNG-RACK CHOI and MOO-JIN JUN*
Department of Chemistry, Yonsei University, Seoul, Korea

(*Received* 1 *February* 1984; *accepted* 9 *May* 1984)

Abstract—Platinum(II) complexes of 2,2′-diaminobiphenyl, $[Pt(R\text{-}pn)(dabp)]Cl_2$ and $[Pt(R,R\text{-}chxn)(dabp)]Cl_2$, where R-pn is the R-1,2-diaminopropane, R,R-chxn, the R,R-*trans*-1,2-diaminocyclohexane, and dabp the 2,2′-diaminobiphenyl, have been prepared. The dabp ligand has been found to coordinate in the λ conformation.

Investigations involving the 2,2′-diaminobiphenyl ligand have so far been limited to the octahedral cobalt(III) complexes.[1–3] The present work was undertaken to prepare pure chiral square planar platinum(II) complexes of 2,2′-diaminobiphenyl and to correlate their stereochemistry to the observed optical activity.

EXPERIMENTAL

2,2′-*Diaminobiphenyl*

A solution of 8.4 g of 2,2′-dinitrobiphenyl[4] in 200 cm^3 of absolute ethanol was shaken with 1.0 g of 10% palladium on charcoal in a Paar's hydrogenation apparatus. The catalyst was filtered off and the alcohol solution concentrated on a rotary evaporator. After recrystallisation from boiling aqueous ethanol the melting point was 76–78°C (m.p. lit.[4] 78–79°C). Found: C, 78.3; H, 6.5; N, 15.2%. Calc. for $C_{12}H_{12}N_2$: C, 78.2; H, 6.6; N, 15.2%. The yields were usually greater than 90%.

Resolution of 1,2-*diaminopropane*

This was resolved according to the method of Dwyer *et al.*[5] using *d*-tartaric acid. It was then converted to the dihydrochloride according to the procedure of Bailar *et al.*[6]

Resolution of trans-1,2-*diaminocyclohexane*

The method of Asperger and Liu[7] was modified to resolve *trans*-1,2-diaminocyclohexane. Equimolar amounts of *trans*-1,2-diaminocyclohexane and *d*-tartaric acid were dissolved in warm water, and then the two solutions were poured together and stirred. The laevorotatory compound precipitated when the solution was cooled in an ice bath. The R,R-*trans*-1,2-diaminocyclohexane-*d*-tartarate was recrystallized from hot water. It was suspended in ethanol and agitated. HCl gas was allowed to bubble through the mixture. Slowly the salt dissolved and after about one hour white crystals of the dihydrochloride began to form. Addition of HCl gas was continued for another hour. The mixture was cooled, filtered, washed successively with ethanol and ether, and then air dried. It was recrystallized from minimal water. The IR spectrum showed that the R,R-(−)-*trans*-1,2-diaminocyclohexane was free of tartaric acid. $[\alpha]_D = -29.6$. (Lit.[8] $\alpha_D = -26.4$.)

$[Pt(R\text{-}pn)Cl_2]$

This was prepared according to the method used for $[Pr(en)Cl_2]$[9] using R-1,2-diaminopropane in place of ethylenediamine. Found: C, 10.4; H, 2.9; N, 8.3; Cl, 20.8%. Calc. for $Pt(C_3H_{10}N_2)Cl_2$: C, 10.6; H, 3.0; N, 8.2; Cl, 20.8%.

* Authors to whom correspondence should be addressed.

[Pt(*R,R-chxn*)Cl_2]

This was prepared by the same method as that used for [Pt(en)Cl_2][7] using R,R-*trans*-1,2-diaminocyclohexane in place of ethylenediamine. Found: C, 18.9; H, 3.7; N, 7.2; Cl, 18.7%. Calc. for Pt($C_6H_{14}N_2$)Cl_2: C, 19.0; H, 3.7; N, 7.4; Cl, 18.6%.

[Pt(*R-pn*(*dabp*)]Cl_2

0.79 g of [Pt(R-pn)Cl_2] and 0.42 g of 2,2'-diaminobiphenyl were suspended in 500 cm^3 of water in a 1000-cm^3 three-neck flask equipped with a mechanical stirrer, thermometer, and condenser. The mixture was stirred and heated at a temperature of 60–70°C for 8 h. Gradually the suspension dissolved and the solution changed from yellow to almost colourless. The solution was cooled and filtered. It was concentrated on a rotary evaporator until crystallisation occurred. The mixture was placed in an ice bath. The white crystals were collected on a sintered glass funnel, washed successively with ice-cold water, ethanol, ether, and air dried. The product was recrystallized from warm water to which one drop of 3 M HCl was added. Yield: 0.57 g (48%). Found: C, 34.1; H, 4.2; N, 9.9; Cl, 12.6%. Calc. for Pt($C_3H_{10}N_2$)($C_{12}H_{12}N_2$)$Cl_2 \cdot H_2O$: C, 33.2; H, 4.5; N, 10.3; Cl, 13.1%.

[Pt(*R,R-chxn*)(*dabp*)]$Cl_2 \cdot 3H_2O$

Procedure was the same as that used for [Pt(R-pn)(dabp)]$Cl_2 \cdot H_2O$ using R,R-*trans*-1,2-diaminocyclohexane in place of R-1,2-diaminopropane. Yield: 0.47 g (55%). Found: C, 35.1; H, 5.2; N, 9.2; Cl, 11.6%. Calc. for Pt($C_6H_{14}N_2$)($C_{12}H_{12}N_2$)-$Cl_2 \cdot 3H_2O$: C, 34.9; H, 5.2; N, 9.1; Cl, 11.5%.

RESULTS AND DISCUSSION

Figure 1 shows the absorption spectra of [Pt(R-pn)(dabp)]Cl_2 and [Pt(R,R-chxn)(dabp)]Cl_2 along with that of 2,2'-diaminobiphenyl. Since the dabp absorbs very little in the 27.5–31.5 kK region, the intensity in this region of the corresponding Pt(II) complexes can be attributed to charge transfer. The dabp ligand has two very strong π–π^* transitions at 34.2 kK (ε = 5,000) and 41.7 kK (ε = greater than 13,00). The absorption bands at these energies for the platinum complexes probably originate from the π–π^* transitions of the ligand.

Examination of the absorption spectra reveals that for Pt(II) complexes some of the *d–d* transitions are buried under the much stronger charge transfer bands in the long wavelength region and the ligand transitions in the near UV. In the dabp complexes

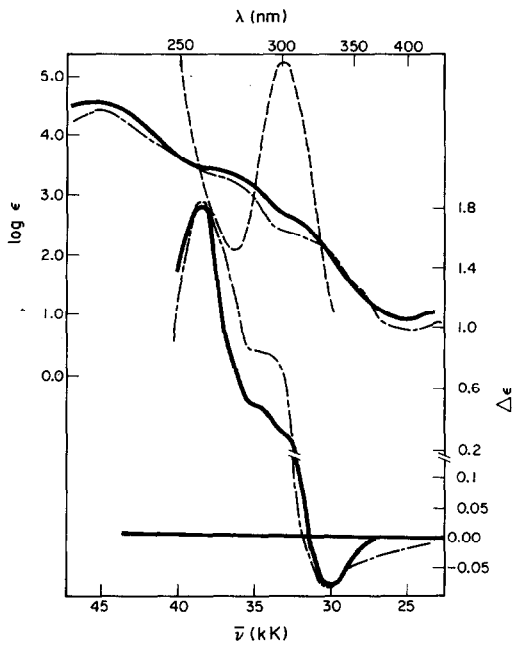


Fig. 1. Electronic absorption spectra of: [Pt(R-pn)(dabp)]Cl_2 (——), [Pt(R,R-chxn)(dabp)]Cl_2 (–·–·–), and electronic absorption spectrum of 2,2'-diaminobiphenyl (– – –).

there is still appreciable intensity in the 22–28 kK region. The bands below 22 kK have been assigned to the $^1A_{1g} \rightarrow {}^3E_g$ and $^1A_{1g} \rightarrow {}^3A_{2g}$ transitions in the $[PtCl_4]^{2-}$ complex.[10] They are weak (log ε less than 1) spin–forbidden transitions. The *d–d* transition of

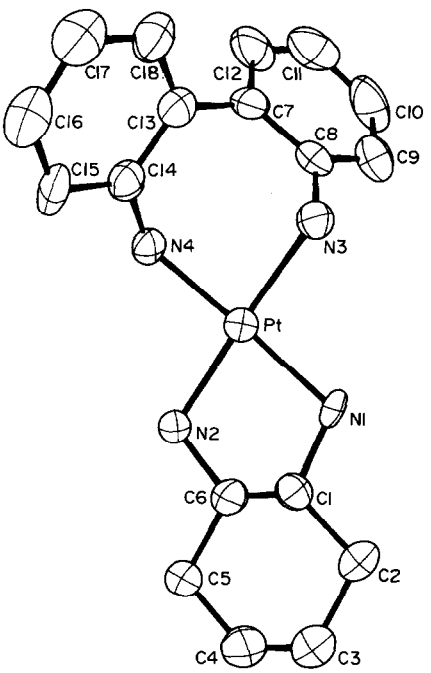


Fig. 2. The molecular structure of the Pt(R,R-chxn)(dabp) unit.

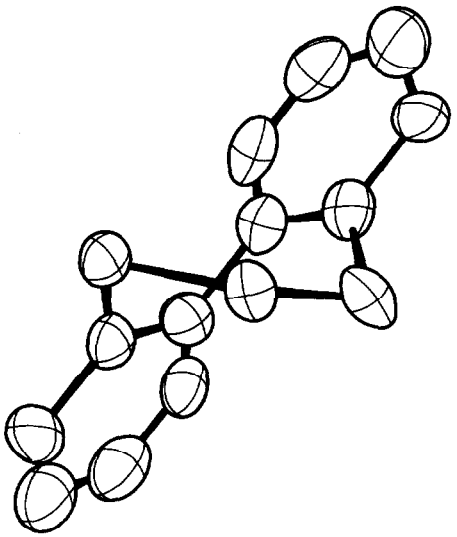


Fig. 3. View through 2,2′-diaminobiphenyl.

the dabp complexes gain intensity through coupling with allowed transitions on the aromatic ligands and charge transfer.

The CD spectrum of $[Pt(R\text{-pn})(dabp)]^{2+}$ and $[Pt(R,R\text{-chxn})(dabp)]^{2+}$ are also seen in Fig. 1. The two spectra are almost identical. Furthermore the intensities are comparable. The R-pn and R,R-chxn ligands should take the λ conformation[11–14] upon coordination to Pt(II) ion. The absolute configuration of $[Pt(R,R\text{-chxn})(dabp)]Cl_2$ has been unambiguously determined from X-ray crystallographic study.[14] As shown in Figs. 2 and 3, the dabp ligand was found to coordinate in the λ conformation. The similarity in the pattern and position of the negative and positive CD bands (Fig. 1) indicates that dabp has the same λ conformation in both complexes. The major contribution to the rotational strength comes from the λ conformation of the two chelate rings in each complex as opposed to the vicinal effect of the asymmetric carbon atom.

The dabp ligand has shown a remarkable stereospecificity upon coordination, considering the fact that statistically there is an equal probability that the freely rotating dabp molecules can assume either the λ or the δ conformation upon complex formation. Such behaviour can be understood from a study using molecular models of R-dabp and S-dabp, λ and δ, respectively, with each of the two Pt(II) complexes. In the diamine complexes containing R-pn and R,R-chxn with R-dabp, the hydrogens on opposing nitrogens are staggered. When the model containing S-dabp is made with those same two ligands in the λ conformation, on the other hand, the hydrogens are almost totally eclipsed. The complete stereospecificity observed should be due to such nonbonded interaction between the hydrogens bonded to nitrogens.

Acknowledgements—Financial support for this work from the National Institute of Health (to CFL) and from the Korea Science and Engineering Foundation (to MJJ) are gratefully acknowledged.

REFERENCES

1. W. Z. Theilacker, *Z. Anorg. Chem.* 1937, **234**, 161.
2. W. T. Jordan, C. Y. Lin and B. E. Douglas, *J. Coord. Chem.* 1973, **3**, 103.
3. T. Tanimura, H. Ito, J. Fujita, K. Saito, H. Hirai and K. Yamasaki, *J. Coord. Chem.* 1973, **3**, 161.
4. N. Kornbulm and D. L. Kendall, *J. Am. Chem. Soc.* 1952, **74**, 5782.
5. F. P. Dwyer, F. L. Garvan and A. Shulman, *J. Am. Chem. Soc.* 1959, **81**, 290.
6. J. C. Bailar, H. B. Jonassen and A. D. Gott, *J. Am. Chem. Soc.* 1952, **74**, 3131.
7. R. G. Asperger and C. F. Liu, *Inorg. Chem.* 1965, **4**, 1492.
8. F. M. Jaeger and J. van Dijk, *K. Ned. Akad. Wet. Proc.* 1936, **B39**, 384; F. M. Jaeger and L. Bijkerk, *K. Ned. Akad. Wet. Proc.* 1937, **40**, 12.
9. G. L. Johnson, *Inorg. Syn.* 1966, **8**, 242.
10. H. Ito, J. Fujita and K. Saito, *Bull. Chem. Soc. Jpn* 1967, **40**, 2548.
11. E. J. Corey and J. C. Bailar, *J. Am. Chem. Soc.* 1959, **81**, 2620.
12. H. Iwasaki and Y. Saito, *Bull. Chem. Soc. Jpn* 1965, **39**, 92.
13. A. Kobayashi, F. Marumo and Y. Saito, *Acta Cryst.* 1972, **B28**, 2709.
14. C. Radlowski, M. Jun and C. Liu, The results of the detailed X-ray crystallographic study will be published elsewhere.

Polyhedron Vol. 4, No. 4, p. 773, 1985
Pergamon Press Ltd. Printed in Great Britain

ERRATUM

J. A. K. Howard, I. D. Salter and F. G. A. Stone, Synthesis and molecular structure of $[Au_3Ru_4(\mu_3\text{-}H)(CO)_{12}(PPh_3)_3$. *Polyhedron* 1984, 3, 567–573.

The publishers regret that the name of the second author of the above article was published incorrectly spelt in the list of authors. His name should have been spelt as follows: Ian D. Salter.

Polyhedron Vol. 4, No. 5, pp. 775–781, 1985
Printed in Great Britain

0277–5387/85 $3.00 + .00
Pergamon Press Ltd

HISTORICAL SKETCH

COS AND C_3S_2: THE DISCOVERY AND CHEMISTRY OF TWO IMPORTANT INORGANIC SULFUR COMPOUNDS

MIHÁLY T. BECK*
Department of Chemistry, Kossuth Lajos University, H-4010 Debrecen, Hungary

and

GEORGE B. KAUFFMAN*
Department of Chemistry, California State University, Fresno, Fresno, CA 93740, U.S.A.

Abstract—Although CO and CO_2 have been known since the dawn of chemistry and although CS_2 was discovered as early as 1796,[1] COS and C_3S_2 were not discovered until 1867 and 1893, respectively. This article considers the circumstances surrounding their discoveries as well as later reports on their chemistries. Both compounds were first prepared by Hungarian chemists, and both are of great theoretical and practical importance. The discovery and preparation of COS by Károly (Karl) Than is a beautiful example of logical chemical thinking, whereas the serendipitous discovery of C_3S_2 by Béla Lengyel is a case study in careful experimentation and keen observation. The sesquicentennial anniversary of the birth of Than, who is regarded as the founder of modern Hungarian chemistry, makes this article of timely significance. Since both he and his student Lengyel and their accomplishments have been neglected by English-speaking chemists and historians of chemistry, they are briefly discussed in this article.

KÁROLY THAN (1834–1908)

Anton Károly Than (Fig. 1), the third son of Janos Than, an estate manager, and his wife Ottilia (née Petény), was born on 20 December 1834 in Óbecse, Hungary (now Bečej, in northeastern Yugoslavia).[2] At the age of fifteen, he enlisted in the Hungarian army during the war of independence (1848–1849) from the Austrian Empire. On returning home at the war's end, he found his mother dead and his father ruined financially. He became apprenticed to pharmacists in several Hungarian towns to earn money while attending school. He completed his secondary school studies in 1855 at Szeged and began to study pharmacy at the University of Vienna in the Faculty of Medicine, but the following year he switched to the Faculty of Liberal Arts to study chemistry. He obtained his doctorate in 1858 under the organic chemist Joseph Redtenbacher (1810–1870), whose personal assistant he became. He spent a *Wanderjahr* studying under Bunsen in Heidelberg and under Wurtz in Paris. Returning to Vienna in 1859, he became an assistant in Redtenbacher's laboratory and a *Privat-Dozent* (unsalaried lecturer) at the university.

By 1860 Hungarian was reintroduced as the language of instruction in Hungarian universities. Because Theodor Wertheim (1820–1864), Professor of Chemistry at the University of Budapest since 1853, was an Austrian and did not have the necessary command of the language, he left to teach at the University of Graz in Austria, and Than was called to Budapest to succeed him. In this post, which he occupied until his retirement in 1908, the year of his sudden and unexpected death on 5 July, Than exerted a great influence on Hungarian science and culture. He served as Director of the Chemistry Laboratory and designed the laboratories of the new Chemical Institute,[3] which opened in 1872, the year of his marriage to Ervina Kleinschmidt, by whom he had five children. He built the institute into an important scientific establishment, which acquired fame throughout Europe, became a model for other institutes, and is still in use today.

* Author to whom correspondence should be addressed.

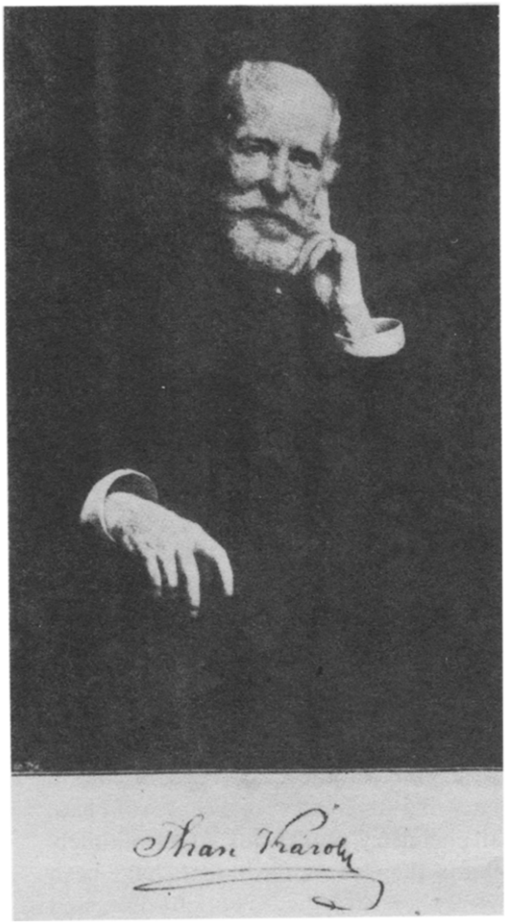


Fig. 1. Károly Than.

Than played a crucial role in the development of the teaching of chemistry in Hungarian universities and was an inspiration to several generations of chemists. He developed a plan for teaching chemistry in Hungarian secondary schools and established the first Pharmacopoeia Hungarica. He founded the Hungarian journal of Chemistry, *Magyar Chémiai Folyóirat*, which is still published today. In 1882, together with his student Loránd (Roland) Eötvös, he founded and edited the *Mathematische und naturwissenschaftliche Berichte aus Ungarn.*

President of the Hungarian Society of Natural Sciences from 1872 until his death, he was active in all of the other Hungarian scientific societies. A recipient of many honors, he was appointed a member of the Upper House of the Hungarian Parliament (House of the Magnates) in 1892 and was made a baron in 1908, shortly before his death.

Than's research embraced many fields of chemistry. His most important work in inorganic chemistry was the discovery of carbon oxide sulfide (COS),[4] but he also investigated platinum complexes[5] and the reaction of metals with alkylene halides.[6] In analytical chemistry he introduced the use of potassium bicarbonate[7] and potassium biiodate[8] as primary titrimetric standards, analyzed numerous mineral waters,[9] and two decades before Arrhenius' theory of electrolytic dissociation suggested that analytical results be reported as the elements rather than as acid or basic anhydrides.[10] In physical chemistry he showed that the anomalous vapor density of ammonium chloride is due to thermal dissociation,[11] he defined the concept of the molar volume of a gas,[12] he made various calorimetric measurements,[13] and he invented various pieces of apparatus.[14] His two-volume textbook, *The Elements of Experimental Chemistry*,[15] was one of the first to be based on concepts of physical chemistry.

COS

The Compromise (in German, *Ausgleich*; in Hungarian, *Kiegyezés*) of 1867 between Austria and Hungary played an important role not only in the history of those two countries and indirectly of all Europe but also in the discovery of carbon oxide sulfide (carbonyl sulfide) as well. In a paper, presented at a meeting of the Hungarian Academy of Sciences on 8 July 1867[4a] and later (dated 20 July 1867) published in German,[4b] Than reported the preparation of COS, which he called carbon oxysulfide (in Hungarian, *szén éleg kéneg*; in German, *Kohlenoxysulfid*) and regarded as the sulfide of the divalent radical CO. For a long time he had presumed the existence of this gaseous compound on the basis of the tetravalent nature of the carbon atom and the existence of the long known compounds carbon dioxide (CO_2) and carbon disulfide (CS_2), between whose compositions the composition of the new compound represents the mean. He also regarded the compound as CO_2 in which one atom of oxygen has been replaced by its congener, sulfur.

The Hungarian Compromise resulted in the imperial and royal Dual Monarchy (*kaiserliche und königliche Doppelmonarchie*) in which an Austrian and a Hungarian half coexisted in equal partnership. It was followed on 8 June 1867 in Buda by the crowning as King of Hungary of the Hapsburg ruler Franz Joseph I, who had been Emperor of Austria since 1848. The connection between this historic event and the discovery of COS is mentioned by Than in the Hungarian but not the German version of his paper:

> About one and half years ago I had already undertaken experiments which, at least partially, proved by guess [of the existence of COS]; however, because of my numerous other activities I was forced to interrupt these experiments until finally the coronation holidays made their successful continuation again possible.[4a]

Also, in the Hungarian version only, he states:

I do not want to bore the Honorable Academy with the enumeration of all those unsuccessful experiments which I have made in order to produce this compound.

Than first prepared COS by leading a mixture of carbon monoxide and excess sulfur vapor through a weakly glowing porcelain tube:

$$CO + S \rightarrow COS.$$

He obtained a "not insignificant" (*nicht unerheblich*) yield of the new compound, but always contaminated with much carbon monoxide, from which it could not be separated. Higher temperatures did not increase the yield because COS thermally decomposes into CO and S.*

Than prepared pure COS by the acid hydrolysis of thiocyanic acid

$$HSCN + H_2O \rightarrow COS + NH_3$$

analogous to the hydrolysis of cyanic acid

$$HOCN + H_2O \rightarrow CO_2 + NH_3.$$

He accomplished this by adding enough powdered KSCN to a cold mixture of 5 volumes of concentrated H_2SO_4 and 4 volumes of H_2O so that the mass remained fluid:

$$KSCN + 2H_2SO_4 + H_2O \rightarrow COS + KHSO_4 + NH_4HSO_4.$$

The evolution of gas began of its own accord, and the rate was controlled by warming or cooling the reaction vessel. The by-products, HCN, H_2O vapor, and CS_2 were removed by passing the product through HgO, chips of unvulcanized rubber, and $CaCl_2$, respectively, and the pure COS was collected over mercury, with which it does not react when dry. Klason[17] later modified this procedure to increase the yield (75%) and used triphenylphosphine to remove the CS_2. Later workers substituted NH_4SCN for KSCN.[18]

Although the discovery of COS is generally attributed to Than,[19,20] the fact that he determined its physical properties and chemical reactions is often overlooked. Than noted its smell (aromatic and similar to carbonated sulfur-containing mineral waters, e.g. those of the Harkány† and Parád springs, but not unpleasant) and the taste of its saturated solution (decidedly sweet with a peculiar pungent sulfur taste, similar to H_2S and H_2SO_3). He determined its density (2.1046 compared to air = 1.0000), molecular weight (60.61), acidity (weaker than CO_2), combustibility (complete combustion yields CO_2 and SO_2; incomplete combustion yields CO_2 and S; some mixtures with air are explosive), and thermal decomposition into CO and S, which he used to analyze the compound. He noted that the gas is absorbed by metal hydroxide solutions, and since such solutions, which are odorless, yield CO_2 and H_2S on acidification, he postulated the following absorption reaction:

$$COS + 4KOH \rightarrow K_2CO_3 + K_2S + 2H_2O.$$

He also observed the reaction of COS with various reagents and attempted unsuccessfully to isolate carbon monosulfide, CS. He acknowledged the assistance of his students Béla Lengyel and Loránd Eötvös in the work on COS. Gas phase reactions for the formation and decomposition reactions of COS are shown in Fig. 2.

Than did not continue to work with COS but left the investigation of its chemistry to his students, who studied it for several decades. For example, the kinetics of its hydrolysis in aqueous solution was thoroughly studied by Buchböck.[22]

Although interest in the new compound remained limited for many years, the number of articles dealing with this theoretically and industrially important gas has increased tremendously during the last two decades[20] (Fig. 3). This renaissance of interest in the chemistry of COS is due primarily to four reasons. (1) As a triatomic molecule consisting of three different atoms, it is ideal for spectroscopic investigations. (2) For the same reason the study of its reactions in the

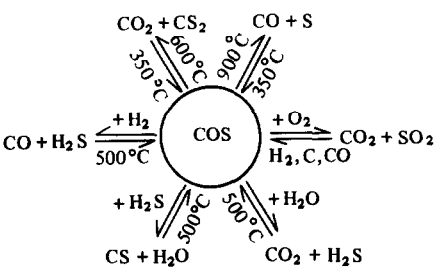


Fig. 2. Gas phase reactions for the formation and decomposition reactions of COS (Ref. 2, p. 40).

* Recent patents have been based on this reaction. For example, CO is led over a mixture of molten sulfur and Na_2S or K_2S at 300–400°C, and the product is obtained in yields > 95% after purification by being led over FeS, CoS, WS_2 or SnS at 250–450°C.[16a] CO is bubbled through molten sulfur at 300–440°C, and the mixture is reacted at 510–650°C. After removing unreacted sulfur, the yield of COS is 97.7%.[16b]

† Than soon discovered COS in Harkány mineral water.[21] He also predicted its occurrence in volcanic gases. Modern analytical techniques have revealed that COS is almost invariably formed whenever organic sulfur compounds are oxidized.

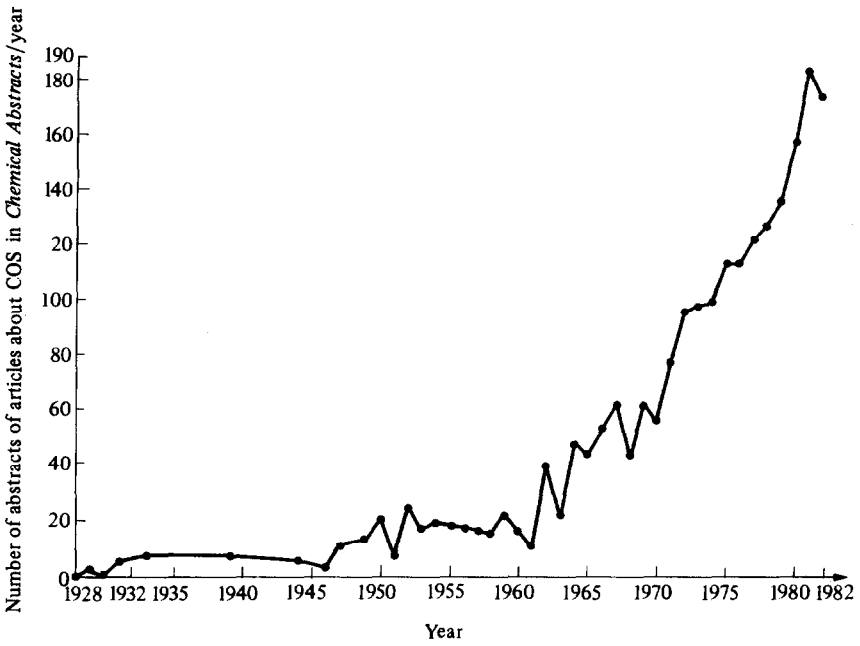


Fig. 3. Number of articles about COS in Chemical Abstracts (1928–1982).

gaseous phase, including photochemical reactions, offers a possibility for a deeper understanding of the details of reactions on a molecular level. (3) Sophisticated analytical methods have revealed that it occurs ubiquitously, e.g. in industrial wastes, cigarette smoke, and biological materials. (4) It is an excellent and versatile raw material for a number of industrially important reactions.

The first steps toward the application of COS to industrial processes were made by Than's students. For example, Izidor Weiser[23] described the reaction between carbon oxide sulfide and aniline:

$$2C_6H_5NH_2 + COS \rightarrow O{=}C(NHC_6H_5)_2 + H_2S$$

and its analogous reactions with toluidine ($CH_3C_6H_4NH_2$) and xylidene ($(CH_3)_2C_6H_3NH_2$). Furthermore, István Weiser and Emil Wolf[24] discovered that is today probably the most important reaction of COS, viz. its reaction with primary and secondary amines to give sulfur-containing organic compounds. Wolf, who founded Chinoin, Hungary's second largest pharmaceutical company, which still is in operation today, was interested in the practical applications of this type of reaction. However, at that time and even for several decades thereafter the compounds produced in these reactions found no practical applications. Today COS is widely used in manufacturing herbicides and pesticides and as a reactant or catalyst in polymerization reactions.

Whereas the discovery of COS is an excellent case study in logical chemical thinking, tricarbon disulfide (C_3S_2) was discovered serendipitously[25] by the careful experimentation and keen observation of Than's former student Béla Lenyel.

BÉLA LENGYEL (1844–1913)

Béla Lengyel (Fig. 4), a distant relative, student and later colleague of Károly Than's, was born on 4 January 1844 in Körösladány, Hungary.[26] In 1865 he began his university studies at Budapest where he became Than's assistant. In 1868 he made a study tour of Heidelberg, where he was Bunsen's assistant, and he became a *Privat-Dozent* (unsalaried lecturer) at the University of Budapest, where he became Professor of the second chair of chemistry in 1872 (Than was Professor of the first chair). Lengyel lectured on general, pharmaceutical and organic chemistry. In 1889 Vol. 1 of Lengyel's textbook on chemistry[27] appeared, which resulted in a bitter, public fight with his former mentor Than, who accused him of plagiarism (the battle was fought in the pages of Hungarian newspapers). A member of the Hungarian Academy of Sciences and an excellent experimenter and artistic glassblower, Lengyel died in Budapest on 11 March 1913.

Like Than, Lengyel carried out thousands of analyses of mineral waters.[28] He was particularly



Fig. 4. Béla Lengyel.

interested in the effects of light and electricity on chemical reactions. He studied the action of metals and gases on photographic plates and found that the effect is due to the reducing action of the hydrogen evolved.[29] He was the first to prepare and characterize calcium hydride[30] and to prepare metallic calcium in large quantites—by electrolysis of anhydrous calcium chloride.[30] He exhibited this calcium at the Paris Universal Exposition in 1900.

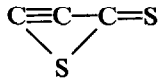
Lengyel prepared what he called "radioactive barium".[31] He fused uranium nitrate with 2–3% of barium nitrate, which he converted by heating to the oxide, fused in an electric arc and dissolved in nitric acid. Barium sulfate, carbonate, and chloride prepared from this barium nitrate was found to be strongly radioactive. Lengyel believed that this "synthesis" of radioactive substances, although preliminary, rendered doubtful the existence of radium and polonium recently discovered by the Curies. He also discovered a new amine of acetone, improved Bertram Boltwood's mercury air pump, and devised a titrimetric determination for nitrous acid. He designed a number of spectacular lecture demonstrations, one of which led to his discovery of what he called tricarbon disulfide.

C_3S_2

While preparing a demonstration of the formation of carbon disulfide, Lengyel observed the formation of a new substance when CS_2 vapors were passed through an electric arc with carbon electrodes.[32] The CS_2 solution became black, and after filtration and distillation *in vacuo* Lengyel obtained a cherry-red liquid with a remarkably strong odor, which caused great irritation to the eyes and mucous membrane. He removed free sulfur from the liquid by allowing it to stand over metallic copper for 6–8 days and then evaporating it with a current of dry air. Analysis showed the deep red liquid to have the composition C_3S_2,*† and Lengyel showed it to be monomeric by cryoscopically determining its molecular weight in benzene solution. The compound was later prepared by the thermolysis of CS_2 streaming through a quartz tube heated to 900–1100°C.[34]

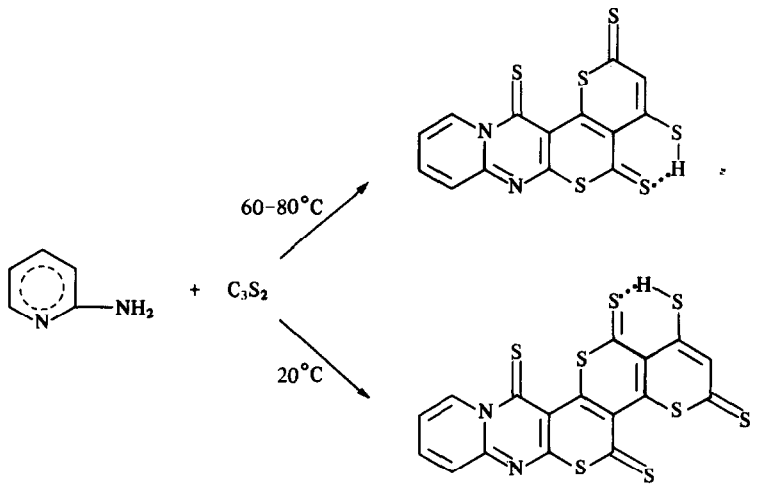
Lengyel determined the physical properties of C_3S_2 (e.g. density = 1.27389 g ml^{-1}) and studied almost all of its known chemical reactions. He found that even at room temperature it slowly polymerizes to a hard, black solid; the rate of polymerization increases sharply with increasing temperature, and rapid heating causes polymerization with explosive violence. The liquid is immiscible with water but readily dissolves in ethanol, ether, chloroform, benzene and carbon disulfide. It burns with a luminous, smoky flame and yields carbon dioxide and sulfur dioxide. Concentrated sulfuric acid causes violent hissing and conversion to the solid modification, which is insoluble in water and all ordinary solvents. However, the polymer dissolves completely in aqueous potassium hydroxide, from which it is reprecipitated unchanged on addition of acid. It decomposes on heating with formation of sulfur.

Lengyel found that when bromide is added to a solution of C_3S_2 in chloroform, heat is evolved, and an aromatic-smelling, yellow precipitate, $C_3S_2Br_2$, insoluble or only slightly soluble in all solvents, is formed. Based on the reaction of this compound, whose structure is still unknown, with silver(I) oxide, he concluded that the bromide derivative has an unsymmetrical structure and that therefore C_3S_2 has the structure



* Several names have been given to this compound. *The Gmelin Handbuch der Anorganischen Chemie*, 8th edn, System No. 14, Part D4, pp. 1–7. Springer, Berlin (1977), which devotes only 6 pp. to the chemistry of this compound and its polymer, lists it as tricarbon disulfide, the name given to it by Lengyel. Its commonest, but ambiguous, name is carbon subsulfide, while *Chem. Abstr.* lists it as 1,2-propanediene-1,3-thione.

† Tricarbon disulfide, C_3O_2, the oxide analogue of C_3S_2, was later discovered by Otto Diels, of Diels–Alder fame, and Bertram Wolf,[33] but they neither mentioned the analogy nor referred to Lengyel's paper.



rather than the linear structure S=C=C=C=S.[35] Later structural determinations, however, have shown C_3S_2 to possess the symmetrical structure.[36] Reaction of chlorine with C_3S_2 yields a compound of the composition $C_3S_2Cl_4$.[37]

In the nine decades following Lengyel's discovery of C_3S_2 only a few studies of the compound were made. In a recent excellent review on conjugated inorganic carbon-based polymers only a few paragraphs are devoted to this compound.[38] At present only one or two articles dealing entirely or partially with the chemistry of C_3S_2 are published annually. However, there is some indication that an exponential increase in research on monomeric and polymeric C_3S_2, similar to that which had occurred with COS, may be about to begin. We predict three main areas for future research. (1) C_3S_2 is a promising reagent for producing highly condensed sulfur-containing compounds. For example, the reactions shown above take place with 2-amino-pyridine.[39] (2) C_3S_2 reacts with different transition metal complexes and is captured in the coordination sphere of the central ion.[40] Some of these complexes may have interesting catalytic properties. (3) The electrical conductivity of doped and undoped C_3S_2 polymers certainly deserves a thorough study, the results of which may contribute to the harnessing of solar energy.

The low yields in cumbersome procedures in the various syntheses of C_3S_2 may further delay the study and application of this intriguing compound. However, it is possible that the polymeric modification may be prepared in a simpler way by heating mixtures of graphite and sulfur. In 1961 different carbon- and sulfur-containing solids were obtained by heating a mixture of anthracene and sulfur.[41] This result was corroborated, together with a measurement of the relatively high electrical conductivity of the solids with higher sulfur content.[42] These species are probably related to polymeric C_3S_2.

Acknowledgements—We wish to thank Yoli Luna, Mary Lou Cancio, Robert Michelotti, George McCann and Prof. Elemer Nagy of the California State University, Fresno for technical assistance and Dr Béla Legyel, himself a chemist and a member of the Hungarian Academy of Sciences, for the photograph of his grandfather. One of us M.T.B.) acknowledges the Council for the International Exchange of Scholars (CIES) for a Fulbright Senior Scholarship (academic year 1983/1984) which made possible the collaboration resulting in this article.

REFERENCES

1. W. A. Lampadius, *Neues J. Physik Gren.* 1796, 306.
2. For details of Than's life and work see F. von Konek-Norwall, *Chem. Ztg* 1908, **32**, 673; F. Szabadváry, In C. C. Gillispie (Editor), *Dictionary of Scientific Biography*, Vol. XIII, pp. 298–299. Charles Scribner's Sons, New York (1976); *History of Analytical Chemistry*, pp. 252–254 and 361. Pergamon Press, Oxford (1966); *Than Károly*. Akadémiai Kiadó, Budapest (1972) (in Hungarian); J. R. Partington, *A Text-book of Inorganic Chemistry*, 6th edn, pp. 115 and 634. Macmillan, London (1950); G. B. Kauffman, *J. Chem. Educ.*, in press.
3. K. Than, *Das chemische Laboratorium der königlichen Univesität in Pest*. Braunmüller, Vienna (1872).
4. K. Than, (a) *Akadémiai Ertekezések* 1867, 3 (in Hungarian); (b) *Annalen* 1867, Suppl. V, 236 (in German).
5. C. Than, *Ann.* 1858, **107**, 315. See also D. F. Evans, D. Jones and G. Wilkinson, *J. Chem. Soc.* 1964, 3167.
6. C. von Than and J. A. Wanklyn, *J. Chem. Soc.* 1859, **12**, 258.
7. K. Than, *Math. Naturwiss. Ber. Ungarn* 1889, **6**, 127.
8. K. Than, *Kir. Magyar Természettud. Társ. Közlönye*

1860, **1**, 67 (in Hungarian); *Math. Naturwiss. Ber. Ungarn* 1890, **7**, 298 (in German).
9. C. Than, *Tschermaks Mineral. Petrog. Mitt.* 1890, **11**, 487.
10. K. Than, *Gyógyszerészi Hetilap* 1865, **4**, 1, 33, 81, 97 (in Hungarian); *Sitzber. Wiener Akad.* 1865, **51** (II), 347 (in German); Z. Szőkefalvi-Nagy and F. Szabadváry, *Talanta* 1966, **13**, 503.
11. K. Than, *Ann.* 1864, **131**, 129.
12. K. Than, *Math. Naturwiss. Ber. Ungarn* 1887, **4**, 161.
13. C. von Than, *Ber.* 1877, **10**, 947; *Wiedemanns Ann. Phys.* 1881, **13**, 84; 1881, **14**, 393.
14. C. von Than, *Ber.* 1882, **15**, 2790; *Z. Phys. Chem.* 1896, **20**, 307.
15. K. Than, *A kisérleti chemia elemei.* Magyar Tudományos Akadémia, Budapest, Vol. 1 (1897), Vol. 2 (1906).
16. (a) S. Kanazawa, S. Ogawa, S. Matsui and M. Shimizu, Ihara Chemical Industry Co. Ltd, Japanese Patent 7227632 (1970–1972); *Chem. Abstr.* 1973, **78**, 60314; (b) K. Hirao, S. Matsui, M. Shimizu and N. Takahashi, Ihara Chemical Industry Co. Ltd, U.S. Patent 4250156 (10 February 1981); *Chem. Abstr.* 1981, **94**, 177530.
17. P. Klason, *J. Prakt. Chem.* 1887, **36**, 64.
18. H. Gamsjäger, *Berg- Hüttenmänn. Monatsh. Montan. Hochsch. Leoben* 1963, **108**, 240; H. Horn, Dissertation, Eidgenössische Technische Hochschule, Zürich (1951).
19. R. J. Ferm, *Chem. Rev.* 1957, **57**, 621.
20. *Gmelin Handbuch der Anorganischen Chemie*, 8th edn, System No. 14, Part D5, pp. 2–141. Springer, Berlin (1977) devotes 140 pp. to this compound.
21. K. Than, *Akadémiai Ertekezések* 1867/70, **1**, XIV.
22. G. Buchböck, *Z. Physik. Chem.* 1900, **34**, 229, 242.
23. I. Weiser, *A carbonylsulfid néhány új reactiojáról.* Dissertation, University of Budapest, Budapest (1897).
24. I. Weiser and E. Wolf, *Magy. Chém. Foly.* 1908, **14**, 134.
25. For other cases of chemical and pharmaceutical serendipity see, for example, G. B. Kauffman, *J. Chem. Educ.* 1975, **52**, 155, 777; 1977, **54**, 753; 1979, **56**, 35, 454; *Chemistry* 1978, **51**(7), 11; *Educ. Chem.* 1980, **17**, 180; 1982, **19**, 168; 1984, **21**, 42; G. B. Kauffman and P. M. Priebe, *Ambix* 1978, **25**, 191.
26. For details of Lengyel's life and work see Z. Szőkefalvi-Nagy, *Béla Lengyel*, Akadémiai Kiadö, Budapest (1983).
27. B. Lengyel, *Chem. Tankönyv a felső tanintézetek számara*, Vol. 1. Budapest (1889). Vol. 2 was never published.
28. For example, B. von Lengyel, *Földt. Közl.* 1893, **23**, 293; 1898, **28**, 229, 280; *Jahrb. Min.* 1895, **i**, ref. 66.
29. B. von Lengyel, *Wiedemanns Ann. Phys.* 1898, **66**, 1162; *Jahresber. Fortschr. Chem.* 1898, 152.
30. B. von Lengyel, *Math. Naturwiss. Ber. Ungarn* 1898, **14**, 180; *Chem. Centr.* 1898, **ii**, 262.
31. B. von Lengyel, *Ber.* 1900, **33**, 1237.
32. B. von Lengyel, *Ber.* 1893, **26**, 2960 (in German); *Mathematikai es Termeszettudomanyi Ertekezések* 1893/1894, **12**, 55 (in Hungarian).
33. B. Wolf, *Ber.* 1906, **39**, 689.
34. A. Stock and P. Praetorius, *Ber.* 1912, **45**, 3568.
35. B. Lengyel, *Mathematikai es Termeszettudomanyi Ertekezések* 1893/1894, **12**, 247.
36. A. O. Diallo, *Comptes Rendus* 1965, **261**, 5386; *Can. J. Chem.* 1968, **46**, 2641; W. H. Smith and G. E. Leroi, *J. Chem. Phys.* 1966, **45**, 1778; K. Ramaswamy and K. Srinivasan, *J. Mol. Struct.* 1969, **3**, 473; T. R. Dyke, W. Klemperer, A. P. Ginsberg and W. E. Falconer, *J. Chem. Phys.* 1972, **56**, 3993.
37. E. Chengeri-Papp, *Magy. Chém. Foly.* 1895, **1**, 161.
38. I. V. Krivosej and V. M. Skorobogatov, *Usp. Khim.* 1981, **50**, 746 (in Russian); *Russ. Chem. Rev.* 1981, **50**, 397 (in English).
39. W. Stadlbauer, T. Kappen and E. Ziegler, *Z. Naturforsch.* 1980, **B33**, 89.
40. A. P. Ginsberg and W. Silverthorn, *Chem. Commun.* 1969, 823.
41. H. Akamato and I. Inokuchi, *Symposium on Electrical Conductivity of Organic Solids*, p. 277. Interscience, New York (1961).
42. B. A. Bolto, D. E. Weiss and D. Willis, *Australian J. Chem.* 1965, **18**, 487.

Polyhedron Vol. 4, No. 5, pp. 783–785, 1985
Printed in Great Britain

0277–5387/85 $3.00 + .00
Pergamon Press Ltd

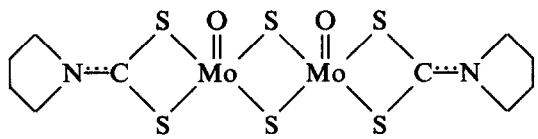
THE UNEXPECTED DECARBONYLATION OF A MOLYBDENUM(0) DITHIOCARBAMATE AND THE FORMATION OF A MOLYBDENUM(V) DIMERIC PRODUCT: CRYSTAL STRUCTURE OF DI-μ-SULFIDO-BIS[OXO(PYRROLIDINEDITHIOCARBAMATO)MOLYBDENUM(V)]

E. C. ALYEA,* G. FERGUSON,* M. PARVEZ and A. SOMOGYVARI
(GWC)[2], Guelph Campus, University of Guelph, Guelph, Ontario, Canada N1G 2W1

(*Received* 3 *March* 1984; *accepted* 9 *May* 1984)

Abstract—The interaction of molybdenum hexacarbonyl with ammonium pyrrolidinedithiocarbamate in warm dimethylsulfoxide solution gives not the expected complex $[NH_4][Mo(CO)_4(S_2CN(CH_2)_4)]$ but the molybdenum(V) dimer, di-μ-sulfido-bis[oxo(pyrrolidinedithiocarbamato)molybdenum(V)]. The structure of this oxidized product $[MoO(S_2CN(CH_2)_4)S]_2$ (1) was determined by single-crystal X-ray diffraction analysis. The crystals are triclinic, space group $P\bar{1}$ with two molecules in a unit cell of dimensions $a = 8.775(1), b = 16.592(2), c = 6.661(1)$ Å, $\alpha = 97.67(1), \beta = 97.89, \gamma = 80.23(1)°$. The structure was solved by the heavy-atom method and refined by block-diagonal least-squares calculations to $R = 0.037$ for 3772 observed data. In the binuclear complex the two Mo atoms are bridged via two S atoms [Mo–S 2.303–2.317(1) Å]. Each Mo atom is also coordinated by a terminal O atom [1.688(4) and 1.682(4) Å] and two S atoms from the bidentate ligand [Mo–S 2.455–2.475(1) Å]. The geometry around the metal atoms is distorted square pyramidal.

Dithiocarbamate complexes of high oxidation states of molybdenum(IV, V, VI) are numerous and their chemistry has been widely studied due to their possible relevance to naturally occurring molybdenum–sulfur systems.[1] In contrast, molybdenum(0) dithiocarbamates have not been isolated, though their existence in dimethyl sulfoxide solution has recently been shown by their IR spectra in the carbonyl stretching frequency region.[2] During our studies to identify a wider range of zero-valent molybdenum complexes of the type $[Mo(CO)_4(L—L)]^-$ (L—L = dithiocarbamato, xanthato, and phosphorodithioato anions) *via* ^{95}Mo NMR spectroscopy[3] we observed that decarbonylation occurs in the reaction of ammonium pyrrolidinedithiocarbamate with molybdenum hexacarbonyl in warm DMSO solution. This paper reports the unexpected formation of a molybdenum(V) dimeric (1) product and its structural elucidation by X-ray analysis.



(1)

EXPERIMENTAL

Preparation of di-μ-sulfido-bis[oxo-(pyrrolidinedithiocarbamato)molybdenum(V)] $[MoO(S_2CN(CH_2)_4)S]_2$

Ammonium pyrrolidinedithiocarbamate (0.62 g, 3.8 mmol) was added under dinitrogen to a dimethylsulfoxide solution (50 cm^3) of molybdenum hexacarbonyl (1.0 g, 3.8 mmol). The reaction mixture was heated to 60–65° for 40 min, and upon cooling a few crystals precipitated from the solution. An X-ray crystal structure determination established the dimeric molybdenum(V) formulation of the title solid product. Infrared and ^{95}Mo NMR

* Authors to whom correspondence should be addressed.

spectroscopy of the solution indicated the absence of carbonyl species such as $[NH_4][Mo(CO)_4(S_2CN(CH_2)_4)]$. This latter complex is identified in solution [IR carbonyl bands at 1995, 1871, 1841 and 1795 cm^{-1}; $\delta(^{95}Mo) = -1388$ ppm (DMSO)][3] if the reaction is performed using potassium pyrrolidinedithiocarbamate or by changing the solvent to N-methylpyrrole.

Crystal data. $C_{10}H_{16}Mo_2N_2O_2S_6$, $M_r = 580.5$, triclinic, $a = 8.775(1)$, $b = 16.592(2)$, $c = 6.661(1)$ Å, $\alpha = 97.67(1)$, $\beta = 97.89(1)$, $\gamma = 80.23(1)°$, $V = 940.58$ Å^3, $D_c = 2.05$ g cm^{-3}, $Z = 2$, $F(000) = 572$, Mo-K_α radiation, $\lambda = 0.71069$ Å, μ(Mo-K_α) = 19.48 cm^{-1}. Space group $P\bar{1}$.

Structure solution and refinement. Data were collected to a maximum θ of 27° on an Enraf–Nonius CAD4 diffractometer by the $\omega/2\theta$ scan technique using monochromatized Mo-K_α radiation. Following machine location and centering of 25 reflections with θ in the range $10 < \theta < 15°$, accurate cell constants and the orientation matrix were obtained by a least-squares refinement. A total of 4094 reflections were collected of which 3772 had intensities greater than $3\sigma(I)$ and were used in structure solution and refinement. The intensities of three standard reflections monitored at regular intervals did not change significantly over the period of data collection. The data were corrected for Lorentz and polarization factors but not for absorption.

The structure was solved by the heavy-atom method. Initial refinement[4] by block-diagonal least-squares calculations with isotropic temperature factors for the non-hydrogen atoms lowered R to 0.110 which further dropped to 0.042 after six cycles of anisotropic refinement. A difference map calculated at this stage revealed maxima corresponding to the 16 hydrogen atoms which were included in the subsequent refinement in geometrically idealized positions (C—H 1.08 Å), and an overall isotropic thermal parameter (0.085 Å^2) was assigned to the hydrogen atoms. In the final cycles of refinement, weights were derived from counting statistics. Scattering factors used in the structure factor calculations were taken from ref. 5 for non-hydrogen atoms and ref. 6 for hydrogen atoms and allowance was made for anomalous dispersion.[7] Refinement converged with $R = 0.037$ and $R_w = [\Sigma w\Delta^2/\Sigma wF_o^2]^{1/2} = 0.045$. A difference map calculated at the conclusion of the refinement showed no significant features. Tables of atomic positional parameters and anisotropic thermal vibrational parameters each with estimated standard deviations, calculated hydrogen coordinates, molecular dimensions and observed structure amplitudes and calculated structure factors have been deposited.*

RESULTS AND DISCUSSION

Ionic complexes of the type [Cat][Mo(CO)$_4$ L—L] (Cat = Na, K, NH_4; L—L = dithiocarbamato, xanthato, phosphorodithioato) are not isolable but can be identified in DMSO solution by IR[2] and ^{95}Mo NMR[3] spectroscopy. In the reaction of ammonium pyrrolidinedithiocarbamate with molybdenum hexacarbonyl in warm DMSO solution, however, we do not observe the four infrared carbonyl bands and ^{95}Mo NMR chemical shift near −1400 ppm that is expected for the $[Mo(CO)_4(S_2CN(CH_2)_4)]^-$ anion. The crystals which precipitated from the reaction mixture are shown by our X-ray analysis to be a binuclear molybdenum(V) complex of a well known type $[(MoO(L—L))_2O_{2-x}S_x]$ ($x = 0$, 1, 2).[8–13] The mechanism of decarbonylation is unknown, though both ammonium ion and dimethylsulfoxide participation are implicated since the reaction does not occur in their absence. Previous examples[8–13] of molybdenum(V) dimers of this type were prepared from Mo(V) and Mo(VI) precursors.

The crystal structure of $[MoO(S_2CN(CH_2)_4)S]_2$ (**1**) consists of dinuclear molecules wherein Mo atoms are linked through a di-μ-sulfido bridge and the molecules have approximate mirror symmetry. A stereoview of the molecule drawn by the Graphics component of the NRC-Crystal Structure Package[4] showing the geometry of the complex is given in Fig. 1. The geometry around each Mo atom is distorted square pyramidal with four S atoms forming the distorted square planes. The Mo atoms lie above the

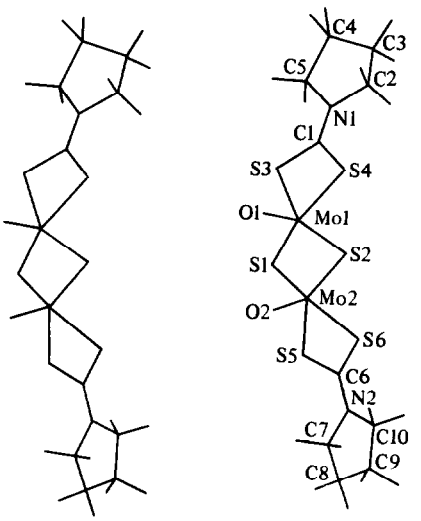


Fig. 1. A stereoview of $[MoO(S_2CN(CH_2)_4)S]_2$ (**1**).

* Copies are avilable on request from the Editor. Atomic co-ordinates have also been deposited at the Cambridge Crystallographic Data Centre.

Table 1. Important molecular dimensions

		Bond distances (Å)			
Mo(1)—S(1)	2.314(1)	Mo(1)—O(1)	1.668(4)	Mo(2)—S(6)	2.455(2)
Mo(1)—S(2)	2.312(1)	Mo(2)—S(1)	2.317(1)	Mo(2)—O(2)	1.682(4)
Mo(1)—S(3)	2.475(1)	Mo(2)—S(2)	2.303(1)	Mo(1) ... Mo(2)	2.803(1)
Mo(1)—S(4)	2.464(1)	Mo(2)—S(5)	2.462(2)		
		Bond angles (°)			
S(1)—Mo(1)—S(2)	100.48(5)	O(1)—Mo(1)—S(4)	108.9(1)	O(2)—Mo(2)—S(5)	106.8(1)
S(1)—Mo(1)—S(3)	86.14(5)	S(1)—Mo(2)—S(2)	100.68(5)	O(2)—Mo(2)—S(6)	105.0(1)
S(1)—Mo(1)—S(4)	137.55(5)	S(1)—Mo(2)—S(5)	83.89(5)	Mo(1)—S(1)—Mo(2)	74.47(4)
S(2)—Mo(1)—S(3)	145.88(5)	S(1)—Mo(2)—S(6)	143.12(6)	Mo(1)—S(3)—C(1)	87.8(2)
S(2)—Mo(1)—S(4)	82.16(5)	S(2)—Mo(2)—S(5)	140.12(6)	Mo(1)—S(4)—C(1)	88.1(2)
S(3)—Mo(1)—S(4)	71.17(4)	S(2)—Mo(2)—S(6)	83.44(5)	Mo(1)—S(2)—Mo(2)	74.80(4)
O(1)—Mo(1)—S(1)	110.3(1)	S(5)—Mo(2)—S(6)	71.05(5)	Mo(2)—S(5)—C(6)	86.7(2)
O(1)—Mo(1)—S(2)	107.9(1)	O(2)—Mo(2)—S(1)	107.9(2)	Mo(2)—S(6)—C(6)	87.4(2)
O(1)—Mo(1)—S(3)	100.8(1)	O(2)—Mo(2)—S(2)	109.2(1)		

respective least-squares planes [Mo(1) 0.706 and Mo(2) 0.701 Å] with the terminal O-atoms in axial positions. The doubly bridged Mo(V) complex has the *syn*-configuration.[11] Important molecular dimensions are given in Table 1. The molecule is folded with an angle between the mean planes S(1), S(2), S(3), S(4) and S(1), S(2), S(5), S(6) of 159.2°. Alternatively, the bent Mo_2S_2 moiety has a dihedral angle between the two MoS_2 planes of 143.2°, as expected for the *syn*-form.[11]

The dimensions of the Mo_2S_2 bridge in (1)

[Mo—S 2.303–2.317(1) Å]

are similar to those in

$\{MoO[S_2CN(C_4H_9)_2]S\}_2$[12] [2.302–2.321(6) Å],

$Mo_2OS(\mu\text{-}S)_2(S_2CN(C_2H_5)_2)_2$[13] [2.309–2.322(7)Å]

and

$[MoS\{SCN(C_3H_7)_2\}\{S_2CN(C_3H_7)_2\}]_2$[14]

[2.242–2.340(2)Å].

Terminal Mo—S_t and Mo—O_t distances observed in (1) [2.455–2.475(1) and 1.668–1.682(4) Å, respectively] are comparable to the corresponding distances reported for

$\{MoO[S_2CN(C_4H_9)_2]S\}_2$[12]

[2.446–2.459(8) and 1.63–1.64(2) Å],

and

$[\{MoO[S_2P(OC_3H_7)_2\}_2OS]$[5]

[2.472–2.505(3) and 1.654(8) Å].

The Mo ... Mo distance of 2.803(1) Å is in the range observed for other complexes with Mo_2S_2 bridges [2.705–2.920(3) Å].[8–14] Similarly, the average Mo—S_b—Mo [74.64(4)°] and S_b—Mo—S_b [100.58(5)°] angles compare favorably with those reported for similar disulfido-bridged Mo(V) complexes.[8–14]

The remaining dimensions in (1) are as expected with mean distances: C—S 1.724(5), C—C 1.496(9), C—N 1.478(7) and C⋯N 1.299(7)Å.

Acknowledgement—E.C.A. and G.F. are grateful to N.S.E.R.C. Canada for continuing financial support.

REFERENCES

1. E. I. Stiefel, *Progr. Inorg. Chem.* 1977, **22**, 1.
2. M. R. Houchin and K. Mitsios, *Inorg. Chim. Acta* 1982, **64**, L147.
3. E. C. Alyea and A. Somogyvari, *Inorg. Chim. Acta* 1984, **83**, L49.
4. E. J. Gabe, A. C. Larson, Y. Wong and F. L. Lee, The NRC Crystal Structure Programs, National Research Council Laboratories, Ottawa, Canada, K1A OR6 (1981).
5. D. T. Cromer and J. B. Mann, *Acta Cryst.* 1968, **A24**, 321.
6. R. F. Stewart, E. R. Davidson and W. T. Simpson, *J. Chem. Phys.* 1965, **42**, 3175.
7. D. T. Cromer and D. Liberman, *J. Chem. Phys.* 1970, **53**, 1891.
8. B. Spivack and Z. Dori, *Coord. Chem. Rev.* 1975, **17**, 99.
9. M. G. B. Drew, P. C. H. Mitchell, A. R. Read and T. Colclough, *Acta Cryst. Sect. B* 1981, **37**, 1758.
10. J. Dirand-Colin, L. Ricard and R. Weiss, *Inorg. Chim. Acta* 1976, **18**, L21.
11. G. Bunzey and J. H. Enemark, *Inorg. Chem.* 1978, **17**, 682.
12. K. Musha, Y. Ohashi, S. Yamazaki, S. Toda and S. Tanaka, *Nippon Kagaku Kaishi* 1983, **5**, 653.
13. W. E. Newton, J. W. McDonald, K. Yamanouchi and J. H. Enemark, *Inorg. Chem.* 1979, **18**, 1621.
14. L. Ricard, J. Estienne and R. Weiss, *Inorg. Chem.* 1973, **9**, 2182.

Polyhedron Vol. 4, No. 5, pp. 787–789, 1985
Printed in Great Britain

0277–5387/85 $3.00 + .00
© 1985 Pergamon Press Ltd

A NEW SYNTHETIC PROCEDURE FOR THE PREPARATION OF PYRIDINIUM TETRAFLUOROBORATE AND HEXAFLUOROSILICATE

R. G. KALBANDKERI, K. SYED MOHAMED, D. K. PADMA* and A. R. VASUDEVA MURTHY

Department of Inorganic and Physical Chemistry, Indian Institute of Science, Bangalore 560 012, India

(*Received* 29 *May* 1984; *accepted* 4 *September* 1984)

Abstract—Pyridinium tetrafluoroborate ($C_5H_5NHBF_4$) and pyridinium hexafluorosilicate [$(C_5H_5NH)_2SiF_6$] have been prepared in good yields and high purity by the reaction of pyridinium poly(hydrogen fluoride) with oxides and acids of boron and silicon respectively. The salts have been characterised by melting points, IR, ^1H and ^{19}F NMR spectroscopy and chemical analysis.

During the course of our investigations in introducing pyridinium poly(hydrogen fluoride) (PPHF) as an efficient and convenient reagent for the preparation of inorganic fluorinated compounds,[1,2] we have observed that it reacts with oxides and acids of boron and silicon to give rise to pyridinium salts of tetrafluoroborate and hexafluorosilicate respectively. This method gives the compounds in almost quantitative yields and of very high purity as compared to the reported methods.[3–6] The details of the investigations are presented in this paper.

EXPERIMENTAL

Materials and methods

All reagents employed in the present study were of LR/AR grade. All operations were carried out using polythene vessels in an efficient hood.

Pyridinium poly(hydrogen fluoride) reagent was prepared in two different concentrations according to the methods described earlier.[1,7] Reagent A contained 40% by wt of hydrogen fluoride and 60% wt of pyridine, and reagent B contained 70% by wt of hydrogen fluoride and 30% wt of pyridine.

The IR spectra of the compounds were recorded both in Nujol mull and as KBr discs using a Perkin–Elmer 599 spectrophotometer, ^1H (TMS standard) and ^{19}F ($CFCl_3$ standard) NMR spectra were recorded on Varian T60 and Varian FT 80A (74.84 MHz) NMR spectrometers using D_2O or DMSO-d_6 as solvent.

Preparation of $C_5H_5NHBF_4$ *and* $(C_5H_5NH)_2SiF_6$

Two procedures (1 and 2) were used for the preparation of the pyridinium salts. The reactions between PPHF and the oxides and acids were found to be highly exothermic and therefore the experiments were carried out around −10°C.

Procedure 1

To a cooled fine suspension of 3 g of boric oxide or 5 g of silicon dioxide or 7.5 g of silicic acid in 100 cm^3 of ether was added dropwise 30 cm^3 of PPHF(A) solution with stirring. The mixture was left aside for 30 min and the remaining ether evaporated. The contents were treated with chloroform to remove excess reagent and the solid separated was filtered, washed with chloroform, dried in vacuum and stored over phosphorus pentoxide. Pyridinium tetrafluoroborate was recrystallised from 95% alcohol while the pyridinium hexafluorosilicate was crystallized from hot methanol. The yields were ca 90% (Table 1).

Procedure 2

To a cooled solution of PPHF (A or B) was added portionwise 6 g of boric acid. To the separated crystalline white solid was added 100 cm^3 of chloroform. The solid was then filtered, washed with

* Author to whom correspondence should be addressed.

Table 1. Preparation of pyridinium tetrafluoroborate and pyridinium hexafluorosilicate from oxides and oxy acids of boron and silicon

Starting material	Compound prepared [yield (%)]	M.p. (°C)	IR spectral data (cm^{-1})	^{19}F NMR spectral data (ppm)
B_2O_3	$C_5H_5NHBF_4$ (87)	210–212[3]	3270, 3185, 3130 3105, 3080, 1630, 1602, 1530, 1480, 1330, 1285, 1248, 1150–1000, 970, 745, 670, 520	−146.5
H_3BO_3	$C_5H_5NHBF_4$ (89)			
SiO_2	$(C_5H_5NH)_2SiF_6$ (95)	154–158[6]	3200, 3140, 3120, 3040, 2985, 2935, 1630, 1600, 1525, 1478, 1330, 1245, 1235, 1185, 1050, 990, 735, 675, 480	−126.13
H_2SiO_3	$(C_5H_5NH)_2SiF_6$ (93)			

chloroform and dried. The compound was recrystallised from 95% ethanol. The yield was *ca* 87% (Table 1).

Analysis

Estimation of $C_5H_5NHBF_4$. Pyridinium tetrafluoroborate was estimated by the methods reported by Tatarskii *et al.*[8] with a slight modification as given below:

(a) About 0.25 g of $C_5H_5NHBF_4$ was treated with 50 cm^3 of 2 M $CaCl_2$ solution and 20 cm^3 of water. The mixture was gently boiled under reflux for 30 min and cooled. About 2 g of mannitol and five drops of phenolphthalein indicator were added and the solution was titrated against standard alkali (0.5 N NaOH). From the volume of the alkali consumed, the purity of the sample was calculated on the basis of the reaction.

$$C_5H_5NHBF_4 + 2CaCl_2 + 3H_2O \rightarrow C_5H_5NHCl + 3HCl + H_3BO_3 + 2CaF_2$$

1 cm^3 of 0.5 N NaOH ≡ 16.68 mg of $C_5H_5NHBF_4$.

(b) In a separate experiment $C_5H_5NHBF_4$ was also estimated by treating a known quantity of the sample dissolved in water with about 5 g of KCl and the contents shaken and cooled in ice. The acidity of the solution was titrated rapidly with 0.1 N NaOH using phenolphthalein as indicator to the first appearance of pink colour.

From both the experiments, the sample was found to be more than 99% pure.

Estimation of $(C_5H_5NH)_2SiF_6$. Pyridinium hexafluorosilicate was estimated by the method of Jacobson[9] with a slight modification. About 0.2 g of the sample was treated with a known excess of standard alkali (15 cm^3 of 0.5 N NaOH) and the solution boiled for 15 min and cooled. About 20 cm^3 of water and five drops of phenolphthalein were added and titrated against standard hydrochloric acid solution (0.5 N). The purity of the sample was calculated on the basis of the reaction.

$$(C_5H_5NH)_2SiF_6 + 6NaOH \rightarrow 2C_5H_5N + 6NaF + SiO_2 + 4H_2O$$

1 cm^3 of 0.5 N HCl ≡ 25.175 mg of $(C_5H_5NH)_2SiF_6$.

The sample was found to be more than 99% pure.

RESULTS AND DISCUSSION

From the results presented in Table 1, it may be inferred that PPHF reacts readily with oxides and acids of boron and silicon giving rise to the respective pyridinium complex fluoro salts of boron and silicon in good yields and of high purity. Pyridinium poly(hydrogen fluoride) acts as a source of hydrogen fluoride and the overall reactions are represented as follows.

$$B_2O_3 + C_5H_5\overset{+}{N}H(HF)_xF^- \xrightarrow{\text{ether}} 2C_5H_5\overset{+}{N}HBF_4^- + 3H_2O,$$

$$H_3BO_3 + C_5H_5\overset{+}{N}H(HF)_xF^- \longrightarrow C_5H_5\overset{+}{N}HBF_4^- + 3H_2O,$$

$$SiO_2 + C_5H_5\overset{+}{N}H(HF)_xF^- \xrightarrow{\text{ether}} (C_5H_5\overset{+}{N}H)_2SiF_6^{2-} + 2H_2O,$$

$$H_2SiO_3 + C_5H_5\overset{+}{N}H(HF)_xF^- \xrightarrow{\text{ether}} (C_5H_5\overset{+}{N}H)_2SiF_6^{2-} + 3H_2O.$$

The IR spectral data of the compounds presented in Table 1 show that the N–H stretching frequencies of $C_5H_5NHBF_4$ and $(C_5H_5NH)_2SiF_6$ appear at 3270 and 3200 cm^{-1} respectively. The very strong, broad band at 1150–1000 cm^{-1} and a strong band at 520 cm^{-1} could be assigned to $\nu_{(B-F)}$ and $\delta_{(B-F)}$ respectively of the BF_4^- anion. The strong bands at 735 and 480 cm^{-1} could be assigned to $\nu_{(Si-F)}$ and $\delta_{(Si-F)}$ respectively of SiF_6^{2-} anion. All the other absorptions are due to the pyridine moiety with the expected shifts due to salt formation. These observations are in good agreement with those reported in the literature for these compounds.[6,10,11]

The ^1H NMR spectra of these compounds show the characteristic pyridine pattern with a shift to lower field due to salt formation. The ^{19}F NMR peaks of BF_4^- and SiF_6^{2-} recorded for the first time appear at −146.5 and −126.13 ppm respectively. These values are in good agreement with those compounds containing the respective anions.[12]

It is of interest to point out that $C_5H_5NHBF_4$ and $(C_5H_5NH)_2SiF_6$ have been used as starting materials for the preparation of other salts of these anions such as alkali metal, ammonium and alkylammonium tetrafluoroborates and hexafluorosilicates respectively.[13]

REFERENCES

1. K. Syed Mohamed, D. K. Padma, R. G. Kalbandkeri and A. R. Vasudeva Murthy, *J. Fluorine Chem.* 1983, **23**, 509.
2. K. Syed Mohamed, D. K. Padma and A. R. Vasudeva Murthy, Paper presented at the International Conference on Phosphorus Chemistry at Nice, France, September 1983—communicated to *J. Fluorine Chem.* for publication.
3. E. Muller and H. H. Emden, *Ann.* 1961, **649**, 70; *Chem. Abstr.* 1962, **56**, 12713b.
4. I. G. Ryss and S. L. Idel's, *Zh. Neorg. Khim.* 1957, **2**, 2270.
5. R. Dotzer and A. Neuwsen, *Z. Anorg. Allg. Chem.* 1961, **308**, 79.
6. J. P. Guertin and M. Onyszchuk, *Can. J. Chem.* 1969, **47**, 1275.
7. G. A. Olah, J. T. Welch, Y. D. Vankar, M. Nojima, I. Kerekos and J. A. Osah, *J. Org. Chem.* 1979, **44**, 3872.
8. S. V. Tatarskii, E. N. Kornilova and F. A. Sheinina, *Tr. Kom. Anal. Khim. Acad. Nauk SSSR* 1951, **3**, 287 *Chem. Abstr.*; 1953, **47**, 2642h.
9. C. A. Jacobson, *J. Phys. Chem.* 1924, **28**, 506.
10. D. Cook, *Can. J. Chem.* 1961, **39**, 2009.
11. D. W. A. Sharp, *Advances in Fluorine Chemistry* (Edited by M. Stacey *et al.*), Vol. 5, p. 70. Butterworth, London (1965).
12. *Annual Reports on NMR Spectroscopy* (Edited by G. A. Webb) 1983, **14**, pp. 331 and 361.
13. K. Syed Mohamed, D. K. Padma and A. R. Vasudeva Murthy, Under communication.

Polyhedron Vol. 4, No. 5, pp. 791–795, 1985
Printed in Great Britain

0277–5387/85 $3.00 + .00
© 1985 Pergamon Press Ltd

3,3′-DICARBOMETHOXY-2,2′-BIPYRIDYL COMPLEXES OF PALLADIUM(II), PLATINUM(II) AND RHODIUM(III)

SMITA DHOLAKIA,* ROBERT D. GILLARD and FRANZ L. WIMMER*†
Department of Chemistry, University College, P.O. Box 78, Cardiff CF1 1XL, Wales, U.K.

(*Received* 15 *September* 1983; *accepted* 13 *September* 1984)

Abstract—3,3′-Dicarbomethoxy-2,2′-bipyridyl (DCMB) reacts with K_2MCl_4 (M = Pd, Pt) to give $M(DCMB)Cl_2$ and with $RhCl_3$ to give the *cis*-$[Rh(DCMB)_2Cl_2]^+$ ion. Attempts to prepare the tris (DCMB) complex with Rh(III) and analogous Co(III) complexes were unsuccessful.

2,2′-Bipyridyl (bpy) may reasonably be expected to coordinate as a monodentate, chelating or bridging ligand. However, in practice, only the chelating mode has been observed.[1] The monodentate form is generally agreed to be involved in the rate-determining step in the formation and dissociation of bipyridyl complexes.[2]

One way to prepare a monodentate bipyridyl complex is to quaternise one of the nitrogen atoms with an alkyl group; the resultant cation forms complexes of the type $M(bpyMe)X_3$ [M(II) = Co–Cu,[3] Zn–Hg,[4] Pd, Pt[5]; bpyMe = *N*-methyl-2,2′-bipyridylium; X = Cl–I]. An alternative route would be to place sufficiently bulky substituents in the 3,3′-positions, so that the ligand cannot attain a planar state, as has been observed for $[MeHg(3,3'\text{-dmbpy})]NO_3$[6,7] (3,3′-dmbpy = 3,3′-dimethyl-2,2′-bipyridyl). However, the dimethyl substituents in 3,3′-dmbpy do not prevent the molecule from coordinating in a bidentate manner.[8–12]

As part of our study of the metal complexes of skewed bipyridyls[3–5,13] we report the coordinating properties of 3,3′-dicarbomethoxy-2,2′-bipyridyl.

RESULTS

Platinum(II) *and palladium*(II) *complexes*

When a suspension of 3,3′-dicarbomethoxy-2,2′-bipyridyl (DCMB) in water was added to a warm solution of K_2PtCl_4 in water (2:1 molar ratio), a dark orange solid, soluble in ethanol, separated initially. This solid was not characterised. When heating was continued for a further 20 min, it did not dissolve completely but was converted to bright orange-yellow crystals.

An orange complex separated when DCMB and K_2PdCl_4 (2:1 molar ratio) in water were gently warmed for 2 min. The same compound is formed when Li_2PdCl_4 is used and the reaction is carried out in ethanol.

Elementary micro-analysis of the complexes gave an empirical formula of $M(DCMB)Cl_2$. The metal residues obtained from the thermogram indicate formula weights of 530 (Pt) and 440 (Pd). The ^1H NMR spectra of these compounds in $CDCl_3$ show only one methyl resonance (at δ 4.2) which suggests that the bipyridyl is coordinating as a chelating or a bridging‡ ligand. The field desorption mass spectra show molecular ions centred at *m/e* 538 (Pt) and 450 (Pd), indicating that the complexes are monomeric and that DCMB acts as a chelating ligand.

The bands due to DCMB in the IR spectra of the complexes $M(DCMB)Cl_2$ are virtually identical to those of the ligand in the region 4000–600 cm^{-1}. $Pt(DCMB)Cl_2$ shows strong bands at 350 and 342 cm^{-1} which are not present in the spectrum of the free ligand. These are assigned to the Pt–Cl stretching vibrations. One of the Pd–Cl stretching vibration for $Pd(DCMB)Cl_2$ can be assigned to the

* School of Natural Resources, University of the South Pacific, P.O. Box 1168, Suva, Fiji.
† Author to whom correspondence should be addressed.

‡ There are no known examples where 2,2′-bipyridyl acts as a bridging ligand (although complexes containing bridging 4,4′-bipyridyl have been described). The blue-green solid formed by the interaction of $[Rh(CO)_2Cl]_2$ with bpy, formulated as $[Cl(OC)_2Rh(\mu\text{-bpy})Rh(CO)_2Cl]$[14] is in fact $[Rh(bpy)(CO)_2][Rh(CO)_2Cl_2]$[15] since a closely similar 1,10-phenanthroline complex has also been prepared.

Table 1. Far-IR spectra* of $MLCl_2$ [M = Pt(II), Pd(II); L = DCMB, bpy]

DCMB	$Pt(DCMB)Cl_2$	$Pt(bpy)Cl_2$	$Pd(DCMB)Cl_2$	$Pd(bpy)Cl_2$
585 sh	585 w		585 w	
575 m				
	540 w		535 w	
525 m	520 m		515 m	
	450 w	460 w	450 w	450 w
410 m		420 m		420 s
	390 m		390 m	
360 m	360 m		370 m	
	350† s	350†‡ s		355†§ s
335 m	342† s	340†‡ s	345† s	348†§ s
				325 m
310 m				
		300 w		
260 m	270 m		280 w	270 w

* sh, shoulder; w, weak; m, medium; s, strong.
† M–Cl stretch.
‡ Literature values[16]: 351 and 338 cm^{-1}.
§ Literature values[16]: 353 and 343 cm^{-1}.

band observed at 345 cm^{-1}, but the other vibration is not clear due to interference from the ligand bands (see Table 1). These M–Cl vibrations do not differ significantly from those for $M(bpy)Cl_2$[16] (M = Pt, Pd; Table 1).

The electronic spectra of $Pt(DCMB)Cl_2$ and $Pd(DCMB)Cl_2$ in chloroform are compared with those of $Pt(bpy)Cl_2$ and $Pd(bpy)Cl_2$ (in chloroform) in Table 2. They differ considerably, and this is probably due to different dihedral angles about the 2,2′-bond. In general, it seems that the absorptions shift to higher wavelengths in going from the bpy complexes to the analogous DCMB complexes, although the relative intensities remain approximately the same.

When a suspension of $Pt(DCMB)Cl_2$ was gently heated with an excess of aqueous pyridine, the solid dissolved gradually to give a pale yellow solution. Addition of solid sodium perchlorate gave white needles of $[Pt(DCMB)(py)_2](ClO_4)_2$. The bands at 350 and 342 cm^{-1} in the IR spectrum of $Pt(DCMB)Cl_2$ are absent in the spectrum of the product. $Pt(bpy)Cl_2$ reacts in a similar mannner: the chloro groups can be substituted with basic ligands such as pyridine, ammonia, ethylenediamine or bpy on mild heating.[17,18]

* This is in sharp contrast to $[Rh(bpy)_2Cl_2]Cl$ which is only slightly soluble in water.

Rhodium(III) *complexes*

DCMB reacts rapidly with $RhCl_3 \cdot nH_2O$ (ligand : metal ratio = 3 : 1) in hot aqueous ethanol to form *cis*-$[Rh(DCMB)_2Cl_2]Cl$. The complex was isolated as a yellow hygroscopic* solid. The non-hygroscopic perchlorate salt can be prepared by metathesis. When the same reaction mixture was boiled for 45 min or when the reactants were heated in the presence of hydrazinium monochloride as a catalyst,[19] the product, isolated as the perchlorate salt, was *cis*-$[Rh(DCMB)_2Cl_2]^+$ in both cases.

Hence, $[Rh(DCMB)_3]^{3+}$ cannot be prepared under these reaction conditions and the bis-complex is the sole product even in the presence of an excess of ligand. A tris complex cannot be prepared from the reaction between 1,10-phenanthroline and $RhCl_3$: this has been attributed[17,19] to the rigidity of phenanthroline. In a similar manner, placing bulky substituents in the 3,3′-positions of bpy would make the ring-closure step more difficult.

The medium intensity bands at 360 and 345 cm^{-1} in the IR spectrum of $[Rh(DCMB)_2Cl_2]Cl$ are assigned to the metal–chlorine stretching modes. The *cis*-isomer of the complex will have C_2 symmetry and therefore will give rise to two IR active M–Cl stretching modes. The analogous bands for $[Rh(bpy)_2Cl_2]Cl$, which is known to have the *cis*-configuration, are at 356 and 349 cm^{-1}.[20]

Attempts to prepare DCMB complexes of cobalt(III) using air oxidation of cobalt(II) chloride, in the presence of charcoal, proved unsuccessful.

Table 2. Absorption spectra* of $MLCl_2$ [M = Pt(II), Pd(II); L = DCMB, bpy]

λ_{nm} ($\varepsilon \times 10^{-5}$ mol^{-1} dm^2)			
Pt(DCMB)Cl_2	Pt(bpy)Cl_2†	Pd(DCMB)Cl_2	Pd(bpy)Cl_2†
445 (0.27)	450 (0.01)		
	398 (0.31)		
370 (0.14)	377 (0.20)	385 (0.12)	
			340 (0.18)
	324 (0.52)	320 (0.89)	
	312 (0.52)		314 (1.4)
300 (1.56)			305 (1.20)
	285 (1.80)		
		275 (1.23)	262 (1.33)

* In chloroform.
† Refs 17 and 18.

DISCUSSION

In the absence of steric effects chelated bpy molecules are essentially planar.[21] When methyl substituents are placed in the 3,3'-positions of bpy, the molecule can still act as a chelating ligand, but with a concomitant increase in the dihedral angle between the pyridyl rings to 30–35°.[10–12] An exception is [MeHg(3,3'-dmbpy)]$^+$ which is two coordinate with a monodentate bpy ligand,[6,7] whereas the complex [MeHg(bpy)]$^+$ is three coordinate.[6]

It follows that if the size of the 3,3'-substituents is increased, a point will be reached at which the ring-closure step will be unlikely and monodentate coordination will result.

EXPERIMENTAL

The carbon, hydrogen, nitrogen and chlorine analyses were determined by the Microanalytical Service, University College, Cardiff. IR spectra were recorded as nujol mulls between caesium iodide plates on a Perkin–Elmer 457 grating IR spectrophotometer and were calibrated with polystyrene. Electronic spectra were recorded with a Beckman Model DK-2A ratio-recording spectrophotometer. Proton NMR spectra were recorded relative to TMS on a 90 MHz Perkin–Elmer R32 Spectrometer at 35°C. Thermogravimetric results were obtained with a Stanton Redcroft TG-750 temperature programmed thermogravimetric balance using samples between 5 and 10 mg. The samples were heated in air at a rate of 5° min^{-1}.

2,2'-Bipyridyl-3,3'-dicarboxylic acid (binicotinic acid)

Synthesis of binicotinic acid was carried out five times by the method of Inglett and Smith,[22] but the yield was 30–40% rather than the reported 85%. Hence the method was modified and binicotinic acid was obtained as follows.

1,10-Phenanthroline (16 g, 0.08 mol), sodium hydroxide (6.4 g, 0.16 mol) and potassium permanganate (38 g, 0.24 mol) were dissolved in water (700 cm^3) and the mixture was boiled in a 1.5 dm^3 Erlenmeyer flask while magnetically stirred. After heating for 2.5 h, the precipitate of manganese dioxide was removed by filtration and the filtrate evaporated to approximately 300 cm^3 on a rotary evaporator. The pH of the concentrate was adjusted to ~ 2 with concentrated hydrochloric acid, decolourising charcoal was added and the solution boiled. The carbon was removed and the filtrate concentrated to 200 cm^3. White needles of binicotinic acid were collected by filtration, washed with cold water and cold ethanol and dried *in vacuo* over P_4O_{10}. Yield = 75%. M.p. = 262°C, literature[22] = 260°C (decomp.).

3,3'-Dicarbomethoxy-2,2'-bipyridyl (DCMB)

To a solution of binicotinic acid (4 g, 0.017 mol) in absolute methanol (20 cm^3) was added concentrated sulphuric acid (4 cm^3; CARE on adding sulphuric acid to methanol). The mixture was heated under reflux for 5 h. The methanol was removed by evaporation, water (5 cm^3) was added and the

solution was neutralised with sodium carbonate. The white needles that separated were collected on a filter, washed with water, a few drops of cold ethanol and dried *in vacuo* (P_4O_{10}). Yield = 86%. M.p. = 152°C, literature[23] = 150°C.

Pt(*DCMB*)Cl_2

A suspension of DCMB (0.49 g, 1.82 mmol) in an aqueous solution of K_2PtCl_4 (0.38 g, 0.92 mmol) was warmed. A dark orange solid initially separates out but heating was continued, with stirring, for a further 30 min. The bright orange-yellow solid was isolated, washed several times with water, warm ethanol, a few drops of chloroform to remove any unreacted ligand, and ether, and air-dried. Found: C, 31.4; H, 2.2; N, 5.4; Cl, 14.2%. $C_{14}H_{12}Cl_2N_2O_4Pt$ requires C, 31.2; H, 2.2; N, 5.2; Cl, 13.2%.

Pd(*DCMB*)Cl_2

To a solution of K_2PdCl_4 (0.42 g, 0.78 mmol) in water was added, with stirring, DCMB (0.25 g, 1.58 mmol) in warm ethanol. An orange precipitate formed immediately; this was separated, washed with water, ethanol, a few drops of chloroform, ether and air-dried. (Found: C, 37.4; H, 2.6; N, 6.7; Cl, 16.5%. $C_{14}H_{12}Cl_2N_2O_4Pd$ requires C, 37.4; H, 2.7; N, 6.2; Cl, 15.8%.)

The platinum(II) and palladium(II) complexes are insoluble in water, ethanol, acetonitrile, slightly soluble in chloroform and extremely soluble in nitromethane.

[Pt(*DCMB*)py_2]$(ClO_4)_2$

Pt(DCMB)Cl_2 (100 mg) was suspended in a solution of pyridine (2 cm^3) in water (10 cm^3). The mixture was heated on a steam bath until all the complex had dissolved to give a pale yellow solution. Solid sodium perchlorate was added and the mixture was stored at 5°C for 3 days. The white needles of [Pt(DCMB)py_2]$(ClO_4)_2$ were collected, washed quickly with cold water and dried *in vacuo* over P_4O_{10}. Found : C, 36.3; H, 3.0; N, 6.7; Cl, 8.3%. $C_{26}H_{22}Cl_2N_4O_{12}Pt$ requires C, 36.8; H, 2.6; N, 6.6; Cl, 8.4%.

[Rh(*DCMB*)$_2Cl_2$]$Cl \cdot 3H_2O$

$RhCl_3 \cdot nH_2O$ (200 mg, 0.76 mmol) in warm water (10 cm^3) was mixed with DCMB (0.61 g, 2.24 mmol) in warm ethanol (10 cm^3) to give an orange solution. On warming for 3 min, a yellow solution was obtained. Heating was continued for 7 min on a steam bath. The solvent was removed by evaporation. The yellow oil obtained was dissolved in absolute ethanol and the solution was concentrated to a minimum volume. Carbon tetrachloride was added and the solution left at 5°C for 1 h. The yellow precipitate of [Rh(DCMB)$_2Cl_2$]$Cl \cdot 3H_2O$ was collected, washed with carbon tetrachloride and ether and recrystallised from ethanol–ether. The pale yellow solid was washed with ether and dried *in vacuo* over P_4O_{10}. Found: C, 41.9; H, 3.5; N, 7.2; Cl, 13.5%. $C_{28}H_{30}Cl_3N_4O_{11}Rh$ requires C, 41.6; H, 3.7; N, 6.9; Cl, 13.1%.

Attempted synthesis of [Rh(*DCMB*)$_3$]$^{3+}$

A solution of $RhCl_3 \cdot nH_2O$ (100 mg, 0.38 mmol) and DCMB (0.32 g, 1.18 mmol) in 50% aqueous ethanol was heated on a steam bath for 45 minutes to give a golden yellow solution. A concentrated aqueous solution of sodium perchlorate was added dropwise to the hot reaction mixture. The yellow oil crystallised on cooling to give pale yellow crystals of *cis*-[Rh(DCMB)$_2Cl_2$]ClO_4, which were collected, washed with water and ethanol and dried *in vacuo* over P_4O_{10}. Found: C, 40.3; H, 3.0; N, 7.0; Cl, 13.3%. $C_{28}H_{24}Cl_3N_4O_{12}Rh$ requires C, 41.1; H, 2.9; N, 6.9; Cl, 12.9%.

REFERENCES

1. J. Van Houten and R. J. Watts, *J. Am. Chem. Soc.* 1976, **98**, 1853; R. D. Gillard, R. J. Lancashire and P. A. Williams, *J. Chem. Soc., Dalton Trans.* 1979, 190; W. A. Wickramasinghe, P. H. Bird and N. Serpone, *J. Chem. Soc., Chem. Commun.* 1981, 1284.
2. R. J. Kazlauskas and M. S. Wrighton, *J. Am. Chem. Soc.* 1982, **104**, 5784; F. Basolo and R. G. Pearson, *Mechanisms of Inorganic Reactions*, 2nd edition, p. 218. John Wiley, London (1967); M. V. Twigg, *Inorg. Chim. Acta* 1974, **10**, 17; A. J. Brown, O. W. Howarth, P. Moore and W. J. E. Parr, *J. Chem. Soc., Chem. Commun.* 1977, 586; *J. Chem. Soc., Dalton Trans.* 1978, 1776.
3. S. Dholakia, R. D. Gillard and F. L. Wimmer, *Inorg. Chim. Acta* 1982, **65**, L121.
4. F. L. Wimmer and S. Wimmer, unpublished results.
5. S. Dholakia, R. D. Gillard and F. L. Wimmer, *Inorg. Chim. Acta* 1983, **69**, 179.
6. A. J. Canty and A. Marker, *Inorg. Chem.* 1976, **15**, 425.
7. A. J. Canty, N. Chaichit, B. M. Gatehouse and A. Marker, *Acta Cryst.* 1978, **B34**, 3229.
8. T. M. Suzuki, *Bull. Chem. Soc. Jpn* 1979, **52**, 433.
9. T. M. Suzuki and T. Kimura, *Bull. Chem. Soc. Jpn* 1977, **50**, 391.

10. S. Sato and Y. Saito, *Acta Cryst.* 1978, **B34**, 3352.
11. S. Ohba, S. Sato and Y. Saito, *Acta Cryst.* 1979, **B35**, 957.
12. S. Ohba, H. Miyamae, S. Sato and Y. Saito, *Acta Cryst.* 1979, **B35**, 1470.
13. S. Dholakia and R. D. Gillard, *Tetrahedron* 1981, **37**, 2929.
14. D. N. Lawson and G. Wilkinson, *J. Chem. Soc.* 1965, 1900.
15. R. D. Gillard, K. Harrison and I. H. Mather, *J. Chem. Soc., Dalton Trans.* 1975, 133.
16. R. A. Walton, *Can. J. Chem.* 1966, **44**, 1480.
17. P. M. Gidney, Ph.D. thesis, University of Kent, Canterbury (1972).
18. E. Beilli, P. M. Gidney, R. D. Gillard and B. T. Heaton, *J. Chem. Soc., Dalton Trans.* 1974, 2133.
19. P. M. Gidney, R. D. Gillard and B. T. Heaton, *J. Chem. Soc., Dalton Trans.* 1972, 2621.
20. R. D. Gillard and B. T. Heaton, *J. Chem. Soc. (A)* 1969, 451.
21. W. Fitzgerald, J. Foley, D. McSweeney, N. Ray, D. Sheahan, S. Tyagi, B. Hathaway and P. O'Brien, *J. Chem. Soc., Dalton Trans.* 1982, 1117 (and references therein).
22. G. E. Inglett and G. F. Smith, *J. Am. Chem. Soc.* 1950, **72**, 842.
23. D. Aziz and J. G. Breckenridge, *Can. J. Chem.* 1950, **28B**, 26.

Polyhedron Vol. 4, No. 5, pp. 797–809, 1985
Printed in Great Britain

0277–5387/85 $3.00 + .00
© 1985 Pergamon Press Ltd

FORMATION OF PARAMAGNETIC MONONUCLEAR IRON NITROSYL COMPLEXES FROM DIAMAGNETIC DI- AND TETRANUCLEAR IRON–SULPHUR NITROSYLS: CHARACTERISATION BY EPR SPECTROSCOPY AND STUDY OF THIOLATE AND NITROSYL LIGAND EXCHANGE REACTIONS

ANTHONY R. BUTLER, CHRISTOPHER GLIDEWELL,*
ANDREW R. HYDE and JOHN C. WALTON
Chemistry Department, University of St. Andrews, St. Andrews, Fife KY16 9ST, U.K.

(*Received* 3 *July* 1984; *accepted* 13 *September* 1984)

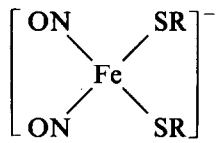
Abstract—The diamagnetic Roussin esters $Fe_2(SR)_2(NO)_4$ readily underwent exchange with thiols R'SH to yield $Fe_2(SR')_2(NO)_4$: the exchange was faster in polar, coordinating solvents where paramagnetic, mononuclear complexes of types $[Fe(NO)_2(solvent)_2]^+$ and $Fe(NO)_2(SR)(solvent)$ were formed. With the corresponding thiolate anions RS^-, the esters $Fe_2(SR)_2(NO)_4$ formed the mononuclear complexes $[Fe(SR)_2(NO)_2]^-$, which were fully characterised by EPR spectroscopy for R = H, Me, Et, *i*-Pr, *t*-Bu and $PhCH_2$: assignments of hyperfine couplings were confirmed by use of ^{15}N. With $Fe_2(SR)_2(NO)_4$ and a different set of thiolate anion, $R'S^-$, in excess, thiol exchange occurred to give $[Fe(SR')_2(NO)_2]^-$. A mechanism for formation of $Fe_2(SR')_2(NO)_4$ from $Fe_2(SR)_2(NO)_4$ has been proposed. The paramagnetic mononuclear complexes $[Fe(SR)_2(NO)_2]^-$ were also readily formed from the diamagnetic clusters $[Fe_4S_3(NO)_7]^-$ and $Fe_4S_4(NO)_4$, together with $[Fe(SR)_3(NO)]^-$, and additionally from $[Fe(CO)_3NO]^-$. $[Fe(SMe)_2(NO)_2]^-$ was found to be a precursor of isolable $Fe_2(SMe)_2(NO)_4$, and $[Fe(SH)_2(NO)_2]^-$ to be the common precursor of both Roussin's red anion $[Fe_2S_2(NO)_4]^-$ and Roussin's black anion $[Fe_4S_3(NO)_7]^-$, interconvertible by appropriate adjustment of pH. The nitrosyl groups in these complexes were freely labile, and mononitrosyliron and dinitrosyliron fragments were readily interconvertible: Fe(NO) fragments were favoured by the dimethyldithiocarbamate ligand ($Me_2NCS_2^-$) and $Fe(NO)_2$ fragments by thiolate ligands, RS^-, regardless of the origin of the $Fe(NO)_x$ ($x = 1, 2$) fragment: both mono- and dinitrosyliron complexes persisted with $[(i\text{-}PrO)_2S_2]^-$ as ligand. Isotopic labelling showed the occurrence of rapid exchange of nitrogen between nitrosyl ligands and added nitrite in $Fe(NO)(S_2CNMe_2)_2$ and $[Fe(SR)_2(NO)_2]^-$.

It was first demonstrated[1] in 1965 that reaction between iron salts and nitric oxide in the presence of anionic ligands gave rise to four-coordinate complexes, of general stoichiometry $[Fe(NO)_2L_2]^{x+}$ and characterised by EPR spectra with isotropic g values of *ca* 2.03. In the specific cases of L = cysteine and penicillamine, the identification of the stoichiometry was particularly clear, and it was further inferred that the iron was formally present as d^9 Fe(−I). Subsequently there have been many studies of the reactions of iron salts with nitric oxide in the presence of a very wide range of additional ligands, including halides and pseudohalides,[2] alcohols and alkoxides,[3] mercaptides,[4,5] and mercapto-purines and mercapto-pyrimidines.[6] In all these cases,[2–6] the g values are close to 2.03, except when the additional ligands are bromide or iodide,[2] when g moves to rather higher values, as observed in other, independent, studies of $[Fe(NO)_2Br_2]^-$ and $[Fe(NO)_2I_2]^-$ and related species.[7,8]

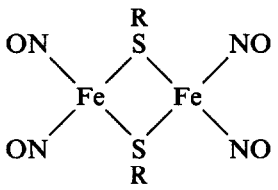
Similar paramagnetic iron–nitrosyl complexes, characterised by usually anisotropic g values around 2.03 have been observed[9–11] in extracts of rat liver following administration of specific chemical carcinogens, such as aminoacetylfluorene[12] and *N*-methyl-*N'*-nitro-*N*-nitrosoguanidine.[13] In addition, $g = 2.03$ complexes have been found[14] in extracts from many of the organs of several species of

* Author to whom correspondence should be addressed.

experimental animals maintained on a normal diet supplemented only by sodium nitrite and iron(II) sulphate. In each of these biological studies[9–11,14] the identification of the $g = 2.03$ species as being complexes of general type $[Fe(NO)_2L_2]^{x+}$ (i.e., the same as those produced from iron salts, nitric oxide and a ligand L) was far from definitive, and was based primarily upon a comparison of their EPR spectra with those of the complexes originally observed[1] by Phillips *et al.*: in each case the $g = 2.03$ complexes were assigned structures of type (I), where R remained unidentified.



I



II

Closely related to complex I are the neutral, diamagnetic complexes II, the esters of Roussin's red salt.[15,16] The methyl ester (II, R = CH_3) has been isolated from vegetable sources, and it has subsequently been implicated in the causation of oesophageal cancer.[17–20] The Fe_2S_2 core of naturally occurring esters II is presumably derived from iron–sulphur proteins, and indeed it has recently been demonstrated[21] that the HIPIP-type iron–sulphur centres in *Clostridium botulinum* are replaced by a $g = 2.03$ complex upon exposure to nitrite, with resultant destruction of the Fe_4S_4 iron–sulphur cluster.

Continuing our general study of iron–sulphur–nitrosyl complexes[8,22–26] we have made a study of the $g = 2.03$ complexes and report in the present paper the definitive characterisation of a range of complexes I, $[Fe(NO)_2(SR)_2]^-$; the ready interconversion of I and II, and consequent facile exchange of R groups in II [eqn (1)]; the ready formation of I and related mononuclear systems from II in polar media; and the

$$Fe_2(SR)_2(NO)_4 + 2R'SH \rightleftharpoons Fe_2(SR')_2(NO)_4 + 2RSH \quad (1)$$

formation of mononuclear complexes, not only from dinuclear precursors, but also from the tetranuclear complexes, $Fe_4S_3(NO)_7^-$ and $Fe_4S_4(NO)_4$.

Our observations provide important points of connection between the existing chemical[1–6] and biological[9–11,14,17–21] studies of these systems.

RESULTS AND DISCUSSION

Reactions of $Fe_2(SR)_2(NO)_4$

A range of esters $Fe_2(SR)_2(NO)_4$ were found to undergo ready exchange of SR groups with added thiols R'SH. Using an approximately 10:1 (w/w) excess of thiol over ester in THF solution, the results recorded in Table 1 were obtained, where the composition of the products was determined by ^1H NMR in $CDCl_3$ solution. The use of a representative range of substituents R,R' showed that exchange is generally complete or almost so. In all cases the total material recovered prior to NMR examination represented $\geqslant 95\%$ recovery, and the spectra showed that the exchange reactions were clean with no decomposition; nor were any products of side-reactions detected. The solvent dependence of the rate of exchange was examined qualitatively for the reaction of $Fe_2(SEt)_2(NO)_4$ with *i*-PrSH in a modest range of solvents, and the results are given in Table 2: as for the data of Table 1, the results represent the composition of the reaction mixtures after 72 h. These qualitative results show clearly that the exchange reaction is faster in polar solvents: we shall return to the question of the possible mechanisms of the exchange below.

Table 1. Results of exchange reactions of $Fe_2(SR)_2(NO)_4$ with added thiols R'SH, in THF

		Product composition (%)	
R	R'	$Fe_2(SR')_2(NO)_4$	$Fe_2(SR)_2(NO)_4$
CH_3	H	90	10
CH_3	*n*-C_3H_7	100	0
C_2H_5	*i*-C_3H_7	100	0
i-C_3H_7	CH_2COOH	95	5
t-C_4H_9	*i*-C_3H_7	60	40

Table 2. Solvent dependence of the exchange between $Fe_2(SEt)_2(NO)_4$ and *i*-PrSH

Solvent	Product composition (%)	
	$Fe_2(SPr\text{-}i)_2(NO)_4$	$Fe_2(SEt)_2(NO)_4$
DMF	100	0
THF	100	0
EtOH	86	14
Toluene	62	38
Cyclohexane	60	40

Table 3. EPR parameters for complexes $[Fe(SR)_2(NO)_2]^-$ in DMF solution, at 240 K

R	g	$A(^{14}N)$ (G)	$A(^1H)$ (G)
H	2.028	2.7	0.5 (2H)
Me	2.028	2.1	2.1 (6H)
Et	2.027	2.0	2.6 (4H)
i-Pr	2.027	2.5	1.3 (2H)
t-Bu	2.027	2.7	— (0H)
$PhCH_2$	2.027	2.4	1.4 (4H)

These alkanethiol exchange reactions are of some synthetic value, as they can provide a very easy route, superior to that described previously[23] and based upon exchange reactions of $Fe_2(SR)_2(CO)_6$, to the formation of esters $Fe_2(SR)_2(NO)_4$ containing functionalised R groups, in particular those containing substituents which render the ester water-soluble.

We have described previously[23,26] the solvent dependence of the ^1H spectra of a range of esters $Fe_2(SR)_2(NO)_4$ and it was the observation[26] of rather broad, poorly resolved ^1H resonances for solutions of $Fe_2(SMe)_2(NO)_4$ in solvents such as DMF, DMSO and pyridine which first indicated the formation of paramagnetic species in these very polar solvents. Examination of these solutions by EPR spectroscopy has revealed the presence of paramagnetic centres.

The esters $Fe_2(SR)_2(NO)_4$ (R = Me, Et, *i*-Pr, *t*-Bu, $PhCH_2$) all gave weak EPR absorptions when dissolved in DMF: the spectra were centred at $g \simeq 2.03$, but no hyperfine coupling was resolvable. The intensity of each of these spectra was somewhat enhanced by addition of the corresponding RSH, although solutions of $Fe_2(SR)_2(NO)_4$ in RSH alone showed no evidence of the presence of paramagnetic species. Upon subsequent addition of a trace of MeS^-, acting as a base, a major enhancement of the spectral intensity occurred: the EPR spectra were all characterised by hyperfine coupling to two equivalent ^{14}N nuclei ($I = 1$) and to the α-hydrogens, where present, of two equivalent RS groups (Table 3), allowing the assignment of these spectra as arising from complexes $[Fe(SR)_2(NO)_2]^-$, formed according to eqn (2):

$$Fe_2(SR)_2(NO)_4 + 2RSH \xrightarrow{\text{base}} 2[Fe(SR)_2(NO)_2]^-. \quad (2)$$

In each example the paramagnetic species contained the alkyl group R from the added thiol, rather than CH_3 from the added base MeS^-.

When a solution of either $Fe_2(SMe)_2(NO)_4$ or $Fe_2(SPr\text{-}i)_2(NO)_4$ in DMF was heated to 350 K for 5 min, and subsequently cooled to 240 K, the spectral intensity was much enhanced over that of the initial solution, and in the case of R = *i*-Pr, at least, it was clear that two paramagnetic complexes were present in approximately equimolar concentrations. Comparison of the spectra obtained from $Fe_2(SPr\text{-}i)_2(NO)_4$ in DMF, DMF-d_7, and dimethyl acetamide (DMA) as solvents, together with the spectrum obtained from $Fe_2(SMe)_2(NO)_4$ in DMF, showed that these two species were $[Fe(NO)_2(DMF)_2]^+$ and $Fe(NO)_2(SR)(DMF)$ in which there is a hyperfine coupling to the unique hydrogen in DMF in addition to those involving the ^{14}N nuclei of the nitrosyl groups and the α-hydrogens of the SR group (Table 4).

Similar solvo-complexes of type $[Fe(NO)_2(solvent)_2]^+$ were formed in a range of heteroaromatic solvents (Table 4), while complexes of type $Fe(NO)_2(SR)(solvent)$ appear to be formed in a range of non-aromatic solvents. In none of the latter class, except when the solvent is DMF (but not however DMF-d_7 or DMA) was any hyperfine coupling observed to either hydrogen or nitrogen in the coordinated solvent molecules. Nevertheless, by analogy with the DMF solvo-complexes $Fe(NO)_2(SR)(DMF)$ where R = Me or *i*-Pr, we have assigned all these species constitution of the same type. In liquid ammonia solution at 200 K, $Fe_2(SMe)_2(NO)_4$ yielded a weak EPR spectrum having $g = 2.029$, in which no hyperfine couplings were resolvable: by analogy with other aliphatic amines, the complex $Fe(NO)_2(SMe)(NH_3)$ may have been formed.

Examination, by EPR spectroscopy at 275 K, of an aqueous solution of $Fe_2(SCH_2COOH)_2(NO)_4$ (which is rendered slightly soluble in water by the carboxylic acid groups) revealed a broad unresolved absorption, centred at $g = 2.030$. In aqueous ethanol solutions, the complex $[Fe(NO)_2(H_2O)_2]^+$ is reported[2] to give a broad unresolved absorption at $g = 2.033$, while in $[Fe(NO)_2(OH)_2]^-$, at $g = 2.027$, the hyperfine coupling to ^{14}N was resolved.[2] By analogy

Table 4. EPR parameters for paramagnetic solvo-complexes

Solvent	Complex	g	$A(^{14}N)$ (G)	$A(^{1}H)(SR)$ (G)	$A(X)$ (G)*
Solvo-complexes from $Fe_2(SPr\text{-}i)_2(NO)_4$					
DMF	$[Fe(NO)_2(DMF)_2]^+$	2.033	2.4 (2N)	—	4.0 (2H)
	$Fe(NO)_2(SPr\text{-}i)(DMF)$	2.027	2.6 (2N)	1.3 (1H)	4.6 (1H)
DMF-d_7	$[Fe(NO)_2(DMF\text{-}d_7)_2]^+$	2.033	2.5 (2N)	—	†
	$Fe(NO)_2(SPr\text{-}i)(DMF\text{-}d_7)$	2.027	2.5 (2N)	1.3 (1H)	†
DMA	$[Fe(NO)_2(DMA)_2]^+$	2.033	2.5 (2N)	—	‡
	$Fe(NO)_2(SPr\text{-}i)(DMA)$	2.027	2.5 (2N)	1.3 (1H)	‡
Pyridine (py)	$[Fe(NO)_2(py)_2]^+$	2.031	2.2 (2N)	—	4.5 (2N)
Solvo-complexes from $Fe_2(SMe)_2(NO)_4$					
DMF	$[Fe(NO)_2(DMF)_2]^+$	2.033	2.4 (2N)	—	4.0 (2H)
	$Fe(NO)_2(SMe)(DMF)$	2.027	2.4 (2N)	4.5 (3H)	4.6 (1H)
DMSO	$Fe(NO)_2(SMe)(DMSO)$	2.032	6.0 (2N)	3.2 (3H)	‡
Pyridine	$[Fe(NO)_2(py)_2]^+$	2.031	2.2 (2N)	—	4.5 (2N)
2,6-Dimethylpyridine	$[Fe(NO)_2(S)_2]^+$§	2.031	2.3 (2N)	—	4.6 (2N)
2,4,6-Trimethylpyridine	$[Fe(NO)_2(S)_2]^+$§	2.030	‖	—	‖
Quinoline	$[Fe(NO)_2(S)_2]^+$§	2.032	2.2 (2N)	—	4.4 (2N)
NH_3¶	‖	2.029	‖	‖	‖
Et_2NH	$Fe(NO)_2(SMe)(Et_2NH)$	2.030	4.0 (2N)	2.0 (3H)	‡
Pyrrolidine (pyr)	$Fe(NO)_2(SMe)(pyr)$	2.029	3.9 (2N)	2.0 (3H)	‡
Piperidine (pip)	$Fe(NO)_2(SMe)(pip)$	2.029	4.2 (2N)	2.1 (3H)	‡
Solvo-complex from $Fe_2(SCH_2Ph)_2(NO)_4$					
Pyrrolidine	$Fe(NO)_2(SCH_2Ph)(pyr)$	2.029	4.2 (2N)	2.0 (2H)	‡
Solvo-complex from $Fe_2(SCH_2COOH)_2(NO)_4$					
H_2O	‖	2.030	‖	‖	‖

* X represents ^1H or ^{14}N in coordinated solvent molecules.
† No resolution of hyperfine coupling to ^2H or ^{14}N in coordinated solvent molecules.
‡ No resolution of hyperfine coupling to ^1H or ^{14}N in coordinated solvent molecules.
§ S represents 2,6-dimethylpyridine, 2,4,6-trimethylpyridine or quinoline.
‖ No resolution of any hyperfine couplings; identity of paramagnetic complex doubtful (see text).
¶ Spectrum recorded at 200 K.

with these results, and allowing for the change of solvent from aqueous ethanol to pure water, we suggest that the $g = 2.030$ species observed here is $[Fe(NO)_2(H_2O)_2]^+$, or a mono-deprotonated form, resulting from solvolysis of $Fe_2(SCH_2COOH)_2(NO)_4$ by water.

With the exception of the solvo-complexes formed in DMF and DMA solutions, all the other solvo-complexes of Table 4 were formed at room temperature or below. Their formation is significant in that it demonstrates that the diamagnetic esters $Fe_2(SR)_2(NO)_4$ can spontaneously and very readily form paramagnetic centres, simply upon dissolution in a polar, coordinating medium, typical of physiological environments.

Despite any residual uncertainty about the constitution of the solvo-complexes formed by DMA, DMSO, and aliphatic amines, it is clear and unambiguous that there are two major points of difference between the solvo-complexes formed by hetero-aromatic and by aliphatic amines. The hetero-aromatic amines displace both RS groups and the resulting complexes show resolved hyperfine coupling to the coordinated solvent. In contrast, the aliphatic amines displace only one RS group and show no coupling to the solvent in the resulting

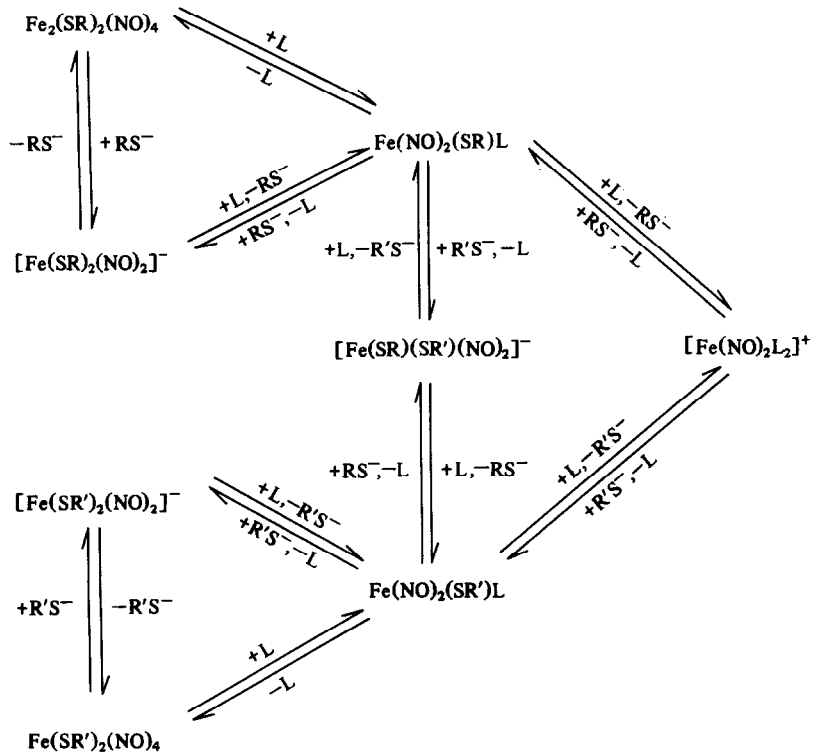
complexes. For a possible rationalisation of these observations we turn to a consideration of the differences in metal–ligand binding aliphatic and hetero-aromatic amines. Although no formation constants appear to be available for the interactions of amines acting both as solvent and as ligand towards a d^9 metal ion, we can nonetheless appeal to the properties of the ligands themselves. The spectrochemical f values for ammonia, the aliphatic amines, and hetero-aromatic amines are very similar[27] and allow no distinction of the several classes of ligand: however, the use of a two-dimensional spectrochemical series[28] shows that whereas aliphatic amines are essentially involved only in σ bonding with central metals, (i.e. $e_\pi \simeq 0$) hetero-aromatic amines such as pyridine, although somewhat weaker σ donors are also strong π acceptors (i.e. $e_\pi < 0$). This difference is expected to be accentuated with electron-rich central metals, and consequently we suggest that metal → ligand π-bonding is the major source of the differences between hetero-aromatic amines and other ligands as solvents. The more powerful metal–ligand interaction in the case of the hetero-aromatic amines is the principal factor underlying the displacement of both RX groups by these amines.

The identification of the two solvo-complexes in DMF solvent then allowed the assignment of the EPR spectra obtained from solutions of the esters $Fe_2(SR)_2(NO)_4$ in mixtures of RSH and DMF to similar pairs of solvo-complexes $[Fe(NO)_2(DMF)_2]^+$ and $Fe(NO)_2(SR)(DMF)$ for each of R = Me, Et and *i*-Pr. When R = *t*-Bu, no resolution of the very weak spectrum was achieved, but it seems unlikely that the composition of this solution was significantly different from those of the lower alkyl esters.

If instead of MeSH, the benzyl mercaptan $PhCH_2SH$ was added to a solution of $Fe_2(SMe)_2(NO)_4$ followed by base, the paramagnetic product identified by EPR spectroscopy was $[Fe(SCH_2Ph)_2(NO)_2]^-$, rather than $[Fe(SMe)_2(NO)_2]^-$. Similarly addition of EtS^- to a DMF solution of $Fe_2(SMe)_2(NO)_4$ gave $[Fe(SEt)_2(NO)_2]^-$ and addition of SH^- to $Fe_2(SPr\text{-}i)_2(NO)_4$ gave $[Fe(SH)_2(NO)_2]^-$ [reaction generalised in eqn (3)]:

$$Fe_2(SR)_2(NO)_4 + 2R'SH \xrightarrow{\text{base}} [Fe(SR')_2(NO)_2]^- . \quad (3)$$

The foregoing series of observations, namely: (i) that the rate of alkanethiol exchange [eqn (1)] is faster in more polar, coordinating, solvents; (ii) that in these solvents the esters $Fe_2(SR)_2(NO)_4$ readily yield mononuclear solvo-complexes; and (iii) that exchange of RS groups occurs readily in the mononuclear complexes $[Fe(SR)_2(NO)_2]^-$, allow the formulation of a tentative mechanism for the exchange reaction (see Scheme 1). Scheme 1 contains



Scheme 1.

all the potentially important equilibria involved in the overall exchange process with converts $Fe_2(SR)_2(NO)_4$ to $Fe_2(SR')_2(NO)_4$, and with the exception of $[Fe(SR)(SR')(NO)_2]^-$, all of the complexes of Scheme 1 and all the individual equilibria have been observed for at least one combination of R,R', and solvent acting as ligand L. Although the mixed anions $[Fe(SR)(SR')(NO)_2]^-$ have not been observed by EPR spectroscopy, we note that the reaction of equimolar quantities of $Fe_2(SMe)_2(NO)_4$ and $Fe_2(SEt)_2(NO)_4$ in DMF solution at room temperature yielded the mixed ester $Fe_2(SMe)(SEt)(NO)_4$, identified by mass spectrometry: in contrast reflux during 4 h of these two pure esters in chloroform solution gave no evidence for mixed ester formation. In solvents such as pyridine, the exchange appears to proceed solely via $[Fe(NO)_2L_2]^+$; in solvents such as Et_3N, solely via $Fe(NO)_2(SR)L$; and in solvent such as DMF, via both routes.

We have recorded elsewhere[8] the observation that $Fe_2(SMe)_2(NO)_4$ reacted, in DMF solution, with an excess of either bromide or iodide ions to yield the complexes $[Fe(NO)_2Br_2]^-$ or $[Fe(NO)_2I_2]^-$ respectively, identical with the species formed[2] by reaction of nitric oxide with mixtures of iron(II) salts and halides. In contrast, fluoride or chloride ions gave no paramagnetic halogeno complexes but rather a mixture, in each case, of the solvo-complexes $Fe(NO)_2(SMe)(DMF)$ and $[Fe(NO)_2(DMF)_2]^+$. The pseudohalide thiocyanate, NCS^-, yielded the complex $[Fe(NO)_2(NCS)_2]^-$ identical with that observed[2] in Fe(II)/NCS^-/NO reactions: cyanate, NCO^-, likewise yielded with $Fe_2(SMe)_2(NO)_4$ the complex $[Fe(NO)_2(NCO)_2]^-$, hitherto unreported, having $g = 2.030$, $A(^{14}N) = 2.6$G ($2 \times NCO$), 1.8 G ($2 \times NO$). Selenocyanate, $NCSe^-$, yielded a very complex spectrum, which we have been unable to interpret.

Reactions of $[Fe_4S_3(NO)_7]^-$ *salts*

The reactions of the Roussin black anion, $[Fe_4S_3(NO)_7]^-$ are inevitably more complex than those of the 2-Fe esters $Fe_2(SR)_2(NO)_4$ since in the anion there are two types of iron:[29,30] the unique apical iron carries a single nitrosyl ligand, whereas the three basal irons each carry two nitrosyl ligands. The structure observed[29,30] by X-ray analysis in crystalline salts is shown by ^{15}N NMR to persist in solution.[25]

Solutions of $[Fe_4S_3(NO)_7]^-$ in water at neutral pH gave no EPR spectrum, but in alkaline solution a weak 3-line EPR spectrum was observed having $g = 2.027$ and $A(^{14}N) = 4.7$ G. The intensity of this spectrum increased as the pH was raised, as previously observed,[1] but at any pH, the intensity decreased with time. No paramagnetic dinitrosyliron complexes were observed in these solutions, despite the fact that on a preparative scale, the reaction of $[Fe_4S_3(NO)_7]^-$ with alkali yields[15,31] Roussin's red anion $[Fe_2S_2(NO)_4]^-$.

In DMF solution, the anion $[Fe_4S_3(NO)_7]^-$ yielded a weak but complex EPR spectrum indicative of the presence of at least three paramagnetic species: we have not achieved a satisfactory interpretation of this spectrum. However if RS^- was then added (R = Me, Et, *i*-Pr, *t*-Bu or $PhCH_2$), this complex spectrum was immediately replaced by a new and much more intense spectrum which indicated the presence of $[Fe(SR)_2(NO)_2]^-$, identified as previously (Table 3), together with, in each case, a mononitrosyl complex having $g = 2.021$ with $A(^{14}N)$ varying from 6.9 G when R = Me to 5.0 G when R = *t*-Bu, but showing no hyperfine coupling to the hydrogens of the R groups. The use of $[Fe_4S_3(^{15}NO)_7]^-$ confirmed these assignments. After two days the spectrum of the mononitrosyl complex had in each case disappeared, leaving only the spectrum of $[Fe(SR)_2(NO)_2]^-$. The reaction of $[Fe_4S_3(NO)_7]^-$ with SH^- yielded similarly a mixture of $[Fe(SH)_2(NO)_2]^-$ (Table 3) and the mononitrosyl complex. The EPR parameters for the mononitrosyl complex produced by reaction of $[Fe_4S_3(NO)_7]^-$ with RS^-, or with[1] aqueous alkali, are essentially identical with those of the mononitrosyl complex produced[1] by reaction of iron(II) salts with nitric oxide in the presence of sulphide. The observation of a variation of A(N) with R, and the assumption of four-coordinate iron, as in $[Fe(SR)_2(NO)_2]^-$ lead then to the tentative assignment of the constitution $[Fe(SR)_3NO]^{x-}$ to these species: if these species were formed from the apical iron of $[Fe_4S_3(NO)_7]^-$ without change of oxidation state, then $x = 1$. The lack of any resolved hyperfine coupling to hydrogen in the SR groups may be the result of a small A(H) value, or a consequence of fast ligand exchange. When R = Me the initial concentration ratio of $[Fe(SMe)_2(NO)_2]^-/[Fe(SMe)_3NO]^-$, measured immediately after reaction, was *ca* 1:2 at 290 K and *ca* 4:1 at 240 K.

We may therefore write, for the reaction of $[Fe_4S_3(NO)_7]^-$ with RS^- the following [eqn (4)]:

$$[Fe_4S_3(NO)_7]^- \xrightarrow{9RS^-} 3[Fe(SR)_2(NO)_2]^- + [Fe(SR)_3(NO)]^- + 3S^{2-}, \quad (4a)$$

[3Fe(−I)(basal), 1Fe(I)(apical)]

$$\rightarrow 3Fe(-I) + Fe(I), \quad (4b)$$

where the dinitrosyl complex is derived from the three basal irons of the 4-Fe anion, and the mononitrosyl complex from the apical iron. When R = alkyl, the complex $[Fe(SR)_2(NO)_2]^-$ appears to be the precursor of the ester $Fe_2(SR)_2(NO)_4$, as reaction of $[Fe_4S_3(NO)_7]^-$ with MeS^- on a preparative scale yielded $Fe_2(SMe)_2(NO)_4$ in 46% purified, isolated yield. On the other hand, reaction of PPN^+ $[Fe_4S_3(NO)_7]^-$ with NaSH yielded $(PPN^+)_2$ $[Fe_2S_2(NO)_4]^{2-}$, for the formation of which we propose the following [eqn (5)]:

$$[Fe_4S_3(NO)_7]^- \xrightarrow{SH^-} [Fe(SH)_2(NO)_2]^- \longrightarrow Fe_2(SH)_2(NO)_4 \xrightarrow[-H_2S]{+SH^-} [Fe_2S_2(NO)_4]^{2-}. \quad (5)$$

In general the anions $[Fe(SR)_2(NO)_2]^-$ lose one mole of RS^- and then dimerise to give $Fe_2(SR)_2(NO)_4$: if R = alkyl, this is the product which is isolated, but when R = H, deprotonation is effected by excess SH^-, followed by precipitation of the salt $(PPN^+)_2[Fe_2S_2(NO)_4]^{2-}$. In support of our suggestion that the initially formed $Fe_2(SH)_2(NO)_4$ is deprotonated in the presence of excess SH^-, we note that this compound has been isolated,[32] but that its formation by protonation of the anion $[Fe_2S_2(NO)_4]^{-2}$ required acids as strong as trifluoroacetic acid or HBF_4.

The complex $[Fe(SH)_2(NO)_2]^-$, produced by reaction of $[Fe_4S_3(NO)_7]^-$ with SH^-, was also formed when hydrogen sulphide was passed into a mixture of hydrated iron(III) chloride and sodium nitrite in DMF: no mononitrosyl was observed in this reaction, but a second dinitrosyl complex was formed, characterised by $g = 2.031$, $A(^{14}N) = 2.00$ G, and $A(^1H) = 1.90$ G, to which we assign the constitution $Fe(SH)(SH_2)(NO)_2$. When acetic acid was added to the foregoing mixture, the concentration of $Fe(SH)(SH_2)(NO)_2$ is increased at the expense of $[Fe(SH)_2(NO)_2]^-$: this was reversed upon addition of base. Substitution of dimethyl sulphide for hydrogen sulphide in the reaction of iron(III) with nitric oxide gave no detectable paramagnetic complexes having g near 2.0. Reaction of the sodium salt of $[Fe_4S_3(NO)_7]^-$, which crystallises from water as a monohydrate, with elemental sulphur in DMF, yielded again an EPR spectrum which indicated a mixture of $[Fe(SH)_2(NO)_2]^-$ and $Fe(SH)(SH_2)(NO)_2$, together with a trace only of the mononitrosyl $[Fe(SH)_3NO]^-$.

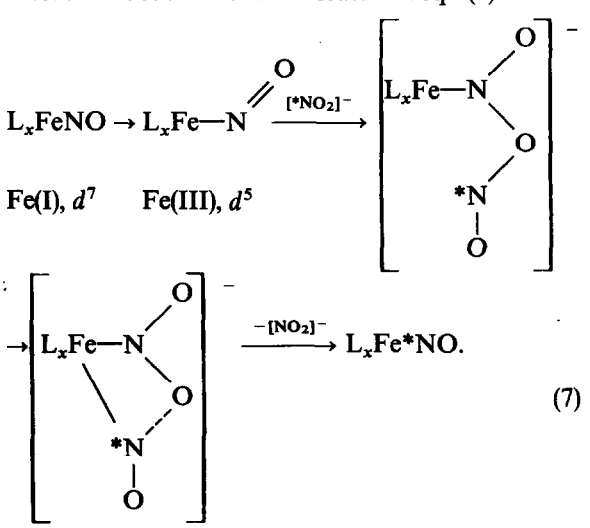
Reaction of $Na[Fe_4S_3(NO)_7]\cdot H_2O$ in DMF with sodium nitrite yielded a mixture of $[Fe(SH)_2(NO)_2]^-$ and $Fe(SH)(SH_2)(NO)_2$, but no mononitrosyl complexes were detected by EPR spectroscopy suggesting that all the Fe(NO) fragments have disproportionated to give $Fe(NO)_2$ species [eqn (6)]:

$$2[Fe(NO)]^{2+} \rightarrow [Fe(NO)_2]^+ + Fe^{3+}, \quad (6a)$$

$$2Fe(I) \rightarrow Fe(-I) + Fe(III). \quad (6b)$$

This conversion of $Fe(NO)^{2+}$ fragments to $Fe(NO)_2^+$ fragments appears to occur also during the ageing of the reaction products from $[Fe_4S_3(NO)_7]^-/RS^-$ reactions (see above). The reverse conversion, of $Fe(NO)_2$ to Fe(NO) fragments, occurs in the presence of the dimethyldithiocarbamate ligand, $[Me_2NCS_2]^-$. The EPR spectrum of a mixture of $[Fe_4S_3(NO)_7]^-$ and $[Me_2NCS_2]^-$ in DMF showed the presence of $Fe(NO)(S_2CNMe_2)_2$ as the sole paramagnetic complex detectable: similarly, this mononitrosyl complex was isolated from such a reaction mixture in 88% yield based upon total iron, i.e. not only the apical Fe(NO) group, but the basal $Fe(NO)_2$ groups in $[Fe_4S_3(NO)_7]^-$ were converted to $Fe(NO)(S_2CNMe_2)_2$.

The lability of the nitrosyl groups was further demonstrated by the use of ^{15}N labelling. When either $[Fe_4S_3(^{14}NO)_7]^-$ and $[^{15}NO_2]^-$, or $[Fe_4S_3(^{15}NO)_7]^-$ and $[^{14}NO_2]^-$ mixtures in DMF, containing similar ratios of $^{14}N/^{15}N$, were treated with $[Me_2NCS_2]^-$, essentially identical EPR spectra, each characteristic of a mixture of $Fe(^{14}NO)(S_2CNMe_2)_2$ and $Fe(^{15}NO)(S_2CNMe_2)_2$, were obtained from the two solutions. The spectra were identical when recorded immediately after mixing, and after one month, and represent an equilibrium distribution of ^{14}N and ^{15}N amongst the nitrosyl ligands. When $Fe(^{14}NO)(S_2CNMe_2)_2$ was treated in DMF solution with a large excess (> 10:1 mol/mol) of $[^{15}NO_2]^-$, its EPR spectrum was replaced, very rapidly and almost completely, by that of $Fe(^{15}NO)(S_2CNMe_2)_2$, indicating fast exchange of the nitrogen, presumably by a mechanism such as that indicated in eqn (7):



(7)

A further example of rapid conversion of a $Fe(NO)_2$ fragment to Fe(NO), combined with isotopic exchange at nitrogen, was observed when $Fe_2(SMe)_2(^{14}NO)_4$ was reacted, in DMF, with $[^{15}NO_2]^-$ and $[Me_2NCS_2]^-$: the resultant EPR spectrum showed the presence of both $Fe(^{14}NO)(S_2CNMe_2)$ and $Fe(^{15}NO)(S_2CNMe_2)_2$. Finally, an example of rapid isotopic exchange in a dinitrosyl species is provided by the reaction of $[Fe(SPr\text{-}i)_2(^{14}NO)_2]^-$ with $[^{15}NO_2]^-$: when the dinitrosyl anion, prepared from $Fe_2(SPr\text{-}i)_2(NO)_4$ in the usual way, was treated with $[^{15}NO_2]^-$ in DMF, its EPR spectrum was rapidly replaced by that of $[Fe(SPr\text{-}i)_2(^{15}NO)_2]^-$, again presumably by the mechanism outlined schematically in eqn (7).

Reactions of $Fe_4S_4(NO)_4$

The tetranuclear complex $Fe_4S_4(NO)_4$ has a structure, in the solid state, based upon two intersecting Fe_4 and S_4 tetrahedra, yielding a distorted cubane skeleton, with a single, essentially linear, terminal nitrosyl ligand on each iron:[33,34] this structure has been shown by ^{15}N NMR spectroscopy[25] to persist in solution. In a variety of reactions of $Fe_4S_4(NO)_4$, the products are essentially the same as those derived from the anion $[Fe_4S_3(NO)_7]^-$, emphasizing again the great ease of migration of nitrosyl groups in these systems, and especially the interconversion of Fe(NO) and $Fe(NO)_2$ fragments.

In DMF solution, $Fe_4S_4(NO)_4$ alone yielded a very weak EPR spectrum which indicates the presence of at least three paramagnetic centres. Addition of RS^- caused replacement of this spectrum with a new spectrum, the principal features of which were those due to $[Fe(SR)_2(NO)_2]^-$ together with those which have been assigned earlier to $[Fe(SR)_3(NO)]^-$, and we postulate their formation according to eqn (8):

$$Fe_4S_4(NO)_4 \xrightarrow{12RS^-} 4[Fe(SR)_3NO]^- + 4S^{2-}, \quad (8a)$$

$$2[Fe(SR)_3NO]^- \rightleftharpoons [Fe(SR)_2(NO)_2]^- + [Fe(SR)_4]^-, \quad (8b)$$

$$2Fe(I) \rightleftharpoons Fe(-I) + Fe(III). \quad (8c)$$

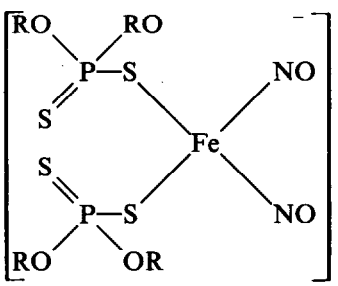
As with the corresponding reactions of $[Fe_4S_3(NO)_7]^-$, the EPR spectrum of the mononitrosyl complex disappears as the solution is aged.

However, when R = H, the observed behaviour is rather different: the initial spectrum indicates the presence of the dinitrosyliron complex $[Fe(SH)_2(NO)_2]^-$ and the mononitrosyl complex $[Fe(SH)_3NO]^-$, having $g = 2.020$ and $A(^{14}N) = 5.0$ G. After one week the $[Fe(SH)_2(NO)_2]^-$ spectrum was still present but that of $[Fe(SH)_3NO]^-$ had been completely replaced by a new mononitrosyl spectrum having $g = 2.040$, $A(^{14}N) = 13.5$ G, but again showing no hyperfine coupling to hydrogen: after a further week, all evidence of the mononitrosyliron species had disappeared from the spectrum which indicated only a mixture of $[Fe(SH)_2(NO)_2]^-$ and $Fe(SH)(SH_2)(NO)_2$. Similar $A(^{14}N) = 13.5$ G mononitrosyliron species have been observed in the reactions of $Fe_4S_4(NO)_4$ with t-BuS^-, where it appeared concurrently with $[Fe(SR)_3NO]^-$; and in the reaction[8] of i-PrSH with $Fe_2I_2(NO)_4$ in mixed THF/Et_3N as solvent: in neither case was any hyperfine coupling to hydrogen resolved. Although we have not identified the 13.5 G species definitively, the alternative routes for its production suggest as a plausible possibility the constitution $[Fe(SR)_3NO]^{-3}$, i.e. a complex of iron(−I), possibly formed by an alternative disproportionation to that defined by eqns (8b) and (8c).

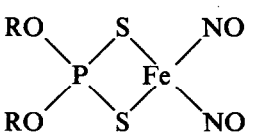
On a preparative scale, reaction of MeS^- with $Fe_4S_4(NO)_4$ in DMF yields the green solution characteristic of $[Fe(SMe)_2(NO)_2]^-$: on addition of a large volume of toluene the solution changed from green to red, and from the red solution the red ester $Fe_2(SMe)_2(NO)_4$ was isolated in 13% overall yield. This experiment demonstrated clearly the reversal of eqn (3) in a non-polar medium, and indicated that any precursor of $[Fe(SR)_2(NO)_2]^-$ can, in the appropriate solvent system, yield $Fe_2(SR)_2(NO)_4$.

Despite the great propensity of $Fe_4S_4(NO)_4$ to form dinitrosyliron complexes in its reactions with RS^-, upon reaction with $[Me_2NCS_2]^-$ in DMF solution, it forms the mononitrosyliron complex $Fe(NO)(S_2CNMe_2)_2$ in almost quantitative (94%) purified yield. Comparison of the reactions of $Fe_4S_4(NO)_4$ and $[Fe_4S_3(NO)_7]^-$ shows that the nature of the principal paramagnetic product (mononitrosyliron or dinitrosyliron complexes) is essentially independent of the structure of the starting complex, but that it depends rather upon the nature of the other ligands available in the system. In the presence of the non-chelating RS^- ligands, dinitrosyliron complexes are strongly favoured, and after an appropriate time interval are the sole detectable paramagnetic products: however if the chelating ligand $[Me_2NCS_2]^-$ is available in the system, the mononitrosyliron complex $Fe(NO)(S_2CNMe_2)_2$ is formed exclusively, and judging by the results of preparative scale experiments, it is formed virtually quantitatively (based upon total iron). However in the presence of a large excess of MeS^-, the complex $Fe(NO)(S_2CNMe_2)_2$ yielded $Fe_2(SMe)_2(NO)_4$ in 24% isolated yield.

In an attempt to explore further the relationship between the nature of the thio-ligands and the stoichiometry of the resulting complexes, we have also studied the reactions of the dialkyl dithiophosphate ion $[(i\text{-PrO})_2PS_2]^-$ with a range of iron nitrosyl substrates. Like $[Me_2NCS_2]^-$ this ligand could in principal act either as a monodentate or as a bidentate chelating ligand: the S···S bite in chelating $[(RO)_2PS_2]^-$ ligands is[35] *ca* 3.28 Å, whereas in $[Me_2NCS_2]^-$ it is[35,36] *ca* 2.97 Å. Reaction of $[(i\text{-PrO})_2PS_2]^-$ with $[Fe_4S_3(NO)_7]^-$ in DMF yielded an EPR spectrum which indicated the presence both of a dinitrosyl complex having $g = 2.033$, $A(^{14}N) = 2.3$ G and a mononitrosyl complex having $g = 2.030$, $A(^{14}N) = 2.2$ G: the spectral analysis was confirmed by use of $[Fe_4S_3(^{15}NO)_7]^-$. Essentially the same spectrum was obtained when $Fe_4S_4(NO)_4$, $Fe_2I_2(NO)_4$, $Fe_2(SMe)_2(NO)_4$ or $Fe_2(SPr\text{-}i)_2(NO)_4$ was employed in place of $[Fe_4S_3(NO)_7]^-$. In none of these systems was any hyperfine coupling to phosphorus (^{31}P, $I = \frac{1}{2}$) resolved. By analogy with $Fe(NO)(S_2CNMe_2)_2$ the mononitrosyl complex may tentatively be assigned the constitution $Fe(NO)[S_2P(OPr\text{-}i)_2]_2$ while in the dinitrosyl complex the dithiophosphate ligand might be monodentate (**III**) or bidentate (**IV**).



III



IV

All attempts to isolate and purify these complexes have been unsuccessful. The complexes derived from $[(RO)_2PS_2]^-$ are clearly less stable chemically than $Fe(NO)(S_2CNMe_2)_2$ derived from the related $[Me_2NCS_2]^-$. In confirmation of this we observed that excess $[(i\text{-PrO})_2PS_2]^-$ effected no displacement of $[Me_2NCS_2]^-$ from $Fe(NO)(S_2CNMe_2)_2$, whereas an excess of RS^- (R = Me, *i*-Pr, *t*-Bu) effected quantitative displacement of $[Me_2NCS_2]^-$, with conversion to the dinitrosyliron complexes $[Fe(SR)_2(NO)_2]^-$: when R = Me, the ester $Fe_2(SMe)_2(NO)_4$ was isolated.

We conclude that the larger $[(i\text{-PrO})_2PS_2]^-$ ligand is less suited to the stabilisation of dinitrosyliron complexes than the non-chelating RS^- ligands, and less suited also to the stabilisation of mononitrosyliron complexes than the chelating ligand $[Me_2NCS_2]^-$ of smaller bite.

Reactions of $[Fe(CO)_3NO]^-$ *salts*

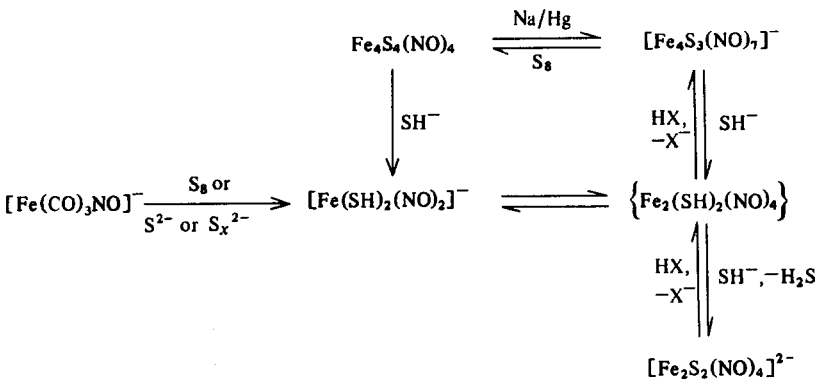
The salt $(PPN)^+[Fe(CO)_3NO]^-$ gives no detectable EPR spectrum in DMF solution either after mixing at room temperature or heating to 350 K before the recording of the spectrum, although we note that several related but paramagnetic complexes are known containing only carbonyl and nitrosyl as ligands, thus: $Fe(NO)_3CO$,[37] $Co(CO)_3NO$,[38] $[Fe(NO)_2(CO)_2]^-$.[39]

Upon addition of elemental sulphur, the above solution readily gave an EPR spectrum characteristic of $[Fe(SH)_2(NO)_2]^-$. When the reaction of this salt with sulphur was carried out on a preparative scale, the presence of the anion $[Fe_4S_3(NO)_7]^-$ was detected by TLC and by IR spectroscopy immediately after mixing the reactants, and $(PPN)^+[Fe_4S_3(NO)_7]^-$ was subsequently isolated from the reaction mixture in 84% yield.

Prolonged reflux of $(PPN)^+[Fe_4S_3(NO)_7]^-$ with elemental sulphur in toluene solution gave no detectable formation of $Fe_4S_4(NO)_4$. This is in contrast both to the reaction of the mercurial $Hg[Fe(CO)_3NO]_2$ with elemental sulphur, under similar conditions, which yields $Fe_4S_4(NO)_4$ in good yield,[33] and to the similar reaction[23] of $Na[Fe_4S_3(NO)_7]$ with sulphur which is in fact our preferred method for the synthesis of $Fe_4S_4(NO)_4$. We note further that reaction of $Hg[Fe(CO)_3NO]$ with sodium polysulphide in methanol gave[23] $Na[Fe_4S_3(NO)_7]$ but no $Fe_4S_4(NO)_4$. Clearly the formation of $Fe_4S_4(NO)_4$ vs $[Fe_4S_3(NO)_7]^-$ from $[Fe(CO)_3NO]^-$ is subject to subtle factors involving the solvent and the solubilities of both the desired products and the by-products.

The observation of $[Fe(SH)_2(NO)_2]^-$ in the reaction mixture of $[Fe(CO)_3NO]^-$ and sulphur, which yields ultimately $[Fe_4S_3(NO)_7]^-$, suggests that just as the reaction of $[Fe_4S_3(NO)_7]^-$ with OH^- or SH^- proceeds via $[Fe(SH)_2(NO)_2]^-$ on its way to $[Fe_2S_2(NO)_4]^{-2}$, so the formation of $[Fe_4S_3(NO)_7]^-$ proceeds via the mononuclear complex $[Fe(SH)_2(NO)_2]^-$. This view is strengthened by the observation by EPR of this complex also in the reaction of $[Fe(CO)_3NO]^-$ with Na_2S, known[23] also to yield $[Fe_4S_3(NO)_7]^-$. Since preparative studies[15,31,32] have shown that $[Fe_2S_2(NO)_4]^-$ and $[Fe_4S_3(NO)_7]^-$ are interconvertible [eqn (9)]:

$$Fe_2S_2(NO)_4]^{2-} \underset{OH^-}{\overset{H^+}{\rightleftharpoons}} [Fe_4S_3(NO)_7]^- \qquad (9)$$



Scheme 2.

the fate of $[Fe(SH)_2(NO)_2]^-$ will in general depend primarily on the pH of the reaction medium. The relationships between all the complexes which are[15,23,31–33] interconnected via $[Fe(SH)_2(NO)_2]^-$ are summarised in Scheme 2.

Just as S^{2-}/SH^- reacts with $[Fe(CO)_3NO]^-$ to give $[Fe(SH)_2(NO)_2]^-$, so also *i*-PrS$^-$ and *t*-BuS$^-$ react to yield $[Fe(SPr\text{-}i)_2(NO)_2]^-$ and $[Fe(SBu\text{-}t)_2(NO)_2]^-$, observed by EPR spectroscopy, while MeS$^-$ yields $Fe_2(SMe)_2(NO)_4$, isolated in 78% yield. These reactions all provide further examples of the conversion of mononitrosyliron sources to dinitrosyliron products by the action of RS$^-$.

CONCLUSIONS

We have demonstrated, for the first time, the ready formation of paramagnetic, mononuclear complexes $[Fe(SR)_2(NO)_2]^-$ from a range of diamagnetic sources, not only from the dinuclear esters $Fe_2(SR)_2(NO)_4$ but also from the tetranuclear clusters $[Fe_4S_3(NO)_7]^-$ and $Fe_4S_4(NO)_4$, and from the mononuclear $[Fe(CO)_3NO]^-$. The characterisation of a range of these complexes $[Fe(SR)_2(NO)_2]^-$, allows definitive identification of the $g = 2.03$ complexes so often observed[9–11,14,21] but never adequately characterised, in biochemical studies related to chemical carcinogenesis. Of particular significance in this context are: (i) the wide range of iron–nitrosyl complexes which we have found to give rise to the $g = 2.03$ species, (ii) the ease of formation of paramagnetic complexes from diamagnetic precursors, by reaction with soft nucleophiles and/or polar solvents, and (iii) the great lability of nitrosyl ligands in these systems. Connected with the first two points is the ready formation, from a range of precursors, via $[Fe(SMe)_2(NO)_2]^-$ of the ester $Fe_2(SMe)_2(NO)_4$. This ester has been isolated[17] from natural vegetable sources in which it appears to be formed by reaction of exogenous nitrite with the natural iron–sulphur clusters of redox proteins, and it has been shown to be a mutagen and a tumour promotor.[18–20] The reaction of $Fe_2(SMe)_2(NO)_4$ as a nitrosating agent with secondary amines[20] has not been elucidated mechanistically, but it is likely to be connected with the lability of the nitrosyl ligands in these systems and possibly also with the ready formation of paramagnetic complexes. We turn our attention next to the mechanism of the nitrosation of amines by $Fe_2(SR)_2(NO)_4$ and related species, and to the formation of such iron–sulphur–nitrosyl complexes from naturally occurring iron–sulphur clusters.

EXPERIMENTAL

Literature methods were used for the preparation of $Fe_2I_2(NO)_4$,[40] $Fe_2(SR)_2(NO)_4$,[23] $Na[Fe_4S_3(NO)_7]$,[15,23] $Na[Fe_4Se_3(NO)_7]$,[23] $Fe_4S_4(NO)_4$,[23] $Fe(NO)(S_2CNMe_2)_2$[41] and $[N(PPh_3)_2][Fe(CO)_3NO]$:[7,42] ^{15}N labelled compounds were prepared by modification of the above procedures, using 99% $Na[^{15}NO_2]$ (MSD Isotopes Inc.).

All manipulations were carried out under an atmosphere of dry nitrogen: all organic solvents were dried and purged with dry nitrogen before use, and all manipulations of solutions were made under dry nitrogen.

EPR spectra were measured, usually at 240 K, in 1 mm quartz capillaries using a Bruker ER200D Spectrometer: di-*t*-butyl nitroxide was used as the standard for the measurement of line positions. NMR spectra were measured at 308 K using a Bruker WP-80 Spectrometer.

Exchange reactions

Samples (0.10 g) of $Fe_2(SEt)_2(NO)_4$ were dissolved in 50 cm^3 portions of DMF, THF, EtOH, or toluene and 1 cm^3 of *i*-PrSH was then added, and the mixtures stirred under nitrogen, at room temperature, during 72 h. The solvent and volatile products

were then removed on the vacuum system, and the residual solid was examined by ^1H NMR spectroscopy in $CDCl_3$ solution.

Samples (0.10 g) of $Fe_2(SR)_2(NO)_4$ were dissolved in 50 cm^3 portions of THF and a 1 cm^3 portion of R'SH was added. The mixtures were stirred under nitrogen, at room temperature, during 72 h, and then worked up and examined as before. The exchange reaction with H_2S was carried out in a sealed 5 dm^{-3} vessel at 1 atm pressure.

Reactions of $Na[Fe_4S_3(NO)_7]$

With CH_3SNa. To 0.10 g of $Na[Fe_4S_3(NO)_7]$ in DMF (30 cm^3) was added 0.10 g of CH_3SNa. The mixture was stirred under nitrogen during 15 min and then diluted with 50 cm^3 of CH_2Cl_2. The solution was washed with water (4×250 cm^3) and then filtered and dried over $MgSO_4$. The solution was reduced to small volume, and methanol was added to precipitate the product, $Fe_2(SMe)_2(NO)_4$, isolated in 46% purified yield, calculated on the basis of $Fe(NO)_2$ fragments.

With Me_2NCS_2Na. To a solution of 0.50 g $Na[Fe_4S_3(NO)_7]$ in 400 cm^3 water was added 2 g of NaOH and 2 g of Me_2NCS_2Na. The mixture was stirred for 10 min, and then quenched by addition of CH_2Cl_2 (100 cm^3). The organic layer was washed, dried, and then evaporated to dryness. Repeated extraction of the aqueous layer with further CH_2Cl_2, followed by washing and drying yielded further portions of solid material. The combined solids were recrystallised from CH_2Cl_2/CH_3OH to yield $Fe(NO)(S_2CNMe_2)_2$ (1.03 g: 88% yield based upon total iron, 354% based upon apical iron).

Preparation of $(PPN)_2[Fe_2S_2(NO)_4]$

To a solution of 0.10 g of $Na[Fe_4S_3(NO)_7]$ in 100 cm^3 water was added 0.5 g NaOH: the mixture was refluxed under nitrogen for 5 min before addition of 2 g of (PPN)Cl dissolved in the minimum volume of water. The whole mixture was cooled and extracted with $CHCl_3$ (1×100 cm^3). The extract was filtered, washed with water (2×100 cm^3), and dried over $MgSO_4$. The volume was reduced somewhat and the product precipitated by addition of cold methanol. Yield 0.031 g (6.7% based upon total iron, 7.5% based upon NO).

Reaction of $Fe_4S_4(NO)_4$ *with* Me_2NCS_2Na

Me_2NCS_2Na (0.27 g) was added to a solution of $Fe_4S_4(NO)_4$ (0.10 g) in DMF (20 cm^3). The mixture was stirred at room temperature, under nitrogen, during 45 min, and then diluted with 50 cm^3 of CH_2Cl_2. The resulting solution was washed with water (4×500 cm^3), filtered, and dried over $MgSO_4$. The solution was reduced to small volume, and methanol was added to precpitate the product, $Fe(NO)(S_2CNMe_2)_2$, isolated in 94% purified yield.

Reaction of $Fe_4S_4(NO)_4$ *with* MeSNa

MeSNa (0.70 g; 10 mmol) was added to a stirred solution of $Fe_4S_4(NO)_4$ (0.47 g; 1.0 mmol) in DMF (20 cm^3). The mixture was refluxed under nitrogen during 2 h, and then cooled. Toluene (100 cm^3) was added dropwise to the *green* solution, via a pressure-equalised dropping funnel, and the resulting *red* solution was filtered through a 1 cm depth bed of silica, and evaporated to dryness. The residue was dissolved in CH_2Cl_2 (30 cm^3), and washed with water (10×200 cm^4): the organic layer was dried over $MgSO_4$. The solution was reduced to small volume, and the product precipitated by addition of ice cold methanol. The product, $Fe_2(SMe)_2(NO)_4$ (0.040 g; 0.13 mmol; 13%) was isolated by filtration and dried *in vacuo*.

Reactions of $(i\text{-PrO})_2PS_2Na$

With $Na[Fe_4S_3(NO)_7]$. To a solution of $Na[Fe_4S_3(NO)_7]$ (0.30 g) in DMF (50 cm^3) under nitrogen was added 1.0 g of $(i\text{-PrO})_2PS_2Na$. The mixture was stirred for 10 h, and then reduced to a solid. This solid was dissolved in CH_2Cl_2 (50 cm^3) and the solution was washed with water, and dried over $MgSO_4$. Removal of the solvent gave a very labile black solid, having ν(NO)($CHCl_3$ solution), 1800 cm^{-1} (sharp and strong absorption). All attempts to purify this material, under nitrogen, proved unsuccessful.

With $Fe_2I_2(NO)_4$. Substitution of $Fe_2I_2(NO)_4$ for $Na[Fe_4S_3(NO)_7]$ yielded the same material as before: no successful purification was achieved.

In $CHCl_3$, very dilute solutions of this black solid gave EPR spectra indicative of the presence of two species, characterised by $g = 2.033$, $A(^{14}N) = 2.3$ G ($2^{14}N$) or $A(^{15}N) = 3.2$ G ($2^{15}N$) and $g = 2.030$, $A(^{14}N) = 2.2$ G ($1^{14}N$) or $A(^{15}N) = 3.1$ G ($1^{15}N$) respectively. Identical spectra were obtained from the reactions of $(i\text{-PrO})_2PS_2K$ with $Fe_4S_4(NO)_4$, $Fe_2I_2(NO)_4$, $Na[Fe_4S_3(NO)_7]$, $Fe_2(SMe)_2(NO)_4$ and $Fe_2(SPr\text{-}i)_2(NO)_4$.

Reaction of $Fe(NO)(S_2CNMe_2)_2$ *with* Na_2S

0.30 g of $Fe(NO)(S_2CNMe_2)_2$ was dissolved in 150 cm^3 of 1:1 (v/v) DMF/H_2O. An approximately 10-fold molar excess of Na_2S was added, and the mixture was refluxed under nitrogen for 60 h. The

solution was cooled, diluted with 850 cm^3 water, filtered, and washed with CH_2Cl_2 (8 × 100 cm^3). The remaining aqueous layer was evaporated to dryness, and the residue dissolved in 100 cm^3 ether: the ether layer was washed with water (4 × 250 cm^3), and then dried over $MgSO_4$. Removal of the solvent yielded 0.015 g of $Na[Fe_4S_3(NO)_7]$ (11% yield based upon Fe, 18% based upon nitrosyl groups).

Reaction of (PPN)[$Fe(CO)_3NO$] *with* MeSNa

To a stirred solution of (PPN)[$Fe(CO)_3NO$] (1.00 g; 1.40 mmol) in DMF (20 cm^3) was added a large excess (2.0 g; 28.6 mmol of MeSNa). The mixture was refluxed under nitrogen for 2 h, cooled, and filtered through silica. After evaporation to dryness, the residue was dissolved in CH_2Cl_2 (30 cm^3) and the resulting solution was washed with water (10 × 200 cm^3). The organic solution was dried over $MgSO_4$ and evaporated to small volume. This solution was applied to a 2.5 cm × 1.2 m silica chromatography column: a red product, $Fe_2(SMe)_2(NO)_4$ was eluted with methanol/CH_2Cl_2 [20:1 (v/v)], and isolated in 78% purified yield.

Reaction of (PPN)[$Fe(CO)_3NO$] *with sulphur*

(PPN)[$Fe(CO)_3NO$] (1.63 g) and elemental sulphur (1.5 g) were dissolved in toluene (200 cm^3). The mixture immediately turned black, and examination by IR spectroscopy and by TLC of an aliquot removed from the fresh mixture revealed the presence of $[Fe_4S_3(NO)_7]^-$. The mixture was then refluxed under nitrogen for 20 h, and then evaporated to dryness. The residue was repeatedly extracted with CH_2Cl_2, and the organic solution reduced to small volume. The product was precipitated by addition of methanol: TLC and UV and IR spectroscopy showed the product to consist solely of (PPN)[$Fe_4S_3(NO)_7$] (yield: 84% based upon NO). Prolonged reflux (1 week) of (PPN)[$Fe_4S_3(NO)_7$] with an excess of sulphur in toluene, caused no detectable conversion to $Fe_4S_4(NO)_4$.

Reaction of $Fe(NO)(S_2CNMe_2)_2$ *with* MeSNa

A solution of $Fe(NO)(S_2CNMe_2)_2$ (1.00 g; 3.1 mmol) and MeSNa (2.0 g; 28.6 mmol) in DMF (20 cm^3) was refluxed during 2 h under N_2. The resulting mixture was cooled and worked up exactly as for the reaction of (PPN)[$Fe/CO)_3NO$] and MeSNa to yield $Fe_2(SMe)_2(NO)_4$ in 24% isolated yield after chromatography.

Acknowledgements—We thank the Cancer Research Campaign for financial support. We thank Professor Wang Guang-hui (Academia Sinica, Beijing, China) for valuable discussions, and in particular for his initial observation that the stability of $Fe_2(SMe)_2(NO)_4$ in solution appeared to be enhanced by the presence of added thiols.

REFERENCES

1. C. C. McDonald, W. D. Phillips and H. F. Mower, *J. Am. Chem. Soc.* 1965, **87**, 3319.
2. L. Burlamacchi, G. Martini and E. Tiezzi, *Inorg. Chem.* 1969, **8**, 2021.
3. G. Martini and E. Tiezzi, *Trans. Faraday Soc.* 1971, **67**, 2538.
4. B. Jezowska-Trzebiatowska and A. Jezierski, *J. Mol. Struct.* 1973, **19**, 635.
5. M. P. Boyer, J. R. Morton and K. F. Preston, *J. Phys. Chem.* 1980, **84**, 2989.
6. R. Basoni, E. Gaggelli, E. Tiezzi and G. Valensin, *J. Chem. Soc., Perkin Trans. 2*, 1975, 423.
7. N. G. Connelly and C. Gardner, *J. Chem. Soc., Dalton Trans.* 1976, 1525.
8. A. R. Butler, C. Glidewell, A. R. Hyde and J. C. Walton, *Polyhedron* (in press).
9. J. C. Woolum and B. Commoner, *Biochim. Biophys. Acta* 1970, **201**, 131.
10. R. W. Chiang, J. C. Woolum and B. Commoner, *Biochim. Biophys. Acta* 1972, **257**, 452.
11. C. Nagata, Y. Ioki, M. Kodama, Y. Tagashira and M. Nakadate, *Ann. N. Y. Acad. Sci.* 1973, **222**, 1031.
12. B. Commoner, J. C. Woolum, L. H. Senturia and J. L. Ternberg, *Cancer Res.* 1970, **30**, 2091.
13. P. D. Lawley, *Nature (London)* 1968, **218**, 580.
14. A. F. Vanin and V. Ya. Varich, *Studia Biophys.* 1981, **86**, 177.
15. F. Z. Roussin, *Ann. Chim. Phys.* 1858, **52**, 285.
16. J. T. Thomas, J. H. Robertson and E. G. Cox, *Acta Cryst.* 1958, **11**, 599.
17. G. H. Wang, W. X. Zhang and W. G. Chai, *Acta Chim. Sinica* 1980, **38**, 95.
18. S. H. Lu, A. M. Camus, L. Tomatis and H. Bartsch, *J. Natl Cancer Inst.* 1981, **66**, 33.
19. S. J. Cheng, M. Sala, M. H. Li, I. Courtois and I. Chouroulinkov, *Carcinogensis* 1981, **2**, 313.
20. W. X. Zhang, M. S. Xu, G. H. Wang and M. Y. Wang, *Cancer Res.* 1983, **43**, 339.
21. D. Reddy, J. R. Lancaster, Jr. and D. P. Cornforth, *Science* 1983, **221**, 769.
22. C. Glidewell and J. McGinnis, *Inorg. Chim. Acta* 1982, **64**, L171.
23. A. R. Butler, C. Glidewell, A. R. Hyde, J. McGinnis and J. E. Seymour, *Polyhedron* 1983, **2**, 1045.
24. A. R. Butler, C. Glidewell, A. R. Hyde and J. McGinnis, *Polyhedron* 1983, **2**, 1399.
25. A. R. Butler, C. Glidewell, A. R. Hyde and J. McGinnis, *Polyhedron* 1984, **3**, 1165.
26. C. Glidewell and A. R. Hyde, *Polyhedron* (in press).
27. C. K. Jørgensen, *Oxidation Numbers and Oxidation States*. Springer, New York (1969).

28. D. W. Smith, *Struct. Bonding (Berlin)* 1978, **35**, 87.
29. G. Johansson and W. N. Lipscomb, *Acta Cryst.* 1958, **11**, 594.
30. C. T.-W. Chu and L. F. Dahl, *Inorg. Chem.* 1977, **16**, 3245.
31. O. Pawel, *Ber. Dtsch. Chem. Ges.* 1882, **15**, 2600.
32. W. Beck, R. Grenz, F. Götzfried and E. Vilsmaier, *Chem. Ber.* 1981, **114**, 3184.
33. R. S. Gall, C. T.-W. Chu and L. F. Dahl, *J. Am. Chem. Soc.* 1974, **96**, 4019.
34. C. T.-W. Chu, F. Y.-K. Lo and L. F. Dahl, *J. Am. Chem. Soc.* 1982, **104**, 3409.
35. S. L. Lawton, C. J. Fuhrmeister, R. G. Haas, C. S. Jarman, Jr and F. G. Lohmeyer, *Inorg. Chem.* 1974, **13**, 135.
36. M. Colapietro, A. Domenicano, L. Scaramuzza and A. Vaciago, *J. Chem. Soc., Chem. Commun.* 1968, 302.
37. N. M. Atherton, J. R. Morton, K. F. Preston and M. J. Vuolle, *Chem. Phys. Lett.* 1980, **70**, 4.
38. J. R. Morton, K. F. Preston and S. J. Strach, *J. Phys. Chem.* 1980, **84**, 2478.
39. C. Couture, J. R. Morton, K. F. Preston and S. J. Strach, *J. Magn. Reson.* 1980, **41**, 88.
40. B. Haymore and R. D. Feltham, *Inorg. Synth.* 1973, **14**, 81.
41. L. Cambi and A. Cagnasso, *Atti Accad. Naz. Lincei* 1931, **13**, 254.
42. R. E. Stevens and W. L. Gladfelter, *Inorg. Chem.* 1983, **22**, 2034.

Polyhedron Vol. 4, No. 5, pp. 811–816, 1985
Printed in Great Britain

0277-5387/85 $3.00 + .00
© 1985 Pergamon Press Ltd

CYCLIC VOLTAMMETRIC STUDIES OF COPPER(II) AMINO ACID COMPLEXES: ELECTROCHEMICAL EVIDENCE FOR THE GENERATION OF COPPER(I) COMPLEX AS AN INTERMEDIATE

GEORGE THOMAS and P. S. ZACHARIAS*
School of Chemistry, University of Hyderabad, Hyderabad 500 134, India

(*Received* 23 *July* 1984; *accepted* 13 *September* 1984)

Abstract—The reduction of the title complexes is studied by cyclic voltammetry in aqueous media. It proceeds through a one-electron process generating the corresponding copper(I) amino acid complexes. The reduced copper(I) species undergo chemical reactions generating Cu(0) at the mercury electrode. The unreacted fraction of the copper(I) species is re-oxidised to the copper(II) complexes. The Cu(0) generated undergo a two-electron oxidation to Cu^{2+} at less cathodic potentials which get reduced to Cu(0) subsequently. pH-dependence of these complexes is also investigated.

The involvement of copper in the redox processes of many biological systems is well established.[1–4] Many of the low-molecular-weight copper(II) chelates of amino acids and peptides are reported to be able to catalyse superoxide dismutation.[5–8] It is reported that type 2 copper(II) undergoes a one-electron reduction[9] at a potential approximately 0.4 V vs NHE. Its optical spectral characteristics are similar to those of the copper(II) amino acid complexes. Several workers have studied the copper(II) amino acid complexes by spectral, analytical, structural etc. methods.[10–20] But there are no detailed studies of the redox behaviour of these low-molecular-weight copper(II) complexes. The cyclic voltammetric behaviour of dipeptide and ternary copper(II) complexes have been investigated.[21] In this context it seemed appropriate to study the redox behaviour of copper(II) amino acid complexes in aqueous media by cyclic voltammetric technique. Our results are presented and discussed in the following sections.

EXPERIMENTAL

Glycine, L-ornithine, L-lysine, L-asparagine and bathocuproin reagents were from Sigma Chemicals. Other amino acids were purchased from BDH, India. Basic copper carbonate was obtained from S.D. Chemicals and was used after estimating the copper content gravimetrically.[22] Analar grade sodium perchlorate was used throughout the work. Water, as well as mercury were used after distilling twice. The copper(II) amino acid complexes were prepared by the following general method. Stoichiometric amounts of the amino acid was added with stirring to a suspension of basic copper carbonate in water for about 1–2 h at about 50°C. The resulting blue solution was filtered to remove unreacted basic copper carbonate and the filtrate on concentration yielded blue crystals. These were filtered, washed several times with water and dried in vacuum at 100–110°C.

Copper(I) bathocuproin complex was prepared by adding a solution of bathocuproin reagent in amyl alcohol, to an aqueous solution of copper(I) ions [obtained by reducing $Cu(NO_3)_2$ with sodium metabisulphite]. The resulting yellow organic layer was separated, washed several times with water to remove bisulphite ions. This solution was used to record CV after adding TEAP (tetraethyl ammonium perchlorate) in acetone to it. The copper(I) ions generated during the electrode processes were trapped by using bathocuproin reagent as described below. A few cm^3 of the bathocuproin reagent solution in amyl alcohol was added to the aqueous solution of the copper(II) amino acid complex, taken in the electrolytic cell and stirred well to mix the two immiscible layers intimately. This mixture was then subjected to controlled potential electrolysis at −0.5 V over mercury pool electrode with stirring. After the completion of the electrolysis the deep yellow

* Author to whom correspondence should be addressed.

organic layer was separated from the aqueous layer. Optical spectra and cyclic voltammograms (CV) of this yellow layer were recorded.

Cyclic voltammetric experiments were carried out in a three-electrode cell with a metrohm E 410 hanging mercury drop electrode (HMDE) as working electrode and a platinum-wire as auxiliary electrode. All the potentials are referred to saturated calomel electrode (SCE) and are uncorrected for liquid-junction potentials. CV were recorded using PAR 175 universal programmer, PAR 174A polarographic analyser, and a PAR RE 0074 X-Y recorder. Controlled potential coulometry was carried out with PAR 173 potentiostat/galvanostat and a PAR 179 digital coulometer over mercury pool electrode. Electronic spectra were recorded on a Shimadzu 2000 S spectrometer and ESR on a JEOL-FE 3X spectrometer.

RESULTS AND DISCUSSION

The copper(II) amino acid complexes studied here are of general composition $[Cu(II)(AA)_2(H_2O)_n]$, where AA represents amino acid anion and n is one or two depending on the complex. The various copper(II) complexes prepared from the amino acids are listed in Table 1. The C, H, N and copper contents of these complexes agreed well with the above composition. The IR and visible spectra were similar to the reported[23,24] spectra of these complexes. Thus the identity of the starting complexes were established before proceeding with the investigations. Cyclic voltammograms were recorded in the potential range +0.1 to −0.6 V in aqueous solution of the complexes [10^{-3} mol dm^{-3}] at 298 K under nitrogen atmosphere with $NaClO_4$ (0.1 mol dm^{-3}) as supporting electrolyte at the dissolution pH ~ 7.5 (pH is not adjusted after dissolving the samples in water). All complexes show similar cyclic voltammetric behaviour and representative voltammograms are shown in Fig. 1. The relevant CV data for all complexes are collected in Table 1. There are no peaks in the positive potential range for any of the copper(II) complexes. None of the amino acids, in the absence of metal ions, show any peak in the potential range +1.0 to −1.0 V.

Table 1. Cyclic voltammetric data of copper(II) amino acid complexes in aqueous media

Compound* (c in mol dm^{-3})	Sweep rate (V s^{-1})	E_p, A† (V)	E_p, B (V)	E_p, C (V)	E_p, D (V)	E_p, $C-E_p$, D (V)	$\frac{E_p, C+E_p, D}{2}$ (V)
$Cu(Gly)_2$	0.02	−0.050	0.010	−0.290	−0.230	0.060	−0.260
(pH = 7.30;	0.05	−0.050	0.010	−0.290	−0.230	0.060	−0.260
c = 1.02)	0.10	−0.055	0.010	−0.300	−0.230	0.070	−0.265
$Cu(L\text{-}Ala)_2$	0.02	−0.030	0.025	−0.280	−0.220	0.060	−0.250
(pH = 7.52;	0.05	−0.035	0.025	−0.290	−0.220	0.070	−0.255
c = 1.09)	0.10	−0.040	0.020	−0.290	−0.215	0.075	−0.253
$Cu(L\text{-}Ile)_2$	0.02	−0.030	0.025	−0.270	−0.210	0.060	−0.240
(pH = 7.68;	0.05	−0.035	0.025	−0.270	−0.200	0.070	−0.235
c = 1.00)	0.10	−0.040	0.020	−0.275	−0.190	0.085	−0.233
$Cu(L\text{-}Pro)_2$	0.02	−0.030	0.045	−0.295	−0.230	0.065	−0.263
(pH = 7.55;	0.05	−0.030	0.045	−0.300	−0.220	0.080	−0.260
c = 1.07)	0.10	−0.030	0.040	−0.305	−0.215	0.090	−0.260
$Cu(L\text{-}Ser)_2$	0.02	−0.025	0.035	−0.265	−0.200	0.065	−0.233
(pH = 7.42;	0.05	−0.030	0.020	−0.270	−0.200	0.070	−0.236
c = 1.16)	0.10	−0.040	0.020	−0.275	−0.195	0.080	−0.235
$Cu(L\text{-}Orn)_2$	0.02	−0.040	0.025	−0.240	−0.165	0.075	−0.203
(pH = 7.71;	0.05	−0.040	0.020	−0.245	−0.160	0.085	−0.203
c = 1.00)	0.10	‡	‡	−0.245	−0.160	0.085	−0.203
$Cu(L\text{-}Lys)_2$	0.02	−0.040	0.030	−0.245	−0.175	0.070	−0.210
(pH = 7.74;	0.05	‡	0.030	−0.245	−0.170	0.075	−0.208
c = 1.12)	0.10	‡	‡	−0.250	−0.170	0.080	−0.210

* A linear dependence on concentration of peak potentials of C and D is observed below 1 mM. The origin of this is not clear.

† Peak observed only during second and subsequent scans.

‡ Broad peak, difficult to measure precisely.

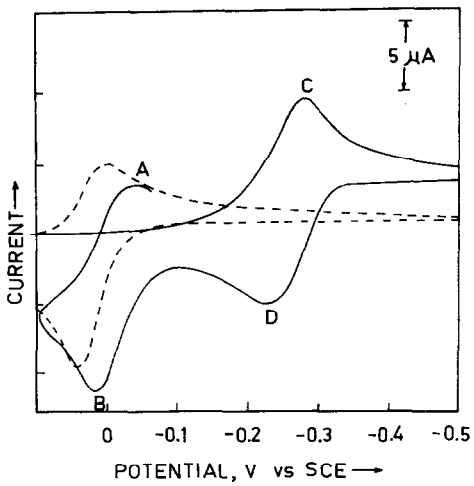


Fig. 1. (——) CV of $Cu(Gly)_2$ in 0.1 mol dm^{-3} $NaClO_4$ at HMDE of area 0.02 cm^2 : (– – –) CV of $Cu(ClO_4)_2$ in 0.1 mol dm^{-3} $NaClO_4$ at HMDE of area 0.02 cm^2.

The following observations are pertinent for discussing the cyclic voltammetric results. (i) During the first cathodic sweep, only one reduction peak C at ~ -0.26 V is observed. (ii) On the reverse scan well-defined anodic peak D at ~ -0.2 V and another peak B at $\sim +0.04$ V appear. (iii) A new cathodic peak A at ~ -0.05 V is apparent from the second scan onwards. (iv) An increase in the scan rate decreases the peak heights of A and B. (v) Holding the potential at a point well past the peak C for a few minutes and on scanning back, peaks A and B increase in height while peaks C and D remain unaffected. Similar effects are observed on multi-scans in the full potential range. (vi) If the potential scan is reversed after the peak A during the second and subsequent scans the heights of A and B decrease considerably. (vii) No CV response is observed if the potential sweep is reversed in the first scan itself before the appearance of peak C.

From an analysis of these observations the electrode processes can be inferred as follows: Since the starting complexes have the composition $Cu(II)(AA)_2$ peak C can originate from a one-electron reduction [$Cu(II) \xrightarrow{1e} Cu(I)$] or a two-electron reduction [$Cu(II) \xrightarrow{2e} Cu(0)$] of the $Cu(II)(AA)_2$ complexes. If the peak C is due to a one-electron reduction process, the generated Cu(I) species can undergo reoxidation to the starting complex giving the peak D. In that case the peak separation between C and D should be $\sim$ 60 mV and it is found to be in the range 60–80 mV (Table 1). These values also suggest that the electron-transfer is nearly reversible. Observations (iii), (v) and (vi) mentioned earlier clearly show that the first electron-transfer is a prerequisite for the observation of peaks B and A. On comparing these peaks with the redox peaks of free copper(II) ions under identical experimental conditions, it can be seen that A–B couple corresponds to the redox peaks of free copper(II) ions. For free copper(II) ions it has been established that the redox couple originates from a reversible two-electron transfer mechanism, $Cu(II) \overset{2e}{\rightleftharpoons} Cu(0)$. This evidence suggests that anodic peak B results from the two-electron oxidation of Cu(0) generated in solution to Cu(II) and the cathodic peak A from the two-electron reduction of the resulting copper(II) ions. Then the question is how is the Cu(0) generated at the electrode? The possibility is that Cu(0) can be the result of the decomposition or disproportionation of a fraction of the Cu(I) species which has not been reoxidised to Cu(II) complex. Thus the overall electrode processes can be represented by eqns (1)–(3):

$$Cu(II)(AA)_2 \overset{1e}{\rightleftharpoons} [Cu(I)(AA)_2], \quad (1)$$

$$[Cu(I)(AA)_2] \xrightarrow[\text{reactions}]{\text{Chemical}} Cu(Hg) + 2AA, \quad (2)$$

$$Cu(Hg) \overset{2e}{\rightleftharpoons} Cu^{2+}(aq). \quad (3)$$

Equations (1)–(3) represent an ECE mechanism.[25]

Equation (1), which generates the copper(I) amino acid complexes, represents the most important step in the overall process. The E_p, $C-E_p$, D values in Table 1 show a one-electron reversible character of this couple. Copper(I) complexes are stable only in tetrahedral or pseudo-tetrahedral geometries. The copper(I) species generated in these experiments can be expected to have a geometry distorted towards tetrahedral since the starting complexes, $Cu(II)(AA)_2$, possess a tetragonally distorted octahedral geometry.[12–16] The extent of stability of the copper(I) species depends on the degree of tetragonality. The transient existence of copper(I) complexes demonstrated by the CV pattern (peak D) shows that it has a life-time long enough to be detected by cyclic voltammetry. Further proof for the generation of copper(I) amino acid complexes as an intermediate was obtained by trapping copper(I) ion using bathocuproin (2,9-dimethyl-4,7-diphenyl-1,10-phenanthroline), a highly specific reagent for cuprous ions in forming stable complexes. The electrochemically generated copper(I) ions were complexed with bathocuproin reagent by adding a few millilitres of the reagent solution in amyl alcohol to an aqueous solution of the copper(II) complex and reducing it electrolytically. The electrochemically generated copper(I) bathocuproin complex is identical with the chemically generated bathocuproin complex (Cu(I) ions generated by chemical reduction of Cu(II) to Cu(I) and subsequently

complexes by bathocuproin reagent) in their spectral and cyclic voltammetric behaviour. Both have a characteristic high intensity band at 479 nm (ε = 14,150 dm^3 mol^{-1} cm^{-1})[21,26,27] and show an irreversibile reduction peak at −0.595 V in amyl alchol/TEAP medium at HMDE. Thus these results give additional evidence for the presence of copper(I) species in the electrode process and hence the first reduction of Cu(II)(AA)$_2$ does proceed by a one-electron process as depicted in eqn (1).

Equation (2) may be the result of a few reactions taking place in steps as in eqns (4) and (5):

$$Cu(I)(AA)_2 \rightleftarrows Cu^+ + 2AA, \quad (4)$$

$$2Cu^+ \rightleftarrows Cu^0 + Cu^{2+}. \quad (5)$$

Under the cathodic potential prevailing in the experimental conditions the predominant species in eqn (5) will be Cu(0) which is continuously removed as Cu(Hg) at the electrode.[28] Cu(0) thus generated can get oxidised by a two-electron process to Cu(II) giving the anodic peak B. Subsequent reduction of Cu(II) ions gives rise to the cathodic peak A and the two processes can be represented by eqn (3). CV of free copper(II) ions in aqueous media under identical experimental conditions give peaks similar to A and B at similar potentials, and its CV profile is shown in Fig. 1 for comparison. It should be noted at this point that peak A appears only from second scan onwards. This is so because there are no free copper(II) ions in solution to start with and they have to be electrochemically generated from Cu(0). This happens during the electrode processes shown in eqns (1)–(3). It is observed that $i_p/V^{1/2}$ for the peaks B and A decrease as the scan rate increases (Fig. 2). This shows that at high scan rates the chemical reaction represented in eqn (2) decreases due to lack of time which in turn decrease the $i_p/v^{1/2}$ value. As noted earlier peaks C and D do not get affected by holding the potential at a point (−0.5 V) well past the peak C, whereas the peaks B and A increase considerably. Such a situation can occur only when a steady concentration of the Cu(I)(AA)$_2$ species is maintained. This means that the process in eqn (1) is faster than that in eqn (2). On the other hand if the processes in eqn (2) are faster than that of eqn (1), the peak D would have decreased in height.[29]

Protonation

It is shown that copper(II) amino acid complexes with different modes of coordination exist in aqueous solution at various pH values. This has been studied by different methods over the years.[17–20] However no systematic study of the cyclic voltammetric behaviour of the copper(II) amino acid complexes in various pH conditions is reported. Here the CV response of these complexes at various pH values is studied and compared with the results discussed in the previous section.

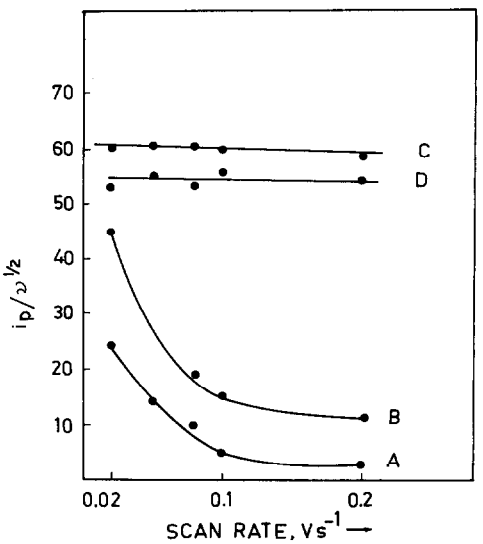


Fig. 2. Comparison of the effect of scan rate on the current function of various peaks of Cu(L-Ser)$_2$ under similar experimental conditions to Fig. 1. A, B, C and D correspond to the peaks in Fig. 1.

A gradual decrease in the pH of the aqueous solution was achieved by the step-wise addition of small amounts (μl) of a strong protonic acid, $HClO_4$, and cyclic voltammograms were recorded at different pH values. All amino acid complexes behave in a similar fashion. Representative cyclic voltammograms at different pH values for one of the complexes, are shown in Fig. 3 and the relevant CV

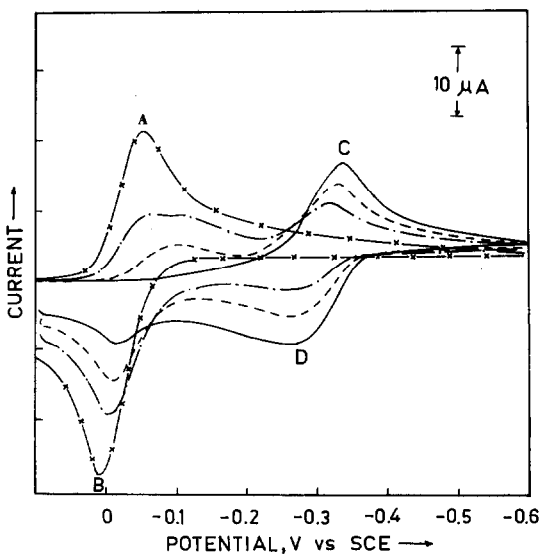


Fig. 3. CV of Cu(L-Pro)$_2$ at various pH values (——), pH = 7.48; (– – –), pH = 6.13; (–·–·–), pH = 5.14; (–×–×–), pH = 3.83.

Table 2. Cyclic voltammetric data* on protonation of $Cu(Gly)_2$

pH	E_p, A	E_p, B	E_p, C	E_p D	i_p, A	i_p, B	i_p, C	i_p, D
7.4	−0.065	0.020	−0.300	−0.235	0.0	4.5	17.5	16.5
7.25	−0.050	0.010	−0.295	−0.230	2.0	8.0	17.0	16.0
6.35	−0.050	0.010	−0.295	−0.230	5.0	11.0	15.0	14.5
5.81	−0.040	0.015	−0.295	−0.230	6.0	14.0	14.0	12.0
5.16	−0.030	0.025	−0.285	−0.235	9.0	21.0	10.0	8.0
4.33	−0.020	0.030	−0.280	−0.225	15.0	29.0	7.0	4.0
3.53	−0.010	0.040	†	†	22.0	36.0	0.0	0.0

* Potentials are expressed in V vs SCE and current in μA. Data collected from CV at scan rate of 0.05 V s^{-1}.

† Peak absent.

data for one compound are collected in Table 2. The major changes of the CV profile occurring on protonation are the following. (i) Heights of C and D decrease gradually and they finally disappear at low pH values. (ii) Peak A begins to appear in the first scan itself. (iii) Peaks A and B increase in height accompanied by a decrease in "peak-broadening" of A along with an anodic shift.

It is known that as the pH is decreased the $Cu(II)(AA)_2$ gets protonated and gives rise to Cu(II)(AA) which on further protonation produces free Cu(II) ions.[17,18,20] Then, as the pH decreases, the Cu(II)(AA) and subsequently the free Cu(II) ions become the major species. The gradual decrease in the heights of peaks C and D with the decrease of pH imply the depletion of $Cu(II)(AA)_2$ because of the protonation and thereby affecting the process in equation (1). The new species, Cu(II)(AA) can undergo a one-electron reduction at a potential less cathodic to peak C. It appears that the "peak-broadening" observed at the peak A is due to the result of the overlap of the reduction peak of Cu(II)(AA) and that of free Cu(II) ions. If so, the "peak-broadening" should disappear with the further decrease of pH as it results in the complete conversion of Cu(II)(AA) to free Cu(II) ions. The generation of more and more free Cu(II) ions with the decrease of pH can shift the peak A anodically. The disappearance of peaks C and D at low pH values (< 4.0), indicate the complete conversion of the starting complex. The CV recorded at various pH conditions for $Cu(II)(L\text{-}Pro)_2$ shown in Fig. 3 show these features clearly.

The peaks A and B have been shown to originate from the process, $Cu(II) \overset{2e}{\rightleftharpoons} Cu(Hg)$. As the concentration of free Cu(II) ions depends on the pH conditions, a gradual increase of the peak heights of A and B with the decrease of pH is expected. Finally at low pH values they should be the only peaks in the CV. These changes are clearly observed. The entire process of protonation can be reversed on raising the pH by adding small amounts of NaOH solution. This cycle can be repeated several times showing the reversibility of the protonation processes. These results from the protonation studies support the electrode mechanism discussed earlier.

Controlled potential coulometry

To distinguish between one or two-electron reduction of the starting complex, $Cu(II)(AA)_2$, controlled potential coulometry (CPC) at a potential −0.6 V, well past the peak C, over mercury pool electrode was carried out. The CPC yielded coulombs which corresponded to $n = 2$. This shows that under the continued influence of the cathodic potential only the overall electron-transfer process, $Cu(II) \overset{2e}{\rightleftharpoons} Cu(0)$, involving two electrons is coulometrically observed. The absence of Cu(II) ions in the electrolysed solution is confirmed by the disappearance of copper ESR signals and the absorption band.

Acknowledgements—We are grateful to Dr J. G. Mohanty and to Miss Janaki Vaidyanathan for their help in the early stages of this project. Financial assistance for this scheme from Department of Science and Technology, New Delhi, is gratefully acknowledged.

REFERENCES

1. J. Cline, B. Reinhammar, P. Jensen, R. Venters and B. M. Hoffman, *J. Biol. Chem.* 1983, **258**, 5124.
2. B. Reinhammar and B. G. Malmstrom, *Metals in Biology* (Edited by T. G. Spiro), Vol. 3, p. 109. Wiley, New York (1981).
3. B. G. Malmstrom, *Annu. Rev. Biochem.* 1982, **51**, 21.
4. D. C. Wharton, *Metal Ions in Biological Systems* (Edited by H. Sigel), Vol. 3, Chap. 5. Marcel Dekker,

New York (1974); R. Lontie and L. Vanquickenborne, *Metal Ions in Biological Systems* (Edited by H. Sigel), Vol. 3, Chap. 6. Marcel Dekker, New York (1974).
5. K. E. Joester, G. Jung, U. Weber and U. Weser, *FEBS Lett.* 1972, **25**, 25.
6. U. Weser, *Struct. Bonding (Berlin)* 1973, **17**, 1.
7. R. Brigelius, R. Spottl, W. Bors, E. Lengfelder, M. Saran and U. Weser, *FEBS Lett.* 1974, **47**, 72.
8. R. Brigelius, H. J. Hartmann, W. Bors, E. Lengfelder, M. Saran and U. Weser, *Hoppe-Seyler's Z. Physiol. Chem.* 1975, **356**, 739.
9. B. Reinhammar, *Biochim. Biophys. Acta* 1972, 275.
10. W. Voelter, G. Sokolowski, U. Weber and U. Weser, *Eur. J. Biochem.* 1975, **58**, 159.
11. T. P. A. Kruck and B. Sarkar, *Can. J. Chem.* 1973, **51**, 3549, 3569.
12. H. C. Freeman, M. R. Snow, I. Nitta and K. Tomita, *Acta Cryst.* 1964, **17**, 1463.
13. M. V. Veidis and G. J. Palenik, *J. Chem. Soc., Chem. Commun.* 1969, 1277.
14. D. Van Der Helm and W. A. Franks, *Acta Cryst. Sect. B*, 1969, **25**, 451; C. M. Weeks, A. Cooper and D. A. Norton, *Acta Cryst. Sect. B* 1969, **25**, 443.
15. W. Camerman, J. K. Fawcett, T. P. A. Kruck, B. Sarkar and A. Camerman, *J. Am. Chem. Soc.* 1978, **100**, 2690.
16. H. C. Freeman, *Adv. Protein Chem.* 1967, **22**, 273, 275, 280.
17. H. Irving and L. D. Pettit, *J. Chem. Soc.* 1963, 1547.
18. R. H. Carlson and T. L. Brown, *Inorg. Chem.* 1966, **5**, 268.
19. J. E. Letter, Jr. and J. E. Bauman, Jr., *J. Am. Chem. Soc.* 1970, **92**, 437.
20. J. P. Greenstein and M. Winitz, *Chemistry of the Amino Acids*, Vol. 1. Wiley, New York (1961).
21. (a) G. Thomas and P. S. Zacharias, *Polyhedron* 1984, **3**, 861; (b) G. Thomas and P. S. Zacharias, *Trans. Met. Chem.* 1984, **9**, 377; (c) G. Thomas and P. S. Zacharias, *Polyhedron* 1985, **4**, 299; (d) G. Thomas and P. S. Zacharias, *Indian J. Chem.* (in press).
22. A. I. Vogel, *A Textbook of Quantitative Inorganic Analysis*, 4th Edn, p. 496. Longmans, Harlow, U.K. (1978).
23. D. P. Graddon and L. Munday, *J. Inorg. Nucl. Chem.* 1961, **23**, 231.
24. O. Yamauchi, T. Sakurai and A. Nakahara, *J. Am. Chem. Soc.* 1979, **101**, 4164.
25. R. S. Nicholson and I. Shain, *Anal. Chem.* 1965, **37**, 179; 190.
26. W. H. McCurdy, Jr. and G. F. Smith, *Analyst* 1952, **77**, 846.
27. L. G. Borchardt and J. D. Butler, *Anal. Chem.* 1957, **29**, 415.
28. J. A. Altermatt and S. E. Manahan, *Anal. Chem.* 1968, **40**, 655.
29. G. N. Collman, J. W. Gesler, F. A. Shirley and J. R. Kuempel, *Inorg. Chem.* 1973, **12**, 1036.

Polyhedron Vol. 4, No. 5, pp. 817–820, 1985
Printed in Great Britain

0277–5387/85 $3.00 + .00
© 1985 Pergamon Press Ltd

REDOX PROPERTIES OF BIS(1,10-PHENANTHROLINE)-(PYRIDINE)RUTHENIUM(II) COMPLEXES

GEOFFREY A. LAWRANCE
Department of Chemistry, The University of Newcastle, New South Wales 2308, Australia

(*Received* 13 *August* 1984; *accepted* 13 *September* 1984)

Abstract—The redox properties of a series of $[Ru(phen)_2(py)X]^{n+}$ cations (X = pyridine, NH_3, Cl, Br, I, CN, SCN, N_3 and NO_2) have been investigated in acetonitrile. Two reversible reduction steps are seen at −1.35 and −1.6 V vs Ag/AgCl; the invariance of these processes with X-group is indicative of electron addition to molecular orbitals mainly of phenanthroline ligand π^* origin. Irreversible multi-electron reductions follow below −2.20 V. The Ru(II)/Ru(III) couple is seen as a reversible wave near +0.8 V vs the normal hydrogen electrode, from calibration with ferrocene, except in the cases of the NO_2 and SCN complexes, where rapid reactions involving these ligands occur.

Ruthenium complexes of the π-conjugated ligands 2,2′-bipyridyl (bpy) and 1,10-phenanthroline (phen) have been extensively studied in recent years,[1] partly as a consequence of their photogalvanic and luminescence properties.[2–4] Mixed ligand complexes of the type $[Ru(bpy)_2L]^{n+}$ and $[Ru(phen)_2L]^{n+}$ have been studied, where L represents a third bidentate ligand, and the redox properties of such systems have been reported.[5–7] In such cases, interest has centred on the effect of the L ligand on the spectroscopic and electrochemical properties of the complexes.

The system $[Ru(phen)_2(py)X]^{n+}$ (py = pyridine), with two unidentate ligands coordinated in addition to two π-conjugated chelates, has been known for some time.[8,9] However, the redox properties of a series of these complexes have not been studied, and it was of interest to observe the variation in these properties with the sixth ligand X.

EXPERIMENTAL

The complexes $[Ru(phen)_2(py)X](ClO_4)_n$, and the method of synthesis, have been described previously.[9] Acetonitrile for electrochemical measurements was dried and distilled by standard methods. Tetra-*n*-butylammonium tetrafluoroborate employed as electrolyte (0.1 M) was recrystallized from acetonitrile.

All electrochemical measurements were made using a conventional three-electrode configuration with a Ag/AgCl(LiCl/acetone) reference electrode and a platinum auxiliary electrode. A conventional controlled-drop dropping mercury electrode (DME), stationary platinum billet or stationary gold billet electrode was employed as working electrode, with solvent-saturated argon as purge gas. Electrochemical controllers were either a BAS Model CV27 or PAR Model 170. Electrochemical measurements at ambient temperature quoted versus the reference electrode are uncorrected for junction potentials, except ferrocene was employed as an internal standard (E^0 + 0.400 V vs the normal hydrogen electrode)[10] for oxidations at stationary electrodes. Half-wave potentials ($E_{1/2}$) for the Ru(II)/Ru(III) couples and electrochemical reversibility was determined by cyclic voltammetry. Half-wave potentials for reductions were determined from d.c. polarograms via the Heyrovsky–Ilkovic equation, or from maxima in low-frequency a.c. polarograms. Complex concentrations were typically 1 mM.

UV–visible spectra were recorded using Varian 635 or Hitachi 220A spectrophotometers at ambient temperature in acetonitrile.

RESULTS AND DISCUSSION

The ruthenium(II) complexes $[Ru(phen)_2(py)X]^{n+}$ exhibit characteristic intense absorption bands in the visible and ultraviolet regions (Table 1). The low-energy metal-to-ligand charge-transfer (MLCT) bands in the visible region exhibit some variation with X-group, but the intense $\pi \rightarrow \pi^*$ phenanthroline intraligand transfers in the ultraviolet at 265 nm are invariant within ex-

Table 1. Electronic spectra maxima for $[Ru(II)(phen)_2(py)X]^{n+}$ complexes in acetonitrile

X-Ligand	λ_{max}, nm ($10^{-4}.\varepsilon_{max}$, $M^{-1}cm^{-1}$) [a]
py	450 (1.12); 414 (1.23); 289 sh; 266 (8.15)
NH_3	475 sh; 452 (1.15); 415 sh; 285 sh; 265 (8.80)
Cl	488 (1.11); 450 sh; 290 sh; 265 (8.39)
Br	484 (1.04); 450 sh; 289 sh; 266 (7.44)
I	485 (1.05); 450 sh; 290 sh; 267 (7.31)
CN	462 (1.16); 435 sh; 290 sh; 264 (8.12)
SCN	465 sh; 430 (1.14); 290 sh; 265 (7.74)
NO_2	450 sh; 415 (1.11); 285 sh; 263 (7.14)
N_3	489 (1.06); 455 sh; 290 sh; 267 (7.38)
$[Ru(phen)_3]^{2+}$	445 (1.90); 420 sh; 285 sh; 262 (12.1) [b]

[a] Distinct shoulders on absorption envelopes = sh.
[b] Literature values are 446 (1.99); 262 (12.5).

Table 2. Redox processes for $[Ru(II)(phen)_2(py)X]^{n+}$ complexes in acetonitrile[a,b]

X-Ligand	Reductions			Oxidation [d]
	I	II	III [c]	
py	-1.35	-1.53	-2.20	+1.44 (+1.29)
NH_3	-1.33	-1.54	-2.15	+1.02 (+0.88)
Cl	-1.39	-1.64	-2.18	+0.92 (+0.78)
Br	-1.37	-1.60	-2.16	+0.94 (+0.80)
I	-1.34	-1.54	-2.15	+0.93 (+0.79)
CN	-1.34	-1.61	-2.18	+0.96 (+0.82)
SCN	-1.32	-1.56	-2.16	~+1.05 (+0.9) [e]
NO_2	-1.34	-1.57	-2.18	~+1.20 (+0.95) [e]
N_3	-1.38	-1.63	-2.20	+0.73 (+0.59)

[a] 0.1 M $(Bu_4N)(BF_4)$ electrolyte; [Ru] 10^{-3} M; ambient temperature; $E_{1/2}$ in V vs Ag/AgCl.
[b] $[Ru(phen)_3]^{2+}$ exhibits waves at −1.20, −1.34, −1.65 and −2.18 V (reduction), and at +1.4 V (oxidation).
[c] Irreversible reduction, associated in each case by a further irreverisble wave at ~ −2.4 V.
[d] Value in parentheses is E^0 vs NHE, calculated from addition of ferrocene (E^0 +0.400 V) as internal standard.
[e] Wave irreversible or complicated by rapid following chemical reaction.

perimental error (±2 nm). The decrease in intensity of the band from 12×10^4 M^{-1} cm^{-1} in $[Ru(phen)_3]^{2+}$ to ~ 8×10^4 M^{-1} cm^{-1} in the $[Ru(phen)_2(py)X]^{n+}$ complexes supports the contention that the absorption arises from a transition of phenanthroline.

The ultraviolet and visible spectra of a large number of $[Ru(bpy)_2L_2]^{2+}$ complexes (L an unsaturated unidentate ligand) have been reported.[5] In these analogues to the present system, the main $t_{2g}(Ru) \rightarrow \pi^*$(ligand) maxima occurs near 450 nm, and distinct shoulders are sometimes observed; a second band of lower intensity is usually reported below 390 nm. Spectra for series of $[Ru(bpy)_2(LL)]^{2+}$ and $[Ru(phen)_2(LL)]^{2+}$ are very similar,[6] and this is a general phenomenon. For $[Ru(bpy)_2L_2]^{2+}$ complexes, no separate $d[Ru(II)] \rightarrow$ L band was detected,[5] although a later study of similar complexes assigned high energy shoulders on the MLCT band as a $d[Ru(II)] \rightarrow \pi^*$(pyridine) transition.[11] The observation of a high energy shoulder in the $[Ru(phen)_2(py)X]^{n+}$ complexes may then be associated with such a $d[Ru(II)] \rightarrow \pi^*$ (pyridine) transition, although the assignment is tenuous.

The electrochemistry of $[Ru(phen)_2(py)X]^{n+}$ in acetonitrile shows a Ru(II)/Ru(III) couple near +0.8 V, and three clear one-electron reductions near −1.35, −1.6 and −2.20 V (Table 2). These reductions correspond to effective ruthenium oxidation states of 1, 0 and −1. A further multielectron wave is associated with the third reduction near −2.4 V in each case. The latter wave is presumably related to ligand dissociation from the nominally low-valent species, since free ligands are reducible to anion radicals at these very negative potentials; such behaviour has been observed in ruthenium complexes of π-conjugated ligands.[4] The various reduced species are not stable on the coulometric timescale, and cannot be isolated by conventional means.

The one-electron reductions show no appreciable variation with X-group. The two reductions at −1.35 and −1.6 V are essentially reversible from d.c. polarographic behaviour (Fig. 1b). Both reductions exhibit strong a.c. polarograms (Fig. 1d); however, adsorption phenomena, as evidenced from the strong quadrature signal in the 400 Hz a.c. polarogram (Fig. 1c) compared with the in-phase 400 Hz a.c. polarogram (Fig. 1d), did not allow assessment of reversibility on the a.c. polarographic timescale from variable-frequency data. The reductions below −2 V are irreversible.

The unpaired electrons in Li(bpy) and $Be(bpy)_2$ occupy molecular orbitals composed mainly of ligand π^* origin, from electron spin resonance evidence.[12–15] However, in low-valent chromium and vanadium complexes of bipyridyl, the highest occupied molecular orbital is a delocalized orbital composed mainly of a metal t_{2g} orbital, since metal hyperfine structure is seen in the electron spin resonance spectra.[12–16] This is not a general observation for metal complexes, since low-valent

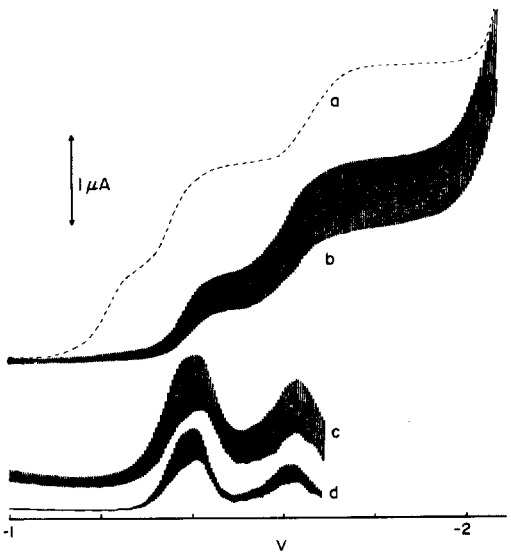


Fig. 1. D.c. polarograms of (a) 1 mM $[Ru(phen)_3]^{2+}$ and (b) 1 mM $[Ru(phen)_2(py)Br]^+$ in acetonitrile, and a.c. polarograms of $[Ru(phen)_2(py)Br]^+$ (400 Hz) in the quadrature (c) and in-phase (d) modes for a 1 mM solution in acetonitrile vs Ag/AgCl.

iron bpy complexes can be described like the Li and Be systems.[17–19] The $[M(bpy)_3]^{2+}$ system (M = Fe, Ru, Os) shows three one electron reduction waves between −1.2 and −1.8 V, which vary by less than 80 mV from Fe to Ru to Os.[20] Substitution on the bpy ligand causes shifts in positions with substituents, but the basic number and shape of waves is preserved. These observations support the view of the added electron occupying a molecular orbital contributed mainly by a ligand π^* orbital.

The highest occupied molecular orbital $[t_{2g}(\pi)]$ and the lowest unoccupied molecular orbital $[t_{1u}(\pi^*)]$ for octahedral Ru(II) will split under the low C_2 microsymmetry of the $[Ru(phen)_2(py)X]^{n+}$ ions into at least e_g and a subsets. Reduction may then lead to successively paramagnetic, diamagnetic and finally paramagnetic species, depending on orbital splitting, as proposed for $[Ru(bpy)_3]^{2+}$.[4] The invariance of the positions of the three reductions with X-group in this system supports the assertion that the available LUMO is dominantly of ligand π^* character, as argued for the $[Ru(bpy)_3]^{2+}$ analogue.[20]

One obvious difference between reduction of $[Ru(phen)_3]^{2+}$ and the $[Ru(phen)_2(py)X]^{n+}$ set is the observation of three one electron reduction waves between −1.2 and −1.8 V in the former and only two in the latter (Fig. 1a and 1b). This result parallels observations for $[Ru(bpy)_3]^{2+}$ vs $[Ru(terpy)_2]^{2+}$, where three waves occur in the former and only two in the latter.[20] The lowest π^* orbital in the bpy or tridentate terpy analogue complex is triply or doubly degenerate and localized in the π-conjugated ligand. In a simple sense, each electron added may occupy one vacant localized conjugated ligand orbital. Electronic repulsions between the added electron and other electron make further electron addition to that locality less facile, evolving a one electron per conjugated ligand rule. The difficulty of adding further electrons is shown in the present experiments, where a third electron is only added at potentials below −2 V, and the process is irreversible. While this simple rule has limited direct theoretical basis, it appears to operate experimentally.

The $[Ru(phen)_2(py)X]^{n+}$ complexes show a one electron and usually reversible oxidation at positive potentials at stationary platinum or gold billet electrodes (Table 2). The typical behaviour is shown in Fig. 2(a). There is some variation in E^0 with X-group, reflecting the differing electronic properties of those ligands, although a majority of values cluster around E^0 of +0.8 V. The difference from the invariance of E^0 for the first two reductions is clear, reflecting electron subtraction from a molecular orbital of metal character for the oxidation and electron addition to one of ligand character for the reductions. Since the five other ligation sites are invariant in this system, variation in the sixth site may be expected to cause only a relatively minor perturbation. The $E_{1/2}$ values have been determined from cyclic responses which usually exhibited $i_{pa} = i_{pc}$, $iv^{1/2}$ constant, and ΔE_p near 70 mV at scan rate at or below 50 mV s^{-1}. The one-electron nature of the couples was confirmed for the X = Cl complex by coulometry.

While most oxidations were well behaved reversible one-electron processes, several ligands offer the opportunity for more complex behaviour. The $X = NO_2$ system is complicated somewhat by disproportionation and oxidation reactions of the ligand on the Ru(III) complex. This system has been

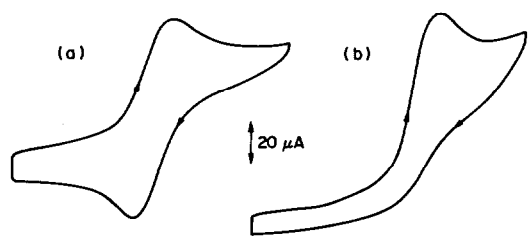


Fig. 2. Cyclic voltammograms at a stationary platinum billet working electrode for $[Ru(phen)_2(py)Br]^+$ [(a), scan rate 200 mV s^{-1}, $+0.6 \rightleftarrows +1.3$ V] and $[Ru(phen)_2(py)(SCN)]^+$ [(b), scan rate 200 mV s^{-1}, $+0.6 \rightleftarrows +1.3$ V].

studied extensively for $[Ru(bpy)_2(NO_2)Cl]$, where coordinated NO_3^- and NO^+ result.[21] The X = SCN complex exhibits a clearly irreversible wave [Fig. 2(b)]. Since the irreversible oxidation of SCN^- in aprotic solvents to NCS–SCN, which is stable in aprotic solvents, occurs at similar potentials,[21] then rapid electron transfer from the Ru(III) complex and ligand dimerization may be involved in this case. The behaviour of coordinated thiocyanate on ruthenium under electrochemical oxidation does not appear to have been studied previously, and detailed characterization of this reaction will be probed.

In closely related series of complexes, correlations of the MLCT band maxima with E^0 have been sought.[5,7,23–27] For the present system, the correlation is poor. Since the MLCT band is apparently a composite of transitions, defining the MLCT band energy is not simple; further, most E^0 values do not vary much. A similar poor correlation was obtained for a series of bis(bipyridyl(isonitrosoketonato)ruthenium(II) complexes,[7] although better correlations do exist for Ru(III) band maxima in that system. The dependence of E^0 on a number of free energy terms not directly related to electronic transitions limits the validity of such correlations which do occur.

Acknowledgements—The assistance of D. Bogsanyi, Research School of Chemistry, The Australian National University, in recording the a.c. polarograms is greatly appreciated. Financial support of the Senate Research Committee of the University of Newcastle is gratefully acknowledged.

REFERENCES

1. J. R. McWhinnie and J. D. Miller, *Adv. Inorg. Chem. Radiochem.* 1969, **12**, 135; W. P. Griffith, *The Chemistry of the Rare Platinum Metals.* Interscience, New York (1967).
2. C. T. Lin and N. Sutin, *J. Phys. Chem.* 1976, **80**, 97.
3. G. B. Porter, P. C. Ford, R. E. Hintze and J. D. Petersen, *Concepts Inorg. Photochem.* 1975, 203.
4. N. E. Tokel-Takvoryan, R. E. Hemingway and A. J. Bard, *J. Am. Chem. Soc.* 1973, **95**, 6582.
5. G. M. Bryant, J. E. Ferguson and H. K. J. Powell, *Aust. J. Chem.* 1971, **24**, 257.
6. R. J. Staniewicz, R. F. Sympson and D. G. Hendricker, *Inorg. Chem.* 1977, **16**, 2166.
7. A. R. Chakravarty and A. Chakravorty, *J. Chem. Soc., Dalton Trans.* 1982, 1765.
8. F. P. Dwyer, H. A. Goodwin and E. C. Gyarfas, *Aust. J. Chem.* 1963, **16**, 544.
9. B. Bosnich and F. P. Dwyer, *Aust. J. Chem.* 1966, **19**, 2229.
10. R. R. Gagné, C. A. Koval and G. C. Lisensky, *Inorg. Chem.* 1980, **19**, 2854.
11. G. M. Brown, T. R. Weaver, F. R. Keene and T. J. Meyer, *Inorg. Chem.* 1976, **15**, 190.
12. E. König and W. Fischer, *Z. Naturforsch.* 1962, **17a**, 1063.
13. J. Dos Santos Veiga, W. L. Reynolds and J. R. Bolton, *J. Chem. Phys.* 1966, **44**, 2214.
14. I. M. Brown and S. I. Weissman, *J. Am. Chem. Soc.* 1963, **85**, 2528.
15. I. M. Brown, S. I. Weissman and L. C. Snyder, *J. Chem. Phys.* 1965, **42**, 1105.
16. E. König, *Z. Naturforsch.* 1964, **19a**, 1139.
17. F. S. Hall and W. L. Reynolds, *Inorg. Chem.* 1966, **5**, 931.
18. C. Mahon and W. L. Reynolds, *Inorg. Chem.* 1967, **6**, 1927.
19. Y. Kaizu, T. Yazaki, Y. Torii and H. Kobayashi, *Bull. Chem. Soc. Jpn* 1970, **43**, 2068.
20. T. Saji and S. Aoyagui, *J. Electroanal. Chem. Interfacial Electrochem.* 1975, **58**, 401.
21. F. R. Keene, D. J. Salmon and T. J. Meyer, *J. Am. Chem. Soc.* 1977, **99**, 2384.
22. D. A. Holtzen and A. S. Allen, *Anal. Chim. Acta* 1974, **69**, 153.
23. J. E. Ferguson, A. W. H. Mau and W. H. F. Sasse, *Chem. Phys. Lett.* 1979, **68**, 21.
24. E. Tfouni and P. C. Ford, *Inorg. Chem.* 1980, **19**, 72.
25. E. C. Johnson, B. P. Sullivan, D. J. Salmon, S. A. Adeyemi and T. J. Meyer, *Inorg. Chem.* 1978, **17**, 2211.
26. J. N. Braddock and T. J. Meyer, *Inorg. Chem.* 1973, **12**, 723.
27. E. V. Dose and L. J. Wilson, *Inorg. Chem.* 1978, **17**, 2660.

Polyhedron Vol. 4, No. 5, pp. 821–827, 1985
ed in Great Britain

0277–5387/85 $3.00 + .00
© 1985 Pergamon Press Ltd

PHOTOSUBSTITUTION REACTIONS IN POTASSIUM OCTACYANOMOLYBDATE(IV) AND OCTACYANOTUNGSTATE(IV) IN THE PRESENCE OF 1,10-PHENANTHROLINE AND 2,2′-BIPYRIDYL

S. I. ALI* and ZAKIR MURTAZA
Department of Chemistry, Jamia Millia Islamia, Jamia Nagar, New Delhi-110 025, India

(*Received* 12 *December* 1983; *accepted after revision* 13 *September* 1984)

Abstract—Substitution reactions take place following the photonic excitation of aqueous $K_4M(CN)_8$ (where M = Mo or W) in the presence of 1,10-phenanthroline and 2,2′-bipyridyl. Changes in absorbance with time show that the overall reaction is dependent on photochemical activation of potassium octacyanomolybdate(IV) and -tungstate(IV). The species $[K_2Mo(CN)_4(OH)_2(phen)]$, $[K_2W(CN)_4(OH)_2(phen)]$, $[K_2Mo(CN)_4(OH)_2(bipy)]$ and $[K_2W(CN)_4(OH)_2(bipy)]$ exist in solution. The final photosubstitution products $[Mo(OH)_3(CN)(phen)_2]\cdot 2H_2O$, $[Mo(OH)_3(CN)(bipy)_2]\cdot 3H_2O$, $[W(OH)_3(CN)(phen)_2]\cdot 2H_2O$ and $[W(OH)_3(CN)(bipy)_2]\cdot H_2O$ have been isolated in the solid state. Their IR spectra have been discussed. The quantum yield of the photosubstitution reactions has been determined and its variation with change of concentration of the complex as well as the H^+ ion concentration has been studied.

Recent studies[1–7] on the photochemical substitution reactions of coordination compounds of chromium, molybdenum and tungsten have been of considerable interest. The cyano complexes of these metals have been investigated in detail. The stoichiometry of the photochemical processes, photochemical kinetics, quantum yield and the electronic excited states responsible for the photoreactions have been studied. Ligand field photochemistry of hexacyanochromate(III), octacyanomolybdate(IV) and octacyanotungstate(IV) arising from continuous irradiation in aqueous medium is photoaquation of one CN^- ligand giving $[Cr(CN)_5H_2O]^{2-}$, $[Mo(CN)_7H_2O]^{3-}$ and $[W(CN)_7H_2O]^{3-}$ respectively. This behaviour is also observed in hexacyanocobaltate(II)[8] and -ferrate(II)[9] which produce aquopentacyanocobaltate(II) and -ferrate(II) respectively. Prolonged irradiation gives rise to secondary photochemical reactions giving the photoproducts $[Cr(CN)_4H_2O]^-$, $[Mo(CN)_4O(OH)]^{3-}$ and $[W(CN)_4O(OH)]^{3-}$.

In $K_4M(CN)_8$ (where M = Mo or W) only four cyanides can be replaced easily because the dodecahedral structure of these complexes is slightly favoured by π-bonding involving the $d_{x^2-y^2}$ orbital so four of the cyanides are better disposed for π-bonding than the others. The four cyanides may be replaced by hydroxide giving[10] the $Mo(CN)_4(OH)_4^{4-}$ ion. Anhydrous compound of molybdenum, $K_4MoO_2(CN)_4$, was first isolated by Steele.[11] The primary photoaquation reactions of $H_4Mo(CN)_8$ and $H_4W(CN)_8$ and the quantum yield of the formation of the photoproducts have been studied by Mohan *et al.*[12,13] Photosubstitution reactions of ferrocyanide ions in the presence of 1,10-phenanthroline and 2,2′-bipyridyl have been reported[14,15] but no work has been done on the photosubstitution reactions of potassium octacyanomolybdate(IV) and -tungstate(IV). In this paper the photosubstitution reactions of these complexes in the presence of 1,10-phenanthroline and 2,2′-bipyridyl have been reported. The stoichiometry of the photochemical reactions, isolation, analysis and IR spectra of the final photoproducts and the quantum yield of the formation of the photoproducts have been determined.

EXPERIMENTAL

Apparatus

Tungsten filament lamp (Wotan ultra vitalux, 300 W) was used whose radiation is centered

* Author to whom correspondence should be addressed.

around ~ 370 nm. The absorbance was recorded on Spectromom 361 using quartz cell. pH of the solution were recorded on Elico pH meter, type L 1/10 No. 305 and IR spectra were recorded by using Pye–Unicam, Sp 1200, grating IR spectrophotometer.

Materials

A.R. 1,10-phenanthroline and 2,2′-bipyridyl were used. $K_4Mo(CN)_8$ and $K_4W(CN)_8$ were prepared by the method of Leipoldt *et al.*[16] Ferrioxalate was used as chemical actinometer, which was prepared by the method of Parker,[17] with quantum yield of 1.21 at 370 nm. Light intensity was calculated by the method given by Murov.[18] The value obtained was 1.08×10^{20} photons A^{-1} cm^{-2} ($\simeq$ 370 nm).

The stoichiometries of the reaction between $K_4M(CN)_8$ and AA ligand (where AA = 1,10-phenanthroline or 2,2′-bipyridyl) were determined by the Job's method of continuous variation and mole ratio method. The solutions of the metal complex were mixed with different concentrations of ligand and the resulting solutions were exposed to UV light for 30 min, the colour of the solutions changed from yellow to green. The absorbance of the green coloured solution was measured at 400 nm for $K_4Mo(CN)_8$–AA complexes and 620 nm for $K_4W(CN)_8$–AA complexes, the maxima of the spectra of the two systems.

Isolation and analysis of the photosubstituted products

The solutions of $K_4M(CN)_8$ and AA ligands were mixed in stoichiometric ratio obtained by the Job's method and mole ratio method. These mixtures were exposed to UV light (~ 370 nm) for about 4 h and the resulting complexes were extracted by adding HCl in the exposed solutions. These coloured precipitates were filtered, washed several times with water and alcohol and dried in a desiccator over calcium chloride. The solid complexes were fused with aqua-regia, molybdenum[19] was estimated as oxinate and tungsten as oxide. The estimations of nitrogen were carried out using Coleman N-analyzer 29. The water of crystalization was estimated by heating the complexes at 100°C for 2 h.

Spectrophotometric determination of the quantum yield

The absorbance of the photolysed solution was measured at 440 nm for the octacyano molybdate complexes and 620 nm for the octacyano tungstate complexes with 1,10-phenanthroline and 2,2′-bipyridyl, these maxima were obtained by mixing the complex with ligand in the stoichiometric ratios obtained by the physical methods and exposing to UV light. The spectra were recorded at different intervals of time. Molar extinction coefficient (ε_{max}) of these complexes, required for the calculation of their concentration, was determined from the maximum absorbance. The absorbance measured for molybdenum and tungsten complexes at 440 and 620 nm respectively increased as more and more of CN^- was released, reached a maximum value and thereafter it decreased. Molar extinction coefficients were calculated from the maximum absorbance. The quantum yield was calculated by the method given by Calvert and Pitts.[20]

RESULTS AND DISCUSSION

The photochemical behaviour of the $Mo(CN)_8^{4-}$ and $W(CN)_8^{4-}$ ions under *d–d* irradiation has been extensively investigated by several workers[21–27] and is found to be very similar. The primary photochemical reactions leads to a red intermediate compound, while prolonged irradiation causes the formation of a blue final product which can be represented by the following photoaquation reactions[22,24,25,28]

$$M(CN)_8^{4-} + 2H_2O \overset{h\nu}{\rightleftharpoons} M(CN)_7(H_2O)^{3-} + HCN + OH^-,$$

$$M(CN)_7(H_2O)^{3-} + H_2O \overset{h\nu}{\rightarrow} M(CN)_4(O)(OH)^{3-} + 3HCN.$$

pH dependent photolysis of the octacyano-tungstate(IV) and kinetics of thermal reactions of the photoproducts were studied recently by Samotus *et al.*[6] and a general reaction scheme for the photochemical and thermal reactions in the irradiated $W(CN)_8^{4-}$ system as well as the over all kinetics equations for the thermal reactions of the photoproducts were proposed.

When $K_4M(CN)_8$ solution was exposed to UV light (~ 370 nm) in the presence of AA ligands, a green colour was developed after a certain time whose absorbance maxima (Figs 1 and 2) was obtained at 440 nm for the $K_4Mo(CN)_8$–(phen) and $K_4Mo(CN)_8$–(bipy) systems and 620 nm for $K_4W(CN)_8$–(phen) and $K_4W(CN)_8$–(bipy) systems.

The absorption spectra of the irradiated $K_4Mo(CN)_8$–AA system (in 1:2 ratio) show one maximum at 440 nm which increases with increase in time, showing the formation of new species in solution. The one at 365 nm which is due to the $K_4Mo(CN)_8$ alone decreases with exposure time.

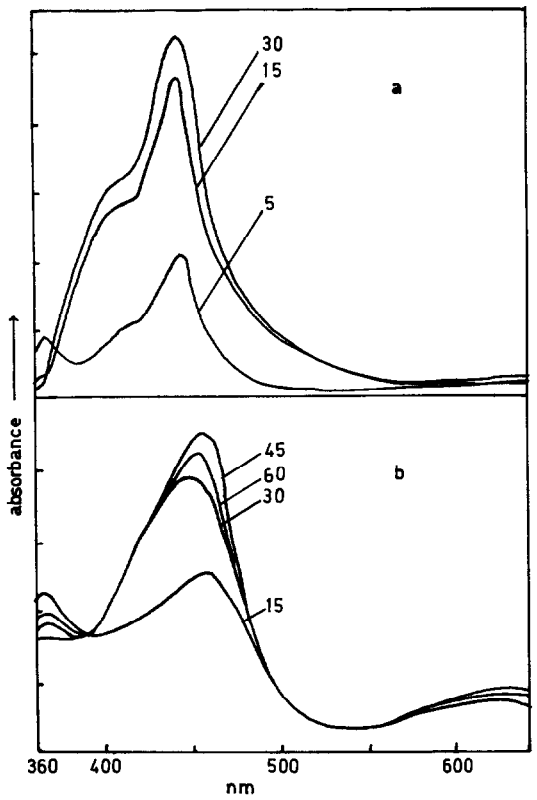


Fig. 1. Variation of absorbance with exposure time (1 cm light path): (a) 0.01 M $K_4Mo(CN)_8$ and 0.02 M 1,10-phenanthroline, (b) 0.01 M $K_4Mo(CN)_8$ and 0.02 M 2,2'-bipyridyl. The numbers indicate irradiation time (min).

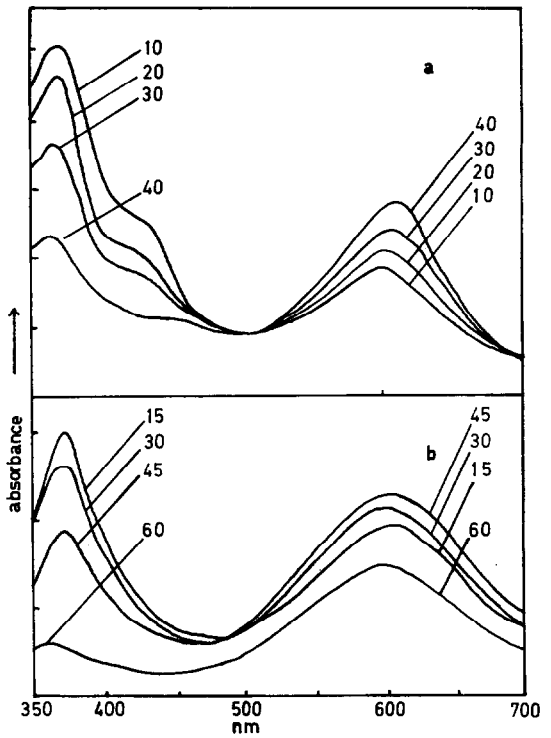


Fig. 2. Variation of absorbance with exposure time (1 cm light path): (a) 0.01 M $K_4W(CN)_8$ and 0.02 M 1,10-phenanthroline, (b) 0.01 M $K_4W(CN)_8$ and 0.02 M 2,2-bipyridyl. The numbers indicate irradiation time (min).

The spectra of the irradiated $K_4W(CN)_8$–AA system (in 1:2 ratio) also show one maximum at 620 nm which increases with increase in time indicating the formation of new species in solution. The maximum at 370 nm due to $K_4W(CN)_8$ decreases with exposure time. The variation of the pH with the exposure time was also studied (Fig. 3). It is found that the pH increases with exposure time which is due to the release of CN^- ions in solution which decompose water to form unionized HCN and OH^- ions in the solution.

The stoichiometry of these complexes was determined with the help of mole ratio and Job's methods. The stoichiometry by mole ratio method is 1:1 and 1:2 for $K_4M(CN)_8$–AA respectively. From Job's method it is 1:2 for the $K_4Mo(CN)_8$–AA systems and 1:1 for the $K_4W(CN)_8$–AA systems respectively.

Several attempts were made to extract these complexes with different organic solvents but without success. These complexes were precipitated as solid by adding dilute HCl in the photolysed system of $K_4M(CN)_8$ and AA in the ratio of 1:2 after development of intense green colour. From the analysis (Table 1), the compositions of the following complexes were established $[Mo(OH)_3(CN)(phen)_2]\cdot 2H_2O$, $[Mo(OH)_3(CN)(bipy)_2]\cdot 3H_2O$, $[W(OH)_3(CN)(phen)_2]\cdot 2H_2O$ and $[W(OH)_3(CN)(bipy)_2]\cdot H_2O$. The results of the analysis supported the stoichiometries obtained by physical methods. The reactions for these systems may be represented by the following equations:

$$M(CN)_8^{4-} + AA \xrightarrow[4H_2O]{h\nu} [M(OH)_2(CN)_4(AA)]^{2-} + 2OH^- + 4HCN, \quad (1)$$

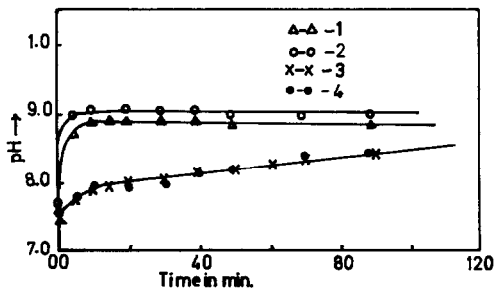


Fig. 3. Variation of pH with irradiation time curve: (1) $K_4Mo(CN)_8$–(phen), (2) $K_4Mo(CN)_8$–(bipy), (3) $K_4W(CN)_8$–(phen) and (4) $K_4W(CN)_8$–(bipy) systems.

Table 1. Analytical data of the complexes

Complex	Colour	Found (calc.) (%) Mo/W	N	H_2O
$[Mo(OH)_3(CN)(phen)_2]\cdot 2H_2O$	Brown powder	16.05 (16.87)	10.25 (12.30)	5.98 (6.33)
$[Mo(OH)_3(CN)(bipy)_2]\cdot 3H_2O$	Pastel brown powder	16.97 (17.81)	12.59 (12.99)	9.80 (10.02)
$[W(OH)_3(CN)(phen)_2]\cdot 2H_2O$	Light brown powder	27.32 (28.01)	11.25 (10.65)	5.20 (5.48)
$[W(OH)_3(CN)(bipy)_2]\cdot H_2O$	Light brown powder	31.20 (31.13)	11.93 (11.84)	3.20 (3.05)

$$[M(OH)_2(CN)_4(AA)]^{2-} + AA \xrightarrow[3H_2O]{h\nu} M(OH)_3(CN)(AA)_2 + 2OH^- + 3HCN. \quad (2)$$

The photochemical substitution reactions of potassium octacyano- molybdate and -tungstate in the presence of 1,10-phenanthroline and 2,2'-bipyridyl take place in two steps. In the first four CN^- ions are replaced by two OH^- and one AA and in the second further substitution of three CN^- ions by one OH^- and one AA.

The quantum yield[21,29] of the formation of the substitution products were determined. Its variation with concentration of the complex $K_4M(CN)_8$ was examined (Tables 2 and 3). The plot of quantum yield vs concentration of $K_4M(CN)_8$ is linear. It is found that the quantum yield increases with increase of the concentration of $K_4M(CN)_8$. The quantum yield was also determined at different pH (6–8.5), it has been found that it is not affected by the pH range studied. It has also been found that the quantum yield is not affected by the variation of the ligand concentration (Tables 2 and 3). The low values of the quantum yield show that the reaction is not a chain reaction and is completed in a few steps.

IR spectra of these complexes are very similar (Figs. 4–6). All the complexes display a broad band in the range 3300–3500 cm^{-1} characteristic of O–H stretching frequency, a single sharp peak in the range of 2100–2140 cm^{-1} characteristic of C≡N stretching, a sharp band 1600 cm^{-1} of H–O–H bending frequency. Bands are obtained at 700–800 cm^{-1} which correspond to the M–O stretching vibrations. Strong bands in the 700–900 cm^{-1} region

Table 2. Values of quantum yield determined using ~ 370 nm radiation for the substitution in $K_4Mo(CN)_8$ with 1,10-phenanthroline or 2,2'-bipyridyl*

System	Concentration of the system ($\times 10^3$ M)	ϕ ($\times 10^2$)
$K_4Mo(CN)_8 + 2$(phen)	4.00	7.00
	2.50	3.00
	1.00	2.00
	0.50	0.80
$K_4Mo(CN)_8 +$ (phen)	4.00	7.00
	0.50	0.80
$K_4Mo(CN)_8 + 2$(bipy)	5.00	8.00
	3.30	5.00
	1.00	2.40
	0.50	1.00
$K_4Mo(CN)_8 +$ (bipy)	5.00	8.00
	0.50	1.00

* $\lambda = 440$ nm, $I_0 = 1.08 \times 10^{20}$, $n_a = 20.01 \times 10^{-4}$, $t = 30°C$, pH = 7.0.

Table 3. Values of quantum yield determined using ~ 370 nm radiation for substitution in $K_4W(CN)_8$ with 1,10-phenanthroline or 2,2'-bipyridyl*

System	Concentration of the system ($\times 10^3$ M)	ϕ ($\times 10^2$)
$K_4W(CN)_8 +$ (phen)	1.00	1.10
	0.80	0.92
	0.50	0.62
	0.30	0.30
$K_4W(CN)_8 + 2$(phen)	0.80	0.89
	0.30	0.38
$K_4W(CN)_8 +$ (bipy)	1.00	0.61
	0.80	0.53
	0.50	0.41
	0.30	0.30
$K_4W(CN)_8 + 2$(bipy)	0.80	0.50
	0.30	0.32

* $\lambda = 620$ nm, $I_0 = 1.08 \times 10^{20}$, $n_a = 20.01 \times 10^{-4}$, $t = 30°C$, pH = 8.5.

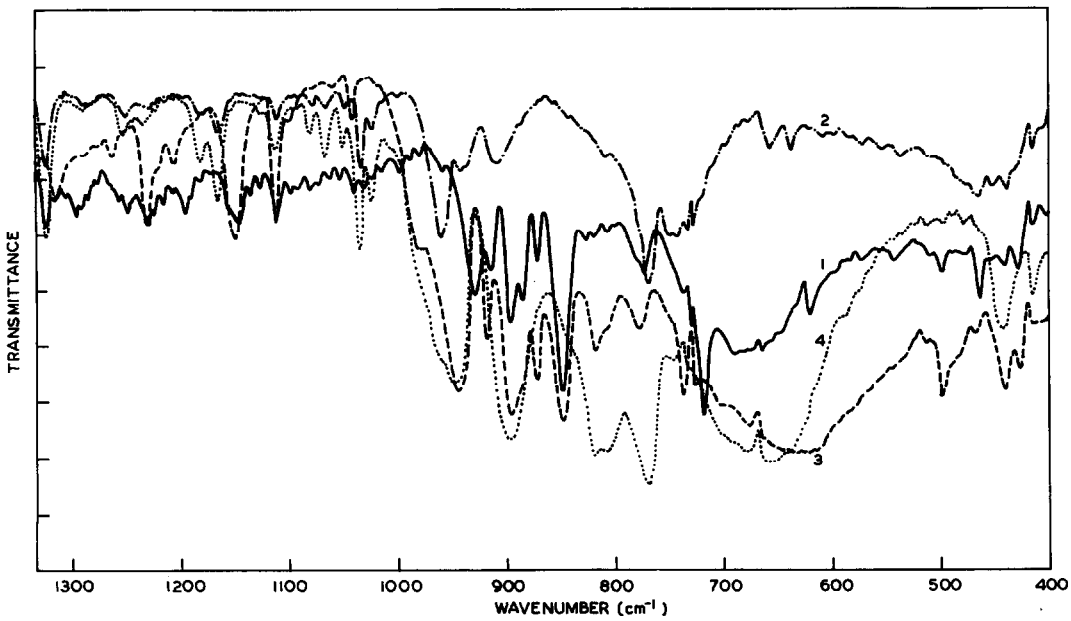


Fig. 4. IR spectra of: (1) $[Mo(OH)_3(CN)(phen)_2]\cdot 2H_2O$, (2) $[Mo(OH)_3(CN)(bipy)_2]\cdot 3H_2O$, (3) $[W(OH)_3(CN)(phen)_2]\cdot 2H_2O$ and (4) $[W(OH)_3(CN)(bipy)_2]\cdot H_2O$.

in spectra of aromatic hydrocarbons[30] have been identified with motions of ring hydrogen atoms moving in phase out of the plane of the ring. In $[Mo(OH)_3(CN)(phen)_2]\cdot 2H_2O$ and $[W(OH)_3(CN)(phen)_2]\cdot 2H_2O$ complexes two strong bands appeared at approximately 725 and 850 cm^{-1}. This is the number expected since there is one group of two and two groups of three adjacent hydrogen atoms in the ring system. In hydrocarbons, the frequency shifts upwards as the number of adjacent atoms in a group decreases. On this basis, the 725 cm^{-1} band is assigned to out of plane motion of the hydrogen atoms on the heterocyclic rings and 850 cm^{-1} band to the hydrogen on the centre ring. In the 2,2'-bipyridyl spectra, only one strong band was observed in this region as expected for two identical groups of four hydrogen atoms each. The pattern of splitting depends on the nature of the coordinated

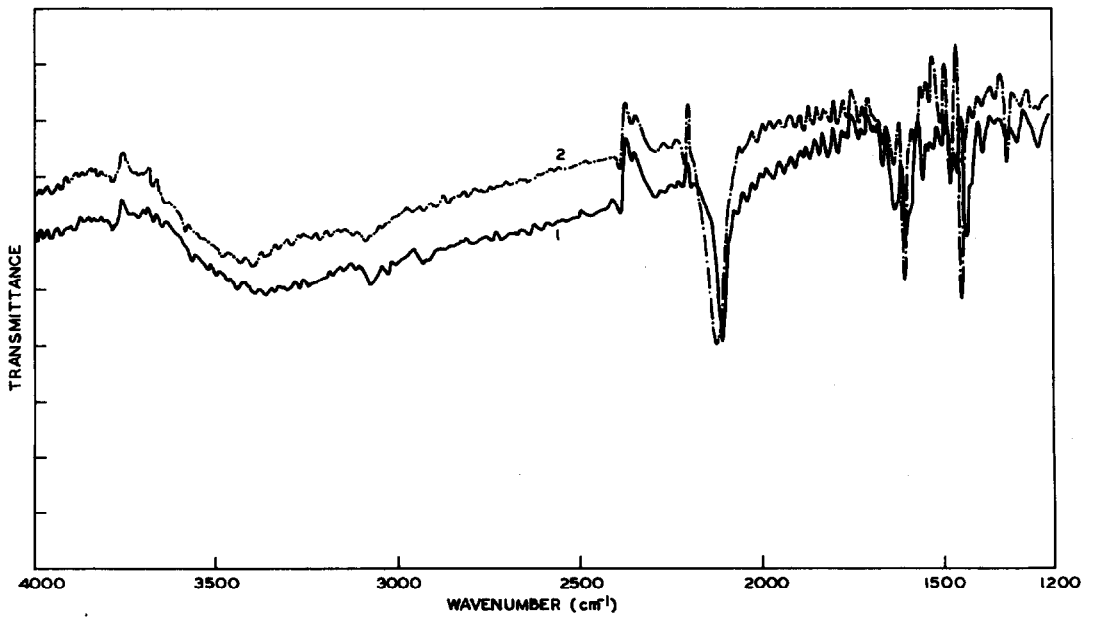


Fig. 5. IR spectra of: (1) $[Mo(OH)_3(CN)(phen)_2]\cdot 2H_2O$ and (2) $[Mo(OH)_3(CN)(bipy)_2]\cdot 3H_2O$.

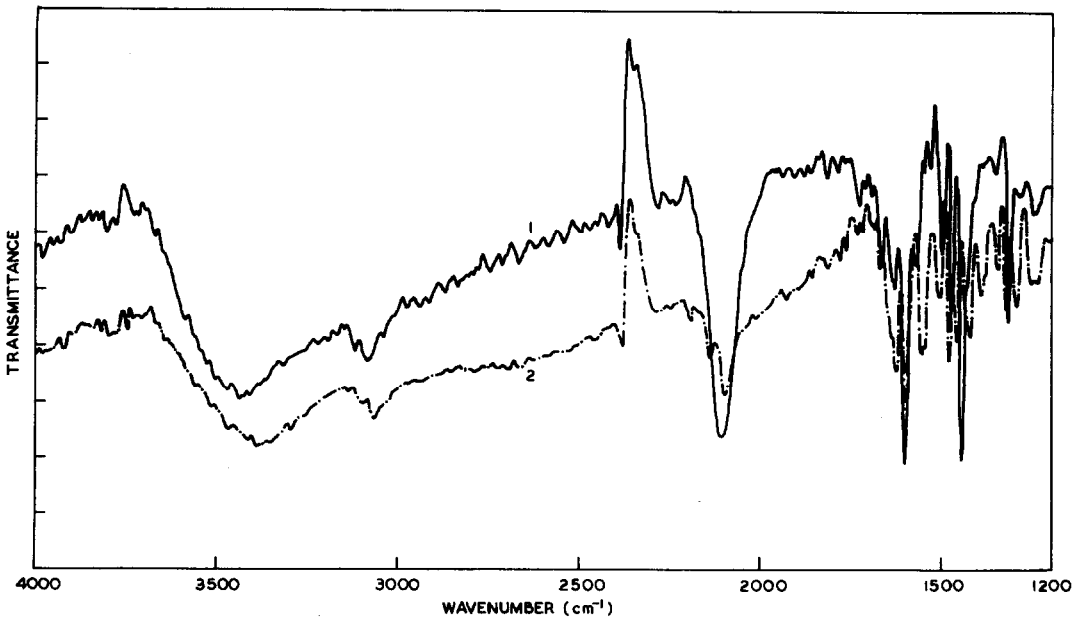


Fig. 6. IR spectra of: (1) $[W(OH)_3(CN)(phen)_2]\cdot 2H_2O$ and (2) $[W(OH)_3(CN)(bipy)_2]\cdot H_2O$.

atom. Two other sharp bands were obtained at ~ 1450 and $\sim 1600\ cm^{-1}$, these bands are most typical and usually the most intense of these ring frequencies. For example, in phenanthroline the first band occurs[31] at approximately $1450\ cm^{-1}$ and the second at $\sim 1605\ cm^{-1}$. The spectrum of 1,10-phenanthroline is quite similar,[30,32] one band is at $1505\ cm^{-1}$, the second appearing as triplet with the center component at $1590\ cm^{-1}$ and the third band shifting to $1423\ cm^{-1}$. All these bands move to higher frequencies on coordination. The $1423\ cm^{-1}$ band was least sensitive but others show shift in the order of 10–25 cm^{-1}. The spectra of $[Mo(OH)_3(CN)(bipy)_2]\cdot 3H_2O$ and $[W(OH)_3(CN)(bipy)_2]\cdot H_2O$ complexes have only three strong bands, one near $770\ cm^{-1}$ ascribed to out of plane bending of ring hydrogen, one near $1450\ cm^{-1}$ which is probably a ring frequency and a ring frequency is also near $1600\ cm^{-1}$. Numerous weak bands were observed between 900 and $1300\ cm^{-1}$. The peak at 1050–1070 cm^{-1} is assigned to out-of-plane M–O–H deformation mode. The cyanide stretching frequencies occur at higher energies for these complexes ($\sim 2100\ cm^{-1}$) than for the corresponding dioxo complexes ($2068\ cm^{-1}$). This suggests that metal–cyanide back-bonding is greater for complexes containing the O–M–O group than for the hydroxo-phenanthroline and hydroxo-bipyridyl complexes.

Acknowledgements—The assistance from the U.G.C. for this work and C.S.I.R., New Delhi for award of P.D.F. to Z.M. is thankfully acknowledged.

REFERENCES

1. A. Marchaj and Z. Stasicka, *Polyhedron* 1983, **2**, 485.
2. K. J. Moore and J. D. Petersen, *Polyhedron* 1983, **2**, 279.
3. M. S. Wrighton, H. B. Abrahamson and D. L. Morse, *J. Am. Chem. Soc.* 1976, **98**, 4105.
4. M. S. Wrighton and H. B. Abrahamson, *Inorg. Chem.* 1978, **17**, 3385.
5. R. M. Dahlgren and J. I. Zinck, *Inorg. Chem.* 1977, **16**, 3154.
6. B. Sieklucka and A. Samotus, *J. Inorg. Nucl. Chem.* 1980, **42**, 1003.
7. B. Sieklucka and A. Samotus, *J. Inorg. Nucl. Chem.* 1978, **40**, 315.
8. L. Mogi, F. Bolletta, V. Balzani and F. Scandola, *J. Inorg. Nucl. Chem.* 1966, **28**, 2589.
9. V. Gaspar and M. T. Beck, *Polyhedron* 1983, **2**, 387.
10. L. E. Orgel, *J. Inorg. Nucl. Chem.* 1960, **14**, 136.
11. M. C. Steele, *Aust. J. Chem.* 1957, **10**, 404.
12. R. P. Mitra, B. K. Sharma and H. Mohan, *Aust. J. Chem.* 1972, **25**, 449.
13. A. E. Nya and H. Mohan, *Polyhedron* 1984, **3**, 743.
14. V. Balzani, V. Carassiti and S. Lass, *Ann. Chim.* 1964, **54**, 103.
15. V. Balzani, V. Carassiti and L. Moggi, *Ann. Chim.* 1964, **54**, 251.
16. J. G. Leipoldt, L. D. C. Bok and P. I. Colliers, *Z. Anorg. Allg. Chem.* 1974, **409**, 343; 1974, **407**, 250.
17. C. A. Parker, *Proc. R. Soc. London* 1952, **A220**, 104; C. A. Hitchard and C. A. Parker, *Proc. R. Soc. London* 1954, **A235**, 518.
18. S. L. Murov, *Hand Book of Photochemistry*, pp. 19 and 122. Marcel Dekker, New York (1973).
19. A. I. Vogel, *Text Book of Quantitative and Inorganic Analysis*, 4th Edn, pp. 472 and 486. Longmans, London (1978).

20. J. G. Calvert and J. N. Pitts, *Photochemistry*, pp. 780, 786 and 796. Wiley, New York (1966).
21. A. W. Adamson, J. P. Welker and M. Volpe, *J. Am. Chem. Soc.* 1950, **72**, 4030.
22. E. L. Goodenow and C. S. Garner, *J. Am. Chem. Soc.* 1955, **77**, 5268, 5272.
23. W. Jakob and Z. Jakob, *Rocz. Chem.* 1962, **36**, 543, 601.
24. A. W. Adamson and J. R. Perumareddi, *Inorg. Chem.* 1965, **4**, 247.
25. S. Asperger, I. Murati and D. Pavolovic, *J. Chem. Soc.* 1960, 730.
26. V. Carassiti and V. Balzani, *Ann. Chim.* 1960, **50**, 630.
27. A. MacDiarmid and N. F. Hall, *J. Am. Chem. Soc.* 1953, **75**, 5204.
28. A. W. Adamson and A. H. Sporer, *J. Am. Chem. Soc.* 1958, **80**, 3865.
29. N. J. Tusro, *Molecular Photochemistry*. Benjamin, New York (1965).
30. A. A. Schilt and R. C. Taylor, *J. Inorg. Nucl. Chem.* 1959, **9**, 211.
31. C. G. Cannon and G. B. B. M. Sulhepland, *Spectrochim. Acta* 1951, **4**, 373.
32. R. N. Jones and C. Sandoify, *Chemical Application of Spectroscopy*, Vol. 9. Interscience, New York (1958).

Polyhedron Vol. 4, No. 5, pp. 829–839, 1985
Printed in Great Britain

0277–5387/85 $3.00 + .00
Pergamon Press Ltd

MIXED METAL $Pt_xM_yL_z$ COMPLEXES OF L = 1-METHYLURACIL AND 1-METHYLTHYMINE: PREPARATION AND SPECTROSCOPIC STUDIES

DAVID M. L. GOODGAME* and ROBERT W. ROLLINS
Chemistry Department, Imperial College of Science and Technology, London SW7 2AY, U.K.

and

BERNHARD LIPPERT
Anorganisch-Chemisches Institut, Technische Universität München, Lichtenbergstrasse 4, D-8046 Garching, F.R.G.

(*Received* 2 *April* 1984; *accepted* 7 *May* 1984)

Abstract—The reactions of *cis*-$(NH_3)_2PtL_2$ (L = 1-MeT or 1-MeU, the anions of 1-methylthymine or 1-methyluracil respectively) in water with various salts of Fe(II), Fe(III), Co(II), Ni(II), Cu(II) or Ag(I) have produced 14 new heteronuclear complexes of the general types: *cis*-$[(NH_3)_2PtL_2ML_2Pt(NH_3)_2]X_n \cdot mH_2O$ or *cis*-$(NH_3)_2PtL_2MX_n \cdot mH_2O$, and also with silver(I) perchlorate a complex of stoichiometry *cis*-$\{(NH_3)_2Pt(1\text{-}MeU)_2\}_2 \cdot 3AgClO_4 \cdot 6H_2O$. Comparisons are made with previously reported heteronuclear species derived from *cis*-$(NH_3)_2PtL_2$ and factors influencing the type of heteronuclear complex formed are discussed, particularly the versatility of binding patterns with Ag(I). A tetranuclear structure is suggested for the compound of stoichiometry *cis*-$(NH_3)_2Pt(1\text{-}MeU)_2 \cdot FeSO_4 \cdot 3H_2O$ involving iron(II) ions linked by sulphate bridges. The electronic spectra of the trinuclear complexes *cis*-$[(NH_3)_2Pt(1\text{-}MeU)_2M(1\text{-}MeU)_2Pt(NH_3)_2](NO_3)_2 \cdot mH_2O$ (M = Fe, Co or Ni) are reported. They show that the *trans*-MO_4Pt_2 geometry results in a very severely *trans*-elongated ligand field about the central metal ion, M. This conclusion is supported by the Mössbauer spectrum in the case of the iron(II) complex. The X- and Q-band EPR spectra of the Fe(III) analogue are also reported.

Complexes containing different metal ions have received considerable attention for reasons such as electron transfer,[1] magnetic exchange,[2] and their possible role in catalysis[3] or in metalloenzymes.[4,5] Heteronuclear complexes are readily formed with bi- or polyfunctional ligands and are usually synthesized in a stepwise manner. Examples of such ligands are acetylacetonates,[6] substituted phosphonites[7] or phosphites,[8] 2-mercaptoethylamine,[9] and many others,[10] including heterocyclic ligands such as pyrazine,[1] deprotonated imidazole,[11] or deprotonated pyrazole.[12]

We have been interested for some time in a group of compounds containing substituted uracils (pyrimidine-2,4-diones) attached through their N3 atom to Pt(II) and through their exocyclic oxygens to a variety of other metal ions. Depending on the Pt starting compound, mixed metal complexes with one or two eight-membered macrochelate rings or with an open structure were obtained (Fig. 1). Specifically, heteronuclear complexes of the following stoichiometries have been obtained and characterized (L = 1-methyluracil or 1-methylthymine anion, 1-MeU and 1-MeT, respectively):

Pt, M, L_2 from *cis*-$(NH_3)_2PtL_2$,[13]

Pt_2, M, L_4 from *cis*-$(NH_3)_2PtL_2$,[14]

Pt_4, M, L_4 from *cis*-$[(NH_3)_2PtL]_2^{2+}$ (*head–head*),[15]

Pt, M, L from *cis*-$[(NH_3)_2PtL(H_2O)]^+$,[16]

* Author to whom correspondence should be addressed.

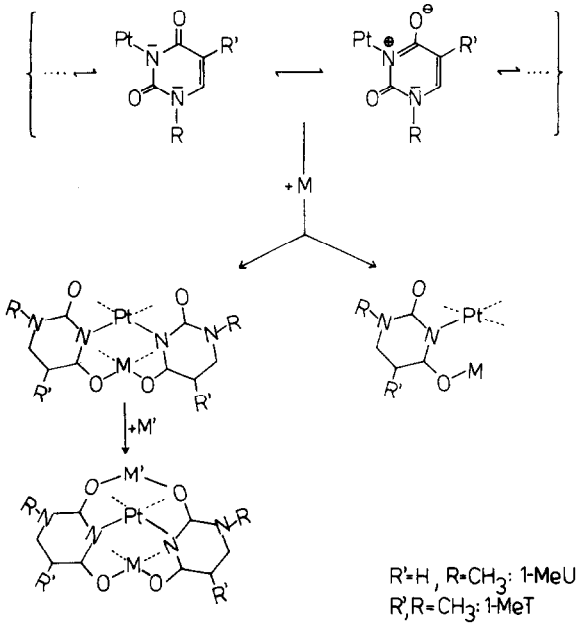


Fig. 1. Formation of heteronuclear complexes containing 1-methyluracil and 1-methylthymine ligands.

Pt_2, M_2, L_2 from *cis*-$[(NH_3)_2PtL]_2^{2+}$ (*head–tail*),[16]

Pt, M_2, L_2 from *trans*-$(NH_3)_2PtL_2$.[17]

There is, at present, no evidence for a biological role of these mixed metal complexes in connection with the mode of action of platinum antitumor drugs.[18] However, there are several observations that suggest that similar binding patterns of the DNA base thymine and the RNA base uracil may indeed play a more important role in nucleic acid–metal ion interactions than anticipated so far. For example, we found that a single L ligand attached through N3 {in *cis*-$[(NH_3)_2PtL(H_2O)]^+$}[16] either alone, or in conjunction with a second nucleobase having no particularly well coordinating site [in *cis*-$(NH_3)_2PtLL'$ with L = 1-MeU, L' = 1-methylcytosine (O2)[19] or 7,9-dimethylhypoxanthine(O6)][20] is sufficient to achieve binding of a second metal. Moreover, Beauchamp and coworkers have demonstrated a similar behaviour with Hg complexes of 1-MeT,[21] and the polymeric structure for Ag(1-MeT) reported by the same authors[22] reflects the tendency of L to use N3 *and* the exocyclic oxygens for metal coordination also. It has been suggested[14(a),23,24] that substitution of the proton at N3 of neutral uracil or its derivatives by the heavy metals Pt, Ag or Hg leads to a delocalization of the electron lone pair at N3 into the ring, thus increasing the basicity of the exocyclic oxygens O4 and O2.

In continuation of our previous work, we have studied in more detail the formation and spectroscopic properties of complexes of the two types Pt, M, L_2 and Pt_2, M, L_4 which were derived from *cis*-$(NH_3)_2Pt(1\text{-}MeU)_2$ and *cis*-$(NH_3)_2Pt(1\text{-}MeT)_2$, respectively. In particular, factors influencing the stoichiometries of the complexes formed, and the effect of the coordination geometry on the electronic state of the heterometals M were of interest. In the course of these studies we obtained, in crystalline form, a compound with yet another stoichiometry (Pt_2, M_3, L_4) with M being Ag(I).

EXPERIMENTAL

Preparation

cis-$(NH_3)_2Pt(1\text{-}MeT)_2 \cdot 2.5H_2O$ (**1**) and *cis*-$(NH_3)_2Pt(1\text{-}MeU)_2 \cdot 4H_2O$ (**2**) were prepared as previously described.[13,14(a)] The heteronuclear complexes were prepared by co-crystallizing *cis*-$(NH_3)_2PtL_2$ with suitable metal salts from aqueous solution. In a typical experiment, to 0.5 mmol of *cis*-$(NH_3)_2PtL_2$, dissolved in 8–15 cm^3 water, 0.25–4 mmol of the metal salt was added, either as solid or dissolved in a small amount of water. With Fe, Co, Ni and Cu salts there was an immediate colour change. The solution was filtered and then allowed to evaporate slowly. In a few cases, the heteronuclear complex precipitated immediately. The compound was collected on a filter, washed with a small amount of water and air dried. No attempts were made to optimize the yields. Reported yields are based on Pt. The following abbreviations are used: 1-MeT = $C_6H_7N_2O_2$ (1-methylthymine anion) and 1-MeU = $C_5H_5N_2O_2$ (1-methyluracil anion).

cis-$[(NH_3)_2Pt(1\text{-}MeT)_2Ni(H_2O)_2](CH_3COO)_2 \cdot 1H_2O$ (**3**) was prepared from **1** and $Ni(CH_3COO)_2 \cdot 4H_2O$ (Pt : Ni = 1) in a solution slightly acidified with CH_3COOH (pH 5.6). After evaporation to dryness, the sample was passed over Sephadex G 10, and the yellow fraction crystallized. Yellow microneedles, checked for absence of unreacted Ni salt by thin layer chromatography on silicagel (Merck 6D F254, methanol as solvent). Yield (after chromatography) 55%. Found: C, 26.08; H, 4.29; N, 11.20; Ni, 8.07%. Calc.: C, 26.03; H, 4.38; N, 11.39; Ni, 7.95%.

cis-$[(NH_3)_2Pt(1\text{-}MeT)_2Cu(H_2O)_2]SO_4 \cdot 1H_2O$ (**4**) was prepared from **1** and $CuSO_4 \cdot 5H_2O$ (Pt : Cu = 1). Evaporation to dryness, chromatography over Sephadex G 10, slow evaporation of yellow fraction gave yellow, transparent crystal plates, up to 1 mm long, losing water of crystallization in air. Yield (after chromatography) 70%. Analysis (of air dried sample). Found: C, 20.08; H, 3.82; N, 11.53; O,

24.47; S, 4.44%. Calc.: C, 19.98; H, 3.64; N 11.66; O, 24.41; S, 4.45%.

Compounds of type cis-$[(NH_3)_2Pt(1\text{-}MeT)_2M(1\text{-}MeT)_2Pt(NH_3)_2]X_n \cdot (H_2O)_m$

M = Co(II); X = CH_3COO^-, $n = 2$, $m = 4$ (**5**) was prepared from **1** and $Co(CH_3COO)_2 \cdot 4H_2O$ (Pt:Co = 1) as for **3**. Crystallization of the blue fraction after Sephadex chromatography gave a light blue microcrystalline material. Yield (after chromatography) 40%. Found: C, 26.50; H, 4.23; N, 13.63; Co, 4.3%. Calc.: C, 26.60; H, 4.31; N, 13.30; Co, 4.66%.

M = Ni(II); X = ClO_4^-, $n = 2$, $m = 2$ (**6**) was prepared from **1** and $Ni(ClO_4)_2 \cdot 6H_2O$ (Pt:Ni = 2). Pale yellow microcrystals, yield 50%. Found: C, 22.42; H, 3.73; Ni, 4.34%. Calc.: C, 22.03; H, 3.40; Ni, 4.49%.

M = Cu(II); X = NO_3^-, $n = 2$, $m = 3$ (**7**) was prepared from **1** and $Cu(NO_3)_2 \cdot 3H_2O$ (Pt:Cu = 2). Tiny, yellow columns, yield 50%. Found: C, 23.01; H, 3.72; N, 15.76; Cu, 5.30%. Calc.: C, 22.94; H, 3.70; N, 15.61; Cu, 5.06%. When $CuSO_4$ was used as starting material with $NaNO_3$ present in an equimolar concentration, **7** was obtained but not the SO_4 product.

cis-$(NH_3)_2Pt(1\text{-}MeU)_2 \cdot FeSO_4 \cdot 3H_2O$ (**8**). 0.5 mmol of **2** and 0.5 mmol $FeSO_4 \cdot 7H_2O$ were dissolved in 5 cm^3 water and the yellow solution (pH 4.4) kept in a partially covered beaker at 22°C. Within 1 day a crystalline precipitate had formed. After 8 days 160 mg (47%) of yellow–olive microplates were collected. In reflecting light the crystals look almost black. Found: C, 17.42; H, 3.03; Fe, 8.17%. Calc.: C, 17.52; H, 3.24; Fe 8.15%.

cis-$(NH_3)_2Pt(1\text{-}MeU)_2 \cdot AgNO_3 \cdot 2H_2O$ (**9**). 0.05 mmol of **2** and 4 mmol $AgNO_3$ were heated in 15 cm^3 water to 70–80°C, filtered, and the solution kept at 22°C for 1 day. As early as 1 h after filtration, **9** starts precipitating as colourless, transparent needles. Yield 200 mg (58%). Found: C, 17.96; H, 3.36; N, 14.03; Ag 15.40%. Calc.: C, 17.52; H, 2.95; N, 14.31; Ag, 15.74%.

cis-$[(NH_3)_2Pt(1\text{-}MeU)_2Zn(H_2O)_3]SO_4 \cdot 2H_2O$ (**10**) was prepared from **2** and $ZnSO_4 \cdot 7H_2O$ (Pt:Zn = 1). Colourless cubes, yield 65%. Found: C, 16.48; H, 3.62; N, 11.61; S, 4.48%. Calc.: C, 16.43; H, 3.59; N, 11.50; S, 4.39%.

Compounds of type cis-$[(NH_3)_2Pt(1\text{-}MeU)_2M(1\text{-}MeU)_2Pt(NH_3)_2]X_n \cdot (H_2O)_m$

M = Fe(II); X = NO_3^-, $n = 2$, $m = 5$ (**11**) was prepared from **2** and $FeSO_4 \cdot 7H_2O$ (Pt:Fe = 1). The yellow solution was filtered, passed through an anion exchange column in the NO_3^- form, the solution concentrated on a rotavaporator to small volume and allowed to evaporate at 3°C. Orange–yellow cubes, yield 45%. Found: C, 19.43; H, 3.39; N, 16.26; Fe, 4.45%. Calc.: C, 19.55; H, 3.45; N, 15.96; Fe, 4.55%.

M = Fe(III); X = NO_3^-, $n = 2$, $m = 4$ (**12**) was prepared from **2** and $Fe(NO_3)_3 \cdot 9H_2O$ (Pt:Fe = 1). The orange–red solution (pH 1.6) was allowed to evaporate at 3°C. Small, red columns losing transparency in air, yield 88%. Found: C, 18.78; H, 3.16; N, 16.37; Fe, 4.63%. Calc.: C, 18.87; H, 3.17; N, 16.51; Fe, 4.39%.

M = Co(II); X = NO_3^-, $n = 2$, $m = 6$ (**13**) was prepared from **2** and $Co(NO_3)_2 \cdot 6H_2O$ (Pt:Co = 1). The purple solution was concentrated to small volume by warming to 35°C. On cooling, light blue crystals formed. Yield 63%. Found: C, 19.33; H, 3.41; N, 16.00; Co, 4.5%. Calc.: C, 19.21; H, 3.56; N, 15.69; Co, 4.71%.

M = Co(II); X = ClO_4^-, $n = 2$, $m = 3$ (**14**) was prepared from **2** and $Co(ClO_4)_2 \cdot 6H_2O$ (Pt:Co = 1). It precipitated immediately on mixing aqueous solutions of the two components. Light blue powder, yield 90%. Found: C, 18.47; H, 2.75; Co, 4.1%. Calc.: C, 18.90; H, 3.02; Co, 4.64%.

M = Ni(II); X = NO_3^-, $n = 2$, $m = 6$ (**15**) was prepared from **2** and $NiSO_4 \cdot 7H_2O$ (Pt:Ni = 3:2). The yellow precipitate obtained after evaporation to dryness was redissolved and passed through an anion exchange column in its NO_3^--form, and the solution crystallized at 22°C. Yellow plates, yield 70%. Found: C, 19.21; H, 3.42; N, 15.79; Ni, 4.83%. Calc.: C, 19.22; H, 3.56; N, 15.70; Ni, 4.70%. An identical product was obtained in 80% yield by reaction of **2** and $Ni(NO_3)_2 \cdot 6H_2O$ (Pt:Ni = 1).

M = Ag(I); X = NO_3^-, $n = 1$, $m = 8$ (**16**) was prepared from **2** and $AgNO_3$ (Pt:Ag = 2). The colourless solution was concentrated to small volume until first signs of formation of a precipitate appeared. The sample was then slightly warmed to dissolve the precipitate and the sample placed in a refrigerator (3°C). Within 1 day colourless, transparent cubes had formed, which lose water of crystallization and their transparency in air. Yield 50%. Found: C, 18.72; H, 3.90; N, 14.31; Ag, 8.2%. Calc.: C, 18.87; H, 3.81; N, 14.31; Ag, 8.47%.

cis-$(NH_3)_2Pt(1\text{-}MeU)_2 \cdot 1.5AgClO_4 \cdot 3H_2O$ (**17**) was obtained as follows: **2** and $AgClO_4 \cdot H_2O$ (Pt:Ag = 1:8) were mixed in water, heated to 70°C, filtered hot, and the colourless solution slowly cooled to 22°C. Colourless, thin needles, yield 75%. Found: C, 14.41; H, 2.59; N, 9.96; Ag, 19.3%. Calc. C, 14.22; H, 2.63; N, 9.95; Ag, 19.16%.

Spectroscopy

IR spectra were recorded as Nujol mulls (CsI windows) on Perkin–Elmer 577 and 580 grating spectrometers. Reference spectra of Cu(II), Cr(II) and Rh(II) acetate were taken and compared with the compounds containing acetate. EPR spectra were obtained as previously reported.[19] Electronic spectra of the powdered samples were measured with a Beckman DK 2 spectrometer and the standard reflectance accessory.

The Mössbauer spectrum of compound **11** was measured at 78 K using the apparatus described previously.[25]

RESULTS AND DISCUSSION

Formation of compounds

Table 1 lists the heteronuclear complexes prepared from *cis*-$(NH_3)_2Pt(1\text{-MeT})_2$ and *cis*-$(NH_3)_2Pt(1\text{-MeU})_2$, respectively. The Pt_2, M, L_4 stoichiometry appears to be the most common one with the metals M and counterions X used in this work. Two examples of this type have previously been examined by us using X-ray crystallography: a silver(I) complex[14(a)] and a manganese(II) complex[14(b)] each with L = 1-MeT. The two compounds differ in the coordination geometry of the heterometal: while Ag adopts a distorted tetrahedral coordination sphere, the Mn is square-planar. This difference leads to markedly different Pt–M–Pt distances, which are shorter in the case of the Mn compound, 2.704(1) Å vs 2.849(1) and 2.884(1) Å. Coordination of the heterometal M in both cases occurs through O4 of the four 1-MeT ligands, while Pt binds through N3. There is little doubt that all the compounds having Pt_2, M, L_4 stoichiometry, which are described in this work, are constructed in this way.

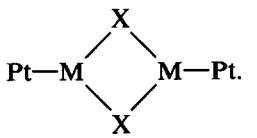
The Pt, M, L_2 stoichiometry is clearly less frequent. The crystal structure of one example, *cis*-$[(NH_3)_2Pt(1\text{-MeU})_2Cu(H_2O)_2]SO_4$, has been determined.[13] In this compound, Pt is coordinated through N3 of 1-MeU, and Cu through two exocyclic O4 oxygens of 1-MeU. Copper completes its coordination sphere by two oxygens from coordinated water molecules. As will be discussed

Table 1. Isolated heteronuclear complexes

		M	X	*n*	No.	Ref.
$[Pt, M, L_2]X_n$	1-MeT	Ni(II)	Acetate	2	**3**	*
		Cu(II)	Sulphate	1	**4**	*
		Ag(I)	Nitrate	1		14(a)
	1-MeU	Fe(II)	Sulphate	1	**8**	*
		Cu(II)	Sulphate	1		13
		Ag(I)	Nitrate	1	**9**	*
		Zn(II)	Sulphate	1	**10**	*
		Na(I)	Nitrate	1		13
$[Pt_2, M, L_4]X_n$	1-MeT	Mn(II)	Chloride	2		14(b)
		Co(II)	Acetate	2	**5**	*
		Ni(II)	Perchlorate	2	**6**	*
		Cu(II)	Nitrate	2	**7**	*
		Ag(I)	Nitrate	1		14(a)
	1-MeU	Fe(II)	Nitrate	2	**11**	*
		Fe(III)	Nitrate	3	**12**	*
		Co(II)	Nitrate	2	**13**	*
		Co(II)	Perchlorate	2	**14**	*
		Ni(II)	Nitrate	2	**15**	*
		Cu(II)	Nitrate	2		13
			Sulphate	1		13
			Chloride	2		13
			$PtCl_4^{2-}$	1		13
		Ag(I)	Nitrate	1	**16**	*
		Na(I)	Nitrate	1		13
$[Pt_2, M_3, L_4]X_n$		Ag(I)	Perchlorate	1	**17**	*

* This work.

subsequently, the formation of dinuclear Pt, M complexes most likely is not the only way to accommodate the Pt, M, L_2 stoichiometry. There exists the possibility of a polymeric arrangement with Pt and M alternating, and coordination of the counterion X to the heterometal may lead to a tetranuclear arrangement of the kind



Finally, with Ag(I) yet another stoichiometry (Pt_2, Ag_3, L_4) has been observed (*vide infra*).

From Table 1 and the details of the preparation of the compounds two conclusions can be drawn.

(1) The relative Pt : M ratio used in the preparation is not the only factor determining the stoichiometry of the product. The choice of the counter ion X has a similar, or even more pronounced, effect, either by influencing the solubility of the product and precipitating the least soluble one, or by coordination to the heterometal M. We have previously noted this in the Pt, Cu, 1-MeU system[13] and find it confirmed here. For example, while at a given Pt : Fe(II) ratio (1 : 1) the NO_3^- salt crystallizes as the Pt_2, Fe, L_4 product, the sulphate crystallizes with Pt, Fe, L_2 stoichiometry. With an excess of $AgNO_3$ over *cis*-$(NH_3)_2Pt(1\text{-MeU})_2$ the Pt, Ag, L_2 product is formed and not Pt_2, Ag, L_4. However, with $AgClO_4$ used in the same excess, Pt_2, Ag_3, L_4 is obtained instead.

(2) There appears to be little or no influence of the nature of the heterometal on the stoichiometry of the compound formed. We attribute this finding to the flexibility of the Pt, L_2 moiety which permits the heterometal in Pt, M, L_2 and Pt_2, M, L_4 to have a tetrahedral, a square-planar, or an octahedral (with Pt occupying a coordination site) coordination sphere. Moreover, in Pt, M, L_2 compounds the coordination sphere of M may be extended from 4 to 5 with the use of coordinated solvent molecules or counter ions.

Versatility of Ag *binding patterns*

With L = 1-MeT, two complexes of Pt, Ag, L_2 and Pt_2, Ag, L_4 stoichiometry have previously been obtained.[14(a)] With L = 1-MeU the two analogues have been prepared and in addition a compound having Pt_2, Ag_3, L_4 stoichiometry. Formation of the first two compounds, of both 1-MeT and 1-MeU, was dictated by the Ag : Pt ratio applied, favouring the Pt_2, Ag, L_4 product at low ratios (1 : 2) and Pt, Ag, L_2 at ratios of 2–8. The Pt, Ag, L_2 product of L = 1-MeU, like the 1-MeT compound, is of a very low solubility in water as compared to the dinuclear Cu(II) or Zn(II) complexes. This suggests that this compound does not consist of isolated dinuclear units but rather is polymeric. A structure as observed for Ag(1-MeT)[22] with Ag binding to N3, O4 and O2 would be consistent with this idea. The principal difference between Ag(1-MeT) and Pt, Ag, L_2 would be the replacement of the Ag binding to two N3 sites of 1-MeT by the $(NH_3)_2Pt(II)$ moiety. Depending on whether the PtL_2 unit assumes a head–head or a head–tail arrangement, a variety of Ag coordination patterns are possible in an assumed polymeric Pt, Ag, L_2 structure: for example, one Ag bound through four O4 sites, the second Ag bound through four O2 sites, or mixed O2, O4 coordination with identical donor atoms in mutual *cis*- or *trans*-positions. Moreover, the coordination geometries of the Ag ions might be tetrahedral as in $\{[(NH_3)_2Pt(1\text{-MeT})_2]_2Ag\}NO_3$[14(a)] or square planar as in $\{[(NH_3)_2Pt(1\text{-MeU})]_4Ag\}(NO_3)_5$;[15] yet it is clear that both Ag ions should have the same geometry.[13]

The stepwise addition of Ag to the Pt_2, Ag, L_4 unit gives a rationale for the other stoichiometries observed (Fig. 2). Formally, a polymeric structure of Pt, Ag, L_2 stoichiometry results if half an Ag ion is added twice to the still available exocyclic oxygens of L in Pt_2, Ag, L_4. Addition of yet another Ag leads to Pt_2, Ag_3, L_4, a product obtained from reaction of *cis*-$(NH_3)_2Pt(1\text{-MeU})_2$ with 8 equivalents of $AgClO_4$. If still another Ag is added, a Pt, Ag_2, L_2 stoichiometry can be expected. A compound of this composition is not yet known for the *cis*-Pt(II) system, but has recently been crystallographically confirmed by us with *trans*-Pt(II).[17] In this compound, the two Ag ions exhibit mixed O2, O4 coordination while Pt binds to two N3 sites of 1-MeU.

Complexes with Pt, M, L_2 *stoichiometry*

As mentioned before, *cis* - $[(NH_3)_2Pt(1\text{-MeU})_2Cu(H_2O)_2]SO_4 \cdot 4.5H_2O$ represents, thus far, the only crystallographically studied example of Pt, M, L_2 stoichiometry. The corresponding 1-MeT complex, **4**, appears to be isostructural with the former. The IR spectrum unambiguously reveals the presence of ionic SO_4^{2-} (ν_3 1115 cm^{-1}, ν_4 620 cm^{-1}). The compound *cis*-$[(NH_3)_2Pt(1\text{-MeU})_2Zn(H_2O)_3]SO_4 \cdot 2H_2O$ (**10**) according to its IR spectrum contains ionic SO_4^{2-} as well, but the coordination geometry is different from that of Cu (square-pyramidyl instead of square-planar).

One alternative to a dinuclear structure of Pt, M, L_2 compounds, a polymeric arrangement of Pt and M has been discussed in the preceding section. A

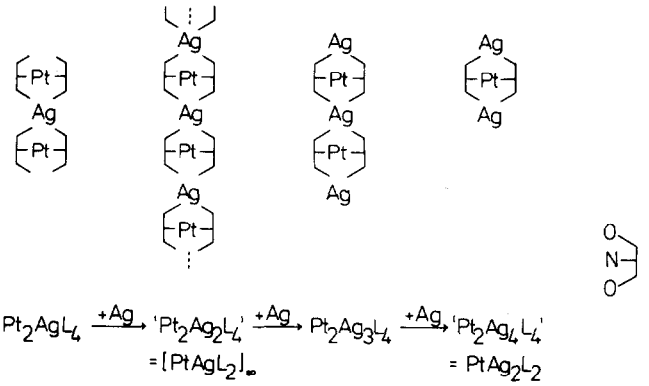


Fig. 2. Stepwise formation of $Pt_xM_yL_z$ stoichiometries, starting with Pt_2AgL_2 (L = 1-MeU).

second alternative, a tetranuclear arrangement with two bridging anions, is also feasible and possibly realized in *cis* - $(NH_3)_2Pt(1 - MeU)_2 \cdot FeSO_4 \cdot 3H_2O$ (**8**). The IR spectrum of this compound clearly demonstrates the presence of SO_4^{2-} in C_{2v} symmetry with bands at 975 cm^{-1}, *s* (ν_1), 1205, *s*, 1110, *s*, 1030 cm^{-1}, *s* (ν_3), and 600, *m*, and 660 cm^{-1}, *m* (ν_4). No straightforward differentiation between chelating and bidentate bridging sulphate is possible,[26] particularly as well characterized examples of Fe(II) sulphato complexes are lacking. Although we cannot, at present, assign the correct structure for *cis* -$(NH_3)_2Pt(1 - MeU)_2 \cdot FeSO_4 \cdot 3H_2O$, a tetranuclear structure as depicted in Fig. 3 seems quite reasonable.

The 1 : 1-product from reaction of *cis*-$(NH_3)_2Pt(1\text{-MeT})_2$ and $Ni(CH_3COO)_2$, compound **3**, was considered another possible candidate containing bridging anion ligands. However, its IR spectrum provides no evidence for bidentate bridging acetate. In the 600–700 cm^{-1} range, its IR spectrum shows no similarity with the spectra of the binuclear acetates of Cr(II), Cu(II) and Rh(II). While these compounds exhibit a characteristic pattern with an intense mode around 685–715 cm^{-1} and a weaker one around 630 cm^{-1}, **3** shows four bands of medium intensity at 615, 650, 670 and 680 cm^{-1}. At least one band (680 cm^{-1}), but possibly also the 670 cm^{-1} band must be assigned to a 1-MeT ring mode, leaving the other two bands to acetate modes. They compare with medium intensity bands at 646 and 615 cm^{-1} for $Na(CH_3COO)$.[27]

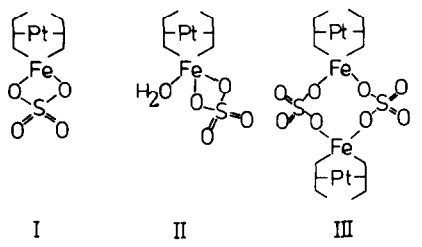


Fig. 3. Feasible geometries of *cis* - $(NH_3)_2Pt(1\text{-MeU})_2 \cdot FeSO_4 \cdot 3H_2O$ (**8**) containing chelating (I, II) and bidentate bridging (III) sulphate.

Electronic spectra of Pt_2, M, L_4 *complexes* [M = Fe(II), Co(II), Ni(II)]

In view of the very unusual ligand fields around the central metal ion M in these compounds we were interested to study their electronic spectra. Earlier work[28] on the EPR spectra of Mn(II) in the trinuclear complex ion *cis* - $[(NH_3)_2Pt(1 - MeT)_2Mn(1 - MeT)_2Pt(NH_3)_2]^{2+}$ showed that the platinum atoms in the axial positions result in a severe axial distortion of the field about the central metal ion. EPR studies on the related copper(II) species *cis* - $[(NH_3)_2Pt(1 - MeU)(1 - MeC)Cu(1 - MeU)(1 - MeC)Pt(NH_3)_2]^{4+}$ and *cis* - $[(NH_3)_2Pt(1 - MeU)_2Cu(1 - MeU)_2Pt(NH_3)_2]^{2+}$ revealed[19] that this distortion was a tetragonal elongation, i.e. that the ligand field effect due to the platinum atoms was less than the in-plane field generated by the exocyclic oxygen atoms of the heterocyclic ligands. Examination of the electronic spectra of the iron(II), cobalt(II) and nickel(II) compounds *cis* - $[(NH_3)_2Pt(1 - MeU)_2M(1 - MeU)_2Pt(NH_3)_2](NO_3)_2$ in the visible and near IR regions would provide an independent check on this conclusion, and also yield spectral information on what would appear to be one of the most distorted examples of a nominally six-coordinate environment for these metal ions.

The microcrystals were too small for single crystal spectroscopy but reflectance spectra of quite good quality were obtained in the 500–2200 nm region (Fig. 4). Sharp bands marked * in the 1400–2200 nm range are ligand vibrational overtones and combinations and these were identified by their invariance on changing the central metal ion, M, and by their presence in the reflectance spectrum of the

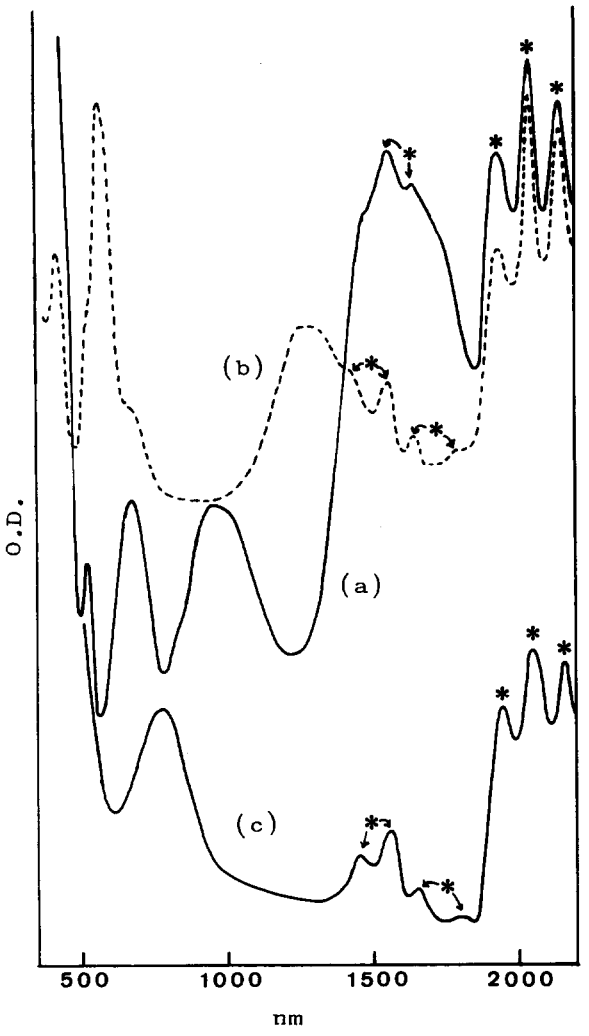


Fig. 4. Electronic reflectance spectra of *cis* - $[(NH_3)_2Pt(1\text{-}MeU)_2M(1\text{-}MeU)_2Pt(NH_3)_2](NO_3)_2(H_2O)_m$: (a) M = Ni(II) (compound **15**); (b) M = Co(II) (compound **13**); (c) M = Fe(II) (compound **11**).

iron(III) compound. Only in the case of the lowest energy *d–d* band of the nickel complex is there significant overlap of the vibrational and d–d bands, and then only by the weak vibrational set at 1400–1700 nm, which are seen as small additional features on that *d–d* band (Fig. 4).

We shall first consider the spectrum of the nickel complex, the *d–d* band energies of which are listed in Table 2. Analysis of the *d–d* spectra of tetragonally distorted six-coordinate nickel(II) complexes is now well documented. Two of the most severely distorted ligand fields are in the compounds $Ni(pyridine)_4I_2$[29] and $Ni(pyrazole)_4Br_2$.[30] The reported band energies and assignments (in D_{4h}) for these compounds are also listed in Table 2 for direct comparison with the results for the Pt–Ni–Pt complex. (An O_h–D_{4h} correlation diagram for the high-spin levels arising for d^7 and d^8 is shown in Fig. 5.)

The ligand fields generated by the exocyclic oxygens in uracil, thymine, and related ligands are known[31] to be low; significantly less than those produced by pyridine or pyrazole. Accordingly, we would expect the average ligand field in the Pt–M–Pt complexes to be quite weak as well as very distorted. The weakness of the overall field is also demonstrated by the electronic spectrum of the cobalt(II) complex (see later).

The strong band at 6250 cm^{-1} in the spectrum of the nickel complex is readily assigned as $^3B_{1g} \rightarrow {}^3E_g(1)$. Three bands [from the transitions $^3B_{1g} \rightarrow {}^3B_{2g}$, $^3A_{2g}(1)$, and $^3E_g(2)$] would then be expected in the 7000–16,000 cm region, but only two were observed, at about 10,000 cm^{-1} and at 14,500 cm^{-1}. The former band is asymmetric and becomes more so on cooling to *ca* 80 K, but the absorption could not be reliably resolved into two components. The $^3B_{2g}$ and $^3A_{2g}(1)$ levels are known to lie close together in $Ni(pyridine)_4I_2$ and $Ni(pyrazole)_4Br_2$, with $^3B_{2g} < {}^3A_{2g}(1)$. The corresponding levels, $^3B_2$ and $^3A_2(1)$ are also closely spaced in the square pyramidal (C_{4v}) complex [Ni(2-methylimidazole)$_4$Br]Br, but in that case $^3B_2$ (at 11,600 cm^{-1}) has moved above $^3A_2(1)$ (at 10,300 cm^{-1}).[32]

The Pt–Ni–Pt complex appears to represent the intermediate situation where the $^3B_{2g}$ and $^3A_{2g}(1)$ levels are too close to be resolved without the use of polarized light. Assignment of the 14,500 cm^{-1} band as either $^3B_{2g}$ or $^3A_{2g}(1)$ would be quite at variance with the results for other compounds given in Table 2. This problem does not arise with our preferred assignment of the 14,500 cm^{-1} band as $^3B_{1g} \rightarrow {}^3E_g(2)$.

The remaining band, at 18,700 cm^{-1}, is probably $^3B_{1g} \rightarrow {}^3A_{2g}(2)$ but, in view of Hitchman's observation[32] of the relatively high intensity of the $^3B_1 \rightarrow {}^1E(1)$ band at 17,300 cm^{-1} in the spectrum of

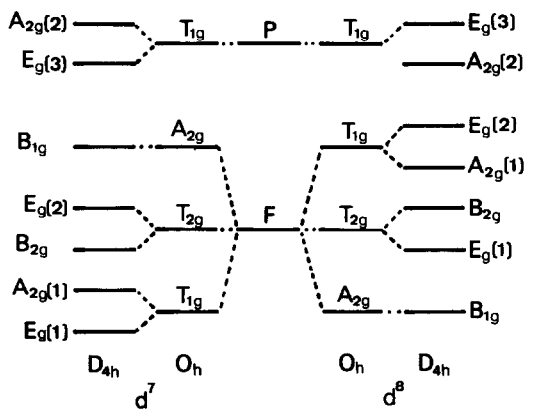


Fig. 5. O_h–D_{4h} correlation for high-spin terms arising from d^7 and d^8.

Table 2. Electronic spectral band energies for the Pt–M–Pt complexes (M = Fe^{II}, Co^{II}, Ni^{II}) and of some reference compounds

Compound	Band maximum (cm^{-1})*					
	$^3E_g(1)$	$^3B_{2g}$	$^3A_{2g}(1)$	$^3E_g(2)$	$^3A_{2g}(2)$	$^3E_g(3)$
Pt–Ni–Pt	6250		10,100†	14,500	18,700	‡
$Ni(pyrazole)_4Br_2$§	7240	10,900	12,000	15,900	25,800‖	
$Ni(pyridine)_4I_2$¶	7905	11,834	13,158	16,393	(23,977)**	(25,164)**
[Ni(2-Meim)$_4$Br]Br††	5150	11,600	10,300	15,300	22,800	24,800
	$^4B_{2g}$	$^4E_g(2)$	$^4B_{1g}$	$^4E_g(3)$	$^4A_{2g}(2)$	
Pt–Co–Pt	‡‡	7750	14,300	17,400	23,500	
$Co(MPZ)_4I_2$§§	(6294)‖‖	8600	¶¶	17,950	24,500	
$Co(s\text{-}Et_2en)_2Br_2$***	6325	9270	17,630	18,700 19,300	21,470	
	$^5A_{1g}$	$^5B_{1g}$				
Pt–Fe^{II}–Pt	‡‡	12,900				
$Fe(MPZ)_4I_2$§§	4700	12,850				
$Fe(IQ)_4I_2$†††	5900	11,750				

* Upper level designations are for D_{4h} symmetry except for [Ni(2-methylimidazole)$_4$Br]Br (C_{4v}) for which g notation in designations should be deleted. Numbers in parentheses indicate the order of increasing energy of the states of same designation.

† Asymmetric band, but components unresolved (see text).

‡ Hidden under strong absorption in UV region.

§ From Ref. 30.

‖ Components not resolved experimentally. Calc. values from Ref. 30: 25,120 cm^{-1} [$^3A_{2g}(2)$], 27,100 cm^{-1} [$^3E_g(3)$].

¶ From Ref. 29.

** Calc. values from Ref. 29; experimental band energies not reported.

†† From Ref. 32; 2-Meim = 2-methylimidazole.

‡‡ Not observed above 4500 cm^{-1}.

§§ From Ref. 35; MPZ = 3(5)-methylpyrazole.

‖‖ Calc. value from Ref. 35.

¶¶ Not reported.

*** From Ref. 37; s-Et_2en = $EtNHCH_2CH_2NHEt$.

††† From Ref. 39; IQ = isoquinoline.

[Ni(2-methylimidazole)$_4$Br]Br, we cannot rule out an alternative assignment as $^3B_{1g} \rightarrow {}^1E_g(1)$ for this 18,700 cm^{-1} band.

The spectrum of the Pt–Co^{II}–Pt complex (Fig. 4b) has only one d–d band in the 4500–12,500 cm^{-1} region and this is at low energy (7750 cm^{-1}) for a nominally six-coordinate Co(II) species.

The spectra of strongly tetragonally distorted six-coordinate cobalt(II) complexes have received less detailed attention than their nickel(II) analogues. The effects of the tetragonal distortion of the ligand field upon the terms arising for the cubic d^7 case and the relative order of the resultant component levels have been discussed, *inter alia*, by Lever.[33]

Splitting of the original $^4T_{2g}$ term into the components $^4E_g(2)$ and $^4B_{2g}$ is quite sensitive to the extent of the distortion of the field from O_h symmetry. The spectra of compounds of the type CoL_4X_2 (L = heterocyclic amine; X = Cl, Br, I), in which the field is quite distorted but of only weak to moderate overall average strength, have the transitions to $^4E_g(2)$ and $^4B_{2g}$ in the 5000–9000 cm^{-1} region. There is, however, some disagreement as to the assignment of the two bands in this region for closely-related compounds. Some workers[34,35] place $^4E_g(2) > {}^4B_{2g}$ while others[36] prefer $^4E_g(2) < {}^4B_{2g}$. From low-temperature single crystal spectroscopy, Lever[37] assigns $^4E_g(1) \rightarrow {}^4B_{2g}$ at 6325 cm^{-1} and $^4E_g(1) \rightarrow {}^4E_g(2)$ at 9270 cm^{-1} for [$Co(EtNHCH_2CH_2NHEt)_2Br_2$], in which the diamine contributes no π-component to the equatorial field.

Notwithstanding the question of the order of the $^4E_g(2)$ and $^4B_{2g}$ levels in the compounds referred to above, our observations of only one band (at 7750 cm^{-1}) Pt–Co^{II}–Pt in the 4500–12,500 cm^{-1} region shows that the ligand field distortion experienced by the cobalt(II) ion in this compound is large, and also that the average field is weak. Making the reasonable assumption that here $DQ_{axial} < DQ_{equatorial}$, we assign the 7750 cm^{-1} band to the transition to $^4E_g(2)$. That to $^4B_{2g}$ either lies below 4500 cm^{-1} or is very weak and is obscured by the vibrational bands in 4500–5250 cm^{-1} region. (The reverse assignment would require a very low value for the equatorial ligand field produced by the exocyclic oxygen atoms.)

Our assignments of the other bands are given in Table 2. The weakness of the transition to $^4B_{1g}$ is as expected,[38] as are the relative intensities of the bands assigned to $^4E_g(3)$ and $^4A_{2g}(2)$. The splitting of the original $^4T_{1g}(P)$ level is large and is similar to those observed for the strongly tetragonally distorted compounds $[Co\{3(5)\text{-methylpyrazole}\}_4X_2]$ (X = Br, I).[35] (Bands for the iodide, from Ref. 35, are given in Table 2 for comparison.)

Assignment of the spectrum of Pt–Fe^{II}–Pt (Fig. 4c) is straightforward. The ^5E_g level arising for high-spin d^6 in O_h symmetry splits into $^5A_{1g} + {}^5B_{1g}$ in D_{4h}, and the effects of a tetragonal distortion on the spectra of six-coordinate iron(II) complexes are well documented.[35,39] In practice both transitions are generally intense enough for them to be detected in the region where vibrational bands also contribute, though the latter can sometimes reduce the precision with which the band maxima can be determined. Examples of compounds in which the tetragonal distortion is particularly large are FeL_4I_2 [L = 3(5)-methylpyrazole[35] or isoquinoline[39]] and the reported band energies for those compounds are listed in Table 2.

As in the case for the nickel and cobalt analogues discussed earlier, the Pt–Fe^{II}–Pt complex represents a more distorted situation than the quoted reference compounds, so that the lower energy component ($^5A_{1g}$) has moved below the limit of our study (4500 cm^{-1}). This $^5A_{1g}$ level is particularly sensitive to the degree of axial distortion and in the limiting case of the high-spin square configuration, as in the mineral gillespite,[40] it becomes the ground state.

These conclusions about the strongly distorted nature of the iron(II) environment in the Pt–Fe^{II}–Pt complex are supported by its Mössbauer spectrum, measured at 78 K (Fig. 6). This consists of a quadrupole split doublet (the peak asymmetry is attributed to partial orientation of the crystallites in the sample) with quadrupole splitting $\Delta = 2.045 + 0.007$ mm^{-1}, and isomer shift $\delta = 0.952 + 0.07$ mm^{-1} with respect to metallic iron. The δ value is particularly informative as it is significantly lower than those generally found[41] (typically *ca* 1.15–1.4 mm^{-1}) for high-spin iron(II) surrounded by an octahedron of oxygen donors. The observed δ value is not as low as that (0.75 mm^{-1}) reported[42] for the planar FeO_4 unit in gillespite, but is in the range for tetrahedral FeO_4 species[41] (a geometry ruled out by

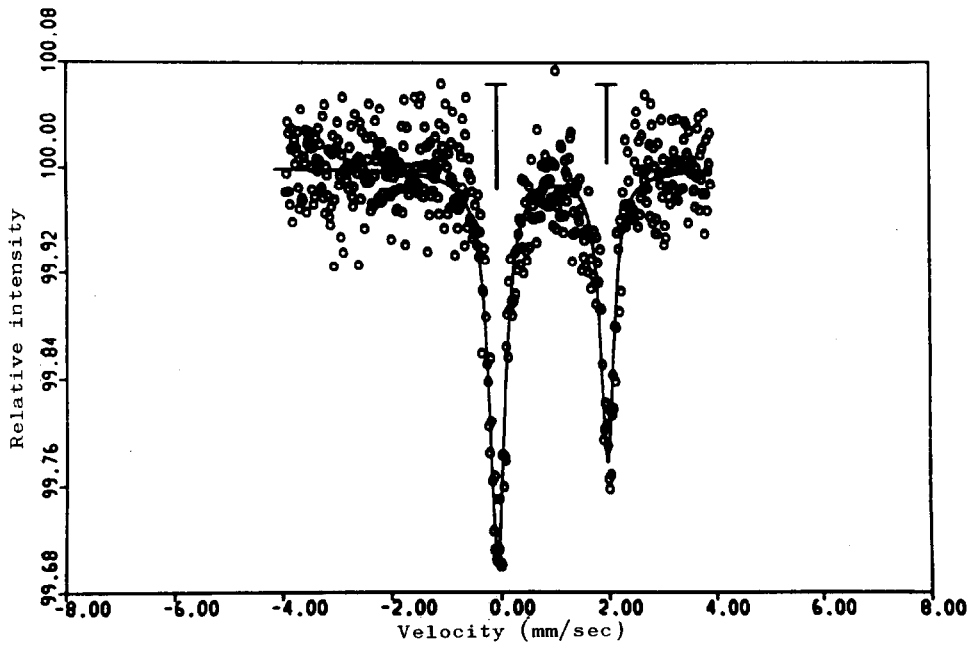


Fig. 6. Mössbauer spectrum (78 K) of *cis*-$[(NH_3)_2Pt(1\text{-MeU})_2Fe(1\text{-MeU})_2\text{-}Pt(NH_3)_2](NO_3)_2 \cdot (H_2O)_6$.

the electronic spectrum) and for very strongly distorted geometries, involving four short Fe–O bonds supplemented by two or more much longer Fe...O distances.[41,43]

The X-band EPR spectrum of a polycrystalline sample of the analogous iron(III) complex consisted of a very strong, asymmetric band in the $g_{eff} = 6$ region and a very weak $g_{eff} = 2$ band, indicative[44] of axial, or nearly axial, symmetry with a large tetragonal distortion (large D), as in the complex *cis*-$[(NH_3)_2Pt(1\text{-}MeT)_2Mn(1\text{-}MeT)_2Pt(NH_3)_2]^{2+}$.[28] The asymmetry in the $g_{eff} = 6$ band suggests that the symmetry about the iron(III) ion is not fully axial ($\lambda \neq 0$). Unlike the Pt–Mn–Pt trinuclear manganese complex, however, the $g_{eff} = 6$ band in Pt–Fe^{III}–Pt was not resolved into two components in the Q-band spectrum. The λ value, representing the rhombic component, must therefore be quite small.

In summary, the electronic spectral results for the Pt–M^{II}–Pt complexes (M = Fe, Co and Ni) substantiate the conclusions drawn from the previous EPR studies in showing a significant axial elongation of the ligand fields experienced by the central metal, M. They would appear to represent some of the most strongly distorted six-coordinate fields known.

Acknowledgements—We thank SERC for a research studentship (to R.W.R.) and for EPR equipment, the Deutsche Forschungsgemeinschaft and the Technische Universität München for financial support. We are indebted to Ian Sayer (Birbeck College, London) for the Mössbauer spectrum obtained under the U.L.I.R.S. service.

REFERENCES

1. For example, S. K. S. Zawacky and H. Taube, *J. Am. Chem. Soc.* 1981, **103**, 3379 and references therein.
2. For example, M. Verdaguer, M. Julve, A. Michalowicz and O. Kahn, *Inorg. Chem.* 1983, **22**, 2624 and references therein.
3. For example, R. Bender, P. Braunstein, J.-M. Jud and Y. Dusausoy, *Inorg. Chem.* 1983, **22**, 3394.
4. J. A. Ibers and R. H. Holm, *Science* 1980, **209**, 223.
5. K. G. Strothkamp and S. J. Lippard, *Acc. Chem. Res.* 1982, **15**, 318.
6. J. Lewis and C. Oldham, *J. Chem. Soc. A* 1966, 1456.
7. R. P. Srerline and D. M. Roundhill, *Inorg. Chem.* 1977, **16**, 2612.
8. W. Kläui, *Z. Naturforsch.* 1979, **34b**, 1403.
9. (a) D. W. Busch and D. C. Jicha, *Inorg. Chem.* 1962, **1**, 884 and references therein. (b) D. P. Strommen, K. Bajdor, R. S. Czernuszewicz, E. L. Blinn and K. Nakamoto, *Inorg. Chim. Acta* 1982, **63**, 151.
10. For example (a) U. Casellato, P. A. Vigato, D. E. Fenton and M. Vidali, *Chem. Soc. Rev.* 1979, **8**, 199. (b) J. Browning, G. W. Bushnell and K. R. Dixon, *Inorg. Chem.* 1981, **20**, 3912. (c) A. F. M. J. Van der Ploeg, G. van Koten and K. Vrieze, *Inorg. Chim. Acta* 1980, **39**, 253.
11. W. M. Davis, J. C. Dewan and S. J. Lippard, *Inorg. Chem.* 1981, **20**, 2928.
12. S. R. Stobart, K. R. Dixon, D. T. Eadie, J. T. Atwood and M. D. Zaworotko, *Angew. Chem.* 1980, **92**, 964.
13. D. Neugebauer and B. Lippert, *J. Am. Chem. Soc.* 1982, **104**, 6596.
14. (a) B. Lippert and D. Neugebauer, *Inorg. Chim. Acta* 1980, **46**, 171. (b) B. Lippert and U. Schubert, *Inorg. Chim. Acta* 1981, **56**, 15.
15. B. Lippert and D. Neugebauer, *Inorg. Chem.* 1982, **21**, 451.
16. B. Lippert, D. Neugebauer and U. Thewalt, *Inorg. Chem.* 1984, **23**, 1713.
17. H. Schöllhorn, U. Thewalt and B. Lippert, *J. Chem. Soc., Chem. Commun.* 1984, 7690.
18. For reviews see, for example, *Platinum, Gold and Other Metal Chemotherapeutic Agents* (Edited by S. J. Lippard), p. 209. ACS Symposium Series (1983).
19. B. Lippert, U. Thewalt, H. Schöllborn, D. M. L. Goodgame and R. W. Rollins, *Inorg. Chem.* 1984, **23**, 2807.
20. B. Lippert, U. Thewalt, H. Schöllhorn, L. G. Marzilli and K. Shinozuka, to be submitted.
21. (a) F. Guay and A. L. Beauchamp, *Inorg. Chim. Acta* 1982, **66**, 57. (b) A. L. Beauchamp, personal communication.
22. F. Guay and A. L. Beauchamp, *J. Am. Chem. Soc.* 1979, **101**, 6260.
23. B. Lippert, *Inorg. Chim. Acta* 1981, **55**, 5.
24. F. Guay, A. L. Beauchamp, C. Gilbert and R. Savoie, *Can. J. Spectrosc.* 1983, **28**, 13.
25. D. M. L. Goodgame, P. B. Hayman and I. Sayer, *Inorg. Chim. Acta* 1984, **92**, L13.
26. K. Nakamoto, *Infrared and Raman Spectra of Inorganic Coordination Compounds*, pp. 239–242. Wiley, New York (1978).
27. Ref. 26, p. 231.
28. D. M. L. Goodgame, R. W. Rollins and B. Lippert, *Inorg. Chim Acta* 1982, **66**, L59.
29. A. F. Schreiner and D. J. Hamm, *Inorg. Chem.* 1973, **12**, 2037, and references therein.
30. C. W. Reimann, *J. Phys. Chem.* 1970, **74**, 561.
31. M. Goodgame and K. W. Johns, *J. Chem. Soc., Dalton Trans.* 1977, 1680; *ibid.* 1978, 1294.
32. M. A. Hitchman, *Inorg. Chem.* 1972, **11**, 2387.
33. A. B. P. Lever, *Coord. Chem. Rev.* 1982, **43**, 63, and references therein.
34. C. D. Burbridge, D. M. L. Goodgame and M. Goodgame, *J. Chem. Soc. (A)* 1967, 349.
35. J. Reedijk, *Rec. Trav. Chim. Pays-Bas* 1970, **89**, 993.
36. A. Bencini, C. Benelli, D. Gatteschi and C. Zanchini, *Inorg. Chem.* 1980, **19**, 1301.
37. A. B. P. Lever, I. M. Walker and P. J. McCarthy, *Inorg. Chim. Acta.* 1980, **39**, 81.
38. A. B. P. Lever, *Inorganic Electronic Spectroscopy*. Elsevier, Amsterdam (1968).
39. D. M. L. Goodgame, M. Goodgame, M. A. Hitchman and M. J. Weeks, *Inorg. Chem.* 1966, **5**, 635.

40. R. G. Burns, M. G. Clarke and A. J. Stone, *Inorg. Chem.* 1966, **5**, 1268.
41. N. N. Greenwood and T. C. Gibb, *Mössbauer Spectroscopy*, Chapman & Hall, London (1971).
42. G. M. Bancroft, A. G. Maddock and A. J. Stone, *Geochim. Cosmochim. Acta.* 1967, **31**, 2219.
43. F. R. Fitch and L. V. C. Rees, *Zeolites* 1982, **2**, 33, and references therein.
44. R. D. Dowsing and J. F. Gibson, *J. Chem. Phys.* 1969, **50**, 294.
45. H. Schöllhorn, U. Thewalt and B. Lippert, to be published.

Polyhedron Vol. 4, No. 5, pp. 841–843, 1985
Printed in Great Britain

0277–5387/85 $3.00 + .00
© 1985 Pergamon Press Ltd

ACTINIDE THERMODYNAMIC PREDICTIONS—II. STABILITIES OF ACTINIDE ANIONS IN LIQUID AMMONIA

STEVEN G. BRATSCH and J. J. LAGOWSKI*
Department of Chemistry, The University of Texas, Austin, TX 78712, U.S.A.

(*Received* 2 *July* 1984; *accepted* 25 *August* 1984)

Abstract—The stabilities (as ΔG_f^0) of monatomic actinide anions in liquid ammonia are estimated from a simple electrostatic model. It is shown that, with the possible exception of Md^-, the existence of actinide anions in this solvent is highly improbable.

This paper is the latest of a series concerning the thermodynamic properties of compounds and ions of the actinides.[1] In a previous paper[2] we have employed a simple electrostatic model to evaluate the thermodynamic stability of monatomic lanthanide anions in liquid ammonia solution. We extend our method here to the actinide anions.

The standard Gibbs free energy of formation of a metal anion M^- in liquid ammonia at 298 K is given by:[2,3]

$$\Delta G_f^0(M^-, am) = \Delta G_f^0(M^-, g) + \Delta G_{am}^0(M^-) + 354 \text{ kJ mol}^{-1}. \quad (1)$$

$\Delta G_f^0(M^-, g)$ can be derived from $\Delta H_f^0(M, g)$, the electron affinities EA(M) and the appropriate enetropy terms; these are given in Table 1 for the elements Fr-104 at 298 K. The scaling factor (354 kJ mol^{-1}) is $\Delta G_f^0(H^+, g) + \Delta G_{am}^0(H^+) = 1517.0–1163$ kJ mol^{-1} at 298 K.[2–4]

$\Delta G_{am}^0(M^-)$, the standard Gibbs free energy of solvation of M^- in liquid ammonia, may be estimated at 298 K by:

$$\Delta G_{am}^0(M^-) = -\frac{50.3}{r - 0.017} \pm 8.7 \text{ kJ mol}^{-1}, \quad (2)$$

where r is the crystal anionic radius expressed in nanometers.[2,3] The latter is estimated by:

$$r_{M^-} = \frac{2.41}{q + 14} + 0.190 \text{ nm} \quad (3)$$

where q is the sum of the $5f$ and $6d$ electrons in the anion and ranges from 0 (Fr^-) to 17 (104^-). Equation (3) is analogous to the equation given previously for lanthanide anions;[2] we estimate the radius of a given actinide anion to be 0.010 nm larger than that of the corresponding lanthanide anion.

Calculated values of r_{M^-}, $\Delta G_{am}^0(M^-)$, $\Delta G_f^0(M^-, am)$ and $E^\circ(M/M^-)$ are given in Table 2. The E^0 values are illustrated in Fig. 1. The stability of Fr^- is predicted to be only slightly less than that of Cs^-.[2,3] The latter species has been detected spectroscopically in cyclic ethers and organic amines, but not in liquid ammonia.[5–7]

Thermodynamic stability for a metal anion in liquid ammonia at 298 K requires that $E^0(M/M^-)$ be more positive than the solvated electron potential, which is -1.93 V.[8a] Of all the metal anions considered in this paper, only Md^- might be stable in liquid ammonia. Unfortunately, the uncertainty in the E^0 value is very large (-1.7 ± 1.0 V) and reflects the uncertainty in EA(Md).[1] It is doubtful whether the order of stability of actinide anions will change appreciably in moving from one solvent to another.

The detection of Md^- in any chemical environment would have to be at the tracer level because the half-life of ^{256}Md is only 77 min and a typical experiment might involve a million atoms or less.[9] We suggest two experiments:

(1) Solutions of alkali metals in liquid ammonia might dissolve Md metal as Md^-. Fm metal could be used as a control because Fm^- is not expected to be stable (Table 2).

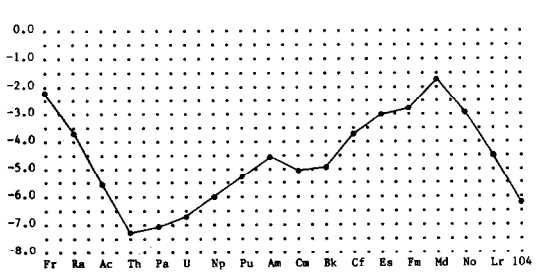


Fig. 1. Predicted $E^0(M/M^-)$ in liquid ammonia (V).

* Author to whom correspondence should be addressed.

Table 1. Thermodynamics of gas-phase ions

M	$\Delta H_f^0(M, g)$* (kJ mol^{-1})	$\Delta H_f^0(M^-, g)$† (kJ mol^{-1})	$S^0(M, c)$‡ (J K^{-1} mol^{-1})	$S^0(M^-, g)$§ (J K^{-1} mol^{-1})	$\Delta G_f^0(M^-, g)$‖ (kJ mol^{-1})
Fr	72	22	95	176	4
Ra	159	182	69	187.9	153
Ac	406	371	62	189.8	339
Th	597.1	543	53.4	188.2	509
Pa	570.7	536	52	197.9	499
U	531.4	496	50.2	198.9	458
Np	464.8	430	50.5	198.3	392
Pu	343.1	366	56.1	189	333
Am	284.1	307	55	197	271
Cm	387.4	352	72	198	321
Bk	310.0	333	78	202	302
Cf	196.2	219	80	203	189
Es	130.5	153	90	202	126
Fm	130	133	88	195	107
Md	130	27	84	178	5
No	130	153	66	189	123
Lr	350	315	56	191	281
104	540	486	48	190	450

* ΔH_f^0(Fr, g and Fm–104, g) estimated by comparison with appropriate elements (this work). ΔH_f^0(Ra, g) from Ref. 11. ΔH_f^0(Ac, g) from Ref. 12. All others from Ref. 13.

† Calculated from:[14a] $\Delta H_f^0(M^-, g) = \Delta H_f^0(M, g) - EA(M) - 2.5RT$. EA(Fr) estimated (0.45 ± 0.02 eV, this work). All other EA from Ref. 1.

‡ S^0(Fr, c) from Ref. 12. S^0(Ra–Es, c) from Ref. 13. S^0(Fm–104, c) estimated (this work) by method of Ward and Hill.[15]

§ Calculated from:[14b] $S^0 = 1.5\,R \ln(\text{at wt}) + R \ln(2J+1) + 108.745$, where J is the total angular momentum quantum number (L–S coupling) ignoring $5f/6d$ electronic interaction.

‖ From $\Delta G_f^0 = \Delta H_f^0 - T\Delta S_f^0$. $S^0(e^-) = 20.87$ J K^{-1} mol^{-1} included in the calculation.[14(c)]

Table 2. Predicted Gibbs free energies in liquid ammonia

M	r_{M^-}* (nm)	$\Delta G_{am}^0(M^-)$† (kJ mol^{-1})	$\Delta G_f^0(M^-, am)$‡ (kJ mol^{-1})	$E^0(M/M^-)$§ (V)
Fr	0.362	−145.7	212	−2.2 ± 0.2
Ra	0.351	−150.7	356	−3.7 ± 0.4
Ac	0.341	−155.4	538	−5.6 ± 0.4
Th	0.332	−159.8	703	−7.3 ± 0.4
Pa	0.324	−163.9	689	−7.1 ± 0.4
U	0.317	−167.8	644	−6.7 ± 0.4
Np	0.310	−171.4	575	−6.0 ± 0.4
Pu	0.305	−174.8	512	−5.3 ± 0.4
Am	0.300	−178.0	447	−4.6 ± 0.4
Cm	0.295	−181.1	494	−5.1 ± 0.4
Bk	0.290	−184.0	472	−4.9 ± 0.4
Cf	0.286	−186.7	356	−3.7 ± 0.4
Es	0.282	−189.3	291	−3.0 ± 0.4
Fm	0.279	−191.8	269	−2.8 ± 1.0
Md	0.276	−194.2	165	−1.7 ± 1.0
No	0.273	−196.4	281	−2.9 ± 0.4
Lr	0.270	−198.6	436	−4.5 ± 0.4
104	0.268	−200.6	603	−6.2 ± 0.4

* Equation (3). † Equation (2). ‡ Equation (1).

§ The quoted uncertainty reflects the cumulative uncertainties in $\Delta H_f^0(M, g)$, $EA(M)$ and eqns (1)–(3).

(2) The similarities in the crystal anionic radii of Md^- (0.276 nm) and Na^- (0.263 nm)[8b] may allow $Na^+C_{222}Md^-$ to cocrystallize with $Na^+C_{222}Na^-$ (C_{222} = 4,7,13,16,21,24-hexaoxa-1,10-diazabicyclo [8.8.8]hexacosane).[10] The short half-life of Md would require the development of a rapid crystallization technique. Also, as Na^- has not yet been detected in liquid ammonia,[3] it would be necessary to carry out this experiment in an organic amine.[10]

Acknowledgement—We are grateful to The Robert A. Welch Foundation (Grant Number F081) for their generous support of this research.

REFERENCES

1. S. G. Bratsch and J. J. Lagowski, *Chem. Phys. Lett.* 1984, **107**, 136.
2. S. G. Bratsch and J. J. Lagowski, *Polyhedron* 1984, **3**, 133.
3. S. G. Bratsch and J. J. Lagowski, *J. Phys. Chem.* 1984, **88**, 1086.
4. N. A. Izmailov, *Dokl. Akad. Nauk SSSR* (*English Translation*) 1963, **149**, 288.
5. J. L. Dye, C. W. Andrews and S. E. Mathews, *J. Phys. Chem.* 1975, **79**, 3065.
6. J. L. Dye, *J. Chem. Educ.* 1977, **54**, 332.
7. J. L. Dye, *Angew. Chem. Int. Ed.* 1979, **18**, 587.
8. W. J. Peer, Ph.D. dissertation: (a) p. 260, (b) p. 313. The University of Texas, Austin, TX (1979).
9. E. K. Hulet, in *Lanthanide and Actinide Chemistry and Spectroscopy* (Edited by N. M. Edelstein), pp. 239–263. American Chemical Society, Washington, DC (1980).
10. U. Schindewolf, L. D. Le and J. L. Dye, *J. Phys. Chem.* 1982, **86**, 2284.
11. NBS Technical Note 270-6. National Bureau of Standards, Washington, DC (1971).
12. NBS Technical Note 270-8. National Bureau of Standards, Washington, DC (1981).
13. J. W. Ward, *J. Less-Common Met.* 1983, **93**, 279.
14. D. A. Johnson, *Some Thermodynamic Aspects of Inorganic Chemistry*, 2nd Edn: (a) p. 251, (b) p. 8, (c) p. 25. Cambridge University Press, London (1982).
15. J. W. Ward and H. H. Hill, in *Heavy Element Properties* (Edited by W. Müller and H. Blank), pp. 65–78. American Elsevier, New York (1976).

Polyhedron Vol. 4, No. 5, pp. 845–852, 1985
Printed in Great Britain

0277–5387/85 $3.00 + .00
© 1985 Pergamon Press Ltd

SYNTHESIS OF NOVEL TERMETALLIC ISOPROPOXIDES

M. AGGRAWAL* and R. C. MEHROTRA†
Chemical Laboratories, University of Rajasthan, Jaipur 302004, India

(*Received* 2 *July* 1984; *accepted* 24 *September* 1984)

Abstract—Novel termetallic isopropoxides are reported which may be represented by the general formulae: $[(Pr^iO)_3M(\mu\text{-}OPr^i)_2Be(\mu\text{-}OPr^i)_2Al(OPr^i)_2]$, $[(Pr^iO)_2M(\mu\text{-}OPr^i)_2Be(\mu\text{-}OPr^i)_2Al(OPr^i)_2]_2$ [where M = Ti(IV), Zr(IV) and Hf(IV)] and $[(Pr^iO)_4M(\mu\text{-}OPr^i)_2Be(\mu\text{-}OPr^i)_2Al(OPr^i)_2]$ [where M = Nb(V) and Ta(V)]. Attempts to synthesize derivatives with the general formula, $[(Pr^iO)_7M_2(\mu\text{-}OPr^i)_2Be(\mu\text{-}OPr^i)_2Al(OPr^i)_2]$ [where M = Ti(IV), Zr(IV) or Hf(IV)], were unsuccessful and in all such cases a mixture of $M(OPr^i)_4$ and $[(Pr^iO)_3M(\mu\text{-}OPr^i)_2Be(\mu\text{-}OPr^i)_2Al(OPr^i)_2]$ was obtained. All these derivatives are soluble in common organic solvents and with the exception of titanium(IV) derivatives, they can be volatilised without noticeable disproportionation. These products have been characterized by elemental analyses, molecular weights, IR, ^1H NMR and (in representative cases) mass spectral studies also.

Amongst the interesting series of compounds with more than one metallic centre,[1] bimetallic alkoxides which were initially considered as alkoxo salts[2,3] have been shown to be coordination compounds stabilized by alkoxo bridges.[4] Special interest has been aroused in these derivatives by the exceptional stability and volatility of bimetallic alkoxides of strongly electropositive alkali, alkaline earth and lanthanide metals such as $[M\{Zr_2(OPr^i)_9\}]$,[5,6] $[M\{Ta(OR)_6\}]$,[7] $[M'\{Nb(OR)_6\}_2]$[8] and $[M'\{Al(OR)_4\}_2]$,[9] and in $[Ln\{Al(OPr^i)_4\}_3]$[10] (where M = Li, Na, K, Rb, Cs; M′ = Mg, Ca, Sr, Ba; Ln = lanthanides and R = Me, Et, Pr^i, Pr^n, Bu^n etc.) and the same has been sustained by the synthesis of soluble, monomeric, volatile bimetallic alkoxides $[M\{Al(OR)_4\}_2]$ of metals (M = Be,[11,12] Zn,[11] Cd,[11] Hg,[11] Mn,[13] Co,[14] Ni[15] and Cu[16]), the simple alkoxides of which are all insoluble, polymeric, non-volatile compounds. A novel interest in these compounds is indicated by the use of bimetallic μ-oxoalkoxides as catalysts for the polymerization of propylene oxide, lactones, oxiranes, epoxides etc.[17,18]

In view of the interest in stable derivatives[1] with more than two metallic centres, it was considered worthwhile to try to synthesize some termetallic alkoxides with bridging ligands like $[Al(OPr^i)_4]^-$ and $[Zr_2(OPr^i)_9]^-$. The strategy planned for this was to synthesize 1:1 derivatives like $[(Pr^iO)M(\mu\text{-}OPr^i)_2Al(OPr^i)_2]$ and replace the terminal isopropoxy group attached to the metal "M" with other chelating alkoxy ligands involving metals other than aluminium. It has already been reported[11] that attempts to synthesize $[(Pr^iO)M(\mu\text{-}OPr^i)_2Al(OPr^i)_2]$ derivatives (M = Be, Zn, Cd and Hg) by a reaction of the following type:

$$MCl_2 + 2KOPr^i + Al(OPr^i)_3 \rightarrow [(Pr^iO)M(\mu\text{-}OPr^i)_2Al(OPr^i)_2] + 2KCl$$

gave equimolar mixtures of insoluble $M(OPr^i)_2$ and soluble $[M\{(\mu\text{-}OPr^i)_2Al(OPr^i)_2\}]$ in all other cases except for the case of beryllium, in which a soluble and volatile product $[(Pr^iO)Be(\mu\text{-}OPr^i)_2Al(OPr^i)_2]$ was isolated as a viscous liquid.

The species $[(Pr^iO)Be(\mu\text{-}OPr^i)_2Al(OPr^i)_2]$, on interaction with isopropoxides of titanium, zirconium, hafnium, niobium and tantalum results in the formation of a number of stable novel termetallic isopropoxides which are being reported for the first time. Amongst the characteristics of these new types of derivatives are their solubility in common organic solvents and volatility (in the majority of the derivatives) on heating under reduced pressure.

EXPERIMENTAL

Stringent precautions were taken to maintain anhydrous conditions throughout the experimental work in view of the extremely hydrolysable nature of

* Present address: Department of Chemistry, SLP College, Morar, Gwalior 474001, India.
† Author to whom correspondence should be addressed.

the newly synthesized derivatives. The general method of synthesis is as follows.

All of these derivatives were synthesized (Table 1) by dissolving each constituent metal alkoxide $Ti(OPr^i)_4$,[19] $Zr(OPr^i)_4 \cdot Pr^iOH$,[20] $Hf(OPr^i)_4Pr^iOH$,[21] $Nb(OPr^i)_5$,[22] $Ta(OPr^i)_5$[22] $[(Pr^iO)Be(\mu\text{-}OPr^i)_2Al(OPr^i)_2]$[11] in benzene, mixing them together and refluxing the total contents for ~ 1 h in each case. As $[ClBe(\mu\text{-}OPr^i)_2Al(OPr^i)_2]$[23] is insoluble in benzene, its solution was prepared in isopropanol; on adding a benzene solution of $[K\{M_2(OPr^i)_9\}]$[6,24] (where M = Ti, Zr or Hf) to it, an exothermic reaction took place and the white insoluble product (identified as KCl) was separated out in this case by filtration. Excess solvent was stripped off under reduced pressure. With the exception of the titanium derivatives (which disproportionate), the products obtained distil unchanged on heating under reduced pressure (Table 1). All these termetallic derivatives are soluble in common organic solvents, e.g. benzene, chloroform and isopropanol.

Metal estimations (as mixed oxides) were carried out by standard methods.[25] Isopropoxy groups were estimated by dichromate oxidation[26] (Table 1).

IR and ^1H NMR spectra were recorded on a Perkin–Elmer 577 and R-32 spectrophotometer respectively. $CDCl_3$ was made anhydrous by storing over molecular sieves (type 4A) for ~ 24h. TMS was used as internal standard. Mass spectra were recorded on a JEOL DMX-300.

Molecular weights were measured in a semimicro ebulliometer (Gallenkamp) equipped with a thermistor sensor using benzene or isopropanol as solvent.

RESULTS AND DISCUSSION

During the successful synthesis of a 1 : 1 bimetallic isopropoxide of beryllium and aluminium $[(Pr^iO)Be(\mu\text{-}OPr^i)_2Al(OPr^i)_2]$, it was observed that this derivative exhibits a strong tendency to dimerize even on standing. This has been explained by the tendency of the tri-coordinate beryllium in the monomeric species to attain four-coordinate environment through dimerization.[17]

In view of the above tendency of beryllium atoms, it was conjectured that it might be possible to satisfy it by formation of new bridges with alkoxides of other metals, leading to the synthesis of stable termetallic alkoxides, with three different metals in the same molecule. This has been achieved by carrying out the reactions of the product $[(Pr^iO)Be(\mu\text{-}OPr^i)_2Al(OPr^i)_2]$ with the isopropoxides of titanium, zirconium, hafnium, niobium and tantalum resulting in the preparation of a number of stable novel termetallic isopropoxides for the first time. The results obtained are discussed under the following heads:

Termetallic isopropoxides of titanium, zirconium or hafnium with beryllium and aluminium with the general formulae $[(Pr^iO)_3M(\mu\text{-}OPr^i)_2Be(\mu\text{-}OPr^i)_2Al(OPr^i)_2]$ *and* $[\{(Pr^iO)_2M\{(\mu\text{-}OPr^i)_2Be(\mu\text{-}OPr^i)_2Al(OPr^i)_2\}_2]$

These derivatives have been synthesized as represented by the following equations:

$$[(Pr^iO)Be(\mu\text{-}OPr^i)_2Al(OPr^i)_2] + M(OPr^i)_4{}^* \xrightarrow{C_6H_6} [(Pr^iO)_3M(\mu\text{-}OPr^i)_2 Be(\mu\text{-}OPr^i)_2Al(OPr^i)_2], \quad (1)$$
$$(T_1)$$

$$2[(Pr^iO)Be(\mu\text{-}OPr^i)_2Al(OPr^i)_2] + M(OPr^i)_4{}^* \xrightarrow{C_6H_6} [(Pr^iO)_2M\{(\mu\text{-}OPr^i)_2 Be(\mu\text{-}OPr^i)_2Al(OPr^i)_2\}_2], \quad (2)$$
$$(T_2)$$

where M = Ti(IV), Zr(IV) or Hf(IV).

Both types of derivatives, T_1 and T_2, synthesized as shown above are soluble in common organic solvents (Table 1). In the case of titanium, both the 1 : 1 (T_1) and 1 : 2 (T_2) products are pale yellow viscous liquids which disproportionate on heating under reduced pressure into $Ti(OPr^i)_4$ (45°C/0.05 mm) and $[(Pr^iO)Be(\mu\text{-}OPr^i)_2Al(OPr^i)_2]$ (128°C/0.05 mm). By contrast, the corresponding derivatives in the cases of zirconium and hafnium, both (T_1 and T_2) types can be volatilised unchanged under reduced pressure to colourless viscous liquids at 139 and 137°C for the T_1 derivatives and at 132 and 129°C for T_2 derivatives (all at 0.05 mm pressure), the hafnium products exhibiting slightly lower boiling points compared to zirconium analogues for the both types of derivatives.

Ebullioscopic measurements indicate that the titanium derivative T_1 like all T_2 derivatives exhibits monomeric nature in benzene while their T_1 type zirconium and hafnium analogues depict dimeric behaviour (Table 1); these derivatives, expectedly depict monomeric nature in isopropanol: 683 obs. (616 calc). 698 (659) and 734 (746) for titanium, zirconium and hafnium derivatives respectively.

The above observations can be easily understood on

*In the cases of zirconium and hafnium isopropoxides, their crystalline adducts $M(OPr^i)_4 \cdot Pr^iOH$ were taken, but for simplicity these are represented by the reactive species $M(OPr^i)_4$.

Table 1. Synthetic details of termetallic isopropoxides

Sl. no.	Reactants;* molar ratio/ reflux time (h)	Product	Volatility (°C/torr)	Yield of distilled product (g/%)	Analysis: % found (calc.)			Molecular weight obs. (calc.)
					Individual metal	Mixed oxide of metals	OPr^i	
1	A = 1.91 g, B = 1.64 g; 1:1/1	$TiBeAl(OPr^i)_9$	†	3.52/99‡	—	25.41 (25.31)	85.94 (86.37)	632 (616)
2	A = 1.54 g, C = 1.80 g; 1:1/1	$ZrBeAl(OPr^i)_9$	139/0.05	1.91/62	13.99 Zr (13.84)	30.28 (30.23)	80.26 (80.70)	1232 (659)
3	A = 1.04 g, D = 1.50 g; 1:1/1	$HfBeAl(OPr^i)_9$	137/0.05	1.29/55	24.01 Hf (23.91)	38.19 (38.38)	70.72 (71.27)	1412 (746)
4	A = 2.57 g, D = 1.10 g; 2:1/1	$TiBe_2Al_2(OPr^i)_{14}$	†	3.64/99‡	—	24.42 (24.47)	87.18 (87.34)	963 (947)
5	A = 2.11 g, C = 1.25 g; 2:1/1	$ZrBe_2Al_2(OPr^i)_{14}$	132/0.05	1.12/58	9.31 Zr (9.21)	27.89 (27.78)	82.99 (83.51)	943 (991)
6	A = 1.88 g, D = 1.38 g; 2:1/1	$HfBe_2Al_2(OPr^i)_{14}$	129/0.05	1.18/58	16.59 Hf (16.56)	33.24 (33.63)	76.50 (76.76)	1093 (1078)
7	A = 1.68 g, E = 1.97 g; 1:1/1	$NbBeAl(OPr^i)_{10}$	112/0.05	3.3/92	—	28.47 (29.02)	81.72 (82.09)	688 (720)
8	A = 1.45 g, F = 2.12 g; 1:1/1	$TaBeAl(OPr^i)_{10}$	120/0.05	3.0/85	—	36.50 (36.75)	72.66 (73.15)	789 (808)

* A = $Pr^iOBe(\mu\text{-}OPr^i)_2Al(OPr^i)_2$; B = $Ti(OPr^i)_4$; C = $Zr(OPr^i)_4 \cdot Pr^iOH$; D = $Hf(OPr^i)_4 \cdot Pr^iOH$; E = $Nb(OPr^i)_5$; F = $Ta(OPr^i)_5$. All reactants dissolved in 30 cm^3 benzene.

† Disproportionated on heating under reduced pressure.

‡ Undistilled product.

the basis of known differences in the properties of titanium on the one hand and zirconium or hafnium on the other.

Of the termetallic isopropoxides described in Table 1 both the titanium derivatives (T_1 and T_2) disproportionate on heating under reduced pressure yielding volatile $Ti(OPr^i)_4$ (49°C/0.1 mm),[27] but the zirconium and hafnium products (both T_1 and T_2 type distil unchanged around 129–139°C/0.05 mm.

In fact, the extraordinarily low boiling point of $Ti(OPr^i)_4$ might actually facilitate the dissociation of termetallic isopropoxides, which might be represented by the following types of equilibria:

$$[(Pr^iO)_3Ti(\mu\text{-}OPr^i)_2Be(\mu\text{-}OPr^i)_2Al(OPr^i)_2] \rightleftharpoons [Pr^iOBe(\mu\text{-}OPr^i)_2Al(OPr^i)_2] + Ti(OPr^i)_4,$$

$$[(Pr^iO)_2Ti\{(\mu\text{-}OPr^i)_2Be(\mu\text{-}OPr^i)_2Al(OPr^i)_2\}_2] \rightleftharpoons 2[(Pr^iO)Be(\mu\text{-}OPr^i)_2Al(OPr^i)_2] + Ti(OPr^i)_4.$$

It appears that the extent of dissociation even in the titanium species (Table 1) is insignificantly low under ambient conditions to be detected by the traditional molecular weight measurements (which normally have an accuracy of ±5%), but during attempts to distil these products under reduced pressure, the equilibrium is gradually shifted to the right as the comparatively more volatile titanium isopropoxide is removed by distillation.

Conversely, the higher volatility of the termetallic T_1 isopropoxides of zirconium and hafnium [e.g. b.ps for T_1:Zr derivative, 139°C/0.05 mm, Hf derivative 137°C/0.05 mm as compared to the constituent simple isopropoxides (b.ps: $Zr(OPr^i)_4$, 172°C/0.35 mm and $Hf(OPr^i)_4$, 170°C/0.35 mm][20,21] would tend to shift the equilibria preferably to the formation of termetallic species as shown below:

$$[(Pr^iO)Be(\mu\text{-}OPr^i)_2Al(OPr^i)_2] + M(OPr^i)_4 \rightleftharpoons [(Pr^iO)_3M(\mu\text{-}OPr^i)_2Be(\mu\text{-}OPr^i)_2Al(OPr^i)_2], \quad (T_1)$$

$$2[(Pr^iO)Be(\mu\text{-}OPr^i)_2Al(OPr^i)_2] + M(OPr^i)_4 \rightleftharpoons [(Pr^iO)_2M\{(\mu\text{-}OPr^i)_2Be(\mu\text{-}OPr^i)_2Al(OPr^i)_2\}_2], \quad (T_2)$$

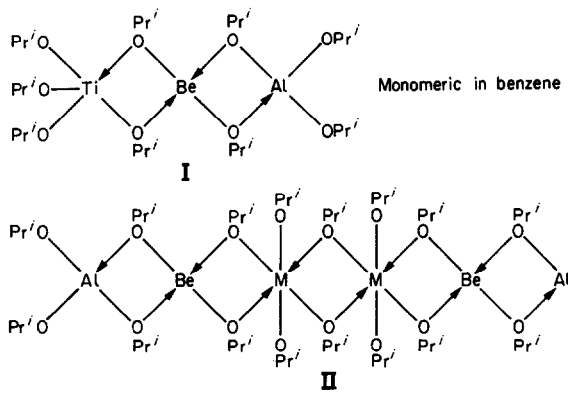
where M = Zr(IV) or Hf(IV).

The slightly higher boiling points of T_1 than T_2 derivatives may easily be understood by the observed dimeric nature of T_1.

The slightly lower boiling points of hafnium compared to zirconium ternary analogues are similar to the earlier reported[21] differences in boiling points of simple alkoxides of the two metals.

IR spectra of these derivatives mainly depict absorptions in four regions of interest, i.e. 1175–930 cm^{-1} {four or five [very strong (vs) or strong (s)] absorptions}: 850–800 cm^{-1} {two [vs, s or medium (m)] absorptions}: 770–630 cm^{-1} {three or four [vs, s or m] absorptions} and 630–530 cm^{-1} {two [vs, s, m or weak] absorptions}, which have been assigned [27–30] to ν_{OPr^i}, ν_{Be-O}, ν_{Al-O} and ν_{M-O}, are indicative of different modes of bonding. Though no definitive assignments have been made yet in general the higher ones are assignable to terminal while lower ones to bridging groups.[27–30]

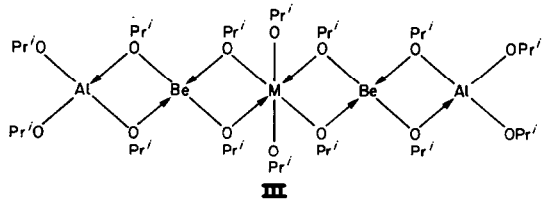
On the basis of the above discussions, the following tentative structures (I–III) may be proposed for these derivatives:



I

Dimeric in benzene M = Zr(IV) or Hf(IV)

II



Monomeric in benzene M = Zr(IV) or Hf(IV)

III

Table 2. PMR spectral data of termetallic isopropoxides of Ti(IV), Zr(IV), Hf(IV), Nb(V) and Ta(V) with Be(II) and Al(III)

Sl. No.	Compound	Chemical shift* (δ) (ppm)
1	$TiBeAl(OPr^i)_9$	4.85m, 4H(OCH-B); 4.30m, 5H(OCH-T); 1.62d† (CH_3-B) and 1.52d,† (CH_3-T) 54‡
2	$ZrBeAl(OPr^i)_9$	4.15m, 9H(OCH-BT); 1.32d† (CH_3-B), 1.15d† (CH_3-T) 54H‡
3	$HfBeAl(OPr^i)_9$	4.15m, 9H(OCH-BT); 1.32d† (CH_3-B), 1.08d† (CH_3-T) 54H‡
4	$TiBeAl(OPr^i)_{14}$	4.20m, 14H(OCH-BT); 1.40m, 84H(CH_3-BT)
5	$ZrBe_2Al_2(OPr^i)_{14}$	4.18m, 14H(OCH-BT); 1.25d† (CH_3-B), 1.10d† (CH_3-T) 84H‡
6	$HfBe_2Al_2(OPr^i)_{14}$	4.15m, 14H(OCH-BT); 1.25d† (CH_3-B), 1.05d† (CH_3-T) 84H‡
7	$NbBeAl(OPr^i)_{10}$	4.95m, 4H(OCH-B); 4.35m, 6H(OCH-T); 1.47d, 24H(CH_3-B); 1.33d, 36H(CH_3-T)
8	$TaBeAl(OPr^i)_{10}$	4.80m, 4H(OCH-B); 4.17m, 6H(OCH-T); 1.48d† and 1.28d† (CH_3-B), 1.21d‡ and 1.14d† (CH_3-T), 60H‡

* Solvent $CDCL_3$: m, multiplet; d, doublet; B, bridging; T, terminal.

† Overlapped each other and appeared to be a triplet.

‡ Integration could not be differentiated between bridging and terminal groups.

The ^1H NMR spectral data of all the products of the T_1 and T_2 (Table 2) show that as expected the spectra for zirconium and hafnium derivatives are similar in nature. In all the cases for T_1 derivatives, signals due to methine protons appear as the septets centred at 4.85 and 4.30 δ for titanium; and at 4.15 δ for zirconium as well as hafnium derivatives; these are as usual not so well defined. However, the methine protons in the spectrum for the titanium derivative T_1 (Table 2) showed rather a clear separation of almost two septets centred, as indicated above at 4.85 and 4.30 δ, with an integration ratio of $\sim 4:5$ in accordance with the structure I for the same. The absorptions occurring in the higher side may be assigned to terminal groups.[31–33] The relative ratio of the methyl signals (Table 2) assignable to terminal and bridging isopropoxy groups are in general (although not exact) conformity with the tentative structures suggested for the T_2 products except in the spectrum of titanium (T_2) product (Table 2) in which case a symmetrical unresolved spectrum only could be recorded. This might indicate the presence of more than one species, presumably due to dissociation of

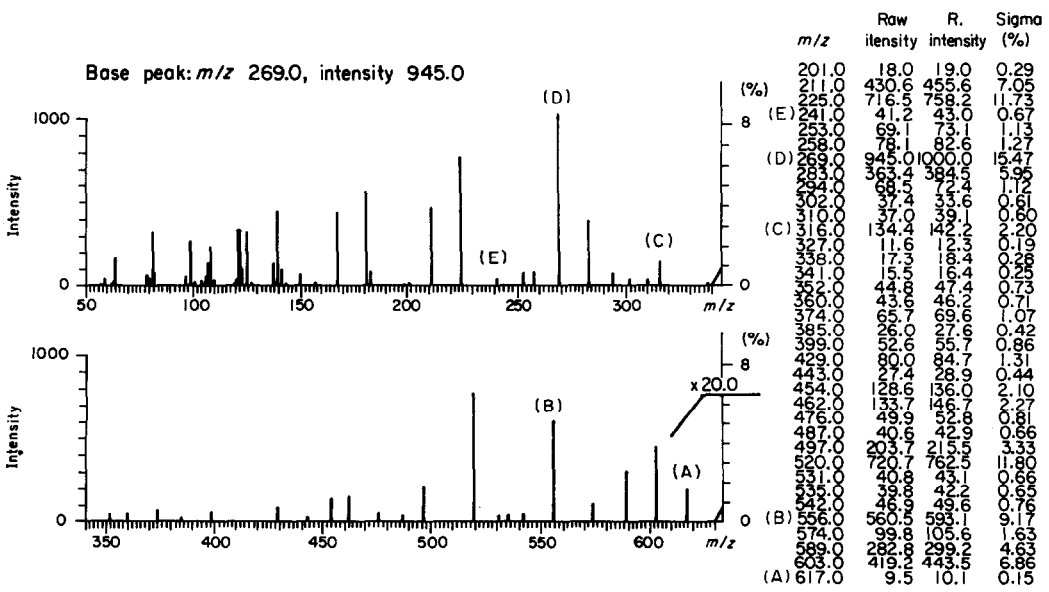


Fig. 1. Mass spectrum of $[(Pr^iO)_3Ti(\mu\text{-}OPr^i)_2Be(\mu\text{-}OPr^i)_2Al(OPr^i)_2]$.

this product to some extent, even at ambient temperatures (which might not be detectable by the ebullioscopic method) may be ascribed to the steric strain produced on the central titanium atom bonded to six isopropoxy groups. Thus, the pmr spectra also support the proposed structures for these derivatives.

Mass spectral studies of the product $[(Pr^iO)_3Ti(\mu\text{-}OPr^i)_2Be(\mu\text{-}OPr^i)_2Al(OPr^i)_2]$ have been carried out and tentative assignments have been made. The mass spectral data of the derivative exhibited (Fig. 1) a weak signal of molecular ion at 617* (A) [molecular weight M = 615; (M + 2H)] and an intense signal at 556*(B) [M − 59(OPr^i)] (a usual fragment reported in isopropoxy derivatives of metals).[34–37] The identity of the termetallic product is also corroborated[37] by non-appearance of signals for the constituent alkoxides at 331* $[(Pr^iO)Be(\mu\text{-}OPr^i)_2Al(OPr^i)_2]$ or at 284* $[Ti(OPr^i)_4]$. However, signals at 316*(C) [331 − 15(CH$_3$)], 269*(D) [(284 − 15(CH$_3$)] and 241*(E) [(284 − 43(Pr^i)] etc. were observed in notable intensity. These would have resulted either as fragments from termetallic species or could be due to fragmentation of products resulting from slight dissociation of the parent derivative to its constituent alkoxides. Assignments of other signals have been deliberately avoided as these would be more speculative in nature.

Attempted syntheses of the derivatives with the general formula $[(Pr^iO)_7M_2(\mu\text{-}OPr^i)_2Be(\mu\text{-}OPr^i)_2Al(OPr^i)_2]$ *(where* M = Ti(IV), Zr(IV) *or* Hf(IV)

By analogy with the derivatives of the general formulae $[K\{Zr_2(OPr^i)_9\}]$[6] or $[Mg\{Zr_2(OPr^i)_9\}_2]$[38] etc. the synthesis of the derivatives with the composition $[(Pr^iO)_7M_2(\mu\text{-}OPr^i)_2Be(\mu\text{-}OPr^i)_2Al(OPr^i)_2]$ was also attempted as represented by the following two different routes:

Instead of obtaining a single compound T_3 as represented by eqn (3) or (5), mixtures of two products were obtained in both the cases as represented by eqns (4) and (6); this was indicated by the observed apparent molecular weights of these products being almost half the theoretical values for T_3. Attempts were made to separate both constituents by dissolving them in limited amounts of isopropanol. The tetraisopropoxide isopropanolates, $M(OPr^i)_4 \cdot Pr^iOH$ (M = Zr or Hf) crystallized out in the cases of the zirconium and hafnium derivatives, eqns (4) and (6), due to their poor solubility in isopropanol; the remaining products were identified as derivatives T_1 as shown above. However, $Ti(OPr^i)_4$ could not be separated in the case of titanium derivative as it does not form a sparingly soluble isopropanolate. When the complex T_3 was heated under reduced pressure, it disproportionated and the total $Ti(OPr^i)_4$ contents distilled out 45°C/0.05 mm) followed by $[(Pr^iO)Be(\mu\text{-}OPr^i)_2Al(OPr^i)_2]$ (128°C/0.05 mm).

Termetallic isopropoxides of niobium or tantalum with beryllium and aluminium with the general formula $[(Pr^iO)_4M(\mu\text{-}OPr^i)_2Be(\mu\text{-}OPr^i)_2Al(OPr^i)_2]$

These derivatives have been synthesized by the interaction of $Nb(OPr^i)_5$ or $Ta(OPr^i)_5$ with $[(Pr^iO)Be(\mu\text{-}OPr^i)_2Al(OPr^i)_2]$ in 1 : 1 molar ratios as indicated by the equation:

$$M(OPr^i)_5 + [(Pr^iO)Be(\mu\text{-}OPr^i)_2Al(OPr^i)_2] \xrightarrow{C_6H_6} [(Pr^iO)_4M(\mu\text{-}OPr^i)_2Be(\mu\text{-}OPr^i)_2Al(OPr^i)_2], \quad (T_4)$$

where M = Nb(V) or Ta(V).

The derivatives T_4 could be distilled (Table 1) unchanged as colourless viscous liquids in almost quantitative (85–92%) yields at 112 and 120°C respectively at 0.05 mm for the niobium and

$$[(Pr^iO)Be(\mu\text{-}OPr^i)_2Al(OPr^i)_2] + 2M(OPr^i)_4 \text{*} \xrightarrow{C_6H_6} [(Pr^iO)_7M_2(\mu\text{-}OPr^i)_2Be(\mu\text{-}OPr^i)_2Al(OPr^i)_2] \quad (T_3) \quad (3)$$

$$(T_3) \xrightarrow{C_6H_6} [(Pr^iO)_3M(\mu\text{-}OPr^i)_2Be(\mu\text{-}OPr^i)_2Al(OPr^i)_2] + M(OPr^i)_4 \quad (T_1) \quad (4)$$

$$[Cl\,Be(\mu\text{-}OPr^i)_2Al(OPr^i)_2] + [K\{M_2(OPr^i)_9\}] \xrightarrow{Pr^iOH} [(Pr^iO)_7M_2(\mu\text{-}OPr^i)_2Be(\mu\text{-}OPr^i)_2Al(OPr^i)_2] + KCl\downarrow \quad (T_3) \quad (5)$$

$$(T_3) \xrightarrow{C_6H_6} [(Pr^iO)_3M(\mu\text{-}OPr^i)_2Be(\mu\text{-}OPr^i)_2Al(OPr^i)_2] + M(OPr^i)_4 + KCl\downarrow \quad (6)$$

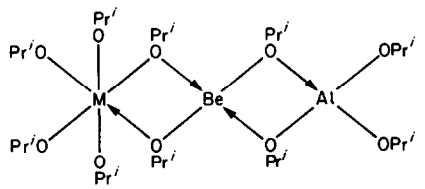
where M = Ti(IV), Zr(IV) or Hf(IV).

* See footnote to eqn (2).

tantalum derivatives. Both these derivatives are soluble in benzene in which they are monomeric.

IR spectra of these complexes are similar to those of T_1 and T_2 derivatives, showing terminal and bridging ν_{OPr^i}, ν_{Be-O} and ν_{Al-O} in the same regions. ν_{Nb-O} and ν_{Ta-O} absorptions have also been observed in the expected regions [for T_4: 560vs, 530vs; 580m, 530w for Nb(V) and Ta(V) derivatives respectively], the higher ones being assigned to terminal and the lower ones to bridging isopropoxy groups.[27–30]

On the basis of molecular weight and IR spectral data, the derivatives T_4 could be assigned the following plausible structure:



IV

M = Nb(V) or Ta(V)

The ^1H NMR spectrum of $[(Pr^iO)_4Nb(\mu\text{-}OPr^i)_2Be(\mu\text{-}OPr^i)_2Al(OPr^i)_2]$ (Table 2) appears to be in conformity with the above plausible structure. The methine signals appear in the form of two septets at δ-values of 4.95 and 4.35 in the ratio of $\sim 2:3$. Similarly the methyl signals appear in the form of two doublets centred at values of 1.47 and 1.33 in the ratio of $\sim 2:3$. For the tantalum analogue, the two septets for methine protons appeared (Table 2) at δ-values of 4.80 and 4.17 again in the ratio of $\sim 2:3$, which also corroborates with structure **IV**.

The methyl protons in the pmr spectrum of the latter tantalum product T_4, $[(Pr^iO)_4Ta(\mu\text{-}OPr^i)_2Be(\mu\text{-}OPr^i)_2Al(OPr^i)_2]$, however, are more complicated (Table 2). Although exact integration for terminal and bridging groups was not possible individually yet the spectrum could be considered to be consisting of two doublets centred at 1.40 and 1.28 δ with considerable overlapping at 1.21 and 1.14 δ in the ratio of roughly 2:3. Similar differences have been recorded[39] in the ^1H NMR spectra of niobium and tantalum pentaisopropoxides. The spectrum of tantalum penta-isopropoxide[39] showed three doublets in the methyl portion of the spectrum and nineteen peaks (about three septets) in the methine portion of the spectrum, in contrast to that of niobium penta-isopropoxide, which gave only a broad methine signal at 4.70 δ and an averaged doublet due to methyl portions at 1.20 δ.

Mass spectral studies have also been carried out in the case of $[(Pr^iO)_4Nb(\mu\text{-}OPr^i)_2Be(\mu\text{-}OPr^i)_2Al(OPr^i)_2]$. The mass spectral data of this derivative exhibited (Fig. 2) a molecular ion peak at 717*(A') [molecular weight M = 719; (M − 2H)] followed by a weak signal at 704*(B') [M − 15(CH_3)] and an intense signal at 660*(C') [M − 59(OPr^i)] which supported formation of the product.[35–38] Other notable signals can be tentatively explained as arising from the fragmentation of termetallic derivative according to the following assignments:

* *m/z* values.

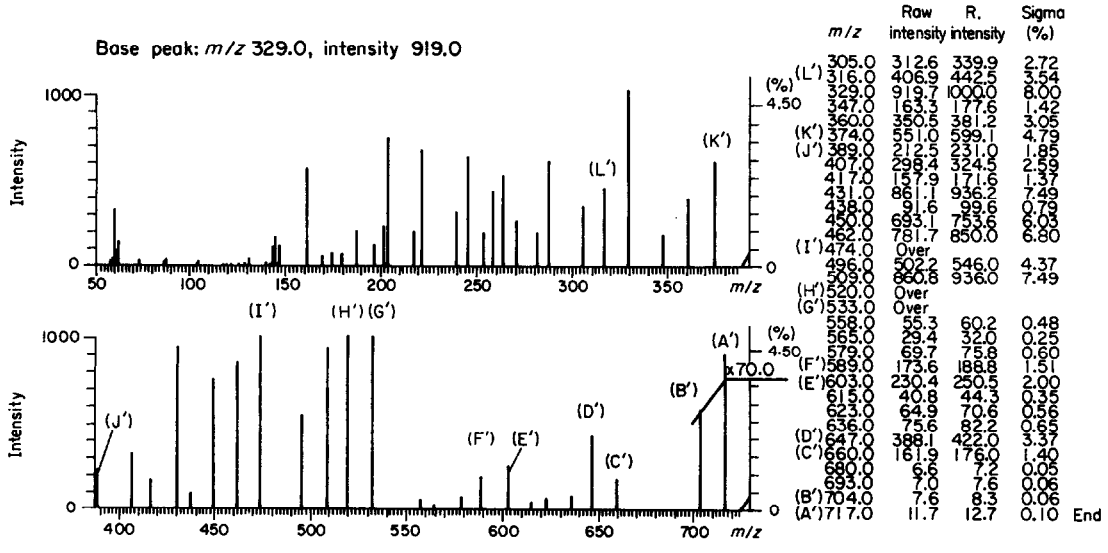


Fig. 2. Mass spectrum of $[(Pr^iO)_4Nb(\mu\text{-}OPr^i)_2Be(\mu\text{-}OPr^i)_2Al(OPr^i)_2]$.

647*(D') [M − 59(OPr^i) − 13(CH)], 603*(E') [647(Pr^i + 1H)], 589*(F') [603 − 14(CH_2)], 533*(G') [589 − 56(C_4H_8)], 520*(H') [533 − 13(CH)], 474*(I') [533 − 59(OPr^i)], 389*(J') [388{Nb(OPr^i)$_5$} + 1H], 374*(K') [388 − 14(CH_2)] and 316*(L') [331 − 15(CH_3)] etc. It may be emphasized that the spectrum did not exhibit signals for the constituent alkoxides, i.e. at 331* for [(Pr^{i}O)Be(μ-OPr^i)$_2$Al(OPr^i)$_2$] or at 388* for Nb(OPr^i)$_5$ which corroborates the identity of T_4 and shows that the termetallic product is not merely a mixture of the constituent alkoxides.[37]

Acknowledgements—We are grateful to Dr P. Ramachandran, Director, Defence Research and Development Establishment, Gwalior for providing facilities for spectroscopic studies at his Centre. A Teacher Fellowship to one of the authors (M.A.) by the University Grants Commission is also gratefully acknowledged.

REFERENCES

1. J. C. Jeffery, A. G. Orpen, W. T. Robinson, F. G. A. Stone and M. J. Went, *J. Chem. Soc., Chem. Commun.* 1984, 396.
2. H. Meerwein, *U.S. Patent* 1929, 1, 689, 356; *Chem. Abstr.* 1929, **23**, 156.
3. H. Meerwein and T. Bersin, *Ann.* 1929, **476**, 113; *Chem. Abstr.* 1930, **24**, 586.
4. R. C. Mehrotra and A. Mehrotra, *Inorg. Chim. Acta Rev.* 1971, **5**, 127.
5. W. G. Bartley and W. Wardlaw, *J. Chem. Soc.* 1958, 422.
6. R. C. Mehrotra and M. M. Agrawal, *J. Chem. Soc.* 1967, 10; 26.
7. R. C. Mehrotra, M. M. Agrawal and P. N. Kapoor, *J. Chem. Soc.* 1968, 2673.
8. S. Govil, P. N. Kapoor and R. C. Mehrotra, *J. Inorg. Nucl. Chem.* 1976, **38**, 172.
9. R. C. Mehrotra, S. Govil, A. B. Goel, R. B. King and K. C. Nainan, *Inorg. Chim. Acta* 1978, **29**, 131.
10. R. C. Mehrotra, M. M. Agrawal and A. Mehrotra, *Synth. React. Inorg. Met.-Org. Chem.* 1973, **3**, 181.
11. M. Aggrawal, C. K. Sharma and R. C. Mehrotra, *Synth. React. Inorg. Met.-Org. Chem.* 1983, **13**, 571.
12. M. Aggrawal and R. C. Mehrotra, *Synth. React. Inorg. Met.-Org. Chem.* 1984, **14**, 139.
13. J. V. Singh, N. C. Jain and R. C. Mehrotra, *Synth. React. Inorg. Met.-Org. Chem.* 1979, **9**, 79.
14. R. C. Mehrotra and J. Singh, *J. Coord. Chem.* (in press).
15. R. C. Mehrotra and J. Singh, *Can. J. Chem.* 1984, **62**, 1003.
16. R. C. Mehrotra and J. Singh, *Z. Anorg. Allg. Chem.* (in press).
17. P. Teyssie, J. P. Bioul, L. Hocks and T. Ouhadi, *Chemtech.* 1977, **7**, 192; *Chem. Abstr.* 1977, **86**, 171914.
18. M. Osgan and P. Teyssie, *Polym. Lett.* 1967, **5**, 789.
19. N. M. Cullinane and S. J. Chard, *Nature (London)* 1949, **164**, 710.
20. D. C. Bradley and W. Wardlaw, *J. Chem. Soc.* 1951, 280.
21. D. C. Bradley, R. C. Mehrotra and W. Wardlaw, *J. Chem. Soc.* 1953, 1634.
22. D. C. Bradley, B. N. Chakravarti, A. Chatterjee, W. Wardlaw and A. Whitley, *J. Chem. Soc.* 1958, 99.
23. M. Aggrawal and R. C. Mehrotra, under communication.
24. M. M. Agrawal, Ph.D. thesis, University of Rajasthan, Jaipur, India (1966).
25. A. I. Vogel, *A Text Book of Quantitative Inorganic Analysis*. Longman, London (1973).
26. D. C. Bradley, F. M. A. Halim and W. Wardlaw, *J. Chem. Soc.* 1950, 3450.
27. D. C. Bradley, R. C. Mehrotra and D. P. Gaur, *Metal Alkoxides*. Academic Press, New York (1978).
28. C. J. Barraclough, D. C. Bradley, J. Lewis and I. M. Thomas, *J. Chem. Soc.* 1961, 2601.
29. K. Nakamoto, *Infrared Spectra of Inorganic and Coordination Compounds*. Wiley, New York (1963).
30. V. A. Sipachev and A. I. Grigorev, *Russ. J. Inorg. Chem.* 1972, **17**, 176.
31. J. G. Oliver and I. J. Worrall, *J. Chem. Soc.* (*A*) 1970, 845.
32. R. C. Mehrotra and A. Mehrotra, *J. Chem. Soc., Dalton Trans.* 1972, 1203.
33. S. Govil, P. N. Kapoor and R. C. Mehrotra, *Inorg. Chim. Acta* 1975, **15**, 43.
34. W. Fieggen, H. Gerding and N. M. M. Nibbering, *Rec. Trav. Chim.* 1968, **87**, 377.
35. J. G. Oliver and I. J. Worrall, *J. Chem. Soc.* (*A*) 1970, 2347.
36. A. Mehrotra, Ph.D. thesis, University of Rajasthan, Jaipur, India (1975).
37. L. G. Hubert-Pfalzgraf and J. G. Riess, *Inorg. Chem.* 1975, **14**, 2854.
38. S. Govil and R. C. Mehrotra, *Aust. J. Chem.* 1975, **28**, 2125.
39. D. C. Bradley and C. E. Holloway, *J. Chem. Soc.* (*A*) 1968, 219.

* *m/z* values.

Polyhedron Vol. 4, No. 5, pp. 853–856, 1985
Printed in Great Britain

0277–5387/85 $3.00 + .00
© 1985 Pergamon Press Ltd

DIOXOURANIUM(VI) COMPLEXES OF SOME SULPHUR DONOR LIGANDS

A. O. BAGHLAF,* M. ISHAQ, O. A. S. AHMED and M. A. AL-JULANI
King Abdulaziz University, College of Science, Department of Chemistry, P.O. Box 9028, Jeddah, Kingdom of Saudi Arabia

(*Received* 13 *March* 1984; *accepted after revision* 26 *September* 1984)

Abstract—Complexes of uranyl chloride and uranyl nitrate of the type $UO_2X_2 \cdot 2L$ and $[UO_2X_2 2L']$, where X = Cl or NO_3 and L = *N,N'*-tetramethylthiourea (TMTU); *N,N'*-dimethylthiourea (DMTU); monomethylthiourea (MMTU), monoethylthiourea (METU), pyridine-2-thiol (PYT) and L' = 4,6-dimethylpyrimidine-2-thiol (PYMT), have been prepared. The complexes were characterised on the basis of IR spectroscopy and by elemental analysis. In some cases Raman spectra are also reported.

Although there is a considerable amount of information available on coordination complexes of *d*-transition metals with ligands containing sulphur as the donor atom,[1] very little work has been reported on actinide complexes with such ligands. Among the ligands, sulphur donor substituted thiourea complexes of molybdenum carbonyl of the type $Mo(CO)_5L$ have recently been reported from these laboratories.[2] In our continued research into the nature of chemical bonding in such systems, we now report the preparation and characterisation of uranyl chloride and uranyl nitrate complexes with substituted thiourea as well as other ligands such as pyridine-2-thiol and 4,6-dimethylpyrimidine-2-thiol. Since these ligands are known to exist in the tautomeric form, the ambidentate nature of these ligands on coordination cannot be overlooked.

The IR spectra of these complexes show that the mode of metal–ligand coordination is through sulphur in the case of substituted thioureas and in pyridine-2-thiol, whereas in the case of 4,6-dimethylpyrimidine-2-thiol the possibility of coordination through nitrogen cannot be entirely ruled out. The complexes have the composition $UO_2X_2 \cdot 2L$ (where X = Cl or NO_3 and L = substituted thioureas or pyridine-2-thiol) and $[UO_2X_2 \cdot 2L'] \cdot H_2O$ (where L' = 4,6-dimethylpyrimidine-2-thiol).

* Author to whom correspondence should be addressed.

EXPERIMENTAL

Materials

UO_2Cl_2 and $UO_2(NO_3)_2 \cdot 6H_2O$ were obtained from B.D.H. Chemicals Ltd, U.K. Methyl, monoethyl, *N,N'*-dimethyl-, *N,N'*-tetramethylthioureas, pyridine-2-thiol and 4,6-dimethyl pyrimidine-2-thiol were purchased from Aldrich Chemical Co. and were used without further purification. Ethanol and other solvents were dried by conventional methods before use.

Physical measurements

IR spectra were measured (KBr pellets or nujol mulls) using a Perkin–Elmer Model 683 IR spectrophotometer. Raman spectra of powdered samples were recorded using a Cary 82 Laser Raman spectrometer.

Elemental analyses. These were carried out by the Microanalysis Laboratory of King Abdulaziz University, Jeddah.

Preparation of the compounds

Preparation of $UO_2Cl_2 \cdot 2TMTU$. The complex was prepared by dissolving UO_2Cl_2 (100 mg/0.29 mmol) and TMTU (77 mg/0.58 mmol) separately in absolute ethanol. On mixing the two solutions a yellow solution was obtained which was stirred for

Table 1. Normal vibrational modes of the NO_3 ion

Point group	NO_3 bonding	Assignment
D_{3h}	Ionic	$\nu_1(A_1)$, $\nu_2(A_2)$, $\nu_3(E)$IR, $\nu_4(E)$IR
		↓ ↓ ↓ ↘ ↘ ↘
C_{2v}	Bidentate	$\nu_2(A)_1$, $\nu_6(B_1)$, $\nu_1(A_1)$, $\nu_4(B_2)$, $\nu_3(A_1)$, $\nu_5(B_2)$

1 h at room temperature. The solvent was reduced to a minimum volume under vacuum and left overnight, giving an orange crystalline solid. This was washed twice with carbon tetrachloride and finally dried under vacuum.

Preparation of $UO_2(NO_3)_2 \cdot 2PYT$. This complex was prepared by dissolving $UO_2(NO_3)_2 \cdot 6H_2O$ (100 mg/0.2 mmol) and pyridine-2-thiol (44 mg/0.4 mmol) separately in absolute ethanol. The solutions were then mixed and stirred for about 2 h at room temperature. The colour of the solution changed to orange red. The solvent was reduced to minimum volume under vacuum and left overnight, giving a red crystalline solid. This was washed twice with carbon tetrachloride and finally dried under vacuum.

The rest of the compounds shown in Table 3 were prepared by the same general method by taking the uranyl salt and the corresponding ligand in a 1:2 mole ratio respectively.

RESULTS AND DISCUSSION

The nature of the NO_3 *ion*

The NO_3 ion of D_{3h} symmetry has four fundamental vibrations, three of which are IR active, $\nu_2(A_2)$, $\nu_3(E)$ and $\nu_4(E)$, while $\nu_1(A)$, $\nu_3(E)$ and $\nu_4(E)$ are Raman active. On coordination, its three-fold symmetry is lost giving C_{2v} symmetry when all six normal modes of vibration become IR active[3] as shown in Tables 1 and 2.

The nature of the UO_2^{2+} *ion*

The linear ion UO_2^{2+} has $D_{\infty h}$ symmetry with four normal modes of vibration. The non-degenerate, symmetric stretching frequency ν_1 is IR forbidden but is Raman active and appears at 871 cm^{-1} in UO_2Cl_2, while the non-degenerate antisymmetric stretching frequency ν_3 is IR allowed and occurs at 960 cm^{-1}.[2] Thus bands at 912 and 922 cm^{-1} can be assigned for $UO_2Cl_2 \cdot 2TMTU$ and $UO_2(NO_3)_2 \cdot 2TMTU$ respectively. These two bands are absent in the Raman spectra. In contrast, the bands at 820 and 840 cm^{-1} in the Raman spectra can be assigned for $UO_2Cl_2 \cdot 2TMTU$ and $UO_2(NO_3)_2 \cdot 2TMTU$ (non-degenerate, symmetrical stretching, frequency ν_1) respectively. See Table 4.

The nature of the C=S *stretching frequency*

The IR spectra of thiourea and *N*-methylthiourea complexes of transition metals have been reported.[4,5] Most of the internal ligand vibrations are mixed, the spectra are difficult to assign, and the mode of coordination is often uncertain. Lane and coworkers[6] have suggested that in *N*-methylthiourea complexes of Zn(II) and Cd(II) the mode of coordination to the metal is through sulphur, while in cases of Pd(II), Pt(II) and Cu(I) it is through a nitrogen atom. Two or three closely spaced bands usually appear near 1490 cm^{-1} in the spectra of the ligands. One contains some C=S stretching character and all of them C—N modes. If one of these bands shows an increase in frequency, coordination through the S atom could be indicated, in which case the band at 1060 cm^{-1}, with considerable C=S character, should show a large decrease in frequency. While both these changes are sometimes observed, in others the 1060 cm^{-1} vibration decreases in frequency only slightly. A band around 1120 cm^{-1} said to contain CN

Table 2. Tentative assignments of NO_3 vibrations (cm^{-1})

Complex		1	2	3	4	5	6	Ref.
$UO_2(NO_3)_2 \cdot 2TMTU$	IR	1525	1025	757	1270	—	808	—
	Raman	1525	1030	753	1269	—	—	—
$UO_2(NO_3)_2 \cdot 2PYT$	IR	1530	1020	748	1268	—	815	—
$UO_2(NO_3)_2 \cdot 2PY$	IR	1500	1028	741	1282	752	812	3

symmetrical stretching and N—CH_3 rocking character usually shows a small decrease in frequency. In the absence of pure C=S and C—N vibrations it is difficult to assign confidently the mode of coordination of the ligand. However, Schafer and Curran[7] have suggested for tetramethylthiourea complexes that an increase in the frequency of the 1504 cm^{-1} band (which they claim is mainly due to N—C—N antisymmetrical stretching vibration) and a decrease in the frequency at ν 1126 cm^{-1}, which is mainly due to a C=S band, means that the ligand–metal coordination is through sulphur. A similar trend showing M—S bond has been reported recently with substituted thiourea complexes of the type $Mo(CO)_5L$[2] (see the IR spectra of the complexes in Table 4).

The nature of the U—S *stretching frequency*

Far IR spectra of complexes showing a metal–sulphur bond feature have been reported[8] but the uranium–sulphur stretching frequency was not detected in these complexes. Presumably the U—S bond is long and therefore weak.

Uranyl–pyridine-2-thiol complexes. Pyridine-2-thiol is known to exist in a tautomeric form as "thione", as shown in Fig. 1(a).[9] Its complexes with various metals have also been reported.[10,11]

The IR spectra of all uranyl–pyridine-2-thiol complexes show that the "thione" form predominates and the coordination with the metal uranium is through sulphur. These findings are based on the following observations: (a) the N—H stretching feature in the complexes is more distinct and occurs ~ 25 cm^{-1} higher than that in the free ligand; and (b) the νC=S stretching feature is ~ 10 cm^{-1} lower as compared to the free ligand.

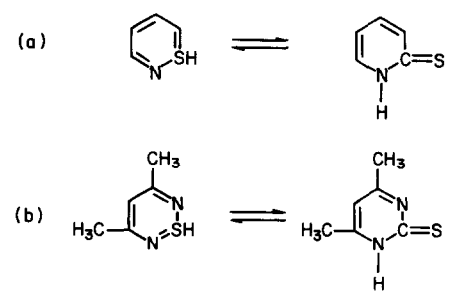


Fig. 1. Tautomeric structure of: (a) pyridine-2-thiol and (b) 4,6-dimethylpyrimidine-2-thiol.

However, uranyl–4,6-dimethylpyrimidine-2-thiol complexes do not show any noticeable change in νC=S frequency while the typical band in the region of 1600–1400 cm^{-1} which are due to the "ring breathing" modes, show very broad strong bands. Therefore the possibility of its coordination to the metal through one of the *N* atoms cannot be ruled out. Also, the presence of a broad and strong band around 3600–3500 cm^{-1} may be due to the free H_2O in these complexes.

Table 3. Analytical data found (required)

S. No.	Compound	Analytical data (%) C	H	N	Colour
1	$UO_2Cl_2 \cdot 2TMTU$	19.5 (19.8	3.8 3.9	8.9 9.2)	Orange
2	$UO_2(NO_3)_2 \cdot 2TMTU$	18.3 (18.2	3.7 3.6	12.7 17.7)	Red
3	$UO_2Cl_2 \cdot 2DMTU$	12.6 (13.1	2.9 2.9	9.8 10.2)	Yellow
4	$UO_2(NO_3)_2 \cdot 2DMTU$	11.3 (11.9	2.8 2.6	12.7 13.9)	Orange
5	$UO_2Cl_2 \cdot MMTU$	10.6 (10.2	2.7 2.3	10.5 10.7)	Yellow
6	$UO_2Cl_2 \cdot 2METU$	13.3 (13.1	3.0 2.9	10.5 10.2)	Yellow
7	$UO_2Cl_2 \cdot 2PYT$	22.0 (21.3	1.8 1.7	4.9 4.9)	Yellow
8	$UO_2(NO_3)_2 \cdot 2PYT$	19.6 (19.4	1.7 1.6	9.3 9.1)	Orange
9	$UO_2Cl_2 \cdot 2PYMT \cdot H_2O$	22.7 (22.5	2.8 2.8	8.9 8.7)	Yellow
10	$UO_2(NO_3)_2 \cdot 2PYMT \cdot H_2O$	21.9 (20.8	2.6 2.6	12.4 12.1)	Orange-red

Table 4. IR spectra (in KBr pellet) (cm^{-1})*

Compound	N—H		C=S		O=U=O
MMTU	3227(w)	3189(w)	1145(w)	1120(w)	—
METU	3370	3150(b,s)	1130(m)	1108(w)	—
DMTU	3240(s)	3040(w)	1035(3)		—
TMTU	—	—	1055(w)		
PYT	3155–3040(b,w)		1140(s)		
PYMT	3200–2800(b,s)		1180(s)		
$UO_2Cl_2 \cdot 2MMTU$	3300–3100(b,m)		1122(s)		912(vs)
$UO_2Cl_2 \cdot 2METU$	3420(m), 3200(s)		1125(m)		914(vs)
$UO_2Cl_2 \cdot 2DMTU$	— —		1030(s)		928(vs)
$UO_2(NO_3)_2 \cdot 2DMTU$			1031(s)		940(vs)
$UO_2Cl_2 \cdot TMTU$			1055(s)		912(s)
$UO_2(NO_3)_2 \cdot 2TMTU$			1058(s)		922(s)
$UO_2Cl_2 \cdot 2PYT$	3175(m), 3120(m)		1131(s)		925(s)
$UO_2(NO_3)_2 \cdot 2PYT$	3215(m), 3110(w)		1131(s)		928(s)
$UO_2Cl_2 \cdot 2PYMT \cdot H_2O$	3210–3800(b,s) (3600–3400)†(b,s)		1180(s)		910(vs)
$UO_2(NO_3)_2 \cdot 2PYMT \cdot H_2O$	3210–2800(b,s) (3600–3400)†(b,s)		1182(s)		940(vs)

* w, weak; m, medium; b, broad; s, strong; vs, very strong.
† Strong broad band can be attributed to H_2O.

Finally the IR spectra of all the complexes, 1–10 show a strong band around 925 cm^{-1} indicating the presence of the UO_2^{2+} moiety (see Table 4). The elemental analyses of the complexes are given in Table 3 and are consistent with the proposed formulations.

Acknowledgements—We are grateful to Prof. K. W. Bagnall (Department of Chemistry, University of Manchester) for his invaluable suggestions in preparing this manuscript and for the help in obtaining the Raman spectra for this research. O. Ahmed and M. Al-Julani also wish to thank KAAU for scholarships.

REFERENCES

1. E. W. Abel and B. C. Crosse, *Organomet. Chem. Rev.* 1967, **2**, 443 (and references therein).
2. A. O. Baghlaf, M. Ishaq and A. S. Daiffulah, *Polyhedron* 1984, **3**, 235.
3. J. I. Bullock, *J. Inorg. Nucl. Chem.* 1967, **29**, 2257.
4. A. Yamaguchi, R. B. Penland, S. Mizushima, T. J. Lane, C. Curran and J. V. Quagliano, *J. Am. Chem. Soc.* 1958, **80**, 527.
5. Yu. Ya. Kharitonov, V. D. Brega, A. V. Ablov and N. N. Proskina, *Russ. J. Inorg. Chem.* 1974, **19**, 1187.
6. T. J. Lane, A. Yamaguchi, J. V. Quagliano, J. A. Ryan and S. Mizushima, *J. Am. Chem. Soc.* 1959, **81**, 3824.
7. M. Schafer and C. Curran, *Inorg. Chem.* 1966, **5**, 265.
8. A. O. Baghlaf and A. Thompson, *J. Less Common. Met.* 1977, **291**, 5453.
9. R. A. Jones and A. R. Katritzky, *J. Chem. Soc.* 1958, 3610.
10. B. P. Kennedy and A. B. P. Lever, *Can. J. Chem.* 1972, **50**, 3488.
11. P. Evans and G. Wilkinson, *J. Chem. Soc., Dalton Trans.* 1974, 946.

Polyhedron Vol. 4, No. 5, pp. 857–867, 1985
Printed in Great Britain

0277–5387/85 $3.00 + .00
© 1985 Pergamon Press Ltd

METAL COMPLEXES OF 2-(2′-CARBOXYMETHYLTHIO-PHENYLAZO)-5-NITROTOLUENE—II. COMPLEX FORMATION EQUILIBRIA WITH COPPER(II) ION IN SEVERAL DIOXANE–WATER SOLVENT MIXTURES

E. CASASSAS*
Department of Analytical Chemistry, Facultat de Química, Universitat de Barcelona, Av. Diagonal, 647, 08028-Barcelona, Spain

and

J. ALIO
Department of Analytical Chemistry, Facultat de Ciències, Universitat Autònoma de Barcelona, Bellaterra, Barcelona, Spain

(*Received* 13 *August* 1984; *accepted* 26 *September* 1984)

Abstract—Stability constants of copper(II) complexes formed by 2-(2′-carboxymethylthiophenylazo)-5-nitrotoluene in dioxane–water solvent mixtures of several different compositions [50, 60 and 75% dioxane (v/v)] were determined from EMF measurements, at 25°C and 0.1 mol dm^{-3} $NaClO_4$ ionic medium. Graphical treatment of experimental data gives for the equilibria $nA^- + Cu^{2+} = CuA_n^{(2-n)+}$ ($n = 1$ or 2), in a solvent with $X\%$ (v/v) dioxane, the following values of $\log \beta_1$ and $\log \beta_2$ (given here successively). $X = 50$: 2.41, 6.77; $X = 60$: 3.36, 7.45; $X = 75$: 4.33, 7.64. The relation between solvent composition and the values found for the stability constants is discussed. From EMF measurements made with the copper(II) ion-selective electrode, at constant pH, the nature of the effective donor groups in this potentially terdentate ligand is inferred.

The study of metal-complex formation equilibria with the potentially terdentate ligand 2-(2′-carboxymethylthiophenylazo)-5-nitrotoluene raises two kinds of problems: those of a conceptual type, derived from the use of mixed solvents, such as dioxane–water mixtures, required because of the water-insolubility of the ligand and its complexes; and the others, of a structural type, derived from the presence in the ligand molecule of three donor groups, although two of them, the thioether sulphur and the azo bridge, show a relatively low coordinating power towards metal ions.

In a mixed solvent, such as dioxane–water, which contains an organic constituent with a low relative permittivity, changes in the content of this constituent, deeply modify the values of the stability constants of metal complexes. Although the theoretical study of the effect on these values of the composition of binary solvent mixtures has been the subject of relatively little attention, the changes in the stability constants were initially assigned to the variation of the relative permittivity of the medium with the contents of its organic constituent, variation which modifies the electrostatic interactions between the complex formers; the well-known Born equation[1] and other similar expressions[2,3] describe linear correlations between the log of stability constants and the reciprocal of the relative permittivity, or the mole fraction of dioxane in the system. Many experimental results, however, deviate from these correlations. Changes shown by stability constants in binary solvent mixtures, as a consequence, have to be assigned to other causes. Some of them must be mentioned here.

One of them is the change in the ligand protonation constant with solvent composition, already studied in the case of the present ligand;[4,5] another one stems from the changes introduced by the organic constituent in the solvation sphere of the implied ions, especially of the metal ion.[6,7] The hypothesis that ions are solvated virtually only by

* Author to whom correspondence should be addressed.

water molecules is no longer acceptable, since it was shown[8] that dioxane (solvating through its oxygen atoms) can form dioxane solvates or mixed solvates with metal ions, its effect on the anion sphere being much weaker. Furthermore, for a solvated ion in a mixed solvent, the complex formation reactions are substitution equilibria in which ligand molecules displace coordinated solvent molecules: the expressions for the corresponding equilibrium constants must include, besides the activities (or concentrations) of the ions and the complex, those of water and the second solvent.[9,10] This means that different contents in the second solvent can alter the values of the formation constant simply by modifying the concentration of the aqua-complex as a result of the change in the water activity in the system.

It seems, therefore, that the observed effects on the formation constants are due to several concurrent causes whose relative weights depend on the nature of the system under study.[11,12] It is in this context that the experimental determination of the log β variation for the copper(II) ion complexes with 2-(2'-carboxymethylthiophenylazo)-5-nitrotoluene as a function of dioxane content in the solvent has been undertaken. Complex formation can be followed by the usual pH titration technique, using either the glass electrode or a copper(II) ion-selective electrode, or both. The use of the latter at constant pH to obtain free copper(II) concentrations in solutions with different ligand-to-metal ratios gives some insight into the afore-mentioned structural problems, in this case derived from the presence of three potential donor centres in the ligand molecule. Although equilibria studies do not usually afford information of a structural nature, such as, for instance, information about the groups which are effectively acting as donors, in the present case the use of the copper electrode to follow the changes in free-metal ion concentration with changes in ligand concentration while working at constant pH, at suitable pH values, affords direct experimental information on the participation or not in complex formation of the donor groups which are prone to undergo protonation (in the case of the present ligand, the carboxylate ion).

EXPERIMENTAL

Reagents and solutions

2 - (2' - *Carboxymethylthiophenylazo*) - 5 - *nitrotoluene.* Synthethized and purified as described earlier.[5] A 10^{-3} mol dm^{-3} stock solution in anhydrous dioxane was prepared and titrated as in ref. [13].

Sodium perchlorate, sodium hydroxide, copper(II) *perchlorate, dioxane and other reagents.* Grade, preparation and standardization as described in ref. [13].

Apparatus

Metrohm compensator potentiometer, E 368 (precision ± 0.1 mV). Indicator glass electrode combined with a calomel reference electrode (Radiometer GK 2311C), with salt bridge containing 0.1 mol dm^{-3} NaCl solution in dioxane–water (with the same dioxane content as the test solution). Copper(II) ion-selective electrode (Orion, 94-98A). Indicator electrodes calibration was performed without buffer solutions by application of Gran's technique to the proper test solutions. Titration cell, which includes pure-nitrogen inlet and outlet, and magnetic stirring, was thermostatted at 25 ± 0.1°C.

Procedure

Complex formation equilibria in the system copper(II) ion and 2-(2'-carboxymethylthiophenylazo)-5-nitrotoluene in dioxane–water mixed solvents with different dioxane contents [50, 60 and 75% (v/v)] were studied through EMF measurements along the course of titrations performed in an ionic medium containing 0.1 mol dm^{-3} $NaClO_4$, at 25.0 ± 0.1°C, under a nitrogen atmosphere (N_2 purified by bubbling through an acidic vanadium solution and through sodium hydroxide solution, and equilibrated with a solution of the same ionic medium in the same mixed solvent as the test solution). EMF measurements were performed according to one of the following procedures.

Procedure A. A volume, V_o of the test solution (TS), with the following initial composition:

TS = $A_o$mol dm^{-3} HA, H_o mol dm^{-3} H^+,

B_o mol dm^{-3} $Cu(ClO_4)_2$, 0.1 mol dm^{-3} $NaClO_4$

is titrated with a sodium hydroxide solution, T_1 (aqueous solution, containing the proper concentration of $NaClO_4$). During the titration, ionic medium, solvent composition, total copper(II) concentration and total ligand (designed in the following HA) concentration are kept constant by adding from burettes, after each titrant addition, suitable volumes of a copper ion aqueous solution, T_2, and of a ligand solution T_3 in anhydrous dioxane. The free hydrogen ion concentration is measured from a reading obtained with the glass electrode (GE, cell I); the free copper(II) ion concentration with an ion-selective electrode (Cu–SpE, cell II). Both indicator electrodes are soaked in the same TS

solution, against the same reference electrode, RE:

Cell I GE/TS//0.1 mol dm^{-3} NaCl/RE

Cell II Cu–SpE/TS//0.1 mol dm^{-3} NaCl/RE

Before starting the titration, the initial hydrogen ion concentration H_o and standard electrode potential for the glass electrode, E°_H, are determined according to Gran's method:[14] a volume of a 0.1 mol dm^{-3} $NaClO_4$ solution in dioxane–water, slightly acidified with perchloric acid, is titrated with sodium hydroxide solution; then, the copper(II) ion selective electrode is standardized through emf measurements after successive additions into the former solution of small volumes of a standard solution of copper(II) perchlorate. Finally, the suitable volume of ligand solution is added, and the TS solution is now ready for titration with T_1 NaOH solution. Reversiblity of equilibria involved in establishment of electrode potential was checked by the usual technique[13] of "back titration" with an acid solution until the initial point was reproduced. Absence of polynuclear species was proved from titrations of several TS solutions covering a range of metal-to-ligand concentration ratios from 0.076 to 0.32 (a wider range was not used because of solubility limitations).

Procedure B. A cell similar to cell II is used, with a test solution TS containing copper(II) ion, but no ligand. This solution is titrated at constant pH with a ligand solution T_1. During the titration, solvent composition [a mixed solvent with 60% (v/v) dioxane was only used], ionic medium, total copper(II) ion concentration and free hydrogen ion concentration are kept constant through addition of suitable volumes (after each titrant addition) of a T_2 copper(II) ion solution and a T_3 hydrogen ion solution, containing both suitable concentrations of ionic medium and dioxane. Before starting titration, free acid in TS solution is determined, and both indicator electrodes (glass electrode only to be used to check pH constancy) are standardized by Gran's method, as described.

In both procedures, A and B, emf measurements are taken, after each titrant and associated additions, when equilibrium is reached, i.e. when potential readings reach stable values. Stabilization of electrode potentials was achieved in every case within less than 5–7 min.

DATA TREATMENT

Procedure A: glass electrode measurements

The experimental values $(V_{T_1}, E_H)_{A_o,B_o}$ obtained from the titrations of the TS with sodium hydroxide (T_1 solution) are transformed into the pairs $(\bar{n}, \log a)_{A_o,B_o}$ in order to build the formation curve which corresponds to each experiment. Calculation details have been described elsewhere.[13] The free hydrogen ion concentration, h, is calculated from the expression $E_H = E^\circ_H - g \log h$ ($g = 59.16$ mV at 25°C). E°_H values for the indicator glass electrode in the different mixed solvents, obtained from standardization according to Gran's technique, are given in Table 1. In Table 1 experimental data from some typical titrations are collected; in Figs 1–3 the evaluated formation curves are shown.

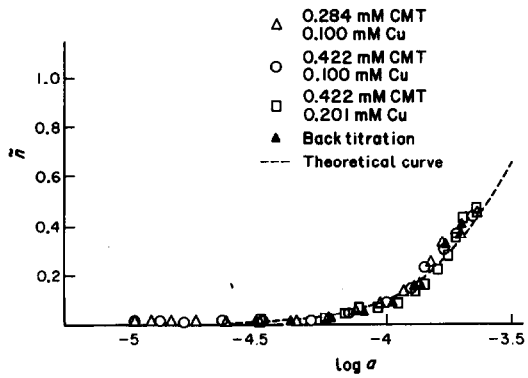


Fig. 1. Formation curve for the system 2-(2'-carboxymethylthiophenylazo)-5-nitrotoluene (CMT)–copper(II) ion in 50% (v/v) dioxane–water.

Data pairs $(\bar{n}, \log a)$ have been treated graphically by a curve-fitting method[15] and by a method of elimination introduced by Schwarzenbach,[16] according to usual procedures, as already described,[13] under the assumption that only the 1:1 and 1:2 complexes are formed. Figure 4 shows the bundle of straight lines resulting from application of the Schwarzenbach method to the data obtained for the present system in a solution in 75% (v/v) dioxane–water.

Procedure A: copper(II) ion-selective electrode measurements

Titrations of TS with sodium hydroxide are performed after checking the Nernstian behaviour of the copper(II) ion-selective electrode and determining its standard potential, E°_{Cu} (its values in the different solvent used are given in Table 2, where the experimental results from several typical titrations are collected). From the measured E_{Cu} for this electrode in each point of the titrations, the free copper(II) ion concentration, b, is first calculated from the expression $E_{Cu} = E^\circ_{Cu} - g \log b$ (where $g = 29.6$ mV at 25°C) and then the numerical value of the function $\eta = \log (B/b)$ (where B is the analytical total metal ion concentration) is evaluated. If only 1:1 and 1:2 complexes co-exist in solution, the

Table 1. Titration with sodium hydroxide of 2-(2′-carboxymethylthiophenylazo)-5-nitrotoluene in the presence of copper(II) ion, in dioxane–water solution (0.10 mol dm^{-3} $NaClO_4$, 25°C)

(A) In 50% (v/v) dioxane–water

TS: $A_o = 0.284$, $B_o = 0.100$, $H_o = 0.578$ (all concentrations in mmol dm^{-3})
T_1: 21.00 mmol dm^{-3} NaOH
$V_o = 74.75$ mol, $E_o = 514.0$ mV

V_{T_1} (ml)	E_H (mV)	pH	$\bar{n}$	log a
1.00	256.6	4.350	0.001	−4.50
1.10	246.6	5.519	0.012	−4.36
1.20	236.6	4.689	0.028	−4.22
1.30	227.7	4.844	0.055	−4.11
1.40	219.0	4.986	0.088	−4.02
1.50	210.5	5.130	0.125	−3.94
1.60	202.5	5.266	0.175	−3.87
1.70	194.3	5.404	0.251	−3.82
1.80	185.1	5.559	0.338	−3.78
1.90	173.3	5.758	0.375	−3.73
2.00	157.9	6.019	0.442	−3.62
2.10	132.0	6.457	1.030	—

Back titration (with 10.5 mmol dm^{-3} $HClO_4$)

0.00	132.0	6.457	1.030	—
0.25	164.1	5.914	0.421	−3.70
0.50	181.9	5.614	0.333	−3.76
0.75	194.6	5.339	0.251	−3.82
1.00	204.9	5.224	0.166	−3.89
1.25	214.9	5.055	0.099	−3.98
1.50	225.3	4.879	0.063	−4.09
1.75	236.0	4.699	0.030	−4.22
2.00	247.1	4.511	0.013	−4.37
2.25	258.0	4.327	0.005	−4.53

(B) In 60% (v/v) dioxane–water

TS: $A_o = 0.800$, $B_o = 0.100$, $H_o = 0.831$ (all concentrations in mmol dm^{-3})
T_1: 27.06 mmol dm^{-3} NaOH
$V_o = 70.00$ ml, $E_o = 356.6$ mV

V_{T_1} (ml)	E_H (mV)	pH	$\bar{n}$	log a
0.00	112.2	4.131	0.129	−4.52
0.20	95.9	4.406	0.283	−4.27
0.40	81.5	4.645	0.503	−4.06
0.60	70.1	4.843	0.759	−3.91
0.80	59.9	5.015	1.006	−3.78
1.00	50.7	5.117	1.217	−3.70
1.20	43.5	5.292	1.595	−3.63

Back titration (with 10.01 mmol dm^{-3} $HClO_4$)

0.00	43.5	5.292	1.595	−3.63
0.50	52.9	5.133	1.261	−3.71
1.00	62.4	4.973	0.969	−3.82
1.50	72.5	4.802	0.695	−3.94
2.00	82.7	4.648	0.443	−4.07
2.50	95.5	4.413	0.286	−4.26
3.00	108.1	4.200	0.150	−4.45
3.50	119.6	4.006	0.097	−4.63

(C) In 75% (v/v) dioxane–water

TS: $A_o = 0.650$, $B_o = 0.200$, $H_o = 0.839$ (all concentrations in mmol dm^{-3})
T_1: 25.25 mmol dm^{-3} NaOH
$V_o = 100.0$ ml, $E_o = 354.0$ mV

V_{T_1} (ml)	E_H (mV)	pH	$\bar{n}$	log a
0.00	134.0	3.719	0.002	−5.79
0.25	123.9	3.889	0.016	−5.63
0.50	109.0	4.140	0.039	−5.38
0.75	86.3	4.525	0.103	−5.01
1.00	67.3	4.846	0.276	−4.72
1.25	48.7	5.160	0.434	−4.45
1.50	35.1	5.390	0.597	−4.26
1.75	23.9	5.579	0.745	−4.12
2.00	13.5	5.755	0.872	−4.00
2.25	4.3	5.911	0.980	−3.90
2.50	−5.1	6.069	1.078	−3.81

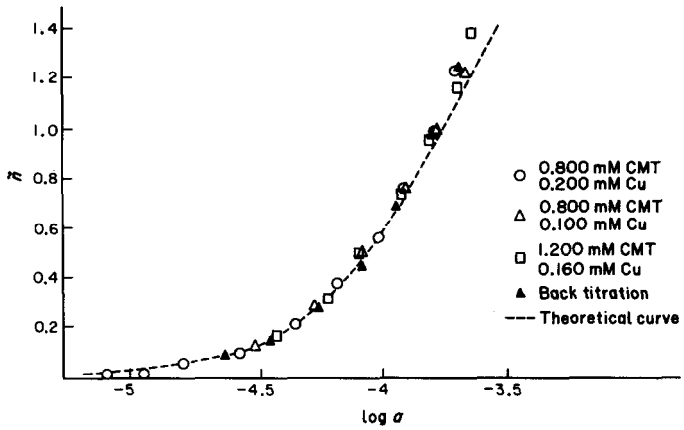


Fig. 2. Formation curve for the system 2-(2′-carboxymethylthiophenylazo)-5-nitrotoluene (CMT)–copper(II) ion in 60% (v/v) dioxane–water.

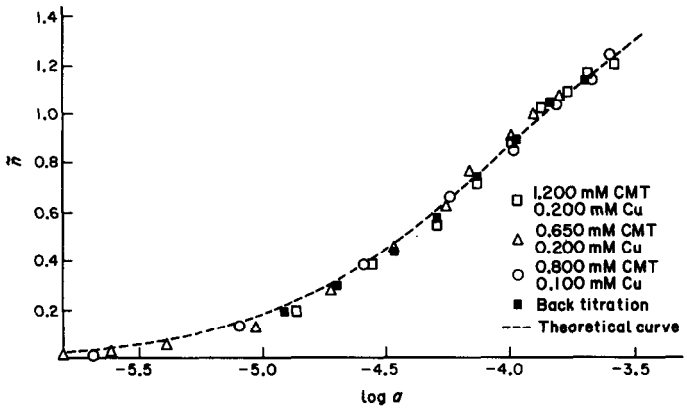


Fig. 3. Formation curve for the system 2-(2′-carboxymethylthiophenylazo)-5-nitrotoluene (CMT)–copper(II) ion in 75% (v/v) dioxane–water.

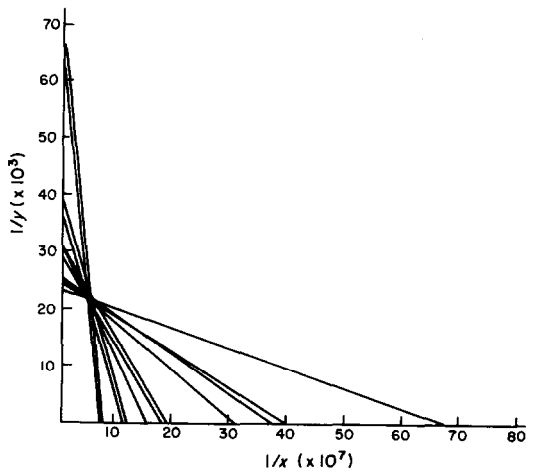


Fig. 4. Schwarzenbach elimination method applied to the determination of stability constants in the system 2-(2′-carboxymethylthiophenylazo)-5-nitrotoluene (CMT)–copper(II) ion in 75% dioxane–water. ($y = (1-\bar{n})a/\bar{n}$; $x = (2-\bar{n})a^2/\bar{n}$; $p_1 = \beta_1$; $p_2 = \beta_2$).

expression $10^{n} = B/b = 1+\beta_1 a+\beta_2 a^2$ holds, from which it is seen that, if a linear plot of B/b vs a is obtained, the 1 : 1 complex is strongly predominant in the solution, whereas a linear plot of B/b vs a^2 shows the predominancy of the 1 : 2 complex. In the general case of co-existence of noticeable amounts of both complexes, this expression can be put in the form $(B-b)/ab = \beta_1+\beta_2 a$, which shows that the plot of the left term vs a will be linear, and that β_2 can be evaluated from the slope and β_1 from the intercept of the resulting straight line.

In the calculation of the free ligand concentration, a, allowance must be made for the fraction of non-bound-to-copper ligand which is bound to hydrogen ion. Under the assumption that, under the experimental conditions used, the concentration of 1 : 1 species is, in a first approximation, negligible in comparison with that of the 1 : 2 species (assumption justified by the type of formation curves obtained in applying the curve-fitting method), the con-

centration of non-bound-to-copper ligand is: $[A^-]+[HA] = A_{tot}-2(B-b) = a+\beta_H ha$, where β_H is the protonation constant of the ligand. Consequently, and within the field of validity of the former assumption, the free ligand concentration (non-bound-to-copper, unprotonated) is: $a = [A_{tot} - 2(B-b)]/(1+\beta_H h)$.

Figures 5 and 6 show the plots of $(B-b)/ab$ vs a

Table 2. Titration with sodium hydroxide of 2-(2'-carboxymethylthiophenylazo)-5-nitrotoluene in the presence of copper(II) ion, in dioxane–water solution (0.10 mol dm^{-3} $NaClO_4$, 25°C): measurements with glass electrode (E_H) and copper(II) ion-selective electrode (E_{Cu})

(A) In 50% (v/v) dioxane–water

TS: $A_o = 0.422$, $B_o = 0.100$, $H_o = 0.710$ (all concentrations in mmol dm^{-3})
T_1: 6.00 mmol dm^{-3} NaOH
$V_o = 60.00$ ml, $E_o^H = 344.0$ mV, $E_o^{Cu} = 185.45$ mV

V_{T_1} (ml)	E_H (mV)	E_{Cu} (mV)	pH	$\bar{n}$	log a	b
2.00	106.9	—	4.000	0.003	−4.66	—
2.50	96.7	—	4.180	0.016	−4.49	—
3.00	84.5	—	4.386	0.008	−4.30	—
3.50	73.3	66.0	4.576	0.050	−4.14	9.05×10^{-5}
4.00	64.0	65.6	4.732	0.101	−4.02	8.77×10^{-5}
4.50	54.6	65.2	4.892	0.155	−3.91	8.50×10^{-5}
5.00	47.1	64.7	5.019	0.228	−3.84	8.18×10^{-5}
5.50	40.0	64.2	5.139	0.305	−3.77	7.94×10^{-5}
6.00	33.3	63.7	5.251	0.380	−3.72	7.56×10^{-5}
6.50	26.4	63.3	5.358	0.459	−3.67	733×10^{-5}
7.00	20.3	62.8	5.474	1.610	−3.61	7.05×10^{-5}

(B) In 60% (v/v) dioxane–water

TS: $A_o = 1.200$, $B_o = 0.160$, $H_o = 1.229$ (all concentrations in mmol dm^{-3})
T_1: 21.65 mmol dm^{-3} NaOH
$V_o = 75.00$ ml, $E_o^H = 372.10$ mV, $E_o^{Cu} = 21.1$ mV

0.00	132.9	−92.1	4.043	0.151	−4.43	15.00×10^{-5}
0.25	120.0	−92.8	4.261	0.313	−4.23	14.21×10^{-5}
0.50	108.1	−93.8	4.452	0.508	−4.05	13.15×10^{-5}
0.75	98.7	−96.0	4.621	0.737	−3.93	11.08×10^{-5}
1.00	90.4	−98.1	4.762	0.962	−3.82	9.41×10^{-5}
1.25	82.9	−100.1	4.888	1.165	−3.72	8.05×10^{-5}
1.50	76.6	−102.6	4.995	1.388	−3.65	6.63×10^{-5}

(C) In 75% (v/v) dioxane–water

TS: $A_o = 1.200$, $B_o = 0.200$, $H_o = 1.18$ (all concentrations in mmol dm^{-3})
T_1: 25.25 mmol dm^{-3} NaOH
$V_o = 90.00$ ml, $E_o^H = 379.0$ mV, $E_o^{Cu} = 11.4$ mV

0.00	117.4	—	4.424	0.198	−4.85	—
0.25	99.0	—	4.733	0.377	−4.56	—
0.50	82.9	—	5.005	0.556	−4.31	—
0.75	70.9	−126.9	5.208	0.721	−4.13	12.55×10^{-5}
1.00	60.9	−127.3	5.377	0.867	−3.99	12.45×10^{-5}
1.25	53.1	−130.4	5.509	1.016	−3.88	9.56×10^{-5}
1.50	45.6	−133.0	5.635	1.087	−3.79	7.80×10^{-5}
1.75	38.7	−135.2	5.752	1.167	−3.69	6.57×10^{-5}
2.00	32.4	−137.8	5.858	1.215	−3.61	5.37×10^{-5}

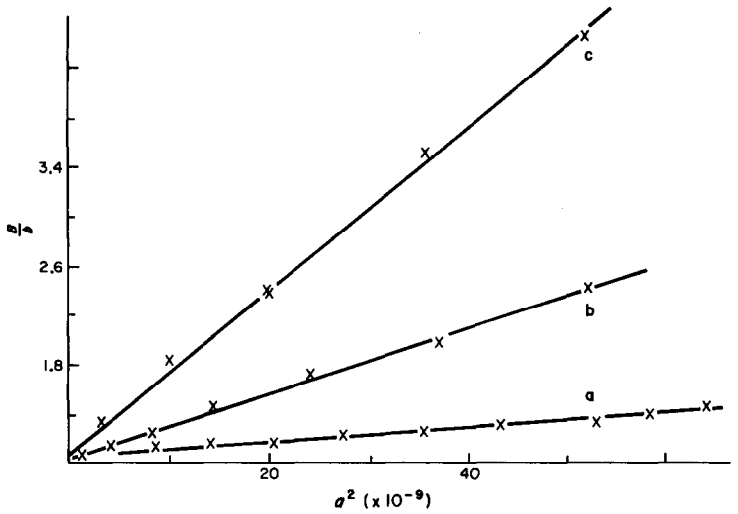


Fig. 5. Plot of the ratio total metal/free metal, B/b vs a^2 for the system 2-(2'-carboxymethylthiophenylazo)-5-nitrotoluene (CMT)–copper(II) ion in dioxane–water. Curve a: 50% (v/v) dioxane; curve b: 60% (v/v) dioxane; curve c: 75% (v/v) dioxane.

and B/b vs a^2, for the system under study, in several dioxane–water solvents: (a) 50% (v/v) dioxane; (b) 60% (v/v) dioxane, and (c) 75% (v/v) dioxane.

Procedure B: copper(II) ion-selective electrode measurements at constant pH

In contrast with procedure A, the total ligand concentration is now not constant and must be evaluated for each experimental point. Calculation is made from known initial values and successive titrant and other additions made.

Experiments have been performed at pH 2.59 and 6.35. Data from typical titrations are given in Table 3. In the solvent used in these experiments [60% (v/v) dioxane–water] the acid dissociation constant of the arylthioacetic acid under study is $K_a = 2.95 \times 10^{-6}$ ($pK_a = 5.33$).[5] Thus, in solutions at pH 2.59, free ligand contains the carboxylate group practically only in its protonated form; in solutions at pH 6.35, free ligand is present in both forms, the greater fraction being that in unprotonated form. Let A' be the unprotonated ligand concentration, and A the total ligand concentration: from the expression for K_a it is found that, at pH 2.59, $A' = 1.15 \times 10^{-3} A$, and at pH 6.35, $A' = 0.868 A$.

For data treatment two alternative models can, in

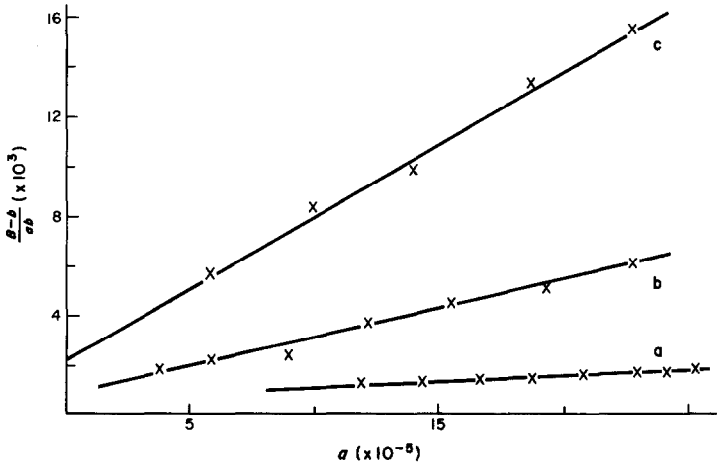


Fig. 6. Plot of the function $(B-b)/ab$ vs a for the system 2-(2'-carboxymethylthiophenylazo)-5-nitrotoluene (CMT)–copper(II) ion in dioxane–water. Curve a: 50% (v/v) dioxane; curve b: 60% (v/v) dioxane; curve c: 75% (v/v) dioxane.

Table 3. Experimental data for the constant-pH potentiometric study of complex-forming equilibria in the system copper(II) ion–2-(2'-carboxymethylthiophenylazo)-5-nitrotoluene in 60% (v/v) dioxane–water (0.10 mol dm^{-3} $NaClO_4$, 25°C): TS: $B_o = 0.150$ mmol dm^{-3}; T_1: 0.375 mmol dm^{-3} Cu(II); T_2: 8.320 mmol dm^{-3} ligand

(A) At constant pH 2.59

$V_o = 85.0$ ml, $E_o^{Cu} = 54.8$ mV

V_{T_1} (ml)	V_{T_2} (ml)	E_{Cu} (mV)	b
0.50	0.75	−59.9	1.32×10^{-4}
1.00	1.50	−61.3	1.18×10^{-4}
1.50	2.25	−62.4	1.09×10^{-4}
2.00	3.00	−63.5	1.00×10^{-4}
2.50	3.75	−64.6	0.92×10^{-4}
3.00	4.50	−65.6	0.85×10^{-4}
3.50	5.25	−66.6	0.79×10^{-4}
4.00	6.00	−67.5	0.73×10^{-4}
4.50	6.75	−67.6	0.72×10^{-4}
5.00	7.50	−67.8	0.71×10^{-4}
5.50	8.25	−68.2	0.69×10^{-4}
6.00	9.00	−68.3	0.68×10^{-4}

(B) At constant pH 6.35

$V_o = 40.0$ ml, $E_o^{Cu} = 133.0$ mV

0.50	0.75	7.33	5.63×10^{-4}
1.00	1.50	2.2	3.96×10^{-4}
1.50	2.25	−1.2	2.90×10^{-4}
2.00	3.00	−4.5	2.25×10^{-4}
2.50	3.75	−8.6	1.63×10^{-4}
3.00	4.50	−13.0	1.16×10^{-4}
3.50	5.25	−16.1	0.91×10^{-4}
4.00	6.00	−18.3	0.77×10^{-4}
4.50	6.75	−20.6	0.64×10^{-4}
5.00	7.50	−22.2	0.57×10^{-4}

principle, be assumed. In the first one, it is the unprotonated ligand (i.e. the ligand form which contains an anionic carboxylate group) that is assumed to take part in complexation. Since at pH 2.59 its concentration is extremely small, the 1:1 complex will predominate at this pH (unless the formation constant for the 1:2 complex be abnormally high), and the expression $B/b = 1 + \beta_1 a$ will hold. Since the 1:1 complex is not very stable one can, as a first approximation, take $a \simeq A'$. Plotting B/b vs A' does give a straight line (Fig. 7), but its slope yields a value of $\log \beta_1 = 6.21$. This value is too high and strongly deviates from the value previously obtained from the well-proven pH titration method (procedure A).

In the second model to be tested it is assumed that, at pH 2.59, the protonated form HA of the ligand

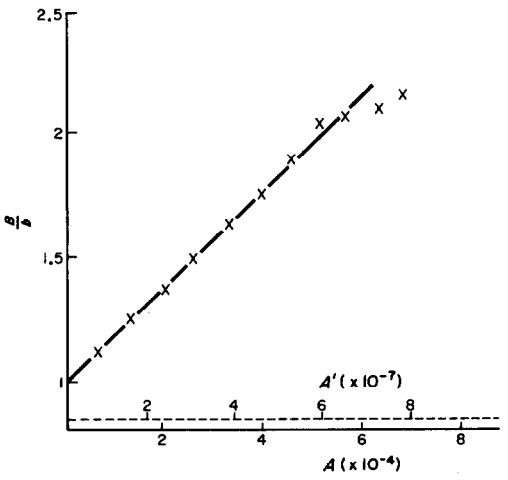


Fig. 7. Plot of the ratio total-metal/free-metal, B/b vs total ligand concentration, A, and unprotonated ligand concentration, A', in 60% (v/v) dioxane–water, at constant pH, 2.59.

is the form involved in copper(II) ion complexation; i.e. the complex formation equilibrium is: Cu + HA ⇄ Cu(HA). In the expression for B/b given before, the total concentration A (or, more exactly, $A - A'$, the true total concentration of protonated ligand) can now be substituted for a. The plot of B/b vs A is a straight line too (Fig. 7), but its slope yields now a value of $\log \beta_1 = 3.27$, which does agree with the value obtained from the procedure A.

Data from experiments performed in solutions at pH 6.35, where ligand fraction in unprotonated form

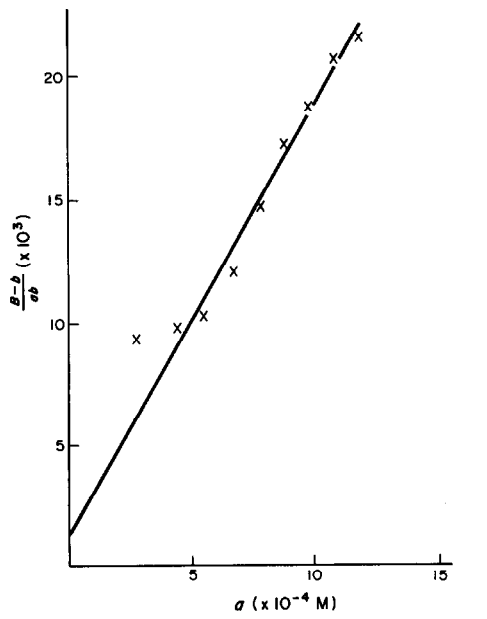


Fig. 8. Plot of the function $(B-b)/ab$ vs free-ligand concentration, a, in 60% (v/v) dioxane–water, at constant pH, 6.35.

Table 4. Overall summary of results for formation constants of copper(II) complexes with 2-(2'-carboxymethylthiophenylazo)-5-nitrotoluene in dioxane–water mixed solvents (0.10 mmol dm^{-3} $NaClO_4$, 25°C)

From glass electrode measurements	From copper(II) ion electrode measurements
(A) In 50% (v/v) dioxane	
$\log \beta_1 = 2.41 \pm 0.01$	$\log \beta_1 = 2.35 \pm 0.15$
$\log \beta_2 = 6.82 \pm 0.02$	$\log \beta_2 = 6.70 \pm 0.08$
(B) In 60% (v/v) dioxane	
$\log \beta_1 = 3.47 \pm 0.01$	$\log \beta_1 = 3.27 \pm 0.13$
$\log \beta_2 = 7.54 \pm 0.02$	$\log \beta_2 = 7.19 \pm 0.07$
(C) In 75% (v/v) dioxane	
$\log \beta_1 = 4.32 \pm 0.02$	$\log \beta_1 = 3.67 \pm 0.30$
$\log \beta_2 = 7.68 \pm 0.04$	$\log \beta_2 = 7.57 \pm 0.14$

is important, show co-existence of both 1:1 and 1:2 complexes. Thus, the plot of $(B-b)/ab$ vs a (as shown in Fig. 8) is a straight line which yields the values $\log \beta_1 = 3.27$ and $\log \beta_2 = 7.24$, as is to be expected from procedure A results.

The values for the stability constants in the different mixed solvents (50, 60 and 75% dioxane) are collected in Table 4.

DISCUSSION

Variation of $\log \beta_i$ *with dioxane content in the mixed solvents*

As is already known,[4] log values of protonation constants for 2-(carboxymethylthiophenylazo)-5-nitrotoluene (in 0.1 mol dm^{-3} $NaClO_4$, at 25°C) in dioxane–water mixed solvents change with dioxane content according to the Born equation. This is not the case with the stability constants of the copper(II) complexes of this ligand in the same ionic medium; neither $\log \beta_1$ nor $\log \beta_2$ show linear variation with the reciprocal of relative permittivity of the solvent; linearity is not observed either as a function of the dioxane mole fraction in the solvent. This behaviour shows, as it has been repeatedly observed,[17,18] although not as a general rule,[19] that complex formation is not governed by electrostatic factors alone. It is observed, however, that the stability of the copper complexes (1:1 and 1:2) grows bigger the higher is the dioxane content in the solvent, paralleling what happens with the observed stability of the proton–ligand complex. This is not a general behaviour of all known systems.[20,22]

Changes in $\log \beta$ [for protonation and copper(II) complex formation] in going through a range of dioxane content from 50 to 75% (v/v) in the solvents, all of them containing 0.1 mol dm^{-3} $NaClO_4$, cannot be assigned to the variation in the ionic strength of the medium caused by the different degree of ionic association which can be present in media with rather different relative permittivities. According to the classical Bjerrum expression for ionic association,[23] on account of the rather high value of the perchlorate ionic radius, ionic association effects in these solutions containing a moderate concentration of background electrolyte are of a minor importance, and their variation with relative permittivity cannot explain the observed deviations from linearity.

Other effects directly deriving from the varying dioxane content in the solvent can modify, even at constant ionic strength, the activity coefficients for the species involved in the equilibria under study, and hence the numerical values of their equilibrium constants. The effect of some solvent properties on the ionic atmosphere can be accounted for using the Davies equation to convert to zero ionic strength the values determined at 0.1 mol dm^{-3} ionic strength. If the value of the ion-size parameter a is taken as equal to 6 for copper(II) ion and to 8 for the arylthioacetate anion and the 1:1 cationic complex, and the appropriate values for the relative permittivity of the solvent mixture are introduced into the Davies equation, ionic activity coefficients can be evaluated. For the complex-forming equilibria (ionic solvation ignored): $M + iL \rightleftarrows ML_i$, the "thermodynamic" stability constants will be given, for the 1:1 complex, by: $\log(\beta_1)_{therm} = \log(\beta_1)_{conc} - \log \gamma_{Cu^{2+}}$, and for the 1:2 complex, by: $\log(\beta_2)_{therm} = \log(\beta_2)_{conc} - \log \gamma_L - 2 \log \gamma_{Cu^{2+}}$. Substitution yields the following values: in 50% dioxane–water, $\log(\beta_1)_{therm} = 3.39$ and $\log(\beta_2)_{therm} = 8.22$; in 60% dioxane–water, 4.73 and 9.47, respectively; and in 75% dioxane–water, 7.03 and 11.66, respectively. These values show a correlation with the reciprocal of relative permittivity which approaches linearity much more than the concentration constants, but it is not yet a linear correlation.

Dioxane content affects too the activity coefficients of both constituents of the solvent, particularly that of water. Since in the complex formation reaction water molecules are displaced by the ligand from the solvation sphere of metal ions, water should not be ignored in the formulation of equilibria and of equilibrium constants. Thus, for the 1:1 complex, the equilibrium would be: $Cu(H_2O)_x^{2+} + L^- \rightleftarrows [Cu(H_2O)_{x-n}L]^+ + nH_2O$, and in the formulation of equilibrium constants, water activity (with activity coefficients which vary from one solvent to another) would be explicitly included.

There are not in the literature the data needed for the evaluation of water activity coefficients in mixed solvents of the type studied here.[24] Another further complicating effect arises from the displacement of water by dioxane in the solvation sphere of the copper(II) ion.[25]

Inferences about the donor groups involved in 1:1 *and* 1:2 *complexes*

The fact that the maximum copper(II) complex detected is the 1:2 complex strongly suggests that the ligand acts as a bidentate one. To elucidate which groups in the ligand molecule effectively act as donors is a difficult matter.

If these groups were the carboxylate anion and the thioether sulphur, stability constants for the 1:2 complexes would be of about the same magnitude as those for other 1:2 copper(II) complexes of aryl- and alkylthioacetates. Since in the literature only a few of these constants are found, obtained from aqueous solutions and at several different ionic strengths, comparison cannot be made in a direct way. By a rough extrapolation of the results obtained here to a zero-dioxane content, an approximate value of $\log \beta_2 = 4.8$ is found, which can be considered to be in agreement with published values.[26]

It is surprising that the results suggest that the azo-group is not involved in the co-ordination of copper(II) ion, when it is well known that this group acts as a co-ordinating centre in the rather stable copper(II) complexes formed by azocompounds with *ortho*-substituents with donor properties. It could be assumed that the present ligand could act as terdentate in the 1:1 complex, the azo group being involved in this complex in the binding of copper ion. When this complex would add a new ligand molecule to form the 1:2 complex, the new carboxylate and thioether groups would displace the azo-nitrogen of the first co-ordinated molecule (and one solvent molecule) from the coordination sphere of copper(II) ion. If this assumption is valid, the stability of the 1:1 complex (which would contain two chelate rings) should be much higher than that of 1:1 copper(II) complexes of aryl- and alkylthioacetates (which form only one chelate ring). In aqueous solution, the latter have $\log \beta_1$ in the range 2.4–2.6; the extrapolation to zero-dioxane content of the results obtained in the present work for the former yields a very much lower value. The extrapolated value is very uncertain but, anyway, the underlying assumption must be rejected.

The lower stability of the 1:1 complex as compared with 1:1 copper complexes of aryl- and alkylthioacetates can be explained from the results obtained from the experiments performed at constant pH [procedure B, copper(II) ion-selective electrode measurements]. As has been shown, the results obtained for $\log \beta_1$ at pH 6.35 agree with those obtained from the acid–base titration technique; in contrast, the interpretation of results from experiments at pH 2.59 offer some difficulty. If it is assumed that at this pH 2.59 the 1:1 complex is predominantly formed (*vide infra*), and that practically all the ligand in the solution is present in its protonated form (its pK_a in 60% dioxane–water solution is 5.53), complex formation will be represented by the equation: $Cu + HA = Cu(HA)$. Under this assumption, data treatment yields a value of $\log \beta_1$ which coincides with that obtained from acid–base titrations. If the carboxyl group is not ionized, it does not participate in binding of copper(II) ion, and complex formation will take place through the thioether-sulphur and the azo-nitrogen donors. If the assumption were made that in the presence of copper(II) ion, this one displaces the carboxylic proton, even at pH 2.59, so that the complex-forming process is: $Cu + HA = CuA^- + H^+$, then, data treatment would require the use of the free unprotonated ligand concentration, and the result for $\log \beta_1 = 6.32$.

It must be noted that in the titrations performed at constant pH 2.59 (using as titrant a ligand solution), the formation degree $\bar{n} = 0.5$ for the system is never exceeded. It is difficult to accept that at this pH under the used conditions the 1:2 complex is formed in any noticeable amount. Experimental data treatment for a two-complex model yields very deficient results for $\log \beta_2$.

REFERENCES

1. M. Born, *Z. Physik* 1920, **1**, 45.
2. H. Irving and H. S. Rossotti, *Acta Chem. Scand.* 1956, **10**, 72.
3. L. G. Van Uiter, C. G. Hass, W. C. Fernelius and B. E. Douglas, *J. Am. Chem. Soc.* 1953, **75**, 455.
4. E. Casassas and J. Alió, *Anales (B)* 1984, **80**, 361.
5. J. Alió and E. Casassas, *Quim. Anal.* 1983, **2**, 145.
6. F. Gaizer, T. B. Tran and K. Burger, *J. Inorg. Nucl. Chem.* 1974, **36**, 1601.
7. A. Gergely, I. Nagypál, T. Kiss and R. Kiraly, *Magy. Kém. Foly.* 1974, **80**, 181.
8. E. Grunwald, in *Electrolytes* (Edited by B. Pesce), p. 62. Pergamon, Oxford (1962).
9. W. A. E. McBryde, K. K. Mui and E. Nieboer, *Abstracts* IV *Inter. Conf. Non-Aq. Solutions* (Edited by V. Gutman), p. 10. Vienna (1974).
10. K. K. Mui and W. A. E. McBryde, *Can. J. Chem.* 1974, **52**, 1821.
11. I. Nagypál and M. Y. Beck, *Magy. Kém. Foly.* 1975, **81**, 117.

12. F. Gaizer and H. B. Silber, *J. Inorg. Nucl. Chem.* 1980, **42**, 1317.
13. E. Casassas and J. Alió, *Anales (B)* 1984, **80**, 498.
14. G. Gran, *Analyst* 1952, **77**, 661.
15. L. G. Sillén, *Acta Chem. Scand.* 1956, **10**, 203.
16. F. J. C. Rossotti and H. S. Rossotti, *The Determination of Stability Constants*, p. 90. McGraw-Hill, New York (1916).
17. T. F. Rudometkina, V. M. Ivanov and A. I. Busev, *Zh. Anal. Khim.* 1977, **32**, 1674.
18. A. K. Chaudhury and N. Kole, *J. Indian Chem. Soc.* 1981, **58**, 368.
19. K. Burger, *Solvation, Ionic and Complex Formation Reactions in Non-Aqueous Solvents*, p. 231. Elsevier, Amsterdam (1983).
20. F. Gazier, P. Buxbaum, E. Papp-Molnar and K. Burger, *J. Inorg. Nucl. Chem.* 1974, **36**, 859.
21. F. Gazier, T. T. Binh and K. Burger, *J. Inorg. Nucl. Chem.* 1974, **36**, 1601.
22. Y. K. Agrawai, *Monatsh. Chem.* 1977, **108**, 713.
23. N. Bjerrum, *Z. Anorg. Allgem. Chem.* 1921, **119**, 179.
24. G. Garaglia, F. J. C. Rossotti and H. S. Rossotti, *Inorg. Chim. Acta* 1970, **4**, 488.
25. Ref. 19, p. 211.
26. L. D. Pettit *et al.*, *J. Chem. Soc.* (*A*) 1968, 2204; 1968, 3078; 1969, 2073; 1971, 2883; 1972, 1763.

Polyhedron Vol. 4, No. 5, pp. 869–873, 1985
Printed in Great Britain

0277-5387/85 $3.00 + .00
© 1985 Pergamon Press Ltd

SYNTHESIS OF CHLORO-CARBONYL DERIVATIVES OF RHENIUM, RUTHENIUM, RHODIUM, IRIDIUM AND PLATINUM VIA REACTION OF THE METAL ATOMS WITH OXALYL CHLORIDE

PAUL R. BROWN, F. GEOFFREY N. CLOKE and MALCOLM L. H. GREEN*
Inorganic Chemistry Laboratory, South Parks Road, Oxford OX1 3QR, U.K.

(*Received* 29 *August* 1984; *accepted* 26 *September* 1984)

Abstract—Co-condensation of atoms of Re, Ru, Rh, Ir and Pt with oxalyl chloride gives metal chloro-carbonyl derivatives which may be used as precursors to the compounds $[Re(CO)_4Cl]_2$, $[Ru(PMe_3)_3(CO)Cl_2]$, α-$[Ru(CO)_3Cl(\mu\text{-}Cl)]_2$, $[Ru(PPh_3)_2(CO)_2Cl_2]$, $[Rh(CO)_2(\mu\text{-}Cl)]_2$, $[Rh(PPh_3)_2COCl]$, $[Ir(PPh_3)(CO)_2Cl_3]$ and *cis*-$Pt(CO)_2Cl_2$. Molybdenum atoms with oxalyl chloride give molybdenum-chloro derivatives.

Atoms of the more refractory transition metals are highly reactive. We have studied their reactions with oxalyl chloride in the expectation that chloro-carbonyl derivatives would be formed. This work is described here: a brief communication of part of this work has already appeared.[1]

RESULTS AND DISCUSSION

Co-condensation of rhenium atoms with oxalyl chloride and extraction of the products with tetrahydrofuran (THF) gave a red–brown solution which contained little unreacted metal. A large quantity of white crystals of the dimer $[Re(CO)_4(\mu\text{-}Cl)]_2$ (**1**)[2] were obtained from the reaction mixture in high yield, > 80%. This reaction represents a very convenient synthesis of **1** on a scale of 5–10 g per experiment.

Co-condensation of ruthenium atoms with oxalyl chloride gave a red THF extract and some insoluble green solid (**2**). When the THF solution was left standing for several days, or was treated with chloroform, a green solid separated. Removal of the THF gave a red oil which gave a green solid upon heating *in vacuo* or when washed with chloroform. The red oil showed bands in the IR spectrum assignable to terminal CO groups at 2150m, 2085s, 2025s and 1960s,br (mull). Due to the inability to further purify the compound it was not further characterised. The IR spectrum (mull) of the green solid (**2**) gave CO stretches at 2142w, 2079s, 2018s and 1970m,br. Microanalysis of the precipitated green solid showed the consistent presence of about 1.8% hydrogen and corresponded approximately to a stoichiometry of $[Ru(CO)_2Cl_2(THF)]_n$. Insolubility and involatility precluded further purification and obtaining NMR and mass spectral data.

Compound **2** was treated with carbon monoxide to give the dimer α-$[Ru(CO)_3Cl(\mu\text{-}Cl)]_2$ (**3**) in good yield. **3** was identified by the mass spectrum and by comparison of the IR spectrum with that of an authentic sample.[3] Treatment of **2** with triphenyl-phosphine gave white, air-stable, crystals of $[Ru(PPh_3)_2(CO)_2Cl_2]$ (**4**).[4]

Co-condensation of rhodium atoms with oxalyl chloride gave a bright red solid (**5**) which was highly reactive towards acetone and THF. It was unchanged by dichloromethane, chlorobenzene and hydrocarbons in which it was insoluble. Solutions in chloroform gave a brown precipitate within minutes.

The observation of seven distinct bands assignable to terminal carbonyl ligands suggests that **5** is complex or a mixture. Because of the reactivity and insolubility of **5** it was not possible to obtain sufficient information to characterize it further. Repeated microanalysis of **5** gave variable results showing *ca* 2% of hydrogen present. The only source of hydrogen was the dichoromethane used to wash the product from the metal vapour synthesis apparatus.

Treatment of **5** with carbon monoxide gave the well-known dimer, $[Rh(CO)_2(\mu\text{-}Cl)]_2$ (**6**).[5] Treatment of **5** with triphenylphosphine gave yellow, air-stable $[Rh(PPh_3)_2(CO)Cl]$ (**7**). The IR spectrum of compound **7** showed a band at 1969 cm^{-1},

* Author to whom correspondence should be addressed.

assignable to a terminal CO stretch. This compares well with the literature value.[6]

Co-condensation of iridium atoms with oxalyl chloride gave an orange solution together with a large quantity of an insoluble orange solid (**8**). Compound **8** was insoluble in all common solvents except acetone and THF, with which it instantly reacted. The IR spectrum of **8** showed bands at 2155w, 2120s and 2080s cm^{-1}. Since **8** could not be purified or further characterised spectroscopically some reactions were studied.

Treatment of **8** with triphenylphosphine gave white, air-stable crystals which were insoluble in hydrocarbon solvents but soluble in chlorobenzene, THF, diethyl ether and dichloromethane. The IR spectrum (mull) showed the bands assignable to $\nu(C{\equiv}O)$ at 2140s, 2103s and 2096s. However, the solution IR (THF) shows two bands assignable to terminal carbonyl stretching frequencies, at 2060 and 2036 cm^{-1} and the small separation of 24 cm^{-1} is unusually low. Normally the separation would be expected to be 60–80 cm^{-1}. However, the few compounds of this class which have been reported have been shown to have such a difference between the two terminal carbonyl stretching frequencies. For example, for $Ir(PPh_3)(CO)_2D_3$, where the difference between the carbonyl frequencies is only 17 cm^{-1}.[7] Microanalysis corresponded to the compound $[Ir(PPh_3)(CO)_2Cl_3]$ (**9**). Only a few dicarbonyl compounds of this type are known.[8,9]

Co-condensation of platinum atoms with oxalyl chloride gave colourless crystals of *cis*-$Pt(CO)_2Cl_2$ (**10**) in high yield. This compound was accidently described as the *trans*-isomer in Ref. 1. The authentic *trans*-$Pt(CO)_2Cl_2$ has recently been described.[10]

Co-condensation of molybdenum atoms with pure oxalyl chloride followed by extraction of the products with THF gave an orange–brown solution and there was no evidence for the presence of unreacted metal. The product could be separated into a THF-soluble orange–brown solution and a pink solid (**11**). The IR spectrum of **11** showed no evidence for the presence of carbonyl ligands. The data show the compound **11** to be the previously described $MoCl_3(THF)_3$.[11]

The IR spectrum of the solid obtained by removal of THF from the orange extract showed no bands assignable to carbonyl ligands. The solid was treated with PEt_3 giving dichroic, blue, crystals, which were identified (IR spectrum) as the binuclear compound $[MoCl_2(PEt_3)_2]_2$ (**12**).[12]

The metals were vapourised from a positive-hearth electron-gun furnace using a "bell-jar" reactor vessel, as described elsewhere.[13] In all the reactions no difficulty was experienced in vaporising the elements on a scale of several grams. In the metal atom reactions with oxalyl chloride it is not possible to identify whether the reactions involve simply isolated atoms, or, whether metal aggregates are formed upon warming and which subsequently react with the oxalyl chloride. Whatever the case, in all the reactions there was none or very little unreacted metal recovered from the initial reaction mixtures. In contrast, metal atom reactions often result in recovery of up to half of the metal vaporised from the furnace. Except for the platinum and rhenium atom reactions the initial metal-carbonyl products, although formed in high yield, were extremely sensitive to common solvents, involatile and rather intractable. However, in every case they could be reacted with donor ligands such as tertiary phosphines giving discrete chloro-carbonyl derivatives, again in high yields. It is clear that the initial carbonyl species are likely to be useful precursors for the synthesis of a range of carbonyl derivatives. In this work we were primarily concerned with finding whether oxalyl chloride provided a source of metal-carbonyl compounds and we have not tried further to study derivatives of the initial reactive products.

We conclude that compounds **1** and **10** are very conveniently available by this metal atom route. Further, the reactive chloro-carbonyl derivatives of ruthenium, niobium and iridium formed initially in the atom reactions with oxalyl chloride are useful synthetic precursors.

EXPERIMENTAL

All preparations, reactions and purifications, other than metal vapour synthesis reactions, were carried out under an inert atmosphere of nitrogen or argon unless otherwise stated.

The drying and purification of solvents was achieved by refluxing over a suitable drying agent followed by distillation under an atmosphere of nitrogen. Oxalyl chloride was purified by distillation under vacuum. Precious metal samples were received as powders and, in a separate operation, were melted into ingots, using the positive-hearth electron gun furnace, before use in the co-condensation experiments. The apparatus used in the metal atom synthesis experiments and the general procedures are described in Ref. 13.

Microanalyses were performed by the analytical department of the Inorganic Chemistry Laboratory or at Alfred Bernhardt Laboratory, in the case of very air-sensitive samples. IR spectra were recorded on a Pye–Unicam SP2000 double beam, grating spectrophotometer in the range 4000–200 cm^{-1} and were calibrated using polystyrene film. Proton NMR spectra were recorded on a JEOL MX60 (60 MHz) or a Brucker WH300 (300 MHz) spectrometer. Mass

spectra were recorded using an A.E.I. MS 902 spectrometer calibrated using PFK.

Reaction of rhenium atoms with oxalyl chloride: the preparation of **1**

Rhenium atoms (1.84 g, 9.9 mmol), evaporated from a rhenium ingot of 11.55 g at a power of 2.1 kW (6 kV at 350 mA), were co-condensed with oxalyl chloride (50 g, 0.40 mol) for 3.5 h. The vacuum during the co-condensation was 4×10^{-5} mbar. During the co-condensation the matrix slowly became orange–red but on warming at the end of the experiment the co-condensate became pale green. However, the product of the reaction emerged from the reaction chamber as a red solution in the excess oxalyl chloride together with some red solid. The product was washed from the reaction chamber with dichloromethane (200 cm^3) in which the product was slightly soluble. There appeared to be no unreacted metal present so the extract was not filtered. After the removal of the volatile components under reduced pressure there remained an oily red–brown solid.

Chlorobenzene (150 cm^3) was then added giving a slightly red solution which was heated to 70°C for 4 h. The solution was filtered from the residual solids, whilst still at 70°C, giving a red–orange solution. On cooling, a large quantity of pale crystals were deposited. The solution was allowed to cool to room temperature (r.t.) and left overnight. The supernatant liquor was then decanted from the crystals which were washed with chlorobenzene (2×10 cm^3) and petroleum ether (10 cm^3 : 100–120°C) and finally dried *in vacuo*.

This material was further purified by sublimation (140°C, 10^{-2} mbar), giving a white sublimate of pure **1**. IR spectrum, CCl_4: 2114w, 2025s, 1999m, 1967m.

Reaction of ruthenium atoms with oxalyl chloride: preparation of α-$Ru_2(CO)_6Cl_4$ *and* $Ru(PPh_3)_2(CO)_2Cl_2$

In a typical experiment, ruthenium atoms (1.40 g, 13.9 mmol) generated from a ruthenium ingot of 8.65 g at a power of 900 W (4.5 kV at 200 MA) were co-condensed with oxalyl chloride (45 g, 0.35 mol) for 4 h. The vacuum in the apparatus during the co-condensation was poor (*ca* 3×10^{-4} mbar) presumably due to the formation of carbon monoxide. The matrix during the co-condensation was orange–brown and colour persisted on warming to r.t. The product emerged from the apparatus as a deep red oxalyl chloride solution together with a small quantity of light green solid (**2**). The remaining product was washed from the apparatus with THF (200 cm^3), giving a red solution. In some of the preparations all of the light green solid would dissolve, in others a small quantity of this solid would persist. In no case was any unreacted metal observed in the extracts.

The volatile components were then removed from the solution under reduced pressure giving a red oil. This was redissolved in THF (100 cm^3) and the solution filtered free from residual solids. Chloroform (100 cm^3) was added to the filtrate causing the solution to become cloudy. After 1 h a green precipitate had separated and the solution became colourless. The solution was then decanted from the solid which was washed with 60–80°C petroleum ether (2×20 cm^3). The solid was dried *in vacuo*, giving a light green powder (**2**). Analysis (%): C, 17.7; H, 1.8; Cl, 27.1.

Preparation of **3**. The green solid (**2**) (200 mg) in THF (40 cm^3) was placed under carbon monoxide (1 atm). There was no immediate reaction at r.t. but after 1 day the solution had become light brown. Over 6 days the intensity did not change but the green solid slowly dissolved. The volatile components were removed under reduced pressure giving a light brown, waxy solid. This was sublimed (100°C, 10^{-2} mbar) giving a white sublimate of pure $[Ru(CO)_3Cl_2]_2$. IR in chloroform: 2132s, 2066s, 2016w cm^{-1}, which is identical to an authentic sample.[3]

Preparation of **4**. A suspension of the green solid (**2**) (0.2 g) in THF (50 cm^3) was treated with triphenylphosphine (1 g, 4 mmol) in THF (10 cm^3). The green solid rapidly dissolved and after 5 min the solution was concentrated (to 10 cm^3). Petroleum ether (40–60°C, 300 cm^3) was added causing precipitation of a white solid. This was collected and washed with petroleum ether (2×50 cm^3, 40–60°C) and dried *in vacuo*. The solid was dissolved in THF (30 cm^3), the solution filtered and the filtrate was concentrated (to 10 cm^3). On cooling to −30°C white crystals separated which were collected, were washed with diethyl ether (2×5 cm^3) at −30°C and dried *in vacuo*.

IR spectrum (mull): 2065 and 1997 cm^{-1} (cf. published values,[4] 2064 and 2001 cm^{-1}). Analysis (%): C, 60.6 (59.3); H, 4.0 (3.9); Cl, 9.4 (9.7).

Reaction of rhodium atoms with oxalyl chloride: preparation of $[Rh(CO)_2(\mu\text{-}Cl)]_2$

In a typical experiment, rhodium atoms (0.63 g, 6.1 mmol), generated from a rhodium ingot of 5.8 g at a power of 800 W (4 kV at 200 mA), were co-condensed over 3.5 h with oxalyl chloride (55 g, 0.43 mol). The vacuum during the co-condensation was very good (4×10^{-5} mbar). The co-condensate was red but on warming became light green. The colour of the

matrix again changed as it melted to a deep red. The product emerged from reaction chamber as an insoluble red solid suspended in the excess of oxalyl chloride. The chamber was flushed with dichloromethane (200 cm^3) to extract the insoluble solid. The product solids contained no visible evidence of metal. The solvents were removed under reduced pressure giving a slightly oily solid. This was washed with petroleum ether (2 × 50 cm^3, 40–60°C) and dried *in vacuo*, giving a scarlet powder (**5**) which was used in the experiments described below. Analysis (%): Cl, 32.7; C, 11.0; H, 2.2.

Preparation of **6**. A scarlet suspension of **5** (200 mg) in chloroform (50 cm^3) was treated with carbon monoxide (1 atm). Immediately the mixture turned orange–red and after 5 min all the solid dissolved. The volatile components were removed under reduced pressure and the resulting orange–red waxy solid was sublimed (100°C, 10^{-2} mbar), giving an orange–red sublimate of pure **6**, *ca* 80%.

Preparation of **7**. A suspension of **5** (500 mg) in chlorobenzene (30 cm^3) was treated with triphenylphosphine (3 g, 11.5 mmol) in chlorobenzene (20 cm^3). The mixture was then stirred at r.t. and the solution rapidly became orange. Within 90 min all the solid dissolved. The solution was filtered into petroleum ether (300 cm^3, 40–60°C), giving an orange precipitate. This was washed with petroleum ether (2 × 50 cm^3, 40–60°C) and dried *in vacuo*. The orange powder was dissolved in hot acetonitrile (200 cm^3, 60°C) and after filtration the filtrate was cooled giving crystals of $Rh(PPh_3)_2(CO)Cl$. These were washed with acetonitrile (2 × 5 cm^3) and dried *in vacuo*. Yield > 80%.

The reaction of iridium atoms with oxalyl chloride

Iridium atoms (1.62 g, 8.4 mmol), generated from an iridium ingot of 10.36 g at a power of 1.5 kW (5 kV at 300 mA), were co-condensed for 4 h with oxalyl chloride (35 g, 0.28 mol). During the co-condensation the pressure in the apparatus was 8×10^{-5} mbar and the matrix slowly developed a deep orange colour. This colour persisted as the matrix warmed and melted. The product emerged from the apparatus as an orange solid suspended in the unreacted oxalyl chloride. The solids were flushed from the reaction chamber with dichloromethane (300 cm^3). The product receiver was then changed and the chamber was flushed with THF (200 cm^3). This produced a deep grey–green solution. The two product mixtures were treated separately. The volatile components of the orange extract were removed under reduced pressure giving a slightly sticky orange solid (**8**). This was washed with petroleum ether (2 × 50 cm^3, 40–60°C) and dried *in vacuo*.

The volatile components were then removed from the grey–green solution giving a dark green oily solid. This was washed with toluene (2 × 50 cm^3) and petroleum ether (50 cm^3, 40–60°C) and dried *in vacuo*. However, the product remained as a dark green oily solid.

Preparation of **9**. A suspension of **8** (500 mg) in chlorobenzene (50 cm^3) was treated with triphenylphosphine (2 g, 7.6 mmol) in chlorobenzene (20 cm^3), giving a pale orange solution. This was filtered into petroleum ether (300 cm^3, 40–60°C) giving a light orange precipitate, which was collected and the solid was washed with petroleum ether (2 × 50 cm^3, 40–60°C) and dried *in vacuo*. The solid was dissolved in chlorobenzene (100 cm^3) at 60°C and after filtration the filtrate was allowed to slowly cool to r.t. giving silvery-white crystals which were washed with petroleum ether (2 × 20 cm^3, 100–120°C) and dried *in vacuo*, yield 750 mg. Analysis (%): C, 39.9 (38.9); H, 2.4 (2.4); Cl, 16.9 (17.2).

The reaction of patinum atoms with oxalyl chloride: preparation of **10**

Platinum atoms (1.32 g, 6.8 mmol), generated from a 9.87 g ingot of platinum at a power of 1.5 kW (5 kV at 300 mA), were co-condensed with oxalyl chloride (35 g, 0.28 mol) over 4 h. The matrix was pale orange but on warming became colourless. The product emerged from the reaction chamber as a colourless solution and was washed out with benzene (200 cm^3). There was only a trace of unreacted metal. The volatile components were removed under reduced pressure giving a very pale orange solid. This was sublimed (60°C, 10^{-4} mbar), giving a white sublimate. The compound was characterised by comparison of the IR spectrum with an authentic sample and by the mass spectrum [M/z (^{195}Pt, ^{35}Cl) 322].

Reaction of molybdenum atoms with oxalyl chloride: preparation of **11** *and* **12**

Molybdenum atoms (1.01 g, 10.5 mmol) were evaporated from a 7.7 g ingot of molybdenum and co-condensed with an excess of oxalyl chloride (45 g, 0.35 mol) for 4.5 h. The power used to generate the molybdenum atoms was 800 W (4 kV at 200 mA) and the vacuum in the apparatus during the co-condensation was *ca* 4×10^{-4} mbar. The resulting co-condensate matrix was deep red–brown and this colour persisted when the matrix was warmed to r.t. The product emerged from the reaction chamber as a slurry of red–brown solid in the excess oxalyl chloride. Initially, the reaction chamber was washed with toluene, in which the product appeared to be

insoluble. Further washing with THF (250 cm^3) was found to dissolve the product. The volatile components were removed from the combined washing under reduced pressure leaving a red–brown oil, This was washed with toluene (2 × 50 cm^3) and 40–60°C petroleum ether (2 × 50 cm^3) and dried *in vacuo*. THF (100 cm^3) was then added to the resulting oil giving a deep orange–brown solution and an insoluble pink solid. The solid was filtered and the residual solid was washed with THF and dried *in vacuo*. The pink solid and the filtrate were then treated separately.

The pink solid was recrystallized from hot THF (100 cm^3) giving red, microcrystalline **11** by comparison with an authentic sample.[11] IR data, Nujol mull: 1355w, 1258w, 1186w, 1050m, 1009s, 965, 930m, 859s. Analysis (%): C, 18.6; H, 3.5; Cl, 29.3.

Triethylphosphine (3 g, 25 mmol) was added to the orange–brown solution. The mixture was warmed to 60°C for 2 days and became dichroic red–blue. After filtration the solution was concentrated and cooled to −30°C for 12 h giving blue crystals, which were washed with THF and dried *in vacuo*. The yield of **12**[12] was *ca* 35%.

Acknowledgements—We thank Johnson–Matthey plc for a generous loan of precious metal samples. We thank the donors of the Petroleum Research Fund, administered by the American Chemical Society for partial support. We thank the British Petroleum (Chemicals) plc for support (to P.R.B.).

REFERENCES

1. P. R. Brown, F. G. N. Cloke, M. L. H. Green and R. C. Tovey, *J. Chem. Soc., Chem. Commun* 1982, 519.
2. J. C. Hileman, D. K. Huggins and H. D. Kaesz, *Inorg. Chem.* 1962, **1**, 933.
3. B. F. G. Johnson, R. D. Johnston and J. Lewis, *J. Chem. Soc. (A)* 1969, 792.
4. K. Stephenson and G. Wilkinson, *J. Inorg. Nucl. Chem.* 1966, **28**, 945.
5. J. A. McCleverty and G. Wilkinson, *Inorg. Synth.* 1966, **8**, 211.
6. J. A. McCleverty and G. Wilkinson, *Inorg. Synth.* 1966, **8**, 213.
7. L. Malatesta, M. Angoletta and F. Conti, *J. Organomet. Chem.* 1971, **33**, 543.
8. J. P. Collman, F. D. Vastine and W. R. Roper, *J. Am. Chem. Soc.* 1968, **90**, 2282.
9. A. J. Drakesmith and R. Wyman, *J. Chem. Soc., Dalton Trans.* 1973, 362.
10. D. B. Dell'Amico, F. Calderrazzo, C. A. Veracini and N. Zandona, *Inorg. Chem.* 1984 (in press).
11. M. A. Anker, J. Chatt, G. J. Leigh and A. G. Wedd, *J. Chem. Soc., Dalton Trans.* 1975, 2639.
12. M. L. H. Green, G. Parkin, J. K. Bashkin, J. Fail and K. Prout, *J. Chem. Soc., Dalton Trans.* 1982, 2519.
13. F. G. N. Cloke and M. L. H. Green, *J. Chem. Soc., Dalton Trans.* 1981, 1938; M. L. H. Green, *J. Organomet. Chem.* 1980, **200**, 119.

Polyhedron Vol. 4, No. 5, pp. 875–877, 1985
Printed in Great Britain

0277–5387/85 $3.00 + .00
© 1985 Pergamon Press Ltd

A NEW METHOD FOR THE PREPARATION OF Ru(IV) IN NON-COMPLEXING ACID MEDIUM: EVIDENCE FOR TETRAMERIC Ru(IV)

J. P. DELOUME,* G. DUC and G. THOMAS-DAVID
Laboratoire de Chimie Analytique II, Université Claude Bernard, Lyon I, 43 Boulevard du 11 Novembre 1918, 69622 Villeurbanne Cedex, France

(*Received* 20 *June* 1984; *accepted* 10 *October* 1984)

Abstract—A new method for the preparation of Ru(IV) in acid solutions is described. This method, avoiding the preparation of the highly reactive RuO_4, is based on the stoichiometric oxidation of Br^- ion of K_2RuBr_6 by BrO_3^- ion. Easy to control and reproducible the process leads to solutions of a well-known composition consisting of the tetrameric Ru(IV) ion.

Lack of reproductibility in Ru(IV) studies arise in most cases from the ruthenium(IV) solutions themselves, owing to their method of preparation. The main method consists in distilling and dissolving ruthenium tetroxide in either aqueous acid solutions or organic solvent. The Ru(VIII) is then reduced by electrochemical[1,2] or chemical[3,4] means. Hydrogen peroxide is currently the most used reducing agent. The reaction is uncontrollable and despite the slow addition of the reagent, oxygen evolves and sweeps some tetroxide. The knowledge of the composition of the final solution requires the titration of total ruthenium and titration of the oxidizing power of the solution, operations which are not very accurate. Nevertheless this method leads to solutions containing only Ru(IV) ion and the counter-ion of the strong acid.

We have worked out a new method avoiding the preparation of RuO_4, leading to a solution of known composition and a procedure which is easily reproducible.

PRINCIPLE OF THE METHOD

The potassium hexabromo ruthenate(IV) (K_2RuBr_6) is used as starting material. The method is based on the stoichiometric oxidation of bromide ions of $RuBr_6^{2-}$ by bromate ion in acid medium. Bromine, the resulting product of the oxidation is evolved from the solution and is displaced by a flow of inert gas. It is worth noting that the balance of the reaction depends on the nature of Ru(IV) ions in the solution. From previous results[2,3,5] on Ru(IV) ion we can write three overall reactions:

$$5RuBr_6^{2-} + 6BrO_3^- + 36H^+ \rightarrow 5Ru^{4+} + 18H_2O + 18Br_2 \quad (1)$$

$$5RuBr_6^{2-} + 6BrO_3^- + 26H^+ \rightarrow 5RuO^{2+} + 13H_2O + 18Br_2 \quad (2)$$

$$5RuBr_6^{2-} + 6BrO_3^- + 21H^+ \rightarrow \tfrac{5}{4}Ru_4O_6^{4+} + \tfrac{21}{2}H_2O + 18Br_2. \quad (3)$$

If titration of protons can be made with sufficient accuracy, we can get direct knowledge of Ru(IV) ion in such solutions.

EXPERIMENTAL

(a) Preparation of K_2RuBr_6: this salt is prepared according to the method of Ferguson and Greenaway.[6] Purity controls are provided by two different ways. First, X-ray powder diffraction photographs show a single phase ($a = 10.299$ Å) without $K_3Ru_2Br_9$[6] or $K_4Ru_2OBr_{10}$. Secondly, we estimate potassium, which is the easiest element to determine, by flame emission spectroscopy. The standardization of the spectrometer is achieved with solutions of potassium bromide containing ruthenium (from hydrated ruthenium trichloride) in the ratio [K]/[Ru] = 2.

(b) The oxidizing solution is prepared from sodium bromate (analytical reagent grade) by weighing known amounts of dried salt and dissolving in

* Author to whom correspondence should be addressed.

the appropriate volume to obtain a solution of *ca* 1 mol l^{-1}.

The acid medium is prepared in the usual way with the selected acid (methanesulfonic acid, analytical reagent grade).

Experiment leads as follows to a final solution 6×10^{-2} mol l^{-1} in Ru(IV); oxidizing solution (1.005 mol l^{-1}) is placed in an automatic titrator Tacussel EXB provided with a 5 cm^3 syringe (rather than a 10 cm^3 one, because of the speed of the plunger). 60.0 cm^3 of acid solution (2.000 mol l^{-1}) are introduced from a pipette into the reaction flask, stirred and bubbled with a nitrogen flow, the needle of the syringe being level with the solution. Then, we quickly pour K_2RuBr_6 salt into the solution as we start adding the bromate ion at the rate of 1 μl per second.

Here, we introduce 4.9965 g of K_2RuBr_6 (658.7 g/mol^{-1}), e.g. 7.585×10^{-3} mol which needs 9.102×10^{-3} mol of bromate ion contained in 9.057 cm^3 of solution.

Bromine vapour appears quickly and evolves continuously during the addition. As stoichiometry is reached we stop the titrator. Nitrogen is bubbled for one hour, then the solution is heated to 50–60°C for one further hour. This solution is cooled to room temperature and transferred, with rinsing water in a 125 cm^3 flask. At this time we can add an exact quantity of acid to obtain the required acidity, since we know the exact number of consumed protons in the reaction. Here the required final acidity is 1.5 mol l^{-1}. The flask is then adjusted to the mark.

ANALYTICAL

We need to know the bromine content which can exist as bromide ion, bromine or bromate ion. Consequently we have to use a reducing agent, which does not interfere with the titration method, to convert higher oxidation states of bromine into bromide ions. This ion is titrated by argentimetric (coulometric) method with an ordinary silver/mercurous sulphate potentiometric detector in 50–50 water–methanol medium. Synthetic solutions of known amounts of bromide and bromate ions were used to check the efficiency of the reducer (hydrazine) and of the electrolytic current. Ruthenium must be eliminated from the solution before titration by precipitation of ruthenium hydroxide and filtration; the basic solution is then acidified and processed as a synthetic one.

The oxidation state of ruthenium is determined after reduction of ruthenium(IV) by iodide ion. The classical method[1] is made easier by distillation of iodine under nitrogen in a solution of iodide ion and then titrated by thiosulphate standardized in the same way.

The acidity measurement is carried out by the Gran's method. Before each run we take care to determine correspondence between the pH read and $-\log [H^+]$ by titrating solutions of strong acid of the same ionic strength as the one of the ruthenium solution.

RESULTS AND DISCUSSION

(*a*) *Bromine content*

The results obtained with four different preparations are summarized in Table 1. They show that the average content in bromine is 3 or 4 bromine atoms per 100 ruthenium atoms. The ratio of this bromine concentration to the theoretical initial bromine concentration is 0.5% which corresponds to the accuracy of a volumetric method as the one used for this preparation.

(*b*) *Oxidation state*

In this new method, total concentration of ruthenium is exactly known from the weight of K_2RuBr_6 introduced (any unexpected loss by

Table 1. Percentage of bromine remaining in different ruthenium(IV) solutions (concentration in mol l^{-1})

Solution	No. 1	No. 2	No. 3	No. 4
[Ru(IV)]	1.01×10^{-2}	0.99×10^{-2}	1.00×10^{-2}	9.8×10^{-2}
[Br^-]	6.06×10^{-2}	5.94×10^{-2}	6.00×10^{-2}	5.98×10^{-1}
Theoretical from weighted K_2RuBr_6 [Br^-] in the Ru(IV) solution	3.3×10^{-4}	4.8×10^{-4}	2.6×10^{-4}	2.4×10^{-3}
(Br/Ru)·100	3.0	4.8	2.6	2.4

Table 2. Experimental oxidation number of ruthenium (concentration in mol l^{-1})

Solution	No. 1	No. 2	No. 3
[Ru(IV)]	3.56×10^{-2}	3.56×10^{-2}	3.57×10^{-2}
[oxidizer]	3.59×10^{-2}	3.59×10^{-2}	3.61×10^{-2}
oxidation	4.01	4.01	4.01

oxidation as RuO_4 is immediately made perceptible by the black powder it forms on rubber or grease). In this case we have only to titrate the oxidizing power of the solution. The results for three preparations are given in Table 2. They prove that ruthenium does not change oxidation state during elimination of bromide ion. Our method is convenient for the preparation of non-complexed ruthenium(IV) solution.

(c) *Existence of a* $Ru_4O_6^{4+}$ *or* $Ru_4(OH)_{12}^{4+}$ *species*

As we have already written, only three species can be suggested in those solutions, namely Ru^{4+}, RuO^{2+}, $Ru_4O_6^{4+}$ which need, respectively the consumption of 7.2, 5.2, 4.2 protons per ruthenium atom in the total reactions.

Unlike previous preparation methods, the titration of proton becomes valid because the yield in ruthenium is 100% in this method. The only source of errors lies in the Gran's method itself. The major one arising from ionic strength. The results for three identical preparations are 0.90, 0.88, 0.89 mol l^{-1}. They are reproducible within 1% from the mean value of acidity but to take into account the basic errors of the method, we assume the accuracy to be less, in the order of 3%. Thus the final acidity ranges from 0.86 to 0.92 mol l^{-1}. The calculation of consumed proton per ruthenium atom leads to:

$$(0.975-0.86)/2.47 \times 10^{-2} = 4.6\ H^+/Ru$$

$$(0.975-0.92)/2.47 \times 10^{-2} = 2.2\ H^+/Ru$$

Those equations show that the high acidity of the solutions is not favourable for a great accuracy. Nevertheless the calculated value does not reach the 5.2 H^+/Ru corresponding to the RuO^{2+} ion. The starting material being mononuclear ion, in which we only oxidize bromide ion, then the produced ion should be RuO^{2+} if this ion had some chance to exist. But as it does not, that proves the stability of the tetrameric form in strong acid medium. We state that the total reaction of the preparation is described by equation (3). This result agrees with the recently published one by Schauwers *et al.*[4]

This method is satisfactory fast, clean and accurate. Another advantage is the ability to work in acid solution other than perchloric acid without the trouble encountered sometimes by workers who try sulphuric or methanesulphonic acids. In any case, the composition of the solution is given by:

$$[Na^+] = 1.2[Ru(IV)]$$

$$[K^+] = 2[Ru(IV)]$$

$$[Br] = 3 \times 10^{-2}[Ru(IV)]$$

$$[H^+] = (H^+)_0 - 4.2[Ru(IV)]$$

$$[Anion] = [H^+]_0$$

where [Ru(IV)] is known by weighing K_2RuBr_6.

REFERENCES

1. P. Wehner and J. C. Hindman, *J. Am. Chem. Soc.* 1950, **72**, 3911.
2. C. Bremard, G. Nowogrocki and G. Tridot, *Bull. Soc. Chim. Fr.* 1968, **5**, 196.
3. R. M. Wallace and R. C. Propst, *J. Am. Chem. Soc.* 1969, **91**, 3779.
4. J. Schauwers, F. Meuris, L. Heerman and W. D'Olieslager, *Electrochim. Acta* 1981, **26**, 1065.
5. F. P. Gortsema and J. W. Cobble, *J. Am. Chem. Soc.* 1961, **83**, 4317.
6. J. E. Ferguson and A. M. Greenaway, *Aust. J. Chem.* 1978, **31**, 497.

Polyhedron Vol. 4, No. 5, pp. 879–883, 1985
Printed in Great Britain

0277–5387/85 $3.00 + .00
© 1985 Pergamon Press Ltd

CHARACTERIZATION OF Cr(III)–Zr(IV) MIXED AND Sn(II) DOPED HYDROUS OXIDES

S. K. SRIVASTAVA* and C. K. JAIN
Department of Chemistry, University of Roorkee, Roorkee-247667, India

(*Received* 2 *April* 1984; *accepted* 9 *November* 1984)

Abstract—Surface and structural properties of chromium–zirconium mixed and Sn(II) doped hydrous oxide gels have been compared with chromium oxide hydrate gel by the use of thermal analysis, IR spectroscopy, X-ray diffraction, electron microscopy and magnetic measurements. The mixed and doped oxide gels were found to have a hexagonal close packed stacking of O, OH and H_2O ligands with chromium ions distributed in octahedral sites with little degree of order among them. The microstructure of the gels are characterized by the presence of large aggregates of chromium hydroxides, fine granular sheets due to $HCrO_2$ phase and $Cr(OH)_3$ microcrystallites. Magnetic susceptibility measurements indicate antiferromagnetic behaviour of these gels.

Chromium oxide hydrate gels find wide applications as advance technology materials apart from their traditional use in the manufacture of pigments, glasses, cement colourants, ceramic oxide coatings, absorbents and catalysts.[1,2] CrO_2 is the only transition metal oxide which is strongly ferromagnetic and is used in magnetic tapes.[3,4] The influence of the precipitation rate on the properties of porous chromia have been summarized by Sonnemans and Keijzer[5] while the effect of pH of the reactant solutions on the texture and surface properties are reported by Siddiq, Gilanyi and Zettlemoyer.[6] Electrical conductivity and thermal analysis studies have recently been reported by Natrajan and Secco[7] while structural evolution of α-Cr_2O_3 from chromium oxide hydrate gel has been studied by Ratnasamy and Leonard.[8] Extensive literature, available on this compound, reveals that its texture and surface properties depend on the conditions of preparation and heat treatment.

We have been working on the sorption characteristics of some pure and mixed hydrous oxides and have also investigated the electrochemical performance of their membranes. It is observed that the mixed oxide of chromium and zirconium (with chromium as a major constituent) exhibits manifold increase in its sorption capacity as compared to individual oxides, therefore it is essential to characterize these systems completely in relation to their utility in various processes involving ion-exchange adsorption etc.

In this paper we have made an attempt to characterize structurally the chromium–zirconium mixed hydrous oxide vis-à-vis the pure one and have also observed the doping effect of Sn(II).

EXPERIMENTAL

Reagents

Chromium chloride (BDH), zirconium oxychloride (AR) and stannous chloride (AR) were used as such and their solutions were prepared in double distilled water.

Preparation of mixed and doped hydrous oxide gels

Chromium chloride (0.2 M) and zirconium oxychloride (0.2 M) were mixed to give a molar ratio of 8:1 (optimum conditions at which the product show maximum anion as well as cation exchange capacity). The mixed hydrous oxide was coprecipitated slowly under constant stirring. The precipitate was left to stand with the mother liquor for two days at room temperature, washed several times with distilled water, filtered and dried at 80°C for 24 h. Doped oxide was prepared by adding 0.075 g of $SnCl_2$ to a 450 ml solution of chromium chloride and zirconium oxychloride in a molar ratio of 8:1 and was precipitated with ammonium hydroxide.

* Author to whom correspondence should be addressed.

Technique used

Thermal analysis, IR spectroscopy, X-ray diffraction, electron microscopy and magnetic measurements are the techniques used to characterize the gels.

Differential thermal curves were recorded on a Fisher Differential Thermalyzer model 260 P and thermogravimetric curves on a Stanton Redcroft TG-770 model instrument. Samples were passed through 100 mesh size sieves and heated in air atmosphere in platinum crucible from room temperature to 1000°C at a rate of 10° min^{-1}.

IR spectrum were recorded with a Beckman model IR-20 spectrophotometer operated in double beam mode. The samples were taken in the form of KBr pellets.

Diffraction patterns were recorded at room temperature at a speed of 2θ degree per minute (ranging from 1° to 2° min^{-1}) in Phillips Type PW 1140/9P X-ray diffractometer using Zr-filtered Mo-K_α radiation = 0.711 Å.

Transmission electron micrographs were recorded with Phillips EM-400 transmission electron microscope of 80–100 KV voltage. Samples were prepared by dilution of a small quantity of it in absolute alcohol after dispersing the sample in ultrasonic bath. Droplets of the diluted sample were taken from the middle of the test tube and put on a 200 mesh copper grid covered with a thin film of formvar. All the grids had been examined in the electron microscope prior to the sample deposition.

Magnetic susceptibility measurements were performed using Vibrating Sample Magnetometer model 155. Samples (0.05–0.10 g) were taken in the form of cylindrical pellets. The system was calibrated using the 3/32″ × 3/32″ cylindrical sample of high purity nickel. The saturated moment of Ni sample was found to be about 55 emu g^{-1} with a saturation flux of about 8000 G.

RESULTS AND DISCUSSION

Thermal analysis

Differential thermal and thermogravimetric curves for chromium oxide, zirconium oxide, Cr–Zr mixed oxide and Sn(II) doped oxide hydrate gels are shown in Figs. 1 and 2 respectively.

DTA curve of chromium oxide hydrate gel [Fig. 1(a)] apparently show three endothermic effects with their peaks centred at 120, 200 and 330°C. These are followed by the appearance of an exothermic effect at 400°C. The splitting of the exothermic effect of dehydration into distinct peaks possibly points to the structural inhomogeneity of the sample thereby

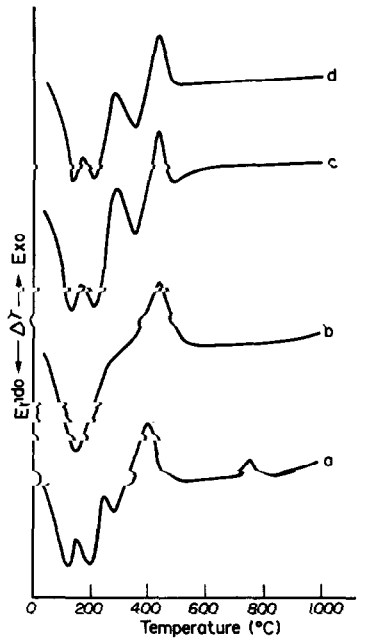


Fig. 1. DTA curves of hydrate gels: (a) chromium oxide; (b) zirconium oxide; (c) Cr–Zr mixed oxide; (d) Sn(II) doped oxide.

suggesting more than one type of phase possessing distinct structural features, being present in the gel. Observation of an exothermic effect at 400°C corresponds to crystallization of the disordered colloidal structure related to dehydrated skeleton of the gel to well developed α-Cr_2O_3. Features beyond 500°C in the DTA curve may be accounted for by the sintering

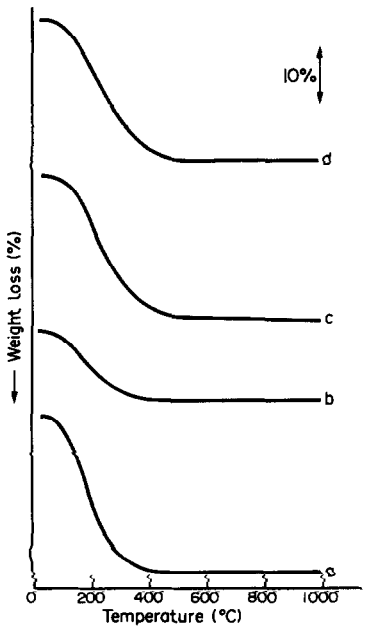


Fig. 2. TGA curves of hydrate gels: (a) chromium oxide; (b) zirconium oxide; (c) Cr–Zr mixed oxide; (d) Sn(II) doped oxide.

and grain growth of α-Cr_2O_3 with concomitant removal of lattice defects and inhomogeneities. A weak but distinct exothermic effect at 750°C is identifiable with the delayed start of crystallization of α-Cr_2O_3.[9] The DTA curve of zirconium oxide hydrate gel [Fig. 1(b)] shows an initial endothermic peak at 150°C, corresponding to dehydration, followed by a strong sharp exothermic peak at 430°C due to the transition of ZrO_2 from an amorphous state to crystalline variety.[10]

DTA curves of Cr–Zr mixed and Sn(II) doped oxide hydrate gels [Fig. 1(c), (d)] show endothermic effects with peaks at 130, 210 and 350°C associated with the removal of adsorbed water molecules and structural hydroxyl groups indicating the presence of more than one type of phase possessing distinct features. Exothermic effect around 430°C corresponds with the onset of crystallization of the mixed oxides. DTA curves of mixed and doped oxide hydrate gel are devoid of any peaks beyond 500°C in contrast to the curve obtained for pure chromium oxide hydrate gel that gave weak exothermic effect at 750°C due to crystallization of α-Cr_2O_3 formed from microcrystalline $Cr(OH)_3$ fraction. The variations in intensity and width of the endotherms suggest considerable variations in water content and microstructures of the gels.

The TG results (Fig. 2) show that the loss in weight takes place in different steps in a continuous manner at temperatures corresponding to the endothermic and exothermic peaks in DTA curves. The TG curves show a total weight loss of 27.0% for chromium oxide, 12.0% for zirconium oxide, 25.4% for Cr–Zr mixed and 25.0% for Sn(II) doped oxide hydrate gels respectively.

IR spectroscopy

IR spectra of chromium oxide hydrate gel show a very strong absorption band at 3440 cm^{-1}, a weak broad absorption extended over the region 2100–1600 cm^{-1}, sharp bands at 1640, 1470 and 1300 cm^{-1} and again an intense broad band centred at 530 cm^{-1} and some inflections in the region 1200–650 cm^{-1}. Absorption bands at 3440 and 1640 cm^{-1} are characteristic of stretching and bending modes of vibrations for water and structural hydroxyl groups.[11,12] The bands around 1380 and 1470 cm^{-1} are due to the presence of some CO_3^{2-} ions that may be incorporated in the gel due to absorption of CO_2 from the atmosphere at the time of precipitation.[13] Weak absorptions in the region 2000–1600 cm^{-1} and around 1200 cm^{-1} are observed in the spectrum which correspond with the presence of some rhombohedral $HCrO_2$ fraction.[14] The bands present in the region 1100–1000 cm^{-1} are due to Cr=O stretching vibrations which arise from the sorbed oxygen on coordinatively unsaturated chromium sites available in the gel.[14] The bands in the lattice vibration region at 530 cm^{-1} all the more indicate for a distribution of Cr^{3+} ions in octahedral sites available in hexagonal close packed structure of oxygen sublattice in the gel with a small degree of order among the chromium ions.

The IR spectra of Cr–Zr mixed and Sn(II) doped oxide hydrate gels compare well with the IR characteristics of chromium oxide hydrate gel. IR spectrum of chromium oxide hydrate gel is characterized by a broad band with absorption centred at 530 cm^{-1}. The IR spectrum of zirconium oxide hydrate gel is characterized by a broad band with absorption centred at 500 cm^{-1}. Inspection of the IR spectra of Cr–Zr mixed and Sn(II) doped oxide hydrate gels show that an increasing amount of chromium ions result in sharpening of the peak in the low frequency region. Incorporation of chromium ions in the mixed oxide cause displacement of IR absorptions towards higher frequencies. These features indicate the formation of Zr-substituted chromium oxide hydrate gel as dominant phase along with some Cr-substituted zirconium oxide hydrate gel.

X-Ray powder diffraction studies

X-Ray diffraction pattern of the chromium oxide hydrate gel shows the mainly amorphous nature of the product. However, some weak reflections at d-values associated with the presence of α-$Cr(OH)_3 \cdot xH_2O$ (bayerite like) and of rhombohedral $HCrO_2$ are observed.

The X-ray diffraction patterns of mixed and Sn(II) doped oxide hydrate gels compare well with the X-ray pattern of chromium oxide hydrate gel. Some weak reflections due to the presence of $Cr(OH)_3$ with Zr(IV) and Sn(II) incorporation are also observed showing some crystallinity in the gel.

Transmission electron microscopy

Selected electron micrographs of chromium oxide, Cr–Zr mixed oxide and Sn(II) doped oxide hydrate gels are displayed in Fig. 3(a–c) respectively.

The electron micrographs of chromium oxide hydrate gel show that the gel is composed of large aggregates and small discrete sub-unit particles with well separated edges. The microstructure of the gel is characterized by the simultaneous presence of three types of phase. The large canonical wedge-shaped opaque aggregates with irregular edges represent the formation of $Cr(OH)_3 \cdot xH_2O$. The second phase is the large fraction of chromium oxyhydroxide,

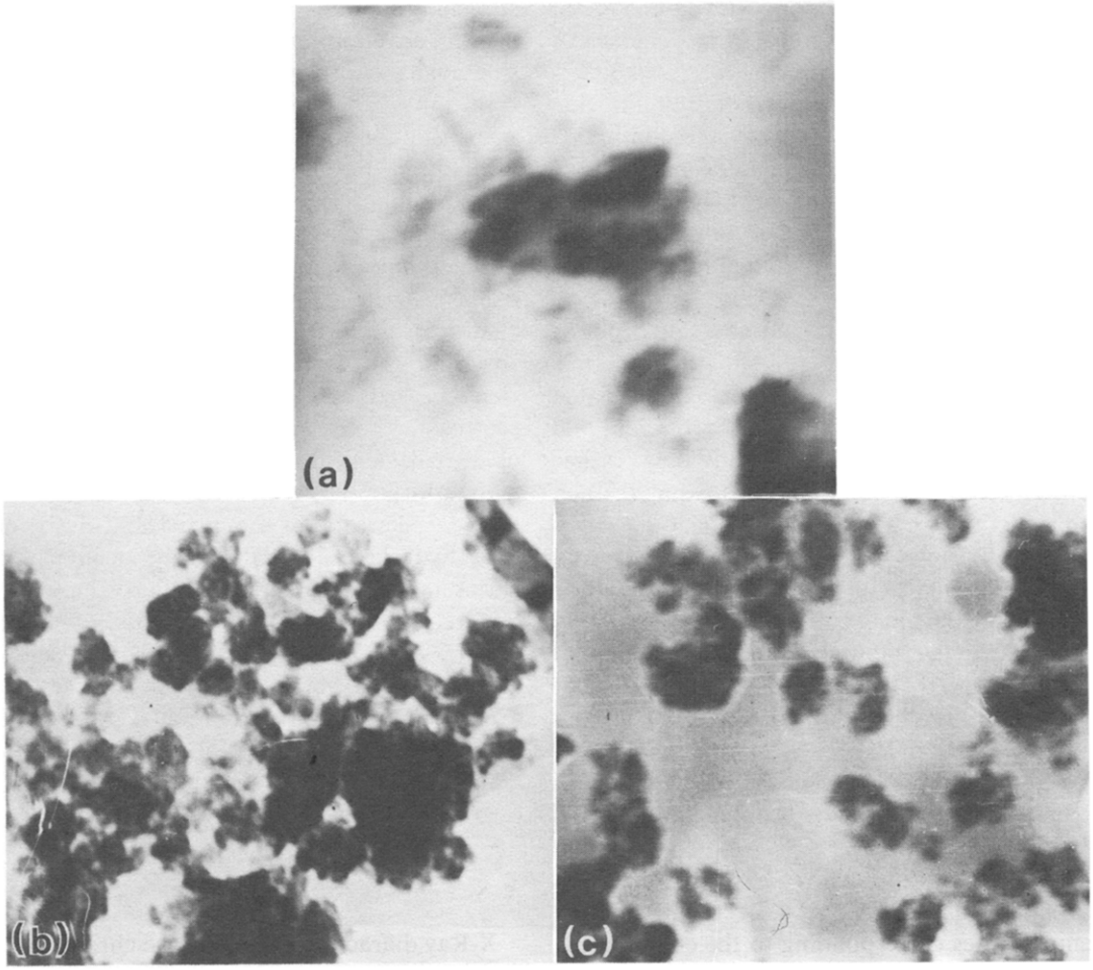


Fig. 3. Electron micrographs of hydrate gels: (a) chromium oxide, × 45,000; (b) Cr–Zr mixed oxide, × 58,000; (c) Sn(II) doped oxide, × 58,000.

$HCrO_2$. A small fraction of polygonal particles with well separated edges indicate the presence of some better defined microcrystallites of $Cr(OH)_3 \cdot xH_2O$.

Electron micrographs of Cr–Zr mixed and Sn(II) doped oxide hydrate gels show much resemblance to chromium oxide hydrate gel. These show the presence of large aggregates of chromium hydroxide, fine granular sheets due to $HCrO_2$ phase and $Cr(OH)_3$ microcrystallites. Incorporation of zirconium and tin in the chromium oxide hydrate gel probably results in a better definition of primary particles and microcrystallites. The coherency of these gels is comparable to that of chromium oxide.

Magnetic measurements

Figure 4 shows the variation of specific magnetization with varying field strength for chromium oxide, zirconium oxide, Cr–Zr mixed and Sn(II) doped oxide hydrate gels. A summary of the results of magnetic measurements is presented in Table 1. Room temperature magnetization of the gels are proportional to the applied field and increases with field values.

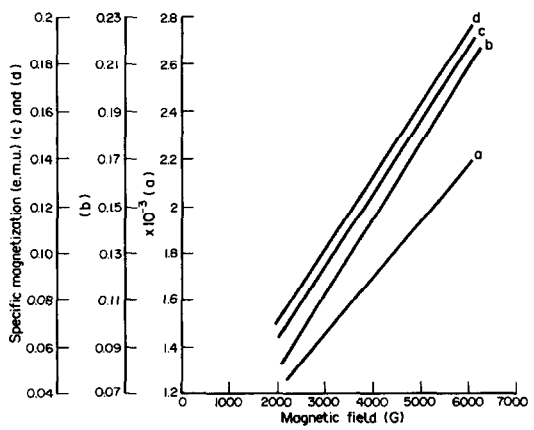


Fig. 4. Least squares fitted linear plots of specific magnetization vs. magnetic field for hydrate gels: (a) zirconium oxide; (b) chromium oxide; (c) Cr–Zr mixed oxide; (d) Sn(II) doped oxide.

Table 1. Values of specific magnetization (σ) with varying magnetic field (H) for chromium oxide, zirconium oxide, Cr–Zr mixed oxide and Sn(II) doped oxide hydrate gels

Field (G)	Specific magnetization (emu)			
	Cr oxide	Zr oxide	Cr–Zr mixed oxide	Sn(II) doped oxide
2500	0.097	1.340×10^{-3}	0.080	0.086
3700	0.139	1.650×10^{-3}	0.116	0.121
4800	0.171	1.880×10^{-3}	0.152	0.160
5800	0.200	2.180×10^{-3}	0.180	0.190
χ_g ($\times 10^{-6}$)[a]	34.8	0.241	30.6	31.3

[a] Values of χ_g have been calculated from the linear plots of specific magnetization vs field strength.

The field dependence and the magnetic susceptibility per gram, χ_g of the chromium oxide, Cr–Zr mixed oxide and Sn(II) doped Cr–Zr mixed oxide hydrate gels indicate antiferromagnetic behaviour for all these samples. The magnetic susceptibility value of the chromium oxide hydrate gel is in good agreement to that reported for chromia gel by Selwood.[15] In the case of α-Cr_2O_3, the spins are aligned antiparallel within the (111) planes. While antiferromagnetism of α-Cr_2O_3 is brought about by weak direct spin–spin interactions between Cr^{3+} ions over common faces and edges leading to relatively short Cr^{3+}–Cr^{3+} distance along the hexagonal axis. The antiferromagnetism of α-Cr_2O_3 is caused by spin–spin interactions between π antibonding t_{2g} electrons. As regards the structure of chromium hydrate gel, it consists of a hexagonal close packed stackings of O, OH and H_2O ligands with chromium ions distributed in octahedral sites with little degree of order among them. Occurrence of planar layers of octahedra $Cr(O, OH, H_2O)_6$ lack three-dimensional order because of the restricted number of unit cells. This is essentially responsible for poorly crystalline character of chromia gel. Low values of magnetic susceptibility for mixed and doped oxide hydrate gels correspond to an antiferromagnetic mixed phase with high surface area.

Acknowledgement—One of the authors (C.K.J.) is grateful to Council of Scientific and Industrial Research, New Delhi, India for financing this research project.

REFERENCES

1. S. K. Bhattacharya, V. S. Ramachandran and J. C. Ghosh, *Advan. Catal.* 1957, **9**, 114.
2. E. Herrmann, *Inorganic Coloured Pigments in Characterization of Powder Surface With Special Reference to Pigments and Fillers* (Edited by G. D. Parfit and K. S. W. Singh), p. 209. Academic Press, New York (1976).
3. G. Bates, *Magnetic Oxides* (Edited by D. J. Craik), p. 689. Wiley, New York (1975).
4. G. Basile, G. C. Boero, F. Garbassi, E. M. Ceresa and F. Montino, *Mat. Res. Bull.* 1982, **17**, 1179.
5. J. Sonnemans, H. de Keijzer and P. Mars, *J. Coll. Interf. Sci.* 1975, **51**, 335.
6. M. Siddiq, T. Gilanyi and A. C. Zettlemoyer, *J. Coll. Interf. Sci.* 1978, **64**, 192.
7. M. Natrajan and E. A. Secco, *Phys. Stat. Solidi A* 1975, **30**, K169.
8. P. Ratnasamy and A. J. Leonard, *J. Phys. Chem.* 1972, **76**, 1838.
9. R. B. Fahim, R. M. Gabr, M. I. Zaki and S. A. A. Mansour, *J. Coll. Interf. Sci.* 1981, **81**, 468.
10. F. G. R. Ginblet, A. A. Rahman and K. S. W. Singh, *J. Chem. Tech. Biotech.* 1980, **30**, 51.
11. Y. I. Ryskin, *The Infrared Spectra of Minerals* (Edited by V. C. Farmer), p. 137. Mineralogical Society, London (1974).
12. R. A. Nyquist and R. O. Kagel, *Infrared Spectra of Inorganic Compounds*. Academic, New York (1971).
13. A. Zechina, S. Coluccia, E. Guglielminotii and G. Ghiotti, *J. Phys. Chem.* 1971, **75**, 2774.
14. R. M. Douglass, *Acta Cryst.* 1957, **10**, 423.
15. P. W. Selwood, *Magnetochemistry*, p. 338. Interscience, London (1956).

Polyhedron Vol. 4, No. 5, pp. 885–892, 1985
Printed in Great Britain

0277–5387/85 $3.00 + .00
© 1985 Pergamon Press Ltd

THE SYSTEM POTASSIUM-GRAPHITE/ METHYLBORONDIBROMIDE/ALKYNE: QUERY ABOUT THE INTERMEDIACY OF METHYLBORYLENE

ROBERT SCHLÖGL
Institut für Physik, Universität Basel, Klingelbergstraße 82, CH-4056 Basel, Switzerland

and

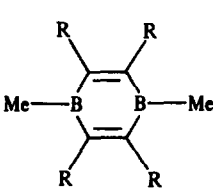
BERND WRACKMEYER*
Institut für Anorganische Chemie der Universität München, Meiserstraße, 1, D-8000 München 2, FRG

(*Received* 5 *November* 1984; *accepted* 18 *December* 1984)

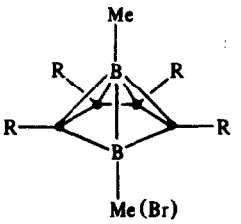
Abstract—Attempts to reproduce the reported synthesis of peralkylated 1,4-dibora-2,5-cyclohexadienes (1) using the so-called "methylborylene-generating system", $2\,C_8K/MeBBr_2$, in the presence of 3-hexyne and 5-decyne were not successful. The *nido*-2,3,4,5-tetracarbaboranes(6) (2) contaminated with other carbaboranes and various organoboronhalides were obtained instead, irrespective of the nature of the C_8K used. Different samples of C_8K were prepared and characterized by X-ray diffraction and XPS spectra. The yields of the carbaboranes were much better when the well ordered stage 1 potassium graphite in hexane was used. In all experiments the first compounds identified from the reaction mixtures are the 1,2-haloboration products (3) and there is no indication for the intermediacy of methylborylene. Most of the organoboranes present in the reaction solution and in the final products could be readily assigned on the basis of ^{11}B- and ^{13}C NMR data, supported by GC/MS analysis.

The synthesis of unsaturated cyclic organoboranes has been a major challenge to many boron chemists for more than two decades.[1,2] The heteroaromatic character of neutral or anionic compounds of this type (e.g. borirenes,[3] borepines[4] and borine-anions[5] or borol-dianions,[6] respectively) has been shown in numerous studies.[2,7] The interest in those heterocycles which do not obey the Hückel rules has been focused on the boroles[2,6a,7,8] and on the 1,4-dibora-2,5-cyclohexadienes (1).[2,7,9]

Among the various synthetic strategies[2] monomeric boranediyles ("borylenes") have been frequently invoked.[10] Although it proved possible to trap monomeric fluoroborylene, BF, from the gas phase[9a] and to generate Ph_3SiB in a hydrocarbon matrix at −196°C,[10c] convincing evidence for the intermediacy of borylenes in solution is still lacking. However, in preliminary communications,[3a,11] and, more recently, in two full papers[12,13] the interaction between potassium-graphite, C_8K, and methylborondibromide, $MeBBr_2$, has been proposed as a methylborylene, MeB, generating system. We became intrigued by these reports mainly for two reasons: (i) We are interested in the application of potassium-graphite in synthesis.[14] (ii) Our own and other attempts to prepare polyalkylated[15] or peralkylated 1,4-dibora-2,5-cyclohexadienes[16] (1) have not been successful, whereas it is claimed[13] that these compounds 1 are the main products from the



1



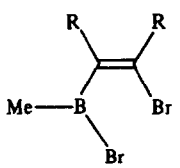
2

* Author to whom correspondence should be addressed.

reaction of C_8K with $MeBBr_2$ in the presence of alkynes (3-hexyne, 3-decyne, 4-decyne, 5-decyne, 6-dodecyne). With these alkynes the formation of *nido*-hexaalkyl-2,3,4,5-tetracarbahexaboranes (6) (2) is said to be of minor importance.

Unfortunately, various important experimental details which would help to reproduce these results[13] have been omitted. Thus, the potassium-graphite, C_8K, has not been fully described or characterized which can be a crucial point[17] considering the manyfold influences controlling heterogeneous reactions. Clearly, the electronic and, therefore, the chemical properties of the potassium-graphite will depend greatly on the amount of the residual non-intercalated potassium invariably present in the frequently used *in situ* preparation.[18] The diffusion-controlled gas phase-solid state reaction of potassium vapour with graphite may lead to products which are not in the thermodynamic equilibrium, meaning that the galleries between the graphite sheets are only partially filled depending on reaction conditions. Thus, it is possible that non-intercalated potassium may induce decomposition of the reactants and/or the products. Furthermore, the degree of undersaturation seems to determine the amount of charge transfer from potassium to graphite (ionicity) and, indirectly, it influences the stability of the intercalated state under reaction conditions. Furthermore, it has been shown that many organic compounds, i.e. commonly used solvents, are capable of forming ternary graphite intercalates.[19] The properties of these intercalates, which seem to contain solvated cations rather than metalloid potassium, are drastically different from the parent binary potassium-graphite, and several irreversible chemical reactions of potassium-graphite with solvents have been reported.[19,20]

The organoboranes reported to result from the reaction of C_8K with $MeBBr_2$ and various alkynes were not completely characterized:[13] Some MS data have been discussed, ^1H-, ^{13}C NMR data have been mentioned but only very few data have been given, and, most regrettably, ^{11}B NMR data which could provide decisive information on the structure of the organoboranes[21,22] have not been reported. We were also puzzled by contradictory statements on the mechanism: Although the title of the paper[13] as well as most of the discussion emphasizes the intermediacy of methylborylene, the authors finally conclude that they are unable to decide between methylborylene addition to alkynes and reduction of the haloboration products (3) by potassium. This unsatisfactory situation prompted us to undertake this study in order to characterize the system $C_8K/MeBBr_2$/alkynes, and to look for evidence for one or the other mechanism. In addition, we wanted to assess the composition and structure of the organoboranes in more detail.



3

RESULTS

Potassium-graphite

In order to obtain reproducible results in this study, first stage potassium-graphite was prepared in three different ways (**A** to **C**) (see Experimental). Although they all exhibited the same golden colour, the properties of these three preparations as determined by XRD and XPS are quite different (Table 1).

Figure 1 shows two energy dispersive X-ray diffractograms[17] of the parent potassium-graphite (method **A**) and of the same material after reaction with $MeBBr_2$ and 3-hexyne in hexane after 4 days.[23] The colour of the particles had changed from uniform golden to a mixture of gold, steel blue and black, typical for higher stage potassium-graphite intercalates. The XRD traces supported by energy-dispersive elemental X-ray analysis clearly indicate transformation of the ordered intercalate into a highly disordered state with potassium still present between the graphite layers. Neither the expected[14d] ordered higher stage structure nor pure graphite has been formed.[24]

Reactions

The arguments discussed so far strongly indicate that the reactivity of C_8K depends critically on the method of preparation. Therefore, two parallel sets of experiments were carried out. The reaction of the characterized compound C_8K (method **A**, **B**) with $MeBBr_2$ in the presence of alkynes (3-hexyne, 5-decyne) was studied under various conditions (solvent, temperature), and the mixture "C_8K" (method **C**) was treated in the same way.

In benzene

With C_8K (**A**, **B**) in the presence of 5-decyne, there was a visible change in the appearance of the solid after heating to reflux. The colour of the liquid turned reddish and the solid became dark. Slow addition of $MeBBr_2$ in benzene caused a vigorous reaction and

Table 1. Properties of potassium-graphite prepared via different methods

Method[a]	Preparation	Stage	J_C [pm]	K2p$_{\frac{3}{2}}$BE FWHM [eV]	"Ionicity"[b]
A	Vapour phase, 320°, 300°C powder graphite	1 (> 99%) only well-ordered	534.8	291.0 1.3	Metallic
B	Vapour phase, 310°, 290°C graphite stabs	1 (93%) + 2 (7%) well ordered	539.2 874.0	291.6 1.2	Partly ionic
C	"*In situ*" preparation in S40 flakes of natural graphite	1 (59%) + 2 (19%) + 3 (22%)[c] poorly ordered	541.7 877.2	291.0 292.4 1.6 1.2	Potassium metal on the surface and ionic states

[a] See Experimental.
[b] As defined by the shift in binding energy of K2p relative to the K metal.
[c] Disordered.

the powdery solid (**A**) became lumpy. The ^{11}B NMR spectrum taken of the reaction mixture immediately after addition of $MeBBr_2$ showed only traces of $MeBBr_2$, Me_2BBr. This indicates that essentially all $MeBBr_2$ has been converted into insoluble or highly polymeric material. The mixture was heated to reflux for 20 h but there was no change in the ^{11}B NMR spectrum of the solution.

The analogous reaction with the mixture "C_8K" (**C**) was somewhat different. There was no marked change in the appearance of the solid material before the $MeBBr_2$ was added. On addition of the $MeBBr_2$ a reaction took place, the solid went black and potassium metal could be seen. The ^{11}B NMR spectrum recorded immediately after the addition of $MeBBr_2$ showed only two resonances, one for $MeBBr_2$ and the other for the haloboration product **3b** ($R^1 = R^2 = Bu^n$). After heating the mixture to reflux for 18 h (lit.[13]: 20 h) the ^{11}B NMR spectrum showed no detectable resonances for organoboranes except very weak signals for traces of the *nido*-2,3,4,5-tetracarbahexaborane(6) (**2b**).

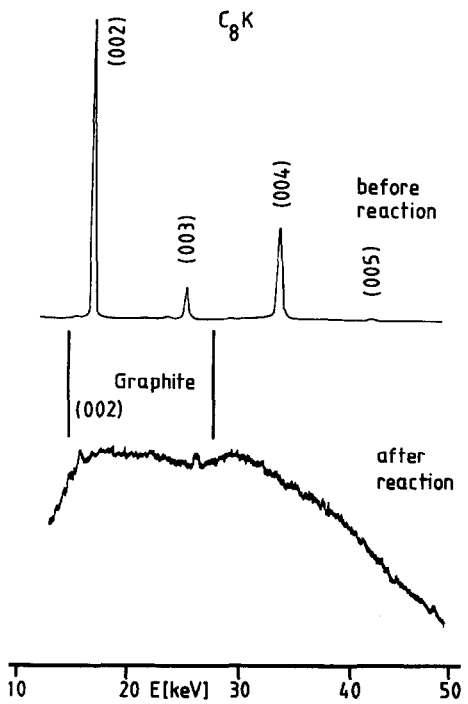


Fig. 1. Energy dispersive X-ray diffractograms[17] of powdered C_8K (method **A**) before reaction and after reaction with 3-hexyne and $MeBBr_2$ in hexane. The solid bars represent the positions of the two strongest reflections of pure graphite.

In hexane

After these disappointing results we decided to use a different solvent since it was reported that the 1,4-dibora-2,5-cyclohexadienes could also be obtained in cyclohexane.[13] We studied the reactions in hexane both at room temperature and under reflux since, according to literature,[13] the reactions under these conditions should afford either carbaboranes or diboracyclohexadienes, respectively. Furthermore, it is well known that benzene forms ternary intercalation products with potassium-graphite[14b,19] whereas hexane or cyclohexane do not react with C_8K.

The reaction of C_8K (**A**, **B**) with $MeBBr_2$ and the alkyne (3-dexyne or 5-decyne) proceeds slowly at room temperature and somewhat more rapidly when heated to reflux. There was no appreciable difference in the product distribution for the different

reaction conditions, and the two alkynes gave analogous products as could be deduced from the ^{11}B NMR spectra. At no stage of the reaction a significantly intense ^{11}B NMR signal could safely be assigned to the peralkylated 1,4-diboracyclohexadienes (**1**). Instead the ^{11}B NMR signals of various carbaboranes were steadily growing as the reaction proceeded whereas the ^{11}B resonances for the haloboration products **3a, b** decreased in relative intensity. In the room temperature reaction after 24 h there was a ^{11}B resonance of minor intensity (δ ^{11}B 58.8) which we cannot explain. This signal vanished after 48 h at room temperature and it was not found when the reaction mixture was heated to reflux.

The mixture "C_8K" (**C**) as a suspension in hexane together with 5-decyne was heated to reflux and $MeBBr_2$ in hexane was added. No visible change occurred. The ^{11}B NMR spectrum showed the presence of $MeBBr_2$ and the haloboration product **3b**. After 18 h in boiling hexane the typical ^{11}B resonances for carbaboranes, **2b**, appeared together with an intense signal for Me_2BBr and there was still much left of $MeBBr_2$ and **3b**. After 48 h the carbaborane ^{11}B-resonances are dominant but the overall intensity had much decreased which indicates decomposition and/or polymerisation.

Finally, we looked at the reaction between $MeBBr_2$ and C_8K (**B**) in hexane. The golden solid was attacked very slowly and a black powdery solid was formed. The ^{11}B NMR spectrum of the colourless supernatant solution taken after 4 days showed only the resonance of unreacted $MeBBr_2$.

The ^{11}B NMR data of the organoboranes identified are given in Table 2, together with data of known compounds for comparison. The haloboration reactions have been carried out independently and the ^{11}B NMR parameters are identical with those measured from the reaction solutions.

Further identification relies on ^{13}C NMR data of the reaction products which can be compared with known data of compounds synthesized independently. The various ^{11}B resonances have been related to the broad ^{13}C resonances of the boron-bonded carbon atoms by selective ^{11}B

Table 2. δ ^{11}B data of organoborane identified in the reaction solutions $C_8K/MeBBr_2$/alkyne and data for comparison

Nr.	Compound	δ ^{11}B	Solvent
2a	*nido*-2,3,4,5-Et_4-1,6-Me_2-2,3,4,5-C_4B_2	−45.5 (B(1)) 17.8 (B(6))	hexane
		−45.3 (B(1)) 17.6 (B(6))	C_6D_6
2b	*nido*-2,3,4,5-Bu^n_4-1,6-Me_2-2,3,4,5-C_4B_2	−45.3 (B(1)) 17.8 (B(6))	hexane
		−45.2 (B(1)) 17.6 (B(6))	C_6D_6
	nido-Et_6-2,3,4,5-C_4B_2[b]	−44.4 (B(1)) 18.6 (B(6))	$CDCl_3$
2c	*nido*-2,3,4,5-Et_4-1-Me-6-Br-2,3,4,5-C_4B_2	−45.1 (B(1)) 14.1 (B(6))	hexane
		−45.1 (B(1)) 13.8 (B(6))	C_6D_6
2d	*nido*-2,3,4,5-Bu^n_4-1-Me-6-Br-2,3,4,5-C_4B_2	−45.3 (B(1)) 14.0 (B(6))	hexane
	nido-1,3,4-Et_3-6-Br-2,3,4,5-C_4B_2[c]	−44.7 (B(1)) 13.9 (B(6))	$CDCl_3$
3a	(*Z*)-Me(Br)B(Et)C=C(Et)Br	72.2[d]	hexane
3b	(*Z*)-Me(Br)B(Bu^n)C=C(Bu^n)Br	72.2[d]	hexane
4a	(*E*)-Me(Br)B(Et)C=C(Et)Br	74.5[d]	hexane
4b	(*E*)-Me(Br)B(Bu^n)C=C(Bu^n)Br	74.0[d,e]	hexane
8a	$Et_4C_4B_4Me_4$[f]	−6.5	hexane
		−6.6	C_6D_6
8b	$Bu^n_4C_4B_4Me_4$	−6.5	hexane
		−6.5	C_6D_6

[a] Relative to external Br_3-OEt_2, 27°C, a positive sign denotes shifts to higher frequency (lower field).

[b] Ref. 16(b).

[c] B. Wrackmeyer and L. Killian, unpublished results.

[d] ^{11}B-resonances from the reaction solutions are identical to those found for mixtures of the alkyne with $MeBBr_2$.

[e] Strong overlap with the ^{11}B-resonance of the (*Z*)-isomer.

[f] Ref. 27 reports δ ^{11}B −6.3 in CS_2.

decoupling in heteronuclear triple resonance experiments ^{13}C $\{^{1}H, ^{11}B\}$. There are two ^{11}B resonances in the typical range for carbaboranes[22] at δ ^{11}B 6.9 and −13.7 for which no assignment is possible at present. Their intensity is much reduced after distillation and the identification of the compounds in the GC/MS analysis was not possible. However, selective ^{13}C $\{^{1}H, ^{11}B\}$ experiments[16b] related the ^{11}B resonance at −13.7 to a ^{13}C resonance of a quaternary carbon atom at δ ^{13}C 65.4. In the same experiment the ^{13}C resonances in the alkyl-region were not affected which indicates that the ^{11}B resonance at −13.7 belongs to B–Br units. Irradiating the ^{11}B resonance at δ ^{11}B 6.9 led to sharpening of ^{13}C resonances at δ ^{13}C −6.3 and δ ^{13}C 134.0. The ^{13}C resonances for C(2, 3, 4, 5) in the carbaboranes **2** are found in the same region as reported in the literature,[16b] between δ ^{13}C 99–110.

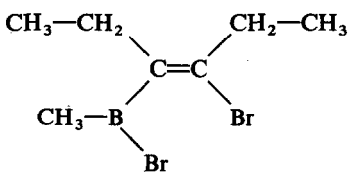
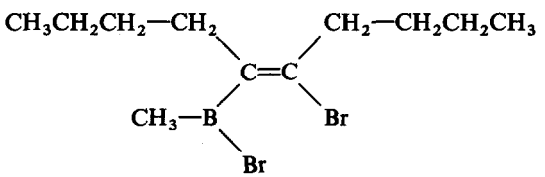
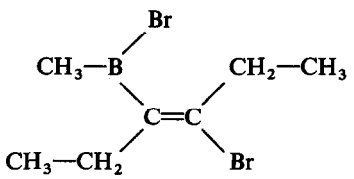
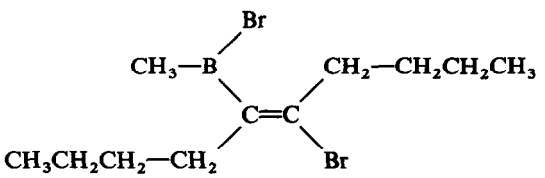
In order to enable stereochemical assignments of 1,2-haloboration products relevant δ ^{13}C-data of the (*Z*, *E*)-isomers **3a, b, 4a, b** are given in Table 3. The assignments rely on known substituent effects[25] and on ^{11}B decoupling which removes residual broadening due to $^{3}J(^{13}C^{11}B)$ across the double bond assuming that $^{3}J(^{13}C^{11}B)_{trans} > {}^{3}J(^{13}C^{11}B)_{cis}$.

The GC/MS analysis of the distilled products from the reaction of C_8K (**A, B**) in hexane with $MeBBr_2$ in the presence of 5-decyne confirmed the results from the ^{11}B- and ^{13}C NMR spectra. Apart from hexabutylbenzene the mixture contains mainly the carbaborane **2b** and small amounts of other carbaboranes. One of the other carbaboranes present in minor quantity is shown in the ^{11}B NMR and in the GC/MS analysis as a peralkylated C_4B_4-system, (**8**), which has been previously reported.[27]

DISCUSSION

All observations in this study are in support of the 1,2-haloboration[26] as the first step of the reaction leading to the compounds **3**. Under the reaction conditions the (*E*)-isomer, **4**, is also formed to a minor

Table 3. Some ^{13}C NMR data for the 1,2-haloboration products **3a, b** and **4a, b**

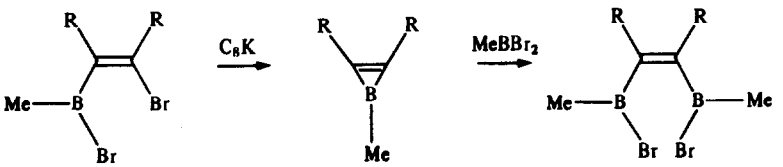
Nr.	Compound	δ ^{13}C[a]			
	(b) (a)	BC=	=CBr	CH_2(a)	CH_2(b)
3a		146.8	134.9	30.2	24.9
3b		146.5	125.7	36.3	31.7
4a		146.3	137.8	36.1	29.5
4b		146.5	136.1[b]	42.1	36.2

[a] In C_6D_6, internal Me_4Si, 27°C.
[b] In $CDCl_3$ (δ ^{13}C 77.0), 27°C.

extent. When the reaction is followed by ^{11}B- or ^{13}C NMR it is evident that the amount of the (*Z*)-isomer, **3**, decreases whereas the (*E*)-isomer seems to be more stable in the reaction solution. The appearance of signals for Me_2BBr shows that complex exchange reactions take place in addition to the reduction reactions. This is also evident from the fact that *nido* - 1,2,3,4,5 - pentaalkyl - 6 - bromo - 2,3,4,5 - tetracarbahexaboranes(6), (**2c, d**), are observed in the ^{11}B NMR spectra and in the GC/MS analysis. There are no ^{11}B resonances in the range expected[22] for the 1,4-dibora-2,5-cyclohexadienes, **1** (δ ^{11}B 55–65). We have no direct proof that the reduction of **3** leads to a borirene, **5**, which has been characterized for R = tert.-Bu[3,13] from the same type of reaction. However, the intermediacy of **5a, b** could explain the presence of various organoboranes identified in the reaction solutions. It can be expected that **5** reacts very fast with excess of $MeBBr_2$ by ring opening to give **6** [Eqn (1)]. Compounds of type **6** are precursors

As has been pointed out[13] the dimerization of the borirenes, **5**, can lead either to the 1,4-dibora-2,5-cyclohexadienes, **1**, or to the carbaboranes, **2**. If the formation of **1** is considered to take place ring opening of **1** in the presence of $MeBBr_2$ to give **7** has to be taken into account too [Eqn (2)], and this will lead to **2** again.

We are unable to account for the major differences between our results and those previously published.[13] Although, as has been mentioned, the preparation of the potassium-graphite may explain some differences, our failure to observe any 1,4-dibora-2,5-cyclohexadienes (**1**) at all is noteworthy. We may add that the mixtures obtained by fractional vacuum distillation had the same appearance as described[13], viscous, yellow, air and moisture sensitive. The GC/MS analysis of these mixtures revealed that the main organoborane component is the carbaborane **2** (proved by ^{11}B- and ^{13}C NMR) which, of course, has the same composition as **1**. The

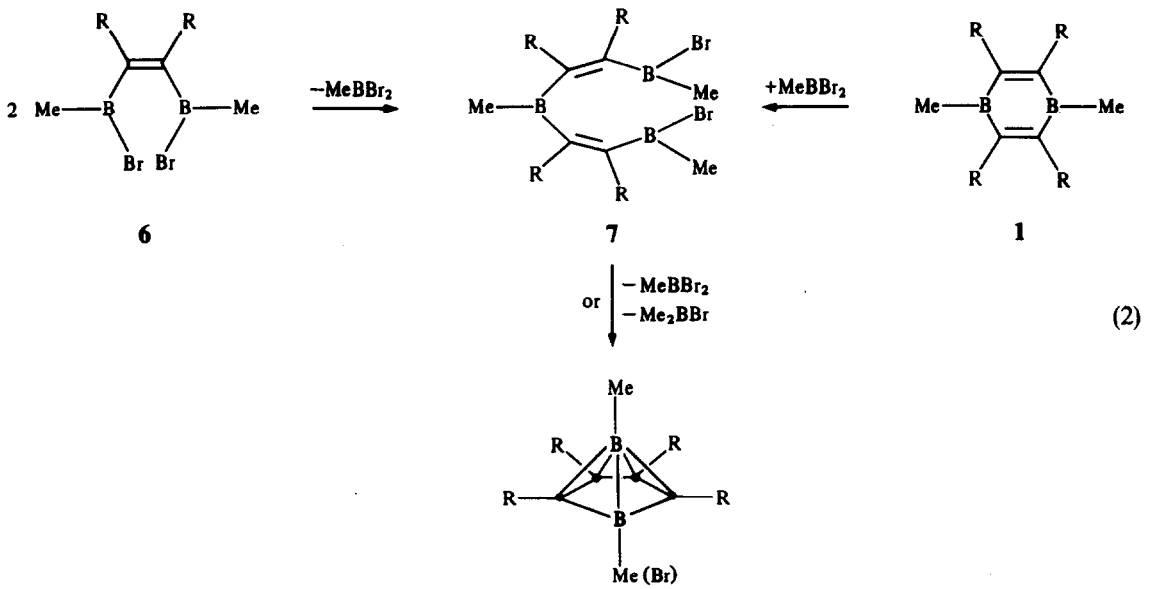


(1)

3 **5** **6**

of carbaboranes **2** and **8**, either via direct reduction of **6** (leading to **8** in case of R = Et, Bu, and to a 1,3-diboretene in case of R = tert.-Bu[13,28]) or via compounds **7** (which tend to rearrange and to boron halides[15,16b]) [Eqn (2)].

air and moisture sensitivity, as well as the yellow colour was traced to small amounts of organoboron bromides like **3** or **4**. Therefore, it is concluded that the reported[13] synthesis of hexaalkyl-1,4-dibora-2,5-cyclohexadienes (**1**) is not firmly established. We



(2)

6 **7** **1** **2**

emphasize that ^{11}B NMR, in particular in combination with ^{13}C NMR, is very convenient to analyse complex mixtures of organoboranes.

EXPERIMENTAL

NMR spectra were recorded with a BRUKER WP-200 spectrometer operating in PFT-mode at 50.3 MHz (^{13}C) and 64.2 MHz (^{11}B). The ^{13}C-probehead was modified to perform $^{13}C\{^1H, ^{11}B\}$ heteronuclear triple resonance experiments. Energy dispersive X-ray diffractograms were recorded on a home-built apparatus.[17] The XPS data were obtained on a Leybold-Heraeu spectrometer with the EA 10 analyser. Spectra were taken at 80 K in a vacuum of 2×10^{-10} torr.

All operations were carried out under dry and oxygen-free nitrogen or argon. Solvents were carefully dried, degassed and saturated with nitrogen. The alkynes were commercial products, $MeBBr_2$ was prepared from Me_4Sn and BBr_3.[29] The purity of $MeBBr_2$ (BBr_3 and $Me_2BBr < 3\%$) was checked by ^{11}B NMR.

Potassium-graphite, C_8K

Method A. 25 g synthetic graphite powder (Lonza, KS 2.5) was filled in a two-bulb tube of 28 mm diameter and *ca* 55 cm length. After heating to 300°C/10^{-6} torr for 3 h the tube was transferred to an argon-filled box (water level *ca* 0.4 ppm). 10.1 g potassium (Merck, doubly distilled before use) to form $C_{8.05}K$ was added. The tube was then sealed under vacuum (10^{-6} torr) and placed for 24 h in a two-zone furnace with the graphite side at 320°C and the potassium side at 300°C. The resulting potassium-graphite was filled into various flasks for further reactions.

Method B. The preparation was carried out in a similar way as in A. Quadratic pieces of $5 \times 5 \times 0.2$ mm grafoil (Union Carbide) were used and the reaction was conducted at temperatures of 310°C (graphite) and 290°C (potassium) for 36 h.

Method **C**. The preparation was carried out as described.[18] Flakes (S40) of natural graphite were used.

Reactions of C_8K *with* $MeBBr_2$ *in the presence of alkynes*

6.75 g (50 mmoles) of C_8K (**A, B, C**) were suspended in 25 cm^3 benzene or hexane and 20 mmole 3-hexyne or 5-decyne were added. According to the experimental conditions required (see results) solutions of 3.72 g $MeBBr_2$ (20 mmole) in 10 cm^3 benzene or hexane were added dropwise over a period of *ca* 0.5 h. When the proceeding of the reaction had been checked by ^{11}B NMR the solid was separated by filtration and volatile materials were removed *in vacuo* from the dark brown liquid. Fractional distillation (40–80°C/10^{-3} torr) in case of potassium-graphite (**A, B**) gave mixtures of compounds as described (results), whereas in case of potassium-graphite (**C**) only traces of the carbaboranes **2a, b** could be recovered. For C_8K (**A, B**) the yield of **2a, b** (based on $MeBBr_2$) was *ca* 35%.

Acknowledgements—Support of this work by the Deutsche Forschungsmeinschaft (B.W.), by the Fonds der Chemischen Industrie (B.W.) and by the Swiss National Science Foundation (R.S.) is gratefully acknowledged. We thank Prof. Dr. R. Köster for the GC/MS analysis.

REFERENCES

1. M. E. Vol'pin, Yu. D. Koreshkov, V. G. Dulova and D. N. Kursanov, *Tetrahedron* 1962, **18**, 107.
2. (a) J. H. Morris, *Comprehensive Organometallic Chemistry* (Edited by G. Wilkinson, F. G. A. Stone and E. W. Abel), Vol. 1, p. 311. Pergamon Press, Oxford (1982); (b) R. Köster, *Olefinische Triorganoborane*, in Houben-Weyl, Methoden der Organischen Chemie (Edited by R. Köster), Vol. 13/3a, pp. 174–235. Thieme Verlag, Stuttgart (1982).
3. (a) S. M. van der Kerk, P. H. M. Budzelaar, A. van der Kerk-van Hoof, G. J. M. van der Kerk and P. v. R. Schleyer, *Angew. Chem.* 1983, **95**, 61; *Angew. Chem. Int. Ed. Engl.* 1983, **22**, 48; (b) C. Pues and A. Berndt, *Angew. Chem.* 1984, **96**, 306; *Angew. Chem. Int. Ed. Engl.* 1984, **23**, 313; (c) C. Habben and A. Meller, *Chem. Ber.* 1984, **117**, 2531.
4. (a) A. J. Leusink, W. Drenth, J. G. Noltes and G. J. M. van der Kerk, *Tetrahedron Lett.* 1967, 1263; (b) G. Axelrod and D. F. Halpern, *J. Chem. Soc. Dalton Trans.* 1971, 291; (c) J. J. Eisch and J. E. Galle, *J. Am. Chem. Soc.* 1975, **97**, 4436; (d) S. M. van der Kerk, J. Boersma and G. J. M. van der Kerk, *J. Organomet. Chem.* 1981, **215**, 303.
5. (a) A. J. Ashe III and P. Shu, *J. Am. Chem. Soc.* 1971, **93**, 1804; (b) G. E. Herberich, H. J. Becker, K. Carsten, C. Engelke and W. Koch, *Chem. Ber.* 1976, **109**, 2382.
6. (a) G. E. Herberich, B. Buller, B. Hessner and W. Oschmann, *J. Organomet. Chem.* 1980, **195**, 253; (b) G. E. Herberich and H. Ohst, *Z. Naturforsch. Teil B* 1983, **38**, 1388.
7. G. E. Herberich, *Comprehensive Organometallic Chemistry* (Edited by G. Wilkinson, F. G. A. Stone and E. W. Abel), Vol. 1, p. 381. Pergamon Press, Oxford (1982) (and references cited therein).
8. (a) J. J. Eisch, N. K. Hota and S. Kozima, *J. Am. Chem. Soc.* 1969, **91**, 4575; (b) L. Killian and B. Wrackmeyer, *J. Organomet. Chem.* 1978, **148**, 137.
9. (a) P. L. Timms, *Acc. Chem. Res.* 1973, **6**, 118 (and references cited therein); (b) G. E. Herberich and B. Hessner, *J. Organomet. Chem.* 1978, **161**, C36; (c) B.

Wrackmeyer, *Revs. Silicon, Germanium, Tin, Lead Compds.* 1982, **6**, 75.
10. (a) B. G. Ramsey and D. M. Anja, *J. Am. Chem. Soc.* 1977, **99**, 3182; (b) J. J. Eisch and H. P. Becker, *J. Organomet. Chem.* 1979, **171**, 141; (c) B. Pachaly and R. West, *Angew. Chem.* 1984, **96**, 444; *Angew. Chem. Int. Ed. Engl.* 1984, **23**, 454.
11. (a) S. M. van der Kerk, G. J. M. Boersma and G. J. M. van der Kerk, *Tetrahedron Lett.* 1976, 4765; (b) S. M. van der Kerk and G. J. M. van der Kerk, *J. Organomet. Chem.* 1980, **190**, C11; (c) S. M. van der Kerk, A. L. M. van Eekeren and G. J. M. van der Kerk, *J. Organomet. Chem.* 1980, **190**, C8.
12. S. M. van der Lerk, J. C. Roos-Venekamp, A. J. M. van Beijnen and G. J. M. van der Kerk, *Polyhedron* 1983, **2**, 1337.
13. S. M. van der Kerk, P. H. M. Budzelaar, A. L. M. van Eekeren and G. J. M. van der Kerk, *Polyhedron* 1984, **3**, 271.
14. (a) M. S. Whittingham and L. B. Ebert, in *Physics and Chemistry of Layered Materials* (Edited by F. Levy), Vol. 6, p. 533. Dordrecht, Reidel (1979); (b) R. Setton, F. Beguin and S. Piroelle, *Synth. Met.* 1982, **4**, 299; (c) W. C. Forsman, T. Dziemianowicz, F. Leong and D. Carl, *Synth. Met.* 1983, **5**, 77; (d) M. E. Vol'pin, Yu. N. Novikov, V. M. Kopylov, L. M. Khananashvili and T. B. Kakuliya, *Synth. Met.* 1982, **4**, 331.
15. H.-O. Berger, H. Nöth and B. Wrackmeyer, *Chem. Ber.* 1979, **112**, 2884.
16. (a) P. Binger, *Tetrahedron Lett.* 1966, 2675; (b) B. Wrackmeyer, *Z. Naturforsch. Teil B* 1982, **37**, 412.
17. M. S. Dresselhaus and G. Dresselhaus, *Adv. in Physics*, 1981, **30**, 139.
18. H. Podall, W. E. Foster and A. P. Giraitis, *J. Org. Chem.* 1958, **23**, 82.
19. F. Beguin, R. Setton, L. Facchini, A. P. Legrand, G. Merle and Ch. Mai, *Synth. Met.* 1980, **2**, 161.
20. (a) J. Jegondez, C. H. Mazieres and R. Setton, *Synth. Met.* 1983, **7**, 85; (b) R. Schlögl, Dissertation, University of Munich (1982).
21. (a) L. J. Todd and A. R. Siedle, *Progr. NMR Spectrosc.* 1979, **13**, 87; (b) A. R. Siedle, *Ann. Rep. NMR Spectrosc.* 1982, **12**, 177.
22. B. Wrackmeyer and R. Köster, *Analytik der Organobor-Verbindungen*, in Houben-Weyl, Methoden der organischen Chemie (Edited by R. Köster), Vol. 13/3c, pp. 377–611. Thieme Verlag, Stuttgart (1984).
23. The X-ray diffractogram of the solid in contact with the reaction solution was identical to that obtained after separation and drying of the solid (shown in Fig. 1).
24. A detailed analysis of the solid products which are complex ternary intercalates will be presented elsewhere. A large portion of the potassium-metal is still inside the graphite, KBr was detected at the surface and the presence of boron has been shown by energy dispersive X-ray analysis and electron energy loss spectroscopy.
25. H.-O. Kalinowski, S. Berger and S. Braun, *^{13}C NMR-Spektroskopie*, pp. 115, 263. Georg Thieme Verlag, Stuttgart (1984).
26. (a) R.-J. Binnewirtz, H. Klingenberger, R. Welte and P. Paetzold, *Chem. Ber.* 1983, **116**, 1271; (b) M. F. Lappert and B. Prokai, *J. Organometal. Chem.* 1964, **1**, 384; (c) S. Hara, H. Dojo, S. Takinami and A. Suzuki, *Tetrahedron Lett.* 1983, 731.
27. W. Siebert, M. El-Din and M. El-Essawi, *Chem. Ber.* 1979, **112**, 1480.
28. R. Wehrmann, C. Pues, H. Klusik and A. Berndt, *Angew. Chem.* 1984, **96**, 372; *Angew. Chem. Int. Ed. Engl.* 1984, **23**, 372.
29. H. Nöth and H. Vahrenkamp, *J. Organomet. Chem.* 1968, **11**, 399.

Polyhedron Vol. 4, No. 5, pp. 893–895, 1985
Printed in Great Britain

0277–5387/85 $3.00 + .00
© 1985 Pergamon Press Ltd

COMMUNICATION

A DIPHOSPHIDE ADDUCT OF DITUNGSTEN-HEXAISOPROPOXIDE: X-RAY CRYSTAL STRUCTURE OF $W_2(OPr^i)_6(py)(\mu\text{-}P_2)$

MALCOLM H. CHISHOLM,* KIRSTEN FOLTING, JOHN C. HUFFMAN and J. J. KOH
Department of Chemistry and Molecular Structure Center, Indiana University, Bloomington, IN 47405, U.S.A.

(*Received* 21 *January* 1985; *accepted* 1 *February* 1985)

Abstract—From the reaction between $W_2(OPr^i)_6(py)_2$ and $Co_2(\mu\text{-}P_2)(CO)_6$ in hexane at room temperature a black crystalline product has been shown to be $W_2(OPr^i)_6(py)(\mu\text{-}P_2)$ by a single crystal X-ray determination. There is a central pseudo tetrahedral W_2P_2 moiety with W—W = 2.695(1) Å, P—P = 2.154(4) Å and W—P = 2.45(2) Å (averaged) corresponding to essentially single bond distances. This new compound is an analogue of the ethyne adducts $W_2(OR)_6(py)(\mu\text{-}C_2H_2)$, where R = Bu^t and CH_2Bu^t, and these in turn are related to $Co_2(CO)_6(\mu\text{-}X)$ compounds (X = P_2, C_2R_2) by isolobal relationships.

There are many complementary aspects of the chemistry of the alkoxide and carbonyl ligands. Alkoxides may act as π-donors and stabilize high oxidation state early transition metal ions, which are d^n electron-poor, while carbonyl ligands are π-acceptors and stabilize the d^n electron-rich later transition elements in their low oxidation states. Both ligands may act as bridging ligands (μ_2 and μ_3) and often bridge $\rightleftharpoons$ terminal site exchange is rapid on the NMR time scale. The 15-electron fragment $Co(CO)_3$ and the d^3-fragments $W(OR)_3$ and $W(OR)_3(py)$ are isolobal.[1,2] The templates $Co_2(CO)_6$ and $W_2(OR)_6$ both support perpendicular alkyne adducts[3,4] and the alkylidyne capped compounds $Co_3(\mu_3\text{-}CR)(CO)_9$[5] and $W_3(\mu_3\text{-}CMe)(OPr^i)_9$[6] may also be viewed as isolobal analogues. We describe here our fortuitous discovery of $W_2(OPr^i)_6(py)(\mu\text{-}P_2)$, which provides a further extension of the $(W{\equiv}W)^{6+}$ and "$(CO)_3Co{\equiv}Co(CO)_3$" relationships.

We recently found that, in hexane at room temperature, the reaction between $W_2(OPr^i)_6(py)_2$[7] and $Fe_2(\mu\text{-}S_2)(CO)_6$[8] yields $W_2Fe_2S_2(OPr^i)_6(CO)_5(py)$.[9] This compound contains a planar W_2Fe_2 unit with two W—Fe bonds and one W—W and one Fe—Fe bond supported by two $\mu_3\text{-}S^{2-}$ ligands. This prompted us to investigate the reaction between the structurally related and isoelectronic compound $Co_2(CO)_6(\mu\text{-}P_2)$[10] and $W_2(OPr^i)_6(py)_2$. Under analogous conditions in hexane at room temperature the black crystalline compound $W_2(OPr^i)_6(py)(\mu\text{-}P_2)$ was isolated in *ca* 30% yield by cooling the solution to −15°C. The fate of the $Co(CO)_3$ fragments, which quite plausibly form $Co_4(CO)_{12}$, are currently not known. Further studies of this reaction and possible alternate, more direct synthetic routes to $W_2(OPr^i)_6(py)(\mu\text{-}P_2)$, such as a direct reaction between P_4 (one half equivalent) and $W_2(OPr^i)_6(py)_2$, are currently under investigation.

A view of the molecular structure of $W_2(OPr^i)_6(py)(\mu\text{-}P_2)$ deduced† from a single crystal

* Author to whom correspondence should be addressed.

† Crystal data for $W_2(OPr^i)_6(py)(\mu\text{-}P_2)$ at −162°C; a = 9.021(3) Å, b = 20.174(10) Å, c = 16.824(6) Å, β = 92.70(2)°, Z = 4, $d_{calc.}$ = 1.826 g cm^{-3}, and space group $P2_1/n$. Of the 7375 reflections collected using Mo-K_α, $6° \leqslant 2\theta \leqslant 45°$, 4120 were unique and the 3447 having $F > 3\sigma(F)$ were used in the least-squares refinement. H atoms were included as fixed-atom contributors in idealized positions. All other atoms were refined anisotropically. Final residuals are $R(F)$ = 0.0359 and $R_w(F)$ = 0.0352.

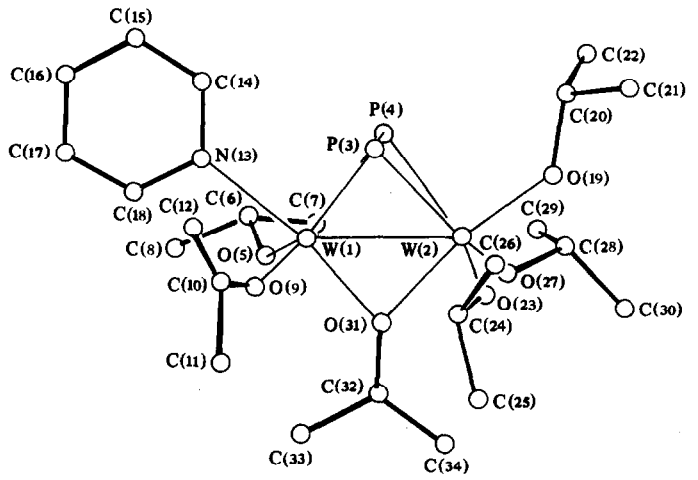


Fig. 1. A ball-and-stick drawing of the $W_2(OPr^i)_6(py)(\mu\text{-}P_2)$ molecule giving the number scheme for the atoms. Pertinent distances (Å) are: W(1)—W(2) = 2.695(1), W(1)—P(3) = 2.432(3), W(1)—P(4) = 2.428(3), W(1)—O(5) = 1.902(7), W(1)—O(9) = 1.892(7), W(1)—O(31) = 1.989(6), W(1)—N(13) = 2.258(8), W(2)—P(3) = 2.491(3), W(2)—P(4) = 2.462(3), W(2)—O(19) = 1.919(7), W(2)—O(23) = 1.901(7), W(2)—O(27) = 1.932(7), W(2)—O(31) = 2.074(7), P(3)—P(4) = 2.154(4).

X-ray determination is shown in Fig. 1. There is a central pseudo-tetrahedral W_2P_2 unit with W—W = 2.69 Å, P—P = 2.15 Å and W—P = 2.45(2) Å (averaged). The presence of one alkoxide bridge and one supporting pyridine ligand make this P_2 adduct a structural analogue of the compounds $W_2(OR)_6(py)(\mu\text{-}C_2H_2)$, where R = Bu^t[4] and CH_2Bu^t.[11] The compound $W_2(OPr^i)_6(py)_2(\mu\text{-}C_2H_2)$ also contains a central pseudo-tetrahedral W_2C_2 core but this is supported by two alkoxide bridges and has one pyridine ligand bonded to each W atom.[4] The presence of one or two OR bridges and one or two pyridine ligands is believed to reflect subtle steric differences between the various OR ligands. Since the alkoxide ligands can act as σ- and π-donors the total valence electron count for each tungsten atom is "buffered" with respect to the EAN rule and the presence of supplemental pyridine ligands. Thus the present compound is viewed as an analogue of $Co_2(CO)_6(\mu\text{-}P_2)$[10] and $Co_2(CO)_5(PPh_3)(\mu\text{-}P_2)$.[12]

The P—P distance in $W_2(OPr^i)_6(py)(\mu\text{-}P_2)$ is close to the single P—P distance, 2.21 Å, in P_4[13] and notably longer than the P—P distance, 2.019(9) Å, observed in $Co_2(CO)_5(PPh_3)(\mu\text{-}P_2)$.[12] This parallels the longer C—C distances seen in alkyne adducts of $W_2(OR)_6$ relative to "$Co_2(CO)_6$" and reflects the greater reducing power of the $(W{\equiv}W)^{6+}$ moiety.[4] The compounds $(Bu^tO)_3W{\equiv}P$ and $(Pr^iO)_9W_3(\mu_3\text{-}P)$, analogues of $(Bu^tO)_3W{\equiv}N$[14] and $(CO)_9(Co_3(\mu_3\text{-}P))$[15], may also be accessible.

Further studies are in progress.

Supplementary materials available

Tables of fractional coordinates have been deposited with the Cambridge Crystallographic Data Centre. Complete structural information is available from the Editor at Queen Mary College and, in microfiche form, from the Indiana University Chemistry Library, Bloomington, IN 47405 at a cost of $2.50 per report. Request MSC Report No. 84112.

Acknowledgements—We thank the National Science Foundation and the Wrubel Computing Center for support.

REFERENCES

1. R. Hoffmann, *Angew. Chem., Int. Ed. Engl.* 1982, **21**, 711.
2. R. Hoffmann, *Science* 1981, **211**, 995.
3. W. G. Sly, *J. Am. Chem. Soc.* 1959, **81**, 18.
4. M. H. Chisholm, K. Folting, D. M. Hoffman and J. C. Huffman, *J. Am. Chem. Soc.* 1984, **106**, 6794.
5. B. R. Penfield and B. H. Robinson, *Acc. Chem. Res.* 1973, **6**, 73.
6. M. H. Chisholm, D. M. Hoffman and J. C. Huffman, *Inorg. Chem.* 1984, **23**, 3683.
7. M. Akiyama, M. H. Chisholm, F. A. Cotton, M. W. Extine, D. A. Haitko, D. Little and P. E. Fanwick, *Inorg. Chem.* 1979, **18**, 2266.
8. C. H. Wei and L. F. Dahl, *Inorg. Chem.* 1965, **4**, 1.
9. M. H. Chisholm, J. C. Huffman and J. J. Koh, results to be published.

10. A. Vizi-Orosz, G. Palyi and L. Marko, *J. Organomet. Chem.* 1973, **60**, 625.
11. M. H. Chisholm, B. Conroy, D. M. Hoffman and J. C. Huffman, results to be published.
12. C. F. Campara, A. Vizi-Orosz, G. Palyi, L. Marko and L. F. Dahl, *Inorg. Chem.* 1979, **18**, 3054.
13. D. E. C. Corbridge, *The Structural Chemistry of Phosphorus*. Elsevier, Amsterdam (1974).
14. M. H. Chisholm, D. M. Hoffman and J. C. Huffman, *Inorg. Chem.* 1983, **22**, 2303.
15. A. Vizi-Orosz, *J. Organomet. Chem.* 1976, **111**, 614.

Polyhedron Vol. 4, No. 5, pp. 897–898, 1985
Printed in Great Britain

0277–5387/85 $3.00 + .00
© 1985 Pergamon Press Ltd

COMMUNICATION

SPECTROPHOTOMETRIC DETERMINATION OF STABILITY CONSTANTS OF Ni(II) AND Cu(II) COMPLEXES WITH *N*-SUBSTITUTED HYDRAZINEDITHIOCARBOXYLIC ACIDS

A. IZQUIERDO*
Departamento de Química Analítica, Facultad de Química, Universidad de Barcelona, Diagonal 647, Barcelona-8, Spain

and

J. GUASCH and F. X. RIUS
Departamento de Química Analítica, Facultad de Química en Tarragona, Universidad de Barcelona, Pl. Imperial Tárraco s/n, Tarragona, Spain

(*Received* 8 *February* 1985; *accepted* 26 *February* 1985)

Abstract—The stability constants of Ni(II) complexes with 2-methylhydrazinedithiocarboxylic and 3,3-dimethylhydrazinedithiocarboxylic acids and Ni(II) and Cu(II) complexes with 3-methyl-3-phenylhydrazinedithiocarboxylic acid have been determined in aqueous solution at 25°C and $I = 0.01$ M. The Bjerrum method of corresponding solutions has been applied, revealing the simultaneous presence of 1:1 and 1:2 complexes in solution.

The study of metallic complexes, in the solid state, of hydrazinedithiocarboxylic acids (dithiocarbazic acids)[1–3] and their derivatives[4–6] is currently drawing considerable attention. These compounds are extensively used as surfactants, pharmaceuticals, fungicides and in vulcanization processes. However, there is little information concerning their chemical equilibria in solution. Byr'ko *et al.*[7] found two ionization constants for the acid–base equilibrium of hydrazinium dithiocarbazate ($pK_1 = 3.87$ and $pK_2 = 8.90$) whilst Izquierdo *et al.*[8] recently reported the existence of only one protonation constant for the ligands: 2-methyldithiocarbazate ($pK = 5.42$), 3,3-dimethyldithiocarbazate ($pK = 4.73$) and 3-methyl-3-phenyldithiocarbazate ($pK = 6.18$). No data have been found in the literature relating to the stability constants of the dithiocarbazate metallic complexes.

In the present work, the spectrophotometric determination of the stability constants at 25°C and $I = 0.01$ M of 2-methyldithiocarbazate and 3,3-dimethyldithiocarbazate complexes with Ni(II) and 3-methyl-3-phenyldithiocarbazate complexes with Ni(II) and Cu(II) is reported.

EXPERIMENTAL

The synthesis of the ligands has been described elsewhere.[8] The Cu(II) (1.55×10^{-2} M) and Ni(II) (1.908×10^{-1} M) stock solutions were obtained by diluting the proper amount of $Cu(NO_3)_2 \cdot 3H_2O$ and $NiCl_2 \cdot 6H_2O$ respectively in distilled water. Their concentrations were determined electrogravimetrically.[9] Buffer solutions ($I = 0.01$ M) were prepared according to Perrin and Dempsey.[10]

A Beckman UV5260 spectrophotometer, equipped with 1.00-cm quartz cells was used for spectrophotometric measurements. pH values were measured in a Radiometer PHM-64 pHmeter using a G-202 glass and a K-401 saturated calomel Radiometer electrodes, standardized with buffer solutions of pH = 4.008 and 6.865 (25°C) according to the NBS.[11]

The absorbance of five different series of solutions for each complex studied was measured at two wavelengths in the region where the free ligands do

* Author to whom correspondence should be addressed.

Table 1. Equilibrium constants ($\log \beta_n$) for the formation of species (metal ion)(dithiocarbazate)$_n$ at $I = 0.01$ M and 25°C which minimize the error-square sum (U)*

Ligand	Equilibrium	N	$\log \lvert\beta \pm s(\beta)\rvert$	U_{min}	W_{min}† (%)
2-Methyldithiocarbazate $[NH_2N(CH_3)CS_2]^-$	Ni+L = NiL Ni+2L = NiL_2	18	7.20±0.03 14.02±0.03	2.29E−3	2.95
3,3-Dimethyldithiocarbazate $[(CH_3)_2NNHCS_2]^-$	Ni+L = NiL Ni+2L = NiL_2	20	6.32±0.07 12.64±0.03	3.00E−3	1.91
3-Methyl-3-phenyldithiocarbazate $[(C_6H_5)(CH_3)NNHCS_2]^-$	Ni+L = NiL Ni+2L = NiL_2	19	5.77±0.05 12.61±0.05	9.04E−3	2.28
	Cu+L = CuL Cu+2L = CuL_2	22	4.66±0.06 11.49±0.03	2.99E−3	1.69

* $U = \sum_1^N (\bar{n}_{exp.} - \bar{n}_{calc.})^2$.

† $W = \left\{ \sum_1^N |(\bar{n}_{exp.} - \bar{n}_{calc.})100/\bar{n}_{exp.}|^2/(N-1) \right\}^{1/2}$.

not absorb. In each series, the analytical concentration of metal ion (M_T) was kept constant within the range 0.18×10^{-5}–5.3×10^{-5} M, while the analytical concentration of ligand (L_T) was varied within the range 0.6×10^{-6}–1.2×10^{-4} M, being the pH controlled by means of a buffer solution of I = 0.01 M. All solutions have been thermostatted at 25±0.1°C. The optimum conditions for the spectrophotometric study to be carried out were established beforehand.

The Bjerrum method of corresponding solutions was applied.[12] The preliminary overall stability constants (β_n), determined by means of graphical analysis from $[L]$ and $\bar{n}$ pairs of values, were used as input data for the MINI1W program computer for nonlinear minimax optimization,[13] by using a Digital PDP 11 | 60 computer.

RESULTS

Since, for all complexes studied, the most favourable pH range spans the interval 5.1–9.3, a phosphate buffer, pH = 7.70, was chosen on account of the small stability constants of the Ni(II) and Cu(II) complexes with this ligand.[14] The overall stability constants found are given in Table 1. When comparing the values found in the present work with those corresponding to Cu(II) complexes with several *N*-substituted dithiocarbamic acids,[15] greater values of the last-named ($\log \beta_1$ = 11–12.5, $\log \beta_2$ = 21–24) are noticed. On the contrary, Hulanicki[15] has found a value of the stability constant for the Ni(II) complex with bis(carboxymethyl)dithiocarbamic acid much lower ($\log \beta_2 = 7.9$) than those reported in this paper for the Ni(II)–dithiocarbazate complexes.

REFERENCES

1. R. A. Haines and W. J. Louch, *Inorg. Chim. Acta* 1983, **71**, 1.
2. N. V. Mel'nikova, A. T. Philipenko and V. P. Badekla, *Ukr. Khim. Zh.* 1981, **47**, 42.
3. G. Dessy and V. Fares, *Cryst. Struct. Commun.* 1980, **9**, 1111.
4. A. Monaci, F. Tarli, G. Chiozzini and M. Zugarini, *Thermochim. Acta* 1982, **53**, 309.
5. M. T. H. Tarafder, M. A. J. Miah, R. N. Bose and M. A. Ali, *J. Inorg. Nucl. Chem.* 1981, **43**, 3151.
6. A. Monaci and F. Tarli, *J. Chem. Soc., Dalton Trans.* 1980, 499.
7. V. M. Byr'ko, A. I. Busev, T. I. Tikhonova, N. V. Baibakova and L. I. Shepel, *Zh. Anal. Khim.* 1975, **30**, 1885.
8. A. Izquierdo, J. Guasch and F. X. Rius, *Talanta* 1985, **32**, 78.
9. A. I. Vogel, *Textbook of Quantitative Inorganic Analysis*, 4th edition. Longman, London (1978).
10. D. D. Perrin and B. Dempsey, *Buffers for pH and Metal Ion Control*, 4th edition, Table 3.8. Chapman & Hall, London (1974).
11. R. G. Bates, *J. Res. Nat. Bur. Stand.* 1962, **A66**, 179.
12. W. A. E. McBryde, *Talanta* 1974, **21**, 979.
13. K. Madsen and H. Schjaer-Jacobsen, Report 76-15, Electromagnetics Institute, Technical University of Denmark, Lyngby, Denmark (1975).
14. L. G. Sillén and A. E. Martell, *Stability Constants for Metal Ion Complexes*. The Chemical Society, London (1964).
15. A. Hulanicki, *Talanta* 1967, **14**, 1371.

Polyhedron Vol. 4, No. 5, p. 000, 1985
Pergamon Press Ltd. Printed in Great Britain

ANNOUNCEMENT

THE SECOND INTERNATIONAL CONFERENCE ON THE BASIC AND APPLIED CHEMISTRY OF *f*-TRANSITION (LANTHANIDE AND ACTINIDE) AND RELATED ELEMENTS

1–5 September 1986

PROVISIONAL LIST OF TOPICS

(1) Coordination and organometallic chemistry
(2) Theory and spectroscopy
(3) Reactivity and catalysis
(4) Solid-state chemistry
(5) Analytical chemistry
(6) Industrial applications

Organizing committee: K. W. Bagnall (Chairman), Manchester; U. Croatto, Padova; N. Edelstein, Berkeley; R. D. Fischer, Hamburg; A. Pires de Matos (Scientific Secretary), Lisboa; Changtao Qian, Shanghai; G. Vicentini, São Paulo.

All requests for information should be addressed to:

A. Pires de Matos,
Departmento de Química,
Instituto de Energia, LNETI,
Estrada Nacional 10,
2686 Sacavem Codex,
Portugal
Tel. 2550021, telex 12/2/NUCLAB P.

Polyhedron Vol. 4, No. 6, pp. 901–927, 1985
Printed in Great Britain

0277–5387/85 $3.00 + .00
Pergamon Press Ltd

POLYHEDRON REPORT NUMBER 11

ARENE–CHROMIUM TRICARBONYL COMPLEXES: BONDING AND BEHAVIOUR

A. SOLLADIÉ-CAVALLO
Laboratoire de Stéréochimie Organometallique, ERA No. 687, Université Louis Pasteur, 1, rue Blaise Pascal, 67008 Strasbourg, France

CONTENTS

I. NATURE OF BONDING 901
A. Spectroscopic properties 901
(a) IR 901
(b) NMR 903
B. Electronic effects. 904
(a) Dipole moments 904
(b) Inductive effects. 906
(c) Stabilization of a positive charge in α- or β-position 907
(d) Stabilization of a negative charge in α- or β-position 909
(e) Basicity of benzylic protons vs aromatic protons 911
(f) Metallation 912
C. Theoretical calculations 913
(a) SCCC MO 913
(b) CNDO/2 914
(c) *Ab initio* 914
II. CHARGE-TRANSFER COMPLEXES 915
III. CONFORMATIONS 916
A. Conformation of the tripod 916
B. Conformation of substituents 919
IV. STEREOELECTRONIC CONTROL OF THE REGIOSELECTIVITY 920
A. Nucleophilic reactions. 920
B. Electrophilic reactions. 922
V. COMPLEXATION SITE ON DIAROMATIC LIGANDS 923

I. NATURE OF BONDING

A. Spectroscopic properties

(*a*) *IR.* The IR spectra of substituted and nonsubstituted benzene chromium tricarbonyl complexes have been extensively studied and reviewed.[1] This paper will focus on the carbonyl stretching frequencies and will give only the main conclusions.

All the complexes have two IR active stretching vibrations for the terminal carbonyl groups in agreement with the C_{3v} local symmetry (Tables 1 and 2). However, when high-resolution spectra are studied, and when unsymmetrically substituted arenes are involved, this C_{3v} local symmetry is of more restricted validity.

Here the degenerate $(E)\nu_{CO}$ band is split[2,3] but the splitting is small [$\leqslant 10\ cm^{-1}$ (Table 3)].

The IR absorptions of the $Cr(CO)_3$ groups are sensitive to the electronic effects of the substituent of the arene ligand transmitted through the metal to the carbonyls of the $Cr(CO)_3$ group[2,4–12] (Tables 1

Table 1. ν_{CO} of $Cr(CO)_3$ group in $(C_6H_5R)Cr(CO)_3$

R	A_1 (cm^{-1})	E (cm^{-1})	Ref.	Solvent
CO_2Me	1992	1930	8	Isooctane
Cl	1992	1931	6	Cyclohexane
H	1987	1918	6	Cyclohexane
CH_3	1983	1914	2	Cyclohexane
$CH{=}CH_2$	1980	1913	9	Cyclohexane
$CH_2{-}CH{=}CH_2$	1977	1906	11	Cyclohexane
OMe	1975	1903	5	CCl_4
OMe	1983	1914	6	Cyclohexane
$OCH_2CH{=}CH_2$	1976	1906	11	Cyclohexane
NH_2	1974	1902	6	Cyclohexane

Table 2. ν_{CO} of $Cr(CO)_3$ group in $(C_6H_4R_1R_2)Cr(CO)_3$

R_1	R_2	A_{1max} (cm^{-1})	E_{max} (cm^{-1})	Ref.	Solvent
CO_2Me	2-Cl	1996 vs	1936 s	4	CCl_4
CO_2Me	H	1990 vs	1926 s	4	CCl_4
CO_2Me	H	1992 vs	1930 s	8	Isooctane
CO_2Me	2-Me	1984 vs	1920 s	4	CCl_4
CO_2Me	2-Me	1988 vs	1925 s	8	Isooctane
CO_2Me	2-OMe	1984 vs	1920 s	4	CCl_4
CO_2Me	2-OMe	1987 vs	1924, 1917	8	Isooctane
CO_2Me	4-NH_2	1978 vs	1912 s	4	CCl_4
H	$CH{=}CH_2$	1980 vs	1913 vs	9	Cyclohexane
OMe	2-OMe	1969 vs	1894 vs	5	CCl_4
NH_2	4-NH_2	1942 vs	1855 vs	12	THF
NH_2	2-NH_2	1942 vs	1848–1808	12	Br
CHO	H	1970 vs	1895 s	10	$CHCl_3$
CHO	2-Me	1970 vs	1895 s	10	$CHCl_3$
CHO	2-OMe	1975 vs	1900 s	10	$CHCl_3$

Table 3. ν_{CO} of $Cr(CO)_3$ group in $LCr(CO)_3$

L	A_{1max} (cm^{-1})	E_{max} (cm^{-1})	Solvent
C_6H_6	1983 vs	1915 vvs	Cyclohexane (A)
	1970 vs	1891 vvs	CH_2Cl_2 (B)
C_6H_5F	1990 vs	1926 vs, 1923 vs	A
	1979 vs	1902 vvs	B
C_6H_5Me	1977 vvs	1911 vs, 1909 vs	A
	1968 vs	1886 vvs	B
1,2-MeC_6H_4	1973 s	1906 s, 1901 vs	A
	1964 vs	1884 vs	B
1,2,3-MeC_6H_3	1969 vs	1902 vs, 1895 vs	A
	1958 vs	1877 vvs	B

Table 4. ν_{CO} of $CrCO_2$ in $ArCO_2L$

Ar	L	A_1 (cm^{-1}) ($\Delta\nu$)*	E (cm^{-1}) ($\Delta\nu$)*	Solvent	Ref.
$Me_3C_6H_3$	$P(Ph)_3$	1886 (76)	1830 (48)	C_6H_6	14
$Me_3C_6H_3$	$CH_2{=}CH_2$	1901 (61)	1852 (26)	C_6H_6	14
$Me_3C_6H_3$	Cyclopentene	1893 (69)	1842 (36)	C_6H_6	14
Me_6C_6	$P(Ph)_3$	1873 (75)	1810 (51)	C_6H_6	14
Me_6C_6	$CH_2{=}CH_2$	1890 (58)	1835 (26)	C_6H_6	14
		1883 (65)	1835 (26)	C_6H_6	14, 18
$C_6H_5(CH_2)_2CH{=}CH_2$	$P(Ph)_3$	1905 (72)	1856 (50)	Hexane	15
$C_6H_5(OCH_2)CH{=}CH_2$	$P(Ph)_3$	1905 (71)	1854 (52)	Hexane	15
$C_6H_5CO_2Me$	$P(Ph)_3$	1896 (89)	1844 (41)	Nujol	16
	$P(OMe)_3$	1910 (75)	1848 (37)	Nujol	16

* $\Delta\nu = \nu[ArCr(CO)_3] - \nu[ArCr(CO)_2L]$.

and 2). The frequencies and the force constants calculated using the approach proposed by Cotton[13] are found to decrease slightly as the electron-donating power of the substituent increases. However there is practically no influence due to the relative position of the substituents within the ring.[4,5] Good correlations are also found between the force constant of the carbonyl (or the stretching frequencies) and the different Hammett constants of the substituents.[4,5,7] This behaviour indicates that an increase in π-electron density enables the chromium atom to transfer electrons into the antibonding orbitals of the C≡O groups, thus decreasing the CO bond order.

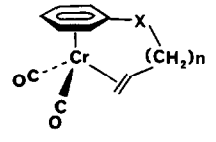
A decrease in the ν_{CO} frequencies is also observed when one of the C≡O is replaced by a phosphine,[14–16] an imine[17] or an olefin[11,14,18] (see Tables 4 and 5). Phosphines, imines and olefins are electron-releasing substituents which increase electron density on the chromium atom. Back-donation from the chromium atom occurs into the antibonding orbitals of the two remaining C≡O and thus decreases the CO bond order. Empty *d*-orbitals of the phospine as well as π-antibonding orbitals of the imines or olefins are obviously less available than those of C≡O for such back-bonding.

However, it must be noticed that replacement of one C≡O by malic anhydride increases the frequency of the *E* band by 20–28 cm^{-1}, the *A*-band being constant.[19,20]

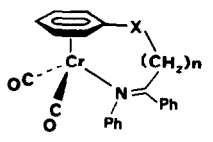
(*b*) *NMR.* The most obvious characteristic of the ^1H, ^{13}C and ^{19}F NMR spectra is the upfield shift of the corresponding resonance upon complexation.

Table 5. ν_{CO} of $Cr(CO)_2$ in $(ArL)Cr(CO)_2$

	A_1 (cm^{-1}) ($\Delta\nu$)	E (cm^{-1}) ($\Delta\nu$)	Solvent	Ref.
(a) $[C_6H_5(CH_2)_2CH{=}CH_2]Cr(CO)_2$	1930 (43)	1878 (28)	C_6H_{12}	11
(b) $[C_6H_5OCH_2CH{=}CH_2]Cr(CO)_2$	1938 (38)	1885 (21)	C_6H_{12}	11
(c) $[C_6H_5(CH_2)_3CH{=}CH_2]Cr(CO)_2$	1923 (54)	1871 (35)	C_6H_{12}	11
(d) $[C_6H_5(CH_2)_2CH(Ph){=}NPh]Cr(CO)_2$	1890 (75)	1830 (55)	C_6H_6	17
(e) $[C_6H_5(CH_2)_3CH(Ph){=}NPh]Cr(CO)_2$	1888 (82)	1830 (65)	C_6H_6	17

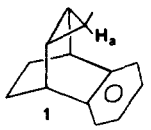


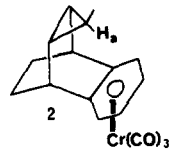
X = CH_2 n = 1 a
X = O n = 1 b
X = CH_2 n = 2 c



X = CH_2 n = 1 d
X = CH_2 n = 2 e

On complexation with $Cr(CO)_3$ aromatic protons undergo an upfield shift of about 1.5–2.5 ppm.[4–6,21,22] Some hypotheses were proposed to explain this diamagnetic shift. The upfield shift could be ascribed to a decrease of the "ring current" contribution to the chemical shift.[23] However, it has been shown that vinylic protons also undergo a 3–3.7 ppm upfield shift on complexation,[11] and that complexation with $Cr(CO)_3$ of compound **1** (to **2**) does not disrupt the aromatic ring current as the chemical shift of $H_a(\delta_a)$ does not change.[24]





Some recent X-ray and neutron diffraction data[25,26] showed a slightly distorted ring, the hydrogen being displaced by $2\text{–}4 \times 10^{-2}$ Å from the ring towards the chromium; however, the ^1H proton spectrum with ^{13}C satellites of benzene–$Cr(CO)_3$ oriented in a nematic phase does not allow the detection of such a deviation.[27] Hence, a change in hybridization may not be the only factor responsible for the shielding. It has been proposed that the magnetic anisotropy of the $Cr(CO)_3$ moiety and of the electrons in the ring–metal bond could produce an upfield shift of the ring proton resonance of the same order of magnitude as the observed shift.[28] This last hypothesis has not yet been refuted.

The most obvious features of the ^{13}C spectra are the large upfield shift—30–40 ppm—of the ring-carbon resonances, and the large downfield shift of the carbonyl-carbon resonances (relative to the uncomplexed C≡O).[29–31] This ring-carbon diamagnetic shift was first related to the change in mobile bond order.[29] Then changes in hybridization of the carbons (associated with the use of π-orbitals for σ-bonding with metal *d*-orbitals) were invoked.[30] It is also possible to account for the observed chemical shifts by postulating the presence of a negative charge on the complexed aromatic ring. But this approach requires the transfer of approximately one electron from the metal to the arene ligand.[31] More recently ^{13}C NMR paramagnetic shielding constants have been calculated using the SCCO MO method and the Pople–Karplus equation.[32] Although only a fair agreement is obtained between the calculated σ^p-values and observed shifts, it is gratifying to note that, in the case of benzene, an upfield shift is predicted as observed on complexation and that a downfield shift is predicted for the carbonyl carbon as observed (relative to free CO).

It is interesting to note that the ^{13}C resonance of methyls substituted in the ring are almost unaffected by the complexation.[24–31] It must be noted also that on complexation olefinic carbon resonances are also usually shielded, the same mechanisms being invoked to explain this behaviour.[33–37]

A correlation has been observed between the ^{13}C carbonyl chemical shifts and either the weighted average of the force constant[31] (calculated using the approach of Cotton[13]) or the carbonyl stretching frequencies[38] for a series of arene–$Cr(CO)_3$. The carbonyl resonance is deshielded when the electron-donating power of the substituent increases, that is with increasing electron density on the $Cr(CO)_3$ group. Thus, it has been proposed that the carbonyl chemical shift reflects the extent of transition metal $\rightarrow \pi^*$ carbonyl back-donation. The study of the transmission of the substituent effects from the arene ring to the $Cr(CO)_3$ group via an analysis of the carbonyl resonance shows a slight predominance of inductive effects and agrees with an important overlap of the metal orbitals with the σ-framework of the arene.[39]

A large upfield shift of about 20 ppm has been observed on complexation with $Cr(CO)_3$ of fluorobenzene[40] for the ^{19}F resonance signal. Such a large shift cannot be explained by the magnetic anisotropy of the $Cr(CO)_3$ moiety alone, which should equivalently contribute to the chemical shift of ^{19}F and ^1H (~ -2 ppm). However, as for ^{13}C, the paramagnetic term of the shielding constant contributes much to the chemical shift of ^{19}F, and changes in hybridization of the vicinal carbon upon complexation might also have a large influence on the ^{19}F chemical shift.

B. Electronic effects

(*a*) *Dipole moments.* Electric dipole moments of arene–$(CO)_3$ complexes, measured in benzene solution, are quite large: ranging from 3.5 to 6.3 D[41–45] (Tables 6 and 7).

Table 6. Dipole moments of arene–$Cr(CO)_3$ measured in benzene solution

Ligand	Dipole moment (D) (Ref.)	Averaged value
C_6H_6	4.81 (43) 4.92 (41) 5.08 (42) 5.03 (44)	4.96
C_6H_5Cl	4.25 (43) 5.08 (42)	4.66
C_6H_5F	4.75 (41) 4.91 (42)	4.83
C_6H_5Me	5.20 (41) 5.26 (42)	5.23
C_6H_5OMe	5.26 (41) 5.43 (42)	5.34
$C_6H_5NMe_2$	6.30 (42) 6.18 (44)	6.24
$C_6H_5NH_2$	5.40 (41) 5.50 (44)	5.45
C_6H_5COMe	4.97 (44)	4.97
$C_6H_5CO_2Me$	4.47 (41)	4.47

According to the IR results (see above), to the numerous studies of the inductive effect of the $Cr(CO)_3$ group and to theoretical data (see below) it is well accepted that in arene–$Cr(CO)_3$ complexes there is a transfer of electrons from the arene ligand through the metal to the carbonyl groups. Hence, owing to the molecular structure, as revealed by X-ray diffraction studies,[46] benzene–$Cr(CO)_3$ has a dipole moment directed along the tricarbonyl C_3-axis and oriented from the arene group to the tripod.[42,44]

The dipole moment of a monosubstituted-benzene–$Cr(CO)_3$ complex is not an additive vector, in that it differs from the vectorial sum μ[benzene–$Cr(CO)_3$] + $\mu(C_6H_5X) = \mu_o + \mu_x$. Both components μ_o and μ_x adopt modified values in the complex.[44]

According to the values of the dipole moments obtained for symmetrically *p*-disubstituted benzene–$Cr(CO)_3$ complexes, where the μ_x-component is 0 (Table 7), it is quite clear that electron-donating

Table 7. Dipole moments of arene–$Cr(CO)_3$ measured in benzene solution

Ligand	Dipole moment (D) (Ref.)
C_6H_6	4.81 (43) 4.92 (41) 5.08 (42) 5.03 (43)
p-$Me_2C_6H_4$	5.39 (41) 5.52 (42) 5.41 (43)
p-$(NH_2)_2C_6H_4$	5.52 (44)
p-$(CO_2Me)_2C_6H_4$	3.52 (43)

Table 8. pK_A[46]

$C_6H_5—CO_2H$ **3** 5.68	$\|C_6H_5—CO_2H\|Cr(CO)_3$ **4** 4.77	$p\text{-}NO_2—C_6H_4—CO_2H$ **5** 4.48
$C_6H_5—CH_2CO_2H$ **6** 5.64	$\|C_6H_5—CH_2CO_2H\|Cr(CO)_3$ **7** 5.02	$p\text{-}NO_2—C_6H_4—CH_2CO_2H$ **8** 5.01

substituents increase the μ_o-component while electron-withdrawing substituents decrease the μ_o-component.[42–44]

Hence the μ_o dipole moment component reflects the electron transfer from the ring to the carbonyls through the metal. However, in the case of disymmetric complexes the μ_x-component must be estimated first.[44]

(*b*) *Inductive effects.* Since the first synthesis of $C_6H_6Cr(CO)_3$ by Fischer[47(a)] and Nicholls[47(b)] the $Cr(CO)_3$ group has often been compared with the NO_2 group.

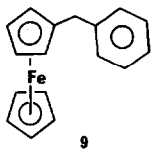
In 1959 the comparison of pK_A values of uncomplexed, complexed and p-NO_2-substituted acids (Table 8) led Whiting *et al.*[46] to the conclusion that the $Cr(CO)_3$ group has the same inductive effect as the NO_2 group.

However, the NO_2 group must have an extra capability to stabilize negative charges by resonance as the pK_A of **5** (4.48) is smaller than the pK_A of **4** (4.77).

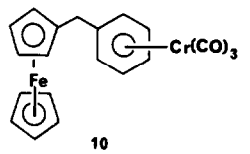
It was already known that the $Cr(CO)_3$ group exerted a net electron-withdrawing effect on the ring as aniline–$Cr(CO)_3$ is a weaker base than aniline.[48]

Studying the polarographic oxidation of ferrocenyl compounds **9** and **10** according to eqn (1) Khandkarova *et al.*[49] found that the redox potential increases by 90–100 mV from **9** to **10** which confirms the inductive effect of the $Cr(CO)_3$ group:

$$\mathbf{9} \text{ or } \mathbf{10} \xrightarrow{-e} \mathbf{9}^+ \text{ or } \mathbf{10}^+. \tag{1}$$



9



10

A highly positive inductive aromatic constant, $\sigma_i = +0.31$, has been calculated for the $C_6H_5Cr(CO)_3$ group, close to that of strong electron-withdrawing substituents such as COMe (+0.28) and CHO (+0.31), but the main result of this study is the fact that coordination of the phenyl ring in **9** with the $Cr(CO)_3$ group giving **10** considerably influences the effective positive charge of the aromatic ring σ-carbon orbitals, thus increasing its electronegativity. Therefore, it should be accepted that coordination with the metal concerns the σ- rather than the π-orbitals of the ligand. This would be consistent with the general theory of the bond in the transition metal π-complexes developed by Chatt and Duncanson,[50] where there might be mutual compensation between direct donor–acceptor interaction from the ligand to the metal and back-donation from the metal to the ligand, resulting in an almost invariant π-electron density in the benzene molecule upon coordination.

The changes in chemical shifts of the fluorine atom in fluorobenzene on substitution with a $C_6H_5Cr(CO)_3$ group[51] (Table 9) are consistent with an electron-withdrawing effect of a $C_6H_5Cr(CO)_3$ group.

Table 9. ^{19}F NMR: $FC_6H_5 \rightarrow FC_6H_4—R$

R	*m*-C_6H_5	*p*-C_6H_5	*m*-$C_6H_5Cr(CO)_3$	*p*-$C_6H_5Cr(CO)_3$
$\Delta\delta_F$*	+0.05	+2.97	−0.66	−0.55

* $\Delta\delta_F = \delta_F$ (fluorobenzene) $- \delta_F$ (substituted fluorobenzene) (ppm).

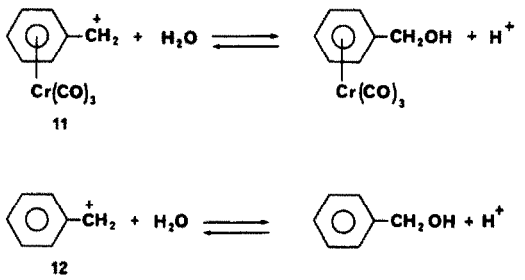
Table 10.

Ligand	Log k_{sol} (free)	Log k_{sol} (complexed)
p-NO_2—$C_6H_4CO_2Me$	−0.1952	
p-Cl—$C_6H_4CO_2Me$	−1.5952	+0.1072
m-Cl—$C_6H_4CO_2Me$	−1.3686	+0.3483
o-Cl—$C_6H_4CO_2Me$	−1.8996	
$C_6H_5CO_2Me$	−2.0969	−0.2034
p-Me—$C_6H_4CO_2Me$	−2.5100	−0.5045
p-NH_2—$C_6H_4CO_2Me$	−3.5686	−1.5467

Estimation of the σ_i inductive and σ_R resonance constants gives +0.21 and −0.04. Comparison with the values obtained for C_6H_5 (+0.10 and −0.09) leads to the conclusion that there is a significant increase in the phenyl electron-withdrawing ability of the inductive type, whereas its tendency to conjugation is almost the same. In other words these results again suggest that coordination of benzene with the $Cr(CO)_3$ group essentially changes the effective positive charge on the σ-carbon orbitals of the aromatic ring while the total π-electron density changes negligibly.

Base-catalyzed hydrolysis of a number of substituted methyl benzoates uncomplexed and complexed with $Cr(CO)_3$[52] (Table 10) showed that the chromium complexes reacted considerably faster than the uncomplexed arene. The effect of the $Cr(CO)_3$ group on ester hydrolysis is almost exactly equal to that of a p-NO_2 group ($\log k = -0.2034$ and -0.1952 respectively). The enhanced reactivity of complexed benzoic esters can be best explained by a decreased electron density at the electrophilic centre and so by an increasing effective positive charge of the aromatic ring σ-carbon orbitals.

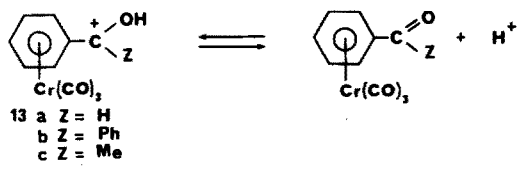
(*c*) *Stabilization of a positive charge in α or β-position.* Electronic spectra of complexed cation **11** have been measured in degassed 80% sulphuric acid and dilute solutions.[53] Determination of pK_{R^+}, eqn (2), by Deno's method[54] shows that the complexed cation **11** is more stable ($pK_{R^+} = -11.8$) than the uncomplexed cation **12** ($pK_{R^+} = -17.3$) and that a donor substituent in the *para* position on the complexed ring again increases the stability of cation **11** (p-Me, $pK_{R^+} = -11.0$; p-OMe, $pK_{R^+} = -10.2$):



(2)

with K_{R^+} = [alcohol][H^+]/[cation].

Complex cations such as **13a** and **13b** also proved to be more stable than the uncomplexed one[55] [eqn (3) and Table 11]:



(3)

Table 11.

Z	pK_{BH^+} (free)*	pK_{BH^+} (complexed)*
H	−7.11	−5.46
Ph	−6.13	−5.68
Me	−5.91	−5.96

* $K_{BH^+} = [B][H^+]/[BH^+]$, B = aldehyde or ketone.

However, the behaviour of methyl is not very clear.

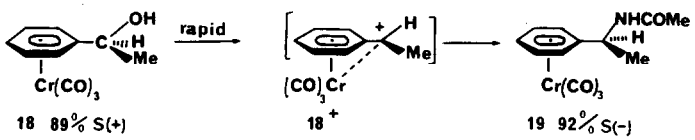
In solvolysis reactions (SN_1) a positive charge develops at the carbon which undergoes the reaction in the transition state and they provide good models to study the stabilization of a positive charge in the α-position.

Holmes *et al.*[56] have shown that solvolysis of benzyl chloride–$Cr(CO)_3$ is 10^5 faster than the solvolysis of the uncomplexed benzyl chloride, the most reasonable explanation for this rate enhancement being a preferential stabilization of the cation intermediate due to increased back-donation from the chromium atom to the ligand.

Solvolysis of π-(tricarbonyl chromium) cumyl chloride (**14**) and *p*-[π-(tricarbonyl chromium)phenyl] cumyl chloride (**16**)[57] (Table 12) shows also that the $C_6H_5Cr(CO)_3$ group stabilizes an α-carbonium ($k_{compl.}/k_{lig.} = 28$). However the $C_6H_5Cr(CO)_3$ substituent, when separated from the reaction centre by a phenyl, stabilizes the cation less than the uncomplexed phenyl ($k_{compl.}/k_{lig.} = 0.4$), probably because of its known electron-withdrawing ability.

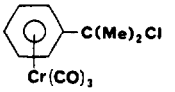
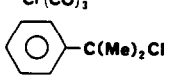
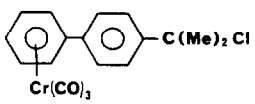
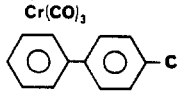
INDO molecular orbital calculations have been carried out on the free benzyl carbonium ion and on the coordinated cation $[(benzyl)Cr(CO)_3]^+$. The stability of the coordinated benzyl cation was shown to arise mainly via back-bonding from the chromium $d_{x^2-y^2}$ orbital into the non-bonding π-orbital of the benzyl ligand.[58]

The remarkable stabilization of a positive charge on the α-carbon via back-bonding from the chromium is confirmed by ^{13}C NMR results. At −50°C the *ortho*-carbons as well as the three carbonyl carbons of carbonium 18^+ display complete non-equivalence: 103.2, 106.7, 226, 226.5 and 227.[59(a)] And more recently Top and Jaouen[59(b)] found that the Ritter reaction on optically active complex **18** leads to an optically active complex, **19**, with complete retention of configuration [eqn (4)]:

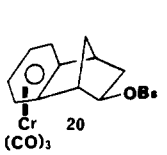


18 89% S(+) 18+ 19 92% S(−) (4)

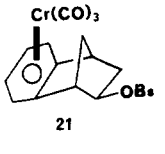
Table 12.

		10^5k (s^{-1})	Temperature (°C)	
14		360	25	$k_{compl.}/k_{lig.} = 28$
15		13	25	
16		33.4	25	$k_{compl.}/k_{lig.} = 0.4$
17		83.3	25	

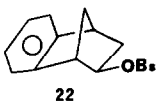
Solvolysis of the *syn-exo*-2 isomer of (benzonorbornen-2-yl) tricarbonyl chromium *p*-bromobenzenesulphonate, **20**, is 300 times faster than the solvolysis of **21**, the *anti-exo*-2 isomer, but the solvolysis of **21** is 400 times slower than the solvolysis of the free ligand **22**.[60(a)] The enhancement of the rate of solvolysis from isomer **21** to isomer **20** may be attributed to a direct interaction of *d*-filled non-bonding orbitals of the metal with the (+)β-carbon in the transition state. And the decrease of the rate of solvolysis from the free ligand **22** to the complex **21** may be explained by the fact that in complex **21** the π-electrons of the aromatic ring are less available for an hyperconjugative interaction with the vacant *p*-orbital of the (+)β-carbon than in the free ligand **22**.



20

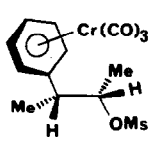


21

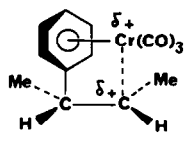


22

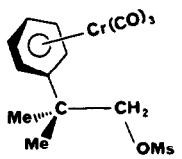
Ninety-four per cent retention of configuration obtained upon acetolysis of L-*threo*-3-[(phenyl) chromium tricarbonyl]-2-butyl methanesulfonate **23**[60(b),(c)] has also been attributed to a direct interaction of filled non-bonding *d*-orbitals of the metal with the (+)β-carbon, **23'**. However, the almost complete migration of the (phenyl) chromium tricarbonyl group during acetolysis of 2-[(phenyl) chromium tricarbonyl]-2-methyl-1-propyl methanesulphonate **24** must involve the cation **25**.



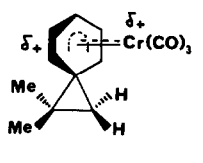
L(+) 23



23'

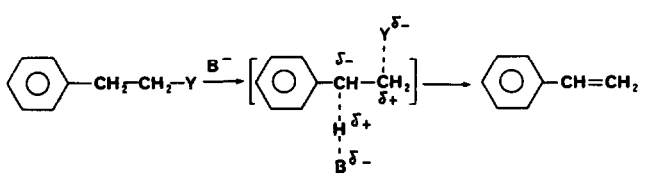


24



25

(*d*) *Stabilization of a negative charge in the* α- *or* β-*position.* Base-catalysed elimination of 2-phenylethyl bromides and tosylates (E_2 type reaction) which develop a negative charge on the α-carbon in the transition state [eqn (5)] are good models for such studies:

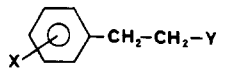


(5)

Kinetic studies of such elimination reactions on compound **26**[61] [Table 13 shows that the $Cr(CO)_3$ group must be regarded, like NO_2, as a strong electron-withdrawing group as the olefin percentage increases from 38% (X = H, Y = OTs) to 97% (X = π-$Cr(CO)_3$, Y = OTs) and 100% (X = NO_2, Y = OTs)].

Complexing the phenyl group with $Cr(CO)_3$ strongly increases the rate of elimination and the extent of the acceleration is not the same in both cases: $k_{Cr(CO)_3}/k_H$ = 142 for OTs and 37 for Br. This difference probably originates in the different amount of negative charge present on the α-carbon in the transition states. The same effect occurs with NO_2; k_{NO_2}/k_H = 4020 for OTS and 1970 for Br. However there is a substantial difference between the kinetic effects of $Cr(CO)_3$ and NO_2; $k_{Cr(CO)_3}/k_H$ = 142 but k_{NO_2}/k_H = 4020 for OTs and $k_{Cr(CO)_3}/k_H$ = 37 but k_{NO_2}/K_H = 1970 for Br. This arises from a lower capacity of

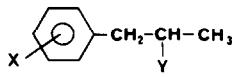
Table 13. E2 on compound **26**



X	Y	Temperature (°C)	$10^3 k_{el.}$ ($l\ m^{-1}\ s^{-1}$)
H	Br	40	1.20
NO_2	Br	40	2370
π-$Cr(CO)_3$	Br	96	290
H	OTs	40	0.16
NO_2	OTs	40	643
π-$Cr(CO)_3$	OTs	42	29.1

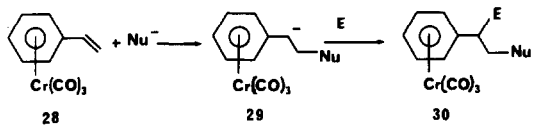
$Cr(CO)_3$ to stabilize a developing negative charge at the α-carbon. A direct resonance interaction between the negative charge on the α-carbon and the substituent is present in the case of the NO_2 group but is absent when $Cr(CO)_3$ is involved. Hence it seems again that the transmission of the electronic effect through the ring involves mainly the σ-framework rather than the π-electron cloud. Kinetic studies of elimination reactions on compound **27** (Table 14) give consistent results.[62,63]

Table 14. E2 on compound **27**



X	Y	% olefin	$10^4 k_{el.}$ ($l\ m^{-1}\ s^{-1}$)	*Cis/trans*	$k_{Cr(CO)_3}/k_H$
H	Br	100	4.8	3/96	45
π-$Cr(CO)_3$	Br	100	221	3/95	
H	OTs	91	1.4	8/79	48
π-$Cr(CO)_3$	OTs	100	67.5	8/86	

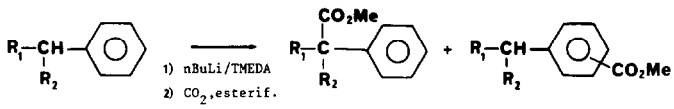
Nucleophilic additions on η^6-styrene–$Cr(CO)_3$ complex **28** [eqn (6)],[64,65] which generates a negative charge on the α-carbon in the intermediate **29** also provide good models for this study:



28 **29** **30** (6)

The reactions, which do not occur on the free ligand, have been shown to give complex **30** in good yields,[64] a reasonable explanation being the stabilization of the intermediate benzylic anion **29** by the $C_6H_5Cr(CO)_3$ group.

Table 15.



B **A**

R_1	R_2	Time (h)	B (%) Benzylic	A (%) *Ortho*	A (%) *Meta*	A (%) *Para*
H	H	0.5	89	3	9	—
H	H	2	92	3	6	—
CH_3	H	0.5	38	9	36	17
CH_3	H	1	37	9	36	17
CH_3	CH_3	2	3	10	57	30

Table 16. Reactivities of benzylic protons relative to benzene with change in base system

Base	Toluene	Ethylbenzene	Cumene
n-BuLi/TMEDA	6* (9†)	1* (0.61†)	0.1* (0.03†)
KNH_2/NH_3	70	9.8	2.1
t-BuOK/DMSO	10^6	2.2×10^5	2.5×10^4

* From Ref. 66.
† From Table 15.

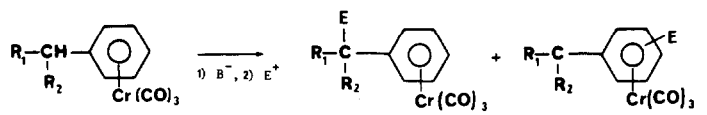
(*e*) *Basicity of benzylic protons vs aromatic protons.* The reactivities of benzylic protons vs aromatic protons in free aromatic ligands has received considerable attention and two general trends must be pointed out.[66] First, with *n*BuLi as base, α-alkyl substitution decreases the reactivity of benzylic protons relative to aromatic protons (Table 15).[66] Second, reactivities of benzylic protons relative to benzene decrease markedly according to the base in the order: BuOK/DMSO ≫ potassium amide > *n*-BuLi/TMEDA (Table 16).[66]

When the phenyl ring is complexed with a $Cr(CO)_3$ group, the results (Table 17)[67–69] show that with *n*-BuLi[67,68] at low temperature the reactivity of benzylic protons decreases relative to the free ligand [14 and 13% (Table 17) vs 89% (Table 16) and < 1% (Table 17) vs 37% (Table 16)]. However when the base is changed to *t*-BuOK[69,70] the only protons removed are the benzylic protons and, apparently, no reaction on the aromatic ring has been detected.

Nevertheless it is noteworthy that, as in the free ligand, α-alkyl substitution decreases the reactivity of benzylic protons relative to aromatic protons (14/69 when $R_1 = R_2 = H$ but < 1/80 when $R_1 = CH_3$ and $R_2 = H$) and that reactivity of benzylic protons relative to aromatic protons decreases markedly according to the base in the order: *t*-BuOK/DMSO ≫ *n*-BuLi.

In the presence of *t*-BuOK/DMSO Trahanovsky *et al.*[71] have shown that deuteration occurs only in the α-position of the complexed phenyl ring in complex **31** [eqn (7)], which indicates that under those

Table 17.

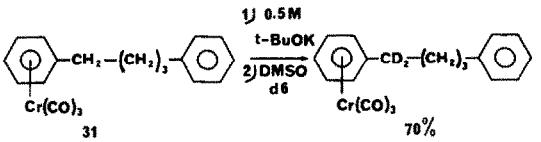


B A

R_1	R_2	Base/method/Ref*	B (%)† Benzylic	A (%)† *Ortho*	*Meta*	*Para*
H	H	*n*-BuLi/A/67	14	6	41	22
H	H	*n*-BuLi/B/68	13	5	24	24
CH_3	H	*n*-BuLi/A/67	< 1	5	41	16
H	H	*t*-BuOK/D/70	86	—	—	—
CH_3	H	*t*-BuOK/C/69	72‡	—	—	—
CH_3	H	*t*-BuOK/D/70	72	—	—	—
CH_3	H	*t*-BuOK/E/70	72§	—	—	—

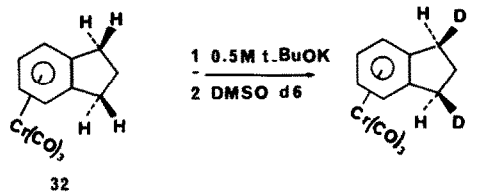
* A: *n*-BuLi/THF, −10°C, MeI, Ce(IV). B: *n*-BuLi/ether, −78°C, CO_2, diazomethane, Ce(IV). C: *t*-BuOK/DMSO, room temperature, MeI. D: *t*-BuOK/DMSO, room temperature, PhCHO. E: *t*-BuOK/DMSO, room temperature, $(CD_3)_2CO$.
† Complexes A and B are analyzed before decomplexation.
‡ A mixture of mono- and dialkylation was observed (71/7).
§ A mixture of mono- and dideuteration was observed (55/17).

conditions the benzylic protons α to a $CrCO_3$-complexed ring are more acidic than those which are situated α to an uncomplexed phenyl ring:

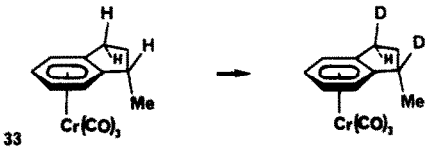


(7)

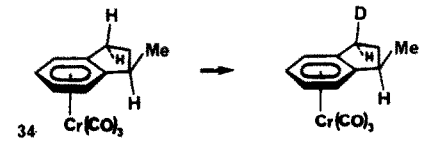
No deuteration on the ring was observed. It is noteworthy that in complex **32** only one proton of each $CH_2\alpha$ to the complexed ring was exchanged [eqn (8)]. In complexes **33** and **34** [eqn (9) and (10)] the *anti*-benzylic protons are preferentially removed. One possible explanation is that the back lobes of the sp^3 orbitals of the antibenzylic C—H bond are closer to the chromium atom and thus participation of the chromium moiety should be easier when these *anti*-protons are removed:



(8)



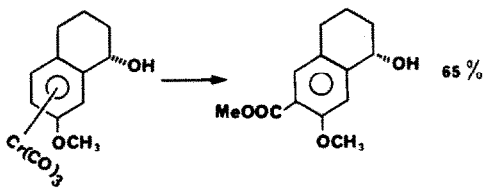
(9)



(10)

(*f*) *Metallation.* Alkyllithium compounds like MeLi, *n*-BuLi and *s*-BuLi can abstract aromatic protons in arene–$Cr(CO)_3$ complexes under mild conditions.[72–74] The main results are given in Table 18.

The selectivity proved to be high (and interesting for synthetic purpose) only in the case of OMe, F, Cl and *N*-disubstituted with large groups (entries 1–15) but quite poor in the other cases: Me, Et, *t*-Bu and $N(Me)_2$ substituents. When there are two possibilities, lithiation occurs at the less hindered position[74] as shown below



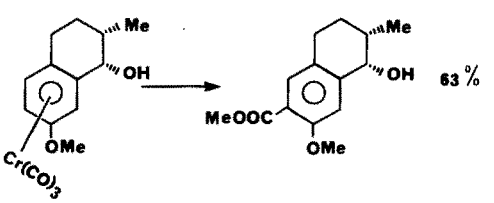
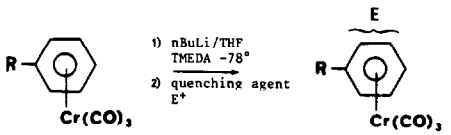


Table 18.



Entry	R	E^+	% *Ortho*	% *Meta*	% *Para*	Yield (%)
1	OMe	CO_2	86	—	—	86
2	OMe	CH_3OSO_2F	65	—	—	65
3	OMe	MeI	14	—	—	80
4	OMe	CH_3COCH_3	85	—	—	85
5	OMe	PhCHO	94	—	—	94
6	OMe	$(CH_3)_3SiCl$	70	—	—	70
7	F	CO_2	99	—	—	99
8	F	CH_3OSO_2F	68	—	—	68
9	F	MeI	71	—	—	71
10	Cl	CO_2	98	—	—	98
11	Cl	CH_3OSO_2F	81	—	—	81
12	N(Me)Si(Me)$_2$*t*-Bu	MeI	—	63	10	73
13	N(Me)Si(Me)$_2$*t*-Bu	CH_3CHO	—	55	2	57
14	N(Me)Si(Me)$_2$*t*-Bu	PhCHO	—	68	1	69
15	N(Et)CH_2*t*-Bu	MeI				
16	$N(Me)_2$	MeI	19	32	11	62
17	Me	MeI	6	41	22	69
18	Me	EtBr	10	34	13	57
19	Et	MeI	5	49	26	80
20	*t*-Bu	MeI	—	32	22	54

C. Theoretical calculations

The nature of the bonding in arene–$Cr(CO)_3$ complexes has been a topic of considerable interest since 1959.[75] Different methods have been used which appeared not to be quite as reliable as some calculations involve σ- and π-orbitals, and others only π-orbitals, and they do not emphasize the same parameters.

(*a*) *SCCC MO.* Carrol and McGlynn[76] reported in 1968 the results of semi-empirical molecular orbital calculations in which all the valence orbitals of the complex were included. Charge and configuration self-consistent Mulliken–Wolfsberg–Helmholz calculations were performed on $XC_6H_5Cr(CO)_3$ complexes (X = H, NH_2). The importance of the σ-orbitals of the ring in the metal–ring bonding was pointed out for the first time. The final charge distributions are shown in Fig. 1.

There is a net charge-transfer from the ring to the metal; despite this, the chromium is positively charged because of the electron-withdrawing effect of the carbonyl groups. The charge-transfer from the ring all the way to the oxygen of the carbonyls is more important in the case of aniline than for benzene, which leads to the prediction that the dipole moment of the aniline complex should be greater than that of the benzene complex, in agreement with the experiment. It is also pointed out that the π-back-donation from the metal to the carbonyl groups is larger (0.64e per CO) than the forward σ-donation from the carbonyl groups to the metal (0.534e per CO).

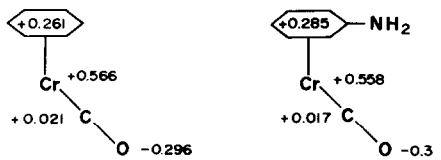


Fig. 1.

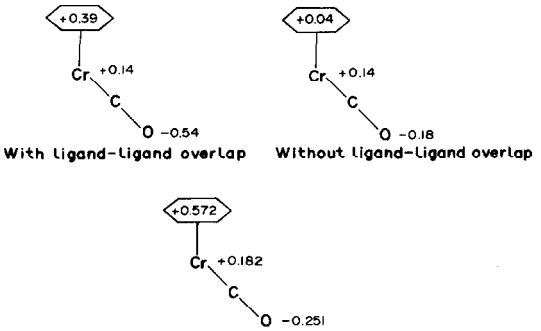


Fig. 2.

Application of SCCC MO theory by Brown[77,78] led to a somewhat different charge distribution (Fig. 2) but gave a satisfactory prediction of the first ionization potential (7.54 and 7.10 eV) compared to the known mass spectroscopic value of 7.39 eV.[79]

It is noteworthy that a charge transfer from the benzene ring (positively charged) to the metal towards the oxygen of the carbonyls (negatively charged) is also pointed out. When σ- and π-orbitals are involved in the calculations[80,81] it is found that the complexed aromatic ring is more negatively charged than before complexation (Fig. 3).

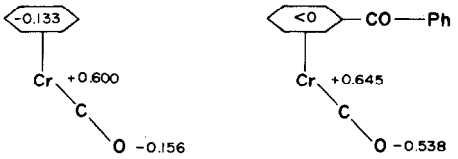


Fig. 3.

These results allowed the prediction of the upfield shift of the carbon atoms of the complexed ring using the Pople–Karplus equation[82] and assuming that changes in the paramagnetic term (σ^P) are alone responsible for the observed shifts.

(*b*) *CNDO/2.* The CNDO/2 formalism has been used by Kaufmann *et al.*[83] and Fitzpatrick *et al.*[84] They obtained quite different results for the charge distribution (Fig. 4) but they both concluded that the highest occupied orbitals are essentially metal orbitals in agreement with P.E. spectroscopic studies.[85] The metal–ring bond is apparently dominated by carbon-$2p_\pi$/chromium-$4p_\pi$ and -$3d_\pi$ interactions according to Kaufmann's results.

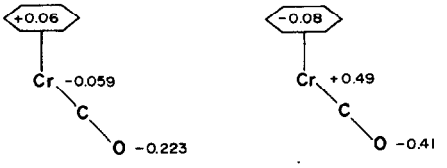


Fig. 4.

(*c*) Ab initio. *Ab initio* SCF MO calculations on a $C_6H_6Cr(CO)_3$ complex described by Guest *et al.*[86] led to very different charge distributions (Fig. 5) with net electron density on the ring, leading to the conclusion that the benzene ring is an acceptor of electron density into the π-orbitals in agreement with

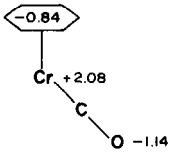


Fig. 5.

the neutron–X-ray diffraction study of Rees and Coppens,[27] but in disagreement with the known reactivity of the ring towards nucleophilic additions. However it was possible to correlate the calculated orbitals and the observed I.P. of the p.e. spectra with only minor adjustments of the level positions. It was also pointed out that metal-3*d*/ligand-2p_π interaction dominates the metal–ring bonding.

II. CHARGE-TRANSFER COMPLEXES

Although the effects of the $Cr(CO)_3$ group on the chemical properties of π-coordinated benzene ring are more like those of an electron-withdrawing group like NO_2, arene–$Cr(CO)_3$ complexes form charge-transfer complexes with electron acceptors such as 1,3,5-trinitro-benzene (TNB) and tetracyanoethylene (TCNE) but not with electron donors such as *N*,*N*,*N*′,*N*′-tetramethyl-*p*-phenylenediamine (TMPD).[87]

TNB forms a molecular complex with arene–$Cr(CO)_3$ by a charge-transfer interaction toward the π-coordinated benzene ring in face-to-face contact of the counterpart benzene rings, as revealed by X-ray crystal structures[88,89] (Fig. 6).

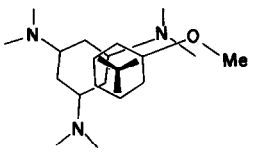


Fig. 6.

Until now structures of molecular complexes between TCNE and arene–$Cr(CO)_3$ have not been determined as they have not been isolated yet, but the presence of charge-transfer absorption bands in the UV indicates that there is formation of a molecular complex in solution.[87–91]

Since TCNE is a stronger acceptor (electron affinity 1.8[92]) than the TNB (electron affinity 0.7[92]) the charge-transfer band of toluene–$Cr(CO)_3$ with TCNE is shifted to a lower wave number (13,500 cm^{-1}) compared to the charge-transfer band of toluene–$Cr(CO)_3$ with TNB (20,200 cm^{-1}). Also, complex formation constants of 1 : 1 molecular complexes of arene–$Cr(CO)_3$ have been shown to be larger with TCNE than with TNB[87] (Table 19).

The stability of the TCNE complexes increases with the decrease in the ionization potential of the arene–$Cr(CO)_3$ evaluated from these charge-transfer bands, while the reverse holds for TNB molecular complexes. This suggests that TCNE forms charge-transfer molecular complexes with arene–$Cr(CO)_3$ with structures different from the TNB molecular complexes, and an inner-sphere charge-transfer interaction of TCNE with the central chromium atom of arene–$Cr(CO)_3$ has been proposed by Kobayashi *et al.*[87]

It has been concluded [section I(c)] that coordination of the benzene ring with the $Cr(CO)_3$ group affects essentially the σ-framework while the total π-electron density changes negligibly. However P.E.

Table 19. *K* (l mol^{-1}) at 25°C of 1 : 1 molecular complexes of arene–$Cr(CO)_3$ with TCNE and TNB, and corresponding evaluated ionization potentials (IPs) (eV) of the arene–$Cr(CO)_3$

	TCNE		TNB	
Donor	*K*	IP	*K*	IP
$C_6H_6Cr(CO)_3$	1070	7.33	67	7.23
$C_6H_5MeCr(CO)_3$	661	7.40	70	7.18
o-$C_6H_4(Me)_2Cr(CO)_3$	952	7.42	56	7.16
$C_6H_5OMeCr(CO)_3$	265	7.47	76	7.17
$C_6H_5N(Me)_2Cr(CO)_3$	139	7.77	79	6.99

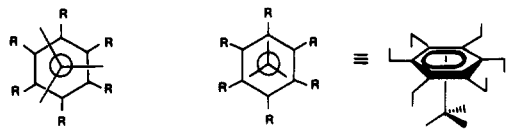
spectroscopy[85,93] shows that aromatic π-type orbitals in the complex are $\sim$ 1.06 eV lower (second ionization potential) than in the free ligand (first ionization potential), in good agreement with Hoffman's model.[94] On the other hand polarographic reduction of complexed acetophenone[95] shows that addition of the first electron is facilitated in the complex ($E_{1/2} = 0.5$ eV) in agreement with the Hoffmann model[94] which proposes that the LUMO (essentially localized on the metal) is slightly lowered in the complex. These arene–$Cr(CO)_3$ complexes are also electron-rich with a first ionization potential of about 7.2 eV[85,93] mainly due to metal *d*-lone pair. Hence the formation of charge-transfer complexes with electron acceptors is not so surprising. However the face-to-face structure found in the case of methoxyphenyl–$Cr(CO)_3$/TNB[88–90] should not have the best geometry and could be affected by symmetry and packing forces.

III. CONFORMATIONS

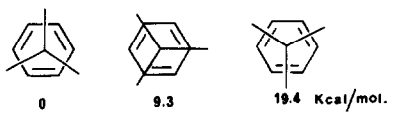
A. Conformation of the tripod

Since the beginning of modern structural chemistry conformation and magnitudes of rotational barriers in molecules have been of much concern to chemists.

In arene–$Cr(CO)_3$ complexes it has been found that the orientation of the $Cr(CO)_3$ tripod relative to the aromatic ring varies according to the nature of the substituents. X-ray[96,97] and neutron diffraction[27] showed that the staggered conformation **I** is preferred with benzene and hexamethylbenzene (D_{6h}) but that the eclipsed conformation **II** is preferred with hexaethylbenzene[98] (D_{3d}), where the methyl groups project alternately above and below the plane of the arene ring.

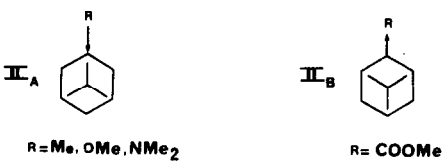


EHT calculations performed by Hoffmann *et al.*[94] on benzene–$Cr(CO)_3$ (postulating a delocalized structure for the benzene) showed that the staggered conformation **I** (R = H) was indeed more stable than the eclipsed conformation **II** (R = H). However the difference is only 0.3 kcal mol^{-1} in accord with electron diffraction[99] and NMR results,[100,101] which shows that the molecule is nearly an unhindered rotor in the gas phase. If the bonds in the benzene fragment were considered completely localized the relative energies calculated for the three possible conformations would have been too large to be

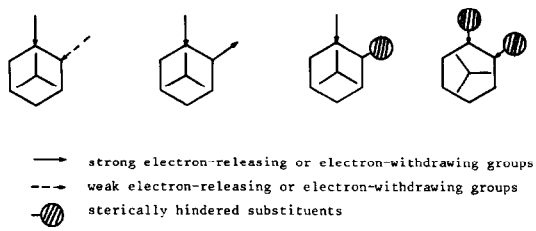


consistent with electron diffraction result. In the solid state mono- and disubstituted benzene–$Cr(CO)_3$ complexes have a tendency to adopt the eclipsed conformation[102–111] **II** unless strong steric effects are involved.[112–115]

In monosubstituted benzene electron-releasing groups favour the *syn*-eclipsed conformation **IIA** over the *anti*-eclipsed conformation **IIB**[88,89,102,103] while the reverse holds for the electron withdrawing CO_2Me group,[104] but an exception has been found for the $COCH_3$ group,[105] for which a staggered conformation was found.



In disubstituted benzene–$Cr(CO)_3$ complexes (Fig. 1) the conformation of the $Cr(CO)_3$ tripod reflects the electron-releasing character of the substituents, and is *syn*-eclipsed with the more releasing substituent,[106,111] as well as the steric effect, which tends to twist the $Cr(CO)_3$ tripod[112–115] away from

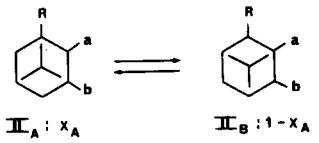


the substituent. Two exceptions, which are not clearly understood, have been found with staggered conformations; *ortho*- and *meta*-toluate complexes (in which the minus charge may play an important role)[116] and paracyclophane complexes,[117] where the aromatic rings are known to be bent.[118]

Carter *et al.*[88,89,106] and, more recently, Hoffmann *et al.*[94] have proposed models which allow this behaviour to be rationalized by relating the conformation of the $Cr(CO)_3$ tripod either to the electronic density at the atoms of the aromatic ring or to the HOMO coefficient of the aromatic ring. These EHT calculations predict that the *syn*-eclipsed conformation **IIA** for aniline–$Cr(CO)_3$ is more stable than **IIB** by 1.3 kcal mol^{-1} (90% **IIA**/10% **IIB**).

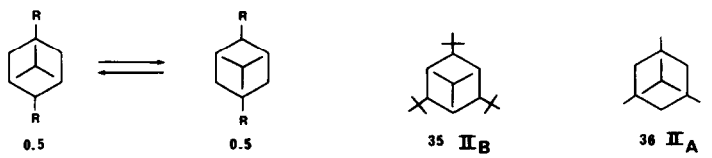
Conformation in solution can be described by equilibrium 1, and have been studied by ^1H[119–124] and ^{13}C NMR[125,126] but most of these studies are not reliable[119–123,125,126] as the effects of substituents were ignored or considered to be invariant from the free ligand to the complexed ligand. This explains the discrepancies between those NMR results and the results predicted by the theoretical models (or obtained by X-ray). It should be noted also that a few studies have been confined to the effects of substituents, disregarding the conformational effect.[127–130]

In fact the averaged non-equivalence measured between *a*- and *b*-protons (or ^{13}C) depends not only on the conformers' populations but also on the difference in the substituent effect at the *ortho* and *meta* positions (equilibrium 1). Disubstituted symmetrical complexes where the conformers' populations are known (equilibrium 2) have been studied by Solladié-Cavallo and Suffert[124] leading to an *estimation* of the substituent effects for ^1H NMR. It was found that the effect of alkyl substituents (and OMe) were nil.



Equilibrium 1.

The difference in proton chemical shifts between 1,3,5-tri-*t*-butylbenzene–$Cr(CO)_3$, **35** (6.10 ppm[120,122]) and 1,3,5-trimethylbenzene–$Cr(CO)_3$, **36** (5.22 ppm[122,131]) could then be attributed to different conformations (**IIA** for **36** and **IIB** for **35**), showing that the aromatic proton is deshielded by 0.88 (d_6-acetone)–0.84 ($CDCl_3$) ppm when the C—H bond is eclipsed by the Cr–CO vector.



Equilibrium 2.

Table 20. Population x_A (%) of conformer **IIA** [evaluated with eqn (11)] in monosubstituted benzene–$Cr(CO)_3$

	CHO	COMe	CO_2Me	Me	Et	*n*-Pr	*n*-Bu	*t*-Bu	OMe	NH_2
$CDCl_3$	30		37	64		61	62	33	80	90
d_6-Acetone		37	43	63	58			32	73	

Using estimated substituent effects, $\Delta\delta_{max} = 0.84$–$0.88$ ppm (according to the solvent) and eqn (11) the population x_A of conformer **IIA** (equilibrium 1) has been calculated (Table 20) for different substituents:

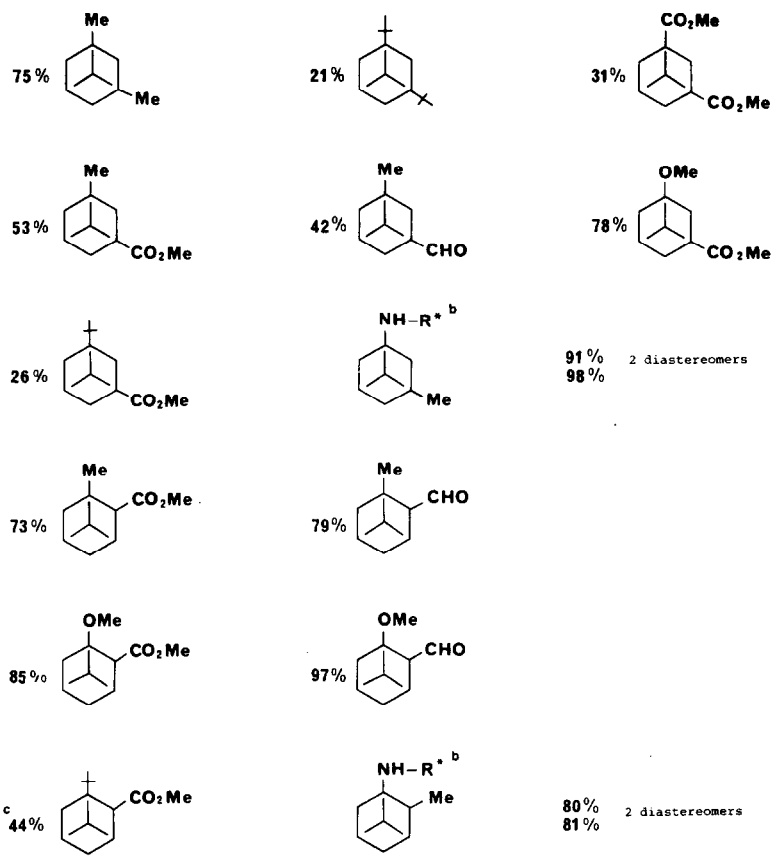
$$\langle\Delta\delta\rangle_{b-a} = (2x_A - 1)\Delta\delta_{max} + (m-o)_{compl.}, \quad \text{with} \quad \Delta\delta_{max} > 0, \quad \langle\Delta\delta\rangle_{b-a} > 0 \quad \text{or} \quad < 0. \tag{11}$$

These results now show that, according to the models of Carter[88,89,106] and Hoffmann,[94] electron-releasing substituents favour the *syn*-eclipsed conformation **IIA** while the reverse holds for electron-withdrawing substituents which favour the *anti*-eclipsed conformation **IIB**.

It should be noted too that there is, for these compounds, no dramatic change between the solid state and the solution; i.e. the conformer present in the solid state is the preferred one in solution.

The same kind of calculations[132] using eqn (11) may be performed on disubstituted complexes in solution. Proton chemical shifts were found in the literature.[122,123,127,128] Assignment of signals in symmetrically 1,3-disubstituted complexes is straightforward and the results (Table 21, line 1) are

Table 21.[a]

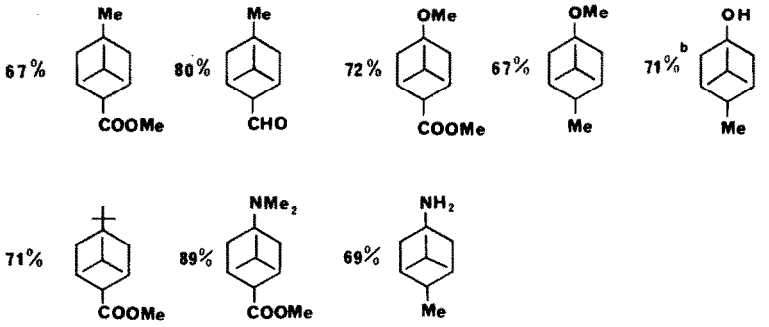


[a] The percentages correspond to the conformer drawn on the table and are averaged values obtained either by the use of $\Delta\delta_{5-6}$ and $\Delta\delta_{4-5}$ or by the use of $\Delta\delta_{4-3}$, $\Delta\delta_{4-5}$ and $\Delta\delta_{6-5}$.

[b] R* = $CH(CH_3)Ph$.[133]

[c] $\delta_4 \simeq \delta_5$.

Table 22.[a]



[a] The percentages correspond to the conformer drawn in the table.
[b] Substituent effects of OH are supposed to be nil, like for OMe.

consistent with the previous results on monosubstituted complexes.[124] In unsymmetrically 1,3-, 1,2- and 1,4-disubstituted complexes assignment of some of the signals are not straightforward. Nevertheless this can be done using the above conclusions that the conformation of the $Cr(CO)_3$ tripod reflects the electron-releasing character of the substituents and that an aromatic proton eclipsed by a Cr–CO vector is deshielded. The results (Table 21, lines 2–4, and Table 22) are self-consistent.

The substituents as far as their ability to favour a *syn*-eclipsed conformation can be classified in the order: $N(Me)_2$, NHR, NH_2 > OMe ≫ Me ≫ *t*-Bu ~ CO_2Me > CHO.

B. Conformation of substituents

In the solid state, X-ray results show that the methyl of the methoxy group in (C_6H_5OMe)–$Cr(CO)_3$ stays in the plane of the aromatic ring (with a C_1–O length of 1.33 Å indicative of the presence of a partial double-bond character).[88] In the 1,2,3-trimethoxybenzene–$Cr(CO)_3$ complex the conformation is as shown in Fig. 7, with two methyls in the plane and one out of the plane of the aromatic ring.[10] The *N*,*N*-diethylaniline–$Cr(CO)_3$ complex exhibits a conjugative effect of the nitrogen with the arene ring with a N–C_1 distance of 1.357 Å characteristic of a partial double bond; hence the CH_2 are in the plane of the arene ring, but the methyls are alternatively up and down out of the arene plane.[103]

A few other X-ray results give information on the conformation of C(O)R groups in substituted arene–$Cr(CO)_3$ complexes. The COMe group[107] with an OH group in the *ortho* position, and COOMe group[104] remain in the plane of the aromatic ring. However, in the presence of an OMe group in the *ortho* position the COMe group is twisted out of the aromatic plane by 21°[107] (both steric and dipolar effects are responsible for the conformation), while the methyl of the methoxy stays in the plane of the aromatic ring (Fig. 7).

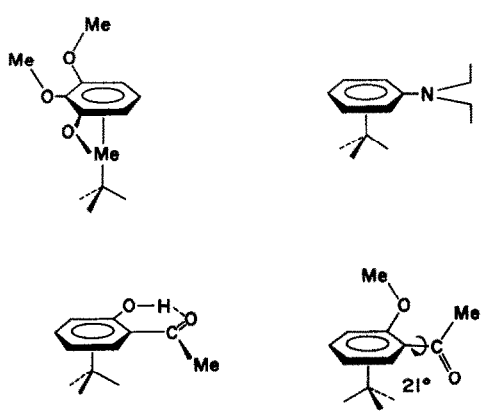


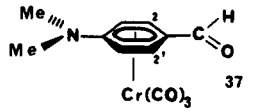
Fig. 7.

In solution conformations have been determined from dipole moments and electric birefrigence studies.[44,45]

Experimental and computed molar Kerr constants[45] lead to the conclusion that in each of the complexes, acetophenone–, benzaldehyde– and methylbenzoate–$Cr(CO)_3$ the preferred conformations are such that the substituent has a near-planar arrangement with the aromatic ring plane ($\phi \sim 0°$, CHO: $\phi \sim 5°$, $COCH_3$: $\phi \sim 10°$, COOMe). For aniline and *N,N*-dimethylaniline complexes the nitrogen was postulated to be pyramidal with rapid inversion; agreements between experimental and computed molar Kerr constants are less good but the best agreement is achieved when the nitrogen lone pair is *trans* to the $Cr(CO)_3$ group and perpendicular to the arene ring as has already been found by comparison of experimental and predicted dipolar moments.[44]

Ester carbonyl stretching vibrations have been reported[134] for several methyl benzoate–$Cr(CO)_3$ complexes and indicate that no loss of conjugation occurs in the complexes.

The barrier to internal rotation around the bond between the formyl group and the complexed ring in compound **37** was determined by ^{13}C NMR spectroscopy at variable temperature and complete line shape analysis.[135] The $\Delta G^{\ddagger}$ value (8.6 kcal mol^{-1}) is 1.6 kcal mol^{-1} lower than in the free ligand. However observation of de-coalescence indicates that the more stable conformation is planar:



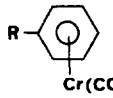
37

$T_c = -82°C$, $\Delta\delta_{2-2'} = 7.4$ ppm.

IV. STEREOELECTRONIC CONTROL OF THE REGIOSELECTIVITY

A. Nucleophilic reactions

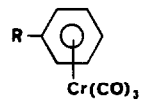
Complexation with a $Cr(CO)_3$ group provides a temporary and powerful means of polarity inversion for aromatic rings and can lead to interesting synthetic applications. Shortly after the first synthesis of an arene–$Cr(CO)_3$ complex[46(a),(b)] was performed it was reported that halobenzene–$Cr(CO)_3$ complexes readily undergo nucleophilic substitution.[136–142] However, we will focus our attention on addition/oxidation reactions which provide overall substitution of a nucleophile for a hydrogen. Such carbanion additions on arene–$Cr(CO)_3$ complexes occur under mild conditions[143–145] and the

Table 23. Nucleophilic addition on 

R	Nu^-Li^+	*Ortho*	*Meta*	*Para*	Yield (%)	x_A (%)*
Me	$LiCH_2CO_2t$-Bu	28	70	0	89	64
	$LiC(Me)_2CO_2t$-Bu	3	97	0	96	
	$LiCH_2CN$	35	63	2	88	
	$LiC(Me)_2CN$	2	96	2	58	
Et	LiC(OR)(CN)Me†	0	94	6	88	58
OMe	$LiCH_2CO_2t$-Bu	6	94	0	86	80
	$LiC(Me)_2CO_2t$-Bu	0	100	0	76	
	$LiCH_2CN$	3	97	0	38	
	$LiC(Me)_2CN$	3	97	0	93	
$N(Me)_2$	$LiC(Me)_2CN$	1	99	0	92	90
CF_3	LiC(OR)(CN)Me†	0	30	70	33	30
t-Bu	LiC(OR)(CN)Me†	0	35	65	85	33

* Population of conformer **IIA**.

† R = 1-ethoxyethyl.

Table 24. Nucleophilic addition on 

R	Nu^-Li^+	*Ortho*	*Meta*	*Para*	Yield (%)
Me	$LiCH_2CN$	35	63	2	88
t-Bu	$LiCH_2CN$	28	48	24	51
Me	$LiC(Me)_2CN$	1	97	2	95
t-Bu	$LiC(Me)_2CN$	0	55	45	78
Me	LiC(OR)(CN)Me	0	96	4	75
Et	LiC(OR)(CN)Me	0	94	6	88
i-Pr	LiC(OR)(CN)Me	0	80	20	88
t-Bu	LiC(OR)(CN)Me	0	35	65	86

approach of the nucleophile may be considered *trans* to the $Cr(CO)_3$ group.[146] It should be remembered here, however, that, with certain alkyllithium species (like MeLi, *n*-BuLi and *s*-BuLi), proton abstraction from the ring occurs[67–69,145] and compete with the addition reaction. Nevertheless the regioselectivity of these nucleophilic additions on substituted arene–$Cr(CO)_3$ complexes were soon recognized[143,147–149] and used for synthetic purposes.[150–153] The main results are given in Tables 23 and 24.

Postulating that these reactions are mainly orbital-controlled, the regioselectivity has been first related to the LUMO coefficients of the free arene ligand,[148] leading to a quite good explanation for the inversion of regioselectivity between electron-releasing substituents (mainly *meta*) and electron-withdrawing substituents (mainly *para*). A close correlation was then observed between *meta* addition and the population (x_A) of the conformer **IIA** in solution, even for the *t*-butyl group[154] (Table 23). In general the products of nucleophilic attack are thought to be kinetically controlled. Hence, as the rotation of the $Cr(CO)_3$ tripod is fast, the Curtin–Hammett principle[155] must hold and (Fig. 8)

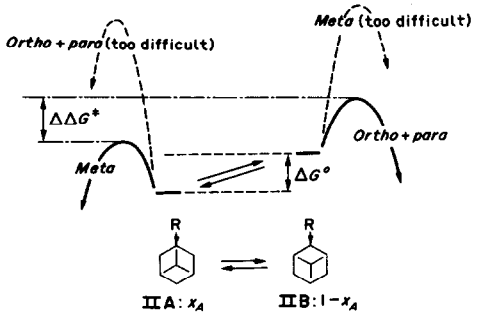


Fig. 8.

$\Delta\Delta G^+ \sim \Delta G^\circ$ is suggested for these reactions. However, the conformation of the $Cr(CO)_3$ tripod could have a strong effect on the arene-centred LUMO of the complexes. HET calculations for two types of substituents, NH_2 and CF_3,[154] led to the following conclusions (Fig. 9). The nature of the

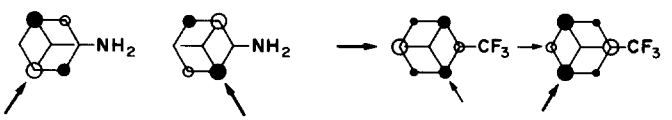
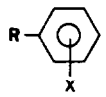


Fig. 9.

Table 25. Acetylation of 

	X = $Cr(CO)_3$			X = H		
R	*Ortho*	*Meta*	*Para*	*Ortho*	*Meta*	*Para*
Me	43	17	40	1	2	97
Et	24	33	43	0	3	97
i-Pr	5	59	36	0	3	97
t-Bu	0	87	13	0	4	96
OMe	77	0	23	0	0	100

arene LUMO is not changed by the introduction of the $Cr(CO)_3$ group, whatever the conformation is. Polarization occurs with the greatest coefficients situated on the carbons eclipsed by a Cr–CO vector. Under orbital-controlled reactions attack will occur at the carbons eclipsed by a Cr–CO vector.

Hence a simple consideration of the first arene-centred LUMO could explain the quasi absence of *para* addition found in the case of electron-releasing substituents and the preferred *para* attack with the presence of *meta* attack in the case of CF_3 (Table 14). However, examination of charge-π, total-charge or consideration of the two closest arene-centred LUMOs to explain the absence of *ortho* addition in the case of CF_3 does not improve the model.

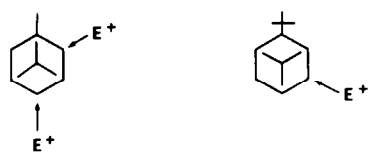
More sophisticated calculations published simultaneously[156] reached the same conclusions, that is: (1) the regioselectivity of attack on the arene should be controlled not only by the substituent on the arene but also by the conformation of the $Cr(CO)_3$ group; and (2) the arene carbons which are eclipsed with a Cr–CO vector are prefentially attacked by nucleophiles.

It was then pointed out by Semmelhack *et al.*[149] that, when the size of the substituent and/or when the size and the reactivity of the nucleophile change, the regioselectivity changes (Table 24). A rationalization based on a balance of orbital control and charge control was proposed. When the energy of the HOMO of the nucleophile is lowered (more stabilized carbanion) charge control begins to dominate and *para* addition can occur even with electron-releasing substituents.

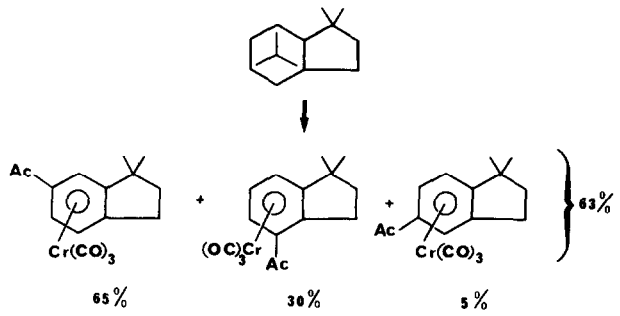
B. Electrophilic reactions

While Nicholls and Whiting[136] mentioned that benzene–$Cr(CO)_3$ was rather inert toward electrophilic substitution ($CH_3COCl/AlCl_3/CS_2$ reflux), Reimschneider *et al.*[157] succeeded in the acetylation of this complex at 10°C under nitrogen (75%). Acetylation of toluene–$Cr(CO)_3$ led to a mixture of 39% *ortho*-, 15% *meta*- and 46% *para*-acylated complex while uncomplexed toluene gives, on acetylation, 9% *ortho*, 2% *meta* and 89% *para*.[158] Jackson and Jennings[159] noticed that alkylbenzene–$Cr(CO)_3$ complexes react much more slowly than the free ligand; their results (Table 25) demonstrate that the presence and orientation of the $Cr(CO)_3$ group strongly affect the regioselectivity.

Here again the inversion of the regioselectivity from a methyl group (*ortho* + *para*) to a *t*-butyl group (*meta*) can be observed, suggesting that the attack of the electrophile occurs at the staggered arene carbons, as predicted by Albright and Carpenter.[156]



The dominance of the conformational effect in directing the regioselectivity of attack of both electrophilic and nucleophilic reagents has recently been pointed out.[160]



V. COMPLEXATION SITE ON DIAROMATIC LIGANDS

It is known that formation of arene–$Cr(CO)_3$ complexes according to eqn (12) is facilitated by electron-donating substituents.[136] This was confirmed by the study of dicomplexation of diaromatic ligands like diphenylamine and benzophenone:[161]

$$\text{arene} + Cr(CO)_6 \xrightarrow{\Delta} \text{arene–}Cr(CO)_3 + 3CO. \tag{12}$$

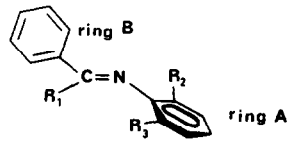
To compare the effects of electron-withdrawing and -donating substituents, complexation of imines (**38**) has been examined[162] (Table 26). In these compounds it is well accepted that ring A (with an η–π

Table 26. Complexation site in diaromatic imines (**38**)

	$R_1 = H$			$R_1 = Me$		
	$R_2 = H$ $R_3 = H$	H Me	Me Me	$R_2 = H$ $R_3 = H$	H Me	Me Me
Global yield (%)	28	58	45	68	43	83
Unreacted imine (%)	70	—	55	32	57	—
Complex						
On ring A	0	81	100	8	38	100
On ring B	0	10	0	81	0	0
On rings A and B	100	9	0	11	62	0

interaction) is electron-rich, whereas ring B (with a π–π interaction) is electron-deficient.[163,164] However, it has been shown that, in the absence of methyl substituents on ring A, the electron-deficient ring B is preferred or that mainly dicomplexation occurs. It thus appears that electron density is not a unique determining factor and that the methyl group has a dramatic influence on complexation.

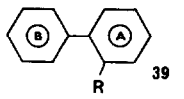
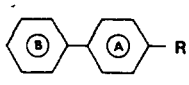
38



R_1=H R_2=R_3=H
R_2=H, R_3=CH_3
R_2=R_3=CH_3

R_1=CH_3 R_2=R_3=H
R_2=H, R_3=CH_3
R_2=R_3=CH_3

Table 27. Complexation site in biphenyls **39** and **40**

	R	Complex on ring (%) A	B	AB	Yield (%)
 **39**	NH_2	84	10	6	69
	OMe	15	81	4	78
	OH	0	100	0	58
	COMe	8	92	0	63
 **40**	NH_2	93	7	0	47
	OMe	35	56	9	52
	OH	61	39	0	38
	COMe	37	63	0	45

Monosubstituted biphenyls, **39** and **40**, provide good models to study substituent effects on complexation. It has been shown that complexation of these biphenyls are thermodynamically controlled under the reaction conditions and the results[165] (Table 27) show that an electron-donating substituent favours complexation on the substituted ring, an electron-withdrawing substituent disfavours complexation on the substituted ring (the unsubstituted ring being preferred) and that OMe behaves like a weak "electron-withdrawing" substituent (the unsubstituted ring being slightly preferred) in accordance with Top and Jaouen's observation.[161]

The 100% complexation on ring B in the *ortho*-substituted biphenyl, **39c**, when R = OH may be atttributed to the presence (in the complex) of an intramolecular H-bond between the OH group and a carbonyl of the tripod, which is not possible in the *para*-substituted biphenyl, **40c**.

This substituent behaviour is in agreement with the fact that the σ-framework of the arene is mainly involved in complexation with $Cr(CO)_3$.

Acknowledgements—Thanks are due to Professor H. Walborsky for his stimulating interest and the fruitful discussions we had during my 2 months stay in his laboratory (Florida State University, Tallahassee, FL), during the summer of 1983.

REFERENCES

1. G. Davidson, *Organomet. Chem. Rev.* 1972, **A8**, 303; P. S. Braterman, *Metal Carbonyl Spectra.* Academic Press, London (1975).
2. R. D. Fischer, *Chem. Ber.* 1960, **93**, 165.
3. G. Davidson and E. M. Riley, *Spectrochim. Acta A* 1971, **27**, 1649.
4. G. Klopman and K. Noack, *Inorg. Chem.* 1968, **7**, 579.
5. W. McFarlane and S. O. Grim, *J. Organomet. Chem.* 1966, **5**, 147.
6. D. A. Brown and J. R. Raju, *J. Chem. Soc. A* 1966, 1617.
7. E. W. Neuse, *J. Organomet. Chem.* 1975, **99**, 287.
8. F. Van Meurs, J. M. A. Baas and H. Van Bekkum, *J. Organomet. Chem.* 1977, **129**, 347.
9. M. D. Rausch, G. A. Moser, E. J. Zaiko and A. L. Lipman, *J. Organomet. Chem.* 1970, **23**, 188.
10. A. Solladié-Cavallo, G. Solladié and E. Tsamo, *J. Org. Chem.* 1979, **44**, 4189.
11. A. N. Nesmeyamov, V. V. Krivykh, P. V. Petrovski, V. S. Kaganovich and M. I. Rybinskaya, *J. Organomet. Chem.* 1978, **162**, 323.
12. W. Cho and J. E. Fernandez, *Synth. React. Inorg. Met.-Org. Chem.* 1974, **4**, 403.
13. F. A. Cotton and C. S. Kraihanzel, *J. Am. Chem. Soc.* 1962, **84**, 4432.
14. W. Strohmeir and H. Hellmann, *Chem. Ber.* 1965, **98**, 1598.
15. G. P. Donnini and A. Shaver, *Can. J. Chem.* 1978, **56**, 1477.
16. G. Jaouen and R. Dabard, *J. Organomet. Chem.* 1973, **61**, C36.
17. A. Solladié-Cavallo and J. Suffert, *J. Organomet. Chem.* 1982, **236**, 83.
18. R. J. Angelici and L. Busetto, *Inorg. Chem.* 1968, **7**, 1935.
19. M. Herberhold and C. Jablonski, *J. Organomet. Chem.* 1968, **14**, 457.
20. M. Herberhold and C. Jablonski, *Inorg. Chim. Acta* 1973, **7**, 241.
21. D. A. Brown, *Advances in Transition Metal Chemistry*, Vol. 3. M. Decker, New York.

22. H. P. Fritz and C. G. Kreiter, *J. Organomet. Chem.* 1967, **7**, 427.
23. A. Mangini and F. Taddei, *Inorg. Chim. Acta* 1968, **2**, 8.
24. L. S. Keller, *Tetrahedron Lett.* 1978, 2361.
25. B. Rees and P. Coppens, *J. Organomet. Chem.* 1972, **102**, 42C.
26. B. Rees and P. Coppens, *Acta Cryst.* 1973, **B29**, 2516.
27. P. Diehl and A. Kunwar, *Org. Magn. Reson.* 1978, **11**, 47.
28. R. V. Emanuel and E. W. Randall, *J. Chem. Soc. A* 1969, 3002.
29. B. E. Mann, *J. Chem. Soc., Chem. Commun.* 1971, 976.
30. L. F. Farnel, E. W. Randall and E. Rosemberg, *J. Chem. Soc., Chem. Commun.* 1971, 1078.
31. B. E. Mann, *J. Chem. Soc., Dalton Trans.* 1973, 2012.
32. D. A. Brown, J. P. Chester, N. J. Fitzpatrick and I. J. King, *Inorg. Chem.* 1977, **16**, 2497.
33. G. M. Bodner, B. N. Storhoff and L. J. Todd, *J. Chem. Soc., Chem. Commun.* 1970, 1530.
34. M. H. Chisholm, H. C. Clark, L. E. Manzer and J. B. Stothers, *J. Am. Chem. Soc.* 1972, **94**, 5087.
35. K. R. Aris, V. Aris and J. M. Brown, *J. Organomet. Chem.* 1972, **42**, C67.
36. H. L. Retcofsky, E. N. Frankel and H. S. Gutowsky, *J. Am. Chem. Soc.* 1966, **88**, 2711.
37. H. G. Preston and J. C. Davis, *J. Am. Chem. Soc.* 1966, **88**, 1585.
38. G. M. Bodner and L. J. Todd, *Inorg. Chem.* 1974, **13**, 1335.
39. G. M. Bodner and L. J. Todd, *Inorg. Chem.* 1974, **13**, 360.
40. V. S. Khandkarova, S. P. Gubin and B. A. Kvasov, *J. Organomet. Chem.* 1970, **23**, 509.
41. E. O. Fischer and S. Schreiner, *Chem. Ber.* 1959, **92**, 938.
42. E. W. Randall and L. E. Sutton, *Proc. Chem. Soc.* 1959, 93.
43. W. Strohmeier and H. Hellmann, *Chem. Ber.* 1963, **96**, 2859.
44. H. Lumbroso, C. Segard and B. Roques, *J. Organomet. Chem.* 1973, **61**, 249.
45. M. J. Aroney, M. K. Cooper, P. A. Englert and R. K. Pierens, *J. Mol. Struct.* 1981, **77**, 99.
46. B. Nicholls and H. C. Whiting, *J. Chem. Soc.* 1959, 551.
47. (a) E. O. Fischer and K. Öfele, *Angew. Chem.* 1957, **69**, 715; *Chem. Ber.* 1957, **90**, 2532; (b) B Nicholls and H. C. Whiting, *Proc. Chem. Soc.* 1958, 152.
48. E. O. Fischer, K. Öfele, H. Essler, W. Frohlich, J. P. Mortensen and W. Semmlinger, *Chem. Ber.* 1958, **91**, 2763.
49. S. P. Gubin and V. S. Khandkarova, *J. Organomet. Chem.* 1970, **22**, 449.
50. J. Chatt and L. A. Duncanson, *J. Chem. Soc.* 1953, 2939.
51. V. S. Khandkarova, S. P. Guvin and B. A. Kvasor, *J. Organomet. Chem.* 1970, **23**, 509.
52. G. Klopman and F. Calderazzo, *Inorg. Chem.* 1967, **6**, 977.
53. W. S. Trahanovsky and D. K. Wells, *J. Am. Chem. Soc.* 1969, **91**, 5870.
54. N. C. Deno, J. J. Jaruzelski and A. Schriesheim, *J. Am. Chem. Soc.* 1955, **77**, 3044.
55. D. K. Wells and W. S. Trahanovsky, *J. Am. Chem. Soc.* 1959, **91**, 5871.
56. J. D. Holmes, D. A. K. Jones and R. Pettit, *J. Organomet. Chem.* 1965, **4**, 324.
57. S. P. Gubin, V. S. Khandkarova and A. Z. Kreinlin, *J. Organomet. Chem.* 1974, **64**, 229.
58. D. W. Clack and L. A. P. Kane-Maguire, *J. Organomet. Chem.* 1978, **145**, 201.
59. (a) M. Acampora, A. Ceccon, M. Dal. Farra, G. Giacometti and G. Rigatti, *J. Chem. Soc., Perkin* II 1977, 483; (b) S. Top and G. Jaouen, *J. Org. Chem.* 1981, **46**, 78.
60. (a) D. K. Wells and V. S. Trahanovsky, *J. Am. Chem. Soc.* 1970, **92**, 7461; (b) R. S. Bly and R. L. Veazey, *J. Am. Chem. Soc.* 1969, **91**, 4221; (c) R. S. Bly, R. C. Strickland, R. T. Swindell and R. L. Veazey, *J. Am. Chem. Soc.* 1970, **92**, 3722.
61. A. Ceccon and G. S. Biserni, *J. Organomet. Chem.* 1972, **39**, 313.
62. A. Ceccon and G. Catelani, *J. Organomet. Chem.* 1974, **72**, 179.
63. A. Ceccon, *J. Organomet. Chem.* 1974, **72**, 189.
64. M. F. Semmelhack, W. Seufert and L. Keller, *J. Am. Chem. Soc.* 1980, **102**, 6584.
65. G. R. Knox, D. G. Leppard, P. L. Pauson and W. E. Watts, *J. Organomet. Chem.* 1972, **34**, 347.
66. C. Broaddus, *J. Org. Chem.* 1970, **35**, 10.
67. R. J. Card and W. S. Trahanovsky, *J. Org. Chem.* 1980, **45**, 2556, 2560.
68. M. F. Semmelhack, J. Bisaha and M. Czarny, *J. Am. Chem. Soc.* 1979, **101**, 768.
69. G. Jaouen, A. Meyer and G. Simmonneaux, *J. Chem. Soc., Chem. Commun.* 1975, 813.
70. J. Brocard, J. Lebibi and D. Couturier, *J. Chem. Soc., Chem. Commun.* 1981, 1264; J. Lebibi, J. Brocard and D. Couturier, *Bull. Soc. Chim.* II 1982, 357.
71. W. S. Trahanovsky and R. J. Card, *J. Am. Chem. Soc.* 1972, **94**, 2897.
72. M. F. Semmelhack, G. R. Clark, J. L. Garcia, J. J. Harrison, Y. Thebtaranonth, W. Wulf and A. Yamashita, *Tetrahedron* 1981, **37**, 3957.
73. M. Fukui, T. Ikeda and T. Oishi, *Tetrahedron Lett.* 1982, 1605.
74. M. Uemura, N. Nishikawa and Y. Hayashi, *Tetrahedron Lett.* 1980, 2069; M. Uemura, N. Nishikawa, K. Take, M. Ohnishi, K. Hirotsu, T. Higuchi and Y. Hayashi, *J. Org. Chem.* 1983, **48**, 2349.
75. D. A. Brown, *J. Inorg. Chem.* 1959, **10**, 39, 49.

76. D. G. Carroll and S. P. McGlynn, *Inorg. Chem.* 1968, 7, 1285.
77. D. A. Brown and R. M. Rawlinson, *J. Chem. Soc. A* 1969, 1534.
78. D. A. Brown, N. J. Fitzpatrick and N. J. Mathews, *J. Organomet. Chem.* 1975, **88**, C27.
79. S. Pignataro and F. P. Lossing, *J. Organomet. Chem.* II 1968, 571.
80. D. A. Brown, J. P. Chester, N. J. Fitzpatrick and I. J. King, *Inorg. Chem.* 1977, **16**, 2497.
81. N. J. Fitzpatrick, N. J. Gogan and I. J. King, *J. Organomet. Chem.* 1979, **166**, 45.
82. M. Karplus and J. A. Pople, *J. Chem. Phys.* 1963, **38**, 2803.
83. J. Y. Saillard, D. Grandjean, F. Chopplin and G. Kaufmann, *J. Mol. Struct.* 1974, **23**, 363.
84. N. J. Fitzpatrick, J. M. Savariault and J. F. Labarre, *J. Organomet. Chem.* 1977, **127**, 325.
85. S. D. Worley and T. R. Webb, *J. Organomet. Chem.* 1980, **192**, 139.
86. M. F. Guest, I. H. Hillier, B. R. Higginson and D. R. Lloyd, *Mol. Phys.* 1975, **29**, 113.
87. H. Kobayashi, M. Kobayashi and Y. Kaizu, *Bull. Chem. Soc. Jpn* 1973, **46**, 3109; *Bull. Chem. Soc. Jpn* 1975, **48**, 1222.
88. O. L. Carter, A. T. McPhail and G. A. Sim, *J. Chem. Soc. A* 1966, 822.
89. G. Huttner, E. O. Fischer, R. D. Fischer, O. L. Carter, A. T. McPhail and G. A. Sim, *J. Organomet. Chem.* 1966, **6**, 288.
90. R. Lalde, J. Von Seyerl, L. Zsolnai and G. Huttner, *J. Organomet. Chem.* 1979, **175**, 185.
91. P. G. Sennikov, V. A. Kuznetsov, A. N. Egorochkin, N. I. Sirotkin, R. G. Nakarova and G. A. Razuvaev, *J. Organomet. Chem.* 1980, **190**, 167.
92. G. Brieglet, *Angew. Chem.* 1964, **44**, 326.
93. C. Guimon, G. Pfister-Guillouzo and E. Rose, *J. Organomet. Chem.* 1982, **227**, 125.
94. T. A. Albright, P. Hofmann and R. Hoffmann, *J. Am. Chem. Soc.* 1977, **99**, 7546.
95. V. S. Khandkarova and S. P. Gubin, *J. Organomet. Chem.* 1970, **22**, 149.
96. P. Corradini and G. Allegra, *J. Am. Chem. Soc.* 1959, **81**, 2271.
97. M. F. Bailey and L. F. Dahl, *Inorg. Chem.* 1965, **4**, 1298, 1314.
98. D. J. Iverson, G. Hunter, J. F. Blount, J. R. Damewood and K. J. Mislow, *J. Am. Chem. Soc.* 1980, **102**, 5942; *J. Am. Chem. Soc.* 1981, **103**, 448.
99. N. S. Chiu, L. Schäfer and R. Seys, *J. Organomet. Chem.* 1975, **101**, 331.
100. C. Barbieri and F. Tadder, *J. Chem. Soc., Chem. Commun.* 1970, 312.
101. W. R. Jackson, W. B. Jennings and R. Spratt, *J. Chem. Soc., Chem. Commun.* 1970, 593.
102. F. Van Mews and H. Van Konigsveld, *J. Organomet. Chem.* 1977, **131**, 423.
103. P. Lemaux, J. Y. Saillard, D. Grandjean and G. Jaouen, *J. Org. Chem.* 1980, **45**, 4524.
104. O. L. Carter, A. T. McPhail and G. A. Sim, *J. Chem. Soc. A* 1967, 1619; J. Y. Saillard and D. Grandjean, *Acta Cryst.* 1967, **B23**, 2285.
105. Y. Dusausoy, J. Protas, J. Besançon and J. C. Tirouflet, *C. R. Acad. Sci.* 1970, **C270**, 1722.
106. O. L. Carter, A. T. McPhail and G. A. Sim, *J. Chem. Soc. A* 1967, 228.
107. Y. Dusausoy, J. Protas, J. Besançon and J. Tirouflet, *Acta Cryst.* 1973, **B29**, 469.
108. Y. Dusausoy, C. Leconte, J. Protas and J. Besançon, *J. Organomet. Chem.* 1973, **63**, 321.
109. Y. Dusausoy, J. Protas, J. Besançon and J. Tirouflet, *Acta Cryst.* 1972, **B28**, 3183.
110. Y. Dusausoy, J. Protas and J. Besançon, *J. Organomet. Chem.* 1973, **59**, 281.
111. Y. Dusausoy, J. Besançon and J. Protas, *C. R. Acad. Sci.* 1972, **C274**, 774.
112. F. Van Meurs and H. Van Kenigsveld, *J. Organomet. Chem.* 1976, **118**, 295.
113. F. Van Meurs and H. Van Kenigsveld, *J. Organomet. Chem.* 1974, **78**, 229.
114. Y. Dusausoy, J. Protas, J. Besançon and S. Top, *J. Organomet. Chem.* 1975, **94**, 47.
115. I. F. Taylor, E. A. Griffiths and E. L. Amma, *Acta Cryst.* 1976, **B32**, 653.
116. M. A. Bush, T. A. Dullforce and G. A. Sim, *J. Chem. Soc., Chem. Commun.* 1969, 1491.
117. Y. Kai, N. Yasuoka and N. Kasai, *Acta Cryst.* 1978, **B34**, 2840.
118. C. L. Coulter and K. N. Trueblood, *Acta Cryst.* 1963, **16**, 667.
119. D. E. F. Gracey, W. R. Jackson, W. B. Jennings, S. C. Rennison and R. Spratt, *J. Chem. Soc. B* 1969, 1210.
120. W. R. Jackson, W. B. Jenning, S. C. Renninson and R. Spratt, *J. Chem. Soc. B* 1969, 1214.
121. C. Segard, B. Roques, C. Pommier and G. Guiochon, *Anal. Chem.* 1971, **43**, 1146.
122. F. Van Meurs, J. M. Van der Toorn and H. Van Bekkum, *J. Organomet. Chem.* 1976, **113**, 341.
123. F. Van Meurs and H. van Bekkum, *J. Organomet. Chem.* 1977, **133**, 321.
124. A. Solladié-Cavallo and J. Suffert, *Org. Magn. Reson.* 1980, **14**, 426.
125. B. Roques and C. Segard, *J. Organomet. Chem.* 1974, **73**, 327.
126. W. R. Jackson, C. F. Pincombe, I. D. Rae and S. Thapebinkarn, *Aust. J. Chem.* 1975, **28**, 1535.
127. H. P. Fritz and C. G. Kreiter, *J. Organomet. Chem.* 1967, 7, 427.
128. G. Klopman and K. Noak, *Inorg. Chem.* 1968, 7, 579.
129. A. Gangini and F. Taddei, *Inorg. Chim. Acta* 1968, 8.
130. G. M. Brodner and L. T. Todd, *Inorg. Chem.* 1974, **13**, 360.
131. R. V. Emmanuel and E. W. Randall, *J. Chem. Soc. A* 1969, 3002.

132. A. Solladié-Cavallo, unpublished results.
133. A. Solladié-Cavallo and E. Tsamo, *J. Organomet. Chem.* 1979, **172**, 165.
134. F. Van Meurs, M. A. Baas and H. Van Bekkum, *J. Organomet. Chem.* 1977, **129**, 347.
135. B. P. Roques, *J. Organomet. Chem.* 1977, **136**, 33.
136. B. Nicholls and M. C. Whiting, *J. Chem. Soc.* 1959, 551.
137. D. A. Brown and J. R. Raju, *J. Chem. Soc. A* 1956, 40.
138. D. A. Brown, *J. Chem. Soc.* 1963, 4389.
139. G. Jaouen and R. Dabard, *J. Organomet. Chem.* 1970, **21**, P42.
140. J. F. Bunnett and H. Hermann, *J. Org. Chem.* 1971, **36**, 4081.
141. M. F. Semmelhack and H. T. Hall, *J. Am. Chem. Soc.* 1974, **96**, 7091, 7092.
142. M. F. Semmelhack, *Ann. N.Y. Acad. Sci.* 1977, **295**, 36.
143. R. J. Card and W. S. Trahanovsky, *Tetrahedron Lett.* 1973, 3823.
144. M. F. Semmelhack, H. T. Hall, M. Yoshifuji and G. Clark, *J. Am. Chem. Soc.* 1975, **97**, 1247.
145. M. F. Semmelhack, G. R. Clark, J. I. Garcia, J. J. Harrison, Y. Thebotaranonth, W. Wulff and A. Yamashita, *Tetrahedron* 1981, **37**, 3957.
146. M. F. Semmelhack, H. T. Hall and M. Yoshifuji, *J. Am. Chem. Soc.* 1976, **98**, 6387.
147. M. F. Semmelhack and G. R. Clark, *J. Am. Chem. Soc.* 1977, **99**, 1674.
148. M. F. Semmelhack, G. R. Clark, R. Farina and M. Saeman, *J. Am. Chem. Soc.* 1979, **101**, 217.
149. M. F. Semmelhack, J. L. Garcia, D. Cortes, R. Farina, R. Hong and B. K. Carpenter, *Organometallics* 1983, **2**, 467.
150. M. F. Semmelhack, J. J. Harrison and Y. Thebtaranonth, *J. Org. Chem.* 1979, **44**, 3275.
151. M. F. Semmelhack and A. Yamashita, *J. Am. Chem. Soc.* 1980, **102**, 5924.
152. A. P. Kozikowsky and R. Isobe, *J. Chem. Soc., Chem. Commun.* 1978, 1076.
153. J. C. Boutonnet, L. Mondenti, E. Rose, O. Le Martret and G. Precigoux, *J. Organomet. Chem.* 1981, **221**, 147.
154. A. Solladié-Cavallo and G. Wipff, *Tetrahedron Lett.* 1980, 3047.
155. D. Y. Curtin, *Rec. Chem. Prog.* 1954, **15**, 111.
156. T. A. Albright and B. K. Carpenter, *Inorg. Chem.* 1980, **19**, 3092.
157. R. Reimschneider, O. Becker and K. Franz, *Monatsschr.* 1959, **90**, 551.
158. G. E. Herberich and E. O. Fischer, *Chem. Ber.* 1962, **95**, 2803.
159. W. R. Jackson and W. B. Jennings, *J. Chem. Soc. B* 1969, 1221.
160. W. R. Jackson, I. D. Rae, M. G. Wong, M. F. Semmelhack and J. N. Garcia, *J. Chem. Soc., Chem. Commun.* 1982, 1359.
161. S. Top and G. Jaouen, *J. Organomet. Chem.* 1979, **182**, 381.
162. A. Solladié-Cavallo, G. Solladié and E. Tsamo, *J. Organomet. Chem.* 1978, **144**, 181.
163. E. Haselbach and E. Heilbronner, *Helv. Chim. Acta* 1968, **51**, 16; H. B. Bürgi and J. D. Dunitz, *Helv. Chim. Acta* 1970, **53**, 1747; *Helv. Chim. Acta* 1971, **54**, 1255.
164. A. Solladié-Cavallo and G. Solladié, *Org. Magn. Reson.* 1977, **10**, 235; W. J. Hehre, L. Radom and J. A. Pople, *J. Am. Chem. Soc.* 1972, **94**, 1496.
165. A. Solladié-Cavallo and J. Suffert, unpublished results [J. Suffert, Thèse 3ème cycle, Strasbourg (1979)].

Polyhedron Vol. 4, No. 6, pp. 929–932, 1985
Printed in Great Britain

0277–5387/85 $3.00 + .00
Pergamon Press Ltd

NMR STUDY OF EXTRACTED COMPOUNDS OF TRIOCTYLALKYLAMMONIUM WITH RARE EARTH NITRATES

VLADIMIR V. BAGREEV and SERGEY O. POPOV*
V. I. Vernadsky Institute of Geochemistry and Analytical Chemistry, U.S.S.R. Academy of Sciences, Kosygin str., 19, Moscow, U.S.S.R.

(*Received* 20 *August* 1984; *accepted* 26 *September* 1984)

Abstract—^{1}H and ^{13}C NMR was used to investigate the structure of ion pairs formed by trioctylalkylammonium (alkyl = CH_3–C_8H_{17}) cation and rare earth-containing anions in nitrobenzene. The cation–anion distance in the investigated compounds increases from trioctylmethyl to trioctylbutylammonium salt, remaining constant with further growth of the *n*-alkyl chain. The ion pair formation changes the conformation equilibrium of the cation alkyl radicals to make easier the cation–counter-ion contact.

The NMR of paramagnetic complexes is now prominently placed in the arsenal of NMR approaches to the elucidation of molecular structure in solution.[1,2] This method has been used in conformational studies of ligand molecules and in studies of the coordination state of ions. It is applicable to a wide variety of molecules (including ion pairs) in organic solvents.[3–6] The method is based on the fact that the paramagnetic ion situated close to the nucleus under investigation can exert considerable influence on the signal position of this nucleus in the NMR spectrum. The difference between the positions of signals belonging to paramagnetic and diamagnetic compounds of similar structure is termed the paramagnetic shift. Although the paramagnetic shift is a three-component sum,[7] it was noted[2–4] that for ion pairs, formed by quaternary ammonium base (QAB) cations with rare earth pentanitrates, a shift observed in the ^{1}H NMR spectrum is due to only one of these components—an axial component of the dipolar shift. This component, δ_{ax}, is expressed by the McConnell–Robertson equation:[8]

$$\delta_{ax} = f(\chi)(3\cos^2\alpha - 1)/r^3, \quad (1)$$

where r is the distance between the paramagnetic ion and the nucleus studied, α is the angle formed by the vector r and the line connecting counter-ion centers. The expression $(3\cos^2\alpha - 1)/r^3$ is called the "geometric factor" denoted as GF. As the magnetic susceptibility function $f(\chi)$ is unknown, the ratio of axial shifts of different nuclei, equal to the ratio of corresponding geometric factors, is usually used:

$$\delta_{ax,i}/\delta_{ax,j} = GF_i/GF_j. \quad (2)$$

Using ^{13}C NMR studies of ion pairs it is impossible to use eqn (1) for structure calculation without proving the absence of a contact component of the overall paramagnetic shift value. To prove this, paramagnetic shifts of carbon nuclei of a compound under investigation are usually measured using different rare earths. Europium, erbium and ytterbium pentanitrates were used in our case.

It is known that the contribution of the contact shift into the overall paramagnetic shift value varies widely for different rare earths. This contribution is almost maximal in europium compounds, minimal in ytterbium ones, while erbium occupies the middle position. If δ_j denotes the experimentally obtained shift and δ_j/δ_i ratios are approximately constant for all the metals used, then we may safely assume that the Fermi contact shift is negligible and that eqn (1) may be used to calculate the structure of the compounds investigated.[1,2,9,10]

In the present work we have studied the structure of ion pairs formed by trioctylalkylammonium (with alkyl radicals CH_3–C_8H_{17}) cations with europium, erbium and ytterbium pentanitrates in nitrobenzene. Nitrobenzene was used because of its high dielectric constant, which minimizes possible QAB salt self-association in the organic solvent.[11]

EXPERIMENTAL

Trioctylmethyl (TOMA), trioctylethyl (TOEA), trioctylpropyl (TOPA), trioctylbutyl (TOBA), trioctylamyl (TOAA) and tetraoctylammonium (TetOA)

* Author to whom correspondence should be addressed.

nitrates were synthesized and purified according to our previous work.[12] Europium, erbium, ytterbium and lutecium (analytical grade) nitrates were extracted from their 0.4 M solutions in 8.2 M $LiNO_3$ (pH = 2) with 0.01 M trioctylalkylammonium nitrate in *n*-hexane (analytical grade) at $21 \pm 1°C$. The phase volume ratio was 5:1, the equilibration time was 20 min. Metal concentrations and QAB/metal ratios in the extracts were estimated radiometrically using a NRG-603 apparatus (Tesla, Czechoslovakia). After phase separation, hexane was vacuum-distilled off (15 mm Hg, 75–80°C). The investigated compounds were dissolved in the distilled nitrobenzene (analytical grade) and then additionally dried over molecular sieves (d = 5 Å) for 24 h.

^1H NMR spectra were obtained on a Varian NV-14 spectrometer, operating frequency 60 MHz, and ^{13}C spectra on a Bruker HX-270 spectrometer, operating frequency 70 MHz, at $37.0 \pm 0.1°C$. The accuracy of paramagnetic shift measurements was about ± 0.2 Hz.

The parameters of investigated compounds structure were calculated by a Videoton EC 1010 computer (Hungary) using a specially prepared computer program.

RESULTS AND DISCUSSION

Experimental data on the QAB/metal ratios in extracts are presented in Table 1. These ratios are close to 2 in all the cases. Therefore, the composition of the studied QAB–rare earth nitrate compounds corresponds to the formula $(TOAlkA)_2Ln(NO_3)_5$, where Ln is a rare earth metal, and TOAlkA denotes trioctylalkylammonium cation.

The dependence of the paramagnetic shifts on the ion pair concentrations for CH_3, α-CH_2 and β-CH_2 group signals in ^1H NMR spectra of TOMA cations are presented as an example in Table 2. These dependences point to dissociation of investigated ion pairs in nitrobenzene but constancy of the paramagnetic shifts ratio of α- and β-CH_2 groups allows us to neglect this process in the calculation of compound structure.

Table 1. The QAB/metal ratio in the extracts obtained

QAB	Eu	Er	Yb	Lu
TOMA	2.06	2.09	2.04	2.06
TOEA	2.06	2.03	2.08	2.03
TOPA	2.11	2.08	2.13	2.10
TOBA	2.04	2.03	2.09	2.07
TOAA	2.01	2.04	2.13	2.08
TetOA	2.04	2.07	2.02	2.06

Table 3 contains paramagnetic shift values of various groups of TOAlkA cations as regards the paramagnetic shift of β-CH_2 groups of octyl radicals. Approximate constancy of the paramagnetic shift ratios in NMR spectra of compounds, that differ only in the metal involved leads to the conclusion that the contribution of Fermi contact interaction to the overall shift value is negligible and can be ignored in further calculations.

For the sake of simplicity, let us introduce a system of Carthesian coordinates relevant to a QAB cation (Fig. 1). The nitrogen atom of the QAB cation is the origin of the coordinates. The Ox axis is directed along the N—α-carbon bond of the alkyl radical (one asterisk in Fig. 1), while one of the other three α-carbon atoms of the octyl chains (two asterisks) is located in the Oxy plane of symmetry. Therefore, the space around the nitrogen atom is divided into four sectors by the N—C bonds. Due to Coulomb attraction between the cation and anion and steric hindrances due to alkyl radicals, the anion is situated inside one of these sectors. Since the paramagnetic

Table 2. Dependences of paramagnetic shifts (Hz) of ^1H NMR signals in the TOMA complex with erbium pentanitrate on ion pair concentration, C (M), in nitrobenzene

C	δ_{CH_3}	δ_{av}*	$\delta_{\alpha\text{-}CH_2}$	$\delta_{\beta\text{-}CH_2}$	$\delta_{av}/\delta_{\beta\text{-}CH_2}$
0.25	136	113	102	63	1.79
0.20	†	102	†	56	1.80
0.15	†	88	†	49	1.79
0.10	†	68	†	38	1.80
0.05	†	62	†	34	1.79
$\delta_j/\delta_{\beta\text{-}CH_2}$	2.16	—	1.62	—	—

* Average shift of all the α-protons.

† CH_3 and α-CH_2 group signals cannot divide because of their significant broadening.

Table 3. Ratios of paramagnetic shifts of signals in ^{13}C NMR spectra of different atomic groups of trioctylalkylammonium cations in respect to the shift of the β-CH_2 group of the octyl radical of the same cation

QAB	Radical	Atomic group	Eu	Er	Yb
TOMA	Methyl	α-CH_3	1.95	1.98	2.00
	Octyl	α-CH_2	1.46	1.47	1.47
		γ-CH_2	0.88	0.88	0.88
TOEA	Ethyl	α-CH_2	1.89	1.86	1.92
		β-CH_3	1.31	1.29	1.33
	Octyl	α-CH_2	1.46	1.46	1.47
		γ-CH_2	0.88	0.87	0.88
TOPA	Propyl	α-CH_2	1.80	1.81	1.83
		β-CH_2	1.25	1.25	1.26
	Octyl	α-CH_2	1.46	1.46	1.46
		γ-CH_2	0.88	0.88	0.87
TOBA	Butyl and octyl	α-CH_2	1.51	1.52	1.53
		γ-CH_2	0.90	0.89	0.89
TOAA	Amyl and octyl	α-CH_2	1.44	1.43	1.46
		γ-CH_2	0.89	0.90	0.89
TetOA	Octyl	α-CH_2	1.43	1.44	1.44
		γ-CH_2	0.89	0.89	0.89

shifts of protons and carbon atoms of the short alkyl chain are maximal in TOMA, TOEA and TOPA compounds, the anion of these compounds cannot be located inside the sector formed by three octyl radicals. Let us now assume that the anion is located in one of other three identical sectors corresponding to positive values of x and y coordinates. Meanwhile according to shift values of protons and α-carbon atoms, all the four sectors in TOBA, TOAA and TetOA compounds are absolutely identical so that the anion is placed into one of them only for the convenience of the calculations. It is quite clear that a sufficiently symmetrical anion such as a rare earth pentanitrate[13] should be located in the Oxy plane of symmetry, as any deviation from this plane will prove unprofitable due to increasing steric hindrance. The problem of determining the geometry of ion pairs is therefore reduced to determining two polar anion coordinates R and ϕ (Fig. 1).

Let us consider a QAB cation in the Newman projection along the N—CH_2 bond (Fig. 2). The anion is located in the vicinity of the central axis of the sector which is situated opposite the **CH_2—N bond. The formation of the ion pair may influence the conformation equilibrium of the cation alkyl radicals due to the fact that the conformation (A) is sterically less profitable as compared to the others (Fig. 2). To analyse this phenomenon, we had to study four theoretical models:

(1) all possible conformations of the carbon skeleton are equally probable;

(2) carbon chains are in "zig-zag" *trans*-positions, and the factor that has to do with the formation of the ion pair is ignored;

(3) carbon skeleton conformation is governed only by the formation of the ion pair;

(4) alkyl radicals are in "zig-zag" *trans*-positions influenced by the ion pair formation.

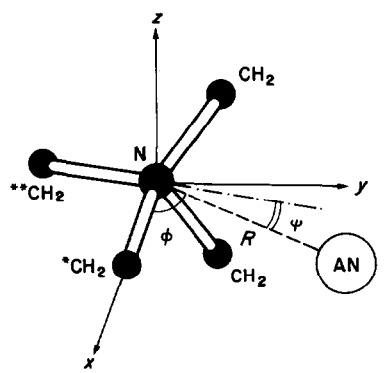


Fig. 1. The system of coordinates connected with the central part of trioctylalkylammonium cation. The α-carbon atom of the alkyl chain is marked by one asterisk, and the α-carbon atom located in the Oxy plane of symmetry opposite the anion is marked by two asterisks. R and ϕ are polar anion coordinates; ψ is an angle characterizing anion deviation from the central axis of the sector.

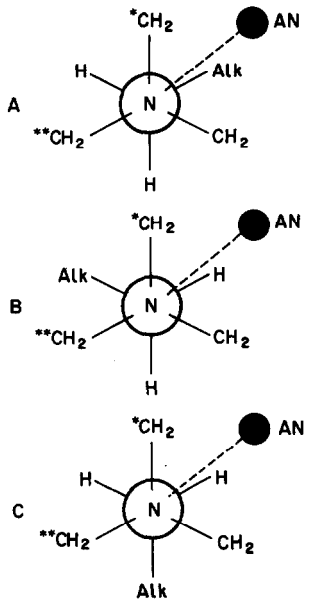


Fig. 2. Non-eclipsed conformation of a QAB cation as regards the N—CH_2 bond.

For each of these models, geometric factors of protons and carbon nuclei were determined in a prearranged area of change of R and ϕ values. Ratios of geometric factors were compared to experimentally obtained ratios of paramagnetic shifts. The following value served as a criterion of correspondence:

$$Q = \left(\sum_j [(\Delta_{obs.,j} - \Delta_{calc.,j})2/\Delta^2_{calc.,j}]\right)^{1/2},$$

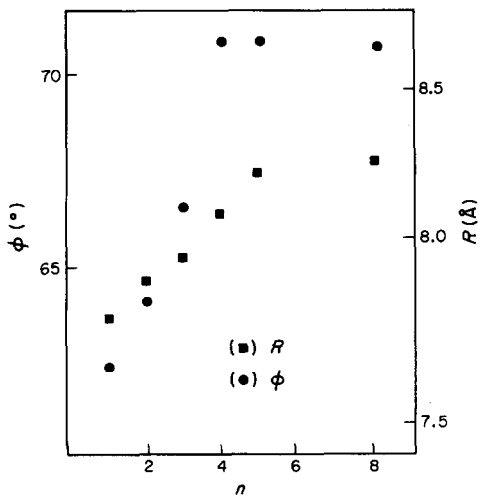


Fig. 3. Geometric parameters of the ion pairs in nitrobenzene depending on the number of carbon atoms (n) in the alkyl chain of the trioctylalkylammonium cation.

where

$$\Delta_{obs.,j} = \delta_j/\delta_{\beta\text{-}CH_2}$$

and

$$\Delta_{calc.,j} = GF_j/GF_{\beta\text{-}CH_2}.$$

As it turned out for compounds investigated only the last two of the above four models correspond to the experimental data. As the difference between energies of *trans*- and *gauche*-conformations constitutes approximately 1 kcal mol^{-1}; at room temperature, about 80% of the molecules are in the *trans*-conformation as regards the chosen bond, which is why model (4) is most probable.

The results of the geometry calculations for the ion pairs are given in Fig. 3. It should be noted that the found values of an angle ψ between the N—*CH_2 bond and the line connecting counter-ion centres in TOMA, TOEA and TOPA compounds are somewhat smaller than the value drawn from a suggestion that the anion is located in the sector axis (70.7°). This may be explained by the fact that the anion rotates around the axis Oz in such a way (Fig. 1) that the short alkyl group approaches the anion, while the sterically hindering long alkyl radicals are drawn away from it. Figure 3 shows that the steric hindrances for the counter-ion created by the alkyl radical increase from methyl to butyl, remaining about the same with a further lengthening of the alkyl chain.

REFERENCES

1. H. G. Hertz, *Pure Appl. Chem.* 1982, **54**, 2297.
2. J. Reuben, *J. Magn. Reson.* 1982, **50**, 233.
3. M. S. Quereshe and I. M. Walker, *Inorg. Chem.* 1974, **13**, 2896.
4. M. S. Quereshe and I. M. Walker, *Inorg. Chem.* 1975, **14**, 2187.
5. R. J. Abraham, *Anal. Proc.* 1981, **18**, 364.
6. C. Chachaty, B. Perly and G. Langlet, *J. Magn. Reson*, 1982, **50**, 125.
7. J. R. Ascenso and A. V. Xavier, *Systematics and Properties of the Lanthanides* (Edited by S. P. Sinha), p. 501. D. Reidel, Dordrecht (1983).
8. H. M. McConnell and R. E. Robertson, *J. Chem. Phys.* 1958, **27**, 1361.
9. S. Spiliadis and A. A. Pinkerton, *Inorg. Chim. Acta* 1983, **75**, 125.
10. L. Vincze and S. Papp, *Acta Chim. Acad. Sci. Hung.* 1982, **110**, 163.
11. Yu. A. Zolotov, V. V. Bagreev and S. O. Popov, *Proc. Int. Solvent Extraction Conf.*, p. 428. Denver (1983).
12. S. O. Popov, V. V. Bagreev and Yu. A. Zolotov, *Zh. Neorg. Khim.* 1982, **27**, 2628.
13. J.-C. G. Bunzli and B. Klein, *Proc. 15th Rare Earth Res. Conf.*, p. 97. Rolla (1981).

Polyhedron Vol. 4, No. 6, pp. 933–941, 1985
Printed in Great Britain

0277–5387/85 $3.00 + .00
© 1985 Pergamon Press Ltd

COBALT(II) PERCHLORATE, TETRAFLUOROBORATE, NITRATE AND SULPHATE COMPLEXES WITH 4,6-DIMETHYLPYRIMIDINE-2(1H)-THIONE

RAFFAELE BATTISTUZZI
Istituto di Chimica Generale e. Inorganica, Università di Modena, 41100 Modena, Italy

(*Received* 13 *August* 1984; *accepted* 26 *September* 1984)

Abstract—Contrary to earlier reports in which no adducts of Co(II) metal ion with 4,6-dimethylpyrimidine-2(1H)-thione (HL) could be isolated starting from $Co(ClO_4)_2 \cdot 6H_2O$, we now report bis- and tris-ligand Co(II) complexes of the type $[Co(HL)_2(H_2O)_2]X_2 \cdot H_2O$ ($X = ClO_4$, BF_4), $[Co(HL)_2NO_3]NO_3$, $[Co(HL)_2SO_4] \cdot 0.5H_2O$ and $[Co(HL)_3]X_2 \cdot 0.5H_2O$ ($X = ClO_4$, BF_4). They have been synthesized by refluxing 2:1 and 3:1 mixtures of HL and $CoX_2 \cdot nH_2O$ in ethanol–triethyl orthoformate. We also describe new $Co(HL)_2X_2 \cdot nH_2O$ complexes in which for $X_2 = ClBr$, ClI and BrI, $n = 2$; for $X_2 = I_2$, $n = 1$ and for $X_2 = (SCN)_2$, $n = 0$. Structural characterization of the complex species is made from electronic and vibrational spectra, magnetic susceptibility measurements in the solid state and conductivity measurements in DMF solution. The magnetic and electronic spectral data together with ligand-field parameters suggest a pseudo-octahedral environment for all the Co(II) complexes, with the exception of $Co(HL)_2SO_4 \cdot 0.5H_2O$ in which the Co(II) ion appears to be pentacoordinated. The IR spectra are consistent with a coordination involving N,S-chelation of the ligand through the non-protonated ring nitrogen atom and the exocyclic sulphur atom.

It has previously been reported[1] that the interaction of 4,6-dimethylpyrimidine-2(1H)-thione (HL) with anhydrous Co(II) chloride and bromide in dry acetone, affords blue $Co(HL)_2X_2$ complexes containing tetrahedral $[Co(HL)_2]^{2+}$ units involving N,S-chelation, whereas the hydrated cobalt(II) salts in the same solvent, lead to the formation of Co(II) or Co(III) complexes depending on the counter-ion. In fact, in the presence of suitable coordinating anions such as chloride and bromide the oxidation state of the Co(II) ion is preserved with the formation of pink six-coordinated $Co(HL)_2X_2 \cdot 2H_2O$ sparingly soluble complexes. On the contrary, with weakly coordinating anions as perchlorate, on account of deprotonation, the HL ligand gives rise to the very soluble dark-green *fac*-octahedral $Co(III)L_3 \cdot$ acetone complex.[2]

From the above results, it seems that the reaction of Co(II) salts with HL ligand is rather complicated. Therefore the effect of solvating and/or coordinating H_2O-molecules of the starting Co(II) salts and solubility of the reaction products, are important factors in determining the coordination stereochemistry and the stabilization of a preferred electronic configuration of the central metal ion, together with chemical environment of the thioamido group thione $\rightleftharpoons$ thiol equilibrium, cobalt(II) counter-ion and atmospheric oxygen.[3]

In this context we report on the preparation and characterization of $Co(HL)_2X_2 \cdot nH_2O$ ($X = ClO_4$, BF_4, $n = 3$; $X = \frac{1}{2}SO_4$, $n = 0.5$; $X = NO_3$, $n = 0$) cobalt(II) complexes by reaction of HL with the corresponding hydrated salts in dehydrating media. New thiocyanate, iodide and mixed-halide $Co(HL)_2X_2 \cdot nH_2O$ complexes were also prepared and their stereochemistry and electronic structure discussed in relation to the 4,6-dimethylpyrimidine-2(1H)-one ligand[4,5] and of previously reported HL complexes.[1] The new complexes have been characterized using IR, optical and magnetic measurements as well as conductivity data.

EXPERIMENTAL

The ligand was prepared by the method previously reported.[6] The complexes were prepared as follows.

$Co(HL)_3X_2 \cdot 0.5H_2O$ ($X = ClO_4$, BF_4)

Three millimoles of hydrated salt were dissolved in 5 cm^3 of anhydrous EtOH and 15 cm^3 of triethyl

orthoformate (TEOF) as dehydrating agent, and the mixture allowed to stand at room temperature for 3 days in a stoppered flask. The initial violet solutions immediately turned to olive–green and finally to purple–brown on addition of the solid ligand (9 mmol) under stirring at 60–80°C for 4 h, and deposited the red–brown complexes.

$Co(HL)_2X_2 \cdot nH_2O$ ($X = ClO_4$, BF_4, $n = 3$; $X = NO_3$, $n = 0$)

These complexes were prepared as above using a metal–ligand molar ratio 1:2. Subsequent combination of the solid ligand (8 mmol) with the salt (4 mmol) solution at 60–80°C under stirring, led to the following behaviour with the variation of anion: nitrate, precipitation occurs after complete addition of the ligand to the salt solution; perchlorate and tetrafluoroborate, precipitation is obtained by reducing the initial volume (20 cm^3) of the solutions and cooling.

$Co(HL)_2SO_4 \cdot 0.5H_2O$

A suspension of 4 mmol of $CoSO_4 \cdot 7H_2O$ in 10 cm^3 of anhydrous EtOH and 15 cm^3 of TEOF was stirred at 60°C for 20 min and left to rest in a stoppered flask for 3 days at room temperature. On addition of the solid ligand (8 mmol) under stirring at 60–80°C the initial pink suspension changed rapidly to cream and at last after 1 h to purple giving a violet compound.

All the above reported compounds were filtered, thoroughly washed with ether–TEOF [3:1 (v/v)] and dried in an evacuated desiccator over phosphorus pentoxide.

$Co(HL)_2I_2 \cdot H_2O$

The compound was prepared by dissolving with stirring at room temperature the solid ligand (8 mmol) in a filtered acetone solution (15 cm^3) of the stoichiometric amount (4 mmol) of $CoI_2 \cdot 4H_2O$. The yellow precipitate was filtered off, washed with acetone and *vacuum* dried over KOH.

$Co(HL)_2XY \cdot 2H_2O$ ($X = Cl$, $Y = Br$; $X = Cl$, $Y = I$; $X = Br$, $Y = I$)

The appropriate hydrated cobalt dihalides (2 mmol : 2 mmol) were either dissolved in 15 cm^3 of acetone and refluxed for 1 h. The stoichiometric amount (8 mmol) of the solid ligand was added and the solutions left with stirring for 2 h at 70–80°C. After cooling at room temperature, the homogeneous compounds were filtered, washed with cold acetone and dried over KOH.

$Co(HL)_2(SCN)_2$

Anhydrous solid $Co(SCN)_2$ (3 mmol) was added to a suspension of ligand (6 mmol) in ethyl acetate (20 cm^3) and the green resultant solution, refluxed for 8 h and allowed to stand at room temperature for three days in a stoppered flask. The brick-red product was separated by filtration, washed with copious amounts of ethyl acetate and ether. The use of acetone as solvent gave an intractable dark-green oil.

Cobalt was determined by complexometric titration with EDTA, after destruction of the complexes with aqua regia. Carbon, hydrogen, nitrogen and sulphur were analyzed using a Carlo Erba Mod. 1106 Elemental Analyzer. Conductivity measurements were performed on freshly prepared 10^{-3} M solutions in DMF at 25°C with a WTW conductivity bridge LBR type.

IR spectra were obtained on the solids in KBr pellets and Nujol mulls on KBr disks (4000–250 cm^{-1}) and in Nujol mulls on polythene (500–50 cm^{-1}) with a Perkin–Elmer 180 spectrophotometer. Solid state electronic spectra were performed with a Shimadzu MPS-50L spectrophotometer as Nujol mulls on filter paper. Magnetic susceptibilities were measured at room temperature by the Gouy method and corrected for diamagnetism using the Pascal constants.

Thermogravimetric studies were carried out on a Mettler TG 50 Thermobalance in conjunction with a direct Mettler TC 10 TA Processor recorder.

RESULTS AND DISCUSSION

General

The elemental analyses, colours and molar conductivities in DMF solution are shown in Table 1. Analytical results demonstrate that, under the experimental conditions, HL forms 3:1 and 2:1 Co(II) complexes with relatively non-coordinating anions as perchlorate and tetrafluoroborate and only 2:1 Co(II) complexes with sulphate, nitrate, thiocyanate, iodide and mixed halides. Attempts to synthesize adducts of HL with $Co(CH_3COO)_2 \cdot 4H_2O$, $Co(CF_3COO)_2 \cdot 4H_2O$ and Co(acetylacetonate)$_2 \cdot 2H_2O$, under different experimental conditions (molar ratio 1:1, 2:1 and 3:1) in EtOH, MetOH, acetone, $CHCl_3$ or their mixtures, were unsuccessful and led invariably to the formation of an inner diamagnetic tris-chelate $Co(III)L_3 \cdot S$ (S = solvent molecule) complex.

All the solid complexes are sensitive to atmospheric moisture, but are stable if stored under an inert atmosphere with the exception of the nitrate complex which slowly decomposes with loss of NO_2

Table 1. Colour, analytical data and molar conductivities, Λ_M (Ω^{-1} mol^{-1} cm^2), in 10^{-3} M DMF solution at 25°C of HL complexes

Complex	Colour	Found (calc.) (%)					Λ_M
		Co	C	H	N	S	
$Co(HL)_2ClBr \cdot 2H_2O$	Green–brown	11.91 (12.01)	29.28 (29.35)	4.10 (4.11)	11.40 (11.41)	12.98 (13.07)	63
$Co(HL)_2ClI \cdot 2H_2O$	Cream	10.83 (10.96)	26.70 (26.78)	3.68 (3.75)	10.40 (10.41)	11.92 (11.93)	73
$Co(HL)BrI \cdot 2H_2O$	Yellow	10.07 (10.12)	24.63 (24.74)	3.45 (3.46)	9.59 (9.62)	11.00 (11.07)	123
$Co(HL)_2I_2 \cdot H_2O$	Yellow	9.59 (9.64)	23.53 (23.56)	2.89 (2.97)	9.15 (9.16)	10.47 (10.49)	145
$Co(HL)_2(SCN)_2$	Brick-red	12.85 (12.94)	36.81 (36.88)	3.53 (3.54)	18.44 (18.44)	28.12 (28.15)	60
$Co(HL)_2(NO_3)_2$	Cream	12.60 (12.72)	31.06 (31.08)	3.46 (3.48)	18.04 (18.13)	13.61 (13.84)	131
$Co(HL)_2SO_4 \cdot 0.5H_2O$	Violet	13.20 (13.26)	32.35 (32.40)	3.85 (3.85)	12.31 (12.60)	21.58 (21.64)	46
$Co(HL)_2(ClO_4)_2 \cdot 3H_2O$	Brick-red	9.86 (9.95)	24.30 (24.31)	3.65 (3.74)	9.46 (9.46)	10.82 (10.82)	144
$Co(HL)_3(ClO_4)_2 \cdot 0.5H_2O$	Red-brown	8.56 (8.57)	31.40 (31.41)	3.63 (3.66)	12.15 (12.22)	13.94 (13.99)	144
$Co(HL)_2(BF_4)_2 \cdot 3H_2O$	Hazel	10.38 (10.39)	25.39 (25.40)	3.87 (3.91)	9.66 (9.87)	11.25 (11.31)	151
$Co(HL)_3(BF_4)_2 \cdot 0.5H_2O$	Red-brown	8.86 (8.90)	32.52 (32.62)	3.80 (3.81)	12.63 (12.68)	14.49 (14.53)	147

and probable oxidation of the central metal ion to Co(III) and/or of the ligand to disulphide or sulphenate or sulphinate anions.[3]

From electrolytic conductance measurements (Table 1) the iodide, bromo-iodide, nitrate and both the bis- and tris-ligand perchlorate and tetrafluoroborate complexes may be formulated as 1:2 electrolytes[7] indicating that in DMF solution these anions are not bound directly to the central metal ion. The chloro-bromide, chloro-iodide and thiocyanate complexes behave as 1:1 electrolytes, while the low molar conductance value observed for sulphate complex suggests that it is a non-electrolyte. Since the greater part of the solid complexes suffer change in colour in DMF solution, indicating extensive solvolysis with probable variation in the nature of the coordination sphere about the Co(II) centre, physical measurements in the solid state were mainly used to tentatively infer the probable structures of the compounds.

Table 2 shows the results of thermogravimetric dehydration studies performed on the hydrated complexes isolated from the ethanol–TEOF mixture. The good agreement between the observed and expected weight losses confirms the compounds stoichiometries.

For $Co(HL)_3X_2 \cdot 0.5H_2O$ ($X = ClO_4$, BF_4) and $Co(HL)_2SO_4 \cdot 0.5H_2O$ complexes water loss occurs gradually in a single step up to *ca* 200°C. This behaviour, in agreement with IR data, suggests that the water is involved in hydrogen bonding with the anions.[8] The thermogravimetric analysis data of the $Co(HL)_2X_2 \cdot 3H_2O$ ($X = ClO_4$, BF_4) complexes reveal that the weight loss corresponding to three water molecules takes place in two steps in the 50–180°C temperature range. Consideration of the relative molar masses involved for $Co(HL)_2X_2 \cdot 3H_2O$ complexes, indicate that two for perchlorate, and one-half for fluoroborate, of the three water molecules are lost in the first stage; the remaining water fractions are lost in the second step. This dissimilar behaviour for apparently similar complexes, suggests that caution must be taken in using thermal information to determine the nature of the water molecules involved in metal complexes. This would seem particularly true when the anions are capable of hydrogen bonding to water as is the case in this study.

IR SPECTRAL STUDIES

The ligand

The IR spectral data of the reported Co(II) complexes when compared with those of the free HL, give positive indication of the donor atoms of the

Table 2. Results of thermogravimetric dehydration studies

Complex	Temperature range (°C)	Weight loss (%) Found	Weight loss (%) Calc.	No. of water molecules lost
$Co(HL)_2SO_4 \cdot 0.5H_2O$	50–193	1.99	2.02	0.5
$Co(HL)_3(ClO_4)_2 \cdot 0.5H_2O$	50–210	1.28	1.30	0.5
$Co(HL)_3(BF_4)_2 \cdot 0.5H_2O$	50–210	1.30	1.35	0.5
$Co(HL)_2(ClO_4)_2 \cdot 3H_2O$	50–110	6.07	6.07	2
	110–175	3.03	3.04	1
$Co(HL)_2(BF_4)_2 \cdot 3H_2O$	50–110	1.54	1.58	0.5
	110–180	7.90	7.94	2.5

ligand, the mode of bonding of the counter-ion and the presence in the solid complexes of possible solvent molecules.

As reported in Table 3 all the water-containing complexes present in the IR spectra one or two broad bands in the 3300–3200 cm^{-1} region characteristic of ν(OH) absorptions. In addition, the presence of aqua-ligand is demonstrated by the identification of the metal-sensitive bands attributable to $\nu(Co—O)_{aqua}$ modes in the range 390–370 cm^{-1}.[5] Bands corresponding to δ(H—O—H), rocking and wagging modes of coordinated or hydration water are presumably masked, in most cases, by the ligand absorptions.

Since it is known that in a large number of metal complexes HL coordinates to metal ions *via* both the unprotonated ring nitrogen atom (strongly) and exocyclic sulphur atom (more weakly), giving a four-

Table 3. Principal IR bands (cm^{-1}) of HL and its cobalt(II) complexes

	ν(O—H)	ν(C=C) + ν(C=N)	ν(NCS) + ν(NCN) + ν(C=S)
HL		1623vs 1567vs 1545ms	1232vs 1220vs 1185vs
$Co(HL)_2ClBr \cdot 2H_2O$	3290s,br	1621vs 1570vs 1530m,sh	1242vs 1210m 1180ms
$Co(HL)_2ClI \cdot 2H_2O$	3295s,br	1621vs 1570vs 1525m,sh	1243vs 1213m 1182s
$Co(HL)_2BrI \cdot 2H_2O$	3310vs 3280s,br	1620vs 1570vs 1525m,sh	1240vs 1212vs 1180s
$Co(HL)_2I_2 \cdot H_2O$	3330vs 3270vs	1620vs 1565vs 1525m,sh	1238vs 1210ms 1178ms
$Co(HL)_2(SCN)_2$		1612vs 1560vs 1520m,sh	1228vs 1202m 1168ms
$Co(HL)_2(NO_3)_2$		1622vs 1570vs 1525m,sh	1240vs 1210m 1175mw
$Co(HL)_2SO_4 \cdot 0.5H_2O$	3300vs 3240vs	1622vs 1565vs 1525m,sh	1240vs 1212m,sh 1180m
$Co(HL)_2(ClO_4)_2 \cdot 3H_2O$	3310vs 3250vs	1620vs 1570vs 1525mw	1240vs 1210m 1180m
$Co(HL)_3(ClO_4)_2 \cdot 0.5H_2O$	3310vs 3240vs	1620vs 1569vs 1525m,sh	1240vs 1210m,sh 1180m
$Co(HL)_2(BF_4)_2 \cdot 3H_2O$	3310vs 3250vs	1620vs 1570vs 1523mw	1240vs 1210m 1180m
$Co(HL)_3(BF_4)_2 \cdot 0.5H_2O$	3310vs 3250vs	1622vs 1570vs 1525m,sh	1240vs 1212m,sh 1181m

membered chelate ring,[1,6] and since it is known that the C=S and C=N stretching frequencies of the S ‖ —C—N=C— group change upon coordination to metal ions, we have looked in more detail at the region in the IR where the C=N and C=S stretching frequencies are to be expected.

In the 1650–1500 cm^{-1} range the ligand spectrum displays three very strong bands at 1623, 1567 and 1545 cm^{-1} which may be assigned to a combination of C=C and C=N bonds stretching vibrations which do not form part of an aromatic skeleton.[9]

In all the complexes the first two bands remain almost unchanged, while the third one, with prevailing ν(C=N) contribution, decreases both in frequency (15–20 cm^{-1}) and intensity indicating N-coordination of the ligand through the non-protonated ring nitrogen atom. Furthermore, only the bands at 1220 and 1185 cm^{-1} [with prevailing of ν(C=S) mode], out of the three HL bands in the 1240–1160 cm^{-1} region, to which a ν(NCN) + ν(CNS) + ν(C=S) contribution was previously assigned,[6] are shifted upon complexation to lower frequency. This indicates an involvement of exocyclic sulphur in the metal coordination.

The anions

As regards the behaviour of the anions, the IR spectra of the bis- and tris-ligand complexes of both perchlorate and tetrafluoroborate (1 : 2 electrolytes in DMF solution), show splitting of the ν_3 and ν_4 (ClO_4, BF_4) modes, while ν_1 and ν_2 modes are IR active (Table 4). This fact clearly indicates that some distortion for ClO_4 and BF_4 groups from T_d symmetry occurs in the solid complexes caused by solid state effect and/or most probably by hydrogen bonding with water molecules present in the complexes[10] rather than to anion–Co(II) interaction. This would explain why the water is not completely eliminated in the presence of TEOF in $Co(HL)_3X_2 \cdot 0.5H_2O$ (X = ClO_4, BF_4) complexes, in which the Co(II) ion achieves an octahedral coordination through the three N,S-chelate ligands. These two complexes do not show IR bands at 400–350 cm^{-1} attributable to $\nu(Co—O)_{aqua}$.[5,11]

This would also explain why the bis-ligand complexes have three water molecules while, in such a case, only two aqua ligands are required, together with the two N,S-chelate ligands, for the completion of the octahedral coordination.

On the basis of the previous evidence, of the thermogravimetric analyses results and of the fact that the $Co(ClO_4)_2$ and $Co(BF_4)_2$ complexes appear to be hexacoordinated (*vide infra*), the bis- and tris-ligand complexes may be formulated as $[Co(HL)_2(H_2O)_2]X_2 \cdot H_2O$ and $[Co(HL)_3]X_2 \cdot 0.5H_2O$ respectively, with ionic counter-ions interacting with water molecules.

The IR spectrum of the sulphato complex clearly shows the presence of the coordinate sulphate group. In fact, both the ν_4 and ν_3 fundamental vibrational modes of sulphate group are split into two and four components respectively, and ν_1 and ν_2 modes are IR active (Table 4). This behaviour is indicative of a bidentate sulphate group of C_{2v} symmetry,[12] and furthermore the absence of a band around 1250 cm^{-1} suggests that this group is bridging rather than chelating.[12,13] Therefore in this complex the metal ion is probably six-coordinated with the sulphate group bridging two Co(II) ions of two $[CoN_2S_2]$ units or five-coordinated (*vide infra*) with the SO_4 group in direct contact with the cobalt ion of a $[CoN_2S_2]$ unit and at the same time engaged in hydrogen bonding with lattice water[8] as in perchlorate and tetrafluoroborate complexes.

The observed IR spectral absorptions of

Table 4. IR band wavenumbers attributed to the SO_4, ClO_4 and BF_4 groups of HL–cobalt(II) complexes

Assignments for XY_4 (T_d)		$Co(HL)_2A_2 \cdot nH_2O$			$Co(HL)_3A_2 \cdot 0.5H_2O$	
		A = $\frac{1}{2}SO_4$	A = ClO_4	A = BF_4	A = ClO_4	A = BF_4
ν_3	ν_d(X—Y)	1175vs	1140vs	1110vs	1140vs	1115vs
		1150vs	1110vs	1080vs	1114vs	1082vs
		1105vs	1085vs	1033vs	1085vs	1055vs
		1085vs				1032vs
ν_1	ν_s(X—Y)	982ms	920w	770w	940w	770w
ν_4	δ_d(YXY)	645m	634s	521ms	635ms	519s
		610m	625vs	513ms	620s	512m,sh
ν_2	δ_d(YXY)	434m,sh	Masked	344m	Masked	354w

Table 5. IR band wavenumbers attributed to the SCN group for the $Co(HL)_2(SCN)_2$ complex

ν(CN)	2090vs
ν(CS)	805m,sh
δ_d(NCS)	470m,sh

thiocyanate anion in the $Co(HL)_2(SCN)_2$ complex are the well-known fundamentals ν(CN), ν(CS) and δ(NCS) (Table 5). According to Nakamoto,[12] usually the position of ν(C=S) at *ca* 800 cm^{-1} is taken as indicative of the *N*-coordination mode of the thiocyanate anion. In addition the presence of a single sharp band due to δ(NCS) at 470 cm^{-1} and a single ν(Co—NCS) mode at 241 cm^{-1} suggests[14] that the metal ion has most probably a six-coordinated octahedral environment achieved through two equatorial N,S-chelate ligands and two axial N-bonded NCS groups.

Also the IR spectrum of the nitrato complex was investigated to obtain evidence for ionic or coordinated nitrate ions, the bands due to these groups together with probable assignments are included in Table 6.

Since in the case under study all modes (ν_1, ν_2, ν_3 and ν_4 in D_{3h} symmetry) are IR active, shifts in band positions and intensities are observed and there is splitting of the ν_3 and ν_4 bands, this suggests that the nitrate groups are present in some coordinated form. The presence of the band at 1385 cm^{-1} indicates again the existence of some ionic species.[15] The coordination mode of the nitrato group cannot be unequivocally deduced from these data, but all the physicochemical characteristics of this complex are compatible with a polymeric structure with a nitrato group bridging two $[CoN_2S_2]$ units and an ionic nitrato group in the lattice.

Metal–ligand and metal–anions vibrations

Additional information about the coordination of HL–Co(II) compounds and about the strength of the metal–ligand and metal–anions bonds can be

Table 6. IR band wavenumbers attributed to the NO_3 group for the $Co(HL)_2(NO_3)_2$ complex

		NO_3 (D_{3h})	NO_3 (C_{2v})
ν_3	ν_d(NO)	1385vs	1478s
			1292vs
ν_1	ν_s(NO)		1000s
ν_2	$\pi(NO_3)$	816m	808m
ν_4	δ_d(ONO)	728w	740w
			710w

Table 7. Far-IR spectral bands (400–50 cm^{-1}) of cobalt(II)–HL complexes and their tentative assignments

Compound	ν(Co—OH_2)	ν(Co—X)	ν(Co—N)	ν(Co—S)		Ligand and other bands
HL						289mw 269mw 230mw 177mbr 91w 84s
$Co(HL)_2ClBr\cdot 2H_2O$	395mbr		295ms	226s	190w	277mbr 164m,sh 145ms 131ms 97w 86w
$Co(HL)_2ClI\cdot 2H_2O$	396mbr		292ms	227s	191w	277mbr 165m,sh 147s 137s 98w 88w
$Co(HL)_2BrI\cdot 2H_2O$	383mbr		298ms	226s	188w	281mbr 157sbr 134w 97m 82w
$Co(HL)_2I_2\cdot H_2O$	372mbr	(169ms)	297ms	234s	190w	279m 158w 142s 118ms 83ms
$Co(HL)_2(ClO_4)_2\cdot 3H_2O$	368mbr		295ms	239s	196w	274mbr 226m,sh 168w 141mbr 127w 100mbr
$Co(HL)_2(BF_4)_2\cdot 3H_2O$	375mbr		300ms	239s	192w	279m 269m 228m,sh 174w 147m 101s 81m
$Co(HL)_2(NO_3)_2$		242vs,br	302ms	232s,sh	195w	277mbr 152mbr 143m,sh 97w 88w
$Co(HL)_2(SCN)_2$		241vs,br	302ms 268s,sh	241vs,br	196s	275m,sh 151mbr 138w 113w 104w 88w
$Co(HL)_2SO_4\cdot 0.5H_2O$		255vs,br	301ms 267m,sh	236m	204m	291s,sh 222mbr 178s,sh 167vs 139s,sh 98w
$Co(HL)_3(ClO_4)_2\cdot 0.5H_2O$			298ms 260s	215vs,br	192w	276m,sh 178m,sh 150w 138w 106mbr
$Co(HL)_3(BF_4)_2\cdot 0.5H_2O$			295s 258s	216vs,br	193w	277m,sh 175m,sh 151w 125w 102mbr

reached from far-IR spectra; the main results are listed in Table 7.

Tentative metal–ligand band assignments were based on the previous ν(M—L) assignments for other metal complexes with HL[4,5,16] and in agreement with the fact that unprotonated ring nitrogen atom, which is the protonated site in the H_2L^+ cation,[17] has a donor tendency greater than that of the exocyclic sulphur atom.

Except the sulphate, all the bis-ligand hydrated complexes, show a broad band in the 395–370 cm^{-1} region assignable to the ν(Co—OH_2) mode of the coordinated water.[5]

The presence, in the far-IR spectra, of only one ν(Co—N) mode for all the bis-ligand complexes, except the thiocyanate and sulphate complexes, in conjunction with the low intensity of the electronic bands, indicates a probable *trans*-ligand arrangement leading to a centrosymmetric octahedral coordination geometry.

In agreement with medium IR spectra, only nitrate, thiocyanate and sulphate, of the bis-ligand complexes, exhibit any pronounced ν(Co—anion) activity. The band positions are in the expected ranges for ν(Co—NCS),[14] ν(Co—ONO_2),[18,19] and ν(Co—OSO_3)[19,20] stretching modes for Co(II) in octahedral complexes.

The low frequency IR spectra of the mixed halides compounds are similar to each other and to those of the pink $Co(HL)_2X_2 \cdot 2H_2O$ (X = Cl, Br),[1] showing in the 300–150 cm^{-1} region, no halogen dependent bands, and this fact suggests that the complexes should be formulated as $[Co(HL)_2(H_2O)_2]X_2$.

On the basis of electronic spectra, no splitting of ν_1 band, the $Co(HL)_3X_2 \cdot 0.5H_2O$ (X = ClO_4 and BF_4) compounds appear to be similar to the $CoL_3(ClO_4)_2$ (L = 2-thio-1,4,6-trimethylpyrimidine or 2-thio-1-methylpyrimidine) for which a *fac*-octahedral arrangement of the ligands was proposed.[21,22] In addition the presence in the far-IR of two ν(Co—N) and two ν(Co—S) modes, $A_1 + E$ in C_{3v} symmetry group,[23] is consistent with a *fac*-octahedral $[Co(HL)_3]^{2+}$ cation.

Magnetic moments and ligand field spectra

Room temperature magnetic moments and diffuse reflectance spectral band energies with their assignments, as well as derived ligand field parameters are listed in Table 8.

The magnetic moment of the iodo-complex occurs in the range associated with octahedral cobalt(II), whereas the remaining values occur in the upper portion of the range observed for tetrahedral Co(II) complexes.[24] However, room temperature magnetic moments of the order of 4.4–4.6 B.M. have been also reported for pseudo-octahedral complexes of Co(II) with *N*- and *S*-coordinating heterocyclic molecules.[25,26]

The reported cobalt(II)–HL complexes, except the sulphate, exhibit solid state spectra typical of octahedral species.[27] Two main absorptions are observed in the 7200–9500 cm^{-1} and 18,000–20,700 cm^{-1} ranges respectively, which are assigned to the $^4T_{1g}(F) \rightarrow {}^4T_{2g}(F)$ and $^4T_{1g}(F) \rightarrow {}^4T_{1g}(P)$ transitions.

In all the octahedral cobalt(II) complexes the ν_3 and ν_1 bands are split in two or three components of almost equal intensities, except for the tris-ligand perchlorate, fluoborate and bis-ligand thiocyanate complexes, where only ν_3 band is split. It seems plausible to believe that the splitting shown by both

Table 8. Electronic bands* and parameters *Dq* and *B* (cm^{-1}) ($\beta = B/971$) and magnetic moments [μ_{eff} (B.M.)] at room temperature of HL complexes

Compound	$^4T_{1g}(F) \rightarrow$ $^4T_{1g}(P)$ ν_3	$^4A_{2g}(F)$ ν_2	$^4T_{2g}(F)$ ν_1	*Dq*	B	β	ν_2/ν_1	μ_{eff} (B.M.)
$Co(HL)_2(SCN)_2$	18,812	17,700sh	8333	943	771.6	0.79	2.13	4.64
$Co(HL)_2ClBr \cdot 2H_2O$	19,442	(17,577)	8228	934	822.3	0.85	2.13	4.47
$Co(HL)_2ClI \cdot 2H_2O$	19,461	(17,539)	8209	933	824.8	0.85	2.13	4.56
$Co(HL)_2BrI \cdot 2H_2O$	19,462	(17,533)	8206	932	825.1	0.85	2.13	4.69
$Co(HL)_2I_2 \cdot H_2O$	18,797	17,513sh	8200	929	779.3	0.80	2.13	5.08
$Co(HL)_2(BF_4)_2 \cdot 3H_2O$	18,894	(17,552)	8225	934	782.7	0.81	2.13	4.46
$Co(HL)_2(ClO_4)_2 \cdot 3H_2O$	18,732	17,395sh	8163	925	777.6	0.80	2.13	4.45
$Co(HL)_2(NO_3)_2$	18,629	(17,361)	8139	922	771.5	0.79	2.13	4.68
$Co(HL)_3(BF_4)_2 \cdot 0.5H_2O$	18,591	(17,340)	8130	921	769.4	0.79	2.13	4.65
$Co(HL)_3(ClO_4)_2 \cdot 0.5H_2O$	18,496	(17,072)	8000	907	771.2	0.79	2.13	4.65

* Averaged values; calc. values in parentheses.

ν_1 and ν_3 bands in most of the complexes as well as the lower magnetic moment values are due to the presence of the low symmetry ligand field components.[28]

Ligand field parameters were calculated on the basis of octahedral geometry from the averaged values of the ν_1 and ν_3 bands taking the centre of gravity of the total intensity[29] by using Konig's method,[30] the ν_2 frequencies were calculated from the equation $\nu_2 = \nu_1 + 10Dq$.

In agreement with the rule of the average environment[31] the Dq values of the tris-ligand complexes $[CoN_3S_3]$, and the Dq of bis-ligand thiocyanate complex $[CoN_2S_2N'_2]$, are intermediate between the values given for $[CoN_6]$ (higher than 1000 cm^{-1}) and $[CoS_6]$ (770–860 cm^{-1}) chromophores.[32]

In the case of the $Co(HL)_2I_2 \cdot H_2O$ complex, besides the electronic spectrum consistent with an octahedral geometry, a low-energy charge-transfer band is present at *ca* 23,000 cm^{-1}; this fact is normal when iodide ions are coordinated to cobalt(II).[4] Moreover, in the far-IR spectrum, there is a band at 169 cm^{-1} not present in the spectra of the other complexes and assignable to a ν(Co—I) mode; these observations are consistent with the presence of a $[CoN_2S_2OI]$ chromophore.

For the bis-ligand perchlorate, tetrafluoroborate, nitrate and mixed-halide complexes, the visible and IR spectral data suggest the existence of a common $[CoN_2S_2O_2]$ chromophore. Consequently in the mixed-halide complexes $Co(HL)_2XY \cdot 2H_2O$ the X or Y groups would not be coordinated to the cobalt as pointed out above, and the low conductivity data for the chloro–bromo and the chloro–iodo complexes would be explained by considering strong —N—H$\cdots$Cl or $OH_2\cdots$Cl hydrogen bonds.

The spectral parameters Dq, B, β, and ν_2/ν_1 are consistent with the proposed pseudo-octahedral stereochemistries and the results strongly support the IR conclusions.

The reflectance spectrum of the violet $Co(HL)_2SO_4 \cdot 0.5H_2O$ differs significantly from the spectra of the other complexes. The number of the bands and their characteristic energies enable us to exclude tetrahedral and octahedral environment for the cobalt ion. The low magnetic moment (4.30 B.M.) and the characteristics of the reflectance spectrum [bands at 19,584m and 18,587sh, 17,035m and 15,330m, 10,810m, 5405sh, assignable to the transitions $^4A_2(F) \rightarrow {}^4E''(P)$, $\rightarrow {}^4A'_2(P)$, $\rightarrow {}^4E'(F)$, $\rightarrow {}^4E''(F)$ respectively] are similar to those corresponding to $CoL_2X_2 \cdot nH_2O$ (L = acetone-thiosemicarbazone, cyclohexanone-thiosemicarbazone; X = Cl, Br, I) complexes for which cobalt coordination number is five and the structures are trigonal bipyramidal.[33,34] Presumably a similar coordination in this complex is achieved through two N,S-chelate ligand molecules and one oxygen atom of the monodentate sulphato group.

Acknowledgement—The IR spectra were recorded in the Centro Strumenti of University of Modena.

REFERENCES

1. D. M. L. Goodgame, I. Jeeves and G. A. Leach, *Inorg. Chim. Acta* 1980, **39**, 247.
2. B. A. Cartwright, D. M. L. Goodgame, I. Jeeves, P. O. Langguth and A. C. Skapski, *Inorg. Chim. Acta* 1977, **24**, L45.
3. M. Lunden, L. R. Firor and K. Seff, *Inorg. Chem.* 1978, **17**, 701.
4. M. Goodgame and K. W. Johns, *Inorg. Chim. Acta* 1981, **55**, 15.
5. R. Battistuzzi and G. Peyronel, *Z. Anorg. Allg. Chem.* 1984, **509**, 192.
6. R. Battistuzzi and G. Peyronel, *Transition Met. Chem.* 1978, **3**, 345.
7. W. J. Geary, *Coord. Chem. Rev.* 1971, **7**, 81.
8. M. Sakamoto, *Polyhedron* 1984, **3**, 451.
9. E. Spinner, *J. Chem. Soc.* 1960, 1237.
10. J. C. Bayon, M. C. Brianso', J. L. Brianso' and P. G. Duarte, *Inorg. Chem.* 1979, **18**, 3478.
11. L. S. Gelfand, L. L. Pytlewski, D. Cosgrove, C. M. Mikulski, A. N. Speca and N. M. Karayannis, *Inorg. Chim. Acta* 1979, **32**, 59.
12. K. Nakamoto, *Infrared and Raman Spectra of Inorganic and Coordination Compounds.* Wiley–Interscience, New York (1977).
13. C. G. Barraclough and M. L. Tobe, *J. Chem. Soc.* 1961, 1993.
14. B. C. Cornilsen and K. Nakamoto, *J. Inorg. Nucl. Chem.* 1974, **36**, 2467.
15. M. R. Rosenthal, *J. Chem. Educ.*, 1973, **50**, 331.
16. R. Battistuzzi and G. Peyronel, *Spectrochim. Acta* 1980, **36A**, 113.
17. A. Albert and G. Barlin, *J. Chem. Soc.* 1962, 3129.
18. D. X. West and S. Huslander, *J. Inorg. Nucl. Chem.* 1981, **43**, 947.
19. I. S. Ahuja, D. H. Brown, R. H. Nuttal and D. W. A. Sharp, *J. Chem. Soc.* (*A*) 1966, 938.
20. L. V. Konovalov and I. S. Maslennikova, *Russ. J. Inorg. Chem.* 1975, **20**, 903.
21. D. M. L. Goodgame and G. A. Leach, *Inorg. Chim. Acta* 1977, **25**, L127.
22. D. M. L. Goodgame and G. A. Leach, *J. Chem. Soc., Dalton Trans.* 1978, 1705.
23. R. J. H. Clark and C. S. Williams, *Inorg. Chem.* 1965, **4**, 350.
24. B. N. Figgis, *Introduction to Ligand Field Theory.* Interscience, New York (1966).
25. M. C. Jain, R. K. Sharma and P. C. Jain, *Gazz. Chim. Ital.* 1979, **109**, 601.
26. B. K. Gupta, D. S. Gupta and U. C. Agarwala, *Bull. Chem. Soc. Jpn* 1978, **51**, 2724.

27. A. B. P. Lever, *Inorganic Electronic Spectroscopy.* Elsevier, Amsterdam (1968).
28. B. N. Figgis, *Introduction to Ligand Fields.* Interscience, New York (1966).
29. F. A. Cotton, D. M. L. Goodgame and M. Goodgame, *J. Am. Chem. Soc.* 1961, **83**, 4690.
30. E. Konig, *Struct. Bonding (Berlin)* 1971, **9**, 175.
31. K. C. Jorgensen, *Absorption Spectra and Chemical Bonding in Complexes.* Pergamon Press, Oxford (1964).
32. C. Preti and G. Tosi, *Aust. J. Chem.* 1979, **32**, 989.
33. C. Bellitto, A. A. G. Tomlinson, C. Furlani and G. De Munno, *Inorg. Chim. Acta* 1978, **27**, 269.
34. G. Dessy, V. Fares, L. Scaramuzza and A. A. G. Tomlinson, *J. Chem. Soc., Dalton Trans.* 1978, 1549.

Polyhedron Vol. 4, No. 6, pp. 943–946, 1985
Printed in Great Britain

0277–5387/85 $3.00 + .00
© 1985 Pergamon Press Ltd

BENZOYLATION OF MACROCYCLIC JÄGER TYPE Ni(II) COMPLEXES AND AN EFFICIENT DEMETALATION OF γ,γ'-DIBENZOYLATED PRODUCTS

JULITA EILMES
Institute of Chemistry, Jagiellonian University, Karasia 3, 30-060 Cracow, Poland

(*Received* 27 *July* 1984; *accepted* 26 *September* 1984)

Abstract—The reaction of [Bzo_2Me_4[14]hexaenato(2−)N_4]Ni(II) and [$Bzo_2Me_2Ph_2$[14]hexaenato(2−)N_4]Ni(II) with benzoyl chloride leading to mono- and disubstituted derivatives is reported. The condition of the reliable demetalation of γ,γ'-dibenzoylated complexes by means of gaseous HCl are described. The Cu(II) complexes are synthesized from free ligands. All new compounds are characterized by elemental analysis, IR, ^{1}H NMR and MS data.

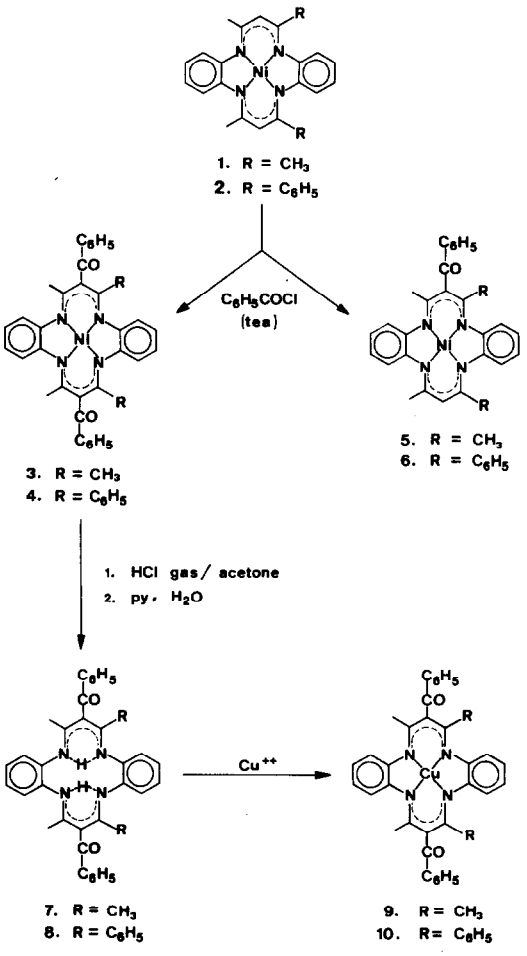
The reactivity of macrocyclic tetraaza metal complexes towards various reagents can be employed to introduce a large number of substituents into macrocyclic ligands. These substituents appended to macrocyclic complexes provide points of attachment for further structural modifications. Consequently, they offer the possibility of producing the more complex compounds which can serve as models for biologically important macrocyclic systems. For many macrocyclic ligands the presence of the coordinated metal greatly assists in these transformations.

From the synthetic point of view such a way of construction of peripherally substituted compounds is especially useful when the starting macrocyclic complexes are easily accessible (e.g. by high-yield, one-step template synthesis) and when the new, modified products can be successfully demetalated. Thus, replacement of the central metal atom by other transition metals is possible and the usually laborious, multi-step, non-template syntheses of peripherally substituted ligands can be avoided.

Very often, however, as it arises from many reports, numerous difficulties with the demetalation and the free ligand isolation procedure renders such synthetic approach unpractical. For example, the destruction of macrocyclic ring[1,2] and the loss of substituents,[2,3] caused by the standard conditions of this reaction, has been observed. Recently, Jäger has mentioned an extreme resistance of the γ,γ'-dicarbonyl derivatives of tetraaza macrocyclic complexes towards strong demetalation agents.[4]

This paper reports benzoylation of [Bzo_2Me_4[14]hexaenato(2−)N_4]Ni(II) (**1**)[2] (Scheme 1) and [$Bzo_2Me_2Ph_2$[14]hexaenato(2−)N_4]Ni(II) (**2**)[6] and a non-destructive demetalation of their γ,γ'-dibenzoylated derivatives.

Further experiments suggest that the conditions



Scheme 1.

reported here of removing of a metal atom are more general and can be successfully applied to other meso-disubstituted macrocyclic complexes.

RESULTS

Benzoylation

The reaction between **1** and benzoyl chloride in a 1 : 2 molar ratio in the presence of triethylamine was carried out in boiling benzene and led to the γ,γ'-dibenzoylated product **3** in 92% yield. A 1 : 1 molar ratio of these reagents produce a mixture of approximately equal quantities of the parent complex **1**, the monobenzoylated product **5** and the dibenzoylated compound **3**. The separation of products of the crude reaction mixture can be achieved by means of column chromatography (silicagel).

In the case of starting complex **2** the reaction with benzoyl chloride in 1:2 molar ratio was accomplished identically as for **1**. This reaction proceeds, however, with lower yield and results in a mixture of about 40, 20, 40% of **2**, **4** and **6** respectively. Similarly a chromatographic procedure allowed the separation of the products **6** and **4**.

A very useful, quick control of the composition of a crude benzoylation product is performed by TLC [silicagel, chloroform–benzene (1 : 1)].

Demetalation

The passage of anhydrous hydrogen chloride through a suspension of γ,γ'-dibenzoylated Ni(II) complexes in acetone produced the change of colour from green to orange–red and resulted in the abundant precipitation of a yellow, crystalline solid. This solid is a mixture of the disubstituted macrocyclic ligand hydrochloride and the nickel chloride. The metal-free hydrochloride of the dibenzoylated macrocyclic ligands was separated from the nickel salt by treatment with dilute hydrochloric acid.

The hydrochlorides of γ,γ'-dibenzoylated ligands are insoluble in water and are unchanged in cold solutions of acids and alkalis. They can be conveniently liberated from HCl by two procedures:

(i) dissolving of a crude hydrochloride in cold pyridine followed by precipitation of a free base with water;

(ii) dissolving of a crude hydrochloride in the solution of chloroform and triethylamine (ratio 2 : 1) followed by dilution with *n*-hexane. Isolation of the solid triethylamine hydrochloride and concentration of the filtrate results in crystallization of a free base, which, after washing with water, becomes completely HCl-free.

The hydrochlorides of γ,γ'-dibenzoylated ligands are insoluble in water and in this respect they differ from the water-soluble hydrochlorides of mono- and non-substituted ligands. Therefore, it is not necessary to purify chromatographically a crude product of the benzoylation reaction before a demetalation procedure. A successful separation of ligand hydrochlorides can be easily achieved.

Synthesis of Cu(II) *complexes*

Cu(II) complexes **9** and **10** were formed in fair yield when the macrocyclic ligands **7** and **8** were subjected to the action of a small excess of copper(II) acetate monohydrate in refluxing ethanol.

EXPERIMENTAL

General

Melting points are uncorrected. IR spectra were recorded in Nujol and hexachlorobutadiene on a Zeiss UR-10 spectrometer. ^{1}H NMR spectra were taken on a JEOL 100 MHz and on a Tesla BS487 80 MHz in $CDCl_3$ using TMS as internal standard. Mass spectra were taken on an LKB 900 instruments.

Parent complexes **1** and **2** were prepared by the template syntheses reported earlier.[5,6]

[2,3 : 9,10 - *dibenzo* - 6,13 - *dibenzoyl* - 5,7,12,14 - *tetramethyl* - 1,4,8,11 - *tetraazacyclotetradeca* - 2,4,6,9,11,13 - *hexaenato*(2−)]*nickel*(II) ([*Bz*$_2$*bzo*$_2$ *Me*$_4$[14]*hexaenato*(2−)]Ni(II)) (**3**). A slurry of 6 g (0.015 mol) of [Bzo$_2$Me$_4$[14]hexaenato(2−)N$_4$] Ni(II) (**1**) and triethylamine (7 cm^3) in dry benzene (100 cm^3) was treated with a solution of 4.2 g (0.03 m) of benzoyl chloride in benzene (10 cm^3), then refluxed for 1.5 h with stirring and protecting from the moisture. The reaction mixture was then allowed to stand at room temperature for 24 h.

A grey-green crystalline precipitate, consisting of the dibenzoylation product and triethylamine hydrochloride, was filtered off, dried and treated with hot water with stirring. Black, crystalline material (cubes) with slightly blue, metallic sheen was collected, washed carefully with hot water and dried *in vacuo*.

A small amount of the product can be additionally isolated from the reaction filtrate by concentration to small volume followed by precipitation with *n*-hexane.

Yield 8.3 g (92%). The product can be recrystallized from chloroform–acetone, xylene or benzene (as a solvate). M.p. > 320°C.

Found: C, 70.47; H, 5.0; N, 9.4; Ni, 9.2%.

Calc. for $C_{36}H_{30}N_4O_2Ni$: C, 70.96; H, 4.96; N, 9.2; Ni, 9.64%.

MS: 608 (P^+, ^{58}Ni) (calc. 609.29); IR: 1650 cm^{-1} (s) ($\nu_{C=O}$). ^1H NMR (δ, ppm): 1.9s (12H)—CH_3, 6.6b.s (8H) *o*-C_6H_4, 7.6m (6H) —CO—C_6H_5, 8.2m (4H) —CO—C_6H_5.

[6 - *benzoyl* - 2,3:9,10 - *dibenzo* - 5,7,12,14 - *tetramethyl* - 1,4,8,11 - *tetraazacyclotetradeca* - 2,4,6,9,11,13 - *hexaenato*(2−)]*nickel*(II) ([*Bzbzo*$_2$ *Me*$_4$[14]*hexaenato*(2−)N_4]Ni(II)) (**5**). A reaction of [Bzo_2Me_4[14]hexaenato(2−)N_4]Ni(II) (**1**) with benzoyl chloride in a 1:1 molar ratio was performed similarly to the procedure described above. After standing for 24 h, a small amount of solid was separated and treated as above. The filtrate was evaporated under reduced pressure to a small volume, cooled and diluted with *n*-hexane. A green, solid material was collected, dried, then treated with hot water with stirring, filtered off and washed carefully. The whole amount of a crude product of the reaction, dissolved in the minimum quantity of chloroform was chromatographed on a column of silicagel (0.05–0.2 mm, Merck). Three fractions—the unreacted complex **1**, the monosubstituted complex **5** and the disubstituted complex **3**—were eluted successively by means of benzene, benzene–chloroform (1:1) and chloroform. Yield of **5** 20%. Analytical sample of **5** was recrystallized from chloroform–acetone (cubes). M.p. 266°C.

Found: C, 68.4; H, 5.0; N, 11.4; Ni, 11.1%.

Calc. for $C_{29}H_{26}N_4ONi$: C, 68.94; H, 5.18; N, 11.09; Ni, 11.62%.

MS: 504 (P^+, ^{58}Ni) (calc. 505.2); IR: 1650 cm^{-1} (s) ($\nu_{C=O}$); ^1H NMR (δ, ppm): 1.9s(6H)—CH_3, 2.1s (6H) —CH_3, 6.6m (8H) *o*—C_6H_4, 7.6m (3H) —CO—C_6H_5, 8.2m (2H) —CO—C_6H_5, 4.86s (1H) =CH.

[2,3:9,10 - *dibenzo* - 6,13 - *dibenzoyl* - 7,12 - *dimethyl* - 5,14 - *diphenyl* - 1,4,8,11 - *tetraazacyclotetradeca* - 2,5,7,9,11,13 - *hexaenato*(2−)]*nickel*(II) ([*Bz*$_2$*bzo*$_2$*Me*$_2$*Ph*$_2$[14]*hexaenato*(2−)N_4]Ni(II)) (**4**) *and* [6-*benzoyl*-2,3:9,10 - *dibenzo* - 7,12 - *dimethyl* - 5,14 - *diphenyl* - 1,4,8,11 - *tetraazacyclotetradeca* - 2,5,7,9,11,13 - *hexaenato*(2−)]*nickel*(II) ([*Bzbzo*$_2$ *Me*$_2$*Ph*$_2$[14]*hexaenato*(2−)N_4]Ni(II)) (**6**). The reaction of 5.24 g (0.01 m) of [$Bzo_2Me_2Ph_2$[14] hexaenato(2−)N_4]Ni(II) (**2**), 3.3 g (0.023 mol) of benzoyl chloride and 10 cm^3 of triethylamine in dry benzene (150 cm^3) was conducted in the same manner as for complex **1**.

A grey, crystalline solid which was filtered off from the reaction mixture was composed of triethylamine hydrochloride and the unconverted starting complex (0.7 g).

A deep-green filtrate was worked-up identically as in the case of monosubstituted complex **5**. A bright-green solid (6 g) dissolved in a minimum amount of chloroform was chromatographed by the usual procedure [silicagel (0.05–0.2 mm, Merck)]. Elution with benzene, benzene–chloroform (1:1), chloroform, allowed the isolation of the parent complex **2**, the monosubstituted product **6** (yield 1 g) and the disubstituted complex **4** (yield 2.9 g, 39.5%). The product **4** was recrystallized from aqueous ethanol, m.p. 320°C, **6** from chloroform–acetone, m.p. 310°C.

Found (**4**): C, 74.82; H, 4.26; N, 7.52; Ni, 7.5%.

Calc. for $C_{46}H_{34}N_4O_2Ni$: C, 75.33; H, 4.67; N, 7.64; Ni, 8.0%.

MS: 732 (P^+, ^{58}Ni) (calc. 733.42); IR: 1640 cm^{-1} (s) ($\nu_{C=O}$); ^1H NMR (δ, ppm): 2.2s (6H)—CH_3, 5.7m (4H)AA'BB' *o*-C_6H_4, 6.7m (4H) *o*-C_6H_4, 7.0m (10H) —C_6H_5, 7.7m (6H) —CO—C_6H_5, 8.2m (4H) —CO—C_6H_5.

Found (**6**): C, 74.05; H, 5.12; N, 8.8; Ni, 8.85%.

Calc. for $C_{39}H_{30}N_4ONi$: C, 74.43; H, 4.8; N, 8.9; Ni, 9.33%.

MS: 628 (P^+, ^{58}Ni) (calc. 629.33); IR: 1640 cm^{-1} (s) ($\nu_{C=O}$); ^1H NMR (δ, ppm): 2.17s (3H)—CH_3, 2.22s(3H)—CH_3, 5.0s (1H)=CH, 5.7m (4H)AA'BB' *o*-C_6H_4, 6.7m (4H) *o*-C_6H_4, 7.0m (5H)—C_6H_5, 7.3m (8H) —C_6H_5, —CO—C_6H_5, 7.7m (2H) —CO—C_6H_5.

2,3:9,10 - *dibenzo* - 6,13 - *dibenzoyl* - 5,7,12,14 - *tetramethyl* - 1,4,8,11 - *tetraazacyclotetradeca* - 2,4,6,9,11,13 - *hexaen* (*Bz*$_2$*bzo*$_2$*Me*$_4$[14]*hexaen* N_4) (**7**). A stream of anhydrous hydrogen chloride gas was bubbled through a magnetically stirred suspension of 5 g (0.0082 mol) of **3** in 150 cm^3 of acetone. The solution slowly turned yellow and a yellow precipitate began to separate. The reaction was complete after about 15 min, when the solution became orange–yellow and an abundant, orange–yellow solid accumulated. The reaction mixture, sealed carefully in the reaction flask, was left overnight, at room temperature with magnetic stirring.

The quantity of the solid diminishes in time. It seems that diacetone alcohol which forms in considerable amount partially dissolves the nickel chloride precipitate, whereas the metal-free product remains insoluble.

The crystalline solid which consisted of the macrocyclic ligand hydrochloride (orange–yellow crystals) and the nickel chloride (pale-yellow precipitate) was filtered off. After washing with acetone and drying it was treated with 100 cm^3 of cold, dilute (1:10) hydrochloric acid, stirred vigorously and quickly filtered off. It was then washed carefully with dilute hydrochloric acid and then immediately with acetone, while still wet.

The free macrocyclic base was isolated by

dissolving the crude material (4 g) in cold pyridine (50 cm^3), followed by dropwise addition of water (50 cm^3) with continuous magnetic stirring. Such a procedure was repeated three times. The method (ii) of the conversion of the hydrochloride into the free base can also be applied with similar result. Yellow cubes, m.p. 265°C. Yield 3.4 g (75.5%). The product **7** can be recrystallized from chloroform–hexane.

Found: C, 78.1; H, 5.33; N, 10.1%.

Calc. for $C_{36}H_{32}N_4O_2$; C, 78.24; H, 5.93; N, 10.14%.

MS: 552 (P^+) (calc. 552.6); IR: 1640 cm^{-1} (s) ($\nu_{C=N}$), 1660 cm^{-1} (s) $\nu_{C=O}$), 2800 cm^{-1} (w, broad) (ν_{N-H}); ^1H NMR (δ, ppm): 2.0s (12H) —CH_3, 7.2s (8H) *o*-C_6H_4, 7.65m (6H) —CO —C_6H_5, 8.2m (4H) —CO—C_6H_5, 14.2s (2H) NH.

2,3:9,10-*dibenzo*-6,13-*dibenzoyl*-7,12-*dimethyl*-5,14-*diphenyl*-1,4,8,11-*tetraazacyclotetradeca*-2,5,7,9,11,13-*hexaen* (*Bz*$_2$*bzo*$_2$*Me*$_2$*Ph*$_2$[14]*hexaen* N_4) (**8**). 2.5 g (0.0034 mol) of **4** in acetone (100 cm^3) was demetalated in the same manner as for complex **3**. The change of colour of the reaction mixture from green to orange–red was significantly slower than for complex **3** and took about 30 min. The orange–red crystalline hydrochloride of the ligand was obtained, from which 1.65 g of the free macrocyclic base **8** was obtained [method (ii)]. Orange–yellow needles, m.p. 278°C. Yield 72%. It can be recrystallized from chloroform–acetone.

Found: C, 81.43; H, 5.12; N, 8.2%.

Calc. for $C_{46}H_{36}N_4O_2$; C, 81.64; H, 5.36; N, 8.28%.

MS: 676 (P^+) (calc. 676.72); IR: 1640–1650 cm^{-1} (s) ($\nu_{C=N}$, $\nu_{C=O}$), 2700 cm^{-1} (w, broad) (ν_{N-H}); ^1H NMR (δ, ppm): 2.3s (6H) —CH_3, 6.4 m (4H)AA'BB' *o*-C_6H_4, 7.0–7.5 m (20H) —CO—C_6H_5, —C_6H_5, *o*-C_6H_4, 7.9m (4H) —CO—C_6H_5, 13.9s (2H) —NH.

[2,3:9,10-*dibenzo*-6,13-*dibenzoyl*-5,7,12,14-*tetramethyl*-1,4,8,11-*tetraazacyclotetradeca*-2,4,6,9,11,13-*hexaenato*(2−)N_4]*copper*(II) ([*Bz*$_2$*bzo*$_2$*Me*$_4$[14]*hexaenato*(2−)N_4]Cu(II)) (**9**). A solution of 0.25 g (0.00125 mol) of copper(II) acetate monohydrate in ethanol (25 cm^3) was added to a suspension of 0.5 g (0.0009 mol) of **7** in ethanol (50 cm^3). An immediate colour change to brownish-green was produced and a dark crystalline precipitate began to separate. The reaction mixture was heated under gentle reflux for 1 h with magnetic stirring. After cooling 0.6 g of black, crystalline product was collected, washed with water, dried and recrystallized from chloroform–acetone. Black, metallic-looking cubes, m.p. > 320°.C. Yield 92%.

Found: C, 70.2; H, 4.52; N, 9.1; Cu, 9.8%.

Calc. for $C_{36}H_{30}N_4O_2Cu$: C, 70.40; H, 4.92; N, 9.12; Cu, 10.35%.

MS: 613 (P^+, ^{63}Cu) (calc. 614.12); IR: 1650–1660 cm^{-1} (s) ($\nu_{C=O}$).

[2,3:9,10-*dibenzo*-6,13-*dibenzoyl*-7,12-*dimethyl*-5,14-*diphenyl*-1,4,8,11-*tetraazacyclotetradeca*-2,5,7,9,11,13-*hexaenato*(2−)N_4] *copper*(II) ([*Bz*$_2$*bzo*$_2$*Me*$_2$*Ph*$_2$[14]*hexaenato*(2−)N_4] Cu(II)) (**10**). The complex **10** was synthesized in the same manner as **9**. It was characterized without further purification. Olive-green microcrystalline product, m.p. 310°C. Yield 75%.

Found: C, 74.52; H, 4.64; N, 7.6; Cu, 8.05%.

Calc. for $C_{46}H_{34}N_4O_2Cu$: C, 74.83; H, 4.64; N, 7.59; Cu, 8.6%.

MS: 737 (P^+, ^{63}Cu) (calc. 738.25); IR: 1630–1640 cm^{-1} (s) ($\nu_{C=O}$).

REFERENCES

1. E. G. Jäger, *Z. Chem.* 1968, **8**, 30.
2. E. G. Jäger, *Z. Anorg. Allg. Chem.* 1969, **364**, 177.
3. D. P. Riley and D. H. Busch, *Inorg. Synth.* 1978, **18**, 41.
4. E. G. Jäger and D. Seidel, *Z. Chem.* 1983, **23**, 31.
5. F. A. L'Eplattenier and A. Pugin, *Helv. Chim. Acta* 1975, **58**, 917.
6. J. Eilmes, D. Pelan and E. Śledziewska, *Bull. Acad. Pol. Sci.* 1980, **28**, 371.

Polyhedron Vol. 4, No. 6, pp. 947–953, 1985
Printed in Great Britain

0277–5387/85 $3.00 + .00
© 1985 Pergamon Press Ltd

ADDUCT FORMATION OF COPPER(II) CHELATES OF 1-HYDROXYPYRAZOLE 2-OXIDES WITH SUBSTITUTED PYRIDINES

FUMIAKI KAI* and HIDEAKI HARAGA
Department of Chemistry, Faculty of Science, Kumamoto University, Kumamoto 860, Japan

and

HIROSHI KOBAYASHI
Chemical Laboratory, Kumamoto Prefectural Daiichi Senior High School, Kumamoto 860, Japan

(*Received* 30 *August* 1984; *accepted* 26 *September* 1984)

Abstract—Equilibrium constants have been determined for the adduct formation of 10 copper(II) chelates of the derivatives of 1-hydroxypyrazole 2-oxide with nine substituted pyridines at room temperature in chloroform solution. These adducts were shown to have 1 : 1 stoichiometry. All the stabilities of the adducts were governed by : (1) σ-donating ability of the nitrogen atom in the substituted pyridines to the copper(II) chelates, (2) electron-attracting forces of substituents at the 3- and 4-positions of the phenyl ring in the chelate ligands, and (3) the magnitude of the polar substituent constant of the substituents in the pyrazole ring of the chelate ligands.

It is well known that the square planer copper(II) chelates behave as Lewis acids and react with a variety of Lewis bases in the axial positions to form either five-coordinate 1 : 1 or six-coordinate 1 : 2 adducts, and many papers on the adduct formation of the copper(II) chelates are now available.

In the present investigation, we have undertaken to obtain more detailed information on the effect of the substituents in both the ligands of the copper(II) chelates and Lewis bases on adduct formation. The derivatives of 1-hydroxypyrazole 2-oxide, which were first reported by Hansen *et al.*[1] as the conjugate ligands of the bivalent metal complexes, were chosen as the ligands of the copper(II) chelates because a variety of the derivatives could be synthesized according to the method proposed by Freeman *et al.*[2] Nine substituted pyridines (pys) were used as Lewis bases. Bases were selected so as to cover the effects of different basicities.

EXPERIMENTAL

Synthesis of derivatives of 1-*hydroxypyrazole* 2-*oxide*

The ligands synthesized in this investigation, according to the literature,[2] and their abbreviations are listed in Table 1. The analytical data and ^{1}H NMR spectral data of the ligands are as follows.

PhMeMe. Found: C, 64.93; H, 5.91; N, 13.50%. $C_{11}H_{12}N_2O_2$ requires C, 64.69; H, 5.92; N, 13.72%. ^{1}H NMR ($CDCl_3$): δ = 2.06 (*s*, 3H); 2.26 (*s*, 3H); 7.3–7.6 (*m*, 5H); 12.36 (*s*, 1H).

2Cl-*PhMeMe.* Found: C, 55.44; H, 4.48; N, 11.60%. $C_{11}H_{11}N_2O_2Cl$ requires C, 55.36; H, 4.65; N, 11.74%. ^{1}H NMR (DMSO-d_6): δ = 1.86 (*s*, 3H); 2.13 (*s*, 3H); 7.3–7.6 (*m*, 4H).

3Cl-*PhMeMe.* Found: C, 55.38; H, 4.67; N, 11.70%. $C_{11}H_{11}N_2O_2Cl$ requires C, 55.36; H, 4.65; N, 11.74%. ^{1}H NMR ($CDCl_3$): δ = 2.10 (*s*, 3H); 2.31 (*s*, 3H); 7.4–7.7 (*m*, 5H); 14.30 (*s*, 1H).

4Cl-*PhMeMe.* Found: C, 55.51; H, 4.47; N, 11.55%. $C_{11}H_{11}N_2O_2Cl$ requires C, 55.36; H, 4.65; N, 11.74%. ^{1}H NMR ($CDCl_3$): δ = 2.07 (*s*, 3H); 2.28 (*s*, 3H); 7.47 (*s*, 4H); 12.50 (*s*, 1H).

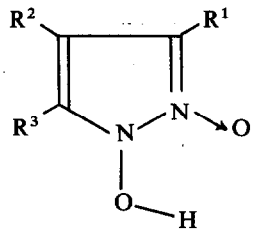
2CH_3O-*PhMeMe.* Found: C, 61.60; H, 6.01; N, 11.77%. $C_{12}H_{14}N_2O_3$ requires C, 61.53; H, 6.02; N, 11.96%. ^{1}H NMR ($CDCl_3$): δ = 1.91 (*s*, 3H); 2.25 (*s*, 3H); 3.77 (*s*, 3H); 6.7–7.6 (*m*, 4H); 14.01 (*s*, 1H).

4CH_3O-*PhMeMe.* Found: C, 61.59; H, 5.94; N, 11.52%. $C_{12}H_{14}N_2O_3$ requires C, 61.53; H, 6.02; N, 11.96%. ^{1}H NMR ($CDCl_3$): δ = 2.05 (*s*, 3H); 2.26 (*s*, 3H); 3.83 (*s*, 3H); 6.9–7.6 (*m*, 4H); 14.44 (*s*, 1H).

4CH_3-*PhMeMe.* Found: C, 66.23; H, 6.47; N,

* Author to whom correspondence should be addressed.

Table 1. Ligands synthesized and their abbreviations



Ligand	Abbreviation	Substituent		
		R^1	R^2	R^3
1-Hydroxy-3-phenyl-4,5-dimethylpyrazole 2-oxide	PhMeMe	Phenyl	Methyl	Methyl
1-Hydroxy-3-(2-chlorophenyl)-4,5-dimethylpyrazole 2-oxide	2Cl-PhMeMe	2-Chlorophenyl	Methyl	Methyl
1-Hydroxy-3-(3-chlorophenyl)-4,5-dimethylpyrazole 2-oxide	3Cl-PhMeMe	3-Chlorophenyl	Methyl	Methyl
1-Hydroxy-3-(4-chlorophenyl)-4,5-dimethylpyrazole 2-oxide	4Cl-PhMeMe	4-Chlorophenyl	Methyl	Methyl
1-Hydroxy-3-(2-methoxyphenyl)-4,5-dimethylpyrazole 2-oxide	$2CH_3O$-PhMeMe	2-Methoxyphenyl	Methyl	Methyl
1-Hydroxy-3-(4-methoxyphenyl)-4,5-dimethylpyrazole 2-oxide	$4CH_3O$-PhMeMe	4-Methoxyphenyl	Methyl	Methyl
1-Hydroxy-3-(4-methylphenyl)-4,5-dimethylpyrazole 2-oxide	$4CH_3$-PhMeMe	4-Methylphenyl	Methyl	Methyl
1-Hydroxy-3,5-diphenyl-4-methylpyrazole 2-oxide	PhMePh	Phenyl	Methyl	Phenyl
1-Hydroxy-3,4,5-trimethylpyrazole 2-oxide	MeMeMe	Methyl	Methyl	Methyl
1-Hydroxy-3-(1-ethylpropyl)-4,5-dimethylpyrazole 2-oxide	1Et-PrMeMe	1-Ethylpropyl	Methyl	Methyl

12.37%. $C_{12}H_{14}N_2O_2$ requires C, 66.04; H, 6.47; N, 12.84%. ^{1}H NMR ($CDCl_3$): δ = 2.05 (*s*, 3H); 2.26 (*s*, 3H); 2.38 (*s*, 3H); 7.1–7.5 (*m*, 4H); 14.05 (*s*, 1H).

PhMePh. Found: C, 71.56; H, 5.24; N, 10.56%. $C_{16}H_{14}N_2O_2$ requires C, 72.16; H, 5.30; N, 10.52%. ^{1}H NMR ($CDCl_3$): δ = 2.19 (*s*, 3H); 7.3–7.9 (*m*, 10H); 9.99 (*s*, 1H).

MeMeMe. Found: C, 50.54; H, 6.75; N, 19.75%. $C_6H_{10}N_2O_2$ requires C, 50.69; H, 7.09; N, 19.71%. ^{1}H NMR ($CDCl_3$): δ = 1.93 (*s*, 3H); 2.18 (*s*, 6H); 15.32 (*s*, 1H).

1Et-PrMeMe. Found: C, 60.33; H, 9.08; N, 13.99%. $C_{10}H_{18}N_2O_2$ requires C, 60.58; H, 9.15; N, 14.13%. ^{1}H NMR ($CDCl_3$): δ = 0.82 (*t*, 6H); 1.5–2.0 (*m*, 4H); 1.93 (*s*, 3H); 2.21 (*s*, 3H); 2.75 (*t*, 1H); 15.06 (*s*, 1H).

Preparation of copper(II) *chelates*

Ten kinds of copper(II) chelates were prepared by shaking a mixture of a chloroform solution of the ligand and an aqeuous solution of copper(II) nitrate in a mole ratio of 2 : 1 for 20 min. After the chloroform solution containing the chelate formed was washed with water to remove excess copper(II) ion, a crude product was obtained by evaporating the solvent under reduced pressure. The resulting precipitate was filtered, recrystallized from chloroform–ethanol and air-dried. The analytical data are shown in Table 2.

Reagents and apparatus

Analytical-grade py and 4-dimethylaminopyridine (4DMAP) were used without further purification. Liquid bases, 3-methylpyridine (3MP), 4-methylpyridine (4MP), 3,4-dimethylpyridine (3,4DMP) and 3,5-dimethylpyridine (3,5DMP), were dried over a molecular sieve (Type 4A) for 2–3 days, then fractionally distilled under reduced pressure prior to use. Among the solid bases, 3-aminopyridine (3AP) and 4-aminopyridine (4AP) were recrystallized from benzene, and 3-cyanopyridine (3CP) from ether. Chloroform as a solvent

Table 2. Elemental analyses of copper(II) chelates

Complex	Found (%)	Calc. (%)
[Cu(PhMeMe)$_2$]	C: 56.37 H: 4.57 N: 11.87	C: 56.22 H: 4.72 N: 11.92
[Cu(2Cl-PhMeMe)$_2$]	C: 49.07 H: 3.73 N: 10.30	C: 49.04 H: 3.74 N: 10.40
[Cu(3Cl-PhMeMe)$_2$]	C: 49.10 H: 3.58 N: 10.42	C: 49.04 H: 3.74 N: 10.40
[Cu(4Cl-PhMeMe)$_2$]	C: 48.94 H: 3.60 N: 10.40	C: 49.04 H: 3.74 N: 10.40
[Cu(2CH$_3$O-PhMeMe)$_2$]	C: 54.12 H: 4.64 N: 10.52	C: 54.39 H: 4.94 N: 10.57
[Cu(4CH$_3$O-PhMeMe)$_2$]	C: 53.99 H: 4.66 N: 10.56	C: 54.39 H: 4.94 N: 10.57
[Cu(4CH$_3$-PhMeMe)$_2$]	C: 57.06 H: 5.13 N: 11.12	C: 57.88 H: 5.26 N: 11.25
[Cu(PhMePh)$_2$]	C: 64.03 H: 4.23 N: 9.45	C: 64.69 H: 4.41 N: 9.43
[Cu(MeMeMe)$_2$]	C: 41.79 H: 5.27 N: 16.33	C: 41.68 H: 5.25 N: 16.20
[Cu(1Et-PrMeMe)$_2$]	C: 52.23 H: 7.39 N: 12.30	C: 52.44 H: 7.48 N: 12.23

for the equilibrium study was purified by the usual method. Electronic spectra were recorded on a Hitachi EPS-3T spectrophotometer equipped with a constant temperature cell housing. Correction of wave-number was done with benzene. Vapour proof 5 cm cells were used. Temperature was controlled at 20 ± 1°C. Chloroform was used as the reference. ESR spectra (X-band) were measured with a JES-FE 3X ESR instrument. ^{1}H NMR spectra were recorded with tetramethylsilane as an internal reference with a Hitachi R-24 spectrometer.

Calculation of equilibrium constant

The equilibrium constant of a 1:1 adduct, K, formed between a copper(II) chelate and a substituted py was determined spectrophotometrically using the following Lang's equation:[3]

$$\frac{ab}{d-d_0} = \frac{1}{\varepsilon_{add}}\left(a+b-\frac{d-d_0}{\varepsilon_{add}-\varepsilon_c}+\frac{\varepsilon_c ab}{d-d_0}\right)+\frac{1}{K\varepsilon_{add}},$$

where a and b are the initial concentrations of the copper(II) chelate and the substituted py, respectively, ε_c and ε_{add} are the molar extinction coefficients of the copper(II) chelate and the adduct, respectively, d_0 is the absorbance of the copper(II) chelate only and d is the absorbance of the adduct at a certain wavelength. In this equation, the values for ε_{add} and K are unknown; accordingly, a tentative value of ε_{add} is determined by using data from two solutions and solving the equation simultaneously for ε_{add} and K. This procedure is repeated until a consistent set of values for both ε_{add} and K has been obtained from two successive plots. In this study, the consistent values for ε_{add} and K were yielded by three-times repetition of a computation procedure. In determining the equilibrium constants of the adducts, absorbance measurements were carried out by using 5 cm cells at 825 nm, where the substituted py and chloroform as a solvent do not absorb.

RESULTS AND DISCUSSION

Copper(II) chelate

As summarized in Table 2, the composition of all copper(II) chelates was Cu(ligand)$_2$. These chelates were soluble in chloroform but not so soluble in other usual organic solvents. The *d–d* absorption bands measured in chloroform solution were in the region of 14,200–14,500 cm^{-1} (molar extinction coefficient 30–50), showing no appreciable differences in the spectral features due to the kind of substituent in the ligands.

Composition of adduct

As a typical example, successive absorption curves of chloroform solutions containing [Cu(PhMeMe)$_2$] at constant concentration and py at variable concentrations are shown in Fig. 1. At least seven different py concentrations were used to provide data for each determination. They pass through a clear isosbestic point, showing an equilibrium between two absorbing species in solution. Accordingly, the following equilibrium is expected to be present:

$$\text{chelate} + \text{py} \rightleftharpoons \text{chelate} \cdot \text{py}, \qquad \text{(A)}$$

or

$$\text{chelate} + 2\text{py} \rightleftharpoons \text{chelate(py)}_2. \qquad \text{(B)}$$

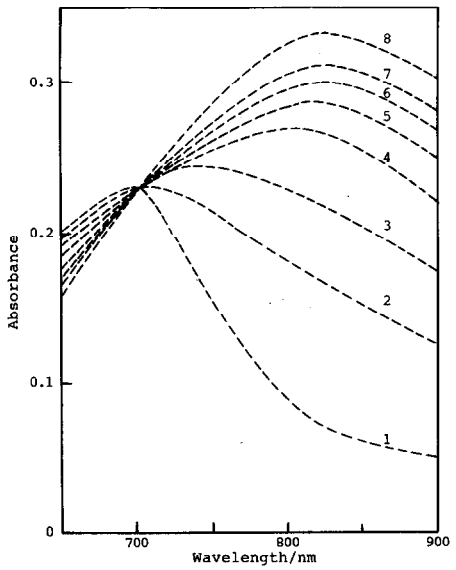


Fig. 1. Spectral change of $[Cu(PhMeMe)_2]$–py mixture in chloroform. Concentration of $[Cu(PhMeMe)_2] = 5.488 \times 10^{-3}$ mol dm^{-3}, concentrations of py: (1) 0, (2) 0.177, (3) 0.354, (4) 0.708, (5) 1.062, (6) 1.416, (7) 1.770, (8) 3.504 mol dm^{-3}.

To confirm equilibrium (A) or (B), the following two independent methods were used: Rose–Drago's[4] and Benesi–Hildebrand's methods.[5] As illustrated in Fig. 2, the curves calculated by the Rose–Drago's method have a common point by an assumption of 1 : 1 adduct formation.

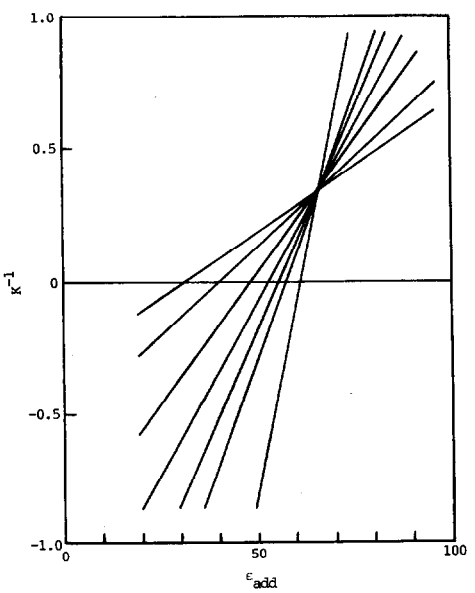


Fig. 2. Graphical solution of Rose–Drago equation[4] for the $[Cu(PhMeMe)_2]$–py system by assuming 1 : 1 adduct formation from the data in Fig. 1.

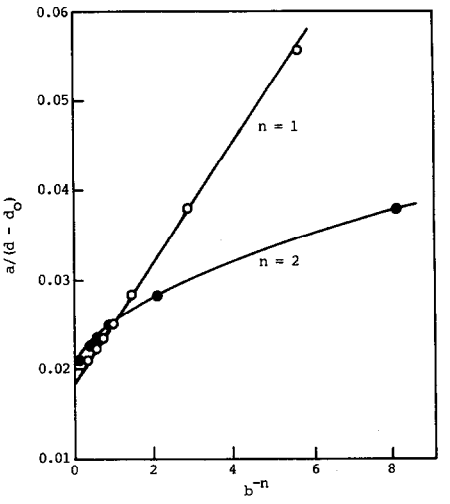


Fig. 3. Plots of Benesi–Hildebrand equation[5] for the $[Cu(PhMeMe)_2]$–py system using the data in Fig. 1.

Furthermore, in the case of equilibrium (C), Benesi and Hildebrand have proposed that the plots of b^{-n} vs $a/(d-d_0)$

$$\text{chelate} + n \cdot \text{py} \rightleftharpoons \text{chelate(py)}_n \qquad \text{(C)}$$

should give a straight line. As shown in Fig. 3, the straight line was obtained when $n = 1$. Hence equilibrium (A) is clearly confirmed to be present by this method too.

ESR spectra of copper(II) chelate and its adduct

The ESR spectra of $[Cu(2Cl\text{-}PhMeMe)_2]$, as a typical example, in chloroform (a) at room temperature and py (b) at liquid nitrogen

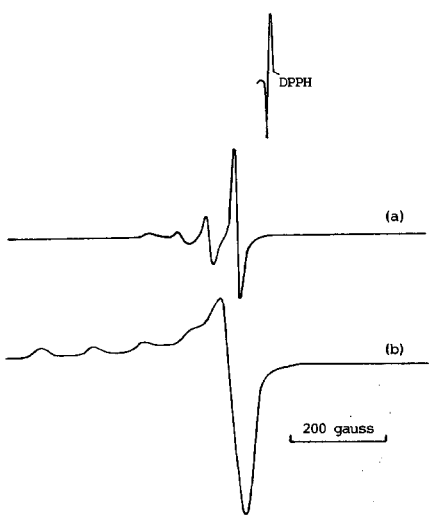


Fig. 4. ESR spectra of $[Cu(2Cl\text{-}PhMeMe)_2]$ in chloroform (a) at 293 K and py (b) at 77 K.

temperature are given in Fig. 4. As can be seen from spectrum (a), a hyperfine structure of the copper nuclei was observed in chloroform solution, indicating that the copper(II) chelate existed as a monomeric structure. In addition, it was seen from spectrum (b) that the py adduct possessed a tetragonal structure.

Kogane *et al.*[6] investigated the ESR spectra of the adducts of $Cu(acac)_2$ (acac = aetylacetonato) with Lewis bases, and reported that a new signal due to 1:2 adduct formation appeared on the lower-field side of the signal corresponding to the 1:1 adduct. However, such a signal was not observed in this study, showing no 1:2 adduct formation for the present systems studied.

Equilibrium constant of adduct

In Table 3, the equilibrium constants for the 1:1 adduct formation between 10 kinds of copper(II) chelates and nine substituted pys are listed, and the Hammett's σ-values of the substituted pys are also listed for illustration in Figs 5–7. The equilibrium constants for the set of 3CP were obtained only for the five adducts having relatively large equilibrium constants.

An effect on the adduct formation due to the substituents in the ligands of the copper(II) chelates and the py derivatives was discussed from the following three viewpoints.

Effect of the substituents in py derivatives. As can be seen from Table 3, it is apparent that the differences in the substituents in py derivatives are largely reflected in the equilibrium constants. Generally, the electronic effect of a substituent bound to aromatic nuclei, including heterocyclic aromatic rings,

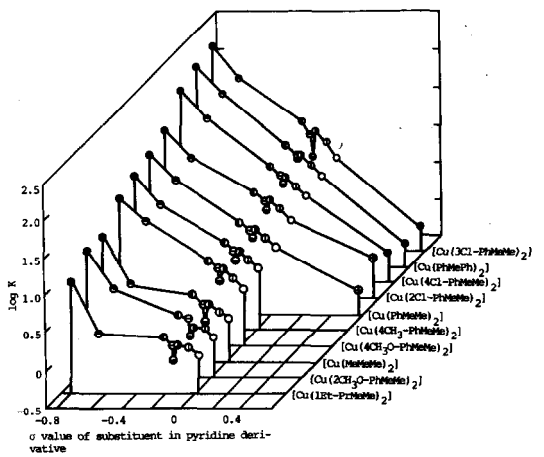


Fig. 5. Plots of Hammett's σ-values of substituents in pyridine derivatives vs equilibrium constants. (●) 4DMAP; (◒) 4AP; (◐) 3,4DMP; (⊖) 4MP; (◒) 3AP; (◑) 3,5DMP; (⊙) 3MP; (○) py; (⊕) 3CP.

Table 3. Equilibrium constants of adducts

Chelate	4DMAP $\sigma = -0.83$	4AP $\sigma = -0.66$	3,4DMP $\sigma = -0.24$	4MP $\sigma = -0.17$	3AP $\sigma = -0.16$	3,5DMP $\sigma = -0.14$	3MP $\sigma = -0.07$	py $\sigma = 0.00$	3CP $\sigma = 0.56$
[Cu(3Cl-PhMeMe)$_2$]	177	67.2	17.7	12.0	6.08	13.8	9.45	5.86	0.67
[Cu(4Cl-PhMeMe)$_2$]	119	50.5	11.8	8.62	6.62	8.07	6.12	4.75	0.79
[Cu(PhMeMe)$_2$]	46.2	20.5	5.55	4.32	3.21	4.31	3.28	2.56	0.67
[Cu(4CH$_3$-PhMeMe)$_2$]	39.8	15.1	4.87	3.73	2.65	3.62	2.81	2.17	
[Cu(4CH$_3$O-PhMeMe)$_2$]	30.7	14.9	4.41	3.44	2.30	3.39	2.61	1.89	
[Cu(PhMePh)$_2$]	153	68.3	14.0	10.2	8.84	9.90	7.58	5.26	0.64
[Cu(2Cl-PhMeMe)$_2$]	61.7	24.0	8.48	6.56	4.75	6.57	5.06	3.65	1.14
[Cu(MeMeMe)$_2$]	15.4	3.35	2.47	1.90	1.06	1.89	1.52	1.24	
[Cu(2CH$_3$O-PhMeMe)$_2$]	16.3	4.98	2.21	1.96	1.17	1.48	1.47	1.14	
[Cu(1Et-PrMeMe)$_2$]	9.56	2.02	1.82	1.41	0.88	1.44	1.31	1.03	

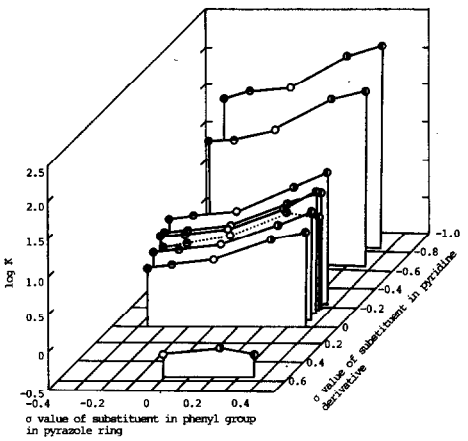


Fig. 6. Plots of Hammett's σ-values of substituents X in [Cu(X-PhMeMe)$_2$] type chelates against equilibrium constants. (●) X = 4CH$_3$O; (◒) X = 4CH$_3$; (○) X = H; (◑) X = 4Cl; (◐) X = 3Cl.

appears as the sum of the induced and resonance effects. Quantitative representation of these effects can be made by Hammett's rule.

The stabilization of the adduct will occur both by contributions from σ-donation, which is an electron transfer from the nitrogen atom in py to the copper(II) chelate, and from π-back donation from the copper atom to the nitrogen. Silva *et al.*[7] reported that, if the back donation is predominant, there is not so good a correlation between the equilibrium constant of the adduct and the Hammett's σ-values, which is a measure of σ-bonding ability, and, in that case, a better correlation of the Hammett's σ-values vs π-stabilization factors, defined as a measure of π-back donation ability, is present.

The plots of the σ-values of the substituted pys vs equilibrium constants of the 1 : 1 adducts obtained in this study are illustrated in Fig. 5. In all cases, the plots had a strong correlation, especially the [Cu(PhMePh)$_2$] and the substituted pys system showed a good correlation, with a coefficient of 0.9989. These results indicate that the stabilization of the adduct studied is thoroughly governed by the electron-donating ability of the nitrogen atom in the substituted py rings, and hence the adduct formation can be carried out by coordinating the nitrogen atom to the square planar copper(II) chelate without steric hindrance.

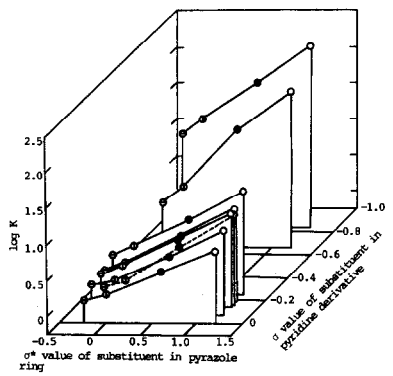


Fig. 7. Plots of Taft's σ^*-values of substituents in pyrazole ring vs equilibrium constants. (⊖) 1Et-PrMeMe; (◑) MeMeMe; (●) PhMeMe; (○) PhMePh.

Among the substituted pys studied, the equilibrium constants for 3AP and 4AP with [Cu(MeMeMe)$_2$], [Cu(2CH$_3$O-PhMeMe)$_2$] and [Cu(1Et-PrMeMe)$_2$] systems deviated slightly from each plot of log K vs σ-value. We cannot explain this deviation so clearly, but it is likely that some interaction of these pys with the copper(II) chelates affected spectral features.

Effect of substituent X in [Cu(*X-PhMeMe*)$_2$] *type chelates.* In all adducts studied, the equilibrium constants increase in the order of X: 2CH$_3$O < 4CH$_3$O < 4CH$_3$ < H < 2Cl < 4Cl < 3Cl. Except for the 2-substituted phenyl group in the copper(II) chelates {[Cu(2CH$_3$O-PhMeMe)$_2$] and [Cu(2Cl-PhMeMe)$_2$]}, this order agreed well with the electron-attracting abilities of X. A substituent in the 2-position of the phenyl group is usually considered to hinder sterically the copper(II) chelate formation. The order H < 2Cl, however, obtained in this study also indicated that the trend of the equilibrium constants of this series should be dependent primarily on the electronic effect of X, and not on the steric factor of X.

Figure 6 shows the plots of the Hammett's σ-values of the substituent X vs the equilibrium constants for the series [Cu(X-PhMeMe)$_2$] other than X = 2CH$_3$O and 2Cl. As can be seen from Fig. 6, correlations of the σ-values against log K are not as good compared to those in Fig. 5, presumably because the electronic effect of X would be transported to the copper atom via the pyrazole ring. As a whole, however, it is clear that the stabilization of the adducts is governed by the electron-attracting ability of the substituent X.

Effect of the substituents R^1 *and* R^3 (R^1 *and* R^3 = *phenyl or alkyl group in pyrazole ring*) *in* [Cu(R^1MeR^3)$_2$] *type chelates.* On changing the methyl group in the [Cu(MeMeMe)$_2$] chelate to [Cu(PhMeMe)$_2$] and [Cu(PhMePh)$_2$], the equilibrium constants of the adduct formation increased linearly for all the substituted pys. This shows that the substituent effect of R^1 and R^3 is considered to be additive for the equilibrium constants, because the positions of R^1 and R^3 in the conjugating pyrazole ring are electrically equivalent.

Taft *et al.*[8] proposed that the polar substituent constant, σ^*, as a measure of an inductive effect of an aliphatic substituent. That is, when $\sigma^* > 0$, the substituent is more electron-attracting than the methyl group, and, if $\sigma^* < 0$, the substituent possesses an electron-donating ability compared to that of the methyl group.

The relations between the σ^* values and the equilibrium constants of the adducts for $[Cu(1EtPrMeMe)_2]$, $[Cu(MeMeMe)_2]$, $[Cu(PhMeMe)_2]$ and $[Cu(PhMePh)_2]$ are illustrated in Fig. 7, in which σ^* values of $C_6H_5 = 0.600$, $H = 0.490$, $CH_3 = 0.000$ and $(C_2H_5)_2CH = -0.225$ were used for illustration. As is apparent from Fig. 7, positively linear correlations are obtained. This tendency shows that the electron density on the copper atom would also be governed by the inductive effect of the substituents in the pyrazole ring.

Acknowledgements—We wish to express our thanks to Professor Sigeo Kida and Associate Professor Hisashi Ōkawa of Kyushu University for help in obtaining the ESR data. The present work was partially supported by a Grant-in-aid for Scientific Research (No. 59540396) from the Ministry of Education, Science and Culture, Japan.

REFERENCES

1. (a) J. F. Hansen and D. E. Vietti, *J. Org. Chem.* 1975, **40**, 816; (b) J. F. Hansen and D. E. Vietti, *J. Org. Chem.* 1976, **41**, 2871; (c) J. F. Hansen, S. P. McCormick and D. X. West, *J. Inorg. Nucl. Chem.* 1977, **39**, 1231; (d) J. F. Hansen, S. P. McCormick and D. X. West, *J. Inorg. Nucl. Chem.* 1977, **39**, 2086.
2. (a) J. P. Freeman and J. J. Gannon, *J. Heterocycl. Chem.* 1966, **3**, 544; (b) J. P. Freeman, J. J. Gannon and D. L. Surbey, *J. Org. Chem.* 1969, **34**, 187; (c) J. P. Freeman and J. J. Gannon, *J. Org. Chem.* 1969, **34**, 194.
3. R. P. Lang, *J. Am. Chem. Soc.* 1962, **84**, 1185.
4. N. J. Rose and H. S. Drago, *J. Am. Chem. Soc.* 1959, **81**, 6138.
5. H. A. Benesi and J. H. Hildebrand, *J. Am. Chem. Soc.* 1949, **71**, 2703.
6. T. Kogane, H. Yukawa and R. Hirota, *Chem. Lett.* 1974, 477.
7. J. J. R. Da Frausto Silva and J. G. Caladao, *J. Inorg. Nucl. Chem.* 1966, **28**, 125.
8. R. W. Taft, Jr, *Steric Effects in Organic Chemistry*. Wiley, New York (1956).

Polyhedron Vol. 4, No. 6, pp. 955–958, 1985
Printed in Great Britain

0277–5387/85 $3.00 + .00
© 1985 Pergamon Press Ltd

SYNTHESIS, CHARACTERISATION AND REACTIONS OF PENTACOORDINATED IRIDIUM(I) COMPLEXES*

SARADA GOPINATHAN, K. JOSEPH and C. GOPINATHAN†
Inorganic Chemistry Division, National Chemical Laboratory,
Poona 411 008, India

(*Received* 13 *August* 1984; *accepted* 1 *October* 1984)

Abstract—Stable, pentacoordinated iridium(I) complexes have been synthesised by the replacement of the chlorine in $IrCO(PPh_3)_2Cl$ by bidentate chelating ligands such as β-diketones, *N*-benzoyl-*N*-phenyl hydroxylamine, salicylaldehyde, 8-hydroxyquinoline, 2-hydroxybenzophenone and 2-hydroxy 4-methoxybenzophenone. Most of them gave stable oxygen adducts $IrCO(PPh_3)_2(L)O_2$ and all of them underwent oxidative addition with bromine in methylene chloride giving $IrCO(PPh_3)_2(L)Br_2$. These chelated iridium(I) compounds reacted with liquid sulphur dioxide to produce two types of SO_2 insertion products.

Square planar iridium(I) complexes are well known for their catalytic activities.[1–4] Although these sixteen electron systems have been studied in detail,[5] the corresponding pentacoordinated iridium(I) derivatives have been only briefly explored.[6–10] Our interest lies in the synthesis of stable electron rich iridium(I) complexes derived from monobasic bidentate chelating ligands having varying degrees of Lewis basicity. Here we report the synthesis and reactions of pentacoordinated iridium(I) complexes.

EXPERIMENTAL

The Vaska complex *trans*-$IrCO(PPh_3)_2Cl$ was prepared as mentioned in the literature.[11] The organic ligands were of the highest purity available in the market. Organic solvents were dried, distilled and degassed before use. All experiments were carried out under oxygen-free nitrogen atmosphere.

The IR spectra were recorded on a Perkin–Elmer IR spectrophotometer Model 599 using CsI optics, and the UV spectra on a Pye Unicam SP8-100 UV–VIS spectrophotometer. ^1H and ^{31}P NMR spectra were recorded on a Bruker-90 Fourier Transform Spectrometer operating at 90 MHz. Chemical shifts are reported relative to TMS for ^1H and 85% H_3PO_4 for ^{31}P. The XPS were recorded using an ESCA-3MK-11 Electron Spectrometer (VG Scientific Ltd, U.K.), equipped with Mg-K_α (1253.6 eV) and Al-K_α (1486.6 eV) anodes at 50 eV analyser energy and 4 mm entrance slit width. The core electron binding energies of Ir $4f_{5/2}$, $4f_{7/2}$ were referred to C_{1s} level of carbon present in the complexes. The binding energy of C_{1s} line was taken as 285.0 eV. The magnetic susceptibility measurements were carried out on a CAHN-1000 Research Model instrument with a Faraday type balance.

Preparation of the 8-hydroxyquinolinato complex

Sodio-derivative of 8-hydroxyquinoline was prepared by stirring a mixture of the ligand (0.145 g; 1 mmol) and sodium hydride (0.027 g; 1.1 mmol) in ether (25 cm^3) at room temperature for 3 h. Ether was then removed under reduced pressure and benzene (25 cm^3) was added along with the Vaska compound $IrCO(PPh_3)_2Cl$ (0.780 g; 1 mmol) and the mixture was refluxed for 12 h. The contents were then cooled, centrifuged and the clear solution was concentrated *in vacuo* to obtain orange crystals of the product, which were washed with hexane and again dried under reduced pressure at room temperature. The crystalline product weighed 0.63 g (yield 70%). M.p. 191°C.

Other compounds listed in Table 1 were prepared similarly.

Preparation of the oxygen adduct

Pure oxygen was slowly bubbled through the reaction flask while refluxing the sodio-derivative of the ligand with the Vaska complex (12 h). The contents were cooled, centrifuged, and the clear

* NCL Communication No. 3575.
† Author to whom correspondence should be addressed.

solution concentrated under reduced pressure to obtain the desired product as a micro-crystalline solid. It was washed with hexane and dried *in vacuo*. Yields were nearly quantitative.

Preparation of the bromine addition compound

The iridium complex $IrCO(PPh_3)_2$(oxinate) (0.088 g; 0.1 mmol) dissolved in methylene chloride (5 cm^3) and bromine (0.016 g; 0.1 mmol) in methylene chloride (5 cm^3) were mixed and stirred for 30 min at room temperature. The solution was concentrated *in vacuo* to get crystals of the product in quantitative yield.

The sulphur dioxide insertion reaction

Sulphur dioxide gas was dried using concentrated sulphuric acid and condensed into liquid in a long-necked flask, in which the complex $IrCO(PPh_3)_2$(Ba) about 0.3 g was kept, by keeping the flask immersed in ice–salt mixture. Moisture was rigorously excluded. After 1 h, when about 10 cm^3 of liquid sulphur dioxide had collected over the sample in the flask, the flow of gas was discontinued. The contents were allowed to remain for 2 h with occasional shaking. The green crystals separated from the liquid were isolated by decantation from the yellow solution. The crystals were washed with hexane and dried *in vacuo*; the portion soluble in liquid sulphur dioxide was separated by evaporating the liquid followed by washing the yellow solid with hexane and drying *in vacuo*. For the green solid $[IrCO(PPh_3)_2SO_2]_2O$. Found: C, 53.80; H, 3.58; P, 7.40; SO_2 8.01%. Calc. for $C_{74}H_{60}O_7P_4S_2Ir_2$: C, 54.40; H, 3.70, P, 7.58; SO_2, 7.84%. For the yellow solid $[IrCO(PPh_3)_2SO_2(Ba)]$. Found: C, 57.92; H, 3.95; P, 6.02; SO_2, 6.85%. Calc. for $C_{47}H_{39}O_5P_2SIr$: C, 58.19; H, 4.05; P, 6.38; SO_2, 6.60%.

RESULTS AND DISCUSSION

The chlorine atom of the Vaska complex $IrCO(PPh_3)_2Cl$ was readily replaced by chelating ligands containing potential hydroxyl group employing sodium hydride as a base:

$$IrCO(PPh_3)_2Cl + NaL \rightarrow IrCO(PPh_3)_2L + NaCl.$$

The products separated from benzene as orange yellow micro-crystalline solids were stable in nitrogen atmosphere (Table 1). When oxygen was bubbled through their solutions (in chloroform or benzene) most of them were oxidized to the corresponding oxygen addition compounds. Some of them were considerably stable in solution as seen from their IR and UV spectral data. For example, the iridium(I) complexes of benzoylacetone, 8-hydroxyquinoline and *N*-benzoyl-*N*-phenyl hydroxylamine did not dissociate in chloroform suggesting these ligands to be harder bases compared to the remaining ones. All the new complexes underwent oxidative addition reaction with bromine in methylene chloride as indicated by the IR stretching frequencies of the products in the carbonyl stretching region ($\sim 2000\ cm^{-1}$).

IR spectra of the complexes were run as Nujol mulls and in chloroform solutions (Table 2). The Vaska complex $IrCO(PPh_3)_2Cl$ shows absorption bands at

Table 1. Analytical data for new iridium(I) carbonyl compounds

No.	Compound*	Colour m.p. (°C)	Analysis: found (calc.) (%) C	H	P
1	$Ir(CO)L_2$(oxinate)	Orange, 191	62.28(62.15)	4.08(4.08)	7.05(7.16)
2	$Ir(CO)L_2$(Bpha)	Yellow, 229	62.66(62.75)	4.19(4.21)	6.75(6.48)
3	$Ir(CO)L_2$(Acac)	Pale yellow, 104	59.59(59.77)	4.78(4.41)	7.44(7.34)
4	$Ir(CO)L_2$(Ba)	Yellow, 240	62.41(62.30)	4.59(4.33)	6.69(6.83)
5	$Ir(CO)L_2$(Dbm)	Brown, 91	64.49(64.51)	4.31(4.26)	6.51(6.39)
6	$Ir(CO)L_2$(Tftac)	Orange, 236	56.02(55.95)	3.83(3.54)	6.52(6.41)
7	$Ir(CO)L_2$(Benph)	Yellow, 94	63.63(63.95)	4.35(4.17)	6.42(6.52)
8	$Ir(CO)L_2$(Me-benph)	Yellow, 117	62.91(63.02)	4.23(4.25)	6.22(6.37)
9	$Ir(CO)L_2(Sal)O_2$	Pale yellow, 192	58.92(58.85)	4.02(3.93)	6.99(6.89)
10	$Ir(CO)L_2(Naph)O_2$	Pale yellow, 178	60.72(60.81)	4.08(3.93)	6.40(6.53)

* L, triphenylphosphine; oxinate, 8-hydroxyquinoline; Bpha, *N*-benzoyl-*N*-phenyl hydroxylamine; Acac, acetylacetone; Ba, benzoylacetone; Dbm, dibenzoylmethane; Tftac, trifluorothenoylacetone; Benph, 2-hydroxybenzophenone; Me-benph, 2-hydroxy-4-methoxybenzophenone; Sal, salicylaldehyde; Naph, 2-hydroxynaphthaldehyde.

Table 2. IR spectra data for new iridium(I) carbonyl compounds*

S. No.	ν(C≡O)	ν(C=O)/(C=N)	ν(Ir–C)	ν(Ir–P)
	(cm^{-1})			
1	1935	1575	655	450
2	1930	1545	630	440
3	1950	1565, 1520	620	455
4	1960	1515	625	450
5	1965	1525	620	455
6	1950	1625	620	450
7	1945	1530	645	455
8	1945	1545	630	440
9	2010	1615	640	440
10	2010	1620	640	440

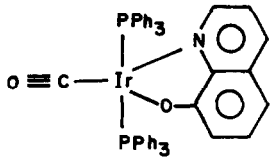
* Serial numbers same as in Table 1.

1955(s) and 1900(sh) cm^{-1} due to terminal carbonyl vibrations. In the chlorine free complexes, however, this band is observed mostly in the lower frequency region; this can be attributed to stronger metal–CO interaction as a result of change in the hybridization of the metal from square planar to trigonal bipyramidal and increased donating property of oxyanions compared to chlorine.

The IR spectrum of the 8-hydroxyquinolinato complex $IrCO(PPh_3)_2$(oxinate) shows ν (C≡O) at 1935 cm^{-1}. The band due to the phenolic ν (C–O) is observed at 1320 cm^{-1}, 40 units to higher frequency, suggesting an increased C–O bond order as the result of proton replacement. In the far IR region, the ν (Ir–CO) is seen at 655 cm^{-1} which is 45 units higher than that of the Vaska complex. The electronic spectrum of the 8-hydroxyquinolinato complex in chloroform shows three well-defined absorption bands in the UV–Visible spectral region; λ_{max} = 430 nm (ε = 8000), 372 nm (ε = 8000), 320 nm (ε = 8600), suggesting iridium in its +1 oxidation state.[12] The large molar extinction coefficient of the absorption bands when compared to those of the Vaska complex, λ_{max} = 438 nm (ε = 683), 386 nm (ε = 4239), 336 nm (ε = 320), has been assigned to strong metal–ligand charge-transfer interaction. Similar features are observed in the case of benzoylacetonate and *N*-benzoyl-*N*-phenyl hydroxylaminate complexes. The stability of these complexes was tested by leaving their dilute chloroform solutions for 24 h in an inert atmosphere; they retained all the absorptions in the UV–Visible region.

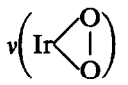
The X-ray photoelectron spectrum of the 8-hydroxyquinolinato complex [$IrCO(PPh_3)_2$(oxinate)] gives Ir 4*f* binding energies at $4f_{5/2}$ = 64.4 and $4f_{7/2}$ = 61.8, and the total electronic charge on iridium in this complex is nearly the same as that of Vaska, $4f_{5/2}$ = 64.6, $4f_{7/2}$ = 61.6.[13] Substitution of chlorine by oxine could have increased total electron density on iridium atom thereby reducing the Ir 4*f* binding energies. The electronic changes due to substitution are obviously compensated by the presence of CO as has been observed from the reduction in the stretching frequency of the C≡O band.

All this evidence suggests that the structure of the oxinate complex is:



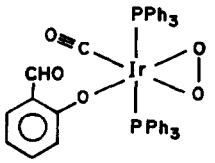
I

Salicylaldehyde and 2-hydroxynaphthaldehyde when reacted with the Vaska complex always gave unstable iridium(I) compounds. However, stable oxygen adducts of the type $IrCO(PPh_3)_2(Sal)O_2$ and $IrCO(PPh_3)_2(Naph)O_2$ could be separated as pale yellow micro-crystalline diamagnetic solids. The IR spectrum of the salicycladehyde derivative shows ν(C≡O) at 2010 cm^{-1} suggesting a higher oxidation number for iridium. The aldehydic carbonyl stretching mode is shifted to lower wave number (1615 cm^{-1}) which could be attributed to conjugative electron drain from carbonyl to oxidised iridium. The phenolic ν (C–O) observed in free salicylaldehyde at 1280 cm^{-1} has been shifted to 1295 cm^{-1} due to complex formation. The presence of a medium band at 835 cm^{-1} due to



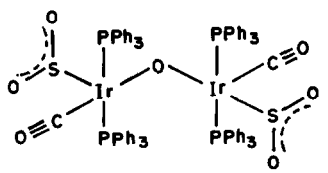
confirms the oxygen adduct formation. Proton decoupled ^{31}P NMR spectrum of the salicylaldehyde derivative [$IrCO(PPh_3)_2(Sal)O_2$] shows a singlet at δ −7.24 ppm. This downfield shift when compared to that of the Vaska complex (δ −24.43 ppm) is indicative of the higher oxidation state for iridium. The Ir 4*f* binding energies for the salicylaldehyde complex are $4f_{5/2}$ = 65.16 and $4f_{7/2}$ = 62.40. These values are nearly one unit higher than those for iridium(I) complexes and suggest an increased positive charge on iridium.

Hence the structure of the salicylaldehyde complex is suggested to be:



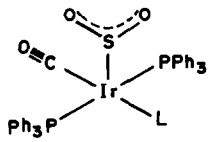
II

Iridium(I) chelates when reacted with liquid sulphur dioxide gave two types of insertion products. A green crystalline solid separated from liquid sulphur dioxide solution (in all cases) did not show the presence of bidentate chelating ligand as confirmed from elemental analysis and spectral data. The IR spectrum shows ν (C≡O) at 2020 cm^{-1} which can be interpreted as a reflection of the oxidaton of the univalent iridium complex. In the SO_2 stretching region, two strong bands are seen due to ν_{as} (SO_2) and $\nu_s(SO_2)$ at 1195 and 1050 cm^{-1}, suggesting the coordination of sulphur to iridium. The presence of an additional medium broad band at 810 cm^{-1} could be attributed to the presence of an Ir—O—Ir linkage.[14,15] The conversion of Ir(I) to Ir(III) in the liquid sulphur dioxide medium with the simultaneous cleavage of the bidentate chelating ligand can be explained by the presence of traces of moisture in the cryogenic system. Hence the structure of the green product is proposed to be:



III

The portion soluble in liquid sulphur dioxide upon isolation in each case gave yellow powdery substances. In their IR spectra, bands associated with chelating ligands are retained with slight increase in the stretching frequency region of the ketonic group in the case of β-diketone derivatives. The ν(C≡O) is shifted to 2000 cm^{-1} which suggests a higher oxidation state for iridium. The $\nu_{as}(SO_2)$ and $\nu_s(SO_2)$ are seen at 1195 and 1050 cm^{-1} respectively. These data support the structure given below:



IV

REFERENCES

1. J. P. Collman, *Acc. Chem. Res.* 1968, **1**, 136.
2. L. Vaska, *Acc. Chem. Res.* 1968, **1**, 335.
3. L. Vaska, *Inorg. Chim. Acta* 1971, **5**, 295.
4. D. Forster, *J. Chem. Soc., Dalton Trans.* 1979, 1639.
5. G. Wilkinson, Ed., *Comprehensive Organometallic Chemistry*, Vol. 5, p. 541. Pergamon Press, Oxford (1982).
6. F. Bonati and R. Ugo, *J. Organomet. Chem.* 1968, **11**, 341.
7. J. S. Miller and K. G. Caulton, *Inorg. Chem.* 1975, **14**, 2296.
8. R. Uson, L. A. Oro, M. A. Ciriano and R. Gonzalez, *J. Organomet. Chem.* 1981, **205**, 259.
9. S. S. Bath and L. Vaska, *J. Am. Chem. Soc.* 1963, **85**, 3500.
10. W. O. Siegel, S. J. Laporte and J. P. Collman, *Inorg. Chem.* 1971, **10**, 2158.
11. W. L. Jolly, Ed., *Inorganic Synthesis* Vol. 11, p. 103. McGraw-Hill, New York (1968).
12. R. Brady, B. R. Flynn, G. L. Geoffrey, H. B. Bray, J. Peone, Jr and L. Vaska, *Inorg. Chem.* 1976, **15**, 1485.
13. F. Holsboer, W. Beck and H. D. Bartunk, *J. Chem. Soc., Dalton Trans.* 1973, 1828.
14. P. Carty and A. Walker, *J. Chem. Soc., Chem. Commun.* 1969, 1374.
15. W. P. Griffith, *J. Chem. Soc.* (*A*) 1969, 211.

Polyhedron Vol. 4, No. 6, pp. 959–966, 1985
Printed in Great Britain

0277–5387/85 $3.00 + .00
© 1985 Pergamon Press Ltd

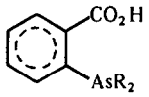
STABILISATION OF COPPER(II) TERTIARY-PHOSPHINE OR -ARSINE COMPLEXES—II. ROLE OF INDUCTIVE EFFECT AND REACTION CONDITIONS IN STABILISING COPPER(II)–ARSINE COMPLEXES OF HYBRID OXYGEN–ARSENIC LIGANDS FROM *o*-$R_2AsC_6H_4CO_2H$

SWARN S. PARMAR,* HARKEERAT K. BHARAJ and MANOHAR L. SEHGAL
Chemistry Department, Guru Nanak Dev University, Amritsar-143 005, India

(*Received* 5 *July* 1984; *accepted* 1 *October* 1984)

Abstract—The characterization of the products of reactions between anhydrous/hydrated copper(II) acetate and the title acids having R = Me, C_6H_{11}, Ph and *p*-tolyl in different solvents and at different temperatures with the help of elemental analysis, TGA, DTA, room temperature magnetic susceptibility, IR, and UV–VIS and EPR spectral data reveal that a competition exists between the chelation of arsine to copper(II) on one side and the reduction of copper(II) to copper(I) and the subsequent chelation of the arsine to copper(I) and/or that of the arsine oxide to copper(II) on the other. This competition which is expected to be normally governed by the inductive effect of group R is disturbed by the change in reaction conditions leading to the conclusion that the reaction conditions rather than the inductive effect of the group R control the mode of reaction.

All earlier attempts[1–8] to prepare copper(II)–arsine complexes of tertiary arsines invariably yielded either a copper(I)–arsine or a copper(II)–arsine oxide complex due to the rapid reduction of copper(II) to copper(I) and simultaneous oxidation of arsine to arsine oxide. In 1968 we reported the preparation of two copper(II)–arsine complexes, $Cu(o\text{-}R_2AsC_6H_4CO_2)_2$, by reacting copper(II) acetate monohydrate with the title acids (A) having R = Ph and *p*-tolyl.[9] Subsequent attempts[10–15] yielded only four



A

copper(II)–arsine complexes, $Cu(hfac)_2(AsPh_3)_n$ (hfac = hexafluoroacetylacetonate; $n = 1$ or 2)[13] and $[Cu(o\text{-}H_2NC_6H_4AsR_2)_2](ClO_4)_2$ (R = Me or Ph).[14] Recently we have reported 20 such complexes using ligand A with R = Ph and its *p*-isomer and have also accounted for the earlier failures.[16] In continuation, we now report the characterization of the products of reactions between anhydrous/hydrated copper(II) acetate and ligands having R = Me, C_6H_{11}, Ph and *p*-tolyl in different solvents and at different temperatures in order to determine whether the reaction conditions or inductive effect of group R controls the stabilization of copper(II)–arsine complexes. The present work is altogether different from the reported[17] limited role of the different sets of the solvents and anions in determining the relative stability of copper(II) and copper(I) since here the ligand anion ($o\text{-}R_2AsC_6H_4CO_2^-$) itself is a reducing agent whose strength depends upon the inductive effect of group R.

EXPERIMENTAL

Preparation of ligands, their sodium salts and complexes **1a**, **1b**, **2a**, **2b**, **3** and **11**, the elemental analysis and other physical measurements have been described earlier.[9,16,18] EPR spectra of the copper(II) complexes isolated in the present investigation were recorded on a Varian EPR spectrophotometer at IIT, Madras.

$Cu(o\text{-}Ph_2AsC_6H_4CO_2)\cdot 0.5H_2O$ (4)

Stirring of a reaction mixture of a solution of the acid (A) (0.1 g, 2 mmol) in 95% EtOH (20 cm^3) with a suspension of copper(II) acetate monohydrate (0.2 g,

* Author to whom correspondence should be addressed.

1 mmol) in 95% EtOH (10 cm^3) resulted in the separation of a green solid, after 15 min, whose colour gradually changed to chocolate brown and finally to white on continuous stirring (5–6 h). It was filtered, washed with 95% EtOH and dried *in vacuo* (yield 82%). The same compound was also obtained on prolonged stirring of each of the copper(II)–arsine complexes **1a**, **1b**, **2a**, **2b** and **3**.

$Cu(o\text{-}Me_2AsC_6H_4CO_2)\cdot 0.5H_2O$ (**5**)

Boiling of a reaction mixture containing **A** (1.8 g, 8 mmol) in *n*-PrOH (30 cm^3) and a suspension of copper(II) acetate monohydrate (0.8 g, 4 mmol) under reflux for 30 min gave a creamy white solid which was filtered, washed with *n*-PrOH and dried *in vacuo* (yield 52%).

$CuO(o\text{-}Me_2As(OH)C_6H_4CO_2)_2$ (**6**)

A blue–green solid was obtained when the dark green filtrate from the above reaction was concentrated to 2–3 cm^3 and treated with ether (30–40 cm^3). It was filtered, washed with ether and dried *in vacuo* (yield 15%).

Stirring of the reaction mixture of **A** (0.9 g, 4 mmol) in 95% EtOH (20 cm^3) and a suspension of copper(II) acetate monohydrate (0.4 g, 2 mmol) in 95% EtOH (3 cm^3) for 2 h gave a green solution which was evaporated to dryness. The whitish green solid residue when treated with hot *n*-PrOH (20 cm^3) gave a white solid which was filtered, washed with *n*-PrOH and dried *in vacuo*. Addition of ether into the green filtrate after concentration to 2–3 cm^3 yielded a green solid which was filtered, washed with ether and dried *in vacuo*. The white and green solids were found to be identical with **5** and **6** respectively.

$Cu(o\text{-}Me_2AsC_6H_4CO_2)_2\cdot H_2O$ (**7a**)

Refluxing of the reaction mixture containing **A** (1.8 g, 8 mmol) in EtOH (30 cm^3) and anhydrous copper(II) acetate (0.74 g, 4 mmol) in the same solvent (10 cm^3) for 15 min afforded a dark green solution. A green solid separated out on the addition of ether to the concentrated solution. It was filtered, washed with ether and dried *in vacuo* (yield 60%).

$Cu(o\text{-}Me_2AsC_6H_4CO_2)_2\cdot H_2O$ (**7b**)

Stirring of the mixture of **A** (1.35 g, 6 mmol) solution in *n*-PrOH (30 cm^3) with a suspension of copper(II) acetate monohydrate (0.6 g, 3 mmol) in the same solvent (10 cm^3) for 30 min gave a dark green solution which was concentrated to 2–3 cm^3. Its treatment with ether yielded a green compound which was filtered washed with ether and dried *in vacuo* (yield 60%).

$Cu(o\text{-}(C_6H_{11})_2AsC_6H_4CO_2)\cdot 0.5H_2O$ (**8a**)

Stirring of the reaction mixture obtained by mixing **A** (0.72 g, 2 mmol) in 95% EtOH (12 cm^3) with a suspension of copper(II) acetate monohydrate (0.2 g, 1 mmol) in 95% EtOH (10 cm^3) yielded a dirty green solid which gradually changed to dirty white during 6 h. It was filtered, washed with 95% EtOH and dried *in vacuo* (yield 81%).

$Cu(o\text{-}(C_6H_{11})_2AsC_6H_4CO_2)\cdot 0.5H_2O$ (**8b**)

Refluxing of a reaction mixture obtained by mixing a solution of **A** (1.4 g, 4 mmol) in MeOH (30 cm^3) with a methanolic solution (20 cm^3) of copper(II) acetate monohydrate (0.4 g, 2 mmol) for 1 h afforded a dirty white solid which was filtered, washed with MeOH and dried *in vacuo* (yield 70%).

$Cu_2O(o\text{-}(C_6H_{11})_2AsC_6H_4CO_2)_2\cdot 2H_2O$ (**9**)

Boiling of a mixture containing **A** (1.45 g, 4 mmol) solution in EtOH (25 cm^3) and a suspension of copper(II) acetate (0.37 g, 2 mmol) in the same solvent (10 cm^3) under reflux for 45 min gave a brown solid, which was filtered washed with EtOH and dried *in vacuo* (yield 73%).

$Cu_2O(o\text{-}(p\text{-tolyl})_2AsC_6H_4CO_2)_2\cdot 2H_2O$ (**10**)

Refluxing of the reaction mixture containing a solution of copper(II) acetate monohydrate (0.4 g, 2 mmol) in MeOH (20 cm^3) and of **A** (1.5 g, 4 mmol) in MeOH (40 cm^3) for 2 h afforded a light green solid which was filtered washed with MeOH and dried *in vacuo* (yield 57%).

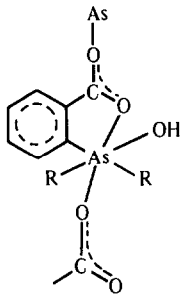
RESULTS AND DISCUSSIONS

The complexes obtained here can be classified as: (i) copper(I)–arsine complexes **4**, **5**, **8a** and **8b**; (ii) copper(II)–arsine complexes **7a**, **7b**, **9** and **10**; and (iii) a copper(II)–arsine oxide complex **6**. The presence of water in these complexes is supported by the appearance of IR bands[19] due to ν(OH) and δ(HOH) at 3000–3400 and 1620–1635 cm^{-1} respectively, and their TGA and DTA data (Table 1). The assignment of formula **6** is based on the appearance of bands at 2350 [ν(AsOH)], 1310, 1195, 765 and 700 cm^{-1} (sh) which are missing in the spectra of arsine and arsine complexes and are present in the spectrum of the

Table 1. Analytical data of copper(I) and copper(II) complexes

Complex [colour, m.p. (°C)]	Found (calc.) (%) C	H	As(III)	Cu	Decomposition stage	Temperature range (°C)	Stepwise % loss found (calc.)	DTA peak* (°C)
Cu(*o*-$Me_2AsC_6H_4CO_2$)·0.5H_2O (**5**) (creamy white, 230)	36.9 (36.2)	3.6 (3.7)	25.0 (25.1)	21.4 (21.3)	1	100–180	3.0 (3.0, 0.5H_2O)	—
Cu(*o*-(C_6H_{11})$_2$$AsC_6H_4CO_2$)·0.5$H_2O$ (**8a**) (dirty white, 181)	51.1 (51.5)	6.6 (6.3)	16.5 (16.9)	14.5 (14.4)	1	80–120	2.0 (2.05, 0.5H_2O)	92 (endo)
					2	160–280	9.0 (10.0, CO_2)	170 (exo)
Cu(*o*-(C_6H_{11})$_2$$AsC_6H_4CO_2$)·0.5$H_2O$ (**8b**) (dirty white, 171)	53.2 (52.6)	6.5 (6.3)	17.4 (17.3)	14.9 (14.6)	1	120–170	2.5 (2.05, 0.5H_2O)	146 (endo)
Cu(*o*-$Ph_2AsC_6H_4CO_2$)·0.5H_2O (**4**) (creamy white, 205)	52.9 (54.0)	3.5 (3.5)	17.2 (17.8)	14.6 (14.8)	1	80–100	2.0 (2.1, 0.5H_2O)	—
					2	125–350	10.5 (11.0, CO_2)	—
CuO(*o*-$Me_2As(OH)C_6H_4CO_2$)$_2$ (**6**)	38.3 (37.7)	4.4 (4.0)	— —	11.3 (11.1)	1	80–180	3.0 (3.1, H_2O)	—
					2	220–280	8.0 (8.0, CO_2)	—
Cu(*o*-$Me_2AsC_6H_4CO_2$)$_2$·H_2O (**7b**) (green, 190)	40.3 (40.6)	4.0 (4.1)	26.2 (28.2)	11.9 (11.9)	1	100–240	4.0 (3.4, H_2O)	100, 190, 220 (endo)
Cu(*o*-$Me_2AsC_6H_4CO_2$)$_2$·H_2O (**7a**) (green, 198)	38.60 (40.6)	4.1 (4.1)	26.7 (28.2)	11.9 (11.9)	1	80–200	3.0 (3.4, H_2O)	125 (endo)
Cu_2O(*o*-(C_6H_{11})$_2$$AsC_6H_4CO_2$)$_2$·2$H_2O$ (**9**) (dirty green, 179)	50.6 (50.6)	6.4 (6.2)	16.8 (16.6)	13.7 (14.1)	1	70–100	2.5 (2.0, H_2O)	—
					2	160–200	6.0 (5.0, CO_2)	177 (exo)
Cu_2O(*o*-(*p*-tolyl)$_2$$AsC_6H_4CO_2$)$_2$·2$H_2O$ (**10**)	54.7 (54.0)	4.1 (4.30)	16.9 (16.1)	13.8 (13.6)	1	80–160	4.0 (3.0, 2H_2O)	120 (endo)

* Position of DTA peak corresponding to dehydration or decarboxylation. The remaining DTA peaks have been mentioned in the Discussion.

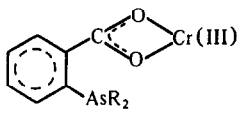


B

arsine oxide which has been assigned structure **B** on the basis of UV and IR data.[20,21]

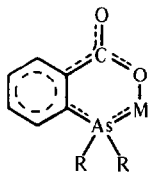
The DTA curve of isomer **8a** shows a phase transformation at 135°C and contains two exothermic peaks instead of the one observed in that of isomer **8b**. The main difference in the DTA curves of isomers **7a** and **7b** is in the number of exothermic peaks which are three in **7a** (310, 373, 400°C) and two in **7b** (156 and 280°C). The identical positions of all the IR bands of both isomers in complexes **7** and **8** and the different DTA curves may be explained in terms of some type of conformational difference. The TGA and DTA data of complexes **9** and **10**, $Cu_2O(o\text{-}R_2AsC_6H_4CO_2)_2 \cdot 2H_2O$, show that only the former loses a molecule of CO_2 between 160 and 200°C while the latter suffers two phase transformations (*endo*-197 and 222°C). The dehydration appears to be followed by decarboxylation in complexes **6** and **8a** also. Thermal decarboxylation of copper carboxylates leading to the formation of various aryl copper species is well documented in literature.[22–25]

Recently the lowering of $\nu_{as}(CO_2)$ of the ligand sodium salts from 1595 to 1520–1535 cm^{-1} and a slight lowering or raising of $\nu_s(CO_2)$ in the complexes of these ligands with chromium(III)[18] and lead(II)[20] has been explained in terms of the chelation of the carboxylate ion with the metal ion (**C**) leaving the



C

arsenic(III) uncoordinated. On the other hand the appearance of $\nu_{as}(CO_2)$ close to that of the sodium salt has been attributed to the simultaneous coordination of carboxylate ion and arsenic(III) leading to the formation of structures **D**[26] in complexes of these ligands with zinc(II), cadmium(II) and mercury(II). These results have also been supported on the basis of UV and PMR data.[20] Application of these criteria to the IR data (Table 2)



D

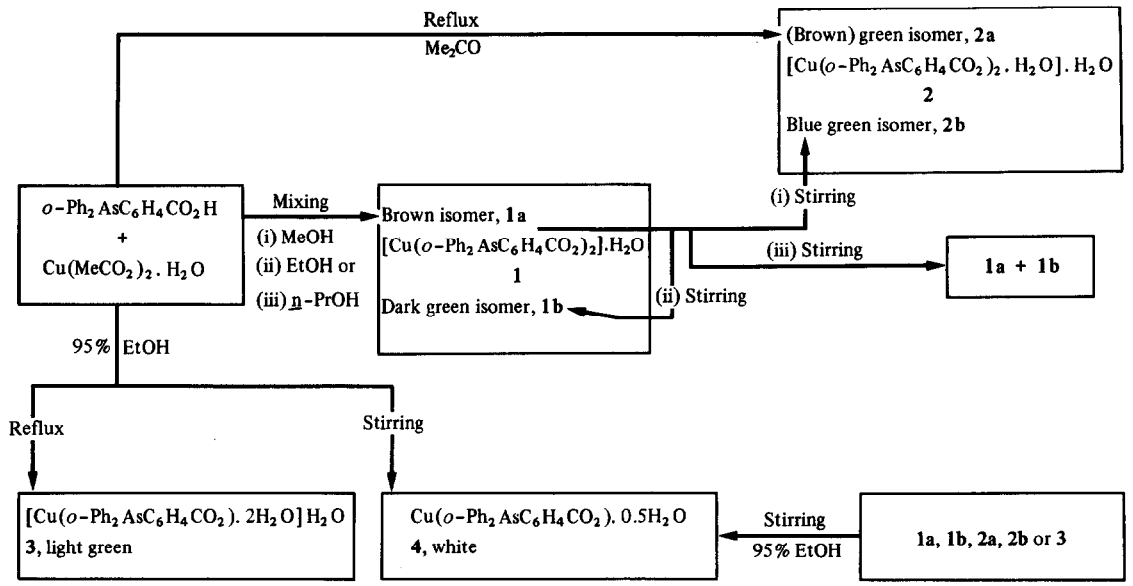
of the copper(II)–arsine and copper(I)–arsine complexes favour the chelation of the ligand (**D**) in both the types of complexes. Splitting of both the $\nu_{as}(CO_2)$ and $\nu_s(CO_2)$ bands observed in the spectra of copper(I)–arsine complexes suggests the presence of two coordination bonding modes of the carboxylate ion[27–30] leading to polymerisation as evidenced by their insolubility in common organic solvents. Their insolubility handicapped the recording of PMR spectra.

The IR spectra of complex **6** and the arsine oxide (**B**) are almost identical in the range 3000–200 cm^{-1}. This appears to indicate that copper(II) ion fits in the interstices without disturbing the solid structure of the oxide with adjacent chains facing each other so that the metal ion is surrounded by four planar carboxylate oxygens. The cationic charge of the metal ion being neutralised by the oxide ion acting as an axial bridge between the adjacent planar CuO_4 chromophores.

The experimental room temperature μ_{eff} values of all the copper(II) complexes are almost normal with the exception of complex **9** which possesses a highly subnormal value of 1.4 B.M. equal to that of the copper(II) acetate monohydrate known to possess a dimeric bridged structure. Its complete EPR spectrum could not be recorded due to the limitation of the instrument used. However, the partial spectrum resembles the corresponding part of the reported[31] spectrum of copper(II) acetate monohydrate. These results favour some type of structure involving spin–spin interaction leading to antiferromagnetism. The EPR spectral data of complexes **7a** ($g_{\|} = 2.378$, $g_{\perp} = 2.04$, $A = 120$ G) and **10** ($g_{\|} = 2.387, g_{\perp} = 2.06, A = 120$ G) suggest an elongated octahedral coordination around copper(II) with $d_{x^2-y^2}$ ground state and C_{4v} axial symmetry. Slightly higher experimental $g_{\|}$ values may be attributed in terms of large amount of distortions leading to the mixing of $d_{x^2-y^2}$ and d_{z^2} under the action of second order spin orbit coupling. The EPR spectra of complexes **6** and **7a** need scanning at 77 K since appreciable absorption could not be obtained at room temperature. The appearance of a broad *d–d* band in the UV–VIS spectra of all the copper(II) complexes at 12,000–13,000 cm^{-1} ($10Dq$) favour a distorted octahedral

Table 2. Spectral data (cm^{-1}) and physical measurements of copper(I) and copper(II) complexes

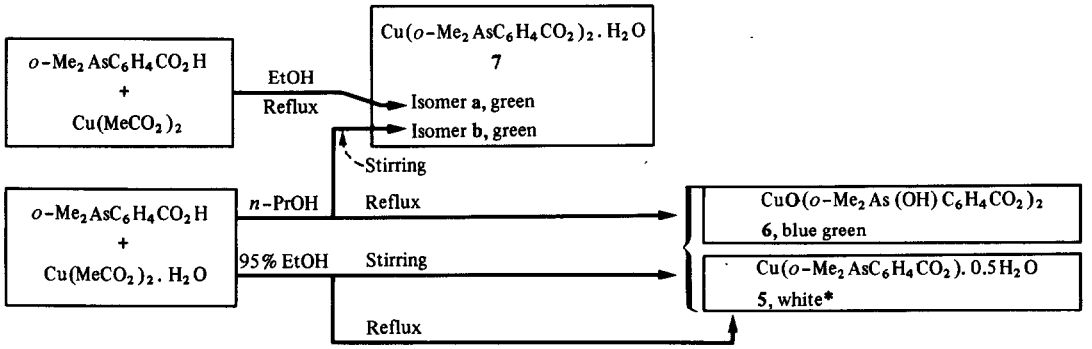
Complex	ν(OH) δ(HOH)	$\nu_{as}(CO_2)$	$\nu_s(CO_2)$	δ(COO)	μ_{eff} (B.M.)	Reflectance band	Conductance in CH_2Cl_2 ($ohm^{-1}\ mol^{-1}\ cm^2$)
o-$R_2AsC_6H_4CO_2Na$	—	1595	1400	—	—	—	Insoluble
Cu(o-$Me_2AsC_6H_4CO_2$)·0.5H_2O (**5**)	3410 (1620)	1585 1545	1415 1395 1355	803sh	dia	—	Insoluble
Cu(o-$(C_6H_{11})_2AsC_6H_4CO_2$)·0.5$H_2O$ (**8a**)	3390 (1620)	1610 1575	1400 1390	848ms	dia	—	Insoluble
Cu(o-$(C_6H_{11})_2AsC_6H_4CO_2$)·0.5$H_2O$ (**8b**)	3400 (1620)	1610 1575	1400 1378	848ms	dia	—	Insoluble
Cu(o-$Ph_2AsC_6H_4CO_2$)·0.5H_2O (**4**)	3300 (1630)	1585 1555	1410 1385	858m	dia	—	Insoluble
CuO(o-$Me_2As(OH)C_6H_4CO_2)_2$ (**6**)	—	1622	1397	830sh	1.71	12,820	Insoluble
Cu(o-$Me_2AsC_6H_4CO_2)_2$·H_2O (**7b**)	3300 (1635)	1620	1385	830sh	1.67	12,820	1.60
Cu(o-$Me_2AsC_6H_4CO_2)_2$·H_2O (**7a**)	3305 (1635)	1615	1385	830sh	1.71	12,820	2.14
Cu_2O(o-$(C_6H_{11})_2AsC_6H_4CO_2)_2$·2$H_2O$ (**9**)	3400 (1620)	1570	1403 1390	848ms	1.40	12,820 22,230	1.75
Cu_2O(o-(p-tolyl)$_2AsC_6H_4CO_2)_2$·2H_2O (**10**)	3400 (1630)	1587	1390	842sh	1.79	12,500	1.50



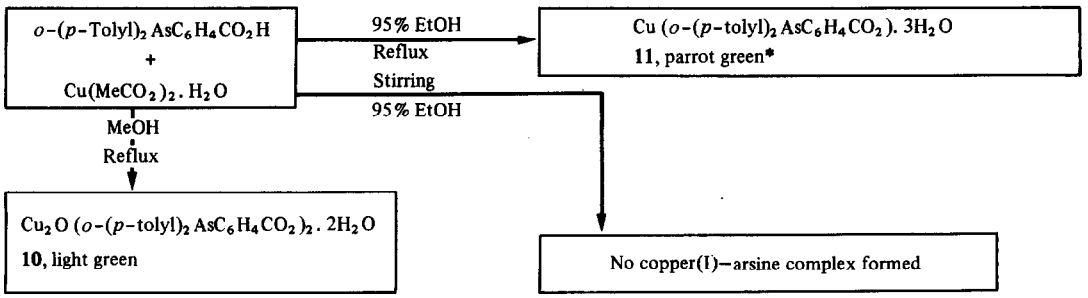
Scheme 1. Reactions of o-$Ph_2AsC_6H_4CO_2H$.

stereochemistry. These experimental $10Dq$ values are slightly lower than normally found (14,000–16,000 cm^{-1}) for octahedral copper(II) complexes. However these lower values are consistent with their experimental higher $g_{\|}$ values.

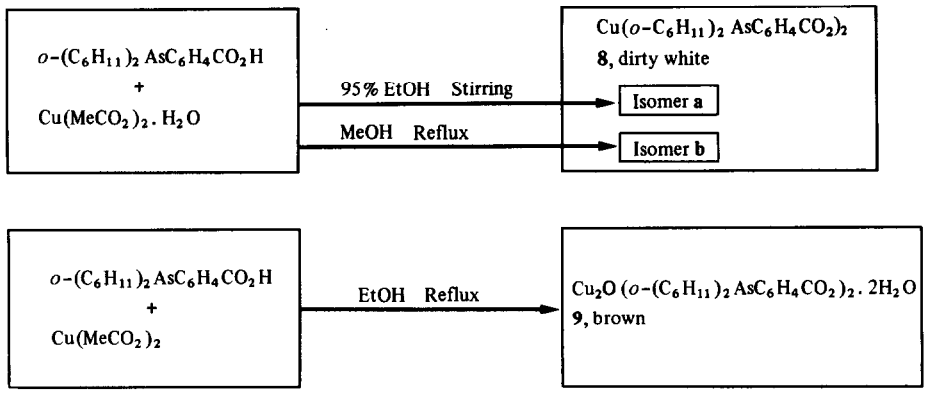
A with R = Ph, reported[16] to yield a variety of copper(II)–arsine complexes (**1a**, **1b**, **2a**, **2b** and **3**) (Scheme 1),[9,16] now reacts, on stirring, with a suspension of copper(II) acetate monohydrate in 95% EtOH to give a green compound that slowly changes to a white copper(I)–arsine complex which can also be obtained by prolonged stirring of all the



Scheme 2. Reactions of o-$Me_2AsC_6H_4CO_2H$. *Previously, the compositions of **5** and **11** have been erroneously reported[9] to be $Cu(o\text{-}Me_2AsC_6H_4CO_2)\cdot 2H_2O$ and $Cu(o\text{-}(p\text{-tolyl})_2AsC_6H_4CO_2)_2$ respectively in the absence of C and H analyses.



Scheme 3. Reactions of o-$(p\text{-tolyl})_2AsC_6H_4CO_2H$. *See caption to Scheme 2.



Scheme 4. Reactions of o-$(C_6H_{11})_2AsC_6H_4CO_2H$.

said copper(II)–arsine complexes. Conversely the ligand with R = Me, under similar conditions, yields a mixture of copper(I)–arsine complex (**5**) and a copper(II)–arsine oxide complex (**6**), and complex **5** alone, under reflux. However, a copper(II)–arsine complex (**7a**) is formed on refluxing a suspension of anhydrous copper(II) acetate and **A** in EtOH alone. These observations (Scheme 2) suggest that the presence of water in the reaction medium initiates the reduction of copper(II) to copper(I) which is partial at room temperature and is complete at the solvent boiling point. The formation of copper(II)–arsine complex **7b** from the reaction of the ligand with copper(II)–acetate monohydrate in n-PrOH at room temperature and that of a mixture of **5** and **6** under reflux indicate that the water of crystallization is not effective in initiating the reduction of copper(II) to copper(I) at room temperature which takes place only partially at higher temperature.

The observations outlined in Scheme 1 suggest that the inductive effect of R = Ph is such that even in the presence of water in the reaction medium, chelation of the arsine to copper(II) precedes the reduction of copper(II) to copper(I) to yield a kinetically more stable copper(II)–arsine complex (**3**) that changes to a thermodynamically more stable copper(I)–arsine complex (**4**) on prolonged stirring. On the other hand, the electron releasing property of R = Me (Scheme 2) facilitates the reduction of copper(II) to copper(I), which takes precedence over the chelation of arsine to copper(II), in the presence of water in the reaction medium, to afford a copper(I)–arsine complex (**5**) and/or copper(II)–arsine oxide complex (**6**). However, in the absence of water it is the chelation of the arsine to copper(II) that takes the lead to yield a copper(II)–arsine complex (**7a**).

Consideration of the inductive effect alone predicts the formation of copper(II)–arsine complexes with the chelating agents for R = Ph and p-tolyl and those of copper(I)–arsine and/or copper(II)–arsine oxide complexes with the remaining two. The formation of both the types of complexes with all the ligands except the one with **R** = p-tolyl (Schemes 1–4) by changing experimental condition leads to the conclusion that the suitable reaction conditions rather than the favourable inductive effect of group R play a crucial role in determining the mode of the reaction.

Acknowledgement—We thank Prof. S. Subramanian R.S.I.C. Madras (IIT), for fruitful discussions of ESR data.

REFERENCES

1. R. S. Nyholm, *J. Chem. Soc.* 1951, 1767 (and references therein).
2. A. Kabesh and R. S. Nyholm, *J. Chem. Soc.* 1951, 38.
3. W. Cochran, F. A. Hart and F. G. Mann, *J. Chem. Soc.* 1957, 2816.
4. B. Chiswell and S. E. Livingstone, *J. Chem. Soc.* 1959, 2931.
5. H. A. Goodwin and F. Lions, *J. Am. Chem. Soc.* 1959, **81**, 311.
6. B. Chiswell and S. E. Livingstone, *J. Inorg. Nucl. Chem.* 1961, **23**, 327.
7. G. A. Barclay, C. M. Harris and J. V. Kingston, *Chem. Ind.* 1965, 227.
8. R. D. Feltham, H. G. Metzger and W. Silverthorn, *Inorg. Chem.* 1968, **7**, 2003.
9. S. S. Sandhu and S. S. Parmar, *J. Chem. Soc., Chem. Commun.* 1968, 1335.
10. H. A. Tayim, A. Bouldoukian and F. Awad, *J. Inorg. Nucl. Chem.* 1970, **32**, 3799.
11. F. H. Jardine and F. J. Young, *J. Chem. Soc. A* 1971, 2444.
12. F. H. Jardine, A. C. Vohra and F. J. Young, *J. Inorg. Nucl. Chem.* 1971, **33**, 2941.
13. R. A. Zelonka and M. C. Baird, *J. Chem. Soc., Chem. Commun.* 1971, 780; *Can. J. Chem.* 1972, **50**, 1269.
14. B. Chiswell, R. A. Plowmann and K. Verrall, *Inorg. Chim. Acta* 1972, **6**, 113.
15. H. J. Gysling, *Inorg. Synth.* 1979, **19**, 92.

16. S. S. Parmar, T. S. Basra and S. S. Sandhu, *J. Chem. Soc., Dalton Trans.* 1982, 1939.
17. F. A. Cotton and G. Wilkinson, *Advanced Inorganic Chemistry*, 4th Edn., p. 800. Wiley–Interscience, New York (1980) (and references therein).
18. S. S. Parmar and H. Kaur, *Transition Met. Chem.* 1982, **7**, 79.
19. K. Nakamoto, *Infrared Spectra of Inorganic and Coordination Compounds*, 2nd Edn., p. 150. Wiley–Interscience, New York (1970).
20. H. Kaur, M.Phil thesis, *Complexes of Lead*(II) *with Oxygen–Arsenic Hybrid Ligands* (o-$R_2AsC_6H_4CO_2H$). Guru Nanak Dev University, Amritsar, India (1983).
21. R. K. Modi, M.Sc. thesis, *Phase Studies of Binary Mixtures of* o-*Carboxyphenyltertiaryarsines with Their Respective Oxides.* Guru Nanak Dev University, Amritsar, India (1981).
22. A. Cairncross, J. R. Roland, R. M. Henderson and W. R. Sheppard, *J. Am. Chem. Soc.* 1970, **92**, 3187.
23. T. Cohen and R. A. Shamback, *J. Am. Chem. Soc.* 1970, **92**, 3189.
24. J. Chodowska-Palicka and M. Nilsson, *Acta Chem. Scand.* 1971, **25**, 3451.
25. T. Tsuda, T. Nakatsuka, T. Hirayama and T. Saegusa, *J. Chem. Soc., Chem. Commun.* 1974, 557; T. Tsuda, Y. Chujo and T. Saegusa, *J. Chem. Soc., Chem. Commun.* 1975, 963.
26. S. S. Parmar and H. Kaur, *Polyhedron* 1982, **1**, 667.
27. J. Catterick and P. Thornton, *Adv. Inorg. Chem. Radiochem.* 1977, **20**, 291 (and references therein).
28. N. W. Alcock, V. M. Tracy and T. C. Waddington, *J. Chem. Soc., Dalton Trans.* 1976, 2243.
29. N. M. Karayannis, C. M. Mikulski, M. J. Strocko, L. L. Pytlewski and M. M. Labes, *J. Inorg. Nucl. Chem.* 1971, **33**, 3185.
30. G. Nardin, L. Randoccio, R. P. Bonomo and E. Rizzarelli, *J. Chem. Soc., Dalton Trans.* 1980, 369.
31. J. Lewis, F. E. Mabbs, L. K. Royston and W. R. Smail, *J. Chem. Soc. A* 1969, 291.
32. B. J. Hathaway and A. A. G. Tomlinson, *Coord. Chem. Rev.* 1970, **5**, 1.
33. B. J. Hathaway and D. E. Billing, *Coord. Chem. Rev.* 1970, **5**, 43.
34. B. J. Hathaway, *J. Chem. Soc., Dalton Trans.* 1972, 1196; *Struct. Bonding (Berlin)* 1973, **14**, 49.

Polyhedron Vol. 4, No. 6, pp. 967–970, 1985
Printed in Great Britain

0277–5387/85 $3.00 + .00
© 1985 Pergamon Press Ltd

SYNTHESIS OF VANADIUM SPINELS BY HYDROGEN-REDUCTION OF OXIDE PRECURSORS

A. MANTHIRAM
Department of Chemistry, Madurai Kamaraj University, P.G. Extension Centre,
St. John's College Campus, Palayamkottai 627 002, India

(*Received* 29 *August* 1984; *accepted* 6 *October* 1984)

Abstract—Two series of vanadium spinels, viz. AV_2O_4 and $A_{1.5}V_{1.5}O_4$ (A = Mg, Mn and Zn) have been prepared at significantly lower temperatures (700–850 K) by hydrogen-reduction of the corresponding oxide precursors, AV_2O_6 and $A_2V_2O_7$ respectively. The cation distribution in these phases have been determined by X-ray powder diffraction intensity analysis. The former vanadium(III) spinels have a cation distribution of $(A^{2+})_t[V_2^{3+}]_oO_4$ while the latter mixed-valence vanadium spinels have a distribution of $(A^{2+})_t[A^{2+}_{0.5}V^{3+}_{1.0}V^{4+}_{0.5}]_oO_4$.

Spinel oxides of vanadium constitute an interesting class of compounds as they exhibit a wide variety of electronic properties[1–3] depending upon the cation–cation distances; when the V–V distance is less than the critical distance of 2.97 Å a collective-electron behaviour is observed and when it is greater than the critical distance a localised-electron behaviour is encountered.

Vanadium spinels such as AV_2O_4 and $A_{1.5}V_{1.5}O_4$ (A = Mg, Mn and Zn) have generally been prepared by high temperature (~ 1450 K) reaction between the component oxides in an inert atmosphere or in evacuated sealed silica tubes.[1,4–6] The synthesis of pure vanadium spinels by this method is especially difficult as the starting component oxides are refractory and relatively unstable with respect to oxidation by air; also this traditional ceramic method requires prolonged and repeated high temperature heating with frequent regrindings. To avoid these harsh reaction conditions, it is necessary to look for alternative simple preparative methods.

Recently there has been considerable interest in the low-temperature preparation of complex metal oxides employing solid state precursors[7,8] in view of obtaining higher-surface-area materials. It is worthwhile to synthesise vanadium spinels by hydrogen-reduction of oxide precursors and thereby avoiding the severe reaction conditions involved in the conventional ceramic method. In the present investigation, attempts have been made to synthesize two series of vanadium spinels, viz. AV_2O_4 and $A_{1.5}V_{1.5}O_4$ (A = Mg, Mn and Zn) by hydrogen-reduction of the precursors AV_2O_6 and $A_2V_2O_7$ respectively with an aim to obtain these spinels at low temperature and in pure condition. This method was successful in giving single-phase materials and the results are reported in this paper.

EXPERIMENTAL

AV_2O_6 and $A_2V_2O_7$ for A = Mg, Mn and Zn were obtained by reaction between required quantities of AO (A = Mg and Zn) or $AC_2O_4 \cdot 2H_2O$ (A = Mn) and V_2O_5 first at 750 K and later at 900 K for about 48 h with one grinding in between. The formation of these oxides was confirmed by X-ray powder diffraction. AV_2O_6 oxides so obtained were reduced in a stream of oxygen-free, dry hydrogen at about 850 K for 20 h to give AV_2O_4 and $A_2V_2O_7$ oxides were reduced at about 700 K for 20 h to give $A_{1.5}V_{1.5}O_4$. The reduction reaction was monitored by determining the weight loss. The reduction products were analysed for total and lower-valent vanadium by a potentiometric method using Ce(IV) as oxidant.[9] The composition of the reduction product as well as the oxidation state of vanadium in the reduction product was fixed from the weight loss and chemical analysis data. Crystal-chemical characterisation of the reduction products was carried out by X-ray powder diffraction using a Philips X-ray diffractometer (PW 1050/70) employing Cu-K_α or Fe-K_α radiation.

RESULTS AND DISCUSSION

Weight loss and chemical analysis results (Table 1) show that AV_2O_6 (A = Mg, Mn and Zn) oxides can be reduced to give stable vanadium(III) oxides of

Table 1. Weight loss and chemical analysis data for the reduction products of AV_2O_6

A	% weight loss: Expected for reaction (1)	% weight loss: Observed	Reducing power of V* (equivalents/mole)
Mg	14.40	14.3	1.99
Mn	12.66	12.7	2.0
Zn	12.16	12.1	1.98

* Expected value for AV_2O_4 is 2.0.

composition AV_2O_4 at 850 K:

$$A^{2+}V_2^{5+}O_6 + 2H_2 \rightarrow A^{2+}V_2^{3+}O_4 + 2H_2O. \quad (1)$$

Hydrogen-reduction of $A_2V_2O_7$ (A = Mg, Mn and Zn) may be expected to give ilmenite type AVO_3 oxides similar to the hydrogen-reduction of $A_2V_2O_7$ (A = Sr and Ba) yielding AVO_3 perovskites:[10]

$$A_2^{2+}V_2^{5+}O_7 + H_2 \rightarrow 2A^{2+}V^{4+}O_3 + H_2O. \quad (2)$$

However, quite surprisingly, the hydrogen-reduction of $A_2V_2O_7$ (A = Mg, Mn and Zn) gives mixed-valence compounds of composition

$$A_{1.5}^{2+}V_{1.0}^{3+}V_{0.5}^{4+}O_4$$

as indicated by the weight loss and chemical analysis data (Table 2):

$$3A_2^{2+}V_2^{5+}O_7 + 5H_2 \rightarrow 4A_{1.5}^{2+}V_{1.0}^{3+}V_{0.5}^{4+}O_4 + 5H_2O. \quad (3)$$

Prolonged hydrogen-reduction of $A_2V_2O_7$ at 700 K does not result in any further weight loss indicating that complete reduction to V^{3+} state is not possible and $A_2V_2O_7$ can be reduced to yield stable mixed-valence compounds of formula $A_{1.5}^{2+}V_{1.0}^{3+}V_{0.5}^{4+}O_4$. These results are in agreement with that found by Palanisamy *et al.*[11] with $Zn_2V_2O_7$.

X-ray powder diffraction data (Table 3) of the reduction products of AV_2O_6 and $A_2V_2O_7$ are characteristic of a spinel structure. There were no reflections corresponding to the precursors or the component oxides AO, V_2O_3 or VO_2 revealing that the hydrogen-reduction of AV_2O_6 and $A_2V_2O_7$ yields monophasic spinel type AV_2O_4 and $A_{1.5}V_{1.5}O_4$ respectively. The diffraction patterns could be indexed on the basis of a cubic spinel type unit cell. The lattice parameters given in Table 4 agree closely with those reported in the literature.[2] In the case of A = Mn and Zn, there is an increase in lattice parameter from AV_2O_4 to $A_{1.5}V_{1.5}O_4$ but no such increase is observed with A = Mg. This can be explained on the basis of effective ionic radii[12] of A^{2+} and vanadium ions. As we go from $A^{2+}V_2^{3+}O_4$ to $A_{1.5}^{2+}V_{1.0}^{3+}V_{0.5}^{4+}O_4$, 50% of V^{3+} (r = 0.64 Å) ions are replaced by equal amounts of A^{2+} ($r_{Mg^{2+}}$ = 0.72 Å, $r_{Mn^{2+}}$ = 0.83 Å, $r_{Zn^{2+}}$ = 0.74 Å) and V^{4+} (r = 0.58 Å) ions. The average radii of Mn^{2+} and V^{4+} or Zn^{2+} and V^{4+} are slightly higher than the radius of V^{3+}, while the average radius of Mg^{2+} and V^{4+} is almost identical to that of V^{3+}. Hence in the former cases, a definite increase in lattice parameter is found from AV_2O_4 to $A_{1.5}V_{1.5}O_4$ while in the latter case no detectable increase is observed.

Cation distribution in spinel oxides is sensitive to the temperature at which the phases are prepared. As the phases in the present study have been prepared at fairly low temperatures, it is of interest to investigate the cation distributions in these phases. Cation distributions in spinels can be fixed by comparing the calculated and observed X-ray diffraction intensity ratios of certain pairs of (*hkl*) reflections[13,14] such as I_{400}/I_{220}, I_{220}/I_{311} and I_{220}/I_{440}. The calculated intensity ratios for the possible cation distributions are given in Table 4 along with the observed ratios for all the six compounds. The results indicate a cation distribution of $(A_{1.0}^{2+})_t[V_2^{3+}]_oO_4$ for AV_2O_4 and $(A_{1.0}^{2+})_t[A_{0.5}^{2+}V_{1.0}^{3+}V_{0.5}^{4+}]_oO_4$ for $A_{1.5}V_{1.5}O_4$ oxides (where the subscripts t and o refer to tetra-

Table 2. Weight loss and chemical analysis data for the reduction products of $A_2V_2O_7$

A	% weight loss: Expected for reaction (2)	% weight loss: Expected for reaction (3)	% weight loss: Observed	Reducing power of V* (equivalents/mole)
Mg	6.10	10.16	10.2	1.68
Mn	4.94	8.24	8.29	1.67
Zn	4.64	7.74	7.69	1.66

* Expected values for AVO_3 and $A_{1.5}V_{1.5}O_4$ are 1.0 and 1.67 respectively.

Table 3. X-ray powder diffraction data of MnV_2O_4 and $Mn_{1.5}V_{1.5}O_4$

			MnV_2O_4				$Mn_{1.5}V_{1.5}O_4$			
h	k	l	d_{obs} (Å)	d_{calc}* (Å)	I_{obs}	I_{calc}	d_{obs} (Å)	d_{calc}† (Å)	I_{obs}	I_{calc}
1	1	1	4.94	4.926	9	3.0	4.95	4.942	10	4.0
2	2	0	3.021	3.016	57	60.3	3.029	3.026	55	57.9
3	1	1	2.572	2.572	100	100	2.580	2.581	100	100
4	0	0	2.134	2.133	40	38.9	2.141	2.140	35	40.0
4	2	2	1.744	1.742	19	22.6	1.748	1.747	16	21.5
3	3	3	1.642	1.642	33	7.3	1.648	1.647	31	7.2
5	1	1		1.642		21.9		1.647		21.7
4	4	0	1.507	1.508	85	91.7	1.512	1.513	84	90.9

* Calculated with $a_o = 8.532$ Å.
† Calculated with $a_o = 8.560$ Å.

hedral and octahedral sites respectively). The distributions are the same as that observed for the phases prepared at high temperatures.[2] These cation distributions are compatible with that expected on the basis of crystal field stabilisation energies (CFSE); $V^{3+}(d^2)$ and $V^{4+}(d^1)$ ions having definite CFSE values in octahedral weak fields prefer octahedral sites while Mg^{2+} (d^0), Mn^{2+} (d^5) and Zn^{2+} (d^{10}) having no CFSE either in tetrahedral or in octahedral weak fields occupy tetrahedral (in the case of AV_2O_4) or both tetrahedral and octahedral (in the case of $A_{1.5}V_{1.5}O_4$) sites.

Considering the hydrogen-reduction reactions, it is found that in the case of AV_2O_6 oxides, all the V^{5+} ions are completely reduced to V^{3+} ions while in the case of $A_2V_2O_7$ oxides, part of the V^{5+} ions are reduced to V^{4+} and the remaining to V^{3+}. This difference in behaviour appears to be controlled by the structural stability of the oxide formed. Spinel structure is one of the versatile structures adopted by

Table 4. Lattice parameters and cation distributions of AV_2O_4 and $A_{1.5}V_{1.5}O_4$

Compound	Lattice parameter (Å)	Cation distribution	Calculated intensity ratio		
			I_{400}/I_{220}	I_{220}/I_{311}	I_{220}/I_{440}
MgV_2O_4	8.421	$(Mg)_t[V_2]_oO_4$	5.26	0.22	0.19
		$(V)_t[MgV]_oO_4$	0.61	0.73	0.70
		Observed ratio	4.8	0.14	0.20
MnV_2O_4	8.532	$(Mn)_t[V_2]_oO_4$	0.65	0.60	0.66
		$(V)_t[MnV]_oO_4$	1.06	0.48	0.50
		Observed ratio	0.70	0.57	0.67
ZnV_2O_4	8.412	$(Zn)_t[V_2]_oO_4$	0.30	0.78	0.89
		$(V)_t[ZnV]_oO_4$	1.38	0.42	0.43
		Observed ratio	0.37	0.72	0.92
$Mg_{1.5}V_{1.5}O_4$	8.421	$(Mg)_t[Mg_{0.5}V_{1.5}]_oO_4$	4.40	0.27	0.22
		$(V)_t[Mg_{1.5}V_{0.5}]_oO_4$	0.46	0.89	0.79
		Observed ratio	5.2	0.19	0.16
$Mn_{1.5}V_{1.5}O_4$	8.560	$(Mn)_t[Mn_{0.5}V_{1.5}]_oO_4$	0.69	0.58	0.64
		$(V)_t[Mn_{1.5}V_{0.5}]_oO_4$	1.13	0.46	0.49
		Observed ratio	0.64	0.55	0.65
$Zn_{1.5}V_{1.5}O_4$	8.421	$(Zn)_t[Zn_{0.5}V_{1.5}]_oO_4$	0.38	0.70	0.80
		$(V)_t[Zn_{1.5}V_{0.5}]_oO_4$	1.60	0.37	0.39
		Observed ratio	0.47	0.64	0.73

several ternary oxides.[15] The preponderant stability associated with the spinel lattice favours the formation of a spinel oxide in both the cases thus causing the reduction to proceed completely to the 3+ state in the case of AV_2O_6 and to a mixed valence state of average oxidation state 3.33+ in the case of $A_2V_2O_7$. The formation of a mixed-valence spinel oxide, $(A^{2+}_{1.0})_t[A^{2+}_{0.5}V^{3+}_{1.0}V^{4+}_{0.5}]_oO_4$ from $A_2V_2O_7$ rather than an ilmenite-type vanadium(IV) phase, $A^{2+}V^{4+}O_3$ or a new vanadium(III) phase of composition $A^{2+}V^{3+}O_{2.5}$ seems to be controlled by the basicity of the A cation in addition to the above stability considerations. A previous study[10] has indicated that the stabilisation of V^{4+} in hydrogen-reduction reactions can be achieved only in the presence of strongly basic cations like Sr^{2+} and Ba^{2+} (hydrogen-reduction of $Sr^{2+}_2V^{5+}_2O_7$ gives $Sr^{2+}V^{4+}O_3$ perovskite) and even the slightly less basic Ln^{3+} (Ln = lanthanide) cations cause the reduction to proceed to the 3+ state (hydrogen-reduction of $Ln^{3+}V^{5+}O_4$ gives $Ln^{3+}V^{3+}O_3$ perovskites and not $Ln^{3+}_2V^{4+}_2O_7$ pyrochlores). In the present investigation, the comparatively less basic nature of the A (A = Mg, Mn and Zn) cations together with the structural stability of the product oxide formed favour the formation of a mixed-valence spinel from $A_2V_2O_7$.

The present hydrogen-reduction study suggests that complex oxides of lower valence vanadium can conveniently be obtained in pure condition at significantly lower temperatures and shorter times by the hydrogen-reduction of suitable oxide precursors. This kind of low-temperature preparation from solid state precursors would be particularly useful to obtain higher-surface-area materials required in catalytic applications.

Acknowledgements—I am grateful to Professor C. N. R. Rao, FRS and to Dr J. Gopalakrishnan, Indian Institute of Science, Bangalore for providing part of the experimental facilities and for their keen interest and encouragement.

REFERENCES

1. D. B. Rogers, R. J. Arnott, A. Wold and J. B. Goodenough, *J. Phys. Chem. Solids* 1963, **24**, 347.
2. *Landolt–Bornstein Tabellen, New Series*, Vol. III/4b, p. 422. Springer, New York (1970).
3. J. B. Goodenough, *Progress in Solid State Chemistry* (Edited by H. Reiss), Vol. 5, p. 301. Pergamon Press, Oxford (1971).
4. B. Reuter, *Bull. Soc. Chim. Fr.* 1965, 1053.
5. B. Reuter, W. Laquo, E. Riedel and J. Jaskowsky, *Ber. Bunsenges. Phys. Chem.* 1966, **70**, 194.
6. B. Reuter and E. Riedel, *Ber. Bunsenges. Phys. Chem.* 1967, **71**, 189.
7. J. M. Longo, H. S. Horowitz and L. R. Clavenna, *Advances in Chemistry Series, No.* 186, *Solid State Chemistry: A Contemporary Overview* (Edited by S. L. Holt, J. B. Milstein and M. Robbins), p. 139. The American Chemical Society (1980).
8. K. Vidyasagar, J. Gopalakrishnan and C. N. R. Rao, *Inorg. Chem.* (in press).
9. T. Palanisamy, J. Gopalakrishnan and M. V. C. Sastri, *J. Solid State Chem.* 1974, **9**, 273.
10. T. Palanisamy, J. Gopalakrishnan and M. V. C. Sastri, *Z. Anorg. Allg. Chem.* 1975, **415**, 275.
11. T. Palanisamy, J. Gopalakrishnan and M. V. C. Sastri, *J. Inorg. Nucl. Chem.* 1976, **38**, 1372.
12. R. D. Shannon, *Acta Cryst.* 1976, **A32**, 751.
13. R. K. Datta and R. Roy, *J. Am. Ceram. Soc.* 1967, **50**, 578.
14. A. Manthiram and J. Gopalakrishnan, *Mater. Res. Bull.* 1980, **15**, 207.
15. O. Muller and R. Roy, *The Major Ternary Structural Families*, p. 38, Springer, Berlin (1974).

Polyhedron Vol. 4, No. 6, pp. 971–977, 1985
Printed in Great Britain

0277–5387/85 $3.00 + .00
© 1985 Pergamon Press Ltd

SELECTIVE REAGENTS FOR SOLVENT EXTRACTION OF METALS—I. QUINALDIC ACIDS

A. G. SVERKER HÖGBERG,*† KHORSHED MADAN, CHRISTINA MOBERG, BIRGER SJÖBERG and MICHAEL WEBER*
Royal Institute of Technology, Department of Organic Chemistry, S-100 44 Stockholm, Sweden

and

MAMOUN MUHAMMED
Royal Institute of Technology, Department of Inorganic Chemistry, S-100 44 Stockholm, Sweden

(*Received* 10 *September* 1984; *accepted* 6 *October* 1984)

Abstract—Alkyl- and alkoxy-substituted quinoline-2-carboxylic acids were synthesized and tested for metal extraction. Zn^{2+} and Cu^{2+} were extracted from aqueous sulphate solutions by reagents containing 8-alkoxy substituents at lower pH values than were Fe^{2+} or Fe^{3+}. Reagents without this substituent were unselective in this respect. A possible explanation for the selectivity may be that the 8-substituent influences the coordination geometry of the metal chelates in favour of tetrahedral complexes.

The development of chelating reagents for metal extraction has attracted much interest in recent years. Various ligands have been designed for selective recovery of metal ions using solvent extraction,[1,2] liquid membrane extraction and adsorption on chelating resins.

Quinoline-2-carboxylic acid (quinaldic acid) is known to form stable complexes with several metal ions. This reagent can be used for the gravimetric determination of, e.g. Cu^{2+}, Zn^{2+}, Cd^{2+} and UO_2^{2+} and colorimetric analysis of Fe^{2+}.[3] Quinaldic acid reagents have also been developed for solvent extraction.[4,5]

We have studied substituted quinaldic acids with the objective of preparing reagents that can extract Zn^{2+} and Cu^{2+} in the presence of Fe^{2+} and Fe^{3+}. This paper reports the syntheses and extractant properties of some new substituted quinaldic acids.

RESULTS

Alkyl- and alkoxy-substituted quinoline compounds were prepared by various routes using known reactions (Scheme 1). (1) O-Alkylation of hydroxyquinoline-2-carbonitriles afforded the 8-substituted reagents **1–6** and the 6- and 7-alkoxyquinaldic acids **14** and **15** (Table 1). (2) The

Table 1. $pH_{1/2}$ values for the extraction of metals with quinaldic acid reagents*

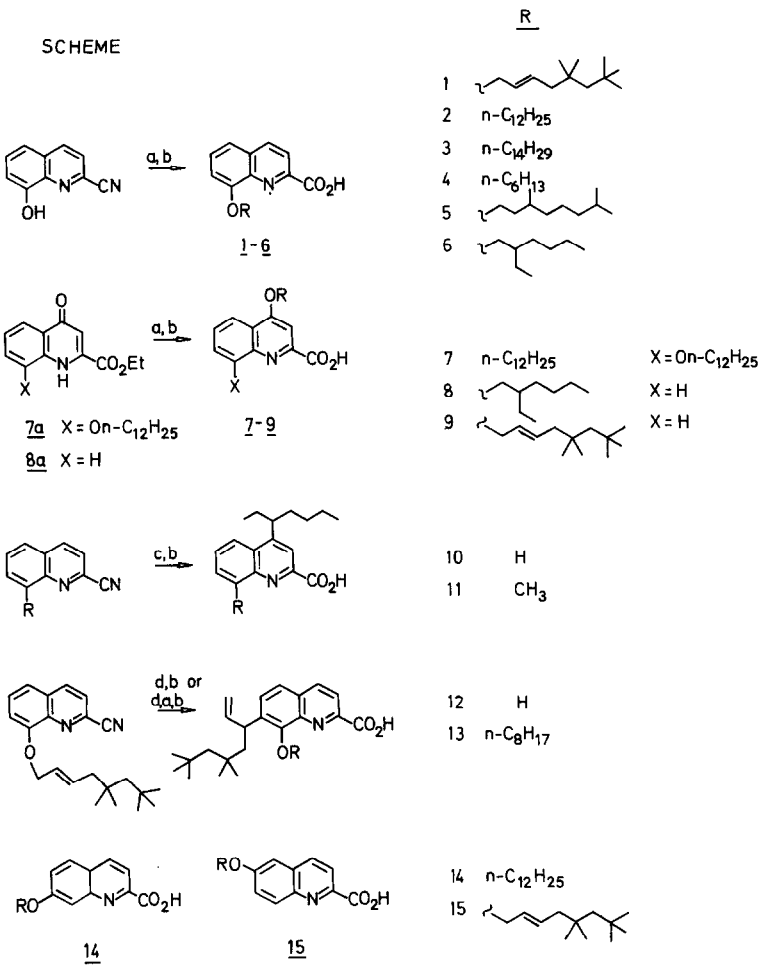
Reagent	Cu^{2+}	Zn^{2+}	Fe^{2+}	Fe^{3+}	Cd^{2+}
1	0.7	2.1	†	2.8	3.1
2	0.9	2.4	†	†	—
3	1.0	2.4	†	†	—
5	1.3	2.7	†	†	—
6	1.5	3.0	†	†	—
7	< 0.8	2.0	†	†	—
8	< 0.7	2.6	2.1	2.0	—
9	0.7	†	1.0	1.1	†
10	0.7	2.9	2.0	1.5	†
11	3.0	†	—	†	†
12	3.0	†	†	†	†
13	2.2	2.6	2.3	2.1	†

* The extractions were performed with equal volumes of a water phase containing initially 2 mM metal sulfates and a 20 mM chloroform solution of the reagent.

† Less than *ca* 3% extraction at pH 2, corresponding to $pH_{1/2} > 2.8$ for divalent metal ions.

* Authors to whom correspondence should be addressed.

† Present address: Boliden Kemi AB, Box 902, S-251 09 Helsingborg, Sweden.



Scheme 1.

ethyl 1,4-dihydro-4-oxoquinaldates **7a** and **8a** were alkylated to give the 4-alkoxy-substituted reagents **7–9**. (3) Radical alkylation[6] yielded the 4-(3-heptyl)quinaldic acid extractants **10** and **11**. (4) Reagents **12** and **13** were prepared by Claisen rearrangement[7] of 8-dodecenyloxyquinoline-2-carbonitrile.

The reagents **1–15** (Scheme 1) were assessed for their ability to extract Cu^{2+}, Zn^{2+}, Fe^{2+}, Fe^{3+}, Ni^{2+}, Co^{2+}, Cd^{2+} and K^+ from aqueous sulphate solutions at pH 2 and 4 into a chloroform phase. The metal concentrations in the water phase were measured by atomic absorption spectrophotometry and are reported here as $pH_{1/2}$ values (Table 1). These values were calculated from mixed metal extraction tests and in three cases, **1–3**, from single metal extraction experiments. The results of systems where the formation of a third phase was noticed are not included in Table 1. Only small amounts of Ni^{2+}, Co^{2+} and Cd^{2+} were extracted at the low pH used.

The 6-, 7- and 8-alkoxyquinaldic acids **14**, **15** and **1** were also tested for Cu, Zn and Fe extraction using 20 mM chloroform solutions of the reagents and 10 mM metal sulphate solutions. The results for reagent **14** were (% extracted, pH_{eq}): Cu^{2+} (86%, 1.7), Fe^{2+} (5%, 2.0), Zn^{2+} (24%, 2.5) (precipitates were formed in the first and last case). Reagent **15** extracted Cu^{2+} (85%, 1.9), Fe^{3+} (36%, 1.7) and Zn^{2+} (22%, 2.6) and reagent **1** Cu^{2+} (72%, 1.7), Fe^{2+} (0%, 2.0) and Zn^{2+} (34%, 2.3).

Metal complexes of some substituted quinaldic acids were studied by ^1H NMR and electronic spectroscopy. Chloroform solutions of isolated chelates were examined by electronic spectroscopy

Table 2. Metal(II) complexes of substituted quinaldic acid reagents

Reagent	M.p. (°C)	ν_{max} (cm^{-1}) [ε ($dm^3\ mol^{-1}\ cm^{-1}$)]
1	Fe 152–153	22,400(830), 19,900(780), ≈ 11,000(sh),* 8300(33), 6450(46)
	Co 161–162	19,000(79), 17,300(103), 6250(12)
	Ni 195–198	15,200(18), 8850(49)
	Cu 185–186	12,100(87)
	Zn 171–173	
2	Fe —	24,000(1090) (sh), 20,300(850)
	Cu† —	12,300
10	Fe† —	21,500(sh), 20,900(sh)
	Cu† —	15,900
9	Fe ≈ 200	23,300(1095) (sh), 21,300(1020) (sh), 11,500(15) (sh), 8130(15)
	Cu 239	15,400(70)

* sh, shoulder.

† The complex was not isolated but obtained by extraction.

in the range 5000–25,000 cm^{-1} (Table 2). Cu^{2+} and Fe^{2+} complexes formed by extraction with reagent **1** were found to have the same absorption bands as the isolated chelates.

The number of ligands coordinating Zn^{2+} in its complex with **1** was determined by ^1H NMR. The H-3 and H-4 peaks of the free ligands and of the zinc complex had different chemical shifts, i.e. δ, 8.28 and 8.35 ppm in the free ligand and 8.63 and 8.65 ppm in the complex. Zinc acetate dissolved in CD_3OD was added in portions to a $CDCl_3$ solution of **1** and the separate peaks from H-3 and H-4 in the free ligand and in the zinc complex were integrated. The results show that a 2:1 complex was formed. In the ^1H NMR spectrum of the Co(II) complex of **1** the geminal methyl groups appeared at −2.09 and −2.25 ppm. The OCH_2-protons in reagent **1** appeared as a doublet (J = 5.8 Hz) at 4.80 ppm. However, these peaks in the zinc complex were shifted upfield and were separated into two doublets of doublets at 4.14 ppm (J = 6.1 and 13.4 Hz) and 4.30 ppm (J = 5.1 and 13.4 Hz).

DISCUSSION

For assessing the Zn/Fe and Cu/Fe selectivity the reagents may be divided into main groups: I, those having alkoxy groups in the 8-position and II, 8-unsubstituted compounds. Reagents which extract Zn^{2+} and Cu^{2+} selectively in the presence of Fe^{2+} and Fe^{3+} belong to group I, whereas group II reagents lack this selectivity. The selectivity of group I reagents may be due to interligand repulsion of the 8-alkoxy substitutents. Steric crowding in the metal chelates is expected to favour the formation of tetrahedral coordination compounds over *trans*-planar complexes and octahedral tris-complexes. The lower extraction of iron with group I reagents may be ascribed to steric factors since Fe(II) prefers octahedral coordination whereas zinc(II) has little sterochemical preference and may readily form 4-coordinate tetrahedral complexes.

The extractant properties of group I reagents also depends on the structure of the alkoxy substituent. The decreasing order of extraction ability of, e.g. zinc: **1** > **5** > **6** may be a result of the higher stability of the chelates where the alkyl branch points are far away from the coordination site. These extractants have branch points at C(5), C(3) and C(2) respectively. The length of the alkyl chain is also of importance for the extractants performance. On extraction with **4** which has a linear C_6 alkoxy substituent a third phase was formed.

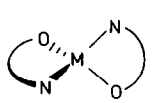
The introduction of an alkoxy group in the 4-position in the quinoline ring improved the extraction ability, as shown by comparison of **7** with **2**. This substitution may have changed the electron donor and π-acceptor properties as well as the pK_a values of the quinaldic acid. The presence of a branched alkyl group in the 7-position resulted in poor extraction with the type I reagent **12**. A possible explanation may be the steric interference of the 7- and 8-substituents in the metal chelates. The 8-methyl substituted quinaldic acid **11** showed poor extractant ability. Hence the low stability of its metal complexes may be attributable to metal–CH_3

interactions. The red colour of chloroform solutions of Fe(II) chelates of the group I reagents **1** and **2** is stable for about one day in the presence of air.[8] However, the red Fe(II) complexes of reagents **9** and **10** turn yellow rapidly (15–30 min) in chloroform solution in the presence of air due to oxidation to Fe(III). Also, in an extraction test with reagent **9** (20 mM in chloroform) and $FeSO_4$ (2 mM, initial pH 2.1), the extracted iron was found to be (partly) oxidized to Fe(III).

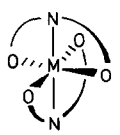
Electronic absorption studies of Cu(II) chelates with N_2O_2 donor atom sets have shown that a distortion from planar towards pseudo-tetrahedral geometry is accompanied by red shifts of the main *d–d* bands.[9]

The Cu(II) complexes of **1** and **2** have absorption maxima at higher wavelengths than Cu(II) complexes of the group II reagents **9** and **10** (Table 2) These data are in agreement with pseudo-tetrahedral structures of the Cu(II) complexes with **1** and **2** and with more flattened structures of the complexes with **9** and **10**.

The stereochemistry of metal chelates has previously been studied by ^1H NMR spectroscopy using methylene groups and geminal dimethyl groups as diastereotopic probes.[9] The separate proton resonances from the geminal methyl groups in the paramagnetic Co(II) chelate of **1** show that a *trans*-planar structure does not form. The two quinoline rings are twisted out of plane thereby decreasing the steric interference of the opposite alkoxy and carboxyl groups. A tetrahedral structure **A** and a bisected octahedral structure **B** offer the least



A



B

steric hindrance. In the diamagnetic Zn(II) chelate of **1** the OCH_2-protons had different chemical shifts, most likely due to the magnetic anisotropy of the aromatic rings in a tetrahedral arrangement. The large upfield shifts (0.9 ppm) observed for the olefinic protons in this complex are also in agreement with a perpendicular orientation of the quinoline rings.

EXPERIMENTAL

Instrumentation

All melting points are uncorrected. Infrared spectra were recorded on a Perkin–Elmer 257 spectrophotometer, and mass spectra were run on an LKB 9000 mass spectrometer. A Varian EM-360 instrument or a Bruker WP 200 spectrometer were used for ^1H NMR spectra at 60 and 200 MHz, respectively. Visible and near IR spectra were recorded on Varian Cary 219 (400–900 nm) and Beckman DK-2 spectrophotometers. A Perkin–Elmer 603 atomic absorption spectrophotometer was used for metal determinations.

Elemental analyses were performed by Mikroanalyslaboratoriet, Centrala Analyslaboratoriet or Mikro Kemi AB in Uppsala, Sweden and were within 0.4% unless otherwise noted.

Metal extraction tests

Aqueous solutions of a mixture of equal parts of metal sulfates: Cu^{2+}, Zn^{2+}, Ni^{2+} and Co^{2+} or Cu^{2+}, Zn^{2+}, Ni^{2+}, Co^{2+} and Cd^{2+} or Cu^{2+}, Zn^{2+}, Fe^{3+}, Cd^{2+} and K^+ were prepared by dissolving the metal salts in dilute sulfuric acid. The metal concentrations were about 2 mM and the pH was adjusted to a value of *ca* 2 or 4. A 20 mM chloroform solution of the reagent was prepared and equal volumes of the two phases were agitated until equilibrium was reached. The two phases were then separated by centrifugation and the amount of metal present in the aqueous phase was determined by atomic absorption spectrophotometry.

Preparation of substituted quinaldic acids

8-(5,5,7,7-Tetramethyl-2-octenyloxy)quinoline-2-carbonitrile (**1a**). A mixture of 8-hydroxyquinoline-2-carbonitrile[10] (34 g, 0.20 mol), K_2CO_3 (28 g, 0.20 mol) and DMF (150 cm^3) was stirred at 60°C for 20 min, then 1-chloro-5,5,7,7-tetramethyl-2-octene (40 g, 0.20 mol) was added. After 17 h at 60°C the mixture was poured into water (0.8 cm^3) and extracted with ether. The organic phase was washed with 2% *aq.* KOH and water. The solvent was evaporated to yield a brown oil (60.0 g). Recrystallization from petroleum ether yielded white crystals, m.p. 63–6°C.

IR (KBr): 2950, 2870 (C–H), 2240 (C≡N), 1550, 1500 (aromat.), 1260 (C–O), 970 cm^{-1} (CH=CH-*trans*). ^1H NMR (CCl_4): δ 0.93 (s, CH_3), 0.97 (s, CH_3), 1.2 (s, CH_2), 2.0 (d, CH_2), 4.7 (d, CH_2), 5.4–6.2 (m, CH=CH), 7.1 (dd, J = 6.8 and 2.2 Hz, H-7), 7.35 (dd, J = 8 and 2.2 Hz, H-5), 7.5 (dd, J = 8 Hz, H-6), 7.6 (d, J = 8.2 Hz, H-3) and 8.2 (d, J = 8.2 Hz, H-4). MS *m/z* (rel. int.): 336 (3, M^+), 223(9), 209(6), 171(16), 170(100), 142(6), 110(9), 95(11), 57(31), 41(7).

8-(5,5,7,7-Tetramethyl-2-octenyloxy)quinoline-2-carboxylic acid (**1**). The crude nitrile **1a** (60 g) was hydrolyzed by heating under reflux (11 h) with KOH (113 g) in EtOH (805 cm^3) and water (140 cm^3). *Ca.* 200 cm^3 of solvent was evaporated and the solution

was washed with petroleum ether. The ethanol solution was acidified with 2 M HCl (700 cm^3) and extracted with ether. The organic phase was washed with water and dried. The solvent was removed and cyclohexane was added yielding the product as white crystals (37.8 g, 53% yield), m.p. 78–82°C. IR (CCl_4): 3300 (O–H), 1780 (C=O), 970 cm^{-1} (CH=CH-*trans*). ^1H NMR ($CDCl_3$): δ 0.98 (15 H, s, CH_3), 1.26 (2 H, s, CH_2), 2.10 (2H, d, J = 7 Hz, CH_2), 4.80 (2 H, d, J = 5.8 Hz, CH_2O), 5.81 (1 H, dt, J = 16 Hz and 5.7 Hz, CH=C<u>H</u>CH_2O), 6.00 (1 H, dt, J = 16 Hz and 7.1 Hz, C<u>H</u>=CHCH_2O), 7.18 (1 H, dd, J = 7.8 Hz and 1.2 Hz, H-7), 7.3 (1 H, bs, OH), 7.49 (1H, dd, J = 8.3 Hz and 1.2 Hz, H-5), 7.60 (1 H, dd, H-6), 8.28 (1 H, d, J = 8.5 Hz), 8.35 (1 H, d, J = 8.5 Hz).

8-(*Dodecyloxy*)*quinoline*-2-*carboxylic acid* (**2**), 8-(*tetradecyloxy*)*quinoline*-2-*carboxylic acid* (**3**) *and* 8-(*hexyloxy*)*quinoline* - 2 - *carboxylic acid* (**4**). These reagents were prepared in analogy with **1** by alkylation with 1-bromoalkanes. The nitriles and carboxylic acids precipitated out on addition of water and 1 M H_2SO_4 respectively to the reaction mixtures.

2: M.p. 95–96°C (EtOH–H_2O).

3: 68% yield, m.p. 98–100°C (EtOH–H_2O).

4: 72% yield, m.p. 73–76°C (MeOH).

8-(3,7-*Dimethyloctyloxy*)*quinoline*-2-*carboxylic acid* (**5**) and 8 - (2 - *ethylhexyloxy*)*quinoline* - 2 - *carboxylic acid* (**6**). These reagents were prepared in analogy with **1** by alkylation with toluene-4-sulphonate esters. The nitriles were obtained by extraction with CH_2Cl_2 and purified by column chromatography (SiO_2/CH_2Cl_2).

6-*Hydroxyquinoline*-2-*carbonitrile* (**14a**).[4] 6-Hydroxyquinoline (2.64 g, 18 mmol) was treated with 90% 3-chloroperbenzoic acid (4.0 g) in chloroform (200 cm^3) over 2 h at room temperature. The solvent was evaporated and 3-chlorobenzoic acid was removed by sublimation at 80°C *in vacuo*. To the residue (mostly *N*-oxide) was added dimethyl sulfate (2.30 g, 18 mmol) and a few cm^3 of acetonitrile, and the mixture heated at 70°C for about 4 h. Evaporation of the solvent *in vacuo* gave 5.25 g of methylated *N*-oxide. This product was dissolved in water (13 cm^3) and was added over 45 min to an ice-cooled solution of sodium cyanide (2.6 g) in water (13 cm^3) under a nitrogen atmosphere. Acetic acid–water 1 : 1 (6 cm^3) was then added after an additional 4 h in the cold. The product was filtered off and washed with water to give **14a** (1.70 g, 56% yield), m.p. 217–219°C (toluene), lit.[11] 218–219°C.

6-*Dodecyloxyquinoline*-2-*carbonitrile* (**14b**). This compound was prepared by alkylation of 6-hydroxyquinoline-2-carbonitrile as described for **3**. M.p. 86–87.5°C (MeOH).

6 - *Dodecyloxyquinoline* - 2 - *carboxylic acid* (**14**). The above nitrile (**14b**) was hydrolyzed with KOH in 80% EtOH to give the carboxylic acid (79% yield based on **14a**), m.p. 148–150°C (toluene). IR ($CHCl_3$): 2920 (C–H), 1765, 1755 cm^{-1} (C=O). ^1H NMR ($CDCl_3$): δ 0.88 (3H, m, CH_3), 1–1.7 (18 H, m, alkyl). 1.88 (2 H, m, CH_2), 4.12 (2 H, t, J = 6.3 Hz, CH_2O), 7.14 (1 H, d, J = 2.6 Hz, H-5), 7.47 (1 H, dd, J = 2.6 and 9.2 Hz, H-7), 8.04 (1 H, d, J = 9 Hz, H-8), 8.21 (1 H, d, J = 8.5 Hz, H-3 or H-4), 8.24 (1 H, d, J = 8.5 Hz, H-3 or H-4), 10.5 (1 H, s, OH).

7 - *Hydroxyquinoline* - 2 - *carbonitrile* (**15a**). Compound **15a** was prepared analogously to **14a** starting from 7-hydroxyquinoline[12] in a yield of 54%, m.p. 248–250°C. IR (KBr): 3100 (O–H), 2220 (C≡N), 1240, 1230 cm^{-1} (C–O). ^1H NMR (acetone-d_6): δ 7.38–7.44 (2 H, m, H-6, H-8), 7.70 (1 H, d, J = 8.3 Hz, H-3), 7.98 (1 H, d, J = 9.5 Hz, H-5) and 8.47 (1 H, d, J = 8.1 Hz, H-4).

7-(5,5,7,7-*Tetramethyl*-2-*octenyloxy*)*quinoline*-2 - *carbonitrile* (**15b**). This compound was prepared from 7-hydroxyquinoline-2-carbonitrile in analogy with the 8-hydroxy compound. M.p. 109–111°C (cyclohexane). IR (KBr): 2950 (C–H), 2240 (C≡N), 1620, 1500 (aromatic), 1220 (C–O), 970 cm^{-1} (CH=CH-*trans*). The ^1H NMR spectrum is consistent with the suggested structure.

7-(5,5,7,7-*Tetramethyl*-2-*octenyloxy*)*quinoline*-2 - *carboxylic acid* (**15**). The acid was obtained by hydrolysis of the nitrile as described for the 8-substituted compound. Yield ≈ 51% based on **15a**, m.p. 96–98.5°C (petroleum ether b.p. 80–110°C). IR (KBr): 3100–2600 (O–H), 1700 (C=O), 970 cm^{-1} (CH=CH-*trans*). ^1H NMR ($CDCl_3$): 0.96 (9 H, s, *t*-Bu), 0.98 (6 H, s, CMe_2), 1.25 (2 H, s, CH_2), 2.08 (2 H, d, J = 7.2 Hz, CH_2), 4.73 (2 H, d, J = 5.9 Hz, CH_2O), 5.75 (1 H, dt, J = 6 and 15.3 Hz, C=C<u>H</u>CH_2O), 5.99 (1 H, dt, J = 7.5 and 15.1 Hz, C=C<u>H</u>CH_2C), 7.38 (1 H, dd, J = 2.2 and 9.1 Hz, H-6), 7.57 (1 H, bs, H-8), 7.83 (1 H, d, J = 9.1 Hz, H-5), 8.17 (1 H, d, J = 8.1 Hz, H-3), 8.34 (1 H, d, J = 8 Hz, H-4 and 9.22 (1 H, bs, OH).

Ethyl 8 - *dodecyloxy* - 1,4 - *dihydro* - 4 - *oxoquinoline* - 2 - *carboxylate* (**7a**). 2-Dodecyloxyaniline hydrochloride[13] (2.01 g, 6.4 mmol) was stirred at room temperature with diethyl oxalacetate sodium salt (1.37 g, 6.4 mmol), anhydrous Na_2SO_4 (2 g) and absolute ethanol (10 cm^3) for two days. Workup by ether extraction gave 2.71 g (95% yield) of the condensation product. This product was added to boiling diphenyl ether over 6–7 min and the resultant solution heated under reflux (15–30 min). Most of the solvent was distilled off at reduced pressure and column chromatography on silica gel (CH_2Cl_2 and CH_2Cl_2–EtOH 20 : 1) yielded a partially crystalline product (1.79 g, 70% yield). ^1H NMR ($CDCl_3$): δ 0.6–2.4 (26 H, m, alkyl), 4.15

(2 H, t, $J = 6$ Hz, $C\underline{H}_2OAr$), 4.5 (2 H, q, $J = 7$ Hz, CH_2O), 6.95 (1 H, d, $J = 3$ Hz, H-3), 7–7.4 (2 H, m, H-6, H-7), 7.9 (1 H, dd, $J = 8$ Hz and 1 Hz, H-5), 9.4 (1 H, bs, NH).

Ethyl 1,8 - *bis(dodecyloxy)quinoline* - 2 - *carboxylate* (**7b**). The above quinolone (**7a**) (1.64 g, 4.1 mmol) and K_2CO_3 (0.6 g) were stirred in DMF (6 cm^3) at 75–80°C, and 1-bromododecane (1.1 g, 4.4 mmol) was added. The reaction mixture was worked up by ether extraction after $2\frac{1}{2}$ h to give 1.7 g (73% yield), m.p. 62–63.5° (petroleum ether). IR (KBr): 2920, 2850 (C–H), 1740, 1720 (C=O), 1595 cm^{-1} (aromat.). ^1H NMR (CCl_4): δ 0.6–2.3 (48 H, m, alkyl), 4–4.6 (6 H, m, CH_2O), 6.9 (1 H, dd, $J = 8$ and 1 Hz, H-7), 7.3 (1 H, dd, $J = 8$ Hz and 8 Hz, H-6), 7.35 (1 H, s, H-3), 7.6 (1 H, dd, $J = 8$ Hz and 1 Hz, H-5).

1,8 - *Bis(dodecyloxy)quinoline* - 2 - *carboxylic acid* (**7**). This compound was obtained by hydrolysis of the ethyl ester with 5% KOH in 80% EtOH at reflux (3 h). Yield: 67%, m.p. 77–78.5°C. IR (CCl_4): 2920, 2850 (C–H), 1770 cm^{-1} (C=O). ^1H NMR (CCl_4); δ 0.5–2.3 (46 H, m, alkyl), 3.9–4.3 (4 H, m, CH_2O), 6.7–7.7. (4 H, m, aromat.), 10.0 (1 H, s, OH).

4 - (2 - *Ethylhexyloxy)quinoline* - 2 - *carboxylic acid* (**8**) *and* 4 - (5,5,7,7 - *tetramethyl* - 2 - *octenyloxy)-quinoline* - 2 - *carboxylic acid* (**9**). These reagents were prepared by alkylation of ethyl 1,4-dihydro-4-oxoquinaldate[14] with 2-ethylhexyl toluene-4-sulphonate and dodecenyl chloride (K_2CO_3/DMF, 40°C and 70°C respectively, 20 h). Alkaline hydrolysis of the esters afforded **8**: 53% yield, m.p. 106–107.5°C (MeOH). IR (KBr): 3360 (O–H), 1630 cm^{-1} (C=O). ^1H NMR ($CDCl_3$): δ 0.8–1.1 (6 H, CH_3), 1.1–1.8 (8 H, CH_2), 1.99 (1 H, m, $C\underline{H}(CH_2)_3$), 4.37 (1 H, d, $J = 5.5$ Hz, CH_2O), 7.73 (1 H, dd, $J = 8$ Hz, H-6 or H-7), 7.91 (1 H, s, H-3), 7.99 (1 H, ddd, $J = 1.5$, 8.8 Hz, H-6 or H-7), 8.31 (1 H, d, $J = 8$ Hz, H-5 or H-8), 8.86 (1 H, d, $J = 8$ Hz) and 9.37 (1 H, s, OH).

9: 76% yield, m.p. 85–87°C (EtOH–H_2O). IR ($CHCl_3$): 1770 (C=O), 970 cm^{-1} (CH=CH-*trans*). ^1H NMR ($CDCl_3$): δ 0.98 (s, CH_3), 1.00 (s, CH_3), 1.27 (s, CH_2), 2.11 (d, $J = 7.5$ Hz, CH_2), 4.95 (d, $J = 6$ Hz, CH_2O), 5.8 (m, CH=CH), 6.03 (m, CH=CH), 7.7 (dd, $J = 8$ Hz, H-6/7), 7.82 (s, H-3), 7.92 (dd, $J = 8$ Hz, H-6/7), 8.33 (d, $J = 8$ Hz, H-4/8), 8.56 (d, $J = 8.6$ Hz, H-4/8).

8 - *Methylquinoline* - 2 - *carbonitrile* (**11a**). 8-Methylquinoline-*N*-oxide[15] (1.78 g, 11 mmol) was heated with dimethyl sulphate (1.41 g, 11 mmol) for 3 h at 75°C. The product was dissolved in water (7 cm^3), the solution filtered and added dropwise to sodium cyanide (1.65 g, 34 mmol) in water (7 cm^3) at 0°C. After 2 h stirring at 0°C the product was filtered off and recrystallized from cyclohexane to give **11a** (0.90 g, 48% yield), m.p. 125–127°C. IR (KBr): 2940 (C–H), 2230 (C≡N), 1495, 1585 cm^{-1} (aromat.). MS *m/z* (% rel. int.): 168 (100, M^+), 169 (2.8), 167 (8.4), 166 (1.7), 141 (2.3), 140 (2.4), 114 (1.4), 70 (1.8), 63 (1.4), 39 (1.2). ^1H NMR ($CDCl_3$): δ 2.8 (3 H, m, CH_3), 7.8 (3 H, m, aromat-H), 7.79 (1 H, d, $J = 8.4$ Hz, H-3) and 8.35 (1 H, d, $J = 8.4$ Hz, H-4).

4 - (3 - *Heptyl)* - 8 - *methylquinoline* - 2 - *carbonitrile* (**11b**).[6] 8-Methylquinoline-2-carbonitrile (0.84 g, 5 mmol), 2-ethylhexanoic acid (3.60 g, 25 mmol), 1 M H_2SO_4 (5 cm^3), CH_3CN (5 cm^3) and $AgNO_3$ (0.17 g, 0.1 mmol) were heated to 70°C. To this mixture was added $(NH_4)_2S_2O_8$ (3.42 g, 15 mmol) in water (8 cm^3) over 0.5 h with stirring. Stirring was continued for 40 min, then the mixture was poured into ice-water and ammonia and extracted with ether. The organic phase was washed with 2 M NaOH and water. Chromatography on silica gel (60 g) with ethyl acetate–petroleum ether 1:10 as the eluant gave the product (0.59 g, 44% yield) together with unreacted starting material (0.11 g). The product was distilled at 175°C/23 Pa. IR (film): 2960, 2930 (C–H), 2230 (C≡N), 1585, 1505 cm^{-1} (aromat.). ^1H NMR (CCl_4) δ 0.5–2 (14 H, m, alkyl-H), 2.8 (3 H, s, C(8)–CH_3), 3.4 (1 H, m, Ar–CH) and 7.3–8.1 (4 H, m, aromat-H).

4 - (3 - *Heptyl)* - 8 - *methylquinoline* - 2 - *carboxylic acid* (**11**). The above nitrile was hydrolyzed with KOH in ethanol–glycol to give the acid (yield 82%) as a yellow oil. IR (CCl_4): 3300 (O–H), 2960, 2930 (C–H), 1770 (C=O) cm^{-1}. ^1H NMR (CCl_4): δ 0.6–2.2 (14 H, m, alkyl-H), 2.9 (3 H, s, C(8)–CH_3), 3.5 (1 H, m, ArCH), 7.4–8.2 (4 H, m, aromat-H) and 10.8 (1 H, s, CO_2H).

4 - (3 - *Heptyl)quinoline* - 2 - *carboxylic acid* (**10**). This compound was obtained from quinoline-2-carbonitrile and 2-ethylhexanoic acid, followed by hydrolysis of the nitrile group.[6] Yield: 57%, m.p. 102–103°C.

7 - (1 - *Ethenyl* - 3,3,5,5 - *tetramethylhexyl)* - 8 - *hydroxyquinoline* - 2 - *carbonitrile* (**12a**). Crude 8-dodecenyloxyquinoline-2-carbonitrile (**1a**) (29.5 g) in decalin (290 cm^3) was heated under reflux (5.5 h) then most of the decalin was distilled off under reduced pressure. The product was filtered off and recrystallized from petroleum ether (b.p. 40–60°C) yielding 19.2 g (57% yield based on 8-hydroxyquinoline-2-carbonitrile), m.p. 96–98°C. Additional recrystallization gave a product with m.p. 98–99°C. IR (KBr): 3360 (O–H), 2950 (C–H), 2240 (C≡N), 1505 (aromat.), 1250 (C–O aryl), 990, 910 cm^{-1} (vinyl). ^1H NMR ($CDCl_3$): δ 0.92 (3 H, s, CH_3), 0.94 (3 H, s, CH_3), 0.96 (9 H, s, *t*-Bu), 1.31 (1 H, d, $J = 14$ Hz, CH_2), 1.34 (1 H, d, $J = 14$ Hz, CH_2), 1.91 (2 H, d, $J = 6.1$ Hz, $C\underline{H}_2$–CH), 4.23 (1 H, m, $J = 6.1$, 7, 1.5 and 1.3 Hz, CH-aryl), 4.99 (1 H, m, $J = 9.9$, 1.6, 1.5 Hz, $=CH_2$), 5.02 (1 H, m, $J = 17.2$, 1.6, 1.3 Hz, $=CH_2$), 6.08 (1 H, m, $J = 17.2$, 9.9, 7 Hz, vinyl-H), 7.39 (1 H, d, $J = 8.5$ Hz, H-5), 7.59 (1 H, d, J

= 8.5 Hz, H-6), 7.67 (1 H, d, J = 8.5 Hz, H-3), 8.044, 8.047 (1 H, O–H) and 8.26 (1 H, d, J = 8.5 Hz, H-4). MS m/z (rel. int.) 336 (18, M^+), 279(7), 265(7), 224(19), 223(100), 210(27), 209(100), 195(15), 183(9), 57(25).

A small amount of the 5-alkenyl isomer, 5-(5,5,7,7-tetramethyl-2-octenyloxy)quinoline-2-carbonitrile (**12b**) was also isolated, m.p. 104–106°C. IR (KBr): 3370 (O–H), 2950 (C–H), 2240 (C≡N), 1630, 1560, 1505 (aromat.), 1240 ($C–O_{aryl}$), 965 cm^{-1} (–CH=CH-*trans*). ^1H NMR ($CDCl_3$): δ 0.905 (s, CH_3), 0.942 (s, CH_3), 1.187 (s, CH_2), 1.957 (m, CH_2), 3.710 (m, CH_2), 5.55 (m, CH=CH), 7.22 (d, J = 7.8 Hz, H-7), 7.47 (d, J = 7.8 Hz, H-6), 7.73 (d, J = 8.5 Hz, H-3), 7.84 (s, OH), 8.51 (d, J = 8.5 Hz, H-4). MS m/z (rel. int.) 336 (21, M^+), 225 (17), 224 (100), 223 (20), 209 (24), 207 (9), 183 (36), 113 (11), 57 (94), 41 (9).

7 - (1 - *Ethenyl* - 3,3,5,5 - *tetramethylhexyl*) - 8 - *octyloxyquinoline* - 2 - *carboxylic acid* (**13**). Alkylation of **12a** with 1-bromo-octane and subsequent hydrolysis of the nitrile group gave the above product in 87% yield.

7 - (1 - *Ethenyl* - 3,3,5,5 - *tetramethylhexyl*) - 8 - *hydroxyquinoline* - 2 - *carboxylic acid* (**12**). The corresponding nitrile (**12a**) (2.0 g, 6.0 mmol), was hydrolyzed in 10% KOH in EtOH at reflux during two days. The carboxylic acid (2.1 g) separated after addition of water and 2 M HCl. Found: C, 73.35; H, 8.17; N, 3.81. Calc. for $C_{22}H_{29}NO_3$: C, 74.33; H, 8.22; N, 3.94%. IR (CCl_4): 3380 (O–H), 1730 (C=O), 915 cm^{-1} (vinyl). ^1H NMR ($CDCl_3$): δ 0.9 (CH_3), 1.3 (2 H, s, CH_2), 1.9 (2 H, d, J = 6 Hz, CH_2), 4.3 (1 H, m, CH-aryl), 4.8–5.2 (2 H, m, $C=CH_2$), 6.1 (1 H, m, vinyl-H), 7.35 (1 H, d, J = 8 Hz, H-5 or H-6), 7.5 (1 H, d, J = 8 Hz, H-5 or H-6), 8.3 (2 H, s, H-2, H-3) and 10.1 (2 H, s, O–H, CO_2H).

Preparation of metal complexes

Metal complexes of the reagents **1** and **9** were prepared by adding aqueous solutions of Cu(II) or Co(II) acetate or $FeSO_4$ to hot ethanol solutions of the appropriate quinaldic acid, neutralized by NaOH. The molar ratio of metal: ligand was 1:2. The precipitates were filtered off, washed with water and dried *in vacuo*. The Fe(II) complexes were prepared under nitrogen atmosphere. The Zn(II) and Ni(II) complexes were obtained from the acetates using $MeOH/CHCl_3$ and CH_2Cl_2, respectively as solvents. These chelates were recrystallized from toluene and toluene–$CHCl_3$ respectively.

Acknowledgements—Financial support from the Swedish Board for Technical Development is gratefully acknowledged. We thank Professors Torbjörn Norin and Ingmar Grenthe for stimulating discussions and Kerstin Högberg, Peter Fäldt and Ann-Chatrin Nilsson at the Department of Inorganic Chemistry for technical assistance.

Table 3. Elemental analysis of metal complexes of reagent **1**

	% calculated / % found			
	Metal	C	H	N
Zn	8.44	68.25	7.29	3.62
	9.0	68.21	7.27	3.63
Cu	8.23	68.41	7.31	3.63
	8.3	67.37	7.32	3.59
Ni	7.65	68.85	7.35	3.65
	7.2	68.25	7.35	3.55
Co	7.67	68.83	7.35	3.65
	7.7	68.55	7.25	3.63
Fe	7.30	69.10	7.38	3.66
	8.1	69.07	7.39	3.64

REFERENCES

1. M. J. Hudson, *Hydrometallurgy* 1982, **9**, 149.
2. A. R. Burkin, *Chem. and Ind.* 1983, 690.
3. I. M. Kolthoff and E. B. Sandell, *Textbook of Quantitative Inorganic Analysis*. Macmillan, New York (1952).
4. M. Pang, U.S. Patents 3 637 476 (1972), 3 697 400 (1972), 3 787 418 (1974).
5. N. Ackerley and P. A. Mack, *Ger. Offen.* 2 339 240 (1974).
6. F. Minisci, R. Bernardi, F. Bertini, R. Galli and M. Perchinummo, *Tetrahedron* 1971, **27**, 3575.
7. W. M. Budde and J. A. Hartlage, U.S. Patent 3 637 711 (1972).
8. The red Fe(II)–quinaldic acid complex has been used for colourimetric determination of Fe(II): P. Ray and M. K. Bose, *Z. Anal. Chem.* 1933, **95**, 400. For a study of the electronic spectra, see: M. Kral, *Coll. Czech. Chem. Commun.* 1972, **37**, 46.
9. D. H. Gerlach and R. H. Holm, *Inorg. Chem.* 1970, **9**, 588; R. C. Rosenberg, C. A. Root, P. K. Bernstein and H. B. Gray, *J. Am. Chem. Soc.* 1975, **97**, 2092. D. M. Roundhill, *Polyhedron* 1983, **2**, 959.
10. I. A. Krasavin, V. M. Dziomko and Y. P. Radin, *Metody Polucheniya Khim. Reaktivov i Preparatov* 1965, **13**, 68, 94; *Chem. Abstr.* 1966, **65**, 5437b, 7139a.
11. C. Kaneko, H. Hasegawa, S. Tanaka, K. Sunayashiki and S. Yamada, *Chem. Lett.* 1974, 123.
12. L. Bradford, T. J. Elliott and F. M. Rowe, *J. Chem. Soc.* 1947, 437.
13. R. Kuhn and D. Jerchel, *Ber.* 1940, **73**, 1100.
14. B. Riegel, C. J. Albisetti, Jr., G. R. Lappin and R. H. Baker, *J. Am. Chem. Soc.* 1946, **68**, 2685; G. F. Lisk and G. M. Stacy, *J. Am. Chem. Soc.* 1946, **68**, 2686.
15. P. Hamm and W. von Philipsborn, *Helv. Chim. Acta* 1971, **54**, 2363.

Polyhedron Vol. 4, No. 6, pp. 979–981, 1985
Printed in Great Britain

0277–5387/85 $3.00 + .00
© 1985 Pergamon Press Ltd

MÖSSBAUER SPECTRA AND ELECTRIC CONDUCTIVITIES OF BIDENTATE BASE BRIDGED IRON(II) PHTHALOCYANINE

HO-HSIANG WEI*
Department of Chemistry, Tamkang University, Tamsui, Taiwan

and

HUEY-LIH SHYU
Chungtai Junior College of Medical Technology, Taichung, Taiwan

(*Received* 13 *August* 1984; *accepted* 6 *October* 1984)

Abstract—Bidentate bridging base polymer complexes of iron(II) phthalocyanine FePcL, where L = pyrazine (pyz), 4,4′-bipyridine (bpy), *trans*-1,2-bis(4-pyridyl)ethylene (bpe), 1,2-bis(4-pyridyl)ethane (bpa) and 4,4′-trimethylene bipyridine (tmbpy), have been prepared, characterized and oxidized by iodine to give a range of iron(II) and iron(III) complexes $(FePcL)_n \cdot I_x$. The electrical conductivities and Mössbauer parameters both change with respect to the kinds of bidentate bridging bases. The conjugation of bridged ligand markedly effects the conductivity of the complexes.

Recently, several face-to-face linked metallophthalocyanines have been studied.[1–7] Hanack *et al.* reported that phthalocyaninato–iron(II) which polymerized via a bidentate bridging heterocyclic amine, has an electrical conductivity higher than that of the monomer species. However, the electronic properties of the iron atom in these complexes was not known.

In the course of our studies of the iron(II) polymer complexes which is relevant to this type of material,[6] we now report independently the preparation and characterization of several additional neutral and iodine-oxidized bidentate-base bridged iron(II) phthalocyanine complexes $(FePcL)_n$ (Fig. 1) together with the results of their Mössbauer spectra and electrical conductivities.

EXPERIMENTAL

Iron phthalocyanine (FePc) was prepared by the reaction of phthalonitrile and iron pentacarbonyl in a solution of 1-chloro-naphthalene at 258°C and recrystallized from chlorobenzene.[7] Bidentate bridged complexes of iron(II)phthalocyanine, $(FePcL)_n$

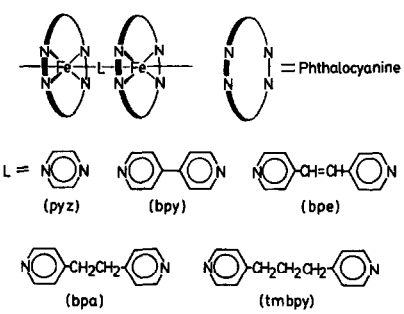


Fig. 1. Structural formula for $(FePcL)_n$.

(L = pyz, bpe, bpy, bpa and tmbpy) were prepared under nitrogen according to the following method.

Bidentate base ligand (10 mmol) was dissolved in chlorobenzene (30 cm^3) and iron phthalocyanine (10 mmol) in chlorobenzene was added dropwise with stirring at 110°C. The mixture was refluxed for 2 h and filtered. The solid residue was washed several times with methanol and dried under high vacuum.

Poly-salts of $(FePcL)_nI_x$ were prepared by oxidizing the neutral complexes with I_2 in chlorobenzene solution for 2 days to give a series of products with a range of stoichiometries.

* Author to whom correspondence should be addressed.

Table 1. Electronic spectral data for $(FePcL)_n$ complexes at 298 K

Compound	λ_{max} (nm)							
$[FePc(pyz)]_n$	1280,	1080,	795,	718,	630,	559,	398,	363
$[FePc(bpe)]_n$	1235,	1060,	700,	624,	538,	404,	360	
$[FePc(bpy)]_n$	1240,	1100,	760,	625,	573,	402,	358	
$[FePc(bpa)]_n$	1260,	1050,	715,	614,	556,	410,	365	
$[FePc(tmbpy)]_n$	1215,	1030,	680,	606,	570,	415,	368	

Electronic spectra were recorded on a Hitachi 330 UV-visible-NIR spectrophotometer. Solid samples were examined as pellets between quartz plates.

The conductivities of the compressed pellets of the complexes at room temperature were obtained with Gen-Rad 1657 RCL digibridge.

The Mössbauer spectra of the complexes at room temperature were measured with an Austin S-600 constant acceleration type Mössbauer spectrometer, using a $^{57}Co(pd)$ source. Isomer shifts are quoted with respect to the centroid of the iron foil. The spectral fittings were performed by a microcomputer least squares method. The line-shape was assumed to be Lorentzian.

RESULTS AND DISCUSSION

The electronic spectra for the adducts are reported in Table 1 to provide a convenient means for identifying them. The weak absorptions in the near infrared 1215–1280 nm, medium absorptions at 795–680 nm and strong absorptions at 630–360 nm in $(FePcL)_n$ can be assigned to metal *d–d* transition, charge-transfer of $d\pi$–$L\pi^*$ (between metal and Pc or bidentate ligand) and ligand-centred π–π^* (Pc and L) transitions respectively.[8–10]

Typical Mössbauer spectra of $(FePcL)_n$ and iodinated $(FePcL)_nI_x$ at 298 K are shown in Figs. 2 and 3 and Table 2 summarizes the Mössbauer parameters.

From the data in Table 2, it can be seen that I.S. and Q.S. values of the divalent iron(II) ion for these iron complexes, $(FePcL)_n$ with respect to ligands (L) increase in the order: pyz > bpe > bpy > bpa > tmbpy. A possible explanation for the lower I.S. and Q.S. values of iron for the first two ligands (pyz and bpe) lies in the greater participation of π-acceptor property, since $3d\pi$-electrons of iron are

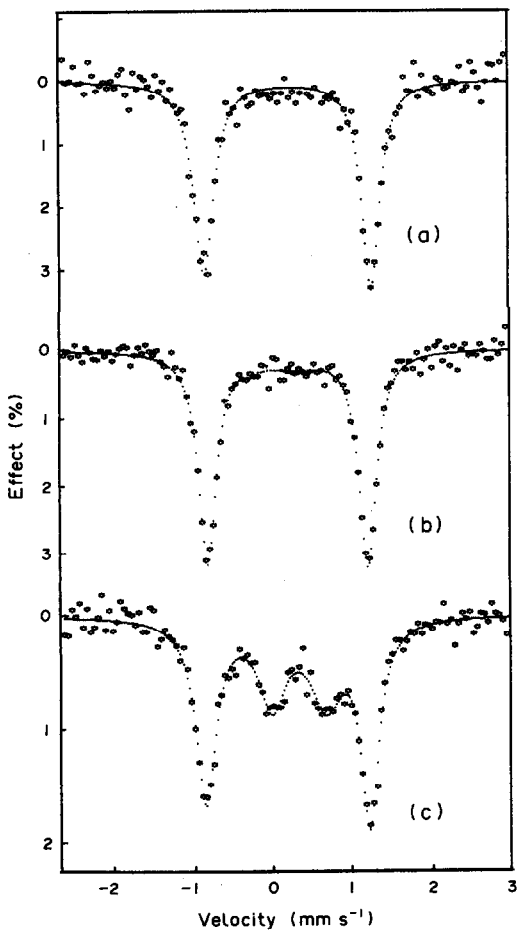


Fig. 2. Mössbauer spectra at 298 K for: (A) $[FePc(pyz)]_n$, (B) $[FePc(bpy)]_n$, and (C) $[FePc(bpe)]_nI_x$.

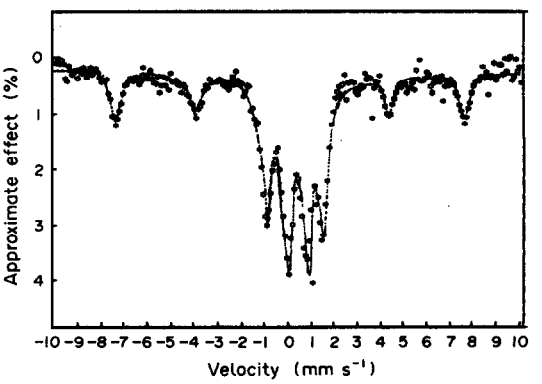


Fig. 3. Mössbauer spectrum at 298 K for coordinated $[FePc(pyz)]_nI_x$ (50% I_2).

Table 2. Mössbauer parameters and electric conductivities for $(FePcL)_n$ complexes at room temperature (298 K)

Complexes	I.S. (mm s^{-1})*	Q.S. (mm s^{-1})†	σ (Ω^{-1} cm^{-1})
FePc	0.48	2.62	2.0×10^{-10}
$FePc(py)_2$	0.20	2.06	7.6×10^{-9}
$[FePc(pyz)]_n$	0.18	1.98	2.5×10^{-6}
$[FePc(bpe)]_n$	0.20	2.01	2.0×10^{-7}
$[FePc(bpy)]_n$	0.24	2.00	9.0×10^{-8}
$[FePc(bpa)]_n$	0.28	2.04	1.0×10^{-8}
$[FePc(tmbpy)]_n$	0.28	2.06	9.5×10^{-9}

* Precision on all runs ± 0.01 mm s^{-1}.
† Precision on all runs ± 0.02 mm s^{-1}.

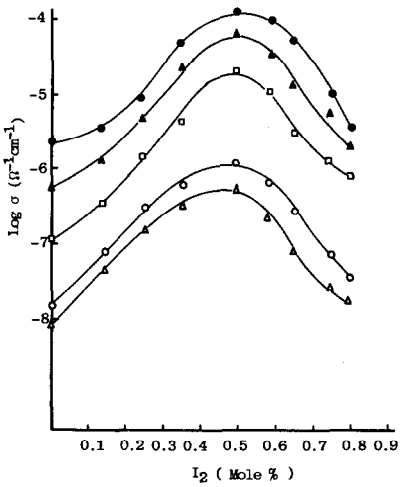


Fig. 4. Conductivity vs mole fraction of I_2 for $[FePc(pyz)]_nI_x$ (●), $[FePc(bpe)]_nI_x$ (▲), $[FePc(bpy)]_nI_x$ (□), $[FePc(bpa)]_nI_x$ (○) and $[FePc(tmbpy)]_nI_x$ (△).

delocalized onto the bridged ligand. This in turn leads to a decrease in *d*-electron population and decrease the shielding of *s*-character for the iron atom. The ~ 50% iodinated $[FePc(pyz)]_nI_x$ at 298 K have two kinds of Mössbauer absorption spectra characterizing mixed-valence of Fe(III)·Fe(II), the trivalent Fe(III) species has Mössbauer parameters of I.S. = 0.37, Q.S. = 0.80 mm s^{-1} and a small contribution of magnetic hyperfine component (an internal magnetic field of *ca.* 458 K Oe, cf. Fig. 3) which is unambiguously assigned to high-spin Fe(III) species.

Table 2 lists the results from four-probe conductivity measurements on the $(FePcL)_n$. The plots of conductivity versus the mole fraction of iodine are shown in Fig. 4. For all samples; the conductivity maximized at *ca.* 50% iodine. The general trend in conductivity as a function of base ligands is: pyz > bpe > bpy > bpa > tmbpy. This trend correlates with increasing conjugation of ligands (going from tmbpy to pyz). It is known from Mössbauer studies that the positive charge in the π-conjugated bidentate base complexes of $(FePcL)_n$ is preferentially localized on iron atom. Thus, conjugate assistance of electron transfer through the π-system markedly effects the conductivity.

Acknowledgement—We wish to thank the National Science Council, Republic of China, Taiwan, for a grant supporting this research.

REFERENCES

1. K. F. Schoch, Jr., B. R. Kundalkar and T. Marks, *J. Am. Chem. Soc.* 1979, **101**, 7071.
2. R. S. Nohr, P. M. Kuznesof, K. J. Wynne, M. E. Kenney and P. G. Siebenmann, *J. Am. Chem. Soc.* 1981, **103**, 4371.
3. C. W. Dirk, T. Inabe and K. F. Schoch, Jr. and T. J. Marks, *J. Am. Chem. Soc.* 1983, **105**, 1539.
4. O. Schneider and M. Hanack, *Angew. Chem., Int. Ed. Engl.* 1982, **21**, 79; 1983, **22**, 784.
5. J. Metz and M. Hanack, *J. Am. Chem. Soc.* 1983, **105**, 828.
6. H.-H. Wei and H.-L. Shyu, *Transition Met. Chem.* 1984, **9**, 211.
7. D. H. Busch, *Inorg. Synth.* 1980, **20**, 155.
8. B. D. Berezin, *Coordination Compounds of Porphyrins and Phthalocyanines.* Wiley, New York (1981).
9. T. J. Marks and D. R. Stojakovic, *J. Am. Chem. Soc.* 1978, **100**, 1695.
10. M. J. Powers and T. J. Meyer, *Inorg. Chem.* 1978, **17**, 2955.

Polyhedron Vol. 4, No. 6, pp. 983–987, 1985
Printed in Great Britain

0277–5387/85 $3.00 + .00
© 1985 Pergamon Press Ltd

NEUTRAL COMPLEXES OF Ga_2X_4 (X = Cl, Br) CONTAINING Ga–Ga BONDS: THE CRYSTAL AND MOLECULAR STRUCTURE OF $Ga_2Cl_4 \cdot 2$PYRIDINE

JOHN C. BEAMISH, ALAN BOARDMAN, RONALD W. H. SMALL and IAN J. WORRALL*

Department of Chemistry, The University, Lancaster LA1 4YA, U.K.

(*Received* 13 *August* 1984; *accepted* 6 *October* 1984)

Abstract—The complexes $Ga_2X_4 \cdot 2L$ (L = pyridine, 3-methylpyridine, 4-methylpyridine, morpholine, 1,4-thioxane, 1,4-dithiane, tetrahydropyran, tetrahydrofuran, tetrahydrothiophene and dimethylsulphide) have been prepared. Vibrational spectra indicate that they all contain Ga–Ga bonds and this is confirmed for $Ga_2Cl_4 \cdot 2$pyridine by a crystal structure determination which shows it to be isostructural with the bromide analogue. We were unable to synthesize complexes of stoichiometry $Ga_2X_4 \cdot 4L$ which had previously been reported.

Complexes of the ionic gallium halides were first reported by Brewer *et al.* in 1959. They reported the synthesis of many complexes of stoichiometry $Ga_2X_4 \cdot 2L$ for ligands with two donor sites and $Ga_2X_4 \cdot 4M$ for monodentate ligands. They concluded that the complexes were ionic with structures $GaL_2^+GaX_4^-$ and $GaM_4^+GaX_4^-$.[1,2] More recently we have shown that $Ga_2X_4 \cdot 2$dioxane (X = Cl, Br) and $Ga_2Br_4 \cdot 2$pyridine have ethane-like structures with Ga–Ga bonds.[3–5] In view of the conflict between Brewer's conclusions and our structural findings a further investigation is desirable.

EXPERIMENTAL

All reactions were carried out in a nitrogen filled dry-box or *in vacuo*. We began the synthetic work using the previous methods fully described by Brewer *et al.*[1,2] involving benzene solutions of the gallium dihalides, with a representative sample of ligands reported to form stable complexes. The ligands used were anisole, 1,4-dioxane, morpholine, acetylacetone, ethylamine, triethylamine, R_2S (R = methyl, ethyl), and selanophane. Isolable compounds were obtained for only two ligands, dioxane and morpholine. The remainder generally produced mixtures of gallium and gallium(III) halide complex. Our successful synthetic methods generally involve either the direct reaction of the ligand and dihalide or ligand displacement reactions.

Synthesis of $Ga_2X_4 \cdot 2L$ (X = Cl, Br; L = 1,4-*dioxane, morpholine, tetrahydrofuran, tetrahydropyran, tetrahydrothiophene, dimethylsulphide,* 1,4-*thioxan) and* $Ga_2Cl_4 \cdot 2$*diethylsulphide.*

The dihalide was cooled in liquid nitrogen and excess pure dry ligand was condensed on to it *in vacuo*. The temperature was allowed to slowly rise to the melting point of the ligand and the resulting slurry rapidly stirred until a colourless solution formed. The excess ligand was then slowly removed under vacuum and white compounds remained. Analytical data are given in Table 3.

Synthesis of $Ga_2X_4 \cdot 2L$ (X = Cl, Br; L = *pyridine,* 3-*methylpyridine and* 4-*methylpyridine*)

These could not be prepared by the method described above and were synthesized by ligand replacement reactions on $Ga_2X_4 \cdot 2$dioxane. Excess pyridine was condensed on the liquid nitrogen-cooled dioxane complex *in vacuo* and the temperature allowed to rise slowly to the melting point of the ligand. The resulting slurry was vigorously stirred until a clear solution formed; excess solvent was removed under vacuum and the remaining white powders analysed as shown in Table 3. The powders are soluble in excess ligand and crystals suitable for X-ray diffraction were obtained for the pyridine complex.

Synthesis of $Ga_2Cl_4 \cdot 2$*dithiane*

A dilute solution of dithiane in CS_2 was slowly added dropwise to a well cooled suspension of

* Author to whom correspondence should be addressed.

Ga_2Cl_4 in CS_2. After a slight excess of ligand had been added the precipitate was stirred for four hours, filtered and dried *in vacuo*; analytical data are given in Table 3.

Raman spectra were recorded on solid samples using a Carey–Anaspec 81L spectrometer and IR on a Nicolet MX-1 Fourier transform spectrometer.

X-Ray structure analysis of $Ga_2Cl_4 \cdot 2$*pyridine*

Crystal data (measured at room temperature). $C_{10}H_{10}Cl_4Ga_2N_2$, $M = 439.5$, monoclinic, $C2/m$, $a = 15.43(2)$ Å, $b = 7.527(5)$ Å, $c = 7.350(5)$ Å, $\beta = 113.49(3)°$, $z = 2$, $U = 782.8$ Å^3, $D_c = 1.86$ mg m^{-3}, $D_m = 1.85$ mg m^{-3}, $F(000) = 428$, $\mu = 3.96$ mm^{-1}, Mo-K_α-radiation, $\lambda = 0.7107$ Å.

Data collection and solution

Stoe STADI-2 circle diffractometer; layers $l = 0$–8 were measured with the crystal set about the c-axis. Absorption corrections and scaling of data were carried out using SHELX.[6] After elimination of those for which $I < 3\sigma(I)$ there remained 1108 reflections. An E map, obtained by the MULTAN program,[7] revealed the positions of the Ga and Cl atoms; $F_o - F_c$ maps then gave the positions of the remaining atoms (apart from H). Using unit weights, full matrix least squares refinement of all atomic positions and anisotropic U_{ij} values was carried out until convergence was reached at $R = 0.0426$, $R_w = 0.0426$. Atomic scattering factors are given in Refs 8 and 9. Final atomic coordinates, anisotropic thermal parameters and lists of structure factors have been deposited with the Editor,* from whom copies are available on request.

DISCUSSION

Stoichiometry of complexes

The analytical data given in Table 3 shows that without exception the complexes have stoichiometry $Ga_2X_4 \cdot 2L$ regardless of the potential monodentate or bidentate nature of the ligand. This is in direct conflict with the findings of Brewer *et al.*[1,2] They reported 1:4 complexes with a number of monodentate O, N, S and Se ligands. We were unable to repeat this work and only with dimethylsulphide and diethylsulphide could stable compounds be isolated and these had 1:2 stoichiometry. Both 1:2 and 1:4 complexes are known for the indium analogues.[12]

Vibrational spectroscopy

This is a valuable technique for distinguishing between ionic type complexes containing the GaX_4^- ion proposed by Brewer *et al.* and Ga–Ga bonded species found in $[Ga_2X_6]^{2-}$,[10] $Ga_2X_4 \cdot 2$-pyridine and $Ga_2X_4 \cdot 2$dioxane (X = Cl, Br).[3–5] We have previously reported that the dioxane complexes have similar spectra to the anions $[Ga_2X_6]^{2-}$; in particular their Raman spectra each contain a very intense band in a similar position. This band has been assigned by Taylor *et al.*[10] to a totally symmetrical mode in which the Ga–Ga bond stretches in phase with Ga–halogen bonds. The presence of this intense band may be used to identify compounds containing Ga–Ga bonds.[11] Similar spectra are observed for analogous indium compounds.[12]

Raman spectra were recorded for all complexes over the range 0–3500 cm^{-1} and IR 210–3500 cm^{-1}. A few complexes produced poor quality IR spectra and these are not included. The discussion below is restricted to the region 100–400 cm^{-1} which is the useful region for Ga–Ga bonded compounds and contains Ga–Ga and Ga–halogen frequencies.† Bands due to the simple GaX_4^- ions are absent in all cases thus eliminating the structures previously proposed. It would be expected that Ga–Ga bonded species with ethane-like structures would contain an intense band associated mainly with Ga–Ga stretching, four bands associated with Ga–halogen stretching and two bands arising from Ga–ligand stretching. The vibrational spectra in the region 100–400 cm^{-1} are given in Tables 2 and 3 together with possible assignments which are based mainly upon those of Taylor *et al.* for $[Ga_2X_6]^{2-}$.[10] Although the assignments are labelled ν(Ga–Ga), ν(Ga–X) and ν(Ga–L) mixing of these modes as found in $[Ga_2X_6]^{2-}$ will occur. It is seen that the overall pattern of the spectra are similar and with few exceptions contain a very intense band close to the position of the intense band observed in $[Ga_2X_6]^{2-}$. These bands are assigned ν(Ga–Ga); they vary over the range 145–170 cm^{-1} for bromide complexes and 214–258 cm^{-1} for chloride complexes. The wider range of the latter may be partly associated with mass effects since the formal replacement of X^- in $[Ga_2X_6]^{2-}$ by ligand is larger and it has been shown that mass effects contribute substantially to band position in the mixed halide complexes, e.g.

* Atomic coordinates have also been deposited with the Cambridge Crystallographic Data Centre.

† Detailed spectroscopic data are given in Ref. 13.

$[Ga_2X_{6-r}Y_r]$.[11] Although the intensity of the band is much reduced in pyridine and substituted pyridine complexes of Ga_2Cl_4, the crystal structure described below confirms the Ga–Ga bonded structure for the pyridine complex.

Bands in the range 300–400 cm^{-1} and 200–330 cm^{-1} may be assigned to ν(Ga–Cl) and ν(Ga–Br) respectively; generally where both Raman and IR spectra have been recorded the required number of bands is observed.

The four crystal structures so far determined have revealed two structural types: C_{2h} in $Ga_2X_4 \cdot 2$-pyridine (X = Cl, Br) in which the *trans* conformation is adopted and C_1 in $Ga_2X_4 \cdot 2$dioxane (X = Cl, Br). Since mutual exclusion should be operative in the former type, spectroscopy should distinguish between the *trans* and lower symmetry structures. It is seen that although mutual exclusion is not strictly adhered to, fewer bands and simpler Raman and IR spectra are observed. Considering other complexes where both Raman and IR spectra were obtained it is possible to predict tentatively that substituted pyridine complexes are *trans* and $Ga_2Cl_4 \cdot 2L$, (L = thioxane, tetrahydrothiophene, dithiane and dimethylsulphide) have structures of lower symmetry. The structure is a possible consequence of the packing in the solid state. In the pyridine complexes the *trans* conformation allows chain-like packing of the planar pyridine rings.[5]

A comparison of Cl and Br complexes of the same ligand allows the tentative assignment of Ga–ligand modes, these are also given in Tables 1 and 2. ν(Ga–N) lies in the range 218–276 cm^{-1} and there are many examples known which support our assignment.[16] The range 255–274 cm^{-1} for ν(Ga–S) is lower than observed in $GaX_3 \cdot SR_2$ complexes[16] (297–328 cm^{-1}) and may be a consequence of mixing. Bands due to ν(Ga–O) are to be expected in the region 400–550 cm^{-1} [17,18] but usually are very weak, broad and often not observed.[17] Since many of the ligands used in this work have bands in this region no reliable assignments could be made.

In complexes containing ambidentate ligands, i.e. morpholine and thioxane, ligand attachment is believed to occur via N in the former and S in the latter. This view is supported by the presence of bands at 275 and 254 cm^{-1} (ν(Ga–N)) in the morpholine complexes with a shift in ν(N–H) of -56 cm^{-1} (Cl) and -44 cm^{-1} (Br)[14] from the free ligand value (3340 cm^{-1}). For the thioxane complexes small

Table 1. Vibrational spectra of $Ga_2Cl_4 \cdot 2L$ in the range 200–400 cm^{-1}*

L		ν(Ga–Ga)	ν(Ga–Cl)	ν(Ga–L)
Dioxane	R	238vs	337w 375m 395m	
	IR		336vs 365 vs	
Pyridine	R	223m	344m 388m	276s
	IR		343vs 360vs	236s
3-Me-pyridine	R	223m	344m 389m	267s
	IR		338vs 357 vs	228s
4-Me-pyridine	R	214s	343m 386m	267s
	IR		342vs 357vs	225s
Morpholine	R	221s	331w 348w 379m	275m
Thioxane	R	237vs	351m 383m	
	IR		348s 363s 385m 396s	
THT	R	243vs	358m 385m	265m
	IR		339s 354s 367s 398s	268m
DMS	R	245vs	359w 365w 385m	267m
	IR		339s 351s 369s 383m	266m
DES	R	213vs	338m 353m 383s	274w
Dithiane	R	238vs	351s 362m 389s	
	IR		331s 350s 361s 388m	
THF	R	258s	366m 396m	
THP	R	236vs	363m 384m	
$Cl^-(Ga_2Cl_6^{2-})$[10]	R	233vs	314w 385m	
	IR		302s 327vs	

* R, Raman, THT, tetrahydrothiophene; DMS, dimethylsulphide; DES, diethylsulphide; THF, tetrahydrofuran; THP, tetrahydropyran; vs, very strong; s, strong; m, medium; w, weak.

Table 2. Vibrational spectra of $Ga_2Br_4 \cdot 2L$ in the range 100–400 cm^{-1}*

L		ν(Ga–Ga)	ν(Ga–Br)	ν(Ga–L)
Dioxane	R	168vs	238m 274m 285m 325m	
	IR		241vs 273s 289vs	
Pyridine	R	163vs	241m 334w	254m
	IR		255s 265vs	231s
3-Me-pyridine	R	163vs	240m 330w	257m
	IR		253s 266vs	228s
4-Me-pyridine	R	153s	233m 324m	265m
	IR		249vs 269vs	218s
Morpholine	R	169vs	235w 304w	254w
Thioxane	R	170vs	264m 326w	
THT	R	145vs	227w 271w 318w	255m
	IR		243s 274s	
DMS	R	155m	233w 274w 321m	259s
	IR		234s 272s	
THF	R	167vs	273m 332w	
THP	R	170vs	274w 322w	
$Br^-(Ga_2Br_6^{2-})$[10]	R	164vs	228m 236m 316m	
	IR		228s 237vs	

* Abbreviations as in Table 1.

shifts of $-10\ cm^{-1}$ are observed in the ν(C–S) at 655 and 688 cm^{-1} in the free ligand with no shift in ν(C–O) indicating a monodentate S attachment.[15]

Crystal structure of $Ga_2Cl_4 \cdot 2pyridine$

$Ga_2Cl_4 \cdot 2$pyridine exists as a single discrete molecule (Fig. 1) with a *trans* configuration and has $2/m$ (C_{2h}) symmetry (by space group requirement); it is isostructural with the bromide analogue.[5] Important bond distances and angles are given in the Table 4; the Ga–Ga bond length is 2.403(1) Å, and compares with 2.406(1) Å found in $Ga_2Cl_4 \cdot 2$-dioxane, 2.395(6) Å in $Ga_2Br_4 \cdot 2$dioxane and 2.421(3) Å in $Ga_2Br_4 \cdot 2$pyridine.

Table 3. Analytical data

Compound	Found (calc.) (%) Ga	Cl	Br
$Ga_2Cl_4 \cdot 2$pyridine	31.7(31.7)	32.3(32.3)	
$Ga_2Br_4 \cdot 2$pyridine	22.4(22.6)		51.8(51.8)
$Ga_2Cl_4 \cdot 2$(3Me-pyridine)	29.7(29.8)	30.1(30.3)	
$Ga_2Br_4 \cdot 2$(3Me-pyridine)	21.7(21.6)		49.3(49.5)
$Ga_2Cl_4 \cdot 2$(4Me-pyridine)	29.7(29.8)	29.6(30.3)	
$Ga_2Br_4 \cdot 2$(4Me-pyridine)	21.3(21.6)		50.1(49.5)
$Ga_2Cl_4 \cdot 2$morpholine	31.2(31.1)	30.6(30.6)	
$Ga_2Br_4 \cdot 2$morpholine	22.0(22.0)		50.5(50.5)
$Ga_2Cl_4 \cdot 2$thioxane	28.0(28.5)	28.7(29.0)	
$Ga_2Br_4 \cdot 2$thioxane	20.6(20.9)		47.6(47.9)
$Ga_2Cl_4 \cdot 2$tetrahydrothiophene	31.3(30.5)	31.7(31.0)	
$Ga_2Br_4 \cdot 2$tetrahydrothiophene	22.1(21.9)		50.0(50.3)
$Ga_2Cl_4 \cdot 2$dimethylsulphide	34.8(34.4)	34.6(35.0)	
$Ga_2Br_4 \cdot 2$dimethylsulphide	23.7(23.9)		54.5(54.8)
$Ga_2Cl_4 \cdot 2$diethylsulphide	30.4(30.2)	31.5(30.7)	
$Ga_2Cl_4 \cdot 2$dithiane	26.7(26.8)	27.0(27.2)	
$Ga_2Cl_4 \cdot 2$tetrahydrofuran	33.1(32.8)	33.5(33.3)	
$Ga_2Br_4 \cdot 2$tetrahydrofuran	23.3(23.1)		53.3(53.0)
$Ga_2Cl_4 \cdot 2$tetrahydropyran	30.8(30.8)	30.8(31.3)	
$Ga_2Br_4 \cdot 2$tetrahydropyran	22.5(22.2)		51.3(50.6)

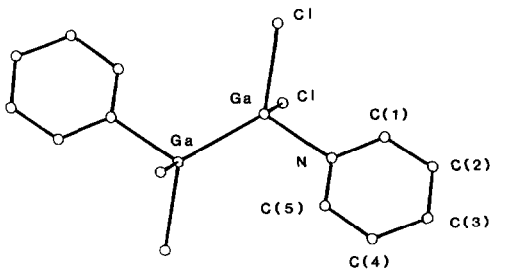


Fig. 1. The molecular structure of $Ga_2Cl_4 \cdot 2$pyridine.

Table 4. Bond lengths and angles for $Ga_2Cl_4 \cdot 2$pyridine

Bond length (Å)		Bond angle (°)	
Ga–Ga	2.403(1)	Ga–Ga–Cl	117.2(1)
Ga–Cl	2.200(2)	Cl–Ga–Cl	105.7(1)
Ga–N	2.003(5)	Ga–Ga–N	110.9(1)
N–C(1)	1.354(8)	Cl–Ga–N	102.5(1)
N–C(5)	1.351(9)	N–C(1)–C(2)	120.8(7)
C(1)–C(2)	1.397(10)	C(1)–C(2)–C(3)	119.8(7)
C(2)–C(3)	1.376(12)	C(3)–C(4)–C(5)	118.8(8)
C(3)–C(4)	1.391(12)	C(4)–C(5)–N	121.5(7)
C(4)–C(5)	1.397(11)	C(5)–N–C(1)	119.7(6)
		C(2)–C(3)–C(4)	119.3(7)

CONCLUSION

A series of neutral Ga–Ga bonded complexes, $Ga_2X_4 \cdot 2L$ has been synthesized with monodentate and bidentate ligands containing O, N, and S. No evidence was found to support previous reports of the existence of ionic 1 : 4 complexes.

REFERENCES

1. S. M. Ali, F. M. Brewer, J. Chadwick and G. Garton, *J. Inorg. Nucl. Chem.* 1959, **9**, 124.
2. F. M. Brewer, J. R. Chadwick and G. Garton, *J. Inorg. Nucl. Chem.* 1961, **23**, 45.
3. J. C. Beamish, R. W. H. Small and I. J. Worrall, *Inorg. Chem.* 1979, **18**, 220.
4. R. W. H. Small and I. J. Worrall, *Acta Cryst.* 1982, **B38**, 250.
5. R. W. H. Small and I. J. Worrall, *Acta Cryst.* 1982, **B38**, 86.
6. G. M. Sheldrick, *SHELX 76. A Program for Crystal Structure Determination.* University of Cambridge, England (1976).
7. P. Main, L. Lessinger, M. M. Woolfson, G. Germain and J. P. Declercq, *MULTAN. A System of Computer Programs for the Automatic Solution of Crystal Structures from X-ray Diffraction Data.* University of York, England (1977).
8. D. T. Cromer and D. Liberman, *J. Chem. Phys.* 1970, **53**, 1891.
9. D. T. Cromer and J. B. Mann, *Acta Cryst.* 1968, **A24**, 321.
10. C. A. Evans, K. H. Tan, S. P. Tapper and M. J. Taylor, *J. Chem. Soc. (Dalton)* 1973, 998.
11. K. H. Tan and M. J. Taylor, *Inorg. Nucl. Chem. Lett.* 1974, **10**, 267.
12. I. Sinclair and I. J. Worrall, *Can. J. Chem.* 1982, **60**, 695.
13. A. Boardman, Ph.D. Thesis, University of Lancaster, England (1984).
14. G. Marcotrigiano and G. C. Pellacani, *Spect. Acta* 1975, **31A**, 1865.
15. R. A. Walton, *Inorg. Chem.* 1966, **5**, 643.
16. N. N. Greenwood, N. S. Srivastava and B. P. Straughan, *J. Chem. Soc. (A)* 1966, 699.
17. M. T. Bories, J. Roziere, A. Manteghetti and A. Potier, *Can. J. Chem.* 1974, **52**, 3274.
18. A. J. Carty, H. A. Patel and P. M. Boorman, *Can. J. Chem.* 1970, **48**, 492.
19. J. Lewis, J. R. Miller, R. L. Richards and A. Thompson, *J. Chem. Soc.* 1965, 5850.

Polyhedron Vol. 4, No. 6, pp. 989–992, 1985
Printed in Great Britain

0277–5387/85 $3.00 + .00
© 1985 Pergamon Press Ltd

PALLADIUM(II) HALIDE COMPLEXES WITH 2,5-DIMETHYL-, 2-AMINO-, 2-AMINO-5-METHYL-, 2-ETHYLAMINO- AND 2-MERCAPTO-5-METHYL-1,3,4-THIADIAZOLE

ANTONIO C. FABRETTI, GIANCARLO FRANCHINI, WANDA MALAVASI and GIORGIO PEYRONEL*

Istituto di Chimica Generale e Inorganica, Università di Modena, 41100 Modena, Italy

(*Received* 4 *May* 1984; *accepted after revision* 6 *October* 1984)

Abstract—Some palladium(II) halide complexes with 2,5-dimethyl- (DTZ), 2-amino- (ATZ), 2-amino-5-methyl- (MATZ), 2-ethylamino- (EATZ) and 2-mercapto-5-methyl-1,3,4-thiadiazole (MTTZ) have been prepared and studied: $PdX_2 \cdot 2L$ (L = DTZ, ATZ, MATZ: X = Cl, Br, I; L = EATZ: X = Br, I; L = MTTZ: X = I), $PdCl_2 \cdot 2.5EATZ$, $PdCl_2 \cdot 3MTTZ$, $PdBr_2 \cdot 1.5MTTZ$ and $PdX_2 \cdot L$ (L = DTZ, ATZ, MATZ, EATZ: X = Cl, Br; L = MTTZ: X = $Cl(H_2O)$, Br). In the $PdX_2 \cdot 2L$, $PdCl_2 \cdot 2.5EATZ$ and $PdCl_2 \cdot 3MTTZ$ complexes the palladium ions are *cis*-(2X, 2L)-coordinated, the coordination sites being N_{ring} for DTZ, NR_2 for ATZ, MATZ, EATZ and C = S for MTTZ. $PdBr_2 \cdot 1.5MTTZ$ may be formulated as *cis*$[PdBr_2 \cdot 2L] \cdot [PdBr_2 \cdot L]$. In the $PdX_2 \cdot L$ complexes the ligand very likely acts as bidentate by using a ring-nitrogen atom as the second coordination site.

Mono- and di-substituted 1,3,4-thiadiazoles have pharmacological properties[1–3] and are potential coordinating agents. The 2,5-dimethyl-1,3,4-thiadiazole (DTZ) has three possible coordinating endocyclic sites (2N, S). Besides them the 2-amino- (ATZ), 2-amino-5-methyl- (MATZ) and 2-ethylamino-1,3,4-thiadiazole (EATZ) have an exocyclic amino nitrogen atom and the 2-mercapto-5-methyl-1,3,4-thiadiazole (MTTZ) has an exocyclic sulphur atom as possible coordination sites. In order to establish the coordination behaviour of these ligands toward palladium(II) some of their complexes with this metal ion were prepared and investigated.

EXPERIMENTAL

All the reagents were of the highest purity commercial grade.

$PdCl_2 \cdot 2L$ (L = DTZ, ATZ, MATZ), $PdCl_2 \cdot 2.5EATZ$ *and* $PdCl_2 \cdot 3MTTZ$

A warm solution of $PdCl_2$ (1 mmol) and NaCl (2 mmol) in H_2O (2 cm^3) and EtOH (2 cm^3) was slowly added to a warm solution of the ligand (4 mmol) in EtOH (4 cm^3) and H_2O (4 cm^3) for DTZ and EATZ, in EtOH (12 cm^3) and H_2O (12 cm^3) for ATZ, in EtOH (16 cm^3) for MATZ and in EtOH (16 cm^3) and conc. HCl (2 cm^3) for MTTZ. The EATZ derivative was precipitated by adding Et_2O and was recrystallized from $CHCl_3$.

$PdBr_2 \cdot 2L$ (L = DTZ, ATZ, MATZ, EATZ) *and* $PdBr_2 \cdot 1.5MTTZ$

A warm solution of $PdBr_2$ (1 mmol) in H_2O (10 cm^3) was slowly added to a warm solution of the ligand (4 mmol) in EtOH (4 cm^3) and H_2O (4 cm^3) for DTZ and EATZ, in EtOH (12 cm^3) and H_2O (12 cm^3) for ATZ, in EtOH (16 cm^3) for MATZ and in EtOH (16 cm^3) and conc. HBr (2 cm^3) for MTTZ.

$PdI_2 \cdot 2L$ (L = DTZ, ATZ, MATZ, EATZ, MTTZ)

A warm solution of PdI_2 (0.25 mmol) and KI (10 mmol) in H_2O (4 cm^3) was slowly added to a warm solution of the ligand (1 mmol) in EtOH (1 cm^3) and H_2O (1 cm^3) for DTZ and EATZ, in EtOH (3 cm^3) and H_2O (3 cm^3) for ATZ, in EtOH (4 cm^3) for MATZ and in EtOH (4 cm^3) and conc. HI (1 cm^3) for MTTZ.

* Author to whom correspondence should be addressed.

$PdX_2 \cdot L$ (L = DTZ, ATZ, MATZ, EATZ: X = Cl, Br; L = MTTZ: X = Cl(H_2O), Br)

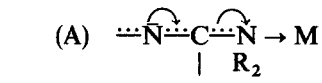
A warm solution of L (1 mmol) in EtOH (1 cm^3) and H_2O (1 cm^3) for DTZ and EATZ, in EtOH (4 cm^3) and H_2O (4 cm^3) for ATZ, in EtOH (4 cm^3) for MATZ and in EtOH (4cm^3) and conc. HX (0.5 cm^3) for MTTZ was slowly added to a warm solution of PdX_2 (1 mmol) and NaCl or KBr (2 mmol) in H_2O (2 cm^3) and EtOH (2 cm^3).

Elemental analyses are reported in Table 1. The molar conductivities were determined with a WTW conductivity bridge. Infrared spectra (Tables 2 and 3) were recorded with a Perkin–Elmer 180 spectrophotometer on the solid compounds in KBr disks (4000–250 cm^{-1}) and as Nujol mulls in polythene (500–50 cm^{-1}).

RESULTS AND DISCUSSION

In DMF solution all the soluble complexes behave as non-electrolytes except the MTTZ complexes which have molar conductivities close or corresponding to those of 1:1 electrolytes (Λ_M = 65–90)[5] probably because MTTZ may act as (N, S) chelating ligand and therefore favours the ionization of one halide ion in solution.

Some infrared bands observed (Table 2) in the 1545–1507 cm^{-1} region for ATZ, MATZ and EATZ may be assigned to ring vibration modes containing a high ν(C=N) contribution. For all the $PdX_2 \cdot 2L$ complexes their frequencies increase in agreement with the electronic shift (A) from the ring nitrogen

(A) 

atom toward the aminic nitrogen atom due to its coordination to the metal ion. For EATZ also the band at 1198 cm^{-1}, lying in the range of ν(C–NR_2) frequencies,[4] is shifted in the complexes to lower frequencies in agreement with the electronic shift (A).

The bands observed at 642 cm^{-1} for DTZ, 680 and 610 cm^{-1} for ATZ, 685 and 649 cm^{-1} for MATZ and 610 cm^{-1} for EATZ, lying in the frequency range given for C–S stretching frequencies (720–570 cm^{-1}),[4] are in agreement with the ν(C–S) frequencies given for 2-amino-5(*o*-hydroxyphenyl)-1,3,4-

Table 1. Analytical data, colour and molar conductivities, Λ_M, of the complexes

Complex	Found (calc.) % N	C	H	S	Colour	Λ_M*
$PdCl_2 \cdot 2DTZ$	13.8 (13.8)	23.8 (23.7)	2.92 (2.98)	15.4 (15.8)	Yellow	Insoluble
$PdCl_2 \cdot DTZ$	9.4 (9.6)	16.6 (16.5)	2.02 (2.07)	10.8 (11.0)	Yellow	5.2
$PdBr_2 \cdot 2DTZ$	11.2 (11.3)	19.5 (19.4)	2.38 (2.45)	12.9 (13.0)	Yellow	Insoluble
$PdBr_2 \cdot DTZ$	7.2 (7.4)	12.6 (12.6)	1.53 (1.59)	8.5 (8.4)	Brown	4.3
$PdI_2 \cdot 2DTZ$	9.3 (9.5)	16.2 (16.3)	2.00 (2.06)	10.5 (10.9)	Green–grey	Insoluble
$PdCl_2 \cdot 2ATZ$	22.0 (22.1)	12.7 (12.7)	1.63 (1.59)	17.0 (16.9)	Yellow	5.1
$PdCl_2 \cdot ATZ$	14.8 (15.1)	8.6 (8.6)	1.09 (1.09)	11.3 (11.5)	Apricot	5.6
$PdBr_2 \cdot 2ATZ$	17.9 (17.9)	10.7 (10.3)	1.22 (1.29)	13.2 (13.7)	Dark yellow	3.9
$PdBr_2 \cdot ATZ$	11.3 (11.4)	6.9 (6.5)	0.79 (0.82)	8.4 (8.7)	Brick-red	6.5
$PdI_2 \cdot 2ATZ$	14.6 (14.9)	8.6 (8.5)	1.09 (1.08)	11.2 (11.4)	Brown	4.9
$PdCl_2 \cdot 2MATZ$	20.6 (20.6)	18.0 (17.7)	2.43 (2.47)	15.9 (15.7)	Yellow	3.1
$PdCl_2 \cdot MATZ$	14.1 (14.4)	12.6 (12.3)	1.69 (1.72)	10.9 (11.0)	Yellow	4.3
$PdBr_2 \cdot 2MATZ$	16.8 (16.9)	14.7 (14.5)	2.01 (2.03)	12.9 (12.9)	Mustard	4.9
$PdBr_2 \cdot MATZ$	10.7 (11.0)	9.8 (9.5)	1.27 (1.32)	8.2 (8.4)	Ochre	5.0
$PdI_2 \cdot 2MATZ$	14.4 (14.2)	12.2 (12.2)	1.73 (1.71)	10.6 (10.9)	Brown	8.6
$PdCl_2 \cdot 2.5EATZ$	20.7 (21.0)	24.2 (24.0)	3.49 (3.53)	15.9 (16.0)	Yellow	3.9
$PdCl_2 \cdot EATZ$	13.5 (13.7)	15.8 (15.7)	2.40 (2.30)	10.3 (10.5)	Dark yellow	3.8
$PdBr_2 \cdot 2EATZ \cdot H_2O$	15.5 (15.5)	17.8 (17.7)	2.83 (2.97)	11.7 (11.8)	Dark yellow	4.0
$PdBr_2 \cdot EATZ$	10.8 (10.6)	12.4 (12.2)	1.78 (1.78)	8.1 (8.1)	Light brown	4.8
$PdI_2 \cdot 2EATZ$	13.5 (13.6)	15.9 (15.5)	2.32 (2.28)	10.1 (10.4)	Orange brown	4.2
$PdCl_2 \cdot 3MTTZ$	14.7 (14.6)	19.2 (18.8)	1.97 (2.11)	33.7 (33.5)	Orange	55.1
$PdCl_2 \cdot MTTZ \cdot H_2O$	8.4 (8.5)	10.9 (11.0)	1.60 (1.85)	18.9 (19.6)	Red brown	Insoluble
$PdBr_2 \cdot 1.5MTTZ$	9.0 (9.0)	11.7 (11.6)	1.30 (1.30)	20.7 (20.7)	Sienna	67.3
$PdBr_2 \cdot MTTZ$	7.0 (7.0)	9.2 (9.0)	0.93 (1.01)	16.4 (16.1)	Light brown	35.5
$PdI_2 \cdot 2MTTZ$	9.0 (9.0)	11.8 (11.5)	1.40 (1.29)	20.8 (20.5)	Deep red	87.6

* Ω^{-1} mol^{-1} cm^2 in 10^{-3} M DMF solutions.

Table 2. Principal infrared bands (cm^{-1}) of the ligands and their complexes

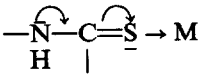
		L	$PdX_2 \cdot 2L$	$PdX_2 \cdot L$
DTZ	ν(C–S)	642vs	693–690 (sm-m) 663–660 (vs-s)	690–685 (ms-mw)
ATZ	ν(C=N)	1507vs	1590–1582 (vs) 1520–1512 (vs-s)	1595 (sh) 1530–1528 (s)
	ν(C–S)	680s 610m	720–717 (ms-wm) 635–628 (w)	720–717 (m-sh) 630 (w)
MATZ	ν(C=N)	1540ms	1586–1583 (vs)	1548 (s-sm)
	ν(C–S)	685m 649m	723–720 (m) 682–680 (w) 658–650 (m)	725–718 (s-ms) 695–690 (m)
EATZ	ν(C=N)	1545s 1517vs	1580–1560 (vs) 1555–1540 (sh)	1587–1582 (vs)
	ν(C–N)	1198s	1150–1148 (s-m)	1150 (m)
	ν(C–S)	610w	690 (m-w) 632–628 (w)	665 (w) 625 (wm)
MTTZ	ν(C–N)	1268vs	1290–1280 (s-ms)	1265–1223 (w)
	ν(C=S)	740vs	740–680 (m)	715–690 (w)

thiadiazole (650 cm^{-1})[6] and 2-amino-5-phenyl-1,3,4-thiadiazole (648 cm^{-1}).[7] Their frequencies increase for the $PdX_2 \cdot 2L$ and for most of the $PdX_2 \cdot L$ complexes in agreement with an electronic shift from the ring sulphur atom toward the ring, excluding a coordination of this atom to the metal ion. For DTZ the coordination site(s) is or are therefore the ring nitrogen atom(s).

Table 3. Principal far-infrared bands of the complexes

	ν PdX		ν PdN_{ring}		ν $PdNR_2$		ν PdS	
$PdCl_2 \cdot 2DTZ$	340vs	306s	306s	250mw				
$PdBr_2 \cdot 2DTZ$	283vs	245mw	303s	247wm				
$PdI_2 \cdot 2DTZ$	183mw	160s	298s	244mw				
$PdCl_2 \cdot 2ATZ$	354s	314m			354s	275sm		
$PdBr_2 \cdot 2ATZ$	277sm	262sm			344sm	277sm		
$PdI_2 \cdot 2ATZ$	229vs	158m			364vs	276m		
$PdCl_2 \cdot 2MATZ$	354vs	321vs			321vs	252ms		
$PdBr_2 \cdot 2MATZ$	285s	249m			314s	249m		
$PdI_2 \cdot 2MATZ$	184mw	159mw			315vs	262m		
$PdCl_2 \cdot 2.5EATZ$	353vs	303mw			353vs	274mb		
$PdBr_2 \cdot 2EATZ \cdot H_2O$	276s	260vs			352wm	276s		
$PdI_2 \cdot 2EATZ$	224s	148s			376s	278s		
$PdCl_2 \cdot 3MTTZ$	335m	326m					375vs	335m
$PdBr_2 \cdot 1.5MTTZ$	278sm	243w					375vs	333ms
$PdI_2 \cdot 2MTTZ$	220s	175m					374vs	332ms
$PdCl_2 \cdot DTZ$	352vs			250m				
$PdBr_2 \cdot DTZ$	275sm	205s	319vs	248w				
$PdCl_2 \cdot ATZ$	345vs	300m		250sm	345vs			
$PdBr_2 \cdot ATZ$	278mw	201vs	300vs		380sb			
$PdCl_2 \cdot MATZ$	352vs			248s	324sh			
$PdBr_2 \cdot MATZ$	277ms	201vs			328s			
$PdCl_2 \cdot EATZ$	349vs		300w		349vs			
$PdBr_2 \cdot EATZ$	278mw		300s		353w			
$PdCl_2 \cdot MTTZ \cdot H_2O$	334vs			280wm				334vs
$PdBr_2 \cdot MTTZ$	274sm			262sm				334w

The ligand MTTZ does not show any ν(SH) band in the 2600–2500 cm^{-1} region in which this stretching frequency is generally expected[4] and is therefore mainly in its thioketo form.[8] Its band at 1268 cm^{-1} may be assigned to the ν(C–N) mode while the band at 740 cm^{-1} may be assigned to the ν(C=S) mode. The frequencies of these bands increase and decrease, respectively, in the $PdX_2 \cdot 2L$ complexes in agreement with he electronic shift due to the coordination of the ligand through the thiocarbonylic sulphur atom.

(B) 

In the $PdX_2 \cdot 2DTZ$ complexes DTZ is bonded as N-monodentate ligand, the resulting unsymmetrical molecule showing two ν(C–S) bands at higher frequencies than the single ν(C–S) band of the symmetrical free ligand molecule. In the $PdX_2 \cdot DTZ$ complexes DTZ acts as a N,N-bridging ligand re-establishing the molecular symmetry with two equivalent C–S bonds having the same ν(C–S) frequency.

In the other $PdX_2 \cdot 2L$ complexes ATZ, MATZ and EATZ are bonded through the exocyclic amino nitrogen atom and MTTZ through the exocyclic thiocarbonylic sulphur atom. Their $PdX_2 \cdot L$ complexes may achieve the square planar coordination by bridging either the halide ions or the ligand molecule. Some of the infrared bands of these complexes are different in frequency and/or intensity from those of the corresponding $PdX_2 \cdot 2L$ complexes, indicating a different coordination of the ligand molecule in the two cases.

Some new bands in the far-infrared spectra may be assigned to ν(PdX) or ν(PdL) modes. The $PdX_2 \cdot 2L$, $PdCl_2 \cdot 2.5EATZ$, $PdCl_2 \cdot 3MTTZ$ and $PdBr_2 \cdot 1.5MTTZ$ complexes show two ν(PdX) bands with normal frequencies for terminal PdX bonds[9–12] and two ν(PdL) bands corresponding to a square planar *cis* coordination. Some of the ν(PdX) bands are superimposed or coupled with ν(PdN) or ν(PdS) bands. The $\nu(PdN_{ring})$ frequencies are, as expected, lower than those of the $\nu(PdNR_2)$ bands involving exocyclic nitrogen atoms. The ν(PdS) frequencies are in agreement with those observed for PdS bonds involving thiocarbonylic sulphur atoms.[9,13,14] The $PdCl_2 \cdot 2.5EATZ$, $PdCl_2 \cdot 3MTTZ$ and $PdBr_2 \cdot 1.5MTTZ$ complexes may therefore have the constitution $[PdCl_2 \cdot 2EATZ]0.5EATZ$, $[PdCl_2 \cdot 2MTTZ]MTTZ$ and $[PdBr_2 \cdot 2MTTZ][PdBr_2 \cdot MTTZ]$.

For the $PdX_2 \cdot DTZ$ complexes, in which DTZ acts as N,N-bidentate ligand, the number of ν(PdX) and $\nu(PdN_{ring})$ bands (Table 3) indicates that the chloride and the bromide could have a *trans* and *cis* 2X, 2N)-coordination, respectively. For most of the other $PdX_2 \cdot L$ complexes besides the band due to the coordination of the exocyclic atom another band due to the coordination of an endocyclic nitrogen atom may be assigned, supporting the view that L acts as a bidentate ligand in these complexes.

Acknowledgement—Infrared spectra were recorded in the Centro Strumenti of the University of Modena.

REFERENCES

1. G. Maffii, E. Testa and R. Ettorre, *Il Farmaco, Ed. Scientifica* 1958, **13**, 187.
2. E. Testa, G. G. Gallo, F. Fava and G. Weber, *Gazz. Chim. Ital.* 1958, **88**, 812.
3. M. M. Ciotti, S. R. Humphreys, J. M. Venditti, N. Kaplan and A. Goldin, *Cancer Research* 1960, **20**, 1195.
4. C. N. R. Rao, *Chemical Applications of Infrared Spectroscopy*, pp. 251, 297. Academic Press, New York (1963).
5. W. J. Geary, *Coord. Chem. Rev.* 1971, **7**, 81.
6. N. B. Singh, J. Singh and K. K. Pathak, *Transition Met. Chem.* 1980, **5**, 60.
7. N. B. Singh and J. Singh, *J. Inorg. Nucl. Chem.* 1979, **41**, 1384.
8. A. C. Fabretti, G. C. Franchini and G. Peyronel, *Spect. Acta* 1980, **36A**, 517.
9. G. Peyronel, A. C. Fabretti and G. C. Pellacani, *J. Inorg. Nucl. Chem.* 1973, **35**, 973.
10. A. C. Fabretti, G. C. Pellacani and G. Peyronel, *Gazz. Chim. Ital.* 1973, **103**, 397.
11. D. A. Duddell, P. L. Goggin, R. J. Goodfellow, M. G. Norton and J. G. Smith, *J. Chem. Soc. (A)* 1970, 545.
12. E. Allen, N. P. Johnson, D. T. Rosevear and W. Wilkinson, *J. Chem. Soc. (A)* 1970, 2137.
13. A. C. Fabretti, G. C. Franchini and G. Peyronel, *Transition Met. Chem.* 1978, **3**, 355.
14. I. Ojima, T. Iwamoto, T. Onichi, N. Inamoto and K. Tamaru, *J. Chem. Soc., Chem. Commun.* 1969, 150.

Polyhedron Vol. 4, No. 6, pp. 993–997, 1985
Printed in Great Britain

0277-5387/85 $3.00 + .00
© 1985 Pergamon Press Ltd

THE TRIS(PICOLINATE)VANADATE(II) ION: REDOX PROPERTIES AND ELECTRON TRANSFER KINETICS WITH COBALT(III) AMINES

HENRIQUE E. TOMA* and FERNANDO T. P. LELLIS
Instituto de Quimica, Universidade de São Paulo, CP 20780, São Paulo, SP, Brazil

(*Received* 2 *July* 1984; *accepted after revision* 6 *October* 1984)

Abstract—Vanadium(II) ions form with the pyridine-2-carboxylate ligand a deep blue, tris-substituted complex absorbing at 660 nm ($\varepsilon = 7.2 \times 10^3\ M^{-1}\,cm^{-1}$) with a shoulder at 450 nm. Reversible spectroelectrochemistry and cyclic voltammetry were observed for this complex, with $E_{1/2} = -0.448$ V vs NHE, and $\Delta S^{\circ}_{rc} = -6\ cal \cdot mol^{-1} \cdot deg^{-1}$. Electron transfer kinetics with $[Co(en)_3]^{3+}$ led to $k_{12} = 3100\ M^{-1}\,s^{-1}$, $\Delta H^{+} = 12.4\ kcal \cdot mol^{-1}$ and $\Delta S^{+} = -0.9\ cal \cdot mol^{-1} \cdot deg^{-1}$ ($I = 0.10$ M). For the related $[Co(NH_3)_6]^{3+}$ complex, $k_{13} = 1.9 \times 10^4\ M^{-1}\,s^{-1}$. The self-exchange rate constant and activation parameters were analysed in terms of relative Marcus theory.

This work deals with the properties and reactivity of the tris(picolinate)vanadate(II) ion.[1] Vanadium(II) complexes are extraordinary in terms of redox reactivity, particularly with respect to oxygen, water and dinitrogen. Because of this, however, only a few complexes have been investigated in aqueous solution.

The $[V(pic)_3]^-$ complex is not an exception in terms of reactivity; however, its unusual deep blue color, in addition to a long life-time in aqueous solution, stimulate spectroscopic and electrochemical studies which are particularly important in vanadium(II) chemistry. The π-conducting picolinate ligand is expected to improve the electron transfer characteristics of the vanadium(II) complex, e.g. increasing the adiabaticity making it useful as a strongly reducing probe in studies of redox reactivity of inorganic and biological complexes.[2,3] To evaluate this point, we have studied the kinetics of the $[Co(en)_3]^{3+}[V(pic)_3]^-$ and $[Co(NH_3)_6]^{3+}$ $[V(pic)_3]^-$ electron transfer reactions, including a relative Marcus theory evaluation of the self-exchange rate constants and the corresponding activation parameters.

EXPERIMENTAL

Aqueous vanadium(II) ions were generated from vanadium(III) trichloride (Alfa) or vanadyl trifluoroacetate solutions, in the presence of zinc amalgam, under argon atmosphere. Lithium picolinate was prepared by reacting picolinic acid (Aldrich) and lithium hydroxide (Fisher), and recrystallized several times from aqueous solution, after a treatment with activated charcoal to remove eventual oxidizing impurities. The tris(picolinate)vanadate(II) complex was always freshly prepared by reacting aqueous vanadium(II) ions with an excess of the picolinate ligand, under argon atmosphere. The ionic strength was adjusted with lithium trifluoroacetate, because vanadium(II) ions are not stable in perchlorate solutions. The complexes $[Co(NH_3)_6](ClO_4)_3$, $[Co(en)_3]I_3$ and $[Co(en)_3]Cl_3$ were prepared as described in the literature.[4,5]

All the measurements in this work were carried out under argon atmosphere. Cyclic voltammetry was performed with a Princeton Applied Research Corporation instrument, consisting of a 173 potentiostat and a 175 Universal programmer. A gold disk electrode was employed for the measurements, with Ag/AgCl (1 M KCl) as the reference electrode, using the conventional Luggin capillary arrangement to minimize the ohmic drop. A platinum wire was used as the auxiliary electrode. Temperature dependence studies were performed using a non-isothermic arrangement, as described in the literature.[6]

The electronic spectra of the complexes in the visible and near-UV region were recorded on a Cary 17 spectrophotometer, fitted with thermostatted cell

* Author to whom correspondence should be addressed.

compartments. Spectroelectrochemical measurements were performed with a PAR 173 potentiostat, in parallel with the Cary 17 spectrophotometer. A three electrode system was designed for a rectangular quartz cell of 0.3 mm internal optical pathlength. A gold minigrid was used as transparent working electrode, in the presence of a small Ag/AgCl reference electrode and of a platinum auxiliary electrode.

The stopped-flow kinetics were carried out with a Durrum D-150 instrument, equipped with a Kel-F flow system. The kinetics were studied under pseudo-first order conditions, by following the decay of the absorption band of the $[V(pic)_3]^-$ complex at 660 nm, in the presence of an excess of the oxidizing agent.

RESULTS AND DISCUSSION

Vanadium(II) ions react with picolinate ligands producing violet–blue complexes in aqueous solution. A small excess of the free ligand, e.g. 10^{-3} M, is enough to convert the intermediate successive complexes to the tris(picolinate)vanadate(II) ion, which has a stability constant of 7.6×10^{13} M^{-3}, at 25°C, and $I = 0.6$ M (lithium trifluoroacetate).[1]

The deep blue color of $[V(pic)_3]^-$ fades within a few hours in deaerated solutions, even under continuous flow of argon. For this reason, the spectra of the tris-picolinate ion were obtained spectroelectrochemically, as shown in Fig. 1, with a gold minigrid electrode kept at −800 mV vs Ag/AgCl (1 M KCl). A strong absorption band is observed at 660 nm, with a shoulder around 450 nm. The extinction coefficients are 7.2×10^3 and 4×10^3 $M^{-1}\,cm^{-1}$, respectively. We assigned these bands to charge transfer transitions from the metal d_π orbitals to the ligand p_π orbitals, in comparison to the spectra of the iron(II) picolinates and related complexes.[7]

Spectroelectrochemistry of $[V(pic)_3]^-$ is Nernstian up to −0.600 V, corresponding to a reversible monoelectronic oxidation process, with $E^\circ \cong -0.68$ V vs Ag/AgCl (1 M KCl), at 28°C, in the presence of 0.100 *M* lithium picolinate and 0.400 *M* lithium trifluoroacetate. Oxidation proceeds irreversibly above −0.500 V, generating vanadium(IV) complexes.

Cyclic voltammograms of the tris-substituted complex, in the presence of 0.35 M lithium picolinate and 0.60 *M* lithium trifluoroacetate were reversible, with a linear behaviour of the peak currents vs the concentration of the vanadium complex, and the square root of the scan rates. The peak separation is close to 60 mV, with $E_{1/2} = -0.670$ V vs Ag/AgCl (1 M KCl) or −0.448 V vs NHE, and a diffusion coefficient of 4.8×10^{-6} $cm^2\,s^{-1}$, at 25°C. The

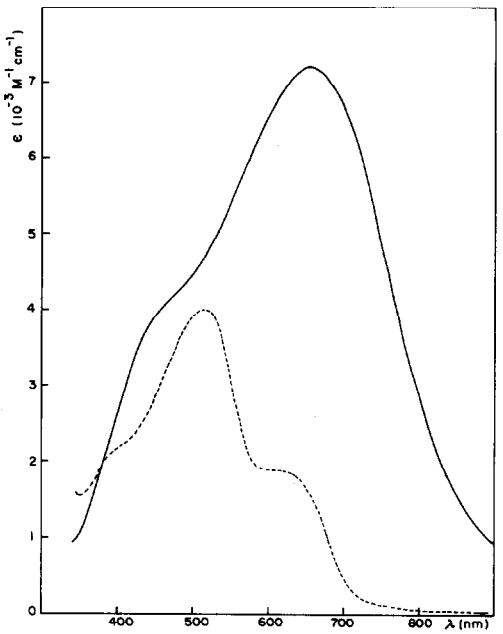


Fig. 1. Electronic spectra of $V(pic)_3^-$ (——) and $V(pic)_3$ (– – –) obtained spectroelectrochemically at −800 and −500 mV vs NHE, respectively, in the presence of 0.10 M lithium picolinate and 0.40 M lithium trifluoroacetate.

half-wave potentials measured at 5, 15, 35 and 45°C were −0.664, −0.667, −0.672 and −0.675 V, respectively. From these values we have calculated the redox couple entropy, $\Delta S^\circ_{rc} = -6$ $cal \cdot mol^{-1} \cdot deg^{-1}$.

The equilibrium constant of the tris(picolinate)vanadium(III) complex, based on equation (1) is 2.1×10^{15} M^{-3}, with $E^\circ_{V(H_2O)_6^{3+/2+}} = -0.253$ V.

$$\Delta E^\circ_{V(pic)_3^{0/-1}} = \Delta E^\circ_{V(H_2O)_6^{3+/2-}} + \frac{RT}{nF} \ln \frac{\beta_{II}}{\beta_{III}}. \quad (1)$$

The electron transfer reaction of $[V(pic)_3]^-$ and $[Co(en)_3]^{3+}$ proceeds according to a first order kinetics for at least three half-lives, in the presence of an excess of the cobalt(III) complex.

$$[V(pic)_3]^- + [Co(en)_3]^{3+} \xrightarrow{k_{12}} V(pic)_3 + [Co(en)_3]^{2+}$$

$$-\frac{d[V(pic)_3^-]}{dt} = k_{12}[V(pic)_3^-][Co(en)_3^{3+}]. \quad (2)$$

The experimental rate law is consistent with an outer sphere mechanism, where $k_{12} = 3100$ M^{-1} s^{-1}, at 25°C, and $I = 0.100$ *M* (KCl, or lithium trifluoroacetate). No evidence for rate saturation has been detected under the conditions employed for the experiments. The kinetics data at several temperatures are shown in Table 1.

Table 1. Kinetic results for the $V(pic)_3^-$–$Co(en)_3^{3+}$ and $V(pic)_3^-$–$Co(NH_3)_6^{3+}$ reactions

T (°C)	I (M)	[Co(III)] (M)	k_{obs}* (s^{-1})	k_{ij} ($M^{-1}\,s^{-1}$)
16.8	0.10†	5.90×10^{-3}‡	9.4	1.59×10^3
20.2	0.10†	5.90×10^{-3}‡	12.6	2.13×10^3
25.0	0.10†	2.04×10^{-3}‡	6.0	2.95×10^3
25.0	0.10†	2.37×10^{-3}‡	7.5	3.16×10^3
25.0	0.10§	5.00×10^{-3}‖	16.5	3.3×10^3
25.0	0.10†	5.90×10^{-3}‡	18.5	3.13×10^3
25.0	1.00†	5.90×10^{-3}‡	15.1	2.6×10^3
25.0	0.10†	9.30×10^{-3}‡	28.9	3.10×10^3
25.0	0.10§	1.00×10^{-2}‖	30.0	3.00×10^3
25.0	0.10§	1.75×10^{-2}‖	53	3.2×10^3
25.0	0.10§	2.50×10^{-2}‖	79	3.16×10^3
30.0	0.10†	5.90×10^{-3}‡	27.4	4.7×10^3
35.0	0.10†	5.90×10^{-3}‡	37.5	6.3×10^3
25.0	0.090§	1.00×10^{-3}¶	22.0	2.2×10^4
25.0	0.090§	2.00×10^{-3}¶	38	1.90×10^4
25.0	0.090§	5.00×10^{-3}¶	91	1.82×10^4

* $[V(pic)_3^-] = 3\times10^{-5}$ M, in the presence of 0.04 M lithium picolinate, pH 6.

† Ionic strength adjusted with KCl.

‡ $[Co(en)_3]Cl_3$.

§ Ionic strength adjusted with lithium trifluoroacetate.

‖ $[Co(en)_3]I_3$.

¶ $[Co(NH_3)_6](ClO_4)_3$.

To evaluate the self-exchange rate constants for the $[V(pic)_3]^-$ complex, we have employed the Marcus theory with the Wherland–Gray[8] formalism for the work terms, W_{ii} and W_{ij}. The reorganization free energies, ΔG_{ii}^{**} are given by the equation,

$$\Delta G_{11}^{**} = 2\Delta G_{12}^{**} - \Delta G_{22}^{**} - \Delta G_r^\circ(1-\alpha_{12}), \quad (3)$$

where

$$\alpha_{12} = \frac{\Delta G_r^\circ}{4(\Delta G_{11}^{**} + \Delta G_{22}^{**})} \quad (4)$$

and

$$\Delta G_{12}^{**} = \Delta G_{12}^{*} - W_{12} \quad (5)$$

$$\Delta G_{11}^{**} = \Delta G_{11}^{*} - W_{11} \quad (6)$$

$$\Delta G_{22}^{**} = \Delta G_{22}^{*} - W_{22} \quad (7)$$

$$\Delta G_r^\circ = \Delta G_{12}^\circ - W_{12} + W_{21}. \quad (8)$$

Analogously to Wherland and Gray,[9] we have used a pre-exponential factor of 6×10^{12} $M^{-1}\,s^{-1}$ (instead of 10^{11} $M^{-1}\,s^{-1}$) in the Marcus equation, as in the semiclassical formalism[10]

$$k = \kappa_{el}\Gamma_n V v_n \exp-(\Delta G^*/RT), \quad (9)$$

where the product of the electronic and nuclear tunneling factors, $\kappa_{el}\Gamma_n$, is close to unity; $V = 4\pi Nr^3/300$; v_n is the nuclear vibration frequency, and $V\cdot v_n \cong kT/h$.

The self-exchange rate constant, k_{22}, for the $[Co(en)_3]^{3+}$ complex has been measured by Lewis *et al.*[11] and by Dwyer and Sargeson[12] as 5.2×10^{-5} $M^{-1}\,s^{-1}$ and 7.7×10^{-5} $M^{-1}\,s^{-1}$ (25°C, $I = 1$ M), respectively. The extrapolated value at $I = 0.1$ M is 2.75×10^{-5} $M^{-1}\,s^{-1}$. The input and output parameters are given in Table 2.

The calculated self-exchange rate constant for the $[V(pic)_3]^{0/-}$ couple, based on the $[Co(en)_3]^{3+}$–$[V(pic)_3]^-$ reaction is 9.7×10^5 $M^{-1}\,s^{-1}$, at $I = 0.100$ M. This value is in good agreement with preliminary data based on Co(sepulchrate)$^{3+}$ and bis(histidinate)–cobalt(III) complexes.[1] In comparison to the self-exchange rate constant for the $[V(H_2O)_6]^{3+/2+}$ couple, ($k_{ii} = 1.0\times10^{-2}$ $M^{-1}\,s^{-1}$ at $I = 1.0$ M), one can see that electron-transfer in the picolinate complex is more effective by seven orders of magnitude. Part of this difference arises from the work term, which is null for $[V(pic)_3]^{0/-}$ and 0.79 kcal mol^{-1} for $[V(H_2O)_6]^{3+/2+}$. The major contribution, however, comes from the smaller reorganization barrier, ΔG_{ii}^{**}, of the $[V(pic)_3]^-$ complex.

The reorganization entropies, ΔS_{ii}^{**} and ΔS_{ij}^{**}, are given by

$$\Delta S_{12}^{**} = \left(\frac{\Delta S_{11}^{**}}{2} + \frac{\Delta S_{22}^{**}}{2}\right)(1-4\alpha_{12}^2) + \frac{\Delta S_r^\circ}{2}(1+2\alpha_{12}), \quad (10)$$

where

$$\Delta S_{11}^{**} = \Delta S_{11}^{*} + \frac{\partial W_{11}}{\partial T} \quad (11)$$

$$\Delta S_{22}^{**} = \Delta S_{22}^{*} + \frac{\partial W_{22}}{\partial T} \quad (12)$$

$$\Delta S_{12}^{**} = \Delta S_{12}^{*} + \frac{\partial W_{12}}{\partial T} \quad (13)$$

$$\Delta S_r^\circ = \Delta S_{12}^\circ + \frac{\partial W_{12}}{\partial T} - \frac{\partial W_{21}}{\partial T}. \quad (14)$$

The reaction entropy ΔS_{12}° can be obtained from the difference of the experimental redox couple entropies:

$$\Delta S_{12}^\circ = \Delta S_{rc[Co(en)_3^{3+/2+}]}^\circ - \Delta S_{rc[V(pic)_3^{0/-}]}^\circ. \quad (15)$$

Derivation of the work terms is given by[10]

$$\frac{\partial W}{\partial T} = -\frac{W}{2T(1+\beta r I^{1/2})}\left[2\left(\frac{\partial \ln D_s}{\partial \ln T}\right) + \beta r I^{1/2}\left(\frac{\partial \ln D_s}{\partial \ln T}\right) - \beta r I^{1/2}\right] \quad (16)$$

Table 2. Self-exchange rate constants and activation parameters for the $V(pic)_3^-$–$Co(en)_3^{3+}$ system at 25°C and $I = 0.10$ M

	V(II)/Co(III)	Co(III)/Co(II)	V(III)/V(II)
r (10^2 pm)	5.6/3.4	3.4/3.5	5.5/5.6
W_{ij}, W_{ii} (kcal·mol^{-1})	−0.604	1.892	0
$\frac{\partial W_{ij}}{\partial T}$, $\frac{\partial W_{ii}}{\partial T}$ (cal·mol^{-1}·deg^{-1})	2.87*	9.07*	0
	2.59†	8.20†	0
ΔE°, E_{rc}° (V vs NHE)	0.228	−0.220	−0.448
		−0.216‡	
k_{ij}, k_{ii} (M^{-1} s^{-1})	3.1×10^3	2.7×10^{-5}	9.7×10^5
ΔG_{ij}^{**}, ΔG_{ii}^{**} (kcal·mol^{-1})	13.28	21.76	9.28
ΔS_{12}°, ΔS_{rc}° (cal·mol^{-1}·deg^{-1})	41	35	−6
		37‡	
ΔS_{ij}^{**}, ΔS_{ii}^{**} (cal·mol^{-1}·deg^{-1})	3.9*	−22.6*	−10.2*
	3.7†	−23.5†	−9.7†
ΔS_{ij}^{*}, ΔS_{ii}^{*} (cal·mol^{-1}·deg^{-1})	−0.9	−33.7§	−12.1*
			−11.6†
ΔH_{ij}^{**}, ΔH_{ii}^{**} (kcal·mol^{-1})	14.4*	15.0*	6.2*
	14.4†	14.7†	6.4†
ΔH_{ij}^{*}, ΔH_{ii}^{*} (kcal·mol^{-1})	12.4	13.6§	5.6*
			5.8†

* Based on eqn (17).
† Eqn (16).
‡ Ref. 18.
§ Ref. 12.

or alternatively,[13] by

$$\frac{\partial W}{\partial T} = Z_1 Z_2 \left(0.868 I^{1/2} + \frac{19.5}{r}\right) \times \exp\left(-0.329 r I^{1/2}\right), \quad (17)$$

where D_s is the static dielectric constant, r is the metal–metal separation in the activated complex, and the other terms have the conventional meanings. For an adiabatic mechanism,[10]

$$\Delta S^* = \Delta S^{**} - \frac{\partial W}{\partial T} - R \quad (18)$$

and

$$\Delta H^* = \Delta H^{**} + W - T\frac{\partial W}{\partial T} - RT. \quad (19)$$

The calculated activation parameters for the $[Co(en)_3]^{3+/2+}$–$[V(pic)_3]^-$ reaction are presented in Table 2. As one can see in Table 2, the use of equations (16) and (17) leads to similar results for the $[V(pic)_3]^-$ complex.

In the present work we assumed an adiabatic mechanism for $[Co(en)_3]^{3+}$, based on recent theoretical calculations[14] and discussion.[15] As a matter of fact, the Franck–Condon or nuclear factors related to ΔG_{ii}^{**} have been estimated as 10^{-4}, in comparison to 10^{-3}–10^{-2} for the electronic factor associated with non-adiabaticity.[14] On the other hand, it has been shown that the electronic factor spans the range 10^{-3}–1 for typical iron and ruthenium complexes.

The reaction of $[V(pic)_3]^-$ with $[Co(NH_3)_6]^{3+}$ follows a rate-law analogous to that for the $[Co(en)_3]^{3+}$ reaction, with $k_{13} = 1.9 \times 10^4$ M^{-1} s^{-1}, as shown in Table 1. According to Marcus theory, the ratio k_{13}/k_{12} for electron transfer with hexaamine and ethylenediamine complexes should be relatively constant.[15] Typical values from the literature for V^{2+}, Cr^{2+}, $Cr(bipy)_3^{2+}$ and Co(sepulchrate)$^{2+}$ reactions with $[Co(NH_3)_6]^{3+}$ and $[Co(en)_3]^{3+}$ complexes vary from 2.9 to 18.1. Our experimental value of k_{13}/k_{12} is 6.1.

Using the calculated self-exchange rate constant for $[V(pic)_3]^-$, we have estimated k_{33} for the $[Co(NH_3)_6]^{3+/2+}$ couple, assuming $r(Co^{II}) = 0.34$ nm, $r(Co^{III}) = 0.32$ nm and $E_{rc}^\circ = 0.057$ V,[16] or 0.018 V.[17] Our result for k_{33} was 2.5×10^{-6} M^{-1} s^{-1}, or 6.7×10^{-7} M^{-1} s^{-1}, respectively. This is in good agreement with the range of values recently proposed in the literature.[15,19]

Acknowledgements—We thank FAPESP and CNPq for support.

REFERENCES

1. F. T. P. Lellis, Thesis, University of Sao Paulo, Brazil, pp. 1–123 (1983).
2. N. Sutin, *Bioinorganic Chemistry II*, *Adv. Chem. Ser.*, *162* (Edited by K. N. Raymond), pp. 157–172. American Chemical Society, Washington (1977).
3. A. Grant Mauk, C. L. Coyle, E. Bordignon and H. B. Gray, *J. Am. Chem. Soc.* 1979, **101**, 5054.
4. W. G. Palmer, *Experimental Inorganic Chemistry*, p. 530. Cambridge University Press, Cambridge (1970).
5. J. A. Broomhead, F. P. Dwyer and J. W. Hogarth, *Inorganic Syntheses*, Vol. 6, p. 183. McGraw Hill, New York (1960).
6. S. Sahami and M. J. Weaver, *J. Electroanal. Chem.* 1981, **122**, 155.
7. H. E. Toma and R. H. U. Borges, *J. Coord. Chem.* 1981, **11**, 143.
8. S. Wherland and H. B. Gray, *Proc. Natl. Acad. Sci. USA* 1976, **73**, 2950.
9. S. Wherland and H. B. Gray, in *Biological Aspects of Inorganic Chemistry* (Edited by D. Dolphin *et al.*), pp. 289–368. Wiley, New York (1977).
10. N. Sutin, in *Inorganic Reactions and Methods* (Edited by J. J. Zuckerman). Springer Verlag, West Berlin (in press).
11. W. B. Lewis, C. D. Coryell and J. W. Irvine, Jr., *J. Chem. Soc.* 1949, S386.
12. F. P. Dwyer and A. M. Sargeson, *J. Phys. Chem.* 1961, **65**, 1892.
13. F. Moattar, J. R. Walton and L. R. Bennett, *Inorg. Chem.* 1983, **22**, 550.
14. N. Sutin, *Acc. Chem. Res.* 1982, **15**, 275.
15. D. Geselowitz and H. Taube, in *Adv. Inorg. and Bioinorg. Mechanisms* (Edited by A. G. Sykes), Vol. 1, pp. 391–407. Academic Press, London (1982).
16. J. Bjerrum, *Metal Ammine Formation in Aqueous Solution*. P. Haase and Son, Copenhagen (1957).
17. A. M. Bond, G. A. Lawrance, P. A. Lay and A. M. Sargeson, *Inorg. Chem.* 1983, **22**, 2010.
18. S. Sahami and M. J. Weaver, *J. Electroanal. Chem.* 1981, **122**, 171.
19. A. Hammershoi, D. Geselowitz and H. Taube, *Inorg. Chem.* 1984, **23**, 979.

Polyhedron Vol. 4, No. 6, pp. 999–1005, 1985
Printed in Great Britain

0277–5387/85 $3.00 + .00
© 1985 Pergamon Press Ltd

CONVERSION OF A PHENYLIMIDO COMPLEX TO A PHENYLAMIDO COMPLEX BY THE POTENTIALLY CHELATING LIGAND 2,3-DIMETHYL-2,3-BUTANDIOL(PINACOL-H_2): THE CRYSTAL AND MOLECULAR STRUCTURES OF $[W_2(NHPh)_2(\mu\text{-PINACOL})(PINACOL)_4]$ AND THE REACTION SIDE-PRODUCT $[W_2(NPh)_2(\mu\text{-O})(PINACOL)_2(PINACOL\text{-}H)_2]$

PAUL A. BATES, ALASTAIR J. NIELSON* and JOYCE M. WATERS†
Chemistry Department, Auckland University, Private Bag, Auckland, New Zealand

(*Received* 8 *August* 1984; *accepted* 6 *October* 1984)

Abstract—The interaction of 2 equivalents of 2,3-dimethyl-2,3-butandiol (pinacol-H_2) with $W(NPh)Cl_4$ in the presence of *t*-butylamine leads to the complexes $W(pinacol)_3$ (**1**), and $[W_2(NHPh)_2(\mu\text{-pinacol})(pinacol)_4]$ (**2**). A side-product of the reaction is $[W_2(NPh)(\mu\text{-O})(pinacol)_2(pinacol\text{-}H)_2]$ (**3**). When 3 or more equivalents of diol are used (**1**) is the sole product. The structures of (**2**) and (**3**) have been determined by single-crystal X-ray diffraction methods. Crystals of (**2**) are monoclinic, space group $C2/c$ with $a = 15.086(3)$, $b = 18.370(5)$, $c = 18.428(5)$ Å and $\beta = 106.04(2)°$; crystals of (**3**) are orthorhombic, space group *Pbca*, with $a = 10.571(1)$, $b = 22.449(12)$, $c = 34.142(5)$ Å. Both structures were solved by Patterson and Fourier methods and refined to an R value of 0.059 for the 1023 observed data of (**2**) and to $R = 0.071$ for the 1212 observed data of (**3**). In the amido complex (**2**) the W–N bond length is 2.02(2) Å with the longest W–O bond length of 2.00(2) Å lying *trans* to it. In the imido complex (**3**) the W–N bond length is 1.75(5) Å; the *trans* W–O bond length at 2.30(4) Å indicates lone-pair donation by the imido N.

Dialkylamido complexes ($M\text{–}NR_2$) of the transition metals are well known[1] but monoalkyl analogues (M–NHR) are less common. Attempts to prepare the latter can lead to polymerisation[2] or to formation of the imido group ($M{\equiv}NR$) by proton loss.[3] However stable complexes have been obtained by reaction of metal halides with amines[4] or silylamines[5] and by reduction of organoimido complexes with sodium–mercury amalgam.[6] Recent work has indicated that the nitrogen of earlier transition metal organoimides might act as a nucleophile[7] so that under appropriate conditions, protonation could lead to an amido complex. The 4-electron donor imido function is however generally robust[3] and apart from the amination of alkenes by osmium(VIII) organoimides,[8] few reactions have been reported.[9]

Recently it has been suggested that a potentially strong π-donating ligand, such as alkoxide, placed *trans* to an organo-imido function might force the M–N bond to act essentially as a 2-electron donor and thus enhance reactivity.[10] To this end we earlier prepared a series of d^0 tungsten phenylimido alkoxides but only lone-pair electron donation was found for ligands in the *trans* position.[11] In this paper we describe the results of our studies with the potentially chelating diol, 2,3-dimethyl-2,3-butandiol.

RESULTS AND DISCUSSION

Reactions of $W(NPh)Cl_4$ were carried out with 2,3-dimethyl-2,3-butandiol(pinacol-H_2), 2,3-butandiol, 2,4-dimethyl-2,4-pentandiol and 2,4-pentandiol using Et_3N or Me_3CNH_2 as proton acceptor to remove HCl and prevent cleavage of the imido function. However we have only been successful in identifying products for the reaction with pinacol-H_2. Thus reaction of 2 equivalents of this diol with $W(NPh)Cl_4$ in the presence of 5 equivalents of

* Author to whom correspondence should be addressed.
† Present address: Chemistry Department, Massey University, Palmerston North, New Zealand.

t-butylamine gave a red solution from which a red crystalline solid was obtained along with both yellow and colourless crystals. Attempts to recrystallise the physically separated red material invariably led to a lightening of solution colour and deposition of further yellow products. The colourless product also formed when the red crystals were reacted with pinacol-H_2.

With 3 or more equivalents of pinacol-H_2 the colourless product formed in good yield and was identified as W(pinacol)$_3$ (**1**). Aniline was produced as a product of the reaction. The complex shows apparent air stability but decomposes above 210°. In the IR spectrum, OH stretches are absent and a strong absorption occurs at 1140 cm^{-1} which is characteristic of ν(C–O).[12] Positive identification of ν(W–O) is not possible due to similarities of complex and free ligand but strong bands occur at 700 and 620 cm^{-1} similar to those in phenylimido tungsten alkoxides.[11] The ^{1}H NMR spectrum shows the absence of hydroxyl protons with the methyl groups appearing as two singlets, the one to higher field at the δ value of the free ligand methyl protons. Similarly the ^{13}C NMR spectrum contains two methyl carbon resonances and a single quaternary carbon resonance shifted 22 ppm downfield from the free ligand. We note that to reduce hydrogen interactions, the chelate rings would adopt a *gauche* conformation with its resulting ring puckering. Molecular models indicate that for this geometry, protons of two methyl groups would experience anisotropy effects from other chelate ring oxygens, leading to a downfield shift for half the methyl group proton resonances. While no attempt has been made to identify optical isomers, a recent report[13] indicates that in the presence of (+)-1-(9-anthryl)-2,2,2-trifluoro ethanol, one methyl group resonance in the ^{1}H NMR spectrum of W(pinacol)$_3$ splits into a doublet demonstrating a racemic mixture of both enantiomers of the chiral complex.

On prolonged standing of the reaction mixture at −20°C, large crystals of the red product formed and were separated manually. The IR spectrum was similar to W(pinacol)$_3$ (ν(C–O), 1130 cm^{-1}, ν(W–O) 620 cm^{-1}) and in addition contained absorbances characteristic of an aromatic ring (3020, 758 and 720 cm^{-1}); a weak band at 3325 cm^{-1} suggested NH or OH groups. Although not stable in $CDCl_3$ the ^{1}H NMR spectrum indicated one phenyl group to approximately 2.5 diols based on the ratio of phenyl and methyl protons. This evidence suggested species such as $W_2(NHPh)_2(pinacol)_5$ or $W_2(NPh)_2(pinacol)_4$(pinacol-H) but whereas C and H analytical data were close for these formulations, nitrogen analyses were always low.

An X-ray crystallographic structural analysis of the complex showed it to be the amido species $W_2(NHPh)_2(pinacol)_5$ (**2**) with one diol ligand bridging two tungsten atoms, the two halves being related by a C_2 crystallographic axis of symmetry. Each tungsten atom adopts a distorted octahedral geometry with the sites occupied by oxygens of two chelating diols and one half of the bridging diol, as well as a nitrogen of the phenylamido ligand. The dimers are loosely packed and there are no significantly short intermolecular contacts. One half of the molecule is shown in Fig. 1 and selected bond distances and angles are given in Table 1.

The bite angles of the bidentate ligands (74.1(8)° and 76.6(8)°) distort the octahedral geometry about the tungsten atom. Chelate ring puckering occurs with the expected *gauche* arrangement being adopted. This ensures that the methyl substituents are well separated with the torsion angle C(92)–C(9)–C(10)–C(102) of 40° being the smallest observed. In spite of this the coordination geometry dictates that the molecule is a sterically crowded one and a number of short intramolecular contacts occur particularly between methyl protons and oxygen atoms.

Although the NH proton was not located the W–N bond distance (2.02(2) Å) and W–N–C bond angle (134(2)°) indicate a phenylamido group. The W–N bond distance shows a small contraction (0.11–0.18 Å) compared with the Re–N distances found in the low valent phenylamido complexes Re(NHPh)$N_2(PMe_3)_4$ (Re–N, 2.200(14)Å) and

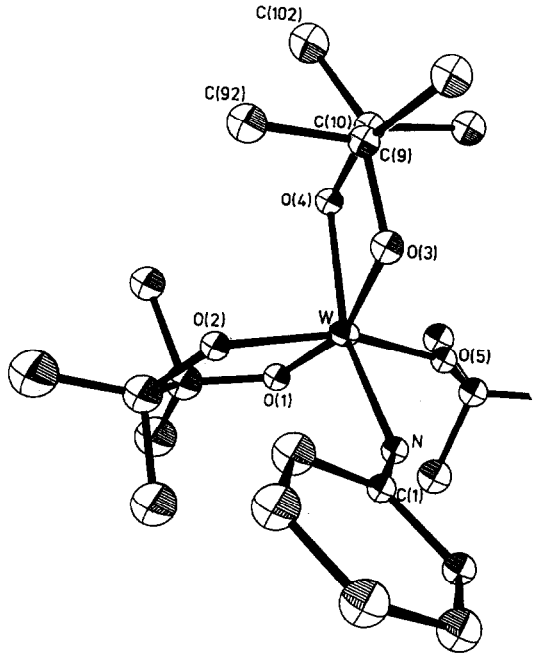


Fig. 1.

Table 1. Selected bond lengths and angles for (2)

Bond lengths (Å)		Bond angles (°)	
W–O(1)	1.92(2)	O(1)–W–O(2)	76.6(8)
W–O(2)	1.85(2)	O(3)–W–O(4)	74.1(8)
W–O(3)	1.96(2)	O(1)–W–O(3)	160.1(8)
W–O(4)	2.00(2)	O(2)–W–O(5)	159.7(8)
W–O(5)	1.80(2)	O–W–O(*cis*)	87.7–107.6(8)
W–N	2.02(2)	N–W–O(4)	157.6(8)
O–C	1.36–1.55(4)	N–W–O(*cis*)	82.1–110.6(9)
N–C(1)	1.39(3)	W–O–C	118–148(2)
C–C	1.42–1.65(5)	W–N–C(1)	134(2)

$Re(NHPh)C_4H_6(PMe_3)_3$ (2.13(3) Å)[6] in which 18 electron configurations are achieved without the need for pπ donation.* However the present W–N bond distance of 2.02(2) Å is similar to that found in $W(NMe_2)_6$ 2.03(3) Å where a degree of amido pπ donation is expected.[15] To achieve an 18 electron configuration O → Wπ donation is necessary in the equatorial plane where the W–O bond lengths range from 1.80(2) to 1.96(2) Å (estimated W–O single bond lengths are *ca.* 2.06 Å†). The W–O(4) bond (2.00(2) Å) which is *trans* to the phenylamido N is the longest of the W–O bonds observed (although not significantly different from W–O(3) at 1.96(2)) and probably involves the smallest amount of π-donation of all the donors. However a delicate balance between oxygen and nitrogen π-donation is likely to exist since both π systems are not necessarily required to satisfy the EAN rule. Since the *cis* W–O bond distances are 0.06–0.22 Å shorter than the W–N bond, whereas the bond radii of N and O differ only by *ca.* 0.05 Å,[14] it appears that oxygen π-bonding is the more dominant.

An X-ray analysis was also carried out on the yellow product obtained in small quantities by crystallisation of the original reaction mixture. The molecular structure consists of two tungsten atoms bridged by a single oxo ligand with further coordination about each metal by one phenylimido and two chelating diol ligands (Fig. 2). The bridging

* The expected reduction due to the difference in single bond metallic radii between W and Re is only 0.02 Å.[14]

† Mo–O bond lengths are calculated at 2.06 Å[16] and W and Mo have similar single bond metallic radii.[14]

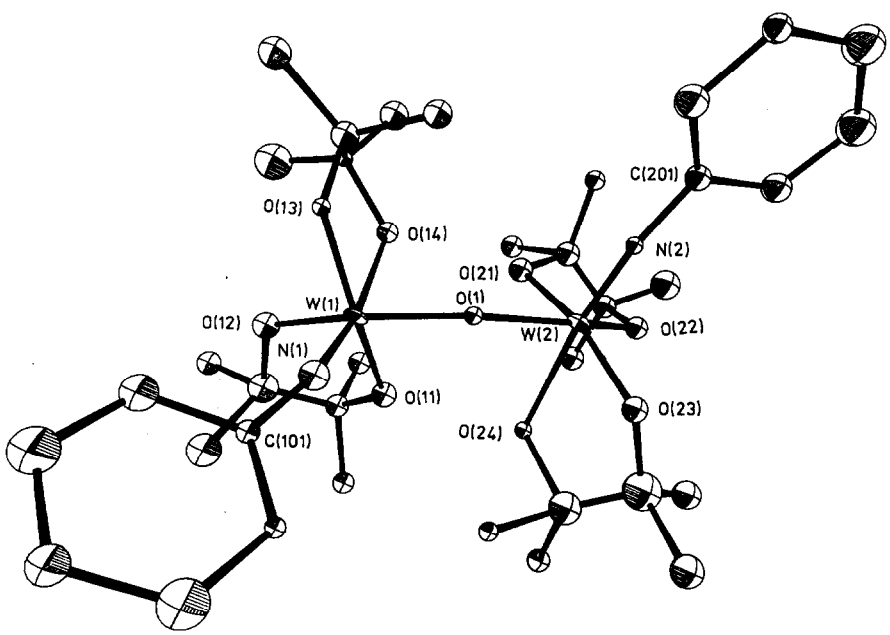


Fig. 2.

oxygen lies on an approximate two-fold rotation axis. Selected bond lengths and angles are given in Table 2.

The bite angles and puckering of the chelate rings are similar to those of the previous structure and again lead to a distorted octahedral geometry. To retain the +VI oxidation state for W, one chelate oxygen in each octahedron remains protonated and these are found to lie *trans* to the imido functions where the considerably longer W–O bond distances of 2.29(4) and 2.30(3) for W(1)–O(14) and W(2)–O(24), respectively, are observed (cf. 2.06 Å, estimated for a W–O single bond[16]). Although the hydroxyl protons were not located, calculated positions indicate the possibility of hydrogen bonding across the dimer (O(14)–H . . . O(21) and O(24)–H . . . O(11) with O . . . O distances of 2.54 and 2.55 Å, respectively, and estimated H . . . O approaches of 1.58 and 1.53 Å, respectively) which may contribute to the size of the W–O–W bond angle (157(2)°) as well as the octahedral distortion. The bridging W–O bond lengths are the same within the limits of accuracy of the structure (1.87(4) and 1.92(4) Å) indicating similar electron donation to both tungstens.

The structure thus shows similarities to [Mo (= O)(pinacol)(pinacol-H)]$_2$O where a symmetric Mo–O–Mo bridging system is observed and where a bent Mo–O–Mo angle of 162° is found.[17] In this molecule similar intramolecular hydrogen-bonding of the pinacol-H proton also occurs. However in the oxo-bridged trimer [W(NPh)(μ-O)Me$_2$(PMe$_3$)]$_3$ the oxygen lies *trans* to the imido function and an asymmetric bridging geometry is observed.[18]

The W–N bond distances (1.75(5) and 1.74(4) Å) shows considerable multiple bond character. Although they do not differ significantly from the value predicted for a W–N triple bond (4-electron donor)[3] and lie within the range observed for other organomido complexes of tungsten[3,11,18–21] their agreement with data for the recently reported complex [W$_2$(NPh)$_2$(OCMe$_3$)$_2$(μ-OCMe$_3$)$_2$] (W–N bond lengths 1.737(5), 1.738(5) Å)[22] is particularly relevant. The bond length agreement is also paralleled by close agreement in the W–N–C bond angles 165.3(5) and 164.2(5)°[22] although the data for complex (3) (164(5), 163(4)) barely differs significantly from that for ideal linear geometry. Thus it seems likely that the W–N bond order is a little less than 3.0.

The imido ligand is clearly the dominant π-bonder although O → W π-bonding must also be present to achieve an 18 electron count. The W–O bond lengths are longer than in the amido complex (**2**) and thus compete less successfully than the imido nitrogen as a π-donor. A similar situation exists in other phenylimido tungsten alkoxides.[11]

Several points emerge from the chemical and

Table 2. Selected bond lengths and angles for (**3**)

Bond length (Å)			
W(1)–O(1)	1.87(4)	W(2)–O(1)	1.92(4)
W(1)–O(11)	2.00(5)	W(2)–O(21)	1.93(5)
W(1)–O(12)	1.82(5)	W(2)–O(22)	1.89(4)
W(1)–O(13)	1.87(3)	W(2)–O(23)	1.80(4)
W(1)–O(14)	2.29(4)	W(2)–O(24)	2.30(3)
W(1)–N(1)	1.75(5)	W(2)–N(2)	1.74(4)
O–C	1.38–1.69(8)		
N(1)–C(101)	1.39(6)	N(2)–C(201)	1.40(5)
C–C	1.30–1.69(9)		
Bond angle (°)			
O(11)–W(1)–O(12)	77(2)	O(21)–W(2)–O(22)	78(2)
O(13)–W(1)–O(14)	74(2)	O(23)–W(2)–O(24)	72(2)
O(1)–W(1)–O(12)	154(2)	O(1)–W(2)–O(22)	154(2)
O(11)–W(1)–O(13)	159(2)	O(21)–W(2)–O(23)	160(2)
O–W–O(*cis*)	79–105(2)		
N(1)–W(1)–O(14)	166(2)	N(2)–W(2)–O(24)	166(2)
N–W–O(*cis*)	93–107(2)		
W(1)–O(1)–W(2)	157(2)		
W–O–C	104–132(4)		
W(1)–N(1)–C(101)	164(5)	W(2)–N(2)–C(201)	163(4)

structural studies. The reaction of pinacol-H_2 with $W(NPh)Cl_4$ in the presence of *t*-butylamine, unlike monohydroxylic alcohols, where only chlorines are replaced,[11] leads to protonation of the imido function. We believe this to be the first example of the formation of the relatively rare amido complexes achieved by this process. Clearly at some stage in the reaction, protonation of the imido function competes with the *t*-butylamine-assisted removal of HCl to finally give aniline [equation (1)]. While it is tempting to postulate a lengthening of the imido function prior to metal-amide bond formation [equation (2)] there is no evidence for this at present.

$$W{\equiv}N{-}Ph \xrightarrow{diol} W{-}NHPh \xrightarrow{diol} NH_2Ph \quad (1)$$

$$W{\equiv}N{-}Ph \longrightarrow W{=}\overset{\displaystyle Ph}{\overset{|}{N}} \longrightarrow W{-}NHPh. \quad (2)$$

However it is likely that electron density at the imido nitrogen would need to be substantially increased before protonation so that distortions within the molecule (structure **2**) and/or potential for W–O single or multiple bonding *trans* to the imido function (structure **2**) may assist the process. The amido group could be formed by protonation from an OH group orientated in the equatorial plane but intermolecular protonation could also occur. In this respect nitrogen reacts essentially as a nucleophile. We note that the reaction is similar to that of pinacol-H_2 with $W(C_2Ph_2)Cl_4$ were the alkyne functions as a strong π-bonding, dianionic, ligand protonating before producing PhCH=CHPh and $W(pinacol)_3$.[13]

One interesting facet of the imido complex described is the origin of the oxygen bridge. Since this complex is only a very minor component of the reaction mixture and molecular oxygen was rigorously excluded, the likely source is a small amount of water present in the undried diol, rather than the diol itself.

We note in passing that several organoimido complexes of tungsten have now been structurally characterised and some trends are apparent. For all d^0 complexes, lone-pair donation has been observed exclusively *trans* to a single terminal organoimido 4-electron donor,[3,11,18–21] but in the d^0 diimido complex, $[W(NPh)(NCMe_3)Cl_2\text{-}(NH_2CMe_3)]_2$ a chloro group lies *trans* to a bridging imido group.[23] In the d^1 and d^2 phenylimido complexes $W(NPh)Cl_3(PMe_3)_2$ and $W(NPh)Cl_2(PMe_3)_3$ a chloro group binds *trans* to a 4-electron donor imido group and only in the former is a *trans* lengthening observed.[20,21] The d^2 complexes $W(NPh)Cl_2(L)_3$ are extremely resistant to reduction and as yet d^3 tungsten organoimides are unknown.[24]

EXPERIMENTAL

Microanalyses were performed by Dr A. C. Campbell and associates, University of Otago, New Zealand.

Spectrometers. IR: Perkin–Elmer 597; spectra in Nujol mulls between CsI plates. NMR: JEOL FX 60 (^1H, 60 MHz, ^{13}C, 15 MHz).

All operations were performed under oxygen-free nitrogen and solvents were dried over sodium and distilled from sodium wire or sodium/benzophenone except for chlorinated hydrocarbons which were dried and distilled from CaH_2. Light petroleum had b.p. 40–60°. $W(NPh)Cl_4$ was prepared by reaction of $WOCl_4$ with phenyl isocyanate.[21] *t*-Butylamine was distilled from CaH_2 and 2,3-dimethyl-2,3-butandiol (K and K) was used as supplied. Melting points were determined in sealed tubes under nitrogen.

$W(pinacol)_3$ (1)

2,3-Dimethyl-2,3-butandiol (0.9 g, 7.6 mmol) in benzene (25 cm^3) was added slowly to a rapidly stirred suspension of phenylimido tungsten tetrachloride (1.0 g, 2.5 mmol) in benzene (30 cm^3) whereupon a homogeneous green solution formed. *t*-Butylamine (1.7 cm^3, 16.2 mmol) in benzene (10 cm^3) was added slowly and the mixture stirred for 3 h to give a pale orange solution and a white crystalline solid of amine hydrochloride. After filtering, the solvent was removed *in vacuo* and the residue held under vacuum for 1 h to remove any excess diol. The white solid was extracted with benzene or chloroform (30 cm^3), the solution filtered and the volume reduced to about one third. Cooling the solutions (benzene: iced-water, chloroform: −20°C) gave the complex as a white crystalline solid. Yield 0.58 g, 46%. M.p.: decomposes above 210°C. Found: C, 39.3; H, 6.8; $C_{18}H_{36}O_6W$ requires: C, 40.6; H, 6.8% (crystallised from benzene).

IR 1360 s, 1242 m, 1202 s, 1140 s, 1002 s, 960 s, 914 m, 880 s, 854 s, 788 m, 708 s, 620 s, 552 w, 498 s, 454 w, 387 s, 328 s, 280 w.

^1H NMR (δ, $CDCl_3$) 1.28 and 1.47 (2s, 12H, Mes). Free ligand 1.28, (s, 12H, Mes) 3.45 (s, 2H (D_2O exchange), OH).

^{13}C NMR (δ, $CDCl_3$) 24.71, (Me), 25.97 (Me), 97.17 (C–O). Free ligand 24.61 (Me), 74.87 (C–O).

Aniline from the reaction was identified as follows: The amine hydrochloride was dissolved in water and made alkaline with 0.1 M NaOH. Concentrated aqueous NaCl was added and the solution extracted with the solvent removed from the original reaction mixture. After separation and drying the solvent was removed. The residue contained aniline (t.l.c. comparison) and was purified (prep t.l.c.).

Reaction of pinacol-H_2 with $W(NPh)Cl_4$

2,3-Dimethyl-2,3-butandiol (0.74 g, 6.3 mmol) and *t*-butylamine (1.65 cm^3, 15.7 mmol) in petroleum ether (50 cm^3) were added slowly to a suspension of finely ground phenylimido tungsten tetrachloride (1.3 g, 3.1 mmol) in petroleum ether (160 cm^3) and the mixture stirred for 8 h whereupon an orange–red coloured solution was obtained along with precipitated amine hydrochloride and some unreacted $W(NPh)Cl_4$. After filtration the solvent was removed *in vacuo* to give an orange–red residue which was extracted with petroleum ether (100 cm^3). The resulting solution was filtered, the volume reduced and on standing for several days at −20°C crystalline products formed which were separated manually from other amorphous material.

(*a*) $[W_2(NHPh)_2(\mu\text{-}pinacol)(pinacol)_4]$ (**2**). This complex formed as large red crystals which were not obtained analytically pure. For example, Found: C, 42.1; H, 7.1; N, 1.5; $C_{42}H_{72}N_2O_{10}W_2$ requires: C, 44.5; H, 6.4; N, 2.4%. Redissolving the sample in petroleum ether, toluene or chloroform led to a lightening of solution colour and on cooling other yellow material deposited along with the red crystals.

IR 3325 w (NH), 3020 w (aromatics) 1594 m and 1585 m (aromatics), 1265 s, 1244 m, 1194 m, 1185 m, 1130 s (C–O), 1080 w, 1000 m, 984 m, 960 s, 890 s, 880 s, 860 s, 830 m, 758 s, 720 s, 708 s, 690 m, 765 m, 620 s (W–O), 510 w, 490 m, 454 w, 390 m, 323 m, 280 w, 270 w, 256 w.

^1H NMR (δ, $CDCl_3$). The solution lightens in colour to become yellow–orange. 1.32 and 1.48 (Mes of coordinated pinacol), 1.37 to 1.45, several resonances (Mes), 7.0 to 7.8, (m, 5H, aromatics). Ratio of aromatic and methyl protons 5:34. The final characterisation of the complex was by X-ray crystallography.

(*b*) $[W_2(NPh)_2(\mu\text{-}O)(pinacol)_2(pinacol\text{-}H)_2]$ (**3**). Very few crystals of this complex formed and these were used for an X-ray crystallographic examination.

(*c*) $W(pinacol)_3$ (**1**). The colourless crystalline material formed had identical decomposition point, IR and ^1H NMR spectra to the previously prepared compound.

Reaction of $W_2(NHPh)_2(\mu\text{-}pinacol)(pinacol)_4$ with pinacol-H_2

Petroleum ether (50 cm^3) was added to the red amido complex (0.2 g, 0.18 mmol) and 2,3-dimethyl-2,3-butandiol (0.05 g, 0.42 mmol) and the solution stirred for 2 h. Removal of the solvent and recrystallisation of the residue from toluene gave colourless crystals of $W(pinacol)_3$ (**1**) which had identical decomposition point, IR and ^1H NMR spectra to the previously prepared compound.

Crystallographic studies

Crystal data. Compound (**2**) $[W_2(NHPh)_2(\mu\text{-pinacol})(pinacol)_4]$: $C_{42}H_{72}N_2O_{10}W_2$, M = 1132.76, monoclinic, a = 15.086(3), b = 18.370(5), c = 18.428(5) Å, β = 106.04(2)°, U = 4908 $Å^3$; space group $C2/c$, Z = 4, D_c = 1.533 g cm^{-1}, $F(000)$ = 2264, μ(Mo-K_α) = 91.7 cm^{-1}.

Crystal data. Compound (**3**) $[W_2(NPh)_2(\mu\text{-O})(pinacol)_2(pinacol\text{-H})_2]$: $C_{36}H_{60}N_2O_9W_2$, M = 1032.59, orthorhombic, a = 10.571(1), b = 22.449(12), c = 34.142(5) Å, U = 8102 $Å^3$; space group $Pbca$, Z = 8, D_c = 1.693 g cm^{-1}, $F(000)$ = 4080, μ(Mo-K_α) = 60.7 cm^{-1}.

Data collection. Compound (**2**). CAD4 diffractometer, Cu-K_α radiation (λ = 1.5418 Å), $\omega/2\theta$ scan mode. Crystal (0.41 × 0.12 × 0.11 mm), sealed under N_2 in a quartz-glass capillary tube, 2532 data measured (θ_{max} = 49°). The intensities of three standard reflections, monitored during the data collection (2 h), showed an overall isotropic decline of 15%; the appropriate corrections were made to the complete data set.[25] Corrections were also made for absorption,[26] minimum and maximum correction factors being 0.876 and 0.999 respectively.

Data collection. Compound (**3**). CAD4 diffractometer, Mo-K_α radiation (λ = 0.7107 Å), graphite monochromator, $\omega/2\theta$ scan mode. Crystal (0.24 × 0.16 × 0.08 mm), sealed under N_2 in a quartz-glass capillary tube, 4872 data measured (θ_{max} = 21°); intensity drop, isotropic, 7% appropriate corrections made.[25] Corrected for absorption[26] minimum and maximum correction factors being 0.806 and 0.999 respectively.

Structural solution and refinement of compounds (**2**) *and* (**3**). Both structures were solved by Patterson and Fourier methods and refined by a full-matrix least-squares technique.[27] The final refinement cycle for compound (**2**) converged to values of 0.059 and 0.060 for R and R_w respectively for the 136 variables and 1023 data for which $F^2 > 3\sigma(F^2)$. The function minimized was $\sum w(|F_o| - |F_c|)^2$ with the weight, w, being defined as $0.9152/[\sigma^2(F) + 0.004549F^2]$. The final cycle for compound (**3**) converged to values of 0.071 and 0.074 for R and R_w respectively for the 231 variables and 1212 data for which $F^2 > 3\sigma(F^2)$; w being defined as $0.6840/[\sigma^2(F) + 0.009672F^2]$.

For compound (**3**) the oxygen atoms *trans* to the imido ligands are expected to be protonated [from the W–O (*trans*) bond lengths and electron counting assuming W(VI)]. However, the hydrogen atoms could not be located with certainty from a final difference Fourier synthesis and they were omitted

from the final refinement cycle; all other hydrogen atoms for both (2) and (3) were included in calculated positions (C–H, N–H; 1.08 Å).

For both complexes isotropic thermal parameters were assumed for all atoms other than tungsten (anisotropic thermal motion was assumed for these). All hydrogen atom temperature factors were fixed at $U = 0.10\,e\,\text{Å}^{-2}$. The amido and imido phenyl groups were treated as ideal C_6 hexagons (C–C 1.395 Å). The atomic scattering factors were taken from the tabulations of Cromer and Mann,[28] anomalous dispersion corrections were by Cromer and Liberman.[29]

Final atomic coordinates for both complexes, tables of anisotropic thermal parameters, complete listings of bond distances and angles and lists of F_o/F_c have been deposited with the Editor as supplementary material.*

REFERENCES

1. D. C. Bradley and M. H. Chisholm, *Acc. Chem. Res.* 1976, **9**, 273; M. F. Lappert, P. P. Power, A. R. Sanger and R. C. Srivastava, *Metal and Metalloid Amides*, Chapter 8, p. 465. Wiley, New York (1980).
2. J. N. Armour, *Inorg. Chem.* 1978, **17**, 203; W. A. Nugent and R. L. Harlow, *Inorg. Chem.* 1979, **18**, 2030.
3. W. A. Nugent and B. L. Haymore, *Coord. Chem. Rev.* 1980, **31**, 123.
4. D. C. Bradley and E. G. Torrible, *Can. J. Chem.* 1963, **41**, 134; T. C. Jones, A. J. Nielson and C. E. F. Rickard, *J. Chem. Soc., Chem. Commun.* 1984, 205; J. A. McCleverty, A. E. Rae, I. Wolochowiez, N. A. Bailey and J. M. A. Smith, *J. Chem. Soc., Dalton Trans.* 1982, 429.
5. W. A. Nugent and R. L. Harlow, *Inorg. Chem.* 1980, **19**, 777.
6. K. W. Chiu, W. Wong, G. Wilkinson, A. M. R. Galas and M. B. Hursthouse, *Polyhedron* 1982, **1**, 37.
7. W. A. Nugent, R. J. McKinney, R. W. Kasowski and F. A. Van-Catledge, *Inorg. Chim. Acta* 1982, **65**, L91.
8. A. O. Chong, K. Oshima and K. B. Sharpless, *J. Am. Chem. Soc.* 1977, **99**, 3420.
9. W. A. Nugent and R. L. Harlow, *J. Am. Chem. Soc.* 1980, **102**, 1759; W. A. Nugent and R. L. Harlow, Abstracts, *179th National Meeting of the American Chemical Society*, Houston, Texas, March (1980), No. PETR-26; E. A. Maatta and R. A. D. Wentworth, *Inorg. Chem.* 1979, **18**, 2409.
10. G. V. Goeden and B. L. Haymore, *Inorg. Chem.* 1983, **22**, 157.
11. A. J. Nielson and J. M. Waters, *Polyhedron* 1982, **1**, 561.
12. D. C. Bradley, R. C. Mehrotra and D. P. Gaur, *Metal Alkoxides*, p. 116. Academic Press, London (1978).
13. K. H. Theopold, S. J. Holmes and R. R. Schrock, *Angew. Chem., Int. Ed. Engl.* 1983, **22**, 1010.
14. L. Pauling, *The Nature of the Chemical Bond*, 3rd Edition, p. 256. Cornell University Press, Ithaca (1960).
15. D. C. Bradley, M. A. Chisholm, C. E. Heath and M. B. Hursthouse, *J. Chem. Soc., Chem. Commun.* 1979, 1261.
16. M. H. Chisholm, *Polyhedron* 1983, **2**, 681.
17. A. J. Matheson and B. R. Penfold, *Acta Cryst.* 1979, **B35**, 2707.
18. D. C. Bradley, M. B. Hursthouse, K. M. A. Malik and A. J. Nielson, *J. Chem. Soc., Chem. Commun.* 1981, 103.
19. M. G. B. Drew, G. W. A. Fowles, B. A. Rice and N. Rolfe, *J. Chem. Soc., Chem. Commun.* 1971, 231; M. G. B. Drew, K. C. Mass and N. Rolfe, *Inorg. Nucl. Chem. Lett.* 1971, **7**, 1219.
20. A. J. Nielson and J. M. Waters, *Aust. J. Chem.* 1983, **36**, 243.
21. D. C. Bradley, M. B. Hursthouse, K. M. A. Malik, A. J. Nielson and R. L. Short, *J. Chem. Soc., Dalton Trans.* 1983, 2651.
22. F. A. Cotton and E. S. Shamshoum, *J. Am. Chem. Soc.* 1984, **106**, 3222.
23. D. C. Bradley, R. J. Errington, M. B. Hursthouse, A. J. Nielson and R. C. Short, *Polyhedron* 1983, **2**, 843.
24. D. C. Bradley and A. J. Nielson (unpublished results).
25. Program CHORTA in the Enraf–Nonius Structure Determination Package (1980).
26. A. C. T. North, D. C. Phillips and F. S. Mathews, *Acta Cryst. Sect. A* 1968, **24**, 351.
27. G. Sheldrick, *SHELX-76, Program for Crystallographic Structure Determination.* University of Cambridge, England (1976).
28. D. T. Cromer and J. B. Mann, *Acta Cryst.* 1968, **A24**, 321.
29. D. T. Cromer and D. Liberman, *J. Chem. Phys.* 1970, **53**, 1891.

* Atomic co-ordinates for these structures have also been deposited with the Cambridge Crystallographic Data Centre for inclusion in their Data Base. Copies are available on request from the Editor at Queen Mary College.

Polyhedron Vol. 4, No. 6, pp. 1007–1011, 1985
Printed in Great Britain

0277–5387/85 $3.00 + .00
© 1985 Pergamon Press Ltd

SYNTHESIS AND CHARACTERISATION OF A NEW MIXED [Si(IV), Al(III)] μ-OXO-ISOPROPOXIDE AND ITS ACID COMPLEXES

R. RAMACHANDRAN, B. SINGH, A. K. NARULA, P. N. KAPOOR, P. K. GUPTA and R. N. KAPOOR*

Department of Chemistry, University of Delhi, Delhi-7, India

(*Received* 4 *January* 1984; *accepted after revision* 10 *October* 1984)

Abstract—Reaction of dimethyldiacetoxysilane with aluminium isopropoxide was carried out in 1:2 molar ratio in refluxing cyclohexane and a mixed [Si(IV), Al(III)] μ-oxo-isopropoxide of the composition $Me_2SiO_2Al_2(OPr^i)_4$ was isolated. This compound was characterised by elemental analysis and IR and NMR spectral studies. The tertiary butanol derivative, $Me_2SiO_2Al_2(OBu^t)_4$, was prepared by alcoholysis. Reactions of this mixed [Si(IV), Al(III)] μ-oxo-isopropoxide with monobasic bidentate carboxylic acids, such as *trans*-cinnamic acid (HCA) and dihydrocinnamic acid (HDCA) and with dibasic tridentate carboxylic acids such as salicylic acid (H_2SA) and benzilic acid (H_2BA) were also studied. Products of the type $Me_2SiO_2Al_2(OPr^i)_{4-n}(L)_n$ [where HL = *trans*-cinnamic acid (HCA), dihydrocinnamic acid (HDCA) and $n = 1, 2, 3$ or 4] and $Me_2SiO_2Al_2(OPr^i)_{4-2n}(L)_n$ [where H_2L = salicylic acid (H_2SA), benzilic acid (H_2BA) and $n = 1$ or 2] were isolated and characterised by elemental and spectral studies.

Metal siloxides have aroused considerable interest in recent years because of their applicability in the synthesis of polymeric substances.[1] Synthesis of alkoxy siloxy derivatives of aluminium has been reported by Mehrotra and Pant[2] starting with trimethylacetoxysilane and aluminium isopropoxide. Preparation of polyaluminoorganosiloxanes reported by Zudanov and Andrianov[3] involves the interaction of aluminium butoxide and dialkyldiacetoxysilane. Reactions of alkylacetoxysilanes with aluminium isopropoxide were carried out by Yasuaki Nakaido[4] and Sugio Otani *et al.*[5] and the compounds so prepared were used for polymer preparation under the name "inorganic polymers". Literature survey reveals that there is no report on the synthesis of mixed [Si(IV), Al(III)] μ-oxo-isopropoxide. It was therefore, considered of interest to synthesise this mixed [Si(IV), Al (III)] μ-oxo-isopropoxide by reacting dimethyldiacetoxysilane with aluminium isopropoxide in 1:2 molar ratio in refluxing cyclohexane. The reaction can be represented as follows:

$$Me_2Si(OAc)_2 + 2Al(OPr^i)_3 \xrightarrow[\text{under reflux}]{\text{Cyclohexane}} Me_2SiO_2Al_2(OPr^i)_4 + 2Pr^iOAc\uparrow.$$

Due to its applicability in the synthesis of polymeric substances,[1] it was considered of interest to study the reactions of mixed [Si(IV), Al(III)] μ-oxo-isopropoxide with monobasic bidentate carboxylic acids like *trans*-cinnamic acid (HCA) and dihydrocinnamic acid (HDCA) and dibasic tridentate carboxylic acids like salicylic acid (H_2SA) and benzilic acid (H_2BA).

EXPERIMENTAL

All-glass apparatus with standard joints was used throughout the work. Utmost care was taken to exclude moisture from the system. Fractionating column of 30 cm length packed with Raschig rings and fitted with a variable reflux ratio still head was used.

Cyclohexane (B.D.H.), benzene (A.R., B.D.H.), isopropanol (B.D.H.), *tert*-butanol (B.D.H.) and ether (Alembic) were dried and purified by standard methods. *Trans*-cinnamic acid (HPC), dihydrocinnamic acid (Fluka), benzilic acid (Sisco) and salicylic acid (A.R., B.D.H.) were purified by recrystallization before use.

Dimethyldiacetoxysilane[6] (b.p. 44–45°C/3 mm) and aluminium isopropoxide[7] were prepared by standard methods.

* Author to whom correspondence should be addressed.

IR spectra were recorded on a Perkin–Elmer-621 spectrophotometer in Nujol mull and in thin film form using potassium bromide plates. NMR spectra were recorded in $CDCl_3$ on a Perkin–Elmer R-32 spectrometer. Isopropanol was estimated by oxidimetric method[8] using 1 N $K_2Cr_2O_7$ in 12.5% sulphuric acid. Aluminium[9] was estimated by titration with EDTA and silicon[10] was estimated gravimetrically as silicon dioxide. Carbon and hydrogen were determined by the microanalytical laboratory of Chemistry Department, Delhi University, Delhi.

Synthesis of mixed [Si(IV), Al(III)] μ-oxo-isopropoxide

Aluminium isopropoxide (22.44 g, 110 mmol) was weighed into a two-necked 250 cm^3 round bottom flask and 50 cm^3 of dry cyclohexane was added to it. To one neck of the flask was fitted a fractionating column and to the other neck of the flask, a dropping funnel containing dimethyldiacetoxysilane (9.68 g, 55 mmol) in 20 cm^3 of dry cyclohexane. The contents of the flask were allowed to reflux at a bath temperature of 110°C before starting the addition of the organo-silicon compound in such a manner that the solvent vapours reached up to the top of the column. The dimethyldiacetoxysilane contained in cyclohexane was now added dropwise from the funnel to the aluminium isopropoxide in the flask and for each drop of silane dropped, a drop of binary azeotrope of isopropyl acetate–cyclohexane was collected at 78–79°C. The addition of silane was completed in 2–3 h and thereafter the contents of the flask were further refluxed for another 2 h and the solvent coming out was collected at the top. The compound remaining in the flask with some cyclohexane was vacuum dried at a temperature of 30°C/0.3 mm. The colourless viscous liquid obtained was purified by vacuum distillation—b.p. 100–105°C/1 mm; yield (13.5 g, 65%).

Found: Al, 13.7; Si, 7.15; C, 44.3; H, 9.3; Pr^iOH, 60.5. Calc. for $Me_2SiO_2Al_2(OPr^i)_4$: Al, 14.2; Si, 7.37; C, 44.2; H, 8.95; Pr^iOH, 63.16%.

IR frequencies of $Me_2SiO_2Al_2(OPr^i)_4$ (cm^{-1}): 2980s, 2920s, 2860s, 2620w, 1740w, 1460s, 1390s, 1370s, 1360s, 1350m, 1330m, 1255s, 1210sh, 1170sh, 1120sb, 1080sb, 1040s, 960m, 945m, 880m, 860m, 835s, 820sh, 780s, 720sh, 680s, 630sb, 615sb, 570s, 540m, 510w, 475m, 450m, 440m, 430m, 420m, 410m, 390m.

^1H NMR of $Me_2SiO_2Al_2(OPr^i)_4$ in $CDCl_3$ solution shows a doublet at δ 1.1–1.35 and multiplet at δ 4.2 due to CH_3 and CH protons of the isopropoxy groups respectively and a singlet at δ 0.00 due to CH_3 protons of the dimethyl silyl group.

Reaction of $Me_2SiO_2Al_2(OPr^i)_4$ with excess of *tert*-butanol:

The mixed [Si(IV), Al(III)] μ-oxo-isopropoxide (1.25 g, 3.29 mmol) was refluxed with excess of *tert*-butanol (~5 cm^3) in 50 cm^3 of benzene for about 8 h at a bath temperature of 110°C and the liberated azeotrope of benzene–isopropanol collected between 72 and 80°C was estimated for isopropanol by oxidimetric method.[8] The *tert*-butanol derivative left in the flask along with some benzene was dried under vacuum at 35°C/0.3 mm for nearly 2 h, whereby a colourless thick liquid was obtained which solidified on keeping. The compound was purified by distillation under vacuum; b.p. 125°/0.6 mm; yield, 80%. The compound was soluble in benzene.

Found: Pr^iOH in azeotrope 0.79 g; Al, 12.25; Si, 6.2; C, 49.0; H, 9.4. Calc. for $Me_2SiO_2Al_2(OBu^t)_4H$: Pr^iOH in azeotrope, 0.79 g; Al, 12.39; Si, 6.42; C, 49.54; H, 9.63%.

Reactions of mixed [Si(IV), Al(III)] μ-oxo-isopropoxide with *trans*-cinnamic acid (1:1 molar ratio):

The mixed [Si(IV), Al(III)] μ-oxo-isopropoxide (1.08 g, 2.84 mmol) was refluxed with (0.428 g, 2.84 mmol) of *trans*-cinnamic acid in approximately 50 cm^3 of benzene for about 4 h using a fractionating column and the liberated azeotrope of isopropanol-benzene was collected at 72–80°C. The isopropanol in the azeotrope was estimated by oxidimetric method.[8] The acid complex left in the flask along with some benzene was dried under vacuum at 35°C/0.4 mm for about 1 h, when a white crystalline solid was obtained; yield, ~70%.

Found: Pr^iOH in azeotrope, 0.18 g; Al, 11.7; Si, 5.73; C, 50.9; H, 6.8. Calc. for $Me_2SiO_2Al_2(OPr^i)_3$ (CA): Pr^iOH in azeotrope, 0.18 g; Al, 11.54; Si, 5.98; C, 51.28; H, 7.26%.

RESULTS AND DISCUSSION

The mixed [Si(IV), Al(III)] μ-oxo-isopropoxide was synthesised taking aluminium isopropoxide and dimethyldiacetoxysilane in 2:1 molar ratio. The μ-oxo-isopropoxide so formed is a colourless, viscous liquid, which distils at 100–105°C/1 mm. The IR spectrum of $Me_2SiO_2Al_2(OPr^i)_4$ shows a band at 1255 cm^{-1}, assigned to the presence of Me_2Si group, a similar band appears at 1240 cm^{-1} in $Me_2Si(OOCCH_3)_2$. The strong absorption in the region 1040–1080 cm^{-1} is presumably due to Si–O bonds.[11]

The ^1H NMR spectrum of dimethyldiacetoxy-silane shows two singlets at δ 2.05 and δ 0.5 due to

Table 1. Reactions of mixed [Si(IV), Al(III)] μ-oxo-isopropoxide with bidentate and tridentate carboxylic acids

Alkoxide (mmol)	Ligand (mmol)	Refluxing time (h)	Product,* state, b.p./m.p. (°C)	Pr^iOH in azeotrope (g) Found (Calc.)	Analysis (%) Si Found (Calc.)	Al Found (Calc.)	C Found (Calc.)	H Found (Calc.)
$M(OPr^i)_4$	HCA	4	$M(OPr^i)_3CA$	0.18	5.73	11.70	50.9	6.8
2.95	2.95		White crystalline solid >300	(0.18)	(5.98)	(11.54)	(51.28)	(7.26)
$M(OPr^i)_4$	HCA	5	$M(OPr^i)_2(CA)_2$	0.37	5.15	9.45	56.90	5.8
3.1	6.2		White crystalline solid >300	(0.37)	(5.03)	(9.71)	(56.11)	(6.1)
$M(OPr^i)_4$	HCA	7	$M(OPr^i)(CA)_3$	0.75	4.10	8.69	59.0	4.90
4.2	12.6		White crystalline solid >300	(0.76)	(4.35)	(8.38)	(59.63)	(5.28)
$M(OPr^i)_4$	HCA	10	$M(CA)_4$	1.11	3.65	7.10	61.3	4.7
4.8	19.2		White crystalline solid >300	(1.14)	(3.82)	(7.38)	(62.29)	(4.64)
$M(OPr^i)_4$	HDCA	4	$M(OPr^i)_3DCA$	0.17	6.04	11.36	50.50	7.0
2.8	2.8		Colourless liquid 110/1 mm	(0.17)	(5.96)	(11.49)	(51.06)	(7.66)
$M(OPr^i)_4$	HDCA	8	$M(OPr^i)_2(DCA)_2$	0.43	5.25	9.0	54.9	6.80
3.58	7.16		Colourless liquid 90–95/1 mm	(0.43)	(5.00)	(9.64)	(55.71)	(6.79)
$M(OPr^i)_4$	HDCA	9	$M(OPr^i)(DCA)_3$	0.75	4.10	7.95	58.2	5.8
4.13	12.39		Colourless liquid 75–78/1.5 mm	(0.74)	(4.31)	(8.31)	(59.08)	(6.15)
$M(OPr^i)_4$	HDCA	10	$M(DCA)_4$	0.84	3.9	7.10	60.90	5.50
3.45	13.80		Colourless liquid 100–105/1.5 mm	(0.83)	(3.78)	(7.3)	(61.62)	(5.67)
$M(OPr^i)_4$	H_2SA	5	$M(OPr^i)_2SA$	0.24	6.94	13.89	46.10	6.8
1.97	1.97		White crystalline solid >300	(0.24)	(7.03)	(13.57)	(45.23)	(6.03)
$M(OPr^i)_4$	H_2SA	8	$M(SA)_2$	1.01	6.60	12.85	43.5	3.7
4.2	8.4		White crystalline solid >300	(1.02)	(6.73)	(12.98)	(46.15)	(3.36)
$M(OPr^i)_4$	H_2BA	6	$M(OPr^i)_2BA$	0.25	5.52	11.30	53.4	6.3
2.05	2.05		Cream coloured solid decomposes >250	(0.25)	(5.74)	(11.06)	(54.1)	(6.15)
$M(OPr^i)_4$	H_2BA	10	$M(BA)_2$	0.51	4.92	9.80	59.7	4.15
2.16	4.32		Cream coloured solid decomposes >250	(0.52)	(4.70)	(9.06)	(60.4)	(4.36)

M = $Me_2SiO_2Al_2$, HCA = *trans*-cinnamic acid, HDCA = dihydrocinnamic acid, H_2SA = salicylic acid, H_2BA = benzilic acid.
* Yield obtained was in the range 60–80%.

the methyl protons of acetoxy and dimethyl silyl groups respectively. However, in the complex absence of peak at δ 2.05 indicates the replacement of acetoxy group and appearance of a doublet and a multiplet in the region δ 1.1–1.3 and δ 4.2 ppm respectively due to CH_3 and CH protons of isopropoxy group, confirming the presence of isopropoxy groups. The methyl proton due to $\begin{matrix}Me\\ \diagdown\\ \diagup\\ Me\end{matrix}$Si of the compound appears as a singlet in the region δ (0.0 ppm), while in the case of dimethyldiacetoxysilane it appears at δ (0.5 ppm). The proton ratio of the methyl protons of $\begin{matrix}Me\\ \diagdown\\ \diagup\\ Me\end{matrix}$Si, methyl protons of isopropoxy group and methine protons of isopropoxy group was found to be 6:24:4 in the μ-oxo-isopropoxide synthesised from aluminium isopropoxide and dimethyldiacetoxysilane. Thus, spectral as well as elemental studies establish the formation of $Me_2SiO_2Al_2(OPr^i)_4$.

Alcoholysis reaction of the mixed [Si(IV), Al(III)] μ-oxo-isopropoxide was carried out with excess of tertiary butanol in refluxing benzene and a compound of the formula $Me_2SiO_2Al_2(OBu^t)_4$ was obtained and characterised by elemental analysis. The reactions of mixed [Si(IV), Al(III)] μ-oxo-isopropoxide with bidentate carboxylic acids like *trans*-cinnamic acid and dihydrocinnamic acid and tridentate carboxylic acids like salicylic acid and benzilic acid in different molar ratios proceed according to the following equation:

$$Me_2SiO_2Al_2(OPr^i)_4 + nHL \xrightarrow[\text{Reflux}]{\text{Benzene}} Me_2SiO_2Al_2(OPr^i)_{4-n}(L)_n + nPr^iOH\uparrow$$

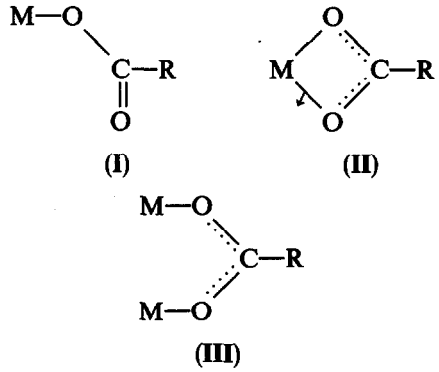
where HL = *trans*-cinnamic acid (HCA), or dihydrocinnamic acid (HDCA) and n = 1, 2, 3 or 4.

$$Me_2SiO_2Al_2(OPr^i)_4 + nH_2L \xrightarrow[\text{Reflux}]{\text{Benzene}} Me_2SiO_2Al_2(OPr^i)_{4-2n}(L)_n + 2nPr^iOH\uparrow$$

where H_2L = salicylic acid (H_2SA) or benzilic acid (H_2BA) and n = 1 or 2.

It was found that the reaction proceeds with the removal of all the four isopropoxy groups from the mixed μ-oxo-isopropoxide. The complexes formed with dihydrocinnamic acid are all liquids and are soluble in chloroform and carbon tetrachloride. All other acid complexes are crystalline solids which are sparingly soluble in benzene, chloroform and carbon tetrachloride. All complexes are soluble in dimethylformamide and dimethylsulphoxide. Other details regarding the physical properties of the complexes are given in Table 1.

The IR spectra of the complexes of *trans*-cinnamic acid (HCA) and dihydrocinnamic acid (HDCA) show no absorption in the region 2700–2500 cm^{-1}, which indicates the replacement of the hydroxylic proton of the carboxylic group from the ligands. Apart from this, ν_{asym}(COO) of *trans*-cinnamic acid and dihydrocinnamic acid complexes which appears in the free acids at 1675 and 1705 cm^{-1} respectively shifts to 1550–1580 cm^{-1} (Δ 125 cm^{-1}) in the complexes, indicating that the carbonyl oxygen of the carboxylic group is strongly coordinated to aluminium in these complexes. The IR spectra of the complexes formed with salicylic acid and benzilic acid show no absorption in the regions 3420 and 3400 cm^{-1}, indicating the absence of hydroxy groups (phenolic, alcoholic) of salicylic and benzilic acid respectively. The disappearance of the band in the region 2700–2500 cm^{-1} indicates the removal of hydroxylic protons of carboxylic group of these two acids. The asymmetric carbonyl stretching frequency which appeared at 1720 cm^{-1} in benzilic acid and at 1665 cm^{-1} in the case of salicylic acid has shifted to lower frequency (1600 cm^{-1}, 1600 cm^{-1}) (Δ 120, 65 cm^{-1}) respectively, indicating the coordination of oxygen of C=O group of carboxylic to aluminium in the complexes. In general, the metal carboxylates can adopt the following modes of coordination:



The difference between the chelated (II) and bridging (III) structures can be understood on the basis of separation (Δ) between ν_{asym}(COO) and ν_{sym}(COO) frequencies. The coordination of both oxygen atoms to the same metal causes OCO angle to decrease and consequently the two CO bonds tend to be more equivalent, resulting in the low separation (Δ) values. In the present case of acid derivatives with $Me_2SiO_2Al_2(OPr^i)_4$, low separation values (125, 120, 65 cm^{-1}) may, therefore, be attributed to the presence of chelate (II) type of coordination. IR spectra of *trans*-cinnamic acid derivatives show no

Table 2. Characteristic IR spectral data for carboxylate derivatives of mixed [Si(IV), Al(III)] μ-oxo-isopropoxide*

Compound	ν(O–H) (cm^{-1})	ν(O–H) of COOH (cm^{-1})	ν(C=O) (cm^{-1})	ν(C=C) (cm^{-1})
HCA	—	2600	1675	1625
$M(OPr^i)_3CA$	—	—	1550	1640
$M(OPr^i)_2(CA)_2$	—	—	1550	1640
$M(OPr^i)(CA)_3$	—	—	1560	1640
$M(CA)_4$	—	—	1550	1640
HDCA	—	2600	1705	—
$M(OPr^i)_3DCA$	—	—	1570	—
$M(OPr^i)_2(DCA)_2$	—	—	1570	—
$M(OPr^i)(DCA)_3$	—	—	1570	—
$M(DCA)_4$	—	—	1570	—
H_2SA	3240	2900	1665	—
$M(OPr^i)_2SA$	—	—	1600	—
$M(SA)_2$	—	—	1600	—
H_2BA	3400	2700	1720	—
$M(OPr^i)_2BA$	—	—	1600	—
$M(BA)_2$	—	—	1600	—

* M = $Me_2SiO_2Al_2$, HCA = *trans*-cinnamic acid, HDCA = dihydrocinnamic acid, H_2SA = salicylic acid, H_2BA = benzilic acid.

noticeable shift in ν(C=C), which suggests that olefinic double bond is not involved in coordination. The other characteristic IR bands are given in Table 2.

^1H NMR spectra of the complexes formed with dihydrocinnamic acid were taken in $CDCl_3$. ^1H NMR spectra of the complexes $Me_2SiO_2Al_2(OPr^i)_3DCA$, $Me_2SiO_2Al_2(OPr^i)_2(DCA)_2$, $Me_2SiO_2Al_2(OPr^i)(DCA)_3$ and $Me_2SiO_2Al_2(DCA)_4$ do not show any signals at δ (10.8 ppm), which indicates the absence of the hydroxylic proton of the carboxylic groups. The resonance due to C_6H_5 and CH_2–CH_2 protons changed relatively little in the spectra of the complexes from their values in the free acid. In addition to the above peaks, these complexes show resonance due to methyl group of isopropoxy in general as a doublet in δ (1.1–1.3 ppm) region. The methine proton of isopropoxy group was observed at δ (4.5–5.0 ppm) as a complex multiplet.

Acknowledgements—One of the authors (R. Ramachandran) is grateful to the Chemistry Department, Delhi University and National Physical Laboratory (India) for providing facilities for the experimental work.

REFERENCES

1. B. Michel, *Acta Chim (Budapest)* 1970, **65**, 239.
2. R. C. Mehrotra and B. C. Pant, *Ind. J. Appl. Chem.* 1963, **26**, 109–111.
3. A. A. Zudanov and K. A. Andrianov, *Vysokomolekul Soedin, Geterotsepnye Vysokomolekul Soedin* 1964, 45.
4. Y. Nakaido, *Kogyo Kagaku Zasshi* 1964, **67**, 236.
5. S. Otani, Y. Nakaido, A. Kojuma and C. Arai, *Kogyo Kagaku Zasshi* 1964, **67**, 239.
6. H. A. Schuyten, J. W. Weaver and J. David Reid, *J. Am. Chem. Soc.* 1947, **69**, 2110.
7. W. G. Young, W. H. Hartung and F. S. Crossley, *J. Am. Chem. Soc.* 1936, **58**, 100.
8. D. C. Bradley, F. M. A. Halim and W. Wardlaw, *J. Chem. Soc.* 1950, 3450.
9. L. V. Myshlyaeva and T. G. Maksimova, *Zh. Anal. Khim.* 1968, **23**, 1584.
10. R. C. Mehrotra and P. Bajaj, *J. Organomet. Chem.* 1971, **22**, 41.
11. *The Infrared Spectra of Complex Molecules* (Edited by L. J. Bellamy). Wiley, New York (1975).

Polyhedron Vol. 4, No. 6, pp. 1013–1017, 1985
Printed in Great Britain

0277-5387/85 $3.00 + .00
© 1985 Pergamon Press Ltd

IDENTIFICATION OF Cu(II)/Cu(III) COUPLES IN BINUCLEAR COPPER(II) COMPLEXES

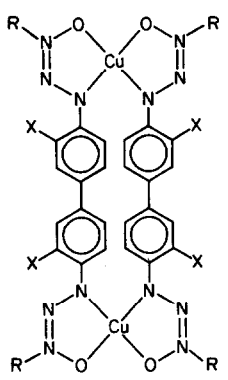
P. S. ZACHARIAS* and A. RAMACHANDRAIAH
School of Chemistry, University of Hyderabad, Hyderabad 500 134, India

(*Received* 17 *July* 1984; *accepted* 10 *October* 1984)

Abstract—A new series of binuclear copper(II) complexes were synthesised and studied by magnetic, spectral, ESR and cyclic voltammetry methods. The μ_{eff} values per copper atom correspond to the values observed for mononuclear copper(II) complexes. ESR spectral data in solution indicate weak interactions resulting from the electron delocalisation through the ligand system. Two nearly reversible red-ox couples are identified at $\tilde{+}0.50$ V and $\tilde{+}0.75$ V vs SCE. They correspond to Cu(II) $\rightleftharpoons$ Cu(III) red-ox processes, successively occurring at the two copper sites in the binuclear complexes.

The electron-transfer properties of binuclear copper(II) complexes are of current interest as models for the oxidoreductive functions of copper proteins.[1] A search for synthetic analogues of binuclear copper(II) systems to mimic the type 3 active site of copper proteins has resulted in the synthesis and study of a large number of binuclear systems.[2–5] Electrochemical studies of such binuclear complexes showed two distinct types of reduction behaviour associated with them. In one case the two copper(II) centres undergo a two-electron transfer involving both the copper centres at identical standard potential,[6–8] while in the other case they have two successive and distinct mono-electronic steps.[9–12]

Although oxidation of Cu(II) $\rightleftharpoons$ Cu(III) is known in many mononuclear tri- and tetra-peptide complexes[13,14] with potentials varying from $\tilde{+}0.40$ to +1.0 V, no examples of synthetic binuclear copper(II) systems with successive single electron oxidation steps are known except for the recent report of single electron oxidation occurring in trinuclear copper(II) systems.[16] Here we wish to report the first example of a binuclear copper(II) system undergoing two successive Cu(II) $\rightleftharpoons$ Cu(III) oxidation-reduction processes. A preliminary report on this system, appeared earlier.[17] The ligand framework and the structure of the copper complex are shown in structure 1. For convenience the complexes will be abbreviated as R–Cu_2–X where R refers to alkyl substituent and X to the substituent on the biphenyl ring. For example, bis {3,3′-dimethoxy-4,4′-bis(3-methyl triazene-3-oxide)biphenyl} di-copper will be represented as Me–Cu_2–OMe.



Structure 1

R–Cu_2–X

R=Me, Et, *n*-Pr, *i*-Pr
X=Me, OMe

EXPERIMENTAL

The CHN analyses were done by the Australian Micro Analytical Service. Molecular weight measurements were carried out using a Knauer Osmometer in chloroform. Electronic spectra were recorded either on Cary 17 D or Shimadzu UV 200 S spectrophotometers. Magnetic susceptibility measurements were done by the Gouy method on a Bruker BM-6 set up. $Hg[Co(SCN)_4]$ was used as the calibrant. ESR spectra were recorded on a JEOL JES PE 3X model spectrometer. Cyclic voltammograms

* Author for correspondence.

were recorded on EG and G Electrochemistry system provided with PAR 174 A Polarographic Analyser and PAR 175 Universal Programmer and PAR X–Y recorder, in acetonitrile with tetraethyl ammonium perchlorate (TEAP) as the supporting electrolyte. Aqueous Saturated Calomel Electrode (SCE) as reference, platinum wire as auxiliary and platinum disc as the working electrodes constituted the three electrode system. Combined ESR-electrolysis experiment was done in an ESR electrolytic cell recording the spectra simultaneously.

Synthesis of the ligands. The ligand systems can be synthesised by adopting the procedure described earlier for the preparation of triazene-1-oxides.[15] It involved the tetrazotisation of the biphenyl diamines followed by coupling with alkylhydroxylamines. In a typical experiment 2.44 g (10 mM) of *o*-dianisidine was tetrazotised using 4.5 cm^3 of conc. HCl and 1.6 g (~ 20 mM) of sodium nitrite at 5–10°C. The tetrazotised solution was added to 1.7 g (~ 20 mM) of N-methyl hydroxylaminehydrochloride in water. The pH of the solution was adjusted to 8.0 by the addition of 10 g of sodium acetate in water, whereby the ligand precipitated instantaneously. The product was filtered and recrystallised from acetone.

Complexation with copper. The copper complexes were prepared by adding an aqueous solution of 200 mg (1 mM) of copper acetate dropwise to a hot acetone solution of 1 mmol of ligand while stirring. The black shining crystals which separated after cooling, were recrystallised from acetone and dichloromethane mixture (2 : 1).

RESULTS AND DISCUSSION

Magnetic and spectral data

The analytical data and molecular weight values of the copper complexes are shown in Table 1. These results agree well with the binuclear structure shown in structure 1. The room temperature magnetic moment values are also given in Table 1. They are comparable to the μ_{eff} values observed for many of the mononuclear copper(II) complexes. Variable low-temperature (14–298 K) magnetic moment measurements showed that the μ_{eff} values are constant, indicating the absence of any strong antiferromagnetic interaction, between the electrons on the two copper centres. The electronic spectral data are also presented in Table 1. There is only one band located at ~ 11,000 cm^{-1}. The similarity of spectra of both X = OCH_3 and X = CH_3 complexes suggests near identical environments for the copper atom in these complexes implying the non-participation of the potentially coordinating OCH_3 group in any observable degree of bond formation. Monomeric planar copper(II) complexes of triazene-1-oxides show only one electronic absorption band[17] at ~ 13,000 cm^{-1}. The shift of the band maxima to longer wave lengths in the binuclear systems compared to mononuclear systems is the

Table 1. Analytical, magnetic and spectral data of R–Cu_2–X complexes

Compound	% C[a]	% H[a]	% N[a]	Molecular weight[a]	μ_{eff}. (BM)[b]		$\nu(\varepsilon)$[d,e]
Me–Cu_2–OMe	45.23	4.53	19.78	790	1.76	solid	10,200
	(45.53)	(4.31)	(19.93)	(843)			10,870(116)
Me–Cu_2–Me	49.57	4.80	21.32	725	1.83	solid	10,750
	(49.26)	(4.66)	(21.56)	(772)			10,810(128)
Et–Cu_2–OMe	48.26	4.72	18.84	953	1.78	solid	10,770
	(48.05)	(4.95)	(18.69)	(899)			10,605(223)
Et–Cu_2–Me	51.62	5.02	19.68	910	1.84	solid	10,700
	(51.73)	(5.26)	(19.98)	(835)			10,638(232)
n-Pr–Cu_2–OMe	49.48	5.51	17.43	[c]	1.83	solid	10,800
	(49.23)	(5.33)	(17.23)	[c]			10,470(244)
n-Pr–Cu_2–Me	52.86	5.84	18.06	[c]	1.83	solid	10,810
	(52.68)	(5.71)	(18.44)				10,580(340)
i-Pr–Cu_2–OMe	49.32	5.57	17.41	[c]	1.80	solid	10,790
	(49.23)	(5.33)	(17.23)				10,360(257)
i-Pr–Cu_2–Me	52.89	5.50	18.22	[c]	1.85	solid	10,790
	(52.68)	(5.71)	(18.44)				10,810(279)

[a] Values in parentheses are calculated; [b] per copper atom; [c] measurement not made; [d] ν in cm^{-1}; ε in 1 $mole^{-1}$; [e] in chloroform solution.

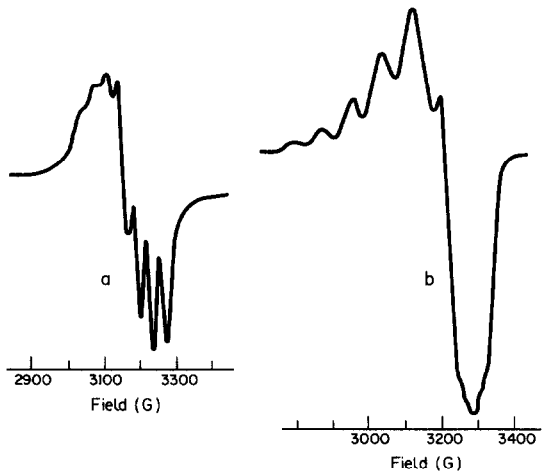


Fig. 1. ESR spectra of Me–Cu_2–OMe in chloroform at $\nu = 9.286$ GHz: (a) solution at 300 K; (b) frozen glass at 100 K.

result of distortion from the planar to tetrahedral environment. An X-ray crystal structure determination carried out on Me–Cu_2–OMe shows that the geometry at the two copper(II) centres is best described as tetrahedrally distorted square planar.[18]

The ESR X-band powder spectra showed a strong absorption at $g \approx 2.080$. In chloroform solution at room temperature they showed seven line spectra with equal spacing between the lines. In frozen solution seven hyperfine components were resolved in the parallel region with no resolution of the hyperfine splitting in the perpendicular region. ESR spectra for a representative compound is shown in Fig. 1. Relevant ESR data calculated from RT and LNT chloroform spectra are presented in Table 2. Since the two copper centres are in the +2 oxidation state (μ_{eff} values are normal) the presence of seven equally spaced lines implies that the unpaired electrons are interacting equally with two copper nuclei. The predicted intensity ratio is 1:2:3:4:3:2:1. The observed intensities are qualitatively consistent with the predicted ratio, the central line being most intense. The deviations may be due to the overlapping of lines and M_I-dependent line width variation of hyperfine components. The g_{iso} of the dimer in solution is close to that of the monomer. The hyperfine spacings of the dimer is approximately half ($A_{iso} \approx 40$ G), of that for the monomer ($A_{iso} \approx 75$ G) as expected from the theory of isotropic exchange involving two equivalent copper ions. It is shown from the X-ray crystal structure data that the two copper centres are separated by ~ 12 Å in these complexes and hence direct copper–copper exchange can be ruled out. The exchange interaction then should be by electron delocalisation through the ligands. This can be expected since the *p* orbital of the nitrogen in the conjugated ligand system partly can overlap with the *d* orbital of the copper atom thereby providing a path for electron movement. The A_o values of these complexes both in liquid as well as frozen solution are much lower than those of planar copper species but slightly higher than the values of tetrahedral species. The lowering of A_o values is an indication of the distortion of the copper environments from planar to pseudotetrahedral.[18] This has been inferred from electronic spectral data and confirmed by X-ray data.

Electrochemical data

Typical cyclic voltammograms of Me–Cu_2–OMe at different scan rates are shown in Fig. 2. The relevant CV data for all complexes are collected in

Table 2. ESR data on R–Cu_2–X

Compound	$g_{\parallel}$	$g_{\perp}$	g_o[a]	g_{iso}[b]	$A_{\parallel}$	$A_{\perp}$	A_o[c]	A_{iso}[b,d]
Me–Cu_2–OMe	2.170	2.043	2.085	2.108	86.67	13.00	37.56	39.17(78.34)
Me–Cu_2–Me	2.161	2.047	2.085	2.103	90.00	12.50	38.33	39.67(79.34)
Et–Cu_2–OMe	2.172	2.047	2.089	2.104	85.25	13.33	37.30	40.00(80.00)
Et–Cu_2–Me	2.161	2.044	2.083	2.099	90.83	15.00	40.27	40.67(81.34)
n-Pr–Cu_2–OMe	2.167	2.046	2.086	2.057	85.00	15.00	38.35	39.67(79.34)
n-Pr–Cu_2–Me	2.163	2.048	2.086	2.060	91.67	11.00	37.89	40.00(80.00)
i-Pr–Cu_2–OMe	2.167	2.047	2.087	2.085	82.50	15.00	37.50	39.17(78.34)
i-Pr–Cu_2–Me	2.161	2.043	2.083	2.060	92.17	15.00	40.72	39.50(79.00)
Me–Cu–OMe[e]	2.177	2.051	2.093	2.110	198.33	16.67	77.22	75.45
Me–Cu–Me[e]	2.168	2.042	2.084	2.101	193.33	13.33	73.33	72.33

[a] $g_o = 1/3(g_{\parallel} + 2g_{\perp})$; [b] room temperature (chloroform solution); [c] $A_o = 1/3(A_{\parallel} + 2A_{\perp})$; [d] the measured spacing for the seven line spectrum is quoted for the dimer. The values in parentheses correspond to double this value; [e] monomeric analogues.

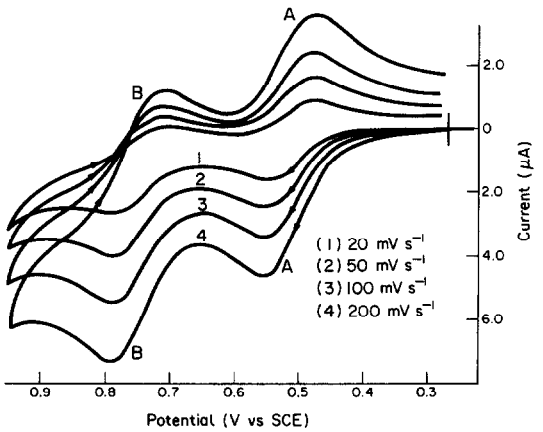


Fig. 2. Cyclic voltammograms of Me–Cu_2–OMe in acetonitrile at different scan rates. Solution concentration $\approx 1 \times 10^{-3}$ M, TEAP concentration $\approx 1 \times 10^{-1}$ M.

Table 3. All the compounds show the presence of two distinct couples *A* and *B* in the positive potential range, *A* being the couple at lower potential. In the negative potential range at ~ -1.1 V an irreversible peak complicated by adsorption was observed. The ligand system of these complexes do not have any cyclic voltammetric peaks in the potential range from 0.0 to +0.90 V. The observed E^o for couples *A* and *B* are at $\tilde{+}0.50$ V and $\tilde{+}0.75$ V respectively. The E_p values show that only a single electron is involved in each couple. The ΔE_p and i_{pa}/i_{pc} values also show the nearly reversible character of these redox couples. It can be seen from Table 3 that the separation between the two couples is 230 mV. It is known that non interacting metal centres of similar environments do not have a separation larger than $\sim$ 50 mV.[19,20] The weak copper–copper interaction in the present binuclear complexes (*vide infra* ESR) can induce CV wave splitting of a magnitude of a few hundred millivolts.

The two couples *A* and *B* can originate from either two Cu(II)$\rightleftharpoons$Cu(I) or two Cu(II)$\rightleftharpoons$Cu(III) one-electron processes. The nature of the elctron transfer process in these complexes has been identified by doing combined electrolysis, ESR and spectral studies in acetonitrile. Three potentials were selected to carry out these experiments: (i) 0.0 V, cathodic to both *A* and *B* couples: (ii) +0.65 V, cathodic to *B* and anodic to *A* (a potential between the two couples); (iii) +0.85 V, anodic to both *A* and *B*. The results of these experiments on one compound *n*-Pr–Cu_2–OMe are shown in Fig. 3. The electrolysis at 0.0 V did not change the ESR signals of the starting

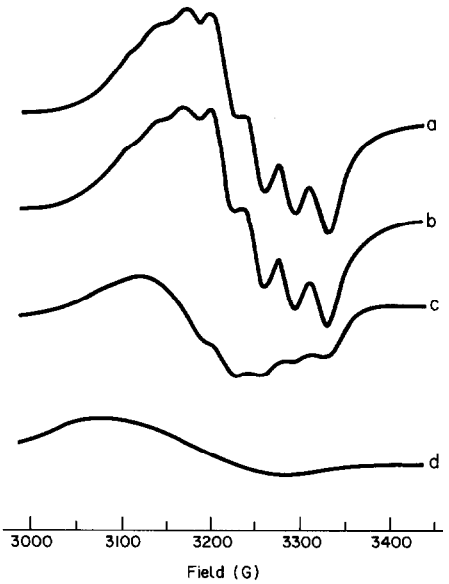


Fig. 3. ESR spectra of 2×10^{-3} M *n*-Pr–Cu_2–OMe in acetonitrile at ν = 9.437 GHz, TEAP concentration $\simeq 1 \times 10^{-1}$ M. (a) Before electrolysis; (b) after electrolysis at 0.0 V; (c) after electrolysis at +0.65 V; (d) after electrolysis at +0.85 V.

Table 3. Cyclic voltammetric data of R–Cu_2–X complexes in acetonitrile

Compound	Scan rate (mV·s^{-1})	Couple *A*				Couple *B*			
		E_{pc} (V)	E_{pa} (V)	ΔE_p (mV)	E^o (V)	E_{pc} (V)	E_{pa} (mV)	ΔE_p (mV)	E^o (V)
Me–Cu_2–OMe	20	0.475	0.550	75	0.512	0.710	0.785	75	0.747
	50	0.475	0.555	80	0.515	0.710	0.790	80	0.750
	100	0.475	0.555	80	0.515	0.710	0.795	85	0.753
	200	0.475	0.560	85	0.517	0.710	0.795	85	0.753
Et–Cu_2–OMe	50	0.55	0.530	75	0.493	0.705	0.780	75	0.743
n-Pr–Cu_2–OMe	50	0.465	0.535	70	0.500	0.725	0.800	75	0.763
i-Pr–Cu_2–OMe	50	0.430	0.495	65	0.463	0.690	0.760	70	0.725

complex even after a prolonged period. If the process at the copper site was a reduction, electrolysis at this potential should have resulted in the disappearance of the ESR signals since Cu(I) species is ESR inactive. This does not happen. Electrolysis at the potential +0.65 V resulted in partial loss of ESR signal intensities. This is expected since electrolysis at this potential will affect only one copper centre. Electrolysis at the potential +0.85 V, completely removed the ESR signals. These observations are compatible only with the oxidation of Cu(II) to Cu(III). The electrode processes can now be visualised as

$$\text{Couple } A: Cu_2(II) \rightleftharpoons Cu(III)Cu(II)$$

$$\text{Couple } B: Cu(III)Cu(II) \rightleftharpoons Cu_2(III)$$

Cu(III) (d^8) can be expected to be ESR inactive in planar or distorted planar configurations.

In another set of experiments, the electronic spectral behaviour of the same complex was analysed while electrolysis was done at the three potentials. The electrolysis at 0.0 V did not change the electronic spectral band at $\sim 11{,}000\ cm^{-1}$ of the starting Cu(II) complex even after a prolonged period. But this band completely disappeared when electrolysed at +0.85 V.

Acknowledgements—We thank Dr. S. Mitra, Tata Institute of Fundamental Research, Bombay for variable temperature magnetic moment measurements. One of us (A.R.) gratefully acknowledges the financial assistance received from Council of Scientific and Industrial Research, New Delhi.

REFERENCES

1. J. A. Fee, *Struct. Bonding* 1975, **23**, 1.
2. D. J. Hodgson, *Prog. Inorg. Chem.* 1975, **19**, 173.
3. R. J. Doedens, *Proc. Inorg. Chem.* 1976, **21**, 209.
4. J. P. Fackler, Jr., *Prog. Inorg. Chem.* 1976, **21**, 55.
5. J. Catterick and P. Thornton, *Adv. Inorg. Chem. Radiochem.* 1977, **29**, 291.
6. D. E. Fenton, R. R. Schroeder and R. L. Lintvedt, *J. Am. Chem. Soc.* 1977, **99**, 8367.
7. J. P. Giselbrecht, M. Gross, A. H. Alberts and J. M. Lehn, *Inorg. Chem.* 1980, **19**, 1386.
8. S. K. Mandal and K. Nag, *Inorg. Chem.* 1983, **22**, 2567.
9. A. W. Addison, *Inorg. Nucl. Chem. Lett.* 1976, **12**, 899.
10. E. F. Hasty, L. J. Wilson and D. N. Hendrickson, *Inorg. Chem.* 1978, **17**, 1834.
11. R. R. Gagne, C. A. Koval, T. J. Smith and M. C. Cimoline, *J. Am. Chem. Soc.* 1979, **101**, 4571.
12. D. Datta and A. Chakravorty, *Proc. Indian Acad. Sci.* 1981, **90**, 1.
13. D. W. Margerum, K. L. Chellappa, F. P. Bossu and G. L. Burce, *J. Am. Chem. Soc.* 1975, **97**, 6894; F. P. Bossu, K. L. Chellappa and D. W. Margerum, *J. Am. Chem. Soc.* 1977, **99**, 2195.
14. T. A. Newbecker, S. T. Krisksey, Jr., K. L. Chellappa and D. W. Margerum, *Inorg. Chem.* 1979, **18**, 444.
15. D. Datta, P. K. Mascharak and A. Chakravorty, *Inorg. Chem.* 1981, **20**, 1673; D. Datta and A. Chakravorty, *Inorg. Chem.* 1983, **22**, 1611.
16. A. Ramachandraiah and P. S. Zacharias, *Inorg. Nucl. Chem Lett.* 1980, **16**, 433.
17. B. Behra and A. Chakravorty, *Inorg. Chem.* 1970, **4**, 372.
18. D. J. Hodgson, *Inorg. Chim. Acta* 1983, **75**, 225.
19. F. Ammar and J. M. Saveant, *J. Electroanal. Chem.* 1973, **47**, 115.
20. J. B. Flamagan, S. Margel, A. J. Bard and F. C. Anson, *J. Am. Chem. Soc.* 1978, **100**, 4248.

Polyhedron Vol. 4, No. 6, pp. 1019–1021, 1985
Printed in Great Britain

0277–5387/85 $3.00+.00
© 1985 Pergamon Press Ltd

THE REACTION OF AQUA-(ETHYLENEDIAMINETETRA-ACETATO)RUTHENIUM(III) WITH *o*-PHENYLENEDIAMINE UNDER AEROBIC CONDITIONS

YUKICHI YOSHINO,*† MICHIO KASAHARA and MASAMI SAITO
College of Arts and Sciences, The University of Tokyo, Meguro-ku, Tokyo 153, Japan

(*Received* 30 *April* 1984; *accepted* 20 *October* 1984)

Abstract—An electron-transfer reaction between [Ru(III)(Hedta)(H_2O)] and *o*-phenylenediamine in the presence of O_2 takes place to give a Ru(II)-edta complex with coordinated (bidentate) *o*-benzoquinone diimine. The complex obtained has been characterized by analysis, magnetic measurements, electronic, IR, ^1H and ^{13}C NMR spectral data.

The extraordinary substitution reactivity of the pentadentate edta complex of ruthenium(III), [Ru(Hedta)(H_2O)], has been reported by several authors.[1–5] In the course of our studies on the substitution reaction of [Ru(Hedta)(H_2O)] with aromatic amines in solution, we have noticed that *o*-phenylenediamine (*o*-pda) gave an unusually intense red colour. A close examination of the reaction product revealed that an unexpected reduction of Ru(III) to Ru(II) and oxidation of *o*-pda to *o*-benzoquinone diimine (*o*-bqdi) had taken place during chelation under aerobic conditions.

EXPERIMENTAL

Preparation of complexes. [Ru(III)(Hedta)(H_2O)]. The complex was prepared by a modification[1] of the method of Mukaida *et al.*[6]

Ru(II)(H_2edta)(*o*-bqdi)]·$2H_2O$. A hot aqueous solution containing 0.817 g (2.0 mmol) of [Ru(III)(Hedta)(H_2O)] and 0.238 g (2.2 mmol) of recrystallized *o*-phenylenediamine was heated for several hours on a water bath. After standing overnight, the reaction mixture was evaporated and concentrated on a water bath. On cooling the solution, the reddish purple crystals separated and they were washed with ethanol and diethyl ether. Yield, 87%. Found: C, 36.31; H, 4.53; N, 10.53. Calc. for $C_{16}H_{24}N_4O_{10}Ru$: C, 36.02; H, 4.53; N, 10.50%.

Physical measurements. The electronic and IR spectra were recorded on a Hitachi 124 spectrophotometer and JASCO 403G IR spectrophotometer, respectively. The magnetic susceptibility was measured by a Gouy magnetic balance at room temperature. ^1H and ^{13}C NMR spectra were obtained by JEOL PMX 60 (60 MHz) NMR spectrometer using DMSO-d_6 and D_2O solutions at an ambient temperature. Tetramethylsilane was used as an internal standard.

RESULTS AND DISCUSSION

When an aqueous solution of

[Ru(III)(Hedta)(H_2O)]

was mixed with a slight excess of *o*-phenylenediamine the reaction mixture gave reddish purple colour and after heating for several hours the electronic spectrum showed an absorption maximum at 480 nm ($\log \varepsilon = 4.14$). The mole ratio plot of the extinction of the reaction mixture revealed that the ruthenium-edta complex and *o*-phenylenediamine react in a 1 : 1 ratio. Together with the analytical data given above, the results suggest that the product is a complex in which Ru, edta and *o*-pda (or its reaction product) are combined in a ratio 1 : 1 : 1.

The magnetic measurements showed that the product complex was diamagnetic. In the IR spectra, besides bands at 1630 cm^{-1} (COORu) and 1723 cm^{-1} (COOH), those at 3216 cm^{-1} (NH) and 1600 cm^{-1} (C=N + C=C) were observed.[7,8] In the

* Author to whom correspondence should be addressed.
† Present address: Faculty of Science, Toho University, Miyama, Funabashi, Chiba Prefecture 274, Japan.

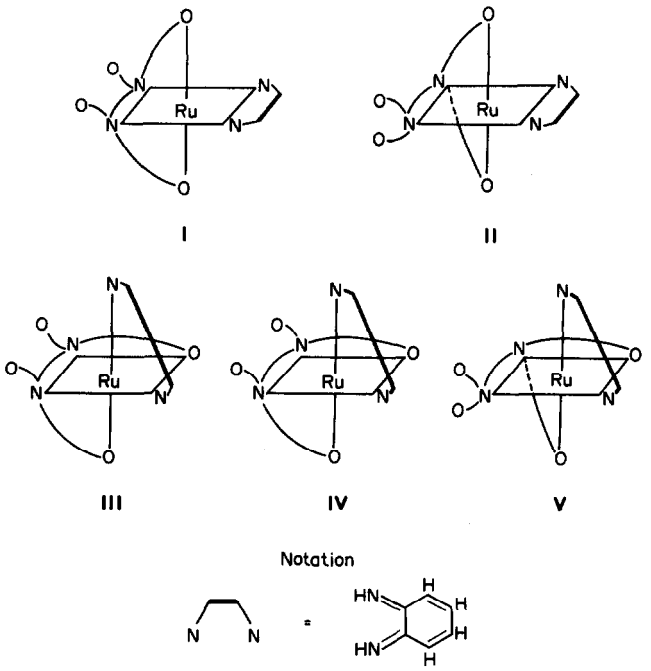


Fig. 1. Possible geometrical isomers for Ru(II) complexes with tetradentate edta and bidentate *o*-benzoquinone diimine.

^{1}H NMR spectrum, the resonance due to imine appeared at 12.7 ppm and this may correspond to that of $K_2[Fe(CN)_4(o\text{-bqdi})]$ at 11.9 ppm.[9] From the pH titration curve, the pK values were calculated as $pK_1 = 3.1$ and $pK_2 = 3.9$ at 30°C and ionic strength 0.1.

On the basis of these observations, it was presumed that, in the reaction of *o*-pda with [Ru(Hedta)(H_2O)], Ru(III) is reduced to Ru(II) and *o*-phenylenediamine is oxidized to *o*-benzoquinone diimine,[7,9] thus

$$[Ru(III)(Hedta)(H_2O)] + o\text{-pda} + \tfrac{1}{4}O_2 \rightarrow [Ru(II)(H_2edta)(o\text{-bqdi})] + \tfrac{3}{2}H_2O.$$

For the octahedral complex with tetradentate edta and bidentate *o*-benzoquinone diimine five geometrical isomers are possible as shown in Fig. 1. When the glycinate arms occupy both equatorial and axial positions (III, IV and V), the ^{13}C NMR spectrum of edta should give seven peaks. In our case, however, only five peaks were observed. It can therefore be presumed that the glycinate arms occupy axial positions (I and II). For the tetradentate edta complex, [Ru(H_2edta)($CH_3CN)_2$], Diamantis and Dubrawski[5] suggested a structure corresponding to I from the stereochemical consideration of the formation route. Similar reasoning will be applicable to the structure of [Ru(H_2edta)(*o*-bqdi)] and we conclude that the most likely isomer is I. The assignments of the observed ^{13}C NMR chemical

Table 1. ^{13}C NMR chemical shifts[a] of Ru(II)(edta) complexes

Complex	Carboxylate C		Methylenic C		Ethylenic C	Ligand C	
	Axial	Free	Axial	Free			
[Ru(H_2edta)(*o*-bqdi)]	180.3	169.8	63.6	59.4	56.1	166.7(C=N)	119.6 116.9
[Ru(H_2edta)($CH_3CN)_2$][b]	188.8	173.7	66.6	64.8	61.8	130.7(C≡N)	5.7(CH_3)

[a] In ppm relative to Me_4Si.
[b] Reference 5.

shifts are shown in Table 1, and may be compared with the values for $[Ru(H_2edta)(CH_3CN)_2]$.[5]

Acknowledgements—The authors thank Prof. Y. Takeuchi and Messrs Nobuo Suzuki and Kazuhiro Uchiki for the NMR measurements.

REFERENCES

1. Y. Yoshino, T. Uehiro and M. Saito, *Chem. Lett.* 1978, 487; *Bull. Chem. Soc. Jpn* 1979, **52**, 1060.
2. T. Matsubara and C. Creutz, *J. Am. Chem. Soc.* 1978, **100**, 6255; *Inorg. Chem.* 1979, **18**, 1956.
3. T. Uehiro, D.Sc. Thesis, The University of Tokyo, March (1978).
4. (a) K. Shimizu, T. Matsubara and G. P. Sato, *Bull. Chem. Soc. Jpn* 1974, **47**, 1651; (b) K. Shimizu, *ibid.* 1977, **50**, 2921.
5. A. Diamantis and J. V. Dubrawski, *Inorg. Chem.* 1981, **20**, 1142.
6. M. Mukaida, T. Ishimori and H. Okuno, *Nippon Kagaku Zasshi* 1965, **86**, 598.
7. L. F. Warren, *Inorg. Chem.* 1977, **16**, 2814.
8. K. Nakamoto, *Infrared Spectra of Inorganic and Coordination Compounds*, p. 193. Wiley, New York (1963).
9. (a) V. L. Goedken, *J. Chem. Soc., Chem. Commun.* 1972, 207; (b) C. G. Christoph and V. L. Goedken, *J. Am. Chem. Soc.* 1973, **95**, 3869.

Polyhedron Vol. 4, No. 6, pp. 1023–1029, 1985
Printed in Great Britain

0277–5387/85 $3.00 + .00
© 1985 Pergamon Press Ltd

AMINOARSOLANES—II. CONFORMATIONAL STUDIES[1]

L. K. KRANNICH, C. L. WATKINS* and R. K. KANJOLIA
Department of Chemistry, University of Alabama at Birmingham, Birmingham, AL 35294, U.S.A.

(*Received* 27 *July* 1984; *accepted after revision* 1 *November* 1984)

Abstract—^{1}H and ^{13}C NMR spectra of six dialkylaminoarsolanes were obtained as a function of solvent, concentration, and temperature. CI mass spectral data were also obtained as a function of retention time for the same compounds. These results suggest that the As–N bond is not labile as compared to the As–Cl bond in chloroarsolanes. No evidence for dimer formation was noted either in solution or the gas phase under the investigated experimental conditions. The averaged solution conformation of the 1,3-dioxarsolane ring is discussed in terms of rapid intramolecular conformational averaging; nature of substituents at the 2, 4, and 5 positions; and effects of temperature, solute concentration and solvent type.

Several NMR studies of 1,3,2-dioxarsolanes (X = Y = O; see Scheme 1) and related five-membered ring compounds (X = Y = S; X = O, Y = S, Z = Cl, OCH_3, SPh, SCH_3, CH_3, OPh, Ph, $N(Ph)_2$, $N(R)_2$, where R = alkyl) have been reported, the primary goal of these studies being to understand the solution conformation of the arsolane ring.[2–14,23]

The study of the solution conformation of these five-membered rings is complicated by the fact that there is often ease of interconversion between several equi-energy conformers. Previous NMR studies have demonstrated that the 1,3,2-dioxarsolane ring adopts a nonplanar conformation with rapid intramolecular averaging between two half-chair (C_2) or twist-envelope forms, the barrier to interconversion being very low.[2–8,12–14] However, inversion at the arsenic is slow on the NMR time scale, the barrier being calculated to be at least 105 kJ/mol.[3,8,9,15–18] Thus, unsymmetrical substitution at the C(4) and C(5) positions can lead to the formation of *cis* and *trans* isomers, which may be detected by ^{1}H and ^{13}C NMR spectroscopy.[4–6,8,9,13]

The appearance of the ^{1}H and ^{13}C NMR spectra of the 1,3,2-dioxarsolanes and related compounds can be directly affected by intermolecular exchange processes, if the processes cause inversion at the arsenic. For such processes to occur in the present study, the As–Z bond must be labile. For example, concentration and temperature dependent ^{1}H NMR studies on solutions of 2-chloro-1,3,2-dioxarsolane and related compounds demonstrate that a rapid bimolecular exchange process occurs that involves chlorine exchange. This leads to apparent inversion at the arsenic.[3–7,9,12,19]

As previously reported, dialkylaminoarsolanes readily undergo transamination at room temperature in the presence of ammonia, primary, or secondary amines,[1] indicating that the As–N bond is quite reactive in the presence of species containing the weakly protonic N–H group. However, the lability of the As–N bond cannot be necessarily inferred from its reactivity. Two preliminary ^{1}H NMR studies on the solution stability of aminoarsolanes have been reported[2,11] in which the ^{1}H NMR spectra were temperature independent, indicating no intermolecular exchange processes occurring on the NMR time scale. In the present study, the ^{1}H and ^{13}C NMR data for compounds I–VI have been obtained as a function of temperature, concentration, solvent, and magnetic field strength in order to assess the relative importance of intramolecular and intermolecular exchange processes in determining the solution conformation of these aminoarsolanes. These studies thus allow a comparison of the As–Cl versus the As–N bond lability in the arsolane ring system. Also, chemical ionization (CI) mass spectral studies were conducted for comparison with the previously reported electron impact (EI) mass spectral studies[1,20] and a CI mass spectral study in which dimerization of the aminoarsolanes in the gas phase was reported.[21]

* Author for correspondence.



Compound	R	X=Y	Z
I	CH_3	O	$N(CH_3)_2$
II	CH_3	O	$N(CH_2CH_3)_2$
III	CH_3	O	$N(CH_2CH_2CH_3)_2$
IV	H	O	$N(CH_3)_2$
V	H	O	$N(CH_2CH_3)_2$
VI	H	O	$N(CH_2CH_2CH_3)_2$

Scheme 1.

EXPERIMENTAL

Synthesis. The aminoarsolanes, compounds **I–VI**, were synthesized as previously reported.[1,22] Satisfactory elemental analyses for C, H, N, and As were obtained.

NMR studies. The ^{13}C and ^{1}H NMR spectral data were obtained on a Nicolet NMC-300/WB Fourier-transform NMR spectrometer operating at 75.475 MHz for ^{13}C and 300.132 MHz for ^{1}H. The ^{1}H NMR spectra for the six compounds were obtained at four concentrations ranging from 0.0032 M to 0.2 M in each of the three solvents benzene-d_6, toluene-d_8, and chloroform-*d*. A temperature dependent ^{1}H NMR study, over the liquid range of the solvent, was conducted for each compound in each solvent and at each concentration. The ^{1}H NMR spectra were also obtained at 25°C for each of the compounds in carbon tetrachloride solution for comparison with previously reported ^{1}H NMR values for compound **IV**.[11] Temperature dependent ^{13}C NMR spectra were obtained for compounds **I–VI** in the solvents benzene-d_6 and chloroform-*d* at a solute concentration of 0.2 M. The ring protons of compounds **IV–VI** exhibit AA'BB' non first-order ^{1}H-NMR spectra. The spectra were analyzed using the Nicolet library program ITRCAL. 400 MHz ^{1}H NMR spectra of compounds **IV–VI** were obtained on a Bruker WH-400 NMR spectrometer (25°C, 0.2 M) in order to verify the accuracy of the calculated ^{1}H chemical shifts and coupling constants. The spectra were analyzed using the Bruker library program PANIC. The two sets of calculated results agree within experimental error. The ^{13}C NMR spectra of the $-OCH_2CH_2O-$ moiety of **IV–VI** were of the AA'BB'X type and were analyzed using the ITRCAL program. The free induction decay in each experiment consisted of 32K data points, yielding a real spectrum of 16K data points. The corresponding digital resolution was 0.50, 0.25, and 0.10 Hz per data point for the decoupled ^{13}C, coupled ^{13}C and ^{1}H NMR experiments, respectively.

Mass spectral studies. Low resolution CI mass spectral data were obtained on a Hewlett–Packard 5985A GC/MS/DS mass spectrometer using isobutane as the ionizing gas. The source temperature was maintained at 200°C with no heating at the probe. The source pressure was 1.0 torr.

RESULTS AND DISCUSSION

^{1}H NMR studies. The ^{1}H NMR spectra of compounds **I–III** are similar, exhibiting two equally intense resonances for the CH_3 groups at the C(4) and C(5) positions. The higher frequency resonance is assigned to R(1) and R(2)—the CH_3 groups *syn* to the $-NR_2$ substituent.[23] The fact that two resonances are present for the methyl group protons indicates that there is rapid intramolecular conformational averaging, presumably between half-chair forms, with no inversion at the arsenic.[2–8,12–14] A static nonplanar structure would be expected to exhibit four methyl resonances whereas one resonance would arise from an averaged planar structure. The ^{1}H NMR chemical shifts of compounds **I–III** are given in Table 1 (0.2 M, 25°C) where Δf(Hz) represents the chemical shift difference between the ring methyl groups.

The ^{1}H NMR spectra of compounds **IV–VI** exhibit a 24-line non first-order pattern for H(1)–H(4), which is analyzed to be that of an AA'BB' type, as previously reported for arsolanes.[11,12,23] The existence of an AA'BB' spectral pattern instead of an ABCD type indicates rapid intramolecular conformational averaging. Analysis of the AA'BB' spectrum leads to two chemical shifts and four coupling

Table 1. Experimentally determined ^{1}H NMR chemical shifts for compounds I–VI[a]

Compound	Solvent	Ring methyls			Alkyl group		
		R(1), R(2)[b]	R(3), R(4)[b]	Δf (Hz)	NCH_2	CH_2	CH_3
I	C_6D_6	1.21	1.17	12.5	—	—	2.56
	$C_6D_5CD_3$	1.18	1.14	12.9	—	—	2.57
	$CDCl_3$	1.28	1.24	11.9	—	—	2.79
II	C_6D_6	1.23	1.18	12.9	3.10	—	0.97
	$C_6D_5CD_3$	1.20	1.15	13.5	3.09	—	0.97
	$CDCl_3$	1.27	1.24	10.0	3.22	—	1.09
III	C_6D_6	1.24	1.18	13.9	3.02	1.40	0.80
	$C_6D_5CD_3$	1.20	1.16	13.9	3.00	1.40	0.81
	$CDCl_3$	1.26	1.24	6.8	3.07	1.49	0.84
IV	C_6D_6				—	—	2.43
	$C_6D_5CD_3$				—	—	2.44
	$CDCl_3$				—	—	2.74
	CCl_4				—	—	2.71
V	C_6D_6				2.94	—	0.91
	$C_6D_5CD_3$				2.95	—	0.92
	$CDCl_3$				3.15	—	1.09
	CCl_4				3.11	—	1.09
VI	C_6D_6				2.87	1.33	0.78
	$C_6D_5CD_3$				2.86	1.34	0.78
	$CDCl_3$				3.00	1.47	0.86
	CCl_4				2.96	1.46	0.86

[a] 0.2 M, 25°C, δ, ppm (TMS), internal reference.
[b] Additional coupling, $^4J(^1H, ^1H) = 0.5$ Hz.

constants. These calculated values for compounds IV–VI are given in Table 2 (0.2 M, 25°C). The downfield ^{1}H NMR chemical shift is assigned to the two protons *syn* to the dialkylamino group. The values of the geminal coupling constant ($^2J(1, 3)$, $^2J(2,4)$) range from −8.92 to −9.12 Hz in agreement with reported values for analogous arsolanes[23] and phospholanes.[24,25] The two *cis* coupling constants ($^3J(1, 2)$, $^3J(3, 4)$), however, are not identical as reported in a previous 1,3,2-dioxarsolane study,[23] but differ slightly (5.2–5.4 vs 5.82–6.05 Hz). A theoretical basis for the nonequivalence of *cis* couplings in five membered ring compounds has been recently proposed.[39] The *trans* coupling constant, $^3J(2, 3)$, is larger than the *cis* coupling constants, as previously observed.[23] The variation in the *cis* and *trans* coupling constants of the –O–CH_2–CH_2–O– moiety reflects changes in the corresponding torsional angle. The *R* factor method of Lambert[26] has been employed to calculate the torsional angle for compounds IV–VI (Table 2). An average value of 46° is obtained in comparison with previous studies on 2-chloro-1,3,2-dioxarsolane[12] (46°), 2-dimethylamino-1,3,2-dioxarsolane in CCl_4 solution[11] (47°), and other 2-substituted dioxarosolanes[23] (46°). *R* value calculations on a series of five-membered rings including dithiarsolanes, dithiaphospholanes, dithiolanes, dioxaphospholanes, dioxolane, diazarsolanes, and diazaphospholanes give torsional angle values in a range of 41–55°.[23]

The CH_3, C_2H_5, and n-C_3H_7 protons in the dialkylamino functional group each exhibit only one set of first-order ^{1}H NMR resonances for compounds I–VI suggesting that the two given alkyl groups are magnetically equivalent and there is no restricted rotation about the As–N bond. The ^{1}H NMR chemical shift values observed are typical values for secondary amines and are listed in Table 1. The ethyl and *n*-propyl groups exhibit typical first-order coupling patterns, where the average $^3J(^1H, ^1H)$ value = 7.2 ± 0.2 Hz.

The ^{1}H NMR spectra of compounds I–VI were determined as a function of concentration in order to determine if any self-association or intermolecular conformational averaging occurred for the solute molecules in the four solvents. Adler and Kober[27] reported that compounds I and IV form dimers in benzene solution as evidenced by vapor pressure osmometry molecular weight measurements. They also argued that as the size of the alkyl substituent was increased, that dimer association would decrease. The ^{1}H NMR chemical shifts for the six solute molecules are essentially concentration independent in each of the solvents, indicating no

Table 2. Calculated ^{1}H NMR parameters for compounds IV–VI based on AA'BB' analysis[a–c]

Compound	Solvent	R(1), R(2)	R(3), R(4)	Δf (Hz)	$^3J(1,2)$	$^2J(1,3)$	$^3J(2,3)$	$^3J(3,4)$	RMS error	$\phi°$
IV	C_6D_6	3.826	3.567	77.7	5.38	−9.01[e]	6.15[f]	5.96	0.022	45.6–47.5
	$C_6D_5CD_3$	3.820	3.553	79.9	5.36	−8.96	6.14	5.97	0.030	45.3–46.3
	$CDCl_3$	4.170	3.894	82.8	5.38	−9.12	6.17	5.82	0.009	46.1–47.5
	CCl_4	4.04	3.768	79.9	5.36	−8.98	6.14	5.94	0.026	45.3–46.3
	CCl_4[d]				5.42	−9.10	6.11	5.42		47
V	C_6D_6	3.840	3.579	78.3	5.39	−8.99	6.11	5.90	0.003	45.7–47.3
	$C_6D_5CD_3$	3.834	3.564	80.8	5.34	−8.95	6.11	5.96	0.025	45.3–46.3
	$CDCl_3$	4.133	3.878	76.5	5.29	−9.07	6.12	5.88	0.014	45.8–47.7
	CCl_4	4.010	3.754	76.7	5.20	−8.95	6.11	6.06	0.082	45.1–46.6
VI	C_6D_6	3.863	3.589	82.2	5.41	−8.98	6.11	5.92	0.006	45.6–47.3
	$C_6D_5CD_3$	3.851	3.570	84.2	5.37	−8.94	6.10	5.99	0.022	45.2–46.3
	$CDCl_3$	4.130	3.876	76.2	5.34	−9.05	6.12	5.85	0.006	45.8–47.5
	CCl_4	4.008	3.756	75.9	5.23	−8.92	6.09	6.09	0.081	45.0–46.5

[a] ^{1}H NMR chemical shifts, δ, ppm (TMS), internal reference; coupling constants, Hz.
[b] 0.2 M, 25°C.
[c] 24 lines assigned in each iterative calculation.
[d] Reference 11.
[e] $^2J(1,3) = {}^2J(2,4)$.
[f] $^3J(2,3) = {}^3J(1,4)$.

intermolecular exchange processes as in 2-chloro-1,3,2-dioxarsolane[3–7,9,12,19] and indicating no measurable monomer–dimer equilibria in solution. Previously reported cryoscopic molecular weight determinations[1] in benzene solution for compounds I–VI indicate monomeric species only to be present.

A comparison of the ^{1}H NMR chemical shift data for a given compound in the four solvents demonstrates general medium effects (Tables 1 and 2). For compounds I–III, the methyl ring and alkyl ^{1}H NMR resonances are shifted to lower frequency (higher field) in the two aromatic solvents, compared with the same resonances in $CDCl_3$ solution. For compounds IV–VI, the ring hydrogen and alkyl ^{1}H NMR resonances are shifted to lower frequency in the aromatic solvents and to higher frequency in $CDCl_3$ in comparison with CCl_4 solution. The Δf value for an individual compound is independent of solvent suggesting no strong preferential solute–solvent interactions. Solvent effects have been previously observed in the ^{1}H NMR spectra of ethylene sulfite, $\overline{OCH_2CH_2OSO}$, and attributed to solvent magnetic anisotropy effects in the case of benzene and intermolecular hydrogen bonding in the case of $CDCl_3$.[25] A comparison of the ring methyl resonances for compounds I–III for a given solvent indicates that the medium effects are dependent on the nature (size) of the R group in the dialkylamino moiety. For example, the ring methyl resonances move to lower frequency in C_6D_6 solution as R is changed from *n*-C_3H_7 to C_2H_5 to CH_3, while the same resonances move to higher frequency in $CDCl_3$ solution. The same trends for R group substitution are observed for the ring hydrogen resonances in compounds IV–VI. However, there is no chemical shift dependence on the R group in CCl_4 solution.

The temperature dependent ^{1}H NMR studies indicate no major changes in the spectral patterns for compounds I–VI in any of the investigated solvents. However, solvent medium effects were observed as discussed above. No intermolecular conformational averaging (amino group exchange) was observed, indicating that the As–N bond, in contrast to the As–Cl bond, is not labile under these experimental conditions. No monomer–dimer equilibria were noted in the temperature studies. The dialkylamino R groups remain magnetically equivalent even at −90°C ($C_6D_5CD_3$ solution) indicating no restricted rotation about the As–N bond. The Δf values are essentially temperature independent and the spin–spin coupling and torsional angle values are temperature independent, suggesting that the intramolecularly exchange averaged half-chair conformation(s) exists over all experimental conditions in the present study. The ^{1}H NMR chemical shifts are mildly temperature dependent for both the ring and alkyl group protons for the six compounds. As would be expected, the ^{1}H NMR resonances move to lower frequency with decreasing temperature in the aromatic solvents and to higher frequency with decreasing temperature in $CDCl_3$ solution, due to the solvent effects previously discussed. No

Table 3. ^{13}C NMR chemical shifts and ^{13}C–^{1}H coupling constants of compounds I–VI[a–c]

Compound	Ring					Alkyl group			
	R(1), R(2)		R(3), R(4)		Δf (Hz)	C(4), C(5)	NCH_2	CH_2	CH_3
I	26.16(126.0)[d]		26.53(126.0)[d]		14.1	80.89	—	—	36.94(134.9)[e]
II	26.36(126.0)[d]		26.40(126.0)[d]		3.1	80.79	39.60(133.4)[h]	—	16.28(125.6)[f]
III	26.42(125.9)[d]		26.43(125.9)[d]		0.9	80.75	47.35(133.4)[i]	22.88(126.1)[j]	11.32(125.0)[g]
	$^{1}J(1,5)$	$^{2}J(2,5)$	$^{1}J(3,5)$	$^{2}J(4,5)$	RMS	C(4), C(5)	NCH_2	CH_2	CH_3
IV	145.6	−0.51	146.1	−0.93	0.065	66.96	—	—	36.81(134.9)[e]
V	145.4	−0.52	146.3	−0.97	0.082	66.55	39.87(134.3)[h]	—	16.09(125.6)[f]
VI	145.4	−0.54	146.3	−0.87	0.089	66.56	47.65(133.7)[i]	22.78(126.0)[j]	11.44(125.0)[g]

[a] 0.2 M, C_6D_6 solution, 25°C, δ, ppm (TMS), internal reference.

[b] The same ^{13}C–^{1}H coupling constant values and only slightly different (0.1–0.3 ppm) chemical shift values were observed in $CDCl_3$ solution.

[c] Values in parentheses represent $^{1}J(^{13}C, ^{1}H)$ values for I–III and the alkyl group in IV–VI, Hz.

Additional coupling:

[d] $^{3}J(CH_3, CH_3)$, 3.8–4.3 Hz (4°).

[e] $^{3}J(CH_3, CH_3)$, 4.5 Hz (4°).

[f] $^{2}J(CH_2CH_3)$, 2.45 Hz (3°).

[g] $^{2,3}J(CH_2CH_2CH_3)$, 3.8 Hz (5°).[k]

[h] $^{2,3}J(CH_2NCH_2CH_3)$, 4.5 Hz (6°).[k]

[i] $^{2,3}J(CH_2NCH_2CH_2CH_3)$, 5.2 Hz (8°).[k]

[j] Complex multiplet.

[k] Selective ^{13}C–^{1}H decoupling performed to verify assignments.

temperature dependence of the ^{1}H NMR chemical shifts was noted in CCl_4 solution.

^{13}C NMR studies. The ^{13}C NMR chemical shifts and ^{13}C–^{1}H coupling constants are given for compounds I–VI in Table 3 (0.2 M, C_6D_6 solution, 25°C). Two methyl ring resonances are observed for I, the difference in their chemical shifts, Δf, being 14.1 Hz in C_6D_6 solution and 6.4 Hz in $CDCl_3$ solution. The ^{13}C chemical shifts at lower frequency are assigned to R(1) and R(2), the methyl groups *cis* to the 2-substituent, based on previous assignments in analogous dioxaphospholanes,[28–30] dioxolanes,[31] and dioxarsolanes.[23] The chemical shift difference between the *cis* and *trans* methyl groups depends on solvent and the nature of the substituent group at the 2-position. As Z changes fron $-N(CH_3)_2$ to $-N(n\text{-}C_3H_7)_2$ in I–III, Δf decreases from 14.1 to 0.9 Hz in C_6D_6 solution. However, only I exhibits two distinct methyl group resonances in $CDCl_3$ solution. The variation in chemical shift of the ring methyl resonances with solvent, temperature, and substituent group at the 2-position is small, indicating that the average solution conformation of the five-membered ring is affected only slightly by these factors.[32] The ^{13}C chemical shifts of C(4) in IV–VI (66.96–66.53 ppm, C_6D_6 solution) are similar to those previously reported for the 1,3,2-dioxarsolanes where Z = Cl (68.7 ppm), OCH_3 (67.8 ppm), OC_6H_5 (67.7 ppm), SCH_3 (67.7 ppm), and SC_6H_5 (67.5 ppm),[23] suggesting that the relative effect of the 2-substituent on the C(4) ^{13}C chemical shift is small. Substitution of four methyl groups at the C(4) and C(5) positions causes a downfield chemical shift of C(4) by 13.9–14.3 ppm in I–III. The chemical shift effect of methyl substitution on the ring carbons in five-membered rings has been previously reported.[31,33,34] Simple α and β effects of methyl group substitution on alkyl chains[35] are not sufficient to explain the observed shifts. Consideration of the parameters of Eliel, Rao, and Pietrusiewicz[33] for 1,3-dioxolanes (α, β, γ, *vic*, *gem*)[34] plus the previously reported data on 1,3,2-dioxarsolanes by Aksnes and Lie[23] indicate that the α,β, *vic* parameters for 1,3,2-dioxarsolanes are very similar to those of 1,3-dioxolanes. (Sufficient data were not available for the evaluation of the γ and *gem* parameters.)

Such evidence implies that substitution on the five-membered ring causes conformational changes dictated by the steric requirements of the substituents.[30,32] An analogous study of methyl group substitution in the 1,3,2-dioxaphospholanes concluded that there was a modification of the geometry about the phosphorus atom and in the $-O-CH_2CH_2-O-$ torsional angle upon introduction of four methyl groups at the C(4) and C(5) positions.[30]

The ^{13}C NMR spectra of the dialkylamino groups in I–VI in each case consist of only one set of equivalent resonances, even at low temperature, further suggesting no restricted rotation about the

As–N bond. The ^{13}C chemical shifts can be adequately explained for the alkyl groups by consideration of simple α, β, and γ intrachain and interchain shielding effects.[35] The one-bond ^{13}C–^{1}H coupling constants for the diakylamino groups in **I–VI** and the ring methyl groups in **I–III** (Table 3) exhibit typical values.[35]

The analysis of the coupled ^{13}C NMR spectra for the C(4) and C(5) carbons in **IV–VI** is rather difficult due to accidental degeneracy and the fact that the analogous ^{1}H NMR spectra are non first-order. The spectra were analyzed as those of the AA'BB'X type (X = ^{13}C) with no correction for isotopic shifts. The data (Table 3) indicate that the $^{1}J(^{13}C, ^{1}H)$ values are slightly different ($^{1}J(1, 5)$ vs $^{1}J(3, 5)$) and large compared to typical aliphatic $^{1}J(^{13}C, ^{1}H)$ values due to the electronegative substituent effect of the directly bound oxygen. The $^{2}J(^{13}C, ^{1}H)$ values are within the range normally expected for aliphatic molecules containing electronegative substituents (−5 to 2 Hz)[23,36] with $^{2}J(4, 5)$ more negative than $^{2}J(2, 5)$ in each case. The data are in excellent agreement with those previously reported for 1,3,2-dioxarsolanes.[23]

The ^{1}H and ^{13}C NMR data are consistent with the proposed model that there is rapid intramolecular conformational averaging of the ring and no inversion at the arsenic. Additionally, there appears to be no restricted rotation about the As–N bond. Interestingly, the ^{1}H NMR chemical shifts of **I–VI** are subject to medium effects, which are reflected in the temperature-dependent spectra. Variation of the substituent at the 2-position has only a small influence on the ^{1}H and ^{13}C NMR spectral parameters. The above factors seem to have little, if any, influence on the average solution conformation. The As–N bond is not labile as is the As–Cl bond in the 2-chloro-1,3,2-dioxarsolanes. **I–VI** exist as monomers in solution under all investigated conditions. The substitution of four methyl groups at the C(4) and C(5) positions alters the average ring geometry in a manner which minimizes steric interaction of the substituent groups.

Mass spectral studies. EI mass spectral investigations on aminoarsolanes have suggested that fragmentation proceeds via amino group elimination to give stable five-membered cyclic arsenium ions.[1,20] The fragmentation pathways have been proposed on the basis of the observed metastable peaks. CI mass spectral data have been previously reported on some of these aminoarsolanes.[21] The results have been interpeted in terms of dimerization of the parent ion.[21,38] Also, molecular weight determinations by vapor pressure osmometry on

Table 4. Chemical ionization mass spectral data on the aminoarsolanes **I–VI**

Compound	RT (min)	*m/e* (relative abundance)
I	0.22	$[M+H]^+$, 236(35); $[M_2-NMe_2]^+$, 426(100)
	0.25	$[M_2-NMe_2]^+$, 426(100)
	0.37	$Me_2COAsNHCH_3]^+$, 163(20); $[(\overline{OCMe_2CMe_2OAs})_2NH_2]^+$, 398(55); $[M_2-NMe_2]^+$, 426(100)
II	0.27	$[M+H]^+$, 264(100)
	0.35	$[M-Et-Me]^+$, 219(20); $[M_2-NEt_2]^+$, 454(100)
	1.03	$[Et_2NH_2]^+$, 74(40); $[M-NEt_2]^+$, 191(28); $[M+H]^+$, 264(100); $[(\underline{OCMe_2CMe_2OAs})_2NH_3]^+$, 399(100)
III	0.28	$[M+H]^+$, 292(100); $[M_2-NPr_2]^+$, 482(20)
	0.50	$[M_2-NPr_2]^+$, 482(100)
	1.15	$[M-16]^+$, 275(60); $[M_2-NPr_2]^+$, 482(100)
IV	0.13	$[M+H]^+$, 180(100); $[M-NMe_2]^+$, 135(65); $[M-1]^+$, 178(19); $[M]^+$, 179(37); $[CH_2CH_2OAs]^+$, 119(30)
	1.33	$[M_2-NMe_2]^+$, 314(100); $[M+H]^+$, 180(50); $[M]^+$, 179(10); $[M-1]^+$, 178(10)
V	1.27	$[M-H]^+$, 208(100); $[M-27]^+$, 180(16); $[Et_2NH_2]^+$, 74(36)
	1.65	$[M_2-MEt_2]^+$, 342(42); $[M+H]^+$, 208(100); $[M-27]^+$, 180(8)
VI	0.23	$[M_2-NPr_2]^+$, 370(36); $[M+H]^+$, 236(100); $[M-Et]^+$, 206(9); $[Pr_2NH_2]^+$, 102(70)
	0.48	$[M_2+1-NPr_2]^+$, 371(11); $[M_2-NPr_2]^+$, 370(100); $[M+41]^+$ or $[CH_2CH_2OAsNPr_2+57]^+$, 276(6); $[M+40]^+$, 275(64)
	0.77	$[M+40]^+$, 275(85); $[M+41]^+$, 276(17); $[M_2-NPr_2]^+$, 370(31); $[M_2-3]^+$, 466(100); $[M_2+1-3]^+$, 467(22)

these and related compounds indicate molecular association to be occurring in benzene solution.[27,37] However, in our previous report on the synthesis of **I–VI** cryoscopic molecular weight determinations in benzene solution indicate the existence of only monomeric species.[1] Furthermore, the present ^1H and ^{13}C NMR studies suggest no self-association (dimerization) to be occurring in solution. CI mass spectral studies have been systematically conducted in order to investigate possible association in the gas phase. The data are given in Table 4.

The CI mass spectral data are dependent on retention time for each compound. The spectra obtained at low retention time exhibit $[M+H]^+$ as the base peak with the other major peak being assignable to $[M-NR_2]^+$. No evidence of $[M_2+H]^+$ or subsequent dimer fragments[21] was noted at low retention time, indicating the absence of dimers in the vapor phase under our experimental conditions. As the retention time is increased, chemical self-ionization ensues and an associated species of the type $[M_2-NR_2]^+$ forms, which becomes the major peak. No species of the type $[M_2+H]^+$ was detected under the present experimental conditions as previously proposed.[21] The formation of $[M_2-NR_2]^+$ via a chemical self-ionization process is further substantiated by single ion monitoring where the ion-current of $[M+H]^+$ remains constant, but the ion-current of $[M_2-NR_2]^+$ increases as a function of time.

REFERENCES

1. L. K. Krannich, *Inorg. Chem.* 1980, **19**, 3300.
2. A. Adler and F. Kober, *Z. Naturforsch.* 1976, **31B**, 472.
3. Yu Yu Samitov, N. K. Tazeeva and N. A. Chadaeva, *J. Struct. Chem.* 1975, **16**, 29; *Zh. Strukt. Khim.* 1975, **16**, 34.
4. D. W. Aksnes, F. A. Amer and K. Bergesen, *Acta Chem. Scand.* 1976, **30A**, 109.
5. D. W. Aksnes and M. Bjoroy, *Acta Chem. Scand.* 1975, **29A**, 672.
6. D. W. Aksnes and O. Vikane, *Acta Chem. Scand.* 1973, **27**, 2135.
7. D. W. Aksnes and O. Vikane, *Acta Chem. Scand.* 1973, **27**, 1337.
8. D. W. Aksnes and O. Vikane, *Acta Chem. Scand.* 1972, **26**, 2532.
9. D. W. Aksnes and O. Vikane, *Acta Chem. Scand.* 1972, **26**, 835.
10. R. Foster and C. A. Fyfe, *Spectrochim. Acta* 1965, **21**, 1785.
11. O. Adler and F. Kober, *J. Prakt. Chem.* 1977, **319**, 313.
12. O. Adler and F. Kober, *Monatsh. Chem.* 1977, **108**, 65.
13. D. W. Aksnes and T. A. Holak, *Org. Magn. Reson.* 1982, **18**, 28.
14. P. A. Morozov, N. K. Tazeeva and N. A. Chadaeva, *J. Struct. Chem.* 1981, **22**, 928; *Zh. Strukt. Khim.* 1981, **22**, 161.
15. J. D. Andose, A. Rauk and K. Mislow, *J. Am. Chem. Soc.* 1974, **96**, 6904.
16. J. P. Casey and K. Mislow, *J. Chem. Soc., Chem. Commun.* 1970, 999.
17. G. H. Senkler, Jr. and K. Mislow, *J. Am. Chem. Soc.* 1972, **94**, 291.
18. R. D. Baechler, J. P. Casey, R. J. Cook, G. H. Senkler, Jr. and K. Misolow, *J. Am. Chem. Soc.* 1972, **94**, 2859.
19. C. L. Watkins, L. K. Krannich and M. Geckle, "Abstract of Papers", Southeast/Southwest Regional Meeting of the American Chemical Society, New Orleans, LA, December 10–13, 1980; *Inorg.* 252.
20. R. H. Anderson and R. H. Cragg, *J. Chem. Soc., Chem. Commun.* 1971, 1414.
21. F. Kober, *Z. Chem.* 1976, **16**, 151.
22. Corrected b.p. for **III** = 148–152°C/13 mm Hg.
23. D. W. Aksnes and A. Lie, *Org. Magn. Reson.* 1983, **21**, 417.
24. K. Bergesen and T. Vikane, *Acta Chem. Scand.* 1972, **26**, 2153.
25. P. Haake, J. McNeal and E. Goldsmith, *J. Am. Chem. Soc.* 1968, **90**, 715.
26. J. B. Lambert, *Acc. Chem. Res.* 1971, **4**, 87.
27. O. Adler and F. Kober, *Z. Anorg. Allg. Chem.* 1976, **420**, 109.
28. H. Tan and W. G. Bentrude, *Tetrahedron Lett.* 1975, 619.
29. D. Besserre and S. Coffi-Nketsia, *Org. Magn. Reson.* 1980, **13**, 235, 313.
30. G. Pouchoulin, J. R. Llinas, G. Buono and E. Vincent, *Org. Magn. Reson.* 1976, **8**, 518.
31. Y. Senda, J. Ishiyama and S. Imaizumi, *Bull. Chem. Soc. Jpn* 1977, **50**, 2813.
32. W. E. Willy, G. Binsch and E. L. Eliel, *J. Am. Chem. Soc.* 1970, **92**, 5394.
33. E. L. Eliel, S. Rao and K. M. Pietrusiewicz, *Org. Magn. Reson.* 1979, **12**, 461.
34. M. Christl, H. J. Reich and J. D. Roberts, *J. Am. Chem. Soc.* 1971, **93**, 3463.
35. G. C. Levy, R. L. Lichter and G. L. Nelson, *Carbon-13 Nuclear Magnetic Resonance Spectroscopy*, 2nd edn. Wiley, New York (1980).
36. D. F. Ewing, In *Ann. Rep. NMR Spectroscopy* (Edited by E. F. Mooney), Vol. **6A**, p. 389. Academic Press, London (1975).
37. O. Alder and F. Kober, *Z. Naturforsch.* 1976, **31B**, 304.
38. F. Kober, W. J. Ruhl and L. Zimmer, *Chem. Ber.* 1976, **109**, 493.
39. F. A. A. M. de Leeuw, A. A. van Beuzekom amd C. J. Altona, *J. Comput. Chem.* 1983, **4**, 438.

Polyhedron Vol. 4, No. 6, pp. 1031–1033, 1985
Printed in Great Britain

0277–5387/85 $3.00 + .00
© 1985 Pergamon Press Ltd

ELECTROCHEMICAL SYNTHESIS OF COPPER(II) CARBOXYLATES

J. S. BANAIT* and P. K. PAHIL
Department of Chemistry, Punjabi University, Patiala-147002, India

(*Received* 2 *July* 1984; *accepted after revision* 1 *November* 1984)

Abstract—A number of copper(II) carboxylates have been synthesized by anodic oxidation of copper. The reactions were found to proceed with current efficiencies of 0.95 to 1.00 eq./Faraday. Reaction products have been characterized by infrared spectral studies and analysis of copper.

Reactions of carboxylic acids at inert anodes have been found to depend upon the nature of the carboxylic acids, e.g., monocarboxylic acids yield hydrocarbons (Kolbe reaction),[1,2] α-substituted carboxylic acids yield aldehydes and ketones,[3,4] unsaturated carboxylic acids yield alkynes[5,6] and dicarboxylic acids yield a number of degradation products.[7] All these reactions proceed through the formation of free radicals at the electrode surface. Recently, Tuck *et al.*[8–10] have shown that the free radicals formed electrochemically react with the active electrodes to yield inorganic and organometallic compounds. In the present communication, reactions of various carboxylic acids at the copper anode are reported.

EXPERIMENTAL

Material and equipment. Conductivity water was prepared by the usual method and had been used as solvent. Carboxylic acids (BDH AnalaR) and tetrabutylammonium chloride (Reidel, pure) were used without further purification.

H-type electrolysis cell made of pyrex glass was used to carry out the electrochemical reactions. The cathode and anode compartments were separated from each other by a sintered disc of G-3 porosity. Volume of one of the compartments was almost three times that of the other one.

Platinum foil, 1 × 1 cm, was used as cathode. A thick layer of copper had been deposited electrochemically[11] on a sheet of copper, 5 × 5 × 0.2 cm, in order to ensure the purity of the anode material.

Direct current was obtained with the help of a Toshniwal electrophoresis power supply.

Procedure. All the carboxylic acids were studied voltametrically using tetrabutylammonium chloride as supporting electrolyte and Radilkis, AC/DC (Type OH-103) polarograph. The cathode and anode were made of platinum and copper respectively.

Solution of the carboxylic acid (5 g) in 250 cm^3 of water was taken in the electrolysis cell. Copper plate freshly electroplated with copper was dipped in the larger compartment and platinum foil in the other one. Necessary connections were made with the power supply and potential across the electrodes was then adjusted so that a current of about 20 mA passed through the cell. Electrolysis was carried out for 6 h. The solution in the anode compartment was then taken out and concentrated under reduced pressure to a volume of 20–30 cm^3. On cooling, crystals separated out which were filtered, washed with methanol and recrystallyzed.

Copper(II) carboxylates of all these acids had been synthesized by the method reported by Graddon and Munday.[12]

Infrared spectra of the products of electrochemical reactions and the synthetic copper(II) carboxylates were scanned on Beckmann IR-20 spectrophotometer in Nujol using sodium chloride plates in the region of 4000–600 cm^{-1} and polythene plates in the region of 600–200 cm^{-1}.

Copper contents in the products were estimated volumetrically.[11]

RESULTS AND DISCUSSION

Solutions of propionic, *n*-butyric, benzoic, oxalic, succinic, phthalic, isobutyric, salicylic, tartaric and crotonic acids in water have been first studied voltametrically. Current–potential curves of these

* Author to whom correspondence should be addressed.

acids show that all the acids react at the copper anode at a potential less than even 2 V. Electrolysis of the acids at a potential corresponding to the plateau of the current–potential curve and under the conditions similar to that of voltametry produce blue/green coloration in the anode compartment. However, several attempts including column chromatography, preparative TLC, fractional crystallization, etc., failed to separate the product from the reaction mixture in the purified form even if the electrolysis have been carried out for 2–3 days. This may be because of the fact that at a potential of less than 2 V, a current of only a few microamperes passes through the cell resulting in the formation of a very small amount of the product and separation of the inorganic compound (which is ionic or highly polar in nature) from a solution containing sufficient quantity of the supporting electrolyte is difficult.

Electrolysis of the acid solutions (5 g/250 cm^3 of water) has therefore been carried out at a sufficiently higher potential[13] so that a current of about 20 mA passes through the cell. As the conductance of the solutions at such a high concentration of the acids is very high, no supporting electrolyte has been added and the solution has also been stirred during electrolysis. Under these modified conditions sufficient amounts of the products have been isolated. The electrolysis characteristics have been summarized in Table 1.

All the compounds formed are soluble in water. Except for the compound of salicylic acid, the solubility of all these compounds is significantly high and the solutions of these compounds in water are highly conducting, showing thereby the ionic nature of these compounds. In commonly used organic solvents, these compounds are almost insoluble. However, in acetone the compound of benzoic acid is highly soluble and those of other carboxylic acids are partially soluble.

Melting points of all these compounds have been found to be higher than 200°C.

Copper contents in these compounds determined volumetrically correspond to the respective copper(II) salts of these acids with appropriate water molecules associated with the crystal lattice of the product. All the relevant data are recorded in Table 1.

Infrared spectra of the products obtained from the electrochemical reactions and the copper(II) salts prepared by the reported methods[12] have been recorded in the region of 4000–200 cm^{-1}.

All the compounds show characteristic absorption bands in the regions; 1650–1550, 1400–1320 and 790–650 cm^{-1} which have been assigned to the asymmetric, symmetric and bending vibrations respectively of the carboxylate ion.[14–16] In addition to the absorption bands in these regions, some of the products show a broad absorption band in the region of 3600–3200 cm^{-1}. This can be attributed to the water molecules associated with the molecules of these salts.

The infrared spectral data thus show that the products of the present electrochemical reactions are copper(II) salts of these acids and thus support the analytical data. This has been further confirmed as the infrared spectra of the electrochemical products and the corresponding synthetic copper(II) carboxylate are superimposable on each other.

In the present studies, electrolysis of aliphatic and aromatic carboxylic acids of different types, i.e., monocarboxylic, dicarboxylic, substituted and unsaturated carboxylic acids have been conducted. The results reveal that all the acids yield copper(II) carboxylates, irrespective of the nature of the acid. The behaviour of carboxylic acids at the copper anode is thus entirely different from that at the inert anode.[1–7]

Current efficiencies of these reactions have also

Table 1. Analytical and related results of electrolysis process

Acid	Voltage (V)	Product	Colour	Current efficiency (eq./Faraday)	Percentage of copper	
					Found	Required
Propionic acid	40	$C_6H_{10}O_4Cu \cdot H_2O$	Bluish green	0.95	27.48	27.91
n-Butyric acid	40	$C_8H_{14}O_4Cu \cdot 2H_2O$	Blue	0.95	23.56	23.22
Benzoic acid	70	$C_{14}H_{10}O_4Cu$	Blue	0.77	20.50	20.78
Oxalic acid	35	$C_2O_4Cu \cdot H_2O$	Light blue	0.27	36.91	37.47
Succinic acid	20	$C_4H_4O_4Cu \cdot H_2O$	Dark blue	1.00	31.22	32.15
Phthalic acid	20	$C_8H_4O_4Cu \cdot H_2O$	Dark blue	1.00	25.29	25.86
Isobutyric acid	50	$C_8H_{14}O_4Cu \cdot H_2O$	Blue	0.78	25.29	24.85
Salicylic acid	40	$C_{12}H_{10}O_6Cu \cdot H_2O$	Green	1.00	17.33	17.86
Tartaric acid	10	$C_4H_4O_6Cu \cdot 3H_2O$	Light blue	1.00	23.04	23.92
Crotonic acid	25	$C_8H_{10}O_4Cu$	Blue	1.00	26.49	27.65

been determined and are recorded in Table 1. Perusal of Table 1 reveals that the current efficiencies for most of these systems vary from 0.95 to 1.00 eq./Faraday showing thereby that the reactions leading to the formation of copper(II) carboxylates are the predominant reactions of these systems. Such a high value of current efficiency of these systems suggest that these electrochemical reactions can be of commercial use for the production of copper(II) carboxylates.

REFERENCES

1. H. Koble, *Annalen* 1849, **69**, 257.
2. F. Fichter, *Bull. Soc. Chem.* 1934, **1**, 1585; *Trans. Amer. Electrochem. Soc.* 1930, **75**, 309.
3. F. Fichter and M. Schmid, *Helv. Chem. Acta* 1920, **13**, 704.
4. F. Fichter and M. Schmid, *Helv. Chem. Acta* 1920, **13**, 103.
5. J. Peterson, *Z. Electrochem.* 1912, **18**, 710; and M. Bouis, *Bull. Soc. Chem.* 1923, **33**, 1081.
6. F. Fichter and A. Petrovich, *Helv. Chem. Acta* 1941, **24**, 549.
7. E. Tommila, *Ann. Acad. Sci. Fenn.* 1932, **36A**, 1.
8. J. J. Habeeb, A. Osman and D. G. Tuck, *Inorg. Chim. Acta* 1979, **35**, 105.
9. F. F. Said and D. G. Tuck, *Inorg. Chim. Acta* 1982, **59**, 1.
10. J. L. Hencher, M. Khan, F. F. Said, R. Sieler and D. G. Tuck, *Inorg. Chem.* 1982, **21**, 2787.
11. A. I. Vogel, *A Text Book of Quantitative Inorganic Analysis.* Longmans, Green and Co. Ltd, London (1961).
12. D. P. Graddon and L. Munday, *J. Inorg. Nucl. Chem.* 1961, **23**, 231.
13. Literature survey in transference number determination by Hittorf's method reveals that the electrolysis is generally carried out at a very high potential ($\approx$ 100 V). Though none of the solvent is stable at such a high potential yet the ions of the electrolyte are oxidized/reduced at the electrode surface and the solvent remains unaffected as far as the ions that are in the solution.
14. J. D. Donaldson, J. F. Knifton and S. D. Ross, *Spectrochim. Acta* 1964, **20**, 847.
15. A. I. Grigor'ev, *Russ. J. Inorg. Chem.* 1963, **8**, 409.
16. N. W. Alcock, V. M. Tracy and T. C. Waddington, *J. Chem. Soc., Dalton Trans.* 1976, 2243.

Polyhedron Vol. 4, No. 6, pp. 1035–1041, 1985
Printed in Great Britain

0277–5387/85 $3.00 + .00
© 1985 Pergamon Press Ltd

η-CYCLOHEPTATRIENYL–MOLYBDENUM CHEMISTRY: TERTIARY PHOSPHINE, ALKYL, HYDRIDO, HALOGENO AND RELATED DERIVATIVES

MALCOLM L. H. GREEN* and RICHARD B. A. PARDY
Inorganic Chemistry Laboratory, South Parks Road, Oxford OX1 3QR, U.K.

(*Received* 24 *September* 1984; *accepted* 7 *November* 1984)

Abstract—The preparation and properties of the compounds $[Mo(\eta\text{-}C_7H_7)(dppe)Y]$ (Y = Cl, I, Me, H), $[Mo(\eta\text{-}C_7H_7)(dppe)Cl]^+A^-$ (A = PF_6, Br or I), $\{[Mo(\eta\text{-}C_7H_7)(dppe)Br]PF_6\}$, $\{[Mo(\eta\text{-}C_7H_7)(dppe)I]PF_6\}$ and $\{[Mo(\eta\text{-}C_7H_7)(dppe)L]PF_6\}$ (L = CO, MeCN, or dppe) are described.

The functional group properties of the η-bonded $\eta\text{-}C_nH_n$ ligands, where $n = 4$–8, in their transition metal complexes are best determined by an exploratory synthetic approach followed by a more quantitative study. As part of a development of the chemistry of the $\eta\text{-}C_7H_7$ ligand we have set out to study derivatives of the system $[Mo(\eta\text{-}C_7H_7)(dppe)]$.

Prior to this work and during the course of these studies there have been reports of other $\eta\text{-}C_7H_7$–molybdenum compounds.[1] In particular, the reactions of $[Mo(\eta\text{-}C_7H_7)(CO)_3]BF_4$ have been studied in considerable detail.[2,3] The $\eta\text{-}C_7H_7$ ring of this cation undergoes nucleophilic addition, e.g. of $P(Pr^i)_3$,[4] CN^-, OMe^- and Ph^-,[5] whilst displacement of carbon monoxide with dppe gives $[Mo(\eta\text{-}C_7H_7)(dppe)CO]BF_4$.[6] Substitution of one CO group by halides ions, X = Cl, Br or I, forms the neutral $Mo(\eta\text{-}C_7H_7)(CO)_2X$.[7] Treatment of the latter with tertiary phosphines causes successive replacement of the two CO groups[8] whilst with cyclopentadienide salts the compound $Mo(\eta^3\text{-}C_7H_7)(CO)_2(\eta\text{-}C_5H_5)$ is isolated.[9] The compound $[Mo(\eta\text{-}C_7H_7)(CO)_3]BF_4$ reacts under photolysis with arenes giving the mixed sandwich compounds $[Mo(\eta\text{-}C_7H_7)(\eta\text{-arene})]BF_4$.[10] However, with acetonitrile the $\eta\text{-}C_7H_7$ ring is displaced, forming $Mo(MeCN)_3(CO)_3$.[5]

The compounds $[Mo(\eta\text{ - }C_7H_7)(\eta\text{ - arene})]A^-$ readily undergo displacement of the η-arene ring leading to many derivatives and, in particular, the compounds $[Mo(\eta\text{-}C_7H_7)L_3]A$, where L = MeCN or Me_2CO.[10,11] These solvate molecules are highly reactive towards substitution of the solvent ligands. Treatment of $[Mo(\eta\text{-}C_7H_7)(\eta\text{-arene})]A$ with methoxide or halides forms the dimers $[(\eta\text{-}C_7H_7)Mo(\mu\text{-}X)_3Mo(\eta\text{-}C_7H_7)]$, X = OR, Cl, Br or I.[12,13] An unusual tetrameric compound $[Mo(\eta\text{-}C_7H_7)(\mu^3\text{-}OH)]_4$ has been described.[14]

It appears that the $Mo(\eta\text{-}C_7H_7)$ moiety is more resistant to ring displacement and to nucleophilic addition reactions in those derivatives where CO ligands are absent.[15]

A preliminary communication of part of this study on the $Mo(\eta\text{-}C_7H_7)$dppe moiety has been published.[16]

RESULTS

Treatment of the compound

$$\{[Mo(\eta\text{-}C_7H_7)(\eta\text{-}C_6H_5Me)]PF_6\},$$

1, in acetone or acetonitrile with one equivalent of bis-1,2-(diphenylphosphino)ethane (dppe) causes displacement of the $(\eta\text{-}C_6H_5Me)$ ligand. The acetonitrile solutions give the red crystalline compound $\{[Mo(\eta\text{-}C_7H_7)(dppe)MeCN]PF_6\}$, **2**. The compound isolated from the acetone solution was a brown oily material. It was not found possible to either obtain consistent analyses or to isolate a crystalline sample. However, the material behaves as though it were the compound $\{[Mo(\eta\text{-}C_7H_7)(dppe)(Me_2CO)]PF_6\}$, **3**. For example, treatment of **3** with carbon monoxide gives $\{[Mo(\eta\text{-}C_7H_7)(dppe)CO]PF_6\}$, **4**. The compound **4** has been described previously and was prepared from $[Mo(\eta$-

* Author to whom correspondence should be addressed.

$C_7H_7)(CO)_2I]$, dppe and NH_4PF_6.[8] Addition of a chloride ion to solution of **3** forms [Mo(η-C_7H_7)(dppe)Cl], **5**, which crystallises from dichloromethane or toluene as green crystals which contain solvent molecules of crystallisation. The crystal structure of the compound [Mo(η-C_7H_7)(dppe)Cl]·toluene has been determined and is presented in Scheme 1 (Mo–Cl, 2.52; Mo–P, 2.50, 2.49 Å).[17] The ^{1}H NMR spectrum of both the dichloromethane and toluene solvate derivatives of **5** in C_6D_6 are anomalous since neither show bands assignable to a η-cycloheptatrienyl ligand although bands due to the dppe ligand are present.

Reduction of the hexafluorophosphate salt of the 17 electron cation [Mo(η-C_7H_7)(dppe)Cl]$^+$ (*vide infra*) with sodium amalgam in dichloromethane gave **5** in high yield. When the reduction was carried out in tetrahydrofuran solution then brown crystals were obtained whose stoichiometry also corresponded to **5** but whose ^{1}H NMR showed all the bands to be expected, including a triplet at δ 4.9 assignable to a η-cycloheptatrienyl group coupled to two equivalent ^{31}P nuclei. The brown isomer may be a polymorph of **5**.

Houk and Beall have described a compound [Mo(η-C_7H_7)(dppe)I].[8] We have prepared a compound **6** of the same stoichiometry from the reaction between **3** and lithium iodide. Initially a light green precipitate forms which redissolves and then brown crystals of **6** separate. Also, treatment of the acetonitrile derivative **2** with lithium iodide in acetonitrile followed by recrystallisation of the involatile products from acetone gives the compound **6**. The IR and NMR spectra of **6** do not correspond to that reported and, as found for the green isomer of **5**, the compound **6** did not show a band in the ^{1}H NMR spectrum assignable to the η-cycloheptatrienyl hydrogens. These anomalous absences of η-C_7H_7 resonances may be due to traces of paramagnetic impurities.

The compounds **5** and **6** are readily oxidised by iodine and, after addition of ammonium hexafluorophosphate, the paramagnetic compounds {[Mo(η-C_7H_7)(dppe)Cl]PF_6}, **7**, and {[Mo(η-C_7H_7)(dppe)I]PF_6}, **8**, are formed.

Addition of lithium iodide to the yellow compound **7** at room temperature resulted in an immediate reaction giving metathesis of the hexafluorophosphate anion and the blue iodide salt {[Mo(η-C_7H_7)(dppe)Cl]I, **9**, was isolated. Similarly, treatment of **7** with lithium bromide forms the compound {[Mo(η-C_7H_7)(dppe)Cl]Br}, **10**. Prolonged reaction between **7** and lithium iodide gave **8**, after addition of ammonium hexafluorophosphate.

In an unexpected reaction, it was found that treatment of **3** with dichloromethane or allyl chloride causes oxidation forming **7**. Similarly **3** undergoes oxidation in the presence of 1,2-dibromoethane giving {[Mo(η-C_7H_7)(dppe)Br]PF_6}, **11**.

The ESR data for the compounds **7**, **11** and **8** are given in Table 1. The spectra of the compound **7** and **11** both show hyperfine structure assignable to coupling of the unpaired electron with two equivalent ^{31}P nuclei, with the ^{95}Mo and ^{97}Mo nuclei and, possibly, also with the hydrogens of the η-cycloheptatrienyl ring and with either the Cl or Br nuclei. The spectra have not been fully assigned due to their complexity. The magnetic susceptibility data for the compounds **7**, **9**, **10** is consistent with the presence of one unpaired electron in the cations.

When **1** was treated with an excess of dppe salmon-pink crystals were obtained which had a stoichiometry corresponding to {[Mo(η-C_7H_7)$(dppe)_2$] PF_6}, **12**. The ^{1}H NMR of **12** in deuterioacetone or CD_3CN showed a *triplet* centered at δ 4.9 (J(P–H) 2.1 Hz) assignable to the η-cycloheptatrienyl hydrogens coupled to only two ^{31}P nuclei. The ^{31}P NMR in $(CD_3)_2CO$ showed two bands assignable to phosphorus in dppe systems. The band at -61.4 ppm has a chemical shift value close to that of the coordinated phosphorus in **2** whilst the second band had a chemical shift value at 13.5 ppm which is close to that of uncoordinated dppe. Thus it seems that the compound **12** dissociates a dppe ligand in acetonitrile or acetone solutions. In support of this observation it was found that treatment of **12** in acetone with carbon monoxide gives the compound **4**.

Reduction of **6** with sodium borohydride in tetrahydrofuran gives highly air sensitive red crystals of the hydrido compound [Mo(η-C_7H_7)(dppe)H], **13**. The compound reacts rapidly with $CDCl_3$ giving **5**. Treatment of **6** with methyllithium in warm tetrahydrofuran gives the expected methyl compound [Mo(η-C_7H_7)(dppe)Me], **14**.

DISCUSSION

The reactions and proposed structures for the new compounds are shown in Scheme 1. The characterising data are given in Table 1.

The question of the formal oxidation state of of the molybdenum centre in these compounds arises. Recently we have reported an extensive chemistry of the η-C_7H_7Ti system[18,19] in which we conclude that the η-C_7H_7 ligand is best described as having a formal trinegative charge so that, for example, the titanium centre in the compound Ti(η-C_7H_7)(dmpe)Cl classifies as d^0 (i.e. Ti(IV)).

By analogy, the molybdenum centre in the com-

Table 1. Analytical and spectroscopic data

Compound and colour	Analytical data (%)[a] C, H, N or Hal[c]	ESR, ^{1}H NMR[b], magnetic susceptibility data
2 {[Mo(η-C_7H_7)(dppe)(MeCN)]PF_6} Red	54.4 4.3 1.7 (54.5) (4.4) (1.8)	2.5, **20**, *c*, 4 Ph; 4.95, **7**, *t*(*J*(P–H) 2), C_7H_7; 7.4 and 7.55, **4**, *c*, $2CH_2$; 8.5, **3**, *t*(*J*(P–H = 1), Me[d,e]
5 [Mo(η-C_7H_7)(dppe)Cl] · C_6H_5Me Green	67.8 5.3 5.2 (67.5) (5.5) (5.0)	2.9, **25**, *c*, 5 Ph; 7.9, **3**, *o*, Me; 8.0, **4**, *m*, *br*, 2 CH_2[f,g]
6 [Mo(η-C_7H_7)(dppe)I] Green–brown	55.9 4.6 18.4 (55.6) (4.4) (18.0)	2.9, **20**, *c*, 4 Ph, 8.0, **4**, *c*, $2CH_2$[f]
7 {[Mo(η-C_7H_7)(dppe)Cl]PF_6} Yellow	52.4 4.3 4.7 (5.18) (4.0) (4.6)	μ_{eff} = 1.26 B.M.; ⟨g⟩ = 1.992(6); a_{iso} = 23;[h] a_{iso} = 5.5;[i] 1w.4[j]
8 {Mo(η-C_7H_7)(dppe)I]PF_6} Scarlet red	45.9 4.1 (46.2) (3.6)	⟨g⟩ = 2.056(8); 1w. = 64[k]
9 {[Mo(η-C_7H_7)(dppe)Cl]I} Blue	53.1 4.1 17.2 (53.0) (4.1) (17.0)	μ_{eff} = 0.450 B.M.
10 {[Mo(η-C_7H_7)(dppe)Cl]Br} Orange–yellow	55.7 4.6 12.0 (56.6) (4.1) (11.4)	μ_{eff} = 0.626 B.M.
11 {[Mo(η-C_7H_7)(dppe)Br]PF_6} Orange–yellow	49.0 4.1 10.4 (48.9) (3.8) (9.9)	⟨g⟩ = 2.015(8); a_{iso}(P) = 45,[h] a_{iso} = 6.3;[i] 1w.7[l]
12 {[Mo(η-C_7H_7)$(dppe)_2$]PF_6} Red	62.3 4.9[m] (62.8) (4.9)	2.45, 2.7, *c*, *br*, 8 Ph; 4.95, **7**, ?(*J*(P–H)2.1)C_7H_7; 7.5, **8**, *c*, *br*, $2CH_2$[d,n]
13 [Mo(η-C_7H_7)(dppe)H] Red	[o]	2.6, **20**, *c*, 4 Ph; 4.9, **7**, *d of t* (*J*(P–H) 2.1, *J*(H–H) 1.2), C_7H_7; 7.8, **4**, *m*, *br*, $2CH_2$; 13.9, **1**, *t*(*J*(P–H) 51), Mo–H[f]
14 [Mo(η-C_7H_7)(dppe)Me] Red	68.0 5.9 (68.0) (5.7)	3.1, **20**, *c*, 4 Ph, 5.5, **7**, *t*(*J*(P–H = 1.8), C_7H_7; 8.7, **4**, *c*, *br*, $2CH_2$; 10.8, **3**, *t*(*J*(P–H) 10.5), Me[f]

[a] Calculated values given in parentheses.

[b] ^{1}H NMR data given as: chemical shift (τ), relative intensity, *multiplicity* (J in Hz), assignment. ESR data; ⟨g⟩; a_{iso} in gauss, assignment; 1w. = average width of main lined (gauss).

[c] Not fluorine.

[d] In $(CD_3)_2CO$.

[e] ^{31}P NMR in CD_3CN: 65.5 (dppe); 144.5, 7 lines (J(P-F) 705.6), PF_6. Specific conductance in CH_2Cl_2 = 0.395 mho cm^{-2}. The CN stretch was at 2275w.

[f] In C_6D_6.

[g] The mass spectrum shows a parent ion peak at *m/e* = 622 (^{96}Mo).

[h] Coupling to two equivalent ^{31}I nuclei (gauss).

[i] Coupling to ^{35}Cl and ^{37}Cl and possibly to the hydrogens of the C_7H_7 ring (gauss).

[j] In acetone : methanol (1 : 1).

[k] In CH_2Cl_2.

[l] In acetone.

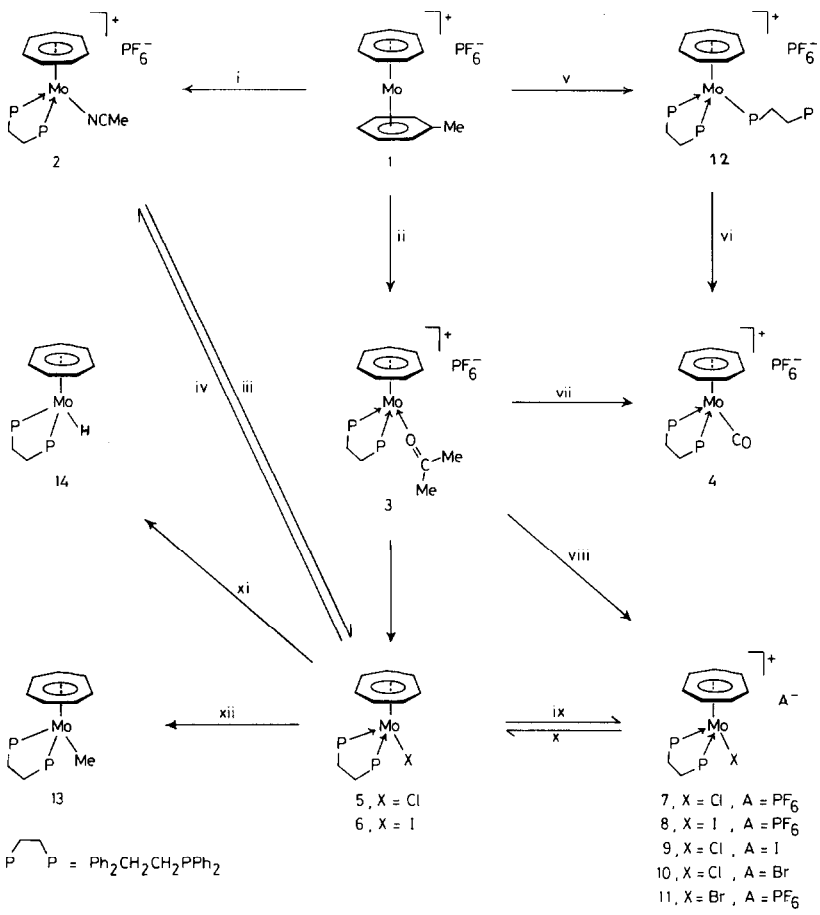
[m] Mo, 8.5 (8.1); P, 13.7 (13.1)%.

[n] ^{31}P NMR in $(CD_3)_2CO$: −61.4, 13.5, dppe; 144, 5$_x$septet (J(P–F) 705.6), PF_6.

[o] The stoichiometry was determined by the mass spectrum, *m/e* = 588 (^{96}Mo), corresponding to the parent ion.

pounds of the type Mo(η-C_7H_7)L_2X, and [Mo(η-C_7H_7)L_3]$^+$, where L = a two electron donor, and X = a one electron donor (e.g. Cl, Me), are described as d^2, i.e. Mo(IV). Correspondingly, the paramagnetic compounds [Mo(η-C_7H_7)L_2Cl]$^+$ are d^1 with Mo(V). This accounts for the observation of ESR spectra which are most characteristic of the presence of only one unpaired electron.

The observed reactivity of the Mo(η-C_7H_7) moiety is consistent with this description. For example, the extreme lability of the η-arene ring in [Mo(η-C_7H_7)(η-arene)]$^+$ and its facile displacement by relatively



Scheme 1.

(i) Dppe (1 equiv.) in acetonitrile at 65°C for 12 h, 74%.
(ii) Dppe (1 equiv.) in acetone at 65°C for 11 h, *ca* 50%.
(iii) Dissolve in acetonitrile at 20°C, 10 min, > 90%.
(iv) Excess of lithium iodide in acetonitrile at 20°C, 10 min, > 90%.
(v) Dppe (2 equivalent) in ethanol at 60°C for 24 h, > 90%.
(vi) Carbon monoxide at 1 atm in acetone at 20°C for 3 h, 42%.
(vii) Halides = Cl, Br or I. Lithium halides in acetone at 20°C for 30 min, > 70%.
(viii) X = Cl, dissolve in CH_2Cl_2 or allylchloride at room temperature for 10 min, > 90%.
X = Br, dissolve in 1,2-dibromoethane at room temperature for 15 min, > 90%.
(ix) X = Cl or I, add iodine at room temperature for 10 min, > 90%.
(x) X = Cl, stir with Na/Hg in CH_2Cl_2 at room temperature for 1 h, > 90%.
(xi) X = I, $Na[AlH_2(OCH_2CH_2OMe)_2]$ in toluene at 80°C for 1 h, 72%.
(xii) Methyllithium in toluene at 80°C for 1 h, 42%.

"hard" ligands such as halide, methoxide, acetone and MeCN is more consistent with a d^2 than a d^4, or, if the η-C_7H_7 ligands was thought to classify as $C_7H_7^+$, as a d^6 centre. The compound $[Mo(\eta\text{-}C_7H_7(CO)_2I]$ undergoes displacement of both CO ligands by the more strongly donor tertiary phosphine ligands.[8] In contrast, the CO ligands in the d^4 compounds $[Mo(\eta\text{-}C_5H_5)(CO)_3X]$ are much less labile.

The dimers $[(\eta\text{-}C_7H_7)Mo(\mu\text{-}X)_3Mo(\eta\text{-}C_7H_7)]$, X = OMe, Cl, Br, I, may be regarded as having formal d^0 centres, if a Mo–Mo bond is assumed, and reduction to the neutral paramagnetic compounds $[(\eta\text{-}C_7H_7)Mo(\mu\text{-}X)_3Mo(\eta\text{-}C_7H_7)]$ would provide a formal d^1 molybdenum centre, which is consistent with the observed ESR data.[12,13]

The chemistry of the system $[Mo(\eta\text{-}C_7H_7)(dppe)]$ compares generally with that of the well-known $Fe(\eta\text{-}C_5H_5)L_2$-moiety, for example, in the formation of the hydrido and alkyl derivatives.

EXPERIMENTAL

All preparations and reactions were carried out under an atmosphere of purified dinitrogen. Solvents were dried and purified by reflux over a suitable drying agent under dinitrogen, followed by distillation under dinitrogen. Microanalyses were performed by the analytical department of this laboratory or by Alfred Bernhardt Ltd.

IR spectra were recorded on a Pye–Unicam SP2000 double beam, grating spectrophotometer or a Perkin–Elmer 457 double beam, grating spectrophotometer.

NMR spectra were recorded on a JEOL PMX60 (^{1}H, 60 MHz), a Bruker WH90 (^{1}H, 90 MHz; ^{31}P, 36.43 MHz). Solvent bands were used as internal standards. Mass spectra were recorded on an A.E.I. MS 902 spectrometer. ESR spectra were determined on a JEOL JES-PE instrument at 9.5 GHz and calibrated against MnO as external standard.

Bis - 1,2 - (diphenylphosphino)ethane(η - cyclo - heptatrienyl)acetonitrilemolybdenum hexafluoro - phosphate, **2**

The compound $\{[Mo(\eta\text{-}C_7H_7)(\eta\text{-}C_6H_5Me)]PF_6\}$ (1.0 g, 2.36 mmol), prepared as described,[12] and dppe (0.91 g, 2.34 mmol) in acetonitrile (40 cm^3) were heated at 65°C for 12 h. The solution was concentrated under reduced pressure at 70°C and allowed to cool. Red crystals separated and were collected washed with toluene and dried under reduced pressure. Yield 74%.

Synthesis of **3** *from* $\{[Mo(\eta\text{-}C_7H_7)(\eta\text{-}C_6H_5Me)]PF_6\}$

The compound

$$\{[Mo(\eta\text{-}C_7H_7)(\eta\text{-}C_6H_5Me)]PF_6\}$$

(0.76 g, 1.8 mmol) in acetone (20 cm^3) was treated with 1,2-bis(diphenylphosphino)ethane (0.71 g, 1.8 mmol) at 65°C for 11 h. The solvent was removed under reduced pressure and the brown frothy residue of the material **3** was used without further purification in the reactions described below, yield 1.55 g. [Found: C, 54.6 (54.9); H, 6.0 (4.7)%.] Crystals obtained from concentrated acetone solutions analysed as C, 52.6 (54.9); H, 5.1 (4.7)%.

Bis - 1,2 - (diphenylphosphino)ethane(η - cyclo - heptatrienyl)carbonylmolybdenum hexafluorophosphate, **4**

Method A. The compound **3** (0.3 g, 0.38 mmol) in acetone (5 cm^3) was treated with carbon monoxide at 1 atm for 3 h. The initially brown solution became red. Ethanol (20 cm^3) was added and the solution was concentrated under reduced pressure giving red crystals. These were recrystallised twice from dichloromethane: petroleum ether (40–60°C) mixture. The resulting red crystals were washed with petroleum ether (40–60°C) (2 × 10 cm^3) and dried *in vacuo*, 0.12 g, 42%. The compound was identified by analysis. [Found (calc.): C, 53.6(53.9); H, 3.9(4.1)%.] Specific conductance in CH_2Cl_2 was 0.435 mho cm^{-2}. The IR spectrum was identical to that described (the CO stretch was at 1952vs cm^{-1}).

Method B. The compound

$$\{[Mo(\eta\text{-}C_7H_7)(dppe)_2]PF_6\}$$

(0.07 g, 0.06 mmol) in dicholoromethane (5 cm^{-3}) was treated with carbon monoxide at 1 atm and at room temperature for 5 h. The solvent was removed under reduced pressure and the residue was recrystallised from acetone: ethanol mixture. The resulting crystals were washed with petroleum ether (40–60°C) (2 × 10 cm^3) and dried *in vacuo*, 0.023 g, *ca* 50%.

Bis - 1,2 - (diphenylphosphino)ethane(η - cyclo - heptatrienyl)chloromolybdenum, **5**

Method A. The compound **3** (0.2 g, 0.25 mmol) in acetone (10 cm^3) was treated with lithium chloride (0.2 g, 4.8 mmol) in acetone (20 cm^3). The initially brown solution turned green. After 2 h the solvent was removed under reduced pressure and the residue was extracted with toluene (10 cm^3). The extract was filtered and petroleum ether (100–120°C) was added to the filtrate. Concentration of the mixture under reduced pressure gave green needle crystals which were collected and dried *in vacuo* 0.13 g, 72%.

Method B. The compound $\{[Mo(\eta\text{-}C_7H_7)(dppe)Cl]PF_6\}$ (0.5 g, 0.65 mmol) in dichloromethane (40 cm^3) was treated with sodium amalgam (10 g of 2% sodium in mercury) and stirred for 1.5 h. The mixture was allowed to stand for 2 h and the green supernatant solution was separated by filtration and the filtrate was treated with petroleum ether (60–80°C: 60 cm^3). After concentration under reduced pressure green crystals separated over a period of several days, 0.2 g, 44%. [Analytical data for $[Mo(\eta\text{-}C_7H_7)(dppe)Cl]\cdot\frac{1}{2}CH_2Cl_2$: Found (calc.): C, 57.9(57.9); H, 4.6(4.6); Cl, 14.9(15.1)%.]

Bis - 1,2 - (diphenylphosphino)ethane(η - cyclo - heptatrienyl)iodomolybdenum, **6**

A solution of the compound **3**, prepared from **1** (0.50 g, 1.18 mmol) in acetone (5 cm^3) and dppe (1 equivalent) in acetone (5 cm^3) was treated with

anhydrous lithium iodide (0.5 g, 3.75 mmol) in acetone (10 cm^3). Fibrous green crystals separated immediately but after 15 min these redissolved and a new precipitate of brown lustrous cubic crystals separated. These were collected, washed with acetone (2 × 5 cm^3) and dried *in vacuo*, 0.73 g, *ca* 87%. The specific conductance in CH_2Cl_2 was 0.0094 mho cm^{-2}. The mass spectrum showed a parent ion peak at $m/e = 714$.

The compound could be recrystallised from toluene: petroleum ether (100–120°C) mixture as yellow–green fibrous crystals whose IR spectrum differed slightly from that of the brown–green cubic crystals.

Bis - 1,2 - (*diphenylphosphino*)*ethane*(*η* - *cyclohepta* - *trienyl*)*chloromolybdenum hexafluorophosphate*, **7**

Method A. The compound **3** (0.5 g) was dissolved in dichloromethane (20 cm^3). After 15 min at room temperature the solution was yellow–orange. The solvent was removed under reduced pressure and the residue was recrystallised from acetone: ethanol mixture, *ca* 90%.

Method B. The compound

$$[Mo(\eta\text{-}C_7H_7)(dppe)Cl]$$

(0.1 g, 0.16 mmol) in dichloromethane was treated with iodine (0.2 g, 0.7 mmol). Addition of petroleum ether (60–80°C) followed by concentration under reduced pressure precipitated black crystals. These were separated and dissolved in aqueous acetone. Aqueous ammonium hexafluorophosphate was added and the mixture was concentrated giving yellow crystals which were collected and dried *in vacuo*, *ca* 90%.

Bis - 1,2 - (*diphenylphosphino*)*ethane*(*η* - *cyclo* - *heptatrienyl*)*iodomolybdenum hexafluorophos* - *phate*, **8**

The compound $[Mo(\eta\text{-}C_7H_7)(dppe)I]$ (0.18 g, 0.25 mmol) in toluene (80 cm^3) was treated with one equivalent of iodine in toluene (10 cm^3) giving a black precipitate. This was collected and extracted with aqueous acetone. The extract was filtered and aqueous ammonium hexafluorophosphate was added. The filtrate was concentrated under reduced pressure giving scarlet red crystals. These were recrystallised from dichloromethane: petroleum ether (40–60°C), yield 90%.

Bis - 1,2 - (*diphenylphosphino*)*ethane*(*η* - *cyclo* - *heptatrienyl*)*chloromolybdenum iodide*, **9**

The compound $\{[Mo(\eta\text{-}C_7H_7)(dppe)Cl]PF_6\}$, **7** (0.2 g, 0.26 mmol), was treated with anhydrous lithium iodide (0.5 g, 3.7 mmol) in acetone (10 cm^3). Blue crystals separated and after 4 h these were collected, washed with ethanol and dried *in vacuo*, *ca* 72%.

Bis - 1,2 - (*diphenylphosphino*)*ethane*(*η* - *cyclo* - *heptatrienyl*)*chloromolybdenum bromide*, **10**

The compound $\{[Mo(\eta\text{-}C_7H_7)(dppe)Cl]PF_6\}$, **7** (0.2 g, 0.26 mmol) was treated with anhydrous lithium iodide (0.5 g, 3.7 mmol) in acetone (10 cm^3). Orange–yellow crystals separated and after 4 h these were collected, washed with ethanol and dried *in vacuo*, *ca* 75%.

Bis - 1,2 - (*diphenylphosphino*)*ethane*(*η* - *cyclohepta* - *trienyl*)*bromomolybdenum hexafluorophosphate*, **11**

The compound was prepared from **3** and 1,2-dibromoethane as described for the chloro analogue **7**, *ca* 90%.

Bis(1,2 - *bis*(*diphenylphosphino*)*ethane*)(*η* - *cyclo* - *heptatrienyl*)*molybdenum hexafluorophosphate*, **12**

The compound

$$\{[Mo(\eta\text{-}C_7H_7)(\eta\text{-}C_6H_5Me)]PF_6\}$$

(0.4 g, 0.94 mmol) and dppe (1.0 g, 2.54 mmol) in ethanol (150 cm^3) were heated at 60°C for 24 h. The mixture was cooled to room temperature and pink crystals separated together with white crystals of dppe. The solid was separated and washed with diethyl ether (2 × 20 cm^3) and the residue was recrystallised from acetone: ethanol mixture. The red crystals were collected, washed with diethyl ether and dried *in vacuo*, 0.6 g, 50%.

Bis - 1,2 - (*diphenylphosphino*)*ethane*(*η* - *cyclo* - *heptatrienyl*)*hydridomolybdenum*, **13**

The compound $Na[AlH_2(OCH_2CH_2OMe)_2]$ (0.6 cm^3 of a 70% solution in benzene, 2.08 mmol) was added to $[Mo(\eta\text{-}C_7H_7)(dppe)I]$ (1.0 g, 1.41 mmol) in toluene (30 cm^3) and the mixture was heated to 90°C for 1.5 h. The initially brown solution became red and, after cooling to room temperature, water (0.5 cm^3) was added. The toluene layer was separated and concentrated under reduced pressure. Addition of petroleum ether (100–120°C) gave red rhombic crystals which were collected and washed with cold petroleum ether (30–40°C) and dried *in vacuo*, *ca* 73%. The compound is pyrophoric in air.

Bis - 1,2 - (*diphenylphosphino*)*ethane*(*η* - *cyclo* - *heptatrienyl*)*methylmolybdenum*, **14**

Methyl-lithium (1.6 cm^3 of a 1.9 M solution in diethyl ether, 3.05 mmol) was added to [Mo(*η*-

C_7H_7)(dppe)I] (0.2 g, 0.28 mmol) in tetrahydrofuran (40 cm^3). The mixture rapidly became red. It was warmed to 65°C for 15 min and then the solvent was removed under reduced pressure. The red residue was extracted with toluene (2 × 20 cm^3) and wet diethyl ether (5 cm^3) was added. Concentration of the mixture and addition of petroleum ether (100–120°C) (20 cm^3) gave deep red prism crystals. These were collected, washed with petroleum ether (30–40°C) and dried *in vacuo*, 0.07 g, *ca* 42%. The mass spectrum show a parent ion peak at $m/e = 602$.

Acknowledgements—We wish to thank the S.E.R.C. for support (to R.B.A.P.) and the Petroleum Research Fund administered by the American Chemical Society for partial support. We thank the Climax Molybdenum Company for a generous gift of chemicals.

REFERENCES

1. S. W. Kirtley, In *Comprehensive Organometallic Chemistry* (Edited by G. Wilkinson, F. G. A. Stone and E. W. Abel), Chapter 27, Volume 3. Pergamon Press, Oxford (1982).
2. R. B. King, *Organometallic Synthesis* 1965, **1**, 141.
3. G. R. Clark and G. J. Palenik, *J. Organomet. Chem.* 1973, **50**, 185.
4. G. R. John, L. A. P. Kane-Maguire and D. A. Sweigart, *J. Organomet. Chem.* 1976, **120**, C47 (and references therein).
5. K. M. Al-Kathumi and L. A. P. Kane-Maguire, *J. Chem. Soc., Dalton Trans.* 1973, 1683.
6. E. E. Isaacs and W. A. G. Graham, *J. Organomet. Chem.* 1976, **120**, 407.
7. R. A. Zelonka and M. C. Baird, *J. Organomet. Chem.* 1972, **44**, 383.
8. T. W. Beall and L. W. Houk, *Inorg. Chem.* 1972, **11**, 915; T. W. Beall and L. W. Houk, *Inorg. Chem.* 1973, **12**, 1979.
9. R. B. King and M. B. Bisnette, *Inorg. Chem.* 1964, **3**, 785.
10. M. Bochmann, M. Cooke, M. Green, H. P. Kirsch, F. G. A. Stone and A. J. Welch, *J. Chem. Soc., Chem. Commun.* 1976, 381.
11. M. L. H. Green and J. Knight, *J. Chem. Soc., Dalton Trans.* 1976, 213.
12. E. F. Ashworth, M. L. H. Green and J. Knight, *J. Less-Common Metals* 1974, **36**, 213; E. F. Ashworth, J. C. Green, M. L. H. Green, J. Knight, R. B. A. Pardy and N. Wainwright, *J. Chem. Soc., Dalton Trans.* 1977, 1693.
13. M. Bochmann, M. Green, H. P. Kirsch and F. G. A. Stone, *J. Chem. Soc., Dalton Trans.* 1977, 714.
14. C. Couldwell and K. Prout, *Acta Cryst. B* 1978, **34**, 2439.
15. B. Kanellakopulos, D. Nothe, K. Weidhammer, H. Wienard and M. L. Ziegler, *Angew. Chem., Int. Ed.* 1977, **16**, 261.
16. M. L. H. Green and R. B. A. Pardy, *J. Organomet. Chem.* 1978, **C13**, 117.
17. A. J. Smith, Part II thesis, Oxford, 1976.
18. M. L. H. Green, N. J. Hazel, P. D. Grebenik, V. S. B. Mtetwa and K. Prout, *J. Chem. Soc., Chem. Commun.* 1983, 356.
19. C. E. Davies, I. Gardner, J. C. Green, M. L. H. Green, N. J. Hazel, V. S. B. Mtetwa and K. Prout, *J. Chem. Soc., Dalton Trans.* 1984, in press.

Polyhedron Vol. 4, No. 6, pp. 1043–1046, 1985
Printed in Great Britain

0277-5387/85 $3.00 + .00
© 1985 Pergamon Press Ltd

SYNTHESIS, CHARACTERIZATION AND CRYSTAL STRUCTURE OF THE ANILINIUM β-OCTAMOLYBDATE DIHYDRATE

P. ROMÁN* and J. M. GUTIÉRREZ-ZORRILLA
Departamento de Química Inorgánica, Univ. del País Vasco, Apartado 644, 48080 Bilbao, Spain

C. ESTEBAN-CALDERÓN, M. MARTÍNEZ-RIPOLL and S. GARCÍA-BLANCO
Departamento de Cristalografía, Instituto Rocasolano, CSIC, Serrano 119, 28006 Madrid, Spain

(*Received* 2 *July* 1984; *accepted* 7 *November* 1984)

Abstract—The anilinium β-octamolybdate dihydrate has been prepared in acidic aqueous solution. TG, DTG, IR and ^{1}H NMR techniques have been used to identify the compound. It belongs to a series of molybdates of alkyl-N- and -N,N-substituted anilinium cations. Single crystals have been analyzed by X-ray diffraction. Crystal data are: $(C_6H_8N)_4[Mo_8O_{26}]\cdot 2H_2O$, space group $P\bar{1}$, $Z = 1$, $a = 10.007(1)$, $b = 8.014(2)$, $c = 14.645(8)$Å, $\alpha = 109.81(3)$, $\beta = 108.59(2)$, $\gamma = 85.44(2)°$, $V = 1052.9(6)$ Å^3, $D_o = 2.49(1)$, $D_x = 2.52$ mg m^{-3}, $R = 0.026$ and $R_w = 0.031$ for 5297 observed reflexions. The crystal structure consists of discrete $[\beta\text{-}Mo_8O_{26}]^{4-}$ polyanions, two crystallographically independent $(C_6H_8N)^+$ cations and one independent water molecule. Polyanions are linked to the cations and to the water molecules by hydrogen bonds of types N–H···O and O–H···O.

In a previous paper[1] we reported on the different types of octamolybdate anions. It seems that in the solid state the most frequent type is the β-isomer. In order to investigate the other types, we have tried with a family of protonated organic bases such as anilinium, N-methylanilinium, N-ethylanilinium, N,N-dimethylanilinium and N,N-diethylanilinium. The first analyzed member, the title compound, corresponds to the β-octamolybdate family. The alkylanilinium polymolybdates have been prepared and they will be reported soon.

EXPERIMENTAL

Aniline (5 cm^3) was added to a stirred suspension of MoO_3 (5 g) in hot water (850 cm^3, 80°C). The slightly turbid solution (pH = 2.5) was filtered. Crystals of anilinium octamolybdate dihydrate (**I**) appeared in the solution after two days. The brownish prismatic crystals were washed with water, ethanol and ether and finally dried in air. They were found to be stable to air, light and X-ray exposure.

Compound **I** appeared to be a dihydrate; Found: Mo, 48.39; C, 18.26; H, 2.19; N, 3.68; weight loss at 570°C, 72.60%; Calc. for $(C_6H_8N)_4[Mo_8O_{26}]\cdot 2H_2O$: Mo, 48.09; C, 18.06; H, 2.27; N, 3.51; weight loss at 570°C, 72.15%.

IR spectra were recorded in KBr pellets or as Nujol mulls on a Beckman IR-4240 (4000–250 cm^{-1}) spectrophotometer. ^{1}H NMR spectra were recorded on a Perkin–Elmer R-12B (60 MHz) instrument in deuterated DMSO solution using TMS as internal standard. TG and DTG analyses were performed with a Perkin–Elmer TGS-2 thermobalance in nitrogen stream under atmospheric pressure.

The cell parameters, as given in the abstract, were determined by least-squares fit from the 2θ values of 35 reflexions measured for both positive and negative Bragg angles. The crystal dimensions were $0.20 \times 0.15 \times 0.20$ mm. An automatic four-circle diffractometer with graphite monochromated Mo-K_α radiation ($\lambda = 0.71069$ Å) was used. Intensity data for 6034 independent reflexions were collected up to $\theta = 30°$ with an $\omega/2\theta$ scan technique. No absorption corrections were applied ($\mu = 23.97$

* Author to whom correspondence should be addressed.

cm^{-1}). After correction for Lorentz and polarization effects, 5297 reflexions with $I > 3\sigma(I)$ were considered as observed and used in the remaining calculations. Scattering factors for neutral atoms and anomalous dispersion corrections for Mo were taken from the literature.[2] The Mo atoms were located on a Patterson synthesis and the structure was expanded by Fourier syntheses. Several cycles of anisotropic least-squares refinement (unit weights and H-atoms as isotropic fixed contributors) gave the disagreement indices $R = 0.026$ and $R_w = 0.031$ for the observed reflexions.

Lists of atomic parameters, observed and calculated structure factors and anisotropic thermal coefficients for non-H atoms have been deposited with the Editor as supplementary material.*

* Supplementary material has also been deposited with the Cambridge Crystallographic Data Centre.

Table 1. Mo–O distances in Å, within the polyanion. For symmetry codes see Table 3

Mo1–O10	1.710(4)	Mo2–O3	1.692(3)
Mo1–O1	1.718(3)	Mo2–O11	1.703(4)
Mo1–O2	1.890(3)	Mo2–O6	1.919(3)
Mo1–O4	1.986(2)	Mo2–O2	1.942(3)
Mo1–O5	2.317(3)	Mo2–O7(v)	2.322(4)
Mo1–O8(v)	2.321(3)	Mo2–O5	2.501(3)
Mo3–O12	1.700(4)	Mo4–O13	1.712(4)
Mo3–O7	1.751(3)	Mo4–O9	1.713(3)
Mo3–O4	1.943(3)	Mo4–O6	1.872(3)
Mo3–O8	1.958(3)	Mo4–O8	2.004(3)
Mo3–O5	2.149(2)	Mo4–O5	2.299(3)
Mo3–O5(v)	2.398(3)	Mo4–O4(v)	2.376(3)

Three families of Mo–O distances:

Short	1.71(2)
Medium	1.94(4)
Long	2.34(10)

Table 2. Bond angles (°) in MoO_6 octahedra. For symmetry codes see Table 3

O1–Mo1–O2	100.6(1)	O2–Mo2–O3	103.6(1)
O1–Mo1–O4	101.2(1)	O2–Mo2–O5	72.2(1)
O1–Mo1–O5	161.4(1)	O2–Mo2–O6	141.2(1)
O1–Mo1–O10	104.8(2)	O2–Mo2–O11	98.7(2)
O1–Mo1–O8(v)	89.7(1)	O2–Mo2–O7(v)	75.8(1)
O2–Mo1–O4	146.3(1)	O3–Mo2–O5	160.4(1)
O2–Mo1–O5	77.5(1)	O3–Mo2–O6	104.2(1)
O2–Mo1–O10	100.3(1)	O3–Mo2–O11	106.0(1)
O2–Mo1–O8(v)	82.3(1)	O3–Mo2–O7(v)	90.9(2)
O4–Mo1–O5	73.6(1)	O5–Mo2–O6	72.6(1)
O4–Mo1–O10	98.6(1)	O5–Mo2–O11	93.7(1)
O4–Mo1–O8(v)	72.4(1)	O5–Mo2–O7(v)	69.5(1)
O5–Mo1–O10	93.7(1)	O6–Mo2–O11	99.1(2)
O5–Mo1–O8(v)	71.6(1)	O6–Mo2–O7(v)	77.2(1)
O10–Mo1–O8(v)	164.4(1)	O11–Mo2–O7(v)	163.1(1)
O4–Mo3–O5	78.4(1)	O5–Mo4–O6	78.4(1)
O4–Mo3–O7	97.2(1)	O5–Mo4–O8	73.3(1)
O4–Mo3–O8	148.7(1)	O5–Mo4–O9	159.1(1)
O4–Mo3–O12	103.3(1)	O5–Mo4–O13	94.4(1)
O4–Mo3–O5(v)	78.1(1)	O5–Mo4–O4(v)	72.3(1)
O5–Mo3–O7	156.5(1)	O6–Mo4–O8	146.5(1)
O5–Mo3–O8	77.7(1)	O6–Mo4–O9	100.4(1)
O5–Mo3–O12	98.2(1)	O6–Mo4–O13	102.6(1)
O5–Mo3–O5(v)	75.0(1)	O6–Mo4–O4(v)	83.8(1)
O7–Mo3–O8	96.7(1)	O8–Mo4–O9	99.7(1)
O7–Mo3–O12	105.2(1)	O8–Mo4–O13	97.2(1)
O7–Mo3–O5(v)	81.5(1)	O8–Mo4–O4(v)	70.9(1)
O8–Mo3–O12	99.9(1)	O9–Mo4–O13	106.1(2)
O8–Mo3–O5(v)	76.3(1)	O9–Mo4–O4(v)	86.8(1)
O12–Mo3–O5(v)	172.7(1)	O13–Mo4–O4(v)	164.0(1)

Most calculations were performed using the XRAY76 System[3] running on a VAX 11/750 computer.

DISCUSSION

Compound I exhibits in the IR spectrum the well known bands for the $[\beta\text{-}Mo_8O_{26}]^{4-}$ polyanion.[4,5] The octamolybdate anion is assumed to have C_{2h} symmetry. This assumption agrees roughly with the X-ray model. The lines at 950 and 910 cm^{-1} have been assigned to the Mo–O_t stretching vibrations, the strong band at 925 cm^{-1} corresponding to the Mo–O stretching. The Mo–O bending and stretching vibrations are represented by the peaks at 845 and 740 cm^{-1}, while the Mo–O–Mo bendings are associated with the lines at 655, 545, 520, 460, 380 and 360 cm^{-1}.

Anilinium cations and water molecules have been detected in the IR spectrum between 3600 and 1000 cm^{-1}. ^1H NMR spectra present a broad singlet (δ = 5.4 ppm, 3H), showing a protonated aniline.

The thermal decomposition of I shows its hydrated state. The two water molecules are lost in two stages corresponding to the ranges 95–130 and 130–176°C. There are nine stages in the total thermal decomposition, the final product being MoO_3 as characterized by IR and powder diffraction. The formation of MoO_3 corresponds to the weight loss given in the chemical analysis.

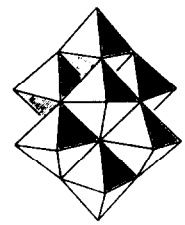


Fig. 1. The $[\beta\text{-}Mo_8O_{26}]^{4-}$ polyanion.

The anionic unit is built up of eight MoO_6 distorted octahedra sharing edges and corners. These centrosymmetric units are the well known $[\beta\text{-}Mo_8O_{26}]^{4-}$ polyanions.[6–9] The Mo–O distances within these units are listed in Table 1, where three families of Mo–O bond lengths are found, short, medium and long. A drawing of this atomic group can be seen in Fig. 1. The O–Mo–O bond angles are shown in Table 2. The distortion of the MoO_6 octahedra has been evaluated in terms of $\Delta = \Sigma |d_i - \bar{d}|/12$, where d_i represents the individual O–O

Table 3. Interatomic contacts

X–H···Y	X···Y (Å)	X–H (Å)	H···Y (Å)	<X–H···Y (°)
	Hydrogen bonds			
N17–H171···O14 W(i)	2.773(6)	0.89	1.92	161°
N17–H172···O1 (ii)	2.914(6)	0.96	2.30	121
N17–H173···O1 (iii)	2.907(6)	1.13	1.79	172
N27–H271···O9 (iv)	3.060(6)	0.89	2.28	146
N27–H272···O13 (ii)	3.015(5)	0.92	2.11	168
N27–H273···O10 (ii)	2.889(6)	1.07	1.94	146
O14 W–H141···O2 (v)	2.832(6)	1.16	2.04	122
O14 W–H142···O8 (vi)	3.127(6)	0.86	2.48	133
	Other contacts			
N17···O9 (vii)	2.950(5)			
N17···O7 (i)	3.143(6)			
N27···O11 (ii)	3.020(6)			
N27···O12 (ii)	2.975(5)			
O14 W···O7	3.167(5)			
O14 W···O14 W (vi)	3.011(7)			

Symmetry codes

(i) 1−x, 1−y, 1−z
(ii) 1+x, y, 1+z
(iii) −x, 1−y, 1−z
(iv) 1+x, 1+y, 1+z
(v) −x, −y, −z
(vi) 1−x, −y, −z
(vii) x, 1+y, 1+z

distances within each octahedra. The values around Mo1, Mo2, Mo3 and Mo4 are 0.09, 0.10. 0.07 and 0.09, respectively.

Anilinium cations, octamolybdate anions and water molecules are linked together through hydrogen bonds of types N–H···O and O–H···O as well as through other interatomic contacts shown in Table 3.

REFERENCES

1. P. Román, M. E. González-Aguado, C. Esteban-Calderón and M. Martínez-Ripoll, *Inorg. Chim. Acta* 1984, **90**, 115.
2. *International Tables for X-ray Crystallography*, Vol. 4, pp. 72–98. Kynoch Press, Birmingham (1974).
3. J. M. Stewart, *The XRAY76 System*, Computer Sci. Center, Univ. of Maryland, College Park, Maryland.
4. L. E. Lyhamn and S. J. Cyvin, *Z. Naturforsch.* 1979, **34a**, 867.
5. W. P. Griffith and P. J. Lesniak, *J. Chem. Soc.* (*A*) 1969, 1066.
6. P. Román, J. Jaud and J. Galy, *Z. Krist.* 1981, **154**, 59.
7. P. Román, M. Martínez-Ripoll and J. Jaud, *Z. Krist.* 1982, **158**, 141.
8. P. Román, A. Vegas, M. Martínez-Ripoll and S. García-Blanco, *Z. Krist.* 1982, **159**, 291.
9. J. Fuchs and J. Knöpnadel, *Z. Krist.* 1982, **158**, 165.

Polyhedron Vol. 4, No. 6, pp. 1047–1050, 1985
Printed in Great Britain

0277–5387/85 $3.00+.00
© 1985 Pergamon Press Ltd

INTERACTIONS BETWEEN EUROPIUM(III) ION AND METHYL GLYCOFURANOSIDES IN AQUEOUS SOLUTION

ANTTI VESALA* and RAINER KÄPPI
Department of Chemistry and Biochemistry, University of Turku, SF-20500 Turku, Finland

(*Received* 24 *September* 1984; *accepted* 9 *November* 1984)

Abstract—The interactions between Eu(III) ion and some methyl glycofuranosides have been studied luminometrically in aqueous solution. The measurements were based on the delayed fluorescence of the Eu(III) ion known to be environmentally sensitive. The reciprocal lifetimes, i.e., the decay constants of this fluorescence, depend on the number of OH bonds in the primary hydration sphere of the ion. These were determined in aqueous glycofuranoside solutions of various concentrations. These data enable us to discuss the effect of ligand configuration on the binding sites in the formed complexes. The formation constants for these complexes have been evaluated with the aid of decay rate equations.

Luminescence excitation spectroscopy of the $^7F_0 \rightarrow {}^5D_0$ transition in the Eu(III) ion has been successfully applied to the study of the environment of the metal ion in solutions of various ligands and biomolecular systems.[1] The luminescence decay constants derived from the excited-state lifetimes have been observed to correlate with the number of OH bonds in the primary solvation sphere of the europium ion.[2,3] The technique has been applied in cases, where ligands are charge bearing and the interactions strong.[4] On the other hand, weak interactions that common anions like Cl^-, NO_3^- and ClO_4^- in aqueous solutions exert on the europium ion have been studied in this way so that even formation constants could be determined.[5,6] The utility of the technique is increased by the fact that in solution the Eu(III) ion functions as a satisfactory model for an ion with noble gas structure even in biological systems.[1]

We have previously studied the interactions that some s-block cations, especially alkaline earth metal cations, exert on monomeric carbohydrates with low molecular weight, methyl aldofuranosides. Employing calorimetric and potentiometric techniques stoichiometries and strengths of the interactions could have been elucidated.[7–12] The results seem to be in agreement with the concept that the interactions are strongest if the ligand has a *cis–cis* triol configuration or its structure is close to that.[13]

The aim of the present study is to apply luminometric measurements in furthering our knowledge about the neighbourhood of a spherical cation in the solutions of neutral ligands with oxygen donors. Since the determined decay constants are dependent on the number of OH oscillators in the solvation sphere of the cation, detectable effects are expected to occur when water molecules with their two OH bonds are replaced by the hydroxyl groups or ether oxygens of the glycoside. Owing to the special character of the OH bonds in the method it is possible to differentiate between bindings *via* hydroxyl and ether oxygens. Also the distinction between inner sphere and outer sphere complexes can be discussed on the basis of the data.

EXPERIMENTAL

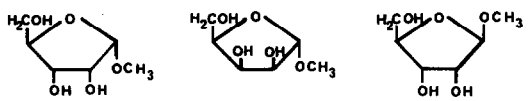
The reagents were commercial ($EuCl_3 \cdot 6H_2O$, Aldrich) or were prepared as described elsewhere (the glycosides).[14–16] Distilled and degassed water was used through all experiments. The concentration of the Eu(III) ion was 0.010 mol dm^{-3} in each solution. The sample solutions were prepared by weighing appropriate amounts of glycoside and determining the density and concentration of the resulting solution by a Parr 45 densitometer. The solid 1:2 europium–glycoside adducts were prepared by dissolving the reagents in minimum amount of water. The mixture was then evaporated in a vacuum desiccator to a constant weight. Because of their hygroscopic nature the adducts were kept in a desiccator until measured.

* To whom correspondence should be addressed.

The intensity of emission of europium fluorescence at 592 nm was followed by a Perkin–Elmer Luminescence Spectrometer LS-5, which was controlled by an Apple II Microcomputer. The excitation was taken place at the wavelength of 395 nm. The intensity of emission falls exponentially. Therefore the exact lifetimes of the excited state can be extracted from semilogarithmic plots of intensity vs. time of delay. The luminescence decay constant is defined as the reciprocal lifetime of the excited state. With the aid of the Apple II Computer it was possible to select measuring conditions and the number of consecutive determinations. Six intensity values were recorded at each time increment. The observed decay constants are collected in Table 1. The values measured in H_2O and D_2O solutions satisfactorily agree with those reported earlier.[2,3,5,6] The experiments with solid samples were carried out by measuring the luminescence emission of a thin sample layer on a cell holder. Because of the great deliquescence of the samples the results proved to be tentative. Temperature was maintained constant in the experiments by a Haake Thermostat. The control was carried out by a thermistor and a Fluke 8860 A Digital Multimeter.

RESULTS AND DISCUSSION

Previous results indicate detectable complex forming abilities of methyl α-D-ribo- (1) and methyl β-D-lyxofuranosides (2) with alkaline earth metal and lanthanum ions, whereas methyl β-D-ribofuranoside (3) shows only a weak ability.[7–12] The present



(1) (2) (3)

luminometric data (Table 1) agree well with this concept. The decay constants remain almost unchanged for β-riboside, while those for the other glycosides decrease clearly even at low ligand concentrations. The magnitudes of this decrease differ with α-riboside and α-lyxoside owing to the stabilities and/or the binding sites of the formed complexes.

In this study the ligand concentrations vary from 2 to 400 times the metal ion concentration. While 1 : 1 stoichiometry was established on the calorimetric basis, where these concentrations had equal magnitudes,[9,10] 1 : 2 stoichiometry has also to be accounted for. This can be seen in Fig. 1, where the curvature of the plots with decreasing $[L]^{-1}$ can be assigned to this phenomenon. The observed k values for the solid 1 : 2 adducts were 4.8–5.1 ms^{-1} for α-

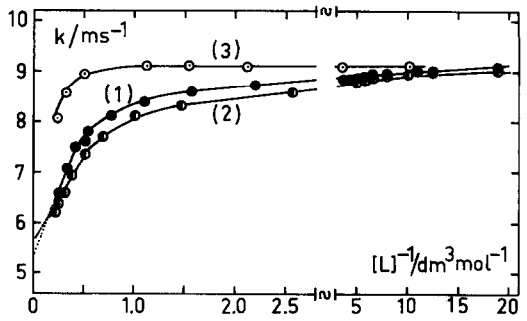


Fig. 1. The observed decay constants for the delayed fluorescence of Eu(III) ion vs reciprocal ligand concentration in solutions of the ligands (1), (2) and (3).

lyxoside and 4.1–4.3 ms^{-1} for α-riboside as ligands. These agree quite well with the intercepts of the curves in Fig. 1, because it has to be noticed that the solid adducts most probably contain one chloride in the inner solvation sphere of the ion, i.e., have the form of $[EuClL_2(H_2O)]^{2+}$.[5] In solution samples the concentration of this form is negligible because of low metal and chloride concentrations.

The hypotheses on the binding sites of the ligands are based on the previous information[7,8] and the recent communication by Angyal.[17] The binding is assumed to take place via MeO-1, HO-2 and HO-3 for methyl α-D-ribofuranoside and via HO-2, HO-3 and HO-5 for methyl α-D-lyxofuranoside. Methyl β-D-ribofuranoside may interact via two oxygens.[7] Accordingly, when the hydrated metal ion and the glycoside ligand are interacting, the loss of three water molecules occurs for both (1) and (2), but the gains of 2 OH and 3 OH, respectively, make the net loss of 2 H_2O for (1) and 1.5 H_2O for (2). If the number of water molecules in the primary hydration sphere of the Eu(III) ion is assumed to be nine,[1] the decay constants for the various forms of complexes can be calculated with the aid of the Horrocks–Sudnick correlation.[2] Here a value of $k(H_2O) - k(D_2O) = 9.12 - 0.41 = 8.71$ ms^{-1} corresponds to 9 H_2O, i.e. we get 0.484 ms^{-1} for each OH bond. By using this value the decay constants of 4.28 ms^{-1} and 5.25 ms^{-1} can be calculated for the solid α-riboside and α-lyxoside adducts mentioned above. In the solution the metal and chloride concentrations are low compared with the ligand concentration. That is why, three emitting forms have to be assumed to exist, viz. $[Eu(H_2O)_n]^{3+}$ (form A),

$$[EuL(H_2O)_{n-x}]^{3+},$$

(form B) and

$$[EuL_2(H_2O)_{n-2x}]^{3+},$$

(form C). The decay constants for the above forms,

Table 1. The determined reciprocal excited state lifetimes (decay constants) of Eu(III) ion along with various ligand concentrations at 298 K

Ligand, L	[L] (mol dm^{-3})	k (ms^{-1})
H_2O soln	—	9.12[a]
D_2O soln	—	0.41
(1) Methyl α-D-ribofuranoside	0.030	9.15
	0.050	9.10
	0.080	9.10
	0.091	9.03
	0.125	8.98
	0.150	8.98
	0.175	8.89
	0.200	8.86
	0.240	8.85
	0.272	8.85
	0.453	8.72
	0.635	8.60
	0.907	8.40
	1.30	8.12
	1.80	7.82
	1.91	7.61
	2.40	7.50
	2.87	7.08
	3.81	6.58
(2) Methyl α-D-lyxofuranoside	0.030	9.07
	0.050	9.05
	0.080	9.02
	0.098	8.98
	0.125	8.94
	0.150	8.91
	0.175	8.87
	0.200	8.83
	0.390	8.58
	0.680	8.29
	0.980	8.05
	1.44	7.70
	1.97	7.37
	2.48	6.95
	3.00	6.60
	3.50	6.36
	4.00	6.22
(3) Methyl β-D-ribofuranoside	0.0985	9.12
	0.289	9.10
	0.471	9.11
	0.644	9.15
	0.892	9.10
	2.00	8.95
	3.00	8.56
	4.00	8.01

[a] The standard errors of the k values varied from 0.02 ms^{-1} to 0.04 ms^{-1}.

k_A, k_B and k_C, based on the assumptions presented have been calculated for the three ligands in Table 2. In conclusion, the data and the binding hypotheses appear to be in agreement.

The complex equilibria (1) and (2) prevail in the solution and are determined by the conventional constants β_1 and β_2.

$$[Eu(H_2O)_n]^{3+} + L = [EuL(H_2O)_{n-x}]^{3+} + xH_2O \quad (1)$$

$$[Eu(H_2O)_n]^{3+} + 2L = [EuL_2(H_2O)_{n-2x}]^{3+} + 2xH_2O. \quad (2)$$

Provided that the equilibria are established in times shorter than the lifetimes of the excited states we can define the observed decay constant with the aid of constants k_A, k_B, k_C, β_1 and β_2.[18,19] If the total concentration of the emitting species is S ($=A+B+C$), the decay rate is defined by eqn (3).

$$-\frac{dS}{dt} = k_A A + k_B B + k_C C. \quad (3)$$

When the concentrations of the emitting species are calculated via the equations for β_1 and β_2, we get

$$-\frac{dS}{dt} = \frac{k_A + k_B\beta_1[L] + k_C\beta_2[L]^2}{1+\beta_1[L]+\beta_2[L]^2} S. \quad (4)$$

The observed decay constant is then

$$k = \frac{k_A + k_B\beta_1[L] + k_C\beta_2[L]^2}{1+\beta_1[L]+\beta_2[L]^2}. \quad (5)$$

Because of the insensitivity of eqn (5) it is not possible to evaluate the whole set of parameters with a reasonable accuracy from the available data. If the 1:1 complex is assumed to be a major form at [L] < 0.2 mol dm^{-3}, eqn (5) is reduced to

$$k = \frac{k_A + k_B\beta_1[L]}{1+\beta_1[L]}. \quad (6)$$

The above equation can be rearranged to give β_1. When this is done, the constants of (0.77 ± 0.12) dm^3 mol^{-1} for (1) and (1.22 ± 0.08) dm^3 mol^{-1} for (2) are derived. These results agree with the previous observation about the order of stability of lanthanum ion–glycofuranoside complexes in methanolic solution.[11] A noticeable matter is that this order is the reverse of the respective Ca^{2+} system. One reliable explanation may be the influence of the greater charge in the central ion. This is able to change the ligand into a favourable configuration. This means especially α-lyxoside, where the binding occurs via the hydroxymethyl group. On the other hand, the calorimetrically determined enthalpies of

Table 2. Calculated decay constants for various metal to ligand species (see text) in aqueous solution

Ligand	k_A (ms^{-1})	k_B (ms^{-1})	k_C (ms^{-1})
(1) Methyl α-D-ribofuranoside	9.12	7.18	5.25
(2) Methyl α-D-lyxofuranoside	9.12	7.67	6.22
(3) Methyl β-D-ribofuranoside	9.12	8.15[a]	

[a] Based on the interaction via two oxygens.

interaction have shown to be more negative for the Ca^{2+} system. As the observed stability constants are roughly of equal magnitude (for Ca^{2+} system $\beta_1 =$ 1.4 and 0.9 $dm^3\,mol^{-1}$, respectively for the ligands (1) and (2)) the complex formation is favoured by entropy in the La^{3+} and Eu^{3+} systems.

The constants β_2 can be roughly evaluated by eqn (5). Values of 0.5 $dm^6\,mol^{-2}$ for α-lyxoside and 0.05 $dm^6\,mol^{-2}$ for α-riboside as ligands can be obtained from the data in ligand concentrations that exceed 0.2 mol dm^{-3}. These constants, although tentative, show that 1 : 2 interactions are meaningful.

It is evident on the basis of the present data that the interactions between the spherical ion and the given ligands occur in the inner solvation sphere of the ion. These are present even at moderately low concentrations depending on the configuration of the ligand. Packing of H_2O molecules towards the inner sphere of the cation that seems to take place, for instance, with ClO_4^- anion[5,6] have not been detected.

To quantify the thermodynamics of the system, measurements are in progress at various temperatures. Despite the insensitivity of the equations derived, the method, however, belongs to the few by which reliable information can be obtained from weak interactions between compounds which are difficult to analyze.

Acknowledgement—Financial aid from the Academy of Finland, the Research Council of Natural Sciences is gratefully acknowledged.

REFERENCES

1. F. S. Richardson, *Chem. Rev.* 1982, **82**, 541.
2. W. DeW. Horrocks Jr. and D. R. Sudnick, *J. Am. Chem. Soc.* 1979, **101**, 334.
3. C. C. Bryden and C. N. Reilley, *Anal. Chem.* 1982, **54**, 610.
4. M. Albin, G. K. Farber and W. DeW. Horrocks Jr., *Inorg. Chem.* 1984, **23**, 1648.
5. P. J. Breen and W. DeW. Horrocks Jr., *Inorg. Chem.* 1983, **22**, 536.
6. F. Tanaka and S. Yamashita, *Inorg. Chem.* 1984, **23**, 2044.
7. H. Lönnberg and A. Vesala, *Carbohydrate Res.* 1980, **78**, 53.
8. H. Lönnberg, A. Vesala and R. Käppi, *Carbohydrate Res.* 1980, **86**, 137.
9. A. Vesala and H. Lönnberg, *Acta Chem. Scand.* 1981, **A35**, 123.
10. A. Vesala, H. Lönnberg, R. Käppi and J. Arpalahti, *Carbohydrate Res.* 1982, **102**, 312.
11. A. Vesala, R. Käppi and P. Lehikoinen, *Finn. Chem. Lett.* 1983, 45.
12. A. Vesala, R. Käppi and H. Lönnberg, *J. Solution Chem.* 1984, **13**, 471.
13. S. J. Angyal, *Chem. Soc. Rev.* 1980, **9**, 415 (and the references therein).
14. H. Lönnberg, A. Kankaanperä and K. Haapakka, *Carbohydrate Res.* 1977, **56**, 277.
15. H. Lönnberg and A. Kulonpää, *Acta Chem. Scand.* 1977, **A31**, 306.
16. H. Lönnberg and L. Valtonen, *Finn. Chem. Lett.* 1978, 209.
17. S. J. Angyal, private communication.
18. Y. Haas and G. Stein, *J. Phys. Chem.* 1971, **75**, 3668.
19. Y. Haas and G. Stein, *J. Phys. Chem.* 1971, **75**, 3677.

Polyhedron Vol. 4, No. 6, pp. 1051–1057, 1985
Printed in Great Britain

0277–5387/85 $3.00 + .00
© 1985 Pergamon Press Ltd

PREPARATION OF NOVEL POLYMER LIGANDS CONTAINING TETRAAZA MACROCYCLIC SCHIFF BASE AS A HIGHLY SELECTIVE EXTRACTANT FOR COPPER(II)

NOBORU KUBOTA, MANABU FUJIWARA, TAKAYUKI MATSUSHITA* and TOSHIYUKI SHONO

Department of Applied Chemistry, Faculty of Engineering, Osaka University, Yamadaoka, Suita, Osaka 565, Japan

(*Received* 24 *September* 1984; *accepted* 9 *November* 1984)

Abstract—Three types of the novel polymer ligands in which 6,8,15,17-tetramethyl-dibenzo-5,9,14,18-tetraaza-cyclotetradecene (L) is present as an integral part of the polymer backbone have been prepared. These polymer ligands are oligomers whose polymerization degree may be about five. Their complexing abilities and extractabilities for copper(II) and nickel(II) have been investigated. Among the polymer ligands, Poly-L3, which contains triethyleneglycol bis(*p*-phenylene) group as a linkage group, was found to be an excellent extractant for copper(II).

Selective separation of heavy metal ions is an important subject in the fields of industrial and analytical chemistry. For this purpose, many extractants and chelating resins have so far been synthesized and some of them have been applied in practice. Zolotov *et al.* have reported that the macrocyclic Schiff base ligand (L, Fig. 1) exhibits a high selectivity for copper(II) in solvent extraction.[1,2] However, its extraction rate was found to be slow compared with those observed for the alkylated derivatives of saturated tetraaza macrocycles.[3] This may be caused by the rigid structure of L itself, which results in a slow rate of the complex formation as found in the case of porphyrins.[4]

We have preliminarily reported that the polymer ligand (Poly-L1, Fig. 1), in which L is present as an integral part of the polymer backbone, exhibits a high selectivity for copper(II) as well as L in the solvent extraction and that the extraction rate by Poly-L1 is much faster than that by L.[5] In the present paper, we describe the preparation of the novel polymer ligands shown in Fig. 1 and their extractabilities for copper(II) and nickel(II).

EXPERIMENTAL

Preparation of dianhydride derivative of L

The monomeric ligand, 6,8,15,17 - tetramethyl - dibenzo - 5,9,14,18-tetraaza-cyclotetradecene (L), was prepared by the method described in the literature.[6] Dianhydride derivative of L was obtained by reacting 4-chloroformylphthalic anhydride with L, by a slight modification of the method described in the literature[7] as follows. A solution of 4-chloroformylphthalic anhydride[8,9] (3.79 g, 18.0 mmol) in 30 cm^3 of acetonitrile was added dropwise to a hot (65°C) solution of acetonitrile (700 cm^3) containing L (3.10 g, 9.0 mmol). After the mixture was stirred for 20 min, it was cooled in an ice-water bath for 2 h to give a brownish orange precipitate. It was collected on a glass filter and dried *in vacuo*. The precipitate was dissolved in 100 cm^3 of chloroform with stirring and filtered off. The reddish orange filtrate was concentrated to about 40 cm^3 and poured into 1000 cm^3 of petroleum ether to give a brownish orange precipitate. It was filtered, washed with petroleum ether, and recrystallized from benzene to give the dianhydride of L as reddish orange crystals in an 18% yield (1.13 g). Found: C, 68.84; H, 4.27; N, 8.04%. Calc. for $C_{40}H_{28}O_8N_4$: C, 69.36; H, 4.07; N, 8.09%.

Preparation of polymer ligands

Three types of polymer ligands were prepared by polycondensation of the above dianhydride of L with diamines such as 1,3-propanediamine, 4,4'-diaminodiphenyl ether, and triethyleneglycol bis(4-aminophenyl) ether.

Preparation of Poly-L1

To a solution of 1,3-propanediamine (0.16 g, 2.15 mmol) in 50 cm^3 of *N*-methyl-2-pyrrolidone (NMP)

* Author to whom correspondence should be addressed.

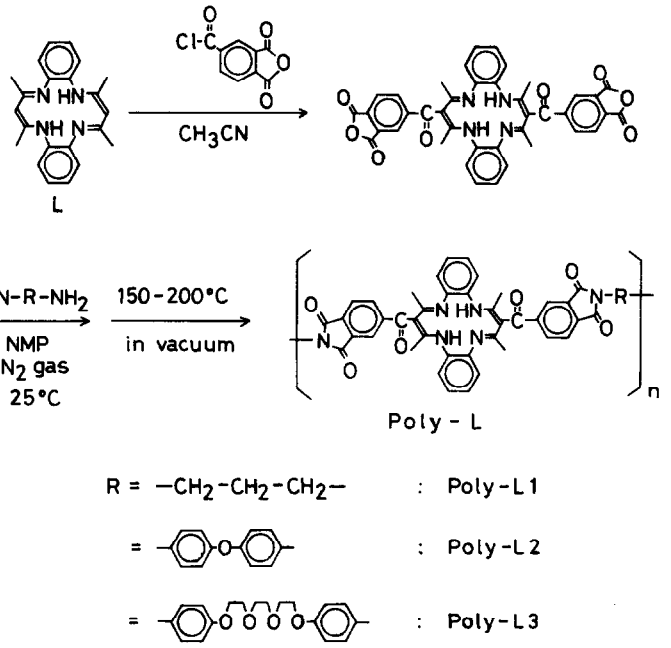


Fig. 1. Synthesis of polymer ligands.

was added a powdered dianhydride of L (1.49 g, 2.15 mmol) at 25°C under nitrogen atmosphere, and the yellowish orange solution was stirred vigorously for 3 h. It was poured into 1200 cm^3 of ether to give a yellow precipitate, which was collected on a glass filter, washed with ether, and dried *in vacuo*. The yield of the product, which was Poly(amic acid)-1, was 1.61 g. Found: C, 65.19; H, 5.27; N, 10.86%. Calc. for $(C_{43}H_{38}N_5O_9)$-$(C_{43}H_{38}N_6O_8)_4$-NH_2: C, 67.04; H, 5.02; N, 10.91%. This Poly(amic acid)-1 was converted to Poly(imide)-1 upon heating near 185°C for 1 h under vacuum. This was confirmed by the IR spectrum of the resulting brownish orange powder: absorption bands due to imide ring appeared at 1770 and 1710 cm^{-1} and those due to amide around 1630 cm^{-1} disappeared. This product, which is abbreviated as Poly-L1 hereafter, is soluble in chloroform and *N*,*N*-dimethylformamide (DMF) but insoluble in methanol (MeOH) and water.

Preparation of Poly-L2

A powdered dianhydride of L (0.48 g, 0.7 mmol) was added to a solution of 4,4′-diaminodiphenyl ether (0.14 g, 0.7 mmol) in 4 cm^3 of NMP under nitrogen atmosphere, and the solution was stirred vigorously at 25°C for 4 h. The highly viscous, yellowish orange solution was poured into 150 cm^3 of MeOH to give a yellow precipitate. It was filtered, washed with MeOH and then ether, and dried *in vacuo*. The yield of the product, which was Poly(amic acid)-2, was 0.60 g. This was converted to Poly(imide)-2 upon heating near 190°C for 1 h under vacuum. The conversion was confirmed by the IR spectrum of the resulting brownish yellow powder as described above. However, this product was partially insoluble in chloroform, so that a soluble part in chloroform was separated from it for use as a solvent extractant. The above Poly(imide)-2 (0.4 g) was added to 80 cm^3 of chloroform and the mixture was stirred at room temperature for 1 h, and the insoluble part was removed by filtration. The reddish orange filtrate was concentrated to about 15 cm^3 and poured into 200 cm^3 of petroleum ether to give a brownish orange precipitate. It was collected on a glass filter, washed with MeOH and then ether, and dried *in vacuo*. The yield was 0.24 g. This Poly(imide)-2 is abbreviated as Poly-L2 hereafter.

Preparation of Poly-L3

Triethyleneglycol bis(4-aminophenyl) ether [m.p.: 94.0–95.0°C, MS (*m/e*): 332 (M^+)] was obtained by hydrogenation of triethyleneglycol bis(4-nitrophenyl) ether [m.p.: 99.5–100°C, MS (*m/e*): 392 (M^+)] which was prepared by the reaction between *p*-nitrophenol and triethyleneglycol dibromide in the presence of K_2CO_3 in acetone.

To a solution of triethyleneglycol bis(4-aminophenyl) ether (0.17 g, 0.5 mmol) in 3 cm^3 of NMP was added a powdered dianhydride of L (0.35

g, 0.5 mmol) at 25°C under nitrogen atmosphere, and the solution was stirred vigorously for 5 h. The highly viscous yellowish orange solution was poured into 125 cm^3 of MeOH to give a yellow precipitate. It was filtered, washed with MeOH and then ether, and dried *in vacuo*. The yield of the product, which was Poly(amic acid)-3, was 0.4 g. This was converted to Poly(imide)-3 upon heating at 150°C for 30 min under vacuum. Its conversion was confirmed by the IR spectrum of the resulting brownish orange powder as described in the above polymer ligands. This Poly(imide)-3 is soluble in chloroform and DMF but insoluble in MeOH and water, which is abbreviated as Poly-L3 hereafter.

The analytical data and ^1H NMR spectral data in $CDCl_3$ for these polymer ligands are summarized in Table 1 along with their intrinsic viscosities in NMP.

Complexation in DMF

The complexation reactions of L and the polymer ligands with copper(II) and nickel(II) were studied in a homogeneous DMF solution. An absorption cell (cell length: 10 mm) with a stopper containing a DMF solution (5 cm^3) of L (5.0×10^{-5} M, 1 M = 1 mol dm^{-3}) or a polymer ligand (5.0×10^{-5} unit M) was thermostated at 25 ± 0.1°C. After the measurement of the absorption spectrum of the DMF solution over the range from 280 to 700 nm, a DMF solution of a metal acetate (0.1 cm^3, 2.5×10^{-3} M) was added to it. The absorption cell was shaken several times and thermostated again. And then the absorption spectra of the mixed DMF solution were measured at regular time intervals. The extent of the complexation was calculated from the absorption spectral changes.

Procedure for solvent extractions

Solvent extractions were carried out by shaking a 10 cm^3 test-tube (inner diameter: 14 mm) with a stopper at room temperature, which contains a chloroform solution (5 cm^3) of the ligand as an organic phase and an equivolume of acetate buffer solution (0.2 M) of the metal acetate as an aqueous phase. After a definite time of shaking, the content of the residual metal ions in aqueous phase was determined by atomic absorption spectrometry.

Measurements

UV and visible absorption spectra were recorded on a Hitachi 340 recording spectrophotometer. IR spectra were recorded on a Hitachi 215 grating spectrophotometer. Atomic absorption spectra were attained by use of a Nippon Jarrel Ash AA-1. ^1H NMR spectra were taken with a JEOL-PS 100 spectrometer, using $CDCl_3$ as the solvent and TMS as the internal standard. A pH value of a sample solution was measured with a Shibata 671 pH meter. Viscosities of the polymer ligands were measured in NMP with an Ostwald viscometer at 25°C, and the solutions of the polymer ligands were prepared in concentration from 0.05 to 0.80 g/100 cm^3 of NMP.

Table 1. Elemental analyses, ^1H NMR spectral data, and intrinsic viscosities of the polymer ligands

Polymer ligand	Found (calc.)[b]			δ (ppm)[c]			
	C	H	N	Methyl	Methylene	Phenyl ring	$[\eta]$[d]
Poly-L1	69.90 (69.98)	5.11 (4.75)	11.51 (11.39)	2.0 (2.14)	2.1, 3.8 (1.00)	7.0–8.5 (2.39)	0.12
Poly-L2[a]	69.39 (72.28)	4.23 (4.29)	8.99 (9.73)				0.17
Poly-L3[a]	68.05 (70.02)	4.78 (5.08)	7.93 (8.49)	2.0 (1.00)	3.8, 3.9, 4.2 (1.25)	7.0–8.5 (1.93)	0.36

[a] Ash was left in the elemental analyses of these polymer ligands.

[b] For Poly-L1 and Poly-L2, calculated on the assumptions that one of the end groups of a polymer chain is an amine moiety and the other a carboxyl moiety and that the polymerization degree (n) is five. For Poly-L3, calculated on the assumptions that both end groups are amine moieties and n is four.

[c] Measured in $CDCl_3$. The values in parentheses are relative ratios calculated from the integrated signal intensities.

[d] Measured in NMP at 25°C. Under the same conditions, the η_{sp}/C values (C = 0.80 g/100 cm^3) for polystyrene oligomers were 0.06 (MW = 1400) and 0.09 (MW = 2500).

Materials

All reagents were of reagent grade. Chloroform and acetonitrile were refluxed over P_2O_5 and distilled. *N,N*-dimethylformamide was distilled over CaH_2 under reduced pressure prior to use. Other solvents were purified by a usual manner. Water was deionized. Acetate buffer solutions (0.2 M) were used for adjusting pH from pH 3.5 to 5.8. The pH values below pH 3.5 or above pH 5.8 were adjusted by addition of an adequate amount of 1 M hydrochloric acid or sodium hydroxide.

RESULTS AND DISCUSSION

Polymerization degree of polymer ligands

Polymerization degree of the polymer ligands was estimated from viscosities, ^1H NMR spectra, and elemental analyses (Table 1). The intrinsic viscosities of the polymer ligands were determined by the extrapolation of the linear η_{sp}/C vs C plots to infinite dilution, where η_{sp} and C denote a specific viscosity and a concentration of the polymer solution, respectively. Specific viscosities of two polystyrene oligomers, whose molecular weights are determined to be *ca.* 1400 and 2500, are included in Table 1 for comparison. The relatively low viscosities of the polymer ligands indicate that these are oligomers whose polymerization degrees may be about five. Of course, they may consist of a mixture of polymer chains having different polymerization degrees.

The ^1H NMR spectrum of the Poly-L1 in $CDCl_3$ exhibited the following resonances: methyl protons at 2.0 ppm, methylene protons at 2.1 and 3.8 ppm, and phenyl ring protons in the 7.0–8.5 ppm region. The integrated intensity ratio $CH_3:CH_2:C_6H_4$ and C_6H_3 is 2.14:1.00:2.39. These values agree reasonably with the calculated values 2.00:1.00:2.33 from the assumption that one of the end groups of a polymer chain is an amine moiety and the other a carboxyl moiety. In addition, the analytical data for Poly-L1 are in best agreement with the calculated values on the basis of the above assumption and the polymerization degree (n) of five (Table 1). On the other hand, the integrated intensity ratio of the signals for Poly-L3 is 1.00 (CH_3): 1.25 (CH_2): 1.93 (C_6H_4 and C_6H_3), which is in agreement with the calculated value 1.00:1.25:2.00 based on the assumptions that both of the end groups of the polymer chain are amine moieties and that the polymerization degree is four. However, the analytical data for Poly-L3 deviate slightly from the calculated value on the basis of the above assumptions. This is believed to be due to the formation of ash in the elemental analysis.

As for Poly-L2, ^1H NMR spectrum could not be measured owing to poor solubility in $CDCl_3$, and also the ash was left in this case. However, this polymer ligand is considered to be an oligomer from the relatively low viscosity as well as Poly-L1 and Poly-L3.

Complexations of L and polymer ligands with copper(II) and nickel(II) in DMF

The complexing abilities of L and the polymer ligands for copper(II) and nickel(II) were studied in a homogeneous DMF solution. These were obtained from the absorption spectral changes of the DMF solution containing each of the ligands and the equimolar amount of the metal ion. Figure 2 shows the absorption spectral changes caused by the complex formation between (A) L and copper (II) and (B) Poly-L1 and copper(II). In the former case, the absorption maximum of L was shifted from 344 to 382 nm with decreasing its intensity and increasing the intensity of the new absorption band. With Poly-L1 the absorption maximum was shifted from 322 to 382 nm. For other systems, similar spectral changes were observed; the absorption maximum of the free ligands around 330 nm was shifted to around 380 and 390 nm by the complex formation with copper(II) and nickel(II), respectively. These results are summarized in Table 2. It should be noted that the pattern in the absorption spectral changes for the polymer ligands is quite similar to that for the monomer ligand, L. This indicates that the metal ions are coordinated with N_4-macrocyclic hole of the polymer ligands to form a square planar complex as well as the case of L.

From these absorption spectral changes the rates of complex formation for all systems were determined. As shown in Fig. 2, however, the rates of complex formation slowed down rapidly after 2 h even in the cases of copper(II). Thus, the final state that means a 100% complexation of the ligand was not obtained under the above conditions. Therefore, the final states for the complexation of L with the metal ions were estimated from the molar extinction coefficients of the isolated complexes; Cu(L) and Ni(L). On the other hand, those for the polymer ligands were obtained from the absorption spectra when excess amounts of the metal ions were further added to the DMF solutions after spectral changes were no longer observed. Figure 3 shows the plots of the extent of complexation of L and the polymer ligands with copper(II) and nickel(II). In each ligand, the complexation rate with copper(II) was found to be much faster than that with nickel(II). Moreover, the complexation rates of the ligands with both metal ions were found to be faster in the order of L $\ll$ Poly-

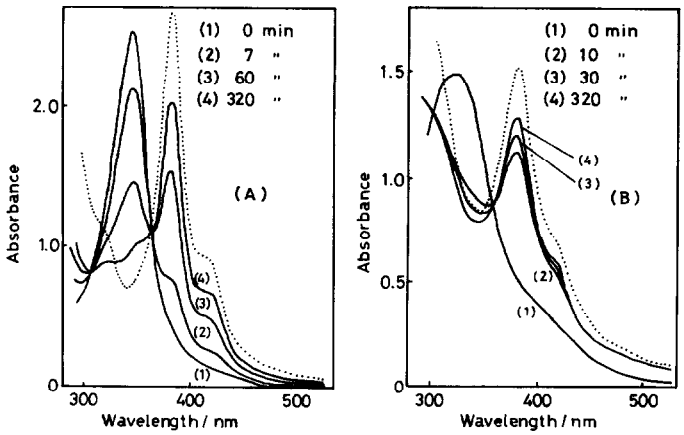


Fig. 2. Absorption spectral changes by complexation of (A) L (5×10^{-5} M) and (B) Poly-L1 (5×10^{-5} unit M) with copper(II) (5×10^{-5} M) in DMF solutions at 25°C. Absorption spectra shown by dotted lines were obtained by the addition of excess copper(II) (5×10^{-4} M). Cell length: 10 mm.

L1 ≃ Poly-L2 < Poly-L3. These results indicate that the polymer ligands possess a high selectivity for copper(II) as well as L and a faster complexation rate than that of L. These findings led us to apply the polymer ligands as selective extractants for copper(II).

Solvent extraction

The extractabilities of the polymer ligands obtained in the present work for copper(II) and nickel(II) have been investigated in comparison with L.

Effect of shaking time on extraction

Figure 4 shows the effect of shaking time on extraction of copper(II) by L and the polymer ligands under the conditions: the pH values of aqueous phase were adjusted to 5.6 with acetate buffer (0.2 M) and the concentration of the ligands in organic phase was ten times as much as that of copper(II) in aqueous phase (1×10^{-4} M). With the polymer ligands a 100% extraction of copper(II) was achieved after shaking within 30 min, whereas with L the extraction attained the equilibrium at *ca* 95% after shaking for 2 h. Noticeably, all of copper(II) in aqueous phase was extracted by Poly-L3 within 10 min. That is to say, the extraction rates of copper(II) by the polymer ligands are much faster than that by L. On the other hand, no nickel(II) was extracted by these ligands after shaking for 8 h (L), for 4 h (Poly-L1 and Poly-L2), and for 2 h (Poly-L3). These results are

Table 2. Absorption maxima of the ligands and their complexes with copper(II) and nickel(II)

Ligand	$\frac{\lambda \text{ max}}{\text{nm}}$ (log ε)		
	Free ligand	Copper(II) complex	Nickel(II) complex
L	344 (4.70)	382 (4.73)	392 (4.53)
Poly-L1	322 (4.48)	382 (4.51)	388 (4.41)
Poly-L2	314 (4.46)	380 (4.46)	386 (4.36)
Poly-L3	320 (4.47)	382 (4.49)	386 (4.41)

The molar extinction coefficients for the polymer ligands and their complexes are determined as per unit mol.

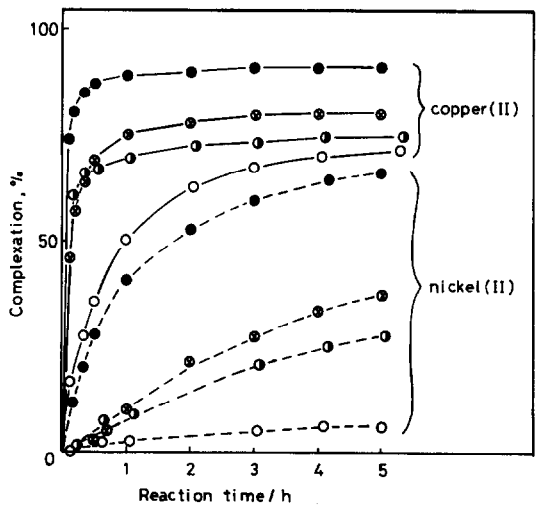


Fig. 3. Time-courses of complexation of L (5×10^{-5} M) and polymer ligands (5×10^{-5} unit M) with copper(II) and nickel(II) (5×10^{-5} M) in DMF solutions at 25°C. (○): L, ◑: Poly-L1, ⊗: Poly-L2, ●: Poly-L3.

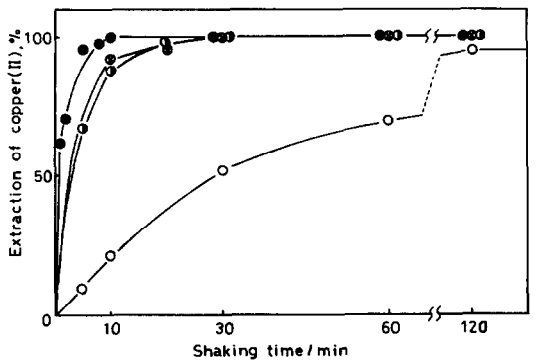


Fig. 4. Effect of shaking time on extraction of copper(II) (1×10^{-4} M) by L (1×10^{-3} M) and polymer ligands (1×10^{-3} unit M) at pH 5.6. ○: L, ◑: Poly-L1, ⊗: Poly-L2, ●: Poly-L3.

consistent with those observed in the complexation reactions described above.

Effect of pH on extraction

Figure 5 shows the pH dependence of extraction of copper(II) by the ligands. The concentrations of the ligands in organic phase and of copper(II) in aqueous phase were the same as those described in the above. The following shaking time was adopted for each system; 2 h for L, 30 min for Poly-L1 and Poly-L2, and 10 min for Poly-L3. These are the adequate time which is needed for attainment of the extraction equilibrium as mentioned above. The efficiency of extraction by these ligands decreases with a decrease in pH of the aqueous phase. In the case of the polymer ligands, the maximal extraction (100%) was observed in the pH range 5–7. Whereas, in the case of L, it was observed in the narrow pH range around 6.75.

Effect of molar ratio of copper(II) to ligand

Figure 6 shows the effect of the molar ratio of copper(II) to the polymer ligands. The concentration of the ligands in the organic phase was kept constant (1×10^{-3} unit M) and that of copper(II) in aqueous phase was varied from 1×10^{-4} to 1×10^{-3} M at pH 5.6. The shaking time was 60 and 30 min for Poly-L1 and Poly-L3, respectively. The efficiency of extraction increases with decrease in the molar ratio of copper(II) to the ligand. It is noticeable that Poly-L3 can extract copper(II) completely at the molar ratio of 1:5 (copper(II): unit M of the ligand), whereas with Poly-L1 and Poly-L2 the molar ratio of 1:10 was needed for its attainment (100%) in the same shaking time, 30 min (see Fig. 4). This indicates that Poly-L3 possesses the highest extractability for copper(II) among the polymer ligands investigated here.

Recovery of copper(II)

The recovery of copper(II) which was transferred into the organic phase by the complex formation with the polymer ligands was carried out by shaking with acidic solution. First, the copper(II) in aqueous phase (1×10^{-4} M) was transferred into the organic phase containing the polymer ligand (1×10^{-3} unit M) at pH 5.6 by shaking for 60 min for Poly-L1 and Poly-L2 and for 30 min for Poly-L3. After the complete extraction of copper(II), conc. hydrochloric acid (0.25 cm^3) was added to the aqueous phase and then shaken for an adequate time. The back-extracted copper(II) into the acidic aqueous solution was determined by atomic absorption spectrometry. The results are shown in Fig. 7. The recovered copper(II) was increased with an increase

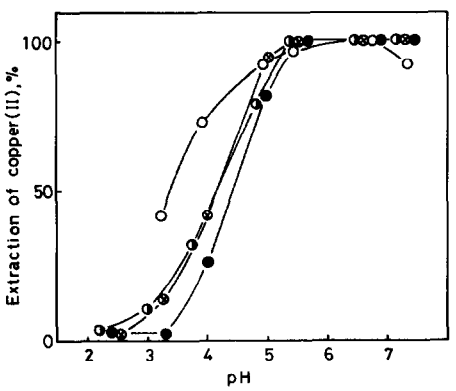


Fig. 5. The pH dependence of extraction of copper(II) (1×10^{-4} M) by L (1×10^{-3} M) and polymer ligands (1×10^{-3} unit M). ○: L (shaking for 2 h), ◑: Poly-L1 (for 30 min), ⊗: Poly-L2 (for 30 min), ●: Poly-L3 (for 10 min).

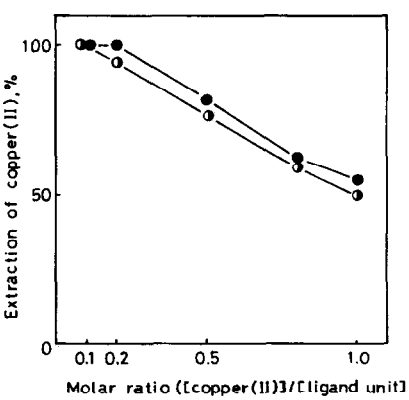


Fig. 6. Effect of the molar ratio of copper(II) to polymer ligands (1×10^{-3} unit M) on extraction at pH 5.6. ◑: Poly-L1 (shaking for 60 min), ●: Poly-L3 (for 30 min).

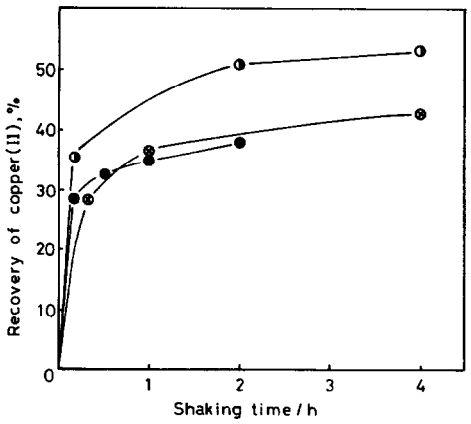


Fig. 7. Back-extraction (recovery) of copper(II) (1×10^{-4} M) with acidic solutions after complete extraction by polymer ligands (1×10^{-3} unit M). ◑: Poly-L1, ⊗: Poly-L2, ●: Poly-L3.

in shaking time. After shaking for 2 h, it was *ca* 50% for Poly-L1 and *ca* 40% for Poly-L2 and Poly-L3. Such a relatively low recovery of copper(II) may be caused by the high stability of the macrocyclic Schiff base complexes formed. It should be noted that some decomposition of these polymer ligands is unavoidable when in contact with acidic solution. Thus, the extent of decomposition of the polymer ligand was determined by measuring absorbances of their chloroform solutions after shaking for definite periods with acidic solutions. These were roughly estimated to be 12 and 8% for Poly-L1 and Poly-L2, respectively, after shaking for 4 h and 5% for Poly-L3 after shaking for 2 h. On the contrary, the monomeric ligand, L was found to be hydrolyzed almost completely within 30 min under the same conditions. These results indicate that the polymer ligands are superior to L for use as extractants.

General discussion

As we have described above, the polymer ligands, Poly-L1, -L2, and -L3 have marked advantages over the monomer ligand, L, in the extraction rate, with high selectivity for copper(II) as well as L. This can be ascribed to the fact that the complexation rate of the polymer ligands is much faster than that of the monomer ligand (L), which is clearly shown in the complexation reaction in a homogeneous DMF solution. These results are mainly caused by "polymer effects", that is, a local increase in concentration of the chelating group (L) is established in the polymer ligands. Morever, with the polymer ligands the recovery of the copper(II) transferred into the organic phase could be achieved by shaking with an acidic aqueous solution, without bringing about extensive decomposition.

As for three polymer ligands investigated here, Poly-L3 was found to display the fastest rate in the extraction and complexation than any others. This may arise from a difference in the nature of the linkage groups in the polymers, namely, which are trimethylene, diphenyl ether, and triethyleneglycol bis(*p*-phenylene) for Poly-L1, -L2, and -L3, respectively. The last group is considered to be much less hydrophobic than the former two groups. Such a less hydrophobic group may provide a thermodynamically preferable environment for the complex formation between a chelating group and a hydrated metal ion. This is a main reason why the extraction rate of Poly-L3 is accelerated, because the extraction rate should be determined by the rate of complex formation in such rigid tetraaza macrocyclic ligands as investigated here. A similar effect may operate for the complex formation of Poly-L3 with copper(II) and nickel(II) in a homogeneous DMF solution. A triethyleneglycol group of Poly-L3 may coordinate weakly to the metal ion by removing some molecules of solvated DMF, which would result in acceleration in the rate of complex formation between the macrocyclic chelating group and the metal ion.

In conclusion, Poly-L3 is the best extractant for copper(II) compared with the other ligands investigated in this work.

REFERENCES

1. Yu. A. Zolotov, V. F. Ionov, V. A. Bodnja, G. A. Larikova, N. V. Niz'eva, G. E. Vlasova and E. V. Rybakova, *Zh. Anal. Khim.* 1982, **37**, 1543.
2. E. A. Krasnushkina and Yu. A. Zolotov, *Trends Anal. Chem.* 1983, **2**, 158.
3. I. Tabushi and M. Fujiyoshi, *Heterocycles* 1977, **7**, 851.
4. D. K. Cabbiness and D. W. Margerum, *J. Amer. Chem. Soc.* 1980, **92**, 2151.
5. T. Matsushita, N. Kubota, M. Fujiwara and T. Shono, *Chem. Lett.* 1984, 657.
6. V. L. Goedken, M. C. Weiss, D. Place and J. C. Dabrowiak, *Inorg. Synth.* 1980, **20**, 115.
7. J. C. Dabrowiak, D. P. Fisher, F. C. McElrory and D. J. Macero, *Inorg. Chem.* 1979, **18**, 2304.
8. E. C. Winslow and A. Laferriere, *J. Polymer Sci.* 1962, **60**, 65.
9. N. Dokoshi, S. Tohyama, S. Fujita, M. Kurihara and N. Yoda, *J. Polymer Sci. A-1* 1970, **8**, 2197.

Polyhedron Vol. 4, No. 6, pp. 1059–1066, 1985
Printed in Great Britain

0277-5387/85 $3.00 + .00
© 1985 Pergamon Press Ltd

THERMAL REACTION OF AQUAAMMINERUTHENIUM(III) COMPLEX WITH AMINO ACID OR IMIDAZOLE DERIVATIVE IN THE SOLID STATE

SUSUMU KOHATA*

Yatsushiro National College of Technology, Yatsushiro 866, Japan

and

KAZUHIRO SAGARA, HITOSHI TAKADA and AKIRA OHYOSHI

Department of Synthetic Chemistry, Faculty of Engineering, Kumamoto University, Kumamoto 860, Japan

(*Received* 3 *October* 1984; *accepted* 9 *November* 1984)

Abstract—Intermolecular thermal-substitution reaction between aquaammineruthenium(III) complex and amino acid or imidazole derivative has been investigated in the solid state by the TG–DTA method. Pentaammineruthenium(III) complexes containing amino acid or imidazole derivative have been obtained directly by the thermal reactions. Glycine, β-alanine, and γ-aminobutyric acid coordinate to Ru(III) through their carbonyl oxygen, and imidazole does through its N(3) atom. Distinct coordination site is provided in the complex with histidine and/or adenine: the bonding site depends on the outer-sphere anion of aquaammine complex. The N(3) atom of the histidine and N(7) atom of the adenine coordinate to Ru(III) taking the paratoluenesulphonate salt of aquaammineruthenium(III) into the reaction. When the methanesulphonate salt is used, the nitrogen atom in the side-chain amino-group participates in complexation. Direct chelation of the glycine, histidine, and adenine to the deaquated *cis*-diaquatetraammineruthenium(III) complex has been confirmed.

The thermal matrix method, proposed by Wendlandt *et al.*,[1,2] was used for the preparation of some cobalt complexes. The method is based on a liberation of the volatile ligand, and followed by the migration of coordinatable solid compound to the position where the ligand had existed. One of the authors has tried this method for the synthesis of the uranyl-citrate complexes,[3] and Oki has also applied it to that of the Cr(III)–amino acid complexes.[4,5] We took up the reaction between the aquaammineruthenium(III) complex and amino acid, and/or imidazole derivative, because it needs many steps as reduction-oxidation of ruthenium to prepare the complex containing the latter ligand by solution reaction.[6] The present work was carried out with the following intentions: (i) investigating the possibility for direct bond-formation of amino acid or imidazole derivative to Ru(III) by intermolecular reaction in the solid phase. Direct chelation of them to the diaqua-Ru(III) complex is particularly interesting; (ii) elucidating the coordination site of the complexed solid ligand.

* Author to whom correspondence should be addressed.

EXPERIMENTAL

Materials

The complexes $[Ru(OH_2)_n(NH_3)_{6-n}]X_3$ ($n = 1$ and X = PTS, MS; $n = 2$ and X = PTS, MS, TFMS) were prepared according to the literature.[7,8] The abbreviations used are as follows: PTS, paratoluenesulphonate ion; MS, methanesulphonate ion; TFMS, trifluoromethanesulphonate ion. Their purity was confirmed by the usual elemental analyses and by electronic spectral measurements. Three kinds of amino acids (glycine, β-alanine, γ-aminobutyric acid) and imidazole derivatives (imidazole, histidine, adenine), purchased from the Wako Pure Chemicals Co. Ltd, were used after the confirmation of their chemical purity.

Procedures and apparatus

A mixture of the aquaammine complex and the amino acid, and that of the aquaammine complex and imidazole derivative with 1:1 mole ratio was ground in a mortar and pestle. Then it was heated

with a rate of 5°C min^{-1} in Ar atmosphere using a Shimadzu DTG-20 type micro differential thermobalance. The abbreviations for the eleven mixture systems taken for thermal analyses are as follows: Gly(1), the complex [n = 1, X = PTS] and glycine; Ala(2), the complex [n = 1, X = PTS] and β-alanine; Aba(3), the complex [n = 1, X = PTS] and γ-aminobutyric acid; Imi(4), the complex [n = 1, X = PTS] and imidazole; His(5), the complex [n = 1, X = PTS] and histidine; Ade(6), the complex [n = 1, X = PTS] and adenine; His(7), the complex [n = 1, X = MS] and histidine; Ade(8), the complex [n = 1, X = MS] and adenine; Gly(9), the complex [n = 2, X = TFMS] and glycine; His(10), the complex [n = 2, X = PTS] and histidine; Ade(11), the complex [n = 2, X = MS] and adenine. The product after the thermal reaction was washed with cold solution of 0.1 mol dm^{-3} $HClO_4$, then with ether. Electronic spectra were measured on a Hitachi Recording Spectrophotometer 323. IR and far-IR spectra were recorded in KBr disks or in Nujol mulls with a JASCO A702 Spectrophotometer. X-ray diffraction patterns were obtained with a Shimadzu XD-3A diffractometer using nickel filtered copper K_α.

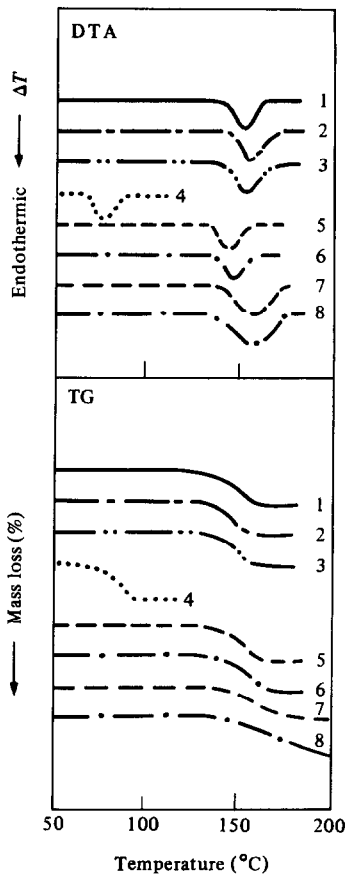


Fig. 1. DTA and TG curves of the mixture systems: 1, Gly(1); 2, Ala(2); 3, Aba(3); 4, Imi(4); 5, His(5); 6, Ade(6); 7, His(7); 8, Ade(8).

RESULTS AND DISCUSSION

Thermal analyses

Figures 1 and 2 show the derivatograms for the eleven mixture systems of aquaammineruthenium(III) complex and solid ligand. The first mass-loss stage in Fig. 1 is the release of one mol water, whose percentage is consistent within ±0.15%. Initiation temperature of deaquation from the aqua complex with PTS ion is observed in the range from 126 to 129°C, except for the Imi(4)-system. On the deaquation step, an endothermic peak is detected at 145, 150, 150, 139, and 140°C for Gly(1), Ala(2), Aba(3), His(5), and Ade(6), respectively. In Imi(4) system, the water liberation was accelerated because the co-melting of imidazole (m.p. = 90°C) and aqua complex occurred at lower temperature (75°C on DTA). On the other hand, the mass loss was initiated at 134 or 136°C with endothermic peak-maximum at 164 or 165°C in the systems of His(7) and Ade(8). The above fact suggests the difference of bond strength between H_2O and Ru(III) in the aqua complex with distinct counter ions and or the occurrence of another type of reaction. In the systems involving the *cis*-diaqua complex, the mass loss was initiated at 110, 113, and 117°C for Gly(9), His(10), and Ade(11), respectively. Continuous liberation of water molecules was found on the first stage but it has occurred by steps since two endothermic changes were separated on the DTA curve at 121, 137°C for Gly(9), at 126, 133°C for His(10), and at 128, 139°C for Ade(11).

In the present thermal reaction, the intermolecular interaction between the aqua complex and the solid compound is suggested strongly for the following reasons: the derivatogram for the mixture is distinguishable from that for the starting mono- or di-aqua complex; a steady line after the first mass-loss stage indicates the existence of a stable compound, and the analytical data of which confirms the completion of the deaquation reaction (see Table 1).

X-ray diffraction

Two typical X-ray diffraction patterns are shown in Fig. 3. The deaquation product A of the unmixed complex $[Ru(OH_2)(NH_3)_5](MS)_3$ reveals many diffractions in the 2θ (Cu, K_α) range of 20–50°, the pattern of which differs from that of the original aqua

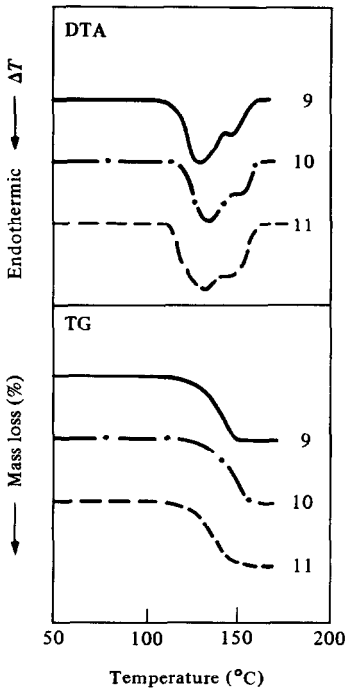


Fig. 2. DTA and TG curves of the mixture systems: 9, Gly(9); 10, His(10); 11, Ade(11).

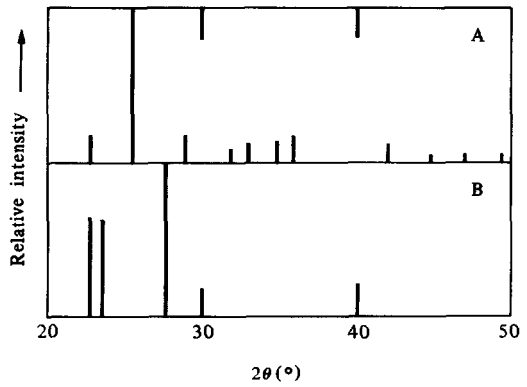


Fig. 3. X-ray diffraction powder patterns of the thermal-deaquation products obtained: A, from the unmixed $[Ru(OH_2)(NH_3)_5](MS)_3$; B, from the mixture between $[Ru(OH_2)(NH_3)_5](MS)_3$ and histidine.

complex. Most of diffractions, however, observed in A and/or original complex has been diminished on the reaction product B of the mixture between the aqua complex and histidine. A simple diffraction pattern, detected in the range of 20–30°, suggests the existence of a single species produced by the intermolecular thermal-reaction between aqua complex and histidine.

Electronic spectra

Electronic spectra of deaquation products observed with 0.1 mol dm^{-3} $HClO_4$ are shown in Table 2. Amino acid systems and imidazole derivative systems show two or three absorption bands λ_1 and λ_3. In amino acid systems, Gly(1), Ala(2), Aba(3), the band λ_1 (287–290 nm, ε = 700–1500 cm^{-1} mol^{-1} dm^3) is assigned to LMCT band contributed from carboxyl oxygen to metal ion.[9,10] The band λ_2 (344–352 nm, ε = 1100–2100) results from the nitrogen atom in amino group.[11,12] The VS-region band λ_3, with a low extinction coefficient 150–410, proved difficult to assign but it may be caused by some electronic interactions between new ligand and Ru metal. Since

Table 1. Analytical data for the reaction product

System	Product[a,b]	Found (calc.)/% C	H	N
Gly(1)	$[Ru(Gly)A_5]X_3$	33.98 (34.07)	5.31 (5.59)	10.41 (10.36)
Ala(2)	$[Ru(Ala)A_5]X_3$	35.14 (34.94)	5.52 (5.74)	9.87 (10.19)
Aba(3)	$[Ru(Aba)A_5]X_3$	35.62 (35.79)	5.59 (5.89)	9.28 (10.02)
Imi(4)	$[Ru(Imi)A_5]X_3$	37.30 (37.54)	5.03 (5.25)	13.14 (12.77)
His(5)	$[Ru(His)A_5]X_3$	36.64 (37.15)	5.23 (5.43)	13.24 (12.84)
Ade(6)	$[Ru(Ade)A_5]X_3$	35.01 (35.86)	4.66 (5.21)	15.84 (16.08)
His(7)	$[Ru(His)A_5]Y_3$	17.70 (17.25)	5.33 (5.31)	17.47 (17.88)
Ade(8)	$[Ru(Ade)A_5]Y_3$	15.65 (15.84)	4.84 (4.82)	23.18 (23.09)
Gly(9)	$[Ru(Gly)A_4]Z_3$	8.73 (8.68)	2.33 (2.46)	9.74 (9.87)
His(10)	$[Ru(His)A_4]X_3$	38.17 (38.70)	4.96 (5.05)	11.24 (11.70)
Ade(11)	$[Ru(Ade)A_4]Y_3$	16.44 (16.30)	4.38 (4.45)	21.10 (21.39)

[a] Chemical formula was assigned from the mass-loss, and UV, IR spectral data.
[b] Abbreviations: A, NH_3; X, PTS; Y, MS; Z, TFMS.

Table 2. Electronic spectral data for the reaction product

Product	λ (nm) [ε (10^{-3} cm^{-1} mol^{-1} dm^3)][a]		
	λ_1	λ_2	λ_3
$[Ru(Gly)A_5]X_3$	287 (1.02)	344 (1.91)	540 (0.14)
$[Ru(Ala)A_5]X_3$	291 (1.55)	345 (2.09)	540 (0.41)
$[Ru(Aba)A_5]X_3$	299 (0.68)	352 (1.12)	546 (0.30)
$[Ru(Imi)A_5]X_3$	302 (1.74)	—	440 (0.28)
$[Ru(His)A_5]X_3$	303 (1.56)	347 (3.55)	538 (0.07)
$[Ru(Ade)A_5]X_3$	306 (1.06)	345 (3.37)	538 (0.83)
$[Ru(His)A_5]Y_3$	263 (3.39)	—	566 (0.48)
$[Ru(Ade)A_5]Y_3$	263 (13.0)	—	—
$[Ru(Gly)A_4]Z_3$	295 (1.22)	357 (0.09)	560 (0.07)
$[Ru(His)A_4]X_3$	295 (1.87)	352 (0.53)	549 (0.91)
$[Ru(Ade)A_4]Y_3$	262 (8.33) 301 (1.74)	356 (0.96)	546 (0.18)

[a] Measured in 0.1 mol dm^{-3} $HClO_4$ at RT.

the intramolecular substitution of aqua ligand for outer-sphere PTS ion hardly proceeds due to steric hindrance, the electronic spectral data indicate the coordination of the amino acid through the carboxylic oxygen atom.

In the imidazole derivative systems, Imi(4), His(5), Ade(6), the band λ_1 (302–306 nm, ε = 1100–1700) has the same absorption as observed in the pentaammineimidazoleruthenium(III) complex,[6,13] or in the pentaamminehistidineruthenium(III) complex.[14] The band λ_1, then, is assigned to LMCT band of the imidazole N-atom to Ru(III). The band λ_2 detected in His(5) and Ade(6) due to the side-chain amino group. The band λ_3 around 440 and 540 nm, in imidazole derivative systems, could be assigned to a CT transition from π-orbital of the ligand to a t_{2g} level of Ru(III).[15,16] It is noteworthy that the spectra of His(7) and Ade(8) with MS ion differ from those of His(5) and Ade(6) with PTS ion. The CT band λ_1 has revealed a blue shift from 303 to 263 nm with enhanced intensity. The λ_2 has diminished and the His(5)'s λ_3 has exhibited a red shift from 538 to 566 nm.

The thermal deaquation–anation reaction has been known in the aquapentaammineruthenium(III) complex with TFMS anions.[17] However, the coordination of the O-atom in TFMS ion and that of the imidazole N-atom have been ruled out by the above spectral changes and by the fact that no characteristic IR-band of ν_{as}(S=O) has been detected in the region 1300–1420 cm^{-1} due to the coordination of TFMS ion.[17] The coordination of the amido N-atom, therefore, is indicated in His(7), and Ade(8).

The CT band λ_1 of the tetraammine complex Gly(9) has revealed a red shift from 287 nm in Gly(1) to 295 nm, while that of His(10) has exhibited a blue shift from 303 nm in His(5) to 295 nm. Spectral feature has been reported[18] for the chelated complexes, the absorption maximum is at 288 nm (ε = 1900) for $[Ru(III)(\underline{N}H_2–CH_2–CO\underline{O})(NH_3)_4]^{2+}$ and 296 nm (ε = 1500) for $[Ru(III)(\underline{N}H_2–CH_2–C(NH_2)–\underline{O})(NH_3)_4]^{3+}$. Two bands are observed as λ_1 on Ade(11)'s spectrum; they are very similar to that found in Ade(6) and Ade(8). The extinction coefficients of λ_2 and λ_3 are deduced in Gly(9), His(10), Ade(11), and the absorption maximum exhibits a red shift of 10–15 nm. The formation of the chelated complex should be suggested by the additional bonding of the amido N-atom in Gly(9) and His(10) and by that of the imidazole N(9)- or N(7)-atom[12] in Ade(11): the electronic charge on the complex ion may be +3.[18]

IR spectra of amino acid system

The characteristic IR bands are shown in Table 3. On the spectra for the deaquated products of Gly(1), Gly(9), Ala(2), and Aba(3), no band assignable to the carboxyl group has been seen around 1750 cm^{-1}. In Gly(1), Ala(2), and Aba(3), the symmetrical and asymmetrical vibrations $\nu(COO^-)$ of the ionized carboxylic group have shifted 10–30 cm^{-1} to lower position. It is clear that the carboxylic group engages in complexation.

When a carboxylate ion coordinate to metal ion as a unidentate ligand, a shifting of $\nu_s(COO^-)$ to lower wavenumber and that of $\nu_{as}(COO^-)$ to higher

Table 3. IR spectral data for the amino acid compound

System	Compound	Band (cm^{-1}) assignments $\nu_{as}(COO^-)$	$\nu_s(COO^-)$	$\nu_s(CCN)$	$\Delta(COO^-)$
Free	Glycine	1603(s)	1405(s)	893(s)	201
Gly(1)	$[Ru(Gly)A_5]X_3$	1575(m)	1395(m)	893(m)	180
Gly(9)	$[Ru(Gly)A_4]Z_3$	1572(m)	1398(s)	889(w)	174
Free	β-Alanine	1628(s)	1403(s)	885(m)	225
Ala(2)	$[Ru(Ala)A_5]X_3$	1572(m)	1395(m)	*	177
Free	γ-Aminobutyric acid	1638(m)	1400(s)	*	238
Aba(3)	$[Ru(Aba)A_5]X_3$	1595(w)	1392(m)	*	203

* Not recorded clearly.

wavenumber has been known.[19] The separation between two $\nu(COO^-)$ will be much larger in the unidentate ligand than in the free ion. The opposite trend should be observed if carboxylate ion plays as a bidentate ligand. Although the separation in Gly(1), Ala(2), and Aba(3) was not so large their mass-loss and analytical data are indicative of unidentate coordination. The reverse shifts to lower wave number of $\nu_{as}(COO^-)$ could be considered that the remaining –C=O bond in COO^- might be released owing to attractive interaction between the O-atom and the H-atom in amino group or in ammine ligand. Such interaction has been noted in the guanine cobalt(III) complex between the amido H-atom and the carbonyl O-atom.[20]

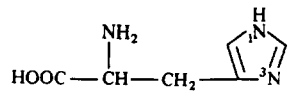
Electronic spectral indication for Gly(9) is the (O, N) chelate. Bidentate coordination, however, remained for carboxylic group, but the band due to ν_s(C–C–N) has shifted with weak intensity from 893 to 889 cm^{-1}, so that direct chelation of glycine (O, N) has been assured in Gly(9).

IR spectra of imidazole derivative system

The result for the Imi(4)-system is shown in Table 4. The strong band of ν(N(3)–H) at 2800 cm^{-1} for imidazole has clearly disappeared. The ring vibration band of ν_{as}(C=N–C=C) for free imidazole exhibits a higher shift of 12 cm^{-1}, while the band of ν_s(C=N–C=C) gives a lower shift of 25 cm^{-1}. The shifts indicate the coordination of imidazole by the N(3)-atom.[21] A weak shoulder also appears at 435 cm^{-1}. According to the Irving–Williams relation,[22] the ratio of $\nu(M-N_{imidazole})/\nu(M-N_{ammine})$ is in the range of 0.7–0.8. The observed one is 0.83, so that the band at 435 cm^{-1} in Imi(4) could be assigned to the stretching vibration mode of Ru–N(3). Additional evidence for N(3) coordination is as follows: the strong band of ν(N(1)–H) remained at 1055 cm^{-1}; the band of δ(N(1)–H) at 935 cm^{-1} has remarkably decreased in intensity and the ring vibration at 662 cm^{-1} also gave reduced intensity, which implies the existence of charge on the imidazole N(1)-atom.[23]

Table 4. IR spectral data for the imidazole compound 

System Compound	Free Imidazole	Imi(4) $[Ru(Imi)A_5](PTS)_3$	Assignments
	2800(s)	—	ν(N(3)–H)
	1575(m)	1586(m)	ν_{as}(C=N–C=C)
	1543(s)	1555(m)	
	1445(s)	1420(m)	ν_s(C=N–C=C)
	1055(s)	1053(m)	ν(N(1)–H)
	935(s)	959(vw)	δ(N(1)–H)
	662(s)	660(vw)	ring vibration
	—	435(w, sh)	ν(Ru–N(3))

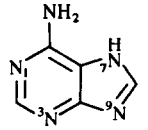
Table 5. IR spectral data for the histidine compounds 

System Compound	Free Histidine	His(5) $[Ru(His)A_5]X_3$	His(7) $[Ru(His)A_5]Y_3$	His(10) $[Ru(His)A_4]X_3$	Assignments
	1632(s)	1633(s)	1635(s)	1633(s)	$\nu_{as}(COO^-)$
	1415(s)	1415(s)	1416(s)	1412(s)	$\nu_s(COO^-)$
	1590(m)	1590(m)	1592(m)	1589(m)	$\delta_{as}(NH_2)$
	1499(m)	1496(m)	1492(w)	1494(w)	$\delta_s(NH_2)$
	1540(w)	1540(w)	1540(w)	1540(w)	δ(N(1)–H)
	1065(w)	1065(w)	1065(w)	1063(w)	ν(N(1)–H)
	1568(m)	1565(m)	1568(w)	1568(w)	ν(C=C)
	1510(m)	1508(w)	1510(m)	1510(vw)	ν(C=N)
	1150(s)	1150(m)	1150(m)	1150(w)	ν(C–N)
	1110(w)	1111(vw)	1110(w)	1115(vw)	ν(C–N)
	925(s)	925(s)	923(w)	920(m)	ν(C–C–N)
	—	—	423(m)	*	ν(Ru–N_{amido})

* Not recorded clearly.

Band assignments[24,25] for His(5), His(7), His(10) are given in Table 5. Characteristic IR-band of ν_{as}(S=O) on the coordination of sulphonate ion[17] was not clear because the band overlaps with other vibrations. The bands ν_s and ν_{as} modes of COO^- do not exhibit any shift, from which the coordination by carboxyl O-atom is excluded in those complexes. The imidazole ring vibrations of ν(C=C), ν(C=N) and the bands ν, δ(N(1)–H) have been detected without any changes, though the former's intensity has markedly decreased. In the spectra of His(5)-system, the bands δ_s, δ_{as} mode of NH_3^+ and ν_s(C–C–N) contributed from amino group appear to be identical with the analogous bands for free histidine. In the spectra of His(7)-system, the vibration modes of $\delta_s(NH_3^+)$, ν_s(C–C–N) have exhibited a shift of band to lower position and a decrease of intensity. The new band at 423 cm^{-1} is assignable to ν(Ru–N_{amido}). In the spectra of His(10)-system, the spectral change of imidazole ring is observed and the same vibrational profile of NH_2 group with the His(7)-system is also found. As a consequence, the coordination of the imidazole N(3)-atom for His(5), the amido N-atom for His(7), and the chelation by the N(3) and N_{amido} atoms for His(10) has been assumed. The results are in agreement with the UV–VS spectral data.

Band assignments for Ade(6) and Ade(8) are shown in Table 6. The in-plane deformation band of

Table 6. IR spectral data for the adenine compounds 

System Compound	Free Adenine	Ade(6) $[Ru(Ade)A_5]X_3$	Ade(8) $[Ru(Ade)A_5]Y_3$	Assignments
	2680(s)	2690(m)	2680(m)	ν(N(9)–H)
	915(m)	918(w)	913(w)	δ(N(9)–H)
	872(m)	875(w)	—	[out plane]
	845(m)	843(m)	845(m)	
	1670(s)	1680(s)	1660(s)	$\delta(NH_2)$
	725(s)	723(m)	718(m)	[in plane]
	940(s)	940(m)	938(m)	$\delta(NH_2)$ [out plane]
	1255(m)	1245(m)	—	$\delta(NH_2)$ [wag.]
	1024(m)	—	1020(m)	ν(N(7)–H)
	1310(s)	1312(s)	1315(w)	ν(C–NH_2)
	—	—	435(w, sh)	ν(Ru–N_{amido})

NH_2 group at 1670 cm^{-1} does not reveal any change, which could be seen when the N(1)-atom is protonated.[26] The band due to ν(N(9)–H) is detected in both Ade(6) and Ade(8),[27,28] whereas the band ν(N(7)–H) is observed not in Ade(6) but in Ade(8). The above information implies that the proton does exist not on the N(1)-atom but on the N(9)-atom in both Ade(6) and Ade(8). In the spectra of Ade(8)-system, the disappearance of $\delta_{wag}(NH_2)$,[29] the lower shifts of δ_s and δ_{as} of NH_2, and the higher shift of ν(C–CH_2) with reduced intensity are observed. This type of IR-spectral change suggests the binding of the amido N-atom,[30] which is in accordance with the UV–VS spectral information, though the coordination of adenine by amido nitrogen is noted in a few cases.[31] The weak shoulder at 435 cm^{-1} is assignable to the Ru–N_{amido} stretching mode. In the spectra of the Ade(6)-system, the unchanged vibrations assigned to NH_2 group indicate that the N_{amido} atom does not coordinate. The N(7)-atom, then, is a most likely coordination site in Ade(6).

With respect to the Ade(11)-system, two possibilities of chelation by N_{amido}–N(7) or N_{amido}–N(9) pairs are provided from the electronic spectra. If the latter pair N_{amido}–N(9) participated in coordination, the complex should be presumably a linear single-bridged structure as reported on the Co(II)–adenine complex.[32] Unfortunately, the mass-loss and analytical data do not support the coordination of such bridging type. Disappearance of the bands ν(N(9)–H), ν(N(7)–H), ν(C=N), and some of $\delta(NH_2)$ may support the chelation by the N_{amido} and N(7) atoms in Ade(11).

Conclusion

The solid-phase thermal reaction for the mixture, taken in this work, was the intermolecular substitution reaction between aqua ligand and solid compound (Y, amino acid; Z, imidazole derivative): $[Ru(OH_2)(NH_3)_5]X_3 + Y$ or $Z \rightarrow [Ru(Y \text{ or } Z)(NH_3)_5]X_3 + H_2O$ (1); *cis*-$[Ru(OH_2)_2(NH_3)_4]X_3 + Y$ or $Z \rightarrow [Ru(Y \text{ or } Z)(NH_3)_4]X_3 + 2H_2O$ (2). The unidentate coordination of amino acid, by eqn (1), has been confirmed, whose site is carboxylic oxygen atom. The chelation of glycine has been completed by eqn 2 with (O, N) coordination. Imidazole coordinates to the complex with its N(3)-atom. Distinct binding site has been found in the histidine and adenine systems: the amido N-atom in the MS-salt, and the imidazole N-atom in the PTS-salt are concerned with the coordination. It was found that the deaquation temperature is higher *ca.* 10°C in the MS-salt than in the PTS-salt, which reflected the bond breaking of H_2O: the hydrogen bonding of outer-sphere ion with the H-atom in aqua- and ammine-ligand is enhanced in the MS-salt than the PTS-salt because the sterical hindrance in crystal lattice and the electrostatic interaction to metal ion of the former ion should be smaller. Nucleophilic attack of the carboxyl group may be predominant in the histidine because its pK value is the smallest. The carboxyl group, however, should have undergone much stronger electronic-repulsion from the PTS-ion than the MS-ion in the mixture; the coordination of the imidazole N-atom may then preponderate in the PTS-salt. The favourable coordination site of the amido N-atom in the MS-salt could be correlated with the fact that a high energy was employed in the thermal reaction. For the adenine systems, similar explanations of the effect of outer-sphere ion could be appropriate, in which the pK value of N(1)-atom is the smallest.

Acknowledgement—The present work was partly supported by a Grant-in-Aid for Scientific Research No. 574237 from the Ministry of Education, Science and Culture of Japan, to one of the authors (SK).

REFERENCES

1. W. W. Wendlandt and C. H. Steinbridge, *J. Inorg. Nucl. Chem.* 1965, **27**, 575.
2. W. W. Wendlandt and L. K. Sveum, *J. Inorg. Nucl. Chem.* 1966, **28**, 393.
3. A. Ohyoshi, J. Oda, T. Odate, H. Kawaguchi and N. Iwasaki, *J. Coord. Chem.* 1976, **5**, 175.
4. H. Oki and K. Otsuka, *Bull. Chem. Soc. Japan* 1976, **49**, 1841.
5. H. Oki and Y. Takahashi, *Bull. Chem. Soc. Japan* 1977, **50**, 2288.
6. R. J. Sundberg, R. F. Bryan, I. F. Taylor, Jr. and H. Taube, *J. Am. Chem. Soc.* 1974, **96**, 381.
7. J. F. Endicott and H. Taube, *J. Am. Chem. Soc.* 1962, **84**, 4984.
8. S. E. Diammond, Ph.D. Thesis, Stanford Univ. 1975.
9. S. W. Lin and A. F. Schreiner, *Inorg. Chim. Acta* 1971, **5**, 290.
10. A. Yeh and H. Taube, *J. Am. Chem. Soc.* 1980, **102**, 4725.
11. S. E. Diammond and H. Taube, *J. Am. Chem. Soc.* 1975, **97**, 5921.
12. A. W. Zanella and P. C. Ford, *Inorg. Chem.* 1975, **14**, 42.
13. R. J. Sundberg, R. E. Shepherd and H. Taube, *J. Am. Chem. Soc.* 1972, **94**, 6558.
14. R. J. Sundberg and G. Gupta, *Bioinorg. Chem.* 1973, **3**, 39.
15. A. B. P. Lever, *Inorganic Electronic Spectroscopy*, pp. 124, 224–248. Elsevier, Amsterdam (1968).
16. I. E. Sutton and H. Taube, *Inorg. Chem.* 1981, **20**, 4021.
17. N. E. Dixon, G. A. Lawrence, P. A. Lay and A. M. Sargeson, *Inorg. Chem.* 1983, **22**, 846.
18. Y. Ilan and H. Taube, *Inorg. Chem.* 1983, **22**, 1655.

19. K. Nakamoto, *Infrared and Raman Spectra of Inorganic and Coordination Compounds*, 3rd Ed., p. 232. Wiley, New York (1978).
20. L. G. Marzilli, T. J. Kistenmacher and C. H. Chang, *J. Am. Chem. Soc.* 1973, **95**, 7507.
21. T. J. Lane, I. Nakagawa, J. L. Walter and A. J. Kandathil, *Inorg. Chem.* 1962, **1**, 262.
22. R. J. H. Clark and C. S. Williams, *Inorg. Chem.* 1965, **4**, 350.
23. W. Otting, *Chem. Ber.* 1956, **89**, 2887.
24. V. Balice and T. Theophanides, *J. Inorg. Nucl. Chem.* 1970, **32**, 1237.
25. M. M. Cordes and J. L. Walter, *Spectrochim. Acta* 1968, **24A**, 1421.
26. T. Fujita and T. Sakaguchi, *Chem. Pharm. Bull.* 1977, **25**, 2419.
27. C. L. Angell, *J. Chem. Soc.* 1961, 504.
28. T. Shimanouchi, M. Tsuboi and Y. Kyogoku, *Adv. Chem. Phys.* 1964, **7**, 435.
29. T. Sakaguchi and M. Tanna, *Nippon Kagaku Kaishi* 1974, **95**, 1637.
30. J. Brigando and D. Colaitis, *Bull. Soc. Chim. France* 1969, 3445.
31. S. M. Wang and N. C. Li, *J. Am. Chem. Soc.* 1968, **90**, 5069.
32. A. N. Speca, C. M. Mikulski, F. J. Iaconianni, L. L. Pytlewski and N. M. Karayannis, *J. Inorg. Nucl. Chem.* 1981, **43**, 2771.

Polyhedron Vol. 4, No. 6, p. 1067, 1985
Printed in Great Britain

0277-5387/85 $3.00 + .00
© 1985 Pergamon Press Ltd

NEW SYNTHESIS OF $K_2[TcF_6]$

R. ALBERTO and G. ANDEREGG
Laboratorium für Anorganische Chemie, ETH Zürich, CH-8092 Zürich, Switzerland

(*Received* 19 *October* 1984; *accepted* 9 *November* 1984)

Abstract—A new high yield synthesis of $K_2[^{99}TcF_6]$ is given. It is based on eqn (1) and uses 40% aqueous HF as solvent.

$$[^{99}TcBr_6]^{2-} + 6F^- + 6Ag^+ \rightarrow [^{99}TcF_6]^{2-} + 6AgBr \quad (1)$$

The hexahalogenotechnetate(IV) anions have been known for a long time.[1] Those with X = Cl, Br, I can be obtained by the reduction of pertechnetate in the corresponding aqueous hydrogen halide solutions. On the other hand, up to now $K_2[TcF_6]$ was prepared by analogy with the synthesis of $K_2[ReF_6]$,[2] i.e., from $K_2[TcBr_6]$ in a melt of KHF_2 ($T = 220°C$), followed by an aqueous work up.[3] This method is lengthy and rather complicated, if radioactive substances are used, and the yields are unsatisfactory.

During the course of our work we became interested in a Tc(IV) starting material which is stable towards hydrolysis over the largest possible pH range. The hexahalogenotechnetate ions with X = Cl, Br, and I, however, are hydrolysed very rapidly in aqueous solution to TcO_2. Since TcF_6^{2-} fulfils these expectations, we developed a simpler and better synthesis. We find that TcF_6^{2-} is formed in a good yield by reacting $TcBr_6^{2-}$ with a 40% HF solution. No hydrolysis takes place at this hydrogen ion concentration and the substitution of Br^- by F^- in the Tc(IV) complex is fully accomplished. After bromide ions are removed from the solution by precipitation with a silver(I) solution, a red intermediate with an absorption band at 552 nm is produced very rapidly. The decrease of the absorbancy of the solution of the red species is accompanied by a parallel increase of the amount of the $[TcF_6]^{2-}$ produced. At room temperature the half-life of this reaction is about 110 h, at 80°C 100 min. After 24 h we obtain a solution containing $[TcF_6]^{2-}$ in 98% yield, the rest, the Tc, being in the form of TcO_4^-.

EXPERIMENTAL

0.4 g (6.09×10^{-4} mol) of $K_2[TcBr_6]$ were suspended in 15 cm^3 of a 40% HF solution. 3.69 mmol Ag^+ in the form of a 1.95 M AgF solution in 40% HF were dropped to the mixture. The black precipitate, which formed initially, changed to white AgBr and the solution became intensely red in colour. After 10 hr the AgBr precipitate was filtered off, dried and weighed. It corresponded to 99% of the calculated value. 14 h later the reaction was complete. The solution was cooled to room temperature, 45 cm^3 of EtOH were carefully added to the reaction mixture and on stirring $K_2[TcF_6]$ precipitated as a white powder (0.158 g, yield 89%).

Characterization

UV/VIS: $\lambda = 352$ nm, $\varepsilon = 15.9$; $\lambda = 291$ nm, $\varepsilon = 20.4$. IR: Tc-Fst 574 cm^{-1}; $R_f = 0.42$ (CH_3CN: H_2O = 2.5:1 v/v).

Elemental analysis

Found: K: 25.2 F: 38.3 Tc: 31.7%. Calc. for $K_2TcF_6 \cdot H_2O$: K: 25.3 F: 36.9 Tc: 32.0%.

^{99}Tc was determined by liquid scintillation; K^+ by complex formation with Kryptat 2.2.2 (Merck, Darmstadt), F^- potentiometrically by titration with $La(NO_3)_3$ solutions and a LaF_3 electrode.

Acknowledgements—We thank the Stiftung Entwicklungsfonds für Seltene Metalle for financial support (R.A.) of these investigations and Professor R. Gut and Dr. K. May (Radiochemie) for technical help.

REFERENCES

1. J. Dalziel, N. S. Gill, R. S. Nyholm and R. D. Peacock, *J. Chem. Soc.* 1958, 4012.
2. E. Weise, *Z. Anorg. Allgem. Chem.* 1956, **283**, 377.
3. K. Schwochau and W. Heer, *Angew. Chem.* 1963, **75**, 95.

Polyhedron Vol. 4, No. 6, pp. 1069–1077, 1985
Printed in Great Britain

0277–5387/85 $3.00 + .00
© 1985 Pergamon Press Ltd

THE STRUCTURE AND DYNAMICS OF THE COPPER(II)–L-PROLINE 1:2 COMPLEX IN SOLUTION

BERNARD HENRY, JEAN-CLAUDE BOUBEL and JEAN-JACQUES DELPUECH*

Laboratoire d'Etude des Solutions Organiques et Colloïdales, UA CNRS 406, Université de NANCY I, B.P. 239, 54506 Vandoeuvre-Les-Nancy Cedex, France

(*Received* 24 *July* 1984; *accepted* 29 *November* 1984)

Abstract—The ^{13}C relaxation times (T_1 and T_2) and isotropic contact shifts ($\Delta\omega$) of a one molar aqueous solution of L-proline at pH = 11 (or pD = 11.4) containing *ca* 10^{-4} M copper(II) perchlorate are measured at 62.86 MHz over a temperature range of 26–70°C. The purely dipolar longitudinal relaxation of carbon-13 nuclei contrasting with purely scalar transverse relaxation allowed us to extract carbon-to-metal distances (through T_1 measurements) and hyperfine coupling constants and dynamic parameters (from T_2 and $\Delta\omega$ measurements). The structure of the complex in solution is found closely similar to that in the solid state. Curve-fitting procedures allowed us to derive the hyperfine electron–carbon coupling constants $A_C = -1.95, +0.42, +1.90$ and -1.70 MHz for carbons $\alpha, \beta, \gamma, \delta$, of the pyrrolidinic ring, the reorientation correlation time of the complex, τ_R (25°C) $= 1.15 \times 10^{-10}$ sec, the L-proline exchange rate, k_M (25°C) $= 4.0 \times 10^5$ sec^{-1} (and the corresponding activation parameters $\Delta H^{\neq} = 9.0$ kcal mol^{-1} and $\Delta S^{\neq} = -0.7$ e.u.), and the electronic relaxation time, $T_{1e} = 1.13 \times 10^{-8}$ sec (at 25°C). The latter value was found in agreement with the one computed from ESR data and the above τ_R value, showing the predominant contributions of spin–rotation interaction and, to a lesser extent, of the effect of g-tensor anisotropy to the electronic relaxation rate.

The structure of aminoacid–paramagnetic ion complexes in aqueous solutions from ^{13}C relaxation studies has been the subject of only a small number of investigations in spite of their possible biological relevance.[1–7] Paramagnetic probes used for such studies are mainly the cobalt(II), manganese(II) and copper(II) ions.[8,9] The latter ion is effectively present in biological tissues, and its transport in the human body seems to involve copper(II)–oligopeptide complexes.[10–13] However NMR investigations on copper(II) complexes seem to be much more difficult than those involving cobalt(II) or manganese(II) ions. This is due to (i) decreased dipolar relaxation rates (which carry all the structural information) as a result of a smaller magnetic moment, (ii) line-broadenings of great amplitude due to long electronic relaxation times[14,15] $T_{1e} \simeq 10^{-9}$ sec, (iii) the difficulty in interpreting electronic relaxation rates in the absence of a mechanism involving the modulation of zero-field splitting tensor, (iv) the plasticity given to the metallic centre by virtue of the Jahn–Teller effect which may result in unexpected distortions of the geometry of Cu^{2+} complexes.[16,17] This explains why detailed NMR relaxation data are available in the literature for a few systems only, such as the hexahydrate ion[14,15,18–21] or complexes with pyridines[22] or acetylacetonate.[23]

As a first step in the NMR studies of copper(II)–peptide systems, we selected the example of the copper(II)–L-proline system for two reasons. This system has been thoroughly investigated in the literature by a variety of methods: potentiometry,[24] X-ray crystallography[25–27] of the solid complex and ESR of solid and aqueous samples. The second reason is that we have studied previously the complex of L-proline with manganese(II) ions and that we have in hand a convenient methodology in this case.[6,7]

Structural parameters were obtained from T_1 and T_2 relaxation times and paramagnetic shifts $\Delta\omega$ of the $\alpha, \beta, \gamma, \delta$ carbon-13 nuclei of the pyrrolidine ring. Experiments were carried out in D_2O solutions at pD = 11.4 using concentrations in the range [Cu^{2+}]

* Author to whom correspondence should be addressed.

$\simeq 10^{-4}$ M and [L-proline] = 1.02 M. Under these conditions, the Cu(II) cation is bound to the aminoacid under the form of a single bis-proline complex Cu(L-Pro$^-$)$_2$.[24] Two species only are existing in solution, the free L-proline molecules and the ligand molecules in the bis-L-proline complex. Carbon nuclei may therefore exist either in a diamagnetic or a paramagnetic site respectively (these two sites are denoted D and M in the following). Ligand exchange is fast at high temperature (60°C) and intermediate at lower temperatures. The measured nuclear parameters T_1, T_2, $\Delta\omega$ therefore depend on their values in the paramagnetic site (T_{1M}, T_{2M}, $\Delta\omega_M$) and in the diamagnetic site (T_{1D}, T_{2D}, $\Delta\omega_D$ respectively), and on the exchange rate $1/\tau_M$ of the bound proline molecule. Extracting T_{1M}, T_{2M}m $\Delta\omega_M$ and $1/\tau_M$ from the experimentally observed quantities T_1, T_2, $\Delta\omega$ is the first point of these investigations. The longitudinal relaxation rates $1/T_{1M}$ in the paramagnetic site are almost exclusively dipolar, thus allowing us in turn to deduce the ion-to-ligand distances r_C and the rotational correlation time τ_R of the complex. The transverse relaxation rate $1/T_{2M}$ are on the contrary predominantly scalar in character, thus allowing us to derive the hyperfine coupling constants A_C between carbon nuclei and the unpaired electron, and the electronic relaxation time T_{1e}.

The purpose of these experiments was to answer some important questions about the structure and dynamics of copper(II) complexes; (i) is the geometry of the solid complex a convenient model for structures in aqueous solutions, (iii) what are the kinetic parameters of ligand exchange about the copper(II) centre, (iii) are NMR data compatible with ESR data (this concerns mainly the experimental electronic relaxation time T_{1e})?

EXPERIMENTAL

L-Proline and hydrated copper(II) perchlorate $Cu(ClO_4)_2 \cdot 4H_2O$ were obtained from Bachem Feinchemikalien and Fluka, respectively, and were used without further purification. Concentrations $C_S = 0, 3.0, 5.0, 10.0, 20.0, 30.0 \times 10^{-5}$ M of the Cu(II) cation and a fixed concentration $C_L = 1.02$ M of L-proline were used in this study. Solutions were added with deuterated soda NaOD to obtain pD = 11.4. Potentiometric measurements were carried out with a Methrom EA436 potentiometer and a combined glass–calomel Ingold microelectrode. All samples were prepared in a nitrogen atmosphere using water which has been purged with nitrogen and NMR tubes equipped with tight-fitting caps. The magnetic susceptibility of the complex $\mu_M = 2.03$ Bohr magnetons in water solution was measured according to the method first described by Evans[29], and then by Crawford and Swanson[30]. Longitudinal relaxation times of ^{13}C nuclei at 62.86 MHz are obtained from partially relaxed Fourier Transform spectra using a CAMECA 250 spectrometer, D_2O as an internal heteronuclear lock, and 180°–τ–90° pulse sequence with the fast inversion-recovery variant.[31] Transverse relaxation times are obtained from linebroadenings $\Delta\nu$ (measured at half width on spectra). Specific relaxation rates: $1/T_{ir} = (1/T_i - 1/T_{iD})/P_M$ (i = 1, or 2) are obtained from the slope of the least squares lines representing the relaxation rates $1/T_1$ and $1/T_2$ measured as a function of the fraction of bound ligand $p_M = 2C_S/C_L$. T_1 and T_2 values were determined at two (33° and 60°C) and at seven (26°, 33°, 38°, 46°, 51°, 60° and 70°C) temperatures, respectively. All calculations were performed on a Texas Instruments 980A minicomputer equipped with a digital plotter, Hewlett–Packard 7210A.

DETERMINATION OF STRUCTURAL AND KINETIC PARAMETERS

Theoretical expressions relating $\Delta\omega$, $1/T_1$, $1/T_2$ to C_S, C_L (or $p_M = 2C_S/C_L$), and T are well-known at the present time[32]. However, the computing path used for this purpose is far from being straight forward and its exact formulation should be reassessed in each particular case. The logical filiation in using the set of theoretical equations (1)–(9) starts from the ligand exchange effect (Swift and Connick equations:[14]

$$1/T_{1r} = (1/T_1 - 1/T_{1D})/p_M = 1/(T_{1M} + \tau_M) \quad (1)$$

$$1/T_{2r} = (1/T_2 - 1/T_{2D})/p_M = \frac{1}{\tau_M} \frac{1/T_{2M}^2 + 1/T_{2M}\tau_M + \Delta\omega_M^2}{(1/T_{2M} + 1/\tau_M)^2 + \Delta\omega_M^2} \quad (2)$$

$$\Delta\omega_r = \Delta\omega/p_M = \frac{\Delta\omega_M}{(1 + \tau_M/T_{2M})^2 + \tau_M^2\Delta\omega_M^2}. \quad (3)$$

Variable concentrations of copper(II) ion are seen to intervene in the obtaining of the normalized relaxation rates and paramagnetic shift, $1/T_{1r}$, $1/T_{2r}$ and $\Delta\omega_r$ (from least squares plots where correlation coefficients are always larger than 0.995). In a second step, the intermediary parameters τ_M, T_{1M}, T_{2M}, $\Delta\omega_M$ are expressed as a function of the temperature T and the resonant frequencies of carbon nuclei ω_C and of the unpaired electron $\omega_e \cdot \tau_M$ is simply assumed to

obey an Arrhenius law

$$\tau_M = \tau_M^{\circ} \exp(E_M/RT). \quad (4)$$

$\Delta\omega_M$ is related to the hyperfine coupling constant A_C through the equation

$$\Delta\omega_M/\omega_C = 2\pi A_C \mu_M \sqrt{S(S+1)}/3kT\gamma_c. \quad (5)$$

Relaxation rates in the paramagnetic site are expressed by classical equations relating $1/T_{1M}$ and $1/T_{2M}$ to ω_e, ω_C, τ_R and T_{1e}.[33] These expressions may be greatly simplified in the present case where

$$\tau_M (\sim 10^{-6} \text{ sec}) \gg T_{1e} (\sim 10^{-8} \text{ sec}) \gg \tau_R (\sim 10^{-10} \text{ sec}),$$

and

$$\omega_e^2 T_{1e}^2 \text{ and } \omega_e^2 \tau_R^2 \gg 1:$$

$$1/T_{1M} = \frac{2\times 10^{-14}}{5} \frac{\mu_M^2 \gamma_c^2}{r_c^6} \tau_R \quad (6)$$

and

$$1/T_{2M} = (7/6)(1/T_{1M}) + 4\pi^2 A^2 S(S+1) T_{1e}/3 \quad (7)$$

(provided that the contribution of the pseudocontact interaction to the overall hyperfine coupling constant is negligible compared to contact shift interactions, see the discussion below).

τ_R is again assumed to obey an Arrhenius law:

$$\tau_R = \tau_R^0 \exp(E_R/RT). \quad (8)$$

The electron relaxation rate may be shown to be inversely proportional to the reorientation correlation time:

$$1/T_{1e} = K/\tau_R \quad (9)$$

where the constant K is independent from T and ω (see Discussion).

We have then to adjust a set of unknown parameters, some of which refer to the whole complex (τ_M^0, E_M^0, τ_R^0, E_R^0, K) or to each ^{13}C nucleus characterized by its own electron-to-nucleus distance r_c ($r_{c\alpha}$, $r_{c\beta}$, $r_{c\gamma}$, $r_{c\delta}$ for carbons α, β, γ, δ, respectively) and hyperfine coupling constants (A_α, A_β, A_γ, A_δ). These parameters are adjusted so as to obtain the best fit between the theoretical and experimental $1/T_{1r}$, $1/T_{2r}$ and $\Delta\omega_r$ values measured at several temperatures according to a generalized least squares procedure. As the great number of unknown parameters makes a one-step adjustment rather hazardous, a stepwise procedure has been devised in a previous investigation.[7] Its adaptation to the present example is schematically described in the following. In a first step, all the adjustable parameters are given an approximate value (denoted by superscript (1) thereafter), which in turn allows us to initiate an iterative procedure of optimization. Thus the hyperfine coupling constants $A_C^{(1)}$ (in fact $A_\alpha^{(1)}$, $A_\beta^{(1)}$, $A_\gamma^{(1)}$, $A_\delta^{(1)}$) are obtained by taking $\Delta\omega_M = \Delta\omega_r$ as a limiting expression for eqn (3) at temperature higher than 50°C. $\tau_M^{(1)}$ and $T_{2M}^{(1)}$ (at any temperature) are then deduced from eqns (2) and (3) which are recast under the form

$$1/T_{2M} = \frac{\Delta\omega_M(1/\tau_M - 1/T_{2r}) - \Delta\omega_r/\tau_M}{\Delta\omega_r} \quad (2\text{bis})$$

$$\Delta\omega_M = \frac{\Delta\omega_r}{(1-\tau_M/T_{2r})^2 + \tau_M^2 \Delta\omega_r^2}. \quad (3\text{bis})$$

Four τ_M values can be computed in this way, and the value finally adopted results from their arithmetic mean. Longitudinal relaxation rates in the paramagnetic site are computed from eqn (1):

$$(T_{1M}^{(1)})^{-1} = (T_{1r} - \tau_M^{(1)})^{-1}.$$

The chemical exchange is in fact fast enough to make $\tau_M^{(1)}$ negligible with respect to T_{1r}. $T_{1M}^{(1)}$ values obtained for carbons α, β, γ, δ of the pyrrolidine ring in the L-proline molecule allows us in turn to position the copper(II) with respect to ligand molecules. The procedure has been fully explained in a previous paper[6,7] and is based on the consideration of the three ratios

$$\lambda_{ij}^6 = \frac{T_{1M}^{(1)}(C_j)}{T_M^{(1)}(C_i)} = \left(\frac{r_{cj}}{r_{ci}}\right)^6, \quad \text{with } i, j = \alpha, \beta, \gamma, \delta.$$

The Cu^{2+} ion is therefore located on three spheres S_{ij} whose diameter M_iM_j is determined by the two points M_i and M_j which share the internuclear vector C_iC_j in a known ratio λ_{ij}. The position of the copper(II) nucleus results from the intersection of three spheres $S_{\alpha\beta}$, $S_{\beta\gamma}$, $S_{\gamma\delta}$. Two positions are actually obtained in this way, one of which can be rejected on account of a too close proximity of the Cu^{2+} ion to the pyrrolidine ring (one distance is less than 1 Å). This allows in turn to compute $\tau_R^{(1)}$ from eqn (6). Similar computations are also performed at 33°C. They yield similar distances r_c (Table 1) and a second value $\tau_R^{(1)}$ (33°C) which, combined with $\tau_R^{(1)}$ (60°C), allows us to deduce the Arrhenius parameters $\tau_R^{0(1)}$ and $E_R^{(1)}$. The longitudinal contribution to the transverse relaxation time is estimated as 7/6 $(T_{1M}^{(1)})^{-1}$ and is subtracted from the overall transverse relaxation rate T_{2M}^{-1} to isolate the scalar contribution

$$(T_{2M}^{(1)})_{RS}^{-1} = 4\pi^2 A^2 S(S+1) T_{1e}/3 \quad (7\text{bis})$$

(in fact the longitudinal contribution was always found to represent less than 1% of the total relaxation rate). The electronic relaxation time $T_{1e}^{(1)}$ is then extracted from eqn (7bis) and then the constant $K^{(1)}$ from eqn (9).

Table 1. The relaxation times T_{1M} (sec) of ^{13}C in bound L-proline molecules at 33 and 60°C; the distances (Å) between the Cu(II) cation and the atoms of L-proline in the complex Cu(L-Pro$^-$)$_2$(H$_2$O)$_2$ (see Fig. 3), and the corresponding values deduced from X-ray crystallography of the solid complex[27]

Atom	Aqueous solution 33°C		60°C		Solid state (room temperature)
	T_{1M}^{-1}	r	T_{1M}^{-1}	r	
C_α	2206±105	2.82±0.20	1304±95	2.91±0.19	2.85
C_β	323±33	3.88±0.29	190±18	4.01±0.28	3.98
C_γ	253±26	4.04±0.26	152±18	4.04±0.26	4.12
C_δ	1862±83	2.88±0.21	1088±73	2.88±0.21	2.96
C_0		2.77		2.93	2.82
N		1.98		2.06	1.96
O_1		1.99		2.03	2.03
O_2		3.97		4.07	4.04

A least squares optimization procedure is then started so as to obtain the best fit between the experimental and theoretical values of the function $1/T_{2r}(T)$ (Fig. 1). In this computational step, the parameters $A_C^{(1)}$ and $r_c^{(1)}$ are kept constant, and the five remaining parameters τ_M^0, E_M, K, τ_R^0, E_R are adjusted in the course of successive iterations, taking as initial values for the first iteration the above approximate set of parameters $\tau_M^{0(1)}$, $E_M^{(1)}$, $K^{(1)}$, $\tau_R^{0(1)}$, $E_R^{(1)}$. Let $\tau_M^{0(2)}$, $E_M^{(2)}$, $\tau_R^{0(2)}$, $E_R^{(2)}$ be the set of adjusted parameters at the end of this first optimization.

The whole cycle of computations is then started again using a slightly modified value of the hyperfine coupling constant A_C until a best value is found by trial and error for A_C (ensuring an absolute minimum of the squares of the residuals of the function $1/T_{2r}(T)$). This approach can be made easier if one decides to perform an auxiliary fit of the function $\Delta\omega_r(T)$ (Fig. 2) where all the parameters except A_C are given constant values equal to the above set $\tau_M^{0(2)}$, $E_M^{0(2)}$, etc.

Four sets of parameters are actually obtained in this way, since we may choose to optimize individual hyperfine coupling constants A_α, or A_β, or A_γ, or A_δ. The differences however are reasonably small (Table 2) and the final values of these parameters are then obtained as their arithmetic mean over the four carbon nuclei.

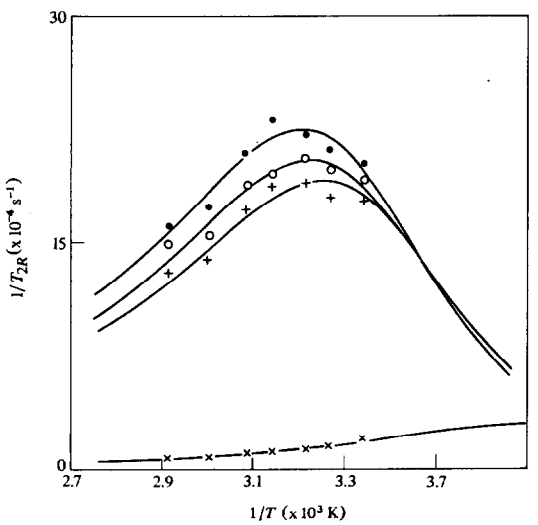


Fig. 1. Temperature variation of the specific relaxation rate $1/T_{2r} = (1/T_2^{obs} - 1/T_{2D})/P_M$ for the L-proline carbons at 62.86 MHz, obtained from 1.02 M solutions of L-proline in D_2O at pD = 11.4 and with $[Cu^{2+}] = 3.0$–30.0×10^{-5} M: (●) C_α, (×) C_β, (○) C_γ, (+) C_δ. The curves were computed using the parameters in Tables 1–3, and correspond to the best fit.

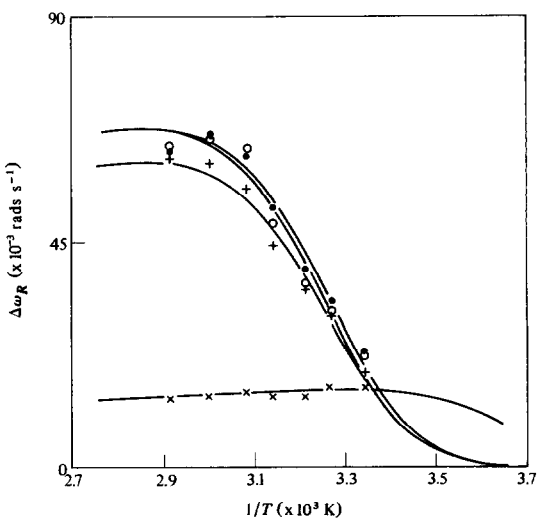


Fig. 2. Temperature variation of the specific paramagnetic shift $\Delta\omega_R = (\omega_{obs} - \omega_D)/P_M$ of the L-proline carbons at 62.86 MHz, using the same conditions and notations as in Fig. 1.

Table 2. Fitted values of the parameters $1/\tau_M^0$ (10^{13} sec^{-1}); τ_R^0 (10^{-14} sec), E_M and E_R (kcal mol^{-1}), and K (10^{22}) for carbons α to δ, and the corresponding mean values

	C_α	C_β	C_γ	C_δ	Mean
$1/\tau_M^0$	1.19±0.24	1.73±0.42	0.78±0.28	1.17±0.32	1.21±0.25
E_M	10.36±0.10	10.30±0.15	10.04±0.06	10.24±0.08	10.23±0.10
τ_R^0	2.77±0.52	3.13±0.27	4.22±0.48	3.91±0.52	3.51±0.56
E_R	4.95±0.09	4.70±0.04	4.80±0.03	4.72±0.06	4.79±0.08
K	1.34±0.25	1.00±0.18	1.02±0.27	0.96±0.32	1.08±0.13

RESULTS

Values of the longitudinal relaxation times T_{1M} are displayed in Table 1, together with the Cu^{2+}–^{13}C distances in the complex. The proline atomic coordinates which serve as a basis for the computation of these distances are taken from crystallographic data relative to the Cu^{2+}–proline complex.[27] Longitudinal relaxation times are determined with an error of *ca* 5%. Ratios such as λ_{ij} are then obtained with an error $\Delta\lambda_{ij}/\lambda_{ij}$ of 1.5%. Values $\lambda_{ij}\pm\Delta\lambda_{ij}$ are then introduced into the computer program to estimate all the possible sets of distance $r_{c\alpha}, r_{c\beta}, r_{c\gamma}, r_{c\delta}$. Each of these distances is given in Table 1 as the mean over the eight sets resulting from the combinations of the $\lambda_{\alpha\beta}$, $\lambda_{\beta\gamma}$, $\lambda_{\gamma\delta}$ ratios, and the corresponding errors are estimated as the difference between the maximum and the minimum values obtained for each parameter. Four sets of adjusted parameters τ_M^0, E_M, τ_R^0, E_R and K are computed for each carbon atom, each one with its own uncertainty (Table 2). Final values of these parameters are given in Tables 2 and 3 as arithmetic means over the four sets of data. These values allow us in turn to extrapolate correlation times and exchange rates for a conventional temperature of 25°C (Table 3).

DISCUSSION

Structure of the complex

X-ray diffraction of solid Cu^{2+}–L-proline[25–27] shows that copper is surrounded by two diagonal oxygens and two diagonal nitrogens at distances of 2.03 and 1.99 Å, respectively, in a square planar arrangement. The tetragonal arrangement is completed by two axial water oxygens at a distance of 2.52 Å. There is a good agreement between the distance found in the solid complex and those deduced from our NMR measurements (Table 1). This is a strong evidence for similar ligand arrangements in the solid and liquid states. The presence of two water molecules in the coordination sphere rapidly exchanging with the bulk solvent is demonstrated by the contact shift and line-broadening for the water protons (see below). The internuclear distances N–Cu^{2+} and O1–Cu^{2+} (1.98 and 1.99 A at 25°C) were computed by

Table 3. Parameters calculated from ^{13}C relaxation and contact shift data

Hyperfine coupling constants (MHz)
$A_{C\alpha} = -1.95\pm0.27$; $A_{C\beta} = 0.42\pm0.08$; $A_{C\gamma} = 1.90\pm0.30$; $A_{C\delta} = 1.70\pm0.30$ MHz

Reorientation correlation times
τ_R (25°C) $= (1.15\pm0.31)\times10^{-10}$ sec
$\tau_R^0 = (3.15\pm0.56)\times10^{-14}$ sec; $E_R = 4.79\pm0.08$ kcal mol^{-1}

Electronic relaxation parameters
T_{1e} (25°C) $= (1.13\pm0.41)\times10^{-8}$ sec; $K = (1.08\pm0.13)\times10^{22}$

Kinetic parameters
τ_M (25°C) $= 2.50\times10^{-6}$ sec or $k_M = 4.00\times10^5$ sec^{-1}
$1/\tau_M^0 = (1.21\pm0.25)\times10^{13}$ sec^{-1}
$E_M = 10.23\pm0.10$ kcal mol^{-1}
$\Delta H^{\neq} = 9.60\pm0.10$ kcal mol^{-1}
$\Delta S^{\neq} = -0.7\pm0.3$ e.u.

positioning first the Cu^{2+} cation with respect to carbons C_α, C_β, C_γ, C_δ of each proline ligand by the method explained above, and then by positioning the other atoms of the proline molecule with respect to the Cu^{2+} cation (using the known geometry of the proline molecule in the solid state). The structure of the whole complex is represented in Fig. 3, obtained from a computer using program ORTEP.[34]

It can be observed that hyperfine coupling constants of the carbon nuclei do not reflect the proximity of the metallic centre. Not only the most remote carbon C_γ is endowed with an abnormally large hyperfine coupling constant, but also there is an alternation in the signs of observed paramagnetic shifts. This could arise from a variable dipolar contribution (pseudo-contact shift) to the overall isotropic shift which we have reduced implicity to its Fermi contact term. This question is also of importance for computing the dynamic parameters of Tables 2 and 3 since eqn (7) is valid only in the absence of pseudo-contact effects. Pseudo-contact shifts (δ_{pc}) can be estimated from the principal components $g_\parallel$ and $g_\perp$ of the g-tensor according to the formula[35]

$$\delta_{pc} = \frac{\bar{g}\beta^2 S(S+1)(g_\parallel - g_\perp)}{9kT}\left(\frac{3\cos^2\theta - 1}{r_c^3}\right), \quad (10)$$

where $\bar{g} = (g_\parallel + 2g_\perp)/3$, β is the Bohr magneton, and θ the angle between the tetragonal axis and the internuclear Cu^{2+}–C vector. Taking $r_c = 2.82$ Å for carbon α (Table 1), $g_\parallel = 2.1853$ and $g_\perp = 2.0669$ from ESR data,[28] the pseudo-contact term at 25°C amount to *ca* 2 ppm compared to an overall paramagnetic shift $\Delta\omega_M = 240$ ppm. This contribution is clearly negligible with respect to the Fermi contact shift, this validates all the rest of calculations.

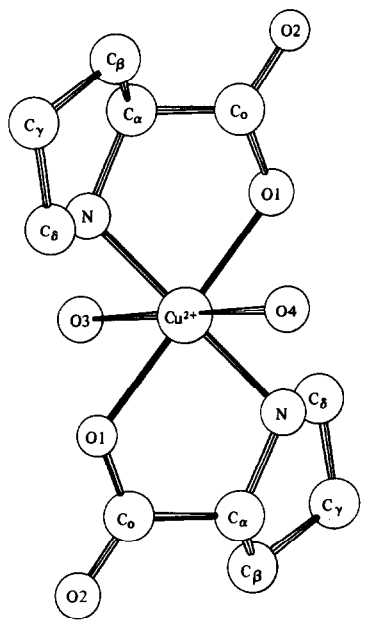


Fig. 3. The structure of the Cu(II)–L-proline complex in D_2O solution at pD = 11.4 and T = 33°C.

The hyperfine coupling constants A_C represent the electron spin density ρ on the observed nucleus according to Fermi formula,[17]

$$A = \frac{8\pi}{3h} g_e\beta_e g_N\beta_N\rho(0)$$

with

$$\rho(0) = (P^\alpha - P^\beta)\,|\varphi_S(0)|^2, \quad (11)$$

where P^α and P^β are the populations of the so called α or β spins (parallel on antiparallel to the magnetic field) and $|\varphi_s(0)|^2$ is the squared amplitude of the electronic wave function at the nucleus. Spin densities may be positive or negative depending on the sign of spin polarization. The value of ρ depends on spin delocalization and spin polarization through σ or π bonding. In copper(II)–proline complex, ESR studies show a fairly covalent bonding between the metal ion and the ligand, involving mainly the $d_{x^2-y^2}$ orbitals of the metal.[28] Theoretical studies show that spin delocalization *via* metal–ligand σ bonding involving filled ligand σ molecular orbitals should be characterized by positive coupling constants which attenuate rapidly as the number of bonds between the lone pair and the observed nucleus increases.[36] However, these predictions were not verified in the σ-electron system of piperidine,[37] in which case the observed chemical shifts alternate in sign, the coupling constant A_C being negative (upfield shifts) or positive (downfield shifts) for α- or β-carbons, respectively. The apparent discrepancy was traced to the neglect of correlation effects. This situation is clearly very similar to the one encountered in the present case for the σ-electron system of the five-membered pyrrolidinic ring of L-proline, where upfield or downfield contact shifts are observed for carbons in an α- or β-position with respect to the nitrogen atom.

The value of the magnetic moment $\mu_M = 2.03 \pm 0.10$ Bohr magnetons is in agreement with the value of 1.82 BM computed for an electron spin number $S = 1/2$ and the $g_\parallel$ and $g_\perp$ values mentioned above according to the formula

$$\mu_M^2 = (g_\parallel^2 + 2g_\perp^2)\beta^2 S(S+1)/3. \quad (12)$$

The NMR value is somewhat larger than the one deduced from ESR measurements[28] and eqn (12); this may be due to slightly modified $g_\parallel$ and $g_\perp$ values by going from the solid state to aqueous solutions of the complex.

Dynamics of the complex

The tumbling correlation time τ_R (25°C) = 1.15×10^{-10} sec is clearly larger than that of the aquo-complex $Cu(H_2O)_6^{2+}$, τ_R (25°C) = 2.0×10^{-11} sec as expected from the different sizes of the two complexes and, on the contrary, is closely similar to the one found for the Mn^{2+}–L-proline complex,[7] $\tau_R = 1.28 \times 10^{-10}$ sec.

Interesting conclusions result from the measured electronic relaxation times, $T_{1e} = 1.13 \times 10^{-8}$ sec at 25°C. For paramagnetic ions with $S = 1/2$, ESR relaxation times depend on anisotropic hyperfine constants and g-tensor, and from spin-rotational effects. The first contribution to the longitudinal relaxation rate $(1/T_{1e})_{g,A}$ has been studied by McConnell[38] and Kivelson[39] as resulting from the interaction of the unpaired electron of copper(II) ion with the copper nuclei with $I = 3/2$ (the two stable isotopes ^{63}Cu and ^{65}Cu each have spin $I = 3/2$ and nearly the same magnetic moment). The magnitude of this contribution can be expressed according to the approximate equation[38]

$$(1/T_{1e})_{g,A} = \frac{8\pi^2}{15}\left(\frac{\Delta g \beta B_0 + bI_z}{h}\right)^2\left(\frac{\tau_c}{1+\omega_e^2\tau_c^2}\right), \quad (13)$$

where $\Delta g = g_{\parallel} - g_{\perp} = 0.1184$, $B_0 = 5.87T$, $b = A_{\parallel} - A_{\perp}$, with $A_{\parallel}$ and $A_{\perp} = 3.134$ and 0.312×10^9 sec^{-1}, respectively.[28] τ_c is the correlation time for the reorientation of the tetragonal axis bearing $g_{\parallel}$. This reorientation may be due either to the random reorientation of the complex in the liquid (in which case $\tau_c = \tau_R$) or to dynamical Jahn–Teller effects as discussed by Lewis and Morgan.[40] However, Jahn–Teller effects are likely to occur only in the case of homogeneous hexacoordinated copper(II) complexes[41] such as $Cu(H_2O)_6^{2+}$. We are then left with the first possibility and $\tau_c = \tau_R$. Using the above values of τ_R and $\omega_e = 1.033 \times 10^{12}$ rad sec^{-1} results into $\omega_e^2\tau_R^2 \gg 1$, so that eqn (13) can be reduced to

$$(1/T_{1e})_{g,A} = \left(\frac{8\pi^2}{15}\right)\frac{1}{\omega_e^2\tau_R}\left(\frac{\Delta g \beta B_0 + bI_z}{h}\right)^2. \quad (14)$$

I_z is the magnetic number of the copper nuclei, $I_z = -3/2$, or $-1/2$, or $+1/2$, or $+3/2$. As pointed by McLachlan[42] and then by Poupko and Luz,[21] there is no single T_{1e} for Cu^{2+}, but rather a multi-exponential law for electronic relaxation whose rate constants are obtained by solving the $(2S+1)(2I+1)$ dimensional (8×8) relaxation matrix. However, according to McLachlan, we can calculate an average longitudinal relaxation rate $(1/T_{1e})^{-1}$ as the arithmetic mean of the four $1/T_{1e}$ values obtained from eqn (14) for each of the four I_z values.

The spin-rotational contribution $(1/T_{1e})_{SR}$ to $1/T_{1e}$ has been studied theoretically by Atkins and Kivelson[43] in the frame of the Hubbard's equations.[44] It can be expressed in terms of the deviations of the principal g-tensor components from the free electron value $g_e = 2.00233$:

$$(1/T_{1e})_{SR} = \delta g^2/9\tau_R, \quad (15)$$

where $\delta g^2 = (g_{\parallel} - g_e)^2 + 2(g_{\perp} - g_e)^2$.

Adding eqns (14) and (15) together results into the expression of the electronic relaxation time

$$1/T_{1e} = (1/T_{1e})_{g,A} + (1/T_{1e})_{SR} = K/\tau_R, \quad (16)$$

where

$$K = \delta g^2/9 + (8\pi^2/15h^2\omega_e^2)(\Delta g^2\beta^2 B_0^2 + b^2 I(I+1)/3). \quad (17)$$

This explains the origin of eqn (9) used to represent the electronic relation rate as mentioned above. With the values of $g_{\parallel}$ and $g_{\perp}$ quoted above, the spin-rotational contribution is in fact predominant, $(1/T_{1e})_{SR} = 4.04 \times 10^7$ sec^{-1} compared to $(1/T_{1e})_{g,A} = 4.49 \times 10^6$ sec^{-1} and $1/T_{1e} = 4.49 \times 10^7$ sec^{-1} at 25°C. More refined treatments following Kivelson *et al.*[39] do not change appreciably the above values of $1/T_{1e}$. The electronic relaxation time $T_{1e} = 1.31 \times 10^{-8}$ sec thus computed from ESR data is relatively close to the one obtained from our NMR data, $T_{1e} = 1.18 \times 10^{-8}$ sec. This consistency strongly supports the validity of the models used. The electronic relaxation time in the Cu^{2+}–L-proline complex is smaller by one order of magnitude than the one measured for the aquo-complex $Cu(H_2O)_6^{2+}$ from dynamic nuclear polarization experiments,[15] $T_{1e} = 1.67 \times 10^9$ sec at 30°C. This difference is probably due to both smaller correlation times τ_c and larger Δg^2 and δg^2 values in eqns (13), (16) and (17).

Kinetic parameters show intermediate ligand exchange rates, e.g. $k_M = 4.0 \times 10^5$ sec^{-1} at 25°C, between those of the Cu^{2+}–DMSO complex[45] ($k_M = 7.9 \times 10^3$ sec^{-1}) on the one hand, and those of $Cu(H_2O)_6^{2+}$ or $Cu(MeOH)_6^{2+}$ on the other hand ($k_M = 2 \times 10^8$ and 7.4×10^7 sec^{-1}, respectively).[14,21] In the first case, the difference arises from a much higher activation enthalpy for the Cu^{2+}–L-proline than for the Cu^{2+}–DMSO complex ($\Delta S^{\neq} = -0.7$ against -13.6 e.u.), more than counterbalancing an unfavorable activation enthalpy increase ($\Delta H^{\neq} =$ 9.60 against 7.25 kcal mol^{-1}). In the second case, the decreased exchange rate for the Cu^{2+}–L-proline complex arises from a higher activation enthalpy ($\Delta H^{\neq} = 9.60$ against 5 or 6.6 kcal mol^{-1}, respectively) and not too different activation entropies ($\Delta S^{\neq} = -0.7$ against -4 and -2.6 e.u.). Another interesting comparison is with the Mn^{2+}–L-proline complex previously studied[7] where ligand

exchange is slower than for the Cu^{2+}/L-proline complex ($k_M = 7.41 \times 10^4$ against 4.0×10^5 sec^{-1}), while the corresponding complexes with DMSO[45] show a reverse sequence of magnitude ($k_M = 2.7 \times 10^6$ and 7.9×10^3 sec^{-1}). These results cannot be rationalized in the present state of these investigations.

The water molecules. Only one line is observed for the protons of water, as the result from either a fast molecule exchange or a fast proton transfer between bond and free water molecules. An upfield shift of 0.0192 ppm and a line-broadening of 16 Hz are observed in a solution containing 0.01 M of the Cu^{2+}–L-proline complex. Pseudo-contact contribution to this shift can still be shown to be negligible using formula (10) with a distance $r_{Cu^{2+}-H}$ of 4.2 Å and cos $\theta = 0.9134$ (computed from the crystallographic data mentioned above). Under these conditions, eqns (1) to (5) are still valid and allow us to compute the electron–proton hyperfine coupling constant, $A_H = -1.7113$ MHz and an exchange rate $1/\tau_M$ (H_2O) $= 1.2 \times 10^8$ sec^{-1} at 25°C, not very far from the one found for the exchange of the axial water molecules in the aquo-complex, $1/\tau_M(H_2O) = 2 \times 10^8$ sec^{-1}. The sign of the paramagnetic shift is in agreement with predictions of Luz and Shulman[19] involving spin density transfer from the metal ion to the oxygen atomic orbital p_x perpendicular to the plane of the water molecule. In the case of the aquo-complex $Cu(H_2O)_6^{2+}$, the hyperfine constant is measured with poor accuracy and seems to be positive, $A \sim 0.1$ MHz;[19] this could result from positive shifts for water molecules in the equatorial plane averaging out the negative shift for the water molecules in axial position (assumed to have a contact shift of the same sign as in the Cu^{2+}–L-proline complex). It should however be emphasized that results pertaining to the aquo-complex are still controversial due to unresolved ESR spectra and to the possibility of dynamic Jahn–Teller effects.

CONCLUSION

These investigations show the importance of the Cu(II) cation as a paramagnetic probe, and the wealth of information resulting from combined NMR, ESR and X-ray crystallographic data. The electron relaxation rate is dominated by spin-rotational interaction and, to a lesser extent, by the effect of g-tensor anisotropy, thus making the electronic relaxation time directly proportional to the reorientation correlation time and almost independent from the magnetic field strength. This points to the possibility of using high magnetic field strengths to increase paramagnetic shifts in copper(II) complexes without extra line-broadening. Ligand exchange about the copper(II) ion is still slow on the NMR timescale, and transverse relaxation is purely scalar, so that selective line-broadening experiments are not sufficient by themselves to determine the binding sites of the ligand. However, the purely dipolar longitudinal relaxation contrasting with purely scalar transverse relaxation makes copper(II) a suitable paramagnetic probe to extract carbon-to-metal distances (through T_1 measurements of ^{13}C nuclei) and hyperfine coupling constants and dynamic parameters (from T_2 and shift measurements).

Acknowledgements—Financial support from the Centre National de la Recherche Schientifique is gratefully acknowledged. All NMR spectra were recorded on spectrometers of the Groupement Régional de Mesures Physiques de l'Académie de NANCY-METZ.

REFERENCES

1. W. G. Espersen and R. B. Martin, *J. Phys. Chem.* 1976, **80**, 161.
2. J. J. Led and D. Grant, *J. Am. Chem. Soc.* 1975, **97**, 6962.
3. J. J. Led and D. Grant, *J. Am. Chem. Soc.* 1977, **99**, 5845.
4. S. Kitagawa, K. Yoshikawa and I. Morishima, *J. Phys. Chem.* 1978, **82**, 89.
5. R. E. Viola, C. R. Hartzell, and J.-J. Villafranca, *J. Inorg. Bioch.* 1979, **10**, 281.
6. B. Henry, M. Rappeneau, J.-C. Boubel, and J.-J. Delpuech, *Adv. Mol. Relax. Inter. Process.* 1980, **16**, 29.
7. B. Henry, J.-C. Boubel and J.-J. Delpuech, *Polyhedron* 1982, **1**, 113.
8. H. Sigel and R. B. Martin, *Chem. Rev.* 1982, **82**, 385.
9. H. Niccolai, E. Tiezzi and G. Walensin, *Chem. Rev.* 1982, **82**, 359.
10. B. Sarkar and Y. Wigfield, *Can. J. Chem.* 1968, **46**, 601.
11. T. P. A. Kruk, S. Lau and B. Sarkar, *Can. J. Chem.* 1976, **54**, 1300.
12. K. S. Iyer, S. Lau, S. H. Laurie and B. Sarkar, *Biochem. J.* 1978, **169**, 61.
13. H. Sigel, *Metal Ions in Biological Systems*, Vol. 12. M. Dekker, New York (1981).
14. T. J. Swift and R. E. Connick, *J. Chem. Phys.* 1962, **37**, 307.
15. D. C. McCain and R. J. Myers, *Mol. Phys.* 1974, **28**, 1109.
16. I. Bertini and A. Scozzafava, in *Metal Ions in Biological Systems* (Edited by H. Sigel), Vol. 12, Chap. 2. M. Dekker, New York (1981).
17. C. Chachaty and P. Rigny, *J. Chem. Phys.* 1982, **79**, 203.
18. L. O. Morgan and A. W. Nolle, *J. Chem. Phys.* 1959, **31**, 365.
19. Z. Luz and R. G. Shulman, *J. Chem. Phys.* 1965, **43**, 3750.

20. W. B. Lewis, M. Alei, Jr and L. O. Morgan, *J. Chem. Phys.* 1966, **44**, 2409.
21. R. Poupko and Z. Luz, *J. Chem. Phys.* 1972, **57**, 3311.
22. A. Boyer and V. Fazakerley, *J. Inorg. Nucl. Chem.* 1981, **43**, 1955.
23. B. R. McGarvey, *J. Phys. Chem.* 1956, **60**, 71.
24. M. M. Petit-Ramel and M. Pâris, *Bull. Soc. Chim. France* 1969, 3070.
25. A. McL. Mathieson and H. K. Welsh, *Acta Crystallogr.* 1952, **5**, 599.
26. R. L. Kaynshina and B. K. Vainhstein, *Sov. Phys. Cryst.* 1966, **10**, 698.
27. N. Samala and K. Venkatesan, *Cryst. Struct. Commun.* 1973, **8**, 5.
28. B. N. Misra and R. Kripal, *Il Nuovo Cimento* 1980, **58B**, 123.
29. D. F. Evans, *J. Chem. Soc.* 1959, 2003.
30. T. H. Crawford and J. Swanson, *J. Chem. Educ.* 1971, **48**, 382.
31. D. Canet, G. C. Levy and I. R. Peat, *J. Magn. Reson.* 1975, **18**, 199.
32. For a review, see (a) R. A. Dwek, *NMR in Biochemistry: Applications to Enzyme Systems.* Clarendon Press, Oxford (1973), (b) Ref. 17.
33. A. Carrington and A. D. McLachlan, *Introduction to Magnetic Resonance.* Harper & Row, New York (1967).
34. C. K. Johnson, ORNL 3794, Oak Ridge National Laboratory, Oak Ridge (Tennessee) ORTEP (1965).
35. J. P. Jesson, in *NMR of Paramagnetic Molecules* (Edited by G. N. La Mar, W. D. Horrocks and R. H. Holm), Chap. 1. Academic Press, New York (1973).
36. G. N. La Mar, in *NMR of Paramagnetic Molecules* (Edited by G. N. La Mar, W. D. Horrocks and R. H. Holm), Chap. 3. Academic Press, New York (1973).
37. I. Morishima, K. Okada, T. Yonezawa and K. Goto, *J. Am. Chem. Soc.* 1971, **93**, 3922.
38. H. M. McConnell, *J. Chem. Phys.* 1956, **25**, 709.
39. D. Kivelson, *J. Chem. Phys.* 1960, **33**, 1094; R. Wilson and D. Kivelson, *J. Chem. Phys.* 1966, **44**, 154, 4440, 4445.
40. W. B. Lewis and L. O. Morgan, *Transition Metal Chemistry* (Edited by R. L. Carlin), Vol. 4. M. Dekker, New York (1968).
41. M. Noack, G. F. Kokoszka and G. Gordon, *J. Chem. Phys.* 1971, **54**, 1342.
42. A. D. McLachlan, *Proc. Roy. Soc.* (*London*) 1964, **A280**, 32.
43. P. W. Atkins and D. Kivelson, *J. Chem. Phys.* 1966, **44**, 169.
44. P. S. Hubbard, *Phys. Rev.* 1962, **131**, 1155.
45. G. S. Vigee and P. Ng, *J. Inorg. Nucl. Chem.* 1971, **33**, 2477.

Polyhedron Vol. 4, No. 6, pp. 1079–1083, 1985
Printed in Great Britain

0277–5387/85 $3.00 + .00
© 1985 Pergamon Press Ltd

POLAROGRAPHIC STUDY OF DIOXO-URANIUM(VI)–8-HYDROXYQUINOLINE–SUCCINATE SYSTEM AND THERMODYNAMIC PARAMETERS

JYOTI SHARMA and ARVIND KUMAR
Department of Chemistry, Agra College, Agra, India

and

B. K. PURI*
Department of Chemistry, Indian Institute of Technology, Hauz Khas, New Delhi—110016, India

(*Received* 16 *October* 1984; *accepted* 29 *November* 1984)

Abstract—The dioxo-uranium(VI)–8-hydroxyquinoline–succinate system has been studied polarographically at constant ionic strength (μ = 0.6 M KCl) in aqueous alcohol (7:3) at different temperatures. The reduction of the simple and mixed complexes is reversible and diffusion controlled. The DeFord–Hume and Schaap–McMaster methods have been applied in the determination of composition and stability constants of the simple and mixed complexes respectively. The thermodynamic parameters ΔG, ΔH and ΔS have also been calculated.

The polarographic behaviours of uranium has been studied in various electrolytes and complexing agents under different conditions.[1–5] Mixed ligand complexes of uranium has only been studied potentiometrically.[6] Recently, dioxo-uranium(VI) complexes of amino acids[7] and hexamethylenetetramine[8] have been studied polarographically. The literature reveals that the mixed complexes with 8-hydroxyquinoline and succinate have not been studied polarographically. In the present communication, the polarographic behaviour of the UO_2^{2+}–8-hydroxyquinoline–succinate system has been studied systematically at different temperatures. The thermodynamic parameters ΔG, ΔH and ΔS have also been calculated.

EXPERIMENTAL

Materials. All the chemicals used were of analytical reagent grade and their solutions were prepared in conductivity water. 8-Hydroxyquinoline (8-HQ) and potassium succinate were used as ligands. Triton X-100 (0.002%) was used as the maximum suppressor. The ionic strength was maintained constant at μ = 0.6 M (KCl).

Apparatus and procedure. Polarograms in all instances were recorded with a manual polarograph (Toshniwal CLO2) in conjuction with a polyflex galvanometer (Toshniwal PL 50). A saturated calomel electrode was used as the reference electrode and was connected to the polarograph cell through a potassium chloride agar–agar-bridge. Oxygen was expelled by passing a slow stream of purified nitrogen into the test solution. The dropping mercury electrode (DME) had the following characteristics:

$h_{corr} = 30$ and

$m^{2/3}t^{1/6} = 2.236\ mg^{2/3}\ sec^{-1/2}$ in 0.1 M KCl

with open circuit.

RESULTS AND DISCUSSION

The reduction of UO_2^{2+} in 8-HQ and succinate, separately, was found to be reversible and diffusion controlled. The slopes of linear plots of log $i/i_d - i$ vs $E_{d.e.}$ were of the order of 59 ± 1 mV indicating one-electron changes. The same value of n was obtained by the millicoulometric studies.[9] Stability constants of simple complexes of UO_2^{2+} with 8-HQ and succinate were determined separately prior to the study of the mixed ligand system. Identical

* Author to whom correspondence should be addressed.

conditions were maintained in both the simple and mixed systems.

UO_2^{2+}–8-*hydroxyquinoline system*

A series of polarograms were obtained with increasing concentration of 8-HQ (0.02–0.10 M) at constant ionic strength, μ = 0.6 M KCl, at 20, 30 and 40°C. In each case, a well-defined reversible one-electron change diffusion controlled wave was obtained. A plot of $E_{1/2}$ vs log [8-HQ] was a smooth curve, indicating the formation of successive complexes. The DeFord and Hume's[10] method was applied to determine the stability constants of successive complexes. At 20°C, UO_2^{2+} forms three complexes with 8-HQ where as at 30 and 40°C it forms only two complexes (Table 1).

UO_2^{2+}–*succinate system*

Similar studies were carried out with increasing concentration of succinate (0.1–0.5 M) at constant ionic strength, μ = 0.6 M (KCl), at 20, 30 and 40°C. In each case, a well defined, reversible one-electron change and diffusion controlled wave appeared. A plot of $E_{1/2}$ vs log [succinate] was a smooth curve indicating the formation of successive complexes. DeFord and Hume's method was applied for the calculation of stability constants. An analysis of the $F(Y)$ functions reveals the formation of three successive complexes at 20°C and two at 30°C and 40°C similar to the UO_2^{2+}–8-HQ system. The results are summarized in Table 2.

UO_2^{2+}–8-*HQ–succinate system*

The concentration of 8-HQ was varied from 0.02–0.10 M keeping [succinate] constant at 0.1 M, at 20, 30 and 40°C. The $E_{1/2}$ values were more negative than those obtained in the absence of succinate showing the formation of mixed complexes. The system was also repeated at another concentration of succinate (0.2 M). These constant concentrations were termed as series 1 and 2. In all the cases, a well-defined diffusion controlled, reversible one-electron change wave appeared. Therefore, the method of Schaap and McMaster[11] was applied to determine the stability constants of the mixed complexes. The $F(X, Y)$ functions (X = 8-HQ, and Y = succinate) of these systems were determined. From the plots of $F(X, Y)$ data vs [8-HQ], the constants A, B, C, D were obtained. The stability constants have been calculated from these constants and are summarized in Table 3. At 20°C only two species $[UO_2(8\text{-HQ})(\text{succinate})]^-$ and $[UO_2(8\text{-HQ})_2(\text{succinate})]^{2-}$ exist in the aqueous solution while the negative values of log β_{12} ruled out the possibility of $[UO_2(8\text{-HQ})(\text{succinate})_2]^{3-}$ in the aqueous solution. At 30

Table 1. Values of $F(X)$ functions for UO_2(II)–(8-HQ) system at different temperatures: UO_2(II) = 0.5 mM, ionic strength μ = 0.6 M (KCl)

Temperature 0°C	[8-HQ] M	$\Delta E_{1/2}$ V vs SCE	log I_s/I_c	$F_0(X)$	$F_1(X)$ $\times 10^{-1}$	$F_2(X)$ $\times 10^{-2}$	$F_3(X)$ $\times 10^{-3}$
20	0.02	0.028	0.0463	3.25	11.25	3.75	—
	0.04	0.042	0.0782	5.99	12.40	4.94	—
	0.06	0.056	0.0709	10.07	15.12	7.70	9.50
	0.08	0.068	0.0732	16.04	18.80	10.37	10.46
	1.00	0.078	0.0792	23.87	22.89	12.39	10.39
30	0.02	0.020	0.0342	2.30	—	—	—
	0.04	0.030	0.0692	3.70	6.75	6.87	—
	0.06	0.042	0.0679	5.85	8.08	6.80	—
	0.08	0.055	0.0648	9.56	10.70	8.31	—
	1.00	0.065	0.0680	14.13	13.13	9.13	—
40	0.02	0.015	0.0342	1.92	—	—	—
	0.04	0.025	0.0564	2.96	4.90	6.62	—
	0.06	0.038	0.0508	4.82	6.36	6.86	—
	0.08	0.050	0.0612	7.82	8.52	7.84	—
	1.00	0.060	0.0628	11.52	10.52	8.27	—

At 20°C, log β_1 = 2.02, log β_2 = 2.30, log β_3 = 4.005.
At 30°C, log β_1 = 1.60, log β_2 = 2.89.
At 40°C, log β_1 = 1.30, log β_2 = 2.86.

Table 2. Value of $F(Y)$ functions in UO_2(II)–(succinate) system at different temperatures: conditions same as in Table 1

Temperature 0°C	[Succinate] M	$\Delta E_{1/2}$ V vs SCE	log I_s/I_c	$F_0(Y)$	$F_1(Y)$ $\times 10^{-2}$	$F_2(Y)$ $\times 10^{-2}$	$F_3(Y)$ $\times 10^{-3}$
20	0.05	0.045	0.1212	7.42	1.28	—	—
	0.10	0.060	0.1244	13.28	1.33	3.34	1.34
	0.15	0.075	0.1402	25.44	1.62	4.19	1.46
	0.20	0.088	0.1282	39.21	1.91	4.55	1.27
	0.25	0.100	0.1302	62.40	2.45	5.80	1.52
30	0.05	0.040	0.1318	6.12	—	—	—
	0.10	0.053	0.1644	12.02	1.10	5.02	—
	0.15	0.070	0.1614	21.18	1.34	4.96	—
	0.20	0.080	0.1761	32.21	1.56	4.80	—
	0.25	0.090	0.1818	47.86	1.87	5.09	—
40	0.05	0.035	0.1348	5.21	—	—	—
	0.10	0.050	0.1369	9.31	8.31	8.31	—
	0.15	0.062	0.1658	15.77	9.84	3.56	—
	0.20	0.072	0.1529	22.44	10.72	3.11	—
	0.25	0.082	0.1512	32.84	12.73	3.29	—

At 20°C, log $\beta_1 = 2.00$, log $\beta_2 = 2.301$, log $\beta_3 = 3.145$.
At 30°C, log $\beta_1 = 1.778$, log $\beta_2 = 2.696$.
At 40°C, log $\beta_1 = 1.653$, log $\beta_2 = 2.530$.

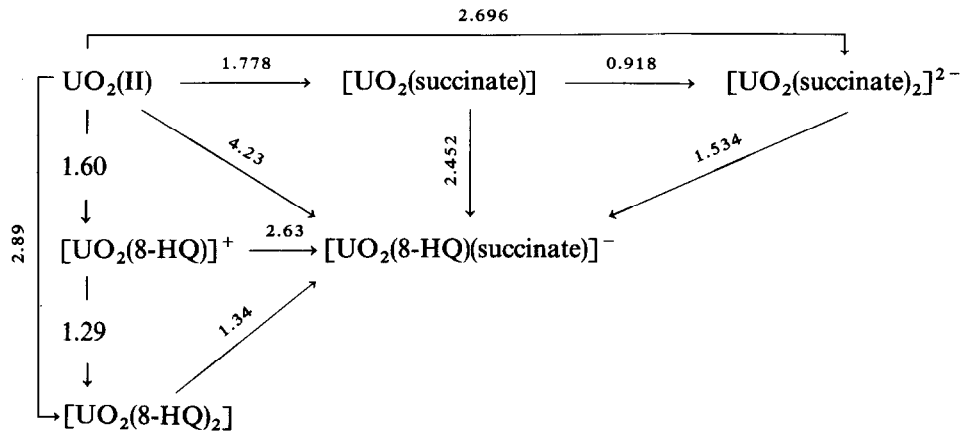
Table 3. Values of $F(X, Y)$ functions of UO_2(II)–(8-HQ)–succinate system at different temperatures: UO_2(II) = 0.5 mM, $\mu = 0.6$ M (KCl), [succinate] = 0.1 M

Temperature °C	[8-HQ] M	$\Delta E_{1/2}$ V vs SCE	log I_s/I_c	$F_{00}(X, Y)$ $\times 10^{-1}$	$F_{10}(X, Y)$ $\times 10^{-3}$	$F_{20}(X, Y)$ $\times 10^{-4}$	$F_{30}(X, Y)$ $\times 10^{-4}$
20	0.02	0.100	0.1700	6.83	1.16	—	—
	0.04	0.110	0.1791	10.24	1.43	1.84	1.60
	0.06	0.125	0.1610	17.46	2.16	2.43	2.05
	0.08	0.128	0.1522	28.17	2.95	2.82	2.02
	0.10	0.148	0.1491	41.04	3.65	2.95	1.71
30	0.02	0.095	0.2998	7.603	—	—	—
	0.04	0.110	0.2739	12.740	24.35	2.337	—
	0.06	0.125	0.2380	20.840	29.73	2.455	—
	0.08	0.138	0.2075	31.990	36.23	2.654	—
	0.10	0.148	0.2025	43.340	43.34	2.834	—
40	0.02	0.085	0.1352	3.59	—	—	—
	0.04	0.095	0.1188	5.01	7.54	1.63	—
	0.06	0.110	0.1108	8.75	11.25	1.70	—
	0.08	0.120	0.1269	13.33	14.16	1.64	—
	0.10	0.130	0.1236	19.41	17.41	1.64	—

At 20°C, log $A = 1.653$, log $B = 2.840$, log $C = 4.079$, log $D = 5.2$, log $\beta_{11} = 3.720$, log $\beta_{12} = -$, log $\beta_{21} = 4.835$.
At 30°C, log $A = 1.477$, log $B = 3.176$, log $C = 4.409$, log $\beta_{11} = 4.164$.
At 40°C, log $A = 1.301$, log $B = 2.00$, log $C = 4.219$, log $\beta_{11} = 2.83$.

and 40°C only the $[UO_2(8\text{-HQ})(\text{succinate})]^-$ exists in the aqueous solution. While the negative value of log β_{12} ruled out the possibility of β_{12} complex in the aqueous solution.

The formation constant of the mixed ligand complex log β_{11} at 30°C is equal to 4.23 (average of the values at 0.1 and 0.2 M succinate, Tables 3 and 4). The results of this study at 30°C are summarized below and the numerical values shown are the log of equilibrium constants of the reactions indicated.



The tendency of the succinate anion to add as the second ligand to $[UO_2(\text{succinate})]$ and $[UO_2(8\text{-HQ})]^+$ can be compared. The log K values are 0.918 and 2.63 respectively. Because the statistical factor is only 2 in favour of mixed complexes, the largest part of the difference in log K values must be attributed to the neutralization of charge. The tendency to add the charged 8-HQ anion as the second ligand to $[UO_2(8\text{-HQ})]^+$ and to $[UO_2(\text{succinate})]$ can also be compared. In this case also charge neutralization effect is expected and, indeed is observed. Log K values are 1.29 and 2.452 respectively.

$$2[UO_2(8\text{-HQ})(\text{succinate})]^- \rightleftharpoons [UO_2(8\text{-HQ})_2] + [UO_2(\text{succinate})_2]^{2-}.$$

The constant for this disproportionation reaction is 0.0013, i.e. log $K = -2.8$; naturally the mixed complex is favoured. Similar conclusion can be drawn from K_M values, i.e. log $K_M = \log \beta_{11} - 1/2$ [log β_{02} + log β_{20}]. The positive value of

Table 4. $F(X, Y)$ functions of UO_2(II)–(8-HQ)–succinate systems at different temperatures [succinate] = 0.2 M: rest of the conditions same as Table 3

Temperature °C	[8-HQ] M	$\Delta E_{1/2}$ V vs SCE	log I_s/I_c	$F_{00}(X, Y)$ $\times 10^{-1}$	$F_{10}(X, Y)$ $\times 10^{-3}$	$F_{20}(X, Y)$ $\times 10^{-4}$	$F_{30}(X, Y)$ $\times 10^{-5}$
20	0.02	0.108	0.1825	9.56	1.782	—	—
	0.04	0.118	0.1867	14.17	2.042	2.35	2.12
	0.06	0.132	0.1902	24.43	3.072	3.28	2.96
	0.08	0.145	0.1945	40.62	4.327	4.02	3.10
	0.10	0.155	0.1956	59.75	5.375	4.27	2.77
30	0.02	0.118	0.2060	14.790	53.95	6.97	—
	0.04	0.136	0.2107	29.850	64.62	6.15	—
	0.06	0.152	0.2234	56.750	87.91	7.98	—
	0.08	0.165	0.2181	92.330	110.13	8.80	—
	0.10	0.175	0.2102	133.030	132.63	9.26	—
40	0.02	0.095	0.1456	5.33	—	—	—
	0.04	0.105	0.1530	7.96	1.24	2.35	—
	0.06	0.120	0.1483	14.00	1.83	2.55	—
	0.08	0.130	0.1530	20.77	2.22	2.40	—
	0.10	0.138	0.1595	28.55	2.55	2.25	—

At 20°C, log A = 1.778, log B = 3.04, log C = 4.17, log D = 5.431, log β_{11} = 3.83, log β_{12} = –, log β_{21} = 4.96.

At 30°C, log A = 1.602, log B = 3.602, log C = 4.894, log β_{11} = 4.296.

At 40°C, log A = 1.477, log B = 2.477, log C = 4.377, log β_{11} = 3.12.

Table 5. Stepwise free energy change ΔG, enthalpy change ΔH and entropy change ΔS in kcal/mole at 30°C

Thermodynamic parameters	UO_2–(8-HQ) system	UO_2(II)–(succinate) system
$-\Delta G_1$	2.208	2.453
$-\Delta G_2$	3.988	3.720
ΔH_1	−15.05	−7.31
ΔH_2	+11.70	+4.80
ΔS_1	−42.409	−16.039
ΔS_2	51.840	+28.11

log K_M (1.44) indicated that the mixed complex $[UO_2(8\text{-HQ})(\text{succinate})]^-$ is more stable than the binary complexes $[UO_2(8\text{-HQ})_2]$ and $[UO_2(\text{succinate})_2]^{2-}$. The value of log β_{11} given in the literature is 3.57.[13] The difference might be due to the experimental conditions, i.e. temperature, medium and the ionic strength.

The thermodynamic constants of the UO_2–(8-HQ) and UO_2–(succinate) have been calculated using the known equations[14] and are summarized in Table 5. The values of free energy change, i.e. ΔG of the above complexes (Table 5) gives an idea of their relative stability. Stepwise enthalpies (ΔH_1, ΔH_2) for the formation of mono and bis 8-HQ complexes of UO_2^{2+} are −15.05 and +11.70 kcal/mole whereas in the case of the UO_2^{2+}–(succinate) system stepwise enthalpies are $\Delta H_1 = -7.31$ kcal/mole and $\Delta H_2 = +4.8$ kcal/mole. The entropy changeΔH which is negative for mono complexes may be due to the loss of transitional degree of freedom by the ligand attached. But this may be off-set by loss of hydration of the metal ion, which may in fact be sufficient to swing the entropy change over to the positive side. The residual positive charge on the central ion may still be sufficient to maintain some degree of ordering of the solvent outside the sphere of the ligand.

Acknowledgements—The authors are thankful to UGC for providing the financial assistance and also to Dr. N. K. Kaushik for useful discussion.

REFERENCES

1. L. Meites, *Polarographic Techniques.* Interscience, New York (1965).
2. A. L. J. Rao and B. K. Puri, *Z. Anal. Chem.* 1971, **255**, 21.
3. V. T. Athavale, R. G. Dhaneshwar and G. S. Padmanaleha Iyer, *Indian J. Chem.* 1976, **5**, 424.
4. T. T. Lai and S. J. Hey, *Rev. Polarog (Japan)* 1967, **14**, 211.
5. V. Almagro, F. S. Garcia and J. Sancho, *Anal. Chim. Acta* 1974, **70**, 237.
6. M. S. Balakrishnan and M. Santappa, *Curr. Sci. (India)* 1972, **41**, 174.
7. V. G. Dongre and D. G. Duley, *Curr. Sci. (India)* 1980, **49**, 8.
8. D. R. Prasad and K. Saraswati, *J. Indian Chem. Soc.* 1980, **57**, 246.
9. T. De Vries and J. L. Kroon, *J. Am. Chem. Soc.* 1953, **75**, 2484.
10. D. N. Hume and D. D. DeFord, *J. Am. Chem. Soc.* 1951, **73**, 532.
11. W. B. Schaap and D. L. McMaster, *J. Am. Chem. Soc.* 1961, **83**, 4699.
12. M. Sharma and M. Singh, *Indian Acad. Sci.* 1983, **92**, 91.
13. P. H. Tedesco and J. Martineg, *J. Inorg. Nucl. Chem.* 1980, **82**, 95.
14. K. B. Yatsimirskii and V. P. Vasiler, *Instability Constants of Complex Compounds.* Pergamon Press, New York (1960).

Polyhedron Vol. 4, No. 6, pp. 1085–1089, 1985
Printed in Great Britain

0277–5387/85 $3.00 + .00
© 1985 Pergamon Press Ltd

SYNTHESIS AND SPECTROSCOPIC STUDIES ON ORGANOTIN DERIVATIVES OF BIOLOGICALLY ACTIVE SCHIFF BASES

ANIL SAXENA* and J. P. TANDON†
Department of Chemistry, University of Rajasthan, Jaipur-302004, India

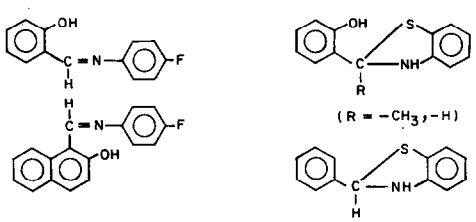
and

A. J. CROWE
Division of Chemistry, International Tin Research Institute, Fraser Road, Greenford UB6 7AQ, U.K.

(*Received* 9 *April* 1984; *accepted after revision* 29 *November* 1984)

Abstract—Some five- and six-coordinated di- and tri-*n*-butyl tin(IV) complexes of the type Bu_2SnL, Bu_2SnL_2 and Bu_3SnL (where L is the anion of a monofunctional bidentate or bifunctional tridentate Schiff base) have been synthesized and characterised on the basis of microanalyses, molecular weight determinations, IR, NMR (^1H, ^{13}C, ^{119}Sn) and ^{119}Sn Mössbauer spectroscopy. These complexes are highly active towards bacteria.

Schiff bases continue to occupy an important position as ligands in metal coordination chemistry even after almost a century since their discovery. Sulphur and fluorine have long been used to increase the biological activity of an organic moiety[1] and organotin compounds have also found applications in medicinal chemistry.[2,3] However, no systematic study has been performed on such complexes. It was therefore considered of interest to prepare organotin complexes of the ligands of the structure given below:



and study their spectral properties and activity on pathogenic bacteria.

EXPERIMENTAL

Chemicals and solvents used were dried and purified by standard methods, and moisture was excluded from the glass apparatus using $CaCl_2$ drying tubes. The ligands were prepared by literature methods,[4,5] The complexes were prepared by methods similar to reported in earlier publications.[6] The details are given in Table 1.

The complexes were analyzed by the literature methods and the molecular weights were determined by the Gallenkamp ebulliometer or cryoscopically in freezing benzene. ^{119}Sn Mössbauer spectra were recorded with $Ba^{119}SnO_3$ source at 77 K and the values relative to SnO_2. The details of spectroscopic measurements are similar to those reported earlier.[7] All the complexes and starting materials were tested for bacterial activity by the method reported earlier.[8]

RESULTS AND DISCUSSION

Reactions of di-*n*-butyl and tri-*n*-butyl tin oxides with these ligands have been carried out in 1:1 and 1:2 molar ratios in refluxing benzene. These reactions proceed with the liberation of water, which is removed azeotropically with benzene.

$$Bu_2SnO + N\begin{matrix}OH\\SH\end{matrix} \rightarrow Bu_2Sn(O\hat{N}\hat{S}) + H_2O$$

$$Bu_2SnO + 2N\hat{X}H \rightarrow 2Bu_2Sn(\hat{XN})_2 + H_2O$$

$$(Bu_3Sn)_2O + 2N\hat{X}H \rightarrow 2Bu_3Sn(N\hat{X}) + H_2O.$$

The above reactions are quite facile and can be completed in 8–10 hr of refluxing. The resulting

* Present address: School of Chemistry and Molecular Science, University of Sussex, Falmer, Brighton BN1 9QJ, U.K.

† Author to whom correspondence should be addressed.

Table 1

Yield %	Product and characteristics (colour and state)	M.p./b.p. °C	Mol. wt. Found Calc.	Analyses % Sn Found Calc.	C Found Calc.	H Found Calc.	S Found Calc.
95	$Bu_2Sn(C_{13}H_9NOF)_2$	234	695.0	18.52	61.67	6.24	—
	Cream yellow solid		660.98	17.99	61.75	5.47	—
90	$Bu_3Sn(C_{13}H_9NOF)$	207/0.6 mm	488.0	22.77	61.58	8.44	—
	Red crystalline solid		503.0	23.22	59.52	7.16	—
85	$Bu_2Sn(C_{17}H_{11}NOF)_2$	118	782.0	22.77	65.03	5.89	—
	Orange red solid		760.98	23.22	66.23	5.25	—
90	$Bu_3Sn(C_{17}H_{11}NOF)$	—	548.0	22.77	61.51	6.05	—
	Dark brown liquid		555.0	21.47	62.70	6.84	—
90	$Bu_2Sn(C_{13}H_{10}NS)_2$	—	672.0	17.85	60.35	5.03	8.52
	Brown semi-solid		656.98	18.11	62.10	5.78	9.74
93	$Bu_3Sn(C_{13}H_{10}NS)$	—	530.0	22.10	57.35	7.08	5.13
	Yellow brown semi-solid		501.0	23.75	59.88	7.38	6.38
92	$Bu_2Sn(C_{14}H_{11}NSO)$	—	488.0	24.65	53.88	6.92	5.92
	Brown red semi-solid		474.09	25.04	55.58	6.10	6.75

complexes are yellow to dark brown in colour. The complexes vary in state from solid to viscous liquids. Solids were recrystallized from a mixture of petroleum ether (30–40°C) and benzene (30:70). These monomeric complexes are soluble in common organic solvents.

A broad and strong band is observed in the region, 3300–2850 cm^{-1}. This band is attributed to ν(OH) and/or ν(NH) which does not appear in the complexes showing the deprotonation of these groups. A sharp and strong band at $\sim$ 1635 cm^{-1} in the complexes, of Schiff bases derived from *p*-fluoroaniline, compared to one at $\sim$ 1620 cm^{-1} in these ligands may be assigned to ν(C=N). However, in ligands derived from *o*-aminothiphenol, a strong band at 1670–1705 cm^{-1} is assigned to the N–H diformation vibrations, and the absence of ν(SH) at 2500–2600 cm^{-1} and ν(C=N) at 1600–1650 cm^{-1} are indicative of the benzothiazoline structure of the ligands and not the Schiff base structure.[9] In the metal complexes a new band appears at $\sim$ 1605 cm^{-1} which is assigned to ν(C=N) vibration.

In all ligands but benzaldehyde benzothiazoline, a band due to phenolic C–O stretching vibrations appears at $\sim$ 1275 cm^{-1} which shifts to the higher frequency indicating the bonding of ligand to the metal atom through phenolic oxygen.

In $Bu_3Sn(\widehat{OX}N)$ and $Bu_2(\widehat{O}N\widehat{S})$ type of complexes

Table 2. ^{1}H NMR data of ligands and orgnotin complexes and ^{119}Sn Mössbauer data for complexes

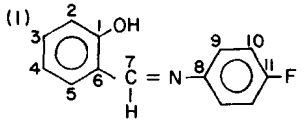
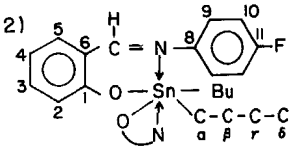
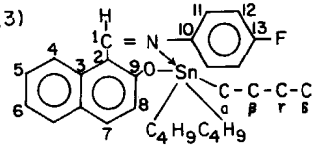
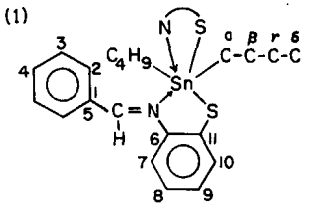
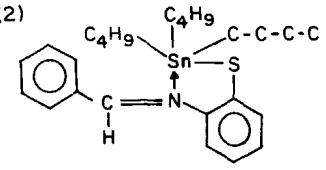
No.	Compound	–OH	$-C_6H_4$	–CH/$-CH_3$	*n*-Bu	*	†
1.	$OH \cdot C_6H_4 \cdot CH{:}N \cdot C_6H_4 \cdot F$	12.05	6.90–8.10	8.75	—	—	—
2.	$Bu_2Sn(OC_6H_4CHNC_6H_4F)_2$	—	6.70–8.15	9.23	0.70–1.90	1.01	2.13
3.	$Bu_3Sn(OC_6H_4(CHNC_6H_4F)$	—	6.75–7.50	8.95	0.7–1.8	—	—
4.	$OH \cdot C_{10}H_6 \cdot CH{:}N \cdot C_6H_4 \cdot F$	12.13	6.80–8.15	9.05	—	—	—
5.	$Bu_2Sn(OC_{10}H_6CHNC_6H_4F)_2$	—	7.0–8.05	9.6	0.55–1.82	0.87	2.26
6.	$Bu_3Sn(OC_{10}H_6CHNC_6H_4F)$	—	6.85–8.10	9.3	0.3–1.93	—	—
7.	$OH \cdot C_6H_4C(CH_3){:}N \cdot C_6H_4 \cdot SH$	11.9	6.50–7.35	2.50			
8.	$Bu_2Sn(OC_6H_4C(CH_3)NC_6H_4S)$	—	6.35–7.20	2.68	0.55–1.90		

Note: NH proton signal is observed at δ4.20 ppm (compound No. 7).

* Isomer shift δ mm sec^{-1}.

† Quadrupole splitting ΔE mm sec^{-1}.

Table 3. ^{13}C NMR data of ligand and metal complexes

Structure	Chemical shifts in δ ppm												
	1	2	3	4	5	6	7	8	9	10	11	12	13
(1) 	162.17	116.5	133.4	120.3	124.0	118.1	150.4	134.3	118.4	123.4	163.5		
(2) 	167.2	114.8	132.5	119.1	123.3	115.6	160.3	133.2	116.6	119.4	163.3		
(3) 	167.4	117.1	128.1	122.0	122.5	133.2	129.5	119.1	156.5	136.1	121.3	123.7	166.4
(1) 	131.1	126.6	126.6	127.0	151.1	128.1	126.1	117.6	119.3	117.0	129.1		
(2) 	$^1J(^{119}Sn–^{13}C) = 465.5$ Hz												

	(1)	(2)	(3)	(4)	(5)
A	—	26.9	16.8	27.4	16.4
B	—	27.5	27.9	27.9	28.4
Y	—	26.1	27.0	26.8	27.2
O	—	13.8	13.5	13.9	13.5

The spectrum was recorded only in –Bu region.

two bands at ~ 595 and 575 cm^{-1} may be assigned to asymmetric and symmetric modes of (Sn–C) vibrations ($Bu_2Sn(\widehat{ON})_2$ show two (Sn–C) bands at ~ 595 and 520 cm^{-1} whereas $Bu_2Sn(\widehat{SN})_2$ show only one band at ~ 595 cm^{-1} due to asym (Sn–C). New bands at ~ 540, 420 and 370 may be assigned to ν(Sn–O), ν(Sn–N) and ν(Sn–S) respectively.[10]

The ^1H NMR data of these complexes have been listed in Table 2. The OH and NH proton signals are present in ligands and which are not observed in the metal complexes indicating the coordination of oxygen or sulphur with tin atom. The phenyl protons are observed in the region, δ 6.35–7.20 ppm and protons due to –CH or $-CH_3$ show marked downfield shift on complex formation. Protons due to butyl groups are also observed in the region δ 0.3–2.10 ppm in all complexes.

^{119}Sn Mössbauer spectra for two complexes of the type $Bu_2Sn(\widehat{NO})_2$ have been obtained and the values are given in Table 2. The observed isomer shift values are indicative of the presence of tin(IV) consistent with six coordinated Sn environments with *cis*-Bu groups.[1] The increase in observed ΔE values may be accounted for by distortion in the field.[12]

The mass spectrum of the compound $Bu_3Sn(OC_6H_4CHNC_6H_4F)$ has been analyzed and the fragmentation scheme is shown in Fig. 1. The molecular ion peak is observed at *m/e* 504 as well as the M^{2+} ion peak.

^{13}C NMR data for a few representative samples have been recorded and given in Table 3. The shifts in the positions of carbons attached with O or S and N are indicative of their coordination with the metal atom. The carbon of Bu groups are observed at

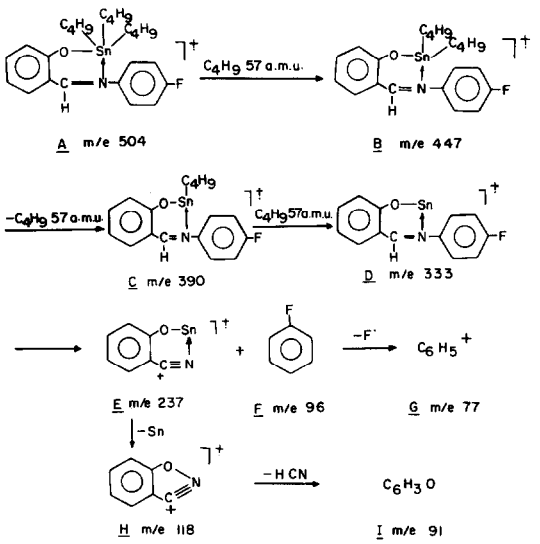


Fig. 1. Mass spectrum of $[C_{25}H_{36}OFNSn]$.

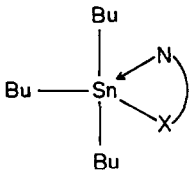
Table 4. Antibacterial activity of organotin Schiff base complexes

Bacteria	Compound	Diameter of inhibition zone (mm)							
		Bu_3Sn $(OC_{17}H_{11}NF)$	Bu_2Sn $(OC_{17}H_{11}NF)_2$	Bu_3Sn $(OC_{13}H_9NF)$	Bu_2Sn $(OC_{13}H_9NF)_2$	$OHC_{17}H_{11}NF$	$OHC_{13}H_9NF$	$(Bu_3Sn)_2O$	Bu_2SnO
Bacillus subtilis		35	22	38	15	10	5	20	12
Staphylococcus aureus		22	17	25	15	6	0	11	8
Escherichia cocii		0	0	0	0	0	0	0	0

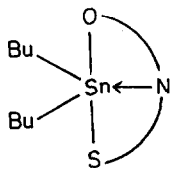
positions comparable to other similar compounds. The compound $Bu_3Sn(C_6H_5CHNC_6H_4S)$ gives a $^1J(^{119}Sn–^{13}C)$ value of 465 Hz, which indicates a five coordination.[13]

The compound $Bu_3Sn(OC_{10}H_6CHNC_6H_4F)$ gives a signal at +125.5 ppm whereas $Bu_3Sn(C_6H_5CHNC_6H_4S)$ gives a signal at +91.3 ppm in ^{119}Sn NMR, indicative of five coordination around tin atom and in agreement with previously reported values.[14,15]

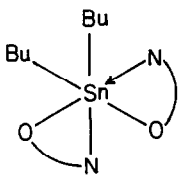
On the basis of the foregoing discussions, the following tentative structures may be proposed.



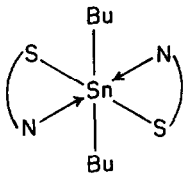
(I)



(II)



(III)



(IV)

A preliminary screening of some of these complexes and ligands has been done and the results are given in Table 4. None of the complexes or ligands is active against Gram (−)ve bacteria whereas all the complexes show marked activity against Gram (+ve) bacteria as compared to their ligands which suggests that the complex formation increases the activity.

Acknowledgements—The authors are thankful to Professor T. N. Mitchell (W. Germany) for kindly recording the spectra. A. Saxena is thankful to CSIR, New Delhi for the award of SRF. The International Tin Research Council is thanked for permission to publish the paper.

REFERENCES

1. K. C. Joshi, V. N. Pathak and P. Panwar, *Agric. Biol. Chem.* 1977, **41**, 543.
2. L. Albanus, N. E. Bjorklund, B. Gustafsson and M. Johsson, *Acta. Pharmacol. Toxicol. Suppl.* 1975, **36**, 93.
3. I. Belsky, D. Gertner and A. Zilkha, *J. Med. Chem.* 1968, **11**, 92.
4. S. M. Tripathi and J. P. Tandon, *Inorg. Nucl. Chem. Lett.* 1978, **14**, 97.
5. E. C. Alyea and A. Malik, *Canad. J. Chem.* 1975, **53**, 2809.
6. A. Saxena and J. P. Tandon, *Polyhedron* 1983, **2**, 443.
7. A. Saxena and J. P. Tandon, *Polyhedron* 1984, **3**, 6.
8. A. Saxena, S. K. Sinha and J. P. Tandon, *J. Antifung. Antibact. Agents* 1981, **9**, 435.
9. P. Pfeiffer, W. Offermann and A. Werner, *J. Prakt. Chem.* 1942, **159**, 313.
10. A. Saxena, K. C. Molloy, J. J. Zuckermann and J. P. Tandon, *Inorg. Chim. Acta* 1982, **63**, 71.
11. R. J. Puddephatt, R. J. H. Clark and A. G. Davies, *J. Chem. Soc. (A)* 1968, 1828.
12. R. R. Berrett and B. W. Fitzsimmons, *J. Chem. Soc. (A)* 1967, 525.
13. T. N. Mitchell, *J. Organomet. Chem.* 1974, **71**, 39.
14. J. D. Kennedy and W. McFarlane, *Reviews on Silicon, Tin, Germanium and Lead Compounds*, Vol. I(3), p. 235 (1974).
15. B. K. Hunter and L. W. Reeves, *Canad. J. Chem.* 1968, **46**, 1399.

Polyhedron Vol. 4, No. 6, pp. 1091–1094, 1985
Printed in Great Britain

0277–5387/85 $3.00 + .00
© 1985 Pergamon Press Ltd

SODIUM: DIBENZO-30-CROWN-10 AGGREGATES IN SOLUTION: Na-23 NMR STUDY

HARALD D. H. STÖVER, LUC J. MAURICE, ALFRED DELVILLE and CHRISTIAN DETELLIER*
Ottawa–Carleton Institute for Chemistry, University of Ottawa Campus, Ottawa K1N 9B4 (Ont.), Canada

(*Received* 11 *July* 1984; *accepted after revision* 29 *November* 1984)

Abstract—$(n+1):n$ sodium : dibenzo-30-crown-10 complexes are formed in nitromethane solutions. A model based on the coexistence in solution of 1 : 1, 2 : 1 and 3 : 2 complexes can account for the observed Na-23 chemical shifts, transverse and longitudinal relaxation rates. Logarithms of the equilibrium constants of formation at (25 ± 1)°C are (2.1 ± 0.3) and (2.5 ± 0.3) for the 2 : 1 and 3 : 2 complexes respectively. The characteristic Na-23 relaxation rates and chemical shifts of the aggregated complexes are compatible with a structure of ion pairs linked by the crown ether.

Large crown ethers form three-dimensional complexes with alkali metal cations in solution: for example, dibenzo-24-crown-8 (DB24C8) wraps around sodium cation and insulates it from solvent molecules or from the counter-anion.[1] A "wrap-around" structure has also been shown for Cs^+–DB30C10 using ^{133}Cs[2] or ^1H and ^{13}C NMR.[3] X-ray structures for the complex K^+–DB30C10 have been published in the case of the iodide[4] and of the thiocyanate.[5] Wrapping of the polyether chain around potassium is mainly accomplished by a change in four C–O bonds conformations, from *trans* to *gauche*.[5] Conformations in solution are consistent with the crystal in the case of K^+, not Na^+.[3]

A flexible thirty membered ring, comprising ten donor atoms, could accommodate two cations if the electrostatic repulsion is not redhibitory. Such 2 : 1 alkali metal cations: crown ethers have been only rarely reported in the literature. Sodium *o*-nitrophenolate,[6] potassium isothiocyanate[7] and DB24C8 form 2 : 1 complexes whose X-ray structures have been determined.[6,7] DB30C10 forms a 2 : 1 complex with sodium isothiocyanate in the solid state.[8] Indications have been given for the formation in solution of 2 : 1 and 3 : 2 sodium tetraphenylborate : DB30C10 complex.[2]

We confirm in this note the formation of 2 : 1 and 3 : 2 Na^+: DB30C10 complexes with tetraphenylborate counter anion, in nitromethane solutions.

* Author to whom correspondence should be addressed.

EXPERIMENTAL

Dibenzo-30-crown-10 was synthesized in two steps from the tetrahydropyranyl monoprotected catechol. Details of the synthesis will appear elsewhere. After recrystallization from ethylacetate, DB30C10 was vacuum-dried at 60°C for several hours. Sodium tetraphenylborate (Aldrich, 99 + %) and sodium hexafluorophosphate (Alfa products) were dried over phosphorus pentoxide under vacuum for three hours prior to use. Nitromethane (Baker) was dried under reflux with calcium hydride under nitrogen and stored after distillation over 4 Å molecular sieves, under nitrogen.

Measurements of Na-23 chemical shifts and bandwidths at half-height were made on a Varian FT-80 NMR spectrometer operating at 21.04 MHz and on a Varian XL-300 NMR spectrometer operating at 79.35 MHz. Chemical shifts are expressed in ppm from $NaBPh_4$ 0.1 M in D_2O solution. An external D_2O lock was used at 21.04 MHz. No lock was used at 79.35 MHz. Longitudinal relaxation times were measured at 79.35 MHz using a 180°–τ–90° pulse sequence (90° pulse width = 22.5 μsec).

Non-linear regression analysis has been performed with a parametric least-squares fitting,[9] incorporating Newton–Raphson iteration.[9] The errors on the calculated values of $\log K_2$, ν_2, $\log K_3$ and ν_3 reported in Table 1 have been determined after several regressions (> 25) with different input parameters. The reported value corresponds to the

Table 1.

$\log K_1$	$\log K_2$	$\log K_3$	ν_1 (Hz)	ν_2 (Hz)	ν_3 (Hz)	δ_1 (ppm)	δ_2 (ppm)	δ_3 (ppm)
>5	2.1 ± 0.3	2.5 ± 0.3	250 ± 30	800 ± 100	500 ± 100	-10.2 ± 0.1	-8	-13

Values of $\log K_1$, $\log K_2$ and $\log K_3$ [eqns (1–3)] at (298 ± 1) K, of ν_2, the bandwidth at half-height and of δ_2, the limiting chemical shift, characterizing the 2:1 Na^+ : DB30C10 complex and the "external" sodium belonging to the 3:2 complex. ν_3 and δ_3 are the corresponding parameters for "internal" sodium of the 3:2 complex and ν_1 and δ_1 for the 1:1 complex. $[NaBPh_4] = 0.050$ M, solvent: nitromethane (see Experimental for discussion of the errors).

best standard deviation obtained (33 Hz). These standard deviations are in the range of the mean of all the experimental errors of the measured linewidths. δ_2 and δ_3 have been calculated by a two parameters regression, using the K values obtained from linewidths. A full five parameters regression on the chemical shifts gave compatible results in the error limits. We found that there is some degree of correlation between the independent variables K_i and ν_i:[10] a standard deviation flat minimum is obtained for a range of K_i and ν_i values, specially in the case of the chemical shifts. This is reflected in the large error limits given in Table 1. Chemical shifts should be considered as only indicative of their order of magnitude.

RESULTS AND DISCUSSION

In Figs 1 and 2, chemical shifts (δ) and bandwidths at half-height ($\nu_{1/2}$) of the lorentzian Na-23 signals are given as a function of the ratio (ρ) DB30C10 : sodium tetraphenylborate in nitromethane.

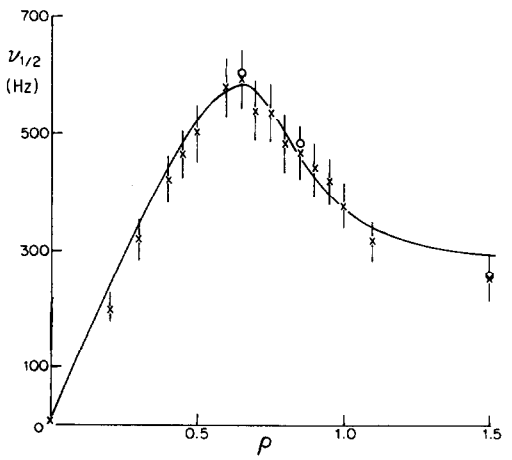


Fig. 1. Na-23 NMR signal bandwidth at half-height ($\nu_{1/2}$) as a function of the ratio $\rho = [DB30C10]/[NaBPh_4]$. $[NaBPh_4] = 0.050$ M. Solvent: nitromethane. (×): $(\pi T_2)^{-1}$ at 21.04 MHz; (○): $(\pi T_1)^{-1}$ at 79.35 MHz. The points are experimental and the curve is calculated following eqns (4)–(6) and values from Table 1.

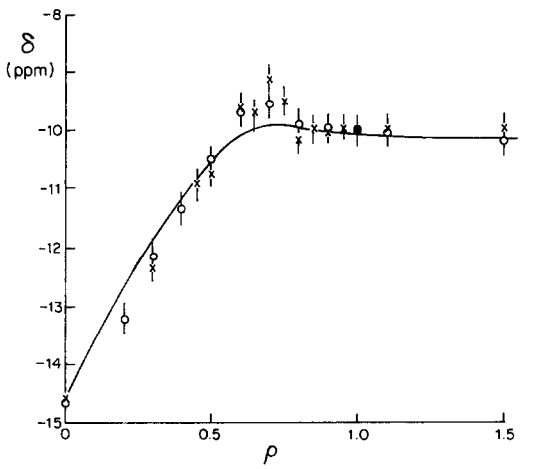


Fig. 2. Na-23 NMR chemical shifts observed in the same conditions as Fig. 1. (×: 21.04 MHz; ○: 79.35 MHz.) The points are experimental and the curve is calculated following eqns (4)–(6) and values from Table 1.

Concentration of $NaBPh_4$ was kept constant at 0.050 M. $\nu_{1/2}$ increases from 9 Hz in nitromethane to a maximum of 590 Hz for $\rho = 0.65$. Chemical shifts vary from -14.5 ppm in nitromethane to a maximum of -9.1 ppm for $\rho = 0.70$. A plateau is reached for $\rho > 0.85$ at a value of -10.0 ppm.

In order to check for the possibility of an exchange contribution to the observed linewidths we made a T_1 study at 79.35 MHz. In the limits of the experimental errors, $(1/\pi T_1)_{79.35} = (1/\pi T_2)_{21.04}$ showing that there is no detectable exchange contribution to the line broadening at 21.04 MHz. The dynamic constants of 1:1 complex formation reaction of DB30C10 with sodium in methanol ($k_c > 1.6\times10^7$ M^{-1} sec^{-1}, $k_{dec} > 1.3\times10^5$ sec^{-1}), as reported by Chock,[11] are consistent with fast exchange conditions. The presence of a maximum associated with an inflexion point suggests the coexistence of 2:1 and 1:1 complexes. The 1:1 complex is characterized by a large equilibrium constant. The 2:1 complex must be characterized by a short relaxation time, due to a dissymetric electronic charge distribution. A model based only

on the presence in solution of those two complexes can not fit the experimental data : in particular, it can not account for the sharp decrease of the chemical shifts observed for $\rho > 0.75$.

Following the proposal by Popov[2] we incorporate the 3:2 complex in our treatment [eqns (1)–(3)] (C = DB30C10)

$$C + Na^+ \rightleftharpoons C, Na^+ \quad (1)$$

$$C, Na^+ + Na^+ \rightleftharpoons Na^+, C, Na^+ \quad (2)$$

$$Na^+, C, Na^+ + Na^+, C \rightleftharpoons Na^+, C, Na^+, C, Na^+. \quad (3)$$

Equations (1), (2) and (3) are characterized by equilibrium constants K_1, K_2 and K_3 respectively. They lead to eqns (4)–(6), where "a" is the concentration of solvated Na^+, C_0 and M_0 are the total concentrations of crown and sodium, X_{obs} is the observed linewidth or chemical shift, X_0, X_1, X_2, are the characteristic linewidths or chemical shifts for the species $(Na^+)_{solv.}$, (C, Na^+), (Na^+, C, Na^+) respectively. For the 3:2 complex, we consider two types of sodium : "external" and "internal" which are characterized respectively by X_2 and X_3. X_0 and X_1 are experimentally determined (at $\rho = 0$, and $\rho = 1.5$ respectively).

$$\begin{aligned} &a^5(4\beta_3 - \beta_2^2) + a^4[\beta_2^2(M_0 - 2C_0) \\ &\quad - 4\beta_3(2M_0 - 3C_0)] + a^3[\beta_1^2 + 2\beta_2 \\ &\quad + \beta_1\beta_2 C_0 + \beta_3(2M_0 - 3C_0)^2] \\ &\quad + a^2[\beta_1^2(C_0 - M_0) + 2\beta_2(3C_0 - M_0) \\ &\quad + 4\beta_1] + a[3 + \beta_1(3C_0 - 4M_0)] - 3M_0 = 0 \end{aligned} \quad (4)$$

where $\beta_i = K_1, \ldots, K_i$. After resolution of eqn (4) for "a", calculation of the free crown concentration "b", is straightforward [eqn (5)]

$$b = \frac{2M_0 - 3C_0 - 2a}{\beta_2 a^2 - \beta_1 a - 3}. \quad (5)$$

X_{obs} is given by :

$$\begin{aligned} M_0 X_{obs} = {} & aX_0 + \beta_1 abX_1 + 2\beta_2 a^2 bX_2 \\ & + \beta_3 a^3 b^2(2X_2 + X_3). \end{aligned} \quad (6)$$

A non-linear regression on eqns (4)–(6) provides the results of Table 1 (see Experimental). We can obtain only a lower estimate for $\log K_1$: the regression is not sensitive to variation of $\log K_1 > 5$. Lower values of $\log K_1$ do not permit to fit the experimental data. The relaxation rate of the 2:1 complex ("external" sodium) reflects a high value of the sodium quadrupolar coupling constant and/or of the reorientational correlation time.[12] It is gratifying to note that the relaxation rate of the "internal" sodium in the 3:2 complex is smaller than the one calculated for "external" sodium. This reflects the expected higher symmetry of the charge distribution around a sodium cation surrounded by two crown molecules, and coordinated by oxygen atoms only. The large quadrupolar coupling constant found in the case of exposed sodium reflects the approach of anion or solvent molecules in the coordination sphere of sodium to form two loose or tight ion pairs linked by the crown ether. This structure which reduces the electrostatic repulsion between the two cations is reminiscent of the dicationic complexes formed with spiro-bis-crown ethers,[13] which are also less disfavored than could have been expected on the basis of electrostatic repulsion.[13] Even if one has to be cautious with the values of δ_2 and δ_3 furnished in Table 1, their trend is significant : δ_2 ("external", exposed, sodium) = −8 ppm has to be compared with −5 ppm and −4 ppm, lower estimates for the Na-23 chemical shifts of the complexes 15C5 : Na^+ and B15C5 : Na^+ [14] and δ_3 ("internal", sandwiched, sodium) = −13 ppm has to be compared with −11 ppm for the sandwiched 15C5 : Na^+ : 15C5 complex.[14] Finally, one should also note a large difference in the values of the linewidths for the 1 : 1 complexes in the cases of different counter anions : tetraphenylborate (250 Hz) and hexafluorophosphate (120 Hz). This result suggests a participation of the anion in the coordination sphere of sodium, a result in contrast with the behaviour of DB24C8.[1]

Acknowledgements—This research has been supported by a grant from National Science and Engineering Research Council of Canada (NSERCC) and by Research Corporation. H.D.H.S. acknowledges an NSERCC postgraduate scholarship (84–85), L.M. an NSERCC undergraduate summer scholarship (1983) and A.D. a NATO travel grant.

REFERENCES

1. M. Bisnaire, C. Detellier and D. Nadon, *Can. J. Chem.* 1982, **60**, 3071.
2. M. Shamsipur and A. I. Popov, *J. Am. Chem. Soc.* 1979, **101**, 4051.
3. D. Live and S. I. Chan, *J. Am. Chem. Soc.* 1976, **98**, 3769.
4. M. A. Bush and M. R. Truter, *J. Chem. Soc., Perkin Trans.* 1972, **2**, 345.
5. J. Hašek, D. Hlavatá and K. Huml, *Acta Cryst., B* 1980, **36**, 1782.
6. D. L. Hughes, *J. Chem. Soc., Dalton Trans.* 1975, 2374.
7. M. Mercer and M. R. Truter, *J. Chem. Soc., Dalton Trans.* 1973, 2469.
8. J. D. Owen and M. R. Truter, *J. Chem. Soc., Dalton Trans.* 1979, 1831.
9. F. R. Ruckdeschel, *Basic Scientific Subroutines*, Vol. II. McGraw-Hill, New York (1981).

10. J. Shorter, in *Correlation Analysis of Organic Reactivity*, p. 22. Research Studies Press, J. Wiley & Sons, Letchworth (1982).
11. P. B. Chock, *Proc. Natl. Acad. Sci., USA* 1972, **69**, 1939.
12. C. Detellier, *Alkali Metals*, in "*NMR of Newly Accessible Nuclei*, Vol. 2: *Chemically and Biochemically Important Elements* (Edited by P. Laszlo), Chapter 5, pp. 105–151. Academic Press, New York (1983).
13. J. Bouquant, A. Delville, J. Grandjean and P. Laszlo, *J. Am. Chem. Soc.* 1982, **104**, 686.
14. J. D. Lin and A. I. Popov, *J. Am. Chem. Soc.* 1981, **103**, 3773.

Polyhedron Vol. 4, No. 6, pp. 1095–1096, 1985
Printed in Great Britain

0277–5387/85 $3.00 + .00
© 1985 Pergamon Press Ltd

PULSED RADIOLYSIS OF PERRHENATE IN NEUTRAL AQUEOUS SOLUTION: COMPARISON WITH PERTECHNETATE

GEOFFREY A. LAWRANCE* and DAVID F. SANGSTER†
* Department of Chemistry, The University of Newcastle, NSW 2308, Australia; and
† Division of Chemical Physics, CSIRO, Lucas Heights Research Laboratories, Sutherland 2232, Australia

(*Received* 25 *October* 1984; *accepted* 18 *December* 1984)

Abstract—Reaction of perrhenate with the aquated electron in neutral aqueous solution yields ReO_4^{2-} (k_f 1.3×10^{10} M^{-1} s^{-1}), with an absorption maximum at 290 nm (ε 1700). This decays by a second-order path (k_d 1.5×10^9 M^{-1} s^{-1}) at a rate ~ 100-fold faster than the decay of TcO_4^{2-} under similar conditions.

The chemistry of the oxyanions of the heavier members of the manganese triad in oxidation states below VII has not been extensively investigated. Reaction of pertechnetate with the hydrated electron (e_{aq}) in neutral aqueous solution has been reported recently,[1] allowing measurement of the formation and decay rates and of the spectrum of TcO_4^{2-} in that medium. Despite the ready availability of perrhenate, and the similarity in the chemistries of rhenium and technecium, there is no report of the pulsed radiolysis of ReO_4^- solutions extant, apart from an uninformative conference abstract.[2] Since we are currently investigating the chemistry, including the pulsed radiolysis, of rhenium complexes, it was of interest to investigate the reaction of ReO_4^- with e_{aq} and to compare this with the data for TcO_4^-.

The 1 MeV pulse radiolysis facility, optical system and process of kinetic analysis have been described previously.[3] Solutions of potassium perrhenate in triply-distilled water ([Re] $\leqslant 10^{-3}$ M) were reacted with e_{aq} using an N_2-purged solution containing 0.1 M *t*-butylalcohol as a radical scavenger of OH. Thiocyanate dosimetry was used for calibration of the system. The formation rate was determined by monitoring decay of e_{aq} at 680 nm in the presence of various concentrations of ReO_4^-. Initial and final optical density changes were measured at 5–25-nm intervals from signal averaged data in the range 250–600 nm, permitting construction of electronic spectra (Fig. 1). Intermediate decay kinetics were followed at several wavelengths.

For the manganese triad, the MO_4^- species may be reduced electrochemically in multielectron steps in aqueous solution. In aprotic solvents, one-electron reductions of all of these anions have been reported, and are increasingly negative down the triad (MnO_4^-, −0.60 V; TcO_4^-, −1.74 V; ReO_4^-, −2.30 V, vs SCE).[4] With the fast kinetic technique of pulsed radiolysis, one-electron reduction with the powerful reductant e_{aq} (E° −2.8 V) allows examination of the fate of the reduction product. Apparently stability of the M(VI) oxyanion decreases down the triad, since MnO_4^{2-} is stable in dilute base, while TcO_4^{2-} generated radiolytically in aqueous base is stable on a timescale greater than 10 ms but less than 50 ms.[5]

When solutions of ReO_4^- were irradiated, the optical density due to e_{aq} disappeared according to a rate law first order in both e_{aq} and ReO_4^-, with $k = 1.3 \times 10^{10}$ M^{-1} s^{-1}. This is consistent with the disappearance of e_{aq} and appearance of the putative species ReO_4^{2-}, which can form via

$$ReO_4^- + e_{aq} \rightarrow ReO_4^{2-} \quad (1)$$

and

$$ReO_4^- + H \rightarrow ReO_4^{2-} + H^+ \quad (2)$$

Since the formation rates in neutral and basic (0.01 M NaOH) solution are essentially the same, presumably eqn (2) does not contribute much above pH 6. The species formed has a maximum at 290 nm, and decays by second-order kinetics. Decay can arise, in the absence of OH, from the following reactions:

$$2Re(VI) \rightarrow Re(VII) + Re(V), \quad (3)$$

$$2Re(V) \rightarrow Re(VI) + Re(IV), \quad (4)$$

Table 1. Comparative data for pulsed radiolysis of TcO_4^- and ReO_4^- in neutral aqueous solution

	TcO_4^-*†	ReO_4^-†‡
k_f	$1.3(\pm 0.2) \times 10^{10}$	$1.3(\pm 0.15) \times 10^{10}$
k_d	$1.5(\pm 0.5) \times 10^{7}$	$1.7(\pm 0.4) \times 10^{9}$
λ_{max} (nm)	325	290
ε_{max} (M^{-1} cm^{-1})	2600	1700

* Reference 1.
† k_f and k_d in M^{-1} s^{-1}.
‡ This work.

$$Re(VI) + H_2O_2 \rightarrow Re(VII) + OH + OH^- \quad (5)$$

Comparison of ReO_4^- and TcO_4^- reacting with e_{aq} in neutral solution appears in Table 1. Formation rates are the same, consistent with reaction of ions of the same symmetry, charge and almost the same size. The absorbance maximum of ReO_4^{2-} is at slightly higher energy than that of TcO_4^{2-}, following the like trend for MO_4^-. Since ReO_4^- does not absorb much above 260 nm, uncorrected observed optical density changes have been used to calculate the spectrum of ReO_4^{2-}. The major difference in the two species is the 100-fold higher rate of decay of ReO_4^{2-} vs TcO_4^{2-}. Disproportionation of MnO_4^{2-} in dilute acid has been studied recently,[6] and a decay rate at pH 6 of $\sim 10^2$ M^{-1} s^{-1} can be estimated from that data. Thus there is clearly an increase in the reactivity of the MO_4^{2-} ion down the triad, which correlates with the increasing negative one-electron reduction potential down the triad.

Acknowledgment—Support from the Australian Institute of Nuclear Science and Engineering is gratefully acknowledged.

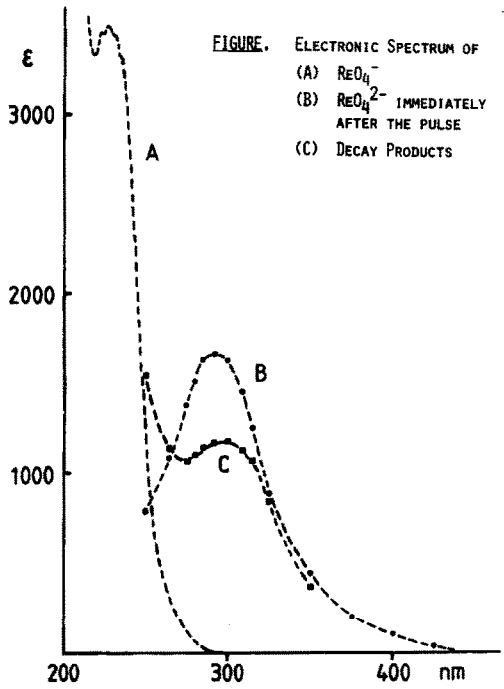


FIGURE. ELECTRONIC SPECTRUM OF
(A) ReO_4^-
(B) ReO_4^{2-} IMMEDIATELY AFTER THE PULSE
(C) DECAY PRODUCTS

Fig. 1.

REFERENCES

1. A. K. Pikaev, S. V. Kryuchkov, A. F. Kuzina and V. I. Spitsyn, *Dokl. Akad. Nauk SSSR* 1977, **236**, 1155.
2. L. V. Ivanitskaya and N. Sh. Tsikhelashvili, *Simp. po radiat. khimii*, p. 147, 1978. INIS Vol. 10/19, 479182.
3. H. A. Boucher, A. M. Sargeson, D. F. Sangster and J. C. Sullivan, *Inorg. Chem.* 1981, **20**, 3719.
4. L. Astheimer and K. Shwochan, *J. Inorg. Nucl. Chem.* 1976, **38**, 1131.
5. E. Deutsch, W. R. Heineman, R. Hurst, J. C. Sullivan, W. A. Mulac and S. Gordon, *J. Chem. Soc., Chem. Commun.* 1978, 1038.
6. J. H. Sutter, K. Colquitt and J. R. Sutter, *Inorg. Chem.* 1974, **13**, 1444.

Polyhedron Vol. 4, No. 6, pp. 1097–1102, 1985
Printed in Great Britain

0277–5387/85 $3.00 + .00
© 1985 Pergamon Press Ltd

SYNTHESIS AND STRUCTURE OF A BINUCLEAR RUTHENIUM 4-CHLOROBENZAMIDATO COMPLEX

AKHIL R. CHAKRAVARTY, F. ALBERT COTTON* and DEREK A. TOCHER
Department of Chemistry and Laboratory for Molecular Structure and Bonding, Texas A & M University, College Station, TX 77843, U.S.A.

(*Received* 15 *October* 1984; *accepted* 18 *December* 1984)

Abstract—The compound $Ru_2Cl(4\text{-}Cl\text{-}C_6H_4CONH)_4$ was prepared by reaction of $Ru_2Cl(O_2CCH_3)_4$ with $4\text{-}Cl\text{-}C_6H_4CONH_2$ at 180°C. Crystals of the composition $Ru_2Cl(4\text{-}Cl\text{-}C_6H_4CONH)_4CH_3OH$ were obtained by slow diffusion of CH_3OH containing Et_4NCl into a Me_2SO solution of the compound. The structure of the crystalline product, which loses solvent of crystallization on removal from the mother liquor, was solved by X-ray crystallography by mounting a single crystal in a capillary containing the mother liquor. The crystals belong to the space group $P\bar{1}$ (triclinic crystal system) with $a = 12.731(3)$ Å, $b = 14.389(3)$ Å, $c = 12.604(3)$ Å, $\alpha = 103.41(2)°$, $\beta = 106.43(2)°$, $\gamma = 64.90(2)°$, $V = 1988.6(8)$ Å^3 and $Z = 2$. There are two half ruthenium dimers linked by a Cl atom and an uncoordinated solvent CH_3OH molecule per asymmetric unit. The ruthenium dimers lie on two centers of inversion at 0, 0, 0 and 1/2, 0, 0. The chloride ions bridge dinuclear cations in the crystal, forming infinite zigzag chains. The average Ru–Ru distance is 2.296[1] Å and each ruthenium atom has a $RuClN_2O_2$ coordination sphere where the average Ru′–Ru–Cl angle is virtually linear (175.68[6]°). The metal oxidation states in the complex are +2 and +3, giving an average value of +2.5. The arrangement of four bridging 4-Cl–benzamidato ligands is of the 2:2 type. The average Ru–N, Ru–O, Ru–Cl distances and Ru(1)–Cl(1)–Ru(2) angle are 2.036[6] Å, 2.044[5] Å, 2.583[2] Å and 117.26(8)°, respectively. The IR spectrum of the compound shows two N–H stretches at 3380 and 3340 cm^{-1}. The electronic spectrum of the compound in Me_2SO exhibits bands at 558 nm ($\varepsilon = 340$ M^{-1} cm^{-1}), 425 nm (1000) and 320 nm (22,700).

Since the report[1] of the first X-ray structural studies on $Ru_2Cl(O_2CC_3H_7)_4$[2] in 1969 from this laboratory, several other diruthenium tetracarboxylato compounds have been prepared[2–8] and subjected to structural studies[3–5] which show that such complexes have short Ru–Ru distances ranging from 2.25 to 2.29 Å. Theoretical calculations[9,10] have also been performed to explain their three electron magnetic moment and the formal oxidation states of +2.5 of ruthenium in such complexes.[11] An SCF–Xα–SW calculation done on $Ru_2(O_2CH)_4Cl$ showed[10] that the ground state configuration should be $\sigma^2\pi^4\delta^2\pi^{*2}\delta^{*1}$.

Recent work from this[12] and other laboratories[13,14] has shown that three-atom bridging ligands with the –NHCO– functionality can be used to prepare a new class of diruthenium(II,III) complexes of the type $Ru_2Cl(RCONH)_4$ which closely resemble the carboxylato species in their physical and chemical properties. While we have reported[12] the synthesis and reactivity of $Ru_2Cl(PhCONH)_4$ having R = aryl group, the work of Bear and coworkers shows[13,14] that other amides, viz. with R = alkyl groups (e.g. CH_3 or CF_3) are also useful in preparing tetraamidato species. These developments in diruthenium chemistry are of considerable interest because previously a systematic study[11] had been done only on the $Ru_2Cl(O_2CR)_4$ complexes. Like carboxylato anions, the anions of the amides, RCONHR′, can be used to study the electronic and steric effects of the R and R′ groups on the physical and chemical properties of the dimeric species. The interesting structural feature[1,3–5] in $Ru_2Cl(O_2CR)_4$ complexes is the presence of infinite zigzag chains in which the diruthenium units are linked by bridging chloride atoms. From the results published to date on the

* Author to whom correspondence should be addressed.

diruthenium amidato species it is apparent that this sort of bonding is also present in these complexes. All other reported[15–20] diruthenium species are known to be discrete dimeric species.

Our report[12] on $Ru_2Cl(PhCONH)_4$ shows that this complex when reacted with PPh_3 forms a novel compound which has been structurally characterized as $Ru_2(Ph)_2(PhCONH)_2[Ph_2POC(Ph)N]_2$. In order to better understand the effect of the bridging benzamidato ligand on the reactivity of the diruthenium unit attempts have been made to crystallize the $Ru_2Cl(PhCONH)_4$ compound. We were unsuccessful with the $PhCONH^-$ ligand, but by using a substituted benzamide, viz. 4-Cl-$C_6H_4CONH_2$, we have been able to isolate single crystals of $Ru_2Cl(4\text{-}Cl\text{-}C_6H_4CONH)_4 \cdot MeOH$. In this paper we report the synthesis and X-ray structure of this complex. Its reactivity and that of other $Ru_2Cl(RCONH)_4$ compounds will be reported in a future paper.

EXPERIMENTAL

Synthesis of $Ru_2Cl(4\text{-}Cl\text{-}C_6H_4CONH)_4 \cdot CH_3OH$

A 1 g quantity of 4-Cl-$C_6H_4CONH_2$ was added to 0.1 g of $Ru_2Cl(O_2CCH_3)_4$.[2] The mixture was heated to 180°C and stirred for 48 h under a dinitrogen atmosphere. Excess ligand was then removed by sublimation under reduced pressure. The residue was dissolved in 10 cm^3 of Me_2SO and filtered. The color of the solution was dark brown. A 5 cm^3 volume of Me_2SO solution was placed in a test tube (diameter 15 mm). A 10 cm^3 volume of methanol containing 0.05 g of Et_4NCl was carefully added on the top of the Me_2SO solution, maintaining a distinct interface between the two solvents. Slow diffusion of the solvents as well as electrolytes gave dark brown crystals in *ca* 50% yield. The compound is but sparingly soluble in common organic solvents other than Me_2SO. On removal from the mother liquor the crystals lose crystallinity due to loss of solvent of crystallization. Found: C, 38.98; H, 2.50; N, 6.53%. Calc. for $Ru_2Cl(4\text{-}Cl\text{-}C_6H_4CONH)_4$: C, 39.27; H, 2.34; N, 6.54%. IR (KBr phase): 3380, 3340, 1590, 1572, 1510, 1475, 1440, 1425, 1275, 1255, 1210, 1175, 1115, 1090, 1010, 945, 842, 820, 800, 742, 725, 655, 625, 585, 488, 435, 335, 300 cm^{-1}. λ_{max} (nm) (ε, M^{-1} cm^{-1}): 558 (340), 425 (1000), 320 (22,700) (in Me_2SO).

Measurements

The elemental analysis was obtained from Galbraith Lab. Inc. The IR spectrum was recorded using a Perkin–Elmer 785 spectrophotometer. The electronic spectrum was obtained from a Me_2SO solution of the compound using a Cary 17D spectrophotometer.

X-ray crystallographic procedures

The structure of the single crystal of $Ru_2Cl(4\text{-}Cl\text{-}C_6H_4CONH)_4 \cdot CH_3OH$ was determined by using procedures described in a general way elsewhere.*[21] A dark-brown single crystal was wedged inside a capillary containing a Me_2SO–CH_3OH mixture in 1:4 proportion. The ends of the capillary were sealed to prevent any loss of solvent. It was observed that the crystals lost crystallinity rapidly when mounted in epoxy on a glass fiber. All geometric and intensity data were taken from this crystal at 5°C by using an automated four-circle Syntex $P\bar{1}$ diffractometer, equipped with graphite-monochromated Mo-$K\alpha$ radiation.

The standards showed a 12.5% decay in intensity during 126 h exposure time. An empirical absorption correction was made based on azimuthal scans of nine reflections with Eulerian angle χ near 90°. Corrections were also made for Lorentz, polarization and decay effects.

The positions of the two Ru atoms in the crystallographic asymmetric unit were found by the direct methods program MULTAN, and refined by least-squares. Successive iterations of difference Fourier maps and least-squares cycles led to the development and convergent refinement of the remainder of the structure.

Towards the end of the refinement, a disordered CH_3OH molecule was identified. There were three pairs of peaks with each pair having a peak-to-peak distance that was reasonable for C–O in CH_3OH. One pair of peaks was refined with a site occupancy factor (SOF) of 0.5. The other two pairs were refined with SOF = 0.25. As a whole there is one CH_3OH molecule per asymmetric unit. The molecule is present as a solvent of crystallization and does not interact with the complex molecule. The C and O atoms of the solvent molecule were refined isotropically. The final difference Fourier map was featureless except for peaks with $e/Å^3$ ranging from 1.4 to 1.7 at positions less than 1.0 Å from the Ru centers.

Crystallographic data and other basic information pertaining to the data collection are summarized in Table 1. Complete tables of bond

* Calculations were done on the VAX-11/780 computer at the Department of Chemistry, Texas A & M University, College Station, Texas with a VAX-SDP software package.

Table 1. Crystallographic data

Formula	$Ru_2Cl(4\text{-}Cl\text{-}C_6H_4CONH)_4 \cdot CH_3OH$
Formula weight	887.94
Space group	$P\bar{1}$
Systematic absences	None
a (Å)	12.731(3)
b (Å)	14.389(3)
c (Å)	12.604(3)
α (°)	103.41(2)
β (°)	106.43(2)
γ (°)	64.90(2)
V (Å^3)	1988.6(8)
Z	2
$d_{calc.}$ (g cm^{-3})	1.483
Crystal size (mm)	0.4 × 0.3 × 0.4
μ(Mo-K_α) (cm^{-1})	11.202
Data collection instrument	Syntex $P\bar{1}$
Radiation (monochromated in incident beam)	Mo-K_α = 0.71073 Å
Orientation reflections, No., range (2θ)	15, $22 < 2\theta < 29$
Temperature (°C)	5
Scan method	ω–2θ
Data collection range 2θ (°)	$5 \leqslant 2\theta \leqslant 50$
No. of unique data, total with $F_o^2 > 3\sigma(F_o^2)$	5364, 4503
No. of parameters refined	412
Trans. factors, max., min. (%)	99.88, 84.31
R*	0.063
R_w†	0.088
Quality-of-fit indicator‡	1.85
Largest shift/esd, final cycle	0.17
Largest peak (e Å^{-3})	1.7

* $R = \sum||F_o|-|F_c||/\sum|F_o|$.
† $R_w = [\sum w(|F_o|-|F_c|)^2/\sum w|F_o|^2]^{1/2}$; $w = 1/\sigma^2(|F_o|)$.
‡ Quality of fit = $[\sum w(|F_o|-|F_c|)^2/(N_{obs}-N_{parameters})]^{1/2}$.

distances and angles as well as atomic positional and anisotropic thermal parameters and structure factors have been deposited as supplementary material with the Editor at Queen Mary College.*

RESULTS AND DISCUSSION

The compound $Ru_2Cl(4\text{-}Cl\text{-}C_6H_4CONH)_4$ was prepared in quantitative yield by reacting $Ru_2Cl(O_2CCH_3)_4$ with molten 4-chlorobenzamide ligand at 180°C under a dinitrogen atmosphere. The resulting product which is dark brown in color is indefinitely stable in air. It is only sparingly soluble in common organic solvents other than Me_2SO. Single crystals of this compound with composition $Ru_2Cl(4\text{-}Cl\text{-}C_6H_4CONH)_4 \cdot CH_3OH$ were obtained by slow diffusion of CH_3OH containing Et_4NCl into a solution of $Ru_2Cl(4\text{-}Cl\text{-}C_6H_4CONH)_4$ in dimethyl sulfoxide. Our interest in structural studies of the diruthenium amidato complexes arises from the recent developments in this chemistry,[12–14] the most noteable feature of which is their reactivity[12] towards PPh_3. Such complexes also display reversible redox behavior which has been extensively studied[13,14] by Bear and coworkers.

Selected bond distances and angles for $Ru_2Cl(4\text{-}Cl\text{-}C_6H_4CONH)_4 \cdot CH_3OH$ are presented in Table 2. The structure of the compound along with the atom labelling scheme is illustrated in Fig. 1 which shows two crystallographically independent dimeric units, at 0, 0, 0 and 1/2, 0, 0 which are bridged by a chloride ion. Each diruthenium unit resides on a

* Atomic co-ordinates have also been deposited with the Cambridge Crystallographic Data Centre.

Table 2. Selected bond distances and angles in $Ru_2Cl(4\text{-}Cl\text{-}C_6H_4CONH)_4 \cdot MeOH$*

Bond distance (Å)			
Ru(1)–Ru(1)	2.299(1)	Ru(2)–Ru(2)	2.292(1)
Ru(1)–Cl(1)	2.603(2)	Ru(2)–Cl(1)	2.563(2)
Ru(1)–O(1)	2.043(5)	Ru(2)–O(3)	2.045(5)
Ru(1)–O(2)	2.047(5)	Ru(2)–O(4)	2.042(5)
Ru(1)–N(1)	2.022(6)	Ru(2)–N(3)	2.030(6)
Ru(1)–N(2)	2.035(5)	Ru(2)–N(4)	2.056(6)
O(1)–C(11)	1.297(9)	O(3)–C(31)	1.286(8)
N(1)–C(11)	1.330(9)	N(3)–C(31)	1.318(9)
O(2)–C(21)	1.278(9)	O(4)–C(41)	1.297(9)
N(2)–C(21)	1.288(9)	N(4)–C(41)	1.296(10)
C(11)–C(12)	1.489(10)	C(31)–C(32)	1.480(10)
C(21)–C(22)	1.492(10)	C(41)–C(42)	1.493(11)
O(5)–C(1)	1.41(2)	O(6)–C(2)	1.43(4)
O(7)–C(3)	1.30(4)		
Bond angle (°)			
Ru(1)–Ru(1)–Cl(1)	175.35(6)	Ru(2)–Ru(2)–Cl(1)	176.01(6)
Ru(1)–Ru(1)–O(1)	91.4(1)	Ru(2)–Ru(2)–O(3)	91.0(1)
Ru(1)–Ru(1)–O(2)	90.2(2)	Ru(2)–Ru(2)–O(4)	90.1(2)
Ru(1)–Ru(1)–N(1)	88.1(2)	Ru(2)–Ru(2)–N(3)	88.1(2)
Ru(1)–Ru(1)–N(2)	88.0(2)	Ru(2)–Ru(2)–N(4)	89.0(2)
Cl(1)–Ru(1)–O(1)	91.9(2)	Cl(1)–Ru(2)–O(3)	92.3(2)
Cl(1)–Ru(1)–O(2)	86.6(2)	Cl(1)–Ru(2)–O(4)	87.8(2)
Cl(1)–Ru(1)–N(1)	88.7(2)	Cl(1)–Ru(2)–N(3)	88.5(2)
Cl(1)–Ru(1)–N(2)	95.3(2)	Cl(1)–Ru(2)–N(4)	93.2(2)
O(1)–Ru(1)–O(2)	89.3(2)	O(3)–Ru(2)–O(4)	88.6(2)
O(1)–Ru(1)–N(1)	179.2(2)	O(3)–Ru(2)–N(3)	178.8(2)
O(1)–Ru(1)–N(2)	89.4(2)	O(3)–Ru(2)–N(4)	89.4(2)
O(2)–Ru(1)–N(1)	91.4(2)	O(4)–Ru(2)–N(3)	90.5(2)
O(2)–Ru(1)–N(2)	177.7(2)	O(4)–Ru(2)–N(4)	177.8(2)
N(1)–Ru(1)–N(2)	89.9(2)	N(3)–Ru(2)–N(4)	91.4(2)
Ru(1)–Cl(1)–Ru(2)	117.26(8)	Ru(2)–O(3)–C(31)	118.8(5)
Ru(1)–O(1)–C(11)	118.2(5)	Ru(2)–O(4)–C(41)	119.6(5)
Ru(1)–O(2)–C(21)	118.9(5)	Ru(2)–N(3)–C(31)	121.6(5)
Ru(1)–N(1)–C(11)	121.8(5)	Ru(2)–N(4)–C(41)	119.8(5)
Ru(1)–N(2)–C(21)	121.5(5)	O(3)–C(31)–N(3)	120.5(7)
O(1)–C(11)–N(1)	120.6(7)	O(4)–C(41)–N(4)	121.4(7)
O(2)–C(21)–N(2)	121.3(7)		

* Numbers in parentheses are estimated standard deviations in the least significant digits.

center of inversion and the asymmetric unit consists of two half dimers linked by Cl, as well as a CH_3OH molecule of crystallization, which is disordered on three sites with 0.5, 0.25 and 0.25 occupancy, and does not interact with the complex.

Each ruthenium dimer is bonded to four bridging amidato ligands which adopt a 2:2 type arrangement (required by inversion symmetry) and to axial chlorine atoms which link the dimetal units. There are four small and slightly different torsional angles for the four bridging ligands, viz.: N(1)–Ru(1)–Ru(1)′–O(1)′ = 0.7°; N(2)–Ru(1)–Ru(1)′–O(2)′ = 1.4°; N(3)–Ru(2)–Ru(2)′–O(3)′ = 0.8°; and O(4)–Ru(2)–Ru(2)′–N(4)′ = 2.0°. Among $Ru_2Cl(O_2CR)_4$ complexes the asymmetric unit consists of only one half of the dimeric unit.[1,3–5] The observed difference between amidato and carboxylato species could be due to the difference in the spatial arrangements of the dimeric units. Since there has been no other structural report on an amidato species, a definitive comparison between the two types of systems is not possible. The two systems resemble each other in the

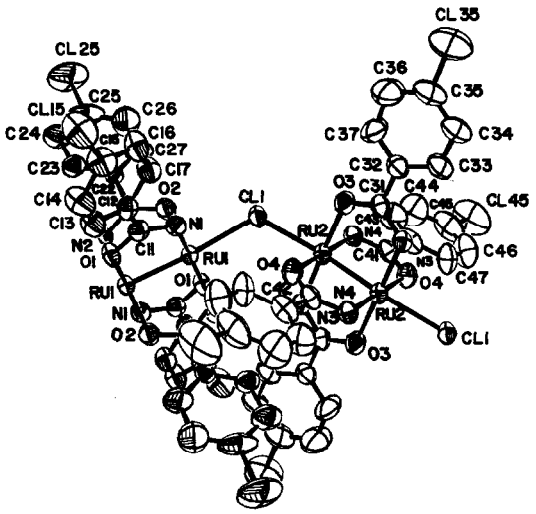


Fig. 1. An ORTEP drawing of the $Ru_2Cl(4\text{-}Cl\text{-}C_6H_4CONH)_4 \cdot CH_3OH$ complex. Atoms are represented by thermal vibration ellipsoids at the 50% level and the atom numbering scheme is defined.

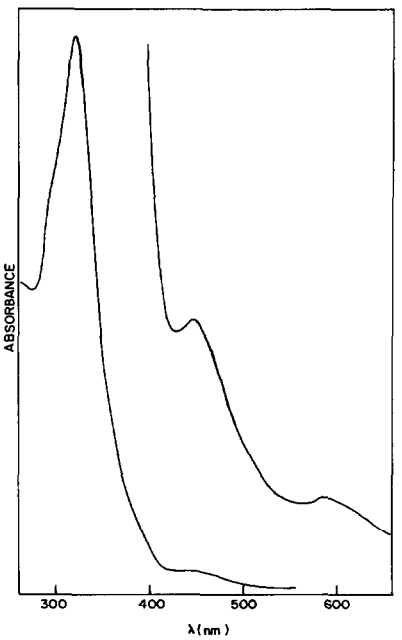


Fig. 3. Electronic spectrum of $Ru_2Cl(4\text{-}Cl\text{-}C_6H_4CONH)_4 \cdot CH_3OH$ in Me_2SO.

formation of infinite zigzag chains[1,3–5] in which dimeric units are linked by bridging chloride atoms. The crystal packing for $Ru_2Cl(4\text{-}Cl\text{-}C_6H_4CONH)_4 \cdot CH_3OH$ is displayed in Fig. 2 which shows the propagation of the chain along the *a*-axis.

The geometry at each ruthenium atom is pseudooctahedral with a $RuClN_2O_2$ coordination sphere. The Ru–Ru distances in the two crystallographically independent dimeric units are 2.299(1) and 2.292(1) Å. The average Ru–Cl, Ru–O and Ru–N distances are 2.583[2], 2.044[5] and 2.036[6] Å, respectively. Each of the Cl–Ru–Ru–Cl chains is essentially linear. The average Ru'–Ru–Cl angle is 175.68[6]°. The angle between two dimeric units, i.e. the Ru(1)–Cl(1)–Ru(2) angle is 117.26(8)°, which is responsible for the zigzag nature of the chain. The Ru–Ru–O angles are all slightly obtuse while the Ru–Ru–N angles are all slightly acute. There is no indication of disordering of O and NH in this case. The angles Cl(1)–Ru(1)–O(1), N(2) and Cl(1)–Ru(2)–O(3), N(4) are considerably greater than 90°. The remaining Cl–Ru–O and Cl–Ru–N angles are acute, ranging from 88.5(2) to 88.7(2)°.

The average Ru–Ru distance, which is 2.296[1] Å, is slightly longer than the distances of 2.250–2.290 Å found in $Ru_2Cl(O_2CR)_4$ complexes but shorter than those in $Ru_2(CH_2Bu^t)_6$ ($Ru^{III}Ru^{III}$ = 2.311(3) Å)[16] and $(Ru(OEP))_2$ ($Ru^{II}Ru^{II}$ = 2.408(1) Å).[15] The Ru–Ru distances in totally polar complexes, viz., in $Ru_2Cl(hp)_4(Hhp)$,[18] $Ru_2Cl(chp)_4$[19] and Ru_2Cl

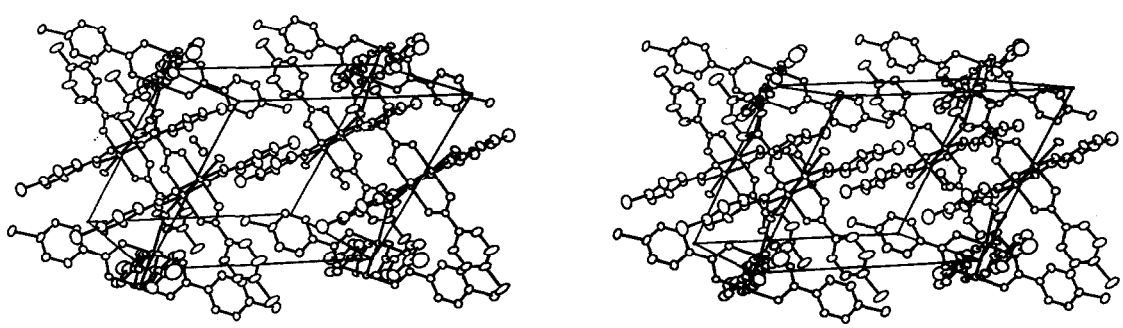


Fig. 2. Stereoscopic view of the crystal packing in $Ru_2Cl(4\text{-}Cl\text{-}C_6H_4CONH)_4 \cdot CH_3OH$ as seen down the *c*-axis with the *a*-axis vertical and the *b*-axis horizontal. The thermal ellipsoids are at the 20% probability level. Only the major orientation of the disordered CH_3OH molecule is shown.

$(PhNpy)_4$,[18] range from 2.275(3) to 2.286(1) Å. The shortest Ru–Ru distance known[17] occurs in $Ru_2(mhp)_4 \cdot CH_2Cl_2$, where it has a value of 2.238(1) Å. The Ru–Cl distance in $Ru_2Cl(4\text{-}Cl\text{-}C_6H_4CONH)_4 \cdot CH_3OH$ is quite long but similar distances are also observed[1,3–5] in $Ru_2Cl(O_2CR)_4$ complexes. In $Ru_2Cl(hp)_4(Hhp)$, the Ru–Cl distance is 2.558(2) Å but in $Ru_2Cl(PhNpy)_4$ and $Ru_2Cl(chp)_4$ the Ru–Cl distances are 2.437(7) and 2.443(2) Å, respectively.[18,19] Elongation of the Ru–Cl bond occurs only when both axial sites of the diruthenium unit are coordinated by ligands. As in the carboxylato species, the Ru–Cl bonds in amidato complexes are weak. From our earlier work[12] and from the work of Bear and co-workers[13,14] it is evident that in polar solvents the amidato species no longer exists in the polymeric form but forms discrete molecular species, with perhaps some loss of Cl^- ligands.

The electronic spectrum of the compound in Me_2SO, shown in Fig. 3, displays three bands. The band at 320 nm is very strong compared to the other two at 558 nm ($\varepsilon = 340\ M^{-1}\ cm^{-1}$) and 425 nm ($\varepsilon = 1000\ M^{-1}\ cm^{-1}$). The visible absorption spectrum of $Ru_2Cl(PhCONH)_4$ in Me_2SO is known[12] to exhibit an intense band at 445 nm. The band observed[13] for $Ru_2Cl(HNOCCF_3)_4$ in Me_2SO is at 459 nm. The diffuse reflectance spectrum of solid $Ru_2Cl(O_2CCH_3)_4$ shows[22] bands at 463 and 559 nm. A polarized absorption spectrum reported[5] for $Ru_2Cl(O_2CCH_3)_4$ shows bands at 558 and 444 nm with a shoulder at 526 nm. Wilson and Taube observed[23] that $Ru_2Cl(O_2CCH_3)_4$ in D_2O displays a sharp band at 425 nm, a broad band at 1000 nm and a shoulder at 310 nm. SCF–Xα–SW calculations on $Ru_2(O_2CH)_4^+$ assigned[10] the band at 425 nm to an allowed $O(\pi) \rightarrow RuRu(\pi^*)$ transition, where the $O(\pi)$ orbital is primarily an Ru–O bonding orbital with appreciable Ru–Ru π-bonding contributions. The lower energy band at 558 nm is assigned[10] to a $Cl \rightarrow \pi^*$ or $Cl \rightarrow \delta^*$ transition. The bands at 558 and 425 nm in $Ru_2Cl(4\text{-}Cl\text{-}C_6H_4CONH)_4$ may have similar origins.

Acknowledgement—We thank the U.S. National Science Foundation for support.

REFERENCES

1. M. J. Bennett, K. G. Caulton and F. A. Cotton, *Inorg. Chem.* 1969, **8**, 1.
2. T. A. Stephenson and G. Wilkinson, *J. Inorg. Nucl. Chem.* 1966, **28**, 2285.
3. A. Bino, F. A. Cotton and T. R. Felthouse, *Inorg. Chem.* 1979, **18**, 2599.
4. T. Togano, M. Mukaida and T. Nomura, *Bull. Chem. Soc. Jpn* 1980, **53**, 2085; 1972, **45**, 2143.
5. D. S. Martin, R. A. Newman and L. M. Vlasnik, *Inorg. Chem.* 1980, **19**, 3404.
6. F. A. Cotton and J. G. Norman, Jr. *Inorg. Chim. Acta* 1972, **6**, 411.
7. P. Legzdins, R. W. Mitchell, G. L. Rempel, J. D. Ruddick and G. Wilkinson, *J. Chem. Soc. A* 1970, 3322.
8. R. W. Mitchell, A. Spencer and G. Wilkinson, *J. Chem. Soc., Dalton Trans.* 1973, 846.
9. J. G. Norman, Jr. and H. J. Kolari, *J. Am. Chem. Soc.* 1978, **100**, 791.
10. J. G. Norman, Jr., G. E. Renzoni and D. A. Case, *J. Am. Chem. Soc.* 1979, **101**, 5256.
11. F. A. Cotton and R. A. Walton, *Multiple Bonds Between Metal Atoms.* Wiley, New York (1982).
12. A. R. Chakravarty, F. A. Cotton and D. A. Tocher, *J. Am. Chem. Soc.* 1984, **106**, 6409.
13. T. Malinski, D. Chang, F. N. Feldmann, J. L. Bear and K. M. Kadish, *Inorg. Chem.* 1983, **22**, 3225.
14. M. Y. Chavan, F. N. Feldmann, X. Q. Lin, J. L. Bear and K. M. Kadish, *Inorg. Chem.* 1984, **23**, 2373.
15. J. P. Collman, C. E. Barnes, P. N. Swepton and J. A. Ibers, *J. Am. Chem. Soc.* 1984, **106**, 3500.
16. R. P. Tooze, M. Motevalli, M. B. Hursthouse and G. Wilkinson, *J. Chem. Soc., Chem. Commun.* 1984, 799.
17. W. Clegg, *Acta Cryst.* 1980, **B36**, 3112.
18. A. R. Chakravarty, F. A. Cotton and D. A. Tocher, *Inorg. Chem.* (in press).
19. A. R. Chakravarty, F. A. Cotton and D. A. Tocher, *Inorg. Chem.* (in press).
20. L. F. Warren and V. L. Goedken, *J. Chem. Soc., Chem. Commun.* 1978, 909.
21. A. Bino, F. A. Cotton and P. E. Fanwick, *Inorg. Chem.* 1979, **18**, 3358; F. A. Cotton, B. A. Frenz, G. Deganello and A. Shaver, *J. Organomet. Chem.* 1973, **50**, 227; A. C. T. North, D. C. Phillips and F. S. Mathews, *Acta Cryst.* 1968, **A24**, 351.
22. R. J. H. Clark and M. R. Franks, *J. Chem. Soc., Dalton Trans.* 1976, 1825.
23. C. R. Wilson and H. Taube, *Inorg. Chem.* 1975, **14**, 2276.

Polyhedron Vol. 4, No. 6, pp. 1103–1108, 1985
Printed in Great Britain

0277–5387/85 $3.00 + .00
© 1985 Pergamon Press Ltd

FURTHER STUDIES OF PHOSPHINE ADDUCTS OF NIOBIUM(IV) AND TANTALUM(IV) CHLORIDES: NEW SEVEN- AND EIGHT-COORDINATE COMPOUNDS WITH TRIMETHYLPHOSPHINE: $NbCl_4(PMe_3)_3$ AND $Ta_2Cl_8(PMe_3)_4$

F. ALBERT COTTON,* MICHAEL P. DIEBOLD and WIESLAW J. ROTH
Department of Chemistry and Laboratory for Molecular Structure and Bonding, Texas A & M University, College Station, TX 77843, U.S.A.

(*Received* 15 *October* 1984; *accepted* 18 *December* 1984)

Abstract—The reaction of $NbCl_4(THF)_2$ with an excess of PMe_3 in toluene solution afforded a 70% isolated yield of green $NbCl_4(PMe_3)_3$. When a slurry of $TaCl_5$ in toluene containing a slight excess of PMe_3 was reduced with sodium amalgam overnight, a 60% yield of orange to red (depending on crystal size) $Ta_2Cl_8(PMe_3)_4$ was obtained. Both compounds have been fully characterized by X-ray crystallography. $NbCl_4(PMe_3)_3$ forms monoclinic crystals ($P2_1/c$) with unit cell dimensions $a = 15.061(3)$ Å, $b = 11.677(4)$ Å, $c = 11.583(4)$ Å, $\beta = 91.71(3)°$, $V = 2036(2)$ Å^3, and $Z = 4$. It is isomorphous with its $TaCl_4(PMe_3)_3$ homolog, and the bond lengths and angles are very similar. $Ta_2Cl_8(PMe_3)_4$ forms cubic crystals ($Im3$) with $a = 16.377(2)$, $V = 4392(2)$ Å^3 and $Z = 6$. It is thus isomorphous with its niobium homolog, and the internal dimensions are quite comparable. The Ta–Ta distance is 2.830(1) Å, consistent with the existence of a single bond.

Studies of the stereochemistry and properties of tertiary phosphine adducts of niobium(IV) and tantalum(IV) chlorides have shown an unexpected variety of structures as well as complex and not fully understood behavior in solution.[1–5] The more sterically demanding phosphines, i.e. PEt_3 and larger ones, seem consistently to give *trans*-octahedral $MCl_4(PR_3)_2$ type complexes, both in solution and in the solid state. For PMe_3 and PMe_2Ph adducts, structural diversity has been observed. Tantalum[3] has given the seven-coordinate $TaCl_4(PMe_3)_3$, as well as *cis*-$TaCl_4(PMe_2Ph)_2$, while in the case of niobium, dinuclear complexes with eight-coordinate metal atoms and four chloride bridges have been reported.[1,2] Two aspects of the chemistry involving these smaller phosphines have been of special interest. First, the structures of the dinuclear complexes, $Nb_2Cl_8L_4$, are unprecedented, for these or any other elements. Second, there was an apparent lack of similarity between the niobium and tantalum chemistry, contrary to what might have been expected for these two metals. We were especially puzzled by the apparent failure of tantalum to form the dinuclear species. To clarify these points, further studies on the PMe_3 adducts have been undertaken. We have now found that both the dinuclear tantalum species, $Ta_2Cl_8(PMe_3)_4$, and the seven-coordinate niobium complex, $NbCl_4(PMe_3)_3$, can, in fact, be prepared in high yield, provided the reaction conditions are chosen correctly.† We present here a summary of our findings on the chemistry of the Nb(IV) and Ta(IV) trimethylphosphine adducts and their relations to similar complexes in lower oxidation states.

EXPERIMENTAL

All manipulations were carried out under an atmosphere of argon. Standard vacuum line techniques were used. The pentachlorides of niobium and tantalum and trimethylphosphine were purchased from Aldrich and Strem Chemicals Inc., respectively, and used as received. $NbCl_4(THF)_2$ was prepared according to the literature method.[4] EPR spectra were recorded on an X-band Varian E-6S EPR spectrometer.

* Author to whom correspondence should be addressed.

† As this manuscript was in preparation a preliminary communication reported that $Ta_2Cl_8(PMe_3)_4$ had been obtained in small quantities as a byproduct when $TaCl_5$ was treated with PMe_3; a preliminary structure report was also given.[6]

Preparation of $Ta_2Cl_8(PMe_3)_4$

Trimethylphosphine (1 cm^3, 11.1 mmol) was added to a slurry of $TaCl_5$ (1.8 g; 5.0 mmol) in 40 cm^3 toluene. Sodium amalgam (0.4%, 0.14 g Na; 5.0 mmol) was added and the solution was stirred overnight. The toluene was decanted off and the reaction mixture was extracted with 3×50 cm^3 of CH_2Cl_2. The combined pale-green extracts were filtered and reduced in volume to *ca* 10 cm^3. An orange precipitate formed slowly and was collected on a frit and dried in vacuum. A yield of 1.3 g (1.5 mmol, 59%) of the red solid was obtained. X-ray quality crystals were grown by carefully layering 25 cm^3 hexane over the concentrated extract. Slow diffusion of the two solvents resulted in the formation of small, red, block-like crystals.

Preparation of $NbCl_4(PMe_3)_3$

$NbCl_4(THF)_2$ (0.76 g, 2.0 mmol) was slowly added with stirring to a solution of PMe_3 (1 cm^3, 11.1 mmol) in 30 cm^3 of toluene. The solution turned green and a solid of the same color precipitated (0.45 g, 50% yield based on $NbCl_4(PMe_3)_3$). Additional product was obtained by cooling the supernatant liquid after filtration. The combined yield of $NbCl_4(PMe_3)_3$ was 0.65 g, *ca* 70%. Crystals suitable for X-ray diffraction were obtained by slow cooling of the post-reaction solution.

X-ray crystallography

Single crystal X-ray analyses were carried out by application of general procedures that have been

Table 1. Summary of crystallographic data

Formula	$NbCl_4(PMe_3)_3$	$Ta_2Cl_8(PMe_3)_4$
Formula weight	462.98	949.76
Space group	$P2_1/c$	$Im3$
Systematic absences	$0k0, k \neq 2n$	$hkl, h+k+l \neq 2n$
	$h0l, l \neq 2n$	
a (Å)	15.061(3)	16.377(2)
b (Å)	11.677(4)	
c (Å)	11.583(4)	
α (°)	90	90
β (°)	91.71(3)	90
γ (°)	90	90
V (Å^3)	2036(2)	4392(2)
Z	4	6
$d_{calc.}$ (g cm^{-3})	1.510	2.154
Crystal size (mm)	$0.2 \times 0.2 \times 0.1$	$0.3 \times 0.3 \times 0.2$
μ(Mo-K_α) (cm^{-1})	13.133	88.08
Data collection instrument	CAD-4	Syntex P1
Radiation (monochromated in incident beam)	Mo-K_α ($\lambda = 0.71073$ Å)	
Orientation reflections, No., range (2θ)	25, $16.5 < 2\theta < 36.2$	15, $20.3 < 2\theta < 33.3$
Temperature (°C)	22	
Scan method	ω–2θ	
Data collection range, 2θ (°)	5, 50	4, 50
No. of unique data, total	2058	678
with $F_o^2 > 3\sigma(F_o^2)$	1285	616
No. of parameters refined	154	57
Empirical absorption correction	0.9996, 0.8435	0.9998, 0.9648
R*	0.0577	0.02229
R_w†	0.0698	0.03205
Quality-of-fit indicator‡	1.654	0.750
Largest shift/esd, final cycle	0.0	0.34
Largest peak (e Å^{-3})	1.016	0.704

* $R = \sum ||F_o| - |F_c|| / \sum |F_o|$.

† $R_w = [\sum w(|F_o| - |F_c|)^2 / \sum w|F_o|^2]^{1/2}$; $w = 1/\sigma^2(|F_o|)$.

‡ Quality of fit $= [\sum w(|F_o| - |F_c|)^2 / (N_{obs} - N_{parameters})]^{1/2}$.

described elsewhere.[7] Numerical data pertaining to the structure determinations are summarized in Table 1. Polarization, Lorentz and absorption corrections were applied to the intensity data for both compounds. A correction for decomposition was also applied to the Nb data. Refinements of the $NbCl_4(PMe_3)_3$ and $Ta_2Cl_8(PMe_3)_4$ structures were initiated by using the positional parameters of the heavy atoms found in the isomorphous compounds of the other metal. The remaining atoms, including hydrogen atoms in the tantalum compound were located in a difference Fourier map. All non-hydrogen atoms were assigned anisotropic thermal parameters and the structures were refined to convergence. A final difference Fourier map for $NbCl_4(PMe_3)_3$ contained two peaks with electron density about 1.0 $e/Å^3$. However they were located *ca* 1.1 Å away from the metal atom and were of no chemical significance.

Tables of observed and calculated structure factors, atomic positional and anisotropic thermal parameters and full lists of bond lengths and angles have been deposited as supplementary material with the Editor at Queen Mary College.†

† Atomic co-ordinates have also been deposited with the Cambridge Crystallographic Data Centre.

RESULTS AND DISCUSSION

Solid state structures

Positional and isotropic equivalent thermal parameters and important interatomic dimensions for $NbCl_4(PMe_3)_3$ and $Ta_2Cl_8(PMe_3)_4$ are presented in Tables 2–4. Complete listings of bond distances and bond angles are included in the supplementary material. ORTEP drawings of the molecules are shown in Figs. 1 and 2.

Each of the new complexes reported here is isomorphous with its niobium or tantalum counterpart, whose structure has been reported previously.[2,3] As seen in Table 3 geometrical parameters of the analogous Nb and Ta molecules are identical in the sense that no difference, Δ, exceeds $3\sigma(\Delta)$. The metal–ligand bond lengths in the dimers are longer than in the seven coordinate monomers, which can be attributed to the higher coordination number of the metal atoms in the former.

Among the complexes of general formula $[MCl_n(PMe_3)_m]_k$, where M = Nb or Ta, structural data are now available for Ta in oxidation states from II to IV. A comparison of bond distances in these compounds is presented in Table 5. For Ta(II) only one complex is known while both monomeric and dimeric species have been isolated for the III and

Table 2. Important bond distances (Å) and angles (°) for $NbCl_4(PMe_3)_3$*

(A) Distances

Nb–Cl(1)	2.409(4)
Nb–Cl(2)	2.476(3)
Nb–Cl(3)	2.449(3)
Nb–Cl(4)	2.433(4)
Nb–P(1)	2.664(4)
Nb–P(2)	2.643(4)
Nb–P(3)	2.647(3)

(B) Angles

Cl(1)–Nb–Cl(2)	120.0(1)	Cl(3)–Nb–Cl(4)	85.3(1)
Cl(1)–Nb–Cl(3)	122.5(2)	Cl(3)–Nb–P(1)	162.1(2)
Cl(1)–Nb–Cl(4)	134.8(1)	Cl(3)–Nb–P(2)	74.3(1)
Cl(1)–Nb–P(1)	75.0(1)	Cl(3)–Nb–P(3)	77.2(1)
Cl(1)–Nb–P(2)	74.0(1)	Cl(4)–Nb–P(1)	78.6(1)
Cl(1)–Nb–P(3)	75.8(1)	Cl(4)–Nb–P(2)	151.2(1)
Cl(2)–Nb–Cl(3)	95.5(1)	Cl(4)–Nb–P(3)	77.3(1)
Cl(2)–Nb–Cl(4)	87.6(1)	P(1)–Nb–P(2)	117.5(1)
Cl(2)–Nb–P(1)	76.1(1)	P(1)–Nb–P(3)	106.5(1)
Cl(2)–Nb–P(2)	74.7(1)	P(2)–Nb–P(3)	116.3(1)
Cl(2)–Nb–P(3)	163.7(1)		

* Numbers in parentheses are estimated standard deviations in the least significant digits.

Table 3. A comparison of equivalent bond distances in isomorphous PMe_3 adducts of Nb(IV) and Ta(IV)*

	Nb	Ta
(A) $M_2Cl_8(PMe_3)_4$		
M–M	2.833(1)	2.830(1)
M–Cl_b	2.541(1)	2.544(2)
M–Cl_t	2.502(1)	2.502(2)
M–P	2.671(1)	2.671(2)
(B) $MCl_4(PMe_3)_3$		
M–Cl_{cap}	2.409(4)	2.417(3)
M–Cl	2.453(13)	2.447(8)
M–P	2.651(6)	2.640(5)

* Numbers in brackets are variances, obtained from the expression $[(\sum \Delta_i^2/n(n-1)]^{1/2}$, where Δ_i is the deviation of the ith value from the arithmetic mean and n is the total number of values averaged.

IV oxidation states. No crystallographic data are available for $TaCl_3(PMe_3)_3$.[11] According to the data in Table 5 oxidation state is only one of several factors determining the lengths of the tantalum to ligand bonds. The presence of metal to metal bonding, steric crowding and disposition of ligands appear to be of comparable importance.

The dinuclear square-antiprismatic geometry of $Ta_2Cl_8(PMe_3)_4$ is also found in another formally Ta(IV) species $[TaCl_2(PMe_3)_2(\mu\text{-H})(\mu\text{-Cl})]_2$. They have comparable M–X distances (see Table 5) but also exhibit some significantly different features. In the former the terminal P_2Cl_2 squares are eclipsed while in the latter P atoms are positioned opposite to Cl atoms at the other end and vice versa. The hydride bridges cause shortening of the metal–metal bond by *ca* 0.2 Å, from 2.830(1) to 2.621(4) Å for the tetra-μ-chloro and di-μ-chloro-di-μ-hydrido complexes, respectively.

Table 4. Important bond angles (°) for $Ta_2Cl_8(PMe_3)_4$*

Ta′–Ta–Cl(1)	56.21(2)
Ta′–Ta–Cl(2)	123.24(4)
Ta′–Ta–P	124.37(4)
Cl(1)–Ta–Cl(1)′	112.43(3)
Cl(1)–Ta–Cl(1)″	71.54(5)
Cl(1)–Ta–Cl(1)‴	72.43(5)
Cl(1)–Ta–Cl(2)	79.40(4)
Cl(1)–Ta–Cl(2)′	142.53(4)
Cl(1)–Ta–P	79.99(5)
Cl(1)–Ta–P′	143.28(4)
Cl(2)–Ta–Cl(2)′	113.52(6)
Cl(2)–Ta–P	71.97(3)
P–Ta–P′	111.26(6)
Ta′–Cl(1)–Ta	67.57(5)

* Numbers in parentheses are estimated standard deviations in the least significant digits.

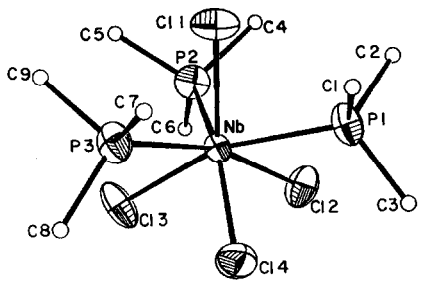


Fig. 1. An ORTEP drawing of the $NbCl_4(PMe_3)_3$ molecule. Thermal ellipsoids enclose 40% of electron density. Methyl carbon atoms were assigned arbitrarily small thermal parameters for the sake of clarity.

Synthesis and properties in solution

Reactions between $NbCl_4(THF)_2$ and PMe_3 can afford any of several adducts of general formula $NbCl_4(PMe_3)_n$, where $n = 2$, 3 and 4, depending on conditions. With $n = 2$ the product is red and dinuclear, $Nb_2Cl_8(PMe_3)_4$, while the one with $n = 3$ is green, seven-coordinate $NbCl_4(PMe_3)_3$. Both of these can be isolated in a pure state. The dimer is best obtained upon addition of the ligand to a suspension of $NbCl_4(THF)_2$ in THF or CH_2Cl_2. Synthesis of the pure tris complex is accomplished by mixing the same reactants in the reverse order. The addition of $NbCl_4(THF)_2$ to a mixture of excess PMe_3 and toluene produces a green solution from which spontaneous crystallization of $NbCl_4(PMe_3)_3$ occurs in about 50% yield. The supernatant solution, from which more of the seven-coordinate complex may be obtained by cooling, was shown, by EPR, to contain the complex $NbCl_4(PMe_3)_4$. The presence of

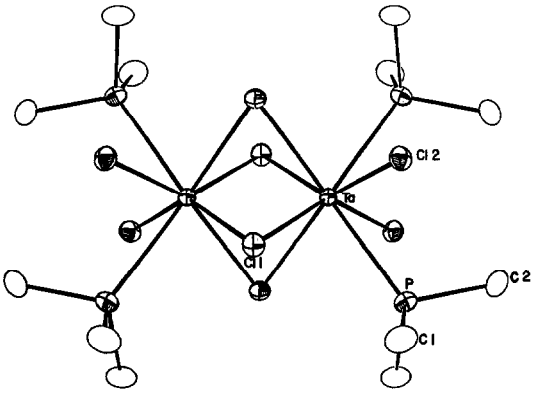


Fig. 2. An ORTEP drawing of the $Ta_2Cl_8(PMe_3)_4$ molecule. Thermal ellipsoids enclose 40% of the electron density. The molecule has crystallographic mmm symmetry. The Cl(2), P and C(2) atoms are in the planes intersecting along the Ta–Ta axis, and the Cl(1) atoms are in the plane perpendicular to the metal–metal vector.

Table 5. Averaged metal–ligand bond lengths in the $[TaCl_n(PMe_3)_m]_k$ complexes*

Oxidation state	Complex	Bond type			Reference
		Ta–Cl_b	$TaCl_t$	Ta–P	
IV	$TaCl_4L_3$	—	2.447(7)	2.640(5)	3
	$Ta_2Cl_8L_4$	2.544(2)	2.502(2)	2.671(2)	This work
	$Ta_2Cl_6H_2L_4$	2.544(4)	2.472(8)	2.639(12)	10
III	$Ta_2Cl_6L_4$†	2.474(4)	2.479(8)	2.657(10)	8
		2.430(3)	2.399(1)	2.608(10)	
II	$TaCl_2L_4$	—	2.464(3)	2.543(2)	9

* Numbers in brackets are variances calculated as defined in footnote in Table 5.
† Non-equivalent sets of ligands were treated separately.

quintets with $A = 25$ G in the spectrum indicates coupling of Nb to four phosphorus atoms. Since pure $NbCl_4(PMe_3)_3$ in solution gives a broad and poorly resolved EPR resonance, it cannot be detected in the supernatant by this method.

The chemical behavior of the $NbCl_4$–PMe_3 system can be qualitatively understood in the following way. The addition of $NbCl_4(THF)_2$ to a solution containing a greater than four-fold molar ratio of PMe_3 to $NbCl_4(THF)_2$ gives rise to the eight-coordinate complex $NbCl_4(PMe_3)_4$, which can be detected in solution by EPR but which we have not yet been able to isolate as a solid. Eight-coordination is not uncommon for Nb(IV) but the well-defined examples containing phosphines are those with bidentate ligands, e.g. $NbCl_4(diphos)_2$.[12] Clearly, with the four separate PMe_3 ligands there will be more ligand–ligand repulsion and a greater tendency to dissociation. An equilibrium between $NbCl_4(PMe_3)_4$ and $NbCl_4(PMe_3)_3$ is thus likely to be established and precipitation of the latter, which is relatively insoluble, occurs.

The compound $Nb_2Cl_8(PMe_3)_4$ is quite stable and rather insoluble and it is therefore the favored solid product at lower PMe_3/Nb ratios, as, for example, when PMe_3 is added to a suspension of $NbCl_4(THF)_2$. Although there is transient formation of a green solution, the red dinuclear complex precipitates promptly and in good yield. Similarly, when the volume of a green solution containing $NbCl_4(PMe_3)_3$ is reduced under vacuum, the red solid crystallizes. Although the dinuclear complex is only slightly soluble, it does afford very dilute solutions in CH_2Cl_2 from which it can be recovered.

Whether a six-coordinate intermediate, $NbCl_4(PMe_3)_2$, ever exists to any appreciable extent or for any length of time is unknown. There is as yet no evidence for it, but it is possible that it might be isolable from some appropriate solvent.

When $Nb_2Cl_8(PMe_3)_4$ is prepared by using stoichiometric amounts of $NbCl_4(THF)_2$ and PMe_3, a pale green solution remains after the product has precipitated. This color is apparently not due to the seven- or eight-coordinate complexes but rather to some species that contain THF. This conclusion is based on the EPR spectra which indicate that a mixture of at least two EPR-active Nb(IV) species is present, neither of which is $NbCl_4(PMe_3)_4$. These spectra display at least eleven (not ten) lines, each a close doublet (presumably due to superhyperfine structure caused by one PMe_3 bound to the Nb atom). When frozen to −196°C these solutions show a long series of signals separated by *ca* 25 G with relative intensities that change from one sample to another.

There are also other color changes that are observed from time to time in the dilute solutions of $Nb_2Cl_8(PMe_3)_4$ which are probably caused by decomposition. The compound is extremely reactive towards traces of oxygen, moisture and other protic materials.

Turning now to tantalum, the fact that both $TaCl_4(PMe_3)_3$ and $Ta_2Cl_8(PMe_3)_4$ can be prepared in good yield and high purity indicates that the chemistry is rather similar to that of niobium, as would be expected. However, a practical difference is that the versatile starting material with labile THF ligands, $NbCl_4(THF)_2$, does not as yet have a known tantalum analog. Consequently, the tantalum chemistry cannot be investigated so thoroughly as that of niobium. Furthermore, all of our attempts to measure EPR spectra for tantalum(IV) phosphine adducts gave only very broad, featureless spectra that were of little use in identifying products.

Synthesis of $Ta_2Cl_8(PMe_3)_4$ in high yield is straightforward, by the method described here, because of its stability and low solubility. Although a stoichiometric ratio of reactants would normally be used, the presence of a moderate excess of phosphine does not appear to affect either yield or purity.

No doubt the $Ta_2Cl_8(PMe_3)_4$ molecule may be assumed to have a Ta–Ta single bond, as we have already suggested for $Nb_2Cl_8(PMe_2Ph)_4$ and $Nb_2Cl_8(PMe_3)_4$; the recent work of Boyd *et al.*[6] provides detailed support for this suggestion.

To obtain the seven-coordinate tantalum complex, $TaCl_4(PMe_3)_3$, loss of PMe_3 from the reaction mixture must be minimized. This can best be done by employing a volatile solvent such as CH_2Cl_2, which can be efficiently removed under vacuum without major loss of PMe_3.

Acknowledgements—We thank the Robert A. Welch Foundation for support under Grant No. A-494. M. P. D. is National Science Foundation Predoctoral Fellow and also holds a Texaco-IUCCP Fellowship from this department.

REFERENCES

1. F. A. Cotton and W. J. Roth, *Inorg. Chem.* 1984, **23**, 945.
2. F. A. Cotton, S. A. Duraj and W. J. Roth, *Inorg. Chem.* 1984, **23**, 3592.
3. F. A. Cotton, S. A. Duraj and W. J. Roth, *Inorg. Chem.* 1984, **23**, 4046.
4. L. E. Manzer, *Inorg. Chem.* 1977, **16**, 525.
5. (a) E. Samuel, G. Labauze and J. Livage, *Nouv. J. Chim.* 1977, **1**, 93; (b) G. Labauze, E. Samuel and J. Livage, *Inorg. Chem.* 1980, **19**, 1384.
6. P. D. W. Boyd, T. C. Jones, A. J. Nielson and C. E. F. Rickard, *J. Chem. Soc., Chem. Commun.* 1984, 1086.
7. See, for example, A. Bino, F. A. Cotton and P. E. Fanwick, *Inorg. Chem.* 1979, **18**, 3558.
8. A. P. Sattelberger, R. B. Wilson and J. C. Huffman, *Inorg. Chem.* 1982, **21**, 2392.
9. M. L. Luetkens, J. C. Huffman and A. P. Sattelberger, *J. Am. Chem. Soc.* 1983, **105**, 4474.
10. A. P. Sattelberger, R. B. Wilson and J. C. Huffman, *Inorg. Chem.* 1982, **21**, 4179.
11. S. M. Rocklage, H. W. Turner, J. D. Fellmann and R. R. Schrock, *Organometallics* 1982, **1**, 703.
12. F. A. Cotton and G. Wilkinson, *Advanced Inorganic Chemistry*, 4th edn, pp. 839–841. Wiley, New York (1980).

Polyhedron Vol. 4, No. 6, pp. 1109–1117, 1985
Printed in Great Britain

0277–5387/85 $3.00 + .00
Pergamon Press Ltd

TRANS-BIS(DIMETHYLGLYOXIMATO) COBALT(III) COMPLEXES CONTAINING IMIDAZOLE AND THIOCYANATE AS AXIAL LIGANDS

JAYANTA K. DAS and KAILASH C. DASH*
Department of Chemistry, Utkal University, Vani Vihar, Bhubaneswar, 751004, India

(*Received* 23 *July* 1984; *accepted after revision* 18 *December* 1984)

Abstract—Imidazole(Im), benzimidazole(BzIm), morpholine (Morph) and their derivatives react with $Co(CNS)_2$ and dimethylglyoxime(DH_2) in ethanolic medium in presence of air to form a number of new cobalt(III) complexes of the type *trans*-$[Co(DH)_2(L)(SCN)]$, which are characterised on the basis of electronic and IR spectra, NMR (^1H and ^{13}C) and mass spectra as well as thermogravimetric (TG–DTA) and conductance measurements. The thiocyanate groups are S-bonded. The NMR observations suggest that in solution these compounds exist as mixtures of the neutral species $[Co(DH)_2(L)(SCN)]$ and the salt $[Co(DH)_2(SCN)_2]^-$ $[Co(DH)_2(L)_2]^+$. The mass spectra does not show the molecular ion peak of the complex. The TG–DTA measurements show that the thermolysis of these complexes proceeds through polymeric intermediates giving Co_3O_4 as the end product.

Bis-(dimethylglyoximato) cobalt(III) complexes (cobaloximes) containing the $Co(DH)_2^+$ moiety (DH is the monoanion of dimethylglyoxime, DH_2) are shown to reproduce the fundamental reactions of cobalamins and are of importance in the study of the mechanism of Vitamin-B_{12} catalysed biochemical processes.[1,2] They closely simulate the reactions of Vitamin B_{12} and are important in Vitamin B_{12} model chemistry.[3–5] The biochemical and other applications of cobaloximes are also known. Simple cyanocobalamins activate and increase the cell membrane permeability.[6] Cobaloximes are useful reagents in synthetic organic chemistry, and are employed as protecting groups in the synthesis of certain amino acids.[7]

Imidazole behaves both as a good σ-donor and as a π-acceptor and is a fundamental component of nucleic acids (*via* the purines) and enzymes or proteins (*via* the amino acid histidine) and provides a potential binding site for metal ions.[8,9] It is one of the choicest ligands in nature. The biological significance of cobaloximes and imidazole prompted us to synthesise imidazole complexes of cobaloximes of the type *trans*-$[Co(DH)_2(Im)(SCN)]$ and study their stereochemical and biochemical characteristics. Earlier work from this laboratory[10–13] and by others[14,15] were centred mostly around homoleptic complexes of imidazoles with divalent first-row transition metals. Attempts to synthesise such homoleptic complexes of cobalt(III) with imidazole met with no success, even though it was possible to synthesise mixed-ligand systems[16,17] using imidazole along with ethylenediamine and acetylacetonate. Synthesis of $[Co(acac)_2(NO_2)(Im)]$[18] and the synthesis and hydrolysis of $[Co(en)_2(Cl)(Im)]Cl_2$[19–21] have also been reported. Reports on mixed-ligand complexes of cobaloximes with imidazole[22–24] and other ligands[25–29] have been made. A series of imidazole derivatives of cobaloximes,

$[Co(DH)_2(X)(Im)]$

(X = Cl, Br, CN, NO_2, OCN, SeCN, SCN),

were reported[23] where the formation of compounds

$$[Co(DH)_2(SCN)(Im)]_2(Im)H_2O$$

and

$$[Co(DH)_2(SeCN)(Im)]_2Im$$

were suggested, primarily on the basis of analytical data. We have prepared not only these two compounds, but a large number of other imidazole derivatives of the thiocyanato cobaloximes and studied their stoichiometry and thermal behaviour very carefully and in no case we obtained evidences in

* Author to whom correspondence should be addressed.

favour of such formulation[23] where the imidazole ligand bridges the two

$$[Co(DH)_2(SCN)(Im)]$$

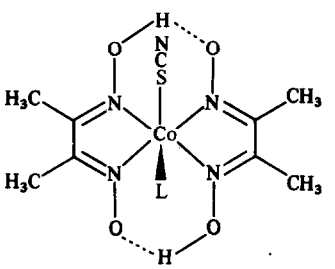
or

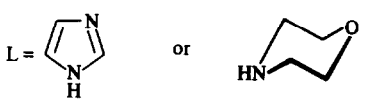
$$[Co(DH)_2(SeCN)(Im)]$$

moieties. The present paper reports systematic studies on mixed-ligand complexes of cobalt(III) with dimethylglyoxime (DH_2) and imidazole (Im), morpholine (Morph) and their various substituted derivatives, where the stereochemistries of the complexes have been deduced on the basis of electronic, IR, NMR (^1H and ^{13}C) and mass spectra as well as their electrical conductivity and thermal analysis measurements.

EXPERIMENTAL

Materials. Imidazole, morpholine and their derivatives were used as supplied by BASF, 2-methyl benzimidazole was prepared by a method analogous to the literature method.[30] Cobalt(II) thiocyanate was obtained by metathetic reaction of hydrated $Co(NO_3)_2$ (BDH) and KCNS (BDH) in ethanolic medium. The precipitated KNO_3 was filtered off and the solution, somewhat reduced in volume, was used as the source of $Co(NCS)_2$.





Synthesis of complexes. Complexes of the type $[Co(DH)_2(SCN)(L)]$ where L = imidazole or morpholine and their derivatives were prepared in 30–70% yield, by bubbling air for a period varying from 1 to 6 h through a solution of $Co(NCS)_2$, dimethylglyoxime (DH_2) and the ligand in 1:2:2 proportions. This was allowed to stand for 1 h and the microcrystalline solid was collected on a frit, washed with small aliquots of EtOH, then with Et_2O and finally dried in a vacuum desiccator. The reaction presumably proceeds in the following manner:

$$2Co(SCN)_2 + 4DH_2 + 4L + \tfrac{1}{2}O_2 \rightarrow 2[Co(DH)_2(SCN)(L)] + 2L \cdot HSCN + H_2O. \quad (1)$$

The time period for bubbling air for oxidation was different for the substituted imidazoles. Generally, the C-2 substituted derivatives of imidazole required more time than others. A typical method of preparation is given below.

$Co(DH)_2(SCN)(Im)$. To a hot ethanolic solution of cobalt(II) thiocyanate (0.002 mole), in a 250 cm^3 Erlenmeyer's flask was added 0.490 g (0.0042 mole) of dimethylglyoxime and 0.286 g (0.0042 mole) of imidazole and boiled for 2–3 min. The solution was then cooled to room temperature and air was bubbled through the solution for 1 h during which period micro-crystalline yellow–brown solid gradually deposited at the bottom. The solid was collected by filtration, washed successively with small portions of EtOH and Et_2O and dried *in vacuo* (yield 0.498 g (60%)).

Analyses. Cobalt was determined by the method of Laitenen and Burdett.[31] Sulphur was estimated gravimetrically as $BaSO_4$, after fusion of the sample with NaOH and Na_2O_2 and extraction of the melt with H_2O. Microanalytical data for nitrogen and (in some cases) carbon and hydrogen were from CDRI, Lucknow.

Electrolytic conductivity measurements, electronic and IR spectra. Electrolytic conductivity measurements were performed at room temperature in $MeNO_2$, Me_2CO and MeOH solution ($\sim 10^{-3}$ M) with an ELICO conductivity bridge type CM82 and a dip type cell with a cell constant of 0.5.

Electronic spectra in dil. MeOH solutions were recorded in a Varian 634 spectrophotometer. IR spectra in the 4000–400 cm^{-1} region were recorded as Nujol mull or KBr pellets in a Perkin–Elmer 337 or 377 grating spectrometer. In some cases, for comparison IR was recorded in $MeNO_2$ medium.

^1H and ^{13}C NMR spectra. The NMR spectra were measured in CD_3NO_2 with respect to internal TMS (4%). The PMR spectrum was recorded in a Varian FT-80A spectrometer operating on Fourier mode using 5 mm insert tubes at a spin rate of 20 rpm. PMR spectrum was recorded at room temperature and at −40°C and the spectra were virtually identical.

Full spectral width (6000 Hz) random-noise ^1H decoupled ^{13}C NMR spectra were measured on the JEOL FX-100 spectrometer operating on Fourier mode at an observed frequency of 25 MHz using 10 mm insert tubes. The field : frequency ratio was stabilized by a time-shared deuterium lock on the solvent. The total number of pulses required for a

reasonably good spectra varied from 14,000 pulses for [Co(DH)$_2$(1-AlIm)(SCN)] to 95,000 pulses for [Co(DH)$_2$(2-MeIm)(SCN)]. For ^{13}C NMR spectra the chemical shifts are reported in δ (ppm) relative to TMS, but they were observed with CD_3NO_2 (δ = 62.8 ppm) as the internal standard.

RESULTS AND DISCUSSION

All the compounds reported in this work are presented in Table 1, along with their analytical data, m.p. and conductance values. The conductance measurements were made in dilute solutions of Me_2CO, $MeNO_2$ and MeOH. The molar conductivity values obtained favour the neutral, non-ionic formulations, although in certain cases higher values are obtained.

The ligand-field spectra of the complexes in MeOH medium show a peak of weak to moderate intensity[32] at around 18,000 cm^{-1}. The two other main bands centred at about 40,000 cm^{-1} and 28,000–30,000 cm^{-1} are due to the intra-ligand $\pi \rightarrow \pi^*$ transition in the coordinated dimethylglyoximato anion and to the imidazole $\rightarrow$ cobalt transitions respectively. The strong band at 47,000 cm^{-1} may be the $d_\pi(Co) \rightarrow \pi^*(DH^-)$ transitions (Fig. 1).[33,34]

The IR absorption frequencies show the main bands due to the coordinated dimethylglyoxime, the ligands (imidazole or morpholine) and the vibrations of the ambidentate 16-electron thiocyanate ligand. The more prominent IR bands were located almost in the same position in all the complexes and not much effective variation was detected. The important IR bands of some typical thiocyanatocobaloximes are shown in Table 2. A comparison of the IR spectra of these complexes was made with those of the free dimethylglyoxime (DH_2) and the bis(dimethylglyoximato) nickel(II) complex [Ni(DH)$_2$] and it was found that while the free DH_2 has no bands at 1240 cm^{-1}, a strong band appears in the Ni(DH)$_2$ complex at 1240 cm^{-1}, due to the ν(N–O) of the ionised N–OH grouping of dimethylglyoxime.[35] For the cobaloxime complexes under discussion this band is seen almost in the same region at 1240–1250 cm^{-1}. The ν(C=N) stretching vibration of free, non-coordinated DH_2 at 1620–1630 cm^{-1} region is shifted to 1560–1570 cm^{-1} region in the complexes. The weak band around 1750 cm^{-1} belongs to the deformation mode of the intramolecular hydrogen bridge and suggests a *trans*-configuration for the complexes.[36,37] This observation was also further substantiated by the chemical behaviour of these cobaloximes in readily forming an O–BF_2–O bonding by the interaction of two O–H . . . O bridges in cobaloximes with $BF_3 \cdot Et_2O$.[38] The characteristic ν(Co–N) frequencies are situated at 515 and 430 cm^{-1} close to the position in well known NH_3 and en containing cobalt(III) complexes.[39]

The IR bands due to the ambidentate thiocyanate groups determine its mode of attachment,[40,41] either through the S-end or the N-end or as a bridging ligand. Class "a" or hard metals are expected to bond through the N-end of the thiocyanate group and class "b" or soft metals through the S-end. Cobalt(III) is an example of a hard acid,[42] but the dimethylglyoximato ligand system, $(DH)_2$, modifies the typical class "a" or "hard" Co(III) centre to such an extent that class "b" or "soft" behaviour is often observed in $Co(DH)_2^+$ moiety.[43–45] This change in behaviour from class "a" to class "b" for the hard cobalt(III) is facilitated by ligands like DH_2 that are soft or have a π-acceptor capacity and imidazole which is also a good π-acceptor inspite of its being a good σ-donor. The thiocyanate group is usually bonded to Co(III) centre in cobaloximes through the S-end,[27,46] although in [Ph_4As][Co(DH)$_2$(SCN)$_2$], Epps and Marzilli[47] were able to isolate all the three isomers, namely S–S, S–N and N–N. The ν(CN) in our complexes was usually obtained as a very intense and sharp peak at 2120 cm^{-1} indicating the coordination of the thiocyanate group. The intensity and sharpness of the ν(CN) band is indicative of Co–SCN bonding.[48]

The NMR spectra

The ^{1}H NMR spectra of some cobaloximes has been discussed in terms of their *trans*-structure.[26,27,47,49] The ^{1}H NMR shifts of the complexes (Table 3) show that on coordination the CH_3 groups of DH_2 at 1.98 ppm undergo a clear downfield shift by about 0.4 to 2.36–2.40 ppm. The imidazole protons also undergo a considerable

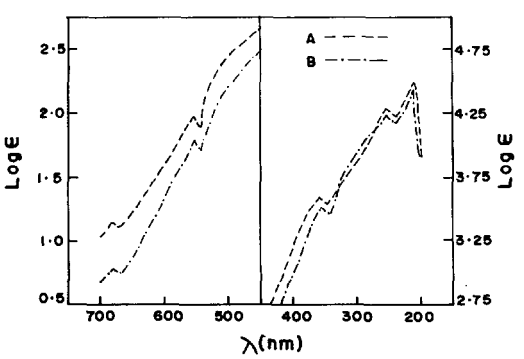


Fig. 1. Electronic spectra of (A) [Co(DH)$_2$(SCN)(2-*i*PrIm)] (– – –) and (B) [Co(DH)$_2$(SCN)(2-MeIm)] (–·–·–) in MeOH.

Table 1. Colour, m.p., analyses, conductivity data and electronic transition of the $[Co(DH)_2(SCN)(Im)]$ type complexes

Compound [A = $Co(DH)_2(SCN)$]	Formula (Mol. wt.)	Colour	M.p. (°C)	Analytical data (%)[a] Co	S	N	Λ_M[b]	L.F. band (cm^{-1}) (log ε)
(1)	(2)	(3)	(4)	(5)	(6)	(7)	(8)	(9)
[A(Im)]	$CoC_{12}H_{18}O_4N_7S$ (414.9)	Brown	> 240	13.87 (14.20)	6.88 (7.71)	23.13 (23.62)	56.65[c] 53.17[e]	18,050 (1.195)
[A(1-MeIm)][f]	$CoC_{13}H_{20}O_4N_7S$ (428.9)	Yellow brown	> 240	12.98 (13.75)	8.06 (7.46)	22.32 (22.80)	64.94[c]	18,018 (1.230)
[A(1-EtIm)]	$CoC_{14}H_{22}O_4N_7S$ (442.9)	Light brown	225	12.92 (13.30)	6.84 (7.22)	22.41 (22.12)	20.54[c] 35.31[d]	18,050 (1.643)
[A(1-ViIm)]	$CoC_{14}H_{20}O_4N_7S$ (440.9)	Yellow brown	208	12.79 (13.37)	6.52 (7.25)	21.95 (22.22)	38.85[c] 15.46[d] 16.09[e]	18,050 (1.769)
[A(1-AlIm)][g]	$CoC_{15}H_{22}O_4N_7S$ (454.9)	Yellow brown	194(d)	12.16 (12.95)	7.71 (7.03)	21.04 (21.54)	37.14[c] 24.43[d]	18,050 (1.708)
[A(1-Vi,2-MeIm)]H_2O	$CoC_{15}H_{24}O_5N_7S$ (472.9)	Yellow brown	178(d)	12.31 (12.46)	7.13 (6.76)	20.82 (20.72)	64.00[c] 87.92[d] 58.81[e]	18,050 (1.814)
[A(1,2-DiMeIm)][h]	$CoC_{14}H_{22}O_4N_7S$ (442.9)	Light brown	185(d)	12.60 (13.30)	7.61 (7.22)	22.68 (22.12)	31.72[c] 22.50[d] 19.10[e]	18,050 (1.849)
[A(2-MeIm)]	$CoC_{13}H_{20}O_4N_7S$ (428.9)	Yellow brown	> 240	14.16 (13.75)	7.04 (7.46)	22.57 (22.82)	50.03[c] 19.93[d] 18.10[e]	18,050 (1.759)
[A(2-EtIm)]	$CoC_{14}H_{22}O_4N_7S$ (442.9)	Yellow brown	162	13.80 (13.30)	6.78 (7.22)	21.80 (22.22)	24.18[c] 27.98[d] 38.38[e]	18,018 (1.855)

[A(2-PrIm)]	$CoC_{15}H_{24}O_4N_7S$ (456.9)	Yellow brown	145	12.55 (12.90)	7.53 (7.00)	21.58 (21.44)	36.48[c] 71.37[d] 93.30[e]	18,018 (2.006)
[A(2-iPrIm)][i]	$CoC_{15}H_{24}O_4N_7S$ (456.9)	Reddish brown	160	12.34 (12.90)	6.80 (7.00)	22.04 (21.44)	1.50[d] 10.15[e]	18,050 (1.916)
[A(2-PhIm)]	$CoC_{18}H_{22}O_4N_7S$ (490.9)	Brown	205	11.89 (12.00)	6.21 (6.52)	20.57 (19.96)	42.66[c] 45.68[e]	18,018 (1.966)
[A(4-MeIm)]	$CoC_{13}H_{20}O_4N_7S$ (428.9)	Yellow brown	235(d)	13.29 (13.75)	7.96 (7.46)	21.85 (22.12)	31.58[c]	
[A(BzIm)]	$CoC_{16}H_{20}O_4N_7S$ (464.9)	Yellow brown	> 240	12.98 (12.68)	7.67 (6.88)	21.49 (21.07)	1.82[c] 4.75[d] 11.80[e]	18,018 (1.764)
[A(2-MeBzIm)]	$CoC_{17}H_{22}O_4N_7S$ (478.9)	Brown	212	12.63 (12.30)	6.92 (6.68)	20.84 (20.46)	78.04[e]	18,018 (2.200)
[A(Morph)]	$CoC_{13}H_{23}O_5N_6S$ (433.9)	Brown	> 240	13.78 (13.58)	7.01 (7.37)	19.02 (19.36)	6.20[c] 13.96[d]	
[A(4-MeMorph)][j]	$CoC_{14}H_{25}O_5N_6S$ (447.9)	Brown	190(d)	12.80 (13.15)	7.38 (7.14)	18.13 (18.75)	49.92[c] 71.42[e]	18,018 (2.374)
[A(4-EtMorph)]	$CoC_{15}H_{27}O_5N_6S$ (461.9)	Dark brown	> 240	12.90 (12.76)	6.54 (6.92)	18.79 (18.18)	43.45[c]	

a. Theoretical values in parentheses; b. All values in $Ohm^{-1}\ cm^2\ mole^{-1}$ at room temperature; c. Nitromethane; d. Acetone; e. Methanol, (d) Decomposition; f. C-36.43(36.37), H-4.24(4.66); g. C-39.05(39.57), H-4.67(4.83); h. C-37.48(37.93), H-4.66(4.96); i. C-39.02(39.39), H-5.10(5.25); j. C-36.95(37.51), H-5.28(5.58).

Abbreviations: Im, imidazole; BzIm, benzimidazole; Morph, morpholine; Me, methyl; Et, ethyl; Pr, propyl; iPr, isopropyl; Vi, vinyl; Al, Allyl; and Ph, phenyl.

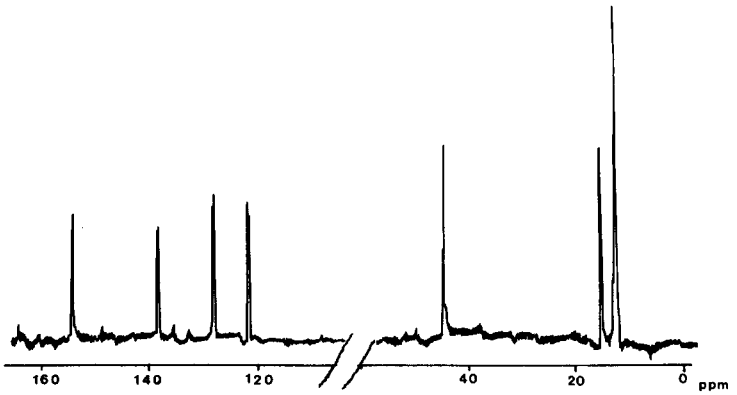


Fig. 2. ^{13}C NMR spectrum of $[Co(DH)_2(SCN)(1\text{-EtIm})]$ in CD_3NO_2.

downfield shift and further the H-4 and H-5 protons of imidazole give rise to separate signals on complexation. The *trans*-structure of the cobaloximes should render the four methyl groups of $(DH)_2$ groups equivalent resulting in only one signal whereas the *cis*-compound, because of lower symmetry should give rise to more number of signals. This is in practice observed for the *trans*-, chloro- and azido-cobaloxime complexes with imidazoles[50] and other N-donor ligands.[36] But, in the present cases, instead of the single peak for the four CH_3 protons as expected for the *trans*-configuration, either two or three signals are observed, indicating the presence of more than one distinct chemical species in solution. Even though the available evidences in solid state favour the formulation as $[Co(DH)_2(Im)(SCN)]$, the complexes are apparently, on the basis of NMR evidences, mixtures of the neutral species

$$[Co(DH)_2(Im)(SCN)]$$

and the salt

$$[Co(DH)_2(Im)_2]^+[Co(DH)_2(SCN)_2]^-$$

in solution. This behaviour is very similar to the observation of Hill and Morallee[49] for $[Co(DH)_2(Ph_3P)(CN)]$ complexes and of Trogler *et al.*[26] for

$$[(t\text{-BuPy})Co(DH)_2X]$$

and $[(Bu_3P)Co(DH)_2X]$

complexes and their corresponding ion-pairs. However, we were unable to observe this tendency of salt formation in the corresponding chloro- and

Table 2. Prominent IR absorption bands of some thiocyanatocobaloximes, $[Co(DH)_2(SCN)(L)]$ (in cm^{-1})

$[Co(DH)_2(SCN)(L)]$	–NCS			$(DH)_2$		
L =	ν(CN)	ν(CS)	δ(NCS)	δ(OH)	ν(C=N)	ν(NO)
Im	2110m	850	440	—	1560	1240 1098
1-MeIm	2130vvs	835	440	1740	1571	1241 1099
1-ViIm	2120vs	842	445	1760	1550	1244 1102
1-Vi,2-MeIm	2110vs	842	442	1760	1570	1250 1100
2-iPrIm	2110vvs	848	450	1752	1575	1250 1102
BzIm	2110vs	845	440	—	1562	1240 1095
Morph	2130vs	849	440	1750	1572	1250 1102
4-MeMorph	2120vvs	835	440	1750	1570	1250 1100

Table 3. Proton chemical shifts for some of $[Co(DH)_2(SCN)(Im)]$ complexes in CD_3NO_2[a]

Compound	Dimethylglyoxime protons $-CH_3$	Imidazole protons H-2	H-4	H-5	R	
Imidazole[b]	—	7.82	7.14	7.14	—	
Dimethylglyoxime[b]	1.98	—	—	—	—	
$[Co(DH)_2(SCN)(1\text{-EtIm})]$						
(A) Room temp.	2.39	7.35	7.15	6.65	3.91q	(1-Et)
	2.33	7.28	6.68	6.50	1.28t	
	2.31					
(B) −40°C	2.41	7.37	7.00	6.66	3.92q	(1-Et)
	2.39	7.21	6.92	6.50	1.31p	
	2.32					
$[Co(DH)_2(SCN)(1\text{-AlIm})]$						
(A) Room temp.	2.40	7.37	6.87	6.63	5.70m	
	2.39	7.14	6.78	6.48	5.04m	(1-Al)
	2.31				4.52m	
(B) −40°C	2.44	7.38	6.93	6.65	5.80m	
	2.41	7.20	6.83	6.50	5.10m	(1-Al)
	2.32				4.71m	
$[Co(DH)_2(SCN)(2\text{-MeIm})]$						
(A) Room temp.	2.41	—	7.29	6.80	2.31	(2-CH_3)
	2.38					
(B) −40°C	2.50	—	7.34	6.80	2.30	(2-CH_3)
	2.43					
	2.41					
$[Co(DH)_2(SCN)(2\text{-iPrIm})]$						
(A) Room temp.	2.42	—	6.81	6.78	1.05d	(2-iPr)
	2.39					
(B) −40°C	2.44	—	6.84	6.73	1.06d	(2-iPr)
	2.41		6.80			
$[Co(DH)_2(SCN)(1,2\text{-DiMeIm})]$						
(A) Room temp.	2.38	—	7.30	6.90	3.46	(1-CH_3)
					2.25	(2-CH_3)

[a] All values in ppm downfield to TMS as internal standard.
[b] In DMF.

azido-cobaloxime complexes with imidazoles,[50] $[Co(DH)_2(Im)(Cl)]$ and $[Co(DH)_2(Im)(N_3)]$, respectively, where clear sharp signals assignable to the neutral species alone were obtained. The PMR signals observed are shown in Table 3. In some cases, the CH_3 protons of $(DH)_2$ are superimposed giving less number of peaks than expected. The imidazole protons are assigned following earlier work[16] and signals of imidazole protons in the neutral and cationic species are also noted. It has been reported[26] that the ion-pair is formed by the cobalt(II) catalysed reactions (Co(II) present as an impurity in trace amounts before oxidation is complete) of $[Co(DH)_2(L)(SCN)]$ giving the following equilibrium:

$$2[Co(DH)_2(L)(SCN)] \overset{Co(II)}{\rightleftharpoons} [Co(DH)_2(L)_2][Co(DH)_2(SCN)_2]$$

which depends markedly on the nature of solvent and the ligand.

The ^{13}C NMR spectra of the thiocyanato-cobaloxime complexes with imidazoles (Table 4) indicate a downfield shift of ^{13}C signals of ligands on complexation and the ^{13}C NMR measurements support the conclusions drawn on the basis of ^1H NMR measurements. The ^{13}C NMR spectra of some

Table 4. ^{13}C chemical shifts for some of $[Co(DH)_2(SCN)(Im)]$ complexes at room temperature in CD_3NO_2[a]

Compound	Dimethylglyoxime carbons		Imidazole carbons				
	$-CH_3$	C=N	C-2	C-4	C-5	R	
Imidazole[b]			136.00	122.38	122.38	—	
Dimethylglyoxime[b]	9.23	154.12	—	—	—	—	
$[Co(DH)_2(SCN)(1\text{-EtIm})]$	13.014	154.59	138.97 138.73	128.73 128.49	122.23 122.06	44.839 15.881	(1-Et)
$[Co(DH)_2(SCN)(1\text{-AlIm})]$	13.131 13.014	155.99 154.649	139.55 139.32	128.849 128.61	122.88 122.70	133.529 120.81 51.918	(1-Al)
$[Co(DH)_2(SCN)(2\text{-MeIm})]$	13.365	155.00 154.82	—	129.258	116.97	13.07	(2-Me)
$[Co(DH)_2(SCN)(2\text{-iPrIm})]$	13.423 13.131	155.17 155.00	—	128.147	117.558	26.296 22.08	(2-iPr)
$[Co(DH)_2(SCN)(1,2\text{-DiMeIm})]$	13.18	155.32 154.14	—	127.74	—	34.53 14.00	(1-Me) (2-Me)

[a] All values in ppm relative to internal CD_3NO_2 resonating at 62.8 ppm downfield to TMS.
[b] In DMF.

cobaloximes was reported by Trogler *et al.*[26] who suggested the the changes of ^{13}C shifts as a function of the axially coordinated anions in cobaloximes are caused by the electronically induced (e.g. through-bond) changes in the electronic environment about the carbon centre. On going from X = Cl to N_3 to NCS in $[Co(DH)_2(Im)(X)]$ complexes (Im = imidazole derivative) the ^{13}C chemical shifts of the CH_3 groups of $(DH)_2$ change progressively from 12.4 to 13.0 to 13.2 ppm and the imine carbon chemical shifts vary from 152.0 to 154.2 to 155.1 ppm.[50] The ^{13}C chemical shifts are tabulated in Table 4. Although a single peak was expected for the ^{13}C of the CH_3 groups of $Co(DH)_2^+$, in practice invariably 2 (or more) signals were obtained indicating the presence of more than one distinct chemical species, i.e. the neutral compound and the ion-pair in variable proportions in solution. In the IR spectra either in the solid state or in solution, we did not get any evidence of this type of behaviour as always only a sharp peak at 2110 cm^{-1} was obtained for the ν(CN). This obviously indicates the Co–SCN bonding in all the species that may be present in solution. As observed in the ^1H NMR, coordination to the cobalt(III) centre also creates some striking changes in the ^{13}C behaviour of imidazole carbons. Even though the ^{13}C of the imidazole carbons are obtained as single peaks in most cases, at least in some cases more than one peak is obtained for each of the carbons again favouring the formulation of the compounds as a mixture of the neutral species and the ion-pair, in solution, as discussed (Fig. 2).

Mass spectra and thermal analysis

The mass spectra of free dimethylglyoxime, the bis(dimethylglyoximato)nickel(II) complex, $Ni(DH)_2$ and the cobaloximes $[Co(DH)_2(SCN)(L)]$ have been studied. While the molecular ion peak of the DH_2 and $Ni(DH)_2$ are obtained, no such peak for the cobaloxime complexes was obtained. The thermal stability of the complexes is also very high and with increase in temperature mass losses are seen corresponding to polymeric intermediates and the ultimate formation of Co_3O_4 as the end product.

Acknowledgements—The authors are thankful to Dr Y. Inoguchi, Gakushuin University, Japan for getting the ^1H and ^{13}C NMR done. One of the authors (JKD) thanks the UGC, Delhi for a teacher-fellowship and the Govt. of Orissa for the leave of absence.

REFERENCES

1. G. N. Schrauzer and G. Klatel, *Angew. Chem.* 1965, **77**, 180.
2. G. N. Schrauzer and R. J. Windgassen, *J. Am. Chem. Soc.* 1966, **88**, 3738.
3. G. N. Schrauzer, *Acc. Chem. Res.* 1968, **1**, 97.
4. J. M. Pratt and P. J. Craig, *Adv. Organomet. Chem.* 1973, **11**, 331.

5. D. G. Brown, *Prog. Inorg. Chem.* 1973, **18**, 177.
6. T. Sasaki, Pat. 7203, 273, Cl. C. 07 cdf, A 61K, 28 Jan 1972, *Chem. Abst.* 1972, **77**, 101625c.
7. H. Eckert, G. N. Schrauzer and I. Ugi, *Tetrahedron*, 1975, **31**, 1399.
8. H. C. Freeman, *Inorganic Biochemistry* (Edited by G. L. Eichhorn), p. 121. Elsevier, Amsterdam (1973).
9. A. R. Norris, E. Buncel and S. E. Taylor, *J. Inorg. Biochem.* 1982, **16**, 279.
10. P. Pujari and K. C. Dash, *J. Inorg. Nucl. Chem.* 1975, **37**, 2061; 1977, **39**, 2167.
11. Ch. K. C. Mohapatra and K. C. Dash, *J. Inorg. Nucl. Chem.* 1976, **38**, 1253.
12. G. Roychaudhury and K. C. Dash, *Transition Met. Chem.* 1977, **2**, 253.
13. K. C. Dash and P. Pujari, *Transition Met. Chem.* 1978, **3**, 53.
14. J. A. C. van Oojen, J. Reedijk and A. L. Spek, *J. Chem. Soc. Dalton Trans.* 1979, 1183.
15. H. M. J. Hendriks and J. Reedijk, *Recl. Trav. Chim. Pays-Bas*, 1979, **98**, 95 (and references cited therein).
16. G. RoyChoudhury and K. C. Dash, *J. Mol. Struct.* 1980, **68**, 319; 1981, **72**, 269.
17. B. Zimmer Gasser and K. C. Dash, *Inorg. Chim. Acta* 1981, **55**, 43.
18. L. J. Boucher, E. J. Batis and N. G. Paez, *J. Inorg. Nucl. Chem.* 1971, **33**, 1373.
19. R. W. Hay, M. Tajik and P. R. Norman, *J. Chem. Soc. Dalton Trans.* 1979, 636.
20. I. J. Kindred and D. A. House, *Inorg. Chim. Acta* 1975, **14**, 185; *Inorg. Nucl. Chem. Lett.* 1974, **10**, 25.
21. D. A. House and J. W. Blunt, *Inorg. Nucl. Chem. Lett.* 1975, **11**, 219.
22. N. Yamazaki and Y. Hohokabe, *Bull. Chem. Soc. Japan* 1971, **44**, 63.
23. T. Sasaki and F. Matsunaga, *Bull. Chem. Soc. Japan* 1969, **42**, 1308.
24. J. K. Das and K. C. Dash, *Proc. Natl. Acad. Sciences*, India (in press).
25. L. A. Epps and L. G. Marzilli, *J. Chem. Soc. Chem. Comm.* 1972, 109.
26. W. C. Trogler, R. C. Stewart, L. A. Epps and L. G. Marzilli, *Inorg. Chem.* 1974, **13**, 1564.
27. A. H. Norbury, P. E. Shaw and A. I. P. Sinha, *J. Chem. Soc. Dalton Trans.* 1975, 742.
28. D. D. Buburoz and Yu. Ya. Kharitonov, *Koord. Khim.* 1975, **1**, 1031.
29. D. D. Buburoz and V. N. Shafranskii, *Koord. Khim.* 1976, **2**, 1504.
30. A. I. Vogel, *A Text Book of Practical Organic Chemistry*, p. 853. Longmans (1961).
31. H. A. Laitenen and L. W. Burdett, *Analyt. Chem.* 1951, **23**, 1268.
32. A. B. P. Lever, *Inorganic Electronic Spectroscopy*. Elsevier, Amsterdam (1963).
33. A. B. Ablov, M. P. Filippov and N. M. Samus, *Dokl. Akad. Nauk. SSSR* 1968, **133**, 575.
34. Y. Yamano, I. Masuda and K. Shimura, *Bull. Chem. Soc., Japan* 1972, **44**, 1581.
35. R. Blinc and D. Hadzi, *J. Chem. Soc.* 1958, 4536.
36. R. D. Gillard and G. Wilkinson, *J. Chem. Soc.* 1963, 6041.
37. D. G. Batyr, M. P. Starysh, V. N. Shafranskii and Yu. Ya. Kharitonov, *Russ. J. Inorg. Chem.* 1974, **19**, 417.
38. J. K. Das and K. C. Dash (to be published).
39. K. Nakamoto, *Infrared Spectra of Inorganic and Coordination Compounds*. Wiley, New York (1963).
40. R. A. Bailey, S. L. Kozak, T. W. Michelsen and W. N. Mills, *Coord. Chem. Rev.* 1971, **6**, 407.
41. J. L. Burmeister, *Coord. Chem. Rev.* 1966, **1**, 205.
42. R. G. Pearson, *J. Am. Chem. Soc.* 1963, **85**, 3533.
43. P. H. Tiwari, R. W. Gaver, H. K. Wilcox and W. K. Wilmarth, *Inorg. Chem.* 1967, **6**, 611.
44. D. N. Hague and J. Halpern, *Inorg. Chem.* 1967, **6**, 2059.
45. L. G. Marzilli, J. G. Salerno and L. A. Epps, *Inorg. Chem.* 1972, **11**, 2050.
46. A. V. Ablov, N. N. Proskina, A. Bologna and N. M. Samus, *Russ. J. Inorg. Chem.* 1970, **15**, 1245.
47. L. A. Epps and L. G. Marzilli, *Inorg. Chem.* 1973, **12**, 1514.
48. C. Pecile, *Inorg. Chem.* 1960, **5**, 210.
49. H. A. O. Hill and K. G. Morallee, *J. Chem., Soc. A* 1969, 554.
50. J. K. Das and K. C. Dash, *Ind. J. Chem.* (in press).

Polyhedron Vol. 4, No. 6, pp. 1119–1130, 1985
Printed in Great Britain

0277-5387/85 $3.00 + .00
© 1985 Pergamon Press Ltd

COORDINATION, OLIGOMERISATION AND TRANSFER HYDROGENATION OF ACETYLENES BY SOME RUTHENIUM AND OSMIUM CARBOXYLATES: CRYSTAL AND MOLECULAR STRUCTURES OF BIS(TRIFLUOROACETATO)CARBONYL-(METHANOL)BIS(TRIPHENYLPHOSPHINE)RUTHENIUM(II) AND (1,4-DIPHENYLBUT-1-EN-3-YN-2-YL)TRIFLUOROACETATO-(CARBONYL)BIS(TRIPHENYLPHOSPHINE)RUTHENIUM(II)[1]

ALAN DOBSON, DAVID S. MOORE and STEPHEN D. ROBINSON*
Department of Chemistry, King's College, Strand, London WC2R 2LS, U.K.

and

MICHAEL B. HURSTHOUSE and LUCY NEW
Department of Chemistry, Queen Mary College, Mile End Road, London E1 4NS, U.K.

(*Received* 20 *November* 1984; *accepted* 18 *December* 1984)

Abstract—The hydrides $[MH(O_2CCF_3)(CO)(PPh_3)_2]$ (M = Ru or Os) react with disubstituted acetylenes PhC≡CPh and PhC≡CMe to afford vinylic products $[M\{C(Ph)=CHPh\}(O_2CCF_3)(CO)(PPh_3)_2]$ and $[M\{C(Ph)=CHMe\}(O_2CCF_3)(CO)(PPh_3)_2]/[M\{C(Me)=CHPh\}(O_2CCF_3)(CO)(PPh_3)_2]$ respectively. Acidolysis of these products with trifluoroacetic acid in cold ethanol liberates *cis*-stilbene and *cis*-PhHC=CHMe respectively thus establishing the *cis*-stereochemistry of the vinylic ligands. The complexes $[M(O_2CCF_3)_2(CO)(PPh_3)_2]$ formed during the acidolysis step undergo facile alcoholysis followed by β-elimination of aldehyde to regenerate the parent hydrides $[MH(O_2CCF_3)(CO)(PPh_3)_2]$ and thereby complete a catalytic cycle for the transfer hydrogenation of acetylenes. The molecular structure of the methanol-adduct intermediate, $[Ru(O_2CCF_3)_2(MeOH)(CO)(PPh_3)_2]$ has been determined by X-ray methods and shows that the coordinated methanol is involved in H-bonding with the monodentate trifluoroacetate ligand [MeO–H---OC(O)CF_3; O···O = 2.54 Å]. The hydrides $[MH(O_2CCF_3)(CO)(PPh_3)_2]$ react with 1,4-diphenylbutadiyne to afford the complexes $[M\{C(C{\equiv}CPh){=}CHPh\}(O_2CCF_3)(CO)(PPh_3)_2]$. The ruthenium product, which has also been obtained by treatment of $[RuH(O_2CCF_3)(CO)(PPh_3)_2]$ with phenylacetylene, has been shown by X-ray diffraction methods to contain a 1,4-diphenylbut-1-en-3-yn-2-yl ligand. The osmium complexes $[Os(O_2CCF_3)_2(CO)(PPh_3)_2]$, $[OsH(O_2CCF_3)(CO)(PPh_3)_2]$ and $[Os\{C(C{\equiv}CPh){=}CHPh\}(O_2CCF_3)(CO)(PPh_3)_2]$ all serve as catalysts for the oligomerisation of phenylacetylene. Acetylene reacts with $[Ru(O_2CCF_3)_2(CO)(PPh_3)_2]$ in ethanol to afford the vinyl complex $[Ru(CH{=}CH_2)(O_2CCF_3)(CO)(PPh_3)_2]$.

Current interest in the chemistry of platinum group metal–acetylene complexes,[2] stimulated by the commercial importance of many transition metal catalysed acetylene reactions,[3] prompted an investigation of the activity of our catalyst system

$[M(O_2CCF_3)_2(CO)(PPh_3)_2]/$
$[MH(O_2CCF_3)(CO)(PPh_3)_2]$ (M = Ru or Os)[4]

towards terminal and non-terminal acetylenes. Reactions examined include the oligomerisation of aryl acetylenes (ArC≡CH), transfer hydrogenation of diarylacetylenes (ArC≡CAr) and the synthesis of a variety of vinylic complexes of ruthenium(II) and

* Author to whom correspondence should be addressed.

osmium(II). We have also determined the crystal and molecular structure of the methanol solvated complex

$$[Ru(O_2CCF_3)_2(CO)(MeOH)(PPh_3)_2]$$

and the 1,4-diphenylbut-1-en-3-yn-2-yl derivative

$$[Ru\{C(C{\equiv}CPh){=}CHPh\}(O_2CCF_3)(CO)(PPh_3)_2]$$

isolated in the course of this investigation. Some of this work has been described in a preliminary report.[5]

EXPERIMENTAL

The ruthenium and osmium precursors were prepared as previously described.[6] Solvents, light petroleum (40–60°C) and acetylenes were used as purchased. Melting points were taken in sealed tubes under nitrogen using a Buchi melting point apparatus. Analyses were performed by the microanalytical laboratories at University College, London. IR spectra were taken on a Perkin–Elmer 457 grating spectrometer using mulls in Nujol. NMR spectra were obtained on a Bruker HFX-90 spectrometer operating in the F.T. mode. The ^{31}P chemical shifts were recorded relative to an external standard of 85% H_3PO_4 and are reported in ppm with positive values indicating a resonance at low field relative to H_3PO_4. The ^{19}F chemical shifts were recorded relative to an internal hexafluorobenzene standard and are reported in ppm with positive values indicating resonances at high field relative to C_6F_6. Samples were examined using deuteriochloroform as solvent.

Physical data for the new complexes presented in this paper are given in Table 1.

Preparation of carbonyl(η^1-1,4-diphenylbut-1-en-3-yn-2-yl) trifluoroacetatobis (triphenylphosphine) ruthenium(II) from phenylacetylene

A mixture of phenylacetylene (0.5 cm^3) and carbonylbis (trifluoroacetato) bis (triphenylphosphine) ruthenium (0.2 g) in ethanol (5 cm^3) was heated under reflux. From the deep yellow solution, a yellow precipitate rapidly deposited. After 30 min the mixture was cooled and the precipitate filtered off, washed successively with methanol, *n*-hexane and methanol, then recrystallised from dichloromethane/methanol as *bright yellow crystals.* These were filtered off and dried *in vacuo.* Yield: 0.15 g, 72.5%.

Carbonyl(η^1-1,4-di-p-tolylbut-1-en-3-yn-2-yl) trifluoroacetatobis (triphenylphosphine) ruthenium(II) was similarly prepared from *p*-tolylacetylene. Yield: 60%.

In the preceding reactions, products identical to the ones described above were also obtained when the complex $[RuH(O_2CCF_3)(CO)(PPh_3)_2]$ was substituted for $[Ru(O_2CCF_3)_2CO(PPh_3)_2]$, and when the ethanol solvent was replaced by benzene. When benzene was employed as solvent, addition of ethanol was necessary to precipitate the product.

Oligomerisation of phenylacetylene in the presence of carbonylbis (trifluoroacetato) bis (triphenylphosphine) osmium(II)

Phenylacetylene (2.0 cm^3) and carbonylbis (trifluoroacetato) bis (triphenylphosphine) osmium (0.05 g) were heated under reflux in benzene (10.0 cm^3) for 2 h, during which time the mixture rapidly darkened. The solution was then evaporated *in vacuo* to leave a dark brown oil which was treated with light petroleum (100 cm^3) to produce a dark brown solution. The solution was filtered then evaporated *in vacuo* and the residue dissolved in benzene (*ca* 5.0 cm^3) and passed down an alumina column. A single band was eluted from the column, and the eluate was evaporated to leave a dark brown powder. This was washed with cold methanol and dried *in vacuo.* Yield: 0.42 g. (Found: C, 91.88; H, 5.67%; M.wt.: 800. Calc. for $C_{64}H_{48}$: C, 94.12; H, 5.88%; M.wt.: 816.)

Oligomerisation of p-*tolylacetylene in the presence of carbonylbis (trifluoroacetato) bis (triphenylphosphine) osmium(II)* was similarly achieved and afforded 0.27 g of product as a dark brown solid. (Found: C, 90.45; H, 6.74%; M.wt.: 1200. Calc. for $C_{90}H_{80}$: C, 93.11; H, 6.89%; M.wt.: 1160.)

Similar oligomers were obtained when the complex $[OsH(O_2CCF_3)CO(PPh_3)_2]$ was substituted for $[Os(O_2CCF_3)_2CO(PPh_3)_2]$ in the above reactions and when the benzene solvent was replaced by ethanol.

Preparation of carbonyl(η^1-1,4-diphenylbut-1-en-3-yn-2-yl) trifluoroacetato (triphenylphosphine) ruthenium(II) from 1,4-*diphenylbutadiyne*

1,4-Diphenylbutadiyne (0.1 g) and carbonylbis (trifluoroacetato) bis (triphenylphosphine) ruthenium (0.2 g) were heated under reflux in ethanol (5 cm^3). A yellow solution rapidly formed from which yellow crystals precipitated. After 30 min the mixture was cooled and the precipitate filtered off, washed with methanol and then recrystallised from dichloromethane/methanol as *bright yellow crystals.* These were filtered off and dried *in vacuo.* Yield: 0.18 g, 79%.

Carbonyl(η^1-1,4-diphenylbut-1-en-3-yn-2-yl) trifluoroacetatobis (triphenylphosphine) osmium(II)

Table 1. Melting point, analytical, IR, Raman, and NMR data for complexes $M(O_2CCF_3)R(CO)(PPh_3)_2$

$M(O_2CCF_3)R(CO)(PPh_3)_2$			Analytical data[a]			IR data		Raman data			NMR data	
M	R	Mp (°C)	% C	% H	% P	ν(CO) (cm^{-1})	$\nu_{(asym)}$ (OCO) (cm^{-1})	ν(C≡C) (cm^{-1})	ν(C=C) (cm^{-1})		δ(M–P) (ppm)	^{19}F (Hz)
Ru	—C(C≡CPh)=CHPh[b]	237–238	67.7 (68.1)	4.7 (4.3)	6.4 (6.4)	1937	1620	2152	1595 1579	1556	+36.86	+7282
Ru	—C(C≡C-*p*-tolyl)=CH-*p*-tolyl	228–229	68.8 (68.6)	4.6 (4.6)	6.3 (6.2)	1942	1612	2157	1607	1543	+36.79	+7294
Ru	—C(Ph)=CHPh	213–214	67.7 (67.4)	4.4 (4.3)	6.7 (6.6)	1938	1615		1595 1589		+33.50	+7285
Ru	—C(Ph)=CHMe/—C(Me)=CHPh	205–207	63.5 (62.9)	4.5 (4.3)	6.8[c] (6.7)	1932	1615		1593 1573		+36.70 +34.00	+7271 +7248
Ru	—C(C≡CPh)=CHPh[d]	235–236	68.1 (68.1)	4.3 (4.3)	6.6 (6.4)	1935	1620	2155	1596 1579	1558	+36.79	+7280
Ru	—CH=CH_2	224–225	62.0 (62.0)	4.2 (4.2)	8.0 (7.8)	1938	1618		1591		+36.72	+7277
Os	—C(Ph)=CHPh	219–220	61.4 (61.5)	4.0 (4.0)	6.2 (5.6)	1918	1612		1590 1550		+14.73	+7240
Os	—C(Ph)=CHMe/—C(Me)=CHPh[c]	198–201	57.6 (57.4)	4.1 (3.9)	6.1 (6.1)	1921	1609		1593		+19.42 +15.18	+7256 +7232
Os	—C(C≡CPh)=CHPh[d]	230–231	62.6 (62.6)	4.1 (3.9)	6.1 (5.8)	1916	1612	2164	1597 1579	1547	+19.17	+7257

[a] Calculated figures in parentheses.
[b] Made from PhC≡CH.
[c] Calculated for ½CH_2Cl_2 solvation.
[d] Made from PhC≡C—C≡CPh.

was similarly prepared from carbonylbis (trifluoroacetato) bis (triphenylphosphine) osmium and obtained as *bright yellow* crystals. Yield: 0.15 g, 70%

Similar procedures employing

$$[MH(O_2CCF_3)CO(PPh_3)_2]$$

in a benzene reaction medium instead of

$$[M(O_2CCF_3)_2CO(PPh_3)_2] \ (M = Ru, Os)$$

in the preceding pair of reactions produced identical results.

Reaction of carbonyl{η^1 - 1,4 - diphenylbut - 1 - en - 3 - yn - 2 - yl} trifluoroacetatobis (triphenylphosphine) ruthenium(II) with trifluoroacetic acid

Trifluoroacetic acid (0.25 cm^3) and carbonyl {η^1 - 1,4 - diphenylbut - 1 - en - 3 - yn - 2 - yl} trifluoroacetatobis (triphenylphosphine) ruthenium(II) (0.2 g) were heated under reflux in benzene (10 cm^3) for 30 min. The mixture was cooled and the solvent removed *in vacuo* to leave an orange oil. This was crystallised and recrystallised from dichloromethane/methanol as *deep yellow crystals.* The product was identified as carbonylbis (trifluoroacetato) bis (triphenylphosphine) ruthenium by its IR spectrum and melting point. Yield: 0.13 g, 71%.

Carbonyl(1 - phenylprop - 1 - en - 1 - yl) trifluoroacetatobis (triphenylphosphine) ruthenium(II) and carbonyl (3 - phenylprop - 2 - en - 2 - yl) - trifluoroacetatobis (triphenylphosphine) ruthenium(II) (ca 1/1 *isomer mixture*)

Methylphenylacetylene (0.5 cm^3) and carbonylbis (trifluoroacetato) bis (triphenylphosphine) ruthenium (0.5 g) were heated under reflux in ethanol (10 cm^3). A yellow solution rapidly formed and yellow crystals precipitated from solution. After 1 h the mixture was cooled and the precipitate filtered off, then washed with methanol, and recyrstallised from dichloromethane/methanol as *bright yellow crystals.* These were filtered off, washed with methanol and dried *in vacuo.* Yield: 0.33 g, 66%.

Carbonyl(1 - phenylprop - 1 - en - 1 - yl) trifluoroacetatobis (triphenylphosphine) osmium(II) and carbonyl (3 - phenylprop - 2 - en - 2 - yl) trifluoroacetatobis (triphenylphosphine) osmium(II) (ca 1/1 *isomer mixture*) was similarly prepared from carbonylbis (trifluoroacetato) bis (triphenylphosphine) osmium and obtained as *bright yellow crystals.* Yield: 0.29 g, 60%.

Carbonyl (cis - 1,2 - diphenylethenyl) trifluoroacetatobis (triphenylphosphine) ruthenium(II)

Diphenylacetylene (0.1 g) and carbonylbis (trifluoroacetato) bis (triphenylphosphine) ruthenium (0.2 g) were heated under reflux in ethanol (5 cm^3). The yellow solution rapidly precipitated yellow crystals; heating was continued for a total of 30 min and then the mixture was allowed to cool. The crystals were filtered off, washed with methanol, and recrystallised from dichloromethane/methanol as *bright yellow crystals.* These were filtered off and dried *in vacuo.* Yield: 0.2 g, 94%.

Carbonyl (cis - 1,2 - diphenylethenyl) trifluoroacetatobis (triphenylphosphine) osmium (II) was similarly prepared from carbonylbis (trifluoroacetato) bis (triphenylphosphine) osmium and obtained as *bright yellow crystals.* Yield: 0.17 g, 80%.

Similar procedures employing

$$[MH(O_2CCF_3)CO(PPh_3)_2] \ (M = Ru, Os)$$

in benzene in place of

$$[M(O_2CCF_3)_2(CO)(PPh_3)_2]$$

produced identical results.

Cleavage of stilbene from carbonyl (cis - 1,2 - diphenylethenyl) trifluoroacetatobis (triphenylphosphine) ruthenium(II)

Carbonyl (*cis* - 1,2 - diphenylethenyl) trifluoroacetatobis (triphenylphosphine) ruthenium (3.6 g) and trifluoroacetic acid (3.0 cm^3) were stirred together in benzene (50 cm^3) at 20°C for 2 h. The initial bright yellow solution rapidly became deep red, and over the period of the reaction slowly became bright yellow again. The benzene was removed by evaporation *in vacuo* and the resultant dark oil was dissolved in dichloromethane (5 cm^3) then diluted with light petroleum (100 cm^3). The solution was allowed to stand for 24 h during which time yellow crystals (A) were precipitated. These were filtered off, and the filtrate reduced *in vacuo* to *ca* 15 cm^3, and again allowed to stand for 24 h. During this time a second crop of yellow crystals (B) precipitated, and were filtered off. The filtrate was further reduced in volume to *ca* 5 cm^3 and then eluted down a short alumina column with dichloromethane. Collection of solution from the column was continued until the eluate became yellow. Evaporation of the initial colourless fraction produced white crystals, these were identified by their IR and NMR spectra as *cis*-stilbene (0.40 g, 53%). The second yellow eluate fraction was found to contain a mixture of *cis*-stilbene and carbonyl-bis (trifluoroacetato) bis (triphenylphosphine) ruth-

enium (by IR and NMR spectroscopy). The crystals (A) and (B) were identified by their IR spectra as carbonylbis (trifluoroacetato) bis (triphenylphosphine) ruthenium (total yield: 3.03 g, 85%).

Catalytic hydrogenation of diphenylacetylene in propan-1-ol

Diphenylacetylene (1.0 g), trifluoroacetic acid (0.33 g) and carbonylbis (trifluoroacetato) bis (triphenylphosphine) ruthenium (0.2 g) were heated together in boiling propan-1-ol (30 cm^3). After 5 min a 1.0 cm^3 sample was withdrawn from the yellow reaction mixture by means of a calibrated syringe. This sample was evaporated *in vacuo* to produce an oily solid and an IR spectrum of this solid was taken. The sampling procedure was repeated at 30 min intervals for a total of 4 h. The spectra obtained in this way all contained, in addition to broad weak bands arising from the presence of carbonylbis (trifluoroacetato) bis (triphenylphosphine) ruthenium, strong sharp vibrations attributable to diphenylacetylene and *trans*-stilbene. The conversion was monitored by comparing the relative intensities of the vibration at 965 cm^{-1} (attributable to *trans*-stilbene) and the vibration at 920 cm^{-1} (attributable to diphenylacetylene) over a period of several hours. Ratios of diphenylacetylene to *trans*-stilbene were estimated by comparison of spectra with those of a standard mixture of diphenylacetylene/*trans*-stilbene. After 4 h the conversion of diphenylacetylene to *trans*-stilbene was approximately half complete.

In an attempt to increase the rate of conversion of diphenylacetylene to *trans*-stilbene, a higher boiling alcohol, butan-1-ol, was employed in place of propan-1-ol. Using a similar procedure to that described above, the conversion of 1.0 g of diphenylacetylene by 0.2 g of carbonylbis (trifluoroacetato) bis (triphenylphosphine) ruthenium in 30 cm^3 of solvent, was found to be complete in *ca* 2 h. From the reaction *trans*-stilbene (0.85 g, 84%) was recovered. Gas-chromatographic analysis of a small sample of the volatiles distilled from the reaction showed the presence of *n*-butyraldehyde.

Carbonyl (ethenyl) (trifluoroacetato) bis (triphenylphosphine) ruthenium(II)

Carbonylbis (trifluoroacetato) bis (triphenylphosphine) ruthenium (0.2 g) was added to cold ethanol (5.0 cm^3), and acetylene bubbled through this solution for 5 min. The mixture was then heated under reflux while passage of acetylene was continued. After *ca* 5 min the initial yellow complex had dissolved and a second pale yellow complex was precipitating from the pale yellow solution. Heating was containued for a further 15 min and the mixture was then cooled. The precipitated solid was filtered off, washed with methanol, then recrystallised from dichloromethane/methanol as fine *pale yellow needles* which were again filtered off and dried *in vacuo*. Yield: 0.12 g, 67%. The reactions of acetylene with $Ru(O_2CCF_3)_2(CO)(PPh_3)_2$ in benzene solution and with $Os(O_2CCF_3)_2(CO)(PPh_3)_2$ in ethanol or benzene solution led to intractable mixtures of products which were not amenable to separation.

X-Ray crystal structure determinations of the complexes $Ru(O_2CCF_3)_2(MeOH)(CO)(PPh_3)_2$ *and* $Ru\{C(C{\equiv}CPh){=}CHPh\}(O_2CCF_3)(CO)(PPh_3)_2$

The preparation and crystallisation

$$(CH_2Cl_2/MeOH)$$

of

$$Ru(O_2CCF_3)_2(MeOH)(CO)(PPh_3)_2$$

have been reported in a previous paper.[6] The preparation and crystallisation (CH_2Cl_2/MeOH) of $Ru\{C{\equiv}CPh){=}CHPh\}(O_2CCF_3)(CO)(PPh_3)_2$ is described above.

The crystals were mounted on glass fibres for X-ray examination, cell dimensions were determined by least squares refinement based on automatically determined diffractometer setting angles.[7]

Crystal data. (I) $Ru(O_2CCF_3)_2(MeOH)(CO)(PPh_3)_2$—compound (I). $C_{42}H_{34}O_6F_6P_2Ru$, M = 911.75, monoclinic, a = 10.519(2), b = 22.108(3), c = 17.393(2) Å, β = 95.33(2)°, V = 4027 $Å^3$, space group $P2_1/n$, D_m = 1.50 g cm^{-3}, Z = 4, D_c = 1.503 g cm^{-3}, $F(000)$ = 1848, μ(Cu-K_α) = 48.13 cm^{-1}, λ(Cu-K_α) = 1.54178 Å.

(II) $Ru(O_2CCF_3)\{C(C{\equiv}CPh):CHPh\}(CO)(PPh_3)_2$—compound (II). $C_{55}H_{41}O_3F_3P_2Ru$, M = 969.54, triclinic, a = 11.526(2), b = 12.469(1), c = 18.025(3) Å, α = 88.44(2), β = 102.41(2), γ = 110.21(2)°, V = 2371 $Å^3$, space group $P\bar{1}$, D_m = 1.34 g cm^{-3}, Z = 2, D_c = 1.358 g cm^{-3}, $F(000)$ = 992, μ(Cu-K_α) = 22.36 cm^{-1}, λ(Cu-K_α) = 1.54178 Å.

Data collection and processing. Intensity data were recorded on a Nonius CAD4 diffractometer using an $\omega/2\theta$ scan mode in a manner previously described in detail.[7] For compound (I) 4088 unique data were recorded, of which 2961 were observed [$I > 2.5\sigma(I)$]. For compound (II) 6964 unique data were measured, of which 5475 had $I > 2.5\sigma(I)$.

Structure analysis and refinement. The structures were solved and refined by standard methods. For both compounds phenyl rings were refined as regular hexagons and hydrogen atoms were included in idealised positions. All non-hydrogen atoms were

assigned anisotropic temperature factors for structure (II), but due to the paucity of data for structure (I), phenyl ring carbons were refined isotropically. Final R values are 0.062(R) and 0.066(R_ω) for compound (I) ($\omega = 1/\sigma^2 F + 0.0002F_o^2$) and 0.054 for compound (II) (unit weights).

Tables of the final atomic coordinates, thermal parameters, observed and calculated structure factors and the full list of bond lengths and angles have been deposited as supplementary material with the Editor from whom copies are available on request. Copies of the atomic coordinates have also been submitted to the Cambridge Crystallographic Data Centre.

RESULTS AND DISCUSSION

In two previous papers we have reported on the fluxional behaviour of the complexes $[M(O_2CCF_3)_2(CO)(PPh_3)_2]$ (M = Ru or Os)[8] and on their ability to catalyse the dehydrogenation of primary and secondary alcohols to aldehydes and ketones respectively.[4] We now describe further work on the interaction of these systems with acetylenic hydrocarbons. The complexes

$$[M(O_2CCF_3)_2(CO)(PPh_3)_2]$$

undergo facile alcoholysis to afford the corresponding hydrides

$$[MH(O_2CCF_3)(CO)(PPh_3)_2],$$

these products in turn react with diphenylacetylene by addition of the M–H group across the acetylenic triple bond to yield the vinylic species

$$[M(PhC{=}CHPh)(O_2CCF_3)(CO)(PPh_3)_2].$$

In similar reactions involving phenylmethylacetylene a finely balanced combination of steric and electronic factors leads to formation of *ca* 1/1 mixture of the isomeric products

$$[M(MeC{=}CHPh)(O_2CCF_3)(CO)(PPh_3)_2]$$

and

$$[M(PhC{=}CHMe)(O_2CCF_3)(CO)(PPh_3)_2]$$

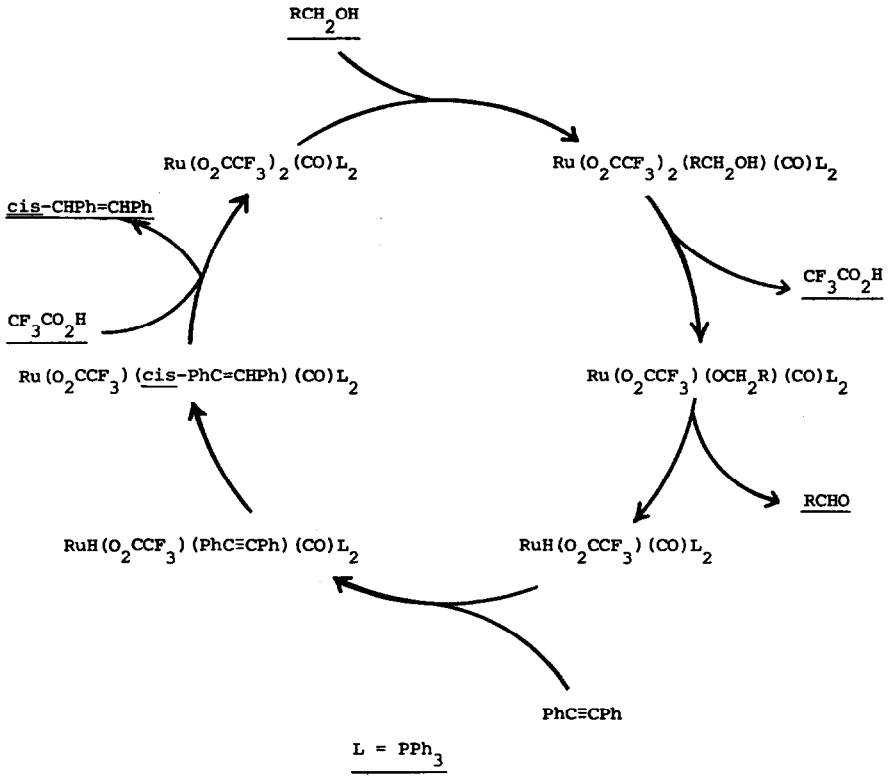
which was analysed on the basis of NMR data given in Table 1. Cleavage of the metal–carbon bonds in their vinylic complexes with cold trifluoroacetic acid affords the vinylic products *cis*-PhCH=CHPh and *cis*-PhCH=CHMe respectively, thereby implying that in each case the original acetylene "insertion" reaction has *cis*-stereochemistry. The stereochemistry of acetylene "insertion" reactions is known to show a critical dependence on the identity of the metal oxidation state, auxiliary ligands and nature of the substituents on the acetylene.[9] Although the complexity of the factors involved has prevented a general interpretation of the mechanism; the occurrence of stereoselective *cis*-insertion is best accounted for in terms of a concerted mechanism involving a four-centre transition state.[2] Such a mechanism is postulated in the present instance. Cleavage of the metal–vinyl linkage under more vigorous conditions is accompanied by isomerisation of the olefinic products to the more thermodynamically stable *trans* form.

The complexes $[M(O_2CCF_3)_2(CO)(PPh_3)_2]$, formed during the cleavage process, undergo alcoholysis, as previously described, to afford the hydrides $[MH(O_2CCF_3)(CO)(PPh_3)_2]$. These hydrides in turn react with more acetylene to regenerate the vinyl complex and thus complete a catalytic cycle (scheme 1) for the transfer hydrogenation of disubstituted acetylenes.

The feasibility of this process has been demonstrated experimentally by the catalytic transfer hydrogenation of diphenylacetylene to *trans*-stilbene using *n*-butanol as the source of hydrogen and $[Ru(O_2CCF_3)_2(CO)(PPh_3)_2]$ as the catalyst. Examination of the volatile products from this reaction by GLC confirmed the formation of *n*-butyraldehyde. If the butyraldehyde is allowed to accumulate within the system the catalyst is converted to the catalytically inactive dicarbonyl species $[Ru(O_2CCF_3)_2(CO)_2(PPh_3)_2]$.

The mechanism proposed for the transfer hydrogenation process (Scheme 1) involves coordination and dehydrogenation of an alcohol substrate and is, therefore, closely akin to that previously advanced for the catalytic dehydrogenation of primary and secondary alcohols.[4] In each mechanism an alcohol is first coordinated to the metal centre, then loses a proton to form an alkoxide ligand which subsequently undergoes β-elimination to generate a molecule of aldehyde (or ketone). Evidence supporting this mechanism has been provided by the results of an X-ray diffraction study performed on a crystal of the catalyst $[Ru(O_2CCF_3)_2(CO)(PPh_3)_2]$ obtained from dichloromethane/methanol solution. The crystal was found to consist of solvated molecules $[Ru(O_2CCF_3)_2(CO)(PPh_3)_2(MeOH)]$ which have the structure shown in Fig. 1. Selected geometric parameters are given in Table 2.

The solvate retains the *cis* arrangement of triphenylphosphine ligands [$\angle$ P–Ru–P = 99.5(1)°, Ru–P 2.341(3) Å (*trans* to MeOH) and 2.361(3) Å (*trans* to $OC(O)CF_3$)] found in the parent complex $[Ru(O_2CCF_3)_2(CO)(PPh_3)_2]$ but has incorporated a molecule of methanol into the coordination sphere [Ru–O 2.174(7) Å] at the expense of the trifluoroacetate ligands, both of which are now monodentate [Ru–O 2.139(6) Å (*trans* to carbonyl) and 2.101(7) Å (*trans* to PPh_3)]. The sixth



Scheme 1.

coordination site is occupied by the carbonyl ligand [Ru–CO 1.81 Å]. The metal–ligand distances are typical for octahedral ruthenium(II). However, the most interesting feature of the structure, and the one most relevant to the present discussion, is the steric relationship between the coordinated methanol and one of the trifluoroacetate ligands. The orientation of this trifluoroacetate relative to the methanol is convenient for the establishment of a hydrogen bond [Me–O–H · · · O–C(O)CF_3] between these two ligands. Moreover the $O_2 \cdots O_3$ distance (2.54 Å) is within the range expected for such an interaction.[10]

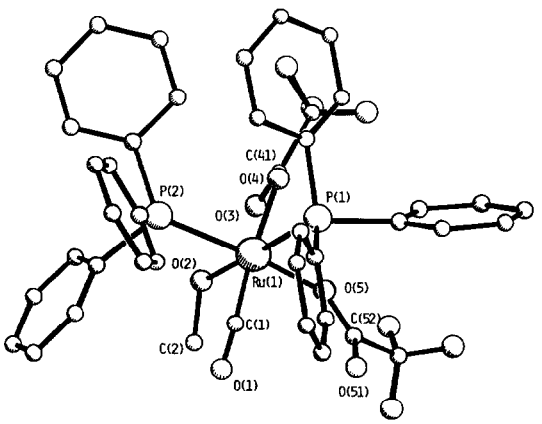
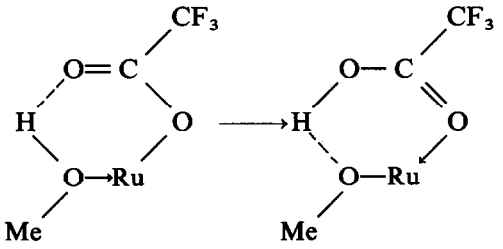


Fig. 1.

The presence of H-bonding, which is confirmed by IR data [hexachlorobutadiene mull, broad band centred at 3000 cm^{-1}], points to a simple and attractive mechanism for the alcoholysis step involving transfer of the H-bonded proton from the alcohol to the carboxylate anion.



Subsequent steps in the catalytic cycle (Scheme 1) are loss of acid CF_3CO_2H, β-elimination of aldehyde (or ketone) coordination of PhC≡CPh, migration of hydride ligand onto coordinated PhC≡CPh, and finally acidolysis of Ru-vinyl linkage to liberate stilbene and regenerate

$$[Ru(O_2CCF_3)_2(CO)(PPh_3)_2].$$

With terminal acetylenes, RC≡CH, a rather different reaction sequence is observed. Arylacetylenes ArC≡CH (Ar = Ph or *p*-tolyl) react with the complexes $[RuH(O_2CCF_3)(CO)(PPh_3)_2]$ and $[Ru(O_2CCF_3)_2(CO)(PPh_3)_2]$ to afford air-stable yellow crystalline products of stoichiometry

Table 2. Selected geometry parameters for $[Ru(O_2CCF_3)_2(CO)(PPh_3)_2(MeOH)]$

(a) Bond lengths (Å)			
Ru(1)–P(1)	2.341(3)	Ru(1)–O(2)	2.174(7)
Ru(1)–P(2)	2.361(3)	Ru(1)–O(4)	2.139(6)
Ru(1)–C(1)	1.808(13)	Ru(1)–O(5)	2.101(7)
C(1)–O(1)	1.159(12)	C(2)–O(2)	1.412(13)
C(41)–O(3)	1.221(13)	C(52)–O(5)	1.210(13)
C(41)–O(4)	1.269(13)	C(52)–O(51)	1.238(13)
(b) Bond angles (°)			
P(1)–Ru(1)–P(2)	99.5(1)	O(2)–Ru(1)–P(2)	86.5(2)
P(1)–Ru(1)–C(1)	93.4(3)	O(2)–Ru(1)–C(1)	93.8(4)
P(1)–Ru(1)–O(4)	87.3(2)	O(2)–Ru(1)–O(4)	84.9(3)
P(1)–Ru(1)–O(5)	94.0(2)	O(2)–Ru(1)–O(5)	79.7(3)
P(2)–Ru(1)–O(4)	97.5(2)	O(5)–Ru(1)–O(4)	79.7(3)
P(2)–Ru(1)–C(1)	88.2(3)	O(5)–Ru(1)–C(1)	94.4(4)
P(1)–Ru(1)–O(2)	170.8(2)	C(1)–Ru(1)–O(4)	174.1(4)
P(2)–Ru(1)–O(5)	166.1(2)	Ru(1)–O(2)–C(2)	121.9(7)

$[Ru(C_4HAr_2)(O_2CCF_3)(CO)(PPh_3)_2]$. In contrast the corresponding osmium complexes catalyse oligomerisation of these aryl acetylenes to yield amorphous light-brown hydrocarbon solids with molecular weights in the range 800–1200 a.m.u. However, the osmium complex

$$[Os(C_4HPh_2)(O_2CCF_3)(CO)(PPh_3)_2]$$

and its ruthenium analogue

$$[Ru(C_4HPh_2)(O_2CCF_3)(CO)(PPh_3)_2]$$

are readily obtained by addition of 1,4-diphenylbutadiyne to the corresponding hydrides

$$[MH(O_2CCF_3)(CO)(PPh_3)_2].$$

An X-ray diffraction study on the ruthenium derivative

$$[Ru(C_4HPh_2)(O_2CCF_3)(CO)(PPh_3)_2],$$

using crystals prepared from phenylacetylene and

$$[Ru(O_2CCF_3)_2(CO)(PPh_3)_2],$$

was undertaken to determine the structure and stereochemistry of the hydrocarbon ligand and thus elucidate the mechanism of its formation. The structure of the complex is shown in Fig. 2. Selected geometric parameters are given in Table 3. The octahedral ruthenium(II) centre is coordinated to a *trans* pair of triphenylphosphine ligands [Ru–P 2.369(2) and 2.372(2)Å], a carbonyl group [Ru–CO 1.79(1) Å], a chelate trifluoroacetate [Ru–O 2.235(6) Å (*trans* to carbonyl) and 2.352(7) Å (*trans* to C_4HPh_2 ligand)] and a 1,4-diphenylbut-1-en-3-yn-2-yl ligand. The geometry of the hydrocarbon ligand is more clearly shown in Fig. 3. The structure of the

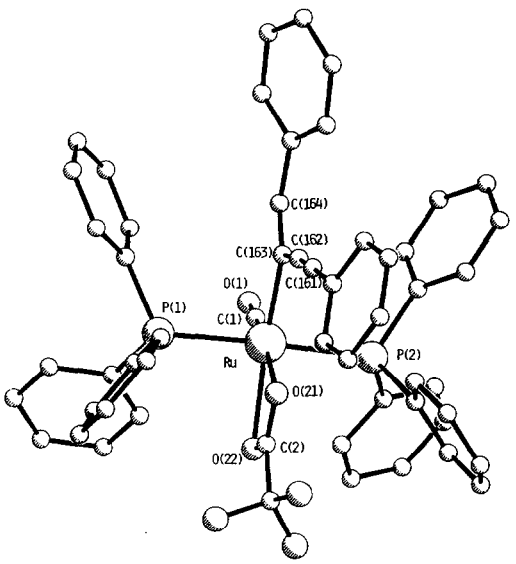


Fig. 2.

hydrocarbon ligand is of particular interest because of relevance to the problems of metal/terminal acetylene interactions and metal catalysed acetylene oligomerisation reactions. Terminal acetylenes are known to undergo oxidative addition reactions at unsaturated metal centres to afford metal acetylide complexes[11] and the subsequent "insertion" of further molecules of acetylene into the M-acetylide linkage has been advanced as a plausible mechanism for acetylene oligomerisation reactions.[2,3] However, it has recently been shown that in their reactions with metal centres terminal acetylenes may also afford vinylidene ligands (M=C=CHR)[12–15] which in

Table 3. Selected geometry parameters for $\{Ru[C(C{\equiv}CPh){=}CHPh](O_2CCF_3)(CO)(PPh_3)_2]$

(a) Bond lengths (Å)			
Ru–P(1)	2.369(2)	Ru–P(2)	2.372(2)
Ru–O(21)	2.235(6)	Ru–O(22)	2.352(7)
Ru–C(1)	1.790(1)	Ru–C(163)	2.076(8)
Ru–C(162)	2.842(7)	Ru–C(161)	3.718(8)
C(2)–O(21)	1.250(10)	C(2)–O(22)	1.248(11)
C(163)–C(164)	1.345(16)	C(163)–C(162)	1.437(12)
C(162)–C(161)	1.208(13)	C(161)–C(16)	1.468(11)
(b) Bond angles (°)			
P(1)–Ru–P(2)	175.9(1)	C(1)–Ru–O(21)	167.9(3)
O(22)–Ru–C(163)	157.9(3)	O(21)–C(2)–O(22)	57.1(2)
P(1)–Ru–C(1)	89.5(3)	P(2)–Ru–C(1)	88.4(3)
P(1)–Ru–C(163)	92.4(3)	P(2)–Ru–C(163)	91.2(3)
P(1)–Ru–O(21)	91.0(2)	P(2)–Ru–O(21)	90.3(2)
P(1)–Ru–O(22)	87.9(2)	P(2)–Ru–O(22)	89.5(2)
O(22)–Ru–C(1)	110.9(3)	C(163)–Ru–O(22)	157.9(3)
C(163)–Ru–O(21)	100.8(3)	C(163)–Ru–C(1)	91.2(4)
Ru–C(163)–C(164)	128.5(6)	Ru–C(163)–C(162)	106.6(6)
C(164)–C(163)–C(162)	124.9(8)	C(163)–C(162)–C(161)	173.0(9)
C(162)–C(161)–C(16)	175.6(10)		

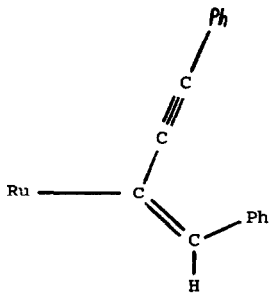


Fig. 3.

turn can react with further molecules of acetylene to build up more complex hydrocarbon structures.[16] Formation of the vinylidene ligand in these systems is thought to involve η^2-coordination of the acetylene followed by conversion to an acetylide intermediate (Scheme 2). This mechanism has recently been confirmed for a rhodium/acetylene system.[17]

The 1,4-diphenylbut-1-en-3-yn-2-yl ligand generated in the

$$[Ru(O_2CCF_3)_2(CO)(PPh_3)_2]/PhC{\equiv}CH$$

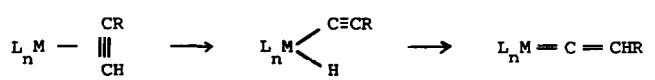
reaction is clearly *not* formed by insertion of a second molecule of acetylene into a metal–acetylide linkage. Therefore the alternative routes given in Scheme 3 were considered. According to the first of these the coordinative unsaturation required to accommodate the incoming acetylene is provided by the chelate trifluoroacetate ligand which relinquishes a coordination site. Subsequent oxidative addition of the coordinated acetylene across the ruthenium centre would afford a seven-coordinate, eighteen electron ruthenium(IV) species which could react further by elimination of acid, CF_3CO_2H, and formation of a ruthenium(II) acetylide complex

$$[Ru(C{\equiv}CAr)(O_2CCF_3)(CO)(PPh_3)_2].$$

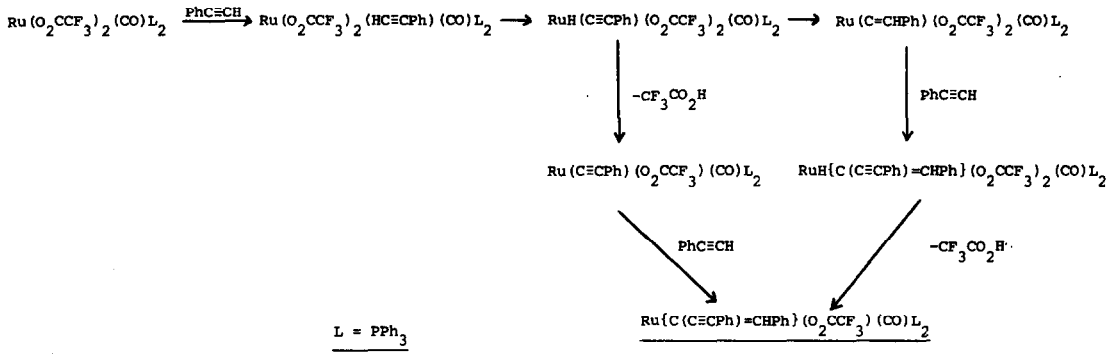
This, in turn, could afford the observed product

$$[Ru\{C(C{\equiv}CAr){=}CHAr\}(O_2CCF_3)(CO)(PPh_3)_2]$$

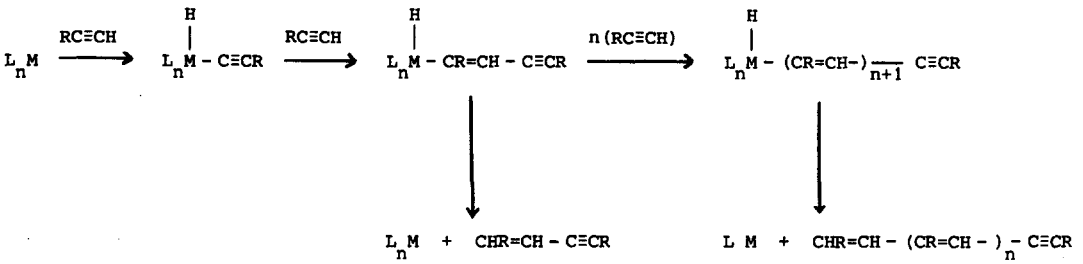
by *trans* addition of a second molecule of acetylene across the triple bond of the acetylide ligand. In a preliminary communication[5] this reaction sequence was advanced as the most probable mechanism for formation of the 1,4-diphenylbut-1-en-3-yn-2-yl ligand. However, the recent work on the formation of vinylidene complexes from terminal acetylenes[14–17]



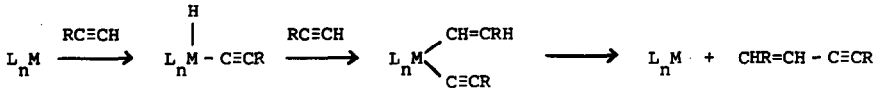
Scheme 2.



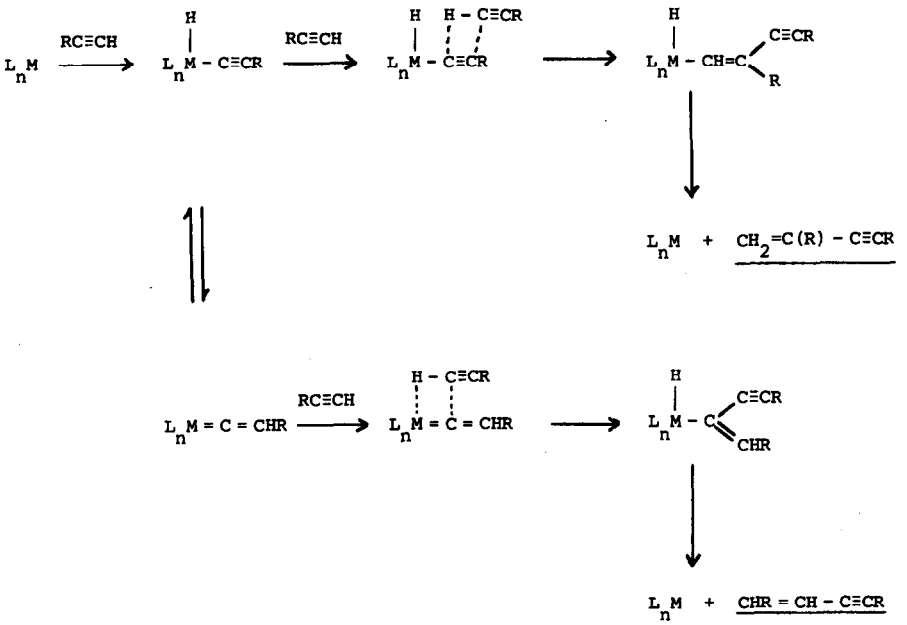
Scheme 3.



Scheme 4.



Scheme 5.



Scheme 6.

points to an alternative mechanism which must now be considered. Rearrangement of the proposed seven-coordinate ruthenium(IV) acetylide intermediate $[RuH(C{\equiv}CAr)(O_2CCF_3)_2(CO)(PPh_3)_2]$ to a more stable six-coordinate ruthenium(II) vinylidene intermediate

$$[Ru(=C{=}CHAr)(O_2CCF_3)_2(CO)(PPh_3)_2]$$

could be followed by *cis*-1,2-addition of a second molecule of acetylene across the ruthenium–vinylidene bond and subsequent elimination of acid, CF_3CO_2H, to afford the observed product. Attack by terminal acetylene on a vinylidene ligand formed by a 1,3-hydrogen shift in a hydrido(ethynyl) ruthenium complex has previously been postulated to account for the ruthenium metallocyclic product obtained from the $RuH_2(CO)(PPh_3)_3/HC{\equiv}C{-}CO_2CH_3$ system.[18]

In an attempt to differentiate between these two possible reaction mechanisms the reactions of $[Ru(O_2CCF_3)_2(CO)(PPh_3)_2]$ with one molecule of $PhC{\equiv}CH$ in dilute benzene or ethanol solution were examined by IR and NMR (^1H, ^{13}C and $^{31}P\{^1H\}$] spectroscopy. The pale yellow product isolated from the evaporated solution displayed strong sharp IR bands attributable to carbonyl [ν(CO) 1986 and 1944 cm^{-1}] acetylide [$\nu(C{\equiv}CPh)$ 2052 cm^{-1}] and vinylidene ligands [$\nu(C{=}CHPh)$ 1680 cm^{-1}]. On the basis of these data we tentatively identify the residue as a mixture of

$$[Ru(O_2CCF_3)_2(C{=}CHPh)(CO)(PPh_3)_2]$$

and

$$[Ru(O_2CCF_3)(C{\equiv}CPh)(CO)(PPh_3)_2].$$

The $^{31}P(^1H)$ NMR spectrum consists of two singlets (δ 29.9 and 33.5 ppm) and is therefore compatible with the proposed formulation. However, the ^{13}C NMR spectrum does not show the resonance at *ca* 360 ppm characteristic of vinylidene ligands[13] and therefore casts some doubt on our interpretation. Either way the result does not enable us to determine which of the two proposed mechanisms is operative.

The transition metal catalysed dimerisation and polymerisation of terminal acetylenes, $RC{\equiv}CH$, has generally been attributed to single and multiple "insertion" of $RC{\equiv}CH$ moieties into the metal–carbon bond of the developing hydrocarbon ligand (Scheme 4).[19–23] The fact that certain group VIII metal catalysts specifically (or predominantly) catalyse dimer production may simply mean that in their systems the "insertion" of acetylenes into the metal-vinylic linkage is kinetically and/or thermodynamically less favourable than "insertion" into a metal acetylide bond, and that for this reason reductive elimination of dimer takes precedent over the second "insertion" step. An alternative mechanism for dimerisation of terminal acetylenes, proposed by Hagihara *et al.*,[24] involves alkenyl-alkynyl intermediates (Scheme 5). However, the present work points to a further possible mechanism based in part on the participation of vinylidene intermediates which may be particularly relevant in systems where steric hindrance inhibits coordination of the second molecule of acetylene at the metal centre. According to this proposal (Scheme 6) addition of the terminal acetylene to the catalyst leads to a mixture of acetylide and vinylidene species. Stereochemically controlled addition of a second molecule of acetylene across the acetylide triple bond and across the metal–vinylidene double bond would afford the head-to-tail ($CH_2{=}CR{-}C{\equiv}CR$) and head-to-head ($CHR{=}CH{-}C{\equiv}CR$) dimers respectively. In each case the reverse mode of addition would be prevented or seriously hindered by stereochemically interactions between the incoming acetylene and the ancillary ligands on the metal.

REFERENCES

1. *Complexes of the Platinum Metals*, Part 28. Part 27: P. Mura, B. G. Olby and S. D. Robinson, *Inorg. Chim. Acta* 1985, **97**, 45.
2. S. Otsuka and A. Nakamura, *Adv. Organometal. Chem.* 1976, **14**, 245 (and references cited therein).
3. M. G. Chauser, Y. M. Rodionov, V. M. Misin and M. I. Cherkaskin, *Uspekhi Khimii* 1976, **45**, 695; *Russian Chem. Rev.* 1976, **45**, 348.
4. A. Dobson and S. D. Robinson, *Inorg. Chem.* 1977, **16**, 137.
5. A. Dobson, D. S. Moore, S. D. Robinson, M. B. Hursthouse and L. New, *J. Organometal. Chem.* 1979, **177**, C8.
6. A. Dobson, S. D. Robinson and M. F. Uttley, *J. Chem. Soc., Dalton Trans.* 1975, 370.
7. M. B. Hursthouse and K. M. A. Malik, *J. Chem. Soc., Dalton Trans.* 1978, 1334.
8. C. J. Creswell, A. Dobson, D. S. Moore and S. D. Robinson, *Inorg. Chem.* 1979, **18**, 2055.
9. See references 2 and 3 for a survey of acetylene "insertion" reactions.
10. J. Emsley, *Chem. Soc. Rev.* 1980, **9**, 91.
11. C. K. Brown, D. Georgiou and G. Wilkinson, *J. Chem. Soc. (A)* 1971, 3120.
12. M. I. Bruce and A. G. Swincer, *Adv. Organometal. Chem.* 1983, **22**, 59.
13. M. I. Bruce and R. C. Wallis, *Aust. J. Chem.* 1979, **32**, 1471.
14. A. B. Antonova, N. E. Kolobova, P. V. Petrovsky, B. V. Lokshin and N. S. Obezyuk, *J. Organometal. Chem.* 1977, **137**, 55.
15. A. N. Nesmeyanov, G. G. Aleksandrov, A. B. Antonova, K. N. Anisimov, N. E. Kolobova and Y. T. Struchkov, *J. Organometal. Chem.* 1976, **110**, C36.

16. M. I. Bruce, R. C. F. Gardner, J. A. K. Howard, F. G. A. Stone, M. Welling and P. Woodward, *J. Chem. Soc., Dalton Trans.* 1977, 621.
17. J. Wolf, H. Warner, O. Serhadli and M. L. Ziegler, *Angew. Chem., Int. Ed. Engl.* 1983, **22**, 414.
18. H. Yamazaki and K. Aoki, *J. Organometal. Chem.* 1976, **122**, C54.
19. L. S. Meriwether, M. F. Leto, E. C. Colthup and G. W. Kennerly, *J. Org. Chem.* 1962, **27**, 3930.
20. H. Singer and G. Wilkinson, *J. Chem. Soc.* (*A*) 1968, 849.
21. R. J. Kern, *J. Chem. Soc., Chem. Commun.* 1968, 706.
22. S. Yoshikawa, J. Kiji and J. Furukawa, *Makromol. Chem.* 1977, **178**, 1077.
23. L. Carlton and G. Read, *J. Chem. Soc., Perkin(I)* 1978, 1631.
24. Y. Tohda, K. Sonogashira and N. Hagihara, *J. Organometal. Chem.* 1976, **110**, C53.

Polyhedron Vol. 4, No. 6, pp. 1131–1134, 1985
Printed in Great Britain

0277-5387/85 $3.00 + .00
Pergamon Press Ltd

SYNTHESIS OF RHODIUM(II) PYRAZOLATE COMPLEXES: CRYSTAL STRUCTURE OF TETRA-μ-3,5-DIMETHYLPYRAZOLATO DIRHODIUM(II) BIS-ACETONITRILE, (Rh–Rh)

ANDREW R. BARRON and GEOFFREY WILKINSON*
Chemistry Department, Imperial College, London SW7 2AY, U.K.

and

MAJID MOTEVALLI and MICHAEL B. HURSTHOUSE*
Chemistry Department, Queen Mary College, Mile End Road, London E1 4NS, U.K.

(*Received* 13 *December* 1984; *accepted* 4 *January* 1985)

Abstract—The reaction of $Rh_2(O_2CMe)_4$ with the sodium salt of 3,5-dimethylpyrazole (3,5-Me_2pzH) in acetonitrile gives $Rh_2(3,5\text{-}Me_2pz)_4 \cdot 2MeCN$. This yellow diamagnetic compound on heating gives $Rh(3,5\text{-}Me_2pz)_4$, which in turn forms adducts with different unidentate ligands, L, to give $Rh_2(3,5\text{-}Me_2pz)_4 \cdot 2L$. The binuclear tetra bridged structure has been established for the acetonitrile complex by X-ray diffraction. The Rh–Rh distance is 2.353(3) Å and the Rh–N (acetonitrile) distance is 2.202(5) Å. Some unsubstituted pyrazolates have been made.

Of the relatively few rhodium(II) compounds known most are binuclear,[1–3] commonly having four carboxylato bridges. Unlike other dimeric complexes,[2] such as the quadruply bonded Cr_2^{4+} and Mo_2^{4+} compounds, there has been little variation in the nature of the bridging ligands, although compounds have been prepared with wide variety of axial ligands.[1]

The chelating ability of pyrazole is well-known, examples being heteronuclear systems such as the polypyrazolylborates.[4] Recently, numerous di-rhodium(I) and di-rhodium(III) compounds with pyrazolato bridges have been reported.[5,6]

We now report the synthesis and characterisation of the first quadruply bridged pyrazolates of di-rhodium, the first for any metal.

RESULTS AND DISCUSSION

3,5-Dimethylpyrazolato compounds. The complex $Rh_2(3,5\text{-}Me_2pz)_4 \cdot 2MeCN$ was first obtained in low yield from the reaction of $[HB(3,5\text{-}Me_2pz)_3RhCl_2]_2$[7] with $NaBH_4$ in THF. The product when recrystallized from MeCN gave bright yellow crystals of $Rh_2(3,5\text{-}Me_2pz)_4 \cdot 2MeCN$. However, an improved procedure is the direct reaction of $Rh_2(O_2CMe)_4$ with $Na(3,5\text{-}Me_2pz)$ in MeCN.

In contrast to exchange reactions of $Rh_2(O_2CMe)_4$ with carboxylic or other similar acids only small yields are obtained using $3,5\text{-}Me_2pzH$ as a melt or in MeCN solution. Use of MeOH or THF as a solvent leads to decomposition, while in water the adduct $Rh_2(O_2CMe)_4 \cdot (3,5\text{-}Me_2pzH)_2$ is formed. The compound $Rh_2(3,5\text{-}Me_2pz)_4 \cdot 2MeCN$ has been fully characterised by elemental analysis and spectral data. The mass spectrum shows $M^+ - 2MeCN$ ($m/e = 586$) but no parent ion (M^+). The IR spectrum shows strong bands at 1560, 1262 and 752 cm^{-1} for a pyrazolate complex with weak ν(CN) bands at 2293 and 2263 cm^{-1} for coordinated MeCN.

The ^1H NMR spectrum in CD_2Cl_2 shows two singlets for the pyrazolyl group indicating that the pyrazoles are in a symmetric environment. This is supported by the X-ray crystal structure (see below).

The acetonitrile complex was sufficiently soluble in CH_2Cl_2 to study its electrochemistry. Cyclic voltametry (CV) measurements show an irreversible oxidation at + 1.1 V *vs* SCE. This is in contrast to the

*Authors to whom correspondence should be addressed.

carboxylates which undergo reversible one-electron oxidation.

The axial MeCN ligands can be removed by heating the solvate under vacuum to yield a deep purple solid which is insoluble in all common solvents. The mass spectrum shows the parent ion ($m/e = 586$). The IR is similar to that of the acetonitrile complex but without the solvent bands.

Other adducts can be obtained by substitution of MeCN in the acetonitrile complex with pyridine or methanol but the latter is unstable and dissociates under vacuum.

Pyrazolate complexes. Similar complexes can be obtained from pyrazole. The reaction of $Rh_2(O_2CMe)_4$, with Napz in MeCN gives the solvated complex which is more soluble in organic solvents than the 3,5-Me_2pz complex. The terminal MeCN molecules also can be removed by heating under vacuum to give $Rh_2(pz)_4$.

X-ray studies. The structure of Rh_2(3,5-$Me_2pz)_4 \cdot 2MeCN$ is shown in Fig. 1; selected bond lengths and angles are given in Table 1. The molecule has a crystallographic centre of symmetry, but neglecting the acetonitriles, the Rh_2(3,5-$Me_2pz)_4$ unit has approximately D_{4h} symmetry. The Rh–Rh distance of 2.353(3) Å is slightly smaller than is common for Rh_2(carboxylate)$_4$ systems (2.386–2.403 Å),[1,2] even though the pyrazolate ligands can bridge metals much further apart than this.[6] There seems, therefore, to be very little weakening of the Rh–Rh system by the CH_3CN molecules, even

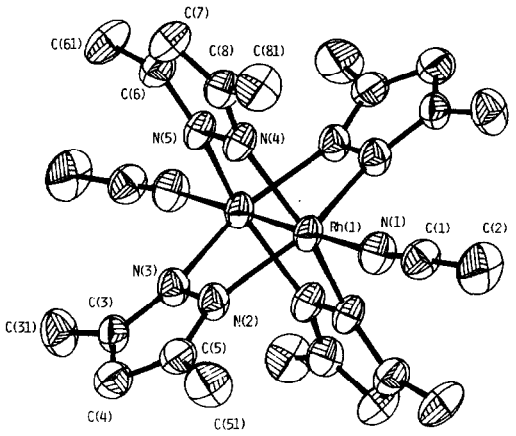


Fig. 1.

though the Rh–N distance of 2.202(5) Å is shorter than that in most axial N-bonded ligands.[8] The Rh–N(pyrazole) bond length of 2.055 and 2.064(5) Å are also slightly smaller than those found in the complex $[Rh(CO)(pz)PPh_3]_2$.[6]

Attempts to make tetra bridged species of other metals have so far been unsuccessful. Interaction of $Mo(CO)_6$, $Mo_2(O_2CMe)_4$, or the blue reduced ruthenium chloride solutions in methanol or tetrahydrofuran with 3,5-dimethylpyrazole or its sodium salt gave intractable products. From $Cu_2(O_2CMe_2)_4$ a deep red highly insoluble product was obtained but this could not be recrystallised.

Table 1. Selected bond lengths (Å) and angles (°) for Rh_2(3,5-$Me_2Pz)_4 \cdot 2MeCN$

N(1)–Rh(1)	2.202(5)	N(2)–Rh(1)	2.064(5)
N(3')–Rh(1)	2.056(5)	N(4)–Rh(1)	2.055(5)
N(5')–Rh(1)	2.050(5)	Rh(1)–Rh(1')	2.353(3)
C(1)–N(1)	1.131(6)	C(2)–C(1)	1.462(6)
N(3)–N(2)	1.378(5)	C(5)–N(2)	1.328(6)
C(3)–N(3)	1.332(6)	N(5)–N(4)	1.370(5)
C(8)–N(4)	1.337(6)	C(6)–N(5)	1.334(6)
C(4)–C(3)	1.380(7)	C(31)–C(3)	1.506(7)
C(5)–C(4)	1.402(7)	C(51)–C(5)	1.502(7)
C(7)–C(6)	1.381(7)	C(61)–C(6)	1.498(7)
C(7)–C(8)	1.389(6)	C(81)–C(8)	1.490(6)
N(1)–Rh(1)–N(2)	106.1(2)	N(2)–Rh(1)–N(4)	87.9(2)
N(1)–Rh(1)–N(4)	104.9(2)	N(2)–Rh(1)–N(5')	86.0(2)
N(1)–Rh(1)–N(3')	101.2(2)	N(3')–Rh(1)–N(4)	85.8(2)
N(1)–Rh(1)–N(5')	102.7(2)	N(3')–Rh(1)–N(5')	87.3(2)
Rh(1)–N(2)–N(3)	103.7(3)	N(2)–N(3)–Rh(1')	103.7(3)
Rh(1)–N(4)–N(5)	103.7(3)	N(4)–N(5)–Rh(1')	103.9(3)
Rh(1)–N(1)–C(1)	170.3(3)	N(1)–C(1)–C(2)	177.3(5)

Key to symmetry operations relating designated atoms to reference atoms at (x, y, z): (') 0.5-x, 0.5-y, 0.5-z.

Table 2. Analytical data for pyrazolato rhodium complexes

Compound	M.p. (°C)	Analysis (%)*		
		C	H	N
$Rh_2(3,5\text{-}Me_2pz)_4$	> 300	40.8 (40.9)	4.8 (4.8)	19.1 (19.1)
$Rh_2(3,5\text{-}Me_2pz)_4 \cdot 2MeCN$	156 dec.	42.9 (43.1)	5.1 (5.1)	21.2 (21.0)
$Rh_2(3,5\text{-}Me_2pz)_4 \cdot 2py$	135–137 dec.	47.6 (48.4)	5.2 (5.1)	18.8 (18.7)
$Rh_2(pz)_4$	> 300	31.0 (30.4)	2.6 (2.5)	24.1 (23.6)
$Rh_2(pz)_4 \cdot 2MeCN$	> 300 dec.	34.5 (34.5)	3.1 (3.2)	25.1 (25.2)
$Rh_2(O_2CMe)_4 \cdot 2(3,5\text{-}Me_2pzH)$	230 dec.	35.4 (34.1)	4.4 (4.4)	8.9 (8.9)

* Required values in parentheses.

EXPERIMENTAL

Microanalyses were by Imperial College and Pascher Laboratories. Melting points were determined in sealed capillaries and are uncorrected. IR spectra were recorded in the region 4000–200 cm^{-1} on a Perkin–Elmer 683 grating spectrometer in Nujol mulls, or on a Perkin–Elmer 983 spectrometer as a KBr disc. ^1H NMR spectra were recorded on a JEOL FX90Q spectrometer (δ values in ppm). Electrochemical studies employed a E.G. and G PAR 174A polarographic analyser and $^nBu_4NBF_4$ solution (0.20 mol dm^{-3}) in CH_2Cl_2 at room temperature and −78°C with Pt working and auxilliary electrodes, and a SCE reference electrode (against which ferrocene is oxidised at $E_{1/2}$ = +0.65 V). Electronic spectra were obtained on a Perkin–Elmer 551 spectrometer. Mass spectra, VG 7070. All manipulations were carried out under argon. Solvents were distilled and degassed before use.

Analytical data are given in Table 2.

1. *Tetra - μ - (3,5 - dimethylpyrazolato)dirhodium(II) bis(acetonitrile)*

To $Rh_2(O_2CMe)_4$ (0.98 g, 2.22 mmol) suspended in MeCN (100 cm^3) was added $Na(3,5\text{-}Me_2pz)$ (1.3 g, 11.02 mmol), either as a solid or in acetonitrile.

After refluxing for 3 h the solution became dark yellow with a white precipitate. The solution was filtered, and residual yellow solid being removed by washing with MeCN and filtered. The solvent was reduced in volume and cooled to give yellow crystals. Yield: 1.25 g, 85%.

Mass spectrum. *m/e*: 586 (M − 2MeCN); 96 ($3,5\text{-}Me_2pz$); 41 (MeCN).

^1H NMR (CD_2Cl_2). 5.207s [4-H(pz)]; 2.475s (CH_3CN); 2.144s [CH_3(pz)].

IR (KBr disc). 3103w, 2295w, 2263w, 1560w, 1522s, 1440s, 1261s, 1150m, 1085s, 1023s, 930m, 866w, 801s, 744s, 648w.

Electronic spectrum. 410 nm, $\varepsilon = 224$ dm^3 cm mol^{-1}.

2. *Tetra-μ-(3,5-dimethylpyrazolato)dirhodium(II)*

$Rh_2(3,5\text{-}Me_2pz)_4 \cdot 2MeCN$ (0.50 g) was heated under vacuum at 150 °C for several h whereupon the yellow solid gradually turned deep purple.

Mass spectrum. *m/e*: 586 (M^+); 96 ($3,5\text{-}Me_2pz$).

IR. 3098w, 1526s, 1440s, 1428m, 1262m, 1150w, 1089m, 1053m, 810m, 760m, 752s, 648w.

3. *Tetra - μ - (3,5 - dimethylpyrazolato)dirhodium(II) bis(pyridine)*

To a suspension of $Rh_2(3,5\text{-}Me_2pz)_4 \cdot 2MeCN$ (0.52 g, 0.88 mmol) in Et_2O (30 cm^3) was added excess pyridine. After 2 h the solution was filtered and the yellow solid dried. Yield: 0.14 g, 62%.

IR. 3082w, 1590s, 1518s, 1435s, 1410m, 1339m, 1228m, 1200s, 1080w, 1058s, 1040w, 1032w, 1000w, 753s, 740s, 710s, 650m, 621w.

4. *Tetra - μ - acetatodirhodium(II)bis(3,5 - dimethylpyrazole)*

To $Rh_2(O_2CMe)_4$ (0.99 g, 2.24 mmol) suspended in H_2O (100 cm^3) was added $Na(3,5\text{-}Me_2pz)$ (1.09 g, 11.4 mmol). The colour rapidly changed from blue/green to purple; on refluxing no further change occurred. The solid was filtered and dried. Yield: 1.20 g, 85%.

Mass spectrum. *m/e*: 442 (M-2 × 3,5-Me_2pz); 96 (3,5-Me_2pz); 60 (O_2CMe).

^{1}H NMR ($CDCl_3$). 6.181s [4-H(pz)]; 2.545s, (CH_3CO_2) 1.879s [CH_3(pz)].

IR. 3220br, 1600s, 1582s, 1560s, 1403m, 1336m, 1278msh, 1140w, 1162m, 1014m, 779m, 717m, 695m, 621w.

5. *Tetra-μ-pyrazolatodirhodium(II)bis acetonitrile*

$Rh_2(O_2CMe)_4$ (0.72 g, 1.63 mmol) was refluxed in MeCN (60 cm^3) with excess Na(pz) (0.63 g). The filtered solution was reduced to yield a fine yellow powder. Yield: 0.61 g, 68%.

^{1}H NMR ($CDCl_3$). 7.27br [3,5-H(pz)]; 6.063 br [4-H(pz)]; 2.081s (MeCN).

IR. 3100w, 2200m, 1560s, 1280m, 1195s, 1172m, 1065s, 972w, 945w, 920w, 845w, 749s, 631m, 440w.

Mass spectrum. *m/e*: 68 (pz); 41 (MeCN).

6. *Tetra-μ-pyrazolatodirhodium(II)*

$Rh_2(pz)_4 \cdot 2MeCN$ (0.40 g, 0.72 mmol) was heated under vacuum at 150°C for several h leaving a dark purple solid.

IR. 2100w, 1283m, 1195s, 1172m, 1060s, 970w, 947w, 920w, 865w, 750s, 631m, 437w.

X-ray crystallography

The crystal used was sealed under argon in a glass capillary. Unit cell and intensity data were obtained at 295 K using a Nonius CAD4 diffractometer, operating in the ω–2θ scan mode and using graphite monochromatized Mo-K_α radiation (λ = 0.71069 Å) in a manner previously described in detail.[10]

The structure was solved and refined via routine heavy atom procedures. Non-hydrogen atoms were refined anisotropically. Methyl hydrogen atoms were placed in idealised positions and the CH_3 groups refined as rigid bodies. The two pyrazolyl hydrogens on C(4) and C(7) were refined freely with isotropic thermal parameters.

Crystallographic data. $C_{24}H_{34}N_{10}Rh_2$, M = 668.41, tetragonal, $a = b = 16.730(1)$, c = 10.488(1) Å, space group $P4_2/n$, $Z = 4$, $D = 1.51$ g cm^{-1}, μ(Mo-K_α) = 10.4 cm^{-1}. Data recorded over $1.5 \leqslant \theta \leqslant 25.0$, giving 2580 unique and 1877 observed [$I > 1.5\sigma(I)$] data. $R = 0.0286$, $R_\omega = 0.0270$ for 191 parameters, with weights of $\omega = 1/[\sigma^2(F_o) + 0.0001(F_o)^2]$.

Final atomic parameters, full lists of bond lengths and angles and F_o/F_c values have been deposited as supplementary material with the Editor from whom copies are available on request. Atomic coordinates have also been deposited with the Cambridge Crystallographic Data Centre.

Acknowledgements—We thank the S.E.R.C. for a studentship (A.R.B.) and for the diffractometer, and Johnson Matthey PLC for the loan of rhodium.

REFERENCES

1. T. R. Felthouse, *Prog. Inorg. Chem.* 1982, **29**, 73; E. B. Boyar and S. D. Robinson, *Coord. Chem. Rev.* 1983, **50**, 109.
2. F. A. Cotton and R. A. Walton, *Multiple Bonds between Metal Atoms*. Wiley, New York (1982).
3. J. Telser and R. S. Drago, *Inorg. Chem.* 1984, **23**, 2599.
4. S. Trofimenko, *Chem. Rev.* 1971, **4**, 17.
5. (a) L. A. Oro, D. Carmona, M. P. Lamata, M. C. Apreda, C. Foces-Foces, F. H. Cano and P. M. Maitlis, *J. Chem. Soc., Dalton Trans.* 1984, 1823 (and references listed therein); (b) B. M. Lovie, S. J. Rettig, A. Storr and J. Trotter, *Can. J. Chem.* 1984, **62**, 1057.
6. R. Uson, L. A. Oro, M. A. Cirianno, M. T. Pinillos, A. Tiripicchio and M. Tiripicchio-Camellini, *J. Organomet. Chem.* 1981, **205**, 247.
7. S. May, P. Reinsalu and J. Powell, *Inorg. Chem.* 1980, **19**, 1582.
8. Y. B. Koh and G. G. Christoph, *Inorg. Chem.* 1978, **17**, 2590.
9. T. A. Stephenson, S. M. Morehouse, A. R. Powell, J. P. Heffer and G. Wilkinson, *J. Chem. Soc.* 1965, 3632.
10. M. B. Hursthouse, R. A. Jones, K. M. Abdul Malik and G. Wilkinson, *J. Am. Chem. Soc.* 1979, **101**, 4238.

Polyhedron Vol. 4, No. 6, pp. 1135–1139, 1985
Printed in Great Britain

0277–5387/85 $3.00 + .00
© 1985 Pergamon Press Ltd

SYNTHESIS AND CRYSTAL STRUCTURE OF THE COMPLEX $[MoW\{\mu\text{-}C_2(C_6H_4Me\text{-}4)_2\}(CO)_4(\eta\text{-}C_5H_5)\{\eta^5\text{-}C_9H_6(COMe)\text{-}1\}]$: AN UNUSUAL PRODUCT OF THE REACTION BETWEEN $[W(\equiv CC_6H_4Me\text{-}4)(CO)_2(\eta\text{-}C_5H_5)]$ AND $[MoMe(CO)_3(\eta^5\text{-}C_9H_7)]$

JOHN C. JEFFERY, JILL C. V. LAURIE and F. GORDON A. STONE*
Department of Inorganic Chemistry, The University of Bristol, Bristol BS8 1TS, U.K.

(*Received* 30 *November* 1984; *accepted* 18 *December* 1984)

Abstract—The compounds $[W(\equiv CC_6H_4Me\text{-}4)(CO)_2(\eta\text{-}C_5H_5)]$ and $[MoMe(CO)_3(\eta^5\text{-}C_9H_7)]$ (C_9H_7 = indenyl) react readily in toluene at 60°C to give the unusual dimetal complex $[MoW\{\mu\text{-}C_2(C_6H_4Me\text{-}4)_2\}(CO)_4(\eta\text{-}C_5H_5)\{\eta^5\text{-}C_9H_6(COMe)\text{-}1\}]$, which has been structurally characterised by an X-ray diffraction study. The metal–metal bond [2.976(1) Å] is transversely spanned by the alkyne ligand $C_2(C_6H_4Me\text{-}4)_2$, formed by coupling of two carbyne fragments. The tungsten atom carries a cyclopentadienyl ring and two carbonyl groups. The molybdenum atom also has two carbonyl ligands, one of which semi-bridges the Mo—W bond [Mo—C—O, 168.7(5)°]. Unexpectedly the indenyl group attached to the molybdenum centre carries a COMe substituent.

The alkylidyne–tungsten compounds $[W(\equiv CR)(CO)_2(\eta\text{-}C_5H_5)]$ (R = C_6H_4Me-4 or Me) are proving to be versatile reagents for the preparation of complexes containing bonds between tungsten and other transition elements.[1,2] As part of our studies in this area, two trimetal species with Mo—W bonds have been prepared. Thus treatment of $[Mo_2(CO)_4(\eta\text{-}C_5H_5)_2]$ with $[W(\equiv CC_6H_4Me\text{-}4)(CO)_2(\eta\text{-}C_5H_5)]$ affords the trimetallatetrahedrane cluster $[Mo_2W(\mu_3\text{-}CC_6H_4Me\text{-}4)(CO)_6(\eta\text{-}C_5H_5)_3]$,[3] while the reaction between the tolylmethylidynetungsten species and $[Mo(CO)_3(NCMe)_3]$ gives $[MoW_2(\mu\text{-}CC_6H_4Me\text{-}4)_2(\mu\text{-}CO)_2(CO)_4(\eta\text{-}C_5H_5)_2]$; a complex with a bent W—Mo—W spine.[4] No dimetal compounds with a Mo—W bond have as yet been obtained *via* reactions between the reagents $[W(\equiv CR)(CO)_2(\eta\text{-}C_5H_5)]$ and suitable organo-molybenum complexes. In an attempt to prepare such a complex, we investigated the reaction between $[MoMe(CO)_3(\eta^5\text{-}C_9H_7)]$ (C_9H_7 = indenyl) and $[W(\equiv CC_6H_4Me\text{-}4)(CO)_2(\eta\text{-}C_5H_5)]$ in the hope of obtaining a bridged-carbene species $[MoW\{\mu\text{-}C(C_6H_4Me\text{-}4)Me\}(\mu\text{-}CO)(CO)_4(\eta\text{-}C_5H_5)(\eta^5\text{-}C_9H_7)]$. In actuality the reaction followed an unexpected and unusual course, as described below. It may be mentioned that the sought for addition of a Mo—Me group across a W≡C bond was prompted by the observation that the complexes $[N(PPh_3)_2][WH(CO)_5]$ and $[W(\equiv CC_6H_4Me\text{-}4)(CO)_2(\eta\text{-}C_5H_5)]$ react to give the salt $[N(PPh_3)_2][W_2\{\mu\text{-}C(C_6H_4Me\text{-}4)H\}(CO)_7(\eta\text{-}C_5H_5)]$,[5] a process formally involving W—H addition to W≡C. The compound $[MoMe(CO)_3(\eta^5\text{-}C_9H_7)]$ was the reagent of choice in the present work, rather than $[MoMe(CO)_3(\eta\text{-}C_5H_5)]$, because indenyl-molybdenum compounds can react *via* an associative mechanism which is assisted by the transformation $Mo(\eta^5\text{-}C_9H_7) \rightarrow Mo(\eta^3\text{-}C_9H_7)$; this slippage creating a vacant site on the metal for attack by a substrate molecule.[6]

RESULTS AND DISCUSSION

The two compounds $[W(\equiv CC_6H_4Me\text{-}4)(CO)_2(\eta\text{-}C_5H_5)]$ and $[MoMe(CO)_3(\eta^5\text{-}C_9H_7)]$ did not react in toluene solution at ambient temperatures, but readily did so when heated to 60°C. Chromatography of the reaction mixture afforded some unreacted starting material, together with a red crystalline compound in *ca* 25% yield. The nature and structure of this product could not be deduced from the microanalytical and spectroscopic data, and hence a single-crystal X-ray diffraction study was undertaken. The results are summarised in Table 1, and the molecular structure is shown in Fig. 1.

* Author to whom correspondence should be addressed.

Table 1. Selected internuclear distances (Å) and angles (°) for [MoW{μ-$C_2(C_6H_4Me\text{-}4)_2$}$(CO)_4(\eta\text{-}C_5H_5)$\{$\eta^5$-$C_9H_6(COMe)$-1}] with estimated standard deviations in parentheses

W—Mo	2.976(1)	W—C(1)	1.982(7)
W—C(2)	1.996(5)	W—C(38)	2.157(5)
W—C(48)	2.190(5)	Mo—C(3)	1.958(5)
Mo—C(4)	1.943(6)	Mo—C(21)	2.314(5)
Mo—C(22)	2.314(5)	Mo—C(23)	2.380(5)
Mo—C(24)	2.517(5)	Mo—C(29)	2.453(5)
Mo—C(38)	2.227(5)	Mo—C(48)	2.169(5)
C(1)—O(1)	1.136(9)	C(2)—O(2)	1.142(7)
C(3)—O(3)	1.174(7)	C(4)—O(4)	1.151(8)
C(21)—C(5)	1.469(9)	C(5)—O(5)	1.221(6)
C(5)—C(6)	1.491(9)		
Mo—W—C(38)	48.3(1)	Mo—W—C(48)	46.7(1)
W—Mo—C(38)	46.3(1)	W—Mo—C(48)	47.2(1)
W—C(1)—O(1)	176.7(5)	W—C(2)—O(2)	175.7(6)
Mo—C(3)—O(3)	168.7(5)	Mo—C(4)—O(4)	176.9(5)
W—C(38)—Mo	85.5(1)	W—C(38)—C(48)	72.9(3)
Mo—C(38)—C(48)	69.5(3)	W—C(38)—C(31)	134.4(3)
Mo—C(38)—C(31)	133.1(4)	C(48)—C(38)—C(31)	135.6(5)
W—C(38)—Mo	86.1(2)	W—C(48)—C(38)	70.3(3)
Mo—C(48)—C(38)	74.1(3)	W—C(48)—C(41)	138.0(4)
Mo—C(48)—C(41)	130.1(3)	C(38)—C(48)—C(41)	132.6(4)
C(21)—C(5)—O(5)	120.6(5)	C(21)—C(5)—C(6)	118.8(5)
O(5)—C(5)—C(6)	120.6(6)		

The compound has a Mo—W bond which is transversely bridged by an alkyne ligand $C_2(C_6H_4Me\text{-}4)_2$. Thus the molecule has a dimetallatetrahedrane core [Mo—W 2.976(1), C(38)—C(48) 1.371(7) Å] of similar dimensions to those found in the species [$Mo_2(\mu\text{-}C_2Ph_2)(CO)_4(\eta\text{-}C_5H_5)_2$] [Mo—Mo 2.956(1), C—C 1.329(6) Å],[7] [$W_2(\mu\text{-}C_2H_2)(CO)_4(\eta\text{-}C_5H_5)_2$] [W—W 2.987(1), C—C 1.33(3) Å],[8] and [$W_2(\mu\text{-}C_2Et_2)(CO)_4$\{$\eta$-$C_5Et_4(C_6H_4Me\text{-}4)$\}$(\eta\text{-}C_5H_5)$] [W—W 3.003(1), C—C 1.361(14) Å].[9] Each metal centre is ligated by two CO groups, one of which [C(3)O(3)] semi-bridges the metal–metal bond [Mo—C(3)—O(3) 168.7(5)°]. This arrangement of the carbonyl ligands, with three terminally bound and one semi-bridging, is a common structural feature of alkyne-bridged di-molybdenum or -tungsten compounds, with the notable exception of [Mo_2\{μ-$C_2(SiMe_3)_2$\}$(CO)_4(\eta\text{-}C_5H_5)_2$].[10]

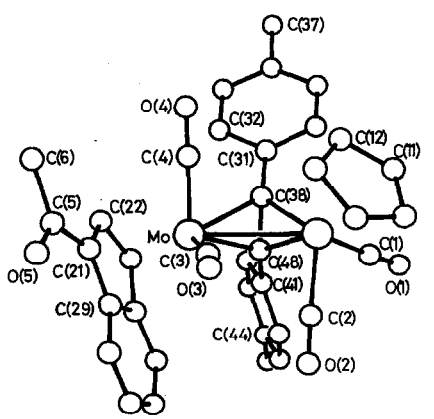


Fig. 1. Molecular structure of the complex [MoW{μ-$C_2(C_6H_4Me\text{-}4)_2$}$(CO)_4(\eta\text{-}C_5H_5)$\{$\eta^5$-$C_9H_6(COMe)$-1}] showing the atom numbering scheme.

The tungsten atom carries a C_5H_5 ligand, and the molybdenum an indenyl group. Surprisingly, however, the latter has an acyl substituent on C(21). Evidently the compound is formed from [$W(\equiv CC_6H_4Me\text{-}4)(CO)_2(\eta\text{-}C_5H_5)$] and [$MoMe(CO)_3(\eta\text{-}C_9H_7)$] *via* a complicated pathway. At some stage, the latter results in a coupling of two alkylidyne–tungsten fragments, to produce a μ-$C_2(C_6H_4Me\text{-}4)_2$ ligand. Many reactions of [$W(\equiv CC_6H_4Me\text{-}4)(CO)_2(\eta\text{-}C_5H_5)$] are now known involving coupling of tolylmethylidyne groups to give either the di-tungsten complex [W_2\{μ-$C_2(C_6H_4Me\text{-}4)$\}$(CO)_4(\eta\text{-}C_5H_5)_2$],[3,11] or cluster compounds containing a μ-$C_2(C_6H_4Me\text{-}4)_2$ ligand.[12] The stoicheiometry of formation of [MoW{μ-$C_2(C_6H_4Me\text{-}4)_2$}$(CO)_4(\eta\text{-}C_5H_5)$\{$\eta^5$-$C_9H_6(COMe)$-1}], however, also implies an unusual cleavage of a carbon–tungsten triple bond. Such a process is not without precedent, having

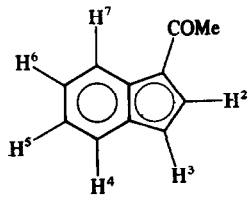
been observed previously in reactions between [W(≡CC_6H_4Me-4)$(CO)_2(\eta\text{-}C_5H_5)$] and the species [W(CO)(alkyne)$_3$],[9] and between [W(≡CC_6H_4Me-4)$(CO)_2(\eta\text{-}C_5H_5)$] and [$Et_3NH$][$Fe_3(\mu$-H)$(CO)_{11}$].[13]

The presence of the acyl-substituted indenyl ligand in [MoW{μ-$C_2(C_6H_4Me\text{-}4)_2$}$(CO)_4(\eta\text{-}C_5H_5)$\{$\eta^5$-$C_9H_6(COMe)$-1}] is surprising, and may imply a process in which [MoMe$(CO)_3(\eta^5\text{-}C_9H_7)$] is attacked by [W(≡$CC_6H_4$Me-4)$(CO)_2(\eta\text{-}C_5H_5)$] to generate an intermediate containing an Mo(COMe)$(\eta^5\text{-}C_9H_7)$ moiety, with the acyl ligand subsequently migrating to the C_9 ring, from which a hydrogen atom is lost. However, the observation[14] that the compound [Mo(COPh)$(CO)_3(\eta\text{-}C_5H_5)$] decarbonylates to give [$Mo_2(CO)_6(\eta\text{-}C_5H_5)(\eta\text{-}C_5H_4Ph)$], and not a product containing a η-C_5H_4(COPh) ligand, suggests that a Mo(COMe)$(\eta^5\text{-}C_9H_7)$ group if formed would release CO and afford a Mo$(\eta^5\text{-}C_9H_6Me)$ system, rather than Mo$\{\eta^5\text{-}C_9H_6(COMe)\}$. Transfer of a σ-bonded alkyl group from molybdenum to a ligated ring system is well established in the pyrolysis of [MoEt$(CO)_3(\eta\text{-}C_5H_5)$], a process which affords [$Mo_2(CO)_6(\eta\text{-}C_5H_4Et)_2$].[15]

Having established the molecular structure of [MoW{μ-$C_2(C_6H_4Me\text{-}4)_2$}$(CO)_4(\eta\text{-}C_5H_5)$\{$\eta^5$-$C_9H_6(COMe)$-1}] it was possible to interpret the spectroscopic data. Bands at 1981, 1921, and 1866 cm^{-1} are observed in the CO stretching region of the IR spectrum; that at 1866 cm^{-1} may be ascribed to the semi-bridging carbonyl ligand.[10] In the ^{1}H NMR spectrum, resonances are observed for the C_5H_5 (δ 5.24), COMe (δ 2.52) and Me-4 (δ 2.37 and 2.35) groups. The presence of the two inequivalent C_6H_4Me-4 substituents is revealed, not only by the two Me-4 signals, but by the presence of several resonances in the aromatic region of the spectrum. Thus an $(AB)_2$ quartet at δ 6.86 and 7.12 [J(AB) 8 Hz] integrates for one C_6H_4 fragment. A broad signal at δ 6.60 and a doublet at 7.04 [J(HH) 8 Hz] may be assigned to two protons of the other C_6H_4 unit; the remaining two protons of this group having their resonances hidden under others in the region. The $(AB)_2$ quartet is typical of a freely rotating μ-C—C_6H_4Me-4 group, but the pattern observed for the other C_6H_4 fragment suggests restricted rotation about a C—C_6H_4 axis, discussed further below, and as observed previously in [CoW{μ-σ:η^3-C(C_6H_4Me-4)C(Me)C(Me)H}$(\mu\text{-}CO)$(CO)$(\eta\text{-}C_5H_5)(\eta\text{-}C_5Me_5)$][$BF_4$].[16]

The signals for the η^5-C_9H_6 protons were assigned (Table 2) by selective homonuclear decoupling experiments. The chemical shift for H^7 is similar to that of the analogous proton in 1-acetyl and 1-formyl naphthalene.[17] Selective irradiation of the resonance at δ 8.37 decoupled the signal at δ 7.20 (H^6) to a doublet and simultaneously sharpened that at δ 6.96 (H^5). Similarly, selective irradiation of the peak at δ 5.89 reduced the triplet at δ 6.96 to a doublet, and also sharpened the signal at 7.20. As the resonances for H^4 and H^5 would be coupled to each other and H^5 would also be coupled to H^6, the peaks at δ 5.89 and 6.96 can be assigned to H^4 and H^5, respectively. This leaves the remaining resonances at δ 6.60 and 4.96 to be assigned to H^3 and H^2, respectively. The broadness of the signals for H^3 and H^4, as well as the resonances of one of the C_6H_4 groups, mentioned above, suggests that these two groups may be sterically interacting. This could lead to restricted rotation about C(48)—C(41); the C(41)—C(47) group being in proximity with the η^5-C_9H_6(COMe) ligand.

Table 2. ^{1}H NMR data for the η^5-C_9H_6(COMe)-1 ligand



Proton	δ* (ppm)
2	4.96 [d, J(H^2H^3) 4]
3	6.60 (br)
4	5.89 (br)
5	6.96 [t, J(H^4H^5) 8, J(H^6H^5) 8]
6	7.20 [t, J(H^5H^6) 8, J(H^7H^6) 8]
7	8.37 [d, J(H^6H^7) 8]

* Measured in CD_2Cl_2, coupling constants in Hz.

The molecule undergoes dynamic behaviour in solution, as revealed by the ^{13}C-{^{1}H} NMR spectrum which, when recorded at −50°C, shows four CO resonances (δ 233.5, 231.0, 215.9 and 209.8 ppm) but when measured at ambient temperatures shows two peaks for these groups. The mechanism of site-exchange of the CO ligands in di-molybdenum and -tungsten alkyne-bridged complexes has been discussed in detail elsewhere.[9,10]

EXPERIMENTAL

The complexes [W(≡CC_6H_4Me-4)$(CO)_2(\eta\text{-}C_5H_5)$][18] and [MoMe$(CO)_3(\eta^5\text{-}C_9H_7)$][19] were prepared by published methods. Solvents were rigorously dried before use, and all reactions were carried out in Schlenk tubes under oxygen-free nitrogen.

Alumina used in chromatography was BDH aluminium oxide (Brockman activity II). Light petroleum refers to that fraction, b.p. 40–60°C.

Reaction between the complexes $[MoMe(CO)_3(\eta^5\text{-}C_9H_7)]$ *and* $[W(\equiv CC_6H_4Me\text{-}4)(CO)_2(\eta\text{-}C_5H_5)]$

A toluene (30 cm^3) solution of $[W(\equiv CC_6H_4Me\text{-}4)(CO)_2(\eta\text{-}C_5H_5)]$ (0.41 g, 1 mmol) and $[MoMe(CO)_3(\eta^5\text{-}C_9H_7)]$ (0.31 g, 1 mmol) was heated at 60°C for 48 h in an evacuated Schlenk tube, fitted with a high pressure stopcock. Removal of solvent *in vacuo* gave a brown residue, which was dissolved in dichloromethane–light petroleum (1 : 1, *ca* 2 cm^3) and chromatographed on an alumina column (2 × 10 cm). Elution with the same solvent mixture afforded an orange band which contained an inseparable mixture of the two starting reagents. Further elution with dichloromethane gave a red eluate. Removal of solvent yielded a red powder which was crystallised from dichloromethane–light petroleum (1 : 3) to give red *crystals* of the complex $[MoW\{\mu\text{-}C_2(C_6H_4Me\text{-}4)_2\}(CO)_4(\eta\text{-}C_5H_5)\{\eta^5\text{-}C_9H_6(COMe)\text{-}1\}]\cdot CH_2Cl_2$ (0.18 g, 23%) (Found: C, 47.8; H, 3.3%. $C_{36}H_{28}MoO_5W\cdot CH_2Cl_2$ requires C, 49.0; H, 3.4%), m.p. 143–144°C, ν_{max}(CO) at 1981s, 1921s, 1914(sh) and 1866s cm^{-1} (in Nujol). NMR: ^1H (CD_2Cl_2), δ 2.35 (s, 3H, Me-4), 2.37 (s, 3H, Me-4), 2.52 (s, 3H, COMe), 5.24 (s, 5H, C_5H_5), for resonances due to η^5-C_9H_6 group see Table 2; $^{13}C\text{–}\{^1H\}$ (CD_2Cl_2—CH_2Cl_2, measured at −50°C), δ 233.5, 231.3, 215.9, 209.8 (CO), 195.8 (*C*OMe), 141.5, 139.5 [$C^1(C_6H_4)$], 136.7, 135.2 [$C^4(C_6H_4)$], 131.0, 129.2, 128.9, 128.5 [C^2 and $C^3(C_6H_4)$], 126.9, 126.3, 125.7, 122.4, 116.6, 113.5, 98.6, 92.0 (η-C_9H_6), 90.8 (η-C_5H_5), 88.3 (η-C_9H_6), 28.0 (CO*Me*), 21.4 and 21.3 ppm (Me-4).

Crystal structure determination for $[MoW\{\mu\text{-}C_2(C_6H_4Me\text{-}4)_2\}(CO)_4(\eta\text{-}C_5H_5)\{\eta^5\text{-}C_9H_6(COMe)\text{-}1\}]$

Crystals grow as red needles from dichloromethane–light petroleum. Diffracted intensities were collected at 200 K on a Nicolet *P3m* four-circle diffractometer using a crystal of dimensions *ca* 0.33 × 0.22 × 0.1 mm. Of the total 5622 reflections, measured to $2\theta \leqslant 50°$ (θ–2θ scans), 4527 had $I \geqslant 2.5\sigma(I)$, and only these were used in the refinement of the structure, after the data had been corrected for Lorentz, polarisation and X-ray absorption effects, the latter by an analytical absorption procedure.[20]

Crystal data. $C_{36}H_{28}MoO_5W\cdot CH_2Cl_2$, M = 905.3, monoclinic, a = 18.531(7), b = 10.368(4), c = 18.668(6) Å, β = 109.73(3)°, U = 3376(2) Å^3, space group $P2_1/c$, Z = 4, D_x = 1.78 g cm^{-3}, $F(000)$ = 1768, Mo-K_α X-radiation (graphite monochromator), $\bar{\lambda}$ = 0.71069 Å, μ(Mo-K_α) = 40.4 cm^{-1}.

The structure was solved by conventional heavy-atom and electron-density difference methods and was refined by blocked-cascade least squares. The asymmetric unit was also found to contain a well ordered dichloromethane molecule of crystallisation. All non-hydrogen atoms were given anisotropic thermal parameters and the cyclopentadienyl and aryl hydrogen atoms were included in calculated positions with isotropic thermal parameters *ca* 1.2 times U_{iso}(equiv.) of their parent carbon atoms. The methyl hydrogen atoms were also included in calculated positions and were given common refined thermal parameters. Refinement converged at R 0.029 (R_w 0.030) with a weighting scheme of the form $w = [\sigma^2(F_o) + 0.001|F_o|^2]^{-1}$ giving a satisfactory weight analysis. A final electron density difference synthesis showed no peaks > 1.2 e Å^{-3}. All computations were carried out on an Eclipse S230 (Data General) computer with the SHELXTL system of programs.[20] Atomic scattering factors, anomalous dispersion corrections and mass absorption coefficients were taken from Ref. 21. The atomic co-ordinates for this work are available on request from the Editor and have been deposited with the Cambridge Crystallographic Data Centre. Any request should be accompanied by the full literature citation for this paper.

REFERENCES

1. F. G. A. Stone, In *Inorganic Chemistry: Toward the 21st Century* (Edited by M. H. Chisholm), ACS Symposium Series 1983, **211**, 383; *Angew. Chem., Int. Ed. Engl.* 1984, **23**, 89.
2. U. Behrens and F. G. A. Stone, *J. Chem. Soc., Dalton Trans.* 1984, 1605; G. A. Carriedo, J. C. Jeffery and F. G. A. Stone, *J. Chem. Soc., Dalton Trans.* 1984, 1597; J. A. Abad, L. W. Bateman, J. C. Jeffery, K. A. Mead, H. Razay, F. G. A. Stone and P. Woodward, *J. Chem. Soc., Dalton Trans.* 1983, 2075.
3. M. Green, S. J. Porter and F. G. A. Stone, *J. Chem. Soc., Dalton Trans.* 1983, 513.
4. G. A. Carriedo, J. A. K. Howard, K. Marsden, F. G. A. Stone and P. Woodward, *J. Chem. Soc., Dalton Trans.* 1984, 1589.
5. D. Hodgson, J. A. K. Howard, F. G. A. Stone and M. J. Went, *J. Chem. Soc., Dalton Trans.* (in press).
6. C. White and R. J. Mawby, *Inorg. Chim. Acta* 1970, **4**, 261; C. White, R. J. Mawby and A. J. Hart-Davis, *Inorg. Chim. Acta* 1970, **4**, 441; D. J. Jones and R. J. Mawby, *Inorg. Chim. Acta* 1972, **6**, 157.
7. W. I. Bailey, M. H. Chisholm, F. A. Cotton and L. A. Rankel, *J. Am. Chem. Soc.* 1978, **100**, 5764.
8. D. S. Ginley, C. R. Bock, M. S. Wrighton, B. E. Fischer,

D. L. Tipton and R. Bau, *J. Organomet. Chem.* 1978, **157**, 41.
9. G. A. Carriedo, J. A. K. Howard, D. B. Lewis, G. E. Lewis and F. G. A. Stone, *J. Chem. Soc., Dalton Trans.* (in press).
10. J. A. Beck, S. A. R. Knox, R. F. D. Stansfield, F. G. A. Stone, M. J. Winter and P. Woodward, *J. Chem. Soc., Dalton Trans.* 1982, 195.
11. M. Green, J. C. Jeffery, S. J. Porter, H. Razay and F. G. A. Stone, *J. Chem. Soc., Dalton Trans.* 1982, 2475.
12. L. Busetto, J. C. Jeffery, R. M. Mills, F. G. A. Stone, M. J. Went and P. Woodward, *J. Chem. Soc., Dalton Trans.* 1983, 101; L. Busetto, M. Green, B. Hessner, J. A. K. Howard, J. C. Jeffery and F. G. A. Stone, *J. Chem. Soc., Dalton Trans.* 1983, 519.
13. M. Green, K. Marsden, I. D. Salter, F. G. A. Stone and P. Woodward, *J. Chem. Soc., Chem. Commun.* 1983, 446.
14. A. N. Nesmeyanov, L. G. Makarova, N. A. Ustynyuk and L. V. Bogatyreva, *J. Organomet. Chem.* 1972, **46**, 105.
15. J. A. McCleverty and G. Wilkinson, *J. Chem. Soc.* 1963, 4096.
16. J. C. Jeffery, I. Moore, H. Razay and F. G. A. Stone, *J. Chem. Soc., Dalton Trans.* 1984, 1581.
17. J. W. Emsley, J. C. Lindon, S. R. Salman and D. T. Clark, *J. Chem. Soc., Perkin Trans.* 2, 1973, 611.
18. E. O. Fischer, T. Selmayr, F. R. Kreissl and U. Schubert, *Chem. Ber.* 1977, **110**, 2574; E. O. Fischer, T. L. Lindner, G. Huttner, P. Friedrich, F. R. Kreissl and J. O. Besenhard, *Chem. Ber.* 1977, **110**, 3397.
19. R. B. King and M. B. Bisnette, *Inorg. Chem.* 1965, **4**, 475.
20. G. M. Sheldrick, *SHELXTL Programs for Use with the Nicolet X-ray System*, Cambridge (1976); updated Göttingen (1981).
21. *International Tables for X-ray Crystallography*, Vol. 4. Kynoch Press, Birmingham (1974).

Polyhedron Vol. 4, No. 6, pp. 1141–1142, 1985
Printed in Great Britain

0277–5387/85 $3.00 + .00
Pergamon Press Ltd

SLOW DIMERIZATION OF ISOPROPOXYBERYLLIUM TETRAISOPROPOXYALUMINATE

R. C. MEHROTRA* and M. AGGRAWAL
Chemical Laboratories, University of Rajasthan, Jaipur 302004, India

(*Received* 2 *July* 1984; *accepted after revision* 18 *December* 1984)

Abstract—An interesting dimerization behaviour has been observed in the freshly distilled monomeric isopropoxy beryllium tetra-isopropoxyaluminate on standing.

The association of metal alkoxides (although subject to steric factors, i.e. size of the metal atom and the nature of the alkyl group) is generally quite facile,[1] but in border-line cases it could be rather slow. For example, freshly distilled trimeric aluminium isopropoxide has been shown[2] to change to the tetrameric form on being allowed to stand (age) for a few days; further association does occur but is comparatively far slower[3] (~ by an order of 2).

Another instance of a similar ageing effect has been observed recently in the case of isopropoxyberyllium tetraisopropoxyaluminate,[4]

$$[(Pr^iO)Be(\mu\text{-}OPr^i)_2Al(OPr^i)_2],$$

which can be distilled (b.p. 156°C/0.3 mm) unchanged and the freshly distilled product shows a molecular weight (347) corresponding to the above formula (332) in chloroform (by ebullioscopic measurements). The above product on being allowed to age in the neat form for a few days at ambient temperatures (~ 20°C) dimerizes to

$$[(Pr^iO)_2Al(\mu\text{-}OPr^i)_2Be(\mu\text{-}OPr^i)_2Be(\mu\text{-}OPr^i)_2Al(OPr^i)_2],$$

which is sufficiently stable to show a dimeric molecular weight (~ 678) in refluxing chloroform. The proton magnetic resonance spectra (Fig. 1) of the two forms lend support to the suggested structures of the two derivatives.

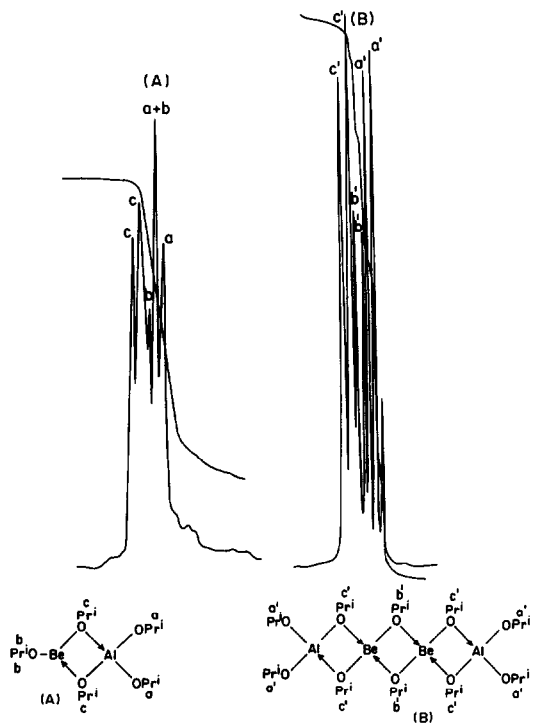


Fig. 1. PMR spectra of methyl protons of $[Pr^iOBe\{Al(OPr^i)_4\}]$ at 90 MHz. (A) Freshly distilled. (B) Aged samples.

Although a 3-coordinated environment around beryllium in some tertiary butoxide derivatives has been previously proposed,[5,6] the stability (cf., the corresponding analogues of Mg, Zn, Cd, and Hg could not be isolated) and rather slow dimerization of $[(Pr^iO)Be\{Al(OPr^i)_4\}]$ may be assigned to steric factors and the strong tendency of beryllium to attain a 4-coordinated state; the same has been exploited in the synthesis of a number of stable volatile termetallic alkoxides, e.g. $[(Pr^iO)_4Nb(\mu\text{-}OPr^i)_2Be(\mu\text{-}OPr^i)_2Al(OPr^i)_2]$, for the first time.[7]

* Author to whom correspondence should be addressed.

REFERENCES

1. D. C. Bradley, R. C. Mehrotra and D. P. Gaur, *Metal Alkoxides*. Academic Press, London (1978).

2. R. C. Mehrotra, *J. Ind. Chem. Soc.* 1953, **30**, 585.
3. R. C. Mehrotra (unpublished results).
4. M. Aggrawal and R. C. Mehrotra, *Synth. React. Inorg. Met.–Org. Chem.* 1983, **13**, 571.
5. G. E. Coates and A. H. Fishwrick, *J. Chem. Soc. A* 1968, 477.
6. H. M. M. Schearer, C. B. Spencer and J. Twiss, Unpublished results quoted by N. A. Bell in *Comprehensive Organometallic Chemistry* (Edited by G. Wilkinson, F. G. A. Stone and E. W. Abel), p. 135. Pergamon Press, Oxford (1982).
7. M. Aggrawal and R. C. Mehrotra, *Polyhedron* 1985, **4**, 845.

Polyhedron Vol. 4, No. 6, pp. 1143–1145, 1985
Printed in Great Britain

0277-5387/85 $3.00 + .00
© 1985 Pergamon Press Ltd

KINETICS OF THE AQUATION OF *CIS*-CHLOROCYANOBIS(2,2′-BIPYRIDINE)COBALT(III) AND *CIS*-CHLOROCYANOBIS(1,10-PHENANTHROLINE)COBALT(III) CATIONS

GAETANO SCHIAVON* and FULVIA MARCHETTI
Istituto Chimico "G. Ciamician", Università di Bologna, Italy

(*Received* 27 *July* 1984; *accepted* 5 *January* 1985)

Abstract—We have studied the kinetics of aquation of *cis*-chlorocyanobis(2,2′-bipyridine)Co(III), and *cis*-chlorocyanobis(1,10-phenanthroline)Co(III) cations, and determined activation parameters, in order to compare the labilities of these cations with the lability of the analogous compounds containing ethylenediamine and other non-participating ligands such as Cl^- and NO_2^-.

We have studied the kinetics of the equation of complexes *cis*-$[Co(bpy)_2(CN)Cl]^+$ and *cis*-$[Co(phen)_2(CN)Cl]^+$, and we have determined the activation parameters to compare the labilities of the chlorocyano complexes containing the two aromatic α-diimines with the lability of the analogous ethylenediamine containing complex.

We have therefore completed the kinetic data collected by Palade *et al.*[1] about the series of compounds of the type *cis*-$[Co(N–N)_2(A)Cl]^+$ where N–N = ethylenediamine (en), 2,2′-bipyridine (bpy), and 1,10-phenanthroline (phen), in order to find out or to exclude a *trans*-labilizing effect of the chelate on the labile ligand Cl^-.

Aquation kinetic studies were carried out by determination of the values of specific conductivity on 5×10^{-3} M solution of the complex, at variable ionic strength. To calculate the values of the first-order rate constants we used the differential method of Guggenheim.

The preparation of *cis*-$[Co(bpy)_2(CN)Cl]^+$ has been described elsewhere,[2] while the preparation of *cis*-$[Co(phen)_2(CN)Cl]^+$ together with preparations of corresponding aquocyano complexes are till now unpublished results. The aquocyano complexes retain the *cis* configuration, since the impossibility of the *trans* form[3] has been shown for all Co(III) complexes containing bpy or phen, due to steric hindrance.

In Table 1 are reported the values of the first-order rate constants and activation parameters of the aquation reactions of two chlorocyano complexes containing bpy or phen, determined in the temperature range 60–90°C. The dependence of the rate constant on the absolute temperature satisfies the Eyring equation. From these data we have calculated the first-order rate constants of aquation at 25°C, which are: $(1.6 \pm 0.9) \times 10^{-7}$ s^{-1}, and $(2.7 \pm 0.5) \times 10^{-7}$ s^{-1} for *cis*-$[Co(bpy)_2(CN)Cl]^+$ and for *cis*-$[Co(phen)_2(CN)Cl]^+$ respectively.

In Table 2 are reported the values of the first-order rate constants and of activation parameters of three chlorocyano complexes containing en, phen, and bpy respectively. While the rate constants are of the same magnitude, activation parameters are different. In particular the value of ΔH^* for the ethylenediamine containing complex is higher than the ΔH^* values of the two analogous complexes containing the aromatic α-diimines. On the other hand the ΔS^* values of the last two complexes are more negative than the value of the first one. This indicates a more associative character in the aquation mechanism for the complexes containing phen or bpy, π-electron acceptor ligands like the cyano-group, respectively in *trans* and in *cis* position to the leaving group.

The same conclusion may be drawn from the data reported in Table 3 for the corresponding aquation of chloronitro complexes. Here we find *k* values of the same magnitude again, but greater difference between ΔH^* and ΔS^* corresponding to aromatic α-diimines containing complexes on the one hand and ethylenediamine containing complex on the other.

* Author to whom correspondence should be addressed.

Table 1. First-order rate constants, and activation parameters of aquation reactions of *cis*-$[Co(N–N)_2(CN)Cl]^+$ (N–N = 2,2′-bipyridine and 1,10-phenanthroline)

Complexes	t °C	10^5K s^{-1}	ΔH^* kcal mol^{-1}	ΔS^* cal K^{-1} mol^{-1}
cis-$[Co(bpy)_2(CN)Cl]^+$	60	0.72±0.03	21.6±0.4	−17.4±0.1
	70	1.90±0.08		
	80	4.90±0.20		
	90	11.80±0.50		
cis-$[Co(phen)_2(CN)Cl]^+$	60	1.26±0.15	19.9±0.1	−21.8±0.3
	70	2.32±0.15		
	80	6.43±0.43		
	90	13.30±0.12		

Table 2. First-order rate constants, and activation parameters of aquation reactions of *cis*-$[Co(N–N)_2(CN)Cl]^+$ (N–N = ethylenediamine, 2,2′-bipyridine, and 1,10-phenanthroline) at 25°C

Complexes	10^7K s^{-1}	ΔH^* kcal mol^{-1}	ΔS^* cal K^{-1} mol^{-1}	Ref.
cis-$[Co(en)_2(CN)Cl]^+$	6.2	24.6	−5.0	4
cis-$[Co(phen)_2(CN)Cl]^+$	2.7	19.9	−21.8	This work
cis-$[Co(bpy)_2(CN)Cl]^+$	1.6	21.6	−17.4	This work

Table 3. First-order rate constants, and activation parameters of aquation reactions of *cis*-[Co $(N–N)_2(NO_2)Cl]^+$ (N–N = ethylenediamine, 2,2′-bipyridine, and 1,10-phenanthroline) at 25°C

Complexes	10^4K s^{-1}	ΔH^* kcal mol^{-1}	ΔS^* cal K^{-1} mol^{-1}	Ref.
cis-$[Co(bpy)_2(NO_2)Cl]^+$	2.5	14.9	−24.9	1
cis-$[Co(phen)_2(NO_2)Cl]^+$	1.3	16.0	−22.6	4
cis-$[Co(en)_2(NO_2)Cl]^+$	1.1	21.8	−3.0	6

Table 4. First-order rate constants, and activation parameters of aquation reactions of *cis*-$[Co(N–N)_2Cl_2]^+$ (N–N = ethylenediamine, 2,2′-bipyridine, and 1,10-phenanthroline) at 25°C

Complexes	10^5K s^{-1}	ΔH^* kcal mol^{-1}	ΔS^* cal K^{-1} mol^{-1}	Ref.
cis-$[Co(en)_2Cl_2]^+$	25.0	22.0	−3.0	7
cis-$[Co(bpy)_2Cl_2]^+$	10.0	21.4	3.1	8
cis-$[Co(phen)_2Cl_2]^+$	6.8	23.7	9.9	9

Values of K, ΔH^*, and ΔS^* reported in Table 4 for dichloro complexes containing respectively en, phen, and bpy, point out, instead, the dissociative character of the aquation's mechanism, due to the presence *cis* to the leaving group of one chloride ion σ and π-donor ligand.

Finally the examination of the values of the first-order rate constants reported in Tables 2, 3, and 4 shows that also with the two chlorocyano complexes containing phen or bpy is verified the rate reducing effect of the cyano-group in respect of the *cis* leaving ligand, made evident by Tobe[4] in the aquation reaction of *cis*-$[Co(en)_2(CN)Cl]^+$. From this examination we can however exclude a *trans*-labilizing effect of the aromatic α-diimines.

REFERENCES

1. D. M. Palade, T. N. Volokh, G. V. Chudaeva and E. G. Saakyan, *Russ. J. Inorg. Chem.* 1975, **20**, 400 (and references therein).
2. G. Schiavon and F. Marchetti, *Polyhedron* (to be published).

3. E. C. Niederhoffer, A. E. Martell, P. Rudolf and C. Clearfield, *Inorg. Chem.* 1982, **21**, 3734.
4. M. L. Tobe and C. K. Williams, *Inorg. Chem.* 1976, **15**, 918.
5. D. M. Palade and T. N. Volokh, *Russ. J. Inorg. Chem.* 1972, **17**, 1960.
6. C. K. Ingold, R. S. Nyholm and M. L. Tobe, *Nature* 1960, **187**, 477.
7. R. G. Pearson, C. R. Boston and F. Basolo, *J. Phys. Chem.* 1955, **59**, 304.
8. D. M. Palade, T. N. Volokh, G. V. Chudaeva, L. Z. Khavina and E. A. Chebysheva, *Russ. J. Inorg. Chem.* 1970, **15**, 1399.
9. D. M. Palade and M. K. Boreiko, *Russ. J. Inorg. Chem.* 1968, **11**, 1556.

Polyhedron Vol. 4, No. 6, pp. 1147–1148, 1985
Printed in Great Britain

0277-5387/85 $3.00 + .00
© 1985 Pergamon Press Ltd

COMMUNICATION

TITANIUM NMR SPECTROSCOPY: A COMMENT ON SOME RECENT ASSIGNMENTS

MICHAEL J. McGLINCHEY*
Department of Chemistry, McMaster University, Hamilton, Ontario, L8S 4M1, Canada

and

DOUGLAS G. BICKLEY*
Department of Chemistry, Mount Allison University, Sackville, New Brunswick, E0A 3C0, Canada

(*Received* 26 *November* 1984; *accepted* 6 *February* 1985)

Abstract—The recently reported ^{47}Ti and ^{49}Ti NMR chemical shift data for Cp_2TiX_2 are reassigned. Arguments based on absolute frequencies and relaxation time data show that the ^{49}Ti peak is always 266 ppm higher frequency than its corresponding ^{47}Ti resonance.

The recent claim[1] to have made the "first NMR observations of the ^{47}Ti and ^{49}Ti nuclei in cyclopentadienyl complexes" prompts us to offer some relevant comments. The statement is made that "the ^{49}Ti resonance exhibits a shielding effect of *ca* 266 ppm relative to the ^{47}Ti signal which, furthermore, always gives the most narrow bandwidth". There then follows a listing of chemical shifts in which the broader peak at higher field (lower frequency) is consistently assigned to the ^{49}Ti nucleus. This assignment is somewhat surprising since the absolute frequencies for $TiCl_4$ (quoted[2] such that the protons in tetramethylsilane resonate at exactly 100 MHz) are $\Xi(^{49}Ti) = 5{,}644{,}259 \pm 10$ and $\Xi(^{47}Ti) = 5{,}642{,}757 \pm 10$ Hz, with the ratio $\Xi(^{49}Ti/\Xi(^{47}Ti) = 1.000266$, a value in excellent accord with previous determinations.[3,4] In short, the ^{49}Ti resonance will always be 266 ppm higher frequency (lower field) than the corresponding ^{47}Ti for the same chemical environment.

The mis-assignment is perhaps understandable since the peak heights are always such that the less shielded (higher frequency) ^{49}Ti peak is the sharper and taller despite the relative abundances (^{49}Ti; 5.51%: ^{47}Ti; 7.28%). However the crucial factor is the relative broadness of the peaks. The peak width at half-height, $W_{1/2}$, is given by:

$$W_{1/2} = \frac{3\pi}{10} \cdot \left(\frac{2I+3}{I^2(2I-1)}\right)\left(1+\frac{\eta^2}{3}\right)\left(\frac{e^2qQ}{h}\right)^2 \tau_c,$$

where I is the nuclear spin, eQ is the nuclear electric quadrupole moment, eq is the electric field gradient and η is the asymmetry parameter which describes the deviation from cylindrical symmetry; τ_c is the correlation time characterising the fluctuation of the electric field. Thus, for molecular systems differing only in the identity of the metal isotope, $W_{1/2}$ varies only with Q and I. Now, for ^{47}Ti, $Q = 0.29 \times 10^{-28}$ m^2 and $I = 5/2$: for ^{49}Ti, $Q = 0.24 \times 10^{-28}$ m^2 and $I = 7/2$.[5] The $f(I)$ terms are 8/25 for the former and 20/147 for the latter. Hence, the nucleus with the *larger* spin gives rise to the narrower lines by a factor of 3.43. It is clear, therefore, that in titanium NMR spectroscopy the less shielded and sharper peak is attributable to the ^{49}Ti resonance.

With this correction, the chemical shift values reported for the series of cyclopentadienyl titanium halide complexes match closely the data already reported on these same complexes by two other groups of workers.[2,6]

* Authors to whom correspondence should be addressed.

REFERENCES

1. A. Dormond, M. Fauconet, J. C. LeBlanc and C. Moise, *Polyhedron* 1984, **3**, 897.
2. N. Hao, B. G. Sayer, G. Dénès, D. G. Bickley, C. Detellier and M. J. McGlinchey, *J. Magn. Reson.* 1982, **50**, 50.
3. C. D. Jeffries, *Phys. Rev.* 1953, **92**, 1262.
4. L. E. Drain and G. W. West, *Philos. Mag.* 1965, **12**, 1061.
5. *Handbook of Chemistry and Physics*, 52nd edn, B-258. Chemical Rubber Co., Cleveland, 1971–1972.
6. P. G. Gassman, W. H. Campbell and D. W. Macomber, *Organometallics* 1984, **3**, 385.

Polyhedron Vol. 4, No. 6, pp. 1149–1150, 1985
Printed in Great Britain

0277–5387/85 $3.00 + .00
© 1985 Pergamon Press Ltd

COMMUNICATION

REINVESTIGATION OF A TRANSMETALLATION SYNTHESIS OF BIS(CYCLOPENTADIENYL)SAMARIUM(II) AND FORMATION OF A NEW SOLUBLE CYCLOPENTADIENYLSAMARIUM(II) COMPOUND

G. B. DEACON,* G. N. PAIN and T. D. TUONG
Chemistry Department, Monash University, Clayton, Victoria 3168, Australia

(*Received* 28 *January* 1985; *accepted* 12 *February* 1985)

Abstract—The transmetallation reaction between $(C_5H_5)_2Hg$ and activated samarium metal in tetrahydrofuran (thf)/ether did not give $(C_5H_5)_2Sm(thf)_2$ but $(C_5H_5)_3Sm(thf)$, whilst reduction of the last compound with potassium in thf gave $KSm(C_5H_5)_3$, a soluble organosamarium(II) complex.

There is currently great interest in the synthesis of soluble divalent organolanthanide complexes, which have potential in catalyst systems utilising the M(III)/M(II) couple,[1] and are useful as reductants in the synthesis of lanthanide(III) organometallics[2] and in organic synthesis.[3] Soluble isolable organosamarium(II) compounds are of special value since samarium(II) is a more powerful reductant than europium(II) or ytterbium(II).[4] Pseudo-Grignard reagents RSmI have been shown to contain large amounts of samarium(III)[5] and the oxidation state in recently prepared thiophen-2-ylsamarium iodide and C_6F_5SmBr[6] has not been established nor have the compounds been isolated. Both $(\eta\text{-}C_5Me_5)_2Sm(thf)_2$[7] and $(\eta\text{-}C_5Me_5)_2Sm$[8] have been isolated and are soluble. However, $(C_5H_5)_2Sm(thf)$[9] and $(C_5H_5)_2Sm(thf)_2$[10] have low solubilities, the latter being reported to leave a colourless solution on deposition from tetrahydrofuran (thf). However, in a recent synthesis from $(C_5H_5)_2Hg$ and activated (by transmetallation with mercuric chloride[11]) samarium metal,[12,13] it was claimed that $(C_5H_5)_2Sm(thf)_2$ was isolated from solution.[13] The oxidation state of the final product is also surprising, since we have shown that the transmetallation between thallous cyclopentadienide and samarium gives $(\eta\text{-}C_5H_5)_3Sm(thf)$ even when an excess of activated samarium metal is used.[14] We now report a reinvestigation of the transmetallation with $(C_5H_5)_2Hg$ and the synthesis of a new soluble and isolable organosamarium(II) compound by reduction of $(\eta\text{-}C_5H_5)_3Sm(thf)$ with potassium.

On reaction of $(C_5H_5)_2Hg$ with activated samarium in thf/ether under the reported conditions [only 0.033 g $(C_5H_5)_2Hg$; 0.075 g Sm used], a yellow solution indicative[14] of $(\eta\text{-}C_5H_5)_3Sm$ [cf. purple and insoluble for $(C_5H_5)_2Sm(thf)_{1\text{ or }2}$[9,10]] was obtained. Filtration to remove excess samarium and mercury and evaporation gave $(\eta\text{-}C_5H_5)_3Sm(thf)$ in approximately quantitative yield. When the reaction was repeated on a more realistic scale [0.50 g $(C_5H_5)_2Hg$; 1.13 g Sm], the trivalent complex was isolated in 88% yield. The compound was identified by its highly characteristic[14] visible/near-IR spectrum. Single crystals grown from thf had an identical microscopic appearance to those (from C_5H_5Tl and Sm) characterized crystallographically.[14] Thus only reaction (1) occurs:

$$3(C_5H_5)_2Hg + 2Sm \rightarrow 2(C_5H_5)_3Sm + 3Hg\downarrow \quad (1)$$

Reduction of $(\eta\text{-}C_5H_5)_3Sm(thf)$ with potassium metal in thf containing a trace of benzophenone gave a purple insoluble solid. This is similar to precipitation of $(C_5H_5)_2Sm(thf)$ when potassium naphthalenide is used as the reductant.[9] After washing with hot thf to remove unreacted $(\eta\text{-}C_5H_5)_3Sm(thf)$ and benzophenone, extraction of the residue with 1,2-dimethoxyethane (dme), filtration and evaporation gave $KSm(C_5H_5)_3$ as a pyrophoric purple solid in 85–90% yield. Qualitative tests and electron microprobe analysis indicated the presence of potassium, and the composition was established by analysis (C, H, K, Sm). The visible/near-IR spectrum in dme, $\lambda_{max}(\varepsilon)$ 370(354), 400(300)

* Author to whom correspondence should be addressed.

and 498(216) nm, was featureless from 500 to 1500 nm, conclusively eliminating samarium(III) species.[5,15,16] On exposure of the purple solution to air, it rapidly turned yellow and the spectrum (λ_{max} 410, 598, 952, 973, 1080, 1098, 1232, 1255, 1268, 1471 and 1538 nm) indicated oxidation to samarium(III). The IR spectrum showed only absorptions attributable to cyclopentadiene, confirming the absence of thf or dme molecules. Although the complex crystallized in what appeared to be clusters of single crystals which were homogeneous on microscopic examination, no X-ray diffraction pattern could be obtained. Further attempts are being made to obtain crystals suitable for a structure determination. The reducing power of the compound can be seen in reduction of mercury and thallium salts and tetraethyllead to the corresponding metals and the synthetic potential of these reactions is being examined.

Acknowledgements—We are grateful to the Australian Research Grants Scheme for support, to Monash University for a Post-Doctoral Fellowship (G.N.P.), to Dallas Wilkinson for X-ray measurements, and to Adrian van den Bergen and Robyn Elliott for electron microprobe measurements.

REFERENCES

1. W. J. Evans, I. Bloom, W. E. Hunter and J. L. Atwood, *J. Am. Chem. Soc.* 1983, **105**, 1401.
2. G. B. Deacon, G. D. Fallon, P. I. MacKinnon, R. H. Newnham, G. N. Pain, T. D. Tuong and D. L. Wilkinson, *J. Organomet. Chem.* 1984, **277**, C21.
3. G. B. Deacon and P. I. MacKinnon, *Tetrahedron Lett.* 1984, **25**, 783.
4. F. A. Cotton and G. Wilkinson, *Advanced Inorganic Chemistry*, 4th edition, Chap. 23. Wiley, New York (1980).
5. D. F. Evans, G. V. Fazakerley and R. F. Phillips, *J. Chem. Soc. (A)* 1971, 1931.
6. O. P. Syutkina, L. F. Rybakova, E. S. Petrov and I. P. Beletskaya, *J. Organomet. Chem.* 1985, **280**, C67.
7. W. J. Evans, I. Bloom, W. E. Hunter and J. L. Atwood, *J. Am. Chem. Soc.* 1981, **103**, 6507.
8. W. J. Evans, L. A. Hughes and T. P. Hanusa, *J. Am. Chem. Soc.* 1984, **106**, 4270.
9. G. W. Watt and E. W. Gillow, *J. Am. Chem. Soc.* 1969, **91**, 775.
10. J. L. Namy, P. Girard, H. B. Kagan and P. E. Caro, *Nouv. J. Chim.* 1981, **5**, 479.
11. G. B. Deacon and A. J. Koplick, *Inorg. Nucl. Chem. Lett.* 1979, **15**, 263.
12. G. Z. Suleimanov, L. F. Rybakova, Ya. A. Nuriev, T. Kh. Kurbanov and I. P. Beletskaya, *J. Organomet. Chem.* 1982, **235**, C19.
13. G. Z. Suleimanov, T. Kh. Kurbanov, Ya. A. Nuriev, L. F. Rybakova and I. P. Beletskaya, *Dokl. Chem.* 1982, **265**, 254.
14. G. B. Deacon, A. J. Koplick and T. D. Tuong, *Aust. J. Chem.* 1984, **37**, 517.
15. G. B. Deacon, A. J. Koplick, W. D. Raverty and D. G. Vince, *J. Organomet. Chem.* 1979, **182**, 121.
16. D. C. Stewart and D. Kato, *Anal. Chem.* 1958, **30**, 164.

Polyhedron Vol. 4, No. 7, pp. 1151–1154, 1985
Printed in Great Britain

0277–5387/85 $3.00 + .00
Pergamon Press Ltd

REACTIONS OF PHOSPHORUS TRICHLORIDE WITH SCHIFF BASES

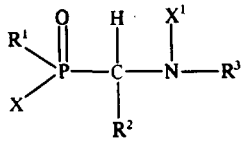
R. P. NARAIN* and MAHTAB Z. SIDDIQUI
Department of Chemistry, University of Gorakhpur, Gorakhpur—273001, India

(*Received* 6 *December* 1983; *accepted after revision* 9 *May* 1984)

Abstract—The reactions of Schiff bases with phosphorus trichloride in the medium of acetone containing pyridine are facile and compounds of the types $RC(PCl_2)=NR'$ and $[RC(PCl_2)=N]_2C_6H_4$ have been prepared.

Much work has been done on the reaction of Schiff bases with silicon tetraacetate,[1] triethylsilane[2] and phosphorus(III) acid chlorides.[3] Singh and Tandon[1] have reported the formation of complexes by the reaction of $Si(OAc)_4$ and bifunctional polydentate ligands.

The reaction of triethylsilane with aromatic azomethines was reported by Andrianov *et al.*[2] Nurtdinov *et al.*[3] have carried out the reaction between phosphinous chlorides and Schiff bases and have reported the formation of phosphinic ester, acids or even tertiary phosphine oxides of the type:



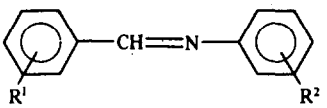
where R^1 = ethyl, phenyl; R^2 = propyl, phenyl; R^3 = butyl, methyl, phenyl; X = ethyl, ethoxy, hydroxy, propoxy; X^1 = acetyl, hydrogen, ethyl, propyl.

The reactions of isocyanates with azomethines in the presence of SO_2 were reported by Arbuzov *et al.*[4]

Deodhar *et al.*[5] have reported the synthesis of 3-substituted 2-styryl-4-3(H) quinazolinones by Schiff bases. The reactions of primary chlorophosphines with azomethines and acetylacetone have been reported by Nurtdinov *et al.*[6]

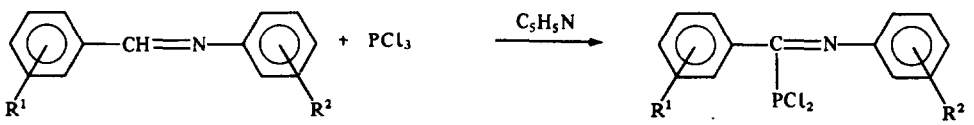
In the present communication we report the substitution of azomethine hydrogen by the Cl_2P-group in various Schiff bases.

Schiff bases of general formula:

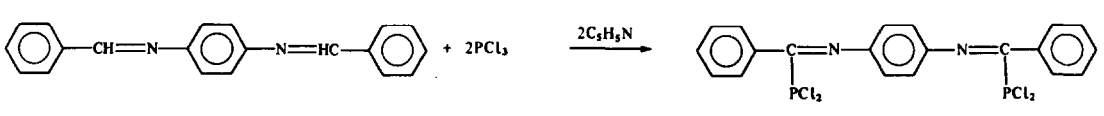


were reacted with phosphorus trichloride in molar ratios 1:1 and 1:2 in the medium of acetone containing pyridine and the reactions may be represented by the following equations:

Molar ratio 1:1



Molar ratio 1:2

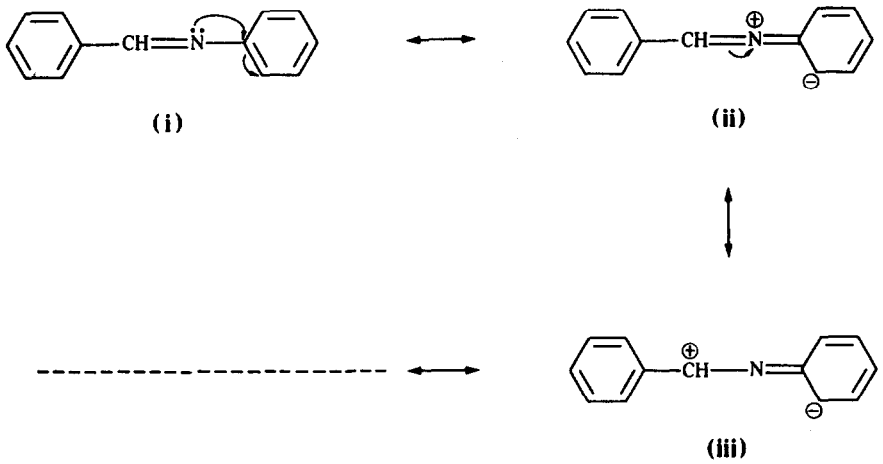


* Author to whom correspondence should be addressed.

where R^1 = H; R^2 = Cl, NO_2, H, PhCH=N—.

It was found that the compounds obtained from benzylidene-*o*-phenylenediamine and PCl_3 in both the molar ratios were white solids, whereas the remaining compounds were of intense yellow/orange coloured crystalline solids. All of them were soluble in alcohol, carbon tetrachloride, chloroform, acetone and acetophenone. They appeared to decompose in their melting point determination.

The formation of these compounds could be explained on the basis that the electrons present on the nitrogen of the azomethine group, may be delocalized with the adjacent phenyl group resulting in a number of canonical forms:



Due to the above resonance effect, the azomethine carbon (iii) becomes a carbonium centre and the hydrogen attached to this electron-deficient carbon becomes acidic and may be replaced under special conditions. The PCl_3 moiety can attack this azomethine carbonium centre or the ring attached to it.

The absence of a peak in NMR spectra in the region (τ value 4.0–5.0) which is characteristic of the presence of an olefinic proton shows the replacement of the azomethine hydrogen by the PCl_3 moiety.

The base-catalyzed nature of the reaction rules out the possibility of the homolytic mechanism and indicates that the rate-determining step involves elimination of a proton.

The longer time for the completion of the reaction between phosphorus trichloride and Schiff bases prepared by the reaction of *o*- and *p*-phenylenediamine and benzaldehyde is due to the presence of PhCH=N— group at the end of the molecule. The reactivity of nitro and chloro derivatives was due to the R and I effect which would facilitate the removal of the proton from azomethine carbon.

EXPERIMENTAL

All-glass apparatus with interchangeable joints was used throughout and special precautions were taken to exclude moisture.

Acetone, pyridine, benzene, ether and acetophenone were purified by standard procedures. Phosphorus trichloride was distilled before use.

Silica gel G (BDH) was used for TLC and spots were detected by UV lamp, iodine chamber and treating the plates in an oven after spraying with 10% H_2SO_4.

Preparation of Schiff bases

Schiff bases were prepared by mixing the corresponding amines with benzaldehyde. The reactions were exothermic. The contents were refluxed over a fractionating column followed by continuous removal of water–benzene azeotrope until the distillate attained a constant temperature of 80°C. Excess solvent was removed and the solid products were purified by crystallization from acetone or acetone–benzene mixture. The melting points of Schiff bases were within 1°C of literature values.

Analysis

Phosphorus was estimated as ammonium phosphomolybdate and chlorine as silver chloride, both gravimetrically by standard methods.[7]

Nitrogen was estimated by the Kjeldhal method.[7] Analytical results are given in Table 1.

Ir spectra [ν_{max} (cm^{-1})] (Table 2) of compounds were recorded on a Perkin–Elmer Spectrophotometer Model 577 in KBr discs and NMR [chemical shifts (τ) (ppm)] (Table 3) were recorded on a EM-360 (60 MHz) NMR Spectrometer in CCl_4 with TMS as internal standard, both working at the Chemical Laboratories of Central Drug Research Institute (Lucknow, India). The values obtained were interpreted by comparing the absorption bands and τ values with those reported in the literature.[8,9]

Molecular weights were determined cryoscopically using acetophenone as a solvent.

Methods of preparation being the same for all the

Table 1. Schiff base derivatives of phosphorus trichloride and their characterization data

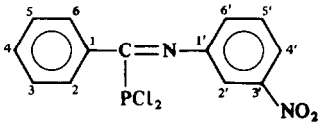
S. No.	Product	% phosphorus		% chlorine		% nitrogen		Molecular weight	
		Calc.	Found	Calc.	Found	Calc.	Found	Calc.	Found
1	$C_{13}H_{10}NPCl_2$	10.99	10.96	25.17	24.94	4.96	4.91	282.0	280.08
2	$C_{13}H_9N_2PCl_2O_2$	9.48	9.49	21.71	21.59	8.56	8.38	327.0	320.92
3	$C_{13}H_9PCl_2O_2$	9.48	9.41	21.71	21.55	8.56	8.48	327.0	322.42
4	$C_{13}H_9N_2PCl_2O_2$	9.48	9.46	21.71	21.56	8.56	8.38	327.0	325.02
5	$C_{13}H_9NPCl_3$	9.79	9.72	33.64	33.60	4.42	4.38	316.5	309.88
6	$C_{13}H_9NPCl_3$	9.79	9.70	33.64	33.59	4.42	4.37	316.5	310.42
7	$C_{13}H_9NPCl_3$	9.79	9.73	33.64	33.61	4.42	4.40	316.5	310.86
8	$C_{20}H_{15}N_2PCl_2$	8.05	7.98	18.44	18.40	7.27	7.14	385.0	380.28
9*	$C_{20}H_{14}N_2P_2Cl_4$	12.73	12.68	29.15	28.99	5.74	5.71	487.0	480.98
10	$C_{20}H_{15}N_2PCl_2$	8.05	8.08	18.44	18.34	7.27	7.18	385.0	380.98
11*	$C_{20}H_{14}N_2P_2Cl_4$	12.73	12.70	29.15	28.88	5.74	5.70	487.0	482.04

* Molar ratio 2:1.

Table 2. Significant bands [ν_{max} (cm^{-1})] in IR absorption spectra

Compound	C=N	C—P	P—Cl	NO_2
$C_{13}H_9N_2PCl_2O_2$	1540	660	540	1340
$C_{13}H_9NPCl_3$	1510	670	540	—
$C_{20}H_{15}N_2PCl_2$	1570	680	500	—

Table 3. Characteristic τ values in NMR spectra (CCl_4)



Assignment	Number of protons	τ value
$C_{2'}$	1 (s)*	1.87
$C_{6'}$	1 (s)	2.32
$C_{4'}$	1 (s)	2.44
$C_{5'}$	1 (s)	2.50
C_5	1 (s)	2.80
C_3	1 (s)	2.87
C_6	1 (s)	2.90
C_2	1 (s)	3.01
C_4	1 (s)	3.70

* s, singlet.

reactions, only one method has been described in detail while a summary of all is given in Table 1.

Reaction of phosphorus trichloride with benzylideneaniline (molar ratio 1 : 1)

To a solution of phosphorus trichloride (0.56 g) taken in acetone (15.00 g) was added a solution of benzylideneaniline (0.75 g) in pyridine. The contents of the flask were cooled and stirred during the addition of the reactants. After addition the contents were subjected to refluxing for 4 h. Acetone was distilled off and the residue was washed several times with dry pyridine to remove the pyridine hydrochloride. Final traces of pyridine hydrochloride were removed by sublimation under reduced pressure. The solid obtained was washed with ether, dried in vacuum and recrystallized from acetone–benzene mixture. The purity of the compound was checked by thin layer chromatography.

THIN LAYER CHROMATOGRAPHY

The chromatoplate was prepared by applying a uniform layer of silica gel in water, drying first at room temperature for 8 h and then at 100°C for 30 min. A 10% solution of the compound in dry acetone was applied over the plate which was then dried at room temperature for 2 h and at 100°C for 10 min.

The plate was then put in the eluant containing ethyl acetate–benzene mixture 1 : 3 by volume.

Finally the spots were located in UV light under a UV lamp, as well as in iodine chamber. A single spot was obtained.

The compound was characterized by elemental analysis, IR and NMR spectra. Found : P, 10.96 ; Cl, 24.94 ; N, 4.91%. $C_{13}H_{10}NPCl_2$ requires : P, 10.99 ; Cl, 25.17 ; N, 4.96%.

Acknowledgements—We express our gratitude to Professor R. P. Rastogi, Head, Department of Chemistry, University of Gorakhpur, Gorakhpur for providing necessary laboratory facilities. One of us (M.Z.S.) is thankful to the State Council of Science and Technology, Lucknow for providing a Junior Research Fellowship.

REFERENCES

1. R. V. Singh and J. P. Tandon, *J. Indian Chem. Soc.* 1978, **55**, 764.
2. K. A. Andrianov, V. I. Sidorov and M. I. Filimonova (*Inst. Element Org. Sovedin., Moscow, USSR*), *Izv. Akad. Nauk SSSR, Ser. Khim.* 1978, **2**, 460 ; *Chem. Abs.* 1978, **88**, 151700.
3. S. Kh. Nurtdinov, V. A. Ryabkov, R. Sh. Gabidullina, N. M. Ismagilova, T. V. Zykova, R. B. Sultanova and V. S. Tsivunin (*Khim. Tekhnol. Inst., Kazan, USSR*), *Zh. Obshch. Khim.* 1981, **51**, 1545 ; *Chem. Abs.* 1981, **95**, 150787.
4. B. A. Arbuzov, N. N. Zobova and N. R. Bubinova (*Kazan Gos. Univ., Kazan, USSR*), *Izv. Akad. Nauk SSSR, Ser. Khim.* 1980, **5**, 1164 ; *Chem. Abs.* 1980, **93**, 95250.
5. K. D. Deodhar, S. D. Samat, S. R. Pednekar and D. S. Kanekar, *Indian J. Chem.* 1982, **21B**, 67.
6. S. Kh. Nurtdinov, I. V. Tsivunina, V. I. Savran, N. M. Ismagilova, T. V. Zykova and V. S. Tsivunin (*Khim. Tekhnol. Inst., Kazan, USSR*), *Zh. Obshch. Khim.* 1981, **51**, 1549 ; *Chem. Abs.* 1982, **96**, 20177.
7. I. Smith Walter, Jr. and R. Shriner, *The Examination of New Organic Compounds.* John Wiley, New York (1956).
8. *Handbook of Chemistry and Physics*, 59th edn. CRC Press, West Palm Beach, FL (1978–1979).
9. J. R. Dyer, *Applications of Absorption Spectroscopy of Organic Compounds.* Offset Press, New Delhi (1974).

Polyhedron Vol. 4, No. 7, pp. 1155–1158, 1985
Printed in Great Britain

0277–5387/85 $3.00 + .00
© 1985 Pergamon Press Ltd

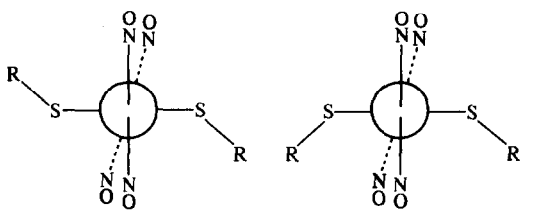
VARIABLE-TEMPERATURE AND SOLVENT NMR STUDY OF BIS(μ_2-METHANETHIOLATO)-BIS(DINITROSYLIRON) AND BIS(μ_2-METHANESELENOLATO)-BIS(DINITROSYLIRON)

CHRISTOPHER GLIDEWELL* and ANDREW R. HYDE
Chemistry Department, University of St. Andrews, St. Andrews, Fife KY16 9ST, U.K.

(*Received* 30 *April* 1984; *accepted* 26 *September* 1984)

Abstract—The ^{1}H NMR spectrum of $Fe_2(SMe)_2(NO)_4$ has been measured in a total of 22 solvents, and the activation barrier ΔG^+ for the $C_{2h} \rightleftharpoons C_{2v}$ isomerisation in nine of these solvents. In aromatic solvents, the solvent-induced shifts are consistent with the formation of charge-transfer complexes, either 1 : 1 or 1 : n; in non-aromatic, non-halogenated solvents of high dipolarity/polarizability the solvent-induced shifts follow the variation of the solvatochromic parameter, π^*. The behaviour of $Fe_2(SeMe)_2(NO)_4$ in a limited range of solvents is similar. The activation barrier ΔG^+ in $Fe_2(SMe)_2(NO)_4$ is *ca* 78 kJ mol^{-1} in the majority of solvents, but that for $Fe_2(SeMe)_2(NO)_4$ is significantly higher.

In the course of an NMR study of the $C_{2h} \rightleftharpoons C_{2v}$, **I** $\rightleftharpoons$ **II**, interconversion of the isomers of esters of Roussin's red salt, of general type $Fe_2(SR)_2(NO)_4$ (R = Me, Et, *n*-Pr, *i*-Pr, *t*-Bu, $PhCH_2$), it was observed[1] that upon changing the solvent from $CDCl_3$ to



I **II**

$C_6D_5CD_3$ at ambient temperature, the ^{1}H chemical shifts all experienced a significant shift to higher field, although the corresponding change in the ^{13}C chemical shift was rather small. For example, in $Fe_2(SMe)_2(NO)_4$ the ^{1}H shift from $CDCl_3$ to toluene-d_8 is *ca* 0.6 ppm, while in $Fe_2(SEt)_2(NO)_4$ the ^{1}H shifts are *ca* 0.4 ppm for the methyl and *ca* 0.5 ppm for the methylene protons: the corresponding ^{13}C shifts are *ca* 0.3, 0.15 and 0.05 ppm, respectively. These observations, and similar findings for other members of the $Fe_2(SR)_2(NO)_4$ series, imply a considerable specificity in the operation of the solvent effect, in discriminating between ^{1}H and ^{13}C shifts in a common methyl or methylene group.

In an attempt to shed further light upon this behaviour we have now carried out a study of the ^{1}H NMR spectrum, as a function of temperature, of the representative ester $Fe_2(SMe)_2(NO)_4$, in a range of solvents. We have also made an outline survey of the behaviour of the selenium analogue $Fe_2(SeMe)_2(NO)_4$ in a limited range of solvents.

EXPERIMENTAL

The ester $Fe_2(SMe)_2(NO)_4$ was prepared as previously described:[1] the selenium ester $Fe_2(SeMe)_2(NO)_4$ was prepared similarly. Purity was established by TLC, IR, and ^{1}H and ^{13}C NMR spectroscopy. All solvents were of the highest available commercial grade and were dried by conventional methods: deuterated solvents were of at least 98.5% isotropic purity.

NMR spectra were recorded for 1% solutions, sealed under vacuum, using a Bruker WP-80 spectrometer. The results for $Fe_2(SMe)_2(NO)_4$ are recorded in Table 1. In addition to the solvents listed in Table 1, an attempt was also made to record similarly the ^{1}H spectrum in CD_3OD: on each of a number of occasions, the sample exploded. It was found for most solvents that the solubility of $Fe_2(SMe)_2(NO)_4$ was too low for the recording of satisfactory ^{13}C NMR spectra. The ^{1}H spectral results for $Fe_2(SeMe)_2(NO)_4$ are recorded in Table 2.

* Author to whom correspondence should be addressed.

Table 1. Solvent dependence of NMR parameters of $Fe_2(SMe)_2(NO)_4$

Solvent	$\delta(^1H)$ (ppm)*	$\Delta\nu$ (Hz)	T_c (K)	ΔG^* (kJ mol^{-1})
Toluene-d_8	2.20	5.8	357	78.3
Benzene-d_6	2.35	4.9	353	77.9
C_6H_5Cl	2.42	3.1	†	
C_6H_5Br	2.45	3.2	†	
C_6H_5I	2.49	3.3	†	
$C_6D_5NO_2$	2.52	1.2	352	77.0
o-$C_6H_4Cl_2$	2.60	4.0	†	
Pyridine	2.72‡§	§	—	
$CCl_2{=}CCl_2$	2.75	2.0	‖	
$(CCl_2{=}CCl)_2$	2.76	2.0	‖	
CCl_4	2.76	2.0	‖	
CD_2Cl_2	2.77	1.2	339	78.7
Cyclohexane-d_{12}	2.78	1.7	344	78.9
$CDCl_3$	2.83	1.6	‖	
CD_3NO_2	2.83	¶	¶	
CD_3CN	2.89	1.3	291	67.0
C_6F_6	2.92	¶	¶	
Acetone-d_6	2.92	1.2	284	65.5
Dioxan-d_8	2.95	1.6	343	78.8
THF-d_8	3.02	1.0	330	77.0
DMSO-d_6	3.31‡**	**	—	
DMF-d_7	3.54‡††	‡	††	

* Mean chemical shift of C_{2h} and C_{2v} isomers, measured at 308 K.

† Not studied.

‡ Broad, unresolved absorption.

§ Mononuclear complex, $[Fe(NO)_2(pyridine)]^+$, detected by EPR spectroscopy.

‖ No coalescence observed even at boiling point of solvent.

¶ No resolution of $\Delta\nu$, even at freezing point of solvent.

** Mononuclear complex, probably $[Fe(NO)_2(SMe)(DMSO)]$, detected by EPR spectroscopy.

†† At elevated temperatures yields the mononuclear complexes $[Fe(SMe)(NO)_2(DMF)]$ and $[Fe(NO)_2(DMF)_2]^+$ (Ref. 3).

Table 2. Solvent dependence of NMR parameters of $Fe_2(SeMe)_2(NO)_4$

Solvent	$\delta(^1H)$ (ppm)*	$\Delta\nu$ (Hz)
Toluene-d_8	2.20	7.2
Benzene-d_6	2.38	6.4
$CDCl_3$	2.83	3.4
CD_2Cl_2	2.84	3.2
Acetone-d_6	2.95	1.7
DMSO-d_6	3.35	†

* Mean chemical shift of C_{2h} and C_{2v} isomers, measured at 308 K.

† No resolution of $\Delta\nu$, even at freezing point of solvent: paramagnetic mononuclear complex, probably $[Fe(NO)_2(SeMe)(DMSO)]$, detected by EPR spectroscopy.

RESULTS AND DISCUSSION

With the exception of solutions in CD_3NO_2, DMSO-d_6, DMF-d_7 and pyridine, the ^1H NMR spectra (Table 1) show that $Fe_2(SMe)_2(NO)_4$ always exists, at ambient spectrometer temperature (308 K), as an equimolar mixture of two isomers, assigned previously[1,2] as having C_{2h} and C_{2v} structures respectively, **I** and **II**. No resolution of the spectrum was achieved at any temperature for solutions in CD_3NO_2, while for solutions in DMSO, DMF and pyridine it was apparent both from the ^1H NMR spectra and subsequently from EPR spectra that paramagnetic species were present. In pyridine, the complex $[Fe(NO)_2(pyridine)_2]^+$ is formed,[3] while in DMSO no definitive identification was achieved, although the paramagnetic complex appears to be $[Fe(NO)_2(SMe)(DMSO)]$: in DMF the two complexes $[Fe(NO)_2(SMe)(DMF)]$ and $[Fe(NO)_2(DMF)_2]^+$ are formed at elevated temperatures.[3] Solutions in benzonitrile and benzaldehyde also underwent major decomposition, as the predominant absorption in the ^1H spectra in these solvents was that of CH_3S^-. Solutions in methanol-d_4 consistently exploded, and so no attempts were made to record spectra in other alcohols.

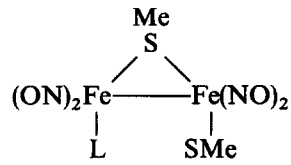
Subject to these limitations, satisfactory ^1H spectra were obtained for all the other solvents listed in Table 1. The ^1H chemical shifts can be divided rather readily into three principal groups. The first group, having $\delta(^1H)$ in the range 2.75–2.83, comprises chlorinated hydrocarbons and cyclohexane: these are all solvents of low polarity, low polarisability and low acid–base potential, and hence the chemical shifts observed in these solvents may be regarded as typical of those in uncoordinated $Fe_2(SMe)_2(NO)_4$ molecules, otherwise unperturbed by any influence of the solvent.

The second group, having $\delta(^1H)$ in the range 2.2–2.7 (together with C_6F_6 having $\delta = 2.92$) comprises aromatic solvents. Aromatic solvent-induced shifts (ASIS) represent a puzzling phenomenon, for which a variety of interpretations have been put forward.[4–7] It has been suggested[7] that the observation of ASIS is restricted to those molecules possessing a permanent electric dipole moment. We note however that if the *anti* isomer (**I**) of $Fe_2(SMe)_2(NO)_4$, and by inference of other $Fe_2(XR)_2(NO)_4$ species also, possesses genuine C_{2h} symmetry in solution, as hitherto supposed,[1] then it cannot exhibit a permanent dipole moment. On the

other hand it is clear from the data of Table 1 that both isomers of $Fe_2(SMe)_2(NO)_4$ exhibit ASIS of similar magnitudes; likewise a range of other $Fe_2(SR)_2(NO)_4$ (R = Et, *n*-Pr, *i*-Pr, *t*-Bu, $PhCH_2$) complexes exhibit comparable ASIS between $CDCl_3$ and toluene-d_8 as solvents.[1] In the solid state[8] the *anti* isomer of $Fe_2(SEt)_2(NO)_4$ exhibits crystallographic $\bar{1}$ (C_i) and molecular symmetry. However if the terminal methyl carbons are discounted (as appropriate for $Fe_2(SMe)_2(NO)_4$), the molecular symmetry then becomes essentially C_{2h}. Consequently it would be of considerable interest, and importance in terms of the ASIS phenomenon, to determine the molecular structure of isolated $Fe_2(SMe)_2(NO)_4$, e.g. by gas-phase electron diffraction. The variation of the ASIS for substituted benzenes as solvents is entirely consistent[9–12] with their acting as electron donors or acceptors towards the solute $Fe_2(SMe)_2(NO)_4$, according as the substituents on the benzene nucleus are themselves $+I$ or $-I$ substituents. The ASIS data are therefore qualitatively consistent with models based upon either specific 1:1 charge-transfer complexes[5] or dynamic 1:*n* complexes,[6] but appear at this stage to be incompatible with any model based upon the permanent dipole moment of the solute.[7]

The third group of solvents, having $\delta(^1H)$ in the range 2.8–3.0, consists (with the exception of C_6F_6) of strongly polar and strongly electron-donating solvents. Each of these aliphatic solvents, being non-protonic and non-polychlorinated, and having a single, predominant bond dipole fulfils Taft's criteria for "select solvents".[13–15] Many quantitative scales of solvent properties for such solvents have been devised,[16–19] which are all linearly related to the solvatochromic parameter, π^*;[13–15] they all describe in fact that the dipolarity/polarizability of a solvent rather than its acid-base properties. Accordingly there is a reasonable correlation between $\delta(^1H)$ and π^* for this group of solvents: in general the chemical shifts induced by the solvents are simply a reflection of the intrinsic properties of the solvents themselves and do not necessarily imply or require any donor–acceptor interactions between solvent and solute.

For a limited number of solvents (toluene, benzene, nitrobenzene, CD_2Cl_2, cyclohexane, CD_3CN, acetone, dioxan and THF) we were able to measure the coalescence temperature, T_c, for the $C_{2h} \rightleftharpoons C_{2v}$ equilibrium, and the coalescence data, together with the derived values of $\Delta G^{\ddagger}$ are given in Table 1: the $\Delta G^{\ddagger}$ values are accurate within ± 0.5 kJ mol^{-1}. No coalescence was observed even at the solvent boiling point for solutions in C_2Cl_4, $(CCl_2{=}CCl)_2$, CCl_4 and $CDCl_3$, while no resolution of the spectra of the two isomers was observed at any temperature down to the solvent freezing point in either CD_3NO_2 or C_6F_6. No attempt was made to carry out a variable-temperature study in C_6H_5X (X = Cl, Br, I) or in dichlorobenzene as deuterated samples were not available and the use of the normal isotopic forms as solvents gave rise to a considerable number of side-bands. In all solvents studied, except CD_3CN and acetone, the value of $\Delta G^{\ddagger}$ found is the same within 2 kJ mol^{-1}, and hence may be taken as constant, so that the same process is being observed in each of these solvents. In both acetonitrile and acetone the $\Delta G^{\ddagger}$ is significantly lower: however, neither of these solutions shows any evidence for the existence of paramagnetic species when freshly prepared although extremely weak EPR signals can be detected in solutions which have been aged for > 2 months. It is therefore unlikely that the lower $\Delta G^{\ddagger}$ reflects any fission of the Fe_2S_2 ring sufficient to yield paramagnetic complexes: nor is it easy to see that formation of a donor–acceptor complex such as **III** (L = solvent) would have an NMR spectrum



III

virtually unchanged from those of **I** and **II**.

In Table 2, we record results for the spectra of the selenium analogue $Fe_2(SeMe)_2(NO)_4$ in a very limited range of solvents. The chemical shifts are very little different from those of $Fe_2(SMe)_2(NO)_4$, but the $\Delta\nu$ values are consistently larger. In all solvents other than DMSO, no coalescence was observed at temperatures up to, or indeed somewhat above, the boiling points of the solvents. For $Fe_2(SMe)_2(NO)_4$ the value of $\Delta G^{\ddagger}$ was essentially constant at 78 kJ mol^{-1} whether the solvent was benzene, toluene or methylene chloride: assuming that this constancy is true also for $Fe_2(SeMe)_2(NO)_4$ (and we have no means at present of proving this), then we estimate as a lower limit for $\Delta G^{\ddagger}$ for the $C_{2h} \rightleftharpoons C_{2v}$ equilibrium in $Fe_2(SeMe)_2(NO)_4$, a value of at least 86 kJ mol^{-1}. This is significantly higher than the value for the sulphur analogue: we do not know why this should be so.

Acknowledgement—We thank the Cancer Research Campaign for financial support.

REFERENCES

1. A. R. Butler, C. Glidewell, A. R. Hyde, J. McGinnis and J. E. Seymour, *Polyhedron* 1983, **2**, 1045.
2. T. B. Rauchfuss and T. D. Weatherill, *Inorg. Chem.* 1982, **21**, 827.

3. A. R. Butler, C. Glidewell, A. R. Hyde and J. C. Walton, *Polyhedron* 1985, **4**, 797.
4. W. G. Schneider, *J. Phys. Chem.* 1962, **66**, 2653.
5. T. Ledaal, *Tetrahedron Lett.* 1968, 1683.
6. E. M. Engler and P. Laszlo, *J. Am. Chem. Soc.* 1971, **93**, 1317.
7. K. Nikki, N. Nakagawa and Y. Takeuchi, *Bull. Chem. Soc. Jpn* 1975, **48**, 2902.
8. J. T. Thomas, J. H. Robertson and E. G. Cox, *Acta Cryst.* 1958, **11**, 599.
9. For a comprehensive review, see: P. Laszlo, in *Progress in NMR Spectroscopy* (Edited by J. W. Emsley, J. Feeney and L. H. Sutcliffe), Vol. 3, p. 231. Pergamon Press, London (1971).
10. R. F. Weiner and J. M. Prausnitz, *Spectrochim. Acta* 1966, **22**, 77.
11. D. V. Fenby, I. A. McLure and R. L. Scott, *J. Phys. Chem.* 1966, **70**, 602.
12. T. G. Beaumont and K. M. C. Davis, *J. Chem. Soc. (B)* 1967, 1131.
13. M. J. Kamlet, J.-L. M. Abboud and R. W. Taft, *J. Am. Chem. Soc.* 1977, **99**, 6027.
14. J.-L. M. Abboud, M. J. Kamlet and R. W. Taft, *J. Am. Chem. Soc.* 1977, **99**, 8325.
15. J.-L. M. Abboud, R. W. Taft and M. J. Kamlet, *J. Chem. Res. (S)* 1984, 98.
16. V. Gutmann, *Electrochim. Acta* 1976, **21**, 661.
17. C. G. Swain, M. S. Swain, A. L. Powell and S. Alluni, *J. Am. Chem. Soc.* 1983, **105**, 502.
18. D. C. Dong and M. A. Winnik, *Photochem. Photobiol.* 1982, **35**, 17.
19. L. R. Snyder, *J. Chromat. Sci.* 1978, **16**, 223.

Polyhedron Vol. 4, No. 7, pp. 1159–1161, 1985
Printed in Great Britain

0277-5387/85 $3.00+.00
© 1985 Pergamon Press Ltd

A FOUR-MEMBERED CHELATE COMPLEX OF Cu(II) WITH CREATININE

M. MITEWA and P. R. BONTCHEV*
Department of Chemistry, University of Sofia, 1126 Sofia, Bulgaria

and

K. KABASSANOV
Institute of Solid State Physics, Bulgarian Academy of Sciences, 1113 Sofia, Bulgaria

(*Received* 13 *August* 1984; *accepted* 26 *September* 1984)

Abstract—The complex formation between Cu(II) and creatinine was studied by means of electronic, IR and EPR spectroscopy. The spectral data show the formation of a Cu(II) four-membered chelate with distorted rhombic structure.

The investigations on the complexation ability of creatinine towards different metal ions might be of interest in connection with the creatinine metabolism studies.[1–3] On the other hand only a few papers are available up to now dealing with complex formation of creatinine with some metal ions, namely Hg(II), Cd(II), Co(II) and Zn(II).[2–4] It has been proved that creatinine coordinates as a monodentate ligand through the cyclic N-atom.[2,3]

The aim of the present work was to synthesize and study the structure of the Cu(II) complex of creatinine.

EXPERIMENTAL

Synthesis of the Cu(II) *complex*

The Cu(II) complex was obtained in neutral medium (pH ~ 6) and isolated as a precipitate. Aqueous 0.1 M solutions of $CuCl_2$(Riedel de Haën AG, p.a.) and creatinine (Loba Chemie, p.a.) in molar ratio 1 : 5 were mixed and then a solution of sodium tetraphenylborate (NaTPB) (Merck, p.a.) was added. The blue precipitate formed was filtered off and washed with water and ethanol.

Analytical data

Elemental analysis of N was provided according to Dumas. Copper was determined by means of atomic absorption analysis after treatment of the complex with conc. HNO_3. The data obtained together with the calculated values for different metal to ligand ratios are represented in Table 1.

Apparatus

The electronic and IR spectra were obtained on recording spectrometers "Specord UV-Vis" (VEB Carl Zeiss, Jena) and on "Perkin–Elmer 580" (KBr disks) respectively. The EPR measurements were provided on an X-band spectrometer ESR 220 (GDR), Mn(II) being used as *g*-marker, the atomic absorption analysis on "Pye–Unicam SP 1950".

RESULTS AND DISCUSSION

The data represented in Table 1 show that a Cu(II) complex with creatinine (creat) is formed with a metal : ligand ratio of 1 : 2, resulting in a blue shift of the *d–d* band from 12,500 to 14,200 cm^{-1}, together with an increase in ε value.

The structure of the complex formed was studied by means of IR and EPR spectroscopy. For our purpose the IR spectra of the free ligand and the $Cu(creat)_2TPB$ were recorded in the 4000–200 cm^{-1} range. The data about the principal bands assigned according to the literature[2–4] are shown in Table 2. It should be noted that new bands are not observed in the range 500–200 cm^{-1}, where the valency vibrations ν_{M-N} or ν_{M-O} are expected to appear.

It is evident that both $\rangle C{=}O$ and cyclic $\rangle NH$

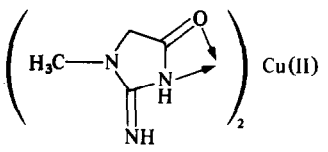
* Author to whom correspondence should be addressed.

Table 1. Elemental analysis and visible spectral data

Compound	N(%) Calc.	N(%) Found	Cu (%) Calc.	Cu (%) Found	λ_{max}	ε ($cm^{-1} M^{-1}$)
Cu(creat)TPB	8.47	13.86	12.81			
$Cu(creat)_2TPB$	13.80	13.92	10.43	10.05*	14,200	38.50
$Cu(creat)_3TPB$	17.46		8.80			

* Average value of five measurements.

groups are involved in the complexation as the corresponding bands are shifted in the $Cu(creat)_2$ complex, while the bands due to =NH and >C=N groups remain unaffected ($\nu_{=NH}$) or slightly affected ($\nu_{C=N}$). On the basis of these data it might be concluded that in $Cu(creat)_2$ complex 4-membered chelate rings are formed (str. I), differing significantly from the corresponding Co(II), Cd(II), Zn(II) and Hg(II) complexes.[2,3] In the latter only the cyclic >NH group coordinates to the metal ions:



In order to obtain additional information about the $Cu(creat)_2$ structure its EPR spectra were recorded—both a polycrystalline sample and frozen glass solutions in several donor solvents: H_2O, pyridine (py), hexamethylphosphortriamide (HMPA) and dimethylsulphoxide (DMSO). The data obtained are summarized in Table 3.

All the spectra are anisotropic with solvent dependent EPR parameters. The four-component $^{63,65}Cu$ ($I = \frac{3}{2}$) hyperfine splitting is readily observed in the $g_{\|}$ component allowing evaluation of $A_{\|}$. The $A_{\perp}$ values were approximated by dividing the maximum and minimum difference by 3.

According to Hathaway and Billing[5] anisotropic EPR spectra with $g_{\|} > g_{\perp}$ are typical for rhombic symmetry with slight misalignment of the tetragonal axes, e.g. a structure close to square-planar. The visible spectral data are consistent with such supposition as the spectrum obtained is similar to those assigned to distorted rhombic or square-planar Cu(II) complexes.[6]

On the basis of numerous experimental data[7–10] it was proved that such complexes tend to form 1:1 adducts with neutral donor molecules connected

Table 2. IR data for creatinine and $Cu(creat)_2$

Compound	$\nu_{(>C=N)}$	$\nu_{(C=O)}$	$\nu_{(=NH)}$	$\nu_{(NH)_{cyclic}}$
Creatinine	1595	1680	3050	3250
$Cu(creat)_2TPB$	1600	1665	3050	3300 (broad)

Table 3. EPR data for $Cu(creat)_2$ complex ($t^0 = -170°C$)

Solvent	$g_{\perp}$	$g_{\|}$	$A_{\perp}$(c.) (10^{-4} cm^{-1})	$A_{\|}$ (10^{-4} cm^{-1})
Polycrystalline sample	2.05 ± 0.01	2.25 ± 0.01	47 ± 5	200 ± 5
H_2O	2.09 ± 0.01	2.28 ± 0.01	36 ± 5	175 ± 5
py	2.10 ± 0.01	2.30 ± 0.01	40 ± 5	174 ± 5
HMPA	2.09 ± 0.01	2.30 ± 0.01	24 ± 5	161 ± 5
DMSO	> 2.14	2.33 ± 0.01		148 ± 5

with an increase in g-values together with a decrease in A values. As can be seen from Table 3 this dependence is valid for the complex studied, thus allowing the α^2 to be determined according to the equation of Kivelson and Neiman.[11] This term is connected with the degree of in-plane σ bonding, being 0.86 for the Cu(creat)$_2$TPB complex. For numerous Cu(II) complexes this value is approximately 0.8,[10,12] showing a square-planar geometry and high degree of ionic bonding. The latter result is in agreement with the lack of $\nu_{(M-O)}$ and $\nu_{(M-N)}$ bands in the IR spectrum. In this case they should be expected at very low frequencies.

In the DMSO spectrum a second EPR signal is observed as well with an approximate g-value of $\sim$ 2.12–2.14. Most probably the latter is due to a Cu(II)–solvato complex, as the system $CuCl_2$–DMSO shows an anisotropic singlet line with g-value 2.14. Recently we have obtained similar results studying the adduct formation of a rhombic Cu(iminopyrophthalone)$_2$ complex.[13,14]

REFERENCES

1. H. Brainerd, S. Margen and M. Shatton, *Current Diagnosis and Treatment*, p. 502. Lang Medical Publications, CA (1968).
2. S. Muralidharan, K. S. Nagaraja and M. R. Udupa, *Polyhedron* 1984, **3**, 619.
3. S. Muralidharan, K. Nagaraja and M. R. Udupa, *Transition Met. Chem.* 1984, **9**, 218.
4. A. J. Canty, M. Fyfe and B. M. Gatehouse, *Inorg. Chem.* 1978, **17**, 1467.
5. B. J. Hathaway and D. E. Billing, *Coord. Chem. Rev.* 1970, **5**, 143.
6. B. J. Hathaway, I. M. Procter, R. C. Slade and A. A. Tomlinson, *J. Chem. Soc. A* 1969, 2219.
7. A. F. Garito and B. B. Wayland, *J. Am. Chem. Soc.* 1969, **91**, 866.
8. B. B. Wayland and V. K. Kapur, *Inorg. Chem.* 1974, **13**, 2517.
9. Yu. Y. Chen, D. E. Chu, B. D. McKinney, L. J. Willis and S. C. Cummings, *Inorg. Chem.* 1981, **20**, 1885.
10. L. G. McDonald, D. H. Brown and W. E. Smith, *Inorg. Chim. Acta* 1982, **63**, 213.
11. D. Kivelson and R. J. Neiman, *J. Chem. Phys.* 1961, **35**, 199.
12. K. Miyoshi, H. Tanaka, E. Kimura, S. Tsuboyama, S. Murata, H. Shimizu and K. Ishizu, *Inorg. Chim. Acta* 1983, **78**, 23.
13. P. R. Bontchev, M. Mitewa, S. Minchev, M. Kashchieva and D. Mechandjiev, *J. Prakt. Chem.* 1983, **325**, 803.
14. M. Mitewa, P. R. Bontchev, A. Malinovski, M. Kashchieva and S. Minchev, *C. R. Acad. Sci. Bulg.* 1983, **36**, 1311.

Polyhedron Vol. 4, No. 7, pp. 1163–1166, 1985
Printed in Great Britain

0277-5387/85 $3.00 + .00
© 1985 Pergamon Press Ltd

TRANSITION METAL COMPLEXES OF HYDROTRIS(IMIDAZOLYL)BORATE ANION

SAIYID AFTAB A. ZAIDI,* TABREZ A. KHAN and S. R. A. ZAIDI
Division of Inorganic Chemistry, Department of Chemistry, Aligarh Muslim University, Aligarh-202001, India

and

ZAFAR A. SIDDIQI
Institut für Anorganisches Chemie, Göttingen, F.R.G.

(*Received* 10 *September* 1984; *accepted* 6 *October* 1984)

Abstract—The preparation and characterization of the ligand potassium hydrotris(imidazolyl)borate and some of its complexes with transition metals is reported. These complexes have apparently an octahedral structure except the Cu(II) complex which seems to have a square planar geometry. The values of the ligand field parameters $10Dq$, B and β have been evaluated for most of these complexes.

Recently we have reported[1,2] the synthesis and characterization of the ligands potassium dihydrobis(imidazolyl)borate and dihydrobis(2-methylimidazolyl)borate and their complexes. In continuation of this work, we now report the synthesis and characterization of potassium hydrotris(imidazolyl)borate, which is comparatively more sterically hindered than its dihydrobis-counterpart and a few of its complexes with transition metal ions with a view to studying its coordinating ability.

EXPERIMENTAL

All the metal chlorides and potassium borohydride used in this study were of BDH quality. The imidazole (sisco) was used after recrystallization from ethanol.

Preparation of the ligand

Imidazole (14.70 mmol) and potassium borohydride (4.90 mmol) in DMF were mixed together and the reaction was completed by refluxing for about twenty four hours. The colourless potassium hydrotris(imidazolyl)borate which crystallizes out on cooling was filtered, washed and finally dried for five hours under reduced pressure at room temperature.

Preparation of the complexes

The complexes were prepared by mixing the stoichiometric amounts of metal chloride solutions (1.39 mmol of $MnCl_2$, $CoCl_2$, $NiCl_2$ and $CuCl_2$ and 0.93 mmol of $FeCl_3$) and the ligand solution (2.78 mmol) and refluxing the mixture for 1–2 h. The solids thus obtained were filtered, washed with ethanol and dried in an electric oven at 70°C.

IR spectra (4000–200 cm^{-1}) were run on a Perkin–Elmer 621 spectrophotometer. Micro-analyses were done in the micro-analytical laboratory. Metal analyses were carried out by chelometric titration with standard EDTA.[3] Prior to titration the metal was liberated from the complex by the addition of a few drops of a mixture of nitric acid, sulphuric acid and perchloric acid to an accurately weighed 0.1 g sample. Diffuse reflectance spectra were taken on Carl–Zeiss VSU-2P spectrophotometer. Magnetic susceptibility measurements were carried on a vibrating sample magnetometer model 155 at room temperature.

RESULTS AND DISCUSSION

In the formation of the ligand potassium hydrotris(imidazolyl)borate the hydrogen atom at

* Author to whom correspondence should be addressed.

Table 1. Colour, % yield and analytical data

Complex	Colour	% yield	Analysis—% found (calc.) C	H	N	M
$K^+[C_9H_{10}N_6B]^-$	—	58	42.56 (42.87)	3.73 (3.99)	33.10 (33.33)	—
$[Mn(C_9H_{10}N_6B)_2]$	Hathi grey	40	44.61 (44.95)	4.59 (4.19)	34.73 (34.95)	11.81 (11.42)
$[Fe(C_9H_{10}N_6B)_3]$	Chinese gold	33	46.93 (46.66)	4.49 (4.35)	36.32 (36.28)	8.40 (8.05)
$[Co(C_9H_{10}N_6B)_2]$	Purple	52	44.98 (44.58)	4.39 (4.16)	34.89 (34.66)	12.45 (12.15)
$[Ni(C_9H_{10}N_6B)_2]$	Black	51	44.81 (44.60)	4.46 (4.16)	34.91 (34.67)	12.37 (12.11)
$[Cu(C_9H_{10}N_6B)_2]$	Harbour blue	55	44.57 (44.16)	4.39 (4.12)	34.73 (34.33)	13.29 (12.98)

position 1 of the imidazole molecules are removed together with the three hydrogen atoms from the potassium borohydride according to the reaction.

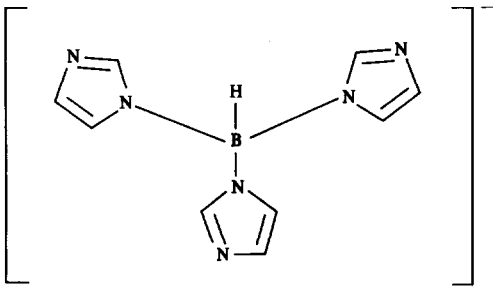
$$KBH_4 + 3C_3H_4N_2 \rightarrow K^+(C_9H_{10}N_6B)^- + 3H_2.$$

This has been ascertained by measuring the volume of the hydrogen gas evolved during the synthesis. The analytical data (Table 1) agrees well with the proposed composition. The IR spectrum (Table 2) does not show any absorption band in the region 3300–3450 cm^{-1}, indicating the absence of the N–H linkage in the molecule, confirming that the imino-hydrogen atoms of the imidazole has been replaced. This has further been characterized by the appearance of the ν(B–N) peak at 1400 cm^{-1}.[4] A strong band at 2440 cm^{-1} may reasonably be assigned to the B–H stretching frequency.[5] Frequencies characteristic of the imidazole ring system[1] also appear in the spectrum. The following structure in which the boron is bonded to three imidazolyl groups through the imino-nitrogen and

Table 2. Important IR bands and their assignments

Complex	B–H stretch (cm^{-1})	B–N stretch (cm^{-1})	Ring stretch (cm^{-1}) R_1	R_2	R_3	R_4
$K^+[C_9H_{10}N_6B]^-$	2440s	1400m	1650m 1660m	1520m	1495m	1330m
$[Mn(C_9H_{10}N_6B)_2]$	2410m	1385m	1650m 1660m	1515m	1490m	1330m
$[Fe(C_9H_{10}N_6B)_3]$	2390m	1390m	1650m 1670m	1520m	1485m	1340m
$[Co(C_9H_{10}N_6B)_2]$	2400s	1385m	1650m 1660m	1510m	1490m	1330m
$[Ni(C_9H_{10}N_6B)_2]$	2395s	1380s	1650s 1660m	1510m,b	1490s	1325m
$[Cu(C_9H_{10}N_6B)_2]$	2410s	1395m	1640s 1670m	1520m	1480s	1340s

to one hydrogen atom may, therefore, be visualized for this ligand.



The complexes prepared are given in Table 1, together with their colour, elemental analyses and % yield. As can be seen, the metal–ligand molar ratios are 1 : 2 and 1 : 3 for divalent and trivalent metal ions, respectively. The ligand studied here would have two possible interaction sites in a molecule to the metal ions. The B–H stretching frequencies of the ligand in the IR spectra shift to lower frequencies by about ~ 30 cm^{-1} upon coordination to the metal chlorides, as shown in Table 2, which indicates that the ligand interacts with the metal ion through the pyrrolic nitrogen atom. The other ring frequencies are affected only slightly from those in the free ligand and the observed shifts, if any, are found to be nearly independent of the metal ion. It is not unusual that there is only a small change in these frequencies after complexation.[6] Metal–ligand stretching frequencies occur in the usual range (250–450 cm^{-1}) for nitrogen donor ligands.[7,8] However, because of the fact that the ligand also has an absorption band in this region the assignments of the M–L stretches are rather uncertain. Considerable mixing between M–L stretching vibrations and ligand modes will certainly be present.

For evidence about the coordination around the metal ions, and the ligand field strength of the ligand, the reflectance spectra and magnetic moment of the solid compound were taken. Band maxima, assignments and calculated values for $10Dq$, B and β are given in Table 3.

The assignment of the electronic spectrum for the Mn(II) compound corresponds with an octahedral ion. The bands at 25,625, 24,775 and 18,822 cm^{-1} are assigned as $^6A_{1g} \rightarrow {}^4A_{1g}(G)$, $^6A_{1g} \rightarrow {}^4E_g(G)$ and $^6A_{1g} \rightarrow {}^4T_{1g}(G)$ respectively. The observed magnetic moment of the Mn(II) complex 5.83 B.M. indicates the formation of a high spin complex.

The electronic spectrum of the Fe(III) complex exhibits well resolved bands at 23,148 and 18,018 cm^{-1} characteristic of the octahedral array of ligands around the metal ion. The magnetic moment of 5.89 B.M. also indicates a high spin complex.

For an octahedral Co(II) complex, three bands are expected corresponding to the three spin-allowed transitions $^4T_{1g}(F) \rightarrow {}^4T_{2g}(F)$ (ν_1), $^4T_{1g}(F) \rightarrow {}^4A_{2g}$ (ν_2) and $^4T_{1g}(F) \rightarrow {}^4T_{1g}(P)$ (ν_3). However, it has been pointed out[9] that the transition $^4T_{1g}(F) \rightarrow {}^4A_{2g}$ corresponds to a two electron jump and as such will have a much lower oscillator strength than the other two bands and will be much weaker. The band at about 10,526 cm^{-1} can, therefore, be assigned to the ν_1 transition and the band at 23,255 cm^{-1} to the ν_3 transition. Using the following equations, which have been derived[10] from the energy matrix of the two

Table 3. Magnetic susceptibility, electronic spectra and ligand field parameters

Complex	μ_{eff} (B.M.)	Electronic bands (cm^{-1})	Possible assignments	$10Dq$	B	β
$[Mn(C_9H_{10}N_6B)_2]$	5.83	25,625	$^4A_{1g}(G) \leftarrow {}^6A_{1g}$	10,400	800	0.83
		24,775	$^4E_g(G) \leftarrow {}^6A_{1g}$			
		18,822	$^4T_{1g}(G) \leftarrow {}^6A_{1g}$			
$[Fe(C_9H_{10}N_6B)_3]$	5.89	23,148	$^4T_{2g}(G) \leftarrow {}^6A_{1g}$	14,337	924	–
		18,018	$^4T_{1g}(G) \leftarrow {}^6A_{1g}$			
$[Co(C_9H_{10}N_6B)_2]$	4.80	23,255	$^4T_{1g}(P) \leftarrow {}^4T_{1g}(F)$	10,625	855	0.76
		21,286	$^4A_{2g} \leftarrow {}^4T_{1g}(F)$			
		10,526	$^4T_{2g}(F) \leftarrow {}^4T_{1g}(F)$			
$[Ni(C_9H_{10}N_6B)_2]$	3.14	26,397	$^3T_{1g}(P) \leftarrow {}^3A_{2g}$	9477	977	0.90
		15,339	$^3T_{1g}(F) \leftarrow {}^3A_{2g}$			
		10,204	$^3T_{2g} \leftarrow {}^3A_{2g}$			
$[Cu(C_9H_{10}N_6B)_2]$	1.82	22,371	$^2A_{1g} \leftarrow {}^2B_{1g}$	15,267	–	–
		15,267	$^2E_g \leftarrow {}^2B_{1g}$			

$^4T_{1g}$ levels, it is possible to obtain the values of Dq and B from the position of the ν_1 and ν_3 bands.

$$Dq = [(2\nu_1+\nu_3)+(\nu_3^2+\nu_1\nu_3-\nu_1^2)^{1/2}]/20,$$

$$B = (\nu_3-2\nu_1+10Dq)/15.$$

Using the relationship $\nu_2 = \nu_1+10Dq$, the ν_2 band would be expected to occur at about 21,150 cm^{-1}, i.e. close to the ν_3 band. A very weak shoulder does occur on the ν_3 band in this region but this may arise from spin–orbit splitting.[9] The reflectance spectrum clearly shows the complex to be octahedral, and this is supported by the magnetic moment which lie in the range normally observed for the Co(II) octahedral complexes. When a solution of the cobalt(II) chloride and the ligand are treated with hydrogen peroxide a dark coloured solution results, indicating the feasibility of making the Co(III) complex.

The solid reflectance spectrum of the Ni(II) complex exhibit three main crystal field transitions at around 10,204 cm^{-1} (σ_1), 15,339 cm^{-1} (σ_2) and 26,397 cm^{-1} (σ_3). An octahedral structure may be inferred for this complex on the basis of the position and intensity of these bands. Moreover, the ratio σ_2/σ_1 for the present complex is 1.60 as predicted for octahedral Ni(II) complexes. The observed μ_{eff} value of 3.14 B.M. also suggests an octahedral environment for the nickel ion.

The electronic spectrum of the Cu(II) complex display two d–d transitions at 15,267 and 22,371 cm^{-1}. These spectral bands may be assigned to the transitions $^2B_{1g} \rightarrow {}^2A_{1g}$ and $^1B_{1g} \rightarrow {}^2E_g$ respectively indicating square planar stereochemistry. The magnetic moment value is 1.82 B.M., corresponding to one unpaired electron.

Acknowledgements—We are thankful to Prof. M. S. Ahmad, Chairman, Department of Chemistry, A.M.U., Aligarh for providing research facilities. One of us (TAK) thanks Department of Atomic Energy, Government of India for financial assistance.

REFERENCES

1. Saiyid Aftab A. Zaidi, Tabrez A. Khan and Zafar A. Siddiqi, *Synth. React. Inorg. Met.-Org. Chem.* 1984, **14**, 717.
2. Saiyid Aftab A. Zaidi, Tabrez A. Khan and Zafar A. Siddiqi, *Bull. Soc. Chim. Fr.* 1984, **5–6**, 149.
3. C. N. Reilley, R. W. Schmid and F. A. Sadak, *Chem. Educ.* 1959, **36**, 555; 619.
4. G. Davidson, *Coord. Chem. Rev.* 1979, **30**, 94.
5. S. A. A. Zaidi and M. A. Neyazi, *Transition Met. Chem.* 1979, **4**, 164.
6. J. Reedijk, *Rec. Trav. Chim.* 1969, **88**, 1451.
7. L. Sacconi, A. Sabatini and P. Gans, *Inorg. Chem.* 1964, **3**, 1772.
8. D. H. Brown, R. H. Nuttal, J. McAvoy and D. W. A. Sharp, *J. Chem. Soc.* 1966, 892.
9. S. Koide, *Phil. Mag.* 1959, **4**, 243.
10. D. E. Billing and A. E. Underhill (unpublished results).

Polyhedron Vol. 4, No. 7, pp. 1167–1184, 1985
Printed in Great Britain

0277-5387/85 $3.00 + .00
© 1985 Pergamon Press Ltd

CLUSTER MOLECULAR ORBITALS AND AN ORBITAL SYMMETRY VIEW OF SOLID PHASE TRANSITIONS IN PEROVSKITES*

YING-NAN CHIU†
Department of Chemistry, The Catholic University of America, Washington, DC 20064, U.S.A.

and

FREDERICK E. WANG
Innovative Technology International, Inc., 10747-3 Tucker Street, Beltsville, MD 20705, U.S.A.

(*Received* 11 *May* 1984; *accepted* 9 *October* 1984)

Abstract—The molecular orbitals, normalization constants and energies of the $M_8(O_h)$, $M_4(T_d)$ and $M_6(O_h)$ clusters are derived and tabulated through the *d*-atomic orbitals. A vector method, adapted to computer application, is devised to compute *s*, *p* and *d* overlap between variously oriented orbitals at atoms that do not have co-directional local axes. Mixing of σ, π and δ orbitals to give the same irreducible representation is also included. As illustrations, the orbitals of Sr_8, La_8, TiO_6 and AlO_6 clusters are computed by the Mulliken–Wolfsberg and Helmholz approximations. During solid phase transitions in the perovskite structures of $SrTiO_3$ and $LaAlO_3$, the TiO_6 octahedron rotates about the C_4 axis whereas the AlO_6 octahedron rotates about the C_3 axis. This difference is explained qualitatively in terms of the relative symmetries of the cluster HOMOs and LUMOs using the second-order Jahn–Teller effect. Allusions are made to the application of this cluster symmetry approach to other systems.

Metal cluster compounds have become of increasing interest to chemists of all disciplines. This interest resulted in two almost consecutive feature articles in *Chemical and Engineering News*, one by Cotton and Chisholm[1] and one by Muetterties.[2] Related books[3,4] and review articles[5–8] are also available. While there are qualitative theories of the bonding of clusters[9,10] and molecular fragments,[4,11] there has been much less work on quantitative, analytical expression for molecular orbitals (MOs) in these clusters.

In 1964, Cotton and Haas[12] treated M_6 *d*-orbital clusters quantitatively. This work was refined[13] later by Cotton's group in 1980. In 1966, Watanabe[14] derived cluster symmetry orbitals using atomic *p*-orbitals (no *d*-orbitals) for $M_4(T_d)$, $M_6(O_h)$ and $M_8(O_h)$ without normalization (in terms of overlap integrals) and without energy expression (in terms of resonance integrals). In 1977, Purcell and Kotz[15] included atomic *d*-orbitals, qualitatively for $M_6(O_h)$ clusters, but again did not include details of overlap or energy expressions. The existing angular overlap model[15] (AOM) of Schaffer[4,16] and Jorgensen[4,17] is concerned mainly with charge overlap between the center metal atom and ligands instead of among ligands clusters *per se*. The tabulated overlaps[4] are for a center atom at the origin and the ligand atom having *codirectional* local axes instead of general relative orientations. As interest increases in larger and larger clusters, there is increasing need for the MOs of basic clusters and for an expedient method to deal with orbitals with arbitrary orientations. The latter is especially true of the bridged complexes[18,22] and unsymmetrical clusters.

In this work we derived quantitative and analytical MOs including *d*-orbitals and energies of the basic clusters, $M_8(O_h)$, $M_6(O_h)$ and $M_4(T_d)$. We also devised a computer-adaptable vector method to

* Contribution No. 0003, ITI Basic Research Laboratory.

† Author to whom correspondence should be addressed.

derive the overlap between *s*, *p* and *d* orbitals with any arbitrary relative orientation. This method supersedes the conventional Euler angle method.[23] Examples of $M_8(O_h)$ clusters[24–27] are $[Cu_8\{S_2C_2(CN)_2\}_6]^{4-}$ and $[Ni_8(CO)_8(\mu\text{-pph})_6]$. An example of an $M_6(O_h)$ cluster[28] is $Ru_6(CO)_{18}H_2$, and $[Fe_4(CO)_{13}]^{2-}$ is an example of an $M_4(T_d)$.[29] Naked clusters are of interest both *per se* and as building blocks. For example, $M_8(O_h)$ and $M_6(O_h)$ can be used to build a face-centered cubic cell. In such a building-up and the subsequent mixing of MOs the complete structure must have the *same* transformation matrix for the degenerate representations of the same symmetry but belonging to *two different clusters* (e.g. M_6 within M_8, both of O_h) under the same operation. We took pains to ascertain this point quantitatively. Within a cluster, e.g. $M_6(O_h)$, irreducible representations with same symmetry (e.g. t_{1u}) but containing different orbitals (σ *vs* π) do not mix in the case of *p*-orbitals (e.g. the overlap between $t_{1u}(P_\sigma)$ and $t_{1u}(P_\pi)$ equals zero). However, this is not generally true. For example, the overlap $s[t_{1u}(d_{z^2})t_{iu}(d_{xz})] \neq 0$. Such mixing between irreducible representations containing $d\sigma$, $d\pi$, and $d\delta$ orbitals is treated in this work for $M_8(O_h)$, $M_4(T_d)$ and $M_6(O_h)$.

Aside from the above mentioned interest in cluster complexes, there is a developing direction in solid state chemistry[4,30,31] toward making use of clusters as building fragments.[32] Band structure calculations[33,34] when extended to three dimensions and cluster calculations[35,36] on minerals, may also require the *d*-overlap methods we have developed here. As another application of the cluster concept in solid state, we note that the phase transition in ferroelectric perovskites ABO_3 which are face-centered cubics involves rotation[37–41] of the inside BO_6 octahedron cluster with respect to the surrounding A_8 cubic cluster. In the case of $SrTiO_3$ the rotation is around the C_4 axis and the transition is from cubic to tetragonal. On the other hand, in the case of $LaAlO_3$ the rotation is around the C_3 axis and the transition is from cubic to rhombohedral (Fig. 1).

Taking inspiration from both Woodward and Hoffmann's[42] success in applying the symmetry of orbitals in a dynamic situation and Pearson's[43] use of symmetry rules to predict molecular structure, we attempt in this work to explore the effect of relative (M_6 vs M_8 cluster) orbital symmetry in determining the axis of rotation during transition. Application of the symmetry of fragments to the determination of the relative barriers of rotation is known from the work of Hoffmann's group on polyene–ML_2 complexes, etc.[44] Our application of a single face-centered cubic unit cell to an infinite system is a drastic theoretical extension. It must be a semi-empirical approach calibrated by known experimental results. The extent of success or failure of the attempt will at least let us know what kind of electronic factors must be included to understand the phase transition. Hopefully, by comparing two parallel systems with the same initial cubic crystal symmetry, $SrTiO_3$ and $LaAlO_3$, the errors of the approximation will balance out and some qualitative trend will emerge.

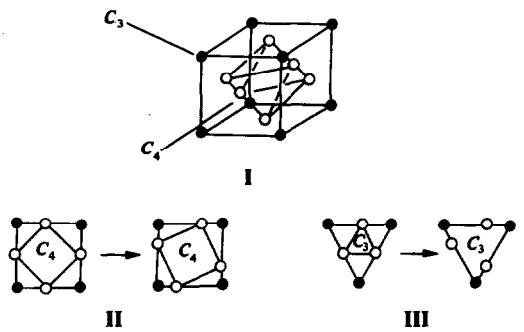


Fig. 1. Phase transition in face-centered cubic ABO_3 perovskite crystals (I). Solid dot for atom "A". Open dots for oxygen atoms. Atom B in the center is not shown. Rotation with respect to C_4 axis corresponds to the cubic to tetragonal transition case of $SrTiO_3$ (II) and rotation with respect to C_3 axis corresponds to the cubic to rhombohedral transition case of $LaAlO_3$ (III).

OVERLAP OF CLUSTER *s*, *p* AND *d* ORBITALS WITH ARBITRARY LOCAL AXIS ORIENTATIONS

Within an M_8 cluster there are $28(={}_8C_2)$ combinations of atomic pairs, each having up to 25 *d*-orbital overlap possibilities. While in $M_6(O_h)$ case, application of symmetry simplifies the calculations, in the general case the prospect of deriving scores of Euler angles[23] and hundreds of overlaps is dizzily discouraging. To expedite and systematize the task, we abandon the Euler angle technique and devise a vector method. First we establish a common origin at the center of $M_8(O_h)$, $M_6(O_h)$ or $M_4(T_d)$ with coordinates system axes along unit vectors $\mathbf{i} = (1, 0, 0)$, $\mathbf{j} = (0, 1, 0)$ and $\mathbf{k} = (0, 0, 1)$. Then we define all local atomic axes in terms of local parallels to **i**, **j** and **k**. Figures 2 and 3 show this choice of atomic labelling and coordinates. Tables 1 and 2 give orientation of local axes. For any given atomic pair *AB*, the relative vector **R** is also defined in terms of the unit vectors **i**, **j** and **k**. **R** is defined as the σ_z overlap direction, with one unique direction instead of the usual two opposite, σ (or *z*) directions for the two overlapping atoms. The overlap π_X and π_Y directions are chosen to be right-handed and mutually

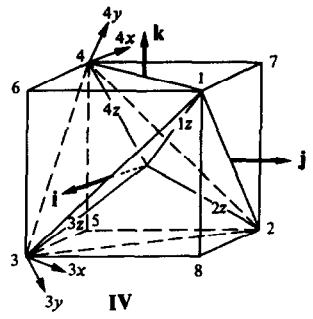


Fig. 2. Local coordinates and atomic labels for $M_4(T_d)$ and $M_8(O_h)$ clusters. The set of numbers 1, 2, 3, and 4 and the set of numbers 5, 6, 7, 8 each compose a tetrahedron. The set of numbers 1, 2, 3, 4, 5, 6, 7, 8 represents a cubic cluster. Unit vectors **i**, **j**, and **k** centered at the origin are common to both clusters.

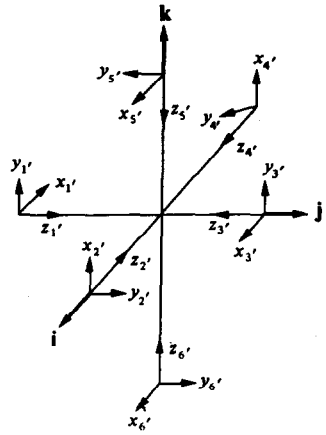


Fig. 3. Local coordinates and atomic labels for $M_6(O_h)$ cluster. The unit vectors **i**, **j** and **k** are common to the $M_8(O_h)$ and $M_4(T_d)$ clusters. These clusters may be superimposed; orbitals of the same symmetry and transformation may be mixed.

perpendicular to **R**, and also expressed in terms of **i**, **j**, **k**. To compute the *p*-overlap, we first project the *p*-orbitals of *A*, $\mathbf{A}_1(=\mathbf{P}_{A_x})$, $\mathbf{A}_2(=\mathbf{P}_{A_y})$ and $\mathbf{A}_3(\mathbf{P}_{A_z})$, onto the $\sigma_z(\equiv \mathbf{R}_3)$, $\pi_x(\equiv \mathbf{R}_1)$, $\pi_y(\equiv \mathbf{R}_2)$ directions, viz. take $\mathbf{A}_1$ (similar projections for $\mathbf{A}_2$, $\mathbf{A}_3$),

$$\mathbf{A}_1 = P_{11}\mathbf{R}_1 + P_{12}\mathbf{R}_2 + P_{13}\mathbf{R}_3. \qquad (1)$$

In as much as $\mathbf{A}_1$, $\mathbf{R}_1$, $\mathbf{R}_2$ and $\mathbf{R}_3$ each has three components (along the common unit vectors), there are three simultaneous linear equations which can be solved by computer for the three projection coefficients, P_{11}, P_{12} and P_{13}. The latter are respectively the π_x, π_y and σ_z components of the orbitals $\mathbf{A}_1(\equiv \mathbf{P}_{A_x})$. Similar projection of **B** (e.g. the $\mathbf{B}_3 = \mathbf{P}_{B_z}$ orbital) gives,

$$\mathbf{B}_3 = Q_{31}\mathbf{R}_1 + Q_{32}\mathbf{R}_2 + Q_{33}\mathbf{R}_3. \qquad (2)$$

In terms of the tabulated π and σ overlaps, the

Table 1. Local coordinates and atomic labels for $M_8(O_h)$ and $M_4(T_d)$ cluster*

$X_5 = (1/\sqrt{2}, -1/\sqrt{2}, 0)$	$X_7 = (1/\sqrt{2}, 1/\sqrt{2}, 0)$
$Y_5 = (1/\sqrt{6}, 1/\sqrt{6}, -2/\sqrt{6})$	$Y_7 = (1/\sqrt{6}, -1/\sqrt{6}, 2/\sqrt{6})$
$Z_5 = (1/\sqrt{3}, 1/\sqrt{3}, 1/\sqrt{3})$	$Z_7 = (1/\sqrt{3}, -1/\sqrt{3}, -1/\sqrt{3})$
$X_6 = (-1/\sqrt{2}, -1/\sqrt{2}, 0)$	$X_8 = (-1/\sqrt{2}, 1/\sqrt{2}, 0)$
$Y_6 = (-1/\sqrt{6}, 1/\sqrt{6}, 2/\sqrt{6})$	$Y_8 = (-1/\sqrt{6}, -1/\sqrt{6}, -2/\sqrt{6})$
$Z_6 = (-1/\sqrt{3}, 1/\sqrt{3}, -1/\sqrt{3})$	$Z_8 = (-1/\sqrt{3}, -1/\sqrt{3}, 1/\sqrt{3})$

* Only coordinates for atoms 5, 6, 7 and 8 are given. The remainder may be obtained by inversion of the physical system as follows:

$$\mathbf{i}X_{5678} = -X_{1234},$$
$$\mathbf{i}Y_{5678} = Y_{1234},$$
$$\mathbf{i}Z_{5678} = Z_{1234},$$

but the vector component changes are just the opposite. For example:

$$\mathbf{i}X_5 = -X_1 \quad \text{means} \quad X_1 = (1/\sqrt{2}, -1/\sqrt{2}, 0) = X_5;$$
$$\mathbf{i}Y_5 = Y_1 \quad \text{means} \quad Y_1 = (-1/\sqrt{6}, -1/\sqrt{6}, 2/\sqrt{6}) = -Y_5;$$
$$\mathbf{i}Z_5 = Z_1 \quad \text{means} \quad Z_1 = (-1/\sqrt{3}, -1/\sqrt{3}, -1/\sqrt{3}) = -Z_5.$$

The choice of coordinate system is the same as that of Watanabe.[14] Note, however, the possible confusion in his footnote on p. 183.

Table 2. Local coordinates and atomic labels for $M_6(O_h)$ cluster*

$X_{1'} = (-1\ 0\ 0)$	$X_{3'} = (1\ 0\ 0)$	$X_{5'} = (1\ 0\ 0)$
$Y_{1'} = (0\ 0\ 0)$	$Y_{3'} = (0\ 0\ 1)$	$Y_{5'} = (0\ -1\ 0)$
$Z_{1'} = (0\ 1\ 0)$	$Z_{3'} = (0\ -1\ 0)$	$Z_{5'} = (0\ 0\ -1)$
$X_{2'} = (0\ 0\ 1)$	$X_{4'} = (0\ 0\ 1)$	$X_{6'} = (1\ 0\ 0)$
$Y_{2'} = (0\ 1\ 0)$	$Y_{4'} = (0\ -1\ 0)$	$Y_{6'} = (0\ 1\ 0)$
$Z_{2'} = (-1\ 0\ 0)$	$Z_{4'} = (1\ 0\ 0)$	$Z_{6'} = (0\ 0\ 1)$

* Choice of coordinate system is the same as Purcell and Kotz.[15]

overlap between P_{A_x} and P_{B_z} is

$$S_{xz}^{A,B} = (P_{11}Q_{31} + P_{12}Q_{32})S^{A,B}(P_\pi P_\pi) - P_{13}Q_{33}S^{A,B}(P_\sigma P_\sigma). \quad (3)$$

The minus sign for σ overlap is due to the unique z (not opposite z) direction for A and B. For a d–d overlap, first project the arbitrarily oriented d-orbital D on A in terms of the five d-orbitals in the coordinate system of the common relative vector $\mathbf{R}_3$, viz. ($\Gamma = \theta = d_{z^2}$, $\Gamma = \varepsilon = d_{x^2-y^2}$, $\Gamma = \xi = d_{yz}$, etc.)

$$D_\Gamma^A = A_\theta \tfrac{1}{2}(2\mathbf{R}_3 - \mathbf{R}_1^2 - \mathbf{R}_2^2) + A_\varepsilon(\sqrt{3}/2)(\mathbf{R}_1^2 - \mathbf{R}_2^2) + A_\xi\sqrt{3}\mathbf{R}_2\mathbf{R}_3 + A_\eta\sqrt{3}\mathbf{R}_1\mathbf{R}_3 + A_\zeta\sqrt{3}\mathbf{R}_1\mathbf{R}_2. \quad (4)$$

The projection coefficients A_Γ are obtained by writing the given $D_\Gamma^A = \sum_{ij} C_{ij}\mathbf{A}_i\mathbf{A}_j$ and expanding $\mathbf{A}_i$ and $\mathbf{A}_j$s in terms of $\mathbf{R}_1$, $\mathbf{R}_2$ and $\mathbf{R}_3$ as in equation (1). Thus,

$$A_\theta = \sum_{ij} C_{ij}P_{i3}P_{j3};$$

$$A_\varepsilon = (2/\sqrt{3})\left[\sum_{ij} C_{ij}P_{i1}P_{j1} + \tfrac{1}{2}A_\theta\right]$$

$$A_\xi = (1/\sqrt{3})\left[\sum_{ij} C_{ij}(P_{i2}P_{j3} + P_{i3}P_{j2})\right]$$

$$A_\eta = (1/\sqrt{3})\left[\sum_{ij} C_{ij}(P_{i1}P_{j3} + P_{i3}P_{j1})\right]$$

$$A_\zeta = (1/\sqrt{3})\left[\sum_{ij} C_{ij}(P_{i2}P_{j3} + P_{i3}P_{j2})\right]. \quad (5)$$

A similar projection for d-orbital at B yields B_θ, B_ε, B_ξ, B_η and B_ζ. The overlap between the D_Γ^A and $D_{\Gamma'}^B$ orbitals in terms of tabulated σ, π and δ overlaps is:

$$S_{\Gamma\Gamma'}^{A,B} = A_\theta B_\theta S^{AB}(d\sigma d\sigma) - (A_\xi B_\xi + A_\eta B_\eta)S^{A,B} \times (d\pi d\pi) + (A_\varepsilon B_\varepsilon + A_\zeta B_\zeta) \times S^{A,B}(d\delta d\delta). \quad (6)$$

After the projections of the p and d orbitals have been calculated it is easy to obtain s–p overlap where the s orbitals combine only with the $\mathbf{R}_3$ projection of p, (namely the P_z orbitals). Similarly the s orbital combines only with the A_θ projection coefficient (the d_{z^2} orbital). To obtain the P_π–d_π overlap combine the P_π projection of P (namely on $\mathbf{R}_1$ and $\mathbf{R}_2$) and the d_π projection on d (namely through A_η and A_ξ) respectively and multiply by -1. For the P_σ–d_σ overlap combine the P_σ projection of P (namely on $\mathbf{R}_3$) and the d_σ projection of d (namely through A_θ). The atomic overlaps are given in Table 5b (s–d, M_8); Table 6 (d–d, M_8); Table 9 (d–d, M_4); Table 12 (d–d, M_6); Table 14 (P–P, M_6). The projection coefficients in equation (5), etc. are basic geometrical properties of the clusters and are independent of the cluster size. The σ, π and δ overlap integrals of equation (6) differ with cluster size and can be fed into the computer program. So can the orientation vector **Rs** which are different for clusters of other than the geometry considered here. General and sample computer programs for the projection coefficients and total overlaps are available on request.

CLUSTER MO ENERGIES AND MIXING OF σ, π AND δ ORBITALS

The d-atomic cluster molecular orbitals $M_8(O_h)$ and $M_4(T_d)$ and their energies appear to have never been obtained. The M_6 orbitals and energies were clarified in 1980 by Bursten, Cotton and Stanley.[13] To insure that the cluster can be superimposed as building blocks, we have used the same coordinates and origin. To insure that the degenerate orbitals of the same symmetry can mix, not only between different clusters but also among s, p and d cluster orbitals, we have maintained consistent phase and transformation properties for *all* of the MOs. To expedite the process of finding MOs for d-orbitals we look for transformation properties of d-orbitals which are similar to those of the p-orbitals which have been given.[14] The following correspondences among atomic orbital transformations were found, after some tedious algebra and anxious anticipation, to be true for operators of the O_h and T_d and point

groups:

$$s \sim z \sim d_{z^2}$$

$$x \sim dxz \sim dxy$$

$$y \sim d_{yz} \sim d_{x^2-y^2}.$$

From there on the construction of MOs was straightforward except for the necessary checking of phases to make sure that the correct and *identical* transformation matrix holds for the three components, e.g. $t_{1u}(s)$, $t_{1u}(P_x, P_y)$, $t_{1u}(P_z)$, $t_{1u}(d_{z^2})$, $t_{1u}(d_{xz}, d_{yz})$ and $t_{1u}(d_{x^2-y^2}, d_{xy})$ in $M_8(O_h)$. Irreducible representations of s, p and d cluster orbitals are summarized in Table 3. Detailed MOs and energy normalizations are given in the Tables 4 (M_8), 7 (M_4) and 10 (M_6). From the atomic overlaps derived in the last section, the normalization factors for these MOs can be obtained. As long as the degenerate orbitals are mutually orthogonal, their energies can be obtained from any one of the degenerate sets in a straightforward manner. We used the Mulliken–Wolfsberg–Helmholz[23,45] method of approximating the Coulomb integral H_{AA} by the valence orbital ionization energy of the corresponding s, p and d orbitals represented symbolically by ε. The resonance integral is assumed to be proportional to the overlap between the two atomic orbitals A and B;

$$\beta_{AB} = KS\tfrac{1}{2}(H_{AA}+H_{BB}). \qquad (7)$$

For mixing between MOs of the same irreducible representation, one needs to take only one of the degenerate components from each set since we have made sure these components share an *identical* transformation matrix. For example, referring to Table 4, we may mix $t_{1uz}(\theta)$ with $t_{1uz}(\varepsilon)$ and $t_{1uz}(\pi)$. The resulting mixing coefficients are equally applicable to $t_{1ux}(\theta)$, $t_{1ux}(\varepsilon)$ and $t_{1ux}(\xi)$. The resonance integral for mixing again may be taken to be proportional to the group overlaps—these are derived and tabulated in Table 5a (d–d, M_8), Table 5b (s–d, M_8), Table 7 (d–d, M_4) and Table 11 (d–d, M_6).

In summary, symmetry orbitals are first generated by group theory as a linear combination of atomic

Table 3. Summary of irreducible representations of s, p and d-orbital clusters*†

	$M_8(O_h)$	$M_4(T_d)$	$M_6(O_h)$
S or P_z or d_{z^2}	$A_{1g}\ A_{2u}$ $t_{1u}\ t_{2g}$	A_1 t_2	$A_{1g}\ e_g\ t_{1u}$
$(P\pi_x P\pi_y)$ or $(d\pi_{xz} d\pi_{yz})$	$e_g\ e_u$ $t_{1g}\ t_{1u}$ $t_{2g}\ t_{2u}$	e t_1 t_2	$t_{1g}\ t_{1u}$ $t_{2g}\ t_{2u}$
$(d\delta_{x^2-y^2}$, $d\delta_{xy})$	$e_g\ e_u$ $t_{1g}\ t_{1u}$ $t_{2g}\ t_{2u}$	e t_1 t_2	$A_{2g}\ A_{2u}$ $e_g e_u$ $t_{2g}\ t_{2u}$

* See Figs 4 and 5 for definitions of the local axes.

† The bonding, non-bonding or anti-bonding characteristic of these orbitals are illustrated by the energy levels of Sr_8, La_8 and O_6 in Tables 15 and 16.

Table 4. $M_8(O_h)$ d-orbital cluster:* MO† normalization constants‡ and energies§

$d\sigma$ orbital: $\theta = d_{z^2} \cong \frac{1}{2}(3z^2-r^2)$

(same form for s-orbital, simply replace θ by s).

$$a_{1g} = (\theta_1+\theta_2+\theta_3+\theta_4+\theta_5+\theta_6+\theta_7+\theta_8)/(8+24s_{\theta\theta}^{1,2}+24s_{\theta\theta}^{1,6})^{1/2}$$

$$E(a_{1g}) = (\varepsilon+3\beta_{\theta\theta}^{1,2}+3\beta_{\theta\theta}^{1,6})/(1+3s_{\theta\theta}^{1,2}+3s_{\theta\theta}^{1,6})$$

$$a_{2u} = (\theta_1+\theta_2+\theta_3+\theta_4-\theta_5-\theta_6-\theta_7-\theta_8)/(8+24s_{\theta\theta}^{1,2}-24s_{\theta\theta}^{1,6})^{1/2}$$

$$E(a_{2u}) = (\varepsilon+3\beta_{\theta\theta}^{1,2}-3\beta_{\theta\theta}^{1,6})/(1+3s_{\theta\theta}^{1,2}-3s_{\theta\theta}^{1,6})$$

$$t_{1ux} = N_{t1u}(\theta_1-\theta_2+\theta_3-\theta_4-\theta_5+\theta_6-\theta_7+\theta_8)$$

$$t_{1uy} = N_{t1u}(\theta_1+\theta_2-\theta_3-\theta_4-\theta_5-\theta_6+\theta_7+\theta_8)$$

$$t_{1uz} = N_{t1u}(\theta_1-\theta_2-\theta_3+\theta_4-\theta_5+\theta_6+\theta_7-\theta_8)$$

$$N_{t1u} = (8-8s_{\theta\theta}^{1,2}+8s_{\theta\theta}^{1,6})^{-1/2}$$

$$E(t_{1u}) = (\varepsilon-\beta_{\theta\theta}^{1,2}+\beta_{\theta\theta}^{1,6})/(1-s_{\theta\theta}^{1,2}+s_{\theta\theta}^{1,6})$$

$$t_{2g\xi} = N_{t_{2g}}(\theta_1-\theta_2+\theta_3-\theta_4+\theta_5-\theta_6+\theta_7-\theta_8)$$

$$t_{2g\eta} = N_{t_{2g}}(\theta_1+\theta_2-\theta_3-\theta_4+\theta_5+\theta_6-\theta_7-\theta_8)$$

$$t_{2g\zeta} = N_{t_{2g}}(\theta_1-\theta_2-\theta_3+\theta_4+\theta_5-\theta_6-\theta_7+\theta_8)$$

$$N_{t_{2g}} = (8-8s_{\theta\theta}^{1,2}-8s_{\theta\theta}^{1,6})^{-1/2}$$

$$E(t_{2g}) = (\varepsilon-\beta_{\theta\theta}^{1,2}-\beta_{\theta\theta}^{1,6})/(1-s_{\theta\theta}^{1,2}-s_{\theta\theta}^{1,6})$$

Table 4 (*continued*).

$d\delta$ orbital: $\varepsilon = d_{x^2-y^2} \cong \sqrt{3}/2(x^2-y^2)$; $\zeta = d_{xy} \cong \sqrt{3}xy$
(same form for $d\pi$- orbital; simply replace ε by $\xi \equiv dyz \cong \sqrt{3}yz$
and replace ζ by $\eta \equiv dxz \cong \sqrt{3}xz$)

$$e_gU = (\varepsilon_1+\varepsilon_2+\varepsilon_3+\varepsilon_4+\varepsilon_5+\varepsilon_6+\varepsilon_7+\varepsilon_8)/(8+16S_{\varepsilon\varepsilon}^{1,2}+8S_{\varepsilon\varepsilon}^{1,4}+16S_{\varepsilon\varepsilon}^{1,6}+8S_{\varepsilon\varepsilon}^{1,8})^{1/2}$$

$$e_gV = (\zeta_1+\zeta_2+\zeta_3+\zeta_4-\zeta_5-\zeta_6-\zeta_7-\zeta_8)/(8+16S_{\zeta\zeta}^{1,2}+8S_{\zeta\zeta}^{1,4}-16S_{\zeta\zeta}^{1,6}-8S_{\zeta\zeta}^{1,8})^{1/2}$$

$$E(e_g) = (\varepsilon+2\beta_{\zeta\zeta}^{1,2}+\beta_{\zeta\zeta}^{1,4}-2\beta_{\zeta\zeta}^{1,6}-\beta_{\zeta\zeta}^{1,8})/(1+2S_{\zeta\zeta}^{1,2}+S_{\zeta\zeta}^{1,4}-2S_{\zeta\zeta}^{1,6}-S_{\zeta\zeta}^{1,8})$$

$$e_uU = (\zeta_1+\zeta_2+\zeta_3+\zeta_4+\zeta_5+\zeta_6+\zeta_7+\zeta_8)/(8+16S_{\zeta\zeta}^{1,2}+8S_{\zeta\zeta}^{1,4}+16S_{\zeta\zeta}^{1,6}+8S_{\zeta\zeta}^{1,8})^{1/2}$$

$$e_uV = (-\varepsilon_1-\varepsilon_2-\varepsilon_3-\varepsilon_4+\varepsilon_5+\varepsilon_6+\varepsilon_7+\varepsilon_8)/(8+16S_{\varepsilon\varepsilon}^{1,2}+8S_{\varepsilon\varepsilon}^{1,4}-16S_{\varepsilon\varepsilon}^{1,6}-8S_{\varepsilon\varepsilon}^{1,8})^{1/2}$$

$$E(e_u) = (\varepsilon+2\beta_{\varepsilon\varepsilon}^{1,2}+\beta_{\varepsilon\varepsilon}^{1,4}-2\beta_{\varepsilon\varepsilon}^{1,6}-\beta_{\varepsilon\varepsilon}^{1,8})/(1+2S_{\varepsilon\varepsilon}^{1,2}+S_{\varepsilon\varepsilon}^{1,4}-2S_{\varepsilon\varepsilon}^{1,6}-S_{\varepsilon\varepsilon}^{1,8})$$

$$t_{1gx} = N_{t1gx}[-\zeta_1+\zeta_2-\zeta_3+\zeta_4+\zeta_5-\zeta_6+\zeta_7-\zeta_8+\sqrt{3}(-\varepsilon_1+\varepsilon_2-\varepsilon_3+\varepsilon_4-\varepsilon_5+\varepsilon_6-\varepsilon_7+\varepsilon_8)]$$

$$t_{1gy} = N_{t1gy}[-\zeta_1-\zeta_2+\zeta_3+\zeta_4+\zeta_5+\zeta_6-\zeta_7-\zeta_8+\sqrt{3}(\varepsilon_1+\varepsilon_2-\varepsilon_3-\varepsilon_4+\varepsilon_5+\varepsilon_6-\varepsilon_7-\varepsilon_8)]$$

$$t_{1gz} = (\zeta_1-\zeta_2-\zeta_3+\zeta_4-\zeta_5+\zeta_6+\zeta_7-\zeta_8)/(8-16S_{\zeta\zeta}^{1,2}+8S_{\zeta\zeta}^{1,4}+16S_{\zeta\zeta}^{1,6}-8S_{\zeta\zeta}^{1,8})^{1/2}$$

$$E(t_{1g}) = (\varepsilon-2\beta_{\zeta\zeta}^{1,2}+\beta_{\zeta\zeta}^{1,4}+2\beta_{\zeta\zeta}^{1,6}-\beta_{\zeta\zeta}^{1,8})/(1-2S_{\zeta\zeta}^{1,2}+S_{\zeta\zeta}^{1,4}+2S_{\zeta\zeta}^{1,6}-S_{\zeta\zeta}^{1,8})$$

$$t_{1ux} = N_{t_{1ux}}[\sqrt{3}(\zeta_1-\zeta_2+\zeta_3-\zeta_4+\zeta_5-\zeta_6+\zeta_7-\zeta_8)-\varepsilon_1+\varepsilon_2-\varepsilon_3+\varepsilon_4+\varepsilon_5-\varepsilon_6+\varepsilon_7-\varepsilon_8]$$

$$t_{1uy} = N_{t_{1ux}}[\sqrt{3}(-\zeta_1-\zeta_2+\zeta_3+\zeta_4-\zeta_5-\zeta_6+\zeta_7+\zeta_8)-\varepsilon_1-\varepsilon_2+\varepsilon_3+\varepsilon_4+\varepsilon_5+\varepsilon_6-\varepsilon_7-\varepsilon_8]$$

$$t_{1uz} = (\varepsilon_1-\varepsilon_2-\varepsilon_3+\varepsilon_4-\varepsilon_5+\varepsilon_6+\varepsilon_7-\varepsilon_8)/(8-16S_{\varepsilon\varepsilon}^{1,2}+8S_{\varepsilon\varepsilon}^{1,4}+16S_{\varepsilon\varepsilon}^{1,6}-8S_{\varepsilon\varepsilon}^{1,8})^{1/2}$$

$$E(t_{1u}) = (\varepsilon-2\beta_{\varepsilon\varepsilon}^{1,2}+\beta_{\varepsilon\varepsilon}^{1,4}+2\beta_{\varepsilon\varepsilon}^{1,6}-\beta_{\varepsilon\varepsilon}^{1,8})/(1-2S_{\varepsilon\varepsilon}^{1,2}+S_{\varepsilon\varepsilon}^{1,4}+2S_{\varepsilon\varepsilon}^{1,6}-S_{\varepsilon\varepsilon}^{1,8})$$

$$t_{2g\xi} = N_{t_{2g\xi}}[\sqrt{3}(\zeta_1-\zeta_2+\zeta_3-\zeta_4-\zeta_5+\zeta_6-\zeta_7+\zeta_8)-\varepsilon_1+\varepsilon_2-\varepsilon_3+\varepsilon_4-\varepsilon_5+\varepsilon_6-\varepsilon_7+\varepsilon_8]$$

$$t_{2g\eta} = N_{t_{2g\eta}}[\sqrt{3}(-\zeta_1-\zeta_2+\zeta_3+\zeta_4+\zeta_5+\zeta_6-\zeta_7-\zeta_8)-\varepsilon_1-\varepsilon_2+\varepsilon_3+\varepsilon_4-\varepsilon_5-\varepsilon_6+\varepsilon_7+\varepsilon_8]$$

$$t_{2g\zeta} = (\varepsilon_1-\varepsilon_2-\varepsilon_3+\varepsilon_4+\varepsilon_5-\varepsilon_6-\varepsilon_7+\varepsilon_8)/(8-16S_{\varepsilon\varepsilon}^{1,2}+8S_{\varepsilon\varepsilon}^{1,4}-16S_{\varepsilon\varepsilon}^{1,6}+8S_{\varepsilon\varepsilon}^{1,8})^{1/2}$$

$$E(t_{2g}) = (\varepsilon-2\beta_{\varepsilon\varepsilon}^{1,2}+\beta_{\varepsilon\varepsilon}^{1,4}-2\beta_{\varepsilon\varepsilon}^{1,6}+\beta_{\varepsilon\varepsilon}^{1,8})/(1-2S_{\varepsilon\varepsilon}^{1,2}+S_{\varepsilon\varepsilon}^{1,4}-2S_{\varepsilon\varepsilon}^{1,6}+S_{\varepsilon\varepsilon}^{1,8})$$

$$t_{2u\xi} = N_{t_{2u\xi}}[-\zeta_1+\zeta_2-\zeta_3+\zeta_4-\zeta_5+\zeta_6-\zeta_7+\zeta_8+\sqrt{3}(-\varepsilon_1+\varepsilon_2-\varepsilon_3+\varepsilon_4+\varepsilon_5-\varepsilon_6+\varepsilon_7-\varepsilon_8)]$$

$$t_{2u\eta} = N_{t_{2u\eta}}[-\zeta_1-\zeta_2+\zeta_3+\zeta_4-\zeta_5-\zeta_6+\zeta_7+\zeta_8+\sqrt{3}(\varepsilon_1+\varepsilon_2-\varepsilon_3-\varepsilon_4-\varepsilon_5-\varepsilon_6+\varepsilon_7+\varepsilon_8)]$$

$$t_{2u\zeta} = (\zeta_1-\zeta_2-\zeta_3+\zeta_4+\zeta_5-\zeta_6-\zeta_7+\zeta_8)/(8-16S_{\zeta\zeta}^{1,2}+8S_{\zeta\zeta}^{1,4}-16S_{\zeta\zeta}^{1,6}+8S_{\zeta\zeta}^{1,8})^{1/2}$$

$$E(t_{2u}) = (\varepsilon-2\beta_{\zeta\zeta}^{1,2}+\beta_{\zeta\zeta}^{1,4}-2\beta_{\zeta\zeta}^{1,6}+\beta_{\zeta\zeta}^{1,8})/(1-2S_{\zeta\zeta}^{1,2}+S_{\zeta\zeta}^{1,4}-2S_{\zeta\zeta}^{1,6}+S_{\zeta\zeta}^{1,8})$$

* p-orbital clusters ($P\sigma P\pi$) without normalization and energy have been given by Watanabe.[14] We use the same coordinate system and atomic numbering of Watanabe (note some confusion in their # 5 and # 8 on the footnote of p. 183 which we clarify). This is so that *orbital mixing of* p *and* d *if desired may be easily made.* It is noted that θ transforms as P_z, dxy and dxz both transform as Px, and $d_{x^2-y^2}$ and dyz both transform as Py. The normalization and energy of the $M_8(O_h)$ p-orbital cluster may be obtained in parallel to the d-cluster.

† Components for degenerate representation are specified exactly and consistently so that mixing with corresponding components of $M_4(T_d)$ and/or $M_8(O_h)$ of the same symmetry may be correctly effected.

‡ Normalized up to nearest neighbor overlap, e.g. between adjacent atoms but not opposite atoms. Only those required for energy computation are given in detail including overlap.

§ Energy expression may be obtained from one of the degenerate levels provided the latter are orthogonal to one another. Only energies for the orbital of a given type (for example, $d\sigma$ or $d\pi$ orbitals) and a given symmetry (for example A_{1g} or t_{1u} symmetry) *per se* are given. Mixing of different types of orbitals of the same symmetry [e.g. $t_{1u}(d\sigma)$ with $t_{1u}(d\pi)$] not included here. For group overlap responsible for such mixing see Table 2.

Table 5a. Group d-orbital overlap for mixing of $M_8(O_h)$ cluster MOs of the same irreducible representation*

Mixing of	
π, δ	$S[t_{1g\zeta}(\eta)t_{1g\zeta}(\zeta)] = N_1N_2(-16S^{1,2}_{\eta\zeta}+8S^{1,4}_{\eta\zeta}+16S^{1,6}_{\eta\zeta}-8S^{1,8}_{\eta\zeta})$
σ, π, δ	$S[t_{1u\xi}(\theta)t_{1u\xi}(\xi)] = N_1N_2(-16S^{1,2}_{\theta\xi}+8S^{1,4}_{\theta\xi}+16S^{1,6}_{\theta\xi}-8S^{1,8}_{\theta\xi})$
	$S[t_{1u\xi}(\theta)t_{1u\xi}(\varepsilon)] = N_1N_2(-16S^{1,2}_{\theta\varepsilon}+8S^{1,4}_{\theta\varepsilon}+16S^{1,6}_{\theta\varepsilon}-8S^{1,8}_{\theta\varepsilon})$
	$S[t_{1u\xi}(\xi)t_{1u\xi}(\varepsilon)] = N_1N_2(-16S^{1,2}_{\xi\varepsilon}+8S^{1,4}_{\xi\varepsilon}+16S^{1,6}_{\xi\varepsilon}-8S^{1,8}_{\xi\varepsilon})$
π, δ	$S[e_gV(\eta)e_gV(\zeta)] = N_1N_2(16S^{1,2}_{\eta\zeta}+8S^{1,4}_{\eta\zeta}-16S^{1,6}_{\eta\zeta}-8S^{1,8}_{\eta\zeta})$
σ, π, δ	$S[t_{2g\zeta}(\theta)t_{2g\zeta}(\xi)] = N_1N_2(-16S^{1,2}_{\theta\xi}+8S^{1,4}_{\theta\xi}-16S^{1,6}_{\theta\xi}+8S^{1,8}_{\theta\xi})$
	$S[t_{2g\zeta}(\theta)t_{2g\zeta}(\varepsilon)] = N_1N_2(-16S^{1,2}_{\theta\varepsilon}+8S^{1,4}_{\theta\varepsilon}-16S^{1,6}_{\theta\varepsilon}+8S^{1,8}_{\theta\varepsilon})$
	$S[t_{2g\zeta}(\xi)t_{2g\zeta}(\varepsilon)] = N_1N_2(-16S^{1,2}_{\xi\varepsilon}+8S^{1,4}_{\xi\varepsilon}-16S^{1,6}_{\xi\varepsilon}+8S^{1,8}_{\xi\varepsilon})$
π, δ	$S[t_{2u\zeta}(\eta)t_{2u\zeta}(\zeta)] = N_1N_2(-16S^{1,2}_{\eta\zeta}+8S^{1,4}_{\eta\zeta}-16S^{1,6}_{\eta\zeta}+8S^{1,8}_{\eta\zeta})$
π, δ	$S[e_uV(\xi)e_uV(\varepsilon)] = N_1N_2(16S^{1,2}_{\xi\varepsilon}+8S^{1,4}_{\xi\varepsilon}-16S^{1,6}_{\xi\varepsilon}-8S^{1,8}_{\xi\varepsilon})$

* N_1 and N_2 symbolically stand for the normalization constants of the two molecular orbitals for which the overlap is derived.

Table 5b. s–d Overlap between $M_8(O_h)$ cluster MOs and cluster atoms*†‡

$S[t_{2g\zeta}(S)t_{2g\zeta}(\theta)] = -N_1N_2 8S^{1,2}_{s\theta}$

$S[t_{2g\zeta}(S)t_{2g\zeta}(\zeta)] = N_1N_2(-16S^{1,2}_{s\xi}+8S^{1,4}_{s\xi}-16S^{1,6}_{s\xi}+8S^{1,8}_{s\xi})$

$S[t_{2g\zeta}(S)t_{2g\zeta}(\varepsilon)] = N_1N_2(-16S^{1,2}_{s\varepsilon}+8S^{1,4}_{s\varepsilon}-16S^{1,6}_{s\varepsilon}+8S^{1,8}_{s\varepsilon})$

$S[t_{1u\xi}(S)t_{1u\xi}(\theta)] = -N_1N_2 8S^{1,2}_{s\theta}$

$S[t_{1u\xi}(S)t_{1u\xi}(\zeta)] = N_1N_2(-16S^{1,2}_{s\xi}+8S^{1,4}_{s\xi}+16S^{1,6}_{s\xi}-8S^{1,8}_{s\xi})$

$S[t_{1u\xi}(S)t_{1u\xi}(\varepsilon)] = N_1N_2(-16S^{1,2}_{s\varepsilon}+8S^{1,4}_{s\varepsilon}+16S^{1,6}_{s\varepsilon}-8S^{1,8}_{s\varepsilon})$

$S^{1,2}_{s\theta} = 0.5000S^{1,2}(Sd\sigma) = S^{1,3}_{s\theta} = S^{1,4}_{s\theta} = 0.0310$

$S^{1,6}_{s\theta} = 0 = S^{1,7}_{s\theta} = S^{1,8}_{s\theta} \approx S^{1,5}_{s\theta}$

$S^{1,2}_{s\varepsilon} = 0.1443S^{1,2}(Sd\sigma) = S^{1,3}_{s\varepsilon} = S^{2,4}_{s\varepsilon} = 0.0089$

$S^{1,4}_{s\varepsilon} = -0.2886S^{1,4}(Sd\sigma) = S^{2,3}_{s\varepsilon} = -0.0178$

$S^{1,6}_{s\varepsilon} = 0.2886S^{1,6}(Sd\sigma) = S^{2,5}_{s\varepsilon} = 0.0482$

$S^{1,8}_{s\varepsilon} = -0.5773S^{1,8}(Sd\sigma) = S^{2,7}_{s\varepsilon} = -0.0964$

$S^{1,2}_{s\xi} = -0.4083S^{1,2}(Sd\sigma) = S^{1,3}_{s\xi} = S^{2,4}_{s\xi} = -0.0253$

$S^{1,4}_{s\xi} = 0.8164S^{1,4}(Sd\sigma) = +S^{2,3}_{s\xi} = 0.0506$

$S^{1,6}_{s\xi} = 0.4083S^{1,6}(Sd\sigma) = S^{2,5}_{s\xi} = 0.0682$

$S^{1,8}_{s\xi} = -0.8164S^{1,8}(Sd\sigma) = S^{2,7}_{s\xi} = -0.1363$

* If one constructs an 8×8 square matrix of atomic labels, the 64 matrix elements representing combinations of atomic orbitals run from 1st row to 8th row as (11, 12, 13, 14) (15, 16, 17, 18) (21 ... 24) (25 ... 28) (31 ... 34) (35 ... 38) (41 ... 44) (45 ... 48) ... (81 ... 84) (85 ... 88). The corresponding overlap integrals have quality patterns as follows: $(0\,s\,s\,s')(\sim 0\,s''\,s''\,s''')(s\,0\,s'\,s)(s''\sim 0\,s'''\,s'')(s\,s'\,0\,s)(s''\,s'''\sim 0\,s'')(s'\,s\,s\,0)$ $(s'''\,s''\,s''\sim 0)(0\,s''\,s''\,s''')(0\,s\,s\,s')(s''\sim 0\,s'''\,s'')(s\,0\,s'\,s)(s''\,s'''\sim 0\,s'')(s\,s'\,0\,s)$ $(s'''\,s''\,s''\sim 0)(s'\,s\,s\,0)$. In the special case of S–d_{z^2} overlap $s = s'$, $s'' = s'''$ $= 0$.

† N_1 and N_2 represent symbolically the first and second normalization constants of the two molecular orbitals.

‡ Numerical values for S–d atomic overlap are for La_8 in $LaAlO_3$ cubic crystal. $a = 3.80$ Å.

orbitals (Tables 4, 7, 10 and 13). The "energies" of these preliminary molecular orbitals are computed from coulomb and atomic resonance integrals. The former is approximated by the valence orbital ionization energies (VOIE) of the atomic orbitals—the latter by the Mulliken–Wolfsberg–Helmholz method, using the atomic overlaps in Tables 6, 9 and 12. When it happens that n of these preliminary molecular orbitals has the same symmetry, these n-symmetry orbitals are again linearly combined. The mixing coefficients and energies of such combinations as final molecular orbitals are obtained by solving the $n \times n$ secular determinant. The group coulomb integral in this secular determinant is approximated by the preliminary molecular orbital energies and the group resonance integral by the group overlaps (Tables 5, 8 and 11), again via the Mulliken–Wolfsberg–Helmholtz method.

RELATIVE ORBITAL SYMMETRY OF CLUSTERS AND THE PEROVSKITE PHASE TRANSITION

Phase transitions in solids have been treated with sophisticated techniques,[39–41] many of which invoke the cooperative Jahn–Teller effect.[38,46] Here

Table 6. Atomic d-overlap*† between $M_8(O_h)$ cluster atomic orbitals

d-Overlap		$\times S(d\sigma d\sigma) +$	$\times S(d\pi d\pi) +$	$\times S(d\delta d\delta)$	La_8 in $LaAlO_3$
$S^{1,6}_{\varepsilon\zeta}$	=	−0.1443	0.1922	−0.0479	0.0033
$S^{1,6}_{\theta\theta}$	=	0.0000	0.6663	0.3331	0.1306
$S^{1,6}_{\varepsilon\varepsilon}$	=	0.0833	0.5553	0.3602	0.1286
$S^{1,6}_{\eta\eta}$	=	−0.5000	−0.1666	−0.3333	−0.1426
$S^{1,6}_{\xi\xi}$	=	0.1666	0.2776	0.5547	0.1030
$S^{1,6}_{\zeta\zeta}$	=	−0.2500	−0.3330	−0.4163	−0.1247
$S^{1,6}_{\theta\varepsilon}$	=	0.0000	−0.1926	0.1922	−0.0274
$S^{1,6}_{\theta\xi}$	=	0.0000	0.1363	−0.1357	0.0194
$S^{1,6}_{\xi\varepsilon}$	=	0.1178	−0.3926	0.2740	−0.0362
$S^{1,6}_{\eta\zeta}$	=	−0.3535	0.2354	0.1176	−0.0252
$S^{1,8}_{\varepsilon\zeta}$	=	0.0000	0.0000	0.0000	0.0000
$S^{1,8}_{\theta\theta}$	=	0.0000	0.6664	0.3333	0.1306
$S^{1,8}_{\varepsilon\varepsilon}$	=	0.3333	0.2221	0.4443	0.1228
$S^{1,8}_{\eta\eta}$	=	0.0000	−0.3333	−0.6665	−0.0833
$S^{1,8}_{\xi\xi}$	=	0.6666	0.1111	0.2221	0.1624
$S^{1,8}_{\zeta\zeta}$	=	0.0000	−0.6667	−0.3332	−0.1306
$S^{1,8}_{\theta\varepsilon}$	=	0.0000	0.3848	−0.3848	0.0546
$S^{1,8}_{\theta\xi}$	=	0.0000	−0.2721	0.2721	−0.0386
$S^{1,8}_{\xi\varepsilon}$	=	0.4714	−0.1571	−0.3142	0.0559
$S^{1,8}_{\eta\zeta}$	=	0.0000	0.4714	−0.4714	0.0669

*Superscripts stand for the numbering of the two atomic d-orbitals in the cluster. Subscripts stand for the orbital type ($\theta = d_{z^2}$, $\varepsilon = d_{x^2-y^2}$, $\xi = d_{yz}$, $\eta = d_{xz}$, $\zeta = d_{xy}$). Accuracy is ± 0.0004.

† $S^{1,2}$ and $S^{1,4}$ are given in the $M_4(T_d)$ case of the same numbering and coordinate system (Table 9). Many overlap integrals between different atomic numbering (labelling) are found to be equal under the coordinate and labelling system used. viz. $S^{1,6}_{ij} = S^{1,7}_{ij} = S^{2,5}_{ij} = S^{2,8}_{ij} = S^{3,5}_{ij} = S^{3,8}_{ij} = S^{4,6}_{ij} = S^{4,7}_{ij} = S^{5,2}_{ij} = S^{5,3}_{ij} = S^{6,1}_{ij} = S^{6,4}_{ij} = S^{7,1}_{ij} = S^{7,4}_{ij} = S^{8,2}_{ij} = S^{8,3}_{ij}$. Similarly, $S^{1,8}_{ij} = S^{2,7}_{ij} = S^{3,6}_{ij} = S^{4,5}_{ij} = S^{5,4}_{ij} = S^{6,3}_{ij} = S^{7,2}_{ij} = S^{8,1}_{ij}$. Also, when four atoms are added to build up to $M_8(O_h)$, the many overlaps in $M_4(T_d)$ case are equal to the new overlaps. viz. $S^{1,2}_{ij} = S^{5,6}_{ij} = S^{5,7}_{ij} = S^{6,5}_{ij} = S^{6,8}_{ij} = S^{7,5}_{ij} = S^{7,8}_{ij} = S^{8,6}_{ij} = S^{8,7}_{ij}$. Similarly, $S^{1,4}_{ij} = S^{5,8}_{ij} = S^{6,7}_{ij} = S^{7,6}_{ij} = S^{8,5}_{ij}$. The overlaps between opposite atoms are assumed negligible, viz. $S^{1,5} = S^{2,6} = S^{3,7} = S^{4,8} = S^{5,1} = S^{6,2} = S^{7,3} = S^{8,4} \cong 0$. The 'overlaps' between the same atom are either zero ($S^{kk}_{ij} = 0$) or one ($S^{kk}_{ii} = 1$).

Table 7. $M_4(T_d)$ d-orbital cluster:* MO† normalization‡ constants and energies§

$d\sigma$ orbital: $\theta = d_{z^2} \cong \frac{1}{2}(3z^2-r^2)$	
$a_1 = (\theta_1+\theta_2+\theta_3+\theta_4)/(4+12S_{\theta\theta}^{1,2})^{1/2}$	$E(a_1) = (\varepsilon+3\beta_{\theta\theta}^{1,2})/(1+3S_{\theta\theta}^{1,2})$
$t_{2\xi} = N(\theta_1-\theta_2+\theta_3-\theta_4)$	$N = (4-4S_{\theta\theta}^{1,2})^{-1/2}$
$t_{2\eta} = N(\theta_1+\theta_2-\theta_3-\theta_4)$	$E(t_2) = (\varepsilon-\beta_{\theta\theta}^{1,2})/(1-S_{\theta\theta}^{1,2})$
$t_{2\zeta} = N(\theta_1-\theta_2-\theta_3+\theta_4)$	
$d\delta$ orbital: $\varepsilon = d_{x^2-y^2} \cong \sqrt{3}/2(x^2-y^2)$; $\zeta = d_{xy} \cong \sqrt{3}xy$ (same form for $d\pi$ orbital, simply replace ε by $\xi \equiv d_{yz} \cong \sqrt{3}yz$ and replace ζ by $\eta = d_{xz} \cong \sqrt{3}xz$)	
$e_u = (\varepsilon_1+\varepsilon_2+\varepsilon_3+\varepsilon_4)/(4+8S_{\varepsilon\varepsilon}^{1,2}+4S_{\varepsilon\varepsilon}^{1,4})^{1/2}$	$E(e) = (\varepsilon+2\beta_{\zeta\zeta}^{1,2}+\beta_{\zeta\zeta}^{1,4})/(1+2S_{\zeta\zeta}^{1,2}+S_{\zeta\zeta}^{1,4})$
$e_v = (\zeta_1+\zeta_2+\zeta_3+\zeta_4)/(4+8S_{\zeta\zeta}^{1,2}+4S_{\zeta\zeta}^{1,4})^{1/2}$	
$t_{1x} = [-\zeta_1+\zeta_2-\zeta_3+\zeta_4+\sqrt{3}(-\varepsilon_1+\varepsilon_2-\varepsilon_3+\varepsilon_4)]$	
$t_{1y} = [-\zeta_1-\zeta_2+\zeta_3+\zeta_4+\sqrt{3}(\varepsilon_1+\varepsilon_2-\varepsilon_3-\varepsilon_4)]$	$E(t_1) = (\varepsilon-2\beta_{\zeta\zeta}^{1,2}+\beta_{\zeta\zeta}^{1,4})/(1-2S_{\zeta\zeta}^{1,2}+S_{\zeta\zeta}^{1,4})$
$t_{1z} = (\zeta_1-\zeta_2-\zeta_3+\zeta_4)/(4-8S_{\zeta\zeta}^{1,2}+4S_{\zeta\zeta}^{1,4})^{1/2}$	
$t_{2\xi} = [\sqrt{3}(-\zeta_1+\zeta_2-\zeta_3+\zeta_4)+\varepsilon_1-\varepsilon_2+\varepsilon_3-\varepsilon_4]$	
$t_{2\eta} = [\sqrt{3}(\zeta_1+\zeta_2-\zeta_3-\zeta_4)+\varepsilon_1+\varepsilon_2-\varepsilon_3-\varepsilon_4]$	$E(t_2) = (\varepsilon-2\beta_{\varepsilon\varepsilon}^{1,2}+\beta_{\varepsilon\varepsilon}^{1,4})/(1-2S_{\varepsilon\varepsilon}^{1,2}+S_{\varepsilon\varepsilon}^{1,4})$
$t_{2\zeta} = (-\varepsilon_1+\varepsilon_2+\varepsilon_3-\varepsilon_4)/(4-8S_{\varepsilon\varepsilon}^{1,2}+4S_{\varepsilon\varepsilon}^{1,4})^{1/2}$	

*†‡§ See the footnotes for Table 4.

we attempt to find a qualitative chemist's way of viewing the transition from orbital symmetry. Our ultimate purpose is to find a qualitative day-to-day guide for the preparation of shape-memory alloys[47] that exhibit martensitic transitions.[47–49] For an illustration of the theory we take the perovskite[37] crystal ABO_3 which consists of one octahedral BO_6 cluster inside a cubic A_8 cluster. We wish to explore the electronic difference between $SrTiO_3$ and $LaAlO_3$ that accounts for their different phase transition characteristics (see Figs. 1, 2 and 3). The cubic crystal dimensions are $a = 3.90$ Å for $SrTiO_3$[50] and $a = 3.790$ Å for $LaAlO_3$.[51] Since for comparison absolute errors are not important, we make the following Mulliken–Wolfsberg–Helmholz approximations.[23] We take for the resonance integral the VOIE of neutral atoms and consider only the atomic orbitals that apply to the neutral atom. The resonance integral is taken to be proportional to the overlap [equation (7)] with a proportionality constant[52] of $K = 1.75$ for all. The VOIEs are obtained or estimated using data from McGlynn's book.[23] For La, they are obtained from the spectroscopic tables of Moore.[53] Single zeta Slater atomic orbitals are used with the zeta value calculated according to Burn's prescription.[54] The overlap integrals are taken from the tables of Boudreaux, Cusachs and Dureau.[55] Energies and orbitals of the clusters are first obtained for $O_6(2p)$, $La_8(6s)$, $La_8(5d)$ and $Sr_8(5s)$. Then the Ti($3d4s4p$) and Al($3s$, $3p$) orbitals are mixed in O_6 for the TiO_6 and AlO_6 octahedrons. Mixing among the orbitals with the same symmetry in La_8 is also effected by using the initial cluster energy as the Coulomb integral. The effect of $6s$ on the $5d$ levels of La_8 is seen to be small. The numerical values of overlaps for specific systems

Table 8. d-Orbital overlap* for mixing of $M_4(T_d)$ cluster MOs of the same irreducible representation

Mixing of	
π, δ	$S[t_{1z}(\eta)t_{1z}(\zeta)] = N_1N_2(-8S_{\eta\zeta}^{1,2}+4S_{\eta\zeta}^{1,4})$
π, δ	$S[eV(\eta)eV(\zeta)] = N_1N_2(8S_{\eta\zeta}^{1,2}+4S_{\eta\zeta}^{1,4})$
σ, π, δ	$S[t_{2\zeta}(\theta)t_{2\zeta}(\xi)] = N_1N_2(8S_{\theta\xi}^{1,2}-4S_{\theta\xi}^{1,4})$
	$S[t_{2\zeta}(\theta)t_{2\zeta}(\varepsilon)] = N_1N_2(8S_{\theta\varepsilon}^{1,2}-4S_{\theta\varepsilon}^{1,4})$
	$S[t_{2\zeta}(\xi)t_{2\zeta}(\varepsilon)] = N_1N_2(-8S_{\xi\varepsilon}^{1,2}+4S_{\xi\varepsilon}^{1,4})$

* N_1 and N_2 symbolically stand for the normalization constants of the two molecular orbitals for which the overlap is derived.

Table 9. Atomic d-overlap*† between $M_4(T_d)$ cluster atomic orbitals

d-Overlap		$\times S(d\sigma d\sigma) +$	$\times S(d\pi d\pi) +$	$\times S(d\delta d\delta)$	La_8 in $LaAlO_3$‡
$S^{1,2}_{\varepsilon\zeta}$	=	0.0361	0.2405	0.5893	0.0085
$S^{1,2}_{\theta\theta}$	=	0.2500	0.6665	0.0834	0.0273
$S^{1,2}_{\varepsilon\varepsilon}$	=	0.0208	−0.1945	−0.3263	−0.0037
$S^{1,2}_{\eta\eta}$	=	0.5000	−0.0833	0.0833	0.0261
$S^{1,2}_{\xi\xi}$	=	0.1667	−0.4721	−0.1944	−0.0008
$S^{1,2}_{\zeta\zeta}$	=	0.0625	0.0834	0.3541	0.0062
$S^{1,2}_{\theta\varepsilon}$	=	0.0721	−0.1924	0.1203	0.0005
$S^{1,2}_{\theta\xi}$	=	−0.2041	0.1360	0.0680	−0.0083
$S^{1,2}_{\xi\varepsilon}$	=	−0.0589	−0.3928	0.4517	−0.0097
$S^{1,2}_{\eta\zeta}$	=	−0.1768	−0.2357	0.4124	−0.0132
$S^{1,4}_{\varepsilon\zeta}$	=	0.0000	0.0000	0.0000	0.0000
$S^{1,4}_{\theta\theta}$	=	0.2500	0.6665	0.0834	0.0273
$S^{1,4}_{\varepsilon\varepsilon}$	=	0.0833	0.2222	0.6944	0.0111
$S^{1,4}_{\eta\eta}$	=	0.0000	−0.6666	−0.3333	−0.0143
$S^{1,4}_{\xi\xi}$	=	0.6665	0.1111	0.2221	0.0395
$S^{1,4}_{\zeta\zeta}$	=	0.0000	−0.3333	−0.6667	−0.0086
$S^{1,4}_{\theta\varepsilon}$	=	−0.1443	0.3848	−0.2406	−0.0009
$S^{1,4}_{\theta\xi}$	=	0.4081	−0.2721	−0.1361	0.0166
$S^{1,4}_{\xi\varepsilon}$	=	−0.2356	−0.1571	0.3928	−0.0149
$S^{1,4}_{\eta\zeta}$	=	0.0000	−0.4713	0.4714	−0.0080

*Superscripts stand for the numbering of the two atomic d-orbitals in the cluster. Subscripts stand for the orbital type ($\theta = d_{z^2}$, $\varepsilon = d_{x^2-y^2}$, $\xi = d_{yz}$, $\eta = d_{xz}$, $\zeta = d_{xy}$).

†Many overlap integrals between different atomic numbering (labelling) are found to be equal in the coordinate and labelling system used, viz. $S^{1,2}_{ij} = S^{1,3}_{ij} = S^{2,1}_{ij} = S^{2,4}_{ij} = S^{3,1}_{ij} = S^{3,4}_{ij} = S^{4,2}_{ij} = S^{4,3}_{ij}$. Similarly $S^{1,4}_{ij} = S^{2,3}_{ij} = S^{3,2}_{ij} = S^{4,1}_{ij}$. In the special case of $d_{z^2}-d_{z^2}$ overlap $S^{1,2}_{\theta\theta} = S^{1,4}_{\theta\theta}$.

‡Last column gives values for La_8 cluster in cubic $LaAlO_3$. La–La distance is 3.80 Å. Note that $M_4(T_d)$ having atoms 1–4 is part of the $M_8(O_h)$ cluster which has the same initial labelling 1–4 but has atoms 5–8 added on.

Table 10. $M_6(O_h)$ d-orbital cluster:* MO normalization constants and energies

$d\sigma$ orbital: $\theta = d_{z^2} \cong \frac{1}{2}(3z^2-r^2)$

$$a_{1g} = (\theta'_1+\theta'_2+\theta'_3+\theta'_4+\theta'_5+\theta'_6)/(6+6S^{1'3'}_{\theta\theta}+24S^{1'5'}_{\theta\theta})^{1/2} \qquad E(a_{1g}) = (\varepsilon+\beta^{1'3'}_{\theta\theta}+4\beta^{1'5'}_{\theta\theta})/(1+S^{1'3'}_{\theta\theta}+4S^{1'5'}_{\theta\theta})$$

$$t_{1ux} = (\theta'_2-\theta'_4)/(2-2S^{1'3'}_{\theta\theta})^{1/2} \qquad E(t_{1u}) = (\varepsilon-\beta^{1'3'}_{\theta\theta})/(1-S^{1'3'}_{\theta\theta})$$

$$t_{1uy} = (\theta'_3-\theta'_1)/(2-S^{1'3'}_{\theta\theta})^{1/2} \qquad E(t_{1u}) = (\varepsilon-\beta^{1'3'}_{\theta\theta})/(1-S^{1'3'}_{\theta\theta})$$

$$t_{1uz} = (\theta'_5-\theta'_6)/(2-S^{1'3'}_{\theta\theta})^{1/2} \qquad E(t_{1u}) = (\varepsilon-\beta^{1'3'}_{\theta\theta})/(1-S^{1'3'}_{\theta\theta})$$

$$e_gU = (\theta'_1+\theta'_2+\theta'_3+\theta'_4-2\theta'_5-2\theta'_6)/(12+12S^{1'3'}_{\theta\theta}-24S^{1'5'}_{\theta\theta})^{1/2} \qquad E(e_g) = (\varepsilon+\beta^{1'3'}_{\theta\theta}-2\beta^{1'5'}_{\theta\theta})/(1+S^{1'3'}_{\theta\theta}-2S^{1'5'}_{\theta\theta})$$

$$e_gV = (\theta'_1-\theta'_2+\theta'_3-\theta'_4)/(4+4S^{1'3'}_{\theta\theta}-8S^{1'5'}_{\theta\theta})^{1/2}$$

Table 10 (*continued*)

$d\pi$ orbital: $\eta = dxz \cong \sqrt{3}xz$; $\zeta = dyz \cong \sqrt{3}yz$	
$t_{2g\xi} = N_{t2g}(-\xi'_1+\xi'_3-\xi'_5-\xi'_6)$	$N(t_{2g}) = (4+8S^{1'5'}_{\xi\xi}-4S^{1'3'}_{\xi\xi})^{-1/2}$
$t_{2g\eta} = N_{t2g}(\eta'_2-\eta'_4+\eta'_5-\eta'_6)$	$E(t_{2g}) = (\varepsilon+2\beta^{1'5'}_{\xi\xi}-\beta^{1'3'}_{\xi\xi})/$
$t_{2g\zeta} = N_{t2g}(\eta_1+\xi_2+\eta_3+\xi_4)$	$(1+2S^{1'5'}_{\xi\xi}-S^{1'3'}_{\xi\xi})$
$t_{1gx} = N_{t1g}(\xi'_1-\xi'_3-\xi'_5-\xi'_6)$	$N(t_{1g}) = (4-8S^{1'5'}_{\xi\xi}-4S^{1'3'}_{\xi\xi})^{-1/2}$
$t_{1gy} = N_{t1g}(\eta'_2-\eta'_4-\eta'_5+\eta'_6)$	$E(t_{1g}) = (\varepsilon-2\beta^{1'5'}_{\xi\xi}-\beta^{1'3'}_{\xi\xi})/$
$t_{1gz} = N_{t1g}(\eta'_1-\xi'_2+\eta'_3-\xi'_4)$	$(1-2S^{1'5'}_{\xi\xi}-S^{1'3'}_{\xi\xi})$
$t_{1ux} = N_{t1u}(\eta'_1-\eta'_3-\eta'_5-\eta'_6)$	$N(t_{1u}) = (4-8S^{1'5'}_{\eta\eta}-4S^{1'3'}_{\eta\eta})^{-1/2}$
$t_{1uy} = N_{t1u}(-\xi'_2+\xi'_4+\xi'_5-\xi'_6)$	$E(t_{1u}) = (\varepsilon-2\beta^{1'5'}_{\eta\eta}-\beta^{1'3'}_{\eta\eta})/$
$t_{1uz} = N_{t1u}(-\xi'_1-\eta'_2-\xi'_3-\eta'_4)$	$(1-2S^{1'5'}_{\eta\eta}-S^{1'3'}_{\eta\eta})$
$t_{2u\xi} = N_{t2u}(-\eta_1+\eta_3-\eta_5-\eta_6)$	$N(t_{2u}) = (4+8S^{1'5'}_{\eta\eta}-4S^{1'3'}_{\eta\eta})^{-1/2}$
$t_{2u\eta} = N_{t2u}(-\xi_2+\xi_4-\xi_5+\xi_6)$	$E(t_{2u}) = (\varepsilon+2\beta^{1'5'}_{\eta\eta}-\beta^{1'3'}_{\eta\eta})/$
$t_{2u\zeta} = N_{t2u}(-\xi_1+\eta_2-\xi_3+\eta_4)$	$(1+2S^{1'5'}_{\eta\eta}-S^{1'3'}_{\eta\eta})$
$d\delta$ orbital: $\varepsilon = d_{x^2-y^2} \cong \sqrt{3}/2(x^2-y^2)$; $\zeta = d_{xy} \cong \sqrt{3}xy$	
$e_gU = (\varepsilon'_1-\varepsilon'_2+\varepsilon'_3-\varepsilon'_4)/$	$E(e_g) = (\varepsilon+2\beta^{1'5'}_{\varepsilon\varepsilon}+\beta^{1'3'}_{\varepsilon\varepsilon})/$
$(4+8S^{1'5'}_{\varepsilon\varepsilon}+4S^{1'3'}_{\varepsilon\varepsilon})^{1/2}$	$(1+2S^{1'5'}_{\varepsilon\varepsilon}+S^{1'3'}_{\varepsilon\varepsilon})$
$e_gV = -(\varepsilon'_1+\varepsilon'_2+\varepsilon'_3+\varepsilon'_4+2\varepsilon'_5+2\varepsilon'_6)/$	
$(12+24S^{1'5'}_{\varepsilon\varepsilon}+12S^{1'3'}_{\varepsilon\varepsilon})^{1/2}$	
$e_uU = -(\zeta'_1+\zeta'_2+\zeta'_3+\zeta'_4+2\zeta'_5+2\zeta'_6)/$	
$(12+24S^{1'5'}_{\zeta\zeta}+12S^{1'3'}_{\zeta\zeta})^{1/2}$	
$e_uV = (-\zeta_1+\zeta_2-\zeta_3+\zeta'_4)/$	$E(e_u) = (\varepsilon+2\beta^{1'5'}_{\zeta\zeta}+\beta^{1'3'}_{\zeta\zeta})/$
$(4+8S^{1'5'}_{\zeta\zeta}+4S^{1'3'}_{\zeta\zeta})^{1/2}$	$(1+2S^{1'5'}_{\zeta\zeta}+S^{1'3'}_{\zeta\zeta})$
$A_{2g} = (\varepsilon'_1+\varepsilon'_2+\varepsilon'_3+\varepsilon'_4-\varepsilon'_5-\varepsilon'_6)/$	$E(A_{2g}) = (\varepsilon-4\beta^{1'5'}_{\varepsilon\varepsilon}+\beta^{1'3'}_{\varepsilon\varepsilon})/$
$(6-24S^{1'5'}_{\varepsilon\varepsilon}+6S^{1'3'}_{\varepsilon\varepsilon})^{1/2}$	$(1-4S^{1'5'}_{\varepsilon\varepsilon}+S^{1'3'}_{\varepsilon\varepsilon})$
$A_{2u} = (\zeta'_1+\zeta'_2+\zeta'_3+\zeta'_4-\zeta'_5-\zeta'_6)/$	$E(A_{2u}) = (\varepsilon-4\beta^{1'5'}_{\zeta\zeta}+\beta^{1'3'}_{\zeta\zeta})/$
$(6-24S^{1'5'}_{\zeta\zeta}+6S^{1'3'}_{\zeta\zeta})^{1/2}$	$(1-4S^{1'5'}_{\zeta\zeta}+S^{1'3'}_{\zeta\zeta})$
$t_{2u\xi} = (\varepsilon_4-\varepsilon_2)/(2-2S^{1'3'}_{\varepsilon\varepsilon})^{1/2}$	
$t_{2u\eta} = (\varepsilon_3-\varepsilon_1)/(2-2S^{1'3'}_{\varepsilon\varepsilon})^{1/2}$	$E(t_{2u}) = (\varepsilon-\beta^{1'3'}_{\varepsilon\varepsilon})/(1-S^{1'3'}_{\varepsilon\varepsilon})$
$t_{2u\zeta} = (\varepsilon_5-\varepsilon_6)/(2-2S^{1'3'}_{\varepsilon\varepsilon})^{1/2}$	
$t_{2g\xi} = N_{t2g}(\zeta_4-\zeta_2)$	$N(t_{2g}) = (2-2S^{1'3'}_{\zeta\zeta})^{-1/2}$
$t_{2g\eta} = N_{t2g}(\zeta_1-\zeta_3)$	$E(t_{2g}) = (\varepsilon-\beta^{1'3'}_{\zeta\zeta})/(1-S^{1'3'}_{\zeta\zeta})$
$t_{2g\zeta} = N_{t2g}(\zeta_5-\zeta_6)$	

* Qualitative symmetry orbitals for $M_6(O_h)$ have been given in Appendix to Chap. 18 of Purcell and Kotz.[15] Their results did not include normalization constants, energy expression, orthogonalization of one $e_g(\sigma)$ component with A_{1g} nor consistent phases and transformation matrices for the degenerate components. All of these we have now included. We used the same coordinate system and atomic labelling as theirs but add a 'prime' to distinguish the atoms from the $M_8(O_h)$ set.

Table 11. Group d-orbital overlap* for mixing of $M_6(O_h)$ cluster MOs of the same irreducible representation

Mixing of	
σ, π	$S[t_{1ux}(\eta)t_{1ux}(\theta)] = N_1N_2 8S_{\eta\theta}^{1'2'} = -N_1N_2 8S_{\eta\theta}^{3'2'}$
σ, δ	$S[e_gU(\varepsilon)e_gU(\theta)] = N_1N_2 24S_{\varepsilon\theta}^{1'2'} = +N_1N_2 24S_{\varepsilon\theta}^{3'2'}$
π, δ	$S[t_{2g\xi}(\xi)t_{2g\xi}(\zeta)] = N_1N_2 8S_{\zeta\xi}^{2'1'} = -8N_1N_2S_{\zeta\xi}^{2'3'}$
π, δ	$S[t_{2u\eta}(\varepsilon)t_{2u\eta}(\xi)] = N_1N_2 8S_{\varepsilon\xi}^{1'2'} = -8N_1N_2S_{\varepsilon\xi}^{3'2'}$

* N_1 and N_2 symbolically stand for the normalization constants of the two molecular orbitals for which the overlap is derived.

Table 12. Atomic d-overlap between $M_6(O_h)$ cluster atomic orbitals*

d-Overlap		$\times S(d\sigma d\sigma) +$	$\times S(d\pi d\pi) +$	$\times S(d\delta d\delta)$	Equivalent orbital; same orbital type	Zero overlap
$S_{\theta\theta}^{1'3'}$	=	1.0000	0.0000	0.0000	$^{2'4'}$; $^{3'1'}$; $^{4'2'}$; $^{5'6'}$; $^{6'5'}$	
$S_{\varepsilon\varepsilon}^{1'3'}$	=	0.0000	0.0000	1.0000	$^{2'4'}$; $^{3'1'}$; $^{4'2'}$; $^{5'6'}$; $^{6'5'}$	
$S_{\eta\eta}^{1'3'}$	=	0.0000	−1.0000	0.0000	$^{3'1'}$; $-(^{2'4'})$; $-(^{4'2'})$; $-(^{5'6'})$; $-(^{6'5'})$	
$S_{\xi\xi}^{1'3'}$	=	0.0000	1.0000	0.0000	$^{3'1'}$; $-(^{2'4'})$; $-(^{4'2'})$; $-(^{5'6'})$; $-(^{6'5'})$	
$S_{\zeta\zeta}^{1'3'}$	=	0.0000	0.0000	−1.0000	$^{2'4'}$; $^{3'1'}$; $^{4'2'}$; $^{5'6'}$; $^{6'5'}$	
$S_{\theta\theta}^{1'5'}$	=	0.0625	0.7500	0.1875	All equal except for $^{1'3'}$ given above	
$S_{\varepsilon\varepsilon}^{1'5'}$	=	0.1875	0.2500	0.5625	All pairs with one labelled $^{5'}$ or $^{6'}$; negative of the rest except $^{1'3'}$ given above	
$S_{\eta\eta}^{1'5'}$	=	0.0000	−0.5000	−0.5000	$^{1'6'}$; $-(^{3'5'})$; $-(^{3'6'})$; $^{5'1'}$; $^{6'1'}$; $-(^{6'3'})$; $-(^{5'3'})$	$^{1'2'}$; $^{1'4'}$; $^{2'1'}$; $^{2'3'}$; $^{3'2'}$; $^{3'4'}$; $^{4'1'}$; $^{4'3'}$
$S_{\xi\xi}^{1'5'}$	=	0.7501	0.0000	0.2500	$^{1'6'}$; $-(^{3'5'})$; $-(^{3'6'})$; $^{5'1'}$; $^{6'1'}$; $-(^{6'3'})$; $-(^{5'3'})$	Ditto
$S_{\zeta\zeta}^{1'5'}$	=	0.0000	−0.5000	−0.5000	All pairs with one labelled $^{5'}$ or $^{6'}$. Negative of the rest except $^{1'3'}$ given above	
$S_{\eta\theta}^{1'2'}$	=	−0.2165	0.0000	0.2165	$^{2'6'}$; $^{3'4'}$; $^{4'6'}$; $^{5'4'}$; $^{6'4'}$; $-(^{4'5'})$; $-(^{1'4'})$; $-(^{2'5'})$; $-(^{3'2'})$; $-(^{5'2'})$; $-(^{6'2'})$	All remaining
$S_{\varepsilon\theta}^{1'2'}$	=	0.1083	−0.4330	0.3247	$^{1'4'}$; $^{2'5'}$; $^{2'6'}$; $^{3'1'}$; $^{3'2'}$; $^{4'5'}$; $^{4'6'}$; $^{5'2'}$; $^{5'4'}$; $^{6'2'}$; $^{6'4'}$; negative of rest	$^{2'4'}$; $^{3'1'}$; $^{1'3'}$; $^{4'2'}$; $^{5'6'}$; $^{6'5'}$
$S_{\zeta\zeta}^{2'1'}$	=	0.0000	−0.5000	0.5000	$^{2'5'}$; $^{2'6'}$; $^{4'3'}$; $^{5'2'}$; $^{5'4'}$; $-(^{2'3'})$; $-(^{4'1'})$; $-(^{4'5'})$; $-(^{4'6'})$; $-(^{6'2'})$; $-(^{6'4'})$	
$S_{\varepsilon\xi}^{1'2'}$	=	−0.3750	0.0000	0.3750	$^{1'5'}$; $^{3'4'}$; $^{3'6'}$; $^{5'1'}$; $^{5'3'}$; $-(^{1'4'})$; $-(^{1'6'})$; $-(^{3'2'})$; $-(^{3'5'})$; $-(^{6'1'})$; $-(^{6'3'})$	
$S_{\eta\eta}^{2'6'}$	=	−0.7501	0.0000	−0.2500	$^{4'5'}$; $^{5'4'}$; $^{6'2'}$; $-(^{6'4'})$; $-(^{2'5'})$; $-(^{4'6'})$; $-(^{5'2'})$	
$S_{\xi\xi}^{2'6'}$	=	0.0000	0.5000	0.5000	$^{4'5'}$; $^{5'4'}$; $^{6'2'}$; $-(^{6'4'})$; $-(^{2'5'})$; $-(^{4'6'})$; $-(^{5'2'})$	

*Overlaps not given are zero and may be checked by inspection of symmetry.

Table 13. $M_6(O_h)$ p-orbital cluster: MO normalization constants and energies

$p\sigma$ orbitals: $z = Pz$	
$a_{1g} = (z'_1+z'_2+z'_3+z'_4+z'_5+z'_6)/(6+6S_{zz}^{1'3'}+24S_{zz}^{1'5'})^{1/2}$	$E(a_{1g}) = (\varepsilon+\beta_{zz}^{1'3'}+4\beta_{zz}^{1'5'})/(1+S_{zz}^{1'3'}+4S_{zz}^{1'5'})$
$t_{1ux} = N_{t1u}(z'_2-z'_4)$	$E(t_{1u}) = (\varepsilon-\beta_{zz}^{1'3'})/(1-S_{zz}^{1'3'})$
$t_{1uy} = N_{t1u}(z'_3-z'_1)$	$N(t_{1u}) = (2-2S_{zz}^{1'3'})^{-1/2}$
$t_{1uz} = N_{t1u}(z'_5-z'_6)$	
$e_gU = (z'_1+z'_2+z'_3+z'_4-2z'_5-2z'_6)/(12+12S_{zz}^{1'3'}-24S_{zz}^{1'5'})^{1/2}$	$E(e_g) = (\varepsilon+\beta_{zz}^{1'3'}-2\beta_{zz}^{1'5'})/(1+S_{zz}^{1'3'}-2S_{zz}^{1'5'})$
$e_gV = (z'_1-z'_2+z'_3-z'_4)/(4+4S_{zz}^{1'3'}-8S_{zz}^{1'5'})^{1/2}$	
$p\pi$ orbitals	
$t_{2g\xi} = N_{t2g}(-y'_1+y'_3-y'_5-y'_6)$	$N(t_{2g}) = (4+8S_{xx}^{2'5'}-4S_{xx}^{2'4'})^{-1/2}$
$t_{2g\eta} = N_{t2g}(x'_2-x'_4+x'_5-x'_6)$	$E(t_{2g}) = (\varepsilon+2\beta_{xx}^{2'5'}-\beta_{xx}^{2'4'})/(1+2S_{xx}^{2'5'}-S_{xx}^{2'4'})$
$t_{2g\zeta} = N_{t2g}(x'_1+y'_2+x'_3+y'_4)$	
$t_{1gx} = N_{t1g}(y'_1-y'_3-y'_5-y'_6)$	$N(t_{1g}) = (4-8S_{xx}^{2'5'}-4S_{xx}^{2'4'})^{-1/2}$
$t_{1gy} = N_{t1g}(x'_2-x'_4-x'_5+x'_6)$	$E(t_{1g}) = (\varepsilon-2\beta_{xx}^{2'5'}-\beta_{xx}^{2'4'})/(1-2S_{xx}^{2'5'}-S_{xx}^{2'4'})$
$t_{1gz} = N_{t1g}(x'_1-y'_2+x'_3-y'_4)$	
$t_{1ux} = N_{t1u}(x'_1-x'_3-x'_5-x'_6)$	$N(t_{1u}) = (4+8S_{yx}^{1'2'}+2S_{xx}^{2'4'})^{-1/2}$
$t_{1uy} = N_{t1u}(-y'_2+y'_4+y'_5-y'_6)$	$E(t_{1u}) = (\varepsilon+2\beta_{yx}^{1'2'}+\beta_{xx}^{2'4'})/(1+2S_{yx}^{1'2'}+S_{xx}^{2'4'})$
$t_{1uz} = N_{t1u}(-y'_1-x'_2-y'_3-x'_4)$	
$t_{2u\xi} = N_{t2u}(-x'_1+x'_3-x'_5-x'_6)$	$N(t_{2u}) = (4-8S_{yx}^{1'2'}+4S_{xx}^{2'4'})^{-1/2}$
$t_{2u\eta} = N_{t2u}(-y'_2+y'_4-y'_5+y'_6)$	$E(t_{2u}) = (\varepsilon-2\beta_{yx}^{1'2'}+\beta_{xx}^{2'4'})/(1-2S_{yx}^{1'2'}+S_{xx}^{2'4'})$
$t_{2u\zeta} = N_{t2u}(-y'_1+x'_2-y'_3+x'_4)$	

are recorded in Tables 6, 9, 12 and 14 where the general projections due to orientation are shown. Energies are given in Tables 15 and 16. The energy of TiO_6 is given next to that of Sr_8, similarly AlO_6 next to La_8.

If the crystal were completely ionic, the $Sr_8^{+16}(5s)$ orbitals would be completely empty as would be the $La_8^{+24}(6s5d)$ orbitals. By contrast, all oxygens now have a charge of -2, each having six $2p$ electrons. The TiO_6^{-8}, AlO_6^{-9} orbitals will both be filled with 36 electrons or up to the slightly antibonding $t_{1g}\pi$ molecular orbital which is essentially the oxygen orbital. The covalent bonding of oxygen to Ti and to Al have been accounted for by the mixing of Ti/Al orbitals in the MO_6 cluster orbital. The orbital ordering is essentially the same in the AlO_6 and TiO_6 clusters. The difference lies in the Sr_8 *vs* La_8 cluster orbitals. For the oxygen cluster to give some electrons to Sr for covalent bonding, the lowest empty orbital must be the $A_{1g}Sr_8(5s)$ orbital [Fig. 4(a)], which features bonding along the edges and favors C_4 rotation of the O_6 octahedron towards the edge. For the oxygen cluster to give some electrons to La for covalent bonding, there is in addition to $A_{1g}La_8(6s)$, another closely lying $A_{1g}La_8(5d\sigma)$ bonding orbital which is now empty. This orbital features bonding through the center [Fig. 4(b)] and favors C_3 rotation bringing all 6 of the octahedral atoms (instead of the 4 atoms in C_4 rotation) inside the cube to seek out the empty $5d_{z^2}$ orbitals lobes [Fig. 4(c)]. This we feel is one reason for the cubic to rhombohedral transition in $LaAlO_3$. The above,

Table 14. Zero group p-orbital overlap for mixing of t_{1u}s in $M_6(O_h)$ cluster MOs and non-zero atomic overlap between the cluster atoms*†

$$S[t_{1ux}(z')t_{1ux}(y')] \equiv 0$$

p-Overlap	$\times S(p_\sigma)$ +	$\times S(p_\pi)$	TiO_6 AlO_6	Equivalent overlap
$S_{zz}^{1'3'}$	1.0000	0.0000	0.002 0.003	$S_{zz}^{2'4'}$; $S_{zz}^{5'6'}$
$S_{zz}^{1'5'}$	0.5000	0.5000	0.0165 0.0195	$S_{zz}^{1'6'}$; $S_{zz}^{1'2'}$
$S_{xx}^{2'5'}$	0.5000	0.5000	0.0165 0.0195	$S_{yx}^{2'1'}$; $S_{xy}^{1'2'}$; $S_{yx}^{2'3'}$
$S_{xx}^{2'4'}$	0.0000	1.0000	0.000 0.000	$S_{yy}^{1'3'}$; $-S_{xx}^{1'3'}$
$S_{yx}^{1'2'}$	0.0000	1.0000	0.004 0.005	$S_{xy}^{2'3'}$; $S_{yy}^{2'6'}$

* Not exhaustive, remaining overlaps easily discerned by symmetry.
† Numerical values: for TiO_6 in $SrTiO_3$ cubic crystal, $a = 3.905$ Å, and for $LaAlO_3$ cubic crystal, $a = 3.79$ Å.

vastly simplified view, explains the experimental facts but suffers from some drawbacks. We do not know exactly how many electrons are transferred back to the M_8 cluster, hence while the LUMO we considered may play a part, higher empty orbitals of M_8 may also be involved. When excitation to higher orbitals is considered, it is tempting to consider the second-order Jahn–Teller effect[4] which was used by Pearson[43] to predict the molecular geometry. The vibration that determines the geometry will have

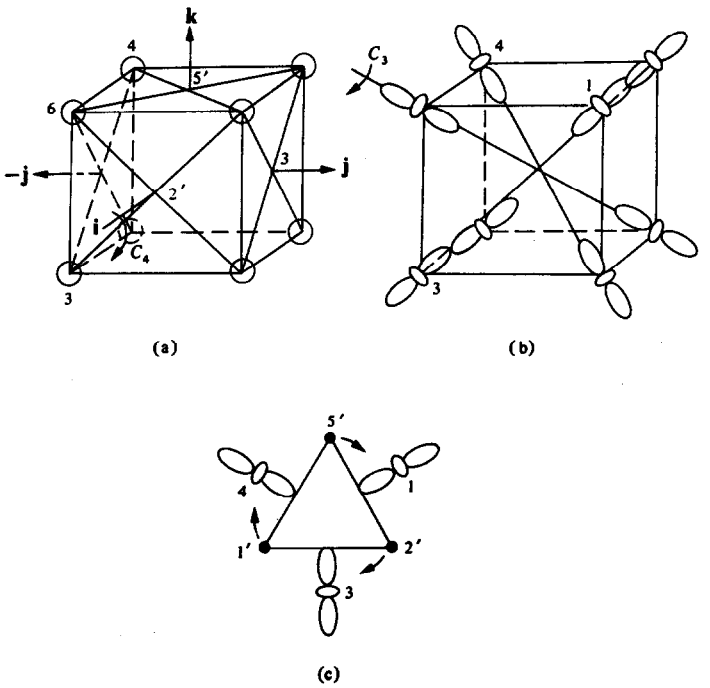


Fig. 4. The 'LUMO' $A_{1g}(6s)$ orbital of Sr_8^{+16} (a) and the 'LUMO' $A_{1g}(dz^2)$ orbital of La_8^{+24} (b). Three-fold rotation allows electrons in the occupied orbitals of the O_6 octahedron (1', 2', 3', 4', 5' and 6') to seek the empty and bonding orbital of La_8 (c).

Table 15. Cluster MO energy levels of $LaAlO_3$

La	$La_8(6S)$	$La_8(5d)$	$La_8(6S, 5d)$	AlO_6	$O_6(2P)$	Al(3S, 3P) O(2P)
			$+4.08A_{2u}$ 6S			
	$3.54A_{2u}$					
			$-2.21t_{2g}$ 6S			
	$-2.76t_{2g}$					
			$-3.56e_u\delta$			
		$-3.57e_u\delta$				
		$-4.10e_u\pi$	$-4.11e_u\pi$			
		$-4.33A_{2u}\sigma$				
			$-4.35A_{2u}\sigma$			
		$-4.73t_{1g}\pi$	$-4.68t_{1g}\pi$	$-4.81A_{1g}$		
				$-5.12t_{1u}$		
			$-5.55t_{2g}\sigma$			
		$-5.61t_{2g}\sigma$				
		$-5.73t_{1g}\delta$				
			$-5.74t_{1g}\delta$			
		$-5.88t_{2g}\delta$				
			$-5.89t_{2g}\delta$			
-5.91 6S						-5.93 3P
-6.52 5d		$-6.51t_{2g}\pi$	$-6.51t_{2g}\pi$			
			$-6.64t_{1u}$ 6S			
	$-6.73t_{1u}$					
		$-6.91t_{1u}\pi$	$-6.93t_{1u}\pi$			
		$-6.96t_{2u}\delta$	$-6.95t_{2u}\delta$			
		$-6.98t_{1u}\sigma$				
			$-7.08t_{1u}\sigma$			
		$-7.11t_{2u}\pi$	$-7.14t_{2u}\pi$			
		$-7.17t_{1u}\delta$	$-7.39t_{1u}\delta$			
			$-7.85e_g\delta$			
		$-7.88e_g\delta$				
		$-7.93e_g\pi$	$-7.96e_g\pi$			
			$-8.06A_{1g}\sigma$			
		$-8.09A_{1g}\sigma$				
	$-8.36A_{1g}$					
			$-8.40A_{1g}$ 6S			
						-11.25 3S
				$-15.31t_{1g}\pi$	$-15.31t_{1g}\pi$	
				$-15.35e_g\sigma$	$-15.35e_g\sigma$	
				$-15.67t_{2u}\pi$	$-15.67t_{2u}\pi$	
					$-15.75t_{1u}\sigma$	
				$-15.77t_{1u}$		
						-15.79 2P
					$-15.90t_{1u}\pi$	
				$-15.92t_{1u}$		
				$-16.23t_{2g}\pi$	$-16.23t_{2g}\pi$	
					$-16.67A_{1g}\sigma$	
				$-17.79A_{1g}$		

the same symmetry as the transition density, and the effect will be inversely proportional to the energy separation between the ground and excited state. The normal vibrations of both the M_8 cube and the M_6 octahedron will have irreducible representations spanned by the $P_{\pi x}$, $P_{\pi y}$, P_z cluster orbitals given in Table 3. Among these, the e_g vibrations of O_h decomposes[56] to the $A_{1g}(+B_{1g})$ irreducible representation of D_{4h} and thus can cause cubic to tetragonal distortion (without determining which is

Table 16. Cluster MO energy levels of $SrTiO_6$ (eV)

Sr(5S)	Sr_8(5S)	TiO_6	O_6(2P)	Ti(4S, 4P, 3d) O(2P)
	$1.04A_{2u}$			
		$-3.24A_{1g}$		
	$-3.57t_{2g}$			
		$-3.89t_{1u}$		
				-4.08 4P
-5.69 5S				
		$-5.79e_g$		
	$-6.41t_{1u}$			
				-7.09 4S
		$-7.18t_{2g}$		
				-7.66 3d
	$-7.82A_{1g}$			
		$-15.38t_{1g}\pi$	$-15.38t_{1g}\pi$	
			$-15.41e_g\sigma$	
		$-15.65e_g$		
		$-15.69t_{2u}\pi$	$-15.69t_{2u}\pi$	
		$-15.76t_{1u}$	$-15.76t_{1u}\sigma$	
				-15.79 2P
		$-15.88t_{1u}$	$-15.88t_{1u}\pi$	
			$-16.16t_{2g}\pi$	
		$-16.21t_{2g}$		
			$-16.54A_{1g}\sigma$	
		$-16.74A_{1g}$		

the axis of rotation or which atom moves etc.). Similarly the T_{2g} vibration contains the $A_{1g}(+E_g)$ irreducible representation of D_{3d} and can cause cubic to rhombohedral distortion. The question is, then, will electronic factors in $SrTiO_3$ yield a transition density of e_g (distorts to tetragonal) symmetry, and in $LaAlO_3$ will they produce a transition density of T_{2g} (distorts to rhombohedral) symmetry? From Tables 15 and 16, it is seen that the energy levels of Sr_8 are higher than those of La_8; therefore, excitation is not favoured. If the charge on Sr is $+1.5$ Sr_8^{+12} has 4 electrons (8×0.5) transferred from TiO_6. The last two give a t_{1u} hole in Sr_8^{+12}. The remaining two electrons in TiO_6 give a t_{1g} hole, then,[5] $t_{1g} \times t_{1u} = A_{1u} + E_u + T_{1u} + T_{2u}$. Neither e_g nor T_{2g} occurs here and no information results. If the charge on La is 2.375, La_8^{+19} has 5 electrons (8×0.625) transferred from AlO_6, all coming from t_{1g}. The acceptor orbitals will become $(A_{1g}6S)^2$, $(A_{1g}3d)^2$, (e_g).[1] The 1 electron going to e_g will result in a transition density of $t_{1g} \times e_g = T_{1g} + T_{2g}$. A T_{2g} vibration is precisely what causes the cubic rhombohedral distortion in a second-order Jahn–Teller effect. The energetic factors are more favorable here, because e_g of La_8 is lower than all of the orbitals of Sr_8. Small variation of charges will not alter the qualitative result. To account for the variation, other charge-transfer states may be mixed in with various coefficients (Fig. 5). Lest we be carried too far by the apparent success of such qualitative arguments, we should add that there are still interesting systems that are not so obviously explained which will be the subject of our next investigation. For example, in the perovskite structure of $PbTiO_3$, the rotation is C_4, but in the perovskite structure $BiFeO_3$ (another trivalent ion, Bi) the rotation is C_3. Yet both Pb_8 and Bi_8 presumably have similar 6p-cluster orbitals. In the closely related perovskite $BaTiO_3$, the rotation is either C_3 or C_4. These will be challenging systems for the application of the cluster orbitals and symmetry views developed in this paper. The methods we used are admittedly crude and qualitative. We would like to mention that similar Mulliken–Wolfsberg–Helmholz MO approximation was also applied to the study[58,59] of superconductivity in A_3B alloys with multiply-bonded A-metal atom chains, and with reasonable success.

Strictly speaking, the second-order Jahn-Teller effect should be discussed in terms of the MOs of the whole cluster A_8MO_6. But note that the energies of the set of empty A_8 orbitals and those of the set of filled MO_6 orbitals are far apart—of the order of 8 eV

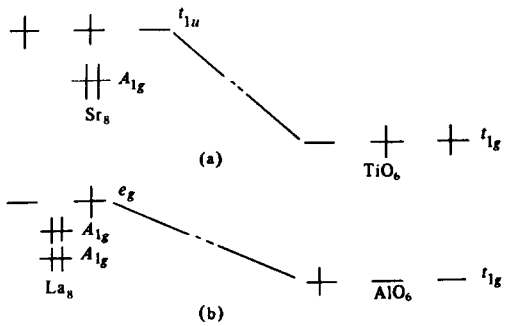


Fig. 5. Idealization of the charge transfer interaction between the donor (MO_6) and acceptor (A_8) clusters. (a) $TiO_6(t_{1g}^6) \rightarrow TiO_6(t_{1g}^2)Sr_8(A_{1g}^2 t_{1u}^2)$. The symmetry of the charge-transfer state and the transition charge density is t_{1g}(hole) $\otimes$ t_{1u}(hole). (b) $AlO_6(t_{1g}^6) \rightarrow AlO_6(t_{1g}^1)$ $La_8(A_{1g}^2 A_{1g}^2 e_g^1)$. The symmetry of the charge-transfer state is $t_{1g} \otimes e_g$. Only the optimum charge-transfer state is given that agrees with experimental observation. Actual transfer of charges may differ by small fractions—this difference can be accounted for by linear combination of other possible charge-transfer states with various coefficients. Note that although the empty states of TiO_6 are close to Sr_8, those states are essentially Ti atomic orbitals further away from Sr, shielded by O_6, and the closer ones don't have the right symmetry (t_{1u}). Same may be said of the AlO_6 and La_8 situation.

and the mixing between them is expected to be small. We have purposely omitted the mixing to see how expedient a qualitative model can be. Instead of mixing, we use the charge-transfer model between the filled HOMO (highest occupied MO) and the empty LUMO (lowest unoccupied MO) to account for deviation from ionicity and to discuss the relative motion between A_8 and MO_6. This is in the spirit of interaction between HOMO and LUMO of the *two reactants* commonly used in the study of inorganic reactions[60] (we have, in parallel, the 'reaction' of *two clusters*). It is also in the spirit of Woodward and Hoffmann's approach based on orbital symmetry.[42] The main purpose of the work is to give analytical expressions of the MOs and the overlaps of M_4, M_6 and M_8 clusters. The qualitative model for phase transition is exploratory. The results of this exploration will serve as encouragment and a guide to future endeavors.

Acknowledgements—Thanks are due Ms. Debora Anderson for her expert and patient typing. The assistance of Kong-seh Chiu with calculations on an IBM home computer is greatly appreciated. YNC wishes to thank the staff, especially Mr. Juan Gallegos, of the Computer Center of the Catholic University of America, for the advice on FORTRAN programming. Also, a word of thanks to Mrs. Vicky Himes of the National Bureau of Standards who very kindly helped with a literature search for crystallographic data.

REFERENCES

1. F. A. Cotton and M. H. Chisholm, *Chem. Eng. News* June 28, 1982, p. 40.
2. E. A. Muetterties, *Chem. Eng. News* Aug. 30, 1982, p. 28.
3. B. F. G. Johnson (ed.), *Transition Metal Clusters*. Wiley, New York (1980).
4. J. K. Burdett, *Molecular Shapes—Theoretical Models of Inorganic Stereochemistry*. Wiley, New York (1980).
5. J. D. Corbett, *Prog. Inorg. Chem.* 1976, **21**, 129; *Acc. Chem. Res.* 1981, **14**, 239.
6. P. Chini, *J. Organometal. Chem.* 1980, **200**, 37.
7. B. F. G. Johnson and J. Lewis, *Adv. Inorg. Chem. Radiochem.* 1981, **24**, 225.
8. B. F. G. Johnson and R. E. Benfield, *Topics in Inorganic and Organo Metallic Stereochemistry* (Edited by G. Geoffrey), p. 253. Wiley, New York (1982).
9. J. W. Lauher, *J. Am. Chem. Soc.* 1978, **100**, 5305; 1979, **101**, 2604.
10. K. Wade, *Adv. Inorg. Chem. Radiochem.* 1976, **18**, 1.
11. J. K. Burdett, *J. Am. Chem. Soc.* 1980, **102**, 450.
12. F. A. Cotton and T. E. Haas, *Inorg. Chem.* 1964, **3**, 10.
13. B. E. Bursten, F. A. Cotton and G. G. Stanley, *Israel J. Chemistry* 1980, **19**, 132.
14. H. Watanabe, *Operator Methods in Ligand Field Theory*. Prentice-Hall, New York (1966).
15. K. F. Purcell and J. Kotz, *Inorganic Chemistry*. W. B. Saunders, PA (1977).
16. C. E. Schäffer, *Proc. Roy. Soc.* 1967, **A297**, 96; *Struct. and Bond.* 1973, **14**, 69.
17. C. K. Jørgenson, R. Pappalardo and H. H. Schmidtke, *J. Chem. Phys.* 1933, **39**, 1422.
18. R. A. Levenson and H. B. Gray, *J. Am. Chem. Soc.* 1975, **97**, 6042.
19. A. B. P. Lever and H. B. Gray, *Acc. Chem. Res.* 1978, **11**, 348.
20. A. Dedius, T. A. Albright and R. Hoffmann, *J. Am. Chem. Soc.* 1979, **101**, 3141.
21. B. E. R. Schilling and R. Hoffmann, *J. Am. Chem. Soc.* 1979, **101**, 3456.
22. E. D. Jemmis, A. R. Pinhas and R. Hoffmann, *J. Am. Chem. Soc.* 1980, **102**, 2576.
23. S. P. McGlynn, L. G. Vanquickenborne, M. Kinoshita and D. G. Carroll, *Introduction to Applied Quantum Chemistry*. Holt, Rinehart and Winston, Inc. (1972).
24. C. D. Garner, *Transition Metal Clusters* (Edited by B. F. G. Johnson), pp. 265–344. Wiley, New York (1980).
25. F. A. Cotton and G. Wilkinson, *Advanced Inorganic Chemistry*. Interscience Publishers, New York (1980).
26. J. P. Fackler, Jr. and D. Coucouvanis, *J. Am. Chem. Soc.* 1966, **88**, 3913; L. E. McCandlish, E. C. Bissell, D. Coucouvanis, J. P. Fackler and K. Knox, *J. Am. Chem. Soc.* 1968, **90**, 7357.
27. L. D. Lower and L. F. Dahl, *J. Am. Chem. Soc.* 1976, **98**, 5046.

28. M. R. Churchill and J. Wormald, *J. Am. Chem. Soc.* 1971, **93**, 5670.
29. See "for example", P. R. Raithby, *Transition Metal Clusters* (Edited by B. F. G. Johnson), pp. 7–192. Wiley, New York (1980).
30. J. K. Burdett, *Nature* 1979, **279**, 121.
31. J. K. Burdett, *J. Solid State Chem.* 1980, **33**, 173.
32. M. Elian and R. Hoffmann, *Inorg. Chem.* 1975, **14**, 1058.
33. M. H. Whangbo and J. J. Foshee, *Inorg. Chem.* 1981, **20**, 113.
34. M. Weger and I. B. Goldberg, *Solid State Phys.* 1973, **28**, 2.
35. J. A. Tossell, *Am. Minerol.* 1976, **61**, 130.
36. J. A. Tossell, *J. Chem. Phys.* 1977, **66**, 5712.
37. W. Cochran and A. Zia, *Phys..Stat. Sol.* 1968, **25**, 273.
38. R. Engleman, *The Jahn–Teller Effect in Molecules and Crystals*, p. 253. Wiley Interscience, New York (1972).
39. R. S. Berry, S. A. Rice and J. Ross, *Physical Chemistry*, p. 887. Wiley, New York (1980).
40. K. A. Müller and H. Thomas (Eds), *Structural Phase Transitions I*, p. 32. Springer Verlag, Berlin (1981).
41. C. N. R. Rao and K. J. Rao, *Phase Transitions in Solids*, p. 316. McGraw-Hill, New York (1978).
42. R. B. Woodward and R. Hoffmann, *The Conservation of Orbital Symmetry*. Verlag Chemie (1970).
43. R. G. Pearson, *J. Am. Chem. Soc.* 1969, **91**, 4947.
44. T. A. Albright, R. Hoffmann, Y.-C. Tse and T. D'ottavio, *J. Am. Chem. Soc.* 1979, **101**, 3812.
45. M. Wolfsberg and L. Helmholz, *J. Chem. Phys.* 1952, **20**, 837.
46. G. A. Gehring and K. A. Ghering, *Rep. Prog. Phys.* 1975, **38**, 1.
47. J. Perkins (ed.), *Shape Memory Effect in Alloys*. Plenum, New York (1975).
48. F. E. Wang, S. J. Pickart and H. A. Alperin, *J. Appl. Phys.* 1972, **43**, 97.
49. F. E. Wang, W. J. Buehler and S. J. Pickart, *J. Appl. Phys.* 1965, **36**, 3232.
50. Landolt-Bornstein, New Series Vol. 3 *Ferro- and Antiferroelectric Substances* (Edited by T. Mitsui *et al.*), Springer Verlag, New York (1969).
51. S. Geller and V. B. Bala, *Acta Cryst.* 1956, **9**, 1019.
52. J. H. Ammeter, H. B. Bürgi, J. S. Thibeault and R. Hoffmann, *J. Am. Chem. Soc.* 1978, **100**, 3686.
53. C. E. Moore, *Atomic Energy Levels*, U.S. Department of Commerce Publication, NSRDS-NBS35, NBS Circular 467, reissued Dec. 1971.
54. G. Burns, *J. Chem. Phys.* 1964, **41**, 1521.
55. E. A. Boudreaux, L. C. Cusachs and L. D. Dureau, *Numerical Tables of Two-Center Overlap Integrals*. W. A. Benjamin, New York (1970).
56. J. S. Griffiths, *The Theory of Transition-Metal Ions* p. 387. Cambridge University Press, New York (1961).
57. G. Herzberg, *Electronic Spectra and Electronic Structure of Polyatomic Molecules*, p. 573. S. Van Nostrand, Princeton, NJ (1966).
58. Y. N. Chiu and F. E. Wang, *J. Solid State Chem.* 1982, **45**, 353.
59. Y. N. Chiu and F. E. Wang, *Inorg. Chem.* 1982, **21**, 4264.
60. R. G. Pearson, *Symmetry Rules for Chemical Reactions: Orbital Topology in Elementary Processes*. Wiley, New York (1976).

Polyhedron Vol. 4, No. 7, pp. 1185–1189, 1985
Printed in Great Britain

0277–5387/85 $3.00 + .00
© 1985 Pergamon Press Ltd

EFFECTS OF ELECTRON DENSITY SHIFT IN FIVE-COORDINATED Pt(II) COMPLEXES WITH OLEFINS: AN XPS STUDY

G. MORELLI
Department of Inorganic Chemistry, University of Naples, Naples, Italy

and

G. POLZONETTI* and V. SESSA
Department of Chemistry, University of Rome, Rome Italy

(*Received* 14 *June* 1984; *accepted* 10 *October* 1984)

Abstract—XP spectra of seven five-coordinated Pt(II) complexes of general formula [Pt(olefin)(N–N)Cl_2] reveal significant differences from analogous four-coordinated Pt(II) complexes. Pt4*f* and N1*s* signals give evidence for π-back-donation from Pt onto both the olefin and the nitrogen chelating ligands, provided the latter belong to conjugated moieties. As a result, π-back-donation is more intense and Pt atoms more positive in 5- than in 4-coordinated complexes with similar ligands; this is in keeping with the previously reported decrease of nucleophilic reactivity of coordinated olefins in 5-coordinated Pt(II) complexes. The above electronic shifts are strongly reinforced by conjugation within the coordinated olefin such as with 2-butenedinitrile.

The chemistry of platinum(II)–olefin complexes is well understood in its usual square-planar coordination. However, in recent years several new olefin complexes have been isolated[1,2] with the general formula [$PtXL_3$(olefin)] and [PtX_2L_2(olefin)] (X = halide or methyl, L_3 = tridentate anionic ligand, L_2 = neutral chelating ligand) where platinum is five-coordinated, and despite the relatively low number of observations on five-coordinated complexes, some significant differences in chemical behaviour between four and five-coordinated Pt(II)–olefin complexes have been pointed out. Coordinated olefins undergo easily nucleophilic addition in square-planar Pt(II) complexes,[3] whereas no such reactivity has been found for trigonal bipyramidal Pt(II)–olefin compounds.[4] Theoretical calculations concerning the reactivity of coordinated olefins toward nucleophiles[5] suggest that olefins are considerably deactivated with regard to a nucleophilic attack on going from a square-planar to a trigonal–bipyramidal coordination in d^8 complexes, and that the unsaturated ligand is not effectively re-activated by the slipping from the η^2 to η^1 coordination mode in the transition state. Such behaviour appears to be strictly connected, on the one hand with coordination geometry, and on the other with electron density on the olefin: theoretical calculations[5] predict a strong increase of the latter quantity owing to back-donation. We undertook the present work with aim at a possible experimental confirmation of such an effect, and to that purpose we resorted to the technique of X-ray photoelectron spectroscopy (XPS or ESCA), which has already proved capable of supplying direct information on charge density shifts in coordination compounds.[6,7] Thus, XPS has been used previously to characterize the oxidation state and charge density in platinum complexes;[8,9] it gives good evidence for π-acceptor properties of olefin ligands,[10,11] (the additive value + 1.0 eV assigned to η^2-olefins in metal complexes by Feltham and Brant[12] points to a highly pronounced characterization of π-back-donation), and has not yet been applied systematically to the study of coordination geometry in metal–olefin complexes. The present

* Author to whom correspondence should be addressed.

work deals with XPS characterization and the corresponding structural implications of a series of five-coordinated Pt(II)–olefin complexes of general formula $[PtCl_2(\eta^2\text{-olefin})(N\text{–}N)]$, where (N–N) is a bidentate nitrogen donor ligand, together with a parallel study, for comparison purposes, of some related four-coordinated Pt(II)–olefin species.

EXPERIMENTAL

Synthesis. The investigated complexes are listed in Table 1, and were prepared by known literature methods;[13–18] further details will appear in a forthcoming paper by Albano *et al.*,[2(c)] and their purity checked by physical constants. Of the three compounds in Table 1 not previously mentioned in the literature, [ethylene)$PtCl_2$(ACIM)] was prepared by addition of the ligand to an acetone solution of $[PtCl_2(C_2H_4)]_2$ in equimolar ratio, and subsequent crystallization from acetone–petrol ether; ^{1}H NMR ($CDCl_3$): $C(CH_3)_3$ 1.80*s*, $=CHCH_3$ 2.94*d*, $=CHCH_3$ 8.2*q*, $CH_2=CH_2$ 4.95*s* (J_{Pt-H} = 60 Hz). $PtCl_2$(DHB) and $PtCl_2$(teten) were obtained from the corresponding five-coordinated olefins complexes by loss of ethylene in benzene solution (for ligand abbreviations, see Table 1).

Spectra measurements. XP spectra were taken on a VG-ESCA 3 spectrometer using the Al-K_α (1486.6 eV) source. No radiation damage was observed even after long irradiation times, so cooling of the samples was not found necessary, and all spectra were run at ambient temperature. The X-ray power level for all present experiments was 120 W (12 kV at 10 mA). Typical ultimate vacuum in the spectrometer chamber, during measurements, was $1\text{–}2 \times 10^{-9}$ torr. Sample charging and spectral calibration were achieved by referring to the C1*s* contamination signal taken as 285.0 eV. The average value of C1*s* contamination level was around 20% in apparent number of atoms, in the upper sampling layer, with respect to the sample. No attempts were made to clean the sample, by ion bombardment, in order to avoid decomposition. The calibration procedure was not straightforward owing to presence of several kinds of C atoms in the ligand moieties; a first rough alignment of the spectra was achieved by assuming either constant Cl2*p* b.e. (which however to a more accurate evaluation turns to vary slightly across the investigated series; see below), or constant C1*s* maximum b.e. of the composite band; in both cases, deviation turned to be quite small (it has to be recalled that overall FWHM of C1*s* is around 2.6–2.7 eV, indicating that individual b.e. differences between various kinds of C atoms are rather small). Subsequently a refinement through gaussian analysis of the C1*s* bands was attempted, aided by quantitative evaluation of atomic ratios from XPS band intensities by means of Scofield's σ values,[19] which allowed more precise identification of the contamination C1*s* signal, never differing however by more than 0.2 eV from the composite band maximum. Reproducibility was good, the standard deviation on aligned spectra not exceeding 0.1 eV for measurements repeated at least six times; however,

Table 1.[a]

Compound[b]	Formula	b.e. Pt4$f_{7/2,5/2}$	b.e. Cl2*p*	b.e. N1*s*
1	DHB	—	—	399.4
2	$PtCl_2$(DHB)	72.5–75.9	198.2	400.1
3	(ethylene)$PtCl_2$(ACIM)	72.8–76.1	198.9	400.3
4	$PtCl_2$(teten)	72.2–75.6	198.3	400.3
5	(ethylene)$PtCl_2$(DEA)	72.4–75.6	198.0	400.3
6	(ethylene)$PtCl_2$(py)	73.5–76.9	198.8	399.2
7	(ethylene)$PtCl_2$(DHBIE)	73.0–76.3	198.6	399.9 broad
8	(ethylene)$PtCl_2$(DHB)	72.9–76.2	198.4	339.9
9	(E-2-butene)$PtCl_2$(DHB)	73.0–76.3	198.6	400.0
10	(E-2-butenedinitrile) $PtCl_2$(DHB)	73.7–76.9	198.5	399.3 {398.8, 399.8}
11	(ethylene)$PtCl_2$(BIE)	73.3–76.6	198.7	399.6
12	(ethylene)$PtCl_2$(BIP)	73.3–76.7	198.7	399.4 {399.2, 399.6}
13	(ethylene)$PtCl_2$(teten)	72.4–75.7	198.4	400.3

[a] Binding energy in eV.
[b] Formulas are given in Fig. 1.

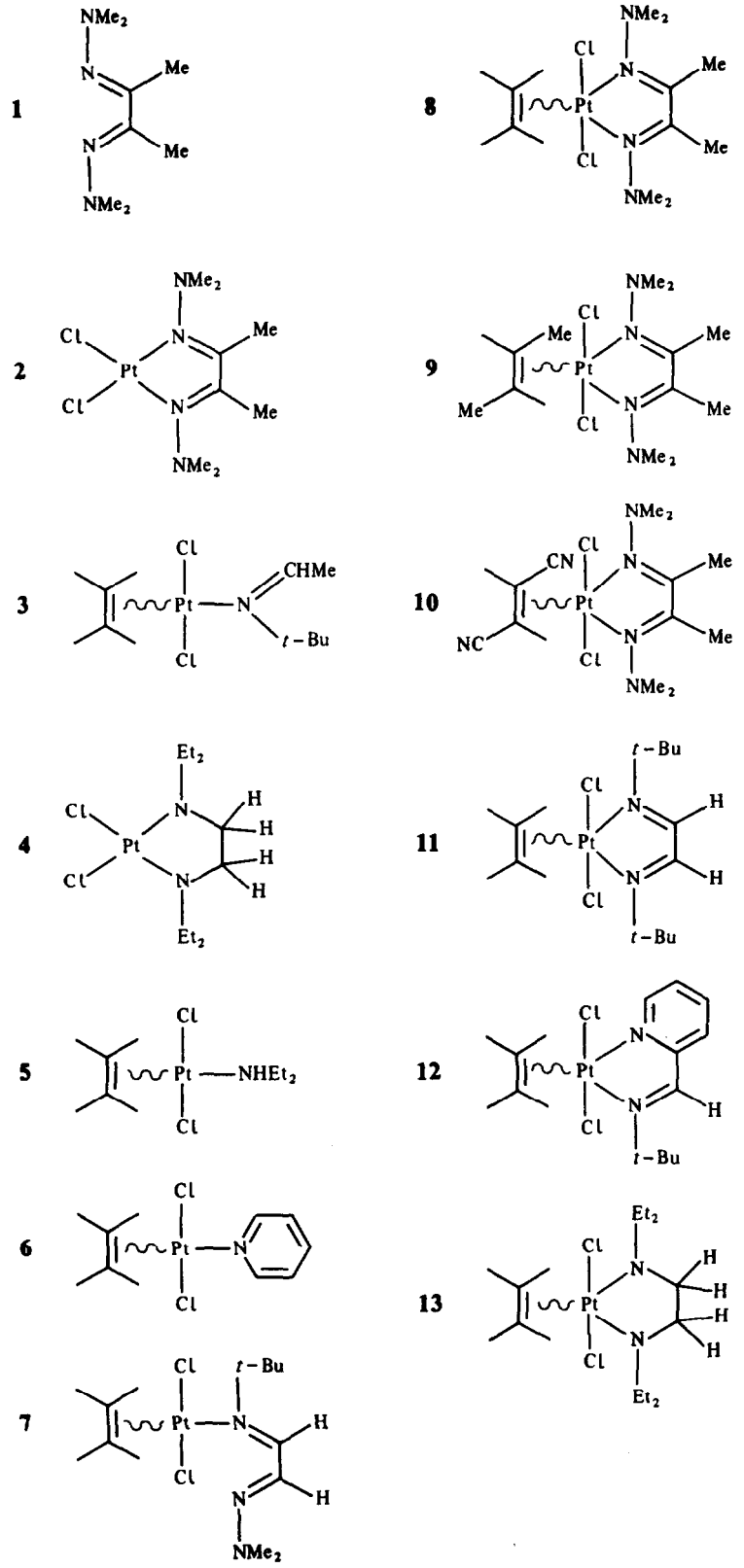


Fig. 1. Formulas (see Table 1).

owing to the composite nature of the C1*s* band and the indirect calibration procedure, the final accuracy of the b.e. values quoted in Table 1 is to be estimated roughly as 0.2 eV.

RESULTS

The relevant XPS data are listed in Table 1 for a series of seven five-coordinated [$PtCl_2$(olefin)(N–N)] complexes where the nature of the olefin ligand is varied (olefin=ethylene, E-2-butene, E-2-butenedinitrile) for (N–N)=glyoxal-bis-dimethylhydrazone (DHB), and the (N–N) ligand is varied at fixed choice of the olefin ligand (C_2H_4) from the wholly saturated teten (=N,N,N′,N′-tetraethylethylenediamine) to conjugated ligands derived from substituted imines (or hydrazones) of diacetyl or glyoxal, and in one case from pyridine-2-aldehyde. For the sake of comparision, the free ligand DHB and five square-planar Pt(II) complexes of related composition were also measured and included in Table 1.

For the five-coordinated complexes we assumed, in agreement with previous X-ray[20–22] and other structural determinations,[15,21,23] a trigonal bipyramidal geometry with both Cl atoms in axial position, the η^2 olefin and both donor atoms of the (N–N) ligand in the equatorial plane. The four-coordinated counterparts belong obviously to the *cis*-[$PtCl_2$(N–N)], respectively to the *trans*-[$PtCl_2N(\eta^2$-olefin)] chromophore type.

The most evident feature emerging from a survey of the XPS data in Table 1 is a trend to higher Pt4*f* b.e. values in the 5- than in the 4-coordinated complexes. This effect is not large, but well defined both from statistical average, and from direct comparisons (such as in the complexes

[$PtCl_2$(DHB)]/[(ethylene)$PtCl_2$(DHB)],

and

[(ethylene)$PtCl_2$(ACIM)]/[(ethylene)$PtCl_2$(BIE)]);

in other cases, such as the couples

[$PtCl_2$(teten)]/[(ethylene)$PtCl_2$(teten)]

and

[(ethylene)$PtCl_2$(DEA)]/[(ethylene)$PtCl_2$(teten)],

the effect is smaller or vanishing. We conclude that Pt(II) is more positive or less electron rich in 5- than in 4-coordinated complexes; in other words, the dominant electronic effect accompanying c.n. expansion from 4 to 5 is enhanced π-back-donation rather than increased σ-donation by the fifth ligand; this conclusion is to be compared with similar theoretical predictions,[5] and with experimental findings on the reduced nucleophilic reactivity of 5-coordinated Pt(II) species.[4]

The acceptors of the increased π-back-donation are both the olefin ligands (e.g. the couples [$PtCl_2$(DHB)]/[(ethylene)$PtCl_2$(DHB)] and [$PtCl_2$(teten)]/[(ethylene)$PtCl_2$(teten)], and the conjugated nitrogen ligands. The latter effect is indeed absent from complexes with saturated nitrogen ligands in [$PtCl_2$(teten)], [(ethylene)$PtCl_2$(DEA)] and [(ethylene)$PtCl_2$(teten)], platinum is more negative with b.e. *ca.* 72.3 eV, and nitrogen more positive with N1*s* b.e. as high as 400.3 eV, but is larger in complexes with imines, hydrazones or pyridine ligands (Pt4*f* b.e. in the 73 eV range; N1*s* around 399 eV), and it is more pronounced with increasing conjugation within the organic ligand: in fact, π-back-donation appears to be larger in [(ethylene)$PtCl_2$(BIE)] than in [(ethylene)$PtCl_2$(ACIM)], and to tend to a limit in the highly conjugated systems [(ethylene)$PtCl_2$(py)] and [(ethylene)$PtCl_2$(BIP)].

It can be debated whether the Pt → olefin or the Pt → N back-donation is larger: the comparison between

[$PtCl_2$(DHB)] and [(ethylene)$PtCl_2$(ACIM)],

and between

[($PtCl_2$(DHB)] and [(ethylene)$PtCl_2$(DHBIE)]

(and indirectly between

[(ethylene)$PtCl_2$)(ACIM)]

and

[(ethylene)$PtCl_2$(DMB)])

suggest the former, although

[$PtCl_2$(teten)]/[(ethylene)$PtCl_2$(DEA)]

indicates that the effect is anyway not large. Probably the π-acceptor effects due to olefins and to $\leftarrow N\!\!\diagup\!\!=$ ligands are of comparable magnitude, the latter varying strongly according to the nature of the conjugated system comprising the nitrogen ligands (e.g. N1*s* varies from 399.2 eV in [(ethylene)$PtCl_2$(py)] to 400.3 eV in [$PtCl_2$(DHB)]). The electronic effect of substituents in the ligated olefin appears to be small between [(ethylene)$PtCl_2$(DHB)] and [(E-2-butene)$PtCl_2$(DHB)], and larger in [(E-2-butenedinitrile)$PtCl_2$(DHB)], where the high Pt4*f* b.e. (73.7 eV) and the low N1*s* b.e. (399.3 eV average, which points to *ca.* 398.8 for —C≡N) are consistent with a push–pull reinforcement of charge shift from Pt until the conjugated nitrogen atoms of the nitrile groups.

As for the electronic structure of nitrogen, XP

spectral data suggest that it is determined almost exclusively by its first neighbours (mainly Pt), and not by remote substituents or by minor variations in the electronics structure of the first neighbours. The donor effect on metal complexation is evident from the N1*s* b.e. shift from 399.4 eV in the free ligand DHB, to 399.8–400.1 eV in [$PtCl_2$(DHB)] and in the three [(olefin)$PtCl_2$(DHB)] complexes in Table 1. Actually, the N1*s* signal in [(ethylene)$PtCl_2$(DHB)] is composite, even if not resolved, owing to presence of two kinds of nitrogen atoms in ratio 1:1; assuming that the signal from $-NR_2$ is not significantly changed, and that the chemical shift on complexation affects only the $\leftarrow N\!\!=$ signals, a possible reconstruction of the N1*s* band components consistent with the experimental data would place $N\text{–}\underline{N}R_2$ at 399.7 eV, free $\underline{N}\text{–}NR_2$ at *ca* 399.2 eV, and complexed $\underline{N}\text{–}NR_2$ at 400.2 eV; replacing $-NR_2$ by a large alkyl groups as in [(ethylene)$PtCl_2$(BIP)] lowers only slightly the b.e. of N1*s* in coordinated $\leftarrow N\!\!=$ (399.6–399.9 eV). Coordinated nitrogen in aliphatic amines as in

[$PtCl_2$(teten)], [(ethylene)$PtCl_2$(teten)]

and

[(ethylene)$PtCl_2$(DEA)]

has relatively high N1*s* b.e. (around 400.3 eV), as noted before, because of lack of Pt → N back-donation effects, as confirmed by the relatively low 4*f* b.e. of platinum in the same complexes. Further N1*s* b.e. regions for nitrogen functions include coordinated pyridine ring nitrogen around 399.2 eV, and nitrile (in coordinated butenedinitrile) at 398.8 eV.

Less evident and less significant structural implications are contained in the Cl2*p* signals, whose b.e. spread is small (between 198.2 and 198.9 eV, with one exception); there seems to be a trend to lower b.e. with increasing proximity of negative ligands, mainly the second coordinated chloride: so the highest b.e.s (198.8–198.9 eV) occur with the quadratic *trans*-dichlorocomplexes

[(ethylene)$PtCl_2$(py)]

and

[(ethylene)$PtCl_2$(ACIM)],

and the lowest ones (198.2–198.3 eV) with the square-planar *cis*-species [$PtCl_2$(DHB)] and [$PtCl_2$(teten)], the 5-coordinated species falling in the intermediate range (*ca* 198.3–198.7 eV) in accordance with the *trans*-position of the two axial Cl ligands, slightly more labilized by the negative charge of three equatorial ligands. [(ethylene)$PtCl_2$(DEA)] has a lower Cl2*p* b.e. value (198.0 eV), which does not fit in the above scheme; we may perhaps suspect hydrogen bond interactions in this case, since [(ethylene)$PtCl_2$(DEA)] is the only complex in the investigated series containing a secondary instead of a tertiary nitrogen ligand.

REFERENCES

1. H. C. Clark and L. E. Manzer, *Inorg. Chem.* 1974, **13**, 1996.
2. (a) H. van der Poel, Ph.D. Thesis, University of Amsterdam; (b) L. Maresca, G. Natile and L. Cattalini, *Inorg. Chim. Acta* 1975, **14**, 79; (c) V. G. Albano *et al.*, *Inorg. Chem.*, in press.
3. R. Palumbo, A. De Renzi, A. Panunzi and G. Paiaro, *J. Am. Chem. Soc.* 1969, **91**, 3874.
4. A. De Renzi and G. Morelli (unpublished results).
5. O. Eisenstein and R. Hoffmann, *J. Am. Chem. Soc.* 1981, **103**, 4308.
6. See, e.g. R. A. Walton, *Coord. Chem. Rev.* 1980, **31**, 83.
7. T. Ibusuki and Y. Saito, *Inorg. Chim. Acta* 1976, **19**, 87.
8. W. E. Moddeman, R. Blackburn, G. Kumas, K. A. Morgan, R. G. Albridge and M. M. Jones, *Inorg. Chem.* 1972, **11**, 1715.
9. M. G. Bancroft, T. Chan, R. J. Puddephatt and M. P. Brown, *Inorg. Chim. Acta* 1981, **53**, L119.
10. C. D. Cook, K. Y. Wan, V. Gelius, K. Hamrin, G. Johansson, E. Olsson, H. Siegbahn, G. Nordling and K. Siegbahn, *J. Am. Chem. Soc.* 1971, **93**, 1904.
11. R. Mason, D. M. P. Mingos, G. Rucci and J. A. Connor, *J. Chem. Soc., Dalton Trans.* 1972, 1729.
12. R. D. Feltham and P. Brant, *J. Am. Chem. Soc.* 1982, **104**, 641.
13. L. Maresca, G. Natile, M. Calligaris, P. Delise and L. Randaccio, *J. Chem. Soc., Dalton Trans.* 1976, 2386.
14. A. De Renzi, G. Morelli, A. Panunzi and S. Wurzburger, *Inorg. Chim. Acta* 1983, **76**, L285.
15. H. van der Poel and G. van Koten, *Inorg. Chem.* 1981, **20**, 2950.
16. A. De Renzi, A. Panunzi and M. Scalone, *Inorg. Synth.* 1982, **21**, 86.
17. P. Cheeseman, A. L. Odell and H. A. Raethel, *J. Chem. Soc., Chem. Comm.* 1968, 1496.
18. S. I. Shupack and M. Orchin, *Inorg. Chem.* 1964, **3**, 374.
19. J. H. Scofield, *J. Electron Spectr. Rel. Phen.* 1976, **8**, 129.
20. M. Calligaris, P. Delise, L. Maresca, G. Natile and L. Randaccio, *J. Chem. Soc., Dalton Trans.* 1976, 2386.
21. A. De Renzi, B. Di Blasio, A. Saporito, M. Scalone and A. Vitagliano, *Inorg. Chem.* 1980, **19**, 960.
22. H. van der Poel, G. van Koten, M. Kokkes and C. H. Stam, *Inorg. Chem.* 1981, **20**, 2941.
23. H. C. Clark and L. E. Manzer, *Inorg. Chem.* 1974, **13**, 1996.

Polyhedron Vol. 4, No. 7, pp. 1191–1196, 1985
Printed in Great Britain

0277-5387/85 $3.00 + .00
© 1985 Pergamon Press Ltd

COPPER(II) AND NICKEL(II) COMPLEXES OF A NEUTRAL PENTADENTATE SCHIFF BASE

EDMUND KWIATKOWSKI* and TADEUSZ OSSOWSKI
Institute of Chemistry, University of Gdańsk, ul. Sobieskiego 18, 80-952 Gdańsk, Poland

and

ANNA JANKOWSKA
Institute of Physics, University of Gdańsk, ul. Sobieskiego 18, 80-952 Gdańsk, Poland

(*Received* 13 *August* 1984; *accepted* 9 *November* 1984)

Abstract—A new pentadentate Schiff base 2,6,10-triaza-1,11-bis(2′-aminophenyl)-undeca-1,10-diene, *abaDPT*, and its complexes of general formula M(*abaDPT*)X_2 where M = Cu(II), Ni(II), X = Cl, Br, I, NO_3, and ClO_4, have been prepared. The complexes have been characterized by electronic and IR spectra, EPR, magnetic moments, molar conductances, and elemental analysis. IR data show an interaction between halide anion of the outer coordination sphere and the complexed amino group. EPR and spectrophotometric data of most of the copper compounds are consistent with a distorted square pyramidal geometry. Single crystal EPR studies of Cu(*abaDPT*)$(NO_3)_2$ and Cu(*abaDPT*)Br_2 revealed that copper atoms in the former compound occupy two magnetically inequivalent places in the lattice while copper atoms in the latter compound take identical sites. Principal g tensor axes of the two compounds have been determined.

Transition metal complexes of Schiff base ligands are of interest since they exhibit a tendency to form various structural types and display a wide variety of magnetic properties. Although numerous linear pentadentate Schiff bases were prepared and investigated in recent years, only a limited number contained a set of five identical donor atoms. Prince and Stotter,[1] Coleman and Taylor,[2] and Simmons *et al.*[3] prepared linear Schiff bases with solely nitrogen donors derived from 2-formylpyridine and polyamines. Copper complexes of some of them functionally resemble hemocyanin in its capacity of reversible binding of oxygen.

Interesting properties of the aforementioned compounds prompted us to study metal complexes with other linear Schiff bases comprising identical sets of donor atoms. Preparative studies in our laboratory have shown that 2-aminobenzaldehyde condenses with bis(3-aminopropyl)amine to give 2,6,10 - triaza - 1,11 - bis(2′ - aminophenyl) - undeca - 1,10-diene, *abaDPT*, a doubly condensed Schiff base with potentially five donor nitrogen atoms. This paper reports the synthesis and properties of *abaDPT* and its complexes with copper(II) and nickel(II).

EXPERIMENTAL

Bis(3-aminopropyl)amine and 2-nitrobenzaldehyde were obtained from Fluka and were used without further purification. All chemicals and solvents were of reagent grade or equivalent. 2-Aminobenzaldehyde was prepared from 2-nitrobenzaldehyde by the literature method.[4]

2,6,10 - *Triaza* - 1,11 - *bis*(2′ - *aminophenyl*) - *undeca* - 1,10 - *diene*, abaDPT

A solution of freshly prepared 2-aminobenzaldehyde (0.05 mol) and bis(3-aminopropyl)amine (0.025 mol) in benzene (1.5 dm^3) was heated in a flask equipped with a Dean–Stark trap and a reflux condenser. After the stoichiometric quantity of water forming in the reaction was collected in trap, the mixture was concentrated under reduced pressure and the oily residue was extracted several times with hot *n*-hexane. Collected extracts deposited upon cooling the Schiff base which was recrystallized from

* Author to whom correspondence should be addressed.

n-hexane to give a white powder of *abaDPT* (30–40% yield).

General preparation of Cu(abaDPT)X_2 (X = Cl, Br, NO_3, ClO_4) *and* Ni(abaDPT)X_2 (X = Cl, Br, I, NO_3, ClO_4) *complexes*

To a hot solution of 5 mmol of the appropriate metal salt in 20 cm^3 of the methanol–water 1:1 mixture (in the case of $CuCl_2$ 10 cm^3 of pure methanol was used) a solution of 5 mmol of *abaDPT* in 20 cm^3 of methanol was added slowly. After 30 min of stirring in room temperature the precipitated complex was filtered off, washed with cold methanol and recrystallized twice from a methanol–water mixture. Crystals of copper complexes were olive-green and those of nickel complexes ranged in colour from green to grey–brown.

Preparation of Cu(abaDPT)I_2

Hot solutions of copper(II) sulphate (0.01 mol in 30 cm^3 of the methanol–water 1:1 mixture) and *abaDPT* (0.01 mol in 20 cm^3 of methanol) were mixed together. To the resulting mixture a solution of barium iodide (0.01 mol in 100 cm^3 of water) was added. After cooling the precipitate was filtered off, washed with cold methanol and extracted with a hot methanol-water mixture. Collected extracts deposited Cu(*abaDPT*)I_2 which was recrystallized twice from methanol–water mixture to give dark-green crystals.

Physical measurements

IR spectra in the 400–4000 cm^{-1} region were obtained using a Perkin–Elmer Model 621 spectrometer. Spectra of solid samples were recorded as Nujol or hexachlorobutadiene mulls. UV visible, and near IR spectra were obtained with a Beckman DK2 spectrometer using 1 cm stoppered silica cells. EPR spectra were recorded on an X-band spectrometer produced by Polish Academy of Science at room temperature; magnetic field was calibrated with DPPH. PMR spectra were obtained using a Tesla BS 487 80 MHz spectrometer in $CDCl_3$ solution with HMDS as internal reference. Electron impact mass spectra were recorded on a Varian MAT 711 spectrometer at 70 eV.

The magnetic measurements were performed by the Gouy method; Diamagnetic corrections were made employing Pascal's constants.[5] Potentiometric titrations were performed using a Radelkis Model OP-205 precision pH-meter. Conductance measurements were made with a K-58 conducting bridge constructed in the Technical University of Warsaw.

RESULTS AND DISCUSSION

Synthesis of the pentadentate ligand *abaDPT* involves refluxing of 1 equivalent of bis(3-aminopropyl)amine with 2 equivalents of 2-aminobenzaldehyde in benzene solution. The results of elemental analysis (Table 1), PMR spectrum, and

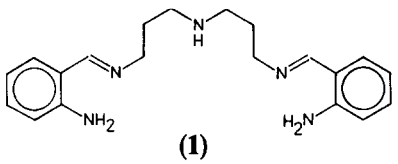
Table 1. Analytical results[a] and molar conductances

Compound	Analysis (%)				λ^c $\left(\frac{cm^2}{\Omega\ mol}\right)$
	C	H	N	X[b]	
abaDPT	71.6 (71.2)	8.08 (8.06)	20.3 (20.7)		
Cu(*abaDPT*)Cl_2	50.7 (50.9)	5.90 (5.77)	14.5 (14.8)	15.1 (15.0)	215
Cu(*abaDPT*)Br_2	42.6 (42.8)	5.00 (4.85)	12.3 (12.5)	28.5 (28.5)	236
Cu(*abaDPT*)I_2	36.7 (36.7)	4.00 (4.16)	10.4 (10.7)	38.5 (38.8)	226
Cu(*abaDPT*)$(NO_3)_2$	45.9 (45.8)	5.00 (5.18)	18.9 (18.7)		217
Cu(*abaDPT*)$(ClO_4)_2$	40.0 (40.0)	4.50 (4.54)	11.4 (11.8)		199
Ni(*abaDPT*)Cl_2	51.4 (51.4)	5.82 (5.82)	15.0 (15.0)	15.1 (15.2)	216
Ni(*abaDPT*)Br_2	43.3 (43.2)	4.88 (4.89)	12.3 (12.6)	28.4 (28.7)	231
Ni(*abaDPT*)I_2	37.2 (37.0)	4.23 (4.18)	10.6 (10.8)	39.4 (39.1)	225
Ni(*abaDPT*)$(NO_3)_2$	46.3 (46.2)	5.30 (5.23)	18.9 (18.9)		212
Ni(*abaDPT*)$(ClO_4)_2$	40.4 (40.4)	4.60 (4.57)	11.9 (11.8)		200

[a] Required values are given in parentheses.

[b] X = Cl, Br, and I.

[c] Molar conductances of 10^{-3} M aqueous solutions at 298 K.



(1)

mass spectrum are consistent with formula (1). A sharp singlet at 8.15 ppm and a broad one at 6.21 ppm in the PMR spectrum are assigned to the azomethine and the NH_2 protons respectively. The bridging methylene protons give rise to three multiplets with baricentres at 3.43, 2.55, and 1.77 ppm respectively. Multiplets of aromatic protons appear in the region of 6.4–7.1 ppm. In the mass spectrum of *abaDPT* a prominent molecular peak is observed at 337 *m/e*, the most abundant fragmentation ions arise from the fissions of C–C bonds within the polyamine chain.

Complexes of empirical formula

$$M(abaDPT)X_2$$

where M = Cu(II), Ni(II), X = Cl, Br, I, NO_3, and ClO_4 are formed when the ligand dissolved in methanol reacts with metal salts MX_2 dissolved in methanol–water mixture. Elemental analysis (Table 1) and conductance measurements (all complexes are electrolytes in water with molar conductances above 200 Ω^{-1} cm^2 mol^{-1} at concentration of 10^{-3} M, Table 1) suggest that the pentadentate Schiff base coordinates copper and nickel ions as a neutral molecule. All the complexes have reasonably good solubility in water, formamide, and N,N-dimethylformamide, but are insoluble in non-coordinating organic solvents. The solubility characteristics are also consistent with salt formulation.

Infrared spectra have been obtained for ligand and complexes (Table 2). Bands in the 3100–3500 cm^{-1} region, which may be assigned to N–H stretching vibrations of both NH_2 and NH groups, are presented in Fig. 1. It is evident from Fig. 1 and Table

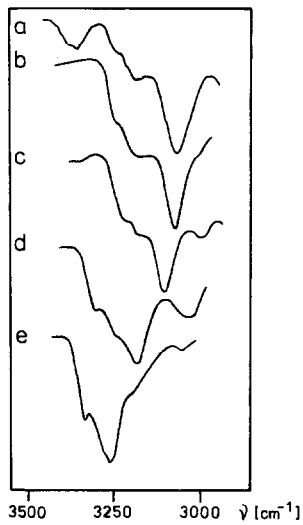


Fig. 1. Part of IR spectra of (a) Cu(*abaDPT*)Cl_2, (b) Cu(*abaDPT*)Br_2, (c) Cu(*abaDPT*)I_2, (d) Cu(*abaDPT*)$(NO_3)_2$, (e) Cu(*abaDPT*)$(ClO_4)_2$ recorded as hexachlorobutadiene mulls.

Table 2. Spectral data for *abaDPT* and complexes

Compound	Infrared[a,b]					Ligand field spectra[a,c]		
	ν_{N-H}			ν_X[d]		ν_{max} (log ε_{max})		
abaDPT	3436m	3272m	3132w					
Cu(*abaDPT*)Cl_2	3370w	3220sh	3172m			16,130 (2.36)	12,120sh	
Cu(*abaDPT*)Br_2	3230sh	3150m				16,130 (2.37)	12,120sh	
Cu(*abaDPT*)I_2	3215sh	3190sh	3100m			16,130 (2.35)	12,120sh	
Cu(*abaDPT*)$(NO_3)_2$	3315w	3260sh	3190m	1742w	1356s	16,130 (2.35)	12,120sh	
Cu(*abaDPT*)$(ClO_4)_2$	3330m	3290sh	3240m	1100s	615m	16,130 (2.35)	12,120sh	
Ni(*abaDPT*)Cl_2	3250sh	3160sh	3140m			18,350 (1.27)	12,200sh	10,530 (0.88)
Ni(*abaDPT*)Br_2	3252m	3190sh	3132m			18,350 (1.30)	12,200sh	10,530 (0.96)
Ni(*abaDPT*)I_2	3230sh	3195m	3130m			18,180 (1.55)	12,200sh	10,530 (0.91)
Ni(*abaDPT*)$(NO_3)_2$	3280m	3246m	3106m	1760w 1365s	1746w	18,350 (1.29)	12,200sh	10,530 (0.89)
Ni(*abaDPT*)$(ClO_4)_2$	3380m	3290m	3230m	1110s	615m	18,350 (1.25)	12,200sh	10,530 (0.99)

[a] Values in cm^{-1}.

[b] Spectra of powdered solids recorded as hexachlorobutadiene mulls.

[c] Measured in aqueous solution.

[d] X = NO_3, ClO_4.

s, strong; m, medium; w, weak; sh, shoulder.

2 data that vibrations of the complexed amino group are influenced by the anions of the outer coordination sphere. A lower frequency of the N–H stretching vibrations in metal halide complexes as compared to metal perchlorate complexes may be due to intramolecular hydrogen bonding between the halide and the NH_2 group, a feature not present in the latter complexes. A similar interaction between the halide and the complexed NH_3 ligand was reported for hexaaminecobalt(III) halides.[6] IR spectra of both copper and nickel perchlorate complexes show a strong band around 1100 cm^{-1} and a medium one at 615 cm^{-1} which indicate a T_d symmetry of ClO_4 and an ionic nature of the complexed metal–ClO_4 bond.[7] Reliable conclusions concerning the bonding of the anion in metal nitrate complexes could not be made from their IR spectra as the main nitrate bands were hidden by the organic ligand bands. However the copper nitrate complex shows a single $\nu_1+\nu_4$ combination band at 1742 cm^{-1} consistent[8] with ionic nitrate group. The spectrum of the nickel nitrate complex exhibits however two weak bands in the 1750 cm^{-1} region separated by 14 cm^{-1}. These bands may accrue from the splitting of $\nu_1+\nu_4$ band, thus indicating the interaction existing between the nitrate and nickel ions[8] in the solid state.

Magnetic moments of solid complexes range from 1.79 to 1.81 B.M. for Cu(*abaDPT*)X_2 and from 2.96 to 2.98 B.M. for Ni(*abaDPT*)X_2 complexes, and show no change with temperature in the 77–298 K range. Magnetic moment data reveal only a small orbital contribution to the predicted spin only value. The evident lack of anomalous moments suggests the absence of appreciable metal–metal interaction in the solid phase.

EPR data of finely powdered Cu(*abaDPT*)X_2 samples are given in Table 3. All the copper complexes show good resolved three g-value spectra (Fig. 2) except of Cu(*abaDPT*)I_2. It had been pointed

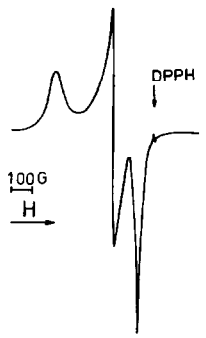


Fig. 2. EPR spectrum of powdered Cu(*abaDPT*)$(ClO_4)_2$.

out earlier[9] that in a three value spectrum with $g_1 < g_2 < g_3$ the value of $R = (g_2-g_1)/(g_3-g_2)$ may indicate the predominant ground state of a mononuclear copper complex containing co-ordinated nitrogen atoms. Calculated R values (see Table 3) suggest that in Cu(*abaDPT*)Cl_2, Cu(*abaDPT*)$(NO_3)_2$, and Cu(*abaDPT*)$(ClO_4)_2$ a predominant $d_{x^2-y^2}$ ground state is present which may be associated with a structure approximate to square pyramidal geometry. A relatively large value of R for Cu(*abaDPT*)Br_2, much exceeding 1, suggests a predominant d_{z^2} ground state and a structure approximate to trigonal bipyramidal.

In order to verify the reliability of the powder g and R values we studied additionally EPR spectra of single crystals of both Cu(*abaDPT*)$(NO_3)_2$ and Cu(*abaDPT*)Br_2.

The former compound crystallizes in the form of rhombic plates while the latter forms small needles. Observation in a polarisation microscope shows that they are not twinned crystals. The angular dependence of the electron spin resonance of Cu(II) measured in single crystal of Cu(*abaDPT*)$(NO_3)_2$ is shown in Fig. 3. It is evident from Fig. 3(b) that the EPR spectrum of a single crystal in a magnetic field oriented perpendicularly to the Z axis [see Fig. 3(a)] consists of two lines which change their separation

Table 3. g-Values for copper complexes[a]

Compound	g_1	g_2	g_3	R[b]	[c]
Cu(*abaDPT*)Cl_2	2.031	2.074	2.202	0.34	$d_{x^2-y^2}$
Cu(*abaDPT*)Br_2	2.028	2.129	2.180	1.81	d_{z^2}
Cu(*abaDPT*)I_2	2.023	[d]	2.171		
Cu(*abaDPT*)$(NO_3)_2$	2.049	2.097	2.182	0.56	$d_{x^2-y^2}$
Cu(*abaDPT*)$(ClO_4)_2$	2.032	2.084	2.207	0.42	$d_{x^2-y^2}$

[a] Measured for powdered samples at room temperature.
[b] Calculated from the relation $R = (g_2-g_1)/(g_3-g_2)$.
[c] Predominant ground state.
[d] Not determined due to a bad resolution.

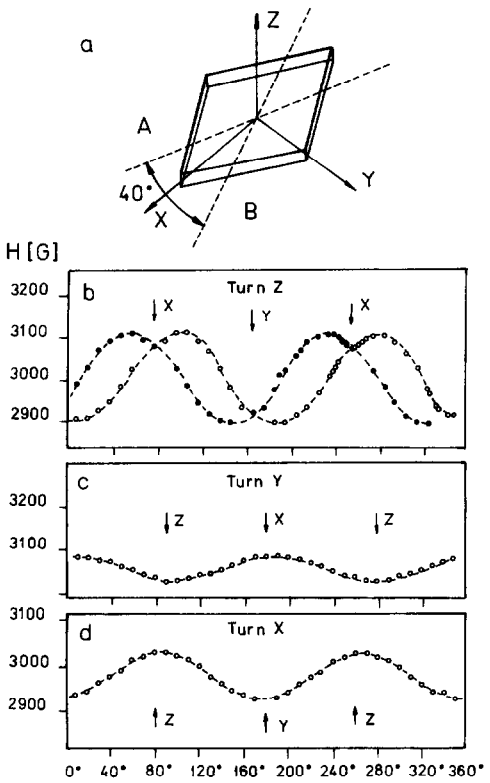


Fig. 3. Angular variation of the EPR of Cu(II) in single crystal of Cu(*abaDPT*)$(NO_3)_2$ on rotation around (b) *Z*, (c) *Y*, (d) *X* axis. (a) Schematic representation of the crystal, *X*, *Y*, *Z*: rotation axes, *A*, *B*: principal *g* tensor axes. The magnetic field was always perpendicular to the axis of rotation. Arrows indicate angles at which one of the axes (*X*, *Y*, or *Z*) is parallel to the magnetic field.

during rotation around the *Z* axis. The two lines of equal intensity indicate that copper atoms in crystalline Cu(*abaDPT*)$(NO_3)_2$ are incorporated in two magnetically inequivalent places. Based on the described earlier method [10] we constructed the $\langle g^2 \rangle$ matrix from the experimental data, which after diagonalization allowed us to calculate the principal *g* tensor values. They are: $g_{11} = 2.037$, $g_{22} = 2.097$, and $g_{33} = 2.188$. It is interesting to note that the principal *g* tensor axes do not coincide with the *X*, *Y*, and *Z* axes [see Fig. 3(a)]. Two of the principal *g* tensor axes of magnetically inequivalent copper atoms in single crystal of Cu(*abaDPT*)$(NO_3)_2$ lie in the *XY* plane [lines *A* and *B* in Fig. 3(a)] forming an angle of approximately 40°. An angular variation study of Cu(*abaDPT*)Br_2 reveals the presence of only one copper centre indicating that Cu(II) occupies identical sites in the lattice. Using the aforementioned method we obtained after processing of the data the following principal *g* tensor values for Cu(*abaDPT*)Br_2: $g_{11} = 2.032$, $g_{22} = 2.121$, and $g_{33} = 2.168$. Comparing EPR spectra of copper complexes with various Schiff bases comprising a set of five nitrogen donors we see that complexes obtained in this work are of much lower symmetry than those reported by Simmons *et al.*[3] for which axial EPR spectra were observed.

Copper complexes dissolved in water display a broad absorption at 16,130 cm^{-1} ($\varepsilon = 220$) with less defined band around 12,120 cm^{-1}. Hathaway[9] summarized the energy ranges covered by the *d–d* transitions of CuN_{4-6} chromophores of different stereochemistry. The *d–d* bands of Cu(*abaDPT*)X_2 complexes fit in well with the range reported for structure of approximate square pyramidal geometry.

Electronic spectra of nickel complexes dissolved in water give bands at 10,530 and 18,350 cm^{-1} which may be interpreted as the spin-allowed transitions $^3T_2 - ^3A_2$ and $^3T_1(F) - ^3A_2$ respectively in approximately octahedral environment. The weak band which appears as a shoulder at *ca* 12,200 cm^{-1} may result from the distortion of octahedral geometry. We consider the octahedral stereochemistry to arise from the coordination of water molecules to give [Ni(*abaDPT*)H_2O]X_2 rather than from the coordination of a counter ion leading to [Ni(*abaDPT*)X]X. This observation is in perfect agreement with the results of our electrochemical studies: molar conductances indicate on 2:1 electrolytes and curves obtained as a result of potentiometric titration of nickel halide complexes with silver nitrate were symmetrical with one inflection point at molar ratio of the complex to Ag(I) as 1:2.

Both copper and nickel complexes are very sensitive towards acids. Solutions of Cu(*abaDPT*)X_2 even slightly acidified by diluted strong acids change the green colour into a yellow which transforms immediately into a very faint blue. The absorption spectrum of the resultant solution shows a weak *d–d* band at 12,600 cm^{-1} ($\varepsilon = 11$) with a shoulder at 9400 cm^{-1} and resembles closely the spectrum of a hydrated copper(II) ion.[11] In the case of Cu(*abaDPT*)I_2 acidification results in the formation of free I_2 and CuI. Absorption spectra of nickel complexes in acidic aqueous solution are very similar to the spectrum of the hydrated nickel(II) ion comprising bands at 15,150 ($\varepsilon = 2$), 13,900 ($\varepsilon = 2$), and 8400 cm^{-1} ($\varepsilon = 3$).[12]

REFERENCES

1. R. H. Prince and D. A. Stotter, *Inorg. Chim. Acta* 1974, **10**, 89.
2. W. M. Coleman and L. T. Taylor, *J. Inorg. Nucl. Chem.* 1979, **41**, 95.

3. M. G. Simmons, C. L. Merrill, L. J. Wilson, L. A. Bottomley and K. M. Kadish, *J. Chem. Soc., Dalton Trans.* 1980, 1827.
4. L. I. Smith and J. W. Opie, *Org. Synth.* 1956, **3**, 56.
5. B. N. Figgis and J. Lewis, *Modern Coordination Chemistry* (Edited by J. Lewis and R. G. Wilkins). Interscience, New York (1960).
6. K. Nakamoto, *Infrared Spectra of Inorganic and Coordination Compounds.* Wiley, New York (1963).
7. A. E. Wickenden and R. A. Krause, *Inorg. Chem.*, 1965, **4**, 404; see also R. H. Balundgi and A. Chakravorty, *Inorg. Chem.* 1973, **12**, 981.
8. A. B. P. Lever, E. Mantovani and B. S. Ramaswamy, *Can. J. Chem.* 1971, **49**, 1957.
9. B. J. Hathaway, *J. Chem. Soc.* 1972, 1196.
10. B. J. Hathaway and D. E. Billing, *Coord. Chem. Rev.* 1970, **5**, 143.
11. J. Bjerrum, C. J. Ballhausen and C. K. Jorgensen, *Acta Chem. Scand.* 1954, **8**, 1275.
12. C. K. Jorgensen, *Adv. Chem. Phys.* 1963, **5**, 33.

Polyhedron Vol. 4, No. 7, pp. 1197–1201, 1985
Printed in Great Britain

0277–5387/85 $3.00 + .00
© 1985 Pergamon Press Ltd

SELECTIVE REAGENTS FOR SOLVENT EXTRACTION OF METALS—II. BIS-QUINALDIC ACIDS

BJÖRN ELMAN, A. G. SVERKER HÖGBERG* and MICHAEL WEBER
Royal Institute of Technology, Department of Organic Chemistry, S-100 44 Stockholm, Sweden

and

MAMOUN MUHAMMED
Royal Institute of Technology, Department of Inorganic Chemistry, S-100 44 Stockholm, Sweden

(*Received* 10 *September* 1984; *accepted* 9 *November* 1984)

Abstract—Bis-quinoline-2-carboxylic acids in which the quinoline rings were joined *via* ether linkages to the 8-position have been synthesized and tested for metal extraction. The reagents extracted Cu^{2+} and Zn^{2+} selectively in the presence of Fe^{2+} and Fe^{3+} from aqueous sulphate solution.

We have previously reported the syntheses and metal extractant properties of substituted quinoline-2-carboxylic acids.[1] This paper presents a study of bis-quinoline-2-carboxylic acids (bis-quinaldic acids) as metal extractants. These tetradentate reagents were prepared with the aim of improved metal ion selectivity and enhanced extractant ability compared with the known bidentate analogues.[1–3]

RESULTS

The bis-quinoline-2-carboxylic acids **1–8** were prepared from 8-hydroxyquinoline-2-carbonitrile by alkylation with ditosylates or dibromoalkanes (Scheme 1, Table 1). The reagents **1–6** were found to be sparingly soluble in chloroform. Hence the more lipophilic reagents **9–11** which possess a dodecenyloxy substituent in the 4-position and the reagents **12** and **13** which have a C_{12}-alkyl group in the 7-position were prepared, as was also the bis-quinaldic acid **7** which has a *n*-decyl group in the triethylene glycol chain.

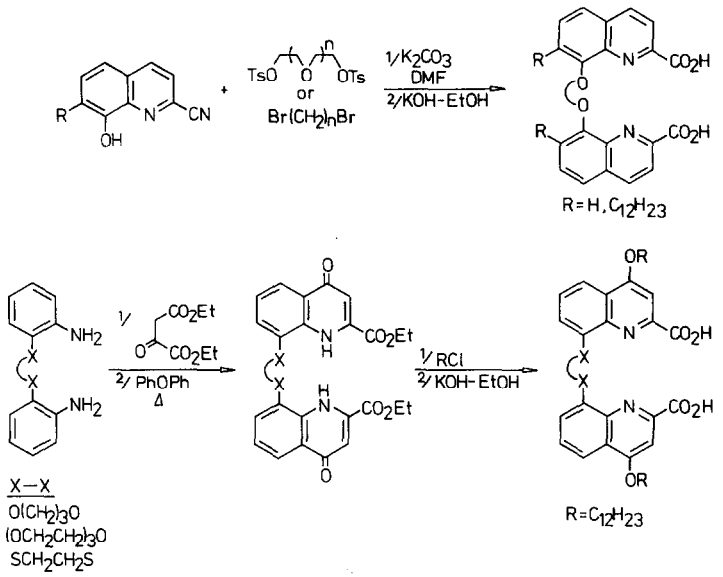
The reagents were tested for the ability to extract Cu^{2+}, Zn^{2+}, Fe^{2+}, Fe^{3+}, Ni^{2+}, Co^{2+}, Cd^{2+} and K^+ from aqueous sulphate solutions at pH 2 or 4 into a chloroform phase. The metal concentrations in the aqueous phase were measured by atomic absorption spectrophotometry. During the extraction tests with reagents **1–4** and **6** a third phase was formed. These reagents formed stable Cu^{2+} and Zn^{2+} complexes but no complex formation with Fe^{2+} was observed at pH 2. The results from mixed metal extraction tests with the more soluble reagents are presented as $pH_{1/2}$ values in Table 2. The reagents **3**, **7**, and **9–11** extracted Cu^{2+} completely at pH 1.8–1.9 but only small amounts of Fe^{3+} were extracted: 11% using reagent **9** at pH 1.9 and less than 5% with the other reagents.

The ^1H NMR spectra of the zinc complexes of **6** and **10** showed significant differences compared to the corresponding spectra of the free ligands. The peaks due to the triethylene glycol part of **6** appeared as an AA'BB' system at 4.41 and 4.10 ppm and a broad singlet at 3.94 ppm from the central glycol unit (Fig. 1). In the Zn^{2+} complex of **6** the signals from the four OCH_2CH_2OAr protons were separated and the OCH_2CH_2O singlet was split into an apparent doublet (J = 10 Hz) at 2.79 and 3.19 ppm. The coupling constants and chemical shifts of the OCH_2CH_2OAr part are indicated in Fig. 2. The Zn^{2+} complex of the reagent **10**, the 4-alkoxy analogue of **6**, had a similar ^1H NMR spectrum in this region.

DISCUSSION

Open-chain oligoethylene glycol ether compounds with 8-quinolinyloxy end groups are known complexing agents for, e.g. alkali metal ions.[4,5] In these ligands the ether oxygen and the quinoline

* Author to whom correspondence should be addressed. Present address: Boliden Kemi AB, Box 902, S-251 09 Helsingborg, Sweden.



Scheme 1.

nitrogen atoms are the donor atoms. Bis-quinaldic acid derivatives have previously been described, but they were not used for metal extraction.[6] Bis-quinaldic acids may form 1 : 1 complexes with two-valent metal ions if the quinoline rings are joined by a chain that permits both carboxylate oxygens and quinoline nitrogen atoms to coordinate to the same metal ion (**A**). The ^{1}H NMR spectrum of the Zn^{2+} complex of **6** is in agreement with a tetrahedral coordination where the triethylene glycol chain is in a synclinal conformation. The bis-thio reagent **11** was found to form a stable Cd^{2+} complex. In this reagent the sulphur atoms may coordinate to the Cd^{2+} in an octahedral structure (**B**).

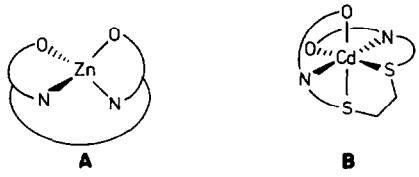


Table 1. Bis-quinaldic acid reagents

Reagent	X–X $R^4 = R^7 = H$	M.p. (°C)	Yield (%)	Anal.
1	$O(CH_2)_3O$	181–2	—	C,H,N,
2	$O(CH_2)_4O$	201–3 (MeOH)	72	C,H,N
3	$O(CH_2)_8O$	177–8 ($HOAc/H_2O$)	82	
4	$O(CH_2)_{10}O$	172–8 ($HOAc/H_2O$)	42	C,H,N
5	$OCH_2CH_2OCH_2CH_2O$	170–2 (EtOH)	23	C,H,N
6	$OCH_2(CH_2OCH_2)_2CH_2O$	148–9 (EtOH)	42	C,H,N,O
7	$OCH_2CH_2OCH_2CH(n\text{-}C_{10}H_{21})OCH_2CH_2O$	93–7 (EtOH)	33	
8	$OCH_2(CH_2OCH_2)_3CH_2O$	132–5 (C_6H_6)	59	C,H,N
	X–X $R^4 = OC_{12}H_{23} R^7 = H$			
9	$O(CH_2)_3O$	167–9	21[a]	—
10	$OCH_2(CH_2OCH_2)_2CH_2O$	93–100 (EtOH)	20[a]	C,H,N[b]
11	SCH_2CH_2S	166–8 ($HOAc/H_2O$)	17[a]	C,H,N[b]
	X–X $R^4 = H R^7 = C_{12}H_{23}$			
12	$OCH_2CH_2OCH_2CH_2O$	115–20 (C_6H_{12})	79	C,H,N
13	$O(CH_2)_8O$	85–7	85	C,H,N

[a] Based on the bis-aniline compound.
[b] Analysis of the monohydrate.

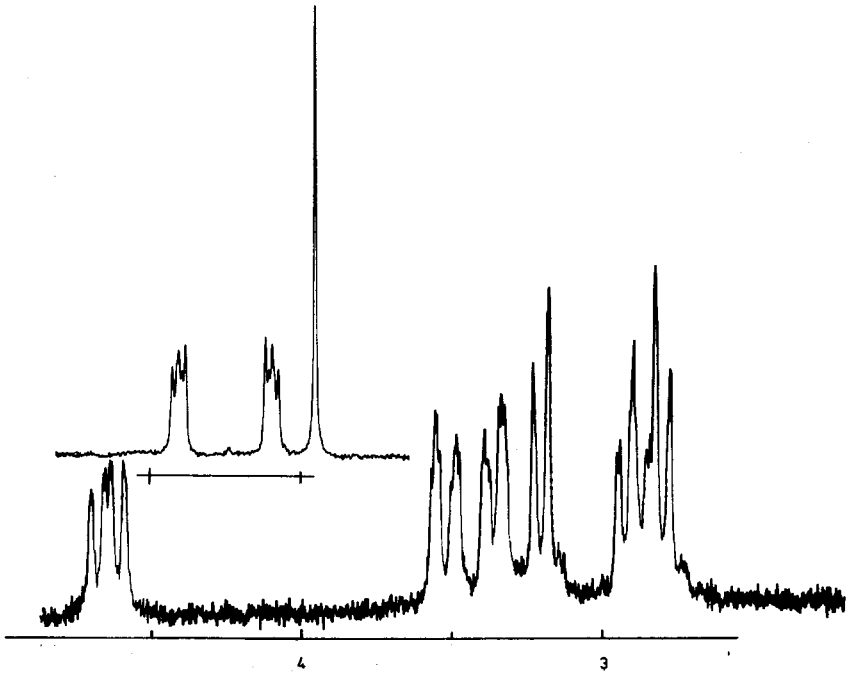


Fig. 1. ^{1}H NMR spectra of 1,8 - bis(2 - carboxy - 8 - quinolinyloxy) - 3,6 - dioxaoctane (**6**) (upper) and its zinc(II) complex (lower).

The metal ion extraction selectivity of the reagents was not greatly influenced by the length of the hydrocarbon chain joining the quinoline rings. The low efficiency of extraction of Fe^{2+} and Fe^{3+} compared with that of Cu^{2+} and Zn^{2+} is a common feature of the bis-quinaldic acid reagents. This selectivity was also observed for bidentate 8-alkoxyquinaldic acids.[1] The reagents **12** and **13** which have a branched C_{12}-alkyl group in the 7-position were poor extractants; this may be due to a steric interference of the 7- and 8-substituents in the complexes.

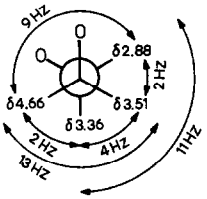


Fig. 2. Proton coupling constants of the $ArOCH_2CH_2O$ part of the zinc(II) complex with reagent **6**.

EXPERIMENTAL

The methods of testing metal extraction are described in an earlier paper.[1]

Preparation of bis-quinaldic acids **1–8**, **12** *and* **13**

8-Hydroxyquinoline-2-carbonitrile[7] (3.40 g, 20 mmol), K_2CO_3 (3.04 g, 22 mmol) and DMF (35 cm^3) were stirred and heated to 75°C. The appropriate

Table 2. $pH_{1/2}$ Values for the extraction of metals[a]

Reagent	Cu^{2+}	Zn^{2+}	Fe^{2+}	Cd^{2+}	Ni^{2+}	Co^{2+}
3[c]	0.9	2.0	[b]	2.7	2.6	2.8
7	1.4	2.9	[b]	2.5	[b]	—
9	< 1.1	2.1	2.7	2.6	3.1	3.1
10	< 0.9	2.2	[b]	—	2.9	[b]
11	< 0.8	1.8	[b]	1.6	[b]	2.3
13	3.2	3.5				3.4

[a] The extractions were performed with equal volumes of an aqueous phase containing initially 2 mM metal sulphates and a 10 mM chloroform solution of the reagent.

[b] Less than 4% extraction at pH 1.9.

[c] Precipitation in the organic phase.

Table 3. 1,*n*-Bis(2-cyano-8-quinolinyloxy)alkanes

Compound	X–X	M.p. (°C)	Yield (%)	Anal.
1a	$O(CH_2)_3O$	221–4 (acetone)	62	C,H,N
2a	$O(CH_2)_4O$	233 (DMF)	75	C,H,N
3a	$O(CH_2)_8O$	166–168.5 (CH_3CN)	98	[a]
4a	$O(CH_2)_{10}O$	150–5 (toluene)	59	C,H,N
5a	$OCH_2CH_2OCH_2CH_2O$	192–4 (acetone)	60	C,H,N
6a	$OCH_2(CH_2OCH_2)_2CH_2O$	143–6 (toluene)	60	C,H,N
7a	$OCH_2CH_2OCH_2CH(n\text{-}C_{10}H_{21})OCH_2CH_2O$	(oil)	80	—
8a	$OCH_2(CH_2OCH_2)_3CH_2O$	137–140 (toluene)	68	[b]
12a	$OCH_2CH_2OCH_2CH_2O$ $R^7 = C_{12}H_{23}$	91–6	83	—
13a	$O(CH_2)_8O$ $R^7 = C_{12}H_{23}$	(oil)	90	C,H,N

[a] Calc. for C,H: C 74.6%, H 5.8%. Found: C 73.6%, H 5.8%.
[b] Calc. for C,H,N: C 67.5%, H 5.3%, N 11.2%. Found: C 68%, H 5.3%, N 11.1%.

ditosylate (11 mmol) for the preparation of reagents **1** and **4–8** or dibromoalkane, for the preparation of reagents **2** and **3**, was then added over 25 min. The reaction mixture was then heated at 75°C for an additional 20 h, cooled and poured into ice-water (300 cm^3). The precipitated product was recrystallized or purified by column chromatography on silica gel (Table 3).

Reagents **12** and **13** were prepared similarly from 7 - (1 - ethenyl - 3,3,5,5 - tetramethylhexyl) - 8 - hydroxyquinoline - 2 - carbonitrile.[1] The dinitrile precursors to reagents **7**, **12** and **13** were isolated by ether or toluene extraction. The ditosylate used in the preparation of reagent **7** was synthesized by a known method.[8]

The dinitriles were hydrolyzed to dicarboxylic acids by KOH in EtOH–H_2O, Claisen's alkali or glycol at 70–140°C until the evolution of ammonia had ceased. The reaction mixture was poured into water, acidified with 2 M HCl, and the product recrystallized.

1,3 - *Bis*(2 - *carbethoxy* - 1,4 - *dihydro* - 4 - *oxo* - 8 - *quinolinyloxy*)*propane* (**9b**)

This compound was prepared by the Conrad–Limpach–Knorr reaction.[9] K_2CO_3 (5.52 g, 40 mmol) was added to 2-nitrophenol (5.56 g, 40 mmol) in DMF (20 cm^3), followed by 1,3-dibromopropane (4.04 g, 20 mmol) and the reaction mixture was kept at 70°C overnight. The reaction mixture was cooled, poured into water and recrystallized from ethanol to give 1,3-di(*o*-nitrophenoxy)propane (4.80 g, 75% yield). This product was reduced with hydrazine (3 cm^3) and Pd(C) (0.2 g) in ethanol (150 cm^3) at reflux for 1.5 h and the resulting diamino compound was converted into its hydrochloride. 1,3-Di(*o*-aminophenoxy)propane hydrochloride (4.38 g, 13 mmol) was stirred at room temperature for two days with diethyl oxalacetate sodium salt (5.56 g, 26.5 mmol), anhydrous Na_2SO_4 (5.8 g) and absolute ethanol (26 cm^3). Water was then added and the product extracted with ether, yielding 6.60 g (85%) of the condensation product. This was dissolved in diphenyl ether (15 cm^3) and the solution added dropwise to 60 cm^3 refluxing diphenyl ether over 7 min. Reflux was continued for an additional 8 min and then most of the solvent was distilled off under reduced pressure. Chromatography on silica gel (90 g) with 5% EtOH in CH_2Cl_2 followed by recrystallization yielded 1.44 g (14% yield based on 2-nitrophenol), m.p. 191–192°C (MeOH). IR (KBr): 3390 (NH), 1720 (C=O), 1630 (C=C—C=O), 1595 cm^{-1} (aromat.). ^1H NMR ($CDCl_3$): δ 1.42 (6H, t, J = 7 Hz, CH_3), 2.58 (2H, m, J = 6 Hz, CCH_2C), 4.45 (4H, q, J = 7 Hz, CH_2OCO), 4.47 (4H, t, J = 6 Hz, CH_2OAr), 6.94 (2H, d, J = 2 Hz, H-3), 7.15 (2H, dd, J = 1 and 8 Hz, H-7), 7.27 (2H, dd, J = 8 Hz, H-6), 7.88 (2H, d, J = 8 Hz, H-5) and 9.34 (2H, bs, NH).

1,3 - *Bis*[2 - *carboxy* - 4 - (5,5,7,7 - *tetramethyl* - 2 - *octenyloxy*) - 8 - *quinolinyloxy*]*propane* (**9**)

This reagent was obtained by alkylation (K_2CO_3/DMF) of **9b** (1.37 g, 2.7 mmol) with 1 - chloro - 5,5,7,7, - tetramethyl - 2 - octene (1.30 g, 6.4 mmol) at 85°C overnight. The crude product was hydrolyzed with KOH–EtOH–H_2O at reflux (5 h). Addition of water and then dilute H_2SO_4 to pH 3 gave the dicarboxylic acid (1.98 g, 94% yield). IR (KBr): 1770, 1720 (C=O), 970 cm^{-1} (CH=CH-*trans*). ^1H NMR ($CDCl_3$): δ 0.98 (18H, s, *t*-Bu), 0.99 (12H, s, CH_3), 1.26 (4H, s, CH_2), 2.10 (4H, d, J = 7 Hz, CH_2–CH=), 2.65 (2H, m, CCH_2C), 4.58 (4H,

CH_2O), 4.87 (4H, d, $OC\underline{H}_2$–CH=), 5.8 (2H, m, CH=CH), 6.0 (2H, m, CH=CH), 7.30 (2H, d, H-7), 7.58 (2H, dd, H-6), 7.71 (2H, s, H-3) and 7.82 (2H, d, H-5).

1,8 - *Bis*(2 - *carbethoxy* - 1,4 - *dihydro* - 4 - *oxo* - 8 - *quinolinyloxy*) - 3,6 - *dioxaoctane* (**10b**)

This compound was prepared in a similar way as **9b** from 2-nitrophenol and triethylene glycol ditosylate. The bis-quinolone **10b** was obtained as a precipitate on addition of petroleum ether to the diphenyl ether solution, m.p. 141–2°C (MeOH), yield 23% based on 2-nitrophenol. IR (KBr): 3400 (NH), 1725 (C=O), 1640 cm^{-1} (C=C—C=O). ^1H NMR ($CDCl_3$): δ 1.41 (6H, t, J = 7 Hz, CH_3), 3.83 (4H, s, CH_2O), 3.97 (4H, m, CH_2O), 4.33 (4H, m, $C\underline{H}_2OAr$), 4.42 (4H, q, J = 7 Hz, $C\underline{H}_2Me$), 6.96 (2H, d, J = 1.9 Hz, H-3), 7.10, (2H, dd, J = 8 and and 1 Hz, H-7), 7.25 (2H, dd, J = 8 Hz, H-6), 7.90 (2H, d, J = 8 Hz, H-5) and 9.49 (2H, bs, NH).

1,8 - *Bis*[2 - *carboxy* - 4 - (5,5,7,7 - *tetramethyl* - 2 - *octenyloxy*) - 8 - *quinolinyloxy*)] - 3,6 - *dioxaoctane* (**10**)

The bis-quinolone compound, **10b**, (2.70 g, 4.66 mmol) was stirred at 60°C (20 min) with K_2CO_3 (1.40 g, 10.2 mmol) in DMF (20 cm^3). 1 - Chloro - 5,5,7,7 - tetramethyl - 2 - octene (2.13 g, 10.5 mmol) was added and the reaction mixture heated at 60°C (40 h). Workup by ether extraction and recrystallization from petroleum ether–ether (3 : 1) gave the 4-alkoxy ester (3.20 g, 75% yield), m.p. 78–80°C. IR (KBr): 1720 cm^{-1} (C=O). Partial ^1H NMR ($CDCl_3$): δ 1.46 (t, CH_3), 4.47 (q, OCH_2) (ethyl ester).

This diethyl ester (3.10 g, 3.4 mmol) was hydrolyzed with KOH in EtOH–H_2O at reflux for 1 h. Yield: 2.29 g (79%). IR ($CHCl_3$): 3500 (O–H), 1760, 1730 cm^{-1} (C=O). ^1H NMR ($CDCl_3$): δ 1.00 (30H, s, CH_3), 1.28 (4H, s, CCH_2C), 2.11 (4H, d, J = 7.3 Hz, $C\underline{H}_2$–CH=), 3.94 (4H, s, CH_2O), 4.08 (4H, m, CH_2O), 4.39 (4H, m, $C\underline{H}_2OAr$), 4.72 (4H, d, J = 5.8 Hz, $C\underline{H}_2$–CH=), 5.76 (2H, dt, J = 5.9 and 15.5 Hz, CH=CH), 6.00 (2H, dt, J = 7.3 and 15 Hz, CH=CH), 7.08 (2H, d, J = 7 Hz, H-7), 7.33 (2H, s, H-3), 7.47 (2H, dd, J = 8 Hz, H-6), 7.60 (2H, d, J = 8 Hz, H-5).

1,2 - *Bis*(2 - *carbethoxy* - 1,4 - *dihydro* - 4 - *oxo* - 8 - *quinolinylthio*)*ethane* (**11b**)

This product was prepared by analogy with **9b** from 1,2-di(*o*-aminophenylthio)ethane dihydrochloride.[10] The bis-quinoline (**11b**) was precipitated on addition of petroleum ether (160 cm^3) to the diphenyl ether solution (80 cm^3). Yield: 26%, m.p. 226–228°C ($CHCl_3$–toluene). IR (KBr): 3330 (NH), 1720 (C=O). 1630 (C=C—C=O), 1590 cm^{-1} (aromat.). ^1H NMR ($CDCl_3$): δ 1.45 (3H, t, J = 7 Hz, CH_3), 2.95 (2H, s, CH_2S), 4.49 (2H, q, J = 7 Hz, CH_2O), 7.00 (1H, d, J = 2 Hz, H-3), 7.31 (1H, dd, J = 8 and 8 Hz, H-6), 7.81 (1H, dd, J = 7 and 1.4 Hz, H-7), 8.34 (1H, ddd, J = 8.1, 1.4 and 0.6 Hz, H-5) and 9.95 (1H, bs, NH).

1,2 - *Bis* - [2 - *carboxy* - 4 - (5,5,7,7 - *tetramethyl* - 2 - *octenyloxy*) - 8 - *quinolinylthio*]*ethene* (**11**)

This reagent was obtained by alkylation with dodecenyl chloride in analogy with **10b**. The 4-alkoxy ester was obtained in 83% yield, m.p. 127–145°C (petroleum ether b.p. 100–125°C). IR (KBr): 2960 (C–H), 1715 (C=O), 1590, 1500 cm^{-1} (aromat.). Partial ^1H NMR ($CDCl_3$): δ 1.45 (t, CH_3), 4.46 (q, CH_2) (ethyl ester).

The diethyl ester (1.51 g, 1.76 mmol) was hydrolyzed with KOH (1 g), EtOH (20 cm^3) and H_2O (4 cm^3) at reflux overnight. Addition of water and acidification gave 1.09 g (77% yield). IR (KBr): 3240 (OH), 2960 (C–H), 1760 (C=O), 1590, 1505 cm^{-1} (aromat.). ^1H NMR ($CDCl_3$): δ 0.99 (30H, s, CH_3), 1.26 (4H, s, CH_2), 2.10 (4H, d, J = 7 Hz, $C\underline{H}_2CH$=), 3.42 (4H, s, CH_2S), 4.85 (4H, d, J = 5 Hz, $OC\underline{H}_2CH$=), 5.79 (2H, m, CH=CH), 6.01 (2H, m, CH=CH), 7.45–7.65 (4H, m, H-6, H-7), 7.66 (2H, s, H-3) and 8.08 (2H, d, J = 8 Hz, H-5).

Acknowledgements—Financial support from the Swedish Board for Technical Development is gratefully acknowledged. We thank Professor Torbjörn Norin and Dr. Christina Moberg for stimulating discussions and Kerstin Högberg and Peter Fäldt for technical assistance.

REFERENCES

1. A. G. S. Högberg, K. Madan, C. Moberg, B. Sjöberg, M. Weber and M. Muhammed, *Polyhedron* **4**, 971.
2. M. Pang, U.S. Patents 3 637 476 (1972), 3 697 400 (1972), 3 787 418 (1974).
3. N. Ackerley and P. A. Mack, *Ger. Offen.* 2 339 240 (1974).
4. E. Weber and F. Vögtle, *Tetrahedron Lett.* 1975, 2415.
5. W. Saenger, I.-H. Suh and G. Weber, *Israel J. Chem.* 1979, **18**, 253.
6. C. M. Hall, H. G. Johnson and J. B. Wright, *J. Med. Chem.* 1974, **17**, 685.
7. I. A. Krasavin, V. M. Dziomko and Y. P. Radin, *Metody Polucheniya Khim. Reaktivov i Preparatov* 1965, **13**, 68, 94; *Chem. Abstr.* 1966, **65**, 5437b; 7139a.
8. M. Cinquini and P. Tundo, *Synthesis* 1976, 516.
9. (a) B. Riegel, C. J. Albisetti, Jr., G. R. Lappin and R. H. Baker, *J. Am. Chem. Soc.* 1946, **68**, 2685. (b) G. F. Lisk and G. W. Stacy, *J. Am. Chem. Soc.* 1946, **68**, 2686.
10. R. D. Cannon, B. Chiswell and L. M. Venanzi, *J. Chem. Soc.* (*A*) 1967, 1277.

Polyhedron Vol. 4, No. 7, pp. 1203–1211, 1985
Printed in Great Britain

0277–5387/85 $3.00 + .00
© 1985 Pergamon Press Ltd

THE MOLYBDENUM–MOLYBDENUM TRIPLE BOND—XVII.* SYNTHESES, SPECTROSCOPIC AND STRUCTURAL CHARACTERIZATIONS OF $Mo_4F_4(O\text{-}t\text{-}Bu)_8$ AND $Mo_2F_2(O\text{-}t\text{-}Bu)_4(PMe_3)_2$ (Mo≡Mo)

MALCOLM H. CHISHOLM,† DAVID L. CLARK and JOHN C. HUFFMAN
Department of Chemistry and Molecular Structure Center, Indiana University, Bloomington, IN 47405, U.S.A.

(*Received* 8 *October* 1984; *accepted* 9 *November* 1984)

Abstract—Hydrocarbon solutions of $Mo_2(O\text{-}t\text{-}Bu)_6$ and PF_3 (2 equiv) yield $Mo_4F_4(O\text{-}t\text{-}Bu)_8$, **I**, and $PF_2(O\text{-}t\text{-}Bu)$. Compound **I** contains a bisphenoid of molybdenum atoms with two short Mo–Mo distances, 2.26 Å, and four long Mo–Mo distances, 3.75 Å, corresponding to localized Mo–Mo triple bonding and non-bonding distances, respectively. The tetranuclear compound may be viewed as a dimer, $[Mo_2(\mu_2\text{-}F)_2(O\text{-}t\text{-}Bu)_4]_2$, and addition of PMe_3 to hydrocarbon solutions of **I** yields $Mo_2F_2(O\text{-}t\text{-}Bu)_4(PMe_3)_2$, **II**, which contains an unbridged Mo–Mo triple bond of distance 2.27 Å. Each molybdenum atom is coordinated to two oxygen atoms, one fluorine atom and the phosphorus atom of the PMe_3 ligand in a roughly square planar manner. The overall central $Mo_2O_4F_2P_2$ skeleton has C_2 symmetry and NMR studies (^1H, ^{19}F and ^{31}P) are consistent with the maintenance of this type of structure in solution. Infrared and electronic absorption spectral data are reported. These are the first compounds containing fluorine ligands attached to the $(Mo{\equiv}Mo)^{6+}$ unit.

As part of our continuing studies of the chemistry associated with compounds containing a central $(Mo{\equiv}Mo)^{6+}$ unit, we reported the fortuitous discovery of two molecules,

$$Mo_4(\mu\text{-}F)_3(\mu\text{-}NMe_2)(O\text{-}t\text{-}Bu)_8$$

and $Mo_4(\mu\text{-}F)_4(O\text{-}t\text{-}Bu)_8$, that cocrystallized in the same unit cell.[2] We describe here the synthesis and characterization of the pure compound $Mo_4(\mu\text{-}F)_4(O\text{-}t\text{-}Bu)_8$ (Mo≡Mo) and its cleavage by trimethylphosphine to yield the dinuclear product $Mo_2F_2(O\text{-}t\text{-}Bu)_4(PMe_3)_2$ (Mo≡Mo).

RESULTS AND DISCUSSION

Synthesis. In hydrocarbon solvents at room temperature $Mo_2(O\text{-}t\text{-}Bu)_6$ reacts with two equivalents of phosphorus trifluoride to give the tetranuclear product $Mo_4(\mu\text{-}F)_4(O\text{-}t\text{-}Bu)_8$ (**I**) as outlined in eqn (1).

$$2Mo_2(O\text{-}t\text{-}Bu)_6 + 4PF_3 \xrightarrow[20°C]{\text{hexane}} Mo_4F_4(O\text{-}t\text{-}Bu)_8 + 4\,PF_2(O\text{-}t\text{-}Bu). \quad (1)$$

The reaction proceeds smoothly at room temperature and appears to be complete within several hours. The ^1H NMR spectra of the products obtained by stripping the reaction mixture *in vacuo* show that formation of **I** is essentially quantitative. If less than two equivalents of phosphorus trifluoride are added, only compound **I** and unreacted starting material are recovered. Recrystallization from hot toluene solution gives the black, crystalline product in 40% yield based on eqn (1). We attribute the orginal isolation[2] of crystals containing a mixture of $Mo_4F_4(O\text{-}t\text{-}Bu)_8$ and $Mo_4F_3(NMe_2)(O\text{-}t\text{-}Bu)_8$ to the presence of $Mo_2(NMe_2)(O\text{-}t\text{-}Bu)_5$ as an impurity in the $Mo_2(O\text{-}t\text{-}Bu)_6$ sample. Presumably the impurity arose from incomplete alcoholysis in the preparation of $Mo_2(O\text{-}t\text{-}Bu)_6$ from $Mo_2(NMe_2)_6$.

Compound **I** is readily cleaved by trimethylphosphine to give the dinuclear compound $Mo_2F_2(O\text{-}t\text{-}Bu)_4(PMe_3)_2$ (**II**) as outlined in eqn (2)

$$Mo_4F_4(O\text{-}t\text{-}Bu)_8 + 4PMe_3 \xrightarrow[20°C]{\text{toluene}} 2Mo_2F_2(O\text{-}t\text{-}Bu)_4(PMe_3)_2. \quad (2)$$

Reduction of the volume of solvent and slow cooling gives compound **II** as a red-brown crystalline product in 60% yield based on eqn (2).

Both **I** and **II** are air and moisture sensitive and

* See Ref. 1 for Part XVI.

† Author to whom correspondence should be addressed.

must be handled in dry and oxygen-free atmospheres and solvents. These compounds are more soluble in aromatic hydrocarbon solvents than in aliphatic ones. A cryoscopic molecular weight determination in benzene indicates that **I** retains its nuclearity in solution.

Solid state and molecular structures of $Mo_4(\mu\text{-}F)_4(O\text{-}t\text{-}Bu)_8$. Structural data for the $Mo_4(\mu\text{-}F)_4(O\text{-}t\text{-}Bu)_8$ molecule has been reported[2] based on the crystallographic characterization of a crystal that contained 2 molecules $Mo_4F_3(NMe_2)(O\text{-}t\text{-}Bu)_8$ and 1 molecule $Mo_4F_4(O\text{-}t\text{-}Bu)_8$ in the unit cell. We have not determined the molecular structure $Mo_4F_4(O\text{-}t\text{-}Bu)_8$ in its pure crystalline state since we believe this will be essentially equivalent to that seen previously.

An ORTEP view of the $Mo_4F_4(O\text{-}t\text{-}Bu)_8$ molecule is shown in Fig. 1. The $Mo_4(\mu\text{-}F)_4(O\text{-}t\text{-}Bu)_8$ molecule contains a bisphenoid of molybdenum atoms. There are two short Mo-to-Mo distances, 2.26 Å (averaged), corresponding to localized Mo-to-Mo triple bonds and four long, nonbonding Mo-to-Mo distances, 3.75 Å (averaged). The local geometry of each $Mo_2F_4O_4$ unit (Mo≡Mo) compares very closely with that observed for the $Mo_2O_4O_4'$ unit in $Mo_2(O\text{-}t\text{-}Bu)_4(O_2CO\text{-}t\text{-}Bu)_2$ (Mo≡Mo).[3] One striking structural feature in this molecule is that the Mo-to-Mo triple bonds are maintained. Indeed, it appears as though the Mo-to-Mo triple bonds are purposefully held apart by the bridging fluoride ligands. Another interesting observation is that these bridging fluoride ligands have Mo–F–Mo angles of 125° (averaged). Fluoride ligands show a strong tendency to form linear bridges[4] as in $[MoF_4(\mu\text{-}F)]_4$, and it has been proposed[5] that this is a result of ligand to metal π-bonding in the bridge. However, one other example of a structurally related dinuclear compound with bent fluoride bridges was recently reported by Crabtree *et al.*:[6] $[(Ph_2MeP)_6H_4Mo_2(\mu_2\text{-}F)_3]^+BF_4^-$.

$Mo_2F_2(O\text{-}t\text{-}Bu)_4(PMe_3)_2$. Selected bond distances and angles are given in Tables 1 and 2, respectively. ORTEP views looking down, and perpendicular to a twofold rotation axis which bisects the Mo≡Mo bond are shown in Figs. 2 and 3 respectively.

It may be seen in Fig. 3 that the rotational conformation is far from eclipsed as in quadruply bonded species (e.g., $Mo_2Cl_8^{4-}$ or $Mo_2Me_8^{4-}$) but at the same time not fully staggered. This partially staggered conformation is seen in other d^3–d^3 dimers of formula $Mo_2X_6L_2$[7] and results from a minimization of steric repulsive interactions.

The following points are worthy of note. (1) The Mo–Mo distance of 2.27 Å is typical of a Mo–Mo triple bond.[8] (2) Two distinct Mo–O distances are observed. Short Mo–O distances of 1.87 Å (averaged) exist for oxygen atoms *trans* to fluoride ligands, and longer Mo–O distances of 1.93 Å for oxygen atoms *trans* to Mo–P bonds.

There are many factors which may influence an

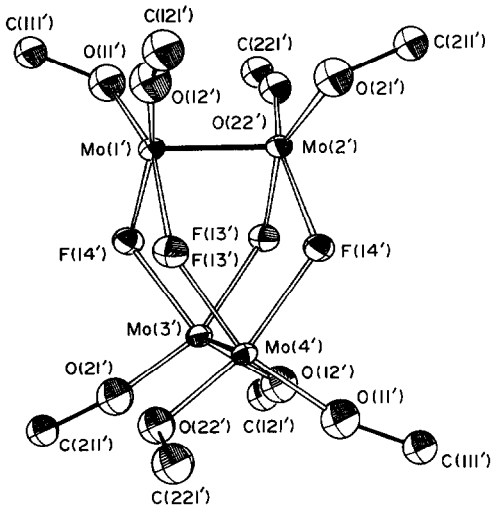


Fig. 1. An ORTEP view of the central skeleton of the $Mo_4(\mu\text{-}F)_4(O\text{-}t\text{-}Bu)_8$ molecule. Pertinent distances (Å) and angles (°) are: Mo(1')–Mo(2') = 2.262(2), Mo(3')–Mo(4') = 2.263(2), Mo(1')–Mo(3') = 3.743(2), Mo(1')–Mo(4') = 3.730(2), Mo(2')–Mo(3') = 3.713(2), Mo(2')–Mo(4') = 3.700(2), Mo–μ-F = 2.10(2) (averaged) and Mo–O = 1.94(2) (averaged), Mo–F–Mo = 125° (averaged).

Table 1. Selected bond distances (Å) for the $Mo_2F_2(O\text{-}t\text{-}Bu)_4(PMe_3)_2$ molecule

A	B	Distance
Mo(1)	Mo(2)	2.2698(11)
Mo(1)	P(4)	2.5879(25)
Mo(1)	F(3)	1.985(5)
Mo(1)	O(8)	1.938(6)
Mo(1)	O(13)	1.879(6)
Mo(2)	P(19)	2.5932(26)
Mo(2)	F(18)	1.981(5)
Mo(2)	O(23)	1.863(6)
Mo(2)	O(28)	1.931(6)
P(4)	C(5)	1.831(10)
P(4)	C(6)	1.806(9)
P(4)	C(7)	1.820(10)
P(19)	C(20)	1.808(10)
P(19)	C(21)	1.799(12)
P(19)	C(22)	1.823(12)
O(8)	C(9)	1.453(11)
O(13)	C(14)	1.427(10)
O(23)	C(24)	1.435(11)
O(28)	C(29)	1.460(10)
C(9)	C(10)	1.461(17)

individual M–O distance, particularly the oxidation state of the metal, the *trans*-ligand and steric and electronic properties of adjacent ligands.[9] The single bond covalent radii for Mo(III) and oxygen have been determined to be 1.40 Å and 0.77 Å respectively.[8] This then sets $d(\text{Mo–O}) = r_{\text{Mo}} + r_{\text{O}} = 2.06$ Å and this value is typical of Mo–μ-OR distances, but considerably longer than any seen for terminal Mo–OR groups which fall in the range 1.80–1.96 Å. In $Mo_2(OCH_2\text{-}t\text{-}Bu)_6$, the average Mo–O distance is 1.88(2) Å.[10] Upon association of other ligands, as in $Mo_2(OR)_6L_2$[7] compounds, the Mo–O distances are in the range 1.90–1.96 Å, consistent with a net decrease in Mo–O π-bonding. In the title compound $Mo_2F_2(O\text{-}t\text{-}Bu)_4(PMe_3)_2$ the alkoxy ligands *trans* to fluorine show a Mo–O bond length of 1.87 Å (averaged) and for alkoxy ligands *trans* to phosphorus a Mo–O bond length of 1.93 Å (averaged).[11] These distances are well within the range where some oxygen-to-molybdenum π-bonding is involved. The alkoxy ligands with short Mo–O bond lengths have Mo–O–C angles of 163.4° (averaged) while those with long Mo–O distances have Mo–O–C angles of 125.1° (averaged). In general the larger M–O–C angle correlates with increased π-donation.[12] We conclude that the Mo–O bonds reflect the *trans*-influence order of the *trans*-ligands: $PMe_3 > F^-$.

Table 2. Selected bond angles (°) for the $Mo_2F_2(O\text{-}t\text{-}Bu)_4(PMe_3)_2$ molecule

A	B	C	Angle
Mo(2)	Mo(1)	P(4)	91.90(6)
Mo(2)	Mo(1)	F(3)	105.49(14)
Mo(2)	Mo(1)	O(8)	102.81(18)
Mo(2)	Mo(1)	O(13)	106.82(18)
P(4)	Mo(1)	F(3)	75.65(14)
P(4)	Mo(1)	O(8)	161.46(19)
P(4)	Mo(1)	O(13)	86.00(19)
F(3)	Mo(1)	O(8)	89.43(23)
F(3)	Mo(1)	O(13)	143.15(24)
O(8)	Mo(1)	O(13)	100.20(26)
Mo(1)	Mo(2)	P(19)	91.03(7)
Mo(1)	Mo(2)	F(18)	105.46(14)
Mo(1)	Mo(2)	O(23)	106.80(21)
Mo(1)	Mo(2)	O(28)	102.48(17)
P(19)	Mo(2)	F(18)	74.91(16)
P(19)	Mo(2)	O(23)	87.71(22)
P(19)	Mo(2)	O(28)	161.48(18)
F(18)	Mo(2)	O(23)	143.43(25)
F(18)	Mo(2)	O(28)	89.16(23)
O(23)	Mo(2)	O(28)	100.20(28)
Mo(1)	P(4)	C(5)	107.5(4)
Mo(1)	P(4)	C(6)	124.1(3)
Mo(1)	P(4)	C(7)	114.9(3)
C(5)	P(4)	C(6)	102.7(5)
C(5)	P(4)	C(7)	102.4(5)
C(6)	P(4)	C(7)	102.6(4)
Mo(2)	P(19)	C(20)	114.6(3)
Mo(2)	P(19)	C(21)	124.3(4)
Mo(2)	P(19)	C(22)	107.6(4)
C(20)	P(19)	C(21)	101.7(5)
C(20)	P(19)	C(22)	102.5(5)
C(21)	P(19)	C(22)	103.8(6)
Mo(1)	O(8)	C(9)	124.8(5)
Mo(1)	O(13)	C(14)	159.2(6)
Mo(2)	O(23)	C(24)	167.5(7)
Mo(2)	O(28)	C(29)	125.2(5)
O(8)	C(9)	C(10)	106.6(9)
O(8)	C(9)	C(11)	106.7(9)
O(8)	C(9)	C(12)	112.0(8)
C(10)	C(9)	C(11)	113.1(13)
C(10)	C(9)	C(12)	111.5(13)
C(11)	C(9)	C(12)	107.0(10)
O(13)	C(14)	C(15)	108.5(8)
O(13)	C(14)	C(16)	110.3(7)
O(13)	C(14)	C(17)	105.7(8)
C(15)	C(14)	C(16)	110.8(8)
C(15)	C(14)	C(17)	110.3(9)
C(16)	C(14)	C(17)	111.2(9)
O(23)	C(24)	C(25)	108.6(9)
O(23)	C(24)	C(26)	109.8(9)

The C_{sp^3}–F distances in CH_3F and C_2H_5F average 1.38 Å.[13] Given that this is a single bond distance and that the radius of C_{sp^3} is 0.77 Å, then the covalent radius of fluorine (single bond) is placed at 0.61 Å (cf. 0.64 Å from reference 13). Given that the single bond covalent radius for molybdenum is 1.40 Å, then this sets $d_{(\text{Mo–F})} = r_{\text{Mo}} + r_{\text{F}} = 2.01$ Å. This value is in fact very close to the observed terminal Mo–F distance of 1.98 Å found in $Mo_2F_2(O\text{-}t\text{-}Bu)_4(PMe_3)_2$. We conclude that there is negligible F-to-Mo π-bonding.

Spectroscopic studies

NMR studies on $Mo_4F_4(O\text{-}t\text{-}Bu)_8$. When the reaction of $Mo_2(O\text{-}t\text{-}Bu)_6$ with PF_3 is carried out at −80°C and monitored by $^{31}P\{^1H\}$ NMR, one initially observes the ^{31}P resonance of free PF_3: there is no evidence for the simple adduct $Mo_2(O\text{-}t\text{-}Bu)_6(PF_3)_2$. Upon warming the NMR tube the PF_3 resonance disappears and the resonance assignable to $PF_2(O\text{-}t\text{-}Bu)$ grows in. By $^{31}P\{^1H\}$, ^{19}F and ^1H NMR spectroscopy the reaction is quantitative based on eqn (1).

The tetranuclear compound $Mo_4F_4(O\text{-}t\text{-}Bu)_8$, as shown in Fig. 1, has idealized D_{2d} symmetry. In the D_{2d} point group, the eight $OC(CH_3)_3$ ligands are all equivalent, and as expected, the room temperature ^1H NMR spectrum shows only one singlet, $\delta = 1.60$ ppm. Similarly, the four bridging fluoride ligands are equivalent and the ^{19}F NMR spectrum shows one singlet at −148.2 ppm, consistent with the solid state molecular structure.

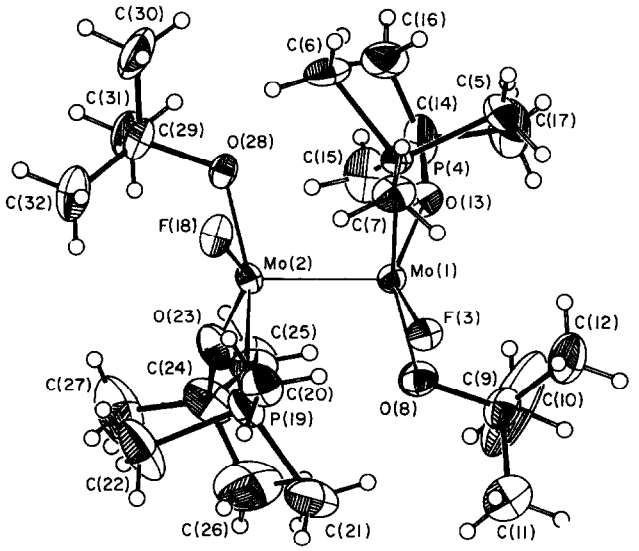


Fig. 2. An ORTEP view looking down the two-fold rotation axis of the $Mo_2F_2(O\text{-}t\text{-}Bu)_4(PMe_3)_2$ molecule giving the numbering scheme used in the tables.

$Mo_2F_2(O\text{-}t\text{-}Bu)_4(PMe_3)_2$. As seen in Figs. 2 and 3, $Mo_2F_2(O\text{-}t\text{-}Bu)_4(PMe_3)_2$ has a twofold rotation axis which makes the fluorine atoms (and phosphines) chemically but not magnetically equivalent, and thus part of an AA'XX' spin system. Both $^{31}P\{^1H\}$ and ^{19}F NMR show half of the expected AA'XX' spectrum shown in Figs. 4 and 5 respectively, but only six of expected ten lines are observed. AA'XX' spin systems have been well studied and their spectra may be regarded as superposition of a_2 and ab subspectra.[14] If there are weak or closely spaced lines, one often observes spectra whose appearance resemble that of a simpler type of spectrum because of the apparent deficiency of lines.[15] Successful spectral simulation at both 40.5 and 340 MHz was based on the assumption of degenerate ab subspectra. The coupling constants

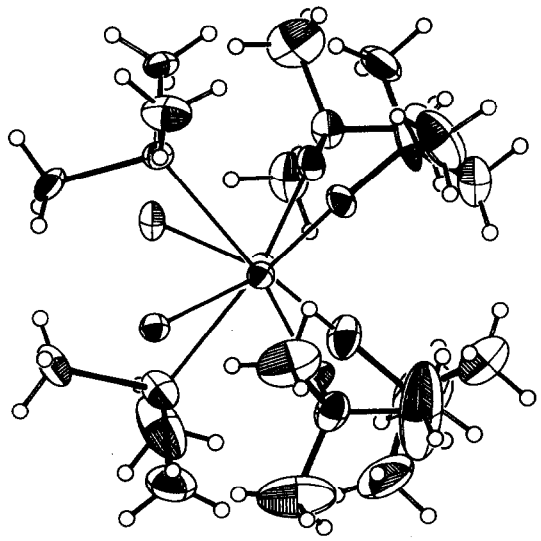


Fig. 3. An ORTEP view looking down the M–M bond and perpendicular to the two-fold rotation axis of the $Mo_2F_2(O\text{-}t\text{-}Bu)_4(PMe_3)_2$ molecule.

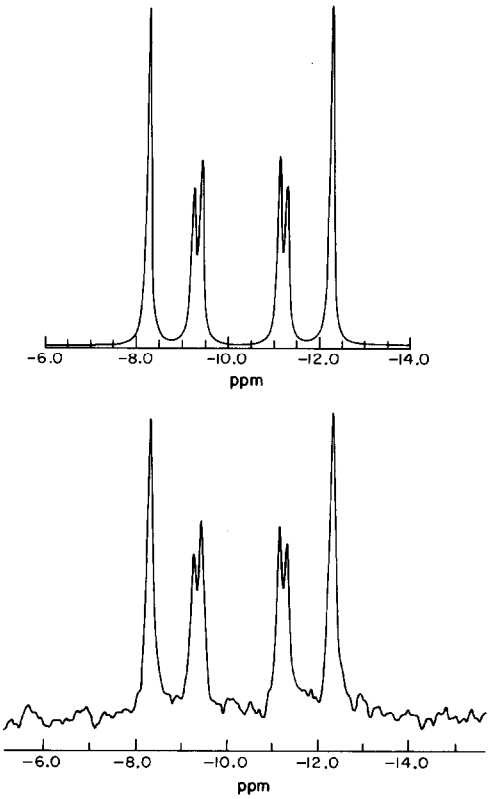


Fig. 4. Observed (bottom) and simulated (top) 40.5 MHz $^{31}P\{^1H\}$ NMR spectra of the $Mo_2F_2(O\text{-}t\text{-}Bu)_4(PMe_3)_2$ molecule.

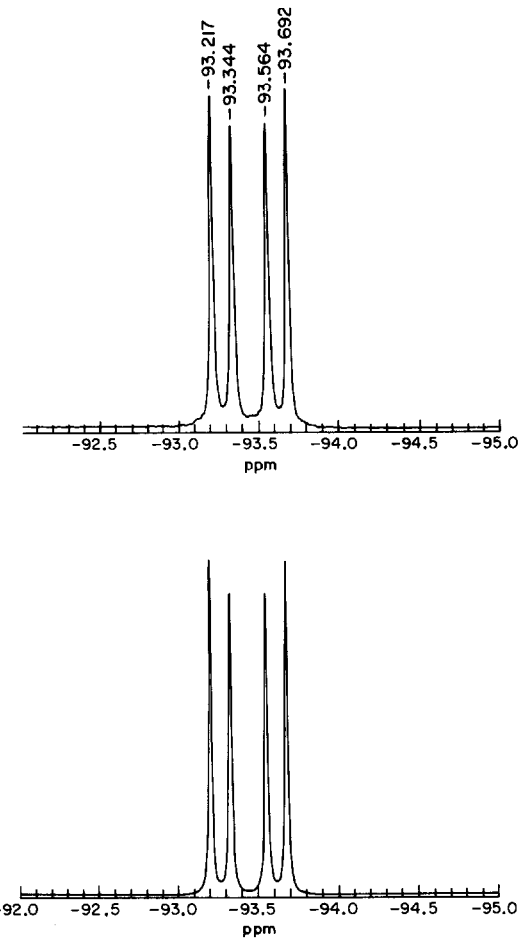


Fig. 5. Observed (top) and simulated (bottom) 340 MHz ^{19}F NMR spectra of the $Mo_2F_2(O\text{-}t\text{-}Bu)_4(PMe_3)_2$ molecule.

were then calculated using the method of Gunther[14] and computer simulation gave the spectra shown in Figs. 4 and 5 for ^{31}P and ^{19}F, respectively. The ^{19}F and ^{31}P spectra should be identical. When 6 Hz of line broadening is applied to the ^{19}F spectrum recorded at 340 MHz (the measured natural line width is 6.1 Hz for ^{19}F) the central lines become too close to be resolved. This simulation gives $^2J_{P-F}$ = 118.6 Hz, $^3J_{P-P}$ = 43.2 Hz, $^3J_{F-F}$ = 6.7 Hz and $^3J_{P-P}$ = 1.0 Hz. $^2J_{P-F}$ and $^3J_{P-F}$ are necessarily of the same sign but the relative signs of J_{F-F} and J_{P-P} cannot be ascertained.

The room temperature ^1H NMR spectra are also consistent with the solid state structure. Two singlets for the $OC(CH_3)_3$ ligands are observed at 1.80 and 1.33 ppm, as well as one doublet for $P(CH_3)_3$ at 1.44 ppm. It is interesting to note that under routine conditions (~60 FT acquisitions) only one rotational isomer is observed by ^1H NMR. Only during ^{19}F data collection (when an extraordinary 700 FT acquisitions were collected) was there any evidence for other rotamers in solution. The major rotamer is consistent with the solid state conformation.

Infrared spectra. Barraclough *et al.*[16] studied the infrared spectra of a number of metal alkoxides and the ν(C–O) and ν(M–O) bands were tentatively assigned. It has been observed that ν(C–O)M and ν(M–O) bands generally appear in the region 900–1150 cm^{-1} and 600–500 cm^{-1}, respectively. The position of the bands is determined by the metal and the nature of the alkoxy groups. The IR spectra of the dimeric $Mo_2(OR)_6$ alkoxides exhibit ν(Mo–O) bands which are higher in energy than those reported by Barraclough presumably because of the strong RO-to-M π-bonding in the former. For example, under D_{3d} symmetry, $Mo_2(O\text{-}i\text{-}Pr)_6$ exhibits two strong bands as expected which can tentatively be assigned as A_{2u} (651 cm^{-1}) and E_u (625 cm^{-1}). The A mode, being totally symmetric, should lie at higher energy. For $Mo_2(O\text{-}t\text{-}Bu)_6$ these two bands are observed at 600 and 560 cm^{-1}. The bands for ν(C–O) come as expected between 900 and 1000 cm^{-1} for all $Mo_2(OR)_6$ compounds. It should be noted, however, that C–O, C–C and M–O coupling will complicate the assignments especially under lower symmetry. For $Mo_4F_4(O\text{-}t\text{-}Bu)_8$, ν(Mo–O) are observed as medium intensity bands at 625 and 555 cm^{-1}, and for $Mo_2F_2(O\text{-}t\text{-}Bu)_4(PMe_3)_2$ ν(Mo–O) are observed at 599 and 540 cm^{-1}.

Terminal M–F stretching bands generally appear in the region of 750–500 cm^{-1}.[17] By comparisons of the IR spectra for I and II we tentatively assign ν(Mo–F) to medium intensity bands at 730 and 740 cm^{-1} for the terminal Mo–F bonds in $Mo_2(O\text{-}t\text{-}Bu)_4(PMe_3)_2$. For the bridging fluorides ν(Mo–F) is observed at 510 cm^{-1} in $Mo_4F_4(O\text{-}t\text{-}Bu)_8$.

Electronic absorption spectra. The electronic

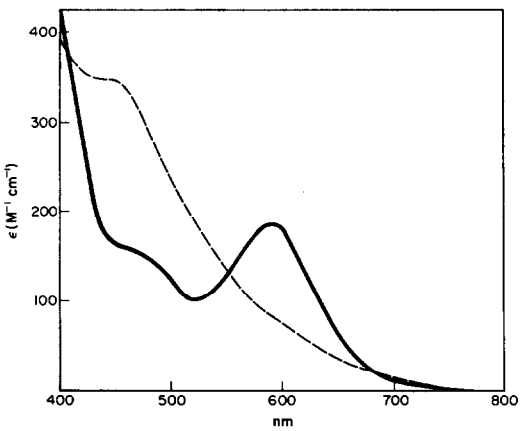


Fig. 6. Comparison of the visible electronic absorption spectra of $Mo_4(\mu\text{-}F)_4(O\text{-}t\text{-}Bu)_8$ (solid line) and $Mo_2F_2(O\text{-}t\text{-}Bu)_4(PMe_3)_2$ (dashed line) in hexane solution.

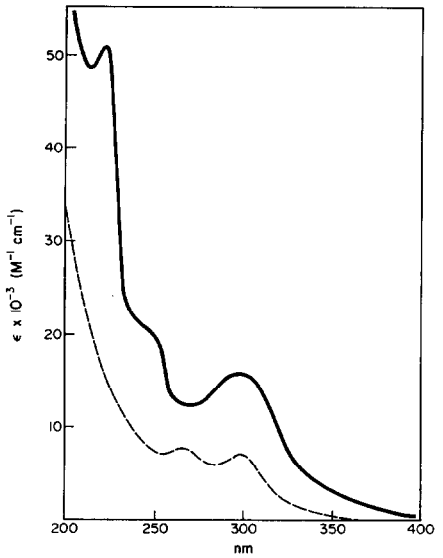


Fig. 7. Comparison of the ultraviolet electronic absorption spectra of $Mo_4(\mu\text{-}F)_4(O\text{-}t\text{-}Bu)_8$ (solid line) and $Mo_2F_2(O\text{-}t\text{-}Bu)_4(PMe_3)_2$ (dashed line) in hexane solution.

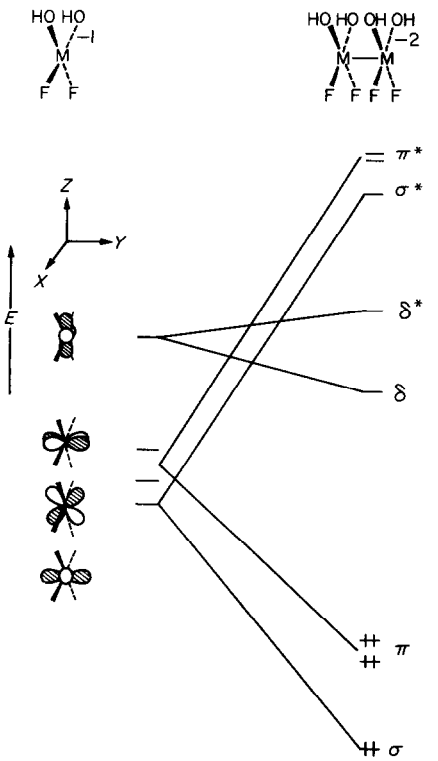


Fig. 8. Schematic drawing showing the derivation of the molecular orbitals of the d^3–d^3 dimer, $Mo_2F_4(OH)_4^{2-}$ (right), from the valence atomic orbitals of a $MoF_2(OH)_2^-$ fragment (left).

spectra of both compounds show weak absorptions ($\varepsilon < 400\ M^{-1}\ cm^{-1}$) in the visible spectra and strong absorptions ($\varepsilon = 10{,}000$–$50{,}000\ M^{-1}\ cm^{-1}$) in the ultraviolet. Visible and ultraviolet absorption spectra are shown in Figs. 6 and 7, respectively. $Mo_4F_4(O\text{-}t\text{-}Bu)_8$ and $Mo_2F_2(O\text{-}t\text{-}Bu)_4(PMe_3)_2$ are green and red–orange because of low energy absorptions at 590 and 480 nm, respectively.

An extended Hückel calculation[18] on the model compound $Mo_2F_4(OH)_4^{2-}$ which can be taken as one half of $Mo_4F_4(O\text{-}t\text{-}Bu)_8$ gives the expected electronic configuration of $\sigma^2\pi^4$ for the M–M bond. A schematic drawing of these molecular orbitals is shown in Fig. 8. In the symmetry groups C_2 and D_{2d} virtually all transitions are allowed. The molecular orbital diagram suggests that the lowest energy transition should be of the type M–M $\pi \rightarrow \delta/\delta^*$. The stronger absorptions in the ultraviolet region are then tentatively assigned M–M $\pi \rightarrow \pi^*$ and LMCT transitions, in increasing order of energy. For comparison we note that for $Mo_2(OR)_6$ compounds[19] there are no absorption maxima in the visible region and that SCF–Xα–SW calculations[20] on $Mo_2(OH)_6$ predict the lowest energy absorption, M–M $\pi \rightarrow \pi^*$, to lie well into the ultraviolet.

CONCLUSIONS

This work demonstrates that replacement of an O-*t*-Bu group by the smaller and more electronegative fluoride ligand promotes a Lewis base association reaction. Probably $Mo_2F_2(O\text{-}t\text{-}Bu)_4$, once formed, associates with itself through the agency of metal–ligand–metal bridges. The choice of bridging ligand is established to be $F > O\text{-}t\text{-}Bu$ which is not what might have been anticipated in view of the well known ability of alkoxides to bridge two or three metal atoms with flexible M–O–M angles.[16]

This work suggests that the choice of bridging ligand $F > O\text{-}t\text{-}Bu$ may be a result of the π-donor properties of the ligands which appear to lie in the inverse order. Through the agency of fluoride bridges, the alkoxide ligands can remain terminal and *cis* in order to maximize π-donation to the metal.

When a strong Lewis base such as trimethylphosphine is added to the fluoride bridged tetramer, the fluoride bridges are readily cleaved to give $Mo_2F_2(O\text{-}t\text{-}Bu)_4(PMe_3)_2$. This supports the view that the tetranuclear compound $Mo_4F_4(O\text{-}t\text{-}Bu)_8$ is best considered $[Mo_2(\mu\text{-}F)_2(O\text{-}t\text{-}Bu)_4]_2$ (M≡M).

At this point it is interesting to speculate about what factors will favor dinuclear compounds containing M–M bonds of multiple order compared with cluster compounds of the same empirical formula in which metal–metal bonding is delocalized.

We note, for example, that molybdenum in oxidation state +3 with halide and alkoxide ligands exists as the tetranuclear compound $Mo_4F_4(O\text{-}t\text{-}Bu)_8$ which contains localized Mo-to-Mo triple bonds, and as square (X = Cl) and butterfly (X = Br, I) clusters $Mo_4X_4(O\text{-}i\text{-}Pr)_8$ with delocalized metal–metal bonding.[21] We also note that molybdenum in oxidation state +3 with halide and dialkylamide ligands exists in dinuclear compounds $Mo_2X_2(NR_2)_4$ with localized Mo-to-Mo triple bonds.[22] There appears to be a subtle balance between the ability of the ligands to π-donate, the ability to bridge, and steric bulk.[23]

Further studies on compounds of these types should provide additional insight to the delicate balance between localized and delocalized bonding in these fascinating molecules.

EXPERIMENTAL

Physical techniques. ^1H NMR spectra were recorded on a Nicolet NT-360 spectrometer at 360 MHz in dry and oxygen-free toluene-d_8 or benzene-d_6. ^{19}F NMR spectra were recorded on the same instrument at 340 MHz in toluene-d_8 or benzene-d_6. ^{31}P NMR spectra were run on a Varian XL-100/Nicolet 1080 FT spectrometer at 40.5 MHz in the same solvents. All ^1H NMR chemical shifts are reported in ppm relative to the CHD_2 quintet of toluene-d_8 set at $\delta = 2.09$ or the ^1H impurity in benzene-d_6 set at $\delta = 7.15$. All ^{19}F NMR chemical shifts are reported in ppm relative to the CF_3 singlet of CF_3COOH used as an external lock and set at $\delta = -78.90$ ppm relative to $CFCl_3$. ^{31}P NMR chemical shifts are reported relative to 85% H_3PO_4.

Infrared spectra were recorded on a Perkin–Elmer 283 spectrophotometer as Nujol mulls between CsI plates. Electronic absorption spectra were obtained with a Perkin–Elmer 330 spectrophotometer. Samples were run versus a solvent blank using matched 1.00 cm or 1.0 mm quartz cells.

Synthesis. All reactions were carried out under an atmosphere of dry and oxygen-free nitrogen using standard Schlenk and glove-box techniques. Hexane and toluene were degassed and eluted from activated copper catalyst and molecular sieve columns and then stored under nitrogen. Phosphorus triflouride was purchased from Pennwalt and used without purification. Trimethylphosphine was purchased from Strem and was stored under a vacuum. Elemental analyses were performed by Alfred Bernhardt Microanalytishes Laboratorium, West Germany.

$Mo_4F_4(OBu^t)_8$. In a Schlenk reaction vessel $Mo_2(O\text{-}t\text{-}Bu)_6$[3] (1.00 g, 1.59 mmol) was completely dissolved in toluene (50 cm^3). The solution was frozen at −196°C and PF_3 (3.18 mmol) was condensed into the flask using a calibrated vacuum manifold. The reaction mixture was allowed to warm to room temperature and left to stir for 12 h. During this time the color of the solution changed from orange to red and finally to red–brown. The volume of toluene was reduced to 1/4 the original volume at which time a green precipitate formed. This solution was heated to 90°C on a hot H_2O bath to force all the precipitate back into solution. The flask was then allowed to slowly cool to room temperature overnight which produced many large black crystals. The flask was then cooled to −15°C for another 2 days. The crystals were collected by filtration and dried *in vacuo*. A second crop of crystals was obtained by reducing the volume of the filtrate and cooling [total yield 0.35 g, 42% based on eqn (1)]. Calc. for $Mo_4F_4O_8C_{32}H_{72}$: C, 36.76; H, 6.95; F, 7.27. Found: C, 36.51; H, 6.82; F, 7.12%.

^1H NMR (22°C): singlet, $\delta = 1.60$.

^{19}F NMR (22°C): singlet, $\delta = -148.24$.

IR (cm^{-1}): 1230 m, 1175s, 1025w, 990s, 915m, 895s, 790m, 775s, 625m, 555m, 510m, 485m, 390w, 370w, 350w, 285w.

UV–visible absorption spectra in hexane solution: λ_{max}, nm (ε, M^{-1} cm^{-1}) 590 (180), 480 (150) sh, 295 (15,000), 245 (21,000) sh, 220 (51,000).

$Mo_2F_2(OBu^t)_4(PMe_3)_2$. In a Schlenk reaction vessel $Mo_4F_4(OBu^t)_8$ (0.25 g, 0.24 mmol) was dissolved in toluene (20 cm^3). The solution was frozen at −196°C and trimethylphosphine (0.98 mmol, 4 equiv) was condensed into the flask using a calibrated vacuum manifold. The reaction mixture was allowed to warm to room temperature. The color of the solution changed from green to red–brown. The volume of solution was reduced by 1/2 and cooled to −15°C. Red–brown crystals were isolated after 6 days. A second crop of crystals was obtained by reducing the volume of the filtrate and cooling [total yield 0.20 g, 61% based on eqn (2)]. Calc. for $Mo_2F_2O_4P_2C_{22}H_{54}$: C, 39.20; H, 8.08; F, 5.64. Found: C, 39.10; H, 7.96; F, 5.48%.

^1H NMR (22°C): δ (O-*t*-Bu) = 1.80 and 1.33, equal intensity singlets; δ (PMe_3) = 1.44, doublet, $^2J_{P-H} = 9.0$ Hz.

$^{31}P\{^1H\}$ NMR (21°C): δ (PMe_3) = −10.26, half of the expected AA'XX' spectrum (Fig. 4). Successful simulation gives $^2J_{P-F} = 118.6$ Hz, $^3J_{P-F} = 43.2$ Hz, $^3J_{F-F} = 6.7$ Hz and $^3J_{P-P} = 1.0$ Hz. See discussion section about signs of coupling constants.

^{19}F NMR (22°C): δ (F) = −93.45; half of the expected AA'XX' spectrum; see Fig. 5. As mentioned in the discussion section, 700 FT acquisitions were collected to observe minor rotational components. To accomplish this a 220 ppm spectral window was

used with 16 K data points, 8 K of which are real. As a consequence, not enough data points were collected to resolve small coupling. For successful ^{19}F spectral simulation $^3J_{P-P} = 0$ Hz and $^3J_{P-F} = 3.0$ Hz was used.

IR (cm^{-1}): 1295m, 1280m, 1230m, 1165s, 1020w, 1000s, 980s, 960s, 920s, 895m, 845w, 785m, 762m, 762s, 740m, 730m, 670w, 599m, 540m, 490s, 385m, 370m, 350m, 290m.

UV–visible absorption spectra in hexane solution: λ_{max}, nm (ε, M^{-1} cm^{-1}) 450 (350) sh, 300 (6500), 265 (6700).

PF_2(O–*t*-Bu). $^{31}P\{^1H\}$ NMR: triplet, $^1J_{P-F} = 1290$ Hz, $\delta = -120$ ppm. ^{19}F NMR: doublet, $^1J_{P-F} = 1290$ Hz, $\delta = -42.2$ ppm. ^1H NMR: singlet, $\delta = 1.13$ ppm.

Crystallographic studies

General operating procedures and listings of programs have been given previously.[24] Crystal data for $Mo_2F_2(O\text{–}t\text{-}Bu)_4(PMe_3)_2$ are given in Table 3. A suitable crystal was transferred to the goniostat using standard inert atmosphere handling techniques employed by the IUMSC and cooled using a gas flow cooling system.

A systematic search of a limited hemisphere of reciprocal space located a set of diffraction maxima of orthorhombic symmetry, with systematic extinctions corresponding to the unique space group Pbca.

The structure was solved by a combination of Patterson and Fourier techniques, and refined by full-matrix least squares refinement. A difference Fourier phased on the non-hydrogen parameters located peaks which could be assigned to 46 of the 54 hydrogen atoms. An attempt was made to refine hydrogen atoms (using calculated positions for the missing eight hydrogens), but those on several methyl groups failed to refine properly, especially those involving C(10), C(11), C(25), C(26) and C(27). For this reason all hydrogen atoms were placed in idealized, fixed positions with dC–H = 0.95 Å for the remainder of the refinement.

A final difference Fourier was featureless, the largest peak being 0.32 e/Å.^{3} No absorption correction was attempted.

Table 3. Crystal data for the $Mo_2F_2(O\text{–}t\text{-}Bu)_4(PMe_3)_2$ molecule

Empirical formula	$Mo_2C_{22}H_{54}F_2O_4P_2$
Color of crystal	red
Crystal dimensions (mm)	0.15 × 0.15 × 0.22
Space group	Pbca
Cell dimensions	
Temperature (°C)	−157
a (Å)	17.883(4)
b (Å)	34.243(12)
c (Å)	10.508(2)
Z (molecules/cell)	8
Volume (Å^3)	6434.74
Calculated density (g/cm^3)	1.392
Wavelength (Å)	0.71069
Molecular weight	674.49
Linear absorption coefficient (cm^{-1})	8.921
Detector to sample distance (cm)	22.5
Sample to source distance (cm)	23.5
Take off angle	2.0
Average omega scan width at half height	0.25
Scan speed (deg/min)	4.0
Scan width (deg + dispersion)	2.0
Individual background (sec)	6
Aperture size (mm)	3.0 × 4.0
Two-theta range (deg)	6–45
Total number of reflections collected	5531
Number of unique intensities	4229
Number of F > 2.33σ(F)	3295
R(F)	0.0579
Rw(F)	0.0573
Goodness of fit for the last cycle	1.109
Maximum delta/sigma for last cycle	0.05

Acknowledgements—We thank the National Science Foundation and the Wrubel Computing Center for support.

Supplementary materials available—Tables of fractional coordinates have been deposited with the Cambridge Crystallographic Data Centre. Complete structural information is available from the Editor at Queen Mary College and, in microfiche form, from the Indiana University Chemical Library, Bloomington, IN, at a cost of $2.50 per structure report. For $Mo_4F_4(O\text{-}t\text{-}Bu)_8$/$Mo_4F_3(NMe_2)(O\text{-}t\text{-}Bu)_8$ request MSC No. 7881 and for $Mo_2F_2(O\text{-}t\text{-}Bu)_4(PMe_3)_2$ request MSC No. 84034.

REFERENCES

1. M. H. Chisholm, K. J. Ahmed and J. C. Huffman, *Organometallics* 1985, in press.
2. M. H. Chisholm, R. L. Kelly and J. C. Huffman, *J. Am. Chem. Soc.* 1979, **101**, 7100.
3. M. H. Chisholm, F. A. Cotton, M. W. Extine and W. W. Reichert, *J. Am. Chem. Soc.* 1978, **100**, 3354.
4. A. J. Edwards, R. D. Peacock and R. W. H. Small, *J. Chem. Soc.* 1962, 4486; A. J. Edwards and B. R. Stevenson, *J. Chem. Soc. (A)* 1968, 2503; A. J. Edwards, D. R. Slim and R. J. Kergoat, *J. Chem. Soc., Dalton Trans.* 1980, 289.
5. F. A. Cotton and G. Wilkinson, *Advanced Inorganic Chemistry*, 4th ed., p. 191. Wiley, New York (1980).
6. R. H. Crabtree, G. G. Hlatky and E. M. Holt, *J. Am. Chem. Soc.* 1983, **105**, 7302.
7. Part 3 of this series. M. H. Chisholm, F. A. Cotton, M. W. Extine and W. W. Reichert, *J. Am. Chem. Soc.* 1978, **100**, 153.
8. For listings and discussions of M–M and M–O distances in the chemistry of molybdenum and tungsten alkoxides see: M. H. Chisholm, *Polyhedron* 1983, **2**, 681.
9. T. G. Appleton, H. C. Clark and L. E. Manzer, *Coord. Chem. Rev.* 1972, **10**, 335.
10. M. H. Chisholm, F. A. Cotton, C. A. Murillo and W. W. Reichert, *Inorg. Chem.* 1977, **16**, 1801.
11. This observation is not unreasonable in view of the higher *trans*-influence of PR_3 relative to F^-. See reference 9.
12. See reference 8 and also: I. P. Rothwell, T. W. Coffindaffer and J. C. Huffman, *Inorg. Chem.* 1983, **23**, 1433.
13. Linus Pauling. *The Nature of the Chemical Bond*, Table 7-2, p. 224. Cornell Press, New York (1960).
14. Excellent reviews exist. See for example (a) H. Gunther, *Angewandte Chemie, Intl. Ed.*, 1972, **11**, 861; (b) E. D. Becker, *High Resolution NMR, Theory and Chemical Applications*, p. 167. Academic Press, New York (1980).
15. A well known case is the deceptively simple AA'XX' system of the protons in furan whose half spectrum degenerates to a triplet. See D. M. Grant, R. C. Hirst and H. S. Gutowsky, *J. Chem. Phys.* 1963, **38**, 470. Triplets are also seen in the ^{13}C spectrum in the η^2-C_2H_2 carbon region of $W_2(OCH_2\text{-}t\text{-}Bu)_6(\mu\text{-}C_4H_4)(^*C_2H_2)$; M. H. Chisholm, D. M. Hoffman and J. C. Huffman, *J. Am. Chem. Soc.* 1984, **106**, 6806.
16. For a general review of metal alkoxides and the physical techniques used to characterize them see: D. C. Bradley, R. C. Mehrotra and D. P. Gaur, In *Metal Alkoxides*. Academic Press, New York (1978).
17. K. Nakamoto, *Infrared and Raman Spectra of Inorganic and Coordination Compounds*, 3rd ed., p. 317. Wiley, New York (1978).
18. Extended Hückel calculations with weighted H_{ij}s were used: R. Hoffmann, *J. Chem. Phys.* 1963, **39**, 1397; R. Hoffmann and W. N. Lipscomb, *J. Chem. Phys.* 1962, **36**, 2179; 1962, **37**, 2872; J. H. Ammeter, H. B. Burgi, J. C. Thibeault and R. Hoffmann, *J. Am. Chem. Soc.* 1978, **100**, 3686. The molybdenum parameters are from P. Kubacek and R. Hoffman, *J. Am. Chem. Soc.* 1981, **103**, 4320.
19. M. H. Chisholm and E. Kober, results to be published.
20. B. E. Bursten, F. A. Cotton, J. C. Green, E. A. Seddon and G. Stanley, *J. Am. Chem. Soc.* 1980, **102**, 4579.
21. M. H. Chisholm, R. J. Errington, K. Folting and J. C. Huffman, *J. Am. Chem. Soc.* 1982, **104**, 2025; and M. H. Chisholm, D. L. Clark and J. C. Huffman, unpublished results.
22. M. Akiyama, M. H. Chisholm, F. A. Cotton, M. W. Extine and C. A. Murillo, *Inorg. Chem.* 1977, **16**, 2407.
23. It has already been shown that decreasing the steric bulk of the alkoxy ligands promotes Lewis base association and the adduct $Mo_2(OSiMe_3)_6(HNMe_2)_2$ has been structurally characterized. See Ref. 7.
24. M. H. Chisholm, K. Folting, J. C. Huffman and C. C. Kirkpatrick, *Inorg. Chem.* 1984, **23**, 1021.

Polyhedron Vol. 4, No. 7, pp. 1213–1217, 1985
Printed in Great Britain

0277–5387/85 $3.00 + .00
© 1985 Pergamon Press Ltd

1,2-DIMETALLACYCLO-1,2-HEXYNE COMPOUNDS OF MOLYBDENUM AND TUNGSTEN

M. J. CHETCUTI, M. H. CHISHOLM,* H. T. CHIU and J. C. HUFFMAN
Department of Chemistry and Molecular Structure Center, Indiana University, Bloomington, IN 47405, U.S.A.

(*Received* 12 *October* 1984; *accepted* 9 *November* 1984)

Abstract—From the reactions between 1,4-dilithiobutane and 1,2-$M_2Cl_2(NMe_2)_4$ compounds in hydrocarbon solvents, the 1,2-dimetallacyclo-1,2-hexyne compounds $M_2(CH_2)_4(NMe_2)_4$(M≡M), where M = Mo and W, have been obtained as yellow–orange, volatile microcrystalline compounds. Spectroscopic data are consistent with expectations based on previous studies of gauche 1,2-$M_2R_2(NMe_2)_4$ compounds in solution and a structural model based on the observed molecular structure of 1,2-$Mo_2Et_2(NMe_2)_4$ is presented and compared with the observed molecular structure of $Mo_2(CH_2)_4(NMe_2)_4$ found in the solid state. Pertinent bond distances (Å) and angles (°) are: Mo–Mo = 2.200(1), Mo–N = 1.96(1) (averaged), Mo–C = 2.165(8) (averaged), Mo–Mo–N = 105(1), Mo–Mo–C = 97(1).

There are a large number of compounds which contain triple bonds between molybdenum and tungsten atoms having a central unit $X_nM{\equiv}MX_n$ where X = a ligand atom directly bonded to the metal and $n = 3, 4, 5$ and 6, e.g., $M_2(NMe_2)_6$ where X = N and $n = 3$ and $W_2(O_2CNMe_2)_6$ where X = O and $n = 6$.[1] Within this group the so-called ethane-like dimers, $X_3M{\equiv}MX_3$, where X = C, N, O, S, have attracted the most study. A subset of the latter group are compounds of formula 1,2-$M_2R_2(NMe_2)_4$, where R = an alkyl[2] or aryl ligands.[3] These exist in solution as a mixture of anti and gauche rotamers and provide an excellent starting point for the study of the chemistry of alkyl/aryl ligands at dinuclear metal centers. One of the reactions we have been particularly interested in studying involves reductive-elimination from the dinuclear center to give M–M quadruple bonded compounds by either C–C or C–H bond formation. This was first observed for molybdenum as shown in eqn. (1)[4] and subsequently extended to tungsten, eqn. (2).[5]

$$1,2\text{-}Mo_2R_2(NMe_2)_4 + CO_2 \rightarrow Mo_2(O_2CNMe_2)_4 + \text{alkene} + \text{alkane} \quad (1)$$

[R = a β-hydrogen containing alkyl]

$$1,2\text{-}W_2R_2(NMe_2)_4 + 4R'COOCOR' \rightarrow W_2(O_2CR')_4 + \text{alkene and alkane} + 4R'CONMe_2. \quad (2)$$

Studies involving the use of labelled alkyls, e.g., CH_2CD_3, showed[4] that the β-H or D atom of one ligand was transferred to the α-carbon of the other alkyl ligand, e.g., CD_3CH_2–Mo≡Mo–CH_2CD_3 → [Mo≡Mo] + $CH_2{=}CD_2$ + CH_2DCD_3. This is consistent with an overall reaction scheme which incorporates an irreversible β-hydrogen abstraction step followed by reductive elimination by C–H bond formation. Just how these steps are achieved at the dimetal center poses several fascinating possibilities and reactions (1) and (2) are rare examples of dinuclear reductive-elimination.[6] In mononuclear chemistry the study of metallacycles of general formula $L_nM(CH_2)_x$, where $x = 3, 4$ and 5, has been helpful in elucidating the nature of the β-hydrogen abstraction step as well as other processes.[7,8] A similar situation could hold for the dinuclear reductive eliminations of the type described in eqns (1) and (2). We describe here the preparation and characterization of 1,2-dimetallacyclo-1,2-hexyne derivatives of molybdenum and tungsten.

RESULTS AND DISCUSSIONS

Synthesis

The new compounds were prepared according to the reaction shown in eqn. (3) and were isolated as microcrystalline yellow or orange solids by sublimation *in vacuo* (80–100°C, 10^{-4} torr) in 40–

* Author to whom correspondence should be addressed.

45% theoretical yield.

$$1,2\text{-}M_2Cl_2(NMe_2)_4 + LiCH_2CH_2CH_2CH_2Li \xrightarrow{\text{hexane}} M_2(CH_2)_4(NMe_2)_4 + 2LiCl. \quad (3)$$

Early problems associated with these reactions centered around the preparation of the 1,4-dilithiobutane and the choice of solvent. We found that the best procedure for the preparation of 1,4-dilithiobutane involved the reaction between lithium sand and 1,4-dichlorobutane. The use of the dichlorobutane is preferable to the dibromobutane and lithium sand is more reactive than the Li wire containing 0.8% Na recommended in the Whitesides' procedure.[8] The use of a non-oxygen containing hydrocarbon solvent in reaction (3), e.g., hexane or toluene, is required since the $M_2Cl_2(NMe_2)_4$ [9] compounds react with THF, ether and other O-donor solvents, etc. This, of course, leads to a rather slow reaction since the dilithiobutane is virtually insoluble in hexane and toluene. Nevertheless the pure compounds can be isolated in reasonable yields in this manner.

Physicochemical and spectroscopic properties

The new compounds of formula $M_2(CH_2)_4(NMe_2)_4$, where M = Mo and W, are yellow–orange, sublimable (80–100°C, 10^{-4} torr), microcrystalline compounds. They are extremely air-sensitive and were handled in dry and oxygen free atmospheres (N_2) and solvents. The compounds showed molecular ions M^+ in the mass spectrometer with characteristic isotope envelopes for the M_2-grouping. The compounds are appreciably soluble in hydrocarbon solvents such as hexane, benzene and toluene. Crystals suitable for detailed X-ray studies were obtained from pentane solutions. Only finely divided micro-crystalline samples were obtained by sublimation.

^{1}H NMR spectra, recorded at 360 MHz and at ambient temperatures, of toluene-d_8 solutions of $M_2(CH_2)_4(NMe_2)_4$ compounds are not very informative because of the complex spin-system (AA'BB'XX'YY') for the methylene protons of the $M_2(CH_2)_4$ ring and the temperature dependent rate of proximal and distal N-methyl exchange.[10] At lower temperatures rotations about M–N bonds are frozen out leading to two types of proximal N–Me resonances and two distal N–Me resonances. These are in agreement with expectations based on the gauche central $M_2N_4C_2$ unit which is imposed by the μ-C_4H_8 ligand. At higher temperatures rotations about M–N bonds become rapid on the NMR time-scale leading to a pairwise collapse of the proximal–distal N–Me signals. Below 110°C in toluene-d_8 gauche $\rightleftharpoons$ gauche isomerization/enantiomerization is not observed on the NMR time-scale.

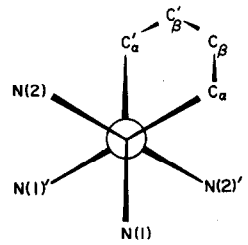


Fig. 1. A Newman projection of the central $M_2C_4N_4$ skeleton of the $M_2(CH_2)_4(NMe_2)_4$ molecules.

The low temperature proton decoupled ^{13}C spectra show four NMe signals assignable to the two proximal and two distal NMe groups. The chemical shift separation of the proximal and distal NMe groups is *ca* 15–20 ppm due to the magnetic anisotropy of the M≡M bond.[1,10] Two other signals of equal intensity are seen and these are assigned to the α,α' and β,β' carbon atoms of C_4-methylene chain. In the case of the ditungsten compound one of these signals shows tungsten satellites, $J_{^{183}W-C} = 113$ Hz, which identifies it as arising from the α,α' carbon atoms. The NMR spectra thus reliably establish the gauche ethane-like geometry depicted by the Newman projection shown in Fig. 1.

A simulated structure

A structure for the $Mo_2(CH_2)_4(NMe_2)_4$ molecule can be simulated from the observed structure of

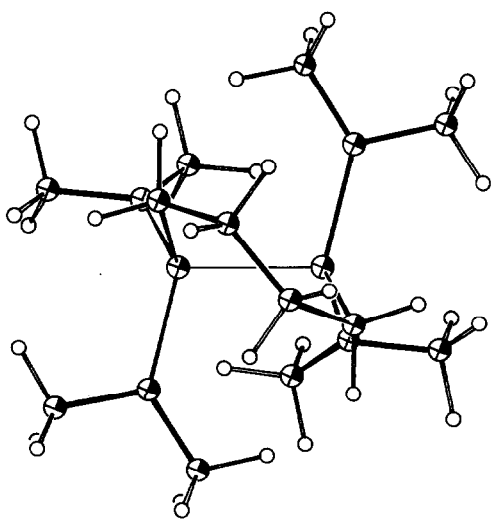


Fig. 2. An ORTEP view showing the anticipated molecular structure of $Mo_2(CH_2)_4(NMe_2)_4$ based on the observed molecular structure for gauche-$Mo_2Et_2(NMe_2)_4$.

gauche $Mo_2Et_2(NMe_2)_4$.[2] The latter molecule has its ethyl groups turned outward from the Mo_2 center. By keeping the Mo–Mo and Mo–C distances and the Mo–C–C angle the same and twisting about the Mo–C bonds one can direct the methyl groups of the ethyl ligands into a proximal position. Then by positioning the β carbon atoms 1.54 Å apart one can replace two C–H bonds by a C–C bond to create the desired four methylene chain spanning the Mo≡Mo bond. A view of the $Mo_2(CH_2)_4$ unit so formed is given in Fig. 2. The hydrogen atoms are positioned on the β,β' carbon atom in idealized tetrahedral sites. The change from Mo-to-W would have little effect since $d_{(W\equiv W)}-d_{(Mo\equiv Mo)} = ca\ 0.08$ Å.

Solid state molecular structure of $Mo_2(CH_2)_4(NMe_2)_4$

An ORTEP view of the molecular structure found for the $Mo_2(CH_2)_4(NMe_2)_4$ in the solid state is given in Fig. 3. Bond distances and bond angles are reported in Tables 1 and 2, respectively.

The observed structure is seen to be very similar to that anticipated from the known structure of gauche-$Mo_2Et_2(NMe_2)_4$. The only significant differences lie in the internal Mo–Mo–C angles which are smaller in the dimetallacycle, 97° vs. 101°. This allows for a greater puckering of the Mo_2C_4 skeleton such that near idealized staggered ethane-like conformations are attained.

Concluding remarks

Metallacycles containing two metal atoms directly bonded to one another are still compara-

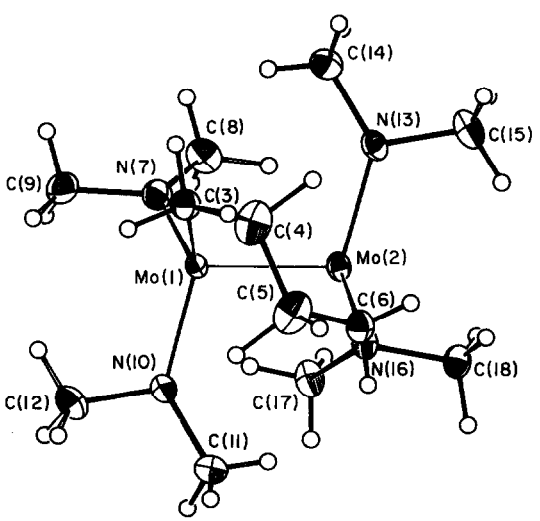


Fig. 3. An ORTEP view of the molecular structure of $Mo_2(CH_2)_4(NMe_2)_4$ giving the atom numbering scheme used in the tables.

Table 1. Bond distances (Å) for the $Mo_2(CH_2)_4(NMe_2)_4$ molecule

A	B	Distance
Mo(1)	Mo(2)	2.2002(8)
Mo(1)	N(7)	1.9587(25)
Mo(1)	N(10)	1.9563(25)
Mo(1)	C(3)	2.165(3)
Mo(2)	N(13)	1.9575(26)
Mo(2)	N(16)	1.9625(25)
Mo(2)	C(6)	2.171(3)
N(7)	C(8)	1.452(4)
N(7)	C(9)	1.457(4)
N(10)	C(11)	1.448(4)
N(10)	C(12)	1.454(4)
N(13)	C(14)	1.457(4)
N(13)	C(15)	1.462(4)
N(16)	C(17)	1.450(4)
N(16)	C(18)	1.457(4)
C(3)	C(4)	1.517(5)
C(4)	C(5)	1.496(5)
C(5)	C(6)	1.530(5)

Table 2. Bond angles (°) for the $Mo_2(CH_2)_4(NMe_2)_4$ molecule

A	B	C	Angle
Mo(2)	Mo(1)	N(7)	105.80(8)
Mo(2)	Mo(1)	N(10)	104.51(8)
Mo(2)	Mo(1)	C(3)	97.49(9)
N(7)	Mo(1)	N(10)	122.44(10)
N(7)	Mo(1)	C(3)	115.36(12)
N(10)	Mo(1)	C(3)	107.61(12)
Mo(1)	Mo(2)	N(13)	104.98(8)
Mo(1)	Mo(2)	N(16)	104.14(8)
Mo(1)	Mo(2)	C(6)	95.79(9)
N(13)	Mo(2)	N(16)	123.38(10)
N(13)	Mo(2)	C(6)	108.95(12)
N(16)	Mo(2)	C(6)	115.08(12)
Mo(1)	N(7)	C(8)	132.26(22)
Mo(1)	N(7)	C(9)	116.68(21)
C(8)	N(7)	C(9)	110.35(26)
Mo(1)	N(10)	C(11)	133.85(21)
Mo(1)	N(10)	C(12)	115.01(21)
C(11)	N(10)	C(12)	111.12(26)
Mo(2)	N(13)	C(14)	133.69(22)
Mo(2)	N(13)	C(15)	115.75(22)
C(14)	N(13)	C(15)	110.30(27)
Mo(2)	N(16)	C(17)	131.70(21)
Mo(2)	N(16)	C(18)	116.96(20)
C(17)	N(16)	C(18)	110.72(25)
Mo(1)	C(3)	C(4)	119.29(22)
C(3)	C(4)	C(5)	115.0(3)
C(4)	C(5)	C(6)	114.9(3)
Mo(2)	C(6)	C(5)	119.89(22)

tively rare in organometallic chemistry, especially when the organic portion of the ring is saturated and composed of methylene groups, viz. $M_2(CH_2)_n$.[7,11] Certainly the compounds reported here are the first of their kind incorporating a M–M triple bond within the 6-membered ring. Further studies of their reactions are planned. The six membered ring clearly imposes restrictions for M–H–C interactions and this may provide mechanistic insights into dinuclear reductive-elimination reactions of type (1) and (2).

EXPERIMENTAL SECTION

General procedures. Dry and oxygen-free solvents and atmospheres (N_2) were used throughout. Bench-top operations were performed by Schlenk and vacuum-line techniques. The preparation of infrared and NMR samples were performed in a Vacuum Atmospheres Co. Dri-Lab assembly.

Infrared spectra were recorded as Nujol mulls between KBr plates on a Perkin–Elmer 283 speetrophotometer. NMR speetra were recorded using a Nicolet 360 spectrometer equipped with a variable temperature probe. The solvent was toluene-d_8 and chemical shifts, δ in ppm, are relative to Me_4Si, $\delta = 0$. Elemental analyses were obtained from Alfred Bernhardt Microanalytisches Laboratorium, West Germany. Mass spectra were obtained courtesy of Mr. Peter Cook, Queen Mary College, London.

Materials. 1,4-$C_4H_8Cl_2$ was purchased from Aldrich Chemical Co. and distilled before use. The compounds $M_2Cl_2(NMe_2)_4$ were prepared by published procedures.[9] 1,4-dilithiobutane, 1,4-$Li_2C_4H_8$, was prepared by a modification of the procedure described by Whitesides and co-workers,[8] employing Li sand rather than Li wire.

Preparations

$Mo_2(CH_2)_4(NMe_2)_4$. $Li_2C_4H_8$ (2.5 cm^3 of a 0.41 M soln in Et_2O) was added via a syringe into a Schlenk

Table 3. Summary of crystal data for $Mo_2(CH_2)_4(NMe_2)_4$

Empirical	$Mo_2C_{12}H_{32}N_4$
Color of crystals	black
Crystal dimensions (mm)	0.25 × 0.28 × 0.21 mm
Space group	$P\bar{1}$
Cell dimensions	
Temperature (°C)	−158
a (Å)	13.581(5)
b (Å)	8.501(3)
c (Å)	7.819(3)
α (deg)	86.16(2)
β (deg)	90.26(2)
γ (deg)	99.03(2)
Z (molecules/cell)	2
Volume (Å^3)	889.52
Calculated density (g/cm^3)	1.584
Wavelength (Å)	0.71069
Molecular weight	424.29
Linear absorption coefficient (cm^{-1})	13.708
Detector to sample distance (cm)	22.5
Sample to source distance (cm)	23.5
Average omega scan width at half height	0.25
Scan speed (deg/min)	4.0
Scan width (deg + dispersion)	2.0
Individual background (sec)	5
Aperture size (mm)	3.0 × 4.0
Two-theta range (deg)	6–45
Total number of reflections collected	2349
Number of unique intensities	2322
Number of F > 3.00σ(F)	2256
R(F)	0.0188
Rw(F)	0.0276
Goodness of fit for the last cycle	1.068
Maximum δ/σ for last cycle	0.05

apparatus and the Et_2O was evaporated by vacuum. The resultant cream–white solid was kept under a dynamic vacuum for *ca* 4 h to be sure all traces of $C_4H_8Cl_2$ were removed. The Schlenk apparatus was then transferred to the Dry Box and $Mo_2Cl_2(NMe_2)_4$ (439 mg, 1 mmol) was added followed by hexane (20 cm^3). The reaction mixture was stirred for 5 h at room temperature by use of a magnetic stirrer/spin bar yielding a dark brown solution with suspended solids. The reaction mixture was filtered through a Celite pad and the filtrate was collected and evaporated to dryness in a dynamic vacuum yielding brown solids. Sublimation of this residue at 100°C, 10^{-4} torr yielded a yellow sublimate $Mo_2(CH_2)_4(NMe_2)_4$ (190 mg, 45% yield based on Mo).

Found: C, 34.03; H, 7.51; N, 13.22. Calc. for $Mo_2N_4C_{12}H_{32}$: C, 33.97; H, 7.60; N, 13.20%.

IR data (cm^{-1}): 2810m, 2766m, 1439m, 1414m, 1390w, 1327vw, 1316vw, 1240s, 1186w, 1147s, 1116w, 1040m, 938vs, 887vw, 793w, 648w, 557w.

^1H NMR data at −40°C: $\delta = 4.30, 3.35, 2.54, 2.40, 2.15$ multiplets: $Mo_2(CH_2)_4$. $\delta = 4.10, 3.88$ singlets: proximal N-methyls; $\delta = 2.51, 2.48$ singlets: distal N-methyls.

^{13}C NMR data (proton decoupled) at −40°C: $\delta = 56.9, 55.0$ proximal N-methyls; $\delta = 41.7$: distal N-methyls (fortuitously degenerate); $\delta = 43.7, 37.6$; $C_\alpha, C_{\alpha'}$, $C_\beta, C_{\beta'}$ carbons of $Mo_2(CH_2)_4$ ring.

A molecular ion at 424 (*m/e*) corresponded to $Mo_2(CH_2)_4(NMe_2)_4^+$.

$W_2(CH_2)_4(NMe_2)_4$ was prepared in a directly analogous manner to that described above employing $W_2Cl_2(NMe_2)_4$.

Found: C, 24.54; H, 5.09; N, 9.61. Calc. for $W_2N_4C_{12}H_{32}$: C, 24.02; H, 5.37; N, 9.34%.

IR data (cm^{-1}): 2810m, 2767m, 1413m, 1390w, 1240s, 1188vw, 1146m, 1120w, 1080vw, 1039m, 1013vw, 938vw, 793m, 657m.

^1H NMR data at −40°C: $\delta = 4.36, 3.48, 2.34, 1.80$ (broad multiplets): $W_2(CH_2)_4$; $\delta = 4.19$, 3.94, singlets: proximal N-methyls; $\delta = 2.39$, 2.38 (singlets): distal N-methyls.

^{13}C NMR data (proton decoupled) at −40°C: $\delta = 60.2, 57.6$: proximal N-methyls; $\delta = 38.5, 38.4$: distal N-methyls; $\delta = 52.7$, $J_{^{183}W-^{13}C} = 113$ Hz: C_α and $C_{\alpha'}$ of $W_2(CH_2)_4$ ring; $\delta = 36.6$, C_β and $C_{\beta'}$ of $W_2(CH_2)_4$ ring.

Crystallographic studies

General operating procedures and listings of programs have been published.[12]

Crystal data are summarized in Table 3. The space group was determined by a reciprocal lattice search on the goniostat and found to be $P\bar{1}$.

The structure was solved by direct methods and Fourier techniques and all atoms (including hydrogen atoms) were located and refined. A final difference Fourier was featureless, the largest peak being 0.34 Å. ψ scans were flat and no absorption correction was performed.

Acknowledgements—We thank the donors of the Petroleum Research Fund administered by the American Chemical Society and the Wrubel Computing Center for support of this work.

Supplementary materials available—Tables of fractional coordinates and thermal parameters have been deposited with the Cambridge Crystallographic Data Centre. Complete structural information is available from the Editor at Queen Mary College and, in microfiche form, from the Indiana University Chemistry Library, Bloomington, Indiana 47405 at a cost of $2.50 per structural report. For $Mo_2(CH_2)_4(NMe_2)_4$ request MSC No. 84074.

REFERENCES

1. M. H. Chisholm and F. A. Cotton, *Acc. Chem. Res.* 1978, **11**, 356.
2. M. H. Chisholm, D. A. Haitko and J. C. Huffman, *J. Am. Chem. Soc.* 1981, **103**, 4046.
3. M. J. Chetcuti, M. H. Chisholm, K. Folting, D. A. Haitko, J. C. Huffman and J. Janos, *J. Am. Chem. Soc.* 1983, **105**, 1163.
4. M. J. Chetcuti, M. H. Chisholm, K. Folting, D. A. Haitko and J. C. Huffman, *J. Am. Chem. Soc.* 1982, **104**, 2138.
5. M. H. Chisholm, H. T. Chiu and J. C. Huffman, *Polyhedron* 1984, **3**, 759.
6. G. Tranquier and R. Hoffmann, *Organometallics* 1984, **3**, 370.
7. S. D. Chappell and D. J. Cole-Hamilton, *Polyhedron* 1982, **1**, 739.
8. J. X. McDermott, J. F. White and G. M. Whitesides, *J. Am. Chem. Soc.* 1973, **95**, 4451; *idem, ibid.* 1976, **98**, 6521; 6529.
9. M. Akiyama, M. H. Chisholm, F. A. Cotton, M. W. Extine and C. A. Murillo, *Inorg. Chem.* 1977, **16**, 2407.
10. M. H. Chisholm, F. A. Cotton, B. A. Brenz, W. W. Reichert, L. W. Shive and B. R. Stults, *J. Am. Chem. Soc.* 1976, **98**, 4469.
11. W. H. Hersh and R. G. Bergman, *J. Am. Chem. Soc.* 1981, **103**, 6992.
12. M. H. Chisholm, K. Folting, J. C. Huffman and C. C. Kirkpatrick, *Inorg. Chem.* 1984, **23**, 1021.

Polyhedron Vol. 4, No. 7, pp. 1219–1222, 1985
Printed in Great Britain

0277-5387/85 $3.00 + .00
© 1985 Pergamon Press Ltd

A STUDY OF MIXED LIGAND COMPLEXES USING DIFFERENTIAL PULSE POLAROGRAPHY

H. M. KILLA,* M. G. ABD EL WAHED and H. A. DESSOUKI
Chemistry Department, Faculty of Science, Zagazig University, Zagazig, Egypt

(*Received* 24 *August* 1984; *accepted* 14 *November* 1984)

Abstract—Differential pulse polarography was used to study the mixed ligand complexes of trimethylenediamine (TMDA) and oxalate (OX) with Cd(II) at constant ionic strength ($\mu = 1$, $NaNO_3$) at 25°C. It has been found that the reduction of complexes is reversible and diffusion-controlled. Three mixed complexes, [Cd(TMDA)(OX)], $[Cd(TMDA)(OX)_2]^{2-}$ and $[Cd(TMDA)_2(OX)]$, are formed. Their overall stability constants are: $\log \beta_{11} = 6.78$, $\log \beta_{12} = 7.53$ and $\log \beta_{21} = 8.20$, respectively.

Electroanalytical methods, and especially polarography have played an important part in investigations of the composition and stability of complexes and of the mechanisms of complex formation. Deford and Hume[1] have derived an expression to study the stepwise formation of complexes while Schaap and McMasters[2] treated the case of mixed ligand complexes.

Heath and Hefter[3] have derived an equation for the determination of stability constants of complex ions by differential pulse (d.p.) polarography. This technique offers a considerable number of advantages[3] compared to DC polarography. On the other hand, the limitations of the original Deford–Hume[1] treatment have been documented.[4–6] Thus, any technique which enables $\Delta E_{1/2}$-values to be measured more accurately than by DC polarography will lead to improved calculations of the stability of complexes and especially the mixed ligand complexes. In the present work, d.p. polarography was extended to study the mixed ligand complexes of Cd(II)–trimethylenediamine–oxalate system which had not been studied before.

EXPERIMENTAL

All current–potential polarograms were obtained using an IBM EC/225 Voltammetric Analyzer with a 7424 M *X–Y* recorder. A conventional three electrode cell with a saturated sodium chloride calomel electrode (SSCE) was employed. A drop time of 1.0 s and sample time of 16.7 ms were used in the case of fast polarography measurements. A potential pulse 50 mV was used throughout the d.p. polarography measurements.

All measurements were made at 25°C and an ionic strength was maintained constant at $\mu = 1$ using $NaNO_3$ as supporting electrolyte. The concentration of Cd^{2+} ions which was used for all the data reported was 1×10^{-4} M.

Reagent grade chemicals, deionized water and triple distilled mercury were employed in all cases. No maximum suppressor was used.

THEORY

Stability constants of polarographically reversible systems may be determined by differential pulse (d.p.) polarography using the Deford–Hume equation[1] as modified by Heath and Hefter.[3] This equation may be expressed as

$$F_0(X) = \Sigma B_j C_X^j = \text{antilog}\left\{\frac{0.4343nF}{RT} \times [(E_p)_s - (E_p)_c] + \log\left[\frac{(I_p)_s}{(I_p)_c}\right]\right\}, \quad (1)$$

where $F_0(X)$ represents the experimentally measured right-hand side of the equation, B_j is the overall stability constant of the jth complex, C_x is the analytical concentration of the ligand, E_p is the peak potential of the d.p. polarography wave, I_p is the peak current of the d.p. wave and the subscripts s and c refer to the free and complexed ions respectively. Other symbols are those used conventionally.

Since Cd^{2+} forms hexacoordinate complexes with

* Author to whom correspondence should be addressed.

(TMDA)[7] and (OX)[2] individually, there can be at most three mixed complex species.

$$F_{00}(XY) = \text{antilog}\left[\frac{0.4343nF}{RT}\Delta E_{1/2} + \log\left(\frac{I_M}{I_C}\right)\right]. \quad (2)$$

Thus, eqn (2) may be changed to the form

$$F_{00}(XY) = \text{antilog}\left\{\frac{0.4343nF}{RT}\Delta E_p + \log\left[\frac{(I_p)_s}{(I_p)_c}\right]\right\}, \quad (3)$$

where $\Delta E_p = (E_p)_s - (E_p)_c$ is the shift in the peak potential due to complexation.

It has been reported,[3] that for a reversible diffusion controlled process, the peak potential (E_p) obtained from d.p. polarography wave is related to the half-wave potential of DC polarography by the expression

$$E_p = E_{1/2} - \frac{\Delta E}{2},$$

where ΔE is the magnitude of the pulse amplitude.

From Leden's approach[8]

$$\begin{aligned} F_{00}(XY) = {} & \{B_{00} + B_{01}[Y] + B_{02}[Y]^2 \\ & + B_{03}[Y]^3\}[X]^0 \\ & + \{B_{10} + B_{11}[Y] + B_{12}[Y]^2\}[X] \\ & + \{B_{20} + B_{21}[Y]\}[X]^2 \\ & + \{B_{30}\}[X]^3 \end{aligned}$$

or

$$F_{00}(XY) = A + B[X] + C[X]^2 + D[X]^3.$$

The original graphical method[1] may be applied to F_{00} if the activity of one of the ligands is held constant while that of the other is varied. The intercept on the F_{00} axis in the plot of F_{00} vs $[X]$ gives A, and

$$F_{10} = \frac{F_{00} - A}{[X]} = B + C[X] + D[X]^2.$$

By a similar plotting of F_{10} vs $[X]$, B is obtained and then C and D by iteration.

From the knowledge of C, the mixed stability constant β_{21} may be calculated. In order to determine β_{11} and β_{21}, B must be evaluated at two concentrations of Y.

RESULTS AND DISCUSSION

Equation (1) by Deford and Hume as modified by Heath and Hefter[3] was applied to determine the stability constants of the simple complexes using d.p. polarography. The stability constants are recorded in Table 1. For Cd(OX) system, the stability constants are in good agreement with previously reported values.[2,9–11] In the case of the Cd(TMDA) system, the results agree well with the values reported by Gupta[7] considering the differences in experimental conditions.

Table 1. Stability constants of simple and mixed complexes

Complex species	Stability constants at 25°C	
$[Cd(OX)]$	$\log \beta_{01}$	2.65
$[Cd(OX)_2]^{2-}$	$\log \beta_{02}$	4.10
$[Cd(OX)_3]^{4-}$	$\log \beta_{03}$	5.07
$[Cd(TMDA)]^{2+}$	$\log \beta_{10}$	5.60
$[Cd(TMDA)_2]^{2+}$	$\log \beta_{20}$	7.54
$[Cd(TMDA)_3]^{2+}$	$\log \beta_{30}$	8.55
$[Cd(TMDA)(OX)]$	$\log \beta_{11}$	6.78
$[Cd(TMDA)(OX)_2]^{2-}$	$\log \beta_{12}$	7.54
$[Cd(TMDA)_2(OX)]$	$\log \beta_{21}$	8.20

It is important to show that for simple and mixed complexes of our work, the ΔE_p values obtained from d.p. polarograms were confirmed using tast polarography ($\Delta E_{1/2}$). It was found that the ΔE_p and $\Delta E_{1/2}$ are not in exact agreement, but in all cases are within the experimental error. The E_p values were generally reproducible to ± 1 mV.

In the mixed ligand system, the concentration of trimethylenediamine was varied while that of the oxalate ions was kept constant at two values, 0.04 M and 0.2 M. The derived functions F_{00}, F_{10}, F_{20} and F_{30} are recorded in Tables 2 and 3.

The half-peak width of a d.p. polarography wave has been reported by a number of workers.[3,12,13] They reported a value of 62 mV for reversible two-electrons reduction with an applied pulse of 50 mV. In the present work, for simple and mixed complexes the d.p. polarograms in nitrate medium had half-peak widths of 62 ± 1 mV, as shown from Tables 2 and 3, indicating the reversibility of the reduction. For further confirmation, tast polarography was used under the same conditions used for d.p. polarography. The plots of $\log [i/(i_d - i)]$ vs $E_{d.e.}$ were linear of 31 ± 1 mV, indicating a high degree of reversibility. Furthermore, the plots of peak current (i_p) of d.p. waves vs $h^{1/2}$ of mercury column were linear, indicating that the reduction of simple and mixed complexes was diffusionally controlled.

The stability constants of the mixed ligand complexes were evaluated using Schaap and McMasters'[2] method using eqn (3) of the d.p. wave. The results of A, B, C and D are presented in Tables 2 and 3.

For the two values of B, the formation constants

Table 2. Derived (F_{i0}) functions for the cadmium (TMDA–oxalate) system. $[Cd^{2+}] = 1 \times 10^{-4}$ M. Ionic strength = 1 M. [Oxalate] = 0.04 M. $(E_p)_s = -0.612$ V

TMDA (M)	$-E_p$ (V) (SSCE)	ΔE_p (mV)	$\log \frac{(I_p)_s}{(I_p)_c}$	Half-peak width (mV)	$F_{00} \times 10^4$	$F_{10} \times 10^5$	$F_{20} \times 10^7$	$F_{30} \times 10^8$
0.03	0.754	142	0.0377	62	6.99	16.63	—	—
0.04	0.761	149	0.0248	61	11.71	24.27	4.32	—
0.05	0.766	154	0.031	62	17.53	31.06	4.81	—
0.06	0.772	160	0.0248	62	27.59	42.65	5.94	—
0.07	0.776	164	0.0345	63	38.54	52.20	6.46	3.51
0.08	0.780	168	0.041	62	53.43	64.29	7.16	3.95
0.10	0.787	175	0.041	62	92.20	90.20	8.32	4.32
0.15	0.799	187	0.0345	62	231.45	152.97	9.73	3.82
0.20	0.808	196	0.0444	61	477.53	237.76	11.50	3.75
0.25	0.816	204	0.0477	62	891.46	355.76	14.00	4.00
0.30	0.822	210	0.0511	62	1444.10	480.70	15.80	3.93
0.35	0.828	216	0.0477	62	2287.17	652.90	18.40	4.13

$A = 2 \times 10^4$, $B = 7 \times 10^5$, $C = 4 \times 10^7$, $D = 3.9 \times 10^8$.

β_{11}, β_{12} were calculated for [Cd(TMDA)(OX)] and $[Cd(TMDA)(OX)_2]^{2-}$ as shown from Table 1. The two values of C gave two values for $\log \beta_{21} = 8.12$, 8.28, in good agreement with each other. On the other hand, the average values of D ($\log \beta_{30}$) from both series is 8.71 ± 0.1. This agrees well with values of $\log \beta_{30} = 8.55$ calculated for the $[Cd(TMDA)_3]^{2+}$ complex from the simple system.

It was observed that the addition of trimethylenediamine to a solution of Cd(II) and oxalate shifts the E_p to more negative side, showing that mixed complexes are formed in solution.

The mixing constant,[14,15] $\log K_m = \log \beta_{11} - \frac{1}{2}(\log \beta_{02} + \log \beta_{20})$ and stabilization constant ($\log K_s = \log K_M - \log 2$)[16] are 0.96 and 0.66 respectively. The positive values of mixing constant and stabilization constant show that the ternary complexes more stable than the binary complexes.

Moreover, the disproportionation reaction

$$2[Cd(TMDA)(OX)] \rightleftharpoons [Cd(TMDA)_2]^{2+} + [Cd(OX)_2]^{2-}$$

has a value of $\log K = -1.92$, which shows the stability of the mixed complexes.

Table 3. Derived (F_{i0}) functions for the cadmium (TMDA–oxalate) system. $[Cd]^{2+} = 1 \times 10^{-4}$ M. Ionic strength = 1 M. [Oxalate] = 0.2 M. $(E_p)_s = -0.612$ V

TMDA (M)	$-E_p$ (V) (SSCE)	ΔE_p (mV)	$\log \frac{(I_p)_s}{(I_p)_c}$	Half-peak width (mV)	$F_{00} \times 10^5$	$F_{10} \times 10^6$	$F_{20} \times 10^8$	$F_{30} \times 10^8$
0.03	0.769	157	0.0345	61	2.23	—	—	—
0.04	0.776	164	0.0444	61	3.94	6.10	—	—
0.05	0.780	168	0.0477	62	5.43	7.85	0.97	—
0.06	0.780	171	0.0511	62	6.91	9.02	1.00	—
0.07	0.787	175	0.0410	61	9.22	11.03	1.15	5.96
0.08	0.790	178	0.0444	62	11.74	12.80	1.22	6.18
0.10	0.796	184	0.0377	62	18.45	16.95	1.39	6.65
0.15	0.807	195	0.0477	62	44.51	28.67	1.71	6.54
0.20	0.816	204	0.0511	62	90.47	44.48	2.07	6.70
0.25	0.823	211	0.0545	62	157.34	62.34	2.37	6.56
0.30	0.829	217	0.0545	62	251.16	83.22	2.37	6.47
0.35	0.835	223	0.0545	62	400.11	113.89	3.17	6.97

$A = 1.5 \times 10^5$, $B = 3 \times 10^6$, $C = 7.3 \times 10^7$, $D = 6.5 \times 10^8$.

The stability constants of mixed complexes have been estimated theoretically using the method of Watters and DeWitt.[17] The values are

$$\log \beta_{11} = 5.32, \quad \log \beta_{12} = 6.70,$$
$$\text{and} \quad \log \beta_{21} = 7.86.$$

These values are less than the observed values by amounts $10^{1.46}$, $10^{0.83}$ and $10^{0.34}$ respectively. The higher experimental values may be due to cooperative effects of electrostatic forces between different kinds of ligands and steric effects as concluded by other workers.[2,10,18]

The equilibrium constants (log values) have been calculated and written against each equilibrium:

		log K
(1)	$Cd^{2+} + (TMDA) + OX^{2-} \rightleftharpoons [Cd(TMDA)(OX)]$	6.78
(2)	$Cd^{2+} + (TMDA) + 2OX^{2-} \rightleftharpoons [Cd(TMDA)(OX)_2]^{2-}$	7.53
(3)	$Cd^{2+} + 2(TMDA) + OX^{2-} \rightleftharpoons [Cd(TMDA)_2(OX)]$	8.20
(4)	$[Cd(TMDA)]^{2+} + OX^{2-} \rightleftharpoons Cd(TMDA)(OX)]$	1.18
(5)	$[Cd(TMDA)_2]^{2+} + OX^{2-} \rightleftharpoons [Cd(TMDA)_2(OX)]$	0.66
(6)	$[Cd(OX)] + TMDA \rightleftharpoons [Cd(TMDA)(OX)]$	4.13
(7)	$[Cd(OX)_2]^{2-} + TMDA \rightleftharpoons [Cd(TMDA)(OX)_2]^{2-}$	3.43
(8)	$[Cd(OX)_3]^{4-} + TMDA \rightleftharpoons [Cd(TMDA)(OX)_2]^{2-} + OX^{2-}$	2.46
(9)	$[Cd(TMDA)(OX)] + OX^{2-} \rightleftharpoons [Cd(TMDA)(OX)_2]^{2-}$	0.75
(10)	$[Cd(TMDA)(OX)] + TMDA \rightleftharpoons [Cd(TMDA)_2(OX)]$	1.42
(11)	$[Cd(TMDA)(OX)_2]^{2-} + TMDA \rightleftharpoons [Cd(TMDA)_2(OX)] + OX^{2-}$	0.67
(12)	$[Cd(TMDA)_2(OX)] + TMDA \rightleftharpoons [Cd(TMDA)_3] + OX^{2-}.$	0.35

It is seen from the above equilibria that TMDA adds to [Cd(TMDA)(OX)] complex more easily than OX^{2-} [equilibria (9) and (10)]. The saturated mixed complexes can accommodate TMDA in place of OX^{2-} [equilibria (8), (11) and (12)]. Thus, the complexing tendency of TMDA is much more than OX^{2-}. These observations are in line with the weaker nature of the oxalate ligand. Equilibrium (8) favours mixed complexation over the simple. In the same way there are many other reactions which favour mixed complexation over the simple ones [equilibria (4)–(7)].

Acknowledgements—One of the authors (H.M.K.) is grateful to Prof. R. H. Philp, Chemistry Dept., University of South Carolina (U.S.A.), for his assistance.

REFERENCES

1. D. D. Deford and D. N. Hume, *J. Am. Chem. Soc.* 1951, **73**, 5321.
2. W. B. Schaap and D. L. McMasters, *J. Am. Chem. Soc.* 1961, **83**, 4699.
3. G. A. Heath and G. Hefter, *J. Electronal. Chem.* 1977, **84**, 295.
4. H. Irving, *Advances in Polarography*, Vol. 1, p. 42. Pergamon Press, New York and London (1960).
5. A. M. Bond, *J. Electroanal. Chem.* 1969, **20**, 223.
6. L. N. Klatt and R. L. Rouseff, *Analyt. Chem.* 1970, **42**, 1234.
7. K. D. Gupta, S. C. Baghel and J. N. Gaur, *Monatsh.* 1979, **110**, 657.
8. I. Leden, *Z. Phys. Chem.* 1941, **188A**, 160.
9. S. C. Khurana and C. M. Gupta, *J. Inorg. Nucl. Chem.* 1973, **35**, 209.
10. R. G. Bidkar, D. G. Dhuley and R. A. Bhobe, *Indian J. Chem.* 1977, **15A**, 63.
11. S. C. Khurana, J. K. Gupta and C. M. Gupta, *Electrochimica Acta* 1973, **18**, 59.
12. J. W. Dillard and K. W. Hanck, *Analyt. Chem.* 1976, **48**, 218.
13. J. W. Dillard, J. A. Turner and R. A. Osteryoung, *Analyt. Chem.* 1977, **49**, 1246.
14. R. Sundaresan and A. K. Sundaram, *Proc. Indian Acad. Sci.* 1974, **79A**, 161.
15. S. L. Jain, J. Kishan and R. C. Kapoor, *Indian J. Chem.* 1979, **18A**, 133.
16. A. A. Aggarwal, K. B. Pandeya and R. P. Singh, *Indian J. Chem.* 1981, **20**, 752.
17. J. I. Watters and De Witt, *J. Am. Chem. Soc.* 1960, **82**, 1333.
18. A. A. Aggarwal, A. K. Arora, K. B. Pandeya and R. P. Singh, *J. Inorg. Nucl. Chem.* 1981, **43**, 601.

Polyhedron Vol. 4, No. 7, pp. 1223–1229, 1985
Printed in Great Britain

0277–5387/85 $3.00 + .00
© 1985 Pergamon Press Ltd

ORGANOTELLURIUM CATIONS: ORGANOTELLURIUM PERCHLORATES AND THEIR COMPLEXES WITH LEWIS BASES

T. N. SRIVASTAVA, V. K. SRIVASTAVA and R. C. SRIVASTAVA*
Chemistry Department, Lucknow University, Lucknow 226007, India

(*Received* 6 *September* 1984; *accepted* 14 *November* 1984)

Abstract—Solutions of diorganotellurium(IV) diperchlorates $R_2Te(ClO_4)_2$ (where R = Ph, *p*-$CH_3OC_6H_4$, $R_2Te = \overline{C_4H_8Te}$) may be prepared by the reaction of R_2TeCl_2 and $AgClO_4$ or by the reaction of diorganyltelluroxide with excess of 70% $HClO_4$. IR and conductivity data indicate that $Ph_2Te(ClO_4)_2$ possesses covalently bonded perchlorate groups in solution. Interaction of the freshly prepared solutions with Lewis bases affords cationic complexes of the types $[R_2Te(ClO_4)(L)][ClO_4]$ and $[R_2Te(L)_2][ClO_4]_2$ which have been characterised by IR elemental analyses and conductivity measurements.

Triorganotelluronium salts containing the monocation $[R_3Te]^+$ are numerous (but see Ref. 1) but the dications $[R_2Te]^{2+}$ are yet to be prepared. displacement of the halide groups (X) from R_2TeX_2 by poorly coordinating groups may be expected to yield the dication. The only attempt in this direction seems to have been made by Lowry and Gilbert who isolated dimethyltellurium diperchlorate and formulated it as $[Me_2Te(OClO_3)]^+[ClO_4]^-$ on the basis of only conductivity data.[2]

In this paper we report (a) the solution behaviour of $Ph_2Te(ClO_4)_2$ and (b) the preparation of a few cationic complexes of diorganotellurium diperchlorates. A complex of $[Ph_2TeMe][ClO_4]$ has also been included for comparison. Lewis bases used include triphenylarsine oxide (TPAsO), pyridine-N-oxide (PyO), 4-picoline-N-oxide (γ-PicO), lutidine-N-oxide (LutO), dimethyl sulphoxide (DMSO), tetramethyl urea (TMU), tetramethylethylenediamine (TMEN), pyridine (Py), tetramethylpiperidine (TMP) and triphenylphosphine sulfide (TPPS). The analytical data for the complexes are shown in Table 1.

EXPERIMENTAL

Diaryltellurium dichlorides,[3,4] 1-telluracyclopentane diiodide,[5] diphenylmethyltelluronium iodide,[6] diphenyltelluroxide[7] and silver perchlorate[8] were prepared by reported methods. All the Lewis bases were obtained from BDH and were further purified, either by distillation under reduced pressure or by recrystallisation from suitable solvents. Molecular weight was determined cryoscopically using a Beckmann thermometer of ±0.01° accuracy. Molar conductance of 10^{-3} *M* solution was determined at 25°C using a Philips conductivity assembly PR-9500. The IR spectra were recorded on a Perkin–Elmer 577 grating spectrophotometer. Nuclear magnetic resonance spectra in $CDCl_3$ or $(CD_3)_2CO$ were recorded on a Perkin–Elmer R-32 spectrophotometer.

Preparation of complexes

Typical experiments are described below.

All operations were carried out under dry nitrogen.

1. *$Ph_2Te(DMSO)(ClO_4)_2$*. Diphenyltellurium dichloride (0.70 g; 2 mmol) in dichloromethane (~ 30 cm^3) was stirred with $AgClO_4$ (0.83 g; 4 mmol) for ~ 1 h at room temperature. The precipitated silver chloride (0.53 g, 95%) was filtered off and the filtrate containing diphenyltellurium diperchlorate was treated with dimethylsulphoxide (0.15 g; 2 mmol) in dichloromethane (~ 10 cm^3). The mixture was refluxed for ~ 5 h. Excess of the solvent was distilled off and the desired product was obtained as a white crystalline solid by addition of excess pet.-ether (bp 40–60°C). It was recrystallized with a mixture of dichloromethane and pet.-ether (1 : 3) and dried *in vacuo*.

The same complex, $Ph_2Te(DMSO)(ClO_4)_2$, was

* Author to whom correspondence should be addressed.

Table 1. Analytical data of complexes of oranotellurium(IV) perchlorates

S. No.	Complex[a]	M.p. °C	Analyses [Found (calc.)] % Te	C	H	Molar conductance Ω^{-1} mol^{-1} cm^2 CH_3CN	CH_3COCH_3
1.	$[Ph_2Te(TPAsO)(OClO_3)][ClO_4]$	156	(15.90) 15.02	(44.92) 44.99	(3.14) 3.08	157.5	139.2
2	$[Ph_2Te(PyO)(OClO_3)][ClO_4]$	110	(22.15) 22.08	(35.45) 35.58	(2.62) 2.60	158.5	135.1
3.	$[Ph_2Te(\gamma\cdot PicO)(OClO_3)][ClO_4]$	130	(21.63) 21.60	(36.65) 36.62	(2.90) 2.82	158.9	134.8
4.	$[Ph_2Te(LutO)(OClO_3)][ClO_4]$	192	(21.09) 21.12	(37.72) 37.68	(3.16) 3.22	157.8	135.2
5	$[Ph_2Te(DMSO)(OClO_3)][ClO_4]$	140	(22.83) 22.81	(30.08) 31.00	(2.88) 2.79	148.9	132.8
6.	$[Ph_2Te(TMU)(OClO_3)][ClO_4]$	161	(21.37) 22.82	(34.20) 35.12	(3.71) 3.68	149.0	138.9
7.	$[Ph_2Te(Py)(OClO_3)][ClO_4]$	160	(22.79) 22.62	(36.47) 36.85	(2.70) 2.78	147.8	132.8
8.	$[Ph_2Te(TMP)(OClO_3)][ClO_4]$	228	(20.51) 20.50	(40.55) 40.58	(4.69) 4.68	145.2	136.7
9.	$[Ph_2Te(TMEN)(OClO_3)][ClO_4]$	150	(21.37) 21.28	(36.21) 36.33	(4.39) 4.43	121.8	100.4
10.	$[(p\text{-}CH_3OC_6H_4)_2Te(PyO)(OClO_3)][ClO_4]$	102	(20.06) 21.00	(35.88) 35.62	(3.01) 3.12	158.2	139.0
11.	$[(p\text{-}CH_3OC_6H_4)_2Te(\gamma\cdot PicO)(OClO_3)][ClO_4]$	110	(19.63) 18.98	(36.96) 37.12	(3.25) 3.32	155.8	136.2
12.	$[(p\text{-}CH_3OC_6H_4)_2Te(LutO)(OClO_3)][ClO_4]$	120	(19.19) 19.84	(37.93) 37.70	(3.48) 3.50	154.6	136.0
13.	$[(p\text{-}CH_3OC_6H_4)_2Te(DMSO)(OClO_3)][ClO_4]$	150	(20.61) 20.19	(31.05) 31.00	(3.25) 3.22	155.7	137.5
14.	$[(p\text{-}CH_3OC_6H_4)_2Te(TMP)(OClO_3)][ClO_4]$	173	(18.70) 18.52	(40.50) 40.41	(4.87) 4.90	153.4	137.8
15.	$[(p\text{-}CH_3OC_6H_4)_2Te(TMEN)(OClO_3)][ClO_4]$	172	(19.42) 19.00	(36.56) 36.42	(4.60) 4.58	125.8	105.7
16.	$[(p\text{-}CH_3OC_6H_4)_2Te(TPPS)(OClO_3)][ClO_4]$	130	(15.27) 15.25	(46.02) 47.08	(3.50) 3.71	145.5	140.5
17.[b]	$[\overline{C_4H_8Te}(DMSO)_2][ClO_4]_2$	116[c]	(23.67) 23.54	(17.83) 17.82	(3.74) 3.79	270.5	187.7
18.[b]	$[\overline{C_4H_8Te}(Py)_2][ClO_4]_2$	160	(23.59) 23.58	(31.09) 31.00	(3.35) 3.34	265.8	186.8
19.	$[Ph_2MeTe][ClO_4]$	156	(32.19) 32.05	(39.40) 39.18	(3.30) 3.19	150.5	129.8
20.	$[Ph_2MeTe(PyO)][ClO_4]$	128	(25.96) 25.90	(43.99) 43.90	(3.69) 3.66	158.5	138.5

[a] Yields are 90–100%.
[b] Yields are 50–70%.
[c] Explodes at this temperature.

also prepared by refluxing a mixture of diphenyltelluroxide (1.15 g; 4 mmol) in ethanol (80 cm^3), slight excess of perchloric acid (70%) and dimethyl sulphoxide (0.31 g; 4 mmol) for ~ 10 h.

2. *$\overline{C_4H_8Te}(Py)_2(ClO_4)_2$*. $\overline{C_4H_8TeI_2}$ (0.87 g; 2 mmol) in dichloromethane (40 cm^3) was stirred with $AgClO_4$ (0.83 g; 4 mmol) for 1 h at room temperature. The precipitated silver iodide (0.93 g; 98%) was filtered off, and the filtrate was treated with a solution of pyridine (0.31 g; 4 mmol) in dichloromethane (10 cm^3). The mixture was refluxed for ~ 5 h. Excess of the solvent was distilled off and the product was precipitated by addition of an excess of pet.–ether. It was washed several times with the same solvent and dried *in vacuo*.

3. *$Ph_2MeTe(PyO)(ClO_4)$*. Ph_2MeTeI (0.84 g; 2 mmol) was stirred with $AgClO_4$ (0.41 g, 2 mmol) at room temperature for 1 h. The precipitated silver iodide (0.46 g; 98%) was filtered off under dry nitrogen. The filtrate, on concentration, yielded diphenylmethyltelluronium perchlorate, m.p. 156°C (see Table 1).

Diphenylmethyltelluronium perchlorate (0.79 g, 2 mmol) in dichloromethane (50 cm^3) was treated with pyridine-N-oxide (0.19 g; 2 mmol) in the same solvent (20 cm^3) and the solution was refluxed for 5 hr. Excess of the solvent was distilled off and the residual solution was kept overnight in a freezer. Colourless crystals were obtained. The complex was recrystallized from $CHCl_3$/pet.–ether (1:3) and dried *in vacuo*.

RESULTS AND DISCUSSION

Diorganotellurium(IV) dihalides react with silver perchlorate metathetically to give solutions of the corresponding diperchlorates. Dichloromethane solution of $Ph_2Te(ClO_4)_2$ is nonconducting (conductance = 0.78 Ω^{-1} mol^{-1} cm^2) whereas its solution in acetonitrile shows 1:1 electrolytic (conductance = 158.5 Ω^{-1} mol^{-1} cm^2) behaviour.[9] The IR spectrum of $Ph_2Te(ClO_4)_2$ in chloroform shows the presence of monodentately bonded perchlorate groups (*vide infra*). These observations suggest that $Ph_2Te(ClO_4)_2$ possesses covalently bonded perchlorate groups and the Te atom is four coodinated. Unfortunately, our attempts to isolate $R_2Te(ClO_4)_2$ invariably resulted either in its reduction to Te metal or isolation of a crystalline compound (structure of which is under investigation) which shows the presence of strong absorptions due to ν(OH) and δ(OH) in its IR spectra.

In order to get more insight into the nature of the perchlorate groups, the solutions of diorganotellurium diperchlorates were reacted with a number of Lewis bases. Whereas $Ar_2Te(ClO_4)_2$ afforded 1:1 complexes even in the presence of an excess of ligand, the $\overline{C_4H_8Te}(ClO_4)_2$ gave 1:2 complexes.

$$R_2Te(ClO_4)_2 + nL \rightarrow R_2Te(L)_n(ClO_4)_2 \quad (1)$$

$$R = Ph,\ p\text{-}CH_3OC_6H_4;\quad n = 1$$

$$R_2Te = \overline{C_4H_8Te};\quad n = 2.$$

The complexes of diaryltellurium diperchlorates were also obtained by refluxing a mixture of R_2TeO, $HClO_4$ (70%) and the Lewis base in ethanol.

Diphenylmethyltellurium perchlorate also interacts with one mole of pyridine-N-oxide forming the complex $Ph_2MeTe(PyO)(ClO_4)$. Attempts to prepare 1:2 adducts resulted in the decomposition of the complex.

All of the complexes (Table 1) are colourless crystalline solids and generally soluble in dichloromethane, acetone and acetonitrile. The complexes are generally stable towards atmospheric moisture and melt sharply, excepting $[\overline{C_4H_8Te}(DMSO)_2][ClO_4]_2$ which explodes at ~ 116°C; other complexes explode only on strong heating.

The molecular weights of the newly synthesised compounds were determined cryoscopically in freezing nitrobenzene and were found to be approximately one third of the calculated value for the complexes $\overline{C_4H_8Te}(L)_2(ClO_4)_2$ and half of the calculated values for $Ar_2Te(L)(ClO_4)_2$ and $Ph_2MeTe(L)(ClO_4)$.

Molar conductance of 10^{-3} *M* solution of the complexes in acetonitrile and acetone was determined at room temperature; the data are collected in Table 1. The values for the complexes $\overline{C_4H_8Te}(L)_2(ClO_4)_2$ in acetonitrile lie in the range (265–271 Ω^{-1} mol^{-1} cm^2 whereas for $Ar_2Te(L)(ClO_4)_2$ and $Ph_2MeTe(L)(ClO_4)$, the range is 120–160 Ω^{-1} mol^{-1} cm^2. In acetone, the corresponding values are 186–188 and 100–140 Ω^{-1} mol^{-1} cm^2 respectively. The conductivity and molecular weight data indicate that the complexes $\overline{C_4H_8Te}(L)_2(ClO_4)_2$ behave as 1:2 electrolytes whereas $Ar_2Te(L)(ClO_4)_2$ and $Ph_2MeTe(L)(ClO_4)$ are 1:1 electrolytes.[9] Molar conductance of $Ph_2Te(ClO_4)_2$ in $CHCl_3$ was found to be 0.7 Ω^{-1} mol^{-1} cm^2 which corresponds to its non-electrolytic nature.

Perchlorate group. The nature of the bonding of perchlorate groups in the complexes can be distinguished by identifying the number of infrared active bands.[10–12] The ionic perchlorate group belongs to point group T_d having nine vibrational degrees of freedom distributed between four normal

modes of vibration. It shows only two IR active absorption due to ν_3 (1100 cm^{-1}) and ν_4 ($\sim$ 620 cm^{-1}) whereas ν_1 and ν_2 are Raman active.[10] If the perchlorate group is involved in partial covalent bonding between one of its oxygen atom and the cation, the symmetry of the perchlorate group is lowered to C_{3v}. The triple degeneracy is removed with the result that ν_3 and ν_4 both split into two peaks and ν_1 ($\sim$ 930 cm^{-1}) and ν_2 (460 cm^{-1}) modes become IR active.[10,13]

The IR spectra of $Ph_2Te(ClO_4)_2$ in $CHCl_3$ shows the splitting of ν_3 and ν_4 bands into two appearing at (1125, 1080 cm^{-1}) and (630, 620 cm^{-1}) respectively indicating the presence of monodentately bonded perchlorate groups.[10] A medium absorption at 920 cm^{-1} due to ν_1 which has become infrared active (due to reduction of the local symmetry of ClO_4 from T_d to C_{3v}) also supports the presence of covalently bonded perchlorate groups.[14] This observation is also supported by the conductivity data of $Ph_2Te(ClO_4)_2$ in chloroform in which it behaves as a non-electrolyte.

Diphenylmethyltelluronium perchlorate was assigned an ionic structure $[Ph_2MeTe][ClO_4]$ on the basis of conductivity data.[15,16] In the present work this structure has been substantiated by recording its IR spectrum. The IR spectra of $Ph_2MeTe(ClO_4)$ and $Ph_2MeTe(PyO)(ClO_4)$, give rise to a broad absorption band at 1100 cm^{-1} due to ν_3 and a sharp band at 620 cm^{-1} due to ν_4 (Table 2) which indicates the nature of the perchlorate group to be ionic.[10–12] Moreover, the absence of a band at 920 cm^{-1} due to ν_1 mode supports the ionic nature of the perchlorate group.[14] These observations are also supported by conductivity data (Table 1) and are in accordance with Figs. 1 and 2.

An examination of the IR spectra of the complexes $Ar_2Te(L)(ClO_4)_2$ (Ar = Ph, *p*-$CH_3OC_6H_4$) reveals that in the 1100 cm^{-1} region the spectrum is fairly complex. However, it is possible to assign the peaks in this region to ionic and coordinated perchlorate groups. In the spectrum of each of these compounds the peak around 1100 cm^{-1} is assigned to ionic perchlorate group and the peaks around 1140 and 1080 cm^{-1} (Table 2) are attributed to monodentately coordinated perchlorate group. The spectra of these complexes also show a weak but sharp absorption around 910 cm^{-1} due to the ν_1 mode, which has become IR active due to the reduction of the symmetry of one of the two perchlorate groups from T_d to C_{3v}. The band at 625 cm^{-1} is also split showing coordination of one of the perchlorate groups.[10] The extent of the splitting in the latter case is however so small that in several cases the peak due to ionic perchlorate overlaps with one of the two peaks due to coordinated perchlorate with the result that only two peaks are observed. The ν_2 band expected around 450 cm^{-1} is generally obscured by the strong ring vibration in this region.[14]

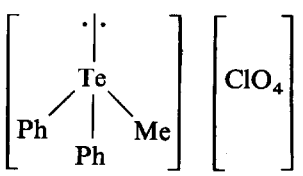


Fig. 1.

Table 2. IR spectra of organotellurium(IV) perchlorate complexes

Compound No.*	Perchlorate absorption (cm^{-1})		
	ν_3	ν_1	ν_4
1.	1140, 1100, 1080	920	630, 620
2.	1140, 1110, 1080	910	630, 620
3.	1140, 1110, 1070	910	630, 620
4.	1140, 1110, 1075	915	630, 620
5.	1140, 1110, 1080	910	630, 620
6.	1140, 1115, 1080	910	645, 635, 625
7.	1140, 1110, 1080	910	630, 620
8.	1135, 1110, 1080	900	630, 620
9.	1140, 1110, 1080	910	630, 620
10.	1140, 1110, 1080	910	630, 620
11.	1138, 1110, 1075	905	630, 620
12.	1140, 1110, 1080	910	630, 620
13.	1140, 1110, 1080	910	630, 620
14.	1140, 1110, 1080	910	630, 620
15.	1135, 1105, 1075	905	630, 620
16.	1140, 1110, 1080	910	630, 620
17.†	1140–1080(br)	—	—
18.	1140–1080(br)	—	625
19.†	1085(br)	—	—
20.	1135–1080(br)	—	625

* Numbers refer to Table 1.

† IR spectra recorded up to 650 cm^{-1}.

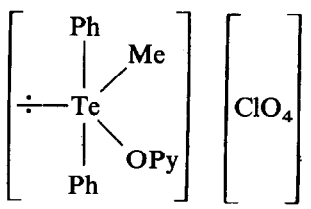


Fig. 2.

The fact that only one perchlorate group is coordinated in the complexes $Ar_2Te(L)(ClO_4)_2$ is also supported by conductivity data (Table 1) of these complexes which behave as 1 : 1 electrolytes even in acetonitrile and acetone in accordance with Fig. 3.

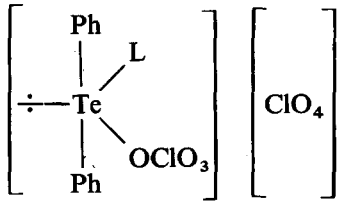


Fig. 3.

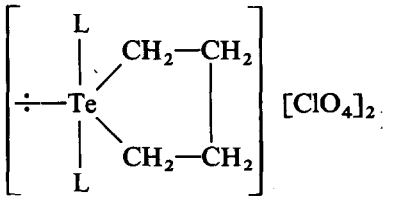


Fig. 4.

In the spectra of the complexes $\overline{C_4H_8Te}(L)_2(ClO_4)_2$, the presence of only one broad band around 1100 cm^{-1} (due to ν_3) and a single sharp band around 625 cm^{-1} (due to ν_4) suggests that both the perchlorate groups are ionic, Fig. 4. The disappearance of the absorption band around 920 cm^{-1} (due to ν_1) rules out the presence of a monodentately coordinated perchlorate group. This

Table 3. Infrared data of complexes of organotellurium(IV) perchlorates

Ligand [L]	Stretching frequencies of ligand affected on coordination	Pure ligand	Stretching frequency (cm^{-1}) in complexes $[Ar_2Te(L)(OClO_3)][ClO_4]$ Ar = Ph	$[Ar_2Te(L)(OClO_3)][ClO_4]$ Ar = *p*-$CH_3OC_6H_4$	$[Ph_2MeTe(L)][ClO_4]$	$[\overline{C_4H_8Te}(L_2)][ClO_4]_2$
Py	ν(C=N)	1578(s)	1595(m)	—	—	1600(s)
	ν(C=C)	1583(s)	1625(s)	—	—	1620(s)
	ring stretch	1439(s)	1480(s)	—	—	1480(s)
TMP	ν(N–H)	3330(m)	3000(m)	3010(w)	—	—
	δ(N–H)	1570(m)	1575(m)	1580(m)	—	—
	ν(C–N)	1240(s)	1220(m)	1225(s)	—	—
		1175(w)	—	—	—	—
TMEN	ν(C–N)	1253(s)	—	—	—	—
		1150(s)	1280(m)	1275(s)	—	—
		1130(m)	—	—	—	—
		1020(s)	—	—	—	—
PyO	ν(N=O)	1265(vs)	1235(vs)	1240(vs)	1230(vs)	—
	δ(N=O)	842(vs)	835(m)	835(m)	840(s)	—
	(C–H) out of plane def.	922(w)	990(s)	995(s)	990(s)	—
γ·PiCO	δ(N=O)	1250(vs)	1220(vs)	1220(vs)	—	—
	δ(N=O)	838(s)	830(s)	830(s)	—	—
	(C–H) out of plane def.	920(s)	990(s)	1000(m)	—	—
LutO	ν(N=O)	1246(vs)	1230(vs)	1225(vs)	—	—
	δ(N=O)	840(vs)	835(m)	830(m)		
	(C–H) out of plane def.	920(s)	990(s)	990(s)		
DMSO	δ(S=O)	1045(vs)	995(s)	990(s)	—	940(s)
	ν(C=S)	705(s)	730(vs)	735(vs)	—	750(m)
TMU	ν(C=O)	1640(vs)	1620(vs)	—	—	—
	ν(C–N)	1499(vs)	1510(vs)			
	δ(C=O)	781(s)	775(w)			
TPAsO	ν(As=O)	885(s)	840(s)	—	—	—
		887(s)				
TPPS	ν(P=S)	639(vs)	—	535(vs)	—	—

s = strong, vs = very strong, m = medium, w = weak.

Table 4. ^{1}H NMR spectral data of some representative complexes

Complexes	δ ppm	Multiplicity	Assignments
$[Ph_2Te(DMSO)(OClO_3)]\cdot[ClO_4]$	7.67(10H)	Multiplet	Phenyl protons
	2.55(6H)	Singlet	–S–CH_3 protons
$[(p\text{-}CH_3OC_6H_4)_2Te(DMSO)(OClO_3)][ClO_4]$	7,40(8H)	Multiplet	Phenyl protons
	3.75(6H)	Singlet	-OCH_3 protons
	2.55(6H)	Singlet	-S-CH_3 protons
$[Ph_2Te(TMEN)(OClO_3)]\cdot[ClO_4]$	7.6(10H)	Multiplet	Phenyl protons
	3.88(4H)	Singlet	-N-CH_2-protons
	3.12(12H)	Singlet	-N-CH_3-protons
$[Ph_2Te(TMP)(OClO_3)]\cdot[ClO_4]$	7.5(10H)	Multiplet	Phenyl protons
	1.68(6H)	Singlet	-CH_2-CH_2-CH_2-protons
	1.35(12H)	Singlet	-C-CH_3 protons
$[\overline{C_4H_8Te}(DMSO)_2][ClO_4]_2$	3.28(4H)	Multiplet	-CH_2-Te-CH_2-protons
	2.55(12H)	Singlet	-S-CH_3-protons
	2.50(4H)	Multiplet	-C-CH_2-protons
$[\overline{C_4H_8Te}(Py)_2][ClO_4]_2$	7.25(4H)	Doublet	Meta protons
	7.67(2H)	Multiplet	Para protons
	8.58(4H)	Doublet	Ortho protons
	3.30(4H)	Multiplet	-CH_2-Te-CH_2-protons
	2.40(4H)	Multiplet	-C-CH_2-protons

observation is also supported by the conductivity data (Table 1). These complexes behave as 1:2 electrolytes in acetonitrile in accordance with Fig. 4.

Coordinated ligands. A critical comparison of the spectra of free ligands with those of the corresponding complexes has been made and the data (Table 3) interpreted in terms of coordination from the Lewis bases.

Oxygen donors. In the complexes with oxygen donors the coordination site was established by a change of $\nu_{E=O}$ frequency (E = N, S, C or As). A negative shift of $\nu_{E=O}$ is taken as a convincing evidence for coordination through the oxygen atom of the bases (Table 3).[17–21]

TPPS. The ν(P=S) mode of vibration has been identified for the free ligand at 630 cm^{-1} by previous workers.[22] Its negative shift to 535 cm^{-1} is attributed to a decrease in double bond character of the (P=S) double bond due to S → Te bonding.

Py. In the free base the C=C, C=N and ring stretchings occur at 1583, 1578 and 1439 cm^{-1} respectively. On complexation these absorptions undergo positive shifts, appearing at ~ 1625, ~ 1595 and ~ 1480 cm^{-1} respectively (Table 3) and thus support the coordination from the nitrogen atom of the base.[23]

TMP. The coordination through the nitrogen atom of the TMP is confirmed by the negative shifts of ν(N–H), δ(N–H) and ν(C–N) appearing at 3330, 1570 and 1240 cm^{-1} in pure ligand to ~ 3000, ~ 1575 and ~ 1220 cm^{-1} respectively in the complexes (Table 3).[24]

TMEN. A comparison of the spectrum of the free ligand (TMEN) with that of its complexes reveals a positive shift of ν(C–N) mode of vibration on complexation (Table 3) indicating coordination from the "N" atom of the ligand.[25] The presence of coordinated base was further confirmed by ^{1}H NMR spectra.

^{1}H NMR spectra of a few representative complexes are listed in Table 4.

Acknowledgement—One of us (VKS) is thankful to the C.S.I.R., New Delhi for an award of S.R.F.

REFERENCES

1. W. R. McWhinnie and J. Mallaki, *Polyhedron* 1982, **1**, 13.
2. T. M. Lowry and F. L. Gilbert, *J. Chem. Soc.* 1929, 2076.
3. R. C. Paul, K. K. Bhasin and R. K. Chadha, *J. Inorg. Nucl. Chem.* 1975, **11**, 2337.
4. J. Bergmann, *Tetrahedron* 1972, **28**, 3323.
5. G. T. Morgan and F. H. Burstall, *J. Chem. Soc.* 1931, 180.
6. K. Lederer, *Ann. Chem.* 1913, **339**, 260.
7. H. Rheinboldt and E. Giesbrecht, *J. Am. Chem. Soc.* 1947, **69**, 2310.

8. R. Macy, *J. Am. Chem. Soc.* 1925, **47**, 1031.
9. W. J. Geary, *Coord. Chem. Rev.* 1971, **7**, 110.
10. B. J. Hathaway and A. E. Underhill, *J. Chem. Soc.* 1961, 3091.
11. B. J. Hathaway, D. G. Holah and M. Hudson, *J. Chem. Soc.* 1963, 4586.
12. K. Nakamoto, *Infrared Spectra of Inorganic and Coordination Compounds*, p. 103. Wiley, New York (1963).
13. F. A. Cotton and D. L. Weaver, *J. Am. Chem. Soc.* 1965, **87**, 4189.
14. S. B. Naikar, N. M. Nanjegowda and G. K. N. Reddy, *Indian J. Chem.* 1981, **20A**, 436.
15. K. J. Irgolic, *The Organic Chemistry of Tellurium.* Gordon and Breach, London (1974).
16. A. Z. Al-Rubaie, W. R. McWhinnie, P. Granger and S. Chapelle, *J. Organometal. Chem.* 1982, **234**, 287.
17. S. Kida, J. V. Quagliano, J. A. Walmsly and S. Y. Tyree, *Spectrochim. Acta* 1963, **19**, 189.
18. N. M. Karayannis, I. I. Pytlewski and O. M. Mikulski, *Coord. Chem. Rev.* 1973, **11**, 93.
19. H. G. Langer and A. H. Blut, *J. Organometal. Chem.* 1966, **5**, 288.
20. J. H. Holloway, G. P. McQuillan and D. S. Ross, *J. Chem. Soc. A* 1971, 1935.
21. M. Schafer and C. Curran, *Inorg. Chem.* 1966, **5**, 265.
22. P. M. Boorman and K. J. Reimer, *Canad. J. Chem.* 1971, **49**, 2926.
23. S. S. Singh and C. B. S. Sengar, *Indian J. Chem.* 1969, **7**, 812.
24. P. J. Asheley and E. G. Torrible, *Canad. J. Chem.* 1969, **47**, 167.
25. T. N. Srivastava and P. C. Kamboj, *Indian J. Chem.* 1980, **19A**, 167.

Polyhedron Vol. 4, No. 7, pp. 1231–1237, 1985
Printed in Great Britain

0277–5387/85 $3.00 + .00
© 1985 Pergamon Press Ltd

BIS(DIMETHYLPHOSPHINO)METHANE (dmpm) COMPLEXES OF IRON, MOLYBDENUM AND CHROMIUM: X-RAY CRYSTAL STRUCTURES OF $FeCr(CO)_6(\mu\text{-dmpm})_2$ AND $Fe_2(CO)_4(\mu\text{-CO})(\mu\text{-dmpm})_2$

WAI KWOK WONG, KWOK W. CHIU and GEOFFREY WILKINSON*
Chemistry Department, Imperial College, London SW7 2AY, U.K.

and

MAJID MOTEVALLI and MICHAEL B. HURSTHOUSE*
Chemistry Department, Queen Mary College, Mile End Road, London E1 4NS, U.K.

(*Received* 6 *November* 1984; *accepted* 29 *November* 1984)

Abstract—The photolysis of $Fe(\eta^1\text{-dmpm})(dmpm)_2$ [dmpm = bis(dimethylphosphino) methane] with $Cr(CO)_6$ and $Fe(CO)_5$ under UV irradiation produces $FeCr(CO)_6(\mu\text{-dmpm})_2$, $Fe_2(CO)_6(\mu\text{-CO})(\mu\text{-dmpm})$ and $Fe_2(CO)_4(\mu\text{-CO})(\mu\text{-dmpm})_2$ respectively. The interaction of $Mo(CO)_3(MeCN)_3$ and $(C_7H_8)Cr(CO)_3$ with dmpm produces $Mo_2(CO)_6(\mu\text{-dmpm})_3$ and *cis*-$Cr(CO)_2(dmpm)_2$ respectively. The X-ray crystal structure of $FeCr(CO)_6(\mu\text{-dmpm})_2$ shows the molecule to contain a trigonal bipyramidal $Fe(CO)_3P_2$ unit plus a square pyramidal $Cr(CO)_3P_2$ unit held closely together by the methylene bridges of the dmpm ligands with steric compression between the CO groups causing distortions from ideal geometry in each case. The Cr . . . Fe distance is 3.111(6) Å and there seems to be little structural evidence of any form of interaction between the 16*e* Cr(0) centre and the Fe-containing unit. The structure of $Fe_2(CO)_4(\mu\text{-CO})(\mu\text{-dmpm})_2$ contains a symmetrical μ_2-carbonyl and a single bond between the two symmetry related (m) iron atoms. The Fe . . . Fe distance is 2.719(4) Å.

We have recently reported the synthesis of the bis(dimethylphosphino)methane complexes $Fe(\eta^2\text{-dmpm})(dmpm)_2$ and $FeR_2(dmpm)_2$ (R = Me and CH_2Ph).[1] Here we report further studies on the reactivity of $Fe(\eta^1\text{-dmpm})(dmpm)_2$, which has a free phosphorus atom available to act as a ligand, towards $Fe(CO)_5$ and $Cr(CO)_6$ to give mixed Fe–Fe or Fe–Cr dimers; the further coordination of η^1-bis(diphenylphosphino)methane(dppm) complexes is already established.[2] We also describe the synthesis of $Mo_2(CO)_6(\mu\text{-dmpm})_3$ and *cis*-$Cr(CO)_2(dmpm)_2$. After completion of these studies, a recent paper has described some similar chemistry of dmpm, including the compounds $Mo_2(CO)_6(dmpm)_3$, $Fe_2(CO)_5(dmpm)_2$ and $Fe_2(CO)_7(dmpm)$ described herein, but no X-ray crystallographic data was obtained.[3]†

RESULTS AND DISCUSSION

Reactions of $Fe(\eta^1\text{-dmpm})(dmpm)_2$

(a) *With hexacarbonylchromium.* When the iron compound in tetrahydrofuran containing excess $Cr(CO)_6$ was irradiated with ultraviolet light at room temperature a red crystalline compound was obtained. Recrystallisation from toluene gave $FeCr(CO)_6(dmpm)_2 \cdot C_7H_8$, which is moderately stable in air. The structure was determined by X-ray diffraction and a molecule is shown in Fig. 1; selected bond lengths and angles are given in Table 1. At the simplest level, the complex can be considered to comprise two $M(CO)_3P_2$ units linked together by the bridged dmpm ligands, with the heterobimetallic nature of the complex giving rise to potential differences in geometries at the metal centres. Furthermore, the differences in electron counts at the metals, 18 at Fe and 16 at Cr, might be expected to

*Authors to whom all correspondence should be addressed.

†The compounds $Fe_2(\mu\text{-CO})(CO)_n(\mu\text{-}R_2pyPR_2)_m$, $n = 6$, $m = 1$, $n = 4$, $m = 2$, including R = Me and Y = CH_2, have also been reported by DeLeew *et al.*, *J. Organomet. Chem.* 1984, **375**, 99.

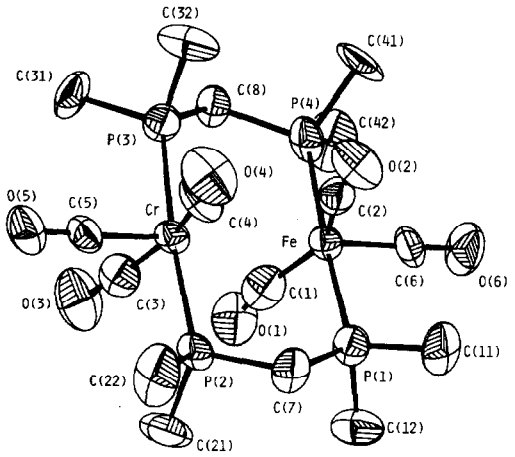


Fig. 1.

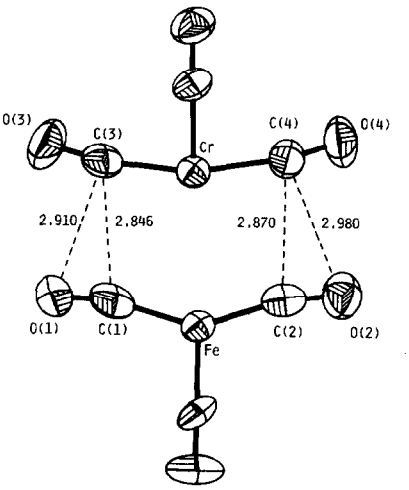


Fig. 2.

lead to some kind of interaction between them. At both centres, the two M–P bonds are mutually *trans* and give P–M–P angles close to 180°; this leaves the arrangement of the "equatorial" carbonyl ligands to reflect any differences in geometry. It is therefore convenient to view the structure in a direction parallel to the P–M–P directions, and this is shown in Fig. 2. The most obvious interpretation of the distribution of the three carbonyls at each metal is that the $Fe(CO)_3P_2$ unit has a distorted trigonal bipyramidal geometry, whilst the $Cr(CO)_3P_2$ unit has a distorted square pyramidal geometry. The main source of the distortion is most likely to be steric compression between those carbonyl groups which are required to point towards each other.

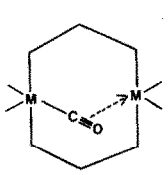
Table 1. Selected bond lengths and angles for $FeCr(CO)_6(dmpm)_2 \cdot C_7H_8$

(a) Bond lengths (Å)			
P(1)–Fe(1)	2.201(4)	P(2)–Fe(1)	2.201(4)
C(1)–Fe(1)	1.931(7)	C(2)–Fe(1)	1.733(8)
C(3)–Fe(1)	1.782(9)	Fe(1)–Fe(1a)	2.719(4)
C(11)–P(1)	1.821(7)	C(12)–P(1)	1.829(10)
C(13)–P(1)	1.811(9)	C(21)–P(2)	1.833(8)
C(22)–P(2)	1.818(10)	C(23)–P(2)	1.853(14)
C(1)–O(1)	1.198(10)	C(2)–O(2)	1.157(8)
C(3)–O(3)	1.135(9)		
(b) Bond angles (°)			
P(2)–Fe(1)–P(1)	171.4(1)	C(1)–Fe(1)–P(1)	90.7(3)
C(1)–Fe(1)–P(2)	91.0(3)	C(2)–Fe(1)–P(1)	85.3(3)
C(2)–Fe(1)–P(2)	86.2(3)	C(2)–Fe(1)–C(1)	103.4(4)
C(3)–Fe(1)–P(1)	91.2(3)	C(3)–Fe(1)–P(2)	93.0(3)
C(3)–Fe(1)–C(1)	139.6(3)	C(3)–Fe(1)–C(2)	117.0(4)
Fe(1)–C(1)–Fe(1a)	89.5(4)	C(11)–P(1)–Fe(1)	114.0(4)
C(12)–P(1)–Fe(1)	116.5(4)	C(12)–P(1)–C(11)	102.0(5)
C(13)–P(1)–Fe(1)	116.2(4)	C(13)–P(1)–C(11)	104.3(5)
C(13)–P(1)–C(12)	102.1(6)	P(1)–C(11)–P(1)	110.9(5)
C(21)–P(2)–Fe(1)	113.8(4)	C(22)–P(2)–Fe(1)	116.2(5)
C(22)–P(2)–C(21)	103.4(5)	C(23)–P(2)–Fe(1)	116.0(5)
C(23)–P(2)–C(21)	103.6(6)	C(23)–P(2)–C(22)	102.0(7)
P(2)–C(21)–P(2)	109.0(6)	O(1)–C(1)–Fe(1)	135.2(2)
O(2)–C(2)–Fe(1)	179.4(6)	O3)–C(3)–Fe(1)	178.0(7)

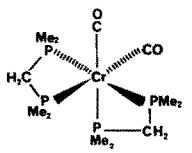
Key to symmetry operations relating designated atoms to reference atoms at (x, y, z): (a) $x, 0.5-y, z$.

Thus, the expected 120° angle between the CO groups C(1), C(2), on the iron atom is increased to 146°, whilst the expected obtuse axial/basal angles C(5)–Cr–C(3), C(4) on the chromium atom have been made acute, with values of *ca* 82°. The close approaches between the CO groups which still remain are seen on Fig. 2.

The "square pyramidal" 16*e* Cr(0) system coordinated by five π-acceptor ligands, might be expected to seek further electron density to achieve an 18*e* configuration. This would occur in one of two ways: (a) by one of the CO groups on Fe acting as a



1



2

σ–π bridge, of the type **1** suggested for $Mn_2(CO)_5(dppm)_2$,[4] or (b) via direct Fe → Cr σ-bonding, using a filled orbital on iron. The former seems most unlikely in view of the arrangement of the CO groups on Fe (Fig. 2) where the Fe–C–O unit is bent at the carbon, directing the C=O bond away from the chromium. Accordingly we assume that any interaction involving the chromium atom is most likely to be of the Fe → Cr type, even though the Fe–Cr distance is long, at 3.111(6) Å.

The IR, ^1H and ^{31}P–$\{^1H\}$ NMR spectra of the compounds (see Experimental) are consistent with the structure as determined.

(b) *With pentacarbonyliron.* Similar photolysis in THF containing excess $Fe(CO)_5$ gave two compounds $Fe_2(CO)_5(dmpm)_2$ and $Fe_2(CO)_7(dmpm)$ both of which are moderately stable in air, slightly soluble in saturated hydrocarbons but soluble in toluene.

The molecular structure of $Fe_2(CO)_5(dmpm)_2$, which has mirror symmetry, is shown in Fig. 3; selected bond lengths and angles are given in Table 2. In this case, if the bridging carbonyl is considered to be "ketonic", and acting as a 1*e* σ ligand for each Fe atom, then completion of 18*e* configuration for the metal requires a single Fe–Fe bond. The closer association of the two metal centres in this complex is seen both in Fig. 3 and in the value of the Fe . . . Fe distance 2.719(4) Å. The structure as found was also proposed on the basis of spectroscopic data.[3]

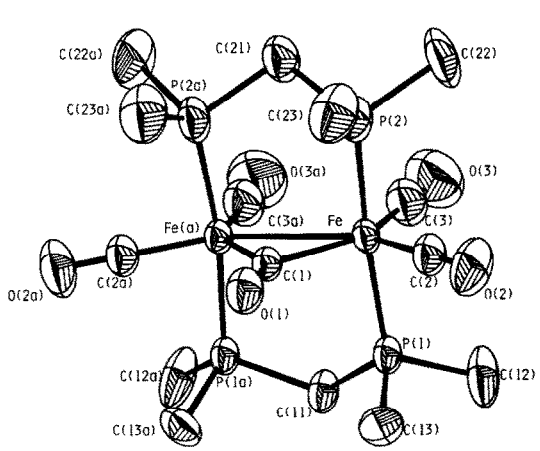


Fig. 3.

The compound $Fe_2(CO)_7(dmpm)$ is readily formulated as $Fe_2(CO)_6(\mu\text{-CO})(\mu\text{-dmpm})$ on the basis of spectra (cf. ref. 3).

$Mo_2(CO)_6(dmpm)_3$ and $Cr(CO)_2(dmpm)_2$

The displacement of cycloheptatriene from $C_7H_8M(CO)_4$, (M = Cr and Mo) gives $M_2(CO)_6(dmpm)_3$.[3] These species were formulated on the basis of NMR spectra as having one bridging and two chelating dmpm ligands; also the reaction of $Mo(CO)_3(MeCN)_3$ with dmpm in *boiling* MeCN is said to give $Mo(CO)_3(dmpm)_3$ that has three unidentate dmpm ligands.[3]

However, we find that interaction of dmpm with $Mo(CO)_3(MeCN)_3$ at *ambient* temperature affords pale yellow prisms (from MeCN) of a compound of the same stoichiometry as King's, namely $Mo_2(CO)_6(dmpm)_3$, but which is evidently an isomer with three bridging dmpm ligands, since the ^1H and ^{31}P NMR spectra differ considerably from King's complex.

Thus the ^1H spectrum in CD_3CN shows two broad singlets at δ1.54 and 2.11 ppm corresponding to the CH_2 and CH_3 protons of dmpm while the ^{31}P spectrum in CD_3CN shows only a singlet at −12.0 ppm. The IR spectrum has two terminal CO stretches at 1930 and 1800 cm^{-1}. Analogous compounds $M_2(CO)_6(P\text{–}P)_3$, M = Cr, Mo, W and P–P = dppe and dmpe, are known[5] but, like King's compound, Connor formulated $Mo_2(CO)_6(dmpe)_3$ as having both chelate and bridging dmpe ligands since two ^{31}P and two ^1H (CH_2) resonances were observed.

The unstable $Cr_2(CO)_6(dmpe)_3$ made in low yield from $C_7H_8Cr(CO)_3$ and dmpe in boiling hexane[3] is said to be converted in solution to $Cr(CO)_3(dmpm)_2$ for which it is proposed that one of the dmpm ligands is unidentate on the basis of NMR spectra.[3]

Again, in the reaction at ambient temperature there appears to be a difference since our product appears to be *cis*-$Cr(CO)_2(dmpm)_2$. The IR spectrum has terminal CO stretches at 1908 and 1800 cm^{-1}. The ^1H NMR spectrum in C_6D_6 shows four doublets at δ1.39 ppm ($^2J_{PH}$ = 6.1 Hz), 1.25 ppm ($^2J_{PH}$ = 7.2 Hz), 1.14 ppm ($^2J_{PH}$ = 6.8 Hz) and 0.83

ppm ($^2J_{PH}$ = 3.5 Hz) for the CH_3 protons; there is a doublet of triplets at 2.6 ppm ($^2J_{PH}$ = 9.2 Hz, 1.3 Hz) and a doublet of doublets at 1.69 ppm ($^2J_{PH}$ = 3.3, 6.13 Hz) for the CH_2 protons. The ^{31}P–$\{^1H\}$ spectrum in C_6D_6 shows two triplets at 20.7 and 0.87 ppm with $^2J_{PP}$ = 35.5 Hz. These spectra suggest that the compound is the *cis* compound **2**. Connor has formulated both the Cr and Mo compounds, $M(CO)_2(dmpe)_2$ as *cis* on the basis of spectroscopic data.[5] The tetracarbonyl *cis*-$Cr(CO)_4(dmpm)$ has also been recently reported[3,6] [cf. *cis*-$M(CO)_4(dmpe)$[5]].

Table 2. Selected bond lengths and angles for $Fe_2(CO)_5(dmpm)_2$

(a) Bond lengths (Å)			
Fe(1)–Cr(1)	3.111(6)	P(2)–Cr(1)	2.284(7)
P(3)–Cr(1)	2.302(7)	C(3)–Cr(1)	1.849(20)
C(4)–Cr(1)	1.900(22)	C(5)–Cr(1)	1.778(20)
P(1)–Fe(1)	2.213(7)	P(4)–Fe(1)	2.215(7)
C(1)–Fe(1)	1.794(22)	C(2)–Fe(1)	1.769(21)
C(6)–Fe(1)	1.759(21)		
C(7)–P(1)	1.833(18)	C(11)–P(1)	1.864(18)
C(12)–P(1)	1.831(19)	C(7)–P(2)	1.853(17)
C(21)–P(2)	1.842(19)	C(22)–P(2)	1.858(18)
C(8)–P(3)	1.848(16)	C(31)–P(3)	1.842(18)
C(32)–P(3)	1.890(20)	C(8)–P(4)	1.826(17)
C(41)–P(4)	1.830(19)	C(42)–P(4)	1.871(19)
C(1)–O(1)	1.159(19)	C(2)–O(2)	1.165(18)
C(3)–O(3)	1.174(18)	C(4)–O(4)	1.129(19)
C(5)–O(5)	1.196(18)	C(6)–O(6)	1.144(18)
(b) Bond angles (°)			
P(2)–Cr(1)–Fe(1)	86.4(2)	P(3)–Cr(1)–Fe(1)	86.6(2)
P(3)–Cr(1)–P(2)	172.9(2)	C(3)–Cr(1)–Fe(1)	98.2(6)
C(3)–Cr(1)–P(2)	90.6(6)	C(3)–Cr(1)–P(3)	89.7(6)
C(4)–Cr(1)–Fe(1)	97.0(6)	C(4)–Cr(1)–P(2)	89.8(6)
C(4)–Cr(1)–P(3)	91.7(6)	C(4)–Cr(1)–C(3)	164.8(7)
C(5)–Cr(1)–Fe(1)	179.0(5)	C(5)–Cr(1)–P(2)	92.8(6)
C(5)–Cr(1)–P(3)	94.3(6)	C(5)–Cr(1)–C(3)	82.4(8)
C(5)–Cr(1)–C(4)	82.4(8)		
P(1)–Fe(1)–Cr(1)	91.8(2)	P(4)–Fe(1)–Cr(1)	91.6(2)
P(4)–Fe(1)–P(1)	176.5(2)	C(1)–Fe(1)–Cr(1)	72.5(6)
C(1)–Fe(1)–P(1)	91.2(6)	C(1)–Fe(1)–P(4)	90.2(6)
C(2)–Fe(1)–Cr(1)	74.0(6)	C(2)–Fe(1)–P(1)	89.1(6)
C(2)–Fe(1)–P(4)	91.6(6)	C(2)–Fe(1)–C(1)	146.5(7)
C(6)–Fe(1)–Cr(1)	177.1(5)	C(6)–Fe(1)–P(1)	88.9(6)
C(6)–Fe(1)–P(4)	87.7(6)	C(6)–Fe(1)–C(1)	104.7(8)
C(6)–Fe(1)–C(2)	108.8(8)		
C(7)–P(1)–Fe(1)	116.4(6)	C(11)–P(1)–Fe(1)	115.2(7)
C(11)–P(1)–C(7)	100.0(8)	C(12)–P(1)–Fe(1)	115.6(7)
C(12)–P(1)–C(7)	106.4(9)	C(12)–P(1)–C(11)	101.0(10)
C(7)–P(2)–Cr(1)	115.5(6)	C(21)–P(2)–Cr(1)	118.4(7)
C(21)–P(2)–C(7)	104.0(9)	C(22)–P(2)–Cr(1)	116.0(7)
C(22)–P(2)–C(7)	98.6(9)	C(22)–P(2)–C(21)	101.5(10)
C(8)–P(3)–Cr(1)	116.1(6)	C(31)–P(3)–Cr(1)	116.0(6)
C(31)–P(3)–C(8)	99.2(9)	C(32)–P(3)–Cr(1)	117.8(7)
C(32)–P(3)–C(8)	102.7(9)	C(32)–P(3)–C(31)	102.2(10)
C(8)–P(4)–Fe(1)	117.3(6)	C(41)–P(4)–Fe(1)	116.1(7)
C(41)–P(4)–C(8)	106.1(9)	C(42)–P(4)–Fe(1)	113.2(8)
C(42)–P(4)–C(8)	99.4(9)	C(42)–P(4)–C(41)	102.5(11)
O(1)–C(1)–Fe(1)	168.6(16)	O(2)–C(2)–Fe(1)	166.6(15)
O(3)–C(3)–Cr(1)	170.6(15)	O(4)–C(4)–Cr(1)	172.2(16)
O(5)–C(5)–Cr(1)	177.4(14)	O(6)–C(6)–Fe(1)	178.2(15)

EXPERIMENTAL

Microanalyses were by Pascher (Bonn). IR spectra were obtained on a Perkin–Elmer 683 spectrometer; data in cm^{-1} for Nujol mulls unless otherwise specified. NMR spectra were recorded on a JEOL FX90Q; data in δ ppm referenced to Me_4Si (^1H) and 85% H_3PO_4 (^{31}P). Molecular weights were determined cryoscopically in benzene.

All operations were carried out under argon, nitrogen or *in vacuo*. All chemicals used were of reagent grade. Solvents were dried by standard procedures, distilled, and deaerated prior to use. Melting points were taken in sealed capillaries and are uncorrected. Fe(η^1-dmpm)(dmpm)$_2$,[1] $Mo(CO)_3(CH_3CN)_3$[7] and $Cr(C_7H_8)(CO)_3$[8] were made by published methods. Irradiations were made using an Applied Photo-Physics Ltd. medium pressure mercury lamp (125 W) type PR 311.0 and a water-cooled reactor.

1. *Hexacarbonyl bis[μ - bis(dimethylphosphino) methane)]iron chromium*(0)

A solution of Fe(dmpm)$_2$(η^1-dmpm) (0.46 g, 1 mmol) and $Cr(CO)_6$ (0.44 g, 2 mmol) in THF (150 cm^3) was photolysed for 18 hr at ambient temperature. The progress of the reaction was monitored by IR spectroscopy and the irradiation was continued until no further change in the spectrum of the reaction mixture was discernable. The orange red solution was evaporated under vacuum, the residue washed with hexane (2 × 50 cm^3) and extracted into toluene (2 × 50 cm^3). The filtered solution was concentrated to *ca* 20 cm^3 and cooled to −20°C to give red crystals. Yield: 0.4 g, 62%; m.p. 75°C (decomp.). The compound is slightly soluble in saturated hydrocarbons but readily soluble in toluene $CHCl_3$ and THF. [Found (required); C, 42.8 (43.1); H, 5.7 (5.7); P, 19.0 (19.4); O, 15.2 (15.0)%.]

IR: 2059w, 1963m, 1916vs, 1880vs, 1878vs, 1832vs, 1805s, 1780s, 1489w, 1411m, 1300m, 1286m, 1277m, 930s, 907w, 893m, 848w, 768m, 743m, 726m, 718m, 688m, 652s, 640m, 630m, 585s.

NMR: $^1H(CDCl_3)$: 2.18m (CH_2); overlapping doublets centred 1.55, $^2J_{PH}$ = 6 Hz; 1.50, $^2J_{PH}$ = 4.4 Hz (CH_3). ^{31}P–{^1H}($CDCl_3$): complex A_2B_2 14 line pattern centred at 36.5 ppm.

2. *Tetracarbonyl(μ - carbonyl)bis[μ - bis(dimethylphosphino)methane]diiron*(0); *hexacarbonyl(μ - carbonyl)μ - bis(dimethylphosphino)methane diiron*(0)

A solution of Fe(dmpm)$_2$(η^1-dmpm)(0.46 g, 1 mmol) and $Fe(CO)_5$ (2 cm^3, 15.2 mmol) in THF (1500 cm^3) was photolysed for 18 hr at ambient temperature and monitored by IR as above. The orange red solution was evaporated under *vacum*. The residue was washed with hexane (2 × 50 cm^3), then extracted with toluene (2 × 40 cm^3) to give a red solution. The residue was extracted with CH_2Cl_2 (2 × 30 cm^3). The CH_2Cl_2 solution was then filtered, concentrated to *ca* 5 cm^3 and cooled to −20°C to give orange crystals of $Fe_2(CO)_6$(μ-CO)(μ-dmpm). Yield: 0.13 g, 30%; m.p., 182°C (decomp.). [Found (required): C, 32.2 (32.5); H, 3.3 (3.2); P, 13.7 (13.9); O, 25.6 (25.3)%.]

IR: 2028s, 1986s, 1955s, 1942s, 1930s, 1907s, 1732s, 1423w, 1415w, 1302w, 1293w, 938m, 853w, 776w, 752w, 729w, 654w, 629m, 603m, 580w, 482w, 452w.

NMR: $^1H[(CD_3)_2CO]$: 2.50 t, $^2J_{PH}$ = 12 Hz, (CH_2); 1.70 pseudo t, $^2J_{PH}+{}^4J_{PH}$ = 9.3 Hz (CH_3). ^{31}P–{^1H}[$(CD_3)_2CO$]: 47.4s.

The above red toluene extract was evaporated *in vacuo*, and residue dissolved in CH_2Cl_2 (*ca* 2 cm^3). To the filtered solution was slowly added Et_2O (*ca* 5 cm^3) until the solution showed slight turbidity when it was cooled to −20°C to yield dark red crystals of $Fe_2(CO)_4$(μ-CO)(μ-dmpm)$_2$. Yield: 0.1 g, 20%; m.p. 210°C (decomp.). [Found (required): C, 34.0 (34.4); H, 5.3 (5.4); P, 23.3 (23.6); O, 15.5 (15.3)%.]

IR: 1940m, 1880s, 1862s, 1846m, 1660s (μ-CO), 1410w, 1406w, 1298w, 1286w, 937s, 850m, 754w, 742w, 722m, 650w, 630m, 615w, 480m.

NMR: $^1H[(CD_3)_2CO]$: 2.24m (CH_2); 1.53br.s (CH_3). ^{31}P–{^1H}[$(CD_3)_2CO$]: 52.7s.

3. *Hexacarbonyl tris[μ - bis(dimethylphosphino) methane]dimolybdenum*(0)

Dmpm (1 cm^3, 6.6 mmol) was added to a solution of $Mo(CO)_3(MeCN)_3$ (1.05 g, 3.46 mmol) in MeCN (50 cm^3) at ambient temperature. The mixture was stirred for 16 hr. After evaporation in vacuo the residue was washed with hexane (2 × 30 cm^3) and extracted into MeCN (40 cm^3). The solution was filtered, concentrated to *ca* 25 cm^3 and cooled to −20°C to give pale yellow crystals, insoluble in alkanes and Et_2O but soluble in MeCN. Yield: 1.2 g, 90%; m.p. 140°C (decomp.). Found (required): C, 32.5 (32.8); H, 5.4 (5.5); P, 23.8 (24.2); O, 12.7 (12.5)%.]

IR: 1930vs, 1800vs, 1435m, 1415m, 1300m, 1282m, 1115m, 940s, 930s, 900s, 865w, 840w, 820w, 792m, 730s, 710s, 680w, 630m, 612m, 600m, 523w, 460w.

NMR: $^1H(CD_3CN)$: 1.54br.s (CH_3); 2.11br.s (CH_2). ^{31}P–{^1H}(MeCN): −12.0s.

4. Cis - *bis(carbonyl)bis[bis(dimethylphosphino) methane]chromium*(0)

Dmpm (0.5 cm^3, 3.3 mmol) was added to a solution of $(C_7H_8)Cr(CO)_3$ (0.2 g, 0.88 mmol) in hexane (60

Table 3. Crystallographic data

(a) Crystal data		
	$FeCr(CO)_6(dmpm)_2 \cdot C_7H_8$	$Fe_2(CO)_5(dmpm)_2$
Formula	$C_{23}H_{36}O_6P_4CrFe$	$C_{15}H_{28}O_5P_4Fe_2$
F. wt.	640.277	523.967
Crystal system	Monoclinic	Orthorhombic
a (Å)	17.392(4)	9.789(1)
b (Å)	12.898(6)	16.656(3)
c (Å)	13.808(2)	114.448(2)
β (deg)	100.35(1)	—
U (Å^3)	3045.91	2355
Space group	$P2_1/n$	*Pnma*
D_c (g cm^{-3})	1.39	1.48
Z	4	4*
$F_{(000)}$	1328	1080
μ (cm^{-1})	10.06	14.40
T (K)	265	295
(b) Data collection		
θ_{min}, θ_{max} (deg)	1.5, 25.0	1.5, 25.0
Total measured	3398	2377
Total unique	3083	2141
Total observed	1566	1331
Significance test	$F_o > 3\sigma(F_o)$	$F_o > 3\sigma(F_o)$
(c) Refinement		
No. of parameters	281	148
Weighting scheme, w =	$1/[\sigma^2(F_o)+0.00008(F_o)^2]$	$1/[\sigma^2(F_o)+0.0005(F_o)^2]$
Final R [$= (\Sigma\Delta F_o)/\Delta(F_o)$]	0.0662	0.0446
Final R_ω $\{= [\Sigma\omega\Delta^2/\Sigma\omega F_o^2]^{1/2}\}$	0.0656	0.0446

* Molecule has *m* symmetry.

cm^3) at ambient temperature. The mixture was then stirred for 16 hr when the colour changed from dark red to pale yellow. The mixture was evaporated under *vacuum* and the residue extracted into hexane (2×30 cm^3). The pale yellow solution was filtered, concentrated to *ca* 5 cm^3 and cooled to -20°C to give pale yellow prisms. Yield: 0.2 g, 65%; m.p., 70°C. [Found (required): C, 37.5 (37.9); H, 7.4 (7.4); P, 32.1 (32.6); O, 8.2 (8.4)%. *M* 360 (380).]

IR: 1908vs, 1800vs, 1420m, 1415m, 1300m, 1280m, 1080m, 940s, 925s, 880m, 840m, 820w, 770m, 720s, 705s, 675m, 635m, 560m.

NMR: see text.

X-ray crystallography

For both compounds, crystals used for X-ray study were sealed under argon in thin-walled glass capillaries. Following preliminary photography, unit cell and intensity data were obtained using an Enraf–Nonius CAD4 diffractometer and graphite monochromatised Mo-K_α radiation ($\lambda = 0.71069$ Å), following standard procedures.[9] The structures were solved and refined *via* use of the heavy atom method and full matrix squares.[10] For the CrFe complex, which gives toluene solvated crystals the crystal quality and accordingly the intensity data were slightly below par. As a result no hydrogen atoms could be located and none were not included in the refinement. For the Fe_2 complex however, all hydrogens were located and freely refined with isotropic thermal parameters. Crystal data and details of the data collections and refinement are given in Table 3. Atomic co-ordinates, thermal parameters, full lists of bond lengths and angles and F_o/F_c values have been deposited as supplementary material with the Editor from whom copies are available on request. Atomic co-ordinates have also been deposited with the Cambridge Crystallographic Data Centre.

Acknowledgement—We thank the SERC for support and for provision of the X-ray diffractometer.

REFERENCES

1. W. K. Wong, K. W. Chiu, G. Wilkinson, A. J. Howes, M. Motevalli and M. B. Hursthouse, *Polyhedron* 1985, **4**, 603. For Fe(η^1-dmpm)(η^2-dmpm)$_2$ see now also H. H. Karsch, *Chem. Ber.* 1984, **117**, 3123.
2. R. J. Puddephatt, *Chem. Soc. Rev.* 1983, **12**, 99; F. Sato, T. Uemura and M. Sato, *J. Organomet. Chem.* 1973, **56**, C27; P. G. Pringle and B. L. Shaw, *J. Chem. Soc., Dalton Trans.* 1984, 1233.
3. R. B. King and K. S. RaghuVeer, *Inorg. Chem.* 1984, **23**, 2482.
4. H. C. Aspinall and A. J. Deeming, *J. Chem. Soc., Chem. Commun.* 1981, 724.
5. F. Zingales and F. Canziani, *Gazz. Chim. Ital.* 1962, **92**, 343; J. A. Connor, G. K. McEwen and J. Rix, *J. Chem. Soc., Dalton Trans.* 1974, 589, *J. Less Comm. Met.* 1974, **36**, 207.
6. H. H. Karsch, *Chem. Ber.* 1983, **116**, 1643.
7. D. P. Tate, W. R. Kripple and J. M. Augl, *Inorg. Chem.* 1962, **1**, 433.
8. E. W. Abel, M. A. Bennett, R. Burton and G. Wilkinson, *J. Chem. Soc.* 1958, 4559.
9. M. B. Hursthouse, R. A. Jones, K. M. A. Malik and G. Wilkinson, *J. Am. Chem. Soc.* 1979, **101**, 4128.
10. SHELX76, G. M. Sheldrick, University of Cambridge (1976).

Polyhedron Vol. 4, No. 7, 1239–1244, 1985
Printed in Great Britain

0277–5387/85 $3.00 + .00
© 1985 Pergamon Press Ltd

SYNTHESIS AND CHARACTERISATION OF SOME SALTS OF THE IONS $[Rh(OXALATO)_2(Rpy)_2]^-$

A. Y. ALI MOHAMED,* R. D. GILLARD† and F. L. WIMMER‡
Department of Chemistry, University College, P.O. Box 78, Cardiff CF1 1XL, Wales, U.K.

(*Received* 7 *November* 1984; *accepted* 29 *November* 1984)

Abstract—Salts of three bisoxalato bis(pyridine) species, *trans*-$[Rh(ox)_2(py)_2]^-$, *trans*-$[Rh(ox)_2(3\text{-Mepy})_2]^-$ and *trans*-$[Rh(ox)_2(4\text{-Mepy})_2]^-$ have been isolated from the substitution of N-heterocycles into trisoxalatorhodate(III) and characterised on the basis of ^1H NMR and ^{13}C NMR spectra, which are similar to that of the *trans*-$[Co(oxalato)_2(R\text{-py})_2]^-$ complex.

Trisoxalatorhodate(III)§ hydrolyses in strong perchloric acid solution (like the analogous chromium(III) species) to a *cis–trans* equilibrium mixture of $[Rh(H_2O)_2(ox)_2]^-$ ions:[1,2] both the *cis*- and *trans*-isomers were isolated[2] after separation by anion exchange chromatography.

This *cis*-diaquoisomer reacts readily[2] with chloride to give the known *cis*-dichlorobisoxalatorhodate(III), which isomerises to *trans*-dichlorobisoxalatorhodate(III) when its solution is boiled, as noted by Delépine.[3]

There is, in the light of the present stereochemical findings, another related area of oxalatometallate(III) complex chemistry, that of dioxalatodipyridine iridate(III). This complex was prepared by Delépine:[4a,b] by heating either *cis*- or *trans*-$K_3[IrCl_2(ox)_2]$ for 1 hr or $K_3[Ir(ox)_3]$ for 4 hr with pyridine in a sealed tube at 130°C, sulphur-yellow crystals of *trans*-$K[Ir(ox)_2py_2]$ were obtained. The mother liquor gave an amorphous, yellow, readily soluble product, presumably containing the *cis*-isomer. The former product was not resolved by natural strychnine (though it gave a solid salt), and Delépine therefore allotted the *trans*-configuration to the ion in the *crystals*.

Although substitution of oxalate in trisoxalatoruthenate(III) by pyridine has been reported,[5–7] substitution in trisoxalatorhodate(III) has not previously been studied. Our aim was to investigate the reactions of $K_3[Rh(ox)_3]$ with pyridine.

EXPERIMENTAL

IR spectra (either in Nujol mulls or KBr discs) were obtained using Perkin–Elmer 257 and 457 double-beam grating spectrophotometers and a Unicam SP 3200 spectrophotometer. Electronic absorption spectra were measured using a Unicam SP 8000 spectrophotometer, using matched silica cells. ^1H NMR spectra were recorded on a Varian R32 spectrometer at 90 MHz, ^{13}C NMR spectra were recorded on a Varian X1-100-12 NMR spectrometer (25.2 MHz). Thermogravimetric analyses were recorded on a Stanton Redcroft VO 750 balance in N_2 atmosphere, with heating rates 2–10°/min. Carbon, hydrogen, nitrogen and halogen analyses were performed by the microanalytical laboratory at University College, Cardiff.

All chemicals (mainly from B.D.H.) were either of reagent grade or of analytical grade purity, and were used without further purification, except N-heterocyclic solvents which were dried over CaH_2, and distilled. "Rhodium trichloride-n-hydrate" was obtained from Johnson Matthey Chemicals Limited.

Preparation of $K_3[Rh(ox)_3]4.5H_2O$. This compound was prepared according to the method[8] of

* Present address: Department of Chemistry, University College of Bahrain, P.O. Box 1082, State of Bahrain.

† Author to whom correspondence should be addressed.

‡ School of Natural Resources, The University of the South Pacific, Laucala Bay, Suva, Fiji.

§ Throughout this paper, the ethane-di-oic acid is called oxalic acid and the second conjugate base is called oxalate rather than the more familiar ethane-di-oate. This paper is based in part on the doctoral thesis of A. Y. Ali Mohamed (Univ. of Wales, 1982) where detailed spectra and the like are to be found.

Werner and Poupardin. A mixture of $RhCl_3 \cdot nH_2O$ (0.997 g), $K_2C_2O_4 \cdot H_2O$ (2.175 g) and water (27 cm^3), was heated on a steam bath for 3 hr. Ethanol was added to the deep red solution, and an oily material formed. On heating, the red oil changed to a yellow solid, which on further heating dissolved. The solution was concentrated by evaporation until yellow crystals began to form. On the addition of ethanol and cooling, a mass of yellow crystals separated. These were collected, washed with ethanol, air dried, and kept over silica gel (yield 3.0 g).

Reaction of $K_3[Rh(ox)_3]4.5H_2O$ *with pyridine.* A mixture of $K_3[Rh(ox)_3]4.5H_2O$ (0.13 g), water (6 cm^3) and pyridine (4 cm^3), was heated under reflux for 18 hr. The colour of the solution changed from orange to lemon yellow. Potassium oxalate was precipitated by the addition of an excess of ethanol, and the solution was concentrated to give yellow crystals of *trans*-$K[Rh(ox)_2py_2]1.5H_2O$ (0.079 g) which were recrystallised from hot water. Analysis for *trans*-$K[Rh(ox)_2py_2]1.5H_2O$ ($C_{14}H_{13}N_2O_{9.5}KRh$): Found: C, 33.58; H, 2.43; N, 4.95; Calc.: C, 33.41; H, 2.6; N, 5.56%.

Reaction of $K_3[Rh(ox)_3]4.5H_2O$ *with aqueous 4-methyl or 3-methyl pyridine.* A mixture of $K_3[Rh(ox)_3]4.5H_2O$ (165 mg), water (8 cm^3) and of either 4- or 3-methyl pyridine was refluxed for 26 hr. The colour of the refluxed mixture changed from yellow orange to yellow. A charge test on Sephadex resin [C25 and A25 columns] showed the product to be anionic. The final refluxed mixture was evaporated to dryness on a steam bath, then dissolved in a small volume of water: ethanol was added to this solution, when $K_2C_2O_4$ separated. This was removed by filtration and the filtrate taken to dryness. The residue was extracted with hot water: the extract, cooled at room temperature, gave fine pale yellow crystals of *trans*-$K[Rh(ox)_2(4\text{-}Mepy)_2]3H_2O$ (yield 65 mg, 39%), or pale creamy yellow fine crystals of $K[Rh(ox)_2(3\text{-}Mepy)_2]3H_2O$ (yield 70 mg, 42%). Analysis for *trans*-$K[Rh(ox)_2(Mepy)_2]3H_2O$ ($C_{16}H_{20}N_2O_{11}KRh$): Found: C, 35.49; H, 3.15; N, 5.5 (for 4-Mepy complex): C, 34.31; H, 3.02; N, 5.89 (for 3-Mepy complex): Calc.: C, 34.4; H, 3.58; N, 5.1%.

RESULTS AND DISCUSSION

Reaction of $[Rh(ox)_3]^{3-}$ *with pyridine.* When a solution of $K_3[Rh(ox)_3]$ in aqueous pyridine was heated under reflux, the colour of the solution changed from orange to lemon-yellow over a period of approximately 18 hr. Monitoring the reaction via the electronic spectrum showed a change in the wavelength of absorption due to the *d–d* transition from 400 to 348 nm. The product was shown to be anionic using ion exchange columns (Sephadex C25 gave no retention but A25 gave strong retention). The new complex ion was isolated as yellow crystals of its potassium salt from warm water and was characterised as $K[Rh(ox)_2py_2]1.5H_2O$.

A solution of $[Rh(ox)_2py_2]^-$ in aqueous pyridine (even with H_3PO_2 (5%) as catalyst) was unchanged after heating under reflux for 8 days. Possible reaction was monitored via the electronic spectrum. Samples were also periodically removed from the reaction mixtures and passed through short columns of Sephadex C25 and A25 resins: anionic starting material remains anionic (*trans*-$[Rh(ox)_2py_2]^-$).

Successive recrystallisation of $K[Rh(ox)_2py_2]$ from aqueous ethanolic solution gave three crops with constant electronic and infrared spectra suggesting the presence of one isomer only. The stereochemistry is established using the ^{13}C NMR spectrum, which shows only one resonance with chemical shift similar to that for $[Rh(ox)_3]^{3-}$ due to the oxalate groups as expected for *trans*-stereochemistry. If the complex were the *cis*-isomer, two resonances are expected from the oxalate C_2 groups. Two such resonances are indeed seen in the case of *cis*-$K[Co(ox)_2py_2]H_2O$.

The preparation of $[Co(ox)_2py_2]^-$ uses mild conditions: the filtrate after isolation of *trans*-isomer was poured on a column of Dowex 50W-X8 resin in the Li form. Then upon concentrating the eluate at low temperature the *cis*-isomer was obtained.

In the early thirties, it was shown that $K_3[Cr(ox)_3]$ precipitates glycine from solution in dilute alcohol. Then, in 1938, Bergman[9] found that $K[Cr(ox)_2py_2]$ forms sparingly soluble salts with some amino acids; the so-called "dioxypyridates".[9] Formation of the insoluble "dioxypyridate" of alanine was used as a means of estimating alanine in protein hydrolysates. A *cis*- and a *trans*-form of "dioxypyridic acid" may be expected. The *cis*-form should exist in two antipodes and therefore yield two series of diastereoisomeric salts with an optically active amino acid. Bergman[9] did not observe the two series of amino acid "dioxypyridates". Our attempt to use this method, for DL-alanine 0.01 M and 0.01 M $[Rh(ox)_2py_2]^-$, gave no precipitation of the *trans*-$[Rh(ox)_2py_2]^-$ ion as its alanine salt.

Reaction of $[Rh(ox)_3]^{3-}$ *with substituted pyridines.* Here, using 3- or 4-methylpyridine in place of pyridine, the reaction conditions were the same as for the parent *trans*-$K[Rh(ox)_2py_2]$. The solutions were evaporated to dryness and the products recrystallised from lukewarm water to give yellow fine solids, characterised as $K[Rh(ox)_2(4\text{-}Mepy)_2]3H_2O$ and $K[Rh(ox)_2(3\text{-}Me\text{-}py)_2]3H_2O$.

Solutions of $K[Rh(ox)_2(4\text{-}Mepy)_2]3H_2O$ and

Table 1. ^1H NMR assignment of the chemical shift (ppm) in the complexes *trans*-$K[Rh(ox)_2(R\text{-}py)_2]$ (R-py = pyridine, 2-methylpyridine, 3-methylpyridine and 4-methylpyridine)

Complexes	Solvent	Pyridines					Reference
		α		β		γ	
trans-$K[Rh(ox)_2py_2]1.5H_2O$	D_2O	8.82–8.72		7.88–7.72		8.28–8.1	this work
trans-$K[Rh(ox)_2(4\text{-}Mepy)_2]3H_2O$	D_2O	8.58–8.49		7.59–7.51		2.45	this work
				(β)	(β′)		
trans-$K[Rh(ox)_2(3\text{-}Mepy)_2]3H_2O$	D_2O	8.45–8.3		2.4	7.68–7.5	8.0–7.9	this work
		(α′)	(α)	(β′)		(β, γ)	
trans-$K[Rh(ox)_2(OH)(2\text{-}Mepy)]$	D_2O	8.65–8.55	2.9–2.7	7.85–7.79		7.42–7.35	this work
cis-$K[Co(ox)_2py_2]2H_2O$	D_2O	8.58–8.50		7.9–7.72		8.45–8.28	this work
		8.4–8.2		7.7–7.4		8.2–7.9	10
trans-$K[Co(ox)_2py_2]3H_2O$	D_2O	8.92–8.82		7.9–7.7		8.3–8.12	this work
		8.9–8.7		8.0–7.6		8.2–8.0	10
Free bases							
Pyridine	CCl_4	8.51		7.14		7.55	14
4-Methylpyridine	CCl_4	8.37		6.99		2.29	14
		(α)		(β)	(β′)		
3-Methylpyridine	CCl_4	8.35		2.27	7.01	7.35	14
					(β′)	(β, γ)	
2-Methylpyridine	CCl_4	(α′)	2.47		6.91	6.91	14
		8.37					

Table 2. ^{13}C NMR assignment of the chemical shift (ppm) in the complexes $K_3[Rh(ox)_3]$ and *trans*-$K[Rh(ox)_2(R\text{-}py)_2]$ (R-py = pyridine, 3-methylpyridine and 4-methylpyridine)

Complexes	Solvent	Oxalato resonance		Pyridine resonance				CH_3	Reference
		(1)	(2)	α		β	γ	substituent	
$K_3[Rh(ox)_3]4.5H_2O$	D_2O	174.292	—	—		—	—	—	this work
cis-$K[Co(ox)_2py_2]2H_2O$	D_2O	171.4	171.8	156		129.25	143.8	—	this work
trans-$K[Rh(ox)_2py_2]1.5H_2O$	D_2O	171	—	155		129.9	143.8	—	this work
				(α)	(α')	(β')			
trans-$K[Rh(ox)_2(3\text{-}Mepy)_2]3H_2O$	D_2O	169.5	—	153.5	151.375	127.375	142.375	139.0	this work
trans-$K[Rh(ox)_2(4\text{-}Mepy)_2]3H_2O$	D_2O	169.0	—	154.5		129	—	151.5	this work
Free bases					δc (ppm)	J (cps)			
Pyridine	CCl_4	—	—	CH-2,6	43.1	180			18
				CH-3,5	69.2	162			
				CH-4	57.3	160			
3-Methylpyridine	CCl_4			CH-2	43.2	178			17b, 18
				C-3	59.9	—			
				CH-4	56.4	156			
				CH-5	69.6	164			
				CH-6	45.9	186			
				3-CH_3	174.8	128			
4-Methylpyridine	CCl_4			CH	43.6	174			17b, 18
				CH-3, 5	67.9	164			
				C-4	46.0	—			
				4-CH_3	172.2	127			

$K[Rh(ox)_2(3\text{-}Mepy)_2]3H_2O$ in aqueous 4-methylpyridine and 3-methylpyridine respectively were heated under reflux for 2 days, but showed no change in spectrum indicating that further addition of 3- or 4-methylpyridine is not possible by this route. Isolation confirmed (by IR and chemical analysis) that the starting material was unchanged.

In the case of 2-methylpyridine, as the reaction proceeded there was a shift during two days in the wavelength of the band of the *d–d* transition from 400 to 362 nm. The product was anionic (retained by Sephadex A25): after removing potassium oxalate by precipitation with ethanol, the product was isolated as a yellow powder, and yellow crystals were obtained by recrystallisation from lukewarm water.

Infrared spectra of the solid product show C=O bands in the region 1700–1665 cm^{-1}, and the bands arising from the complexed 2-methylpyridine show slight shifts from neat 2-methylpyridine and some splitting. Elemental analyses suggest that the product is $K[Rh(ox)_2(OH)(2\text{-}Mepy)]$ although the proton resonance shows two methyl signals. This difference in product (2-methylpyridine ≠ 3- or 4-methylpyridine) probably stems from steric hindrance by the methyl group of the 2-methylpyridine molecule. This case is also reported by Shibata *et al.*[10] for the substitution of oxalate by 2-methylpyridine in $K_3[Co(ox)_3]3H_2O$.

Cis- and *trans*-octahedral bisoxalato–metallate complexes have been distinguished[11a,b] by the presence of four (for *cis*) and three (for *trans*) stretching vibrations of the non-bonded C–O groups occurring near 1700 cm^{-1}. This region is free from absorption by coordinated pyridines, and for the *trans*-compounds (point group D_{2h}), only two IR active non-bonded C–O stretching vibrations of B_{2u} and B_{3u} symmetry are predicted. These stretching vibrations of the non-bonded C–O groups of planar bisoxalato complexes are not affected greatly by coupling (unlike those of octahedral trioxalato complexes). For *cis*-compounds having C_{2v} symmetry, four IR active vibrations are predicted, two of *A* symmetry and two of *B* symmetry.

Pratt[12] reported that PMR spectra may be a tool for the stereochemistry of amine complexes.[12,13] This technique was used by Shibata *et al.*[10] to distinguish between the *cis-* and the *trans*-Co(III) bispyridines. In those, the γ-proton resonates at lower field for the *trans*-isomer, and at slightly higher field for *cis*-isomer. Our work has confirmed that result and applied such techniques to the bispyridinerhodium(III) complexes which are shown in Table 1.

In free pyridine, the α, γ and β protons resonate[14] at 8.51, 7.55, and 7.14 ppm (in CCl_4) respectively. The ^1H NMR analyses of the complexes $[Rh(ox)_2(R\text{-}py)_2]^-$ (R-py = py, 3-methylpyridine and 4-methylpyridine) are summarised in Table 1. There is a marked difference in chemical shift for the γ-protons of these complexes compared to the *cis*-isomer of the *cis*-Co(III) bispyridine as a reference. This clearly suggests that the Rh(III)bis-pyridine or bismethylpyridine complexes prepared here have the *trans*-configuration.

This has been confirmed by ^{13}C NMR spectra for bis(3- and 4-methylpyridine)bisoxalates which show only one resonance due to the oxalate group (Table 2). For bis(3-methylpyridine)bisoxalate, the spectral assignment is unambiguous for C-3 since its resonance appears as a single line in off resonance spectra. All other aromatic carbon resonances appear as doublets due to large one bond C^{13}–H spin–spin couplings. Assignments of the doublets to specific carbon atoms are based upon the known assignment in pyridine[15] and substituent effects established for monosubstituted pyridines.[16,17a,b] These doublets will appear as singlets in the ^1H noise decoupled spectra. Thus 5 bands are expected as shown in Table 2. The sixth singlet at 168.666 ppm is assigned to C-1 of the oxalato group.

As for bis(4-methylpyridine)bisoxalate, in the ^1H noise decoupled spectra one would expect 3 singlets, as found, one for C_2 and C_6 at 154.186 ppm, one for C_3 and C_5 at 128.216 ppm, one for C_4 at 150.684 ppm. The fourth singlet at 168.689 ppm is assigned to C_1 of the oxalato group as shown in Table 2.

REFERENCES

1. D. Barton and G. M. Harris, *Inorg. Chem.* 1962, **1**, 251.
2. R. D. Gillard and G. Wilkinson, *J. Chem. Soc.* 1964, 870.
3. M. Delépine, *An. Espan. Fis. Quim.* 1929, **27**, 485, a reference cited in G. B. Kauffman, *Coord. Chem. Rev.* 1976, **21**, 181.
4. (a) *Gmelins Handbuch der Anorganischen Chemie, Iridium*, 8th edn., system No. 67. Verlag Chemie, Weinheim and Berlin (1939); (b) M. Delépine, *Iridium* (edited by P. Pascal), *Nouveau Traité de Chimie Minérale*, Vol. 19, p. 465. Masson, Paris (1958).
5. P. T. Cheng, B. R. Loescher and S. C. Nyburg, *Inorg. Chem.* 1971, **10**, 1275.
6. D. W. Raichart and H. Taube, *Inorg. Chem.* 1978, **11**, 997.
7. D. L. Key, L. F. Larkworthy and J. E. Salmon, *J. Chem. Soc.* (*A*) 1971, 371, who made aniline complexes $[(\phi NH_2)_2(ox)_2Ru]^-$ by the direct reaction; following R. Charonnat, *Ann. Chim.* (*France*), 1931, **16**, 179, who had used the method for pyridine.
8. A. Werner and J. Poupardin, *Chem. Ber.* 1914, **47**, 1955.
9. M. Bergman, *J. Biol. Chem.* 1937, **122**, 569.
10. M. Shibata, Y. Ida and S. Fujinami, *Bull. Chem. Soc. Japan* 1977, **50**, 2665.

11. (a) J. Gouteron, *J. Inorg. Nucl. Chem.* 1976, **38**, 55; (b) J. P. Mathieu, *Compt Rend. Acad. Sci.* 1961, 2232.
12. L. Pratt and P. Clifton, *Proc. Chem. Soc.* 1963, 339.
13. M. Watabe, K. Onuki and S. Yoshikawa, *Bull. Chem. Soc. Japan* 1975, **48**, 687.
14. *The Sadtler Handbook of Proton Magnetic Resonance Spectra* (Edited by W. W. Simmons). Sadtler Heyden, (1978).
15. C. Levy and G. L. Nelson, *Carbon-13 NMR for Organic Chemists.* Wiley–Interscience, New York, London, Sydney and Canada (1972).
16. H. L. Retcofsky and R. D. Friedel, *J. Phys. Chem.* 1967, **71**, 3592.
17. (a) H. L. Retcofsky and R. D. Friedel, *J. Phys. Chem.* 1968, **72**, 290; (b) H. L. Retcofsky and R. D. Friedel, *J. Phys. Chem.* 1968, **72**, 2619.
18. P. C. Lauterbur, *J. Chem. Phys.* 1965, **43**, 360.

Polyhedron Vol. 4, No. 7, pp. 1245–1251, 1985
Printed in Great Britain

0277–5387/85 $3.00 + .00
Pergamon Press Ltd

NMR INVESTIGATION OF BIS(2,3-ALKANEDIONE DIOXIMATO)-BIS(PYRIDINE)COBALT(III) IODIDE COMPLEXES: ^1H AND ^{13}C NMR SPECTRA AND ^{13}C SPIN–LATTICE RELAXATION TIME MEASUREMENTS

SETSUKO KINOSHITA* and ISAO MASUDA

Department of Chemistry, Faculty of Science, Fukuoka University, Nanakuma, Jonan-ku, Fukuoka 814-01, Japan

(*Received* 8 *June* 1984; *accepted after revision* 29 *November* 1984)

Abstract—The complexes of *trans*-[Co(III)(R,CH_3-dioxH)$_2$(py)$_2$]I† (R = CH_3, C_2H_5, *n*-C_3H_7 and *n*-C_4H_9) were investigated in solution by ^1H and ^{13}C NMR spectra and ^{13}C spin–lattice relaxation time measurements. The ^1H- and ^{13}C-resonances of the R = C_2H_5, *n*-C_3H_7 and *n*-C_4H_9 groups were shifted to higher field than those of the free ligands by the complexation; it was attributable to the ring current shielding due to the axial pyridine ligands of the complexes. ^{13}C spin–lattice relaxation times were interpreted as due to movement of the axial pyridine ligands as if they twist around the Co–N (pyridine nitrogen) bond axis and the above R groups were moving segmentally. These segmental movements allowed the R groups to approach closely toward the axial pyridine ring plane to experience the ring current shielding.

In the thermal, pyridine liberation–anation reactions in the crystalline states of the complexes, *trans*-[Co(III)(R,CH_3-dioxH)$_2$(py)$_2$]I† where R is a long chain alkyl group, the reaction rates were found to be described by Taft's equation.[1] This fact suggests that the reaction rates are controlled not only by electronic effects but also by such a steric arrangement of the R groups locating near to the axial pyridine ring plane in the crystals.

In the similar reactions of these complexes in dimethylsulphoxide (DMSO) solution, the alkyl groups were found to play a role in preventing the reactions.[2] It implies that the alkyl groups are still having a tendency to locate near to the axial pyridine ring plane in the complex molecules in solution. If the alkyl groups were located as above, such structural situation might be reflected in the NMR spectra. In the present research, the same complexes were subjected to investigation by ^1H and ^{13}C NMR and ^{13}C relaxation time measurements. For comparison, the complexes of the type [Co(III)(R,CH_3-dioxH)$_2$(py)I] were also investigated.

* Author to whom correspondence should be addressed.

† The following abbreviations are used. R,CH_3-dioxH$_2$: CH_3–C(=NOH)–C(=NOH)–R (R = CH_3, C_2H_5, *n*-C_3H_7, and *n*-C_4H_9), py: pyridine.

EXPERIMENTAL

Materials

The 2,3-alkanedione dioxime ligands with the general formula, R,CH_3-dioxH$_2$, and their complexes of the two types of the general formulas, [Co(R,CH_3-dioxH)$_2$(py)I] and [Co(R,CH_3-dioxH)$_2$(py)$_2$]I, were prepared as described previously.[1,3]

Measurements

The ^1H NMR, ^{13}C NMR, and $T_1(^{13}C)$ measurements were carried out by use of a JEOL FX-200 spectrometer at 200 MHz for ^1H and at 50 MHz for ^{13}C. The assignments for the ^{13}C resonances were carried out by applying a selective proton decoupling method.[4] Each of the sample solutions was almost saturated with the respective complexes.

RESULTS

^1H NMR spectra

The ^1H NMR spectra of the free ligands and their complexes in DMSO-d_6 solutions are shown in Figs.

1 and 2; the numerical data are tabulated in Table 1. As is seen in Fig. 1, the free CH_3,CH_3-dioxH$_2$ ligand showed two singlet resonances at δ1.97 and 11.37 ppm; these were ascribed to the $C^1H_3(C^4H_3)$ and NOH groups, respectively. The resonances due to the α, β, and γ protons of the free pyridine appeared at *ca* 8.6, 7.4, and 7.8 ppm, respectively. On complex formation, the above $C^1H_3(C^4H_3)$ proton resonance shifted to lower field and appeared at 2.31 ppm for the [Co(CH_3,CH_3-dioxH)$_2$(py)I] and 2.32 ppm for the [Co(CH_3,CH_3-dioxH)$_2$(py)$_2$]I complexes. The proton resonances due to the NOH groups appeared at 18.48 ppm in the former and at 18.18 ppm in the latter, being shifted remarkably to lower field by complexation. In respect of the pyridine, the coordination resulted in lower-field shifts of the β- and γ-proton resonances, but a higher-field shift of the α-proton resonance.

The free C_2H_5,CH_3-dioxH$_2$ ligand showed a singlet resonance at 1.99 ppm, a quartet at 2.61 ppm, and a triplet at 1.03 ppm, as is seen in Fig. 2A; these can be ascribed to the C^1H_3, C^4H_2, and C^5H_3 protons, respectively. By complexing, the C^1H_3 and C^4H_2 proton resonances were shifted to lower field,

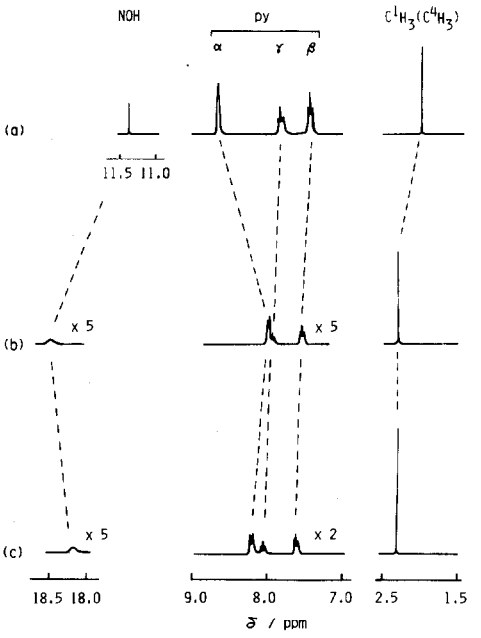


Fig. 1. ^{1}H NMR spectra. (a) CH_3,CH_3-dioxH$_2$ and py; (b) [Co(CH_3,CH_3-dioxH)$_2$(py)I]; (c) [Co(CH_3,CH_3-dioxH)$_2$(py)$_2$]I.

Table 1. ^{1}H NMR data for free R,CH_3-dioxH$_2$ ligands and for their complexes, in DMSO-d_6 solutions

Compound	δ (ppm)					
	$C^1H_3(C^4H_3)$[a]					NOH
CH_3,CH_3-dioxH$_2$	1.97					11.37
[Co(CH_3,CH_3-dioxH)$_2$(py)I]	2.31					18.48
[Co(CH_3,CH_3-dioxH)$_2$(py)$_2$]I	2.32					18.18
	C^1H_3	C^4H_2	C^5H_3			NOH
C_2H_5,CH_3-dioxH$_2$	1.99	2.61	1.03			11.15, 11.22
[Co(C_2H_5,CH_3-dioxH)$_2$(py)I]	2.31	2.76	0.90, 0.91			18.47
[Co(C_2H_5,CH_3-dioxH)$_2$(py)$_2$]I	2.32	2.75	0.80, 0.82			18.20
	C^1H_3	C^4H_2	C^5H_2	C^6H_3		NOH
C_3H_7,CH_3-dioxH$_2$	1.99	2.58	1.50	0.91		11.17, 11.25
[Co(C_3H_7,CH_3-dioxH)$_2$(py)I]	2.31	2.76	1.43	0.71		18.49
[Co(C_3H_7,CH_3-dioxH)$_2$(py)$_2$]I[b]	2.34	2.77	1.34	0.51		18.19
[Co(C_3H_7,CH_3-dioxH)$_2$(NH_3)$_2$]I	2.30	2.71	1.57	0.97		18.26
	C^1H_3	C^4H_2	C^5H_2	C^6H_2	C^7H_3	NOH
C_4H_9,CH_3-dioxH$_2$	1.98	2.60	1.45	1.33	0.89	11.16, 11.24
[Co(C_4H_9,CH_3-dioxH)$_2$(py)I]	2.31	2.78	1.37	1.08	0.76	18.48
[Co(C_4H_9,CH_3-dioxH)$_2$(py)$_2$]I[c]	2.33	2.79	1.27	0.85	0.66	18.18

[a] Each carbon atom of ligands is noted as in following example; C^1H_3–C^2(=NOH)–C^3(=NOH)–C^4H_2–C^5H_2–C^6H_2–C^7H_3.

[b] 2 hydrate.

[c] 4 hydrate.

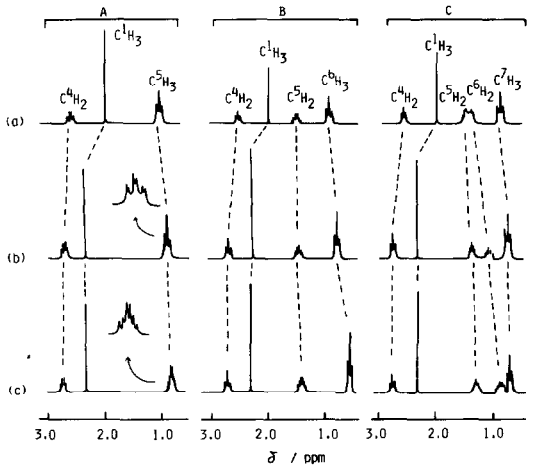


Fig. 2. ^{1}H NMR spectra. A: (a) C_2H_5,CH_3-dioxH$_2$; (b) [Co(C_2H_5,CH_3-dioxH)$_2$(py)I]; (c) [Co(C_2H_5,CH_3-dioxH)$_2$(py)$_2$]I. B: (a) n-C_3H_7,CH_3-dioxH$_2$; (b) [Co(n-C_3H_7,CH_3-dioxH)$_2$(py)I]; (c) [Co(n-C_3H_7,CH_3-dioxH)$_2$(py)$_2$]I. C: (a) n-C_4H_9,CH_3-dioxH$_2$; (b) [Co(n-C_4H_9,CH_3-dioxH)$_2$(py)I]; (c) [Co(n-C_4H_9,CH_3-dioxH)$_2$(py)$_2$]I.

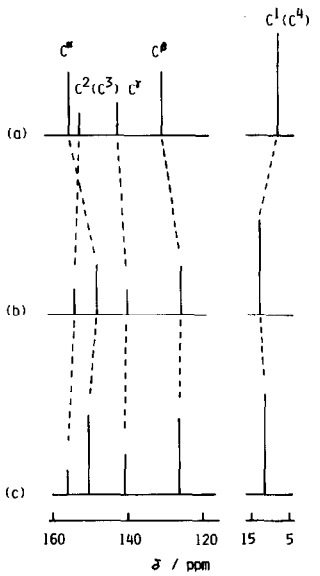


Fig. 3. ^{13}C NMR spectra. (a) CH_3,CH_3-dioxH$_2$ and py; (b) [Co(CH_3,CH_3-dioxH)$_2$(py)I]; (c) [Co(CH_3,CH_3-dioxH)$_2$(py)$_2$]I.

whereas the C^5H_3 proton resonance shifted to higher field. It was found that the resonance due to the C^5H_3 protons for either mono- or bis-pyridine type complex consisted of two triplet peaks; this suggested that each of these complexes included two geometrical isomers.

For the complexes included R = n-C_3H_7 and n-C_4H_9, similar shifts of the alkyl proton resonances caused by complexing were observed, as is shown in Figs. 2B and C.

As for the other complexes excluding those with R = C_2H_5, the existence of their isomeric forms was not suggested by the spectra.

The resonance peaks for the NOH groups of the complexes appeared at nearly same positions with each other among the present series of the complexes. It was similarly said with regard to the position of the resonances of the coordinated pyridines.

^{13}C *NMR spectra*

In Fig. 3, the ^{13}C NMR spectra of the free CH_3,CH_3-dioxH$_2$ and pyridine ligands measured in DMSO-d_6 solution are compared with those of the [Co(CH_3,CH_3-dioxH)$_2$(py)I] and [Co(CH_3,CH_3-dioxH)$_2$(py)$_2$]I complexes. With respect to free CH_3,CH_3-dioxH$_2$, the peaks at δ9.2 and 153.1 ppm could be ascribed to the $C^1(C^4)$ and $C^2(C^3)$ atoms, respectively. The free pyridine showed the peaks at 156.1, 130.3, and 142.5 ppm; these were assigned to the C^α, C^β, and C^γ atoms, respectively. Upon complexing, the $C^1(C^4)$ and $C^2(C^3)$ peaks shifted to lower field, while the C^α, C^β, and C^γ resonances shifted to higher field.

The resonance peaks of the free C_2H_5,CH_3-dioxH$_2$ ligand, shown in Fig. 4A, were assigned as follows; 9.2 ppm to C^1, 152.0 ppm to C^2, 157.7 ppm to C^3, 16.5 ppm to C^4, and 10.8 ppm to C^5 atoms. By complexing, the C^1, C^2, C^3, and C^4 resonances were shifted to lower field, while the C^5 peak was shifted to higher field. The splitting of the C^2 and C^3 peaks seen for its bis-pyridine type [Co(C_2H_5,CH_3-dioxH)$_2$(py)$_2$]I complex would be due to the presence of geometric isomers. This observation is in agreement with that on the ^{1}H NMR spectrum, mentioned already. Although, in the case of the mono-pyridine type [Co(C_2H_5,CH_3-dioxH)$_2$(py)I] complex, similar splitting of the peak for the corresponding carbon atoms was not seen; it differed from the ^{1}H NMR results.

The results of the peak assignments for the free n-C_3H_7,CH_3-dioxH$_2$ ligand are given in Fig. 4B. When it formed the complexes, the C^1, C^2, C^3, and C^4 peaks shifted to lower field, whereas the C^5 and C^6 peaks shifted to higher field. For its mono-pyridine type [Co(n-C_3H_7,CH_3-dioxH)$_2$(py)I] complex, the peak due to the C^6 atom appeared at lower field than that due to the C^1 atom; this trend was in line with the observation for the free ligand. On the other hand, the bis-pyridine type [Co(n-C_3H_7,CH_3-dioxH)$_2$(py)$_2$]I complex, the C^6 atom resonated at the higher field than the C^1 atom.

The resonances observed for the free n-C_4H_9,CH_3-dioxH$_2$ ligand and its complexes were

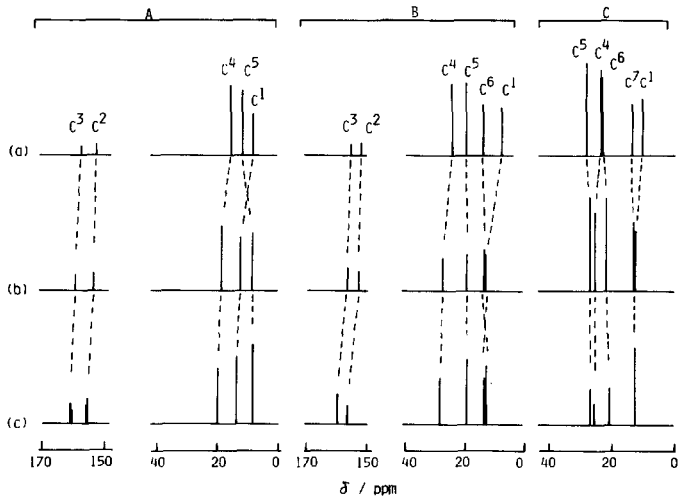


Fig. 4. ^{13}C NMR spectra. A: (a) C_2H_5,CH_3-dioxH$_2$; (b) [Co(C_2H_5,CH_3-dioxH)$_2$(py)I]; (c) [Co(C_2H_5,CH_3-dioxH)$_2$(py)$_2$]I. B: (a) n-C_3H_7,CH_3-dioxH$_2$; (b) [Co(n-C_3H_7,CH_3-dioxH)$_2$(py)I]; (c) [Co(n-C_3H_7,CH_3-dioxH)$_2$(py)$_2$]I. C: (a) n-C_4H_9,CH_3-dioxH$_2$; (b) [Co(n-C_4H_9,CH_3-dioxH)$_2$(py)I]; (c) [Co(n-C_4H_9,CH_3-dioxH)$_2$(py)$_2$]I.

assigned as given in Fig. 4C. The C^1 and C^7 resonances for the bis-pyridine type [Co(n-C_4H_9,CH_3-dioxH)$_2$(py)$_2$]I complex, appeared as one peak, due to overlapping.

T_1 *measurements*

The T_1 measurements were carried out by applying the inversion recovery method[4] for the series of the bis-pyridine type [Co(R,CH_3-dioxH)$_2$(py)$_2$]I complexes, in DMSO-d_6 solution with the concentration of *ca* 5×10^{-2} mol dm^{-3}.* In Fig. 5, the result obtained for [Co(CH_3,CH_3-dioxH)$_2$(py)$_2$]I is given as an example. As is seen in Fig. 5, when the pulse interval, τ, was 0.05 sec, all the peaks were inverted. The time needed for recovery increased in the order of the carbon atoms, $C^\gamma < C^\alpha \simeq C^\beta < C^1(C^4)$. The T_1 value can be obtained as the reciprocal slope of straight line of log $(I_\infty - I_\tau)$ vs τ plot; I_∞ is the equilibrium intensity of a resonance peak, and I_τ, the peak intensities at each τ values. The above plots for all the ^{13}C resonance peaks of the complexes gave good linear relations. As to the [Co(C_2H_5,CH_3-dioxH)$_2$(py)$_2$]I complex which was considered to be composed of two geometric isomers, similar linear relations were observed; this indicated that the isomers have quite similar T_1 values. The T_1 data thus obtained are listed in Table 2. As for free pyridine (*ca* 10% in DMSO-d_6 solution), the T_1 values decreased in the order of its carbon atoms, $C^\beta > C^\alpha > C^\gamma$; as for the coordinated one, these decreased in the order, $C^\beta \simeq C^\alpha > C^\gamma$. Concerning the carbon atoms in the long-chain alkyl groups bound to the dioximato moiety, it was found that the T_1 values increased in the order, $C^4 < C^5 < C^6$. The C^1 atom of the methyl group had rather larger T_1 value than the C^4 atom of the methylene group. The T_1 values of the C^1 and C^7 atoms in the [Co(n-C_4H_9,CH_3-dioxH)$_2$(py)$_2$]I complex were not determined owing to the overlapping of the resonances of these atoms.

In order to investigate temperature dependence of the T_1 values, the [Co(n-C_3H_7,CH_3-dioxH)$_2$(py)$_2$]I complex in CD_2Cl_2 solution was subjected to the measurements at lower temperature. As Fig. 6 shows, with decreasing temperatures, the difference in the T_1 values between C^β ($\simeq C^\alpha$) and C^γ atoms of the pyridine ligand became smaller. However, a small difference was still observed to be present even at -78°C. With regard to the long-chain alkyl groups,

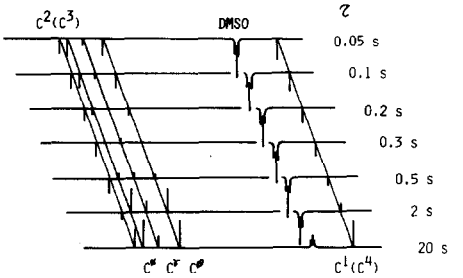


Fig. 5. Relaxation times, T_1, measurements for ^{13}C atoms of [Co(CH_3,CH_3-dioxH)$_2$(py)$_2$]I, in DMSO-d_6 solution.

*For the mono-pyridine type complexes, the T_1 measurements were unsuccessful owing to their scarce solubilities.

Table 2. Relaxation times of ^{13}C atoms for $[Co(R,CH_3\text{-dioxH})_2(py)_2]I$ complexes

Complexes: R	T_1 (s) py C^α	py C^β	py C^γ	R,CH_3-dioxH C^1	C^4	C^5	C^6	C^7
CH_3	0.58	0.64	0.50	1.84	1.84	—	—	—
C_2H_5	0.52	0.52	0.40	1.73	0.36	1.05	—	—
n-C_3H_7	0.39	0.41	0.31	1.33	0.29	0.50	1.49	—
n-C_4H_9	0.34	0.39	0.29	×	0.22	0.48	0.65	×
(free py)	(8.77	9.75	7.60)					

it could be said that the T_1 value of the C^4 atom did not depend so much on temperature, while those of the C^5 and C^6 atoms depended remarkably on it, as shown in Fig. 7. The T_1 value of the C^1 atom also decreased with decreasing temperature.

It may be stated overall that the T_1 values determined in the CD_2Cl_2 solution were appreciably larger than those in the DMSO-d_6 solution.

DISCUSSION

^1H and ^{13}C NMR spectra

Excluding the complexes with $R = C_2H_5$, the complexes examined here showed the ^1H and ^{13}C NMR spectra which were well explained by proposing the structure of the complexes in which the R,CH_3-dioxH ligands are bidentately and planarly coordinated in the manner of *trans* forming two equivalent intramolecular hydrogen bonds;[5] one pyridine molecule and iodide anion of the mono-pyridine type complexes or two pyridine molecules of the bis-pyridine type complexes are coordinated at the axial sites.

As to both types of complex including $R = C_2H_5$, the existence of the two isomeric structures was suggested by the NMR spectra. The ^1H resonance of the C^5H_3 group consisted of two triplet peaks. It can be understood by considering the presence of the two geometric isomers, which may be formed by the *cis*- and *trans*-coordinations of the two C_2H_5,CH_3-dioxH ligands at the equatorial plane. With respect to the C^2 and C^3 atoms, their ^{13}C resonances appeared, respectively, as two peaks for the bis-pyridine type complex, whereas, as one peak for the mono-pyridine type complex due to their incidental overlap.

The lower-field shifts for the ^1H resonances of the C^1H_3 and C^4H_2 groups and for the ^{13}C resonances of the C^1, C^2, C^3, and C^4 atoms caused by the complexation, are considered to be due to the Co(III) atoms which, in general, behave to decrease the electron densities on these proton and carbon atoms.[6] On the other hand, as to the higher field shifts observed for both ^1H and ^{13}C resonances of the C^5, C^6, or C^7 group, it can be attributed to the ring

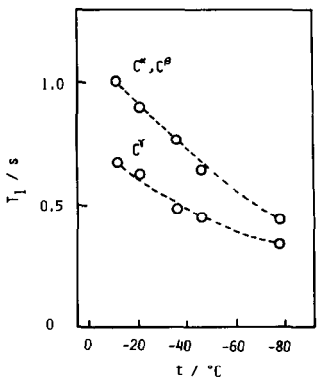


Fig. 6. Temperature dependence of T_1 values for the carbon atoms of the pyridine ligand of $[Co(n\text{-}C_3H_7,CH_3\text{-dioxH})_2(py)_2]I$, in CD_2Cl_2 solution.

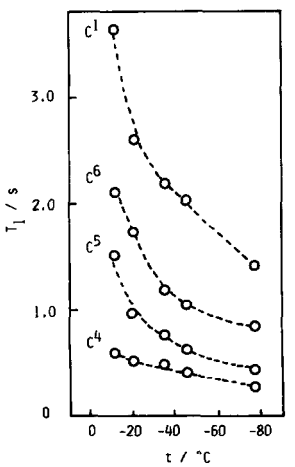


Fig. 7. Temperature dependence of T_1 values of the carbon atoms in the coordinated n-C_3H_7,CH_3-dioxH of $[Co(n\text{-}C_3H_7,CH_3\text{-dioxH})_2(py)_2]I$, in CD_2Cl_2 solution.

current shielding of the axial pyridine ligand.[6] The higher field shifts of the ^1H and ^{13}C resonances were not seen for the C^5 and C^6 groups of the [Co(*n*-C_3H_7,CH_3-dioxH)$_2$(NH_3)$_2$]I complex, in which the shielding due to the axial ammonia ligands could not be expected. Moreover, it is noticed, in Fig. 2, that the amount of the shifts caused by the above ring current effect is larger in the bis-pyridine type complexes than in the corresponding mono-pyridine type ones.

The lower-field shifts for the H^β and H^γ resonances of the pyridine molecules caused by the coordination may be owing to the predominant electron-withdrawing property of the Co(III) atoms, while the higher-field shift for the H^α resonance may be due to the predominant anisotropic effect of the metal chelate rings.[7]

^{13}C *spin–lattice relaxation times,* T_1

It is considered that in such large molecules as those investigated here, the dipole–dipole relaxation is dominant.[8] This assumption was confirmed by measuring the NOE factor (η). The values were found to be within the 2.0 ± 0.1 range for all the carbons of the complexes, indicating the dipole–dipole relaxation mechanism being dominant. Due to probable anisotropical movements, the correlation time could not be calculated. However, molecular movements may be qualitatively discussed on the basis of the T_1 values.

As has been described, the T_1 values for the free pyridine molecule are $C^\beta > C^\alpha > C^\gamma$ (Table 2). This fact is considered to suggest the rotation of the free pyridine molecule taking place a little more preferably around C^γ–N axis than around the other axes. Analogous anisotropic molecular rotation has been known to occur for the several benzene derivatives with the formula C_6H_5X (X = CH_3, NO_2, etc.).[9] Regarding the coordinating pyridine ligands, the T_1 values are also $C^\beta > C^\gamma$, over the four complexes examined. It is of interest that the ratios $T_1(C^\beta)/T_1(C^\gamma)$ are *ca* 1.3 for all of these complexes, being quite similar to the corresponding ratio, 1.3, for the free pyridine molecule. This fact can be explained as follows. If the pyridine ligands were fixed at the axial sites in the complex molecules in such a manner as its ring plane was held at a definite position, the above ratio could be expected to be closer to 1.0. On the other hand, if the puridine ligands were allowed to rotate around the C^γ–N axis, the above ratio could be expected to be much larger than that (1.3) of the free pyridine molecule, since the rotations around the other axes would be inhibited by the coordination. Thus, the fact that the $T_1(C^\beta)/T_1(C^\gamma)$ ratios of the complexes are quite similar to that of the free pyridine molecule is considered to indicate that the pyridine ligand moves as if it twists around the C^γ–N axis.

Regarding the alkyl groups of the complexes, their T_1 values increased in the order of the carbon atoms $C^4 < C^5 < C^6$; this is in line with a prediction that the segmental movement of the R groups would become more brisk along the extended carbon-chains. The similar trend in the movement has been pointed out for the carbon atoms of the *n*-decane or 1-decanol.[10]

As Table 2 indicates, the T_1 value of the C^1 atom in the methyl group is larger than that of the C^4 atom in the methylene group, suggesting more brisk movement in the former than in the latter. In such compound as iso-octane, the CH_3 groups are sterically hindered to rotate within the molecule, and therefore their T_1 values are smaller than that of the CH_2 group.[11]

The T_1 values measured at the lower temperatures for [Co(*n*-C_3H_7,CH_3-dioxH)$_2$(py)$_2$]I in CD_2Cl_2 solution indicate that the coordinated pyridine ligands are still twisting around the C^γ–N axis even at -78°C, though the ratio $T_1(C^\beta)/T_1(C^\gamma)$ decreases from 1.5 at -12°C to 1.3 at -78°C (Fig. 6). The T_1 values of the C^4, C^5, and C^6 atoms become smaller as the temperature decreases (Fig. 7). This is in accordance with an expectation that the segmental movement becomes more stagnant at lower temperature. However, it should be noticed that the changes in the above T_1 values are rather continuous. Hence, the presence of a bonding interaction between the axial pyridine ligand and the prolonged alkyl groups of the complex molecules in the solution has not been substantiated here.[12] With respect to the C^1H_3 group, it is also suggested that the internal rotation becomes more stagnant with the decreasing temperatures.

The larger T_1 values observed in CD_2Cl_2 than in DMSO-d_6 solutions would be ascribed to the smaller viscosity of CH_2Cl_2 than DMSO; the viscosity at 30°C is 0.4 cp for the former and 1.7 cp for the latter.

It is said in conclusion that in the present complexes the axial pyridine ligands are twisting around the Co–N (pyridine nitrogen) bond axis and the long alkyl(R) groups do segmental motions; as the result of these segmental movements, the terminal methyl groups of R may experience the shielding effect of the pyridine ring and the amount of the shifts caused by the above effect is much larger in the bis-pyridine type complexes than in the corresponding mono-pyridine type ones. In the case of the complex including R = *n*-C_3H_7, the chain length is most advantageous for the terminal methyl group to experience the largest shielding effect.

REFERENCES

1. S. Kinoshita, H. Wakita and I. Masuda, *Bull. Chem. Soc. Jpn* 1984, **57**, 1818.
2. S. Kinoshita and I. Masuda, *Bull. Chem. Soc. Jpn* (to be submitted).
3. M. I, H. Wakita and I. Masuda, *Bull. Chem. Soc. Jpn* 1983, **56**, 1627.
4. K. Müllen and P. S. Pregosin, *Fourier Transform NMR Techniques—A Practical Approach.* Academic Press, London (1976).
5. Y. Yamano, I. Masuda and K. Shinra, *J. Inorg. Nucl. Chem.* 1971, **33**, 521, and references therein.
6. M. Tanaka, R. Ryu, I. Masuda and T. Shono, *Bull. Chem. Soc. Jpn* 1977, **50**, 415.
7. H. A. O. Hill and K. G. Moralee, *J. Chem. Soc., A* 1969, 554.
8. A. Allerhand, D. Doddrell and R. Komoroski, *J. Chem. Phys.* 1971, **55**, 189.
9. G. C. Levy, J. D. Cargioli and F. A. L. Anet, *J. Am. Chem. Soc.* 1973, **95**, 1527.
10. D. Doddrell and A. Allerhand, *J. Am. Chem. Soc.* 1971, **93**, 1588.
11. G. C. Levy and G. L. Nelson, *Carbon-13 NMR for Organic Chemists.* Wiley, New York (1972).
12. H. Okawa, K. Ueda and S. Kida, *Inorg. Chem.* 1982, **21**, 1594. On the basis of the conformational characteristics in the structure, these authors proposed the presence of the bonding interaction between the phenyl group and the methyl group in the Co(III), Cr(III), and Mn(III) complexes of 1-*l*-menthyloxy-3-benzoylacetone. Related articles dealing with intramolecular interaction are quoted therein.

Polyhedron Vol. 4, No. 7, pp. 1253–1257, 1985
Printed in Great Britain

0277–5387/85 $3.00 + .00
© 1985 Pergamon Press Ltd

PREPARATION OF METAL BROMOACETATES FROM OTHER SALTS BY SOLVOLYTIC REACTIONS IN FUSED MONOBROMOACETIC ACID

J. K. PURI,* JASWINDER KAUR and VIJAY SHARMA
Department of Chemistry, Panjab University, Chandigarh 160014, India

and

JACK M. MILLER*
Department of Chemistry, Brock University, St. Catharines,
Ontario, Canada L2S 3A1

(*Received* 23 *July* 1984; *accepted after revision* 29 *November* 1984)

Abstract—Solvolytic reactions between monobromoacetic acid and metal oxides, carbonates, oxalates, formates, sulphites, nitrates, nitrites and chlorides form monobromoacetates. In the case of transition metals, a molecule of solvent is also attached to the solvolysed products. The solvolysed products have been investigated by IR, magnetic susceptibility and molar conductance measurements. Lewis bases form adducts with these products. The solvolytic reactions have been explained on the bases of autoionization of monobromoacetic acid reported earlier[1] as,

$$2CH_2BrCOOH \rightleftharpoons CH_2BrCOOH_2^+ + CH_2BrCOO^-.$$

A few bromoacetates of transition metals are reported in the literature. Melnik and co-workers[2] from EPR studies have shown that copper(II) tribromoacetate is mononuclear while copper(II) monobromoacetate and its adducts with dioxane are binuclear. Physico-chemical properties of vanadyl bromoacetate have been investigated by Walter and co-workers,[3] while studies of bridging monobromocarboxylate complexes of palladium(II) and platinum(II) have also been reported.[4] In the present investigations an effort has been made to explore the solvent potentialities of fused monobromacetic acid with various metal oxides, carbonates, oxalates, formates, sulphites, nitrites, nitrates, chlorides and bromides, at approximately 180°C. In most of the cases insoluble anhydrous monobromoacetates were isolated but in some cases extra molecules of the solvent formed solvates with these acetates.

EXPERIMENTAL

Monobromoacetic acid was purified by the method reported earlier.[5] Metal oxides, oxalates, formates, nitrites, nitrates, sulphites, carbonates were dried over phosphorus pentoxide for 48 h in a vacuum desiccator. Partial solvolysis of some of the compounds could be brought about around 100°C by thoroughly mixing the compounds with monobromoacetic acid. However, in most cases the following procedure was required for complete solvolysis. The anhydrous metal compound (2 g) was added to monobromoacetic acid (10 g) and the reaction mixture was heated under anhydrous conditions for one to seven days, depending upon the reaction. In most cases the solvolysed products have been isolated from solution by the addition of an inert solvent such as petroleum ether or carbon tetrachloride.

Molar conductance values of millimolar solutions have been measured at 25 ± 0.1°C using a precision conductivity bridge (Phillips PR-9500) with a cell having a cell constant = 0.678 ohm^{-1} cm^{-1}. IR spectra were recorded using KBr discs and grating infrared spectrophotometers (Perkin–Elmer, Models 337 and 621). Mulls, Nujol and HCB (hexachlorobutadiene), were prepared in dry box.

Magnetic susceptibility measurements were carried out by using standard Gouy method using a permanent magnet and a sample tube calibrated

* Authors to whom correspondence should be addressed.

Table 1. Analytical results of various monobromoacetates

Compound (X = CH_2BrCOO^-)	Colour	M.pt (°C)	Elemental analysis % Metal	[calc.]	% Halogen	[calc.]	Molar conductance ($ohm^{-1}\ cm^{-2}\ mol^{-1}$)
$MgX_2 \cdot HX$	Pink	159–160	5.31	[5.53]	54.48	[54.59]	12.32
$ZnX_2 \cdot HX$	White	203–4	13.53	[13.61]	50.02	[49.92]	2.24
$CdX_2 \cdot HX$	Grey	—	21.00	[21.32]	45.27	[45.47]	—
$CaX_2 \cdot HX$	White	202	8.77	[8.81]	52.74	[52.70]	9.24
$SrX_2 \cdot HX$	White	>230	17.35	[17.43]	47.80	[47.74]	6.45
AlX_3	White	>260	6.22	[6.12]	54.55	[54.39]	6.04*
FeX_3	Reddish	136–37	11.96	[11.87]	51.42	[51.01]	8.64*
$FeClX_2$	Brown	>230	15.39	[15.31]	43.13 9.65(Cl)	[43.52] [9.66]	11.84
CoX_2	Pinkish violet	>260	17.09	[17.58]	47.91	[47.76]	23.78
$CoX_2 \cdot 2(C_6H_5)_3PO$	Light blue	—	6.28	[6.61]	17.66	[17.95]	38.74
$CoX_2 \cdot 2C_5H_5NO$	Blue	—	11.01	[11.23]	29.96	[30.48]	41.88
NiX_2	Dirty yellow	>260	17.52	[17.54]	47.91	[47.76]	19.40
$NiX_2 \cdot 2C_5H_5NO$	Yellowish green	85–87	11.00	[11.18]	30.04	[30.49]	34.50
$NiX_2 \cdot 2(C_6H_5)_3PO$	Light green	70–72	6.46	[6.59]	17.81	[17.96]	43.62
CuX_2	Blue	245(D)	18.65	[18.71]	47.00	[47.12]	29.02
$CuX_2 \cdot 2C_6H_5NO$	Green	—	11.63	[[11.99]	30.02	[30.21]	39.26
$CuX_2 \cdot 2(C_6H_5)_3PO$	Yellowish brown	134(D)	6.90	[7.09]	17.30	[17.81]	43.94

D = decomposed, molar conductance at 25°C ± 0.1°C in DMF, * = in acetonitrile, [ ] = % required.

with mercury(II) tetrathiocyanato cobalt(II) as standard[6] and the diamagnetic corrections were made by a method as reported earlier.[7]

Analysis of these compounds were done partially by the Guelph Chemical Laboratories Ltd., Guelph, Ontario Canada and partially by the usual methods already reported in literature.[8] Analysis of bromine in the presence of chlorine was done as follows. The bromine was first oxidized to bromate by hypochlorite at a pH range 6–6.5. The excess of hypochlorite was removed by sodium formate and the bromate determined iodometrically.

RESULTS AND DISCUSSION

Zinc and cadmium oxides are insoluble in fused monobromoacetic acid at 50°C. On heating these oxides with fused monobromoacetic acid at nearly 180°C for 20–24 hr compounds of composition $Zn(CH_2BrCOO)_2 \cdot CH_2BrCOOH$ and $Cd(CH_2BrCOO)_2 \cdot CH_2BrCOOH$ are obtained (Table 1). The corresponding acetic acid derivatives are known to have a water molecule attached.[9] This difference may be due to the fact that the present reactions have been carried out at about 180°C and water is lost at this temperature. All attempts to remove the extra solvent molecule from these compounds failed. They are not very sensitive to moisture, and are insoluble in most organic solvents including various aprotic solvents such as nitromethane, acetonitrile, suggesting their possible polymeric nature. Both these compounds are soluble in dimethyl formamide in which the molar conductance values of their millimolar solutions indicate them to be non-ionic in nature (Table 1). The broad absorption band at 3360 cm^{-1} assigned to hydrogen bonded-OH group in pure carboxylic acid[10] becomes quite sharp and shifts to 3380 and 3386 cm^{-1} for the zinc and cadmium complexes respectively, ruling out the possibility of free OH groups in these compounds.[11] This suggests that the OH group of the solvating monobromoacetic acid is not hydrogen bonded but is co-ordinated to the metal atom. No band has been observed around 1720 cm^{-1} showing thus that there is no free carbonyl group present in these complexes. The intense absorption bands at 1520 and 1408 cm^{-1} assigned to asymmetric and symmetric stretching modes of carboxylate group have been shifted to lower frequencies when compared to those found in sodium acetate[12] suggesting that the carboxylate ion

is acting as a bidentate ligand. It is further observed that the asymmetric stretching frequencies of these complexes are split which may be attributed either to a slight difference in the force constants for the chelating and the bridging carboxylate groups or to a solid state lattice interaction. Similar observations have been made by Wilkinson and co-workers[13] in molybdenum (II) carboxylate where the acetate group acts both as bridging and a chelating group. That the central atom is six coordinate and monobromoacetic acid attached to the complex acts as a bridging group is also supported by the degree of separation of symmetric and asymmetric carboxy stretching frequencies. These are not very different from those found in other metal complexes where the acetate group acts as a bridging group. This is unlike those acetate complexes where there is a significant difference between the two frequencies and the acetates are known to act as monodentate ligands.[14] Since both the compounds are insoluble in most of the aprotic solvents it may be reasonable to assume a polymeric structure for these adducts. The spectral bands in the region 440–320 cm^{-1} for the adducts which are absent in pure monobromoacetic acid arise from oxygen–metal vibrations and this assignment has been made on the basis of observations made by Briggis.[15]

The oxides of magnesium, calcium and strontium form bromoacetates of composition $M(CH_2BrCOO)_2 \cdot CH_2BrCOOH$ (Table 1), while in case of barium oxide no compound was isolated. By analogy with the solvated bromoacetates of zinc and cadmium, a similar polymeric structure through solvent bridging may be postulated for these bromoacetates, the central metal atom having octahedral coordination.

The oxides of copper, nickel and cobalt also form bromoacetates, $Cu(CH_2BrCOO)_2$, $Ni(CH_2BrCOO)_2$, and $Co(CH_2BrCOO)_2$ respectively (Table 1), i.e. without the extra monobromoacetic acid. The reaction is accompanied by a change in the colour of the reactants. Like the other complexes reported above, these are non-ionic in nature. No spectral band that could be assigned to –OH group is present in these compounds, indicating that no free monobromoacetic acid is present. The ν(C–O) asymmetric and symmetric vibrations in the region 1400–1600 cm^{-1} are shifted to lower frequencies, suggesting that the metal atom has acquired a tetrahedral environment through the bidentate nature of monobromoacetate group. The bands at 450, 418 and 395 cm^{-1} are due to the metal–oxygen bond.

The nature of these compounds has been further deduced from their magnetic susceptibility measurements. The magnetic moment value of 4.76 B.M. at room temperature, which was observed for the cobalt(II) bromoacetate, is much higher than 3.88 B.M., the spin only value corresponding to three unpaired electrons. The values in the range 4.2–4.8 B.M. are generally observed for the tetrahedral stereochemistry and thus a tetrahedral stereochemistry with $^4A_2$ ground state term may be proposed for Co(II) bromoacetate. The magnetic moment of 4.08 B.M. derived for Ni(II) bromoacetate is in good agreement with the tetrahedral stereochemistry for which the values ranging from 3.5–4.1 B.M. are expected because of the orbital contribution by the $^3T_1$ ground state term.[16] In the case of the Cu(II) bromoacetate a magnetic moment of 1.43 at room temperature is consistent with the dimeric structure for this compound as suggested earlier.[17]

Complexes of pyridine N-oxide and triphenyl phosphine oxide with monobromoacetates of cobalt and nickel have been prepared and characterized. The complexes $Co(CH_2BrCOO)_2 \cdot 2(C_6H_5)_3PO$ and $Ni(CH_2BrCOO)_2 \cdot 2(C_6H_5)_3PO$ are non-ionic and monomeric in nature (Table 1). By combining with two molecules of the ligand the metal atom has acquired an octahedral environment. Among the characteristic non-ligand vibrations in the range 1400–1600 cm^{-1} are the ν asymmetric and symmetric carboxylate vibrations which have been found to shift to higher and lower frequency regions respectively. Since the carboxylate stretching frequency is known to be sensitive to the electronic environment, the observed shifts indicate the electron donation by oxygen of the ligand to the metal atom. This is in agreement with the earlier observations on the infrared spectra of the complexes of some metal carboxylates with some oxygen ligands.[6] The spectral bands observed in the region 375 cm^{-1} (for the nickel complex) and at 395 cm^{-1} (for the cobalt complex) arise from metal–oxygen vibrations. Interest has been focused on the change in the P–O stretching frequency on complex formation. It is interesting to note that there is a decrease in P–O stretching frequency of nearly 39 cm^{-1}. Similar observations have already been reported by Cotton and co-workers.[18] In the case of non-ionic pyridine-N-oxide complexes of composition $Ni(CH_2BrCOO)_2 \cdot 2C_5H_5NO$ and $Co(CH_2BrCOO)_2 \cdot 2C_5H_5NO$, the absorption bands due to N–O stretching vibrations originally present at 1250, 835 and 545 cm^{-1} in the pure ligand[19] are shifted to 1195, 815 and 528 cm^{-1} in these complexes.

The solvolysis of metal oxides (MO) in fused monobromoacetic acid may be explained on the basis of the formation of a solvate which rearranges under the conditions of the reaction to form bromoacetates. The overall reactions thus may be

explained as

$$2CH_2BrCOOH + MO \rightarrow (CH_2BrCOOH)_2MO$$
$$\downarrow$$
$$\leftarrow CH_2BrCOOH_2^+ + CH_2BrCOOMO^-$$
$$M(CH_2BrCOO)_2 + H_2O$$

Formation of metal bromoacetates and the elimination of a water molecule suggests that bromoacetate ion and the protonated monobromoacetic acid ($CH_2BrCOOH_2^+$) are the reactive species in fused monobromoacetic acid and supports the mode of ionization of the solvent as proposed earlier.[1]

Metal chlorides also react in fused monobromoacetic acid to form the corresponding monobromoacetates as

$$MCl_3 + 2CH_2BrCOOH$$
$$\rightleftharpoons MCl_3 \cdot CH_2BrCOO^- + CH_2BrCOOH_2^+$$
$$MCl_3 \cdot CH_2BrCOO^- + CH_2BrCOOH_2^+$$
$$\xrightarrow{180°C} MCl_2 \cdot CH_2BrCOO + CH_2BrCOOH + HCl.$$

Further heating of the intermediate replaces the other chlorine atoms bonded to metal and the final product is the completely solvolysed compound $M(CH_2BrCOO)_3$. Compounds of composition $Al(CH_2BrCOO)_3$, $Fe(CH_2BrCOO)_3$ and $FeCl(CH_2BrCOO)_2$ were isolated using the above methods. These compounds are less hygroscopic than the parent metal chlorides. They are insoluble in conventional non-polar organic solvents but are soluble in polar solvents such as nitromethane, nitrobenzene and acetonitrile. Molar conductance values of their millimolar solutions (Table 1) show them to be fairly ionic in character.

The infrared spectra of this latter group of compounds, especially in the region of asymmetric and symmetric carboxylate group vibrations, are similar to those of transition metal acetates, where the acetate groups are supposed to act as bidentate chelating and bridging group. The intense sharp bands observed in the range 1620–1570 cm^{-1} may be assigned to the bridging groups. Bands at 1520 and 1390 cm^{-1}, though of low intensity, are shifted to lower frequency and the difference in the asymmetric and symmetric stretching modes is also reduced suggesting that there are also bidentate carboxylate groups.

A polymeric structure for these carboxylates cannot be ruled out but the extent of bridging appears small as the compounds are soluble in aprotic solvents. The other important bands in the case of $Al(CH_2BrCOO)_3$ is observed at 490 cm^{-1} which may be attributed to the Al–O stretching mode. No spectral band that could be assigned to aluminium–chlorine stretching mode is present. In the case of the compounds $Fe(CH_2BrCOO)_3$ and $FeCl(CH_2BrCOO)_2$ the asymmetric and the symmetric stretching modes of the carboxylate group (Table 2) indicate that iron must be six coordinate. In the case of $FeCl(CH_2BrCOO)_2$, the iron acquires a coordination number of six through chlorine bridging. The iron–chlorine stretching mode is observed at 435 cm^{-1} which could be assigned to bridging clorine rather than a terminal one, the bridging stretching modes being expected at the lower frequency. Since the monobromoacetate group functions as bidentate chelating group, a possible hexa-coordination structure around iron for both the compounds may be postulated.

Sodium and potassium formates, oxalates, nitrates, sulphites, nitrates and carbonates, etc. undergo rapid solvolysis in fused monobromoacetic acid as one of the products of solvolysis escapes, or decomposes and escapes from the solution. Similarly complete solvolysis of the hydrated nitrates of sodium and potassium has also been carried out.

Table 2. Principal infrared bands of some of the solvolysed products (cm^{-1}) of various metal bromoacetates

Compound	Asymmetric $(COO)^-$	Symmetric $(COO)^-$	M–O	M–Cl	O–H
$MgX_2 \cdot HX$	1590	1430, 1365	445, 412	—	3375
$ZnX_2 \cdot HX$	1520, 1515	1400, 1370	438, 345, 545	—	3380
$CdX_2 \cdot HX$	1510, 1505	1408, 1390	440, 320, 520	—	3386
$CaX_2 \cdot HX$	1580, 1560, 1510	1420, 1365, 1295	400, 370	—	3380
$SrX_2 \cdot HX$	1575	1410, 1370	410, 385	—	3377
AlX_3	1622, 1568, 1527	1400	490	—	—
FeX_3	1620, 1575, 1545	1385	425	—	—
$FeClX_2$	1610, 1570, 1538	1390	418	435	—
CoX_2	1570	1390	418	—	—
NiX_2	1565	1405	390	—	—
CuX_2	1580	1395, 1392, 1372	450, 395, 340	—	—

Carbonates of sodium, calcium, zinc and cadmium undergo complete solvolysis within 8 h when heated with excess of monobromoacetic acid at nearly 180°C. The mechanism of all these reactions can be explained through the loss of HX, where X is NO_2^-, NO_3^-, $HCOO^-$, $C_2O_4^{2-}$, SO_3^{2-}, CO_3^{2-}, etc. In most of the reactions, HX escapes from the solutions at higher temperatures.

It may be concluded that all the reactions discussed are consistent with the existence of CH_2BrCOO^- ions in solution, supporting the auto-ionization of $CH_2BrCOOH$ as

$$2CH_2BrCOOH \rightleftharpoons CH_2BrCOOH_2^+ + CH_2BrCOO^-.$$

Acknowledgements—The authors thank the Natural Science and Engineering Council of Canada for financial support to (J.M.M.) and the Panjab University, Chandigarh, India for grant of leave to J.K.P.

REFERENCES

1. J. K. Puri, Jaswinder Kaur, Vijay Sharma and J. M. Miller, *Polyhedron* 1983, **2**, 1287.
2. R. Uggala and M. Melnik, *Suom Kemii* 1970, **44B**, 6.
3. J. P. Walter, Dartiguenava and Y. Dartiguenava, *J. Inorg. Nucl. Chem.* 1973, **35**, 3207.
4. J. J. Powell and T. Jack, *Inorg. Chem.* 1972, **11**, 1039.
5. A. I. Vogel, *A Textbook of Practical Organic Chemistry*, 3rd edition, p. 429. Longman, Green and Co. Ltd., London (1956).
6. R. C. Paul, P. Singh, A. S. Makhni and S. L. Chadha, *J. Inorg. Nucl. Chem.* 1970, **32**, 3694.
7. B. N. Figgis and J. Lewis, *The Magnetic Properties of Transition Metal Complexes. Progress in Inorganic Chemistry* (Edited by F. A. Cotton), Vol. 6, p. 37. Wiley–Interscience, New York (1964).
8. A. I. Vogel, *A Textbook of Quantitative Inorganic Analysis*, 3rd edition, pp. 266, 389, 479, 390, 635, 572, 472, 377, 468. Longman, Green and Co. Ltd., London (1961).
9. S. A. Johnson, H. R. Hunt and H. M. Newmann, *Inorg. Chem.* 1963, **2**, 960.
10. L. J. Pauling, *Nature of the Chemical Bond*, p. 487. Oxford & IBH Publishing Co., New Delhi (1962).
11. L. J. Bellamy, *The Infrared Spectrum of Complex Molecules*, p. 94. Wiley, New York (1969).
12. K. Ito and H. J. Berstein, *Can. J. Chem.* 1956, **34**, 170.
13. T. A. Stephenson, E. Bannister and C. Wilkinson, *J. Chem. Soc.* 1964, 2538.
14. G. Costa, E. Panbizzi and A. Puzeeddu, *Gazz. Chim., Ital.* 1957, **87**, 885.
15. E. M. Briggis and A. E. Hill, *J. Chem. Soc. (A)* 1969, 1835.
16. J. Lewis and R. Wilkinson, *Modern Coordination Chemistry*, p. 429. Interscience, New York (1960).
17. M. Kondo and M. Kubo, *J. Phys. Chem.* 1958, **62**, 1558.
18. F. A. Cotton, R. D. Barness and E. Bannister, *J. Chem. Soc.* 1960, 2199.
19. R. C. Paul, C. L. Arora, R. S. Dass and K. C. Malhotra, *Ind. J. Chem.* 1971, **9**, 985.

Polyhedron Vol. 4, No. 7, pp. 1259–1261, 1985
Printed in Great Britain

0277–5387/85 $3.00 + .00
© 1985 Pergamon Press Ltd

SOLVENT EXTRACTION OF CALCIUM(II) AND STRONTIUM(II) WITH 1-PHENYL-3-METHYL-4-ACYL-5-PYRAZOLONE

K. SATO, Y. AKAMA* and T. NAKAI
Department of Chemistry, Meisei University, Hodokubo, Hino, Tokyo 191, Japan

(*Received* 17 *October* 1984; *accepted* 29 *November* 1984)

Abstract—The extraction of calcium and strontium from aqueous solution with 1-phenyl-3-methyl-4-acyl-5-pyrazolone (C_n) in MIBK and benzyl alcohol has been studied. In the extraction of Sr with 4-acyl derivatives–MIBK systems, the $pH_{1/2}$ values change with increasing the length of acyl chain in the derivatives. The reagent C_3 is more suitable than the other reagents for the separation of Ca and Sr, using MIBK as solvent.

1 - Phenyl - 3 - methyl - 4 - benzoyl - 5 - pyrazolone (PMBP) is a suitable agent for the extraction of metals due to the great reactively and stability of its complex. Numerous studies[1–3] have been made on metal extraction with PMBP. Recently, we have synthesized systematically the 4-acyl derivatives of 1-phenyl-3-methyl-5-pyrazolone. The extraction of Cu(II)[4] and Mn(II)[5] were studied and the compositions and extraction constants for the complex have been determined. Umetani *et al.*[6] developed a method for the extraction of alkaline earth metals using a mixture of 4-acyl derivatives and trioctylphosphine oxide. However, detailed study of the extraction for the system containing the 4-acyl derivatives of the type $(C_{10}H_9N_2O)(C_nH_{2n+1}CO)$ ($n = 2$–11) has received little attention. In the present paper, the extraction of Ca and Sr with these newly synthesized 4-acyl derivatives into MIBK and benzyl alcohol has been measured at 25°C, and studied the effectiveness of these derivatives in the separation of Ca and Sr.

EXPERIMENTAL

Reagents. The calcium and strontium stock solutions were prepared from calcium carbonate and strontium carbonate respectively. 4-Acyl derivatives were synthesized as previously described and these compounds were purified by several recrystallizing from methanol and the purity (of these reagents) was checked by elemental analysis, and used in MIBK and benzyl alcohol solution. All other reagents were of analytical reagents grade.

Extraction and analytical procedure. All the extraction procedure were carried out in a thermostatted room at 25 ± 1°C. Equal volumes (8 cm^3) of the aqueous (4×10^{-4} M Ca and Sr) and organic (0.05 M 4-acyl derivatives) phases were agitated in a 50 cm^3 centrifuge tube during 30 min. In all cases the time necessary to attain equilibrium was established as 1–2 min. After centrifugation the two phases separated and the pH of the aqueous phase was measured by TOA HM-6A pH meter. A 5 cm^3 portion was pipetted from organic phase and Ca and Sr were back-extracted into 0.1 M hydrochloric acid. The concentration of metals in this solution and in the aqueous phase were determined by an atomic absorption method. The ionic strength of the aqueous phase was maintained constant (0.1 M) by adding sodium perchlorate.

RESULTS AND DISCUSSION

The extraction of Ca and Sr from aqueous solution with 4-acyl derivatives in MIBK and benzyl alcohol were studied. The reagents except for the PMBP are shown as C_n, where the subscript n denote number of carbon involved in acyl chain. These 4-acyl derivatives are β-diketone with pK_a of *ca* 4[4] in 10% (v/v) dioxane–water at 25°C. The solubility in organic solvent such as MIBK is relatively high but that is insoluble in aqueous solution. The extraction of Ca and Sr with 0.01 M PMBP into benzene is negligible.[7] However, when MIBK and benzyl alcohol was used as organic phase the extraction is largely enhanced due to the synergistic effect.

Figure 1 shows the influence of pH on the extraction of Ca and Sr by PMBP in MIBK and benzyl alcohol. High extraction of Ca and Sr was

* Author to whom correspondence should be addressed.

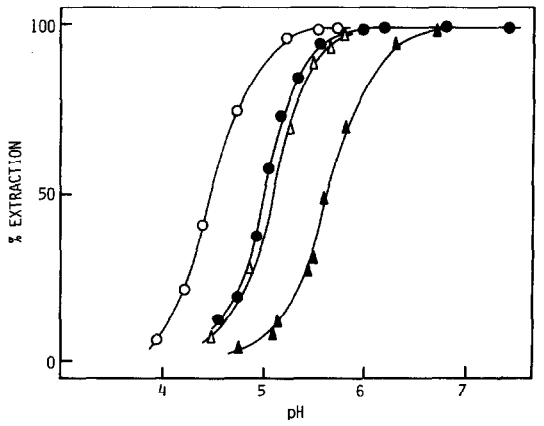


Fig. 1. Effect of pH on the extraction of Ca and Sr with PMBP. —○—, Ca, benzyl alcohol; —●—, Ca, MIBK; —△—, Sr, benzyl alcohol; —▲—, Ca, MIBK.

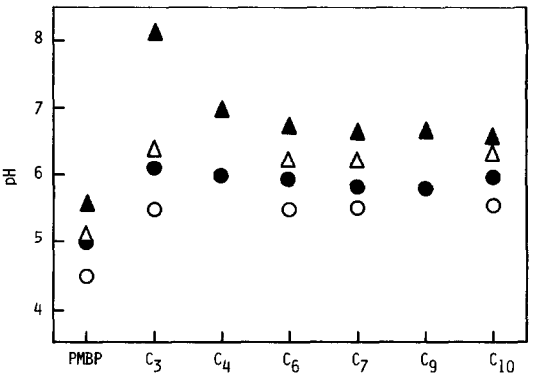


Fig. 3. Comparison of $pH_{1/2}$ for the 4-acyl derivatives. —○—, Ca, benzyl alcohol; —●—, Ca, MIBK; —△—, Sr, benzyl alcohol; —▲—, Sr, MIBK.

obtained utilizing the benzyl alcohol, and Ca is extracted more readily than Sr at lower pH. The plots log D vs pH gave straight line of slope near 2, indicating that under these conditions a 1:2 complex, $Ca(PMBP)_2$ and $Sr(PMBP)_2$, are found in the organic phase. Figure 2(a) shows the extraction percentage as a function of pH for the difference derivatives in MIBK. With increasing number of carbon in acyl chain extraction percentage of Sr increased remarkably whereas in Ca extraction little difference between the extraction curves is observed. This phenomenon has an important effect on the separation of Ca and Sr. When benzyl alcohol was used as organic solvent, the substituent effect of 4-acyl derivatives was not recognized for extraction as shown in Fig. 2(b). Figure 3 shows the pH of the half extraction of Ca and Sr with MIBK and benzyl alcohol as solvents. From these results it can be seen that the reagent C_3 is more suitable than the other reagents for the separation of Ca and Sr, using MIBK as solvent. On the other hand PMBP is much more efficient for the extraction of Ca and Sr than the other derivatives, even at low pH. This appears to be a direct consequence of the relatively low pK_a value of PMBP, viz. 3.80, the pK_a values of the other

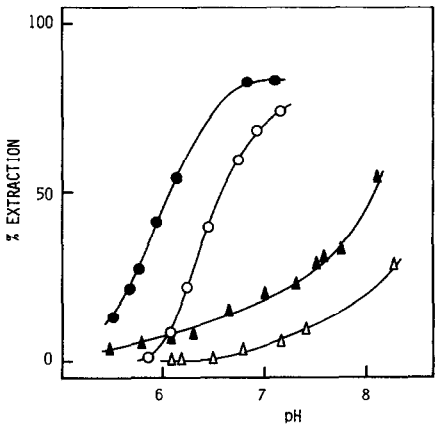


Fig. 4. The extraction behavior of Ca and Sr with C_3 in MIBK at 5 and 25°C. —●—, Ca, 25°C; —○—, Ca, 5°C; —▲—, Sr, 25°C; —△—, Sr, 5°C.

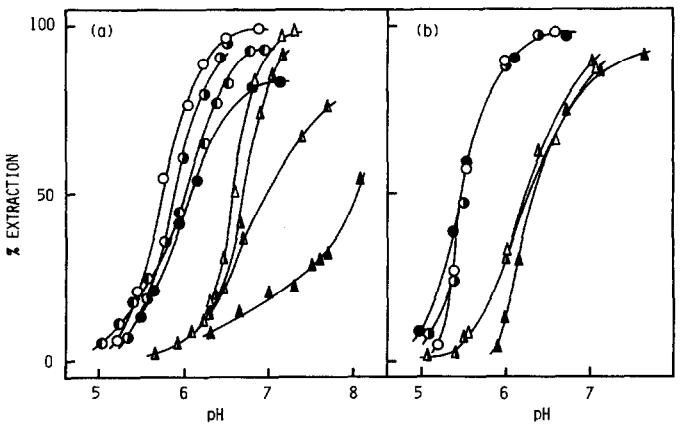


Fig. 2. Effect of pH on the extraction of Ca and Sr with 4-acyl derivatives. (a), MIBK; (b), benzyl alcohol; —●—, Ca, C_3; —◐—, Ca, C_4; —◑—, Ca, C_6; —○—, Ca, C_7; —▲—, Sr, C_3; —◭—, Sr, C_4; —◬—, Sr, C_6; —△—, Sr, C_7.

derivatives (C_3–C_9) all being in the range 4.1–4.2. Figure 4 shows the extraction of Sr and Ca at temperature 5 and 25°C for C_3–MIBK system. The extraction percentage of the Sr and Ca decrease with decreasing temperature. This indicates that the extraction process was found to involve an endothermic reaction. The extraction of Ca at 2×10^{-4} M level with 0.05 M C_3–MIBK solution was studied at 5°C, in the presence of various concentration of Sr (2×10^{-4}–2×10^{-2} M). It was found that the recovery of Ca is about 71% at pH 6.9 while Sr is about 4%.

Further work concerning the use of 4-acyl derivatives for the separation of metals is in progress.

REFERENCES

1. Yu. A. Zolotov and V. G. Lambrev, *J. Anal. Chem. USSR* 1965, **20**, 615.
2. M. Y. Mirza and F. I. Nwabue, *Talanta* 1981, **28**, 49.
3. Y. Akama, T. Nakai and F. Kawamura, *Bunseki Kagaku* 1976, **25**, 496.
4. Y. Akama, K. Sato, M. Ukaji, T. Kawata and M. Kajitani, *Polyhedron* (in press).
5. Y. Akama, H. Yokota, K. Sato and T. Nakai, *Talanta* (in press).
6. S. Umetani, K. Sasayama and M. Matsui, *Anal. Chim. Acta* 1982, **134**, 327.
7. Yu. A. Zolotov and V. G. Lambrev, *Soviet Radiochem.* 1966, **8**, 572.

Polyhedron Vol. 4, No. 7, pp. 1263–1267, 1985
Printed in Great Britain

0277–5387/85 $3.00 + .00
© 1985 Pergamon Press Ltd

THE DIRECT ELECTROCHEMICAL SYNTHESIS AND CRYSTAL STRUCTURE OF SALTS OF $[M_4(SC_6H_5)_{10}]^{2-}$ ANIONS (M = Zn, Cd)

J. LAWRENCE HENCHER, MASOOD A. KHAN, FAROUQ F. SAID and DENNIS G. TUCK*
Department of Chemistry, University of Windsor, Windsor, Ontario, Canada N9B 3P4

(*Received* 3 *October* 1984; *accepted* 29 *November* 1984)

Abstract—The salts $[(C_2H_5)_3NH]_2[M_4(SC_6H_5)_{10}]$ (M = Zn, Cd) can be prepared by the electrochemical oxidation of the metal in an acetonitrile solution of triethylamine and benzenethiol. An X-ray crystal structure determination shows that the anion consists of a tetrahedron of metal atoms, each carrying a terminal $-SC_6H_5$ ligand, and connected to the three other metal atoms by bridging $>SC_6H_5$ groups. The results are compared with those for similar compounds reported in the literature.

Complexes of both main group and transition metals with sulphur-donor ligands are a subject of current interest, not least because of the biochemical significance of such species. In previous papers, we have shown that the electrochemical oxidation of a metal into a non-aqueous solution of a thiol or disulphide is a convenient and direct route to the neutral thiolato complexes of such elements as zinc, cadmium, mercury,[1] tin,[2] lead,[2] gallium,[3] indium[3] and thallium.[3] As reported briefly in an earlier publication,[4] attempts to synthesise an anionic derivative of $Zn(SC_6H_5)_2$ gave the triethylammonium salt of the unusual $[Zn_4(SC_6H_5)_{10}]^{2-}$ anion. We now report full details of the synthesis of this salt, and its cadmium analogue, and of the X-ray crystallographic study of both compounds. The results are compared with those of other workers on a series of related compounds.

EXPERIMENTAL

General

Acetonitrile was distilled from, and stored over, molecular sieves. All other materials were used as supplied. Proton NMR spectra were run in CD_3CN solution at 60 MHz on a Jelco instrument.

Electrochemical synthesis

The electrochemical methods followed those described in previous publications (e.g. Refs. 1, 2, 5) with a 100 cm^3 tall-form beaker containing 50 cm^3 acetonitrile, 3 cm^3 triethylamine (2.2 g, 21.5 mmol), 3 cm^3 benzenethiol (3.2 g, 29 mmol) and 20 mg tetraethylammonium perchlorate. The anode consisted of a piece of metal, approx. 2 cm^2 in area; the cathode was a similar sized platinum sheet. In the case of zinc, an applied voltage of 10–15 V gave a current of 20 mA, and the metal dissolved smoothly (0.28 g in 20 hr). For cadmium, a voltage of 6–12 V gave a satisfactory rate of dissolution (1.22 g in 24 hr); a spongy deposit of cadmium metal formed on the cathode in the latter stages of the experiment. In both cases, the final solution was filtered to remove any particles of metal; the dropwise addition of diethyl ether, with subsequent overnight cooling, produced well-formed crystals. (Yield approx. 90%, based on metal dissolved.) Typical analytical results for the zinc complex $[(C_2H_5)_3NH]_2[Zn_4(SC_6H_5)_{10}]$ were given previously.[4] Analysis of the analogous cadmium complex for metal by atomic absorption spectrophotometry gave, Cd: 25.3%; calc. 25.75%.

Attempts to replicate these syntheses using a zinc anode and an acetonitrile solution of triethylamine and *n*-butanethiol were unsuccessful. The anode rapidly became coated with a black solid, and as the electrolysis proceeded a white solid was also formed. Both of these products were insoluble in common solvents. The solution phase yielded a yellow oil on removal of solvent *in vacuo*, but no useful products could be isolated from this. Similar differences between arene- and alkane-thiols were noted earlier in studies of the electrochemical oxidation of tin and lead.[2]

* Author to whom correspondence should be addressed.

Table 1. Summary of crystal data, intensity collection, and structural refinement for $[(C_2H_5)_3NH]_2[Zn_4(SC_6H_5)_{10}]$, $Zn_4S_{10}N_2C_{72}H_{80}$

Cell constants	$a = 12.819(4)$ Å $\alpha = 108.16(2)°$
	$b = 13.673(4)$ Å $\beta = 96.90(3)°$
	$c = 23.158(7)$ Å $\gamma = 98.78(3)°$
Cell volume (Å^3)	3750(2)
Space group	$P\bar{1}$
Z	2
M_r	1555.6
ρ(calc) (g cm^{-3})	1.377
Absorption coefficient (cm^{-1})	15.09
Crystal dimensions (mm)	$0.10 \times 0.21 \times 0.23$
Radiation	Mo-K_α, $\lambda = 0.71069$ Å
Temp (°C)	22
2θ angle (°)	4–50
Scan type	coupled θ (crystal)/2θ (counter)
Scan width	$K_{\alpha 1} - 1°$ to $K_{\alpha 1} + 1°$
Scan speed (° min^{-1})	2.0–5.0
Background time/scan time	0.5
Total reflections measured	6373
Unique data used (m)	4935
No. of parameters (n)	275 (blocked)
$R = (\Sigma \|\|F_o\| - \|F_c\|\|/\Sigma\|F_o\|)$	0.586
$R_w = [\Sigma w(\|F_o\| - \|F_c\|)^2/\Sigma w\|F_o\|^2]^{1/2}$	0.0634
$\Delta\rho$ max (e Å^{-3})	0.52
Shift: error (max)	0.013

Crystallographic analysis

A pale yellow crystal of

$$[(C_2H_5)_3NH]_2[Zn_4(SC_6H_5)_{10}]$$

mounted directly on a glass fibre was used in obtaining cell constants and diffraction intensities. The details of the experimental conditions for these measurements, carried out on a Syntex $P2_1$ diffractometer, are given in Table 1. The procedures used in data collection and processing were essentially those outlined elsewhere.[6] The space group $P\bar{1}$ was identified from the average $(E^2 - 1)$ and E^2, and subsequently confirmed by the agreement between the observed and calculated densities. Diffraction data were corrected for Lorentz and polarisation effects, and analytically for absorption. Scattering factors, anomalous dispersion and correction terms for zinc and sulphur atoms were taken from Ref. 7. Computer programmes were those quoted in Ref. 8.

The positions of the zinc and sulphur atoms of the Zn_4S_{10} skeleton were obtained by direct methods. The remaining non-hydrogen atoms (C and N) were then identified from difference Fourier maps. In the least-squares analysis, all the zinc and sulphur atoms were refined in each cycle, with the blocks C(11)---C(126), N(1), CE(1)---CE(6) and C(131)---C(346), N(2), CE(7)---CE(12) (where CE identifies a carbon atom of an ethyl group of the cation) being refined in alternate cycles until convergence was found at $R = 0.0586$. Thermal parameters were anisotropic for Zn and S, and isotropic for C and N. Hydrogen atoms were not included in the refinement. The resultant structure is shown in Fig. 1. Table 2 gives selected bond lengths

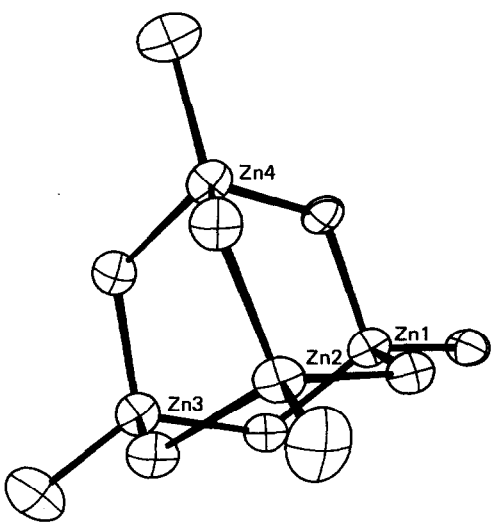


Fig. 1. Zn_4S_{10} core in $[Zn_4(SC_6H_5)_{10}]^{2-}$ anion, showing numbering of zinc atoms. Zinc(1) carries a terminal S(1), and is bonded to S(12) which bridges Zn(1) and Zn(2), etc.

Table 2. Selected interatomic distances (Å) and angles (°) for $[C_2H_5)_3NH]_2[Zn_4(SC_6H_5)_{10}]$

$Zn–S_t$			
Zn(1)–S(1)	2.288(4)	Zn(3)–S(3)	2.278(4)
Zn(2)–S(2)	2.284(4)	Zn(4)–S(4)	2.292(4)
mean 2.286(6)			
$Zn–S_{br}$			
Zn(1)–S(12)	2.399(3)	Zn(2)–S(12)	2.359(3)
Zn(1)–S(13)	2.351(3)	Zn(2)–S(23)	2.373(3)
Zn(1)–S(14)	2.395(3)	Zn(2)–S(24)	2.367(4)
Zn(3)–S(13)	2.376(4)	Zn(4)–S(14)	2.368(4)
Zn(3)–S(23)	2.375(3)	Zn(4)–S(24)	2.364(3)
Zn(3)–S(34)	2.383(3)	Zn(4)–S(34)	2.376(3)
mean 2.37(1)			
$S_t–Zn–S_{br}$			
S(1)–Zn(1)–S(12)	114.9(1)	S(2)–Zn(2)–S(12)	110.3(1)
S(1)–Zn(1)–S(13)	115.4(1)	S(2)–Zn(2)–S(23)	111.8(1)
S(1)–Zn(1)–S(14)	105.0(1)	S(2)–Zn(2)–S(24)	111.9(1)
S(3)–Zn(3)–S(13)	118.0(2)	S(4)–Zn(4)–S(14)	116.7(1)
S(3)–Zn(3)–S(23)	104.8(1)	S(4)–Zn(4)–S(24)	102.2(1)
S(3)–Zn(3)–S(34)	118.4(1)	S(4)–Zn(4)–S(34)	116.7(1)
mean 112(6)			
$S_{br}–Zn–S_{br}$			
S(12)–Zn(1)–S(13)	107.3(1)	S(12)–Zn(2)–S(23)	115.7(1)
S(12)–Zn(1)–S(14)	102.0(1)	S(12)–Zn(2)–S(24)	106.8(1)
S(13)–Zn(1)–S(14)	111.6(1)	S(23)–Zn(2)–S(24)	99.7(1)
S(13)–Zn(3)–S(23)	102.5(1)	S(14)–Zn(4)–S(24)	117.3(1)
S(13)–Zn(3)–S(34)	107.5(1)	S(14)–Zn(4)–S(34)	116.7(1)
S(23)–Zn(3)–S(34)	103.4(1)	S(24)–Zn(4)–S(34)	105.8(1)
mean 108(6)			
$Zn–S_{br}–Zn$			
Zn(1)–S(12)–Zn(2)	112.8(1)	Zn(2)–S(23)–Zn(3)	116.0(1)
Zn(1)–S(13)–Zn(3)	115.0(1)	Zn(2)–S(24)–Zn(4)	111.0(1)
Zn(1)–S(14)–Zn(4)	112.9(1)	Zn(3)–S(34)–Zn(4)	117.5(1)
mean 114(2)			
S–C	1.75(1)–1.80(1)	mean 1.77(1)	
Zn–S–C	107.6(4)–111.3(4)	mean 110(2)	
Zn–S–C	103.2(4)–113.3(4)	mean 107(3)	
C–C	1.34(3)–1.48(2)	mean 1.401(4)	
Et_3NH^+ parameters			
N–C	1.48(2)–1.63(3)	mean 1.55(6)	
C–C	1.48(4)–1.59(4)	mean 1.51(4)	
C–N–C	105(1)–121(2)	mean 110(7)	
N–C–C	108(2)–113(1)	mean 110(2)	

and angles for the anion; other bond lengths, positional and thermal parameters, and structure factors have been deposited as supplementary material with the Editor* from whom copies may be obtained.

The cell constants and space group determined for the cadmium salt $[(C_2H_5)_3NH]_2[Cd_4(SC_6H_5)]_{10}$ are given in Table 3, but no attempt was made to solve the structure when it became known that the

* Atomic coordinates have also been deposited with the Cambridge Crystallographic Data Centre.

Table 3. Cell constants for $[(C_2H_5)_3NH]_2[Cd_4(SC_6H_5)_{10}]$, $Cd_4S_{10}N_2C_{72}H_{80}$

$a = 13.759(2)$ Å
$b = 20.504(5)$ Å
$c = 14.056(4)$ Å
$\beta = 102.32(2)°$
$V = 3874(a)$ Å^3

Space group $P2_1$ ($0k0$; $k = 2n+1$ absent)

crystal structure of

$$[(C_2H_5)_4N][C_2H_5)_3NH][Cd_4(SC_6H_5)_{10}]$$

had been completed.[9] One interesting point is that the triethylammonium salts of the zinc and cadmium complexes crystallize in different space groups ($P1$ and $P2_1$ respectively).

RESULTS AND DISCUSSION

The structure of $[(C_2H_5)_3NH]_2[Zn_4(SC_6H_5)_{10}]$

As reported previously,[4] this compound consists of triethylammonium cations, whose structure requires no further comment, and the cage or cluster anion based on the Zn_4S_{10} kernel, with both bridging and terminal thiolato groups. A number of analogous species have been reported recently, including $[M_4(SC_6H_5)_{10}]^{2-}$ anions for M = Fe(II),[10,11] Co(II),[12,13] Mn(II)[9] and Co(II),[9] and the related

$[Zn_4(SC_6H_5)_8Cl_2]^{2-}$,[14] $[Fe_4(SC_6H_5)_6Cl_4]^{2-}$,[15]

and $[Zn_4(SC_6H_5)_8CH_3OH]_n$.[16] Holm and his co-workers[10] have emphasised the structural similarities between such molecules and the metallothionen proteins, but an equally valid analogy is with those metal sulphides having a zinc blende structure. This is clearly apposite for $[Zn_4(SC_6H_5)_{10}]^{2-}$, since both in this molecule and in zinc blende one finds four-coordinate zinc surrounded by a tetrahedron of sulphur atoms. The usefulness of this model is confirmed by the work of Dance *et al.*, who have shown that extended structures incorporating both $-SC_6H_5$ and S (e.g. $[S_4M_{10}(SC_6H_5)_{16}]^{4-}$, M = Zn, Cd)[17,18] are readily formed from the parent $[M_4(SC_6H_5)10]^{2-}$, thus emphasising that the ligating properties of S^{2-} and SR^- are such as to make these entities interchangeable in such molecules.

The structure of $[Zn_4(SC_{65})_{10}]^{2-}$ consists of four zinc atoms, each coordinated by one terminal and three bridging $-SC_6H_5$ ligands. The zinc atoms themselves are at the corners of a tetrahedron, while the bridging sulphur atoms are at the corners of a slightly distorted octahedron in which the S_{br}–S_{br} distance is slightly greater than twice the van der Waals radius of sulphur (1.85 Å). One of the interesting aspects of the structural results thus far available is the near constancy of the M–M and S_{br}–S_{br} distances, and of the volumes V_{tot}(M) and V_{oct}(S) calculated from these distances, assuming that the four metal atoms and six sulphur atoms define regular polyhedra. The present results (Zn–Zn = 3.98(6) Å; V(Zn) = 7.43 Å^3; S_{br}–S_{br} = 3.80(14) Å; $V(S_{br})$ = 25.87 Å^3) are in good agreement with those reported in earlier publications[10–13]. This constancy may simply arise because of the restricted range of metals with similar ionic radii, and it would be interesting to see whether this effect extends to derivatives of other metal ions. In this context, it is worth noting that the relevant volumes for the cadmium compound[13] are V(Cd) = 9.46 Å^3 and $V(S_{br})$ = 32.23 Å^3, 39% and 31% respectively greater than those for the zinc compound discussed here (cf. ref. 11, footnote (47)).

The Zn–S_{br} and Zn–S_t bond lengths in the present anion are in good agreement with those published by Dance *et al.*,[12,14] and call for no comment. The angles within the $Zn_4(S_{br})_6$ kernel are on average (108°) close to the 109.5° required for exact tetrahedral ZnS_4 coordination, and a similar average applies to the S_t–Zn–S_{br} angles. The bond lengths and angles in the $-SC_6H_5$ ligand are very close to those reported for analogous complexes with other metal ions.

Spectroscopic results

The identification of two relatively broad resonances in the phenyl region of the ^{1}H NMR spectrum served to confirm the presence of bridging and terminal $-SC_6H_5$ ligands for the zinc complex. A more detailed temperature dependent study[11] at 300 MHz has confirmed this result, showing that the intra-molecular rearrangement implied by these broad absorptions is significantly slowed at 239 K. The room temperature spectrum of the cadmium compound is very similar to that of the zinc analogue, with phenyl resonances centred at 7.13 and 6.77 ppm from Me_4Si (relative intensities 1:1.17).

Acknowledgements—This work was supported in part by grants (to DGT) from the Natural Sciences and Engineering Research Council of Canada and from Imperial Oil Research Ltd.

REFERENCES

1. F. F. Said and D. G. Tuck, *Inorg. Chim. Acta* 1982, **59**, 1.
2. J. L. Hencher, M. A. Khan, F. F. Said, R. Seiler and D. G. Tuck, *Inorg. Chem.* 1982, **21**, 2787.
3. J. H. Green and D. G. Tuck, unpublished results.
4. J. L. Hencher, M. A. Khan, F. F. Said and D. G. Tuck, *Inorg. Nucl. Chem. Lett.* 1981, **17**, 287.
5. J. J. Habeeb and D. G. Tuck, *Inorg. Synth.* 1979, **19**, 257.
6. M. A. Khan, R. C. Steevensz, D. G. Tuck, J. G. Noltes and P. W. R. Corfield, *Inorg. Chem.* 1980, **19**, 3407.
7. *International Tables for X-ray Crystallography* (Edited by J. A. Ibers and W. C. Hamilton), Vol. IV, pp. 99, 149. Kynoch Press, Birmingham, England (1974).
8. M. A. Khan and D. G. Tuck, *Acta Cryst.* 1982, **B38**, 803.
9. K. S. Hagen and R. H. Holm, *Inorg. Chem.* 1983, **22**, 3171.
10. K. S. Hagen, J. M. Berg and R. H. Holm, *Inorg. Chim. Acta* 1980, **45**, L17.
11. K. S. Hagen, D. W. Stephan and R. H. Holm, *Inorg. Chem.* 1982, **21**, 3928.
12. I. G. Dance and J. C. Calabrese, *J. Chem. Soc., Chem. Commun.* 1975, 762.
13. I. G. Dance, *J. Am. Chem. Soc.* 1979, **101**, 6264.
14. I. G. Dance, *Inorg. Chem.* 1981, **20**, 2155.
15. D. Coucouvanis, M. Kanatzidis, E. Simhon and N. C. Baenziger, *J. Am. Chem. Soc.* 1982, **104**, 1874.
16. I. G. Dance, *J. Am. Chem. Soc.* 1980, **102**, 3445.
17. A. Choy, D. Craig, I. G. Dance and M. Scudder, *J. Chem. Soc., Chem. Commun.* 1982, 1246.
18. A. Lacelle, W. C. Stevens, D. M. Kurtz, Jr., J. W. Richardson, Jr. and R. A. Jacobson, *Inorg. Chem.* 1984, **23**, 930.

Polyhedron Vol. 4, No. 7, pp. 1269–1270, 1985
Printed in Great Britain

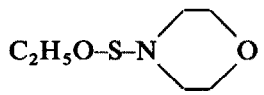
0277–5387/85 $3.00 + .00
© 1985 Pergamon Press Ltd

A CHARACTERISTIC REDOX REACTION FOR N,N′-THIOBISAMINES AND SOME OTHER S(II) COMPOUNDS

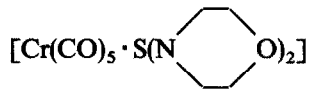
CARLOS DÍAZ
Universidad de Chile, Facultad de Ciencias Básicas y Farmacéuticas Casilla 653, Santiago, Chile

(*Received* 12 *June* 1984; *accepted after revision* 29 *November* 1984)

Abstract—The reaction of copper(II) perchlorate hexahydrate with a number of sulphur(II) compounds in acetonitrile as solvent were studied. It is found that SCl_2, N,N′-thiobisamines $S(NR_2)_2$, ethoxythiomorpholine



and pentacarbonyl (thiobismorpholine) chromium(0)



reduce Cu(II) with formation of the complex $Cu[(CH_3CN)_4]ClO_4$ and SO_2.

The hydrolysis of sulphur(II) compounds such as SCl_2, $S(OC_2H_5)_2$ and $S[N(C_2H_5)_2]_2$ has been investigated by Goering.[1] These hydrolytic reactions are very complex and sulphur, sulphur dioxide, thiosulphurous and polythionic acids are obtained as products. The formation of these compounds has been rationalized by assuming the formation of an unstable intermediate the sulphoxilic acid, by hydrolysis of the S(II) compounds, and subsequent redox reaction of this acid. Such reactions have been investigated in an aqueous medium and therefore—because $S(OC_2H_5)_2$ and $S[N(C_2H_5)_2]_2$ are insoluble—in a heterogeneous phase.

In our laboratory we have studied the redox reaction of thiobismorpholine and N,N′-thiobisdimethylamine with copper(II) salts in the presence of water, in a homogeneous medium.[2] In such conditions the reactions are very much more simple, since the products are easy to separate and identify. In this work is reported the reaction of copper(II) perchlorate hexahydrate, with the following S(II) compounds; sulphur dichloride, N,N′-thiobisamines, ethoxythiomorpholine and the complex pentacarbonyl (thiobismorpholine) chromium(0) in acetonitrile as solvent.

EXPERIMENTAL

N,N′-thiobisamines were prepared from SCl_2 by a known method.[3] Ethoxythiomorpholine was synthesized by ethanolysis of thiobismorpholine in the presence of $CuCl_2$.[2] Pentacarbonyl (thiobismorpholine) chromium(0) was obtained by photochemical substitution of the ligand on $Cr(CO)_6$ in THF.[4] Reactions were made as follows: The calculated amount of sulphur compound (2:1, SB_2:Cu(II) stoichiometry) in CH_3CN was added over the $Cu(H_2O)_6 \cdot (ClO_4)_2$ solution with stirring and ambient temperature. The white solid formed was filtered and dried with a stream of dry nitrogen gas. In some cases a green basic Cu(II) salts was obtained as impurity, which was eliminated by dissolution of the solid in hot acetonitrile followed by filtration of the green solid and evaporation of the solvent to afford the white crystalline product. The IR spectra was identical with that synthesized from CuO and perchloric acid.[5]

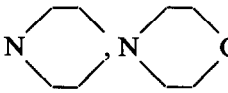
RESULTS AND DISCUSSION

N,N′-thiobisamines react with copper(II) perchlorate hexahydrate in acetonitrile to give the Cu(I)

complex $Cu[(CH_3CN)_4]ClO_4$, sulphur dioxide and the respective ammonium perchlorate salts:

$$2[Cu(H_2O)_6](ClO_4)_2 + S(NR_2)_2 \xrightarrow{CH_3CN} 2[Cu(CH_3CN)_4]ClO_4 + SO_2 + 2[H_2NR_2]ClO_4 + 10H_2O$$

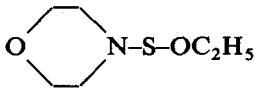
NR_2 = $N(CH_3)_2$, $N(C_2H_5)_2$, $N(CH_2{-}CH{=}CH_2)_2$,



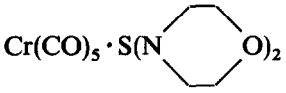
, $N(CH_2{-}C_6H_5)_2$, $N(C_6H_5)_2$.

The Cu(I) complex is a crystalline white solid of easy isolation and identification by IR spectroscopy. The IR spectra show the characteristic bands corresponding to $\nu(C{\equiv}N)$ (2300 and 2260 cm^{-1}), $\nu(ClO_4)$ (ν_{as}, 1000–1120 cm^{-1} and ν_s 922 cm^{-1}) and $\delta(ClO_4)$ (620 cm^{-1}). Further from the filtrate it was possible to identify the $H_2NR_2^+$ species by ^1H NMR. The SO_2 evolved from the reaction was confirmed by the common chemical method.[6]

Similarly from the reaction of SCl_2,



and

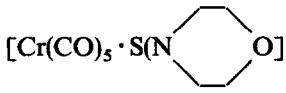


with copper perchlorate in acetonitrile was isolated and identified the sample complex of Cu(I).

The fact that in all reactions the same product is obtained, the Cu(I) complex, suggests that the reduction of Cu(II) could be made by a common intermediate, namely the sulphoxylic acid which is formed in the hydrolysis of the sulphur compound SB_2,

$$SB_2 + 2H_2O \rightarrow S(OH)_2 + 2BH.$$

$S(OH)_2$ could then be oxidized to SO_2 with simultaneous reduction of Cu(II) to Cu(I) and with acetonitrile to yield the complex $[Cu(CH_3CN)_4]ClO_4$. It is interesting to note that the yield of the copper(I) compound is better for the reaction with



than with

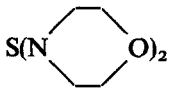
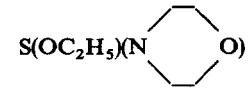
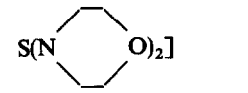
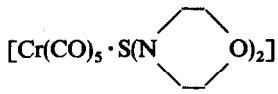


Table 1. Yield of $[Cu(CH_3CN)_4]ClO_4$ with various S(II) compounds

Compound	Yield (%)
SCl_2	50
	60
$S[N(CH_3)_2]_2$	50
$S[N(CH_2{-}CH{=}CH_2)_2]_2$	30
	80
	98

(see Table 1) which could be due to a more facile hydrolysis of thiobismorpholine in the complex than free thiobismorpholine. This is consistent with the greater strength of the S–N bond found in the free thiobismorpholine than in that linked to chromium.[4,7]

In conclusion, the reaction of copper(II) perchlorate hexahydrate with compounds of sulphur in an oxidation state +2 could be considered as characteristic because in all cases the same products namely the complex $[Cu(CH_3CN)_4]ClO_4$ and SO_2 are obtained. On the contrary the reaction of sulphur(II) compounds with other copper(II) salts and solvent affords different products depending of the properties of the substituents on the sulphur.[2]

Acknowledgement—Financial support received by the "Departamento de Investigación y Bibliotecas de la Universidad de Chile" is gratefully acknowledged.

REFERENCES

1. N. Goering, *Angew. Chem.* 1948, **A60**, 147.
2. G. González, C. Díaz and S. Copaja, *Monatsh. Chem.* 1983, **114**, 177.
3. E. S. Blake, *J. Am. Chem. Soc.* 1943, **65**, 1267.
4. C. Díaz and G. González, *Inorg. Chim. Acta* 1984, **85**, 61.
5. P. Hammerich and C. Sigwart, *Experientia* 1963, **19**, 488.
6. A. I. Vogel, *Química Analítica Cuantitativa.* Kapelusz (1974).
7. C. Díaz, E. Clavijo and G. González, *Spectrochim. Acta* 1983, **39A**, 537.

Polyhedron Vol. 4, No. 7, pp. 1271–1273, 1985
Printed in Great Britain

0277–5387/85 $3.00 + .00
© 1985 Pergamon Press Ltd

He I PHOTOELECTRON SPECTRA OF [3]-FERROCENOPHANE AND ITS 7-OXA DERIVATIVE

TOMÁŠ VONDRÁK

ESCA Centre, The J. Heyrovský Institute of Physical Chemistry and Electrochemistry, Czechoslovak Academy of Sciences, Vlašská 9, 118 40 Prague, Czechoslovakia

(*Received* 17 *September* 1984; *accepted* 9 *November* 1984)

Abstract—He I photoelectron spectra of [3]-ferrocenophane and 6,8-dimethyl-7-oxa-[3]-ferrocenophane have been measured. In comparison with ferrocene the energy gap between $^2E'_2(a'^2_1e'^3_2)$ and $^2A'_1(a'^1_1e'^4_2)$ is decreased to 0.28 and 0.22 eV due to the destabilization of the $a'_1(d)$-level originating in its more pronounced mixing with ligand orbitals. The increase of photoionization cross section of the $a'_1(d)$-level in the 6,8-dimethyl-7-oxa-[3]-ferrocenophane spectrum supports this interpretation. The band shapes and ionization potentials of ligand π-levels are strongly influenced by the hydrocarbon bridge.

The electronic structure of bis(η^5-cyclopentadienyl) metal halides, hydrides carbonyls and olefin complexes in which the cyclopentadienyl rings are not coplanar has been extensively studied by ultraviolet photoelectron (PE) spectroscopy[1,2] and by quantum chemical methods.[3,4] The starting point of the bonding schemes of these complexes is the bent bis(η^5-cyclopentadienyl) metal fragment.

In ferrocenophanes the cyclopentadienyls are not coplanar.[5] We have carried out an ultraviolet PE spectroscopic investigation of ferrocenophane species in order to reveal the changes in the electronic structure which come from the bending of the metallocene unit.

Ferrocene is a closed-shell system with fully occupied a'_1 and e'_2 d-levels (D_{5h} symmetry if the eclipsed conformation is assumed for the cyclopentadienyl rings), and the low ionization potential (IP) region of its PE spectrum has been unequivocally assigned.[6] The ring substituents do not introduce any splitting of the doubly degenerate $e'_2(d)$-level.[7,8] Ferrocenophanes seem thus to be excellent model species for the PE spectroscopic investigation of the bent bis(η^5-cyclopentadienyl) metal fragment.

To our knowledge we report the first PE spectra of ferrocenophane species [3]-ferrocenophane (I) (Fig. 1) in which the angle between the planes of cyclopentadienyls is 10°,[5] and that of 6,8-dimethyl-7-oxa-[3]-ferrocenophane (II) (Fig. 2).

In the PE spectrum of ferrocene the bands a and b are assigned to the $e'_2(d)$ and $a'_1(d)$-level, respectively.

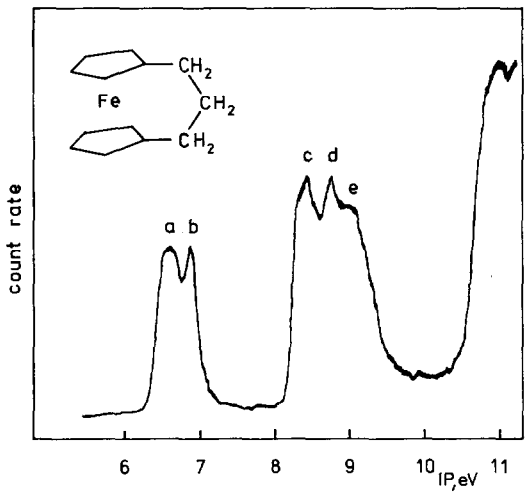


Fig. 1. He I PE spectrum of [3]-ferrocenophane (I).

Since the band shapes of d-ionizations are similar to ferrocene, the same interpretation is adopted here for (I) and (II), though the actual local symmetry is C_{2v}. The IPs of the d-levels of (I) are lowered in comparison with ferrocene due to the weak electrondonor character of the hydrocarbon bridge. The IP of the $e'_2(d)$-level in (I) is exactly between the IP of this level in 1,1′-diethyl and 1,1′-dimethylferrocene whereas the $a'_1(d)$ IP is the same as in 1,1′-diethylferrocene (Table 1). The alkylsubstituents do not affect the energy difference between $^2E'_2(a'^2_1e'^3_2)$ and $^2A'_1(a'^1_1e'^4_2)$ ion states[1,8] (see Table 1). Therefore it may be concluded that tilting of the cyclo-

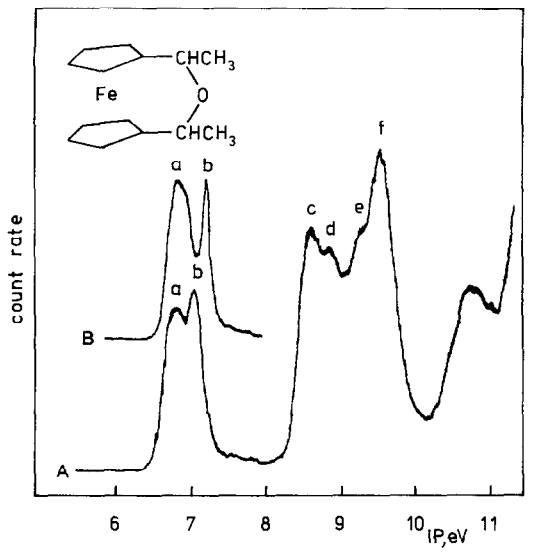


Fig. 2. (A) He I PE spectrum of 6,8-dimethyl-7-oxa-[3]-ferrocenophane (II). (B) He I PE spectrum of ferrocene, *d*-ionizations.

pentadienyl rings is responsible for the decrease of this energy difference to 0.28 eV observed in the spectrum of (I).

The geometry of the 7-oxa derivative (II) is not experimentally determined but the larger tilting of cyclopentadienyls may be anticipated if we take into account the shorter C–O bond length in comparison with that of C–C.[9] The decrease of the energy difference $^2E_2'$–$^2A_1'$ is more pronounced in the PE spectrum of (II) (0.22 eV). The IP of $a_1'(d)$-level is the same as in 1,1′-dimethylferrocene in spite of the electronegative oxygen bridge atom (see Table 1).

The preceding comparison with the IPs of 1,1′-dialkylferrocenes shows that the IP of $a_1'(d)$-level is lowered by bending of the metallocene unit. The increase of the relative photoionization cross-section of $a_1'(d)$-level in comparison with ferrocene indicates its larger mixing with ligand orbitals in (II).

These findings indicate that the $a_1'(d)$-level acquires a slightly antibonding character due to bending of the metallocene unit. The previous calculation of Hoffmann and Lauther[3] support this conclusion.

The band shapes of ligand $e_1'(\pi)$ and $e_1''(\pi)$-ionizations differ significantly from those of parent ferrocene. On the basis of the comparison with the spectra of 1,1′-disubstituted ferrocenes[8] we have tentatively assigned the bands *c* and *d* to the $e_1'(\pi)$-level and the band *e* to the $e_1''(\pi)$-level. In the PE spectrum of (II) the ionization involving oxygen non-bonding orbital n(O) overlaps with the ligand π-ionizations. The intensive band *f* is assigned to the n(O)-orbital. The $e_1'(\pi)$ and $e_1''(\pi)$-orbitals interact directly with the orbitals of the bridge atoms. Hence the influence of bending of the molecule upon the ligand π-levels can be hardly revealed from the PE spectra. Nevertheless, it is worth noting that in the PE spectrum of (I) the band *d* assigned to a component of the doubly degenerate $e_1'(\pi)$-level is shifted to higher IP in comparison with that of ferrocene. It may be assumed that the bending of the molecule is responsible for this increase of the IP since the electron-donating CH_2-groups cannot bring it about.

The first PE investigation of [3]-ferrocenophanes gives evidence on the lowering of the energy gap between the $^2E_2'$ and $^2A_1'$ ion states. A reverse order of ion states could be expected for the ferrocenophane species in which a larger ring tilting occurs.

The He I PE spectra were recorded on the VG Scientific UVG 3 instrument with working resolution of 0.03 eV on the Ar $^2P_{3/2}$ peak. The Ar/Xe mixture was used as the internal calibrant.

Table 1. Vertical ionization potentials (peak maxima) of ferrocenophanes and 1,1′-dialkylferrocenes

Compound* Orbital	(I)	(II)	(III)	(IV)	(V)
			IP, eV†		
$e_2'(d)$	6.66a	6.84a	6.60	6.72	6.85a
$a_1'(d)$	6.94b	7.06b	6.94	7.06	7.21b
$e_1'(\pi)$	8.48c 8.82d	8.62c 8.86d	8.33 8.60	8.63 8.73	8.72
$e_1''(\pi)$	9.06e	(9.35)e	9.05	9.17	9.17 9.38
n(O)		9.53f			

*(I) = [3]-ferrocenophane, (II) = 6,8-dimethyl-7-oxa-[3]-ferrocenophane, (III) = 1,1′-diethylferrocene,[8] (IV) = 1,1′-dimethylferrocene,[7] (V) = ferrocene.

† Standard deviation 0.03 eV, the value in parentheses corresponds to the shoulder and standard deviation is 0.05 eV.

REFERENCES

1. J. C. Green, *Struct. and Bond.* 1981, **43**, 37 (and references therein).
2. H. van Dam, A. Terpstra and A. Oskam, *Z. Naturforsch.* 1981, **36B**, 420.
3. J. W. Lauther and R. Hoffmann, *J. Am. Chem. Soc.* 1976, **98**, 1729.
4. J. L. Petersen, D. L. Lichtenberg, R. F. Fenske and M. B. Hall, *J. Am. Chem. Soc.* 1975, **97**, 6433.
5. C. Lecomte, Y. Dusausoy, J. Protas, C. Moise and J. Tirouflet, *Acta Cryst.* 1973, **B29**, 488.
6. C. Cauletti, J. C. Green, M. R. Kelly, P. Powell, J. van Tilborg, J. Robbins and J. Smart, *J. Electron Spectrosc. Relat. Phenom.* 1980, **19**, 327.
7. S. Evans, M. L. H. Green, B. Jewitt, A. F. Orchard and C. F. Pygall, *J. Chem. Soc., Faraday Trans. II* 1972, **68**, 1847.
8. T. Vondrák, *5th Seminar on Electron Spectroscopy of Socialistic Countries*, Dresden, 26–29 August (1984).
9. *Landolt–Börnstein Numerical Data and Functional Relationships in Science and Technology*, Group II, Vol. 7, *Structure Data of Free Polyatomic Molecules.* Springer, Berlin (1976).

Polyhedron Vol. 4, No. 7, pp. 1275–1277, 1985
Printed in Great Britain

0277–5387/85 $3.00 + .00
© 1985 Pergamon Press Ltd

EPR ON TETRABUTYLAMMONIUM TETRAIODO-NITROSYLTECHNETATE(II), $(Bu_4N)[Tc(NO)I_4]$

R. KIRMSE and J. STACH
Department of Chemistry, Karl-Marx-University, DDR-7010 Leipzig, Liebigstr. 18, G.D.R.

and

U. ABRAM*
Academy of Sciences of the G.D.R., Central Institute of Nuclear Research Rossendorf, DDR-8051 Dresden, PF 19, G.D.R.

(*Received* 18 *July* 1984; *accepted after revision* 29 *November* 1984)

Abstract—An EPR study on tetrabutylammonium tetraiodo-nitrosyltechnetate(II), $(Bu_4N)[Tc(NO)I_4]$, is reported. The frozen solution EPR spectrum is described by an axially symmetric spin Hamiltonian. The ^{99}Tc hyperfine interaction is used to estimate the spin density distribution in the MO of the unpaired electron which is of "in-plane-π-type".

The widespread use of the metastable isotope of technetium, ^{99m}Tc, in diagnostic nuclear medicine procedures is well documented.[1] This is due to the favourable nuclear properties of ^{99m}Tc (γ-emitter with $E_\gamma = 140$ keV, half-life-time $t_{1/2} = 6$ hr) which allow high resolution γ-camera studies.

The chemistry, however, of this first man-made element is still poorly known. During the recent years the availability of the long lived isotope ^{99}Tc ($t_{1/2} = 2.13 \times 10^5$ years) from fission products in macroscopic amounts has lead to substantial progress in development of the technetium chemistry. Most of the well characterized Tc compounds contain the metal in the oxidation states "+4" and "+5", respectively.[2,3] The coordination chemistry of technetium in which Tc occurs in lower formal oxidation states is much less known.[2]

Tc(II) compounds are favoured for EPR studies because the d^5 low-spin ($S = 1/2$) configuration can be detected by EPR at temperatures $T > 77$ K. Nevertheless, only a few studies have been reported on nitrosyltechnetate(II) complexes containing EPR data:

$(n\text{-}Bu_4N)[Tc(NO)Br_4]$,[2,4,5]

$(n\text{-}Bu_4N)_2[Tc(NO)Cl_5]$,[5,6]

$(n\text{-}Bu_4N)_2[Tc(NO)(NCS)_5]$,[5]

$[Tc(NO)(NH_3)_4(H_2O)]^{3+}$[6]

and

$TcCl_3(NO)(PMe_2Ph)_2$.[7]

EPR studies on frozen solutions of the complexes from which the tensor parameters of $\tilde{g}$ and $\tilde{A}^{Tc}$ can be obtained are available for

$[Tc(NO)(NH_3)_4(H_2O)]^{3+}$,[6]

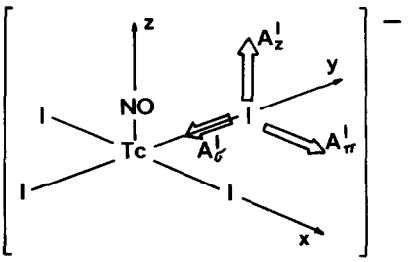
$[Tc(NO)Cl_5]^{2-}$,[6] $TcCl_3(NO)(PMe_2Ph)_2$[7]

and

$(n\text{-}Bu_4N)[Tc(NO)Br_4]$.[4]

Only for $TcCl_3(NO)(PMe_2Ph)_2$ and $[Tc(NO)Br_4]^-$ have they been used to derive the bonding properties of the Tc–ligand bonds.

In this paper we report EPR studies on the Tc(II) low-spin complex tetrabutylammonium tetraiodo-nitrosyltechnetate(II), (I), which has been made in order to get more insight into the bonding properties of the Tc–ligand bonds. In comparison to the corresponding Tc(II) nitrosyl compounds having



Cl^- or Br^- ligands more covalent bonds are to be expected.

* Author to whom correspondence should be addressed.

EXPERIMENTAL

Due to the radioactivity of ^{99}Tc (weak β^--emitter, $E_{max} = 0.29$ MeV) some health precautions have been taken.[8] All operations have been carried out in a fume cupboard with gloves. EPR measurements have been done in sealed glass tubes to avoid contaminations.

(n-Bu_4N)[Tc(NO)I_4] was prepared according to Ref. 9. EPR spectra were recorded at $T = 295$ and 130 K in the X-band ($\nu \approx 9.3$ GHz) using an E-112 spectrometer (VARIAN, U.S.A.). 5×10^{-4} M solutions of (**I**) were used (solvent: acetone).

RESULTS AND DISCUSSION

The room temperature EPR spectrum of (**I**) is only poorly resolved, obviously due to strongly overlapping lines resulting from the hyperfine interactions with the ^{99}Tc (nuclear spin $I = 9/2$) and the ^{127}I ($I = 5/2$) nuclei. The frozen solution spectrum is shown in Fig. 1. The general feature of the spectrum is characteristic for an axially symmetric, randomly oriented $S = 1/2$ system as described by the spin Hamiltonian

$$\hat{H}_{sp} = \beta_e[g_{\parallel}H_z\hat{S}_z + g_{\perp}(H_x\hat{S}_x + H_y\hat{S}_y)] + A_{\parallel}^{Tc}\hat{I}_z\hat{S}_z + A_{\perp}^{Tc}(\hat{I}_x\hat{S}_x + \hat{I}_y\hat{S}_y), \quad (1)$$

where $g_{\parallel}$, $g_{\perp}$, $A_{\parallel}^{Tc}$ and $A_{\perp}^{Tc}$ are the principal values of the $\tilde{g}$ and the ^{99}Tc hyperfine interaction tensor $\tilde{A}^{Tc}$. These parameters were obtained by use of the usual second-order expressions.[10] ^{99}Tc quadrupolar interactions are expected to be small and have been neglected. The spin Hamiltonian parameters obtained are: $g_{\parallel} = 2.262 \pm 0.003$, $g_{\perp} = 2.144 \pm 0.010$, $A_{\parallel}^{Tc} = (155 \pm 3) \times 10^{-4}$ cm^{-1} and $A_{\perp}^{Tc} = (73 \pm 10) \times 10^{-4}$ cm^{-1}. The corresponding average values—$g_{av} = (g_{\parallel} + 2g_{\perp})/3 = 2.183$ and $a_{av}^{Tc} = (A_{\parallel}^{Tc} + 2A_{\perp}^{Tc})/3 = 100 \times 10^{-4}$ cm^{-1} are in good agreement with the values obtained from the liquid solution spectrum: $g_0 = 2.172 \pm 0.005$ and $a_0^{Tc} = (106 \pm 5) \times 10^{-4}$ cm^{-1}, respectively.

Ligand hyperfine structures due to the interaction of the unpaired electron with the equatorial I-ligands are badly resolved. The linewidth of the parallel part ^{99}Tc hfs lines—$\Delta H_{pp} \approx 5$–6 mT—is noticeably larger than those observed for [Tc(NO)Br_4]$^{-4}$ and [Tc(NO)Cl_5]$^{2-}$.[6] From this linewidth consideration the principal value A_z^I of the ^{127}I hfs tensor $\tilde{A}^I$ can be estimated to be $A_z^I = 2.5$–3.0×10^{-4} cm^{-1}. The other components of $\tilde{A}^I$, A_x^I and A_y^I could not be obtained because the complexity of the perpendicular part of the EPR spectrum of (**I**) in frozen solutions.

In accordance with the results obtained earlier for $TcCl_3(NO)(PMe_2Ph)_2$[7] and [Tc(NO)Br_4]$^{-4}$ the EPR spectra of (**I**) suggest an "in-plane-π-type" for the molecular orbital (MO) of the unpaired electron:

$$\psi_{MO}(B_2) = \beta_2|d_{xy}\rangle - \beta_2'|\phi_L\rangle, \quad (2)$$

where $|\phi_L\rangle$ represents a linear combination of 5p orbitals of the four equatorial I ligands, β^2 is a measure of covalency of the equatorial Tc–I bonds in this MO.

The ^{99}Tc hfs can be used to estimate the degree of covalency of the equatorial Tc–I bonds. Applying the formalism given by McGarvey[11]

$$A_{\parallel}^{Tc} = -K - 4/7\beta^2P + (g_{\parallel} - g_e)P + 3/7(g_{\perp} - g_e)P, \quad (3a)$$

$$A_{\perp}^{Tc} = -K + 2/7\beta^2P + 11/14(g_{\perp} - g_e)P, \quad (3b)$$

and

$$a_{av}^{Tc} = -K + (g_{av} - g_e)P, \quad (3c)$$

where K is a measure of the Fermi contact interaction and $P = (+)200 \times 10^{-4}$ cm^{-1},[11] one arrives at a value of $\beta^2 = 0.72$; $K = (+)136.2 \times 10^{-4}$ cm^{-1}.

A comparison of the β^2 values derived for [Tc(NO)Cl_5]$^{2-}$, $\beta^2 = 0.88$,[9] and [Tc(NO)Br_4]$^-$, $\beta^2 = 0.83$,[4] with that obtained for [Tc(NO)I_4]$^-$ shows a considerable increase of covalency for the Tc–

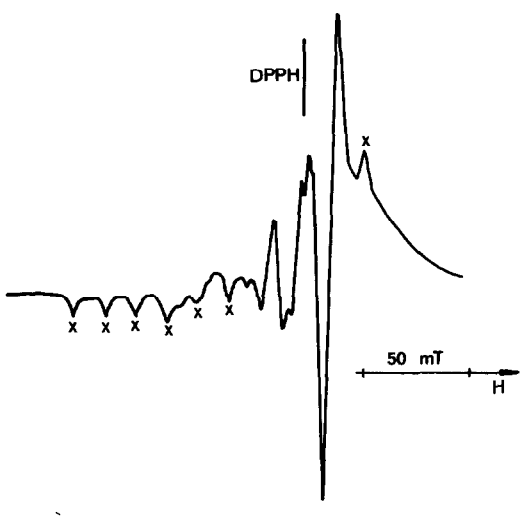


Fig. 1. X-band EPR spectrum of (n-Bu_4N)[Tc(NO)I_4] in acetone, $T = 130$ K (^{99}Tc hfs lines of the parallel part of the spectrum are indicated with (×); remaining parallel lines as well as the perpendicular lines are not detectable unambiguously due to the complexity of the perpendicular part of the spectrum).

(equatorial) ligand bonds if going to the heavier halogenide donors. A similar dependence has been observed for the d^1 type complexes $Mo(V)OX_4Y$ (X = Cl, Br, I; Y = X or solvent).[12]

It should be noted that for pentacyano–nitrosyl complexes of the iron group metals[13] some small hyperfine interactions have been found resulting from the interaction of the unpaired spin density with the ^{14}N nucleus of the NO ligand. For the complexes under study such additional hyperfine splittings have not been resolved, possibly due to the larger linewidths in the EPR spectra of the Tc complexes.

Finally it should be noted that no attempts have been made to interprete the $\tilde{g}$ tensor components in terms of molecular orbital coefficients. Such an interpretation is extremely difficult for the present case because there are more unknown quantities (ordering of energy levels, energy separations between the levels giving important contributions to the $\tilde{g}$ components, the large number of MO coefficients to be considered) than experimentally obtained ones. Results of semiempirical MO calculations which may be very helpful for these purposes[13–15] are not available for Tc compounds of this type up to now.

Acknowledgement—The authors wish to thank Dr. Bernd Lorenz (Leipzig) for his help in preparation of the technetium compounds.

REFERENCES

1. G. Subramanian, B. A. Rhodes, J. F. Cooper and V. J. Sodd, *Radiopharmaceuticals*. The Society of Nuclear Medicine, New York (1975).
2. A. G. Jones and A. Davison, *Int. J. Appl. Radiat. Isot.* 1982, **33**, 867.
3. A. Davison and A. G. Jones, *Int. J. Appl. Radiat. Isot.* 1982, **33**, 875.
4. R. Kirmse, J. Stach, B. Lorenz and I. N. Marov, *Z. Chem.* 1984, **24**, 36.
5. C. Orvig, A. Davison and A. G. Jones, *J. Labelled Compd. Radiopharm.* 1981, **18**, 148.
6. G. C. Yang, M. W. Heitzmann, L. A. Ford and W. R. Benson, *Inorg. Chem.* 1982, **21**, 3242.
7. R. Kirmse, B. Lorenz and K. Schmidt, *Polyhedron* 1983, **2**, 935.
8. R. Kirmse, J. Stach and U. Abram, *Polyhedron*, submitted for publication.
9. R. Kirmse, J. Stach, U. Abram and I. N. Marov, *Z. anorg. allg. Chem.* 1984, **518**, 210.
10. B. Bleaney, *Philos. Mag.* 1951, **42**, 441.
11. B. R. McGarvey, *J. Phys. Chem.* 1967, **71**, 51.
12. I. N. Marov and N. A. Kostromina, *EPR and NMR in the Chemistry of Coordination Compounds* (Russ.). Nauka, Moscow (1979).
13. P. T. Manoharan, S. Vijava, J. R. Shock and M. T. Rogers, *J. Chem. Phys.* 1975, **63**, 2507.
14. C. P. Keijzers and E. de Boer, *Molec. Phys.* 1975, **29**, 1007, 1743.
15. J. Stach, R. Kirmse, S. Wartewig and R. Böttcher, *Z. Chem.* 1979, **19**, 205.

Polyhedron Vol. 4, No. 7, pp. 1279–1282, 1985
Printed in Great Britain

0277–5387/85 $3.00 + .00
© 1985 Pergamon Press Ltd

^{1}H AND ^{13}C NMR OF PLATINUM PORPHYRINS—II. PLATINUM COMPLEXES OF *MESO*-TETRAKIS(3,5-DI-*t*-BUTYL-4-HYDROXYPHENYL)PORPHYRIN AND 2,3,7,8,12,13,17,18-OCTAETHYLPORPHYRIN

LIONEL R. MILGROM

Imperial College of Science and Technology, Department of Chemistry, Exhibition Rd, London SW7 2AZ, U.K.

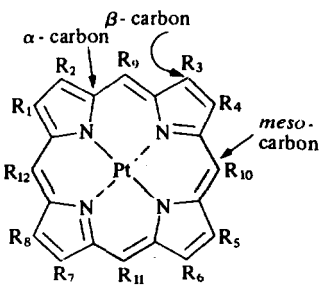
(*Received* 13 *August* 1984; *accepted* 18 *December* 1984)

Abstract—The ^{1}H and ^{13}C NMR spectra of the title compounds are reported. In both porphyrins, long-range spin–spin coupling is observed between platinum and the porphyrin protons and carbon atoms. Two-bond Pt–"α-pyrrole" carbon couplings are less than the three-bond Pt–"β-pyrrole" carbon and Pt–"*meso*-carbon" couplings. Also, large upfield shifts of the pyrrole α-carbon resonances are noted. The coupling mechanism appears to proceed via Fermi contact through the porphyrin σ-framework for the carbons, and the π-system for the protons.

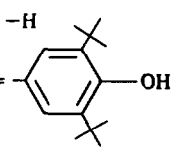
The previous paper in this series[1] attempted to rectify a deficiency of NMR data[2] on platinum porphyrins[3,4] by describing, for the first time, long-range coupling between platinum and the porphyrin protons and carbon atoms in platinum *meso*-tetraphenylporphyrin (PtTPP). Also observed were large upfield shifts in the α-carbon resonances of both PdTPP and PtTPP.[1] As thallium(III)[5,6] and phosphorus(V)[6(c)] complexes are the only extensively studied metalloporphyrins which demonstrate ^{1}H–M and ^{13}C–M spin–spin coupling in their NMR spectra, it was decided to extend observation of these couplings into other platinum porphyrin systems. This paper, therefore, reports the ^{1}H and ^{13}C NMR spectra of platinum porphyrins **1** and **2**, and attempts to obtain such spectra for the platinum complex of the naturally-occurring porphyrin protoporphyrin IX dimethyl ester [PtPPIXDME (**3**)] (Fig. 1).

RESULTS AND DISCUSSION

Platinum was inserted into the porphyrins using the method of Büchler and Puppe.[4] Unreacted free-base porphyrins were separated as reported earlier.[1] The synthesis of the free-base porphyrin (**1**) has been described elsewhere.[7]



1 $R_1 - R_8 = -H$

$R_9 - R_{12} =$ 

2 $R_1 - R_8 = -CH_2CH_3$
$R_9 - R_{12} = -H$

3 $R_1 = R_3 = R_5 = R_8 = -CH_3$
$R_2 = R_4 = -CH{=}CH_2$
$R_6 = R_7 = -CH_2CH_2CO_2CH_3$
$R_9 - R_{12} = -H$

Fig. 1.

Table 1.

	Pyrrole β-H[a]	Aryl *ortho*-H	Aryl-OH	Aryl *t*-butyl-H
Free-base porphyrin (1)	8.92[b] (8.75)[c]	8.03 (8.30)	5.52	1.62
Zinc porphyrin (1)	9.04	8.04	5.50	1.62
Platinum porphyrin (1)	8.84[d] (8.74)	7.96 (8.14)	5.50	1.60

[a] Spectra recorded in $CDCl_3$ with TMS as internal reference.
[b] Chemical shifts in δ ppm.
[c] Figures in parentheses are the equivalent chemical shifts for the TPP complex.[1]
[d] Satellites are 5.5 Hz either side of this peak; $^4J_{^1H-^{195}Pt}$ is 10.9 Hz compared to 3–17 Hz.[8]

Pt *complex* **1**

The free-base porphyrin undergoes a facile two-electron oxidation[7] and metal complexes, including the zinc and platinum compounds, are currently under investigation as electrocatalysts for the reduction of oxygen. The ^1H NMR spectrum of the platinum complex **1** was similar to those of the free-base porphyrin and its zinc complex (see Table 1). As with PtTPP,[1] the two satellites flanking the pyrrole β-proton resonance are due to long-range ^1H–^{195}Pt coupling over four bonds. The coupling constant (10.9 Hz) is consistent with this,[8] although slightly smaller than for PtTPP (12.5 Hz[1]). This may reflect small differences in the steric "ruffling" of the macrocycles, induced by the bulky *t*-butyl groups on the *meso*-aryl substituents.

The ^{13}C NMR spectrum of platinum porphyrin **1** is assigned, once again, by comparison with the free-base porphyrin, the zinc complex, and the TPP complexes (see Table 2). The porphyrin macrocyclic carbons are readily assigned. The aryl carbons, being part of a polysubstituted aromatic system, are for the most part predictable on the basis of additivity of chemical shifts of monosubstituted benzenes.[9] On this assumption, the C-3″ carbons appear at higher field than expected. This may be due to aryl-ring distortion brought about by steric interactions of the *t*-butyl and OH substituents.

The large $^{13}C_{meso}$–Tl couplings found in thallium porphyrins[5,6] prompted a reexamination of the ^{13}C NMR spectrum of PtTPP which revealed a ^{13}C–^{195}Pt coupling to the *meso*-carbons (three-bond, 37 Hz) consistent with similar couplings reported elsewhere. In complex **1**, besides the coupling to the β-pyrrole carbons, no other ^{13}C–^{195}Pt couplings are observed due to a poor signal-to-noise ratio.

The large upfield shift of the α-carbons is accounted for[1] by steric "ruffling"[12] of the porphyrin nucleus and/or metal *d*-porphyrin π*-back-bonding.

Pt *complex* **2** (PtOEP)

The ^1H NMR spectrum of this porphyrin is similar to those of the free-base porphyrin and other metallo-OEP complexes[13] (see Table 3). An earlier observation of the ^1H NMR spectrum of **2**[2] failed to note the near-resolution of Pt satellites on the methine-proton resonance. Unlike TlOEP,[5] no coupling was observed between platinum and the methylene protons of the β-pyrrole-substituted ethyl groups.

Table 2.

	C-α[a]	C-β	C-*meso*	C-1″	C-2″	C-3″	C-4″	*t*-Butyl	
Free-base (1)	147[b]	131	121	133.7	134.2	131.8	153.5	34.6	30.8
	(145.8)[c]	(130.6)	(119.6)	(141.7)	(134.0)	(126.1)	(127.5)	—	—
Zinc (1)	150.7	132.0	122.1	134.1	134.0	131.7	153.4	34.6	30.8
	(150.8)	(132.5)	(121.6)	(143.4)	(134.9)	(127.5)	(128.0)	—	—
Platinum (1)	141.3	130.6[d]	123.2	132.8	134.3	131.1	153.5	34.6	30.8
	(140.9)	(130.7)	(122.3)	(141.5)	(133.9)	(126.8)	(127.8)	—	—

[a] Spectra recorded in $CDCl_3$ with TMS as internal reference.
[b] Chemical shifts in δ ppm.
[c] Figures in parentheses are equivalent chemical shifts for TPP complexes.[1]
[d] Satellites are 15.9 Hz either side of this peak; $^3J_{^{13}C-^{195}Pt}$ is 31.9 Hz, cf. 34–70 Hz.[10,11]

Table 3.

	Methine-H[a]	Ethyl-CH_2	Ethyl-CH_3
OEP	10.18[b]	4.14(q)	1.95(t)
PdOEP	10.12[c]	4.06(q)	1.91(t)
PtOEP	10.02[c]	4.07(q)	1.95(t)
PtOEP	10.01[d]	4.01(q)	1.90(t)

[a] Spectra recorded in $CDCl_3$ with TMS as internal reference and chemical shifts in δ ppm.

[b] See Ref. 13.

[c] Values reported at 60 MHz.

[d] Values in this work, peak nearly resolved into 1:4:1 triplet with $^4J_{^1H-^{195}Pt} = 4.5$ Hz.

The ^{13}C NMR spectrum of **2** is similar to OEP and other metallo-OEP complexes[6(a)] in that it consists of five main peaks (see Table 4). All the macrocyclic carbons are accompanied by Pt satellites. Unusually for metalloporphyrins,[13] the pyrrole α-carbon resonance is assigned to higher field than the pyrrole β-carbon resonance. This is based on the previously-recorded large high-field shift of the α-carbons in PtTPP[1] and the magnitude of long-range ^{13}C–^{195}Pt coupling, which is greater for β-carbons than for α-carbons. A similar inversion in the resonance position of these carbons is seen in the dication of OEP.[6(a)]

In order to confirm this, a fully proton-coupled ^{13}C NMR spectrum of PtOEP was recorded. It was hoped that long-range ^{13}C–^{1}H coupling (between the pyrrole α-carbons and the *meso*-protons, and the pyrrole β-carbons and the ethyl protons) could be resolved. In the event, only unresolvable multiplets of similar bandwidth were obtained for these carbons. However, the *meso*-carbons were split into a large doublet (155.6 Hz), of which each peak is further split into a 1:4:1 triplet (36.2 Hz). The one-bond ^{13}C-*meso*–^{1}H-methine coupling constant is close to that found for benzene (157.65 Hz).[15] This would indicate little ring strain in the macrocycle even though the Pt cation is too large for central cavity. Further studies are investigating how this coupling constant varies with central metal cation and could act as a probe of porphyrin ring strain.[9]

Although the magnitude of the coupling constants for PtTPP and **2** is smaller than the thallium porphyrins, the data (see Table 5) suggest that the coupling mechanisms are the same. Transmission of long-range coupling is attributed to Fermi contact through the macrocyclic σ-framework while coupling to the *meso*-protons is transmitted through the π-system via a σ–π interaction.[5,6,16] Also ^{13}C–^{195}Pt coupling over three bonds is larger for the pyrrole *meso*-carbons than for the β-carbons. This is because there are two equivalent *cis*-three-bond pathways for the *meso*-carbons, but only one *trans*-three-bond pathway for the β-carbons.

Replacement of haem [Fe(II)PPIX] with PtPPIX could, by virtue of these couplings, act as a sensitive NMR probe for the active sites of haemoproteins. Therefore, **3** was prepared but both the ^{1}H and ^{13}C NMR spectra suffered severe line-broadening. As both solvent and TMS peaks were sharp, this was attributed to extensive aggregation in solution, a conclusion supported by the UV/vis spectrum of **3** (all bands broadened and reduced in intensity).[17,18] If such aggregation is mediated by mutual overlap of d_{z^2} orbitals of Pt then PtPPIXDME would make an ideal one-dimensional conductor.

EXPERIMENTAL

All spectra were obtained, in the FT mode, on a Bruker WM 250 NMR spectrometer. UV/vis spectra

Table 4.

	C-α[a]	C-β	C-*meso*	$-\underline{C}H_2-$	$-\underline{C}H_3$
OEP[b]	143.5[c]	140.9	96.0	19.7	18.3
OEP($2H^+$)[d]	143.1	147.0	100.3	21.4	18.1
ZnOEP[b]	146.7	141.1	96.2	19.8	18.3
TlOEP(OH, H_2O)[b]	146.6(18)[e]	142.7(104)	97.7(147)	19.9(13)	18.4
PtOEP	138.5(12.2)[e]	140.7(27.8)	99.2(37.6)	19.7	18.2

[a] Spectra recorded in $CDCl_3$ using TMS as internal reference, chemical shifts in δ ppm.

[b] See Ref. 6(a).

[c] See Ref. 14 for this value.

[d] In TFA.

[e] Figures in parentheses refer to long-range ^{13}C–M coupling constants; values for TlOEP taken from Ref. 6(a).

Table 5.

	H-β	C-α	C-β	C-*meso*	H-*meso*	C-α	C-β	C-*meso*
TlTPP[a]	65.4[b]	13	119	141 TlOEP[c]	44.4	18	104	147
PtTPP	12.5	12.6[d]	25.2	37[d] PtOEP	4.5[e]	12.2	27.8	37.6

[a] With OH and H_2O axial ligands.[5,6(b)]
[b] Couplings in Hz.
[c] With OH and H_2O axial ligands, see Refs 5 and 6(b).
[d] Coupling constants tentative here due to poor signal-to-noise ratio.
[e] This value approximate due to poor resolution of Pt satellites.

were obtained on a Pye–Unicam SP8-400 spectrophotometer in $CHCl_3$ using approximately 10^{-5} M solutions. Platinum was inserted according to a literature method[2] and the porphyrins purified by column chromatography on silica gel, eluting with $CHCl_3$/TFA [2%(v/v)].[1]

Pt *complex* 1

Obtained as an orange amorphous powder from *n*-hexane, m.p. 300°C. Yield = 288 mg (65%). Found: C, 68.7; H, 7.13; N, 4.17%. $C_{76}H_{92}N_4O_4Pt \cdot \frac{1}{2}H_2O$ requires: C, 68.7; H, 7.0; N, 4.2%. λ_{max} (nm)[ε (mmol l^{-1})]: 411(302), 514(26.2), 542(s, 1.5).

Black microcrystals from methanol (360 mg, 71%). Found: C, 56.71; H, 4.52; N, 7.72%. $C_{36}H_{36}N_4O_4Pt \cdot \frac{1}{2}C_6H_5CN$ requires: C, 56.8; H, 4.6; N, 7.6%. λ_{max} (nm)[ε (mmol l^{-1})] 387(69), 506(6.8), 541(12.3).

Acknowledgements—I thank Dr R. Shepherd, Ms S. Johnson and Mr P. Booth for NMR spectra and the SERC for support.

REFERENCES

1. L. R. Milgrom, *Polyhedron* 1984, **3**, 879.
2. J. W. Büchler and L. Puppe, *Ann. Chem.* 1974, 1046.
3. J. R. Darwent, P. Douglas, A. Harriman, G. Porter and M.-C. Richoux, *Coord. Chem. Rev.* 1982, **44**, 83.
4. B. M. Hoffman and J. A. Ibers, *Acc. Chem. Res.* 1983, **16**, 15.
5. R. J. Abraham, G. H. Barnett and K. M. Smith, *J. Chem. Soc., Perkin Trans.* I. 1973, 2142.
6. (a) R. J. Abraham, G. E. Hawkes and K. M. Smith, *J. Chem. Soc., Perkin Trans.* II. 1974, 627; (b) R. J. Abrahams, G. E. Hawkes, M. F. Hudson and K. M. Smith, *J. Chem. Soc., Perkin Trans.* II. 1975, 204; (c) C. A. Marrese and C. J. Carrano, *Inorg. Chem.* 1983, **22**, 1858.
7. L. R. Milgrom, *Tetrahedron* 1983, **39**, 3895.
8. F. Bonati, H. C. Clark and C. S. Wong, *Can. J. Chem.* 1980, **58**, 1435.
9. G. C. Levy, R. L. Lichter and G. L. Nelson, In *Carbon-13 Nuclear Magnetic Resonance Spectroscopy*, 2nd edition, Chap. 4, p. 109. John Wiley, New York (1980).
10. H. C. Clark and J. E. H. Ward, *J. Am. Chem. Soc.* 1974, **96**, 1741.
11. C. A. Wilkie and D. T. Haworth, *J. Inorg. Nucl. Chem.* 1978, **40**, 195.
12. E. B. Fleischer, C. K. Miller and L. E. Webb, *J. Am. Chem. Soc.* 1964, **86**, 2342.
13. T. R. Janson and J. J. Katz, In *The Porphyrins* (Edited by D. Dolphin), Vol. 4, pp. 1–59. Academic Press, New York (1979).
14. A. R. Battersby, J. Moron, E. McDonald and J. Feeney, *J. Chem. Soc., Chem. Commun.* 1972, 920.
15. H. Günther, H. Seel and M.-E. Günther, *Org. Magn. Reson.* 1978, **11**, 97.
16. J. P. Maher and D. F. Evans, *J. Chem. Soc.* 1964, 637.
17. J.-H. Führop, In *Porphyrins and Metalloporphyrins* (Edited by K. M. Smith), p. 619. Elsevier, New York (1974).
18. L. R. Milgrom, *J. Chem. Soc., Perkin Trans.* I. 1983, 2535.

Polyhedron Vol. 4, No. 7, pp. 1283–1292, 1985
Printed in Great Britain

0277–5387/85 $3.00 + .00
© 1985 Pergamon Press Ltd

S-ALKYL AND S-ALKYLARYL CYSTEINE COMPLEXES WITH PLATINUM(II) AND THEIR INTERACTIONS WITH NUCLEOSIDES

V. THEODOROU
University of Athens, Department of Chemistry, Organic Chemistry Laboratory, Navarinou 13A, Athens, Greece

and

N. HADJILIADIS*
University of Ioannina, Department of Chemistry, Laboratory of Inorganic and General Chemistry, Ioannina 45332, Greece

(*Received* 5 *November* 1984; *accepted* 18 *December* 1984)

Abstract—The reactions of K_2PtCl_4 with the aminoacids, S-methyl-L-cysteine, S-ethyl-L-cysteine, S-benzyl-L-cysteine, S-para-nitro-benzyl-L-cysteine, S-diphenyl-methyl-L-cysteine, S-tribenzyl-L-cysteine and S-4′,4′-dimethoxy-diphenylmethyl-L-cysteine were studied in neutral or acidic aqueous solutions. Complexes of the formulae $PtLCl_2$, $[PtL_2]Cl_2$ and $Pt(L–H^+)_2$, where L = aminoacid, were isolated in the solid state and their structures investigated with elemental analysis, conductivity measurements, IR, ^1H NMR and ^{13}C NMR spectra. The results show that the coordination sites of Pt(II) with the amino-acids are the N and S atoms, producing two diastereoisomers around the chiral sulphur atom, which were identified in the ^1H NMR and ^{13}C NMR spectra. The complexes $PtLCl_2$ further react with the nucleosides guanosine and inosine. The complexes $[PtL(nucl)_2]Cl_2$ were isolated from these reactions and studied with the same methods. They showed a $Pt–N_7$ bonding with the nucleosides and retained the N, S bondings with the aminoacids. As a result of the higher *trans* influence of S than N, the nucleoside molecule coordinated to the metal through N_7 and *trans* to S has a weaker bond strength than the other, as it is revealed from the ^1H NMR and ^{13}C NMR spectra of these complexes.

Recently, we reported the syntheses, spectroscopic studies and X-ray crystal structure determination of the complex *cis*-(S-ethyl-L-cysteine) platinum(II) dichloride.[1] This complex, which was among a number of other similar complexes prepared by us with S-alkyl- and -alkylaryl derivatives of cysteine, was shown to occur in two diastereoisomeric forms (R, S), both in solution and in the solid state, due to the chiral sulphur atom. Pd(II) and Pt(II) complexes of S-methyl-L-cysteine also exist in two diastereoisomeric forms in solution[2,3] and in the solid state for Pd(II).[4] The S-methyl-L-cysteine sulphoxide complex of Pd(II) however, was found in only one diastereoisomeric form in the solid state.[3]

Reports on complexes of S-alkyl cysteine derivatives of Pd(II) and Pt(II) are mainly limited to S-methyl cysteine and methionine.[2–8] Recently, Kozlowski *et al.*[9] reported on complexes of Pd with S-benzyl-cysteine and glycyl-S-benzyl-L-cysteine and found also two diastereoisomers on sulphur (R, S). Some S-alkylaryl cysteines on the other hand (e.g. S-trityl cysteine) are antitumor agents in their own right.[10,11] The study therefore of the interactions of Pt(II) with S-alkyl or S-alkylaryl cysteine derivatives presents interests, both from the chemical point of view (e.g. binding sites of the ligands with the metal (S, N, O), stoichiometry of the complexes, possibility for the existence of diastereoisomers around the sulphur atom, etc.) and the possibility of preparing new antitumor agents. (Preliminary screening tests of all the *cis*-Pt(II) complexes with cysteine derivatives prepared in this study, showed them inactive.)

* Author to whom correspondence should be addressed.

Also the study of the reactions of all the new complexes having the *cis* structure, like the *cis*-(S-ethylcysteine) platinum(II) dichloride with nucleosides are comparable to the ones of the antitumor complex *cis*-$Pt(NH_3)_2Cl_2$. Analogous studies of Pt(II) and Pd(II) with cysteine[12] and the reactions of a Pt(II)–cysteine complex with nucleosides[13] were also reported.

This paper describes the reactions of Pt(II) with the above mentioned cysteine derivatives and the interactions of certain of these complexes with a *cis* configuration, with nucleosides.

RESULTS

The L-amino acids used in this study were, S-methyl-L-cysteine (S-MeCys), S-ethyl-L-cysteine (S-EtCys), S-benzyl-L-cysteine (S-BzlCys), S-para-nitro-benzyl-L-cysteine (S-*p*-NO_2-BzlCys), S-diphenyl-methyl-L-cysteine (S-DpmCys), S-tribenzyl-L-cysteine (S-TrtCys) and S-4′,4′-dimethoxydiphenylmethyl-L-cysteine (S-DmbCys).

These amino acids (presented with L) react with K_2PtCl_4 in aqeuous solutions, to produce complexes of various empirical formulae, as follows:

$$K_2PtCl_4 + L \rightarrow PtLCl_2 + 2KCl. \quad (1)$$

The complexes with S-TrtCys and S-DmbCys, were not isolated, due to the hydrolysis of the bulky Trt and Dmb groups, producing complexes of the type PtL'_2Cl_2, with L′ = cysteine[12] (see Experimental).

The 1:2 metal to ligand ratio complexes were prepared either from the 1:1 or directly from the starting materials.

$$PtLCl_2 + L \rightarrow [PtL_2]Cl_2 \quad (2)$$

or

$$K_2PtCl_4 + 2L \rightarrow [PtL_2]Cl_2 + 2KCl. \quad (3)$$

Reaction (3) failed to give pure products, due to the liberated KCl. On the other hand, both reactions (2) and (3) produce soluble and to a lesser extent insoluble materials of the same empirical formulae. A polymeric structure was attributed to the latter (see Discussion).

When the soluble $[PtL_2]Cl_2$ complexes react with freshly prepared Ag_2O, complexes of the empirical formulae $[Pt(L–H^+)_2]$ are prepared:

$$[PtL_2]Cl_2 + Ag_2O \rightarrow [Pt(L–H^+)_2] + 2AgCl + H_2O. \quad (4)$$

The same complexes may also be produced upon neutralization of aqueous solutions of $[PtL_2]Cl_2$ with dilute NaOH solutions, although not in pure condition, due to the inability to separate them from the liberated NaCl, in this case.

$$[PtL_2]Cl_2 + 2NaOH \rightarrow [Pt(L–H^+)_2] + 2NaCl + 2H_2O. \quad (5)$$

Finally, the nucleoside complexes were prepared according to

$$[PtLCl_2] + 2nucl \rightarrow [PtL(nucl)_2]Cl_2. \quad (6)$$

The isolated complexes correspond to the above empirical formulae, as their elemental analysis show (see Table 1).

DISCUSSION

1. $PtLCl_2$ *type complexes*

The molar conductances of these complexes in DMF solutions show that they are non-electrolytes, as expected[1] (see Table 1). The water soluble complex *cis*-(S-MeCys)platinum(II) dichloride as well as the *cis*-(S-EtCys)platinum(II)dichloride has a molar conductance[1] of 280 ohm^{-1} cm^2 $mole^{-1}$, in aqueous solutions. This may be explained by their easy aquation, especially at the position *trans* to the sulphur atom,

$$[PtLCl_2] + H_2O \rightarrow [PtL(H_2O)Cl]Cl \xrightarrow{+H_2O} [PtL(H_2O)_2]Cl_2 \quad (7)$$

and the ionization of the free carboxylate group.[1,14,15] A 10^{-3} M aqueous solution of the complexes has a pH ~ 3. On the other hand, the complex $[Pt(MtH)Cl_2]$, with MtH = methionine has a $pK_a = 2.3$, of the same order with the hydrochloric acid salt of methionine (MtH·HCl), while the $[Pd(MtH)Cl_2]$ presents $\Lambda_M = 365$ ohm^{-1} cm^2 $mole^{-1}$.[5,15]

In the IR spectra of all these complexes, there is a strong band at ~ 1720 cm^{-1} which is assigned to the $\nu_{as}C{=}O$, of a free carboxylate group. For the ionized free carboxylate group, this vibration occurs in the range of 1550–1620 cm^{-1}, while for a coordinated one, it is seen at 1580–1660 cm^{-1}.[1,12,13] This suggested an S, N coordination in the case of *cis*-(S-EtCys)platinum(II)dichloride complex, which was confirmed with its X-ray crystal structure determination[1] and suggests the same, for all the similar $PtLCl_2$ complexes, isolated in the present study.

The amino group participation in the bonding with Pt(II) is confirmed here also from the examination of the νNH_2 and the δNH_2 frequencies of the complexes, identified with deuteration at ~ 3200 and ~ 1600 cm^{-1}, respectively (see Table 2). The observed frequencies compare favorably with the ones of other similar complexes like, $Pt(MtH)Cl_2$, $Pt(L–H^+)_2$, where L = CysOEt,

Table 1. Analytical data and molar conductances of the complexes

Complex	% Pt		% Cl		% C		% H		% N		% S		Λ_M
	Calc	Found	Calc	Found	Calc	Found	Calc	Found	Calc	Found	Calc	Found	$ohm^{-1}\ cm^2\ mole^{-1}$
cis-Pt(S-Me-L-Cys)Cl_2	48.7	48.6	17.6	17.7	12.0	12.0	2.3	2.3	3.5	3.5	8.0	8.0	19(DMF), 280(H_2O)
cis-Pt(S-Et-L-Cys)Cl_2	47.2	47.0	16.4	17.1	14.1	14.5	2.6	2.7	3.3	3.4	7.7	7.7	11(DMF), 280(H_2O)
cis-Pt(S-Bzl-L-Cys)Cl_2	40.8	40.9	13.7	13.9	26.0	25.2	2.8	2.7	3.0	2.9	6.8	6.7	22(DMF)
cis-Pt(S-*p*-NO_2-Bzl-L-Cys)Cl_2	37.6	37.4	13.8	13.6	22.1	23.0	2.3	2.3	5.1	5.4	5.8	6.1	22(DMF)
cis-Pt(S-Dpm-L-Cys)Cl_2	35.0	35.2	11.9	12.8	36.0	35.7	3.1	3.1	2.6	2.5	6.0	5.8	23(DMF)
Pt(S-Me-L-Cys)$_2Cl_2$	36.3	36.4	12.4	13.2	17.6	17.9	3.3	3.4	—		—		680(H_2O)
Pt(S-Et-L-Cys)$_2Cl_2$	34.8	34.6	13.0	12.6	21.1	21.3	3.8	3.9	—		—		695(H_2O)
Pt(S-Bzl-L-Cys)$_2Cl_2$	28.1	28.3	10.2	10.3	33.6	33.9	3.5	3.8	—		—		655(H_2O)
Pt(S-*p*-NO_2-Bzl-L-Cys)$_2Cl_2$	25.3	25.1	9.2	9.1	30.6	30.8	3.0	3.1	—		—		—
Pt(S-Dmp-L-Cys)$_2Cl_2$	24.5	23.9	8.7	8.4	—		—		—		—		—
Pt(S-Me-L-Cys-H^+)$_2$	41.7	42.1	0.0	0.0	20.2	20.7	3.3	3.5	—		—		16(H_2O)
Pt(S-Et-L-Cys-H^+)$_2$	40.4	39.7	0.0	0.0	—		—		—		—		14(H_2O)
Pt(S-Bzl-L-Cys-H^+)$_2$	31.5	31.7	0.0	0.0	—		—		—		—		8(H_2O)
Pt(S-*p*-NO_2-Bzl-L-Cys-H^+)$_2$	27.4	27.6	0.0	0.0	—		—		—		—		8(H_2O)
[Pt(S-Me-L-Cys)(Guo)$_2$]Cl_2	21.3	20.9	6.9	7.3	—		—		—		—		349(H_2O)
[Pt(S-Me-L-Cys)(Ino)$_2$]Cl_2	21.3	20.8	7.5	7.6	—		—		—		—		356(H_2O)
[Pt(S-Et-L-Cys)(Guo)$_2$]Cl_2	19.0	19.9	7.1	7.2	—		—		—		—		398(H_2O)
[Pt(S-Et-L-Cys)(Ino)$_2$]Cl_2	19.5	20.1	7.2	7.4	—		—		—		—		348(H_2O)
[Pt(S-Bzl-L-Cys)(Guo)$_2$]Cl_2	19.5	18.8	6.1	6.8	—		—		—		—		305(H_2O)
[Pt(S-*p*-NO_2-Bzl-L-Cys)(Guo)$_2$]Cl_2	18.7	17.9	5.9	6.4	—		—		—		—		301(H_2O)

All the complexes decomposed at temperatures higher than 200°C, without melting.

Table 2. Characteristic IR frequencies of the complexes in cm^{-1}

Compound	νNH	δNH	$\nu_{as}CO$	δNH_2 wag	δNH_2 twist	δNH_2 rock	νPt–Cl
S-Me-L-Cys	~ 3000 br	1600	1565	1245, 1108	850	510	—
Pt(S-Me-L-Cys)Cl_2	3190, 3090	1575	1733	1220	1085	640	329, 314
Pt(S-Me-L-Cys)$_2Cl_2$	3200, 3090	1585	1735	1210	1085	670	—
Pt(S-Me-L-Cys-H^+)$_2$	3240, 3100	1585	1620	1240	1065	—	—
S-Et-L-Cys	3140, 3040	1575	1610	1250, 1120	877	535	—
Pt(S-Et-L-Cys)Cl_2	3240, 3100	1580	1720	1230	1075	670	328, 310
Pt(S-Et-L-Cys)$_2Cl_2$	3250, 3100	1585	1735	1210	1088	680	—
Pt(S-Et-L-Cys-H^+)$_2$	3240, 3100	1585	1620	1240	1065	—	—
S-Bzl-L-Cys	3150, 3055	1610	1580	1230, 1150	—	520	—
Pt(S-Bzl-L-Cys)Cl_2	3220, 3160	1570	1725	1215	—	—	330, 310
Pt(S-Bzl-L-Cys)$_2Cl_2$	3200	1580	1730	1200	1080	—	—
Pt(S-Bzl-L-Cys-H^+)$_2$	3240, 3200	1585	1620	1200	1080	—	—
S-*p*-NO_2-L-Bzl-Cys	3150 br	1625	1595	1250, 1110	890	525	—
Pt(S-*p*-NO_2...)Cl_2	3240–3150	1590	1720	1200, 1080	—	—	330, 310
[Pt(S-*p*-NO_2...)]Cl_2	3200, 3120	1580	1735	1200, 1080	—	—	—
S-Dpm-L-Cys	3100 br	1610	1590	1220, 1100	880	—	—
Pt(S-Dmp-L-Cys)Cl_2	3205–3070	1587	1730	1230	800	620	322
[Pt(S-Dpm-L-Cys)$_2$]Cl_2	3220, 3200	1585	1735	1210, 1080	—	—	—

br = broad.

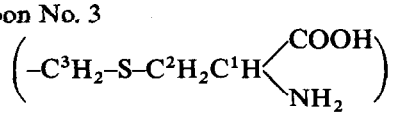
etc.[7,8,12,14,15] Also, the $\delta_t(NH_2)$ twisting motion of the free S-EtCys which occurs at 1120 cm^{-1} is seen at 1085 cm^{-1} in its complex with Pt(II), while the $\delta_r(NH_2)$ rocking motion at 535 and 600 cm^{-1} respectively, identified with deuteration. The negative shift of the former and the positive one of the latter, once again confirm the amino group participation with Pt(II).[16] All the complexes present also two Pt–Cl bands, confirming their *cis* configuration.

The ^1H NMR spectra of the complexes are useful for assigning the bonding sites and confirming the existence of two diastereoisomers in all the complexes. They were recorded either in D_2O or DMSO-d_6 according to their solubilities. All the protons near the bonding sites (N, S) of the ligands are shifted down- or up-field upon complexation with Pt(II), while the observed two sets of protons for the various methylene or methine protons, confirm the existence of the two diastereoisomers[1] (see Table 3). Similar results were also found in the work of Erickson *et al.*[17] on the interaction of Pt(II) with S-

Table 3. ^1H NMR chemical shifts of the aminoacids and the complexes in ppm

Compound	^1CH	$^2CH_2$	$^3CH_2$	$^4CH_3$	CH aromatic	Solvent
S-Me-L-Cys	0.90	3.03	2.15	—	—	D_2O
Pt(S-Me-L-Cys)Cl_2	3.99, 3.60	3.05	3.05	—	—	D_2O
Pt(S-Me-L-Cys)Cl_2	5.47, 5.80	3.30	3.00, 2.83	—	—	DMSO-d_6
[Pt(S-Me-L-Cys)$_2$]Cl_2	4.30, 4.01	3.28	2.80	—	—	D_2O
Pt(S-Me-L-Cys-H^+)$_2$	3.70, 4.03	3.15	2.67	—	—	D_2O
S-Et-L-Cys	3.90	3.08	2.61	1.24	—	D_2O
Pt(S-Et-L-Cys)Cl_2	4.02, 3.72	3.17	3.08	1.44	—	D_2O
Pt(S-Et-L-Cys)Cl_2	5.25, 5.78	3.20	3.00	1.33, 1.37	—	DMSO-d_6
[Pt(S-Et-L-Cys)$_2$]Cl_2	4.33, 4.01	3.43	3.33	1.45	—	D_2O
Pt(S-Et-L-Cys-H^+)$_2$	3.80, 4.00	3.22	3.10	1.42	—	D_2O
Pt(S-Bzl-L-Cys)Cl_2	5.60	3.33, 3.54	4.87	—	7.33	DMSO-d_6
Pt(S-*p*-NO_2...)Cl_2	5.00	3.00, 3.24	4.87, 4.57	—	8.20, 7.72	DMSO-d_6
Pt(S-Dpm-L-Cys)Cl_2	5.00	3.24	6.06	—	7.38, 7.50	DMSO-d_6

MeCys and others.[18,19] It is worthwhile mentioning that the down-field chemical shifts of the protons at the carbon No. 3



are larger in the complexes with S-BzlCys and S-DpmCys than in the other ligands, due to the large shielding constants of the phenyl groups (see Table 3).

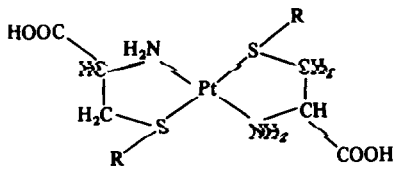
The conclusion of the ^1H NMR spectra was further reconfirmed more clearly with the ^{13}C NMR spectra of the ligands S-methyl and S-EtCys and their complexes with Pt(II)[1] and this was also in agreement with the results of Kozlowski *et al.*[2,3,9,20]

2. PtL_2Cl_2 type complexes

The molar conductances of these complexes in aqueous solutions, range from 650 to 700 ohm^{-1} cm^2 mole^{-1}, much higher than the values for the 1:2 electrolytes (~ 200). This is obviously due to the ionizations of the two free carboxylate groups. A 10^{-3} M aqueous solution of the complexes has a pH ~ 2.5. This compares favorably with the pH ~ 2.9 for the complex $[Pt(MtH)_2]Cl_2$ found by Chernova *et al.*,[14] as well as the values of the Λ_M for the same complex, which is found[14] near 600 ohm^{-1} cm^2 mol^{-1}.

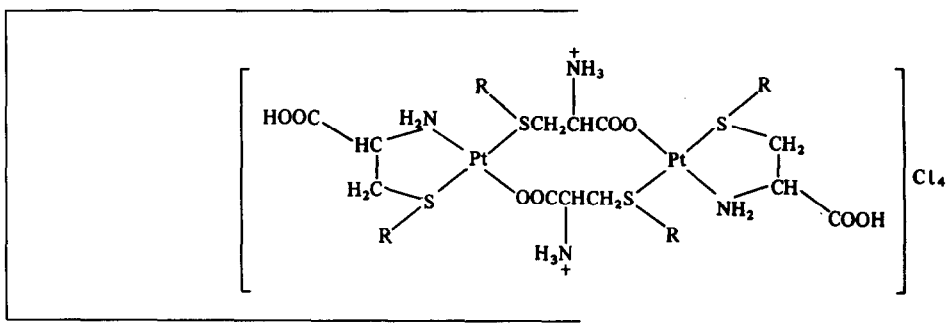
From the IR spectra of these complexes, which closely resemble those of the $PtLCl_2$ series, it is again concluded that the carboxylate groups are free, as the strong band at ~ 1730 cm^{-1} assigned to the $\nu_{as}C{=}O$, shows. The amino groups are coordinated with Pt(II), since the νNH occurs at 3100–3200 cm^{-1} and the δNH at 1580–1585 cm^{-1} (see Table 2), identified with deuteration. The characteristic feature in the far IR spectra of these complexes, is the absence of the doublets observed at 300–330 cm^{-1} in the $PtLCl_2$ series, indicating ionic chloride ions, in this case.

Since the PtL_2Cl_2 series is easily prepared from the $PtLCl_2$ series and the S and N atoms are the coordination sites in the latter and taking into account the large *trans* influence of the sulphur atom, the observations of free carboxylate groups and coordinated amino groups as well as the absence of Pt–Cl bonds in the former, the following structures for them are suggested.



(a) (b)

The insoluble products of the reactions (2) and (3) which correspond to the same empirical formulae, present a strong band at 1630–1640 cm^{-1}, which may be assigned to the νC=O of a coordinated carboxylate group (–COO–Pt), beside the other νC=O strong band at 1730 cm^{-1}. These observations suggest an oligomeric or polymeric structure for these materials.



Similar polymeric structures cannot be excluded. Similar oligomeric or polymeric structures were also found in the complexes $Pt(Cys)_2$ and $Pd(Cys)_2$,[12,21] as well as the $Pt(MtH)_2Cl_2$.[14]

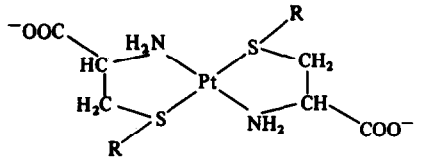
The ^1H NMR spectra in these series of complexes further shows the S, N coordination with Pt(II). The protons near the coordination sites shift downfield by 0.2–0.7 ppm (see Table 3). Several diastereoisomers are expected theoretically in the PtL_2Cl_2 series of complexes. However, taking into account that in the crystal structure of *cis*-Pt(S-EtCys)Cl_2, we found only two diastereoisomers, namely the S and R around the chiral sulphur centre, with the chelate ring in the λ conformation[1] and if we assume that the second chelate ring takes also a λ configuration, then the expected isomers will be only the R(λ)R(λ), R(λ)S(λ) and S(λ)S(λ) combinations.

A detailed analysis, however, of all the diastereoisomers formed cannot be done with certainty in the present case, like in the case of other similar Pd(II) complexes,[9] due to the low solubility of most of the complexes of the PtL_2Cl_2 series. Most of the proton resonances are broad and not well resolved in an 80 MHz spectrometer and may

suggest the presence of more than one diastereoisomer (see Table 3).

3. $Pt(L–H^+)_2$ *type complexes*

Since the complexes are prepared according to the reactions (4) and (5), their expected structures are



These complexes are non-electrolytes in water solutions, with molar conductances ranging from 8–16 $ohm^{-1}\ cm^2\ mole^{-1}$ (Table 1), as expected.

The structures **III** are further substantiated from their IR spectra, where we observe the νNH of a coordinated amino group, in the range 3020–3280 cm^{-1} and the δNH of the same at $\sim$ 1580 cm^{-1}, both identified with deuteration. Also with the absence of the characteristic band near 1730 cm^{-1} assigned to the νC=O of a free and protonated carboxylate group. There is instead a strong absorption near 1620 cm^{-1} not removed upon deuteration, assigned to the νC=O of a free ionized carboxylate group. [1,12,13] This was substantiated from the IR spectra of the residue of a sample of a $Pt(L–H^+)_2$ in 0.1 N HCl aqueous solution, obtained after evaporation, which showed again the band at 1730 cm^{-1} and not the one at 1620 cm^{-1}. Obviously, the HCl addition is reversible and the following reaction occurred:

$$Pt(L–H^+)_2 + 2HCl \rightarrow PtL_2Cl_2. \qquad (8)$$

The structure **III** was also proposed by Chernova *et al.*[14] for the complex $Pd(Mt)_2$, with Mt = the methionine anion, which showed the νC=O at 1575 cm^{-1} and the νNH at 3150 and 3004 cm^{-1}. In these complexes again, the νPt–Cl bands, are not observed in their far IR spectra, as expected.

The ^{1}H NMR spectral data have been included in Table 3. These indicate once again as coordination sites the S and N atoms (shift of the adjacent protons). Only the methine protons of C_1 are shifted to a larger extent here than in the other series of complexes, shielded by the adjacent $-COO^-$ group. The broadness of the observed ^{1}H NMR resonances also suggests several diastereoisomers here, as in the PtL_2Cl_2 series.

4. $PtL(nucl)_2Cl_2$ *type complexes*

The nucleosides used for the preparation of these complexes, according to reaction (6), were guanosine = Guo and inosine = Ino. These complexes have molar conductances in aqueous solutions ranging from 300–400 $ohm^{-1}\ cm^2\ mole^{-1}$ (see Table 1), due to the ionization of the free carboxylate group of the amino acids.

The IR spectra of these complexes are quite complicated, due to the presence of the nucleosides and it is not easy to identify the νNH and δNH motions of the amino-acids or the nucleosides, whenever present, because they overlap in several cases. The only observation worth mentioning is that the νC=O motions of the free carboxylate groups of the amino acid complexes without nucleosides, occurring near 1730 cm^{-1}, are now observed near 1700 cm^{-1} as broad bands, obviously coupled with the νC=O of the carbonyl groups of the nucleosides guanosine and inosine. Also there are no bands assignable to νPt–Cl in the far IR spectra of the complexes, as expected.

The ^{1}H NMR spectral data are given in Table 4. The H_2 and H_8 aromatic proton resonances of free inosine, appearing at 8.07 and 8.17 ppm respectively,[22] shift to higher fields and show two resonances for each proton near 8.30 and 9.00 ppm, in the complexes (see Table 4). The larger shift of the H_8 resonance (near 9.00 ppm) suggests an N_7 coordination with Pt(II), as expected.[23] The two sets of resonances observed for each proton are most probably due to the inequivalence of the two inosine molecules, in the $[PtL(Ino)_2]Cl_2$ complexes, the one being *trans* to a sulphur atom, with a higher *trans*-influence than the other, *trans* to a nitrogen atom. The protons less shifted to higher fields are assigned to the inosine molecule coordinated through N_7, *trans* to the sulphur atom. Similar behaviour was also observed in the complex Pt(Cys–

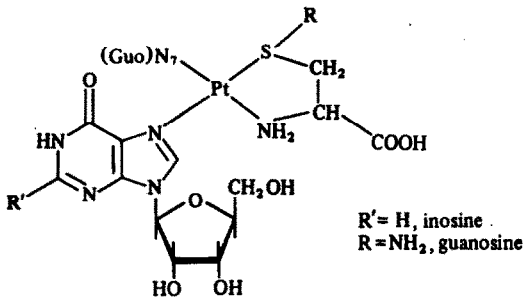
Table 4. ^{1}H NMR chemical shifts of the nucleosides in the complexes $PtL(nucl)_2Cl_2$ in ppm

Compound	H_2	H_8	H'_1	H'_2	H'_3	H'_4	H'_5
$[Pt(S\text{-}Me\text{-}L\text{-}Cys)(Guo)_2]Cl_2$	—	8.56, 8.35	5.92	4.65	4.41	4.28	3.86
$[Pt(S\text{-}Et\text{-}L\text{-}Cys)(Guo)_2]Cl_2$	—	8.65, 8.41	5.99	4.75	4.35	4.35	3.90
$[Pt(S\text{-}Me\text{-}L\text{-}Cys)(Ino)_2]Cl_2$	8.29, 8.32	9.02, 8.86	6.12	4.75	4.31	4.31	3.88
$[Pt(S\text{-}Et\text{-}L\text{-}Cys)(Ino)_2]Cl_2$	8.30 (doublet)	8.98, 8.81	6.12	4.65	4.34	4.34	3.90

OMe)(Ino)Cl[13] where the H_8 proton of inosine opposite to the sulphur atom, was shifted only by 0.28 ppm, while in the *cis*-$Pt(Ino)_2Cl_2$[23] the same proton was shifted by 0.62 ppm.

The same behaviour is also found in the complexes with Guo, $[PtL(nucl)_2]Cl_2$, e.g. two resonances for the H_8 protons (see Table 4). The ^{195}Pt–H coupling satellites are also seen in the spectra of the complexes, although not well enough resolved to allow measurements of the coupling constants.

The ^{13}C NMR spectral data finally, are given in Table 5 and Fig. 1. The chemical shifts of the carbons of the amino acids are shown as doublets and this indicates that the S, N coordination and the two diastereoisomers of the starting complexes are retained also in the complexes $[PtL(nucl)_2]Cl_2$. The chemical shifts of the nucleoside carbon resonances on the other hand, confirm once again the N_7 coordination, in both Ino and Guo (see Table 5). The C_2 and C_4 resonances of the nucleosides are the more sensitive in the different Pt–N_7 bond strength, and are shown up as doublets, like in the ^1H NMR spectra. The two diastereoisomeric forms of the starting complexes would result also in two different isomers in the complexes with the nucleosides. However, the chemical shifts, both in the ^1H NMR and the ^{13}C NMR spectra of the nucleosides due to the two isomers are exactly the same. The only differentiation comes out from the different Pt–N_7 bond strengths of the nucleosides *trans* to sulphur or nitrogen atoms. The suggested structures for these complexes are



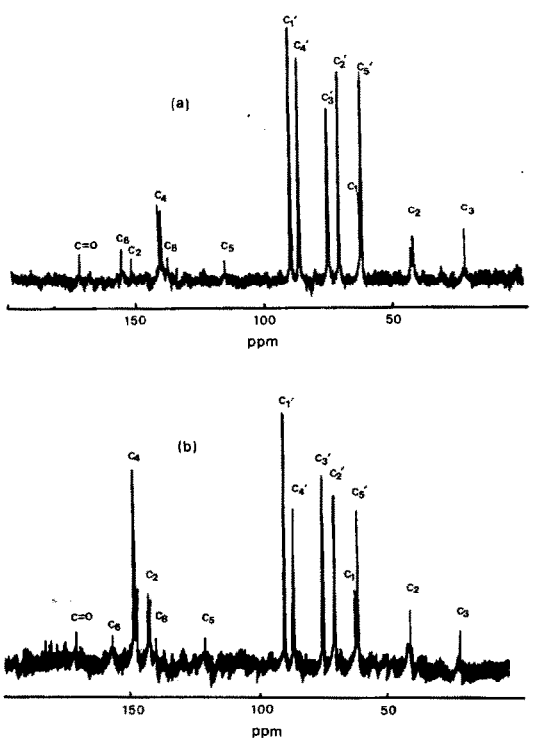


Fig. 1. ^{13}C NMR spectra of the complexes (a) [Pt(S-Me-Cys)$(Guo)_2$]Cl_2 and (b) [Pt(S-Me-Cys)$(Ino)_2$]Cl_2, in D_2O.

EXPERIMENTAL

Materials. S-Ethyl-L-cysteine, S-methyl-L-cysteine and S-benzyl-L-cysteine were purchased from Aldrich Chem. Comp, Fluka A.G. and ICN Pharmaceuticals Inc. A part of S-benzyl-L-cysteine together with S-*p*-nitro-benzyl-L-cysteine, S-trityl-L-cysteine, S-diphenyldimethyl-L-cysteine and S-4',4'-dimethoxyphenyl-methyl-L-cysteine were prepared in our laboratory, according to known methods.[24,25] The nucleosides guanosine and inosine were also from Fluka A.G.

Potassium tetrachloplatinate(II) was from Johnson Matthey and Mallory Ltd., Fluka A.G. and Ventron GmbH.

Methods. (1) The elemental analysis of Pt and Cl were performed in our laboratory, while those of C, H, N, and S in the laboratories of F. Hoffman–La Roche and Co., Basel, Switzerland.

(2) The IR spectra were recorded in a Perkin–Elmer model 283 spectrophotometer, covering the region of 4000–200 cm^{-1} in KBr pellets, Nujol mulls and CaF_2 cells in D_2O solutions.

(3) The ^1H NMR and ^{13}C NMR spectra were recorded using a Varian F.T.80A spectrometer, with TMS as internal standard.

(4) The conductivity measurements were performed in an E365B Conductoscope, Metrohm Ltd., Herisau, Switzerland.

Preparation of the complexes

1. $PtLCl_2$ *type complexes.* (a) In the case of the amino acids, S-Me-L-Cys, S-Et-L-Cys, S-Bzl-L-Cys and S-(*p*-NO_2-Bzl)-L-Cys, soluble in 0.1–0.5 N HCl, the reactions with K_2PtCl_4 were carried out in this solvent, by using equimolar amounts (1 mmol) of each, either at room temperature or in the water bath at 40–50°C for the first two aminoacids or in the

Table 5. ^{13}C NMR chemical shifts of the ligands and the complexes

Compound	Purine carbons				
	C_2	C_4	C_5	C_6	C_8
cis-Pt(S-Et-L-Cys)Cl_2	—	—	—	—	—
cis-Pt(S-Me-L-Cys)Cl_2	—	—	—	—	—
[Pt(S-Et-L-Cys)(Guo)$_2$]Cl_2	151.2	140.8, 140.3	114.9	155.2	137.3
[Pt(S-Me-L-Cys)(Guo)$_2$]Cl_2	151.3	140.7, 140.2	115.0	155.1	137.6
Guo	153.9	151.5	117.3	157.0	135.8
[Pt(S-Et-L-Cys)(Ino)$_2$]Cl_2	143.1, 142.6	148.6, 147.4	121.8	155.1	140.4
[Pt(S-Me-L-Cys)(Ino)$_2$]Cl_2	142.9, 141.7	148.5, 147.2	120.8	155.9	140.2
Ino	145.9	148.2	124.5	156.6	138.7

water bath for the other two. The reactions with the first two aminoacids could also be performed in aqueous solutions, in the water bath.

The heating in the water bath at 40–50°C lasted for 4–5 h, whereupon standing at room temperature, yellow crystals of the complexes of Pt(II) with the first two aminoacids were obtained. The other two aminoacids produce yellow powders. Yellow powders are also obtained in the reactions carried out in aqueous solutions, overnight. The yellow crystals or powders are filtered off by suction, washed with small quantities of ice cold water, ethanol and finally with ether. They are first dried in a desiccator at room temperature and then at 110°C under vacuum, until constant weight. The complexes with the first two aminoacids could also be obtained after evaporation of the reaction mixtures until dryness, dissolution of the residue in THF, filtration from the insoluble KCl and precipitation with excess of ether. Yields 70–80%.

(b) In the case of the insoluble S-Dpm-L-Cys, the reaction is carried out in the same solvent (0.1 N HCl) with equimolar amounts of the reactants (1 mmol), by suspending the aminoacid in the solvent and heating in the water bath, at 40–50°C and 3–4 h time. After one day the precipitate is obtained with filtration, using the same procedure as in (a). The reaction is facilitated by using a small excess of K_2PtCl_4 (5–10%). Yield 80%.

(c) In the case of the aminoacids S-Trt-L-Cys and S-Dmb-L-Cys and using the same procedure as in (a), the obtained final products corresponded to the empirical formula $Pt_2L_2Cl_2$, where L = cysteine anion[12] with a platinum content of 58.5%. It seems that the bulky trityl and dimethoxydiphenylmethyl groups hydrolyze after metal complexation with sulphur and this is verified with the TLC identification of the corresponding carbinoles, Trt–OH and Dmb–OH, in the washing liquids of the complexes after filtration.

2. PtL_2Cl_2 *type complexes.* (a) Using equimolar amounts (0.5 mmol) of the $PtLCl_2$ complexes, prepared above, and the corresponding aminoacids (L), in the minimum amount of water or 0.1 HCl and heating in the water bath at 40–50°C for 30 min, in the case of S-Me-L-Cys and S-Et-L-Cys or at 70–80°C for 2–3 h, in the case of the other aminoacids, the solutions become colourless. The complexes are obtained upon evaporating the solutions to dryness, in quantitative yields. They are dried first at room temperature and then at 110°C under vacuum.

(b) The same complexes could also be obtained, starting with K_2PtCl_4 and the corresponding aminoacid (L) in 1:2 molar ratio, in water or 0.1 N HCl solutions upon slight heating (40–70°C) in the water bath. In this case however, it is difficult to isolate pure complexes without KCl, due to their high water solubility. Only in the case with S-Me-L-Cys, where the complex is soluble in DMF, can it be separated from the insoluble form in this solvent, KCl.

Note. In the case of the complexes with the aminoacids, S-Bzl-L-Cys, S-(*p*-NO_2-Bzl)-L-Cys and S-Dmp-L-Cys and upon heating at 70–80°C in the water bath, small amounts of a yellow precipitate is obtained, which is not further soluble in the reaction mixture. This is filtered off, prior to the evaporation of the solutions to dryness. To this insoluble precipitate, which corresponds to the same elemental analysis, an oligomeric or polymeric structure was assigned (Structure **III**).

3. $Pt(L–H^+)_2$ *type complexes.* (a) These complexes were obtained by reacting the PtL_2Cl_2 type complexes with freshly prepared Ag_2O in (1:1.95) molar ratios, in aqueous solutions. The Ag_2O is prepared with titration of 0.1 N $AgNO_3$ solutions

Table 5 (*continued*).

Sugar carbons					Aminoacids carbons					
C'_1	C'_2	C'_3	C'_4	C'_5	C_1	C_2	C_3	C_4	C=O	Solvent
—	—	—	—	—	64.5, 64.0	39.5	34.5, 35.6	15.6, 16.3	171.7	D_2O
—	—	—	—	—	62.1, 62.6	41.0	21.9, 23.3	—	169.5	D_2O
89.8	70.5	74.4	86.2	61.6	62.8, 62.6	38.7	33.6, 32.6	12.3	171.4	D_2O
89.5	70.5	74.6	86.1	61.6	62.6, 62.2	42.1, 42.2	20.9	—	171.5	D_2O
87.0	70.6	74.4	85.0	61.8	—	—	—	—	—	DMSO-d_6
90.4	70.4	75.2	86.4	61.4	62.3	38.3, 39.1	32.8, 33.9	12.3	170.9	D_2O
90.2	70.1	74.9	86.1	61.1	62.3	40.5 (doublet)	20.0, 20.8	—	171.3	D_2O
87.6	70.4	74.2	85.6	61.4	—	—	—	—	—	DMSO-d_6

with 0.1 N NaOH, filtration and drying of the precipitate at 110°C under vacuum, in the dark. After stirring the PtL_2Cl_2 and Ag_2O mixtures for 30 min at room temperature, in the dark, the AgCl precipitate formed, is filtered off and the resulting solution is evaporated to dryness. The complex is then obtained by dissolving the residue in a small amount of MeOH or EtOH, filtering and adding excess of ether. After filtration and drying at 110°C under vacuum, the yields of the hygroscopic products, were of the order of 50%.

(b) The same compounds can also be obtained upon neutralization of 10^{-3} M solution of the PtL_2Cl_2 complexes with 0.1 N NaOH and evaporation to dryness, or from the starting materials (K_2PtCl_4 and L) in 1 : 2 molar ratios and pH = 9.5. However, the complexes obtained in these ways, were not 100% pure, containing amounts of KCl or NaCl salts.

4. $[PtL(nucl)_2]Cl_2$ *type complexes.* These complexes were prepared from the $PtLCl_2$ complexes and the corresponding nucleosides (inosine or guanosine) in 1 : 2 molar ratios, in aqueous solutions. The solutions were stirred with heating at 50–60°C over night and they became colourless. After evaporation to a small volume of the resulting colourless solutions, the complexes were precipitated by adding an excess of acetone. They were then filtered and dried first at room temperature and then at 110°C in vacuum, in the presence of P_2O_5. The yields were quantitative.

5. *Deuterated complexes and ligands.* The deuterated complexes were prepared according to the above described corresponding method in D_2O, instead of H_2O solutions, or by equilibrating in an atmosphere saturated with D_2O, in a desiccator.

The ligands were dissolved in D_2O and reprecipitated with excess of acetone.

Acknowledgement—This research was supported by the Greek National Committee for Research and Technology.

REFERENCES

1. V. Theodorou, I. Photaki, N. Hadjiliadis, R. W. Gellert and R. Bau, *Inorg. Chim. Acta* 1982, **60**, 1.
2. H. Kozlowski, Z. Siatecki, B. J. Trzebiatowska and A. Allain, *Inorg. Chim. Acta* 1980, **46**, L25.
3. A. Allain, M. Kubiak, B. J. Trzebiatowska, H. Kozlowski and T. Glowiak, *Inorg. Chim. Acta* 1980, **46**, 127.
4. L. P. Battaglia, A. Bonarmantini-Corradi, C. Grasselli-Palmieri, M. Nardelli and M. E. Yidoni Tani, *Acta Cryst.* 1973, **B29**, 762.
5. L. M. Volshtein and M. F. Mogilevkina, *Russ. J. Inorg. Chem.* 1963, **8**, 304.
6. C. A. McAuliffe, *Inorg. Chem.* 1973, **12**, 1699.
7. O. Vigol, N. Hurduk and J. A. Schneider, *J. Inorg. Nucl. Chem.* 1979, **41**, 309.
8. C. A. McAuliffe, *J. Chem. Soc. A* 1967, 641.
9. H. Kozlowski, B. Decock-le-Reverend, J. L. Delaruelle, C. Loucheux and B. Ancian, *Inorg. Chim. Acta* 1983, **78**, 31.
10. B. Shohat, H. Schlesinger, N. Grossowicz and N. Lichtenstein, *Isr. J. Med. Sci.* 1972, **8**, 29.
11. L. Cheng, Y. Kwang and C. C. Cheng, *J. Med. Chem.* 1972, **15**, 13.
12. G. Pneumatikakis and N. Hadjiliadis, *J. Inorg. Nucl. Chem.* 1979, **41**, 429.
13. N. Hadjiliadis and G. Pneumatikakis, *Inorg. Chim. Acta* 1980, **46**, 255.
14. N. Chernova, I. Kurskii and V. Strukov, *Russ. J. Inorg. Chem.* 1978, **23**, 239.
15. M. Chandrasekharan, M. R. Udupa and G. Aravamudan, *J. Inorg. Nucl. Chem.* 1974, **36**, 1417.
16. D. Kovala-Demertzi, J. M. Tsangaris and N. Hadjiliadis, *Transition Met. Chem.* 1983, **8**, 140.
17. L. E. Erickson, J. W. McDonald, J. K. Howie and R. P. Clow, *J. Am. Chem. Soc.* 1968, **90**, 6371.

18. W. Kitching, C. Moore and D. Dodrell, *Inorg. Chem.* 1970, **9**, 541.
19. F. Hartley, S. Murray, W. Levason, H. Soutter and C. A. McAuliffe, *Inorg. Chim. Acta* 1979, **35**, 265.
20. B. J. Trzebiatowska, A. Allain and H. Kozlowski, *Inorg. Nucl. Chem. Lett.* 1979, **15**, 279.
21. L. M. Volshtein and L. E. Krylova, *Russ. J. Inorg. Chem.* 1976, **21**, 1237.
22. (a) P. C. Kong and T. Theophanides, *Inorg. Chem.* 1974, **13**, 1167. (b) *Inorg. Chem.* 1974, **13**, 1981.
23. N. Hadjiliadis and T. Theophanides, *Inorg. Chim. Acta* 1976, **16**, 77.
24. M. Bachi and K. Peterson, *J. Org. Chem.* 1972, **37**, 2550.
25. I. Photaki, J. Papadimitriou, C. Sakarellos, P. Mazarakis and L. Zervas, *J. Chem. Soc. C* 1970, 2683.

Polyhedron Vol. 4, No. 7, pp. 1293–1295, 1985
Printed in Great Britain

0277–5387/85 $3.00 + .00
© 1985 Pergamon Press Ltd

THERMAL DECOMPOSITION OF INORGANIC AND ORGANOMETALLIC COMPOUNDS OF TIN—I. TRIPHENYLTIN HYDROXIDE

JOHN D. DONALDSON, SUSAN M. GRIMES,* ARTHUR F. LeC. HOLDING and MICHELLE HORNBY

Department of Chemistry, The City University, Northampton Square, London EC1V 0HB, U.K.

(*Received* 8 *August* 1984; *accepted after revision* 18 *December* 1984)

Abstract—The thermal decomposition of triphenyltin hydroxide in the temperature range 25–400°C has been studied. The decomposition products formed at each stage have been isolated and characterised. A decomposition scheme involving a reductive-elimination reaction is proposed. The proportions of this reaction and the accompanying reaction are dependent on the mode of heating.

The literature contains very few reports on the thermal decomposition of organotin(IV) compounds. The interpretation of pyrolysis reactions involved in the decomposition of a series of organotin(IV) adducts and carbohydrate derivatives has been shown to be difficult[1] because of the lack of information on the thermal decomposition of simple organotin(IV) compounds. This is particularly true of organotin–oxygen-containing derivatives and for this reason we have investigated the thermal behaviour of a number of relatively simple oxygen-containing compounds by simultaneous thermogravimetry and differential thermal analysis (TG/DTA).

Triphenyltin hydroxide was chosen as the first example for a detailed thermal analytical study including the identification of the product(s) formed at each stage of the decomposition by the use of appropriate techniques including IR, UV and ^{119}Sn Mössbauer spectroscopy, thin layer chromatography, X-ray powder diffraction data and elemental analyses.

EXPERIMENTAL

The thermal decompositions were carried out under a N_2 atmosphere in a vertical electrically heated furnace (temperature control ±5°C). The sample was contained in a small pyrex dish and a glass probe, which could be cooled if necessary, was inserted into the furnace such that the bottom tip of the probe was about 5 mm above the sample. The slow stream of N_2 gas issuing from the furnace was passed through a trap cooled in liquid nitrogen to collect any volatile products. The sample was heated stepwise at 85, 310 and 400°C and maintained at each temperature for 2.5 h. After each heating stage the furnace was cooled to room temperature, the volatile product on the probe was collected and a sample of the non-volatile product removed for analysis.

The TG/DTA data were recorded using a Stanton Redcroft STA 780 simultaneous thermal analyser, IR data, as KBr discs, on a Perkin–Elmer 599 IR Spectrophotometer and UV spectra, in absolute ethanol, using a Perkin–Elmer 402 UV/visible Spectrophotometer. ^{119}Sn Mössbauer data were recorded at 78 K using a $BaSnO_3$ source as previously described.[2]

RESULTS AND DISCUSSION

The TG/DTA data show that Ph_3SnOH decomposes in three stages as detailed in Table 1, and the decomposition products identified are listed in Table 2.

From the percentage weight loss data, the first decomposition corresponds to the reaction

$$2Ph_3SnOH \xrightarrow{75°C} Ph_3SnOSnPh_3 + H_2O \quad (1)$$

and the second to

$$nPh_3SnOSnPh_3 \xrightarrow{290°C} (Ph_2SnO)_n + nPh_4Sn. \quad (2)$$

* Author to whom correspondence should be addressed.

Table 1.

Decomposition reaction	Temperature (°C)	Weight loss (%)	DTA feature
1	75	2.5	Endothermic
2	290	59.5	Endothermic
3	362	16.5	Endothermic

However, no simple decomposition reaction can be inferred from the percentage weight loss recorded in the third decomposition. In order to determine the products formed in the third decomposition, and to confirm the products postulated in the reactions (1) and (2), the pyrolysis of approximately 0.2 g Ph_3SnOH was carried out stepwise at temperatures slightly in excess of those recorded in Table 1 with product isolation and characterisation at each stage.

The IR and C, H analysis of (**I**) and the TG data are consistent with reaction (1) being the first decomposition step. The O–H bands at 3610 and 895 cm^{-1} in the IR spectrum of Ph_3SnOH are absent in (**I**); the percentage weight loss of 2.5 is close to that required (2.45). Characterisation of the non-volatile product (**II**) by IR and C, H analysis, and of the volatile product (**III**) by IR and UV spectroscopy identified them as $(Ph_2SnO)_n$ and Ph_4Sn respectively. For reaction (2) the percentage weight loss required is 59.3, and that found is 59.5.

The third decomposition reaction gives three final products, a non-volatile residue (**IV**), whose IR spectrum shows the absence of any organic species, and two volatile fractions (**V**) and (**VI**) of different volatility. Component (**VI**) was identified as Ph_4Sn from its IR spectrum. The IR spectrum of (**V**) was similar to that of (**VI**), but with one extra band at 749 cm^{-1}. The absorption band λ_{max} 250 nm in the UV spectrum of (**V**) suggested the presence of Ph–Ph. A TLC study using a 100:50:5 mixture of *n*-butanol:water:acetic acid[3,4] showed that (**V**) consisted of Ph–Ph with a small amount of Ph_4Sn, whereas (**VI**) consisted mostly of Ph_4Sn with a small amount of Ph–Ph (Ph–Ph, R_f 1.00; Ph_4Sn, R_f 0.00).

^{119}Sn Mössbauer spectroscopy on the non-volatile residue (**IV**) gave the following data, a Sn(II) doublet ($\delta = 2.76 \pm 0.02$ mm s^{-1}, $\Delta = 1.41 \pm 0.02$ mm s^{-1}), assignable to SnO, and a Sn(IV) singlet ($\delta = 0.12 \pm 0.01$ mm s^{-1}) assignable to SnO_2.

Table 2.

Temperature (°C)	Non-volatile product	Volatile product
85	$(Ph_3Sn)_2O$ (**I**)	H_2O
310	$(Ph_2SnO)_n$ (**II**)	Ph_4Sn (**III**)
400	Tin oxide (**IV**)	Ph–Ph*: Ph_4Sn (**V**)
		Ph–Ph: Ph_4Sn* (**VI**)

* Major component of (**V**) > (**VI**).

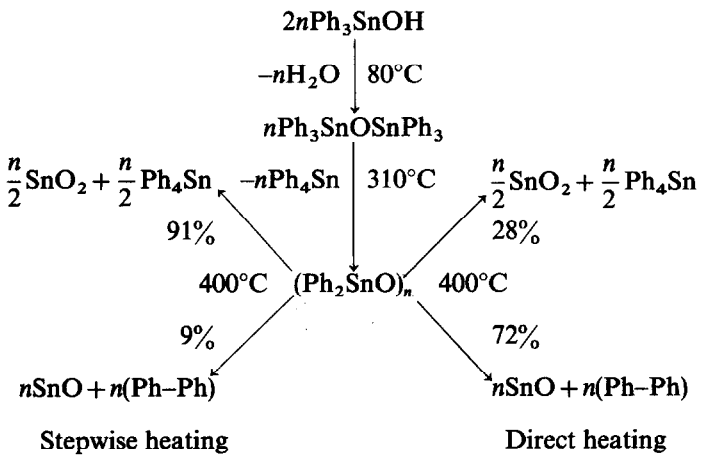


Fig. 1.

The volumetric determination of Sn(II) in the residue using ceric sulphate showed that the Sn(II) : Sn(IV) ratio was approximately 1 : 5.

When a sample of Ph_3SnOH was heated directly to 400°C more Ph–Ph and SnO were produced than when it was heated stepwise to the same temperature. By titrimetry the Sn(II) : Sn(IV) ratio in the residue in this case was approximately 5 : 1.

Thus for the third decomposition reaction, the contribution of the reductive elimination reaction

$$(Ph_2SnO)_n \xrightarrow{400°C} n(Ph\text{–}Ph) + SnO$$

to the overall decomposition of $(Ph_2SnO)_n$ when Ph_3SnOH is heated stepwise to 400°C is less than when it is heated directly to the same temperature.

The results show that the thermal decomposition of Ph_3SnOH by the two modes of heating are as shown in Fig. 1.

The results clearly show that the products of the thermal decomposition of even a simple compound such as Ph_3SnOH do depend on the exact conditions of pyrolysis.

Acknowledgement—The authors thank the International Tin Research Institute for the generous gift of organotin(IV) compounds.

REFERENCES

1. S. M. Grimes, PhD. Thesis, The City University, London (1982).
2. J. D. Donaldson and B. J. Senior, *J. Chem. Soc.* (*A*) 1966, 1769.
3. A. H. Chapman and J. W. Price, *Int. Pest Contr.* 1972, **14**, 11.
4. Y. Tanaka and T. Morikawa, *Japan Analyst* 1964, **13**, 753.

Polyhedron Vol. 4, No. 7, pp. 1297–1299, 1985
Printed in Great Britain

0277–5387/85 $3.00 + .00
© 1985 Pergamon Press Ltd

C^3-BONDED HETERO-β-DIKETONATES OF PALLADIUM(II)

G. C. DASH, R. C. MISHRA, D. PANDA and B. K. MOHAPATRA*
Department of Chemistry, B.J.B. College, Bhubaneswar-14, India

(*Received* 24 *July* 1984; *accepted* 4 *January* 1985)

Abstract—Reactions of PdL_2 complexes, where LH = benzoylacetone, dibenzoyl methane, or dipivaloyl methane, with pyridine and neat β-diketones (L^1H trifluoroacetylacetone, hexafluoroacetylacetone, thenoyltrifluoroacetone and pivaloyltrifluoroacetone) in toluene resulted in the formation of central carbon (C^3) bonded hetero-β-diketonate complexes of the formula [Pd(L)(C^3-L')py]. These were characterized by microanalyses, IR and ^1H NMR spectral data.

As a part of the general programme of "studies on the linkage modes of β-diketones in transition metal complexes" the chelation of the terminal carbon (C^1) bonded acetylacetonato complex [Pd(C^1-acac)Cl · bpy] to form bi- and tri-nuclear complexes with another metal ion involving the bridging of the terminal carbon bonded acetylacetone dianion has been reported by us.[1] The ionic C^3-bonded acetylacetonato complex K[PtCl(acac)$_2$] reacts[2] with several divalent metal ions to form neutral complexes of the type [MPtCl(acac)$_2$]. On the otherhand, the neutral palladium(II) [Pd(acac)(C^3-acac)(γ-pic)][3] contains the central carbon bonded acetylacetone molecule in the keto form. Such a compound can have ketonic coordination with other metal ions or form O,O'-chelate if the proton at the C^3-atom can be abstracted. Reaction of this compound with divalent metal halides and acetates results in the cleavage of the Pd–C bond, but reaction with [Pd(hfac)bpy]Hfac produces[4] a mixed β-diketonate like [Pd(acac)(bpy)]Hfac and a central carbon bonded β-diketonato complex. Reaction of similar compounds [Pd(acac)(C^3-acac)py] and [Pt(acac)(C^3-acac)py] with substitution labile compounds like Pd(tfac)$_2$, Pd(hfac)$_2$ resulted[5] in the formation of central carbon bonded hetero β-diketonate complexes like [M(acac)(C^3-X)py] where M is Pd(II) or Pt(II) and XH is trifluoro- or hexafluoroacetylacetone. Such compounds are also produced by reaction with neat β-diketones. It has also been observed that the Pt–C bond of [Pt(acac)(C^3-acac)(PPh_3)] is cleaved[6] on treatment with either an organic halide or $NaBH_4$ (in the presence of PPh_3). The results suggested that the C^3-acac ligand is more labile than the chelate acac ligand towards electrophilic attack. Yamamoto *et al.* studied the reactions of complexes [M(acac)(C^3-acac)(PPh_3)], where M = Pd(II) or Pt(II), with a series of β-diketones and found that some β-diketones replaced the chelated acac ligand selectively, leaving the C^3-acac ligand intact. Thus three kinds of products, i.e. [Pt(acac)(C^3-dik)(PPh_3)], [Pt(dik)(C^3-dik)(PPh_3)] and [Pt(dik)(C^3-acac)(PPh_3)] were obtained depending on the nature of the β-diketones employed. To study further about these selective replacement reactions, this communication describes the reaction of Pd(bzac)$_2$, Pd(dbm)$_2$ and Pd(dpm)$_2$ with a number of halogen substituted β-diketones to produce C^3-bonded hetero β-diketonate complexes of palladium(II).

EXPERIMENTAL

To warm aqueous solution of potassium tetrachloro palladate(II) methanol solutions of the respective β-diketones, i.e. benzoylacetone, dibenzoylmethane and dipivaloylmethane in 1 : 2 proportion were added, followed by dropwise addition of aqueous sodium acetate solution. The solution was stirred for 30 min and the precipitate filtered, washed with ethanol followed by ether and dried in vacuum.

PdL_2 (1 mmol) was dissolved in 3 cm^3 dichloromethane, 5 cm^3 of dichloromethane solutions of L'H (more than 3 mmol) and pyridine (1 mmol) were added to it, followed by 10 cm^3 of toluene. The resulting orange–yellow solutions were stirred magnetically for 3 h at 40°C in a closed vessel. Volume of the solution was reduced to 3 cm^3 by a

* Author to whom correspondence should be addressed.

Table 1. Analytical data of complexes

Compounds	C		H		N		Λ_M
	Found	Calc.	Found	Calc.	Found	Calc.	mhos·cm^2
1. Pd(bzac)(C^3-tfac)py	48.25	48.05	3.25	3.60	2.62	2.8	8.4
2. Pd(bzac)(C^3-hfac)py	43.12	43.34	2.64	2.71	2.41	2.53	8.5
3. Pd(bzac)(C^3-tta)py	48.51	48.64	3.26	3.17	2.32	2.47	6.8
4. Pd(bzac)(C^3-pta)py	48.64	48.76	4.31	4.43	2.41	2.59	7.2
5. Pd(dbm)(C^3-tfac)py	53.58	53.44	3.25	3.38	2.36	2.49	6.5
6. Pd(dbm)(C^3-hfac)py	48.63	48.75	2.64	2.76	2.11	2.27	8.8
7. Pd(dbm)(C^3-tta)py	53.48	53.38	3.25	3.18	2.01	2.22	8.4
8. Pd(dbm)(C^3-pta)py	53.61	53.69	4.22	4.31	2.14	2.32	10.2
9. Pd(dpm)(C^3-tfac)py	48.36	48.33	5.16	5.37	2.45	2.68	6.5
10. Pd(dpm)(C^3-hfac)py	43.66	43.78	4.06	4.34	2.32	2.43	6.0
11. Pd(dpm)(C^3-tta)py	48.72	48.86	4.52	4.75	2.46	2.38	8.0
12. Pd(dpm)(C^3-pta)py	48.75	48.98	6.26	6.03	2.59	2.48	8.5

bzac = anion of benzoylacetone.
dpm = anion of dipivaloylmethane.
hfac = anion of hexafluoroacetylacetone.
pta = anion of pivaloyltrifluoroacetone.
dbm = anion of dibenzoylmethane.
tfac = anion of trifluoroacetylacetone.
tta = anion of thenoyltrifluoroacetone.

rotary vacuum evaporator and 10 cm^3 of hexane was added to it and kept overnight in a refrigerator. The yellow–brown crystals were filtered off, dried in vacuum and recrystallised from toluene–hexane. Yield was about 65–72%.

C, H, N, of the compounds were determined by microanalysis and molar conductances were measured using M/1000 acetone solution of the complexes by a Toshniwal conductance meter. IR spectra were recorded in Nujol mulls by Perkin–Elmer 337 and 620 spectrophotometers. ^{1}H NMR spectra were recorded in $CDCl_3$ solution by JEOL-JNM MHz-100 spectrometer using tetramethyl silane as internal reference. All the relevant analytical data are presented in Table 1 and spectral data in Table 2.

Table 2. IR spectra (cm^{-1}) and ^{1}H NMR spectra δ (ppm)

ν(C=O)+ν(C=C)			CH of	
O-bonded β-dik.	C^3-bonded β-dik.	Pyridine	O-bonded β-dik.	C^3-bonded β-dik.
1. 1585, 1540, 1510	1728, 1668	1615	6.04	5.8
2. 1580, 1545, 1510	1735, 1693	1618	6.02	5.32
3. 1585, 1540, 1515	1712	1612	6.04	5.44
4. 1580, 1540, 1510	1715	1615	6.02	5.04
5. 1585, 1530, 1520	1730, 1665	1612	6.77	5.8
6. 1585, 1535, 1520	1735, 1690	1618	6.76	5.3
7. 1580, 1535, 1515	1715	1615	6.76	5.44
8. 1585, 1530, 1515	1718	1610	6.72	5.04
9. 1590, 1530, 1500	1730, 1670	1618	5.67	5.8
10. 1585, 1525, 1505	1732, 1665	1615	5.66	5.3
11. 1590, 1525, 1500	1718	1615	5.64	5.44
12. 1585, 1530, 1500	1715	1612	5.64	5.04

RESULTS AND DISCUSSION

Complexes reported have the general composition [Pd(L)(L')py] where LH is benzoylacetone, dibenzoylmethane or dipivaloylmethane and L'H is trifluoroacetyetone, hexafluoroacetylacetone, thenoyltrifluoroacetone or pivaloyltrifluoroacetone. These are yellow–brown crystalline solids. Acetone solution of the complexes have low molar conductance values indicating non-electrolytic nature.

The IR spectra of the compounds reveals the presence of two types of carbonyl frequencies in two different regions. Comparison of these with those of PdL_2 and the C^3-bonded β-diketonate complexes of palladium(II)[8–10] and platinum(II) [11–13] made the assignments easier. In all the compounds three bands were observed around 1580–1590, 1525–1545, and 1500–1520 cm^{-1} regions attributable to ν(C=O) + ν(C–C) modes of the O,O'-chelated β-diketones (L). The other set of bands were observed around 1715–1730 and 1660 cm^{-1} regions assignable to the ν(C=O) modes of the central carbon (C^3) bonded β-diketones (L'). Hence the infrared spectra show the presence of the β-diketone (L) in the O,O'-chelated form and the fluorine substituted β-diketones (L') in the central carbon (C^3) bonded form. The characteristic band of pyridine is observed in the 1610–1618 cm^{-1} region. The other important band due to pyridine ring vibrations undergoes a marked shift and is observed at 635 cm^{-1}. In the far IR region ν(Pd–O), ν(Pd–C) and ν(Pd–N) are observed at 470, 500 and 330 cm^{-1} confirming the bonding of the respective ligand donor atoms.

The presence of chelated β-diketone (L) and central carbon bonded β-diketone (L') has been corroborated by ^1H NMR spectra. Two types of CH proton signals of the β-diketones have been observed (Table 2). One is ascribed to the methine proton signal of the oxygen bonded β-diketone (L) and the other to the methine proton signals of the central carbon bonded β-diketones (L'). These assignments have been made by comparison with the methine proton signals of the chelated β-diketones (L) and the central carbon bonded β-diketones (L') in earlier reported[9–11] compounds.

Methine protons of pyridine resonate in the 7–8.5 ppm region. Factors governing such selectivity of the β-diketones to be present in the O,O'-chelated or carbon bonded form is the keto-enol character of these compounds. A great difference in the keto-enol character of each β-diketone was observed and the diketones may be divided into two categories. One is a highly keto predominant type such as Htfac, Hhfac, Htta, Hpta and the other is rich in enol form such as Hbzac, Hdbm, or Hdpm. Keto-predominant β-diketones replace the chelated β-diketones either by a direct attack of the carbanion (dik^-) to the metal centre or by the process involving the ionic intermediate in which the β-diketonate anion is coordinated to the complex in the outer sphere.[14]

REFERENCES

1. B. K. Sahu, S. B. Mishra and B. K. Mohapatra, *Indian J. Chem.* 1982, **21A**, 823.
2. J. Lewis and C. Oldham, *J. Chem. Soc. A* 1966, 1456.
3. B. K. Sahu and B. K. Mohapatra, *J. Indian Chem. Soc.* 1982, **59**, 732.
4. B. K. Sahu and B. K. Mohapatra, *Curr. Sci.* 1982, **51**, 193.
5. B. K. Sahu and B. K. Mohapatra, *Indian J. Chem.* 1982, **21A**, 730.
6. T. Ito, T. Kiriyana and A. Yamamoto, *Bull. Chem. Soc. Jpn* 1976, **49**, 3250.
7. T. Ito and A. Yamamoto, *J. Organometal. Chem.* 1979, **174**, 237.
8. S. Baba, T. Ogura and S. Kawaguchi, *Bull. Chem. Soc. Jpn* 1974, **47**, 665.
9. S. Okeya, H. Sazaki, M. Ogita, T. Takemoto, Y. Onuki, Y. Nakamura, B. K. Mohapatra and S. Kawaguchi, *Bull. Chem. Soc. Jpn* 1981, **54**, 1978.
10. (a) S. Okeya, S. Ooi, K. Matsumoto, Y. Nakamura and S. Kawaguchi, *Bull. Chem. Soc. Jpn* 1981, **54**, 1085; (b) T. Ito, T. Kiriyama, Y. Nakamura and A. Yamamoto, *Bull. Chem. Soc. Jpn* 1976, **49**, 3257.
11. D. Gibson, J. Lewis and C. Oldham, *J. Chem. Soc. A* 1966, 1453.
12. G. T. Behnke and K. Nakamoto, *Inorg. Chem.* 1968, **7**, 330.
13. Y. Nakamura and K. Nakamoto, *Inorg. Chem.* 1975, **14**, 63.
14. S. Okeya, Y. Oniku, Y. Nakamura and S. Kawaguchi, *Chem. Lett. Jpn* 1977, 1305.

Polyhedron Vol. 4, No. 7, pp. 1301–1309, 1985
Printed in Great Britain

0277–5387/85 $3.00 + .00
© 1985 Pergamon Press Ltd

LINKAGE ISOMERISM OF THE OXIMATO GROUP: THE CHARACTERIZATION OF SOME MONO- AND BINUCLEAR SQUARE PLANAR NICKEL(II) COMPLEXES OF VICINAL OXIME-IMINE LIGANDS*

M. M. ALY,†‡ A. O. BAGHLAF† and N. S. GANJI
Chemistry Department, Faculty of Science, King Abdulaziz University, Jeddah, Saudi Arabia

(*Received* 15 *March* 1984; *accepted after revision* 4 *January* 1985)

Abstract—The reactions of the Schiff-base N,N-ethylenebis-(isonitrosoacetylacetoneimine), (H_2L), with Ni(II) acetate led to the formation of the yellow–orange complex LNi (**I**) in water and the red complex LNi (**II**) in ethanol. Both oximato groups in **I** are coordinated to the metal through the oximino-oxygen whereas in **II** one group is similarly coordinated while the other is coordinated through the oximino-nitrogen. Complex **I** was converted to complex **II** by boiling in chloroform and the conversion was reversed by reacting complex **II** with either piperidine or ethylenediamine. H_2L neutralized by ammonia reacted with Ni(II) chloride (1 : 1) and the complex formed was characterized as the red square planar bis-(4-iminopentane-2,3-dione 3-oximato)Ni(II); (**III**). This *trans* complex reacted with piperidine (1 : 4) to produce its *cis* configuration (**IV**). Complex **III** reacted with ethylenediamine (2 : 1) and 1,3-diaminopropane (1 : 1) to produce complexes **II** and **V** respectively of the identical structure. Attempted similar reaction (1 : 1) with either 1,4-diaminobutane or 1,5-diaminopentane led to the formation of the binuclear complexes **VI** and **VII** in which two molecules of complex **III** are linked together by $-(CH_2)_4-$ and $-(CH_2)_5-$ moieties respectively. The suggested structures of the square planar Ni(II) complexes are based on analytical, spectral and magnetic moment evidence.

Recently the versatile chemistry of square planar Ni(II) complexes was subjected to extensive studies based on two main aspects. The first one deals with the geometrical interconversions of the metal complexes of the Schiff-bases N-substituted salicylaldiminates[1] through the effect of heat or reactions with organic solvents. The second aspect concentrates on linking two of the square planar bis(α-dioximato) nickel(II) complexes by linking reagents to produce binuclear complexes whereby the metal ions are not in one plane.[2] These observations prompted us to pursue our interest in the chemistry of square planar complexes of the metal ion[3,4] by investigating the possible interconversions and linking in the Ni(II) complexes of the Schiff-base N,N′ - ethylenebis - (isonitrosoacetylacetoneimine) and the related ligand 4-iminopentane-2,3-dione 3-oxime taking into consideration the above mentioned two points in addition to the interesting isomeric linkage behaviour of the latter ligand.[5] This phenomenon had resulted from the ability of the oximato group to coordinate through either the oximino-oxygen or the oximino-nitrogen forming thereby six- and five-membered chelate rings respectively.[6]

EXPERIMENTAL

Reagent grade chemicals were used. The ligands N,N′ - ethylenebis - (isonitrosoacetylacetaneimine)[3] and authentic sample of bis-(4-iminopentane-2-3-dione 3-oximato)nickel(II)[7] were prepared by published methods. The IR spectra of the metal complexes were measured as KBr pellets using a Perkin–Elmer 683 spectrophotometer. The electronic spectra were obtained using a Pye–Unicam S.P. 8000 spectrophotometer. ^1H NMR spectra were obtained in $CDCl_3$ solution using a Varian EM 390 spectrometer at 25°C. Chemical shifts are reported in

* This paper is part of the M.Sc. thesis of N. S. Ganji.

† Authors to whom correspondence should be addressed.

‡ Present address: Chemistry Department, Faculty of Science, Shebin El-Kom, El-Menoufia University, Egypt.

ppm relative to internal tetramethylsilane (τ = 10.00). Magnetic susceptibilities were measured at 25°C by the Gouy method. Mercuric tetrathiocyanotocobaltate(II) was used as the magnetic susceptibility standard. Diamagnetic corrections were effected by employing Pascal's constants.[8] The magnetic moments were calculated from the equation $\mu_{eff} = 2.84\sqrt{\chi_M^{Corr.} \cdot T}$. Carbon, hydrogen and nitrogen analyses were determined at the analytical unit of our department. A standard method was used for the determination of the metal ion. The metal complexes were dried under vacuum over phosphorus pentoxide.

Preparation of the Ni(II) *complexes*

1. *Reaction of the ligand* (H_2L) *with* $Ni(OAc)_2 \cdot 6H_2O$. (a) Complex **I**. The filtered aqueous solution (50 cm^3) of the metal acetate (0.0071 mol) was added, while stirring, to a suspension of the equimolar concentration of the powdered ligand in water (100 cm^3). The warmed reaction mixture was stirred for 3 h, filtered, and washed several times with water. The same complex was obtained when the molar ratio of the metal acetate to the ligand was varied from 1 : 1 up to 5 : 1.

(b) Complex **II**. This red complex was prepared as described in (a) using absolute ethanol as a solvent instead of water. The same complex was obtained on changing the molar ratio of the metal acetate to ligand from 1 : 1 up to 5 : 1.

2. *Reaction of complex* **I** *with chloroform to produce complex* **II**. A suspension of the powdered complex **I** (0.003 mol) in chloroform (100 cm^3) was boiled for 2 h whereby the solvent turned red. The unreacted complex **I** (yellow–orange) was filtered off and complex **II** was obtained from the filtrate by evaporating the solvent.

3. *Reaction of complex* **II** *with piperidine or ethylenediamine to produce complex* **I**. This reaction was carried out by refluxing the chloroform solution (100 cm^3) with either piperidine (1 : 4 molar ratio) or ethylenediamine (1 : 1 molar ratio) for 1 h. The precipitated yellow–orange complex was filtered off and washed with chloroform.

4. *Reaction of the ligand* (H_2L) *with* Ni(II) *ion in the presence of ethylenediamine.* This reaction was carried out in absolute ethanol using the molar ratios for NiX_2 (0.0071 mol; X = chloride, nitrate or acetate) ethylenediamine and the ligand of 2 : 4 : 1, 2 : 1 : 1, 4 : 2 : 1 and 1 : 2 : 1. The ethylenediamine was added to the ethanol solution (100 cm^3) of the metal ion and the resulting amine complex was added to the warmed suspension of the ligand in ethanol (100 cm^3). The reaction solution was stirred for 2 h and the precipitated yellow material was filtered off and washed with ethanol. The crude product was boiled in water (50 cm^3) for 1 h in order to separate complex **I** from the water soluble organic amine salts formed in the reaction. The yellow complex **I** was filtered off, washed with water and dried.

5. *Reaction of the neutralized ligand with* $NiCl_2 \cdot 6H_2O$. The powdered suspension of the ligand (0.014 mol) in water (150 cm^3) was neutralized by dil. ammonia to pH 9 and added to the aqueous solution (50 cm^3) of the equimolar concentration of the metal chloride. The reaction solution was warmed for 3 h. The precipitated complex was filtered off, washed with ethanol and crystallized from chloroform (complex **III**).

6. *Reactions of complex* **III**. (a) With piperidine. The chloroform solution (50 cm^3) of the base (0.028 mol) was added to the red chloroform solution (100 cm^3) of the Ni(II) complex (0.007 mol) and the resulting reaction solution was refluxed for 5 h. A dark brown precipitate was formed on cooling which was filtered off, washed with benzene and dried (complex **IV**).

(b) With ethylenediamine. The chloroform solution (30 cm^3) of the base was added to that of the Ni(II) complex (0.014 mol) in the same solvent (100 cm^3). The molar ratios of the base to Ni(II) complex were either 1 : 1, 2 : 1, 3 : 1 or 4 : 1. The reaction solution was refluxed for 2 h to precipitate the yellow complex **I**. This was filtered off, washed with benzene and dried. The orange–red complex **II** was formed when the molar ratio of the base was lower than that of the Ni(II) complex (1 : 2). Mixtures of complexes **I** and **II** were obtained from the other molar ratios with shorter reaction times.

(c) With either 1,3-diaminopropane, 1,4-diaminobutane or 1,5-diaminopentane (1 : 1 molar ratio). These reactions were carried out as described in (b). The reaction solution was boiled for 2 h in the case of 1,3-diaminopropane to precipitate complex **V**. The formation of complexes **VI** and **VII** from the reaction with 1,4-diaminobutane and 1,5-diaminopentane respectively, had required boiling the reaction solutions for 12 h. The unreacted complex **III** was precipitated from shorter reaction times.

RESULTS AND DISCUSSION

The reactions of the ligand N,N′-ethylenebis-(isonitrosoacetylacetoneimine) with Ni(II) ion and the reactivity of the formed complexes are schematically represented in Fig. 1. Thus, the analytical (Table 1) and spectral data (Tables 2 and 3) are compatible with regarding the reaction of the ligand with Ni(II) acetate in water to produce the yellow–orange complex **I** which is structurally

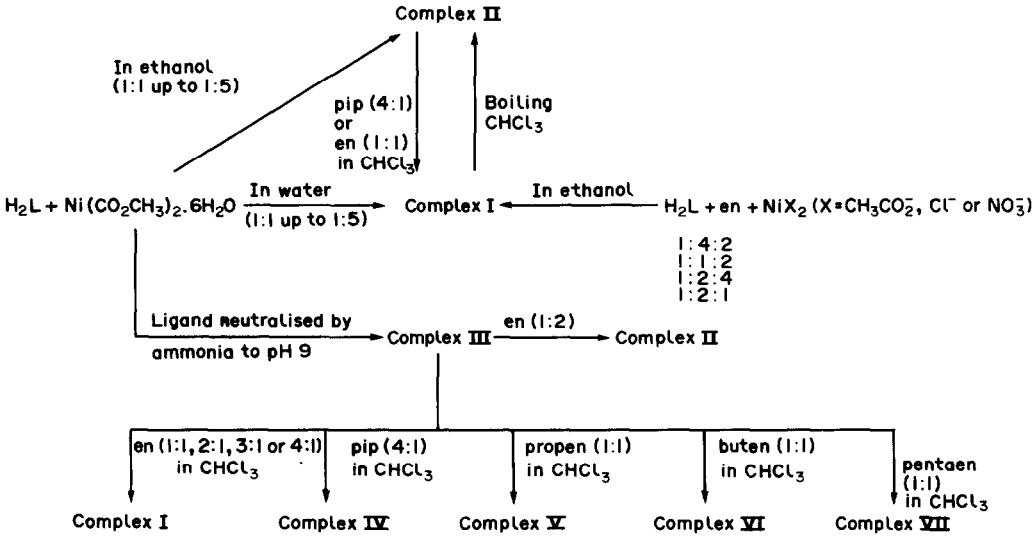


Fig. 1. Schematic representation for the reactions of the ligand (H_2L) with Ni(II) and the reactivity of the metal complexes (en = ethylenediamine, propen = 1,3-diaminopropane, buten = 1,4-diaminobutane, pentaen = 1,5-diaminopentane and pip = piperidine).

different from the red complex **II**, obtained when the same reaction was carried out in absolute ethanol (Fig. 2), although they have the same analytical data.

The IR spectrum of complex **I** revealed the presence of a splitting ν(C=O) in the 1670–1690 cm^{-1} region. This band is located at comparable frequency to that observed from the ligand itself which indicated that the carbonyl group is not coordinated to the metal atom. Furthermore, this region for ν(C=O) is associated[9] with the six-membered chelate ring in the Ni(II) complexes of vicinal oxime-imine ligands which implied, in turn, coordination of the oxime group through the oximino-oxygen. Since there are no other vibrational frequencies in this region, as well as in the frequency region (1660–1630 cm^{-1}) ascribed to the five-membered chelate ring in the vicinal oxime-imine Ni(II) complexes,[9] it is suggested therefore that

Table 1. Analytical data and colour of metal complexes

Complex C = calculated F = found		Elemental analyses (%) C	 H	 N	 Ni	Colour
$C_{12}H_{16}N_4O_4Ni$	(C)	42.52	4.76	16.53	17.32	Yellow–orange
(I)	(F)	42.93	4.68	16.25	17.18	
$C_{12}H_{16}N_4O_4Ni$	(C)	42.52	4.76	16.53	17.32	Red
(II)	(F)	42.28	4.71	16.41	17.28	
$C_{10}H_{14}N_4O_4Ni$	(C)	38.38	4.50	17.90	18.75	Red
(III)	(F)	38.12	4.57	17.68	18.63	
$C_{10}H_{14}N_4O_4Ni$	(C)	38.38	4.50	17.90	18.75	Brown
(IV)	(F)	38.35	4.52	18.15	18.50	
$C_{13}H_{18}N_4O_4Ni$	(C)	44.23	5.14	15.87	16.63	Orange–red
(V)	(F)	44.45	5.21	16.16	16.47	
$C_{24}H_{34}N_8O_8Ni_2$	(C)	42.39	5.04	16.48	17.26	Red–brown
(VI)	(F)	42.06	5.18	16.70	17.27	
$C_{25}H_{36}N_8O_8Ni_2$	(C)	43.27	5.23	16.15	16.92	Red–brown
(VII)	(F)	42.98	5.13	16.39	16.76	

Table 2. Vibrational features (cm^{-1}) of the metal complexes

Assignment / Ref. No.	ν(NH)	ν(C=O) 6-membered	ν(C=O) 5-membered	ν(C=N)	ν(N–O) 6-membered O-coordination	ν(N–O) 5-membered N-coordination	δ(N–O)	ν(Ni–N)
I	—	1685(s) 1680(s)	—	1572(m)	1153(s) 1145(m)	—	835(w) 788(w)	603(m) 593(s)
II	—	1685(s) 1680(s)	1654(s) 1642(s)	1592(m) 1570(m)	1127(m)	1188(m)	830(w) 790(w)	603(m) 590(m) 575(m)
III	3250(s)	1685(s) 1672(s)	1642(s) 1632(s)	1597(m) 1593(m)	1202(m)	1202(m)	812(w) 780(w)	638(m) 630(m)
IV	3250(s)	1685(s) 1673(s)	1643(s) 1635(s)	1597(m) 1587(m)	1202(m)	1232(m)	810(w) 780(w)	635(m) 630(m)
V	—	1685(m) 1680(m)	1648(s) 1640(s)	1570(m) 1560(m)	1127(m)	1185(m)	845(w) 788(w)	597(m)
VI	3318(m) 3160(m)	1687(s) 1680(s)	1655(s) 1648(s)	1597(m) 1580(m) 1565(m)	1124(m) 1108(m); Δ = 16	1192(s) 1172(s); Δ = 20	825(w) 805(w) 780(w)	632(m) 604(m) 580(w)
VII	3160(m)	1688(s) 1680(s)	1655(s) 1650(s)	1600(m) 1580(m) 1565(m)	1125(m) 1115(m); Δ = 10	1185(s) 1170(s); Δ = 15	810(w) 780(w)	632(m) 610(w) 578(w)

s = strong, m = medium, w = weak, Δ = higher ν(N–O), — = lower ν(N–O).

Table 3. Electronic spectra of metal complexes as Nujol mulls and in chloroform

Ref. No.	Solvent	λ_{max} (nm); values in parentheses are molar absorptives in 1 mol cm^{-1}
I	N.M. $CHCl_3$(a)	510, 450, 364 500, 440, 354, 290
II	N.M. $CHCl_3$	515, 440, 360 490(71), 440(2810), 354(5610), 292(31,000)
III	N.M. $CHCl_3$	590(sh), 510, 440, 360 430(2800), 345(19,600), 298(18,700), 275(22,600)
IV	N.M. $CHCl_3$	590(sh), 500, 450, 355 590(sh,34), 445(2670), 343(17,000), 298(17,500), 280(22,800)
V	N.M. $CHCl_3$	610(sh), 562, 465, 375 610sh(476), 548(812), 430(3810), 364(7180), 320(10,900), 288(14,700)
VI	N.M. $CHCl_3$	505, 466, 430, 364 448(4810), 345(26,300), 304(24,600), 280(33,400)
VII	N.M. $CHCl_3$	505, 455, 425, 355 445(4720), 344(25,500), 304(25,100), 280(34,400)

N.M. = Nujol mull, a = saturated solution of the sparingly soluble complex, sh = shoulder.

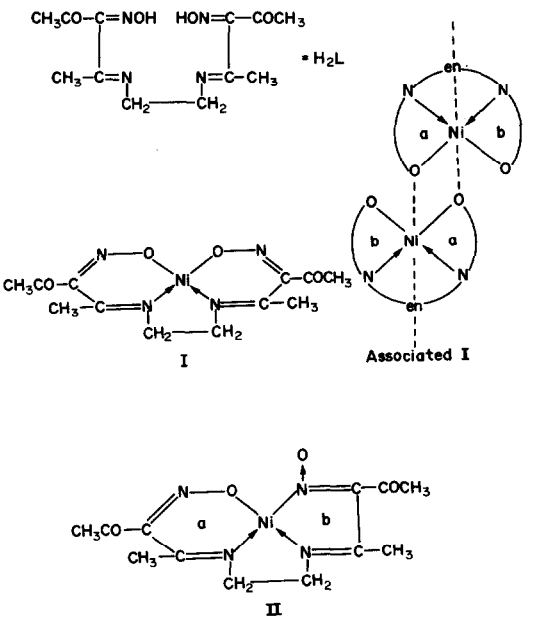


Fig. 2. Suggested formulation for complexes I (and its associated form) and II.

both chelate rings in complex I are six-membered. The 1153 and 1145 cm^{-1} bands in the IR spectrum of this complex are assigned to ν(N–O) of the oxygen-bonded oxime group (shifted from the 1060–975 cm^{-1} bands of the ν(N–O) in the hydrogen bonded –NOH group[3] to the imino-nitrogen of the ligand). These bands are located at lower frequency than the 1200 cm^{-1} band of the oximino-nitrogen coordination in the Ni(II) complex of pyridine-2-aldehyde oxime and could be compared with those reported for the ν(N–O) in the oximino-oxygen coordination in the mononitrosation product of N,N′-ethylenebis-(acetylacetoneimine)Ni(II) (ν(N–O) 1171 cm^{-1})[11] and the Cu(II) complex[12] (ν(N–O) 1143 cm^{-1}); see Fig. 3. for complexes **B** and **C**. The structure of the Ni(II) complex was investigated by isotopic labelling of the oxygen and nitrogen atoms of the oximato group in isomers **A** and **B** whereas that of the Cu(II) complex was determined from X-ray structural data.

Coordination by the oximino-oxygen would lead to more single bond character for the N–O bond and therefore lower the frequency of the stretching vibration.[13] This splitting of the ν(N–O) band to two bands (separated by 8 cm^{-1}) is compatible with the non-equivalence of the two six-membered chelate rings in the square planar structure of the complex.

This behaviour could be explained by the possible weak molecular association in the solid state as a result of side coordination of the oxygen of chelate ring (a) to the metal ion of adjacent molecules. This bridging behaviour is expected to increase the constraint on the N–O bond in chelate ring (a) relative to that in chelate ring (b) and should produce ν(N–O) with higher frequency [1153 cm^{-1} for chelate ring (a)] in a similar manner to

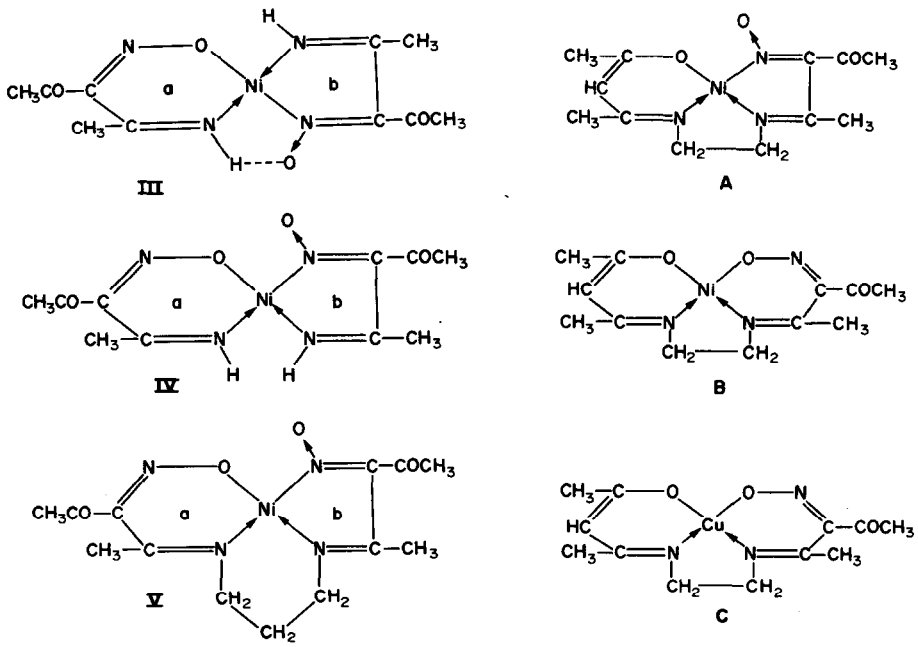


Fig. 3. Suggested formulations for complexes III, IV and V and their relation to the formulated mononitrosation products (complexes A, B and C) of the Ni(II) and Cu(II) complexes of N,N′-ethylenebis-(acetylacetoneimine).

that reported[14] for the ν(C–O) with the oxygen bridging coordination in the adducts of either N,N′-ethylenebis-(salicylideneimine)Ni(II) or N,N′-ethylenebis-(acetylacetoneimine)Ni(II) with transition and non-transition metal ions.

The insolubility of complex **I** in organic solvents (ethanol, chloroform, methylenedichloride) is consistent with the molecular association suggested in this case. This formulation is compatible with the formation of complex **II** from complex **I** by refluxing the chloroform suspension of the latter complex. Under such conditions, molecular dissociation of complex **I** on dissolution in chloroform should produce a separated reactive molecule, allowing thereby for the rearrangement of the coordination mode of the oximato group of chelate ring (a) from the oxygen cordination of complex **I** to the isomeric nitrogen coordination in complex **II** (see Fig. 2). Two distinct ν(C=O) vibrations were observed from complex **II** at the higher (1680 cm^{-1}) and lower (1640 cm^{-1}) regions. The higher frequency vibration is assigned[9] to the ν(C=O) in the six-membered chelate ring (a) and the lower frequency vibration is ascribed to ν(C=O) in the five-membered chelate ring (b) (see Fig. 2). This implied coordination for the oximato group through the oximino-oxygen and the oximino-nitrogen in chelate rings (a) and (b) respectively. Consequently, those bands at 1127 and 1188 cm^{-1} in complex **II** which replaced the ν(N–O) band in complex **I**, are associated with the ν(N–O) in chelate rings (a) and (b) of the former complex. Since the N–O bond of chelate (b) (N-coordination) is expected to have more double bond character than the corresponding bond for chelate ring (a) (O-coordination) it is, therefore, suggested that the higher frequency band (1188 cm^{-1}) is associated with ν(N–O) of oximino-nitrogen coordination of chelate ring (b) and the lower frequency band (1127 cm^{-1}) is attributed to ν(N–O) of the oximino-oxygen coordination in chelate ring (a).

Complex **II** (soluble in chloroform) was converted to complex **I** (insoluble in chloroform) through its reaction with piperidine or ethylenediamine, Fig. 1. This reaction involves the change in the coordination mode of the oximato group in chelate ring (b) of complex **II** from the oximino-nitrogen to oximino-oxygen followed by molecular association of the formed complex to produce the associated form of complex **I**. A process of this type should involve the dissociation of the Ni–N bond (oximato-nitrogen) of chelate ring (b), in the presence of piperidine or ethylenediamine, followed by charge redistribution in the oximato group to allow for the coordination through the oximino-oxygen. The formation of complex **I** in this reaction, is related to the suggested weak molecular association as a stabilizing factor.

Complex **II** was also prepared from the reaction of the ligand with Ni(II) acetate (1 : 1 up to 1 : 5 molar ratios) in ethanol. Under this condition a clear red reaction solution was obtained before the precipitation of complex **II** whereas the yellow complex **I** was formed from the suspension of the ligand in water. The formation of either complexes is thus related to the dissociation of the dimeric ligand in the solvent as well as to the hydrolyses of the monomeric ligand itself to isonitrosoacetylacetone and ethylenediamine in a similar manner to that suggested[15] for N,N′-ethylenebis-(acetylacetoneimine). In order to investigate this and other possible template reactions, several reactions were carried out, in ethanol, for the ligand with NiX_2 (X = acetate, chloride or nitrate) in the presence of ethylenediamine; see Fig. 1 for molar ratios. These reactions led to the formation of complex **I** instead of complex **II** which is formed in the absence of ethylenediamine. The formation of the latter complex is explained by either the shift of the dissociation equilibrium by the presence of the diamine or the reaction of the diamine with the complex **II** to form complex **I**.

The reaction of the hydrolysed ligand (by ammonia to pH 9) with Ni(II) chloride produced a red complex which was characterized by analytical and spectral evidence as the previously reported[3] square planar bis-(4-iminopentane-2,3-dione 3-oximato)Ni(II), complex **III** (Fig. 3). This complex comprises chelate rings (a) and (b) of complex **II** with the oximato group in the *trans* position rather than the *cis* position of complex **II**. The reaction of the red complex **III** with piperidine (1 : 4 molar ratio) led to the formation of a dark brown complex **IV**. These two complexes have the same analytical data. The IR spectrum of the latter complex is identical with that of complex **III** except that a new band appeared at 1232 cm^{-1} in addition to the weakened vibration at 1202 cm^{-1} which was assigned[11] to the coupled ν(N–O). This spectral feature is reproducible after crystallization from boiling chloroform in which the complex is sparingly soluble in contrast with the soluble complex **III**. Complex **IV** is formulated as the *cis* structure of the *trans* complex **III** and the band at 1232 cm^{-1} is assigned to the pure ν(N–O) of the oximino-nitrogen coordination in chelate ring (b). It is of interest to note that the coupled ν(N–O) band at 1202 cm^{-1} of complex **III** was broad which is not the case in complex **IV**. It could be safely assumed, therefore, that the band at 1202 cm^{-1} in the case of complex **IV** is associated with the pure ν(N–O) of the oximino-oxygen coordination of chelate ring (a) in complex **IV**.

The visible spectra of complexes **I**, **II** and **IV** are similar to that of complex **III**, which is known to be square planar,[5] and other square planar Ni(II)

complexes[6] (Table 3). Furthermore, these complexes are spin-paired which is additional evidence for the square planar structure. It is assumed therefore that 180° rotation of either chelate rings (a) or (b) of complex **III** to the fixed position of the other one produced the *cis* complex **IV**. The action of piperidine in this process should involve (i) breaking of the hydrogen bonding between the two chelate rings and (ii) dissociation of one of the coordinate bonds between the metal and the imino-nitrogen, in order to allow for the free rotation of one of the chelate rings to the position of the other one. Reaction of piperidine with the metal in the axial position, as an intermediate step, is less probable.[16] The location of ν(N–H) is identical in both complexes **III** and **IV** which implied that the hydrogen bonding between chelate rings (a) and (b) is weak and therefore had insignificant effect on the ν(N–H). However, this weak hydrogen bonding had observable influence on the ν(N–O) of the chelate ring (b) to the extent that the ν(N–O) of both chelate rings were coupled in complex **III** and the removal of the hydrogen bonding had separated the ν(N–O) vibrations of the oximino-nitrogen from the oximino-oxygen. The locations of ν(C=O), ν(C=N) and ν(Ni–N) are identical in complexes **III** and **IV** as expected since the 180° rotation of one of the chelate rings does not involve them. The reaction of piperidine with complex **III**, that led to the formation of complex **IV**, produced no change when attempted with bis-(dimethyl glyoximato)Ni(II) of the established[17,18] hydrogen bonding [ν(O–H ... O) at 2300 cm^{-1}]. The stability of the latter complex in the presence of piperidine appears to be compatible with the known square planar structure of this complex with the added stability of the hydrogen bonding and the layer structure of the complex.[18]

The conversion of the *trans* complex **III** to *cis* complex **IV** as well as the suggested coordination modes in chelate rings (a) and (b) of complexes **I** and **II** are substantiated from the reaction of complex **III** with aliphatic diamines. These reactions are based on the following factors: (i) The conversions of complexes **II** to **I** and **III** to **IV** were effected through the reaction of complexes **II** and **III** with the basic nitrogen of piperidine, (ii) The reactions of ethylenediamine with complex **II** did not lead to condensation with the carbonyl group of the chelate rings in the complex but produced, instead, a change in the coordination mode of the oximato group (from the oximino-oxygen to the oximino-nitrogen) in one of the chelate rings, and (iii) The mode of coordination of the oximato groups in chelate rings (a) and (b) of complex **III** are identical with those suggested for complex **II** and therefore transamination of the latter complex with ethylenediamine should provide direct evidence for its suggested structure as well as for the role of the basic nitrogen in converting complex **III** to complex **IV** before allowing for the transamination reaction.[16] Thus, the 1:2 molar ratio reaction of ethylenediamine with complex **III** led to the formation of complex **II** which was characterized by analytical and spectral data and compared with complex **II** prepared from the reaction of Ni(II) acetate with the ligand N,N′-ethylenebis-(isonitrosoacetylacetoneimine) in ethanol. The formation of this complex could only take place through satisfying the requirements of factor (iii) and provided, thereby, a conclusive evidence for the structure of complex **II** (and indirectly complex **I**) in addition to clarifying the role of basic nitrogen of ethylenediamine in converting complex **III** to complex **IV** (in a similar manner to the conversion produced by piperidine) which is the preceding step to the transamination reaction. Moreover, the 1:1, 2:1, 3:1 and 4:1 molar ratio reactions of ethylenediamine with complex **III** led to the formation of a mixture of complexes **I** and **II** after a reaction time of 1 h. The IR spectrum of the product was a superimposition of the IR spectra of both complexes. However, complex **I** was the only product when the reaction time was increased to 3 h. This observation is explained by the reaction of the formed complex **II** with the unreacted ethylenediamine which is present in the reaction solution in higher molar ratio than complex **III** in accordance with factors (i) and (ii).

It is note-worthy in this connection that Bose *et al.* had reported[19] the reaction of ethylenediamine with complex **III** using the molar ratio 1.5:1, and the proposed structure was that of both chelate rings of complex **II** to be five-membered with the oximato group coordinated to the metal through oximino-nitrogen. This structure was based on the similarity of their IR spectrum of the complex with those of authentic samples prepared by either the direct[13,20] nitrosation of N,N′-ethylenebis-(acetylacetoneimine)Ni(II) or by the condensation[13,21] of isonitrosoacetylacetone with ethylenediamine in the presence of Ni(II) acetate. This suggestion[19] assumes that the mode of coordination of the oximato group in chelate ring (a) of complex **III** had changed from the oximino-oxygen to the oximino-nitrogen coordination in the reaction of complex **III** with ethylenediamine. An investigation of the reported IR spectrum[13,20] showed that it is identical with that of complex **I**. Furthermore, the ν(N–O) of the complex reported by Bose *et al.*[19] was located around 1150 cm^{-1} and not around 1200 cm^{-1} used by the same authors[19] for the N-coordinated oximato group in vicinal oxime-imino complexes of Ni(II) with ligands of isomeric linkage. Accordingly, it is suggested that

the structure of the Ni(II) complex reported[19] by Bose *et al.* is identical with that of complex I (Fig. 2) and resulted from the reaction of ethylenediamine with the initially formed complex II and not the proposed structure with the two five-membered chelate rings. The same structure of complex I is also applicable to the complex prepared from the nitrosation[13,20] of N,N'-ethylenebis-(acetylacetoneimine)-Ni(II) or from the condensation of isonitrosoacetylacetone with ethylenediamine in the presence of Ni(II) acetate (2:2:1 molar ratio) in methanol. The presence of ethylenediamine in the latter reaction in a higher molar ratio than required by condensation reaction produced the conversion of complex II to complex I. Attempted similar reaction with a molar ratio of 2:1:1 in water or ethanol led to the formation of a mixture of complexes I and II.

The reaction of complex III with aliphatic diamino ligands was extended to include the 1:1 molar ratio reactions with either 1,3-diaminopropane, 1,4-diaminobutane or 1,5-diaminopentane. The reaction with 1,3-diaminopropane in chloroform produced complex V. The analytical and spectral data (Tables 1, 2 and 3) are compatible with the suggested formulation in Fig. 3. Thus, two ν(C=O) bands are located at comparable locations to those of complexes II, III and IV indicating the presence of two carbonyl groups attached to a six-membered [higher ν(C=O)] and five-membered chelate rings[9] [lower ν(C=O)]. Two bands were detected at 1185 and 1127 cm^{-1} corresponding to those of complex II and are assigned accordingly to ν(N–O) of the oximino-nitrogen (five-membered chelate ring) and oximino-oxygen (six-membered chelate ring) respectively. The ν(Ni–N) band is located near 600 cm^{-1} as in complex II which accords with the formulation shown in Fig. 3. The alternative formulation which comprises linking two molecules of complex III by $-(CH_2)_3-$ moiety after the transamination reactions appears to be energetically less favourable than the chelate ring formation of the diamine suggested in Fig. 3.

The analytical and spectral data are consistent with regarding the products of the reaction (1:1 molar ratio) between complex III and either 1,4-diaminobutane or 1,5-diaminopentane to be formulated as shown in Fig. 4. This formulation considers that the transamination reaction had involved the imino group of the five-membered chelate rings and led to linking two molecules of complex III through the $-(CH_2)_n-$ moiety (n = 4 or 5 for complexes VI and VII respectively). Thus, ν(C=O) of the six-membered and five-membered chelate rings in complex VI and VII are located at comparable locations to those of complexes II–V (Table 2). The splitting of these bands in the latter

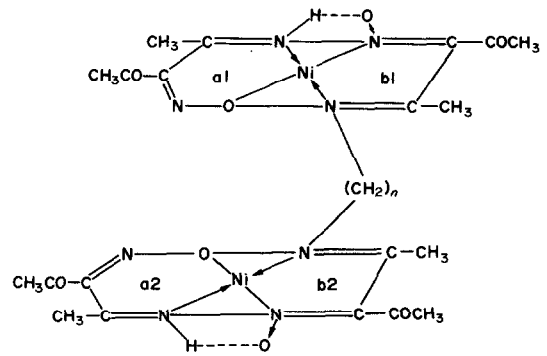


Fig. 4. Suggested formulations for complexes VI (n = 4) and VII (n = 5).

complexes was identical with those observed from complexes VI and VII (Table 2). The ν(NO) bands observed from complexes II and V (Figs. 2 and 3 respectively), which are ascribed to oximino-oxygen [chelate ring (a)] and oximino-nitrogen [chelate ring (b)], have their counterparts in complex VI and VII. Under such conditions the higher frequency band is associated with the N-coordination and the lower frequency is related to the O-coordination. The splitting of each of these bands to two bands in complexes VI and VII is indicative of the presence of steric interactions between the linked square planar mononuclear Ni(II) complex III. This suggestion accords with the observed decrease of the extent of separation between the ν(N–O) bands of the same mode of coordination as the linking moiety is increased from $-(CH_2)_4-$ in complex VI to $-(CH_2)_5-$ in complex VII (compare values of Δ for ν(N–O) in Table 2).

It seems that these steric interactions did not allow linking with the $-(CH_2)_3-$ moiety (and consequently $-(CH_2)_2-$) and led to the more stable complex V. The formulation of complexes VI and VII assumes that linking takes place between the imino-nitrogen of chelate ring (b-1) and the imino-nitrogen of chelate ring (b-2) which allows for the least possible steric interactions and consequently accounts for the absence of another link between the imino-nitrogen of chelate ring (a-1) and that of chelate ring (a-2) although the reaction solution (1:1 molar ratio) of complex III and the diamine was refluxed for 12 h. The ν(N–H) vibrations of complexes VI and VII are another evidence for the steric interactions between the linked square planar Ni(II) complex III. Thus, two well resolved ν(N–H) vibrations (separated by 150 cm^{-1}) were detected from complex VI of the higher steric interactions whereas only one of these bands was detected from complex VII.

The ^1H NMR spectra of complexes VI and VII are diagnostic for the linked imino-nitrogen. Thus, two

NH proton resonances were detected from complex **III** at $\tau = 1.35$ and $\tau = 2.32$ where the downfield resonance is associated[9] with the hydrogen bonded –N–H and the second resonance is attributed to the –N–H of the six-membered chelate ring. In the case of complexes **VI** and **VIII** a downfield resonance ($\tau = 1.23$) only was observed, indicating, therefore, that the hydrogen bonded –N–H (Fig. 4) of chelate rings (a1) and (a2) was not involved in the transamination reaction. The absence of the higher field –NH proton resonance ($\tau = 2.32$) indicated, thereby, that the two molecules of the square planar Ni(II) complex **III** are linked together through the imino-nitrogen of the five-membered chelate rings [(b1) and (b2) in Fig. 4] of each molecule. The proposed structures for complexes **VI** and **VII** are useful for locating the rotating chelate ring in the conversion of complex **III** to **IV**. Thus, the suggestion that the unreacted molecule of either 1,4-diaminobutane or 1,5-diaminopentane (in the 1 : 1 molar ratio reaction of complex **III** with diamines) did not lead to rotation of either chelate ring (a1) or (a2) implied that the imino-nitrogen of the five-membered chelate ring (b) in complex **III** is the reactive site not only for the transamination reaction (complexes **VI** and **VII**) but also for the rotation of chelate ring (b); complexes **IV**, **II** and **I**. The latter step could not occur after the transamination reaction that led to complexes **VI** and **VII**.

The electronic spectra of the metal complexes as Nujol mulls and in chloroform are summarized in Table 3. The observed peaks in the visible region are typical *d–d* transition peaks of square planar Ni(II) complexes.[22] There are slight shifts from the positions of the absorption maxima when comparing the spectra of Nujol mulls with those in chloroform. Furthermore, the intensities of the maxima are somewhat higher than expected.[22] This is accounted for by the intermolecular interactions which are operative in the solid state as well as the intramolecular interactions taking place between the mononuclear square planar units of complexes **VI** and **VII**. Accordingly, it could be suggested that the *d–d* transitions have been overlapped by some charge-transfer absorption peaks. This observation, which is most noticeable in the spectra of complexes **VI** and **VII**, is consistent with our interpretation for their IR spectra regarding steric interactions and accords with similar behaviour reported[13] for the Cu(II) analogue of complex **I** (intermolecular interactions).

REFERENCES

1. S. Yamada and A. Takeuchi, *Coord. Chem. Rev.* 1982, **43**, 187 (and cited references); E. D. McKenzie and F. S. Stephens, *Inorg. Chim. Acta* 1979, **32**, 253.
2. M. L. Bowers and C. L. Hill, *Inorg. Chim. Acta* 1983, **72**, 149.
3. M. M. Aly and F. A. El-Said, *J. Inorg. Nucl. Chem.* 1981, **43**, 287.
4. M. C. R. Symons, M. M. Aly and D. X. West, *J. Chem. Soc., Chem. Commun.* 1979, 51; *J. Chem. Soc., Dalton Trans.* 1979, 1744.
5. M. J. Lacey, C. G. Macdonald, J. S. Shannon and P. J. Collin, *Aust. J. Chem.* 1970, **23**, 2279; M. J. Lacey, C. G. Macdonald, J. F. McConnell and J. S. Shannon, *J. Chem. Soc., Chem. Commun.* 1971, 1206.
6. A. Chakravotry, *Coord. Chem. Rev.* 1974, **13**, 1.
7. C. Djordjevic, J. Lewis and R. S. Nyholm, *J. Chem. Soc.* 1962, 4778.
8. J. Lewis and R. G. Wilkins, *Modern Coordination Chemistry*, p. 403. Interscience, New York (1960).
9. M. J. Lacey, J. S. Shannon and C. G. Macdonald, *J. Chem. Soc., Dalton Trans.* 1974, 1215.
10. R. A. Krause, N. B. Colthup and D. H. Busch, *J. Phys. Chem.* 1961, **65**, 2216.
11. M. J. Lacey, C. G. Macdonald and J. S. Shannon, *Aust. J. Chem.* 1973, **26**, 263.
12. M. B. Cingi, A. C. Villa, A. G. Manfredotti, C. Guastini and M. Nardelli, *Acta Cryst.* 1972, **28B**, 1075.
13. K. S. Bose and C. C. Patel, *J. Inorg. Nucl. Chem.* 1971, **33**, 2947.
14. M. Koto, Y. Muto, H. B. Jonassen, K. Imai and T. Tokii, *Bull. Chem. Soc. Japan* 1970, **43**, 1066; L. G. Armstrong, H. C. Lip, L. F. Lindoy, M. McPartlin and P. A. Tasker, *J. Chem. Soc., Dalton Trans.* 1977, 1771.
15. P. J. McCarthy, R. J. Hovey, K. Ueno and A. E. Martell, *J. Am. Chem. Soc.* 1955, **77**, 5820.
16. S. Yamada, E. Ohno, Y. Kuge, A. Takenehi, K. Yamanouchi and K. Iwasaki, *Coord. Chem. Rev.* 1968, **3**, 247.
17. R. Blinc and D. Hadzi, *J. Chem. Soc.* 1958, 4536.
18. L. G. Godycki and R. E. Rundle, *Acta Cryst.* 1953, **6**, 487.
19. K. S. Bose, B. C. Sharma and C. C. Patel, *Inorg. Chem.* 1973, **12**, 120.
20. I. Masuda, M. Tamaki and K. Shinra, *Bull. Chem. Soc. Japan* 1969, **42**, 157.
21. A. V. Ablov and V. N. Zubarev, *Russ. J. Inorg. Chem.* 1968, **13**, 1563.
22. A. B. P. Lever, *Inorganic Electronic Spectroscopy*, p. 343. Elsevier, Amsterdam (1968).

Polyhedron Vol. 4, No. 7, pp. 1311–1313, 1985
Printed in Great Britain

0277–5387/85 $3.00 + .00
© 1985 Pergamon Press Ltd

COORDINATION BEHAVIOUR OF BENZOTHIAZOLINES TOWARDS STANNOUS ION

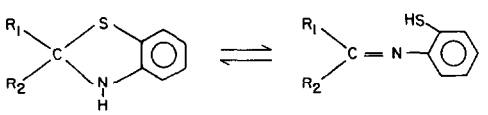
ANIL VARSHNEY and J. P. TANDON*
Department of Chemistry, University of Rajasthan, Jaipur-302004, India

(*Received* 19 *October* 1984; *accepted* 4 *January* 1985)

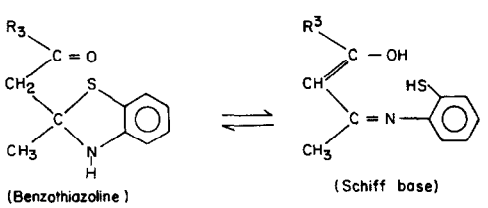
Abstract—Equimolar reactions of tin(II) methoxide with benzothiazolines result in the isolation of a new series of tin(II) complexes, which further undergo 1 : 1 adduct formation with pyridine. The electronic, IR and ^{1}H NMR spectral studies indicate coordination of tin to the oxygen, azomethine nitrogen and sulphur of the ligand moiety.

The condensation of a *o*-aminothiophenol with a carbonyl compound does not normally lead to the isolation of the corresponding Schiff-base, but a benzothiazoline is formed.[1,2] However, in the presence of a metal ion, the cyclic structure of thiazoline or benzothiazoline rearranges to give the Schiff-base metal chelate quantitatively.[3,4] During the course of the present investigations, an attempt has been made to synthesize tin(II) derivatives by interacting tin(II) methoxide with benzothiazolines derived by the condensation of salicylaldehyde (**I**), 2-hydroxy-1-naphthaldehyde (**II**), *o*-hydroxy acetophenone (**III**), acetylacetone (**IV**) or benzoyl acetone (**V**) with *o*-aminothiophenol.

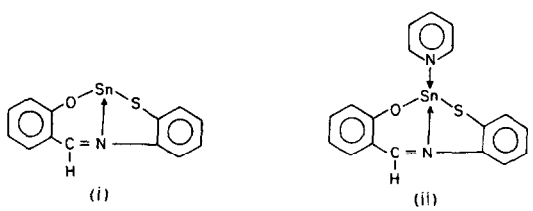
The benzothiazolines used can be structurally depicted as follows:



I, R_1 = C_6H_4OH and R_2 = H (H_2SSP)
II, R_1 = $C_{10}H_6OH$ and R_2 = H (H_2NSP)
III, R_1 = C_6H_4OH and R_2 = CH_3 ($H_2A'SP$)



IV, R_3 = CH_3 (H_2ASP)
V, R_3 = C_6H_5 (H_2BSP)



EXPERIMENTAL

Tin(II) methoxide was prepared by the reaction of anhydrous $SnCl_2$ with an excess of triethylamine in methanol as described by Gsell and Zeldin.[5] The ligands were prepared by the condensation of aldehydes/ketones with *o*-aminothiophenol as described earlier.[6,7] These were purified by recrystallization from ethanol.

The complexes were analysed as reported earlier[8] and the infrared spectra were recorded on a Perkin–Elmer 577 IR spectrophotometer in the region, 4000–200 cm^{-1} using KBr optics. The electronic spectra (in methanol) were taken on a Toshniwal spectrophotometer. A Perkin–Elmer (Model RB-12) spectrometer was used for obtaining the PMR spectra employing DMSO-d_6 as the solvent and TMS as the internal standard. Molar conductance measurements were made in anhydrous dimethylformamide at 36 ± 1°C using a Systronics Conductivity Bridge Model-305. Molecular weight determinations were carried out by the Rast Method.

Synthesis of tin(II) complexes

To a weighed amount of tin(II) methoxide was added the calculated amount of the ligand in 1 : 1 molar ratio using methanol as the reaction medium

* To whom all correspondence should be addressed.

Table 1. Synthesis and characteristics of tin(II) complexes

	Reactant					Analysis observed (cal.)			Mol. wt. observed (cal.)
	Tin compound	Ligand	Molar ratio	Compound, colour and state	M.P. °C	Sn	N	S	
1.	$Sn(OMe)_2$	H_2SSP	1:1	SnSSP	205s	33.93	3.85	8.86	330
				Yellow solid		(34.34)	(4.05)	(9.26)	(345.7)
2.	$Sn(OMe)_2$	H_2NSP	1:1	SnNSP	280d	29.73	3.02	7.89	370
				Green solid		(29.99)	(3.54)	(8.09)	(395.7)
3.	$Sn(OMe)_2$	$H_2A'SP$	1:1	SnA'SP	180d	32.56	3.42	8.43	372
				Yellow solid		(32.99)	(3.89)	(8.89)	(359.7)
4.	$Sn(OMe)_2$	H_2ASP	1:1	SnASP	230d	35.93	3.86	9.43	340
				Yellow solid		(36.67)	(4.33)	(9.89)	(323.7)
5.	$Sn(OMe)_2$	H_2BSP	1:1	SnBSP	195s	30.53	3.31	7.86	400
				Orange solid		(30.78)	(3.63)	(8.29)	(385.7)
6.	SnSSP	Pyridine	1:1	SnSSP · Py	260s	27.85	5.86	6.94	405
				Yellow solid		(27.95)	(6.59)	(7.54)	(424.7)
7.	SnNSP	Pyridine	1:1	SnNSP · Py	315s	24.82	5.35	6.34	440
				Green solid		(25.01)	(5.89)	(6.74)	(474.7)
8.	SnA'SP	Pyridine	1:1	SnA'SP · Py	310s	26.84	5.86	6.82	415
				Yellow solid		(27.06)	(6.38)	(7.29)	(438.7)
9.	SnASP	Pyridine	1:1	SnASP · Py	210s	28.86	6.53	7.64	385
				Yellow solid		(29.48)	(6.95)	(7.95)	(402.7)
10.	SnBSP	Pyridine	1:1	SnBSP · Py	200s	24.98	5.86	6.34	443
						(25.54)	(6.03)	(6.89)	(464.7)

Where: H_2SSP = salicylaldehyde-2-mercaptoanil
H_2NSP = 2-hydroxy-1-naphthaldehyde-2-mercaptoanil
$H_2A'SP$ = 2 -hydroxy acetophenone-2-mercaptoanil
H_2ASP = acetyl acetone-2-mercaptoanil
H_2BSP = benzoylacetone-2-mercaptoanil
s = sharp
d = decomposition.

in an oxygen-free nitrogen atmosphere. Immediately, the colour of the solution changed and it was then stirred magnetically for *ca* 2 h. The excess of the solvent was removed and the compound finally dried *in vacuo* at a bath temperature of 35 ±5°C after being repeatedly washed with dry cyclohexane.

Synthesis of 1 : 1 *adducts*

To a weighed amount of tin(II) complex was added the calculated amount of pyridine in 1 : 1 molar ratio in methanol under an oxygen-free nitrogen atmosphere. The above solution was stirred magnetically for *ca* ½ h. The excess solvent was removed and the compound finally dried *in vacuo* after being repeatedly washed with dry cyclohexane.

RESULTS AND DISCUSSION

The formation of tin(II) complexes by the equimolar reactions of tin(II) methoxide and benzothiazoline and their further adduct formation with pyridine can be depicted by the following equations:

$$Sn(OMe)_2 + ONSH_2 \rightarrow Sn(ONS) + 2\,MeOH$$

$$Sn(ONS) + Py \rightarrow Sn(ONS) \cdot Py$$

(where $ONSH_2$ and Py represent the benzothiazoline and pyridine molecules respectively).

The resulting new derivatives are coloured solids and found to be soluble in DMF and DMSO. The molar conductance of 10^{-3} M solutions of the adducts in DMF lies in the range, 8–14 $ohm^{-1}\,cm^2\,mol^{-1}$, indicating their non-electrolytic behaviour and the molecular weight determinations indicate their monomeric nature.

Electronic spectra

The electronic spectra of the ligands show two bands around 250 nm and 315 nm. These bands are consistent with the typical spectrum of benzothiazoline[2] (cyclic form) and may be attributed to

the ϕ–ϕ^* and π–π^* benzenoid transitions.[9,10] In the corresponding tin(II) complexes, an additional band around 410 nm due to the n–π^* electronic transitions of the azomethine group is also observed.[11] This new band may be due to the isomerization of the ligands on complexation.

IR spectra

A comparison of the characteristic IR absorption bands of the benzothiazolines with those of the corresponding tin(II) complexes reveals the following important features:

(1) In the IR spectra of ligands, a strong broad band at 3400–3250 cm^{-1} is observed which can be assigned to the association of ν (NH) with the phenolic OH vibrations.[12] In the spectra of metal complexes, these bands disappear, indicating the chelation of oxygen as well as nitrogen to the metal atom.

(2) A strong band at 1670–1705 cm^{-1} may be assigned to the N–H deformation vibrations and the absence of ν (SH) at $\sim$ 2500–2600 cm^{-1} is indicative of the benzothiazoline rather than the Schiff-base structure of the ligands. In the spectra of complexes, a new band at $\sim$ 1605 cm^{-1} is observed and which can be assigned to ν (C=N) vibrations. The presence of this band clearly indicates that the resulting metal complexes are Schiff-base derivatives and these are formed by the rearrangement of the benzothiazoline structure.

(3) New bands at $\sim$ 405 and 360 cm^{-1} may be attributed to ν(N $\rightarrow$ Sn) and ν(S $\rightarrow$ Sn) bands, while ν (O $\rightarrow$ Sn)[14] is observed at 645 cm^{-1} in the complexes.

(4) The formation of the pyridine adduct is evidenced by the appearance of new bands in the region, 650–700 cm^{-1}.

Proton magnetic resonance spectra

The proton magnetic resonance spectra of salicylaldehyde-2-mercaptoanil (H_2SSP) and its 1:1 (SnSSP) derivatives have been recorded in DMSO-d_6. The signals at δ 9.25 ppm and δ 4.20 ppm in the case of the ligand are due to the phenolic and NH protons respectively. These, however, disappear from the spectra of tin(II) complexes indicating the deprotonation of the functional groups during complexation with the tin atom.

The ligand shows a complex multiplet in the region δ 7.40–6.40 ppm for the benzene protons, and it remains at almost the same position in the spectra of the tin(II) complexes. The proton signal for the azomethine proton at δ 8.30 ppm in the ligand shifts downfield in the spectra of complexes due to the donation of a lone pair of electrons by the nitrogen to the central tin atom on account of the formation of a coordinate linkage.

Thus on the basis of the above spectral evidence, the following structures can be proposed for the resulting tin(II) complexes and in which the tin atom is probably in tri- (i) and tetra-coordinated (ii) environments.

Acknowledgement—One of us (A.V.) thanks the U.G.C., New Delhi (India) for the financial support.

REFERENCES

1. H. Jadamus, R. Fernando and H. Freiser, *J. Am. Chem. Soc.* 1964, **86**, 3056.
2. R. G. Charles and H. Freiser, *J. Org. Chem.* 1953, **18**, 422.
3. P. Pfeiffer, W. Offermann and A. Werner, *J. Prakt. Chem.* 1942, **159**, 313.
4. L. F. Lindoy and S. E. Livingstone, *Inorg. Chim. Acta* 1967, **1**, 365.
5. R. Gsell and M. Zeldin, *J. Inorg. Nucl. Chem.* 1975, **37**, 1133.
6. M. Aggrawal, J. P. Tandon and R. C. Mehrotra, *J. Inorg. Nucl. Chem.* 1981, **43**, 1070.
7. E. C. Alyea and Abdul Malik, *Can. J. Chem.* 1975, **53**, 939.
8. A. Varshney and J. P. Tandon, *Indian J. Chem.* (in press) (1984).
9. N. S. Biradar, V. B. Mohale and V. H. Kulkarni, *Inorg. Chim. Acta* 1973, **7**, 267.
10. B. Bosnich, *J. Am. Chem. Soc.* 1968, **90**, 627.
11. G. E. Mecasland and E. C. Horswill, *J. Am. Chem. Soc.* 1951, **73**, 3923.
12. R. K. Sharma, R. V. Singh and J. P. Tandon, *J. Inorg. Nucl. Chem.* 1980, **42**, 1267.
13. M. Consiglto, F. Maggio, T. Pizzno and V. Romano, *Inorg. Nucl. Chem. Lett.* 1978, **14**, 135.
14. A. Varshney and J. P. Tandon, *Proc. Indian Acad. Sci. (Chem. Sci.)* (in press) (1984).

Polyhedron Vol. 4, No. 7, pp. 1315–1318, 1985
Printed in Great Britain

0277–5387/85 $3.00 + .00
© 1985 Pergamon Press Ltd

PLATINUM(II) COMPLEXES OF HYDRAZIDES OF ASPARTIC AND GLUTAMIC ACIDS

P. R. BONTCHEV* and M. BONEVA
Faculty of Chemistry, University of Sofia, 1 Anton Ivanov Str., 1126 Sofia, Bulgaria

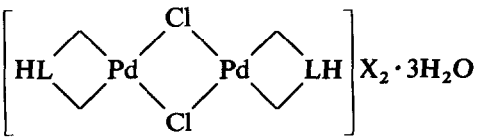
and

V. I. NEFEDOV and YA. V. SALIN
Institute of General and Inorganic Chemistry, USSR Academy of Sciences, Moscow, U.S.S.R.

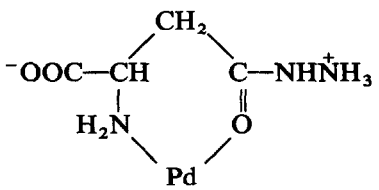
(*Received* 22 *October* 1984; *accepted* 6 *February* 1985)

Abstract—Mononuclear platinum(II) complexes of the hydrazides of aspartic and glutamic acids have been synthesized and studied. The 1:1 complexes are of the type $[Pt(HL)Cl_2] \cdot 3H_2O$, while the 1:2 complexes are $[Pt(HL)_2]Cl_2 \cdot 3H_2O$. In DMF solutions the water molecules are substituted completely by DMF, while in 1:1 (v/v) water–DMF solutions complexes with one DMF and two water molecules are formed. The complexes are characterized using spectroscopic methods (IR, electronic spectra, ESCA), DTA, elemental analysis and titration curves, on the basis of which the ligands are thought to coordinate through the amino- and the hydrazide groups, the carboxylic one remaining deprotonated and non-coordinated.

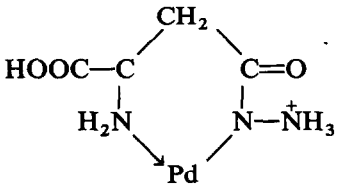
Recently we have synthesized and studied complexes of mono- and dihydrazides of aspartic and glutamic acids firstly with copper(II),[1] nickel(II) and cobalt(II)[2] and then with palladium(II).[3,4] The complexes of the last metal ion were most interesting, because in this case two types of complexes were synthesized, that differ in the way of bonding between the metal and the ligand. In the first type, denoted conventionally as type B complexes, binuclear species were formed



where $X = Cl^-$ or OH^-, depending on the acidity. The ligands are bonded through the amino group and the hydrazide group via its carbonyl oxygen, the carboxylic groups being not engaged in coordination:



In the second group of complexes (type C) the ligands are bonded *via* the amino group and through the deprotonated hydrazide nitrogen



In this case, depending on the pH of the solution and the excess of the ligand either mononuclear complexes PdL_2 and $[Pd(HL)_2]Cl_2$ are formed, or the binuclear species $[Pd_2(HL)_2Cl_2]Cl_2$.

The present work is dedicated to the synthesis of the corresponding platinum complexes with the same ligands and to the investigation of the type of bonding in them.

EXPERIMENTAL

The hydrazides of aspartic and glutamic acids and the dihydrazide of aspartic acid (AH, GH and DH correspondingly) were synthesized and purified, according to the literature data.[5]

The formation of the complexes was studied in slightly acidic aqueous solutions, where the formation of type B complexes is favoured, and in

* Author to whom correspondence should be addressed.

acetone–water, DMF–water and pure DMF media as well. As in the case of Pd(II) complexes with DH and of Cu(II) with the three ligands, only complexes of type B were obtained with platinum(II). The complexes were synthesized according to the following procedure.

Aqueous 0.2 M solutions of K_2PtCl_4 (0.415 g in 5.00 cm^3) and of the ligands (AH—0.147 g and GH—0.161 g in 5.00 cm^3) were prepared, adjusted to *ca.* pH 4.5 and mixed. The reaction mixture with AH was stirred and heated on water bath for 10 min and after cooling a yellow precipitate was formed. The reaction system with GH was kept for 24 hr at room temperature, because heating of the system leads to slow reduction of Pt(II) to metal. The complexes thus obtained were filtered off, washed with ethanol and diethyl ether successively and vacuum-dried at room temperature. The complexes with M : L = 1 : 2 were synthesized in the same way using 0.4 M solutions of the ligands.

In the case of Pt(II) complexes with DH the IR data also indicate the formation of a type B complex, but the elemental analysis showed a variable non-reproducible content of the precipitates. After many experiments we were not able to obtain pure platinum complexes of this ligand with a well defined constant composition. For that reason the data for the platinum complexes of DH are not presented in the paper.

All the reagents and solvents used throughout the work were of A.R. grade and were used without any additional purification.

The elemental analysis was performed in a standard way. Palladium was determined gravimetrically with dimethylglyoxime after destruction of the complexes by heating with conc. HNO_3. Nitrogen was determined by the Dumas' method, the total chlorine assay—after destruction of the complexes with hot conc. HNO_3—gravimetrically as AgCl. The ionic chloride was titrated potentiometrically with $AgNO_3$ after dissolution of the complexes.

The IR spectra were recorded on a Perkin–Elmer, model 580 spectrophotometer in KBr pellets and the electronic reflectance spectra—on a VSU 2P spectrophotometer (Carl Zeiss). The DTA data were obtained with a microdifferential thermoanalyser MIKRO ATD M4 and the ESCA measurements were carried out on a VIEE-15 spectrometer using the carbon 1*s* photoelectron line (285.0 eV) for energy calibration.

RESULTS AND DISCUSSION

The complexes of Pt(II) with AH and GH were obtained from solutions with M : L = 1 : 1 and 1 : 2. In aqueous media the pH of the solution over the precipitate was 3.8–4.2, depending on the metal to ligand ratio. The complexes obtained in such conditions represent white to light yellow precipitates.

Table 1. Bonding energy (eV)

Complexes with	Pt $4f_{7/2}$	Cl 2*p*	N 1*s*
AH	73.3	198.7	400.9
GH	73.5	198.9	400.9
DH	73.4	198.9	401.0

Using the ESCA method it was found that in all complexes platinum is in oxidation state +2. The values for the energy of electron detachment determined for the complexes studied vary from 73.3 to 73.5 eV, while from literature data it is known that usually in Pt(II) complexes the value for Pt $4f_{7/2}$ is in the range 72.4–73.9 eV.[6] In contrast with palladium(II) complexes chlorine is present in all complex species obtained as follows from the appearance of the Cl 2*p* line. The data for the complexes synthesized with AH, GH and DH in aqueous solutions with M : L = 1 : 1 are summarized in Table 1. The N 1*s* line is broadened to a considerable extent indicating the different types of nitrogen atoms present in the complexes. In the same samples no indication was found for the presence of potassium.

With DTA it was found that all the complexes obtained in aqueous solutions contain crystallohydrate water, which in the 1 : 1 complexes was removed at *ca.* 130°C, while in the 1 : 2 species formed in

Table 2. IR spectral frequencies (cm^{-1})

Free ligands	Complexes with AH	Complexes with GH	Assignment
3460[a]	3450[a]	3460[a]	(NH) uncoord.
3280	—	—	(NH_2)
—	3170[a]	3160[a]	(NH_2) coord.
1650–1670	1670	1670	(COO^-) asym.
1610–1630	1620	1620	amide(I)
1535–1550	1540	1540	amide(II)
1510	1510	1510	$(\overset{+}{N}H_3)$
1400	1400	1400	$(COO^-)_{sym.}$
1310	1340	1340	amide(III)
1020	1080	1090	(N–N)
—	530	540	(Pd–NH_2)
—	330+340[b]	330+340[b]	(Pd–Cl)

[a] Broad band.

[b] Only in 1 : 1 complexes.

aqueous medium it was determined at *ca.* 135°C. The amount of crystallohydrate water is three mols per mol of platinum(II). It was found, that when the synthesis is carried out in H_2O+DMF solutions (1:1 v/v), one mol of the crystallohydrate water is replaced by DMF, and if pure DMF is used as a reaction medium, water is completely substituted in the complex by an equivalent amount of DMF. The presence of DMF in the complexes was proved by IR spectra and by the elemental analysis data combined with determination of water in these samples.

The direct potentiometric titration of the complexes in solution showed that the 1:1 complexes do not contain ionic chloride, while in the 1:2 species the chlorine assay is due completely to ionic chloride. At the same time the electronic reflectance spectra of the 1:1 complexes do not show absorption bands at wavelengths $\lambda > 350$ nm. This fact excludes the presence of units such as $PtCl_4^{2-}$ or $Pt_2Cl_6^{2-}$ in the solid phase.

The IR data (Table 2) have indicated that the carboxylic groups are deprotonated and not engaged in coordination. This follows from the absence of ν(COOH) = 1720 cm^{-1} observed in complexes with protonated carboxylic groups, and from the appearance of $\nu(COO^-)_{sym}$ = 1400 cm^{-1} and $\nu(COO^-)_{asym}$ = 1670 cm^{-1}.[3] The position of the amide(I), amide (II) and amide(III) bands[3,7–9] shows that most probably the hydrazide group is bonded to platinum through oxygen as in type B complexes of palladium(II), and not through nitrogen, as is the case with type C complexes of Pd(II).[3] This is confirmed also by the absence of the typical bands indicating bonding through the hydrazide nitrogen—at 1375 cm^{-1} and 385+405 cm^{-1}.[3] The protonation of the hydrazide amino group is shown by the presence of the band at 1510 cm^{-1} and confirmed also by titration of the complexes with NaOH. It was shown, that while the 1:1 complexes with AH and GH consume one mol NaOH per mol complex, the 1:2 complexes consume two mols NaOH per mol complex, i.e. in both complexes the ligand contains one protonated group, namely $-CONH\overset{+}{N}H_3$.

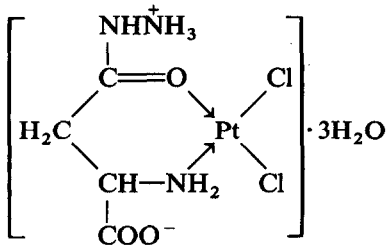
The presence of two chlorine atoms in *cis*-positions in the 1:1 complexes was shown by the presence of the doublet band 330+340 cm^{-1},[10–12] that is observed only in the 1:1 and not in 1:2 complexes. The coordination of NH_2 from the aminocarboxylic group follows from the appearance of ν(Pt–NH_2) at 540 cm^{-1} [3,10] and from the shift of the band at 3280 cm^{-1} of the free ligands to 3170–3160 cm^{-1} in the complexes.[3]

The experimental data thus obtained are consistent with the following structure of the complexes. In the 1:1 complexes there is one ligand with deprotonated carboxylic and protonated hydrazide groups, coordinated to platinum(II) through the amino group and the carbonyl oxygen of the hydrazide group. Two chlorides are also present

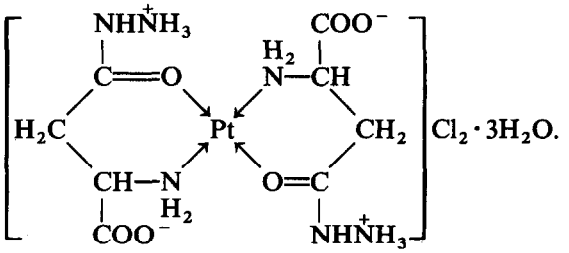
Table 3. Elemental analysis data

M:L ratio in the solution	Complex formed	Found (calc.)%				
		Pt	Cl	N	C	H_2O
1:1 in H_2O	$[Pt(AH)Cl_2]\cdot 3H_2O$	41.50 (41.76)	15.08 (15.20)	9.24 (8.99)	10.42 (10.28)	11.38 (11.56)
1:2 in H_2O	$[Pt(AH)_2]Cl_2\cdot 3H_2O$	32.04 (31.76)	11.37 (11.56)	13.56 (13.68)	15.70 (15.63)	8.60 (8.79)
1:2 in H_2O +DMF(1:1)	$[Pt(AH)_2]Cl_2\cdot 2H_2O\cdot DMF$	29.30 (29.15)	10.78 (10.61)	14.52 (14.65)	19.60 (19.73)	5.54 (5.38)
1:2 in DMF	$[Pt(AH)_2]Cl_2\cdot 3DMF$	25.14 (25.03)	9.10 (9.11)	16.41 (16.17)	25.96 (26.19)	— —
1:1 in H_2O	$[Pt(GH)Cl_2]\cdot 3H_2O$	40.70 (40.54)	14.48 (14.76)	8.88 (8.73)	12.56 (12.47)	11.10 (11.23)
1:2 in H_2O	$[Pt(GH)_2]Cl_2\cdot 3H_2O$	30.56 (30.37)	10.92 (11.06)	13.12 (13.08)	18.60 (18.69)	8.30 (8.41)
1:2 in H_2O +DMF(1:1)	$[Pt(GH)_2]Cl_2\cdot 2H_2O\cdot DMF$	28.14 (27.98)	9.96 (10.19)	14.12 (14.06)	22.40 (22.38)	5.28 (5.16)
1:2 in DMF	$[Pt(GH)_2]Cl_2\cdot 3DMF$	24.36 (24.16)	8.62 (8.80)	15.40 (15.61)	28.17 (28.25)	— —

in the inner coordination sphere and three crystallohydrate water molecules are bonded to the complex:



The 1:2 complexes contain two molecules of the ligand, bound in the same way and as the complex thus formed is positively charged it contains also two chlorides as counter ions:



In a mixed DMF+H_2O (1:1 v/v) reaction medium the 1:2 complexes obtained have the formulae $[Pt(HL)_2]Cl_2 \cdot 2H_2O \cdot DMF$, and those synthesized in a pure DMF correspond to $[Pt(HL)_2]Cl_2 \cdot 3DMF$.

All the conclusions stated above were confirmed by the elemental analysis data presented in Table 3. The values given there are average from the analysis of three parallel samples.

Summarizing the results of the present work it must be mentioned first of all that in contrast with Pd(II) complexes, where we were also able to obtain complexes in which the ligand is bonded through $-NH_2$ from the aminocarboxylic group and through the deprotonated hydrazide nitrogen, the complexes of Pt(II) with the ligands studied are only of type B. Another significant difference between the complexes of Pt(II) and Pd(II) studied is that all the platinum complexes obtained with these ligands are mononuclear, while in most cases the corresponding palladium(II) complexes were binuclear with chloride bridges.

REFERENCES

1. P. R. Bontchev, M. Boneva, M. Mitewa, D. Mehandjiev and E. Golovinsky, *J. Inorg. Nucl. Chem.* 1981, **43**, 3163.
2. M. Boneva, P. R. Bontchev, M. Mitewa, S. Zahariev and E. Golovinsky, *Compt. Rend. Acad. Bulg. Sci.* 1980, **33**, 1091.
3. P. R. Bontchev, M. Boneva, M. Arnaudov and V. I. Nefedov, *Inorg. Chim. Acta* 1984, **81**, 75.
4. P. R. Bontchev, M. Boneva and M. Arnaudov, *Compt. Rend. Acad. Bulg. Sci.* (in press).
5. K. Narita and J. Ohta, *Bull. Chem. Soc. Jpn* 1959, **32**, 1023.
6. G. M. Bancroft, T. Chan, R. J. Puddenphatt and M. P. Brown, *Inorg. Chim. Acta* 1981, **53**, L119.
7. R. C. Aggarwal and B. Singh, *J. Inorg. Nucl. Chem.* 1978, **40**, 1174.
8. H. A. O. Hill and K. A. Raspin, *J. Chem. Soc. (A)* 1969, 619.
9. R. K. Steinhaus and D. J. Brown, *Inorg. Chim. Acta* 1981, **53**, L253.
10. S. Mylonas, A. Valvanidis, V. Voukouvalidis and M. Polyssiou, *Inorg. Chim. Acta* 1981, **55**, 125.
11. A. Finch, D. N. Gates, K. Radcliffe, F. N. Dickson and F. F. Bentley, *Chemical Applications of Far Infrared Spectroscopy*. Academic Press, London (1970).
12. A. A. Danopoulos and S. M. Paraskewas, *Inorg. Chim. Acta* 1981, **55**, 141.

Polyhedron Vol. 4, No. 7, pp. 1319–1321, 1985
Printed in Great Britain

0277-5387/85 $3.00 + .00
© 1985 Pergamon Press Ltd

HIGH-RESOLUTION SOLID-STATE NMR MEASUREMENTS OF OLIGOMERIC POLYSILANES

R. K. HARRIS*† and K. METCALFE‡
School of Chemical Sciences, University of East Anglia, Norwich NR4 7TJ, U.K.

and

E. HENGGE
Institut für Anorganische Chemie der Technischen Hochschule, Graz, Austria

(*Received* 15 *November* 1984; *accepted* 6 *February* 1985)

Abstract—High-resolution solid-state ^{13}C and ^{29}Si NMR spectra have been obtained for $(Ph_3Si)_2$, $(Ph_2Si)_4$ and $(Ph_2Si)_5$ under conditions of high-power decoupling, cross-polarization and magic-angle rotation. The spectra reveal crystallographic inequivalences for $(Ph_2Si)_5$ but not for the other two compounds. There are significant ^{29}Si chemical shift variations.

Polysilanes are now well-known, and their spectroscopic properties have been reported. In particular, ^{29}Si-NMR chemical shifts have been measured for a range of oligomeric polysilanes in solution.[1–5] However, difficulties are sometimes encountered because of the low solubility of phenyl-substituted polysilanes, combined with the poor sensitivity of ^{29}Si-NMR. Recently, the high-power-decoupling/cross-polarisation/magic-angle-rotation suite of techniques has enabled NMR spectra of dilute spins (e.g. ^{13}C or ^{29}Si) to be obtained in high-resolution for solids, and this is clearly an attractive possibility for relatively insoluble organometallic compounds. Much use has been made of these methods for ^{29}Si spectra of zeolites and other silicate species (see, for example, ref. 6). This has been extended to polysiloxanes,[7] but has scarcely been used for polysilanes. There is, however, one report[8] of a high-resolution solid-state NMR spectrum for $Me_3SiSiPh_3$, which showed that the two types of silicon could be distinguished. This note presents results for both ^{13}C and ^{29}Si solid-state NMR for three perphenylpolysilanes, namely hexaphenyldisilane (HPDS), $Ph_3SiSiPh_3$; octaphenylcyclotetrasilane (OPTS), $(Ph_2Si)_4$; and decaphenylcyclopentasilane (DPPS) $(Ph_2Si)_5$.

EXPERIMENTAL

The ^{29}Si solid-state NMR spectra were obtained at 39.76 MHz using a Bruker *CXP 200* spectrometer. The ^{13}C spectra were recorded at 50.3 MHz using a specially-constructed spectrometer based on a 4.7 T Oxford Instruments superconducting magnet, a Nicolet 1180 computer, Bruker gating and phase-shifting units for both high- and low-frequency channels, and a Bruker CP/MAR probe. In all cases, the high-power-decoupling (HPD), cross-polarization (CP) and magic-angle-rotation (MAR) techniques were used. Proton relaxation characteristics were measured in order to assist choice of operating parameters for the ^{29}Si and ^{13}C spectra. They were found to be in the region of 3–4 s for T_1 and 2–6 ms for $T_{1\rho}$. Additional ^{13}C spectra were obtained using the non-quaternary suppression (dipolar dephasing) pulse sequence[9] in order to locate the signal(s) arising from the *ipso* carbon of the phenyl rings. Chemical shifts were measured by replacement and are reported with respect to the ^{29}Si and ^{13}C signals of tetramethylsilane using the high-frequency-positive convention. Ambient probe temperature (*ca.* 22°C) was used for all NMR experiments. The compounds used were prepared by known preparative routes. HPDS is formed in a

* Author to whom correspondence should be addressed.
† Present address: Department of Chemistry, University of Durham, South Road, Durham DH1 3LE, U.K.
‡ Present address: Unilever Research, Port Sunlight Laboratory, Bebington, Wirral, Merseyside L63 3JW, U.K.

Table 1. Silicon-29 NMR chemical shifts for polysilanes

Compound	δ_{Si} (ppm) Solution[a]	Solid
Si_2Ph_6 (HPDS)	−26.61 (2)	−25.2
Si_4Ph_8 (OPTS)	−20.93 (13)	−23.8
Si_5Ph_{10} (DPPS)	−34.41 (1)	−31.8
	−34.14 (14)	−33.9
		−36.8[b]
		−39.1

[a] Reference in parentheses.
[b] Of greater intensity than the other lines (see Fig. 1).

coupling reaction from triphenylchlorosilane.[10] Diphenyldichlorosilane reacts to form OPTS[11] and DPPS[12] in good yields.

RESULTS AND DISCUSSION

Signals were observed in all cases and the results are given in Tables 1 and 2. The ^{29}Si spectra are displayed in Fig. 1. Single resonances were seen for the proton-decoupled ^{29}Si spectra of HPDS and OPTS. The crystal structure of OPTS shows[12] that although there are four molecules per unit cell, the asymmetric unit consists of half a molecule. Evidently NMR cannot resolve the difference between the two silicon atoms in the asymmetric unit. Indeed, the environments of these atoms revealed by the X-ray diffraction studies are very similar.

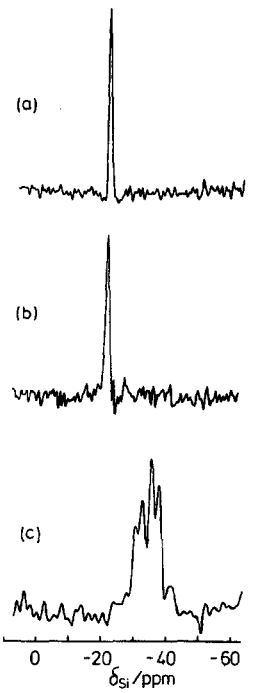


Fig. 1. 39.8 MHz ^{29}Si-{^1H} cross-polarization/magic-angle-rotation NMR spectra of solid (a) $Ph_3SiSiPh_3$, (b) $(Ph_2Si)_4$, and (c) $(Ph_2Si)_5$. Spectrometer conditions: contact time 5 ms; recycle time 10 s; number of transients (a) and (c) ~ 5000, (b) ~ 1000.

Table 2. Carbon-13 chemical shifts for solid polysilanes

Compound	δ_C (ppm) Normal experiment	NQS experiment
Si_2Ph_6 (HPDS)	135.9	
	134.1	134.1
	129.5	
	127.5	
Si_4Ph_8 (OPTS)	136.0	
	134.1	133.9
	129.5	
	127.8	
Si_5Ph_{10} (DPPS)	138.2	138.6
	136.1	
	134.3	134.9[a]
	132.0	132.1
	127.3	
	126.0	125.6

[a] Of greater intensity than the other NQS peaks (see Fig. 2).

On the other hand, DPPS gives four ^{29}Si signals. It is not easy to determine the relative intensities of these resonances, in spite of using a long accumulation time. However, one signal appears to be more intense (possibly twice as intense) as the others, though this may be an artefact of the particular contact time used. The crystal structure of DPPS has been published,[16] and shows eight molecules per unit cell. The asymmetric unit appears to be a complete molecule, thus allowing all five silicon atoms to be different—consistent with the NMR result if this contains an accidental equivalence.

The spread of ^{29}Si chemical shifts for DPPS is substantial (7.3 ppm), indicating a considerable diversity of environment, though whether this arises from inter- and intra-molecular effects is difficult to establish. The molecule is known[16] to have a puckered ring, intermediate between C_s and C_2 symmetry. The solution-state ^{29}Si NMR shows a single resonance (see Table 1), which falls within the solid-state range. The solution-state ^{29}Si shifts for HPDS and OPTS are also known (Table 1), and represent only small (< 3 ppm) deviations from the solid-state values. There is a substantial effect of ring

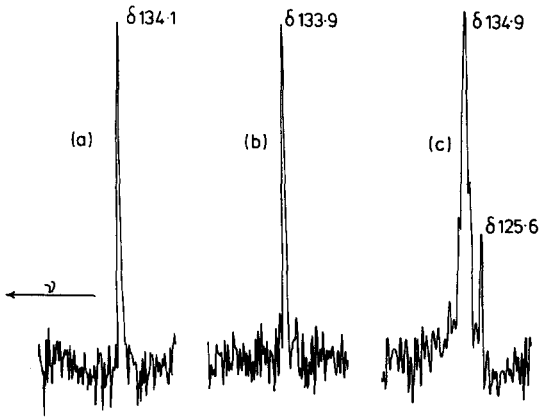


Fig. 2. 50.3 MHz ^{13}C–{^{1}H} cross-polarization/magic-angle-rotation NMR spectra of solid (a) $Ph_3SiSiPh_3$, (b) $(Ph_2Si)_4$, and (c) $(Ph_2Si)_5$, obtained using the non-quaternary suppression (dipolar dephasing) pulse sequence. Spectrometer conditions: contact time (a) 5 ms, (b) 4 ms, (c) 2 ms; recycle time 10 s; number of transients (a) and (b) 3000, (c) 4000; dephasing delay 40 μs.

size on the shifts, as already thoroughly reported from solution-state work.[17]

The solid-state ^{13}C spectra support the ^{29}Si results. The non-quaternary suppression (NQS) experiment is particularly helpful in this regard, since it gives very clearly only one signal for both HPDS and OPTS. As for the ^{29}Si spectra, the theoretical non-equivalences for OPTS are not revealed by ^{13}C NMR, indicating that the various environments are very similar. On the other hand, the solid-state ^{13}C spectra of DPPS are more complex (Fig. 2). Although the quality of these spectra in terms of resolution is not high, the NQS experiment clearly reveals more than one peak, and a possible interpretation is that there are four peaks, with one of double intensity.

CONCLUSIONS

The work reported here demonstrates that solid-state NMR is a valuable adjunct to both X-ray diffraction studies and solution-state NMR for organometallic systems. In the present cases, although the compounds are not very soluble, their solution-state ^{29}Si spectra were obtainable. Obviously, for even less soluble systems, solution-state NMR is not an option. Moreover for glassy (or otherwise amorphous) materials, or those which, though crystalline, do not give suitable crystals, X-ray studies may not be feasible or informative. On the other hand, solid-state NMR suffers few limitations.

Acknowledgements—We would like to thank K. J. Packer for allowing the use of his spectrometer for the ^{13}C spectra. We are grateful to the U.K. Science and Engineering Research Council for the award of a Research Assistantship to KM under research grant GR/C/04376 (Cooperative Award involving ICI PLC) and for financial support to purchase the CXP 200 spectrometer under research grant GR/B/81298.

REFERENCES

1. D. Kovar, K. Utvary and E. Hengge, *Monatsh. Chem.* 1979, **110**, 1295.
2. H. Söllradl and E. Hengge, *J. Organomet. Chem.* 1983, **243**, 257.
3. R. C. Helmer and R. West, *J. Organomet. Chem.* 1982, **236**, 21.
4. H. C. Marsmann, W. Raml and E. Hengge, *Z. Naturforsch.* 1980, **35b**, 35.
5. H. C. Marsmann, W. Raml and E. Hengge, *Z. Naturforsch.* 1980, **35b**, 1541.
6. R. K. Harris, *NATO Advanced Study Institute* 1983, **C103**, 361.
7. G. Engelhardt, D. Zeigan, D. Hoebbel, A. Samoson and E. Lippmaa, *Z. Chem.* 1982, **22**, 314.
8. B. C. Gerstein, *Anal. Chem.* 1983, **55**, 781A.
9. S. J. Opella and M. H. Frey, *J. Am. Chem. Soc.* 1979, **101**, 5854.
10. M. V. Georg, D. J. Peterson and H. Gilman, *J. Am. Chem. Soc.* 1960, **82**, 403.
11. A. W. P. Jarvie, S. H. Winkler, D. J. Peterson and H. Gilman, *J. Am. Chem. Soc.* 1961, **83**, 1921.
12. E. Hengge and H. Marketz, *Monatsh. Chem.* 1969, **100**, 890.
13. E. Hengge (unpublished).
14. R. K. Harris, unpublished work, 1975.
15. L. Parkanyi, K. Sasvari and I. Barta, *Acta Cryst.* 1978, **B34**, 883.
16. L. Parkanyi, K. Sasvari, J. P. Declercq and G. Germain, *Acta Cryst.* 1978, **B34**, 3678.
17. H. C. Marsmann, *NMR Basic Principles and Progress* 1981, **17**, 65.

NOTE ADDED IN PROOF

Since the submission of this article a further publication involving high-resolution solid-state NMR spectra of polysilanes has come to our attention, viz. W. J. Welsh, K. Beshah, J. L. Ackerman, J. E. Mark, L. D. David and R. West, *Polym. Prepr.* 1983, **24**, 131.

Polyhedron Vol. 4, No. 7, pp. 1323–1327, 1985
Printed in Great Britain

0277–5387/85 $3.00 + .00
© 1985 Pergamon Press Ltd

THE ASSOCIATION CONSTANT OF THE FIRST CHLORO-COPPER(II) COMPLEX IN WATER TO 100°C

LESLEY A. ASHTON, JOSEPH I. BULLOCK* and PETER W. G. SIMPSON
Cecil Davies Laboratory, Department of Chemistry, University of Surrey, Guildford, Surrey GU2 5XH, U.K.

(*Received* 12 *November* 1984; *accepted* 6 *February* 1985)

Abstract—The equilibrium constant, K_1, for the reaction $Cu^{2+} + Cl^- \rightleftharpoons [CuCl]^+$ has been determined in the range 15–100°C from spectrophotometric data. The method of analysis, which is widely used, requires both slope and intercept from a reciprocal plot of absorbance against total metal ion concentration. The calculated values of K_1, particularly at low temperature, are very sensitive to the chosen method of data treatment such that the application of weighting factors to the absorbance data for a given photometric accuracy can halve the values. The large variations in K_1 found in the literature are likely to be caused by underestimation of the instability inherent in the method as much as by the neglect of chemical effects such as the formation of higher complexes. By appropriate weighting of the absorbance data an increase in K_1 is apparent above 30°C and the method may have limited usefulness at high temperatures.

Complexes of the 3*d*-transition elements with simple inorganic anions are often difficult to study in water at high temperatures. Hydrolysis sets in at a progressively lower pH as the temperature is raised, complexes with thermally stable anions of technological interest, e.g. Cl^- and SO_4^{2-}, are often weak although the formation constants should increase with temperature, reduction of a metal ion is more favourable at high temperature, and a non-complexing, thermally stable supporting electrolyte is difficult to find.

Spectrophotometry is a commonly used method for the study of weak metal–ion complexes[1–6] and we have previously shown it to be a convenient method for the acid dissociation complexes of organic acids,[7] the protonation constants of heterocyclic bases,[8] and the stability constants of some strong iron(II) complexes[9–10] in water at temperatures above 100°C. The present work is an evaluation of a spectrophotometric method for the determination of the first chloro-copper(II) complex to 100°C. The equilibrium has been studied extensively at low temperatures but with widely differing results.

RESULTS AND DISCUSSION

The chosen method[1,2,5,6] involves the use of a large excess of a metal ion M over a ligand L in order to prevent the formation of all but the first complex and to allow the simplification that the variable, total metal concentration M_T equals the free metal ion concentration M_F.

$$Cu^{2+} + Cl^- \rightleftharpoons [CuCl]^+ \qquad K_1.$$

This results in a high ionic strength, I, if the complexes are weak. The total ligand concentration L_T is held constant and for a 1 cm cell eqn (1) results

$$1/(A - A_0) = 1/L_T \varepsilon K_1 M_T + 1/\varepsilon L_T, \qquad (1)$$

where ε ($dm^3\ mol^{-1}\ cm^{-1}$) is the molar extinction coefficient of the first complex ML at a chosen analytical wavelength, K_1 ($dm^3\ mol^{-1}$) is the required formation constant and $(A - A_0)$ is the measured absorbance using a reference solution of absorbance A_0 containing all the components of the system except L. It is also assumed that the formation of complexes between L and cations from the supporting electrolyte can be ignored.

A plot of $1/(A - A_0)$ against $1/M_T$ should give a straight line of intercept $1/\varepsilon L_T$ and gradient $1/L_T \varepsilon K_1$. Since ε cannot be found from an independent experiment under the same conditions, ε and K_1 are highly correlated through the use of eqn (1). The analysis depends on the complex formed, e.g. $[CuCl]^+$, having an absorption maximum for which the absorptions of the free metal ion, ligand, and other components are slight. Such bands are usually associated with ligand to metal ion charge-transfer

* Author to whom correspondence should be addressed.

so that the metal ion may be readily reduced at higher temperature. On the other hand, a non-absorbing, non-complexing mineral acid, e.g. $HClO_4$, can be conveniently added to prevent hydrolysis and perchlorate salts can be used to make up the necessary high ionic strengths.

In the present work, two series of experiments were performed, in series 1 the ionic strength was brought to 1.00 mol dm^{-3} with $NaClO_4$ while in series 2 with $HClO_4$. In common with most previous spectroscopic experiments[1,2,5,6] absorbances were measured to long wavelength of $\lambda_{max}[CuCl]^+$ which occurs[2] at 251 nm at 25°C. As the temperature was raised the absorption of a given solution increased and λ_{max} shifted to longer wavelength. The results in Table 1 were obtained by linear regression to find the straight line of best fit. Errors in intercept and slope of one standard deviation, obtained from the linear regression analysis, were combined to estimate the deviations in K_1 shown in Table 1 and are thus not dependent on any predefined photometric accuracy. The way in which deviations were calculated in previous work[1,2,5,6] is not clear but more likely tolerances might be obtained by at least doubling those quoted by us and others to allow for systematic spectrophotometric and other errors. In these terms there was little real variation with temperature (except perhaps at 90°C and above), wavelength, or nature of the ionic medium.

A selection of literature data with I close to 1 mol dm^{-3} are compared with ours in Table 2. A wide variation in K_1 and ε is apparent. It has been stated[3,5] that the variations arise at least in part by interference of higher complexes, $[CuCl_n]^{(2-n)+}$, for example in Nasanen's work[4] with $CuCl_2$ since ε, $CuCl_2$ is apparently[3] greater than ε, $[CuCl]^+$ near 270 nm and by neglect[6] of the polymeric form, $[Cu_2Cl]^{3+}$, see footnote *b*, Table 2. With the copper concentration at 5×10^{-3} mol dm^{-3} and chloride in the range 0–0.25 mol dm^{-3} it is possible[3] to find K_1 and K_2 simultaneously but the values obtained can be altered considerably by adjusting the minimisation procedure. Preliminary determination of K_1 through eqn (1) can be used[1] to find K_2 from a second set of experiments. In our work at 25°C M_F was 98.9–99.3% of M_T in Series 1 and 99.2–99.4% of M_T in Series 2 and in either case, if K_2 is[1,3] about 0.25 K_1, the amount of chloride contained in $CuCl_2$ was less than 0.1% of the total. An iterative loop could be added to take account of the small difference between M_T and M_F but little is to be gained by this in view of other likely errors. In addition, Libus[2] has suggested that the variation in K_1 is caused by ignored variation in the activity coefficients of the reacting species and recommends the use of $Mg(ClO_4)_2$ as the supporting electrolyte if one of the reacting species is divalent when better control should be obtained. The interaction of magnesium ions with chloride is not well understood at high temperature so it was not used in our study. At 25°C our K_1 values (Table 1) fall within the values reported previously (Table 2).

Table 1. Equilibrium constant K_1 for the formation of the first chloro-copper(II) complex

Series 1. I = 1.00 mol dm^{-3} ($NaClO_4$), Cl^- = 5.04×10^{-3} mol dm^{-3}, Cu^{2+} = 1.80×10^{-2}–0.2544 mol dm^{-3}, 12 solutions

T (°C)	λ (nm)	εK_1	ε	K_1 (dm^3 mol^{-1})
15.0	270	442	277	1.58 (0.20)
	272	396	199	2.00 (0.18)
25.0	270	564	272	2.09 (0.10)
	272	493	249	2.00 (0.20)
30.0	270	608	343	1.78 (0.13)
	272	541	277	1.95 (0.13)
45.0	270	852	476	1.78 (0.08)
	272	754	399	1.91 (0.09)
60.0	270	1175	629	1.86 (0.08)
	272	1040	552	1.91 (0.13)
75.0	270	1620	738	2.19 (0.05)
	272	1455	640	2.29 (0.05)
90.0[a]	270	2935	543	5.37 (0.40)
	272	2580	530	4.90 (0.40)

Series 2. I = 1.00 mol dm^{-3} ($HClO_4$), Cl^- = 5.00×10^{-3} mol dm^{-3}, Cu^{2+} = 2.00×10^{-2}–0.2500 mol dm^{-3}. 6 solutions

T (°C)	λ (nm)	εK_1	ε	K_1 (dm^3 mol^{-1})
24.0	270	526	321	1.64 (0.30)
49.0	270	935	471	1.98 (0.30)
75.0	270	1413	604	2.34 (0.35)
100.0[a]	280	1330	482	2.78 (0.50)

[a] High temperature cell (see Experimental).

At 40°C, values[6] of K_1 (2.00 mol dm^{-3}, $NaClO_4$) of 1.35 (265 nm), 1.38 (270 nm) and 1.29 (275 nm) are reported and at 46.9°C (1.00 mol dm^{-3}, $HClO_4$) a value[1] of 1.39 ± 0.05 (270 nm) was found.

A striking feature of Table 2 is the fair agreement in the value of the product εK, obtained from the slope of the plot which gave, however, wide variation in K_1. This has been mentioned before[3] when the importance of the chosen method of evaluation was noted. In view of the calculated value[1,2] of K_2 it is unlikely that neglect of higher complexes is alone the cause of the variation in K_1 since, as is shown above, a very small amount of the second complex is present

Table 2. Selected literature values[a] of K_1 for the formation of the first chloro-copper(II) complex at 25°C

Ref. No.	I(mol dm^{-3})	λ (nm)	εK_1	ε	K_1 (dm^3 mol^{-1})
4	1.0, $LiClO_4$	272	503	1478	0.34 (0.03)
3	1.0, $HClO_4$	272	428	186	2.3 (0.4)
2	1.22, $Mg(ClO_4)_2$	272	455	1115	0.44 (0.03)
Table 1	1.00, $NaClO_4$	272	493	249	2.00 (0.20)
Mean	$\varepsilon K_1 = 470 \pm 35$				
1	1.0, $HClO_4$	270	416	326	1.30 (0.06)
6	2.0, $NaClO_4$	270	591	477	1.24[b]
Table 1	1.0, $HClO_4$	270	526	321	1.64 (0.30)
Table 1	1.0, $NaClO_4$	270	564	272	2.09 (0.10)
Mean	$\varepsilon K_1 = 524 \pm 23$				
6	2.0, $NaClO_4$	265	870	669	1.30
This work	1.0, $HClO_4$	265	720	426	1.69 (0.30)
5[c]	1.0, $HClO_4$	250	1030	3800	0.27

[a] A kinetic method (Ref. 11) gave $K_1 = 1.41 \pm 0.33$ at 25°C, $I = 1.00$ mol dm^{-3} ($NaClO_4$).

[b] 5.47 if the polynuclear $[Cu_2Cl]^{3+}$ is included in the calculation.

[c] 22°C.

in our experiments and those of others[1,2,5,6] because of the relative concentrations of copper and chloride. However the method of evaluation should take note of the photometric accuracy. It is usual[11] in the determination of rate constants by spectrophotometric methods to weight the data used in linear regression analysis for a constant photometric accuracy in absorbance. Weighting factors are not usually applied to the time data.

Weighting factors are particularly appropriate here since in a given set of experiments $(A - A_0)$ might vary from, say 0.1 to 1 or above and reciprocals are used for the plot. Following the usual procedures,[12] weighting factors, w_i, proportional to $1/\sigma^2(A - A_0)$, where $\sigma(A - A_0)$ was set at 0.002 (0.004 at 90°C), were applied through a locally written program to the absorbance data from the Series 1 experiments (Table 1). The program calculated the slope, intercept, ε, and K_1 and their standard deviations. As can be seen from Table 3 the values of K_1 were much reduced as a result and there was on average a smaller standard deviation. This derived from a very much better defined intercept. The actual numerical values of the product εK_1 was little changed at any temperature and at 25°C remained well within the range reported previously (Table 2), e.g. at 25°C, εK_1 was 523 compared with 564 for the unweighted data at 270 nm. The standard deviation in slope was worsened by a few percent through the use of weighting factors. This alternative use of the absorbance data highlights the fragiligy of the method itself. As widely differing values of K_1 can be obtained from a single set of data, the variation in Table 2 becomes more understandable. The general instability is also indicated by the large increase in K_1 to what would seem to be an unacceptable value by the inclusion[5] of a few percent of the polymeric $[Cu_2Cl]^{3+}$ (Table 2).

The method relies on a non-linear relationship between $(A - A_0)$ and M_T. While, from visual

Table 3. Equilibrium constant K_1 using a weighting scheme for the absorbance data

Series 1 data $\lambda = 270$ nm, 12 solutions

T (°C)	15.0	25.0	30.0	45.0	60.0	75.0	90.0
K_1^a	1.24 (0.08)	1.18 (0.08)	1.24 (0.05)	1.41 (0.03)	1.62 (0.04)	1.95 (0.04)	4.79 (0.20)

[a] K_1, dm^3 mol^{-1}, standard deviation in parentheses.

inspection, plots of $(A-A_0)$ against M_T were invariably non-linear the degree of curvature is in all cases slight. As an example, the unweighted Series 1 results at 25°C and 270 nm were plotted as $(A-A_0)$ against M_T for 12 data points to give through linear regression the best fit straight line which had a correlation coefficient of 0.9982. The corresponding unweighted reciprocal fit [eqn (1)] had a correlation coefficient of 0.9998. The degree of curvature must be governed by the values of ε and K_1 as well as the concentrations M_T and L_T required to obtain acceptable absorbance data. An attempt to use the program SQUAD,[13,14] successful in our other studies,[7-9] failed to calculate K_1 or K_1 and K_2 simultaneously through non-convergence which was caused by the near linear relationship between $(A-A_0)$ and M_T. It seems likely that the use of eqn (1) cannot lead to a definitive value of K_1 at 25°C.

Interestingly, the use of a weighting scheme produced a more noticeable trend in the variation of K_1 with temperature (Table 3). Bearing in mind the expected large increase in K_1 at high temperature, it would appear that the use of the method with weighted data is an appropriate route to the high temperature determination of weak metal ion complexes with simple inorganic ions. Unfortunately, above 100°C perchloric acid reacted with the cell materials used to construct our high temperature cell.

It is possible to calculate the thermodynamic parameters ΔH^0, ΔS^0, etc. from the temperature variation in K_1. There is little profit in doing so when the total inaccuracies of the method are considered particularly as a plot of $\log_{10} K_1$ against $1/T$ is clearly non-linear (Table 3).

EXPERIMENTAL

Series 1 experiments

Copper(II) perchlorate was prepared[15] from Analar copper(II) oxide and Analar perchloric acid and recrystallised from perchloric acid (0.25 mol dm^{-3}). Stock solutions of copper(II) perchlorate ($\sim$1 mol dm^{-3}) were prepared in Analar perchloric acid (0.25 mol dm^{-3}). The Cu(II) and hydrogen ion concentrations of the stock solutions were determined by standard methods. The test solutions (100 cm^3) were prepared by taking appropriate aliquots of the Cu(II) stock solution, standardised Analar hydrochloric acid, and Analar sodium perchlorate solution to bring all the solutions to an ionic strength (I) of 1.00 mol dm^{-3}. No chloride ion was detectable in either the Cu(II) or sodium perchlorate stock solutions. The reference solutions were identical except they contained no hydrochloric acid.

Except at 90°C (see later), absorbances were measured on a Pye–Unicam SP8-100 spectrophotometer calibrated for absorbance with solutions from Pye–Unicam traceable to National Physical Laboratory Standards with matched 1 cm silica cells to give $(A-A_0)$ directly. Both sample and reference cells were thermostatically controlled to $\pm$0.05°C.

Series 2 experiments

Copper(II) perchlorate stock solutions ($\sim$ 1 mol dm^{-3}) were prepared from Analar copper(II) oxide and Analar perchloric acid and analysed for copper and acid concentrations by standard methods. Test and reference solutions were prepared as for Series 1 except that perchloric acid was used to make up the ionic strength to 1.00 mol dm^{-3}. Analar reagents were used throughout.

Except at 100°C (see later), absorbances were measured on a Unicam SP3000 spectrophotometer with the same cells as for Series 1.

If a reference solution had an absorbance greater than 0.2, the photometric accuracy worsened so that all $(A-A_0)$ values were obtained by separate measurements on the test and reference solutions using a water blank to give an overall accuracy of $\pm$0.004 units in absorbance. The cell temperature was controlled to $\pm$0.05°C and the instrument calibrated in absorbance as before.

High temperature cell

This has been described previously.[16] The cell has a pathlength of 1 cm with a teflon body and sapphire windows. A modified SP1800 spectrometer is used to measure absorbance. Absorbance measurements became unreliable above 2.0 so that in Series 2, Table 1 at 100°C, 280 nm became the lowest acceptable wavelength for accurate data. Because the reference beam is air-filled and sealed off, separate measurements on the test and reference solutions are necessary. The instrument was calibrated with neutral density filters which were first measured on the calibrated SP3000 and SP8-100 spectrometers. Under these conditions the spectrophotometric accuracy is about $\pm$0.004 overall. This cell was used at 90°C and above. Above 110°C absorbance readings increased rapidly with time and subsequent experiments showed that an absorbing material (λ_{max} 236 nm) was produced by reaction between teflon and acidic perchlorate solutions at high temperature.

Acknowledgements—Financial support from the Central Electricity Research Laboratories, Leatherhead, and the SERC is gratefully acknowledged.

REFERENCES

1. H. McConnell and N. Davidson, *J. Am. Chem. Soc.* 1950, **72**, 3164.
2. Z. Libus, *Inorg. Chem.* 1973, **12**, 2972.
3. B. Carlsson and G. Wettermark, *J. Inorg. Nuclear Chem.* 1976, **38**, 1525.
4. B. Nasanen, *Acta Chem. Scand.* 1950, **4**, 140.
5. B. Kruh, *J. Am. Chem. Soc.* 1954, **76**, 4865.
6. M. W. Lister and P. Rosenblum, *Canad. J. Chem.* 1960, **38**, 1827.
7. L. A. Ashton and J. I. Bullock, *J. Chem. Soc., Faraday 1* 1982, **78**, 1177.
8. L. A. Ashton, J. I. Bullock and P. W. G. Simpson, *J. Chem. Soc., Faraday 1* 1982, **78**, 1961.
9. J. I. Bullock and P. W. G. Simpson, *J. Chem. Soc., Faraday 1* 1981, **77**, 1991.
10. R. D. Alexander, D. H. Buisson, A. W. L. Dudeney and R. J. Irving, *J. Chem. Soc., Faraday 1* 1978, **74**, 1081.
11. M. H. Hutchison and W. C. E. Higginson, *J. Chem. Soc., Dalton Trans.* 1973, 1247.
12. See, for example, *Comprehensive Chemical Kinetics* (Edited by C. H. Bamford and C. F. H. Tipper), Volume 1, p. 372. Elsevier, Amsterdam (1969).
13. D. J. Leggett and W. A. E. McBryde, *Talanta* 1975, **22**, 781.
14. D. J. Leggett and W. A. E. McBryde, *Analyt. Chem.* 1975, **47**, 1065.
15. R. A. Matheson, *J. Phys. Chem.* 1969, **73**, 3229.
16. R. D. Alexander, A. W. L. Dudeney and R. J. Irving, *J. Phys. E.* 1980, **13**, 22.

Polyhedron Vol. 4, No. 7, pp. 1329–1331, 1985
Printed in Great Britain

0277–5387/85 $3.00 + .00
© 1985 Pergamon Press Ltd

SOME COMMENTS ON THE MECHANISM OF THE PREPARATION OF $(Et_4N)_2B_{10}H_{10}$ BY THERMOLYSIS OF Et_4NBH_4

DEIRDRE POWER and TREVOR R. SPALDING*
Department of Chemistry, University College, Cork, Ireland

(*Received* 11 *December* 1984; *accepted* 6 *February* 1985)

Abstract—The volatile intermediate Et_3NBH_3 was isolated during the thermolysis of Et_4NBH_4 at 185°C for 16 hr under dynamic vacuum. The rate of decomposition of Et_4NBH_4 was studied. Separate thermolyses of Et_4NBH_4 (or Et_3NBH_3) with *closo* $B_9H_9^{2-}$, *nido* $B_9H_{12}^-$, or *arachno* $B_9H_{14}^-$ did not produce $B_{10}H_{10}^{2-}$ as the major product. These results are inconsistent with the "build-up" mechanism previously proposed for the thermolytic convertion of BH_4^- to $B_{10}H_{10}^{2-}$ and a new mechanism is required.

The remarkable formation of the $[B_{10}H_{10}]^{2-}$ cluster by thermolysis of Et_4NBH_4 in the solid state at 185°C under atmospheric pressure was first reported almost 20 years ago.[1] The stoichiometry of the reaction is given in eqn (1). The yield of $B_{10}H_{10}^{2-}$ was 94%. No mechanism for the reaction has been established and any proposed mechanism has to explain the following,

(i) the production of only one borane product in high yield, $[B_{10}H_{10}]^{2-}$;

(ii) the conversion of monoanionic to dianionic species;

(iii) a sequence of steps from $[BH_4]^-$ to $[B_{10}H_{10}]^{2-}$ and recognise the possible intermediates involved;

(iv) effects due to the cation (note, when Me_4NBH_4 was thermolysed under identical conditions, methane and Me_3NBH_3 were the major products with only residual amounts of $[B_{10}H_{10}]^{2-}$, $[B_{11}H_{14}]^-$, and $[B_{12}H_{12}]^{2-}$).[1]

$$10Et_4NBH_4 \xrightarrow[16\,hr]{185°C} (Et_4N)_2B_{10}H_{10} + 8Et_3N + 8C_2H_6 + 11H_2 \quad (1)$$

In their original work, Makhlouf *et al.* proposed eqn (2) as the first step of the reaction,

$$Et_4NBH_4 \rightarrow Et_3NBH_3 + EtH. \quad (2)$$

They did not report the isolation of the Et_3NBH_3 intermediate or obtain any evidence for it. However the same reaction was later assumed to occur in a proposed sequential mechanism which involved BH_3 additions to $[BH_4]^-$ to give $[B_nH_{n+7}]^-$ and $[B_nH_{n+5}]^-$ anions (n = 2–12).[2] These anions were suggested to convert to the dianions $[B_nH_n]^{2-}$ (n = 6–12), but the mechanism was not discussed. It was also suggested that BH_3 reacted with $[B_nH_n]^{2-}$ (n = 6–10) to produce finally $[B_{12}H_{12}]^{2-}$. The observed selectivity to $[B_{10}H_{10}]^{2-}$ in the thermolysis of Et_4NBH_4 was not expained.

We have attempted to isolate and identify neutral intermediates in the thermolysis of Et_4NBH_4 and to investigate the steps from B_9-species to $[B_{10}H_{10}]^{2-}$. We compare our results with the previously proposed mechanism.

RESULTS AND DISCUSSION

The original thermolysis of Et_4NBH_4 was carried out at atmospheric pressure.[1] We decided to modify the experiment to study the thermolysis under dynamic vacuum conditions. Accordingly the reaction vessel was connected to a vacuum line *via* a liquid N_2 cooled trap which would retain the volatile compounds other than H_2 which are produced during the reaction. Thermolysis under these conditions produced $(Et_4N)_2B_{10}H_{10}$ as the major ionic product (> 85%) and Et_3NBH_3 (confirmed by IR, NMR and mass spectrum) which was the only volatile boron containing compound to be trapped. Triethylamine was also trapped as expected from eqn (1). There was no evidence for any other neutral borane being produced during the reaction. This is consistent with the reported lack of observation of $(Et_3NH)_2B_{10}H_{10}$ which may have been anticipated

* Author to whom correspondence should be addressed.

Table 1. Thermolysis of Et_4NBH_4 (185°C, vacuum)

Time (h)	% Et_4NBH_4 remaining
0.0	100.0
1.0	85.0
2.3	73.6
4.0	63.5
8.0	44.2
16.0	5.8

by deprotonation by Et_3N of the neutral borane $B_{10}H_{14}$ (which would be an expected product of thermolysis of lower boranes at 185°C).[1] In confirmation of the previous results,[1] no Et_3NH^+ salts were observed in the present study. It would appear that Et_3NBH_3 is the only neutral intermediate species responsible for the transformation of $[BH_4]^-$ to $[B_{10}H_{10}]^{2-}$ and all other intermediates are presumably ionic species.

The rate of loss of Et_4NBH_4, i.e. rate of production of Et_3NBH_3, was studied. The results shown in Table 1 were obtained by stopping the thermolysis at various time intervals and analysing the solid mixture for Et_4NBH_4 by IR and acid hydrolysis (H_2 gas evolution). The only compounds identified by IR were unreacted Et_4NBH_4, $(Et_4N)_2B_{10}H_{10}$ and $(Et_4N)_2B_{12}H_{12}$ as a minor product. Possible anionic intermediates such as $[B_2H_7]^-$, $[B_3H_8]^-$, etc. were not observed at any stage. Clearly Et_4NBH_4 is present during the 16 hr reaction time, suggesting that the production of Et_3NBH_3 is continuous.

A previously suggested mechanism contained steps involving the addition of "BH_3" to both mono- and dianions from $[BH_4]^-$ to $[B_{12}H_{12}]^{2-}$.[2] In order to explore the feasibility of some of these steps we studied the thermolyses of $[B_9H_9]^{2-}$, $[B_9H_{12}]^-$, and $[B_9H_{14}]^-$ salts and their cothermolyses with Et_4NBH_4 or Et_3NBH_3.

The *closo* $[B_9H_9]^{2-}$ system can be prepared by thermolysis of CsB_3H_8 at 200–230°C,[4] and hence is stable to thermolysis at 185°C. The dicaesium salt $Cs_2B_9H_9$ was recovered unchanged after heating at 185°C for 16 h with a 10-molar excess of Et_3NBH_3. This indicates that the conversion of $[B_9H_9]^{2-}$ to $[B_{10}H_{10}]^{2-}$ is not feasible under the conditions of the thermolysis of Et_4NBH_4. This result was somewhat surprising since previous work showed that reaction of $(NH_4)_2B_{10}H_{10}$ with excess Et_3NBH_3 at 190°C for 2 h gave a 27% yield of $(NH_4)_2B_{12}H_{12}$.[5] Similarly in the present work reaction of $(Et_4N)_2B_{10}H_{10}$ with excess Et_3NBH_3 at 185°C for 16 h gave 66% of the $[B_{12}H_{12}]^{2-}$ salt. The reason for the difference in the reactivity of $[B_9H_9]^{2-}$ and $[B_{10}H_{10}]^{2-}$ is not immediately obvious.

Thermolysis of the *nido* borane $Et_4NB_9H_{12}$ at 185–190°C produced only $(Et_4N)_2B_{12}H_{12}$. Cothermolysis of an equimolar mixture of $Et_4NB_9H_{12}$ and Et_4NBH_4 gave mainly $[B_{12}H_{12}]^{2-}$ with a proportion of $[B_{10}H_{10}]^{2-}$ equivalent to that expected from the thermolysis of Et_4NBH_4 alone. It appears probable that the borane anions reacted separately.

An alternative B_9-system, the *arachno* $[B_9H_{14}]^-$ ion was also studied. Thermolysis of either CsB_9H_{14} or $Et_4NB_9H_{14}$ alone produced $[B_{12}H_{12}]^{2-}$ salts as the predominant species. This result agrees with previously published work.[6] Cothermolysis of CsB_9H_{14} with a ten molar excess of $NaBH_4$ gave $CsB_{12}H_{12}$ and the $NaBH_4$ did not react. Cothermolysis of an equimolar mixture of $Et_4NB_9H_{14}$ and Et_4NBH_4 produced $(Et_4N)_2B_{12}H_{12}$ and an amount of $(Et_4N)_2B_{10}H_{10}$ equivalent to that expected from the thermolysis of Et_4NBH_4 alone.

In conclusion, during this investigation we have isolated Et_3NBH_3 as the only volatile boron containing intermediate in the thermolysis of Et_4NBH_4. With regard to the suggested build-up mechanism for the conversion of $[BH_4]^-$ to $[B_{10}H_{10}]^{2-}$ (and on to $[B_{12}H_{12}]^{2-}$) there does not appear to be a step involving conversion of a *closo*, *nido* or *arachno* B_9-species to $[B_{10}H_{10}]^{2-}$. Moreover the suggested mechanism would not explain the selective production of $(Et_4N_2)B_{10}H_{10}$ from $(Et_4N)BH_4$.

EXPERIMENTAL

Physical measurement

Infrared spectra were recorded as KBr disks or thin films between KBr plates on Perkin–Elmer 457 and 1310 spectrometers. Proton NMR were recorded on a Perkin–Elmer R20A spectrometer and ^{13}C spectra on a Jeol FX-60 spectrometer using Me_4Si as internal standard. Mass spectra were recorded on an AEI-Kratos 30–74 double beam spectrometer. Elemental analyses were carried out by the Analytical Laboratory, University College, Cork. Hydrogen gas analysis was carried out with a gas burette after samples had been hydrolysed by addition of 1.5 M sulphuric acid.

Materials

Tetraethylammonium borohydride,[7] Et_3NBH_3,[8] $(Et_4N)_2B_{10}H_{10}$, $(Et_4N)_2B_{12}H_{12}$,[1] $Cs_2B_9H_9$,[5] $(Et_4N)B_9H_{12}$,[9] CsB_9H_{14}, and $(Et_4N)B_9H_{14}$[10] were prepared as described in the literature.

Thermolyses

Reaction involving solids were carried out in a vacuum oven at $187 \pm 2°C$. Volatile products were collected in a liquid N_2 trap. Reactions involving Et_3NBH_3 were carried out at atmospheric pressure at 185°C. Separation of $B_{10}H_{10}^{2-}$ salts from $B_{12}H_{12}^{2-}$ was achieved using the method described in the literature.[1]

REFERENCES

1. J. M. Makhlouf, W. V. Hough and G. T. Hefferan, *Inorg. Chem.* 1966, **6**, 1196.
2. E. L. Muetterties and W. H. Knoth, *Polyhedral Boranes*, p. 87. M. Dekker Inc., New York (1968).
3. H. C. Brown, *Science* 1946, **103**, 385.
4. F. Klanberg and E. L. Muetterties, *Inorg. Chem.* 1966, **5**, 1955.
5. H. C. Miller, N. E. Miller and E. L. Muetterties, *Inorg. Chem.* 1964, **3**, 1456.
6. L. I. Isaenko, K. G. Myakiskev and V. V. Volkov, *Izv. Akad. Nauk SSSR, Ser. Khim.* 1982, 19; L. I. Isaenko, K. G. Myakishev, I. S. Posnaya and V. V. Volkov, *Izv. Sib. Otd. Akad. Nauk SSSR, Ser. Khim. Nauk* 1982, 73.
7. A. G. MacDiarmid (Ed.), *Inorganic Synthesis*, Vol. XVII, Chap. 1, p. 23. McGraw-Hill Co., New York (1977).
8. S. Y. Tyree (Ed.), *Inorganic Synthesis*, Vol. IX, Chap. 1, p. 10. McGraw-Hill Co., New York (1967).
9. B. M. Graybill, J. K. Ruff and M. F. Hawthorne, *J. Am. Chem. Soc.* 1967, **83**, 2669.
10. L. E. Benjamin, S. E. Stafiej and E. A. Takacs, *J. Am. Chem. Soc.* 1963, **85**, 2674.

Polyhedron Vol. 4, No. 7, pp. 1333–1334, 1985
Printed in Great Britain

0277–5387/85 $3.00 + .00
© 1985 Pergamon Press Ltd

THE ^{35}Cl NQR SPECTRA AND STRUCTURE OF PENTAFLUOROPHENYLTETRACHLOROPHOSPHORANE, $C_6F_5PCl_4$

KEITH B. DILLON* and JAMES LINCOLN
Chemistry Department, University of Durham, South Road, Durham DH1 3LE, U.K.

(*Received* 9 *October* 1984; *accepted* 6 *February* 1985)

Abstract—The low temperature structure of $C_6F_5PCl_4$ was confirmed by ^{35}Cl NQR measurements as ψ-trigonal bipyramidal, with the C_6F_5 group axial. Discrepancies were found with previously reported data, and possible causes of these are discussed.

Pentafluorophenyltetrachlorophosphorane, i.e. $C_6F_5PCl_4$, may be readily prepared by chlorination of $C_6F_5PCl_2$; its ^{31}P NMR shift of -70.9 ppm in CH_2Cl_2/CD_2Cl_2 (50:50) suggests a five-coordinate molecular structure.[1] Fild and co-workers reported ^{35}Cl NQR signals for the compound at 34.4 and 27.1 MHz (77 K), in an approximately 3:1 intensity ratio, which they ascribed to the equatorial and axial chlorines respectively in a ψ-trigonal bipyramidal structure, with the C_6F_5 group occupying the remaining axial position.[1] We have recently reprepared $C_6F_5PCl_4$ (Experimental section), and obtained a ^{31}P NMR signal from the liquid (307.2 K) at -69.5 ppm, in very good agreement with the previous value. The compound is a liquid at room temperature, so ^{35}Cl NQR spectra can only be recorded at lower temperatures from the frozen material. At 77 K three equally intense signals were observed near 34.4 MHz (Table 1), with an average frequency of 34.38 MHz, but we could find no resonance near 27.1 MHz. A careful search showed the presence of a fourth, equally intense signal at 25.300 MHz, ascribed to the axial chlorine. The results are thus compatible with the previously deduced structure but there are significant differences, particularly for the lower frequency line. The most probable explanation is that the signal seen by Fild *et al.* at 27.1 MHz[1] is the ^{37}Cl resonance from the equatorial chlorines. The ^{37}Cl frequency calculated[2] from a ^{35}Cl resonance at 34.4 MHz is 27.1 MHz, and the isotopic ratio for $^{35}Cl:^{37}Cl$ is 3.07:1, in excellent agreement with the reported signal intensities. The reasons for our observation of three signals instead of one for the equatorial chlorines are less apparent. Our instrument may have shown better resolution, but the possibility of two different structural modifications of this compound at 77 K cannot be discounted, one form having all three chlorines crystallographically equivalent, and one showing three types of equatorial chlorines with minor crystallographic differences between them.

Four weak equally intense signals were also detected at 195 K (Table 1); the average frequency for the equatorial chlorines is 33.92 MHz. All resonances showed a normal temperature dependence, and there was no evidence of a phase transition between these temperatures. The structure of $C_6F_5PCl_4$ at 77 and 195 K is thus confirmed as ψ-trigonal bipyramidal, with the electronegative C_6F_5 group occupying an axial position.

EXPERIMENTAL

All manipulations, including NMR sample preparation, were carried out either *in vacuo* or under an inert atmosphere of dry nitrogen. Pentafluorophenyldichlorophosphine, $C_6F_5PCl_2$, was prepared via reaction of the Grignard reagent C_6F_5MgCl (obtained from C_6F_5Cl and Mg in Et_2O, with a small quantity of 1,2-dibromoethane as an initiator[3]) with PCl_3. The Grignard reaction was very slow. The ^{31}P NMR of the product showed the presence of some C_6F_5PClBr as well as $C_6F_5PCl_2$,

Table 1. ^{35}Cl NQR frequencies for $C_6F_5PCl_4$

T (K)	77	195
ν ^{35}Cl (MHz)	34.480	34.100
	34.380	33.900
	34.290	33.749
	25.300	25.085

* Author to whom correspondence should be addressed.

presumably because of the initiator used, but the former was converted to $C_6F_5PCl_2$ by treatment with Et_4NCl, followed by removal of tetraethylammonium salts. $C_6F_5PCl_2$ was then chlorinated in CH_2Cl_2 solution, and the product $C_6F_5PCl_4$ was obtained as a colourless liquid after removal of the solvent.

^{31}P NMR spectra were recorded at 307.2 K as described previously; [4] chemical shifts are quoted relative to external 85% H_3PO_4, with the downfield direction taken as positive. ^{35}Cl NQR spectra were also recorded as described in previous papers.[5,6]

REFERENCES

1. M. Fild, R. Kurpat and T. Stankiewicz, *Z. anorg. allgem. Chem.* 1978, **439**, 145.
2. Decca N.Q.R. Spectrometer Handbook, Decca Radar Ltd., Instrument Division, Walton-on-Thames (1973).
3. G. M. Brooke (personal communication).
4. K. B. Dillon and A. W. G. Platt, *J. Chem. Soc., Dalton Trans.* 1982, 1199.
5. K. B. Dillon, R. J. Lynch and T. C. Waddington, *J. Chem. Soc., Dalton Trans.* 1976, 1478.
6. K. B. Dillon, R. J. Lynch, R. N. Reeve and T. C. Waddington, *J. Chem. Soc., Dalton Trans.* 1976, 1243.

Polyhedron Vol. 4, No. 7, p. 1335, 1985
Pergamon Press Ltd. Printed in Great Britain

BOOK REVIEW

Gmelin Handbook of Inorganic Chemistry. Fe—Organoiron Compounds. Part B12, Mononuclear Compounds. Edited by U. Krüerke and W. Petz, Springer, Berlin, 1984, ISBN 0-387-93500-2, 340 pp. 34 illus., DM1188, approx. $443.20.

It is nearly 30 years since the synthesis of the first cyclopentadienyl iron carbonyl compounds. Within the space of a generation, a vast number of these compounds have been prepared. The present volume represents a continuation of series B on the mononuclear organoiron compounds; the preceding volume, B11, concluded with compounds of type $(C_5H_5)Fe(CO)_2X$, where X represents a ligand bound through a group V element. Volume B12 completes the treatment of this type of compound by examining the derivatives where iron is bound to elements within groups IV (Si, Ge, Sn, Pb), III (B, Al, Ga, In), II (Mg) and transition metals, in successive sections. The impressive volume of derivatives involving the group IV elements could well present a considerable and indigestible bulk; this book, however, adopts a lucid treatment (aided by both empirical formula and ligand formula indexes). It successively examines synthetic routes, spectroscopic data, and reactions of the derivatives themselves. The properties of individual compounds are listed in clearly-arranged tables (appearance, m.p., b.p., NMR, IR, Mössbauer and UV parameters). Intelligibility is further aided by good structure diagrams, with molecular dimensions and angles, where appropriate. Compared to 77 pp. of compounds with iron—group IV bonds, the next section takes a mere 11 pp., which are mainly taken up with derivatives where the cyclopentadienyl iron carbonyl group is bound to a borane or carborane fragment.

The field of metal—metal bonds is now vast, but of the relatively small number involving the $(C_5H_5)Fe(CO)_2$ fragment, most involve bonds to Hg and Co. The IR data, necessary to comprehend structural possibilities particularly for bridged and non-bridged isomers of the cobalt compounds, are easily found.

The subsequent section involves compounds of the $^5LFe(CO)_2X$ type which do not contain unsubstituted cyclopentadienyl rings (e.g. methylcyclopentadienyl, 1,3-dimethylcyclopentadienyl, pentamethylcyclopentadienyl etc.), which are treated in a similar way (30 pp.), followed by 5 pp. dealing with derivatives with other dienyl ligands.

The importance of compounds containing the $[(C_5H_5)Fe(CO)_2L]^+$ *ion (and related systems)* is indicated by the 60 pp. that deal with them, again further subdivided according to the donor atom in the ligand L (successively O, S, N, P, As and Sb). Again the compounds are tabulated clearly, yet with further discussion of particular facets of the preparation and properties of individual compounds given subsequently.

The closing section (92 pp.) contains the immense number of σ-bonded organometallic compounds of type $(C_5H_5)Fe(CO)_2{}^1L$. Subdivision is according to the type of substituent, successively R = alkyl, halogen-substituted alkyl, alkyl groups containing group VI elements, then group V and group IV elements (presumably the remaining derivatives and aryls are to be continued in Vol. B13). Treatment follows that previously outlined, this time including compendia of kinetic data.

In summary, this volume, as usual, presents the accumulated material in readily assimilated form with literature coverage complete to the end of 1981 and with many key references into 1983. Iron is fortunate in its Gmelin treatment of organometallics; only the elements Au, Cu, Sb, Sn, Ti, U, Sc, Y and the lanthanides are anything like so up-to-date. The continued expansion in published research makes it increasingly difficult for the Gmelin philosophy of literature coverage on a "global" scale to be fulfilled, but that is no reason for criticism of their attempts to succeed.

Stanground School **SIMON COTTON**
Peterborough, U.K.

Polyhedron Vol. 4, No. 8, pp. 1337–1351, 1985
Printed in Great Britain

0277-5387/85 $3.00 + .00
Pergamon Press Ltd

HISTORICAL SKETCH

THE EARLY HISTORY OF COORDINATION CHEMISTRY IN AUSTRALIA

ANTHONY T. BAKER and STANLEY E. LIVINGSTONE*
School of Chemistry, University of New South Wales, Kensington, N.S.W. 2033, Australia

Although Prussian blue was discovered by the Berlin artists' colour maker, Diesbach, during the first decade of the eighteenth century and Lewis in 1763[1] reported the sparingly soluble potassium chloroplatinate, coordination chemistry is considered to have begun with the discovery of the cobaltammine $CoCl_3 \cdot 6NH_3$ by Tassaert in 1798.[2] During the next 50 years many "complex" compounds were reported, including potassium ferricyanide in 1822, Magnus's green salt, $[Pt(NH_3)_4][PtCl_4]$, in 1828, and the nitroprussides in 1849. In the ensuing 40 years large numbers of these "complex" compounds were reported, particularly by Jørgensen in Copenhagen, but it was not until 1893 that Werner[3] put forward a satisfactory explanation of the type of bonding present in these compounds. He proposed that in addition to the "primary" valency, which satisfied the chemical equivalence, a metal atom displayed a "secondary" valence, directed in space around the metal atom. This secondary valence or coordination number, usually 4 or 6, was satisfied by the requisite number of neutral molecules, such as NH_3, or negative ions, such as Cl^-, which were accommodated in an inner sphere about the metal atom. For his work Werner was awarded the Nobel Prize in 1913 and, although his active career spanned only 25 years, he published 174 papers and supervised some 200 PhD students. His concepts have remained the basis of coordination chemistry since 1893.[4]

Perhaps it is germane to review briefly the beginnings of science and chemistry in Australia. It now seems likely that the Portuguese naval captain Cristovão de Mendonça charted the entire east coast of Australia in 1524,[5,6] but the Dutchman Dirk Hartog is usually considered to be the first European to set foot in Australia. Hartog landed in 1616 on what is still a remote and arid region of Western Australia. However, it is to the English navigator James Cook that credit is given for the discovery of the fertile east coast of Australia. His voyage had been financed by the Royal Society, of which he was made a Fellow in 1776, in order to observe the transit of Venus in Tahiti on 3 June 1769. Having accomplished this, he was directed by the Royal Navy to explore the east Coast of New Holland, the name by which Australia was then known. He was accompanied by two botanists, the Swede Dr Solander and Joseph Banks, later to become President of the Royal Society for nearly 40 years. A tablet on the shore of Botany Bay, just south of Sydney, bears the inscription: "A.D. MDCCLXX. Under the auspices of British science, these shores were discovered by James Cook and Joseph Banks, the Columbus and Maecenas of their time. This spot once saw them ardent in the pursuit of knowledge..."

European colonization of Australia began with the establishment of a British convict settlement at Sydney Cove in January 1788. The Philosophical Society of Australasia was formed in 1821 and a few months later the newly arrived sixth governor of New South Wales, Sir Thomas Brisbane, became President of the Society. He was a keen astronomer and set up the first observatory in the colony. The Philosophical Society in 1866 became the Royal Society of New South Wales and continues to this day as a viable scientific society.

The University of Sydney was established in 1850 and one of the four Foundation Professors was John Smith, the first Professor of Chemistry in Australia. In 1874 Archibald Liversidge was appointed Professor of Chemistry, although Smith retained his Chair until 1881. Liversidge, in an academic career which extended until 1907, was active in research, particularly in the area which we would now call geochemistry, and he did much for the development of chemistry in Australia.[7] The University of Melbourne was founded in 1853. Chemistry instruction was begun in 1855 by Frederick McCoy, Professor of Geology and Mineralogy, but it was not

* Author to whom correspondence should be addressed.

until 1882 that John D. Kirkland was appointed to the first Chair of Chemistry in Melbourne.[8] In 1878 William A. Dixon was requested by the Committee of the newly formed Sydney Technical College to set up a chemical laboratory. In 1879 he commenced courses in chemistry and thus began the Sydney Technical College Chemistry Department, which in 1950 became the School of Chemistry in the University of New South Wales. Dixon remained in charge until his retirement in 1896 and published a number of papers on the chemical constituents of minerals and natural waters. One of his students in 1889 was Henry G. Smith who was the father of Australian phytochemistry.[9]

The University of Adelaide was established in 1874 and in 1885 the University appointed Edward H. Rennie as its Foundation Professor of Chemistry, the first Australian-born occupant of a chair of chemistry. Rennie was an organic chemist and worked on essential oils of Australian flora.[7] Other Australian universities were established: Tasmania (1890), Queensland (1909), Western Australia (1911), Australian National University (ANU) (1946) and New South Wales (1949). Between 1954 and 1974 another 11 were founded, so that there are now 19 universities in Australia, all of which have Departments or Schools of Chemistry.

It seems that the earliest research in coordination chemistry performed in Australia was by Masson and Steele at the University of Melbourne in 1898. Professor Sir David Orme Masson (1858–1937) was born and educated in Britain; he occupied the Chair of Chemistry in the University of Melbourne from 1886 to 1924. In his inaugural lecture in March 1887 he stated: *A School of Chemistry*! That is what it should be. Not a mere adjunct to one particular technical training . . . a school . . . permeated by the atmosphere of Research."[8] He did much to raise the status of chemistry in Australia and was the founder of the Royal Australian Chemical Institute in 1917. In their paper "The blue salt of Fehling's solution and other cuprotartrates" published in 1899, Masson and Steele[10] proved by electrolytic experiments that the deep blue colour of Fehling's solution was due to an anionic copper species. They isolated the K, Ag, Ba and Pb salts of the complex anion $[Cu_4C_{12}H_9O_{19}]^{3-}$. Apparently this early work on coordination chemistry was not extended further until 1920 (see below). Bertrand Dillon Steele later worked with William Ramsay at University College, London, and became the Foundation Professor of Chemistry at the University of Queensland.

Coordination chemistry can be said to have begun in Sydney in 1919 when E. E. Turner was appointed Lecturer in Chemistry at the University of Sydney. Eustace Ebenezer Turner (1893–1966) (Fig. 1) during

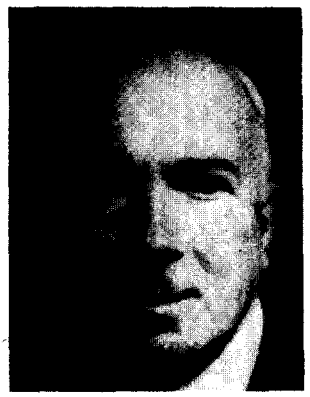


Fig. 1. Eustace Turner.

the First World War had been research assistant at Cambridge to Professor W. J. (later Sir William) Pope, who was a member of the Chemical Warfare Committee. The German Army had begun to use shells containing phenylarsonic acid, $PhAsO(OH)_2$, diphenylarsinous chloride, Ph_2AsCl, and phenylarsinous dichloride $PhAsCl_2$. Turner and Pope worked on the synthesis of arsines but the work was confidential and was not published until 1920 when it appeared in a paper entitled "Triphenylarsine and diphenylarsenous salts".[11] In Sydney Turner began a collaborative research effort with George Joseph Burrows (1888–1950) who had been appointed to the staff at the University of Sydney in 1919. Chemistry in Sydney at that time was under Charles Edward Fawsitt (1878–1960), a former pupil at Ostwald. Fawsitt succeeded Liversidge to the Chair of Chemistry in 1907 and retained it until 1946. Although no longer doing original work himself, he encouraged his staff to do research.

The first conjoint work by Burrows and Turner, "The constitution of the nitroprussides. Part I. Conductivity and cryoscopic measurements", was published in *J. Chem. Soc.* in 1919.[12] They showed conclusively that the nitroprussides contain the $[Fe(CN)_5NO]^{2-}$ ion and not a dimeric anion as had been previously proposed. Another paper, "A new type of compound containing arsenic", described addition compounds of the type $R_1R_2R_3As \cdot RAsI_2$.[13] In their next publication, "Compounds containing arsenic as a centre of optical activity",[14] they reported the optical resolution of phenyl-α-naphthylbenzylmethylarsonium ion, the first resolution of an arsenic compound to be achieved. A short paper entitled "Some additive compounds derived from arsines" reported the isolation of $PhMe_2As \cdot MI_3$ (M = P, As, Sb, Bi), $2PhMe_2As \cdot SnI_4$, $[PhMe_3As]_2[CdI_4]$ and $[PhMe_2EtAs][MI_3]$ (M = Hg, Pb).[15]

Although metal–arsine complexes had been reported in 1854,[16] this was the first work done in Australia in this area and Turner had aroused in Burrows a deep interest in metal–arsine complexes which was to be further developed in Sydney. Burrows and Turner published two more papers, one on the alkylation of nitroprussic acid[17] and the other on ferrioxalates.[18]

In 1921 Turner returned to England. In 1923 he became Senior Lecturer in Chemistry at East London (later Queen Mary) College, where he and his energetic research student Raymond J. W. Le Fèvre worked on the orientation of electrophilic substitution in biphenyl compounds, publishing 11 papers together in the period 1926–1928. Le Fèvre was later to become a Fellow of the Royal Society and Professor of Chemistry at Sydney from 1946 to 1970. Thus, although Turner spent only 2 years in Sydney, his influence was profound. In 1928 Turner went to Bedford College for Women, London, as Head of the Department of Organic Chemistry and his research interests thereafter were concentrated in organic chemistry. He was elected FRS in 1939 and became Professor and Head of Department at Bedford College in 1946 until his retirement in 1960; he was the author of 164 publications.[19]

Meanwhile at the University of Melbourne Masson in 1920 put his research students Packer and Wark to work on cupritartrates, the problem on which he and Steele had worked 22 years before. This resulted in a publication, "Cupritartrates",[20] which confirmed Masson and Steele's results and reported the isolation and identification of several complex cupritartrates. John Packer (1899–1971) entered the University of Melbourne in 1917 and became a Lecturer in Chemistry at Canterbury University College, Christchurch, New Zealand, in 1923 and its Professor in 1944.

Ian William (later Sir Ian) Wark was to become one of Australia's most distinguished scientists. He was born in 1899 and, like Packer, entered the University of Melbourne in 1917. In 1921 he was awarded an 1851 Exhibition Overseas Scholarship to University College, London, where, under the supervision of Professor F. G. Donnan, he gained his PhD in 1923, doing further research on copper complexes of hydroxy acids. This work was published in three papers: "Cuprilactates", "Cuprimalates", and "Constitution of cuprimalates and analogous compounds".[21] In the third paper of this series Wark made the somewhat remarkable statement: "Ordinary views of primary valance lead to a satisfactory explanation of the structure (of these complexes) without recourse to Werner's ideas on inner complexes". Wark spent a short time in Bragg's laboratory gaining some knowledge of X-ray crystallography. In 1924 he worked with Professor G. N. Lewis at the University of California, Berkeley, where he increased his understanding of thermodynamics and its application to solution chemistry. In 1925 he spent a year as Lecturer in Chemistry at the University of Sydney and collaborated with Burrows on salicylato complexes.[22]

In 1926 Wark returned to Melbourne as research chemist with the Electrolytic Zinc Company, where he completed his investigations on copper complexes of hydroxy acids.[23,24] In a paper in 1927 he applied the concept of free energy to galvanic cells.[25] He also investigated the distribution coefficients of inorganic compounds such as $Fe(NCS)_3$ and $HgCl_2$ in water and organic solvent mixtures.[26] However, in 1929 his interests changed to surface chemistry and his work on flotation processes for sulfide ores was widely recognized throughout the world. His book *Principles of Flotation*[27] became the standard work on the subject. In 1939 he was appointed Chief of the Australian Commonwealth Scientific and Industrial Research Organization (CSIRO) Division of Industrial Chemistry and was Director of CSIRO (1958–1960). He was H. G. Smith Medallist (1933) and Leighton Medallist (1966) of the Royal Australian Chemical Institute (see Fig. 2) of which he was President in 1958.

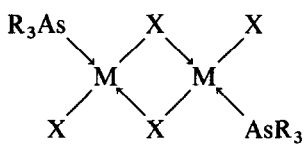
In Sydney Burrows continued research on metal complexes. Following on from his work with Turner on ferrioxalates,[18] Burrows established the exact constitution of $Na_3[M(C_2O_4)_3]\cdot 5H_2O$ (M = Fe, Cr, Al)—over which there had been some confusion in the literature—and investigated their dissociation.[28] Several iodobismuthites, $[BiI_6]^{3-}$, of organic bases[29] and further work on complex oxalates of aluminium were reported, including an unsuccessful attempt to resolve the ion $[Al(C_2O_4)_3]^{3-}$.[30]

In 1933 Burrows took up work again on metal–arsine complexes, a line of research he had begun with Turner some 13 years previously and which he was to follow for the remainder of his career. The silver complexes $[Ag(Ph_2MeAs)_2]X$ (X = Cl, Br, I)[31] and the copper complexes $[Cu(Ph_2MeAs)X]$ (X = Cl, Br, NO_3), $[Cu(PhMe_2As)X]$ (X = Br, I), $[Cu(PhMe_2As)_2]X$ (X = Cl, I) and $Cu_2X_3(Ph_2MeAs)_3$ (X = Cl, Br)[32] were isolated and the platinum complexes $[Pt(Ph_2MeAs)_2Cl_2]$ and $[Pt(PhMe_2As)_2X_2]$ (X = Cl, Br) were obtained in two isomeric forms, one soluble in toluene, the other in chloroform.[33] Complexes of zinc, cadmium and mercury were prepared: viz. $[Zn(R_3As)_2X_2]$ (R_3As = Ph_2MeAs, $PhMe_2As$; X = Br, I), $PhMe_2As\cdot ZnCl_2$,[34] $R_3As\cdot CdX_2$ (X = Cl, Br, I),[35] $[Hg(R_3As)_2X_2]$ and $R_3As\cdot HgX_2$ (X = Cl, Br, I).[36] The 1:1 complexes $R_3As\cdot MX_2$ (M = Zn, Cd, Hg)



Fig. 2. The Governor General of Australia, Lord Casey (left) presenting the Leighton Medal to Dr I. W. Wark, Canberra, 19 August 1966.

are probably dimeric with the tetrahedral halogen-bridged structure (**I**):



I

Complexes of 8-aminoquinoline with iron, cobalt, nickel and copper and the phthalic acid complexes $Na_2[M(C_6H_4C_2O_4)_2]\cdot 2H_2O$ (M = Co, Cu) were described.[37] Apart from this work and some papers dealing with arsines,[38] Burrows did not publish any more research papers. However, in 1940 he was the Royal Society of New South Wales Liversidge Lecturer and his published lecture, "Organic arsenicals in peace and war", is an excellent review of arsines and arsine–metal complexes.[39] In the 1930s Burrows lectured on coordination chemistry to third-year undergraduates at the University of Sydney and he so interested one of these students in 1936 that he worked with Burrows on an honours project on metal–arsine complexes in 1937. The student's name was Ronald Nyholm, who was to have a significant influence on coordination chemistry in Australia, Britain and elsewhere. Burrows' health was declining and he retired on medical grounds in 1941.

David Paver Mellor (1903–1980) (Fig. 3) was born in Launceston, Tasmania, and graduated from the University of Tasmania in 1924. He was appointed Lecturer in Chemistry in the University of Sydney in 1929 and promoted to Reader in Inorganic Chemistry in 1946. His lifelong interest was in the structure of inorganic compounds and metal complexes. In 1931 he undertook supervision of a brilliant graduate student, Francis Patrick Dwyer (1910–1962) (Fig. 4). Dwyer's initial interest was in organic chemistry in which he hoped to specialize. As an undergraduate he had investigated the reaction of potassium dichromate, aniline and sodium nitrite



Fig. 3. David Mellor.



Fig. 4. Frank Dwyer.

which led to an improved method for the preparation of pure diazoaminobenzene;[40] this work was published 2 years later.[41] Mellor and Dwyer were to do a great deal in the development of coordination chemistry in Australia.

Mellor's early interest lay in X-ray crystallography and his first three papers—all with Dwyer—viz. "The crystal structure of indium", "The occurrence of β-cristabolite in Australian opals", and "An X-ray study of opals",[42] were in this area. For his MSc degree Dwyer worked on glyoximato complexes of palladium and succeeded in isolating *cis* and *trans* isomers of bis(benzylmethylglyoximato)palladium(II).[43] This was an important contribution to coordination chemistry, since controversy still existed concerning the stereochemistry of four-coordinate palladium(II) and platinum(II). In 1934 Dwyer became Lecturer in Inorganic Chemistry at Sydney Technical College where he commenced active research in chemistry; little research had been done in chemistry at Sydney Technical College since William Clunies Ross's death in 1914.[9]

Mellor and his students continued work on metal complexes, using a variety of physical techniques including refractive index, X-ray diffraction, optical resolution and magnetic susceptibility measurements and stability determinations.[44–50] In 1938 Mellor went to California to work with Linus Pauling. Upon his return to Sydney in 1940 he introduced the ideas contained in Pauling's book *The Nature of the Chemical Bond* into the teaching of inorganic chemistry and into his own research and subsequently his writings show Pauling's influence. In two papers of a five-part series, "Magnetic studies of coordination compounds",[51–53] Mellor and Craig reported the magnetic moments of 37 nickel and 21 cobalt complexes with the chromophores: O_4, O_2N_2, N_4, N_2S_2, O_2S_2 and S_4. These were important data at the time, as the authors attempted to explain the preference for high- or low-spin behaviour on the basis of the chromophore (i.e. the donor atom grouping). David Parker Craig did his MSc under Mellor's supervision; later he occupied chairs of Physical Chemistry at the University of Sydney, University College, London, and the Research School of Chemistry, ANU, Canberra, and became a Fellow of the Royal Society and of the Australian Academy.

In three papers, "The significance of large angle distortions in relation to the stereochemistry and magnetic properties of quadricovalent metals", "The stereochemistry of some metallic complexes with special reference to their magnetic properties and the Cotton effect", and "A study of the magnetic behaviour of complexes containing the platinum metals", Mellor gave a lead in the clarification of the rather muddy area of the magnetic behaviour of transition metals.[54] His review, "The stereochemistry of square complexes",[55] based on his Presidential Address to the Royal Society of New South Wales in 1942,[56] became the standard reference work in this area for many years. For this and his other work on metal complexes Mellor was awarded the DSc degree by the University of Tasmania.

In two important publications[57] Mellor and Maley established that the stability sequence for bivalent metals in complexes with oxygen and nitrogen donors is: Pd > Cu > Ni > Co > Zn > Cd > Fe > Mn > Mg. These papers preceded the publication of the classic work of Irving and Williams,[58] who showed that the sequence for the first transition series is: Mn < Fe < Co < Ni < Cu > Zn. Additional papers followed reporting the paramagnetism of tungsten bronzes[59] and the crystal structures of $K_2[PtF_6]$,[60] $K_2[RuCl_6]$[61] and Zeise's salt, $K_2[PtCl_3(C_2H_4)] \cdot H_2O$, in which it was shown that the C—C axis of the ethylene ligand is perpendicular to the plane containing the $PtCl_3$ grouping.[62]

In 1955 Mellor accepted the Foundation Chair of Inorganic Chemistry in the University of New South Wales and the following year became Head of the School of Chemistry, a position he held until his retirement in 1968. During this period this was the largest School of Chemistry in Australia and this position took up much of his time so that he did no more active research. He was the author of several books, including *The Rôle of Science and Industry in Australia in the War of 1939–1945*;[63] the writing singlehanded of this large work of 738 pages occupied his efforts over several years in the early 1950s. Upon Dwyer's death he took over the editing of *Chelating Agents and Metal Chelates*,[64] a book

with contributions by Mellor, Dwyer, Nyholm, and a number of their former students and colleagues. His historical work, *The Evolution of the Atomic Theory*,[65] was published in 1971 and his "Chemistry of chelation and chelating agents"[66] was published just prior to his death in January 1980. Mellor made considerable contributions to education and held many honorary positions in this field, such as Chief Examiner for Science and Chairman, Syllabus Committee, N.S.W. Higher School Certificate. He was the recipient of many honours, including the H. G. Smith Medal (1949), the Liversidge Medal (1951), and the Leighton Medal (1969) of the Royal Australian Chemical Institute and the Dwyer Memorial Medal (1969) of the University of New South Wales Chemical Society. An earnest and quietly spoken man not without a sense of humour, he and his contributions to education are commemorated by the endowment in 1972 by the University of New South Wales of the Mellor Lecture and Medal for Chemical Education.

Shortly after his appointment as Head Teacher of Inorganic Chemistry at Sydney Technical College in 1934, Frank Dwyer began an investigation of the reactions of diazoamino compounds with metallic salts to produce highly coloured "lakes", which are loose coordination complexes chemisorbed at the surface of metal hydroxides.[67] Using these reactions, Dwyer devised a number of micro-analytical tests for metals such as magnesium, cobalt, copper, zinc and cadmium; the work was reported in 18 papers in *J. Soc. Chem. Ind.* and *J. Proc. Aust. Chem. Inst.* in the period 1936–1939. This was followed by four papers on furfuraldoxime as a ligand[68] and two papers on diazoaminobenzene complexes.[69]

In 1940 Ronald Sydney Nyholm (1917–1971) (Fig. 5) was appointed to the chemistry staff at Sydney Technical College. He was born in Broken Hill, an isolated mining town in a semi-desert area in New South Wales, some 1200 km west of Sydney. In Broken Hill streets have the names of minerals, metals and acid radicals: *inter alia*, Blende, Cobalt, Chloride, Bromide and Sulphide Streets are to be found there. Nyholm's grandfather, Erik Nyholm (1850–1887), was born in Nykaleby, Finland, and had migrated to Adelaide, South Australia, in 1873. Ronald Nyholm valued this Finnish connection and he took great pleasure in his election in 1959 as a Corresponding Member of the Finnish Chemical Society.[70]

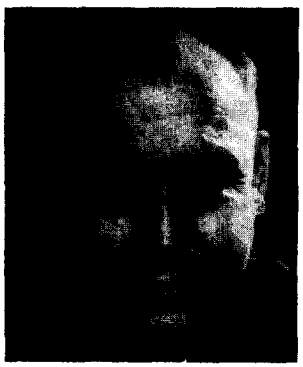


Fig. 5. Sir Ronald Nyholm.

Dwyer with his enthusiasm and experimental skills and Nyholm with his keen interest in coordination chemistry and experience with arsines, gained from Burrows, developed not only a good working combination, but a close personal friendship. With a heavy teaching load, very limited resources, and a small quantity (5 g) of rhodium they set to work. In a 10-part series, "The chemistry of bivalent and trivalent rhodium",[71,72] they reported a number of Rh(III) and Rh(II) complexes with arsines, pyridine, dimethylglyoxime and dimethylsulfide. The Rh(II) complexes, prepared by reduction with hypophosphorous acid, included such compounds as the halogen-bridged dimeric compounds $[RhX_2(Ph_2MeAs)_3]_2$ (X = Cl, Br, I). The presence of Rh(II) in these diamagnetic complexes was later questioned, since Rh(II) would be expected to have one unpaired electron, and a reinvestigation in 1960 by Lewis, Nyholm and Reddy[73] showed that at least some of these compounds are hydrido complexes of Rh(III). This should not be taken as a criticism of the early work of Dwyer and Nyholm, since hydrides of transition metals were unknown at that time. It is noteworthy that hydride complexes of rhodium have been extensively used as catalysts in the organic chemical industry. The Rh(IV) complex $Cs_2[RhCl_6]$, which was found to be isomorphous with $(NH_4)_2[PtCl_6]$, was also reported.[72] In a four-part series, "The chemistry of bivalent and trivalent iridium",[74,75] Dwyer and Nyholm reported the Ir(III) complexes $[IrX_3(Ph_2MeAs)_2]_2$ and $H[IrX_4(Ph_2MeAs)_2]$ and the Ir(II) complexes $[IrX_2(Ph_2MeAs)_3]_2$ (X = Cl, Br, I); the latter are no doubt hydrido complexes of Ir(III). The standard redox potentials for $[IrCl_6]^{3-}/[IrCl_6]^{4-}$ and $[IrBr_6]^{3-}/[IrBr_6]^{4-}$ were reported as 1.017 and 0.99 V, respectively.

Some papers with Gibson followed, describing the use of quaternary arsonium salts and their coordination compounds with bismuth, cadmium and cobalt as analytical reagents.[76] Neville Gibson later joined the staff of Sydney University and became an Associate Professor of Inorganic Chemistry. Nyholm and Dwyer continued work on arsines, reporting complexes of Ru(III), Ru(II), Os(III) and Os(II) with Ph_2MeAs.[77,78] The stability constant of $[Fe(phen)_3]^{2+}$ and the redox potentials of the systems $[Ru(phen)_3]^{3+}/[Ru(phen)_3]^{2+}$,

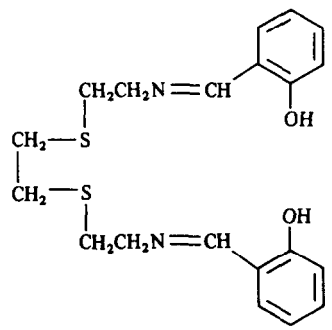
$[OsBr_6]^{3-}/[OsBr_6]^{4-}$ and $[OsCl_6]^{3-}/[OsCl_6]^{4-}$ were determined.[79–81] This work brought to a close the collaboration of Dwyer and Nyholm at Sydney Technical College. It had been a most fruitful collaboration, not only because of the intrinsic value of the work but also because of the pattern it set within the Chemistry Department, which soon after became the School of Chemistry in the University of New South Wales. Ever since the early 1940s research in coordination chemistry has been vigorously pursued within this Department.

In 1945 the University of Sydney awarded the DSc degree to Dwyer for his thesis entitled "The diazoamino compounds and their metallic salts and metallic hydroxide lakes". It was the first DSc in chemistry awarded by the University in nearly 20 years. In January 1946 Dwyer accepted a position as Senior Lecturer in Inorganic Chemistry at Sydney University. And in 1947 Nyholm was awarded an Imperial Chemical Industries Fellowship to work with Professor C. K. Ingold, later Sir Christopher Ingold, in the William Ramsay and Ralph Forster Laboratories at University College, London.

Soon after his arrival at the University of Sydney Dwyer began a productive collaboration with Frank Lions. Francis Lions (1901–1972) was Dux of Sydney High School in 1918, coming first in Chemistry and second in Physics in the New South Wales Leaving Certificate examinations. He won an Exhibition bursary to the University of Sydney, where he represented the university at rugby football and graduated in 1923 with First Class Honours and the University Medal in Chemistry and also in Organic Chemistry. He was awarded an 1851 Science and Research Scholarship to the University of Manchester where he gained his PhD in organic chemistry. He then spent a year on post-doctoral research at Brasenose College, Oxford. He was appointed Lecturer in Chemistry at Sydney University in 1926 and promoted to Senior Lecturer in 1944 and to Reader in 1946, retiring in 1966.

Lions was a popular lecturer, emphasizing the essential points with clarity. He had breadth of vision not only in science but also in humanity. He was considerate of students needs, being an elected representative of the graduates on the University Senate (1949–1959) and a strong and early advocate of the establishment of a Student Health Service.

In 1946 Lions was President of the Royal Society of New South Wales and had published 56 papers in its journal. All but two of these were in the area of organic chemistry, the two exceptions being "1-Hydroxyacridine as a chelate compound"[82] and "Coordination compounds derived from nicotinylacetone".[83] Dwyer, Lions and others had discussed the possibility of synthesizing a sexadentate chelating agent. Owing to the Second World War many European journals of the war period were not available in Australia in 1946 and the work of Brinzinger on the sexadentate function of ethylenediaminetetraacetic acid was not known to the group at Sydney University. Accepting the challenge, Lions set out to synthesize a sexadentate and soon succeeded in producing 1,8-bis(salicylideneamino)-3,6-dithiaoctane (**II**) ($H_2ONSSNO$).[40] Dwyer reacted **II** with cobalt acetate and isolated the Co(III) complexes [Co(ONSSNO)]X (X = Cl, I, NO_3, ClO_4) and succeeded in resolving the cation by treating the chloride with silver *d*-α-bromocamphor-π-sulfonate and precipitating the *d*- and *l*-iodides, which, after several recrystallizations, gave molar rotations of $\pm 50{,}160°$.[84] This was the highest molar rotation recorded up to that time.



II

Dwyer became interested in complexes of group VIII metals with 1,10-phenanthroline and 2,2′-bipyridyl.[85–87] He then began in earnest to develop his skill in resolving metal complexes into their optical isomers. He was fortunate in acquiring Nora Gyarfas as a research student. Eleonora Clara Gyarfas was born in Hungary and was a graduate of the University of Budapest; she had migrated to Australia after the war. In 1948 she began work with Dwyer and in 1951 was one of the first two PhD graduates from the University of Sydney. (The first Australian PhD was awarded in 1948 by the University of Melbourne to R. H. Myers, later Sir Rupert Myers, Vice-Chancellor, University of New South Wales, 1969–1981.) After gaining her PhD degree, she worked as a Teaching Fellow in the School of Chemistry and between 1949 and 1957 no less than 32 papers appeared under the name of Dwyer and Gyarfas. She left Australia in 1955 to go to the University of Illinois, where she worked with Professor John C. Bailar, Jr. She married Dr C. Liu of the University of Michigan and they now live in Chicago.

In their first paper Dwyer and Gyarfas reported the resolution of $[Ru(phen)_3]^{2+}$ and showed that the

enantiomorphous forms were stable and could be oxidized to $[Ru(phen)_3]^{3+}$ with retention of optical activity.[88] The resolutions of $[Ru(bipy)_3]^{2+}$, $[Ni(phen)_3]^{2+}$, $[Fe(phen)_3]^{2+}$ and $[Os(bipy)_3]^{2+}$ were also achieved.[89,90] The optical resolution of $[Os(bipy)_3]^{2+}$ was the first recorded resolution of an osmium compound. In an ingenious experiment they showed the existence of electron transfer and dynamic equilibrium between oxidized and reduced forms of complex ions.[91] Previously this had been demonstrated with the ions $[Co(en)_3]^{2+}$ and $[Co(en)_3]^{3+}$ by the use of radioactive cobalt. Dwyer and Gyarfas mixed equimolar solutions of *d*-$[Os(bipy)_3]^{2+}$ and *l*-$[Os(bipy)_3]^{3+}$. In the absence of electron transfer the optical rotation of the mixture would be expected to be the algebraic sum of the rotations of the two solutions before mixing. It was found that the mixture rapidly lost all optical activity, indicating the existence of the following equilibria:

$$d\text{-}[Os(bipy)_3]^{2+} \rightleftarrows d\text{-}[Os(bipy)_3]^{3+} + e,$$

$$l\text{-}[Os(bipy)_3]^{3+} + e \rightleftarrows l\text{-}[Os(bipy)_3]^{2+}.$$

By lowering the temperature they were able to slow down the rate of exchange and show how such a technique could be used to determine reaction rates. They also prepared the optical isomers of $[Fe(bipy)_3]^{2+}$, $[Os(phen)_3]^{3+}$ and $[Os(bipy)_3]^{3+}$ by oxidation of the *d*- and *l*-forms of the bivalent metal complexes.[92]

Dwyer and Gyarfas discovered the phenomenon of configurational activity: briefly, the phenomenon is that, although both *d*- and *l*-forms of a complex ion normally have the same thermodynamic activity coefficient, in the presence of another optically active ion these activity coefficients are different. They predicted that configurational activity should be of biological importance, since the rates of many enzyme processes should be changed by the addition of inert optically active complex ions.[93] With these thoughts in mind, Dwyer became interested in what is now called bioinorganic chemistry and reported on a preliminary investigation of the biological activity (toxicity to mice) of some complex ions such as the *d*- and *l*-forms of $[Co(en)_3]^{3+}$ and $[Os(bipy)_3]^{2+}$.[94]

Dwyer and Lions did further work on sexadentates, preparing ligands similar to **II** but with three in place of two methylene groups in the N—S chains and resolving the metal complexes and measuring their magnetic moments.[95] One of the research students engaged in this work was Naida Gill who became a Senior Lecturer in Chemistry at the School of General Studies, Australian National University, Canberra. Another of Dwyer's students at this time was Alan McLeod Sargeson who is now Professor of Inorganic Chemistry, Research School of Chemistry, ANU and a Fellow of the Australian Academy and a Fellow of the Royal Society (London).

In 1954 Dwyer spent a year as Visiting Professor at Northwestern University, Evanston, Illinois, and was also George Fisher Baker Lecturer at Cornell University. Not long after his return to Sydney he was appointed to a new Chair at Pennsylvania State University. This was a major blow to inorganic chemistry in Australia. Many of his contemporaries thought that his work had not been fully recognized in Australia; nevertheless he had been awarded the Rennie Medal (1940) and the H. G. Smith Medal (1945) of the R.A.C.I. and the David Syme Medal of the University of Melbourne (1953) and he was Liversidge Lecturer in 1959. A group of people including Dr I. W. Wark of CSIRO sought means of retaining Dwyer in Australia and, with financial assistance from CSIRO, the Australian National University offered him the position of Reader in Biological Inorganic Chemistry within the John Curtin School of Medicine. Dwyer accepted this position without ever taking up the post in Pennsylvania. At a farewell function at Sydney University prior to his departure for Canberra Dwyer was presented with a caricature of himself as a sexadentate coordinated to a cobalt atom (see Fig. 6). It was drawn on the spot by Graham Hunt, a postgraduate student working with Dr Ian Ross.

As it is our intention in this historical review to deal with matters only up until 1954, Dwyer's subsequent career will be briefly summarized. In 1960 he was offered a Personal Chair at ANU and in 1961 he was elected Fellow of the Australian Academy. He continued his research on optical activity and stereospecificity while at the same time

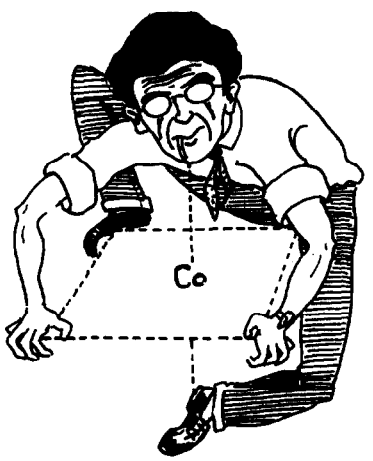
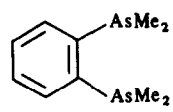


Fig. 6. Frank Dwyer as a sexadentate.

becoming involved in investigating the biological activity of complex ions. He died suddenly at his home in June 1962 at the age of 51. During his career he was the author of 160 papers and his book *Chelating Agents and Metal Chelates*[64] was published posthumously in 1964.

Frank Dwyer above all else was a highly skilled experimenter and spent long periods at the laboratory bench. His enthusiasm was infectious and, as Keith Sutherland once said, he gloated over each new compound establishing a record for optical rotation. He was admired and respected by colleagues and students for his depth of chemical knowledge and his sense of humour. His friends and former students in the University of New South Wales Chemical Society established the Dwyer Memorial Lecture Fund. Table 1 lists eminent chemists who have delivered the Dwyer Lectures. The first was given by his close friend and former colleague Ron Nyholm (see also Fig. 7).

Nyholm was awarded his PhD by the University of London in 1950 for research on metal complexes of tertiary arsines. In 1948 he met Joseph Chatt, a former student of F. G. Mann, who had prepared the diarsine *o*-phenylenebisdimethylarsine (**III**) in 1939.[96] Nyholm wanted to prepare dimeric halogen-bridged complexes of Fe(III) which would be soluble in organic solvents; he had attempted to make such complexes with arsines R_3As but without success. Chatt suggested that he use the diarsine **III**. Nyholm prepared the diarsine but he did not obtain the iron complexes he was seeking. However, he did obtain a range of transition metal complexes of the diarsine, including complexes of Ni(III) and Ni(IV), thus opening up a new area of coordination chemistry.[97]



III

In 1950 Ingold appointed Nyholm on his staff as a lecturer. On 21–22 September 1950 he attended a Discussion on Coordination Chemistry, organized by Joe Chatt at the Butterwick Research Laboratories of ICI Ltd at The Frythe, Welwyn, U.K. Papers were read by N. V. Sidgwick (Oxford), F. G. Mann (Cambridge), G. Schwarzenbach (Zürich), H. Irving (Oxford), R. S. Nyholm (University College, London), J. Chatt (ICI), R. G. Wilkins (ICI), K. A. Jensen (Copenhagen), L. E. Orgel (Oxford), A. F. Wells (ICI) and L. E. Sutton (Oxford); others in attendance included A. Albert (ANU), D. P. Craig (University College, London) and J. S. Anderson (AERE, Harwell, U.K.). This historic meeting came to be regarded as the Ist International Conference on Coordination Chemistry. These conferences have been held at approximately 2-year intervals ever since at venues all around the world, including XII Sydney, Australia (1969), XVIII São Paulo, Brazil (1977), and XX Calcutta, India (1979).

In February 1952 Nyholm returned to the University of New South Wales School of Chemistry, which until 1950 had been the Chemistry Department, Sydney Technical College. His effect on the inorganic chemistry staff was immediate and profound. He brought back the fresh ideas of what he called the "Renaissance of inorganic chemistry" taking place overseas. The teaching of inorganic chemistry was updated and a new enthusiasm for

Table 1. Dwyer Memorial Lecturers and Medallists

I	1963	R. S. Nyholm, University College London
II	1964	M. Calvin, University of California
III	1965	J. C. Bailar, University of Illinois
IV	1966	F. A. Cotton, Massachusetts Institute of Technology
V	1967	H. B. Jonassen, Tulane University
VI	1968	F. Lions, University of Sydney
VII	1969	D. P. Mellor, University of New South Wales
VIII	1972	J. F. Duncan, Victoria University of Wellington
IX	1973	H. Taube, Stanford University
X	1975	J. A. Ibers, Northwestern University
XI	1975	G. Schwarzenbach, Eidgenössische Technische Hochschule, Zürich
XII	1976	F. Basolo, Northwestern University
XIII	1977	G. Wilkinson, Imperial College London
XIV	1977	L. Sacconi, University of Florence
XV	1978	D. H. Busch, Ohio State University
XVI	1980	R. J. Gillespie, McMaster University, Ontario
XVII	1980	J. Chatt, Sussex University
XVIII	1982	J. Lewis, Cambridge University



Fig. 7. David Mellor, President of the University of New South Wales Chemical Society presenting the Dwyer Memorial Medal to Frank Lions, 23 July 1968.

research was engendered. The lecturers and research students affected were: G. A. Barclay, C. M. Harris, S. E. Livingstone, R. L. Martin, R. J. Irving, L. N. Short, G. J. Sutton, J. R. Backhouse, B. N. Figgis, B. M. Gatehouse, E. A. Magnusson and N. C. Stephenson. Gordon Barclay became Foundation Professor of Chemistry and later Pro-Vice-Chancellor, Macquarie University; Ray Martin became, in turn, Professor of Inorganic Chemistry at the University of Melbourne and the Research School of Chemistry, ANU, Canberra, and Vice-Chancellor, Monash University; Stanley Livingstone succeeded David Mellor as Professor of Inorganic Chemistry, University of New South Wales; Laurence Short became Professor of Education and later Pro-Vice-Chancellor, Newcastle University (N.S.W.); and Brian Figgis became Professor of Inorganic Chemistry, University of Western Australia. All owe a heavy debt to Nyholm. Martin's and Figgis's interest in magnetochemistry stemmed from Nyholm's influence in this period.

Nyholm was promoted to Associate Professor in 1953 and in the same year received the Corday Morgan Medal of The Chemical Society. In 1954 he was President of the Royal Society of New South Wales and received his DSc (London). In February 1955 he left Australia to accept a Chair of Chemistry at University College London. He had spent only 3 years in Sydney, yet in that time he had taken coordination chemistry out of one rut and put it in another. During that period he supervised several PhD students and published four important reviews, viz. "Stereochemistry and valence states of nickel",[98] "Magnetism and inorganic chemistry",[99] "The stereochemistry of complex compounds",[100] and "Magnetism and stereochemistry".[101]

At University College Nyholm soon built up a flourishing research group which attracted PhD and postdoctoral students not only from Britain but from the United States, Australia, New Zealand, India and elsewhere. After Ingold's retirement and the early death of his successor Edward Hughes in 1963, Nyholm became Head of the Chemistry Department. He received many honours: Tilden Lecturer (1961), Liversidge Lecturer of The Chemical Society (1967), and President of The Chemical Society (1968–1970); during his tenure of office he saw the amalgamation of the Society with the Faraday Society, the Royal Institute of Chemistry and the Society for Chemical Industry. He was knighted in 1967. He also became active in the area of chemical education and played a leading rôle in the launching of a new journal, *Education in Chemistry*, and in the organization of the large (6000 pp.) work, *Comprehensive Inorganic Chemistry*.[102] His publications numbered 278. He was killed in a motor car accident near Cambridge in December 1971 at the age of 54.

Many tributes were paid to Nyholm. Sir Jack Lewis once said to one of the authors (S.E.L.): "When you talk to him (Nyholm), he makes you feel that you are the most important guy around." Professor Jim Millen of University College, London, wrote: "He

was the master of the general survey and could condense and bring order to the large areas of chemical knowledge." Lord Annan, Provost of University College said at Nyholm's Memorial Service: "Ron Nyholm never entered a room, he bubbled into it and exploded into good fellowship, mirth and happiness." David Craig wrote: "He had warmth, sympathy, humour, great kindness and vitality. He had star quality... and reserves of energy seemingly without limit."[70] One of us stated: "He was probably the noblest person associated with this School (of Chemistry at the University of New South Wales) and he always maintained a close relationship with it."[9]

Let us return to Melbourne. After Wark's work on copper complexes of hydroxy acids in the 1920s, interest in coordination chemistry died. In 1939 John Stuart Anderson was appointed Senior Lecturer. He had a brilliant record as an undergraduate and research student at Imperial College, London, and had done research on nitrosyl–carbonyl complexes and isotopic exchange reactions of cobaltammines.[103] In 1941 he was awarded the Grimwade Prize in Industrial Chemistry for work on the recovery of indium from industrial by-products. In 1942 he and Keith Sutherland were engaged on research for the Defence Department's munitions laboratory at Maribyrnong, Victoria. He published two papers on the kinetics of interchange of hydrogen isotopes with cobaltammines and tetrammine complexes of Pd(II) and Pt(II), although some of this work was done at Imperial College.[104] However, during this period in Melbourne Anderson's main interests were in solid state chemistry, including crystal lattice defects, semi-conductors and non-stoichiometric compounds. Among his research students were Norman N. Greenwood and Thomas A. O'Donnell, now Professor of Inorganic Chemistry at Melbourne. In 1942 he delivered the Liversidge Lecture entitled, "Chemistry of the earth".[105] In 1947 Anderson left Melbourne to take up a senior position at the AERE (Harwell, U.K.).

The arrival of Gordon M. Harris from Saskatchewan as Senior Lecturer in 1947 introduced radiochemistry into the Department. Harris's research was concerned with radio-isotopic studies of exchange mechanisms, particularly in regard to cobaltammines.[106] He attracted among his students Donald Richard Stranks and they published several papers on the mechanism of exchange reactions of $^{14}CO_3^{2-}$ with $[Co(NH_3)_4CO_3]^+$.[107,108] In 1953 Harris left Melbourne to go to the University of Buffalo, New York. James F. Duncan was appointed Senior Lecturer in 1953 and continued research, in radiochemistry but not in the same area. Stranks became Professor of Inorganic Chemistry, first at the University of Adelaide (1964–1973), then at the University of Melbourne (1973–1977) and Vice-Chancellor, University of Adelaide (1977).

Anderson, now a Fellow of the Royal Society, returned to Melbourne in 1954 as Professor of Chemistry. His research interests were still mainly in the area of solid state chemistry rather than coordination chemistry. He resigned the Chair in 1959 and went to the National Chemical Laboratory (Teddington, U.K.). He became Professor of Inorganic Chemistry at Oxford and was awarded the Davy Medal of the Royal Society in 1973.

Stuart Walter Pennycuick (1887–1966) was born in Blackall, Queensland, and graduated MSc from the University of Queensland in 1920. He was appointed Lecturer in Physical Chemistry at the University of Adelaide in 1922 and was later promoted to Reader, retiring in 1952. He carried out research on colloidal sols of platinum and gold, confirming that $H_2[Pt(OH)_6]$ is the strong acid present in solutions of colloidal platinum prepared by the Bredig method.[109] In a later paper[110] he showed that $H_2[Pt(OH)_6]$ is present in the micelles of a sol prepared by the Bredig method, accounting for 27% of the total mass of the micelle. Although this work was essentially physical chemistry, it was the first research relating to coordination chemistry done at the University of Adelaide.

Inorganic chemistry at Adelaide was taught by William Ternent Cooke from around 1910 until 1948. Cooke was an analytical chemist and taught applied chemistry without any reference to coordination chemistry. It is therefore somewhat surprising that Bruce West, who graduated from Adelaide in 1948, should have become interested in coordination chemistry. West was appointed Lecturer in Inorganic Chemistry at the University of Adelaide in 1950. He did research under the formal supervision of Pennycuick, working on stabilities of cobalt complexes and exchange reactions with radioactive ^{60}Co and gained his PhD in 1953. He then took leave to go to Cambridge to work in Professor H. J. Emeléus's laboratory under the supervision of Robert N. Haszeldine.[111] He obtained his Cambridge PhD in 1955 and upon his return to Adelaide worked on Schiff-base complexes.[112,113] His subsequent work included pyrromethene complexes, solvent extraction and electron-transfer reactions.[114] He was promoted to Reader in 1962 and in 1964 accepted the Chair of Inorganic Chemistry at Monash University, Clayton, Victoria.

At the University of Queensland in 1950 coordination chemistry was taught by Ian Lauder to Chemistry III students but it appears that no research in coordination chemistry was done before

the arrival of Ronald Arthur Plowman as Senior Lecturer in June 1951. Plowman was a graduate of Sydney Technical College (1941) and was appointed to the staff of Sydney Technical College in 1945. He gained his BSc (London) by external study. With Dwyer's encouragement he began research in 1948 on complexes of platinum and palladium[115,116] and obtained his PhD (London) externally in 1951, after travelling to London to be given a *viva voce* by W. Wardlaw. After his arrival in Queensland, Plowman worked on polarography of platinum complexes[117] and synthesis of substituted 1,10-phenanthrolines.[118]

There seems to have been no research in genuine coordination chemistry at the University of Western Australia before 1962. However, with the arrival of Donald W. Watts (1962), Brian N. Figgis (1963), David L. Kepert (1965) and Allan H. White (1966) research in this area rapidly developed in Perth. Similarly, at the University of Tasmania it began after the return of Peter W. Smith in 1960 after working with Nyholm at University College.

No history of the development of coordination chemistry in Australia would be complete without the name of Adrien Albert, FAA. Albert was born in 1907 and was educated at Scots College, Sydney, and gained his BSc from the University of Sydney and PhD Med. from London University. He was on the staff of the School of Pharmacy at the University of Sydney (1938–1947) before going to London to join the research staff at the Wellcome Research Institute. In 1949 he was appointed Professor of Medical Research in the John Curtin School of Medical Research, ANU, Canberra, a post he held until his retirement in 1973. Subsequently he was Research Professor at the State University of New York at Stony Brook (1975–1977). Albert's research interests were primarily in pharmacology as indicated by his book *Selective Toxicity—The Physico-Chemical Basis of Therapy*,[119] yet he has made considerable contributions to coordination chemistry.

As early as 1944 Albert had suggested[120,121] that oxine (8-hydroxyquinoline) owes its bactericidal and fungicidal action to metal chelation, a hypothesis which struck an unfamiliar note at the time. It was shown that the antibacterial activity of 1-hydroxyacridine was also due to its ability to chelate to metabolically important metals.[122,123] He determined stability constants for complexes of a number of metals with the amino acids cysteine and histidine and the anti-tuberculosis drug isoniazid.[124,125] In the mid-1950s Douglas D. Perrin, a New Zealander, joined Albert's staff and determined stability constants of Fe(III) and Fe(II) complexes of amino acids.[126]

On 25–26 May 1953 a Conference on Coordination Compounds was held at the University of Sydney. After an introduction by I. W. Wark (CSIRO), review-type papers were presented by D. P. Craig (Sydney), R. S. Nyholm (N.S.W.), L. N. Short (N.S.W.), D. P. Mellor (Sydney), D. D. Brown (Colonial Sugar Co. Ltd), N. R. Davies (N.S.W.), E.C. Gyarfas (Sydney), G. A. Barclay (N.S.W.), B. J. Ralph (N.S.W.), W. A. Rawlinson (Melbourne) and N. A. Gibson (Sydney). The full text of these reviews was published.[127] The fact that over 100 people attended all the sessions showed that coordination chemistry was being actively pursued at least in the state of New South Wales. It is at this point that we have chosen to end our detailed historical narrative.

Within the next decade research in coordination chemistry was going on in all six states of Australia and in Canberra. Consequently, on 18–19 May 1964 an Australian Conference on Coordination and Metal–Organic Chemistry was held at the Royal Society of Victoria Building in Melbourne. It was

Table 2. Royal Australian Chemical Institute Coordination and Metal–Organic Chemistry Division Conferences

I	University of New South Wales, Kensington, August 1965
II	Australian National University, Canberra, August 1966
III	Monash University, Clayton, Victoria, May 1968
IV	Sydney University Agricultural Research Station, Camden, May 1972
V	Broadbeach, Queensland, February 1974
VI	University of Adelaide, South Australia, May 1975
VII	La Trobe University, Bundoora, Victoria, February 1977
VIII	University of Western Australia, Perth, May 1978
IX	University of New South Wales, Kensington, February 1980
X	Queenstown, New Zealand, May 1981
XI	Australian National University, Canberra, August 1982
XII	University of Tasmania, Hobart, January 1984

Table 3. C. J. Burrows Award Winners

I	1975	A. M. Sargeson
II	1977	D. R. Stranks
III	1978	R. L. Martin
IV	1980	H. C. Freeman
V	1981	B. O. West
VI	1983	C. J. Hawkins
VII	1984	D. L. Kepert

decided at this conference to form within the Royal Australian Chemical Institute a Coordination and Metal–Organic Chemistry Division, which would organize regular conferences. The first conference was held the following year. Table 2 lists the venues and dates of these conferences.

In 1974 it was decided to make an award for scientific work in the field of inorganic chemistry, the major portion of which was done in Australia, published in the previous 10 years. The successful candidate is required to deliver a lecture at the Division Conference. The lecture was to be known as the G. J. Burrows Lecture. The Burrows Lecturers are listed in Table 3. It is fitting that Burrows should be remembered in this way. And in the School of Chemistry at the University of New South Wales in 1972 three lecture theatres were named: Dwyer, Nyholm and Mellor.

REFERENCES

1. W. Lewis, *Commercium Philisophico-technium.* London (1763).
2. Tassaert, *Ann. Chim.* 1798, **28**, 92.
3. A. Werner, *Z. Anorg. Chem.* 1893, **34**, 267.
4. Werner Centennial, *Adv. Chem. Ser.* 1967, **62**, 1.
5. T. M. Perry, *The Discovery of Australia.* Nelson, Melbourne (1982).
6. R. Ward, *Australia Since the Coming of Man.* Landsdowne, Sydney (1982).
7. R. J. W. Le Fèvre, In *A Century of Scientific Progress: The Centenary Volume of the Royal Society of New South Wales*, p. 332. Royal Society of New South Wales, Sydney (1966).
8. J. Radford, *The Chemistry Department of the University of Melbourne: Its Contribution to Australian Science, 1854–1959.* Hawthorn Press, Melbourne (1978).
9. S. E. Livingstone, *Chem. Aust.* 1979, **46**, 471.
10. O. Masson and B. D. Steele, *J. Chem. Soc.* 1899, **75**, 725.
11. W. J. Pope and E. E. Turner, *J. Chem. Soc.* 1920, **117**, 1447.
12. C. J. Burrows and E. E. Turner, *J. Chem. Soc.* 1919, **115**, 1429.
13. G. J. Burrows and E. E. Turner, *J. Chem. Soc.* 1920, **117**, 1373.
14. G. J. Burrows and E. E. Turner, *J. Chem. Soc.* 1921, **119**, 426.
15. G. J. Burrows and E. E. Turner, *J. Chem. Soc.* 1921, **119**, 1448.
16. Cahours and Ritchie, *C. R.* 1854, **39**, 541.
17. G. J. Burrows and E. E. Turner, *J. Chem. Soc.* 1921, **119**, 1450.
18. G. J. Burrows and E. E. Turner, *J. Proc. R. Soc. N.S.W.* 1921, **55**, 263.
19. C. K. Ingold, *Biogr. Mem. Fellows R. Soc.* 1968, **14**, 449.
20. J. Packer and I. W. Wark, *J. Chem. Soc.* 1921, **119**, 1248.
21. I. W. Wark, *J. Chem. Soc.* 1923, **123**, 1815; 1924, **125**, 2994.
22. G. J. Burrows and I. W. Wark, *J. Chem. Soc.* 1928, 222.
23. I. W. Wark, *J. Chem. Soc.* 1927, 1753.
24. I. W. Wark, *Chem. Eng. Min. Rev.* 1926, **19**, 76.
25. I. W. Wark, *Chem. Eng. Min. Rev.* 1927, **20**, 64.
26. I. W. Wark, *J. Proc. R. Soc. N.S.W.* 1929, **63**, 47.
27. I. W. Wark, *Principles of Flotation.* Australasian Institute of Mining and Metallurgy, Melbourne (1938); revised with K. L. Sutherland (1955).
28. G. J. Burrows and G. Walker, *J. Chem. Soc.* 1928, **123**, 2738.
29. E. M. Bartholomew and G. J. Burrows, *J. Proc. R. Soc. N.S.W.* 1926, **60**, 208.
30. G. J. Burrows and K. H. Lauder, *J. Am. Chem. Soc.* 1931, **53**, 3600.
31. G. J. Burrows and R. H. Parker, *J. Am. Chem. Soc.* 1933, **55**, 4133.
32. G. J. Burrows and E. P. Sandford, *J. Proc. R. Soc. N.S.W.* 1935, **69**, 182.
33. G. J. Burrows and R. H. Parker, *J. Proc. R. Soc. N.S.W.* 1934, **68**, 39.
34. G. J. Burrows and A. Lench, *J. Proc. R. Soc. N.S.W.* 1936, **70**, 222.
35. G. J. Burrows and A. Lench, *J. Proc. R. Soc. N.S.W.* 1936, **70**, 218.
36. J. J. Anderson and G. J. Burrows, *J. Proc. R. Soc. N.S.W.* 1936, **70**, 63.
37. G. J. Burrows and E. Ritchie, *J. Proc. R. Soc. N.S.W.* 1938, **72**, 113; 175.
38. G. J. Burrows and A. Lench, *J. Proc. R. Soc. N.S.W.* 1936, **70**, 294, 300, 437.
39. G. J. Burrows, *J. Proc. R. Soc. N.S.W.* 1940, **74**, M1.
40. D. P. Mellor, VIIth Dwyer Memorial Lecture, "Dwyer's contribution to coordination chemistry", *Proc. R. Aust. Chem. Inst.* 1970, **37**, 199.
41. F. P. J. Dwyer, D. P. Mellor and V. M. Trikojus, *J. Proc. R. Soc. N.S.W.* 1932, **66**, 315.
42. F. P. Dwyer and D. P. Mellor, *J. Proc. R. Soc. N.S.W.* 1932, **66**, 234, 378; 1934, **68**, 47.
43. F. P. Dwyer and D. P. Mellor, *J. Proc. R. Soc. N.S.W.* 1934, **68**, 107; *J. Am. Chem. Soc.* 1934, **56**, 1551; 1935, **57**, 605.
44. D. P. Mellor and F. M. Quodling, *J. Proc. R. Soc. N.S.W.* 1935, **69**, 107; 1936, **70**, 205.

45. D. P. Mellor and B. S. Morris, *J. Proc. R. Soc. N.S.W.* 1937, **71**, 536.
46. D. P. Mellor, *J. Proc. R. Soc. N.S.W.* 1941, **75**, 157; 1943, **77**, 145.
47. D. P. Mellor and D. P. Craig, *J. Proc. R. Soc. N.S.W.* 1942, **76**, 281; 1944, **78**, 258.
48. H. A. McKenzie, D. P. Mellor, J. E. Mills and L. N. Short, *J. Proc. R. Soc. N.S.W.* 1944, **78**, 70.
49. D. P. Mellor and J. B. Willis, *J. Proc. R. Soc. N.S.W.* 1945, **79**, 141.
50. J. A. Friend and D. P. Mellor, *J. Proc. R. Soc. N.S.W.* 1947, **81**, 154.
51. D. P. Mellor and R. J. Goldacre, *J. Proc. R. Soc. N.S.W.* 1939, **73**, 233.
52. D. P. Mellor and W. H. Lockwood, *J. Proc. R. Soc. N.S.W.* 1940, **74**, 141.
53. D. P. Mellor and D. P. Craig, *J. Proc. R. Soc. N.S.W.* 1940, **74**, 475, 495; 1941, **75**, 27.
54. D. P. Mellor, *J. Proc. R. Soc. N.S.W.* 1940, **74**, 107; 1941, **75**, 157; 1943, **77**, 145.
55. D. P. Mellor, *Chem. Rev.* 1943, **33**, 137.
56. D. P. Mellor, *J. Proc. R. Soc. N.S.W.* 1942, **76**, 1.
57. D. P. Mellor and L. Maley, *Nature* (*London*) 1947, **159**, 370; 1948, **161**, 436.
58. H. Irving and R. J. P. Williams, *Nature* (*London*) 1948, **162**, 746; *J. Chem. Soc.* 1953, 3192.
59. P. M. Stubbin and D. P. Mellor, *J. Proc. R. Soc. N.S.W.* 1948, **82**, 225.
60. D. P. Mellor and N. C. Stephenson, *Aust. J. Sci. Res.* 1951, **A4**, 406.
61. C. A. Adams and D. P. Mellor, *Aust. J. Sci. Res.* 1952, **A5**, 577.
62. J. A. Wunderlich and D. P. Mellor, *Acta Cryst.* 1954, **7**, 130.
63. D. P. Mellor, *The Rôle of Science and Industry*, Series 4, Vol. 5, In *Australia in the War of 1939–45*. Australian War Memorial, Canberra (1958).
64. F. P. Dwyer and D. P. Mellor (Eds) *Chelating Agents and Metal Chelates*. Academic Press, New York (1964).
65. D. P. Mellor, *The Evolution of the Atomic Theory*. Elsevier, Amsterdam (1971).
66. D. P. Mellor, In *The Chelation of Heavy Metals* (Edited by W. C. Levine), *International Encyclopedia of Pharmacology and Therapeutics*, Section 20. Pergamon Press, Oxford (1979).
67. F. P. Dwyer, *J. Proc. R. Soc. N.S.W.* 1940, **74**, 99.
68. A. Bryson and F. P. Dwyer, *J. Proc. R. Soc. N.S.W.* 1940, **74**, 107, 240, 455, 471.
69. F. P. Dwyer, *J. Am. Chem. Soc.* 1941, **63**, 78; F. P. Dwyer and D. P. Mellor, *J. Am. Chem. Soc.* 1941, **63**, 81.
70. D. P. Craig, *Biogr. Mem. Fellows R. Soc.* 1972, **18**, 445.
71. F. P. Dwyer and R. S. Nyholm, *J. Proc. R. Soc. N.S.W.* 1942, **75**, 122, 127, 140; 1942, **76**, 129, 133, 275; 1944, **78**, 67, 266; 1945, **79**, 126.
72. F. P. Dwyer, R. S. Nyholm and L. E. Rogers, *J. Proc. R. Soc. N.S.W.* 1947, **81**, 267.
73. J. Lewis, R. S. Nyholm and G. K. Reddy, *Chem. Ind.* 1960, 1386.
74. F. P. Dwyer and R. S. Nyholm, *J. Proc. R. Soc. N.S.W.* 1943, **77**, 116; 1945, **79**, 121.
75. F. P. Dwyer, H. A. McKenzie and R. S. Nyholm, *J. Proc. R. Soc. N.S.W.* 1944, **78**, 260; 1947, **81**, 216.
76. F. P. Dwyer, N. A. Gibson and R. S. Nyholm, *J. Proc. R. Soc. N.S.W.* 1944, **78**, 118, 226; 1945, **79**, 118.
77. F. P. Dwyer, J. E. Humpoletz and R. S. Nyholm, *J. Proc. R. Soc. N.S.W.* 1946, **80**, 217, 242.
78. F. P. Dwyer, R. S. Nyholm and B. T. Tyson, *J. Proc. R. Soc. N.S.W.* 1947, **81**, 272.
79. F. P. Dwyer and R. S. Nyholm, *J. Proc. R. Soc. N.S.W.* 1946, **80**, 28.
80. F. P. Dwyer, H. A. McKenzie and R. S. Nyholm, *J. Proc. R. Soc. N.S.W.* 1946, **80**, 183.
81. F. P. Dwyer, J. E. Humpoletz and R. S. Nyholm, *J. Proc. R. Soc. N.S.W.* 1946, **80**, 212, 242.
82. D. H. Freeman and F. Lions, *J. Proc. R. Soc. N.S.W.* 1940, **74**, 520.
83. F. Lions, B. S. Morris and E. Ritchie, *J. Proc. R. Soc. N.S.W.* 1942, **76**, 294.
84. F. P. Dwyer and F. Lions, *J. Am. Chem. Soc.* 1947, **69**, 2917.
85. F. P. Dwyer and H. A. McKenzie, *J. Proc. R. Soc. N.S.W.* 1947, **81**, 93, 97.
86. F. P. Dwyer, *J. Proc. R. Soc. N.S.W.* 1949, **83**, 134.
87. J. R. Backhouse and F. P. Dwyer, *J. Proc. R. Soc. N.S.W.* 1949, **83**, 138, 146.
88. F. P. Dwyer and E. C. Gyarfas, *J. Proc. R. Soc. N.S.W.* 1949, **83**, 170; *Nature* (*London*) 1949, **163**, 918.
89. F. P. Dwyer and E. C. Gyarfas, *J. Proc. R. Soc. N.S.W.* 1949, **83**, 174, 232, 263.
90. F. H. Burstall, F. P. Dwyer and E. C. Gyarfas, *J. Chem. Soc.* 1950, 953.
91. F. P. Dwyer and E. C. Gyarfas, *Nature* (*London*) 1950, **166**, 481.
92. F. P. Dwyer and E. C. Gyarfas, *J. Am. Chem. Soc.* 1951, **73**, 2322; 1952, **74**, 4699.
93. F. P. Dwyer, E. C. Gyarfas and M. F. O'Dwyer, *Nature* (*London*) 1951, **167**, 1036; F. P. Dwyer and E. C. Gyarfas, *Nature* (*London*) 1951, **168**, 29.
94. F. P. Dwyer, E. C. Gyarfas, W. P. Rogers and J. H. Koch, *Nature* (*London*) 1952, **170**, 190.
95. F. P. Dwyer and F. Lions, *J. Am. Chem. Soc.* 1950, **72**, 1545; F. P. Dwyer, F. Lions and D. P. Mellor, *J. Am. Chem. Soc.* 1950, **72**, 5037; F. P. Dwyer, N. A. Gill, E. C. Gyarfas and F. Lions, *J. Am. Chem. Soc.* 1952, **74**, 1188; J. Collins, F. P. Dwyer and F. Lions, *J. Am. Chem. Soc.* 1952, **74**, 3134; F. P. Dwyer, N. S. Gill, E. C. Gyarfas and F. Lions, *J. Am. Chem. Soc.* 1953, **75**, 1526, 2243; 1954, **76**, 383.
96. J. Chatt and F. G. Mann, *J. Chem. Soc.* 1939, 1622.
97. R. S. Nyholm, *J. Chem. Soc.* 1950, 851, 857, 2061, 2070; 1951, 38, 2602.
98. R. S. Nyholm, *Chem. Rev.* 1953, **53**, 263.
99. R. S. Nyholm, *Q. Rev. Chem. Soc.* (*London*) 1953, **7**, 263.
100. R. S. Nyholm, *Prog. Stereochem.* 1954, **1**, 322.
101. R. S. Nyholm, *J. Proc. R. Soc. N.S.W.* 1955, **59**, 8.
102. *Comprehensive Inorganic Chemistry* (Edited by J. C. Bailar, H. J. Emeléus, R. S. Nyholm and A. F. Trotman-Dickenson). Pergamon Press, Oxford (1973).

103. F. W. James, J. S. Anderson and H. V. A. Briscoe, *Nature (London)* 1937, **139**, 109; J. S. Anderson, N. L. Spoor and H. V. A. Briscoe, *Nature (London)* 1937, **139**, 508; L. O. Brockway and J. S. Anderson, *Trans. Faraday Soc.* 1937, **33**, 1233.
104. J. S. Anderson, H. V. A. Briscoe and N. L. Spoor, *J. Chem. Soc.* 1943, 361; J. S. Anderson, H. V. A. Briscoe, L. H. Cobb and N. L. Spoor, *J. Chem. Soc.* 1943, 367.
105. J. S. Anderson, *J. Proc. R. Soc. N.S.W.* 1942, **76**, 329.
106. G. M. Harris, *J. Chem. Phys.* 1950, **18**, 764; *J. Proc. R. Aust. Chem. Inst.* 1950, **17**, 227; *Rev. Pure Appl. Chem. (Aust.)* 1952, **2**, 57.
107. G. M. Harris and D. R. Stranks, *J. Chem. Phys.* 1951, **19**, 257; *Trans. Faraday Soc.* 1952, **48**, 137, 911; *J. Phys. Chem.* 1952, **56**, 906.
108. D. R. Stranks, *Trans. Faraday Soc.* 1955, **51**, 492, 505.
109. S. W. Pennycuick, *J. Chem. Soc.* 1927, 2600; 1928, 2108; 1929, 618, 623; R. J. Best and S. W. Pennycuick, *J. Chem. Soc.* 1928, 551.
110. S. W. Pennycuick, *J. Am. Chem. Soc.* 1939, **61**, 2234.
111. R. N. Haszeldine and B. O. West, *J. Chem. Soc.* 1956, 3631; 1957, 3880.
112. C. S. Hocking, W. G. P. Robertson and B. O. West, *Nature (London)* 1955, **176**, 832.
113. B. O. West, *Rev. Pure Appl. Chem. (Aust.)* 1960, **10**, 207.
114. T. Kurcucsev, A. M. Sargeson and B. O. West, *J. Phys. Chem.* 1957, **61**, 1567; R. W. Cattrall, J. R. McKellar and B. O. West, *Proc. Aust. At. Energy Symp.* 1958, 628.
115. R. A. Plowman, *J. Proc. R. Soc. N.S.W.* 1949, **83**, 216; 1950, **84**, 38, 41.
116. S. E. Livingstone and R. A. Plowman, *J. Proc. R. Soc. N.S.W.* 1950, **84**, 107, 188; 1951, **85**, 116.
117. J. R. Hall and R. A. Plowman, *Aust. J. Chem.* 1955, **8**, 158; 1956, **9**, 14, 143.
118. E. J. O'Reilly and R. A. Plowman, *Aust. J. Chem.* 1960, **13**, 145.
119. A. Albert, *Selective Toxicity—The Physico-Chemical Basis of Therapy.* Chapman & Hall, London (1951); 6th edn (1979).
120. A. Albert, *Med. J. Aust.* 1944, **1**, 245.
121. A. Albert, S. D. Rubbo, R. J. Goldacre and B. Balfour, *Br. J. Exp. Path.* 1947, **28**, 69.
122. A. Albert and R. J. Goldacre, *J. Chem. Soc.* 1946, 706.
123. A. Albert and R. J. Goldacre, *Nature (London)* 1948, **161**, 95.
124. A. Albert, *Biochem. J.* 1950, **47**, 531; 1952, **50**, 690; *Nature (London)* 1956, **177**, 525.
125. A. Albert, *Aust. J. Sci.* 1967, **30**, 1.
126. D. D. Perrin, *J. Chem. Soc.* 1958, 3120, 3125; 1959, 290.
127. *Rev. Pure Appl. Chem. (Aust.)* 1954, **4**, 1.

Polyhedron Vol. 4, No. 8, pp. 1353–1355, 1985
Printed in Great Britain

0277-5387/85 $3.00 + .00
© 1985 Pergamon Press Ltd

MOLECULAR COMPLEXES OF ARYLTELLURIUM(IV) CHLORIDES

M. V. GARAD
Department of Chemistry, University of Poona, Pune 411 007, India

(*Received* 30 *April* 1984; *accepted* 13 *September* 1984)

Abstract—The synthesis and spectroscopic study of molecular complexes of type $[RTeCl_3 \cdot L]$ and $[RTeCl_3 \cdot 2L]$, where R = phenyl, 4-phenoxyphenyl and L = pyridine, pyridine-*N*-oxide, tri-*n*-octylphosphine oxide, 1,10-phenanthroline and 2,2′-bipyridyl are reported. These compounds were characterised by their IR spectra, elemental analysis and conductivity data. The conductivities in acetonitrile shows the non-electrolytic behaviour of these hygroscopic compounds which are monomeric in boiling benzene.

Tellurium tetrachloride, like tin and titanium tetrachlorides, forms molecular addition complexes with various neutral molecules containing O, S, N and P donor atoms with sites available for coordination by base.[1,2] Tellurium tetrachloride forms 1:1 and 1:2 molecular complexes. Several workers in this field have inferred the structure of these compounds on the basis of their X-ray crystallographic, spectroscopic conductivity and elemental analysis data. The octahedral configuration with *trans*-tetramethylthiourea groups around tellurium has been found in hexacoordinated derivatives of tellurium tetrahalides with tetramethylthiourea, which was studied earlier.[3,4]

Though several reports are found for molecular addition complexes of tellurium tetrachloride very little literature is available for alkyl- and aryltelluriumtrichloride. Molecular complexes of tetramethylthiourea with methyltelluriumtrihalide have been reported.[5] These monomeric complexes have been suggested to have a square pyramidal structure and are examples of five-coordinated tellurium. We have undertaken the study of molecular complexes of phenyltelluriumtrichloride and 4-phenoxyphenyltelluriumtrichloride with various O, N, P donor molecules, in continuation of our earlier work on chelated derivatives of aryltellurium chlorides.[6]

The geometry around tellurium in 1:1 complexes, i.e. M:L, where M = phenyltelluriumtrichloride, L = bidentate ligand, and 1:2 complexes, i.e. M:L, where M = 4-phenoxyphenyltelluriumtrichloride, L = monodentate ligand, is found to be octahedral. The coordination of the ligand is confirmed by IR spectra and conductivity data. All these compounds are readily obtained by mixing and refluxing solutions of the reactants in benzene in suitable molar ratios.

EXPERIMENTAL

All experiments were carried out using dry and distilled solvents and N_2 atmosphere. IR spectra were recorded as Nujol mulls on a Perkin–Elmer 599 B grating spectrometer. The conductivity measurements in acetonitrile were carried out using a modified Toshniwal conductivity bridge. Molecular weight was determined using Gallenkamp semimicro ebulliometer in the concentration range 0.3–1% (w/v).

The phenyltelluriumtrichloride and 4-phenoxyphenyltelluriumtrichloride were prepared as reported earlier.[7,8] The molecular complexes were prepared as follows.

Preparation of phenyltelluriumtrichloride bis-pyridine complex (1:2 *complex*)

Phenyltelluriumtrichloride (0.622 g, 0.002 mol) and pyridine (0.316 g, 0.004 mol) were mixed in benzene (50 cm^3) and refluxed for 3 h. The solution was then concentrated under reduced pressure to obtain crystals of desired product, which were washed with hexane and dried in vacuum at 60°C. The compound is hygroscopic, soluble in benzene and chloroform, insoluble in hexane. Yield: 0.75 g (79.95%).

Found: C, 40.50; H, 3.05; Te, 27.15; Cl, 22.7%. Calc. for $C_6H_5TeCl_3 \cdot 2C_5H_5N$: C, 40.94; H, 3.19; Te, 27.21; Cl, 22.68%.

Other molecular complexes were prepared using 1 : 2 molar ratios in case of monodentate donors.

Preparation of 4-phenoxyphenyltelluriumtrichloride 1,10-phenanthroline complex (1 : 1 complex)

4-Phenoxyphenyltelluriumtrichloride (0.80 g, 0.002 mol) and anhydrous 1,10-phenanthroline (0.36 g, 0.002 mol) were mixed in benzene (60 cm^3) and refluxed for 2.5 h. The solution was then concentrated under reduced pressure to obtain crystals of product which were washed with 3 cm^3 of hot benzene 3–4 times in order to remove some unreacted ligand impurity. The compound is dried under reduced pressure at 60°C.

The compound is hygroscopic, insoluble in benzene, chloroform and in hexane, sparingly soluble in hot benzene. Yield: 0.90 g (77.6%).

Found: C, 49.23; H, 2.90; Te, 21.85; Cl, 18.21%. Calc. for $C_6H_5OC_6H_4TeCl_3 \cdot C_{12}H_8N_2$: C, 49.40; H, 2.91; Te, 21.88; Cl, 18.22%.

Other molecular complexes were prepared using 1 : 1 molar ratio in the case of a bidentate donor like 2,2′-bipyridyl.

Analytical data of all these compounds are as reported in Table 1.

RESULTS AND DISCUSSION

Vibrational spectra

Compounds of the type $RTeCl_3 \cdot 2L$, R = *phenyl*, L = *pyridine*. The C=C and C=N stretching vibrations of pyridine were seen at 1590 cm^{-1}, after the complex formation the C=N and C=C stretching vibrations are split to 1615 and 1590 cm^{-1} which indicates the coordination of the C=N group to the central tellurium atom and hexacoordinated structure resulted.

L = *pyridine-N-oxide*. In pyridine-*N*-oxide C=C vibrations are observed at 1580 cm^{-1}, C=N at 1500 cm^{-1} and N–O at 1260 cm^{-1}. There is no appreciable change in the C=C absorption after the complex formation, but the C=N and N–O bands are seen at 1490 and 1245 cm^{-1} respectively as a result of coordination of the ligand through its oxygen to the metal atom.

L = *tri-n-octylphosphine oxide*. The absorption due to P=O of the ligand is seen in the region 1350–1260 cm^{-1}. This band is shifted to 1220 cm^{-1} as a result of complex formation. The coordination of the ligand to the central tellurium atom takes place through phosphoryl oxygen.

Compounds of the type $RTeCl_3 \cdot L$, L = *2,2′-bipyridyl*. In the free 2,2′-bipyridyl molecule, the C=C and C=N are observed at 1570 and 1420 cm^{-1}. New bands are observed at 1575 and 1405 cm^{-1} as a result of complex formation. The out-of-plane C–H bonding vibrations of the ligand are seen at 750 cm^{-1}. This band is split and seen at 715 and 760 cm^{-1}. This observation indicates the bidentate nature of 2,2′-bipyridyl. Similar behaviour is also observed in the 1,10-phenanthroline complex.

The hybridization of the tellurium atom in aryltellurium trichloride changes from sp^3d to sp^3d^2 in these complexes. It was observed that pyridine, pyridine-*N*-oxide and tri-*n*-octylphosphrine oxide formed 1 : 2 complexes while 1,10-phenanthroline and 2,2′-bipyridyl formed 1 : 1 complexes. The lone pair of electrons on tellurium act in an inert way in

Table 1. Molecular complexes of aryltellurium chlorides*

S. No.	Ligand	Product	Physical characteristics, color and m.p. (°C)	Elemental analysis data			
				Te		Cl	
				Found	Calc.	Found	Calc.
1	Pyridine	$C_6H_5TeCl_3 \cdot 2py$	Dull white, 130	27.15	27.21	22.70	22.68
2	Pyridine-*N*-oxide	$C_6H_5TeCl_3 \cdot 2pyo$	White, 107	25.45	25.47	20.99	21.22
3	Tri-*n*-octylphosphine oxide	$C_6H_5TeCl_3 \cdot 2topo$	Yellow, liquid	11.74	11.79	9.80	9.82
4	1,10-Phenanthroline	$C_6H_5TeCl_3 \cdot phen$	Pink, 175	26.00	25.97	21.56	21.64
5	2,2′-Bipyridyl	$C_6H_5TeCl_3 \cdot bipy$	Pink, 160	27.25	27.32	22.61	22.76
6	Pyridine	$C_6H_5OC_6H_4TeCl_3 \cdot 2py$	Brown, low melting	22.69	22.75	18.87	18.95
7	Pyridine-*N*-oxide	$C_6H_5OC_6H_4TeCl_3 \cdot 2pyo$	Brown, low melting	21.44	21.52	17.88	17.93
8	Tri-*n*-octylphosphine oxide	$C_6H_5OC_6H_4TeCl_3 \cdot 2topo$	Pale yellow liquid	10.83	10.86	9.03	9.05
9	1,10-Phenanthroline	$C_6H_5OC_6H_4TeCl_3 \cdot phen$	White, 87	21.85	21.88	18.21	18.22
10	2,2′-Bipyridyl	$C_6H_5OC_6H_4TeCl_3 \cdot bipy$	Brown, 103	22.80	22.82	19.00	19.01

* Aryl group = phenyl or 4-phenoxyphenyl.

these complexes and geometry remains octahedral, which is also evidenced in bis-tetramethylthiourea-telluriumtetrachloride complex.[4] X-ray crystal structure of above complexes will be reported in a forthcoming communication of this series. All reactions gave well defined products, which are hygroscopic and sparingly soluble in organic solvents. The conductivity measurement on modified Toshniwal conductivity bridge in acetonitrile shows that these complexes are non-ionic in nature. Similar behaviour was also observed for 4-phenoxyphenyltelluriumtrichloride complexes.

Acknowledgements—I am indebted to Drs Sarada Gopinathan and C. Gopinathan Scientists, National Chemical Laboratory, Pune 8, for helpful discussion. I thank Council of Scientific and Industrial Research for award of Scientist Pool. My sincere thanks are due to Prof. A. J. Mukhedkar for his encouragement and to the Head, Department of Chemistry for giving necessary facilities.

REFERENCES

1. S. Prasad and B. Khandelwal, *J. Indian Chem. Soc.* 1961, **38**, 837.
2. S. Prasad and B. Khandelwal, *J. Indian Chem. Soc.* 1962, **39**, 112.
3. S. Husebye and J. W. George, *Inorg. Chem.* 1969, **8**, 313.
4. S. Husebye and J. W. George, S. Husebye and O. Mikalsen, *Acta Chem. Scand. A*, 1975, **29**, 141.
5. K. J. Wynne and P. S. Pearson, *J. Chem. Soc., Chem. Commun.* 1970, 556.
6. M. V. Garad, S. Gopinathan and C. Gopinathan, *Indian J. Chem.* 1979, **18A**, 267.
7. R. C. Paul, K. K. Bhasin and R. K. Chadha, *J. Inorg. Nucl. Chem.* 1975, **37**, 2337.
8. H. D. K. Drew, *J. Chem. Soc.* 1926, 223.

Polyhedron Vol. 4, No. 8, pp. 1357–1363, 1985
Printed in Great Britain

0277–5387/85 $3.00 + .00
© 1985 Pergamon Press Ltd

REACTION OF *TRANS*-$[Co(en)_2(SO_3)(H_2O)]^+$ WITH IMIDAZOLE AND IMIDAZOLE CONTAINING LIGANDS

H. F. REXROAT and N. S. ROWAN*
Department of Chemistry, The American University, Washington, DC 20016, U.S.A.

(*Received* 13 *March* 1984; *accepted after revision* 24 *September* 1984)

Abstract—*trans*-$[Co(en)_2(SO_3)(H_2O)]^+$ reacts with imidazole (ImH) and imidazole containing ligands (L) to form *trans*-$[Co(en)_2(SO_3)L]^+$ in the pH range 6.0–9.0. The complex seems to react both in the hydroxy and in the aquo form. The rate constant for the reaction of imidazole with the aquo form is 6.0 ± 0.7 and $4 \pm 1\ M^{-1}\ s^{-1}$ for the reaction with the hydroxy form at 25°C. The apparent equilibrium constant for formation of the imidazole complex at pH 7 is consistent with the value of 3×10^2 measured previously. Appreciable amounts of complex form only in the pH 6–9 range. Above pH 9 NMR spectra show that even the immediate products are different. In aged solutions at all pHs other products form.

Because of the interest in labelling proteins with substitution inert metal ions,[1–5] we have investigated the reaction of *trans*-$[Co(en)_2(SO_3)(H_2O)]^+$ with imidazole and other imidazole containing ligands. Although the *trans* effect is more common in square planar complexes, it is found for some octahedral cobalt(III) complexes,[6] and the sulfite group produces a strong *trans* effect in *trans*-$[Co(en)_2(SO_3)(H_2O)]^+$ and causes it to react rapidly with ligands. In fact, sulfite has been found to have the strongest *trans* effect of a number of sulfur containing ligands.[7] Yandell and Tomlins have already investigated the reaction of *trans*-$[Co(en)_2(SO_3)(H_2O)]^+$ with imidazole and other ligands at pH 7.00.[8] Based on the curvature of their rate plots at high ligand concentration, they suggested that the reaction occurs by an ion-pair dissociative interchange mechanism. Stranks and Yandell have investigated the reactivity of *trans*-$[Co(en)_2(SO_3)(OH)]$[9] and Harris *et al.* have investigated the reaction of $[Co(en)_2(H_2O)(OH)]^{2+}$ with SO_2 to form O bonded sulfite.[10] In order to be useful for labelling proteins, the complex must bind rapidly to the protein at a reasonable pH, and then become substitution inert. With this in mind, we looked at the products of the reaction of the *trans*-$[Co(en)_2(SO_3)(H_2O)]^+$ with imidazole and imidazole-containing compounds in the pH range 7–10 both immediately and after ageing, studied the kinetics of the reaction with imidazole in the pH range 6–9 and finally looked at the ease of oxidation of coordinated sulfite to sulfate.

* Author to whom correspondence should be addressed.

EXPERIMENTAL

Synthesis

trans-$[Co(en)_2(SO_3)(H_2O)]ClO_4$, was prepared by the method of Baldwin.[11] The *trans*-$[Co(en)_2(SO_3)(ImH)]ClO_4$ was prepared by the action of 1.5 mole excess of imidazole on the aquo complex dissolved in a minimum volume of water. Crystals formed after adding solid $NaClO_4$ to the solution and letting it cool in ice for several minutes. The crystals were filtered and washed with ethanol and ether. Purity of the crystals was determined by Co(II) analyses by the method of Kitson,[12] and spectrophotometrically. The λ_{max} for the Co(III) imidazole complex was 452 nm ($\varepsilon = 162$).[8] Our values of ε were within 5% of this value. Reagent grade imidazole and sodium perchlorate were used.

Ion exchange

Ion exchange chromatography using Dowex 50-X4 100–200 mesh resin in the Na^+ form was chosen for product analysis of aged solutions. Known solutions of

$$[Co(en)_2(SO_3)(ImH)]^+, [Co(en)_2(SO_3)(H_2O)]^+$$

and $[Co(en)_2(ImH)(H_2O)]^{3+}$ were chromatographed using 0.1–1 M sodium perchlorate as eluant at pH = 7.5 and then UV–VIS spectra were run to determine the absorption maximum of each fraction. These results were compared to solutions of $[Co(en)_2(SO_3)(H_2O)]^+$ plus imidazole, at equal concentrations at pH 7.5 or pH 8.4, which were aged 20 days, chromatographed and the spec-

trum of the resulting fractions determined with a UV–VIS spectrophotometer. Solutions of $[Co(en)_2(SO_3)(H_2O)]^+$ plus *N*-methylimidazole, l-histidine or methyl l-histidine were aged at pH 7 and 9 and then treated as the imidazole-containing solutions.

Potentiometric determinations

pK_a determinations of imidazole and *trans*-$[Co(en)_2(SO_3)(H_2O)]^+$ were done by potentiometric titration with standard hydrochloric acid and sodium hydroxide. Generally, solutions were maintained at 1.0 M ionic strength with sodium perchlorate. A Fisher Accumet pH Meter with a NaCl combination electrode was used for all measurements. The electrode was standardized with buffers at the temperature of the titration. A constant temperature bath was used to maintain constant temperature through the titration.

Kinetics

Rate constants were measured by using a Durrum stopped flow apparatus. Experiments were done using 4.00×10^{-3} M *trans*-$[Co(en)_2(SO_3)(H_2O)]^+$ and varying the imidazole concentration between 0.050 and 0.40 M. Most solutions were 1.0 M in $NaClO_4$. Absorbance changes were measured at 430 nm and the rate constants were calculated by computer. Reported rate constants are the average of at least six determinations. All solutions were adjusted for pH prior to the reaction and checked afterwards.

Proton NMR spectra were obtained on a Bruker WP-80 spectrometer. Chemical shifts are reported in δ relative to trimethylsilylpropanesulfonic acid (DSS) as internal standard. All spectra were run in D_2O and pH adjustments were done with NaOD and DCl. (pH values are uncorrected for D_2O solution.)[13]

Equilibrium studies were done using Job's method where the total imidazole plus complex concentration was 5.0×10^{-3} M. The wavelength used for the determinations was 433 nm. All UV–VIS spectra were run on either a Cary 14 or a Varian DMS 90 Spectrophotometer.

RESULTS AND DISCUSSION

trans-$[Co(en)_2(SO_3)(H_2O)]^+$ reacts rapidly with imidazole, *N*-methylimidazole, l-histidine and methyl l-histidine, according to eqn (1):

$$[Co(en)_2(SO_3)(H_2O)]^+ + L \rightleftharpoons [Co(en)_2(SO_3)L]^+ + H_2O. \quad (1)$$

Only the reaction of the aquo complex with imidazole had been studied before[8] and a crystal structure of the product had been determined. The crystal structure showed the bond distance for the *trans* ligand was 0.04 Å greater than the *cis* ligand bond distance.[14] Because spectral changes were small, the products for the reaction of *trans*-$[Co(en)_2(SO_3)(H_2O)]^+$ with L were difficult to characterize by UV–VIS spectroscopy. For the bisethylenediamine sulfito complexes, the range for λ_{max} is between 475 and 430 nm for the lowest energy ligand field band. The λ_{max} for each of the above complexes was respectively 452, 451, 454 and 455 nm. It was easier to identify the coordinated ligands using ^1H NMR spectroscopy. The ^1H spectrum of each ligand with *trans*-$[Co(en)_2(SO_3)(H_2O)]^+$ was measured at pH 8. The chemical shifts of the coordinated imidazoles are given in Table 1. The chemical shifts found in Table 1 are at lower field positions than those found for *trans*-$[Co(en)_2(OH)(ImH)]^{2+}$ where for C_2–H δ equals 8.15, C_4–H, $\delta = 7.40$ and C_5–H, $\delta = 7.12$ ppm,[15] which may be due to electron donating effect of the sulfite ligand or the longer Co–N bond. At pH 8 the reaction with imidazole appears to be complete yielding only the imidazole complex. The same results are found for *N*-methylimidazole. With l-histidine the NMR spectrum showed very little coordination through the pyridine type nitrogen of the imidazole ring (about 16%) even though the reactions with imidazole and *N*-methylimidazole were favorable. However, at pH 8 the carboxyl group of the histidine is deprotonated and also probably binds to the Co(III) center, although this product cannot be detected spectrophotometrically or by NMR spectroscopy. To prevent coordination with the carboxyl group, methyl l-histidine was used. Once the carboxyl group was blocked, the product formed by coordination almost exclusively through the pyridine type nitrogen of the imidazole group. Little competition from the amine nitrogen was

Table 1. ^1H NMR chemical shifts for L in *trans*-$[Co(en)_2(SO_3)L]$ at pH 8

	Chemical shift*		
L	C_2–H	C_4–H	C_5–H
Imidazole	8.40	7.56	7.47
N-methylimidazole	8.29	7.48	7.41
l-Histidine	8.34		7.28
Methyl l-histidine	8.31		7.25

* Ppm relative to DSS.

found as it is mostly protonated at this pH. Consequently, the Co–sulfito complex might be expected to react with imidazole nitrogens in proteins as long as there are few deprotonated carboxyl groups to compete with.

A more thorough study of the reaction of *trans*-$[Co(en)_2(SO_3)(H_2O)]^+$ with imidazole was done and compared to the earlier work done by Yandell and Tomlins.[8] From their kinetic results they had found an equilibrium constant at 25°C and pH 7 of 3×10^2 for reaction (1). The equilibrium was studied three different ways in this work, kinetically, by ^1H NMR and spectroscopically by Job's method. The expression for K_{app} is given in eqn (2):

$$K_{app} = \frac{[trans\text{-}Co(en)_2(SO_3)(ImH)^+]}{[Co(III)_{free}][Im_t]} \quad (2)$$

$$Co(III)_{free} = trans\text{-}[Co(en)_2(SO_3(H_2O)]^+ + trans\text{-}[Co(en)_2(SO_3)OH];$$

$$Im_t = ImH + ImH_2^+$$

and the reaction in eqn (3):

$$Co(III)_{free} + ImH \underset{k_r}{\overset{k_f}{\rightleftharpoons}} trans\text{-}[Co(en)_2(SO_3)(ImH)]^+. \quad (3)$$

The kinetic results (below) show that $k_f \gg k_r$ in the pH 6–9 range and therefore K_{app} is large. Errors in the Job's method determinations are high because absorbance changes were small but K_{app} was found to be 3×10^2 at pH 6.15, 2×10^3 at pH 7.1, 3×10^2 at pH 7.70 and 3×10^2 at pH 8.8. Temperature seemed to have little effect on the equilibrium position.

Again, ^1H NMR studies gave the most detailed analysis of the products of the reaction although minor imidazole containing species were not detected. For the range pH 6–9.0, the only imidazole resonances apparent in the NMR spectrum in freshly prepared solutions of *trans*-$[Co(en)_2(SO_3)(ImH)]^+$ are those characteristic of free imidazole and those of the complexed imidazole (Table 2). At pHs 7 and 8 no free imidazole is apparent in the spectrum, indicating that K_{app} is >300, assuming the minimum amount of free imidazole that can be detected is 5% of the initial complex concentration. The chemical shifts of the complexed imidazole peaks do not change in the pH range 6–10 although new peaks start to appear in the spectrum at pHs above 9.0. (See Table 2.)

From the relative intensities of the peaks at pH 9.5, we suggest that the second set may be due to bridging imidazole. Above pH 10, the peaks of the original coordinated imidazole are absent. Between pH 10 and 11, a third set of peaks appears, all of which have approximately equal intensities and constant chemical shifts. This implies the formation of a third type of imidazole complex. Above pH 11, very little imidazole complex of any kind forms and the NMR spectrum shows mostly free imidazole. The imidazole sulfito complex does not show the usual NMR titration behavior for coordinated imidazole where there is a gradual change in chemical shift of the imidazole protons with change in pH.[15,16] Instead, it appears that the deprotonated imidazole, if it forms, is an excellent ligand and undergoes further coordination in the solution. Bridging imidazoles with Ru(II) and Co(III) have been synthesized in basic solutions.[17]

The NMR spectra of the freshly prepared solutions of *trans*-$[Co(en)_2(SO_3)(H_2O)]^+$ and imidazole showed that in the pH range 6–9 only free imidazole and $[Co(en)_2(SO_3)(ImH)]^+$ were present. Therefore, the kinetics of reaction (1) could be studied in this pH range.

The results of the kinetics runs showed the rate law is rate $= k_{obs}[Im_t][Co(III)_{free}]$ at all pHs in this range and all temperatures with no limiting rate at high ligand concentration or dependence of rate on

Table 2. ^1H NMR chemical shifts and intensities for the imidazole hydrogens of *trans*-$[Co(en)_2(SO_3)(ImH)]^+$ as a function of pH

Complex	pH range	Chemical shifts (ppm from DSS)*		
trans-$[Co(en)_2(SO_3)(H_2O)]^+$	6–10	8.40 (1)	7.56 (1)	7.46 (1)
Possible dimer	9.5–11	8.30 (1)	7.63 (2)	
Basic form	10.5–11	8.0 (1)	7.40 (1)	7.32 (1)

* Value in parentheses is the integral of the peak.

Table 3. Observed rate constants for the reaction of $[Co(en)_2(SO_3)(H_2O)]^+$ with imidazole

pH*	$[ImH]_t$	k_{obs} (s^{-1})†		
		20°C	25°C	30°C
6.0	0.10	0.031±0.001	0.065±0.005	0.151±0.004
	0.20	0.057±0.002	0.12±0.02	0.21±0.05
	0.30	0.089±0.006	0.169±0.002	0.26±0.01
	0.40	0.11±0.01	0.24±0.06	0.5±0.2
	0.40‡		0.21±0.01	
7.0	0.050	0.068±0.002	0.14±0.01	0.20±0.01
	0.10	0.14±0.02	0.27±0.01	0.52±0.06
	0.20	0.27±0.05	0.55±0.01	1.1±0.1
	0.30	0.39±0.01	0.82±0.01	1.7±0.2
	0.40	0.56±0.02	1.12±0.03	1.98±0.03
	0.40‡		1.23±0.04	
7.8	0.050	0.153±0.005	0.297±0.007	0.46±0.03
	0.10	0.33±0.02	0.55±0.01	0.85±0.06
	0.20	0.61±0.03	1.07±0.09	1.75±0.04
	0.30	0.91±0.02	1.6±0.2	2.6±0.2
	0.40	1.19±0.03	2.06±0.06	3.3±0.1
8.9	0.050	0.166±0.005	0.385±0.005	0.38±0.01
	0.10	0.346±0.004	0.56±0.07	0.74±0.02
	0.20	0.74±0.05	1.1±0.2	1.53±0.03
	0.30	1.05±0.02	1.6±0.1	2.2±0.2
	0.40	1.30±0.05	2.2±0.2	3.0±0.1

* Error on pH is ±0.1.

† Each rate constant is the average of at least six individual determinations; errors are standard deviations on the average values.

‡ These experiments were done to check the effect of ionic strength.

ionic strength in the 1.0–1.4 M range (Table 3). Rate constants at pH 7 and 25°C agree with those found previously by Yandell and Tomlins.[8] Plots of k_{obs} vs $[Im_t]$ appear to have a zero intercept which implies no contribution to k_{obs} from the aquation reaction (k_r). Slopes of the k_{obs} vs $[Im_t]$ plots gave values of the forward rate constant, k_f (Table 4). The immediate reaction seems to proceed according to eqn (3) which can be written as a two-path reaction:

$$trans\text{-}[Co(en)_2(SO_3)(H_2O)]^+ + ImH \underset{k_{r'}}{\overset{k_{f'}}{\rightleftharpoons}} trans\text{-}[Co(en)_2(SO_3)(ImH)]^+ + H_2O; \quad K' \quad (4)$$

$$trans\text{-}[Co(en)_2(SO_3)(OH)] + ImH \underset{k_{r''}}{\overset{k_{f''}}{\rightleftharpoons}} trans\text{-}[Co(en)_2(SO_3)(ImH)]^+ + OH^-; \quad K'' \quad (5)$$

$$trans\text{-}[Co(en)_2(SO_3)(H_2O)]^+ \rightleftharpoons trans\text{-}[Co(en)_2(SO_3)(OH)] + H^+; \quad K_c \quad (6)$$

but $k_{r'} \ll k_{f'}$ and $k_{r''} \ll k_{f''}$. The expression for k_{obs} for this mechanism shows that:

$$k_{obs} = \frac{k_f K_a}{K_a + [H^+]}[Im_t] \quad (7)$$

$$k_{obs} = \left[\frac{k_{f'}[H^+] + k_{f''}K_c}{K_c + [H^+]}\right]\left[\frac{K_a}{K_a + [H^+]}\right][Im_t] \quad (8)$$

$$K_a = \frac{[ImH][H^+]}{[ImH_2^+]}. \quad (9)$$

pK_a values for imidazole and *trans*-$[Co(en)_2(SO_3)(H_2O)]^+$ in 1.0 M sodium perchlorate were measured under the conditions of the kinetics experiments. At 20, 25 and 30°C, the values were 7.05, 7.02 and 6.98, respectively, for imidazole, and 9.04, 8.96 and 8.95, respectively, for *trans*-$[Co(en)_2(SO_3)(H_2O)]^+$. They had previously been determined to be 7.12[18] and 9.27[19] at 25°C. ΔH^0 for both dissociations was small.

Using experimental values of K_c, K_a and k_f, values of $k_{f'}$ and $k_{f''}$ can be calculated, and are reported in

Table 4. Rate constants for the reaction of *trans*-$[Co(en)_2(SO_3)(H_2O)]^+ + ImH$

pH	Temperature (°C)	Slope* ($M^{-1}\,s^{-1}$)	k_f† ($M^{-1}\,s^{-1}$)	$k_{f'}$‡ ($M^{-1}\,s^{-1}$)	$k_{f''}$§ ($M^{-1}\,s^{-1}$)	k_M‖ ($M^{-1}\,s^{-1}$)
6.0	20	0.26±0.02	3.2±2	2.9±0.3	4.2±0.5	3.4
7.0	20	1.36±0.09	2.6±0.2			2.5
7.8	20	2.92±0.07	3.4±0.1			3.8
8.9	20	3.3±0.2	3.4±0.2			5.5
6.0	25	0.56±0.07	5.6±0.7	5.9±0.7	4±1	6.5
7.0	25	2.78±0.04	6.2±0.1			6.4
7.8	25	5.1±0.3	5.9±0.3			6.7
8.9	25	5.2±0.3	5.2±0.3			11
6.0	30	1.0±0.3	8.1±0.2	8.9±0.9	6±1	6.5
7.0	30	5.4±0.5	9.6±0.9			10
7.8	30	8.4±0.3	10.1±0.4			11
8.9	30	7.3±0.3	7.4±0.3			15

* Slope from graph of k_{obs} vs Im_t concentration and calculated from a linear least squares program. In this work:

$$\text{slope} = \frac{k_f K_a}{K_a + [H^+]} = \left(\frac{k_{f'}[H^+] + k_{f''}K_c}{K_c + [H^+]}\right)\frac{K_a}{K_a + [H^+]}.$$

From Yandell and Tomlin's assumption:

$$\text{slope} = \left(\frac{k_M[H^+]}{[H^+] + K_c}\right)\frac{K_a}{K_a + [H^+]}.$$

† Calculated from slope $\frac{K_a + [H^+]}{K_a}$ (see *).

‡ Average of k_f for pH 6 and 7.

§ Calculated from $\frac{k_f(K_c + [H^+]) - k_{f'}[H^+]}{K_c}$ at pH 8.9.

‖ Calculated from second equation in *.

Table 4. The results show that k_f reaches a maximum between pH 7 and 8 and then decreases at pH 9. Yandell and Tomlins' mechanism which does not account for the reaction of $[Co(en)_2(SO_3)(OH)]$ with the incoming ligand, consequently predicts that k_f will increase with increasing pH although at pH 7 their value of k_f is $5.5 \pm 0.3\ M^{-1}\,s^{-1}$ and ours is $6.2 \pm 0.1\ M^{-1}\,s^{-1}$ (see Table 4). Yandell and Tomlins studied the reaction between *trans*-$[Co(en)_2(SO_3)(H_2O)]^+$ and a number of ligands at pH 7 and neglecting the reaction with the hydroxy complex can be justified for several reasons. First, the value of the K_c shows that very little hydroxy complex exists at this pH and, secondly, comparisons between the aquo (positively charged) complex and hydroxy (neutral) complex show negatively charged ligands react with the aquo complex with a rate constant that is two orders of magnitude larger.[9] At pH 7, imidazole was the only neutral ligand in the previous study and the rate constant for the reaction with the neutral ligand was two orders of magnitude less than the reaction with negative ligands.[8] Because of this slower reaction with a neutral ligand and because at pHs 8 and 9 substantial amounts of the hydroxy complex were present, the reaction with the hydroxy form also had to be considered in our studies. For many complexes both the aquo and hydroxy forms react with incoming ligands.[6]

Ion-pairing constants for the neutral ligand, imidazole, with the positive aquo complex and neutral hydroxo complex have been estimated to be similar (about 0.1).[20] Therefore, the difference in reactivity between the aquo and hydroxy species would depend on the rates of dissociation of H_2O and OH^- from the complexes. The rate of dissociation of H_2O from the aquo complex has been estimated to be $13.0\ s^{-1}$ at 25°C and we find reasonable agreement with Stranks and Yandell with our $k_{f'} = 6\ M^{-1}\,s^{-1}$. The rate constants found in this work for the reaction of the hydroxy complex ($k_{f''} = 4\ M^{-1}\,s^{-1}$) are comparable also to the limiting rate constant of OH^- dissociation from

trans-$[Co(en)_2(SO_3)(OH)]$ of $> 3\ M^{-1}\ s^{-1}$ at 25°C found by Stranks and Yandell.[9]

Our activation energy for the substitution of ImH in the aquo complex of 22 ± 2 kcal mol^{-1} is consistent with other values for similar systems; for example, 16.5 kcal mol^{-1} for $[Co(en)_2(SO_3)(H_2O)]^+$[9] and 21.3 kcal mol^{-1} for $[Co(en)_2(SO_3(OH)]$,[9] and 11.5 kcal mol^{-1} reported for the forward reaction of $[Co(en)_2(SO_3)(H_2O)]^+$ with SCN^-.[8] The activation energy for the hydroxy species of roughly 7 ± 5 kcal seems lower than expected, but this is only an estimate because the error of $k_{f''}$ is so large.

Equation (1) shows the immediate reaction between *trans*-$[Co(en)_2(SO_3)(H_2O)]^+$ and L, but aging solutions of $[Co(en)_2(SO_3)L]^+$ yielded spontaneous production of SO_4^{2-} and formation of new Co(III) complexes. The λ_{max} of aged solutions shifts to longer wavelengths and the higher the pH (7–9) the more rapid is the color change. In the ion exchange chromatography of the aged solutions two or three fractions were found. The first behaved like $[Co(en)_2(SO_3)(H_2O)]^+$ with a similar λ_{max}. For the imidazole and *N*-methylimidazole solutions, the second fraction behaved like $[Co(en)_2(H_2O)(ImH)]^{3+}$ with a similar λ_{max} and the third fraction behaved like a dimer because it required concentrated sodium perchlorate to remove it from the column indicating that it was highly charged. For the imidazole product ^1H NMR showed, from intensities and chemical shifts, that the solution contained 60% *trans*-$[Co(en)_2(SO_3)(H_2O)]^+$, 11% *cis*-$[Co(en)_2(H_2O)(ImH)]^{3+}$ and 21% *trans*-$[Co(en)_2(H_2O)(ImH)]^{3+}$ and 6% unidentified product. In the histidine and methylhistidine solutions the second fraction had a λ_{max} greater than 500 nm which does not correlate with any of our known solutions and the third fraction behaved like the $[Co(en)_2(H_2O)(ImH)]^{3+}$ complex. ^1H NMR spectra of some of the column fractions do not seem to contain ethylenediamine in the product complex. From these data, it seems that $[Co(en)_2(SO_3)L]^+$ aged in slightly basic solution loses sulfite or L and/or perhaps forms a dimer.

It was also found that thermal oxidation of sulfite in the complex could be accomplished with sodium bismuthate. Qualitative analysis for SO_4^{2-} and Co(II) showed substantial production of free sulfate without concurrent production of Co(II) indicating sodium bismuthate does not destroy the Co(III) complex. Milder oxidizing agents like MnO_4^-, $Cr_2O_7^{2-}$ and H_2O_2 had no effect on the sulfite or the complex.

Both the aging studies and oxidation study show that it is possible to convert the substitution labile complex $[Co(en)_2(SO_3)L]^+$ to a substitution inert one.

In summary we find that *trans*-$[Co(en)_2(SO_3)(H_2O)]^+$ reacts with imidazole and imidazole-containing ligands (L) rapidly to form *trans*-$[Co(en)_2(SO_3)L]^+$. The kinetics and the equilibrium constant for the reaction with imidazole were measured. The product forms via two paths with $k_{f'} = 6\ M^{-1}\ s^{-1}$ and $k_{f''} = 4\ M^{-1}\ s^{-1}$ at 25°C. The activation energy for $k_{f'}$ is 22 ± 2 kcal mol^{-1} and K_{app} at pH 7 is $> 3 \times 10^2$. Our equilibrium studies show that appreciable amounts of the complex form only in the pH 6–9 range. The initial product deteriorates on aging to a mixture of products and above pH 9 the immediate products are different possibly forming bridged complexes. Complexes of other imidazole containing ligands also form other products on aging. Oxidation of the coordinated sulfite with sodium bismuthate does not affect the Co(III) center. As a result, we have shown that it might be possible to react *trans*-$[Co(en)_2(SO_3)(H_2O)]^+$ with a protein by having it react with the imidazole in histidine and then convert the resulting Co(III) complex to a substitution inert one, although the conditions for the oxidation of the sulfite are too harsh for use with proteins. We have also extended the studies on the mechanism of the reaction of imidazole with *trans*-$[Co(en)_2(SO_3)(H_2O)]^+$.

REFERENCES

1. E. P. Kang, C. B. Storm and F. W. Carson, *J. Am. Chem. Soc.* 1975, **97**, 6723.
2. J. I. Legg, *Coord. Chem. Rev.* 1978, **25**, 103.
3. N. S. Rowan, C. B. Storm and J. B. Hunt, *Inorg. Chem.* 1978, **17**, 2853.
4. S. S. Isied, G. Worosila and S. J. Atherton, *J. Am. Chem. Soc.* 1982, **104**, 7658.
5. N. M. Kostic, R. Margalit, C. M. Che and H. B. Gray, *J. Am. Chem. Soc.* 1983, **105**, 7765.
6. J. E. Byrd and W. K. Wilmarth, *Inorg. Chem. Acta Rev.* 1971, **5**, 7; Basolo and R. G. Pearson, *Mechanisms of Inorganic Reactions*, 2nd Edn, pp. 175–176. Wiley, New York (1967).
7. J. N. Cooper, J. D. McCoy, M. G. Katz and E. Deutsch, *Inorg. Chem.* 1980, **19**, 2265.
8. J. K. Yandell and L. A. Tomlins, *Aust. J. Chem.* 1978, **31**, 561.
9. D. R. Stranks and J. K. Yandell, *Inorg. Chem.* 1970, **9**, 751.
10. T. P. Dasgupta and G. M. Harris, *Inorg. Chem.* (in press).
11. M. E. Baldwin, *J. Chem. Soc.* 1961, 3123.
12. R. E. Kitson, *Anal. Chem.* 1950, **22**, 664.
13. J. L. Markley, *Acc. Chem. Res.* 1975, **8**, 70.
14. C. L. Raston, A. H. White and J. K. Yandell, *Aust. J. Chem.* 1978, **31**, 993.
15. N. R. Brodsky, N. M. Nguyen, N. S. Rowan, C. B. Storm, R. J. Butcher and E. Sinn, *Inorg. Chem.* 1984, **23**, 891.

16. N. S. Rowan, C. B. Storm and R. Rowan III, *J. Inorg. Biochem.* 1981, **14**, 59.
17. S. S. Isied and C. G. Kuehn, *J. Am. Chem. Soc.* 1978, **100**, 6754.
18. *Stability Constants* 1964. Chemical Society of London.
19. K. L. Scott, R. S. Murray and W. C. E. Higginson, *J. Chem. Soc., Dalton Trans.* 1975, 1339.
20. R. G. Wilkins, *The Study of Kinetics and Mechanism of Reaction of Transition of Metal Complexes*, pp. 182–183. Allyn & Bacon, Boston, MA (1974).

Polyhedron Vol. 4, No. 8, pp. 1365–1369, 1985
Printed in Great Britain

0277-5387/85 $3.00 + .00
© 1985 Pergamon Press Ltd

PHOTOCHEMISTRY OF PLANAR FOUR-CO-ORDINATE PALLADIUM(II) COMPLEXES—III.* PHOTOSYNTHESIS AND CRYSTAL STRUCTURE OF $[Pd_2(PPr^n_3)_2(NCS)(SCN)_2(\mu\text{-}CN)]$

G. BOMBIERI, G. BRUNO, M. CUSUMANO,† G. GUGLIELMO and V. RICEVUTO

Dipartimento di Chimica Inorganica e Struttura Molecolare, University of Messina, Via dei Verdi, 98100 Messina, Italy

(*Received* 13 *August* 1984; *accepted* 16 *October* 1984)

Abstract—U.V. irradiation of MeOH and CH_3CN solutions of *trans*-$[Pd(PPr^n_3)_2(NCS)_2]$ causes a stepwise photochemical reaction. When the solvent is CH_3CN the photoproduct can be conveniently isolated in a crystalline form. This compound has been shown, by X-ray analysis, to be a cyano bridged palladium(II) complex.

In the last few years we have been concerned with the study of the photochemical behaviour of several square planar palladium(II) complexes.[1,3] In particular, we have investigated the nitro–nitrito linkage isomerization in $[Pd(Et_4dien)NO_2]^+$ (Et_4dien = 1, 1, 7, 7-tetraethyldiethylenetriamine) and the *cis–trans* isomerization of the substrates *trans*-$[Pd(PPr^n_3)_2Cl_2]$ (X = Cl, Br, I). In the case of the latter complexes the derivatives formed in the early stage of irradiation, by further prolonged irradiation, can be transformed into the bridged complexes $[Pd_2(PPr^n_3)_2X_4]$. This photoreaction is an easy alternative to the thermal synthesis of these complexes. We have now extended our study to the complex *trans*-$[Pd(PPr^n_3)_2(NCS)_2]$ which could undergo both *cis–trans* and NCS–SCN linkage isomerization. In this paper we report the results of a spectrophotometric investigation of the photoreactivity of *trans*-$[Pd(PPr^n_3)_2(NCS)_2]$ in MeOH and CH_3CN. Furthermore the crystal structure of the photoproduct isolated from acetonitrile is described.

EXPERIMENTAL

The complex *trans*-$[Pd(PPr^n_3)_2(NCS)_2]$ was prepared by methatetic exchange from *trans*-$[Pd(PPr^n_3)_2Cl_2]$ obtained in turn by standard procedure.[4]

The photoproduct was obtained by irradiation of a saturated CH_3CN solution of *trans*-$[Pd(PPr^n_3)_2(NCS)_2]$ at 320 nm. The solvent was evaporated off and the resulting oily substance was washed with diethyl ether and subsequently crystallized from *n*-hexane.

Methanol and acetonitrile were of spectrophotometric grade.

The electronic spectra were recorded by means of a Cary 219 spectrophotometer.

Conductivity measurements were performed with a Radiometer CDM 3 conductivity bridge.

The solutions were irradiated by using a high intensity Bausch–Lomb monochromator or an Applied Photophysics MLU 18 photoreactor in the case of the preparative stage.

Determination of crystal structure

Crystal data. $C_{39}H_{65}N_3P_3S_3Pd_2$, orthorhombic, $a = 16.129(3)$, $b = 18.937(5)$, $c = 28.836(10)$ Å, $U = 8807.5$ Å, space group *Pbca*, $Z = 8$, $D_c = 1.47$ mg m^{-3}, $F(000) = 3696$, μ(Mo-K_α) = 9.9 cm^{-1}.

The data were collected on a Siemens–Stoe diffractometer, ω/θ scan 0.5 s count at each of 120 steps of 0.01° for each reflection and 10 s background count. Mo-K_α (λ radiation = 0.71069 Å) $1.5 \leqslant \theta \leqslant 25°$. Three standard reflections monitored every 100 to check crystal and electronic stability. No decay in intensity. 4428 reflections measured, 3063 observed [$I \geqslant 2.5\sigma(I)$]. The structure was solved by Patterson and Fourier methods and refined by full-matrix least squares procedure. Function $\sum W(|F_o|-|F_c|)^2$ was minimized; $W = 2.46/[\sigma^2(F_o)+1.1\times10^{-3}(F_o)^2]$. In the last refinement cycles all non-hydrogen atoms (except the

* For Part II see Ref. 2.

† Author to whom correspondence should be addressed.

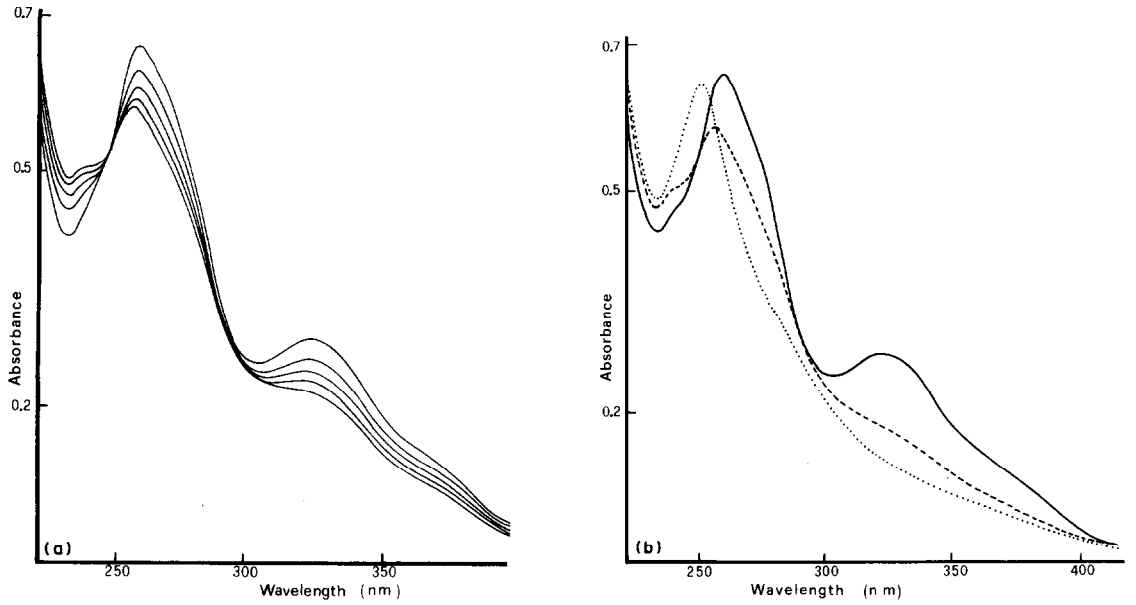


Fig. 1. Spectral variations on irradiation of a CH_3CN solution of *trans*-$[Pd(PPr^n_3)_2(NCS)_2]$ (4×10^{-5} M). Left: spectra of the complex at various irradiation times at 325 nm in the first photochemical step. Right: ——, complex; - - - -, intermediate photoproduct; ····, final photoproduct.

disordered propyl chains to which isotropic thermal parameters were assigned) were refined anisotropically. A general high thermal motion is present in the structure which is associated with a disordering in the propyl chains. For this reason some of the C–C bond distances were refined with fixed geometry [d(C–C = 1.53(2) Å] taking into account also the alternative positions for C(18), C(19), C(28), C(29), C(35) and C(36) atoms (labelled with additional Fig. 1 i.d. C(181), etc.). From relative peak heights in the electron density map and comparison of the isotropic thermal parameters an occupancy ratio 0.6/0.4 for C(18)/C(181), etc. was estimated. The final model reached convergence with $R = 0.059$ and $R_w = 0.065$. Relevant bond lengths and valence angles are reported in Table 1. Thermal parameters, F_o/F_c values, as well as final coordinates for non-hydrogen atoms have been deposited with the Editor as supplementary material. Atomic coordinates have also been deposited with the Cambridge Crystallographic Data Centre. The calculations were carried out on the IBM 4341 of the "Centro di Calcolo" at University of Messina with the SHELX-76 program.[5] Atomic scattering factors and anomalous dispersion terms (for Pd only) were from Reference 6.

RESULTS AND DISCUSSION

Irradiation of CH_3CN and MeOH solutions of *trans*-$[Pd(PPr^n_3)_2(NCS)_2]$ at the wavelengths relative to the absorption band of the complex (254, 325 and 370 nm) leads to a well defined spectral variation characterized by an isosbestic point respectively at 248 and 246 nm in the case of the former and the latter solvent. At this stage the process is thermally reversible; however, if the irradiation is prolonged, new thermally irreversible photoreactions occur. In the case of CH_3CN this new process is very clean and the spectral variation is characterized by only one absorption band, in the range 230 to 270, centred at 252 nm ($\varepsilon = 18{,}700\ M^{-1}\ cm^{-1}$). When the solvent is MeOH, however, the irradiation causes decomposition of the complex to give various unidentified products. Attempts to isolate the photoproduct in the early stage of irradiation failed and only the starting complex could be recovered from the reaction mixture. Nevertheless we have been able to isolate the final stable photoproduct of irradiation in CH_3CN. The availability of crystals of this substance suitable for X-ray analysis has allowed us to determine its structure.

Photoproduct crystal structure

The crystal of the photoproduct consists of the packing of discrete dimeric molecules $[Pd_2(PPr^n_3)_3(NCS)(SCN)_2(\mu\text{-}CN)]$. The molecular structure is shown in Fig. 2 together with the atom numbering scheme (only one of the alternate positions in the propyl chains is reported). The coordination geometry about the two palladium

Table 1. Selected bond distances (Å) and angles (°)

a. Distances			
Pd(1)–P(1)	2.252(3)	Pd(2)–P(2)	2.320(3)
Pd(1)–S(1)	2.316(5)	Pd(2)–P(3)	2.334(3)
Pd(1)–S(2)	2.334(6)	Pd(2)–N(3)	2.023(12)
Pd(1)–N(4)	2.066(9)	Pd(2)–C(4)	1.945(11)
S(1)–C(1)	1.647(18)	N(3)–C(3)	1.097(19)
C(1)–N(1)	1.110(23)	C(3)–S(3)	1.617(12)
S(2)–C(2)	1.542(21)	P(2)–C(21)	1.848(12)
C(2)–N(2)	1.132(29)	P(2)–C(24)	1.860(12)
P(1)–C(11)	1.842(16)	P(2)–C(27)	1.839(15)
P(1)–C(17)	1.800(22)	P(3)–C(40)	1.843(24)
P(1)–C(14)	1.789(18)	P(3)–C(37)	1.864(15)
C(4)–N(4)	1.124(15)	P(3)–C(34)	1.813(18)
b. Angles			
S(1)–Pd(1)–S(2)	175.3(2)	C(4)–Pd(2)–N(3)	178.8(5)
S(1)–Pd(1)–N(4)	92.5(3)	C(4)–Pd(2)–P(3)	90.2(3)
S(1)–Pd(1)–P(1)	89.1(2)	C(4)–Pd(2)–P(2)	88.7(3)
S(2)–Pd(1)–N(4)	91.7(3)	P(3)–Pd(2)–N(3)	88.9(3)
S(2)–Pd(1)–P(1)	86.7(2)	P(3)–Pd(2)–P(2)	178.9(1)
P(1)–Pd(1)–N(4)	177.3(3)	P(2)–Pd(2)–N(3)	92.1(3)
Pd(1)–S(1)–C(1)	105.2(6)	Pd(2)–N(3)–C(3)	168.0(12)
Pd(1)–S(2)–C(2)	109.6(8)	Pd(2)–P(2)–C(27)	112.1(5)
Pd(1)–N(4)–C(4)	168.2(9)	Pd(2)–P(2)–C(21)	113.9(4)
Pd(1)–P(1)–C(11)	116.3(5)	Pd(2)–P(2)–C(24)	113.0(4)
Pd(1)–P(1)–C(4)	110.9(6)	Pd(2)–P(3)–C(40)	122.4(7)
Pd(1)–P(1)–C(17)	112.8(7)	Pd(2)–P(3)–C(37)	118.2(5)
S(1)–C(1)–N(1)	174.5(16)	Pd(2)–P(3)–C(34)	110.3(7)
S(2)–C(2)–N(2)	173.8(20)	N(3)–C(3)–S(3)	177.8(15)

atoms of each dimeric unit is approximately square planar. Palladium(1) is coordinated to two isothiocyanates *trans* related, to one phosphorus atom of the PPr^n_3 ligand and to the nitrogen of the bridging cyano group, whereas palladium(2) is coordinated to two phosphorus atoms of the PPr^n_3 ligands *trans* related, to one isothiocyanate ligand and to a carbon of the bridging cyano group. The

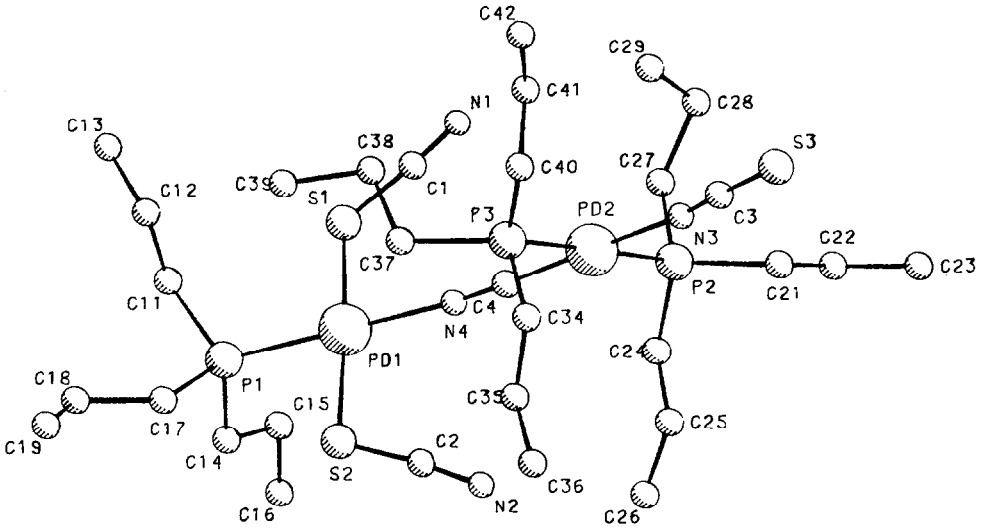


Fig. 2. Molecular configuration and atom naming scheme.

deviations from planarity for the atoms coordinated to Pd(1) are in a tetrahedral direction [S(1) 0.033(6), S(2) 0.048(7), P(1) 0.013(4) and N(4) 0.068(9) Å]; for those related to Pd(2) the deviations are lower [N(3) 0.014(12), P(2) 0.004(3), P(3) 0.08(5) and C(4) 0.010(11) Å] and in an approximately square pyramidal direction with the Pd(2) atom at the apex of the very flattened square pyramid. The two planes form a dihedral angle of 66°. Because of the very high thermal motion present in the structure (probably related to the way in which the crystal has been obtained) a clear distinction between nitrogen and carbon atom positions of the cyano group is impossible; however, the values of the bond distances to the respective palladium atoms suggests as highly probable the assignment made.

The major interest of this compound is related to the presence of thiocyanate ligands bound to the metal in both the bonding modes (S and N). The bonding mode of the thiocyanate ion to "soft" metals such as Pt(II) and Pd(II) is still a matter of controversy as electronic[7,8] effects and/or steric[9,10] effects have been suggested to play a determining role in the S or N coordination mode to the metal. The presence of phosphine ligands as possible π-acceptors in such complexes has also been thought to influence the thiocyanate coordination mode.[11,13] Recently it has been pointed out that Pd(II) is ambivalent[14] towards the thiocyanate ion and small changes in steric and electronic factors are sufficient in determining its coordinating mode as well as the geometry of the complex. This is in relation to a study on $[PdL_2(CNS)_2]$ complexes ($L = R_nP(C_6H_5)_{3-n}$; $n = 0$–3, $R = CH_3$ and $C_6H_5CH_2$) while in the phosphole complexes $[PdL_2(SCN)_2]$ the steric effects seem to be determinant. As a conclusion the authors said that the *cis*-$[PdL_2(SCN)_2]$ complexes S-bound are stable with small ligands, as was the case with L = 1,3,4-trimethylphosphole. On increasing the bulk of the phosphorus substituent the *trans*-N-bound thiocyanates are favoured: by substitution of a methyl group with a phenyl group in the previously quoted ligand a *cis* complex with both N and S bonded thiocyanate ligands present is obtained[15] and this suggests again the importance of the electronic effects as factors controlling the thiocyanate bonding mode in square planar complexes of the type $[Pd(PPr_3)_2(CNS)_2]$ because they favour *cis* coordination and the S-bonding mode. Here around Pd(1) we have a distortion in a pseudotetrahedral sense of the coordinated ligands (this is considered an unfavourable arrangement[16] for palladium). This means a relief from steric constraints and noticeable influence on the coordination geometry of the electronic factors. This is in agreement with the S-bonding mode of the thiocyanate ligand while for the *trans* disposition of the SCN ligands we have to consider the bulk of PPr^n_3 ligand which is in favour of the *trans* disposition. The Pd–P bond length of 2.252(4) Å is at the lower end of the range of Pd–P bond distances commonly found[17] showing that the *d*–*d* back bond is significant. Its value agrees well with those of 2.247(4) Å and 2.248(4) Å found in

$$[Pd_4(P(C_3H_7)_3)_4(NO_2)_4(ONO)_4]^{18}$$

and also with that of 2.243 Å found in

$$[Pd(C_6H_5\text{–}P\text{–}(CH_2)_2\text{–}C_6H_5)(SCN)(NCS)]^{19}$$

for a Pd–P bond distance *trans* to a Pd–N(NCS) bond of 2.062(10) Å which is again in agreement with the Pd–N(4) bond length of 2.07(1) Å for bridging the cyano groups (cf. also bond length of 2.078(7) Å in dithiocyanato bis-hydrogen bis-diphenylphosphinato dipalladium(II).)[20] The Pd–P bond distances (2.2334(6) and 2.316(5) Å) have the values expected for *trans* SCN group as in *trans*-dithiocyanato bis-(3,3-dimethylbuthynyl)diphenylphosphinepalladium(II).[21] The distance Pd–S of 2.323 Å is in agreement also with the averaged value of 2.323 Å found[22] in the anion $[Pt(SCN)_4]^{2-}$. The Pd(2) environment is more planar, the steric effects are important due also to the two *trans*-coordinated PPr^n_3 phosphines, and the N bonding mode of the thiocyanate ligand is fully justified. The Pd–P distances, 2.333(4) and 2.320(4) Å, are in very good agreement with those reported in *trans*-$[Pd(PPh_3)_2(CH_3CN)Cl]$. The Pd–N(NCS) and Pt–C(CN) lengths of 2.02(1) and 1.94(1) Å compare well with the corresponding values of 2.024(9) and 1.921(12) Å for Pt–N(NCS) and Pt–C(CN) in $[Pt(NCS)(PEt_3)_2]_2$-*p*-$C_6H_4(C{\equiv}C)_2$[24] as well as the Pd–P compared with the Pt–P bond lengths which average 3.30(1) Å.

From this structural analysis it can be seen that the old question concerning the factors influencing the (CNS) coordination mode cannot easily be rationalized because of the influence of both electronic and steric effects. Nevertheless it appears that while in a crowded geometry, as in the case of the Pd(2) environment, the N-bonding mode of (CNS) ligand is favoured; with less hindering about Pd(1) the S-mode is more likely.

Although at this stage we have no quantitative photochemical data, on the basis of the trend of the spectral variations upon irradiation and taking into account the structure of the product $[Pd_2(PPr^n_3)_2(NCS)(SCN)_2(\mu\text{-}CN)]$, we can tentatively propose a mechanism for the photoprocess. The presence of two (CNS) groups bound to palladium through sulphur suggests that in a first

step the complex *trans*-$[Pd(PPr^n_3)_2(NCS)_2]$ converts to its linkage isomer *trans*-$[Pd(PPr^n_3)_2(SCN)_2]$. Further reaction of two molecules of the S-bound isomer with direct participation of the solvent CH_3CN yields $[Pd_2(PPr^n_3)_2(NCS)(SCN)_2(\mu\text{-}CN)]$. It is significant in this respect that no stable photoproduct is obtained when the reaction is performed in MeOH. On the other hand we cannot exclude that the CN group bridging the two palladium atoms comes from fragmentation of (CNS) bound to metal, though, to our knowledge, such a fragmentation has never been reported.

REFERENCES

1. L. Costanzo, A. Giuffrida, G. Guglielmo and V. Ricevuto, *Inorg. Chim. Acta* 1984, **33**, 29.
2. M. Cusumano, G. Guglielmo, V. Ricevuto, O. Traverso and J. Kemp, *J. Chem. Soc., Chem. Commun.* 1979, 775.
3. M. Cusumano, G. Guglielmo, V. Ricevuto, S. Sostero, O. Traverso and J. Kemp, *J. Chem. Soc., Dalton Trans.* 1981, 302.
4. F. G. Mann and D. Purdie, *J. Chem. Soc.* 1935, 1549.
5. G. M. Sheldrick, SHELX Computing System, University of Cambridge (1976).
6. D. D. Cromer and D. Liberman, *J. Chem. Phys.* 1970, **53**, 1891.
7. D. A. Redfield and J. H. Nelson, *Inorg. Nucl. Chem. Lett.* 1974, **10**, 931.
8. D. A. Redfield and J. H. Nelson, *J. Am. Chem. Soc.* 1974, **96**, 6219.
9. D. A. Redfield, J. H. Nelson, R. A. Henry, D. W. Moore and H. B. Jonassen, *J. Am. Chem. Soc.* 1974, **96**, 6298.
10. J. L. Burmeister and F. Basolo, *Inorg. Chem.* 1964, **3**, 1587.
11. H. A. Pidcock, R. E. Richards and L. M. Venanzi, *J. Chem. Soc. A* 1966, 1707.
12. L. M. Venanzi, *Chem. Brit.* 1968, **4**, 162.
13. S. S. Zumdahl and R. S. Drago, *J. Am. Chem. Soc.* 1968, **30**, 6669.
14. J. J. MacDougall, J. H. Nelson, M. W. Babich, C. C. Fuller and R. A. Jacobsen, *Inorg. Chim. Acta* 1978, **27**, 201.
15. J. J. McDougall, E. M. Halt, P. de Meester, N. W. Alcock, F. Mathey and J. H. Nelson, *Inorg. Chem.* 1980, **19**, 1439.
16. D. R. Eaton, *J. Am. Chem. Soc.* 1968, **90**, 4272.
17. L. Manojlovic'-Muir, K. W. Muir and T. Solumun, *J. Organometal. Chem.* 1977, **142**, 265.
18. G. Bombieri, G. Bruno, M. Cusumano and G. Guglielmo, *Acta Cryst.* 1984, **C40**, 409.
19. G. J. Palenik, M. Mathew, W. L. Steffen and G. Beran, *J. Am. Chem. Soc.* 1975, **97**, 1059.
20. V. D. Naik, G. J. Palenik, S. Jacobson and A. J. Carty, *J. Am. Chem. Soc.* 1974, **96**, 2286.
21. G. Beran, A. J. Carty, P. G. Chieh and H. A. Patel, *J. Chem Soc., Dalton Trans.* 1973, 488.
22. H. J. Gysling and H. R. Luss, *Organometallics* 1984, **3**, 596.
23. R. McCriddle, G. Ferguson, A. J. McAless and M. Parvez, *J. Chem. Soc., Dalton Trans.* 1982, 1699, and references therein for related complexes.
24. U. Beherens, H. Hoffmann, J. Kopf and J. Moritz, *J. Organometal. Chem.* 1976, **117**, 91.

Polyhedron Vol. 4, No. 8, pp. 1371–1378, 1985
Printed in Great Britain

0277–5387/85 $3.00 + .00
© 1985 Pergamon Press Ltd

REACTIONS OF MOLYBDENUM(III) WITH MACROCYCLIC POLYTHIAETHERS

D. SEVDIĆ* and L. FEKETE
Rudjer Bošković Institute, 41001 Zagreb, Yugoslavia

(*Received* 14 *May* 1984; *accepted* 20 *October* 1984)

Abstract—Reactions of $MoCl_3(THF)_3$ and $MoCl_3(PrCN)_3$ with the macrocyclic polythiaethers: 1,4,8,11-tetrathiacyclotetradecane (TTP) and 1,4,7,10,13,16-hexathiacyclooctadecane (HTO) were studied. The type of reaction and the complexes formed depend on reactant concentration and nature of the solvent. The complexes: $[MoCl_3(HTO)]$, $[(MoCl_3)_2(HTO)(THF)_3]$, $[MoCl_3(TTP)(THF)]$ and $[MoCl_3(TTP)]$ in which the macrocyclic polythiaethers are coordinated to the molybdenum through sulphur atoms were isolated. Some new mixed-valence complexes were formed in reactions where a partial change in the molybdenum oxidation state and a cleavage of the macrocyclic ring took place. The following complexes were isolated: $[Mo_3Cl_9(PHT)_2(PrCN)] \cdot CH_2Cl_2$, $[Mo_3Cl_9(PHT)_2(THF)] \cdot CH_2Cl_2$, $[Mo_2Cl_6(PHT)] \cdot CH_2Cl_2$, $[Mo_3Cl_9(TTT)_2(THF)] \cdot CH_2Cl_2$, where PHT = 3,6,9,12,15-pentathiaheptadec-16-ene-1-thiolato(1-) and TTT = 4,7,11-trithiatridec-12-ene-1-thiolato(1-). The complexes were characterized on the basis of elemental analyses, magnetic measurements, IR, ^1H NMR, ^{13}C NMR and mass spectra.

A variety of metalloproteins characterized by X-ray diffraction are known to contain sulphur atoms as a part of the coordination environments of metal ions. Molybdenum, together with iron and copper ions, is specially common in metalloenzymes containing sulphur ligands.[1] Among the other oxidation states, molybdenum(III) has also been suggested as a participant in biological and catalytic processes.[2]

The development of bioinorganic chemistry has also been an important factor in spurring the growth of interest in complexes of macrocyclic compounds since they may serve as models for biologically important species.[3]

In comparison to molybdenum(VI), (V) and (IV) complexes, the compounds of molybdenum(III) have been scantily investigated, especially those with sulphur-containing ligands.[4–11]

Previous studies have been concentrated on complex formation of molybdenum(VI), (V) and (IV) with potentially tetradentate and hexadentate polythiaethers TTP and HTO, respectively.[12] Now our studies are extended to the reactions of molybdenum(III) with the macrocyclic polythiaethers TTP and HTO.

EXPERIMENTAL

Starting materials

The ligands 1,4,8,11-tetrathiacyclotetradecane (TTP) and 1,4,7,10,13,16-hexathiacyclooctadecane (HTO) were prepared as described previously.[13,14] Reagent grade chemicals were used without further purification except in the cases noted. All solvents were purified by standard methods, dried and saturated with dry argon before use. Tetrachlorobis(propionitrile)molybdenum(IV) and tetrachlorobis(acetonitrile)molybdenum(IV) were obtained by the reaction of pentachloromolybdenum(V) with the corresponding alkylcyanide.[15] Trichlorotris(tetrahydrofuran)molybdenum(III) was prepared from $MoCl_4(RCN)_2$ following the method reported by Anker *et al.*[16] $Mo(CO)_4Cl_2$ was prepared by the reaction of hexacarbonylmolybdenum(0) with liquid chlorine at −78°C.[17] Trichlorotris(propionitrile)molyb-

* Author to whom correspondence should be addressed.

denum(III) was obtained by the reaction of $Mo(CO)_4Cl_2$ with the propionitrile.[6]

Preparation of complexes

All reactions and manipulations were performed under a dry argon atmosphere using a standard dry-box technique except in the case noted.

Trichloro(1,4,7,10,13,16 - *hexathiacycloocta* - *decane*)*molybdenum*(*III*) (**I**). $MoCl_3(THF)_3$ (0.418 g, 1 mmol) was dissolved in dichloromethane (15 cm^3) and the ligand HTO (2.164 g, 6 mmol) dissolved in the same solvent (15 cm^3) was added. After a few minutes the product started to precipitate. The next day the orange crystalline product formed was filtered off, washed with dichloromethane and dried.

IR cm^{-1}: 1199s, 1143w, 905s, 856s, 843s, 745(sh), 736m, 701s, 690w, 462vw, 441vw, 411vw, 322vs (sh), 312vs.

Bis(*trichloro*)(*μ*-1,4,7,10,13,16 - *hexathiacyclo* - *octadecane*)*tris*(*tetrahydrofuran*)*dimolybdenum*(*III*) (**II**). $MoCl_3(THF)_3$ (0.837 g, 2 mmol) was suspended in tetrahydrofuran (20 cm^3) and HTO (0.361 g, 1 mmol) dissolved in THF (25 cm^3) was added. The reaction mixture was stirred at room temperature in a stoppered reaction flask. After 2 h the reaction vessel was stored in a dry-box and the next day the orange crystalline product was filtered off, rinsed with THF and dried. The same product was obtained with the metal/ligand ratios 3:1 and 5:1.

IR cm^{-1}: 1209m, 1156vw, 1010s, 925vw, 917vw, 855vs, 745m, 688w, 452vw, 407vw, 320vs, br.

Trichloro(1,4,8,11 - *tetrathiacyclotetra* - *decane*)(*tetrahydrofuran*)*molybdenum*(*III*) (**III**). The TTP ligand (0.537 g, 2 mmol) and $MoCl_3(THF)_3$ (0.837 g, 2 mmol) were suspended in diethyl ether (50 cm^3). The reaction mixture was stirred 7 h in a stoppered flask and stored overnight in a dry-box. The pink–orange product formed was separated, washed with diethyl ether and dried.

IR cm^{-1}: 1204m, 1138w, 1009s, 922w, 849vs, 689w, 415vw, 403vw, 325vs, br.

Trichloro(1,4,8,11 - *tetrathiacyclotetra* - *decane*)*molybdenum*(*III*) (**IV**). A solution of TTP (1.611 g, 6 mmol) in dichloromethane (15 cm^3) was added to a solution of $MoCl_3(THF)_3$ (0.418 g, 1 mmol) in CH_2Cl_2 (15 cm^3). After two days orange crystals were formed on the walls of the reaction flask together with a fluffy brown precipitate. The brown product was separated by filtration. The filtrate was poured into the reaction flask and allowed to stand overnight in order to achieve further crystallisation of orange hemispherical crystals. The orange crystals were filtered off, washed with dichloromethane and dried.

IR cm^{-1}: 1124vw, 928m, 915w, 907m, 857s, 840m, 761s, 734m, 724m, 479m, 445(sh), 439vw, 407vw, 333(sh), 310vs, br.

A powder diffractogram showed that the orange agglomerates of the complex $[MoCl_3(TTP)]$ are crystalline. It was shown that the IR spectrum of the brown precipitate is identical to the spectrum of the complex **VIII**.

Nonachlorobis(*μ*-3,6,9,12,15-*pentathiaheptadec*-16-*ene*-1-(*thiolato*)(*propionitrile*)*molyb*-*denum*(*III*)*dimolybdenum*(*IV*) - *dichloro* - *methane*(1/1) (**V**). A solution of HTO (0.360 g, 1 mmol) in CH_2Cl_2 (25 cm^3) was added to a solution of $MoCl_3(CH_3CH_2CN)_3$ (0.735 g, 2 mmol) in CH_2Cl_2 (25 cm^3). Although a product started to form after 30 min, the stoppered reaction flask was allowed to stand two days in a dry-box to complete the reaction. The red–brown precipitate was filtered off, rinsed with dichloromethane and dried.

IR cm^{-1}: 2275vw, 1600vw, br, 1203w, 972m, 915w, 730m.

Nonachlorobis(*μ*-3,6,9,12,15-*pentathiaheptadec*-16-*ene*-1-(*thiolato*)(*tetrahydrofuran*)*molyb*-*denum*(*III*)*dimolybdenum*(*IV*) - *dichloro* - *methane*(1/1) (**VI**). $MoCl_3(THF)_3$ (1.256 g, 3 mmol) was dissolved in CH_2Cl_2 (20 cm^3). The solution was filtered and the HTO (0.721 g, 2 mmol) dissolved in CH_2Cl_2 (15 cm^3) was added. After two days the red–brown crystalline product formed was filtered off, washed with CH_2Cl_2 and dried.

IR cm^{-1}: 1610vw, br, 1207m, 1153vw, 1008vw, 986vw, 913w, 851m, 731vs, 698m, 455vw, 435vw, 415vw, 317vs, br.

Hexachloro(*μ*-3,6,9,12,15-*pentathiaheptadec*-16-*ene*-1-*thiolato*)*molybdenum*(*III*)*molybdenum*(*IV*)-*dichloromethane*(1/1) (**VII**). A solution of HTO (0.360 g, 1 mmol) in CH_2Cl_2 (20 cm^3) was added to a filtered solution of $MoCl_3(CH_3CH_2CN)_3$ (1.470 g, 4 mmol) in CH_2Cl_2 (25 cm^3). The reaction went on very slowly and after six days the main part of the brown crystalline product formed was separated and rinsed with dichloromethane.

IR cm^{-1}: 1600vw, br, 1208w, 983m, 929w, 730m, 698vw.

On the walls of the reaction vessel there remained dark-red (like rubies) hemispherical crystalline agglomerates. Their identification is in progress.

Nonachlorobis(*μ*-4,7,11-*trithiatridec*-12-*ene*-1-*thiolato*)(*tetrahydrofuran*)*molybdenum*(*III*)*dimolyb*-*denum*(*IV*) - *dichloromethane*(1/1) (**VIII**). $MoCl_3(THF)_3$ (0.837 g, 2 mmol) was dissolved in CH_2Cl_2 (25 cm^3) and TTP (0.268 g, 1 mmol) dissolved in CH_2Cl_2 (20 cm^3) was added. After four days the orange–brown crystalline product formed was filtered off, washed with CH_2Cl_2 and dried.

IR cm^{-1}: 1610vw, br, 1004vw, 984m, 918w,

908vw, 861m, 844vw, 743(sh), 732m, 697vw, 470vw, 455vw, 417w, 334vs, 312vs, br.

Trichloro(acetone)bis(tetrahydrofuran)molybdenum(III) (**IX**). Trichlorotris(tetrahydrofuran) molybdenum(III) (2 g) was dissolved in technical grade acetone (20 cm^3) without any precaution with regard to air. After a few minutes the product started to precipitate. The orange needle crystals formed were filtered off, washed with acetone and dried. The complex is stable for several days.

IR cm^{-1}: 1656vs, 1013vs, 924m, 917m, 854vs, br, 322vs.

Physical measurements

IR spectra of the complexes were recorded as Nujol mulls on a Perkin–Elmer 580 B (4000–180 cm^{-1}) spectrophotometer. Mass spectra were obtained on a Varian CH-7 mass spectrometer. ^1H NMR spectra for solutions in DMSO-d_6 were measured on a JEOL FX 90 Q spectrometer with tetramethylsilane as the internal standard.

^{13}C NMR were measured with a JEOL JNM-FX 100 spectrometer. Magnetic susceptibilities were determined by the standard Gouy method at 295 K using $CuSO_4 \cdot 5H_2O$ as calibrant.

RESULTS AND DISCUSSION

Investigations of the reactions of trichloromolybdenum(III) with macrocyclic polythiaethers TTP and HTO have shown that depending on the reactant concentration and the nature of the solvent used different types of complexes were formed.

The first type of complexes, in which macrocyclic polythiaethers are coordinated to the molybdenum(III) only through sulphur atoms, were formed when the reaction was carried out in tetrahydrofuran with the concentration of molybdenum higher than that of the ligand. The same reaction occurred in CH_2Cl_2 as solvent only when the concentration of the ligand was in excess of the molybdenum concentration.

When the reaction was carried out in CH_2Cl_2 with the metal–ligand ratio from 1 : 1 to 4 : 1, new mixed-valence complexes were formed. In this case a partial change in the molybdenum oxidation state and a cleavage of the macrocyclic ring took place leading to the formation of molybdenum thiolate complexes.

The complexes were formulated on the basis of elemental analysis and physical measurements. Most of the complexes were prepared several times. The analyses are presented as the mean of the results with different preparations. Conditions of preparation and analytical data for the complexes obtained are given in Tables 1 and 2. Some complexes were obtained as solvates, from which the solvate molecules were not removable by prolonged pumping at room temperature. The presence of dichloromethane was confirmed by examination of mass spectra. The complexes were not sufficiently soluble in suitable solvents, or their solutions were too unstable, for molecular-weight determinations. The air and moisture sensitivity of the complexes further limited their characterisation.

Complexes of trichloromolybdenum(III)

Although the complexes of $MoCl_3L_3$ have been widely investigated, only a few studies were performed on $MoCl_3$ complexes with sulphur-containing monodentate ligands.[4,6] Until now no complexes of $MoCl_3$ with multidentate sulphur-containing ligands have been prepared. However, we were able to obtain new complexes of trichloromolybdenum(III) with multidentate macrocyclic polythiaethers.

It has been found that HTO as ligand forms with $MoCl_3$ two different complexes depending on the experimental conditions.

One type of complex was formed in the reaction of $MoCl_3(THF)_3$ and HTO in CH_2Cl_2 as a solvent with the metal–ligand ratio 1 : 6. In this case the HTO ligand displaced all of the tetrahydrofuran and the new complex, according to the analyses, corresponds to the formula $[MoCl_3(HTO)]$ (complex **I**). This complex has a magnetic moment of 3.44 B.M., consistent with the results published for $MoCl_3L_3$ complexes, where L is an oxygen or sulphur donor.[6] These values are consistent with quasi-octahedral complexes containing a $4d^3$ ion. A comparison of the IR spectrum of the precursor molecule $MoCl_3(THF)_3$ with that of complex **I** shows that the IR band of the $MoCl_3$ unit at 325 cm^{-1}, assigned to the Mo–Cl stretching vibration, is affected by the complexation. In the spectrum of the complex $[MoCl_3(HTO)]$ two very strong bands at 322 and 312 cm^{-1} are present. Coordination of a sulphur from the ligand to the metal atom causes both a decrease in the frequencies and a lowering of the intensity of C–S–C stretching modes. The HTO ligand has four strong bands at 713, 699, 683 and 660 cm^{-1}, assigned to the C–S–C stretching vibrations, while in the spectrum of the complex only two bands at 701 and 690 cm^{-1} are present. Two weak bands at 462 and 441 cm^{-1} most probably correspond to Mo–S stretching vibrations. On the basis of these results we propose that the complex $[MoCl_3(HTO)]$ has an expected octahedral coordination in which chlorine and sulphur atoms have the meridional arrangement. The HTO ligand acts as a bridge between two molybdenum units. However, to

Table 1. Conditions of preparation of molybdenum complexes

	Compound	Starting compound	Ligand	Metal/ligand ratio	Solvent
I	$[MoCl_3(HTO)]$	$MoCl_3(THF)_3$	HTO	1:6 2:1	CH_2Cl_2
II	$[(MoCl_3)_2(HTO)(THF)_3]$	$MoCl_3(THF)_3$	HTO	3:1 5:1	THF
III	$[MoCl_3(TTP)(THF)]$	$MoCl_3(THF)_3$	TTP	1:1	Ether
IV	$[MoCl_3(TTP)]$	$MoCl_3(THF)_3$	TTP	1:6	CH_2Cl_2
V	$[Mo_3Cl_9(PHT)_2(PrCN)]\cdot CH_2Cl_2$	$MoCl_3(CH_3CH_2CN)_3$	HTO	2:1 3:2	CH_2Cl_2
VI	$[Mo_3Cl_9(PHT)_2(THF)]\cdot CH_2Cl_2$	$MoCl_3(THF)_3$	HTO	2:1 3:2	CH_2Cl_2
VII	$[Mo_2Cl_6(PHT)]\cdot CH_2Cl_2$	$MoCl_3(CH_3CH_2CN)_3$	HTO	4:1	CH_2Cl_2
VIII	$[Mo_3Cl_9(TTT)_2(THF)]\cdot CH_2Cl_2$	$MoCl_3(THF)_3$	TTP	2:1 1:1	CH_2Cl_2

achieve six coordination HTO probably behaves as a bidentate and monodentate ligand at the same time (Fig. 1, Structure **I**).

When the reaction between $MoCl_3(THF)_3$ and HTO was carried out in tetrahydrofuran as solvent with the metal–ligand ratios 2 : 1, 3 : 1 or 5 : 1 another complex $[(MoCl_3)_2(HTO)(THF)_3]$ was formed. The magnetic moment of this complex is 3.46 B.M. per molybdenum atom. The analytical data for this complex are listed in Table 2. As can be seen in the case where the molybdenum was in excess in comparison to the HTO, the ligand was not able to displace all molecules of tetrahydrofuran from the $MoCl_3(THF)_3$ compound. The presence of tetrahydrofuran is confirmed by the IR spectrum (complex **II**) which exhibits two very strong bands at 1010 and 855 cm^{-1}, assignable to ν(C–O–C) of coordinated tetrahydrofuran. The complex $[(MoCl_3)_2(HTO)(THF)_3]$, contrary to the $[MoCl_3(HTO)]$ complex, exhibits only one very strong band at 320 cm^{-1} corresponding to ν(Mo–Cl). The very weak band in its IR spectrum at 452 cm^{-1} can be assigned to the Mo–S stretching vibration. The complex also exhibits only one band at 688 cm^{-1}, which can be attributed to the ν(C–S). The results suggest that for the complex $[(MoCl_3)_2(HTO)(THF)_3]$ an alternative structure (**II**) (Fig. 1) involving coordination of tetrahydrofuran molecules is more acceptable. It can be expected that in this complex HTO, in order to retain six coordination, acts as a bridge between two molybdenum units in a bidentate and monodentate manner.

With TTP as a ligand we could not isolate any

Table 2. Analytical data for molybdenum complexes

	Compound	Mo %	Cl %	S %	C %	H %
I	$[MoCl_3(HTO)]$	17.00 (17.04)[a]	18.61 (18.89)	32.19 (34.17)	24.62 (25.60)	4.08 (4.30)
II	$[(MoCl_3)_2(HTO)(THF)_3]$	19.55 (19.55)	21.67 (21.76)	19.50 (19.60)	28.23 (29.37)	4.29 (4.93)
III	$[MoCl_3(TTP)(THF)]$	17.45 (17.67)	19.66 (19.59)	20.07 (23.68)	28.75 (30.97)	5.11 (5.20)
IV	$[MoCl_3(TTP)]$	20.18 (20.38)	22.17 (22.59)	26.12 (27.24)	25.90 (25.51)	4.29 (4.28)
V	$[Mo_3Cl_9(PHT)_2(PrCN)]\cdot CH_2Cl_2$	19.66 (19.63)	21.76 (21.76)	26.39 (26.24)	22.15 (22.94)	3.60 (3.64)
VI	$[Mo_3Cl_9(PHT)_2(THF)]\cdot CH_2Cl_2$	19.67 (19.40)	21.19 (21.51)	27.16 (25.94)	22.15 (23.48)	3.81 (3.81)
VII	$[Mo_2Cl_6(PHT)]\cdot CH_2Cl_2$	22.54 (22.60)	23.19 (25.05)	22.57 (22.65)	19.37 (18.38)	3.28 (2.97)
VIII	$[Mo_3Cl_9(TTT)_2(THF)]\cdot CH_2Cl_2$	21.40 (22.12)	24.94 (24.53)	19.20 (19.71)	21.37 (23.08)	3.66 (3.87)
IX	$[MoCl_3(THF)_2(CH_3COCH_3)]$	23.05 (23.71)	26.09 (26.29)	—	30.15 (32.65)	5.16 (5.48)

[a] Calculated percentage in parentheses.

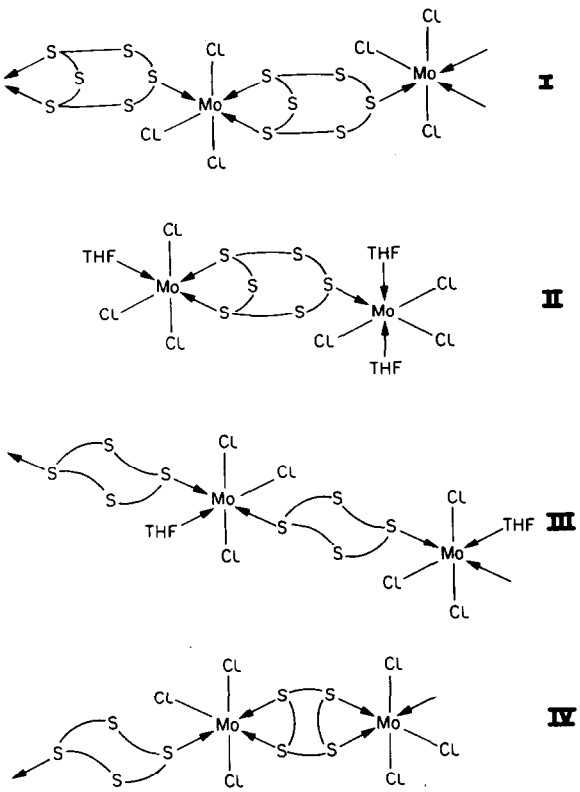


Fig. 1. Proposed structures of molybdenum(III) complexes with macrocyclic polythiaethers.

complex in tetrahydrofuran as solvent. However, we were able to prepare the complex of molybdenum(III) with TTP in the reaction of $MoCl_3(THF)_3$ and TTP in ether as solvent. With the metal–ligand ratio 1:1, a yellow–orange complex was formed whose analyses correspond to the formula $[MoCl_3(TTP)(THF)]$ (complex **III**). The presence of THF was also confirmed by the IR spectrum which shows two bands at 1009 and 849 cm^{-1} corresponding to the C–O–C stretching vibrations of coordinated THF. The C–S–C stretching vibrations which are present in the IR spectrum of the TTP ligand at 722, 715, 690 and 674 cm^{-1} disappeared completely by complexation, except one very weak band at 689 cm^{-1} which remained in the spectrum of the complex. The complex **III** has a very strong band at 325 cm^{-1} which corresponds to ν(Mo–Cl) and one very weak band at 415 cm^{-1} presumably arising from Mo–S stretching vibrations. $[MoCl_3(TTP)(THF)]$ has a magnetic moment of 3.47 B.M. and there is little doubt of an octahedral structure in the complex (**III**) (Fig. 1). In order to achieve this coordination around the molybdenum atom the TTP ligand should probably act as a bridge between two molybdenum units in a double monodentate manner.

When the reaction of $MoCl_3(THF)_3$ and TTP was carried out in CH_2Cl_2 with the metal–ligand ratio 1:6 the complex $[MoCl_3(TTP)]$ (complex **IV**) was formed, which does not contain THF. The IR spectrum of this complex has no bands which correspond to the coordinated or noncoordinated tetrahydrofuran. In contrast to the spectrum of $[MoCl_3(TTP)(THF)]$, in the IR spectrum of $[MoCl_3(TTP)]$ there are two strong bands at 333 and 310 cm^{-1} corresponding to ν(Mo–Cl), and three bands at 479, 445 and 439 cm^{-1} which can be assigned to Mo–S stretching vibrations. While free TTP ligand exhibits a very strong band at 1203 cm^{-1}, attributed to the *trans*-CH_2-wagging vibrations, in the spectrum of complex (**IV**) this band disappeared completely as well as the bands corresponding to the C–S stretching vibrations. On the other hand, two new bands at 857 and 849 cm^{-1}, corresponding to the *gauche*-CH_2-rocking vibrations, appeared in the spectrum. All these changes indicate that considerable conformation changes of the TTP ligand appeared upon complexation. The complex has a magnetic moment of 3.42 B.M. Therefore, it is reasonable to propose the structure (**IV**) (Fig. 1) in which one ligand molecule acts as a bridge between two molybdenum units as a double bidentate while the other molecule acts as a double monodentate in order to achieve 6 coordination around the molybdenum atom.

Mixed-valence complexes

During our investigation of the complex formation of molybdenum(III) with macrocyclic polythiaethers we have observed that under certain experimental conditions a new type of mixed-valence complexes was formed. These reactions were accompanied by a cleavage of the macrocyclic ring.

DeSimone *et al.*[18] have also observed that in the reaction of $[Mo_2(CF_3SO_3)_2(H_2O)_4](CF_3SO_3)_2$ with the cyclic polythiaether 1,5,9,13-hexathiacyclohexadecane some cleavage of the macrocycle ring occurred. Koray *et al.*[19–21] have also observed that in the reaction of 2,6,15,19-tetrathia(7,7)paracyclophane with metal carbonyls, the reaction products demonstrate the tendency of the 1,3-dithiapropane unit to be cleaved off under the influence of the metal carbonyl.

When the reactions between molybdenum(III) and macrocyclic polythiaethers were carried out in CH_2Cl_2 as solvent with a higher concentration of molybdenum in relation to the concentration of the ligand a new type of mixed-valence complexes was formed.

The reaction of HTO ligand with $MoCl_3(THF)_3$ or $MoCl_3(CH_3CH_2CN)_3$ at metal–ligand ratio 2:1

or 3:2 leads to the formation of red–brown complexes. The elemental analyses correspond to the formulae $[Mo_3Cl_9(PHT)_2(PrCN)]\cdot CH_2Cl_2$ (complex **V**) and $[Mo_3Cl_9(PHT)_2(THF)]\cdot CH_2Cl_2$ (complex **VI**), where PHT is 3,6,9,12,15 - penta - thiaheptadec - 16 - ene - 1 - thiolato(1-). These complexes have magnetic moments of 2.57 and 2.65 B.M. per molybdenum atom which are consistent with the proposed structures. The presence of CH_2Cl_2 was confirmed by examination of the mass spectra. In the complex **V** the presence of coordinated CH_3CH_2CN was confirmed by the IR spectrum in which a ν(C≡N) band at 2275 cm^{-1}, corresponding to the coordinated cyanide, is present. The complex **VI** contains THF as part of the composition. This can be seen from the IR spectrum which exhibits ν(C–O–C) bands at 1008 and 851 cm^{-1}, assignable to the coordinated THF. In the spectrum of the complex **VI** there is a very strong band at 317 cm^{-1} which corresponds to the ν(Mo–Cl) and two very weak bands at 455 and 435 cm^{-1}, presumably arising from M–S stretching vibrations.[22]

The IR spectra of both complexes differ significantly from the spectra of the previously mentioned complexes of molybdenum(III). The bands at 1152, 929, 843 and 743 cm^{-1}, corresponding to *trans*-CH_2-twisting, *gauche*-CH_2-rocking, and *trans*-CH_2-rocking of the ligand, disappeared completely in the spectra of these new complexes indicating that a drastic change in the ligand was taking place. At the same time new bands appeared in the spectra of these complexes. The complex **V** has three bands at 1600, 972 and 915 cm^{-1} and the complex **VI** at 1610, 986 and 913 cm^{-1}, respectively. These bands are normal characteristic vibrations of the vinyl group. The band at 1600 cm^{-1} corresponds to the stretching vibrations of the C=C group. The absorptions at 972 and 915 cm^{-1} for the complex **V** and at 986 and 913 cm^{-1} for the complex **VI** obviously represent the out-of-plane vinyl C–H deformation vibrations which are normally found near 990 and 910 cm^{-1} in hydrocarbons.[23–25] The appearance of the ν(C=C) band at 1600 cm^{-1} indicates that the ligand is not attached to the metal through this bond. The presence of the vinyl group is also confirmed by the ^1H and ^{13}C NMR spectra (peaks centred at 5.74 ppm and 117.39 ppm, respectively).

These results allow us to propose that during the reactions of macrocyclic polythiaethers with molybdenum, cleavage of the macrocyclic ring takes place with formation of $-S^-$ and $-CH{=}CH_2$ groups at the ends of the ligand chain. The thiol ligands have bands assigned to the S–H stretching vibrations at *ca* 2600 cm^{-1}. Since in the IR spectra of the investigated complexes there are no bands in this region, it could be considered that the bonding occurs through the ionised thiolato group accompanied by a partial change from the molybdenum(III) oxidation state to the molybdenum(IV) oxidation state. Since the complexes were prepared with careful exclusion of air we are confident that there was no change in the oxidation state of molybdenum owing to the formation of Mo=O or Mo–O–Mo bonds. The stability of the starting compound $MoCl_3(THF)_3$ towards air oxidation was confirmed by the preparation of the complex

$$[MoCl_3(THF)_2(CH_3COCH_3)]$$

(complex **IX**) which has a magnetic moment of 3.74 B.M. Namely, this preparation was carried out without any precaution with regard to air. On the basis of the fact mentioned it can be proposed that the complexes most probably have the structures **V** and **VI** (Fig. 2) in which all molybdenum atoms retain 6 coordination.

When the HTO reacted with

$$MoCl_3(CH_3CH_2CN)_3$$

in CH_2Cl_2 as solvent with the metal–ligand ratio 4:1 the brown complex $[Mo_2Cl_6(PHT)]\cdot CH_2Cl_2$ was formed (complex **VII**). This complex has a magnetic moment of 2.25 B.M. per molybdenum atom and does not contain CH_3CH_2CN molecules. In the IR spectrum of this complex there are also three bands at 1600, 983 and 920 cm^{-1} which arise from the vinyl group present. Two bands at 730 and 698 cm^{-1} which correspond to the C–S stretching vibrations are also present in the spectrum of this complex. For this complex structure (**VII**) (Fig. 2), in which all sulphur atoms from the ligand are engaged in bonding with two molybdenum atoms, is more likely to be acceptable.

Investigations have shown that the TTP ligand is less stable than HTO. It was possible to isolate only one well defined complex. This complex was obtained in the reaction of TTP and $MoCl_3(THF)_3$ in CH_2Cl_2 with metal–ligand ratio 2:1 or 1:1. The orange–brown complex formed has a magnetic moment of 2.58 B.M. per molybdenum atom. The elemental analyses correspond to the formula $[Mo_3Cl_9(TTT)_2(THF)]\cdot CH_2Cl_2$ (complex **VIII**), where TTT is 4,7,11 - trithiatridec - 12 - ene - 1 - thiolato(1-). The presence of THF was confirmed by the IR spectrum in which two bands at 1004 and 861 cm^{-1} corresponding to the coordinated THF are present. In comparison to the spectra of the complexes with HTO, in the spectrum of the complex with TTP there are some differences. Namely, bands at 908, 844 and 743 cm^{-1} arising from *gauche*-CH_2-

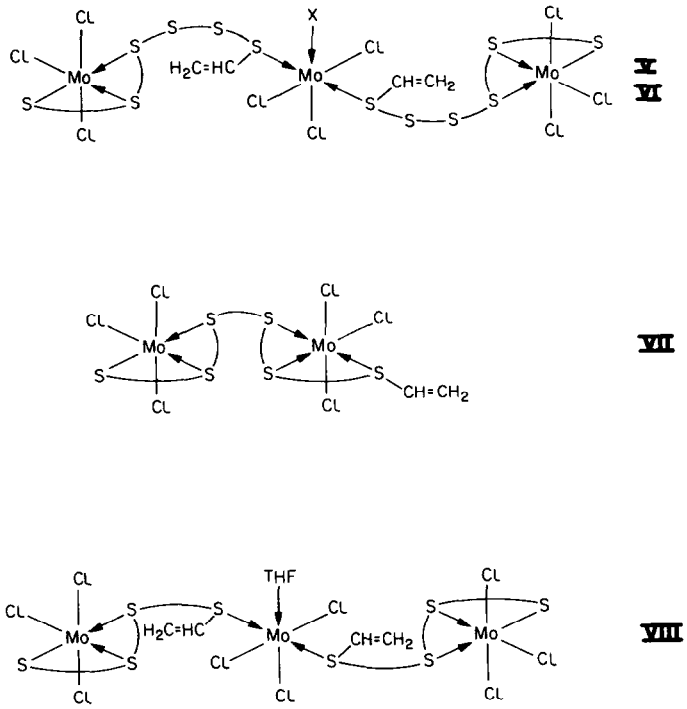


Fig. 2. Proposed structure of molybdenum mixed-valence complexes. X = THF or CH_3CH_2CN.

rocking and *trans*-CH_2-rocking remained in the spectrum of the complex **VIII**. This complex has three bands at 470, 455 and 417 cm^{-1} which probably arise from Mo–S stretching vibrations and two bands at 334 and 312 cm^{-1} corresponding to Mo–Cl stretching vibrations. In spectrum of the complex **VIII** there are also three bands at 1610, 984 and 918 cm^{-1}, arising from the vinyl group present, which confirm that during the complexation the cleavage of the TTP ring is also taking place. For this complex the structure **VIII** is proposed (Fig. 2) in which all sulphur atoms from two ligand units are engaged in complexation with three molybdenum units. The 6 coordination of the central molybdenum atom is maintained by one molecule of THF.

These different reactions between molybdenum(III) and macrocyclic polythiaethers, depending on the nature of the solvent used and the concentration of the molybdenum, can be explained by the great affinity of molybdenum(III) toward the sulphur from the investigated ligands. In the case where the reactions were carried out in a donor solvent such as THF, with a higher concentration of molybdenum, donor molecules of the solvent soften the reaction between molybdenum and ligands and formation of normal complexes of molybdenum(III) occurs. Similar reactions occur in the neutral solvent CH_2Cl_2 only when the ligand is in higher concentration. In this case there are enough sulphur atoms for molybdenum(III) to achieve the corresponding coordination. On the other hand, when the reactions were carried out in CH_2Cl_2 with a higher molybdenum concentration there was a lack of sulphur atoms to coordinate all the molybdenum atoms present in the reaction solution. Because of the strong affinity of molybdenum(III) toward the sulphur, cleavage of the macrocyclic ring occurs accompanied by a partial change from the oxidation state of molybdenum(III) to molybdenum(IV) and the formation of new types of mixed-valence complexes.

Acknowledgement—The authors thank the Foundation for Scientific Research of SR Croatia, Zagreb, for financial support.

REFERENCES

1. C. G. Kuehn and S. S. Isied, *Prog. Inorg. Chem.* 1980, **27**, 153.
2. E. I. Stiefel, *Prog. Inorg. Chem.* 1977, **22**, 1.
3. G. A. Melson, *Coordination Chemistry of Macrocyclic Compounds*. Plenum Press, New York (1979).
4. V. B. Evdokimov, V. V. Zelencov, I. D. Kolli, T. Ven-sja and I. Spicyn, *Dokl. Akad. Nauk SSSR* 1962, **145**, 1282.
5. L. F. Lindoy, S. E. Livingstone and T. N. Lockyer, *Aust. J. Chem.* 1965, **18**, 1549.
6. A. D. Westland and N. Muriithi, *Inorg. Chem.* 1972, **11**, 2971.

7. D. A. Brown, W. K. Glass and C. O'Daly, *J. Chem. Soc., Dalton Trans.* 1973, 1311.
8. P. C. H. Mitchell and R. D. Scarle, *J. Chem. Soc., Dalton Trans.* 1975, 110.
9. M. Rakowski DuBois, R. C. Haltiwanger, D. J. Miller and G. Glatzmaier, *J. Am. Chem. Soc.* 1979, **101**, 5245.
10. B. A. Averill and H. W. Orme-Johnson, *Inorg. Chem.* 1980, **19**, 1702.
11. A. W. Edelblut and R. A. D. Wentworth, *Inorg. Chem.* 1980, **19**, 1117.
12. D. Sevdić and L. Fekete, *Inorg. Chim. Acta* 1982, **57**, 111.
13. D. Sevdić, L. Fekete and H. Meider, *J. Inorg. Nucl. Chem.* 1980, **42**, 885.
14. D. Sevdić and H. Meider, *J. Inorg. Nucl. Chem.* 1981, **43**, 153.
15. E. A. Allen, B. J. Brisdon and G. W. A. Fowles, *J. Chem. Soc.* 1964, 4531.
16. M. W. Anker, J. Chatt, G. J. Leigh and A. G. Wedd, *J. Chem. Soc., Dalton Trans.* 1975, 2639.
17. R. Colton and I. B. Tomkins, *Aust. J. Chem.* 1966, **19**, 1143.
18. J. Cragel, Jr., V. B. Pett, M. D. Glick and R. E. DeSimone, *Inorg. Chem.* 1978, **17**, 2885.
19. A. R. Koray and M. L. Ziegler, *J. Organomet. Chem.* 1979, **169**, C34.
20. A. R. Koray and M. L. Ziegler, *J. Organomet. Chem.* 1980, **202**, 13.
21. B. K. Balbach, A. R. Koray, A. Okur, P. Wülknitz and M. L. Ziegler, *J. Organomet. Chem.* 1981, **212**, 77.
22. A. Müller, H. Bögge and U. Schimanski, *Inorg. Chim. Acta* 1983, **69**, 5.
23. D. Barnard, L. Bateman, A. J. Harding, H. P. Koch, N. Sheppard and G. B. B. M. Sutherland, *J. Chem. Soc.* 1950, 915.
24. B. L. Ross, J. G. Grasselli, W. M. Ritchey and H. D. Kaesz, *Inorg. Chem.* 1963, **2**, 1023.
25. R. L. Downs and A. Wojcicki, *Inorg. Chim. Acta* 1978, **27**, 91.

Polyhedron Vol. 4, No. 8, pp. 1379–1381, 1985
Printed in Great Britain

0277–5387/85 $3.00 + .00
© 1985 Pergamon Press Ltd

CRYSTAL AND MOLECULAR STRUCTURE OF THE TETRACHLOROPALLADATE OF THE DICATION *MESO*-3,7-DIAZONIA TRICYCLO[4.2.2.2^{2,5}]DODECA-3,7,9,11-TETRAEN-4,8 DIAMINE OBTAINED BY COUPLING REACTION OF 2-AMINOPYRIDINES

M. CARMEN NAVARRO-RANNINGER
Departamento de Química Inorgánica, Universidad Autónoma de Madrid, Canto Blanco, 28049 Madrid, Spain

SAGRARIO MARTINEZ-CARRERA and SEVERINO GARCIA-BLANCO*
Departamento de Rayos X, Instituto de Química-Física "Rocasolano" Consejo Superior de Investigaciones Científicas, Serrano, 119, 28006 Madrid, Spain

(*Received* 11 *July* 1984; *accepted* 1 *November* 1984)

Abstract—A solution of *trans*-bis(2-aminopyridine)dichloropalladium(II) in DMF and HCl 2 N was left for several weeks. The compound isolated from this solution was identified by X-ray structural analysis as the tetrachloropalladate of *meso*-3,7-diazonia tricyclo[4.2.2.2^{2,5}] dodeca-3,7,9,11-tetraen-4,8 diamine, which contains a dication not previously described in literature. The organic dication is formed by two aminopyridine rings linked by C–C bonds whose length is greater (1.61 Å) than a normal single C–C bond.

The title compound has been synthesized as a result of a series of experiments carried out in order to investigate the chemical behaviour of *trans*-dichlorobis(2-aminopyridine)palladium(II), as part of a research project on amino–halogen complexes of Pd(II).[1,2]

The crystalline form and the unexpected stoichiometric composition of the compound obtained have led us to determine its structure by X-ray diffraction.

The anion $PdCl_4^{2-}$ and an organic dication were identified. No references for this dication or similar forms have been found for what we suggest as a mechanism of formation under the working conditions.

EXPERIMENTAL

The compound of general formula $PdCl_4C_{10}N_4H_{14}$ whose structure has been proved to be that of the tetrachloropalladate of *meso*-3,7-diazonia tricyclo[4.2.2.2^{2,5}]dodeca-3,7,9,11-tetraen-4,8 diamine is obtained as a result of the slow evolving of a solution of *trans*-bis(2-aminopyridine) dichloropalladium(II) in DMF and HCl 2N (volume ratio 1:5). After several weeks light yellow needles are made visible.

X-ray data collection and refinements. Crystallographic data collection and processing parameters are given in Table 1. Intensities were measured on an Enraf–Nonius CAD-4 diffractometer with Mo-K_α radiation ($\lambda = 0.7107$ Å). Two standard reflexions were monitored at frequent intervals but showed no evidence of sample decomposition. Intensities were corrected for Lorentz and polarization, but not for absorptions.

The structure has been solved and developed by the heavy-atom method, and refined by least squares with anisotropic temperature factors assigned to all non-hydrogen atoms. The hydrogen atoms belonging to N(1) and N(2) were assumed geometrically. All other hydrogen atoms were found from difference Fourier syntheses. Each H atom was assigned the B ef. of the atom to which it was attached and included in all further calculations, but the parameters were not refined. Calculations were carried out with the X-ray system[3] and program PARST[4] on a Univac 1100/80 computer; scattering factors and anomalous dispersion corrections were from *International*

* Author to whom correspondence should be addressed.

Table 1. Summary of X-ray data collection and processing parameters

Molecular formula	$PdCl_4C_{10}N_4H_{14}$
Formula weight	438.46
Crystal class	Monoclinic
Space group	$P2_1/a$
Absences	h0l, h = 2n, 0k0, k = 2n
a (Å)	12.442(2)
b (Å)	8.810(1)
c (Å)	6.687(1)
β (°)	101.94(1)
V (Å^3)	717.2(2)
Z	2
F(000)	432
D_x (mg m^{-3})	2.03
Absorption coefficient (cm^{-1})	$\mu = 20.2$
Radiation (Mo-K_α)	$\lambda = 0.7107$ Å
Collection range	$4° \leqslant 2\theta \leqslant 60°$
No. of independent reflections	2218
No. of observed data	1717
Criteria for data inclusion	$I \geqslant 2\sigma(I)$
Total variables	1717/103
$R = \Sigma[\|F_o\|-\|F_c\|]/\Sigma\|F_o\|$	0.027
$R_\omega = [\Sigma(\omega\|F_o-F_c\|)^2/\Sigma\omega\|F_o\|^2]^{1/2}$	0.029
Weights	1

Tables for X-ray Crystallography (1974).[5] The final agreement factors were R = 0.027, R_ω = 0.029 (ω = 1) for 1717 reflections ($I \geqslant 2\sigma(I_0)$).

Atomic positional parameters, observed and calculated structure factors as well as final anisotropic thermal parameters and coordinates for the H atoms are listed in Supplementary Material, deposited with the Editor.

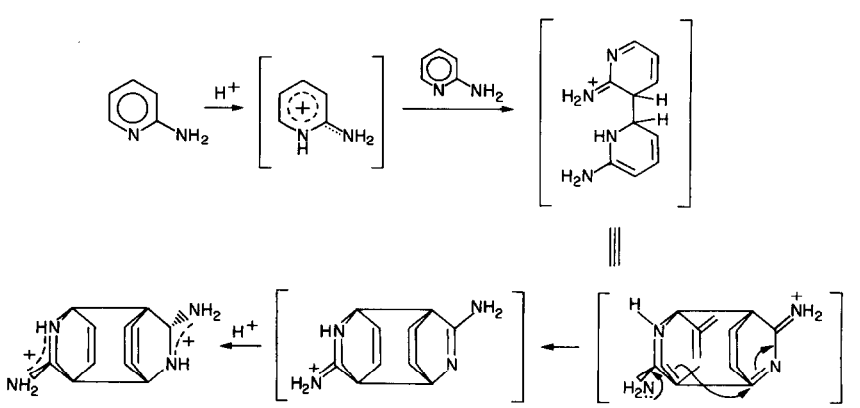
Atomic coordinates have also been deposited with the Cambridge Crystallographic Data Centre.

RESULTS AND DISCUSSION

An ORTEP drawing of the structure is shown in Fig. 1.

The complex consists of discrete $PdCl_4^{2-}$ anions and dimeric $[C_{10}N_4H_{14}]^{2+}$ cations. Relevant interatomic distances and bond angles are listed in Table 2. The structure clearly shows the presence of $PdCl_4^{2-}$ ions in the lattice without appreciable Pd... N, Pd... C interaction. The coordination around the Pd(II) ion is square planar, with almost equal Pd–Cl bonds (2.302(2)) and angles Cl $\hat{Pd}$ Cl of 90.04(6)°. These bond distances are similar to those observed in other Pd compounds.

During the process of formation of the dication cleavage of the Pd–N bond takes place so that the 2-aminoypridine molecule is released. This molecule evolves under the medium conditions according to the following scheme:



Scheme 1.

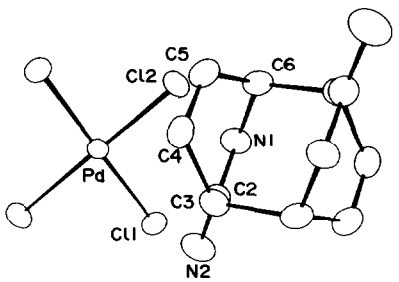


Fig. 1. An ORTEP view at the complex showing the numbering scheme used. The hydrogen atoms are omitted for clarity.

The protonated 2-aminopyridine behaves like an electrophilic agent in front of another molecule of non-protonated 2-aminopyridine forming an intermediate which evolves by a reaction of nucleophilic addition of an enamine to an imine type double bond. The dication observed in the crystal is finally generated by protonation of the resulting product of this addition. However the same dication could also be formed if the protonation took place previously to the nucleophilic addition.

Although the proposed mechanism seems chemically acceptable it demands further examination. The folding of the system which allows the spatial arrangement observed is entropically disfavoured. Probably, the palladium is involved in the process by complexing.

Table 2. Bond lengths (Å) and bond angles (°). E.s.d.s in parentheses

Pd–Cl1	2.303(2)	Cl1–Pd–Cl2	90.04(6)
Pd–Cl2	2.302(2)	C2–N1–C6	119.9(4)
N1–C2	1.310(4)	N1–C2–C3	116.7(3)
C2–C3	1.512(4)	C2–C3–C4	107.3(3)
C3–C4	1.517(5)	C3–C4–C5	117.5(3)
C4–C5	1.320(4)	C4–C5–C6	117.6(4)
C5–C6	1.509(5)	C5–C6–N1	107.5(3)
C6–N1	1.466(4)	N1–C2–N2	122.6(4)
C2–N2	1.311(4)	N2–C2–C3	120.7(3)
C6–C'3	1.610(5)	C5–C6–C3	111.8(3)
C3–C'6	1.610(5)	N1–C6–C'3	111.5(3)

The C3–C'6 and C'3–C6 bonds (1.610(5)) are long, indicating that cleavage of the dimer should occur easily. Similar long dimer C–C bond distances have been found in other compounds.[6–8]

The fact that C2–N2 and N1–C2 bond lengths are almost identical is an evidence for the existence of delocalization of positive charge between both nitrogen atoms.



The protonation of the pyridine nitrogen and not on the amino group is thus confirmed. Otherwise charge delocalization would not be possible and bond order for C2 with each nitrogen would be different.

Acknowledgements—We thank Professor Masaguer, Director del Departamento de Química Inorgánica de la Universidad Autónoma de Madrid for his help, and Professor García Ruano, del Departamento de Química Orgánica for many useful discussions.

REFERENCES

1. C. Gómez-Vaamonde, A. Alvarez-Valdés, M. C. Navarro-Ranninger and J. R. Masaguer, *Trans. Met. Chem.* 1984, **9**, 52.
2. M. C. Navarro-Ranninger, S. Martínez-Carrera and S. García-Blanco, *Acta Cryst.* 1985, **C41**, 21.
3. J. M. Stewart, *The XRAY 76 System*, Tech. Rep. TR-446. Computer Science Center, Univ. of Maryland, College Park, Maryland (1976).
4. M. Nardelli, *Computer and Chemistry* 1983, **7**, 95.
5. *International Tables for X-ray Crystallography*, Vol. IV. Kynoch Press, Birmingham (1974).
6. M. Whitefield, K. Hendrick and P. G. Owston, *Acta Cryst.* 1982, **B38**, 1248.
7. M. Ehrenberg, *Acta Cryst.* 1966, **20**, 177.
8. M. Ehrenberg, *Acta Cryst.* 1967, **22**, 482.

Polyhedron Vol. 4, No. 8, pp. 1383–1389, 1985
Printed in Great Britain

0277–5387/85 $3.00 + .00
© 1985 Pergamon Press Ltd

REDOX PROPERTIES OF NN′-X-PHENYLENEBIS(Y-SALICYLIDENEIMINATO)IRON(II) COMPLEXES AND REACTIVITY OF THE CORRESPONDING IRON(III) COMPLEXES TOWARDS CATECHOLATES

PIERO ZANELLO,* RENZO CINI and ARNALDO CINQUANTINI
Dipartimento di Chimica dell'Università di Siena, Pian dei Mantellini, 44, 53100 Siena, Italy

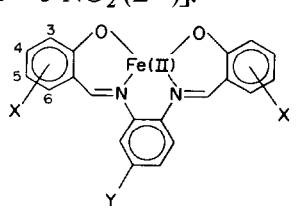
(*Received* 2 *October* 1984; *accepted* 29 *November* 1984).

Abstract—The electrochemical behaviour of a series of iron(II) complexes with the tetradentate ligand NN′-1,2-phenylenebis(salicylideneimine), [Fe(II)L], was studied in non-aqueous solvents. The redox properties of the complexes were related to the nature of the substituents in the aromatic rings. Attention was devoted to dioxygen reactivity of the complexes. The electrode activity of the catechol–[NN′-1,2-phenylenebis(salicylideneiminato) iron(III)] system, [Fe(III)L(catH)], was also studied; the results gave evidence that both the electrochemical oxidation and the chemical oxidation by dioxygen of [Fe(II)L] in the presence of catechol lead to the complex [Fe(III)L(catH)].

The electrochemistry of Schiff-base transition metal complexes is a field of research of wide interest, since redox potentials of central metal ions are often related to the functions of metal-containing molecules of biological interest[1–3] and for their importance in catalytic processes.[4]

In previous studies we investigated by electrochemical techniques the redox properties of complexes of trigonal bipyramide coordination geometry between quinquedentate ligands having N_3O_2 atom donor set and cobalt(II),[5,6] iron(II),[2,6] nickel(II),[2,6] copper(II)[2,6] and manganese(II)[6] ions.

We now report the results of the electrochemical investigation on planar complexes of iron(II) ion with the N_2O_2 tetradentate ligand NN′-1,2-phenylenebis(salicylideneimine) and its derivatives [see below: Y = H, X = H (L^1); Y = H, X = 3-OMe (L^2); Y = H, X = 4-OMe (L^3); Y = H, X = 5-OMe (L^4); Y = H, X = 5-Cl (L^5); Y = H, X = 5-NO_2 (L^6); Y = NO_2, X = H (L^7); Y = Cl, X = H (L^8); Y = OMe, X = H (L^9); Y = OMe, X = 5-OMe (L^{10}); Y = Cl, X = 5-OMe (L^{11}); Y = NO_2, X = 5-NO_2 (L^{12})].



* Author to whom correspondence should be addressed.

The first aim of the present study is to get information about electronic effects able to affect the redox potentials of the metal centre; in fact, except for manganese complexes,[7] previous electrochemical investigations on copper(II),[1,8–10,12] and cobalt(II) complexes[1,11,13] have been mainly devoted to unsubstituted NN′-1,2-phenylenebis(salicylideneiminato) derivatives.

This study is also devoted to test the ability of these complexes to act as oxygen carriers.

Finally we intend to study the interaction of these complexes with catecholates/semiquinones/benzoquinones redox systems in order to gain information on derivatives able to mimic important biological functions.[14–18]

RESULTS AND DISCUSSION

Voltammetric behaviour of [Fe(II)L] (L = L^1–L^{12}) *derivatives.* Figure 1 reports the responses in cyclic voltammetry, both at mercury and platinum microelectrodes, of [Fe(II)L^1], in dimethyl sulphoxide (DMSO) solution.

The anodic process gives rise to a well-formed anodic peak, *I*, with a cathodic one, *L*, directly associated in the reverse scan. Controlled potential coulometric tests performed at 0.0 V indicated the process to involve a one-electron charge-transfer, The analysis of the cyclic voltammetric responses with scan rates ranging from 0.02 to 50 V sec^{-1} revealed the following features:[19] the difference

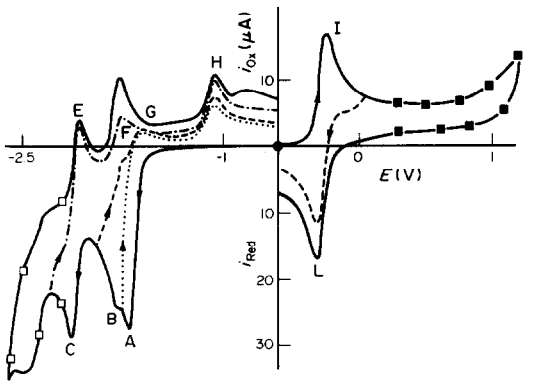


Fig. 1. Cyclic voltammetric responses recorded for a DMSO solution containing [Fe(II)L^1] (1.6×10^{-3} mol dm^{-3}) and [NEt_4][ClO_4] (0.1 mol dm^{-3}). (——) Both platinum and mercury electrode; (■■■) platinum microelectrode; (□□) mercury microelectrode. (●) Starting potential. Scan rate 0.2 V sec^{-1}.

between the peak potential value of the anodic and cathodic peaks, $E_p^a - E_p^c$, which is 61–63 mV at low scan rates (0.02–0.20 V sec^{-1}), progressively increases and reaches a value of 270 mV at 50 V sec^{-1}; the cathodic to anodic peak current ratio, $i_p^c : i_p^a$, is constantly equal to unity; the quotient of the anodic peak current and the square root of the scan rate, $i_p^a/v^{1/2}$, remains almost constant (a decrease of less than 10% was obtained in the cited scan rate range). All these findings are typical of an uncomplicated charge-transfer process characterized by a high degree of reversibility at low scan rates, which however decreases with increasing the scan rate. In the likely hypothesis that the transfer coefficient α ranges between 0.3 and 0.7, the reversible half-wave potential, $E_{1/2}^r$, which can be assumed as the formal electrode potential, $E^{o\prime}$, can be computed as the average of the potentials of the anodic peak and of its directly associated cathodic peak; in addition, the standard electron-transfer constant, k_s, can be evaluated by Nicholson's treatment,[20] if diffusion coefficients of both oxidized and reduced forms of the reactant are known. Under previous assumptions,[5] the electrochemical characteristics of the charge transfer formally attributable to the iron(II)–iron(III) couple have been computed, and they are reported in Table 1, together with the values relevant to all the studied complexes.

The cathodic behaviour of [Fe(II)L^1] is characterized in cyclic voltammetry by two successive cathodic peaks *A* and *B*. At mercury electrodes other peaks at more cathodic potentials (> -2 V), are also present, which, for comparison with the cathodic behaviour of [Na_2L^1], have to be attributed to the reduction of the deprotonated ligand. We attribute the two cathodic processes *A* and *B* to the successive one-electron reduction of the central iron(II) ion of the complex to formally iron(I) and iron(0) derivatives, respectively. In fact, controlled potential coulometric tests at -1.71 V, i.e. at the peak potential of peak *A*, indicate the consumption of one electron per molecule of [Fe(II)L^1]. The peak system *A–G* is attributable to the redox couple [Fe(II)L^1] | [Fe(II)L^1]$^-$. The $(i_p)_G : (i_p)_A$ ratio clearly

Table 1. Electrochemical characteristics for the electrode activity of [Fe(II)L] (L = L^1–L^{12}) at a mercury electrode in DMSO solution

Complex	$E^{o\prime}$ (V) Fe(III)/Fe(II)	k_s (cm sec^{-1})	$E^{o\prime}$ (V*) Fe(II)/Fe(I)	$t_{1/2}$ (sec) [Fe(I)L]$^-$	$E^{o\prime}$ (V*) Fe(I)/Fe(0)
[Fe(II)L^1]	−0.28	1.9×10^{-2}	−1.66*	1	−1.75
[Fe(II)L^2]	−0.38	3.1×10^{-3}	−1.68†	—	−1.68†
[Fe(II)L^3]	−0.32	2.6×10^{-2}	−1.76	1	−1.92
[Fe(II)L^4]	−0.32	2.5×10^{-2}	−1.62	1	−1.75
[Fe(II)L^5]	−0.19	1.8×10^{-2}	−1.60†	—	−1.60
[Fe(II)L^6]	+0.02	3.3×10^{-3}	—	—	—
[Fe(II)L^7]	−0.20	2.8×10^{-2}	—	—	—
[Fe(II)L^8]	−0.27	7.3×10^{-3}	−1.66	—	−1.71
[Fe(II)L^9]	−0.29	1.1×10^{-2}	−1.67	0.5	−1.83
[Fe(II)L^{10}]	−0.34	1.9×10^{-2}	−1.65	0.5	−1.78
[Fe(II)L^{11}]	−0.29	7.0×10^{-3}	−1.62†	—	−1.71
[Fe(II)L^{12}]	+0.06	1.4×10^{-2}	–	–	–

* The usual computation of formal electrode potentials as the average value between the peak potential of a response and that of the directly associated one can give in this case only approximate values, because the closeness of the two cathodic processes prevents a separate analysis with the scan rate in order to overcome the complications coupled to the charge transfers (see text), i.e. to reach the condition $i_p^a/i_p^c = 1$.

† Peak potential values at 0.2 V sec^{-1}.

shows that a chemical reaction follows the charge transfer; assuming an irreversible first-order reaction to be coupled to the charge transfer,[21] a half-life of about 1 sec was estimated for $[Fe(II)L^1]^-$. The further coulometric reduction at -1.95 V, in correspondence to peak *B*, consumes another mol of electrons per mol of starting compound. The peak system *B–F* is hence attributable to the redox couple $[Fe(I)L^1]^-|[Fe(0)L^1]^{2-}$. Also in this case the electrogenerated Fe(0)-complex is unstable in the macroelectrolysis time scale; its half-life is about 9 sec.

It must be pointed out that the electrogeneration of Fe(I)-complexes is not unusual.[22,23]

In acetonitrile solvent the electrochemistry of $[Fe(II)L^1]$ resulted less encouraging. In fact, the cathodic picture follows the same trend as in DMSO: two ligand-based processes at $E_p^c = -1.93$ V and -2.19 V, respectively, and two metal-based processes at $E_p^c = -0.96$ *V* and -1.68 V, respectively, were observed. On the contrary in the anodic range a response attributable to the charge transfer $[Fe(II)L^1] \overset{-e^-}{\rightarrow} [Fe(III)L^1]^+$ was detected at an $E^{\circ\prime} = -0.05$ V, but it resulted less well defined than in DMSO and followed by other electrode-poisoning anodic processes at potentials higher than $+1.3$ V.

The electrochemistry in DMSO of all other derivatives studied is qualitatively similar to that reported for $[Fe(II)L^1]$ except for nitro-compounds, because of the interference due to the cathodic reduction of the nitro-group. Table 1 summarizes the most significant features of the electrode behaviour of all studied compounds.

Electronic effects of the phenyl substituents. As expected, electron-donating groups favour the access to the Fe(III)-complex, where electron-withdrawing groups stabilize the Fe(II)-complex. As in the case of previously studied pentadentate ligands,[2,5,6] a linear correlation holds between oxidation potentials and the Hammett constants of X-type substituents only considering the 3-, 4-, 5-positions to be *ortho*, *meta*, *para* with respect to the phenolic oxygen atom, thus indicating that the electron density on the metal centre is enhanced or diminished by phenyl substituents chiefly *via* the Ph–O–Fe–O–Ph pathway. In this connection it must be noted that potential values are affected by electronic effects of Y-type substituents at an extent lower than that of X-type substituents.

The available set of data for the reduction potentials Fe(II)/Fe(I) is not sufficient for a reliable evaluation of relevant electronic effects.

The effect of dioxygen on the electrochemical behaviour of $[Fe(II)L](L = L^1–L^{12})$ *derivatives.* The oxygenation reaction of all [Fe(II)L] derivatives in

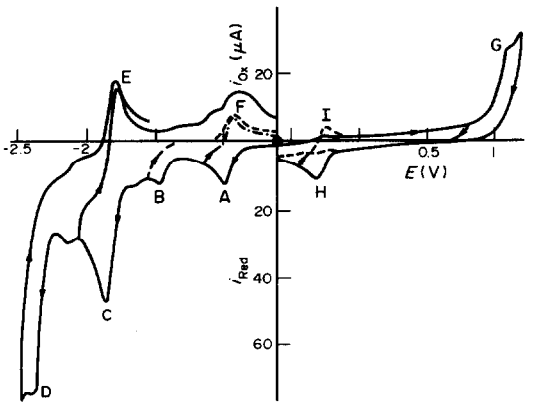


Fig. 2. Cyclic voltammograms recorded on a DMSO solution of $[Fe(II)L^1]$ (1.6×10^{-3} mol dm^{-3}) and $[NEt]_4[ClO_4]$ (0.1 mol dm^{-3}) upon oxygenation and subsequent deaeration. Cathodic scan at a mercury electrode. Anodic scan at a platinum electrode. Scan rate 0.2 V sec^{-1}.

DMSO solution was performed under the following experimental conditions: (a) bubbling of dioxygen ($p_{O_2} = 1$ atm) for 30 min in previously deaerated solution of the Fe(II)-complex; (b) subsequent bubbling of nitrogen for 30 min in order to purge from free dioxygen.

After the bubbling of dioxygen the voltammetric behaviour of $[Fe(II)L^1]$ reveals that the well-known catho–anodic system relevant to the $O_2 + e^- \rightleftarrows O_2^-$ process ($E_{1/2}^r \simeq -0.76$ V) gives an $i_p^a | i_p^c$ ratio equal to 0.86 at 0.2 V sec^{-1}, indicating that the electrogenerated superoxide ion is involved at a low extent in a reaction with species present in solution.

The voltammetric picture of the oxygenation product, after deaeration, is illustrated in Fig. 2.

Since it is ascertained that upon oxygenation $[Fe(II)L^1]$ is irreversibly oxidized to the μ-oxo dimer $[Fe(III)L^1]_2O$,[15,17,24] we try to explain the voltammogram in Fig. 2 on this basis. As it can be seen the response is complicated by the presence of a lot of peaks, however, a comparison with that of $[Fe(II)L^1]$ reported in Fig. 1, allows some interesting conclusions. The peak system *A–F* is likely attributable to the electrode process

$$[Fe(III)L^1\text{–O–}Fe(III)L^1] \underset{-e^-}{\overset{+e^-}{\rightleftarrows}} [Fe(II)L^1\text{–O–}Fe(III)L^1]^-.$$

Tests at different scan rates show that the charge transfer is complicated by following chemical reactions; however, the use of scan rates of the order of 10 V sec^{-1} allows to prevent the chemical complication ($i_p^a/i_p^c = 1$) and to compute a formal electrode potential of -0.97 V for the quasi-reversible charge transfer. The assignment of peak *B*

Table 2. Potential values for both the reduction of one Fe(III) center and the oxidation of the μ-oxo group in $[Fe(III)L]_2O$ ($L = L^1$–L^{12}), together with the lifetime of electrogenerated superoxide ion in the presence of oxygenation products

Compound subjected to dioxygenation reaction	$E^{\circ\prime}$ (V) $[Fe(III)L]_2O/[Fe(II)L–O–Fe(III)L]^-$	Oxo-group oxidation E_p (V)	$t_{1/2}$ (sec)† $[O_2]^-$
$[Fe(II)L^1]$	−0.97	+1.10	8
$[Fe(II)L^2]$	−0.92	+0.97	13
$[Fe(II)L^3]$	−1.01	+1.05	23
$[Fe(II)L^4]$	−1.05	+0.86	12
$[Fe(II)L^5]$	−0.85	+1.10	10
$[Fe(II)L^6]$	−0.63	>1.15	4
$[Fe(II)L^7]$	−0.77	>1.15	11
$[Fe(II)L^8]$	−0.91	+1.13	—
$[Fe(II)L^9]$	−0.98	+1.07	2
$[Fe(II)L^{10}]$	−1.05	+0.86	3
$[Fe(II)L^{11}]$	−0.98	+0.94	2
$[Fe(II)L^{12}]$	—	—	4

* Peak potential values at 0.2 V sec^{-1}.

† Lifetimes computed assuming a pseudo-first order chemical reaction with respect to superoxide ions to be involved in the consumption of the electrogenerated superoxide ions.

presents some difficulty because it can be attributed both to the subsequent Fe(II)/Fe(I) charge transfer and to the reduction of the second Fe(III) centre in the mixed-valence compound primarily electrogenerated. As regards the anodic scan, it is well evident the occurrence of an anodic process, irreversible in character, followed by a chemical reaction leading to the oxidized form of the precursor; we attribute peak *G* to the oxidation of the oxo group which causes the breakage of the μ-oxo dimer with formation of $[Fe(III)L^1]^+$, responsible for the peak system *H–I*.

It must also be pointed out that both the existence of some cathodic current at the starting potential (−0.6 V) and the cited presence of some species able to react with electrogenerated superoxide ions testify for the formation of an oxygenation by-product (very likely $[Fe(III)L^1]^+$ which can react with O_2^- to give the superoxo species $[Fe(III)L^1(O_2)^-]$).

A qualitatively similar voltammetric trend was also observed for the oxygenation of Fe(II)–Schiff base pentadentate complexes.[2,6]

The voltammetric picture illustrated for the oxygenation of $[Fe(II)L^1]$ is common to all other derivatives under investigation; Table 2 summarizes the relevant parameters, significant because rarely found.

As expected, the charge transfer $[Fe(II)L]_2O/[Fe(II)L–O–Fe(III)L]^-$ is favoured by the presence of electron-withdrawing groups and disfavoured by the presence of electron-donating groups in the aromatic portions of the ligand.

The electrochemical behaviour of the catechol/$[Fe(II)L^1]$ *system.* The first approach to the study of the catechol/$[Fe(II)L^1]$ system and its oxidation product was accomplished by a voltammetric investigation on the iron complex with monodentate catecholate coordination, $[Fe(III)L^1(catH)]$, which has been proposed as a model for the dioxygenases.[15,16]

Figure 3(a) illustrates the cyclic voltammetric response of $[Fe(II)L^1(catH)]$ in deaerated DMSO solution. For comparison, the responses relevant to both catechol and Na[catH] are also reported in Figs. 3(b) and 3(c), respectively. The peak system *A–D* is just coincident with the one of the redox couple $[Fe(III)L^1]^+/[Fe(II)L^1]$; the peak systems *E–G* and *F* are to be attributed to the oxidation of Hcat group to semiquinone and quinone, respectively, according to electrode mechanisms reported by Sawyer.[25] It must be remarked the anodic potential shift of peak *E* ($\Delta E_p = 0.38$ V) in respect to the one-electron oxidation of free $[Hcat]^-$, due to the complexation of Hcat with the iron substrate. The processes occurring at peaks *C* have been previously described in the reduction of $[Fe(II)L^1]$. About peak *B* it must be pointed out that the successive addition of increasing amount of $[Hcat]^-$ to the solution of $[Fe(III)L^1(catH)]$ causes the peak system *A–D* to decrease up to its disappearance and the peak *B* to increase up to a maximum ($E_p = -1.24$ V). On the contrary the addition of catechol to $[Fe(III)L^1(catH)]$ does not cause changes in the starting voltammetric response, except

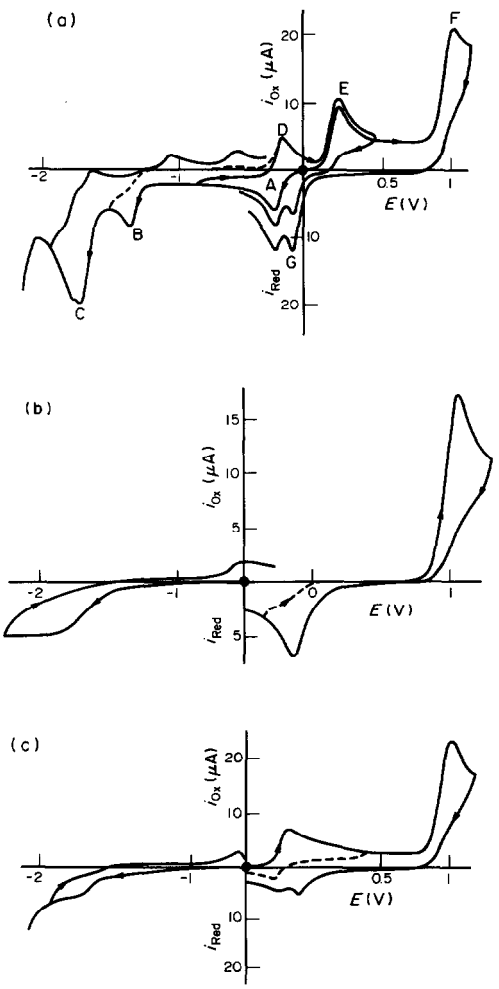


Fig. 3. Cyclic voltammetric responses of deaerated DMSO solutions containing $[NEt_4][ClO_4]$ (0.1 mol dm^{-3}) and: (a) $[Fe(III)L^1(catH)]$ (1.32×10^{-3} mol dm^{-3}); (b) catechol (1.11×10^{-3} mol dm^{-3}); (c) $[Hcat]^-$ (1.45×10^{-3} mol dm^{-3}). Platinum working microelectrode. Scan rate 0.2 V sec^{-1}.

for peak *F*. This behaviour suggests peak *B* must be attributed to the cathodic reduction $[Fe(III)L^1(catH)]/[Fe(II)L^1(catH)]^-$. The ligand exchange reaction in the presence of an excess of $[Hcat]^-$ to form $[Fe(III)(cat)_3]^{3-}$ has to be disregarded, as this anion reduces at a potential of -2.2 V (Hg electrode). In addition these data suggest that in DMSO solution the following equilibria hold:

$$[Fe(III)L^1(catH)] \rightleftarrows [Fe(III)L^1][catH]$$
$$\rightleftarrows [Fe(III)L^1]^+ + [catH]^-.$$

This equilibria could constitute a further reason, together with the hydrolytic formation of the μ-oxo dimer, for the differences noted between the properties of $[Fe(III)L^1(catH]$ in the solid state and in dichloromethane solution,[16] even if the relatively high polarity of DMSO can strengthen this dissociating process at an extent higher than in CH_2Cl_2.

Electrochemically induced reactivity of $[Fe(II)L^1]$ *towards catecholate.* A preliminary examination of the effect of addition of either catechol or $[Hcat]^-$ to a deaerated solution of $[Fe(II)L^1]$ indicated that complexation of the catecholate occurred upon electrode oxidation, the reactivity of electrogenerated $[Fe(III)L^1]^+$ towards $[Hcat]^-$ being much more effective than towards catechol. Figure 4 illustrates the most significant complexation steps of $[Fe(II)L^1]$ by $[Hcat]^-$.

As it can be seen the addition of $[Hcat]^-$ causes the appearance of both the peak system *D–E*, attributable to the one-electron oxidation of coordinated Hcat to the semiquinone form cited above, and peak *C* ($E_p = -0.59$ V), which more and more takes the place of the peak system *A–B* of the redox couple $[Fe(II)L^1]/[Fe(III)L^1]^+$. It must be further observed [see Fig. 4(d)] that in the reverse scan after traversing the anodic processes, peak *F* arises just at the potential of peak *B* of Fig. 3, which has been attributed to the couple $[Fe(III)L^1(catH)]/[Fe(II)L^1(catH)]^-$. The anodic peak *C* is hence attributable to the process:

$$[Fe(II)L^1] + [Hcat]^-(\text{excess}) \rightarrow$$
$$[Fe(III)L^1catH] + e^-.$$

In agreement with this hypothesis, controlled potential coulometric tests at -0.3 V (Pt macroelectrode) on DMSO solution containing the system $[Fe(II)L^1]$–$[Hcat]^-$ in a ratio of about 1:4.5 give a black–green solution displaying the already described voltammetric response of $[Fe(III)L^1(catH)]$ in the presence of excess of $[Hcat]^-$, and showing an IR spectrum superimposable to that of a DMSO solution of $[Fe(II)L^1(catH)]$ prepared according to Ref. 15.

Reactivity of the $[Fe(II)L^1]$*–catecholate system towards dioxygen.* The voltammetric investigation on DMSO solutions of catechol or catecholate monoanion as function of the addition of dioxygen showed that catechol does not undergo oxidation processes, while the catecholate monoanion is oxidized to quinone.

By bubbling dioxygen ($p_{O_2} = 1$ atm) in deaerated DMSO solutions containing $[Fe(II)L^1]$ and catechol (in a 1:2.5 ratio) a black–green solution forms, able to give cyclic voltammetric responses similar to those reported in Figure 3(a). This accounts for the formation of $[Fe(III)L^1(catH)]$, and demonstrates that the usual irreversible oxidation of the Fe(II)-complex by dioxygen to the μ-oxo dimer is prevented by the presence of catechol.

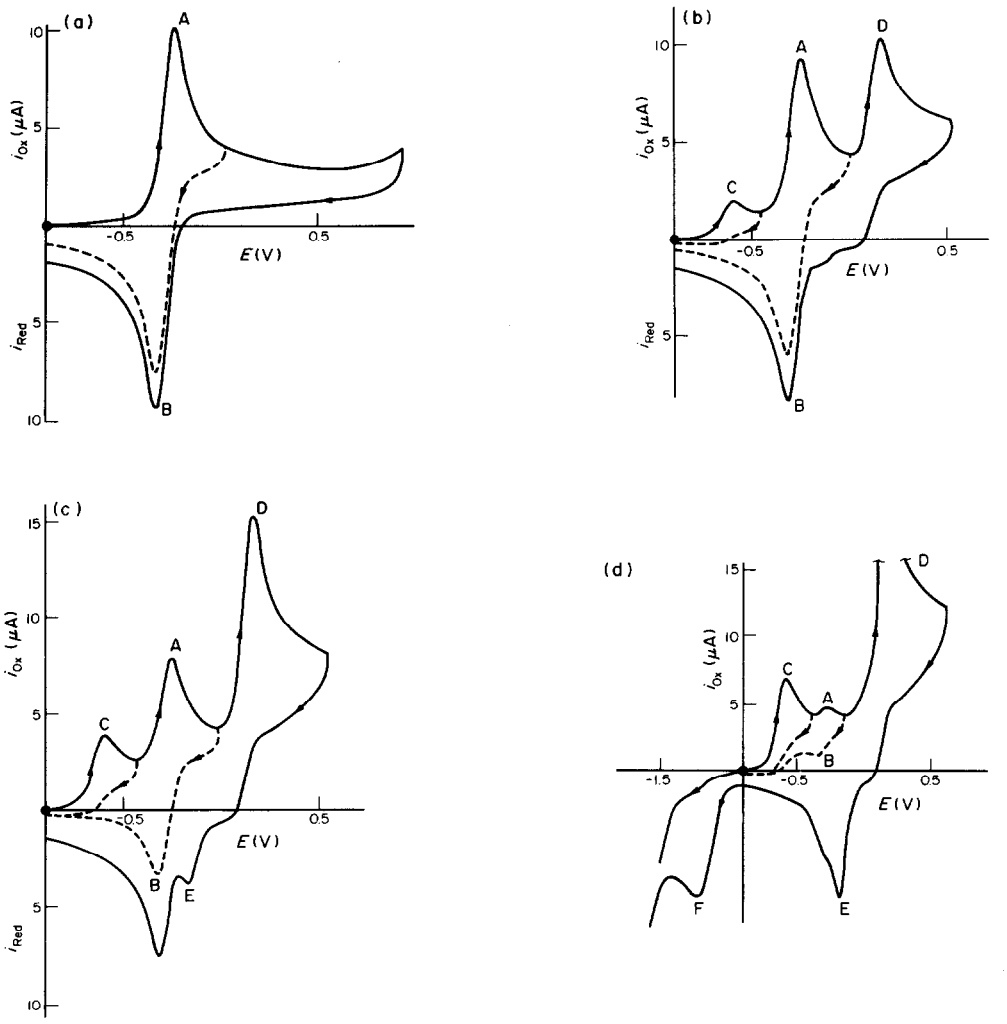


Fig. 4. Cyclic voltammetric responses of a deaerated DMSO solution containing $[NEt_4][ClO_4]$ (0.1 mol dm^{-3}) and $[Fe(II)L^1]$ (1.61×10^{-3} mol dm^{-3}) as a function of the addition of catecholate monoanion. (a) Before the addition of $[Hcat]^-$; (b) after the first addition ($[Hcat]^- = 1.74 \times 10^{-3}$ mol dm^{-3}); (c) after the second addition ($[Hcat]^- = 3.18 \times 10^{-3}$ mol dm^{-3}); (d) after the third addition ($[Hcat]^-$ 6.5×10^{-3} mol dm^{-3}). Platinum working microelectrode. Scan rate 0.2 V sec^{-1}.

In addition we thought this reaction could be an alternative route to the synthesis of $[Fe(III)L^1(catH)]$ if performed in acetonitrile solution. In this connection a deaerated acetonitrile solution of catechol and $[Fe(II)L^1]$ (in a ratio of about 3:1) leads to crystalline $[Fe(III)L^1(catH)]$ when dioxygen is bubbled through it.

These results suggest that, under the present experimental conditions, the oxidizing power of dioxygen stops at the level of iron(II) centre oxidation. A confirmation of this comes from the fact that the bubbling of air in a deaerated DMSO solution of $[Fe(III)L^1(catH)]$, followed by deaeration, does not cause changes with respect to the starting voltammetric picture, i.e. no chemical oxidation occurs. This is in marked contrast to the dioxygen reactivity of [NN′-ethylenebis (salicylideneiminato)] (3,5-di-*tert*-butylcatecholato) iron(III).[26]. Hence, at least for $[Fe(III)L^1(catH)]$ as dioxygenases model,[15,16,26] the enzyme mechanism, which attributes to iron the role of binding and activation of dioxygen after substrate reduction of the ferric centre to the ferrous oxidation state,[27] could be preferred over the one which assumes the coordination of the catechol to the ferric centre to activate the catechol to attack by oxygen, with the formation of semi-quinone and superoxide.[26,28]

EXPERIMENTAL

Materials. *o*-Phenylenediamine, *o*-hydroxobenzaldehyde (salicylaldehyde) and their derivatives, as

well as catechol, were reagent grade products and were used without further purifications.

Ferrous acetate was prepared as previously described.[2]

Dimethyl sulphoxide and acetonitrile solvents (Burdick and Jackson, distilled in glass, UV grade) were used as received.

Tetraethylammonium perchlorate ($[NEt_4][ClO_4]$) supporting electrolyte (Carlo Erba) was dried in a vacuum oven and used without further purification.

Deaeration or oxygenation of solutions, when necessary, were performed by using ultrapure dinitrogen or dioxygen.

Synthesis of the complexes. [Fe(II)L] (L = L^1–L^{12}) derivatives were prepared according to the method described in Ref. 17 for [Fe(II)L^1], and identified by IR spectroscopy and elemental analyses.

[Fe(III)L^1(catH)] was prepared either according to Ref. 15, or by the following method (see text): a deaerated acetonitrile solution containing [Fe(II)L^1] and catechol (in a molar ratio of about 1:3) was refluxed for 1 hour under a dioxygen atmosphere (p_{O_2} = 1 atm). The black solid was filtered and washed three times with acetonitrile. The product was characterized by IR spectroscopy and microanalysis. The yield was about 40%.

$[Fe(cat)_3]^{3-}$ was prepared according to Ref. 29.

$[H_2L^1]$ was synthesized by condensation of salicylaldehyde and *o*-phenylenediamine in dry methanol. $[Na_2L^1]$ was obtained by neutralizing a methanol solution of $[H_2L^1]$ with a methanol solution of sodium methoxide, and identified by its IR spectrum.[30]

$[Hcat]^-$ was prepared by mixing equimolar amounts of catechol and sodium methoxide in deaerated methanol solution.

Apparatus. The electrochemical apparatus used has been previously described.[5] All potential values refer to an aqueous saturated calomel electrode (SCE). The temperature was controlled at 20 ± 0.1°C.

The IR absorption spectra, both in solution and in the solid state, were recorded on a Model 782 Perkin–Elmer grating spectrophotometer.

Acknowledgement—Financial support from the Italian C.N.R. is gratefully acknowledged.

REFERENCES

1. D. F. Rohrbach, W. R. Heineman and E. Deutsch, *Inorg. Chem.* 1979, **18**, 2536, and references therein.
2. P. Zanello, R. Cini and A. Cinquantini, *Inorg. Chim. Acta* 1983, **74**, 89, and references therein.
3. P. Zanello, P. A. Vigato, U. Casellato, S. Tamburini and G. A. Mazzocchin, *Transition Met. Chem.* 1983, **8**, 294, and references therein.
4. J. E. Lyons, *Fundamental Research in Homogeneous Catalysis.* Plenum Press, New York (1977).
5. P. Zanello, R. Cini, A. Cinquantini and P. L. Orioli, *J. Chem. Soc., Dalton Trans.* 1983, 2159.
6. R. Cini, P. Zanello, A. Cinquantini, A. Colligiani, C. Pinzino and G. Valentini, *Inorg. Chim. Acta* 1984, **88**, 105.
7. R. K. Bogess, J. W. Hughes, W. M. Coleman and L. T. Taylor, *Inorg. Chim. Acta* 1980, **38**, 183.
8. M. Calvin and R. H. Bailes, *J. Am. Chem. Soc.* 1946, **68**, 949.
9. G. S. Patterson and R. H. Holm, *Bioinorg. Chem.* 1975, **4**, 257.
10. R. R. Gagne, J. L. Allison and D. M. Ingle, *Inorg. Chem.* 1979, **18**, 2767.
11. A. V. Benedetti, E. R. Dockal, H. L. Chum and T. Rabockai, *J. Electroanal. Chem. Interfacial Electrochem.* 1982, **142**, 191.
12. H. Doine, F. F. Stephens and R. D. Cannon, *Inorg. Chim. Acta*, 1983, **75**, 155.
13. G. Costa, A. Puxeddu and E. Reisenhofer, *J. Chem. Soc., Dalton Trans.* 1972, 1519, and references therein.
14. P. Cassoux and A. Gleizes, *Inorg. Chem.* 1980, **19**, 665.
15. R. H. Heistand, A. L. Roe and L. Que, *Inorg. Chem.* 1982, **21**, 676.
16. R. H. Heistand, R. B. Lauffer, E. Fikrig and L. Que, *J. Am. Chem. Soc.* 1982, **104**, 2789.
17. J.-P. M. Tuchagues and D. N. Hendrickson, *Inorg. Chem.* 1983, **22**, 2545.
18. S. D. Pell, R. B. Salmonsen, A. Abelleira and M. J. Clarke, *Inorg. Chem.* 1984, **23**, 385.
19. E. R. Brown and R. F. Large, *Physical Methods of Chemistry, Part IIA, Electrochemical Methods* (Edited by A. Weissberger and B. W. Rossiter), Vol. 1, p. 423. Wiley–Interscience, New York (1971).
20. R. S. Nicholson, *Anal. Chem.* 1965, **37**, 1351.
21. R. S. Nicholson and I. Shain, *Anal. Chem.* 1964, **36**, 706.
22. L. F. Warren, *Inorg. Chem.* 1977, **16**, 2814.
23. L. A. Bottomley and K. M. Kadish, *Inorg. Chem.* 1981, **20**, 1348.
24. R. H. Niswander and A. E. Martell, *Inorg. Chem.* 1978, **17**, 2341.
25. M. D. Stallings, M. M. Morrison and D. T. Sawyer, *Inorg. Chem.* 1981, **20**, 2655.
26. R. B. Lauffer, R. H. Heistand and L. Que, *J. Am. Chem. Soc.* 1981, **103**, 3947.
27. M. Nozaki, *Molecular Mechanisms of Oxygen Activation* (Edited by O. Hayaishi), Chapter 4. Academic Press, New York (1974).
28. L. Que, J. D. Lipscomb, E. Munck and J. M. Wood, *Biochim. Biophys. Acta* 1977, **485**, 60.
29. K. N. Raymond, S. S. Isied, L. D. Brown, F. R. Fronczek and J. H. Nibert, *J. Am. Chem. Soc.* 1976, **98**, 1767.
30. C. S. Marvel, S. A. Aspey and E. A. Dudley, *J. Am. Chem. Soc.* 1956, **78**, 4905.

Polyhedron Vol. 4, No. 8, pp. 1391–1401, 1985
Printed in Great Britain

0277–5387/85 $3.00 + .00
© 1985 Pergamon Press Ltd

PREPARATION OF NIOBIUM AND TANTALUM ORGANO-IMIDO COMPLEXES FROM REACTIONS OF THE PENTAHALIDES WITH AMINES: THE CRYSTAL AND MOLECULAR STRUCTURE OF BIS(*t*-BUTYLAMINE)BIS(*t*-BUTYLIMIDO)BIS(*μ*-ETHOXY)TETRACHLORODITANTALUM

PAUL A. BATES, ALASTAIR J. NIELSON* and JOYCE M. WATERS†
Department of Chemistry, University of Auckland, Private Bag, Auckland, New Zealand

(*Received* 29 *October* 1984; *accepted* 29 *November* 1984)

Abstract—MCl_5 (M = Nb, Ta) reacts with 2 equivalents of $Me_3SiNHCMe_3$ to give $[M(NCMe_3)Cl_3(NH_2CMe_3)]$ from which $[M(NCMe_3)Cl_3(PMe_3)_2]$ is obtained on addition of PMe_3. One equivalent of $Me_3SiNHCMe_3$ reacts with MCl_5 in the presence of 3 equivalents of PMe_3 to give $[M(NCMe_3)Cl_3(PMe_3)_2]$ and PMe_3HCl. MCl_5 reacts with excess RNH_2 (R = CMe_3, $CHMe_2$, CH_2Me) to give $[M(NR)(NHR)Cl_2(NH_2R)]$ and 3 equivalents of RNH_3Cl. One equivalent of alcohol replaces the amido ligand in $[M(NCMe_3)(NHCMe_3)Cl_2(NH_2CMe_3)]$ to give $[M(NCMe_3)(OR)Cl_2(NH_2CMe_3)]_2$ (M = Nb, R = $OCMe_3$; M = Ta, R = OEt). The structure of $[Ta(NCMe_3)(\mu\text{-}OEt)Cl_2(NH_2CMe_3)]_2$ was determined by single-crystal X-ray diffraction methods. Crystals are triclinic, space group $P\bar{1}$ with $a = 9.900(5)$, $b = 10.161(17)$, $c = 9.017(6)$ Å and $\alpha = 103.91(8)$, $\beta = 97.77(4)$, $\gamma = 64.40(7)°$. The structure was solved by Patterson and Fourier methods and refined to an R value of 0.062 for 1319 observed data. The Ta–N_{imido} and Ta–N_{amino} bond lengths are 1.70(2) Å and 2.28(2) Å, respectively; the bridging Ta–O bond lengths are 2.01(2) Å and 2.32(2) Å, the longer one lying *trans* to the imido function.

Organo-imido complexes of the heavier group V transition metals (Nb, Ta) are generally less well known than those of group VI and VII.[1] Early methods of preparation included thermolysis of dialkylamido complexes[2] and reaction of the pentachlorides with lithium dialkylamides[3] or lithium dialkylamide–monoalkylamide mixtures.[4] More recently the imido function has been generated by reaction of low valent complexes with PhN=NPh[5] or Me_3SiN_3[6] and by elimination of methane from species containing both alkyl and monoalkylamido groups.[7] To date, the most convenient method has been the reaction of *neo*pentylidene complexes with imines.[6,8]

With the aim of obtaining both niobium and tantalum organo-imides by simpler and more direct methods, we believed that by analogy with high-valent metal–alkyl–alkylidene chemistry,[9] proton abstraction from one of two coordinated mono-alkylamido ligands [eqn (1)] or base promoted deprotonation of a single monoalkylamido ligand [eqn (2)] might lead to the required imido linkage. These reactions are likely in view of the greater acidity of an NH proton in comparison with a CH proton.

$$M(NHR)_2Cl_3 \rightarrow M(NR)Cl_3 + RNH_2 \quad (1)$$

$$M(NHR)Cl_4 + \text{base} \rightarrow M(NR)Cl_3 + \text{base, HCl.} \quad (2)$$

These ideas were further encouraged by a recent report that bridging imido complexes

$$(M{-}\overset{\overset{R}{|}}{N}{-}M)$$

could be prepared by thermolysis or addition of primary amine to $CpTiCl_2(NHR)$ complexes.[10] Monoalkylamido complexes are relatively rare but are known for titanium,[10,11] molybdenum,[12] tungsten[13] and rhenium (phenylamido complexes).[14] For group V, $[Ta(NHR)_2Cl_2(NH_2R)]$ (R = Me, Et, "propyl, "butyl)[15] and $Nb(NHR)_3Cl_2$

* Author to whom correspondence should be addressed.
† Present address: Department of Chemistry, Massey University, Palmerston North, New Zealand.

($R = Me$)[16] have been claimed on the basis of analytical data.

We report here some reactions of niobium and tantalum pentachlorides with $Me_3SiNHCMe_3$ and primary amines. A brief report of this work has appeared.[17]

RESULTS AND DISCUSSION

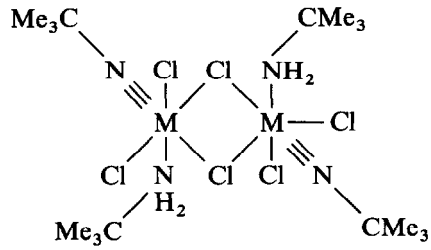
Addition of slightly more than two equivalents of $Me_3SiNHCMe_3$ to $NbCl_5$ in benzene solution leads to dissolution of the niobium halide and development of an orange red colouration after approximately 2 h. After a further 6 h the solution pales to a light yellow–brown and a yellow precipitate is deposited. This air-sensitive product analyses as $Nb(NHCMe_3)_2Cl_3$ but was shown to be the imido complex $[Nb(NCMe_3)Cl_3(NH_2CMe_3)]$ on the basis of spectroscopic data. Sharp NH absorbances in the IR spectrum at 3243 and 3175 cm^{-1} as well as NH resonances in the ^1H NMR spectrum at 3.90 and 7.01 ppm are similar to those found for $[W(NPh)(NCMe_3)Cl_2(NH_2CMe_3)]_2$ for which an X-ray structure determination has shown terminal *t*-butylimido and amine ligands.[18] By ^{13}C NMR spectral comparisons with other complexes we have prepared (see Table 2), the position of the *t*-butyl group quarternary carbon resonance is conveniently found to distinguish between imido, amido and amine ligands (see Table 2). For $[Nb(NCMe_3)Cl_3(NH_2CMe_3)]$ there are imido resonances at 71.6 and 70.4 ppm as well as two amine resonances at 54.8 and 53.7 ppm, suggesting two forms of the complex in solution. In addition there are three *t*-butyl group methyl resonances in both ^{13}C and ^1H NMR spectra, the NH protons in the latter being of unequal intensity.

The reaction of $TaCl_5$ and $Me_3SiNHCMe_3$ also gave a product which analysed as $[Ta(NCMe_3)Cl_3(NH_2CMe_3)]$ and had similar IR, ^1H and ^{13}C NMR spectra to the niobium analogue. Insolubility has precluded molecular weight determinations but the complexes are most likely chloro-bridged dimers with lone pair donation from a ligand lying *trans* to the imido function as found in the X-ray structure determination of $[Ta(NCMe_3)Cl_3(PEt_3)(THF)]$.[19] For the $[M(NCMe_3)Cl_3(NH_2CMe_3)]$ complexes, two forms [(a) and (b)] are then possible depending on the nature of the *trans* ligand. We have been unable to separate the two cleanly by recrystallization but the product obtained from reacting $NbCl_5$ with one equivalent of $Me_3SiNHCMe_3$ shows only the ^{13}C NMR spectral features of one isomer.

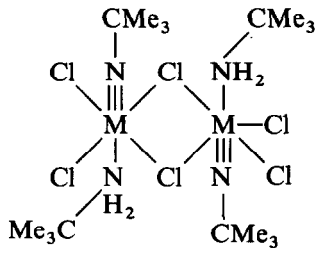
The $[M(NCMe_3)Cl_3(NH_2CMe_3)]$ complexes reacted with PMe_3 to give yellow gums which failed to crystallise but, after extensive washing and pumping down, flaky solids were obtained which gave analytical data that were close to the formulation $[M(NCMe_3)Cl_3(PMe_3)_2]$ (for example, see $[Nb(NCMe_3)Cl_3(PMe_3)_2]$ in Table 1). The ^1H NMR spectra contained PMe_3 and ^{t}butyl methyl resonances (2:1 ratio) as did the ^{13}C NMR spectrum which additionally showed the quaternary carbon of a *t*-butylimido group. For example $[Nb(NCMe_3)Cl_3(PMe_3)_2]$ shows a quaternary carbon at 70.3 ppm, a single resonance for the *t*-butyl methyl group at 30.0 ppm, and PMe_3 doublets at 15.5 and 14.3 ppm. The spectrum is essentially the same as that of $[Ta(NCMe_3)Cl_3(PMe_3)_2]$ prepared from $[Ta(NCMe_3)Cl_3(THF)_2]$ where one PMe_3 was assigned *trans* to the imido function.[6,8] The ^1H NMR of $[Nb(NCMe_3)Cl_3(PMe_3)_2]$ shows a doublet for the PMe_3 groups indicating a *cis* orientation.

We have found that a variety of $M(NCMe_3)Cl_3L_2$ complexes can be prepared from the $[M(NCMe_3)Cl_3(NH_2CMe_3)]$ species but they generally persist as gummy materials which fail to crystallise and are best characterised by NMR spectroscopy. For example the ^{13}C NMR spectrum of $Nb(NCMe_3)Cl_3 \cdot$ bipyridyl contains *t*-butylimido resonances at 76.3 and 30.0 ppm. The proton spectrum shows α,α-dipyridyl and a *t*-butyl group in the required ratio as well as a downfield shift of the bipyridyl α-protons, compared with the free ligand.

In attempting an alternative preparation of $[Nb(NCMe_3)Cl_3(PMe_3)_2]$ by deprotonation of a single coordinated monoalkylamido ligand, 3 equivalents of PMe_3 were added to $NbCl_5$



(a)



(b)

Table 1. Analytical data[a,b]

	C	H	N	Cl
$Nb(NCMe_3)Cl_3(NH_2CMe_3)\cdot(C_6H_6)_{0.33}$	33.2	6.5	8.1	29.8
	(32.5)	(6.0)	(7.6)	(29.8)
$Ta(NCMe_3)Cl_3(NH_2CMe_3)\cdot(C_6H_6)_{0.17}$	24.1	5.0	6.3	24.1
	(24.3)	(4.8)	(6.3)	(23.9)
$[Nb(NCMe_3)Cl_3(PMe_3)_2]$	29.3	6.8	4.2	24.1
	(28.4)	(6.4)	(3.3)	(25.3)
$[Nb(NCMe_3)(NHCMe_3)Cl_2(NH_2CMe_3)]$	37.3	7.7	10.8	18.5
	(37.9)	(8.0)	(11.1)	(18.7)
$[Ta(NCMe_3)(NHCMe_3)Cl_2(NH_2CMe_3)]$	32.7	7.4	8.8	14.9
	(30.8)	(6.5)	(9.0)	(15.1)
$Ta(NCHMe_2)(NHCHMe_2)Cl_2(NH_2CHMe_2)\cdot(C_6H_6)_{0.22}$	28.2	6.5	10.0	16.0
	(28.0)	(5.8)	(9.5)	(16.0)
$Ta(NEt)(NHEt)Cl_2(NH_2Et)\cdot(C_6H_6)_{0.17}$	21.3	5.6	10.6	17.6
	(21.2)	(4.9)	(10.6)	(17.9)
$[Nb(NCMe_3)(OCMe_3)Cl_2(NH_2CMe_3)]$	37.6	7.4	7.0	18.4
	(37.8)	(7.7)	(7.4)	(18.6)
$[Ta(NCMe_3)(\mu\text{-}OEt)Cl_2(NH_2CMe_3)]_2$	27.4	5.8	5.7	15.4
	(27.2)	(5.7)	(6.3)	(16.1)

[a] Formulations with added benzene are supported by ^1H NMR spectra.
[b] Calculated figures in parentheses.

in benzene followed by one equivalent of $Me_3SiNHCMe_3$, whereupon the solution turned dark red, lightening to yellow after several hours and depositing PMe_3HCl. Unsatisfactory analytical data were again obtained for the yellow flaky material isolated but it was formulated as $[Nb(NCMe_3)Cl_3(PMe_3)_2]$ on the basis of the 2:1 ratio of PMe_3 and *t*-butyl methyl groups in the ^1H NMR spectrum; IR and ^{13}C NMR spectra were similar to those of $[Nb(NCMe_3)Cl_3(PMe_3)_2]$ formed from $[Nb(NCMe_3)Cl_3(NH_2CMe_3)]$. $TaCl_5$, PMe_3 and $Me_3SiNHCMe_3$ also reacted to give a yellow flaky solid which was somewhat contaminated but the ^1H NMR spectrum clearly showed a 2:1 ratio of PMe_3 and *t*-butyl methyl resonances while the IR and ^{13}C NMR spectra were similar to those of $[Ta(NCMe_3)Cl_3(PMe_3)_2]$ prepared from either

$$[Ta(NCMe_3)Cl_3(NH_2CMe_3)]$$

or

$$[Ta(NCMe_3)Cl_3(THF)_2].^{6,8}$$

The reactions described so far demonstrate that the *t*-butylimido function may be generated from the pentahalides and $Me_3SiNHCMe_3$. Monoalkylamido species are the most likely intermediates involved during the initial darkening of solution colour, so that the possibility arises during the formation of the $[M(NCMe_3)Cl_3(NH_2CMe_3)]$ complexes that a steric effect may be responsible for deprotonation of one of two *cis* coordinated monoalkylamido ligands.* However our ongoing investigations have shown that $[Ta(NEt)Cl_3(NH_2Et)]$ is the result of using $Me_3SiNHEt$. For base promoted deprotonation of a single monoalkylamido species it is apparent that a strong base such as PMe_3 is required to direct the reaction course since reacting $NbCl_5$ with NEt_3 and $Me_3SiNHCMe_3$ does not appear to produce NEt_3HCl while ^1H and ^{13}C NMR spectra suggest the presence of $[Nb(NCMe_3)Cl_3(NH_2CMe_3)(NEt_3)]$ and $NbCl_5(NEt)_x$.

Niobium and tantalum pentachlorides also react with excess *t*-butylamine in benzene to produce colourless to slightly yellow solutions and 3 equivalents of insoluble *t*-butylamine hydrochloride based on the amount of pentahalide used. Crystalline complexes analysing as $M(NHCMe_3)_3Cl_2$ were obtained from these solutions but the alternative formulation

$$[M(NCMe_3)(NHCMe_3)Cl_2(NH_2CMe_3)]$$

* *cis* oriented alkylamido ligands are not without precedent. Crystal structure determinations have shown that dialkylamido ligands are orientated *cis* in $Ta(NMe_2)_3Cl_3(NHMe_2)$, $[Ta(NMe_2)Cl_2(NHMe_2)]_2O$ and $[Ta(NMe_2)_3Cl_2]_2$.[20] Ligands with a high *trans* influence always prefer a mutual *cis* configuration irrespective of their π-acceptor or donor properties.[20,21]

Table 2. NMR data

Complex	^{13}C NMR: α-Carbon (N–C) Imido	Amido	Amino	^{13}C NMR: Others	^{1}H NMR
$[Nb(NCMe_3)Cl_3(NH_2CMe_3)]$	71.6 70.4	—	54.8 53.7	30.7, 29.7, 28.1 (CMe_3)	1.17s, 1.23s, 1.3s (CMe_3) 3.45b, 6.47b (NH)
$[Ta(NCMe_3)Cl_3(NH_2CMe_3)]$	67.5 (broad)	—	54.7 53.8	31.8, 30.6, 28.0 (CMe_3)	1.42s, 1.48s, 1.55s (CMe_3) 4.0b, 6.9b (NH)
$[Nb(NCMe_3)Cl_3(PMe_3)_2]$	70.3	—	—	30.0 (CMe_3) 15.5 and 14.3, d ($^1J_{P-C}$ = 18.0 Hz,[a] *cis* PMe_3)	1.42s (CMe_3) 1.55d ($^2J_{P-H}$ = 9.2 Hz, *cis* PMe_3)
$[Ta(NCMe_3)Cl_3(PMe_3)_2]$	65.6	—	—	32.2 (CMe_3) 16.8 and 15.2, d ($^1J_{P-C}$ = 24.1 Hz,[a] *cis* PMe_3) 14.5 & 13.4, d ($^1J_{P-C}$ = 16.5 Hz,[a] *cis* PMe_3)	1.40s (CMe_3) 1.56b (PMe_3)
$[Nb(NCMe_3)(NHCMe_3)Cl_2(NH_2CMe_3)]$	69.5	59.4	52.3	32.4, 30.8, 30.6 (CMe_3)	1.30s, 1.35s (CMe_3) 4.0b, 8.5b (NH)
$[Ta(NCMe_3)(NHCMe_3)Cl_2(NH_2CMe_3)]$	66.6 66.5	57.6	53.2 52.8		2.32s, 2.35s, 2.38 (CMe_3) 3.70b (NH_2), 8.5 b (NH)
$[Ta(N^i prop)(NH^i prop)Cl_2(NH^i_2 prop)]$	66.0	59.8	49.2	27.6, 26.3, 24.6 ($-CMe_2$)	1.05d, 1.15d, 1.24d, 1.30d, J = 7 Hz (CMe_2) 3.45b, 7.37b, 7.56b (NH_3) 3.5 (obscured), 4.2–5.0 (CH)
$[Ta(NEt)(NHEt)Cl_2(NH_2Et)]$	52.9	53.7	42.6	20.7, 19.0, 17.4 (Me_s)	1.0–1.6m (CH_3) 3.2m, 4.3q (CH_2) 3.41b, 7.68b (NH)
$[Nb(NCMe_3)(NHCMe_3)Cl_2(PMe_3)_2]$	66.8	58.2	—	34.1, 32.1 (CMe_3) 15.9t ($^1J_{P-C}$ = 11.5 Hz,[a] *trans* PMe_3)	1.35s (CMe_3) 1.50t ($^2J_{P-H}$ = 4 Hz, *trans* PMe_3) 10.91b (NH)
$[Ta(NCMe_3)(NHCMe_3)Cl_2(PMe_3)_2]$	64.7	56.6	—	34.9, 33.7 (CMe_3) 16.0t ($^1J_{P-C}$ = 11.5 Hz,[a] *trans* PMe_3)	1.35s (CMe_3) 1.50t ($^2J_{P-H}$ = 4 Hz, *trans* PMe_3) 10.91b (NH)
$[Nb(NCMe_3)(\mu\text{-}OCMe_3)Cl_2(NH_2CMe_3)]_2$	69.6	—	52.3	85.2 (OC) 31.0, 30.6 (CMe_3)	1.36, 1.39, 1.50 (CMe_3) 3.84, 4.67 (NH_2)

[a] Values taken from noise decoupled spectra.

is consistent with spectral data. Thus the niobium complex exhibited 3 *t*-butylmethyl resonances of equal intensity in the ^{1}H NMR spectra as well as NH proton resonances at 4.0 and 8.5 ppm in an approximate 2:1 ratio. The ^{13}C NMR spectrum contained quaternary carbons of *t*-butylimido and amino ligands as found for

$[Nb(NCMe_3)Cl_3(NH_2CMe_3)]$

but also an additional resonance (59.4 ppm) attributable to a *t*-butylamido ligand. The ^{13}C NMR spectrum of

$[Ta(NCMe_3)(NHCMe_3)Cl_2(NH_2CMe_3)]$

showed the presence of two species in solution which appear to persist in the same ratio after successive recrystallisations. So far variable temperature studies have been inconclusive but we believe that dissociation of a chloro-bridged dimer gives rise to these features.

The complexes react with two equivalents of PMe_3 to form $[M(NCMe_3)(NHCMe_3)Cl_2(PMe_3)_2]$ species again obtained as non-crystalline flaky solids which were characterised by NMR spectroscopy. Thus the ^{1}H NMR of the niobium analogue exhibited PMe_3 and *t*-butyl group methyl resonances in a ratio of 2:1 and a single broadened NH proton at 10.9 ppm. The ^{13}C NMR spectrum

contained *t*-butyl quaternary carbon resonances characteristic of imido and amido ligands whereas the *t*-butylamino quaternary carbon observed for the parent complex was absent.

The amido proton in these species apparently resists abstraction as we have been unable to obtain diimido species by reaction with excess PMe_3. The

$$[M(NCMe_3)(NHCMe_3)Cl_2(NH_2CMe_3)]$$

complexes may also be prepared by adding two equivalents of Me_3CNH_2 to the

$$[M(NCMe_3)Cl_3(NH_2CMe_3)]$$

complexes but no further reaction occurs when excess of the amine is present. The compound

$$[Nb(NCMe_3)(NHCMe_3)Cl_2(NH_2CMe_3)]$$

does, however, react with two equivalents of $LiNHCMe_3$ but convincing analytical data for the petroleum ether soluble material have not yet been obtained. Chlorine is absent from the product and the ^{13}C NMR spectrum shows two *t*-butylimido quaternary carbons so that a diimido species may be present.

We were also interested in determining the role of steric factors in the formation of the $[M(NCMe_3)(NHCMe_3)Cl_2(NH_2CMe_3)]$ complexes. Reactions of $TaCl_5$ with the less sterically demanding amines Me_2CHNH_2 and $EtNH_2$ again led to deposition of 3 amine hydrochloride equivalents and colourless complexes analysing as $[Ta(NR)(NHR)Cl_2(NH_2R)]$ were obtained from solution. The formulation is again supported by NMR spectra, particularly the appearance of α-carbon resonances attributable to an amino ligand in the ^{13}C NMR spectrum of each complex. The imido and amido α-carbons have approximately the same shift downfield and we are further investigating this facet of their chemistry at present.

An X-ray structure determination of $[Ta(NCMe_3)(NHCMe_3)Cl_2(NH_2CMe_3)]$ reported earlier,[17] showed the molecule to be a chloro-bridged dimer containing *t*-butylimido, amido and amino ligands orientated about each tantalum. Several points emerged from this structure and these are presented more fully here. The short Ta–N bond distance [1.86(3) Å] and large Ta–N–C bond angle [160(2)°] observed for the amido ligand are of particular interest. An 18 electron count for the complex requires $Ta–N_{amido}$ π-bonding and this is reflected by the comparatively short $Ta–N_{amido}$ bond distance and lengthening of the *trans* Ta–Cl(2) bond to 2.66(1) Å. This latter distance is similar to the Ta–Cl(1) bond length [2.69(1) Å] *trans* to the imido function where the essentially linear $Ta–N–C_{imido}$ bond angle indicates significant π-bonding. However, the $Ta–N_{amido}$ π-bonding situation may well be further complicated since a calculation of the amido proton position places it approximately 2.2 Å from the metal centre.*

In alkylidene complexes of tantalum, short Ta–C bond distances and large $Ta–C_\alpha–C_\beta$ bond angles are important in identifying metal . . . H–C interactions.[23] A neutron study of $[Ta(CHCMe_3)Cl_3(PMe_3)_2]_2$[24] has shown the above bond length and angle to be 1.898(2) Å and 161(1)°, respectively, values which are similar to the present tantalum–amido ligand data. With a Ta–C–H bond angle of 84.8° the alkylidene proton was located only 2.12 Å from the metal suggesting a 2-electron-3 centre bond or "protonated" triple bond.[24]

Distorted alkylidene ligands in tantalum complexes are simply identified from $^1J_{C-H\alpha}$ values[23] but the only easily obtainable NMR data for the amido ligand is the NH proton shift. Table 3 contains structural data for known monoalkylamido complexes as well as ^1H NMR NH proton shifts. A relationship between M–N–C bond angles or M–N bond lengths with the NH proton shift is not apparent but within the limits of structure refinement, the largest bond angle and shortest bond length are shown by the Ta–amido complex where the NH proton resonates upfield compared with the low valent molybdenum amido complex.[12] The proton is observed even further upfield in

$$[W(NCMe_3)_2(NHCMe_3)_2]$$

and

$$[WO(NEt)(NHEt)Cl]$$

for which structural data are not available. Clearly precise structural information is now needed to determine the extent of the Ta . . . H–N interaction as well as possible Cl . . . H–N interactions especially as both may be important in proton abstraction processes.

The reactivity of the metal–monoalkylamido bond in the

$$[M(NCMe_3)(NHCMe_3)Cl_2(NH_2CMe_3)]$$

complexes was also investigated. The complexes do not react with excess Me_3SiCl to produce the

$$[M(NCMe_3)(NH_2CMe_3)Cl_3]$$

species but the amido group may be replaced by an

* For $(adamantyl–NH)_2Mo(OSiMe_3)_4$ a modified extended Hückel calculation predicted a Mo–N–H bond angle of 77°.[22] If the Ta–N–H bond angle of the present complex is allowed to range from 77 to 91°, the calculated Ta . . . H approach has the limiting values of 1.96 and 2.20 Å.

Table 3. Structural and ^{1}H NMR data for amido complexes [M(NHR)]

	M–N–C (°)	M–N (Å)	Calc. M . . . H (Å)	δNH	Ref.
$[Ta(NCMe_3)(NHCMe_3)Cl_2(NH_2CMe_3)]$	161(2)	1.86	2.20	8.0	17
$Mo(NHadamantyl)_2(OSiMe_3)_4$	150.8	2.057	2.50 (2.097)[a]	—	22
$Mo[HB(3,5\text{-}Me_2C_3HN_2)_3](NO)I(NHEt)$	146.9(18)	1.954(23)	2.46	12.80	12
$Re(NHPh)N_2(PMe_3)_4$	141(1)	2.200(14)	2.76	2.3	14
$Re(NHPh)(\eta^4\text{-}C_4H_6)(PMe_3)_3$	140(3)	2.13(14)	2.71	2.74	14
$[W_2(NHPh)_2(\mu\text{-pinacol})(pinacol)_4]$	134(2)	2.02	2.69	—	32
$[W(NCMe_3)_2(NHCMe_3)_2]$	—	—	—	5.0	13b
[WO(NEt)(NHEt)Cl]	—	—	—	5.4	13a

[a] Value for Mo–N–H angle of 77°.

alkoxide. One equivalent of *t*-butanol reacted with the niobium complex to give a crystalline material analysing as

$$[Nb(NCMe_3)(OCMe_3)Cl_2(NH_2CMe_3)],$$

the imido and amine ligands being confirmed by *t*-butyl group quaternary carbons at 69.6 and 52.3 ppm in the ^{13}C NMR spectrum. The ^{1}H NMR spectrum shows two amino protons at 3.8 and 4.7 ppm but no amido NH proton.

Addition of one equivalent of EtOH to $[Ta(NCMe_3)(NHCMe_3)Cl_2(NH_2CMe_3)]$ initially gave a gummy material which NMR spectral analysis indicated to be a mixture. However, crystals were obtained from the sample, one of which was examined by X-ray crystallography. The molecule was found to be an ethoxy-bridged dimer with the two halves centrosymmetrically related (see Fig. 1). Each tantalum atom adopts a distorted octahedral coordination geometry with the bridging ethoxides lying *trans* to both *t*-butylimido and chloro ligands. The remaining chloro group lies *trans* to a *t*-butylamino ligand. Selected bond lengths and angles are given in Table 4.

The Ta–N bond distance of 1.70(2) Å and Ta–N–C(1) bond angle of 171(2)° indicate a linear *t*-butylimido ligand involving multiple bonding between tantalum and nitrogen. The bond length is

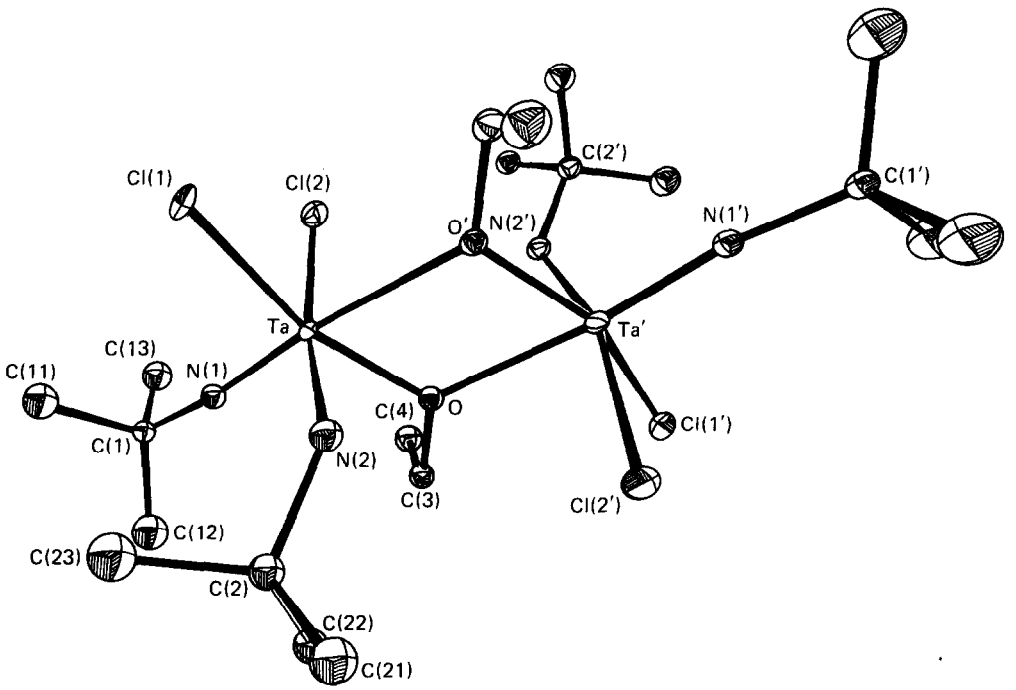


Fig. 1. The molecular structure of $[Ta(NCMe_3)(\mu\text{-}OEt)Cl_2(NH_2CMe_3)]_2$. Hydrogen atoms have been omitted for clarity. Thermal ellipsoids have been drawn at the 15% probability level.

Table 4. Selected bond lengths and angles for $[Ta(NCMe_3)(\mu\text{-}OEt)Cl_2(NH_2CMe_3)]_2$

(a) Bond lengths (Å)			
Ta–Cl(1)	2.421(6)	Ta–O′	2.32(2)
Ta–Cl(2)	2.407(7)	Ta–N(1)	1.70(2)
Ta–O	2.01(2)	Ta–N(2)	2.28(2)
Ta . . . Ta	3.58		
(b) Bond angles (°)			
Ta–N(1)–C(1)	167(2)	Cl(2)–Ta–N(1)	95.3(7)
Ta–N(2)–C(2)	130(2)	O′–Ta–N(1)	171.1(8)
N(2)–Ta–N(1)	101.7(8)	Cl(2)–Ta–N(2)	161.5(5)
O–Ta–N(1)	102.7(8)	O–Ta–O′	68.5(6)
Cl(1)–Ta–N(1)	98.6(7)	Ta–O–Ta′	111.5(7)
N(2)–Ta–Cl(1)	81.6(6)		
N(2)–Ta–O	88.4(7)		
N(2)–Ta–O′	80.4(7)		

in accord with that predicted for a Ta–N triple bond (4-electron donor)[1] and lies within the range of values found for other organo-imido complexes of tantalum.[1,17,19,20,25] The Ta–N(2) bond distance of 2.28(2) Å is indicative of σ lone pair donation to the metal whereas the two terminal Ta–Cl bond distances [2.421(6) and 2.407(7) Å] are not significantly different from others reported,[19,20,25] the shorter distance occurs *trans* to the amino N.

A significant *trans* lengthening (*ca* 0.31 Å) occurs for the Ta–O bond *trans* to the imido function and this results in the asymmetric bridge linking the two tantalum atoms, a feature which also prevails in other tungsten phenylimido alkoxide complexes.[26] The shorter Ta–O bond distance [2.01(2) Å] is not significantly different from the sum of the covalent radii (2.08 Å) so that a normal Ta–O single bond is present. This absence of Ta–O π-interactions is noted in other bridging alkoxide complexes.[27] The molecule $[Ta(NCMe_3)(\mu\text{-}OEt)Cl_2(NH_2CMe_3)]_2$ is thus a 16 electron species as are

$$[Ta(NPh)Cl_3(PEt_3)(THF)]^{19}$$

and

$$[TaCl_3(THF)_2]_2(=NC(Me)=C(Me)N=).^{28}$$

They are in contrast to

$$[Ta(NCMe_3)(NHCMe_3)Cl_2(NH_2CMe_3)]$$

where the possibility of π-bonding from the amido nitrogen allows an 18-electron count.

The distorted octahedral geometry about each metal centre is shown by the relatively large distance (0.37 Å) the tantalum atoms lie above the plane perpendicular to the Ta–N(1) vector. Similar deviations are observed in other organo-imido and the related nitrido complexes as a result of the short M–N bond distance.[29] It may be contrasted with the distance (0.05 Å) of the Ta from the plane containing N(1), Cl(1), O and O′. Calculation of the proton positions of the amino group indicates a weak interaction [H . . . Cl(2), 2.27 Å] across the dimer to an adjacent chloride. (This hydrogen bond is as strong as that observed in

$$[W(NPh)(NCMe_3)Cl_2(NH_2CMe_3)]_2.^{18}$$

There is also an even weaker interaction (2.6 Å) between a *cis* chloro group (H . . . Cl(1)) and the second amino proton. The combined effect apparently causes the *t*-butyl group to face the *t*-butylimido ligand which would otherwise not be a favoured orientation.

In conclusion we summarise the similarities of some of the chemistry presented here to features found in metal–carbon multiple and single bonded d^0 transition metal complexes. In particular, the deprotonation of NH groups has analogies to that of α-CH groups of bulky alkyl ligands.[9] Three types of metal–nitrogen bonding occur about the same metal centre in the

$$[M(NCMe_3)(NHCMe)Cl_2(NH_2CMe_3)]$$

complexes which may be compared with the three types of metal–carbon bonding in

$$[W(CCMe_3)(CHCMe_3)(CH_2CMe_3)(dppm)].^{30}$$

The close approach of an amido NH proton to the metal centre in the amido complex is similar to that observed in alkyl[31] and alkylidene[23] chemistry where metal–proton interactions are now a well established feature.

EXPERIMENTAL

Microanalyses were performed by Dr. A. C. Campbell and associates, University of Otago, New Zealand.

Spectrometers—IR: Perkin–Elmer 597; spectra in Nujol mulls between CsI plates. NMR: Varian T60 (^{1}H, 60 MHz), JEOL FX60 (^{13}C, 15.04 MHz).

All operations were performed under oxygen-free nitrogen and solvents were dried over sodium and distilled from sodium wire or sodium/benzophenone except for chlorinated hydrocarbons which were dried and distilled over CaH_2. Amines were dried and distilled over CaH_2. Silylamines and PMe_3 were prepared by literature methods.[33,34] Niobium and tantalum pentachlorides (Riedel de-Haën) were sublimed prior to use. Melting points were determined in sealed tubes under nitrogen and are uncorrected. Analytical data are collected in Table 1.

t-*Butylamine*-t-*butylimidotrichloroniobium*

Trimethylsilyl-*t*-butylamine (1.9 cm^3, 9.8 mmol) in benzene (40 cm^3) was added to a suspension of $NbCl_5$ (1.3 g, 4.8 mmol) in benzene (50 cm^3). After 2 h the solution was an orange–red colour and after a further 12 h the colour was yellow–brown and a yellow precipitate was deposited. The volume was reduced to *ca* 20 cm^3 and the solid filtered followed by washing with cold benzene (2 × 5 cm^3) to give the complex as yellow microcrystals. Yield: 1.2 g (67%). M.p. 237–240°C.

IR 3243m; 3175m; 2560w; 1560m; 1395m; 1355m; 1280m; 1210s; 1160s; 1140m; 1104m; 1022w; 923w; 890m; 842w; 801w; 740w; 720w; 678m; 646m; 584w; 542m; 530m; 444w; 418m; 370s; 350s; 322s; 302s; 280s cm^{-1}.

Further complex is obtained by removal of solvent from the filtrate but the product is less pure.

Addition of trimethylsilyl-*t*-butylamine (1.2 cm^3, 6.3 mmol) in benzene (30 cm^3) to $NbCl_5$ (1.6 g, 5.9 mmol) suspended in benzene (40 cm^3) gave a yellow precipitate, containing only one species by ^{13}C NMR [δ, CD_3CN, 71.8, 55.5 (CMe); 29.5, 27.5 (CMe_3) ppm].

t-*Butylamine*-t-*butylimidotrichlorotantalum*

Trimethylsilyl-*t*-butylamine (1.6 cm^3, 8.3 mmol) in benzene (30 cm^3) and $TaCl_5$ (1.4 g, 3.9 mmol) suspended benzene (50 cm^3) were reacted as before to give at first a yellow orange solution which paled to light yellow brown. The solution was filtered, the solvent reduced to *ca* 20 cm^3 and the white solid filtered off and washed with cold benzene as before. Yield: 1.45 g (83%). M.p. 258–262°C.

IR 3240m; 3180m; 2700m; 2580w; 2480w; 2050w; 1600m; 1560m; 1400m; 1360s; 1290s; 1258s; 1210s; 1170s; 1140w; 1020w; 880s; 805s; 735s; 670s; 655s; 558m; 535m; 522m; 522w; 422m; 417w; 345s; 340s; 314s; 260s cm^{-1}.

t - *Butylimidotrichlorobis(trimethylphosphine)niobium*

(a) Trimethylphosphine (0.92 cm^3, 8.4 mmol) in benzene (30 cm^3) was added to a suspension of $NbCl_5$ (0.75 g, 2.7 mmol) in benzene (50 cm^3). To the red solution obtained was added trimethylsilyl-*t*-butylamine (0.57 cm^3, 2.9 mmol) in benzene (20 cm^3) and the mixture was stirred for 12 h. The solution was filtered from the precipitate of PMe_3HCl and the solvent removed to give a yellow–orange gum which was washed several times with petroleum ether (20 cm^3 aliquots) and finally with diethyl ether (20 cm^3). After holding the product *in vacuo* for several hours the complex was obtained as a yellow, flaky solid. Yield: 1.0 g (85%). Found: Cl, 25.8. $C_{10}H_{27}NP_2Cl_3Nb$ requires Cl, 25.3%.

(b) Trimethylphosphine (0.7 cm^3, 6.4 mmol) in petroleum ether (30 cm^3) was added slowly to a rapidly stirring suspension of *t*-butylamine-*t*-butylimidotrichloroniobium (1.0 g, 2.9 mmol) in petroleum ether (30 cm^3) and the solution stirred for 18 h. The resulting yellow solution was filtered from a small amount of white solid material and the solvent removed to give a gum which after extensive washing with cold petroleum ether and pumping on the residue gave the impure complex as a yellow, flaky solid (see analytical data in Table 1). Yield: 0.9 g (73%).

IR (KEL-F) 2950s; 2890s; 1410m; 1400m; 1375w; 1358m. (Nujol) 1410m; 1400m; 1355m; 1300w; 1280m; 1245s; 1215m; 1145m; 1124m; 960s; 844w; 800w; 730s; 720s; 645w; 320s; 300s cm^{-1}.

t - *Butylimidotrichlorobis(trimethylphosphine)tantalum*

(a) Trimethylsilyl-*t*-butylamine (0.7 cm^3, 3.6 mmol) in benzene (25 cm^3) was added to $TaCl_5$ (1.3 g, 3.6 mmol) and trimethylphosphine (1.3 cm^3, 11.8 mmol) in benzene (50 cm^3) and the mixture stirred for 18 h. The solution was filtered and the solvent removed to give a gum which was washed extensively with petroleum ether (20 cm^3) and finally diethylether. After a prolonged pumping a flaky, off-white solid was obtained. Yield: 1.4 g (78%). Borderline analytical data were obtained. Found: C, 24.7; H, 5.6; N, 2.1. $C_{10}H_{27}Cl_3NP_2Ta$ requires C, 23.5; H, 5.3; N, 2.7%.

(b) Trimethylphosphine (0.7 cm^3, 6.4 mmol) in petroleum ether (30 cm^3) was added slowly to a rapidly stirring suspension of *t*-butylamine-*t*-butylimidotrichlorotantalum (1.0 g, 2.9 mmol) in petroleum ether (30 cm^3) and the solution stirred for 16 h. The reaction was worked up as the niobium reaction to give the complex as a white solid. Yield: 0.9 g (73%).

IR 1410m; 1400m; 1355m; 1300w; 1280m; 1245s; 1215m; 1145m; 1124m; 960s; 844w; 800w; 730s; 720s; 645w; 320s; 310s; 300s cm^{-1}.

Bis(t - *butylamido*)*bis*(t - *butylamine*)*bis*(t - *butylimido*)*tetrachlorodiniobium*

t-Butylamine (3.7 cm^3, 35.3 mmol) in benzene (25 cm^3) was added to a rapidly stirring suspension of $NbCl_5$ (1.2 g, 4.4 mmol) in benzene (50 cm^3) and the mixture stirred for 6 h. The solution was filtered from the precipitated *t*-butylamine hydrochloride (1.5 g, 3 equivalents based on $NbCl_5$) and the solvent removed to *ca* 10 cm^3 to give the complex as light yellow crystalline solid. Yield: 1.3 g (76%). M.p.: decomposes above 220°C.

IR 3295w; 3230w; 3178m; 3108w; 2705w; 2595w; 2500w; 2070w; 1610w; 1568m; 1510w; 1403m; 1360s; 1340w; 1300w; 1280m; 1240s; 1210s; 1165m; 1132m; 1027m; 977m; 925m; 895m; 805w; 785m; 730m; 674m; 645m; 610w; 553m; 535w; 450w; 424w; 370w; 348w; 308s; 285m cm^{-1}.

The complex was also prepared by adding *t*-butylamine (0.85 cm^3, 8.1 mmol) in benzene (25 cm^3) to a suspension of *t*-butylamine-*t*-butylimidotrichloroniobium (0.7 g, 2.0 mmol) in benzene (30 cm^3) and working up as above.

Bis(t-*butylamido*)*bis*(t-*butylamine*)*bis*(t-*butylimido*)-*tetrachloroditantalum*

t-Butylamine (6 cm^3, 57 mmol) in benzene (30 cm^3) was reacted with $TaCl_5$ (2.0 g, 5.6 mmol) in benzene (60 cm^3) for 12 h to give *t*-butylamine hydrochloride (1.8 g, 3 equivalents based on $TaCl_5$) and a colourless solution which gave the complex as colourless crystals. Yield: 2.1 g (78%). M.p. decomposes above 270°C.

IR 3300w; 3250w; 3200m; 2710m; 2600m; 2500m; 2225w; 2075w; 1610m; 1580m; 1555m; 1512m; 1400m; 1360m; 1302m; 1280m; 1255s; 1215s; 1164m; 1140m; 1025w; 984w; 930m; 910m; 900m; 740s; 650w; 600w; 558w; 540w; 455m; 426w; 350m; 295w; 260w cm^{-1}.

The complex was also prepared by adding *t*-butylamine (1.2 cm^3, 11.4 mmol) in benzene (25 cm^3) to a suspension of *t*-butylamine-*t*-butylimidotrichlorotantalum (1.1 g, 2.6 mmol) in benzene (30 cm^3) and working up as above.

Crystallinity of both tantalum and niobium complexes is lost when the solid is not in contact with solution.

Bis(i - *propylamido*)*bis*(i - *propylamine*)*bis*(i - *propylimido*)*tetrachloroditantalum*

i-Propylamine (2.0 cm^3, 23 mmol) in benzene (30 cm^3) was reacted with $TaCl_5$ (1.1 g, 3.1 mmol) in benzene (50 cm^3) to give *i*-propylamine hydrochloride (0.9 g, 3 equivalents based on $TaCl_5$) and the complex. Yield: 0.9 g, (64%) after crystallisation. M.p.: decomposition above 220°C.

IR 3300w; 2340m; 3150w; 3125w; 2725w; 1560m; 1550m; 1355m; 1320w; 1280s; 1238s; 1170m; 1122m; 1090s; 1068w; 995w; 948w; 850w; 818w; 725w; 680m; 650w; 620w; 540w; 470w; 415w; 390w; 260w cm^{-1}.

Bis (*ethylamido*) *bis* (*ethylamine*) *bis* (*ethylimido*) *tetrachloroditantalum*

Ethylamine (2.5 cm^3, 38.3 mmol) in benzene (30 cm^3) was reacted with $TaCl_5$ (1.75 g, 4.9 mmol) in benzene (60 cm^3) to give ethylamine hydrochloride and the complex as a white solid. Yield: 1.2 g (63%) after crystallisation. M.p.: decomposes above 180°C.

IR 3200m; 2740m; 2500w; 2340; 2050w; 1578m; 1360m; 1324w; 1292m; 1215m; 1196m; 1110m; 1050s; 960w; 910w; 880w; 790m; 720m; 660m; 615m; 415w; 390w; 260m cm^{-1}.

t - *Butylamido* - t - *butylimidodichlorobis*(*trimethylphosphine*)*niobium*

Trimethylphosphine (0.7 cm^3, 6.4 mmol) in benzene (30 cm^3) was added to bis(*t*-butylamido)bis(*t* - butylamine)bis(*t* - butylimido)tetrachloroditantalum (1.0 g, 2.6 mmol) in benzene (50 cm^3) and the mixture stirred for 4 h. After filtering the solution, the solvent was removed *in vacuo* to give a flaky solid. Yield: 1.1 g, (92%). Borderline analytical data were obtained (e.g. Found: N, 5.3; Cl, 16.4. $C_{14}H_{37}N_2P_2Cl_2Nb$ requires N, 6.1; Cl, 15.5%) but the complex was characterised by ^1H and ^{13}C NMR spectroscopy (see Table 2). Product melts at 96–100°C.

IR (KEL-F) 3200m; 3150m; 2925s; 2880s; 2850s; 1560w; 1442m; 1400s; 1345s. (Nujol) 3250m; 3200m; 2900w; 2700w; 1560w; 1560w; 1405s; 1442s; 1300m; 1285s; 1240s; 1210s; 1180s; 1130s; 1030w; 960s; 858m; 805s; 790s; 740s; 680s; 610m; 580m; 570m; 550m; 445w; 380w; 300s; 260s cm^{-1}.

t - *Butylamido* - t - *butylimidodichlorobis(trimethylphosphine)tantalum*

Trimethylphospine (0.4 cm^3, 3.6 mmol) in benzene (30 cm^3) was added to bis(*t*-butylamido)bis(*t*-butylamine)*bis(t-butylimido)tetrachloroditantalum* (0.5 g, 0.5 mmol) in benzene (30 cm^3) and the mixture stirred for 5 h. The solution was worked up as for the niobium analogue to give the complex as colourless crystals. *Yield: 0.5 g (86%). M.p. 142–145°C.* Boron-free analytical data were obtained. Found: C, 27.8; H, 6.5; N, 5.2. $C_{14}H_{36}Cl_2N_2P_2Ta$ requires C, 30.8; H, 6.6; N, 5.1%.

IR 3250w; 2700w; 2600w; 2500w; 2075w; 1610w; 1515w; 1418m; 1358m; 1305m; 1284m; 1260s; 1218m; 1208m; 1180w; 960s; 850w; 808w; 786w; 742m; 720w; 660w; 610w; 576w; 558w; 540w; 550w; 350w; 265m cm^{-1}.

t-Butylamine - t - butylimido - t - butoxydichloroniobium

t-Butanol (0.3 g, 4.1 mmol) in benzene (30 cm^3) was added to bis(*t*-butylamido)bis(*t*-butylamine)bis(*t*-butylimido)tetrachlorodiniobium (*1.35 g, 3.6 mmol*) in benzene (40 cm^3) and the mixture stirred for 12 h. The resulting solution was filtered from a small amount of precipitate and the solvent removed giving a white crystalline solid. Recrystallisation from toluene at −5°C gave the complex as large, light yellow crystals. 0.4 g (30%). M.p.: decomposes above 235°C.

IR 3300w; 3190m; 3100w; 2700w; 2600w; 2500w; 2050w; 1610m; 1570s; 1510m; 1502s; 1360s; 1340w; 1300w; 1280m; 1240s; 1220s; 1180vs; 1125m; 1020s; 980vs; 930w; 900m; 804w; 790m; 740m; 674m; 650m; 560m; 485w; 450w; 420w; 370m; 348m; 310s cm^{-1}.

Bis(t - *butylamine*)*bis*(t - *butylimido*)*bis*(*μ-ethoxy*)*tetrachloroditantalum*

Ethanol (0.068 cm^3, 11.8 mmol) in benzene (25 cm^3) was added slowly to bis(*t*-butylamido) bis(*t*-butylamine) bis (*t*-butylimido)tetrachloroditantalum (0.55 g, 11.8 mmol) and the mixture was stirred for 5 h. The solution was filtered from a small amount of solid and the solvent removed to give a gum which partly solidified on pumping. The crude product had the following physical data.

IR 3250w; 3160w; 2700w; 2590w; 2500w; 2050w; 1610m; 1560w; 1510m; 1400m; 1358m; 1300m; 1264s; 1215m; 1290m; 1250m; 1210m; 1075m; 1020m; 925m; 875s; 840m; 802m; 740m; 720s; 670m; 550m; 520m; 445m; 420w; 345m; 320w; 280m cm^{-1}.

^{1}H NMR (δ, $CDCl_3$) 1.19s, CMe_3; 1.30s CMe_3; 1.0–1.5 several poorly defined methyl resonances of OCH_3CH_3; 4.2–4.8 broad multiplet OCH_2 and NH_2.

^{13}C NMR (δ, $CDCl_3$) 72.6, 71.4, OCH_2; 66.6, imido CMe_3; 53.5, 51.8, amino CMe_3; 32.1, 31.9, 31.0, 30.9, imido and amino Me_3; 19.4, 18.2 alkoxide Me.

Recrystallisation of the complex from toluene at −20°C gave a small quantity of colourless crystals, one of which was used for an *X*-ray crystallographic study.

Crystallographic study

Crystal data.

$[Ta(NCMe_3)(\mu\text{-}OEt)Cl_2(NH_2CMe_3)]_2$,

$C_{20}H_{50}Cl_4N_4O_2Ta_2$,

M = 888.36, triclinic, *a* = 9.900(5), *b* = 10.161(17), *c* = 9.017(6) Å, α = 103.91(8), β = 97.77(4), γ = 64.40(7)°, *U* = 794 $Å^3$, space group $P\bar{1}$, *Z* = 1, D_c = 1.859 g cm^{-3}, *F*(000) = 428, μ(Mo-K_α) = 76.3 cm^{-1}.

Data collection. CAD4 diffractometer, Mo-K_α radiation (λ = 0.71073 Å), $\omega/2\theta$ scan mode. Crystal (approx. dimensions 0.28 × 0.22 × 0.10 mm), sealed under N_2 in a glass capillary tube, 2357 data measured (θ_{max} = 23°). The intensities of three standard reflections were monitored during the data collection (1 h intervals) but any variation was less than 3%. Empirical absorption corrections were applied,[35] minimum and maximum transmission factors being 0.891 and 0.998, respectively.

Structural solution and refinement. The structure was solved by Patterson and Fourier methods and refined by a full matrix least-squares technique.[36] The final refinement cycle converged to a value of 0.062 for both *R* and R_w, for the 101 variables and 1319 data for which $F^2 > 3\sigma(F^2)$. The function minimized was $\sum w(|F_o|-|F_c|)^2$ with the weight, *w*, being defined as $0.1756/[\sigma^2(F)+0.005600F^2]$. In the final refinement cycle all hydrogen atoms were included in calculated positions (C–H, N–H; 1.08 Å) and only the tantalum and chlorine atoms were refined assuming anisotropic thermal motion; all hydrogen atom temperature factors were fixed at $U = 0.10\ e\ Å^{-2}$. The atomic scattering factors were taken from the tabulations of Cromer and Mann,[37] anomalous dispersion corrections were by Cromer and Liberman.[38]

Final atomic coordinates, anisotropic thermal parameters and thermal parameters for the complex as well as listings of calculated hydrogen atom coordinates, complete lists of bond distances and

angles and F_o/F_c values have been deposited with the Editor as supplementary material.*

REFERENCES

1. W. A. Nugent and B. L. Haymore, *Coord. Chem. Rev.* 1980, **31**, 123.
2. D. C. Bradley and I. M. Thomas, *Can. J. Chem.* 1962, **40**, 449.
3. D. C. Bradley and I. M. Thomas, *Can. J. Chem.* 1962, **40**, 1355.
4. W. A. Nugent and R. L. Harlow, *J. Chem. Soc., Chem. Commun.* 1978, 579.
5. O. A. Lemenovskii, S. A. Konde and E. G. Perevalova, *J. Organomet. Chem.* 1982, **226**, 223; D. A. Lemenovskii, V. P. Fedin, Y. L. Slovohotov and Y. T. Struchkov, *J. Organomet. Chem.* 1982, **228**, 153.
6. S. M. Rocklage and R. R. Schrock, *J. Am. Chem. Soc.* 1980, **102**, 7808.
7. J. M. Mayer, C. J. Curtis and J. E. Bercaw, *J. Am. Chem. Soc.* 1983, **105**, 2651.
8. S. M. Rocklage and R. R. Schrock, *J. Am. Chem. Soc.* 1982, **104**, 3077.
9. R. R. Schrock and J. P. Fellman, *J. Am. Chem. Soc.* 1978, **100**, 3359; J. D. Fellman, G. A. Rupprecht, C. D. Wood and R. R. Schrock, *J. Am. Chem. Soc.* 1978, **100**, 5964; D. N. Clark and R. R. Schrock, *J. Am. Chem. Soc.* 1978, **100**, 6774.
10. C. T. Vroegop, J. H. Teuben, F. Van Bolhuis and J. G. M. van der Linden, *J. Chem. Soc., Chem. Commun.* 1983, 550.
11. G. W. A. Fowles and F. H. Pollard, *J. Chem. Soc.* 1953, 2588; R. T. Cowdell and G. W. A. Fowles, *J. Chem. Soc.* 1960, 2522.
12. J. A. McCleverty, A. E. Rae, I. Wolochowicz, N. A. Bailey and J. M. Smith, *J. Chem. Soc., Dalton Trans.* 1982, 429.
13. (a) A. A. Kuznetsova, Y. G. Podzolko and Y. A. Buslaev, *Russ. J. Inorg. Chem.* 1969, **14**, 393; (b) W. A. Nugent and R. L. Harlow, *Inorg. Chem.* 1980, **19**, 777.
14. K. W. Chiu, W. Wong, G. Wilkinson, A. M. R. Galas and M. B. Hursthouse, *Polyhedron* 1982, **1**, 37.
15. P. J. H. Carnell and G. W. A. Fowles, *J. Chem. Soc.* 1959, 4113.
16. G. W. A. Fowles and C. M. Pleass, *J. Chem. Soc.* 1957, 2078.
17. T. C. Jones, A. J. Nielson and C. E. F. Rickard, *J. Chem. Soc., Chem. Commun.* 1984, 205.
18. D. C. Bradley, R. J. Errington, M. B. Hursthouse, A. J. Nielson and R. L. Short, *Polyhedron* 1983, **2**, 843.
19. M. R. Churchill and H. J. Wasserman, *Inorg. Chem.* 1982, **21**, 223.
20. M. H. Chisholm, J. C. Huffman and L. S. Tan, *Inorg. Chem.* 1981, **20**, 1859.
21. T. G. Appleton, H. C. Clark and L. E. Manzer, *Coord. Chem. Rev.* 1973, **10**, 335.
22. W. A. Nugent and R. L. Harlow, *Inorg. Chem.* 1980, **19**, 777.
23. A. J. Shultz, R. K. Brown, J. M. Williams and R. R. Schrock, *J. Am. Chem. Soc.* 1981, **103**, 169.
24. A. J. Schultz, J. M. Williams, R. R. Schrock, G. A. Rupprecht and J. D. Fellmann, *J. Am. Chem. Soc.* 1979, **101**, 1593.
25. D. C. Bradley, M. B. Hursthouse, K. M. A. Malik, A. J. Nielson and G. B. Vuru, *J. Chem. Soc., Dalton Trans.* 1984, 1069.
26. A. J. Nielson and J. M. Waters, *Polyhedron* 1982, **1**, 561.
27. M. H. Chisholm, *Polyhedron* 1983, **2**, 681.
28. F. A. Cotton and W. T. Hall, *Inorg. Chem.* 1978, **17**, 3525.
29. D. Bright and J. A. Ibers, *Inorg. Chem.* 1969, **8**, 703, 709.
30. M. R. Churchill and W. J. Youngs, *J. Chem. Soc., Chem. Commun.* 1979, 321.
31. Z. Dawoodi, M. L. H. Green, V. S. B. Mtetwa and K. J. Prout, *J. Chem. Soc., Chem. Commun.* 1982, 802 and 1410.
32. P. A. Bates, A. J. Nielson and J. M. Waters, *Polyhedron* 1985, **4**, 999.
33. R. M. Pike, *J. Org. Chem.* 1961, **26**, 232 (and references therein).
34. W. Wolfsberger and H. Schmidbaur, *Synth. React. Inorg. Metal-Org. Chem.* 1974, **4**, 149.
35. A. C. T. North, D. C. Phillips and F. S. Mathews, *Acta Cryst.* 1968, **24A**, 351.
36. G. Sheldrick, SHELX-76, Program for Crystal Structure Determination, University of Cambridge, England (1976).
37. D. T. Cromer and J. B. Mann, *Acta Cryst.* 1968, **24A**, 321.
38. D. T. Cromer and D. L. Liberman, *J. Chem. Phys.* 1970, **53**, 1891.

* Atomic coordinates for the structure have also been deposited with the Cambridge Crystallographic Data Centre for inclusion in their Data Base. Copies are available on request from the Editor at Queen Mary College.

Polyhedron Vol. 4, No. 8, pp. 1403–1406, 1985
Printed in Great Britain

0277-5387/85 $3.00 + .00
© 1985 Pergamon Press Ltd

PENTACHLORO-NITRIDOTECHNETATE(VI), $[TcNCl_5]^{2-}$—AN EPR STUDY

R. KIRMSE and J. STACH
Department of Chemistry, Karl-Marx-University, DDR-7010 Leipzig, Liebigstr. 18, G.D.R.

and

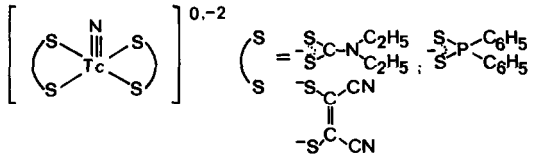
U. ABRAM*
Academy of Sciences of the G.D.R., Central Institute of Nuclear Research Rossendorf, DDR-8051 Dresden, PF 19, G.D.R.

(*Received* 18 *July* 1984; *accepted after revision* 27 *November* 1984)

Abstract—By oxidation of nitridotechnetate(V) complexes of the type $[TcN(\hat{S}\hat{S})_2]^{0,2-}$ ($\hat{S}\hat{S}$ = diethyldithiocarbamate, diphenyldithiophosphinate and maleonitrile-dithiolate) with chlorine the Tc^{6+} complex anion $[TcNCl_5]^{2-}$ was created and studied by EPR in liquid and frozen solutions. The EPR spectra are in agreement with a d^1 ($S = 1/2$) system. The hyperfine interactions are used to characterize the bonding properties in the molecular orbital of the unpaired electron.

The availability of the long lived isotope of technetium (^{99}Tc), half-life $t_{1/2} = 2.13 \times 10^5$ years, from fission products lead to a more intensive exploration of the chemistry of this element.[1,2] Nevertheless, the coordination chemistry in which the metal possesses the formal oxidation state "+6" is almost unknown. Up to now only two EPR studies on Tc(VI) compounds have been reported, made on the trigonal prismatic complexes tris(toluene dithiolato)technetium(VI), $Tc(tdt)_3$,[3] and tris(*o*-aminobenzene thiolato)technetium(VI), $Tc(abt)_3$.[4] In the former case only the liquid solution EPR spectrum was reported; for $Tc(abt)_3$ studies in frozen solution have been made. In the EPR spectra of $Tc(tdt)_3$ and $Tc(abt)_3$ only very small ^{99}Tc hyperfine splittings (hfs) are observable due to their trigonal-prismatic structure.[4,5] For Tc(VI) complexes in which the ligand arrangement comes close to C_{4v} symmetry well resolved ^{99}Tc hfs should be observed in the spectra as found for some d^5 low-spin nitrosyl complexes of Tc recently reported.[6–9] The EPR behaviour of Tc(VI) compounds ($4d^1$, $S = 1/2$) having symmetries which differ from the trigonal-prismatic one is unknown up to now.

In this paper we report an EPR investigation of the reaction between $[TcN(\hat{S}\hat{S})_2]^{0,2-}$ complexes (**I**), containing Tc in the oxidation state "+5" and molecular chlorine dissolved in $CHCl_3$.



(**I**)

The $\hat{S}\hat{S}$-ligands used are diethyldithiocarbamate, et_2dtc^-, diphenyldithiophosphinate, ph_2dtpi^-, and 1,2-dicyanoethylene-1,2-dithiolate, mnt^{2-} [see (**I**)].

The preparation of the Tc(V)N(dialkyldithiocarbamate)$_2$ complexes has been reported previously.[10] Since $TcN(ph_2dtpi)_2$ and $(Et_4N)_2[TcN(mnt)_2]$ have not yet been reported in the literature, the synthesis of these complexes will be briefly described.

EXPERIMENTAL

All solvents were reagent grade and used without further purification. The ligands Hph_2dtpi[11] and Na_2mnt[12] have been prepared by literature methods.

Preparation of the complexes

$TcN(ph_2dtpi)_2$. (a) 100 μl of a 0.3 M NH_4TcO_4 solution (30 μmole) was added to 1 cm^3 6 M HCl.

* Author to whom correspondence should be addressed.

Reduction with 100 μl hydrazine hydrate (25%) yields a clear yellow solution. After neutralization with concentrated NaOH solution 0.5 g Hph_2dtpi in 5 cm^3 acetone was added. The mixture was stirred for 1 hr and after cooling yellow crystals deposited.

(b) 100 mg $TcNCl_2(PPh_3)_2$[13] was stirred in 10 cm^3 acetone containing 1 g Hph_2dtpi for 1 hr. The resulting mixture was filtered and cooled to 0°C. The deposited crude product was recrystallized from $CHCl_3$/iso-propanol solutions.

M.pt. 268°C; elemental analysis, $C_{24}H_{20}NSP_2Tc$ (calc./found): C: 47.14/47.03, H: 3.27/3.03, N: 2.29/2.10, S: 20.95/21.11, P: 10.15/9.85, Tc: 16.20/15.41%.

$(Et_4N)_2[TcN(mnt)_2]$. According to procedure (b) 100 mg of $TcNCl_2(PPh_3)_2$ was stirred with 1 g Na_2mnt in 10 cm^3 boiling acetone for 1 hr. After addition of an excess Et_4NBr in 5 cm^3 EtOH and cooling $(Et_4N)_2[TcN(mnt)_2]$ could be obtained. After recrystallization from acetone/iso-propanol the product has a melting point of 167–168°C.

Elemental analysis, $C_{24}H_{40}N_7S_4Tc$ (calc./found): C: 44.10/43.97, H: 6.13/6.12, N: 15.01/14.84, S: 19.60/19.98, Tc: 15.16/15.16%.

$TcN(et_2dtc)_2$ was prepared according to Ref. 10.

EPR measurements

EPR spectra were recorded in the X-band ($\nu \approx 9.3$ GHz) on an E-112 spectrometer (VARIAN, U.S.A.) at $T = 295$ and 140 K. The solutions used for the EPR experiments have been prepared as follows: 0.5–1 mg of the corresponding $Tc(V)N(\hat{S}\hat{S})_2$ complex was dissolved in about 1 cm^3 $CHCl_3$. To the solution obtained a small amount (1–3 drops) of a saturated solution of Cl_2 in $CHCl_3$ is added. The reaction mixtures were measured immediately after mixing.

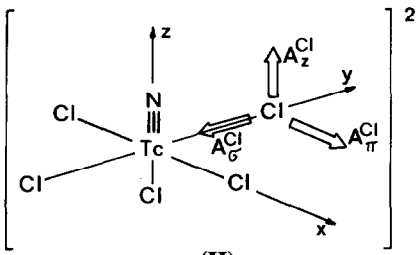
Health precautions

Due to the radioactivity of ^{99}Tc some health precautions have been made. All operations have been carried out in a fume cupboard with gloves. EPR spectra have been measured in sealed glass tubes to avoid contamination.

^{99}Tc is a only weak β^--emitter ($E_{max} = 0.29$ MeV; specific activity of 17 μCi/mg) and so no further precautions are necessary provided some elementary ones are taken and no volatile compounds are being produced during the reaction. Normal glassware gives adequate protection against the weak β^--emission. Secondary X-rays (bremsstrahlung) become important if handling ^{99}Tc in a larger scale (> 20 mg) only.

RESULTS AND DISCUSSION

In all cases the solutions of the $[Tc(V)N(\hat{S}\hat{S})_2]^{0,2-}$ complexes oxidized by Cl_2 give intense EPR spectra which are typical for d^1 complexes ($S = 1/2$) having a well separated orbital state occupied by the unpaired electron. The spectra are found to be strongly dependent on the experimental conditions applied for the oxidation. The oxidation of the systems in cooled solutions (253–273 K) with small amounts of Cl_2 results in very complex EPR spectra showing the presence of 2–4 different mixed-ligand Tc(VI) complexes. However, if the Tc(V) complexes are oxidized with a large excess of Cl_2 at room-temperature, in all cases the same spectrum was observed consisting of the EPR signals of one Tc(VI) compound only. Since very different Tc(V) complexes have been used, the common oxidation product is expected to be $[TcNCl_5]^{2-}$ **(II)**.



(II)

The X-band EPR spectrum of a $CHCl_3$ solution of **(II)** recorded at $T = 295$ K is shown in Fig. 1. It consists of 10 hyperfine lines resulting from the hyperfine interaction of the unpaired electron with the ^{99}Tc nucleus (^{99}Tc, nuclear spin $I = 9/2$). In Fig. 2 the EPR spectrum of a frozen solution of **(II)** at $T = 140$ K is reproduced. The general feature of the spectrum is characteristic for an axially symmetric, randomly oriented $S = 1/2$ system with parallel and perpendicular sets of ^{99}Tc-hyperfine lines, as described by the spin Hamiltonian

$$\hat{H}_{sp} = \beta_e[g_\parallel H_z\hat{S}_z + g_\perp(H_x\hat{S}_x + H_y\hat{S}_y)] + A_\parallel^{Tc}\hat{S}_z\hat{I}_z + A_\perp^{Tc}(\hat{S}_x\hat{I}_x + \hat{S}_y\hat{I}_y), \quad (1)$$

where $g_\parallel$, $g_\perp$, $A_\parallel^{Tc}$ and $A_\perp^{Tc}$ are the principal values of the $\tilde{g}$ and the ^{99}Tc hfs tensor $\tilde{A}^{Tc}$. Quadrupolar interactions are expected to be small and will be neglected. The principal values of $\tilde{g}$ and $\tilde{A}^{Tc}$ obtained by second-order expressions outlined in Ref. 14 are given in Table 1.

Ligand hyperfine interactions due to the coupling of the unpaired electron with the $^{35,37}Cl$ nuclei and, possibly, the ^{14}N nucleus of the nitrido-nitrogen could not be observed. The noticeably different line widths found in the parallel and perpendicular parts of the spectrum suggest, however, the presence of unresolved ligand hyperfine interactions. In Table 1

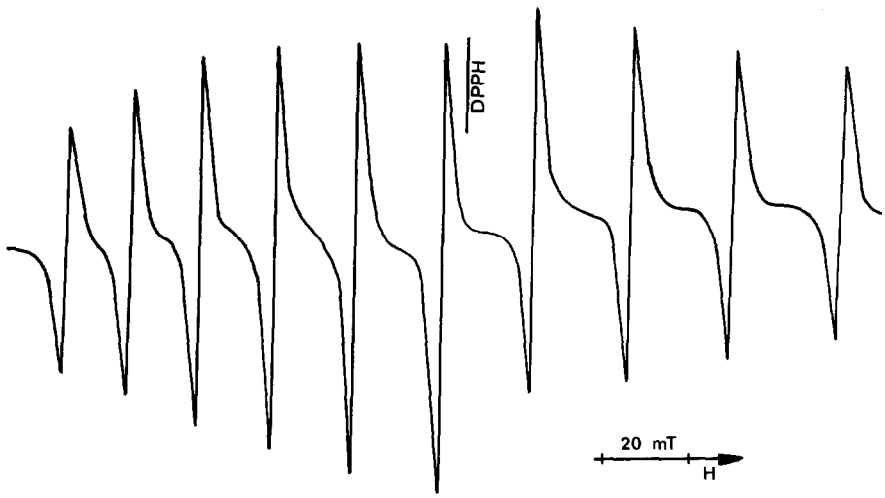


Fig. 1. Room-temperature EPR spectrum of $[TcNCl_5]^{2-}$, solvent: $CHCl_3$.

the upper limits of the ^{35}Cl hfs tensor components estimated from linewidth considerations for the equatorial (x, y) ligands are given using the notation illustrated in (II).

The EPR spectra are in agreement with an "in-plane-π-type" ground state for the molecular orbital (MO) of the unpaired electron (C_{4v} symmetry assumed):

$$\psi_{MO}(B_2) = \beta_2|d_{xy}\rangle - \beta_2'|\phi_L\rangle. \quad (2)$$

$|\phi_L\rangle$ represents a linear combination of $3p$ orbitals of the equatorial Cl ligands; contributions of the Cl $3s$ orbitals are expected to be very small because of symmetry considerations.

The ^{99}Tc hfs can be used to estimate the degree of covalency of the equatorial Tc–Cl bonds. Using the familiar eqns (3a–c):[15]

$$A_{\parallel}^{Tc} = -K - 4/7\beta_2^2 P + (g_{\parallel} - g_e)P + 3/7(g_{\perp} - g_e)P, \quad (3a)$$

$$A_{\perp}^{Tc} = -K + 2/7\beta_2^2 P + 11/14(g_{\perp} - g_e)P, \quad (3b)$$

and

$$a_0^{Tc} = -K + (g_{av} - g_e)P, \quad (3c)$$

where K is a measure of the Fermi contact interaction and $P = g_e g_N \beta_e \beta_N \langle r^{-3}\rangle_{4d} = 230 \times 10^{-4}$ cm^{-1},[16] a value of $\beta_2^2 = 0.81$ will be obtained. β_2^2 is a measure of covalency of the equatorial Tc–Cl bonds in the MO of the unpaired electron.

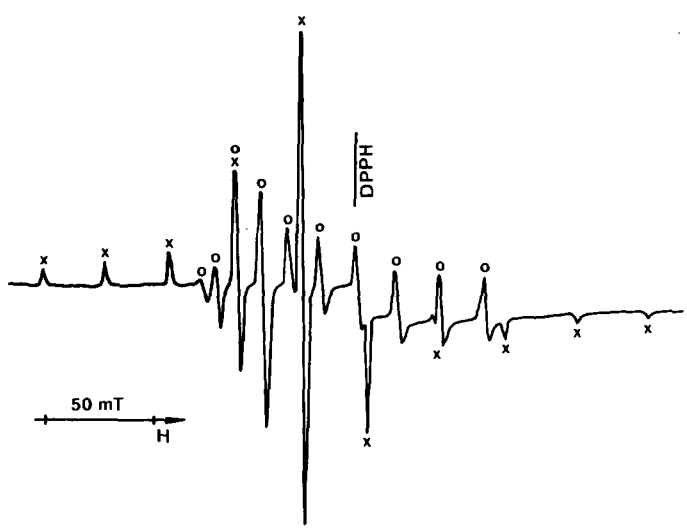


Fig. 2. X-band EPR spectrum of $[TcNCl_5]^{2-}$ in $CHCl_3$ at $T = 140$ K [parallel part of the spectrum is indicated with (×), perpendicular part with (○)].

Table 1. EPR parameters[a] for $[TcNCl_5]^{2-}$ (hyperfine coupling constants are given in 10^{-4} cm^{-1})

$\tilde{g}$	$\tilde{A}^{Tc}$	$\tilde{A}^{Cl}$
$g_{\parallel} = 2.016 \pm 0.003$	$A_{\parallel} = 295.0 \pm 2.0$	$A_{\pi}^{Cl} \leqslant 5.4$
$g_{\perp} = 2.003 \pm 0.005$	$A_{\perp} = 136.8 \pm 5.0$	$A_{z}^{Cl} \leqslant 0.9$
g_{av}[b] $= 2.007$	A_{av}[b] $= 189.5$	
g_0[c] $= 2.006 \pm 0.003$	a_0[c] $= 188.0 \pm 3.0$	$a_0^{Cl} \leqslant 1.5$

[a] Principal values of the Cl-hfs tensor are obtained from linewidth considerations.

[b] $\langle g_{av} \rangle = (g_{\parallel} + 2g_{\perp})/3$; $\langle A_{av} \rangle = (A_{\parallel} + 2A_{\perp})/3$.

[c] Obtained from the liquid solution spectrum.

Additional information about delocalization of unpaired spin density can be obtained from the $^{35,37}Cl$ hyperfine interactions. Neglecting the very small contributions of the Cl 3*s* orbitals $(\beta')^2$ can be estimated by eqn (4):

$$A_{\parallel}^{Cl} - a_0^{Cl} = (4/5) g_e g_N \beta_e \beta_N \langle r^{-3} \rangle_{3p} \times (\beta'^2/4). \quad (4)$$

Using $(4/5) g_e g_N \beta_e \beta_N \langle r^{-3} \rangle_{3p} = 78 \times 10^{-4}$ cm^{-1},[17] $(\beta')^2$ is found to be ≈ 0.2 which corresponds to an overall spin density of about 20% in the four equatorial Cl 3*p* orbitals. It should be noted that the parameters derived are close to those found for $Mo(V)OCl_5^{2-}$.[18]

In addition, the experimentally obtained hyperfine parameters have been analyzed using the following atomic parameters recently calculated by Morton and Preston:[19] ^{35}Cl; $a_{0,calc.}^{Cl} = 1909 \times 10^{-4}$ cm^{-1}; $b_{calc.}^{Cl} = (A_{\parallel}^{Cl} - a_0^{Cl})/2 = 58.6 \times 10^{-4}$ cm^{-1}; $a_{0,calc.}^{Tc} = 3149.8 \times 10^{-4}$ cm^{-1} and $b_{calc.}^{Tc} = (A_{\parallel}^{Tc} - a_0^{Tc})/2 = 65.4 \times 10^{-4}$ cm^{-1}. By means of eqns (5a–d) the following bonding parameters were obtained: $\beta'^2 = 0.14$, $n_{Cl}^2 = 0.98$, $\beta^2 = 0.88$ and $n_{Tc}^2 = 0.93$ (n_{Cl}^2 and n_{Tc}^2 are the Cl 3*s*/3*p* and Tc 5*s*/4*d* hybridization degrees, respectively).

$$a_{0,exp.}^{Cl}/a_{0,calc.}^{Cl} = 1/4(\beta')^2(1 - n_{Cl}^2), \quad (5a)$$

$$b_{exp.}^{Cl}/b_{calc.}^{Cl} = 1/4(\beta')^2 n_{Cl}^2, \quad (5b)$$

$$a_{0,exp.}^{Tc}/a_{0,calc.}^{Tc} = \beta^2(1 - n_{Tc}^2) \quad (5c)$$

and

$$b_{exp.}^{Tc}/b_{calc.}^{Tc} = \beta^2 n_{Tc}^2. \quad (5d)$$

As expected the contributions of the Cl 3*s* orbitals to the MO of the unpaired electron are very small ($n_{Cl}^2 \approx 1$); the covalency degree of the Tc–Cl bonds is smaller than that estimated using the atomic parameters given by Wertz and Bolton.[17] It is, however, difficult to use these values for comparison purposes because up to now in the literature the values given in the outlined procedure were used for interpretation of hyperfine data in nearly all cases.

Finally, it should be noted that all attempts made to isolate the $[TcNCl_5]^{2-}$ anion were without success because of its instability. The EPR spectra recorded from the reaction mixtures after standing for two hours are much less intense than those obtained for the freshly prepared solutions.

Acknowledgement—The authors wish to thank Prof. Dr. I. N. Marov (Vernadskij Institute, Academy of Sciences, Moscow) for helpful discussions.

REFERENCES

1. K. Schwochau, *Radiochim. Acta* 1983, **32**, 139.
2. R. Münze, *Isotopenpraxis* 1983, **19**, 401.
3. M. Kowashima, M. Koyama and T. Fujinaga, *J. Inorg. Nucl. Chem.* 1976, **38**, 801.
4. R. Kirmse, J. Stach and H. Spies, *Inorg. Chim. Acta* 1980, **45**, L251.
5. E. I. Stiefel, R. Eisenberg, R. C. Rosenberg and H. B. Gray, *J. Am. Chem. Soc.* 1966, **88**, 2956.
6. C. Orvig, A. Davison and A. G. Jones, *J. Labelled Compd. Radiopharm.* 1981, **18**, 148.
7. G. C. Yang, M. W. Heitzmann, L. A. Ford and W. R. Benson, *Inorg. Chem.* 1982, **21**, 3242.
8. R. Kirmse, B. Lorenz and K. Schmidt, *Polyhedron* 1983, **2**, 935.
9. R. Kirmse, J. Stach, B. Lorenz and I. N. Marov, *Z. Chem.* 1984, **24**, 36.
10. U. Abram and H. Spies, *Inorg. Chim. Acta* 1984, **94**, L3.
11. W. A. Higgins, P. W. Vogel and W. G. Graig, *J. Am. Chem. Soc.* 1955, **77**, 1864.
12. G. Bähr and G. Schleitzer, *Chem. Ber.* 1957, **90**, 438.
13. L. Kaden, B. Lorenz, K. Schmidt, H. Sprinz and M. Wahren, *Isotopenpraxis* 1981, **17**, 174.
14. B. Bleaney, *Phil. Mag.* 1951, **42**, 441.
15. B. R. McGarvey, *J. Phys. Chem.* 1967, **71**, 51.
16. R. Kirmse, J. Stach and U. Abram, *Z. anorg. allg. Chem.* (to be published).
17. J. E. Wertz and J. R. Bolton, *Electron Spin Resonance—Elementary Theory and Practical Applications*, Appendix E. McGraw-Hill, New York (1972).
18. I. N. Marov and N. A. Kostromina, *EPR and NMR in the Chemistry of Coordination Compounds* (Russ.), p. 138. Nauka, Moscow (1979).
19. J. R. Morton and K. F. Preston, *J. Magn. Reson.* 1978, **30**, 577.

Polyhedron Vol. 4, No. 8, pp. 1407–1412, 1985
Printed in Great Britain

0277-5387/85 $3.00 + .00
© 1985 Pergamon Press Ltd

STRUCTURAL STABILITY INDEX OF HETEROPOLY- AND ISOPOLYANIONS—IV. APPLICATION TO SITE-VACANT KEGGIN POLYANIONS, MIXED-TYPE KEGGIN POLYANIONS, SOME MOLYBDO- AND TUNGSTO-VANADATES AND JEANNIN-TYPE POLYANION

KENJI NOMIYA and MAKOTO MIWA*
Department of Industrial Chemistry, Faculty of Engineering, Seikei University, Musashino, Tokyo 180, Japan

(*Received* 4 *October* 1984; *accepted* 29 *November* 1984)

Abstract—The theory of structural stability, being based on the number of closed loops per MO_6 octahedral unit in the polyanion-cage, has been applied to a variety of heteropoly- and isopoly-compounds with previously unreported structures. The discussion includes the prediction of the structure of lacunary Keggin heteropoly-compound, $Cs_7Na_2[PW_{10}O_{37}]\cdot 8H_2O$, recently obtained by Knoth and Harlow, the reinvestigation of mixed-type Keggin polyanions, $[SiW_9Co_3(H_2O)_3O_{37}]^{10-}$ and $[SiW_{11}CoO_{39}]^{6-}$, recently prepared by Pope's group, the interpretation of chemical behaviours of some molybdo- and tungsto-vanadates, the structural stabilities of Jeannin-type $[As_2W_{21}O_{69}(H_2O)]^{6-}$ polyanion and its related compounds, and some remarks on Weakley-type $[X(W_5O_{18})_2]^{n-}$ polyanions and Flynn–Stucky-type $[X(Nb_6O_{19})_2]^{n-}$ complexes belonging to the hybrid-complex of polyanion.

As an attempt at rationalizing the structures of heteropolyanions (HPA) and isopolyanions (IPA), we have proposed the idea of structural stability on the basis of the number of closed loops in the polyanion-cage.[1–3] The closed loop can be counted as a geometrical circuit of the interpenetrating linkage –O–M–O–M–O–, which is formed by a junction of M ion and mutually-*trans* bridged oxygens (edge-sharing and/or corner-sharing) around the polyanion-cage. The structural stability index (η) has been defined as the number of closed loops per MO_6 octahedral unit and estimated from $\eta = (\Sigma B \cdot C)/A$, where A is the number of MO_6 octahedral units constituting the polyanion-cage, B the number of MO_6 units constituting the closed loop and C the number of closed loops. The index represents not only a topological feature of the polyanions, but also the degree of condensation and the relative stability of them. Furthermore, it clarifies the phenomenological classification of the structural types according to the number of terminal oxygens attached to each M atom, which has been proposed by Pope in 1972.[4,5] There is no precedent for the idea and its application is available for a variety of polyanions. The properties of the structural stability indexes determined in some fundamental structures of HPA (Keggin-, Dawson-, Anderson-, Waugh-, Silverton- and Evans–Showell-type) and IPA ($[M_6O_{19}]^{n-}$, $[W_{10}O_{32}]^{4-}$, $[Mo_7O_{24}]^{6-}$, α- and β-$[Mo_8O_{26}]^{4-}$, $[H_2W_{12}O_{40}]^{6-}$ and $[H_2W_{12}O_{42}]^{10-}$) have been summarized as general rules; (1) the polyanions with the larger index are more stabilized, (2) the polyanions with an identical index within the same series of M ion and heteroatom can be interconverted, or converted from one polyanion to another, (3) the index reveals the degree of condensation, (4) when an HPA decomposes, or degradates, into some IPA under an appropriate condition, the IPA possessing the largest index is predominantly produced, and (5) the real heteropoly- and isopoly-compounds with the small index are stabilized by some supporting factors other than the structural one. Incidentally, it should be noted that the comparison of the structural stability is limited within the polyanion-series comprising identical heteroatom and identical M atom. Only if this is observed can these rules be conveniently

* Author to whom correspondence should be addressed.

applied to some interesting polyanions. For example, it has been previously elucidated that a molybdo-HPA with the reverse Keggin structure, a vanado-HPA with "*trans*"-bicapped Keggin structure, and a Finke-type HPA formed by an interpenetration of two trisubstituted Keggin subunits are more stabilized than the respective parent Keggin HPA.[1,2] In Pope's recently published book,[6] which reviews all important or representative papers published by the beginning of 1982 in the chemistry of HPA and IPA, we found a number of polyanions with previously unreported structures. Here we intend to discuss, according to our stability index, the structural stabilities of some important polyanions, which include (1) some site-vacant Keggin HPA, (2) mixed-type Keggin HPA, (3) Jeannin-type HPA and related compounds, (4) some molybdo- and tungsto-vanadates, and (5) Weakley-type HPA as hybrid-complex of polyanion.

RESULTS AND DISCUSSIONS

1. *Divacant Keggin polyanions.* Of many site-vacant polyanions derived from Keggin structure including α-, β-, γ-, δ- and ε-isomers, the lacunary structures from α- and β-$[XM_{12}O_{40}]^{n-}$ by removal of one MO_6 octahedron or a trigonal group of three adjacent MO_6 octahedra have been well-known (Fig. 1).[6] They have been usually called α-XM_{11} and β-XM_{11} (containing three isomers of β_1-, β_2- and β_3-) for monovacant species and α-*A*-XM_9, α-*B*-XM_9, β-*A*-XM_9 and β-*B*-XM_9 for trivacant species. Our theory has indicated that their structural parameters are $A = 11$, $(B, C) = (6, 2)$; $\eta = 1.09$ for the monovacant species, and $A = 9$, $(B, C) = (6, 1)$; $\eta = 0.67$ for the trivacant species, independent of α- and β-isomers.[1,3]

Knoth and Harlow have recently determined the crystal structure of $Cs_7[PW_{10}O_{36}]\cdot 7H_2O$, which is the divacant species of hypothetical γ-Keggin structure formed by each 60° rotation of two W_3O_{13} units (Fig. 1C).[7] Two octahedra of "new" edge-shared contact between WO_6 octahedra are lost. There is no isomer with such lacunary sites. Using the molecular model of γ-Keggin structure, we can find two closed loops and estimated the index η of 1.2 from $A = 10$ and $(B, C) = (6, 2)$. Since this is only one species with the largest index of all γ-divacant Keggin polyanions, it is reasonable that such a compound has been actually isolated. Knoth and Harlow have also obtained the crystals of

$$Cs_7Na_2[PW_{10}O_{37}]\cdot 8H_2O,$$

the composition of which has been only determined from elemental analyses, but its structure has been unreported.[7] As far as all divacant Keggin HPA are concerned, the largest structural stability can be observed in the HPA with the parameters of $A = 10$ and $(B, C) = (6, 2)$. Our theory predicts the latter crystals will be 1,11-vacant species, α-$[PW_{10}O_{38}]^{11-}$, if the species is a derivative of α-Keggin HPA (Fig. 1A), otherwise it will be a "1,8"-vacant species, β-$[PW_{10}O_{38}]^{11-}$, if it is a derivative of β-Keggin HPA (Fig. 1B). The numbering of vacant site is performed according to the Pope's manner.[8] In these cases, the vacant sites are nonadjacent. If this is the case, the isolated species will be a protonated form of such α- or β-divacant species, $[PW_{10}O_{38}H_2]^{9-}$,

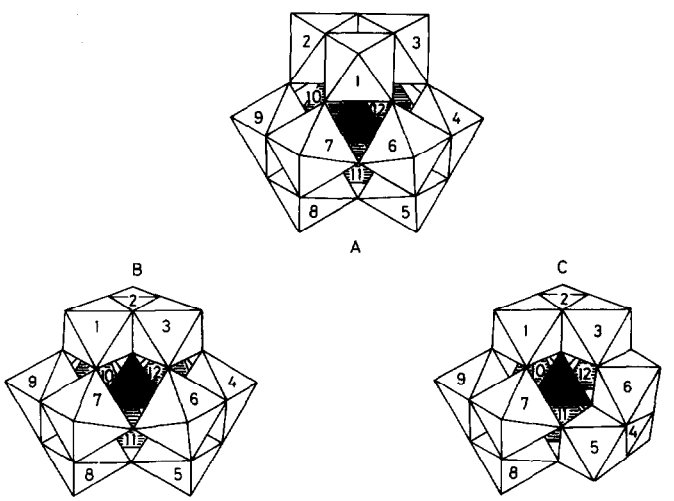


Fig. 1. Polyhedral models of three of five isomers of idealized α-Keggin structure (A) and the numbering according to Pope.[8] In B (β-isomer) and C (γ-isomer), one and two M_3O_{13} groups have been rotated by 60°.

and the formula will be rewritten as

$$Cs_7Na_2[PW_{10}O_{38}H_2]\cdot 7H_2O,$$

where the analytical data are unchanged. Of course, the forms derived from hypothetical δ- and ε-Keggin structures could be considered as divacant species with $\eta = 1.2$. However, in these cases, the formula should become $[PW_{10}O_{36}]^{7-}$ or its protonated form, but not $[PW_{10}O_{37}]^{9-}$, because two vacant sites are adjacent as observed in the γ-divacant polyanion.

2. *Mixed-type Keggin polyanions.* In the mixed-Keggin structures, e.g. $[XM_{12-x}M'_xO_{40}]^{n-}$ and $[XM_{11}Z(H_2O)O_{39}]^{n-}$ (X: heteroatom, Z: metal ion other than Mo and W, M and M′: Mo or W), there exist two kinds of closed loop, which are "homo"-type loop such as –O–M–O–M–O– and "hetero"-type loop such as –O–M–O–Z–O– and –O–M–O–M′–O–.[2] For the estimation of stability index, they have been treated as equivalent loops. Therefore, the stability index of mixed-Keggin HPA is identical with that of normal Keggin HPA [$A = 12$, $(B, C) = (6, 4)$ and $\eta = 2$]. This accounts for the fact that the closed loop itself is derived from the topological or geometrical consideration, even though the actual chemical bonds along the closed loops are different. The trisubstituted Keggin HPA $[SiW_9Co_3(H_2O)_3O_{37}]^{10-}$, recently prepared by Pope's group,[9] has also the same index as that of parent Keggin HPA. If the compound is the 1,2,3- or 1,6,7-trisubstituted derivative of $[SiW_{12}O_{40}]^{4-}$ by Co(II) ion, it will be probably what Finke *et al.* have initially desired to prepare.[10] The Finke-type HPA,

$$[P_2W_{18}Co_4(H_2O)_2O_{68}]^{10-},$$

which Finke *et al.* have unexpectedly obtained, is a dimeric and interpenetrating form of two trisubstituted Keggin HPA.[10,11] By such a condensation, two new closed loops of "hetero"-type passing through two Keggin subunits are generated besides some local closed loops belonging to each subunit. This leads to the larger stability index than that of the trisubstituted Keggin HPA at which they have initially aimed. The structural parameters are $A = 22$ and $(B, C) = [(6, 2)_{homo} + (6, 4)_{hetero} + (10, 2)_{hetero}]$ and the index is $\eta = 2.55$.[2] Pope's group have also obtained a new HPA containing unsaturated coordination of surface atoms represented as $[SiW_{11}CoO_{39}]^{6-}$.[9] This is derived from a mixed-Keggin HPA $[SiW_{11}Co(H_2O)O_{39}]^{6-}$ in anhydrous nonpolar solvents and contains the square-pyramidal Co(II) moiety, which is provided by elimination of a coordinated water molecule and can be saturated by a variety of donors such as alcohols, acetone, acetonitrile, pyridine etc. In this case, the "hetero"-loops passing through the five-coordinate Co(II) moiety may well be counted and they can be treated as that of parent HPA $[SiW_{11}Co(H_2O)O_{39}]^{6-}$.

3. *Molybdo- and tungsto-vanadates.* Some molybdovanadates as mixed-metal polyanions show interesting behaviours in the standpoint of the structural stability. The skeletal cage of $[V_5Mo_8O_{40}]^{7-}$, in yellow acicular crystals obtained as $K_7[V_5Mo_8O_{40}] \sim 8H_2O$, consists of a puckered ring of eight edge-sharing MoO_6 octahedra to which are attached four VO_5 trigonal bipyramids (Fig. 2A).[6,12] Since a centrally buried VO_4 tetrahedron and the four external VO_5 polyhedra, the latter of which are described as bridging tetrahedra in Pope's book, can be treated as "heteroatoms", we can find no closed loop passing through Mo atoms and the equatorial oxygens. Thus, the stability index η is zero and this compound is predicted to be unstable. As a matter of fact, the structure is stabilized in the crystals by two potassium ions which are coordinated to surface cavities of the polyanion. This is compatible with the rule (5) described earlier. By slow recrystallization of the V_5Mo_8 compound from water, the salt of $K_8[V_8Mo_4O_{36}]\cdot 12H_2O$ has been obtained.[13] The structure of $[V_8Mo_4O_{36}]^{8-}$ has been described as an arrangement of four MoO_6 octahedra, six VO_5 square pyramids and two VO_4 tetrahedra (Fig. 2B).[6] In this skeletal cage, although one closed loop passing through two MoO_6 octahedra and VO_5 polyhedra seems to be present, it is unrealized because of attaching two external VO_4 tetrahedra.

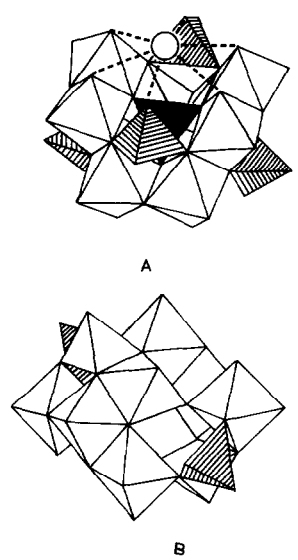


Fig. 2. Polyhedral models of the $[V_5Mo_8O_{40}]^{7-}$ (A) and the $[V_8Mo_4O_{36}]^{8-}$ (B) polyanions illustrated according to Pope.[6] In A, the open circle shows the position of one of two potassium ions.

Since each of two external VO_4 tetrahedra is binding only by two oxygens to the cage, the stabilization of crystal structure by potassium ions is also expected as observed above. This polyanion will be also unstable in solution. In fact, when the mother liquor from the crystallization of the V_8Mo_4 polyanion is allowed to stand for some months, the brown cubic crystals of the partially-reduced salt

$$K_6[V_3Mo_{10}O_{40}]\cdot 13H_2O$$

are formed. It has been confirmed by X-ray investigation that it contains a Keggin HPA $[V(V)V(IV, V)_2Mo_{10}O_{40}]^{6-}$ with a central tetrahedral vanadium(V) atom.[14] The Keggin structure is in the state with the degree of polymerization more progressed, as expected from the stability index ($\eta = 2$). Thus, these observations reveal the validity of rule (1).

On the other hand, one of the tungsto-vanadates, $[V_2W_4O_{19}]^{4-}$, is a vanadium-substituted species of the $[W_6O_{19}]^{2-}$ IPA and its stability index η becomes 2, since $(B, C) = (4, 3)_{hetero}$ or $[(4, 1)_{homo} + (4, 2)_{hetero}]$ and $A = 6$ (Fig. 3) Interesting reactions have been reported; acidification and heating of solutions of orange V_2W_4 leads to the darker coloured polyanions of the Keggin-series $[VV_xW_{12-x}O_{40}]^{(3+x)}$ $(x = 2, 3)$.[15] These polyanions are vanadium-substituted species of the hypothetical Keggin $[VW_{12}O_{40}]^{3-}$ HPA and also belonging to the mixed-type Keggin HPA. Although each of these polyanions exists as mixtures of several isomers with different distributions of V and W atoms in the $[M_{12}O_{40}]$-cage, all of them have the stability index identical with that of the parent structure ($\eta = 2$) as described in the preceding section. Thus, the reaction of $[V_2W_4O_{19}]^{4-}$ to $[VV_xW_{12-x}O_{40}]^{(3+x)-}$ will become an example compatible with the rule (2), since both of them are belonging to the same series of the polyanions comprising V, W and O.

Apart from the oxidation state of vanadium, the $[V(IV)_{18}O_{42}]^{12-}$ polyanion has been obtained as deep red–brown crystals of $Na_{12}[V_{18}O_{42}]\cdot 24H_2O$ by Johnson and Schlemper from combining solutions of $VOSO_4$ with appropriate hydroxide at 60–70°C under nitrogen or argon.[16] The structure consists of almost spherical shell of edge- and corner-sharing VO_5 square pyramids with the axial V–O bonds directed outwards. This polyanion results from the considerably high degree of polymerization. In fact, a number of closed loops can be counted and its structural stability is expected to be extremely large. It will be reasonable, as mentioned by Johnson and Schlemper, that this polyanion occupies a position in the aqueous chemistry of vanadium(IV) analogous to that of $[V(V)_{10}O_{28}]^{6-}$ in the chemistry of vanadium(V).

4. *Jeannin-type polyanion and related compounds.* In 1981, Jeannin and Martin-Frère reported the synthesis and the structural study by X-ray and ^{183}W NMR techniques of

$$H_2Rb_4[As_2W_{21}O_{69}(H_2O)]\cdot 34H_2O.^{17}$$

The

$$[As_2W_{21}O_{69}(H_2O)]^{6-} \text{ HPA } (As_2W_{21})$$

is made of two α-*B*-As(III)W_9O_{33} subunits, joined together in an asymmetrical way by three W atoms among which one is octahedrally surrounded and two are in a square-pyramidal environment. The former W atom accompanies with the coordination of one water molecule (Fig. 4). This HPA is one of the new type HPA with As(III) as a heteroatom and some of them have been already known as

$$[H_2AsW_{18}O_{60}]^{7-}$$

and inorganic cryptate-like

$$[As_4W_{40}O_{140}]^{28-} \text{ HPA.}^{18,19}$$

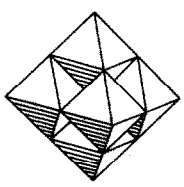


Fig. 3. Polyhedral model of the $[W_6O_{19}]^{2-}$-structure.

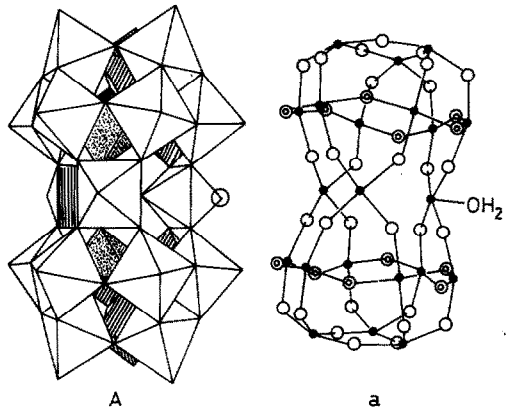


Fig. 4. Polyhedral model of the Jeannin-type HPA $[As_2W_{21}O_{69}(H_2O)]^{6-}$ (A) and its framework bond model (a). In A, the circle shows the position of coordinating water molecule and two tetrahedra of As(III) are stippled. In a, open circles are bridged-oxygens and filled ones are tungsten atoms. The oxygens illustrated by double circles represent local closed loops. Heteroatoms, terminal oxygens and triply bridged oxygens to which are attached the heteroatoms are omitted.

The consideration of structural stability for the As_2W_{21} HPA can be performed as usual (Fig. 4a). We can find two local closed loops belonging to each subunit, or $(B, C) = (6, 2)$, and one overall closed loop passing through two subunits, $(B, C) = (30, 1)$; the latter is a very large and continuous loop passing two times through each central bridging W atom. Thus, the stability index is $\eta = (6 \times 2 + 30 \times 1)/(18 + 3) = 2$. It is beyond imagination and very interesting that the index is identical with that of Keggin- and Dawson-structures.[1]

As related compounds, the mixed-type polyanions $As_2W_{20}M$, $As_2W_{19}M_2$ and $As_2W_{18}M_3$ have been reported, where three W atoms bridging between two subunits in the As_2W_{21} are replaced, one by one, with metal ion M.[20,21] One of them,

$$[Cu_3As_2W_{18}O_{66}(H_2O)_2]^{12-}$$

polyanion, is also introduced in Pope's book.[6] Since the "hetero"-loop through the bridging M atoms can be treated equivalently as the "homo"-one through the bridging W atoms in the parent HPA as described above, the structural stability of these mixed-type HPA is unchanged by the metal-substitution. As other related compounds, the lacunary species of As_2W_{21}, such as As_2W_{19} and As_2W_{20} polyanions, have also been known. They have been used as reactants producing the mixed-type $As_2W_{19}M_2$ and $As_2W_{20}M$ HPA.[22] However, their structures have been unreported yet. If the bridging W atoms in the As_2W_{21} are removed, the large closed loop of $B = 30$ is broken and only the local loops of $(B, C) = (6, 2)$ remain. This leads to the remarkable decrease of structural stability; $\eta = 0.63$ for the As_2W_{19} and 0.60 for the As_2W_{20}.

5. *Weakley-type HPA as hybrid-complex of polyanion.* The variety of tri- and tetravalent metals of rare-earth group has constituted two interesting groups of HPA, because of the large ionic radii and the high oxidation state. One is eight-coordination compounds represented as $[X(W_5O_{18})_2]^{n-}$ and $[XL_2]^{n-}$ (L: monovacant HPA of Keggin- and Dawson-structures such as $[PW_{11}O_{39}]^{7-}$, $[SiW_{11}O_{39}]^{8-}$, $[P_2W_{17}O_{61}]^{10-}$, etc.), which have been first characterized by Peacock and Weakley,[23,24] and the other is twelve-coordination compounds known as the Silverton-type $[XMo_{12}O_{42}]^{n-}$ HPA,[25] the structural stability of which has been previously described.[1,2] The $[X(W_5O_{18})_2]^{n-}$ polyanion is a predominantly "ionic" coordination complex incorporating two quadridentate $[W_5O_{18}]^{6-}$ ligands, which may be regarded as lacunary derivatives of the $[W_6O_{19}]^{2-}$ structure (Fig. 3), and the central XO_8 moiety is confirmed to be approximately square antiprismatic (Fig. 5A).[26–29] Analogous coordination of X has been also provided in the $[XL_2]^{n-}$ polyanion, where the lacunary Keggin and Dawson polyanions act as quadridentate ligand L.[30,31] These are attributed exclusively to the largeness of ionic radius of X and contrast to the examples of the mixed-IPA $[MW_5O_{19}]^{n-}$ (M = Mo, V, Nb) and the mixed-type Keggin and Dawson HPA $[ML]^{n-}$ such as $[PW_{11}M(H_2O)O_{39}]^{n-}$, $[SiW_{11}M(H_2O)O_{39}]^{n-}$ and $[P_2W_{17}M(H_2O)O_{61}]^{n-}$. Thus, these rare-earth compounds are, rather than the normal HPA, close to the metal complex with polyanions as ligand and may be classified to the category of the hybrid-complex of polyanion, to which the complex $[X(Nb_6O_{19})_2]^{n-}$ [X = Mn(IV) and Ni(IV)], first characterized by Flynn and Stucky,[32,33] belongs as a typical example (Fig. 5B). Since the Weakley-type HPA and the Flynn–Stucky-type complex have no polyanion-cage as an overall skeleton, the application of the structural stability theory is not suitable to such compounds. Only the structural stability of the "ligand" moiety can be discussed. From this point of view, the Weakley-type HPA is distinct from the Silverton-type HPA with the heteroatom of rare-earth metal. The latter has no closed loop, although it has the polyanion-cage.[1,2] Here, it should be noted that the $[XL]^{n-}$ as mixed-type Keggin and Dawson HPA and the $[XL_2]^{n-}$ as hybrid-complex of polyanion are quite distinguished in the discussion of the structural stability. Generally, whether the compound is belonging to a mixed-type HPA or to a hybrid-complex will be readily judged from the possibility of replacing X with Mo(VI), W(VI) and V(V) ions. Recently, the curious copper complex $[Cu_2(SiMo_9O_{33})_2]^{12-}$, which contains two $SiMo_9$ units formally derived from hypothetical β-*B*-$SiMo_9$, has been established by X-ray investigation.[34] This compound may be considered to be a hybrid-complex.

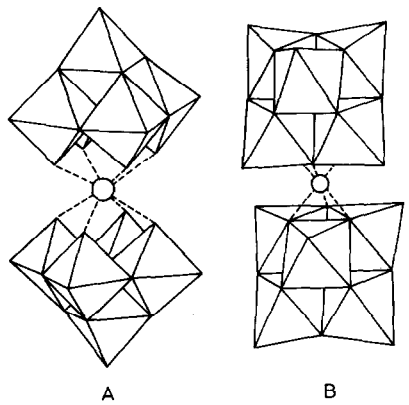


Fig. 5. Polyhedral models of the Weakley-type HPA $[X(W_5O_{18})_2]^{n-}$ (A) and the Flynn–Stucky-type complex $[X(Nb_6O_{19})_2]^{n-}$ (B).

Acknowledgement—This work was partially supported by a Grant-in-Aid for Scientific Research No. 59540402 from the Ministry of Education, Science and Culture of Japan.

REFERENCES

1. K. Nomiya and M. Miwa, *Polyhedron* 1984, **3**, 341, 1161.
2. K. Nomiya and M. Miwa, *Polyhedron* 1985, **4**, 89.
3. K. Nomiya and M. Miwa, *Polyhedron* 1985, **4**, 675.
4. M. T. Pope, *Inorg. Chem.* 1972, **11**, 1973.
5. K. Nomiya and M. Miwa, *Technology Reports of the Seikei University*, 1985 (No. 39), 2551.
6. M. T. Pope, *Heteropoly and Isopoly Oxometalates*. Springer-Verlag, New York (1983).
7. W. H. Knoth and R. L. Harlow, *J. Am. Chem. Soc.* 1981, **103**, 1865.
8. M. T. Pope, *Inorg. Chem.* 1976, **15**, 2008.
9. D. E. Katsoulis and M. T. Pope, *J. Am. Chem. Soc.* 1984, **106**, 2737.
10. R. G. Finke, M. Droege, J. R. Hutchinson and O. Gansow, *J. Am. Chem. Soc.* 1981, **103**, 1587.
11. T. J. R. Weakley, H. T. Evans, J. S. Showell, G. F. Tourné and C. M. Tourné, *J. Chem. Soc., Chem. Commun.* 1973, 139.
12. A. Björnberg, *Acta Cryst.* 1979, **B35**, 1989.
13. A. Björnberg, *Acta Cryst.* 1980, **B36**, 1530.
14. A. Björnberg and B. Hedman, *Acta Cryst.* 1980, **B36**, 1018.
15. C. M. Flynn and M. T. Pope, *Inorg. Chem.* 1971, **10**, 2745.
16. G. K. Johnson and E. O. Schlemper, *J. Am. Chem. Soc.* 1978, **100**, 3645.
17. Y. Jeannin and J. Martin-Frère, *J. Am. Chem. Soc.* 1981, **103**, 1664.
18. Y. Jeannin and J. Martin-Frère, *Inorg. Chem.* 1979, **18**, 3010.
19. F. Robert, M. Leyrie, G. Hervé, A. Tézé and Y. Jeannin, *Inorg. Chem.* 1980, **19**, 1746.
20. C. M. Tourné, A. Revel, G. F. Tourné and M. Vendrell, *C.R. Acad. Sci.* 1973, **C277**, 643.
21. C. M. Tourné and G. F. Tourné, *C.R. Acad. Sci.* 1975, **C281**, 933.
22. M. Leyrie, J. Martin-Frère and G. Hervé, *C.R. Acad. Sci.* 1974, **C279**, 895.
23. R. D. Peacock and T. J. R. Weakley, *J. Chem. Soc. A* 1971, 1836.
24. R. D. Peacock and T. J. R. Weakley, *J. Chem. Soc. A* 1971, 1937.
25. D. D. Dexter and J. V. Silverton, *J. Am. Chem. Soc.* 1968, **90**, 3589.
26. J. Iball, J. N. Low and T. J. R. Weakley, *J. Chem. Soc., Dalton Trans.* 1974, 2021.
27. A. M. Golubev, L. P. Kazanskii, E. A. Torchenkova, V. I. Simonov and V. I. Spitsyn, *Dokl. Akad. Nauk SSSR* 1975, **221**, 351; *Dokl. Chem.* (Engl. Trans.) 1975, **221**, 198.
28. A. M. Golubev, L. A. Muradyan, L. P. Kazanskii, E. A. Torchenkova, V. I. Simonov and V. I. Spitsyn, *Koord. Khim.* 1977, **3**, 920; *Sov. J. Coord. Chem.* (Engl. Trans.) 1977, **3**, 715.
29. L. P. Kazanskii, M. A. Fedotov and V. I. Spitsyn, *Dokl. Akad. Nauk SSSR* 1977, **233**, 152; *Dokl. Phys. Chem.* (Engl. Trans.) 1977, **233**, 250.
30. S. C. Termes and M. T. Pope, *Trans. Met. Chem.* 1978, **3**, 103.
31. V. N. Molchanov, L. P. Kazanskii, E. A. Torchenkova and V. I. Simonov, *Kristallografiya* 1979, **24**, 167; *Sov. Phys. Cryst.* (Engl. Trans.) 1979, **24**, 96.
32. C. M. Flynn and G. D. Stucky, *Inorg. Chem.* 1969, **8**, 332.
33. C. M. Flynn and G. D. Stucky, *Inorg. Chem.* 1969, **8**, 335.
34. H. F. Fukushima, A. Kobayashi and Y. Sasaki, *Acta Cryst.* 1981, **B37**, 1613.

Polyhedron Vol. 4, No. 8, pp. 1413–1417, 1985
Printed in Great Britain

0277-5387/85 $3.00 + .00
© 1985 Pergamon Press Ltd

THE CRYSTAL AND MOLECULAR STRUCTURE OF $Rh_2(CH_3CO_2)_4[HCON(CH_3)]_2$—EFFECT OF LIGANDS ON METAL–METAL BONDING

MONIKA MOSZNER, TADEUSZ GŁOWIAK and JÓZEF J. ZIÓŁKOWSKI*
Institute of Chemistry, University of Wrocław, 50-383 Wrocław, Poland

(*Received* 22 *October* 1984; *accepted* 18 *December* 1984)

Abstract—The structure of $Rh_2(CH_3CO_2)_4(DMF)_2$ {DMF = $HCON(CH_3)_2$} has been determined by single crystal X-ray methods. The compound crystallizes with eight formula units in a cell of dimensions: $a = 29.438(7)$ Å, $b = 7.978(2)$ Å, $c = 20.279(5)$ Å, $\beta = 113.20(4)°$, $V = 4377.5$ Å^3, space group $C2/c$. The structure has been refined by full-matrix least-squares method to a final $R = 0.030$ for the 4156 observed data. Two Rh(II) atoms are linked by four acetate groups forming a dimeric unit, where the Rh–Rh distance is 2.383(1) Å. The coordination sphere about each Rh atom is completed by a DMF molecule; the average Rh–O(DMF) distance is 2.296(3) Å.

$Rh_2(CH_3CO_2)_4(DMF)_2$ is one of the rhodium(II) dimer carboxylates of a general formula $Rh_2(CH_3CO_2)_4L_n$ ($n = 1, 2$)[1,2] where the problem of correlation between the Rh–Rh distance, its bond order and electronic structure of Rh–Rh core is still unresolved.[3–9]

It is known that the Rh–Rh bonding distance in $Rh_2(CH_3CO_2)_4L_n$ complexes is determined by the donor–acceptor properties of the terminal ligands L and of the bridging ligands RCO_2^-. Some authors who have reported the electronic structure of this type rhodium dimers believed that the influence of the L ligands on Rh–Rh bond distance was limited by their σ donor ability only.[4,5] The X-ray data[1,2] revealed that the Rh–Rh distance in the presence of ligands L of σ-donor and π-acceptor properties was longer ($d_{Rh-Rh} = 2.449$ Å in $Rh_2(CH_3CO_2)_4(PPh_3)_2$; $pK_bPPh_3 = 11.3$) than that found in the presence of ligands regarded as typical σ donors ($d_{Rh-Rh} = 2.402$ Å in $Rh_2(CH_3CO_2)_4(NHEt_2)_2$, $pK_bNHEt_2 = 3.51$).[3]

From the crystallographic data it follows that the Rh–Rh distance in $Rh_2(CH_3CO_2)_4L_n$ increases with decrease of donor properties of bridging ligands RCO_2^- ($d_{Rh-Rh} = 2.371$ Å in $Rh_2(Me_3CCO_2)_4(H_2O)_2$, $d_{Rh-Rh} = 2.409$ Å in $Rh_2(CF_3CO_2)_4(H_2O)_2 \cdot 2DTMN$).[1] The effect of structural elements of $Rh_2(RCO_2)_4L_n$ complexes on the Rh–Rh distance may suggest that, in interactions between the Rh–Rh core and the surrounding ligands, both σ and π interactions should be taken into account.

EXPERIMENTAL

Dark blue–green single crystals of $Rh_2(CH_3CO_2)_4(DMF)_2$ were obtained by slow evaporation at room temperature of the solvent after dissolving a small amount of $Rh_2(CH_3CO_2)_4$ (prepared according to Ref. 10) in neat DMF.

Found: C, 28.3; H, 4.3; N, 4.5. Calc. for $Rh_2(CH_3CO_2)_4(DMF)_2$; C, 28.57; H, 4.42; N, 4.76%.

X-RAY STUDY

All measurements for a crystal $0.3 \times 0.3 \times 0.35$ mm were made on a Syntex $P2_1$ computer-controlled four-circle diffractometer equipped with a scintillation counter and graphite monochromator. Indexing of 15 intense reflections in the range $22.0° \ll 2\theta \ll 29.5°$ produced a unit cell in the monoclinic system with dimensions: $a = 29.438(7)$ Å, $b = 7.978(2)$ Å, $c = 20.279(5)$ Å, $\beta = 113.20(4)°$, $V = 4377.5$ Å^3, $M = 588.2$, $D_m = 1.78(1)$ g cm^{-3} (by flotation), $D_c = 1.78$ g cm^{-3}, $Z = 8$, μ(Mo-K_α) = 15.2 cm^{-1}.

Systematic absences (khl; $h + k = 2n + 1$ and $h0l$, $l = 2n + 1$) established the space group as $C2/c$.

Intensities of 4865 independent reflections were

* Author to whom correspondence should be addressed.

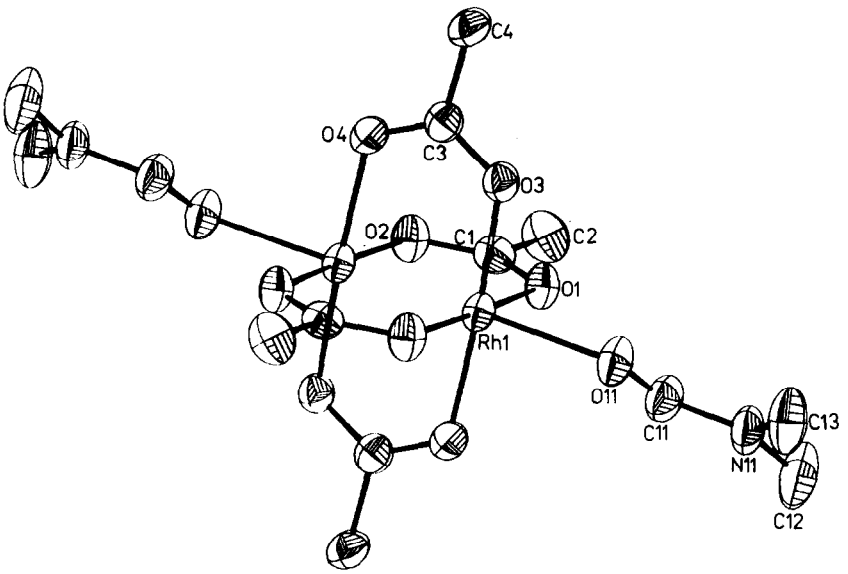


Fig. 1. Structure of the $Rh_2(CH_3CO_2)_4(DMF)_2$ molecule.

measured up to $2\theta = 55.0°$ with the variable θ–2θ scan technique. The scan rate varied from 2.0 to 29.0° min^{-1}. The intensities of two standard reflections were monitored during the data collection but the maximum variation was less than 2%.

The structure was solved by Patterson and Fourier methods and refined by a full-matrix least squares technique. The final refinement cycle converged to values of 0.030, 0.036 and 2.457 for R, R_ω and S respectively for 4256 data for which $I \geqslant 1.96\sigma(I)$. The H atoms and their isotropic thermal factor ($B = 4.5$ Å^2) were not refined.

The function minimised was $\Sigma\,\omega(|F_o| - |F_c|)^2$ with $\omega = 1/\sigma^2(F)$. The atomic scattering factors were taken from the tabulations of Cromer and Waber.[11] All calculations were performed with the Syntex XLT system.[12]

RESULTS AND DISCUSSION

Interatomic distances and bond angles for $Rh_2(CH_3CO_2)_4(DMF)_2$ are reported in Tables 1 and 2.*

A stereoscopic diagram of the unit cell contents of $Rh_2(CH_3CO_2)_4(DMF)_2$ is depicted in Fig. 1.

The structure of $Rh_2(CH_3CO_2)_4(DMF)_2$ is centrosymmetric with an Rh–Rh of 2.383(1) Å and axially bound *N,N*-dimethylformamide ligands at a distance of 2.296(3) Å (average). The Rh–Rh–O(DMF) linkage is not quite linear, being 177.46°. The Rh–O bond is approximately 0.256 Å longer than expected on the basis of covalent radii of oxygen and Rh(II) or in comparison with the literature data.

Average Rh–O and C–O ($CH_3CO_2^-$) bond distances are 2.038(3) Å and 1.261(5) Å, respectively; average Rh–Rh–O($CH_3CO_2^-$), Rh–O–C and O–C–O angles are 88.33(9)°, 118.92(30)° and 126.1(44)°, respectively.

Correlations between Rh–Rh, Rh–L distances, Rh–Rh–O, Rh–O–C and O–C–O ($CH_3CO_2^-$) angles and the basicity of L ligands measured by the pK_b values and donor number DN are listed in Table 3.

Comparison of the Rh–Rh bond distances in $Rh_2(CH_3CO_2)_4L_n$ type complexes, where L = CH_3OH, DMF, H_2O, shows the slight increase of the Rh–Rh distance as the ligand L acidity increases: CH_3OH (2.377 Å) < DMF (2.383 Å) < H_2O (2.386 Å).

The data in Table 3 indicate that the Rh–Rh bond distances in fact could be correlated with acidity of the ligand L (expressed by pK_b or DN) only within the determined group of donors, i.e. ligands coordinating via the same atom (O, N, S, C, P). It is striking, that the Rh–Rh bond distance increases with increase of the π acceptor ability of ligands L. This trend is in agreement with a position of the donor atom of the ligand L in the nephelauxetic series.[13]

From the crystallographic data it is known that the Rh–Rh bond distances in $Rh_2(RCO_2)_4L_2$ complexes depends on the R and increases in the order: $(CH_3)_3C$ (2.37 Å) < CH_3 (2.386 Å) < CF_3 (2.409 Å), i.e. according to the ability of the RCO_2^-

* Atomic positional and thermal parameters and lists of F_o/F_c have been deposited as supplementary material with the Editor, from whom copies are available on request. Atomic co-ordinates have also been deposited with the Cambridge Crystallographic Data Centre.

Table 1. Bond lengths (Å, with e.s.d.s in parentheses) in $Rh_2(CH_3CO_2)_4(DMF)_2$

Rh(1)–Rh(1^i)	2.383(3)	Rh(2)–Rh(2^i)	2.383(0)
Rh(1)–O(1)	2.041(3)	Rh(2)–O(5)	2.038(1)
Rh(1)–O(2)	2.036(3)	Rh(2)–O(6)	2.031(3)
Rh(1)–O(3)	2.038(3)	Rh(2)–O(7)	2.045(3)
Rh(1)–O(4)	2.045(3)	Rh(2)–O(8)	2.032(3)
Rh(1)–O(11)	2.308(4)	Rh(2)–O(21)	2.285(3)
O(1)–C(1)	1.267(6)	O(5)–C(5)	1.256(5)
O(2)–C(1)	1.254(5)	O(6)–C(5)	1.260(6)
O(3)–C(3)	1.257(6)	O(7)–C(7)	1.266(6)
O(4)–C(3)	1.265(6)	O(8)–C(7)	1.263(5)
O(11)–C(11)	1.217(7)	O(21)–C(21)	1.215(6)
N(11)–C(11)	1.328(7)	N(21)–C(21)	1.316(6)
N(11)–C(12)	1.438(7)	N(21)–C(22)	1.491(9)
N(11)–C(13)	1.447(9)	N(21)–C(23)	1.467(8)
C(1)–C(2)	1.494(7)	C(5)–C(6)	1.497(7)
C(3)–C(4)	1.493(7)	C(7)–C(8)	1.490(8)

ligand to decrease the electron density in the Rh–Rh core.[14]

Comparison of the Rh–Rh distances in complexes:

$Rh_2(CH_3CO_2)_4(H_2O)_2$ (2.386 Å),[15]

$Rh_2(CH_3CO_2)_4(DMSO)_2$ (2.406 Å),[16]

$Rh_2(CH_3CO_2)_4(THT)_2$ (2.413 Å)[16]

and

$Rh_2(CH_3CSO)_4(CH_3COSH)_2$ (2.550 Å)[17]

revealed that substitution of oxygen by sulphur in the carboxylate ligands resulted in elongation of the Rh–Rh bond distance like the replacement of oxygen by sulphur in the terminal ligands. The differences in the Rh–Rh distances in the case of thioacetate and

Table 2. Bond angles (° with e.s.d.s in parentheses) in $Rh_2(CH_3CO_2)_4(DMF)_2$

Rh(1^i)–Rh(1)–O(1)	87.37(9)	Rh(2^i)–Rh(2)–O(5)	87.43(9)
Rh(1^i)–Rh(1)–O(2)	88.86(9)	Rh(2^i)–Rh(2)–O(6)	88.65(9)
Rh(1^i)–Rh(1)–O(3)	87.97(9)	Rh(2^i)–Rh(2)–O(7)	88.68(9)
Rh(1^i)–Rh(1)–O(4)	88.16(9)	Rh(2^i)–Rh(2)–O(8)	87.43(9)
Rh(1^i)–Rh(1)–O(11)	178.16(9)	Rh(2^i)–Rh(2)–O(21)	176.76(9)
Rh(1)–O(1)–C(1)	119.22(30)	Rh(2)–O(5)–C(5)	119.22(29)
Rh(1)–O(2)–C(1)	118.18(30)	Rh(2)–O(6)–C(5)	118.24(29)
Rh(1)–O(3)–C(3)	119.40(30)	Rh(2)–O(7)–C(7)	118.19(30)
Rh(1)–O(4)–C(3)	118.69(30)	Rh(2)–O(8)–C(7)	120.19(30)
Rh(1)–O(11)–C(11)	113.74(30)	Rh(2)–O(21)–C(21)	122.89(34)
O(1)–Rh(1)–O(2)	176.23(13)	O(5)–Rh(2)–O(6)	175.99(13)
O(1)–Rh(1)–O(3)	91.39(13)	O(5)–Rh(2)–O(7)	91.45(13)
O(1)–Rh(1)–O(4)	89.03(13)	O(5)–Rh(2)–O(8)	89.15(13)
O(1)–Rh(1)–O(11)	93.38(13)	O(5)–Rh(2)–O(21)	92.30(13)
O(2)–Rh(1)–O(3)	88.42(13)	O(6)–Rh(2)–O(7)	87.59(13)
O(2)–Rh(1)–O(4)	90.91(13)	O(6)–Rh(2)–O(8)	91.54(13)
O(2)–Rh(1)–O(11)	90.39(13)	O(6)–Rh(2)–O(21)	91.66(13)
O(3)–Rh(1)–O(4)	176.09(13)	O(7)–Rh(2)–O(8)	176.06(13)
O(3)–Rh(1)–O(11)	93.68(13)	O(7)–Rh(2)–O(21)	94.55(13)
O(4)–Rh(1)–O(11)	90.17(13)	O(8)–Rh(2)–O(21)	89.34(13)
O(1)–C(1)–O(2)	126.17(44)	O(5)–C(5)–O(6)	126.26(43)
O(3)–C(3)–O(4)	126.77(44)	O(7)–C(7)–O(8)	125.22(44)
O(11)–C(11)–N(11)	126.54(51)	O(21)–C(21)–N(21)	126.16(50)
C(11)–N(11)–C(12)	119.69(47)	C(21)–N(21)–C(22)	120.28(47)
C(11)–N(11)–C(13)	121.44(49)	C(21)–N(21)–C(23)	122.39(50)

Table 3. Effect of ligands basicity on crystal structure data of $Rh_2(CH_3CO_2)_4L_2$ complexes

Ligand parameters			Crystal data							
L	pK_b	DN[24]	d_{Rh-Rh} (Å)	d_{Rh-L} (Å)	d_{Rh-O} (Å)	d_{C-O} (Å)	Rh–Rh–O (°)	Rh–O–C (°)	O–C–O (°)	Ref.
CH_3CH	16.05[21]	19	2.377	2.254						1
DMF		26.6	2.383(1)	2.296(3)	2.038(3)	1.262(5)	88.33(9)	118.92(30)	126.1(44)	This work
H_2O		~33	2.3855(5)	2.310(3)	2.039(8)	1.269(4)	88.1(3)	119.9(3)	124.8(3)	15
CH_3CN	24.12[23]	14	2.384	2.254						1
py	8.75	33.1	2.3963(2)	2.227(3)	2.039(2)	1.266(3)	88.0(3)	119.1(3)	125.7	9
$NHEt_2$	3.51	~60	2.4020(7)	2.301(5)	2.038(3)	1.260(6)	87.9(1)	118.6(3)	127.0(4)	3
DMSO			2.406(1)	2.451(1)	2.036(3)	1.265(6)	87.82(9)	119.6(2)	125.5(4)	16
THT	18.52[23]		2.413(1)	2.517(1)	2.039(3)	1.273(6)	87.83(6)	119.4(3)	125.5(4)	16
CO			2.419(3)	2.091(3)	2.032(2)	1.266(3)	87.6(1)	119.6(2)	125.5(2)	3
PPh_3	11.3		2.449(2)	2.497(3)	2.044(4)	1.268(7)	87.1(1)	118.9(4)	126.4(4)	3
$P(OMe)_3$	~ 10.5[3]		2.455	2.973						3

acetate could be explained by the steric effects (longer S ... O distance in CH_3CSO, compared with O ... O distance in CH_3COO);[18] increase of the Rh–Rh bond distance in complexes

$$Rh_2(CH_3CO_2)_4(DMSO)_2$$

and

$$Rh_2(CH_3CO_2)_4(THT)_2$$

compared with the $Rh_2(CH_3CO_2)_4(H_2O)_2$ dimer requires the consideration of π-acceptor properties of coordinated sulphur.

This observation suggests that not only the steric effect but also the replacement of one oxygen atom in acetate ion by the sulphur capable of greater delocalization of the electron density could be responsible for elongation of the Rh–Rh distance in the $Rh_2(CH_3CO_2)_4(CH_3COSH)_2$ complex. The data presented here point out that while the influence of donor properties of bridging carboxylate ligands on the Rh–Rh bond distance was reversible compared to the influence of the donor properties of the terminal ligands L, the influence of acceptor power of both ligands on the Rh–Rh distance was the same.

Elongation of the Rh–Rh bond distance in the presence of ligands able to decrease the electron density in the Rh–Rh core (e.g., $CF_3CO_2^-$, CO, PR_3, DMSO, coordinating via S atom) could be caused by the increase of the positive charge on metal ions, and, simultaneously by contraction of the *d* orbitals, and in consequence, by their weaker mutual overlapping.[19]

Analysis of the crystallographic data seems to point out that in discussion of interactions between the Rh–Rh core and the bridging and terminal ligands, the σ and π interactions should be considered equally.

REFERENCES

1. F. R. Felthouse, *Prog. Inorg. Chem.* 1982, **29**, 73.
2. E. B. Boyar and S. D. Robinson, *Coord. Chem. Rev.* 1983, **50**, 109.
3. G. G. Christoph and Y. B. Koh, *Inorg. Chem.* 1979, **18**, 1122; *J. Am. Chem. Soc.* 1979, **101**, 1422.
4. J. G. Norman, Jr. and H. J. Kolari, *J. Am. Chem. Soc.* 1978, **100**, 791.
5. J. G. Norman, Jr., G. E. Renzoni and D. A. Case, *J. Am. Chem. Soc.* 1979, **101**, 5256.
6. B. E. Bursten and F. A. Cotton, *Inorg. Chem.* 1981, **14**, 2776.
7. T. Sowa, T. Kawamura, T. Shida and T. Yonezawa, *Inorg. Chem.* 1983, **22**, 56.
8. H. Nakatsuji, Y. Onishi and T. Yonezawa, *Inorg. Chem.* 1983, **22**, 103.
9. Y. B. Koh and G. G. Christoph, *Inorg. Chem.* 1978, **17**, 2590.
10. G. A. Rempel, P. Legadius, H. Smith and G. Wilkinson, *Inorg. Synth.* 1971, **13**, 90.
11. D. T. Cromer and I. T. Waber, *International Tables for X-ray Crystallography*, Vol. IV. Birmingham, Kynoch Press (1974).
12. Syntex (1976) XTL Structure Determination System, Syntex Analytical Instruments, Cupertino, California.
13. C. K. Jørgensen, *Modern Aspects of Ligand Field Theory*. North-Holland, Amsterdam–London (1971).
14. K. Das, K. M. Kadish and J. L. Bear, *Inorg. Chem.* 1978, **17**, 930.
15. F. A. Cotton, B. G. DeBoer, M. D. LaPrade, J. R. Pipal and D. A. Ucko, *Acta Cryst., Sect. 3* 1971, **97**, 4884.

16. F. A. Cotton and T. R. Felthouse, *Inorg. Chem.* 1980, **19**, 323.
17. L. M. Dikareva, M. A. Porai-Koshits, G. G. Sadikov, I. B. Baranovskii, M. A. Golubnichaya and R. N. Shchelokov, *Zh. Neorg. Khim.* 1978, **23**, 1044; *Russ. J. Inorg. Chem.* 1978, **23**, 578.
18. L. M. Dikareva, G. G. Sadikov, M. A. Porai-Koshits, I. B. Baranovskii, S. S. Adbullaev and R. N. Shchelokov, *Zh. Neorg. Khim.* 1982, **27**, 417.
19. F. A. Cotton, *Chem. Soc. Rev.* 1983, **1**, 35.
20. *Handbook of Chemistry and Physics* (Edited by R. C. Weast), 53rd ed. Chemical Rubber Publishing Co., Cleveland, Ohio (1973).
21. G. Perdoncin and G. Scorrano, *J. Am. Chem. Soc.* 1977, **99**, 6983 (calculated from data given there).
22. W. P. Jencks and J. Carriuolo, *J. Am. Chem. Soc.* 1960, **82**, 1778.
23. *Organic Solvents, Techniques of Chemistry* (Edited by J. A. Riddick and W. B. Bunger), Vol. II, Third Ed. Wiley–Interscience, New York (1970).
24. V. Gutmann, *Electrochimica Acta* 1976, **2**, 661.

Polyhedron Vol. 4, Vol. 8, pp. 1419–1424, 1985
Printed in Great Britain

0277–5387/85 $3.00 + .00
© 1985 Pergamon Press Ltd

RUTHENIUM(II) COMPLEXES WITH TRIPHENYLPHOSPHINE OR TRIPHENYLARSINE AND OTHER MONODENTATE LIGANDS

RAJ K. PODDAR,* K. P. SARMA and U. C. SARMA
Department of Chemistry, North-Eastern Hill University, Bijni Complex, Shillong—793 003, India

(*Received* 24 *October* 1984; *accepted* 18 *December* 1984)

Abstract—Synthesis and studies on some five-coordinate ruthenium(II) complexes, viz. $[Ru(MPh_3)(C_6H_5CHO)_2Cl_2]$ and $[Ru(MPh_3)_2(CO)Cl_2]$ (where M = P or As) have been described. Reactions of $[Ru(MPh_3)(C_6H_5CHO)_2Cl_2]$ with *N*,*N*-dimethylformamide, dimethylsulphoxide and pyridine and of $[Ru(MPh_3)_2(CO)Cl_2]$ with pyridine are described.

The chemistry of the complexes of ruthenium(II) and ruthenium(III) containing strong donor ligands such as mono-tertiary-phosphine, arsine or stibine has been studied extensively.[1–23] The chemistry of the complexes of ruthenium(II) and ruthenium(III) with relatively weak donor ligands, such as dimethylsulphoxide, pyridine and acetonitrile has been relatively less studied.[24–28] Complexes of ruthenium(II) and ruthenium(III) containing both strong and weak donor ligands where the coordination around metal ion is generally six have also been studied in detail.[2,9,13,19,21,22,29–37] Complexes of ruthenium(II) containing weak donor ligands or having both strong and weak donor ligands have a strong potential to act as catalysts in various homogeneous reactions.[24]

Most of the complexes of ruthenium(II) and ruthenium(III) of the type discussed above involve six coordinated metal ions. Complexes having pentacoordination have a strong potential to act as catalysts in various homogeneous reactions. Here, some pentacoordinated complexes of ruthenium(II) containing triphenylphosphine or triphenylarsine and benzaldehyde are reported. Some of their reactions to substitute the coordinated benzaldehyde by weak donor ligands are also described.

EXPERIMENTAL

All the chemicals used were reagent grade. Ruthenium trichloride hydrate was supplied by Aurora-Matthey Limited, Calcutta.

$[RuCl_2(PPh_3)_2]_n$,[20]

$[RuCl_2(PPh_3)_3]$[2]

and

$[RuCl_2(AsPh_3)_2]_2$[20]

were prepared according to reported methods.

Preparations

$[RuCl_2(MPh_3)(C_6H_5CHO)_2]$ (M = P *or* As). To a solution of ruthenium trichloride hydrate ($RuCl_3 \cdot xH_2O$) (0.1 g) in *n*-butanol (10 cm^3), benzaldehyde (2 cm^3) was added. A solution of triphenylphosphine (0.5 g) or triphenylarsine (0.6 g) in *n*-butanol (5 cm^3) was added to the hot solution of ruthenium trichloride mentioned above. The resulting solution was then refluxed for about 30 min or 2 h, in the case of triphenylphosphine or triphenylarsine respectively. The reaction mixture was cooled overnight when a brownish-yellow crystalline compound in the case of triphenylarsine and a light green compound in the case of triphenylphosphine was obtained. The compound was separated by centrifugation and washed first with methanol and then with diethylether and dried under vacuum. The compounds were analysed for $[RuCl_2(MPh_3)(C_6H_5CHO)_2]$.

$[RuCl_2(CO)(AsPh_3)_2]$. (i) To a clear solution of ruthenium trichloride hydrate (0.1 g) in *n*-butanol (10 cm^3) and benzaldehyde (2 cm^3) mixture, a solution of triphenylarsine (1 g) in *n*-butanol (5 cm^3) was added

* Author to whom correspondence should be addressed.

and the mixture was refluxed for about 20 h. Initially, benzaldehyde complex was formed which went into solution and finally an orange solution was obtained which on cooling yielded a yellow compound. The mother liquor upon concentration under reduced pressure and cooling yielded more of the yellow compound, which was centrifuged, washed first with acetone and then with ether and dried under vacuum. It was analysed for $[Ru(CO)(AsPh_3)_2Cl_2]$.

(ii) $[RuCl_2(CO)(AsPh_3)_2]$ could be obtained also by boiling under reflux $[RuCl_2(AsPh_3)_2]_2$ (0.2 g) in benzaldehyde (2 cm^3) and *n*-butanol (10 cm^3) mixture for about 8 h or by boiling under reflux $[RuCl_2(C_6H_5CHO)_2(AsPh_3)]$ (0.2 g) and triphenylarsine (0.2 g) in *n*-butanol (10 cm^3) for about 10 h and cooling the orange–red solution obtained.

$[RuCl_2(CO)(PPh_3)_2]$ *(reddish-brown).* To a solution of ruthenium trichloride hydrated (0.2 g) in *n*-butanol (20 cm^3) and benzaldehyde (4 cm^3) mixture, a solution of triphenylphosphine (1.5 g) in *n*-butanol (10 cm^3) was added and the mixture was boiled under reflux for 6–8 h, when a reddish-brown crystalline compound (m.p. 195–200°C) separated out which was separated by centrifugation and washed first with methanol and then with diethylether and dried under vacuum. It was analysed for $[RuCl_2(CO)(PPh_3)_2]$.

$[RuCl_2(CO)(PPh_3)_2]$ *(yellow).* (i) The reaction was carried out in a way similar to that for the reddish-brown compound mentioned above, except that the reaction mixture was refluxed for 15–20 h, when the red crystalline compound obtained as an intermediate went into solution and finally a reddish-yellow solution was obtained, which on cooling resulted in the separation of a yellow compound. The compound was separated and washed first with acetone and then with ether. Concentration of the mother liquor resulted in the separation of more yellow compound. The compound was analysed for $[RuCl_2(CO)(PPh_3)_2]$.

(ii) The yellow compound could also be obtained by boiling under reflux $[RuCl_2(PPh_3)_2]_n$ or $[RuCl_2(PPh_3)_3]$ (0.2 g) in benzaldehyde (2 cm^3) and *n*-butanol (10 cm^3) mixture for about 8 h or by boiling under reflux $[RuCl_2(C_6H_5CHO)_2(PPh_3)]$ (0.2 g) and triphenylphosphine (0.2 g) in *n*-butanol (10 cm^3) for about 10 h and cooling the reddish-yellow solution obtained.

Reactions of $[Ru(MPh_3)(C_6H_5CHO)_2Cl_2]$ (M = P, *or* As) *with* L = *pyridine,* N,N-*dimethylformamide (DMF) and dimethylsulphoxide (DMSO).* $[Ru(MPh_3)(C_6H_5CHO)_2Cl_2]$ (0.2 g) was taken with L (0.5 cm^3) and heated on a water-bath for about 1 h, when a clear solution was obtained. To the cold solution, methanol was added in the case of DMF or DMSO and the diethylether in the case of pyridine reaction and the mixture was kept overnight when crystalline compound separated out. It

Table 1. Some physical and analytical data of new ruthenium(II) complexes

Compound	Colour	m.p. °C	% C (calc.)	% H (calc.)	% N (calc.)	% Cl (calc.)
$[Ru(AsPh_3)(benz)_2Cl_2]$	Brownish-yellow	188–192	55.28 (55.65)	3.94 (3.91)	—	10.15 (10.29)
$[Ru(PPh_3(benz)_2Cl_2]$	Light-green	175–182	59.21 (59.44)	4.44 (4.18)	—	10.73 (10.99)
$[Ru(CO)(PPh_3)_2Cl_2]$	Reddish-brown	195–200	61.60 (61.32)	4.32 (4.14)	—	10.00 (9.81)
$[Ru(CO)(AsPh_3)_2Cl_2]$	Yellow	260–267	54.92 (54.68)	3.85 (3.69)	—	8.38 (8.74)
$[Ru(CO)(PPh_3)_2Cl_2]$	Yellow	270–275	61.49 (61.32)	4.36 (4.14)	—	10.05 (9.81)
$[Ru(AsPh_3)(py)_3Cl_2]$	Reddish-brown	198–200	54.95 (55.38)	3.95 (4.20)	6.12 (5.87)	9.62 (9.93)
$[Ru(AsPh_3)(DMF)_3Cl_2]$	Reddish-brown	205–210	46.05 (46.48)	4.69 (5.16)	6.41 (6.03)	9.76 (10.19)
$[Ru(PPh_3)(DMF)_3Cl_2]$	Yellowish-brown	215–220	50.06 (49.62)	5.12 (5.51)	6.11 (6.43)	11.24 (10.87)
$[Ru(CO)(py)_2(AsPh_3)Cl_2]$	Yellow	208–210	52.73 (52.41)	3.42 (3.77)	4.54 (4.22)	11.12 (10.69)
$[Ru(CO)(py)_2(PPh_3)Cl_2]$	Yellow	180–185	55.67 (56.13)	3.86 (4.03)	4.28 (4.52)	11.69 (11.45)

benz = benzaldehyde; py = pyridine.

Table 2. Electronic absorption and important IR spectral data of ruthenium(II) complexes

Compound	Electronic spectral bands: λ_{max} in nm (ε_{max})	Important IR absorptions in cm^{-1}
$[Ru(AsPh_3)(benz)_2Cl_2]$	810 (220) 520 sh 410 (1460)	1615 m 1595 m 1575 m 1450 m 1218 m 670 m 330 s
$[Ru(PPh_3)(benz)_2Cl_2]$	765 (225) 420 (1500)	1615 m 1597 m 1580 m 1452 m 1220 m 675 m
$[Ru(AsPh_3)(py)_3Cl_2]$	450 (1105) 390 (2300)	1445 m
$[Ru(AsPh_3)(DMF)_3Cl_2]$	510 (250) 405 (1050)	1640 s 1360 m
$[Ru(PPh_3)(DMF)_3Cl_2]$	550 (240) 415 (1250)	1642 s 1358 m
$[Ru(CO)(py)_2(PPh_3)Cl_2]$	—	1962 m–s 1945 m–s 1442 m
$[Ru(CO)(py)_2(AsPh_3)Cl_2]$	—	1952 m 1940 s 1923 m 1445 m

benz = benzaldehyde; py = pyridine; DMF = dimethylformamide.

was centrifuged, washed with ether and dried under vacuum. The compounds obtained had the composition $[RuCl_2(MPh_3)L_3]$ (where M = P or As and L = pyridine or DMF) and $[RuCl_2(DMSO)_4]$.

Reaction of $[Ru(MPh_3)_2(CO)Cl_2]$ *with pyridine.* $[Ru(MPh_3)_2(CO)Cl_2]$ (M = P or As) (0.2 g) was taken with pyridine (1 cm^3) and heated on a water bath when a clear yellow solution was obtained. After cooling the solution, ether was added when yellow compound precipitated out, which was centrifuged, washed with ether and dried under vacuum. The compounds had the composition $[RuCl_2(CO)(MPh_3)(py)_2]$.

Carbon, hydrogen and nitrogen analyses were obtained from the Microanalytical Laboratory, I.I.T., Kanpur. Chloride estimations were carried out according to standard methods[38] gravimetrically after decomposing the complexes using KNO_3, KOH mixture. IR spectra were recorded in KBr as pellets in the region 4000–600 cm^{-1} on a Perkin–Elmer 297 IR spectrophotometer, and on Perkin–Elmer 580 spectrophotometer in the region 600–250 cm^{-1} for some complexes. Visible electronic spectra were recorded in chloroform in the region 800–350 nm on a Beckmann-26 spectrophorometer. Proton magnetic resonance spectra were recorded on a Varian EM-390, 90 MHz spectrometer in $CDCl_3$, with TMS as reference. Magnetic susceptibility measurements were carried out using a Gouy balance at room temperature. Mercury tetrathiocyanatocobaltate(II) was used as calibrant. All the melting points are uncorrected. The conductivity measurements were made using an Elico type CM 82 conductivity bridge in nitrobenzene.

RESULTS AND DISCUSSION

(a) $[Ru(MPh_3)(C_6H_5CHO)_2Cl_2]$ (M = P *or* As)

Ruthenium compounds containing triphenylphosphine or triphenylarsine and benzaldehyde have the composition $[Ru(MPh_3)(C_6H_5CHO)_2Cl_2]$ (M = P or As). Benzaldehyde is easily oxidised to benzoic acid. As the reactions were carried out in the presence of air, the possibility of benzaldehyde getting oxidised to benzoic acid and coordinating to the ruthenium can not be eliminated. However, a similar reaction under nitrogen atmosphere also gave the same products. The PMR of $[Ru(AsPh_3)(C_6H_5CHO)_2Cl_2]$ in dueterated chloroform showed signals at 10, 7.31 and 7.23δ. The signals at 10 and at 7.31 and 7.32δ were in the ratio 2:25. The aryl aldehyde proton is normally observed in the 10.1–9.5δ range.[39] In the benzaldehyde complex containing triphenylarsine, a proton signal at 10δ can unambiguously be assigned as due to the proton of the aldehyde functional group of benzaldehyde. The signals at 7.31 and 7.23δ are due to the phenyl groups of triphenylarsine and benzaldehyde respectively. The ratio of the proton signals for aldehydic proton and the phenyl protons is as expected (2:25). Similarly, the triphenylphosphine analogue, viz. $[Ru(PPh_3)(C_6H_5CHO)_2Cl_2]$, gave proton signals at 10, 7.5 and 7.23δ. The ratio of 10δ to 7.5 and 7.23δ signals is again 2:25 as expected for two aldehyde protons and 25 phenyl protons. The signals at 7.5 and 7.23δ are due to the phenyl groups of triphenylphosphine and benzaldehyde respectively. Thus, the PMR spectra of $[Ru(MPh_3)(C_6H_5CHO)_2Cl_2]$ (M = P or As) confirmed the presence of three phenyl groups due to triphenylphosphine or arsine, two phenyl groups and two aldehydic protons due to two benzaldehyde molecules.

The IR spectra of the two complexes discussed above showed all the bands due to triphenylphosphine or triphenylarsine and benzaldehyde. Among the important IR bands due to benzaldehyde are three bands of medium intensity at 1615, 1595 and 1575 cm^{-1} and bands at 1450, 1220 and 670 cm^{-1}. ν_{CO} for free benzaldehyde occurs at 1698 cm^{-1}. Due to coordination of benzaldehyde to the metal, the stretching frequency of ν_{CO} goes down and one of the bands around 1600 cm^{-1} could be due to ν_{CO} of benzaldehyde coordinated to ruthenium. Other IR bands are present in free benzaldehyde too but with a slight shift in the position. A strong band at 330 cm^{-1} was observed for $[Ru(AsPh_3)(C_6H_5CHO)_2Cl_2]$. Triphenylarsine also shows absorption around 330 cm^{-1}. Hence this band cannot be assigned unambiguously; however, it may be due to the coupled vibrations of ν_{Ru-Cl} and the characteristic vibrations of triphenylarsine.[20] The complexes discussed above are diamagnetic, thereby confirming the presence of bivalent ruthenium. These complexes are probably pentacoordinated as suggested by the electronic absorption spectra in chloroform. These spectra (Fig. 1) show one absorption band in the region 760–810 nm and another around 410 nm. The band around 800 nm is observed in ruthenium(II) pentacoordinated square-pyramidal complexes, viz. $[RuCl_2(PPh_3)_3]$ and $[RuCl_2(AsPh_3)_2]_2$.[20] Electronic absorption in this region is generally not observed for octahedrally coordinated complexes of ruthenium(II). Hence, the benzaldehyde complexes seem to have a distorted square-pyramidal structure. The diamagnetic behaviour thus suggests that the six electrons in ruthenium(II) are probably distributed as $(d_{xz}, d_{yz})^4$, d_{xy}.[2] The band around 800 nm could be assigned to $d_{xy} \rightarrow d_{z^2}$ and around 400 nm to $(d_{xz}, d_{yz}) \rightarrow d_{z^2}$ transitions. The complexes are non-conducting in nitrobenzene, thereby confirming non-ionic type of structure for the complexes.

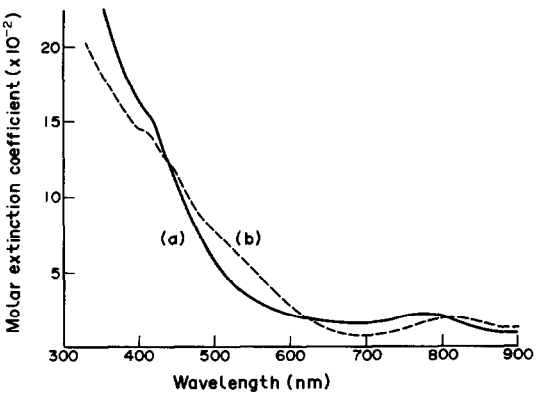


Fig. 1. Electronic spectra of (a) $[RuCl_2(PPh_3)(C_6H_5CHO)_2]$ and (b) $[RuCl_2(AsPh_3)(C_6H_5CHO)_2]$ in chloroform.

(b) $[Ru(MPh_3)(CO)Cl_2]$

The reaction of ruthenium trichloride, benzaldehyde and triphenylphosphine in *n*-butanol for a period of about 6–8 h yielded a reddish-brown crystalline compound of the composition $[Ru(PPh_3)_2(CO)Cl_2]$. It is diamagnetic in nature and shows a strong and sharp IR absorption at 1980 cm^{-1} assignable to ν_{CO} (terminal). A compound with the same molecular formula and yellow in colour was reported by James *et al.*[19] which showed IR absorptions at 1931 and 1921 cm^{-1} in Nujol and at 1940 cm^{-1} in methylene chloride solution for

ν_{CO} (terminal). It was characterised as a pentacoordinated complex, which apparently isomerized in methylene chloride solution showing a broad band at 1970 cm^{-1}. The reddish-brown compound may be an isomer of the yellow compound reported by James *et al.*[19]

Prolonged reaction ($\sim$ 20 h) of ruthenium trichloride, benzaldehyde and triphenylphosphine or triphenylarsine resulted in the formation of yellow compounds of the composition $[Ru(CO)(MPh_3)_2Cl_2]$ (M = P or As). These compounds could also be obtained by the reaction of $[RuCl_2(PPh_3)_3]$, $[RuCl_2(PPh_3)_2]_n$ or $[RuCl_2(AsPh_3)_2]_2$ with benzaldehyde in *n*-butanol or by the reaction of $[RuCl_2(MPh_3)(C_6H_5CHO)_2]$ with the corresponding triphenylphosphine or arsine in *n*-butanol. Formation of these carbonyl containing complexes is due to the extraction of a carbonyl group from a benzaldehyde molecule, either coordinated to the metal or free (present in the reaction medium). The infrared spectra of these yellow carbonyl complexes show a strong and sharp band at 1940 cm^{-1} assignable to ν_{CO} (terminal), and all other bands due to triphenylphosphine or triphenylarsine. Yellow $[Ru(CO)(PPh_3)_2Cl_2]$ obtained by us may be same as reported by James *et al.*[19]

(c) *Reactions of* $[Ru(MPh_3)(C_6H_5CHO)_2Cl_2]$ (M = P *or* As) *with donor solvents*

Reactions of $[Ru(MPh_3)(C_6H_5CHO)_2Cl_2]$ (M = P or As) with donor solvents were carried out to find out the ease of substitution of the coordinated benzaldehyde. The donor solvents used were pyridine, *N,N*-dimethylformamide (DMF), and dimethylsulphoxide (DMSO).

Reactions with pyridine or DMF results in the formation of the six coordinate species $[Ru(MPh_3)L_3Cl_2]$ (L = py or DMF) because two molecules of benzaldehyde in the original complexes are replaced by three molecules of pyridine or DMF. The inability to form hexacoordinate complexes with benzaldehyde may be due to partial blocking of the sixth coordination site by the phenyl groups of the two benzaldehyde molecules or the triphenylarsine or phosphine molecule. The IR spectra of the complexes containing DMF showed a very strong band at 1640 cm^{-1} which is due to ν_{CO} of DMF coordinate through the oxygen atom.[22] In the case of pyridine complexes, all bands due to coordinated pyridine were observed besides bands due to triphenylphosphine or triphenylarsine in the IR region. A medium-sharp band at 1445 cm^{-1} characteristic of pyridine was also observed.

Pyridine or DMF containing complexes are diamagnetic, thereby confirming that ruthenium(II) is present in the low-spin state. The electronic absorption spectra of these complexes showed two bands one in the region 450–550 nm and other one in the region 415–390 nm, with a molar extinction coefficient of the order of 10^2–10^3. These bands may be assigned to $^1A_{1g} \rightarrow {}^1T_{1g}$ and $^1A_{1g} \rightarrow {}^1T_{2g}$ transitions respectively. The values of the molar extinction coefficient ($\sim 10^3$) are relatively high but this may be due to the mixing of the energy levels with the charge-transfer band(s) in that region.[22] These complexes are non-electrolytes in nitrobenzene, thereby confirming their non-ionic character.

Reaction of DMSO with

$$[Ru(MPh_3)(C_6H_5CHO)_2Cl_2]$$

resulted in the substitution of all the benzaldehyde and triphenylphosphine or triphenylarsine molecules by DMSO and gave $[Ru(Cl_2(DMSO)_4]$. The DMSO complex showed strong IR absorptions at 1120, 1090 and 915 cm^{-1}. The former two absorptions could be due to $\nu_{S=O}$ of the S-bonded DMSO and the later one due to $\nu_{S=O}$ of the O-bonded DMSO. The complex was same as reported by Evans *et al.*[27]

(d) *Reactions of* $[Ru(CO)(MPh_3)_2Cl_2]$ (M = P *or* As) *with pyridine*

Reddish-brown or yellow compounds of the composition $[Ru(CO)(MPh_3)_2Cl_2]$ (M = P or As), on treatment with pyridine resulted in the formation of $[Ru(CO)(MPh_3)(py)_2Cl_2]$, which showed all IR absorptions due to triphenylphosphine or triphenylarsine and pyridine. A band at 1444 cm^{-1} characteristic of pyridine was observed. Besides, two or three bands in the region 1965–1920 cm^{-1} due to ν_{CO} were also observed.

The potential of some of the above mentioned pentacoordinated complexes to act as homogenous catalysts is being examined.

REFERENCES

1. F. P. Dwyer, J. E. Humpoletz and R. S. Nyholm, *J. Proc. Roy. Soc. N. S. Wales* 1946, **80**, 217.
2. T. A. Stephenson and G. Wilkinson, *J. Inorg. Nucl. Chem.* 1966, **28**, 945.
3. R. S. Nyholm and G. J. Sutton, *J. Chem. Soc.* 1958, 567.
4. J. Chatt and R. G. Hayter, (i) *J. Chem. Soc.* 1961, 896; (ii) *J. Chem. Soc.* 1963, 6017.
5. J. Chatt, B. L. Shaw and A. E. Field, *J. Chem. Soc.* 1964, 3466.
6. J. Chatt, G. J. Leigh, D. M. P. Mingos and R. J. Paske, *J. Chem. Soc. (A)* 1968, 2636.

7. J. N. Jenkins, M. S. Lupin and B. L. Shaw, *J. Chem. Soc.* (*A*) 1966, 1787.
8. M. S. Lupin and B. L. Shaw, *J. Chem. Soc.* (*A*) 1968, 741.
9. L. Vaska, *Chem. & Ind.* 1961, 1402.
10. L. Vaska and J. W. Diluzio, *J. Am. Chem. Soc.* 1961, **83**, 1262.
11. J. Halpern, B. R. James and L. W. Kemp, *J. Am. Chem. Soc.* 1966, **88**, 5142.
12. J. K. Nicholson, *Angew Chem.* (*Int. Ed.*) 1967, **6**, 264.
13. T. A. Stephenson, (i) *Inorg. Nucl. Chem. Lett.* 1968, **4**, 687; (ii) *J. Chem. Soc.* (*A*) 1970, 889.
14. J. J. Levison and S. D. Robinson, *J. Chem. Soc.* (*A*) 1970, 2947.
15. N. Ahmed, S. D. Robinson and M. F. Uttley, *J. Chem. Soc., Dalton Trans.* 1972, 843.
16. K. G. Caulton, *J. Am. Chem. Soc.* 1974, **96**, 3005.
17. P. R. Hoffman and K. G. Caulton, *J. Am. Chem. Soc.* 1975, **97**, 4221.
18. R. C. J. Vriends, G. V. Koten and K. Vrieze, *Inorg. Chim. Acta* 1978, **26**, L29.
19. B. R. James, L. D. Markhan, B. C. Hui and G. L. Rempel, *J. Chem. Soc., Dalton Trans.* 1973, 2247.
20. R. K. Poddar and U. Agarwala, (i) *Ind. J. Chem.* 1971, **9**, 477; (ii) *J. Inorg. Nucl. Chem.* 1973, **35**, 567.
21. R. K. Poddar, I. P. Khullar and U. Agarwala, *Inorg. Nucl. Chem. Lett.* 1974, **10**, 221.
22. K. Natarajan, R. K. Poddar and U. Agarwala, (i) *Inorg. Nucl. Chem. Lett.* 1976, **12**, 749; (ii) *J. Inorg. Nucl. Chem.* 1976, **38**, 249; (iii) *J. Inorg. Nucl. Chem.* 1977, **39**, 431.
23. R. K. Poddar, R. Parshad and U. Agarwala, *J. Inorg. Nucl. Chem.* 1980, **42**, 837.
24. J. A. Davies and F. R. Hartley, *Chem. Rev.* 1981, **81**, 79.
25. J. Chatt, G. J. Leigh and A. P. Storace, *J. Chem. Soc.* (*A*) 1971, 1380.
26. J. D. Gilbert, D. Rose and G. Wilkinson, *J. Chem. Soc.* (*A*) 1970, 2765.
27. I. P. Evans, A. Spencer and G. Wilkinson, *J. Chem. Soc., Dalton Trans.* 1973, 204.
28. N. V. Sidwick, *The Chemical Elements and their Compounds*, pp. 1468, 1479. Clarendon Press, Oxford (1950).
29. S. Cenini, A. Fusi and G. Capparella, *Inorg. Nucl. Chem. Lett.* 1972, **8**, 127.
30. E. S. Switkes, L. Ruiz Ramirez, T. A. Stephenson and J. Sinclair, *Inorg. Nucl. Chem. Lett.* 1972, **8**, 593.
31. L. Ruiz Ramirez, T. A. Stephenson and E. S. Switkes, *J. Chem. Soc., Dalton Trans.* 1973, 1770.
32. J. D. Gilbert, M. C. Baird and G. Wilkinson, *J. Chem. Soc.* (*A*) 1968, 2198.
33. J. D. Gilbert and G. Wilkinson, *J. Chem. Soc.* (*A*) 1969, 1749.
34. M. Yagupsky and G. Wilkinson, *J. Chem. Soc.* (*A*) 1968, 2183.
35. K. R. Grundy, R. O. Harris and W. R. Roper, *J. Organomet. Chem.* 1975, **90**, C34.
36. R. K. Poddar and U. Agarwala, *J. Inorg. Nucl. Chem.* 1973, **35**, 3769.
37. J. C. Muscarella and J. R. Crook, *J. Chem. Soc., Dalton Trans.* 1978, 1152.
38. J. Bassett, R. C. Denney, G. H. Jeffery and J. Mendham, *Vogel's Text Book of Quantitative Inorganic Analysis*. ELBS and Longman (1979).
39. J. R. Dyer, *Applications of Absorption Spectroscopy of Organic Compounds*, p. 88. Prentice-Hall (1978).

Polyhedron Vol. 4, No. 8, pp. 1425–1428, 1985
Printed in Great Britain

0277–5387/85 $3.00 + .00
© 1985 Pergamon Press Ltd

ESR STUDIES ON THE REACTIONS OF SULPHITE RADICAL ANION, $SO_3^{\dot{-}}$, WITH NITROALKANE COMPOUNDS IN AQUEOUS SOLUTIONS

TOSHIHIKO OZAWA* and TAKAO KWAN†
Faculty of Pharmaceutical Sciences, University of Tokyo, Hongo, Bukyo-ku, Tokyo 113, Japan

(*Received* 9 *October* 1984; *accepted* 4 *January* 1985)

Abstract—The reactions of the sulphite radical anion, $SO_3^{\dot{-}}$ (generated from the Ti^{3+}–H_2O_2–Na_2SO_3 system at pH 9), in aqueous solutions with some nitroalkane compounds were investigated by using a rapid-mixing flow technique coupled with electron spin resonance (ESR) which can detect the radicals having a lifetime of 5–100 ms. The $SO_3^{\dot{-}}$ radical added to the double bond of C=N in the nitroalkane *aci*-anions which are the main form of nitroalkanes in aqueous alkaline solutions. From the observed hyperfine splitting constants of the $SO_3^{\dot{-}}$ adducts of nitroalkane *aci*-anions, the preferred conformation of the adducts was deduced.

It is well known that the rapid-mixing flow technique coupled with electron spin resonance (ESR) is very useful to detect the short-lived radicals having a lifetime longer than a few msec. In previous papers, by the use of this technique we have reported that the sulphite radical anion, $SO_3^{\dot{-}}$, which is generated from Ce^{4+}–$NaHSO_3$ system in acidic solutions, can add to the compounds having C=C,[1] C≡C[2] and C=S[3] bonds to give the corresponding secondary radicals, respectively. Also, in the alkaline aqueous solutions at pH 9, the same radical species, $SO_3^{\dot{-}}$, which is obtained from a Ti^{3+}(ethylenediaminetetraacetic acid)–H_2O_2–Na_2SO_3 system, can add to uracil derivatives having the C=S bond.[4] Further, we have found that the reactive characteristics of the oxy anion radicals of sulphur, $SO_2^{\dot{-}}$, $SO_3^{\dot{-}}$ and $SO_4^{\dot{-}}$, are different from each other and reported that these differences of reactivity towards the organic substrates may be caused by the difference in the distribution of the unpaired electron density in each radical anion.[5] It was also found that the $SO_3^{\dot{-}}$ radical could not react with aromatic nitro compounds.[3] However, Norman *et al.* briefly reported that in aqueous alkaline solutions, the $SO_3^{\dot{-}}$ radical could add to the nitroalkane compounds.[6] Therefore, we have further examined in detail the reactions of the $SO_3^{\dot{-}}$ radical with the nitroalkane compounds in alkaline aqueous solutions by use of the rapid-mixing flow technique.

EXPERIMENTAL

Materials. $TiCl_3$ (20% v/v), ethylenediaminetetraacetic acid (EDTA) and Na_2SO_3 were purchased from Wako Pure Chemical Ind. Ltd. and used without further purification. H_2O_2 (30%) was obtained from Mitsubishi Gas Chemical. Nitroalkane compounds were purchased from Tokyo Kasei Kogyo Co. Ltd. and used without further purification. Other chemical reagents were of commercial GR grade.

ESR measurements. ESR measurements were carried out on a JEOL-PE-1X ESR spectrometer (X-band) with 100 kHz field modulation in conjunction with a JEOL mixing chamber and T-shaped cell which enabled three reagents to mix almost simultaneously.[4] This apparatus enabled us to detect radicals having lifetimes of 5–100 ms. The hyperfine coupling constants and g-values were calibrated by comparison with an aqueous solution of Fremy's salt ($g = 2.0055$, $a^N = 13.0$ G)[7] in a capillary tube attached to the sample.

Procedure. All solutions were prepared from triply distilled water, and their pH was adjusted by aqueous ammonia solution.

* Author to whom correspondence should be addressed. Present address: National Institute of Radiological Sciences, 9-1, Anagawa-4-chome, Chiba-shi 260, Japan.

† Present address: Faculty of Pharmaceutical Sciences, Teikyo University, Sagamiko-cho, Tsukui-gun, Kanagawa 199-01, Japan.

For the generation of the $SO_3^{\dot{-}}$ radical in alkaline aqueous solutions,[6] $TiCl_3$ (20%), H_2O_2 (30%) and Na_2SO_3 were used. The conditions for oxidation with and without an added organic substrate were the same except that, in the latter case, only two of the three entry of ports into the mixing chamber were employed and the third solution referred to below was omitted. Three solutions were prepared: the first solution contained 0.01 M Ti^{3+}, 0.01 M EDTA, and 0.1 M Na_2SO_3; the second contained 0.05 M H_2O_2; and the third contained the organic compound (0.1 M). Aqueous ammonia was added to the first and the third solution to give a pH of 9.

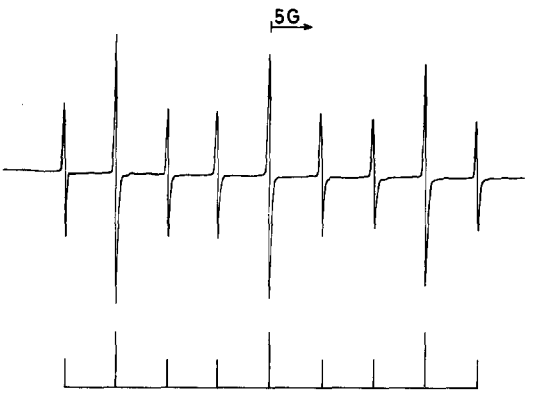


Fig. 1. ESR spectrum and its stick diagram observed by the reaction of nitromethane *aci*-anion with the $SO_3^{\dot{-}}$ radical at pH 9.

RESULTS

It is well known that nitroalkane compounds exist as *aci*-anion forms ($R_1R_2C{=}NO_2^-$) in alkaline aqueous solutions, and that these *aci*-anions from several nitroalkanes react rapidly enough with various radicals such as hydroxyl,[8] amino,[8] methyl[9] and α-aminoalkyl[10] to give the corresponding secondary radical anion adducts

$$[R_1R_2C(X)\text{–}NO_2^{\dot{-}}]$$

in sufficient concentration for ESR detection. The formation of the same radical anion adduct was expected during the reaction of the $SO_3^{\dot{-}}$ radical with nitroalkane *aci*-anions.

When solutions of Ti^{3+} and EDTA, H_2O_2, and Na_2SO_3 were mixed in the cavity of the ESR spectrometer, the pH after mixing being 9, a singlet absorption line at $g = 2.0028$, which has been assigned to the $SO_3^{\dot{-}}$ radical,[4] was observed. Since when either Ti^{3+} or H_2O_2 was omitted no ESR spectrum could be observed, the $SO_3^{\dot{-}}$ radical may be formed by one-electron oxidation of the sulphite ion by the hydroxy radical which is generated by the reaction of Ti^{3+} ion with H_2O_2[11] [eqns. (1)–(3)], taking into consideration the pK of HSO_3^- of 7.2.[12]

$$Ti^{3+} + H_2O_2 \rightarrow Ti^{4+} + HO^- + HO\cdot \quad (1)$$

$$HSO_3^- \rightleftarrows SO_3^{2-} + H^+ \quad (2)$$

$$HO\cdot + SO_3^{2-} \rightarrow HO^- + SO_3^{\dot{-}}. \quad (3)$$

Nitromethane aci-*anion.* When nitromethane was added as the third solution and allowed to react with the solution mentioned above, the absorption line due to the $SO_3^{\dot{-}}$ radical was completely consumed, and a new ESR signal appeared at $g = 2.0050$ (Fig. 1). This spectrum can be analyzed in terms of parameters: $a^N(1) = 22.22$ G and $a^H(2) = 7.53$ G. Since these parameters are different from those of nitromethane radical anion[9] or those of OH adduct of nitromethane *aci*-anion,[8] the radical species observed is assignable to the $SO_3^{\dot{-}}$ adduct, $H_2C(SO_3^-)NO_2^{\dot{-}}$.

Nitroethane aci-*anion.* When nitroethane was mixed with the $SO_3^{\dot{-}}$ radical, the ESR signal due to the latter disappeared and a new ESR signal was observed at $g = 2.0050$ (Fig. 2), This spectrum can be analyzed in terms of the parameters: $a^N(1) = 22.80$ G, $a^H(1) = 3.33$ G and $a^H(3) = 0.42$ G. Since the spectral pattern is similar to that of OH adduct of nitroethane *aci*-anion, but the parameters are different from each other, the radical species observed can be assigned to the $SO_3^{\dot{-}}$ adduct, $MeCH(SO_3^-)NO_2^{\dot{-}}$.

1-*Nitropropane* aci-*anion.* When 1-nitropropane was reacted with the $SO_3^{\dot{-}}$ radical at pH 9, only the ESR spectrum as shown in Fig. 3 was observed. This newly observed spectrum can be analyzed in terms of the parameters: $a^N(1) = 22.08$ G, $a^H(1) = 2.18$ G and $a^H(1) = 0.70$ G. Since these parameters are different from those of OH adduct of 1-nitropropane *aci*-anion, the observed radical species is assignable to the $SO_3^{\dot{-}}$ adduct, $EtCH(SO_3^-)NO_2^{\dot{-}}$. In this case, only

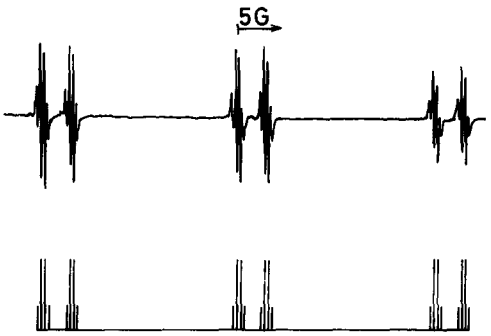


Fig. 2. ESR spectrum and its stick diagram observed during the reaction of the $SO_3^{\dot{-}}$ radical with nitroethane *aci*-anion at pH 9.

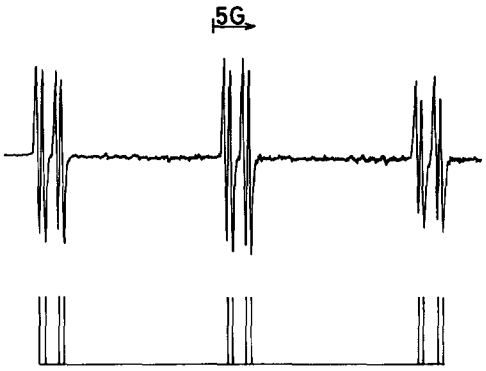


Fig. 3. ESR spectrum and its stick diagram observed during the reaction of the $SO_3^{\dot{-}}$ radical with 1-nitropropane *aci*-anion at pH 9.

one hyperfine splitting attributable to a γ-proton was observed. Possibly the other splitting was small enough to be marked by the line-widths (*ca* 0.3 G). This type of the magnetic non-equivalency is ascribed to the chirality of the adjacent carbon atom.[13]

2-*Nitropropane* aci-*anion*. The similar $SO_3^{\dot{-}}$ adduct of 2-nitropropane *aci*-anion, $(Me)_2C(SO_3^-)NO_2^{\dot{-}}$, was observed when 2-nitropropane was reacted with the $SO_3^{\dot{-}}$ radical at pH 9. The spectrum can be analyzed as follows: $a^N(1) = 22.83$ G and $a^H(6) = 0.42$ G.

The ESR parameters observed during the reaction of the $SO_3^{\dot{-}}$ radical with some nitroalkanes are summarized in Table 1.

DISCUSSION

From Table 1, it is apparent that the $SO_3^{\dot{-}}$ radical can easily add to the C=N bond of nitroaklane *aci*-anions to yield the $SO_3^{\dot{-}}$ adducts.

The β-proton splitting constants of the radical anions as shown in Table 1 are less than that of nitromethane radical anion, $CH_3NO_2^{\dot{-}}$ (12.0 G).[9] The sensitivity of the hyperfine splitting from a β-proton

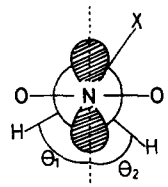


Fig. 4. Possible model of the nitroxide radical. θ represents the dihedral angle.

to the dihedral angle between the orbital of the unpaired electron and the β C–H bond has continued to provide a useful probe for the study of the radical conformation.

Generally, the hyperfine splitting constant due to the β-protons could be represented by the following eqn (4).

$$a(\beta\text{-H}) = \beta_0 + B\cos^2\theta \qquad (4)$$

where θ is dihedral angle made between the orbital of the unpaired electron and the β C–H bond, and B_0 and B are constants. In this equation, since B_0 is approximately zero, $a(\beta$-H) is mainly dependent on $\cos^2\theta$.

Now, consider the conformation of the model as shown in Fig. 4.[14] Since methyl group in the nitromethane radical anion (X = H) is thought to be freely rotating around the C–N bond, $\cos^2\theta$ in the eqn (4) is averaged to be 1/2. That is, θ is 45°. On the other hand, $a(\beta$-H) in the $SO_3^{\dot{-}}$ adduct (X = SO_3^-) is less than that of nitromethane radical anion. Then, from the eqn (4),

$$1/2(\cos^2\theta_1 + \cos^2\theta_2) = \text{average of } \cos^2\theta < 1/2.$$

Consequently, $\theta > 45°$. This result shows that the preferred conformation of the $SO_3^{\dot{-}}$ adduct is the conformation in which the dihedral angle between the β C–H bond and the p_z orbital of nitrogen atom is larger than 45°.

Also, the larger reduction in the hyperfine splitting of the β-proton in the other $SO_3^{\dot{-}}$ adducts when substituent (R_2) is replaced by a methyl and ethyl group is observed (Table 1). These results are

Table 1. Hyperfine splitting constants (Gauss) and *g*-factors for radicals, $R_1R_2C(SO_3^-)NO_2^{\dot{-}}$

R_1	R_2	a^N	$a(\beta$-H)	$a(\gamma$-H)	*g*
H	H	22.22	7.53(2H)	—	2.0050
H	Me	22.80	3.33(1H)	0.42(3H)	2.0050
H	Et	22.08	2.18(1H)	0.70(1H)	2.0050
Me	Me	22.83	—	0.42(6H)	2.0051

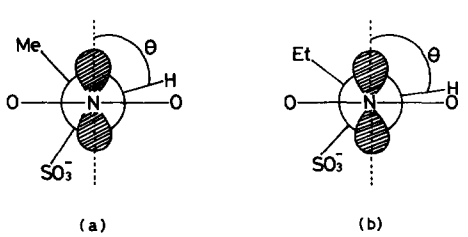


Fig. 5. Conformational preferences for the radicals (a) $MeCH(SO_3^-)NO_2^{\dot{-}}$ and (b) $EtCH(SO_3^-)NO_2^{\dot{-}}$.

explained by the idea that the bulky substituents such as methyl and ethyl further affect the conformation of the $SO_3^{\pm}$ adduct. That is, in these adducts, the dihedral angle (θ) gradually approaches 90° as shown in Fig. 5, dependent on the substituents.

REFERENCES

1. T. Ozawa, M. Sato and T. Kwan, *Chem. Lett.* 1972, 591.
2. T. Ozawa and T. Kwan, *J. Chem. Soc., Chem. Commun.* 1983, 80.
3. T. Ozawa, M. Setaka, H. Yamamoto and T. Kwan, *Chem. Pharm. Bull.* 1974, **22**, 962.
4. T. Ozawa and T. Kwan, *J. Chem. Soc., Chem. Commun.* 1983, 1295.
5. T. Ozawa and T. Kwan, *Polyhedron* 1983, **2**, 1019.
6. R. O. C. Norman and P. M. Storey, *J. Chem. Soc.* (*B*) 1971, 1009.
7. J. Q. Adams, S. W. Nicksick and J. R. Thomas, *J. Chem. Phys.* 1966, **45**, 654.
8. D. J. Edge and R. O. C. Norman, *J. Chem. Soc.* (*B*) 1969, 182.
9. M. McMillan and R. O. C. Norman, *J. Chem. Soc.* (*B*) 1968, 590.
10. N. H. Anderson and R. O. C. Norman, *J. Chem. Soc.* (*B*) 1971, 993.
11. W. T. Dixon and R. O. C. Norman, *J. Chem. Soc.* 1963, 3119.
12. A. Albert and E. P. Serjent, *Ionization Constants of Acids and Bases*, p. 151. Methuen, London (1962).
13. B. C. Gilbert, J. P. Larkin and R. O. C. Norman, *J. Chem. Soc., Perkin II* 1972, 1508.
14. In this type of nitroxide radical, an unpaired electron is mainly located on the p_z orbital of nitrogen atom.

Polyhedron Vol. 4, No. 8, pp. 1429–1431, 1985
Printed in Great Britain

0277-5387/85 $3.00 + .00
© 1985 Pergamon Press Ltd

THE REACTIONS BETWEEN TETRACHLOROPLATINATE(II) ANION AND BIDENTATE SULPHUR–NITROGEN CHELATING AGENTS: A DIRECT ROUTE FOR THE SYNTHESIS OF THE NEUTRAL DICHLORO SPECIES

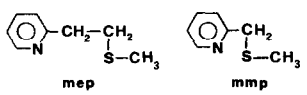
A. BALDO, G. CHESSA, G. MARANGONI* and B. PITTERI
University of Venice, Department of Chemistry, 30123 Venice, Italy

(*Received* 9 *October* 1984; *accepted* 6 *February* 1985)

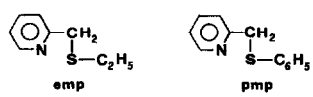
Abstract—A direct route for the synthesis of the neutral dichloro complexes $[Pt(N–S)Cl_2]$, (N–S = 2-[(ethylthio)methyl]pyridine and 2-[(phenylthio)methyl]pyridine) in dimethylformamide, which avoids the formation of bis-chelate cations, is reported.

In the general context of a program dealing with kinetic studies on planar tetracoordinate complexes, we faced the problem of synthesizing neutral dichloro complexes containing sulphur–nitrogen chelating ligands, of general formula $[Pt(N–S)Cl_2]$.

It is reported that the reaction between tetrachloroplatinate(II) anion and 2-[(methylthio)-ethyl]pyridine (mep) in aqueous-methanol solution, gives the neutral tetracoordinate $[Pt(mep)Cl_2]$,[1] in which the organic ligand forms a six-membered chelate ring containing the metal. Attempts to obtain the analogous $[Pt(mmp)Cl_2]$ (mmp = 2-[(methylthio)methyl]pyridine) in which the ligand is expected to form a five-membered chelate ring, under the same experimental conditions, yielded only the insoluble Magnus type salt $[Pt(mmp)_2][PtCl_4]$[2].



We have now confirmed this observation on reacting $[PtCl_4]^{2-}$ with the parent ligands 2-[(ethylthio)methyl]pyridine (emp) and 2-[(phenylthio)methyl]pyridine (pmp). The Magnus type salts $[Pt(emp)_2][PtCl_4]$ and $[Pt(pmp)_2][PtCl_4]$ are the products when the reactions are carried out in water or methanol–water.



* Author to whom correspondence should be addressed.

In this report we describe a new synthetic route which allows the direct preparation of the neutral dichloro species by carrying out the reactions in dimethylformamide (dmf).

EXPERIMENTAL

Physical measurements

IR spectra as KBr discs and Nujol mulls were recorded on a Perkin–Elmer 683 spectrophotometer. Electronic spectra were measured in the 250–370 nm range on a Varian-Cary 219 spectrophotometer. ^1H NMR spectra in CD_3NO_2 were obtained with an FT-80 Varian spectrometer. Conductivity measurements were performed on a Radiometer Copenhagen CDM 83 conductivity meter.

Preparation of 2-[*(phenylthio)methyl*]*pyridine hydrochloride* (*pmp*)

This compound was obtained according to the method of Bauer *et al.*[3] by condensation of sodium thiophenolate with 2-chloromethylpyridine in refluxing 95% ethanol. The product was converted to the hydrochloride salt which was crystallized from ethanol–diethylether. Yield 85%; m.p. 136–137°C (Lit. 137°C). Found: C, 60.3; H, 5.1; N, 5.9; Cl, 14.9; S, 13.5. $C_{12}H_{12}NClS$ requires: C, 60.3; H, 5.0; N, 5.8; Cl, 15.0; S, 13.5%.

Preparation of 2-[*(ethylthio)methyl*]*pyridine hydrochloride* (*emp*)

This was prepared in a similar way to pmp and crystallized from hot acetone. Yield 70%; m.p. 101–

102°C. Found: C, 50.8; H, 6.3; N, 7.2; Cl, 18.7; S, 16.7. $C_8H_{12}NClS$ requires: C, 50.7; H, 6.4; N, 7.4; Cl, 18.7; S, 16.9%.

Preparation of bis(2-[(ethylthio)methyl]pyridine)-platinum(II) tetrachloroplatinate(II), $[Pt(emp)_2][PtCl_4]$

K_2PtCl_4 (0.415 g, 1 mmol) in water (10 cm^3) was added to a warm solution of 2-[(ethylthio)methyl]-pyridine hydrochloride (0.189 g, 1 mmol), previously neutralized with 1 M KOH, in water (20 cm^3). The pink precipitate of the complex salt which was obtained, was filtered off, washed with water, ethanol and diethyl ether and dried under vacuum. Yield 95%. Found: C, 22.9; H, 2.5; N, 3.3; Cl, 17.1; S, 7.4. $C_{16}H_{22}N_2Cl_4S_2Pt_2$ requires: C, 22.9; H, 2.6; N, 3.3; Cl, 16.9; S, 7.6%.

Preparation of bis(2-[(phenylthio)methyl]pyridine)-platinum(II) tetrachloroplatinate(II), $[Pt(pmp)_2][PtCl_4]$

This was prepared following the same procedure as in the previous case. Yield 95%. Found: C, 30.7; H, 2.2; N, 3.3; Cl, 15.4; S, 6.7. $C_{24}H_{22}N_2Cl_4S_2Pt_2$ requires: C, 30.8 ; H, 2.35; N, 3.0; Cl, 15.2; S, 6.85%.

Preparation of cis*-dichloro-2-[(phenylthio)methyl]-pyridine platinum(II)*, $[Pt(pmp)Cl_2]$

A solution of 2-[(phenylthio)methyl]pyridine hydrochloride (0.238 g, 1 mmol) in dmf (10 cm^3) was neutralized with an aqueous solution of 1 M KOH (1 cm^3) and then dried with anhydrous Na_2SO_4. The filtered solution was slowly dropped under vigorous stirring into a solution of K_2PtCl_4 (0.415 g, 1 mmol) in dmf (50 cm^3) at room temperature. The temperature was then raised to 60°C and the mixture left to react for 6 hr. During that time the initially deep red solution became orange yellow and KCl precipitated. It was then cooled to room temperature, acetone was added (10 cm^3) and any solid filtered. The clear solution was concentrated to 5 cm^3 and a microcrystalline yellow product recovered by adding diethyl ether. It was filtered off, washed with diethyl ether and dried under vacuum. Yield 0.33 g (70%), m.p. (decomp) 175°C. Found: C, 30.2; H, 2.3; N, 3.1; Cl, 15.2; S, 6.9. $C_{12}H_{11}NCl_2SPt$ requires: C, 30.85. H, 2.4; N, 3.0; Cl, 15.2; S, 6.85%. A 1×10^{-3} molar solution of the complex in nitromethane is non-conducting. ^1H NMR (CD_3NO_2, δ from TMS as internal standard: 7.14–9.65 (complex multiplets, 9H, pyridyl and phenyl residues), 3.09–5.28 (m, 2H, $-C\underline{H}_2-$). The IR spectrum shows significant bands at: 1610s, ν(C=N); 328, 340m, ν(Pt–Cl).

Preparation of cis*-dichloro-2-[(ethylthio)methyl]-pyridine platinum(II)*, $[Pt(emp)Cl_2]$.

This complex was prepared following the same procedure as in the previous case. Yield 70%, m.p. (decomp) 175°C. Found: C, 22.9; H, 2.6; N, 3.4; Cl, 16.7; S, 7.7. $C_8H_{11}NCl_2SPt$ requires: C, 22.9; H, 2.6; N, 3.3; Cl, 16.9; S, 7.6%. A 1×10^{-3} molar solution of the complex in nitromethane is non-conducting. ^1H NMR (CD_3NO_2, δ from TMS as internal standard): 7.04–9.77 (complex multiplets, 4H, pyridyl residue), 2.37–3.49 (m, 2H, $-C\underline{H}_2-$), 4.38 (q, 2H, $-C\underline{H}_2-CH_3$), 1.38 (t, 3H, $-CH_2-C\underline{H}_3$). The IR spectrum shows significant bands at: 1612s, ν(C=N); 318, 333m, ν(Pt–Cl).

RESULTS AND DISCUSSION

When potassium tetrachloroplatinate(II) is reacted with an equimolar amount of emp or pmp in aqueous solution at room temperature, the pink, very insoluble Magnus type salts $[Pt(emp)_2][PtCl_4]$ and $[Pt(pmp)_2][PtCl_4]$, which can be easily recognized by IR spectra, are obtained quantitatively. IR spectra of both the salts show a medium to strong single band at 312 cm^{-1}, typical of the Pt–Cl stretching vibration of the symmetric $[PtCl_4]^{2-}$ anion.[4] All attempts to obtain the neutral dichloro monochelated species under the same experimental conditions were unsuccessful.

It is known[5] that, when equimolar amounts of K_2PtCl_4 and ethylenediamine are allowed to react in water, a mixture of $[Pt(en)Cl_2]$ and $[Pt(en)_2][PtCl_4]$ precipitates. Furthermore, treatment of K_2PtCl_4 with two equivalents of trialkylphosphine gives a precipitate of $[Pt(PR_3)_4][PtCl_4]$.[6] However in that case, the product can be transformed into a mixture of the neutral dichloro species *cis-* and *trans-* $[Pt(PR_3)_2Cl_2]$ by boiling in water for several hours. The polydentate molecules, pyridine-2,6-dicarboxylic acid and 2-pyridine-carboxylic acid behave similarly, giving the neutral compounds containing two chelating ligands per molecule.[7] In the case of the ligands emp and pmp, the transformation of the Magnus type salts by prolonged boiling in water does occur, but only partially, and the final product is a mixture which is difficult to handle and decomposes, probably as a consequence of the very low solubility of the first product in water. Very pure neutral dichloro species, $[Pt(emp)Cl_2]$ and $[Pt(pmp)Cl_2]$ can be directly obtained by reacting K_2PtCl_4 with an equimolar amount of the appropriate ligand in dmf at 60°C. The K_2PtCl_4 is soluble in dmf at this temperature and, on addition of the ligand, the colour of the solution gradually changes from cherry-red to orange–yellow

with simultaneous precipitation of KCl and the formation of the neutral dichloro species, which is also soluble in dmf. The neutral dichloro species can be easily recovered from the dmf solution as microcrystalline yellow products by adding diethyl ether after a preliminary concentration. They are, as expected, non-conducting and their IR spectra show two well separated absorption bands in the 340–315 cm^{-1} range, which are the typical stretching vibrations of *cis*-dichloro platinum species. ^1H NMR resonances are in full agreement with the proposed formulation. In particular the complex multiplet in the range 3.49–2.27 for the emp complex and 5.28–3.09 for the pmp complex indicate, as expected, the magnetic non-equivalence of the methylene protons. Methanolic solutions of the two neutral complexes closely follow Beer's law.

The fact that the dichloro neutral species can be directly obtained in dmf is probably related to the different solubility of the Magnus type salt intermediate in the two solvents. This is in agreement with the observation that these intermediates, prepared in water and isolated as pure solids, are soluble in dmf where, on heating, they are transformed into the dichloro species.

Acknowledgements—We thank the Italian Ministry of Education and CNR for financial support.

REFERENCES

1. P. S. K. Chia, S. E. Livingstone and T. N. Lockyer, *Aust. J. Chem.* 1966, **19**, 1835.
2. P. S. K. Chia, S. E. Livingstone and T. N. Lockyer, *Aust. J. Chem.* 1967, **20**, 239.
3. L. Bauer and L. A. Gardella, *J. Org. Chem.* 1963, **28**, 1323.
4. P. J. Hendra, *J. Chem. Soc.* (*A*) 1967, 1298.
5. G. L. Johnson, *Inorg. Synth.* VIII, 242.
6. K. A. Jensen, *Z. Anorg. Allg. Chem.* 1936, **229**, 237.
7. G. Marangoni, private communication.

Polyhedron Vol. 4, No. 8, pp. 1433–1437, 1985
Printed in Great Britain

0277-5387/85 $3.00 + .00
© 1985 Pergamon Press Ltd

FORMATION EQUILIBRIA OF COPPER(II) COMPLEXES WITH SOME PYRIDINOLS IN VARIOUS SOLVENTS

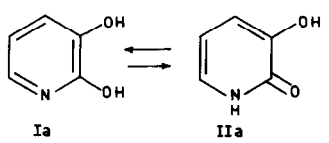
R. BUCCI, V. CARUNCHIO,* A. M. GIRELLI and A. MESSINA
Dipartimento di Chimica, Università degli Studi "La Sapienza",
P. le Aldo Moro 5, 00185 Roma

(*Received* 26 *November* 1984; *accepted* 6 *Febraury* 1985)

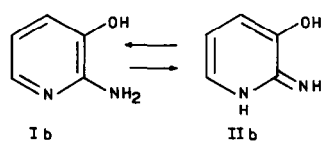
Abstract—Complexation of copper(II) with two different pyridinols in three solvents has been studied by visible spectrophotometry and flow-microcalorimetry. The influence of the solvent on tautomeric equilibrium of the ligand, on distribution, on stability and on formation enthalpies of the main complex species is discussed.

The thermodynamic properties of complexes in solution are remarkably influenced by the interactions of the solvent with both metal and the ligand.[1–3] These interactions are generally interpreted on the basis of donor power (DN), acceptor power (AN), dielectric constant values (DEC) and hydrogen bonding ability which all influence the solvation and/or ionization of the species present.

In the present work the solvent effect on the complexation equilibria of copper(II) with 2,3-dihydroxypyridine (HHP) and 2-amino-3-hydroxypyridine (AHP) is evaluated having chosen the following media: ethanol (EtOH), dimethylacetamide (DMA) and dimethylsulphoxide (DMSO). These solvents can influence also the tautomeric equilibria of the considered ligands:



Ia IIa



Ib IIb

Moreover the results may be discussed considering also those obtained in the copper(II)–aminopyridine systems[4] to formulate some hypothesis concerning the influence of the substituents of the heterocyclic ring on complexation equilibria.

EXPERIMENTAL

All products used were of analytical grade. Solvents were dehydrated and purified in the usual way.[5] The water content of the products was determined using Karl–Fischer reagent and found to be less than 0.05% in all cases.

The ligands were recrystallized from EtOH : ligroin (1 : 1) until their proper melting points.

The metal solutions, prepared from $Cu(ClO_4)_2 \cdot 6H_2O$, were analyzed by complexometric titration.

The spectrophotometer was a Perkin–Elmer 559. Quartz cells of different lengths (5 cm, 3 cm, 1 cm) were used.

The flow microcalorimeter was a LKB 10700 apparatus with two glass syringes on an injection pump. All measurements were carried out at 25 ± 0.1°C.

NMR measurements were carried out with a Bruker WP 80 at 25°C in DMSO-d_6 solutions, using TMS as reference.

RESULTS

2,3-*Dihydroxypyridine* (HHP)

The addition of HHP to a solution of constant metal concentration (1×10^{-3} M) led to the appearance of a new absorption band at $\lambda = 440$ nm

* Author to whom correspondence should be addressed.

Table 1. Absorbance values at certain wavelengths (A_λ) of copper(II)-2,3-dihydroxypyridine system in ethanol, dimethylacetamide, dimethylsulphoxide at constant metal concentration $C_M = 1 \times 10^{-3}$ M and various initial molar concentration ratios $C_L/C_M = 0.5$–40. Blank: solvent; $b = 1$ cm; $T = 25°C$

EtOH		DMA		DMSO	
C_L/C_M	$A_\lambda = 440$ nm	C_L/C_M	$A_\lambda = 460$ nm	C_L/C_M	$A_\lambda = 440$ nm
0.2	0.070	0.2	0.10	2.0	0.10
0.4	0.130	0.4	0.185	4.0	0.130
0.6	0.195	0.6	0.275	6.0	0.150
0.8	0.253	0.8	0.345	8.0	0.165
1.0	0.288	1.0	0.394	10.0	0.177
1.2	0.300	1.2	0.410	15.0	0.193
1.4	0.304	1.4	0.419	20.0	0.210
1.6	0.308	1.6	0.425	25.0	0.230
2.0	0.311	2.0	0.428	30.0	0.243
3.0	0.325	3.0	0.434	35.0	0.250
4.0	0.340	4.0	0.440	40.0	0.255

in EtOH and DMSO and at $\lambda = 460$ nm in DMA, in the range $C_L/C_M = 0$–40.

Optical densities measured at these wavelengths were constant for at least one day, and the ionic strength was maintained at 0.05 M with tetrabutylammonium perchlorate.

Mathematical elaboration[6] of the absorbance variation vs C_L/C_M (Table 1) has evidenced the formation of only one species, in all the solvents characterized by a complexation ratio L/M = 1 : 1.

Equilibrium constants and the molar absorptivities have been calculated using Rose and Drago's method.[7] A graphical procedure, based on plotting several curves obtained from equation (1), was used. The eqn (1) which is applicable only when one complex is formed and when the donor molecule does not absorb in the region studied, is that of a straight line with two unknowns, K^{-1} and ε_c:

$$K^{-1} = A/b\varepsilon_c - C_M - C_L + C_M C_L \varepsilon_c b/A, \quad (1)$$

where b = path length; C_M = initial concentration of the metal; C_L = initial concentration of ligand; ε_c = molar absorptivity of the constant; A = total absorbance.

The stability constant and molar absorptivities, determined intersection of the curves, are reported in Table 2.

Calorimetric investigations, carried out in the same experimental conditions, have given suitable data in all the solvents considered. In particular

Table 2. Concentration quotients at equilibrium, β_i ($mol^{-i}\ l^{-i}$), molar absorptivities, ε_i ($mol^{-1}\ l\ cm^{-1}$), and formation enthalpies ΔH_{β_i} (kcal mol^{-1}) for the copper(II)-2,3-dihydroxypyridine and copper(II)-2-amino-3-hydroxypyridine systems in ethanol, dimethylacetamide and dimethylsulphoxide at 25°C

Solvents	EtOH	DMA	DMSO
Parameters of the solvent	DN = 24.0 AN = 37.9 DEC = 25.3	DN = 27.8 AN = 13.6 DEC = 37.9	DN = 29.8 AN = 19.3 DEC = 45.0
Copper(II)-2,3-dihydroxypyridine	$\log \beta_1 = 4.41$ $\varepsilon_1 = 71$ ($\lambda = 440$ nm) $\Delta H_1 = -4.6$	$\log \beta_1 = 4.56$ $\varepsilon_1 = 86$ ($\lambda = 460$ nm) $\Delta H_1 = -2.7$	$\log \beta_1 = 2.54$ $\varepsilon_1 = 52$ ($\lambda = 440$ nm) $\Delta H_1 = -2.2$
Copper(II)-2-amino-3-hydroxypyridine	$\log \beta_2 = 6.13$ $\log \beta_3 = 12.12$	$\log \beta_3 = 12.18$	$\log \beta_2 = 7.08$

the calculated values were: $\Delta H_1 = -4.6$ in EtOH; $\Delta H_1 = -2.7$ in DMA; $\Delta H_1 = -2.2$ in DMSO.

Although NMR measurements did not provide any useful results it is reasonable to suppose the formation of a chelating ring, through the oxygen atoms of hydroxylic groups.

2-*Amino*-3-*hydroxypyridine* (AHP)

For all the solvents considered the complexation reactions are not instantaneous. In fact it required 4 hr in EtOH, 5 hr in DMA and 7 hr in DMSO to reach constant values of the absorbances. Therefore it was impossible to carry out calorimetric investigations.

Spectrophotometric measurements have been performed on solutions of different metal concentrations ($1–10 \times 10^{-5}$ M).

In EtOH the spectra behaviour shows the change in the absorption curve of a copper perchlorate solution on the addition of AHP. With increasing AHP concentrations the absorption maximum is displaced to shorter wavelengths, indicating that more than one complex is formed in solution.

Mathematical elaboration[6] of the absorbance values allowed the identification of two complex species with complexation ratios L/M = 2:1 and 3:1 and the determination of concentration quotients at equilibrium β_2 and β_3. The trend of the curves C_L/C_M vs A (Fig. 1) suggests the presence of a 1:1 complex species.

In DMA only one species, characterized by complexation ratio L/M = 3:1 exists in significant amounts in the range $C_L/C_M = 0–10$.

In DMSO only the species with complexation ratio L/M = 2:1 has been found in the range $C_L/C_M = 0–40$ at $\lambda = 510$ nm.

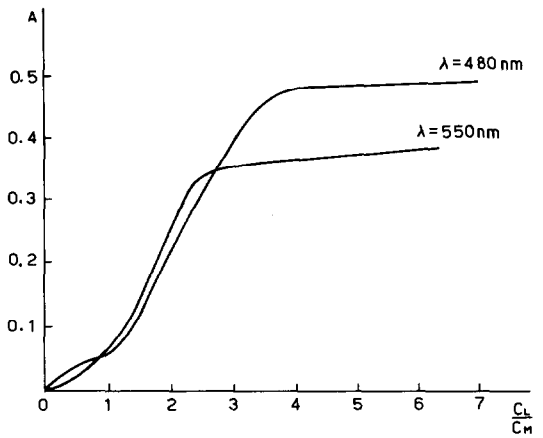


Fig. 1. Absorbance values of the copper(II)-2-amino-3-hydroxypyridine system in ethanol, at constant metal concentration $C_M = 5 \times 10^{-5}$ M and various initial molar concentration ratios $C_L/C_M = 0–7$ at two different wavelengths $\lambda_1 = 480$ nm, $\lambda_2 = 550$ nm. Blank: solvent, $b = 3$ cm, $T = 25°C$.

In Table 3 the absorbance values at different C_L/C_M are reported for all the solvents.

In this case, NMR measurements have confirmed that the coordinating centre on the ligand is the heterocyclic nitrogen atom. NMR spectra of AHP and its copper complex (Fig. 2) indicate that the signal of proton 6 and in less amount the proton 5 are perturbed by the presence of copper ion.

DISCUSSION

The data obtained allow us to formulate some hypotheses concerning the influence of the solvent

Table 3. Absorbance values at certain wavelengths (A_λ) of the copper(II)-2-amino-3-hydroxypyridine system, at constant metal concentration $C_M = 5 \times 10^{-5}$ M and various initial molar concentration ratios $C_L/C_M = 0.5–40$. Blank: solvent, $b = 3$ cm, $T = 25°C$

EtOH			DMA		DMSO	
C_L/C_M	$A_\lambda = 480$ nm	$A_\lambda = 550$ nm	C_L/C_M	$A_\lambda = 520$ nm	C_L/C_M	$A_\lambda = 510$ nm
0.5	0.040	0.035	0.5	0.105	2.0	0.125
1.0	0.060	0.062	1.0	0.210	4.0	0.140
1.5	0.160	0.160	1.5	0.306	6.0	0.230
2.0	0.223	0.272	2.0	0.390	8.0	0.277
2.5	0.320	0.337	2.5	0.471	10.0	0.320
3.0	0.398	0.355	3.0	0.540	15.0	0.371
3.5	0.457	0.360	3.5	0.585	17.5	0.380
4.0	0.480	0.364	4.0	0.600	20.0	0.385
4.5	0.483	0.367	4.5	0.606	25.0	0.392
5.0	0.485	0.373	5.0	0.615	30.0	0.400
6.0	0.486	0.378	6.0	0.621	35.0	0.404
7.0	0.486	0.380	7.0	0.621	40.0	0.404

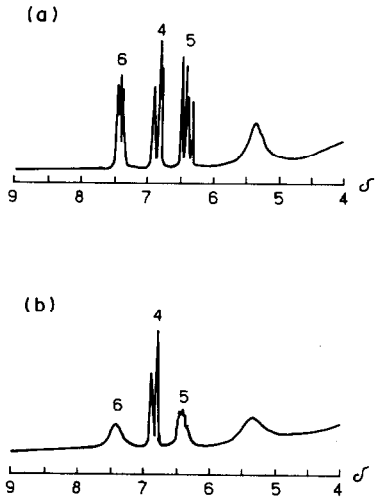


Fig. 2. ^{1}H NMR spectrum in DMSO-d_6 of: (a) 2 amino-3-hydroxypyridine, (b) copper(II)-2-amino-3-hydroxypyridine system.

on formation equilibria of complex species in the systems examined.

Regarding the 2,3-dihydroxypyridine, the values of concentration quotients at equilibrium are very similar in EtOH and DMA while in DMSO the value is considerably lower (Table 2). This order does not agree with that of the ΔH_1 values; in fact the ΔH_{EtOH} is twice as great as ΔH_{DMA}. This discrepancy suggests that the "model system" changes, in particular that in EtOH the ligand is in the oxo-hydroxy-form (**IIa**) whereas in DMSO and in DMA it is in the diol-form (**Ia**).

This hypothesis is in agreement with the assumption that the hydrogen bonding ability of the solvent plays an obvious role as hydrogen bond donors stabilize the oxo-hydroxy-form and hydrogen bond acceptors stabilize the diol-form.[8]

The stability sequence EtOH $\simeq$ DMA > DMSO can be explained if we consider that besides the metal solvation (DN) an important role is played by the ligand solvation. In fact we must consider that the ability of the ligand to give intermolecular (HHP-solvent) or intramolecular hydrogen bonding depends on the solvent. In particular in DMSO and DMA, that are good acceptors of hydrogen bonding the intermolecular bonds are favoured, while in EtOH the favoured intramolecular bond determines a decrease in the basicity of the two oxygen atoms involved in the chelating ring.

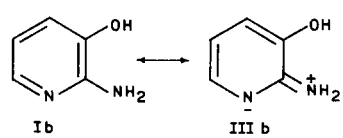
The values of concentration quotients at equilibrium, that are remarkably higher than those of corresponding complexes concurs with the assumption that the ligand is chelating.

In the system copper(II)–AHP the influence of solvent is evident both from thermodynamic and kinetic results.

It is reported in the literature[9] that the formation of complex species with this ligand is not instantaneous. Our results obtained in various media have evidenced that the rate of complex formation is strongly influenced by the nature of solvent. In particular the time needed for the reaction to be complete increases with increasing donor number of the solvent. In fact, increasing DN of the solvent causes a decrease in acceptor strength of the coordination centre (metal) and hence in formation rate of the intermediate. Moreover the donor power of the ligand decreases as solvation of AHP increases (EtOH > DMA > DMSO). This sequence agrees with the observed solubility order of the ligand.

With regard to the stability of the evidenced complex species the results obtained (Table 2) can be explained if we consider that the solvent influences the concentration quotients at equilibrium because of various factors: (i) the solvation of the metal and the ligand; (ii) the dielectric constant; (iii) the possibility of π-interactions between solvent and ligand.

In fact while the solvation order of ligand and metal (DMSO > DMA > EtOH) favours the stabilization of complex species in EtOH, the effect of dielectric constant and π-interactions (DMSO > DMA > EtOH) favours the stabilization of complex species in DMSO and DMA respectively. In fact if we consider the resonance forms of the ligand it is evident that the form **IIIb**, in which the basicity of the nitrogen atom is higher, is the prevailing one in the solvents characterized by high DEC and stronger π-interactions. The two effects act in opposition causing a levelling of complex stability.



Ib III b

The data obtained compared with those reported in a previous paper[4] allow us to formulate some considerations on the influence of substituents in the pyridine ring:

(i) In HHP the presence of hydroxy groups in the 2- and 3-positions allows the formation of a very stable five-membered chelate with the copper ion.

(ii) In AHP the presence of a hydroxy group in α-position to the amino group increases the resonance and hence the basic strength of the heterocyclic nitrogen atom increases. In such a way the complex species are more stable than those ones of the aminopyridine.

(iii) The presence of chlorine and bromine atoms in *para*-positions to the amino group decreases the basic strength of nitrogen atom because of the inductive effect ($-I$). The stability order agrees with the Lewis basicity of the ligands: CuApy > CuBrApy > CuClApy.

Acknowledgments—This work was carried out with financial support by the Consiglio Nazionale delle Ricerche (C.N.R., Rome), which also gave a grant for one of us (A.M.G.). The authors thank Mr. G. Frachey for NMR measurements.

REFERENCES

1. V. Gutmann, *Coordination Chemistry in Non-aqueous Solutions*. Springer-Verlag, New York (1968).
2. *The Chemistry of Non-aqueous Solvents* (Edited by J. J. Lagowski), Vo. 1. Academic Press, New York (1966).
3. K. Burger, *Solvation, Ionic and Complex Formation Reactions in Non-aqueous Solvents*. Elsevier, Amsterdam (1983).
4. S. Balzamo, V. Carunchio, R. Galvani and A. Messina, *Inorg. Chim. Acta* 1985, **97**, 13.
5. J. A. Riddick and W. B. Burger, *Techniques of Chemistry*, Vol. 2. Wiley–Interscience (1970).
6. E. Asmus, *Z. Anal. Chem.* 1960, **178**, 104.
7. N. J. Rose and R. S. Drago, *J. Am. Chem. Soc.* 1959, **81**, 6138.
8. J. Elguero, C. Marzin, A. R. Katritzky and P. Linda, *The Tautomerism of Heterocycles* (Edited by A. R. Katritzky). Academic Press, New York (1976).
9. V. Kaushwaha, M. Katyal and R. P. Singh, *Talanta* 1974, **21**, 63.

Polyhedron Vol. 4, No. 8, pp. 1439–1442, 1985
Printed in Great Britain

0277–5387/85 $3.00 + .00
© 1985 Pergamon Press Ltd

REACTION OF COPPER POWDER WITH TETRAALKYLTHIURAM DISULPHIDES

T. TETSUMI* and M. SUMI
Department of Pharmaceutical Sciences, Setsunan University, Nagao Tohge-cho, Hirakata-shi, Osaka 573-01, Japan

and

M. TANAKA and T. SHONO
Department of Applied Chemistry, Faculty of Engineering, Osaka University, Yamada-oka, Suita, Osaka 565, Japan

(*Received* 12 *November* 1984; *accepted* 6 *February* 1985)

Abstract—Copper powder reacts photochemically with tetraalkylthiuram disulphides [$(R_2NCS_2)_2$, TRTD] in chloroform. The effect of different alkyl substituents (R) on the reaction was studied systematically by means of both high-performance liquid chromatography (HPLC) and spectrophotometry. The results obtained show that the reactivity of $(R_2NCS_2)_2$ increases with increase of R in the order butyl > propyl > ethyl > methyl. In addition, this reaction is applicable to the analysis of the copper content in copper powder, copper oxides, copper(II) hydroxides, and basic copper carbonates.

The direct reaction of β-diketones with metals has been known for a long time.[1] Kamimori *et al.*[2,3] examined the reaction of β-diketones, mainly of acetylacetone, with several metals and compared their reactivity. Sievers *et al.*[4–6] applied the direct reaction of fluoro derivatives of β-diketones with many metals and the resultant formation of complexes to the analysis of metallic elements by gas chromatography. We previously confirmed the formation of metal(II) dialkyldithiocarbamate complexes [$M(R_2NCS_2)_2$] when TRTD was injected into gas chromatographic columns containing metal powder.[7] This fact suggested that metal powders and TRTD might react with each other, even in solution. Contrary to this expectation, no complex-forming reactions occurred at all. However, it is found that copper powder reacts with TRTD under irradiation by light. Hence the complex-forming reactions were run under irradiation with a mercury-arc lamp set at a constant distance. Then, the decreasing quantity of TRTD and the quantity of copper complexes formed were measured by means of liquid chromatography and ultraviolet spectroscopy, and the effect of alkyl substituents (R) of TRTD on their reactivity was examined. The reaction of copper powder with tetrabutylthiuram disulphide [$(Bu_2NCS_2)_2$, TBTD], was satisfactorily applied to the quantitative analysis of copper in copper powder, copper oxides, copper hydroxides and basic copper carbonates.

EXPERIMENTS AND RESULTS

(a) *Materials.* TRTD and $Cu(R_2NCS_2)_2$ were purified as previously reported.[7] The other materials were of analytical-reagent grade available in the market.

(b) *Apparatus.* A Shimadzu UV-240 spectrophotometer equipped with a thermoelectric cuvette temperature controller was used to record absorption spectra at 25 ± 0.5°C. HPLC was performed using a Shimadzu LC-4a HPLC system fitted with a variable-wavelength detector. The column was a stainless-steel tube (25 cm × 4.6 mm I.D.) packed with Zorbax ODS and was held at 20°C. A Toshiba mercury-arc lamp H-400-PL with a stabilizer was utilized to irradiate with light at a constant distance from the cuvette. A Yanagimoto CHN recorder (MT-Model 2) was used for elemental analyses, and a Nippon Jarrel–Ash A-8100 atomic absorption spectrophotometer for copper analysis. Each sample weight was measured with a Shiebel–Mettler ME-Model 22 balance.

* Author to whom correspondence should be addressed.

Table 1. Results of elemental analyses

Compound	Elemental analyses				
	C Found/Calc.	H Found/Calc.	N Found/Calc.	S Found/Calc.	M[a] Found/Calc.
Cu+TMTD } $Cu(Me_2NCS_2)_2$ }	23.72/23.71	4.03/3.98	9.26/9.22	41.86/42.19	20.90/20.91
Cu+TETD } $Cu(Et_2NCS_2)_2$ }	33.42/33.36	5.64/5.60	7.76/7.78	35.49/35.61	17.65/17.65
Cu+TPTD } $Cu(Pr_2NCS_2)_2$ }	40.38/40.41	6.91/6.78	6.67/6.73	29.98/30.81	15.27/15.27
Cu+TBTD } $Cu(Bu_2NCS_2)_2$ }	45.89/45.78	7.76/7.68	5.71/5.93	27.08/27.15	13.46/13.46

[a] Titrating with 0.01-M EDTA solution.

(c) *Reaction between metallic powder and* TRTD. We found that the yield of copper complex formed by reaction of copper powder with a TRTD in chloroform varied considerably from day to day and was dependent upon positions where the reaction flask was set. These facts strongly suggest the participation of the light in the reaction. Moreover, no copper complex was formed at all when the flask was covered with aluminium foil to shield it from the light. The products formed were isolated by filtering the reacted solutions, and recrystallized from chloroform for elemental analyses. As shown in Table 1, the values found are in good agreement with the calculated ones as $Cu(R_2NCS_2)_2$; therefore, copper powder is considered to react with TRTD in chloroform to form $Cu(R_2NCS_2)_2$. On the other hand, iron, cobalt, and lead powders did not react with TRTD at all; neither did nickel nor zinc powders.

(d) *Calibration curves of* TRTD *and* $Cu(R_2NCS_2)_2$. The calibration curves were constructed by plotting the peak areas of TRTD or $Cu(R_2NCS_2)_2$ vs their concentrations in chloroform. In this chromatography, the column of ODS and both eluents of methanol– and acetonitrile–water mixtures were used. In the case of the methanol–water system, the satisfactory, good separation of TMTD and $Cu(Me_2NCS_2)_2$, or $Cu(Pr_2NCS_2)_2$ and $Cu(Bu_2NCS_2)_2$ could not be attained with isocratic elution. In the case of the acetonitrile–water (99:1) system, the calibration curves are straight lines passing through the origin. The correlation coefficients of TRTD and $Cu(R_2NCS_2)_2$ were more than 0.997. The flow rate of the eluents was 1.0 cm^3/min, and the wavelength utilized for detection was 290 nm. The spectrophotometric calibration curve for each $Cu(R_2NCS_2)_2$ was also a straight line passing through the origin.

(e) *Effect of alkyl substituents on reactivity.* The determination of the copper complexes produced was performed as follows. After the addition of each of 15, 30, 45 or 100 mg of copper powder to 3 cm^3 of 1.5×10^{-4} mol dm^{-3} TRTD which had been put in a 1.0 cm wide quartz cell for spectrophotometry, the changes of absorbance at 437 nm were measured with irradiation of light with a constant intensity to the cell in the thermostat. The amount of the copper complexes produced was also determined together with that of unreacted TRTD by withdrawing 1 μl of the reaction mixture with a microsyringe and by injecting it into the liquid chromatograph under the conditions as in (d). Figure 1 shows a typical example of the reaction behaviours of copper powder and

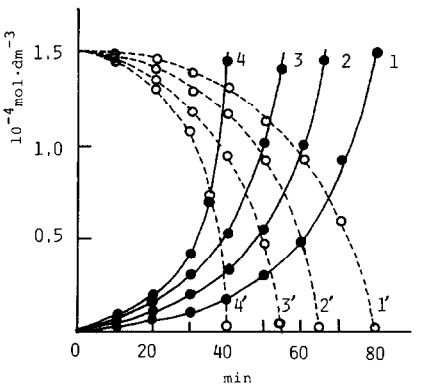


Fig. 1. Reaction behaviour between Cu and TETD. $Cu(Et_2NCS_2)_2$: —●——●—, TETD: --○---○--. 1, 15 mg; 2, 30 mg; 3, 40 mg; 4, 100 mg.

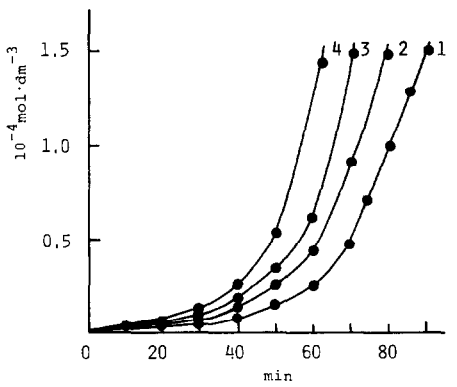


Fig. 2. Reaction behaviour between Cu (15 mg) and TRTD [$(R_2NCS_2)_2$]. 1, TMTD; 2, TETD; 3, TPTD; 4, TBTD.

TETD. The reaction rate is relatively slow at the beginning of the reaction, but rapidly increases as the time proceeds. As can be seen in Fig. 2, the relative reactivity of TRTD increases in the order of TBTD > TPTD > TETD > TMTD, and the amount of complex formed, of course, increases with increase of the quantity of copper powder added.

(f) *Application to the determination of copper.* By taking advantage of the selective photochemical reaction of TRTD with copper, an attempt was made to determine the copper content in the samples such as copper powder, copper oxides, copper hydroxides and basic copper carbonates. In a 30 cm^3 weighing bottle, 0.5–10 mg of each sample was weighed out accurately, and then TBTD two or three times by weight as much as each sample was added together with chloroform to the sample in the bottle. The mixture in the bottle was allowed to react for 1 hr under irradiation.

At the end of the reaction period, the reaction mixture was transferred into a 100 cm^3 measuring flask, and the flask was made up to the mark with chloroform. Further dilution with chloroform was performed, if necessary. The copper content of the reacted solution put in the 1.0 cm wide quartz cell was calculated from the following regression equation, the calibration curve of $Cu(Bu_2NCS_2)_2$:

$$C\,(10^{-4}\ \text{mol dm}^{-3}) = 0.9198 \times abs + 0.0018,$$

where C and abs are the concentration of $Cu(Bu_2NCS_2)_2$ and the absorbance, respectively. The results are given in Table 2. As can be seen in the table, the values obtained by the above-mentioned method agree well with those from atomic absorption spectrophotometry.

DISCUSSION

The elemental analyses (Table 1) for the reaction products of copper powder with TRTD are in good agreement with the ones calculated for $Cu(R_2NCS_2)_2$. It is, therefore, evident that copper powder reacts with TRTD under irradiation of light to form $Cu(R_2NCS_2)_2$. By the irradiation of the light, TRTD is presumed to become $R_2NCS_2\cdot$ which subsequently reacts selectively with copper. The relative reactivity of TRTD is in the order of TBTD > TPTD > TETD > TMTD. This is reasonably interpreted as follows. With an increase in R (butyl > propyl > ethyl > methyl) of TRTD, the electron-

Table 2. Analytical results of copper in practical samples

Sample	Sample taken (mg)	Copper determined (%) Atomic absorption method	c.v.	Spectrophotometric method	c.v.
Copper powder	0.516	99.98		99.98	
	0.783	99.97	0.8	99.98	0.5
	1.823	99.99		99.97	
Copper(II) oxide	0.563	79.38		79.38	
	0.832	79.37	1.2	79.35	1.2
	1.811	79.35		79.37	
Copper(II) hydroxide	0.562	64.80		64.78	
	0.893	64.83	1.2	64.81	1.7
	1.790	64.82		64.82	
Copper(II) carbonate	0.546	52.91		52.87	
	0.961	52.92	0.8	52.96	4.9
	2.298	52.93		52.88	

donating power of R increases. This results in the increase of electron density around the S atoms. The same tendency of relative reactivity is also observed in the reaction of copper powder with TRTD in the gas phase or in the reaction of metal powder with R_2NCS_2Na.

Table 2 shows that the coefficients of variation are less than 5.0%. It is apparent that good agreement is found between the spectrophotometric and atomic absorption spectrophotometric methods.

Acknowledgement—The authors are indebted to Mr. M. Iwasaki for his assistance in the experiments.

REFERENCES

1. K. Yamakawa, *Kagaku no Ryoiki* 1962, **16**, 905.
2. O. Kamimori, K. Sato, K. Takimoto and K. Arakawa, *Bunseki Kagaku* 1966, **15**, 561.
3. O. Kamimori, N. Yamaguchi and K. Sato, *Bunseki Kagaku* 1966, **15**, 1043.
4. R. E. Sievers and J. W. Connolly, *Inorg. Syntheses* 1970, **12**, 72.
5. R. E. Sievers, J. W. Connolly and W. D. Ross, *J. Gas Chromatogr.* 1967, **5**, 241.
6. W. D. Ross and R. E. Sievers, *Anal. Chem.* 1969, **41**, 1109.
7. T. Tetsumi and T. Matsumoto, *Nippon Kagaku Kaishi* 1983, 1906.

Polyhedron Vol. 4, No. 8, pp. 1443–1448, 1985
Printed in Great Britain

0277-5387/85 $3.00+.00
© 1985 Pergamon Press Ltd

METAL–(PHENYLTHIO)ACETIC ACID INTERACTIONS—VI.* THE CRYSTAL AND MOLECULAR STRUCTURES OF DIAQUABIS[(PHENYLSULFINYL)ACETATO]BIS(PYRIDINE)COPPER(II) AND BIS[(BENZYLTHIO)ACETATO]BIS(PYRIDINE)COPPER(II)

WING HONG CHAN
Department of Chemistry, Hong Kong Baptist College, Kowloon, Hong Kong

THOMAS C. W. MAK
Department of Chemistry, The Chinese University of Hong Kong, Shatin, New Territories, Hong Kong

GRAHAM SMITH† and ERIC J. O'REILLY
Department of Chemistry, Queensland Institute of Technology, Brisbane, Q4000, Australia

and

COLIN H. L. KENNARD
Department of Chemistry, University of Queensland, Brisbane, Q4067, Australia

(*Received* 26 *October* 1984; *accepted* 6 *February* 1985)

Abstract—The crystal structures of diaquabis[(phenylsulfinyl)acetato]bis(pyridine)-copper(II), (**1**), and bis[(benzylthio)acetato]bis(pyridine)copper(II) (**2**) have been determined using X-ray diffraction. In (**1**), the copper atom is at the centre of a distorted octahedron with the equatorial sites occupied in a *trans* configuration by two unidentate (phenylsulfinyl)acetate oxygens [Cu–O, 1.97(2), 2.01(2) Å] and two pyridine nitrogens [Cu–N, 1.99(2), 2.05(2) Å] with water molecules completing the polyhedron [Cu–O, 2.51(2), 2.58(2) Å]. The copper atom in (**2**) is at the inversion centre of a distorted octahedron having in the equatorial sites, *trans*-related pyridine nitrogens [Cu–N, 1.993(3) Å] and four oxygens from two asymmetric bidentate (benzylthio)acetate ligands [Cu–O, 2.012(3), 2.510(5) Å].

In a survey of the crystal structures of metal–(phenylthio)alkanoic acid complexes determined so far, all the copper(II) complexes have been tetracarboxylate bridged dimers of the copper acetate type.[1–3] This paper reports two examples of other stereochemistries for copper(II). The compounds studied are diaquabis[(phenylsulfinyl)-acetato]bis(pyridine)copper(II),

$$[Cu(PSA)_2(py)_2(H_2O)_2], \text{ (1)}$$

and bis[(benzylthio)acetato]bis(pyridine)copper(II), $[Cu(BTA)_2(py)_2]$, (**2**).

EXPERIMENTAL

a. *Preparation of complexes*

(**1**) and (**2**) were prepared by reacting an ethanolic solution of (phenylsulfinyl)acetic acid, PSAH, or (benzylthio)acetic acid, BTAH, respectively and pyridine with excess copper(II) carbonate as previously described.[4] (**1**) crystallised as light blue prisms, elongated along the *b* axis, m.p. 125.7°C. Crystals of (**2**) were deep purple in colour and formed diamond shaped plates which decomposed on melting at 125.1°C.

b. *Crystallography*

Details of unit cell parameters, intensity data collection and structure solution and refinement for

* For Part V see Ref. 1.
† Author to whom correspondence should be sent.

Table 1. Crystal data for $[Cu(PSA)_2(py)_2(H_2O)_2]$, (1), and $[Cu(BTA)_2(py)_2]$, (2)

Formula	(1) $C_{26}H_{28}CuN_2O_8S_2$	(2) $C_{28}H_{28}CuN_2O_4S_2$
Mr	624.2	584.2
a (Å)	23.58(1)	8.413(2)
b (Å)	7.747(3)	8.370(3)
c (Å)	16.082(8)	10.988(3)
α (°)		98.14(3)
β (°)	107.05(3)	84.43(2)
γ (°)		119.62(2)
V (Å^3)	2808(2)	665.5(3)
Z	4	1
Dc (g cm^{-3})	1.475	1.457
Do (g cm^{-3})	1.486	1.470
F(000)	1292	303
μ (cm^{-1})	10.0	10.4
λ (Å)	0.7107	0.7107
Space group	*C*2	$P\bar{1}$
Data collection:		
a. diffractometer	Nicolet R3m	Nicolet R3m
b. radiation	Mo-K_α	Mo-K_α
c. $2\theta_{max}$ (°)	50	50
d. crystal size (mm)	0.36 × 0.30 × 0.20	0.36 × 0.36 × 0.10
e. unique reflections:		
measured	2437	2279
used	1653	1690
discrimination	$I > 2.5\sigma(I)$	$I > 2.5\sigma(I)$
Structure solution, refinement:		
a. method used	Patterson	Heavy atom/Fourier
b. *R*	0.054	0.052
c. *Rw*	0.055	0.061
d. ω^a A	1.58	1.71
B	7.43×10^{-4}	1.44×10^{-3}

[a] $\omega = A/[\sigma^2(Fo) + B(Fo^2)]$.

(1) and (2) are given in Table 1. For (1), systematic absences (*h*0*l* absent for $l = 2n+1$) suggested either *C*2/*c* or *Cc*, while a statistical analysis of intensities indicated a noncentrosymmetric space group $[(E^2-1) = 0.64]$. The copper atom was located from the Patterson synthesis but the subsequent model obtained using the heavy atom method failed to reduce *R* below 0.22 (*C*2/*c*, with all non-hydrogen atoms anisotropic) or 0.23 (*Cc*, isotropic atoms). Using the *C*2/*c* model in the space group *C*2, the remaining atoms related by a pseudo centre of symmetry at 0, 0, $\frac{1}{4}$ were located by difference methods. The atomic positions were refined by blocked-matrix least-squares with anisotropic thermal parameters for only the copper, sulphurs, the thiophinyl oxygens and the atoms of the coordination sphere. The pseudo symmetry means that positions *x*, *y*, *z* and $-x$, $-y$, $\frac{1}{2}-z$ are related. The two-fold axis generates $-x$, *y*, $-z$ and *x*, $-y$, $\frac{1}{2}+z$. Thus there is a pseudo *c* glide operation (*h*0*l*, $l = 2n+1$ weak or absent). Structure factor calculations for these odd reflections gave amplitudes which could be considered close to background.

For (2), with $Z = 1$ in a triclinic space group, the copper atom was placed at the origin and initially gave $R = 0.53$. The weighted difference-Fourier gave the remainder of the non-hydrogen atoms. Blocked-matrix least-squares refinement was used with anisotropic thermal parameters for all non-hydrogen atoms. For both complexes, hydrogen atoms were located in difference-Fourier syntheses and included in the refinements at fixed positions with the isotropic *U* values also fixed (0.05 Å^2). Program systems used were SHELX 76,[5] PLUTO[6] and APPLECRYST 83.[7]

Neutral atom scattering factors were used and Cu and S were corrected for anomalous dispersion. Atomic coordinates, thermal parameters, observed and calculated structure factors and intra-ligand

Table 2. Bond distances (Å) and angles (degrees) about the coordination sphere for (1) and (2)

(i) distances

(1)				(2)	
Cu–O(11)A	1.97(2)	Cu–OwB	2.51(2)	Cu–O(10)	2.012(3)
Cu–O(11)B	2.01(2)	Cu–N(1)pA	1.992)	Cu–O(11)	2.510(5)
Cu–OwA	2.58(2)	Cu–N(1)pB	2.05(2)	Cu–N(1)p	1.993(3)

(ii) angles

(1)				(2)	
O(11)A–Cu–O(11)B	179.2(7)	OwA–Cu–N(1)pB	93.0(8)	O(10)–Cu–O(11)	57.5(1)
O(11)A–Cu–OwA	92.5(7)	OwB–Cu–N(1)pA	95.2(7)	O(10)–Cu–N(1)p	91.4(1)
O(11)A–Cu–OwB	87.1(6)	OwB–Cu–N(1)pB	84.8(7)	O(11)–Cu–N(1)p	89.7(2)
O(11)A–Cu–N(1)pA	91.9(7)	N(1)pA–Cu–N(1)pB	178.9(8)	Cu–O(10)–C(9)	96.7(4)
O(11)A–Cu–N(1)pB	89.1(7)	Cu–O(11)A–C(9)A	128.4(12)	Cu–O(11)–C(9)	78.3(4)
O(11)B–Cu–OwA	86.8(7)	Cu–O(11)B–C(9)B	125.9(10)	Cu–N(1)p–C(2)p	122.3(3)
O(11)B–Cu–OwB	93.6(6)	Cu–N(1)pA–C(2)pA	120.5(12)	Cu–N(1)p–C(6)p	119.9(3)
O(11)B–Cu–N(1)pA	88.3(7)	Cu–N(1)pA–C(6)pA	123.2(12)		
O(11)B–Cu–N(1)pB	90.6(6)	Cu–N(1)pB–C(2)pB	120.9(12)		
OwA–Cu–OwB	177.8(6)	Cu–N(1)pB–C(6)pB	118.7(11)		
OwA–Cu–N(1)pA	87.0(6)				

bond distances and angles have been deposited with the Editor as supplementary material; copies are available on request from the Editor or the Authors. Atomic coordinates have also been deposited with the Cambridge Crystallographic Data Centre. Bond distances and angles about the coordination polyhedrons for both compounds are given in Table 2.

DISCUSSION

$[Cu(PSA)_2(py)_2(H_2O)_2]$, (1) (Fig. 1), is an example of a copper(II) complex in which the metal is at the centre of a distorted octahedron, with the equatorial sites occupied in a *trans* configuration by two unidentate PSA ligands bonding through carboxyl oxygens [Cu–O, 1.97(2), 2.01(2) Å] and two pyridines [Cu–N, 1.99(2), 2.05(2) Å]. Water molecules complete the octahedron [Cu–Ow, 2.51(2), 2.58(3) Å]. One half of the molecule is related to the other half by a pseudo centre of inversion at 0, 0, $\frac{1}{4}$. The difference between comparable atoms ranges up to 0.35 Å in x for C(4), and 0.23 Å in y for the acetate and pyridine atoms. The structure of the deep green coloured complex, diaquabis[ethylthio)-acetato]-copper(II) has ligands similar to (1), bonded through unidentate carboxylate oxygens [Cu–O, 1.916(2) Å]. However, the complex is centrosymmetric with each ligand forming a five-membered chelate ring through the sulphur atom [Cu–S, 2.381(1) Å], with the distorted octahedron completed by two water molecules [Cu–O, 2.457(1) Å].

Leiserowitz *et al.* have determined the structures for acids similar to PSAH, (1-naphthylsulfinyl)acetic acid,[10] and (4-chlorophenylsulfinyl)acetic acid.[11] Unlike most carboxylic acids which form cyclic

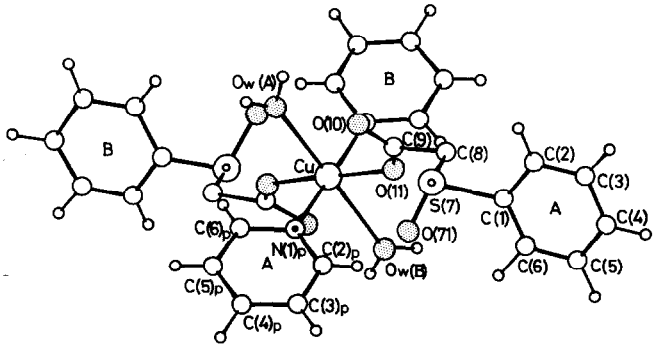


Fig. 1. Molecular configuration and atom naming scheme for $[Cu(PSA)_2(py)_2(H_2O)_2]$ (1). Ligands A and B and related by pseudo inversion symmetry.

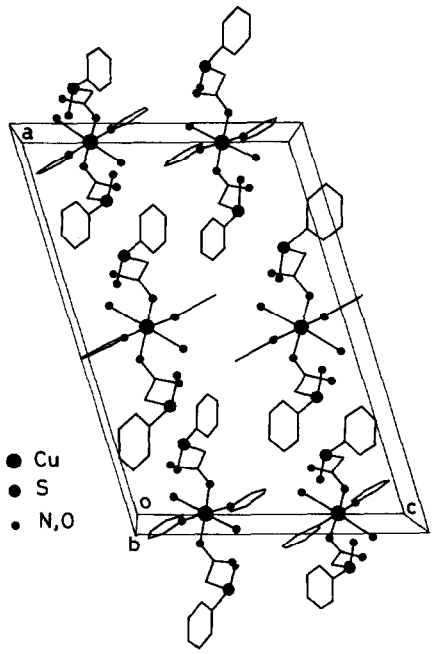


Fig. 2. The packing of (**1**) in the unit cell viewed down the *b* axis.

hydrogen-bonded dimers,[12] these compounds have extended hydrogen bonded arrays formed through single OH···O=S bonds [2.58 Å,[10] 2.64 Å[11]]. In (**1**), the sulfinyl oxygen is hydrogen bonded to waters from a neighbouring complex molecule [O(71)···Ow, 2.59(1), 2.88(1) Å for ligands A and B respectively]. In (**1**), the sulfinyl oxygen is hydrogen bonded to waters from neighbouring molecules [O(71)···Ow, 2.59(1), 2.88(1) Å for ligands A and B respectively]. These are the only significant intermolecular interactions involved in the packing of the complex in the unit cell (Fig. 2). Within the complex, stability is enhanced by the presence of hydrogen bonding contacts between the waters and the uncoordinated carboxyl oxygens [2.72(1), 2.67(1) Å for A and B respectively]. In addition, the presence of the tetrahedral sulfinyl oxygen significantly changes the stereochemistry of the side chain compared to (phenylthio)acetic acid (PTAH),[13] [C(2)–C(1)–S(7)–C(8): (**1**), −99, +93°; PTAH, −170°, C(1)–S(7)–C(8)–C(9): (**1**), −174, +165°; PTAH, +177°. S(7)−C(8)−C(9)−O(10): (**1**), −41, +56°; PTAH, −4°].

The copper atom in (**2**) is at a centre of symmetry, and has a distorted octahedral ($CuN_2O_2+O_2$) coordination (Fig. 3). This is made up of two nitrogen atoms from *trans* pyridines [Cu–N, 1.993(3) Å] and two oxygens from BTAH ligands [Cu–O(10), 2.012(3) Å] in the equatorial plane. The six-coordination is completed by the BTAH carboxyl group behaving as an asymmetric bidentate ligand [Cu–O(11), 2.510(5) Å]. There are a number of other examples in which bidentate carboxylate groups form four-membered chelate rings with the same copper atom. These may be categorized according to the coordination number of the copper atom.

a. *Five-coordinate*

$CuN_2O_2+O^*$. In green-blue (*o*-phthalato)bis (pyridine)copper(II), Cingi *et al.*[14] describe the metal coordination as square pyramidal for both of the two independent molecules. The square base comprises a pyridine nitrogen, [Cu–N, 2.028(5), 2.015(5) Å], two oxygens from the bidentate carboxylate group, [Cu–O, 1.954(5), 2.285(4) and 1.967(5), 2.316(4) Å], and an oxygen from a

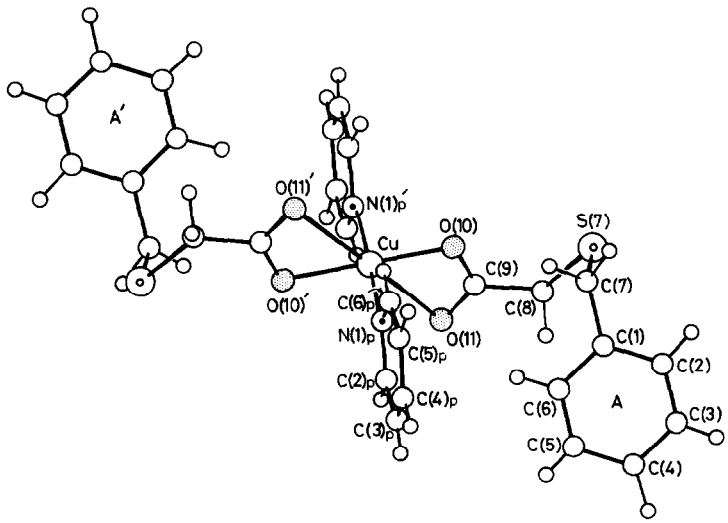


Fig. 3. Molecular configuration and atom naming scheme for $[Cu(BTA)_2(py)_2]$, (**2**). Primed atoms are related by inversion symmetry.

unidentate carboxylate group [Cu–O, 1.921(4), 1.922(4) Å]. The other nitrogens, in the apical positions, and coppers, are at 2.428, 0.265 and 2.442, 0.343 Å respectively above the square plane.

b. *Six-coordinate*

(i) CuN_4O+O^*. These are essentially five-coordinate with the second oxygen at a considerable distance from the metal. Typical examples belong to the [CuX_2(acetate)] Y series, where X = bipyridine, Y = ClO_4^-;[15] X = phenanthroline, Y = ClO_4^-;[16] and X = phenanthroline, Y = BF_4^-.[16,17]

(ii) $CuN_2O_2+O^*N^*$. Violet bis[(isopropylthio)-acetato]tris(isoquinoline)copper(II)[22] has tetragonally distorted octahedral coordination for the metal atom with *trans*-related oxygens from the two acetate groups and two isoquinoline nitrogens forming the square plane. The other two carboxylate oxygens are 2.642(10) Å and 3.282(10) Å from the metal while the third isoquinoline nitrogen is at 2.359(11) Å. Although this was considered "potentially hepta-coordinated", it is being classified in this discussion as six-coordinate.

(iii) $CuN_2O_2+O^*O^*$. Complex (**2**), which is deep purple in colour, represents one of the few examples in this category. Ogawa *et al.*[9] claim that colour in such complexes is possibly due to a charge transfer band caused by the presence of the strong Cu–S bond, while Bonomo[21] attributes the coordination between copper and sulphur to both electronic and steric effects. Cu–S bonding [2.697(1) Å] occurs in blue [aqua(2,2′-bipyridine)(thiodiacetato)-copper(II)] tetrahydrate and deep green diaquabis-[(ethylthio)acetato]copper(II) [2.381(1) Å][22] but no bonds are found in bright green [(2,2′,6′,2″-terpyridine)(thiodiacetato)copper(II)]. Similarly, compound (**2**) (purple) has no bonds involving the sulphur atom, nor do any other examples of the copper(II) (phenylthio)acetate complexes investigated to date.[1–3] Only with the cadmium complex, *catena*-aquabis[(phenylthio)acetato)]cadmium(II)[13] is a M–S bond found but this involves only one ligand [Cd–S, 2.738(5) Å]. In comparable copper(II) phenoxyalkanoate complexes, there are a number of examples involving copper-O(ether) links, e.g. [Cu(*p*-X-phenoxyacetate)$_2$(H_2O)$_n$], where $n = 0$, X = H;[18] $n = 2$, X = H;[19] $n = 2$, X = Cl;[4] $n = 2$, X = F;[23] $n = 2$, X = CH_3O;[20] $n = 2$, X = NO_2.[20] With the exception of the anhydrous complex,[18] which is a hexamer, these compounds are tetragonally distorted octahedral monomers with the axial positions invariably occupied by ether oxygens.

There are no significant intermolecular distances for (**2**), the molecules packing as unassociated monomers in the unit cell (Fig. 4). The additional carbon atom in the side chain compared to (phenylthio)acetic acid prevents the benzene ring from influencing significantly the metal stereochemistry.

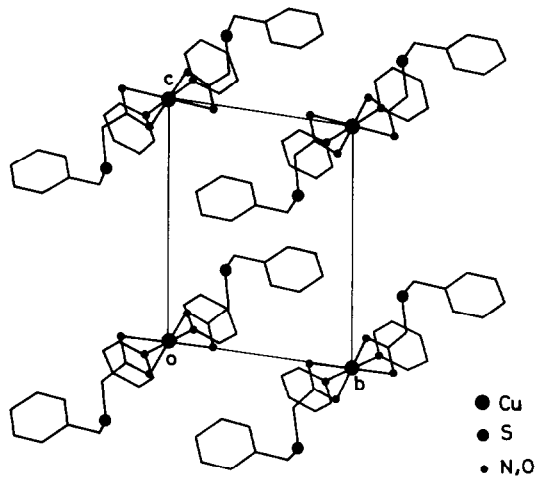


Fig. 4. The packing of (**2**) in the unit cell viewed down the *a* axis.

Acknowledgements—The authors wish to thank the Chinese University of Hong Kong for provision of data collection facilities, the University of Queensland and the Queensland Institute of Technology for financial support and data preparation services.

REFERENCES

1. C. H. L. Kennard, G. Smith, E. J. O'Reilly, T. C. W. Mak and W.-H. Yip, *Polyhedron* 1985 (in press).
2. E. J. O'Reilly, G. Smith, C. H. L. Kennard, T. C. W. Mak and W.-H. Yip, *Inorg. Chim. Acta* 1984, **83**, L63.
3. C. H. L. Kennard, G. Smith, E. J. O'Reilly, T. C. W. Mak and W.-H. Yip, *Inorg. Chim. Acta* 1985, **98**, L31.
4. G. Smith, E. J. O'Reilly, C. H. L. Kennard, K. Stadnicka and B. Oleksyn, *Inorg. Chim. Acta* 1981, **47**, 111.
5. G. M. Sheldrick, *SHELX-76, Program for Crystal Structure Determination.* University of Cambridge, England (1976).
6. S. Motherwell, "*PLUTO*", *Molecular Plotting Program.* University of Cambridge (1971).
7. C. H. L. Kennard, "*APPLECRYST 83*", *A Set of Crystallographic Programs for an Apple II.* University of Queensland, Australia (1983).
8. *International Tables for X-ray Crystallography*, Vol. IV. Kynoch Press, Birmingham (1974).
9. T. Ogawa, M. Shimoi and A. Ouchi, *Bull. Chem. Soc. Jpn* 1982, **55**, 126.
10. L. Leiserowitz, G. Salem and M. Weinstein, *Cryst. Struct. Commun.* 1975, **4**, 85.
11. L. Leiserowitz, G. Salem, C.-P. Tang and M. Weinstein, *Cryst. Struct. Commun.* 1975, **4**, 89.

12. G. Smith and C. H. L. Kennard, *J. Agric. Food Chem.* 1979, **27**, 779.
13. T. C. W. Mak, W.-H. Yip, G. Smith, E. J. O'Reilly and C. H. L. Kennard, *Inorg. Chim Acta* 1984, **84**, 57.
14. M. G. Cingi, A. M. M. Lanfredi, A. Tiripicchio and M. T. Camellini, *Acta Cryst.* 1981, **B37**, 2159.
15. B. J. Hathaway, N. Ray, D. Kennedy, N. O'Brien and B. Murphy, *Acta Cryst.* 1980, **B36**, 1371.
16. F. Clifford, E. Counihan, W. Fitzgerald, K. Seff, C. Simmons, S. Tyagi and B. Hathaway, *J. Chem. Soc. Chem. Commun.* 1982, 196.
17. W. Fitzgerald and B. Hathaway, *Acta Cryst.* 1984, **C40**, 243.
18. J. R. Carruthers, K. Prout and F. J. C. Rossotti, *Acta Cryst.* 1975, **B31**, 2044.
19. C. K. Prout, M. J. Barrow and F. J. C. Rossotti, *J. Chem. Soc. A* 1971, 3326.
20. C. K. Prout, P. J. Grove, B. D. Harridine and F. J. C. Rossotti, *Acta Cryst.* 1975, **B31**, 2047.
21. R. P. Bonomo, E. Rizzarelli, N. Bresciani-Pahor and G. Nardin, *J. Chem. Soc., Dalton Trans.* 1982, 681.
22. A. Ouchi, Y. Sato, Y. Yukawa and T. Takeuchi, *Bull. Chem. Soc. Jpn* 1983, **56**, 2241.
23. E. J. O'Reilly, G. Smith and C. H. L. Kennard, *Inorg. Chim. Acta* 1984, **90**, 63.

Polyhedron Vol. 4, No. 8, pp. 1449–1450, 1985
Printed in Great Britain

0277–5387/85 $3.00 + .00
© 1985 Pergamon Press Ltd

POTASSIUM TRIFLUOROPEROXOTITANATE(IV) TRIHYDRATE, $K[Ti(O_2)F_3]\cdot 3H_2O$

M. K. CHAUDHURI* and B. DAS
Department of Chemistry, North-Eastern Hill University, Shillong 793003, India

(*Received* 24 *September* 1984; *accepted after revision* 6 *February* 1985)

Abstract—Potassium trifluoroperoxotitanate(IV) trihydrate, $K[Ti(O_2)F_3]\cdot 3H_2O$, with the peroxide (O_2^{2-}) being bonded to the Ti(IV) centre in a triangular bidentate manner (C_{2v}) as evidenced from the IR and laser Raman spectroscopic studies, has been synthesised from the reaction of a solution of TiO_2 in 40% HF with an excess of 30% H_2O_2 and KOH, followed by the addition of aqueous HF to adjust the pH of the reaction solution between 8 and 9.

It has been known that Ti(IV) produces a characteristic colour reaction, with H_2O_2, which is used for the detection of either reagent.[1] Some solid peroxotitanate complexes have been reported, however, there is little agreement over their composition let alone their structure.[1,2] Pentafluoroperoxotitanate(IV) complex, $[Ti(O_2)F_5]^{3-}$, is rather well studied, and constitutes the only example of fluoroperoxotitanate(IV) known to date. Reported herein are the synthesis and assessment of molecular structure by IR and laser Raman spectroscopic studies of a new fluoroperoxotitanate(IV), potassium trifluoroperoxotitanate(IV) trihydrate, $K[Ti(O_2)F_3]\cdot 3H_2O$.

EXPERIMENTAL

The chemicals used were all reagent grade products. IR spectra were recorded on a Perkin–Elmer Model 983 spectrophotometer. The laser Raman (LR) spectra were recorded on a SPEX Ramalog Model 1403 spectrometer. The 4880 Å laser line from the Spectra-Physics Model 165 Argon laser was used as the excitation source. The scattered light at 90° was detected with the help of a cooled RCA 31034 photomultiplier tube followed by photon counting processsing system. The spectra were recorded at ambient temperatures by making a freshly prepared solution of the sample, or a pressed pellet of the compound. Molar conductance was measured using a Philips PR9500 conductivity bridge. The pH of the reaction solution was measured with a Systronic Type 335 digital pH meter, and also with pH indicator (BDH) paper. Magnetic susceptibility was measured by the Gouy method, using $Hg[Co(NCS)_4]$ as the calibrant.

Synthesis of potassium trifluoroperoxotitanate(IV) trihydrate, $K[Ti(O_2)F_3]\cdot 3H_2O$. An amount of 1.0 g (12.5 mmol) of TiO_2 was dissolved in 10 cm^3 (200 mmol) of 40% HF by heating for *ca* 10 min over a steam-bath. The clear solution was cooled to 20°C, and 20 cm^3 (176.4 mmol) of 30% H_2O_2 was added under stirring, followed by the addition of 17.5 g (311.9 mmol) of powdered potassium hydroxide. The colourless solution thus obtained was maintained at *ca* 20°C for 15 min. Dropwise addition of 40% HF to the solution, until the pH of the medium was reduced to 8–9, changed colour of the reaction solution to yellow and afforded yellow microcrystalline potassium trifluoroperoxotitanate(IV) trihydrate, $K[Ti(O_2)F_3]\cdot 3H_2O$. Addition of hydrofluoric acid was stopped at this stage and the product was isolated by centrifugation, washed 3–4 times with ethanol, and finally dried *in vacuo* over concentrated sulphuric acid. Yield of $K[Ti(O_2)F_3]\cdot 3H_2O$ was 2 g (69%).

Elemental analysis. Peroxide, fluoride and potassium were estimated by the methods described in earlier papers.[3] Titanium content in the compound was determined gravimetrically by estimating as TiO_2, after precipitation with cupferron.[4] Found: K, 17.3; Ti, 20.45; O_2^{2-} (active oxygen), 14.2; F, 24.3%. Calc. for $K[Ti(O_2)F_3]\cdot 3H_2O$: K, 17.0; Ti, 20.82; O_2^{2-} (active oxygen), 13.91; F, 24.78%.

RESULTS AND DISCUSSION

The pentafluoroperoxotitanate(IV), $[Ti(O_2)F_5]^{3-}$, was synthesised from the reaction of TiF_6^{2-} with

* Author to whom correspondence should be addressed.

H_2O_2. It was expected, however, that a viable synthesis of fluoroperoxotitanates(IV) may be possible from TiO_2 under suitable conditions. In view of this and also considering the importance of pH in the syntheses of peroxometalates,[3,5] the reaction of a solution of TiO_2 in 40% HF with hydrogen peroxide and KOH was conducted followed by adjusting the pH of the reaction medium between 8 and 9 by the addition of 40% HF. This has led to the successful synthesis of potassium trifluoroperoxotitanate(IV) trihydrate,

$$K[Ti(O_2)F_3]\cdot 3H_2O,$$

in a high yield. It is believed that TiO_2 dissolves in 40% HF producing fluorotitanate(IV) in solution which subsequently undergoes peroxygenation in the presence of H_2O_2 and KOH ultimately leading to the synthesis of the complex $[Ti(O_2)F_3]^-$ ion at a pH 8–9. Further lowering of pH to 6 by the addition of 40% HF produced the already known complex $K_3[Ti(O_2)F_5]$.[6,7]

Potassium trifluoroperoxotitanate(IV) trihydrate, $K[Ti(O_2)F_3]\cdot 3H_2O$, is stable in the absence of moisture, and in water it decomposes slowly as evident from the comparatively higher molar conductance at room temperature. The results of a magnetic susceptibility measurement show that the compound is diamagnetic suggesting the occurrence of titanium(IV). Estimation of peroxide, accomplished by red-ox titrations separately involving standard potassium permanganate and Ce^{4+} solutions, conspicuously suggested the presence of one O_2^{2-} per titanium atom in the compound.

The IR spectrum of the compound showed bands at 900vs and 860s cm^{-1}, at 610s cm^{-1}, at 535s cm^{-1}, at 440 m and 310 cm^{-1}, while the laser Raman spectra, recorded in the solid state as well in a solution, were similar exhibiting peaks at 900 and 860 cm^{-1}, at 610 cm^{-1}, at 530 cm^{-1} and at 285 cm^{-1}. The peaks, at 900 and 860 cm^{-1} assigned to ν_{-O-O-} (ν_1), at *ca* 530 cm^{-1} to ν_{Ti-O_2} (ν_2), at 610 cm^{-1} to ν_{Ti-O_2} (ν_3), and at *ca* 300 cm^{-1} to δ_{Ti-F}, are in order and well precedented in the literature.[3,5–7] The additional bands in the IR spectrum are assigned to ν_{Ti-F} (440 cm^{-1}), ν_{O-H} (3450 cm^{-1}), and δ_{H-O-H} (1640 cm^{-1}) modes respectively of un-coordinated water.[8–10] The fact that the ν_{-O-O-} (ν_1) and the complementary ν_{Ti-O_2} (ν_2 and ν_3) modes in the IR and LR spectra were observed in the positions stipulated for a triangularly bonded peroxide, renders it certain that the peroxide (O_2^{2-}) is bonded to the Ti(IV) centre in a triangular bidentate (C_{2v}) manner.

Thus, it may be inferred that potassium trifluoroperoxotitanate(IV) trihydrate,

$$K[Ti(O_2)F_3]\cdot 3H_2O,$$

with the peroxide ligand being bonded to the metal in a triangular bidentate fashion, can be synthesised directly from TiO_2. The complex $[Ti(O_2)F_3]^-$ may be a penta-coordinated monomer; however, it is more likely that it has an octahedral or a distorted octahedral structure through –Ti–F–Ti– interactions.

Acknowledgement—We thank the Department of Atomic Energy for financial assistance.

REFERENCES

1. J. A. Connor and E. A. V. Ebsworth, *Adv. Inorg. Chem. Radiochem.* 1964, **6**, 286.
2. R. J. H. Clark, D. C. Bradley and P. Thornton, *The Chemistry of Titanium, Zirconium and Hafnium, Pergamon Texts in Inorganic Chemistry*, Vol. 19, p. 378. Pergamon Press, Oxford (1975).
3. M. K. Chaudhuri and S. K. Ghosh, *Inorg. Chem.* 1982, **21**, 4020; *J. Chem. Soc., Dalton Trans.* 1984, 507.
4. A. I. Vogel, *A Text Book of Quantitative Inorganic Analysis*, p. 544. Longman-Green, London (1962).
5. M. K. Chaudhuri and S. K. Ghosh, *Inorg. Chem.* 1984, **23**, 534.
6. W. P. Griffith, *J. Chem. Soc.* 1964, 5248.
7. W. P. Griffith and T. D. Wickins, *J. Chem. Soc.* 1967, 590; 1968, 397.
8. A. J. Edwards, *J. Chem. Soc.* (*A*) 1971, 2653.
9. M. N. Bhattacharjee, M. K. Chaudhuri, H. S. Dasgupta and D. T. Khathing, *J. Chem. Soc., Dalton Trans.* 1981, 2587.
10. N. F. Curtis, *J. Chem. Soc.* (*A*) 1968, 1584.

Polyhedron Vol. 4, No. 8, pp. 1451–1456, 1985
Printed in Great Britain

0277-5387/85 $3.00 + .00
© 1985 Pergamon Press Ltd

THE EFFECT OF LIGAND DONOR ATOMS ON TERNARY COMPLEX STABILITY

C. R. KRISHNAMOORTHY,* S. SUNIL and K. RAMALINGAM
Department of Chemistry, Indian Institute of Technology, Madras 600036, India

(*Received* 26 *October* 1984; *accepted after revision* 6 *February* 1985)

Abstract—Formation constants of mixed ligand complexes of Cu^{2+}, Zn^{2+}, Ni^{2+}, Co^{2+}, and Mn^{2+}, with cytidine-5′-monophosphoric acid (CMP) and various primary ligands such as 1,10-phenanthroline (phen), glycylglycine (glygly) and salicylic acid (sal) have been determined in aqueous solution at 35°C and 0.1 M (KNO_3) by potentiometric measurements. The acid dissociation constants of all the above mentioned ligands together with their 1 : 1 binary metal complex formation constants were also measured at 35°C. In general all the 1 : 1 binary complexes follow the Irving–Williams order of stability. Further the binary metal complexes of primary ligands are more stable than their ternary complexes with CMP. For ternary complexes, $\Delta(\log K)$ values seem to change from positive to highly negative as the coordinating atoms of the primary ligands were varied from *N,N* to *N,O*$^-$ to *O*$^-$,*O*$^-$. The higher stability of ternary complexes involving phen is due to its Π-bonding interaction with the above metal ions and the relative decrease in the stability of other ternary systems is due to the coulombic repulsion of donor oxygen atoms of primary and secondary ligands. Thus for ternary complexes the stabilities follow a decreasing order of M–phen–CMP > M–glygly–CMP > M–sal–CMP.

Ternary complexes play a predominant role in many biological systems because of their involvement in enzyme–metal–substrate complexes and also due to their participation in the storage and transport of active substrates through membranes. Nucleotides and nucleosides are commonly used as ligands because many enzyme reactions need the presence of nucleotides like ATP, ADP, AMP, CMP, etc. In addition, metal ions seem to affect the structure of nucleic acids[1] *in vivo* and also the structure of nucleic acid–protein complexes.[1,2] Besides, specific interaction between nucleotides and amino acids must have been significant during the first steps of biochemical evolution.[3] Several reviews[2,4,5] have appeared on these lines. But most of them are confined to adenine nucleosides and nucleotides.[6–11] In the present study CMP is chosen as the secondary ligand because of the relatively fewer studies done on cytosine nucleosides in comparison to adenine nucleosides. Choice of phen, glygly and sal as primary ligands is because of their tendency to form stable metal complexes even in high acid medium and also to assess the influence of factors such as: (1) nature of coordinating atom; (2) steric factors; and (3) Π-bonding effects on the stabilities of these metal complexes. Moreover stabilities of the 1 : 1 binary complexes of the above mentioned primary ligands and metal ions are also determined for the sake of completion.

Thus the present investigation is the first attempt to study the formation of binary and ternary complexes of transition metal ions such as Cu^{2+}, Zn^{2+}, Ni^{2+}, Co^{2+}, and Mn^{2+} and the above mentioned primary and secondary ligands in aqueous solution.

EXPERIMENTAL

Reagents. Chromatographically pure samples of cytidine monophosphoric acid (CMP), 1,10-phenanthroline (S. Merck), glycylglycine (BDH) and salicylic acid (BDH) were employed in this study. For each measurement fresh solid ligand was weighed out to avoid possible photochemical decomposition or hydrolysis. The metal nitrates were analar grade samples (BDH), and stock solutions of these metal nitrates were estimated volumetrically by EDTA

* Author to whom correspondence is to be addressed at: Department of Chemistry, Georgia State University, Atlanta, GA 30303, U.S.A.

titrations.[12] Carbonate free sodium hydroxide was prepared by known procedure and standardized by titration with pure potassium acid phthalate.

Procedure. Potentiometric titrations of various ligands (1.5×10^{-3} M) in the presence and absence of metal ions (1 : 1 ratio) were carried out with standard sodium hydroxide solution to calculate the disssociation constants of various ligands and the stability of their 1 : 1 binary metal complexes. The ionic strength of the solution was maintained at 0.1 M (KNO_3). A stream of nitrogen was passed throughout the course of the experiment to exclude the adverse effect of atmospheric carbon dioxide and the temperature was maintained at 35 ± 0.1°C. The reactants were equilibrated before commencing the titration and between each further addition of sodium hydroxide. The conditions used for the titration of ternary systems were the same as for binary ones (and for the determination of dissociation constants) but the solution contained both primary and secondary ligands and respective metal ions all in 1 : 1 ratio.

An Elico model LI-120 digital pH meter with a combined electrode was used to measure the hydrogen ion concentration. The electrode system was calibrated as previously described.[13]

Calculations. Acid dissociation constants of the ligands are calculated by a direct algebraic method.[14,15]

The stability of 1 : 1 binary complexes pertaining to equilibrium $M + A \rightleftharpoons MA$ was calculated by the method developed by Martell.[14] Stepwise formation of the ternary complex was assumed to take place as shown below and the respective formation constants were calculated by the method described earlier.[16]

$$MA + B \overset{K^{MA}_{MAB}}{\rightleftharpoons} MAB. \qquad (1)$$

The formation constants of 1 : 1 binary metal complexes of the secondary ligand (CMP) were calculated by the usual algebraic method corresponding to the following reaction, $M + B \rightleftharpoons MB$. The stability of the ternary complex characterized by its $\Delta(\log K)$ value can be defined by eqn (2).

$$\Delta(\log K) = \log K^{MA}_{MAB} - \log K^{M}_{MB}, \qquad (2)$$

where M = Cu^{2+}, Zn^{2+}, Ni^{2+}, Co^{2+} or Mn^{2+}; A = primary ligands such as phen, glygly or sal; B = secondary ligand, CMP. Charges on the complexes are omitted for simplicity. In the case of phen, sal and CMP the predominant equilibria involved in the binary complexation is $M + L \rightleftharpoons ML$, at the pH employed in our calculation. For glygly, the species M(H-1L) is excluded in our calculation for the sake of simplicity, and all other species such as M(H-1L)OH, $M(H\text{-}1L)(OH)_2$, ML_2, etc., are negligible in concentration at the pH employed in our calculations.

RESULTS AND DISCUSSION

Acid dissociation constants of both primary and secondary ligands calculated by a direct algebraic method are presented in Table 1. From the potentiometric titration curves shown (for Cu^{2+} alone) in Figs. 1–3, the stability of binary complexes were calculated assuming the equilibria indicated above and presented in Table 2. In all the cases the metal–ligand interaction was confirmed by checking the possibility of metal hydrolysis using titration procedure described earlier.[17,18] Stabilities of the ternary complexes were calculated in the region of titration curve, a = 3–4 based on the reaction shown above and the values are given in Table 3. So also $\Delta(\log K)$ values calculated from eqn (2) are presented in Table 4.

Proton ionization sites of primary ligands are assigned to the two ring nitrogen atoms in phen, COOH and NH_3^+ groups in glygly and carboxylate and phenolic oxygens in sal respectively. The corresponding dissociation constants presented in Table 1 are consistent with earlier published results.[19–21]

In the case of CMP the deprotonation takes place from N_3 and phosphatic oxygen respectively and

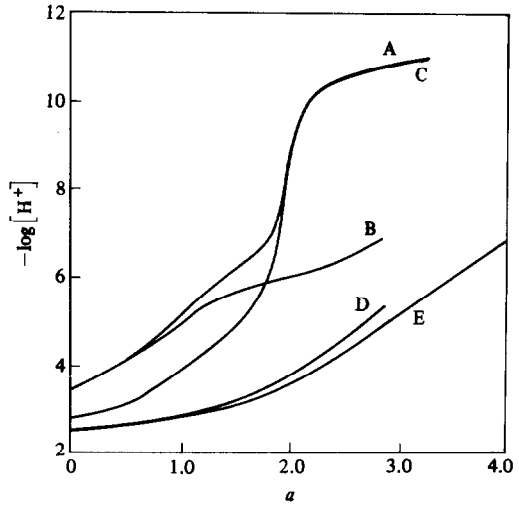


Fig. 1. Potentiometric titration curves of 1:1 binary and 1:1:1 ternary complexes involving Cu^{2+}, 1,10-phenanthroline and cytidine-5′-monophosphoric acid (CMP). A = CMP; B = 1:1 Cu^{2+}–CMP; C = 1,10-phenanthroline; D = 1:1 Cu^{2+}–1,10-phenanthroline; E = 1:1:1 Cu^{2+}–1,10-phenanthroline–CMP; a = moles of base added per mole of ligand; t = 35°C; μ = 0.1 M (KNO_3).

Table 1. Acid dissociation constants of various ligands investigated. $t = 35°C$, $\mu = 0.1$ M (KNO_3)

Ligand	pK_{a}	pK_{2a}
Cytidine-5′-monophosphoric acid	4.27±0.01	6.30±0.02
1,10-Phenanthroline	1.95±0.02	4.77±0.02
Glycylglycine	3.16±0.02	7.91±0.02
Salicylic acid	2.75±0.01	12.87±0.02

Table 2. Stability of 1:1 binary complexes of transition metal ions with various ligands. $t = 35°C$, $\mu = 0.1$ M (KNO_3)

Metal ion	M–phen log K	M–glygly log K	M–sal log K	M–CMP log K
Cu^{2+}	7.20±0.10	5.70±0.10	9.84±0.05	3.90±0.10
Co^{2+}	6.75±0.05	3.10±0.10	6.83±0.10	3.50±0.10
Ni^{2+}	7.30±0.10	4.10±0.10	6.80±0.10	2.36±0.06
Zn^{2+}	6.25±0.05	3.50±0.10	7.10±0.10	2.25±0.10
Mn^{2+}	3.95±0.05	2.60±0.10	6.10±0.10	2.65±0.03

Phen = 1,10-phenanthroline, glygly = glycylglycine, sal = salicylic acid, CMP = cytidine-5′-monophosphoric acid.

Table 3. Formation constants of the 1:1:1 ternary complex of transition metal ions with various primary ligands and CMP. $t = 35°C$, $\mu = 0.1$ M (KNO_3)

Metal ion	M–phen–CMP log K	M–glygly–CMP log K	M–sal–CMP log K
Cu^{2+}	4.60±0.10	4.30±0.10	2.84±0.10
Co^{2+}	3.74±0.10	1.59±0.10	0.84±0.05
Ni^{2+}	3.77±0.10	2.15±0.10	0.84±0.05
Zn^{2+}	3.76±0.10	2.06±0.10	1.61±0.05
Mn^{2+}	3.65±0.10	1.44±0.10	0.15±0.03

Phen = 1,10-phenanthroline, glygly = glycylglycine, sal = salicylic acid, CMP = cytidine-5′-monophosphoric acid.

Table 4. $\Delta(\log K)$ values of the 1:1:1 ternary metal complexes of CMP with various primary ligands. $t = 35°C$, $\mu = 0.1$ M (KNO_3)

Metal ion	M–phen–CMP	M–glygly–CMP	M–sal–CMP
Cu^{2+}	+0.70	+0.40	−1.06
Co^{2+}	+0.24	−1.91	−2.66
Ni^{2+}	+1.41	−0.21	−1.52
Zn^{2+}	+1.51	−0.21	−0.64
Mn^{2+}	+1.00	−1.21	−2.50

Phen = 1,10-phenanthroline, glygly = glycylglycine, sal = salicylic acid, CMP = cytidine-5′-monophosphoric acid.

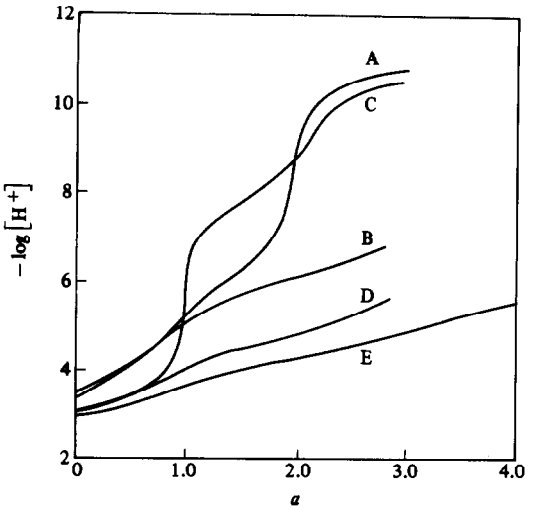


Fig. 2. Potentiometric titration curves of 1 : 1 binary and 1 : 1 : 1 ternary complexes involving Cu^{2+}, glycylglycine and cytidine-5'-monophosphoric acid (CMP). A = CMP; B = 1 : 1 Cu^{2+}–CMP; C = glycylglycine; D = 1 : 1 Cu^{2+}–glycylglycine; E = 1 : 1 : 1 Cu^{2+}–glycylglycine–CMP; a = moles of base added per mole of ligand; t = 35°C; μ = 0.1 M (KNO_3).

the corresponding dissociation constants reported agree well with the previous studies.[20] Stability of all binary metal complexes follow the Irving–Williams order and also agree well with earlier studies.[19–23] The enhanced stabilities of all the primary ligand–metal complexes are due to the chelate forming

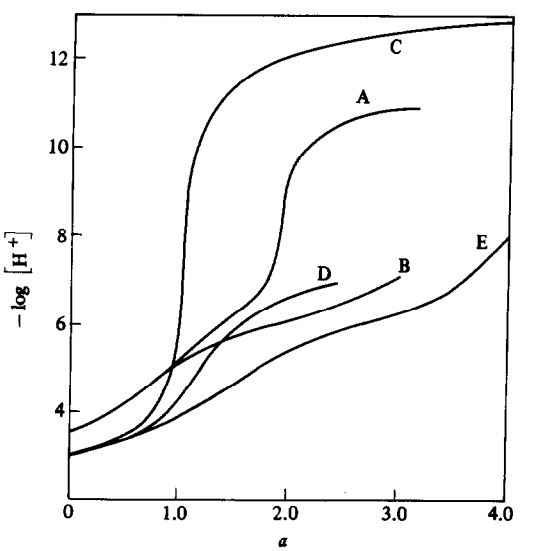


Fig. 3. Potentiometric titration curves of 1 : 1 binary and 1 : 1 : 1 ternary complexes involving Cu^{2+}, salicylic acid and cytidine-5-monophosphoric acid (CMP). A = CMP; B = 1 : 1 Cu^{2+}–CMP; C = salicylic acid; D = 1 : 1 Cu^{2+}–salicylic acid; E = 1 : 1 : 1 Cu^{2+}–salicylic acid–CMP; a = moles of base added per mole of ligand; t = 35°C; μ = 0.1 M (KNO_3).

tendency of these primary ligands using their donor atoms. For glycylglycine the presence of metal ion induces the deprotonation of the amide group proton. This makes the ionised amide nitrogen more basic than the amide oxygen and thereby metal chelation in glycylglycine occurs via aminonitrogen, deprotonated amide nitrogen and carboxylate oxygen.[24]

There are conflicting statements in literature about the metal ion binding sites in CMP especially in regard to the base nitrogen. Studies with Ni^{2+}, Mn^{2+}, and Mg^{2+} using magnetic resonance techniques have shown that there is a very weak interaction with the cytosine ring.[25] So also in other nucleotide–metal systems, the evidence for metal binding through the pyrimidine ring, apart from the phosphatic oxygen is indicated.[26] The relatively higher stabilities of Cu^{2+} and Co^{2+} complexes of CMP may be due to the simultaneous binding of cytosine ring nitrogen and phosphate oxygen to the metal ions.

In the case of ternary complexes the stabilities decrease in the order M–phen–CMP > M–glygly–CMP > M–sal–CMP. The $\Delta(\log K)$ values given in Table 4 show that in general the change is from positive to weakly negative to highly negative when the primary ligand is varied from phen, glygly to sal. This effect in turn is due to the change in the coordinating atoms from N,N to N,O^- and O^-,O^- respectively in these ligands.

Thus M–phen–CMP systems uniformly show positive $\Delta(\log K)$ in all the cases and this is expected when the primary ligand is an aromatic amine like phen or bipyridyl and the secondary ligand is a potential oxygen donor.[27] This is due to the back-donation from the metal d orbital into vacant Π-orbital of the aromatic amine and when the secondary ligand has oxygen donor that will neutralize the charge on the central atom resulting in the enhancement of the stability of the ternary complexes. This increased stability of the ternary complexes can also be explained in another way, namely, that the aromatic amine and transition metal ions are borderline cases according to Pearson HSAB principle and the drain of electron from metal to aromatic amine ligands increases the effective nuclear charge on the central metal ion thereby making it harder. This enables the metal ions to have a selective interaction with harder oxygen ligands.[28]

Except in the case of Cu^{2+}, the ternary systems of M–glygly–CMP have weakly negative $\Delta(\log K)$ values, which is due to the change of ligand donors to N,O^- in glygly. Similar observations were noticed for other ternary systems of glygly.[29] The positive $\Delta(\log K)$ value for Cu–glygly–CMP may be due to the fact that Cu^{2+} can also bind to N_3 of cystosine

ring and thus form stable square planar ternary chelate with glygly. This might also account for the weakly negative values for Ni^{2+} and Zn^{2+} which can form similar stable square planar and tetrahedral complexes respectively.

The literature information available is scanty regarding the ternary metal complexes involving phenolic acids as primary ligands and biologically significant ligands such as nucleotides as secondary ligands. Hence, it is of interest to examine the effect of these primary ligands on the interaction of nucleotides with metal ions, as some of these phenolic compounds are known to occur in biological systems.

In the present study it is noticed that there is very little interaction for CMP with metal ions already bound to salicylic acid as compared to its interaction with free (hydrated) metal ions. In fact the ternary systems of M–sal–CMP show large negative $\Delta(\log K)$ values in all the cases. This is because of the very high stability of the binary metal–sal complexes due to chelation and conjugation effects which detract from its tendency to interact further. Another reason could be due to the increased coulombic repulsion between the donor oxygen atoms of sal and CMP resulting in the destabilization of their ternary complexes. The situation in which sal acts as primary ligand the electronic repulsion is maximum from its two donor oxygen atoms with that of the oxygen atoms of CMP. Thereby the stability of their ternary complex will be much less with $\Delta(\log K)$ being most negative. However, glygly has only one such donor oxygen carrying a lone pair of electrons and their ternary complexes will be more stable [$\Delta(\log K)$ small and negative]. Whereas phen has no such coulombic repulsion and the greater stability of its ternary systems are shown by its large positive value for $\Delta(\log K)$. These marked differences in the stability of the ternary metal complexes could be directly related to the nature of primary ligands with varying donor atoms such as N,N, N,O^- and O^-,O^- in phen, glygly and sal respectively. This discriminating behavior of M–CMP complexes towards other ligands will have a significant role in many biological systems.

CONCLUSION

Thus as the donor atoms in the primary ligands are changed from N,N to N,O^- to O^-,O^- the stability of their corresponding ternary complexes show a drastic decrease. The added stability in the case of ternary complexes involving aromatic N,N donor ligands is due to Π-interaction with the central metal ion. The least stability seen in the ternary systems with O^-,O^- donor ligands is due to the coulombic repulsion of highly charged oxygen ions coming together to coordinate with the central metal ion thus leading to repulsion. Hence apart from Π-backbonding and chelation the nature of coordinating atoms of the primary ligands also influence the stabilities of the ternary systems. Since the stability of ternary complex is one of the major factors deciding its concentration in biological systems, the above discrimination of metal–CMP and similar systems towards primary ligands with varying donor atoms such as N,N, N,O^- and O^-,O^- will be helpful to have selectivity of carrier bases in biological systems. Besides this will help in designing suitable model systems for various reactions involving metalloenzymes. Further study on similar systems is in progress in our laboratory.

Acknowledgements—The award of research fellowship to one of the authors (K.R.) by C.S.I.R. New Delhi, is gratefully recognized. We wish to thank Yueh-Hwa Wang of Georgia State University for drawing the figures and for carefully reading the manuscript.

REFERENCES

1. G. L. Eicchorn (Ed.), *Inorganic Biochemistry*, Vol. 1. Elsevier, New York (1973).
2. (a) L. G. Mazilli, *Prog. Inorg. Chem.* 1977, **23**, 255; (b) D. J. Hodgson, *Prog. Inorg. Chem.* 1977, **23**, 211.
3. J. Orenberg, H. Sigel and B. E. Fischer, *J. Inorg. Nucl. Chem.* 1980, **42**, 785.
4. R. Phillips, *Chem. Rev.* 1966, **66**, 501.
5. R. M. Izatt, J. J. Christensen and J. H. Rything, *Chem. Rev.* 1971, **71**, 439.
6. M. Taqui Khan and A. E. Martell, *J. Am. Chem. Soc.* 1962, **84**, 3037.
7. M. M. Taqui Khan and A. E. Martell, *J. Am. Chem. Soc.* 1966, **88**, 688.
8. M. M. Taqui Khan and A. E. Martell, *J. Am. Chem. Soc.* 1967, **89**, 5585.
9. E. Walaas, *Acta Chem. Scand.* 1958, **12**, 528.
10. J. Bar-Tana and W. W. Cleland, *J. Biol. Chem.* 1974, **249**, 1271.
11. H. Sigel and C. F. Naumann, *J. Am. Chem. Soc.* 1976, **98**, 730.
12. A. I. Vogel, *A Textbook of Quantitative Inorganic Analysis*. ELBS & Longman (1975).
13. M. M. Taqui Khan and C. R. Krishnamoorthy, *J. Inorg. Nucl. Chem.* 1971, **33**, 1417.
14. S. Chaberek, Jr. and A. E. Martell, *J. Am. Chem. Soc.* 1952, **74**, 5052.
15. G. F. Condike and A. E. Martell, *J. Inorg. Nucl. Chem.* 1969, **31**, 2455.
16. K. Ramalingam and C. R. Krishnamoorthy, *Inorg. Chim. Acta* 1982, **67**, 167.
17. M. M. Taqui Khan and Amjad Hussian, *Ind. J. Chem.* 1981, **194**, 44.

18. M. M. Taqui Khan and S. Satyanarayana, *Ind. J. Chem.* 1981, **204**, 814.
19. A. E. Martell and R. M. Smith, *Critical Stability Constants*, Vol. 1, p. 294. Plenum Press, New York (1974).
20. A. E. Martell and R. M. Smith, *Critical Stability Constants*, Vol. 2, p. 251. Plenum Press, New York (1974).
21. A. E. Martell and R. M. Smith, *Critical Stability Constants*, Vol. 3, p. 186. Plenum Press, New York (1977).
22. D. D. Perrin, *Nature* 1958, **182**, 741.
23. R. P. Martin, L. Mosoni and B. Sarkar, *J. Biol. Chem.* 1971, **246**, 5944.
24. Hemlut Sigel and R. B. Martin, *Chem. Rev.* 1981, **82**, 385.
25. M. J. Heller, *Biochemistry* 1970, **9**, 4981.
26. G. L. Eicchorn, *Biochemistry* 1966, **5**, 245.
27. P. J. Patel, V. K. Patel and P. K. Bhattachanya, *Inorg. Chem.* 1982, **21**, 3163.
28. H. Griesser and H. Sigel, *Inorg. Chem.* 1970, **9**, 1238.
29. H. Sigel, Bernard Prijs and R. Bruce Martin, *Inorg. Chim. Acta* 1981, **56**, 45.

Polyhedron Vol. 4, No. 8, pp. 1457–1460, 1985
Printed in Great Britain

0277–5387/85 $3.00 + .00
© 1985 Pergamon Press Ltd

MIXED-VALENCE ELECTRON DELOCALIZED THIOCYANATO BRIDGED RUTHENIUM DINUCLEAR COMPLEX $[\{Ru(NH_3)_5\}_2SCN]^{4+}$

V. PALANIAPPAN, S. K. S. YADAV* and U. C. AGARWALA†
Department of Chemistry, Indian Institute of Technology, Kanpur 208 016, India

(*Received* 16 *October* 1984; *accepted after revision* 6 *February* 1985)

Abstract—The thiocyanato bridged mixed-valence ruthenium dinuclear species $[\{Ru(NH_3)_5\}_2SCN]^{4+}$ has been prepared and characterized. A solvent independent, low intensity intervalence transfer band was observed in the near IR absorption spectrum suggesting a delocalized limit in the [Ru(II)–SCN–Ru(III)] unit.

The syntheses of ligand bridged mixed-valence dinuclear complexes of transition metals have stimulated a great deal of interest[1–7] in the process of electron exchange in binuclear redox reactions and in getting information about the character of electron transmission through chemical systems. There also exists a possibility of thiocyanate ion acting as a bridging ligand in such systems. In this paper we would like to communicate the synthesis and characterization of a thiocyanato bridged mixed-valence ruthenium ammine complex and the behaviour of the intervalence transfer (IT) absorption band in the near IR region in different solvents.

EXPERIMENTAL

[A] *Chemicals*

All the chemicals used were of chemically pure or of Analar grade. $[Ru(NH_3)_5N_2]Br_2$ and $[Ru(NH_3)_5SCN]X_2$ (X = Br, ClO_4) were prepared by known procedures.[8,9] The purities of $[Ru(NH_3)_5SCN]X_2$ were confirmed by passing them through a Sephadex G-10 column (25 × 1 cm) and eluting with 10^{-4} M HBr or $HClO_4$.[10]

[B] *Preparation of complexes*

[B.1] *Preparation of* $[\{Ru(NH_3)_5\}_2SCN]Br_4$. Aqueous solutions of stoichiometric amounts of $[Ru(NH_3)_5N_2]Br_2$ and $[Ru(NH_3)_5SCN]Br_2$ (2×10^{-4} mole in 10 cm^3 each) were mixed. The resulting solution was stirred for about 14–15 hr at room temperature (~ 37°C), whereby the colour of the solution turned from red to reddish-yellow. It was centrifuged and a few cm^3 of conc. HBr was added to the centrifugate to precipitate a reddish-brown compound. It was filtered, washed with ethanol and ether and dried under vacuum; It was analysed for $[Ru_2(NH_3)_{10}SCN]Br_4$ (yield 60–70%).

Found: C, 1.8; H, 4.4; N, 20.2; S_{tot}, 4.7; S_{cat}, 4.3; Br_{tot}, 42.8; Br_{ion}, 42.5.

Calc.: C, 1.6; H, 4.0; N, 20.5; S_{tot}, 4.2; S_{cat}, 4.2; $Br_{tot} = Br_{ion}$, 42.6%.

[B.2] *Preparation of* $[\{Ru(NH_3)_5\}_2SCN](ClO_4)_4$. The procedure for the synthesis of the complex was the same as that described in B.1 except that (i) $[Ru(NH_3)_5SCN](ClO_4)_2$ was used in place of $[Ru(NH_3)_5SCN]Br_2$ and (ii) conc. $HClO_4$ was used to precipitate the reddish-violet perchlorate salt. The reddish-violet compound was analysed for $[Ru_2(NH_3)_{10}SCN](ClO_4)_4$ (yield 60–70%).

Found: C, 1.6; H, 3.4; N, 18.8; S_{tot}, 4.2; S_{cat}, 4.0; Cl_{tot}, 17.6; $ClO_{4\,ion}$, 49.0.

Calc.: C, 1.4; H, 3.6; N, 18.5; S_{tot}, 3.8; S_{cat}, 3.8; Cl_{tot}, 17.1; $ClO_{4\,ion}$, 48.1%.

[C] *Physico-chemical measurements*

Carbon, hydrogen and nitrogen present in the samples were analysed by the Microanalytical Laboratory, I.I.T., Kanpur (India). Analytical methods of sulphur (total and cationic) and bromide/chloride (total and ionic) were given

* Present address: Chemist, Thapar Research Group, Karwar, India.

† Author to whom correspondence should be addressed.

elsewhere.[10] Spectra were obtained using the following intruments: IR; Perkin–Elmer model-521 IR Diffraction Grating Spectrophotometer; UV and Visible, Beckmann DB, UV and Visible Recording Spectrophotometer; near IR, Cary 17 model spectrophotometer using 1 cm matched quartz cells. The apparatus used for cyclic voltammetric studies was assembled in our laboratory using a triangular wavefunction generator potentiostat having three electrode operational amplifier assembly. All the measurements were made on platinum electrodes in the range of 0–0.9 V using KCl as supporting electrolyte. The values are with respect to saturated calomel electrode and are uncorrected for junction potentials.

RESULTS AND DISCUSSION

The analyses of both the complexes indicate that only one SCN group per two ruthenium atoms is present in the cation. Since NH_3 cannot form a bridge between two $[Ru(NH_3)_5]$ units, the only possibility is that the thiocyanate group must be the bridging ligand and is proved by the following studies.

Conductance measurements

Extensive conductance measurements at different concentrations were carried out to establish the charge type on the water soluble complex $[\{Ru(NH_3)_5\}_2SCN]Br_4$. Equivalent conductance vs $\sqrt{C_{eq}}$ graphs were plotted. Equivalent concentration (C_{eq}) of the species was calculated by the method suggested by Feltham *et al.*[11] Conductance at infinite dilution, λ_0, was determined from the plots by extrapolation from which the molar conductance value was found to be 423 Ω^{-1} cm^2 M^{-1} and that of λ_0, 232 Ω^{-1} cm^2 eq.$^{-1}$ Plots of $(\lambda_0 - \lambda_e)$ vs $\sqrt{C}_{eq}$ (cf. Onsager equation) were made and the slope of the straight line was found to be 1200, a value which was quite comparable to those reported for +4 charged species[11] (Fig. 1).

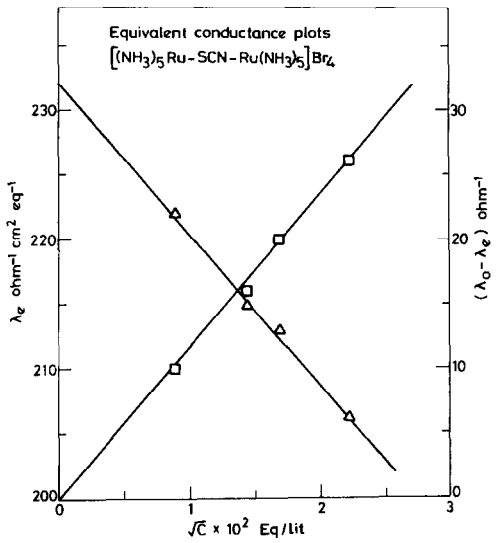


Fig. 1. Equivalent conductance plots.

Magnetic measurements

At room temperature, the dimer exhibited a μ_{eff} of 1.1 BM per ruthenium atom, which suggests the presence of one unpaired electron in the system. The fact that the two ruthenium sites are in different oxidation states, viz. +2 and +3, is also obvious.

IR spectroscopy

The IR spectra of the dimer $[\{Ru(NH_3)_5\}_2SCN]^{4+}$ is similar to the one of $[Ru(NH_3)_5SCN]^{2+}$ reported earlier,[10,12] except for a small shift in the position of the band due to ν(CN). A broad, intense band due to ν(CN) of the dimer was observed at 2060 cm^{-1} with a shoulder at 2090 cm^{-1}; the monomer exhibited the ν(CN) band at 2073 cm^{-1}.[12] The broadness of the band ($\Delta\nu_{1/2}$ = 120 cm^{-1}) suggests the presence of a bridging thiocyanato group.[13,14] Besides, all the characteristic bands of the coordinated NH_3 were observed around 3400(w), 3200, 1600, 1300, 800 and 450 cm^{-1}. The masking of the relatively weak band due to ν(CS) of SCN in the region 820–750 cm^{-1} by the broad and moderately intense band due to the rocking mode of the NH_3 around 800 cm^{-1} left some uncertainty in assigning the ν(CS) band. Although, due to the asymmetry of the bridging thiocyanato group, the IR studies are not strongly evidential as in the case of μ-pyrazine ion,[4] the slight shift in the positions of ν(CN) bands of the monomer and dimer does help. The shift may be attributed to the nitrogen end coordination of [Ru(III)–SCN] unit on Ru(II) and is understandable as the π-acceptor ability of the S-bonded thiocyanato group is only slightly higher than that of an N-bonded one.[15]

Electronic spectra

Analogous to most of the other mixed-valence species, the electronic spectra of the dinuclear species $[\{Ru(NH_3)_5\}_2SCN]^{4+}$ exhibited a near IR transition. The position of the absorption maximum of the band was found to be independent of solvent, similar to μ-pyrazine,[16] μ-cyanogen[17] and μ-dinitrogen[18] complex ions (Table 1).

Ignoring the asymmetry of the bridging

Table 1. Solvent independent near IR spectral data

Solvent	$\left(\frac{1}{n^2}-\frac{1}{D}\right)$	λ_{max} (nm)
H_2O	0.551	1690
DMF	0.464	1610
Chlorobenzene[a]	0.254	1600
Formamide	0.468	1640

[a] ε_{max} in chlorobenzene: 331 M^{-1} cm^{-1}.
(n and D are refective index and dielectric constant of the solvent.)

thiocyanato group, the bandwidth was calculated within the limits of the conceptual model proposed by Hush,[19,20] which is applicable to systems having trapped integral valences with a moderately small delocalization. For a symmetrical one-electron transfer, the absorption maximum and the bandwidth can be calculated from each other. In the high temperature limit at 300 K:

$$\nu_{max} = (\Delta\nu_{1/2})^2/2310 \qquad (\nu_{max} \text{ and } \Delta\nu_{1/2} \text{ in } cm^{-1}). \tag{1}$$

The weak band (ε_{max} = 331 M^{-1} cm^{-1} in C_6H_5Cl) is narrower than expected from eqn (1) ($\Delta\nu_{1/2}$ = 929 cm^{-1} compared to the calculated value of 3800 cm^{-1}; Fig. 2). The weak intensity, narrowness compared to the bands of other systems having largely trapped integral valences and the solvent independence of the absorption maximum of the band can be attributed to a comparatively higher delocalized limit rather than to trapped integral valences; i.e., in the classification of Robin and Day[21] the dimer can be designated as a class III system.

The d-levels of the dimer can be best described by molecular orbitals delocalized over both the metal centres as has been assumed for the $[\{Ru(NH_3)_5\}_2N_2]^{4+}$ dimer.[22] Assuming the linearity of the SCN bridge, the tentative ordering of the molecular orbitals of the dimer in C_{4v} symmetry can be given as $E(xz_1+xz_2,\ yz_1+yz_2) < B_2(xy_1+xy_2) \sim B_2(xy_1-xy_2) < E(xz_2-xz_2-yz_1-yz_2) < \pi^*(SCN)$ with an unpaired electron in the $E(xz_1-xz_2, yz_1-yz_2)$ level. From the above ordering, the two transitions $(xz_1-xz_2,\ yz_1-yz_2)E \leftarrow B_2$ and $(SCN)\pi^* \leftarrow B_2$ may be attributed to the near IR and the 490 nm charge transfer bands, respectively (Fig. 3).

Cyclic voltammetric studies

The cyclic voltammogram showed two one-electron reduction waves (Fig. 4), one having a maximum around 0.325 V and the other around 0.575 V with practically no anodic peaks in the first scan (scan rate 120 mV s^{-1}). The cathodic maximum around 0.575 V exhibited the anodic counterpart around 0.5 V after the second scan, suggesting quasi-irreversibility of the process (E_{pc} = 0.575 V; E_{pa} = 0.500 V; $E_{1/2}$ = 0.538; ΔE_p = 0.075 V). After the third scan, the cathodic peak around 0.325 V started disappearing with the appearance of a new peak around 0.2 V. It suggested the formation of an intermediate which was possibly disproportionating, with one of the disproportionation products, having ruthenium in the +3 oxidation state. The aquation of the electrogenerated intermediate may lead to the formation of $[Ru(NH_3)_5SCN]^{2+}$. This inference is understandable by the fact that after the third scan the system was showing the same redox behaviour as that of $[Ru(NH_3)_5SCN]^{2+}$.[10,12]

The equilibrium between the mixed-valence, completely oxidized and completely reduced

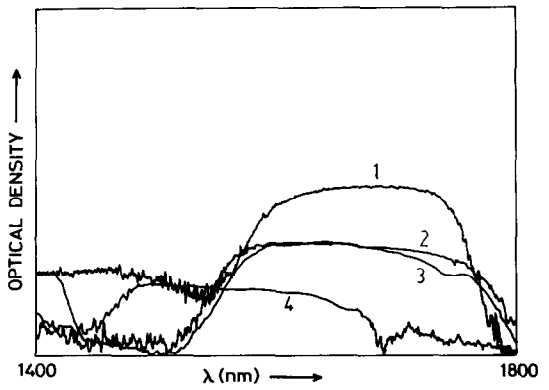


Fig. 2. NIR spectra in different solvents: 1. Water (2.7×10^{-4} M); 2. chlorobenzene (6.3×10^{-4} M); 3. formamide (8.3×10^{-4} M); 4. DMF (6.0×10^{-4} M).

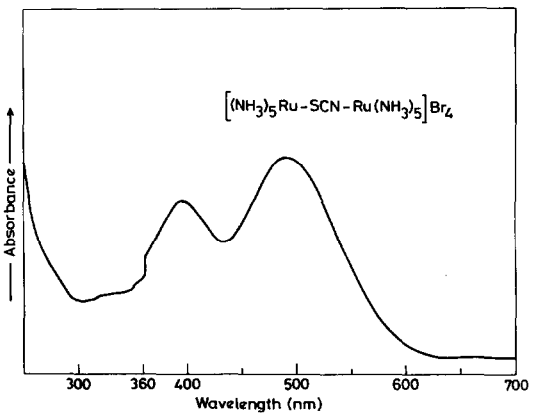


Fig. 3. Electronic spectrum.

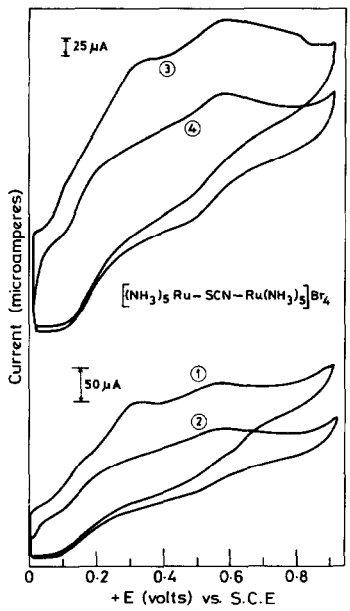


Fig. 4. Cyclic voltammograms.

moieties is also a possibility if the half-wave potentials of the two one-electron redox processes are close enough.[23] Such an equilibrium between mixed-valence and completely oxidized moieties can explain the following tentative scheme:

$$\text{Ru(III)–SCN–Ru(III)} \xrightarrow{0.325\,V} \text{Ru(II)–SCN–Ru(III)}$$

$$\text{Ru(II)–SCN–Ru(III)} \underset{}{\overset{0.575\,V}{\rightleftharpoons}} \text{Ru(II)–SCN–Ru(II)}$$

$$\text{Ru(II)–SCN–Ru(II)} \xrightarrow[\text{Disproportionation}]{} \text{Ru(III)–SCN}$$

$$\text{Ru(III)–SCN} \xrightarrow{0.2\,V} \text{Ru(II)–SCN}.$$

The confirmation of such a scheme was not possible because of the lack of coulometric data. Besides, the efforts to synthesize the completely reduced moiety failed and the product invariably decomposed to $[Ru(NH_3)_5SCN]^{2+}$. The instability of the Ru(II)–SCN–Ru(II) species can tentatively be attributed to the comparatively weaker π-acidities of the nitrogen and sulphur ends of the thiocyanate group.[15]

Acknowledgement—The financial aid (JRF) to one of the authors (VP) by C.S.I.R., New Delhi, India is acknowledged.

REFERENCES

1. C. Creutz and H. Taube, *J. Am. Chem. Soc.* 1969, **91**, 3988.
2. G. M. Tom, C. Creutz and H. Taube, *J. Am. Chem. Soc.* 1974, **96**, 7827.
3. R. W. Callahan, G. M. Brown and T. J. Meyer, *Inorg. Chem.* 1975, **14**, 1443.
4. R. W. Callahan, F. R. Keene, T. J. Meyer and D. J. Salmon, *J. Am. Chem. Soc.* 1977, **99**, 1064.
5. B. P. Sullivan and T. J. Meyer, *Inorg. Chem.* 1980, **19**, 752.
6. Diana Sedney and A. Ludi, *Inorg. Chem. Acta* 1981, **47**, 153.
7. A. Vogler and J. Kisslinger, *J. Am. Chem. Soc.* 1982, **104**, 2311.
8. A. D. Allen, F. Bottomley, V. P. Remsolu and C. V. Senoff, *J. Am. Chem. Soc.* 1967, **89**, 5595.
9. S. K. S. Yadav and U. C. Agarwala, *Indian J. Chem.* 1982, **21A**, 175.
10. R. Parashad, S. K. S. Yadav and U. C. Agarwala, *J. Inorg. Nucl. Chem.* 1981, **43**, 2359.
11. R. D. Feltham and R. G. Hayter, *J. Chem. Soc.* 1964, 4587.
12. S. K. S. Yadav and U. C. Agarwala, *Polyhedron* 1984, **3**, 1.
13. S. Fronaeus, *Acta Chem. Scand.* 1962, **16**, 1447.
14. C. Pecile, *Inorg. Chem.* 1966, **5**, 210.
15. H. S. Lim, D. J. Barclay and F. C. Anson, *Inorg. Chem.* 1972, **11**, 1460.
16. C. Creutz and H. Taube, *J. Am. Chem. Soc.* 1973, **95**, 1086.
17. G. M. Tom and H. Taube, *J. Am. Chem. Soc.* 1975, **97**, 5310.
18. R. H. Magnuson and H. Taube, *J. Am. Chem. Soc.* 1972, **94**, 7213.
19. N. S. Hush, *Prog. Inorg. Chem.* 1967, **8**, 391.
20. N. S. Hush, *Electrochim. Acta* 1968, **13**, 1005.
21. M. B. Robin and P. Day, *Adv. Inorg. Chem. Radiochem.* 1967, **10**, 247.
22. I. M. Treitel, M. T. Flood, R. E. Marsh and H. B. Gray, *J. Am. Chem. Soc.* 1969, **91**, 6512.
23. R. W. Callahan and T. J. Meyer, *Chem. Phys. Lett.* 1976, **39**, 82.

Polyhedron Vol. 4, No. 8, pp. 1461–1466, 1985
Printed in Great Britain

0277–5387/85 $3.00 + .00
© 1985 Pergamon Press Ltd

A STUDY OF 4-CARBA-*ARACHNO*-NONABORANE(14) AND THE DERIVED TRIDECAHYDRO-4-CARBA-*ARACHNO*-NONABORANE(−1) ANION: STRUCTURE AND C–H BOND ACTIVATION AS SHOWN BY 1- AND 2-D NMR

O. W. HOWARTH, M. J. JASZTAL, J. G. TAYLOR and M. G. H. WALLBRIDGE*
Department of Chemistry, University of Warwick, Coventry CV4 7AL, U.K.

(*Received* 16 *November* 1984; *accepted* 6 *February* 1985)

Abstract—The ^{11}B and ^{1}H NMR spectra of the carbaborane CB_8H_{14}, and its anion $CB_8H_{13}^-$, have been recorded and assigned unambiguously by decoupling and COSY techniques. The results indicate the presence of unsymmetrical bridging hydrogen atoms in both the neutral and anionic species. More significantly the *endo*-hydrogen attached to the carbon atom is involved in exchange with all the three bridging hydrogen atoms in the $CB_8H_{13}^-$ anion, whereas no such exchange is observed in the neutral CB_8H_{14}.

The use of NMR spectroscopy in the study of boranes and their derivatives has been well documented.[1] More recently two-dimensional (2D), and homonuclear chemical shift correlation spectroscopy (COSY)[2] data have also been shown to be useful in providing additional information.[3] For example, the application of homonuclear 2D NMR techniques have been utilised to elucidate boron hydride cluster connectivity.[4–7]

The spectra produced exhibit diagonal symmetry with cross peaks due to scalar spin–spin coupling, indicating adjacent nuclei. Boron atoms connected by a bridging hydrogen have been found, in general, not to give rise to such coupling.[5,6] This is explained in terms of the negligible electron density along the B–B vector predicted in the theoretical description of three-centre bridging hydrogen bonds. However, some exceptions have been noted, as in

nido-2-$(C_5H_5)CoB_4H_8$

and

nido-$[C_6(CH_3)_6]Fe(C_2H_5)_2C_2B_3H_5$.[5]

We have applied these techniques to the monocarbaborane systems *arachno*-CB_8H_{14}, and the $CB_8H_{13}^-$ anion, to obtain more information about their properties, and to extend the current knowledge of the type of results to be expected using these techniques.

EXPERIMENTAL

The neutral carbaborane CB_8H_{14} was prepared as described elsewhere,[12] with spectra being obtained from a benzene-d_6 solution. The anion $CB_8H_{13}^-$ was prepared by a different route to that reported,[11] as follows. In a dry-box with a nitrogen atmosphere, a 10 mm diameter NMR tube, containing 0.82 cm^3 of a 0.16 mol dm^{-3} lithium butyl solution (0.13 mmol), was pumped under vacuum to remove the hexane solvent. The residue was dissolved in 1.0 cm^3 of tetrahydrofuran-d_8. To this solution was added 0.15 g of CB_8H_{14} (0.13 mmol), dissolved in the same solvent, and the mixture agitated for 15 min, whereupon reaction to form the anionic derivative, $CB_8H_{13}^-$, was complete.

The ^{11}B COSY and ^{1}H spectra were recorded on a Bruker WH-400 NMR spectrometer, at 128.0 and 400.1 MHz respectively. COSY 2D spectra typically required a 128 × 128 point spectrum matrix, with 64 transients per 64 time-domain points taking *ca.* 1 hr in total. ^{1}H–^{11}B shift-correlated 2D spectra required a similar matrix, but overnight accumulation of typically 256 transients with inter-transient delays of 1–2 s. A double sine-bell window function was used for COSY, and a double Lorentz-to-Gaussian function for shift correlation, in which the interpulse spacings were a compromise between the optima for terminal H–B couplings and bridging H–B couplings.

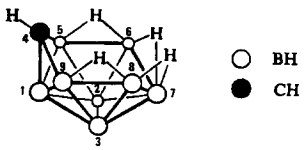
The ^{1}H–(^{11}B) spectra were recorded at 360 MHz on a similar spectrometer. The ^{1}H and ^{11}B spectra

* Author to whom correspondence should be addressed.

are referenced to $Si(CH_3)_4$ and $BF_3 \cdot OEt_2$ respectively, shifts to high frequency being positive.

RESULTS AND DISCUSSION

Neutral CB_8H_{14}. The application of Wade's rules to the neutral monocarborane, CB_8H_{14}, leads to a predicted *arachno* structure based on an octadecahedron.[9] The absence of the most highly connected vertex and one adjacent vertex, as indicated by Williams' rules,[10] with the four bridging hydrogens positioned symmetrically in the open face of the cluster, yields the predicted structure, as shown below.



Proposed structure of CB_8H_{14}.

The ^{11}B NMR spectrum shows five resonances [relative intensities 1:1:2:2:2, denoted *a*, *b*, *c*, *d*, *e*, Fig. 1(a)] compatible with this structure. A complete assignment of the ^{11}B resonances has been proposed by Baše *et al.* based upon both $J(B–H_{bridge})$ couplings and experience of chemical shifts in related systems,[11] as follows: B(7), 17.0 ppm; B(1), −3.7 ppm; B(5, 9), −6.3 ppm; B(6, 8), −34.9 ppm; B(2, 3), −41.1 ppm.

We have recorded the ^{11}B COSY spectrum of CB_8H_{14} [Fig. 1(a)] and the two possible alternative assignments of skeletal connectivity are as indicated [Figs. 1(b,c)].

The two possible assignments arise because of the high symmetry of the carborane; similar difficulties in assignment have been noted in the ^{11}B COSY of the 1,2- and 1,7-$C_2B_{10}H_{12}$ isomers.[5] The correct structure of CB_8H_{14} may be deduced by examining the ^1H NMR spectra obtained with selective ^{11}B decoupling as shown in Fig. 2.

The fully coupled ^1H NMR spectrum consists of a series of quartets at lower field arising from the $B–H_{(terminal)}$ bonds, while at higher field there are two resonances (−0.13 and −2.06 ppm) from the CH_2 group, and two broad resonances (centred at −0.64 and −3.76 ppm) from the two sets of bridging hydrogen atoms. These four higher field resonances have been previously reported, but not the complete ^1H spectrum, and no assignment of individual sets of bridging hydrogens exists.[11,12]

We have found that the broad band decoupled

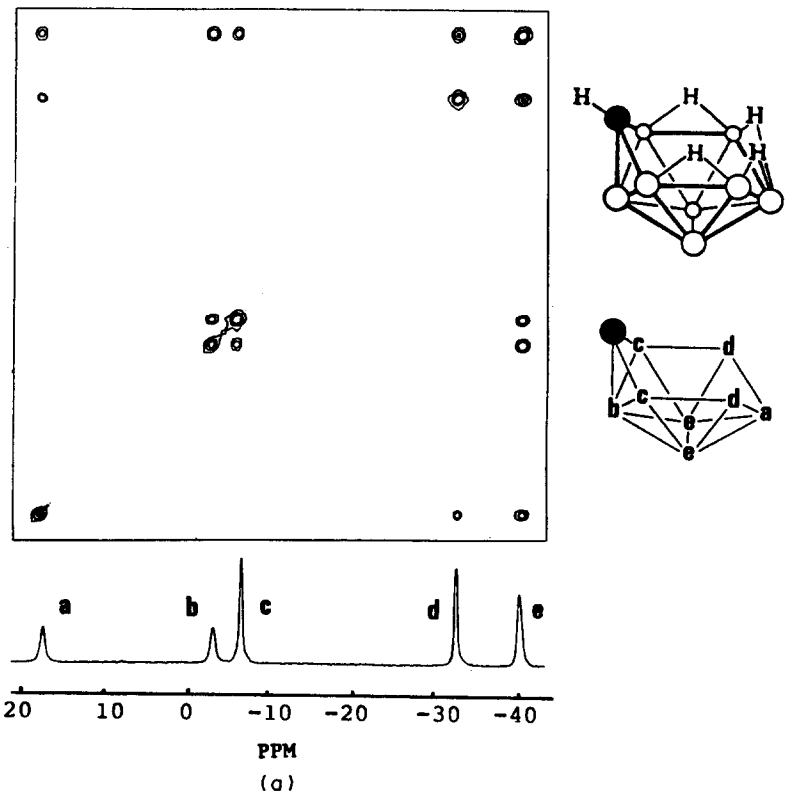
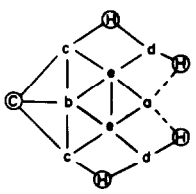
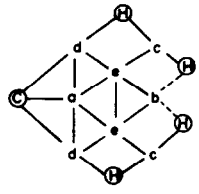


Fig. 1(a). ^{11}B COSY spectrum of CB_8H_{14}.



(b)



(c)

Fig. 1(b). Correct skeletal connectivity (see text).

Fig. 1(c). Alternative COSY connectivity.

spectrum gives little information, but selective decoupling at resonance *a* [assigned as in Fig. 1(a)] partially decouples the set of bridging hydrogens at −0.64 ppm, while the same treatment at resonance *b* only decouples the terminal proton at 3.17 ppm. On further decoupling at resonance *c* one of the CH resonances becomes sharpened, indicating that the resonance *c* is assignable to the boron atoms B(5, 9) adjacent to the carbon atom. The same effect does not result from decoupling at the ^{11}B frequency of resonance *d*. The unambiguous skeletal connectivity is therefore deduced as shown in Fig. 1(b), with the boron atoms being assigned as *a* = B(7), *b* = B(1), *c* = B(5, 9), *d* = B(6, 8) and *e* = B(2, 3).

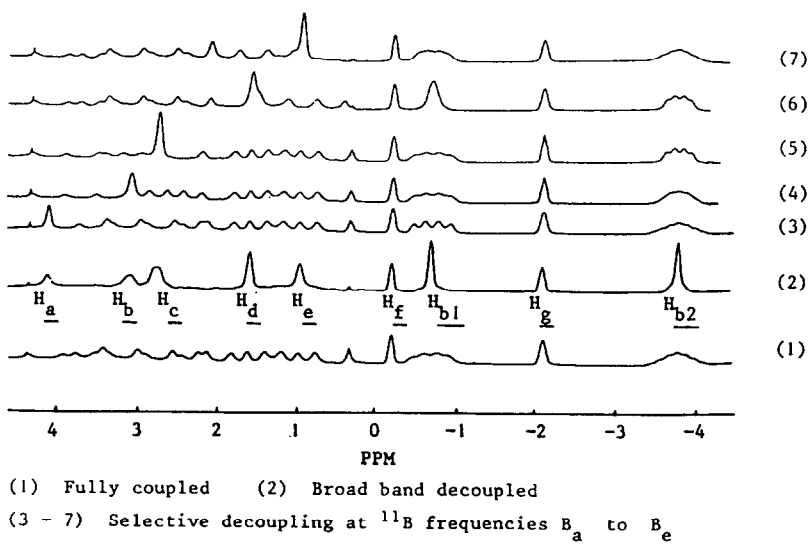
Using the above information, the complete assignment of the resonances in the ^1H NMR spectrum of CB_8H_{14} is as follows: *terminal*: $H_a = H_{B(7)}$, 4.20 ppm; $H_b = H_{B(1)}$, 3.17 ppm; $H_c = H_{B(5,9)}$, 2.83 ppm; $H_d = H_{B(6,8)}$, 1.66 ppm; $H_e = H_{B(2,3)}$, 1.0 ppm; *bridging*: $H_{b1} = H_{B(6,8)-B(7)}$, −0.6 ppm; $H_{b2} = H_{B(5,9)-B(6,8)}$, −3.7 ppm. C—H: $H_f = H_{exo}$, −0.1 ppm; $H_g = H_{endo}$, −2.0 ppm. The $^1H_{(terminal)}$ resonances follow the same pattern as in the ^{11}B NMR spectrum.

Closer inspection of the ^{11}B COSY spectrum reveals that a coupling between B(6, 8) and B(7) is observed, though they are connected by a bridging hydrogen. This is in contrast to the absence of coupling between B(5, 9) and B(6, 8), which are also connected by bridging hydrogens.

The theoretical justification for the absence of such coupling is based on an ideal symmetrical bridging hydrogen bond where there is negligible electron density along the B–B vector. In an unsymmetrical bridge there may be significant electron density along the B–B vector, enabling scalar spin–spin coupling. The present results indicate therefore that CB_8H_{14} contains two distinctly different types of bridging hydrogen atoms, and further evidence in support of this proposal is seen in the ^1H–^{11}B shift correlation map (Fig. 3). The correlations between the ^{11}B resonances and the resonances due to the attached hydrogen atoms are as shown.

All of the hydrogen resonances are readily assignable and are in agreement with that deduced above. The high field symmetrical bridging hydrogens exhibit coupling to *c*[B(5, 9)] and *d*[B(6, 8)] as expected. The lowfield resonance due to the proposed unsymmetrical bridging hydrogens give an observable coupling to *d*[B(6, 8)] only and not to *a*[B(7)]. From this information the bridging group is deduced to be displaced towards the *d*[B(6, 8)] boron atoms; similar conclusions have been reached following theoretical CNDO/2 calculations.[11]

Corroborating evidence for the unsymmetrical bridge is provided by the ^1H–($^{11}B_{selective}$) NMR spectra (Fig. 2). Decoupling at both *c*[B(5, 9)] and



(1) Fully coupled (2) Broad band decoupled

(3 - 7) Selective decoupling at ^{11}B frequencies B_a to B_e

Fig. 2. ^1H–($^{11}B_{selective}$) NMR of CB_8H_{14}.

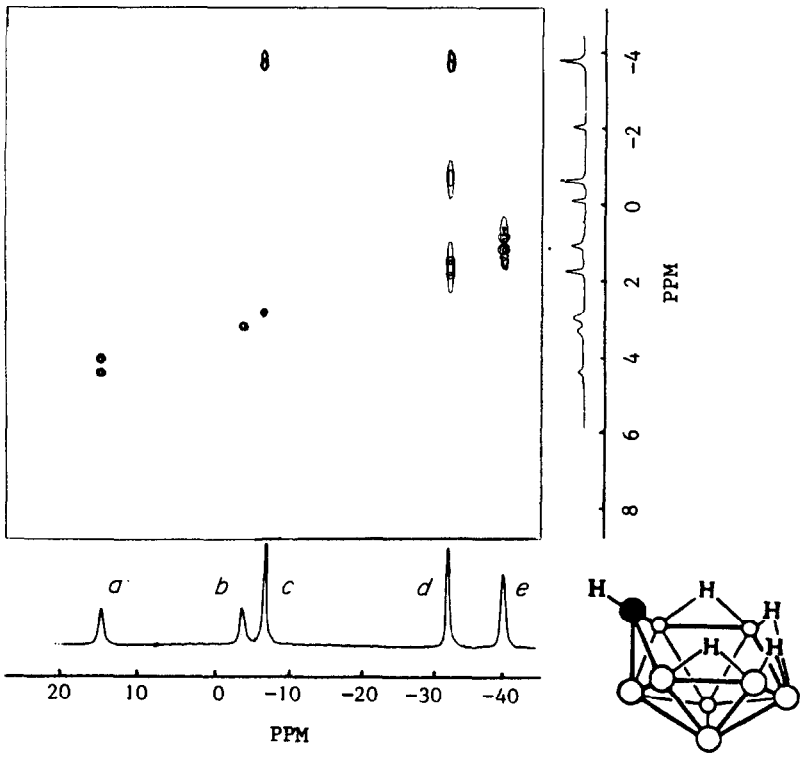


Fig. 3. ^{1}H–^{11}B correlation map of CB_8H_{14}.

d[B(6, 8)] resonance frequencies has an identical effect upon the highfield bridging hydrogen resonance, compatible with that expected for a symmetrical bridge. In comparison, decoupling at the *d*[B(6, 8)] frequency, results in a near-singlet resonance for the lowfield bridging hydrogen resonance, whereas decoupling at the *a*[B(7)] frequency has considerably less effect. The differential effect of selective decoupling reflects a larger association of the *d*[B(6, 8)] boron atoms with the bridging hydrogen atom compared to that of the *a*[B(7)] boron atom, as expected for an unsymmetrical bridging hydrogen displaced closer to the *d*[B(6, 8)] boron atoms. The refined structure is therefore as shown in Fig. 1(a).

Anion $CB_8H_{13}^-$. The ^{11}B–(^{1}H) NMR spectrum of the anion $CB_8H_{13}^-$ is similar to that of the neutral CB_9H_{14} showing five resonances (relative intensities 2:1:1:2:2, denoted *a**, *b**, *c**, *d**, *e**, Fig. 4), indicating that symmetry of the framework is preserved, in agreement with the model proposed by Base *et al.*[12]

The highest field resonance, *e**, shows the largest $J(B–H_{bridge})$ coupling, and can be assigned to the B(6, 8) pair of boron atoms. Further assignments cannot be made with confidence from this spectrum alone, since the relative chemical shifts of the resonances have changed substantially compared with those from CB_8H_{14}. Thus to date no complete assignment of the ^{1}H and ^{11}B resonances for the anion have been made. The connectivity in the skeleton of the anion is derived in a similar manner to that used for the neutral precursor, namely, from the ^{11}B COSY spectrum (Fig. 4) and the ^{1}H–($^{11}B_{selective}$) spectra to give the following ^{11}B NMR resonance assignments: *a** = B(5, 9), 4.0 ppm; *b** = B(7), −3.9 ppm; *c** = B(1), −21.5 ppm; *d** = B(2, 3), −30.4 ppm; *e** = B(6, 8), −35.2 ppm.

Notable features of the ^{11}B COSY spectra of the neutral CB_8H_{14} and the anionic $CB_8H_{13}^-$ are now evident, as follows. Firstly, in the anion, a strong coupling is observed between B(5, 9) and B(6, 8), which is absent in the neutral precursor, suggesting the symmetrical bridges in CB_8H_{14} are now unsymmetrical in $CB_8H_{13}^-$. Secondly, for the three boron atoms B(6, 8) and B(7) in the anion, now connected by a single unique bridging hydrogen, a weak coupling is still observed, and is a clear indication of significant electron density along the B–B vector in this four-centre bond. Thirdly, an unexpected reduction in the observed coupling between B(1) and B(5, 9) of the anion is also found, which is presumably produced by the shift of electron density on the open face of the cluster towards the B(6, 8) positions, resulting in a reduced electron density between those boron atoms adjacent to the carbon atom.

From the assignment shown in Fig. 4, the order of

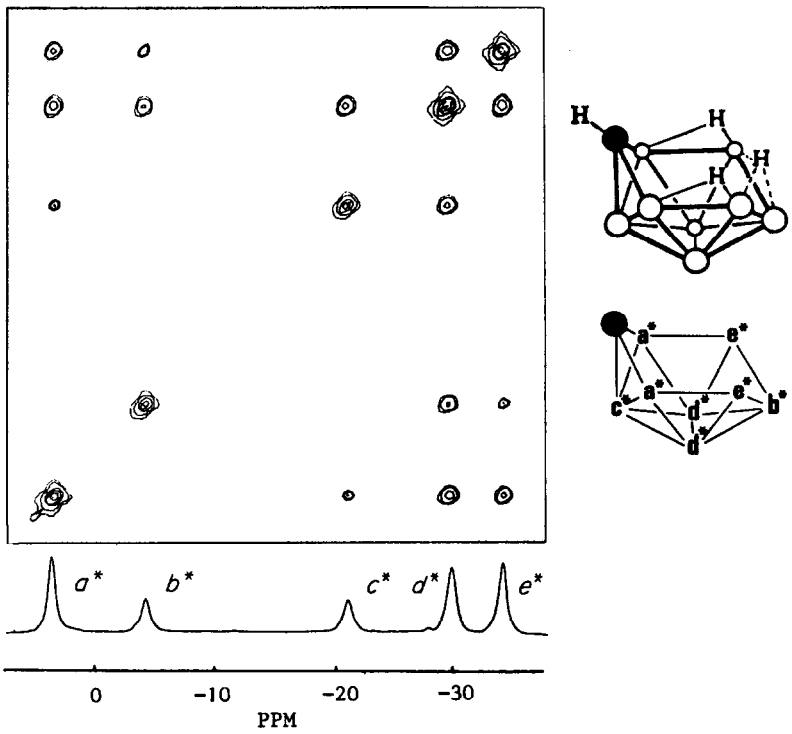


Fig. 4. ^{11}B COSY of $CB_8H_{13}^-$.

the resonances has changed in a way that confirms the electron density shift, such that the lowest-field resonance is now attributable to the relatively less electronegative boron atoms B(5, 9) adjacent to the carbon atom, though the major factor may be the relative up-field shift of the B(7) boron atom due to the reduction in co-ordination.

The practical difficulties involved in the preparation of the anion, namely the elimination of hexane residues from the lithium butyl solution, lead to impurity peaks in the ^1H spectrum. However, assignment of the lowfield resonances from the terminal hydrogen atoms was made possible by a series of difference spectra produced by subtracting the spectra obtained by selective ^{11}B decoupling from the fully decoupled spectrum.

The impurities do not interfere with the more important upfield CH_2 and bridging hydrogen resonances, which appear as two singlets (C–H), a distorted quartet and a broad multiplet, of ratio 1:1:2:1 respectively. The unique bridging hydrogen resonance, at highfield, is complex because of the coupling to three boron atoms. The distorted quartet resonance is due to greater coupling to the B(6, 8) boron atoms than to the B(5, 9) boron atoms in the unsymmetrical bridge. The complete assignment of the resonances in the ^1H NMR spectrum of $CB_8H_{13}^-$ is as follows: *terminal*: $H_a^* = H_{B(5,9)}$, 3.93 ppm; $H_b^* = H_{B(7)}$, 3.05 ppm; $H_c^* = H_{B(1)}$, 2.52 ppm; $H_d^* = H_{B(2,3)}$, 1.44 ppm; $H_e^* = H_{B(6,8)}$, 1.29 ppm; *bridging*: $H_{b1}^* = H_{B(5,9)-B(6,8)}$, −1.04 ppm; $H_{b2}^* = H_{B(6,8)-B(7)}$, −2.0 ppm. C—H: $H_f^* = H_{exo}$, 0.34 ppm; $H_g^* = H_{endo}$, −0.36 ppm. The $^1H_{(terminal)}$ resonances again follow the same pattern as in the ^{11}B NMR spectrum.

Confirmation of the unsymmetrical nature of both types of hydrogen bridge is provided by subtraction spectra. A significant effect on both bridging resonances is observed by decoupling at the *e**[B(6, 8)] frequency, whilst decoupling at *a**[B(5, 9)] and *b**[B(7)] frequencies has only a marginal effect on both bridging hydrogen resonances. The refined structure of the anion, $CB_8H_{13}^-$, to show the unsymmetrical bridging groups is shown in Fig. 4.

The highfield *endo*-CH resonance has a broader linewidth (50 Hz) than either the *exo*-CH resonance (24 Hz) of the anion, or the *endo*-CH resonance (33 Hz) in the neutral precursor. Saturation transfer experiments show that the *endo*-CH hydrogen, and all three bridging hydrogens, are in exchange at room temperature. The *exo*-CH hydrogen is not involved in the exchange process. Similar saturation transfer experiments also show that the neutral precursor does not exhibit such exchange. Linewidth broadening observed during variable temperature NMR studies yields a very approximate activation energy for this process of 50 kJ mol^{-1}. The removal of a proton has therefore significantly activated the open face of the cluster, including the *endo*-hydrogen on the carbon atom. While fluxional behaviour of

bridging hydrogen atoms in boranes and carboranes is well established, to our knowledge this is the first observation of such a process incorporating a C–H hydrogen atom.

Attempts to produce and identify the di-anion by further removal of a proton have been unsuccessful. This may be due to the insolubility of the product in a range of solvents, or more likely the probable cage degradation expected on further activation of the open cluster face.

CONCLUSIONS

The structure of the neutral monocarborane CB_8H_{14} is confirmed to be that proposed previously,[12] with the further refinement that the presence of both symmetrical and unsymmetrical bridging hydrogens on the open face of the cluster is indicated. Boron atoms connected by unsymmetrical bridges have been shown to give rise to observable coupling in the ^{11}B COSY spectrum, a feature so far found only in two metallo-borane derivatives, one of which results from tautomeric exchange between bridged and directly bound boron atoms.[5]

The removal of a proton from the open face of the *arachno* monocarborane, CB_8H_{14}, to yield the anion $CB_8H_{13}^-$, results in a significant activation of the open face of the cluster, involving exchange of all three $B–H_{(bridging)}$ hydrogen atoms and the *endo*-C–H hydrogen atom.

Acknowledgements—We thank the S.E.R.C. for support and Drs. I. H. Sadler and D. Reed (University of Edinburgh) for the decoupled proton spectra.

REFERENCES

1. G. R. Eaton and W. N. Lipscomb, *NMR Studies of Boron Hydrides and Related Compounds.* Benjamin, New York (1969); L. J. Todd and A. R. Siedle, *Progress in NMR Spectroscopy* 1979, **13**, 87.
2. A. Bax and R. Freeman, *J. Magn. Reson.* 1981, **42**, 164; 1981, **44**, 542.
3. I. J. Colquhoun and W. McFarlane, *J. Chem. Soc., Dalton Trans.* 1981, 2014.
4. T. Venable, W. Hutton and R. Grimes, *J. Am. Chem. Soc.* 1982, **104**, 4716.
5. T. Venable, W. Hutton and R. Grimes, *J. Am. Chem. Soc.* 1984, **106**, 29.
6. D. Reed, *J. Chem. Research* 1984, 198.
7. N. W. Alcock, J. G. Taylor and M. G. H. Wallbridge, *J. Chem. Soc., Chem. Commun.* 1983, 1168.
8. B. Štíbr, K. Baše, S. Heřmánek and J. Plešek, *J. Chem. Soc., Chem. Commun.* 1976, 150.
9. K. Wade, *Adv. Inorg. Chem. and Radiochem.* 1976, **18**, 1.
10. R. E. Williams, *Adv. Inorg. Chem. and Radiochem.* 1976, **18**, 67.
11. J. Dolanský, S. Heřmánek and R. Zahradnik, *Coll. Czech. Chem. Commun.* 1981, **46**, 2479.
12. K. Baše, B. Štíbr, J. Dolanský and J. Duben, *Coll. Czech. Chem. Commun.* 1981, **46**, 2345.

Polyhedron Vol. 4, No. 8, pp. 1467–1470, 1985
Printed in Great Britain

0277–5387/85 $3.00 + .00
© 1985 Pergamon Press Ltd

STABILITY CONSTANTS OF ZINC HALIDE COMPLEXES IN DMSO–WATER AND DMF–WATER MIXTURES

F. GAIZER*
Department of Inorganic and Analytical Chemistry, A. József University, Szeged, P.O. Box 440, Hungary

H. B. SILBER
Division of Earth and Physical Sciences, The University of Texas at San Antonio, TX 78285, U.S.A.

and

J. LÁZÁR
Department for Pharmaceutical Chemistry, The Medical University, Szeged, Hungary

(*Received* 6 *December* 1984; *accepted* 6 *February* 1985)

Abstract—The overall stability constants of zinc bromide and iodide complexes in DMSO–water and those of zinc chloride, bromide and iodide in DMF–water mixtures have been determined potentiometrically at mole ratios about 0.2–1 for the organic solvents at 25°C and in a 0.5 M ammonium perchlorate ionic medium. The complex formation is much stronger in DMF and its mixtures than in DMSO and the log βs are generally higher in solvent mixtures than those expected from the values measured in the pure components.

In our previous study[1] the change of the stability constants of the zinc chloride complexes has been observed in DMSO–water mixtures. It was pointed out that the values of the constants change in response to the change of the composition of the solvent mixtures, but the constants are greater than could be expected from the values measured in pure DMSO and water. The above studies were extended to zinc bromide and zinc iodide systems in DMSO and to all the three zinc halides in DMF–water mixtures.

EXPERIMENTAL

Chemicals. Zinc perchlorate was examined according to our previous descriptions.[1] The ammonium halides were of analytical grade. DMSO was purified by vacuum distillation and DMF was purified by fractional distillation after the addition of 10% benzol and 5% water.

Titrations and *computer evaluation* of the results were carried out by the MAXIPOT program[2] corresponding to the previous paper.[1]

RESULTS

The titrations were performed at constant zinc ion concentration. Since only small differences were observed between the shapes of potentiometric curves obtained in either system, for the sake of conciseness, potentiometric results of the study of the zinc chloride and zinc iodide systems in DMF–water mixtures are presented as two extreme cases (Fig. 1).

The log β values showing the best agreement between the measured and calculated potentials are summarized in Tables 1 and 2. The standard deviations of the constants calculated from the residuals of the individual titration curves are given in brackets. However, it must be noted that these are the standard deviations of the fit of only one experimental curve and, considering reproducibility, the errors of the log β_2 and β_3 values amount to approximately 0.05–0.1. As can be seen from the data, the uncertainty of the constants of complexes (1, 1) is considerably greater than for the other complexes. Therefore, in Figure 2 illustrating the data of Table 2, the log β_1 values are displayed with their errors calculated from individual titration curves. It is worth mentioning that, because of the

* Author to whom correspondence should be addressed.

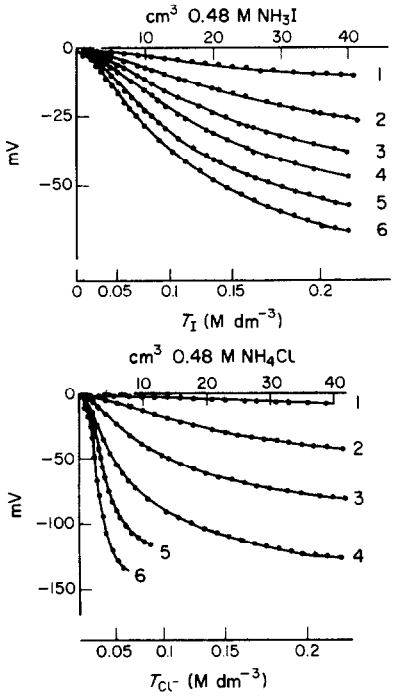


Fig. 1. Potentiometric titration curves of 50.0 cm³ 0.01 M zinc perchlorate in DMF–water mixtures, A: with 0.48 M ammonium chloride and B: with 0.48 M ammonium iodide. One half of the experimental points chosen randomly are plotted. The solid curves are the calculated ones using the formation constants summarized in Table 2.

minor solubility of ammonium chloride, measurements could be made in DMF only in mixtures containing more than 5% water.

From the experimental data it could be stated that the values of all the equilibrium constants are greater by several orders of magnitude in DMF than in DMSO. It is also obvious that the zinc iodide system can well be measured in DMF, but in DMSO a rather slight interaction can be experienced: the value of ΔE is only about 2 mV in response to the 0.2 mol iodide. Systems containing chloride or bromide can definitely be described by the supposition of the formation of complexes (1, 1), (1, 2) and (1, 3). Among systems containing iodide the formation of these three species could definitely be detected only in DMF and values with relatively great experimental errors were only obtained in the case of log β_1 values. However, in DMSO the formation of the diiodo complex was found to be minor and that of the triiodo complex cannot be substantiated on the basis of measurements.

DISCUSSION

The stability constants of zinc halide complexes obtained in the course of measurements made in solutions of 0.5 molar ionic strength with NH_4ClO_4 at 25°C are summarized in Table 3.

The values obtained in DMSO approximately correspond to the literature results,[3] the deviations are probably due to the difference in ionic strengths. Accessible data[4] are not available for the constants measured in DMF.

The difference between the measured values of equilibrium constants and those expected from the composition of the solvent mixtures is never negative in any system, i.e. the solvent mixtures usually have a stabilizing effect on the complex formation. In mixtures in which there are detectable deviations between the measured values and those expected from constants obtained in pure solvents, generally the maximum of the deviations is approximately at $\alpha = 0.5$ and the shapes of difference-curves are symmetrical. Deviations from this were detected

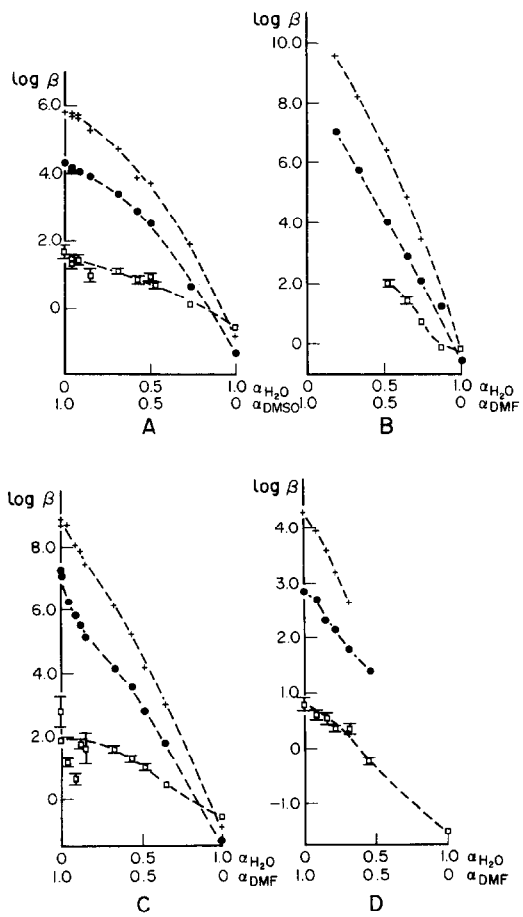


Fig. 2. The plot of the measured log β_1 (lines), log β_2 (points) and log β_3 (crosses) values of zinc halide complexes as a function of molar fraction of organic solvent. A: Zn^{2+}–Br^- in DMSO–water mixtures and B: Zn^{2+}–Cl^-, C: Zn^{2+}–Br^- and D: Zn^{2+}–I^- in DMF–water mixtures. The dotted lines are the probable runnings of the constants.

Table 1. Formation constants and their errors (in parentheses) of zinc halide complexes in DMF–water solvent mixtures

System	α_{DMSO}	log β_1	log β_2	log β_3	K_3	σ, mV	No. of expt. points
	0.81		7.06 (0.02)	9.57 (0.04)	324	0.87	55
	0.67		5.77 (0.02)	8.22 (0.02)	282	0.55	97
	0.48	2 (0.15)	4.05 (0.04)	6.39 (0.05)	219	1.13	99
Zn^{2+}–Cl^-	0.35	1.42 (0.05)	2.89 (0.13)	4.87 (0.07)	95.5	0.26	87
	0.35	0.5 (0.42)	3.01 (0.09)	4.66 (0.03)	45	0.4	80
	0.26	0.72 (0.05)	2.07 (0.07)	3.47 (0.02)	25.1	0.12	77
	0.13	−0.13 (0.1)	1.21 (0.04)	—	—	0.11	62
	1	1.90 (0.4)	7.24 (0.1)	8.91 (0.1)	47	2.97	36
	1	2.78 (0.54)	7.03 (0.06)	8.70 (0.07)	47	3.23	73
	0.96	1.19 (0.3)	6.22 (0.03)	8.72 (0.01)	316	0.86	96
	0.91	0.67 (0.2)	5.78 (0.07)	8.07 (0.02)	195	1.35	77
Zn^{2+}–Br^-	0.88	1.77 (0.17)	5.49 (0.06)	7.88 (0.03)	245	0.71	100
	0.85	1.63 (0.5)	5.12 (0.05)	7.45 (0.01)	214	0.65	79
	0.67	1.63 (0.11)	4.12 (0.09)	6.15 (0.02)	107	0.77	95
	0.56	1.30 (0.08)	3.55 (0.05)	5.26 (0.02)	51	0.37	99
	0.48	1.03 (0.07)	2.77 (0.05)	4.22 (0.02)	28	0.22	82
	0.35	0.46 (0.03)	1.77 (0.04)	3.01 (0.01)	17.5	0.06	82
	1	0.79 (0.11)	2.85 (0.04)	4.30 (0.01)	28	0.27	90
	0.91	0.59 (0.11)	2.72 (0.04)	3.94 (0.02)	17	0.18	90
Zn^{2+}–I^-	0.84	0.55 (0.1)	2.30 (0.06)	3.61 (0.02)	20	0.17	93
	0.78	0.36 (0.04)	2.13 (0.02)	3.0 (0.15)	7	0.1	84
	0.68	0.36 (0.1)	1.77 (0.05)	2.65 (0.1)	8	0.08	100
	0.55	−0.22 (0.1)	1.38 (0.1)	—	—	0.12	82

only in zinc bromide and zinc iodide systems in DMF, but only in the case of log β_2.

In order to aid in the interpretation of the constants, we have measured the relative permittivity of the solvent mixtures. They differ from additivity only to such a small extent, that the equilibrium constants variations could not be interpreted in terms of relative permittivity.

By means of the equilibrium constants the number of halide ions coordinated to the zinc ion ($\bar{n}$) was calculated and plotted against the composition of the solvent mixtures. In the case of all the systems studied

Table 2. Formation constants and their errors (in parentheses) of zinc halide complexes in DMSO–water solvent mixtures

System	α_{DMSO}	log β_1	log β_2	log β_3	K_3	σ, mV	No. of expt. points
	1.0	1.68 (0.2)	4.27 (0.05)	5.8 (0.03)	34	0.75	37
	0.96	1.38 (0.2)	4.05 (0.06)	5.69 (0.04)	43.6	0.82	36
	0.96	1.45 (0.12)	4.13 (0.02)	5.78 (0.02)	44.7	0.20	44
	0.92	1.46 (0.15)	4.02 (0.03)	5.64 (0.02)	41.7	0.37	35
	0.92	1.44 (0.15)	4.02 (0.02)	5.73 (0.02)	51	0.23	44
Zn^{2+}–Br^-	0.85	0.98 (0.20)	3.90 (0.03)	5.28 (0.03)	24	0.40	37
	0.69	1.11 (0.07)	3.38 (0.03)	4.69 (0.10)	20	0.15	44
	0.58	0.85 (0.13)	2.88 (0.03)	3.86 (0.04)	9.5	0.36	35
	0.5	0.94 (0.10)	2.52 (0.03)	3.69 (0.04)	15	0.18	37
	0.47	0.69 (0.10)	1.41 (0.06)	2.85 (0.02)	27	0.1	29
	0.27	0.1 (0.06)	0.56 (0.14)	1.91 (0.06)	22	0.08	22
Zn^{2+}–I^+	1.0	0.12 (0.05)	—	—	—	0.19	20

Table 3. The logarithm of overall stability constants of zinc halide complexes in DMF and DMSO in 0.5 M (NH_4ClO_4) ionic medium

Solvent		Cl^-	Br^-	I^-
DMF	$\log \beta_1$	3±0.25	2±0.5	0.8±0.3
	$\log \beta_2$	8.2±0.1	7.1±0.1	2.8±0.1
	$\log \beta_3$	10.7±0.15	8.8±0.12	4.3±0.1
DMSO	$\log \beta_1$	—	1.7±0.2	0.12±0.5
	$\log \beta_2$	6.16±0.1	4.27±0.07	—
	$\log \beta_3$	8.76±0.1	5.8±0.1	—

a curve similar to that of the zinc chloride system was obtained,[1] the limiting value of which cannot exceed $\bar{n} = 3$ even in the case of the most stable systems. On this basis, in accordance with our earlier supposition, for the geometry of the complexes a tetrahedral configuration is predicted in which three of the coordination sites are occupied by one halide ion each and the fourth coordination site is occupied by a solvent molecule. This result is consistent with the ultrasonic absorption measurements in $ZnCl_2$ systems in aqueous methanol, DMSO and DMF.[5,6] This supposition is also supported by electron-diffraction measurements recently made on the $LiZnBr_3$ solution.[7]

The experimental technique used in the course of experiments provided reliable values only for the stability constants of the (1,2) and (1,3) complexes. Generally, the stability constants of the (1,1) complex were determined only with relatively great experimental errors, moreover, in solutions in which the complex formation is rather strong they could not be treated as parameters of fits and the determination of their values was not possible by graphical treatment either. In spite of this, it would be difficult to exclude the possibility of the formation of this species.

Acknowledgement—The authors graciously acknowledge the Robert A. Welch Foundation of Houston, Texas, U.S.A. for partial support under Grant AX-659.

REFERENCES

1. F. Gaizer and H. B. Silber, *J. Inorg. Nucl. Chem.* 1980, **42**, 1317.
2. F. Gaizer, *Acta Chim. Acad. Sci. Hung.* 1980, **103**, 397.
3. S. Ahrland and N. O. Björk, *Acta Chem. Scand. A* 1965, **30**, 265.
4. K. G. Ashurst, *Natl. Inst. Metall., S. Afr. Rep.* 1974, 1626; *Chem. Abstr.* 1974, **81**, 159816q.
5. H. B. Silber, L. U. Kromer and F. Gaizer, *Inorg. Chem.* 1981, **20**, 3323.
6. H. B. Silber, D. Simon and F. Gaizer, *Inorg. Chem.* 1984, **23**, 2844.
7. G. Kabisch, E. Kálmán, G. Pálinkás, T. Radnai and F. Gaizer, *Chem. Phys. Letts.* 1984, **107**, 463.

Polyhedron Vol. 4, No. 8, pp. 1471–1473, 1985
Printed in Great Britain

0277–5387/85 $3.00 + .00
© 1985 Pergamon Press Ltd

COMPLEXING PROPERTIES OF AN *N,N'*-METHYLATED DIAZA-CROWN-ETHER

P. CORBAUX and B. SPIESS
Laboratoire de Chimie Analytique, Faculté de Pharmacie 74, route du Rhin, 67048 Strasbourg Cedex, France

and

F. ARNAUD* and M. J. SCHWING
Laboratoire de Chimie Physique, UA AU CNRS 405, ENSCS, 1, rue Blaise Pascal, 67000 Strasbourg, France

(*Received* 11 *December* 1984; *accepted* 6 *February* 1985)

Abstract—The nature and stability of some transition and heavy metal cation complexes of an *N,N'*-methylated diaza-crown-ether have been determined in 0.1 M Et_4NClO_4 aqueous solution by means of pH metric measurements. The results are compared to previous ones concerning the homologous unmethylated ligand.

As part of our general study on the complexing properties of cryptands in different solvents,[1,2] we present here the results concerning the stability of some metallic complexes ($M^{n+} = Co^{2+}$, Ni^{2+}, Cu^{2+}, Zn^{2+}, Ag^{+}, Cd^{2+}, Pb^{2+} and Hg^{2+}) of the ligand 1,10-diaza-4,7,13,16 tetraoxacyclooctadecane, abbreviated Me_2-(2.2) according to the usual cryptand nomenclature. The nature of the species formed in 0.1 M Et_4NClO_4 aqueous solution and their stability constant β_{xyz} referring to the general equilibrium of complexation:

$$xM^{n+} + yL + zH^{+} \rightleftharpoons M_xL_yH_z^{(nx+z)+}$$

have been determined by following the pH changes resulting from successive additions of Me_4NOH to acidic solutions of ligand diperchlorate and of metallic perchlorate, of various stoichiometries. Details of the experimental procedure, the glass electrode conditioning and the calculation methods using the numerical program SCOGS[3] have been previously reported.[1] The results are summarized in Table 1: values of log β_{xyz} are given with their confidence interval $\pm 2\sigma$ (σ being the standard deviation calculated by the program). Previously determined values for the homologous (2.2) cryptates are also mentioned for comparison.

The two protonation constants β_{011} and β_{012} have been first determined from solutions without metallic cation ($x = 0$). The results corresponding to three experiments, summing up 138 experimental points, are in good agreement with the previous determinations of Gramain *et al.*[4] and Vitali.[5] They show that methylation of (2.2) slightly increases the basicity of the first protonation site but decreases the second one. The electrostatic interactions are greater in Me_2-(2.2) than in (2.2) as shown by the differences log K_1 − log K_2,† respectively 1.97 and 1.18.

Only 1:1 complexes have been found in the pH range explored, except for Cu^{2+} where an additional protonated species had to be taken into account to improve the calculation fit. In most cases results given in Table 1 correspond to a minimum of two experiments for which the ratio of the metal to ligand concentrations, $R = C_M/C_L$, was generally about 1 and 0.5. Some of our values have already been determined by Vitali[5] in 0.1 M Me_4NBr aqueous solution. Our values are generally slightly lower than theirs, except for Co^{2+} and Pb^{2+} which are higher. Most of the constants are rather low and hydrolysis of the metallic cations strongly competes with the complexation. In these cases hydrolysis equilibria were considered in the calculations.[6]

From the differences $\Delta \log \beta = \log \beta_{110}$ [Me_2-(2.2) − log β_{110} (2.2)], given in Table 1, it can be seen that Ag^{+}, Cd^{2+} and Hg^{2+} complexes with Me_2-(2.2)

* Author to whom correspondence should be addressed.
† $K_1 = \beta_{011}$ and $K_2 = \beta_{012}/\beta_{011}$.

Table 1. Logarithms of the stability constants β_{xyz} for metallic complexes of Me_2-(2.2), at 25°C, $I = 0.1$ M (Et_4NClO_4), pH's range explored, $R = C_M/C_L$, N: number of experimental points

Cations (r (Å))	pH range	R	N	Complexes	Ligands: Me_2-(2.2)	Ligands: (2.2)[a]	$\Delta \log \beta$
H^+	7.1–10.4		138	HL^+	9.58 ± 0.02 (9.62)[b] (9.56)[c]	9.20	0.38
				H_2L^{2+}	17.19 ± 0.02 (17.36)[b] (17.15)[c]	17.24	
Co^{2+} (0.82)[d]	7.5–8.1	0.5	6	CoL^{2+}	4.42 ± 0.14	⩽ 2.5	
		0.4			(4.01)[b]		
Ni^{2+} (0.78)[d]	7.9–8.6	0.5	13	NiL^{2+}	3.85 ± 0.14	⩽ 2.5	
	8.4–8.9	0.4			(4.10)[b]		
Cu^{2+}	6.0–6.7	1	16	CuL^{2+}	6.82 ± 0.05 (6.92)[b]	6.18	0.64
(0.72)[d]	6.3–7.2	0.5		$CuHL^{3+}$	13.99 ± 0.08		
Zn^{2+} (0.83)[d]	7.5–7.6	1	10	ZnL^{2+}	3.77 ± 0.19	3.19	0.58
	7.3–7.7	0.5			(4.88)[b]		
Pb^{2+} (1.18)[e]	5.8–6.4	1	32	PbL^{2+}	8.39 ± 0.01	6.90	1.49
	5.7–6.2	0.5			(7.90)[b]		
Cd^{2+} (0.95)[e]	6.9–8.5	1	55	CdL^{2+}	4.38 ± 0.01	5.31	−0.93
	6.9–8.5	0.5			(4.61)[b]		
Ag^+ (1.15)[e]	6.2–7.3	1.2	37	AgL^+	7.27 ± 0.01	7.90	−0.63
	6.3–7.8	0.7					
Hg^{2+} (1.02)[e]	2.9–3.4	0.6	53	HgL^{2+}	15.38 ± 0.02	17.85[f]	−2.47
	2.8–3.7	0.8					
	3.0–3.5	0.4					

[a] Ref. 1.
[b] Ref. 5: 0.1 M Me_4NBr.
[c] Ref. 4: 20°C, 0.1 M Me_4NCl.
[d] Ref. 8.
[e] Ref. 9.
[f] Ref. 10: 25°C, 0.1 M Me_4NBr.

are less stable than their homologs with (2.2). On the contrary, the presence of the methyl groups on the ring leads to a stabilization of the complexes of transition metal cations and particularly of Pb^{2+} for which $\Delta \log \beta = 1.49$. The same behaviour was already observed for the complexes of these ligands with alkaline-earth cations in water as well as in methanol.[7]

Methylation of the ligand (2.2) can affect the complexation mainly by inducing (i) a less important hydration of the ligand, (ii) a greater availability of the electrons in N–CH_3 than in N–H,[7] (iii) a steric hindrance caused by the two substituents.

The first two effects which would lead to a stabilization of the complexes, certainly prevail for the transition metal cations, overcoming the third one which would lead to a destabilization. This last effect must be therefore predominant for Ag^+, Hg^{2+} and Cd^{2+} complexes. These results could be expected from size considerations, the latter cations, which are much larger than the first ones, being more strongly affected by steric effects. Nevertheless the opposite behaviour displayed by the large Pb^{2+} and alkaline-earth cations suggests that another factor should be considered besides the sizes of the cations.

Acknowledgement—The authors thank Prof. J. M. Lehn who provided a sample of the ligand.

REFERENCES

1. F. Arnaud-Neu, B. Spiess and M. J. Schwing, *Helv. Chim. Acta* 1977, **60**, 2633.

2. (a) B. Spiess, F. Arnaud-Neu and M. J. Schwing-Weill, *Helv. Chim. Acta* 1979, **5**, 1531; (b) 1980, **8**, 2287; F. Arnaud-Neu, B. Spiess and M. J. Schwing-Weill, *J. Amer. Soc.* 1982, **104**, 5641.
3. I. G. Sayce, *Talanta* 1968, **15**, 1397.
4. P. Gramain and Y. Frere, *Nouveau Journal de Chimie* 1979, **3**, 1, 53.
5. P. Vitali, Thèse de Doctorat de 3ème cycle, Strasbourg (1975).
6. L. G. Sillén and A. E. Martell, *Stability Constants of Metal-Ion Complexes*. The Chemical Society, London (1964).
7. B. G. Cox, P. Firman and H. Schneider, *Inorg. Chim. Acta* 1983, **69**, 161.
8. U. M. Goldschmidt, *Skrifter Norske Tidenskaps*, Akad. Oslo, Mat.-Naturv., Kl. 1 (1926).
9. J. E. Huheey, *Inorganic Chemistry: Principles of Structure and Reactivity*. Harper & Row, New York (1972).
10. G. Anderegg, *Helv. Chim. Acta* 1975, **58**, 1218.

Polyhedron Vol. 4, No. 8, pp. 1475–1478, 1985
Printed in Great Britain

0277–5387/85 $3.00 + .00
© 1985 Pergamon Press Ltd

ELECTROCHEMICAL STUDIES ON THREE POLAR DIRUTHENIUM(II,III) COMPLEXES

AKHIL R. CHAKRAVARTY, F. ALBERT COTTON,* DEREK A. TOCHER and JOANNE H. TOCHER

Department of Chemistry and Laboratory for Molecular Structure and Bonding, Texas A & M University, College Station, TX 77843, U.S.A.

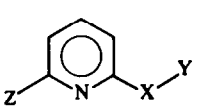
(*Received* 5 *October* 1984; *accepted* 7 *February* 1985)

Abstract—Electrochemical studies on a new class of diruthenium(II,III) compounds were done. The complexes having a polar arrangement of ligands across the diruthenium unit in $Ru_2Cl(hp)_4(Hhp)$, $Ru_2Cl(chp)_4$ and $Ru_2Cl(PhNpy)_4$ where Hhp, Hchp and PhNHpy are 2-hydroxypyridine, 6-chloro-2-hydroxypyridine, and 2-anilinopyridine, respectively, undergo two or more oxidations and reductions. The metal centered reductions in the range of +0.1 to −0.75 V and oxidations in the range +0.5 to +1.2 V are discussed and compared with diruthenium carboxylato and amidato complexes.

Unsymmetrical ligands of the type **1** bridging across a pair of metal atoms are known[1] to form complexes $M_2(NX)_4$ with short metal–metal bond distances. The arrangement of bridging ligands is usually[1–3] of the type **2**. In some dirhodium compounds, a type **3** arrangement was observed.[4,5] The type **4** arrangement was first found[6,7] in Hfhp complexes of Cr_2, Mo_2, W_2 and Rh_2. With these metals all other ligands are known[1] to form either type **2** or type **3** complexes. Recently we have reported[8,9] the syntheses and X-ray structures of three diruthenium(II,III) complexes having bridging ligands hp, chp and PhNpy in a totally polar arrangement as shown in **4**.

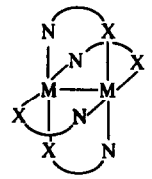
* Author to whom correspondence should be addressed.

In $Ru_2Cl(O_2CR)_4$[10–16] and $Ru_2Cl(RCONH)_4$[17–20] complexes, the formal oxidation state of the ruthenium is +2.5 and the coordination environments of the two metal centers are the same. In our compounds, **5**–**7**, the coordination environments of two ruthenium atoms are different.[8,9] We have previously[9] discussed the probable reasons for the occurrence of this polar type of arrangement, citing a combination of steric and electronic factors. The electronic character of the two metals is expected to be somewhat different, but the question is whether their different environments will lead to any gross differences in properties. With that question in mind we have been motivated to carry out electrochemical studies on these complexes and the results of this investigation will be reported here.

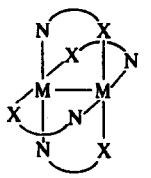


X	Y	Z	
O	H	H	Hhp
O	H	F	Hfhp
O	H	Cl	Hchp
O	H	CH_3	Hmhp
N	C_6H_5	H	PhNHpy

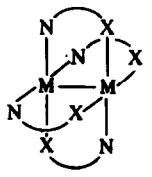
1



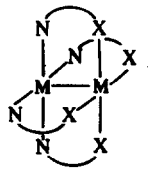
2a



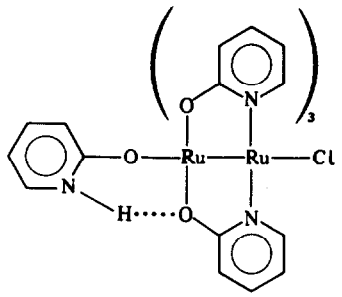
2b



3

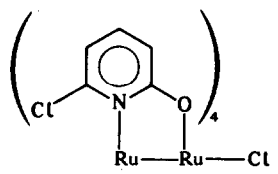


4



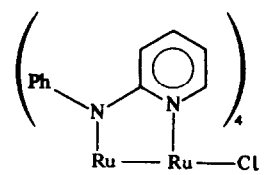
$Ru_2Cl(hp)_4(Hhp)$

5



$Ru_2Cl(chp)_4$

6



$Ru_2Cl(PhNpy)_4$

7

EXPERIMENTAL

The preparations of these complexes have been already reported.[8,9] Tetra-*n*-butylammonium tetrafluoroborate ($TBABF_4$) was used as a supporting electrolyte in electrochemical measurements. All solvents were freshly distilled under a dinitrogen atmosphere and measurements were carried out under an argon atmosphere. Redox studies were done with a Bioanalytical Systems, Inc. Model BAS 100 Electrochemical Analyser instrument in connection with a Bausch and Lomb, Houston Instruments Model DMP 40 digital plotter. In a three-electrode cell system, a platinum disk, Model BAS MF 2032, and a platinum wire were used as working and auxiliary electrodes, and a BAS MAF 2020 Ag–AgCl cell was used as reference electrode. All potentials were referenced to the Ag–AgCl electrode at $22 \pm 2°C$ and are uncorrected for junction potentials.

RESULTS AND DISCUSSION

Electrochemical data in different solvents are presented in Table 1. Cyclic voltammograms of $Ru_2Cl(PhNpy)_4$ in tetrahydrofuran are shown in Fig. 1. The complexes undergo one nearly reversible one-electron reduction in the potential range +0.1 to −0.8 V. On the positive side of the reference electrode one reversible one-electron oxidation in the range +0.5 to +1.2 V is observed in all complexes. The one-electron stoichiometry of the electron-transfer processes was verified by controlled-potential coulometry done on

Table 1. Electrochemical data[a]

Complex	Solvent	Scan rate, mV s^{-1}	$E_{1/2}$, V(ΔE_p, mV)[b]
$Ru_2Cl(hp)_4(Hhp)$	CH_3CN	50–500	−1.45,[c] −0.29(70), +0.94(60), +1.11(70), +1.48[d]
	$HCONMe_2$[e]	10	−0.47, −0.31, +1.12, +1.25
$Ru_2Cl(chp)_4$	CH_2Cl_2	100	−1.70,[c] +0.10(73), +1.13(300)[f]
	CH_3CN	100	−1.70,[c] +0.09(80), +0.34(60), +1.61[d]
$Ru_2Cl(PhNpy)_4$	CH_2Cl_2	250	−1.57,[c] −0.75(67), +0.50(60), +1.45(100)
	C_4H_8O	500	−1.57,[c] −0.71(60), +0.65(60), +1.20[d]

[a] Cyclic voltammetry with 0.1 M $TBABF_4$ as supporting electrolyte.
[b] Volts vs Ag/AgCl reference electrode.
[c] Cathodic peak ($E_{p,c}$).
[d] Anodic peak ($E_{p,a}$).
[e] Differential pulse voltammetry.
[f] Ill-defined response.

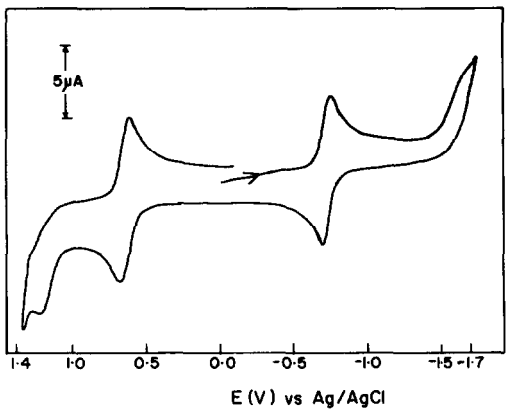


Fig. 1. Cyclic voltammograms of $Ru_2Cl(PhNpy)_4$ in tetrahydrofuran–0.1 M $TBABF_4$ at scan rate 200 mV s^{-1}.

$Ru_2Cl(chp)_4$ and $Ru_2Cl(PhNpy)_4$. For both the processes the $i_{p,c}/i_{p,a}$ ratio is $\simeq 1$ for sweep rates between 50 and 500 mV s^{-1}. The peak-to-peak separation, $E_{p,a} - E_{p,c} = \Delta E_p$, of 60–80 mV indicates a reversible electron-transfer process. In all complexes one further reduction is observed at higher negative potential. The process is irreversible since there is no anodic counterpart of the cathodic wave. Similarly all complexes display one or more oxidation waves at higher positive potentials and these processes are irreversible or quasireversible in nature.

In our earlier reports[8,9] we have mentioned that these complexes resemble $Ru_2Cl(O_2CR)_4$[10–16] and $Ru_2Cl(RCONH)_4$[17–20] in having magnetic moments corresponding to three unpaired electrons. For the carboxylates this has been attributed to a ground electronic configuration of

$$(\sigma)^2(\pi)^4(\delta)^2(\pi^*)^2(\delta^*)^1,$$

in which the π^* and δ^* orbitals are essentially degenerate.[12] One-electron oxidation of such compounds is expected to give either

$$(\sigma)^2(\pi)^4(\delta)^2(\pi^*)^2(\delta^*)^0$$

or

$$(\sigma)^2(\pi)^4(\delta)^2(\pi^*)^1(\delta^*)^1$$

as electronic configuration. Similarly one-electron reduction will add one electron either to the π^* or to the δ^* orbital. Comparing the electrochemical results of **5–7** we see a cathodic shift of the first reduction and oxidation potentials in the order PhNpy > hp > chp. This indicates that the energy of the antibonding π^* and δ^* levels follows the same order.

$Ru_2Cl(chp)_4$ in CH_3CN displays two reduction peaks at +0.09 and +0.34 V. The one at higher potential is less prominent and could be due to the couple $Ru_2(chp)_4^+ + e \rightleftharpoons Ru_2(chp)_4$. X-ray structural studies[8,9] on these compounds show that the Ru–Cl bond lengths in **6** and **7** are short (*ca.* 2.45 Å) compared to the ones in $Ru_2Cl(O_2CR)_4$[11,15,16] and $Ru_2Cl(4\text{-}Cl\text{-}C_6H_4CONH)_4$[20] (*ca.* 2.56 Å). The amidato and carboxylato species thus have weak Ru–Cl bonds which can be easily cleaved by strong polar solvents. Electrochemical studies on these compounds do show[13,17,18] the presence of an equilibrium between dissociated and undissociated species. A similar phenomenon is also noticed in **5**. The compound is slightly soluble in CH_3CN. In DMF, it exhibits two reductions at −0.31 and −0.47 V and two oxidations at +1.12 and +1.25 V. The waves at −0.31 and +1.25 V are more prominent and they could be due to reduction and oxidation of the $[Ru_2(hp)_4(Hhp)]^+$ cation which is in equilibrium with $Ru_2Cl(hp)_4(Hhp)$.

The potential difference, $\Delta E_{1/2}$, between the first oxidation and the first reduction processes is *ca.* 1.3 V. In $Ru_2Cl(HNOCCH_3)_4$ the oxidation and two reductions takes place in Me_2SO at +0.47, −0.96 and −1.22 V, respectively.[18] The $\Delta E_{1/2}$ value is *ca.* 1.5 V. In $Ru_2Cl(O_2CC_3H_7)_4$, the reduction process is known[13] to occur in the range of 0.0 to −0.34 V vs SCE depending on the solvent. From our electrochemical studies, it is apparent that the redox behavior of the polar compounds is similar to that of other carboxylato and amidato species. We conclude that the completely polar arrangement of the ligands in **5–7** does not lead to any pronounced electronic difference from the carboxylato or amidato species, such as might be expected if there was a tendency to localize the +2 and +3 oxidation states.

Acknowledgement—We thank National Science Foundation for support.

REFERENCES

1. F. A. Cotton and R. A. Walton, *Multiple Bonds Between Metal Atoms.* John Wiley and Sons, New York (1982).
2. (a) F. A. Cotton and J. L. Thompson, *J. Am. Chem. Soc.* 1980, **102**, 6437; (b) W. Clegg, *Acta Crystallogr.* 1980, **B36**, 3112.
3. A. R. Chakravarty, F. A. Cotton and E. S. Shamshoum, *Inorg. Chem.* 1984, **23**, 4216.
4. F. A. Cotton and T. R. Felthouse, *Inorg. Chem.* 1981, **20**, 584.
5. M. Berry, C. D. Garner, I. H. Hiller and W. Clegg, *Inorg. Chim. Acta* 1980, **45**, L209.
6. F. A. Cotton, L. R. Falvello, S. Han and W. Wang, *Inorg. Chem.* 1983, **22**, 4106.

7. F. A. Cotton, S. Han and W. Wang, *Inorg. Chem.* 1984, **23**, 4762.
8. A. R. Chakravarty, F. A. Cotton and D. A. Tocher, *Inorg. Chem.* 1985, **24**, 172.
9. A. R. Chakravarty, F. A. Cotton and D. A. Tocher, *Inorg. Chem.* in press.
10. P. Legzdins, R. W. Mitchell, G. L. Rempel, J. D. Ruddick and G. Wilkinson, *J. Chem. Soc. A* 1970, 3322.
11. M. J. Bennett, K. G. Caulton and F. A. Cotton, *Inorg. Chem.* 1969, **8**, 1.
12. J. G. Norman, Jr., G. E. Renzoni and D. A. Case, *J. Am. Chem. Soc.* 1979, **101**, 5256.
13. F. A. Cotton and E. Pedersen, *Inorg. Chem.* 1975, **14**, 388.
14. T. A. Stephenson and G. Wilkinson, *J. Inorg. Nucl. Chem.* 1966, **28**, 2285.
15. A. Bino, F. A. Cotton and T. Felthouse, *Inorg. Chem.* 1979, **18**, 2599.
16. D. S. Martin, R. A. Newman and L. M. Vlasnik, *Inorg. Chem.* 1980, **19**, 3404.
17. T. Malinski, D. Chang, F. N. Feldman, J. L. Bear and K. M. Kadish, *Inorg. Chem.* 1984, **23**, 2373.
18. M. Y. Chavan, F. N. Feldman, X. Q. Lin, J. L. Bear and K. M. Kadish, *Inorg. Chem.* 1984, **23**, 2373.
19. A. R. Chakravarty, F. A. Cotton and D. A. Tocher, *J. Am. Chem. Soc.* 1984, **106**, 6409.
20. A. R. Chakravarty, F. A. Cotton and D. A. Tocher, *Polyhedron* 1985, **4**, 1097.

Polyhedron Vol. 4, No. 8, pp. 1479–1484, 1985
Printed in Great Britain

0277-5387/85 $3.00 + .00
© 1985 Pergamon Press Ltd

A BINUCLEAR TANTALUM(III) COMPLEX WITH A BRIDGING CARBOXYLATO LIGAND

F. ALBERT COTTON,* MICHAEL P. DIEBOLD, STAN A. DURAJ and WIESLAW J. ROTH

Department of Chemistry and Laboratory for Molecular Structure and Bonding, Texas A & M University, College Station, TX 77843, U.S.A.

(*Received* 26 *November* 1984; *accepted* 7 *February* 1985)

Abstract—$Ta_2Cl_6(SMe_2)_3$ reacts with one equivalent of $C_4H_9CO_2Li$ to give a complex with a bridging carboxylate ligand, $Ta_2Cl_5(O_2CC_4H_9)(SMe_2)(THF)_2$. The product was isolated in two crystalline forms, **1** and **2**, from a THF/hexane and benzene/hexane solvent mixture, respectively. The following are the unit cell parameters, for **1**: monoclinic ($P2_1/n$), $a = 10.537(5)$ Å, $b = 22.015(4)$ Å, $c = 11.663(4)$ Å, $\beta = 107.80(3)°$, $V = 2576(3)$ Å^3, and $Z = 4$; for **2**: monoclinic ($P2_1/c$), $a = 15.584(4)$ Å, $b = 15.647(4)$ Å, $c = 11.275(3)$ Å, $\beta = 106.04(5)°$, $V = 2642(3)$ Å^3 and $Z = 4$. The complex is a dimer with a distorted octahedra-sharing-an-edge geometry. The Ta–Ta distances in **1** and **2** were 2.766(1) Å and 2.779(1) Å, respectively, which is somewhat longer than in previously reported Nb(III) and Ta(III) dinuclear compounds. Diamagnetism of the complex is shown by NMR. Fenske–Hall calculations, which correctly predict an electronic transition at about 16,000 cm^{-1}, indicate a double Ta–Ta bond. The observed elongation of the metal–metal bond is attributed mainly to steric crowding. The complex is the first proven low-valent Ta species with a coordinated carboxylate ion.

The chemistry of metal–metal bonded complexes of group V transition elements is not particularly well developed, especially when compared to that of their neighbors to the right in the periodic table.[1] One of the major lacunae in this area is the lack of unequivocally established carboxylato complexes of Nb and Ta.[2] The majority of other metals have extensive chemistry with RCO_2^- ligands, which play a very important role in the area of metal–metal multiple-bonded complexes of groups VI and VII. The reported non-monomeric carboxylates of Nb and Ta include $[CpNbO_2CH]_3(OH)_2(O)$,[3] $Nb_3O_2(O_2CR)_6(THF)_3^+$,[4] and $Ta_2Cl_4(O_2CBu)_4 \cdot 2BuCO_2H$.[5] The exact nature of the last compound is uncertain as no structural verification, which in this particular case would be desirable, has been carried out.

The chemistry of Nb and Ta in oxidation states lower than +5 with oxygen donors is in general not very rich.[6] A major reason seems to be the affinity of these elements for oxygen and consequently their tendency to abstract oxygen atoms from otherwise stable ligands, such as alkoxide, carboxylate, ketonate, etc. It appears that frequently mixtures of products are obtained in such systems, and this adversely affects the isolation of tractable products.

Following the characterization of bi-oxo-capped trimers[4] of niobium we began a similar study in tantalum chemistry, one result of which has been the isolation and characterization of a green intermediate which is seen with both metals when $M_2Cl_6L_3$, where $L = (CH_3)_2S$ or C_4H_8S, are reacted with an alkali metal carboxylate. The compound is a dimer, approximating to an edge-sharing bi-octahedron with a bridging pivalate anion. It is the first proven low-valent carboxylate of tantalum.[2] Its structural features are unique and in many respects different from those observed in previously reported Nb(III) and Ta(III) dimers.[7]

EXPERIMENTAL

All manipulations were carried out under an atmosphere of argon. Standard vacuum line techniques were used. $TaCl_5$ was purchased from Pressure Chemicals, Inc. and used as received. $Ta_2Cl_6(SMe_2)_3$ was prepared according to the literature method.[8] $C_4H_9CO_2Li$ was prepared by reacting pivalic acid with *n*-BuLi. The salt was

* Author to whom correspondence should be addressed.

recrystallized from THF and stored in the dry box. The spectra were recorded using the following instruments: UV–visible—Cary 17D spectrophotometer; ^{1}H NMR—Varian EM390 NMR spectrometer.

Preparation. $C_4H_9CO_2Li$ (0.07 g, 0.165 mmol) was added to a suspension of $Ta_2Cl_6(SMe_2)_3$ (0.5 g, 0.165 mmol) in 10 mL of THF (the observed precipitate was probably $Ta_2Cl_6(SMe_2)(THF)_2$).[7b] Within a few minutes the solution became dark green and stirring was maintained for *ca.* 0.5 hr. The solvent was removed under vacuum and the residue redissolved in 2–3 cm^3 of benzene. Excess hexane, about 20 cm^3, precipitated a green product which was contaminated with a reddish material. Purification involved extraction with 5–10 cm^3 aliquots of 2:1 hexane–THF mixture, which dissolved the complex leaving behind a brown, oily material. 30–40 cm^3 of hexane was added to each extract. On storing at −20°C a crystalline complex was obtained, with a combined yield varying between 30 and 50%.

The compound was obtained in two crystalline forms, **1** and **2**, by using THF/hexane and benzene/hexane solvent mixtures, respectively, for recrystallization. ^{1}H NMR ($CDCl_3/Me_4Si$), δ in ppm: 1.18—$C(CH_3)_3$, 3.03—$S(CH_3)_2$ and 3.37—$S(CH_3)_2$ with intensity ratio 3:1:1; 2.17 and 4.57—C_4H_8O. Visible spectrum (400–900 nm, benzene/hexane)—λ_{max} = 610 nm; a strong charge transfer band beginning at 500–600 nm.

X-ray crystallography. Single crystal X-ray analyses have been carried out by application of general procedures that are fully described elsewhere.[9] The relevant data pertaining to the

Table 1. Summary of crystallographic data

	1	**2**
Formula	$Ta_2Cl_5SO_4C_{15}H_{31}$	
Formula weight	846.64	
Space group	$P2_1/n$	$P2_1/c$
Systematic absences	$0k0$, $k \neq 2n$	$0k0$, $k \neq 2n$
	$h0l$, $h+l \neq 2n$	$h0l$, $l \neq 2n$
a, Å	10.537(5)	15.584(4)
b, Å	22.015(4)	15.647(4)
c, Å	11.663(4)	11.275(3)
β, °	107.80(3)	106.04(5)
V, Å^3	2576(3)	2642(3)
Z	4	4
d_{calc}, g/cm^3	2.183	2.128
Crystal size, mm	0.2 × 0.3 × 0.35	0.2 × 0.2 × 0.4
μ(Mo-K_α), cm^{-1}	90.128	87.866
Data collection instrument	CAD-4	
Radiation (monochromated in incident beam)	Mo-K_α (λ = 0.71073 Å)	
Orientation reflections, number, range (2θ)	25, 16.4–34.0	25, 15.3–30.8
Temperature, °C	22	
Scan method	$\omega-2\theta$	
Data collection range, 2θ, °	$4 \leqslant 2\theta \leqslant 50$	
No. of unique data, total with $F_o^2 > 3\sigma(F_o^2)$	3662, 2817	3627, 2612
Number of parameters refined	240	209
Empirical absorption correction, max., min.	0.9977, 0.9010	0.9997, 0.8274
R^a	0.042	0.042
$R_w{}^b$	0.051	0.048
Quality-of-fit indicator^c	1.262	1.168
Largest shift/esd, final cycle	0.41	0.30
Largest peak, e/Å^3	2.1^d	1.3^d

^{a} $R = \sum||F_o|-|F_c||/|F_o|$.
^{b} $R_w = [\sum w(|F_o|-|F_c|)^2/\sum w|F_o|^2]^{1/2}$; $w = 1/\sigma^2(|F_o|)$.
^{c} Quality of fit = $[\sum w(|F_o|-|F_c|)^2/(N_{obs}-N_{parameters})]^{1/2}$.
^{d} See discussion in the text.

structure determination are summarized in Table 1. Polarization, Lorentz and absorption corrections were applied to the intensity data.

The position of one Ta atom in each structure was determined from a three-dimensional Patterson function. The remaining atoms were located by a series of alternating difference Fourier syntheses and least squares refinements. The final difference Fourier maps contained, in both cases, some residual electron density above 1 $e/Å^3$ but it was located in the vicinity of the Ta atoms. No peaks of chemical significance were left in the maps. The following are additional comments pertaining to the individual crystal structure determinations.

(1) Several carbon atoms were found to be disordered. They were assigned the following fractional occupancy factors by trial and error: C(3) to C(5), 0.7; C(3A) to C(5A), 0.3, C(14) and C(14A), 0.65 and 0.35, respectively. The disordered atoms were refined isotropically, while anisotropic thermal vibration parameters were assigned to the remaining atoms. The listing of reflections with the worst match between F_o and F_c showed a strong extinction for the top 20 of them. Since these reflections constituted a small fraction of the data set they were rejected altogether and no correction for extinction was made.

(2) Several carbon atoms had relatively high thermal parameters indicating the possibility of a disorder. However, either there was no residual electron density around them [C(3) to C(5)] or no peaks in the difference Fourier map generated an adequate disorder model (THF ring). Thus, taking into account that these atoms were not crucial for an accurate description of the structure, we did not attempt to find a refinable disordered model.

Tables of structure factors, anisotropic thermal parameters, complete lists of bond distances and bond angles and selected non-bonding intramolecular contacts (37 pages) have been deposited with the Editor at Queen Mary College. Positional parameters and isotropic thermal parameters have been forwarded to the Director, Cambridge Crystallographic Data Centre.

RESULTS AND DISCUSSION

Molecular structure. $[TaCl_2(THF)]_2(\mu\text{-}Cl)(\mu\text{-}SMe_2)(\mu\text{-}O_2CC_4H_9)$ was isolated in two crystalline forms, **1** and **2** (see Table 1), by crystallization from THF/hexane and benzene/hexane mixtures, respectively. Both are monoclinic and have identical composition; they represent a case of polymorphism. The unit cell volumes differ by about 2.5% (66 $Å^3$), apparently as a result of different packing.

Important bond distances and angles are presented in Tables 2 and 3. Full listings of bonding interatomic dimensions are included in the supplementary material. The same atom labeling scheme, defined in Fig. 1, has been adopted for both compounds.

Table 2. Important bond distances (Å) in $Ta_2Cl_5(O_2CC_4H_9)(SMe_2)(THF)_2$

	1	2
Ta(1)–Ta(2)	2.766(1)	2.779(1)
Ta(1)–Cl(1)	2.444(3)	2.444(3)
Ta(1)–Cl(2)	2.393(4)	2.402(4)
Ta(1)–Cl(3)	2.377(3)	2.381(4)
Ta(1)–S	2.349(3)	2.348(4)
Ta(1)–O(1)	2.123(8)	2.127(9)
Ta(1)–O(10)	2.260(9)	2.259(9)
Ta(2)–Cl(1)	2.446(3)	2.449(4)
Ta(2)–Cl(4)	2.403(4)	2.389(4)
Ta(2)–Cl(5)	2.372(3)	2.371(4)
Ta(2)–S	2.355(3)	2.354(4)
Ta(2)–O(2)	2.118(8)	2.125(9)
Ta(2)–O(20)	2.248(9)	2.258(9)

Numbers in parentheses are estimated standard deviations in the least significant digits.

The molecule is an edge-sharing bioctahedron with a meridional disposition of chloride ions in each $TaCl_3SO(THF)$ half. There is a virtual mirror plane perpendicular to the Ta–Ta vector. Table 4 lists values of interatomic dimensions within the coordination sphere averaged for both molecules according to C_s symmetry. The pseudooctahedral environment around each metal atom is distorted to a considerable extent. A view along the Ta–Ta axis shown in Fig. 2 and the torsional angles listed in Table 5 show that SMe_2 is the ligand affected most by the deformation. It bends away from the Cl(2)–Ta(1)–Ta(2)–Cl(4) plane by *ca.* 45° due to spatial crowding, as indicated by short non-bonding S–Cl and Cl–C(7) contacts, which are about 3.25 and 3.45 Å, respectively. Such repulsion between a bridging SMe_2 and terminal Cl atoms in a dimeric Ta complex is seen in $Ta_2Cl_4(dmpe)_2(O)(SMe_2)$.[10] Since the distance from S and C(6) to Cl atoms *trans* to pivalate are also rather short, namely about 3.3 and 3.4 Å, the position of SMe_2 seems to be the optimal one allowed by the proximity of four Cl atoms. The other deformations are smaller, and while caused mainly by the positioning of SMe_2, may be also associated, to a smaller extent, with the terminal THF molecules.

Metal–metal bonding. While the tantalum to ligand bond distances are all very similar to corresponding ones in other Nb and Ta complexes, it is noteworthy that the Ta–Ta distance, 2.766(1) and

Table 3. Important bond angles (°) in $Ta_2Cl_5(O_2CC_4H_9)(SMe_2)(THF)_2$

	1	2		1	2
Ta(2)–Ta(1)–Cl(1)	55.59(8)	55.47(8)	Ta(1)–Ta(2)–Cl(4)	130.1(1)	131.4(1)
Ta(2)–Ta(1)–Cl(2)	130.6(1)	131.8(1)	Ta(1)–Ta(2)–Cl(5)	108.8(1)	108.7(1)
Ta(2)–Ta(1)–Cl(3)	107.5(1)	107.8(1)	Ta(1)–Ta(2)–S	53.89(9)	53.68(9)
Ta(2)–Ta(1)–S	54.09(8)	53.87(9)	Ta(1)–Ta(2)–O(2)	82.6(2)	82.3(3)
Ta(2)–Ta(1)–O(1)	83.2(2)	82.0(3)	Ta(1)–Ta(2)–O(20)	136.2(2)	133.8(3)
Ta(2)–Ta(1)–O(10)	134.6(3)	136.0(3)	Cl(1)–Ta(2)–Cl(4)	164.5(1)	165.0(1)
Cl(1)–Ta(1)–Cl(2)	164.9(1)	166.3(1)	Cl(1)–Ta(2)–Cl(5)	92.6(1)	92.5(1)
Cl(1)–Ta(1)–Cl(3)	90.5(1)	90.6(1)	Cl(1)–Ta(2)–S	105.2(1)	105.2(1)
Cl(1)–Ta(1)–S	105.4(1)	105.5(1)	Cl(1)–Ta(2)–O(2)	82.7(3)	84.4(3)
Cl(1)–Ta(1)–O(1)	83.3(3)	84.6(3)	Cl(1)–Ta(2)–O(20)	83.4(2)	81.3(3)
Cl(1)–Ta(1)–O(10)	81.7(3)	83.6(3)	Cl(4)–Ta(2)–Cl(5)	97.8(1)	96.5(2)
Cl(2)–Ta(1)–Cl(3)	99.1(1)	96.6(1)	Cl(4)–Ta(2)–S	86.7(1)	86.8(2)
Cl(2)–Ta(1)–S	86.6(1)	86.1(1)	Cl(4)–Ta(2)–O(2)	83.9(3)	83.7(3)
Cl(2)–Ta(1)–O(1)	84.0(3)	85.3(3)	Cl(4)–Ta(2)–O(20)	86.0(3)	87.4(3)
Cl(2)–Ta(1)–O(10)	87.5(3)	85.4(3)	Cl(5)–Ta(2)–S	88.4(1)	89.7(2)
Cl(3)–Ta(1)–S	88.8(1)	90.2(1)	Cl(5)–Ta(2)–O(2)	162.3(3)	164.1(3)
Cl(3)–Ta(1)–O(1)	161.5(3)	164.1(3)	Cl(5)–Ta(2)–O(20)	85.2(2)	86.1(3)
Cl(3)–Ta(1)–O(10)	85.2(3)	85.9(3)	S–Ta(2)–O(2)	109.3(2)	106.3(3)
S–Ta(1)–O(1)	109.6(3)	105.7(3)	S–Ta(2)–O(20)	169.6(2)	172.4(3)
S–Ta(1)–O(10)	170.8(3)	170.1(3)	O(2)–Ta(2)–O(20)	77.4(3)	77.9(4)
O(1)–Ta(1)–O(10)	76.7(3)	78.5(4)	Ta(1)–Cl(1)–Ta(2)	68.89(9)	69.21(9)
Ta(1)–Ta(2)–Cl(1)	55.52(8)	55.32(8)	Ta(1)–S–Ta(2)	72.02(9)	72.5(1)

Numbers in parentheses are estimated standard deviations in the least significant digits.

2.779(1) Å, in **1** and **2**, respectively, is somewhat longer (by 0.03–0.05 Å) than those previously reported[7] in dinuclear complexes of Nb(III) and Ta(III) with edge-sharing bioctahedral structures. We believe that this can be attributed principally to the steric crowding in the molecule and that a metal–metal double bond can be postulated here just as in other binuclear complexes of the trivalent metals. It is notable that the compound is shown by its display of a normal NMR spectrum to be diamagnetic.

Table 4. Important interatomic dimensions in $Ta_2Cl_5(O_2CC_4H_9)(SMe_2)(THF)_2$ averaged according to C_s symmetry[a]

	A. Distances (Å)		
Ta–Ta	2.773[7]	Ta–S	2.352[2]
Ta–Cl_b	2.445[2]	Ta–O_{carb}	2.123[2]
Ta–Cl(*trans* Cl_b)	2.397[3]	Ta–O_{THF}	2.256[3]
Ta–Cl(*trans* O_{carb})	2.375[2]		
	B. Angles (°)		
Cl_b–Ta–Cl(*trans* Cl_b)	165.2[4]	Cl(*trans* Cl_b)–Ta–Cl(*trans* O)	97.5[6]
Cl_b–Ta–Cl(*trans* O)	91.6[6]	Cl(*trans* Cl_b)–Ta–S	86.6[2]
Cl_b–Ta–S	105.3[1]	Cl(*trans* Cl_b)–Ta–O_{carb}	84.2[4]
Cl_b–Ta–O_{carb}	83.8[5]	Cl(*trans* Cl_b)–Ta–O_{THF}	86.6[5]
Cl_b–Ta–O_{THF}	82.5[6]	Cl(*trans* O)–Ta–S	89.3[4]
		Cl(*trans* O)–Ta–O_{carb}	163.0[7]
		Cl(*trans* O)–Ta–O_{THF}	85.6[2]
		S–Ta–O_{carb}	107.7[10]
		S–Ta–O_{THF}	170.7[6]
		O_{carb}–Ta–O_{THF}	77.6[4]

[a] Numbers in brackets are variances, obtained from the expression $[\sum \Delta_i^2/n(n-1)]^{1/2}$, where Δ_i is the deviation of the ith value from the arithmetic mean and n is the total number of values averaged.

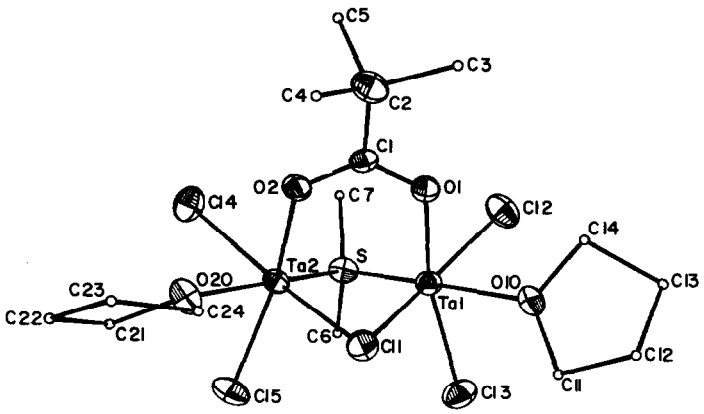


Fig. 1. An ORTEP drawing of the $Ta_2Cl_5(O_5CC_4H_9)(SMe_2)(THF)_2$ molecule. Thermal ellipsoids are drawn at 30% probability level. Selected carbon atoms have been assigned arbitrarily small thermal vibration parameters for the sake of clarity.

Table 5. Selected torsional angles (°) in $Ta_2Cl_5(O_2CC_4H_9)(SMe_2)(THF)_2$

Cl(1)–Ta(1)–Ta(2)–Cl(4)	161.8	162.9
Cl(1)–Ta(1)–Ta(2)–Cl(5)	−79.9	−79.7
Cl(1)–Ta(1)–Ta(2)–S	−153.4	−154.8
Cl(1)–Ta(1)–Ta(2)–O(2)	86.2	88.4
Cl(1)–Ta(1)–Ta(2)–O(20)	23.2	23.3
Cl(2)–Ta(1)–Ta(2)–Cl(1)	−162.6	−165.2
Cl(2)–Ta(1)–Ta(2)–Cl(4)	−0.8	−2.3
Cl(2)–Ta(1)–Ta(2)–Cl(5)	117.6	115.0
Cl(2)–Ta(1)–Ta(2)–S	44.1	39.9
Cl(2)–Ta(1)–Ta(2)–O(2)	−76.3	−76.8
Cl(2)–Ta(1)–Ta(2)–O(20)	−139.3	−141.9
Cl(3)–Ta(1)–Ta(2)–Cl(1)	78.1	78.1
Cl(3)–Ta(1)–Ta(2)–Cl(4)	−120.1	−119.0
Cl(3)–Ta(1)–Ta(2)–Cl(5)	−1.8	−1.7
Cl(3)–Ta(1)–Ta(2)–S	−75.2	−76.8
Cl(3)–Ta(1)–Ta(2)–O(2)	164.3	166.5
Cl(3)–Ta(1)–Ta(2)–O(20)	101.3	101.4
S–Ta(1)–Ta(2)–Cl(1)	153.4	154.8
S–Ta(1)–Ta(2)–Cl(4)	−44.9	−42.2
S–Ta(1)–Ta(2)–Cl(5)	73.5	75.1
S–Ta(1)–Ta(2)–O(2)	−120.4	−116.7
S–Ta(1)–Ta(2)–O(20)	176.6	178.2
O(1)–Ta(1)–Ta(2)–Cl(1)	−86.5	−89.0
O(1)–Ta(1)–Ta(2)–Cl(4)	75.3	73.9
O(1)–Ta(1)–Ta(2)–Cl(5)	−166.3	−168.7
O(1)–Ta(1)–Ta(2)–S	120.2	116.2
O(1)–Ta(1)–Ta(2)–O(2)	−0.2	−0.6
O(1)–Ta(1)–Ta(2)–O(20)	−63.3	−65.7
O(10)–Ta(1)–Ta(2)–Cl(1)	−22.7	−24.8
O(10)–Ta(1)–Ta(2)–Cl(4)	139.1	138.1
O(10)–Ta(1)–Ta(2)–Cl(5)	−102.6	−104.5
O(10)–Ta(1)–Ta(2)–S	−176.1	−179.6
O(10)–Ta(1)–Ta(2)–O(2)	63.5	63.6
O(10)–Ta(1)–Ta(2)–O(20)	0.5	−1.5

The existence of a Ta=Ta bond is supported by the results of a Fenske–Hall[11] calculation, carried out on a simplified model,

$$Nb_2Cl_5(O_2CH)(SH_2)(H_2O)_2,$$

in which the experimental bond lengths and angles were retained. The results are summarized in the MO digram shown in Fig. 3. The σ and π orbitals each have predominant metal *d*-orbital parentage. The δ and δ^* orbitals, which are empty, are mainly localized on individual metal atoms. The calculation yields a π to δ orbital energy difference of about 16,000 cm^{-1}, which is in fortuitous agreement with the observed band in the visible spectrum at 16,400 cm^{-1} (610 nm).

Synthesis and properties. $C_4H_9CO_2Li$ readily

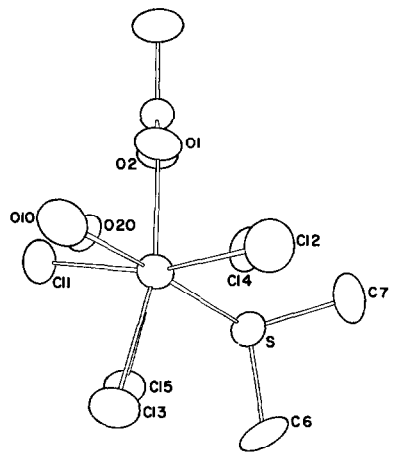


Fig. 2. A view of the $Ta_2Cl_5(O_2CC)(SMe_2)(O_{THF})_2$ skeleton along the Ta–Ta vector.

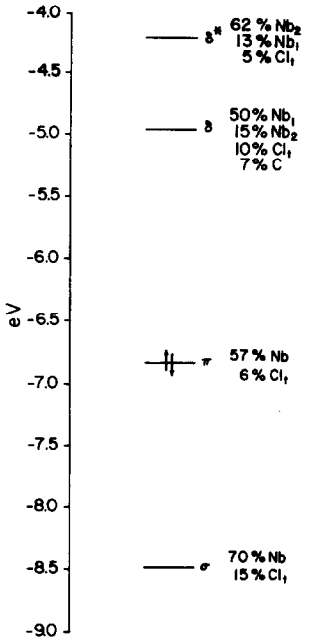


Fig. 3. An MO diagram for the model $Nb_2Cl_5(O_2CH)(SH_2)(H_2O)_2$ compound.

replaces one Cl ion in $Ta_2Cl_6L_3$ forming a green complex containing the bridging carboxylate. The product has to be isolated promptly as it undergoes further changes. If the reaction is carried out in a benzene/THF mixture the green color changes to brown after several hours. A small amount of the green species may still be obtained from this solution by solvent removal and extraction with THF/hexane but a brown, waxy material is the major product. When the latter is crystallized from a benzene/hexane mixture crystals with unit cell parameters matching those of $Ta_2Cl_6(SMe_2)(THF)_2$[7(b)] are obtained. This would indicate reversibility of the reaction but at this point it would not be appropriate to venture any specific explanation. With neat THF as the reaction medium the green color persists much longer but the brown material is also observed in the early stages of the workup. However, after purification the complex is quite stable in solution. The use of sodium pivalate instead of the lithium salt gives similar results but the reaction takes 1–2 weeks. The proton NMR spectrum was taken in $CDCl_3$ and is normal with respect to chemical shifts and line widths, in accord with the diamagnetism of the molecule. The *t*-Bu signal is at 1.18 ppm, which is only slightly different from the position for the free acid (1.21 ppm). The SMe_2 gives two signals at 3.03 and 3.37 ppm, consistent with the non-equivalence of the methyl groups. Their relatively large shift with respect to the free ligand (2.06 ppm) may be due to their proximity to the chlorine atoms. THF resonances are observed at 2.17 and 4.57 ppm. Based on intensity it is concluded that there is free THF in solution, as a result of crystallization from that solvent, and it undergoes exchange with the coordinated THF molecules. The spectrum in benzene is similar except that the chemical shifts for THF protons are somewhat different.

Although the reported complex is simply a product of ligand substitution in the starting material it is of importance in the area of multiple bonded complexes of Nb and Ta. As the first carboxylato complex of Ta(III) it shows that such species are stable and oxidation of low valent complexes of the heavier group V elements by oxo ligands can be avoided. It is also the first Nb(III) and Ta(III) dimer containing a bridging bidentate ligand. Such a species was not obtained with bis(diphenylphosphino)methane which instead bonded to Nb(III) in a chelating mode.7[a] The persistence of the Ta=Ta bond despite steric stress is notable. This compound may have potential as a reactant for synthesis of other binuclear compounds of low-valent tantalum.

Acknowledgements—We thank the Robert A. Welch Foundation for support under Grant No. A-494. M.P.D. is a National Science Foundation Predoctoral Fellow and also holds a Texaco–IUCCP Fellowship from this department.

REFERENCES

1. F. A. Cotton and R. A. Walton, *Multiple Bonds Between Metal Atoms*. Wiley, New York (1982).
2. R. C. Mehrotra and R. Bohra, *Metal Carboxylates*. Academic Press, New York (1983).
3. V. T. Kalinnikov, A. A. Pasynskii, G. M. Larin, V. M. Novotortsev, Y. T. Struchov, A. I. Gusev and N. I. Kirilova, *J. Organomet. Chem.* 1974, **74**, 91.
4. F. A. Cotton, S. A. Duraj and W. J. Roth, *J. Am. Chem. Soc.* 1984, **106**, 3527.
5. J. L. Morancais and L. G. Hubert-Pfalzgraf, *Inorg. Chim. Acta* 1983, **71**, 119.
6. D. L. Kepert, *The Early Transition Metals*. Academic Press, New York (1972).
7. Structurally characterized dimers of Nb(III) and Ta(III) are discussed in: (a) F. A. Cotton and W. J. Roth, *Inorg. Chem.* 1983, **22**, 3654; (b) F. A. Cotton, S. A. Duraj and W. J. Roth, *Acta Cryst. Section C* (in press).
8. F. A. Cotton and R. C. Najjar, *Inorg. Chem.* 1981, **20**, 2716.
9. See, for example, A. Bino, F. A. Cotton and P. E. Fanwick, *Inorg. Chem.* 1979, **18**, 3558.
10. F. A. Cotton and W. J. Roth, *Inorg. Chem.* 1983, **22**, 868.
11. M. B. Hall and R. F. Fenske, *Inorg. Chem.* 1972, **11**, 768.

Polyhedron Vol. 4, No. 8, pp. 1485–1491, 1985
Printed in Great Britain

0277–5387/85 $3.00 + .00
© 1985 Pergamon Press Ltd

PREPARATION, MOLECULAR STRUCTURE AND ELECTRONIC STRUCTURE OF THE RHOMBIC, SIX-COORDINATE NIOBIUM(IV) COMPLEX $NbCl_2(Bu^tC(O)CHC(O)Bu^t)_2$

F. ALBERT COTTON,* MICHAEL P. DIEBOLD and WIESLAW J. ROTH
Department of Chemistry and Laboratory for Molecular Structure and Bonding, Texas A & M University, College Station, TX 77843, U.S.A.

(*Received* 10 *December* 1984; *accepted* 20 *February* 1985)

Abstract—The compound *trans*-$NbCl_2(dpm)_2$, Hdpm = 2,2,6,6-tetramethylheptane-3,5-dione, has been prepared and the molecular structure determined in each of two crystalline polymorphs by X-ray diffraction. The visible spectrum and the EPR spectrum have been measured and a Fenske–Hall calculation performed. The combined results give a reasonable and internally consistent picture of the electronic structure of the molecule. The HOMO is a b_{3g}-orbital (predominantly d_{yz}), while the two lowest-lying unoccupied orbitals (*ca* 16,000 cm^{-1} higher) are $b_{2g}(\sim d_{xz})$ and $a_g(\sim d_{x^2-y^2})$ orbitals, all in the D_{2h}-symmetry. The $b_{3g} \rightarrow b_{2g}$ and $b_{3g} \rightarrow a_g$ transitions are observed at 588.4 and 626.7 nm. The EPR spectrum in solution is a decet; the measured value of $\langle g \rangle$ is 1.930 and $\langle A_{iso} \rangle$ is 149 G. For the crystalline polymorph **1** the crystal data are: orthorhombic ($P2_12_12_1$), $a = 13.649(3)$ Å, $b = 18.166(4)$ Å, $c = 11.425(4)$ Å, $V = 2833(2)$ Å^3 and $Z = 4$. Polymorph **2** is monoclinic ($P2_1/n$) with $a = 12.288(5)$ Å, $b = 9.226(4)$ Å, $c = 12.545(4)$ Å, $\beta = 94.24(3)°$, $V = 1418(2)$ Å^3 and $Z = 2$. The molecule in **2** is centrosymmetric with virtual D_{2h}-symmetry. In **1** there are distortions in the chelate plane postulated to be due to packing forces. The two forms have comparable averaged values of interatomic dimensions.

Although the number of chemically and structurally well-defined complexes of niobium(IV) and tantalum(IV) has been growing rapidly in recent years,[1–3] their electronic structure and spectroscopic properties are still poorly defined,[4] even for the six-coordinate species with "octahedral" structures. These complexes have the simplicity of being d^1-systems, but they have the disadvantage that the metal atoms are in a high formal oxidation state, which means that charge-transfer transitions may occur at as low, or lower, energies than some *d–d* transitions, thus obscuring them. They also have rather large spin–orbit coupling constants [J = 750 cm^{-1} for Nb(IV) and a much higher, though imprecisely known, value for Ta(IV)].

We have isolated and structurally characterized the complex *trans*-$NbCl_2(dpm)_2$, where dpm represents the anion of dipivaloylmethane (Hdpm), $(CH_3)_3CC(O)CHC(O)C(CH_3)_3^-$, which has rhombic ($D_{2h}$) molecular symmetry. By combining the results of EPR and visible spectral measurements with a molecular orbital calculation (by the Fenske–Hall procedure[5]) we have been able to establish clearly at least some features of its electronic structure.

EXPERIMENTAL

All manipulations were performed under an atmosphere of argon using standard inert atmosphere techniques. $NbCl_5$ and 2,2,6,6-tetramethylheptane-3,5-dione (Hdpm) were purchased from Aldrich. $Nb_2Cl_6(SMe_2)_3$ was prepared as described previously.[6] Hdpm was stored over molecular sieves and degassed by a freeze–thaw method before use. The lithium salt, Lidpm, was obtained by reaction of *n*-BuLi with Hdpm.

Synthesis of $NbCl_2(dpm)_2$

A solution of Hdpm (0.7 cm^3, 3.4 mmol) in the 5 cm^3 of CH_2Cl_2 was added to a solution of $Nb_2Cl_6(SMe_2)_3$ (0.56 g, 1 mmol) in 20 cm^3 of CH_2Cl_2. The purple solution turned to deep blue after several minutes of stirring. After filtration the solvent was removed under vacuum, leaving a blue,

* Author to whom correspondence should be addressed.

waxy residue. Approximately 200 mg portions of the product were placed in glass tubes, which were then evacuated to about 10^{-3} torr and sealed. The sample end of an ampoule was placed in a furnace and the temperature was raised gradually in the course of 1 week to about 100°C. The sublimation afforded large blue crystals in *ca* 50% yield. A small amount of white non-volatile material was also observed in the tube.

Examination of the crystals on a diffractometer showed that two different forms were present, namely orthorhombic and monoclinic, **1** and **2**, respectively. The unit cell volume of **1** was almost exactly twice that of **2**, and the abundance of the former type of crystals was roughly twice the latter. Full crystallographic analysis showed that both types of crystals contain the same complex, $NbCl_2(dpm)_2$.

EPR spectra were recorded on an X-band Varian E-6S spectrometer. DPPH was used as a standard for the calculation of g values. To obtain the spectrum of pure $NbCl_2(dpm)_2$ the compound was prepared as described, sublimed and dissolved in toluene.

X-ray crystallography

Single-crystal X-ray analyses were carried out by application of general procedures that have been described elsewhere.[7] Relevant crystallographic data are summarized in Table 1. Polarization and Lorentz corrections were applied to the intensity data. No correction for absorption was made.

A Delaunay reduction (program TRACER) performed on both cells with the largest permissible

Table 1. Crystallographic data

	1	**2**
Formula	$NbCl_2O_4C_{22}H_{38}$	
Formula weight	530.36	
Space group	$P2_12_12_1$	$P2_1/n$
Systematic absences	$00l$, $l \neq 2n$	$0k0$, $k \neq 2n$
	$0k0$, $k \neq 2n$	$h0l$, $h+l \neq 2n$
	$h00$, $h \neq 2n$	
a (Å)	13.649(3)	12.288(5)
b (Å)	18.166(4)	9.226(4)
c (Å)	11.425(4)	12.545(4)
α (°)	90	90
β (°)	90	94.24(3)
γ (°)	90	90
V (Å^3)	2833(2)	1418(2)
Z	4	2
$d_{calc.}$ (g cm^{-3})	1.243	1.242
Crystal size (mm)	0.4 × 0.4 × 0.35	0.35 × 0.3 × 0.25
μ(Mo-K_α) (cm^{-1})	6.168	6.160
Data collection instrument	Syntex P$\bar{1}$	
Radiation (monochromated in incident beam)	Mo-K_α (λ = 0.71073 Å)	
Orientation reflections, number, range (2θ)	15, 24.6–29.1	15, 21.6–27.1
Temperature (°C)	22	
Scan method	ω–2θ	
Data collection range (2θ) (°)	$4 \leqslant 2\theta \leqslant 50$	
Number of unique data, total with $F_o^2 > 3\sigma(F_o^2)$	2445, 1542	1798, 1297
Number of parameters refined	262	137
R*	0.0522	0.0493
R_w†	0.0631	0.0635
Quality-of-fit indicator‡	1.271	1.281
Largest shift/esd, final cycle	0.07	0.02
Largest peak (e Å^{-3})	0.522	0.331

* $R = \sum||F_o|-|F_c||/\sum|F_o|$.

† $R_w = [\sum w(|F_o|-|F_c|)^2/\sum w|F_o|^2]^{1/2}$; $w = 1/\sigma^2(|F_o|)$.

‡ Quality of fit $= [\sum w(|F_o|-|F_c|)^2/(N_{obs.}-N_{parameters})]^{1/2}$.

difference between any two reduced cell scalar products equal to 4.0 ruled out the possibility of transforming one cell into the other. In both cases the position of the Nb atom was derived from a three-dimensional Patterson function. The rest of the structure was developed by a sequence of alternating least-squares refinements and difference Fourier syntheses. After anisotropic refinement of all non-hydrogen atoms the hydrogen atoms bonded to the ring carbon atoms were located in the difference Fourier maps and included in the full matrix least-squares refinement. The two H atoms in the orthorhombic crystal were refined with an isotropic thermal parameter fixed at 4.0.

Tables of observed and calculated structure factors, anisotropic thermal parameters, complete lists of bond distances and bond angles, selected least-squares planes and short intermolecular contacts (26 pp.) have been deposited with the Editor at Queen Mary College. Positional parameters and isotropic thermal parameters have been forwarded to the Director, Cambridge Crystallographic Data Centre.

Table 3. Important bond angles (°) for the $NbCl_2(dpm)_2$ molecules*

(A) Orthorhombic, **1**	
Cl–Nb–Cl′	178.7(1)
Cl–Nb–O(1)	89.3(3)
Cl–Nb–O(2)	88.9(3)
Cl–Nb–O(1)′	87.4(2)
Cl–Nb–O(2)′	88.7(3)
Cl′–Nb–O(1)	90.7(3)
Cl′–Nb–O(2)	92.3(3)
Cl′–Nb–O(1)′	92.9(2)
Cl′–Nb–O(2)′	90.1(3)
O(1)–Nb–O(2)	82.0(3)
O(1)–Nb–O(1)′	165.9(3)
O(1)–Nb–O(2)′	111.4(3)
O(2)–Nb–O(1)′	84.2(3)
O(2)–Nb–O(2)′	166.4(3)
O(1)′–Nb–O(2)′	82.2(3)
(B) Monoclinic, **2**†	
Cl–Nb–O(1)	90.3(1)
Cl–Nb–O(2)	90.3(1)
O(1)–Nb–O(2)	82.3(1)

* Numbers in parentheses are estimated standard deviations to the least significant digits.

† Angles related due to the presence of an inversion center have been omitted.

RESULTS

Molecular structure

Important bond distances and angles are presented in Tables 2 and 3, respectively. The atom-labelling scheme is defined in Fig. 1.

As can be seen in Table 2 the molecules of $NbCl_2(dpm)_2$ in both crystallographic forms are quite similar in terms of average values of bond distances and angles. In detail, however, there are some real differences between them. The monoclinic $NbCl_2(dpm)_2$, **2**, has a crystallographically imposed inversion center and its actual symmetry is very close

Table 2. A comparison of selected interatomic dimensions in the orthorhombic, **1**, and monoclinic, **2**, form of $NbCl_2(dpm)_2$

	1			**2**
	(A) Distance (Å)			
			Average*	
Nb–Cl	2.413(4)	2.410(4)	2.412[2]	2.410(2)
Nb–O(1)	1.954(7)	2.021(6)		1.981(4)
			1.980[24]	
Nb–O(2)	2.043(7)	1.959(7)		1.984(4)
	(B) Angle (°)			
Cl–Nb–Cl′		178.7(1)	178.7(1)	180.0
Cl–Nb–O†	88.6[4]	91.5[7]	90[1.6]	90.0
O–Nb–O′ chelate	82.0(3)	82.2(3)	82.1[1]	82.3(1)
O–Nb–O′ *trans*	165.9(3)	166.4(3)	166.2[3]	180.0
O–Nb–O′ *cis*	111.4(3)	84.2(3)	97.8[13.6]	97.7(1)

* Numbers in brackets are variances, obtained from the expression $[\sum\Delta_i^2/n(n-1)]^{1/2}$, where Δ_i is the deviation of the ith value from the arithmetic mean and n is the total number of values averaged.

† Average of four angles between Cl–Nb–O and Cl′–Nb–O, respectively, given.

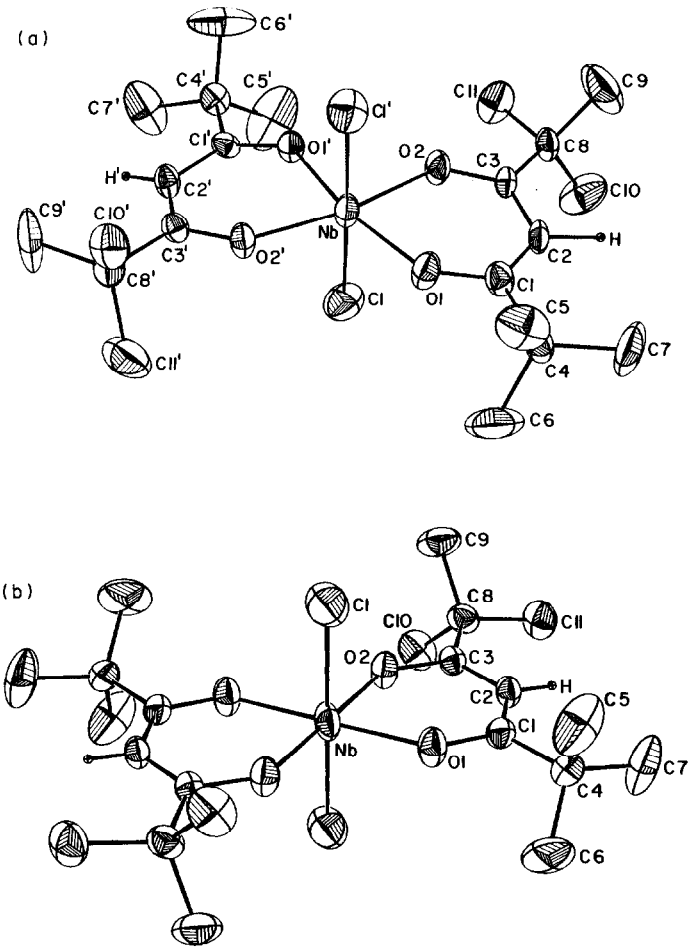


Fig. 1. ORTEP drawing of the $NbCl_2(dpm)_2$ molecules defining the labeling scheme. Thermal ellipsoids are drawn at 30% probability level. (a) Orthorhombic, **1**. (b) Monoclinic, **2**.

to D_{2h}. In the orthorhombic cell the molecule resides on a general position and owing to distortion in the NbO_4 plane, shown in Fig. 2, its symmetry is, at best, C_{2v}, even if the methyl groups are disregarded. The most prominent distortion is a 27° difference between the two O—Nb—O′ angles where O and O′ are in different chelate rings. The Nb—O bond lengths also differ by 0.1 Å. However, average values of the two quantities are comparable to those in the undistorted molecule in **2**, as is clear in Table 2.

Examination of unit cell packing (Fig. 3) and intermolecular contacts leads us to the conclusion that the deformations found in **1** are caused by packing forces, but we find that magnitude of the effects somewhat surprising. The orientation of methyl carbon atoms is quite revealing in this respect. In **2** the set of four *t*-butyl (*t*-Bu) groups has an approximate *mmm* symmetry. Such an arrangement seems to be the preferred one since, as discussed[8] for $Ni(dpm)_2$, where it also occurs, it minimizes the intramolecular contacts. The closing of the O(1)–Nb–O(2) angle in **1** results in a small separation between two of the C_4H_9 groups, which apparently prevents them from orienting so as to be related by a mirror plane. The shortest contact is between C(11) and C(5)′ and it is equal to 4.48 Å. On the other side, the two *t*-Bu groups are oriented as in **2** and there is a cavity between two pairs of methyl groups. That space is occupied by C(10) and C(11) atoms from another molecule. The intermolecular contacts between carbon atoms in this region are around 4 Å, which compares well with the accepted van der Waals' radius for a methyl group, viz. 2 Å. Naturally, in **2** there are also intermolecular contacts of the order of 4 Å, but they are directed away from the chelate ring.

Apart from the distortion in **1** the $NbCl_2(dpm)_2$ molecules are normal in terms of features expected for octahedral β-diketonate complexes. The $Nb(chelate)_2$ unit is essentially planar with somewhat more pronounced deviations in the orthorhombic form. The average Nb–O distance of

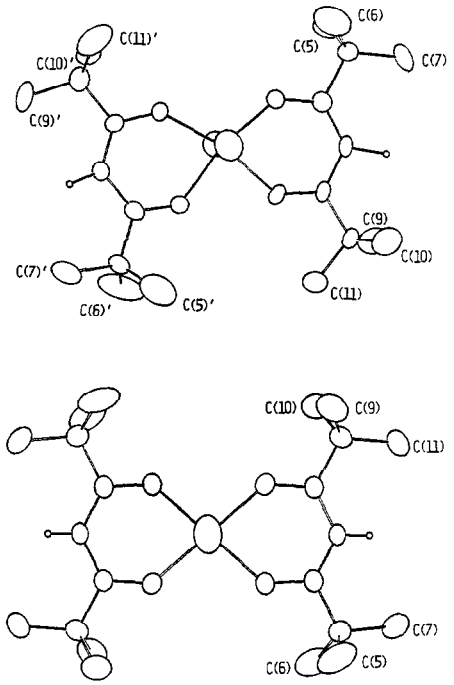


Fig. 2. A view of the $NbCl_2(dpm)_2$ molecules from above the chelate plane: upper—orthorhombic, **1**; lower—monoclinic, **2**.

ca 1.98 Å is 0.15 Å shorter than in the eight-coordinate $Nb(dpm)_4$ complex.[9] Steric crowding is clearly the major factor contributing to the lengthening of the bond in the latter case. We believe it is reasonable to assume, for purposes of analyzing the spectra and bonding, that the molecule in solution has true D_{2h}-symmetry.

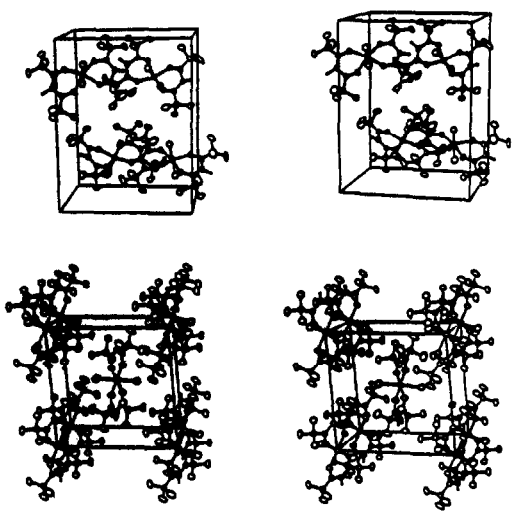


Fig. 3. A unit cell packing for $NbCl_2(dpm)_2$; upper—orthorhombic, **1**; lower—monoclinic, **2**.

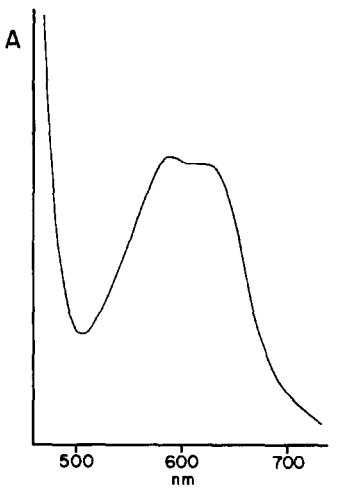


Fig. 4. The UV–visible spectrum of $NbCl_2(dpm)_2$ in toluene.

Spectroscopic data and Fenske–Hall calculations

The UV–visible spectrum of $NbCl_2(dpm)_2$ is shown in Fig. 4. The doublet band with maxima at 588.4 and 626.7 nm is very similar to that in $NbCl_2(acac)_2$.[10] In the latter an additional doublet is observed at higher energy but an intense charge-transfer band beginning around 500 nm covers this region in the dpm derivative.

The blue solutions obtained by reacting $Nb_2Cl_6(SMe_2)_3$ with Hdpm and Lidpm contained several paramagnetic species as evidenced by the complexity of low-temperature EPR spectra shown in Fig. 5. $NbCl_2(dpm)_2$, purified by sublimation, gives at room temperature the expected 10-line signal with $\langle g \rangle = 1.930$ and $\langle A_{iso} \rangle = 149$ G. At −196°C a well-resolved EPR spectrum consistent with the rhombic symmetry of the complex is obtained. It is noteworthy that spectrum C in Fig. 5 appears to be due to superposition of the signal from $NbCl_2(dpm)_2$ (predominant) and some other paramagnetic complex.

A Fenske–Hall calculation[5] has been performed on the model compound $NbCl_2(acac)_2$. Atomic parameters from the centrosymmetric $NbCl_2(dpm)_2$, **2**, crystal structure, idealized to D_{2h}-symmetry, were used, and a right-handed coordinate system was chosen with the Z-axis along a Nb–Cl bond vector and the X-axis directed from the niobium atom to the central carbon atom of a dpm ligand. As seen in Fig. 6, these calculations place the d_{yz}-orbital lowest in energy and singly occupied. The d_{xz} and $d_{x^2-y^2}$ orbitals are 2.223 and 2.470 eV higher in energy, respectively, and the a_u and b_{3g} combinations of the C=O π^*-orbitals are above these. The other two combinations of C=O π^*-

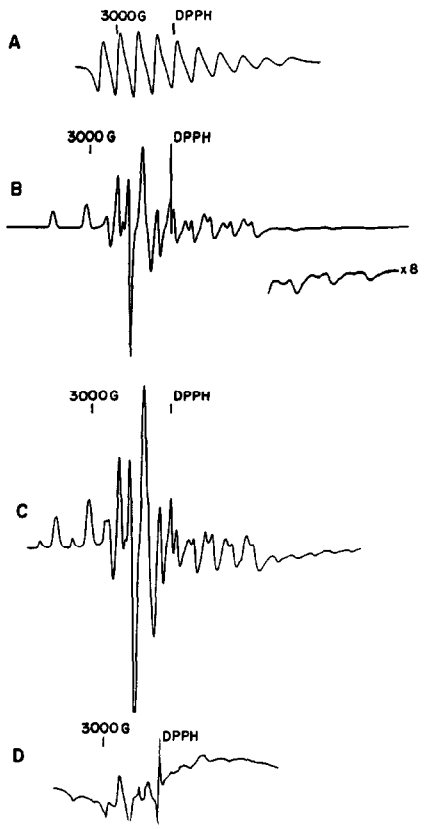


Fig. 5. ESR spectra: (a) $NbCl_2(dpm)_2$ at 22°C; (b) $NbCl_2(dpm)_2$ at −196°C; (c) reaction mixture $Nb_2Cl_6(SMe_2)_3$ + Lidpm at −196°C; (d) reaction mixture $Nb_2Cl_6(SMe_2)_3$ + Hdpm at −196°C.

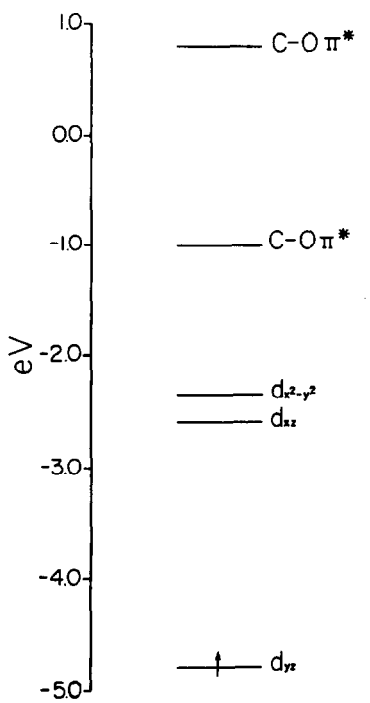


Fig. 6. The MO diagram of the model compound $NbCl_2(acac)_2$, where acac = $CH_3C(O)CHC(O)CH_3$.

orbitals, as well as the remaining *d*-orbitals, are much higher in energy (> 15 eV above the d_{yz}-orbital).

DISCUSSION

Synthesis

The work reported here was begun in response to a recent report[11] describing the synthesis and properties of several β-diketonato complexes of niobium(III), which were assigned structures rather different from those previously recognized[12] for compounds with the metal atoms in oxidation state III. We were particularly interested in the reported compound $Nb_2Cl_3(dpm)_3$ and attempted to prepare it in crystalline form by the recommended method. Our attempts to obtain crystals from solution failed and we therefore tried to obtain them by sublimation. It was in this way that we obtained the two crystal forms of the title compound. There have been a few β-diketonato complexes of niobium and tantalum reported previously.[3,9,10,13,14] The +4 oxidation state is represented by a postulated nine-coordinate $Nb(LL)_4 \cdot$dioxane,[13] eight-coordinate $Nb(LL)_4$[9,13] and octahedral $NbCl_2(LL)_2$[10,13] species. Apparently no Ta(IV) β-diketonato complex has been characterized. So far a complete structural analysis has been carried out only for the dodecahedral $Nb(dpm)_4$.

Both the eight-coordinate $M(LL)_4$ and *trans*-$MX_2(LL)_2$ complexes, where X may be a mono-anionic or neutral ligand, are common types of β-diketonato compounds.[14]

Electronic structure and interpretation of the spectra

There are now three reported complexes of the stoichiometry $NbCl_2$(β-diketonate)$_2$, with acetylo-acetonate,[10] dibenzoylmethane (dbm)[13] and dpm. It is reasonable to expect that they would have analogous structures, and the similarity of the UV–visible spectra for the acac and dpm compounds supports this. For the dbm complex the diffuse reflectance spectrum was reported. Although it shows a band at 17.4 kK, which correlates well with what is seen for the other two compounds, the rest of the spectrum is somewhat more complicated. Since no information concerning the solution spectrum is available and only the band positions were reported we shall not try to explain this apparent discrepancy.

The results of the Fenske–Hall calculation provide an excellent basis for interpreting both the visible and EPR spectra. The doublet observed in the visible spectrum with maxima at *ca* 16,000 cm^{-1} and *ca* 17,000 cm^{-1} can be assigned to the following calculated $d \rightarrow d$ transitions: $yz \rightarrow xz$ (calc. 17,700

cm^{-1}) and $yz \rightarrow x^2-y^2$ (calc. 20,200 cm^{-1}). In view of the well-known tendency of the Fenske–Hall method to place virtual orbitals at energies that are too high, the agreement here is very satisfactory. No higher $d \rightarrow d$ transitions are expected until energies well above the onset of ligand-to-metal charge-transfer transitions. Because of the difficulties in handling solutions of this extremely air-sensitive compound, we have not attempted to record the spectrum in the charge-transfer region.

The EPR spectrum is also nicely accounted for by the results of the calculation. Using the standard method of calculating g values for a d^1-ion with spin–orbit coupling[15] the expressions for the three components of the diagonalized g tensor are:

$$g_x = 2 - \frac{6\lambda}{\Delta E(z^2)} - \frac{2\lambda}{\Delta E(x^2-y^2)},$$

$$g_y = 2 - \frac{2\lambda}{\Delta E(xy)},$$

$$g_z = 2 - \frac{2\lambda}{\Delta E(xz)},$$

where an expression like $\Delta E(xz)$ means the orbital energy difference between the lowest d-orbital (d_{yz}) and an upper one such as the d_{xz}-orbital. For Nb(IV) the free-ion value of λ is 750 cm^{-1} but the effective value in the complex is surely no more than 80% of this. We may also use the experimental values of $\Delta E(xz)$ and $\Delta E(x^2-y^2)$ and take the true values of $\Delta E(z^2)$ and $\Delta E(xy)$ to be about 50% of those calculated. On this basis we obtain the following calculated g values:

$$g_x = 1.877, \quad g_y = 1.988 \text{ and } g_z = 1.925,$$

from which a $\langle g \rangle$ value $[(g_x^2+g_y^2+g_z^2)/3]^{1/2}$ of 1.931 is obtained, in good agreement with the measured value of 1.930. The measured $\langle A_{iso} \rangle$ value of 149 G is quite reasonable when compared to such parameters in some other Nb(IV) complexes.[3,16]

Acknowledgements—We thank the Robert A. Welch Foundation for support of this research under Grant No. A-494. M.P.D. is the recipient of a National Science Foundation Predoctoral Fellowship and a Texaco–IUCCP Fellowship from this department.

REFERENCES

1. F. A. Cotton, M. P. Diebold and W. J. Roth, *Polyhedron* 1985, **4**, 1103.
2. M. L. Luetkens, W. L. Elcesser, J. C. Huffman and A. P. Sattelberger, *Inorg. Chem.* 1984, **23**, 1718.
3. D. A. Miller and R. D. Bereman, *Coord. Chem. Rev.* 1972, **9**, 107.
4. A. B. P. Lever, *Inorganic Electronic Spectroscopy*, 2nd edition, p. 392. Elsevier, Amsterdam (1984).
5. M. B. Hall and R. F. Fenske, *Inorg. Chem.* 1972, **11**, 768.
6. F. A. Cotton, S. A. Duraj and W. J. Roth, *J. Am. Chem. Soc.* 1984, **106**, 3527.
7. See, for example, A. Bino, F. A. Cotton and P. E. Fanwick, *Inorg. Chem.* 1979, **18**, 3558.
8. F. A. Cotton and J. J. Wise, *Inorg. Chem.* 1966, **5**, 1200.
9. T. J. Pinnavaia, B. L. Barnett, G. Podolsky and A. Tulinsky, *J. Am. Chem. Soc.* 1975, **97**, 2712.
10. R. Gut and W. Perron, *J. Less-common Metals* 1972, **26**, 369.
11. L. G. Hubert-Pfaltzgraf, M. Tsunoda and D. Katoch, *Inorg. Chim. Acta* 1981, **51**, 81.
12. Structurally characterized Nb(III) and Ta(III) dimers are discussed in: (a) F. A. Cotton and W. J. Roth, *Inorg. Chem.* 1983, **22**, 3654; and (b) F. A. Cotton, S. A. Duraj and W. J. Roth, *Acta. Cryst. C* (in press).
13. R. L. Deutscher and D. L. Kepert, *Inorg. Chim. Acta* 1970, **4**, 645.
14. R. C. Mehrotra, R. Bhora and D. P. Gaur, *Metal β-Diketonates and Allied Derivatives*. Academic Press, New York (1978).
15. B. A. Goodman and J. B. Raynor, *Adv. Inorg. Chem. Radiochem.* 1970, **13**, 135.
16. D. P. Johnson and R. D. Bereman, *J. Inorg. Nucl. Chem.* 1972, **34**, 2957.

Polyhedron Vol. 4, No. 8, pp. 1493–1498, 1985
Printed in Great Britain

0277–5387/85 $3.00 + .00
© 1985 Pergamon Press Ltd

SYNTHESIS, SPECTROSCOPIC PROPERTIES AND CRYSTAL STRUCTURE OF THE EIGHT-COORDINATED LEAD COMPLEX BIS[THIOCYANATO]-1,4,7,10,13-PENTAOXACYCLOPENTADECANO LEAD(II)

H. J. BRÜGGE, R. FÖLSING and A. KNÖCHEL*
Institut für Anorganische und Angewandte Chemie, Universität Hamburg,
Martin-Luther-King-Platz 6, D-2000 Hamburg 13, F.R.G.

and

W. DREIßIG
Institut für Kristallographie, Freie Universität Berlin, Takustr. 6, D-1000 Berlin 33, F.R.G.

(*Received* 13 *August* 1984; *accepted after revision* 12 *February* 1985)

Abstract—The complex [Pbc[15]crown-5]$(SCN)_2$ was synthesized and characterized spectroscopically (IR and FIR range) and the crystal structure was determined by X-ray diffraction on a single crystal (orthorhombic space group $Pmc2_1$). The structure was solved by Patterson synthesis with least-square refinement. The final R-value is 0.0328. Two Pb-atoms and two unidentical halves of the ligand were found in the asymmetric unit. For each complexed lead cation and each half of the crown ether there exists a plane of reflexion, whereby C18 and C28 are disordered. There is, however, no centre of inversion between these unidentical halves. The elementary cell comprises four units and two different types of two centrally coordinated Pb cations. Both lead cations are eight-coordinated. In the case of Pb1 the eight donor centres are the five O-atoms of the ligand and three N-atoms of the thiocyanates. For Pb2 these are five oxygens of the ligand, one nitrogen and two sulphurs of the three thiocyanates. In this complex the thiocyanate ligands occur in both ionic and covalent states. The complexation of the crown ether and the two different species of thiocyanate anions are indicated too by typical shifted absorption bands in the IR spectra. The vibrations in the FIR region can be assigned to the interactions between lead and the donor groups.

The complexation of main-group elements of the periodic system, especially the alkali and earth-alkali metals, by substituted and unsubstituted crown ethers has been widely studied.[1,2] However there is very little analogous work on other elements (metals); in particular the few investigations on the complexation with the ligands [18]crown-6, [15]crown-5 and [12]crown-4 have seldom ended in X-ray structural analysis.[5,6] The lanthanides[3,4,7] and uranium[11] are exceptions. In spite of that there are sufficient data indicating the capability of all metal ions to form complexes with polyethers of different sizes.

In the course of the systematic investigation of the complexation behaviour of the main group elements in the presence of [15]crown-5 we obtained the 1:1 or more correctly the 2:2 complex of $Pb(SCN)_2$.

To elucidate the structural and conformational features of the complex one has to resort to other complexes involving the same ligand for comparison since the necessary information from X-ray diffraction are lacking. Important complexes in this connection are those with direct metal–oxygen interactions such as $[Co(II)L(NO_3)_2]$,[5] $[Eu(III)L(NO_3)_3]$,[7] [NaL SCN][9] and $[Ba(L_2)Br_2]$[8] (L = [15]crown-5).

EXPERIMENTAL

The complex was prepared by reacting freshly distilled [15]crown-5 (Fluka) with $Pb(SCN)_2$ in

* Author to whom correspondence should be addressed.

Table 1. IR and FIR absorptions of the complex [Pbc[15]crown-5]$(SCN)_2$[a]

Wavenumber[b] [cm^{-1}]	Vibration	Assignment
2060 vs	ν C≡N	N-coordinated or ionic SCN
2090 sh	ν C≡N	S-coordinated SCN
1115 m	ν C–O–C	Characteristic ether bands for
1090 vs	ν C–O–C	coordinated cyclic polyethers
1020 m	ν C–O–C	
975 s	d CH_2	Methylene rocking vibration
860 m	ν C–C	Hydrocarbon bridge
568 s	d C–C–O	Deformational vibrations
555 m	d C–C–O	of the ligand
521 s	d C–C–O	
509 m	d C–C–O	
470 s	d SCN	Deformational vibration of
460 s	d SCN	thiocyanate anion
389 m	ν Pb–S	Cation SCN-vibrations
360 s	ν Pb–S	
323 s	ν Pb–N	Cation NCS-vibrations
296 m	ν Pb–N	
281 s	ν Pb–N	
266 m	ν Pb–N	
below 250	ν Pb–O	Stretching and deformational vibrations of the Pb–O-coordination polyhedron

[a] Absorptions below 700 cm^{-1} are recorded with an FT-IR spectrometer.

[b] vs = very strong, s = strong, m = medium, sh = shoulder.

purified methanol. The $Pb(SCN)_2$ was obtained by dissolving freshly precipitated $Pb(OH)_2$ in 5% aqueous HSCN, which in turn was prepared from $Mg(SCN)_2 \cdot 4H_2O$ over an ion exchanger (in the H_3O^+ form). Crystallization took place in methanol/ether (80/20) by gradually lowering the temperature of a thermostat. The compound was characterized by elemental analysis: Calc. (found) Pb: 38.11 (38.2); C: 26.51 (26.42); H: 3.72 (3.80); N: 5.15 (5.18)%; by m.p. (480 K) as well as IR, FIR, ^1H and ^{13}C NMR spectroscopy. The typical IR and FIR bands are listed in Table 1. For IR spectrometry we used a Perkin–Elmer 683 grating spectrometer (Nujol mulls) and a Bruker FT-IR spectrometer (polystyrene matrix).

The NMR spectra were recorded on a Bruker WH 80 spectrometer in about 0.01 M solution in CD_3CN (^1H) and saturated solution in CH_3OH/CH_3OD (^{13}C) at room temperature with TMS as internal standard.

The colourless compound crystallizes in the orthorhombic system with $a = 1236.6 \pm 0.2$ pm, $b = 865.1 \pm 0.1$ pm, $c = 1679.9 \pm 0.2$ pm and belongs to a space group $Pmc2_1$. $V = 1797.13$ nm^3, $Z = 4$ ($8 \times 1/2$), crystal size = $0.11 \times 0.2 \times 0.5$ mm; density (calc.) = 2.009 g cm^{-3}.

The crystal was measured at room temperature on a STOE four-circle automatic diffractometer using Ni-filtered Cu-K_α radiation. From the 1667 reflexes collected ($2.5 < 2\theta < 64.5$) 1649 were found to be independent of symmetry.

The structure was solved by the Patterson synthesis. Programs used and structural factors are cited in the appendix.[10] The refinement was accomplished with the help of the least squares method employing an isotropic extinction function which is based on the absorption-corrected data ($\mu = 204$ cm^{-1}). All hydrogen atoms were placed at calculated positions, with a temperature factor of $u = 5.7$ pm^2 and at a distance of 105 pm from the

Table 2. Bonding distances of selected atoms and selected angles in the molecule—standard deviations are given in parentheses

Pb1–O11	284.3(1.4)	N1–Pb1–N3	83.4(0.6)
Pb1–O14	274.0(1.0)	N3–Pb1–N3′	91.5(0.6)
Pb1–O17	285.2(1.3)	N2–Pb2–S3	74.0(0.5)
Pb2–O21	253.1(1.4)		
Pb2–O24	265.9(1.0)	SCN1	178.6(2.1)
Pb2–O27	282.2(1.2)	C1–N1–Pb1	165.3(1.9)
C1–S1	165.1(1.9)	SCN2	179.5(2.5)
C1–N1	110.9(2.6)	C2–N2–Pb2	176.4(2.0)
N1–Pb1	249.5(2.0)		
C2–S2	159.0(2.1)	SCN3	174.9(1.7)
C2–N2	113.1(3.1)	N3–S3–Pb2	115.5(0.6)
N2–Pb2	243.6(3.5)	C1–N3–Pb1	168.9(1.6)
C3–S3	161.3(1.8)	C12′–O11–C12	113.9(1.2)
C3–N3	121.9(2.5)	O11–C12–C13	105.7(1.3)
N3–Pb1	253.2(1.9)	C12–C13–O14	110.7(1.3)
S3–Pb2	324.3(0.4)	C13–O14–C15	112.1(2.5)
		O14–C15–C16	110.3(1.4)
O11–C12	146.9(1.7)	C15–C16–O17	107.8(1.5)
C12–C13	145.0(2.3)	C16–O17–C181	130.8(2.1)
C13–O14	142.0(2.0)	C16–O17–C182	98.6(1.8)
O14–C15	146.4(2.0)	O17–C181–C182′	103.8(2.7)
C15–C16	143.4(2.5)	O17–C182–C181′	97.3(2.1)
C16–O17	142.8(2.6)		
O17–C181	146.5(4.3)	C22–O21–C22′	113.0(1.4)
O17–C182	151.7(3.9)	O21–C22–C23	106.6(1.3)
C181–C182	160.9(5.6)	C22–C23–O24	108.5(1.2)
		C23–O24–C25	115.0(1.1)
O21–C22	138.9(2.0)	O24–C25–C26	112.1(1.2)
C22–C23	149.3(2.5)	C25–C26–O27	107.7(1.4)
C23–O24	146.8(2.4)	C26–O27–C281	129.5(1.6)
O24–C25	138.0(1.8)	C26–O27–C282	100.4(1.8)
C25–C26	149.8(2.4)	O27–C281–C282′	103.8(2.9)
C26–O27	143.8(2.2)	O27–C282–C281′	101.0(2.4)
O27–C281	155.8(4.0)		
O27–C282	152.3(3.9)		
C281–C282′	142.0(3.6)		

C-atoms. The final R-value is 0.033. In Table 2 are listed interatomic distances and interbond angles. Relevant dihedral angles are presented in Table 3.*

DISCUSSION

When $Pb(SCN)_2$ complexes the polyether [15]crown-5 eight-coordination around Pb is retained. The occupation and therefore the geometry of the coordination polyhedron are however altered.

The IR-absorption bands of the thiocyanate indicate a change of coordination of the SCN^- in $Pb(SCN)_2$ upon complexation with crown ether, i.e. from S to N. A shoulder at higher wave number represents SCN^- coordinated through sulphur. In the crystal structure this can be correlated well with the position of the SCN found generally (No. 3) (Fig. 1).

Furthermore, the intensities of these bands reveal that there has been a change in the ratio of coordination of the anions between N and S.

The C–O–C valence vibrations of the crown ether are shifted to lower wave numbers upon complexation. Noteworthy in this connection. is the appearance of three bands which can be correlated with the three different cation–oxygen donor distances shown by the X-ray diffraction analysis.

* Final atomic coordinates, thermal parameters and lists of F_o/F_c values have been deposited as supplementary data with the Editor, from whom copies are available on request. Atomic coordinates have also been deposited with the Cambridge Crystallographic Data Centre.

Table 3. Selected torsion angles (°)

O11–C12–C13–O14	58.5(1.6)
O14–C15–C16–O17	69.2(2.1)
O17–C181–C182′–O17′	75.3(2.2)
O21–C22–C23–O24	61.4(1.6)
O24–C25–C26–O27	66.0(1.8)
O27–C281–C282′–O27′	77.4(1.7)
C12′–O11–C12–C13	173.1
C12–C13–O14–C15	(−)165.0
C13–O14–C15–C16	83.2
C15–C16–O17–C182	(−)170.9
C15–C16–O17–C181	162.2
C16–O17–C181–C182′	92.1
C16–O17–C182–C181′	173.3
C22′–O21–C22–C23	167.1
C22–C23–O24–C25	(−)167.3
C23–O24–C25–C26	84.1
C25–C26–O27–C281	170.6
C25–C26–O27–C282	(−)165.3
C26–O27–C281–C282′	84.0
C26–O27–C282–C281′	177.9

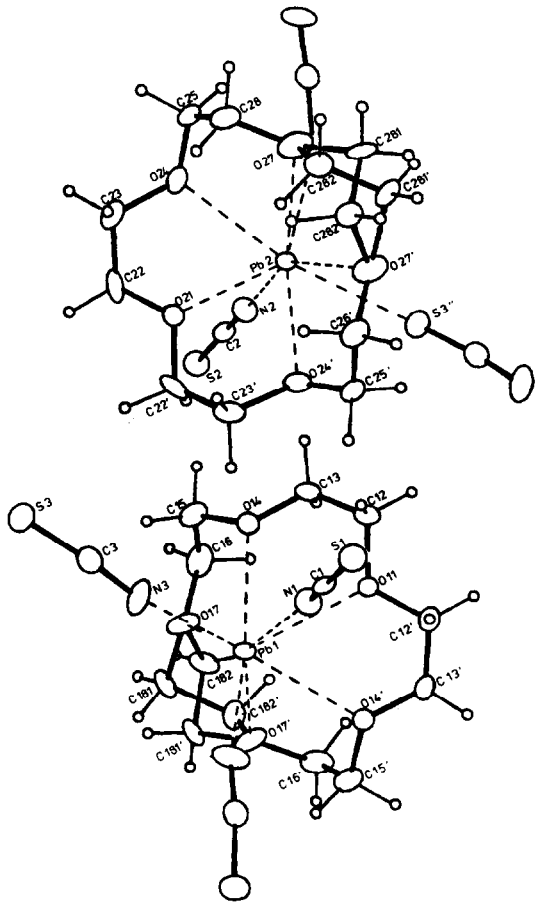


Fig. 1. ORTEP drawing of the asymmetric unit.

Complexes with approximately equal cation–donor distances do not exhibit such large splittings.

In the FIR region, between 700 and 100 cm^{-1} (Fig. 3) several absorptions appear, which cannot be assigned unambiguously. Absorptions between 568 and 509 cm^{-1} represent deformational vibrations of the macrocyclic ligand. The split strong band at 470/460 cm^{-1} again shows the deformation of the two types of thiocyanate. Bands below 400 cm^{-1} represent the different vibrations between the lead cation and sulphur (389, 360 cm^{-1}) and nitrogen (323, 296, 281, 266 cm^{-1}). This attribution of thiocyanate-cation vibrations is analogous to attributions in the cited literature.[13]

The bands below 250 cm^{-1} can be assigned to the stretching vibrations between Pb^{2+} and the ether oxygens and the deformation vibrations of the coordination sphere of the cation.

In the uncomplexed $Pb(SCN)_2$, lead is coordinated in a distorted tetragonal antiprism, in which each plane is formed by two nitrogen and two sulphur atoms.[12] Upon complexation to the crown ether the coordination polyhedron of the metal is changed to a pseudo-antiprism the base of which is formed by the five O-atoms of the polyether and the upper surface by the donors of the thiocyanates. In the case of Pb1 only N-donors form the upper surface of the pseudo-antiprism whereas two S and one N

Table 4. Comparison of the torsion angles with those of some other crown ether complexes

Torsion angle (atom number)	(L = [15]crown-5) (°) Pb1 L1	Pb2 L2	Ba L1 [8]	Ba L2	NaL [9][a]	NaL	Eu L [7]
1, 2, 3, 4	58.5	61.4	53	57	61	62	64
4, 5, 6, 7	69.2	66.0	61	81	66	62	4
7, 8, 8′, 7′	75.3	77.9	67	60	58	58	38
7′, 6′, 5′, 4′	69.2	66.0	62	33	65	66	53
4′, 3′, 2′, 1	58.5	61.4	57	66	59	55	69

[a] The two columns represent the disorder in the ligand.

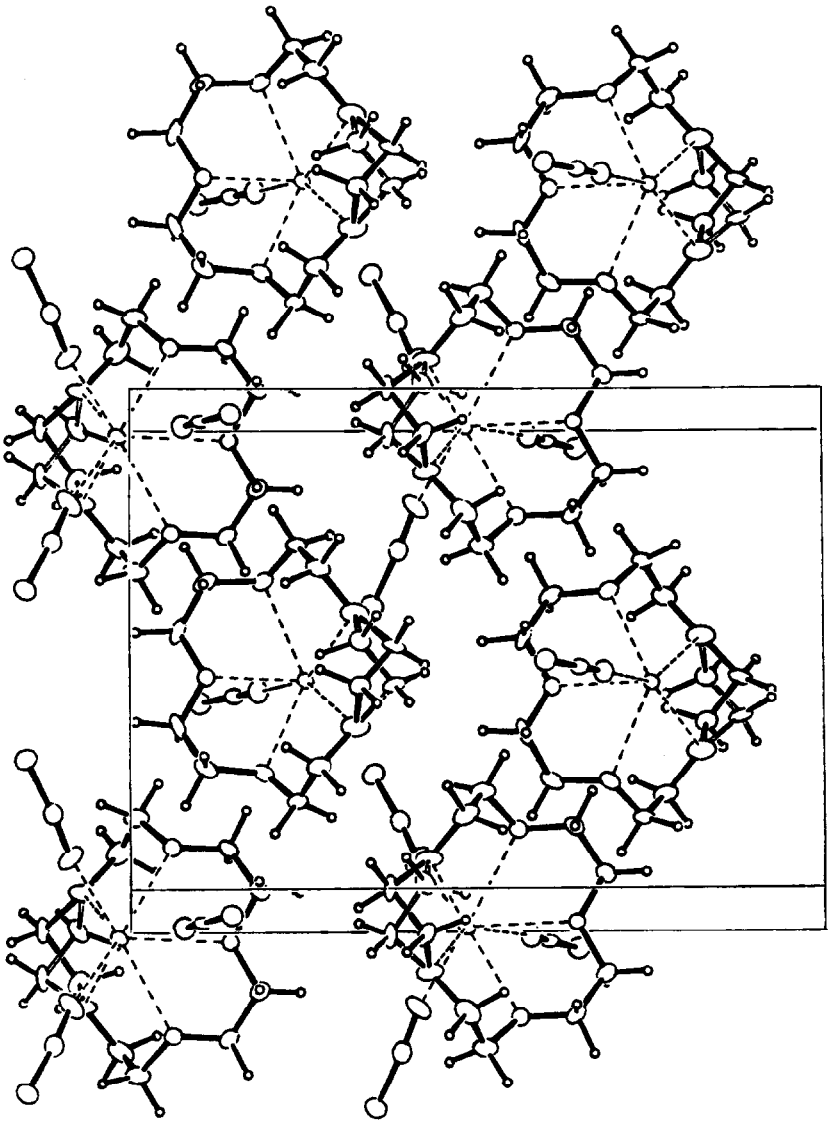


Fig. 2. ORTEP drawing of the unit cell contents.

atom are involved in the case of Pb2. This situation explains the splitting and the ratio of the intensities of the ν_{CN} bands encountered in the IR spectrum.

The ^{1}H NMR spectrum of the complex shows two signals at 3.74 and 3.81 ppm which were slightly shifted to lower field compared to the uncomplexed ligand (3.58 ppm). These two signals represent the two different species of macrocyclic ligand in the complex.

In contrast to the ^{1}H NMR, the ^{13}C NMR signal of the complex shows no significant change in chemical shift compared with that of the free polyether.

A conspicuous feature of this structure is that the asymmetric unit contains two halves of the crown ether and two lead cations and so, despite the formal 1 : 1-stoichiometry, both central cations have different environments. It is not uncommon that in sandwich complexes like $[Ba(L_2)Br_2]$[8] two different conformations of the ligand about a central atom are possible. The occurrence in the crystal lattice of two alternative conformations, each bearing a central atom is, on the contrary, unprecedented (Fig. 2: elementary unit cell). The two ligands in the Ba^{2+} complex have different energies as can be deduced from the deviation of the dihedral angle of the O–C–C–O unit from the theoretical 60°.

A comparison of the dihedral angles of the $Pb(SCN)_2$ complex with those of the complexes in Table 4 reveals that the conformation of the ligand in the lead complex assumes an intermediate position, although the C18 and C18′ as well as the C28 and

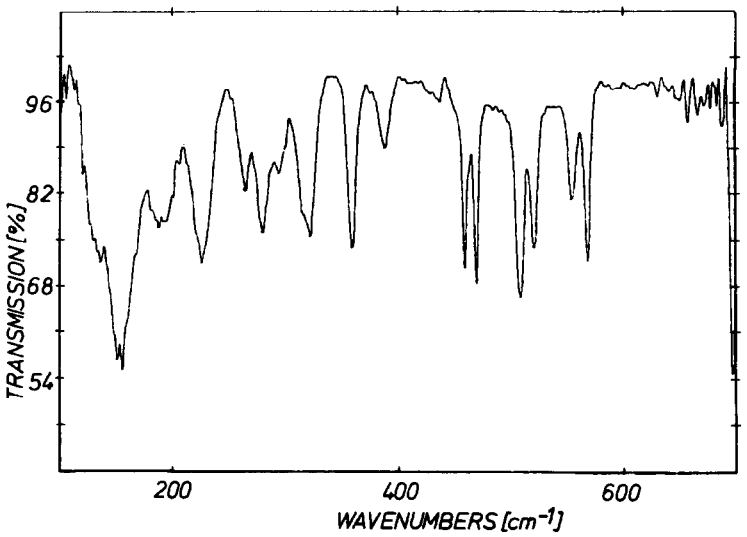


Fig. 3. FT-IR-spectrum of [Pbc[15]crown-5](SCN)$_2$.

C28′ are disordered. A special characteristic of the complex is the alternating position of the disorder in the crystal lattice (Fig. 2). A look at the planes described by the polyether shows a displaced sandwich structure in which the enclosed lead atoms are facing themselves. In spite of that there are no direct Pb–Pb interactions; the Pb–Pb distance is 775 pm. The deviations of the atoms and the distance of the lead atoms from the best planes are summarized in Table 5.

Table 5. Deviations of the oxygens from the plane and some other distances in the coordination sphere of lead

Ring 1 (O11, O14, O17, O14′ and O17′)	
O11	−47.9 pm
O14 (O14′)	34.3 pm
O17 (O17′)	−10.4 pm
distance of Pb from ringplane	
Pb1	157.4 pm
distance of coordinated nitrogen	
N1	261.2 pm
N3 (N3′)	327.7 pm
Ring 2 (O21, O24, O27, O27′ and O24′)	
O21	39.9 pm
O24 (O24′)	−29.0 pm
O27 (O27′)	9.0 pm
distance of Pb from ringplane	
Pb2	−135.9 pm
distance of coordinated nitrogen and sulfur	
N2	−277.9 pm
S3 (S3′)	375.8 pm

The angle between ring 1 and ring 2 amounts to 0.5°.

Acknowledgements—We thank Prof. P. Gütlich (Mainz, F.R.G.) for performing the FT–IR spectra and the Fond der Chemischen Industrie for financial support.

REFERENCES

1. J. D. Dunitz, M. Dobler, P. Seiler and R. P. Phizackerley, *Acta Cryst. B* 1974, **30**, 2733.
2. R. Hilgenfeld and W. Sänger, *Top. in Curr. Chem.* 1982, 101.
3. J. C. G. Bünzli, B. Klein and D. Wessner, *Inorg. Chim. Acta Lett.* 1980, **44**, L147.
4. M. E. Harman, F. A. Hart, M. B. Hursthouse, G. P. Moss and P. R. Raithby, *J. Chem. Soc., Chem. Commun.* 1976, 396.
5. E. M. Holt, N. W. Alcock, R. R. Hendrixson, G. D. Malpass, Jr., R. G. Ghirardelli and R. A. Palmer, *Acta Cryst. B.* 1981, **37**, 1080.
6. A. Knöchel, J. Kopf, J. Oehler and G. Rudolph, *Inorg. Nucl. Chem. Lett.* 1978, **14**, 61.
7. J. C. G. Bünzli, B. Klein, D. Wessner and N. W. Alcock, *Inorg. Chim. Acta* 1982, **59**, 269.
8. J. Feneau-Dupont, E. Arte, J. P. Declerq, G. Germain and M. V. Meersche, *Acta Cryst. B* 1979, **35**, 1217.
9. P. Groth, *Acta Chem. Scand.* 1981, **A35**, 721.
10. (a) M. Steward, *The XRAY 76 System*, Techn Reports TN 446; Comp. Sc. Cent., Univ. of Maryland, Coll. Park, Maryland; (b) *International Tables for X-Ray Crystallography*, Vol. III. Kynoch Press, Birmingham (1974); (c) D. T. Cromer and J. B. Mann, *Acta Cryst. A* 1968, **24**, 321; (d) R. F. Steward, E. R. Davidson and W. T. Simpson, *J. Chem. Phys.* 1965, **42**, 3175.
11. G. Bombieri, G. DePaoli, A. Cassol and A. Immirzi, *Inorg. Chim. Acta* 1976, **18**, L23.
12. J. A. A. Macuolu and J. C. Speakman, *Acta Cryst. B* 1975, **31**, 172.
13. (a) D. Forster and D. M. L. Goodgame, *Inorg. Chem.* 1965, **4**, 715; (b) J. Weidlein, U. Mueller and D. Dehnicke, *Schwingungsspektroskopie.* Verlag Thieme, Stuttgart (1982).

Polyhedron Vol. 4, No. 8, pp. 1499–1505, 1985
Printed in Great Britain

0277–5387/85 $3.00 + .00
© 1985 Pergamon Press Ltd

SPECTROSCOPIC INVESTIGATION OF ADSORBED 7-(4-ETHYL-1-METHYLOCTYL)-8-QUINOLINOL (KELEX 100) AND OF ITS GALLIUM(III) COMPLEX: COMPARISON WITH THE BEHAVIOURS OBSERVED IN SOLVENT EXTRACTION SYSTEMS

LILIANE BOKOBZA
Laboratoire de Physico-Chimie Structurale et Macromoléculaire, E.S.P.C.I., 10 rue Vauquelin, 75231 Paris Cedex 05, France

and

GÉRARD COTE*
Laboratoire de Chimie Analytique (Unité de Recherche Associée au C.N.R.S. 437), E.S.P.C.I., 10 rue Vauquelin, 75231 Paris Cedex 05, France

(*Received* 2 *January* 1985; *accepted* 12 *February* 1985)

Abstract—The adsorption of a long hydrocarbon chain oxine derivative, 7-(4-ethyl-1-methyloctyl)-8-quinolinol, on the macromolecular Amberlite XAD-7 support is shown by FT-IR spectroscopy to be the result of only weak extractant–support interactions. It is also shown that the chelation ability of the extractant towards gallium(III) does not suffer from the presence of the solid support. Finally the stereochemistry (*fac* or *mer* configuration) of the tris-7-(4-ethyl-1-methyloctyl)-8-quinolinato gallium(III) complex formed either in solution in an organic diluent or on the support is discussed on the basis of ^{1}H and ^{13}C NMR and FIR data.

Solvent-impregnated resins have attracted considerable attention since selective liquid ion-exchangers such as LIX 63 (an aliphatic alpha-hydroxyoxime), Kelex 100 (an 8-quinolinol derivative), etc., and high specific area macroreticular adsorbents have become commercially available. Indeed, the combination of appropriate extractants, adsorbents and eventually additives allows the formulation of efficient reactive resins for both analytical and industrial purposes.

In the present work we consider the chelation of gallium(III) in alkaline media (0.5 to 4 M NaOH) by a long hydrocarbon chain oxine derivative, 7-(4-ethyl-1-methyloctyl)-8-quinolinol, adsorbed on a macromolecular resin, the Amberlite XAD-7 support. The 7-alkyl-8-quinolinols are important in the hydrometallurgy of gallium[1] and germanium,[2–4] and their impregnated forms could be particularly well adapted for the recovery of traces of these two metals from zinc sulphate (Ge), zincate (Ga) or aluminate (Ga) solutions. Up to date, little has been done to elucidate the behaviours of impregnated extractants. Two papers published recently have proposed the use of ESR spectroscopy for elucidating the properties of grafted[5] or impregnated[6] chelating agents. However, the technique is limited to the study of the paramagnetic complexes such as those of copper(II). EXAFS spectroscopy has also been proposed,[7] but has not yet been widely used. Our investigation of the 7-(4-ethyl-1-methyloctyl)-8-quinolinol impregnated support is mainly based on FT-IR spectroscopy.

7-(4-Ethyl-1-methyloctyl)-8-quinolinol, a pale yellow viscous liquid at room temperature easily soluble in the organic solvents but insoluble in water,[8] is the main active component of a commercially available product (post-1976) Kelex 100 from Shering. The first spectroscopic investigation of Kelex 100 was reported by Ashbrook in 1975.[9] At that time, the active substance of Kelex 100 was 7-(1-ethenyl-3,3,5,5-tetramethylhexyl)-8-quinolinol. The IR evidence then given concerned only the presence of a C=C double bond in the substituent group and the involvement of the phenolic OH function in intramolecular hydrogen bonding. More recently, Demopoulos and Distin[10]

* To whom the correspondence should be addressed.

have identified the major constituents of post-1976 Kelex 100 by GLC, mass spectrometry and IR spectroscopy. The IR absorption spectra of vacuum distilled Kelex 100 (a two component-product) and of its copper chelate have been reported (4000–500 cm^{-1}), but some of the assignments given are speculative. Kelex 100 has not yet received much attention from the NMR spectroscopists. Indeed, only its ^1H NMR spectrum (for pre-1976 Kelex 100) has been partially reported.[9] On the other hand, an interesting literature has been published on ^1H and ^{13}C NMR spectroscopy of various oxine derivatives.[11–17]

In liquid–liquid systems (e.g. water/dodecane), 7-(4-ethyl-1-methyloctyl)-8-quinolinol forms with gallium(III) a three-liganded complex, GaL_3, the structure of which is assumed, as the one of the tris-chelated metal oxinates to be octahedral.[18] Nevertheless, no spectroscopic evidence of this has been given.

Due to the absence of comprehensive bibliographical data, the IR spectra of non-adsorbed 7-(4-ethyl-1-methyloctyl)-8-quinolinol and of its gallium(III) complex have been carefully examined in this work, preliminary to the study of the adsorbed species. This IR investigation has been complemented by Raman spectroscopy.

EXPERIMENTAL

(1) *Reagents*

7-(4-Ethyl-1-methyloctyl)-8-quinolinol (HL) was isolated from Kelex 100 (Shering) by: (i) vacuum distillation, (ii) precipitation and recrystallization of its lead complex, (iii) regeneration with 2 M H_2SO_4, and finally (iv) vacuum distillation.[18] Found (calc.): C, 80.27 (80.27); H, 9.82 (9.70); N, 4.51 (4.68); O, 5.16 (5.35)%.

Gas chromatography revealed that the product so obtained contained only one component, whereas Kelex 100 purified by a mere vacuum distillation was a three-component product (approx. percentage: 87, 10 and 3%). The molecular mass deduced from the mass spectrum of completely purified Kelex 100 (one component) was 299 as expected.

Tris-7-(4-ethyl-1-methyloctyl)-8-quinolinato gallium(III) complex (GaL_3) was obtained by mixing a 0.12 M solution of HL in hexane with a 0.4 M aqueous alkaline (1 M NaOH) solution of gallium(III). At the equilibrium, the two phases were separated. The hexane solution was then filtered on Whatman ^{1}PS phase separator and pumped dry to give a bright yellow compound. All attempts at recrystallization have failed to produce a crystalline solid. Found (calc.): C, 74.96 (74.71); H, 8.63 (8.72); N, 4.19 (4.36); Ga, 6.74 (7.23)%; Na < 50 ppm (0).

Tris-8-quinolinato aluminium(III) complex [$Al(Ox)_3$] was prepared by precipitation from homogeneous solution.[19] Found (calc.): C, 70.10 (70.53); H, 4.02 (3.92); N, 9.07 (9.14); Al, 5.75 (5.88)%.

The Amberlite XAD-7 resin (Serva) of practical grade quality was carefully washed with ethanol and water, and impregnated with HL in a classical way.[20,21] For gallium(III) fixation, the impregnated support was equilibrated with an aqueous alkaline (0.5 to 4 M NaOH) solution of gallium(III) prepared from gallium oxide (Rhône-Poulenc Co). After separation of the two phases, the gallium loaded resin was rinsed with water and dried before spectroscopic investigation.

The other reagents from Prolabo were all analytical grade.

(2) *Apparatus*

The spectroscopic instruments used were a Nicolet 7199 Fourier transform infrared spectrometer (4000–400 cm^{-1}) [32 co-added interferograms were scanned at 2 cm^{-1} resolution] and an IFS 113 V Bruker Fourier transform infrared spectrometer (400–60 cm^{-1}) [100 co-added interferograms were scanned at 4 cm^{-1} resolution] for FT-IR and far FT-IR spectroscopy, respectively; a T 800 Coderg model for Raman spectroscopy; a Varian EM 390 model (^1H) and a Varian FT 80 A model (^{13}C) for NMR measurements. The chemical shifts (δ) are referenced to Me_4Si (^1H and ^{13}C). Gas chromatography analyses were performed with an IGC 16 Intersmat chromatograph equipped with a 1.50 m 10% SE 30/PAW 60/100 column ($\phi = 1/8$). Mass spectra were recorded by the Laboratoire de Spectrométrie de Masse (E.N.S.C.P., Paris) with a Ribermag 10-10 mass spectrometer.

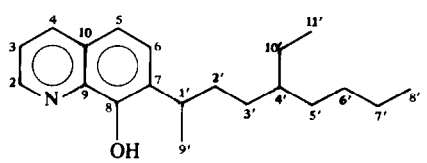
(3) *Analytical*

Microanalyses were performed by the Service Central d'Analyse (CNRS, Vernaison). Gallium(III) titrations in aqueous phases were carried out by atomic absorption spectrophotometry (at 294.4 nm) in an air–acetylene flame with a Varian AA6 spectrophotometer.

RESULTS AND DISCUSSION

(1) 7-(4-*Ethyl*-1-*methyloctyl*)-8-*quinolinol* (HL)

The formula of 7-(4-ethyl-1-methyloctyl)-8-quinolinol is given below:



The structure of the alkyl chain has been confirmed by selective irradiation NMR measurements.[22]

(a) *The non-adsorbed molecule.* The IR spectra of HL (spectrum 1 in Fig. 1 and 1 in Fig. 2) differ significantly from the one reported by Demopoulos and Distin[10] for vacuum distilled Kelex 100 (a two component product), especially in the range of the C–H stretching frequencies. Our spectrum exhibits four strong bands (*c*, *d*, *e* and *f* in Fig. 1) at 2957, 2927, 2871 and 2858 cm^{-1}, ascribed to the stretching modes of the methyl and methylene groups, and a weak band (*b*) at 3055 cm^{-1} corresponding to an aromatic C–H stretching vibration.

The band (*a*) at 3386 cm^{-1} is due to the stretching frequency of the intramolecularly hydrogen-bonded O–H group. Upon dilution of HL in carbon tetrachloride to 5×10^{-3} mole l^{-1} (2 mm cell path) this band still located at 3395 cm^{-1} confirms the presence of the chelate species.

By comparison with other heteroatomic cycles like pyridine, naphthalene, quinolines and phenols,[23] the bands observed at 1576 (*g*), 1505 (*h*), 1463 (*i*), 1435 (*j*), 1408 (*k*), 1376 (*l*) and 1331 (*m*) cm^{-1} are assigned to ring vibrations. These modes give rise to strong Raman lines. The 1463 and 1376 cm^{-1} bands also contain contributions due to the bending modes of the methyl and methylene groups.

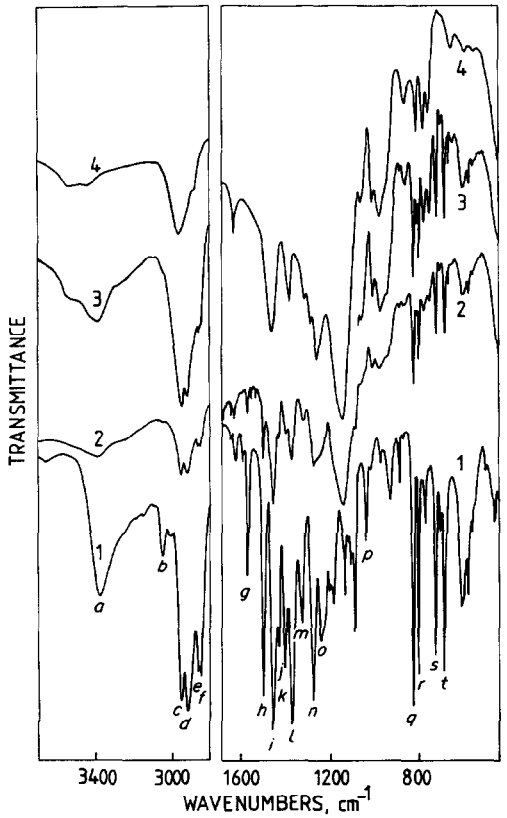


Fig. 1. IR spectra of (1) HL as a film on a CsBr disc; (2) HL 0.73 g/g on Amberlite XAD-7 [KBr pellet]; (3) HL 0.31 g/g on Amberlite XAD-7 [KBr pellet]; (4) Amberlite XAD-7 [KBr pellet].

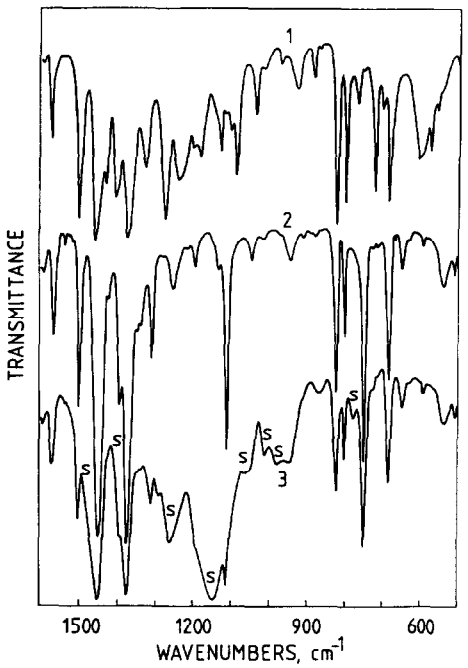


Fig. 2. IR spectra of (1) HL as a film on a CsBr disc; (2) GaL_3 as a film on a CsBr disc; (3) HL 0.73 g/g on Amberlite XAD-7 after complete reaction with gallium(III) [KBr pellet]. (S = support.)

The two bands occurring in substituted phenols between 1200 and 1300 cm^{-1} represent O–H deformation and C–O stretch which interact somewhat. Following Sharma *et al.*[23] and Mecke and Rossmy,[24] but in disagreement with Demopoulos and Distin,[10] the highest of the two frequencies located at 1279 cm^{-1} (*n*) is assigned to the C–O stretching mode whereas the band at 1244 cm^{-1} (*o*) is attributed to the O–H in-plane bending mode.

The ring breathing vibration is well known to give rise to a very strong and polarized band in the Raman spectrum. It is the reason why we assign this mode to the strongest Raman band at 724 cm^{-1} and, at the same frequency, to the strong band (*s*) observable on the IR spectrum. In the same spectral range, the IR bands at 826 (*q*), 803 (*r*) and 687 (*t*) cm^{-1} correspond to the out-of-plane C–H bending vibrations of the aromatic ring.

The Raman spectrum presents a strong band at 1040 cm^{-1} corresponding probably to a ring vibration and four bands at 429, 460, 501 and 560 cm^{-1}. The first two bands are assigned, by analogy with pyridine, to out-of-plane ring deformations, and the two others to in-plane ring deformations.

(b) *The adsorbed molecule.* Two impregnated supports containing respectively 0.31 and 0.73 g/g of HL (gram of HL per gram of dry Amberlite XAD-7 resin) have been prepared and investigated. It must be pointed out that, in the two cases, the content of HL is significantly lower than the loading capacity of the support (about 1.7 g/g),[3] so that all HL is presumably adsorbed on the inner surface (specific area: 450 m^2/g)[25] of the support, and not merely retained by capillarity in its pores.

The IR spectra of the two impregnated supports have been recorded (spectra 2 and 3 in Fig. 1). Examination of these spectra shows that the retention of the 7-(4-ethyl-1-methyloctyl)-8-quinolinol molecules by the Amberlite XAD-7 support does not involve any significant shift in the frequency of the normal modes of the alkyl chain or of the cycles of these extractant molecules: e.g. band *c* 2957.4[(i)], 2959.8[(ii)], 2959.9[(iii)] and 2958.7[(iv)], band *s* 724.5[(i)], 724.0[(iii)] and 724.1[(iv)] with: (i) HL as a film on a CsBr disc, (ii) HL in solution (5×10^{-3} M) in CCl_4, (iii) HL on XAD-7 (0.31 g/g) and (iv) HL on XAD-7 (0.73 g/g). Such an observation suggests that there is no strong interaction between HL and the support.

(2) *Tris-[7-(4-ethyl-1-methyloctyl)-8-quinolinato] gallium*(III), GaL_3

(a) *The non-adsorbed complex.* In liquid–liquid systems (e.g. water/dodecane), HL has been shown by the slope analysis technique to form a three-liganded complex of gallium(III): GaL_3.[18] Microanalysis obtained for the compound isolated from an hexane solution of HL treated with a large excess of gallium(III) (in solution in aqueous 1 M NaOH) confirm this result (experimental section). The tris-[7-(4-ethyl-1-methyloctyl)-8-quinolinato] gallium(III) complex has been investigated in the present work both by IR spectroscopy and NMR spectrometry.

IR (4000–400 cm^{-1}). The IR spectrum of gallium(III) loaded 7-(4-ethyl-1-methyloctyl)-8-quinolinol shows several modifications compared with the spectrum of the free reagent (spectra 1 and 2 in Fig. 2). The main change is the shift of the C–O stretching frequency from 1279 to 1114 cm^{-1}. The band at 1114 cm^{-1} has already been observed by Rane and Ravi[26] in the IR spectra of cobalt(II) and nickel(II)-8-quinolinates, and is taken by the authors as a characteristic band for the identification of the bond between the metal ion and the 8-quinolinate anion through oxygen.

Apart from the expected effects related to hydrogen replacement in the O–H group, some fundamental frequencies suffer significant shifts on coordination to the metal. As an example, the breathing mode shifts from 724 to 751 cm^{-1}. A similar effect was also observed when pyridine is coordinated and was explained by Filimonov and Bystrov[27] by an increase in the sigma nature of the carbon–nitrogen bonds of the ring, increase which strengthens these bonds.

FIR (500–80 cm^{-1}). In the FIR region, the metal–ligand vibrations ν(Ga–O) and ν(Ga–N) are expected. The vibrational analysis can give information about the structure of the complex and the strength of the metal–ligand bonds. As the normal tris metal oxinates $M(Ox)_3$, GaL_3 is expected to be octahedral. However, the complex can exist in *fac* (1,2,3 isomer) and *mer* (1,2,6 isomer) forms. In the *fac* isomer all three chelate rings are geometrically and magnetically equivalent; conversely, in the *mer* isomer they are not. On the basis of their ^1H NMR spectra, the aluminium(III), cobalt(III) and rhodium(III) oxinates have been shown to contain three unequivalent ligands, and logically to exist in solution in their *mer* configuration.[11] Nevertheless in a previous work[28] based on FIR data, the conclusion was reached that $Co(Ox)_3$ might exist in solution only as the *fac* isomer, whereas the solutions of $Al(Ox)_3$ and $Fe(Ox)_3$ might contain a mixture of the *fac* and *mer* isomers. More recently, Ohkaku and Nakamoto[29] concluded from the presence of only four metal–ligand bands (identified by the metal isotope technique) in the FIR region that $Fe(Ox)_3$ is *fac* in the solid state.

The *fac* configuration of octahedral GaL_3 would be of C_3 symmetry, whereas the *mer* configuration would be of C_1 symmetry. In C_3 symmetry, one expects four IR-active metal–ligand stretching bands ($2A + 2E$), whereas six bands are expected for C_1 symmetry. The IR spectrum of GaL_3 (spectra 1 and 2 in Fig. 3) presents a simple pattern in the FIR region: a strong and large band (a') at 299 cm^{-1} (304 cm^{-1} in solution), a weaker band (b') at 240 cm^{-1} (241 cm^{-1} in solution) and a very weak band (c') at 213 cm^{-1}. The two strongest bands (a' and b') must be assigned to the metal–ligand stretching frequencies since the free ligand exhibits only weak absorptions in that spectral range (spectrum 6 in Fig. 3). The assignment of these two modes were drawn according to the work of Ohkaku and Nakamoto[29] on metal complexes of 8-hydroxyquinoline. Their analysis using the metal isotope technique points out that in the IR absorption spectrum the metal–oxygen stretching band is generally more intense and located at a higher frequency than the metal–nitrogen stretching band. Therefore the strong band (a') at 299 cm^{-1} is assigned to the Ga–O stretching mode, whereas the weaker one (b') at 240 cm^{-1} is assigned to the Ga–N stretching mode. The few

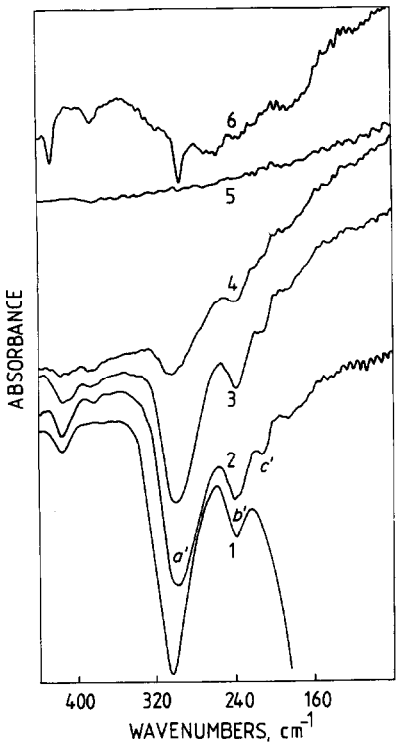


Fig. 3. FIR spectra of (1) GaL_3 in solution (0.3 M) in cyclohexane [recorded in a 5×10^{-5} m width CsI cell with a Perkin–Elmer 983 IR spectrometer]; (2) GaL_3 as a film on a polyethylene disc; (3) HL 0.73 g/g on Amberlite XAD-7 after complete reaction with gallium(III) [polyethylene pellet]; (4) = (3) but with HL 0.31 g/g; (5) = (2) but before reaction with gallium(III); (6) pure HL between two discs of polyethylene.

bands obtained in the spectrum of GaL_3 may support the hypothesis of a *fac* configuration. In this hypothesis, the bands *a'* and *b'* would correspond to the Ga–O (*E*) and Ga–N (*E*) stretching modes, respectively, and the weak band *c'* at 213 cm^{-1} might be attributed to the Ga–N (*A*) vibration. Indeed, the *A* vibration is usually less intense than the *E* vibration.[29] As for the Ga–O (*A*) stretching mode, it could give rise to a band overlapped with the Ga–O (*E*) vibration and appearing in the large and strong band *a'*. The comparison with the spectrum of $Fe(Ox)_3$ which is believed to be *fac* octahedral[29] reveals an interesting similarity: ν(Fe–O) (*E*) 314.9 cm^{-1} (very strong), ν(Fe–O) (*A*) 280.5 cm^{-1} (weak), ν(Fe–N) (*E*) 259.5 (medium), ν(Fe–N) (*A*) 201.5 cm^{-1} (weak and overlapped with a ligand band). In contrast, the spectrum of $Al(Ox)_3$ which is believed to be at least partially *mer* octahedral is more complex.[28]

NMR. The ^1H NMR spectrum of 7-(4-ethyl-1-methyloctyl)-8-quinolinol presents six signals between 7 and 9 ppm (spectrum 1 in Fig. 4), one multiplet at 3.40 ppm corresponding to H'_1 and three groups of multiplets at about 1.68, 1.23 and 0.80 ppm associated with the other aliphatic protons. On coordination with gallium(III), the hydroxyl proton signal disappears and the chemical shift values for some of the aromatic ligand protons are shifted substantially. In fact, the shape of the aromatic part of the ^1H NMR spectrum of GaL_3 greatly depends on the temperature. At low temperature (−14°C), this spectrum presents at least two, possibly three, separate sets of ligand resonances whereas at high temperature (+55°C) there is a collapse to a single set of ligand resonances (spectra 2–4 in Fig. 4). The signals associated with the protons H_2 are the most illustrative. Indeed, at 55°C the three protons H_2 of GaL_3 give rise to a single peak at about 8.2 ppm ($CDCl_3$) but on cooling this signal separates into two different signals, the first at about 8.7 ppm (CD_2Cl_2) corresponding to two protons H_2 and the second appearing between 6.8 and 7.6 ppm and associated with the third proton H_2. Such a phenomenon has already been reported by Baker and Sawyer[11] for the aluminium oxinate $Al(Ox)_3$, but in this latter case the separate sets of ligand resonances were observable at room temperature (spectrum 5 in Fig. 4) and the collapse required a temperature of 115°C.

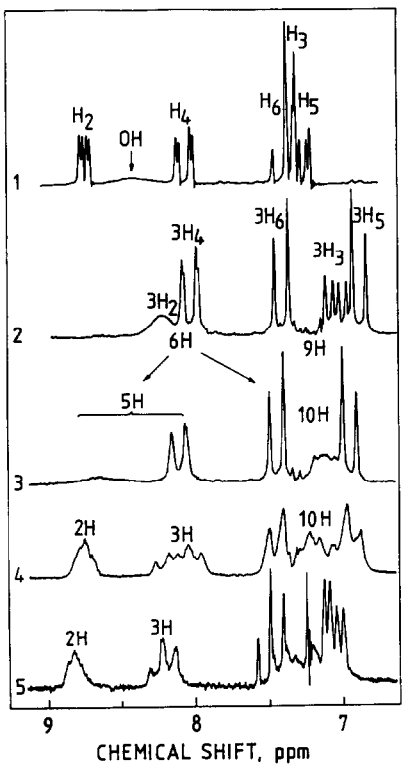


Fig. 4. ^1H NMR spectra of (1) HL in $CDCl_3$ at 33°C; (2) GaL_3 in $CDCl_3$ at 55°C; (3) GaL_3 in CD_2Cl_2 at 33°C; (4) GaL_3 in CD_2Cl_2 at −14°C; (5) $Al(Ox)_3$ in $CDCl_3$ at 33°C.

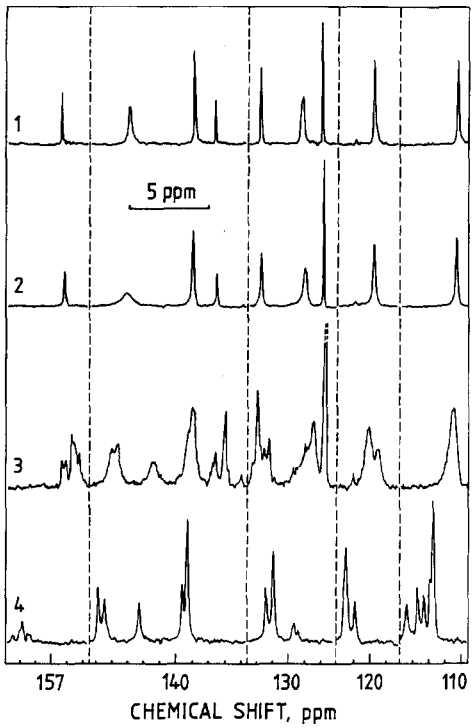


Fig. 5. Proton-decoupled ^{13}C NMR spectra of (1) GaL_3 in $CDCl_3$ at 50°C°;* (2) GaL_3 in $CDCl_3$ at 27°C;* (3) GaL_3 in $CDCl_3$ at −14°C;* (4) $Al(Ox)_3$ in $CDCl_3$ at 27°C. [(*) aromatic part only.]

Examination of the ^{13}C NMR spectra of GaL_3 and $Al(Ox)_3$ exhibits the same type of phenomena (Fig. 5). In particular, the spectrum of $Al(Ox)_3$ contains at least 18 signals which is many more than the 9 peaks expected for a *fac* molecule (spectrum 4 in Fig. 5). In the same way, the aromatic part of the spectrum of GaL_3 is complicated at low temperature but is collapsed to a simple pattern at 50°C (spectra 1–3 in Fig. 5).

Following Baker and Sawyer[11] one can conclude from the NMR data that GaL_3 has a *mer* configuration in solution at low temperature. Moreover, pointing out that the chemical shift for protons H_2 in the collapsed spectrum is about the average of the three corresponding chemical shifts measured at room temperature, the two authors reached the conclusion that the collapse observed when the aluminium chelate solution is heated is due to rapid exchange in the *mer* isomer rather than to conversion to the *fac* configuration. The same argument applies for GaL_3.

For $Al(Ox)_3$, the conclusions drawn from the NMR data are consistent with the ones reached from the FIR study, i.e. the complex $Al(Ox)_3$ can be regarded as actually *mer* octahedral. On the other hand, for GaL_3 the two methods lead to divergent conclusions. Indeed, the FIR spectrum of GaL_3 exhibits a simple pattern (suggesting a *fac* configuration), even when recorded on a film of pure product at the liquid nitrogen temperature. Therefore we cannot conclude as far as the actual stereochemistry of GaL_3. However, since the conclusions of the FIR study are based on the absence of absorption bands whereas the conclusions of the NMR investigation are derived from the presence of NMR signals, one might consider the latter as more likely.

(b) *The adsorbed complex.* The 7-(4-ethyl-1-methyloctyl)-8-quinolinol impregnated Amberlite XAD-7 supports can be used as the traditional chelating resins for the recovery of metal ions, especially gallium(III) and germanium(IV), from aqueous solutions. At saturation in gallium(III), the mol ratio of N/mol of Ga has been found to be close to 3, suggesting that the adsorbed molecules of HL react with gallium(III) to form the three-liganded complex, GaL_3, as they do in solution. IR and FIR spectra (spectra 3 in Fig. 2 and 2 and 3 in Fig. 3) give confirmation of this. In particular, the similarity in the FIR spectral pattern between GaL_3 in solution and the complex formed directly on the support leads us to conclude that the two complexes exhibit the same stereochemistry.

In conclusion, we can say that the adsorption of lipophilic extractants on a macroreticular support such as the Amberlite XAD-7 resin is a convenient technique for obtaining an efficient reactive resin. Indeed, the extractant–support interactions are weak enough to avoid any hindrance in the chelation ability of the extractant, but strong enough to reduce the losses of reagent by solubility in aqueous phases by a factor up to ten compared with what is observed in liquid–liquid systems.[3]

Acknowledgements—The authors are greatly thankful to Prof. D. Bauer (University of Paris VI) for her interest in this work, to M. le Postollec (University of Paris VI) and J. P. Forgerit (C.N.R.S., L.A.S.I.R., Thiais) for running Raman and FIR spectra, respectively, and to C. Chassagnard (E.S.P.C.I., C.N.R.S. UA 476, Paris) for help in analysis of the NMR data.

REFERENCES

1. J. Helgorsky and A. Levêque, "*CIM Special Volume*", *Canadian Institute of Mining and Metallurgy, Montreal*, 1979, **21**, 439.
2. G. Cote and D. Bauer, *Hydrometallurgy* 1980, **5**, 149.
3. P. Mourier, G. Cote and D. Bauer, *Analusis* 1982, **10**, 468.
4. D. Rouillard, G. Cote, P. Fossi and B. Marchon, Jpn. Kokai Tokkyo Koho JP 58 31,048, 23 Feb 1983, US Patent 4,389,379, 21 June 1983.

5. P. J. Hoek and J. Reedijk, *J. Inorg. Nucl. Chem.* 1980, **42**, 1759.
6. H. Hommel and A. P. Legrand, *Reactive Polymers* 1983, **1**, 267.
7. L. Alagna, T. Prosperi and A. A. G. Tomlinson, in *Ion Exchange Technology* (Edited by D. Naden and M. Streat), p. 222. Ellis Horwood Limited, Chichester (1984).
8. G. Cote and D. Bauer, *J. Inorg. Nucl. Chem.* 1981, **43**, 1023.
9. A. W. Ashbrook, *Hydrometallurgy* 1975, **1**, 93.
10. G. P. Demopoulos and P. A. Distin, *Hydrometallurgy* 1983, **11**, 389.
11. B. C. Baker and D. T. Sawyer, *Anal. Chem.* 1968, **40**, 1945.
12. A. Corsini, W. J. Louch and M. Thompson, *Talanta* 1974, **21**, 252.
13. S. A. Osadchii, V. A. Tatarinov, L. Y. Marochkina, N. A. Pankrushina, I. N. Qribanova, A. V. Nikolaev, I. M. Ivanov and L. M. Qindin, *Izv. Sib. Otd. Akad. Nauk SSSR, Ser. Khim. Nauk* 1976, (4), 59.
14. A. A. Fomichev, Yu. S. Ryabokobylko, A. V. Kessenikh, A. Ataev, B. V. Parusnikov, I. A. Krasavin and V. M. Dziomko, *Khim. Geterotsikl. Soedin* 1977, (9), 1235.
15. J. K. Howie, P. Bosserman and D. T. Sawyer, *Inorg. Chem.* 1980, **19**, 2293.
16. J. Kidric, D. Hadzi, D. Kocjan and V. Rutar, *Org. Magn. Reson.* 1981, **15**, 280.
17. E. Uhlemann, W. Mickler, E. Ludwig and G. Klose, *J. Prakt. Chemie* 1981, **323**, 521.
18. P. Fourré, Thèse de doctorat d'Etat ès-Sciences Physiques, Paris VI (1984).
19. G. Charlot, *Chimie Analytique Quantitative*, tome II, p. 327. Masson, Paris (1974).
20. A. Warshawsky and A. Patchornik, *Israel J. Chem.* 1978, **17**, 307.
21. F. Vernon, *Separ. Sci. Technol.* 1978, **13**, 587.
22. F. Lauprêtre (private communication).
23. S. N. Sharma, R. B. Gupta and P. L. Gupta, *Acta Ciencia Indica* 1980, **6**, 58 (and papers cited in references).
24. R. Mecke and G. Z. Rossmy, *Electrochemistry* 1955, **59**, 866.
25. J. Paleos, *J. Colloid Interface Sci.* 1969, **31**, 7.
26. A. T. Rane and V. V. Ravi, *Spectrochim. Acta* 1982, **38A**, 937.
27. V. N. Filimonov and D. S. Bystrov, *Optics and Spectroscopy* 1962, **12**, 31.
28. R. Larsson and O. Eskilsson, *Acta Chem. Scand.* 1968, **22**, 1067.
29. Ohkaku Noburu and Nakamoto Kazuo, *Inorg. Chem.* 1971, **10**, 798.

Polyhedron Vol. 4, No. 8, pp. 1507–1510, 1985
Printed in Great Britain

0277-5387/85 $3.00 + .00
© 1985 Pergamon Press Ltd

EFFECT OF THE SUBSTITUENTS ON THE ENANTIOMERIZATION BARRIER ENERGY OF *N*-ISOPROPYLSALICYLALDIMINATE BERYLLIUM AND ZINC COMPLEXES

F. A. BOTTINO* and P. FINOCCHIARO
Institute of Chemistry, Faculty of Engineering of the University, viale A. Doria 6, 95125 Catania, Italy

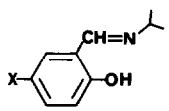
(*Received* 5 *June* 1984; *accepted after revision* 12 *February* 1985)

Abstract—Substituted bis-(*N*-isopropylsalicylaldiminate) complexes of Be(II) and Zn(II) have been prepared and their variable-temperature ^{1}H NMR spectra have been investigated. The variation of the $\Delta G^{\neq}$ values for the enantiomerization process in these complexes was studied as a function of the substituents present in the aromatic ring.

In our preceding works we have investigated the static and dynamic stereochemistry of bis-chelate complexes as a function of the variation of the complexed metal and (or) of the ligand structure.[1–4]

In this work our attention was devoted to the study of the dynamic stereochemistry of Be and Zn bis-chelate *N*-isopropylsalicylaldiminate complexes as a function of the substituents on the aromatic ring of the ligand, with the purpose of investigating the effect of the nature of the substituents on the energy of the enantiomerization process.

For this reason we prepared a series of ligands of general formula **I**:



I

X = H, OCH_3, CH_3, Br, Cl, NO_2

1 2 3 4 5 6

EXPERIMENTAL

The ligands **1**, **2** (b.p. 120°C; 0.2 mmHg) and **4** (m.p. 69–71°C) were prepared treating the commercial grade salicylaldehyde with *N*-isopropylamine in benzene solution. The ligands **3** (b.p. 58°C; 0.015 mmHg) and **5** (m.p. 64–5°C) were obtained by condensation with isopropylamine of the 5-methyl and 5-chloro-salicylaldehyde which were prepared starting from *p*-cresol and *p*-chlorophenol according to the procedure described by Duff.[5] The ligand **6** was obtained by nitration of salicylaldehyde[6] and successive condensation with *N*-isopropylamine of the 5-nitro-salicylaldehyde obtained. The ^{1}H NMR spectra in $CDCl_3$ were in agreement with the proposed structure **I**.

The corresponding Zn-complexes were prepared treating the respective Schiff bases in methanol with zinc acetate dihydrate dissolved in methanol.[7] After 30 min at reflux temperature, a pale yellow crystalline precipitate was obtained from the cooled solution.

The Be-complexes of the substituted ligands were obtained by a method at variance with that described by Green *et al.*[8] The ligand was mixed with an excess of dried $Be(OH)_2$ and maintained at 120°C for 15 min. The slurry was extracted with hot methanol. After concentration of the methanolic solution a crystalline product was obtained. Also the Be-complex of the non-substituted ligand was obtained according to this procedure.

The melting points and the elemental analyses of the complexes obtained are reported in Table 1. NMR spectra were recorded by means of a Bruker WP 80 FT spectrometer equipped with variable temperature accessories. $CDCl_3$ was used as solvent for room and low temperature experiments, while $C_6D_5NO_2$ was used for the high temperature spectra and, when possible, for measurements below room temperature only in some Zn-complexes.

* Author to whom correspondence should be addressed.

Table 1.

Compound No.	M.p. (°C)	Analyses found calc. (%) C	H	N	ΔG^* (kcal/mole) (Tc, K) $CDCl_3$	$C_6D_5NO_2$	σ_p[e]
1a	[a]	—	—	—		22.18 (416)	
2a	178–9	67.39 67.47	7.19 7.21	7.21 7.15		21.36 (404)	−0.27
3a	189–90	73.14 73.09	7.85 7.81	7.71 7.75		21.72 (412)	−0.17
4a	209–10	[b]				22.42 (420)	0.23
5a	176–7	59.61 59.70	5.46 5.51	6.83 6.96		22.10 (417)	0.23
6a	264–5	[b]				23.42 (440)	0.78
1b	[c]	—	—	—	15.50 (292)	15.16 (293)	
2b	220–21	59.08 59.00	5.82 5.85	6.31 6.26	16.01 (306)	16.00 (308)	
3b	233–4	63.20 63.23	6.78 6.75	6.66 6.70	15.69 (300)	15.60 (302)	
4b	203–4	43.79 43.87	4.12 4.05	5.06 5.11	14.89 (285)		
5b	194–5	52.28 52.37	4.72 4.83	6.13 6.11	15.21 (292)		
6b	236–8	[d]			13.32 (252)		

[a] Ref. No. 2.
[b] Ref. No. 12.
[c] Ref. No. 4.
[d] Ref. No. 11.
[e] Ref. No. 13.

RESULTS AND DISCUSSION

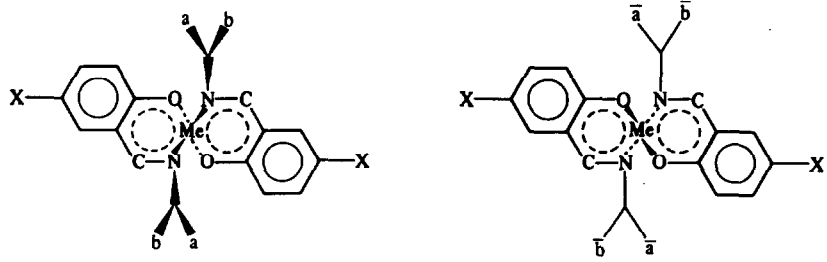
In our previous studies[1,2] compelling evidence has been reported that β-diketonate or bis-chelate salicylaldiminate complexes of beryllium and zinc adopt a tetrahedral idealized D_{2h} structure in solution and in the solid state. Such a conformation, provided that the two ligands are unsymmetrically substituted, is chiral and can exist as only *dl* pair. Therefore the isopropyl groups present in these compounds (structures **IIa** and **IIb**) act as a diastereotopic probe in the sense that under conditions in which the chirality of the structure is preserved the two methyl groups within each isopropyl moiety (labelled a and b in Fig. 1) are magnetically non-equivalent, giving rise to two doublets in the methyl region of the ^1H NMR spectrum. Any process which corresponds to a loss of chirality in the transition state will render the two methyl groups equivalent on the NMR time-scale, and the two doublets will collapse to a single doublet permitting the calculation of the inversion barrier energy at the tetrahedral metal centre.

The ^1H NMR spectra of the Be-complexes at probe temperature show two doublets in the methyl region; the spectra of the Zn complexes have only one doublet at the same temperature.

Lowering the temperature below 250 K caused the Zn-derivatives to show the same pattern (two doublets) as the Be-derivative, due to the two diastereotopic methyl groups of each isopropyl moiety.

This observation is consistent with a tetrahedral configuration of such complexes on the NMR time-scale, with low interconversion of the two enantiomers at probe temperature for the Be-derivatives and at low temperature for the Zn-complexes.

A NMR study at variable temperature shows that when the temperature of the samples is increased the two diastereotopic methyl groups coalesce to a single doublet at temperatures of 306, 300, 292, 285 and 252



IIa **IIb**

Me = Be; X = H, OCH_3, CH_3, Br, Cl, NO_2
1a 2a 3a 4a 5a 6a

Me = Zn; X = H, OCH_3, CH_3, Br, Cl, NO_2
1b 2b 3b 4b 5b 6b

Fig. 1.

K for the compounds **2b**, **3b**, **4b**, **5b** and **6b** respectively ($CDCl_3$ as solvent) and at higher temperatures for the Be-derivatives, 404, 412, 420, 417 and 440 K for the compounds **2a**, **3a**, **4a**, **5a** and **6a** respectively ($C_6D_5NO_2$ as solvent).

The use of $C_6D_5NO_5$ as solvent for the Be-derivatives was necessary owing to the high coalescence temperatures (404–440 K) but only a few Zn-derivatives can be studied in this solvent due to its melting point of 279 K. However, the compounds **1b**, **2b** and **3b**, for which it is possible to obtain the coalescence temperature (Table 1), show practically the same trend as that in $CDCl_3$ solvent. Furthermore, the values of the free-energy of coalescence remain almost unchanged on varying the solvent, and this could be taken as strong evidence that the role of the solvent is trivial in such process.

The Gutowsky–Holm equation[9] was used to derive the rate constant at the coalescence temperature, and this was used to calculate an Eyring free energy of activation for the enantiomerization process. The results are reported in Table 1.

A plot of $\Delta G^{\neq}$ as a function of the σ of Hammett is shown in Fig. 2. Satisfactory linear relationships are observed for both Be (1) and Zn (2) complexes:

$$\Delta G^{\neq} = 1.81\sigma + 21.96 \quad (1)$$

and

$$\Delta G^{\neq} = -2.48\sigma + 15.44 \quad (2)$$

with a correlation coefficient of 0.970 for eqn (1) and 0.978 for eqn (2).

Interestingly, the trend is just opposite for the two series of metal complexes independently of the solvent used for the experiments. Thus, in the Zn-complexes, $\Delta G^{\neq}$ values increase with increasing the electron donor capability of the substituents on the aromatic nucleus, whereas in the Be-complexes a greater free energy of activation for racemization process is associated with electron-withdrawing groups in the aromatic ring.

However, although the trend is opposite, the slopes of the two linear relationships are similar to each other, indicating that the effect of the substituents on the values of such inversion barrier is equally sensed in both series of complexes.

Many effects can be invoked in order to explain such concomitant and opposite trends. A first tentative explanation could be the following.

Literature data[10] indicate that in such complexes the Be–O bond has relatively more covalent character in contrast with the Zn–O bond in the corresponding Zn-complexes.

These differences can account for the greater energy barrier to the racemization encountered in the Be-complexes.

Under these conditions, electron-donating groups should increase the strength of the partially ionic Zn–O bond in agreement with the experimental

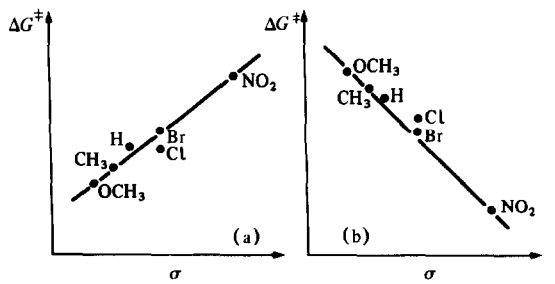


Fig. 2. Plot of $\Delta G^{\neq}$ for the Be(II)-complexes (diagram a) and the Zn(II)-complexes (diagram b) vs σ.

data (see Fig. 2); conversely, considering the differences in the bonds of the two Be- and Zn-complexes, electron-donating groups should reduce the energy necessary for the racemization process (inversion at tetrahedral central atom) in the Be-complexes.

Further experiments by other techniques are in progress in order to verify such a tentative explanation.

REFERENCES

1. F. A. Bottino, P. Finocchiaro, A. Recca and H. G. Brittain, *J. Inorg. Nucl. Chem.* 1978, **40**, 1997.
2. F. A. Bottino, A. Recca and P. Finocchiaro, *J. Organometal. Chem.* 1978, **160**, 373.
3. F. A. Bottino, E. Libertini, O. Puglisi, A. Recca and G. Ronsisvalle, *J. Inorg. Nucl. Chem.* 1980, **42**, 1.
4. F. A. Bottino, A. Recca and P. Finocchiaro, *J. Inorg. Nucl. Chem.* 1980, **42**, 479.
5. J. C. Duff, *J. Chem. Soc.* 1941, 547.
6. H. Ichibagase and S. Terada, *J. Pharm. Soc. Jpn* 1952, **72**, 876.
7. G. E. Batley and D. P. Graddon, *Aust. J. Chem.* 1967, **20**, 877.
8. R. W. Green and P. W. Alexander, *Aust. J. Chem.* 1965, **18**, 1297.
9. H. S. Gutowsky and C. H. Holm, *J. Chem. Phys.* 1956, **25**, 1228.
10. J. P. Oliver, *J. Organometal. Chem.* 1983, **257**, 1.
11. L. E. Nivorozhkim, L. E. Konstantinovskii, M. S. Korobov and V. I. Minkin, *Koord. Khim.* 1979, **5**, 508; *Chem. Abst.* 1979, **91**, 97344e.
12. V. I. Minkin, L. E. Nivorozhkim, L. E. Konstantinovskii and M. S. Korobov, *Koord. Khim.* 1977, **3**, 174; *Chem. Abst.* 1977, **87**, 44697h.
13. H. H. Jaffé, *Chem. Rev.* 1953, **53**, 191.

Polyhedron Vol. 4, No. 8, pp. 1511–1518, 1985
Printed in Great Britain

0277–5387/85 $3.00 + .00
© 1985 Pergamon Press Ltd

SYNTHESIS AND SPECTRAL STUDIES OF COPPER(II) COMPLEXES WITH AMIDE GROUP LIGANDS

V. RAVINDAR, S. J. SWAMY, S. SRIHARI and P. LINGAIAH*
Department of Chemistry, Kakatiya University, Warangal 506 009, Andhra Pradesh, India

(*Received* 13 *March* 1984; *accepted after revision* 12 *February* 1985)

Abstract—Complexes of copper(II) with 2-(acetylamino)benzoic acid, 2-(benzoylamino) benzoic acid, 2-(aminocarbonyl)benzoic acid, 2-[(phenylamino)carbonyl]benzoic acid, 2-[(1-naphthalenylamino)carbonyl]benzoic acid, 2-[(2-aminophenylamino)carbonyl]benzoic acid, 2-aminobenzanilide, 2(aminobenzoyl)benzoic acid, maleanilic acid and malea-1-naphthalanilic acid have been prepared and characterized by chemical analyses, molar conductivity, magnetic susceptibility measurements, thermal data, IR, electronic and ESR spectra. The visible and ESR spectral studies of these complexes (except those of maleanilic acid and malea-1-naphthalanilic acid) indicate that they are monomeric having either square planar or distorted octahedral geometry around Cu(II). The Cu(II) complexes of maleanilic acid and malea-1-naphthalanilic acid have been tentatively assigned dimeric structures. From the ESR spectra of Cu(II) complexes various parameters have been calculated.

An amide group offers two potential binding atoms, the oxygen and nitrogen, for complexation of metal ions. A number of complexes have been reported with amide group ligands which exhibit diverse coordinating behaviour with different metal ions.[1–4] However, studies on the metal complexes of the derivatives of amide groups are limited. Wiersema and Windle,[5] on the basis of ESR spectra of Cu(II)–salicylamide complexes, have reported that the salicylamide coordinates through nitrogen of the amide group. On the other hand, Pannu *et al.*,[6] have proposed the structure for this complex with oxygen, but not nitrogen, of the amide group coordinating. The majority of amide ligands form monomeric complexes with Cu(II) showing a doublet state. But the ESR spectra of Cu(II)–cyclic acid amide complexes are of a dimeric species, in which the two metal ions are exchange-coupled, leading to a paramagnetic triplet state. In view of these differences, investigation of the coordinating behaviour of the amide group containing ligands is worthwhile. In this paper, complexes of copper(II) with 2-(acetylamino)benzoic acid (AABA), 2-(benzoylamino)benzoic acid (BABA), 2-(aminocarbonyl)benzoic acid (ACBA), 2-[(phenylamino)carbonyl]benzoic acid (PACBA), 2-[(2-naphthalenylamino)carbonyl]benzoic acid (NACBA), 2-[(2-aminophenylamino)carbonyl]-benzoic acid (APACBA), 2-aminobenzanilide (ABn), 2-(aminobenzoyl)benzoic acid (ABBA), maleanilic acid (MA) and malea-1-naphthalanilic acid (MNA) are discussed.

* Author to whom correspondence should be addressed.

EXPERIMENTAL

All the chemicals used were of AR grade. The ligands AABA,[7] BABA,[8] ACBA,[9] PACBA,[10] NACBA,[10] APACBA,[11] ABn,[12] MA[13] and MNA[13] were prepared by the literature methods. The purity of these compounds was checked by TLC and melting point determination. ABBA was obtained from Aldrich Chemical Company (U.S.A.) and was used as such.

Preparation of complexes

The complexes were prepared by mixing an aqueous solution of cupric acetate or cupric sulphate and methanolic solution of the ligands in 1 : 2 molar ratio and heating the mixture on a hot water bath for about 30 min. The crystalline complexes formed were suction filtered, washed with hot water and methanol and dried *in vacuo* over anhydrous calcium chloride.

Analyses

Copper in the complexes was estimated by iodometry using sodium thiosulphate. C, H and N analyses were obtained from the Microanalytical Laboratory, Calcutta University, Calcutta, India.

Physical measurements

The magnetic susceptibility measurements were made at room temperature (25°C) on a Gouy balance and corrected for diamagnetism using Pascal's constants. Molar conductivities of the complexes in DMF were measured using a Digisun Digital Conductivity Meter, model D 1-909. The thermal data of the complexes were obtained using a Stanton Thermobalance available at R.R.L., Hyderabad. IR spectra of the ligands and the complexes (4000–200 cm^{-1}) in Nujol mulls or in KBr (using cesium iodide plates in FIR region) were recorded on Perkin–Elmer-283 spectrophotometer. The electronic spectra of the complexes in DMF or in Nujol mulls were obtained using a Shimadzu MPS 5000 spectrophotometer. ESR spectra of the complexes in the solid state and in solution were recorded at 25°C and liquid nitrogen temperature employing JEOL PE-3X- and Varian X-band spectrometers.

RESULTS AND DISCUSSION

All the copper(II) complexes are crystalline powders, their colour being light blue or light green. They (except MA and MNA complexes) are slightly soluble in ethanol and freely soluble in DMF and DMSO. On the basis of analytical data (Table 1) the metal chelates are found to have 1 : 2 (metal : ligand) stoichiometry. The molar conductance values of the complexes in DMF at 10^{-3} molar concentration are low (7–18 Ω^{-1} cm^2 mol^{-1}) suggesting that they are non-electrolytes, but the complex of ABn has a value of 67 Ω^{-1} cm^2 mol^{-1} indicating that it is a 1 : 1 electrolyte.

Table 1. Analytical and physical data of Cu(II) complexes

Complex	Colour	Decomp. temp. (°C)	Analysis (%)[a] M	C	H	N	Molar conductance (Ω^{-1} cm^2 mol^{-1})	μ_{eff} (B.M.)
$(Cu(AABA)_2(H_2O)_2)$	Green	290	14.32 (13.94)	46.93 (47.41)	3.11 (3.51)	6.30 (6.14)	12.0	1.94
$(Cu(BABA)_2(H_2O)_2)$	Green	300	11.12 (10.96)	60.72 (57.97)	4.23 (4.14)	4.91 (4.83)	10.0	1.94
$(Cu(ACBA)_2)$	Light green	245	15.98 (16.22)	48.87 (49.03)	3.15 (3.06)	7.22 (7.15)	16.00	1.84
$(Cu(PACBA)_2)2H_2O$	Light green	290	10.37 (10.96)	58.26 (57.97)	4.28 (4.14)	5.01 (4.83)	18.0	1.86
$(Cu(NACBA)_2)2H_2O$	Green	300	8.96 (0.35)	62.01 (63.57)	3.73 (4.12)	4.24 (4.12)	14.5	1.87
$(Cu(APACBA)_2)$	Green	310	11.19 (11.07)	58.24 (58.58)	3.67 (3.83)	9.63 (9.76)	12.0	1.92
$(Cu(ABH)_2(H_2O)_2)SO_4$[b]	Light green	275	10.36 (10.25)	50.12 (50.35)	4.36 (4.51)	8.92 (9.03)	67.0	1.89
$(Cu(ABBA)_2)$	Light green	300	11.28 (11.69)	61.29 (61.81)	3.52 (3.67)	4.99 (5.15)	13.0	1.90
$(Cu(MA)_2)_2$	Bluish green	330	14.02 (14.32)	54.10 (54.11)	3.50 (3.60)	6.03 (6.31)	—	1.13
$(Cu(MNA)_2)_2$	Light green	320	11.53 (11.69)	61.67 (61.81)	3.52 (3.67)	5.00 (5.15)	—	1.06

[a] Calculated values are given in parentheses.
[b] % Sulphur = 5.03(5.16).

Thermal analysis

The decomposition temperatures of the complexes obtained from their thermograms are recorded in Table 1. The thermograms of Cu(II) complexes of AABA, and ABn show initial weight loss in the temperature range 140–220°C corresponding to two water molecules. The expulsion of water molecules in the above temperature range indicates that they are coordinated.[14] The presence of water molecules in these complexes is further evidenced by their DTA curves which give endothermic peaks in the range 140–200°C. On the other hand, the Cu(II) complexes of PACBA and NACBA show initial weight loss curves in the temperature range 70–130°C, again amounting to two water molecules. The loss of water molecules in this low temperature range indicates that they are present as lattice-held water.[14] Also, each of the DTA curves of these complexes shows an endothermic peak in the range 90–120°C giving additional evidence for the presence of water molecules. The other Cu(II) complexes are thermally stable up to 240°C and are not hydrated. This is confirmed by the absence of an endothermic peak in the range 150–220°C in their DTA curves. The final products of decomposition above 560°C, in all the complexes, correspond to metallic oxide. The decomposition temperatures of the complexes are taken as a measure of their thermal stability. The ligands under study form complexes of varying stability in the order: ACBA < AABA < ABn < PACBA < BABA < NACBA < ABBA < APACBA < MNA < MA.

Despite the good amount of work on thermogravimetry, considerable difficulty still exists in assigning definite reasons for the increase or decrease in thermal stability of complexes with different ligands. One of the reasons advanced in the literature to explain the relative order of thermal stability of complexes formed with different ligands is that the thermal stability of the complexes increases with increase in π-electron delocalization, size of the molecule and also the nature and number of the rings formed.[15–17] The relative order of stability observed for the present complexes (except those of MA and MNA) might well be explained in terms of these reasons. The high decomposition temperatures of the Cu(II) complexes of MA and MNA may be ascribed to their polymeric nature.

IR spectra

The C=O and C–O stretching frequencies at 1700 and 1330 cm^{-1} in uncomplexed ligands containing carboxylic groups[11,18] are shifted to 1550 and 1380 cm^{-1} in complexes and are assigned to ν_{as}(COO) and ν_s(COO) modes respectively.[19] The ν(O–H) of the carboxylic group appearing at 2600 cm^{-1} in free ligands disappears in the IR spectra of their complexes.

The ν(N–H) frequency in AABA and BABA shifts to lower frequency by 100–140 cm^{-1} in complexes indicating that the nitrogen of the amide group is coordinating. A band at 1650 cm^{-1} in these ligands assignable to ν(C=O) of the amide group shows no considerable shift in the complexes, thus ruling out coordination through amide oxygen. In the ACBA, PACBA, NACBA, APACBA, ABn, ABBA, MA and MNA complexes ν(N–H) shifts towards higher frequencies compared with the ligand spectra, indicating non-participation of the nitrogen atom in coordination.[20] On the other hand, ν(C=O) (or the amide-I frequency) in the above set of ligands undergoes a negative shift (40 cm^{-1}) in the complexes, indicating coordination of this group through oxygen.[20] The N–H bands in AABA, BABA, ABn, PACBA, and NACBA complexes are somewhat obscured by ν(O–H) mode of water of crystallization and broadening due to hydrogen bonding. But the spectra of Cu(II) complexes of AABA and BABA recorded after heating them to 200°C for one hour clearly show bands around 3300 cm^{-1}, quite characteristic of N–H group. IR data also indicate that the anion SO_4^{-2} retains its ionic character in the Cu(II)–ABn complex.[21]

The amine ν(N–H) frequency in APACBA, ABn and ABBA undergoes a lower shift in the complexes showing that nitrogen of this group is coordinating. Further, the FIR spectra of the complexes show bands corresponding to ν(M–O) and ν(M–N) vibrations.[19] Some of the stretching frequencies relevant to the characterization of the complexes are listed in Table 2.

Electronic spectra

The electronic spectra of the complexes of ACBA, PACBA and NACBA show absorption bands in the ranges 14,500–15,100 cm^{-1} and 18,200–20,200 cm^{-1} assignable respectively to the transitions $^2B_{2g} \leftarrow {}^2B_{1g}$ and $^2E_g \leftarrow {}^2B_{1g}$ of square-planar structure.[22] Complexes of MA and MNA show a broad band centred at 20,600 cm^{-1} which is characteristic of square-planar geometry. Further, a strong charge-transfer band (CuO) has been observed around 27,000 cm^{-1} in these complexes.[23]

The complexes of AABA and BABA give rise to two bands, one of broad nature at 13,300 and 13,200 and the other as a shoulder of low intensity at 16,400 and 17,200 cm^{-1} respectively. These positions suggest distorted octahedral geometry for the

Table 2. Assignments of some important IR absorption bands of Cu(II) complexes (cm^{-1})

Complex	$-NH_2$	ν(N–H)	–NH–	ν(C=O)	ν(COO) asym	ν(COO) sym	ν(M–N)	ν(M–O)
$(Cu(AABA)_2(H_2O)_2)$	3500		3500–3200 (3380)	1640 (1640)	1560	1385	450	280
$(Cu(BABA)_2(H_2O)_2)$	—		3450–3200 (3460)	1635 (1640)	1545	1370	460	260
$(Cu(ACBA)_2)$	—		3350 (3060)	1620 (1660)	1550	1380	470	290
$(Cu(PACBA)_2)2H_2O$	—		3450–3280 (3300)	1625 (1640)	1560	1375	485	300
$(Cu(NACBA)_2)2H_2O$	—		3480–3280 (3280)	1640 (1660)	1535	1380	470	310
$(Cu(APACBA)_2)$	3340,	3290	3220 (3200)	1615 (1640)	1545	1370	530	470, 300
$(CuABn)_2(H_2O)_2)SO_4$[a]	(3420,	3320)	3500–3200 (3240)	1620 (1640)	—	—	520	410
$(Cu(ABBA)_2)$	3360, (3460,	3280 3340)	—	1640 (1710–1670)	1560	1380	520	470, 280
$(Cu(MA)_2)_2$	—		3350 (3340)	1615 (1630)	1540	1400	—	450, 200
$(Cu(MNA)_2)_2$	—		3300 (3280)	1620 (1640)	1530	1405	—	460, 300

Some of the absorptions in free ligands are given in parentheses.
[a] SO_4^{2-} shows a strong absorption band at 1150–1080 cm^{-1}.

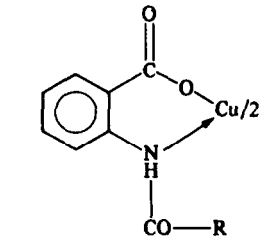
complexes.[24] The complexes of APACBA, ABn and ABBA, on the other hand, exhibit a single broad band in the region 14,500–14,800 cm^{-1} due to $^2T_{2g} \leftarrow {}^2E_g$ of octahedral structure. This band is considerably blue shifted compared to the first band maximum of the corresponding Ni(II) complexes, the ν(Cu)/ν(Ni) being 1.40. This suggests appreciable distortion from octahedral geometry in these Cu(II) complexes.[4]

Magnetic moments

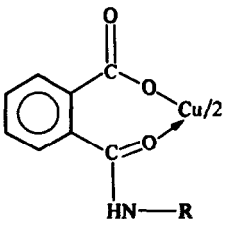
The magnetic moments of Cu(II) complexes at room temperature are given in Table 1. The Cu(II)

Table 3. ESR spectral and bonding parameters of Cu(II) complexes

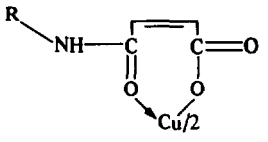
Complex	$g_\parallel$	$g_\perp$	$A_\parallel \times 10^4$ (cm^{-1})	$A_\perp \times 10^4$ (cm^{-1})	α^2	β^2	γ^2
$(Cu(AABA)_2(H_2O)_2)$	2.252	2.065	150	26.0	0.74	0.67	0.83
$(Cu(BABA)_2(H_2O)_2)$	2.243	2.051	163	18.0	0.68	0.69	0.73
$(Cu(ACBA)_2)$	2.253	2.049	132	18.0	0.63	0.90	0.90
$(Cu(PACBA)_2)2H_2O$	2.234	2.044	138	20.0	0.62	0.82	0.71
$(Cu(NACBA)_2)2H_2O$	2.190	2.047	144	14.0	0.62	0.65	0.79
$(Cu(APACBA)_2)$	2.225	2.060	170	38.0	0.78	0.62	0.65
$(Cu(ABn)_2(H_2O)_2)SO_4$	2.220	2.058	166	34.0	0.75	0.64	0.65
$(Cu(ABBA)_2)$	2.206	2.051	185	12.5	0.68	0.65	0.62
$(Cu(MA)_2)_2$	2.371	2.042	—	—	—	—	—
$(Cu(MNA)_2)_2$	2.439	2.100	—	—	—	—	—



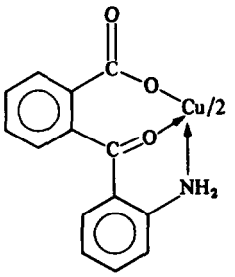
AABA, BABA (R = CH_3Ph)



ACBA, PACBA, NACBA (R = H, Ph)



MA, MNA (R = Ph, naphthyl)



ABBA

Fig. 1. Structures of ligands showing ways of coordination.

complexes with all the ligands are paramagnetic, μ_{eff} value corresponding to the presence of one unpaired electron. But in the case of Cu(II) complexes of MA and MNA, the magnetic moments are found to be 1.13 and 1.06 B.M. respectively. These subnormal moments indicate some metal–metal interaction in solid state, possibly due to the formation of dimeric or polymeric structure.[25]

ESR spectra

The ESR spectral and bonding parameters of the Cu(II) complexes are presented in Table 3. The ESR spectra of Cu(II) complexes of PACBA, ABBA, MA and MNA are given in Figs 1–4.

The spectra of Cu(II) complexes of AABA, BABA, ACBA, PACBA, NACBA and ABn show at room

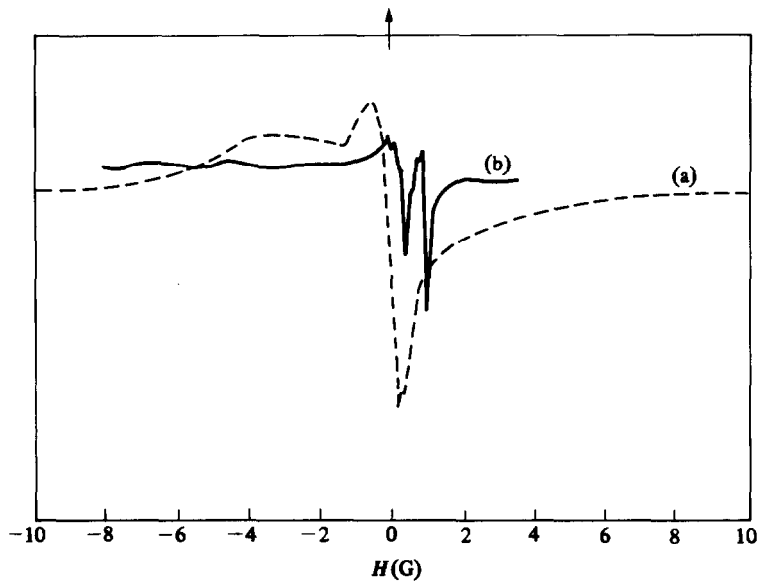


Fig. 2. ESR spectra of Cu(II)–PACBA complex at room temperature (a) and at liquid-nitrogen temperature (b).

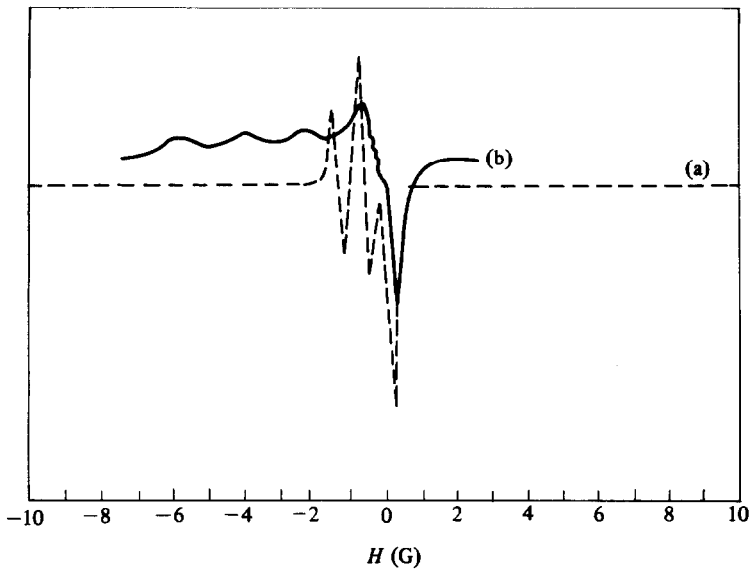


Fig. 3. ESR spectra of Cu(II)–ABBA complex at room temperature (a) and at liquid-nitrogen temperature (b).

temperature two peaks, one of intense absorption at high field and the other of less intensity at low field both in solid and solution states. From these peaks $g_{\|}$ and $g_{\perp}$ have been calculated. Inspection of the ESR data in the solid and in solution shows no significant difference in the room temperature values of $g_{\|}$ and $g_{\perp}$. Therefore, it is quite probable that the arrangement of Cu(II) ion in polycrystalline state and in solution is the same.

The spectrum of Cu(II)–ABBA complex at room temperature is isotropic due to tumbling motion of the molecules. The isotropic value, g_0, is calculated at the centre of the four-line spectrum. The isotropic nuclear hyperfine constant, A_0, expressed in cm^{-1} is calculated from the separation between two adjacent lines of the spectrum. However, this complex in the frozen state at 77 K shows three well resolved peaks of low intensity in the low-field region and one intense

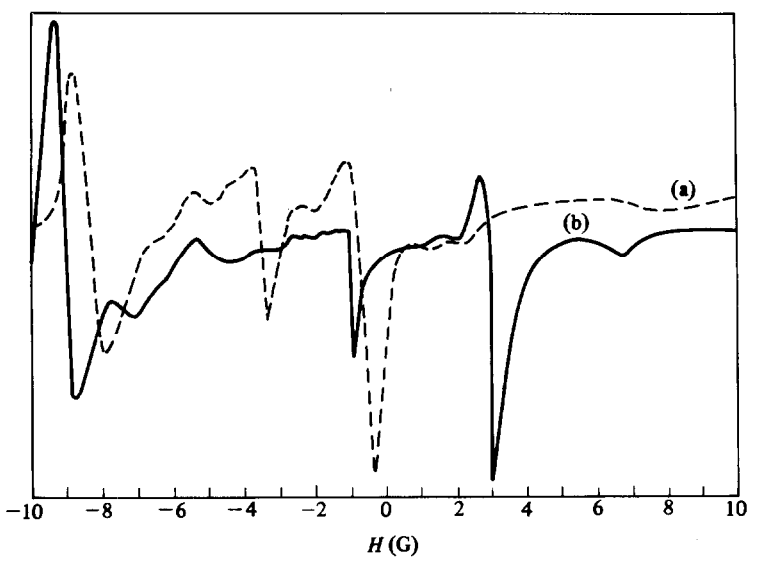


Fig. 4. ESR spectra of Cu(II)–MA complex at room temperature (a) and at liquid-nitrogen temperature (b).

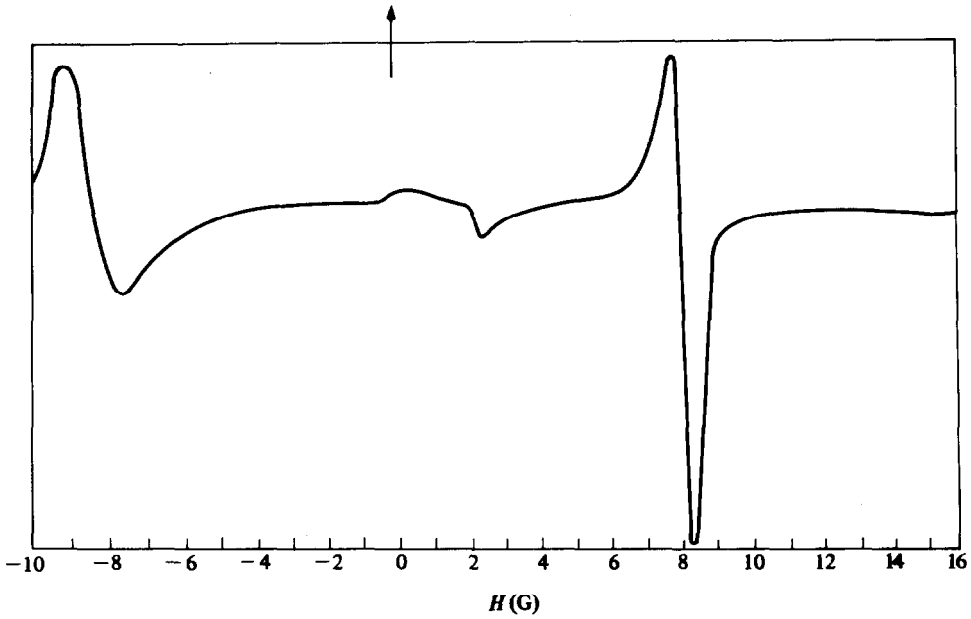


Fig. 5. ESR spectrum of Cu(II)–MNA complex at room temperature.

unresolved peak in the high-field region. The $g_{\|}$ and $A_{\|}$ values were calculated from the spectrum while $g_{\perp}$ and $A_{\perp}$ were evaluated using the following equations.[26]

$$g_{\perp} = \frac{3g_0 - g_{\|}}{2} \quad \text{and} \quad A_{\perp} = \frac{3A_0 - A_{\|}}{2}.$$

The $g_{\|}$ values of these Cu(II) complexes are greater than the corresponding $g_{\perp}$ values (Table 3) and, therefore, they have the unpaired electron in $d_{x^2-y^2}$ molecular orbital.[4]

Kivelson and Neiman[27] have shown that $g_{\|}$ is a moderately sensitive function for indicating covalency; for an ionic environment $g_{\|}$ is normally > 2.3 and for covalent environment it is < 2.3. The $g_{\|}$ for all the complexes (except those of MA and MNA) is found to be < 2.3 and taking these values into consideration the covalency of the M–L bond in the complexes may be formulated in the order AABA > BABA > NACBA > ABBA > ABn > APACBA > PACBA > ACBA.

Further, the bonding parameters, α^2, β^2 and γ^2 have been evaluated and based on the values obtained, the following bonding scheme is proposed for the present complexes: strongly covalent bonding with α^2 values in the range 0.62–0.78; strongly covalent in-plane π-bonding with β^2 values of the order 0.62–0.69 except in the case of Cu(II) complexes of ACBA and PACBA where it is moderate (β^2 = 0.82 and 0.90) and strongly covalent out-of-plane π-bonding with γ^2 values of the order 0.62–0.79 while in Cu(II) complexes of AABA and ACBA it is only moderate with γ^2 = 0.83 and 0.90.

The ESR spectra of Cu(II) complexes of MA and MNA were recorded in the solid state at 25°C and at liquid nitrogen temperature. The spectra consist of a moderately strong absorption at *ca* 250 G, strong absorption at *ca* 4500 G, a weak absorption at *ca* 6450 G and an absorption of varying intensity at *g ca* 2. The intensities of the first three absorptions decrease with a decrease in temperature, while that of the last at *g ca* 2 remains virtually unchanged. The *g ca* 2 absorption has, therefore, been assigned to a small percentage of monomeric impurity present to a different extent in each of the samples. It is noticeable that the linewidth of the three triplet absorptions differ (Figs 4 and 5). The linewidth of the high- and low-field absorptions is *ca* three times that of the absorption at *ca* 4500 G. All these features of the present MA and MNA complexes are similar to those observed in the case of the Cu(II) complexes of unsaturated carboxylic acids[28] and dicarboxylic acids and acid amides[29] for which a dimeric structure was proposed. Based on this, the present two complexes are tentatively assigned a dimeric structure.

Acknowledgements—The authors are grateful to Prof. A. K. Bhatnagar, University of Hyderabad, Hyderabad for providing facilities for recording ESR spectra. VR thanks the CSIR, New Delhi for the award of a Senior Research Fellowship.

REFERENCES

1. R. L. Dutta and A. K. Sarkar, *J. Inorg. Nucl. Chem.* 1981, **43**, 57.
2. I. S. Ahuza, R. SriRamulu and Raghuvir Singh, *Indian J. Chem.* 1980, **19A**, 909.
3. H. Sigel and R. B. Martin, *Chem. Rev.* 1982, **82**, 385.
4. R. C. Agarwal, N. K. Singh and R. P. Singh, *Inorg. Chem.* 1981, **20**, 2794.
5. A. K. Wiersema and J. J. Windle, *J. Phys. Chem.* 1964, **68**, 2316.
6. B. S. Pannu, S. L. Chopra and S. S. Parmer, *Indian J. Chem.* 1971, **9**, 1396.
7. K. Josef, *J. Prakt. Chem.* 1961, **14**, 84.
8. E. R. Steiger, *J. Org. Chem.* 1944, **9**, 396.
9. E. Chapman and H. Stephen, *J. Chem. Soc.* 1925, **127**, 1791.
10. N. V. Subba Rao and C. V. Ratnam, *J. Sci. Ind. Res.* 1962, **21B**, 45.
11. R. P. Young, *J. Heterocycl. Chem.* 1972, **9**, 371.
12. R. H. Clark and E. C. Wagner, *J. Org. Chem.* 1944, **9**, 55.
13. A. D. Gholap, M. V. Patel, R. C. Patil, P. Balasubramaniyan and V. Balasubramaniyan, *Indian J. Chem. Educ.* 1980, **7**, 26.
14. A. V. Nikolaev, V. A. Logvinenko and L. I. Myachina, *Thermal Analysis*, Vol. 2, p. 779. Academic Press, New York (1969).
15. R. S. Bottel and D. Quane, *J. Inorg. Nucl. Chem.* 1964, **26**, 1919.
16. V. Sheshagiri and S. B. Rao, *Z. Anal. Chem.* 1972, **262**, 175.
17. R. Sheshagiri Naidu and R. Raghava Naidu, *Indian J. Chem.* 1977, **15A**, 652.
18. D. Hadzi and M. Pintar, *Spectrochim. Acta* 1959, **8**, 249.
19. K. Nakamoto, *Infrared Spectra of Inorganic and Coordination Compounds*, p. 152. Wiley–Interscience, New York (1970).
20. B. S. Pannu and S. L. Chopra, *J. Indian Chem. Soc.* 1974, **51**, 387.
21. N. B. Colthup, D. H. Daly and S. E. Wiberly, *Introduction to Infrared and Raman Spectroscopy*, p. 311. Academic Press, New York (1964).
22. R. L. Belford and W. A. Teanos, *Molec. Phys.* 1963, **6**, 121.
23. D. X. West and Palaniandavar, *Inorg. Chim. Acta* 1983, **76**, 149.
24. C. B. Mehto, *J. Indian Chem. Soc.* 1980, **57**, 485.
25. B. N. Figgis and J. Lewis, *Progress in Inorganic Chemistry*, p. 37. Interscience Publishers (1964).
26. H. M. McConnel, *J. Chem. Phys.* 1956, **25**, 709.
27. D. Kivelson and R. R. Neiman, *J. Chem. Phys.* 1961, **35**, 149.
28. W. J. Newton and B. J. Tabner, *J. Chem. Soc., Dalton Trans.* 1979, **11**, 1.
29. P. Arrizabalaga, P. Castan and P. Sharrock, *Polyhedron* 1983, **2**, 823.

Polyhedron Vol. 4, No. 8, p. 1519, 1985
Pergamon Press Ltd. Printed in Great Britain

ANNOUNCEMENT

INTERNATIONAL CONFERENCE ON COMPOSITE INTERFACES

The first international conference on composite interfaces (ICCI) is scheduled to be held from 27 to 30 May 1986 at Case Western Reserve University in Cleveland, Ohio. This international conference will provide a forum for discussion on recent advances in the fundamental, scientific understanding of the microstructure of composite interfaces and their influences on macroscopic properties of composite materials.

The first circular including a preregistration form is available from Prof. H. Ishida, General Chairman of ICCI, Department of Macromolecular Science, Case Western Reserve University, Cleveland, OH 44106, tel.: (216) 368-4285. Extended abstracts of two single-spaced pages are due on 1 December 1985 for review purposes. Final papers are due on 31 January 1986.

Polyhedron Vol. 4, No. 9, pp. 1521–1526, 1985
Printed in Great Britain

0277-5387/85 $3.00 + .00
Pergamon Press Ltd

SPECTROPHOTOMETRIC STUDY OF THE COMPLEXATION EQUILIBRIA OF URANIUM(VI) WITH 1,4-BIS(4′-METHYLANILINO)ANTHRAQUINONE AND DETERMINATION OF URANIUM(VI)

K. A. IDRISS,* M. M. SELEIM, M. S. ABU-BAKR and H. SEDAIRA
Department of Chemistry, Faculty of Science, Assiut University, Assiut, Egypt

(*Received* 15 *November* 1983; *accepted* 10 *January* 1984)

Abstract—The reaction of U(VI) with 1,4-bis(4′-methylanilino)anthraquinone (quinizarin green) in water-dimethylformamide medium was investigated spectrophotometrically. The complexation equilibria in solution were demonstrated. The study of the reaction in presence of equimolar concentrations or in solutions containing metal or ligand excess gave evidence for the formation of complexes with stoichiometric ratios of UO_2:L = 1:1 and 1:2 in dependence on the pH of the medium. Their thermodynamic stabilities and the values of their molar absorption coefficients were determined. The optimum conditions for spectrophotometric determination of U(VI) with this reagent were found.

The ligand 1,4-bis(4′-methylanilino)anthraquinone, quinizarin green (QG), has very interesting properties as an analytical reagent. Solid complexes of this ligand with some metal ions have been isolated and characterised,[1,2] but solution studies have not yet been discussed in detail. Recent work from this laboratory involving the acid-base properties of arylaminoanthraquinone dyes in aqueous medium[3] and in water-solvent mixtures[4,5] has led us to obtain information in this area.

The preliminary results of our study showed that QG yields five variously coloured acid-base forms: LH_4^{2+}, LH_3^+, LH_2, LH^- and L^{2-}. In 40% (v/v) DMF at pH 3.2–5 there is a pronounced ionisation from LH_4^{2+} form to the monoprotonated species LH_3^+, and the latter is converted to LH_2 at pH 6–8. It has been spectrophotometrically determined, at the working pH region of solutions and 40% (v/v) DMF, that pK_{a_1} (LH_3^+/LH_2) = 5.15 and pK_{a_2} (LH_2/LH^-) = 9.46. The determination of the first dissociation constant (LH_4^{2+}/LH_3^+) was rather difficult because of the poor solubility of QG in strongly acidic solutions (see Fig. 1). The different acid-base equilibria liable to occur in solutions of QG can be represented as:

$$\underset{(pH \leqslant 2.5)}{LH_2^{2+}} \overset{-H^+}{\rightleftharpoons} \underset{(pH\ 3\text{–}5)}{LH_3^+} \overset{-H^+}{\rightleftharpoons} \underset{(pH\ 6\text{–}8)}{LH_2} \rightleftharpoons \underset{(pH\ 9\text{–}10.5)}{LH^-} \rightleftharpoons \underset{(pH \geqslant 11)}{L^{2-}}.$$

The dissociation constants corresponding to the last three ionisation steps have been calculated by treating the non-linear dependences $A = f(pH^*)$ as described elsewhere.[4] The mean pK_a values are given in Table 1. The experimental data can be obtained from the authors of this work.

The present paper deals with the study of the complexation equilibria of the analytically useful reagent QG and U(VI) in water-DMF medium and the conditions for the spectrophotometric determination of U(VI).

EXPERIMENTAL

Quinizarin green (QG) was purified by recrystallization of commercial reagent. 10^{-3} M solution of QG was prepared by dissolving the accurately weighed amount of the compound in dimethylformamide. 10^{-3} M solution of U(VI) was prepared from the analytically pure uranyl nitrate and standardized by conventional method.[6]

Thiel buffers (boric acid, borax, succinic acid and sodium sulphate) of pH 3–9, sodium acetate-acetic acid buffers of pH 3–6 or tris-(hydroxymethyl)aminomethane–HCl buffer (pH 7–9) were used for pH adjustment and were prepared as recommended.[7,8] The ionic strength, I, of solutions was kept constant at 0.1 ($NaClO_4$). Dimethylformamide was purified by a recommended procedure.[9] The pH-measurement was carried out using on Orion pH-meter (M 601 A). The pH-values in water-solvent mixtures were corrected according to the method of Douheret.[10]

*Author to whom correspondence should be addressed.

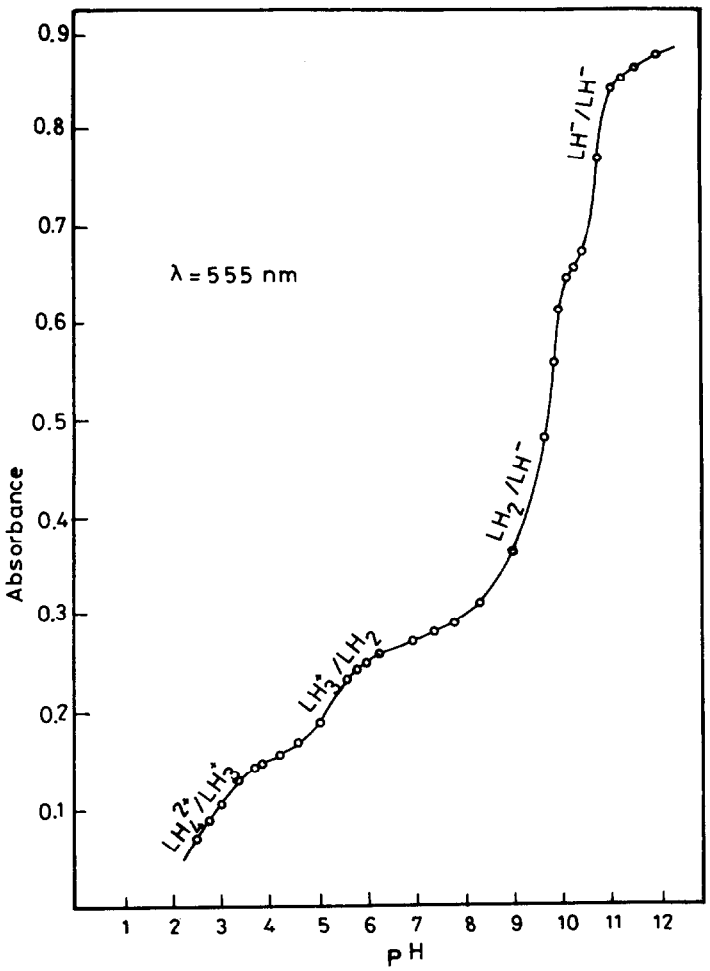


Fig. 1. Variation of absorbance with pH for the QG solution (1.12×10^{-4} M), λ = 555 nm, 40% DMF.

The absorption spectra of solutions were recorded on a Unicam SP 8000 spectrophotometer within the 350–750 nm range using 1 cm matched quartz cells. Measurements were performed at 25 ± 0.1°C.

RESULTS AND DISCUSSION

The absorption spectra of solutions with equimolar amounts of the metal ion and QG or with an excess of one component were investigated at different pH values. The spectra reflect the formation of a complex with a double-headed band (λ_{max} at 600 and 650 nm). The conversion of the orange–yellow protonated form of the ligand LH_3^+ (λ_{max} = 465 nm), which is the predominant species at pH 3–5, to the pink–violet complex of UO_2^{2+} with QG is characterised by a substantial red-shift ($\sim$ 185 nm). Above pH 8, the spectrum of the complex exhibits a more or less symmetrical band with λ_{max} at $\sim$ 650 nm and the colour changes to deep blue. The intensity of the latter band decreases with rise of pH.

Table 1. Dissociation constants of QC in 40% DMF

pK_{a_1} ()	pK_{a_2}	pK_{a_3}
5.15	9.46	10.85

() LH_3^+/LH_2

To explain the complexation equilibria and to establish the stability constant spectrophotometrically, the methods based on the relationship $A = f(pH^*)$ were employed.[11] The absorbance-pH curves in equimolar solutions and with excess metal or with excess ligand (Figs. 2 and 3) exhibit two inflections within the pH range 3–9.5. The two straight line portions of the three curves in the absorbance-pH plots, used for calcu-

Table 2. Data obtained from logarithmic analysis of the absorbance-pH curves, I 0.1

M:L	Slope	Intercept	log K_n(qH)
	(pH range 4-6)		
$C_L = C_M$	1.05[a], 1.00[b]	-2.30[a],-2.50[b]	3.05[a],3.00[b]
C_L/C_M=3	1.05[a], 0.90[b]	-3.75[a],-3.70[b]	3.94[a],2.99[b]
C_M/C_L=3	0.90[a], 0.95[b]	-2.45[a],-2.50[b]	2.98[a],2.93[b]
	(pH range 6-8)		
$C_L = C_M$	1.95[a], 1.90[b]	-11.25[a],-11.50[b]	-5.23[a],-5.39[b]
C_L/C_M=3	1.55[a], 1.60[b]	-12.05[a],-12.00[b]	-5.41[a],-5.36[b]
C_M/C_L=3	2.00[a], 2.00[b]	-11.35[a],-11.55[b]	-5.23[a],-5.34[b]

a) λ = 605 nm,

b) λ = 650 nm.

lations, fall in the pH regions 3.5–5 and 6–8. As indicated in Fig. 4 the absorbance-pH curves indicate the existence of two chelate equilibria. At higher pH values (pH > 8) the absorbance for the U(VI)–QG complex decreases rapidly owing to hydrolysis effect.

The number of protons released during complexation and the equilibrium constants were deduced graphically from the plots obtained with the three metal to ligand mole ratios as follows:

(a) For equimolar solutions, the eqn (1) was applied:

$$K_{eq} = \frac{AA_0^2[H^+]^n}{4C_M^2(A_0 - A)^3} \quad (1)$$

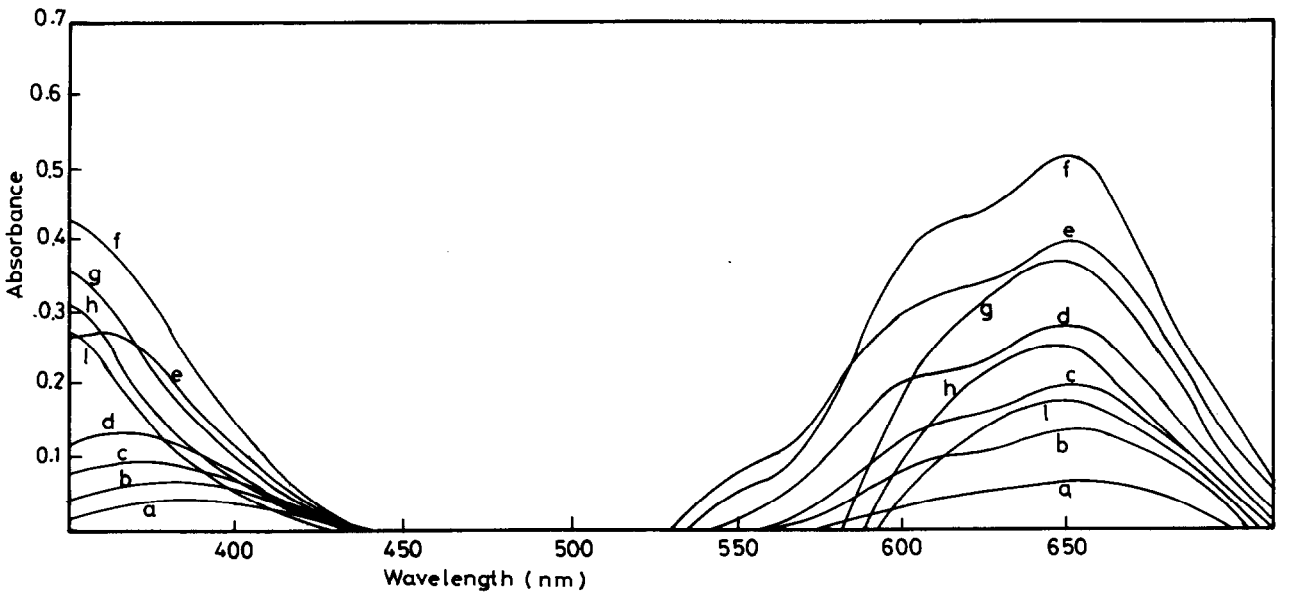


Fig. 2. Absorption spectra of UO_2(II)–QG complexes, $C_L = 2 \times 10^{-4}$ M, $C_M = 2 \times 10^{-4}$ M, I 0.1, 40% DMF; pH: (a) 3.12, (b) 4.36, (c) 5.5, (d) 6.89, (e) 7.22, (f) 7.92, (g) 8.72, (h) 9.39, (i) 9.88.

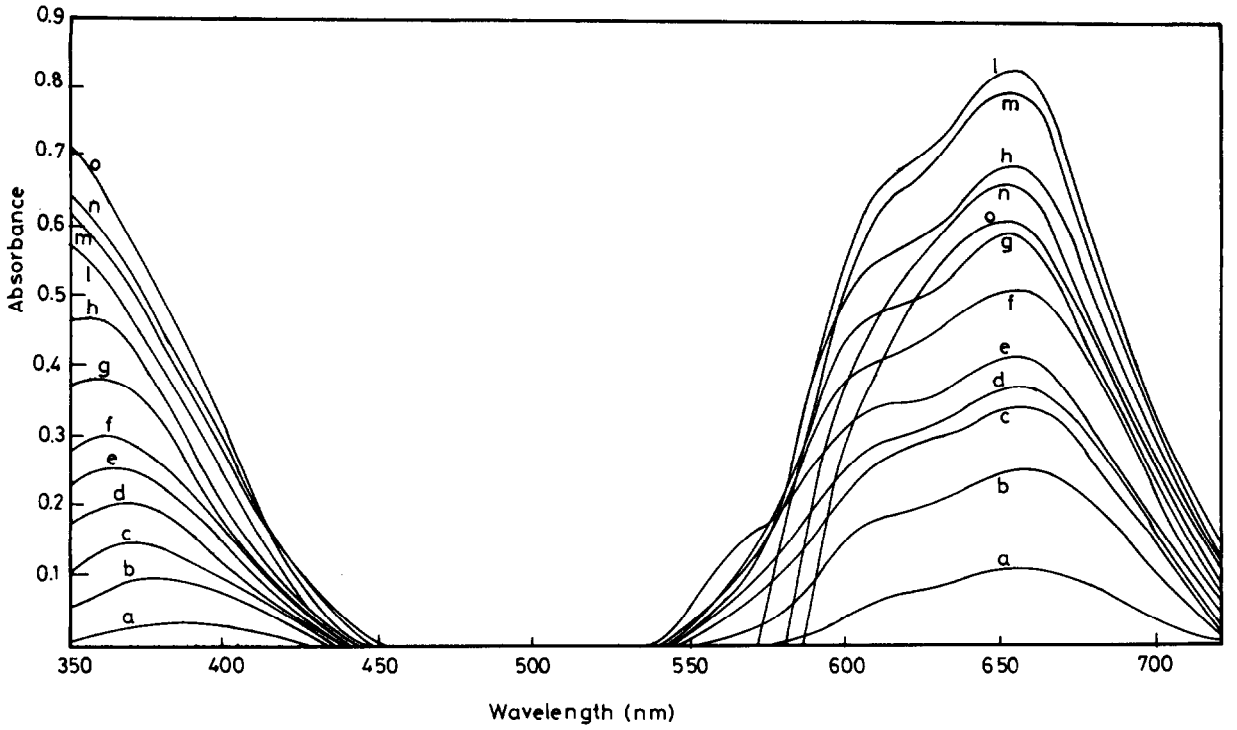


Fig. 3. Absorption spectra of UO_2(II)–QG complexes, $C_L = 4.5 \times 10^{-4}$ M, $C_M = 1.5 \times 10^{-4}$ M, I 0.1, 40% DMF; pH = (a) 3.18, (b) 4.46, (c) 5.4, (d) 6.09, (e) 6.45, (f) 6.95, (g) 7.31, (h) 7.67, (i) 8.19, (m) 8.88, (n) 9.35 (o) 9.65.

where A is the absorbance at given pH value, A_0 is the absorbance maxima and C_M is the total metal concentration. The logarithmic dependence of this equation is a straight line with a slope n and an intercept including K_{eq}:

$$\log \frac{A}{(A_0 - A)^3} = \log K_{eq} - \log \frac{A_0^2}{4C_M^2} + n\text{pH}$$

(b) In the presence of excess metal ion, the following equation is valid

$$K_{eq} = \frac{AA_0^2[H^+]^n}{mC_M^2(2A_0 - mA)(A_0 - A)^2} \qquad (2)$$

where $m = C_L C_m < 1$, C_L being the total ligand concentration. The logarithmic transformation of this equation gives also a straight line.

(c) For solutions with excess of ligand, the logarithmic transformation of the equation:

$$K_{eq} = \frac{\Delta A[H^+]^n}{(\Delta A_0 - \Delta A)C_L^2} \qquad (3)$$

was used.

The stability constants of the complexes β, and values of the molar absorption coefficients ϵ, were found for selected wavelengths from the shape of the non-linear dependences. The number of hydrogen ions released in the reaction

$$M + mLH_n \rightleftharpoons ML_mH_z + qH^+; {}^*B_m$$

were found graphically (the ionic charges were omitted except for protons). In the reaction scheme $n = 3$ or 2 (depending on the pH of the reaction mixtures) and $z + q = nm$.

According to the results of this study, the reaction of U(VI) with QG can be represented by the schemes:

(A) $UO_2^{2+} + LH_3^+ \rightleftharpoons [UO_2(LH_2)]^{2+} + H^+$, $K^*_{1(H^+)}$

(B) $[UO_2(LH_2)]^{2+} + LH_2 \rightleftharpoons UO_2(LH)_2 + 2H^+$, $K^*_{2(2H^+)}$.

In solutions with $C_M = C_L$ or with excess of one component, the logarithmic absorbance-pH curves indicated unambiguously the presence of equilibrium (A) over the entire formation interval pH 4–6. Assuming that LH_3^+ species of QG predominates at this pH range, reaction (A) takes place independently of the metal to ligand ratio and a diprotonated complex is formed.

The complexation equilibrium (B) is attained at pH 6–8.5 in solutions with excess ligand and at pH

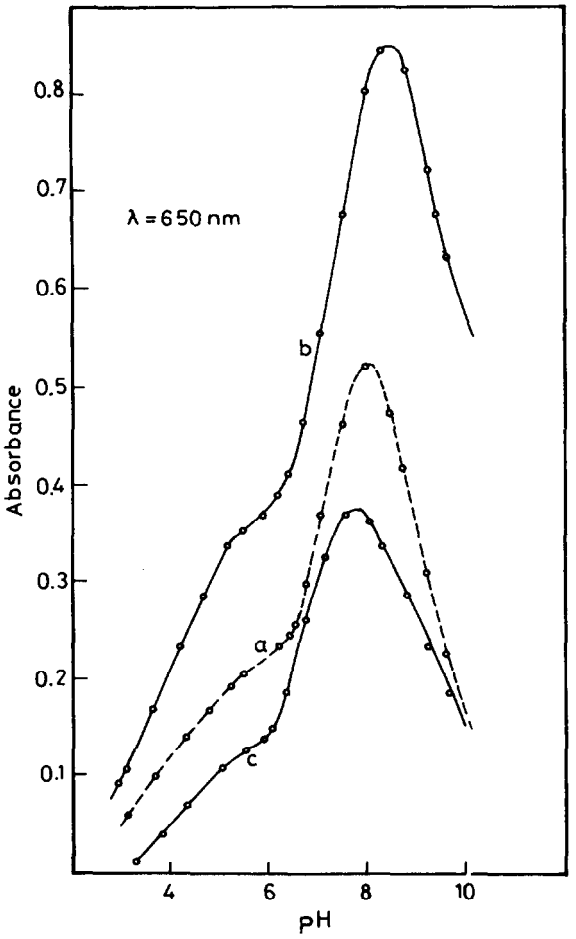


Fig. 4. Absorbance-pH curves in the QG–UO_2(II) system, λ = 650 nm, I 0.1, 40% DMF. (a) $C_L = 2 \times 10^{-4}$ M, $C_M = 2 \times 10^{-4}$ M; (b) $C_L = 4.5 \times 10^{-4}$ M; $C_M = 1.5 \times 10^{-4}$ M; $C_L = 1.67 \times 10^{-4}$ M, $C_M = 5 \times 10^{-4}$ M.

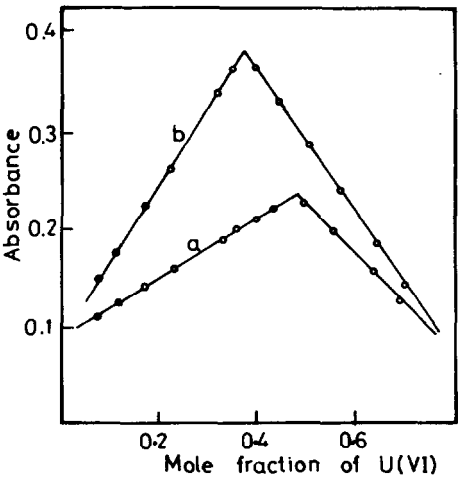


Fig. 5. Continuous variation plots for the QG–UO_2(II) system, λ = 650 nm, 40% DMF, $C_0 = 3.6 \times 10^{-4}$ M. (a) pH = 4.5, (b) pH = 7.8.

6.5–8 in equimolar solution or in presence of excess metal. The component ratios of the complexes was confirmed by the method of continuous variations in equimolar solutions[12] and by the molar ratio method[13] at selected pH values. It follows from the shape of the dependences obtained that U(VI) do not form higher complexes at pH 4.5. It has also been confirmed that the stoichiometry of the complexed ligand at pH 7.8 is 1:2 (M/L) (see Fig. 5).

Equilibrium constants $K_n^*(qH)$ are related to stability constants β_n by the expressions[14]

$$\beta_1 = K^*_{1(H)} \cdot K_{a_1}^{-1}$$

$$\beta_2 = B_1 K^*_{2(2H)} \cdot K_{a_2}^{-1}$$

Table 3. Stability constants and spectral characteristics of U(VI) complexes of QG, 40% (v/v) DMF, 20°C, I 0.1

Log β_1	log β_2	log $K_n(qH)$	λ_{max} nm	ϵ_{max}() l mol^{-1} cm^{-1}	$\Delta\lambda$ nm
8.45	10.29	2.99[a], -5.33[b]	650	3.55×10^3	185(LH_3^+)
					170(LH_2)
					140(LH^-)

() valid for 1:2 complex at 650 nm

a) equilibrium constant for reaction(A), mean value.

b) equilibrium constant for reaction (B), mean value.

$\Delta\lambda$: the difference in the wavelengths of the maximum of the uranium complex and that of the given acid-base form of the reagent.

The constants K_n^* and β_n as concluded from the average values determined at various metal to ligand ratios are given in Table 3.

The effect of buffers

At pH 3–6 sodium acetate-acetic acid, tris-(hydroxymethyl)aminomethane–HCl buffer (pH 7–9) or thiel buffer (boric acid-borax-succinic acid and sodium sulphate) can be employed, as they do not interfere. Buffers based on phosphate, tetraborate, citrate, triethanolamine strongly interfere. Thiel buffer gave the best results.

The effect of DMF

Dimethylformamide affects neither the absorbance of the complexed ligand nor the complex stability at concentrations from 25 to 40% (v/v). At lower concentrations of DMF < 20% the absorbance measurements could not be carried out in acidic solutions owing to the precipitation of the reagent.

The effect of ionic strength

The solution absorbance increases with increasing salt concentration. However, this effect is negligible within I = 0–0.2 ($NaClO_4$).

Determination of uranium (VI) with quinizarin green

The spectrophotometric determination of U(VI) with QG employs the complex with molar ratio M:L = 1:2, which is formed in solutions with equimolar components or with a concentration excess of the ligand, at a pH of 7.5 in a medium of 40% (v/v) DMF. Calibration curves $A = f(C_M)$ are linear up to 49.5 μg U/cm^3 at 605–650 nm, $C_L = 2 \times 10^{-4}$ M ($\epsilon = 3.55 \times 10^3$ for 650 nm).

Procedure. To a 20 cm^3 volumetric flask was gradually added 5 cm^3 of 1×10^{-3} M reagent solution in 40% DMF, 5 cm^3 0.4 M $NaClO_4$, 5 cm^3 thiel buffer (pH = 7.5) and a weakly acidic uranium sample solution containing less than 1 mg U. The solution was diluted to the mark with the required amounts of DMF and doubly-distilled water. After thoroughly mixing the reaction mixture, the absorbance was measured at 650 nm against a reagent blank similarly prepared but containing no uranium.

REFERENCES

1. I. M. Issa, K. A. Idriss and M. M. Seleim, *Monatsh. Chem.* 1977, **108**, 1461.
2. K. A. Idriss, M. M. Seleim and M. M. Khalil, *Monatsh. Chem.* 1978, **109**, 1883.
3. K. A. Idriss and M. M. Seleim, *J. Chem. Tech. Biotech.* 1980, **30**, 136.
4. K. A. Idriss and M. M. Seleim, *Ind. J. Chem.* 1980, **19A**, 771.
5. K. A. Idriss, A. Awad, M. M. Seleim and M. S. Abu-Bakr, *Bull. Soc. Chim. Fr.* 1981, **5**, 1.
6. W. Scott and H. Furman, *Standard Methods of Chemical Analysis*, 6th Edn. Van Nostrand, New York (1962).
7. H. T. S. Britton, *Hydrogen Ions*, 4th Edn. Chapman & Hall, London (1952).
8. D. D. Perrin and B. Dempsey, *Buffers for pH and Metal Ion Control.* Chapman & Hall, London (1974).
9. A. I. Vogel, *Practical Organic Chemistry.* Longman, London (1961).
10. G. Douheret, *Bull. Soc. Chim. Fr.* 1967, 1412.
11. D. Nonova and B. Evtimova, *J. Inorg. Nucl. Chem.* 1973, **35**, 3581.
12. P. Job, *Ann. Chim.* 1928, **9**, 113.
13. J. H. Yoe and H. L. Jones, *Ind. Eng. Chem., Anal. Ed.* 1944, **16**, 111.
14. M. Suchanek and L. Šucha, *Coll. Czech. Chem. Commun.* 1978, **43**, 1393.

Polyhedron Vol. 4, No. 9, pp. 1527–1531, 1985
Printed in Great Britain

0277–5387/85 $3.00 + .00
Pergamon Press Ltd

KINETIC STUDY OF THE REACTION OF *meso*-TETRAKIS (*p*-TRIMETHYLAMMONIUMPHENYL)PORPHINATO-DIAQUORHODATE(III) WITH CHLORIDE, BROMIDE, IODIDE, HEXACYANOCOBALTATE(III) AND THIOCYANATE IONS IN AQUEOUS SOLUTION

J. G. LEIPOLDT* and H. MEYER

Department of Chemistry, University of the Orange Free State, Bloemfontein, Republic of South Africa

(*Received* 4 *September* 1984; *accepted* 18 *December* 1984)

Abstract—The reaction of Cl^-, Br^-, I^-, $Co(CN)_6^{3-}$ and NCS^- with *meso*-tetrakis (*p*-trimethylammoniumphenyl)porphinatodiaquorhodate(III), $[RhTAPP(H_2O)_2]^{5+}$, has been studied at 15, 25 and 35°C in 0.1 M $[H^+]$ with $\mu = 1.00$ M ($NaNO_3$). The value of the acidity constant, K_{al}, at 25°C is 4.39×10^{-9} M. The reactions are first order in anion concentration up to 0.9 M. The values of the stability constants, K_1, and the second order rate constants, k_1, for the reaction with Cl^-, Br^-, I^-, $Co(CN)_6^{3-}$ and NCS^- are respectively 0.23 M^{-1} and 2.5×10^{-3} $M^{-1}\,s^{-1}$, 1.1 M^{-1} and 6.92×10^{-3} $M^{-1}\,s^{-1}$, 40.0 M^{-1} and 17.0×10^{-3} $M^{-1}\,s^{-1}$, 550 M^{-1} and 20.0×10^{-3} $M^{-1}\,s^{-1}$, 3400 M^{-1} and 20.9×10^{-3} $M^{-1}\,s^{-1}$. The porphine greatly labilizes the Rh(III). There has been about a 500-fold increase in the rate constant for substitution compared to that of $[Rh(NH_3)_5H_2O]^{3+}$. The substitution rates are however about the same as for $[Rh(TPPS)(H_2O)_2]^{3-}$, indicating that the overall charge on the complex plays only a minor role. The kinetic results indicate that dissociative activation is occurring in these reactions.

The axial ligand substitution reactions of cobalt(III), rhodium(III) and chromium(III) porphyrins are known to be much faster than for the normal complexes like the metal pentaammineaquo complexes indicating that the porphyrin ligand labilizes the axial positions.[1–7] In the case of the porphine TPPS (TPPS = *meso*-tetra(*p*-sulphonatophenyl)-porphine) the labilization of the axial water molecules was about 10^9 for the cobalt(III) complex,[3,8] about 10^3 and 10^2 for the rhodium(III)[4,8] and chromium(III)[5,8] complexes respectively. The extent of labilization also depends on the porphine. For example the anation reaction of $[Co(TPPS)(H_2O)_2]^{3-}$ are more than 100 times faster than those of $[Co(TMPP)(H_2O)_2]^{5+}$, TMPP = *meso*-tetra(4-N-methylpyridyl)porphine.[1,3] The effect of the different porphines is, as may be expected, not so pronounced in the case of the chromium(III) complexes. The anation reaction of $[Cr(TPPS)(H_2O)_2]^{3-}$ is only 6 times faster than the anation reactions of $[Cr(TMPP)(H_2O)_2]^{5+}$.[5,6] The labilization effect of the porphine ligand is probably due to its ability to donate electron density to the central metal ions, making the metal(III) ions more like the labile metal(II) ions. The fact that the TPPS complexes are more reactive than the TMPP complexes, is in agreement with this view since TPPS is more electron rich and thus a better electron donor than TMPP. The structures of the different porphines are shown in Fig. 1.

The kinetic data that are available, indicate that the labilization of the metal(III) ion is accompanied by promoting a dissociative mechanism. This is probably due to the electron donating capability of the electron rich porphine, not only making the central metal(III) ion more like a metal(II) ion, but also stabilizing the five coordinate intermediate in a dissociative reaction mode. This is also seen in the complete different pressure dependencies found for the anation reactions of $[Co(TPPS)(H_2O)_2]^{3-}$ compared to the results of the substitution reactions of the corresponding metal pentaamineaquo complexes.[8,9] The high-pressure data for the TPPS

* Author to whom correspondence should be addressed.

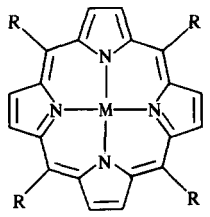
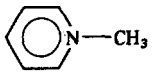
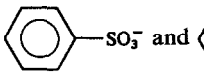
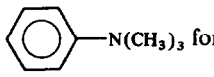


Fig. 1. The structures of the different porphine complexes. M = Co, Rh or Cr. R =   and  for TMPyP, TPPS and TAPP respectively.

complexes suggested a *D* mechanism for the anation reaction of the cobalt(III) complex and an I_d mechanism for the rhodium(III) and chromium(III) complexes.[9]

The formation constants for the $[Rh(TPPS)(H_2O)(X)]^{4-}$ complexes (X = NCS^-, I^-, Br^- and Cl^-) varied by a factor of about 1.6×10^4 whereas the anation reaction rate constants varied only by a factor of about ten.[4] These results also imply a dissociative reaction mode.

This work on the reaction mechanisms of different porphine complexes is extended to the metal complexes of another water soluble porphine TAPP, TAPP = tetrakis(*p*-trimethylammoniumphenyl)-porphine.

EXPERIMENTAL AND RESULTS

The iodide salt of TAPP was synthesized as described by Krishnamurthy.[10] The rhodium complex of this porphine was prepared in the same way as $[Rh(TPPS)(H_2O)_2]^{3-}$:[4] 200 mg of the iodide salt of TAPP was dissolved in 100 cm^3 N,N-dimethylformamide (DMF). The solution was filtered to remove any undissolved impurities. A solution of $[RhCl(CO)_2]_2$ in DMF (prepared by refluxing 100 mg of $RhCl_3 \cdot 3H_2O$ in 20 cm^3 DMF until a yellow solution was obtained;[11] approximately 30 min) was added to the porphine solution. This solution was refluxed for about 60 min until all the free porphine were converted into the rhodium(III) complex as indicated by the visible spectrum. The solution was cooled and about five drops of concentrated $HClO_4$ were added, followed by about 500 cm^3 diethylether to precipitate the rhodium(III) complex. The $[Rh(TAPP)(H_2O)_2](ClO_4)_5$ was washed with ether and allowed to dry in the atmosphere at room temperature. The wavelength of the Soret band for this complex is at 418 nm with molar absorptivity $1.75 \times 10^5\ M^{-1}\ cm^{-1}$.

The determination of the acid dissociation constant, K_{al}, was difficult, as a result of the small change in the absorption spectrum from the acidic form to the basic form. K_{al} was determined at an ionic strength of 1.0 M. In changing the pH between 1 and 13, there was a change in absorbance between about pH 7 and 9 over a pH range of 2. We believe that the absorbance change for the second deprotonation is too small to detect and that the observed absorbance change is the result of the first deprotonation.

Taking into account the mass balance, Beer's law and the definition of K_{al} (Scheme 1), we can write

$$A = \frac{A_b K_{al} + A_a[H^+]}{K_{al} + [H^+]}. \qquad (1)$$

A is the absorbance at a particular $[H^+]$, A_b is the absorbance of the deprotonated form and A_a is the absorbance of the protonated form. The absorbance vs pH data were fitted to eqn (1) by using a nonlinear least squares program.[12] The change in the absorbance at 435 nm as a function of pH is shown in Fig. 2. The solid line is the computer fit of the data. The value of K_{al} at 25°C and μ = 1.0 M is 4.39×10^{-9} M.

The values of the stability constant K_1 (Scheme 1)

$$\begin{array}{ccc} [RhTAPP(H_2O)_2]^{5+} + L^{n-} & \underset{k_{-1}}{\overset{k_1; K_1}{\rightleftharpoons}} & [RhTAPP(H_2O)L]^{(5-n)+} + H_2O \\ K_{al},\ -H^+ \Big\downarrow\Big\uparrow +H^+ & & \\ [RhTAPP(H_2O)(OH)]^{4+} & & \end{array}$$

Scheme 1. Reaction scheme under the experimental conditions

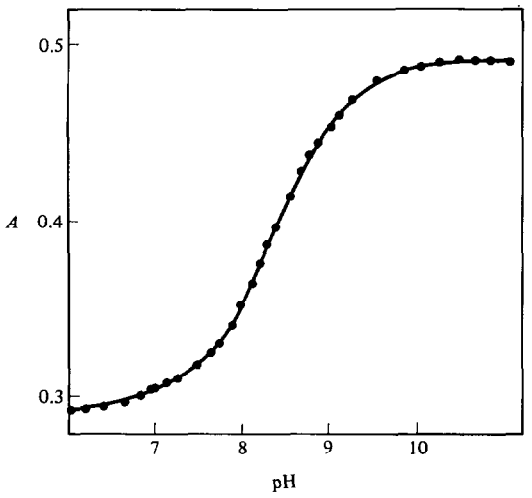


Fig. 2. Change in absorbance as a function of pH at 435 nm. The solid line is the least squares fit of the data using eqn (1).

for the different ligands were determined spectrophotometrically in 0.1 M HNO_3 and an ionic strength of 1.0 M at 25°C. The following equation is derived from the definition of K_1 and Beer's law

$$A = \frac{A_r + A_p K_1[L]}{1 + K_1[L]}. \quad (2)$$

A_r is the absorbance of the reactant, A_p the absorbance of the product and A the absorbance at the particular concentration of the incoming ligand L. The absorbance vs $[L]$ data were fitted to eqn (2) by using a nonlinear least squares program with A_r held constant at the experimental value. Figure 3 is a typical curve, with the solid line the computer calculated line. The results for the various ligands are represented in Table 1.

The anation reaction of $[Rh(TAPP)(H_2O)_2]^{5+}$ by $[Co(CN)_6]^{3-}$, NCS^-, I^-, Br^- and Cl^- were studied at 15, 25 and 35°C in 0.1 M HNO_3 and $\mu = 1.0$ M ($NaNO_3$). It was established that the reaction rates were $[H^+]$ independent at $[H^+] > 10^{-4}$ M.

The rate law under these experimental conditions is

$$-\frac{d[RhTAPP(H_2O)_2^{5+}]}{dt} = (k_1[L] + k_{-1})[Rh(TAPP)(H_2O)_2^{5+}]. \quad (3)$$

All the kinetic studies were performed under pseudo-first order conditions with

$$k_{obs} = k_1[L] + k_{-1}. \quad (4)$$

Figure 4 is a typical plot of k_{obs} vs $[L]$ for L = NCS^-. The kinetic results obtained in this way, are summarized in Table 1. The values of k_{-1} were calculated from the values of K_1 and k_1. The activation parameters were calculated by means of a nonlinear least square program fit of the data to the Eyring–Polanyi equation and are also reported in Table 1.

The accuracy of the rate constants, as well as the equilibrium constants, was not as good as one would like. This was due to the formation of a precipitate near the completion of the reaction. The value of the absorbance at the completion of the reaction was thus accordingly calculated by means of a computer fit of the absorbance vs reaction time data. The rate constants obtained by this method were verified by the Guggenheim method.

The small, but significant change in the absorbance with pH, as well as the determination of the stability constants and the kinetic data, point to a

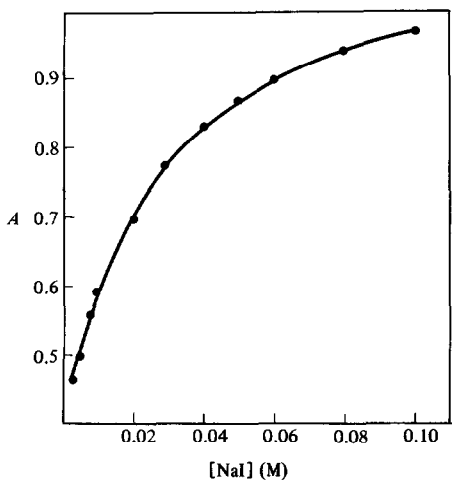


Fig. 3. Plot of absorbance vs $[I^-]$ at 25°C, $\lambda = 418$ nm. The solid line is the computer fit of the data to eqn (2).

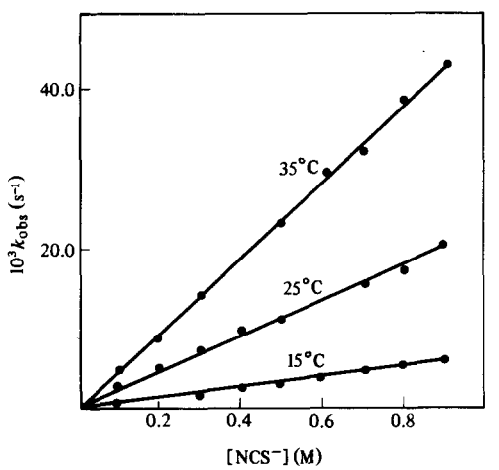


Fig. 4. Plot of k_{obs} vs $[NCS^-]$ at $[H^+] = 0.1$ M, $\mu = 1.0$ M.

Table 1. Kinetic and equilibrium data for the reaction $RhP(H_2O)_2^{5+} + L^{n-} \rightleftharpoons RhP(H_2O)L^{(5-n)+} + H_2O$ (H^+) = 0.1 M, μ = 1.00 M: the rate constants are at 25°C

	$Co(CN)_6^{3-}$	NCS^-	I^-	Br^-	Cl^-
$10^{-3}\,k_1$[a], $M^{-1}\,s^{-1}$	20.0	20.9	17.0	6.92	2.50
k_{-1}[a], s^{-1}	3.64×10^{-5}	6.15×10^{-6}	4.25×10^{-4}	6.29×10^{-3}	1.09×10^{-2}
K_1[a], M^{-1}	550	3400	40	1.1	0.23
$\Delta H^{\#}$[a](k_1)	15.8	15.9	27.4	21.2	15.6
$\Delta S^{\#}$[a](k_1)	−13	−9.3	−13	−8.3	−9.0
$10^{-3}\,k_1$[b], $M^{-1}\,s^{-1}$	—	27.3	20.1	5.7	2.6
k_{-1}[b,c], s^{-1}	—	2.2×10^{-3}	0.49	3.2	3.7
K_1[b], M^{-1}	—	12,200	41	1.8	0.7

[a] P = TAPP.
[b] P = TPPS.
[c] $k_{-1} = k_1/K_1$.
$\Delta H^{\#}$ in kcal $mole^{-1}$.
$\Delta S^{\#}$ in kcal $mole^{-1}$ $degree^{-1}$.

similar reaction scheme as proposed for the anation reactions of $[Rh(TPPS)(H_2O)_2]^{3-}$ [4]— see Scheme 1. The fact that the rate constants were pH independent for $[H^+] > 10^{-4}$ M clearly indicate that $[Rh(TAPP)(H_2O)_2]^{5+}$ is the only reactive species under our experimental conditions.

DISCUSSION

The trend in the values of the stability constants, see Table 1, indicates that the rhodium(III) behaves as a soft acid towards the different ligands. This is the case for all the porphine complexes of rhodium(III), cobalt(III) and chromium(III) studied so far and may be explained in view of the delocalized electron density in the porphine ligand that is apparently available to the central metal ion. The formation constants for the reaction of $[Rh(TAPP)(H_2O)_2]^{5+}$ with the different ligands are about the same as found for the $[Rh(TPPS)(H_2O)_2]^{3-}$ complex—see Table 1. These results indicate that the overall change on the complex plays a minor role and that π-bonding is important in the metal–ligand bonding.

The reaction of $[Rh(TAPP)(H_2O)_2]^{5+}$ with NCS^-, $[Co(CN)_6]^{3-}$, I^-, Br^- and Cl^- shows no deviation from second order kinetics up to 0.9 M in the concentration of the incoming ligand. There is thus no kinetic evidence for an intermediate. As there is also no other evidence for an intermediate, the possibility of a *D* or *A* mechanism for these reactions may be rejected. The comparison of the stability constants and the rate constants, however, gives an indication of the mode of activation. The stability constants vary by a factor of about 1.5×10^4, while the rate constants (k_1) vary by a factor of only about 8. These results indicate that the rate is not sensitive to the nature of the incoming ligand, but very sensitive to the nature of the leaving group. This is indicative of a dissociative reaction mode.

If an I_d mechanism is assumed, see eqns (5) and (6), the observed rate constants are a measure of $K_{os}k_i$.

$$[Rh(TAPP)(H_2O)_2]^{5+} + X^- \overset{K_{os}}{\rightleftharpoons} [Rh(TAPP)(H_2O)_2 \cdot X]^{4+}, \quad (5)$$

$$[Rh(TAPP)(H_2O)_2 \cdot X]^{4+} \overset{k_i}{\rightarrow} [Rh(TAPP)(H_2O)(X)]^{4+} + H_2O. \quad (6)$$

The relative small difference in the values of the observed anation rate constants is thus indicative of a dissociative activation since the values $K_{os}k_i$ are expected to remain fairly constant for similarly charged incoming ligands.[13]

Figure 5 is a plot of log k_{-1} vs log K_1 for the various incoming ligands. The line is drawn with a unit slope. This linear relationship is indicative of a dissociative activation.

The reaction rate constants for the reaction of $[Rh(TPPS)(H_2O)_2]^{3-}$ with the different incoming ligands, are also given in Table 1. It is clear that the anation rate constants and the equilibrium constants for the reaction of $[Rh(TPPS)(H_2O)_2]^{3-}$ and $[Rh(TAPP)(H_2O)_2]^{5+}$ with the different incoming ligands are very similar. The overall charge on the complex thus plays a minor role in the reaction process. In this respect, it is important to note that the overall charge on the complex is spread over a large planar surface area since the negatively charged sulphonato groups and the positively charged trimethylammonium groups are removed far from

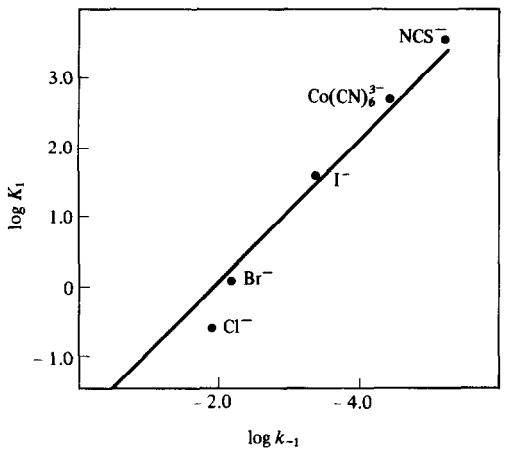


Fig. 5. Plot of log K_1 vs log k_{-1} for the various ligands. The line is drawn with unit slope.

the metal centre. Further evidence for an I_d mechanism for the anation reaction of $[Rh(TAPP)(H_2O)_2]^{5+}$ is this similarity in the anation rate constants for these two complexes and the fact that it was established by means of high-pressure kinetic data that the anation reaction between $[Rh(TPPS)(H_2O)_2]^{3-}$ and NCS^- proceeds via an I_d mechanism.[9] The similarity of the activation parameters for substitution reactions of these two complexes support this hypothesis.

The kinetic data clearly indicate that the porphine ligand labilizes the rhodium(III) ion, although not as much as in the case of the cobalt(III) complexes. The anation rate constants are about 500 times faster than the anation rate constants for $[Rh(NH_3)_5H_2O]^{3+}$. The central metal ion seems thus to control not only the extent to which the porphine ligand modifies the mode of the substitution process, but also the extent of labilization.

Acknowledgements—We thank the South African CSIR and the research fund of this University for financial support.

REFERENCES

1. R. F. Paternack, M. A. Cobb and N. Sutin, *Inorg. Chem.* 1975, **14**, 866.
2. K. R. Ashley and S. Au-Young, *Inorg. Chem.* 1976, **15**, 1937.
3. K. R. Ashley and J. G. Leipoldt, *Inorg. Chem.* 1981, **20**, 2326.
4. K. R. Ashley, Shaw-Bey Shyu and J. G. Leipoldt, *Inorg. Chem.* 1980, **19**, 1613.
5. K. R. Ashley, J. G. Leipoldt and V. K. Joshi, *Inorg. Chem.* 1980, **19**, 1608.
6. J. G. Leipoldt, S. S. Basson and D. R. Rabie, *J. Inorg. Nucl. Chem.* 1981, **43**, 3239.
7. J. G. Leipoldt, S. S. Basson, G. J. Lamprecht and D. R. Rabie, *Inorg. Chim. Acta* 1981, **51**, 67.
8. R. van Eldik, D. A. Palmer and H. Kelm, *Inorg. Chem.* 1979, **18**, 1520.
9. J. G. Leipoldt, R. van Eldik and H. Kelm, *Inorg. Chem.* 1983, **22**, 4146.
10. M. Krishnamurthy, *Indian J. Chem.* 1977, **15B**, 964.
11. A. Rusina and A. A. Vlcek, *Nature* 1965, **206**, 295.
12. R. Moore, Rep. No. La 2367, Los Alamos Scientific Laboratory (1960).
13. A. Haim, *Inorg. Chem.* 1970, **9**, 426.

Polyhedron Vol. 4, No. 9, pp. 1533–1535, 1985
Printed in Great Britain

0277–5387/85 $3.00 + .00
© 1985 Pergamon Press Ltd

THE ^{31}P NMR CHEMICAL SHIFTS OF FOUR-, FIVE- AND SIX-COORDINATE PHOSPHORUS(V) COMPOUNDS

KEITH B. DILLON*
Chemistry Department, University of Durham, South Road, Durham DH1 3LE, U.K.

and

ROGER N. REEVE
Schools of Chemical Engineering, University of Bradford, Bradford, West Yorkshire BD7 1DP, U.K.

(*Received* 23 *November* 1984; *accepted* 20 *February* 1985)

Abstract—There appears to be a correlation between the ^{31}P chemical shift differences between A^+ and AX (Δ_1), and between A^+ and AX_2^- (Δ_2), where A^+ is a phosphonium ion and X is an anionic ligand. This relationship holds for a wide range of substituents on phosphorus, despite the expected changes in hybridisation along the series, and is very useful for predicting the shifts of new or unknown species.

During investigations into the coordination chemistry of phosphorus(V) compounds[1–6] we observed a correlation between Δ_1, the ^{31}P chemical shift difference between a phosphonium ion A^+ and the corresponding phosphorane AX, and Δ_2, the corresponding shift difference between A^+ and AX_2^-, where X is an anionic ligand;[7] further data, both from this research group[8–11] and the literature,[12–20] has shown its wide applicability to a large variety of substituents on phosphorus.

The ^{31}P chemical shifts of some phosphorus(V) compounds A^+, AX and AX_2^- are shown in Table 1, together with Δ_1 and Δ_2. All shifts have been rounded off to the nearest ppm, and are expressed relative to 85% H_3PO_4, with the downfield direction taken as positive. Δ_1 is plotted against Δ_2 in Fig. 1. It is clear that Δ_1 and Δ_2 increase systematically in the same direction; the relationship is not perfectly linear—indeed there is no reason to expect a linear correlation—but appears to tail off for higher values of Δ_1 and Δ_2. The best straight line from a least squares fit of the data, neglecting the last point, is shown.

The occurrence of this relationship is rather unexpected since the change in coordination number is expected to cause a change from sp^3 (ψ-tetrahedral) through sp^3d (trigonal bipyramidal or square pyramidal[21]) to sp^3d^2 (ψ-octahedral) hybridisation. There are also greater possibilities of Π-bonding in the four-coordinate species with suitable substituents present, although Π-bonding may still be possible in special cases even in six-coordinate compounds.[22]

One other system for which the shifts of the four- and six-coordinate species as well as the molecular form have been reported is for addition of Cl to $EtPCl_3^+$.[9] There is a problem, however, in that the chemical shift for $EtPCl_4$ is difficult to establish in $PhNO_2$, the solvent used for recording the shifts of $EtPCl_3^+$ and $EtPCl_5^-$, since it appears to be partially dissociated in this solvent.[9] If δ ^{31}P for $EtPCl_4$ is taken as −24.2 ppm from the results in CH_2Cl_2 and

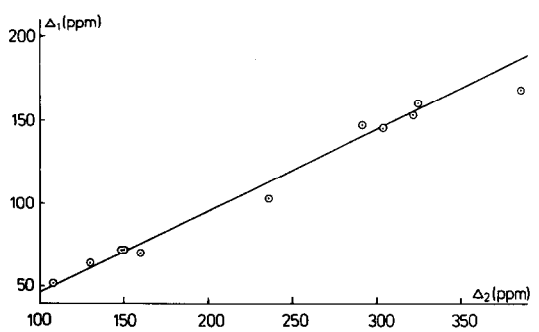


Fig. 1. Relationship between Δ_1 and Δ_2 for some phosphorus(V) species.

* Author to whom correspondence should be addressed.

Table 1. Shift data for A^+, AX and AX_2^-

A	X	δ ^{31}P (ppm) for A^+	AX	AX_2^-	Δ_1	Δ_2	References
$(C_6H_4O_2)_2P$	Cl	42	−10	−66	52	108	6
$(PhO)_4P$	PhO	−22	−86	−152	64	130	8, 12
$(C_6H_4O_2)_2P$	PhO	42	−30	−107	72	149	6, 13, 14
$(MeO)_4P$	MeO	5	−67	−145	72	150	15, 16
$(C_6H_4O_2)_2P$	N_3	42	−28	−113	70	155	6, 17
$(C_6H_4O_2)PCl_2$	Cl	77	−26	−159	103	236	6
Me_2PF_2	F	155	8	−137	147	292	18, 19
$PhPCl_3$	Cl	101	−44	−203	145	304	2, 5
$C_6F_5PCl_3$	Cl	82	−71	−240	153	322	10
$MePCl_3$	Cl	120	−40	−205	160	325	9
PCl_4	Cl	88	−80	−298	168	386	1, 11, 20

C_6H_6,[9] Δ_2 is lower than expected from Fig. 1. It is possible that $EtPCl_5^-$ is always partially dissociated, even at high chloride ion concentrations, and that the shift value of −138.0 ppm, although the highest obtainable in $PhNO_2$,[9] does not represent the limiting shift for this ion. This hypothesis is in accordance with UV results, which suggested that partial formation only of $EtPCl_5^-$ took place when $EtPCl_4$ was treated with either Me_4NCl or Et_3PCl_2.[23] The alternative possibility of a lower field value than −24.2 ppm for molecular $EtPCl_4$ in $PhNO_2$, thus lowering Δ_1, cannot be entirely discounted, however.

Geometrical isomerism is possible in the six-coordinate complexes with two different substituents present and at least two of each type of ligand. For the compounds in Table 1 this applies to the addition of either two Cl, two PhO or two N_3 groups to $(C_6H_4O_2)_2P^+$, but only one shift was reported for the six-coordinate species in each case.[6,14,17] These results imply either preferential formation of one structural isomer or rapid exchange on the NMR time-scale between the possible isomers. $Me_2PF_4^-$ may also exist in isomeric forms, but again only one ^{31}P shift was reported.[19] ^{1}H and ^{19}F NMR data for this anion suggested either a *trans* configuration of the methyl groups or a fluxional species at room temperature, but the limited solubility of the salts at lower temperatures prevented *T*-dependence studies of the ^{19}F NMR,[24] which would have clarified this ambiguity. In any event the shift differences between isomeric six-coordinate phosphorus(V) species are usually small[5,9,22,25–28] compared with the values of Δ_1 and Δ_2 in Table 1, and seem unlikely to affect the graph significantly.

The plot is very useful for predictive purposes. For example, the shift of the ion PF_4^+, which is known in the compound $PF_4^+Sb_3F_{16}^-$[29] but for which no ^{31}P NMR has been recorded, may be predicted as *ca* −15 ppm from the shifts of PF_5[30] and PF_6^-.[25] Similarly the shift of the unknown ion $Ph_2PCl_4^-$ may be derived as *ca* −150 ppm from the data for $Ph_2PCl_2^+$ and Ph_2PCl_3.[11,31]

REFERENCES

1. K. B. Dillon, R. J. Lynch, R. N. Reeve and T. C. Waddington, *J. Inorg. Nuclear Chem.* 1974, **36**, 815.
2. K. B. Dillon, R. J. Lynch, R. N. Reeve and T. C. Waddington, *J. Chem. Soc., Dalton Trans.* 1976, 1243.
3. K. B. Dillon, R. N. Reeve and T. C. Waddington, *J. Chem. Soc., Dalton Trans.* 1977, 1410.
4. K. B. Dillon, R. N. Reeve and T. C. Waddington, *J. Chem. Soc., Dalton Trans.* 1977, 2382.
5. K. B. Dillon, R. N. Reeve and T. C. Waddington, *J. Chem. Soc., Dalton Trans.* 1978, 1318.
6. K. B. Dillon, R. N. Reeve and T. C. Waddington, *J. Chem. Soc., Dalton Trans.* 1978, 1465.
7. R. N. Reeve, Ph.D. Thesis, Durham (1975).
8. M. P. Nisbet, Ph.D. Thesis, Durham (1976).
9. R. M. K. Deng and K. B. Dillon, *J. Chem. Soc., Dalton Trans.* 1984, 1911.
10. R. Ali and K. B. Dillon (unpublished work).
11. K. B. Dillon, M. P. Nisbet and T. C. Waddington, *Polyhedron* 1982, **1**, 123.
12. C. L. Lerman and F. H. Westheimer, *J. Am. Chem. Soc.* 1976, **98**, 179.
13. F. Ramirez, A. J. Bigler and C. P. Smith, *Tetrahedron* 1968, **24**, 5041.
14. D. Hellwinkel and H.-J. Wilfinger, *Chem. Ber.* 1970, **103**, 1056.
15. I. Ruppert, *Z. anorg. Chem.* 1981, **477**, 59.

16. D. B. Denney, D. Z. Denney and C.-F. Ling, *J. Am. Chem. Soc.* 1976, **98**, 6755.
17. A. Skowronska, M. Pakulski and J. Michalski, *J. Am. Chem. Soc.* 1979, **101**, 7412.
18. J. F. Nixon and R. Schmutzler, *Spectrochim. Acta* 1964, **20**, 1835.
19. M. Brownstein and R. Schmutzler, *J. Chem. Soc., Chem. Commun.* 1975, 278.
20. V. Mark, C. H. Dungan, M. M. Crutchfield and J. R. Van Wazer, *Topics Phosphorus Chem.* 1967, **5**, 227.
21. R. K. Brown and R. R. Holmes, *Inorg. Chem.* 1977, **16**, 2294.
22. K. B. Dillon and A. W. G. Platt, *J. Chem. Soc., Dalton Trans.* 1982, 1199.
23. L. M. Sergienko, G. V. Ratovskii, V. I. Dmitriev and B. V. Timokhin, *Zh. Obshch. Khim.* 1981, **51**, 495.
24. W. Stadelmann, O. Stelzer and R. Schmutzler, *J. Chem. Soc. D, Chem. Commun.* 1971, 1456.
25. K. B. Dillon and A. W. G. Platt, *J. Chem. Soc., Dalton Trans.* 1983, 1159.
26. K. B. Dillon, A. W. G. Platt and T. C. Waddington, *J. Chem. Soc., Dalton Trans.* 1980, 1036.
27. K. B. Dillon and A. W. G. Platt, *J. Chem. Soc., Chem. Commun.* 1983, 1089.
28. K. B. Dillon and A. W. G. Platt, *Phosphorus and Sulfur* 1984, **19**, 299.
29. G. S. H. Chen and J. Passmore, *J. Chem. Soc., Chem. Commun.* 1973, 559.
30. L. Maier and R. Schmutzler, *J. Chem. Soc. D, Chem. Commun.* 1969, 961.
31. D. B. Denney, D. Z. Denney and B. C. Chang, *J. Am. Chem. Soc.* 1968, **90**, 6332.

Polyhedron Vol. 4, No. 9, pp. 1537–1542, 1985
Printed in Great Britain

0277–5387/85 $3.00 + .00
Pergamon Press Ltd

OPTICAL ACTIVITY OF COMPOUNDS FORMED BY AMINO-COMPLEXES OF Co(III) AND CARBOHYDRATES—I

S. BUNEL* and C. IBARRA

Departamento de Análisis Químico, Facultad de Ciencias Básicas y Farmacéuticas, Universidad de Chile, Casilla 233, Santiago, Chile

(*Received* 2 *January* 1985; *accepted* 20 *February* 1985)

Abstract—The preparation of aminocomplexes of Co(III) containing D-ribose, L-sorbose or D-glucosamine as second ligand is described. Their spectral features and optical activity are reported. Formation in solution of complex species with other chosen carbohydrates gives ground for discussion as to the origin and sign of the observed Cotton effects.

While the formation of complexes by interaction of carbohydrates with metallic ions has been a subject of ever increasing interest,[1] the generation of optically active species has received little attention as compared with other chiral ligands.

We herein report the results of a study which was originally aimed at finding out whether the asymmetric medium provided by a carbohydrate in solution was able to orient the chelate rings of the complex *cis*-$[Co(phen)_2(H_2O)_2]^{3+}$,[2] (phen = 1,10-phenanthroline), according to a preferred chirality. The presence of a Cotton effect under the Co(III) ion first visible absorption band and the existence of carbohydrate in the compound chromatographically isolated from the reacting mixture revealed that coordination of the carbohydrate to the metallic ion takes place.

Preliminary studies showed that other amino-complexes of Co(III) such as *cis*-$[Co(en)_2(H_2O)_2]^{3+}$, (en = ethylenediamine),[3] and *cis*-$[Co(NH_3)_4(H_2O)_2]^{3+}$ react in the same way with several monosaccharides, incorporating them into the coordination sphere.

We will here show results of measurements performed on compounds formed by reaction between the complex ion *cis*-$[Co(NH_3)_4(H_2O)_2]^{3+}$ and the monosaccharides D-ribose, L-sorbose and D-glucosamine. These last were chosen considering the number of asymmetric carbon atoms per molecule, the series they belong to, and the presence of an amino group which has a good donor atom in the case of D-glucosamine (Fig. 1).

At the same time, studies in solution were carried out with the same Co(III) aminocomplex and other carbohydrates in an attempt to find a correlation between the characteristics of the observed Cotton effects and their structure.

EXPERIMENTAL

Materials

The carbohydrates came from Merck and were used without further purification, but their $[\alpha]_D^t$ values were checked.

The complex *cis*-$[Co(NH_3)_4(H_2O)_2]_2(SO_4)_3 \cdot 3H_2O$ was synthesized in the laboratory following reported methods.[4]

Preparation of $[Co(NH_3)_4(D\text{-}ribose)]_2(SO_4)_3 \cdot 4H_2O$

A mixture of 0.835 g (1.25 mmole) of

cis-$[Co(NH_3)_4(H_2O)_2]_2(SO_4)_3 \cdot 3H_2O$

and 3.750 g (25 mmole) of D-ribose is dissolved in 25 cm^3 of water and the solution pH is adjusted to 6.2 with drops of ammonia solution. The temperature of

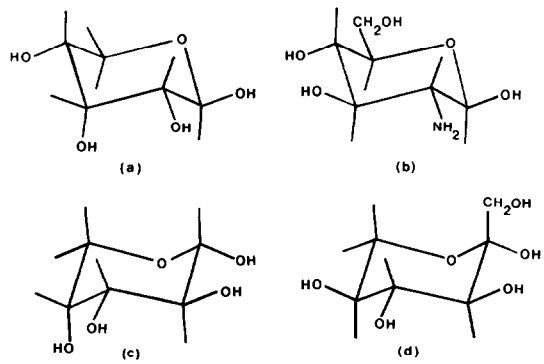


Fig. 1. (a) β-D-ribose; (b) β-D-glucosamine (2-amino-2-deoxy-D-glucose); (c) α-D-arabinose; (d) α-L-sorbose.

* Author to whom correspondence should be addressed.

the reacting mixture is kept at 30°C for 60 min in a thermoregulated water bath. A sample of the solution is placed in a thermostatted polarimetric cell of 0.5 cm pathlength and the course of the reaction is followed through the change of rotation of polarized light at 475 nm. Once the reaction stops the solution is removed from the bath and poured into a beaker, and 25 cm^3 of methanol is added dropwise with constant stirring. The liquid is then centrifuged to eliminate traces of the polynuclear complex

$[Co\{(OH)_2Co(NH_3)_4\}_3](SO_4)_3nH_2O$ (n = 2–9),[5]

which is also formed in the course of the reaction and it was identified by analysis and IR spectrum. Methanol is then added to the clear solution with constant stirring up to a total addition of 100 cm^3. During this process, the formation is observed of a microcrystalline precipitate which adheres to the walls of the beaker. The precipitate is separated by filtration in glass plates, washed with 5 cm^3 methanol and then 5 cm^3 ethanol; it is then quickly removed from the plate and dried under vacuum. The yield is about 350 mg.

The microcrystalline solid is deep pink, very soluble in water, giving a solution of the same colour. The solid compound is stable if kept in a dry atmosphere.

Found: C, 13.18; H, 5.48; N, 12.47; Co, 13.86; SO_4, 31.32. Calc: C, 13.13; H, 5.68; N, 12.25; Co, 12.91; SO_4, 31.51%.

Preparation of $[Co(NH_3)_4$(L-*sorbose*)$]_2(SO_4)_3$

0.835 g (1.25 mmole) of *cis*-$[Co(NH_3)_4(H_2O)_2](SO_4)_3 \cdot 3H_2O$ and 4.5 g (25 mmole) of L-sorbose are dissolved in 25 cm^3 of water; the solution pH is raised to nearly 6.5 with drops of ammonia solution. The procedure previously described is followed, but in this case the maximum value of rotation is reached after 45 min of heating at 30°C. The yield is 400 mg.

The compound is a deep pink microcrystalline solid, stable in a dry atmosphere. It is soluble in water and the solutions decompose slowly. Dissociation of the complex species was checked by measuring the rotation of solutions prepared by successive dilutions.

Found: C, 15.49; H, 5.43; N, 12.67; Co, 14.3; SO_4, 32.63. Calc: C, 15.96; H, 5.32; N, 12.42; Co. 13.8; SO_4, 31.93%.

Preparation of $[Co(NH_3)_3$(D-*glucosamine*)$]_2(SO_4)_3 \cdot 4H_2O$

A mixture of 0.835 g (1.25 mmole), of

cis-$[Co(NH_3)_4(H_2O)_2]_2(SO_4)_3 \cdot 3H_2O$

and 2.69 g (12.5 mmole) of D-glucosamine hydrochloride is dissolved in 55 cm^3 of water; the solution pH is raised to 7 with drops of ammonia solution. The procedure described for the preparation of the complexes previously mentioned is applied with the following modifications: (a) the time needed to reach the maximum value of rotation at 475 nm is 40 min; (b) after addition of the first 25 cm^3 of methanol to the solution and centrifugation, another 50 cm^3 of the same solvent is added. Formation is observed of a viscous dark red product adhering to the walls of the beaker. The supernatant is then separated and residues of methanol and water are evaporated with an air current. The viscous material is redissolved in 3 cm^3 of water and then poured, drop by drop, into 70 cm^3 of 95% methanol containing about 100 mg $NaClO_4$. The liquid is constantly stirred during the process. The yield is 400 mg.

The compound is a violet microcrystalline solid, water soluble, giving deep red solutions. It is a stable compound in the absence of humidity.

Found: C, 15.47; H, 5.52; N, 12.01; Co, 12.45; SO_4, 31.36. Calc: C, 15.38; H, 5.55; N, 11.96; Co, 12.60; SO_4, 30.76%.

Analyses of C, H and N were performed with a Perkin–Elmer 240 microanalyzer. Carbon was also determined from the sugar content and analyzed by oxidation with ceric sulphate,[6] and nitrogen was checked as NH_3 with a specific electrode, after digestion with sulphuric acid.

Cobalt content was iodometrically determined as Co_2O_3.[7]

Sulphate analyses were carried out both gravimetrically and by means of a chloride-exchange resin in a column, the exchanged chloride being measured with an appropriate electrode.

Water of hydration was estimated by variation in whole number multiples to give best agreement with analytical data. Compounds with different number of hydration water molecules are obtained. Results herein reported correspond to one batch in each case. These variations in composition are reflected through bigger or smaller values of the measured optical activity.

Absorption spectra were measured with a Zeiss PMQ-2 spectrophotometer over 10^{-2} to 10^{-3} M solutions of the complexes.

Optical rotatory dispersion measurements were carried out with a modified Perkin–Elmer 141 polarimeter and Bausch and Lomb monochromator over 10^{-2} M water solutions using 2 cm pathlength cells. Variation of the angle of rotation against time was followed employing a 0.5 cm pathlength cell.

Circular dichroism measurements were carried out with a Schimadzu QV-50 spectrophotometer

fitted with circular dichroism attachment, on 10^{-2} M solutions with 1 cm pathlength cells.

RESULTS AND DISCUSSION

Figure 2 is shown as an example of the optical activity of the reaction product in solution between the Co(III) aminocomplex and D- and L-arabinose respectively, once the maximum value of rotation at one wavelength is reached in each case. These carbohydrates were chosen because they are enantiomorphs. They give optical rotatory dispersion curves of opposite sign. It can also be seen that, considering the dispersion curve of the carbohydrate as a base line, two Cotton effects are apparent in the region of Co(III) visible first absorption band. Maximum rotation is attained after 100 min.

The reagent *cis*-$[Co(NH_3)_4(H_2O)_2]^{3+}$ has two visible absorption bands: the first one is located at 505 nm and the second one at 355 nm. Introduction of carbohydrate into the coordination sphere causes a shift of the first absorption band maximum to 525 nm and of the second one to 375 nm. Besides, the second band is overlapped by an intense charge-transfer transition located at 220 nm with an extinction coefficient of 11,600 cm^2 $mole^{-1}$.

From the spectroscopic point of view, complexes of the type $[Co(NH_3)_4(carbohydrate)]^{3+}$ behave like the complex $[Co(NH_3)_4CO_3]^+$,[8] whose first and second absorption bands are located at 522 and 360 nm respectively. The spectra correspond, in both cases, to the coordination of 4 nitrogen and two *cis*-oxygen atoms around the Co(III) ion. Therefore the carbohydrate contribution would turn out to be similar to that of the carbonate ion.

In the complexes formed by D-ribose and L-sorbose the second absorption band keeps its identity (Table 1); but in the complex with D-glucosamine overlapping is broader and the second *d–d* band appears as only a shoulder at 375 nm.

The two Cotton effects with $-+$ sign sequence observed in Fig. 3 are located under the first absorption band of the complexes formed by D-ribose, L-sorbose and D-glucosamine, in agreement with the two signals of opposite sign revealed by the circular dichroism spectra of the same compounds (Table 1).

This pattern of separation is characteristic of complexes of the type *cis*-$[Co(NH_3)_4L_2]$ where L is a bidentate or a non-charged monodentate ligand. The $^1T_{1g}$ transition in C_{2v} symmetry is split in one component with A_2 symmetry and two others with B_1 and B_2 symmetries. The last two components generally intermix, whereas the A_2 state remains invariant.[9] Similar result is obtained under the holohedrized D_{4h} symmetry, where the $^1T_{1g}$ transition is split into the $^1A_{2g}$ and E_g transitions, which have an energy difference $\frac{1}{4}[\Delta_O - \Delta_{NH_3}]$. Considering that Δ_O (O = carbohydrate oxygen atom) is smaller than Δ_{NH_3}, it is possible to deduce that the negative circular dichroism component would correspond to the A_2 state, whereas the positive component would correspond to the E state.[10]

In all three cases the molar amplitudes of the Cotton effects centred at 510 nm are remarkably high: values range from 5900 to 13,350°. They are thus much higher than values given by a complex such as $[Co(NH_3)_4(sarcosinate)]^{2+}$, where the molar amplitude of the positive Cotton effect in the visible region is 1800°.[11]

The complexes formed by D-ribose and L-sorbose show only one positive circular dichroism signal in the charge-transfer spectral zone and they are placed at 300 and 320 nm respectively. The complex formed by D-glucosamine has two circular dichroism signals instead: a positive one at 315 nm and a negative signal at 270 nm.*

Taking account of the fact that the isolated compounds showed the same type of optical rotatory dispersion curve as that of the reaction products in solution, further experiments were performed with other carbohydrates and derivatives. They were selected so that they would permit the correlation of the sign of optical rotation of the complexes formed with the structure of the carbohydrate. In this way, the sign of the Cotton effect centred at 500 nm is positive for the product of the reaction between the tetramino Co(III) complex and 2-deoxy-D-glucose, whereas in the reaction product with α-methyl-D-glucoside the same is negative (Fig. 4).

The signs of the Cotton effects in the visible absorption region are the same for the compounds formed by D-ribose, L-sorbose, D-glucosamine and L-arabinose. This result is striking at first sight in view of the different configurations of these carbohydrates, the number of asymmetric carbon atoms and the possibilities of anomeric mixtures and pyranoidal or furanoidal structures. The constant pattern of optical rotatory dispersion in spite of the diversity of structural possibilities can be accounted for if one admits the requirement of a surrounding of identical chirality around the Co(III) ion in all these compounds.

It is well known that the anomeric equilibrium is

* Circular dichroism spectra in the UV region were measured in Santa Barbara, California with a Cary 60 spectropolarimeter. The complexes could have partially lost their optical activity on travelling; therefore we have omitted the $\Delta\varepsilon$ values obtained.

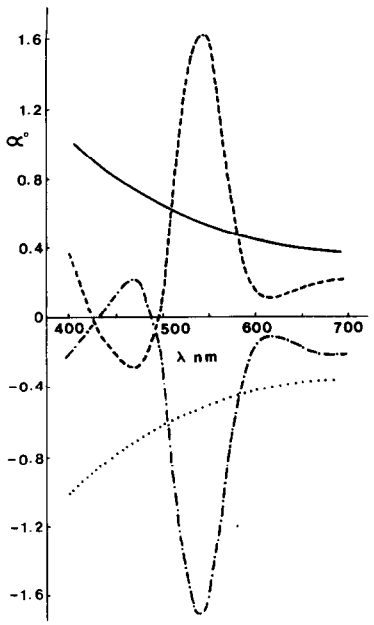


Fig. 2. Optical rotatory dispersion of complex species formed in solution after 100 min at 30°C, pH 6, 0.5 cm pathlength cell: (– – –) *cis*-$[Co(NH_3)_4(H_2O)_2]^{3+}$ 0.1 M/L-arabinose 0.5 M and (— · — · —) *cis*-$[Co(NH_3)_4(H_2O)_2]^{3+}$ 0.1 M/D-arabinose. Optical rotatory dispersion of: (——) L-arabinose 0.5 M and (···) D-arabinose 0.5 M.

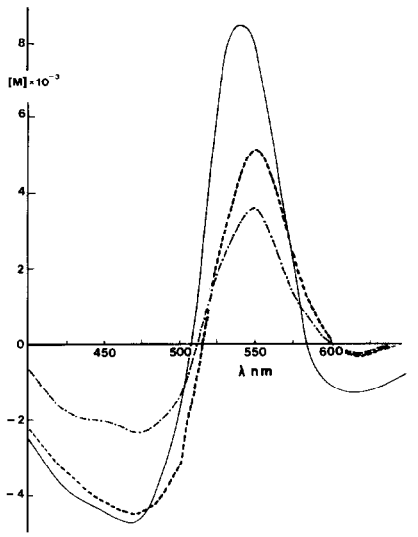


Fig. 3. Optical rotatory dispersion curves of the ions: (—·—·—) $[Co(NH_3)_3(H_2O)$(D-glucosamine)$]^{3+}$, (– – –) $[Co(NH_3)_4$(L-sorbose$)]^{3+}$ and (——) $[Co(NH_3)_4$(D-ribose$)]^{3+}$.

shifted towards the β-form in the carbohydrates D-glucosamine and D-ribose; whereas D-arabinose is mainly an α-anomer.[12] Accepting that the carbohydrates bond to Co(III) preferably through the OH groups of C1 and C2, the chelate rings formed display an arrangement of one carbon atom over and another one under the *xy* plane of the $\{Co(NH_3)_4\}$ species looked at from the metallic centre and moving from left to right, as can be appreciated in Fig. 5. This arrangement of atoms is somehow equivalent to the conformation adopted by the N–C–C–N chain of the ethylenediamine molecule when bonding to the Co(III) ion to form a complex.[13]

Besides the bonding sites already mentioned, other existing possibilities would lead to identical chiral ring, for example the OH groups of C3 and C4 of D-glucosamine; or else, the OH groups of C2 and C3 of D-ribose or of L-sorbose.

The preference for coordination through the donor groups bonded to C1 and C2 is perhaps reflected in the signs of the Cotton effects observed in the reaction product in solution of α-methyl-D-glucoside with the Co(III) aminocomplex, which are

Table 1. Visible-absorption and circular dichroism data

	Absorption		Circular dichroism	
Complex species	λ_{max} (nm)	ε_{max} (nm)	λ_{max} (nm)	$\Delta\varepsilon$
$[Co(NH_3)_4$(D-ribose$)]^{3+}$	530	94	570	−1.9
			505	2.9
	375	166	390	−1.6
$[Co(NH_3)_4$(L-sorbose$)]^{3+}$	530	81	570	−0.9
			505	2.2
	378	134	390	−1.0
$[Co(NH_3)_3(H_2O)$(D-glucosamine$)]^{3+}$	528	76	570	−0.9
			505	1.6
	375 (sh)	111	390	−0.8

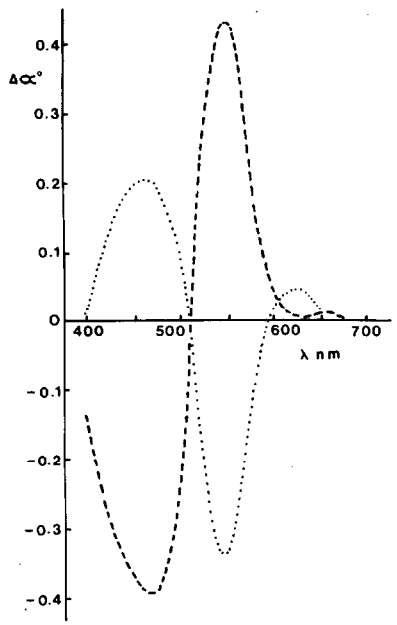


Fig. 4. Optical rotatory dispersion of complex species formed in solution after 30 min at 30°C, pH 6, 0.5 cm pathlength cell. (····) *cis*-$[Co(NH_3)_4(H_2O)_2]^{3+}$ 0.1 M/α-methyl-glucose 0.5 M; (— —) *cis*-$[Co(NH_3)_4(H_2O)_2]^{3+}$ 0.1 M/2-deoxy-glucose 0.5 M. $\Delta\alpha = \alpha_{\text{complex species}} - \alpha_{\text{carbohydrate}}$

opposite to those of the complexes containing D-ribose, L-sorbose and D-glucosamine. Structurally, coordination through sites 1 and 2 of the glucoside gives rise to a ring of the corresponding opposite chirality, although bonding to the metallic ion can also be achieved through the OH groups of C3 and C4.

When 2-deoxy-D-glucose is used for the reaction, the sign of the Cotton effect centred at 510 nm, is the same as that obtained for the complexes formed by D-ribose, L-sorbose and D-glucosamine. According to our proposal this is achieved by coordination through the OH groups of C3 and C4, which are the only sites properly arranged for chelation in this carbohydrate.

The difficulties we have found to isolate a solid compound from the reaction product with 2-deoxy-D-glucose can indicate that bonding through OH groups of carbon atoms other than C1 and C2 leads to unstable species.

In the case of L-sorbose, which is formed in solution by 98% of the α-anomer,[14] coordination is probably established through the OH groups of C2 and C3, since bonding through sites 1 and 2 is sterically hindered, as revealed by a molecular model to scale. Again, decomposition of the complex in solution by dissociation may be reflecting the lability of the bond between the Co(III) aminocomplex and this sugar.

Finally when 2-deoxy-ribose was used for the reaction there was no evidence of coordination. For the pyranoidal structure, the OH groups of C3 and C4 are the only ones that can be used for chelation.

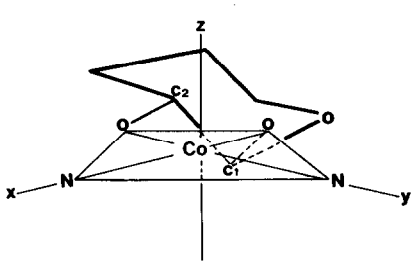


Fig. 5.

Acknowledgements—We thank Dr. C. A. Bunton, Department of Chemistry, University of California, for help with experimental measurements. This research was supported by projects Nr Q 1857-8413, Departamento de Investigación, Universidad de Chile and Nr 1019-84, Fondo Nacional de Investigación.

REFERENCES

1. (a) S. J. Angyal, *Chem. Soc. Rev.* 1980, **9**, 415; (b) C. C. Hinckley, P. S. Ostenburg and W. J. Roth, *Polyhedron* 1982, **1**, 335; (c) S. J. Blunden, P. A. Cusack and P. J. Smith, *Inorg. Chim. Acta* 1983, **72**, 217; (d) M. Tonković, O. Hadzija and I. Nagy-Czako, *Inorg. Chim. Acta* 1983, **80**, 251; (e) A. Cervilla, J. A. Ramirez and A. Beltran-Porter, *Transition Met. Chem.* 1983, **8**, 21; (f) T. Tsubomura, Sh. Yano and S. Yoshikawa, *Polyhedron* 1983, **2**, 123.
2. O. Pavez, Tesis de Licenciatura, Facultad de Ciencias Básicas y Farmacéuticas, Universidad de Chile (1984).
3. O. Cisterna, Tesis de Licenciatura, Facultad de Ciencias Básicas y Farmacéuticas, Universidad de Chile (1984).
4. A. M. Greenaway and R. J. Lancashire, *J. Chem. Educ.* 1982, **59**, 419.
5. G. Blyholder and N. Ford, *J. Phys. Chem.* 1964, **68**, 1496.
6. N. N. Sharma, *Anal. Chim. Acta* 1956, **14**, 423.
7. D. N. Grindley, *An Advanced Course in Practical Inorganic Chemistry*. Butterworths, London (1964).
8. V. S. Sastri and C. H. Langford, *Can. J. Chem.* 1969, **47**, 4237.
9. A. J. McCaffery, S. F. Mason and B. J. Norman, *J. Chem. Soc.* 1965, 5094.
10. C. J. Hawkins, J. A. Stark and C. L. Wong, *Aust. J. Chem.* 1972, **25**, 273.
11. D. A. Buckingham, S. F. Mason, A. M. Sargeson and K. T. Turnbull, *Inorg. Chem.* 1966, **5**, 1649.
12. (a) J. Staneck, M. Cerny, J. Kocourek and J. Pacak, *The Monosaccharides*. Academic Press, New York

(1963); (b) E. L. Eliel, N. L. Allinger, S. J. Angyal and G. A. Morrison, *Conformational Analysis.* Wiley–Interscience, New York (1966); (c) B. Capon, *Chem. Rev.* 1969, **69**, 407; (d) J. F. Kennedy and C. A. White, *Bioactive Carbohydrates.* Ellis Horwood Limited Publishers, Chichester (1983).

13. (a) J. Corey and J. C. Bailar, *J. Am. Chem. Soc.* 1959, **81**, 2690; (b) G. Snatzke, *Optical Activity and Chiral Discrimination* (Edited by S. F. Mason). Reidel Publishing Company, Dordrecht (1978).
14. W. Funcke and C. von Sonntag, *Carbohydr. Res.* 1979, **75**, 305.

Polyhedron Vol. 4, No. 9, pp. 1543–1551, 1985
Printed in Great Britain

0277–5387/85 $3.00 + .00
© 1985 Pergamon Press Ltd

THEORETICAL STUDY OF THE STATIC JAHN–TELLER EFFECT—I. TWO-MODE VIBRONIC COUPLING IN OCTAHEDRAL HALOCOMPLEXES WITH DOUBLY DEGENERATE ELECTRONIC STATES

PETER PELIKÁN, MARTIN BREZA and ROMAN BOČA*
Departments of Physical and Inorganic Chemistry, Slovak Technical University, CS-812 37 Bratislava, Czechoslovakia

(*Received* 11 *December* 1984; *accepted* 20 *February* 1985)

Abstract—A two-mode E_g–$(a_{1g}+e_g)$ vibronic coupling is analyzed for octahedral systems. Analytic formula for the adiabatic potential surface (APS) is obtained considering quadratic vibronic terms and anharmonicities of normal vibrations as well. Potential constants, viz. five elastic force constants and three vibronic constants, are evaluated from the numerical map of the APS applying the non-linear regression analysis. Numerical values are obtained for hexahalocomplexes on the CNDO/INDO level of total energy calculations.

The adiabatic potential surface (APS) represents a principal concept useful in various different areas of chemical physics, connecting together molecular structure, spectroscopy, statistical thermodynamics, chemical thermodynamics and kinetics in a unified manner. The usual procedure is to consider the APS in a parametric form where some constants, specifying its shape, occur. They may be obtained from experimental data. Another approach lies in the direct quantum-chemical calculations of the total molecular energy for fixed positions of nuclei thus yielding a continuous parameteric function of nuclear configurations.

However, the existence of electron degeneracy for certain configurations of nuclei makes the problem of specifying the analytic form of the APS more complex. The electron-vibration (vibronic) interaction manifests itself in new phenomena among which the Jahn–Teller effect plays the dominant role. The generally accepted formulation of the Jahn–Teller theorem[1] consists of the assertion that a non-linear nuclear configuration in the degenerate electronic state is energetically unstable. This theorem implies the existence of at least one stable nuclear configuration in which the electron degeneracy is removed so that the system relaxes to an energetically more advantageous non-degenerate state.[2–9]

Considerations resulting in an analytic form of the APS for doubly degenerate electronic states (mostly in octahedral or tetrahedral reference configurations) have a long history. Among them let us mention the approaches by van Vleck,[10] Öpik and Pryce,[11] Moffitt and Liehr,[12] Liehr and Ballhausen,[13] Coffman,[14] O'Brien[15] and Goodenough.[16] Nevertheless, those considerations seem to be incomplete as they are based on the *E*–*e* single-mode coupling scheme only. In two papers[17,18] we have indicated that the two-mode *E*–(a_1+e) coupling scheme appears to be a more realistic model. In trying to develop our two-mode approach, the conditions yielding the analytic form of the APS were here re-derived. They resulted in a more complex (and hence the more flexible) form of the APS for the case of two-fold degenerate electronic state. Connections with other approaches and possibilities of further extensions are clearly demonstrated.

Several authors have applied the MO–LCAO–SCF method in predicting the Jahn–Teller distortions in metal complexes and organic cation radicals.[19–23] The EHT, CNDO, INDO, MINDO/3 and *ab initio* calculations proved the existence of a stable nuclear configuration with lowered symmetry, the results being in qualitative agreement with the Jahn–Teller theorem. The Jahn–Teller distortions and stabilization energies, however, represent only one aspect of the vibronic coupling. More complete information may be obtained if the elastic force constants and the vibronic coupling constants are evaluated. For this purpose we outlined a non-

* Author to whom correspondence should be addressed.

linear regression method by which the numerical values of the APS were used to fit its analytic form. The semiempirical CNDO–UHF and INDO–UHF methods were applied in order to calculate the total molecular energy of hexahalo complexes $^m[MX_6]^q$.

TWO-STATE STRONG VIBRONIC COUPLING

The non-relativistic electronic Hamiltonian $\hat{H}(r, Q)$ of a molecule may be partitioned into the electronic kinetic energy operator $\hat{T}_e(r)$, the electronic repulsion $\hat{V}_{ee}(r)$, the electron-nuclear potential energy $\hat{V}_{eN}(r, Q)$ and the mutual repulsion of nuclei $\hat{F}_{NN}(Q)$:

$$\hat{H}(r, Q) = \hat{T}_e(r) + \hat{V}_{ee}(r) + \hat{V}_{eN}(r, Q) + \hat{F}_{NN}(Q), \quad (1)$$

r and Q being the electron and nuclear coordinates, respectively. For a fixed set of nuclear coordinates $[Q]$, this Hamiltonian has a set of eigenfunctions $v_n(r; [Q])$:

$$\{\hat{H}(r, Q) - E_n[Q]\} v_n(r; [Q]) = 0, \quad (2)$$

with corresponding eigenvalues $E_n[Q]$. The total Hamiltonian, including the nuclear kinetic energy operator $\hat{T}_N(Q)$, obeys the Schrödinger equation

$$\{\hat{T}_N(Q) + \hat{H}(r, Q) - W\} \Psi(r, Q) = 0, \quad (3)$$

where the electron-nuclear (vibronic) wave function Ψ may be expanded to the form:

$$\Psi(r, Q) = \sum_i v_i(r; [Q^0]) \chi_i(Q). \quad (4)$$

Usually, Q^0 is a configuration of nuclei where the energy $E_n[Q]$ displays a minimum value.

Following Özkan and Goodman,[24] an approximate solution of vibronic equations for W and $\chi_i(Q)$, as they appear by combination of eqns (3) and (4), may be obtained by the partitioning technique. For the two-state strong coupling case the unperturbed (zero-order) wave function stands:

$$\begin{aligned} \Psi^0 &= v_n(r; [Q^0]) \chi_n(Q) + v_m(r; [Q^0]) \chi_m(Q) \\ &= v_n^0 \chi_n + v_m^0 \chi_m \end{aligned} \quad (5)$$

and the perturbation covers the remaining terms, namely:

$$\Psi^1 = \sum_{i \neq m,n} v_i^0 \chi_i. \quad (6)$$

An ordered set of eigenvalues, $E_n^0 \leqslant E_m^0 < E_i^0$, is assumed where a simplified notation of $E_n^0 = E_n[Q^0]$ is used. In a first approximation, the vibrational functions χ_n^0 and χ_m^0 are calculated by means of equation:

$$\begin{bmatrix} \hat{T}_N + U_{nn} - W; & U_{nm} \\ U_{mn}; & \hat{T}_N + U_{mm} - W \end{bmatrix} \begin{bmatrix} \chi_n^0 \\ \chi_m^0 \end{bmatrix} = 0, \quad (7)$$

where the total energy W is measured relative to E_n^0 by

$$W = E_n^0 + \varepsilon_n, \quad (8)$$

thus defining a purely vibrational energy ε_n. The matrix elements U_{nm} contain a Taylor expansion of $H_{nm} = \langle v_n^0 | \hat{H}(r, Q) | v_m^0 \rangle$ (usually up to the quadratic terms) and the second-order energy correction $E^{(2)}$ as it follows from the first-order wave function by the perturbation treatment:

$$\begin{aligned} U_{nm} = E_n^0 \delta_{nm} + H_{nm}^{(1)} + H_{nm}^{(2)} \\ + \ldots + \sum_{i \neq n,m} H_{ni}^{(1)} H_{im}^{(1)} / (E_n^0 - E_i^0) \end{aligned} \quad (9)$$

or

$$\mathbf{U} = E^0 \mathbf{1} + \mathbf{H}^{(1)} + \mathbf{H}^{(2)} + \cdots + \mathbf{E}^{(2)}. \quad (10)$$

Therefore, the U_{nm} elements may be considered as a projection of the electronic Hamiltonian into the subspace spanned by the electronic functions v_n^0 and v_m^0.

The lowest powers of the Taylor series are:

$$\begin{aligned} H_{nm}^{(1)} &= \sum_k \left\langle v_n^0 \middle| \left(\frac{\partial \hat{H}}{\partial Q_k} \right)_0 \middle| v_m^0 \right\rangle \Delta Q_k \\ &= \sum_k \left\{ \left(\frac{\partial \hat{F}_{NN}}{\partial Q_k} \right)_0 \delta_{nm} \right. \\ &\quad \left. + \left\langle v_n^0 \middle| \left(\frac{\partial \hat{V}_{eN}}{\partial Q_k} \right)_0 \middle| v_m^0 \right\rangle \right\} \Delta Q_k \\ &= \sum_k \{ F^k \delta_{nm} + V_{nm}^k \} \Delta Q_k \\ &= F^{(1)} \delta_{nm} + V_{nm}^{(1)}, \end{aligned} \quad (11)$$

$$\begin{aligned} H_{nm}^{(2)} &= \tfrac{1}{2} \sum_{k,l} \left\langle v_n^0 \middle| \left(\frac{\partial^2 \hat{H}}{\partial Q_k \partial Q_l} \right)_0 \middle| v_m^0 \right\rangle \Delta Q_k \Delta Q_l \\ &= \tfrac{1}{2} \sum_{k,l} \left\{ \left(\frac{\partial^2 \hat{F}_{NN}}{\partial Q_k \partial Q_l} \right)_0 \delta_{nm} \right. \\ &\quad \left. + \left\langle v_n^0 \middle| \left(\frac{\partial^2 \hat{V}_{eN}}{\partial Q_k \partial Q_l} \right)_0 \middle| v_m^0 \right\rangle \right\} \Delta Q_k \Delta Q_l \\ &= \tfrac{1}{2} \sum_{k,l} \{ F^{kl} \delta_{nm} + V_{nm}^{kl} \} \Delta Q_k \Delta Q_l \\ &= F^{(2)} \delta_{nm} + V_{nm}^{(2)} \end{aligned} \quad (12)$$

and analogically

$$\begin{aligned} H_{nm}^{(3)} &= \tfrac{1}{6} \sum_{k,l,j} \{ F^{klj} \delta_{nm} + V_{nm}^{klj} \} \Delta Q_k \Delta Q_l \Delta Q_j \\ &= F^{(3)} \delta_{nm} + V_{nm}^{(3)}, \end{aligned} \quad (13)$$

where the derivatives are to be evaluated at the nuclear configuration of Q^0. The quantities $\Delta Q = Q - Q^0$ are the internal displacement coordinates measured relative to Q^0. They may be chosen, within a symmetry point group G_0, each of them belonging

to a γ line of the Γ representation. Thus, the electron-nuclear interaction terms are:

$$V^{(1)}_{nm} = \sum_{\Gamma_1\gamma_1} V_{nm}[\Gamma_1\gamma_1]\Delta Q[\Gamma_1\gamma_1], \tag{14}$$

$$V^{(2)}_{nm} = \tfrac{1}{2}\sum_{\Gamma_1\gamma_1}\sum_{\Gamma_2\gamma_2} V_{nm}[\Gamma_1\gamma_1, \Gamma_2\gamma_2] \times \Delta Q[\Gamma_1\gamma_1]\Delta Q[\Gamma_2\gamma_2]. \tag{15}$$

The last expression is a scalar convolution of two second-rank tensors, their components forming a basis of the $\Gamma_1 \otimes \Gamma_2$ direct product. These considerations are useful in reducing the number of indepedent parameters and in specifying the analytic form of the potential **U**. The matrix elements can be expressed through reduced matrix elements and the respective Clebsh–Gordan coefficients via the Wigner–Eckart theorem or the group theory treatment.[25]

Considering the fixed (frozen) nuclei, the nuclear kinetic energy disappears ($T_N \to 0$) and thus the vibrational energy vanishes ($\varepsilon_n \to 0$). Consequently, the eigenvalues of the secular equation

$$\det\begin{bmatrix} U_{nn}-W; & U_{nm} \\ U_{mn}; & U_{mm}-W \end{bmatrix} = 0 \tag{16}$$

adopt a meaning of the adiabatic potential surface (APS) in the two-state strong coupling case. This is the basic equation which connects various treatments in a unified manner, namely:

(i) the strict degeneracy at the nuclear configuration of Q^0 ($U_{nn} = U_{mm}$) considered in the static Jahn–Teller effect;

(ii) the quasi-degeneracy ($U_{nn} \approx U_{mm}$) considered in the pseudo-Jahn–Teller effect.

Moreover, the method may be simply extended to the three-state strong coupling case and the limiting case for a single state weakly coupled with excited ones is obvious. Having calculated the matrix elements **U**, the solution of vibronic eqn (7) is processed. Notice, **U** looses a meaning of the potential energy in dynamical equations for nuclear motion (7).

ANALYTIC FORM OF APS FOR E_g–($a_{1g}+e_g$) COUPLING

Let us consider an octahedral system ML_6 with the doubly degenerate electronic state E_g. The set of internal displacement coordinates may be represented by 15 normal modes, $Q_1, \ldots, Q_{15}$. Among them, $Q_1(a_{1g})$ is the symmetric stretching, $Q_2(e_g)$ corresponds to the orthorhombic and $Q_3(e_g)$ to the tetragonal distortion. The remaining coordinates span to t_{2g}, t_{2u}, t'_{1u} and t''_{1u} irreducible representations. This assignment allows one to select the non-zero linear integrals in eqn (11), because the Wigner–Eckart theorem states:

$$V^k_{nm} = \left\langle n\left|\left(\frac{\partial \hat{V}(r,Q)}{\partial Q_k}\right)_0\right|m\right\rangle = X(\Gamma_k;\Gamma_n,\Gamma_m)C^{\Gamma_n\Gamma_k\Gamma_m}_{\gamma_n\gamma_k\gamma_m}. \tag{17}$$

The reduced matrix element $X(\Gamma_k;\Gamma_n,\Gamma_m)$ depends only on the irreducible representations Γ_k, Γ_n and Γ_m, and the Clebsh–Gordan (Wigner) coefficients C (or the $3j$-symbols) have been tabulated.[25] For the electronic doublet ($\Gamma_n = \Gamma_m = E_g$) the integral V^k_{nm} is non-zero only if Γ_k will be contained in the symmetrized direct product

$$[\Gamma_n \otimes \Gamma_m] = [E_g \otimes E_g] = A_{1g} + E_g. \tag{18}$$

Thus the integrals V^k_{nm} for $k = 4, 5, \ldots, 15$ (the t-type representation of Q_k) are vanished and for the linear part $\mathbf{V}^{(1)}$ it holds:

$$\mathbf{V}^{(1)} = X_A\Delta Q_1\mathbf{C}_1 + X_E\Delta Q_2\mathbf{C}_2 + X_E\Delta Q_3\mathbf{C}_3, \tag{19}$$

where

$$\mathbf{C}_1 = \begin{pmatrix}1 & 0\\ 0 & 1\end{pmatrix},\quad \mathbf{C}_2 = \frac{1}{\sqrt{2}}\begin{pmatrix}0 & 1\\ 1 & 0\end{pmatrix},\quad \mathbf{C}_3 = \frac{1}{\sqrt{2}}\begin{pmatrix}-1 & 0\\ 0 & 1\end{pmatrix} \tag{20}$$

are the matrices of Wigner coefficients in the doubly degenerate function space. Totally, $2\times 15\times 2 = 60$ linear integrals V^k_{mn} are reduced to the number of six non-zero elements where only two distinct reduced matrix elements, $X_A = X(a_{1g}; E_g, E_g)$ and $X_E = X(e_g; E_g, E_g)$, occur.

The quadratic terms V^{kl}_{nm} in eqn (12) require a successive reduction of the operator part according to the Wigner formula:

$$|\Gamma_k\Gamma_l\gamma_k\gamma_l\rangle = \sum_{\Gamma,\gamma}\begin{pmatrix}\Gamma_k & \Gamma_l & \Gamma\\ \gamma_k & \gamma_l & -\gamma\end{pmatrix}|\Gamma_k\Gamma_l\Gamma_\gamma\rangle \tag{21}$$

where the $3j$-symbols in parentheses again have been tabulated. The summations run over all Γ and γ contained in the reducible representation of the direct product $\Gamma_k \otimes \Gamma_l$.[26]

Applying the above procedure, the quadratic part $\mathbf{V}^{(2)}$ can be partitioned into three terms:

$$\begin{aligned}\mathbf{V}^{(2)} &= \mathbf{V}^{(2)}[a+e,a+e] + \mathbf{V}^{(2)}[t,t] + \mathbf{V}^{(2)}[a+e,t]\\ &= \tfrac{1}{2}\sum_{k=1}^{3}\sum_{l=1}^{3}\mathbf{V}^{kl}[a+e,a+e]\,\Delta Q_k\Delta Q_l\\ &\quad + \tfrac{1}{2}\sum_{k=4}^{15}\sum_{l=4}^{15}\mathbf{V}^{kl}[t,t]\,\Delta Q_k\Delta Q_l\\ &\quad + \tfrac{1}{2}\sum_{k=1}^{3}\sum_{l=4}^{15}\mathbf{V}^{kl}[a+e,t]\,\Delta Q_k\Delta Q_l.\end{aligned} \tag{22}$$

For the first term it may be written:

$$\mathbf{V}^{(2)}[a+e,a+e]$$
$$= \left\{\frac{1}{2}X_{AA}\Delta Q_1^2 + \frac{1}{2\sqrt{2}}X_{EE}(\Delta Q_2^2+\Delta Q_3^2)\right\}\mathbf{C}_1$$
$$+\left\{X_{AE}\Delta Q_1\Delta Q_2 + \frac{1}{\sqrt{2}}X_{EE}\Delta Q_2\Delta Q_3\right\}\mathbf{C}_2$$
$$+\left\{X_{AE}\Delta Q_1\Delta Q_3 + \frac{1}{2\sqrt{2}}X_{EE}(\Delta Q_2^2-\Delta Q_3^2)\right\}\mathbf{C}_3, \quad (23)$$

where three reduced matrix elements occur (X_{AA}, X_{AE} and X_{EE}). The second term of eqn (22) can be evaluated in an analogous manner but it is not considered within the E_g–$(a_{1g}+e_g)$ coupling model. The last term vanishes exactly by the symmetry. In this way, the number of $2\times15\times15\times2 = 900$ quadratic integrals V_{nm}^{kl} becomes reduced to 16 non-zero elements.

The nuclear–nuclear interaction part of **H** for three relevant vibrational modes is:

$$F^{(1)} = \sum_{k=1}^{3} F^k \Delta Q_k = F_A \Delta Q_1, \quad (24)$$

$$F^{(2)} = \tfrac{1}{2}\sum_{k=1}^{3}\sum_{l=1}^{3} F^{kl}\Delta Q_k\Delta Q_l$$
$$= \tfrac{1}{2}F_{AA}\Delta Q_1^2 + \tfrac{1}{2}F_{EE}(\Delta Q_2^2+\Delta Q_3^2), \quad (25)$$

$$F^{(3)} = \tfrac{1}{6}\sum_{k=1}^{3}\sum_{l=1}^{3}\sum_{j=1}^{3} F^{klj}\Delta Q_k\Delta Q_l\Delta Q_j$$
$$= F_{AAA}\Delta Q_1^3 + F_{AEE}\Delta Q_1(\Delta Q_2^2+\Delta Q_3^2)$$
$$+F_{EEE}(3\Delta Q_2^2\Delta Q_3 - \Delta Q_3^3). \quad (26)$$

Notice, that the contribution from the nuclear vibrations has to be of a_1 symmetry. The procedure outlined by Goodenough[16] may be used in order to derive eqns (25) and (26).

Omitting the weak vibronic coupling of the ground-state electronic doublet E_g with excited states (the second-order perturbation correction $\mathbf{E}^{(2)}$), the potential U adopts the general form of

$$\mathbf{U} = E^0\mathbf{1} + \mathbf{H}^{(1)} + \mathbf{H}^{(2)} = c_1\mathbf{C}_1 + c_2\mathbf{C}_2 + c_3\mathbf{C}_3 \quad (27)$$

and its eigenvalues, according to eqn (16), are:

$$W = c_1 \pm \sqrt{(c_2^2+c_3^2)/2}. \quad (28)$$

The explicit form of the Wigner matrices (20) has to be considered in order to prove eqn (28). After simple algebraic manipulations, inspection of eqns (19) and (22)–(28) proves, that it is legitimate to consider the adiabatic potential surface in the analytic form of:

$$W = E^0 + (F_A+X_A)\Delta Q_1 + \frac{1}{2}(F_{AA}+X_{AA})\Delta Q_1^2$$
$$+\frac{1}{2}\left(F_{EE}+\frac{1}{\sqrt{2}}X_{EE}\right)(\Delta Q_2^2+\Delta Q_3^2)$$
$$\pm\left\{\frac{1}{2}(X_E+X_{AE}\Delta Q_1)^2(\Delta Q_2^2+\Delta Q_3^2)\right.$$
$$+\frac{1}{16}X_{EE}^2(\Delta Q_2^2+\Delta Q_3^2)^2$$
$$+\frac{1}{2\sqrt{2}}X_{EE}(X_E+X_{AE}\Delta Q_1)$$
$$\left.\times\Delta Q_3(3\Delta Q_2^2-\Delta Q_3^2)\right\}^{1/2}. \quad (29)$$

PHYSICAL MEANING OF POTENTIAL CONSTANTS

The reduced matrix elements X_A, X_{AA}, X_E, X_{EE} and X_{AE}, as well as F_A, F_{AA} and F_{EE} are constants (evaluated at the configuration of Q^0); they determine the shape of the adiabatic potential surface. Their physical meaning will be here briefly discussed.

First of all, $\Delta Q_2 = Q_2$ and $\Delta Q_3 = Q_3$ are valid since the reference configuration Q^0 is a regular octahedron where $Q_2^0 = Q_3^0 = 0$ holds. The matrix element

$$H_{mm}^1 = H_{nn}^1 = \left\{\frac{\partial}{\partial Q_1}\langle n|\hat{H}(r,Q)|n\rangle\right\}_0$$
$$= \left\{\frac{\partial E_n}{\partial Q_1}\right\}_0 = F_A + X_A = 0 \quad (30)$$

vanishes because of the condition of minimum energy in the optimum octahedral configuration. Thus, F_A and X_A are cancelled at the configuration Q_1^0. The matrix element

$$H_{mm}^{11} = H_{nn}^{11} = \left\{\frac{\partial^2 E_n}{\partial Q_1^2}\right\}_0 = F_{AA} + X_{AA} = K_{AA} \quad (31)$$

is positive and represents a harmonic force constant. In reality, the observable quantity is lowered by an additional term following from the $E_{nn}^{(2)}$ correction—the interaction (weak coupling) with excited electronic states. The reduced matrix element X_E usually is named as a linear vibronic coupling constant. It provides the existence of lower sheet of W referring to E^0 in directions of Q_2 and Q_3, which leads to a well-known "Mexican hat"-type behaviour of W. The reduced matrix element X_{EE} appears in two parts of the APS. In combination with F_{AA} it defines a

harmonic force constant K_{EE}:

$$K_{EE} = F_{EE} + \frac{1}{\sqrt{2}} X_{EE} > 0. \quad (32)$$

Standing under the square root of W, the quadratic vibronic coupling constant X_{EE} is responsible for a warping of the "Mexican hat"-type of potential. Finally, the reduced matrix element X_{AE} couples the a_{1g} and e_g modes and it means the two-mode vibronic coupling constant.

CONNECTIONS WITH OTHER APPROACHES

Works dealing with the static Jahn–Teller effect mostly are based on the potential W, where only the single mode E_g–e_g coupling is considered. Within this more approximative approach the coupling constant X_{AE} is omitted and the APS is simplified as:

$$W = E^0 + \tfrac{1}{2}K_{AA}\Delta Q_1^2 + \tfrac{1}{2}K_{EE}\rho^2 \pm \rho\{A^2 + B^2\rho^2 + 2AB\rho\cos(3\phi)\}^{1/2}, \quad (33)$$

where the following substitutions were used:

$$A = -X_E/\sqrt{2}, \quad B = X_{EE}/4, \quad \rho = (Q_2^2 + Q_3^2)^{1/2}, \quad Q_2 = \rho\sin\phi, \quad Q_3 = \rho\cos\phi. \quad (34)$$

Taking into account the term

$$Z = X_{AE}/\sqrt{2} \quad (35)$$

our formula (29) relaxed to:

$$W = E^0 + \tfrac{1}{2}K_{AA}\Delta Q_1^2 + \tfrac{1}{2}K_{EE}\rho^2 \pm \rho\{(A - Z\Delta Q_1)^2 + B^2\rho^2 + 2(A - Z\Delta Q_1)B\rho\cos(3\phi)\}^{1/2}. \quad (36)$$

It is seen that eqn (36) has the same form as eqn (33) usually used in interpreting the experimental data. Only the term $A \to A - Z\Delta Q_1$ needs a slight re-interpretation.

Several authors[7,11,15] tried to include a third-order term $F^{(3)} = F_{EEE}(3Q_2^2Q_3 - Q_3^3) = -F_{EEE}\rho^3\cos(3\phi)$ where the parameter F_{EEE} has a dimension of energy per volume. This term is responsible for warping the "Mexican hat"-type potential too. The corresponding function

$$W = E^0 + \tfrac{1}{2}K_{EE}\rho^2 \pm A\rho - F_{EEE}\rho^3\cos(3\phi) \quad (37)$$

has the extreme points (three absolute minima and three saddle points) for angular coordinates $\phi = n\pi/3$, being the same as for eqn (33).

The most complex potential within the E_g–e_g coupling model was considered by Goodenough[16] in the form:

$$W = E^0 + \tfrac{1}{2}K_{EE}\rho^2 \pm \rho\{A^2 + B^2\rho^2 + 2AB\rho\cos(3\phi)\}^{1/2} - F_{EEE}\rho^3\cos(3\phi). \quad (38)$$

Its counterpart within the E_g–$(a_{1g} + e_g)$ coupling scheme, proposed here, is

$$W = E^0 + \tfrac{1}{2}K_{AA}\Delta Q_1^2 + \tfrac{1}{2}K_{EE}\rho^2 + F_{AAA}\Delta Q_1^3 + F_{AEE}\Delta Q_1\rho^2 - F_{EEE}\rho^3\cos(3\phi) \pm \rho\{(A - Z\Delta Q_1)^2 + B^2\rho^2 + 2(A - Z\Delta Q_1)B\rho\cos(3\phi)\}^{1/2}. \quad (39)$$

This is the most complex analytic form of the APS derived up to now where five force constants (K_{AA}, K_{EE}, F_{AAA}, F_{AEE} and F_{EEE}) as well as three vibronic constants (A, B and Z) occur. The necessity to include a cubic term $F^{(3)}$ was discussed elsewhere.[27]

The potential (39) may be still a subject of extensions, e.g.:

(i) to include some $V^{kl}[t,t]$ terms in eqn (22), as well as the corresponding $F^{kl}[t,t]$ terms;

(ii) to consider relevant third-order terms V^{klj};

(iii) to take into account the second-order energy correction $E^{(2)}$ as it follows from the first-order wave function by the perturbation theory treatment.

Finally, it must be mentioned that the formula (39) is valid not only for octahedral systems; it is also fulfilled for the E–$(a_1 + e)$ coupling scheme of tetrahedral systems. This is a consequence of the relation $O_h = C_i \otimes O$. Since the groups O and T_d are izomorphous, they exhibit the same form of the vibronic coupling.

CALCULATION OF POTENTIAL CONSTANTS

For practical applications it is useful to evaluate the potential constants occuring in eqn (39). A direct integration approach requires knowledge of the corresponding derivatives of the $\hat{V}_{eN}$ operator. Such calculations were presented only for simple qualitative methods, like the angular overlap model.[28]

Our treatment is based on a qualitatively new idea. The numerical map of the APS values is to be calculated using certain quantum-chemical method. Then, the least-squares method is applied in order to fit the numerical map $W^c(Q_i)$ to the analytic form. Actually, the set of approximate values $W^a(Q_i)$ is produced so that the functional

$$\mathcal{F} = \sum_i w_i^2\{W^c(Q_i) - W^a(Q_i)\}^2 \quad (40)$$

adopts a minimum value. The values of $W^q(Q_i)$ are calculated by eqn (39) for a trial set of potential constants. The statistical weights w_i were chosen in accordance with the metric weighing concept:

$$w_i = 1 \Big/ \left\{ \sum_k Q_k^2 \right\}^{1/2}, \qquad (41)$$

where Q_k is a set of displacement coordinates for the given APS point. The established minimization procedure is not a numerically trivial problem. The gradient minimization was used by the Newton–Raphson method and, alternatively, the Fletcher–Powell algorithm.[29] In order to accelerate a convergence the process may be split into two, linear and non-linear optimizations. Good starting values of potential constants may be obtained considering $Q_2 = 0$. This leads to a simpler, polynomial form of the APS[27] which can be fit by the linear optimization only, as outlined elsewhere.[18]

The quality of the regression was measured by statistical characteristics. The standard deviations of individual potential constants, the correlation coefficient and the discrepancy R-factor belong to them.

NUMERICAL APPLICATION

For numerical application a series of hexahalo complexes was chosen. Eighteen complexes of the $^m[MX_6]^q$ type covered systems having a doubly degenerate electronic state E_g in octahedral configuration. The semiempirical CNDO–UHF method was used[30–32] for the total energy calculations of above complexes. The numerical map of the APS was obtained in this way, considering *ca* 50 points for each system. The energy cut-off was 10^{-4}–10^{-5} eV.

Table 1 shows the calculated potential constants (three vibronic and five elastic force constants) which are presented in significant number of digits (the order of the last number being higher than the standard deviation). Calculated statistical characteristics ($\rho > 0.9999$ and $R < 0.01$) show that the regression is fairly good. The cubic terms of eqn (39), however, partly include vibronic coupling terms, i.e. those which are reduced by the Wigner matrix $\mathbf{C}_1$. Therefore, we leave both, the F_{ijl} and K_{ijl} notation and T_{ijl} is used in this sense.

From Table 1 it can be seen that the two-mode vibronic constant Z is higher than the quadratic vibronic constant B. This demonstrates a considerable role of the a_{1g} vibration in the two-mode E_g–$(a_{1g}+e_g)$ coupling model. It is obvious that the single-mode E_g–e_g coupling model is obtained for vanishing value of Z. Since K_{AA} is much higher relative to K_{EE}, the e_g-mode may be considered as a "soft" mode. In other words, the tetragonal or orthorhombic distortions are much easier than the symmetric stretching.

The characteristics of the extremal points of individual APS are collected in Table 2. It is registered that the calculated Jahn–Teller distortions are too small (*ca* 10^{-12} m) and they do not approach the experimental values (of order of 10^{-11} m) found in solid-state compounds. Also the corresponding Jahn–Teller stabilization energies are underestimated. This indicates that solid-state influences may be responsible for amplification of the static Jahn–Teller effect. Preliminary calculations show that a certain arrangement of cations around the primary coordination sphere raises the degree of distortion.[33] On the other hand, a more sophisticated method (*ab initio* in good basis set) is to be used in order to clear up this particular problem.

A more detailed analysis of Table 2 shows that the fluoro-complexes exhibit the greatest degree of distortion. Consequently, the Jahn–Teller stabilization energies are much higher so that the strength of the static Jahn–Teller effect increases with increasing polarity of the metal–ligand bond. The interesting fact is that free fluoro-complexes have the energy minimum for compressed tetragonal bipyramid (the tetragonality parameter $T > 1$) unlike the chloro- and bromo-complexes.

Application of the INDO–UHF method[34] shows that the characteristics of the APS do not change significantly when compared with CNDO results. The Jahn–Teller stabilization energy, however, increases for the complex $^1[NiF_6]^{4-}$.

The central atom effect—the influence of $^mM^q$ characteristics—manifests itself in a great variability of the strength of the static Jahn–Teller effect. Comparing two central atoms with the same number of d-electrons (e.g. d^4 in Cr(II) and Mn(III) or d^7 in Co(II) and Ni(III)) it is registered that the Jahn–Teller distortions and stabilization energies increase with increasing oxidation state of the central atom. Evidently, it is a consequence of a higher polarity of the M–X bond. Also another effect takes place as follows from comparison of ^{2}Co(II), ^{1}Ni(II) and ^{2}Cu(II) systems. Although the ^{2}Cu(II) complexes exhibit a usual behaviour when compared with ^{2}Co(II) systems (a weakening of the Jahn–Teller effect is registered), the ^{1}Ni(II) complex displays the greatest distortion and stabilization, respectively. Its unique feature lies in the high assymetry of the corresponding electronic configuration $(e_g)_n^2(e_g)_m^0$ compared with configuration $(e_g)_n^2(e_g)_m^1$ for ^{2}Cu(II) or configuration $(e_g)_n^1(e_g)_m^0$ for ^{2}Co(II) complexes. This effect clearly predominates over the oxidation state influence as follows from comparison of ^{1}Ni(II) and ^{2}Ni(III) systems.

Table 1. The calculated values of vibration and vibronic constants of the first row transition metal hexahalo complexes with double degenerate E_g terms[a]

System	A	B	Z	K_{AA}	K_{EE}	T_{AAA}	T_{AEE}	T_{EEE}	Correl. coeff.	R-factor
$^5CrF_6^{4-}$	−0.43108	−0.13	−0.6777	16.3036	10.625	−3.934	−6.91	−1.976	0.999999	0.00110
$^5CrCl_6^{4-}$	−0.2878	0.0003	−0.157	14.8287	8.8368	−3.898	−3.943	−0.798	0.999999	0.00127
$^5CrBr_6^{4-}$	−0.376	−1.44	−2.531	19.038	10.286	−1.92	−85.7	−47.80	0.999847	0.01078
$^2CoF_6^{4-}$	−0.975	−0.328	−1.701	33.520	23.854	−7.896	−21.349	−4.947	0.999999	0.00164
$^2CoCl_6^{4-}$	−0.4575	0.22	−2.133	30.289	19.2532	−2.81	−52.88	6.26	0.999991	0.00408
$^2CoBr_6^{4-}$	−0.4599	0.19	−2.03	34.4780	20.5916	−6.535	−46.21	1.30	0.999999	0.00120
$^5MnF_6^{3-}$	−1.565	−0.65	−2.387	28.676	20.370	−6.900	−23.323	−4.80	0.999991	0.00276
$^5MnCl_6^{3-}$	−0.9008	−0.064	−1.219	25.5600	17.4198	−5.290	−20.95	−3.036	0.999999	0.00113
$^5MnBr_6^{3-}$	−1.005	0.11	−1.56	29.5599	18.953	−5.533	−30.31	−1.69	0.999999	0.00154
$^1NiF_6^{4-}$[b]	−2.2547	−0.74	−4.236	41.320	29.521	−9.656	−28.643	−7.074	0.999997	0.00246
$^1NiF_6^{4-}$[c]	−2.5410	−1.5148	−3.565	42.535	28.966	−8.58	−22.64	−11.46	0.999985	0.00212
$^1NiCl_6^{4-}$	−0.94212	−0.040	−1.484	35.7291	22.5557	−8.214	−26.882	−4.849	0.999999	0.00110
$^1NiBr_6^{4-}$	−0.9016	−0.70	−2.66	39.981	23.432	−0.005	−59.17	−26.78	0.999975	0.00725
$^2NiF_6^{3-}$	−2.2967	−0.29	−2.758	50.3358	36.578	−13.707	−42.21	−1.01	0.999998	0.00194
$^2NiCl_6^{3-}$	−1.1546	0.49	−1.040	42.3973	30.334	−10.023	−34.1	−8.34	1.000000	0.00041
$^2NiBr_6^{3-}$	−1.1468	0.30	−0.962	46.2489	28.4073	−10.457	−28.27	−4.30	0.999998	0.00157
$^2CuF_6^{4-}$	−1.0362	−0.80	−3.385	45.872	32.428	−10.68	−40.81	−10.97	0.999979	0.00738
$^2CuCl_6^{4-}$	−0.4497	−0.06	−1.649	39.157	24.891	−8.67	−33.11	−5.843	0.999996	0.00267
$^2CuBr_6^{4-}$	−0.3676	−1.03	−9.105	42.748	22.02	11.58	−130.2	−24.05	0.999967	0.00768

[a] Units used: A is in 10^{10} eV m^{-1}; B, Z, K_{AA} and K_{EE} are in 10^{20} eV m^{-2}; T_{AAA}, T_{AEE} and T_{EEE} are in 10^{30} eV m^{-3}. The R-factor is defined as $R = [\sum_i (E_i - E_i^c)^2 / \sum_i E_i^2]^{1/2}$.

[b] Results obtained from CNDO energy hypersurface.

[c] Results obtained from INDO energy hypersurface.

Table 2. The calculated characteristics of energy hypersurface extreme points for hexahalo complexes of the 1st row transition metals with double degenerate E_g terms[a]

System	Q_1^0	ΔQ_1	ρ	ϕ	T	ΔE	ΔQ_1	ρ	ϕ	T	ΔE
$^5CrF_6^{4-}$	2.35980	−0.0008	0.04	0	1.015	−0.00884	−0.0012	0.041	π	0.985	−0.008664
$^5CrCl_6^{4-}$	2.63259	−0.00007	0.03	π	0.983	−0.00482	−0.00006	0.032	0	1.011	−0.00473
$^5CrBr_6^{4-}$	2.73511	−0.0004	0.04	0	1.010	−0.00672	−0.0002	0.034	π	0.991	−0.00652
$^2CoF_6^{4-}$	2.05971	−0.0009	0.041	0	1.017	−0.02016	−0.001125	0.041	π	0.983	−0.01974
$^2CoCl_6^{4-}$	2.37111	−0.001	0.02	π	0.991	−0.00548	−0.0006	0.024	0	1.009	−0.00540
$^2CoBr_6^{4-}$	2.52905	−0.0007	0.023	π	0.992	−0.005224	−0.00059	0.022	0	1.008	−0.00506
$^5MnF_6^{3-}$	2.10266	−0.0010	0.077	0	1.033	−0.0618	−0.0021	0.076	π	0.969	−0.0585
$^5MnCl_6^{3-}$	2.40786	−0.0004	0.052	π	0.981	−0.02355	−0.00017	0.0507	0	1.019	−0.02305
$^5MnBr_6^{3-}$	2.55364	0.00004	0.055	π	0.919	−0.0273	−0.0001	0.052	0	1.018	−0.0261
$^1NiF_6^{4-}$[b]	1.98918	−0.00334	0.0760	0	1.034	−0.0876	−0.00425	0.0767	π	0.967	−0.0852
$^1NiF_6^{4-}$[c]	1.98095	−0.0032	0.0877	0	1.081	−0.1156	−0.0033	0.0876	π	0.927	−0.1078
$^1NiCl_6^{4-}$	2.31097	−0.00048	0.0428	π	0.984	−0.01997	−0.00037	0.0408	0	1.016	−0.01941
$^1NiBr_6^{4-}$	2.48222	−0.0004	0.042	π	0.986	−0.01795	−0.0003	0.036	0	1.013	−0.01693
$^2NiF_6^{3-}$	1.89971	−0.00002	0.0635	0	1.030	−0.07302	−0.00029	0.0621	π	0.972	−0.07121
$^2NiCl_6^{3-}$	2.23953	−0.0003	0.04	π	0.984	−0.0232	−0.00017	0.0358	0	1.014	−0.02088
$^2NiBr_6^{3-}$	2.42030	0.00019	0.0421	π	0.985	−0.02396	0.00014	0.0389	0	1.014	−0.02241
$^2CuF_6^{4-}$	1.97356	−0.0013	0.033	0	1.014	−0.01707	−0.00157	0.0314	π	0.986	−0.01615
$^2CuCl_6^{4-}$	2.28895	−0.0005	0.018	π	0.993	−0.00408	−0.00045	0.018	0	1.007	−0.00405
$^2CuBr_6^{4-}$	2.46500	−0.00230	0.0178	0	1.006	−0.00341	−0.00303	0.0167	π	0.994	−0.00305

[a] $\Delta Q_1 = Q_1 - Q_1^0$, $\rho = (Q_2^2 + Q_3^2)^{1/2}$, $\phi = \text{arctg}\,(Q_2/Q_3)$. ΔE is the Jahn–Teller stabilization energy: $\Delta E = E^{ext}(Q) - E(Q^0)$. T is parameter of tetragonality: $T = R_e/R_a$, where R_e (R_a) is the equatorial (axial) distance transition metal–ligand. Distances are in 10^{-10} m; energies in eV.

[b] Results obtained from CNDO energy hypersurface.

[c] Results obtained from INDO energy hypersurface.

CONCLUSIONS

Some theoretical aspects of the static Jahn–Teller effect were studied in the present communication. Using the group theory treatment the analytic formula for the adiabatic potential surface of octahedral and/or tetrahedral systems was derived. Actually, the non-linear, two-mode E–(a_1+e) vibronic coupling was considered. The potential constants may be evaluated if a numerical map of APS values is known where for the total energy calculations an arbitrary quantum-chemical method is applicable. Consequently, the potential constants (three vibronic constants and five elastic force constants) are to be enumerated by the least-squares method. Their physical meaning is discussed in detail.

The above procedure was applied for the hexahalo complexes over the first transition metal series having a doubly degenerate electronic state E_g in octahedral configuration. Actually, the CNDO method was used for the total energy calculations. The most important results may be summarized as follows:

(i) The inclusion of the total symmetric vibrational mode manifests itself in significant values of corresponding vibronic constants.

(ii) In the light of CNDO calculations the Jahn–Teller distortions are small when compared with distortions found for solid-state complexes. It indicates that solid-state influences may prevail over the net Jahn–Teller effect. However, this result stimulates subsequent studies where some solid-state influences are to be included into the model calculations.

(iii) The e_g-vibrational modes are much more softer than the non-degenerate a_{1g} ones as follows from the calculated force constants. This fact may play an important rôle in deformations of the solid-state systems.

(iv) The central atom effect of the metal centre has significant consequences on the static Jahn–Teller effect.

REFERENCES

1. H. A. Jahn and E. Teller, *Proc. Roy. Soc.* 1937, **161**, 220.
2. A. D. Liehr, *J. Phys. Chem.* 1963, **67**, 389.
3. A. D. Liehr, *J. Phys. Chem.* 1963, **67**, 471.
4. I. B. Bersuker, *Coord. Chem. Rev.* 1975, **14**, 357.
5. M. D. Sturge, in *Solid State Physics* (Edited by F. Seitz, D. Turnbull and H. Ehrenreich), Vol. 20. Academic Press, New York (1967).
6. F. S. Ham, in *Electron Paramagnetic Resonance* (Edited by J. Geschwind). Plenum Press, New York (1971).
7. D. Reinen and C. Friebel, *Struct. Bonding* 1979, **37**, 1.
8. R. Englman, *The Jahn–Teller Effect in Molecules and Crystals*. Wiley–Interscience, New York (1971).
9. I. B. Bersuker and V. Z. Polinger, *Adv. Quantum Chem.* 1982, **15**, 85.
10. J. H. Van Vleck, *J. Chem. Phys.* 1939, **7**, 72.
11. U. Öpik and M. H. L. Pryce, *Proc. Roy. Soc.* 1957, **A238**, 425.
12. W. Moffitt and A. D. Liehr, *Phys. Rev.* 1957, **106**, 1195.
13. A. D. Liehr and C. J. Ballhausen, *Ann. Phys.* 1958, **3**, 304.
14. R. E. Coffman, *J. Chem. Phys.* 1966, **44**, 2305.
15. M. O'Brien, *Proc. Roy. Soc.* 1964, **A281**, 323.
16. J. Goodenough, *J. Phys. Chem. Solids* 1964, **25**, 151.
17. P. Pelikán, M. Breza and M. Liška, *Inorg. Chim. Acta* 1980, **45**, L1.
18. R. Boča, P. Pelikán, M. Breza and J. Gažo, *Polyhedron* 1983, **2**, 921.
19. L. L. Lohr and W. N. Lipscomb, *Inorg. Chem.* 1963, **2**, 911.
20. D. W. Clack and W. Smith, *Mol. Phys.* 1975, **29**, 1615.
21. D. W. Clack and D. Reinen, *Solid State Commun.* 1980, **34**, 395.
22. J. R. Bews and C. Glidewell, *J. Mol. Struct.* 1980, **64**, 87.
23. J. Demuynck, A. Veillard and U. Wahlgreen, *J. Am. Chem. Soc.* 1973, **95**, 5563.
24. I. Özkan and L. Goodman, *Chem. Rev.* 1979, **79**, 275.
25. J. S. Griffith, *The Theory of Transition Metal Ions*. Dickens, Northampton (1964).
26. Notice the identities of $e_g \otimes e_g = a_{1g}+a_{2g}+e_g$, $e \otimes t_1 = e \otimes t_2 = t_1+t_2$ and $t_1 \otimes t_1 = t_2 \otimes t_2 = a_1+e+t_1+t_2$.
27. If only the tetragonal distortion is considered, $Q_2 = 0$ and $\cos(3\phi) = \pm 1$ are valid. Consequently the square root in eqn (36) has an explicit solution and the APS relaxes to $W = c_1 \pm c_3/\sqrt{2} = E^0 + \frac{1}{2}K_{AA}\Delta Q_1^2 + \frac{1}{2}K_{EE}Q_3^2 \pm \{(A - Z\Delta Q_1)Q_3 + BQ_3^2\}$. A behaviour of such a paraboloid potential is better visualized in the basis set of internal coordinates, say two axial (R_a) and four equatorial (R_e) metal–ligand distances. The corresponding harmonic potential has the form of $W = E^0 + bR_a + cR_a^2 + dR_e + eR_aR_e + fR_e^2$ and it leads to the following condition for the local energy minima: $(\partial E/\partial R_a)_{R_e} = b + eR_e + 2cR_a = 0$ so that an R_a vs R_e dependence[18] adopts a form of a descending straight line. This yields an unacceptable prediction of $R_e \leqslant 0$ for larger displacements of R_a. Therefore, at least the cubic or higher degree terms must be considered in order to obtain a correct form of the R_a vs R_e dependence.
28. M. Bacci, *Biophys. Chem.* 1980, **11**, 39.
29. R. F. Fletcher and M. J. D. Powell, *Computer J.* 1963, **6**, 163.
30. J. A. Pople and D. L. Beveridge, *Approximate Molecular Orbital Theory*. McGraw-Hill, New York (1970).
31. D. W. Clack, N. S. Hush and J. R. Yandle, *J. Chem. Phys.* 1972, **57**, 3503.
32. R. Boča, *Program MOSEM2*. Slovak Technical University, Bratislava (1980).
33. M. Breza, P. Pelikán and R. Boča, *Proc. 9th Conference on Coord. Chem.* p. 51. Smolenice, Bratislava (1983).
34. R. Boča, *Program PCILO3, QCPE, No 462* (1983).

Polyhedron Vol. 4, No. 9, pp. 1553–1558, 1985
Printed in Great Britain

0277-5387/85 $3.00 + .00
© 1985 Pergamon Press Ltd

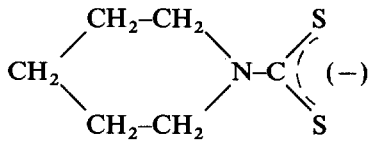
COORDINATING ABILITY OF METHYLPIPERIDINE DITHIOCARBAMATES TOWARDS PLATINUM GROUP METALS

GIAN CARLO FRANCHINI, ALEARDO GIUSTI, CARLO PRETI, LORENZO TASSI and PAOLO ZANNINI*
Istituto di Chimica Generale ed Inorganica, University of Modena, 41100 Modena, Italy

(*Received* 18 *December* 1984; *accepted* 20 *February* 1985)

Abstract—New rhodium(III), iridium(III), palladium(II) and platinum(II) dithiocarbamate complexes of the types $M(Rdtc)_3$ and $M(Rdtc)_2$ (Rdtc = 2-, 3- and 4-methylpiperidine dithiocarbamate) have been prepared and characterized by chemical analyses, conductance measurements, electronic and IR spectral studies, magnetic measurements and thermal analyses (TG and DTG techniques). From the electronic absorption spectra the values of the ligand field parameters were determined; the nephelauxetic parameters are indicative of a strong covalency in the metal–ligand bond. All the complexes here reported are diamagnetic and nonconducting both in the solid state and in DMF solution.

As a part of our study on the coordinating behaviour of the heterocyclic containing dithiocarbamate ligands toward transition and *p*-block metals we report in this study the synthesis and characterization of new complexes of rhodium(III), iridium(III), palladium(II) and platinum(II) with three derivatives of the piperidine dithiocarbamate



i.e. 2-, 3-, 4-methylpiperidine dithiocarbamate sodium salts, hereafter abbreviated as 2-MePipdtc, 3-MePipdtc, and 4-MePipdtc.

We have previously described the complexes of other cyclic dithiocarbamates with many *d*- and *p*-block metals, the reactivity of the obtained complexes towards nitrogen donor ligands, the mass spectral investigations and the structural characterization by XPS techniques.[1–6]

This paper extends our previous studies on the dithiocarbamates in which dialkyl groups are replaced by heterocycles and, as a further extension, the heterocycle bears aryl or alkyl groups in different positions on the ring. It is of interest to study the influence of the substituent in the ring on the C···N and C···S bonds and on the electronic structure of the complexes. The nature and the position of the substituent can also influence the behaviour of the dithiocarbamate ligands through variation in the electronic releasing ability of the different amines.

RESULTS AND DISCUSSION

The analytical data of the compounds are listed in Table 1 and show that the complexes possess 1 : 3 and 1 : 2 metal to ligand stoichiometry in the case of rhodium and iridium, and of palladium and platinum derivatives respectively. They are soluble in common organic solvents, particularly in *N*,*N*′-dimethylformamide (DMF), chloroform, acetone, benzene and nitrobenzene. The molar conductances of 10^{-3} M solutions of all these compounds in DMF lie below 40 ohm^{-1} cm^2 $mole^{-1}$, indicating their non-electrolytic nature; all the complexes are non-conducting even in the solid state. The solid state electronic spectra are given in Table 2, while the most important IR bands are summarized in Table 3.

Electronic spectra

The trisdithiocarbamate derivatives of rhodium(III) and iridium(III) are low-spin type (t_{2g}^6) and their solid state electronic spectra suggest an octahedral configuration of the central atom, Table 2. The band positions are similar to those reported for other sulphur containing ligands; the dia-

* Author to whom correspondence should be addressed.

Table 1. Analytical data

Compounds	Colour	N% found (calc.)	C% found (calc.)	H% found (calc.)	S% found (calc.)
$Pd(2\text{-}MePipdtc)_2$	Dark yellow	6.4 (6.2)	37.3 (37.0)	5.5 (5.3)	28.2 (28.2)
$Pd(3\text{-}MePipdtc)_2$	Yellow	6.3 (6.2)	37.4 (37.0)	5.5 (5.3)	28.2 (28.2)
$Pd(4\text{-}MePipdtc)_2$	Light yellow	6.3 (6.2)	37.1 (37.0)	5.5 (5.3)	28.0 (28.2)
$Pt(2\text{-}MePipdtc)_2$	Yellow	5.2 (5.2)	30.8 (30.9)	4.5 (4.4)	23.1 (23.6)
$Pt(3\text{-}MePipdtc)_2$	Bright yellow	5.2 (5.2)	31.0 (30.9)	4.4 (4.4)	23.7 (23.6)
$Pt(4\text{-}MePipdtc)_2$	Light yellow	5.2 (5.2)	30.7 (30.9)	4.4 (4.4)	23.6 (23.6)
$Rh(2\text{-}MePipdtc)_3$	Hazel-brown	6.5 (6.7)	40.2 (40.3)	5.7 (5.8)	30.6 (30.7)
$Rh(3\text{-}MePipdtc)_3$	Hazel-brown	6.6 (6.7)	40.0 (40.3)	5.8 (5.8)	30.5 (30.7)
$Rh(4\text{-}MePipdtc)_3$	Hazel-brown	6.3 (6.7)	39.9 (40.3)	5.6 (5.8)	30.3 (30.7)
$Ir(2\text{-}MePipdtc)_3 \cdot 2H_2O$	Hazel-brown	5.3 (5.6)	33.2 (33.6)	5.2 (5.4)	25.3 (25.6)
$Ir(3\text{-}MePipdtc)_3 \cdot 2H_2O$	Hazel-brown	5.3 (5.6)	33.0 (33.6)	5.0 (5.4)	25.3 (25.6)
$Ir(4\text{-}MePipdtc)_3 \cdot 2H_2O$	Dark yellow	5.5 (5.6)	33.0 (33.6)	5.1 (5.4)	25.4 (25.6)

magnetic behaviour of these metal complexes indicates octahedral surroundings of the donor atoms around the metal ions producing a strong field.

Rhodium and iridium derivatives (Table 2) show a band at 19,120–22,200 cm^{-1} ($^1A_{1g} \rightarrow {}^1T_{1g}$) and a second band in the 23,800–28,200 cm^{-1} range, ($^1A_{1g} \rightarrow {}^1T_{2g}$). These two peaks at lower energy are the two expected spin allowed transitions to the $t_{2g}^5 e_g^1$ configuration and they are not obscured by charge-transfer absorptions. The values of $10Dq$ and B' as calculated from the positions of these bands by means of the available methods are reported in Table 2 and are well within those found for other trivalent rhodium and iridium complexes,[8] indicating the presence of RhS_6 and IrS_6 chromophores and suggesting a considerable orbital overlap with a strong covalency in the metal ligand σ bond.

The effective ionic charges for the rhodium complexes studied here, calculated using the available methods,[7] are in the 0.27–0.30 range, considerably below the formal +3 oxidation state.

The bands at somewhat higher energies, Table 2, can be attributed to charge-transfer transitions,[10,11] see below.

The electronic spectra of the diamagnetic palladium(II) and platinum(II) derivatives, recorded in the solid state as Nujol mulls, are indicative of square planar geometry,[12,13] Table 2. The bands at 16,700 cm^{-1} in the palladium derivatives may be assigned to a *d–d* transition.[14]

The solid state electronic spectra of all the complexes reported in this study show absorption bands at high energy values due to the chromophore group NCS_2;[15] these absorptions are indicated as bands I, II and III.

Band I is assigned to an intramolecular charge-transfer in the ligand of the type $\pi^* \leftarrow \pi$ located on the N···C···S group.[16,17] The band II is attributed to a second transition of the type $\pi^* \leftarrow \pi$ in the S···C···S group.[18] The position of these bands is affected by the nature of the central atom and it is not sensitive to the position of the methyl group in the piperidine ring.

Band III may be due to an electronic transition $\pi^* \leftarrow n$ located on the sulphur atom.[19–21]

In the palladium(II) and platinum(II) complexes band IV at some 22,500 and 25,300 cm^{-1} respectively is present, which can be assigned either to a charge-transfer transition of the type M → L or to a *d–d* transition.

IR spectra

The most important IR peaks of the free ligand sodium salts and of the complexes are reported in Table 3.

The thioureide band near 1450 cm^{-1} indicates considerable double-bond character in the C···N bond; this behaviour, already observed for many other dithiocarbamates, may be attributed to the electron releasing ability of the amines, which forces high electron density towards the sulphur atoms, via the π system, thus producing greater double-bond character in the carbon–nitrogen bond, and shifting ν(C···N) to higher energy.

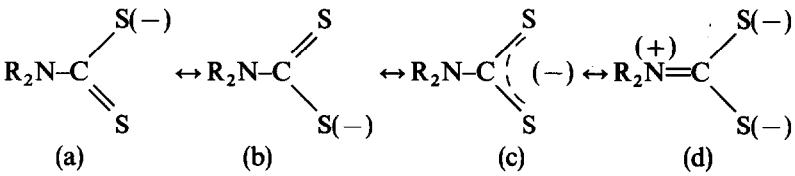
As regards the influence of the position of the methyl group on the piperidine ring, the ν(C···N) value increases in the order 2-MePipdtc < 3-MePipdtc < 4-MePipdtc. Furthermore, the position of this band is affected by the nature of the central atom in the complexes and is shifted to lower

frequencies as follows: Ir > Rh and Pt > Pd; this is a reflection of the higher electron acceptor ability of Ir than Rh and of Pt than Pd.

The band in the region 965–940 cm^{-1} is attributed to the stretching vibration of the C⋯S bonds.

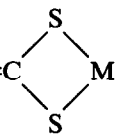
The ν(C⋯S) mode indicates whether the diothiocarbamato moiety is mono- or bidentate; the presence in our complexes of only one strong band in this region strongly supports bidentate coordination of the dithioligand, a doublet being expected in the 1000 ± 70 cm^{-1} region for monodentate behaviour.[22–24] Further confirmation comes from the analysis of the position of the ν(C⋯N) mode; this band undergoes a blue shift in all the complexes while for unidentate coordination this stretching would be shifted towards lower wavenumbers or remain unchanged at the value of the free dithiocarbamate sodium salt.[25]

The structure of the dithioligands can be represented by the following formalism



and we can suggest, according to our previous studies, that the contribution of the structure (d), greatest for the dialkylderivatives, is lower for more complex aliphatic chains and relatively small for the heterocyclic derivatives. Perhaps because of the rigid heterocyclic ring system which shows less tendency to release electrons to the carbon–nitrogen bond, this bond has a less double-bond character. This tendency to release electrons is less in the compounds reported here than in the piperidine dithiocarbamate complexes; this fact is quite surprising taking into account the inductive effect of the methyl group which should cause an increase in the carbon–nitrogen bond order.

As for the 600–500 cm^{-1} region, where the bands arise with mainly ν(CS) and δ(SCS) character, it is interesting to point out that the bands in this range

must entail some  M ring deformation and

stretching modes involving ν(CS) and δ(SCS), as demonstrated by a detailed IR isotopic study.[2]

In the far IR region the bands of the ligands appear unchanged in spectra of the complexes. New bands appear in the rhodium derivatives at 327–331 cm^{-1} and at some 320 cm^{-1} in the iridium complexes, Table 3. These absorption bands, absent in the spectra of the free ligands and in those of the palladium and platinum derivatives, are probably due to a metal–ligand interaction; we can assign these bands to ν(Rh–S) and ν(Ir–S) stretching vibrations respectively.[9]

Passing to the palladium and platinum derivatives, the vibration modes in the 373–359 cm^{-1} range can be assigned to Pt–S stretching vibrations (λ_8), whereas the second band at some 340 cm^{-1} could be attributed to complex normal modes involving both metal–sulphur bond and ring vibration modes. The band in the 315–296 cm^{-1} range is assigned to the NCS bending mode (λ_9).[26]

The methyl group absorptions both in the free ligands and in the complexes can be assigned without ambiguity; the medium strong bands in the 2970–2960 cm^{-1} range can be attributed to the asymmetric CH_3 stretching vibration, while the two series of bands at 1380–1373 cm^{-1} and at 1189–1175 cm^{-1} are evidently due to the degenerate symmetric and rocking vibrations of the methyl group.

Thermal analyses

The rhodium(III) derivatives were stable up to 375°C; beyond this temperature a rapid mass loss up to 500°C occurs, corresponding to the decomposition of the dithiocarbamato complexes to the metal. The next step over 500°C corresponds to the oxidation of metallic rhodium to the black Rh_2O_3 oxide.

The iridium(III) complexes, stable up to 360°C, undergo decomposition in the 360–500°C range, giving metallic iridium as a product. From this last temperature, up to 800°C, the Ir_2O_3 is obtained.

The palladium(II) derivatives were thermally stable up to 400°C. Above this temperature decomposition sets in and continues transforming the dithiocarbamates into polysulphides of the type Pd_xS_y, which slowly give PdO.

The platinum(II) complexes were also stable up to 400°C, but, beyond this point, a single step decomposition starts and proceeds with the loss of the ligands giving metallic platinum sponge as the end-product.

Table 2. Electronic spectra and ligand field parameters (cm^{-1})

Compounds	I	II	III	IV	*d–d*						
					ν_2	ν_1	ν_2/ν_1	Δ	B'	β
Pd(2-MePipdtc)$_2$	35,100	32,800 31,250 sh	29,400	22,600	16,700					
Pd(3-MePipdtc)$_2$	35,100	32,500, 31,250 sh	29,000	22,500	16,700					
Pd(4-MePipdtc)$_2$	34,500	32,700, 31,700 sh	29,400	22,500	16,700					
Pt(2-MePipdtc)$_2$	38,900, 37,000 sh	34,500	28,200	25,300						
Pt(3-MePipdtc)$_2$	38,900; 37,000 sh	34,500	28,200	25,300						
Pt(4-MePipdtc)$_2$	38,900, 37,000 sh	34,500	28,500	25,300						
					ν_2	ν_1	ν_2/ν_1	Δ	B'	β
Rh(2-MePipdtc)$_3$	39,200	31,300	28,300		23,800	19,120	1.24	19,958	319	0.44
Rh(3-MePipdtc)$_3$	39,500	31,100	27,400		23,800	19,230	1.24	20,059	311	0.43
Rh(4-MePipdtc)$_3$	39,100	31,300	27,900		23,800	19,160	1.24	19,995	316	0.44
Ir(2-MePipdtc)$_3 \cdot 2H_2O$	37,700	35,700	30,000		28,200	22,200	1.27	23,220	414	0.63
Ir(3-MePipdtc)$_3 \cdot 2H_2O$	37,700	36,000	29,900		27,300	22,200	1.23	23,139	346	0.52
Ir(4-MePipdtc)$_3 \cdot 2H_2O$	37,700	36,100	29,900		26,700	22,200	1.20	23,068	302	0.46

B is taken to be 720 and 660 cm^{-1} for the free gaseous Rh^{3+} and Ir^{3+} ions respectively.

EXPERIMENTAL

Preparation of the ligands

The sodium salts of the ligands were prepared by treating 2-methyl-, 3-methyl- or 4-methylpiperidine (reagent grade) in dry diethylether with CS_2 and adding NaOH with vigorous stirring over a 5 h period. Molar ratio amine: CS_2 : NaOH = 1 : 1 : 1. The crude products were recrystallized from isopropyl alcohol.

Analyses. For 2-MePipdtcNa · $2.5H_2O$. Found: C, 34.4; H, 7.0; N, 5.8; S, 26.2%. For 3-MePipdtcNa · $2.5H_2O$. Found: C, 34.1; H, 7.1; N, 5.7; S, 26.0%. For 4-MePipdtcNa · $2.5H_2O$. Found: C, 34.9; H, 7.0; N, 5.9; S, 26.3%. Calc. for $C_7H_{12}NS_2Na \cdot 2.5H_2O$: C, 34.7; H, 7.1; N, 5.8; S, 26.5%.

Preparation of the complexes

The complexes were obtained by reaction of an aqueous solution of rhodium trichloride, ammonium hexachloroiridate(III), palladium nitrate, potassium tetrachloroplatinate(II) with the dithiocarbamate sodium salt dissolved in methanol or water at room temperature, in 1 : 3 or 1 : 2 molar ratios. The products were filtered off, washed several times with cold water and dried over P_4O_{10} *in vacuo*. Repeated syntheses and elemental analyses gave reproducible results.

Electronic spectra

The electronic spectra were recorded with a Shimadzu MPS-50L spectrophotometer in the solid state in the 5000–45,000 cm^{-1} region. Samples were prepared by grinding the complexes on a filter paper as support.

IR spectra

The IR spectra have been recorded in the 4000–50 cm^{-1} range with a Perkin–Elmer 180 spectrophotometer of the Instruments Centre of Modena University. The spectra in the 4000–400 cm^{-1} range were measured for KBr discs or Nujol mulls. Far IR spectra were measured for Nujol mulls supported between polyethylene sheets. Atmospheric water was removed from the spectrophotometer housing by flushing with dry nitrogen.

Magnetic susceptibility measurements

These measurements were carried out by Gouy's method at room temperature. The molecular

Table 3. IR absorption bands (cm^{-1})[a]

Compounds	$\nu(C\cdots N)$	$\nu(C\cdots S)$	$\nu(CS)+\delta(SCS)$	$\nu(M-S)$
$Pd(2\text{-MePipdtc})_2$	1436 vs	950 ms	582 m, 538 m	359 sh, 341 s
$Pd(3\text{-MePipdtc})_2$	1439 vs	952 ms	554m, 514 m	365 sh, 343 s
$Pd(4\text{-MePipdtc})_2$	1446 vs	960 vs	580 w, 545 w, 526 m	364 sh, 342 s
$Pt(2\text{-MePipdtc})_2$	1440 vs	950 ms	578 m, 538 m	367 m, 341 s
$Pt(3\text{-MePipdtc})_2$	1441 vs	951 ms	547 m, 513 m	366 sh, 344 s
$Pt(4\text{-MePipdtc})_2$	1450 vs	962 vs	580 w, 540 w, 526 m	373 w, 338 s
$Rh(2\text{-MePipdtc})_3$	1435 vs	957 ms	576 m, 538 m	331 s
$Rh(3\text{-MePipdtc})_3$	1438 vs	953 ms	568 w, 547 w, 514 w	334 s
$Rh(4\text{-MePipdtc})_3$	1449 vs, 1442 vs	965 s	580 vw, 546 w, 528 m	327 s
$Ir(2\text{-MePipdtc})_3 \cdot 2H_2O$	1437 vs	957 s	574 m, 537 ms	323 s
$Ir(3\text{-MePipdtc})_3 \cdot 2H_2O$	1440 vs	953 s	565 mw, 543 mw, 513 mw	323 s
$Ir(4\text{-MePipdtc})_3 \cdot 2H_2O$	1451 vs, 1445 sh	964 s	572 w, 541 mw, 526 m	321 s

[a] 2-MePipdtcNa: $\nu(C\cdots N)$ 1407 vs; $\nu(C\cdots S)$ 943 s. 3-MePipdtcNa: $\nu(C\cdots N)$ 1418 vs; $\nu(C\cdots S)$ 951 s. 4-MePipdtcNa: $\nu(C\cdots N)$ 1424 vs; $\nu(C\cdots S)$ 950 s.

susceptibilities were corrected for the diamagnetism of the component atoms by use of Pascal's constants. All the complexes were diamagnetic.

Conductivity measurements

These measurements were carried out with a WTW LBR type conductivity bridge for freshly prepared 10^{-3} M solutions in DMF at 25 ± 0.1°C. The solid state measurements were performed using the four probes method.

Thermal analyses

Thermogravimetric analyses (TG and DTG) were performed in air on a Mettler TG50 thermobalance equipped with a Mettler TC10TA processor. A scan rate of 10°C min^{-1} was used.

Analyses

Carbon, nitrogen, hydrogen and sulphur were determined with a Carlo Erba 1106 elemental analyzer.

Acknowledgements—We thank Mr. G. Goldoni for elemental analyses, the Instruments Centre of Modena University for recording the IR spectra and the Consiglio Nazionale delle Ricerche (C.N.R.) of Italy for the financial support.

REFERENCES

1. A. C. Fabretti, F. Forghieri, A. Giusti, C. Preti and G. Tosi, *Inorg. Chim. Acta* 1984, **86**, 127 (and references therein quoted).
2. H. O. Desseyn, A. C. Fabretti, F. Forghieri and C. Preti, *Spectrochim. Acta A* (in press).
3. A. Benedetti, C. Preti and G. Tosi, *J. Mol. Struct.* 1983, **98**, 155.
4. A. Benedetti, C. Preti, L. Tassi, G. Tosi and P. Zannini, *J. Mol. Struct.* (in press).
5. C. Furlani, G. Polzonetti, C. Preti and G. Tosi, *Inorg. Chim. Acta* 1983, **73**, 105.
6. C. Furlani, G. Polzonetti, C. Preti and G. Tosi, *Gazz. Chim. Ital.* 1983, **113**, 609.
7. C. K. Jorgensen, *Prog. Inorg. Chem.* 1962, **4**, 73.
8. A. Benedetti, C. Preti and G. Tosi, *J. Mol. Struct.* 1984, **116**, 397 (and references therein quoted).
9. G. Marcotrigiano, G. C. Pellacani, C. Preti and G. Tosi, *J. Chem. Soc. Jpn* 1975, **48**, 1018 (and references therein quoted).
10. C. K. Jorgensen, *Absorption Spectra and Chemical Bonding in Complexes*. Pergamon Press, London (1964).
11. J. A. Broomhead and W. Grumley, *Inorg. Chem.* 1971, **10**, 2002.
12. A. B. P. Lever, *Inorganic Electronic Spectroscopy*. Elsevier, Amsterdam (1984).
13. P. L. Goggin, R. J. Goodfellow and F. J. S. Red, *J. Chem. Soc., Dalton Trans.* 1972, 1298.
14. A. R. Latham, V. Hascall and H. B. Gray, *Inorg. Chem.* 1965, **4**, 788.
15. C. K. Jorgensen, *Inorganic Complexes*. Academic Press, London (1963).
16. C. K. Jorgensen, *J. Inorg. Nucl. Chem.* 1962, **24**, 1571.
17. F. Takami, S. Wakahara and T. Maeda, *Tetrahedron Lett.* 1971, **28**, 2645.
18. M. J. Janssen, *Rec. Trav. Chim. Pays-Bas* 1960, **79**, 1066.
19. M. J. Janssen, *Rec. Trav. Chim. Pays-Bas* 1960, **79**, 454.
20. M. L. Shankaranarayana and C. C. Patel, *Acta Chem. Scand.* 1965, **19**, 1113.

21. D. C. Bradley and M. H. Gitlitz, *J. Chem. Soc.* (*A*) 1969, 1152.
22. F. Bonati and R. Ugo, *J. Organomet. Chem.* 1967, **10**, 257.
23. T. N. Srivastava and V. Kumar, *J. Organomet. Chem.* 1976, **107**, 55.
24. G. St. Nikolov, N. Jordanov and K. Daskalova, *Inorg. Nucl. Chem. Lett.* 1970, **6**, 723.
25. C. O'Connor, J. D. Gilbert and G. Wilkinson, *J. Chem. Soc.* (*A*) 1969, 84.
26. K. Nakamoto, J. Fujita, R. A. Condrate and Y. Morimoto, *J. Chem. Phys.* 1963, **39**, 423.
27. N. B. Colthup, L. M. Daly and S. E. Wiberley, *Introduction to Infrared and Raman Spectroscopy*. Academic Press, New York (1964).

Polyhedron Vol. 4, No. 9, pp. 1559–1562, 1985
Printed in Great Britain

0277-5387/85 $3.00 + .00
© 1985 Pergamon Press Ltd

^{17}O AND ^{183}W NMR STUDIES OF THE PARATUNGSTATE ANIONS IN AQUEOUS SOLUTIONS

R. I. MAKSIMOVSKAYA* and K. G. BURTSEVA
Institute of Catalysis, Novosibirsk 630090, U.S.S.R.; and North-Caucasian Mining and Metallurgical Institute, Ordzhonikidze, U.S.S.R.

(*Received* 17 *January* 1985; *accepted* 20 *February* 1985)

Abstract—^{17}O (40.7 MHz) and ^{183}W (12.5 MHz) NMR spectra of aqueous

$Na_{10}[H_2W_{12}O_{42}]\cdot 27H_2O$ (**1**), $Na_6[W_7O_{24}]\cdot 14H_2O$ (**2**)

and $(NH_4)_6[Mo_7O_{24}]\cdot nH_2O$ solutions, as well as of 2, 1 and 0.1 M Na_2WO_4 and 2 M Li_2WO_4 solutions acidified up to $P = 0.5$, 1 and 1.14 have been measured. The composition of the $W_7O_{24}^{6-}$ anion remains unchanged (**2**), its structure being similar to that of $Mo_7O_{24}^{6-}$. The W_7O_{24} ^{183}W NMR spectrum shows three resonances with the chemical shifts +269.2, −98.8 and −178.9 ppm relative to WO_4^{2-} and intensity ratio 1:4:2. "Paratungstate A" produced during polycondensation of WO_4^{2-} at $P \leqslant 1.17$ is identical with heptatungstate $W_7O_{24}^{6-}$. The $[H_2W_{12}O_{42}]^{10-}$ ^{183}W NMR spectrum in the acidified 2 M Li_2WO_4 solution has four resonances with the chemical shifts in the range −105–145 ppm and intensity ratio 1:2:1:2. As suggested by NMR data, the $H_2W_{12}O_{42}^{10-} \rightleftarrows W_7O_{24}^{6-}$ transformations occur, which depend upon concentration and temperature.

The formation of two types of paratungstate anions in aqueous Na_2WO_4 solutions acidified up to $P = 1.17$ is well known.[1] Crystalline paratungstate $Na_{10}[H_2W_{12}O_{42}]\cdot 27H_2O$, containing a discrete anion, is deposited from such solutions. The structure of $Na_{10}[H_2W_{12}O_{42}]\cdot 27H_2O$ has been determined by X-ray method crystallography.[2] The existence of this anion (paratungstate B) in solutions has been proved by various methods.[1,3] The other polyanion, the so-called paratungstate A, is regarded as a hexameric particle $HW_6O_{21}^{5-}$ on the basis of potentiometric and spectrophotometric acidity measurements.[1] However, no direct experimental evidence for such composition of these anions has been obtained. From solutions with $P \sim 1.14$ the crystalline paratungstate, $Na_6[W_7O_{24}]\cdot nH_2O$ ($n =$ 14 or 21), has been obtained recently and has been shown to contain the discrete polyanion too.[4–6] The question arises whether the polyanion retains its integrity upon dissolution in water and whether it is the first product of WO_4^{2-} polycondensation, i.e. paratungstate A, as follows from the thermodynamic analysis of the polycondensation reactions.[7] To answer these questions, we have used ^{17}O and ^{183}W NMR methods, which can give structural information about polycomplexes in solutions.[8–10]

EXPERIMENTAL

Solutions of crystalline sodium paratungstates and ammonium paramolybdate, as well as acidified aqueous solutions of Na_2WO_4 and Li_2WO_4 were studied. Paratungstates,

$$Na_{10}[H_2W_{12}O_{42}]\cdot 27H_2O \text{ (1)}$$

and

$$Na_6[W_7O_{24}]\cdot 14H_2O \text{ (2)},$$

were prepared as described.[4–6] The concentrated solutions of **1** were prepared by rapid dissolution in hot water; paratungstate (**2**) and paramolybdate were dissolved in cool water. The spectra were taken immediately after the preparation of the solutions. Aqueous solutions of Na_2WO_4 (2, 1 and 0.1 M) and a 2 M solution of Li_2WO_4 were acidified with 5 N HCl up to $P = 0.5$, 1 and 1.14. 0.1 M Na_2WO_4 solutions were prepared using water enriched with ^{17}O ($\sim 1\%$). ^{17}O and ^{183}W NMR spectra were taken on a Bruker CXP-300 spectrometer at 40.7 and 12.5 MHz, respectively, over the temperature range 280–345 K. The chemical shifts (δ) were given relative to

* Author to whom correspondence should be addressed.

H_2O (^{17}O) and WO_4^{2-} in the solution of Na_2WO_4 (^{183}W). The downfield shift was taken as positive.

RESULTS AND DISCUSSION

Crystalline paratungstate (2) has the $W_7O_{24}^{6-}$ polyanions with the structure of heptamolybdate anions, $Mo_7O_{24}^{6-}$.[5,11] The seven MO_6 polyhedra fall into three structural types 4 M_I, 2 M_{II} and 1 M_{III} (Fig. 1). The anion contains oxygens of the following types: 12 *cis*-dioxo terminal (two types), 8 doubly bridging (four types), 2 threefold bridging and 2 fourfold bridging oxygens. A single M_{III} atom is not bound with the terminal oxygens; however, the lengths of its bonds with two oxygens O_E in the bridge M_{III}–O_E–M_{II} ($\sim$ 1.75 Å) are close to the lengths of the bonds of M_I and M_{II} atoms with the terminal oxygens $O_{F,G}$ (1.71–1.74 Å).

A comparison of ^{17}O NMR spectra of paratungstate (2) and paramolybdate (Fig. 1) in solutions indicates that they correspond to polyanions of the same structural type. The spectrum of the solution of paratungstate (2) completely corresponds to the structure described. The peaks A, B, C, D and G (Fig. 1, Table 1) were assigned using the ^{17}O chemical shift scale for polyoxotungstates and the "δ ^{17}O NMR–O–W bond length correlation",[9,10] and taking into account the line intensities. This correlation is insufficient for attribution of three lines of the same intensity at 590, 595 and 624 ppm (from four O_F oxygens and two O_E oxygens) because the corresponding bonds have nearly the same lengths. As usual,[8] the resonances of oxygen atoms bound with tungsten atoms are shifted to the high field, as compared with the resonances of the corresponding oxygen atoms bound with molybdenum atoms. The difference in the chemical shifts of the two spectra becomes less pronounced as the coordination number of oxygen atoms increases, and, correspondingly, the paramagnetic contribution to the screening decreases. However, in the case of $Mo_7O_{24}^{6-}$, the resonances of the oxygens O_D and O_F bound with the Mo_{II} atoms appear in the

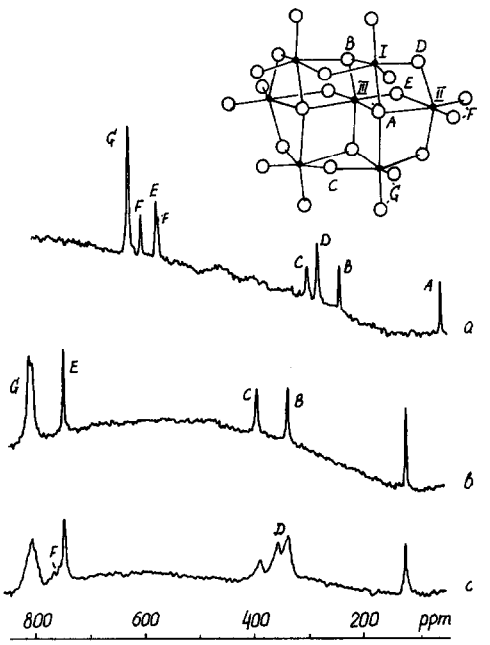


Fig. 1. ^{17}O NMR spectra of aqueous solutions of $Na_6[W_7O_{24}]\cdot 14H_2O$, 330 K (a), $(NH_4)_6Mo_7O_{24}\cdot nH_2O$, 293 K (b) and 283 K (c); and idealized bond structure of the polyanion.

Table 1. Chemical shifts of the ^{17}O and ^{183}W NMR lines of polyoxoanions

Anion	δ ^{17}O NMR ($\pm$3) of O atoms of different types (ppm)							
	O=M			M–O–M		OM_3OM_4		
$Mo_7O_{24}^{6-}$	821, 817 (8)		750	757 (2)	397 (2)	354 (4)	340 (2)	122 (2)
$W_7O_{24}^{6-}$	648 (8)	624 (2)	590 (2)	595 (2)	314 (2)	295 (4)	254 (2)	71 (2)
$H_2W_{12}O_{42}^{10-}$	663, 651 (6)	613* (12)	607*	457 (4)	398 (4)	343, 323*	271	
δ NMR ^{183}W, ppm								
$W_7O_{24}^{6-}$	+269.2 (1)			−91.8 (4)		−178.9 (2) Na, pH 7		
$H_2W_{12}O_{42}^{10-}$	−108.2 (2)			−110 (4)		−114.5 (2)–141.4 (4) Li, pH 6		

( ) is the relative line intensity.

* The lines enhanced during oxygen exchange with water enriched with ^{17}O.

spectra at temperatures below 286 K [Fig. 1(c)]. At higher temperatures, the lines from O_D and O_F are broadened rapidly and then disappear. This indicates chemical exchange between these atoms, which leads to the broadening of their resonances separated by a 400 ppm interval. The exchange appears to be the result of the rotation of the $Mo_{II}(O_FO_D)_2$ fragments weakly bound with the Mo_{III} atom (the lengths of the Mo_{II}–O_A and Mo_{II}–O_E bonds are 2.16 and 2.42 Å, respectively).[11] With increase in temperature (310–320 K), the other lines of the $Mo_7O_{24}^{6-}$ spectrum are broadened too and become unobservable.

For $W_7O_{24}^{6-}$, a small linewidth indicates a very slow rotation, if any, even at 330 K. However, if the temperature of the solution is raised to 345–350 K, the broadening of the line from O_D and of the lines at 590 and 624 ppm can be observed. Therefore, by analogy with $Mo_7O_{24}^{6-}$, these lines can be attributed to four O_F atoms and, the line at 595 ppm to the O_E atoms. A 34 ppm difference in δ of the two pairs of the O_F atoms corresponds to *ca* 0.015 Å difference in the lengths of two O_F–W_{II} bonds in *cis*-positions.

Thus, the ^{17}O NMR spectra suggest retention of the composition and structure of the $W_7O_{24}^{6-}$ anion in aqueous solutions. This conclusion is supported by the ^{183}W NMR spectrum of the solution containing, according to ^{17}O NMR, the $W_7O_{24}^{6-}$ anions solely: three peaks with the ratio of intensities 1:4:2 from W atoms of three types are observed. The line positions of the spectrum are similar to those of the ^{51}V NMR spectrum of the $V_{10}O_{28}^{6-}$ polyanion, which has the V atoms of the same three types but with the ratio 2:4:4.[11]

During aging of the concentrated $Na_6[W_7O_{24}]$ solutions, crystalline $Na_{10}[H_2W_{12}O_{42}]\cdot 27H_2O$ is deposited. The crystals of this compound appear on the ampoule walls even an hour after the preparation of the solution. The concentration of the $W_7O_{24}^{6-}$ anions in the solution gradually decreases, and the line intensities also decrease. However, new lines do not appear, which points to a very low concentration of the $H_2W_{12}O_{42}^{10-}$ anions in the solution.

^{17}O NMR spectra of the paratungstate (1) solution were taken at 315–330 K immediately after its dissolution in hot water. The spectrum has no lines from polytungstates observed previously by ^{17}O NMR.[8–10] All lines seem to belong to the $H_2W_{12}O_{42}^{10-}$ anions, which remain in freshly prepared solutions of paratungstate (1), as evidenced by Raman spectra.[1,3] $H_2W_{12}O_{42}^{10-}$ has a complex structure.[2,11] The WO_6 polyhedra of four structural types (Fig. 3) have several different groups of oxygens: 18 terminal (4 types); 18 doubly bridging (3 or 4 types), and 6 threefold bridging (two types) atoms. The chemical shifts, corresponding to the lengths of the W–O bonds of approx. 1.75–1.77 Å, and the ratio of line intensities (~ 2:4:4:8) of the terminal oxygens, as well as the number, and the integrated intensity of the resonances of the bridging oxygens, are in good conformity with the $H_2W_{12}O_{42}^{10-}$ structure.

The lines corresponding to $W_7O_{24}^{6-}$ gradually appear in the spectrum of the solution of paratungstate (1). Their part comprises *ca* 25% at 330 K in 30 min after dissolution and tends to increase. Upon cooling the solutions down to 293 K, the reverse transformation occurs, and the major part of tungsten(VI) progressively crystallizes in the form of paratungstate (1), the remainder being in the form of $W_7O_{24}^{6-}$ in the solution. At higher temperatures, the solubility of paratungstate (1) and the concentration of $H_2W_{12}O_{42}^{10-}$ in the solution increases, but simultaneously the rate of $W_7O_{24}^{6-}$ formation also increases.

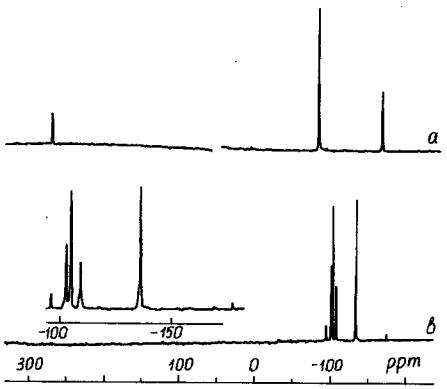


Fig. 2. ^{183}W NMR spectra of $W_7O_{24}^{6-}$ in the acidified Na_2WO_4 solution, pH ~ 7 (293 K) (a), and of $H_2W_{12}O_{42}^{10-}$ in the acidified Li_2WO_4 solution, pH ~ 6 (293 K) (b).

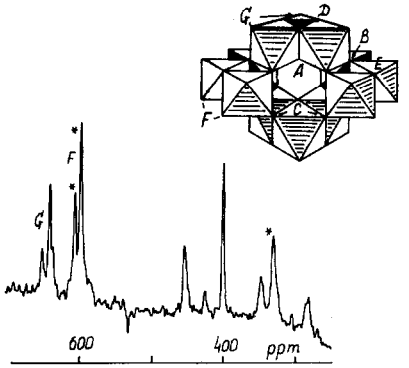


Fig. 3. ^{17}O NMR spectrum of the freshly prepared aqueous solution of $Na_{10}[H_2W_{12}O_{42}]\cdot 27H_2O$ (330 K) and polyhedral model of the polyanion structure.

At the natural abundance of ^{17}O ($\sim 0.04\%$), ^{17}O NMR measurements can be made at tungsten concentrations approx. equal to or higher than 1 M. It is essential that at such concentrations the system is a two-phase one due to the very low solubility of $Na_{10}[H_2W_{12}O_{42}]$. We have succeeded in registering ^{17}O NMR spectra of $H_2W_{12}O_{42}^{10-}$ anions in such solutions because freshly prepared supersaturated solutions of paratungstate (1) were studied, and also because its transformation to $W_7O_{24}^{6-}$ occurs rather slowly. The enhanced sensitivity of modern high-field NMR spectrometers provides the possibility to quite rapidly accumulate ^{17}O NMR spectra at the natural abundance of ^{17}O and to register the state of the solution even in 10–15 min after dissolution. When operating on the previously used spectrometers, the preliminary enrichment with ^{17}O in the heated solution and a prolonged accumulation of spectra were necessary. As a result, the equilibrium state of the solutions, in which $W_7O_{24}^{6-}$ prevailed, was registered.[9] Moreover, in the case of enrichment of anions via dissolution of preliminary prepared samples of paratungstate (1) in the enriched water, we observed only three lines—from the oxygens in the side fragments of $H_2W_{12}O_{42}^{10-}$, because of the non-uniform enrichment of oxygens of the polyanion (Fig. 3, Table 1).

Thus, the heating of the solutions of sodium paratungstate (1) accelerates the formation of the $W_7O_{24}^{6-}$ anions in the solution. Using the concentrated solutions prepared by prolonged heating of $Na_{10}[H_2W_{12}O_{42}]\cdot 27H_2O$ with water accompanied by their rapid cooling and acetone addition, it is possible to obtain almost pure, crystalline heptatungstate.[4]

From ^{17}O NMR spectra of freshly acidified 1 and 2 M Na_2WO_4 solutions one may judge about the presence of $W_7O_{24}^{6-}$ anions solely. At $P = 0.5$ and 1 excess WO_4^{2-} anions are also observed. During aging, paratungstate (1) was crystallized from the solutions, however no $H_2W_{12}O_{24}^{10-}$ anions were detected in their spectra. By using water enriched with ^{17}O, it was possible to measure ^{17}O NMR spectra of 0.1 M Na_2WO_4 solutions. In freshly acidified solutions ($P = 1$), only $W_7O_{24}^{6-}$ and excess WO_4^{2-} anions were observed. The composition of the solution remained unchanged during a 3-months storage at 293 K. On the contrary, in the solution with the same concentration of W(VI) prepared from $Na_{10}[H_2W_{12}O_{42}]\cdot 27H_2O$ and stored for 3 months at 293 K, nearly complete conversion to heptatungstate occurred.

In freshly acidified 2 M Li_2WO_4 solutions, $W_7O_{24}^{6-}$ was also registered. At room temperature $W_7O_{24}^{6-}$ transforms to $H_2W_{12}O_{42}^{10-}$ rather quickly (for several hours). At elevated temperatures this transformation is incomplete and occurs more slowly. In the presence of Li^+ the $H_2W_{12}O_{42}^{10-}$ anions remain in the solution. Their ^{183}W NMR spectra (Fig. 2, Table 1) show four resonances with the intensity ratio 1:2:1:2, which corresponds to the anion structure in the crystalline state. The chemical shifts of the ^{183}W NMR depend upon pH of the solution and differ from those in the presence of sodium by 10–15 ppm toward the high field. This seems to indicate a stronger association of Li^+ with polyanions, as compared with Na^+. Upon heating the solution, the $H_2W_{12}O_{42}^{10-}$ anions partly transform to $W_7O_{24}^{6-}$. The lower the concentration of tungsten the larger the extent of such transformation.

Thus, using ^{17}O and ^{183}W NMR, we have shown that, when formed in aqueous WO_4^{2-} solutions acidified up to $P \leqslant 1.17$, the complex of paratungstate A (whose composition has long been in question[1]) is actually heptatungstate $W_7O_{24}^{6-}$ rather than hexatungstate. Other isopolyanions of tungsten(VI), except for $W_7O_{24}^{6-}$ and $H_2W_{12}O_{42}^{10-}$, have not been observed in such solutions.

REFERENCES

1. K. H. Tytko and O. Glemser, *Adv. Chem. Radiochem.* 1976, **19**, 239.
2. R. Allman, *Acta Cryst.* 1971, **B27**, 1393.
3. J. Aveston, *Inorg. Chem.* 1964, **3**, 981.
4. P. B. Petrun'kov, K. G. Burtseva and D. P. Semchenko, *Zh. neorgan. khimii* 1976, **21**, 2380.
5. K. G. Burtseva, T. S. Chernaya and M. I. Sirota, *Dokl. AN SSSR* 1978, **243**, 104.
6. K. G. Burtseva, L. A. Kochubei, L. A. Voropanova and B. Kh. Gorbatkova, *Zh. neorgan. khimii* 1981, **26**, 2121.
7. K. G. Burtseva, L. A. Voropanova and L. A. Kochubei, *Zh. neorgan. khimii* 1984, **29**, 1463.
8. M. Filowitz, R. K. C. Ho, W. G. Klemperer and W. Shum, *Inorg. Chem.* 1979, **18**, 93.
9. L. P. Kazanskii, M. A. Fedotov and V. I. Spitsyn, *Dokl. AN SSSR* 1977, **234**, 1376.
10. M. A. Fedotov, L. P. Kazanskii and V. I. Spitsyn, *Dokl. AN SSSR* 1983, **272**, 1179.
11. H. T. Evans, *Persp. Struct. Chem.* 1971, **4**, 2.

Polyhedron Vol. 4, No. 9, pp. 1563–1568, 1985
Printed in Great Britain

0277–5387/85 $3.00 + .00
© 1985 Pergamon Press Ltd

MOLYBDENUM(V) DIMERIC COMPLEXES WITH DIALKYL CARBAMATES

R. LOZANO,* J. ROMAN, M. D. ARMADA and A. DOADRIO
Departamento de Química Inorgánica, Facultad de Farmacia, Universidad Complutense de Madrid, Madrid 28040, Spain

(*Received* 4 *April* 1984; *accepted after revision* 28 *February* 1985)

Abstract—Syntheses are reported for a number of novel oxo and sulphido bridged molybdenum(V) complexes with *N*-methyl-*N*-cyclohexyl carbamate and *N*,*N*-dicyclohexyl carbamate as ligands, and we have compared these complexes with the molybdenum(V) complexes with dialkyldithiocarbamates as ligands. These complexes were identified by IR and electronic spectra, magnetic susceptibility and analytical data, and were assigned the formulae $[Mo_2O_3(LL)_4]$, $[Mo_2O_4(LL)_2]$, $[Mo_2O_2S_2(LL)_2]$ and $[Mo_2O_3S(LL)_2]$. IR and electronic spectra of these compounds are sensitive to substitution of sulphur atoms into the bridge system. It is suggested that the low magnetic moments observed are due, at least in part, to intramolecular metal–metal interactions.

In previous communications, we have reported the isolation and study of dimeric molybdenum(V) complexes with xanthates, oxinates and dithiocarbamates as ligands.[1–7]

The object of the present study, has been to obtain binuclear complexes of molybdenum(V) with *N*-methyl-*N*-cyclohexyl carbamate and *N*,*N*-dicyclohexyl carbamate as ligands (O-donor), and to compare these complexes with the molybdenum(V) complexes with dithiocarbamates as ligands (S-donor) and similar structures, obtained previously[6–11] and studied by X-ray diffraction.[12–14]

In this paper, we describe the isolation and characterization of four different dimeric complexes of molybdenum(V):

(a) Molybdenum(V) oxo-complexes with a monoxo bridge $[Mo_2O_3(LL)_4]$;

(b) Molybdenum(V) oxo-complexes with a dioxo bridge $[Mo_2O_4(LL)_2]$;

(c) Molybdenum(V) oxo-complexes with a disulphido bridge $[Mo_2O_2S_2(LL)_2]$;

(d) Molybdenum(V) oxo-complexes with oxo-sulphido bridge $[Mo_2O_3S(LL)_2]$.

EXPERIMENTAL

Materials. $Na_2MoO_4 \cdot 2H_2O$ was Merck commercial product used as supplied. Potassium *N*-methyl-*N*-cyclohexyl carbamate and potassium *N*,*N*-dicyclohexyl carbamate were prepared by the reaction of potassium hydroxide with carbon dioxide and *N*-methyl-*N*-cyclohexyl amine or *N*,*N*-dicyclohexyl amine in water, and were recrystallized from water : methanol. The solvents used to prepare the complexes were Carlo Erba or Merck; the solutions for absorption spectra were prepared with dimethylsulphoxide (DMSO) spectral grade Merck-Uvasol and water.

Analytical procedures. Elemental analyses were performed on a Perkin–Elmer Analyzer model 240 B. Molybdenum was determined by atomic absorption spectrophotometry, with a Perkin–Elmer model 430 atomic absorption spectrophotometer after the complexes had been decomposed with a 1:1 mixture of concentrated nitric and sulphuric acids. Analytical data are collected in Table 1.

Magnetic susceptibilities. Measurements were made using the Gouy method at room temperature on a Mettler H-51 A.R. balance and an Oxford electromagnet. Molar susceptibilities given are corrected for the diamagnetism of the constituent molecules. The magnetic moments were calculated according to the formula $\mu = 2.84\ (\chi'_M \cdot T)^{0.5}$ BM, where χ'_M is the corrected molar susceptibility.[15] Table 1 shows the results obtained for the molybdenum(V) oxo-complexes with dialkylcarbamates as ligands.

The IR spectra were obtained using a Perkin–Elmer spectrophotometer model 283. The samples

* Author to whom correspondence should be addressed.

Table 1. Elemental analyses, and magnetic moments of molybdenum(V) oxo-complexes

Compound	Calculated %				Found %				
	C	H	N	Mo	C	H	N	Mo	μ(BM)
$Mo_2O_3\{O_2CN(CH_3)(C_6H_{11})\}_4$	44.44	6.48	6.48	22.22	45.00	6.95	6.67	22.29	0.51
$Mo_2O_3\{O_2CN(C_6H_{11})_2\}_4$	50.70	7.70	4.92	16.90	51.01	7.85	5.00	16.86	0.38
$Mo_2O_4\{O_2CN(CH_3)(C_6H_{11})\}_2$	33.80	4.92	4.92	33.80	34.01	5.00	5.10	33.75	0.22
$Mo_2O_4\{O_2CN(C_6H_{11})_2\}_2$	40.90	6.25	3.97	27.27	41.10	6.53	4.06	27.24	0.24
$Mo_2O_2S_2\{O_2CN(CH_3)(C_6H_{11})\}_2$	32.00	4.66	4.66	32.00	32.17	4.80	4.77	32.05	0.08
$Mo_2O_2S_2\{O_2CN(C_6H_{11})_2\}_2$	39.13	5.97	3.80	26.08	40.05	6.00	3.97	26.04	0.00
$Mo_2O_3S\{O_2CN(CH_3)(C_6H_{11})\}_2$	32.87	4.79	4.79	32.87	33.00	4.91	4.88	32.82	0.12
$Mo_2O_3\{O_2CN(C_6H_{11})_2\}_2$	40.00	6.11	3.88	26.66	41.17	6.23	4.00	26.64	0.04

were run as KBr pellets. Important IR absorption peaks for the complexes prepared in this study are listed in Table 2.

The visible–near UV spectra of the compounds, were measured in the range 200–900 nm on a Beckman recording spectrophotometer model 5240, over dissolutions of the complexes in DMSO and water. The results obtained in this study and the ones obtained for the complexes with dialkyl dithiocarbamates as ligands (only *d–d* transitions), are given in Table 3.

Preparation of the complexes. $Mo_2O_3\{O_2CN(CH_3)(C_6H_{11})\}_4$. $Na_2MoO_4 \cdot 2H_2O$ (2.42 g) was dissolved in water (40 cm^3) and it was depolymerized with NaOH. The solution was added to a solution of potassium *N*-methyl-*N*-cyclohexyl carbamate (3.90 g) in water (50 cm^3), with vigorous stirring, and a solution (freshly prepared) of sodium dithionite (0.5 g) in water (20 cm^3) was added. Lastly, drop-by-drop, glacial acetic acid was added to give pH = 5. There was an immediate brown precipitate. The suspension was set aside for 1 hr and then filtered *in vacuo* and dried over P_4O_{10}. Yield: 53%.

$Mo_2O_4\{O_2CN(CH_3)(C_6H_{11})\}_2$. A solution of $Na_2MoO_4 \cdot 2H_2O$ (2.42 g) in water (40 cm^3) was treated with concentrated sodium hydroxide. The resulting solution was added to a solution of potassium *N*-methyl-*N*-cyclohexyl carbamate (1.95 g) in water (30 cm^3). A solution of sodium dithionite (0.5 g) in water (20 cm^3) was prepared and this solution was added to the previous one. Diluted hydrochloric acid was added dropwise until precipitation of the complex was complete. The precipitate was filtered by suction and the green residue was dried *in vacuo* over P_4O_{10}. Yield: 60%.

$Mo_2O_2S_2\{O_2CN(CH_3)(C_6H_{11})\}_2$. 2.42 g of $Na_2MoO_4 \cdot 2H_2O$ was dissolved in water (40 cm^3) and to this solution was added concentrated sodium hydroxide to give pH = 8–9. The resulting solution was treated with potassium *N*-methyl-*N*-cyclohexyl carbamate (1.95 g) in water (40 cm^3). Hydrogen sulphide was passed through the resulting solution with simultaneous cooling in freezing mixture for 30 min. The solution gradually takes a brown colour. Drop-by-drop, glacial acetic acid was added to give pH = 6, and a brown solid precipitates. The residue was filtered *in vacuo* and dried over P_4O_{10}. Yield: 64%.

$Mo_2O_3S\{O_2CN(CH_3)(C_6H_{11})\}_2$. A solution of $Na_2MoO_4 \cdot 2H_2O$ (2.42 g) in 2 M sodium hydroxide (40 cm^3) was treated with dilute hydrochloric acid to give pH = 6. Hydrogen sulphide was bubbled slowly through the resulting solution for 1 hr. The solution gradually takes a brown colour, and it was added to a solution of potassium *N*-methyl-*N*-cyclohexyl carbamate (1.95 g) in water (40 cm^3). Lastly, glacial acetic acid was added dropwise until the precipitation of the complex was complete. The precipitate was filtered *in vacuo* and the brown residue was dried over P_4O_{10}. Yield: 80%.

A similar preparation was carried out for the complexes with *N*,*N*-dicylohexyl carbamate as ligand.

DISCUSSION

According to the analytical results and spectroscopic data, the four synthesized complexes have dimeric structures. If we carry out the precipitation at pH = 5, with acetic acid, the complexes present a monoxo bridge, the stoichiometry is 2:1, and the molybdenum is six-coordinated. The formula which most closely fits the analyses is $Mo_2O_3(LL)_4$:

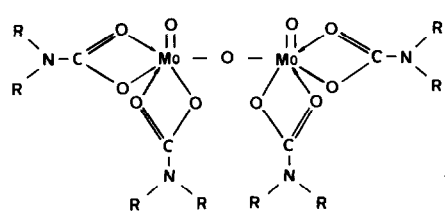
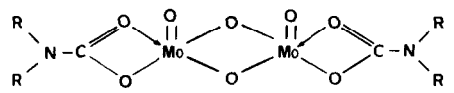


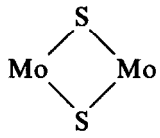
Table 2. IR absorption maxima, in cm^{-1}, of molybdenum(V) oxo-complexes

Compound	ν(C–N)	ν(C–O)	ν_s(Mo=O)	ν_a(Mo–O_b)	ν_s(Mo–O_b)	ν_a(Mo–S_b)	ν_s(Mo–S_b)	ν(Mo–O_t)
$Mo_2O_3\{O_2CN(CH_3)(C_6H_{11})\}_4$	1415	1580	940	640	480	—	—	317
$Mo_2O_4\{O_2CN(CH_3)(C_6H_{11})\}_2$	1405	1625	950	630	475	—	—	310
$Mo_2O_2S_2\{O_2CN(CH_3)(C_6H_{11})\}_2$	1410	1570	932	—	—	605	405	330
$Mo_2O_3S\{O_2CN(CH_3)(C_6H_{11})\}_2$	1412	1580	924	640	—	610	405	332
$Mo_2O_3\{O_2CN(C_6H_{11})_2\}_4$	1390	1635	930	650	480	—	—	310
$Mo_2O_4\{O_2CN(C_6H_{11})_2\}_2$	1385	1620	950	640	560	—	—	300
$Mo_2O_2S_2\{O_2CN(C_6H_{11})_2\}_2$	1380	1580	925	—	—	600	450	320
$Mo_2O_3S\{O_2CN(C_6H_{11})_2\}_2$	1380	1585	920	640	—	600	450	305

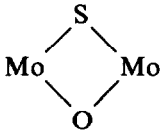
However, if we carry out the precipitation at pH = 2, the stoichiometry of the compounds is 1 : 1, the molybdenum is five-coordinated and these complexes present a dioxo bridge. The formula that we assign to these complexes is $Mo_2O_4(LL)_4$:



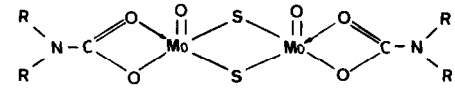
The complexes obtained by bubbling H_2S through $Na_2MoO_4 \cdot 2H_2O$ solution and the corresponding dialkyl carbamate, and the ones synthesized by bubbling H_2S through $Na_2MoO_4 \cdot 2H_2O$ solution in diluted hydrochloric acid, with posterior addition of the dialkyl carbamate, present a 1:1 stoichiometry, the molybdenum being five-coordinated. The union between the molybdenum atoms is realized by means of a disulphido



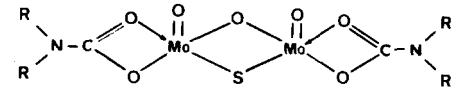
bridge, in the first case, with formula $Mo_2O_2S_2(LL)_2$; and through an oxo-sulphido bridge



in the second case.



The complexes obtained in this paper, gave low values of magnetic moments (see Table 1) that suggest the presence of polymeric species and involve



interaction through the oxygen or sulphur bridges or by direct metal–metal bonding. Similar behaviour has been observed in other dimeric molybdenum(V) complexes.[12–16]

The IR spectra of the four various kinds of complexes studied exhibit a very strong band in the range 920–952 cm^{-1}, which we attribute to the vibration of the symmetric stretching mode of the terminal Mo=O bond. The antisymmetric stretch-

Table 3. Electronic absorption spectra of molybdenum(V) oxo-complexes

Compound	λ (nm)	$\tilde{\nu}$ (*kK*)	ε	Transition
$Mo_2O_3\{O_2CN(CH_3)(C_6H_{11})\}_4$[a]	648	15.4	37	$^2B_2 \rightarrow {}^2E(I)$
	602 (sh)	16.6	218	$^2B_2 \rightarrow {}^2B_1$
	467	21.4	3479	Charge transfer
	422	23.7	8620	Charge transfer
	330	30.3	16,241	Intraligand
	305	32.8	32,943	Intraligand
	240	41.7	51,040	Intraligand
$Mo_2O_3\{S_2CN(CH_3)(C_6H_{11})\}_4$[b]	698	14.3	206	$^2B_2 \rightarrow {}^2E(I)$
	494 (sh)	20.2	333	$^2B_2 \rightarrow {}^2B_1$
$Mo_2O_3\{O_2CN(C_6H_{11})_2\}_4$[a]	645	15.5	78	$^2B_2 \rightarrow {}^2E(I)$
	600 (sh)	16.6	310	$^2B_2 \rightarrow {}^2B_1$
	465	21.5	3192	Charge transfer
	421	23.7	9374	Charge transfer
	330	30.3	15,987	Intraligand
	303	33.0	50,128	Intraligand
	250	40.0	65,403	Intraligand
$Mo_2O_3\{S_2NC(C_6H_{11})_2\}_4$[b]	680	14.7	101	$^2B_2 \rightarrow {}^2E(I)$
$Mo_2O_4\{O_2CN(CH_3)(C_6H_{11})\}_2$[a]	645 (sh)	15.5	82	$^2B_2 \rightarrow {}^2E(I)$
	603 (sh)	16.5	451	$^2B_2 \rightarrow {}^2B_1$
	465	21.5	4916	Charge transfer
	420	23.8	7644	Charge transfer
	332 (sh)	30.9	13,916	Intraligand
	305 (sh)	32.8	25,437	Intraligand
	250	40.0	37,041	Intraligand
$Mo_2O_4\{S_2NC(CH_3)(C_6H_{11})\}_2$[c]	506	19.8	25	$^2B_2 \rightarrow {}^2B_1$
$Mo_2O_4\{O_2CN(C_6H_{11})_2\}_2$[a]	648 (sh)	15.4	81	$^2B_2 \rightarrow 2E(I)$
	602 (sh)	16.6	497	$^2B_2 \rightarrow {}^2B_1$
	470	21.2	1280	Charge transfer
	422	23.6	4753	Charge transfer
	330	30.3	8009	Intraligand
	310	32.2	24,316	Intraligand
	250	40.0	51,493	Intraligand
$Mo_2O_4\{S_2CN(C_6H_{11})_2\}_2$[c]	622	15.1	614	$^2B_2 \rightarrow {}^2E(I)$
$Mo_2O_2S_2\{O_2CN(CH_3)(C_6H_{11})\}_2$[a]	648 (sh)	15.4	150	$^2B_2 \rightarrow {}^2E(I)$
	602 (sh)	16.6	642	$^2B_2 \rightarrow {}^2B_1$
	468	21.3	5243	Charge transfer
	420	23.8	10,724	Charge transfer
	320	31.2	14,961	Intraligand
	295	33.8	31,418	Intraligand
	260	38.4	37,976	Intraligand
$Mo_2O_2S_2\{S_2CN(CH_3)(C_6H_{11})\}_2$[b]	560 (sh)	17.8	17	$^2B_2 \rightarrow {}^2E(I)$
	496 (sh)	20.1	30	$^2B_2 \rightarrow {}^2B_1$
$Mo_2O_2S_2\{O_2CN(C_6H_{11})_2\}_2$[a]	645	15.5	126	$^2B_2 \rightarrow {}^2E(I)$
	605	16.5	459	$^2B_2 \rightarrow {}^2B_1$
	465	21.5	3933	Charge transfer
	420	23.8	7318	Charge transfer
	335	29.8	12,356	Intraligand
	300	33.3	28,907	Intraligand
	260	38.4	36,514	Intraligand
$Mo_2O_2S_2\{S_2NC(C_6H_{11})_2\}_2$[b]	—	—	—	—

Table 3 (*continued*).

Compound	λ (nm)	$\tilde{\nu}$ (*kK*)	ε	Transition
$Mo_2O_3S\{O_2CN(CH_3)(C_6H_{11})\}_2$[a]	648	15.4	112	$^2B_2 \rightarrow {}^2E(I)$
	602	16.6	480	$^2B_2 \rightarrow {}^2B_1$
	468	21.3	4654	Charge transfer
	420	23.8	9243	Charge transfer
	350	31.2	17,418	Intraligand
	310	32.2	41,243	Intraligand
	275	36.3	60,128	Intraligand
$Mo_2O_3S\{S_2CN(CH_3)(C_6H_{11})\}_2$[b]	500	20.0	34	$^2B_2 \rightarrow {}^2B_1$
$Mo_2O_3\{O_2CN(C_6H_{11})_2\}_2$[a]	645 (sh)	15.5	105	$^2B_2 \rightarrow {}^2E(I)$
	602 (sh)	16.6	519	$^2B_2 \rightarrow {}^2B_1$
	465	21.5	5986	Charge transfer
	420	23.8	12,123	Charge transfer
	330	30.3	17,012	Intraligand
	295	33.8	36,904	Intraligand
	262	38.1	45,098	Intraligand
$Mo_2O_3S\{S_2CN(C_6H_{11})_2\}_2$[b]	—	—	—	—

(sh) = shoulder.

[a] This work.

[b] Reference 7.

[c] Reference 6.

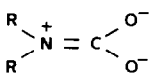
ing mode has not been observed. However, the appearance of the symmetric stretching mode is sufficient to designate, in the dimeric complexes, a *cis* disposition of the two terminal Mo=O.[12]

The complexes with monoxo bridge, dioxo bridge and oxo-sulphido bridge exhibit two bands in the IR spectra between 640 and 480 cm^{-1}, which we attribute to the vibration of the antisymmetric and symmetric stretching mode, respectively, of the Mo–O bridge bond.

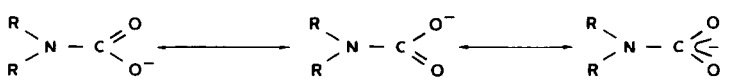
The IR spectra of the complexes with disulphido and oxo-sulphido bridges show two bands between 605 and 450 cm^{-1}, which we attribute to the vibration of the antisymmetric and symmetric stretching mode, respectively, of the Mo–S–M bridge bond.

The IR spectra of the analogous molybdenum(V) complexes with *N*-methyl-*N*-cyclohexyl dithiocarbamate and *N*,*N*-dicyclohexyl dithiocarbamate as ligands show the vibration of the symmetric stretching mode of the terminal Mo=O bond displaced to lower frequencies and the vibration of the antisymmetric stretching mode of the Mo–O bridge bond displaced to greater frequencies[6,7] than the molybdenum(V) carbamates studied here. These differences can be attributed to the more covalent character of the Mo(V)–S bond in the dithiocarbamates than the Mo(V)–O in the carbamates.

If we compare the IR spectra of the molybdenum(V) carbamate complexes with the IR spectra of potassium carbamates, we observe that the molybdenum(V) complexes exhibit the band of the stretching mode of the C–N bond displaced to higher frequencies than potassium carbamates. The IR spectra of molybdenum(V) complexes exhibit this band in the range 1415–1380 cm^{-1} (see Table 2) while the IR spectra of potassium *N*-methyl-*N*-cyclohexyl carbamate and potassium *N*,*N*-dicyclohexyl carbamate exhibit this band at 1365 and 1360 cm^{-1}, respectively. This difference may be attributed to a substantial contribution of resonance form:



in the molybdenum(V) carbamate complexes, while in potassium carbamates, the following resonance forms take place:



Consequently, the frequencies of the stretching mode of the C–O bond must be lower in molybdenum(V) carbamate complexes than in potassium salts, because the C–O bond is not so strong in the complexes due to the stronger C–N bond. The IR spectra of molybdenum(V) complexes exhibit the band of the C–O stretching mode in the range 1635–1570 cm^{-1}, while in the IR spectra of potassium carbamates this band appears at 1650 cm^{-1}. A similar behaviour has been observed in the frequencies of the stretching mode of the C–S bond and C–N bond to the molybdenum(V) complexes with dithiocarbamates as ligands and the potassium dithiocarbamates.[6,7]

The IR spectra of all carbamate complexes show also other bands between 332–300 cm^{-1}, attributed to molybdenum–oxygen ligand frequencies.

All the complexes studied here show, in the electronic spectra, two bands in the 645–600 nm region which we attribute to *d–d* transitions. We cannot observe appreciable differences between the six-coordinated dimeric complexes with monoxo bridge and the five-coordinated dimeric complexes with dioxo, disulphido and oxo-sulphido bridge, which can be attributed to a distortion of octahedral structure for a d^1 ion in the complexes with monoxo bridge, due to a Jahn–Teller effect (Ballhausen–Gray scheme).[17]

We assign the two bands to $^2B_2 \rightarrow {}^2E(I)$ and $^2B_2 \rightarrow {}^2B_1$ transitions, respectively, for a distorted octahedral structure[17] for the monoxo bridge complexes and for a square pyramidal structure[18] for the complexes with dioxo, disulphido and oxo-sulphido bridges.

If we compare the electronic spectra in the visible region of the Mo(V) carbamate complexes obtained in this study with the electronic spectra of the Mo(V) dithiocarbamate complexes previously studied,[6,7] we observe that the $^2B_2 \rightarrow {}^2E(I)$ transition is displaced to greater frequencies (750 cm^{-1}) in the carbamate complexes, while the $^2B_2 \rightarrow {}^2B_1$ transition is displaced to greater frequencies (3000 cm^{-1}) in the dithiocarbamate complexes. These differences may be attributed to the greater distortion of the octahedral structure in the Mo(V) carbamate complexes and to the more covalent character of the Mo(V)–S bond (see Table 3).

In the visible region we detect two bands over 470 and 420 nm that we attribute to charge transfer transitions. We observe no significant differences between these transitions and the charge transfer transitions observed in Mo(V) complexes with dithiocarbamates as ligands.[6,7]

In the UV region, three transitions are detected at 330, 300 and 250 nm, that we attribute to intraligand transitions.

REFERENCES

1. A. Doadrio Villarejo, A. Doadrio, R. Lozano and M. P. Alonso, *An. Quim.* 1980, **76B**, 80.
2. R. Lozano, A. Doadrio and A. L. Doadrio, *Polyhedron* 1982, **1**, 163.
3. R. Lozano, J. Román, E. Alarcón, A. L. Doadrio and A. Doadrio, *Rev. Chimie Minerale* 1983, **20**, 173.
4. A. Doadrio López, A. L. Doadrio and R. Lozano, *An. Quim.* 1978, **74**, 566.
5. R. Lozano, J. Román, E. Alarcón and A. L. Doadrio, *An. Quim.* 1983, **79B**, 187.
6. A. L. Doadrio, M. P. Alonso, R. Lozano and A. Doadrio, *An. Quim.* 1983, **79B**, 195.
7. A. L. Doadrio, M. P. Alonso, A. Doadrio and R. Lozano, *An. Real Acad. Farmacia* 1983, **49**, 501.
8. D. Couvouvanis, *Prog. Inorg. Chem.* 1979, **26**, 301.
9. W. E. Newton, J. L. Corbin, D. C. Bravard, J. E. Searle and J. W. McDonald, *Inorg. Chem.* 1974, **13**, 1100.
10. G. Bunzey and J. H. Enemark, *Inorg. Chem.* 1978, **17**, 682.
11. L. Ricard, J. Estienne, P. Karagiannidis, P. Toledano, J. Fisher, A. Mitschler and R. Weiss, *J. Coord. Chem.* 1974, **3**, 277.
12. F. A. Cotton, D. L. Hunter, L. Ricard and R. Weiss, *J. Coord. Chem.* 1974, **3**, 259.
13. L. Ricard, C. Martin, R. Wiest and R. Weiss, *Inorg. Chem.* 1975, **14**, 9, 2300.
14. L. Ricard, J. Estienne, P. Karagiannidis, P. Toledano, J. Fisher and A. Mitschler, *J. Coord. Chem.* 1974, **3**, 277.
15. P. W. Selwood, *Magnetochemistry*. Interscience, New York (1956).
16. H. B. Blake, F. A. Cotton and J. S. Wood, *J. Am. Chem. Soc.* 1964, **86**, 3024.
17. C. J. Ballhausen and H. B. Gray, *Molecular Orbital Theory*. Benjamin, New York (1965).
18. H. B. Gray and C. R. Hare, *Inorg. Chem.* 1962, **1**, 363.

Polyhedron Vol. 4, No. 9, pp. 1569–1572, 1985
Printed in Great Britain

0277–5387/85 $3.00 + .00
© 1985 Pergamon Press Ltd

SYNTHESIS AND CHARACTERISATION OF CHELATED (1-CYANOETHYL)RUTHENIUM(II) CARBONYL COMPLEXES*

SARADA GOPINATHAN, I. R. UNNY and C. GOPINATHAN†
Inorganic Chemistry Division, National Chemical Laboratory, Poona 411 008, India

(*Received* 1 *February* 1985; *accepted* 28 *February* 1985)

Abstract—The reaction between acrylonitrile and the Ru–H bond in $HRu(CO)Cl(PPh_3)_3$ results in the formation of a binuclear ruthenium(II) complex having chlorine bridges which are easily broken by sodio-derivatives of bidentate chelating ligands giving mononuclear hexacoordinated ruthenium(II) compounds. The Ru–C bond in these new complexes has been found to be stable towards nucleophilic reagents. The stereochemistry for these complexes has been suggested on the basis of IR, ^1H and ^{31}P NMR spectra.

Binuclear ruthenium(II) complexes of the type $[Ru(CO)Cl(CH_3CHCN)(L)_2]_2$, where L = triphenyl phosphine or picoline, have been synthesised and studied by Hiraki *et al.*[1] Our interest in the synthesis of stable ruthenium–alkyl σ-bonded compounds[2] prompted us to isolate several 1-cyanoethyl derivatives of ruthenium(II) containing monobasic bidentate chelating ligands.

EXPERIMENTAL

Experiments were carried out in an atmosphere of dry, oxygen-free nitrogen. Solvents were carefully purified, dried, distilled and degassed before use. Other reagents used were of the highest purity available.

(a) *Preparation of* $HRu(CO)Cl(PPh_3)_3$

This compound was prepared from ruthenium trichloride trihydrate, triphenyl phosphine and formaldehyde in 2-methoxyethanol medium as previously reported.[3] The yield of the brown crystalline powder was 95%.

(b) *Preparation of the* 1-*cyanoethyl complex*, $[Ru(CO)Cl(CH_3CHCN)(PPh_3)_2]_2$

$HRu(CO)Cl(PPh_3)_3$ (1.95 g; 2 mmol) in THF (30 cm^3) was reacted with freshly distilled acrylonitrile (0.85 g; 15.5 mmol) in a Schlenk tube by stirring the contents for 24 h at room temperature. The solvent was then removed under reduced pressure, the residue washed with cold hexane and the product dried *in vacuo*. Nearly white crystals, m.p. 154°C. Yield 1.45 g (95%).

(c) *Preparation of chelated complexes of* (b), $[Ru(CO)(CH_3CHCN)(PPh_3)_2(chelate)]$

(i) 8-*Hydroxyquinoline complex.* The sodio-derivative of 8-hydroxyquinoline was prepared by reacting the ligand (0.08 g; 0.55 mmol) and oil-free sodium hydride (0.013 g; 0.55 mmol) in refluxing ether (8 h). Ether was then removed, THF (30 cm^3) added to it and, to this stirred suspension, $[Ru(CO)Cl(CH_3CHCN)(PPh_3)_2]_2$ (0.37 g; 0.5 mmol) was introduced. The reaction was completed at room temperature within 12 h. THF was then replaced with benzene, the contents centrifuged and the benzene solution concentrated to crystallisation. The yellow crystals obtained were washed with hexane and dried *in vacuo* at room temperature. Yield 0.36 g (80%).

(ii) *Acetylacetone complex.* This was obtained similarly to the above complex from 0.55 mmol of the sodio-derivative of acetylacetone and 0.5 mmol of the chlororuthenium complex prepared in (b). Yield of the cream coloured crystalline product was 0.32 g (80%).

Other chelated complexes (Table 1) were similarly prepared.

RESULTS AND DISCUSSION

Treatment of a THF solution of $HRu(CO)Cl(PPh_3)_3$ with an eight-fold excess of acrylonitrile

* NCL Communication No. 3676.

† Author to whom correspondence should be addressed.

Table 1. Chelated (1-cyanoethyl)ruthenium(II) carbonyl complexes

No.	$Ru(CO)(CH_3CHCN)(PPh_3)_2(L)$* where LH =	Colour	m.p. (°C)	Analysis: % found (calc.) C	H	P
1.	Acetylacetone	Cream	103	66.98 (67.01)	5.12 (5.03)	7.67 (7.84)
2.	Benzoylacetone	Brown	107	69.11 (68.99)	4.98 (5.01)	7.13 (7.09)
3.	Dibenzoylmethane	Yellow	150	70.95 (71.00)	4.87 (4.91)	6.65 (6.58)
4.	Trifluorothenoylacetone	Yellow	105	62.06 (61.90)	4.12 (4.06)	6.66 (6.81)
5.	2-Hydroxy-4-methoxybenzophenone	Yellow	99	69.36 (69.89)	4.85 (4.75)	6.62 (6.50)
6.	*N*-benzoyl-*N*-phenyl hydroxylamine	Grey	132	69.19 (68.97)	4.82 (4.79)	6.73 (6.85)
7.	8-Hydroxyquinoline	Yellow	177	69.08 (68.91)	4.73 (4.89)	7.27 (7.18)

* Product yield 75–85% in all cases.

at room temperature resulted in the complete conversion into a binuclear (1-cyanoethyl)ruthenium(II) derivative with chlorine bridges.[1] This complex, $[Ru(CO)Cl(CH_3CHCN)(PPh_3)_2]_2$, is sparingly soluble in common organic solvents. Stable octahedral mononuclear derivatives have been prepared by chlorine bridge cleavage reaction using sodio-derivatives of potential bidentate chelating ligands in THF at ambient temperatures. The chelating ligands used were β-diketones, 8-hydroxyquinoline, 2-hydroxy-4-methoxybenzophenone and *N*-benzoyl-*N*-phenyl hydroxylamine. These complexes were coloured solids soluble in common organic solvents. Unlike other Ru–C (alkyl/aryl) bonded compounds, the metal–carbon bond in these complexes is found to be remarkably stable. The products isolated contain both 1-cyanoethyl and bidentate chelating ligand. The unusual stability of the Ru–C bond could be attributed to the proximity of the cyanoethyl group which controls the electronic effect. The Ru–C bond in these derivatives, $[Ru(CO)(CH_3CHCN)(PPh_3)_2(chelate)]$, did not undergo insertion reactions; there was no reaction with liquid SO_2. Likewise treatment of a chloroform solution of the compound with carbon monoxide at room temperature as well as at refluxing temperature did not produce the corresponding acyl derivative.

IR spectra

The IR spectrum of the binuclear complex $[Ru(CO)Cl(CH_3CHCN)(PPh_3)_2]_2$ shows $\nu(C{\equiv}N)$ at 2220 cm^{-1} and $\nu(C{\equiv}O)$ at 1930 cm^{-1}. In the chelated ruthenium(II) complexes,

$$[Ru(CO)(CH_3CHCN)(PPh_3)_2(chelate)],$$

the $\nu(C{\equiv}N)$ is observed at 2200 cm^{-1}. The observed reduction of carbon–nitrogen bond order could be attributed to the increased electronic charge on the nitrile carbon as a result of chlorine bridge cleavage by the electron-rich bidentate chelating ligand. A similar reduction ($\Delta \sim 15$ cm^{-1}) is observed for the carbonyl stretching frequency of most of the complexes. All these new products show bands due to chelated bidentate moiety (Table 2).

NMR spectra

^1H NMR spectra (Table 2) of mononuclear chelated derivatives,

$$[Ru(CO)(CH_3CHCN)(PPh_3)_2(chelate)],$$

exhibit resonances associated with methyl and > CH protons of the 1-cyanoethyl group. The acetylacetonato complex

$$[Ru(CO)(CH_3CHCN)(PPh_3)_2(acac)]$$

exhibits a doublet centred at δ 0.75 [$^3J(HH) = 8$ Hz] due to the methyl protons of the 1-cyanoethyl group and a multiplet at δ 2.30 assignable to > CH protons. Similar doublets for methyl protons are observed in the case of other β-diketone derivatives. The resonances due to CH_3–CO groups are seen at δ 1.25 and 1.50 with equal intensity, indicative of chelated acetylacetone bonded to an asymmetric ligand pair. A high field shift is seen for the γ-CH

Table 2. IR and proton NMR data for the complexes, $[Ru(CO)(CH_3CHCN)(PPh_3)_2(chelate)]$

Compound	IR ν in cm^{-1}			^1H NMR δ ppm			
				(1-cyanoethyl)			
	C≡N	C≡O	C=O/ C=N	$-CH_3$*	> CH	CH_3CO-	–CH
1. $[Ru(CO)Cl(PPh_3)_2(acac)]$	2200	1920	1585 1520	0.75d	2.3q	1.15 1.25	3.85
2. $[Ru(CO)Cl(PPh_3)_2(bzac)]$	2200	1915	1560 1510	0.75d	2.3q	1.25 1.30	4.45 4.50
3. $[Ru(CO)Cl(PPh_3)_2(dbm)]$	2200	1930	1545 1520	0.83	2.4q	—	5.20
4. $[Ru(CO)Cl(PPh_3)_2(tftac)]$	2200	1920	1595 1535	0.80d	2.3m	—	4.55
5. $[Ru(CO)Cl(PPh_3)_2(8\text{-}Hq)]$	2200	1915	1550	0.65d 0.90d	2.4q	—	3.65 3.70 ($-OCH_3$)
6. $[Ru(CO)(CH_3CHCN)(PPh_3)_2(acac)]$	2200	1920	1530	0.90	2.40	—	—
7. $[Ru(CO)(CH_3CHCN)(PPh_3)_2(bzac)]$	2200	1925	1575	—	—	—	—

* $^3J(HH) = 8$ Hz in all cases for $-CH_3$.

Table 3. Proton decoupled ^{31}P NMR data for some ruthenium(II) derivatives

Compound	^{31}P δ ppm
1. $[Ru(CO)Cl(PPh_3)_2(acac)]$	29.22
2. $[Ru(CO)Cl(PPh_3)_2(bzac)]$	28.60, 29.80
3. $[Ru(CO)Cl(PPh_3)_2(dbm)]$	28.80
4. $[Ru(CO)Cl(PPh_3)_2(tftac)]$	52.55, 55.66
5. $[Ru(CO)Cl(PPh_3)_2(8\text{-}Hq)]$	31.37
6. $[Ru(CO)(CH_3CHCN)(PPh_3)_2(acac)]$	31.89
7. $[Ru(CO)(CH_3CHCN)(PPh_3)_2(bzac)]$	31.22, 32.23
8. $[Ru(CO)(CH_3CHCN)(PPh_3)_2(dbm)]$	31.44

resonance of the ligand which appears as a singlet at δ 3.85 possibly due to the diamagnetic anisotropy of the neighbouring phosphine phenyl rings. A similar upfield shift is observed for the γ-CH proton of other β-diketone derivatives.

The proton decoupled ^{31}P NMR spectrum of the acetylacetone derivative (Table 3) comprises a singlet at δ 31.90 (lower field from 85% H_3PO_4 as external standard), suggesting a *trans* disposition of the phosphine ligands as shown in Fig. 1.

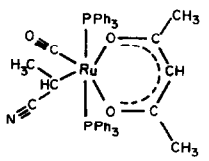


Fig. 1.

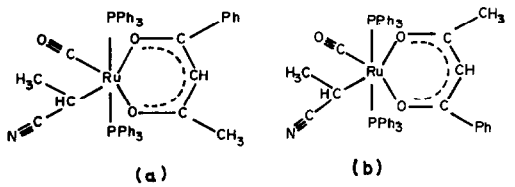


Fig. 2.

A singlet is observed for the phosphorus resonance in the case of the dibenzoylmethane derivative suggesting equivalent nature of both the phosphorus atoms. The corresponding chloro complexes

$[Ru(CO)Cl(PPh_3)_2(acac)]$

and

$[Ru(CO)Cl(PPh_3)_2(dbm)]$

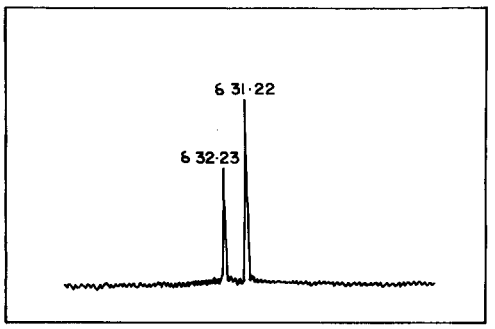


Fig. 3. ^{31}P NMR spectrum of $[Ru(CO)(PPh_3)_2(CH_3CHCN)(bzac)]$.

also show singlets at δ 29.22 and 28.80 respectively. The down field shift observed for the phosphorus resonance in these chlorine substituted derivatives could be attributed to the increased electronegativity of the cyano group attached to the α-carbon atom.

The ^{1}H NMR spectrum of the benzoylacetone complex $[Ru(CO)(CH_3CHCN)(PPh_3)_2(bzac)]$ exhibits two methyl resonances at δ 1.25 and 1.30 with relative intensities 1 : 1.7 due to the CH_3CO protons. The proton decoupled ^{31}P NMR spectrum (Fig. 3) comprises two singlets at δ 31.22 and 32.23 arising from two isomers shown in Figs. 2(a) and 2(b). A similar doublet is observed in the case of the trifluorothenoylacetone derivative. Attempts to isolate these isomers using chromatographic techniques did not succeed.

REFERENCES

1. K. Hiraki, N. Ochi, T. Kitamura, Y. Sasada and S. Shinoda, *Bull. Chem. Soc. Jpn* 1982, **55**, 2356.
2. S. Gopinathan, K. Joseph and C. Gopinathan, *J. Organomet. Chem.* 1984, **269**, 273.
3. S. D. Robinson, J. J. Levason, N. Ahmad and M. F. Uttley, *Inorganic Syntheses* Vol. 15, p. 48. McGraw-Hill, New York (1974).

Polyhedron Vol. 4, No. 9, pp. 1573–1578, 1985
Printed in Great Britain

0277–5387/85 $3.00 + .00
© 1985 Pergamon Press Ltd

COMPLEXES OF SILVER(III) WITH OXOANIONS

JAMES D. RUSH* and LOUIS J. KIRSCHENBAUM†
Department of Chemistry, University of Rhode Island, Kingston, RI 02881, U.S.A.

(*Received* 17 *January* 1985; *accepted* 28 *March* 1985)

Abstract—Silver(III) has a half-life at pH 11 of several hundred seconds in aqueous solutions in the presence of 0.1–1.0 M concentrations of certain basic oxoanions (Oxo) (phosphate, carbonate, borate, pyrophosphate, and arsenate). This compares with a lifetime of a few seconds at pH 11 in the absence of these oxoanions. UV–visible spectra and kinetic data for these solutions are interpreted as evidence for the following equilibria in the pH range 9–13.

$$Ag(OH)_4^{-1} + H_2O \rightleftharpoons Ag(OH)_3H_2O + OH^- \quad (1)$$

$$Ag(OH)_4^{-1} + Oxo \rightleftharpoons Ag(OH)_3Oxo + OH^- \quad (2)$$

$$Ag(OH)_3Oxo + H_2O \rightleftharpoons Ag(OH)_2(Oxo)H_2O + OH^- \quad (3)$$

Values of K_3 lie in the range $10^{-3} < K_3 < 10^4$ M for the systems studied. K_2 is estimated to be $\sim 10^2$ for phosphate and slightly smaller for the other systems. $Ag(OH)_4^-$ undergoes an unusual reaction with pyrophosphate at pH $\sim$ 8 to form a novel silver(II) complex, $[Ag(P_2O_7)_2]^{6-}$, for which EPR and electronic absorption spectral parameters are reported.

The tetrahydroxo-argentate(III) ion, $Ag(OH)_4^-$, is a square-planar complex of tervalent silver that is highly oxidizing and metastable in aqueous solution at pH > 13 ($t_{1/2} \sim 1.5$ h in 1.2 M NaOH at room temperature). Its solutions decompose to AgO with resulting oxidation of water. $Ag(OH)_4^-$ solutions are prepared electrochemically by oxidizing a silver metal anode in 1.2 M NaOH.[1,2]

We have previously investigated the kinetics of $Ag(OH)_4^-$ reactions with a number of reductants and complexing agents.[3–8] When coordinated by strong ligands, such as periodate or tellurate,[2] silver(III) is quite stable even near pH neutrality. The redox stability of $Ag(OH)_4^-$ solutions decreases as the pH is lowered[2,7] suggesting that substitution of OH^- by solvent water [eqn (1)] is the principal mechanism for decay of $Ag(OH)_4^-$.

$$Ag(OH)_4^- + H_2O \underset{k_{-1}}{\overset{k_1}{\rightleftharpoons}} Ag(OH)_3(H_2O) + OH^- . \quad (1)$$

The aquo species, $Ag(OH)_3(H_2O)$ rapidly oxidizes the solvent ($k = 142\ s^{-1}$).[7] Its instability arises from the poor electron-donating properties of solvent water.

At pH $\sim$ 11 decomposition of Ag(III) is controlled by the rate of aquation ($k_1 = 2 \pm 1\ s^{-1}$)[5] of $Ag(OH)_4^-$. The reverse reaction in eqn (1), abstraction by OH^- of a proton from the aquo complex, is relatively slow, presumably because of internal hydrogen bonding. This accounts for the importance of the solvent path for ligand substitution on Ag(III) even at pH > 13.[8]

In this report we describe some labile complexes of silver(III) with oxoanions (phosphate, borate, carbonate, arsenate, and pyrophosphate—general designation "Oxo"), which show enhanced kinetic stability at pH < 13. The preparation of these species provides new approaches to the study of silver(III) reactivity under conditions where the hydroxyl ion concentration is significantly reduced.

We also report here the first trapping of an intermediate silver(II) complex, resulting from the decomposition of the Ag(III) pyrophosphate complex. This suggests that the oxidation of water to oxygen by Ag(III) may proceed by one-electron processes.

* Present address: Department of Chemistry, Building 555, Brookhaven National Laboratory, Upton, L.I., NY 11937, U.S.A.

† Address correspondence to this author at the University of Rhode Island.

EXPERIMENTAL

The electrochemical preparation of $Ag(OH)_4^-$ has been described previously.[1] Stock solutions for the present study generally contained $3–5 \times 10^{-4}$ M $Ag(OH)_4^-$ as determined at its absorbance maximum at 267 nm ($\varepsilon_{267} = 1.17 \times 10_4\ M^{-1}\ cm^{-1}$). Dilution of $[OH^-]$ at a constant ionic strength was made using 1.2 M $NaClO_4$.

The chemicals used in all preparations were of reagent grade. The sodium hydroxide used was Mallinckrodt 50% solution (low carbonate), and the water was doubly-distilled. Oxoanion solutions were made from the sodium salts, and pH adjustments were made with perchloric acid or NaOH. The pH was measured with a Markson Electromark pH meter calibrated at pH 10 with standard buffers.

Solutions of Ag(III) with oxoanions at pH 9–13 were prepared in two ways: (1) slow addition of perchloric acid to an $Ag(OH)_4^-$ solution containing the oxoanion ([Oxo] > 0.1 M) while the solution was stirred rapidly, and (2) addition of a neutral or slightly acidic oxoanion solution to $Ag(OH)_4^-$ in NaOH. The final pH was adjusted by varying [NaOH] in the Ag(III) component prior to mixing. This method was used exclusively in the kinetic and spectral studies because the loss of Ag(III) during mixing due to local regions of low pH is minimal.

Concentrations of Oxo in excess of 0.1 M were necessary to neutralize the excess OH^-. Because ionic strength could not be uniform for all experiments (the speciation and charges of the oxoanion vary over the pH range of the study), the Ag(III) Oxo preparations were made to a final μ (1 M < μ < 2 M) over which ionic strengths effects are expected to be small.

Electronic spectra were obtained on a Cary 15 or a Varian DMS-90 UV-Vis spectrometer with a thermostated reaction cell. The decomposition kinetics of Ag(III) solutions were measured at 20°C. Observed decay rate constants, k_d, were calculated from plots of $\ln(A - A_\infty)$ vs time which were linear for most runs. In cases where catalytic effects from solid reaction products were evident, k_d was obtained from the initial slope of the absorbance vs time data. Absorbance changes were generally monitored at 270 nm.

Fast reactions were monitored in an Aminco–Morrow stopped-flow apparatus.[1] A solution of the oxoanion was mixed with $Ag(OH)_4^-$, and absorbance changes were recorded on a storage oscilloscope.

Analysis for the +2 oxidation state of silver was done by EPR of frozen solution samples on a Bruker ER200 spectrometer. The interaction of the unpaired spin in the d^9 electronic configuration with the $Ag^{107,109}$ ($I = 1/2$) gives a characteristic spectrum.[9(a),(b)] The diamagnetic trivalent oxidation state in solution was detected by addition of sodium periodate. The bis periodatoargentate(III) complex is bright yellow and indefinitely stable.[2]

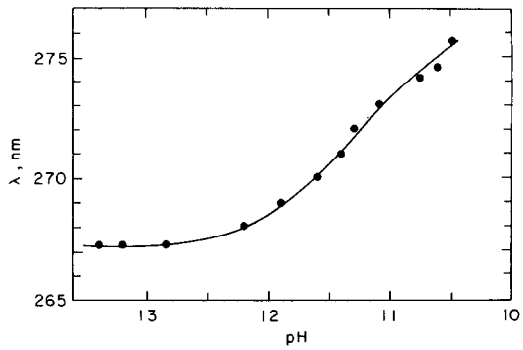


Fig. 1. pH dependence of the absorbance maximum of Ag(III) phosphate solutions: [phosphate] = 0.35 M; 20°C. The solid curve is calculated using eqn (4) (see Discussion).

RESULTS

Spectra of oxoanion solutions. The addition of an oxoanion causes a pH-dependent shift in the absorption maximum of Ag(III). For Oxo = borate, phosphate, arsenate, and pyrophosphate, λ_{max} changes from 267 to ~ 276 nm as the pH is lowered from 13 to 10. The spectral data for phosphate shown in Fig. 1 are typical of the other systems as well. At pH > 12.5, the spectrum is indistinguishable from that of $Ag(OH)_4^-$. In the pH range 11–12 the spectrum broadens and exhibits a small shoulder near 280 nm which merges into a single peak at ~ 276 nm as the pH is further reduced (Fig. 2). These pH-dependent shifts are reversible upon addition of NaOH. The presence of labile complexes of tervalent silver was confirmed by the addition of sodium periodate.

Over the same pH range, solutions, containing 0.2 M carbonate become orange coloured owing to the formation of a Ag(III) carbonate complex with the spectrum shown in Fig. 2. The colour change seems to be associated with the pK_a of the complex. Ag(III) borate solutions have spectra similar to that of phosphate when pH > 10. At lower pH, further reactions result in a new spectrum which is also shown in Fig. 2. As with carbonate, the change in spectrum appears to be associated with the pK_a of the oxoanion complex. The extinction coefficients of the spectra in Fig. 2 are approximate (± 15%).

The addition of 0.2 M pyrophosphate to $Ag(OH)_4^-$ with $HClO_4$ sufficient to reduce the pH to ~ 8 (a

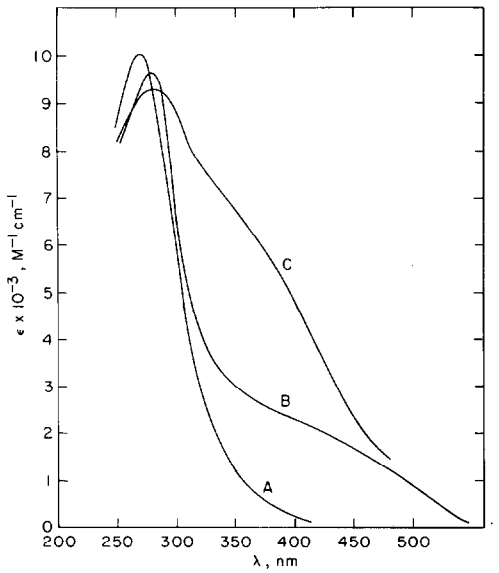


Fig. 2. Solution spectra of Ag(III) oxoanion complexes at selected pHs. (A): 0.35 M phosphate at pH 10.5. Borate, arsenate, and pyrophosphate solutions are similar at this pH; (B): 0.4 M carbonate at pH 10.5; (C): 0.6 M borate at pH ~ 9.5.

buffer region for $P_2O_7^{4-}/HP_2O_7^{3-}$) causes the immediate formation of a pale yellow-brown solution containing a silver(II) species with the absorption spectra shown in Fig. 3. Spectrum A is indefinitely stable in 0.1 M pyrophosphate at pH 6–8. Its stability decreases at lower pH. At pH 2–2.5 a species with the spectral peak shown in B predominates which has a half-life of ~3 s. A spectrum identical to A is obtained when an Ag(I) solution is oxidized with sodium persulphate under the same conditions. The silver in solutions prepared

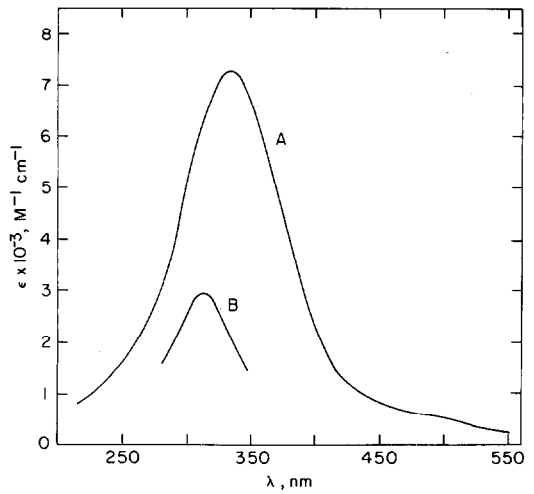


Fig. 3. Spectra of Ag(II) complexes in 0.1 M pyrophosphate at (A): pH 7.8, and (B): pH 2.2.

from $Ag(OH)_4^-$ (frozen at −100°C, pH = 8.2) had the following EPR parameters: $g_\perp = 2.051$, $g_\parallel = 2.269$, and $A_\perp = 32.3$ G, $A_\parallel = 39.3$ G. These parameters are typical of many tetragonal Ag(II) complexes.[9] At pH 8, the complex is predominately $[Ag(II)(P_2O_7)_2]^{6-}$ by analogy with the Cu(II) pyrophosphate system.[10]

Products of Ag(III) oxoanion decomposition. With the exception of pyrophosphate, Ag(III) oxoanion solutions of pH < 12 decay almost entirely to silver(I) products. Black precipitates which result from slow decomposition of $Ag(OH)_4^-$ contain mostly AgO, a mixed Ag(I)/Ag(III) oxide which, in base, may form from the fast disproportionation of Ag(II)[11] or the very slow reaction between $Ag(OH)_2^-$ and $Ag(OH)_4^-$.[12] However, the rapid decomposition of $Ag(OH)_4^-$ at reduced pH gives Ag(I),[7] suggesting that AgO is formed via the latter pathway in strongly alkaline solution. By contrast, the addition of pyrophosphate causes Ag(III) to be reduced entirely to Ag(II) over the pH range 8–14, and eventually results in precipitates of AgO at pHs where the decompositions of other Ag(III) Oxo systems yield Ag(I) as a product. AgO is detected by its reaction with bipyridine in acid to give the red bis-bipyridyl Ag(II) complex.[9(b)]

Formation of Ag(III) Oxo complexes. Qualitative observations of the reactions between $Ag(OH)_4^-$ and some oxoanions were made in the stopped-flow apparatus in the pH range 10–13. Concentrated Oxo solutions (0.4 M phosphate, 0.6 M borate and carbonate) which produced a final pH > 12.5 caused no discernable spectral changes when mixed with $Ag(OH)_4^-$. At lower pH a fast decrease in the absorbance ($t_{1/2}$ ~ 8–15 ms) was monitored at 270 nm in all three systems. The amplitude of the absorbance changes, though not the rates, depended upon the pH. In the cases of borate (pH < 10) and carbonate (pH 10–11.5), the spectra of Fig. 2 were attained by slower processes ($t_{1/2}$ ~ 3 s and 75 ms, respectively) following the initial, much faster, reaction. Only the faster reaction was observed for the phosphate system.

These kinetic observations and the solution spectra (Figs. 1 and 2) show that $Ag(OH)_4^-$ is in a pH-dependent equilibrium with silver(III) oxoanion complexes where one or more hydroxyl ligands have been substituted by the oxoanion as in eqn (2).

$$Ag(OH)_4^- + n\text{Oxo} \overset{K_2^n}{\rightleftharpoons} Ag(OH)_{4-n}(\text{Oxo})_n + nOH^- . \quad (2)$$

The relatively small spectral shifts and the single step formation reaction suggest that $n = 1$ when Oxo = phosphate. At pH > 10 this condition also seems to hold for all except the carbonate system where

further substitution may occur. These substitution reactions are reversible upon changing the pH.

In the case of oxoanions which have protolytic equilibria in this pH range, a proton ambiguity exists as to the source of the spectral changes upon which eqn (2) is, so far, based. In eqn (2) we have treated "Oxo" without regard to its degree of deprotonation. Some justification for this exists. In the range $12 \lesssim \text{pH} \lesssim 10$ the spectral shifts which occur on the phosphate system (Fig. 1) are qualitatively similar to spectral changes in the borate and pyrophosphate systems, in which the ligands have pK_as below this range. Thus, we have attributed the speciation to a single equilibrium, eqn (2), with the realization that ligand protonations might also contribute to the complexity of the systems. It should be noted that the rather pronounced spectral changes due to protonations in the borate and carbonate systems may arise from further substitutions or chelation, rather than protonation at a remote site which would not result in a structural change in the complex.

Kinetics of the decomposition of Ag(III) Oxo solutions. The first-order rate constants for decomposition of Ag(III) in oxoanion solutions, k_d, were measured over the range $9 < \text{pH} < 13$ at 20°C. At $\text{pH} > 12.5$ half-lives generally exceeded $\frac{1}{2}$ h (except for pyrophosphate preparations) and are very susceptible to the catalytic effects of solids (e.g. AgO) which often complicate the slower reactions of $Ag(OH)_4^-$.[4] At lower pH the decay remains first-order in [Ag(III)], although values of k_d varied by as much as 50% over repeat runs due to impurities or the effect of solid products. Rate constants were selected to minimize these effects.

The Ag(III) phosphate system shows typical characteristics and was the most extensively studied. Values of k_d obtained at different phosphate concentrations are shown in Table 1. At pH 11 k_d is virtually independent of [phosphate] in the range 0.065–0.5 M. Lower concentrations could not be achieved because of limitations imposed by the preparative procedure. However, in the absence of stabilizing ligands, Ag(III) decomposes within a few seconds[7] at this pH.

Table 1. Phosphate dependence of k_d (pH 11, 20°C, 1 M $< \mu <$ 2 M)

[Phosphate], M	$10^3\ k_d$, s^{-1}
0.5	2.6
0.46	2.5
0.35	1.3
0.21	2.3
0.175	1.6
0.1	2.0
0.065	1.9

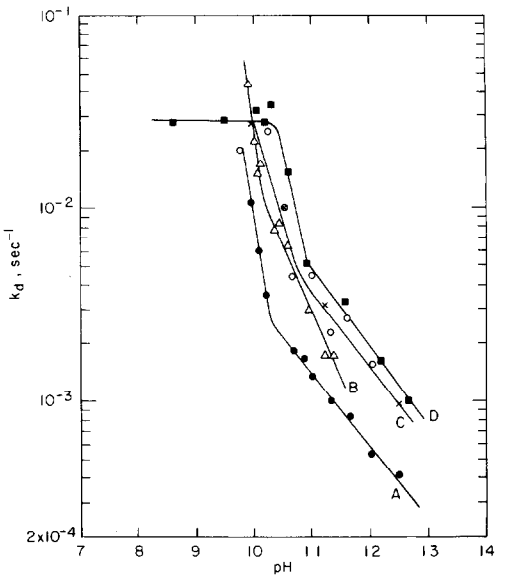


Fig. 4. pH dependence of the rate constant for decay of Ag(III) Oxoanion systems at 20°C: A, ●, 0.35 M phosphate; B, △, 0.40 M carbonate; C, ×, 0.10 M pyrophosphate; D, ■, 0.33 M borate; ○, 0.2 M arsenate. Ionic strengths vary between 1 and 2 M.

The pH dependence of k_d at constant [Oxo] is shown in Fig. 4 for several systems. For Ag(III) phosphate, log k_d varies linearly with pH with a slope of -0.4 in the range $10.3 < \text{pH} < 12.5$. The slopes increase sharply at a "break point" which occurs between pH 10 and 11 for all of the systems studied. Values of k_d for the different systems (except for arsenate) are correlated with solid lines in Fig. 4. In the pH range of greater stability the values of k_d vary by less than an order of magnitude between the least stable (borate) and the most stable (phosphate) systems. This presumably reflects differences in the stability constants (K_2) of the Ag(III) Oxo complexes. The pH dependence of k_d in the Ag(III) carbonate system reflects the combined effect of two complex pK_as on Ag(III) speciation. This produces a more pronounced dependence above pH 10.5 than is seen in the other systems. The Ag(III) arsenate system appears to have intermediate stability. However, the scatter in the data obtained for this system causes us to present several observations of k_d in Fig. 4 without attempting to correlate them.

The acid/base properties of the ligand have no specific effect upon the pH dependence of k_d except in those systems where pronounced spectral changes appear to be associated with a pK_a of the ligand. The rapid increase in k_d between pH 10 and 11 in these

Table 2. Equilibrium constants for aquation of Ag(III) oxoanion complexes (K_3) (20°C, 1 M < μ < 2M)

Oxo	Log K_3
Phosphate	-3.75 ± 0.2
Borate	-3.2 ± 0.2
Pyrophosphate	-3.25 ± 0.2
Carbonate	-3.7 ± 0.2

systems indicates a protonic equilibrium in this range which we suggest is due to reaction (3).

$$Ag(OH)_3Oxo + H_2O \overset{K_3}{\rightleftharpoons} Ag(OH)_2(Oxo)(H_2O) + OH^- \quad (3)$$

The qualitatively similar variations in k_d (at pH > 10) observed in the phosphate, borate, and pyrophosphate systems support the contention that the acid/base properties of the $Ag(OH)_3$ moiety in $Ag(OH)_3Oxo$, rather than those of the ligands, are the primary cause of the decreasing stability of the systems as pH is lowered. Values of $\log K_3$ for the various systems were evaluated at the inflection points of the data in Fig. 4 and are listed in Table 2.

In the borate system, k_d reaches a constant value of $\sim 3\ s^{-1}$ to pH $\sim$ 10. A complex (spectrum C in Fig. 2) which decays at a rate almost independent of pH is formed in competition with the pH-dependent decay of its precursor.

DISCUSSION

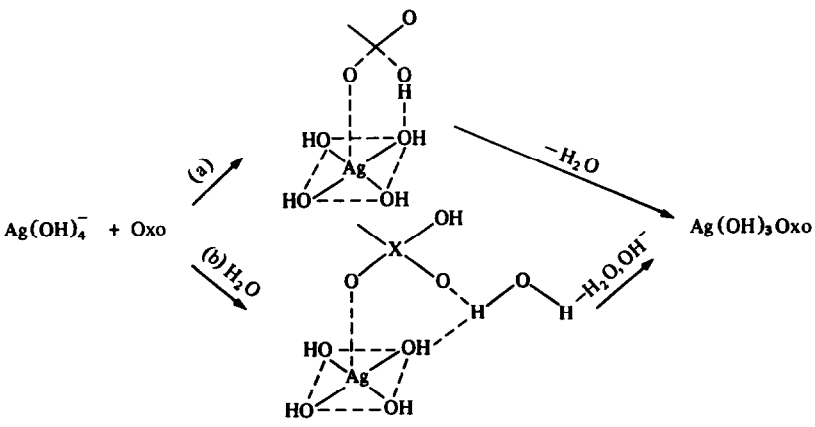
Formation reactions. The fast reactions observed in the stopped-flow experiments between $Ag(OH)_4^-$ and the Oxo ligands are too rapid to be mediated by the aquation of $Ag(OH)_4^-$ [eqn (1)]; $k_1 \sim 2\ s^{-1}$,[5] indicating that a direct reaction occurs. Although the oxoanions differ in structure as well as other properties, their common ability to form hydrogen bonds at several sites suggests a possible mechanism for complex formation. If, as in other reactions of $Ag(OH)_4^-$,[3,5] the axial attack on Ag(III) by the entering nucleophile occurs, the oxoanion might assist in transferring a proton to a hydroxyl ligand via a sequence such as those shown in Scheme 1.

Path (a) would result in deprotonation of protonated ligands (e.g. $B(OH)_4^-$, $H_2PO_4^{2-}$, $HAsO_4^{2-}$) while path (b) would be possible for most species throughout our pH range. Path (b) would be required for pyrophosphate (which is $P_2O_7^{4-}$ down to about pH 8) and would be inaccessible to borate both as $B(OH)_4^-$ and $B(OH)_3$.

The five-coordinate Ag(III) transient may be stabilized by the formation of a chelate ring which effectively protonates a hydroxyl ligand. Tetrahedral oxoanions might indeed form two such rings within the five-coordinate intermediate. The formation of the four-coordinate entity $Ag(OH)_3Oxo$ is then assisted by elimination of an aquo rather than a hydroxyl ligand. Similar hydrogen bond assisted pathways are important, e.g. in the complexation of molybdate and tungstate with catecholate dianion.[13]

Transient silver(III) species in which one OH^- ligand is replaced by a monodentate ligand have spectra very similar to that of the parent $Ag(OH)_4^-$,[4,5] whereas multidentate ligands typically produce charge-transfer bands at longer wavelengths.[6,14] The formation of a monosubstituted complex, as in Scheme 1, appears to be common to all the oxoanions studied. However, as the pH is reduced, slower processes are observed in the borate and carbonate systems which appear to be further substitutions.

Decomposition reactions. Our analysis of the pH stability data will be qualitative and is based on assumptions which seem to be in accord with the



Scheme 1.

experimental observations. These are (1) decay of Ag(III) proceeds mainly through steady-state amounts of aquated Ag(III) species, (2) Ag(III) speciation is basically described by eqns (1)–(3), and (3) coordination by either OH^- or Oxo should affect the hydrolysis properties of the silver(III) moiety similarly.

At pH > 11, where decomposition is slow, the speciation of an Ag(III) Oxo solution is described approximately by eqn (4).

$$\frac{[Ag(OH)_3Oxo]}{[Ag(III)]_{Tot.}} = \frac{K_2^1[Oxo]}{[OH^-]+K_2^1[Oxo]}. \quad (4)$$

If it is allowed that the spectral shifts shown in Fig. 1 arise from two species, $Ag(OH)_4^-$ and the silver(III) phosphate complex, which contribute to the shift in peak maximum proportionately to their concentrations, eqn (4) can be applied to obtain a rough estimate for K_2. Using values of $\lambda_{max} = 267$ nm for $Ag(OH)_4^-$ and $\lambda_{max} \sim 276$ nm for $Ag(OH)_3(PO_4)$ the data in Fig. 1 yields $K_2^1 = 10^{-2}$ and the calculated curve.

The reaction of excess Oxo with aquo Ag(III) species in equilibrium with $Ag(OH)_4^-$ and $Ag(OH)_3Oxo$ [eqns (1) and (3)] prevents the rapid decomposition of the solutions even at pH < pK_1 or pK_3. Still, when the pK_as of the complexes are approached the concentration of reactive aquo complex, and hence k_d, increases. The values of K_3 obtained for these systems (see Table 2) suggest that 10^{-3} M > K_1 > 10^{-5} M, in agreement with earlier estimates.[7]

The above interpretations of the formation, speciation, and decay of the Ag(III) oxoanion complexes is qualitative and accounts only for general features. The differences among the oxoanion systems have not been emphasized. However, it is clear from Fig. 4 that K_2 and K_3, and hence k_d, depend on the nature of the oxoanion ligand.

The reaction of $Ag(OH)_4^-$ with pyrophosphate. This reaction, which at pH < 8 results in the one-electron Ag(II) reduction product rather than Ag(I) warrants further discussion. This system differs from the others in the sequence of reactions which follow eqn (3), aquation of the monosubstituted complex, since the pH dependence of k_d is quite similar to that of the other oxoanion systems. Evidently, closure of the pyrophosphate ring must follow aquation at a *cis*-position resulting in a chelated Ag(III) transient which is reduced (by solvent) to form an Ag(II) species. In base (pH > 9) this complex hydrolyzes to produce AgO precipitates, but at pH 6–8 (following probable addition of a second pyrophosphate ligand) the complex is quite stable. In contrast to this system, the addition of bipyridyl (which also forms strong Ag(II) complexes) to $Ag(OH)_4^-$ solutions does not result in spontaneous one-electron reduction.[15] This is probably because the weakly basic bipyridyl nitrogens are unable to mediate a proton transfer to OH^- and thus cannot complex Ag(III) in strong base.

Acknowledgements—We wish to thank Professor P. H. Rieger for his help with the EPR experiments and Professor E. Mentasti for helpful discussions under the NATO Collaborative Grants Program (RG 803/83).

REFERENCES

1. L. J. Kirschenbaum, J. H. Ambrus and G. Atkinson, *Inorg. Chem.* 1973, **12**, 2832.
2. G. L. Cohen and G. Atkinson, *J. Electrochem. Soc.* 1968, **115**, 1236.
3. L. J. Kirschenbaum and J. D. Rush, *Inorg. Chem.* 1983, **22**, 3304.
4. E. T. Borish and L. J. Kirschenbaum, *Inorg. Chem.* 1984, **23**, 2355.
5. J. D. Rush and L. J. Kirschenbaum, *Inorg. Chem.* (in press).
6. L. J. Kirschenbaum and J. D. Rush, *J. Am. Chem. Soc.* 1984, **106**, 1003.
7. L. J. Kirschenbaum and L. Mrozowski, *Inorg. Chem.* 1978, **17**, 3718.
8. L. J. Kirschenbaum, *J. Inorg. Nucl. Chem.* 1976, **38**, 881.
9. (a) H. N. Po, *Coord. Chem. Rev.* 1976, **20**, 1971 (and references therein); (b) W. G. Thorpe and J. K. Kochi, *J. Inorg. Nucl. Chem.* 1971, **33**, 3962.
10. O. E. Schupp, P. E. Sturrock and J. I. Watters, *Inorg. Chem.* 1963, **2**, 106.
11. A. Kamar and P. Neta, *J. Phys. Chem.* 1979, **83**, 3091.
12. Addition of dilute Ag(I) (slightly soluble in base as $Ag(OH)_2^-$) to an $Ag(OH)_4^-$ solution results in the slow ($t_{1/2} \sim 15$ min) formation of AgO precipitates. AgO itself is insoluble in base. E. T. Borish (unpublished results).
13. K. Gilbert and K. Kustin, *J. Am. Chem. Soc.* 1976, **98**, 5502.
14. A. Balikungieri and M. Pelletier, *Inorg. Chim. Acta* 1978, **29**, 141.
15. Bipyridyl reduces solutions of $Ag(OH)_4^-$ very slowly. The rate of many such redox reactions correlates strongly with the nucleophilicity of the reductant (Ref. 5).

Polyhedron Vol. 4, No. 9, pp. 1579–1584, 1985
Printed in Great Britain

0277-5387/85 $3.00 + .00
© 1985 Pergamon Press Ltd

SOME MIXED-LIGAND PALLADIUM(II) COMPLEXES AND COMPARISON OF THEIR PHOTOSENSITIZING ABILITY WITH ANALOGOUS PLATINUM(II) COMPLEXES

K. H. PUTHRAYA and T. S. SRIVASTAVA*
Department of Chemistry, Indian Institute of Technology, Powai, Bombay 400 076, India

(*Received* 3 *October* 1984; *accepted after revision* 5 *March* 1985)

Abstract—Three new palladium(II) complexes of formula [Pd(bipy)(XX)] [where bipy is 2,2′-bipyridine and XX are dianions of catechol (CAT), 4-*tert*-butylcatechol (BCAT) and 3,4-dimercaptotoluene (DMT)] have been prepared and characterized by physical methods. A ligand–ligand charge-transfer band in each complex was observed between 16–21 kK (ε_{max} = 1500–2200 l mol^{-1} cm^{-1}) which is negatively solvochromic. These palladium(II) complexes in dimethylformamide photosensitize the formation of singlet oxygen and their ability to photosensitize triplet oxygen ($^3O_2$) to singlet oxygen ($^1O_2$) are compared with analogous platinum(II) complexes. In addition, 2,2′-bipyridine-platinum(II) complex of 3,4-dimercaptotoluene also undergoes self-sensitized photooxidation.

Several mixed-ligand complexes of beryllium(II),[1] zinc(II),[2] nickel(II)[3] and platinum(II)[4,5] having 2,2′-bipyridine, 1,10-phenanthroline and other related ligands show absorption bands corresponding to ligand-to-ligand charge-transfer (LLCT) transitions to low energies if one ligand is reducing and the other is oxidizing. This intense LLCT transition in [Pt(bipy)(DMT)] is involved in its photooxidation in $CHCl_3$ solution.[4] This and other related complexes show the formation of $^1O_2$ by energy transfer from their triplet LLCT excited states to $^3O_2$.[5] In view of the importance of mixed-ligand metal complexes in inorganic photochemistry, we report here the synthesis and characterization of some new [Pd(bipy)XX] complexes. These complexes show intense LLCT transitions in the visible region. They also photosensitize $^3O_2$ to $^1O_2$ and their propensity to form $^1O_2$ are compared with analogous platinum(II) complexes.

EXPERIMENTAL

Chemicals

Potassium tetrachloroplatinate, palladium dichloride, 2,2,6,6-tetramethyl-4-piperidinol and 2,2′-bipyridine were purchased from Strem Chemical Co. (U.S.A.), Johnson Matthey (U.K.), Aldrich Chemical Co. (U.S.A.), SISCO (India) respectively. Catechol, 4-*tert*-butylcatechol, thiosalicylic acid and 3,4-dimercaptotoluene were bought from B.D.H. (England). The solvents were of reagent grade and were purified before use by the standard methods.[6] Other chemicals used were of analytical reagent grade and used as such.

Synthetic procedures

[Pd(bipy)Cl$_2$] and [Pt(bipy)Cl$_2$]. These complexes were prepared by the following methods as given elsewhere.[7,8]

[Pt(bipy)(CAT)], [Pt(bipy)(BCAT)] and [Pt(bipy)(DMT)]. They were synthesized by following the procedures published earlier.[5]

[Pd(bipy)(DMT)]. [Pd(bipy)Cl$_2$] (333 mg, 1 mmol) was dissolved in 20 cm^3 of dimethyl sulphoxide. 3,4-Dimercaptotoluene (155 mg, 1 mmol) was dissolved in 2 cm^3 of 1 N NaOH, which was added to the above solution with stirring. The reaction mixture was stirred at room temperature for 30 min and diluted with 100 cm^3 of chloroform. The chloroform layer containing the desired complex was repeatedly washed with fresh water. The chloroform layer, was finally separated and dried over anhydrous sodium sulphate. Sodium sulphate was later removed by filtration. The chloroform from dry chloroform layer was removed under vacuum at room temperature. The complex was recrystallized

* Author to whom correspondence should be addressed.

from chloroform. The crystals were filtered, washed with small quantity of cold chloroform and finally with petroleum ether. The violet red crystals were dried in vacuum at room temperature. The whole process was carried out in the absence of light. Visible max. (CH_3OH) 20.79, (DMF) 20.08, ($CHCl_3$) 18.18 and (C_6H_6) 16.72 kK; ^{1}H NMR (DMSO-d_6) δ 8.72 (m, 2, H-6,6'), 7.84 (m, 2, H-5,5'), 6.96 (d, 1, H_A), 6.64 (d, 1, H_B), 2.20 (s, 3, H_C) and 6.86 ppm (s, 1, H_D).

[*Pd(bipy)(BCAT)*]. This compound was prepared by following the procedure as given for [Pd(bipy)(DMT)] except 4-*tert*-butylcatechol was used in place of 3,4-dimercaptotoluene. The complex was recrystallized from acetone and petroleum ether mixture. The violet crystals obtained were filtered, washed with acetone and finally with petroleum ether. They were dried in vacuum at room temperature. Visible max. (CH_3OH) 20.74; (DMF) 17.84, ($CHCl_3$) 16.62 and (C_6H_6) 16.08 kK; ^{1}H NMR (DMSO-d_6) 8.66 (m, 2, H-6,6'), 7.84 (m, 2, H-5,5'), 6.39 (d, 1, H_A), 6.26 (d, 1, H_B), 1.20 (s, 9, H_C) and 6.24 ppm (s, 1, H_D).

[*Pd(bipy)(CAT)*]. This violet crystalline compound was prepared by following the procedure as given for [Pd(bipy)(BCAT)] except the catechol was used in place of 4-*tert*-butylcatechol. Visible max. (CH_3OH) 21.36, (DMF) 18.59 and ($CHCl_3$) 17.48 kK; ^{1}H NMR (DMSO-d_6) δ 8.68 (m, 2, H-6,6'), 7.80 (m, 2, H-5,5') and 6.30 ppm (m, 4, H_A, H_B, H_C and H_D).

Photochemical measurements

(a) *Photosensitized oxidation of 2,2,6,6-tetramethyl-4-piperidinol using 2,2'-bipyridine-palladium(II) and -platinum(II) complexes as sensitizers.* These experiments were carried out on a merry-go-round apparatus. The stabilized light source of 150 W × 24 V tungsten halogen lamp operating at 18 V was housed at the centre of merry-go-round apparatus in a double jacketted pyrex vessel thermostatted at 28° ± 1°C by circulating water through the jacket. The solutions to be irradiated were taken in pyrex glass tubes (20 cm × 1 cm) and kept on the merry-go-round apparatus.

The photoproduction of singlet oxygen ($^1O_2$) was measured by electron paramagnetic resonance (EPR) method using 2,2,6,6-tetramethyl-4-piperidinol as singlet oxygen acceptor.[9,10] Typically a 200 μmol l^{-1} solution of the above complex in dimethylformamide (DMF) was bubbled for 15 min with solvent saturated molecular oxygen. Then 2,2,6,6-tetramethyl-4-piperidinol was added to a final concentration of 10 mM. The mixture was irradiated on the merry-go-round apparatus at different irradiation times.

The nitroxide free radicals thus formed by reaction of 2,2,6,6-tetramethyl-4-piperidinol with singlet oxygen were recorded at room temperature in aqueous EPR cell on a Varian E-112 ESR spectrometer (X-band) using TCNE as g marker (g = 2.00277). The quantitative EPR measurements were made by comparison with the EPR spectrum of a solution of nitroxide free radicals of known concentration.

(b) *Self-sensitized photooxidation of some 2,2'-bipyridine-palladium and -platinum complexes.* A stabilized beam of light from 200 W × 24 V tungsten halogen lamp operating at 22 V was directed through a dichroic heat filter having range of transmission between 400 and 710 nm. This filter was placed 14 cm from the light source. The filtered light coming out from this filter was directed through a solid clear cast acrylic cylinder (16 × 4 cm) placed 45 cm from the light source. A stoppered 1 cm path length quartz cuvette having solution of the complex in DMF was placed on the other side of the cylinder. The course of the photolysis was followed by difference absorption spectroscopy in the visible region.

Other physical measurements were carried out as described earlier.[11,12]

RESULTS AND DISCUSSION

Three new neutral mixed-ligand palladium(II) complexes of general formula [Pd(bipy)(XX)] (where bipy is 2,2'-bipyridine and XX are dianions of catechol, 4-*tert*-butylcatechol and 3,4-dimercaptotoluene were prepared. The colour, yield, molar conductance and chemical analysis of these complexes are given in Table 1. The molar conductance values of these complexes in dimethylformamide (10^{-3} M) lie between 4.2 to 8.6 $cm^2\ \Omega^{-1}\ mol^{-1}$. These small values of molar conductance suggest that these complexes are non-electrolytes.[13]

UV–visible spectra

The UV–visible absorption spectra of palladium(II) complexes recorded in dimethylformamide solution show several band maxima in the UV–visible region, the positions of which along with their extinction coefficients (ε_{max}) are given in Table 1. These bands are assigned following the band assignments of [Pd(bipy)Cl_2].[14] The band 2 between 25 and 30 kK is due to a charge-transfer band from palladium d-orbital to π-antibonding orbital of 2,2'-bipyridine. The band 4 is due to charge-transfer transition from same palladium orbital to a higher π-antibonding orbital of 2,2'-bipyridine. The bands 1, 3 and 5 are assigned to the first, second and higher internal π–π^* type transitions of 2,2'-bipyridine respectively. Each of these complexes has shown an

Table 1. Colour, yield, molar conductance, chemical analysis data, and electronic absorption spectra of [Pd(bipy)(XX)]

Compound (colour; yield; molar conductance)[a]	Calculated (found)			Band maxima (λ_{max}) in DMF[b]					
	% C	% H	% N	Band 1	Band 2	Band 3	Band 4	Band 5	
1. [Pd(bipy)(CAT)] (violet; 60%; 4.2)	51.84 (51.90)	3.26 (3.21)	7.56 (7.50)	18.59 (2.20)[c]	27.78 (0.84)	31.35 (14.10)	32.47 (18.64)	33.56 (15.24)	37.31 (9.70)
2. [Pd(bipy)(BCAT)] (violet; 65%; 8.6)	56.28 (56.23)	4.72 (4.79)	6.56 (6.60)	17.89 (2.06)	27.78 (0.95)	31.25 (14.59)	32.47 (18.14)	33.33 (16.47)	39.31 (10.14)
3. [Pd(bipy)(DMT)] (red; 80%; 5.8)	48.98 (48.92)	3.39 (3.43)	6.72 (6.79)	20.08 (1.60)	27.78 (0.51)	31.06 (9.64)	32.89 (18.76)	35.34 (17.12)	37.31 (20.03)

[a] $cm^2\ \Omega^{-1}\ mol^{-1}$.
[b] kK ($1 \times 10^{-3}\ cm^{-1}$).
[c] Extinction coefficients in $l\ mol^{-1}\ cm^{-1} \times 10^{-3}$ are given in parentheses.

additional strong band in the visible region between 17 and 21 kK (ε_{max} = 1600–2200 $l\ mol^{-1}\ cm^{-1}$). This band has comparable intensity to the charge-transfer band 2 and is strongly solvent dependent. The maximum of this band for these complexes in different solvents is given in the experimental section. This peak experiences a bathochromic shift with decrease in polarity of the solvent. Similar shift was earlier observed in [Pt(bipy)(DMT)] and other related complexes[4,5] and thus this band is assigned to ligand-to-ligand charge-transfer (LLCT) band.

IR spectra

In order to characterize the palladium(II) complexes and throw light on the mode of binding of ligands to palladium, the IR of these complexes were recorded between 4000 and 300 cm^{-1}. There were, in general, spectral changes in ligands of these complexes as compared to the free ligands. This suggests the coordination of these ligands to palladium ion. The IR spectrum of [Pd(bipy)Cl_2] shows two vibrational bands at 342 and 354 cm^{-1} (shoulder).[15] These bands due to ν(Pd–Cl) vibrations are absent in the [Pd(bipy)(XX)] complexes as expected.

The IR spectrum of [Pd(bipy)(CAT)] complex shows two strong bands at 1490 and 1270 cm^{-1}. This suggests the bonding of ionized hydroxyl groups of catechol to palladium(II).[16] In the [Pd(bipy)(BCAT)] complex, the bands at 1480 and 1265 cm^{-1} have also been observed and assigned to the bonding of ionized hydroxyl groups to palladium(II). The IR spectrum of 3,4-dimercaptotoluene shows ν(S–H) vibration at 2540 cm^{-1} which is absent in the spectrum of [Pd(bipy)(DMT)] complex. This suggests that the –SH groups are present in the ionized form in the palladium(II) complex.[17]

^1H NMR spectra

The ^1H NMR spectra of [Pd(bipy)(XX)] complexes in deuterated dimethyl sulphoxide (DMSO-d_6) were measured using tetramethyl silane (TMS) as internal reference. The chemical shifts of H-6,6′ and H-5,5′ protons of 2,2′-bipyridine and various protons of XX ligands in the above palladium(II) complexes have been given in the experimental section. The numbering scheme of the ligand protons is followed as published elsewhere.[5] The information regarding the bonding of ligand (XX) to palladium is based on the downfield chemical shifts of the protons of ligand in the [Pd(bipy)(XX)] complex as compared to proton chemical shifts of the free ligand.[18] The protons H-6,6′ and H-5,5′ resonate at 9.18 and 7.86 ppm respectively in [Pd(bipy)Cl_2]. In [Pd(bipy)(XX)] complexes these protons show upfield shifts as compared to [Pd(bipy)Cl_2]. The upfield shifts can be interpreted in terms of stronger bonding of ligands (XX) to palladium(II) as compared to bonding of chloride ions.[11] This effect is more dominant on the H-6,6′ protons, indicating that they are better shielded.

The ^1H NMR spectra of [Pd(bipy)(CAT)], [Pd(bipy)(BCAT)] and [Pd(bipy)(DMT)] show down-field shifts of H_A, H_B and H_C and in the former compound also of H_D in coordinated ligands as compared to corresponding protons in the free ligands. Similar observations have been made earlier for analogous platinum(II) complexes.[5] The above observations suggest that the ligands are coordinating to palladium(II) by $-O^-$, $-O^-$ or $-S^-$, S^- groups.

Photooxidation of 2,2,6,6-tetramethyl-4-piperidinol

The aerated DMF solutions of [Pd(bipy)(XX)] (where XX are CAT, BCAT and DMT) and [Pt(bipy)(XX)] (where XX are CAT, BCAT and

DMT) were irradiated in presence of 2,2,6,6-tetramethyl-4-piperidinol by light at different irradiation times. The singlet oxygen thus formed combines with 2,2,6,6-tetramethyl-4-piperidinol forming nitroxide free radical. Nitroxide radicals are detected by EPR spectroscopic method.[9,10] The 2,2,6,6-tetramethyl-4-piperidinol does not react with O_2^-, H_2O_2 and .OH radicals.[19] Figure 1 shows the amount of nitroxide free radical measured by EPR spectroscopy for various complexes such as [Pd(bipy)(CAT)], [Pd(bipy)(BCAT)], [Pd(bipy)(DMT)], [Pt(bipy)(CAT)] and [Pt(bipy)(BCAT)], as a function of irradiation time. Since the amount of nitroxide free radical measured by the EPR method bears a direct relationship to the singlet oxygen produced possibly via energy transfer from triplet excited LLCT state of the above complexes, the slopes calculated from experimental plots in Fig. 1, are 0.047 for [Pt(bipy)(BCAT)], 0.015 for [Pt(bipy)(CAT)], 0.036 for [Pd(bipy)(BCAT)], 0.012 for [Pd(bipy)(CAT)] and 0.01 for [Pd(bipy)(DMT)]. These data suggest that [Pt(bipy)(BCAT)] is the best photosensitizer of singlet oxygen because of its largest slope. Thus the efficiency of these complexes to photosensitize the formation of singlet oxygen is [Pt(bipy)(BCAT)] > [Pt(bipy)(BCAT)] > [Pt(bipy)(CAT)] > [Pd(bipy)(CAT)] > [Pd(bipy)(DMT)]. If comparison is made with Rose-Bengal as photosensitizer, the [Pt(bipy)(BCAT)] is about 10 times less efficient than Rose-Bengal to photosensitize the formation of singlet oxygen.

Self-sensitized photooxidation

The oxygenated solutions of [Pt(bipy)(BCAT)], [Pd(bipy)(BCAT)], [Pt(bipy)(CAT)] and [Pd(bipy)(CAT)] complexes were stable to light after five hours of irradiation. However, the oxygenated solution of [Pd(bipy)(DMT)] was slightly decolorized after irradiation with light for five hours. On the other hand the oxygenated solution of [Pt(bipy)(DMT)] was very much affected by light irradiation. This self-sensitized photooxidation of [Pt(bipy)(DMT)] and [Pd(bipy)(DMT)] is now discussed below:

(a)*Pt(bipy)(DMT)*]. An oxygen saturated solution of [Pt(bipy)(DMT)] (200 μM) in DMF was irradiated with light of wavelength greater than 400 nm. The course of photolysis was followed by

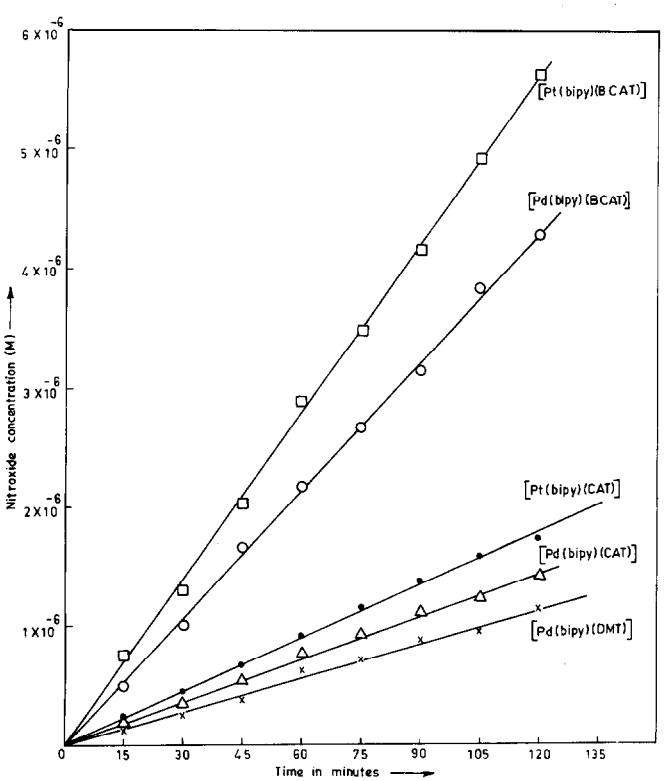


Fig. 1. Nitroxide concentrations as measured by EPR measurements against different times of light irradiation of DMF solutions of [M(bipy)(XX)] (200 μM) in presence of 2,2,6,6-tetramethyl-4-piperidinol at 27 ± 1°C.

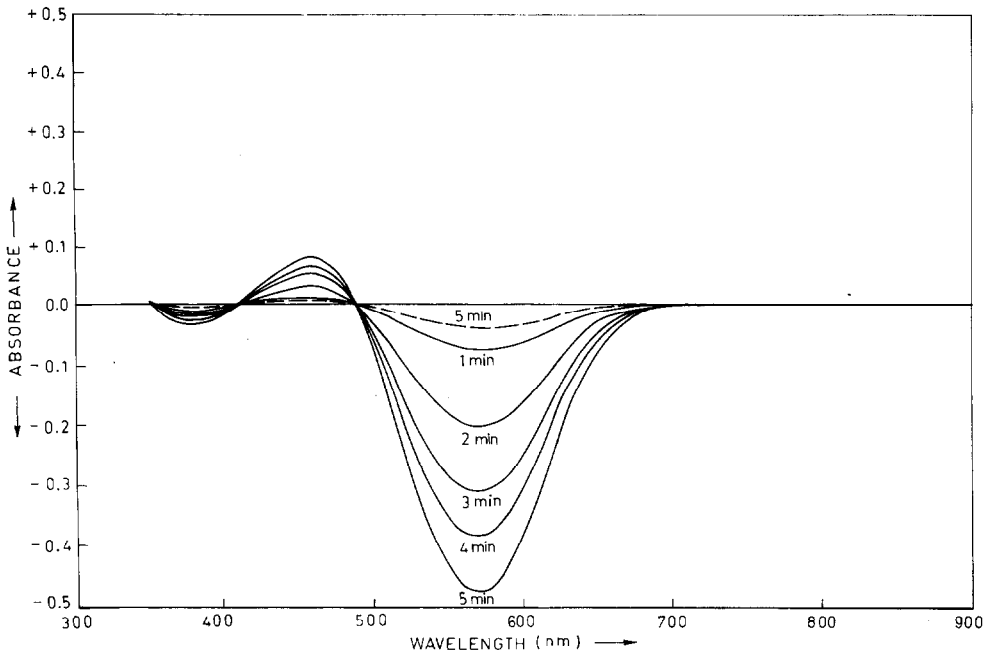
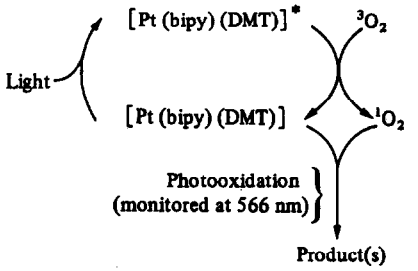


Fig. 2. Difference UV–visible spectra of DMF solutions of [Pt(bipy)(DMT)] (200 μm) (——) at different times of irradiation and of [Pt(bipy)(DMT)] (– – –) at 5 min of light irradiation in presence of sodium azide (500 μM) with light of wavelength greater than 400 nm.

difference absorption spectrophotometry in the visible region. The difference absorption spectra at different times of light irradiation (1–5 min) are given in Fig. 2. The photolysis was accompanied by bleaching of the colour of the complex. New positive (456 nm) and negative (378 and 570 nm) peaks were observed in the difference spectra. Thus, these spectral changes have been accounted for the loss of [Pt(bipy)(DMT)] complex as a result of photolysis. The above reaction was retarded by about 90% in presence of sodium azide, a known singlet oxygen quencher,[20] under similar light irradiation conditions.

The solution was quite stable when either molecular oxygen saturated solution of [Pt(bipy)(DMT)] was kept in dark or irradiated with light while oxygen free molecular nitrogen was bubbled through it. This suggests that the observed decay of [Pt(bipy)(DMT)] was due to the combined action of light and molecular oxygen. The quenching of reaction in presence of sodium azide indicates the involvement of singlet oxygen in the above reaction. This suggests that the [Pt(bipy)(DMT)] sensitizes the generation of singlet oxygen which in turn reacts with the [Pt(bipy)(DMT)] causing the observed change. Figure 3 shows a plot of log (logarithm) of concentration vs time of photolysis. This plot is linear which suggests a first order kinetics for the above reactions. A similar plot of self-sensitized photooxidation of bilirubin was observed earlier.[21,22] Thus the above observations can be explained by the following proposed mechanism.



All the efforts to isolate the product(s) of photolysis met with failure. The absorption spectra of [Pt(bipy)(DMT)] before photolysis and after all [Pt(bipy)(DMT)] complex has been converted to product(s) as a result of photolysis suggest that the LLCT band of [Pt(bipy)(DMT)] at 566 nm is shifted to 478 nm due to photolysis. Since the [Pt(bipy)(CAT)] and [Pt(bipy)(BCAT)] complexes are not photooxidized even after irradiation for five hours in presence of molecular oxygen, it suggests that 2,2'-bipyridine molecule is not photooxidized in [Pt(bipy)(DMT)] complex. The possibility left is the photooxidation of dimercaptotoluene molecule in [Pt(bipy)(DMT)]. The position of LLCT spectrum of [Pt(bipy)(TSA)] compares favourably with photooxidized product of [Pt(bipy)(DMT)],[5] and,

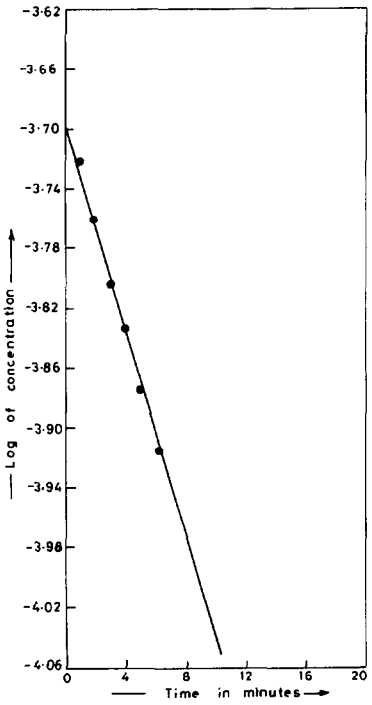


Fig. 3. Plot of log of concentration against time of light irradiation of DMF solution of [Pt(bipy)(DMT)] (200 μM) with light of wavelength greater than 400 nm.

thus, it seems one of the sulphur atoms of dimercaptotoluene is oxidized.[23]

(b) [*Pd(bipy)(DMT)*]. An oxygenated solution of [Pd(bipy)(DMT)] (200 μM) in DMF was quite stable to light during two hours of irradiation under identical irradiation conditions as used for [Pt(bipy)(DMT)] and [Pt(bipy)(TSA)]. The decrease of absorbance during irradiation for three hours was only 5% of initial absorbance. This suggests that [Pd(bipy)(DMT)] undergoes very poor self-sensitized photooxidation by singlet oxygen.

The neutral 2,2'-bipyridine-palladium(II) and -platinum(II) derivatives of catechol and 4-*tert*-butylcatechol are found to be good photosensitizers of the singlet oxygen while their 3,4-dimercaptotoluene derivatives are poor photosensitizers due to self-sensitized photooxidation.

Acknowledgements—We are grateful to Dr. S. S. Talwar for valuable help and stimulating discussions. This work has been supported in part by a grant from the DST, Govt. of India, New Delhi.

REFERENCES

1. G. E. Coates and S. I. E. Green, *J. Chem. Soc.* 1962, 3340.
2. V. J. Koester, *Chem. Phys. Lett.* 1975, **32**, 575.
3. T. R. Miller and I. G. Dance, *J. Am. Chem. Soc.* 1973, **95**, 6970.
4. A. Vogler and H. Kunkley, *J. Am. Chem. Soc.* 1981, **103**, 1559.
5. L. Kumar, K. H. Puthraya and T. S. Srivastava, *Inorg. Chim. Acta* 1984, **86**, 173.
6. A. I. Vogel, *A Textbook of Practical Organic Chemistry*, 3rd Edn., pp. 163–179. Longman, London (1956).
7. B. J. McCormick, E. N. Jaynes, Jr. and R. I. Kaplan, *Inorg. Syn.* 1971, **13**, 217.
8. F. A. Palocsay and J. V. Rund, *Inorg. Chem.* 1969, **8**, 524.
9. Y. Lion, M. Delmelle and A. Van de Vorst, *Nature* 1976, **263**, 442.
10. Y. Lion, E. Gandin and A. Van de Vorst, *Photochem. Photobiol.* 1980, **31**, 305.
11. L. Kumar, N. R. Kandasamy and T. S. Srivastava, *Inorg. Chim. Acta* 1982, **67**, 139.
12. L. Kumar and T. S. Srivastava, *Inorg. Chim. Acta* 1983, **80**, 47.
13. W. J. Geary, *Coord. Chem. Rev.* 1971, **7**, 81.
14. P. M. Gidney, R. D. Gillard and B. T. Heaton, *J. Chem. Soc., Dalton Trans.* 1973, 132.
15. A. N. Norbury and A. I. P. Sinha, *J. Inorg. Nucl. Chem.* 1973, **35**, 1211.
16. D. G. Brown, J. T. Reinprecht and G. C. Vogel, *Inorg. Nucl. Chem. Letters* 1976, **12**, 399.
17. G. Soerates, *Infrared Characteristics Group Frequencies*, p. 11. Wiley, New York (1980).
18. L. E. Erickson, J. W. McDonald, J. K. Howie and R. P. Clow, *J. Am. Chem. Soc.* 1976, **90**, 6373.
19. A. Rigo, E. Argese, R. Selvanto, E. F. Orsega and P. Vigliano, *Inorg. Chim. Acta* 1977, **24**, L71.
20. C. S. Foote, *Free Radicals in Biology* (Edited by W. A. Pryor), Vol. II, pp. 85–133. Academic Press, New York (1976).
21. I. Diamond, S. G. Granelli and A. F. McDonough, *Biochem. Medicine* 1977, **17**, 121.
22. I. B. C. Matheson, N. U. Curry and J. Lee, *Photochem. Photobiol.* 1980, **31**, 115.
23. C. S. Foote, *Oxygen and Oxy Radicals in Chemistry and Biology* (Edited by M. A. J. Rodgers and E. L. Powers), p. 431. Academic Press, New York (1981).

Polyhedron Vol. 4, No. 9, pp. 1585–1588, 1985
Printed in Great Britain

0277-5387/85 $3.00 + .00
© 1985 Pergamon Press Ltd

FLUORINATED BARRELENE–RUTHENIUM(II) COMPLEXES WITH ANIONIC CHELATING LIGANDS

M. VALDERRAMA,* M. SCOTTI and A. ROJAS
Facultad de Química, Pontificia Universidad Católica de Chile, Casilla 6177, Santiago, Chile

(*Received* 31 *January* 1985; *accepted* 28 *February* 1985)

Abstract—Reaction of ruthenium(III) chloride with the barrelene diolefins (tetrafluorobenzobarrelene (TFB) or (trimethyltetrafluorobenzobarrelene) (Me_3TFB) leads to the formation of the polymeric complexes $[RuCl_2(barrelene)]_n$. These compounds react with anionic chelating ligands with formation of new hexacoordinated neutral complexes of the general formulae [Rh(chelate)$_2$(barrelene)], where chelate = acetylacetonate, tropolonate, salicylaldehydate and 8-oxyquinolinate. The IR and ^{1}H NMR spectra of the complexes are given and discussed.

The synthesis of polymeric halogen bridged complexes of ruthenium(II) of the type $[RuX_2(diolefin)]_n$, where diolefin = 1,5-cyclooctadiene (COD) or bicyclo[2.2.1]hepta-2,5-diene (NBD) have been described by Wilkinson *et al.*[1,2] These complexes show a marked insolubility in most common organic solvents and only a few of their reactions have been reported.[1,3,4] Interestingly, hexacoordinated complexes of formula [Ru(acac)$_2$(diolefin)] (acac = acetylacetonate, diolefin = COD or NBD) have been prepared by Pannetier *et al.*[5,6] using an oxalate intermediate. On the other hand Powell[7] has reported an alternative and general route for the synthesis of [Ru(chelate)$_2$(diolefin)] complexes where the anionic chelating ligands present as donor atoms O–O, O–N, N–S or S–S. In particular the formation of geometrical isomers was found for the benzoylacetonate ligand.[7] As a continuation of studies on rhodium complexes containing tetrafluorobenzobarrelene ligands[8–11] we report new polymeric chloride ruthenium(II) complexes with tetrafluorobenzobarrelene (TFB) and trimethyltetrafluorobenzobarrelene (Me_3TFB) (see Fig. 1), along with a high yield synthesis under mild conditions of hexacoordinated barrelene ruthenium(II) derivatives with the anionic ligands acac, tropolonate (trop), salicylaldehydate (sal) and 8-oxyquinolinate (oq).

EXPERIMENTAL

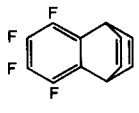
Carbon and hydrogen analyses were made with a Heraeus Mikro Standard microanalyser. IR spectra were recorded on a Perkin–Elmer 567 spectrophotometer using Nujol mulls between KBr discs, or dichloromethane solutions between KBr plates. ^{1}H NMR spectra were recorded on a Varian XL-100 intrument relative to tetramethylsilane.

Molecular weight measurements were obtained in chloroform solutions at 37°C with a Knauer vapour pressure osmometer calibrated with benzil. Melting points were determined with a Büchi apparatus and are uncorrected.

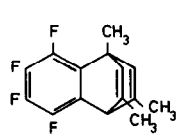
Ruthenium(III) chloride hydrate was obtained from commercial sources. Reagent grade solvents were dried, distilled and stored under nitrogen. Tetrafluorobenzobarrelene (TFB), the trimethyl derivative (Me_3TFB) and the polymeric complex $[RuCl_2(NBD)]_n$ were prepared according to literature procedures.[12,13]

Preparation of the complexes $[RuCl_2(diolefin)]_n$ (diolefin = TFB, Me_3TFB)

1 g (3.83 mmol) of the starting compound $RuCl_3 \cdot xH_2O$ was treated with 2.6 g (11.5 mmol) of TFB in ethanol solutions, and the mixture was stirred



TFB



Me_3TFB

Fig. 1.

* Author to whom correspondence should be addressed.

for 4 h at room temperature. The red–brownish solid obtained was filtered and washed with ethanol, acetone and diethylether. Yield 98% (1.49 g). Refluxing conditions (24 h) were required for the Me_3 TFB derivative (1.5 g, 5.60 mmol), due to the low solubility of this diolefin.

Preparation of the complexes [Ru(chelate)$_2$(diolefin)]

The compounds were prepared by the two general routes described below:

(i) *Synthesis of* [Ru(chelate)$_2$(diolefin)] (chelate = trop; diolefin = TFB, Me_3TFB, NBD). To a suspension of the polymeric complex [$RuCl_2$(diolefin)]$_n$ (100 mg, 0.25 mmol) in chloroform (50 cm^3) was added the stoichiometric amount of Tltrop (163 mg, 0.50 mmol). The mixture was boiled under reflux for 2 h. The TlCl formed was filtered off through kieselguhr, and the red filtrate was evaporated to dryness. The solid obtained was crystallized from dichloromethane–diethylether.

(ii) *Synthesis of* [Ru(chelate)$_2$(diolefin)] (chelate = acac, sal, oq; diolefin = TFB, Me_3TFB). A slurry of [$RuCl_2$(diolefin)]$_n$ (100 mg, 0.25 mmol), a large excess of chelating ligand [0.5 cm^3 (acetylacetone), 0.5 cm^3 (salicylaldehyde), 0.75 mmol (8-hydroxyquinoline)] and an excess of sodium carbonate (0.25 g) in dimethylformamide (10 cm^3) was boiled under reflux for 10 min. The mixture was cooled to room temperature, filtered and the sodium salts washed with methanol. Careful addition of distilled water precipitated the complexes which were washed with water and dried *in vacuo*.

The acac complexes were purified by column chromatography on activated silica-gel using hexane as eluant.

RESULTS AND DISCUSSION

The reaction of an ethanolic solution of $RuCl_3 \cdot xH_2O$ with TFB or Me_3TFB gave rise to the formation of [$RuCl_2$(barrelene)]$_n$ complexes. These polymeric compounds react, in refluxing dimethylformamide, with the potentially bidentate ligands acetylacetone, tropolone, salicylaldehyde or 8-hydroxyquinoline, in the presence of sodium carbonate, yielding hexacoordinated neutral complexes of general formula [Ru(chelate)$_2$(barrelene)] (chelate = acac, trop, sal, oq).

An alternative high yield method used for the tropolonate derivatives, involves the reaction of chloroform or diethylether suspensions of [$RuCl_2$(barrelene)]$_n$ complexes with a slight excess of thallium(I) tropolonate.

All the complexes are stable in air at room temperature and are non-conducting in organic solvents. Molecular weight measurements in chloroform solutions confirm the mononuclear

Table 1. Analytical results, colour, melting points and yields of the isolated complexes

Complex	Colour	Found (calc.) % C	Found (calc.) % H	M.p. (°)	Yield (%)
[$RuCl_2$(TFB)]$_n$ (I)	Red–brownish	36.72 (36.20)	1.88 (1.52)	218[a]	98
[$RuCl_2$(Me_3TFB)]$_n$ (II)	Red	40.37 (40.97)	2.84 (2.75)	258–259[a]	81
[Ru(acac)$_2$(TFB)] (III)	Yellow	50.83 (50.28)	3.84 (4.20)	136–138[b]	73
[Ru(trop)$_2$(TFB)][c] (IV)	Red	54.01 (54.70)	2.70 (2.82)	291–292	92
[Ru(acac)$_2$(Me_3TFB)] (V)	Yellow	52.83 (52.91)	4.67 (4.62)	178–179[b]	71
[Ru(trop)$_2$(Me_3TFB)] (VI)	Red	56.88 (56.96)	3.65 (3.62)	259–260[b]	87
[Ru(sal)$_2$(Me_3TFB)] (VII)	Brown	57.97 (56.96)	3.63 (3.62)	142–146[a]	52
[Ru(oq)$_2$(Me_3TFB)] (VIII)	Green–yellow	59.87 (60.27)	3.39 (3.68)	248–250[b]	45
[Ru(trop)$_2$(NBD)] (IX)	Pale-brown	58.20 (57.64)	4.26 (4.15)	236–238[a]	88

[a] Decomposes without melting.
[b] Melts under decomposition.
[c] Molecular weight: found, 596; calculated, 571.

Table 2. IR and ^{1}H NMR data for [Ru(chelate)$_2$(barrelene)] complexes

	Representative IR data	^{1}H NMR[a] (δ)	
Complex	1300–1600 cm^{-1}	Chelate protons	Barrelene protons
III	1515, 1590	1.94, 2.30 (CH_3) 5.43 (CH)	4.28, 4.54 (CH=CH) 5.28 (CH)
IV	1380, 1505, 1585	7.2–7.5 (H-ring)	3.80, 4.90 (CH=CH) 5.40 (CH)
V	1510, 1575	1.92, 2.32 (CH_3) 5.43 (CH) 1.83, 2.24 (CH_3) 5.56 (CH)	1.20, 1.43 (CH_3C=C) 2.29 (CH_3C) 3.26, 4.05 (CH=C) 4.58 (CH)
VI	1330, 1505, 1585	6.7–7.0 (H-ring) 7.1–7.7 (H-ring)	1.16, 1.76 (CH_3C=C) 2.31 (CH_3C) 3.23, 4.28 (CH=C) 4.67 (CH)
VII	1330, 1600	7.1–7.5 (H-ring) 8.84, 8.91 (H-ald.)	1.19, 1.60 (CH_3C=C) 2.38 (CH_3C) 3.70, 4.23 (CH=C) 4.72 (CH)
VIII	1110, 1330, 1560, 1580	6.82–7.47, 7.79–7.87, 8.40–8.56 (H-ring)	0.82, 1.53 (CH_3C=C) 2.56 (CH_3C) 3.24, 4.15 (CH=C) 4.89 (CH)
IX	1335, 1505, 1585	7.2–7.6 (H-ring)	1.78 (CH_2) 4.10 (CH=CH) 5.20 (CH)

[a] Data obtained using $CDCl_3$ solutions.

formulation. Elemental analyses, melting points, colour and yields are collected in Table 1.

The IR spectra of the complexes (Table 2) show absorptions of the coordinated diolefins (TFB at 1500 s, 1040 s, 885 s, 850 s, 670 m; Me_3TFB at 1500 s, 1490 s, 1060 s, 970 s, 930 s, 850 s and NBD at 1310 s cm^{-1}) together with the bands due to the coordinated chelating ligands. The acetylacetonate complexes show two strong bands in the range 1505–1515 cm^{-1} and 1575 cm^{-1} which are probably due to the combination of ν(C=O) and ν(C=C).[14] In the same range, the tropolonate complexes show two absorptions tentatively assigned to ν(C=O) + ν(C=C) and ν(C=C), whereas the absorptions located in the *ca* 1330–1340 cm^{-1} range is assigned to ν(C–O).[15,16] The salicylaldehyde complex shows the expected bands ν(C–O) and ν(C=O) at 1330 and 1600 cm^{-1} respectively.[17,18] The 8-oxyquinolinate derivative shows bands at ~1110 and 1330 cm^{-1} assigned to ν(C=N) and ν(C–O) together with strong bands at 1560 and 1580 cm^{-1}, characteristic of the heteroaromatic ring.[19,20]

The ^{1}H NMR spectrum of the [Ru(acac)$_2$(TFB)] complex (III) shows the presence of non-equivalent methyl groups and the related tropolonate compound (IV) presents a multiplet for the protons of the tropolonate ring (Table 2). In both cases the coordinated TFB diolefin presents two resonances for the vinyl protons and one resonance corresponding to the protons bonded to the tertiary carbons. These non-equivalent methyl groups of the ligand (acac) and the resonances corresponding to the vinyl protons of the TFB are due to the unsymmetrical coordination of the anionic chelate ligands (Fig. 2).[21,22]

Lack of symmetry is generally observed for the Me_3TFB complexes, due to the 1,3,8 disposition of the methyl groups in the ligand [Me_3TFB = 1,3,8 - trimethyl(tetrafluorobenzo[5,6])bicyclo - [2.2.2]octa-2,5,7-trieno] (Table 2). Thus the ^{1}H

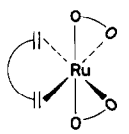


Fig. 2.

NMR spectrum of complex **V** show signals indicating non-equivalent acetylacetonate ligands. On the other hand, the tropolonate ligand in complex **VI** shows two multiplets of aromatic ring protons, whilst the complex obtained with NBD (**IX**) shows only one multiplet, indicating that the non-equivalence of the anionic bidentate ligands is probably due to the presence of the Me_3TFB diolefin.

Finally the complexes with the sal or oq ligand show an unsymmetrical coordination. In particular the ^1H NMR spectrum of the complex $[Ru(sal)_2(Me_3TFB)]$ (**VII**) shows two signals at δ 8.89 and 8.91 ppm, indicating the non-equivalence of the salicylaldehydate ligand. Although the presence of geometrical isomers cannot be completely excluded, we believe that only one geometric isomer is present because no chromatographic separation was observed (Fluorisil).[23] Therefore, the observed low symmetry has most probably the same origin as that in the above-mentioned complexes.

Acknowledgements—The authors thank Dirección de Investigación de la Pontificia Universidad Católica de Chile (DIUC) and Stiftung Volkswagenwerk for financial support.

REFERENCES

1. E. W. Abel, M. A. Bennett and G. Wilkinson, *J. Chem. Soc.* 1959, 3178.
2. M. A. Bennett and G. Wilkinson, *Chem. Ind.* 1959, 1516.
3. J. Powell and B. L. Shaw, *J. Chem. Soc. A* 1968, 159.
4. T. V. Ashworth, E. Singleton and J. J. Hough, *J. Chem. Soc., Dalton Trans.* 1977, 1809.
5. C. Potvin and G. Pannetier, *J. Less-Common Metals* 1970, **22**, 91.
6. C. Potvin, J. M. Manoli, A. Dereigne and G. Pannetier, *J. Less-Common Metals* 1971, **23**, 373.
7. P. Powell, *J. Organometal. Chem.* 1974, **65**, 89.
8. R. Usón, L. A. Oro, R. Sariego, M. Valderrama and C. Rebullida, *J. Organometal. Chem.* 1980, **197**, 87.
9. R. Usón, L. A. Oro, C. Foces-Foces, F. Cano, S. García-Blanco and M. Valderrama, *J. Organometal. Chem.* 1982, **229**, 293.
10. L. A. Oro, C. Foces-Foces, F. H. Cano and S. García-Blanco, *J. Organometal. Chem.* 1982, **236**, 385.
11. R. Usón, L. A. Oro, D. Carmona, M. Esteruelas, C. Foces-Foces, F. H. Cano and S. García-Blanco, *J. Organometal. Chem.* 1981, **254**, 249.
12. D. M. Roe and A. G. Massey, *J. Organometal. Chem.* 1971, **28**, 273.
13. E. W. Abel, M. A. Bennett and G. Wilkinson, *J. Chem. Soc.* 1959, 3178.
14. K. Nakamoto, *Infrared Spectra of Inorganic and Coordination Compounds*, second ed, p. 247. Wiley–Interscience, New York (1970).
15. L. G. Hulett and D. A. Thornton, *Spectrochimica Acta* 1971, **27A**, 2089.
16. M. Valderrama, H. Rafart and L. A. Oro, *Transition Met. Chem.* 1981, **6**, 221.
17. G. C. Percy and D. A. Thornton, *J. Inorg. Nucl. Chem.* 1973, **35**, 2719.
18. M. Valderrama and L. A. Oro, *J. Organometal. Chem.* 1981, **218**, 241.
19. R. Usón, L. A. Oro, M. A. Ciriano and R. González, *J. Organometal. Chem.* 1981, **205**, 259.
20. R. Ugo, G. La Monica, S. Cenini and F. Bonati, *J. Organometal. Chem.* 1968, **11**, 159.
21. D. St. C. Black, G. B. Deacon and N. C. Thomas, *Aust. J. Chem.* 1982, **2**, 409.
22. D. St. C. Black, G. B. Deacon and N. C. Thomas, *Polyhedron* 1983, **2**, 409.
23. Powell[7] has previously reported the chromatographic separation of geometrical isomers of the complex $[Ru(Bzac)_2(COD)]$.

Polyhedron Vol. 4, No. 9, pp. 1589–1594, 1985
Printed in Great Britain

0277-5387/85 $3.00 + .00
© 1985 Pergamon Press Ltd

PREPARATION AND CHARACTERIZATION OF COPPER(II) AND NICKEL(II) COMPLEXES WITH NOVEL TETRAAZA-MACROCYCLIC SCHIFF BASES

MANABU FUJIWARA, YASUHIRO NAKAJIMA, TAKAYUKI MATSUSHITA* and TOSHIYUKI SHONO

Department of Applied Chemistry, Faculty of Engineering, Osaka University, Yamadaoka, Suita, Osaka 565, Japan

(*Received* 9 *November* 1984; *accepted* 6 *March* 1985)

Abstract—Novel tetraaza-macrocycles with *N*-substituted carbamoyl groups were prepared by the reaction of 5,7,12,14-tetramethyl-1,4,8,11-tetraazacyclotetradeca-1,5,7,12-tetraene with isocyanates (R–N=C=O, R = CH_3 and C_6H_5). Their copper(II) and nickel(II) complexes were characterized by magnetic susceptibilities, electronic absorption spectra, and electrochemical properties. The complexing abilities and extractabilities of the ligands for the metal ions were investigated.

Many reports on the displacement reactions of a methine hydrogen of β-diketone derivatives by various electrophilic reagents have been presented.[1–9] For example, the methine hydrogen can be displaced by several substituents such as nitro,[1] thiocyanate,[2] chloro, bromo,[3,4] alkyl[5] and carbonyl[6] groups. Recently, Tokumitsu *et al.*[7] have reported the preparation and characterization of the disubstituted derivatives of 5,7,12,14-tetramethyl-1,4,8,11 - tetraazacyclotetradeca - 1,5,7,12 - tetraene, $(N_4)H_2$, with Cl, $SC_6H_4NO_2(o)$, $N_2C_6H_5$ and COC_6H_5 and their complexes with copper(II), nickel(II) and palladium(II). On the other hand, Nelson *et al.*[8] have found that [*N*,*N*′-bis(1-methyl-3-oxo-1-butenyl) ethylenediaminato]copper(II) reacts with various isocyanates to give mono- and diamide derivatives. In a preceding paper,[9] we have described the preparation of the dinitro-substituted macrocycle of $(N_4)H_2$ which possesses an excellent extractability for copper(II).

In this paper, we wish to describe the preparation of novel tetraaza-macrocyclic Schiff bases having carbamoyl groups (Fig. 1) and their copper(II) and nickel(II) complexes. The complexing abilities and extractabilities of these ligands for the metal ions are also described.

* Author to whom correspondence should be addressed.

EXPERIMENTAL

Materials

All reagents were of reagent grade, and isocyanates were distilled prior to use. Chloroform was refluxed over P_4O_{10} and distilled. Benzene was refluxed over sodium and distilled. *N*,*N*-dimethylformamide (DMF) was distilled over CaH_2 under reduced pressure prior to use. Other solvents were purified in the usual manner. Water was deionized.

Measurements

UV and visible absorption spectra were recorded on a Hitachi 340 recording spectrophotometer. IR

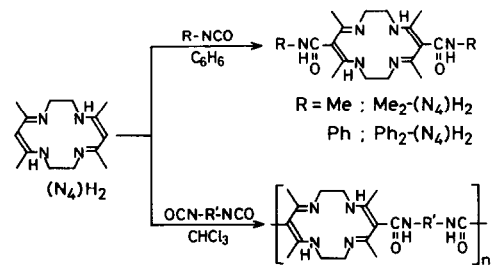


Fig. 1. Synthetic scheme for the novel tetraaza-macrocycles studied.

spectra were recorded on a Hitachi 215 grating spectrophotometer. Atomic absorption spectra were obtained using a Nippon Jarrell Ash AA-1. ^{1}H NMR spectra were taken with a JEOL JNM-PS 100 spectrometer, using DMSO-d_6 as the solvent and TMS as the internal standard. Polarograms were measured in DMF at 25°C by use of a Yanaco P-8 polarograph. A dropping mercury electrode and a mercury pool were used as the working and counter electrodes, respectively. Tetrabutylammonium perchlorate (0.1 mol dm^{-3}) was used as the supporting electrolyte. The pH of a sample solution was measured with a Shibata 671 pH meter. Magnetic susceptibilities were measured by the Gouy method at room temperature.

Procedure for solvent extraction

Solvent extractions were carried out by using a 10-cm^3 test tube with a stopper in which an aqueous solution (5 cm^3) of metal acetate (copper(II) and nickel(II)) and a chloroform solution (5 cm^3) of Me_2–$(N_4)H_2$ were contained as aqueous and organic phases, respectively. The test tube was shaken for an adequate time, from 2 min to 24 h, at room temperature by use of a shaker. After shaking, the concentrations of metal ions remained in the aqueous phase were determined by atomic absorption spectrometry.

The preparative scheme for tetraaza-macrocyclic Schiff base ligands is shown in Fig. 1.

Preparation of 6,13-*bis*(*N-methylcarbamoyl*)-5,7,12,14-*tetramethyl* - 1,4,8,11 - *tetraazacyclotetradeca* - 1,5,7,12 - *tetraene* (Me_2–$(N_4)H_2$)

To a benzene solution (20 cm^3) of the parent macrocycle[7] (1.0 g, 4.0 mmol) was added methyl isocyanate (0.57 g, 10 mmol). The mixture was stirred vigorously at room temperature for 24 h. The solution turned to milky yellow and then a turbidity appeared. It was collected on a glass filter and washed with dry benzene several times. The pale yellow solid was dissolved in a very small amount of ethanol and reprecipitated with benzene. It was filtered and dried *in vacuo*. The yield was 30%. This compound is very soluble in ethanol and DMF, slightly soluble in chloroform, and insoluble in ether and benzene. M.p.: 160.7–161.0°C (decomp.). Found: C; 59.21, H; 8.56, N; 23.48. Calc. for $C_{18}H_{30}N_6O_2$: C; 59.64, H; 8.34, N; 23.19%. MS found: *m/z* 362. Calc. for $C_{18}H_{30}N_6O_2$: 362. IR (in KBr disk): 3320, 1615, 1560, 1440, 1260, 1160, 810 and 730 cm^{-1}. ^{1}H NMR (in DMSO-d_6): δ 1.80 (6H, s, C$\underline{H}_3$), 2.48 (12H, s, C$\underline{H}_3$) and 3.36 (8H, s, C$\underline{H}_2$) ppm.

Preparation of 6,13 - *bis*(*N* - *phenylcarbamoyl*) - 5,7,12,14 - *tetramethyl* - 1,4,8,11 - *tetraazacyclotetradeca* - 1,5,7,12 - *tetraene* (Ph_2–$(N_4)H_2$)

To a benzene solution (100 cm^3) of the parent macrocycle (1.0 g, 4.0 mmol) was added phenyl isocyanate (1.2 g, 10 mmol). The mixture was stirred vigorously at room temperature for 48 h to give a precipitate gradually. It was collected on a glass filter, washed with dry benzene several times, and dried *in vacuo*. The yield was 55%. This compound is very soluble in ethanol and DMF, but insoluble in chloroform and benzene. M.p.: 254.5–256.0°C (decomp.). Found: C; 68.97, H; 7.24, N; 17.06. Calc. for $C_{28}H_{34}N_6O_2$: C; 69.10, H; 7.06, N; 17.27%. IR (in KBr disk): 3280, 1630, 1590, 1500, 1435, 1310, 1250, 1130, 750 and 690 cm^{-1}. ^{1}H NMR (in DMSO-d_6): δ 2.48 (12H, s, C$\underline{H}_3$), 3.36 (8H, s, C$\underline{H}_2$) and 7.30 (10H, m, $C_6\underline{H}_5$) ppm.

Preparation of copper(II) and nickel(II) complexes, Cu[Me_2–(N_4)], Cu[Ph_2–(N_4)], Ni[Me_2–(N_4)] *and* Ni[Ph_2–(N_4)]

The copper(II) complex, Cu[Me_2–(N_4)], was prepared by the reaction of Cu(N_4)[7] with methyl isocyanate as follows.

Cu(N_4) (1.0 g, 3.2 mmol) and methyl isocyanate (0.5 g, 8.7 mmol) were dissolved in a mixture of benzene and chloroform (1 : 1, 50 cm^3). It was stirred for 12 h at room temperature under a nitrogen atmosphere in the dark. A green precipitate formed gradually. It was collected on a glass filter, washed with dry benzene and then chloroform, and dried *in vacuo*. The yield was 50%. IR (in KBr disk): 3370, 1610, 1545, 1405, 1335, 1270, 1175, 800 and 720 cm^{-1}. Found: C; 50.92, H; 6.81, N; 19.64. Calc. for $CuC_{18}H_{28}N_6O_2$: C; 50.98, H; 6.67, N; 19.82%. Magnetic moment: μ_{eff} = 1.61 BM.

Other complexes were prepared by a method similar to that for Cu[Me_2–(N_4)].

Cu[Ph_2–(N_4)] was obtained in a similar manner to that described for Cu[Me_2–(N_4)], using phenyl isocyanate in place of methyl isocyanate. The yield was 70%. IR (in KBr disk): 3270, 1630, 1590, 1500, 1430, 1335, 1250, 1130, 750 and 690 cm^{-1}. Found: C; 61.09, H; 6.11, N; 15.17. Calc. for $CuC_{28}H_{32}N_6O_2$: C; 61.34, H; 5.90, N; 15.33%. Magnetic moment: μ_{eff} = 1.99 BM.

Ni[Me_2–(N_4)] was obtained in 55% yield. Found: C; 51.43, H; 6.99, N; 19.84. Calc. for $NiC_{18}H_{28}N_6O_2$: C; 51.57, H; 6.75, N; 20.05%. IR (in KBr disk): 3380, 1610, 1550, 1410, 1345, 1280, 1175, 800 and 725 cm^{-1}. The complex is diamagnetic.

Ni[Ph_2–(N_4)] was obtained in 80% yield. Found:

C; 62.02, H; 5.98, N; 15.21. Calc. for $NiC_{28}H_{32}N_6O_2$: C; 61.89, H; 5.95, N; 15.47%. IR (in KBr disk): 3280, 1625, 1590, 1500, 1425, 1345, 1255, 1135, 745 and 690 cm^{-1}. The complex is diamagnetic.

These complexes were also prepared by the reaction between copper(II) or nickel(II) acetate and the corresponding free ligands, and identified by the IR and UV spectra. However, their yields were lower than those obtained by the reaction between the metal complexes of $(N_4)H_2$ and the isocyanates, because it was difficult to purify the complexes.

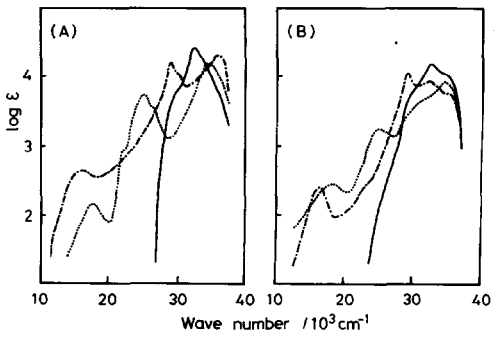


Fig. 2. Electronic spectra in DMF. (A) (——) Me_2–$(N_4)H_2$, (— · — · —) Cu[Me_2–(N_4)], (· · ·) Ni[Me_2–(N_4)]. (B) (——) Ph_2–$(N_4)H_2$, (— · — · —) Cu[Ph_2–(N_4)], (· · ·) Ni[Ph_2–(N_4)].

RESULTS AND DISCUSSION

Electronic spectra

Figure 2 shows the electronic spectra of the ligands Me_2–$(N_4)H_2$ (Fig. 2A) and Ph_2–$(N_4)H_2$ (Fig. 2B) and their copper(II) and nickel(II) complexes in DMF. The band positions of the absorption maxima are listed in Table 1, together with the molar extinction coefficients.

Both spectra of Me_2–$(N_4)H_2$ and Ph_2–$(N_4)H_2$ resemble that of the parent ligand.[9] The spectrum of Me_2–$(N_4)H_2$ exhibits three absorption bands centred at 309 nm, which can be assigned to π–π^* transitions.[10] The spectrum of either Cu[Me_2–(N_4)] or Ni[Me_2–(N_4)] shows an absorption band with moderate intensity in the visible region. The absorption band at 620 nm for Cu[Me_2–(N_4)] and at 558 nm for Ni[Me_2–(N_4)] can be assigned to the ligand field transitions. The band positions and intensities of the absorption bands of these complexes in the visible region are quite similar to those for the corresponding complexes of the parent macrocycle, indicating that the carbamoyl groups have little effect on the electronic state of the central metal ions.

The spectrum of Ph_2–$(N_4)H_2$ exhibits slightly broad absorption bands centred at 311 nm. The band positions and intensities are similar to those of Me_2–$(N_4)H_2$, suggesting that the phenyl rings of the ligand are not conjugated with the tetraaza ring. The spectra of Cu[Ph_2–(N_4)] and Ni[Ph_2–(N_4)] resemble those of Cu[Me_2–(N_4)] and Ni[Me_2–(N_4)], respectively, and the band positions for the former complexes due to the ligand field transitions are slightly shifted to shorter wavelengths than those for the latter.

Electrochemical properties

The reduction potentials of the complexes measured in DMF are summarized in Table 1. The polarograms of Cu[Me_2–(N_4)] and Ni[Me_2–(N_4)] show one cathodic wave at half-wave potentials of

Table 1. Absorption maxima and half-wave potentials of the macrocycles and their copper(II) and nickel(II) complexes

Compound	λ_{max} (log ε)[a] (nm)	$-E_{1/2}$ (vs Hg pool)[a] (V)
Me_2–$(N_4)H_2$	309 (4.42)	
Cu[Me_2–(N_4)]	620 (2.60), 346 (4.19), 269 (4.47)	2.05
Ni[Me_2–(N_4)]	558 (2.16), 402 (3.73), 293 (4.22)	2.28
Ph_2–$(N_4)H_2$	311 (4.18)	
Cu[Ph_2–(N_4)]	609 (2.40), 346 (4.05), 308 (3.95)	2.09
Ni[Ph_2–(N_4)]	542 (2.47), 401 (3.29), 290 (3.93)	2.26
$(N_4)H_2$[b]	308 (4.48)	
Cu(N_4)[b]	615 (2.15), 343 (4.34), 302 (4.03)	2.23
Ni(N_4)[b]	562 (2.40), 399 (3.87), 292 (4.26)	2.50

[a] Measured in DMF at 25°C.
[b] Measured in chloroform. Previous work, Ref. 9.

−2.05 and −2.28 V (vs Hg pool), respectively. These values are slightly positive (*ca* 0.20 V) compared with those of the parent complexes. Moreover, the polarograms of Cu[Ph_2–(N_4)] and Ni[Ph_2–(N_4)] also show one cathodic wave at half-wave potentials of −2.09 and −2.26 V, respectively. These slightly positive shifts may be caused by the carbamoyl groups which were introduced into the parent ligand; they act as weakly electron-attracting groups, which cause a decrease in the electron density on the central metal ion of the complexes. Previously, we have pointed out that the introduction of nitro groups into $(N_4)H_2$ results in a large positive shift (*ca* 1.0 V) of the half-wave potentials of the copper(II) and nickel(II) complexes.[9] Therefore, it can be said that the carbamoyl derivatives are similar to the parent ligand based on the spectral and electrochemical properties.

Complexation of copper(II) and nickel(II) with Me_2–$(N_4)H_2$ *and* Ph_2–$(N_4)H_2$

The rates of complexation of copper(II) and nickel(II) with Me_2–$(N_4)H_2$ and Ph_2–$(N_4)H_2$ were spectrophotometrically determined in a homogeneous DMF solution at 25°C. A DMF solution of each ligand (8.0×10^{-5} mol dm^{-3}) and a DMF solution of the equimolar amount of each metal ion were mixed in a UV cell (light-path length: 10 mm) with a stopper under an atmosphere of prepurified nitrogen, and then its absorption spectra were measured in a closed system over the range 290–420 nm at regular time intervals. In the case of copper(II) with Me_2–$(N_4)H_2$, the absorption spectrum changes remarkably during the initial 2 min and then gradually until 120 min: the absorption maximum of the ligand at 309 nm decreases in intensity and the new absorption bands which appear at 269 and 346 nm increase in intensity, having isosbestic points at 292 and 322 nm (Fig. 3A). These spectral changes indicate the formation of Cu[Me_2–(N_4)] complex. Similar spectral changes were observed for other cases: with Ph_2–$(N_4)H_2$ and copper(II) the absorption maximum of the ligand was shifted from 311 to 346 nm, having an isosbestic point at 321 nm, with Me_2–$(N_4)H_2$ and nickel(II) it was shifted from 309 to 402 nm, having an isosbestic point at 357 nm (Fig. 3B), and with Ph_2–$(N_4)H_2$ and nickel(II) it was shifted from 311 to 401 nm, having an isosbestic point at 342 nm.

The extent of complexation for these systems was calculated from these spectral changes. The results are shown in Fig. 4. Clearly, the rates of complexation of copper(II) with both ligands were found to be much faster than those for nickel(II), and the rates of complexation of both metal ions with

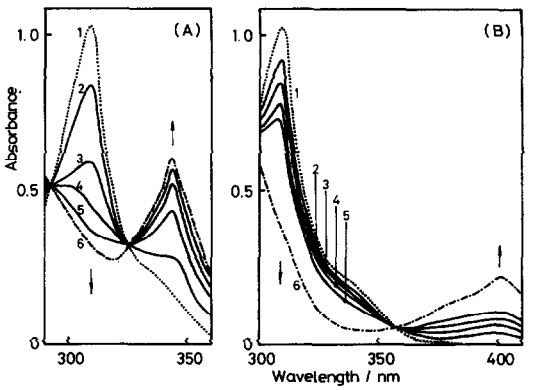


Fig. 3. Absorption spectral changes caused by complexation of copper(II) (A) and nickel(II) (B) with Me_2–$(N_4)H_2$ in DMF at 25°C. [Me_2–$(N_4)H_2$] = [metal]: 4.0×10^{-5} mol dm^{-3}; cell length = 10 mm. (A) 1, Me_2–$(N_4)H_2$; 2, 3, 4 and 5, after 2, 20, 60 and 90 min, respectively; 6, Cu[Me_2–(N_4)]. (B) 1, Me_2–$(N_4)H_2$; 2, 3, 4 and 5, after 20, 120, 240 and 360 min, respectively; 6, Ni[Me_2–(N_4)].

Me_2–$(N_4)H_2$ were faster than those with Ph_2–$(N_4)H_2$. The rate of the complexation of copper(II) with Me_2–$(N_4)H_2$ was fastest among them and its extent reached *ca* 100% (exactly 97%) after 2 h. This value is better than those observed for the complexation of copper(II) with $(N_4)H_2$ and its nitro derivatives.[9] The advantage of this tetraaza-macrocyclic ligand in the complex formation may arise from the formation of more stable complex than the parent macrocycle and the nitro derivative because the electron density on the nitrogen atoms of Me_2–$(N_4)H_2$ is richer than the nitro derivative and its copper(II) complex is more stable against oxygen and light than that of $(N_4)H_2$.

The extent of the complexation of copper(II) with

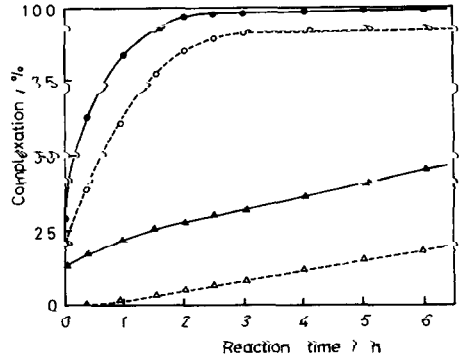


Fig. 4. The time-courses of complexation of copper(II) and nickel(II) with either Me_2–$(N_4)H_2$ or Ph_2–$(N_4)H_2$ in DMF at 25°C. [ligand] = [metal]: 4.0×10^{-5} mol dm^{-3}. (—●—) Cu(II)–Me_2–$(N_4)H_2$, (—▲—) Ni(II)–Me_2–$(N_4)H_2$, (– – ○ – –) Cu(II)–Ph_2–$(N_4)H_2$, (– – △ – –) Ni(II)–Ph_2–$(N_4)H_2$.

Ph_2-$(N_4)H_2$ reached *ca.* 90% after 3 h, which was slightly lower than that with Me_2-$(N_4)H_2$.

Generally, a nickel(II) ion is known to possess lower complexation rates and smaller formation constants with ordinary ligands than a copper(II) ion.[11–13] In fact, we have previously shown that with both of $(N_4)H_2$ and the nitro derivative ligands a copper(II) ion reached to the equilibrium of complexation faster than a nickel(II) ion.[9] And also the rates of the complexation of nickel(II) with the carbamoyl derivatives were late: after 6 h, the extent of the complexation of nickel(II) was 45 and 17% for Me_2-$(N_4)H_2$ and Ph_2-$(N_4)H_2$, respectively. These results suggest that the carbamoyl substituted tetraaza-macrocycles selectively form complexes with copper(II) rather than nickel(II). Thus, we have applied Me_2-$(N_4)H_2$, which can complex with copper(II) very fast and completely, as a selective extractant for copper(II).

Solvent extraction of copper(II) and nickel(II) by Me_2-$(N_4)H_2$

Solvent extractions of copper(II) and nickel(II) by Me_2-$(N_4)H_2$ were carried out under the conditions mentioned in the Experimental section. Figure 5 shows the plots of the percentages of two metal ions extracted by Me_2-$(N_4)H_2$ against the shaking time. The concentrations of Me_2-$(N_4)H_2$ in chloroform and of the metal ions in water were 2.0×10^{-3} and 2.0×10^{-4} mol dm^{-3}, respectively, and pH of the aqueous phase was adjusted to nearly 5.7 without using a buffer solution. Expectedly, the extraction rate of copper(II) by Me_2-$(N_4)H_2$ was found to be much faster than that of nickel(II). The copper(II) ion extracted into the chloroform phase was 78% within 30 min and its percentage was kept to be constant until 24 h. As for nickel(II), its extraction rate was late: after shaking for 30 min, the nickel(II) ion transferred into the chloroform phase was only 11%. The extraction equilibrium was not attained after 24 h, and the percentage of the extracted nickel(II) increased gradually.

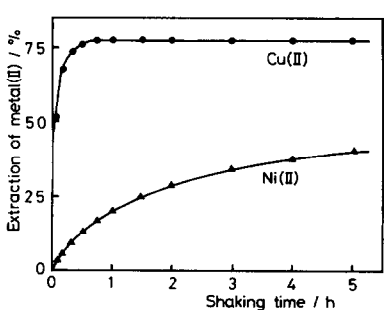


Fig. 5. Extractabilities of Me_2-$(N_4)H_2$ (2.0×10^{-3} mol dm^{-3}) for copper(II) and nickel(II) (2.0×10^{-4} mol dm^{-3}).

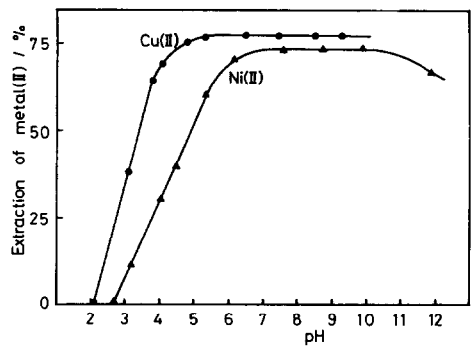


Fig. 6. Effect of pH on extraction of copper(II) and nickel(II) (2.0×10^{-4} mol dm^{-3}) by Me_2-$(N_4)H_2$ (2.0×10^{-3} mol dm^{-3}).

However, the percentage of the extracted copper(II) is lower than that expected from the results obtained on the complexation. This may be caused by the solubility of Me_2-$(N_4)H_2$ in water. In fact, the distribution ratio of Me_2-$(N_4)H_2$, ($[Me_2$-$(N_4)H_2]_{org}/[Me_2$-$(N_4)H_2]_{aq}$), was determined to be 0.02 and 0.85 at pH 5.0 and 7.7, respectively, after shaking for 2 h. Therefore, appreciable amounts of the ligand and the formed complex may be distributed into the aqueous phase.

Effect of pH on extraction

Figure 6 shows the effects of the pH of the aqueous phase on the extraction of copper(II) and nickel(II) by Me_2-$(N_4)H_2$. The extractions were made under the following conditions: the concentrations of the extractant and metal ions were 2.0×10^{-3} and 2.0×10^{-4} mol dm^{-3}, respectively, and the shaking time was 2 and 24 h for copper(II) and nickel(II), respectively. The pH of the aqueous solution was adjusted by addition of an adequate amount of

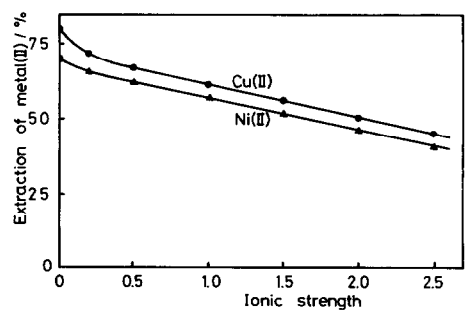


Fig. 7. Effect of ionic strength on extraction of copper(II) and nickel(II) (2.0×10^{-4} mol dm^{-3}) by Me_2-$(N_4)H_2$ (2.0×10^{-3} mol dm^{-3}). Ionic strength was adjusted by addition of sodium nitrate.

1.0 mol dm^{-3} hydrochloric acid, acetic acid, sodium acetate or sodium hydroxide. Because the extractability of Me_2–$(N_4)H_2$ was found to be influenced strongly by ionic strength, buffer solutions could not be used.

No extractions of copper(II) and nickel(II) were observed below pH 2.1 and 2.7, respectively. The percentage of the extracted copper(II) increased linearly with increasing pH of the aqueous phase, and came up to constant (78%) in the pH range from 5.7 to 9.0. On the other hand, the percentage of the extracted nickel(II) increased similarly with increasing pH of the aqueous phase in a higher pH region than the copper(II) case, and reached a constant value (73%) in the pH range from 7.5 to 10.0.

Effect of ionic strength on extraction

Figure 7 shows the effect of the ionic strength of the aqueous phase on the extractions of copper(II) and nickel(II) by Me_2–$(N_4)H_2$. The extractions were carried out under the following conditions: the concentrations of the extractant and metal ions and shaking time were the same as those described above. The pH of the aqueous phase was adjusted to be 5.7. The ionic strength of aqueous phase was varied from 0.0 to 2.5 by addition of sodium nitrate. Both extractions of copper(II) and nickel(II) were strongly influenced by the ionic strength of the aqueous phase. The percentage of the extracted copper(II) decreased linearly from 78 to 45% as the ionic strength was increased from 0.0 to 2.5. A similar behavior was obtained for the extraction of nickel(II).

REFERENCES

1. J. P. Collman, R. L. Marshall, W. L. Young and S. D. Goldby, *Inorg. Chem.* 1962, **1**, 704.
2. R. W. Kluiber, *J. Am. Chem. Soc.* 1961, **83**, 3030.
3. R. W. Kluiber, *J. Am. Chem. Soc.* 1960, **82**, 4839.
4. J. P. Collman, R. A. Moss, H. Maltz and C. C. Heindel, *J. Am. Chem. Soc.* 1961, **83**, 531.
5. D. F. Martin, W. C. Fernelius and M. Shamma, *J. Am. Chem. Soc.* 1959, **81**, 130.
6. J. A. Streeky, D. G. Pillsbury and D. H. Busch, *Inorg. Chem.* 1980, **19**, 3148.
7. T. Tokumitsu and T. Hayashi, *Bull. Chem. Soc. Jpn* 1981, **54**, 2348.
8. N. Howells, J. W. Kenney, J. H. Nelson and R. A. Henry, *Inorg. Chem.* 1976, **15**, 124.
9. M. Fujiwara, T. Matsushita and T. Shono, *Polyhedron* 1984, **3**, 1357.
10. Y. Nishida, K. Hayashida, A. Sumita and S. Kida, *Inorg. Chim. Acta* 1978, **31**, 19.
11. M. J. Bain-Ackerman and D. K. Lavellee, *Inorg. Chem.* 1979, **12**, 3358.
12. W. Steinmann and T. A. Kaden, *Helv. Chim. Acta* 1975, **58**, 1358.
13. R. H. Voss and R. B. Jordan, *J. Am. Chem. Soc.* 1976, **98**, 6926.

Polyhedron Vol. 4, No. 9, pp. 1595–1602, 1985
Printed in Great Britain

0277–5387/85 $3.00 + .00
© 1985 Pergamon Press Ltd

SYNTHESIS AND SPECTRAL STUDIES ON PALLADIUM AND PLATINUM COMPLEXES WITH MONO- AND BIDENTATE *N*-DONOR ORGANIC LIGANDS AND THEIR INTERACTION WITH CALF THYMUS DNA IN SOLUTION*

P. UMAPATHY,† RASHIDA A. HARNESSWALA and C. S. DORAI
National Chemical Laboratory, Poona 411008, India

(*Received* 17 *September* 1984; *accepted after revision* 6 *March* 1985)

Abstract—Palladium(II) and platinum(II) complexes of the types $PdLX_2$, PdL_2X_2, PtL_2X_2 and the Pt(IV) complexes $PtLX_2Y_2$, $PtL_2X_2Y'_2$ (where L = mono- or bidentate organic ligand containing nitrogen donor atoms; X = Cl or Br; Y = Br and Y′ = OH) have been synthesized and characterized by elemental analysis, IR and X-ray photoelectron spectral data. The Pd $3d_{5/2}$ binding energies indicate that the 8-aminoquinoline ligand is a better electron donor to the metal than other ligands studied. The Cl $2p_{3/2}$ binding energies in the square planar Pd(II) complexes are observed in the range 198.0–199.56 eV. The ν(Pd–Cl) vibrations (*ca* 340 and 320 cm^{-1}) corresponding to two *cis*-Cl ligands were observed in the IR spectra. Binding through probably N-7 of the guanine residue and the phosphate oxygen in a chelate form is implied from UV difference spectral data.

The discovery that some platinum compounds, especially *cis*-$Pt(NH_3)_2Cl_2$, exhibit anti-tumour properties[1] has stimulated considerable research in the area of metal ion interactions with nucleic acid constituents.[2–4] A majority of the recent studies on platinum drugs have been directed towards an understanding of their biological mode of action and their toxic side-effects. Studies in cultured cells have indicated the relevance of platinum–DNA binding to cytotoxicity. The bulk of evidence at present favours the view that damage to DNA leads to the inhibition of DNA synthesis and that this in turn results in cell death.[5] The anticancer action of *cis*-$Pt(NH_3)_2Cl_2$ is thought to involve coordination to a guanosine residue in DNA. Little is precisely known about the specific covalent attachment sites of *cis*-$Pt(NH_3)_2Cl_2$ and platinum uracil blues on DNA. Nevertheless, numerous studies have implicated N-7 and possibly O-6 of guanine.[2,3,6,7] Other atoms in nucleic acid bases which have been shown to have affinity for platinum include the deprotonated N-1 and N-3 positions of guanine and thymine respectively, as well as the N-3 position of cytosine and the deprotonated NH_2 group of cytosine.[8] Furthermore, scant attention has been given to the binding of *cis*-$Pt(NH_3)_2Cl_2$ to the oxygen atoms of phosphate groups despite the fact that early experimental studies of the binding of platinum complexes to DNA and nucleosides produced evidence that suggested platinum–phosphate binding was a significant factor in these systems.[9–11] In order to further explore the nature of the metal ion binding sites in DNA, we have in continuation of our earlier work,[12] synthesized several new Pt(II) and Pd(II) complexes of the types PtL_2X_2, $PdLX_2$ PdL_2X_2 and Pt(IV) complexes $PtLX_2Y_2$, $PtL_2X_2Y'_2$ (where L = mono- or bidentate ligand, such as 8-aminoquinoline, 1,8-naphthalenediamine or a derivative of 1,10-phenanthroline, theophylline, cytidine, etc., X = Cl or Br, Y = Br and Y′ = OH) and studied in solution the reactions of two complexes, namely, *cis* - dichlorobis(theophyllinato) - *trans* - dihydroxoplatinum(IV), *cis*-$PtCl_2(theoph)_2(OH)_2$, and *cis*-dichlorobis(cytidine)palladium(II), *cis*-$Pd(cytd)_2Cl_2$, with calf thymus DNA by recording UV difference spectra at various concentrations, pHs and temperatures. Solubility problems precluded the study of other Pt- or Pd-complexes.

* NCL Communication No. 3629.

† Author to whom correspondence should be addressed.

EXPERIMENTAL

K_2PtCl_4, K_2PdCl_4, K_2PtBr_4 and $K_2PtCl_4(OH)_2$ were prepared by the reported methods.[13–15] The cis- and trans-isomers of dichlorodiammine palladium(II) were prepared by following the procedure of Layton *et al.*[16] and later modified by Coe and Lyons.[17] The ligands 5-nitro-1,10-phenanthroline, theophylline, 7-methyltheophylline were synthesized by the known procedures.[18,19] Their purity was checked by elemental analysis, m.p.s and spectral data. Calf thymus DNA (Type 1), 8-aminoquinoline, 1,8-naphthalenediamine, *o*-phenylenediamine were purchased (Sigma Chemical Co., Fluka AG, Buchs SG, Switzerland, Aldrich Chemical Company, Inc., U.S.A. and E. Merck AG, Darmstadt). All other chemicals used were of reagent grade. Solvents were purified and dried prior to use. IR spectra were recorded on a Perkin–Elmer model 599B IR spectrophotometer.

X-ray photoelectron spectra were recorded using a VG Scientific ESCA-3MK-2 electron spectrometer. Powdered samples were mounted on a nickel sample holder. Magnesium K_α radiation (1253.6) was used as a source. Nitrogen 1*s*, Pt 4*f*, Pd 3*d*, Cl 2*p*, Br 3*p*, K 2*p* binding energies were referred to C 1*s* line of adventitious carbon at 285.0 eV. The final values of the binding energies for each sample were determined from measurements in triplicate on several sample preparations and their accuracy is within ± 0.20 eV. Visual examination of the samples after measurements revealed no evidence of radiation damage.

The experimental details concerning the preparation of stock solutions of DNA and the aquated platinum complex and recording of UV difference spectra were described before.[12] The difference spectra reported at 30°C were obtained on a 1.00 expanded absorbance scale on a Pye Unicam Model SP8-100 spectrophotometer.

The Pd(II) complexes of the type $Pd(II)LX_2$, $Pd(II)L_2X_2$ were synthesized by following the general procedure given below:

Clear (filtered if necessary) solutions of K_2PdCl_4 in water (10 cm^3) and the appropriate organic ligand in excess hot water (25–30 cm^3) in 1 : 1 or 1 : 2 mole ratios were mixed together and heated on a water bath for about 8–12 h. (In the case of 5-nitro-1,10-phenanthroline, solvent acetone–water mixture, 1 : 1, was used and refluxed for 8 h.) The solid products separated out were collected on a filter under suction, washed with hot water (5 cm^3 portions) and dried under vacuum. Yield ~ 80%.

The platinum complexes of the types $Pt(II)L_2X_2$, $Pt(IV)LX_2Y_2'$ were prepared in an analogous manner starting with K_2PtCl_4 or $K_2PtCl_4(OH)_2$ and refluxing the mixtures for about 8 h. The tetrabromo(8-aminoquinoline)platinum(IV) was obtained by bromination, in $CHCl_3$ solution, of Pt(8-aminoQ)Br_2.[12] The analytical data of platinum and palladium complexes are given in Table 1.

RESULTS AND DISCUSSION

The interactions of platinum and palladium complexes, *cis*-dichlorobis(theophyllinato) - *trans* - dihydroxoplatinum(IV) and *cis* - dichlorobis-(cytidine)palladium(II) with calf thymus DNA were followed by UV difference spectral technique. The UV difference spectrum for the DNA solution mixed with *cis*-$Pt(theoph)_2Cl_2(OH)_2$ did not change, indicating no reaction with DNA bases. However, when the aquated Pt-complex was mixed with DNA, the spectrum exhibited large hyperchromism with a wavelength shift of the peak absorption from 259 to 280 nm initially. Over several days, at the end of the reaction apparently, the observed shift was from 259 to 263–4 nm (Figs 1 and 2). It seems well established now[3,20] that the interaction between Pt-compounds and DNA takes place through the complex aquated charged species of platinum and the high concentration of chloride ions (> 0.01 M) inhibits the reaction to an appreciable extent. The aquo complexes bind more readily to cellular targets such as DNA since water is relatively a good leaving group. It was postulated[21,22] that reactions of compounds such as *cis*-$Pt(NH_3)_2Cl_2$ with DNA bases and even DNA itself *in vivo* go through an aquation product supposedly

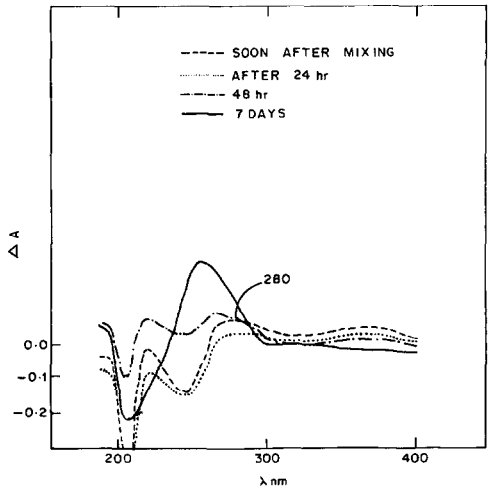


Fig. 1. UV difference spectra resulting from aquated *cis*-$Pt(theoph)_2(OH)_2(H_2O)]^{2+}$–DNA interaction: pH = 6.9, T = 30°C, 0.2 mg DNA/10 cm^3 phosphate buffer, Pt(IV) = 1×10^{-4} M (phosphate buffer).

Table 1. Analytical data of platinum and palladium complexes

Complex	M.p. (°C) (decomp.)	C	H	N	(Cl or Br)	(Pd or Pt)
				(%)		
1. Dichloro(8-aminoquinoline)palladium(II)	270	33.83	2.70	8.30	23.20	32.80
		(33.62)	(2.51)	(8.70)	(22.05)	(33.10)
2. Dichloro(5-nitro-1,10-phenanthroline)palladium(II)	260	36.54	1.84	10.50	17.02	26.30
		(35.81)	(1.75)	(10.44)	(17.62)	(26.44)
3. Dichloro(O-phenylenediamine)palladium(II)	300	25.65	3.20	10.20	24.85	37.77
		(25.25)	(2.82)	(9.82)	(24.84)	(37.29)
4. Dichloro(1,8-naphthalenediamine)palladium(II)	290	34.61	3.20	8.10	22.12	31.23
		(35.80)	(3.00)	(8.35)	(21.13)	(31.73)
5. Dichlorobis(theophylline)palladium(II)	295	30.55	3.30	20.58	13.70	20.10
		(31.27)	(3.00)	(20.84)	(13.18)	(19.79)
6. Dichlorobis(7-methyltheophylline)palladium(II)	> 270	34.32	4.00	19.40	12.88	18.06
		(33.96)	(3.56)	(19.81)	(12.53)	(18.81)
7. Dichlorobis(cytidine)palladium(II)	236	33.61	4.31	12.10	11.03	15.80
		(32.57)	(3.95)	(12.67)	(10.68)	(16.03)
8. Dichlorobis(5-azacytosine)palladium(II)	> 270	17.50	2.52	26.92	17.08	26.26
		(17.95)	(2.01)	(27.92)	(17.66)	(26.51)
9. Dichlorobis(5-azacytosine)platinum(II)dihydrate	~ 340	12.86	2.80	20.06	12.90	38.00
		(13.70)	(2.30)	(21.29)	(13.47)	(37.07)
10. Cytidinium trichloro cytidine platinum(II)	160	27.11	3.80	10.49	13.14	25.30
		(27.40)	(3.45)	(10.65)	(13.49)	(24.73)
11. Tetrabromo(8-aminoquinoline)platinum(IV)	~ 300	16.86	1.67	4.26	50.74	29.31
		(16.41)	(1.22)	(4.25)	(48.53)	(29.61)
12. *cis*-Dichlorobis(8-aminoquinoline)-*trans*-dihydroxoplatinum(IV)	~ 345	36.47	3.02	9.09	12.10	33.00
		(36.74)	(3.08)	(9.52)	(12.07)	(33.15)
13. *cis*-Dichloro(7-methyltheophylline)-*trans*-dihydroxoplatinum(IV)	230	26.17	3.31	15.48	10.27	29.02
		(27.90)	(3.22)	(16.23)	(10.30)	(28.33)
14. *cis*-Dichlorobis(theophylline)-*trans*-dihydroxoplatinum(IV)	220	25.13	3.08	16.07	10.16	28.86
		(25.46)	(2.75)	(16.97)	(10.74)	(29.54)

Values in parentheses are the calculated values.

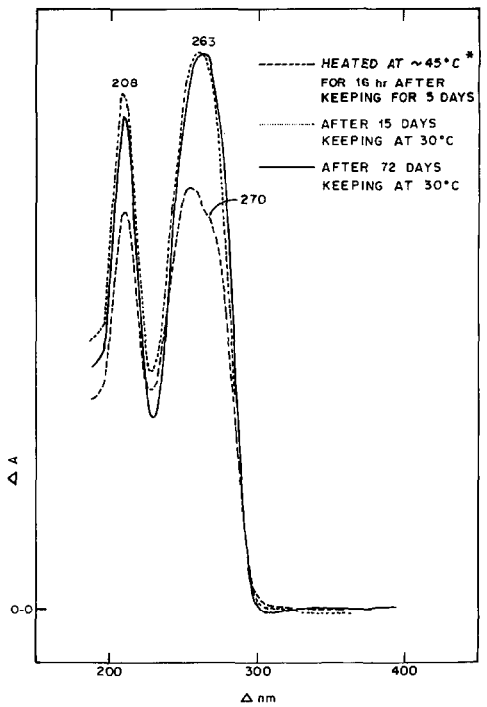


Fig. 2. UV difference spectra resulting from aquated *cis*-Pt(theoph)$_2$(OH)$_2$–DNA interaction: concentrations same as in Fig. 1. *Recorded on 2.00 full scale.

$[Pt(NH_3)_2(H_2O)_2]^{2+}$. Rosenberg *et al.*[23–26] recently have shown that aqueous solutions of the aquation product are very complex and in addition to such species as above contain substantial amounts of hydroxide bridged species containing two, three or four platinum atoms. A ^{195}Pt and ^{15}N NMR spectral studies of aqueous solutions of *cis*-$Pt(NH_3)_2Cl_2$ and its hydrolysis and oligomerization products showed[27] that, in the blood substitute Hanks' medium, conversion of

$$cis\text{-}[Pt(^{15}NH_3)_2(H_2O)_2](NO_3)_2$$

into

$$cis\text{-}PtCl_2(^{15}NH_3)_2,$$

$$cis\text{-}[PtCl(H_2O)(^{15}NH_3)_2]^+,$$

$$[Pt(^{15}NH_3)_2(OH)_3]^{3+}$$

and

$$[Pt(^{15}NH_3)_2(OH)_2]^{2+}$$

takes place, the reaction taking several hours at 30°C. The aquated *cis*-$PtCl_2$(theoph)$_2$(OH)$_2$ solution may contain presumably *cis*-$[Pt(theoph)_2(OH)_2(H_2O)_2]^{2+}$ species. The extent of the reaction depends on pH, time, temperature and the mole ratio of Pt/DNA system. The time required to reach the end of the reaction under optimum conditions (pH 6.89–7.6, mole ratio 1 : 1) is of the order of 48 h at 30°C for the initial reaction and several days for the slow reaction. A rapid reaction occurred within hours and then a slow reaction extending over several days. The binding of a bifunctional Pt-complex to DNA probably occurs in two stages. The UV difference spectrum in the reaction with aquated species of Pt(IV) complex with DNA at pH 6.89 exhibits λ_{max} at *ca* 280 nm (broad band) probably consisting of two bands (the reaction mixture after 5 days showed a shoulder at 270 nm) while λ_{min} was observed at 248 nm and at *ca* 210 nm. ΔA at 280 nm increased with increased concentration of DNA as well as Pt-concentration. In citrate buffer, pH 7.59 the reactions of Pt(IV) and Pd(II) complexes with DNA appear to be sluggish. The DNA secondary structure undergoes a very profound alteration upon binding of *cis*-$[Pt(theoph)_2(OH)_2(H_2O)_2]^{2+}$ and the hyperchromism observed has been attributed to a denaturation of the double helical structure caused by breaking of one hydrogen bond at O-6-Guo for each Pt-bound by the first binding process.[28,29] The increments of ΔA at 280 nm (and at 263–4 nm) in the initial fast reaction and the final reaction may be due to change in the electron distribution of base moieties.[30,31] It is also possible that the aquated species binds to guanine residues at N-7 position with the resulting liberation of proton at N-1 position as has been postulated.[32] Scovell and O'Connor[33] observed in their studies of aquated *cis*-$Pt(NH_3)_2Cl_2$ with nucleic acid constituents that deprotonation of the guanosine does not occur and that in the complexation reaction monodentate coordination occurs with displacement of water. Millard *et al.*[34] have suggested that in the *cis*-Pt(II)$(NH_3)_2$ interaction with DNA, guanine acts as a chelate binding through the N-7 and O-6 positions. The shift of the 259 nm band of DNA to 280 nm (or 263–4 nm) in the UV difference spectrum of aquated *cis*-(theoph)$_2$(OH)$_2$Pt–DNA interaction is indicative of the involvement of N-7 of the guanine residues in DNA. The UV difference spectral pattern and the shift are similar approximately to those previously reported.[20,30,33]

It is interesting to note that the UV difference spectra in the reaction with aquated *cis*-Pt(IV)(theoph)$_2$(OH)$_2$Cl$_2$ with DNA recorded after several days (Fig. 2) exhibit a well defined intense positive peak at 208 nm. The UV spectrum of calf thymus DNA in buffer, pH 6.89 (recorded against appropriate blank) shows an intense absorption peak at 196 nm in the far UV region. The phosphate groups are known to absorb in this region.[35] The shift of the phosphate group absorption peak of DNA from 196 to 208 nm indicates

direct involvement of the phosphate oxygen with platinum in a Pt–OPO_3^{2-} type interaction. The formation of the charged aquo complex *cis*-$[Pt(theoph)_2(OH)_2(H_2O)_2]^{2+}$ equally may raise the affinity of the complex to phosphate group. The interaction between aquated *cis*-$[Pt(theoph)_2(OH)_2(H_2O)_2]^{2+}$ and DNA results in the denaturation of the double helical structure caused by breaking of the hydrogen bonds. The domain of this part of this helix can unwind itself over the planar base in such a way that the nitrogen of the base and the phosphate oxygen are in close proximity—an ideally placed configuration—for eventual coordination. Szent-Györgyi[36] has postulated a quadridentate chelate between ATP and Mg^{2+} in which the bonding involves the 6-amino group, the nitrogen atom at position 7 and one oxygen atom of each of the terminal phosphate groups.

FT–IR spectral studies[37] of the adenosine-5′-monophosphate complexes of Pt(II) and Mg(II) metal ions reveal that Mg(II) complexes synthesized in acid solution show direct Mg–phosphate interactions as well as N-7 bonding. However, no direct metal phosphate interaction was observed for the Pt(II) complexes. Crystal structure data for the complex $[Pt(en)(5'\text{-CMP})]_2 \cdot 2H_2O$ confirm the presence of direct platinum–phosphate bonding.[38] The CMP ligands are linked in a head-to-tail fashion by two Pt(en) fragments such that each Pt-atom is bonded to the N-3 atom of one nucleotide and to a phosphate oxygen of the other. The structure of this complex is consistent with those of other metal–CMP complexes.[39,40]

The UV difference spectrum for the DNA solution mixed with *cis*-$Pd(cytidine)_2Cl_2$, unlike the Pt(IV) complex, showed changes soon after mixing, indicating immediate reaction with DNA bases (Figs 3 and 4). The spectrum exhibited large hyperchromism with shift of the 259 nm band to 276 nm along with an additional positive peak at 220 nm. At the end of the reaction over several days, the observed shift was from 259 to 263 nm; the other peak appearing at 206 nm. The extent of the reaction depends on time, pH and the mole ratio of Pd/DNA system. The time required to reach the end of the initial reaction under optimum conditions (pH 6.8–7.6) mole ratio (1 : 1) is of the order of 24 h at 30°C. Although Pt- and Pd-complexes would be expected to exhibit similar reactivity towards DNA, the greater reactivity of Pd(II) towards heterocyclic nitrogen is a consequence of the lower affinity of Pd(II) towards Cl^-. Studies by Martin *et al.*[41] have indicated that, in the absence of Cl, Pt(II) is also reactive. The aquated *cis*-$Pd(cytidine)_2Cl_2$ may contain presumably the bifunctional *cis*-

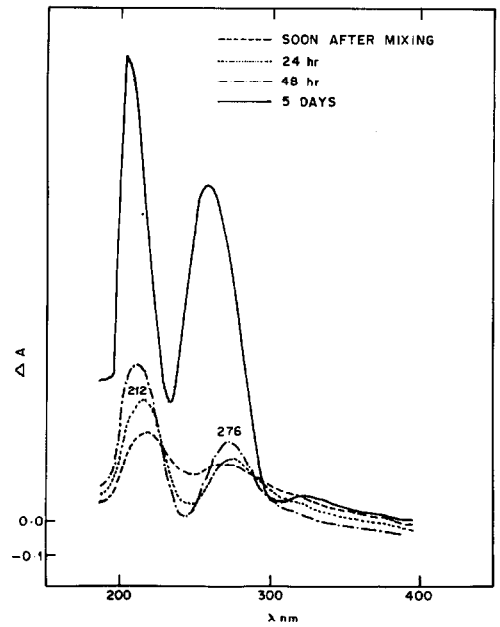


Fig. 3. UV difference spectra resulting from aquated *cis*-$(cytd)_2Pd(II)$–DNA interaction: pH = 6.8, T = 30°C, 0.2 mg DNA/10 cm^3 phosphate buffer, Pd(II) = 1×10^{-4} M (phosphate buffer).

$[Pd(cytidine)_2(H_2O)_2]^{2+}$ species which binds to the DNA in two stages. The shift of the 259 nm band of DNA to 276 nm (or to 263 nm) in the initial and final reactions is indicative of the perturbation of the electronic systems of the bases due to interaction of

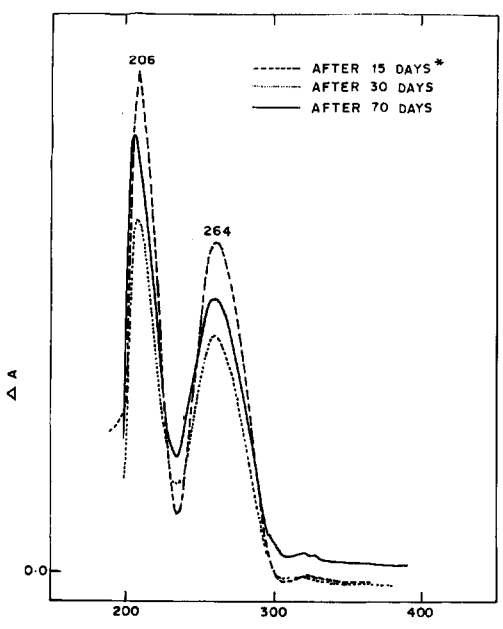


Fig. 4. UV difference spectra resulting from aquated *cis*-$(cytd)_2Pd(II)$–DNA interaction: concentrations same as in Fig. 3. *Recorded on 0.500 full scale.

cis-(cytidine)$_2$Pd^{2+}, possibly at the N-7 of the guanine residues. From a detailed study on the binding of (en)Pd^{2+} and (dien)Pd^{2+} to nucleic bases of nucleosides and nucleotides Martin[42,43] favoured a general rule for metal ion binding to N-7 of purine bases. Though the basicity of N-1 is much greater than that of N-7 in purines, (dien)Pd^{2+} only slightly favours N-1. In the region around neutral pH (en)Pd^{2+} coordinates to both N-7 and N-1 leading to possible polymeric complexes. The shift of the phosphate group absorption of DNA from 196 to 206 nm in the UV difference spectra recorded after several days (as in the case of Pt(IV)–DNA interaction) suggest involvement of phosphate oxygen with palladium. Recent interaction studies of *cysteinato - O - methylesterpalladium(II) - μ* - dichloro - cysteinato - *O* - methylesterpalladium(II) with adenosine-5'-monophosphate disodium, AMP–Na$_2$ indicate that in the complex [Pd(*O*-MeCys)(AMP)]Na, the nucleotide AMP coordinates to palladium through the N-7 atom of the purine ring and the phosphate group, most probably in a chelate form.[44]

The XPS data for the platinum and palladium complexes investigated are given in Tables 2 and 3. The Pd $3d_{5/2}$ binding energies of compounds nos. 2–6 imply a marked decrease in electron density on the metal relative to that in the 8-aminoquinoline complex. All the compounds are formally square planar Pd(II) complexes presumably containing the *cis*-PdCl$_2$ fragment. Variations in relaxation effect should be minimized in this series and the differences in metal binding energies should primarily be due to differences in the electron donating ability of the coordinated ligands.[45] A comparison of the Pd $3d_{5/2}$ binding energies for the complexes indicates that 8-aminoquinoline is a better electron donor, i.e. a better complexing agent, compared to 1,8-naphthalenediamine, 5-nitro-1,10-phenanthroline, theophylline or 7-methyltheophylline. The substantial shift in the binding energy of N(1*s*) clearly confirms a net electron transfer from nitrogen to palladium in these complexes. The change in the Pt $4f_{7/2}$ binding energies shows both the effect of oxidation state and of ligand character. The higher the formal oxidation state, the higher the binding energy. The platinum(II) and (IV) complexes of the type PtL$_2$X$_2$, PtLX$_2$Y$_2$ or PtLX$_2$Y$'_2$ investigated have Pt $4f_{7/2}$ binding energies within the range reported in the literature[46,47] for platinum complexes. The Cl(2*p*) binding energies of these complexes are lower than that of K$_2$PtCl$_4$ or K$_2$PtCl$_6$ indicating partial ionic character of the Pt–Cl bond.

The Cl(2*p*) binding energies for the palladium complexes studied are in the range 198.0–199.56 eV. The observed Cl(2*p*) binding energy for *cis*-Pd(NH$_3$)$_2$Cl$_2$ is lower than the *trans*-Pd(NH$_3$)$_2$Cl$_2$. In complexes where L = a bidentate ligand, the square planar geometry presumably implies *cis*-Cl configuration. The other complexes may also have *cis*-chlorines in view of the close range of observed

Table 2. N(1*s*), Pd(3*d*) and Cl(2*p*) X.p.e. binding energies for palladium complexes[a]

Compound	Pd $3d_{5/2}$	N $1s_{1/2}$	Cl $2p_{3/2}$
1. K_2PdCl_4	338.4 ± 0.2[b]		
2. Pd(methyltheoph)$_2$Cl$_2$	341.12	403.40 (broad)	199.56
3. *trans*-Pd(NH$_3$)$_2$Cl$_2$	340.24	401.64	200.20
4. Pd(1,8-Naphdiam)Cl$_2$	338.24	400.60 400.20	198.56
5. *cis*-Pd(NH$_3$)$_2$Cl$_2$	338.00	400.64	198.60
6. Pd(cytd)$_2$Cl$_2$	336.92	398.88 401.68	198.20
7. Pd(5-nitro-1,10-phen)Cl$_2$	336.80	400.10 400.00	198.00
8. Pd(theoph)$_2$Cl$_2$	336.44	400.20	198.60
9. Pd(*O*-phendiam)Cl$_2$	336.20	399.84 399.76	199.32
10. Pd(8-aminoQ)Cl$_2$	336.12	400.32 399.64	199.20

[a] Binding energies are in electron volts, eV, relative to adventitious carbon C 1*s*, 285 eV.

[b] Value from Gobind Kumar, J. R. Blackburn, R. G. Albridge, W. E. Moddeman and M. M. Jones, *Inorg. Chem.* 1972, **11**, 296.

Table 3. N(1*s*), Pt(4*f*), Cl(2*p*) and K(2*p*) X.p.e. binding energies for platinum complexes[a]

Compound	Pt $4f_{7/2}$	N $1s_{1/2}$	Cl $2p_{3/2}$	Br $3p_{1/2,3/2}$	K $2p_{1/2,3/2}$
1. K_2PtCl_6	76.8±0.2,[c] 75.9[b]	—	201.0[c]	—	295.1[c]
2. K_2PtBr_6	75.8±0.2	—	—	183.5[c]	—
3. K_2PtCl_4	73.4[b]	—	200.7[c]	—	—
			199.4[b]		
4. $K_2PtCl_4(OH)_2$	75.24	—	199.16	—	295.36
					292.84
5. Pt(5-azacyt)$_2Cl_2 \cdot 2H_2O$	73.84	400.36	199.20	—	—
		401.12			
6. Pt(8-aminoQ)Br_4	75.92	400.58	—	189.89	—
		399.04		182.28	
7. Pt(theoph)$_2Cl_2(OH)_2$	73.68	400.80	200.76	—	—
		399.76	198.96		
8. Pt(methyltheoph)$_2Cl_2(OH)_2$	73.56	401.08	198.92	—	—
		400.00			
9. Pt(8-aminoQ)$_2Cl_2(OH)_2$	73.00	400.16	198.60	—	—
		400.36			

[a] Binding energies are in electron volts, eV, relative to adventitious carbon C 1*s*, 285 eV.

[b,c] Data from *Electron Spectroscopy*, D.A. Shirley (Editor), pp. 713, 725, North-Holland, Amsterdam (1972); and from W. M. Riggs, *Anal. Chem.* 1972, **44**, 830.

binding energies compared to *cis*-$Pd(NH_3)_2Cl_2$. The IR spectral data also confirm this. X-ray crystallographic data show quite clearly that there is a considerable increase in metal–halogen bond length in going from the *trans*- to *cis*-isomer in square planar Pt(II) and Pd(II) complexes of the type $(PR_3)_2MX_2$. For X = Cl, NQR data suggest[48] that the bond lengthening is accompanied by a considerable electron drift to chlorine. It is however observed[49] that in a given *cis–trans*-pair the binding energy of the metal is the same but that of the halogen is considerably lower in the *cis*-isomer. The ^{35}Cl resonance signals in the three *trans*-L_2PtCl_2 complexes are found at higher frequencies than in the corresponding *cis*-complex and this difference is related to the charge on the ligands. A tentative suggestion is that the *trans*-influence in the ^{35}Cl quadrupole resonance of the complexes of the type L_2MCl_2 [M = Pt(II) or Pd(II), Ni(II)] manifests itself in a general lowering of the frequencies on going from the *trans*- to the *cis*-complex and the difference being related to the position of the ligand L in the *trans*-series.

The IR spectra of Pd(II) complexes with organic ligands show two medium intense absorptions at *ca* 340 and *ca* 320 cm^{-1} ascribable to ν(Pd–Cl) vibrations—asymmetric and symmetric respectively corresponding to two Cl ligands in the *cis*-arrangement.[50,51] In the spectra of Pt(IV) complexes, the two Pt–Cl stretching vibrations are observed at *ca* 335 and *ca* 350 cm^{-1}. The Pt–Cl stretching vibrations absorb in the range observed for other complexes of Pt(IV) with chloroligands *trans* to (NH_3) group.[52,53] The IR ν(Pt–Cl/Pd–Cl) vibrations and XPS data (Cl $2p_{3/2}$ binding energies) support the view that both the complexes Pd(II) and Pt(IV), contain two Cl ligands in the *cis*-arrangement, in their respective geometries. XPS data also confirms the oxidation state of the metals involved in the study. It is well known that *cis*-$Pt(NH_3)_2Cl_2$ is effective against various tumour systems while *trans*-$Pt(NH_3)_2Cl_2$ is inactive. The activity of Pt(IV) complexes involves reduction inside the cell to the corresponding Pt(II) complex with the loss of the two *trans*-ligands. The profound spectral changes observed in the spectra of the interaction products of *cis*-Pt(IV) and *cis*-Pd(II) complexes with DNA are consistent with the observation[30] that the changes in the DNA secondary structure induced by antitumour active platinum complexes are greater than those of inactive platinum complexes.

Acknowledgements—The authors thank Dr. S. Badrinarayan for the help in recording the XP spectra. One of the authors, (Miss) R.A.H., thanks CSIR, New Delhi, for placement in the Scientist's Pool. The authors also thank the referees for helpful suggestions.

REFERENCES

1. B. Rosenberg, L. Van Camp, J. E. Trosko and V. H. Mansour, *Nature (London)* 1969, **222**, 385.
2. L. G. Marzilli, *Prog. Inorg. Chem.* 1977, **23**, 255.
3. S. J. Lippard, *Acc. Chem. Res.* 1978, **11**, 211.

4. J. J. Roberts and A. J. Thomson, The mechanism of action of antitumour platinum compounds, in *Progress in Nucleic Acid Research and Molecular Biology* (Edited by W. E. Cohn), Vol. 22, p. 71. Academic Press, New York (1979).
5. J. J. Roberts, Cisplatin in *Cancer Chemotherapy Annual* (Edited by B. A. Chabner and H. M. Pinedo), p. 95. Excerpta Medica, Amsterdam (1983).
6. S. Mansy, R. Rosenberg and A. J. Thomson, *J. Am. Chem. Soc.* 1973, **95**, 1633.
7. A. B. Robins, *Chem. Biol. Interactions* 1973, **6**, 35.
8. R. Bau, in *Proceedings, International Conference on the Chemistry of Platinum Group Metals*, Bristol, P.A5, Royal Society of Chemistry (1981).
9. F. E. Wood, C. T. Hunt and A. L. Balch, *Inorg. Chim. Acta* 1982, **67**, L19.
10. A. B. Robins, *Chem. Biol. Interactions* 1973, **11**, 6.
11. P. Horáček and J. Drobník, *Biochim. Biophys. Acta* 1971, **254**, 341.
12. P. Umapathy and R. A. Harnesswala, *Polyhedron* 1983, **2**, 129.
13. G. Brauer, *Handbook of Preparative Inorganic Chemistry*, 2nd edn., Vol. 2, pp. 1572, 1584. Academic Press, New York (1965).
14. G. A. Shagisultanova, *Russ. J. Inorg. Chem.* 1961, **6**, 904.
15. L. E. Cox and D. G. Peters, *Inorg. Chem.* 1970, **9**, 1927.
16. R. Layton, D. W. Sink and J. R. Durig, *J. Inorg. Nucl. Chem.* 1966, **28**, 1965.
17. J. S. Coe and J. R. Lyons, *Inorg. Chem.* 1970, **9**, 1775.
18. J. Mtochowski and Z. Skrowaczewska, *Rocniki Chem.* 1973, **47**, 2255.
19. *BIOS report*, 1404.
20. M. C. P. Gillet, C. Houssier and E. Fredericq, *Chem. Biol. Interactions* 1979, **25**, 87.
21. H. J. S. King, *J. Chem. Soc.* 1938, 1338.
22. M. J. Cleare, *Coord. Chem. Rev.* 1974, **12**, 349.
23. R. Faggiani, B. Lippert, C. J. L. Lock and B. Rosenberg, *J. Am. Chem. Soc.* 1977, **99**, 777.
24. R. Faggiani, B. Lippert, C. J. L. Lock and B. Rosenberg, *Inorg. Chem.* 1977, **16**, 1192.
25. R. Faggiani, B. Lippert, C. J. L. Lock and B. Rosenberg, *Inorg. Chem.* 1978, **17**, 1941.
26. B. Lippert, C. J. L. Lock, B. Rosenberg and M. Zvagulis, *Inorg. Chem.* 1978, **17**, 2971.
27. C. J. Boreham, J. A. Broomhead and D. P. Fairlie, *Aust. J. Chem.* 1981, **34**, 659.
28. L. L. Munchaussen and R. O. Rahan, *Biochim. Biophys. Acta* 1975, **414**, 242.
29. J. P. Macquet and L. L. Butour, *J. Clin. Hematol. Oncol. Wadley Med. Bull.* 1977, **7**, 469.
30. K. Inagaki and Y. Kidani, *Inorg. Chim. Acta* 1980, **46**, 35.
31. G. Onori and D. Blidaru Salandi, *Inorg. Chim. Acta* 1983, **80**, 197.
32. G. Y. H. Chu and R. S. Tobias, *J. Am. Chem. Soc.* 1976, **98**, 2641.
33. W. M. Scovell and T. O'Connor, *J. Am. Chem. Soc.* 1977, **99**, 120.
34. M. M. Millard, J. P. Macquet and T. Theophanides, *Biochim. Biophys. Acta* 1975, **402**, 166.
35. E. A. Johnson, Inorganic systems, in *U.V. Atlas of Organic Compounds* (Edited by H. H. Perkampus, I. Sandeman and C. J. Timmons), Vol. V, K_2/ I. Butterworths, London (1971).
36. A. Szent-Györgyi, *Enzymes: Units of Biological Structure and Functions* (Edited by O. H. Gaebler), p. 393. Academic Press, New York (1956).
37. H. A. Tajmir-Riahi and T. Theophanides, *Inorg. Chim. Acta* 1983, **80**, 183.
38. S. Louie and R. Bau, *J. Am. Chem. Soc.* 1977, **99**, 387.
39. G. R. Clark and J. D. Orbell, *J. Chem. Soc., Chem. Commun.* 1975, 697.
40. R. Bau, R. W. Gellert and S. K. Shiba, *Abstracts of the Seventh International Conference on Organometallic Compounds*, p. 238. Venice, Italy (1975).
41. M. C. Lim and R. B. Martin, *J. Inorg. Nucl. Chem.* 1976, **38**, 1915.
42. U. K. Häring and R. B. Martin, *Inorg. Chim. Acta* 1983, **80**, 1.
43. K. H. Scheller, V. Scheller-Krattigev and R. B. Martin, *J. Am. Chem. Soc.* 1981, **103**, 6833.
44. G. Pneumatikakis, *Inorg. Chim. Acta* 1983, **80**, 89.
45. P. Brant, J. H. Enemark and A. L. Balch, *J. Organometal. Chem.* 1976, **114**, 99.
46. W. M. Riggs, *Anal. Chem.* 1972, **44**, 830.
47. W. E. Moddeman, J. R. Blackburn, G. Kumar, K. A. Morgan, R. G. Albridge and M. M. Jones, *Inorg. Chem.* 1972, **11**, 1715.
48. C. W. Fryer and J. A. S. Smith, *J. Chem. Soc.* (*A*) 1970, 1029.
49. D. T. Clark, D. B. Adams and D. Briggs, *J. Chem. Soc., Chem. Commun.* 1971, 602.
50. J. R. Durig, R. Layton, D. W. Sink and B. R. Mitchell, *Spectrochim. Acta* 1965, **21**, 1367.
51. C. H. Perry, D. P. Athans, E. F. Young, J. R. Durig and B. R. Mitchell, *Spectrochim. Acta* 1967, **23A**, 1137.
52. D. M. Adams and P. J. Chandler, *J. Chem. Soc.* 1967, A, 1009.
53. R. Faggiani, H. E. Howard-Lock, C. J. L. Lock, B. Lippert and B. Rosenberg, *Can. J. Chem.* 1982, **60**, 529.

Polyhedron Vol. 4, No. 9, pp. 1603–1609, 1985
Printed in Great Britain

0277-5387/85 $3.00 + .00
© 1985 Pergamon Press Ltd

ROLE OF SECONDARY LIGANDS IN THE STRUCTURE AND STABILITY OF METAL–CYTIDINE COMPLEXES IN SOLUTION

PULIMAMIDI RABINDRA REDDY* and V. B. MALLESWARA RAO
Department of Chemistry, Osmania University, Hyderabad—500007, India

(*Received* 18 *February* 1985; *accepted* 27 *March* 1985)

Abstract—The interaction of Cu(II), Ni(II), Zn(II), Mn(II), Co(II), Mg and Ca ions with cytidine and the biologically important ligands histidine, histamine, glycine and oxalic acid in a 1:1:1 ratio have been investigated by potentiometric equilibrium measurements at 35°C and 0.10 M (KNO_3) ionic strength. These investigations were undertaken to assess the influence of the secondary ligands on the structure and stability of the 1:1 metal–cytidine system. The stability of the binary and ternary complexes has been compared. The enhanced stability of the ternary complexes was measured in terms of Δ log K, the difference between the ternary and binary complexes. The involvement of various donor sites of histidine in metal binding was specially discussed. A general conclusion drawn from this investigation is that aromatic ligands formed more stable complexes than aliphatic ligands. This is attributed to the stacking phenomenon.

Mixed-ligand complexes are gaining importance because they provide models for metalloenzyme reactions in biological systems.[1–3] The ternary complexes of nucleosides and nucleotides in particular have attracted the attention of many scientists throughout the world.[4–11] This is mainly because of the fact that metal ions participate in almost all biological processes involving nucleic acids, the winding and unwinding of the DNA helix being controlled by certain metal ions, apart from their being involved in other important biochemical processes like replication,[12,13] transcription[14,15] and translation[16] reactions. These studies (on the metal–nucleoside and metal–nucleotide interactions) have explained to some extent the specific and selective interactions that take place in many biological systems. However, much more information is needed before one can come to clear conclusions about the reactions that occur *in vivo*. One of the important aspects concerned with the ternary complexes is the influence of secondary ligands on the 1:1 metal–ligand complex. This influence becomes much more important when the secondary ligands are capable of participating in electrostatic,[17] hydrophobic[18] and stacking[19,20] interactions. We have been involved for some time in the study of ternary complexes involving nucleosides and nucleotides, which act as model systems for metal–nucleic acid interactions. The study of metal–nucleic acid interactions at the monomer level has a definite advantage over polymeric species because one can selectively eliminate or modify certain groups to obtain the necessary information about these reactions in solution.

Earlier work on the ternary complexes of cytidine was confined mainly to Th(IV) and UO_2(II),[21] and EPR and electronic absorption studies on the interaction of Cu(II)–glyglyglycine complexes.[22]

In the present paper we describe a detailed physicochemical investigation of the interaction of transition and alkaline earth metal ions with cytidine and biologically important secondary ligands to see the role of these ligands (secondary) on the structure and stability of metal–cytidine complexes in solution.

EXPERIMENTAL

Cytidine, glycine, histidine and histamine were obtained from Sigma (U.S.A.) and oxalic acid from Fluka (Switzerland). For every titration, fresh solid ligands were weighed out into the reaction cell to avoid possible hydrolysis. Transition and alkaline earth metal ions [Cu(II), Ni(II), Zn(II), Co(II), Mn(II), Mg and Ca] were of AnalaR grade and were standardized volumetrically by titration with the

* Author to whom correspondence should be addressed.

disodium salt of ethylenediamine tetraacetic acid in the presence of a suitable indicator as outlined by Schwarzenbach.[23] Carbonate-free sodium hydroxide was prepared by the method of Schwarzenbach and Biedermann.[24]

The experimental method employed consisted of potentiometric titration of the ligands with standard sodium hydroxide solution, in the absence and presence of the above-mentioned metal ions. The ionic strength was maintained constant by using 0.10 M (KNO_3) as the supporting electrolyte and relatively low concentrations of the ligand and metal ion (1×10^{-3} M). During the course of the titrations a stream of nitrogen was passed over the solution to eliminate the adverse effect of atmospheric carbon dioxide.

A Digisun digital pH meter (model DI-707) with a combination electrode was used to determine the hydrogen ion concentration. The electrode system was calibrated by direct titration of acetic acid, the observed pH meter reading was compared with the actual hydrogen ion concentration, and the pH regions below 3.5 and above 10.5 were calibrated by measurement in HCl and NaOH solutions, respectively.

CALCULATIONS

Dissociation constants

The acid dissociation constants of the primary ligand cytidine and the secondary ligands glycine, histidine, histamine and oxalic acid were calculated by the usual algebraic method.

Formation constants

To calculate the stability constants of the ternary complexes of Cu(II), Ni(II), Zn(II) and Co(II) with cytidine and histidine in a 1 : 1 : 1 ratio the following equations were employed [eqns (1)–(11)] (charges are omitted for clarity):

$$M + HL + H_2A \overset{K_1'}{\rightleftharpoons} MLA + 3H^+, \quad (1)$$

$$M + L + A \overset{K^M_{MLA}}{\rightleftharpoons} MLA, \quad (2)$$

$$K^M_{MLA} = \frac{T_M - [M]}{[M][L][A]}, \quad (3)$$

$$[M] = QL \quad \text{or} \quad PA \quad (4)$$

$$[L] = \frac{P\alpha}{QX + PY}, \quad (5)$$

$$[A] = \frac{Q\alpha}{QX + PY}, \quad (6)$$

$$\alpha = AX + LY, \quad (7)$$

$$X = \frac{3[H]^2}{K_aK_{2a}} + \frac{2[H]}{K_{2a}} \quad (8)$$

$$P = \frac{[H]^2}{K_aK_{2a}} + \frac{[H]}{K_{2a}} + 1 \quad (9)$$

(8), (9): using K_a and K_{2a} values of histidine

$$Y = \frac{3[H]}{K_a} + 2 \quad (10)$$

$$Q = \frac{[H]}{K_a} + 1 \quad (11)$$

(10), (11): using K_a values of cytidine

Equations (1)–(11) were also employed to calculate the stability constants of the ternary complexes of Cu(II), Ni(II), Zn(II) and Co(II) with cytidine and histamine, the ternary complex of Cu(II) with cytidine and glycine and the ternary complexes of Cu(II), Ni(II), Zn(II), Co(II), Mn(II), Mg and Ca with cytidine and oxalic acid in a 1 : 1 : 1 ratio.

For the ternary complexes of Mn(II), Ca and Mg with cytidine and histidine in a 1 : 1 : 1 ratio eqns (12)–(27) were used. In the buffer region between $a = 0$ and $a = 2$:

$$M + HL + H_2A \overset{K_2'}{\rightleftharpoons} [M(HA)L] + 2H^+, \quad (12)$$

$$M + HA + L \overset{K^M_{M(HA)L}}{\rightleftharpoons} [M(HA)L], \quad (13)$$

$$K^M_{M(HA)L} = \frac{T_M - [M]}{[M][HA][L]}, \quad (14)$$

$$[M] = QL \quad \text{or} \quad PA, \quad (15)$$

$$L = \frac{P\alpha}{QX + PY}, \quad (16)$$

$$A = \frac{Q\alpha}{QX + PY}, \quad (17)$$

$$\alpha = AX + LY, \quad (18)$$

$$X = \frac{2[H]^2}{K_aK_{2a}} + \frac{[H]}{K_{2a}} \quad (19)$$

$$P = \frac{[H]^2}{K_aK_{2a}} + \frac{[H]}{K_{2a}} \quad (20)$$

(19), (20): using K_a and K_{2a} values of histidine

$$Y = \frac{2[H]}{K_a} + 1, \quad (21)$$

$$Q = \frac{[H]}{K_a} + 1. \quad (22)$$

In the buffer region between $a = 2$ and $a = 3$ the following equations are used:

$$[M(HA)L] \overset{K_2'}{\rightleftharpoons} MLA + H^+, \quad (23)$$

$$M + L + A \overset{K^{M(HA)L}_{MLA}}{\rightleftharpoons} MLA, \quad (24)$$

$$K^{M(HA)L}_{MLA} = \frac{T_M - M}{[M][A]}, \quad (25)$$

$$[M] = A\left[\frac{H}{K_{2a}} + 1\right] \quad \text{using } K_{2a} \text{ values of histidine} \quad (26)$$

$$A = \frac{\alpha}{H/K_{2a}} \quad (27)$$

$$\alpha = (1-a)T_M - H^+ + OH^-. \quad (28)$$

In eqns (25) and (26) "M" equals M(HA)L.

For eqns (1)–(27) HL = monoprotonated cytidine, H_2A = monoprotonated histidine, and T_M = total metal ion species present in solution.

Equations (12)–(27) were also employed to calculate the stability constants of the ternary complexes of Mn(II), Mg and Ca with cytidine and histamine and the ternary complexes of Ni(II), Zn(II), Co(II), Mn(II), Mg and Ca with cytidine and glycine in a 1 : 1 : 1 ratio.

RESULTS

The proton dissociation constants of the ligands cytidine, glycine, histidine, histamine and oxalic acid are presented in Table 1.

Table 1. Acid dissociation constants of the ligands: temperature = 35°C, μ = 0.10 mol dm^{-3} (KNO_3)

Ligand	pK_a	pK_{2a}
Cytidine	4.15±0.04	—
Glycine	2.50±0.02	9.75±0.02
Histidine	6.00±0.04	9.00±0.04
Histamine	5.87±0.04	9.63±0.04
Oxalic acid	2.18±0.05	4.20±0.05

Metal : cytidine : glycine system (1 : 1 : 1)

The mixed-ligand titration curve of Cu(II)–cytidine–glycine given in Fig. 1(e) shows an inflection at m = 3 (where "m" is mol of base added per mol of metal ion), indicating simultaneous formation of a 1 : 1 : 1 mixed-ligand complex in the entire buffer region between m = 0 and m = 3. The constant K^M_{MLA} was calculated with the help of eqn (3) and presented in Table 2. The titration curve for all the other metal ions resulted in an inflection at m = 2, indicating the formation of a monopronated complex and the constant $K^M_{M(HA)L}$ was calculated with the help of the eqn (14). The constant $K^{M(HA)L}_{MLA}$ was, however, calculated in the buffer region between m = 2 and m = 3 using eqn (24). All the constants so calculated are listed in Table 2.

Metal : cytidine : histidine system (1 : 1 : 1)

The mixed-ligand titration curve of Cu(II) with cytidine and histidine in a 1 : 1 : 1 ratio is given in Fig. 1(d), resulting in an inflection at m = 3, indicating the simultaneous formation of a 1 : 1 : 1 complex in the

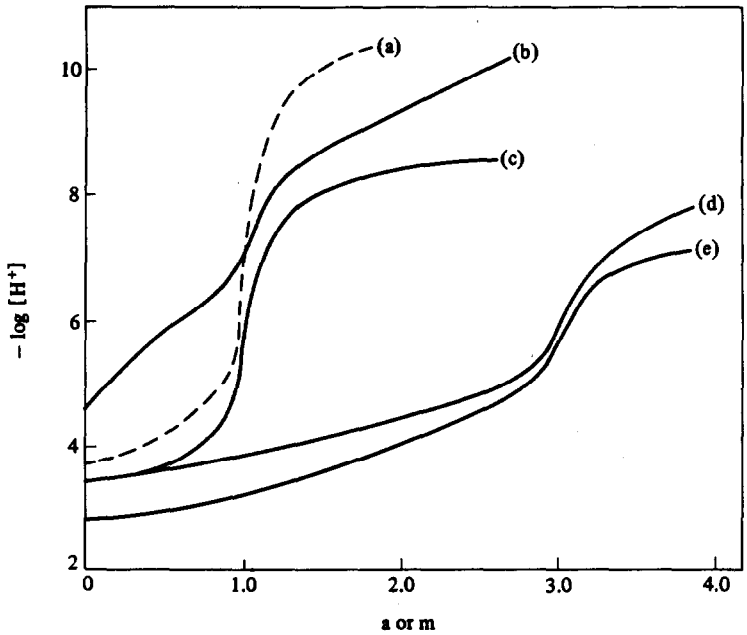


Fig. 1. Potentiometric titration curves for Cu(II)–cytidine–glycine and Cu(II)–cytidine–histidine systems in a 1 : 1 : 1 ratio at 35°C, μ = 0.10 M (KNO_3). (a) Free cytidine, (b) free histidine, (c) free glycine, (d) Cu(II)–cytidine–histidine, and (e) Cu(II)–cytidine–glycine. m, mol of base added per mol of metal ion [for curves (d) and (e); a, mol of base added per mol of ligand [for curves (a)–(c)].

Table 2. Stability constants[a] of the binary and ternary complexes of cytidine (HL) with glycine (H_2A) and oxalic acid (H_2A): temperature = 35°C, μ = 0.10 mol dm^{-3} (KNO_3)

Metal ion	Metal:cytidine (1:1)	Metal:glycine (1:1)	Metal:cytidine:glycine (1:1:1)			Metal:oxalic acid (1:1)	Metal:cytidine:oxalic acid (1:1:1)
	K^{M}_{ML}	K^{M}_{MA}	$K^{M}_{M(HA)L}$	$K^{M(HA)L}_{MLA}$	K^{M}_{MLA}	K^{M}_{MA}	K^{M}_{MLA}
Cu(II)	3.19	8.61			13.85	6.16	9.93
Ni(II)	2.94	5.92	8.56	5.72		5.23	9.31
Zn(II)	2.60	5.22	8.23	5.54		5.31	9.40
Co(II)	2.74	5.50	8.03	5.10		4.97	9.17
Mn(II)	2.51	3.85	8.16	3.79		5.14	9.53
Mg	2.42	3.40	8.19	3.59		4.65	8.81
Ca	2.47	3.58	8.24	3.63		4.85	8.80

[a] Deviations are omitted for clarity.

entire buffer region between $m = 0$ and $m = 3$. The constant K^{M}_{MLA} was calculated with the help of the eqn (3). Similar trends were observed for Ni(II), Zn(II) and Co(II). The constants so calculated are presented in Table 3.

However, in the case of the other metal ions [Mn(II), Mg and Ca] an inflection was obtained at $m = 2$, indicating the formation of a monoprotonated complex in the region between $m = 0$ and $m = 2$. The constant $K^{M}_{M(HA)L}$ was calculated using eqn (14). The constant $K^{M(HA)L}_{MLA}$ was also calculated in the buffer region between $m = 2$ and $m = 3$ with the help of eqn (24). All the constants thus calculated are listed in Table 3.

Metal:cytidine:histamine (1:1:1)

This system is exactly similar to the metal:cytidine:histidine system. The constants thus calculated are presented in Table 3.

Metal:cytidine:oxalic acid system (1:1:1)

The titration curve of all the metal ions showed an inflection at $m = 3$, indicating the simultaneous formation of a 1:1:1 mixed-ligand complex in the entire buffer region between $m = 0$ and $m = 3$. The constants were calculated with the help of eqn (3) and presented in Table 2.

DISCUSSION

In the ternary system there exist two types of complexes: (i) complexes in which interligand interactions (electrostatic, hydrophobic and stacking) occur; and (ii) complexes in which there is no such interaction. These interligand interactions have been found to be most effective in deciding the stability of the ternary complexes in solution along with other factors like the nature of the metal ion, the geometry of the metal complex and the solvent effects

Table 3. Stability constants[a] of the binary and ternary complexes of cytidine (HL) with histidine (H_2A) and histamine (H_2A): temperature = 35°C, μ = 0.10 mol dm^{-3} (KNO_3)

Metal ion	Metal:cytidine (1:1)	Metal:histidine (1:1)		Metal:cytidine:histidine (1:1:1)			Metal:histamine (1:1)		Metal:cytidine:histamine (1:1:1)		
	K^{M}_{ML}	$K^{M}_{M(HA)}$	K^{M}_{MA}	$K^{M}_{M(HA)L}$	$K^{M(HA)L}_{MLA}$	K^{M}_{MLA}	$K^{M}_{M(HA)}$	K^{M}_{MA}	$K^{M}_{M(HA)L}$	$K^{M(HA)L}_{MLA}$	K^{M}_{MLA}
Cu(II)	3.19		10.02			14.23		8.98			14.42
Ni(II)	2.94		8.42			13.48		6.36			12.65
Zn(II)	2.60		6.35			11.95		6.11			11.73
Co(II)	2.74		7.00			12.69		5.98			11.87
Mn(II)	2.51		6.26	8.43	3.91		3.02		8.36	3.48	
Mg	2.42	3.35		8.90	2.58		2.44		8.48	2.96	
Ca	2.47	3.10		8.72	2.79		2.32		8.63	3.13	

[a] Deviations are omitted for clarity.

etc. These interactions (interligand) become more pertinent when the ligands participate in stacking interactions, but what is intriguing is that even this stacking interaction is neither automatic nor universal. Our experience[9–11,19] shows that this phenomenon (stacking) not only varies from ligand to ligand but also from metal ion to metal ion, indicating the high selectivity and specificity of the reactants in solution. Usually, the role of secondary ligands on the stability of 1:1 metal–ligand complexes is quantified in terms of $\Delta \log K$. $\Delta \log K$ is the difference between the overall 1:1:1 ternary complexes and the corresponding 1:1 binary complexes. Thus, if the $\Delta \log K$ values are positive, the ternary complexes are more stable than the binary complexes and, if they are negative, the binary complexes are more stable than the ternary complexes. However, it should be noted here that negative values of $\Delta \log K$ do not preclude the formation of ternary complexes in solution. A detailed discussion on the subject is found elsewhere.[11,25]

It was mentioned in one of the recent papers[26] that $\Delta \log K$ values are influenced by the stability constants of simple complexes. As there is no ambiguity about this observation (since ternary complexes are the combination of individual binary systems also) what is important here is the extent to which the two ligands influence the metal in the presence of each other compared to simple 1:1 parent complexes, affecting the coordination modes of the ligands and geometry of the complex as a whole. Therefore whatever information one gets out of $\Delta \log K$ values is still worthwhile.

Table 4 presents the $\Delta \log K$ values for the various systems studied. It can be seen that $\Delta \log K$ values are positive for all the systems studied. Various factors like charge neutralization, the π-accepting capacity of the secondary ligands and stacking interaction are reponsible for this extra stability found in ternary complexes.

First, let us compare the $\Delta \log K$ values for the

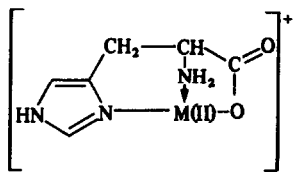


Fig. 2. Tentative structure of 1:1 metal–histidine showing the involvement of all available donor sites in metal coordination.

systems where interligand interactions are absent (glycine and oxalic acid systems). The $\Delta \log K$ values in the case of the glycine system are reported (Table 4) only for Cu(II) and the corresponding values for the other metal ions could not be computed owing to the formation of different types of complexes in binary and ternary systems. The $\Delta \log K$ value of the Cu(II)–cytidine–glycine system is more positive compared to the corresponding value of the oxalic acid system, although both ligands are aliphatic. This is due to the involvement of hetero-donor atoms in metal coordination in the case of the glycine system. The enhancement of the stability when mixed-donor atoms are involved has been reported for other related systems.[9,10,27] This is also supported by electrostatic molecular potential calculations.[28] In the case of the systems where interligand interactions are expected (the histidine and histamine systems), the $\Delta \log K$ values of histidine are less positive than the corresponding values of histamine complexes for all the metal ions investigated. This is exactly the reverse trend to that observed for their 1:1 complexes. In 1:1 complexes histidine forms more stable complexes than histamine, suggesting a different mode of coordination [involving amino, imidazole and carboxylate groups (Fig. 2)], but in ternary complexes the closeness in the values of $\Delta \log K$ (though a little more positive in the case of histamine) suggests that the mode of binding in ternary complexes is most probably similar in both of the ligands. This means

Table 4. $\Delta \log K$ values for various metal–ligand systems in solution: temperature = 35°C, $\mu = 0.10\ \text{mol dm}^{-3}$ (KNO_3)

Metal ion	Metal:cytidine: glycine (1:1:1)	Metal:cytidine: histidine (1:1:1)	Metal:cytidine: histamine (1:1:1)	Metal:cytidine: oxalic acid (1:1:1)
Cu(II)	+2.05	+2.02	+2.25	+0.58
Ni(II)	—	+2.12	+2.35	+1.14
Zn(II)	—	+2.98	+3.02	+1.49
Co(II)	—	+2.95	+3.15	+1.46
Mn(II)	—	—	+2.83	+1.88
Mg	—	+3.13	+3.62	+1.74
Ca	—	+3.15	+3.84	+1.48

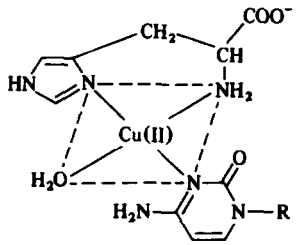


Fig. 3. Tentative structure of 1:1:1 Cu(II)–cytidine–histidine showing the histamine-like coordination: R = ribose.

that, in ternary complexes, histidine is acting in a histamine-like way, involving only amino and imidazole groups in metal coordination (Fig. 3). The interesting question that then arises is what is the status of the carboxylate group. It is likely that a hydrogen-bonding type of interaction between the

and NH_2 of cytidine takes place, as a result of

which the C—O group is kept away from the metal coordination.

It is significant to mention here the very recent work of Arena *et al.*,[26] where similar observations were made in the case of the Cu(II)–ATP–histidine system. Such an interaction disfavours the formation of ternary complexes in solution by an entropy factor, as the ligands become more rigid as a consequence of the bridge between the two-noncoordination groups and also due to the different degree's of solvent interaction with the metal ion. This may be the reason for the less positive values of $\Delta \log K$ in histidine complexes compared to those with histamine.

In general, for the systems under investigation, the $\Delta \log K$ values of Cu(II) are less positive than for the rest of the metal ions studied. This may be due to the lower coordination number of Cu(II) compared to other metal ions whose coordination number is more certain. Finally, the $\Delta \log K$ values are controlled and significantly contributed to by the nature of the secondary ligands, and the ligands which participate in stacking interaction (aromatic ligands) result in the formation of more stable ternary complexes (more positive $\Delta \log K$ values). Within the aromatic ligands the non-coordinating side chain affects the stacking interaction at least to some extent.

Based on the above conclusions we propose the following tentative structure for metal–cytidine–histamine complexes in solution (Fig. 4).

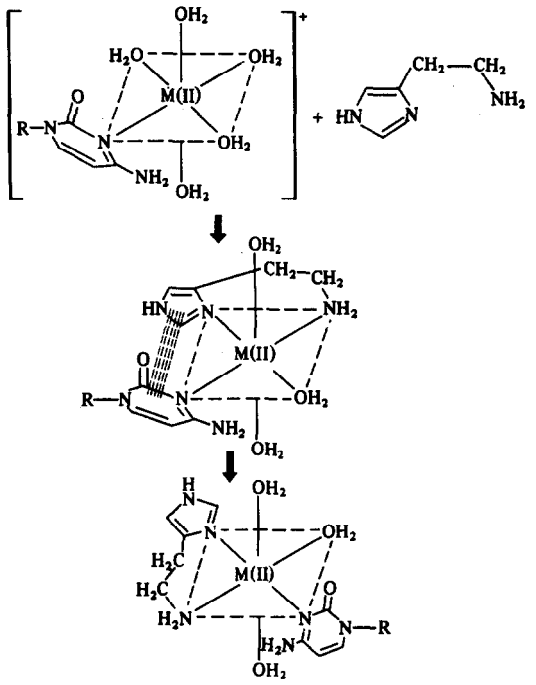


Fig. 4. Model illustrating the stacking interaction followed by coordination in H_2O: R = ribose (metal–cytidine–histamine complex).

Acknowledgement—One of us (V.B.M.R.) is grateful to CSIR, New Delhi, for a junior research fellowship.

REFERENCES

1. H. Sigel, In *Advances in Solution Chemistry* (Edited by I. Bertini, L. Lunazzi and A. Dei), p. 149. Plenum, New York (1981).
2. C. Helene, J. L. Dimicoli and F. Brun, *Biochemistry* 1971, **10**, 3802.
3. C. Helene, *Nucleic Acid Res.* 1975, **2**, 961.
4. R. M. Izzatt, J. J. Christensen and J. J. Rytting, *Chem. Rev.* 1971, **71**, 439.
5. H. Sigel (Ed.), In *Metal Ions in Biological Systems*, Vol. 2, Chap. 2. Marcel Dekker, New York (1973).
6. R. B. Martin and Y. H. Mariam, In *Metal Ions in Biological Systems* (Edited by H. Sigel), Chap. 2. Marcel Dekker, New York (1979).
7. R. P. Martin, M. M. Petit-Ramel and J. P. Scharff, In *Metal Ions in Biological Systems* (Edited by H. Sigel), Vol. 2, Chap. 1. Marcel Dekker, New York (1973).
8. M. M. T. Khan and P. R. Reddy, *J. Inorg. Nucl. Chem.* 1973, **35**, 2821.
9. P. R. Reddy, K. V. Reddy and M. M. T. Khan, *J. Inorg. Nucl. Chem.* 1979, **41**, 423.
10. P. R. Reddy and M. H. Reddy, *Polyhedron* 1983, **2**, 1171.
11. P. R. Reddy and M. H. Reddy, *J. Chem. Soc., Dalton Trans.* 1985, 239.
12. M. J. McCarthy, *J. Gen. Physiol.* 1941, **29**, 123.
13. J. P. Slater, I. Tamir, L. A. Loeb and A. S. Mildman, *J. Biol. Chem.* 1972, **247**, 6784.

14. P. Ballard and H. G. Nathams-Ashman, *Nature (London)* 1964, **203**, 150.
15. C. C. Widnell and R. J. Tata, *Biochem. J.* 1964, **92**, 313.
16. G. L. Eichhorn, In *Inorganic Biochemistry* (Edited by G. L. Eichhorn), Vol. 2, p. 1210. Elsevier, Amsterdam (1973).
17. K. Gopalkirshnan and P. K. Bhattacharya, *J. Chem. Soc., Dalton Trans.* 1981, 543.
18. H. Sigel, B. E. Fisher and E. Farkas, *Inorg. Chem.* 1983, **22**, 925.
19. P. R. Reddy, M. H. Reddy and K. V. Reddy, *Inorg. Chem.* 1984, **23**, 974.
20. K. H. Scheller, F. Hofstetter, P. R. Mitchell, B. Prijs and H. Sigel, *J. Am. Chem. Soc.* 1981, **103**, 247.
21. K. Ramalingam and C. R. Krishnamoorthy, *Inorg. Chim. Acta* 1982, **67**, 167.
22. S. V. Deshpande, R. K. Sharma and T. S. Srivastava, *Inorg. Chim. Acta* 1983, **78**, 13.
23. G. Schwarzenbach, *Complexometric Titrations*, p. 77. Interscience, New York (1957).
24. G. Schwarzenbach and R. Biedermann, *Helv. Chim. Acta* 1948, **31**, 331.
25. H. Sigel, *Angew. Chem., Int. Ed. Engl.* 1975, **14**, 394.
26. G. Arena, R. Coll, V. Cucinolta, S. Musumeci, E. Rizzarelli and S. Sammaratano, *J. Chem. Soc., Dalton Trans.* 1984, 1651.
27. G. Ostacoli, In *Bioenergetics and Thermodynamics Model Systems* (Edited by A. Braibanti), p. 181. D. Reidel, Dordrecht (1980).
28. R. Bonaccorsi, A. Pullman, E. Scrocco and J. Tomasi, *Theor. Chim. Acta* 1972, **24**, 51.

Polyhedron Vol. 4, No. 9, pp. 1611–1615, 1985
Printed in Great Britain

0277–5387/85 $3.00 + .00
© 1985 Pergamon Press Ltd

^{1}H NMR STUDY OF ISOMERIZATION IN CHLOROTIN(IV) TERNARY COMPLEXES OF 8-QUINOLINOL AND 5,7-DICHLORO-8-QUINOLINOL

J. L. NIETO* and F. GALINDO
Instituto de Estructura de la Materia, Consejo Superior de Investigaciones Científicas, Serrano 119, 28006 Madrid, España

and

A. M. GUTIÉRREZ
Departamento de Química Analítica, Facultad Químicas. Universidad Complutense, 28040 Madrid, España

(*Received* 30 *January* 1985; *accepted* 27 *March* 1985)

Abstract—A complete analysis of the temperature dependence (−30 to 52°C) of the ^{1}H NMR spectra in *d*-chloroform of the ternary complexes, bis-(8-quinolinato)tin(IV) dichloride and bis-(5,7-dichloro-8-quinolinato)tin(IV) dichloride has been performed. The intramolecular character of the exchange process has been established, and the spectra have been analyzed by the total lineshape method in terms of the interconversion of two isomers, the *cis–cis–trans* and the *cis–trans–cis* (with respect to Cl, N and O atoms), including the tin–proton couplings in the simulations. Arrhenius parameters of the process were $E_a = 54 \pm 1$ and $52 + 1$ kJ mol^{-1}, and log $A = 11.8 \pm 0.2$ and 11.7 ± 0.3, respectively, for the two complexes. The similarity of the activation parameters obtained for both complexes indicates that the presence of bulky Cl atoms in the 8-quinolinol ring had no appreciable energetic influence on the isomerization process. Data were compared with those reported for other chlorinated hexacoordinated complexes, involving ligands other than the 8-quinolinol ring.

Descriptions of chelates of tri- and tetravalent metals (including tin) with the ligand 8-quinolinol can be found in the literature.[1–11] However, no activation data on isomerization equilibria have been reported as far as we know, probably due to the difficulties in obtaining NMR spectra of such chelates that show limited solubility, specially when carbon–metal bonds are absent. The structure and ^{1}H NMR spectra at low temperature (−30°C) of the chlorotin(IV) ternary complexes with 8-quinolinol and derivatives have been characterized very recently,[12] and, in view of the scarcity of data, we considered it interesting to study the temperature dependences of the NMR spectra in order to obtain activation parameters of the isomerization equilibrium.

In this work, a complete analysis of the temperature dependence of the ^{1}H NMR spectra of the ternary complexes bis-(8-quinolinato)tin(IV) dichloride (Cl_2SnQ_2) and bis-(5,7-dichloro-8-quinolinato)tin(IV) dichloride [$Cl_2Sn(CQ)_2$] has been carried out and the activation parameters of the isomer exchange process obtained. The total-line shape method, with visual comparison between experimental and computed spectra, has been employed, and the whole ^{1}H NMR spectrum, including the tin–proton couplings, computed.

EXPERIMENTAL

Materials

Details of the preparation of the complexes have been reported previously.[13] Chloroform was chosen as the solvent because it represented a compromise between solubility, availability in a high degree of deuteration, thus reducing dynamic range problems in the NMR spectrum, and the absence of signals in the region of interest (Stholer Isotope Inc., 99.98% $CDCl_3$ was used).

* Author to whom correspondence should be addressed.

NMR spectra

These were recorded at 360 MHz in a Bruker WM-360 Fourier spectrometer. Flip angles of 70°, 16 K of memory, 10,000 scans and 2-s relaxation delays were typical recording conditions. Saturated solutions of the complexes in *d*-chloroform were used. Variable-temperature spectra were obtained with a standard accessory by flushing the sample with cool N_2 or heated air, and the temperature was calibrated with a methanol thermometer.[14] The signal-to-noise ratio of exchange-broadened spectra was somewhat critical in the complex of lowest solubility (Cl_2SnQ_2), so that a moderate digital filtering (line-broadening factor of 1 Hz) was employed in that case.

Spectral simulations

These were carried out by the Binsch program,[15,16] modified by us to include the tin–proton couplings in the calculations. The NMR spectrum of the $Cl_2Sn(CQ)_2$ complex was simulated as the sum of three independent spin subsystems, $H_2H_3H_4H_6$, H_6Sn and $H_2H_3H_4Sn$, with relative intensities in accordance with natural isotopic abundances. In an analogous way, the Cl_2SnQ_2 spectrum was decomposed into four spin subsystems, namely $H_2H_3H_4$, $H_5H_6H_7$, $H_2H_3H_4Sn$ and $H_5H_6H_7Sn$. The whole ^1H NMR spectrum was computed for both complexes and, using an adequate expanded scale, visually compared with the experimental one. The introduction of the tin–proton couplings in the simulations has proved to be necessary to obtain a good agreement between experimental and computed line shapes. Static parameters and isomer populations were those given in Ref. 12; a 2-Hz linewidth in the absence of exchange was used. Tin–proton coupling constants that were not available for the Cl_2SnQ_2 complex were transferred from the $Cl_2Sn(CQ)_2$ one.

The low-temperature spectra evidenced that the chemical shifts were appreciably temperature-dependent only in the case of the Cl_2SnQ_2 complex, so that they were extrapolated in that case through the full temperature range, following the criterion of resemblance with the experimental spectrum recommended by Szymanski *et al.*[17]

RESULTS AND DISCUSSION

In the absence of exchange at low temperature, the NMR spectra of the complexes show sharp lines, corresponding to the presence in solution of only two appreciably populated isomers,[12] namely *cis–cis–trans* and *cis–trans–cis* with respect to the Cl, N and O atoms (see Fig. 1). As the temperature is raised, the NMR lines begin to broaden, indicating that an

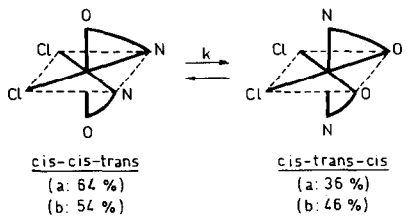


Fig. 1. Isomer exchange and populations of the Cl_2SnQ_2 (a) and $Cl_2Sn(CQ)_2$ (b) complexes.

exchange process is taking place. The intramolecular character of such an exchange is supported by two facts. First, the appearance of sharp NMR signals corresponding to protons of the free ligands when they are added to the complexes, at temperatures where signals of the complexes are extensively exchange-broadened. Second, the absence of appreciable changes in the linewidths of the NMR signals following a significant change in the concentration of the complexes (10-fold dilution, monitored at 2°C where lineshapes are sensitive to rate constant changes).

The analysis of the NMR spectra in terms of an intramolecular exchange between two unequally populated sites, gives the first-order rate constants, *k*, that provide the best fit between experimental and computed spectra. Table 1 lists the best-fit rate constants, at each temperature, obtained for both complexes. The degree of agreement between experimental and computed spectra is illustrated for some of the temperatures, in Figs 2 and 3. It can be seen that the agreement is good in all the spectral regions corresponding to the different protons of the ligand rings.

Arrhenius (see Fig. 4) and Eyring plots were obtained for both complexes. A good linearity was found for $Cl_2Sn(CQ)_2$ in the whole range of

Table 1. Rate constants, *k*, that reproduce the experimental ^1H NMR spectra of the complexes

Cl_2SnQ_2		$Cl_2Sn(CQ)_2$	
T (°C)	*k* (s^{-1})	*T* (°C)	*k* (s^{-1})
−7	4	−30	3
2	20	−15	12
9	50	−7	22
20	110	2	40
27	210	9	100
35	400	20	200
45	650	34	600
51	1000	47	1500

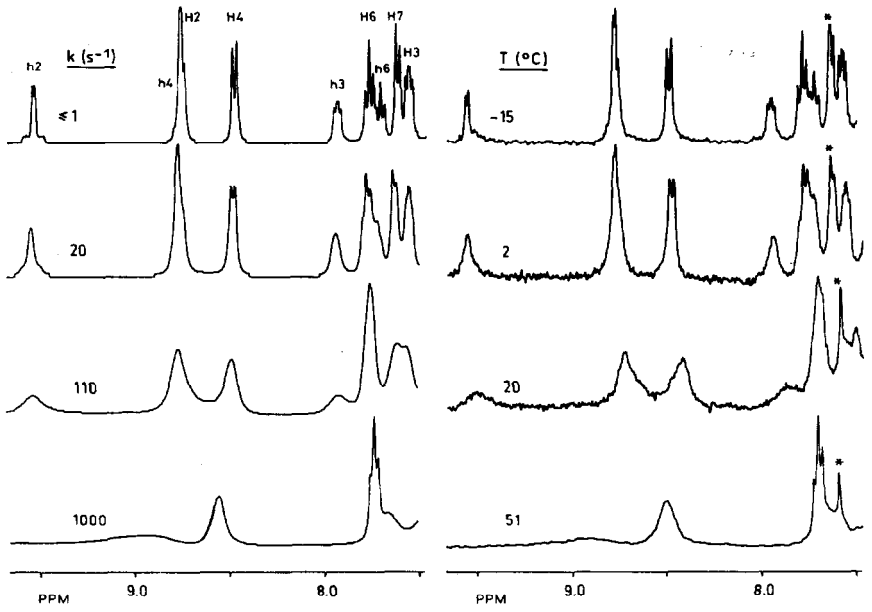


Fig. 2. Experimental and simulated ^{1}H NMR spectra of the Cl_2SnQ_2 complex at selected temperatures. Upper and lower case letters identify *cis–cis–trans* and *cis–trans–cis* isomers respectively. Signals from H5, h5 and h7 protons are not shown due to overlapping with the solvent line. The asterisk marks a solvent impurity.

temperatures, and for Cl_2SnQ_2 at temperatures higher than 2°C (correlation coefficient was 0.998 and 0.999, respectively). However, for the Cl_2SnQ_2 complex at temperatures below 2°C, a slight curvature of the plot can be seen. Although these temperatures are near the slow-exchange limit where rate constants are not very well determined, a change in the slope was apparent. The involvement of the solvent in the activated complex[18] or the existence of two consecutive exchange processes with different activation energies[18,19] are two possible explanations for convex curvatures in Arrhenius plots. It should be noted that an interaction with the solvent could explain the temperature dependence of the

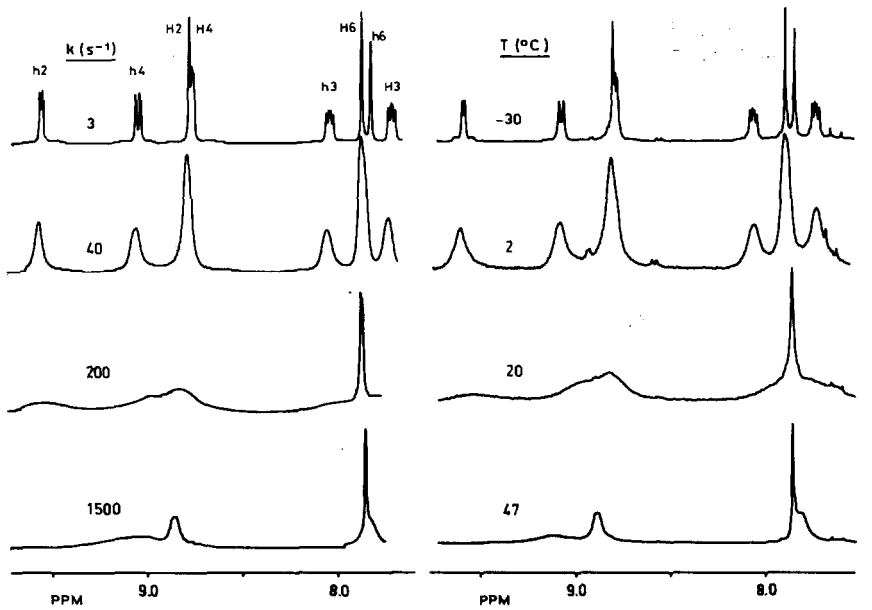


Fig. 3. Experimental and simulated ^{1}H NMR spectra of the $Cl_2Sn(CQ)_2$ complex at selected temperatures. Upper- and lower-case letters identify *cis–cis–trans* and *cis–trans–cis* isomers respectively.

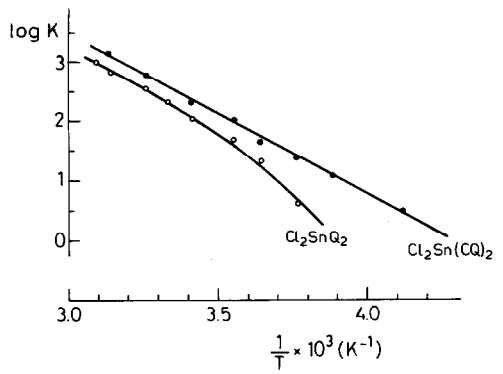


Fig. 4. Arrhenius plots of the Cl_2SnQ_2 and $Cl_2Sn(CQ)_2$ complexes.

chemical shifts in the slow-exchange region and the small curvature of the Arrhenius plots as well, both trends being shown by the same complex, Cl_2SnQ_2.

The Arrhenius (E_a and log A) and Eyring ($\Delta H^{\neq}$, $\Delta S^{\neq}$) parameters obtained are shown in Table 2, where activation data of related chlorinated hexacoordinated complexes of tetravalent metals (including tin) are also included for comparison purposes. It can be seen that the activation energies are very similar for the two complexes, $Cl_2Sn(CQ)_2$ and Cl_2SnQ_2, indicating that the presence of bulky Cl atoms in the 8-quinolinol ring had no appreciable influence on the isomer exchange around the tin atom. Even the substitution of the 8-quinolinol ring by acetylacetonate or dipivaloylmethanide (dpm) ligands, maintaining the Cl and tin atoms, causes only a moderate (~ 15 kJ mol^{-1}) change in activation energies. On the contrary, the substitution of the Sn(IV) atom by Ge(IV), maintaining the Cl and dpm ligands, practically doubled the activation energy of the exchange process.

We would like to point out that, as far as we know, this is the first time that an isomerization process involving a ligand as complex as the 8-quinolinol ring (seven coupled nuclear spins) has been studied by NMR techniques and the activation parameters obtained. Studies on the stereodynamics of complexes of 8-quinolinol with other metals are desirable to fully characterize its behaviour, and further work in that direction will be done in the future.

Acknowledgements—We thank A. Gómez, Mrs C. López and Mr L. de la Vega for excellent technical assistance.

REFERENCES

1. K. Kawakami and R. Okawara, *J. Organomet. Chem.* 1966, **6**, 249.
2. L. Roncucci, G. Faraglia and R. Barbieri, *J. Organomet. Chem.* 1966, **6**, 278.
3. B. C. Baker and D. T. Sawyer, *Anal. Chem.* 1968, **40**, 1945.
4. B. C. Baker and D. T. Sawyer, *Inorg. Chem.* 1969, **8**, 1160.
5. C. D. Barsode, P. Umapathy and D. N. Sen, *J. Indian Chem. Soc.* 1976, **53**, 761.
6. T. S. B. Baul, T. K. Chattopadhyay and B. Majee, *Polyhedron* 1983, **2**, 635.
7. G. S. Sodhi, S. Kumar and N. K. Kaushik, *Acta Chim. Hung.* 1983, **114**, 329.
8. W. Cheng, *J. Coord. Chem.* 1983, **13**, 57.
9. R. K. Bajaj, G. S. Sodhi, N. K. Kaushik and K. N. Johri, *Polyhedron* 1984, **3**, 883.
10. W. Langseth, *Inorg. Chim. Acta* 1984, **87**, 47.
11. P. Zannella, G. Rossetto and G. Paolucci, *Inorg. Chim. Acta* 1984, **82**, 227.
12. J. L. Nieto and A. M. Gutiérrez, *Polyhedron* 1983, **2**, 987.
13. A. M. Gutiérrez, A. Sanz-Medel and R. Gallego, *Anal. Chim. Acta* 1983, **149**, 259.
14. R. Duerst and A. Merbach, *Rev. Sci. Instrum.* 1965, **36**, 1896.
15. G. Binsch, *J. Am. Chem. Soc.* 1969, **91**, 1304.

Table 2. Arrhenius and Eyring activation parameters of the isomer exchange process in the complexes Cl_2SnQ_2 and $Cl_2Sn(CQ)_2$: data reported for other related chlorinated hexacoordinated complexes are also included

Ref.	Complex	E_a (kJ mol^{-1})	log A	$\Delta H^{\neq}$ (kJ mol^{-1})	$\Delta S^{\neq}$ (J K^{-1} mol^{-1})
This work	Cl_2SnQ_2[a]	54±1	11.8±0.2	52±1	−29±4
	$Cl_2Sn(CQ)_2$	52±1	11.7±0.3	51±1	−29±4
20	$Cl_2Sn(acac)_2$	67±2	10.9±0.2		−44±4
20	$Cl_2Sn(dpm)_2$	69±2	12.0±0.3		−24±7
20	$Cl_2Ti(acac)_2$	47±3	11.0±0.5		−42±10
20	$Cl_2Ge(dpm)_2$	105±6	13.0±0.7		−5±13

[a] Data obtained in the range 2–51°C.

16. G. Binsch and D. A. Kleier, *DNMR Program* 140, *Quantum Chemistry Program Exchange*. Indiana University (1969).
17. S. Szymanski and M. Witanowski, *Annu. Rep. NMR Spectrosc.* 1978, **8**, 227.
18. J. R. Hulett, *Q. Rev.* 1964, **18**, 227.
19. D. Bunn, F. S. Dainton and S. Duckworth, *Trans. Faraday Soc.* 1961, **57**, 1131.
20. N. Serpone and D. G. Bickley, *Prog. Inorg. Chem.* 1972, **17**, 391.

Polyhedron Vol. 4, No. 9, pp. 1617–1619, 1985
Printed in Great Britain

0277–5387/85 $3.00 + .00
© 1985 Pergamon Press Ltd

COMPLEXES OF Pt(II) AND Pt(IV) WITH DISUBSTITUTED PURINES

BADAR TAQUI KHAN,* S. VIJAYA KUMARI, K. MURALI MOHAN and G. NARSA GOUD

Department of Chemistry, Osmania University, Hyderabad-7, India

(*Received* 5 *February* 1985; *accepted* 27 *March* 1985)

Abstract—Mixed-ligand complexes of Pt(II) and Pt(IV) with 2,6-diaminopurine and 6-thioguanine were synthesized and characterised. The complexes were prepared in acidic and basic media. The binding of the ligands to the metal ion varies according to the pH of the medium. Thus, in the complexes of 6-thioguanine, the ligand acts as a monodentate ligand coordinating through the neutral C_6-SH group in the acidic medium and in the basic medium as a bidentate ligand binding to the metal ion through C_6S^- and N_7, forming a five-membered chelate ring. In an acidic medium 2,6-diaminopurine forms mononuclear complexes with Pt(II) and Pt(IV) binding through N_7. In a basic medium binuclear hydroxobridged complexes are formed with Pt(IV) and the ligand is monodentate, coordinating through N_7.

There has been a growing interest in the study of various mixed-ligand complexes of platinum group metal ions because of their anti-tumour activity.[1–3] Earlier we have reported on platinum group metal complexes with purines, pyridimidines and nucleosides as ligands.[4–7] In the present paper the preparation and characterisation of Pt(II) and Pt(IV) complexes with 2,6-diaminopurine and 6-thioguanine are reported.

EXPERIMENTAL

Hexachloroplatinic acid was purchased from Alfa–Ventron (U.S.A.). 2,6-Diaminopurine and 6-thioguanine were purchased from Schwarzmann (U.S.A). Hexachloroplatinic acid was converted to potassium hexachloroplatinate(IV) and potassium tetrachloroplatinate(II) by reported procedures.[8] Elemental analysis of the samples was performed at Australian Mineral Development Laboratories (Australia). The percentage of chlorine in the complexes was estimated by a reported procedure.[9] The IR and UV spectra were recorded on Perkin–Elmer (377) and Beckman Model (DB) spectrophotometers, respectively. ^{1}H NMR spectra were recorded on a Varian A-60 spectrometer.

The insolubility of some of the complexes precluded the use of electronic and NMR spectra.

* Author to whom correspondence should be addressed.

Synthesis

Pentachloro-2,6-diaminopurinium platinum(IV) dihydrate. Potassium hexachloroplatinate (0.243 g, 0.5 mM) was dissolved in 10 cm^3 of water and to this a solution of 2,6-diaminopurine (0.075 g, 0.5 mM) in 10 cm^3 of 3 N HCl was added. The resulting solution was stirred at room temperature for 6 h. A yellow precipitate was obtained on cooling, which was filtered, washed with methanol and acetone, and dried.

Hexachloro - μ - dihydroxo - bis(2,6 - diaminopurine) diplatinum(IV). Potassium hexachloroplatinate(IV) (0.243 g, 0.5 mM) was dissolved in 10 cm^3 of water and to this a solution of 2,6-diaminopurine (0.075 g, 0.5 mM) in 10 cm^3 of 3 N KOH was added. The resulting solution was stirred at room temperature for 6 h, when a yellow precipitate was obtained. The precipitate was filtered, washed with methanol and acetone, and dried.

Trichloro 2,6-diaminopurinium platinum(II) dihydrate. Potassium tetrachloroplatinate(II) (0.207 g, 0.5 mM) was dissolved in 10 cm^3 water and to this a solution of 2,6-diaminopurine (0.075 g, 0.5 mM) in 10 cm^3 of 3 N HCl was added. The resulting solution was stirred for 5 h at room temperature, when a yellow-coloured precipitate was obtained. The complex was filtered, washed with water, methanol and acetone, and dried.

Tetrachloro bis(6-thioguanine) platinum(IV) trihydrate. Potassium hexachloroplatinate(IV) (0.243 g,

0.5 mM) was dissolved in 10 cm^3 of water and to this a solution of 6-thioguanine (0.167 g, 1 mM) in 10 cm^3 of acidified water was added. On stirring for 3 h a yellow precipitate was obtained. The compound was filtered, washed with methanol and acetone, and dried.

Dichloro bis(6-thioguaninato) platinum(IV) tetrahydrate. Potassium hexachloroplatinate(IV) (0.243 g, 0.5 mM) was dissolved in 10 cm^3 of water and to this a solution of 6-thioguanine (0.167 g, 1 mM) in 10 cm^3 of 2 N KOH was added. The resulting solution was stirred for 6 h, when a yellow precipitate was obtained. The complex was filtered, washed with methanol and acetone, and dried.

Dichlorobis(6-thioguanine) platinum(II). Potassium tetrachloroplatinate(II) (0.207 g, 0.5 mM) was dissolved in 10 cm^3 of water and to this a solution of 6-thioguanine (0.083 g, 0.5 mM) in 10 cm^3 of acidified water was added, when a yellow precipitate was obtained. The precipitate was stirred for 2 more hours at room temperature. The complex was filtered, washed with methanol and dried.

Bis(6-thioguaninato) platinum(II) pentahydrate. Potassium tetrachloroplatinate(II) (0.207 g, 0.5 mM) was dissolved in 10 cm^3 of water and to this a solution of 6-thioguanine (0.088 g, 0.5 mM) dissolved in 10 cm^3 of 2 N KOH was added. The resulting solution was stirred at room temperature for 15 min, when a yellow precipitate appeared. The stirring was continued for 3 more hours and the reaction mixture was kept in the refrigerator overnight. The precipitate was filtered, washed with methanol and dried.

RESULTS AND DISCUSSION

The analytical and other data for complexes **1**–**7** are presented in Table 1. The IR spectra of 2,6-diaminopurine and 6-thioguanine exhibit a strong band around 1600 cm^{-1} due to the NH_2 deformation mode. 6-Thioguanine exhibits a band at 1060 cm^{-1}, which may be assigned to skeletal vibrations of the pyrimidine ring. The S–H stretching frequency is observed as a strong band in the region around 2100 cm^{-1}. In the free ligands, the C=N and C=C frequencies are observed as strong bands at 1460, 1500 and 1580 cm^{-1}. The band at 1600 cm^{-1} remains unaffected in the spectra of all the complexes, indicating that the NH_2 group is not involved in coordination. Except for complexes **4** and **6** the peaks corresponding to C=N are shifted to a lower frequency by about 50–70 cm^{-1} indicating the involvement of ring nitrogen in bonding. The coordination of the metal ions of the ring nitrogen in these complexes is also ascertained by a band due to M–N vibrations observed around 500–600 cm^{-1}.

Complexes **1** and **3** are prepared in acidic medium at a pH of 3–4. In these complexes, 2,6-diaminopurine binds to the metal ion through N_7, as N_1 is preferentially protonated.[10] Complex **1** shows two M–Cl stretching modes at 340 and 360 cm^{-1}. The former corresponds to the equatorial chlorides in the plane of the metal ion and the latter to the chloride *trans* to the coordinated purine in the sixth position. In complex **3** two M–Cl stretching frequencies are observed around 350 and 330 cm^{-1}, indicating a meridional arrangement of three

Table 1. Analytical and conductivity data

Serial No.	Complex[a]	% Found (calc.) Carbon	Hydrogen	Chlorine	Conductivity (mohs·cm^2·l^{-1}) (in DMSO)
1	$[Pt(2,6\text{-diampuH}_2^+)(Cl)_5]\cdot 2H_2O$	11.03 (10.72)	2.01 (1.98)	31.50 (31.71)	16.1
2	$[Pt_2(2,6\text{-diampu})_2(OH)_2(Cl)_6]$	12.50 (12.80)	1.39 (1.50)	23.10 (22.72)	—
3	$[Pt(2,6\text{-diampuH}_2^+)Cl_3]\cdot 2H_2O$	11.77 (12.27)	1.93 (2.26)	21.40 (21.76)	14.3
4	$[Pt(6\text{-thioguH})_2Cl_4]\cdot 3H_2O$	17.01 (16.54)	2.30 (2.22)	20.37 (19.58)	28.2
5	$[Pt(6\text{-thiogu}^-)_2Cl_2]\cdot 4H_2O$	18.00 (17.92)	2.33 (2.40)	10.21 (10.59)	—
6	$[Pt(6\text{-thioguH})_2Cl_2]$	20.01 (19.98)	1.70 (1.67)	11.40 (11.80)	16.0
7	$[Pt(6\text{-thiogu}^-)_2]\cdot 5H_2O$	19.00 (19.42)	2.81 (2.93)	—	10.0

[a] Abbreviations: 2,6-diampu, 2,6-diaminopurine; 2,6-diampuH$_2^+$, 2,6-diaminopurinium ion; 6-thioguH, 6-thioguanine; 6-thiogu$^-$, 6-thioguaninato ion.

chlorides in the square plane of the metal ion. The 2,6-diaminopurinium ion is coordinated to Pt(II) through N_7 at the fourth coordination position. In both complexes **1** and **3** the proton is associated with N_1, as verified by a peak around 2600 cm^{-1}, which is observed unaltered in the protonated 2,6-diaminopurinium ion.

The electronic spectrum of complex **1** exhibits two peaks at 370 nm ($\varepsilon_{max} = 567$) and 384 nm ($\varepsilon_{max} = 467$), which may be assigned to $^1A_1 \rightarrow {}^1B_2$ and $^1A_1 \rightarrow {}^1A_2$ transitions, respectively based on a C_{4v}-symmetry of the complex. In complex **3** the peaks at 384 nm ($\varepsilon_{max} = 275$) and 272 nm ($\varepsilon_{max} = 1.06 \times 10^4$) are assigned to $^1A_1 \rightarrow {}^1A_1(1)$ transition. The $\pi \rightarrow \pi^*$ transition of the ligand is observed in complexes **1** and **3** in the range of 265–275 nm.

Complex **2** was prepared in a basic medium. The complex is an insoluble hydroxo-bridged dimer with coordinated terminal chlorides and 2,6-diaminopurine coordinated through N_7. The presence of bridging hydroxo groups in the complex is supported by a broad peak at 2900–3000 cm^{-1}. The M–Cl stretch of the terminal chlorides is observed around 350 cm^{-1}.

Complexes **4** and **6** were prepared in an acidic medium. The IR spectra of these complexes exhibit NH_2 stretching modes as a broad band around 3040–3350 cm^{-1}. The NH_2 deformation mode is observed around 1610 cm^{-1}. This mode is not shifted to any appreciable extent in these complexes, indicating its non-involvement in coordination. The ring C=C and C=N stretching frequencies of 6-thioguanine are observed in these complexes around 1470 and 1450 and 1370–1385 cm^{-1}, respectively, and are not shifted to an appreciable extent when compared to the ligand, indicating that the ring nitrogen is not involved in coordination. In both complexes a medium band is observed around 480 cm^{-1}, which may be assigned to an M–S stretching vibration. In the IR spectra of complexes **4** and **6** a single intense peak is exhibited at 330 and 350 cm^{-1} respectively, indicating the presence of *trans*-chlorides in the complexes. In complexes **4** and **6** the S–H stretching frequency is shifted to a lower frequency by about 100 cm^{-1}, indicating the coordination of neutral S–H in these complexes. The NMR spectrum of free 6-thioguanine gives a peak around 7.8 ppm (δ) due to C_8H protons. In complexes **4** and **6** this peak is not shifted and exhibited at 7.75 (δ) and 7.9 ppm, respectively, indicating that N_7 is not involved in coordination. From the above data complex **4** is assigned an octahedral structure with four chlorides in the equatorial position and two 6-thioguanine ligands coordinating to the metal ion in the axial position. The electronic spectrum of complex **4** exhibits *d–d* transitions at 370 and 344 nm assigned to $^1A_{1g} \rightarrow {}^1B_{1g}$ and $^1A_{1g} \rightarrow {}^1B_{2g}$, respectively, in accord with a D_{4h}-symmetry of the complex. The $\pi \rightarrow \pi^*$ transition of 6-thioguanine is observed in complex **4** at 267 nm. In the electronic spectrum of complex, **6**, peaks are observed at 358 nm ($\varepsilon_{max} = 540$) and 370 nm ($\varepsilon_{max} = 700$) which are assigned to $^1A_{1g} \rightarrow {}^1A_{2g}$ and $^1A_{1g} \rightarrow {}^1A_{1g}(1)$ transitions, respectively, for a C_{4h}-symmetry. A band is also observed at 266 nm ($\varepsilon_{max} = 1.5 \times 10^4$) which is assigned to a $\pi \rightarrow \pi^*$ transition of the ligand.

The IR spectrum of complex **5** exhibits two peaks at 330 and 450 cm^{-1}, which may be assigned to stretching frequencies of *trans*-chlorides and ν(M–S) respectively. The insolubility of the complex precludes its studies by other physico-chemical techniques. The SH stretching frequency at 2100 cm^{-1} observed in the ligand disappears in the complex, indicating the coordination of the thiolato S^- group in the complex. Based on the analytical data, IR spectrum and the usual stereochemistry of Pt(IV), complex **5** is assigned an octahedral geometry with the chelated 6-thioguaninato ions in the equatorial position of Pt(IV) and the two axial positions occupied by the chloride ions with a C_{2v}-symmetry.

In complex **7** the coordination of 6-thioguaninato ion is through N_7 and C_6S^- as indicated by the presence of peaks corresponding to M–N and M–S stretching frequencies at 530 and 450 cm^{-1}, respectively. The ν(M–Cl) and ν(S–H) bands are absent in that complex.

Acknowledgement—Two of us, K.M.M. and G.N.G. are thankful to C.S.I.R., New Delhi, for financial support to carry out this work.

REFERENCES

1. B. Rosenberg, L. Van Camp, J. E. Troska and V. H. Mansour, *Nature (London)* 1969, **222**, 385.
2. A. Terzis, N. Hadjiliadis, R. Revert and T. Theophanides, *Inorg. Chim. Acta* 1975, **12**, L5.
3. P. C. Kong, D. Iyansenye and F. D. Rochan, *Bioinorg. Chem. Acta* 1976, **16**, 167.
4. B. T. Khan, S. V. Kumari and G. N. Goud, *J. Coord. Chem.* 1982, **12**, 19.
5. B. T. Khan, A. Mehmood and M. M. T. Khan, *J. Inorg. Nucl. Chem.* 1979, **40**, 1934.
6. B. T. Khan, M. R. Somayajulu and M. M. T. Khan, *J. Inorg. Nucl. Chem.* 1978, **40**, 1251.
7. B. T. Khan, S. V. Kumari and G. N. Goud, *Indian J. Chem.* 1982, **21A**, 264.
8. H. L. Gurbe, In *Handbook of Preparative Inorganic Chemistry* (Edited by G. Brauer), Vol. 2, p. 1571. Academic Press, New York (1965).
9. A. I. Steyermark, R. A. Calancette and E. M. Eontreras, *J. AoAc* 1972, **55**, 680.
10. M. M. T. Khan and C. R. Krishnamurthy, *J. Inorg. Nucl. Chem.* 1973, **35**, 1285.

Polyhedron Vol. 4, No. 9, pp. 1621–1624, 1985
Printed in Great Britain

0277–5387/85 $3.00 + .00
© 1985 Pergamon Press Ltd

THE OXIDATION OF THIOSULPHATE IONS BY OCTACYANOTUNGSTATE(V) IN WEAK ACIDIC MEDIUM

C. R. DENNIS,* J. G. LEIPOLDT, S. S. BASSON and G. J. LAMPRECHT
Chemistry Department, University of the Orange Free State, Bloemfontein (9300), Republic of South Africa

(*Received* 11 *December* 1984; *accepted* 3 *April* 1985)

Abstract—The kinetics of the oxidation of thiosulphate ions by octacyanotungstate(V) ions has been studied in the pH range 3.9–5.0. The reaction showed zero-order kinetics with respect to $[W(CN)_8^{3-}]$ and is consistent with the rate law $R = k[H^+][S_2O_3^{2-}]^2$. A reaction mechanism is proposed for the reaction with a third-order rate constant of 0.26 $M^{-2}\,s^{-1}$ at 25°C.

The oxidation of thiosulphate ions by mild oxidizing agents like iodine and iron(III) yields tetrathionate ions in neutral aqueous medium.[1] Stronger oxidizing agents such as bromine and chlorine yield sulphate ions, whilst hydrogen peroxide gives a mixture of sulphate and tetrathionate ions. In an alkaline medium oxidation by iodine produces some sulphate ions and the ratio of sulphate to tetrathionate increase with increasing pH of the reaction medium. This suggests that the oxidation product of thiosulphate ions is determined by two factors: (i) the reduction potential of the oxidizing agent, and (ii) the pH of the reaction medium.

The kinetics of the oxidation of thiosulphate ions by octacyanotungstate(V) ions in the pH range 3.9–5.0 were investigated as part of a research program on the redox properties of the cyano complexes of iron, molybdenum and tungsten. Sandved and Holte[2] reported the oxidation of thiosulphate by hexacyanoferrate(III) ions to be zero-order in $Fe(CN)_6^{3-}$ with a rate law:

$$-\frac{d[Fe(CN)_6^{3-}]}{dt} = k[H^+][S_2O_3^{2-}]^2. \quad (1)$$

The rate law for the oxidation by octacyanomolybdate(V) ions[3] in a weak acidic medium has been reported to be:

$$-\frac{d[Mo(CN)_8^{3-}]}{dt} = k[Mo(CN)_8^{3-}][S_2O_3^{2-}][M^+]. \quad (2)$$

(M^+ = alkali-metal ion)

A reinvestigation[4] of the oxidation of the thiosulphate by hexacyanoferrate(III) ions confirmed the zero-order kinetics in $[Fe(CN)_6^{3-}]$ and showed the rate to be consistent with a two-term rate law [eqn (3)] of which the second term represents an alkali-metal ion catalysis pathway:

$$R = k[H^+][S_2O_3^{2-}]^2 + k'[H^+][S_2O_3^{2-}]^2[M^+]. \quad (3)$$

The results of both Lamprecht *et al.*[3] and Howlett and Wedzicha[4] show the effect of the alkali-metal ion catalysis to be in the order $Na^+ < K^+ < Rb^+ < Cs^+$.

In view of the above-mentioned results the kinetic study of the octacyanotungstate(V) oxidation of thiosulphate ions was performed for a comparison with those of the hexacyanoferrate(III) and octacyanomolybdate(V) ions.

EXPERIMENTAL

The complex tricesium octacyanotungstate(V) dihydrate, $Cs_3[W(CN)_8]\cdot 2H_2O$, was prepared as described by Leipoldt *et al.*[5,6] All other reagents used were analytical grade and redistilled water was used throughout.

Kinetic measurements were made in acetate buffer solutions ($[CH_3COO^-]_T = 0.01$ M) by monitoring the decrease in $[W(CN)_8^{3-}]$ at 357 nm using a Pye–Unicam SP1700 spectrophotometer. The temperature was controlled to ±0.1°C. Stock solutions of sodium thiosulphate were renewed daily and standardised against potassium iodate.

The concentration of $W(CN)_8^{3-}$ at various times

* Author to whom correspondence should be addressed.

was calculated from the molar absorptivity of $W(CN)_8^{3-}$ and $W(CN)_8^{4-}$, which were determined as 1850 and 230 $M^{-1}\,cm^{-1}$ at 357 nm respectively.

The stoichiometry of the reaction at a pH of 4.5 was determined volumetrically by oxidation of the reaction product, $W(CN)_8^{4-}$, with a Ce(IV) solution using *N*-phenylanthranilic acid as indicator. This indicated that the overall reaction is represented by:

$$2W(CN)_8^{3-} + 2S_2O_3^{2-} \rightarrow 2W(CN)_8^{4-} + S_4O_6^{2-}.$$

RESULTS AND DISCUSSION

Reproducible zero-order reaction rates could only be obtained after addition of Na_2EDTA to reaction mixtures. Similar phenomena were observed for the reaction with $Fe(CN)_6^{3-}$ and $Mo(CN)_8^{3-}$. Addition of 6×10^{-6} M Na_2EDTA to reaction mixtures containing 5×10^{-4} M $W(CN)_8^{3-}$ and 0.10 M $S_2O_3^{2-}$ at 25°C and pH = 4.5 caused the reaction rate to drop by about 20% compared to the rate in the absence of EDTA. No further effect on the reaction rate was observed with a 50-fold increase in [EDTA]. All the reported runs were therefore 1×10^{-5} M in Na_2EDTA to eliminate catalysis by traces of multivalent cations. No reaction between $W(CN)_8^{3-}$ and EDTA was observed under the experimental conditions.

The kinetic results (Table 1) show that the reaction is second order with respect to $[S_2O_3^{2-}]$ and linearly dependent on $[H^+]$. The alkali-metal ion concentration and also the ionic strength of the reaction medium have no significant effect on the reaction rate. These results are consistent with the rate law:

$$R = k_{obsd}[H^+][S_2O_3^{2-}],^2 \quad (4)$$

which was also found for the uncatalysed reaction between $Fe(CN)_6^{3-}$ and thiosulphate ions.

According to the pK_a values of $H_3W(CN)_8$ ($pK_{a1} < 1$, $pK_{a2} = 1.70$, $pK_{a3} = 2.35$)[7] the main octacyanotungstate(V) species under the experimental conditions is the $W(CN)_8^{3-}$ ion. The K_{a2} value[8,9] (1×10^{-2} M) of $H_2S_2O_3$ and the observed hydrogen ion dependence indicate the existence of the association equilibrium:

$$S_2O_3^{2-} + H^+ \overset{K}{\rightleftharpoons} HS_2O_3^-. \quad (5)$$

The formation of colloidal sulphur in acidified thiosulphate solution[10] was found to involve a bimolecular reaction between $HS_2O_3^-$ and $S_2O_3^{2-}$ followed by a first-order decay of the resultant ionic

Table 1. Observed rate constants for the reaction of octacyanotungstate(V) ions with thiosulphate ions: [EDTA] = 1×10^{-5} M, T = 25°C, μ = 0.61

10^4 $[W(CN)_8^{3-}]$ (M)	$[S_2O_3^{2-}]$ (M)	pH	$[Na^+]$ (M)	10^7 k_{obsd} ($M\,s^{-1}$)	k ($M^{-2}\,s^{-1}$)
2.5	0.10	4.32	0.30	1.24	0.26
3.0	0.10	4.32	0.30	1.24	0.26
3.5	0.10	4.32	0.30	1.20	0.25
4.0	0.10	4.32	0.30	1.15	0.24
4.5	0.10	4.32	0.30	1.19	0.25
5.0	0.10	4.32	0.30	1.15	0.26
5.0	0.05	4.32	0.30	0.28	0.23
5.0	0.06	4.32	0.30	0.40	0.23
5.0	0.07	4.32	0.30	0.56	0.24
5.0	0.08	4.32	0.30	0.77	0.25
5.0	0.09	4.32	0.30	0.89	0.23
5.0	0.10	4.32	0.30	1.19	0.25
5.0	0.10	4.98	0.30	0.35	0.34
5.0	0.10	4.84	0.30	0.43	0.30
5.0	0.10	4.54	0.30	0.75	0.26
5.0	0.10	4.34	0.30	1.10	0.24
5.0	0.10	4.17	0.30	1.60	0.24
5.0	0.10	3.88	0.30	2.90	0.22
5.0[a]	0.10	4.32	0.35	1.05	0.22
5.0[a]	0.10	4.32	0.40	1.19	0.25
5.0[a]	0.10	4.32	0.45	1.10	0.23
5.0[a]	0.10	4.32	0.50	1.15	0.24

[a] μ varied between 0.61 and 0.81.

associate. The following reaction mechanism was proposed:

$$HS_2O_3^- + S_2O_3^{2-} \underset{k_{-1}}{\overset{k_1}{\rightleftharpoons}} [HS_2O_3 \cdot S_2O_3]^{3-}, \quad (6)$$

$$[HS_2O_3 \cdot S_2O_3]^{3-} \overset{k_2'}{\rightarrow} HSO_3^- + SO_3^{2-} + 2S. \quad (7)$$

The rate constants k_1 and k_2' are comparable in magnitude.

The reduction of octacyanotungstate(V) by excess thiosulphate ions proceeds with a uniform rate until all the $W(CN)_8^{3-}$ has reacted. The excess $S_2O_3^{2-}$ then decomposes in the acidic medium as shown in eqns (6) and (7). The fact that the experimental rate constants for the oxidation of thiosulphate ions by hexacyanoferrate(III) ions ($k = 0.6\ M^{-2}\ s^{-1}$) and $W(CN)_8^{3-}$ ($k = 0.3\ M^{-2}\ s^{-1}$) are of the same order compared to that of the acid decomposition[10] of thiosulphate ions ($k = 0.5\ M^{-2}\ s^{-1}$), as well as the mutual second-order concentration dependence in $S_2O_3^{2-}$, show the first and rate-determining step of the reaction mechanism to be the same as depicted in reaction (6). This is followed by a series of fast reactions with $W(CN)_8^{3-}$ ions which can be represented by:

$$[HS_2O_3 \cdot S_2O_3]^{3-} + 2W(CN)_8^{3-} \underset{\text{fast}}{\longrightarrow} S_4O_6^{2-} + 2W(CN)_8^{4-}. \quad (8)$$

This reaction mechanism is consistent with a rate law:

$$-\frac{d[W(CN)_8^{3-}]}{dt} = 2k_1[HS_2O_3^-][S_2O_3^{2-}]. \quad (9)$$

From reaction (5) it follows that:

$$[HS_2O_3^-] = \frac{K[H^+][S_2O_3^{2-}]_T}{1 + K[H^+]}. \quad (10)$$

($[S_2O_3^{2-}]_T$ = total thiosulphate concentration)

Substitution of the latter into eqn (9) yields the rate law:

$$-\frac{d[W(CN)_8^{3-}]}{dt} = \frac{2k_1K[H^+][S_2O_3^{2-}]^2}{1 + K[H^+]}. \quad (11)$$

Since $1 \gg K[H^+]$ under the experimental conditions, eqn (11) simplifies to the observed rate law [eqn (4)] with $k_{obsd} = 2k_1K$.

From eqn (11) it is expected that a pH region would be found where the reaction is independent of hydrogen ion concentration. This region could not be reached experimentally because of the acid decomposition of thiosulphate ions.

Qualitative proof for the formation of tetrathionate was performed by comparing an IR spectrum of the yellow precipitate, formed by the reaction of tetrathionate with an excess mercurous nitrate, with that of a precipitate formed by adding an excess mercurous nitrate to a reaction mixture containing an excess of $W(CN)_8^{3-}$ relative to $S_2O_3^{2-}$. The only two peaks at 625 and 1125 cm^{-1} present in the first spectrum were also present in the second and were absent in a third recorded from a precipitate formed with an excess of mercurous nitrate added to a buffered solution of $W(CN)_8^{3-}$ in the absence of thiosulphate ions.

In addition to the above, the formation of a polythionate was proved by a method of Kolthoff and Belcher[11] using the reaction:

$$S_4O_6^{2-} + 3CN^- + H_2O \rightarrow S_2O_3^{2-} + SO_4^{2-} + SCN^- + 2HCN. \quad (12)$$

The polythionate formed by oxidation of thiosulphate ions with excess octacyanotungstate(V) ions was similarly reduced to $S_2O_3^{2-}$ using excess potassium cyanide. Determination of the formed thiosulphate ions yielded only half the originally reacted amount of thiosulphate ions, in accordance with reaction (12).

The reaction mechanisms for the oxidation of thiosulphate ions by the cyano complexes of iron(III) and tungsten(V) compared to that of molybdenum(V) in a weakly acidic medium are clearly different. This may be explained by the difference in the reduction potentials[12,13] of these complexes. Since the reduction potential of the molybdenum complex ($E = 0.80$ V) is high relative to those of the iron ($E = 0.42$ V) and tungsten ($E = 0.54$ V) complexes a difference in reaction pathway as discussed earlier, for the reduction of $Mo(CN)_8^{3-}$ ions by thiosulphate ions, can be expected.

Acknowledgements—We are grateful to the South African C.S.I.R. and the Research Fund of our university for financial assistance.

REFERENCES

1. J. H. Karchmer, *Analytical Chemistry of Sulfur and its Compounds*, Part I. Wiley–Interscience, New York (1970).
2. K. Sandved and J. B. Holte, *Tidsskr. Kjemi Bergves.* 1940, **20**, 106.
3. G. J. Lamprecht, J. G. Leipoldt, C. R. Dennis and S. S. Basson, *React. Kinet. Catal. Lett.* 1980, **13**, 269.
4. K. E. Howlett and B. L. Wedzicha, *Inorg. Chim. Acta* 1976, **18**, 133.
5. J. G. Leipoldt, L. D. C. Bok and P. J. Cilliers, *Z. Anorg. Allg. Chem.* 1974, **409**, 343.
6. L. D. C. Bok, J. G. Leipoldt and S. S. Basson, *Z. Anorg. Allg. Chem.* 1975, **415**, 81.
7. A. Samotus and B. Kosowicz-Czajkowska, *Rocz. Chem.* 1971, **45**, 1623.
8. K. Jellinek, *Z. Phys. Chem.* 1911, **76**, 257.
9. I. Kolthoff, *Recl Trav. Chim.* 1924, **43**, 216.

10. R. H. Dinegar, R. H. Smellie and V. K. la Mer, *J. Am. Chem. Soc.* 1951, **73**, 2050.
11. I. M. Kolthoff and R. Belcher, *Volumetric Analysis*, Vol. 3. Interscience. New York (1957).
12. R. J. Campion, N. Purdie and N. Sutin, *Inorg. Chem.* 1964, **3**, 1091.
13. J. M. Anast and D. W. Margerum, *Inorg. Chem.* 1982, **21**, 3494.

Polyhedron Vol. 4, No. 9, pp. 1625–1635, 1985
Printed in Great Britain

0277–5387/85 $3.00 + .00
© 1985 Pergamon Press Ltd

REACTIONS OF XENON DIFLUORIDE: OXIDATIVE FLUORINATION OF METHYL DERIVATIVES OF THE *p*-BLOCK ELEMENTS

ALAN M. FORSTER and ANTHONY J. DOWNS*
Inorganic Chemistry Laboratory, University of Oxford, South Parks Road, Oxford OX1 3QR, U.K.

(*Received* 6 *January* 1985; *accepted* 20 *February* 1985)

Abstract—A survey has been carried out to determine how xenon difluoride reacts with methyl derivatives of *p*-block elements, Me_nX ($n = 3$, X = N, P, As, or Sb; $n = 2$, X = O, S, or Se; $n = 1$, X = Cl, Br, or I), on the basis of NMR measurements, tensimetric and IR analysis of the gaseous products, and mass balances. The reaction proceeds smoothly in most cases, although a Freon like CCl_3F may be needed as a moderator; the rate of the reaction seems to reflect the basicity of the substrate Me_nX. The difluoride Me_nXF_2 is formed in the cases where X = P, As, Sb, Se, or I. The scope of xenon difluoride in these conditions as a mild selective oxidative fluorinating agent is illustrated by the synthesis of the known compounds $(CF_3)_2XF_2$ (X = S or Se) and the novel compound $Me(CF_3)SeF_2$. By contrast, cleavage of C–H bonds, with the formation of CH_2F derivatives, is the predominant path in the cases where X = N, O, or S, and cleavage of C–X bonds, with the formation of MeF, occurs in the cases where X = Cl or Br.

Oxidative fluorination of an organic derivative of a *p*-block element X can take one of three courses: (i) difluorine-addition at X, (ii) fluorination at one or more carbon atoms of the organic groups with the formation of C–F bonds, and (iii) cleavage of X–C bonds. All three paths are liable to be followed more-or-less indiscriminately when such a derivative reacts with molecular fluorine in normal circumstances. Additional paths are created, moreover, by the increasing range of oxidation states open to the *p*-block elements in the later groups of the Periodic Table: situations such as these accentuate the need for selective methods of fluorination. The search for improved selectivity has led recently to the development of low-temperature procedures involving molecular fluorine diluted with an inert carrier,[1] albeit with varying degrees of success.[2] Receiving considerable attention too have been various fluorides, e.g. SF_4, halogen fluorides, and AgF_2, which have been used for example to promote changes of the type

$$R_nX \rightarrow R_nXF_2,$$

where R = alkyl, aryl, or perfluoro-organo groups; $n = 3$ for X = P, As, or Sb;[3] $n = 2$ for X = S, Se, or Te;[4] and $n = 1$ for X = I.[5] Such studies show that unsubstituted alkyl groups like CH_3 are the organic ligands most susceptible to fluorination.

Xenon difluoride[6] has much to commend it as a selective fluorinating agent of organic[7] as well as inorganic[8] derivatives: it can be prepared, purified, and manipulated with comparative ease and safety; when it acts as a fluorinating agent, moreover, it has the great attraction of affording in elemental xenon a highly volatile, inert co-product. On the other hand, it can be rather sluggish in its action. That it is capable of selective fluorination has been established by the reaction reported to occur with iodomethane,[9] viz.

$$MeI + XeF_2 \rightarrow MeIF_2 + Xe.$$

By contrast, we have shown that the reaction with dimethyl sulphide in a non-acidic medium results in fluorination at carbon with the formation of CH_2FSMe and hence the cation $[Me_2SCH_2SMe]^+$.[10]

$$Me_2S + XeF_2 \rightarrow \underset{\downarrow Me_2S}{\underline{CH_2FSMe + HF}} + Xe$$
$$[Me_2SCH_2SMe]^+[F(HF)_n]^-$$

* Author to whom correspondence should be addressed.

The difference between the behaviours of dimethyl sulphide and iodomethane prompted us to extend our initial investigation to determine the nature and scope of the reactions which occur between xenon difluoride and the methyl derivatives of *p*-block elements in Groups V (N, P, As, and Sb), VI (O, S, and Se), and VII (Cl, Br, and I). Here we report the results of this survey.

RESULTS

(i) *Methyl derivatives of group V elements*

(a) *Trimethylamine.* The attack of trimethylamine by molecular fluorine[11] or cobalt(III) fluoride[12] gives rise to a host of degradation products; with molecular chlorine or bromine, however, it is said to form an adduct formulated as $[Me_3NX]^+X^-$ (X = Cl or Br).[13] We have found that xenon difluoride reacts explosively with trimethylamine even when diluted with trichlorofluoromethane ($Me_3N:CCl_3F$ = *ca* 1:20) at room temperature. However, increased dilution ($Me_3N:CCl_3F$ = *ca* 1:400) results in a smooth reaction with the release of one mole of xenon gas for every mole of xenon difluoride taken. Evaporation of the solvent leaves a sticky solid product which dissolves in liquid sulphur dioxide; the ^1H and ^{19}F NMR spectra of the solution indicate the presence of a complex mixture of products in which the only components to be identified were $[Me_3NH]^+$ and HF arising presumably from attack of the C–H bonds. Chlorination of trimethylamine by vanadium tetrachloride results similarly in the formation of the $[Me_3NH]^+$ cation.[14] With xenon difluoride, as with vanadium tetrachloride, it is likely that trimethylamine is oxidised to the intermediate $[Me_2N{=}CH_2]^+X^-$ (X = F or Cl); this reacts in turn with an excess of the amine with elimination of HX to form $[Me_3NH]^+X^-$ and unidentified products derived possibly from the carbene Me_2NCH.[14,15]

(b) *Trimethyl-phosphine, -arsine, and -stibine.* Controlled oxidative fluorination of the trimethyl derivatives Me_3X (X = P, As, or Sb) to the corresponding difluoride Me_3XF_2 has not been described previously. Instead trimethylphosphorus difluoride has normally been prepared by metathesis involving a trimethylphosphorus(V) precursor, e.g. $Me_3PO + SF_4$[16] or $Me_3PS + SbF_3$,[17] although an unpublished report[18] alludes to its formation from Me_3P by the action of SF_4. Trimethylarsenic and trimethylantimony difluoride have been prepared by the action of aqueous silver fluoride on the corresponding dichloride[19] and dibromide[20] respectively, or, better, by the action of sodium fluoride on the dichloride in an acetonitrile medium.[21]

Xenon difluoride reacts explosively on contact with the liquid trimethyl compounds Me_3X (X = P, As, or Sb) at or near ambient temperatures. However, dilution of the trimethyl compound with trichlorofluoromethane (e.g. $Me_3X:CCl_3F$ = *ca* 1:100) results in a smooth reaction at room temperature with the quantitative evolution of one mole of xenon gas for every mole of xenon difluoride taken. Evaporation of the solvent leaves a colourless residue which is a liquid (X = P) or a solid (X = As or Sb) at room temperature, and which is shown by its ^1H and ^{19}F (and ^{31}P for X = P) NMR spectra to be the difluoride Me_3XF_2. The difluoride is free from any contaminant detectable by its NMR spectrum and a mass balance shows that it can be isolated in greater than 90% yield based on the amount of xenon difluoride taken (see Table 1). Hence xenon difluoride provides a highly efficient single-step route from Me_3X to the corresponding difluoride Me_3XF_2. Previous reports[9b] have established that similar reactions occur, not only with Ph_3P, but also with species like Ph_2PH and *cyclo*-$C_6H_{11}PH_2$ the P–H bonds of which remain intact during oxidative fluorination.

A deuteriochloroform solution of the difluoride Me_3XF_2 in contact with dry caesium fluoride and held in a Teflon-FEP cell[10,22] gives rise to well-resolved NMR spectra at ambient temperatures (35–40°C), as displayed for example in Fig. 1. Previous accounts of the NMR spectra disclosed only

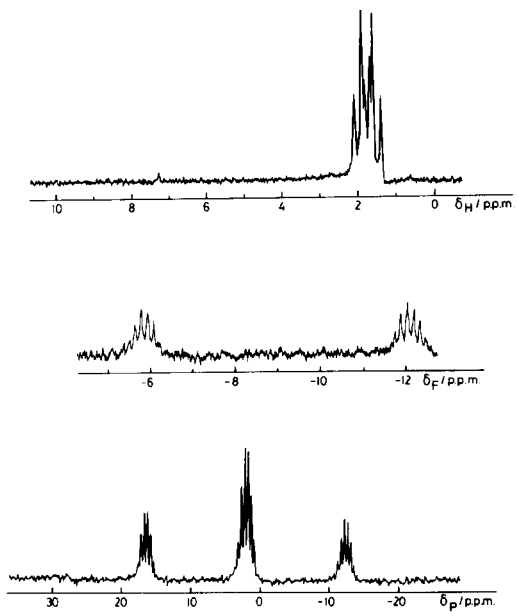


Fig. 1. 60 MHz ^1H, 84.6 MHz ^{19}F and 36.43 MHz ^{31}P NMR spectra of Me_3PF_2 in $CDCl_3$ solution.

Table 1. Reactions of xenon difluoride with methyl and related derivatives of *p*-block elements

Reagent	Amount of XeF_2 taken mg (mmoles)	Diluent	Volatile reaction products: Temperature of vaporisation (K)	Volatile reaction products: Identity	Volatile reaction products: Yield of Xe (%)[a]	Less volatile product: Identity	Less volatile product: Amount mg (mmoles)	Less volatile product: Yield (%)[a]
Me_3N	100 (0.59)	CCl_3F	210	Xe	88	$[Me_3NH]^+$ + unidentified products	[b]	[b]
Me_3P	170 (1.00)	CCl_3F	210	Xe	97	Me_3PF_2	105 (0.92)	92
Me_3As	170 (1.00)	CCl_3F	250	Xe	95	Me_3AsF_2	155 (0.98)	98
Me_3Sb	170 (1.00)	CCl_3F	273	Xe	96	Me_3SbF_2	195 (0.95)	95
Me_2O	100 (0.59)	None	[b]	Xe	[b]	CH_2FOMe	[b]	[b]
Me_2S	65 (0.38)	CCl_3F	250	Xe	99	CH_2FSMe or $[Me_2SCH_2SMe]^+$	[c]	[c]
$MeSCF_3$	130 (0.77)	None	[b]	Xe	[b]	CH_2FSCF_3	[b]	[b]
$(CF_3)_2S$	50 (0.30)	None	178	Xe	[b]	$(CF_3)_2SF_2$	[b]	[b]
Me_2Se	152 (0.90)	CCl_3F	273	Xe	98	Me_2SeF_2	120 (0.82)	91
$MeSeCF_3$	170 (1.00)	None	273	Xe	97	$Me(CF_3)SeF_2$	190 (0.95)	95
$(CF_3)_2Se$	70 (0.41)	None	190	Xe	100	$(CF_3)_2SeF_2$	90 (0.35)	85
MeCl	130 (0.77)	None	178	$Xe + MeF + Cl_2$	[b]	Nil	[b]	[b]
MeBr	153 (0.90)	None	210	Xe + MeF	[b]	Br_2	[b]	[b]
MeI	122 (0.72)	None	228	Xe + MeF	[b]	$MeIF_2$ or I_2	[b]	[b]

[a] Based on the amount of XeF_2 taken.
[b] Not measured quantitatively or not applicable.
[c] See Ref. 10.

Table 2. NMR parameters for fluorination products derived from methyl and related derivatives of *p*-block elements[a]

Species	Medium	Chemical shifts (ppm) δ_H	δ_F	δ_X[b]	Coupling constants (Hz)
Me_3PF_2	$CDCl_3$	1.74 (1.61)[c]	−8.9 (−4.8)[d]	+1.9 (−15.8)[d]	^3J(FH) 13.3 (12.0)[d] ^2J(PH) 17.4 (17.2)[c] ^1J(PF) 530 (542)[d]
$[Me_3PF]^+$	HF	2.1 (2.28)[e]	−139 (−136.6)[e]	(+143.9)[e]	^3J(FH) 10.5 (12.7)[e] ^2J(PH) 11.7 (13.8)[e] ^1J(PF) 960 (955)[e]
Me_3AsF_2	$CDCl_3$	2.08 (2.04)[f]	−53.7 (−53.2)[f]	—	^3J(FH) 8.8 (8.6)[f]
Me_3SbF_2	$CDCl_3$	1.74 (1.71)[g]	−107.0 (−106.1)[g]	—	^3J(FH) 4.6 (5.0)[g]
Me_2SF_2	$CDCl_3$	3.27[h]	+0.1[h]	—	^3J(FH) 12.8[h]
$(CF_3)_2SF_2$	$(CF_3)_2S$	—	CF_3 −57.7 (−58.0)[i] SF_2 −14.2 (−14.2)[i]	—	^3J(FF) 19.5 (19.5)[i]
Me_2SeF_2	$CDCl_3$	3.15 (3.13)[j]	−64.1 (−66.6)[j]	+776	^3J(FH) 9.76 (9.0)[j] ^2J(SeH) 9.52 ^1J(SeF) 634 (650.2)[j]
	HF	3.2	—	—	^3J(FH) 8.5
$Me(CF_3)SeF_2$	$CDCl_3$ or neat liquid	3.30	CF_3 −60.7 SeF_2 −69.5	+834	^3J(FH) 10.2 ^3J(FF) 11.9 ^2J(SeF) 51.2 ^1J(SeF) 505
$(CF_3)_2SeF_2$	$CDCl_3$	—	CF_3 −52.3 (−53.2)[k] SeF_2 −70.7 (−68.8)[k]	(+830)[k]	^3J(FF) 13.0 (13.0)[k] ^2J(SeF) 50.0 ^1J(SeF) 337.5 (377)[k]
CH_2FOMe	Me_2O	CH_3 3.40 CH_2 5.16	−155	—	^2J(FH) 56.7 ^4J(FH) 2.1
CH_2FSMe	$CDCl_3$	CH_3 2.29[h] CH_2 5.43[h]	−189.0	—	^2J(FH) 54.0 ^4J(FH) 2.4
CH_2FSeMe	$CDCl_3$	CH_3 2.20 CH_2 5.79	−196.3	—	^2J(FH) 52.3 ^4J(FH) 2.0
CH_2FSCF_3	$MeSCF_3$	CH_2 5.66	CF −188.2 CF_3 −42.0	—	^2J(FH) 52
$MeIF_2$	MeI	4.13 (4.23)[l]	−174 (−176.4)[l]	—	^3J(FH) 6.8(7)[l]
MeF	MeCl, MeBr or MeI	4.12 to 4.25 (4.26)[m]	−263 to −268 (−272)[m]	—	^2J(FH) 46.5–47 (46.4)[m]

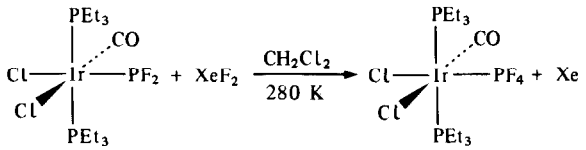
[a] Numbers in parentheses correspond to values reported previously.
[b] X = ^{31}P or ^{77}Se referenced to external 85% H_3PO_4 in D_2O or Me_2Se respectively.
[c] CCl_4 solution, Ref. 17. [d] Neat liquid, Ref. 17.
[e] $[Me_3PF]^+[BF_4]^-$ in SO_2 solution at −30°C, Ref. 16. [f] $CDCl_3$ solution, Ref. 19.
[g] $CDCl_3$ solution, Ref. 23. [h] Ref. 10.
[i] Conditions not specified, Ref. 4(a). [j] Benzene solution, Ref. 4(c).
[k] Neat liquid, Ref. 4(b). See also W. Gombler, *Z. Naturforsch., Teil B* 1981, **36**, 535.
[l] MeI solution, Ref. 9(b). [m] CCl_4 solution, Ref. 33.

unresolved features at ambient temperatures, although the NMR parameters quoted for all three species Me_3XF_2 (X = P,[17] As,[19] or Sb[23]) are close to those we have measured (see Table 2).

(c) *Behaviour in hydrogen fluoride solution.* As reported previously,[10] xenon difluoride reacts with a hydrogen fluoride solution of dimethyl sulphide or the adduct $Me_2S \cdot BF_3$ to form the cation $[Me_2SF]^+$. However, no similar reaction occurs with either trimethylamine or trimethyl-phosphine in hydrogen fluoride solution. No xenon is evolved when xenon difluoride is introduced into such a solution at room temperature, and the ^1H NMR spectrum of the solution shows that the cation $[Me_3XH]^+$ (X = N or P) survives unchanged. A hydrogen fluoride solution of trimethylphosphorus difluoride at ambient temperatures yielded ^1H and ^{19}F NMR spectra consisting of broad resonances; cooling the sample to 0°C caused the resonances to be resolved into the multiplets characteristic[17] of the fluorotrimethylphosphonium cation, $[Me_3PF]^+$ (Table 2). Hence trimethylphosphorus difluoride resembles dimethylsulphur difluoride[10] under these conditions in its ionisation in accordance with the equation

$$Me_3PF_2 + nHF \rightarrow [Me_3PF]^+[F(HF)_n]^-.$$

The immunity of four-coordinate phosphorus, as in the cation $[Me_3PH]^+$, to attack by xenon difluoride is also strikingly illustrated by the very recent report of the following reaction[24]



in which the coordinated PF_2 but not the PEt_3 ligands undergo oxidative fluorination. This is perhaps the most telling example yet of the selectivity which can be achieved through the use of xenon difluoride as a fluorinating agent.

(ii) *Methyl derivatives of group VI elements*

(a) *Dimethyl ether.* In contrast to the potentially explosive reaction between xenon difluoride and either dimethyl sulphide[10] or dimethyl selenide (q.v.), xenon difluoride reacts extremely slowly with liquid dimethyl ether in Teflon apparatus at ambient temperatures. Crystals of xenon difluoride are consumed by the liquid over a period of several days with the evolution of xenon gas. The ^1H and ^{19}F NMR spectra of the liquid showed, in addition to the ^1H resonance associated with the excess of dimethyl ether, resonances attributable to fluoromethyl methyl ether, CH_2FOMe. This compound has been prepared previously by the action of a metal fluoride on chloro- or bromomethyl methyl ether, and characterised by its vibrational and microwave spectra.[25] The relevant NMR parameters which we have determined are listed in Table 2 together with those of the related molecules CH_2FSMe and CH_2FSeMe.

(b) *Methylsulphur compounds.* Xenon difluoride reacts with dimethyl sulphide diluted in trichlorofluoromethane in a matter of minutes at room temperature to form initially CH_2FSMe; the corresponding reaction in hydrogen fluoride solution yields $[Me_2SF]^+$.[10] On the evidence of the ^1H and ^{19}F NMR spectra, methyl trifluoromethyl sulphide, $MeSCF_3$, behaves in a similar fashion yielding either the hitherto unknown CH_2FSCF_3 in non-acidic conditions or the novel sulphonium cation $[Me(CF_3)SF]^+$ in hydrogen fluoride solution. Neat methyl trifluoromethyl sulphide reacts slowly with xenon difluoride at 20°C but not at all in the presence of caesium fluoride. Neat bis(trifluoromethyl) sulphide reacts quantitatively with xenon difluoride in 24 h at 20°C to yield the known compound $(CF_3)_2SF_2$[4(a),26] as the major sulphur-containing product formed in accordance with the reaction

$$(CF_3)_2S + XeF_2 \rightarrow (CF_3)_2SF_2 + Xe.$$

The sulphides Me_2S and $MeSCF_3$ react also with xenon difluoride in hydrogen fluoride solution in the presence of boron trifluoride to give adducts best formulated as $[Me_2SF]^+[BF_4]^-$[10] and $[Me(CF_3)SF]^+[BF_4]^-$;[27] a fuller account of these and related compounds will be given elsewhere.[28]

Thus, provided that neither of the substituents in an organic sulphide RR'S is susceptible to fluorination, xenon difluoride offers a route to the corresponding sulphur(IV) compound $RR'SF_2$, as shown previously in the cases where R = R' = Ph[29] and R = aryl group, R' = CF_3.[30]

(c) *Methylselenium compounds.* Dimethyl selenide has been shown to react with silver(II) fluoride affording dimethylselenium difluoride, Me_2SeF_2, in 22% yield.[4(c)] We have shown that the selenide dissolved in either trichlorofluoromethane or anhydrous hydrogen fluoride reacts with xenon difluoride at room temperature with the quantitative release of xenon and the formation of dimethylselenium difluoride in yields exceeding 90% (based on the amount of XeF_2 taken). At room temperature and in the presence of a small amount of caesium fluoride, a deuteriochloroform solution of the dimethylselenium difluoride gives rise to well-resolved first-order ^1H, ^{19}F, and ^{77}Se NMR spectra

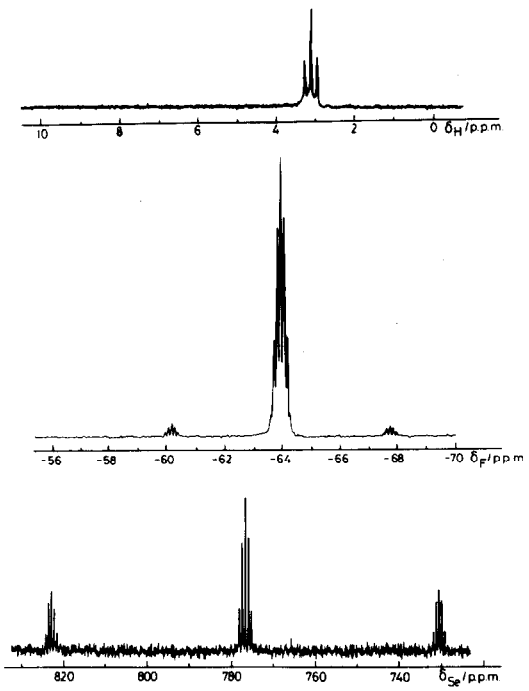
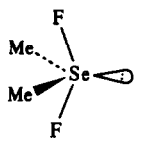


Fig. 2. 60 MHz ^{1}H, 84.26 MHz ^{19}F and 17.04 MHz ^{77}Se NMR spectra of Me_2SeF_2 in $CDCl_3$ solution.

(see Fig. 2). Where comparisons can be made, the NMR parameters thus derived tally closely with those reported earlier;[4(c)] the identity of the neat difluoride has also been confirmed by elemental analysis and Raman spectroscopy.[31] All the spectra are consistent with the presence of Me_2SeF_2 molecules having the structure I with the two methyl groups occupying equatorial sites and the two fluorine atoms axial sites of a trigonal bipyramid centred on the selenium atom, although the comparatively low volatility of the compound at room temperature[4(c)] points to strong intermolecular interactions in the condensed phases.



I

At ambient temperatures a very dilute hydrogen fluoride solution of dimethylselenium difluoride exhibited a single ^{1}H resonance ($\delta_H = 3.3$); at -40°C the resonance was resolved into a triplet ($\delta_H = 3.2$, J(FH) = 8.5 Hz); a more concentrated solution gave a resonance which remained unresolved even at temperatures as low as -70°C. Hence it appears that dimethylselenium difluoride, unlike its sulphur analogue,[10] exists in hydrogen fluoride solution as undissociated molecules.

In a non-acidic medium dimethylselenium difluoride is appreciably more stable than its sulphur analogue[10] with respect to the elimination of hydrogen fluoride. However, decomposition in accordance with the equation

$$Me_2SeF_2 \rightarrow CH_2FSeMe + HF$$

occurs very slowly at ambient temperatures. Thus, after a deuteriochloroform solution of the compound has been allowed to stand for 10 weeks, the ^{1}H and ^{19}F resonances due to Me_2SeF_2 are found to have broadened and lost the multiplicity originating in H–F coupling. In addition, the spectra reveal the simultaneous appearance of new resonances attributable to the novel compound CH_2FSeMe (see Table 2).

Neat methyl trifluoromethyl selenide reacts smoothly with xenon difluoride at room temperature with the near-quantitative formation of the novel compound methyl(trifluoromethyl)selenium difluoride, $Me(CF_3)SeF_2$, in accordance with the equation

$$MeSeCF_3 + XeF_2 \rightarrow Me(CF_3)SeF_2 + Xe.$$

A colourless mobile liquid scarcely volatile at room temperature, the product has been characterised by elemental analysis and by its ^{1}H, ^{19}F, and ^{77}Se NMR spectra (see Table 2 and Fig. 3) and vibrational spectra (see Table 3). It shows no sign of

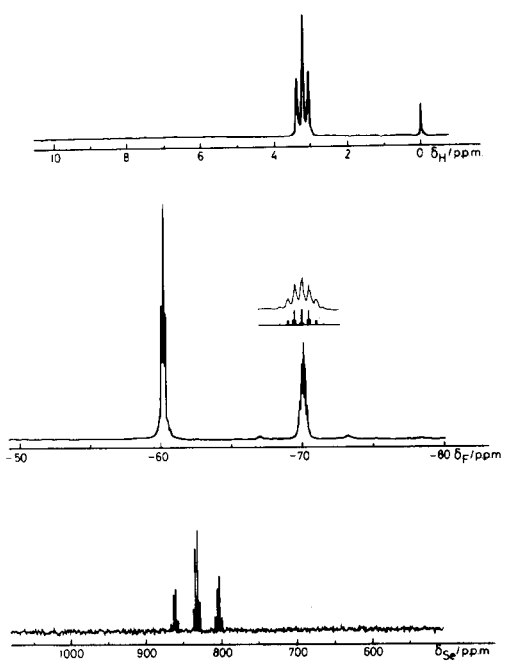


Fig. 3. 60 MHz ^{1}H, 84.26 MHz ^{19}F and 17.04 MHz ^{77}Se–{^{1}H} NMR spectra of $Me(CF_3)SeF_2$ in $CDCl_3$ solution.

Table 3. Principal features in the vibrational spectra of liquid methyl(trifluoromethyl)selenium difluoride

IR (cm^{-1})	Raman (cm^{-1})	Assignment
3050 w 2960 vw	3080 vw, br 2963 m	C–H stretching
1410 m 1290 w	1380 vw	CH_3 def.
1200 vs, br 1100 vs	1100 vw	C–F stretching
1045 w		*ca* 740 + 300
935 m		CH_3 rocking
810 m		*ca* 500 + 300
741 s 731 w	751 s 731 m	sym. CF_3 def. + combination mode
	608 s	Se–CH_3 stretching
490 vs, br	506 s, br	SeF_2 stretching + antisym. CF_3 def.
	384 w	Se–CF_3 stretching + CF_3 rocking
	342 m	CF_3 rocking
	300 s	SeF_2 def. + CF_3 rocking

w = weak, m = medium, s = strong, v = very, br = broad.

decomposition over a period of 5 weeks at room temperature (cf. Me_2SeF_2).

Liquid bis(trifluoromethyl) selenide reacts slowly but quantitatively with xenon difluoride to yield bis(trifluoromethyl)selenium difluoride, $(CF_3)_2SeF_2$. This relatively volatile compound (vapour pressure *ca* 35 mmHg at room temperature) has been produced otherwise by fluorination of the selenide with either chlorine monofluoride[4b] or silver difluoride;[32] the electron-diffraction pattern of the vapour implies that the molecule has a skeleton derived from a trigonal bipyramid with equatorially sited CF_3 and axially sited F ligands.[32] We find that it reacts immediately on contact with borosilicate glass to give the white solid selenoxide $(CF_3)_2SeO$.

On the evidence of these experiments, xenon difluoride appears to be particularly well suited to the preparation of diorgano derivatives of selenium tetrafluoride, $RR'SeF_2$ (where R and R′ may be the same or different organic groups). Where the organic groups contain C–H bonds, the diorganoselenium difluoride is much slower to eliminate hydrogen fluoride than is the corresponding sulphur compound.

(iii) *Methyl derivatives of group VII elements*

Gibson *et al.* have detected methyliodine difluoride, $MeIF_2$, by its ^1H and ^{19}F NMR spectra as a product of the reaction between xenon difluoride and iodomethane.[9] We have confirmed that xenon difluoride reacts smoothly with an excess of liquid iodomethane in the presence of caesium fluoride at room temperature with the quantitative evolution of xenon gas and the development of the resonances associated with methyliodine difluoride[9]

$$MeI + XeF_2 \rightarrow MeIF_2 + Xe.$$

Standing at room temperature for several hours causes the initially colourless iodomethane solution to assume the deep purple colour characteristic of elemental iodine. The ^1H and ^{19}F NMR spectra of the solution testify to the decay of the methyliodine difluoride with the formation of fluoromethane;[33] there are no signs of higher iodine fluorides.

Xenon difluoride reacts much more slowly with liquid chloromethane or bromomethane at room temperature but there is no spectroscopic evidence of the species $MeXF_2$ (X = Cl or Br). The evolution of xenon gas is accompanied by the development of a yellowish-green (MeCl) or yellowish-brown (MeBr) colouration, and fluoromethane is identified as the sole hydrogen- and fluorine-containing product in each case by the ^1H and ^{19}F NMR spectra of the solution[33] and by the IR spectrum displayed by the vapour of the material volatile at −112°C.[34] The evidence available points to cleavage of the C–X bond in accordance with the equation

$$2MeX + XeF_2 \rightarrow 2MeF + X_2 + Xe.$$

DISCUSSION

Xenon difluoride is now well characterised with respect to certain aspects of its chemistry, e.g. in its ability to act as an electrophilic fluorinating agent[7] and its capacity to release fluoride ions with the formation of the cationic species $[XeF]^+$ and $[Xe_2F_3]^+$.[6] Some of its reactions are subject evidently to catalysis by traces of acid.[6,35] However, the response of xenon difluoride to donor species is relatively sparsely charted and attempts to exploit any acidic character in the formation of the trifluoroxenate(II) anion, $[XeF_3]^-$, have proved fruitless.[36]

Xenon difluoride reacts with donor molecules of the type Me_nX, where $n = 1$–3 and X is a *p*-block element belonging to Groups V–VII, and the facility of the reaction appears to parallel the base strength of Me_nX, as illustrated by the following variations of reaction rate: (a) $Me_3As > Me_2Se > MeBr$; (b) $Me_2X \gg MeXCF_3 > (CF_3)_2X$ (X = S or Se). With trichloro fluoromethane or the neat reagent as the solvent in the presence of caesium fluoride, the cation $[XeF]^+$ is unlikely to function as an intermediate. A more plausible mechanism involves interaction between the donor molecule and molecular XeF_2 functioning as a Lewis acid. The lowest unoccupied molecular orbital of XeF_2 possesses σ-symmetry and is anti-bonding in character (see Fig. 4).[6,37] The symmetry of this frontier orbital is expected to encourage the approach of the donor atom X along the principal axis of the F–Xe–F molecule. Such a model is consistent with the changes in energy exhibited by the antisymmetric Xe–F stretching mode when XeF_2 is exposed to different environments.[38] Thus, the energy is reported to decrease from 555 cm^{-1} for the gaseous molecule and 547 cm^{-1} for the solid to 538, 533, 532, or 530 cm^{-1} for the molecule dissolved in CCl_4, MeCN, $MeNO_2$, or dioxan respectively. As the donor capacity of the solvent increases and the molecule relaxes its grip on the electrons occupying the HOMO, the energy gap between this HOMO and the LUMO of XeF_2 is narrowed; as a result charge-transfer from the solvent to XeF_2 is enhanced, but at the expense of the Xe–F bond strength.

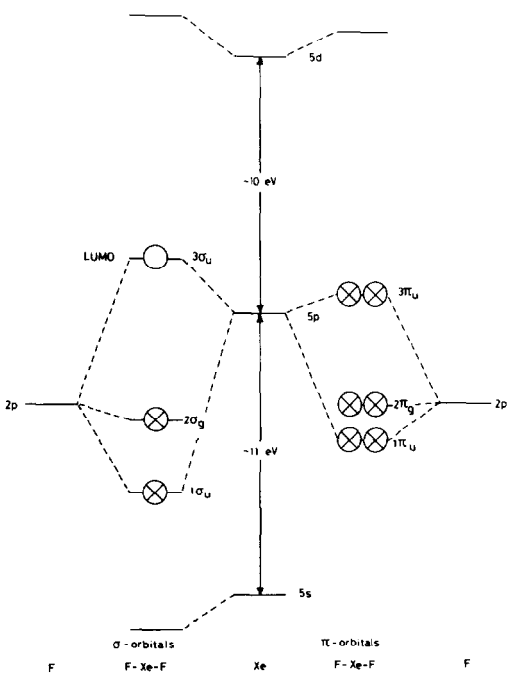


Fig. 4. One-electron orbital energy diagram for XeF_2, adapted from Ref. 37.

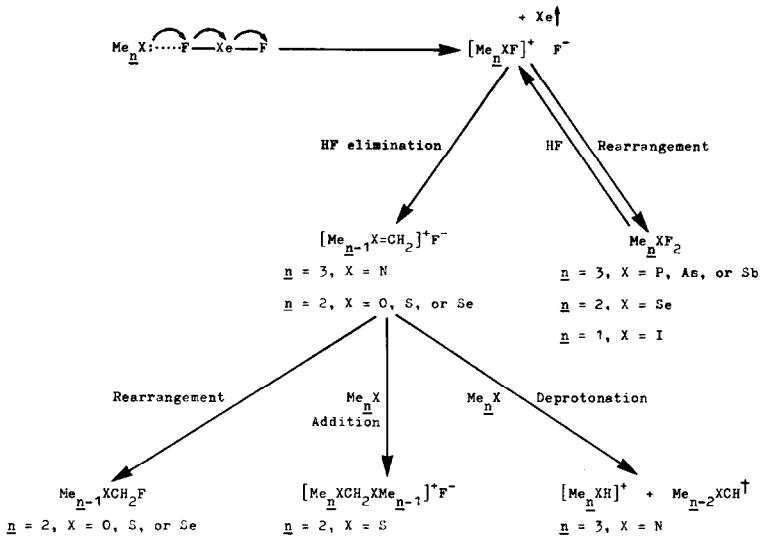
A possible sequence for the subsequent reactions between Me_nX and XeF_2 is depicted in Scheme 1. Transfer of charge proceeds with the formation of the ion-pair $[Me_nXF]^+F^-$ which may then rearrange to form the molecular difluoride Me_nXF_2. Alternatively, depending on the strength of the X–F bond and the basicity of Me_nX, the ion-pair may eliminate HF to form the intermediate $[Me_{n-1}X{=}CH_2]^+F^-$. This in turn may suffer one of three possible fates: (i) rearrangement to give the molecular monofluoromethyl derivative $Me_{n-1}XCH_2F$ (as when $n = 2$ and X = O, S, or Se); (ii) addition to another molecule of Me_nX to give a derivative of the cation $[Me_nXCH_2XMe_{n-1}]^+$ (as when $n = 2$ and X = S);[10] or (iii) elimination of HF in the presence of Me_nX to give the cation $[Me_nXH]^+$ and the carbene $Me_{n-1}XCH$ which is susceptible to polymerisation and other secondary reactions (as seems to be the case when $n = 3$ and X = N).[14,15]

If the molecular difluoride Me_nXF_2 is thermally fragile, there is the risk that the threshold temperature required to initiate selective but highly exothermic fluorination with xenon difluoride is too high to permit the survival of the desired product. Such is the case with X = S ($n = 2$).[10] With the most strongly basic substrates, like Me_3N and Me_3P, protonation yielding the cation $[Me_nXH]^+$ occurs to such an extent in acid solution as to leave insufficient free base to react at an appreciable rate with xenon difluoride.

On the other hand, the feebly basic haloalkane molecules MeX (X = Cl, Br, or I) react very slowly with xenon difluoride, and their pattern of reaction differs from that outlined above. Although iodomethane undergoes oxidative addition initially to form methyliodine difluoride, the mechanism for the overall reaction

$$2MeX + XeF_2 \rightarrow 2MeF + X_2 + Xe$$

(X = Cl, Br, or I)



† Polymerises or undergoes other secondary reactions; see Refs. 14 and 15.

Scheme 1.

is not immediately apparent. We propose that the underlying reaction with a haloalkane molecule involves a simple nucleophilic attack by fluoride anion, either real (formed for example via heterolytic fission of XeF_2) or incipient (in XeF_2 itself). Such a process, although slow at ambient temperatures, is favoured with the haloalkanes partly by default (i.e. for want of the basic properties needed to promote difluorine-addition), partly by the strength of the C–F bond formed and the ease of displacement of halide anions (cf. the corresponding leaving groups $[Me_{n-1}X]^-$; $n = 3$, X = N, P, As, or Sb; $n = 2$, X = O, S, or Se)

$$F^- + MeX \rightarrow MeF + X^-.$$

The halide anions are then oxidized by XeF_2 (or perhaps $MeIF_2$ where X = I) to the elemental halogen

$$2X^- + XeF_2 \rightarrow X_2 + Xe + 2F^-.$$

We cannot account for our results simply on the basis of the elimination of MeF by thermal decomposition of the halogen(III) fluoride $MeXF_2$ since this would be expected also to give rise to the appropriate halogen monofluoride, or at least its disproportionation products (e.g. $Br_2 + BrF_3$ or $I_2 + IF_5$).[39] Furthermore, the cleanliness of the reactions and the absence of molecules such as CH_2FX (X = Cl, Br, or I)[40] counter suggestions that fluorination with xenon difluoride takes place through a predominantly free-radical mechanism.[6,7]

Despite these complications, xenon difluoride emerges as a highly efficient and selective agent for the conversion of several organic derivatives of the *p*-block elements R_nX to the corresponding difluorides R_nXF_2. The specificity of the reactions, combined with the volatility and immunity to side-reactions of the co-product—elemental xenon—offer significant advantages over the use of reagents like elemental fluorine or the halogen fluorides.

EXPERIMENTAL

Caution. Xenon difluoride reacts explosively with the methyl derivatives Me_nX ($n = 3$, X = N, P, As, or Sb; $n = 2$, X = S or Se) in the absence of a diluent. Although the reactions are moderated with CCl_3F or HF as the diluent, suitable shielding should be employed at all times.

Apparatus. Experiments were carried out with a vacuum system constructed in Teflon-FEP tubing with PTFE couplings and needle valves (Production Techniques Ltd.). Apparatus was conditioned before use by exposure overnight to fluorine gas at a pressure of 1 atm.

A conventional glass vacuum system was available for the purification of other reagents and CCl_3F (B.D.H.) prior to its use as a diluent. A nitrogen-filled glove-box was used for the storage and transfer of xenon difluoride and other solid materials.

Chemicals. Xenon difluoride was prepared by exposure to sunlight of a Pyrex bulb containing an equimolar xenon–fluorine mixture, typically for about 1 week.[41] Caesium fluoride (Alfa, 99.9%) was

used as supplied, whereas hydrogen fluoride (B.D.H., 99.8%) was purified before use by double distillation from Teflon-FEP traps held at −63°C. The following reagents were obtained from commercial sources: trimethylamine (B.D.H.), dimethyl ether (B.D.H.), dimethyl sulphide (B.D.H.), dimethyl selenide (Alfa), and the haloalkanes MeX (X = Cl, Br, or I; all B.D.H.). Trimethyl-phosphine, -arsine, and -stibine were prepared by standard procedures.[42] The compounds $(CF_3)_2X$ and $Hg(XCF_3)_2$ (X = S or Se) were kindly made available by Professors A. Haas and W. Gombler; the monomethyl derivatives $MeXCF_3$ were prepared by the reaction between $Hg(XCF_3)_2$ and neat iodomethane at 70°C for 2–4 days. Each volatile reagent was typically purified by fractional condensation *in vacuo* and its purity checked by reference to its vapour pressure at an appropriate temperature and to the IR spectrum of its vapour.

Spectrometers. NMR spectra were recorded with the aid of four different spectrometers, a JEOL PMX-60 (^1H, 60 MHz), a Perkin–Elmer R32 (^1H, 90 MHz; ^{19}F, 84.6 MHz), a JEOL FX-90Q FT spectrometer (^1H, 89.56 MHz; ^{19}F, 84.26 MHz; ^{77}Se, 17.04 MHz), and a Brüker WH-90 FT instrument (^{31}P, 36.43 MHz). Each sample was normally sealed in a section of FEP tubing 5–10 cm long and 4 mm in external diameter which was inserted into a standard 5 mm precision NMR tube.[10,22] Chemical shifts were referenced, where possible, to internal $SiMe_4$ or CCl_3F; ^{77}Se and ^{31}P shifts were measured by sample interchange using as external standards neat Me_2Se and 85% H_3PO_4 in D_2O respectively. With hydrogen fluoride solutions, ^1H shifts were measured by sample interchange using CH_2Cl_2 ($\delta_H = 5.30$ ppm) as a secondary standard.

IR spectra of vapours were measured with a Pye Unicam Model SP 2000 spectrophotometer. Raman spectra of liquid samples, measured with a Spex Ramalog 5 spectrophotometer, were excited at $\lambda =$ 514.5 nm using the output from a Spectra-Physics Model 165 Ar^+ laser.

Reactions with XeF_2. A typical experiment was performed with a vessel constructed from PTFE components (Chemcon, Production Techniques Ltd.) and heat-moulded Teflon-FEP tubing, the internal capacity being 5–10 cm^3. The reaction chamber was loaded with 50–200 mg (0.3–1.2 mmol) of xenon difluoride and *ca* 50 mg (0.33 mmol) of finely powdered caesium fluoride; in addition, *ca* 5 mg of caesium fluoride was introduced into a side-arm intended to contain the NMR sample. The reagent was co-condensed with the xenon difluoride to give the proportions substrate: $XeF_2 > 1:1$, together with CCl_3F (2–5 cm^3) where necessary as a moderator. The mixture was then allowed to warm up to room temperature. With the completion of the reaction, material volatile at low temperatures (−45 to −95°C) could be removed and assayed by tensimetric and IR measurements. The less volatile component remaining in the reaction chamber could then be weighed before transfer either by distillation or by decanting the neat liquid or a solution into the side-arm which was sealed for analysis, typically by NMR spectroscopy. Essential details of the different experiments are summarised in Table 1.

Elemental analysis of some of the less volatile products was performed by the Analytische Laboratorien Elbach, Engelskirchen, West Germany with the following results (%).

Compound		C	H	F	Se
Me_2SeF_2	found	16.18	3.94	25.35	53.45
	calc.	16.34	4.11	25.84	53.70
$Me(CF_3)SeF_2$	found	11.95	1.59	47.11	39.04
	calc.	11.95	1.51	47.26	39.28
$(CF_3)_2SeO$	found	10.15	—	48.69	33.86
	calc.	10.31	—	48.93	33.89

Details of the IR and Raman spectra of liquid methyl(trifluoromethyl)selenium difluoride are given in Table 3; the features may be interpreted by analogy with the vibrational analyses carried out previously on the compounds Me_2SeF_2[31] and $(CF_3)_2SeF_2$.[4b]

Acknowledgements—We thank the S.E.R.C. for research grants and the award of a research studentship (to A.M.F.) and Christ Church, Oxford for the award of a Graduate Scholarship (also to A.M.F.); we are grateful also to Professors A. Haas and W. Gombler for providing samples of the trifluoromethyl compounds $(CF_3)_2X$ and $Hg(XCF_3)_2$ (X = S or Se), and to Dr. M. C. Grossel and Mr. D. R. Parkinson for practical assistance with some of the NMR measurements.

REFERENCES

1. I. Ruppert and V. Bastian, *Angew. Chem., Int. Ed. Engl.* 1977, **16**, 718; 1978, **17**, 214. I. Ruppert, *Chem. Ber.* 1979, **112**, 3023.
2. D. Naumann and H. R. Feist, *J. Fluorine Chem.* 1980, **15**, 541. E. K. S. Liu and R. J. Lagow, *J. Am. Chem. Soc.* 1976, **98**, 8270; *J. Organomet. Chem.* 1978, **145**, 167; *Inorg. Chem.* 1978, **17**, 618.
3. (a) R. Schmutzler, *Halogen Chemistry* (Edited by V. Gutmann), Vol. 2, p. 31, Academic Press, New York (1967); (b) V. I. Popov and N. V. Kondratenko, *J. Gen. Chem. USSR (Engl. Transl.)* 1976, **46**, 2477; (c) W. C. Smith, *J. Am. Chem. Soc.* 1960, **82**, 6176.

4. (a) D. T. Sauer and J. M. Shreeve, *J. Fluorine Chem.* 1971/72, **1**, 1; (b) C. Lau and J. Passmore, *J. Fluorine Chem.* 1976, **7**, 261; (c) K. J. Wynne and J. Puckett, *J. Chem. Soc., Chem. Commun.* 1968, 1532; K. J. Wynne, *Inorg. Chem.* 1970, **9**, 299; (d) D. Naumann and S. Herberg, *J. Fluorine Chem.* 1982, **19**, 205.
5. C. S. Rondestvedt, Jr., *J. Am. Chem. Soc.* 1969, **91**, 3054; O. R. Chambers, G. Oates and J. M. Winfield, *J. Chem. Soc., Chem. Commun.* 1972, 839.
6. A. H. Cockett, K. C. Smith, N. Bartlett and F. O. Sladky, *The Chemistry of the Monatomic Gases*, Pergamon Press, Oxford (1975). Gmelins Handbuch der Anorganischen Chemie, *Edelgasverbindungen*, Verlag Chemie, Weinheim/Bergstrasse (1970); J. H. Holloway, *Noble-gas Chemistry*, Methuen, London (1968); J. G. Malm, H. Selig, J. Jortner and S. A. Rice, *Chem. Rev.* 1965, **65**, 199.
7. R. Filler, *Israel J. Chem.* 1978, **17**, 71 (and references cited therein); M. R. C. Gerstenberger and A. Haas, *Angew. Chem., Int. Ed. Engl.* 1981, **20**, 647.
8. R. C. Burns, I. D. MacLeod, T. A. O'Donnell, T. E. Peel, K. A. Phillips and A. B. Waugh, *J. Inorg. Nucl. Chem.* 1977, **39**, 1737; D. M. Bruce, A. J. Hewitt, J. H. Holloway, R. D. Peacock and I. L. Wilson, *J. Chem. Soc., Dalton Trans.* 1976, 2230; M. J. Atherton and J. H. Holloway, *J. Chem. Soc., Chem. Commun.* 1977, 424; 1978, 254.
9. (a) J. A. Gibson and A. F. Janzen, *J. Chem. Soc., Chem. Commun.* 1973, 739; (b) J. A. Gibson, R. K. Marat and A. F. Janzen, *Can. J. Chem.* 1975, **53**, 3044.
10. A. M. Forster and A. J. Downs, *J. Chem. Soc., Dalton Trans.* 1984, 2827.
11. J. A. Gervasi, M. Brown and L. A. Bigelow, *J. Am. Chem. Soc.* 1956, **78**, 1679.
12. R. W. Rendell and B. Wright, *Tetrahedron* 1979, **35**, 2405.
13. H. Böhme and W. Krause, *Chem. Ber.* 1951, **84**, 170.
14. R. Kiesel and E. P. Schram, *Inorg. Chem.* 1973, **12**, 1090.
15. F. Knoll and U. Krumm, *Chem. Ber.* 1971, **104**, 31.
16. F. Seel and H.-J. Bassler, *Z. Anorg. Allg. Chem.* 1975, **418**, 263.
17. A. J. Downs and R. Schmutzler, *Spectrochim. Acta* 1967, **23A**, 681.
18. See Ref. 3(a), p. 43.
19. M. H. O'Brien, G. O. Doak and G. G. Long, *Inorg. Chim. Acta* 1967, **1**, 34.
20. G. G. Long, G. O. Doak and L. D. Freedman, *J. Am. Chem. Soc.* 1964, **86**, 209.
21. I. A. Steer, D. Phil. thesis, University of Oxford (1969).
22. R. R. Reinhard, *Rev. Sci. Instrum.* 1965, **36**, 549.
23. G. G. Long, C. G. Moreland, G. O. Doak and M. Miller, *Inorg. Chem.* 1966, **5**, 1358.
24. E. A. V. Ebsworth, J. H. Holloway, N. J. Pilkington and D. W. H. Rankin, *Angew. Chem., Int. Ed. Engl.* 1984, **23**, 630.
25. C. T. Mason and C. C. Allain, *J. Am. Chem. Soc.* 1956, **78**, 1682; M. Hayashi and H. Kato, *Bull. Chem. Soc. Jpn* 1980, **53**, 2701; J. Nakagawa, H. Kato and M. Hayashi, *J. Mol. Spectrosc.* 1981, **90**, 467; D. C. McKean, I. Torto and A. R. Morrisson, *J. Mol. Struct.* 1983, **99**, 101.
26. D. A. Coe and J. M. Shreeve, *Spectrochim. Acta* 1977, **33A**, 965; H. Oberhammer, R. C. Kumar, G. D. Knerr and J. M. Shreeve, *Inorg. Chem.* 1981, **20**, 3871.
27. A. M. Forster, D.Phil. thesis, University of Oxford (1983).
28. A. J. Downs and A. M. Forster (paper to be published).
29. R. K. Marat and A. F. Janzen, *Can. J. Chem.* 1977, **55**, 3031.
30. Yu. L. Yagupol'skii and T. I. Savina, *J. Org. Chem. USSR (Engl. Transl.)* 1979, **15**, 386.
31. R. H. Larkin, H. D. Stidham and K. J. Wynne, *Spectrochim. Acta* 1971, **27A**, 2261.
32. P. L. Baxter, A. J. Downs, A. M. Forster, M. J. Goode, D. W. H. Rankin and H. E. Robertson, *J. Chem. Soc., Dalton Trans.* 1985, 941.
33. F. A. Bovey, *NMR Data Tables for Organic Compounds*, p. 8, Interscience, New York (1967); J. W. Emsley and L. Phillips, *Prog. Nucl. Magn. Reson. Spectrosc.* 1971, **7**, 116.
34. R. Mecke and F. Langenbucher, *Infrared Spectra of Selected Chemical Compounds*, Vol. VII, Serial No. 1687, Heyden, London (1965); G. Herzberg, *Molecular Spectra and Molecular Structure. II. Infrared and Raman Spectra of Polyatomic Molecules*, p. 315, Van Nostrand, Princeton, N.J. (1945).
35. N. Bartlett and F. O. Sladky, *J. Chem. Soc., Chem. Commun.* 1968, 1046; M. J. Shaw, H. H. Hyman and R. Filler, *J. Am. Chem. Soc.* 1970, **92**, 6498.
36. I. Sheft, T. M. Spittler and F. H. Martin, *Science* 1964, **145**, 701; G. J. Moody and H. Selig, *Inorg. Nucl. Chem. Lett.* 1966, **2**, 319.
37. C. A. Coulson, *J. Chem. Soc.* 1964, 1442.
38. H. Meinert and G. Kauschka, *Z. Chem.* 1969, **9**, 114.
39. A. J. Downs and C. J. Adams, *The Chemistry of Chlorine, Bromine, Iodine and Astatine.* Pergamon Press, Oxford (1975).
40. I. O. Leipunskii, I. I. Morozov and V. L. Tal'roze, *Dokl. Phys. Chem. (Engl. Transl.)* 1971, **198**, 547.
41. S. M. Williamson, *Inorg. Synth.* 1968, **11**, 147.
42. M. Halmann, *Spectrochim. Acta* 1960, **16**, 407; R. A. Zingaro and A. Merijanian, *Inorg. Chem.* 1964, **3**, 580; G. O. Doak, G. G. Long and M. E. Key, *Inorg. Synth.* 1967, **9**, 92.

Polyhedron Vol. 4, No. 9, pp. 1637–1641, 1985
Printed in Great Britain

0277–5387/85 $3.00 + .00
© 1985 Pergamon Press Ltd

NMR STUDIES OF MIXED-LIGAND IRON(III) DITHIOCARBAMATES

KRZYSZTOF DRABENT* and LECHOSŁAW LATOS-GRAŻYNSKI
Institute of Chemistry, University of Wrocław, 50-383 Wrocław, F. Joliot-Curie 14, Poland

(*Received* 14 *November* 1984; *accepted* 20 *February* 1985)

Abstract—^{1}H NMR studies of mixed-ligand iron (III) dithiocarbamates have been carried out using the following ligands: *N*,*N*-diethyldithiocarbamate, morpholinyl-*N*-, and piperidyl-*N*-carbodithioate. The ligand exchange equilibria gave all species of the general formula $Fe(dtc)_n(dtc')_{3-n}$, where $n = 0$–3 with nearly random statistical distribution of $Fe(Et_2dtc)_n(morphdtc)_{3-n}$ complexes. Magnetic moments of the mixed-ligand complexes have been determined. Both the magnetic moment and isotropic shift temperature dependences confirmed the cross-over properties of these mixed-ligand complexes.

The possibility of preparing mixed-ligand iron(III) dithiocarbamates of type $Fe(dtc)_2(dtc')$ was first suggested by Wickman and Trozzolo.[1] The formation of such complexes in solution has been reported on the basis of NMR[2–6] and electrochemical[7] studies. It has been found that equilibration takes place in a few minutes leading to the mixture of complexes of general formula $Fe(dtc)_n(dtc')_{3-n}$ ($n = 0$–3).[2,6,7] The radioisotopic exchange studies of tris-dithiocarbamate iron(III) complexes had confirmed the previous kinetic observation.[8] Tsipis *et al.*[9] and Wajda *et al.*[10] had prepared the title complexes in the solid state according to the Wickman and Trozzolo's method[1] and had concluded that the discussed compounds showed the "cross-over" behaviour.

The problems in preparation of mixed-ligand dithiocarbamate complexes have been discussed recently.[5,6] Particularly it is not possible to investigate the magnetic properties of the title compounds in the solid. However, an attempt has been made to determine the solution magnetic properties of the mixed-ligand complexes. An application of the ^{1}H NMR spectroscopy makes possible, at least in principle, the determination of the magnetic susceptibility and composition of the equilibrium mixture of $Fe(dtc)_n(dtc')_{3-n}$ ($n = 0$–3) complexes. As a result, the magnetic properties of the particular form could be determined. Additionally, the temperature dependence of isotropic shifts provided some information related to the spin state of each species existing in solution.

* Author to whom correspondence should addressed.

The present investigation has been undertaken to determine the magnetic properties of the mixed-ligand iron(III) dithiocarbamates by means of the ^{1}H NMR spectroscopy.

EXPERIMENTAL

The sodium diethyldithiocarbamate was commercially available (Merck, F.R.G.) and used as received. Sodium morpholinyl-*N*-, and sodium piperidyl-*N*-carbodithioate were prepared as previously described.[11] $Fe(dtc)_2Cl$ complexes were prepared by the reaction of anhydrous $FeCl_3$ and the sodium salt of the dithiocarbamate ligand in anhydrous ethanol.[1] $Fe(dtc)_3$ complexes were prepared by a standard method[12] and recrystallized from chloroform. The mixed-ligand iron(III) dithiocarbamates were prepared by published methods[9,10] by reaction between stoichiometric amounts of the appropriate chloro complex, $Fe(dtc)_2Cl$, and a salt of dtc'. The isolated product was used without purification. The composition of the product is discussed in the Discussion section (see below).

^{1}H NMR spectra were recorded at 100 MHz on a JEOL PS 100 spectrometer. The pulse and/or CW techniques have been used depending on concentration. Magnetic moments were determined by Evans' method[13] with 2% v/v TMS as the internal reference. The corrections for the change in density of the solution with temperature were applied according to the literature.[14] The variable temperature probe was calibrated with ethanol and ethylene glycol using Van Geet's calibrations.[15] All the spectra were measured in $CDCl_3$ solutions with

concentration about 0.01 M of iron(III) complexes. The measurements were repeated three times at various concentrations.

The samples of mixed-ligand complexes were obtained in two ways: by dissolving a suitable quantity of isolated product and by dissolving appropriate $Fe(dtc)_3$ and $Fe(dtc')_3$ complexes in the required molar ratio (2:1 or 1:2). The spectrum pattern and magnetic properties did not depend on the method of the sample preparation.

RESULTS AND DISCUSSION

1. *Resonance assignments*

Equilibrium mixtures of $Fe(Et_2dtc)_3$ and $Fe(morphdtc)_3$ (denoted as FeE_3 and FeM_3, respectively) should contain four compounds with formula FeE_nM_{3-n}, where $n = 0$, 1, 2 or 3. Compounds with $n = 0$ or 3 are expected to exhibit one α-methylene proton resonance,[16] but two resonances with intensity ratio 1:2 and 2:1 are expected for compounds with $n = 1$ or 2, respectively. The metal centred intramolecular rearrangements are expected to be fast in the temperature range studied.[2,3] Therefore, a total of six α-methylene resonances should be observed for an equilibrium mixture, grouped in two groups of three, differing by their isotropic shifts. The α-methylene proton resonance spectra for the equilibrium mixtures of FeE_3 and FeM_3 in chloroform solutions at various values of ligand composition are shown in Fig. 1.

The ligand composition is specified by the quantity f_A which is defined as the molar fraction of total ligand present as Et_2dtc. The identical NMR spectra as those shown for $f_A = 0.333$ and $f_A = 0.666$ were measured for the products of the reactions aimed at the synthesis of the mixed-ligand complexes in the solid (see Experimental). A total of six α-methylene resonances are observed as expected.

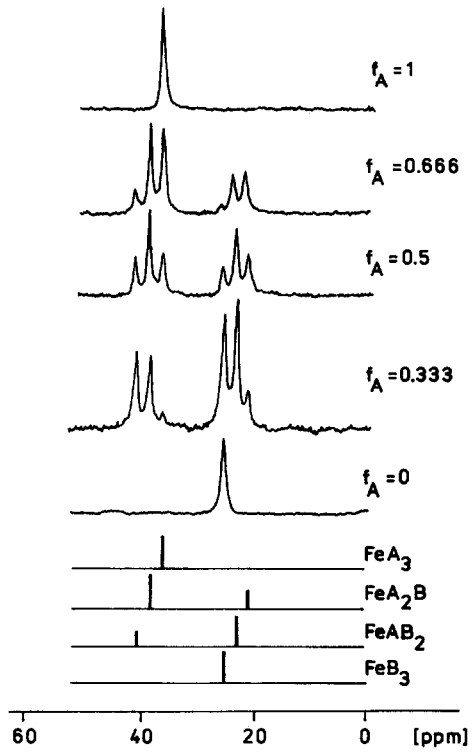


Fig. 1. α-Methylene proton resonance spectra and resonance assignments for equilibrium mixtures of $Fe(Et_2dtc)_3$ and $Fe(morphdtc)_3$ (denoted as FeA_3 and FeB_3, respectively) in $CDCl_3$ at 25°C.

The FeE_3 and FeM_3 singlets have been assigned by comparison with the respective spectra of pure complexes. Based on the dependence of signal intensities on ligand composition and the expected intensity ratios (see above) the resonance assign-

Table 1. Isotropic shifts for iron(III) dithiocarbamate complexes[a]

Compound	α-CH_2[b]	β-CH_2 and/or CH_3[b]
$Fe(Et_2dtc)_3$	36.28	−0.3
$Fe(pipdtc)_3$	25.15	−1.2
$Fe(morphdtc)_3$	27.23	−1.6
$Fe(Et_2dtc)_2(morphdtc)$	E 38.38, M 23.32	E −0.3, M −1.7
$Fe(Et_2dtc)(morphdtc)_2$	E 40.34, M 25.22	E −0.3, M −1.6
$Fe(Et_2dtc)_2(pipdtc)$	E 35.00, P 27.85	E −0.3, P −1.2
$Fe(Et_2dtc)(pipdtc)_2$	E 33.20, P 26.73	E −0.3, P −1.2
$Fe(morphdtc)_2(pipdtc)$	M 24.23, P 31.61	M −1.6, P −1.1
$Fe(morphdtc)(pipdtc)_2$	M 21.37, P 28.15	M −1.7, P −1.2

[a] In $CDCl_3$ at 298 K respective to $Co(dtc)_3$ complexes[21] used as diamagnetic references.

[b] Ligand resonance assignments: E, Et_2dtc; P, pipdtc; M, morphdtc.

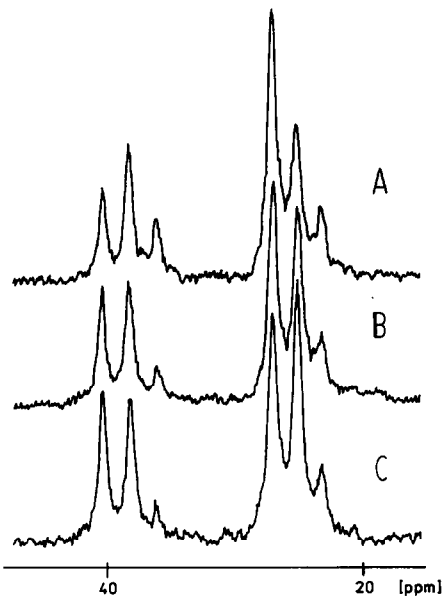


Fig. 2. ^{1}H NMR spectra of FeA_3 and FeB_3 mixture (molar ratio (1 : 2) in $CDCl_3$ at 25°C. A, 3 min; B, 5 min; C, 20 min after dissolving the sample in $CDCl_3$. Resonance assignments and notation—see Fig. 1.

ments have been made as shown in Fig. 1 and Table 1. The resonances due to CH_3 (Et_2dtc) and β-CH_2 (morphdtc) have been observed at -0.3 and -1.6 ppm, respectively (at 298 K). There is no shift differentiation depending on the form composition, so these resonances are of little interest in the present studies.

The assignment of resonances found its confirmation during the studies of equilibration process observed for the FeE_3–FeM_3 system. The NMR spectra of the FeE_3–FeM_3 mixture in $CDCl_3$ were clearly time dependent. The observed intensity changes (Fig. 2) resulted from the equilibration process. The mixed-ligand complexes were formed according to eqn (1):

$$FeE_3 + FeM_3 \rightleftharpoons FeE_2M + FeEM_2. \qquad (1)$$

The equilibrium was established during 20 min, and $t_{1/2}$ of the reaction was estimated to be less than 3 min. The resonance assignment, made in this work, allowed for the detailed determination of the equilibrium mixture composition not discussed before. The NMR spectra of the solid products (see Experimental) indicate that the exchange and equilibration have taken place during the preparation of the complexes.

The equilibrium concentrations of complexes were determined by numerical integration of their α-methylene proton resonance signals. For a completely random statistical distribution of ligands, the dependence of α_i [$i = (3-n)+1$] on ligand composition is given[17] by:

$$\alpha_i = f_A^n(1-f_A)^{3-n}\frac{3!}{n!(3-n)!}, \qquad (2)$$

where f_A is the total molar fraction of ligand A. The observed equilibrium molar fractions of FeE_nB_{3-n} complexes vs ligand composition are shown in Table 2. The values calculated for a random scrambling of ligands according to eqn (2) are also shown. It is readily seen that the FeE_3–FeM_3 system behaves nearly statistically at all temperatures studied.

2. *Magnetic susceptibility measurements*

It was shown in the previous section that the products of reactions between $Fe(dtc)_2Cl$ and Na dtc′ or of FeE_3 and FeM_3 are mixtures of all $Fe(dtc)_n(dtc')_{3-n}$ complexes according to random statistical distribution. As the molar fractions of particular compounds in the mixture were measured it was possible to determine the values and temperature dependence of magnetic moments for FeE_2M and $FeEM_2$ complexes. The magnetic moments of the FeE_3 and FeM_3 complexes as well as the magnetic moments of mixtures denoted $(FeE_2M)^{mix}$ and $(FeEM_2)^{mix}$ were measured for this purpose. Taking into account the determined distribution of compounds in the mixtures the magnetic moments of FeE_2M and $FeEM_2$ complexes were calculated by solution of two linear equations:

$$\mu^2_{(FeE_2M)^{mix}} = \alpha_1\mu^2_{FeE_3} + \alpha_4\mu^2_{FeM_3} + \alpha_2\mu^2_{FeE_2M} + \alpha_3\mu^2_{FeEM_2}$$

$$\mu^2_{(FeEM_2)^{mix}} = \beta_1\mu^2_{FeE_3} + \beta_4\mu^2_{FeM_3} + \beta_2\mu^2_{FeE_2M} + \beta_3\mu^2_{FeEM_2}$$

where α_i and β_i are the molar fractions of particular forms in the mixtures (see Table 2). The results obtained are shown in Table 3.

The magnetic moments for these complexes have shown the cross-over in the temperature range

Table 2. Equilibrium distribution of FeE_nM_{3-n} complexes as a function of ligand composition for $f_E = 0.666$

			α_i^{exp}		
i	Compound	$\alpha_i^{calc.}$	290 K	259 K	248 K
1	FeE_3	0.296	0.293	0.286	0.291
2	FeE_2M	0.444	0.456	0.425	0.439
3	$FeEM_2$	0.222	0.226	0.255	0.232
4	FeM_3	0.038	0.025	0.034	0.038

Table 3. Magnetic moments in $CDCl_3$ solution (μ_B) for FeE_nM_{3-n} complexes ($n = 0$–3)

T(K) \ n	0[a]	3[a]	2[b]	1[b]
210	3.20	3.69	3.53	3.16
228	3.47	3.81	3.62	3.48
233	3.60	3.94	3.76	3.58
248	3.73	4.05	3.94	3.77
259	3.97	4.20	4.23	3.86
278	4.24	4.28	4.34	3.98
290	4.39	4.38	4.34	4.11
300	4.54	4.49	4.34	4.19

[a] Estimated error $\pm 0.03\ \mu_B$.[13]

[b] Error $\pm 0.25\ \mu_B$, calculated by the method of total differential (intensity measurement error assumed as in Ref. 22).

studied, typical for the parental tris-dithiocarbamate iron(III) compounds.[12] It is not possible to correlate the measured magnetic moments and the FeE_nM_{3-n} ($n = 0$–3) complex composition as the error in the magnetic moment calculation is too large.

The analysis of the dependence of isotropic shift vs temperature has shown the very characteristic deviation from the regular Curie behaviour. This conclusion is valid for all species present in the solution. A large increase in isotropic shifts as the temperature increased has been found (Fig. 3) whereas the Curie law requires a decrease in isotropic shifts as the temperature is increased.

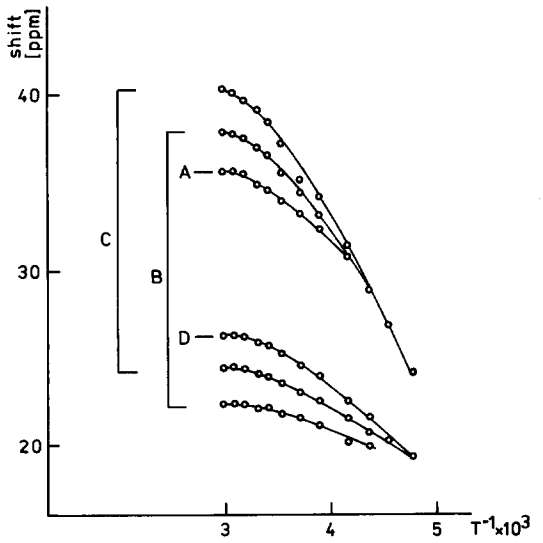


Fig. 3. Temperature dependence of the α-CH_2 chemical shifts for: A, FeA_3; B, FeA_2B; C, $FeAB_2$ and D, FeB_3 complexes. Notation—see Fig. 1.

The increase of the high spin term contribution in the ground state of iron(III) postulated for the cross-over phenomenon[16] is responsible for the observed isotropic shift dependences. This confirms explicitly the magnetic moment studies and provides a strong argument for the cross-over properties of the mixed-ligand complexes.

The pronounced dependence of the isotropic shifts on the complex composition has been found. It reflects the different distribution of the spin density between the A and B ligand depending on the iron dithiocarbamate bond characters, i.e. the total amount of spin delocalized remained constant but as the ligands were different it was shared unequally. It was observed that the sum of the differences of isotropic shifts of mixed-ligand and their parent complexes expressed by the equation:

$$\Delta = (\nu_{FeA_3} - \nu_{FeA_nB_{3-n}})n + (3-n)(\nu_{FeB_3} - \nu_{FeA_nB_{3-n}})$$

was close to zero for each system studied, as expected (see above). The sign of the difference was determined in each case by a pair of two dithiocarbamate ligands. The Et_2dtc α-CH_2 protons have been shifted upfield or downfield in the presence of morphdtc or pipdtc ligand, respectively. The influence of ligand character on the spin distribution has been determined for the variety of complexes of the formula $M(A_2A')$[18] or $M(AA')$.[19] The mechanism of the spin density delocalization of the mixed-ligand complexes is identical to that proposed for FeA_3 and FeB_3 (A and B are dithiocarbamate ligands) as the isotropic shift pattern is similar in each case[20] (see Table 1) and is determined mainly by the contact shift.

3. *Other systems*

The isotropic shifts and resonance assignments for $Fe(Et_2dtc)_n(pipdtc)_{3-n}$ and

$$Fe(pipdtc)_n(morphdtc)_{3-n}\ (n = 0\text{–}3)$$

are shown in Table 1. In this manner all binary systems including Et_2dtc–pipdtc–morphdtc ligands were investigated. The large overlapping of resonances made it impossible to study the magnetic properties of four of the six mixed-ligand complexes observed. The isotropic shift vs temperature dependences could be made in each case. The noted deviation from the Curie law allowed us to conclude that all systems studied belong to the class of cross-over complexes. The distribution of the species in the equilibrium could be measured only in a few cases. The small deviations from random statistical distributions have been found for $Fe(pipdtc)_n(morphdtc)_{3-n}$ and $Fe(Et_2dtc)_n(pipdtc)_{3-n}$ systems.

CONCLUSION

The NMR studies of the mixed-ligand iron(III) dithiocarbamate complexes have clearly demonstrated cross-over properties on the basis of magnetic susceptibility and isotropic shift analysis.

Acknowledgements—We thank Professor Dr. S. Wajda for his interest in this work. Financial support from Polish Academy of Sciences under Problem MR-I-9 is gratefully acknowledged.

REFERENCES

1. H. H. Wickman and A. M. Trozzolo, *Inorg. Chem.* 1968, **7**, 63.
2. M. C. Plazzotto, D. J. Duffy, B. L. Edgar, L. Que and L. H. Pignolet, *J. Am. Chem. Soc.* 1973, **95**, 4537.
3. D. J. Duffy and L. H. Pignolet, *Inorg. Chem.* 1974, **13**, 2045.
4. E. Beinrohr and J. Garaj, *Coll. Czech. Chem. Commun.* 1980, **45**, 1785.
5. N. V. Duffy, *Inorg. Chim. Acta* 1981, **47**, 31.
6. N. V. Duffy, W. G. Movius and D. L. Uhrich, *Inorg. Chim. Acta* 1982, **64**, L91.
7. R. Chant, A. R. Hendrickson, R. L. Martin and N. M. Rohde, *Inorg. Chem.* 1975, **14**, 1894.
8. M. Kostański and S. Magas, *Radiochem. Acta* 1980, **27**, 27.
9. C. A. Tsipis, C. C. Hadjikostas and G. E. Manoussakis, *Inorg. Chim. Acta* 1977, **23**, 163.
10. S. Wajda, K. Drabent and A. Ożarowski, *Inorg. Chim. Acta* 1980, **45**, L201.
11. S. Akerstrom, *Arkiv Kemi* 1959, **14**, 387.
12. A. H. White, R. Roper, E. Kokot, H. Waterman and R. L. Martin, *Aust. J. Chem.* 1964, **17**, 294.
13. D. F. Evans, *J. Chem. Soc.* 1959, 2003; D. F. Evans and T. A. James, *J. Chem. Soc., Dalton Trans.* 1979, 723.
14. C. L. Yaws, *Physical Properties*, Chemical Engineering, p. 222. McGraw-Hill, New York (1977).
15. A. L. Van Geet, *Analyt. Chem.* 1968, **20**, 2227; 1970, **42**, 679.
16. R. M. Golding, W. C. Tennant, J. P. Bailey and A. Hudson, *J. Chem. Phys.* 1968, **48**, 264.
17. T. J. Pinnavia and S. O. Nweke, *Inorg. Chem.* 1969, **8**, 639.
18. G. N. La Mar and G. R. Van Hecke, *J. Am. Chem. Soc.* 1969, **91**, 3442; G. N. La Mar and G. R. Van Hecke, *J. Magn. Reson.* 1971, **4**, 384.
19. M. F. Rudolf, *Bull. Acad. Polon. Sci., Ser. Sci. Chim.* 1979, **27**, 747.
20. A. K. Gregson and D. Doddrell, *Chem. Phys. Lett.* 1975, **31**, 125 (and references cited therein).
21. R. M. Golding, P. Healy, P. Newman, E. Sinn, W. C. Tennant and A. H. White, *J. Chem. Phys.* 1970, **52**, 3105.
22. M. L. Martin, J. J. Delpuech and G. J. Martin, *Practical NMR Spectroscopy*, Chapter 9. Heyden, London–Philadelphia–Rheine (1980).

Polyhedron Vol. 4, No. 9, pp. 1643–1658, 1985
Printed in Great Britain

0277–5387/85 $3.00 + .00
© 1985 Pergamon Press Ltd

A SPECTRAL STUDY OF TRANSITION-METAL COMPLEXES ON A CHELATING ION-EXCHANGE RESIN CONTAINING AMINOPHOSPHONIC ACID GROUPS

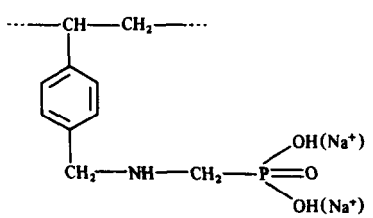
SURESH K. SAHNI, RENE VAN BENNEKOM and JAN REEDIJK*
Department of Chemistry, Gorlaeus Laboratories, State University Leiden, P.O. Box 9502, 2300 RA Leiden, The Netherlands

(*Received* 13 *December* 1984; *accepted* 3 *April* 1985)

Abstract—The coordination mode of a commercial chelating ion-exchange resin, ES 467, containing aminomethylphosphonic acid groups anchored on a macroporous styrene–divinylbenzene copolymer, with several metal ions, such as chromium(III), cobalt(II), nickel(II), copper(II) and zinc(II) has been studied with the aid of IR, ligand field and ESR spectra. The chelating group of ES 467, aminomethylphosphonic acid, appears to bind different metal ions mainly through oxygen atoms of the phosphonic acid group, though, in the case of those species containing low-loading of metal ions, the secondary amine nitrogen atom also appears to take part in coordination. Most of the metal ions studied seem to be present as six-coordinated species in the polymeric matrix, whereas cobalt(II) species show electronic spectra which are consistent with the presence of both four-coordinated (tetrahedral) and six-coordinated (octahedral) structures of these species. The distribution coefficients for cobalt(II), nickel(II), copper(II) and zinc(II) have been determined and it appears that the resin ES 467 binds copper(II) ions selectively. An attempt has been made to find a possible relationship between the selectivity of the chelating resin and the stereochemistry of the adsorbed metal ions.

In recent years, a great deal of research effort has been expended to study the ion-selective properties of chelating ion-exchange resins and quite a few such resins are commercially available now.[1] Some of the salient features of a successful selective ion-exchange resin are its high capacity, selectivity and marked kinetics combined with its chemical and mechanical stability. The selectivity, among other things, depends on the nature of the donor atoms and different steric factors of the chelating group. However, it appears that no attempt has been made to develop a relationship between selectivity and different properties of a chelating group present in a selective ion-exchange resin. A possible approach to develop such a relationship consists in studying the stereochemistry of the chelated/adsorbed species (the term metal complexes will be used throughout this paper) on a selective ion-exchange resin with the aid of their spectral properties. Some scattered studies[2–5] on this subject are available, but much more data are required before any meaningful relationship between selectivity and various properties of ion-exchange resins could be evolved.

In continuation of our previous work on the spectral studies of metal complexes of chelating ion-exchange resins, Chelex-100[6] and Spheron Oxine,[7] the ligating behaviour of a commercial chelating ion-exchange resin (ES 467) containing aminomethylphosphonic acid groups attached to a macroporous styrene–divinylbenzene copolymer, with chromium(III), cobalt(II), nickel(II), copper(II) and zinc(II) ions has been described in this paper. The schematic tentative structure of ES 467 is depicted in Fig. 1.



ES 467

Fig. 1. Schematic structure of ES 467.

* Author to whom correspondence should be addressed.

ES 467 is known to form stable complexes with low-atomic mass cations.[8] Several other chelating ion-exchange resins containing aminoalkylphosphonic acid groups anchored on different types of polymeric matrices have been developed in recent years to explore their potential in preconcentration and selective removal of certain cations and anions.[9,10] The synthesis and ion-selective properties of such chelating ion-exchange resins[11] and also those of several phosphonic acid resins, including their kinetics and ion-exchange equilibria, have been reported.[12–16] Recently, the capacity and ion-separation capabilities of ES 467 have been compared with several other commercially available chelating ion-exchange resins for its applications in hydrometallurgy.[17] It has been found that, like the picolylamine resins XF 4195 and XF 4196,[1] the aminophosphonic acid resin, ES 467, shows a moderate selectivity for copper(II) over iron(III) in acid sulfate solution compared with an iminodiacetic acid resin which shows no or limited selectivity depending on the pH. The thermodynamic aspects[18] and other applications such as maintaining the required level of calcium ions in feed brine for chlorine-alkali cells using ES 467 have recently been reported.[19]

EXPERIMENTAL

Elemental analysis, physical measurements and materials

The elemental analysis (C, H, N and P) was performed by Mikroanalytisches Laboratories of E. Pascher, Bonn, F.R.G., and P. van den Bosch, Technical University, Eindhoven, The Netherlands, and metal analyses were carried out by digesting the metal-containing beads of the resin with nitric and sulfuric acids, by atomic absorption spectroscopy, using a Perkin–Elmer 460 atomic absorption and flame emission spectrometer. IR spectra were recorded in KBr pellets on a Perkin–Elmer 580 spectrophotometer provided with an IR data station; the far-IR spectra were recorded in powdered polyethylene pellets using a freshly prepared polyethylene disc as a reference. The electronic spectra of various complexes have been recorded as diffuse reflectance on Perkin–Elmer 330 spectrophotometer also provided with a data station, using a zinc(II) complex of the same resin, ES 467, as a reference[3,6,7] for both the wet and the dried samples in the region 5000–33,000 cm^{-1}. The electronic spectra of the high-loaded (7–9% metal content) metal complexes have been recorded to find out the geometry around the metal ions under the different conditions of loading and synthesis. In the case of low-loaded complexes (*ca* 0.1–1% of metal content), the *d–d* transitions originating from the metal ions are overshadowed by intense intraligand bands and the assignments appeared to be impossible. However, in the case of high-loaded complexes, the *d–d* transitions could easily be discerned and lead to reliable conclusions. Electron spin resonance spectra at X-band frequencies at room and liquid nitrogen temperature were recorded on a Varian E-3 spectrometer.

Analytical metal salts have been used throughout and all metal-uptake experiments have been carried out in polyethylene bottles. The details of various buffer solutions used are: sodium chloride–hydrochloric acid (pH = 1–2.5), sodium acetate–acetic acid (pH = 3–6) and Tris [tris(hydroxymethyl) aminomethane]–hydrochloric acid (pH = 7). ES 467 was obtained from Duolite International Inc., France. The sodium form of the commercially available resin ES 467 was converted into its hydrogen form by a conventional method using dilute hydrochloric acid.

Determination of distribution coefficients

The distribution coefficients for cobalt(II), nickel(II), copper(II) and zinc(II) were determined by the following procedure. An accurately weighed sample of ES 467 (H^+-form) (200 ± 5 mg) was added to an appropriate metal salt solution (25 cm^3 of 0.001 M solution) buffered at a certain pH, using an appropriate buffer solution (25 cm^3) and the ionic strength of the solution was maintained at 0.3 by addition of potassium chloride or potassium nitrate. The reaction contents were shaken on an automatic shaker for *ca* 48 h at room temperature (*ca* 22°C). However, it was observed that the equilibration was generally achieved within 24 h. The metal-containing beads were filtered and washed with water, ethanol and ether, and dried *in vacuo* at *ca* 80°C for 60–72 h. Both the metal-containing solutions and metal-containing beads were analysed for their metal contents. The distribution coefficients (D) have been calculated using the following relationship:

$$D = \frac{\text{amount of metal ion per gram of dry resin}}{\text{amount of metal ion per cm}^3\text{ of solution}}.$$

Determination of capacity

The capacity of ES 467 for different metal ions was determined by a batch method. To a weighed amount of buffered ES 467 an appropriate metal salt was added in a quantity greater than its theoretical

capacity (*ca* 3 times). The reaction contents were shaken for *ca* 36 h at room temperature. The metal-containing beads were filtered and washed thoroughly with water, ethanol and ether, dried to a constant weight at *ca* 70–80°C *in vacuo* for 24 h, and analysed for their metal contents.

Preparation of different samples used for spectroscopic studies

These samples were prepared both from the sodium and hydrogen forms of ES 467. A general procedure has been adopted for the preparation of both low- and high-loaded samples. To a weighed amount of air-dried resin (200 ± 5 mg) was added the appropriate metal salt (100, 50, 25 and 10% of the theoretical capacity of the resin) and the reaction contents were buffered at a pH between 3 and 5, and shaken for 24–36 h. The samples were thoroughly washed and dried as described above. The samples used for the detection of the presence of counter ions of metal salts on the polymeric matrix were also prepared in demineralised water without using any buffer solutions. For low-loaded samples, the complexes isolated from *D* determination experiments were used.

RESULTS AND DISCUSSION

General

ES 467 has been claimed to be of general use in the removal and recovery of transition and alkaline-earth metal ions from process liquors and relatively dilute solutions.[8,17–19] Besides binding transition-metal ions, this resin also weakly binds calcium and magnesium ions, like Chelex-100 or Dowex A-1 resins containing iminodiacetic acid as functional groups.[1] The stability constants for several divalent metal with several monomeric aminoalkylphosphonic acids and their derivatives are known from the literature.[20–23] The stability constants for divalent metal ions with aminomethylphosphonic acid[20,22] and 2-aminoethylphosphonic acid,[21,23] which can be considered as ideal monomeric analogues for ES 467, have been found to follow the order: $Ca^{2+} < Mg^{2+} < Co^{2+} < Ni^{2+} < Cu^{2+} > Zn^{2+}$, which is in accord with the Irving–Williams order of chelate stability. The *D* for divalent cobalt, nickel, copper and zinc with ES 467 have been determined (Table 1) and the log *D* values for different metal ions appear to follow the same trend as observed in the monomeric systems. This observation has been confirmed by capacity determination of ES 467 for different metal ions. It has been found that this resin, ES 467, takes up the maximum amount of copper; however, more cobalt than nickel is taken up, despite the fact that the nickel chelate has a higher stability than the cobalt chelate[20,22] (Table 2). These results are in accord with those of Milling and West[17] who also found that ES 467 possesses a higher capacity for copper(II) ions compared to nickel(II) and iron(III), and that the capacity is lowered with the lowering of the pH and metal ion concentration of the solutions. The capacities for different metal ions are comparable when either chloride or nitrate salts of these metal ions are used, indicating that these anions do not play any significant role as far as the capacity of ES 467 is concerned.

The solution studies on metal complexes of monomeric analogues of ES 467 reveal that several types of complexes are formed in solution, although the species having a 1:1 metal:ligand stoichiometry have been found to be most stable.[20–23] On the basis of the magnitude of formation constants of copper(II), nickel(II), zinc(II), cobalt(II), magnesium and calcium ions, different binding modes of these monomeric aminoalkylphosphonic acids have been

Table 1. Distribution coefficients of cobalt(II), nickel(II), copper(II) and zinc(II) with ES 467

Metal salt	pH	Metal output ($\mu g\ cm^{-3}$)	Metal uptake (wt %)	log *D*
$CuCl_2$	1.0	22.4	0.076	1.53
	1.4	20.8	0.265	2.11
	3.0	0.185	0.713	4.59
	4.0	0.185	0.713	4.59
	5.0	0.185	0.704	4.58
	6.0	0.100	0.659	4.82
	7.0	0.115	0.577	4.70
$CoCl_2$	1.0	25.8	0.150	1.76
	1.5	25.2	0.231	1.96
	3.0	0.78	1.38	4.24
	4.0	0.46	0.863	4.27
	5.0	0.71	0.915	4.11
	6.0	0.42	0.851	4.31
	7.0	0.02	0.614	5.49
$NiCl_2$	1.0	29.7	0.155	1.72
	1.5	27.4	0.166	1.78
	3.0	0.80	0.533	3.82
	4.0	0.80	0.839	4.02
	5.0	1.11	0.851	3.88
	6.0	0.26	0.942	4.56
	7.0	0.21	0.819	4.59
$ZnCl_2$	1.0	28.0	0.091	1.51
	1.5	23.3	—	—
	3.0	0.44	—	—

Table 2. Capacity of ES 467 for cobalt(II), nickel(II) and copper(II) at different concentrations

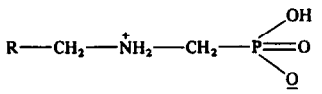
Metal salt	Concentration of solution with respect to theoretical capacity (mmol metal/g resin) (pH)	Wt % metal (dry resin)
$Cu(NO_3)_2$	20.0 (3.5)[a]	14.5
	15.0 (3.5)[a]	12.1
	5.0 (4.5)	8.94
	3.0 (4.5)	4.63
	1.5 (4.5)	2.19
$CuCl_2$	5.0 (4.5)	8.47
	3.0 (4.5)	4.63
	1.5 (4.5)	2.08
$CoCl_2$	5.0 (4.5)	7.25
	3.0 (4.5)	4.17
	1.5 (4.5)	2.20
$Co(NO_3)_2$	5.0 (4.5)	7.31
	3.0 (4.5)	4.18
	1.5 (4.5)	2.55
$NiCl_2$	5.0 (4.5)	6.90
	3.0 (4.5)	3.73
	1.5 (4.5)	2.15
$Ni(NO_3)_2$	5.0 (4.5)	6.00
	3.0 (4.5)	3.98
	1.5 (4.5)	2.25

[a] pH 3.5 was reached by adding a dilute solution of NaOH and for the rest of the solutions a buffer solution of pH = 4.5 was used.

proposed.[20,22,23] These studies were inconclusive, as no light is shed on the structure of the various metal complexes. The spectral properties of transition-metal complexes of aminoalkylphosphonic acids have been studied, but no attempt has been made to analyse the binding mode of the ligands with different metal ions under varied conditions.[24] With a view to ascertaining the binding sites in ES 467, several of its metal complexes have been prepared under different conditions of pH and concentration of metal ions. The extent of metal loading of different species is given in Table 3 and their spectral properties are discussed below.

IR spectra

The IR spectra of aminoalkylphosphonic acids[25,26] and phosphonic acids, including their polymeric derivatives,[27,28] have been reported. The IR spectra of some metal complexes of polymer-supported phosphonic acids,[29] aminoalkylphosphonic acids[24,30–34] and their metal complexes have also been reported. However, no attempt has been made to make a detailed analysis of polymer-supported aminoalkylphosphonic acids and their metal complexes. The important IR spectral bands of ES 467 and its metal complexes recorded under different conditions of pH are given in Tables 4 and 5, respectively. Aminoalkylphosphonic acids, like their carboxylic acid analogues (amino acids), also exist in zwitterion forms and have been shown to possess betaine structure as established on the basis of various analytical and spectral techniques.[33,34] The chelating ion-exchange resin ES 467, which incorporates aminomethylphosphonic acid groups anchored on a polymeric matrix has also been found to possess a zwitterion structure as established on the basis of IR spectra and is depicted in Fig. 2. The IR spectra of ES 467 samples conditioned at lower pH (less than 7) show strong bands at *ca* 1170 and 1070 cm^{-1} due to $\nu_{as}(PO_2)$ and $\nu_s(PO_2)$ vibrations of the PO_3H^- group.[25,26,31,32] A strong band appearing at *ca* 925 cm^{-1} can be assigned to a ν(P—OH) vibration.[25,26] The spectra of the samples conditioned above pH 10 show two strong bands at *ca* 1090 and 975 cm^{-1} assignable to $\nu_{as}(PO_3)$ and $\nu_s(PO_3)$ vibrations of the PO_3^{2-} group, respectively.[31,32,34] However, the spectrum of a sample conditioned between pH 7 and 10 (pH = 7.5) shows two strong bands at *ca* 1088 and 975 cm^{-1} due to asymmetric and symmetric stretching vibrations of the completely ionised PO_3^{2-} group, along with a shoulder at 1170 cm^{-1}, resembling the spectra of the samples conditioned at pH lower than 7. This indicates that the spectra of the samples conditioned between pH 7 and 10 possess the features of completely ionised and zwitterion-like forms of ES 467. The occurrence of asymmetric and symmetric stretching vibrations of the PO_3H group at higher frequencies in the samples conditioned at lower pH has been ascribed to the positive charge on the nitrogen atom.[31] The spectra of all these samples show a band at *ca* 1215 cm^{-1} due to ν(P=O) vibrations.[32] The presence of a protonated $\overset{+}{N}H_2$ group is indicated by the occurrence of bands at *ca* 1660 and 1570 cm^{-1} [24,34] in the spectra of the samples conditioned at lower pH. In fact, the resin acts as an anion-exchanger at lower pH, as indicated



where R = polymeric matrix

Fig. 2. Zwitterion-like structure of ES 467.

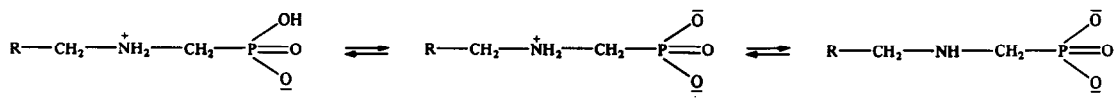
Table 3. Elemental analysis of ES 467 and a selection of its complexes[a]

No.	Sample	% Metal	% C	% H	% N	% P	% Cl	
	ES 467	—	46.20	5.64	3.45	10.4	—	(found)
	(Na form)		46.93	4.65	4.88	10.79	—	(calc.)
							(for 10% divinylbenzene)	
1.	$Cr(NO_3)_3$—100% (pH = 3.5)	14.0	—	—	—	—	—	
2.	$CrCl_3$—100% (pH = 4.3)	12.8	—	—	—	—	Negligible	
3.	$Cr(NO_3)_3$—10% (pH = 2.5)	5.4	—	—	—	—	—	
5.	$Co(NO_3)_2$—100% (pH = 4.5)	7.1	—	—	—	—	Negligible	
7.	$CoCl_2$—100% (pH = 4.5)	7.25	43.94	5.61	3.20	—	Negligible	
9.	$Co(NO_3)_2$—D.C.[b] (pH = 3.0)	0.89	—	—	—	—	—	
10.	$CoCl_2$—D.C. (pH = 5.0)	1.40	—	—	—	—	< 0.5	
12.	$Ni(NO_3)_2$—100% (pH = 4.5)	6.00	46.44	5.71	3.22	—	—	
13.	$NiCl_2$—100% (pH = 4.5)	6.90	—	—	—	—	< 0.5	
14.	$Ni(NO_3)_2$—D.C. (pH = 7.0)	0.54	—	—	—	—	—	
15.	$Ni(NO_3)_2$—D.C. (pH = 5.0)	6.90	—	—	—	—	—	
17.	$Cu(NO_3)_2$—100% (pH = 4.5)	8.94	46.56	5.41	3.13	—	—	
18.	$CuCl_2$—100% (pH = 4.5, dried)	8.97	—	—	—	—	—	
19.	$Cu(NO_3)_2$—50% (pH = 4.5)	4.63	—	—	—	—	—	
20.	$Cu(NO_3)_2$—25% (pH = 4.5)	2.19	—	—	—	—	—	
21.	$Cu(NO_3)_2$—D.C. (pH = 7.0)	0.71	—	—	—	—	—	
22.	$CuCl_2$—D.C. (pH = 4.0)	1.4	—	—	—	—	0.5	
23.	$Cu(NO_3)_2$—D.C. (pH = 2.0)	0.76	—	—	—	—	—	

[a] The number given to each complex corresponds to the number given to a particular sample in Table 6. All the complexes were dried well before estimating their metal content.

[b] Isolated from the distribution coefficient experiments.

by the IR spectrum of a sample of ES 467 treated with potassium nitrate which shows a strong band at *ca* 1380 cm^{-1} due to the ionic nitrate group. The spectra of the samples conditioned at higher pH show a distinct band at *ca* 3260 cm^{-1} due to ν(NH) vibrations of the unprotonated secondary amino group. On the basis of these observations, the dissociation of ES 467 is depicted in Fig. 3. These



(A) pH = 1.0 (B) pH = 6.0 (C) pH = 11.0

where R = polymeric matrix

Fig. 3. Dissociation of ES 467 as a function of pH.

Table 4. Important IR spectra bands (cm^{-1}) of ES 467 at different pH values (1–11.5)

Sample (resin form, pH)	ν_s/ν_{as}(P—OH)	$\nu_s(PO_3)$ (of PO_3^{2-} group)	$\nu_{as}(PO_3)$ group)	$\nu_s(PO_2)$ (of PO_3H^- group)	$\nu_{as}(PO_2)$	ν(P=O)	ν(P—C)	$\delta(PO_3)$
$RCH_2\overset{+}{N}H_2CH_2PO_3H^-$ (H^+, 1.0)	915s	—	—	1085s	1185s	1212sh	758m	550s
$RCH_2\overset{+}{N}H_2CH_2PO_3H^-$ (H^+, 2.5)	925s	—	—	1070s	1170s	1215sh	760m	540s
$RCH_2\overset{+}{N}H_2CH_2PO_3H^-$ (H^+, 4.5)	915s	—	—	1075s	1170s	1215sh	752m	548s
$RCH_2NH_2CH_2PO_3^{2-}$ (H^+, 7.0)	915m	980w	1080s	—	1175s	1215sh	758m	550s
$RCH_2NHCH_2PO_3^{2-}$ (Na^+, 10.5)	910w	975s	1088s	—	1170sh	1212sh	752m	563m
$RCH_2NHCH_2PO_3^{2-}$	—	975s	1090s	—	—	1215sh	755w	568m

[a] The spectra of the samples buffered at pH = 4.5 (acetate buffer) and pH = 1.0 (KNO_3) show bands at 1700 and 1380 cm^{-1}, due to the vibrations of acetate and nitrate groups, respectively.

observations are consistent with the two pK values (pK_1 = 5.38 and pK_2 = 10.4); the first one corresponds to the deprotonation of the hydroxyl group of the phosphonic moiety and the second one to the deprotonation of the amino group.[26] Thus, it appears that the possibility of coordination of the secondary nitrogen atom at lower pH seems extremely remote in view of its protonated nature and also for steric reasons, and the only potential donor or binding sites in ES 467 are the oxygen atoms of the phosphonic groups under these conditions.[32]

The important bands of the metal complexes of ES 467 prepared under different conditions are given in Table 5. It may be pointed out that only the spectra of high-loaded species have been icnluded. In the case of low-loaded samples hardly any discernible changes can be observed in the vibrations of the ligand (in this case polymer-supported aminomethylphosphonic acid) upon coordination to a metal atom. In the spectra of the metal complexes prepared with the acid form of ES 467 below pH 7, a doublet appears at *ca* 1120 and 1080 cm^{-1}, along with three more bands at *ca* 925, 985 and 1165 cm^{-1} due to different symmetric and asymmetric stretching vibrations of the phosphonic group. The occurrence of a doublet in a narrower range (*ca* 40–50 cm^{-1}) supports the coordination of the phosphonic group to the various metal ions.[24,28,29,31] The persistence of a band at *ca* 1165 cm^{-1} indicates that the betaine structure of ES 467 is also retained in the metal complexes prepared at lower pH. This again rules out the possibility of coordination of the secondary nitrogen atom to metal ions. The occurrence of several bands in the region characteristic of $\nu_{as}(PO_3)$ and $\nu_s(PO_3)$ vibrations indicates that the two hydroxyl groups of the phosphonic group are not alike.[24] The spectra of the complexes prepared from the disodium salt of ES 467 (at pH 10) also show a doublet at *ca* 1120 and 1060 cm^{-1} along with a strong band at *ca* 985 cm^{-1}, which supports the coordination of the phosphonic group to metal ions. The spectra of the air-dried samples show a broad band at *ca* 980–1120 cm^{-1}, which changes into a well-defined doublet in the spectra of the dried samples. The conspicuous absence of a band at *ca* 1170 cm^{-1} indicates the absence of a betaine structure of ES 467 in these complexes. In such cases (at higher pH) the possibility of coordination of the secondary nitrogen atom to metal ions cannot be ruled out.

The spectra of ES 467 show a number of bands in the lower region at *ca* 550–565 and 450 and 450–490 cm^{-1} which are assigned to $\delta_{as}(PO_3)$ and $\delta_s(PO_3)$ vibrations, respectively.[25,26] In the spectra of the metal complexes, the bands occurring at high

Table 5. Important IR spectral bands (cm^{-1}) of a selection of metal complexes of ES 467[a]

Sample (resin form, pH)	ν_s/ν_{as}(P—OH)	$\nu_s(PO_3)$ (of PO_3^{2-} group)	$\nu_{as}(PO_3)$	$\nu_s(PO_2)$ (of PO_3H^- group)	$\nu_{as}(PO_2)$	ν(P=O)	(ν(P—C)	$\delta(PO_3)$
$Cr(NO_3)_3$–ES 467 (H^+, 3.5)	920w	—	1070–1130s	1020m	1170sh	1212w	760m	552m
$CrCl_3$–ES 467 (Na^+, 4.3)	925w	980s	1075–1110sb	—	—	1212sh	760m	550m
$FeCl_3$–ES 467 (H^+, 2.0)	925m	—	1075s	1020sh	1170s	1212sh	760m	548m
$Mn(NO_3)_2$–ES 467 (H^+, 4.0)	925s	—	1075s	1020sh	1170s	1212sh	760m	545m
$MnCl_2$–ES 467 (Na^+, 6.0)	—	982s	1080–1120s	—	—	1212sh	760m	565m
$CoCl_2$–ES 467 (H^+, 4.5)	925m	985w	1080–1120	—	1165s	1210sh	760m	560m
$CoCl_2$–ES 467 (Na^+, 11.0)	—	985s	1050–1105s	—	—	1220w	760m	580m
$NiCl_2$–ES 467 (H^+, 4.0)	922m	980w	1080–1125sb	1040sh	1165s	1210w	760m	565m
$NiCl_2$–ES 467 (Na^+, 10.5)	—	980s	1055–1100s	—	—	1212w	760m	580m
$CuCl_2$–ES 467 (H^+, 4.0)	928m	985m	1065–1120s	—	1165m	1215w	762m	585m
$CuCl_2$–ES 467 (Na^+, 11.5)	—	975s	1050–1130s	—	—	1212w	760m	595m
$Zn(NO_3)_2$–ES 467 (H^+, 1.6)	925s	—	1070s	1020sh	1170s	1215sh	760m	548s
$Zn(NO_3)_2$–ES 467 (Na^+, 4.6)	—	998s	1075–1125bs	—	—	1210m	760m	578m

[a] The iron(III) and manganese(II) complexes have been included for comparison only.

frequencies shift to higher frequencies, whereas the band assigned to $\delta_s(PO_3)$ vibrations either remains stationary or disappears altogether. The $\delta_{as}(PO_3)$ band has been found to increase in frequency with the decrease in the ionic radii of divalent metal ions, i.e. Cu^{2+} (590 cm^{-1}) > Zn^{2+} (588 cm^{-1}) > Ni^{2+} (575 cm^{-1}) > Co^{2+} (565 cm^{-1}) ≥ Mn^{2+} (565 cm^{-1}), indicating that the strongest metal–oxygen bond is formed in the case of copper(II) ions, followed by zinc(II) and other metal ions in accord with the Irving–Williams order of metal stability. The band due to the ν(P—C) vibration occurring in the free ligand at *ca* 760 cm^{-1} remains unperturbed in the spectra of the metal complexes. From the preceding discussion, it is evident that the aminomethylphosphonic group of ES 467 exists in a zwitterion form in the lower range of pH and coordinates various metal ions mainly through the oxygen atoms (of the hydroxyl group) of the phosphonic group. The same trend has also been observed in the metal complexes prepared at higher pH; however, the possibility of the coordination of a secondary nitrogen atom cannot be ruled out as it will be shown below. In all these complexes, the possibility of coordination of the oxygen atom of the P=O group has been completely ruled out as no shift is observed in its position in the metal complexes.

An attempt has also been made to establish the presence of counter ions required to maintain the electrical neutrality of the metal complexes present in the polymeric matrix. It has been observed that the counter anions are generally washed away with buffer solutions used to maintain the pH of the reaction medium and, in turn, the electrical neutrality of the metal complexes is either maintained by deprotonation of the ligand or anions coming from the buffer solutions (for instance, acetate ions in the case of sodium acetate–acetic acid buffers) or hydroxide ions present in the polymeric matrix.[35] To solve this problem, some of the complexes of ES 467 have been prepared in an aqueous media without using any buffer solutions, using different salts of metal ions. The IR spectra of the metal complexes prepared from different salts show no trace of counter anions being present in the polymeric matrix. This is also confirmed by the elemental analysis of some of the metal chloride and nitrate complexes. This again indicates that the electroneutrality of the metal ions is maintained by deprotonation of the phosphonic acid moiety of the resin ES 467.

Electronic spectra of chromium(III) complexes

The spectral data of a few chromium(III) complexes of ES 467 are given in Table 6 and those of reference compounds in Table 7. The spectra of all complexes show well-defined, relatively strong bands in the regions 15,700–16,700 and 22,000–23,900 cm^{-1} and two shoulders are also observed on the low-energy side of these bands at *ca* 14,500 and 21,500 cm^{-1}, respectively. The spectra of these complexes bear a close resemblance to typical octahedral chromium(III) complexes, which generally show three spin-allowed bands and the highest-energy band due to the $^4T_{1g}(P) \leftarrow {}^4A_{2g}$ transition occurs above 30,000 cm^{-1}.[36,37] In addition to these spin-allowed transitions, two of the three spin-forbidden transitions have also been observed. In the present complexes, the two spin-allowed bands occurring at *ca* 16,000 and 22,500 cm^{-1} can be assigned to $^4T_{2g} \leftarrow {}^4A_{2g}$ and $^4T_{1g}(F) \leftarrow {}^4A_{2g}$ transitions, respectively.[36,37] The two bands which appear as shoulders can be assigned to the spin-forbidden transitions $^2E_g \leftarrow {}^4A_{2g}$ and $^2T_{1g} \leftarrow {}^4A_{2g}$, in increasing order of energy.[36] These spectra can further be rationalised in terms of various ligand field and nephelauxetic parameters ($10Dq$, B and β_{35}) and the values of these parameters have been computed through procedures given in the literature.[37,38] The values of $10Dq$ and B which lie in the ranges 15,740–16,720 and 593–665 cm^{-1} are comparable to those observed for the chromium(III) complexes of the monomeric aminoethylphosphonic acid and those of other oxygen-containing ligands.[24] This indicates that the functional group, aminomethylphosphonic acid, present in ES 467 coordinates or binds the chromium(III) ions through the oxygen atoms of the phosphonic acid moiety. In fact, the $10Dq$ values for the present complexes are even lower than those observed for the $[Cr(H_2O)_6]^{3+}$ complex which contains the chromosphore CrO_6. The lower $10Dq$ values have also been observed with metal complexes involving rather bulky ligands, as is the case here. In the present complexes, the exclusive coordination through oxygen atoms of the aminophosphonic acid moiety can be explained as follows. Most of the chromium(III) complexes have been prepared in the lower pH range (less than 3) conditions which are subjective to protonation of the secondary nitrogen atom and, moreover, chromium(III) ions have a pronounced tendency to bind to oxygen donors due to their "a"-class character. The monomeric analogue of ES 467, aminomethylphosphonic acid, is reported to form a chromium(III) complex having the formula $[Cr(AEP)(OH)]_2 \cdot 4H_2O$, which has been interpreted in terms of a dimeric structure having two hydroxo bridges as revealed by low magnetic moments (3.37 BM) and the IR spectrum showing characteristic bands for hydroxo bridges between 500 and 550 cm^{-1}.[20] No such observation has been made in the chromium(III) complexes of ES 467 and

Table 6. Electronic and ESR spectral data of a selection of chromium(III), cobalt(II), nickel(II) and copper(II) complexes, along with some reference compounds

Serial No.[a]	Sample (resin form, pH, dried or air-dried)	Ligand field maxima (kK)	ESR parameters			
1.	$Cr(NO_3)_3$—100%[b] (H+, 3.5, air-dried)	14.49sh, 16.26, 21.05sh, 22.22	$g = 1.98$,	$g = 5.10$		
2.	$CrCl_3$—100% (Na^+, 4.3, air-dried)	14.49sh, 16.72, 21.50sh, 23.26	$g = 2.01$,	$g = 5.08$		
3.	$Cr(NO_3)_3$—10% (H+, 2.5, air-dried)	14.70sh, 16.13, 22.73	$g = 1.97$,	$g = 5.20$		
4.	$Co(NO_3)_2$—100% (H+, 4.5, air-dried)	7.63, 16.76, 18.52, 20.41sh	—	—		
5.	$Co(NO_3)_2$—100% (H+, 4.5, dried)	7.00, 16.14, 18.50	—	—		
6.	$CoCl_2$—100% (Na^+, 5.6, air-dried)	6.67, 16.62, 18.50, 21.74	—	—		
7.	$CoCl_2$—100% (Na^+, 5.6, dried)	6.78, 16.48, 18.52, 21.74	—	—		
8.	$CoCl_2$—100% (Na^+, 11.0, dried)	7.22, 17.70, 18.52, 21.17	—	—		
9.	$Co(NO_3)_2$—D.C.[c] (H+, 3.0, air-dried)	7.63, 9.52, 17.86, 20.62	—	—		
10.	$CoCl_2$—D.C. (H+, 5.0, dried)	7.63, 16.28, 18.18, 20.00	—	—		
11.	$Ni(NO_3)_2$—100% (H+, 4.0, air-dried)	8.33, 13.30, 14.50sh, 24.39	—	—		
12.	$Ni(NO_3)_2$—100% (H+, 4.0, dried)	8.00, 12.90, 14.50sh, 23.53	—	—		
13.	$NiCl_2$—100% (Na^+, 10.5, air-dried)	8.45, 13.30, 14.45sh, 24.39	—	—		
14.	$Ni(NO_3)_2$—D.C. (H+, 7.0, air-dried)	9.00, 13.51, 24.40	—	—		
15.	$Ni(NO_3)_2$—D.C. (H+, 5.0, air-dried)	8.87, 13.51, 24.40	—	—		
			$g_\parallel$	$g_\perp$	$A_\parallel$ (G)	
16.	$Cu(NO_3)_2$–100% (H+, 4.5, air-dried)	11.77	2.33	2.12	125	(at RT[d])
			2.33	2.12	130	(at 77 K)
17.	$Cu(NO_3)_2$—100% (H+, 4.5, dried)	11.76	2.35	2.13	125	(at RT)
18.	$CuCl_2$—100% (Na^+, 11.5, air-dried)	11.70	2.28	2.14	140	(at RT)
19.	$Cu(NO_3)_2$—50% (H+, 4.5, air-dried)	11.76	2.33	2.12	130	(at RT)
20.	$Cu(NO_3)_2$—25% (H+, 4.5, air-dried)	12.35	2.32	2.12	135	(at RT)
21.	$Cu(NO_3)_2$—D.C. (H+, 7.0, air-dried)	12.90	2.34	2.09	125	(at RT)
			2.35	2.12	125	(at 77 K for the dried sample)
22.	$CuCl_2$—D.C. (H+, 4.0, dried)	11.43	2.34	2.06	135	(at 77 K)
23.	$Cu(NO_3)_2$—D.C. (H+, 2.0, air-dried)	11.76	2.33	2.07	135	(at RT)

[a] The number of the complex given in this table corresponds to the number of the complex in Table 3.

[b] 100, 50, 25 and 10% indicate that the resin has been equilibrated with the said % of the capacity of the resin using the appropriate metal salt.

[c] Corresponds to the samples isolated from the distribution coefficient experiment.

[d] Room temperature.

Table 7. Electronic and ESR spectral data of some reference chromium(III), cobalt(II), nickel(II) and copper(II) complexes of ion-exchange resins[a] and some model compounds

Sample (resin-form, pH)	Chromophore	Ligand field maxima (kK)	ESR parameters			Reference
$Cr(H_2O)_6^{3+}$	CrO_6	15.00, 17.00, 24.60	—			37
$CrCl_3$–Chelex-100 (Na$^+$, 3.5, air-dried)	$CrNO_5$	14.29sh, 17.24, 21.28sh, 24.29	—			Unpublished
Cr^{3+}–Dowex A-1 (Na$^+$, 3.90, dried)	$CrNO_5$	—	$g = 1.97$, $g = 5.16$			2
Cr^{3+}–UR-50	$CrNO_5$	—				
Cr^{3+}–AEP[b]	CrO_6	16.90, 24.60	—			24(a)
$CoCl_2$–Chelex-100	$CrNO_5$	8.47, 19.12	—			6
Co^{2+}–Dowex A-1	$CoNO_5$	8.50, 19.50	—			3
Co^{2+}–AEP	CoO_4	6.82, 17.12	—			24(a)
$Co(H_2O)_6^{2+}$	CoO_6	8.10, 19.40	—			37
Ni–Chelex-100	$NiNO_5$	9.50, 15.60, 25.50	—			6
Ni–Dowex A-1	$NiNO_5$	9.30, 15.75, 26.60	—			3
Ni–Zeo-Karb-226	NiO_6	8.70, 14.08, 25.60	—			41, 42
Ni^{2+}–AEP	NiO_6	8.70, 14.50, 25.30				24(a)
Ni^{2+}–PhPO[b]	NiO_6	8.20, 13.50, 24.10				24(b)
Cu–Chelex-100	$CuNO_5$	14.50	$g_{av.} = 2.14$			6
			$g_{\parallel}$	$g_{\perp}$	$A_{\parallel}$ (G)	
$CuCl_2$–Chelex-100 (low-loading in HCl)	$CuNO_5$	14.50	2.25	2.06	180	
Cu–Dowex A-1						
hydrated	$CuNO_5$	14.30	2.26	2.06	194	46
dehydrated	$CuNO_5$	—	2.28	2.07	194	46
Cu–BioRex-63						
hydrated	CuO_6	12.50	2.38	2.08	143	47
dehydrated	CuO_4	—	2.42	2.08	113	47
Cu^{2+}–AEP	CuN_2O_2Cl	12.35	$g_1 = 2.08$,	$g_2 = 2.157$,	$g_3 = 2.24$	30

[a] Chelex-100 and Dowex A-1 are commercial chelating ion-exchange resins containing iminodiacetic acid groups attached to styrene–divinylbenzene copolymers. UR-50 is also a commercial chelating resin containing (*o*-hydroxybenzyl)iminodiacetic acid incorporated into a phenol–formaldehyde condensate. BioRex-63 is a commercial resin having PO_3H_2 groups attached to a styrene–divinylbenzene copolymer and Zeo-Karb-226 is another commercial resin having carboxylic groups.

[b] AEP and PhPO stand for 2-aminoethylphosphonic and phenylphosphonic acids, respectively.

thus no exact structural analogy can be made with their monomeric analogue.

The electronic spectra of the chromium(III) complexes of ES 467 have also been compared with other chelating resins such as those containing iminodiacetic acid groups (Chelex-100 and ES 466) and multidentate aminoalkylphosphonic acid groups attached to a cross-linked polystyrene resins. The iminodiacetic acid resins and monomeric ethylenediaminotetrakis(methylenephosphonic) acids are well known to bind transition-metal ions through nitrogen and oxygen donor atoms present in these systems.[2,6,30,33,34] The values of $10Dq$ obtained for chromium(III) complexes of these resin lie around 17,240 (Chelex-100 and ES 466 with coordination of N-atoms) and 16,700 cm^{-1}, respectively, are slightly higher than those observed for our ES 467 complexes.

Electronic spectra of cobalt(II) complexes

The spectral data of a few representative complexes are given in Table 6, whereas some model and reference compounds are listed in Table 7. The ligand field spectra of most of these complexes show a cluster of bands at *ca* 6400–7500 and 15,800–21,000 cm^{-1}. It may be mentioned that most of the cobalt(II) complexes appear pink–purple when air-dried, but a distinct blue color is attained when the samples are dried *in vacuo*. This observation indicates that water may play an important role in the coordination geometry of cobalt(II) complexes of ES 467 and that water is lost upon heating. The spectra of these complexes cannot be rationalised in terms of either tetrahedral or octahedral or an intermediate coordination geometry. Instead, it appears that more than one type of cobalt(II) species is present in the polymeric matrix of ES 467. The presence of a band near 7000 cm^{-1} with multiple components (two–three) and another multi-component band near 16,500 cm^{-1} supports the presence of tetrahedral cobalt(II) species and these two bands can be assigned to $^4T_1(F) \leftarrow {}^4A_2\ (\sigma_2)$ and $^4T_1(P) \leftarrow {}^4A_2\ (\sigma_3)$ transitions in increasing order of energy.[37] Similar bands have also been observed in the spectra of the cobalt complex of monomeric aminoethylphosphonic acid which has been shown to possess a 1:2 metal:ligand stoichiometry and a tetrahedral geometry around the cobalt(II) ions.[24] The occurrence of another band at *ca* 18,500 cm^{-1} indicates that some octahedral cobalt(II) species are also present in the polymeric matrix, which is supported by the presence of a shoulder at *ca* 20,500 cm^{-1}.[37,39] In some of the complexes, the shoulder appears at higher energies, *ca* 21,500 cm^{-1}. The shifting of this band towards a higher energy indicates that cobalt(II) ions may not be exclusively coordinated to oxygen donor atoms (as is the case with chromium complexes), but some of the cobalt(II) ions may also be chelated by a nitrogen donor atom of the chelating group present in ES 467.[5,6,37] This nitrogen atom donor atom may not necessarily come from the aminoethylphosphonic acid group, but it cannot be ruled out that other nitrogen-containing species such as poly(aminomethylstyrene) or other species containing nitrogen used as a starting material for the synthesis of this resin may be present as impurities in the polymeric matrix might also coordinate to metal ions. A similar observation has also been made in the cobalt(II) and copper(II) species adsorbed on Dowex A-1 known to contain a small amount of quaternary nitrogen atoms.[5] The band appearing at *ca* 7500 cm^{-1} also appears to contain a component of octahedral cobalt(II) species, as this band splits to show a well-defined band at *ca* 9000 cm^{-1} in some of the cobalt(II) complexes. This band which occurs particularly in the case of low-loaded cobalt species prepared at relatively high pH also supports the involvement of a nitrogen atom in coordination.

Though there appears to be some overlap in the band position of the tetrahedral and the octahedral cobalt(II) species present in the polymeric matrix of ES 467, the band belonging to the tetrahedral species are clearly discernible because of their high intensity. Some ligand field and nephaulextic parameters (Dq and B) have been evaluated by taking the weighted average of the multiple bands.[37] The values of these parameters are consistently on the lower side (particularly those of Dq) of those observed for oxygen donor ligands and are comparable to those observed for the cobalt(II) complex of monomeric aminoethylphosphonic acid.[24] There is no particular trend in the Dq values of low- or high-loaded and air- or *in vacuo* dried cobalt(II) species. However, the high-loaded well-dried species show Dq values which are consistently lower (*ca* 4100 cm^{-1}) compared to those found for the low-loaded air-dried cobalt(II) samples (*ca* 4450 cm^{-1}). Thus, it appears that the high-loaded cobalt(II) species are exclusively coordinated to oxygen donor atoms, whereas in the case of relatively low-loaded species the coordination of the secondary nitrogen atom cannot be ruled out. One possible reason for the exclusive oxygen coordination in the case of high-loaded cobalt(II) species can be the additional cross-linking caused by cobalt ions resulting in the binding of the secondary nitrogen atom which is relatively close to the polymeric matrix.[40] The B values (700–800 cm^{-1}) of the cobalt complexes are about 20–30% lower than the free-ion value of cobalt and indi-

cate a moderately covalent nature for the metal–ligand bond.[37]

Electronic spectra of nickel(II) complexes

The band maxima for a selection of nickel(II) complexes are given in Table 6 and those of some reference and model compounds are given in Table 7. In general, four bands are observed in the regions 8000–9000, 12,900–13,510, 14,400–14,910 and 23,250–25,000 cm^{-1} which can be interpreted in terms of octahedral geometry for these nickel(II) complexes of ES 467. The band occurring at *ca* 14,500 cm^{-1} appears to have its origin in the spin-forbidden transition $^1E_g \leftarrow {}^3A_{2g}$ and three other bands can be assigned to $^3T_{2g} \leftarrow {}^3A_{2g}$ (σ_1), $^3T_{1g} \leftarrow {}^3A_{2g}(\sigma_2)$ and $^3T_{1g} \leftarrow {}^3A_{2g}(\sigma_3)$ transitions, respectively, in increasing order of energy.[37] The values of different ligand field parameters (*Dq* and *B*) have been calculated through the procedures documented in the literature.[6,37,38] The 10*Dq* values for most of the nickel(II) complexes lie in the range 8330–8700 cm^{-1}, except for two complexes prepared at a relatively higher pH, *ca* 7, with low-loading of the metal ions. The 10*Dq* values for these two complexes lie *ca* 9000 cm^{-1}. The lower 10*Dq* values of these nickel(II) complexes are comparable to those observed for the nickel(II) complexes of aminoethylphosphonic acid and phenylphosphonic acid in which nickel(II) ions have been postulated to be present as a NiO_6 chromophore.[24,29] In view of the comparable 10*Dq* values, it appears that the nickel(II) ions are mainly coordinated by oxygen donor atoms of ES 467 and also possess a chromophore NiO_6 (the coordination sphere is completed by water molecules like cobalt and chromium complexes). However, the 10*Dq* values of the order of *ca* 9000 cm^{-1} observed for two of the nickel(II) complexes are too high to be attributed to a chromophore NiO_6; these are rather close to nickel(II) complexes involving nitrogen and oxygen donor atoms.[6,7,41,42] It appears that, in the case of low-loaded nickel(II) complexes isolated at relatively higher pH, ES 467 behaves as a $(N, O_2)^-$ tridentate ligand. The *B* values observed for the nickel(II) complexes lie in the range 730–860 cm^{-1}, indicating a moderately covalent nature for the metal–ligand bonds present in the complexes of ES 467. However, the low-symmetry components present in these complexes can also be responsible for the very low values of *B*.[37]

Electronic spectra of copper(II) complexes

The spectral data for a selection of copper(II) complexes of ES 467 are given in Table 6 and those of some model and reference compounds in Table 7. Most of the copper(II) complexes show a broad band in the region 11,700–12,900 cm^{-1}, with one or two conspicuous shoulders on the low-energy side at *ca* 9000 and 7500 cm^{-1}. The position of the main broad band is comparable to one found in the copper(II) complexes of monomeric aminoethylphosphonic and phenylphosphonic acids.[24,29] Interestingly, the main *d–d* band assignable to the $^2T_{2g} \leftarrow {}^2B_{1g}$ transition for a distorted octahedral geometry of copper(II) complexes, occurs at a lower energy, *ca* 11,700 cm^{-1}, in the high-loaded complexes, whereas it occurs at a higher energy, *ca* 12,500 cm^{-1}, in the low-loaded complexes. This lowering in the position of the main band might possibly be due to exclusive oxygen donor coordination of the copper(II) ions, as it has been observed that the complexes having a low-loading of the metal content and isolated at higher pH show this band at a relatively higher energy at *ca* 12,900 cm^{-1}, possibly due to involvement of the secondary nitrogen atom in coordination to copper(II) ions.[43–46] Thus, it is apparent that ES 467 coordinates copper(II) ions exclusively through its oxygen donors in the high-loaded species and binds as $(N, O_2)^{2-}$ in a tridentate fashion in the low-loaded species (the coordination sphere is completed by water molecules). Tentative structures of metal complexes involving a bidentate and a tridentate ES 467 are depicted in Figs 4 and 5, respectively.

Electron spin resonance spectra

The electron spin resonance spectra of air-dried and vacuum-dried samples having different loadings of metal ions have been recorded both at room and at liquid-nitrogen temperature. The spectral data obtained for a selection of chromium(III) and copper(II) complexes are given in Table 6 and those of some model and reference compounds in Table 7. No significant difference in the ESR signal positions and their shapes has been observed in air-dried samples and in the samples dried *in vacuo* at 60°C for more than 24 h. The spectra recorded at liquid-

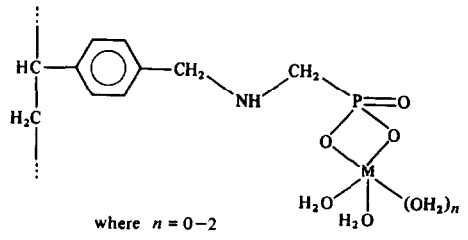


Fig. 4. Schematic structure of a metal complex of ES 467 acting as a bidentate ligand.

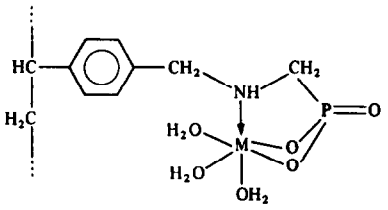


Fig. 5. Schematic structure of a metal complex of ES 467 acting in tridentate fashion.

nitrogen temperature do not show any better resolution than those recorded at room temperature. The low-loaded copper(II) samples show better resolved hyperfine splitting patterns compared to high-loaded samples, apparently because of some weak Cu–Cu interactions resulting in the disappearance of the fine structure in the latter species.

The chromium(III) complexes of ES 467 having different metal loadings show similar ESR spectra, having broad signals with $g = 5.10$–5.20 and 1.97–1.98 values, resulting from zero-field splitting.[2] It is, however, not possible to draw any useful conclusions about the bonding mode of ES 467 with chromium(III) ions.

In the case of copper(II) complexes, it has been found that the low-loaded copper(II) species (*ca* 0.1–1% metal content) show well-resolved spectra both at room and at liquid-nitrogen temperature, facilitating the evaluation of different ESR parameters. The species having a high loading of copper(II) ions (more than 1%) also show some hyperfine splitting which is rather poor and does not show any improvement even at lower temperatures. The values of $A_{\|}$, $g_{\|}$ and $g_{\perp}$ calculated for both the low- and the high-loaded species in air-dried and vacuum-dried states lie in the ranges 125–135 G, 2.31–2.35 and 2.06–2.14, respectively. The values observed for $A_{\|}$ are comparable to copper(II) species absorbed on Amberlite IRC-50 (a carboxylic acid containing resin), Dowex-50W (a resin with sulphonic acid group) and BioRex-63 (a resin having phosphonic acid groups attached to a cross-linked polystyrene copolymer) and hexaaquacopper(II) ions, all having a CuO_6 chromophore.[41,42,47] These values of $A_{\|}$ are much lower than those observed for copper(II) ions adsorbed or chelated to Dowex A-1,[46] Chelex-100,[6] ES 466[48] and Unicellex UR-50[2] (all having iminodiacetic acid or its derivative anchored on different types of polymeric matrices) possessing a common chromophore, $CuNO_5$. On the basis of the results obtained, it appears that ES 467 coordinates mainly through oxygen atoms, whereas the possibility of the secondary nitrogen atom coordinating as well in very low-loaded species cannot be completely ruled out. For such species, rather complex spectra have been obtained and the complexity appears to arise from the presence of more than one type of copper(II) species on the polymeric matrix, in which smaller $g_{\|}$ and larger $A_{\|}$ values can be distinguished, suggesting that some species with chromophore $CuNO_3O_2$ are also present.[7,30]

The fact that the g and A values of air-dried and vacuum-dried copper(II) species present in the ES 467 matrix do not differ significantly from each other indicates that copper(II) ions are chelated by aminomethylphosphonic acid groups of the resin. This behaviour of ES 467 resin differs from that of other resins containing phosphonic acid groups, such as BioRex-63 or Duolite C-63 (ES-63), in which copper(II) ions are present as $[Cu(H_2O)_6]^{2+}$, interacting only by means of electrostatic forces.[47] This is also confirmed by a kinetic study of BioRex-63 in which the rate-determining step for the exchange of uni- and divalent cations has been found to be diffusion through the particle bead.[12,49] The behaviour of copper(II) ions present in the matrix of ES 467 resembles to other chelating resins such as Dowex A-1 or Chelex-100 in which the presence of chelated copper ions has been established by ESR spectra showing almost similar g and A values for hydrated and dehydrated species.[6,46,47]

Stoichiometry and tentative structure of the metal complexes of ES 467

The elemental analysis of ES 467 reveals that it contains about 10% divinylbenzene which makes it a quite rigid structure. It has been pointed out in the case of Dowex A-1 or Chelex-100 containing iminodiacetic acid groups anchored on a styrene–divinylbenzene (2%) copolymer that it cannot form 1:2 (metal:ligand) complexes like monomeric iminodiacetic acid, because of the unfavourable position of two iminodiacetic acid groups caused by its cross-linked structure. Indeed, it has been observed and confirmed by several workers[2,6,41,46,47] that Dowex A-1 or Chelex-100 only form 1:1 (metal:ligand) complexes with several di- and trivalent metal ions. The possibility of the formation of 1:2 (metal:ligand) metal complexes in the case of ES 467 which contains a highly cross-linked matrix seems, therefore, even more unlikely. To confirm this, some of the high-loaded metal complexes of ES 467 have been analysed and it has been found that they conform to 1:1 metal:ligand stoichiometry, keeping in view that all the coordination or exchange sites are not accessible because of the highly cross-linked nature of the

polymeric matrix [10% cross-linking agent (divinylbenzene)]. It has been observed that with an increase in the cross-linking the exchange capacity of styrene–divinylbenzene copolymer-based ion-exchanger resins decreases appreciably and a 10% cross-linked sulfonated styrene–divinylbenzene copolymer takes up only *ca* 51% of tetrabutylammonium ion, for example, relative to Na^+ capacity.[50] In fact, the degree of cross-linking is generally higher than the known weight percentage of divinylbenzene content, because of some additional intrastrand cross-linking which creeps in during the modification of the polymers.[51]

The chelating group, aminomethylphosphonic acid groups present in ES 467, is potentially a tridentate ligand having two bonding sites at a phosphonic acid group and one coordination site at the secondary nitrogen atom. The structures of metal complexes of aminoalkylphosphonic acids have been discussed in detail elsewhere.[33,34] It has been observed that the amino-nitrogen atom normally does not participate under acidic conditions because of its protonated nature[31] and only phosphonic acid groups chelate the metal ions. One of the most favourable mode of chelation of the phosphonic acid group is the formation of a four-membered ring through the deprotonation of two P—OH groups, though the formation of a four-membered ring through bonding of one of the OH groups and the coordination of the oxygen atom (P=O) has also been reported.[29(a)] However, in the present complexes of ES 467, it has been found to be unaffected and thus it appears that it does not take part in coordination or bridging. These complexes are mainly formed by the chelation of two oxygen atoms of the OH groups of the phosphonic acid moiety forming a four-membered group and the rest of the coordination sphere is completed by three or four water molecules, as has been observed in the case of metal complexes of iminodiacetic acid resins.[2,6,41,42,46] This type of chelation by phosphonic acid results in the formation of more stable complexes compared to those formed by the corresponding carboxylic acids, because of the fact that the P—O bond lengths are longer than the C—O bond lengths, which results in a wider "bite", with a more favourable bond angle close to 90°. The higher stability of the metal complexes of the aminomethylphosphonic acid containing chelating resin, ES 467, is also augmented by the formation of hydrogen bonds between coordinated water molecules and the phosphono groups, as observed also in the case of alkylphosphate complexes.[27(b)] However, it appears that ES 467 can also act as a chelating agent in which the secondary nitrogen atom can participate in coordination as well, and the rest of the coordination sphere is again completed by water molecules as discussed in the preceding sections.

The selectivity and stereochemistry of metal complexes of chelating resins

The selectivity of chelating ion-exchange resins generally follows the same order as that of chelate stability suggested by Irving and Williams.[52] However, several deviations have been found from this order in the case of highly selective ion-exchange resins which bind almost exclusively only one metal ion over a given pH range.[48,53] This indicates that there are some other factors which play an important role in imparting selectivity to chelating ion-exchange resins. It is well known that the ultimate stereochemistry of metal complexes depends on several factors such as the denticity, the nature of the donor atoms, steric configurations, the rigidity and distribution of electrical charge on donor atoms of a ligand and the nature of a metal ion. A proper combination of all these factors can lead to enhanced selectivity of chelating systems and this appears to be more true for polymer-supported chelating ligands in which steric factors are expected to play an important role.

ES 467, containing aminomethylphosphonic acid groups, appears to combine some of these properties. This resin has been found to bind copper(II) ions selectively over a range of pH, but it also takes up other metal ions such as cobalt(II), nickel(II), zinc(II), iron(III) and chromium(III) like the chelating resins containing iminodiacetic acid groups. However, ES 467 appears to be more selective for copper(II) ions than iminodiacetic acid type resins because of some fundamental differences in the structure and stereochemistry of the phosphonic acid and carboxy groups. The phosphate ion is almost tetrahedral (distorted tetrahedron) with a three-fold symmetry axis. A carboxylate ion is planar with a two-fold symmetry and different valence angles and bond lengths. Besides, the phosphonic acid group possesses two hydroxyl groups and an extra oxygen atom in the P=O grouping which can coordinate to metal ions in different fashions than the carboxy groups, contributing to enhanced selectivity and coordination capacity.[33,34] The selectivity of ES 467 for copper(II) ions can be attributed to special steric and electronic factors present in aminoalkylphosphonic acid type ligands and also to the flexible nature of the copper(II) ion which can easily adapt different stereochemical features.[44,45] It is this flexibility of copper(II) ion which leads to the formation of different types of polyhedra around it under the different conditions of loading and pH which, in turn, lead to the formation of different types

of species in solution, some of which are taken up selectively and others are not.[48,53,54]

It has been found that the capacity of ES 467 for cobalt(II) ions is higher than that of nickel(II) ions at a given pH (Table 2), though the stability of nickel(II) complexes is higher than those of cobalt(II) complexes of the monomeric aminoalkylphosphonic acids.[21–23] This again points towards the role of some steric factors and the flexible nature of metal ions (in this case cobalt) which can make stable four- and six-coordinated complexes with equal ease with the same set of donor ligands.

Acknowledgements—We thankfully acknowledge the financial support from the Netherlands Organisation for Advancement of Pure Research (Z.W.O.) through grant No. 11-28-17 of the Netherlands Foundation for Chemical Research (S.O.N.) and Stichting Technische Wetenschappen through grant No. LCH 011.0144. The continued interest of and useful suggestions by Dr W. L. Driessen, Mr F. B. Hulsbergen, Mr J. W. F. M. Schoonhoven and Mr W. J. van den Boogert are thankfully acknowledged. Thanks are also due to Duolite International Inc. for supplying a gift sample of ES 467.

REFERENCES

1. S. K. Sahni and J. Reedijk, *Coord. Chem. Rev.* 1984, **59**, 1.
2. A. Nakashima, T. Isobe and T. Tarutani, *Bull. Chem. Soc. Jpn* 1982, **55**, 1811.
3. S. Laitinen and T. Norita, *Suom. Kemistil.* 1970, **B43**, 128.
4. A. Deratani, B. Sebille, H. Hommel and A. P. Legrand, *React. Polym.* 1983, **2**, 261.
5. C. Heirner-Wirguin and N. Ben-Zwi, *Isr. J. Chem.* 1970, **8**, 913.
6. P. J. Hoek and J. Reedijk, *J. Inorg. Nucl. Chem.* 1979, **41**, 401.
7. P. J. Hoek and J. Reedijk, *J. Inorg. Nucl. Chem.* 1980, **42**, 1759.
8. Technical Bulletin of Duolite International Inc., 1972.
9. Y. Kataoka and M. Matsuda, *Sumitomo Kagaku Tokushugo* 1982, 55; *Chem. Abstr.* 1983, **98**, 161924t.
10. Sumitomo Chemical Co. Ltd, *Japan Kokai Tokkyo Koho*, JP 57, 177, 012 (1982); *Chem. Abstr.* 1983, **98**, 162006g; *Japan Kokai Tokkyo Koho*, JP 82, 105, 104 (1982); *Chem. Abstr.* 1982, **97**, 203050s.
11. J. Kennedy and R. V. Davies, *Chem. Ind.* 1956, 378; J. Kennedy and G. E. Ficken, *J. Appl. Chem.* 1958, **8**, 465.
12. C. Heitner-Wirguin and J. Kendler, *J. Inorg. Nucl. Chem.* 1971, **33**, 3119.
13. J. Horyana and V. Vesley, *J. Inorg. Nucl. Chem.* 1972, **34**, 1739.
14. K. E. Becher, S. Lindebaum and G. E. Boyd, *J. Phys. Chem.* 1966, **70**, 3834.
15. J. Persoz and R. Rosset, *Bull. Soc. Chim. Fr.* 1964, 2197.
16. J. Persoz, *Bull. Soc. Chim. Fr.* 1966, 511.
17. J. Milling and D. W. West, *Proceedings of the International Conference on Ion-Exchange*, p. 724. Society of Chemical Industry, Cambridge, England (1984).
18. K. Ashurst, *Proceedings of the International Conference on Ion-Exchange*, p. 189. Society of Chemical Industry, Cambridge, England (1984).
19. J. J. Wolff, *Oslo Symposium on Ion-Exchange and Solvent Extraction*, IV/62-IV/74. Society of Chemical Industry, London (1982).
20. M. Wozniak, J. Nicole and G. Tridot, *Chim. Anal.* 1971, **53**, 512.
21. M. Wozniak, J. Nicole and G. Tridot, *Chim. Anal.* 1972, **54**, 147.
22. M. Wozniak, J. Nicole and G. Tridot, *Bull. Chim. Soc. Fr.* 1972, 4445.
23. M. S. Mohan and E. H. Abbott, *J. Coord. Chem.* 1978, **8**, 175.
24. A. G. Menke and M. Walmsley, *Inorg. Chim. Acta* 1976, **17**, 193.
25. B. Dupuy and C. Garrigon-Lagrange, *J. Chem. Phys.* 1968, **65**, 632.
26. C. Garrigon-Lagrange and C. Destrade, *J. Chem. Phys.* 1970, **67**, 1646.
27. (a) E. Steger and J. Rehak, *Z. Anorg. Allg. Chem.* 1965, **336**, 136; (b) H. Britzinger, *Helv. Chim. Acta* 1965, **48**, 47.
28. (a) R. D. Wittington and J. R. Millar, *J. Appl. Chem.* 1968, **18**, 122; (b) B. N. Laskorin, L. A. Fedorova, I. A. Logvineko and N. P. Stupin, *Zh. Prikl. Khim.* 1969, **42**, 522; (c) V. I. Paranionova, G. P. Nikitina and G. A. Akopov, *Radiokhimiya* 1968, **10**, 638, 646.
29. (a) K. M. Saldadze, V. D. Kopylova, T. V. Mekvabishvili and R. I. Machkhoshvili, *Russ. J. Phys. Chem.* 1972, **46**, 51; (b) E. A. Chuveleva, N. K. Yufryakova, P. P. Nazarova and K. V. Chmutov, *Russ. J. Phys. Chem.* 1971, **45**, 672.
30. W. Wojciechowski and M. Makles, *Russ. J. Inorg. Chem.* 1975, **20**, 570.
31. A. Yu. Kireeva, N. F. Shugal and N. M. Dyatlova, *Russ. J. Inorg. Chem.* 1973, **18**, 409.
32. B. V. Zhadanov and N. M. Dyatlova, *Russ. J. Phys. Chem.* 1973, **43**, 409.
33. M. I. Kabachnik, T. Ya. Medved', N. M. Dyatlova, O. G. Arkhipova and M. V. Rudomino, *Russ. Chem. Rev.* 1968, **37**, 503, and references therein.
34. M. I. Kabachnik, T. Ya. Medved', N. M. Dyatlova and M. V. Rudomino, *Russ. Chem. Rev.* 1974, **43**, 733, and references therein.
35. F. Vernon, *React. Polym.* 1982, **1**, 51.
36. L. S. Forster, *Transition Metal Chemistry* (Edited by R. L. Carlin), Vol. 5, p. 1. Marcel Dekker, New York (1969).
37. A. B. P. Lever, *Inorganic Electronic Spectroscopy*. Elsevier, Amsterdam, The Netherlands (1968).
38. E. König, *Struct. Bonding* 1971, **9**, 175.
39. J. Reedijk, P. W. N. van Leeuwan and W. L. Groeneveld, *Recl Trav. Chim.* 1968, **87**, 129.
40. J. A. Welleman, F. B. Hulsbergen and J. Reedijk, *Makromol. Chem.* 1982, **182**, 768.

41. S. Laitinen and T. Norita, *Suom. Kemistil.* 1970, **B43**, 71.
42. S. Laitinen and T. Norita, *Suom. Kemistil.* 1968, **B41**, 253.
43. N. Palta, B. V. Rao, S. N. Dubey and D. M. Puri, *Polyhedron* 1984, **3**, 527.
44. B. J. Hathaway and D. E. Billing, *Coord. Chem. Rev.* 1970, **5**, 143.
45. B. J. Hathaway, *Coord. Chem. Rev.* 1981, **35**, 211.
46. R. Cohen and C. Heitner-Wirguin, *Inorg. Chim. Acta* 1969, **3:4**, 647.
47. K. Umezawa and T. Yamabe, *Bull. Chem. Soc. Jpn* 1972, **45**, 56.
48. S. K. Sahni and J. Reedijk, unpublished results.
49. C. Heitner-Wirguin and W. Urbach, *J. Phys. Chem.* 1965, **69**, 3400.
50. V. A. Davankov, S. V. Rogozhin and M. P. Tsyurupa, In *Ion Exchange and Solvent Extraction* (Edited by J. A. Marinsky and Y. Marcus), Vol. 7, p. 29. Marcel Dekker, New York (1977).
51. R. M. Wheaton and M. J. Hatch, In *Ion Exchange and Solvent Extraction* (Edited by J. A. Marinsky and Y. Marcus), Vol. 5, p. 191. Marcel Dekker, New York (1968).
52. H. M. N. H. Irving and R. J. P. Williams, *J. Chem. Soc.* 1953, 3192.
53. R. R. Grinstead, *Proceedings of the International Conference on Ion-Exchange*, p. 509. Society of Chemical Industry, Cambridge, England (1984).
54. C. Heitner-Wirguin, In *Ion-Exchange and Solvent Extraction* (Edited by J. A. Marinsky and Y. Marcus), Vol. 7, p. 83. Marcel Dekker, New York (1977).

Polyhedron Vol. 4, No. 9, pp. 1659–1660, 1985
Printed in Great Britain

0277–5387/85 $3.00 + .00
© 1985 Pergamon Press Ltd

COMMUNICATION

THE INTERACTION OF SILVER IONS WITH THE ISOTHIOCYANATOPENTA-AMMINECHROMIUM(III) CATION

HERVINE MILLER
Chemistry Department, University of the West Indies, Cave Hill, Barbados

(*Received* 18 *January* 1985; *accepted* 3 *April* 1985)

Abstract—The reaction of the isothiocyanatochromium(III) ion with silver ions produces adducts of the type $[Cr(NH_3)_5NCSAg_n]X_{n+2}$. For X = ClO_4, $n = 1$ and for NO_3, $n = 2$.

There is significant interaction between silver ions and $[M(NH_3)_5NCS]^{2+}$ cations as in reaction (1):

$$M(NH_3)_5NCS^{2+} + nAg^+ \rightleftharpoons M(NH_3)_5NCAg_n^{(n+2)+}, \quad (1)$$

where M = Cr, Co, Rh. Values of log K for $n = 1$ are approximately 10^3.[1] The complexes thus formed are thought[2,3] to account for the enhanced rates of aquation of the penta-ammines in the presence of silver ions. For $[Cr(NH_3)_5NCS]^{2+}$ there is spectral evidence for the existence of intermediates with $n = 1$–3 at 25°C[2] and the silver-assisted aquation reaction has been reported[2] as proceeding through such an intermediate, with $n = 1$ at higher temperature (76.4°C). Similar observations have also been reported for $[Co(NH_3)_5NCS]^{2+}$[3] and $[Rh(NH_3)_5I]^{2+}$.[4]

The isolation and characterization of two solid adducts of the isothiocyanatopenta-ammine chromium(III) cation is reported here. These adducts are analogous to, but less stable than, those of cobalt previously reported.[3]

EXPERIMENTAL

Analytical grade reagents were used throughout and distilled water was passed through a column of Permutit "Biodeminrolit" before use. Silver perchlorate solution was prepared by neutralizing freshly prepared silver carbonate with perchloric acid. Isothiocyanatopenta-ammine chromium(III) perchlorate was prepared and analysed as previously reported.[1] All reactions were carried out in the dark or in diffused light.

Preparation and analysis of adduct

Silver adducts were precipitated as follows. Solid $[Cr(NH_3)_5NCS](ClO_4)_2$ was added to a 2 mol dm^{-3} solution of silver perchlorate in a mole ratio Cr : Ag of approximately 1 : 10. The resulting suspension was shaken vigorously and allowed to react at room temperature, approximately 25°C, for a few minutes. A peach-yellow powder precipitated. For the nitrate adduct a similar procedure was followed with silver nitrate being used instead of perchlorate. The resulting precipitate was yellow-buff in colour. The adducts were collected at pump, washed with dry ethanol and dried over silica gel in a darkened vacuum desiccator.

The freshly prepared adducts were analysed quantitatively for chromium and silver by atomic absorption spectrophotometry, after decomposition of an accurately known weight of adduct in aqueous perchloric acid (*ca* 10^{-3} mol dm^{-3}). Found: Cr, 8.72; Ag, 17.2. Calc. for $[Cr(NH_3)_5NCSAg](ClO_4)_3$: Cr, 8.64; Ag, 17.93%. Found: Cr, 7.9; Ag, 31.8. Calc. for $[Cr(NH_3)_5Ag_2](NO_3)_4$: Cr, 7.89; Ag, 32.75%. The ratio Cr : Ag in the adducts was confirmed by spectrophotometric analysis using dithiozone.

RESULTS AND DISCUSSION

The reaction of $[Cr(NH_3)_5NCS]^{2+}$ with silver ions in aqueous solution at 25°C is too fast for study by conventional stopped-flow spectrophotometry.[2] However, in the solid state there is very little evidence of reaction between the adducts.

The silver adducts are only partially soluble in

Table 1. Wavenumber (cm^{-1}) and assignments[5] of bands in spectra of silver adducts of $[ML_5NCS]^{2+}$ (L = NH_3) and silver thiocyanate

Compound	ν_{C-N}	ν_{C-S}	δ_{NCS}	Reference
AgSCN	2145	899, 749	445	3
$[CoL_5NCS](ClO_4)_2$	2110	853	502	3
$[CoL_5NCSAg](ClO_4)_3$	2135, 2185	839, 760	505–510	3
$[CoL_5NCSAg_2](NO_3)_4$	2120	825, 735	505, 458	6
$[CrL_5NCS](ClO_4)_2$	2070	858	458	This work
$[CrL_5NCSAg](ClO_4)_3$	2080, 2160	830, 784	492	This work
$[CrL_5NCSAg_2](NO_3)_4$	2080	840, 825	477, 463	This work

water, even at elevated temperatures, and decompose to give a pink solution and a black powder. After filtration and cooling, this solution corresponds quantitatively to $[Cr(NH_3)_5NCS]^{2+}$. The black powder is, presumably silver oxide since the solutions were not acidified.

In the solid state, decomposition of the adducts was evident in a relatively short time—the nitrate in 3 days, the perchlorate in about 2 weeks. This shows that the compounds are less stable than the cobalt(III) analogues. Analyses showed that the perchlorate and nitrate salts were 1 : 1 and 1 : 2,

$$[Cr(NH_3)_5NCSAg](ClO_4)_3$$

and

$$[Cr(NH_3)_5\ NCSAg_2](NO_3)_4,$$

respectively. The differences are probably due to solubility effects.

Special features of the IR KBr disc spectra compared to those of the cobalt(III) analogues and AgSCN are shown in Table 1. Assignments were made according to published data.[5]

Resolved bands in the region 3100–3300 cm^{-1} $[Cr(NH_3)_5NCS](ClO_4)_2$ are undoubtedly due to N–H stretches and, while unaltered in the 1 : 1 adduct, are significantly changed in the 1 : 2 compound. ν_{C-N} for the pure penta-ammine is at 2070 cm^{-1} and the splitting to 2080 and 2060 cm^{-1} for the 1 : 1 adduct is consistent with a simple bridging SCN group.[5,6] A single band at 2080 cm^{-1} is observed for the 1 : 2 adduct as for the analogous cobalt complex.[3] ν_{C-S} values between 830 and 860 cm^{-1} are assigned to MNC–S and lower values to M'S–CN. A large shift is observed for $\rho_{r(NH_3)}$, being 737 cm^{-1} in $[Cr(NH_3)_5NCS]^{2+}$, and 751 and 760 cm^{-1} in the 1 : 1 and 1 : 2 adducts respectively.

REFERENCES

1. G. C. Lalor and H. Miller, *J. Inorg. Nucl. Chem.* 1975, **37**, 1832.
2. G. C. Lalor and H. Miller, *J. Inorg. Nucl. Chem.* 1978, **40**, 305.
3. G. C. Lalor and H. Miller, *J. Inorg. Nucl. Chem.* 1975, **37**, 307.
4. (a) G. C. Lalor and H. Miller, *Rev. Latinoam. Quim.* 1976, **7**, 102; (b) C. StE. Boyce, G. C. Lalor and H. Miller, *J. Inorg. Nucl. Chem.* 1979, **41**, 857.
5. (a) K. Nakamoto, *Infrared Spectra of Inorganic Coordination Compounds*, 2nd Edn, Wiley, New York (1970); (b) C. Pecile, C. Giacometti and A. Turco, *Atti Accad. Naz. Lincei, Cl. Sci. Fis. Mat. Nat., Rend.* 1960, **28**, 189.
6. H. M. Miller, Ph.D. Thesis, University of the West Indies (1977).

Polyhedron Vol. 4, No. 9, pp. 1661–1664, 1985
Printed in Great Britain

0277-5387/85 $3.00 + .00
© 1985 Pergamon Press Ltd

COMMUNICATION

^{1}H AND ^{13}C NMR OF PLATINUM PORPHYRINS—III. PLATINUM DEUTEROPORPHYRIN IX DIMETHYL ESTER

LIONEL R. MILGROM
Imperial College of Science and Technology, Department of Chemistry, Exhibition Rd, London SW7 2AZ, U.K.

(*Received* 14 *November* 1984; *accepted* 3 *April* 1985)

Abstract—^{1}H and ^{13}C NMR spectra of the title compound are reported and peaks assigned by comparison with the free-base porphyrin. Long-range spin–spin coupling is observed between platinum and the macrocyclic protons and carbon atoms. *Meso*-protons are assigned from line-broadening observed for three of the peaks, possibly caused by residual coupling of these protons to the pyrrole β-protons. Allylic coupling of the pyrrole β-protons to adjacent methyl groups is also noted, and supports the tautomeric model of an 18-atom delocalisation pathway around the macrocycle. The ^{1}H NMR spectrum of the title compound is more concentration-dependent than that of the free-base porphyrin and probably reflects additional macrocyclic interactions via the platinum atoms.

Previous papers in this series[1,2] described long-range coupling in the NMR of the symmetric platinum porphyrins, PtTPP[1] and PtOEP.[2] An attempt to observe similar couplings in the NMR of platinum protoporphyrin IX dimethyl ester [PtPPIXDME (**1**)] was unsuccessful,[2] owing to excessive line-broadening of all the peaks. Those due to the internal reference and solvent were, however, sharp and well-defined. These observations were rationalised in terms of the aggregation of **1** in solution to an oligomer of unknown constitution.

If monomers of **1** aggregate via their platinum atoms, then attempts to prepare platinum complexes of other type IX porphyrins should also yield oligomers with line-broadened NMR spectra. If, on the other hand, oligomerisation is due to some, as yet, unspecified interaction involving platinum and porphyrin vinyl groups, then oligomerisation should be confined to **1** only: other type IX platinum porphyrins should give sharp, well-defined NMR spectra.

To test this hypothesis, platinum deuteroporphyrin IX dimethyl ester [PtDPIXDME (**3**)] was chosen because it should demonstrate in the same molecule all the couplings found separately in the NMR of PtTPP[1] and PtOEP.[2] This paper, therefore, reports the ^{1}H and ^{13}C NMR of the type IX platinum porphyrin, **3**.

RESULTS AND DISCUSSION

Platinum was inserted into **2** using the method of Büchler and Puppe[3] and the product (**3**) gave a clear melting point, unlike **1**. In addition, the FAB spectrum of **3** exhibited a discrete molecular ion, (M^+, m/z = 731). The UV/visible spectrum of the orange-coloured **3** gave sharp, well-defined bands, in contrast to the less-intense and broadened bands of the brown-coloured **1**. These data would indicate much less aggregation in solution for **3**, in contrast to that supposed for **1**.

Assignment of the ^{1}H NMR spectrum of **3** depended on data obtained for the free-base porphyrin (**2**) in these laboratories and elsewhere. This will be discussed first.

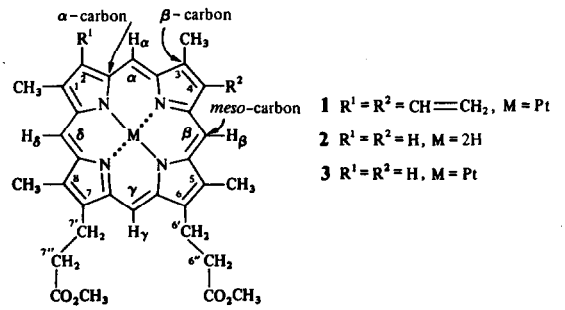


Fig. 1.

Proton assignments for the peripheral substituents and the pyrrole β-positions are in broad agreement with previous results.[5–7] The 5- and 8-methyl groups are to higher field than the 1- and 3-methyls, the latter identifiable by allylic coupling to the pyrrole β-protons (1 Hz). This leads to clearly resolved doublets for these methyl groups in dilute (4 mM) solution and as broadened peaks at a higher (20 mM) concentration. This confirms the results of Clezy *et al.*[6] and Sano *et al.*,[7] but is a feature unremarked on by Janson and Katz[5] who, in the present view, wrongly assign the 1- and 3-methyl groups to higher field.

The pyrrole β-protons appear as two partly-resolved overlapping quartets in dilute solution (allylic coupling to the 1- and 3-methyls), and as a broadened singlet at higher concentration. The *meso*-protons appear as four singlets around 10 ppm (see Table 1).

With this data, the ^{1}H NMR spectrum of **3** can be assigned (see Table 1). In dilute solution (4 mM), the methyl groups appear as a triplet and two singlets at a slightly lower field (assigned to those at the 5- and 8-positions). The triplet, 1- and 3-methyls, arises from two overlapping doublets (J = 1.1 Hz), caused by allylic four-bond coupling to the 2,4-pyrrole β-protons.[6,7] At a higher concentration (20 mM), the triplet becomes two broadened singlets, this time at a lower field to the 5- and 8-methyls.

Again, in dilute solution, the 2,4-pyrrole β-protons are a well-defined quartet[7] (J = 1.2 Hz), presumably due to allylic coupling to the 1,3-methyl groups. Flanking the quartet are partly-resolved Pt satellites ($^4J_{^1H-^{195}Pt}$ = 12.5 Hz) as reported earlier for PtTPP.[1] At a higher concentration, the quartet broadens into two poorly-resolved overlapping quartets (J = 1.2 Hz). Only the Pt satellites outside of them are resolved, giving an apparently larger ^{1}H–^{195}Pt four-bond coupling constant (15.3 Hz).

Assignment of the *meso*-protons is tentative. Three

Table 1.

		DPIXDME				PtDPIXDME	
		4 mM		20 mM		4 mM	20 mM
Assignment		Ref. 5	LRM	Ref. 5	LRM	LRM	LRM
$-CH_2 \cdot C\underline{H}_2 \cdot CO_2CH_3$	7″	3.24[a]	3.30	3.20	3.26	3.22	3.16
	6″	3.24	3.30	3.20	3.26	3.22	3.19
CH_3	1	3.60	3.74[b]	3.55	3.71[c]	3.63[d]	3.56[e]
	3	3.57	3.76[b]	3.54	3.70[c]		3.61[e]
	8	3.70	3.67	3.65	3.60	3.66	3.40
	5	3.68	3.64	3.65	3.59	3.67	3.45
$-CH_2 \cdot CH_2 \cdot CO_2C\underline{H}_3$	7″	3.59	3.65	3.58	3.65	3.51	3.68
	6″	3.59	3.66	3.58	3.64	3.51	3.69
$-C\underline{H}_2 \cdot CH_2 \cdot CO_2CH_3$	7′	4.38	4.36	4.33	4.38	4.25	4.16
	6′	4.38	4.36	4.33	4.38	4.25	4.19
Pyrrole β-H	2	9.06	9.11[f]	8.99	9.04[e]	8.91[g]	8.78[h]
	4	9.04	9.09[f]	8.99	9.04[e]	8.91[g]	8.79[h]
Meso-H	δ	9.99	10.04	9.92	9.97	9.84[i]	9.61[j]
	β	10.03	10.08	9.96	10.01	9.87[i]	9.64[j]
	α	10.06	10.12	9.98	10.02	9.88[i]	9.67[j]
	γ	10.10	10.15	10.01	10.05	9.82	9.74

[a] In ppm.
[b] Doublet, J = 1 Hz.
[c] Almost broadened into doublets.
[d] Triplet from two overlapping doublets, J = 1.1Hz.
[e] Broadened.
[f] Quartet, J = 0.6 Hz.
[g] Quartet, J = 1.2 Hz, and Pt satellites, J = 12.5 Hz.
[h] As *g*, Pt satellites, J = 15.3 Hz.
[i] Broad.
[j] Broad + Pt satellites, J = 4.5 Hz.

of the peaks are broader than the fourth by about 0.5 Hz. This may be due to concentration effects or residual long-range coupling of the three *meso*-protons to the 2,4-pyrrole β-protons. If the latter, the γ-*meso*-proton is assigned to the narrower peak as being furthest from the 2,4-pyrrole β-protons. At low concentration, the γ-*meso*-proton appears to higher field than the α-, β- and δ-*meso*-protons while at higher concentrations the assignment is reversed. In addition, at a higher concentration, Pt satellites are observed on all the *meso*-protons, the coupling constant ($^4J_{^1H-^{195}Pt}$ = 4.5 Hz) being in agreement with the value reported earlier for PtOEP.[2] In dilute solution, the *meso*-protons are too close for individual Pt satellites to be resolved.

Practically all the proton resonances are deshielded by dilution, but the effect is approximately twice as great for the platinum complex (**3**) as for the free-base porphyrin (**2**). This agrees with an earlier report on nickel mesoporphyrin IX dimethyl ester[5(b)] and probably reflects increased dimer formation in solution, presumably mediated via platinum d_{z^2}-orbitals.

The allylic coupling constant, J = 1.2 Hz (cf. 1.5–1.7 Hz in model systems[8]) points to a significantly diminished bond-order for the β–β pyrrolic linkage of **3**.[6] This would implicate the periphery of the molecule in an 18-atom delocalisation pathway,[6] which favours the tautomeric model[9–11] for the platinum porphyrin skeleton as opposed to a 16-atom pathway involving a formal porphyrin dianion.[12] This contradicts the usual dianion formalism for the macrocycle in metalloporphyrins.

The ^{13}C NMR spectrum of **3** differs from **2** in two respects. Firstly, Pt satellites are observed and clearly resolved on all the *meso*-carbons, the 2,4-pyrrole β-carbons, and the 5,6,7,8-pyrrole β-carbons. The coupling constants are similar to those reported for PtTPP[1] and PtOEP[2] (see Table 2). Secondly, the pyrrole α-carbons are shifted upfield so that they overlap with the 1,3-pyrrole β-carbons. Consequently it proved impossible to distinguish the various two- and three-bond ^{13}C–^{195}Pt couplings for these carbons.[1,2]

The *meso*-carbons appear in two groups. The higher-field group is close to that observed for the γ- and δ-carbons of TIDPIXDME(OH,H_2O),[13] themselves assigned on the basis that substitution of the neighbouring pyrrole β-carbons by alkyl groups shifts the *meso*-carbons upfield. The lower-field group are, therefore assigned to the α- and β-*meso*-carbons.

That **3** gives well-defined UV/visible and NMR spectra compared to **1**[2] implies that the latter's vinyl groups are involved in some, as yet, unspecified interaction with Pt. As **1** could be a useful NMR probe for haemoproteins (beause of its potential coupling of Pt to the porphyrin's protons and carbons), synthetic efforts to **1** will in future be directed to modification of 2,4-substituents of an already-existing type IX platinum porphyrin.[14]

EXPERIMENTAL

NMR spectra were obtained in the FT mode on a Bruker WM 250 NMR spectrometer. UV/visible spectra were obtained on a Pye–Unicam SP8-400 spectrophotometer in $CHCl_3$ using approximately 10^{-5} M solutions. The melting point was obtained using a hot-stage microscope. The FAB spectrum was obtained using a Vacuum Generators VG 7070 in a matrix of 2,2′-thiodiethanol. Platinum was

Table 2.

C-α		C-β		C-*meso*		$-CH_3$		$-CH_2CH_2CO_2CH_3$	
(2)	(3)	(2)	(3)	(2)	(3)	(2)	(3)	(2)	(3)
143.3	138.4	128.0[2,4]128.2[a]		95.1[γ]98.2[b]		11.3[5,8]11.3		21.5[C(7′)H_2]21.7	
144.2	138.7	135.5[5,8]135.7[c]		96.2[δ]99.5[d]		13.4[1,3]13.6		36.7[C(7″)$H_2$36.8	
		137.4[6]137.3[a]		98.7[α]101.7[e]				51.4[$-CH_3$]51.6	
		137.7[7]137.5[a]		99.5[β]102.5[f]				172.8[–C=O]173.5	
		139.2[1]139.1							
		139.5[3]139.4							

Numbers in brackets indicate position (see Fig. 1):
[a] $^3J_{^{13}C(\beta)-^{195}Pt}$ = 29.0 Hz.
[b] $^3J_{^{13}C(meso)-^{195}Pt}$ = 37.9 Hz.
[c] $^3J_{^{13}C(\beta)-^{195}Pt}$ = 27.9 Hz.
[d] $^3J_{^{13}C(meso)-^{195}Pt}$ = 36.0 Hz.
[e] $^3J_{^{13}C(meso)-^{195}Pt}$ = 38.2 Hz.
[f] $^3J_{^{13}C(meso)-^{195}Pt}$ = 37.2 Hz.

inserted into **2** by the method of Büchler and Puppe[3] as reported earlier.[1,2] The metalloporphyrin was separated from unreacted **2** by column chromatography on silica-gel (Kieselgel 60, Merck) eluting with $CHCl_3$/TFA [2% (v/v)]. The intense orange band was collected, concentrated, and crystallised with methanol to yield **3** (53 mg, 39% from **2**) as orange micro-crystals, m.p. = 249–251°C. (Found: C, 50.1; H, 4.2; N, 7.3. $C_{32}H_{32}N_4PtO_4 \cdot 2H_2O$ requires: C, 50.1; H, 4.7; N, 7.3%.) λ_{max}(nm) [ε(mmol l^{-1})] in $CHCl_3$: 380(257), 500(10.8), 533(41). FABS: found M^+, m/z = 731, requires m/z = 731.

Acknowledgements—I wish to thank Dr R. Shephard and Ms S. Johnson for obtaining NMR spectra, and Professor D. F. Evans, FRS, and Dr G. B. Young for helpful discussions. Support by the SERC (post-doctoral fellowship) is gratefully acknowledged.

REFERENCES

1. L. R. Milgrom, *Polyhedron* 1984, **3**, 879.
2. L. R. Milgrom, *Polyhedron* 1985, **4**, 1279.
3. J. W. Büchler and L. Puppe, *Justus Liebigs Ann. Chem.* 1974, 1046.
4. K. M. Smith, In *Porphyrins and Metalloporphyrins* (Edited by K. M. Smith), p. 381. Elsevier, New York (1974).
5. (a) T. R. Janson and J. J. Katz, *J. Magn. Reson.* 1972, **6**, 209; (b) D. A. Doughty and C. W. Dwiggins, Jr, *J. Phys. Chem.* 1969, **73**, 423.
6. P. S. Clezy, C. J. R. Fookes and S. Sternhell, *Aust. J. Chem.* 1978, **31**, 639.
7. S. Sano, T. Shingu, J. M. French and E. Thonger, *Biochem. J.* 1965, **97**, 250.
8. M. Barfield, R. J. Spear and S. Sternhell, *Chem. Rev.* 1976, **76**, 593.
9. C. B. Storm and Y. Teklu, *J. Am. Chem. Soc.* 1972, **94**, 1745.
10. M. V. Zehler and R. G. Hughes, *J. Am. Chem. Soc.* 1973, **95**, 3855.
11. J. L. Hoard, In Ref. 4, p. 332.
12. E. B. Fleischerm, *Acc. Chem. Res.* 1970, **3**, 105.
13. R. J. Abraham, G. E. Hawkes and K. M. Smith, *J. Chem. Soc., Perkin Trans. II* 1974, 627.
14. H. Fischer and K. Zeile, *Justus Liebigs Ann. Chem.* 1929, **468**, 98.

Polyhedron Vol. 4, No. 9, pp. 1665–1666, 1985
Printed in Great Britain

0277–5387/85 $3.00 + .00
© 1985 Pergamon Press Ltd

COMMUNICATION

N-METHYL-2,2′-BIPYRIDYLIUM ION (bpyMe) COMPLEXES: SYNTHESIS AND CYCLOMETALLATION OF $[Pd(bpyMe)_2Cl_2]^{2+}$

FRANZ L. WIMMER* and SMITA WIMMER
School of Natural Resources, University of the South Pacific, Suva, Fiji

(*Received* 14 *January* 1985; *accepted* 3 *April* 1985)

Abstract—On prolonged heating in water $Pd(bpyMe)Cl_3$ (bpyMe = *N*-methyl-2,2′-bipyridylium cation) cyclometallates to give monomeric $Pd(bpyMe\text{-}H)Cl_2$, whereas the immediate products are a mixture of *trans*-$[Pd(bpyMe)_2Cl_2]^{2+}$ and anionic palladium species. $[Pd(bpyMe)_2Cl_2]^{2+}$ was synthesised directly from Na_2PdCl_4 and on heating gives $Pd(bpyMe\text{-}H)Cl_2$ with the elimination of bpyMe and H^+.

Two areas of current interest are the metal complexes of cationic ligands[1,2] and cyclometallated compounds.[3] We describe here the facile cyclopalladation of the cationic ligand, the *N*-methyl-2,2′-bipyridylium ion [bpyMe (**1**)]. We have previously shown that **1** forms zwitterionic complexes of the type $M(II)(bpyMe)Cl_3$ with both 3*d* metals[4] and palladium (**2**) and platinum (**3**).[5] $Pt(bpyMe)Cl_3$ (**3**) slowly cyclometallates on heating to give $Pt(bpyMe\text{-}H)Cl_2$ (**5**).[5]

$Pd(bpyMe)Cl_3$ (**2**) is insoluble in all solvents except very hot water, from which it can be recovered unchanged on cooling as brownish orange crystals. However, when the heating is prolonged† **2** cyclometallates readily to give pale yellow needles of $Pd(bpyMe\text{-}H)Cl_2$ (**4**) which is sparingly soluble in boiling water and insoluble in all other solvents.‡

The IR spectrum of **4** is identical to that of **5**.§‖ The medium intensity bands at 335 and 265 cm^{-1} are assigned as Pd—Cl stretching modes. This is consistent with the dichloro ligands being *trans* to a sigma C-donor and an N-donor ligand respectively. However, it is not possible to distinguish between the two isomeric structures for **4** shown in Fig. 1. Both the neutral monomer (**I**) and the dicationic dimer (**II**) should give rise to similar frequencies for their respective Pd—Cl stretching absorptions.[6]

The molar conductivity of a 3.73×10^{-3} M aqueous solution of **2** at 298 K is 1.26×10^{-2} S m^2 mol^{-1}, which is typical of a 1 : 1 electrolyte. Aquation of either **1** or chloride will account for this. Ion-exchange chromatography on Sephadex C25 and

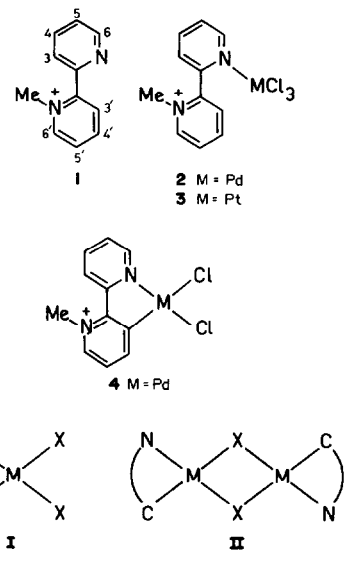


Fig. 1. Generalized structures for cyclometallated compounds of Pd(II).

* Author to whom correspondence should be addressed.

† In a typical experiment $Pd(bpyMe)Cl_3$ (0.36 mmol) is heated under reflux in water (20 cm^3) for 22 h to give $Pd(bpyMe\text{-}H)Cl_2$ in 85% yield. The mother liquor is acidic and gives a positive test for chloride with $AgNO_3$.

‡ Water is necessary for cyclometallation to occur. $Pd(bpyMe)Cl_3$ is recovered unchanged after heating under reflux in solvents with varying boiling points such as ethanol and 2-methoxyethanol (**5**).

§ The IR spectrum on cyclometallation shows changes in both the ring-stretching (1650–1400 cm^{-1}) and the C–H out-of-plane (800–700 cm^{-1}) regions, suggesting cyclometallation at $C^{3'}$ rather than in the methyl group.

‖ Far-IR region: 335 m, 290 wm, 280 wm and 265 m cm^{-1}.

A25 resins shows that the solution contains both cationic and anionic palladium species.

The cationic species was isolated by adding sodium perchlorate to a hot solution of **2**; this gave an immediate pale yellow precipitate which was recrystallized as pale yellow plates from water/acetone (1 : 1) by slow evaporation at room temperature (25–30°C). The elementary analyses indicate the formulation $[Pd(bpyMe)_2Cl_2](ClO_4)_2$ (**6**). The IR spectrum shows a strong band at 348 cm^{-1} which is assigned as a Pd—Cl stretching mode, suggesting that the complex has the *trans*-configuration.

The crude yield of **6** is about 48% based on **2**. The rest of palladium remains in solution as either $[PdCl_4]^{2-}$ or $[Pd(H_2O)Cl_3]^-$ and was not isolated. Presumably the primary process in the dissolution of **2** is aquation of **1** [eqn (1)] followed by substitution [eqn (2)]:

$$Pd(bpyMe)Cl_3 \rightarrow [Pd(H_2O)Cl_3]^- + bpyMe^+ \quad (1)$$

$$Pd(bpyMe)Cl_3 + bpyMe^+ \rightarrow [Pd(bpyMe)_2Cl_2]^{2+} + Cl^-. \quad (2)$$

It should be possible to prepare the bis-complex $[Pd(bpyMe)_2Cl_2]^{2+}$ by direct synthesis. Addition of 2 mol of $(bpyMe)NO_3$ to a warm aqueous solution of Na_2PdCl_4 results initially in an orange precipitate of **2**, which dissolves to a yellow solution. Addition of a dilute sodium perchlorate solution precipitates **6** in 85% yield.* Similarly, treatment of a warm solution of **2** with $(bpyMe)ClO_4$ (1.5 mol) followed by sodium perchlorate gives **6** in 75% yield.†

The facile formation of a four-coordinate bis(bpyMe) complex is unexpected since most complexes with cationic ligands (L) are insoluble zwitterions of type $MLCl_3$. The limited number of first-row transition-metal complexes with two cationic ligands are mainly five-coordinate.[7] There are no known Pd(II) or Pt(II) complexes with two cationic ligands.

On heating **2** in water, the overall reaction is cyclometallation to give **4**, whereas the immediate products are $[Pd(bpyMe)_2Cl_2]^{2+}$ and anionic species [eqns (1) and (2)]. It follows that $[Pd(bpyMe)_2Cl_2]^{2+}$ should cyclometallate with elimination of **1**. Heating **6** under reflux in water for 5 h gives **4** in 88% yield. The **1** produced in the reaction was recovered by precipitation with sodium tetraphenylborate. The IR spectrum of the cyclometallated complex formed in this reaction is free from perchlorate bands, indicating that **4** is monomeric (i.e. has structure **I**) and neutral overall. The cyclometallated bpyMe ligand is now behaving as an internal zwitterion. If **4** was dimeric (i.e. **II**) it would bear a dipositive charge and would be expected to separate from solution as the perchlorate salt if the normal solubility difference between chloride and perchlorate salts is followed.

Most complexes formed as a result of cyclopalladation of a neutral ligand have the dimeric structure **II** so as to produce a neutral compound.[3] In some cases[8] the dimer can be cleaved by halide ions to the monomer **I** which is now anionic.

These results are of interest in the light of recent X-ray studies[9] of $Ir(bpy)_3Cl_3 \cdot 4H_2O$, which have shown the presence of a cyclometallated C^3,N'-bpy ligand similar to cyclometallated bpyMe.‡

REFERENCES

1. G. Marcotrigiani, L. Menabue and G. C. Pellacani, *Inorg. Chim. Acta* 1978, **26**, 57, and references cited therein.
2. W. L. Steffen and G. J. Palenik, *Inorg. Chem.* 1978, **17**, 1338, and references cited therein.
3. For reviews see: J. Dehand and M. Pfeffer, *Coord. Chem. Rev.* 1976, **18**, 327; M. I. Bruce, *Angew. Chem.* 1977, **89**, 75; I. Omae, *Chem. Rev.* 1979, **79**, 287; *Coord. Chem. Rev.* 1980, **32**, 235; 1982, **42**, 245.
4. S. Dholakia, R. D. Gillard and F. L. Wimmer, *Inorg. Chim. Acta* 1982, **65**, L121.
5. S. Dholakia, R. D. Gillard and F. L. Wimmer, *Inorg. Chim. Acta* 1983, **69**, 179.
6. D. M. Adams, J. Chatt, J. Gerratt and A. D. Westland, *J. Chem. Soc.* 1964, 734; J. D. Ruddick and B. L. Shaw, *J. Chem. Soc.* (*A*) 1969, 2801; B. Crociani, T. Boschi, R. Pietropaolo and U. Belluco, *J. Chem. Soc.* (*A*) 1970, 531; J. Dehand, M. Pfeffer and M. Zinsius, *Inorg. Chim. Acta* 1975, **13**, 229.
7. V. L. Goedken, L. M. Vallarino and J. V. Quagliano, *Inorg. Chem.* 1971, **10**, 2682; 1972, **11**, 1466; 1973, **12**, 102.
8. P. Braunstein, J. Dehand and M. Pfeffer, *Inorg. Nucl. Chem. Lett.* 1974, **10**, 581.
9. G. Nord, A. C. Hazell, R. G. Hazell and O. Farver, *Inorg. Chem.* 1983, **22**, 3429, and references cited therein.

* Mixing hot solutions of K_2PtCl_4 and $(bpyMe)ClO_4$ (2 mol) gives a yellow solution. Cooling in the presence of excess perchlorate yields $Pt(bpyMe)Cl_3$ with only a very small amount of $[Pt(bpyMe)_2Cl_2](ClO_4)_2$ which can be extracted with acetone/water (1 : 1).

† The soluble salt $[Pd(bpyMe)_2Cl_2](NO_3)_3$ was prepared by treating $Pd(bpyMe)Cl_3$ with warm $(bpyMe)No_3$ followed by $AgNO_3$ (1 mol), filtering and evaporating to dryness at room temperature. $Pd(bpyMe)Cl_3$ gives a clear solution when treated with (bpyMe)Cl, but on cooling the starting compound crystallises.

‡ Attempts to obtain the crystal structure of $Pt(bpyMeH)Cl_2$ have been unsuccessful due to an unusually large unit cell (M. R. Snow, personal communication). The crystal structure of $[Pd(bpyMe)_2Cl_2](ClO_4)_2$ is currently under investigation.

Polyhedron Vol. 4, No. 9, pp. 1667–1668, 1985
Printed in Great Britain

0277–5387/85 $3.00 + .00
© 1985 Pergamon Press Ltd

COMMUNICATION

AZIDES OF HEAVIER MAIN GROUP ELEMENTS: THE RELUCTANCE OF PHOSPHINE AZIDES TO UNDERGO A CURTIUS-TYPE REARRANGEMENT

EDGAR OCANDO, SAMIA MAJID and JEAN PIERRE MAJORAL*
U.A. 454, Université Paul Sabatier, 118 route de Narbonne, 31062 Toulouse, France

and

ANTOINE BACEIREDO and GUY BERTRAND*
U.A. 477, Université Paul Sabatier, 118 route de Narbonne, 31062 Toulouse, France

(*Received* 18 *December* 1984; *accepted* 3 *April* 1985)

Abstract—Under thermolytic or photolytic conditions, phosphine azide complexes $Ph_2PN_3M(CO)_5$ (M = W, Cr) gave rise to the corresponding isocyanato complexes and not to the expected iminophosphane complexes.

Recently, Curtius-type rearrangements involving an azide group bonded to boron,[1] silicon,[2] germanium[3] or tetracoordinated pentavalent,[4] tetracoordinated tetravalent[5] and pentacoordinated pentavalent[6] phosphorus atoms have been reported. On the other hand, although phosphine azides have received considerable attention in recent years,[7–9] no Curtius rearrangement:

$$R_2PN_3 \xrightarrow[-N_2]{h\nu \text{ or } \Delta} R{-}P{=}N{-}R,$$

which would lead to dicoordinated trivalent phosphorus derivatives, has been observed. Depending on the nature of the substituents, three types of reactions have been described previously:[7–9]

$$Ph_2PN_3 \xrightarrow{\Delta} (Ph_2PN)_{3,n}$$

$$[(Me_3Si)_2N]_2PN_3 \xrightarrow{\Delta} (Me_3Si)_2N{-}P(=N{-}SiMe_3)(=N{-}SiMe_3)$$

$$[(iPr)_2N]_2PN_3 \xrightarrow{h\nu} [(iPr)_2N]_2P{\equiv}N$$

Since all of these reactions involve the phosphorus lone pair electrons, one might anticipate that the complexation of the phosphorus atom might encourage the Curtius-type rearrangement and thereby provide a facile route to iminophosphane complexes (**2**).[10]

Because of the great instability of diphenylphosphine azide which explodes when shocked at −13°C, compounds **1a** and **1b** were prepared by reaction of diphenylchlorophospine complexes with sodium azide [**1a**: ^{31}P NMR (CH_3CN): +88 ppm, $^1J_{PW}$ = 273 Hz; IR (CH_3CN): 2130 cm^{-1} (P—N_3); **1b**: ^{31}P NMR (CH_3CN): +134 ppm; IR (CH_3CN): 2130 cm^{-1} (P—N_3)]:

$$Ph_2PCl \xrightarrow{NaN_3} Ph_2PN_3 \qquad \begin{matrix}\textbf{1a}: M = W\\ \textbf{1b}: M = Cr\end{matrix}$$
$$\quad | \qquad\qquad |$$
$$M(CO)_5 \qquad M(CO)_5$$

Irradiation of a toluene or acetonitrile solution of complexes **1a** and **1b** at 254 nm and ambient temperature for 9 h, using a Rayonet photochemical reactor or heating at 70°C (6 h) gave new complexes, **3a** and **3b**, with release of nitrogen:

$$Ph{-}P{=}N{-}Ph \quad \leftarrow\!\times\!- \mathbf{1} -\!\rightarrow \quad Ph_2P{-}N{=}C{=}O$$
$$\quad | \qquad\qquad\qquad\qquad\quad |$$
$$M(CO)_5 \qquad\qquad\qquad\qquad M(CO)_5$$
$$\mathbf{2} \qquad\qquad\qquad\qquad\quad \mathbf{3}$$

3a: M = W
3b: M = Cr

*Authors to whom correspondence should be addressed.

Complexes **3a** and **3b** were obtained in 33 and 42% yields respectively, as pale yellow powders; **3a**: m.p. 50°C; ^{31}P NMR (CH_3CN): +70 ppm, $^1J_{PW}$ = 276 Hz; IR (CH_3CN): 2250 (N=C=O) 2080, 1950 (CO) cm^{-1}; mass spectrum: M^+ and successive eliminations of CO groups; **3b**: m.p. 42°C; ^{31}P NMR (CH_3CN): +118 ppm; IR (CH_3CN): 2280 (N=C=O), 2080, 1930 (CO) cm^{-1}; mass spectrum: M^+ and successive eliminations of CO groups. Confirmation of the structural assignments of **3** were obtained by their independent synthesis by uniquely different routes:

$$Ph_2PN{=}C{=}O \xrightarrow{M(CO)_5THF} \mathbf{3} \xleftarrow{NaOCN} Ph_2PCl \mid M(CO)_5$$

It seems reasonable that the reaction **1** → **3** proceeds via the transient formation of a phosphinonitrene intermediate, **4**, which combines with carbon monoxide:

$$Ph_2P{-}N \mid M(CO)_5$$

4

Addition of CO to an aryl nitrene has been observed but under drastic conditions (160°C, 150 atm).[11] However, all attempts to trap **4** by classical nitrene reagents failed; in each case **3a** or **3b** was formed.

In conclusion, in marked contrast with other heavier main group element azides, free or complex phosphine azides are reluctant to give Curtius-type rearrangement, although a nitrene type intermediate seems to be formed.

Acknowledgement—Thanks are due to the CNRS (ATP Concepts Nouveaux de l'Objectif Chimie Fine) for financial support.

REFERENCES

1. P. I. Paetzold and H. Grundke, *Synthesis* 1973, 635; W. Pieper, D. Schmitz and P. I. Paetzold, *Chem. Ber.* 1981, **114**, 3801.
2. D. R. Parker and L. H. Sommer, *J. Am. Chem. Soc.* 1976, **98**, 618; M. Elsheikh, N. R. Pearson and L. H. Sommer, *J. Am. Chem. Soc.* 1979, **101**, 2491; A. Baceiredo, G. Bertrand, J. P. Majoral and P. Mazerolles, *Nouv. J. Chim.* 1983, **7**, 645.
3. W. T. Reichle, *Inorg. Chem.* 1964, **3**, 402; A. Baceiredo, G. Bertrand and P. Mazerolles, *Tetrahedron Lett.* 1981, **22**, 2553.
4. G. Bertrand, J. P. Majoral and A. Baceiredo, *Tetrahedron Lett.* 1980, **21**, 5015; J. Wiseman and F. H. Westheimer, *J. Am. Chem. Soc.* 1974, **96**, 4262; R. Breslow, A. Feiring and F. Herman, *J. Am. Chem. Soc.* 1974, **96**, 5937; M. J. P. Harger and M. A. Stephen, *J. Chem. Soc., Perkin Trans.* 1981, 736; M. J. P. Harger and S. Westlake, *Tetrahedron* 1982, **38**, 1511; M. J. P. Harger and S. Westlake, *J. Chem. Soc., Perkin 1* 1984, **10**, 2351; A. Baceiredo, J. P. Majoral and G. Bertrand, *Nouv. J. Chim.* 1983, **7**, 255.
5. M. Mulliez, J. P. Majoral and G. Bertrand, *J. Chem. Soc., Chem. Commun.* 1984, 284.
6. A. Baceiredo, G. Bertrand, J. P. Majoral, U. Wermuth and R. Schmutzler, *J. Am. Chem. Soc.* 1984, **106**, 7065.
7. K. C. Paciorek and R. Kratzer, *Inorg. Chem.* 1964, **3**, 594; G. Tesi, C. P. Haber and C. M. Douglas, *Proc. Chem. Soc.* 1960, 219.
8. H. G. Schäfer, Dissertation, Universität Bielefeld (1981); Wildbredt, Dissertation, Universität Bielefeld (1981), Z. Min Xie and R. H. Neilson, *Organometallics* 1983, **2**, 921.
9. G. Sicard, A. Baceiredo, G. Bertrand and J. P. Majoral, *Angew. Chem., Int. Ed. Engl.* 1984, **23**, 459; A. Baceiredo, G. Bertrand, J. P. Majoral, G. Sicard, J. Jaud and J. Galy, *J. Am. Chem. Soc.* 1984, **106**, 6088.
10. E. Niecke, M. Engelman, H. Zorn, B. Krebs and G. Henkel, *Angew. Chem., Int. Ed. Engl.* 1980, **19**, 710.
11. P. Guiseppe, C. Guiseppe and B. Giampero, *Chim. Ind. (Milan)* 1968, **50**, 1200.

Polyhedron Vol. 4, No. 9, pp. 1669–1671, 1985
Printed in Great Britain

0277–5387/85 $3.00 + .00
© 1985 Pergamon Press Ltd

COMMUNICATION

THE STRUCTURE OF (DICHLORO) (DI-μ-ACETATO)(BIS-TRIPHENYL PHOSPHINE) DIMOLYBDENUM(II)

F. ALBERT COTTON* and GREGORY L. POWELL
Department of Chemistry and Laboratory for Molecular Structure and Bonding, Texas A & M University, College Station, TX 77843, U.S.A.

(*Received* 25 *February* 1985; *accepted* 19 *April* 1985)

Abstract—The title compound was obtained in crystalline form suitable for X-ray structure determination. It forms crystals in the monoclinic space group $P2_1/c$ with two centrosymmetric molecules in a unit cell of dimensions, $a = 10.888(1)$ Å, $b = 10.182(2)$ Å, $c = 17.929(4)$ Å, $\beta = 104.33(1)°$. The central $Mo_2Cl_2(O_2C—)_2P_2$ core has effectively C_{2h}-symmetry with the following principal dimensions: Mo—Mo = 2.091(1) Å, Mo—Cl = 2.405 Å, Mo—P = 2.566(2) Å, Mo—O(av.) = 2.103[4] Å, Mo—Mo—P = 104.38(7)°, and Mo—Mo—Cl = 116.23(8)°.

Molecules of type $Mo_2(O_2CR)_2X_2L_2$, in which X is a halogen and L a phosphine, have been known since the first ones were synthesized by San Filippo *et al.*[1,2] in 1976. At that time the structure of $Mo_2(O_2CC_6H_5)_2Br_2(PBu^n_3)_2$ was determined.[2] In 1982 there were three further reports of the preparation of such compounds[3–5] and structures were reported for $Mo_2(O_2CMe)_2Cl_2(PBu^n_3)_2$[3] and $Mo_2(O_2CCMe_3)_2Cl_2(PEt_3)_2$.[5] Three preparative methods have been used:

$$Mo_2(O_2CMe)_4 + AlCl_3 + PPh_3 \rightarrow Mo_2(O_2CMe)_2Cl_2(PPh_3)_2 \quad \text{(McCarley)},$$

$$Mo_2(O_2CMe)_4 + Me_3SiCl + PR_3 \rightarrow Mo_2(O_2CMe)_2Cl_2(PR_3)_2 \quad \text{(Green } et\ al.\text{)},$$

$$Mo_2X_4(PR_3)_4 + RCOOH \rightarrow Mo_2(O_2CR)_2X_2(PR_3)_2 \quad \text{(San Filippo)}.$$

In two of the earlier studies the title compound of this paper was prepared. This was first done by Ryan and McCarley[4] who characterized it by elemental analysis, visible absorption spectrum and IR spectrum. Green *et al.*[3] also obtained it by their method and added ^1H and ^{31}P NMR data to the characterization. We now report its structure and compare it with the three other structures mentioned above.

* Author to whom correspondence should be addressed.

EXPERIMENTAL

The preparation was by the method of Green *et al.*,[3] but relatively greater amounts of Me_3SiCl and PPh_3 were used, and a technique for obtaining the crystalline compound directly from the reaction mixture was employed. Me_3SiCl (1.0 cm^3, 7.9 mmol) was added to a stirred mixture of $Mo_2(O_2CMe)_4$ (0.42 g, 0.98 mmol) and PPh_3 (1.04 g, 3.97 mmol) in 50 cm^3 of THF. After 2 h of stirring at 22°C the mixture was filtered through a glass frit and the filtrate collected in a large Schlenk tube. A layer of toluene was carefully placed over this solution and after a few days slow interdiffusion of the two liquid phases had caused the formation of red crystals suitable for X-ray analysis.

The crystal structure was determined in the usual way by methods that are routine.[6] The pertinent crystallographic facts are summarized in Table 1. There was no evidence of crystal decay during data collection and absorption corrections were made empirically by scanning nine reflections with χ near 90° at 10° intervals in ψ. The structure was solved and refined without difficulty or any indication of disorder and the final difference map contained no feature of chemical significance. Atomic positional and thermal parameters, structure factors and complete lists of bond angles and distances have been deposited as supplementary material with the Editor, from whom copies are available on request. Atomic coordinates have also been submitted to the Cambridge Crystallographic Data Centre.

Table 1. Summary of crystal data, data collection parameters, and refinement residuals for $Mo_2(OAc)_2Cl_2(PPh_3)_2$

Formula	$Mo_2Cl_2P_2O_4C_{40}H_{36}$
Formula weight	905.46
Spacc group	$P2_1/c$
Systematic absences	$h0l: l = 2n+1$
	$0k0: k = 2n+1$
a (Å)	10.888(1)
b (Å)	10.182(2)
c (Å)	17.929(4)
α (°)	90
β (°)	104.33(1)
γ (°)	90
V (Å^3)	1926(1)
Z	2
$d_{calc.}$ (g cm^{-3})	1.56
Crystal size (mm)	0.07 × 0.20 × 0.21
μ(Mo-K_α) (cm^{-1})	8.958
Data collection instrument	Enraf–Nonius CAD-4
Radiation (monochromated in incident beam)	Mo-K_α, λ = 0.710730
Orientation reflections, number, range (2θ)	25, 17–32°
Temperature (°C)	25
Scan method	ω–2θ
Data collection range, 2θ (°)	5–50
No. of unique data, total with $F_o^2 > 3\sigma(F_o^2)$	1801
Number of parameters refined	226
Transmission factors (max, min) (%)	99.87, 87.35 (9 psi scans)
R^a	0.0521
R_w^b	0.0639
Quality-of-fit indicator^c	1.545
Largest shift/esd, final cycle	0.22
Largest peak (e Å^{-3})	0.80

$^a R = \sum ||F_o| - |F_c|| / \sum |F_o|$.
$^b R_w = [\sum w(|F_o| - |F_c|)^2 / \sum w|F_o|^2]^{1/2}$; $w = 1/\sigma^2(|F_o|)$.
^{c} Quality of fit $= [\sum w(|F_o| - |F_c|)^2 / (N_{obs} - N_{parameters})]^{1/2}$.

RESULTS AND DISCUSSION

A labelled drawing of the molecular structure is presented in Fig. 1. There is a crystallographic inversion center at the midpoint of the Mo—Mo bond. Table 2 lists the important bond lengths and angles. The molecule is qualitatively very similar to the others of the same type whose structures have been reported. In all cases, the virtual symmetry of the central $Mo_2X_2(O_2C—)_2P_2$ core is C_{2h} with the plane of symmetry containing the $Mo_2X_2P_2$ atoms.

We present in Table 3 a comparison of the present structure with the three others. It is clear that changes in the R group of the carboxylic acid, the halogen or the R′ groups in the phosphine have only

Table 2. Selected bond distances and bond angles

Distance (Å)	
Mo—Mo	2.091(1)
Mo—Cl	2.405(2)
Mo—P	2.566(2)
Mo—O(1)	2.009(5)
Mo—O(2)	2.107(5)
Angle (°)	
Mo—Mo—Cl	116.23(8)
Mo—Mo—P	104.38(7)
Mo—Mo—O(1)	91.5(2)
Mo—Mo—O(2)	92.0(2)
Cl—Mo—P	139.36(9)

Table 3. Comparison of structurally characterized $Mo_2(O_2CR)_2X_2(PR'_3)_2$ complexes

Compound	Mo–Mo	Mo–Cl	Mo–P	Mo–O	Mo–Mo–X	Mo–Mo–P	P–Mo–X
1 $Mo_2(O_2CCMe_3)_2Cl_2(PEt_3)_2$[a]	2.0984(4)	2.428(5)	2.513(4)	2.105(0)	117.9(1)	99.8(1)	142.2(2)
2 $Mo_2(O_2CPh)_2Br_2[P(n\text{-}Bu)_3]_2$[b]	2.091(3)	—	2.526(5)	2.11(1)	115.9(1)	101.9(1)	142.1(1)
3 $Mo_2(O_2CMe)_2Cl_2[P(n\text{-}Bu)_3]_2$[c]	2.099(1)	2.427(2)	2.501(3)	2.105(5)	119.00(8)	101.21(8)	139.8(1)
4 $Mo_2(O_2CMe)_2Cl_2(PPh_3)_2$[d]	2.091(1)	2.405(2)	2.566(2)	2.103(4)	116.23(8)	104.38(7)	139.36(9)

[a] Ref. 5.
[b] Ref. 2.
[c] Ref. 3.
[d] This work.

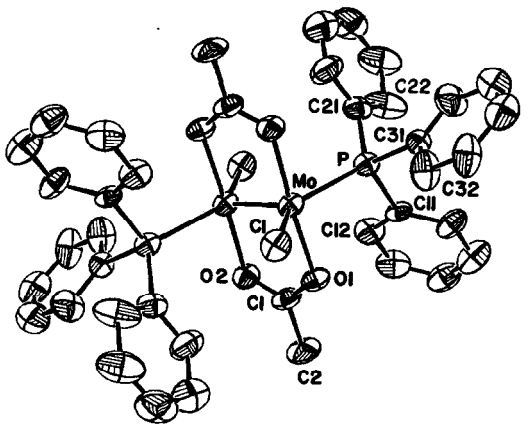


Fig. 1. An ORTEP drawing of the $Mo_2(O_2CCH_3)_2Cl_2(PPh_3)_2$ molecule. Atoms are represented by displacement ellipsoids at the 40% probability level. Unlabeled atoms in one half of the molecule are related by an inversion center to those that are labeled. The numbering of unlabeled ring atoms, C13–C16, C23–C26 and C33–C36, should be evident.

slight effects on the structures. Indeed in comparing compounds **1** and **3** it appears that the change from $MeCO_2^-$ to $Me_3CCO_2^-$ is without any detectable effect. Nor does the replacement of Cl^- by Br^- seem to have any important consequences. Only changes in the bulk and/or the basicity of the phosphines appear to have structural consequences of any size.

The variation in Mo—Mo—P angles correlates with the increasing bulk of the PR_3 ligands. While the variation in Mo—P distances from **1** to **3** is virtually negligible, there is an appreciable increase for **4**. This could be due to the lower basicity of the aryl phosphine but it may also be partly of steric origin since the bulkier PPh_3 ligand may be sterically repelled by the other ligands.

Acknowledgement—We thank the National Science Foundation for support.

REFERENCES

1. J. San Filippo, Jr and H. J. Sniadoch, *Inorg. Chem.* 1976, **15**, 2215.
2. J. A. Potenza, R. J. Johnson and J. San Filippo, Jr, *Inorg. Chem.* 1976, **15**, 2215.
3. M. L. H. Green, G. Parkin, J. Bashkin, J. Fail and K. Prout, *J. Chem. Soc., Dalton Trans.* 1982, 2519.
4. T. R. Ryan and R. E. McCarley, *Inorg. Chem.* 1982, **21**, 2072.
5. J. D. Arenivar, V. V. Mainz, H. Ruben, R. A. Andersen and A. Zalkin, *Inorg. Chem.* 1982, **21**, 2649.
6. A. Bino, F. A. Cotton and P. E. Fanwick, *Inorg. Chem.* 1979, **18**, 3558; F. A. Cotton, B. A. Frenz, G. Deganello and A. Shaver, *J. Organomet. Chem.* 1973, **50**, 227; A. C. T. North, D. C. Phillips and F. S. Mathews, *Acta Cryst. Sect. A* 1968, **A24**, 351.

Polyhedron Vol. 4, No. 9, pp. 1673–1675,
Printed in Great Britain

0277–5387/85 $3.00 + .00
© 1985 Pergamon Press Ltd

COMMUNICATION

CATIONIC DIHYDRIDOIRIDIUM(III) COMPLEXES OF NITRILES

CHONG SHIK CHIN* and HWA-KUN PARK
Department of Chemistry, Sogang University, CPO Box 1142, Seoul, 121 Korea

and

WAN-CHUL JOO
Department of Chemistry, Sung Kyun Kwan University, Suwon, 170 Korea

(*Received* 15 *February* 1985; *accepted* 19 *April* 1985)

Abstract—The reaction of $[IrL(CO)(PPh_3)_2]ClO_4$ (PPh_3 = triphenylphosphine) with H_2 produces new cationic dihydridoiridium(III) complexes of nitriles (L), $[Ir(H)_2L(CO)(PPh_3)_2]ClO_4$ [L = CH_3CN (**1**), CH_3CH_2CN (**2**), $CH_3CH_2CH_2CN$ (**3**) and C_6H_5CN (**4**)], where nitriles are coordinated through the nitrogen atom. Proton NMR spectral data for complexes **1–4** suggest that the two hydrides in each complex are *cis* to each other and *trans* to CO and nitrogen (nitrile), and the two PPh_3 are *trans* to each other.

We recently prepared dihydridoiridium(III) complexes of unsatured nitriles,

$$[Ir(H)_2L(CO)(PPh_3)_2]ClO_4$$

(L = unsaturated nitriles coordinated through the nitrogen) and examined their physical properties and catalytic activities.[1] In this paper, we wish to report the synthesis of new cationic dihydridoiridium(III) complexes of saturated and aromatic nitriles and suggest their structures on the basis of the spectral data.

Stirring the yellow solution of

$$[IrL(CO)(PPh_3)_2]ClO_4$$

(L = CH_3CN, CH_3CH_2CN, $CH_3CH_2CH_2CN$ and C_6H_5CN)† in dichloromethane under hydrogen (P_{H_2} = 1 atm) at 25°C yielded a beige precipitate within 5 min. The addition of hexane to this beige suspension resulted in a more beige solid of $[Ir(H)_2L(CO)(PPh_3)_2]ClO_4$[eqn (1):‡

$$[IrL(CO)(PPh_3)_2]ClO_4 + H_2 \rightarrow [Ir(H)_2L(CO)(PPh_3)_2]ClO_4 \quad (1)$$

[L = CH_3CN (**1**), CH_3CH_2CN (**2**), $CH_3CH_2CH_2CN$ (**3**) and C_6H_5CN (benzonitrile) (**4**)].

Complexes **1–4** are stable in the solid state in air at room temperature, and slightly soluble in chloroform and dichloromethane and insoluble in benzene and hexane. The conductance measurements (110–120 ohm^{-1} cm^2 mol^{-1} for **1–4**)‡ indicate that the complexes are 1:1 electrolytes.§

* Author to whom correspondence should be addressed.

† $[IrL(CO)(PPh_3)_2]ClO_4$ (L = CH_3CN and C_6H_5CN) were prepared as before.[2] $[IrL(CO)(PPh_3)_2]ClO_4$ (L = CH_3CN, CH_3CH_2CN, $CH_3CH_2CH_2CN$ and C_6H_5CN) used in this study, have been prepared in the same manner as described in Ref. 2. The newly prepared compounds, $[IrL(CO)(PPh_3)_2]ClO_4$ (L = CH_3CH_2CN and $CH_3CH_2CH_2CN$) have been identified by the elemental analyses, solution conductance measurements and spectral data (IR, ^1H NMR and electronic absorption) and will be reported elsewhere.

‡ 0.2 mmol (0.18–0.19 g) of $[IrL(CO)(PPh_3)_2]ClO_4$ (L = CH_3CN, CH_3CH_2CN, $CH_3CH_2CH_2CN$ and C_6H_5CN) was used to prepare 0.18 mmol (0.16–0.17 g) of **1–4** whose molar conductance ranged from 110 to 120 ohm^{-1} cm^2 mol^{-1} ($[Ir] = 4.0 \times 10^{-5}$ M) in dichloromethane at 25°C. Calc. for **1** ($IrC_{39}H_{35}NO_5P_2Cl$): C, 52.81; H, 3.98; N, 1.58. Found: C, 52.48; H, 4.11; N, 1.59%. Calc. for **2** ($IrC_{40}H_{37}NO_5P_2Cl$): C, 53.31; H, 4.14; N, 1.55. Found: C, 52.94; H, 4.21; N, 1.51%. Calc. for **3** ($IrC_{41}H_{39}NO_5P_2Cl$): C, 53.81; H, 4.30; N, 1.53. Found: C, 52.98; H, 4.42; N, 1.49%. Calc. for **4** ($IrC_{44}H_{37}NO_5P_2Cl$): C, 55.63; H, 3.93; N, 1.48. Found: C, 55.01; H, 4.02; N, 1.40%.

§ Molar conductance of a standard 1:1 electrolyte $[(C_3H_7)_4N]PF_6$ in dichloromethane is 110 ohm^{-1} cm^2 mol^{-1} at 25°C.

Table 1. IR (Nujol) and ^1H NMR ($CDCl_3$) spectral data for $[Ir(H)_2L(CO)(PPh_3)_2]ClO_4$ [L = CH_3CN (**1**), CH_3CH_2CN (**2**), $CH_3CH_2CH_2CN$ (**3**) and C_6H_5CN (**4**)]

Compound	IR absorption (cm^{-1})			
	$\nu_{CN}(\nu_{CN})^a$	$\nu_{CO}{}^b$	$\nu_{Ir-H}{}^c$	$\rho_{Ir-H}{}^d$
1	2289 (34)	1994	2140, 2243	878, 858
2	2290 (43)	2008	2137, 2236	875, 858
3	2293 (42)	2006	2137, 2241	886, 862
4	2269 (32)	2019	2127, 2224	870
	^1H NMR chemical shift (ppm)[e]			
CH_3CN	1.73 (s, $C\underline{H}_3$)			
CH_3CH_2CN	1.30 (t, $C\underline{H}_3$), 2.38 (q, $C\underline{H}_2$)			
$CH_3CH_2CH_2CN$	0.77 (t, $C\underline{H}_3$), 1.35 (m, $CH_3C\underline{H}_2$), 2.09 (t, $C\underline{H}_2CN$)			
C_6H_5CN	6.95 (m, $C_6\underline{H}_5$)			
1	7.45 (m, $PC_6\underline{H}_5$, 30H), 1.70 (s, $C\underline{H}_3$, 3H), -8.5 (dt, Ir–$\underline{H}_A$, 1H),[f] -18.3 (dt, Ir–$\underline{H}_B$, 1H)[g]			
2	7.45 (m, $PC_6\underline{H}_5$, 30H), 0.74 (t, $C\underline{H}_3$, 3H), 2.16 (q, $C\underline{H}_2$, 2H) -8.4 (dt, Ir–$\underline{H}_A$, 1H),[h] -18.2 (dt, Ir–$\underline{H}_B$, 1H)[i]			
3	7.45 (m, ($PC_6\underline{H}_5$, 30H), 0.47 (t, $3\underline{H}_3$, 3H), 0.94 (m, $CH_3C\underline{H}_2$, 2H), 2.16 (t, $C\underline{H}_2CN$, 2H) -8.4 (dt, Ir–$\underline{H}_A$, 1H),[j] -18.2 (dt, Ir–$\underline{H}_B$, 1H)[k]			
4	7.45 (m, $PC_6\underline{H}_5$, 30H), 6.78 (m, $C_6\underline{H}_5$, 5H) -8.2 (dt, Ir–$\underline{H}_A$, 1H),[l] -17.9 (dt, Ir–$\underline{H}_B$, 1H)[m]			

[a] Weak. ν_{CN} = ν_{CN} of coordinated nitrile $-\nu_{CN}$ of free nitrile. [b] Very strong. [c] Strong. [d] Medium.

[e] In air at 25°C at 60 MHz (Varian 60 MHz EM-360A) for free nitriles and at 80 MHz (Bruker WP 80 MHz FT-NMR) for **1–4**. Chemical shifts are relative to TMS and coupling constants are in Hz.

[f] $J(P, H_A) = 16.5$, $J(H_A, H_B) = 3.9$. [g] $J(P, H_B) = 13.6$, $J(H_A, H_B) = 3.9$.

[h] $J(P, H_A) = 16.5$, $J(H_A, H_B) = 3.9$. [i] $J(P, H_B) = 13.6$, $J(H_A, H_B) = 3.9$.

[j] $J(P, H_A) = 16.5$, $J(H_A, H_B) = 3.9$. [k] $J(P, H_B) = 13.7$, $J(H_A, H_B) = 3.9$.

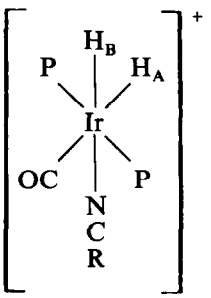
[l] $J(P, H_A) = 16.5$, $J(H_A, H_B) = 3.8$. [m] $J(P, H_B) = 13.6$, $J(H_A, H_B) = 3.8$.

IR spectral data (see Table 1) clearly suggest that the nitriles are coordinated to iridium through the nitrogen atom, rather than through the π-system of the nitrile group. It is well-known that ν_{CN} of a nitrile increases upon coordination through the nitrogen atom,[3–5] and decreases significantly upon coordination through the π-system of the nitrile group,[4,5] A strong and broad absorption band at 1100 cm^{-1} (not listed in Table 1) observed for all complexes is attributable to the tetrahedral (C_{4v}) anion ClO_4^-,[6] which suggests that **1–4** are 1:1 electrolytes as confirmed by the conductance measurements. It is seen in Table 1 that ν_{CO} of **4** is higher than those of **1–3**, which is readily understood by the relative basicity of the nitrogen atoms of the nitriles. It is also noticed in Table 1 that the substituents of the nitriles do not significantly affect the ν_{Ir-H} (ν_{M-H} varies widely from 1700 to 2250 cm^{-1} among various metal complexes[7]).

Electronic absorption spectra of **1–4** show no bands in the visible region as observed for the related six-coordinated dihydridoiridium(III) complexes, $[Ir(H)_2L(CO)(PPh_3)_2]ClO_4$ (L = unsaturated nitrile coordinated through the nitrogen atom).[1]

Proton NMR spectral data (see Table 1) provide more conclusive information on the characterization of **1–4**. The ratios of protons observed clearly indicate that each compound contains the $Ir(H)_2L(PPh_3)_2$ moiety. Practically no changes in coupling constants have been observed in this study for the protons of the nitriles upon coordination to $Ir(H)_2(CO)(PPh_3)_2$ as observed for the unsaturated nitrile complexes.[1] The coupling constants between hydride and *trans* phosphorus are relatively large (53–154 Hz) compared with those between hydride and *cis* phosphorus (10–20 Hz).[1,8–14] The relatively small coupling constants (13.6–16.5 Hz) observed for **1–4** (Table 1) indicate that both hydrides are *cis* to

both phosphorus atoms. The large difference in the chemical shifts of the hydrides implies that the two hydrides are *trans* to different groups, respectively. Accordingly the two hydrides are *cis* to each other and *trans* to CO and nitrogen (nitrile), respectively. For the series of related hydridoiridium(III) complexes, it is well-known that the chemical shift of a hydride depends on the *trans* donor atom.[1,8–16] The shielding at the hydride *trans* to nitrogen (nitrile) is higher (−17 to −20 ppm relative to TMS)[1,11,15] that than at the hydride *trans* to carbon (CO, $C_6H_{11}NC$) (−7 to −13 ppm).[1,10,16] Accordingly the signals at *ca* −8 ppm observed for **1–4** are due to the hydride (H_A) *trans* to CO and those at *ca* −18 ppm are due to the hydride (H_B) *trans* to nitrogen of the nitrile. Accordingly, the following structure is suggested for **1–4**:



P = PPh_3,

R = CH_3— (**1**), CH_3CH_2— (**2**),

$CH_3CH_2CH_2$— (**3**) and C_6H_5— (**4**).

Acknowledgements—We wish to thank the Korea Science and Engineering Foundation and the Ministry of Education for the financial support.

REFERENCES

1. S. Park, H.-K. Park and C. S. Chin, *Inorg. Chem.* 1985, **24**, 1120.
2. C. A. Reed and W. R. Roper, *J. Chem. Soc., Dalton Trans.* 1973, 1365.
3. S. J. Bryan, P. G. Huggett, K. Wade, J. A. Daniels and J. R. Jenning, *Coord. Chem. Rev.* 1982, **44**, 149, and references therein.
4. M. Klinger, *Adv. Organomet. Chem.* 1971, **10**, 115.
5. K. Nakamoto, *Infrared and Raman Spectra of Inorganic and Coordination Compounds*, p. 259, John Wiley, New York (1978).
6. J. Peone, Jr and L. Vaska, *Angew. Chem., Int. Ed. Engl.* 1971, **10**, 511.
7. Ref. 5, p. 304.
8. D. L. Thorn, *Organometallics* 1982, **1**, 197.
9. R. H. Crabtree and R. J. Uriate, *Inorg. Chem.* 1983, **22**, 4152.
10. C. E. Johnson, B. J. Fisher and R. Eisenberg, *J. Am. Chem. Soc.* 1983, **105**, 7772.
11. R. H. Crabtree, G. G. Hlatky, C. P. Parnell, B. E. Segmüller and R. J. Uriate, *Inorg. Chem.* 1984, **23**, 354.
12. R. H. Crabtree, J. W. Faller, M. F. Mellea and J. M. Quirk, *Organometallics* 1982, **1**, 1361.
13. M. Drouin and J. F. Harrod, *Inorg. Chem.* 1983, **22**, 999.
14. M. Basoto, F. Morandini, B. Longato and S. Bresadola, *Inorg. Chem.* 1984, **23**, 649.
15. B. Olgemoller and W. Beck, *Inorg. Chem.* 1983, **22**, 997.
16. A. M. Mueting, P. Boyle and L. H. Pignolet, *Inorg. Chem.* 1984, **23**, 44.

Polyhedron Vol. 4, No. 10, pp. 1677–1681, 1985
Printed in Great Britain

0277–5387/85 $3.00 + .00
Pergamon Press Ltd

STRUCTURE OF DI-μ-*N*-PHENYLANTHRANILATO-DI-1, 5-CYCLOOCTADIENE DIRHODIUM(I)

ANNA M. TRZECIAK,* JÓZEF J. ZIÓŁKOWSKI and TADEUSZ LIS
Institute of Chemistry, University of Wrocław, 14, Joliot-Curie, 50-383 Wrocław, Poland

and

ANDRZEJ BOROWSKI
Institute of Petroleum and Coal Chemistry, Polish Academy of Sciences, 44-100 Gliwice, Poland

(*Received* 15 *November* 1983; *accepted after revision* 4 *May* 1984)

Abstract—The reaction of $[RhCl(COD)]_2$ (COD = 1,5-cyclooctadiene) with sodium *N*-phenylanthranilate leads to the formation of the new crystalline rhodium(I) complex $[RhFA(COD)]_2$ (FA = *N*-phenylanthranilate anion). The compound is a dimer with two *N*-phenylanthranilate ions bridging and COD ligands terminally bonded to rhodium with an Rh . . . Rh distance equal to 3.424(3) Å. Strong intramolecular hydrogen bonding occurs between the hydrogen of the NH group and the closest carbonyl oxygen in the FA ligands. The crystals are monoclinic, space group $P2_1/c$, with $a = 11.246(8)$, $b = 14.999(9)$, $c = 21.82(2)$ Å, $\beta = 105.11(6)°$. The structure was solved by the heavy-atom method and refined by least squares to $R = 0.035$ for 4260 diffractometer data.

Only a few Rh(I) compounds with aminoacids are known.[1] The complex with *N*-phenylanthranilic acid with the formula $H[Rh_2(FA)_2Cl]$ (FA = *N*-phenylanthranilate anion) was synthesized for the first time by Khidekel *et al.*[2] Their studies, as well as the results reported in Ref. 3, revealed it to be a catalyst active in the hydrogenation of aromatic hydrocarbons. The complexes with anthranilic acid, asparagine and L-tyrosine were synthesized by a similar procedure to $H[Rh_2(FA)_2Cl]$.[4] The structural investigations which could resolve their spatial structures have not been made. The formulae were proposed on the basis of analytical studies.[4] Recently, the Rh(I) dicarbonyl complex with anthranilic acid, $Rh(AA)(CO)_2$ (AA = anthranilate ion) has been synthesized and spectroscopically examined.[5] The Rh(I) compounds with aminoacids are still attractive as potential hydrogenation catalysts. Thus, it was reasonable to establish the spatial structure of the complex obtained by us.

RESULTS AND DISCUSSION

The overall structure of the $[Rh(FA)(COD)]_2$ (COD = 1,5-cyclooctadiene) complex is shown in Fig. 1; selected bond distances and angles are listed in Table 1. The compound is a dimer with two bridging *N*-phenylanthranilate ions and two COD molecules terminally coordinated to each rhodium atom via π-olefin interactions.

The complex molecule has approximate C_2-symmetry. The idealized two-fold axis is perpendicular to the plane of four oxygen atoms. Each rhodium atom is tetracoordinated; two sites are occupied by the carboxyl oxygen atoms and two sites by the olefin units of cyclooctadiene. The Rh...Rh distance of 3.424(3) Å is comparable to the Rh...Rh distances in the other dimeric Rh(I) complexes in which there is no direct metal–metal bonding, e.g. 3.5[6] for $[RhCl(COD)]_2$, 3.12[7] for $[Rh(CO)_2Cl]_2$, and 3.396(1) Å[8] for

$$Rh(CO)Cl[(C_6H_5)_2AsCH_2As(C_6H_5)_2]_2.$$

In the Rh(I) and Rh(II) complexes with single metal–metal bonds the Rh—Rh distance is shorter and equal to 2.752(2)[9] and 2.618(5) Å[10] for

$$[(Et_3P)_2Rh(\mu\text{-}PPh_2)_2Rh(COD)]$$

and

$$[Rh(CH_3CO_2)(DMG)(PPh_3)]_2.$$

Two *N*-phenylanthranilate ligands are bonded to Rh

* Author to whom correspondence should be addressed.

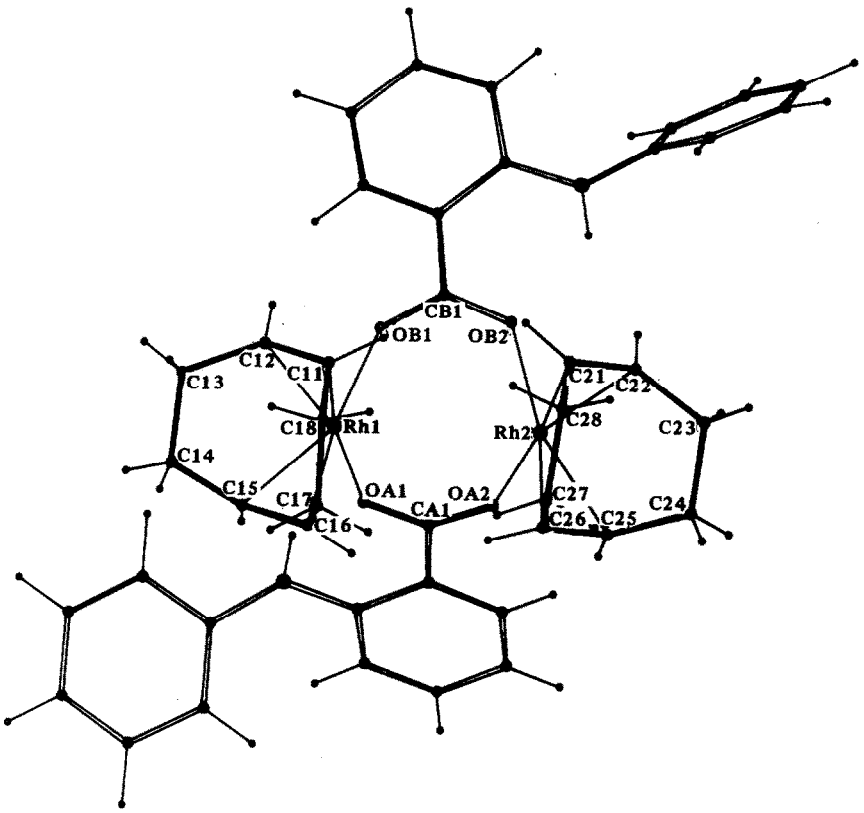


Fig. 1. A view of the complex molecule with the atom core numbering.

atoms via carboxyl oxygens. Comparison of the Rh—O bonding distances shows a small non-equivalence of the two Rh atoms.

Rh(1)—O(A1) and Rh(1)—O(B1) distances are 2.078(4) and 2.062(5) Å, respectively, while the bonds formed by Rh(2) are a little longer, with Rh(2)—O(A2) being 2.107(4) and Rh(2)—O(B2) 2.115(3) Å. These distances are comparable with the Rh—O distances found for Rh(II) carboxylate complexes.[10,11] X-ray studies allowed us to exclude the formation of bonding between the rhodium and the nitrogen of the *N*-phenylanthranilate ligand. The presence of hydrogen bonding within the carboxylic ligand causes the complete disability of nitrogen to the bonding formation with metal ion. Rh—C(COD) bond distances are between 2.080(6) and 2.098(6) Å and are similar to Rh—C(COD) distances in the other complexes of that type.[13,16]

For

$$Rh(C_5H_4CO_2Me)(COD),$$

$$[Rh(Ph_3PC_5H_4)(COD)]BPh_4,$$

$$B(pz)_4Rh(COD)$$

[where $B(Pz)_4$ = poly(1-pyrazolyl)borate] and Rh(ACA)(COD)(ACA = acetylacetone), the Rh—C(COD) bond distances are 2.101(5)–2.129(5),[13] 2.13(1)–2.28(2),[14] 2.124(3)–2.139(2)[15] and 2.092(8)–2.115(7) Å,[16] respectively. The view of *N*-phenylanthranilate ligands respective to the plane of one of two phenyl rings is shown in Fig. 2. Two phenyl rings in each FA molecule are arranged towards each other by approximately equal angles of 50.8(25)° for the A-molecule and 55.0(22)° for the B-molecule, respectively, but the direction of the rotation is the reverse. The hydrogen bond between N and the nearest oxygen atom of the carboxyl group is shown by dotted lines in Fig. 2. The N(1)...O(A1) distance is 2.623(6) and that of N(2)...O(B2) is 2.660(5) Å. These distances are comparable with N...O distances in systems in which hydrogen bonding was classified as strong.[17,19]

In 3,4,6-trichloro-2-diethylamino-methylphenol the N...O distance is 2.58(1),[17] in 2,2′-bis(6-methyl-3-piridinol) 2.568[18] and in salicylaldehyde azine 2.645(3) Å.[19] The C—N—C angles are 128.2(5) [C(A7)—N(1)—C(A8)] and 127.4(6)° [C(B7)—N(2)—C(B8)], respectively. That suggests that hybridization of nitrogen orbitals in *N*-phenylanthranilate ligands is sp^2 rather than sp^3.

Repulsion between two phenyl rings causes an increase in the C—N—C angle to over 120°. The

Table 1. Selected interatomic distances (Å) and angles (°)

Bond distances			
Rh(1)—O(A1)	2.078(4)	Rh(2)—O(A2)	2.107(4)
Rh(1)—O(B1)	2.062(5)	Rh(2)—O(B2)	2.115(3)
Rh(1)—C(11)	2.080(6)	Rh(2)—C(21)	2.093(6)
Rh(1)—C(12)	2.095(5)	Rh(2)—C(22)	2.095(5)
Rh(1)—C(15)	2.087(6)	Rh(2)—C(25)	2.098(6)
Rh(1)—C(16)	2.081(7)	Rh(2)—C(26)	2.094(6)
C(11)—C(12)	1.351(10)	C(21)—C(22)	1.369(8)
C(12)—C(13)	1.488(9)	C(22)—C(23)	1.484(10)
C(13)—C(14)	1.516(10)	C(23)—C(24)	1.508(11)
C(14)—C(15)	1.492(9)	C(24)—C(25)	1.499(9)
C(15)—C(16)	1.365(10)	C(25)—C(26)	1.364(10)
C(16)—C(17)	1.490(11)	C(26)—C(27)	1.483(12)
C(17)—C(18)	1.407(15)	C(27)—C(28)	1.477(15)
C(18)—C(11)	1.496(13)	C(28)—C(21)	1.495(12)
O(A1)—C(A1)	1.232(6)	O(A2)—C(A1)	1.217(6)
O(B1)—C(B1)	1.224(7)	O(B2)—C(B1)	1.247(6)
C(A1)—C(A2)	1.497(7)	C(B1)—C(B2)	1.492(7)
C(A2)—C(A3)	1.391(7)	C(B2)—C(B3)	1.380(7)
C(A3)—C(A4)	1.370(8)	C(B3)—C(B4)	1.359(8)
C(A4)—C(A5)	1.372(9)	C(B4)—C(B5)	1.378(9)
C(A5)—C(A6)	1.355(8)	C(B5)—C(B6)	1.352(8)
C(A6)—C(A7)	1.398(8)	C(B6)—C(B7)	1.402(7)
C(A7)—C(A2)	1.406(7)	C(B7)—C(B2)	1.416(7)
C(A7)—N(1)	1.372(7)	C(B7)—N(2)	1.367(6)
C(A8)—N(1)	1.395(7)	C(B8)—N(2)	1.414(7)
C(A8)—C(A9)	1.372(8)	C(B8)—C(B9)	1.371(7)
C(A9)—C(A10)	1.385(9)	C(B9)—C(B10)	1.380(8)
C(A10)—C(A11)	1.357(9)	C(B10)—C(B11)	1.370(9)
C(A11)—C(A12)	1.355(9)	C(B11)—C(B12)	1.353(10)
C(A12)—C(A13)	1.364(9)	C(B12)—C(B13)	1.384(8)
C(A13)—C(A8)	1.375(8)	C(B13)—C(B8)	1.371(8)
N(1)—H(N1)	0.86	N(2)—H(N2)	0.92
H(N1)...O(A1)	1.95	H(N2)...O(B2)	1.97
N(1)...O(A1)	2.623(6)	N(2)...O(B2)	2.660(5)
Angles			
O(A1)—Rh(1)—O(B1)	89.1(2)	O(A2)—Rh(2)—O(B2)	92.5(1)
Rh(1)—O(A1)—C(A1)	131.6(4)	Rh(2)—O(A2)—C(A1)	140.1(4)
Rh(1)—O(B1)—C(B1)	140.8(4)	Rh(2)—O(B2)—C(B1)	129.3(3)
O(A1)—C(A1)—O(A2)	123.5(5)	O(B1)—C(B1)—O(B2)	124.3(5)
O(A1)—C(A1)—C(A2)	118.0(4)	O(B1)—C(B1)—C(B2)	115.8(5)
O(A2)—C(A1)—C(A2)	118.6(4)	O(B2)—C(B1)—C(B2)	119.9(4)
C(A7)—N(1)—C(A8)	128.2(5)	C(B7)—N(2)—C(B8)	127.4(5)
C(12)—C(11)—C(18)	121.0(8)	C(22)—C(21)—C(28)	121.4(7)
C(11)—C(12)—C(13)	124.4(6)	C(21)—C(22)—C(23)	124.4(6)
C(12)—C(13)—C(14)	113.3(6)	C(22)—C(23)—C(24)	116.2(7)
C(13)—C(14)—C(15)	115.2(6)	C(23)—C(24)—C(25)	113.5(6)
C(14)—C(15)—C(16)	123.5(6)	C(24)—C(25)—C(26)	123.3(6)
C(15)—C(16)—C(17)	123.4(7)	C(25)—C(26)—C(27)	123.9(7)
C(16)—C(17)—C(18)	113.4(9)	C(26)—C(27)—C(28)	114.0(8)
C(11)—C(18)—C(17)	119.0(10)	C(21)—C(28)—C(27)	116.5(9)
N(1)—H(N1)...O(A1)	133	N(2)—H(N2)...O(B2)	130

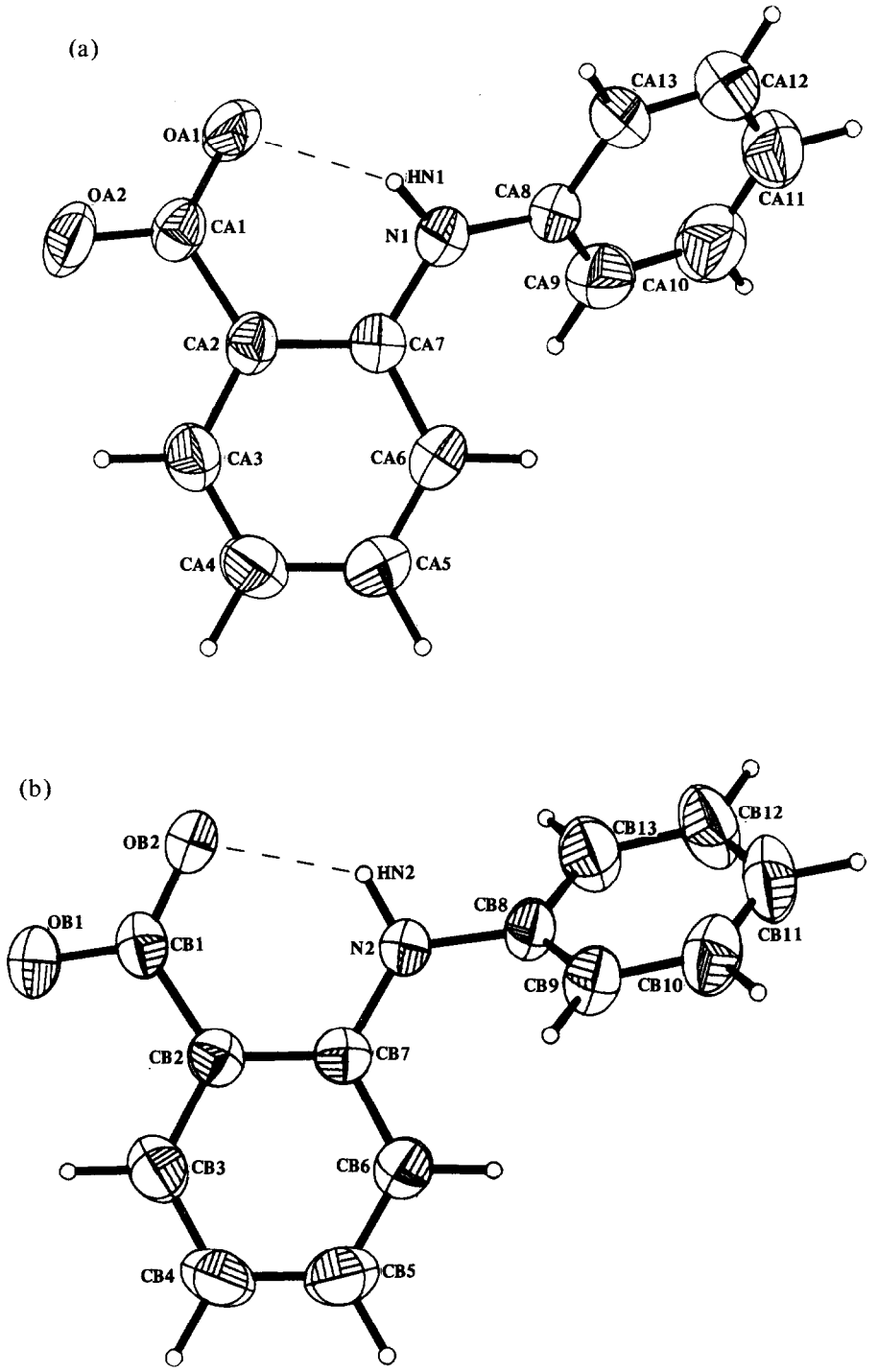


Fig. 2(a) and (b). ORTEP drawings showing different conformations of two *N*-phenylanthranilate crystallographically independent ligands.

N—C bonds are non-equivalent; the nitrogen atoms in both *N*-phenylanthranilate ligands are closer to the carbon adjacent to the carboxyl group. The respective distances are N(1)—C(A7) 1.372(7) and N(2)—C(B7) 1.367(6) Å. The N—C distances to the second phenyl rings are longer, 1.395(7) and 1.414(7) Å, respectively. In both FA ions differences in the C—C bond length in phenyl rings closer to rhodium ions are observed. The longest C—C distances are C(A2)—C(A7) [1.406(7) Å] and C(B2)—C(B7) [1.416(7) Å]. The shortest C—C distances are C(A5)—C(A6) [1.355(8) Å] and C(B5)—C(B6)

[1.352(8) Å]. This indicates a disproportionate electron density distribution in these phenyl rings. The distortion of the phenyl rings and non-equivalence of the N—C distances are caused by electron density delocalization on the carboxyl group, the first phenyl ring and the nitrogen atom. The carboxyl group, two carbon atoms from the phenyl ring and nitrogen atom with hydrogen are almost planar. The phenyl ring and the ring with hydrogen bonding may be treated as conjugated because they are almost coplanar. This is the explanation for the shortening of the C—C bond distances in phenyl rings closer to rhodium ions. The further phenyl ring is not conjugated with the first one, because it is twisted towards its plane. For that reason the electron density delocalization over two phenyl rings in each FA ion does not take place. Therefore the N—C distances to the second phenyl rings are longer and no differences in C—C bond distances are observed.

EXPERIMENTAL

Synthesis

$[RhCl(COD)]_2$ (0.49 g), obtained as reported by Chatt and Venanzi[20] and sodium *N*-phenylanthranilate (0.71 g) were heated in boiling ethanol for 3 h. The precipitate was washed with water until the reaction on Cl^- ceased, then with ethanol, and dried *in vacuo*. Recrystallization of the compound from chloroform and ethyl ether produced yellow crystals suitable for the X-ray examination.

Elemental analysis. Found: C, 59.3; N, 3.1; H, 5.2; Rh, 24.8. Calc. for $C_{42}H_{44}N_2O_4Rh_2$: C, 59.0; N, 3.3; H, 5.2; Rh, 24.8%.

X-ray structure analysis of $[Rh(FA)(COD)]_2$

Crystal data. $C_{42}H_{44}N_2O_4Rh_2$, $M = 846.7$, monoclinic, $a = 11.246(8)$, $b = 14.999(9)$, $c = 21.82(2)$ Å, $\beta = 105.11(6)°$, $U = 3553$ Å^3, $Z = 4$, $D_c = 1.58$ g cm^{-3}, $D_o = 1.54$ g cm^{-3}, space group $P2_1/c$ Mo-K_α radiation $\lambda = 0.71069$ Å, $\mu = 9.5$ cm^{-1}.

A specimen ($0.6 \times 0.4 \times 0.3$ mm) was cut from a large crystal. A Syntex $P2_1$ diffractometer, Mo-K_α radiation and a graphite monochromator were used for lattice-parameter and intensity measurements at $T = 298 \pm 2$ K. Intensities were measured only for reflections above background with a 2θ–ω scan technique. The structure was solved by the heavy-atoms method using 4260 reflections with $I > 3\sigma(I)$. All calculations were performed with the Syntex XTL/XTLE programs.[21] The carbon-bonded hydrogen atoms were placed in geometrically calculated positions at a distance of 1.0 Å and fixed. The nitrogen-bonded hydrogen atoms were found from a difference Fourier synthesis and were not refined. Block-diagonal least-squares refinement, with anisotropic thermal parameters for Rh, N, O and C gave a final R_1 ($\sum ||F_o| - |F_c|| / \sum |F_o|$) of 0.035 and an R_w [$(\sum w\Delta F^2 / \sum wF_o^2)^{1/2}$] of 0.041.

The final difference Fourier synthesis showed the highest peaks located around the Rh atoms with an electron density in the range 0.4–0.7 e Å^{-3}. All other peaks had lower densities. Final atomic positional and thermal parameters and a list of F_o and F_c values have been deposited as supplementary data with the Editor from whom copies may be obtained on request. Atomic coordinates have also been deposited with the Cambridge Crystallographic Data Centre.

REFERENCES

1. D. Dowerach and M. M. Sing, *J. Chem. Res. S* 1979, 38.
2. O. N. Efimov, O. N. Eremienko, A. G. Ovcharenko, M. L. Khidekel and P. S. Cherkij, *Izv. Akad. Nauk USSR* 1969, **4**, 855.
3. V. A. Avilov, O. N. Eremienko, O. N. Efimov, A. G. Ovcharenko, M. L. Khidekel and P. S. Cherkij, Pat. USSR 1970, 215200.
4. I. Rajca, *Pol. J. Chem.* 1981, **55**, 775.
5. E. Kwaskowska-Chęć and J. J. Ziółkowski, *Transition Met. Chem.* 1983, **8**, 103.
6. J. A. Ibers and R. G. Snyder, *J. Am. Chem.* Soc. 1962, **84**, 495.
7. E. F. Dahl, C. Martell and D. L. Wampler, *J. Am. Chem. Soc.* 1961, **83**, 1761.
8. T. J. Mague, *Inorg. Chem.* 1969, **8**, 1975.
9. D. W. Meek, P. E. Kreter and G. G. Christoph, *J. Organomet. Chem.* 1982, **231**, C53.
10. J. Halpern, E. Kimura, J. Molin-Case and C. S. Wong, *J. Chem. Soc., Chem. Commun.* 1971, 1207.
11. B. G. De Boer, M. D. La Prade, J. R. Pipal and D. A. Ucho, *J. Am. Chem. Soc.* 1970, **92**, 2926.
12. P. De Mester and A. C Skąpski, unpublished results.
13. M. Arthurs, M. Nelson and M. G. B. Drew, *J. Chem. Soc., Dalton Trans.* 1977, 779.
14. G. Bombieri, G. Tresoldi, F. Faraone, G. Bruno and P. Cavoli-Belluco, *Inorg. Chim. Acta* 1982, **57**, 1.
15. M. Cocivera, G. Ferguson, B. Kaitner, F. J. Lalor, D. J. O'Sullivan, M. Parvez and B. Ruhl, *Organometallics* 1982, **1**, 1132.
16. P. A. Tucker, W. Scutcher and D. R. Russel, *Acta Cryst. B* 1975, **31**, 592.
17. W. Robien, H. Völlenkle and P. Wolschann, *Z. Phys. Chem., Neue Folge* 1982, **130**, 123.
18. L. H. Vogt and J. C. Wirth, *J. Am. Chem. Soc.* 1971, **93**, 5402.
19. G. Arcovito, M. Bonamico, A. Domenicano and A. Vaciago, *J. Chem. Soc., B* 1969, 733.
20. J. Chatt and L. M. Venanzi, *J. Chem. Soc.* 1957, 4735.
21. Syntex 1976, *XTL/XTLE Structure Determination System.* Syntex Analytical Instruments, Cupertino, CA.

Polyhedron Vol. 4, No. 10, pp. 1683–1688, 1985
Printed in Great Britain

0277–5387/85 $3.00 + .00
© 1985 Pergamon Press Ltd

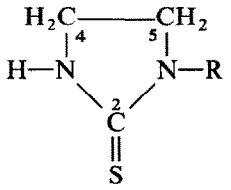
SYNTHESIS, ^{13}C NMR AND IR SPECTROSCOPIC STUDIES OF GOLD(I) COMPLEXES OF IMIDAZOLIDINE-2-THIONE AND ITS DERIVATIVES

ANVARHUSEIN A. ISAB* and M. SAKHAWAT HUSSAIN
Department of Chemistry, University of Petroleum and Minerals, Dhahran, Saudi Arabia

(*Received* 22 *March* 1984; *accepted* 9 *May* 1984)

Abstract—The gold(I) complexes of imidazolidine-2-thione and its derivatives were synthesized and their ^{13}C NMR and IR spectroscopic studies were carried out. When gold(III) was reacted with the ligands using a 1 : 4 metal to ligand ratio, gold(III) was reduced to gold(I), the bis complexes of the general formula AuL_nX (where $n = 2$) were formed. However, when gold(III) was reduced to gold(I) by a reducing agent followed by an addition of the ligand to an aqueous or methanolic solution of gold(I), only mono complexes of the type AuLX were obtained. The structures of the reported complexes are proposed on the basis of their spectroscopic measurements.

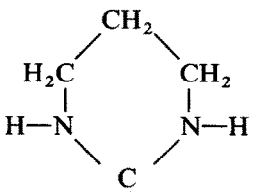
Imidazolidine-2-thione, Imt (**Ia**), its six-membered analog, Eapt (**II**), and its derivatives MeImt (**Ib**) and PrImt (**Ic**) are interesting ligands because of their potential binding sites such as —NH and —C=S. These ligands exist in —N=C—SH or —NH—C=S form exhibiting thiol ⇌ thione equilibrium. However, it has been established that the thione form dominates in the solid state.[1,2] The coordination chemistry of these ligands with various transition metal ions such as Cu(I), Zn(II), Pd(II), Co(II), Ni(II) and Hg(II) has been studied.[1,5]



I

(**Ia**) Imt: R = H; imidazolidine-2-thione
(**Ib**) MeImt: R = CH_3; *N*-methyl-imidazolidine-2-thione
(**Ic**) PrImt: R = $-CH_2CH_2CH_3$; *N*-propyl-imidazolidine-2-thione

By reacting copper(II) chloride or bromide with these ligands, an immediate reduction of copper(II) to copper(I) takes place in MeOH or in aqueous solution[4,6] and the mono as well as the bis complexes of the general formulas CuLX and CuL_2X are formed. The mono complexes are polymeric in nature whereas the bis complexes are dimeric.[4,6] The reduction of gold(III) to gold(I) with Imt was studied by Morgan and Burstall.[7] Usually a gold(III) to ligand ratio of 1 : 4 resulted in a bis complex of the formula AuL_2X ($X = Cl^-, Br^-$). However, we have recently demonstrated[8] that, if the reduction of gold(III) is carried out in aqueous solution using SO_2 gas, gold(I) is stabilized by the ligand forming only monomeric AuLX species.



II

(**II**) Eapt: 1,3-bis(ethylamino)propane-2-thione

*Author to whom all correspondence should be addressed.

We have extended our studies on gold(I)–Imt systems, as a part of our continuing research program on synthetic and structural studies of crystalline gold(I)–thiol complexes as model compounds for anti-arthritic drugs[9,10] such as Myocrisin or Solganol which are polymeric in nature as identified by NMR and CD spectroscopy.[11,12] In the present paper we report the synthesis and spectroscopic studies of some mono and bis gold(I)–imidazolidine-2-thione complexes. Most of these complexes were obtained in pure crystalline forms and the single crystal X-ray studies on some of them are currently in progress.

EXPERIMENTAL

All chemicals were obtained from Fluka Chemical Co. except $^{12}CD_3OD$ which was obtained from BDH. The ligands were prepared by the procedures described in the literature.[13,14]

Preparation of complexes of formula L_nAuX

The ligands were dissolved in MeOH and the gold(III) halides were dissolved in double deionized distilled water. The L : M ratio was kept at 4 : 1. As soon as gold(III) was added to the ligand, an orange coloured residue was immediately formed which dissolved on stirring to give a colourless precipitate. The precipitate was dissolved in boiling MeOH to obtain crystalline products. In some cases the complexes could only be obtained in the form of a powder.

Preparation of mono complexes of formula LAuX

The gold(III) halides were reduced to gold(I) by passing SO_2 gas as described earlier.[15] As soon as the solution became colourless, the ligand was added, keeping the gold(I) to ligand ratio close to 1 : 1. Usually a white residue was obtained. The elemental analyses of the products were carried out on a Carlo Erba (Italy) elemental analyzer.

Using the above general procedures the following complexes were prepared:

Gold(I)–imidazolidine - 2 - thione bromide: (Imt)AuBr.

Bis(imidazolidine - 2 - thione)gold(I) chloride hydrate: $(Imt)_2AuCl \cdot H_2O$.

Gold(I)–*N* - methyl - imidazolidine - 2 - thione chloride: (MeImt)AuCl.

Gold(I)–*N* - methyl - imidazolidine - 2 - thione bromide: (MeImt)AuBr.

Bis(*N* - methyl - imidazolidine - 2 - thione)gold(I) chloride: $(MeImt)_2AuCl$.

Bis(1,3 propyl - imidazolidine - 2 - thione)gold(I) chloride: $(Eapt)_2AuCl$.

Bis(*N* - propyl - imidazolidine - 2 - thione)gold(I) chloride: $(PrImt)_2AuCl$.

Spectroscopic measurements

IR spectra of the pure ligands and their gold(I) compounds were obtained on a Perkin–Elmer IR 180 or on a Beckman Microlab IR spectrophotometer using KBr pellets. ^{13}C NMR spectra were obtained on a Varian XL-200 NMR spectrometer operating at a 50.3 MHz frequency. The ligands and gold(I) complexes were dissolved in a 50 : 50 (v/v) $D_2O/^{12}CD_3OD$ solvent. The complexes were not very soluble but enough dissolved to yield spectra except $(Eapt)_2AuCl$ and (MeImt)AuCl which are extremely insoluble in the above solvents. The chemical shifts were measured relative to 1,4-dioxane as internal reference having resonance at +67.4 ppm relative to DSS. ^{13}C NMR spectra of PrImt, (PrImt)AuCl and $(PrImt)_2AuCl$ were measured in d_6-acetone.

RESULTS AND DISCUSSION

Mono and bis gold(I) complexes were formed by Imt and its *N*-methyl derivative, all of which were in pure crystalline state. In the case of Eapt only the bis complex was formed as indicated by the analytical data given in Table 1.

^{13}C *NMR studies*

A representative ^{13}C NMR spectrum is shown in Fig. 1 and Table 2 lists the ^{13}C NMR chemical shifts of the ligands and their complexes. As reported earlier,[8] in the case of mono complexes, the C-2 resonance is shifted by about 8 ppm compared to the free ligand but a less dramatic shift (−0.768 ppm) was observed for C-4 and C-5 resonances. In the bis Imt complexes, the C-2 resonance is shifted by +6.764 ppm whereas the C-4,5 resonance shows a slight shift of only −0.836 ppm. The most significant shift for the $(MeImt)_2AuCl$ complex is also for the C-2 resonance (+7.644 ppm). The C-4, C-5 and CH_3 resonances are only shifted by −1.43, −0.96 and −0.627 ppm, respectively. The shift in the C-2 resonance of the $(PrImt)_2AuCl$ complex is only about 2 ppm, which is significantly less than 8.292 ppm observed for the mono complex (PrImt)AuCl or about 7 ppm observed for any of the bis complexes. This variation in the C-2 shift (Fig. 2) can be explained on

Table 1. Analytical data for the ligands and gold(I) complexes*

Complex	Melting point (°C)	Colour	H	C	N
(Imt)AuBr	198–199	Pale yellow powder	1.53	9.22	7.86
			(1.58)	(9.55)	(7.38)
$(Imt)_2AuCl \cdot H_2O$	247–249	White crystalline	2.98	15.70	12.80
			(3.08)	(15.84)	(12.32)
(MeImt)AuCl	186–187	White powder	2.33	14.36	13.92
			(2.29)	(13.77)	(14.92)
(MeImt)AuBr	167–168	Yellow powder	1.98	12.29	7.21
			(2.04)	(12.21)	(7.12)
$(MeImt)_2AuCl$	246–247	Light brown crystalline	3.24	20.12	11.77
			(3.44)	(20.66)	(12.05)
$(Eapt)_2AuCl$	286–288	White crystalline	3.39	20.64	11.94
			(3.44)	(20.66)	(12.05)
$(PrImt)_2AuCl$	92–93	White crystalline	4.75	28.08	11.03
			(4.66)	(27.66)	(10.76)

* The corresponding calculated values are given in parentheses.

the basis of the shielding effects on C-2 which is least shielded in the bis complexes and is most shielded in the mono compounds. An appreciable shift of the C-2 resonance in the ^{13}C NMR spectra clearly indicates that, in all of these complexes, gold(I) is bonded to the ligand through sulfur atom only and the —NH group is not involved in any kind of bonding. Any bonding through —NH would have resulted in a considerable shift of the C-4 resonance in the $(MeImt)_2AuCl$ complex. A significant shift in ^{13}C NMR for C=S carbon atoms consistently observed in these complexes can be used as a diagnostic NMR observation for the location of bonding sites in solution phase of these and similar gold(I) complexes. The sulfur coordination of gold(I) in chloro (*N* - ethyl - 1,3 - imidazolidine - 2 - thione)gold(I) and chloro(*N* - propyl - 1,3 - imidazolidine - 2 - thione) gold(I) complexes[8] was confirmed by the single crystal X-ray analysis in the solid state and a similar ^{13}C shift for the C=S carbon was observed in both complexes. The +1 oxidation state for gold in the $(PrImt)_2AuCl$ was assumed on the basis of its white

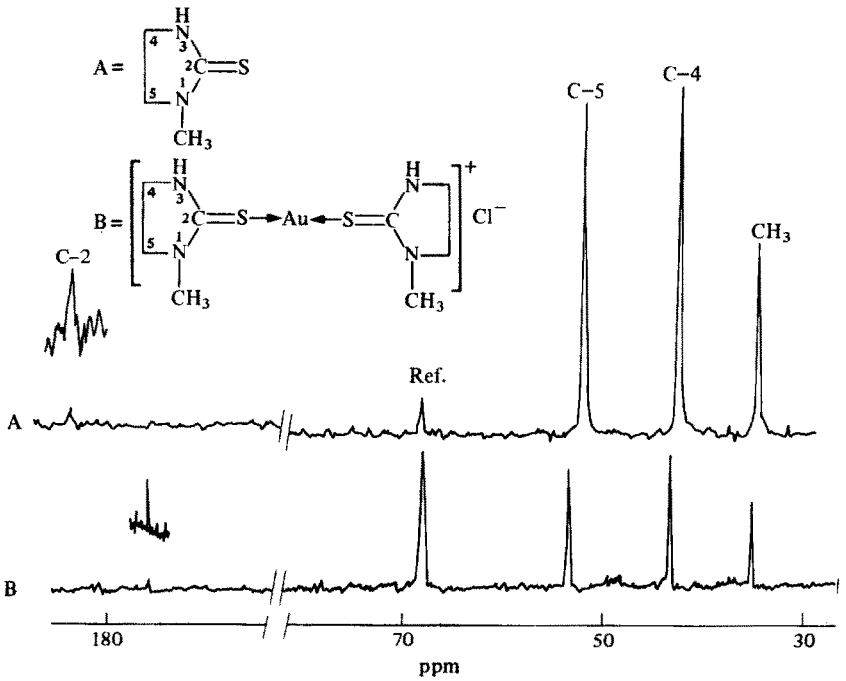


Fig. 1. Representative ^{13}C NMR spectra of MeImt ligand and its bis-gold(I) complex.

Table 2. ^{13}C NMR chemical shifts of gold(I) complexes of imidazolidine-2-thione and its derivatives*

Complex	C-2	C-4	C-5	α-CH_2	β-CH_2	γ-CH_3
Imt	182.69	45.205	45.205	—	—	—
(Imt)AuBr	†	45.973	45.973	—	—	—
		(−0.768)	(−0.768)			
$(Imt)_2AuCl$	175.926	46.041	46.041	—	—	—
	(6.764)	(−0.836)	(−0.836)			
MeImt	183.084	41.661	51.461	—	—	33.828
$(MeImt)_2AuCl$	175.44	42.641	52.891	—	—	34.455
	(7.644)	(−1.43)	(−0.96)			(−0.627)
PrImt	184.469	48.539	48.851	41.763	20.801	11.306
$(PrImt)_2AuCl$	182.508	48.749	49.175	42.012	20.857	11.173
	(1.961)	(−0.21)	(−0.324)	(−0.249)	(−0.056)	(0.133)
(PrImt)AuCl	176.181	50.616	49.505	42.712	20.795	11.067
	(8.282)	(−2.077)	(−0.654)	(−0.49)	(0.006)	(0.239)

* ^{13}C NMR resonances are assigned as given in Faure *et al.*, *Org. Magn. Reson.* 1977, **9**, 688. The numbers in parentheses indicate shifts with respect to the free ligands. A positive value indicates a high-field shift whereas a negative value shows a low-field shift. The spectrum of (MeImt)AuBr could not be recorded due to its insolubility in the 50/50 (v/v) CD_3OD/D_2O solvent.

† The resonance could not be detected in the spectrum.

colour. Both mono and bis complexes are white in colour. In the case of the mono complexes the reduction of gold(III) to gold(I) was carried out by SO_2, whereas an excess of the ligand was used for the reduction of the bis complexes. The Mössbauer and single crystal X-ray studies are planned to identify the oxidation state of gold and to elucidate the solid state structures of these complexes.

The $(Eapt)_2AuCl$ complex is very insoluble in water and its analytical data (Table 1) show that no

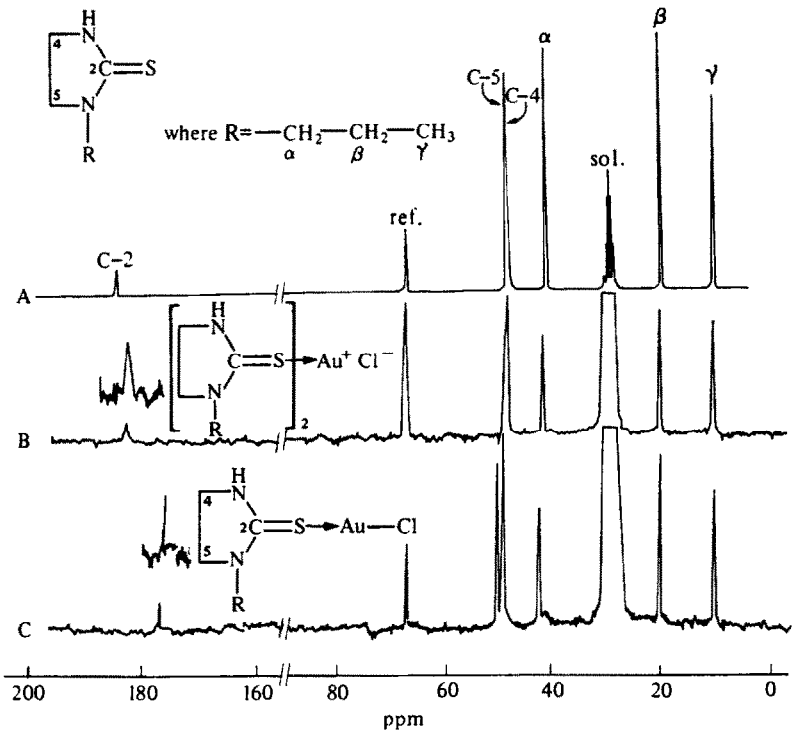


Fig. 2. ^{13}C NMR spectra of PrImt ligand and its mono- and bis-coordinated species showing variations in the chemical shift of C-2 as a function of shielding.

Table 3. Significant IR bands for the ligands and their complexes in the region 4000–200 cm^{-1}

Compound	ν(N—H)	ν(C—N) + δ(N—H)	Δ(N—H)	ν(C=S)	Vibrations below 450 cm^{-1}
Imt	3300	1500	680 sh	510 w	—
(Imt)AuBr	3300 sh	1520 sh	660 sh	530 sh	345 w, 320 w, 295 w, 275 sh, 240 w, 210 w
$(Imt)_2AuCl$	3260 sh	1525 sh	665 sh	490 sh	385 w, 345 w, 290 w
MeImt	3200 sh	1520 sh	670 sh	520 sh	390 w
(MeImt)AuCl	3200 sh	1555 sh	635 sh	495 sh	415 w, 350 w, 320 sh
(MeImt)AuBr	3300 sh	1555 sh	635 sh	490 sh	415 w, 275 w, 225 w
$(MeImt)_2AuCl$	3100 sh	1550 sh	640 sh	490 sh	420 w, 345 w, 275 sh
Eapt	3300 sh	1560 sh	640 sh	510 w	415 sh, 340 sh
$(Eapt)_2AuCl$	3200 sh	1565 vs	635 sh	520 sh	415 sh, 385 sh, 345 w, 315 sh
PrImt	3300 sh	1510 vs	610 sh	515 vs	375 vw
$(PrImt)_2AuCl$	3200 sh	1530 sh	670 sh	515 sh	350 w

H_2O molecule is present. In contrast to this, the 5-membered analog of Eapt forms the complex $(Imt)_2AuCl \cdot H_2O$ which is water soluble[16] and its X-ray analysis revealed an ionic structure with linear gold(I) coordination through sulfur atoms. Due to the high insolubility of $(Eapt)_2AuCl$, its ^{13}C NMR spectrum could not be recorded.

IR absorption spectral studies

The IR spectra of the free ligands and their gold(I) complexes (Table 3) do not show S—H absorption in the region of 2500 cm^{-1} nor a C=N band at 1700–1590 cm^{-1} but exhibit a strong absorption around 3300 cm^{-1} corresponding to N—H stretch.[17] The presence of the band at 3300 cm^{-1} in the free ligand as well as in the gold(I) complexes clearly indicates the existence of thione forms in the solid state.

A band at 375 w cm^{-1} in the gold(I)–diisobutyl dithiocarbamate dimer[18] and a band at 342 cm^{-1} for $Au(SMe)_2^-$ anion[19] have been assigned to the Au—S vibration. On a correlative basis the band at 345 cm^{-1} found in all complexes of the present study can be assigned to the Au—S vibration. A shift of about 40 cm^{-1} in the C=S band in all complexes is consistent with our conclusion that the gold(I) is bonded through sulfur. The band at 210 cm^{-1} for (Imt)AuBr and at 225 cm^{-1} for (MeImt)AuBr can be assigned to the Au—Br stretching.[20] The Au—Cl absorption is usually found in the region of 310–320 cm^{-1} for various gold(I) complexes[20] with coordinated chloride ion. This band was observed in the (MeImt)AuCl complex but was absent for $(Imt)_2AuCl$, $(MeImt)_2AuCl$ and $(PrImt)_2AuCl$ complexes. This is consistent with the ionic nature of the chloride in the last three complexes which, of course, will not exhibit any Au—Cl stretching vibrations.[16] The presence of an Au—Cl vibration at 315 cm^{-1} in $(Eapt)_2AuCl$ complex indicates that the gold(I) is three coordinated. The fact that this complex is insoluble in water/methanol solvent further indicates that the complex is neutral or polymeric in nature.

CONCLUSIONS

On the basis of ^{13}C NMR and IR spectral data, the following conclusions can be drawn for gold(I) geometries in its complexes with imidazolidine-2-thiones and its derivatives:

(1) Imt and its derivatives exist in the thione forms both in the solution as well as in the solid phase.

(2) When these ligands react with gold(I), different complexes of types AuLX and AuL_2X are formed, in all of which the ligands exist in the thione form.

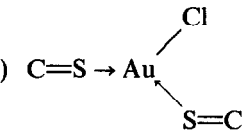
(3) The IR and ^{13}C NMR spectral studies revealed three coordination of the following kinds for the gold(I) complexes with the above ligands:

(a) C=S → Au—X

for all mono complexes.

(b) $[C{=}S \rightarrow Au \leftarrow S{=}C]^+$

for all bis complexes which are soluble in water or methanol.

(c)


for L_2AuX neutral complex such as $Au(Eapt)_2Cl$.

Acknowledgements—This research was supported by the UPM Research Committee Project No. CY/METALION/54. One of us (A.A.I) is thankful to the UPM for providing facilities under the above project.

REFERENCES

1. C. Preti and G. Tosi, *Can. J. Chem.* 1976, **54**, 1558.
2. L. M. Butler, J. R. Creighton, R. E. Oughtred, E. S. Raper and I. W. Nowell, *Inorg. Chim. Acta* 1983, **75**, 149.
3. M. E. O'Neil, E. S. Raper and J. A. Daniels, *Inorg. Chim. Acta* 1981, **54**, L3.
4. L. P. Battagalia, A. B. Corradi, F. A. Devillanova and G. Verani, *Transition Met. Chem.* 1979, **4**, 264.
5. E. S. Raper and P. H. Crakett, *Inorg. Chim. Acta* 1981, **50**, 159.
6. F. A. Devillanova and G. Verani, *Transition Met. Chem.* 1977, **2**, 120.
7. G. T. Morgan and F. H. Burstal., *J. Chem. Soc.* 1928, 143.
8. M. S. Hussain and A. A. Isab, *J. Coord. Chem.* 1985, **14**, 17.
9. P. J. Sadler, *Struct. Bonding (Berlin)* 1976, **29**, 171.
10. C. F. Shaw, *Inorg. Perspect. Biol. Med.* 1978, **2**, 287.
11. A. A. Isab and P. J. Sadler, *J. Chem. Soc., Dalton Trans.* 1981, 1657.
12. D. H. Brown, G. McKinaly and W. E. Smith, *J. Chem. Soc., Dalton Trans.* 1977, 1874.
13. G. D. Thorn, *Can. J. Chem.* 1955, **33**, 1278.
14. L. Maier, *Helv. Chim. Acta* 1970, **53**, 1417.
15. A. A. Isab and P. J. Salder, *Biochim. Biophys. Acta* 1977, **492**, 322.
16. P. G. Jones and G. M. Sheldrick, *Acta Crystallogr.* 1976, **B32**, 3321.
17. L. H. Little and R. H. Ottewill, *Can. J. Chem.* 1962, **40**, 2110.
18. F. J. Farrell and T. G. Spiro, *Inorg. Chem.* 1971, **10**, 1606.
19. G. A. Bowmaker and B. C. Dobson, *J. Chem. Soc., Dalton Trans.* 1981, 267.
20. G. E. Coates and C. Parkin, *J. Chem. Soc.* 1963, 421.

Polyhedron Vol. 4, No. 10, pp. 1689–1695, 1985
Printed in Great Britain

0277–5387/85 $3.00 + .00
© 1985 Pergamon Press Ltd

SYNTHESIS OF DINUCLEAR PHOSPHIDO OR ARSENIDO BRIDGED COMPLEXES OF MOLYDENUM VIA REACTION OF SECONDARY PHOSPHINES OR ARSINES WITH $[Mo(\eta^5\text{-}C_5H_5)(CO)_3]_2$: X-RAY STRUCTURES OF $\{[Mo(\eta^5\text{-}C_5H_5)(CO)_2]_2(\mu\text{-}H)(\mu\text{-}ER_2)\}$ (E = P, R = *t*-Bu; OR E = As, R = Me)

RICHARD A. JONES,* STUART T. SCHWAB, ANTHONY L. STUART, BRUCE R. WHITTLESEY and THOMAS C. WRIGHT
Department of Chemistry, The University of Texas at Austin, Austin, TX 78712, U.S.A.

(*Received* 17 *July* 1984; *accepted* 8 *October* 1984)

Abstract—Reaction of $[Mo(\eta^5\text{-}C_5H_5)(CO)_3]_2$ with $t\text{-}Bu_2PH$ or Me_2AsH yields $\{[Mo(\eta^5\text{-}C_5H_5)(CO)_2]_2(\mu\text{-}H)(\mu\text{-}ER_2)\}$, where E = P, R = *t*-Bu (**1**) (45%); or E = As, R = Me (**2**) (35%). The X-ray crystal structures of **1** and **2** have been determined. Each complex contains a central planar $Mo_2(E)(H)$ core and the co-ordination geometry about each Mo is best described as a "four-legged stool" in which adjacent H and P (or As) atoms are shared. The positions of the bridging hydrogen atoms are symmetrical to within experimental error.

A variety of dinuclear phosphido or arsenido bridged complexes of molybdenum have been reported. These include

$[Mo(CO)_4PR_2]_2$ (R = Me,[1] Et,[2] Ph[2]),
$[Mo(CO)_5]_2PMe_2$,[3] $[Mo(CO)_4(AsPh_2)]_2$,[2]
$[Mo(CO)_3(PR_3)(PMe_2)]_2$,[4]
$[Mo(\eta^5\text{-}C_5H_5)(CO)_2(EMe_2)]_2$ (E = P,[5] As[6]),
$[Mo(\eta^5\text{-}C_5H_5)(CO)_2As(CF_3)_2]_2$,[7]
$[Mo(\eta^5\text{-}C_5H_5)(CO)_2(PMe_3)(\mu\text{-}AsMe_2)Mo(PMe_3)(CO)_2(\eta^5\text{-}C_5H_5)]^+[Mo(CO)_3(\eta^5\text{-}C_5H_5]^-$,[8]
$[Mo(CO)_3(\eta^5\text{-}C_5H_5)(\mu\text{-}AsMe_2)Mo(CO)_5]$,[9]
$\{CpMo(CO)_2[\mu\text{-}o\text{-}C_6H_4\text{-}(PPh)(PPhH)](\mu\text{-}H)(MoCp(CO)]\}$,[10]

and

$[Mo(\eta^5\text{-}C_5H_5)(CO)_2(\mu\text{-}H)(\mu\text{-}Me_2P)]$.[5] The last two complexes in this list are two of a number of dinuclear phosphido bridged complexes of the *d*-block transition metals in which the two metals are bridged both by an R_2P^- (or R_2As^-) group and by a hydrogen atom. Other examples include

$\{[Fe(\eta^5\text{-}C_5H_5)CO]_2(\mu\text{-}H)(\mu\text{-}PR_2)\}$,[6]
$\{[Mn(CO)_4]_2(\mu\text{-}H)(\mu\text{-}Ph_2P)\}$,[11]
$\{[Mn(CO)_4]_2(\mu\text{-}H)[\mu\text{-}P(CF_3)_2]\}$,[12]
$\{[Co(\eta^5\text{-}C_5H_5)(\mu\text{-}PMe_2)]_2(\mu\text{-}H)\}^+BF_4$,[13]

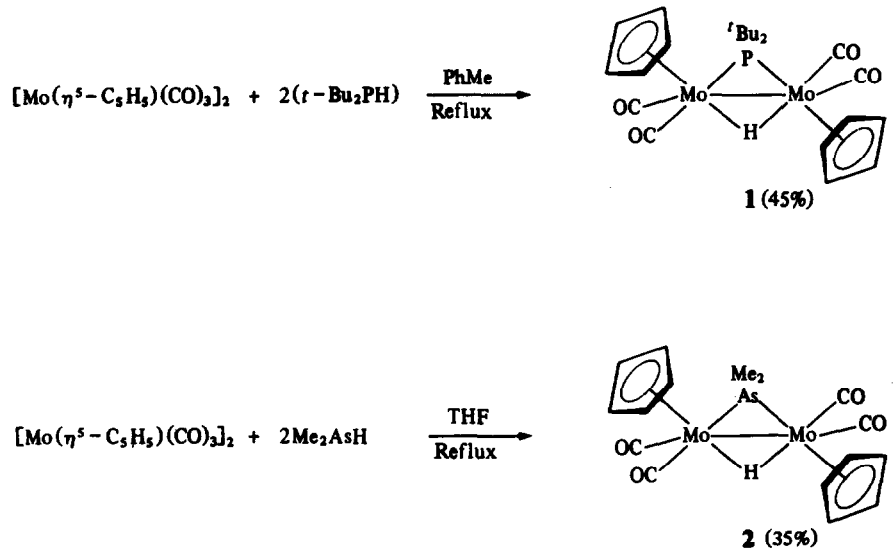
and $[Mn_2(\mu\text{-}H)(\mu\text{-}PPh_2)(CO)_8]$.[14]

$\{[Mo(\eta^5\text{-}C_5H_5)(CO)_2]_2(\mu\text{-}H)(\mu\text{-}Me_2P)\}$ was originally prepared by Hayter[5] via the interaction of Me_2PH with $[Mo(\eta^5\text{-}C_5H_5)(CO)_3]_2$ and several structural studies have also been reported.[15–17] The key structural feature of this molecule is a central, planar $Mo_2P(H)$ core with an Mo–Mo distance of *ca* 3.2 Å consistent with a fairly long single metal–metal bond. This is bridged by both the PMe_2 unit and the H atom. We felt that complexes of this type might prove to be useful starting materials for further studies of the chemistry of dinuclear phosphido or arsenido bridged complexes. However, we were surprised to find that, to our knowledge, the Me_2P bridged complex is the only one of this type for Mo to have been reported so far.[10]

In order to prepare other analogues we investigated the reaction of $[Mo(\eta^5\text{-}C_5H_5)(CO)_3]_2$ with $t\text{-}Bu_2Ph$ and Me_2AsH. Under refluxing conditions both the phosphine and arsine gave complexes analogous to

$\{[Mo(\eta^5\text{-}C_5H_5)(CO)_2]_2(\mu\text{-}H)(\mu\text{-}PMe_2)\}$

* Author to whom all correspondence should be addressed.



Scheme 1.

(see Scheme 1) suggesting that this may be a general reaction for the preparation of complexes of this type.

Neutron diffraction studies[16] on

$$\{[Mo(\eta^5\text{-}C_5H_5)(CO)_2]_2(\mu\text{-}H)(\mu\text{-}PMe_2)\}$$

have shown that the bridging hydrogen atom occupies a symmetrical position between the two molybdenum atoms. We expected our X-ray studies on **1** and **2** to reveal similar symmetrical μ-H atoms if they could be detected. In both cases the X-ray studies show symmetrical bridging hydrides.

We report here the syntheses, characterizations and X-ray crystal structures of **1** and **2**.

RESULTS AND DISCUSSION

Synthesis of $\{[Mo(\eta^5\text{-}C_5H_5)(CO)_2]_2(\mu\text{-}H)(\mu\text{-}ER_2)\}$ (**1** *and* **2**)

The reaction of t-Bu_2PH or Me_2AsH with $[Mo(\eta^5\text{-}C_5H_5)(CO)_3]_2$ in refluxing toluene or THF yields the phosphido or arsenido bridged dinuclear complexes **1** and **2** in 45 and 35% yields respectively (see Scheme 1). These red (**1**) or orange (**2**) crystalline materials are air-stable both in the solid state and in solution for prolonged periods. Spectroscopic data are in accord with the solid state structures as determined by X-ray diffraction studies. Thus IR spectra for both **1** and **2** show two strong bands in the terminal CO region (see Experimental). The ^1H NMR spectra are also quite straightforward with the unique bridging hydrides giving high field resonances: (**1**) δ −13.1 d ($^2J_{P-H}$ = 35.4 Hz), (**2**) δ −12.09 s (C_6D_6, RT). The $^{31}P\{^1H\}$ NMR spectrum of **1** shows a low field resonance (δ 267.53 ppm) indicative of a phosphide bridging a metal–metal bond.* Both complexes are also sufficiently volatile to yield molecular ions as the highest observable peaks in their mass spectra. In order to confirm the geometries and formulations of each complex and to study the $Mo_2E(H)$ cores in these molecules, single-crystal X-ray diffraction studies were undertaken for both **1** and **2**.

X-ray structures of $\{[Mo(\eta^5\text{-}C_5H_5)(CO)_2]_2(\mu\text{-}H)(\mu\text{-}ER_2)\}$ (**1** *and* **2**)

General views of each molecule are shown in Figs 1 and 2. Relevant bond lengths and angles are presented in Tables 1–4. As found for

$$\{[Mo(\eta^5\text{-}C_5H_5)(CO)_2]_2(\mu\text{-}H)(\mu\text{-}Me_2P)\}$$

the structures of **1** and **2** consist of a central $Mo_2(R_2E)(H)$ core (E = P, As) which is virtually planar.† Each molybdenum atom bears one η^5-C_5H_5 ligand and two carbonyls. Ignoring the position

* Downfield shifts in the δ 50–200 range in the ^{31}P NMR of Ph_2P groups bridging metal–metal bonds have been noted by several groups of workers. See Ref. 18. Similar downfield shifts have been noted for μ-t-Bu_2P complexes, see Ref. 1 and references therein.

† Deviations from the least-squares plane through Mo1–Mo2–H1B–P1 are Mo1 −0.074(1), Mo2 −0.080(1), H1B 0.10(9), P1 0.046(2). (**2**) Deviations (Å) from the least-squares plane through Mo1–As–Mo2–HY1 are Mo1 −0.002(1), As −0.001(1), Mo2 −0.002(1), HY1 0.003(1).

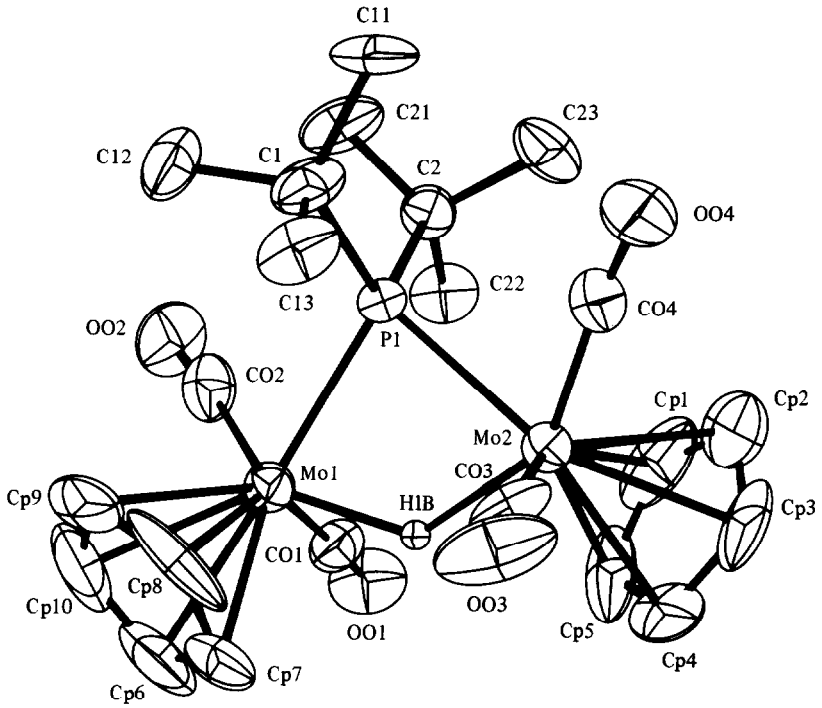
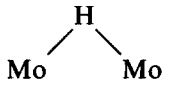


Fig. 1. General view of $[Mo(\eta^5\text{-}C_5H_5)(CO)_2](\mu\text{-}H)(t\text{-}Bu_2P)$ (**1**). Hydrogen atoms except for the bridging hydride have been omitted for clarity.

of the μ-H atom there is a pseudo-two-fold axis passing through the P or As atom and the mid-point of the Mo–Mo vector. The geometry about each Mo atom can be described in terms of a "four legged stool"[15] with the overall dinuclear geometry resulting from a sharing of adjacent H and P (or As) atoms. A reasonable electron-counting scheme for each Mo has been proposed for

$$\{[Mo(\eta^5\text{-}C_5H_5)(CO)_2]_2(\mu\text{-}H)(\mu\text{-}Me_2P)\}$$

which involves a bent 3*c*–2*e*



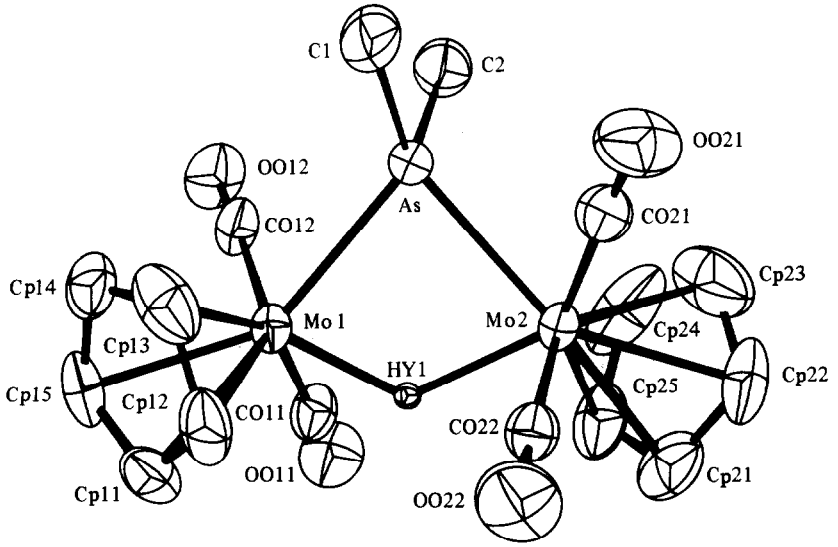


Fig. 2. General view of $[Mo(\eta^5\text{-}C_5H_5)(CO)_2]_2(\mu\text{-}H)(\mu\text{-}Me_2As)$ (**2**). Hydrogen atoms, except for the bridging hydride have been omitted for clarity.

Table 1. Bond distances (Å) for compound **1**

Mo1–Mo2	3.247(1)	P1–C1	1.948(8)
Mo1–P1	2.497(2)	P1–C2	1.936(8)
Mo1–CO1	1.907(9)	OO1–CO1	1.169(9)
Mo1–CO2	1.947(10)	OO2–CO2	1.161(9)
Mo1–Cp6	2.335(9)	OO3–CO3	1.153(9)
Mo1–Cp7	2.318(10)	OO4–CO4	1.136(9)
Mo1–Cp8	2.344(9)	C1–C11	1.551(11)
Mo1–Cp9	2.312(10)		
Mo1–Cp10	2.301(10)		
Mo1–H1B	1.91(8)		
Mo2–P1	2.497(2)		
Mo2–CO3	1.907(8)		
Mo2–CO4	1.972(9)		
Mo2–H1B	1.74(8)		

Table 3. Bond distances (Å) for compound **2**

Mo1–Mo2	3.329(1)	Mo2–CO21	1.948(3)
Mo1–As	2.508(1)	Mo2–CO22	1.934(12)
Mo1–HY1	1.824(2)	Mo2–Cp21	2.334(2)
Mo2–As	2.520(1)	As–C1	1.960(3)
Mo2–HY1	1.888(2)	As–C2	1.958(13)
As–HY1	2.706(2)	OO11–CO11	1.156(5)
Mo1–As	2.508(1)	OO12–CO12	1.154(12)
Mo1–HY1	1.824(2)	OO21–CO21	1.156(4)
Mo1–CO11	1.952(3)	OO22–CO22	1.170(14)
Mo1–CO12	1.953(9)	Mo2–As	2.520(1)
Mo1–Cp11	2.335(9)	Mo2–HY1	1.888(2)

interaction involving a substantial Mo–Mo bonding component despite the fairly long Mo–Mo distances [e.g. 3.247(1) Å in **1**]. The key structural features of the central cores of **1** and **2** are similar to those of $\{[Mo(\eta^5\text{-}C_5H_5)(CO)_2]_2(\mu\text{-}H)(\mu\text{-}Me_2P)\}$ and are tabulated in Table 5. In both cases the X-ray data was of sufficient quality to permit the location and isotropic thermal refinement of the bridging hydrides. It is well known that the apparent positions of the hydrogen nuclei in metal hydrides when obtained from X-ray data may deviate substantially from their true positions obtained via neutron diffraction studies.[17] For both **1** and **2** however the μ-H atoms *appear* to occupy fairly symmetrical positions (to within the limits of error inherent in locating them). This is consistent with the more reliable positions of the non-hydrogen atoms in **1** and **2**, which also adopt quite symmetrical positions and we feel that this is a reasonably good indication that the μ-H units are symmetrically bridging.

The chemistry of these and related complexes will be described in future papers.

EXPERIMENTAL

All reactions were performed under oxygen-free nitrogen. Microanalyses were by the Schwartzkopf Microanalytical Laboratory (Woodside, NY). Hexane and THF were dried over sodium and distilled from sodium/benzophenone under nitrogen before use. Toluene was distilled from sodium under nitrogen. Melting points were in sealed capillaries under nitrogen (1 atm) and are uncorrected.

Instruments

IR: Perkin–Elmer 1330. NMR: Nicolet NT200 (^{1}H and ^{31}P), Varian EM-390 (^{1}H, 90 MHz), FT80 (^{31}P, 32.384 MHz). IR spectra were as Nujol mulls (KBr plates) or in solution (matched KBr or CaF_2

Table 2. Bond angles (°) for compound **1**

P1–Mo1–CO1	105.8(3)	P1–Mo2–CO4	77.7(2)
P1–Mo1–CO2	79.3(3)	P1-Mo2–H1B	77(3)
P1–Mo1–Cp6	134.4(4)	CO3–Mo2–CO4	77.3(4)
P1–Mo1–Cp7	164.7(3)	CO3–Mo2–H1B	72(3)
P1–Mo1–Cp8	108.3(3)	CO4–Mo2–H1B	135(3)
P1–Mo1–Cp9	112.7(4)	Mo1–P1–Mo2	81.11(6)
P1–Mo1–Cp10	141.3(6)	Mo1–P1–C1	113.2(3)
P1–Mo1–H1B	74(2)	Mo1–P1–C2	121.2(3)
CO1–Mo1–CO2	77.9(4)	Mo2–P1–C1	121.1(3)
CO1–Mo1–Cp6	103.6(5)	Mo2–P1–C2	110.9(3)
Mo1–CO2–OO2	175.0(8)	C1–P1–C2	108.0(4)
P1–C2–C21	113.7(6)	P1–C1–C11	116.2(6)
Mo1–H1B–Mo2	126(4)	P1–Mo2–CO3	102.8(3)
Mo1–CO1–OO1	177.2(8)	CO1–Mo1–H1B	85(2)

Table 4. Selected bond angles (°) for compound **2**

Mo2–Mo1–As	48.70(1)	As–Mo2–Cp22	142.2(3)
Mo2–Mo1–HY1	26.75(7)	Mo1–As–Mo2	82.91(1)
As–Mo1–HY1	75.45(7)	Mo1–As–C1	116.6(2)
Mo1–Mo2–As	48.39(1)	Mo1–As–C2	121.2(1)
Mo1–Mo2–HY1	25.78(6)	Mo2–As–C1	122.5(2)
As–Mo2–HY1	74.17(6)	Mo2–As–C2	115.93(9)
Mo1–As–Mo2	82.91(1)	Cl–As–C2	99.3(3)
Mo1–As–HY1	40.74(5)	Mo1–CO11–OO11	177.0(3)
Mo2–As–HY1	42.17(5)	Mo1–CO12–OO12	177.5(4)
Mo1–HY1–Mo2	127.5(1)	Mo2–CO21–OO21	178.1(7)
Mo1–HY1–As	63.81(6)	Mo2–CO22–OO22	177.5(4)
Mo2–HY1–As	63.66(6)	Mo1–Cp11–Cp12	74.4(5)
As–Mo1–HY1	75.45(7)	Mo1–Cp11–Cp15	70.2(5)
As–Mo1–CO11	111.7(2)	HY1–Mo2–CO21	125.9(2)
As–Mo1–CO12	77.4(1)	HY1–Mo2–CO22	73.2(1)
As–Mo1–Cp11	146.9(1)	HY1–Mo2–Cp21	97.6(1)
HY1–Mo1–CO11	74.0(1)	CO21–Mo2–CO22	77.9(3)
HY1–Mo1–CO12	130.3(2)	CO21–Mo2–Cp21	128.7(1)
HY1–Mo1–Cp11	94.9(1)	CP21–Mo2–Cp22	35.2(1)
As–Mo2–HY1	74.17(6)	Mo1–Cp12–Cp11	71.0(5)
As–Mo2–CO21	77.3(1)	CO22–Mo2–Cp21	92.5(2)
As–Mo2–CO22	113.8(1)		
As–Mo2–Cp21	147.8(2)		

cells). NMR spectra were recorded in C_6D_6 at ambient temperature and are referenced to Me_4Si (δ 0.0, ^1H) or 85% H_3PO_4 (aq.) (δ 0.0, ^{31}P). Mass spectra were run on a Bell and Howell 21-491 (EI) at U.T. Austin or on a VG ZAB-1HF (FAB) at the University of Illinois using xenon as the fast atom beam.

$[CpMo(CO)_3]_2$,[5] $(t\text{-Bu})_2PH$,[19] and Me_2AsH[20] were prepared as previously described.

$\{[Mo(\eta^5\text{-}C_5H_5)(CO)_2]_2(\mu\text{-}H)(\mu\text{-}t\text{-}Bu_2P)\}$ (**1**)

A solution containing $[Mo(\eta^5\text{-}C_5H_5)(CO)_3]_2$ (1.0 g, 2.04 mmol) and HP^tBu_2 (0.596 g, 4.08 mmol) was refluxed (8 h) in toluene (95 cm^3) during which time the colour changed from red to brown. Volatile residues were removed under vacuum and the residue was extracted into Et_2O (2×15 cm^3) and

Table 5. Comparison of structural data for the central $Mo_2(ER_2)(\mu\text{-}H)$ core in $[CpMo(CO)_2]_2(\mu\text{-}H)(\mu\text{-}ER_2)$ complexes

Complex	Mo–Mo (Å)	Mo–E (Å)	Mo–E–Mo (°)	Mo–H (Å)	Mo–H–Mo (°)	Reference
$[Mo(\eta^5\text{-}C_5H_5)(CO)_2]_2(\mu\text{-}H)(\mu\text{-}Me_2P)$ (X-ray)	3.2715(5)	2.431(1)	84.81(4)	1.94(6)	133.0(3)	15, 17
		2.420(1)		1.63(6)		
$[Mo(\eta^5\text{-}C_5H_5)(CO)_2]_2(\mu\text{-}H)(\mu\text{-}Me_2P)$ (neutron)	3.267(2)	2.432(3)	84.8(1)	1.851(4)	122.9(2)	16
		2.411(3)		1.869(4)		
$[Mo(\eta^5\text{-}C_5H_5)(CO)_2]_2(\mu\text{-}H)(\mu\text{-}t\text{-}Bu_2P)$ (**1**)	3.247(1)	2.497(2)	81.11(6)	1.91(8)	126.0(4)	This work
		2.497(2)		1.74(8)		
$[Mo(\eta^5\text{-}C_5H_5)(CO)_2]_2(\mu\text{-}H)(\mu\text{-}Me_2As)$ (**2**)	3.329(1)	2.508(1)	82.91(1)	1.824(2)	127.5(1)	This work
		2.520(1)		1.888(2)		
$[Mo(\eta^5\text{-}C_5H_5)(CO)][\mu\text{-}o\text{-}C_6H_4\text{-}(PPh)(PPhH)(\mu\text{-}H)Mo(\eta^5\text{-}C_5H_5)(CO)$	3.282(1)	2.398(1)	86.0(5)	1.96(6)	122.5(5)	10
		2.417(1)		1.78(6)		

filtered. Cooling the red Et_2O solution (−20°C) yielded red prisms of **1** over 72 h which were collected and dried under vacuum. The compound is air-stable in solution and in the solid state. Yield 0.53 g (45%); m.p. 177–185°C (dec); IR (CaF_2, toluene) 1935 *s*, 1857 *s*, 1800 *w* (cm^{-1}); IR (Nujol, NaCl) 1915 *s*, 1831 *s*, 1257 *m*, 1009 *m*, 807 *s* (cm^{-1}). ^1H NMR (C_6D_6, 200 MHz) δ 4.95 *s* (10 H) (C_5H_5), δ 1.28 *d*, J = 13.5 Hz (18H), (μ-P^{t}Bu$_2$), δ −13.1 *d*, $^2J_{PH}$ = 35.4 Hz (μ-H); $^{31}P\{^1H\}$ NMR (C_6D_6) δ 267.53 *s*, (μP^tBu_2); M.S. using fast atom bombardment; positive ion, thioglycerol matrix. The molecular ion (M^+) was observed as the highest peak at 580.08(58) a.m.u. (based on $_{42}Mo^{96}$). $^{92}Mo_2PC_{22}H_{29}O_4$ peak matching was also good: m/z measured = 571.9926; m/z calculated = 571.9940. Other peaks (relative intensity in parentheses): 552 (78) ($M^+ - CO$); 525 (32) ($M^+ - 2CO$); 495 (20) ($M^+ - 3CO$); 467 (50) ($M^+ - 4CO$); 437 (100) [$M^+ - (t\text{-}Bu_2P)$]; 407 (70) [$M^+ - (t\text{-}Bu_2P$, $CO)$]; 382 (75) [$M^+ - (t\text{-}Bu_2P$, $2CO)$]; 353 (70) [$M^+ - (t\text{-}Bu_2P$, $3CO)$]; 323 (40) [$M^+ - (t\text{-}Bu_2P$, $4CO)$]. Found: C, 45.43; H, 4.89%. Calc. for $C_{22}H_{29}Mo_2O_4P$: C, 45.53; H, 5.04%.

$\{[Mo(\eta^5\text{-}C_5H_5)(CO)_2]_2(\mu\text{-}H)(\mu\text{-}Me_2As)\}$ (**2**)

To a solution of $[Mo(\eta^5\text{-}C_5H_5)(CO)_3]_2$ (1.23 g, 2.50 mmol) in THF (100 cm^3) was added two equivalents (0.437 cm^3, 5.0 mmol) of neat Me_2AsH. The mixture was then heated under reflux 40 h. Volatile materials were removed under vacuum, the dark brown residue extracted with toluene (30 cm^3) and the solution filtered. The volume was reduced (*ca* 20 cm^3) and cooled overnight (−20°C). **2** is obtained as air-stable orange rods. Yield 0.51 g (35%), m.p. 185–192°C (dec); IR (THF solution, CaF_2 cells) 1935 *s*, 1870 *s* (cm^{-1}); (Nujol, KBr plates) 1920 *s*, 1850 *s*, 1260 *w*, 890 *w*, 850 *vw*, 810 *m*, 790 *m*, 710 *vw*, 590 *m*, 555 *vw*, 525 *vw*, 500 *m*, 460 *m* (cm^{-1}). NMR: ^1H δ 4.65 *s* (10H) (C_5H_5); δ 1.54 *s* (6H) (Me_2As); δ −12.09 *s*, 1 *H* (μ-*H*) M.S. (EI). The parent ion (M^+ = 540 a.m.u.) was the highest observable peak. Found: C, 35.62; H, 3.10%. Calc. for $C_{16}H_{17}AsMo_2O_4$: C, 35.58; H, 3.17%

X-ray experimental data

X-ray quality crystals of **1** and **2** were grown from toluene solutions at −20°C. Crystals were mounted in thin-walled glass capillaries under nitrogen. Data were collected by the $\omega/2\theta$ scan technique at 23 ± 2°C on an Enraf–Nonius CAD-4 diffractometer. Final lattice parameters were determined from 25 carefully centered high angle reflections ($26.0 > 2\theta > 30.0$). Details of crystal data and a summary of intensity data collection parameters for **1** and **2** are given in Table 1. Details of data collection were similar to those outlined in Ref. 21. For **1** the space group was uniquely determined by systematic absences to be *Pbca* and this was confirmed by the successful refinement. For **2** the stucture was solved successfully in $P\bar{1}$. The data for **1** and **2** were corrected for Lorentz and polarization effects. Both structures were solved using standard heavy-atom methods or direct methods and successive difference Fourier maps using the Enraf–Nonius software package "SDP-PLUS" (B. A. Frenz and Associates, College Station, TX 77840, 4th edition, 1981) on a PDP 11/44 computer. Scattering factors were taken from Ref. 22. Empirical absorption corrections (psi scans) were applied [% trans: min. 73.6, max. 99.9 (**1**); min. 64.9, max. 99.8 (**2**)]. Hydrogen atoms on the Cp rings were placed in idealized positions with fixed temperature factors (sp^2 geometry, 0.95 Å bond lengths) and were used in structure factor calculations but not refined. The bridging hydride was located and refined isotropically in both cases. The methyl hydrogen atoms in both structures were not located. Crystal data: (**1**) $C_{22}H_{29}Mo_2PO_4$, M = 580.33, orthorhombic, *Pbca* (No. 61), a = 18.085(7) Å, b = 16.637(5) Å, c = 15.423(6) Å, U = 4640.5(5) Å^3, D_c = 1.661 g cm^{-3}, Z = 8, λ(Mo-K_α) = 0.71069 Å (graphite monochromator), μ(Mo-K_α) = 11.47 cm^{-1}, from 2064 observed reflections [$I > 2\sigma(I)$], 4548 measured. (**2**) $C_{16}H_{17}AsMo_2O_4$, M = 540.11, triclinic, $P\bar{1}$ (No. 2), a = 9.246(1) Å, b = 9.493(1) Å, c = 11.625(1) Å, α = 83.04(9)°, β = 82.239(9)°, γ = 61.976(10)°, U = 890.9(5) Å^3, D_c = 2.013 g cm^{-3}, Z = 2, λ(Mo-K_α) = 0.71069 Å (graphite monochromator), μ(Mo-K_α) = 32.29 cm^{-1}, 3120 observed reflections [$I > 3\sigma(I)$], 3332 measured. Final full-matrix least-squares refinements with anisotropic thermal parameters for all non-hydrogen atoms gave final values of R = 0.0407 and R_w = 0.0463 for **1** and R = 0.0258 and R_w = 0.0373 for **2**

$$\{R = \Sigma(|F_o| - |F_c|)/\Sigma|F_o|$$

and

$$R_w = [\Sigma w(|F_o| - |F_c|)^2/\Sigma w|F_o|^2]^{1/2}\}.$$

Final difference Fourier maps showed no chemically significant peaks. Tables of atomic coordinates, thermal parameters, complete bond lengths and angles and F_o/F_c values (65 pages) have been deposited as supplementary materials with the Editor from whom copies are available on request. Atomic coordinates have also been deposited with the Cambridge Crystallographic Data Centre.

Acknowledgements—We thank the Robert A. Welch Foundation (F-816) and the National Science Foundation

(CHE82-11883) for support. The X-ray diffractometer was purchased with funds from the NSF (CHE82-058712) and the University of Texas. We thank Professor E. P. Kyba of this Department for helpful discussions of his work prior to publication.

REFERENCES

1. R. G. Hayter, *Inorg. Chem.* 1964, **3**, 711.
2. J. Chatt and D. A. Thornton, *J. Chem. Soc.* 1964, 1005; L. R. Nassimbeni, *Inorg. Nucl. Chem. Lett.* 1971, **7**, 909.
3. W. Ehrl and H. Vahrenkamp, *Chem. Ber.* 1971, **104**, 3261.
4. R. H. B. Mais, P. G. Owston and D. T. Thompson, *J. Chem. Soc. (A)* 1967, 1736.
5. R. G. Hayter, *Inorg. Chem.* 1963, **2**, 1031.
6. R. G. Hayter, *J. Am. Chem. Soc.* 1963, **85**, 3120.
7. W. R. Cullen and R. G. Hayter, *J. Am. Chem. Soc.* 1964, **86**, 1030.
8. R. Janta, W. Albert, H. Rossner, W. Malisch, H. J. Langenbach, E. Rottinger and H. Vahrenkamp, *Chem. Ber.* 1980, **113**, 2729.
9. R. Müller and H. Vahrenkamp, *Chem. Ber.* 1977, **110**, 3910.
10. E. P. Kyba, Personal communication.
11. R. G. Hayter, *J. Am. Chem. Soc.* 1964, **86**, 823; R. J. Doedens, W. T. Robinson and J. A. Ibers, *J. Am. Chem. Soc.* 1967, **89**, 4323.
12. H. J. Emeleus and J. Grobe, *Angew. Chem.* 1962, **74**, 467; J. Grobe, *Angew. Chem.* 1963, **75**, 1113.
13. R. Zolk and H. Werner, *J. Organomet. Chem.* 1983, **252**, C53 (and references therein).
14. J. A. Iggo, M. J. Mays and P. R. Raithby, *J. Chem. Soc., Dalton Trans.* 1984, 633.
15. R. J. Doedens and L. F. Dahl, *J. Am. Chem. Soc.* 1965, **87**, 2576.
16. J. L. Petersen, L. F. Dahl and J. M. Williams, *J. Am. Chem. Soc.* 1974, **96**, 6610.
17. See J. L. Petersen and J. M. Williams, *Inorg. Chem.* 1978, **17**, 1308 (and references therein); R. Bau (Ed.), *ACS Adv. Chem. Ser.* 1978, 167.
18. P. E. Garrou, *Chem. Rev.* 1981, **81**, 229; A. J. Carty, *Adv. Chem. Ser.* 1982, **196**, 163; P. E. Kreter and D. W. Meek, *Inorg. Chem.* 1983, **22**, 319; A. D. Harley, G. J. Guskey and G. L. Geoffroy, *Organometallics* 1983, **2**, 53 (and references therein).
19. H. Hoffman and P. Schellenbeck, *Chem. Ber.* 1966, **99**, 1134.
20. R. D. Feltham and W. Silverthorn, *Inorg. Synth.* 1967, **10**, 159.
21. R. A. Jones and T. C. Wright, *Organometallics* 1983, **2**, 1842.
22. *International Tables for X-Ray Crystallography*, Vol. 4. Kynoch Press, Birmingham, U.K. (1974).

NOTE ADDED IN PROOF

Compound **2** has been reported as being formed in 1% yield from the photolysis of $Cp(CO)_2Mn(\mu\text{-}AsMe_2)Mo(CO)_3Cp$ [see U. Richter and H. Vahrenkamp, *J. Chem. Res. (S)* 1977, 156].

Polyhedron Vol. 4, No. 10, pp. 1697–1700, 1985
Printed in Great Britain

0277–5387/85 $3.00 + .
© 1985 Pergamon Press L

COMPLEXING PROPERTIES OF 1,2-DIHYDROXY-3,4-DIKETOCYCLOBUTENE WITH IRON AND NICKEL IN ETHANOL

O. ST. C. HEADLEY and L. A. HALL*
Department of Chemistry, University of the West Indies, St. Augustine, Trinidad

(*Received* 29 *August* 1983: *accepted after revision* 19 *February* 1985)

Abstract—The divalent chlorides of iron and nickel were reacted with 1,2-dihydroxy-3,4-diketocyclobutene (squaric acid) in ethanolic solution to form complexes of molecular formula $[M(HC_4O_4)(Cl)(C_2H_5OH)]_2 \cdot C_2H_5OH$ in which the metal ions show penta-coordination. Both complexes are hygroscopic and on exposure to air undergo changes indicating change of coordination number. However, only the iron complex undergoes a change in oxidation state as well.

A number of complexes of squaric acid have been reported previously, but so far all have been octahedral and have been obtained from aqueous solution.[1–5] Tetrahedral complexes have been obtained by the vacuum dehydration of their octahedral analogues,[6] but, as far as we know, this is the first direct synthesis of five-coordinate inorganic squarate complexes.

EXPERIMENTAL

Chemicals. The squaric acid was obtained from the Aldrich Chemical Company, Milwaukee, Wisconsin. It was recrystallised once from water and dried at approximately 100°C. The ethanol used was absolute ethanol (which was redistilled over calcium oxide) obtained from BDH. The nickel(II) and iron(II) chlorides were used in their hydrated form.

Preparation of the complexes (squarate chlorides). The method of preparation of the iron(II) and nickel(II) squarate chlorides is identical and therefore only the preparation of the nickel(II) complex is described.

Approximately 1.48 g (6.2 mmol) of nickel(II) chloride-6-water was dissolved in 200 cm^3 of hot ethanol through which a continuous stream of nitrogen was being passed. A hot ethanolic solution (200 cm^3) containing 0.71 g (6.3 mmol) of squaric acid was then added to the nickel(II) chloride solution and the resulting mixture evaporated for a few minutes in an atmosphere of nitrogen. The mixture was then quickly transferred to a dry bag filled with nitrogen, filtered and the complex placed in a vacuum manifold, which was then removed from the dry bag and connected to a drying pistol containing phosphorus pentoxide. The complex was then dried at approximately 0.1 mm pressure for four hours and sealed *in vacuo*.

Yield: nickel(II) squarate chloride, 2.10 g (61.3%); iron(II) squarate chloride, 2.25 g (66.4%).

Found: C, 30.32; H, 5.12; Cl, 13.20; Ni, 21.18. Calc. for $C_{14}H_{20}Cl_2Ni_2$: C, 30.38; H, 3.62; Cl, 12.84; Ni, 21.34%.

Found: C, 30.16; H, 5.02; Cl, 13.05; Fe, 20.18. Calc. for $C_{14}H_{20}Cl_2Fe_2$: C, 30.71; H, 3.66; Cl, 12.98; Fe, 20.48%.

Instrumentation. A Perkin–Elmer 237B grating spectrophotometer was used to record the spectra between 4000 and 625 cm^{-1} while the spectra in the 600–180 cm^{-1} region were done with a Perkin–Elmer model 983 spectrophotometer. Nujol was used in the preparation of the mulls for both types of spectra and "saran wrap" was used as window material for the spectra between 600 and 180 cm^{-1}. The UV–visible–near IR reflectance spectra were recorded on a Varian 2300 spectrophotometer. The magnetic susceptibility measurements were done on a Newport magnetic balance using mercury tetrathiocyanatocobalt(II) as calibrant. Thermal weight loss curves were obtained on a Netzsch STA 409 thermogravimetric analyser.

* Author to whom correspondence should be addressed.

Analyses. The carbon and hydrogen microanalyses were done by Huffman Laboratories, Inc., Colorado, U.S.A. The metal determinations were done with the use of a Pye–Unicam SP9 atomic absorption spectrophotometer, while the chlorine was determined gravimetrically as silver chloride using the method described by Vogel.[7]

RESULTS AND DISCUSSION

Iron(II) squarate chloride and nickel(II) squarate chloride

The IR spectra of the two complexes are almost superimposable (Table 1). The peak at 1775 cm^{-1} in the IR spectrum of both complexes is attributed to C=O stretching and the fact that it is observed a few wave numbers below 1800 cm^{-1} where it is expected is most likely due to hydrogen bonding involving the ketonic oxygen. The broad band around 3400 cm^{-1} is characteristic of hydrogen bonded hydroxyl groups and has been assigned to the O–H stretch in ethanol and the hydroxyl groups on the squarate rings. The peaks at 884, 1050, 1100, 1270 and 1925 cm^{-1} are due to ethanol since they all appear in the spectrum of neat ethanol.[8] The peak at 2200 cm^{-1} is an overtone of the peak at 1100 cm^{-1}. The band between 2600 and 2700 cm^{-1} and the peak at 725 cm^{-1} are also present in the spectra of the both complexes and have been identified as squarate bands.[9] The broad band between 1500 and 1700 cm^{-1} is due to a mixture of C–C and C–O stretchings.[3] The strong absorption at 525 cm^{-1} is assigned to M–O stretching.[10] The peaks at 180–250, 280 and 300 cm^{-1} in the iron complex and those at 225–250, 305, 317 and 330 cm^{-1} in the nickel complex are assumed to be due to the bridging chlorine atoms.[11]

Ciampolini[12] calculated the splittings of the terms of the free nickel(II) ion in the fields of five point dipoles arranged in trigonal–bipyramidal configurations. The predicted electronic spectrum resembles closely the observed spectra of [Ni(dienMe)Cl]Cl,[13] to which a distorted trigonal–bipyramidal structure has been assigned (see Fig. 1), and $[Ni(HC_4O_4)(Cl)(C_2H_5OH)]_2 \cdot C_2H_5OH$. The band at 8000 cm^{-1} in the electronic spectrum of nickel(II) squarate chloride has been assigned to $^3E' \rightarrow {}^3E''$, the band at 12,500 cm^{-1} to $^3E' \rightarrow {}^3A_1''$, and the shoulders at 14,300 and 20,600 cm^{-1} to $^3E' \rightarrow {}^3A_2'$ and $^3E' \rightarrow {}^3E''$ respectively. The band at 23,500 cm^{-1} has been assigned to $^3E' \rightarrow {}^3A_2'$.

The electronic spectrum of the iron(II) complex shows bands which can be interpreted in terms of the ligand-field model for trigonal–bipyramidal iron(II) proposed by Norgett *et al.*[14] The broad band between 8700 and 12,500 cm^{-1} has been assigned to $(e'')^4(e')^2 \rightarrow (e'')^3(e')^3$. The bands at 20,000 and 26,300 cm^{-1} have been assigned to $(e'')^4(e')^2 \rightarrow (e'')^4(e')^1a_1'$ and $(e'')^4(e')^2 \rightarrow (e'')^3(e')^2a_1'$ respectively. In addition, the spectrum compares favourably with that of the five-coordinate iron(II) complex $[Fe(NO_3)(QP)]^+$; $[QP = (OPh_2P \cdot C_6H_4)_3P]$. The electronic spectra of the two complexes appear in Fig. 2.

Table 1. IR spectroscopic data [ν (cm^{-1})]

$Fe_2(C_4O_4HCl)_2 \cdot 2C_2H_5OH$	$Ni_2(C_4O_4HCl)_2 \cdot C_2H_5OH$
3400 s, b	3400 s, b
2600–2700 w, b	2600–2700 w, b
2200 m, sh	2200 m, sh
1925, 1950 vw	1925, 1950 vw
1775 w, sh	1775 w, sh
1500–1700 b	1500–1700 b
1270 m, sh	1270 m, sh
1100 s, sh	1100 s, sh
1050 s, sh	1050 s, sh
884 s, sh	884 s, sh
725 s, sh	725 s, sh
525 s, b	525 s, b
300 sh	330 sh
280 sh	317 sh
180–250 b	305 sh
	225–250 s, sh

s: strong; sh: sharp; w: weak; vw: very weak; b: broad; m: medium.

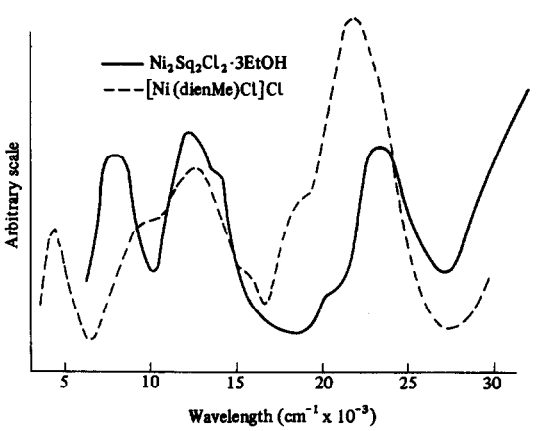


Fig. 1. Comparison of the electronic spectrum of [Ni(dienMe)Cl]Cl with that of $Ni_2Sq_2Cl_2 \cdot 3EtOH$ ($Sq = C_4O_4H^-$).

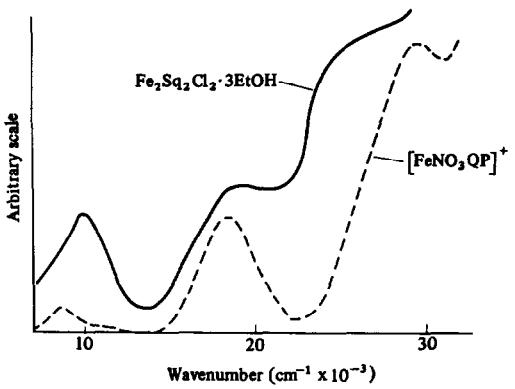
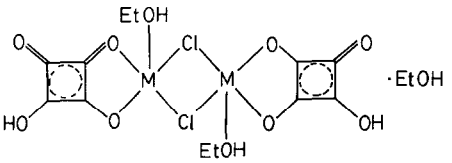


Fig. 2. Comparison of the electronic spectrum of $[Fe(NO_3)QP]^+$ with that of $Fe_2Sq_2Cl_2 \cdot 3EtOH$ ($Sq = C_4O_4H^-$).

The evidence tends to suggest that both the iron(II) and nickel(II) complexes are five-coordinate and most likely trigonal–bipyramidal. The following structure is therefore proposed.



The thermal weight loss curve for

$$[Fe(HC_4O_4)(Cl)(C_2H_5OH)]_2 \cdot C_2H_5OH$$

shows an inflection at about 150°C which corresponds to a 19.4% weight loss and another at about 200°C which corresponds to a weight loss of 9.9%. The first weight loss probably corresponds to the loss of coordinated ethanol while the second is apparently due to the loss of "lattice" ethanol.

Wrobleski and Brown[15,16] have postulated that hydrogen bonding between squarate and lattice solvent may be so strong that solvent coordinated to the metal is more easily lost from the complex.

The calculated weight losses of 16.8% and 8.4% are lower than those observed. This disparity may possibly be attributed to contamination by ethanol and/or water molecules, an occurrence which would also lead to the high H analysis recorded. A similar solvent contamination was observed[17] when $NiC_4O_4 \cdot 2H_2O$ was prepared from a 50:50 ethanol/water mixture. In that case, H analysis yielded values that were 50% higher than calculated.

The first inflection in the thermal weight loss curve for $[Ni(HC_4O_4)(Cl)(C_2H_5OH)]_2 \cdot C_2H_5OH$ occurs at about 175°C and corresponds to a weight loss of 28%. The theoretical weight loss for 3 molecules of ethanol is 25%. It appears that nickel(II) squarate chloride looses the coordinated and "lattice" ethanol simultaneously. This could be due to a weaker binding of the "lattice" ethanol in this complex. The disparity between the theoretical and experimental weight loss is again attributed to solvent contamination which could also explain the difference between the calculated and found H values.

Subsequent steps in the decomposition of the two squarate complexes seem to follow a complicated mechanism as observed for other squarates.[15] On exposure to the atmosphere, the nickel(II) complex changes from yellow to green. The electronic spectrum of the exposed complex shows the bands shifting with time until the spectrum becomes similar to that of $[Ni(H_2O)_6]^{2+}$.[18] The nickel(II) complex thus appears to become octahedral on taking up water from the atmosphere.

Iron(II) squarate chloride, when exposed to the atmosphere, undergoes two colour changes. The first change from faint yellow–brown to brown is accompanied by a weight loss and probably corresponds to the replacement of ethanol by water. Some atmospheric oxidation to iron(III) also takes place. The second colour change to deep red–brown is definitely due to rapid atmospheric oxidation to iron(III) since addition of hydrogen peroxide to the original faint yellow–brown complex produces the same change immediately.

The two complexes are apparently high spin since they have magnetic moments of 3.25 and 4.96 BM at 298 K which suggest spin-free Ni^{2+} and Fe^{2+} respectively.

Relative molecular mass and conductivity measurements could not be done since the complexes are insoluble in all the common solvents. Work is now being done to prepare crystals suitable for X-ray investigation.

REFERENCES

1. G. Maahs and P. Hegenberg, *Angew. Chem., Internat. Ed. Engl.* 1966, **5**, 890.
2. S. M. Condren and H. O. McDonald, *Inorg. Chem.* 1973, **12**, 57.
3. N. R. West and Y. Niu, *J. Am. Chem. Soc.* 1963, **85**, 2589.
4. A. Ludi and P. Schlindler, *Angew. Chem., Internat. Ed. Engl.* 1968, 638.
5. D. N. Hendrickson *et al.*, *Inorg. Chem.* 1973, **12**, 985.
6. R. A. Bailey, W. N. Mills and W. J. Tangredi, *J. Inorg. Nucl. Chem.* 1971, **33**, 2387.
7. A. I. Vogel, *A Textbook of Quantitative Inorganic Analysis*, 3rd Edn, pp. 461, 462. Longmans, London (1961).
8. Data from the *Aldrich Library of Infrared Spectra*, 2nd Edn, (Edited by C. J. Pouchert), copyright 1975, Aldrich Chemical Co., Milwaukee.
9. F. G. Baglin and C. B. Rose, *Spectrochimica Acta* 1970, **26A**, 2298.

10. D. M. Adams, *Metal–Ligand and Related Vibrations*, p. 260. Edward Arnold Ltd., London (1967).
11. K. Nakamoto, *Infrared Spectra of Inorganic and Coordinated Compounds*, 2nd Edn, pp. 216–218. Wiley–Interscience, New York (1970).
12. M. Ciampolini, *Inorg. Chem.* 1966, **5**, 40.
13. M. Ciampolini and N. Nardi, *Inorg. Chem.* 1966, **5**, 45.
14. M. Norgett *et al.*, *J. Chem. Soc.* (*A*) 1967, 540.
15. J. T. Wrobleski and D. Brown, *Inorg. Chem.* 1978, **17**, 2959.
16. J. T. Wrobleski and D. Brown, *Inorg. Chem.* 1979, **18**, 2738.
17. B. C. Gerstein and M. Habenschuss, *J. Appl. Phys.* 1972, **12**, 5155.
18. F. A. Cotton and G. Wilkinson, *Advanced Inorganic Chemistry*, 3rd Edn, p. 894. Wiley–Interscience, New York (1972).

Polyhedron Vol. 4, No. 10, pp. 1701–1705, 1985
Printed in Great Britain

0277–5387/85 $3.00 + .00
© 1985 Pergamon Press Ltd

INVERSION OF TETRAHEDRAL CONFIGURATION OF BIS-{4-AMINOMETHYLENEPYRAZOLE-5-THION(SELENO)ATO} NICKEL(II) COMPLEXES

L. E. NIVOROZHKIN, A. L. NIVOROZHKIN, M. S. KOROBOV, L. E. KONSTANTINOVSKY and V. I. MINKIN*
Institute of Physical and Organic Chemistry, Rostov-on-Don University, 344711 Rostov-on-Don, U.S.S.R.

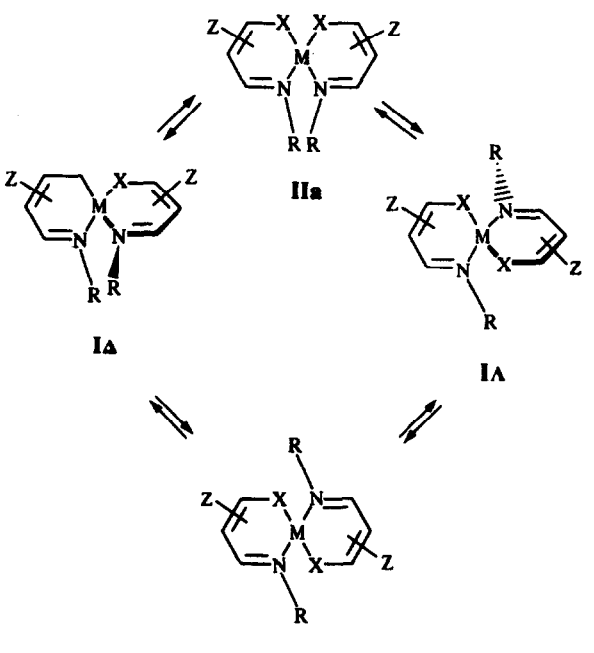
(*Received* 15 *January* 1985; *accepted* 28 *March* 1985)

Abstract—Novel bis-chelate Ni(II) complexes with a series of 1,3-disubstituted 4-aminomethylenepyrazole-5-thion(seleno) derivatives have been prepared. An inversion of the tetrahedral configuration at the metal centre in these complexes proceeds in solution *via* the intramolecular diagonal twist rearrangement on the NMR time scale which was followed by coalescence studies on several pairs of diastereotopic protons. The activation barriers are: $\Delta G^{\ddagger}(T_c) = 41$–$74$ kJ mol^{-1}, $T_c = 218$–373 K. The bulky substituents R_3 at the aldimine nitrogen give rise to significant increases in the energy barriers to enantiomerization of tetrahedral complexes owing to the steric hindrance involving an intermediate square planar form.

Inversion of tetrahedral configuration ($\Delta \rightleftarrows \Lambda$) at four-coordinated metal centres in the MN_2X_2 (X = O, S, Se; M = Zn, Cd, Be) complexes **I** derived from unsymmetrical ligands has been studied in detail using dynamic NMR spectroscopy, without requiring the separation of enantiomers.[1–5] The same method was also found to be efficient in evaluation of the energy barriers to enantiomerization of tetrahedral B (**III**) mono-chelates with similar ligands.[6,7]

Two competing reactions were found to occur to complexes **I** in solution, both leading to the $\Delta \rightleftarrows \Lambda$ interconversion. These include the degenerate bond rupture-bond closure ligand exchange process and more rapid intramolecular digonal twist rearrangements via square planar *trans* **IIa** or *cis* **IIb** configurational isomers.

By applying the quantitative line-shape analysis and the two-dimensional FT–NMR technique to the study of ^{111}Cd isotopomeric complexes it became recently possible to evaluate rate constants and activation parameters for each of these reactions.[8,9] It was shown that the digonal twist rearrangements **IΔ** ⇄ **IΛ** are the purely intramolecular processes which are 10^2–10^3 times faster than the degenerate

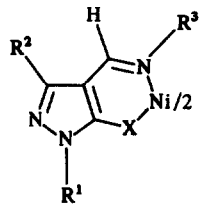


ligand exchange reactions. Unlike the Be(II), Zn(II) and Cd(II) type **I** chelates isoligand Ni(II) complexes exist in solution as equilibrium mixtures of

* Author to whom correspondence should be addressed.

diamagnetic square planar **II** and paramagnetic tetrahedral **I** isomers, free energy of equilibrium (ΔG°_{298}) lying ordinarily in the range of 4–12 kJ mol^{-1}.[10] The rates of interconversion between planar and tetrahedral forms and, therefore, of the enantiomerization processes **IΔ** ⇄ **IΛ** are normally extremely high and are beyond the limits of the NMR time scale.

An approach to paramagnetic Ni(II)bis-chelates with sufficiently rigid chiral tetrahedral structure was first presented by Knorr *et al.*[11,12] By substituting X in **I** by the NR group these authors succeeded in destabilizing the square planar structure **II** as compared to the tetrahedral isomer **I** which led to the increase of square planar–tetrahedral energy gap up to 70–120 kJ mol^{-1}. Another way to achieve such a high energy difference between these isomeric forms of Ni(II) complexes was found in annelating various π-acceptor moieties (benzofurane, benzothiophene, pyrazole) to their chelate rings which results in a complete shift of the **I** ⇆ **II** equilibria to the left.[13–16] Therefore a considerable thermodynamic contribution to the energy barriers for the interconversion of the Ni(II)bis-chelate complexes might be expected. In the present paper the results of dynamic ^1H NMR investigation of enantiomerization kinetics of previously unknown paramagnetic tetrahedral Ni(II) complexes **III** are reported.



RESULTS AND DISCUSSION

The presence of prochiral isopropyl and benzyl groups R^1 and R^2 in chiral tetrahedral complexes **III** allows the investigation of the tetrahedral inversion by use of the NMR method without prior separation of enantiomers. Any process which leads to the inversion at the metal centre on the ^1H NMR time scale will result in averaging signals belonging to the diastereotopic methyl groups (*i*-Pr) or to the methylene protons (CH_2Ph). The ^1H NMR spectra of paramagnetic Ni(II) complexes **III** exhibit moderately broadened lines ($\Delta\nu^0_{1/2} \simeq 10$ Hz). The values of isotropic contact shifts originated from delocalization of the electron spin density to the ligands are very near to those measured earlier for some of type **IIIa** Ni(II) complexes.[15]

The typical spectrum for one of the complexes is given in Fig. 1.

In the slow exchange region at low temperatures diastereotopic methyls in both isopropyl groups R^3

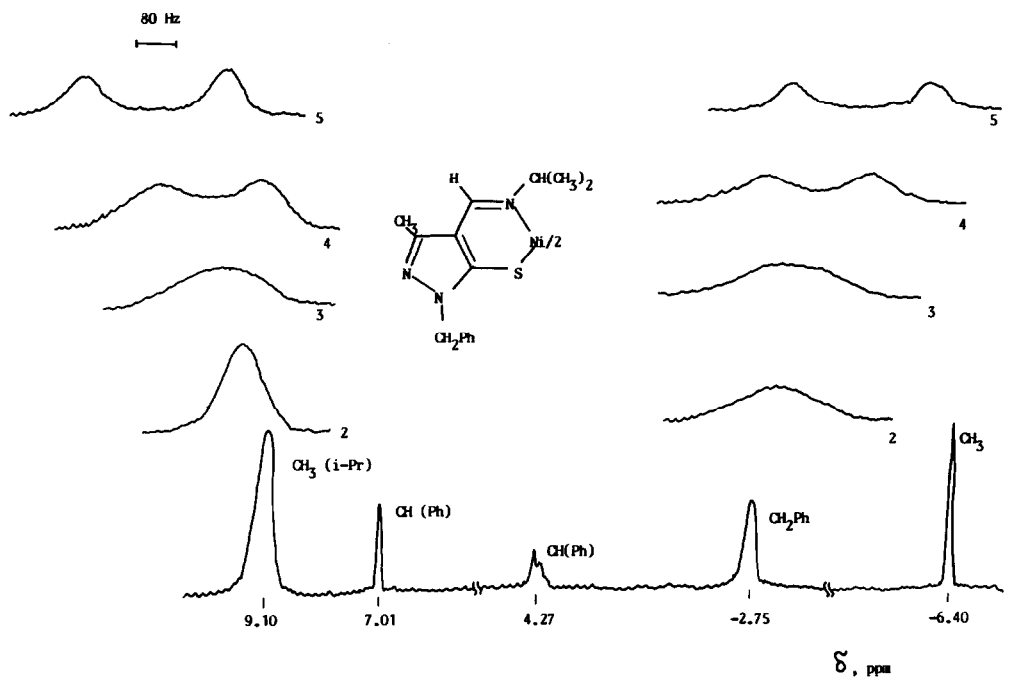


Fig. 1. ^1H NMR spectrum of bis-chelate complex **IIIc** (R^3 = *i*-Pr) in $CDCl_3$ solution at 25°C (1) and temperature dependent methyl (R^3 = *i*-Pr, X = S) and methylene ($R^1 = CH_2Ph$) resonances in the intermediate-exchange region: −10° (2), −20° (3), −30° (4) and −50° (5).

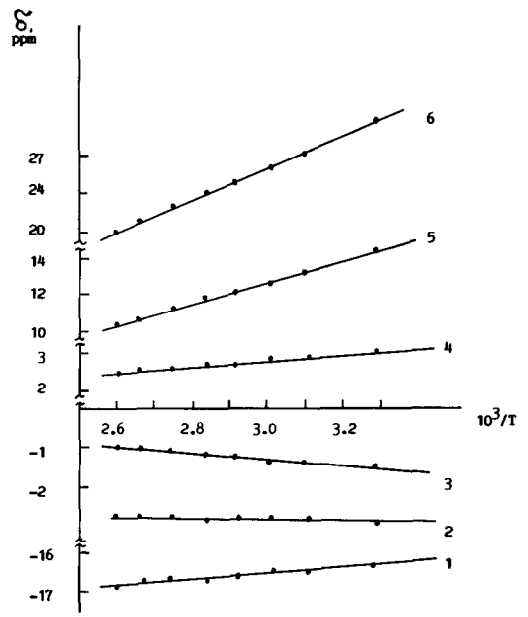


Fig. 2. Temperature dependence of isotropic chemical shifts of protons for bis-chelate complex **IIId** (R^3 = *t*-Bu, X = S) in DMSO solution: (1) CH, (2) CH_3 (*i*-Pr), (3) *m*-H, (4) *p*-H, (5) *o*-H, (6) CH_3 (*t*-Bu).

are rendered anisochronic, showing two unresolved six-proton peaks. Such broadened lines are typical for paramagnetic Ni(II) complexes ($\Delta\nu^0_{1/2} > {}^3J_{HH}$), while characteristic splitting (${}^3J_{HH}$ = 6.5–7 Hz) is observed in ^{1}H NMR spectra of both free ligands and diamagnetic tetrahedral complexes of Zn(II) and Cd(II). A linear contact shift vs 1/T dependence was observed for various protons in **III** in accordance with the Curie law. This is shown in Fig. 2.

At elevated temperatures the methyl proton peaks become broadened and then coalesce. A similar reversible temperature dependence was observed for the N_1-benzyl diastereotopic methylene protons. The AB type spectrum of this pair of protons is perturbed by significant paramagnetic broadening and a loss of terminal components of the AB quartet due to very large AB chemical shift. Thus, the dynamic ^{1}H NMR spectra of paramagnetic tetrahedral Ni(II) complexes **III** reveal the existence of the $\Delta \rightleftarrows \Lambda$ interconversions in solution manifesting themselves in a loss of chirality of the tetrahedral structure.

Since the total line-shape analysis of the temperature dependent NMR spectra of Ni(II) complexes **III** could not be carried out because of paramagnetic broadening and of large signal drifts (see also[17,18] for similar cases) the free energies of activation for the $\Delta \rightleftarrows \Lambda$ interconversion $\Delta G^{\ddagger}(T_c)$ were calculated at coalescence temperatures. They are listed in Table 1. The table includes also the values of magnetic moments of complexes **III** which were determined in chloroform solution by Evans' method.

The measured values of effective magnetic moments remained constant over a temperature interval covering the range of reversible line-shape evolution of prochiral group signals which indicates that no appreciable amounts of equilibrium diamagnetic isomers of **III** appeared. Neither contact shifts, even more sensitive to rather small concentrations of diamagnetic isomer,[17] nor coalescence temperatures depended on the concentration in the accessible range of 10^{-2}–10^{-4} mol l^{-1}. These values were not influenced either by varying solvent polarity ($CDCl_3$, CH_2Cl_2, acetone-d_6, DMSO-d_6). It may be concluded, therefore, that the mechanism and kinetics of the **III**(Δ) $\rightleftarrows$ **III**(Λ) interconversion is determined by the intramolecular digonal twist rearrangement, while the intermolecular degenerate ligand exchange reactions, if they proceed, are slow enough relative to the former process.

Although the free energies of activation for **III**(Δ) $\rightleftarrows$ **III**(Λ) interconversion could not have been calculated and compared at a single temperature relatively small differences in the coalescence temperatures and a compensation effect (see ref. 19) make possible a comparison of the energy barrier values given in Table 1. This is also justified by a good coincidence of the $\Delta G^{\ddagger}(T_c)$ values calculated for different pairs of diastereotopic groups within the same molecule (compounds under numbers 2, 3, 22 in Table 1).

It may be seen from the data given in Table 1 that the main structural factor influencing the height of the energy barrier against the digonal twist in tetrahedral complexes **III** is a steric volume of the R^3 substituent attached to the aldimine nitrogen atom coordinated to the metal centre. The bulkier the R^3 substituent the higher the **III**(Δ) $\rightleftarrows$ **III**(Λ) energy barrier. The following sequence of the energy barriers was found, for instance, for complexes relating to the **IIIb** series (X = S)

R^3 = *t*-Bu (no. 1 in Table 1);	*i*-Pr (no. 2);	CH_2Ph (no. 4);	aryl (nos. 10–15);	Me (no. 8)
73.6 kJ mol^{-1}	50.6	47.7	45.6–47.7	44.4

This sequence is similar to the one proved for the increasing relative stability of the square planar isomeric forms of various bis-chelate Ni(II)

Table 1. NMR parameters, magnetic moments, rate constants and free activation energies at coalescence temperature for $\Delta \rightleftarrows \Lambda$ interconversion of tetrahedral complexes **IIIb–d**

No.	Compound Type	X	R	Chemical shift of diastereotopic group[a], ppm	$\Delta\nu_{1/2}$, Hz	T_c, K	$\Delta G^{\neq}(T_c)$, kJ mol^{-1}	$k(T_c)$, s^{-1}	μ_{eff}, B.M.
1	**IIIb**	S	*t*-Bu[b]	5.10	160	373	73.6	4.0	3.43
2		S	*i*-Pr	3.70	86	243	50.6	1.9	3.37
		S	*i*-Pr[c]	9.17	360	268	50.6	8.0	
3		Se	*i*-Pr	4.05	87	263	52.7	1.9	3.51
		Se	*i*-Pr[c]	11.05	260	283	54.4	5.8	
4		S	C_6H_{11}	4.31	72	263	55.6	0.74	3.54
5		S	CH_2Ph	3.33	130	243	47.7	2.9	3.35
6		Se	CH_2Ph	3.59	143	258	50.6	3.2	3.27
7		S	Et	3.29	132	223	43.5	2.9	3.21
8		S	Me	3.20	200	223	44.4	2.2	3.25
9		Se	Me	3.25	160	248	48.1	6.0	3.29
10		S	$C_6H_4NO_2$-*p*	3.45	36	223	45.6	0.9	[d]
11		S	$C_6H_4COOCH_3$-*p*	3.45	36	228	46.9	0.9	3.35
12		S	C_6H_4Cl-*p*	3.45	28	223	46.0	0.73	3.25
13		S	C_6H_4F-*p*	3.45	28	218	45.2	0.73	3.30
14		S	C_6H_5	3.45	25	218	46.4	0.31	3.33
15		S	$C_6H_4CH_3$-*p*	3.49	37	233	47.7	0.91	3.38
16		Se	$C_6H_4CH_3$-*p*	3.89	52	253	53.1	0.55	3.30
17		S	$C_6H_4OCH_3$-*p*	3.75	36	243	50.2	0.89	3.21–3.38
18		S	$C_6H_4NMe_2$-*p*	3.45	60	253	51.0	1.4	3.27–3.39
19		S	$C_{10}H_7$-1	3.95	220	273	52.7	4.9	3.30
20	**IIIc**	S	C_6H_{11}	−2.35	180	263	51.0	3.8	3.32
21		Se	C_6H_{11}	−5.75	170	272	53.1	3.8	3.57
22		S	*i*-Pr	−2.75	225	253	48.1	5.6	3.51
		S	*i*-Pr[e]	9.10	210	253	48.5	4.7	
23		Se	*i*-Pr	−3.95	180	223	51.9	4.0	3.42
24		S	CH_2Ph	−1.40	260	243	46.0	5.8	3.31
25		Se	CH_2Ph	−2.35	294	248	46.9	6.5	3.33
26		S	Me	−1.25	500	238	43.9	11.0	3.15
27		S	$C_6H_4OCH_3$-*p*	−1.75	172	263	51.0	3.8	3.38
28	**IIId**	S	*t*-Bu[b]	−2.52	25	333	70.7	0.56	3.36 (3.32)[e]
29		S	*i*-Pr	3.90	60	230	47.3	0.88	3.30 (3.02)[e]
30		Se	*i*-Pr	0.13	33	225	42.3	0.74	3.37 (3.18)[e]
31		S	C_6H_{11}	4.39	40	218	41.4	0.83	3.53 (3.21)[e]

[a] Chemical shifts for the following diastereotopic groups at fast exchange conditions are given (solvent $CDCl_3$): R^1 = *i*-Pr (nos. 1–19), $R^1 = CH_2Ph$ (nos. 20–27), R^2 = *i*-Pr (nos. 28–31).

[b] In DMSO-d_6.

[c] Averaging diastereotopic methyls in R^3 = *i*-Pr group.

[d] Not measured because of very poor solubility.

[e] The values obtained in solid at 298 K.

complexes **I** with respect to their tetrahedral forms.[10,20,21]

In contrast to the steric factors, electronic properties of R^3 substituents slightly affect the rates of **III**(Δ) $\rightleftarrows$ **III**(Λ) interconversion which are almost insensitive to the origin of *para*-substituent in *N*-aryl ring (R^3 = aryl). The only exceptions are complexes nos. 17, 18 (**IIIb**) and no. 27 (**IIIc**) containing very strong π-donor groups (*p*-OMe, *p*-NMe_2) in *N*-aryl moieties. It is noteworthy, however, that a nonlinear contact shift vs $1/T$ plot and a small decrease of the effective magnetic moment values upon cooling the solution were observed in the cases of all the above mentioned complexes which may be accounted for by the presence of measurable quantities of polymeric associates in an equilibrium with tetrahedral monomeric forms. Replacement of the sulphur atom in the chelate rings of complexes **IIIb,c**

by selenium results in a small increase in the energy barriers to the tetrahedral inversion. This trend, however, is not observed in the case of complexes **IIId**.

EXPERIMENTAL

^{1}H NMR spectra were obtained using a Varian XL-100 (100 MHz) spectrometer equipped with a variable-temperature probe. The temperature in the samples was controlled with an accuracy of ± 1 K. The rate constants at coalescence temperatures were calculated according to the usual equation: $k(T_c) = \pi/\sqrt{2}\Delta\nu_{1/2}$, where $\Delta\nu_{1/2}$ stands for a linewidth at half height for diastereotopic group signals.

Magnetic moments of complexes in solution were determined by Evans' method.[22]

Complexes **III** were prepared by refluxing (5–10 min) equimolecular quantities of nickel acetate with the respective 4-aminomethylene derivatives of 1,3-substituted 5-thio(seleno)pyrazoles in ethanol solution. All the complexes thus obtained were purified by repeated crystallization from benzene. The experimental details of synthetic procedure and some additional characteristics of complexes **III** will be reported elsewhere.[23]

REFERENCES

1. S. S. Eaton and R. H. Holm, *Inorg. Chem.* 1971, **10**, 1446.
2. V. I. Minkin, L. E. Nivorozhkin, L. E. Konstantinovsky and M. S. Korobov, *Koord. Khim.* 1977, **3**, 174.
3. L. E. Nivorozhkin, L. E. Konstantinovsky, M. S. Korobov and V. I. Minkin, *Koord. Khim.* 1979, **5**, 508.
4. L. E. Nivorozhkin, M. S. Korobov, R. Ya. Olekhnovich, L. E. Konstantinovsky and V. I. Minkin, *Koord. Khim.* 1982, **8**, 1080.
5. F. A. Bottino, A. Recca and P. I. Finocchiaro, *J. Organomet. Chem.* 1978, **160**, 373.
6. M. S. Korobov, L. E. Nivorozhkin, L. E. Konstantinovsky and V. I. Minkin, *J. Chem. Soc., Chem. Commun.* 1982, 169.
7. A. J. Boulton and C. S. Prado, *J. Chem. Soc., Chem. Commun.* 1982, 1008.
8. L. E. Nivorozhkin, V. I. Minkin, N. I. Borisenko, L. E. Konstantinovsky, M. S. Korobov and R. Ya. Olekhnovich, *Dokl. Akad. Nauk SSSR* 1981, **261**, 1176.
9. L. E. Nivorozhkin, Yu. E. Czernysh, G. S. Borodkin, R. Ya. Olekhnovich, Yu. A. Zhdanov and V. I. Minkin, *Dokl. Akad. Nauk SSSR* 1983, **273**, 144.
10. R. H. Holm and M. I. O'Connor, *Progr. Inorg. Chem.* 1971, **14**, 241.
11. R. Knorr, A. Weiss, H. Polzer and E. Räpple, *J. Am. Chem. Soc.* 1977, **99**, 650.
12. R. Knorr and A. Weiss, *Chem. Ber.* 1981, **114**, 2104.
13. V. I. Usacheva, V. A. Bren, L. O. Atovmyan, V. V. Tkachev and V. I. Minkin, *Koord. Khim.* 1976, **2**, 1578.
14. V. A. Bren, O. A. Isipov, V. I. Minkin, Zh. A. Bren, L. S. Minkina, L. O. Atovmyan, S. M. Aldoshin and O. A. Dyachenko, *Koord. Khim.* 1979, **5**, 1058.
15. L. E. Nivorozhkin, L. E. Konstantinovsky, V. I. Minkin, O. A. Osipov, A. D. Garnovsky, V. P. Kurbatov and I. Ya. Kvitko, *Zh. Neorg. Khim.* 1975, **20**, 3012.
16. L. E. Nivorozhkin, L. E. Konstantinovsky, V. I. Minkin, M. S. Korobov and I. Ya. Kvitko, *Koord. Khim.* 1980, **6**, 568.
17. G. W. Everett and R. H. Holm, *Inorg. Chem.* 1968, **7**, 776.
18. T. J. Swift, in *NMR of Paramagnetic Molecules* (edited by G. N. LaMar, W. Horrocks and R. H. Holm), p. 69. Academic Press, New York (1973).
19. G. Binsch, in *Dynamic Nuclear Magnetic Resonance Spectroscopy* (edited by L. M. Jackson and F. A. Cotton), p. 77. Academic Press, New York (1975).
20. R. H. Holm, in *Dynamic Nuclear Magnetic Resonance Spectroscopy* (edited by L. M. Jackson and F. A. Cotton), p. 317. Academic Press, New York (1975).
21. O. A. Osipov, A. D. Garnovsky, V. I. Minkin and V. A. Kogan, *Dipole Moments in the Chemistry of Coordination Compounds*, Ch. 3. Rostov University Publishing House, Rostov-on-Don (1976).
22. D. F. Evans, *J. Chem. Soc.* 1959, 2003.
23. A. L. Nivorozhkin, M. S. Korobov, L. E. Konstantinovsky, L. E. Nivorozhkin and V. I. Minkin, *Zh. Obshch. Khim.* 1985, **55**, 849.

Polyhedron Vol. 4, No. 10, pp. 1707–1710, 1985
Printed in Great Britain

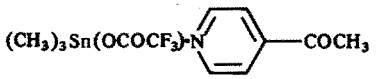
0277–5387/85 $3.00 + .00
© 1985 Pergamon Press Ltd

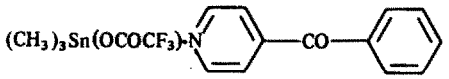
REACTIONS OF THE PYRIDINE ADDUCTS OF ORGANOTIN HALIDES: SYNTHESIS AND SPECTRAL PROPERTIES OF SOME SUBSTITUTED PYRIDINE ADDUCTS OF $(CH_3)_3SnOCOCF_3$ AND $(CH_3)_2Sn(OCOCF_3)_2$

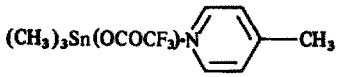
J. J. BONIRE
Department of Chemistry, Ahmadu Bello University, Zaria, Nigeria

(*Received* 23 *November* 1984; *accepted after revision* 3 *April* 1985)

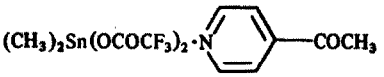
Abstract—A study of the reactions of the pyridine aducts of organotin halides has led to the synthesis of







and



which were characterised by elemental analysis and spectroscopy.

Studies of the substitution reactions of organotin and organosilicon halides and pseudohalides[1–5] have indicated that the reactions occur by an associative route. Therefore, while triorganotin halide pyridine adducts might undergo associative substitution reactions, the hexacoordinated diorganotin dihalide pyridine adducts might not, due to steric factors. However, Van der Berghe's observation[6] that the trimethyltin chloride pyridine adduct ionizes in polar media suggests that organotin chloride pyridine adducts could undergo dissociative substitution reactions.

Reactions of organotin halide pyridine adducts have not attracted much interest apparently because of their poor solubility in many organic solvents.

Organotin carboxylate pyridine adducts appear to be a new class of compounds. Graddon and Rana[7] have reported their apparent existence in solution, and Saxena *et al.*[8] have reported the synthesis of some tridentate Schiff base complexes of Sn(IV) acetate.

This paper reports the synthesis and some spectroscopic properties of some methyltin trifluoroacetate pyridine adducts in the study of the reactions of organotin halide adducts.

EXPERIMENTAL

"Dry" acetone was prepared by refluxing the analytical grade of acetone with *p*-toluenesulphonylchloride (2 g l^{-1}) for $\frac{3}{4}$ h and distilling the acetone.

All m.p. temperatures (°C) are uncorrected.

IR spectra (KBr disc) were obtained using Perkin–Elmer SP 700 and 800 spectrometers.

^1H NMR spectra were obtained using a T-60 spectrometer at an operating temperature of 38°C; the δ values (ppm, reference TMS) were recorded.

Elemental analyses (C, H and N) were done by the Scandinavian Analytical Laboratories. Sn contents were determined locally, using the methods reported by Farnsworth and Pekola.[9]

All reagents were obtained from BDH, Alfa or Aldrich.

$Me_3Sn(OCOCF_3)\cdot L$: L = *4-acetylpyridine* (*4-AcPy*), *4-benzoylpyridine* (*4-BzPy*) *or* *4-picoline* (*4-Pic*)

Equimolar amounts (0.01 mol) of Me_3SnCl and L were mixed after dissolving both solutes in CCl_4 (10 and 15 cm^3 respectively). Each mixture was cooled (5°C) overnight. Crystals of $Me_3SnCl\cdot L$ separated out, and were removed, washed with the cold solvent, and dried over silica gel. Each product was recrystallized twice from CCl_4.

Equimolar amounts (0.005 mol) of $Me_3SnCl\cdot L$ and $AgO\cdot CO\cdot CF_3$, both in portions of dry acetone (30 cm^3), were mixed. The ensuing white precipitate was coagulated by boiling the mixture under reflux for 10 min under a covering of aluminium foil, and then removed by filtration. The filtrate was concentrated by evaporation until a yellow oil was left. This solidified on standing, and was dried *in vacuo*. The product was recrystallised 3 times from CCl_4 and dried *in vacuo*.

$Me_2Sn(OCOCF_3)_2\cdot 4$-AcPy

Me_2SnCl_2 (2.21 g, 0.01 M) in CH_2Cl_2 (50 cm^3) and 4-AcPy (2.42 g, 0.02 M) in CH_2Cl_2 (50 cm^3) were mixed. The resulting clear solution was left to stand overnight. Light yellowish granular crystals of $Me_2SnCl_2\cdot$ bis-4-AcPy were produced. The product was removed by filtration, dried *in vacuo*, and recrystallised 3 times from dry acetone (m.p. 117–118°C, lit.[10] 117–118°C).

$Me_2SnCl_2\cdot$bis-4-AcPy (2.32 g, 0.005 M) and $AgOCOCF_3$ (2.21 g, 0.01 M) each in (50 cm^3) of hot, dry acetone, were mixed. The ensuring white precipitate of AgCl was coagulated by boiling the mixture under reflux for 10 min under aluminium sheet cover, and filtered off. The filtrate was evaporated until a thick brownish oil was left. This, on cooling (5°C), yielded yellowish crystals. The mass of crystals was removed and dried *in vacuo* (2.05 g, dry), and recrystallised 3 times from toluene.

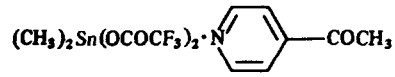
RESULTS AND DISCUSSION

The reactions of the methyltin chloride pyridine adducts with silver trifluoroacetate occurred smoothly in hot, dry acetone. The insoluble silver chloride, after coagulation by boiling, was easily removed by filtration.

Elemental analysis results show all the complexes (Table 1) to be 1:1 complexes, including $Me_2Sn(OCOCF_3)_2\cdot 4$-AcPy. They generally have lower m.ps than the corresponding methyltin chloride adducts.

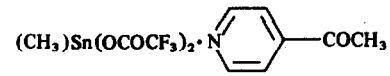
The ^1H NMR spectra of the complexes, obtained in deuterodimethyl sulphoxide and shown in Table 2, show that the chemical shift (δ) values for the Sn—CH_3 protons are generally lower for the methyltin carboxylate than for the methyltin chloride pyridine adducts. The other signals are not remarkably different from those given by the independent Lewis acids and bases, except that the shift values for the pyridyl protons decreased slightly with the complexation of the pyridine.

Table 3 shows the IR spectra. The pronounced bands at ~1650 and 1200 cm^{-1}, assignable to OCO and C—F stretch respectively, confirm the presence of the trifluoroacetate group in the complexes. The broad OCO band in the spectrum of

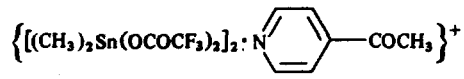


suggests that the OCO is of a bridging type.

A mass spectrum of the



gave the highest mass unit of 873, assignable to

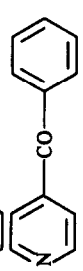


which is twice the molecule of the complex minus a molecule of the Lewis base. This strongly suggests that the adduct exists as a dimer with the structural

Table 1. Melting points, yield and elemental analysis results for the organotin trifluoroacetate substituted pyridine adducts

Compound	Yield (%)	m.p. (°C)	Found (%) C	H	N	Sn	Calc. (%) C	H	N	Sn
$Me_3Sn(OCOCF_3)\cdot 4$-AcPy	82.0	91–92	35.85	3.92	3.49	29.91	36.21	4.02	3.52	29.84
$Me_3Sn(OCOCF_3)\cdot 4$-BzPy	75.6	80–81	43.87	3.96	3.06	25.95	44.38	3.91	3.04	25.81
$Me_3Sn(OCOCF_3)\cdot 4$-Pic	66.8	66–67	35.81	4.40	3.80	32.50	35.70	4.32	3.78	32.10
$Me_2Sn(OCOCF_3)_2\cdot 4$-AcPy	60.2	88–89	31.50	2.81	2.73	24.10	31.47	2.62	2.82	23.94

Table 2. ^{1}H NMR chemical shifts of the methyltin trifluoroacetate substituted pyridine adducts.[a]

Compound	δ (ppm) (*d*-DMSO)				
	Sn—CH_3	—$COCH_3$	Pyridyl-*m*-H	Pyridyl-*o*-H	—CO—
$(CH_3)_3Sn(OCOCF_3)\cdot$ 	0.50s	2.65s	7.90m	8.95d	—
$(CH_3)_3Sn(OCOCF_3)\cdot$ 	0.50s	—	7.90m	9.00d	7.80m
$(CH_3)_3Sn(OCOCF_3)\cdot$ 	0.50s	—	7.40d	8.50d	—
$(CH_3)_2Sn(OCOCF_3)_2\cdot$ 	0.92s	2.65s	7.85m	8.86d	—

[a] s, singlet; d, doublet; m, multiplet.

formula shown in Fig. 1, which explains why the 4-AcPy adduct of $(CH_3)_2Sn(OCOCF_3)_2$ is obtained as a 1 : 1 Lewis acid : Lewis base.

This work therefore shows that at least some organotin halide pyridine adducts can undergo associative substitution reactions, and also establishes the existence of at least some organotin carboxylate pyridine adducts. It also suggests that interconversion reactions between the adducts of methyltin (and perhaps other organotin) halides and pseudohalides might be possible, as commonly known[1–5] with organosilicon and organotin halides and pseudohalides.

The route of synthesis of the complexes given in this report could be summarized as follows:

$$(CH_3)_3SnCl\cdot L + AgOCOCF_3 \xrightarrow{\text{in hot, dry acetone}} (CH_3)_3Sn(OCOCF_3)\cdot L + AgCl, \quad (1)$$

where L = 4-AcPy, 4-BzPy or 4-Pic.

$$(CH_3)_2SnCl_2\cdot \text{bis-4-AcPy} + AgOCOCF_3 \xrightarrow{\text{in hot, dry acetone}} (CH_3)_2Sn(OCOCF_3)_2\cdot \text{4-AcPy} + AgCl. \quad (2)$$

However, the complexes were also synthesized by the direct reaction of the methyltin trifluoroacetate with the Lewis base in a dry acetone medium. Equimolar amounts of the Lewis acid and Lewis base when mixed in hot dry acetone (heated to ensure the dissolution of the reactants) yielded the complexes, which were obtained from the medium in the manner described above for the complexes prepared from the organotin chloride adducts. Alternatively, the methyltin trifluoroacetates, prepared from the reaction of the methyltin chloride with silver trifluoroacetate in dry acetone, reacted *in situ* with the Lewis bases to yield the complexes.

The route of synthesis of the organotin carboxylate complexes from the organotin chloride complexes being reported cannot be called a general

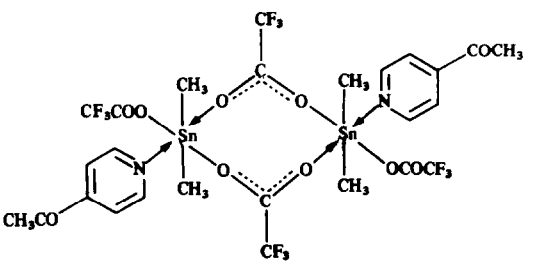
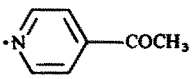
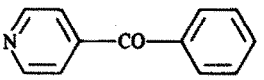
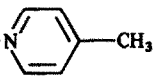
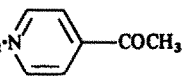


Fig. 1. The suggested structural formula of $(CH_3)_2Sn(OCOCF_3)_2\cdot$4-AcPy, thought to exist in the dimeric form.

Table 3. IR absorption frequencies of the methyltin trifluoroacetate substituted pyridine adducts

Compound	Stretching vibration frequencies (cm^{-1})					
	C—H aromatic	C=O and OCO	C=C aromatic	C—O	C—F (CF_3)	Sn—CH_3 rock
$(CH_3)_3Sn(OCOCF_3)\cdot$  —$COCH_3$	3050w	1650–1710w	1600w	1410m	1200s	795s
$(CH_3)_3Sn(OCOCF_3)\cdot$  —CO—	3030w	1650–1710s	1600m	1410m	1200s	790s
$(CH_3)_3Sn(OCOCF_3)\cdot$  —CH_3	3075w	1640–1750s	1608m	1410m	1200s	790s
$(CH_3)_2Sn(OCOCF_3)_2\cdot$  —$COCH_3$	3100w	1620–1720s	1600m	1410m	1200s	795m

one; attempts to isolate the $(CH_3)_2Sn(OCOCF_3)_2$ complexes of other pyridine Lewis bases than 4-AcPy have so far failed. Also, only organotin trifluoroacetate complexes have so far been isolated; there is not enough evidence to believe at this stage that all organotin carboxylates complex with the pyridines to give isolable products.

REFERENCES

1. A. S. Mufti and R. C. Poller, *J. Chem. Soc.* 1965, 5055.
2. M. Frankel, D. Gertner, D. Wagner and A. Zilkha, *J. Organomet. Chem.* 1967, **9**, 83.
3. R. J. P. Corriu, J. M. Fernandez and C. Guerin, *J. Organomet. Chem.* 1978, **152**, 21.
4. L. H. Sommer, J. McLick and C. M. Golino, *J. Am. Chem. Soc.* 1972, **94**, 669.
5. C. Eaborn and S. P. Hopper, *J. Organomet. Chem.* 1979, **170**, C51.
6. E. V. Van der Berghe and G. P. Van der Kelen, *J. Organomet. Chem.* 1968, **11**, 479.
7. D. P. Graddon and B. A. Rana, *J. Organomet. Chem.* 1977, **136**, 19.
8. A. Saxena, J. P. Tandon, K. C. Molloy and J. J. Zuckerman, *Inorg. Chim. Acta* 1982, **63**, 7.1.
9. N. Farnworth and J. Pekola, *Analyt. Chem.* 1959, **31**, 410.
10. J. J. Bonire, *Niger. J. Sci.* (in press).

Polyhedron Vol. 4, No. 10, pp. 1711–1715, 1985
Printed in Great Britain

0277–5387/85 $3.00 + .00
Pergamon Press Ltd

PREPARATION AND PROPERTIES OF VANADYL(IV) HYPOPHOSPHITE, $VO(PO_2H_2)_2 \cdot H_2O$

ENRIQUE J. BARAN* and SUSANA B. ETCHEVERRY
Departamento de Química, Facultad de Ciencias Exactas, Universidad Nacional de La Plata, 1900-La Plata, Argentina

and

EKKEHARD DIEMANN
Fakultät für Chemie der Universität Bielefeld, D-4800 Bielefeld 1, F.R.G.

(*Received* 9 *October* 1984; *accepted in revised form* 3 *April* 1985)

Abstract—The preparation of $VO(PO_2H_2)_2 \cdot H_2O$ was possible by direct reduction of V_2O_5 with hypophosphorous acid or by interaction of $VOSO_4$ and H_3PO_2 solutions, and subsequent crystallization. The compound was characterized by IR, electronic and ESR spectroscopy and X-ray powder diffractometry. Magnetic susceptibilities were measured in the temperature range between 100 and 300 K. The thermal decomposition was also investigated in detail, showing a very complex sequence of degradation steps which finally generate a polymeric V(III) phosphite.

As part of a current research program devoted to the study of simple and not well-characterized compounds of the vanadyl(IV) cation, VO^{2+}, we have recently prepared and investigated the corresponding hypophosphite.

This research is also of more general interest, because very little is known up to now about the structural, spectroscopic and thermal properties of transition-metal hypophosphites. On the other hand, it extends previous work of our laboratory on different complex compounds containing other phosphate ligands (cf, for example, Refs 1–3).

EXPERIMENTAL

The only earlier literature reference about vanadyl hypophosphite is a 1907-dated paper by Mawrow.[4] He prepared this compound by direct reaction between V_2O_5 and hypophosphorous acid. By subsequent crystallization, a blue powder of composition $VO(PO_2H_2)_2 \cdot H_2O$ was obtained. We could also obtain the same product by direct interaction between vanadyl sulfate and hypophosphorous acid solutions. The following procedure, which we have worked out, allows an easy and quick preparation of the compound.

* Author to whom correspondence should be addressed.

Method A

1.5 g of V_2O_5 are suspended in 10 cm^3 of distilled water. 4 cm^3 of a 50% H_3PO_2 solution are dropwise added to this suspension under continuous stirring. The solution is heated until all the V_2O_5 is dissolved and the heating continued for a few minutes more. The resulting blue solution is then concentrated in a vacuum desiccator over conc. H_2SO_4. After a few days a blue compact mass is deposited. It is filtered, washed 3 times with hot water and finally dried again over H_2SO_4.

Method B

4.5 g of $VOSO_4 \cdot 5H_2O$ are dissolved in 20 cm^3 of hot distilled water. 4.5. cm^3 of a 50% H_3PO_2 solution are dropwise added to this solution. The mixture is heated for 10 min and then stored in a vacuum desiccator over conc. H_2SO_4. The remaining steps of the operation are similar to those described in method A.

The solid product is very insoluble in water. Chemical analyses of the obtained samples, performed as described in Ref. 4, confirm the formula $VO(PO_2H_2)_2 \cdot H_2O$. Found: V, 23.7; P, 28.7. Calc.: V, 23.72; P, 28.83%.

Spectroscopic measurements

IR spectra were recorded with a Perkin–Elmer 580 B spectrophotometer, using the KBr pellet technique. The UV/VIS spectra were recorded with a Shimadzu UV-600 model spectrophotometer. The ESR spectrum was obtained by means of a Brucker-ER 10 type spectrometer, working at room temperature and employing a microwave frequency of 9.6 GHz; DPPH was used as an internal calibration standard.

Magnetic measurements

Magnetic susceptibility measurements were performed using the Gouy method in the temperature range between 100 and 300 K. The instrument was calibrated with $HgCo(SCN)_4$. The molar magnetic susceptibilities were corrected by the diamagnetism of the sample.[5]

Diffractometric measurements

X-ray powder data were obtained on a Philips 1732/10 diffractometer using Cu-K_α radiation (Ni filter) and employing NaCl as an external calibration standard.

Thermal studies

The TG/DTA measurements were performed with a Linseis L-81 thermoanalytical system, working in air, at a heating rate of 5°C/min. Al_2O_3 was used as a DTA standard. Studies were also performed at constant controlled temperatures in a crucible furnace in air.

RESULTS AND DISCUSSION

The formula of the compound and the physicochemical properties clearly support the structural arrangement shown in Fig. 1.

This implies that the $H_2PO_2^-$ anion acts as a bidentate ligand of the vanadyl ion occupying four coordination positions about the vanadium atom. The fifth position is obviously occupied by the oxygen atom and the remaining one by the water molecule. The free hypophosphorous acid has a C_{2v} point symmetry,[6,7] but this symmetry is probably reduced in the complex.

Physicochemical studies

IR spectrum. The IR spectrum of the compound is reproduced in Fig. 2 and the corresponding band assignment is given in Table 1.

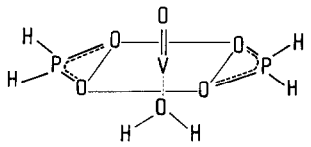


Fig. 1. Proposed structural arrangement for vanadyl(IV) hypophosphite.

Some interesting features of this spectrum are worth further comments.

In this case, the values of the P—H frequencies are displaced to higher wavenumbers, whereas those of the P—O bonds show a shift to lower wavenumbers, in comparison with that reported for the free hypophosphorous acid and for some ionic hypophosphites.[7,8] This behaviour clearly indicates that the $H_2PO_2^-$ moieties act as bidentate ligands of the metallic centre. Its coordination produces a weakening of the P—O bonds and a concomitant increase of the strength of the P—H bonds.

The shift of the $\nu_{as}(PO_2)$, which in the free acid is found at 1184 cm^{-1},[7] produces a partial overlap with the PH_2-scissor band, which appears only as a weak shoulder on the higher-frequency side of the $\nu_{as}(PO_2)$ band.

It is very interesting to observe a weak band placed at 912 cm^{-1} assignable to the PH_2-twisting mode.

Table 1. Assignments of the IR spectrum of $VO(PO_2H_2)_2 \cdot H_2O$

Band position (cm^{-1})	Assignment
3520	ν(OH)
3470	
3242	(?)
3218	$2\delta(H_2O)$
2448	$\nu_s(PH_2)$
2420	$\nu_{as}(PH_2)$
2270	$2(PH_2)_{scis.}$
2145	$2(PH_2)_{wag.}$
1938	$(PH_2)_{scis.} + (PH_2)_{rock.}$
1618	$\delta(H_2O)$
1135	$(PH_2)_{scis.}$
1112	$\nu_{as}(PO_2)$
1074	$(PH_2)_{wag.}$
1043	$\nu_s(PO_2)$
975	ν(VO)
921	$(PH_2)_{twist.}$
811	$(PH_2)_{rock.}$
590 sh	$(H_2O)_{wag.}$
518	$(PO_2)_{scis.}$
436 sh	$(H_2O)_{rock.}$(?)
412	$\nu(V–OH_2)$

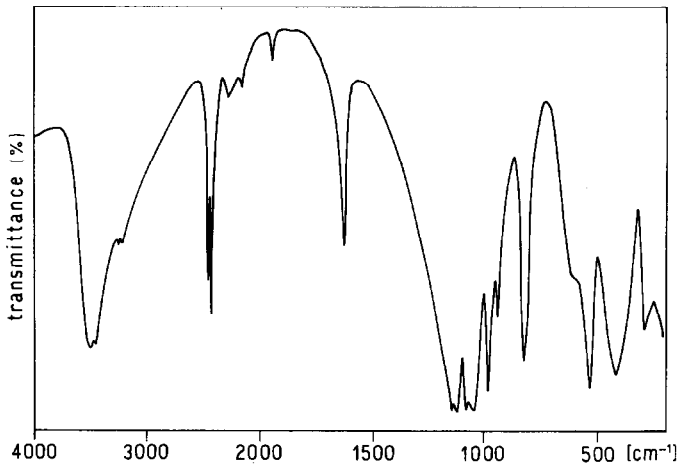


Fig. 2. IR spectrum of $VO(PO_2H_2)_2 \cdot H_2O$.

This band is forbidden for C_{2v}-symmetry[7] and its appearance is indicative of a further lowering in symmetry of the ligands in the complex.

One of the two very weak bands at 3242 and 3218 cm^{-1} can be assigned to the first overtone of the water bending mode, whereas the origin of the other one remains uncertain.

The fact that the $\delta(H_2O)$ band shows a certain asymmetry (a weak shoulder is clearly identified at *ca* 1623 cm^{-1}) can probably be related to the presence of two crystallographically non-equivalent water molecules in the unit cell. If this were true, the presence of two overtones of this bending mode could be explained.

The bands due to the coordinated water (wagging, rocking and V–OH_2 stretch) have been assigned by comparison with the spectra of other aquo complexes.[8,9]

The typical V=O stretching band appears as a very well defined and intense band at 975 cm^{-1}. For comparative purposes we have also measured the IR spectrum of pure $VOSO_4 \cdot 5H_2O$ under the same experimental conditions; in this case the ν(VO) band was found at 980 cm^{-1}. The variations of this stretching mode are commonly associated with changes in the electronic density in the metal *d*-orbitals due to ligand-to-metal $p_\pi \rightarrow d_\pi$ donation (cf. for example, Ref. 10) which indirectly affects the strength of the V—O bond. The present results would imply that the $p_\pi \rightarrow d_\pi$ donation of the $H_2PO_2^-$ ligands is not very different from that of the water oxygen atoms, although a little stronger.

Electronic spectrum. Although the band assignments of the electronic spectra of vanadyl complexes are still not settled (cf. Refs 11 and 12) there seems to be enough evidence favouring the level ordering proposed by Ballhausen and Gray.[13,14] According to their treatment, three "*d–d*" bands related to the $b_2 \rightarrow e_\pi^*$, $b_2 \rightarrow b_1^*$ and $b_2 \rightarrow a_1^*$ transitions, could be observed, although the third one is frequently obscured by the tail of more intense, charge-transfer bands. This is also the situation in our case, in which only two "*d–d*" transitions located at 12,300 cm^{-1} ($\varepsilon = 19.5$) and 15,600 cm^{-1} ($\varepsilon = 8.9$) are observed. In addition, two change-transfer bands, placed at 40,160 cm^{-1} ($\varepsilon \sim 270$) and 48,310 cm^{-1} ($\varepsilon \sim 700$), have been measured.

The crystal field splitting parameter $10Dq$ can be directly obtained from the $b_2 \rightarrow b_1^*$ transition.[13,14] The observed value of 15,600 cm^{-1} is in agreement with those obtained for other simple VO^{2+} complexes with a similar VO^{2+} environment.[15]

ESR spectrum and magnetic susceptibility. In order to obtain a wider insight into the electronic properties and the metal–ligand interactions in this complex, we have also measured its ESR spectrum and investigated its magnetic behaviour at different temperatures.

The first derivative of the ESR spectrum of a powdered sample gives practically an isotropic pattern from which a g_0 value of 1.97 is obtained. This value clearly lies in the region which is considered as typical for a $VO(O_4)$ environment (cf. Ref. 16).

The magnetic susceptibilities were measured in the range between 100 and 300 K. The substance obeys the Curie–Weiss law and a least-squares refinement of the experimental data shows that the Weiss constant, θ, has a value of -7.86 K, whereas the Curie constant is equal to 0.373.

X-ray diffraction measurements. The compound shows a very complex powder pattern, which is given in Table 2. The intensities of the peaks included in Table 2 are relative values, obtained by setting the

Table 2. X-ray powder diagram of $VO(PO_2H_2)_2 \cdot H_2O$

d (Å)	I/I_o	d (Å)	I/I_o
6.32	3	2.868	22
5.48	100	2.749	6
4.05	41	2.532	10
3.90	5	2.394	6
3.76	1	2.341	4
3.74	1	2.309	2
3.59	9	2.257	2
3.425	9	2.236	4
3.305	16	2.122	7
3.200	25	2.077	5

value of the most intense line as equal to 100 and referring the intensity of all other lines to this value. No attempts have been done to index this powder diagram.

Thermal behaviour. TG and DTA diagrams have been recorded and the spectroscopic behaviour of the decomposition residues and intermediates, collected at different temperatures, were investigated.

As it has been already shown by Mawrow,[4] the heating of the vanadyl hypophosphite at 135–145°C causes a colour change from the characteristic bluish coloration to a light green tint, which he associates with the release of water. A further heating, up to 180°C, should produce the decomposition of the substance, which is accompanied with a new colour change from greenish to grey.

The DTA curve shows a very strong endothermic peak at 170°C, which is associated with a mass loss of *ca* 9.5%. This loss extends up to *ca* 200°C in the TG curve; above this temperature and up to 400°C neither new mass changes nor clearly defined DTA signals could be observed.

The controlled heating of samples in a crucible furnace in air, at different temperatures between 130 and 500°C, shows the following behaviour.

The mass loss is strongly dependent on the heating time, heating rate and final temperature.

If one places a sample in the warm furnace at 400°C a very violent reaction with spontaneous inflammation is observed, suggesting the rapid generation of PH_3 and/or H_2.

The characteristic $\nu(OH)$ and $\delta(H_2O)$ IR bands are present, even if the mass loss was greater than 8.4% (which is the percentage of H_2O in the compound). Although it is impossible to formulate a stoichiometric schema for the overall decomposition process, it is evident that, simultaneously with the loss of water, part of the $H_2PO_2^-$ ligand is decomposed, generating HPO_3^{2-} (or $H_2PO_3^-$) and PH_3 in a similar way as for pure H_3PO_2 (cf. Ref. 17).

In a second stage, the remaining hypophosphite is also transformed to phosphite, whereas the primarily generated phosphite is further degraded, probably with the loss of H_2. In this stage the VO^{2+} is probably reduced to V(III) and as a final consequence of this process some type of polymeric V(III) phosphite is formed. These last possibilities are in agreement with the well-known behaviour of V_2O_5 when it is heated with conc. H_3PO_4,[18–20] a process in which its gradual reduction to V(IV) and V(III) takes place. On the other hand, the IR spectra of the residues collected after heating treatments of $VO(PO_2H_2)_2 \cdot H_2O$ at 400°C closely resemble that of $V(PO_3)_3$.[20]

Acknowledgements—This work is supported by CONICET (Programa QUINOR) and CIC–PBA and is also a part of a special research program devoted to the chemistry and biochemistry of vanadium which is sponsored by the Foundation Volkswagenwerke (Hannover, F.R.G.). We are also indebted to G. Minelli (Istituto di Chimica Generale ed Inorganica, Universitá di Roma, Italy) for the magnetic susceptibility measurements.

REFERENCES

1. S. B. Etcheverry and E. J. Baran, *Z. Anorg. Allg. Chem.* 1979, **457**, 197.
2. S. B. Etcheverry, E. J. Baran and E. Diemann, *Z. Anorg. Allg. Chem.* 1982, **486**, 215.
3. S. B. Etcheverry and E. J. Baran, *Thermochim. Acta* 1984, **72**, 387.
4. F. Mawrow, *Z. Anorg. Allg. Chem.* 1907, **55**, 147.
5. A. Weiss and H. Witte, *Magnetochemie.* Verlag Chemie, Weinheim (1972).
6. W. H. Zachariasen and R. C. L. Mooney, *J. Chem. Phys.* 1954, **22**, 162.
7. R. W. Lovejoy and E. L. Wagner, *J. Phys. Chem.* 1964, **68**, 544.
8. H. Siebert, *Anwendungen der Schwingungsspektroskopie in der Anorganischen Chemie.* Springer, Berlin (1966).
9. K. Nakamoto, *Infrared and Raman Spectra of Inorganic and Coordination Compounds*, 3rd edition. John Wiley, New York (1978).
10. J. Selbin, L. H. Holmes, Jr and S. P. McGlynn, *J. Inorg. Nucl. Chem.* 1963, **25**, 1359.
11. J. Selbin, *Coord. Chem. Rev.* 1966, **1**, 293.
12. G. A. Kolawole and K. S. Patel, *J. Chem. Soc., Dalton Trans.* 1981, 1241.
13. C. J. Ballhausen and H. B. Gray, *Inorg. Chem.* 1962, **1**, 111.
14. E. J. Baran and S. B. Etcheverry, *Acta Sud Am. Quim.* 1983, **3**, 1.

15. A. B. P. Lever, *Inorganic Electronic Spectroscopy*. Elsevier, Amsterdam (1968).
16. L. J. Boucher, E. C. Tynan and T. F. Yen, in *Electronic Spin Resonance Spectra of Metal Complexes* (Edited by T. F. Yen). Plenum Press, New York (1969).
17. J. C. Bailar, H. J. Emeléus, R. Nyholm and A. F. Trotman-Dickenson (Eds), *Comprehensive Inorganic Chemistry*, Vol. 2, p. 470. Pergamon Press, Oxford (1973).
18. B. C. Tofield, G. R. Crane, G. A. Pasteur and R. C. Sherwood, *J. Chem. Soc., Dalton Trans.* 1975, 1806.
19. B. Nador, *Acta Chim. Sci. Hung.* 1964, **40**, 1.
20. A. V. Lavrov, L. S. Guzeeva and P. M. Fedorov, *Izv. Akad. Nauk SSSR, Neorg. Mater.* 1974, **10**, 2180.

Polyhedron Vol. 4, No. 10, pp. 1717–1719, 1985
Printed in Great Britain

0277–5387/85 $3.00+.00
© 1985 Pergamon Press Ltd

DITHIOPHOSPHINATES OF TRIVALENT IRON, RUTHENIUM AND OSMIUM

R. N. MUKHERJEE,* S. SHANKAR, V. S. VIJAYA and P. K. GOGOI
Department of Chemistry, Indian Institute of Technology, Powai, Bombay 400 076, India

(*Received* 31 *January* 1985; *accepted* 3 *April* 1985)

Abstract—Dithiophosphinates of Fe(III), Ru(III) and Os(III) have been prepared and their ESR studies indicate distortion from octahedral geometry. The tetragonal and rhombic splittings and the orbital reduction factors were calculated from the experimental g values for low-spin Ru(III) and Os(III) complexes. The metal–ligand covalency increases in the order Ru < Os.

There are few reports on ESR studies of low-spin d^5 Ru(III) and Os(III) complexes[1,2] and, in particular, complexes of these metals with sulphur donors have received much less attention.[3,4] These investigations are of interest because of the sensitive nature of the g values to small changes in the structure and also to the metal–ligand covalency and are found to be a good probe for molecular structure and bonding. In continuation of our earlier work[5,6] on dithiophosphinates of transition metals, we wish to report the synthesis and spectral studies on di-(2,4-dimethylphenyl)dithiophosphinato derivatives of trivalent iron, ruthenium and osmium. Detailed ESR studies were also carried out on a few other dithio compounds of ruthenium and osmium (doped in the corresponding rhodium matrix) which were briefly reported earlier.[7,8]

EXPERIMENTAL

All the chemicals used were of chemically pure grade. Dithiophosphinic acids were prepared by the procedure reported in the literature.[9]

Preparation of the complexes

$Fe(2,4\text{-}Me_2dtpi)_3$. A concentrated aqueous solution of ferric chloride was treated with a slight excess of $Na(2,4\text{-}Me_2dtpi)$ in methanol. The dark green complex which separated out was washed with a water–methanol (80:20) mixture and dried in vacuum. Found: C, 59.12; H, 5.26; S, 19.62; Fe, 5.66; $C_{48}H_{54}P_3S_6Fe$ requires: C, 59.31; H, 5.60; S, 19.79; Fe, 5.75%.

$Ru(2,4\text{-}Me_2dtpi)_3$. Ruthenium trichloride trihydrate (0.5 g) in methanol was mixed with a methanolic solution of sodium salt of the ligand (2 g). On evaporation a chocolate brown complex was precipitated out. This was filtered, washed with methanol and recrystallised from a chloroform–methanol mixture. Found: C, 56.32; H, 5.25; S, 18.68; $C_{48}H_{54}P_3S_6Ru$ requires: C, 56.67; H, 5.35; S, 18.91%.

$Os(2,4\text{-}Me_2dtpi)_3$. The chocolate brown complex was prepared by mixing a methanolic solution of $(NH_4)_2OsCl_6$ (0.5 g) and the sodium salt of the ligand (1.5 g). The complex which separated out was washed with methanol and recrystallised from a chloroform–methanol mixture. Found: C, 51.87; H, 4.70; S, 17.32; $C_{48}H_{54}P_3S_6Os$ requires: C, 52.11; H, 4.92; S, 17.39%.

Physical measurements

The electronic spectra were recorded on a Varian Super Scan 3 UV visible spectrophotometer. The IR spectra were obtained on a Pye–Unicam SP-2000 IR spectrophotometer. ESR spectra of the powdered samples were carried out at $\approx$ 77 K on a Varian E-112 ESR spectrometer (X-band) by using TCNE ($g = 2.00277$) as g marker. Magnetic measurements were made either by Gouy's method or by Evan's NMR technique.

RESULTS AND DISCUSSION

$Fe(2,4\text{-}Me_2dtpi)_3$

The room temperature magnetic moment is 5.80 BM, indicating a d^5 high-spin complex. The

* Author to whom correspondence should be addressed.

Table 1. Typical g values for Ru(III) and Os(III) complexes

Complex[a]	g_1	g_2	g_3
Ru(2,4-Me_2dtpi)$_3$	2.102	2.026	1.962
Ru(3,4-Me_2dtpi)$_3$	2.125	2.071	1.987
Ru(MeCldtpi)$_3$	2.110	2.034	1.978
Ru(Cl_2dtpi)$_3$	2.080	2.050	1.983
Ru(Medtpi)$_3$	2.257	2.077	1.948
Os(2,4-Me_2dtpi)$_3$	2.084	2.029	1.962
Os(MeCldtpi)$_3$	2.054	2.019	1.939
Os(Medtpi)$_3$	2.059	2.007	1.965

[a] 2,4-Me_2dtpi, di(2,4 - dimethylphenyl)dithiophosphinate; 3,4-Me_2dtpi, di(3,4 - dimethylphenyl)dithiophosphinate; MeCldtpi, di(2 - methyl - 5 - chlorophenyl)-dithiophosphinate; Cl_2dtpi, di(3,4 - dichlorophenyl)dithiophosphinate; Medtpi, di(p - tolyl)dithiophosphinate.

electronic spectrum shows bands at 16,300, 19,100, 23,250, 28,250, 28,600 and 40,650 cm^{-1} and is similar to that of other dithio complexes.[10,11] The spectra of Fe(III) complexes are likely to be influenced by charge-transfer transitions in the visible region[12] and therefore no attempt has been made to assign the observed bands. The IR spectrum shows a P—S stretching frequency at 632 cm^{-1}.

ESR spectrum of the complex at liquid-nitrogen temperature gave a broad signal at $g = 8.24$; in addition, a signal at $g = 4.46$ and a weak signal at $g = 1.87$ were obtained. This observation is similar to those reported for high-spin octahedral Fe(III) complexes.[13]

M(2,4-Me_2dtpi)$_3$ (M = Ru *or* Os)

The room-temperature magnetic moments for these complexes were observed to be 1.67 and 1.79 BM, respectively. The absorption spectrum of the ruthenium compound shows bands at 23,600, 28,500, 34,700 and 40,000 cm^{-1}, while for the osmium compound bands were observed at 17,500, 21,750, 25,600 and 39,400 cm^{-1}. The electronic spectra of Ru(III) and Os(III) complexes have not been fully understood and in most cases it is dominated by charge-transfer bands.[14,15] The bands at 640 and 638 cm^{-1} in the IR spectrum were assigned to P—S stretching vibrations for ruthenium and osmium compounds, respectively.

The ESR data have been interpreted by using the theory described by various authors.[16–18] The observation of three principal g values showed magnetic anisotropy, with $g_1 = 2.080$–2.257, $g_2 = 2.026$–2.077, and $g_3 = 1.948$–1.987 for ruthenium complexes and $g_1 = 2.054$–2.084, $g_2 = 2.007$–2.029, and $g_3 = 1.939$–1.965 for osmium complexes. The g values are given in Table 1.

The paramagnetic resonance experiments give only the absolute principal g values and so neither their signs nor the correspondence of g_1, g_2 or g_3 to g_x, g_y or g_z are known. There are 48 possible combinations depending on the labelling (x, y, z) and signs chosen for the experimental g values. We consider all the possible combinations of experimental g values and their signs for acceptable results. In the present case we have taken g_1 and g_2 to be negative, g_3 to be positive and $g_1 > g_2 > g_3$ to get a reasonable value of k (< 1.0). For other solutions k values are not within the limit and have been rejected. This yielded values of A (0.048–0.094), B (0.995–0.999), C (-0.010 to -0.038), k (0.33–0.76), V/λ (-4.68 to -11.09), Δ/λ (9.57 – 16,14), V/Δ (0.36–0.86), $\Delta E_1/\lambda$ (10.44–16.60) and $\Delta E_2/\lambda$ (12.56–18.50) for ruthenium complexes and A (0.085–0.117), B (0.993–0.996), C (-0.017 to -0.028), k (0.20–0.29), V/λ (-2.08 to -6.86), Δ/λ (6.57–9.85), V/Δ (0.32–0.70), $\Delta E_1/\lambda$ (6.37–10.45) and $\Delta E_2/\lambda$ (7.46–12.48) for osmium complexes. All of these values have been calculated by using a Fortran-IV computer programme and are given in Table 2.

Table 2. Parameters calculated from ESR data

Complex[a]	A	B	C	k	V/λ^b	Δ/λ^b	V/Δ	$\Delta E_1/\lambda^b$	$\Delta E_2/\lambda^b$
Ru(2,4-Me_2dtpi)$_3$	0.087	0.996	−0.030	0.33	−7.12	9.76	0.73	10.44	12.56
Ru(3,4-Me_2dtpi)$_3$	0.048	0.999	−0.0115	0.76	−7.99	16.14	0.50	16.60	18.50
Ru(MeCldtpi)$_3$	0.064	0.998	−0.025	0.45	−11.09	13.64	0.81	15.09	18.01
Ru(Cl_2dtpi)$_3$	0.058	0.998	−0.010	0.44	−4.68	13.03	0.36	12.99	14.36
Ru(Medtpi)$_3$	0.094	0.995	−0.038	0.71	−8.20	9.57	0.86	10.59	13.05
Os(2,4-Me_2dtpi)$_3$	0.089	0.996	−0.023	0.29	−4.94	8.99	0.55	9.18	10.77
Os(MeCldtpi)$_3$	0.117	0.993	−0.017	0.20	−2.08	6.57	0.32	6.37	7.46
Os(Medtpi)$_3$	0.085	0.996	−0.028	0.20	−6.86	9.85	0.70	10.45	12.48

[a] Abbreviations as in Table 1.

[b] In units of spin–orbit coupling constant, λ.

The orbital reduction factor, k, cannot be equated purely with delocalisation or covalency but other unaccounted for effects are to be considered.[19] These effects were taken into account by some authors[1,20,21] and, in particular, Cotton[22] has shown that for $Fe(dtc)_3$ and $Fe(exan)_3$ complexes k can be reduced from 1.07–1.08 to 0.83–0.87 by considering $t_2^4(^3T_1)e$ and $t_2^4(^1T_2)e$ configurations mixed into $t_{2g}^5(^2T_2)$ by electrostatic interactions. However, spin–orbit and charge-transfer mixing have not been taken into account. Further, Desimone[4] has concluded that out of two fits for some ruthenium and osmium dithio compounds the one with a lower value of k is more likely to be an acceptable solution, even though the second one cannot be rejected out of hand. It is clear from Table 2 that the low values of k for Os(III) complexes compared to their corresponding Ru(III) analogues indicate that the metal–ligand covalency increases in the order Ru < Os.

X-ray and Mössbauer studies of iron dithio compounds[23,24] show considerable distortion from O_h-symmetry. Ru(III) and Os(III) complexes show low, relatively temperature-independent magnetic moments,[2,14] indicating a considerable distortion from idealised symmetry. From hyperfine splitting analysis Desimone[4] has concluded that the sulphur compounds of ruthenium and osmium have distorted structures. The ratio V/Δ gives information about the rhombicity of the complex. In the present case V/Δ is less than 1.0 indicating that the tetragonal splitting is greater than the rhombic splitting. Table 2 shows that ruthenium compounds have larger V/Δ values compared to their corresponding osmium analogues. The V/λ and Δ/λ values also follow the same trend except for $Ru(Medtpi)_3$ and $Os(Medtpi)_3$ in which Δ/λ value is almost equal. The high values of Δ/λ indicate considerable distortion of the complexes and the ground state consists of the d_{xy}-hole. Geometric factors and anisotropy in covalent bonding may contribute for this distortion. The latter factor probably plays an important role in distorting the molecules.

The relative energies of the ground and two excited Kramer's doublet states were calculated and it is found that the orbital reduction factor decreases as ΔE_2 decreases. As ΔE_2 is related to bond length,[3] the lower value of k is indicative of the increased covalency of the metal–ligand bond. For these compounds the values of $\Delta E_1/\lambda$ and $\Delta E_2/\lambda$ are in the order Ru > Os, which confirms that osmium complexes are somewhat more covalent than the corresponding ruthenium analogues.

REFERENCES

1. S. Sakaki, N. Hagiwara, Y. Yanse and A. Ohyoshi, *J. Phys. Chem.* 1978, **82**, 1917.
2. O. K. Medhi and U. Agarwala, *Inorg. Chem.* 1980, **19**, 1381.
3. A. Hudson and M. J. Kennedy, *J. Chem. Soc. A* 1969, 1116.
4. R. E. Desimone, *J. Am. Chem. Soc.* 1973, **95**, 6238.
5. R. N. Mukherjee and M. D. Zingde, *J. Inorg. Nucl. Chem.* 1973, **35**, 696.
6. R. N. Mukherjee and R. Raghunand, *J. Inorg. Nucl. Chem.* 1981, **43**, 171.
7. R. N. Mukherjee and P. K. Gogoi, *Indian J. Chem.* 1980, **19A**, 455.
8. R. N. Mukherjee and V. S. Vijaya, *Indian J. Chem.* 1982, **21A**, 427.
9. W. A. Higgins, P. W. Vogel and W. G. Craig, *J. Am. Chem. Soc.* 1955, **77**, 1864.
10. C. K. Jorgensen, *J. Inorg. Nucl. Chem.* 1962, **24**, 1571.
11. E. Cervone, F. D. Camassei, M. L. Luciani and C. Furlani, *J. Inorg. Nucl. Chem.* 1969, **13**, 1101.
12. A. H. Ewald, R. L. Martin, E. Sinn and A. H. White, *Inorg. Chem.* 1969, **8**, 1837.
13. G. R. Hall and D. N. Hendrickson, *Inorg. Chem.* 1976, **15**, 607.
14. G. A. Heath and R. L. Martin, *Aust. J. Chem.* 1970, **23**, 1721.
15. L. Dubicki, J. Ferguson, E. R. Krauusz, P. A. Lay and M. Maeder, *J. Phys. Chem.* 1984, **88**, 3940.
16. K. W. H. Stevens, *Proc. R. Soc.* 1953, **A219**, 542.
17. B. Bleaney and M. C. M. O'Brien, *Proc. Phys. Soc.* 1956, **69**, 1216.
18. J. S. Griffith, *The Theory of Transition Metal Ions*, pp. 364–373. Cambridge University Press, Cambridge (1961).
19. J. B. Raynor and B. G. Jeliazkowa, *J. Chem. Soc., Dalton Trans.* 1982, 1185.
20. N. J. Hill, *J. Chem. Soc., Faraday Trans.* 1972, **2**, 427.
21. D. Kaplan and G. Navon, *J. Phys. Chem.* 1974, **78**, 700.
22. S. A. Cotton, *Inorg. Nucl. Chem. Lett.* 1972, **8**, 371.
23. B. F. Hoskins and B. P. Kelley, *J. Chem. Soc., Chem. Commun.* 1970, 45.
24. R. Beckett, G. A. Heath, B. F. Hoskins, B. P. Kelly, R. L. Martin, I. A. G. Roos and P. L. Weickhardt, *Inorg. Nucl. Chem. Lett.* 1970, **6**, 257.

Polyhedron Vol. 4, No. 10, pp. 1721–1726, 1985
Printed in Great Britain

0277–5387/85 $3.00 + .00
© 1985 Pergamon Press Ltd

CAN THE PENTAZOLE ANION (N_5^-) BE ISOLATED AND/OR TRAPPED IN METAL COMPLEXES?

M. T. NGUYEN, M. A. McGINN and A. F. HEGARTY†
Department of Chemistry, University College, Belfield, Dublin 4, Ireland

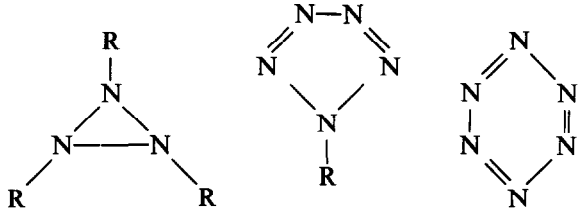
and

J. ELGUÉRO
Instituto de Química Médica, CSIC, Juan le la Cierva 3, 28006-Madrid, Spain

(*Received* 19 *February* 1985; *accepted* 3 *April* 1985)

Abstract—The 1,3-dipolar cycloreversion pathway of the pentazole anion (N_5^-) to the azide anion (N_3^-) plus dinitrogen (N_2) has been investigated using *ab initio* methods. At the MP4SDQ/6-31 + G* level of theory plus zero-point energy contributions, the pentazole anion is predicted to lie at 31 kcal mol^{-1} above the $N_3^- + N_2$ system but the energy barrier for decomposition is 22 kcal mol^{-1}. This indicates that the pentazole anion could be isolated in an inert matrix at low temperature. Comparison between extended Hückel calculations on the $(N_5)M(CO)_3$ and $(C_5H_5)M(CO)_3$ complexes (with M = Fe^{2+}, Mn^+ and Cr) suggests that the N_5^- complexes would be formed if the fragments could be brought together. Predicted vibrational frequencies of the N_5^- anion are also reported.

The chemistry of homocycles containing exclusively nitrogen atoms is only in its first stage of development. For instance, triaziridines (**I**)[1–3] and pentazoles (**II**)[4,5] are at present the only stable or isolable saturated and unsaturated *N*-homocycles, respectively, for which some spectroscopic data and *ab initio* calculations on model molecules (N_3H_3[6] and N_5H[7]) are available.

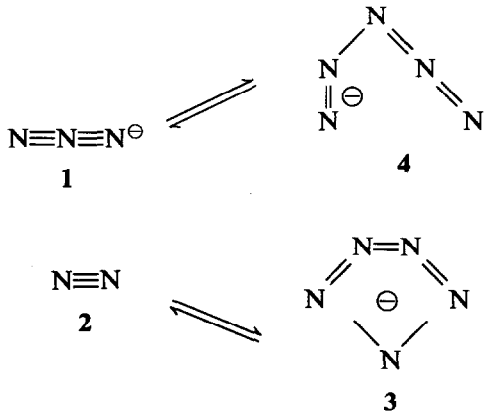


I **II** **III**

The question of whether hexazine (**III**), the all-nitrogen analogue of benzene, is stable enough to be detected has recently attracted the interest of several groups.[8–13] However, experimental[8] and theoretical[9–13] studies have as yet been inconclusive as to the existence of this intriguing species.[12]

We have recently reported an *ab initio* study of the structure and reactivities towards cycloreversion and cycle-chain isomerisation of the pentazole anion, N_5^- (**3**) (the all-nitrogen analogue of the cyclopentadienyl anion) (Scheme 1).

This study suggested that **3** is of higher energy than the azide anion (**1**) plus molecular nitrogen (**2**) system, but much more stable than the pentazene anion (**4**) and might constitute a reasonable synthetic target. Nevertheless, this prediction should be regarded with caution, because the calculations on



1 **4**

2 **3**

Scheme 1.

† Author to whom correspondence should be addressed.

which it is based were performed at the SCF level using a rather limited basis set (4-31G).

In order to gain further insight into the stability of the pentazole anion, it seems useful to reinvestigate the **3** supersystem at higher levels of accuracy by extending the basis set and including the effects of electron correlation in the wave functions.

In addition, the possibility of trapping the anion in a metal complex such as $(N_5)Mn(CO)_3$ (mentioned in our earlier work,[14] but with theoretical support) is also worth examining.

The aims of the present work are twofold: firstly, to determine the effects of basis set and electron correlation on the energy differences between stationary points in the 1,3-dipolar cycloaddition (or cycloreversion) pathway connecting fragments N_3^- (**1**) plus N_2 (**2**) to the anion **3**. Because of the large energy differences between **3** and **4** (68 kcal mol^{-1} at 4.31 G[14]), we have excluded the two remaining pathways of Scheme 1 involving **4** from this study. Secondly, to examine whether **3** is a possible candidate for metal complexation by performing some extended Hückel (EH) calculations[15] on the systems $(N_5)M(CO)_3$ with M = Fe^{2+}, Mn^+ and Cr.

We used the Gaussian-82 program[16] for *ab initio* calculations and the FORTICON-8 program[17] for EHT calculations. Details of the choice of semi-empirical parameters used for the latter calculations are given in the appendix. We will present the results obtained in two separate sections.

RESULTS AND DISCUSSION

Ab initio *calculations*

The molecular geometries of stationary points in the N_5^- (**3**) supersystem determined using the force method with analytical gradients and the 3-21 G basis set[18] are displayed in Fig. 1. This basis set has been shown to provide reasonable geometries for anions.[19]

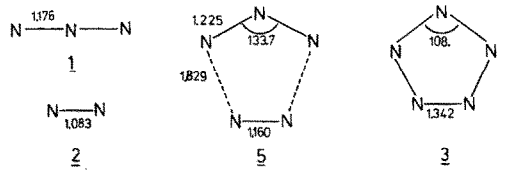


Fig. 1. 3-21G optimized geometries of species considered: N_3 (**1**), N_2 (**2**), transition state (**5**) and pentazole anion (**3**). Bond lengths in Å and bond angles in degrees.

Structure **5** is the transition state connecting isolated fragments **1**+**2** to **3**. The N—N bond lengths of 1.176 Å in **1** are comparable to the experimental values of 1.15–1.18 Å found in various ionic azides.[20] By comparison with previous 4-31 G geometries,[14] the 3-21G N—N bond lengths are somwhat shorter for **1** (4-31G: 1.20 Å), but slightly larger in both **3** (4-31G: 1.32 Å) and **5**.

It is also worth noting that the energy surface near the D_{5h}-minimum of **3** is not flat, in contrast to that of the corresponding point for the hexazine (N_6) molecule.[11] An energy increase of about 2 kcal mol^{-1} accompanies a shift of 0.02 Å in the N—N bond length.

In order to obtain improved relative energies, we have carried out single point SCF calculations on **1**, **2** and **5** employing the 3-21G optimized geometries and three basis sets: 6-31G, 6-31+G[21] (6-31G plus a set of diffuse *s*- and *p*-functions), 6-31G*[22] (plus a set of polarization *d*-functions) and 6-31+G* (including both diffuse and polarization functions; this basis set thus consists of 19 contracted Gaussian functions for each nitrogen atom). The correlation energies have been taken into account using Møller–Plesset perturbation theory to second, third and fourth order[23] (denoted MP2–MP4) making use of the HF/6-31G wave functions as references. The calculated total energies of the species considered at

Table 1. Calculated total energies of species considered at different levels (a.u.)

Method[a]	1	2	3	4
HF/3-21G	−162.27962	−108.30095	−270.52728	−270.57699
HF/6-31G	−163.15674	−108.86793	−271.94368	−271,99039
HF/6-31+G	−163.17957	−108.87166	−271.96162	−272.00822
HF/6-31G*	−163.25936	−108.94382	−272.10066	−272.17283
HF/6-31+G*	−163.28161	−108.94695	−272.12023	−272.19141
MP2/3-21G	−162.66638	−108.53298	−271.15879	−271.16499
MP2/6-31G	−163.54616	−109.10020	−272.58438	−272.58551
MP3/6-31G	−163.49379	−109.07850	−272.51482	−272.55068
MP4SDQ/6-31G	−163.52035	−109.09257	−272.55668	−272.57021

[a] Using HF/3-21G-optimized geometries given in Fig. 1.

Table 2. Relative energies (kcal mol^{-1}) of N_5^- species

	1+2	5	4	$\Delta E^{\neq}$ (5−4)
HF/3-21G	0.0	33.4	2.2	31.2
HF/6-31G	0.0	50.8	21.5	29.3
HF/6-31+G	0.0	56.0	27.0	29.0
HF/6-31G*	0.0	64.3	19.0	45.3
HF/6-31+G*	0.0	68.0	23.3	44.7
MP2/3-21G	0.0	25.5	21.6	3.9
MP2/6-31G	0.0	38.9	38.2	0.7
MP3/6-31G	0.0	36.0	13.6	22.4
MP4SDQ/6-31G	0.0	35.3	26.8	8.5
MP4SDQ/6-31+G*[a]	0.0	52.5	28.6	23.9
Estimated[b]	0.0	53.6	31.3	22.3

[a] Estimated from MP4SDQ/6-31G (see text).

[b] Including MP4SDQ/6-31+G* and ZPVE. The corrected zero-point vibrational energies are (kcal mol^{-1}): **1**, 6.1; **2**, 3.3; **4**, 12.1 and **5**, 10.5. The imaginary frequency of **5** is 646*i* (cm^{-1}).

different levels are collected in Table 1. The relative energy differences between stationary points as well as the energy barrier for the cycloreversion of **3** to fragments **1** and **2** are summarized in Table 2.

Firstly one sees that at all levels, the separate **1**+**2** system is calculated to be of lower ion energy than **3**. The 3-21G basis set overestimated the stability of the ring. In comparison with that determined by 6-31G for **3**, it is seen that diffuse functions and polarization functions act in opposite directions: the former destabilizes by 5.5 kcal mol^{-1} with respect to **1**+**2** whereas the latter stabilizes by 2.5 kcal mol^{-1}. The trend in the Møller–Plesset calculations is not continuous: MP2 raises the energy appreciably (16.2 kcal mol^{-1}), MP3 reduces it significantly (7.9 kcal mol^{-1}), while MP4SDQ raises it again (5.3 kcal mol^{-1}).

The situation concerning **5** is rather more homogeneous, both diffuse and polarization functions increasing the energy barrier for the 1,3-dipolar cycloaddition of **1** to **2**, while the correlation energies at all orders tend to reduce it.

For both structures **4** and **5**, we can note a certain additivity of the basis set effect. For example, the global modifications found at the HF/6-31+G* level are slightly smaller than the sum of the changes observed in separate calculations.

More interesting perhaps is the variation in magnitude of the energy barrier for the 1,3-dipolar cycloreversion of **4** ($\Delta E^{\neq}$, Table 2). An interesting feature is that diffuse functions do not modify this quantity. As is usually observed, the modifications created by polarization functions and correlation energies cancel each other, the former increasing the barrier while the latter decreases it.

As an estimation considering both basis set and electron effects, the MP4SDQ/6-31G* values reported in Table 2 were obtained from the additivity relationship:[24,25]

$$\Delta E(\text{MP4SDQ/6-31G*}) \approx \Delta E(\text{MP4SDQ/6-31G}) + \Delta E(\text{HF/6-31+G*}) - \Delta E(\text{HF/6-31G}).$$

These values, together with the addition of a contribution for zero-point vibrations, thus constitute our best relative energies. The zero-point vibrational energy contributions have been determined from HF/3-21G and scaled by a factor of 0.95 (see Table 3). Hence our best values in this work predict that **3** lies about 31 kcal mol^{-1} above the **1**+**2** system and can be decomposed to the latter by means of an energy barrier of 22 kcal mol^{-1}. This indicates that **3** could hardly be isolated in solution or even in the gas phase. Nevertheless, such an energy barrier seems to be sufficiently large for this species to be isolated, for example in an ethanol matrix at low temperature.[8] Under such conditions, intermolecular hydrogen bonds of the O—H...N type

Table 3. Predicted vibrational frequencies (cm^{-1}) for **3** compared with those of **1**

3				**1**			
	HF/3-21G		Predicted[a]		HF/3-21G		Experimental[b]
E_1'	1210	1150	Stretching	Σ_u	2007	2020	Asymmetric stretch
E_2'	1188	1129	Stretching	Σ_g	1396	1350	Symmetric stretch
A_1'	1185	1126	Breathing				
E_2'	878	834	Bending	Π_u	673	640	Bending
E_2''	806	766	Out-of-plane				

[a] From HF/3-21G and scaled by 0.95 (see text).

[b] Taken from Ref. 26.

might be expected to occur, reducing the destabilizing interaction between nitrogen lone pairs of **3** and hence favouring the existence of the anion.

On the other hand, the energy barrier for the 1,3-dipolar cycloaddition turns out to be 53 kcal mol^{-1}. It can be concluded that **3** would not be involved in a hypothetical process of molecular nitrogen fixation by azide.

This discussion raises the question to what extent the above estimation is definitive. The answer to this is somewhat equivocal, because the geometries of stationary points were not optimized at higher levels of accuracy. As seen in Table 2, the energy differences change significantly and unhomogeneously in going from one level to another. A definite estimation can only be provided from a determination of stationary-point geometries at the MP4SDQ/6-31G* level (diffuse functions can be omitted). At the present time, our computational resource precludes such calculations.

In summary, the present theoretical study suggests that **3** could be isolated in a matrix at low temperature. In order to assist eventual further experiment, the predicted vibrational frequencies for **3** are collected in Table 3. A comparison between HF/3-21G and experimental frequencies of **1** (see Table 3) emphasizes that the calculated frequencies were overestimated by about 4–5%. To provide more realistic frequencies, the HF/3-21G values can thus be reduced by an average scale factor of 0.95. The N—N stretching frequencies in **3** are a little smaller than those relevant to the symmetric stretching mode of **1**. The out-of-plane mode (E_2'') frequency is about twice those in the hypothetical hexazine (318 cm^{-1}, DZP[11]) or benzene (404 cm^{-1}, IR).

EH calculations

The results of EH calculations show that in transforming the cyclopentadienyl into **3** by successive replacement of the C—H groups by N atoms, the σ-character MOs become destabilized by "lone pair–lone pair" type repulsions, while there is a steady decrease in the energy of the π-MOs. In consequence, the $1e_1''$ MO, which constitutes the HOMO of $(C_5H_5)^-$ lies below the occupied $2e_2'$ and $2e_1'$ σ-type MOs in **3** (Fig. 2). The σ-character of the pentazole anion HOMO is in agreement with the results of the *ab initio* study, but the ordering of the $1e_1''$ and $2e_2'$ levels is the reverse of that obtained from the more rigorous treatment (see Table 4).

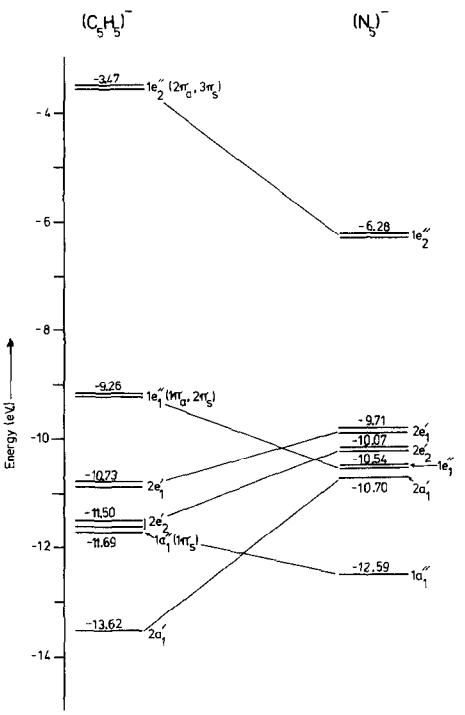


Fig. 2. Energy level diagram comparing the ordering of frontier MOs for $(C_5H_5)^-$ and N_5^-, calculated using the EH method (energies in eV).

The ability of transition metal bearing fragments to "trap" otherwise unknown organic species by formation of isolable complexes is well known, the

Table 4. Comparison of MO energy levels (eV) of **3** calculated by *ab initio* and EH methods

MO level[a]	HF/6-31G*	HF/6-31+G*	EH
Occupied			
$7a_1'$	−11.86	12.37	−10.70 ($2a_1'$)
$2e_2'$	−7.58	−8.09	−10.54 ($1e_1''$)
$1e_1''$ (π)	−7.01	−7.51	−10.07 ($2e_2'$)
$2e_1'$	−5.53	−6.64	−9.71 ($2e_1'$)
Virtual			
$1e_2''$ (π^*)	10.34	8.39	−6.28 ($1e_2''$)
$3e_2'$	17.47	8.42	6.45 ($3a_1'$)

[a] *Ab initio* MO levels.

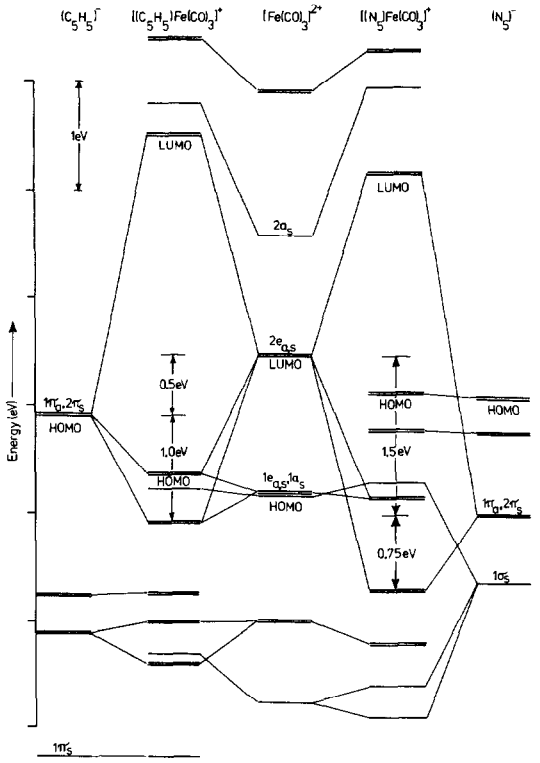


Fig. 3. Energy level diagram comparing the $[(C_5H_5)Fe(CO)_3]^+$ and $[(N_5)Fe(CO)_3]^+$ complexes (energies in eV).

classic example being that of cyclobutadienes, which may be isolated as the cationic complexes $[(C_4R_4)Fe(CO)_3]^+$.[27] To determine whether such a stabilization of **3** would be possible, calculations were performed on $(N_5)M(CO)_3$ complexes where $M = Fe^{2+}$, Mn^+ and Cr [analogous to the $(C_5H_5)M(CO)_3$ complexes which are known to exist]. An energy level diagram comparing the cyclopentadienyl and pentazole tricarbonyliron structures is shown in Fig. 3, with the levels traced to show their parentage in the MOs of the ring and $M(CO)_3$ fragments. The important frontier levels are labelled "s" or "a" depending upon whether they are symmetric or antisymmetric with respect to the plane of symmetry of the complex.

The bonding in $(C_5H_5)M(CO)_3$ species has been the subject of previous discussions.[28,29] A fragment MO analysis shows that the principal interaction occurs between the $1\pi_a$, $2\pi_s$ ($1e_1''$) HOMOs of the ring and the $2e_{a,s}$ and $1e_{a,s}$ LUMOs and HOMOs of the $M(CO)_3$ fragment. In the case of the iron complex, where the energy gap between these levels is ~ 0.5 eV, the stabilization is ~ 1 eV (see Table 5). In comparison, in the pentazole complex, the drop in energy of the $1\pi_a,2\pi_s$ MOs of **3** relative to $(C_5H_5)^-$ widens the energy separation from the $2e$ levels to 1.5 eV, and this reduces the stabilization to 0.75 eV. Nevertheless, this suggests that such a complex would be stable. Note that the HOMOs of $[(N_5)Fe(CO)_3]^+$ are composed of the non-bonding σ-HOMOs of **3**.

The calculations on the pentazole complex also show a very strong stabilisation of the $2a_1'$ ("σ_s") level of N_5 which has a very strong contribution from the nitrogen lone pairs by interaction with the $1a_s$ and another low-lying $M(CO)_3$ orbital of *s*-symmetry. This should be treated with caution in view of the fact that the EH method is known to underestimate the degree to which filled orbitals repel each other. However, if it is a genuine effect, it would greatly enhance the stability of the pentazole system.

The bonding pattern exhibited by the analogous chromium and manganese complexes is identical to the iron complex, but because the *e* LUMO lies at higher energy in the $Cr(CO)_3$ and $Mn(CO)_3^+$ fragments, they are predicted to be less stable (see Table 5).

These results suggest that the complexes would be stable if the fragments could be brought together, possibly by diffusion in an inert matrix at low temperature.

Table 5. Energy separation between $2e$ (LUMO) of $M(CO)_3$ and $1\pi_a,2\pi_s$ ($1e_1''$) MOs of $(C_5H_5)^-$ and N_5^- vs stabilization (eV)

Complex	ΔE $[2e_{a,s}-(1\pi_a,2\pi_s)]$	Stabilization from interaction of $2e_{a,s}$ and $1\pi_a,2\pi_s$
$[(C_5H_5)Fe(CO)_3]^+$	0.5	1.0
$[(N_5)Fe(CO)_3]^+$	1.5	0.75
$[(C_5H_5)Mn(CO)_3]$	1.25	0.65
$[(N_5)Mn(CO)_3]$	2.15	0.40
$[(C_5H_5)Cr(CO)_3]^-$	2.05	0.40
$[(N_5)Cr(CO)_3]^-$	2.75	0.25

Acknowledgements—We are indebted to the Department of Education (Irish Government) for financial support. A computer time grant provided by the UCD Computer Centre is gratefully acknowledged.

REFERENCES

1. L. Hoesch, C. Leuenberger, H. Hilpert and A. S. Dreiding, *Helv. Chim. Acta* 1982, **65**, 2682.
2. R. Prewo and J. H. Bieri, *Acta Cryst., Sect. A* 1981, **37**, C-208.
3. Y. Kim, J. N. Giljie and K. Seff, *J. Am. Chem. Soc.* 1977, **99**, 7075.
4. M. Witanwowski, L. Stefanisk, H. Januszewski, K. Bahadur and G. I. Webb, *J. Cryst. Mol. Struct.* 1975, **5**, 137.
5. J. D. Wallis and J. D. Dunitz, *J. Chem. Soc., Chem. Commun.* 1983, 910, and references therein.
6. M. T. Nguyen, J. Kaneti, L. Hoesch and A. S. Dreiding, *Helv. Chim. Acta* 1984, **67**, 1918.
7. M. Sana, G. Leroy, M. T. Nguyen and J. Elguéro, *Nouv. J. Chim.* 1979, **3**, 607.
8. A. Vogler, R. E. Wright and H. Kunkley, *Angew. Chem.* 1980, **92**, 745.
9. T. K. Ha, R. Cimiraglia and M. T. Nguyen, *Chem. Phys. Lett.* 1981, **83**, 317.
10. H. Huber, *Angew. Chem.* 1982, **94**, 71.
11. P. Saxe and H. F. Schaefer III, *J. Am. Chem. Soc.* 1983, **105**, 1761.
12. H. Huber, T. K. Ha and M. T. Nguyen, *J. Mol. Struct. Theochem.* 1983, **105**, 351.
13. M. Ramek, *J. Mol. Struct. Theochem.* 1984, **109**, 391.
14. M. T. Nguyen, M. Sana, G. Leroy and J. Elguéro, *Can. J. Chem.* 1983, **61**, 1435.
15. R. Hoffmann, *J. Chem. Phys.* 1963, **39**, 1397; R. Hoffmann and W. N. Lipscomb, *J. Chem. Phys.* 1962, **32**, 2872.
16. J. S. Binkley, M. J. Frisch, D. J. DeFrees, K. Raghavachari, R. A. Whiteside, R. Seeger, H. B. Schlegel and J. A. Pople, Gaussian-82 Program.
17. J. Howell, A. Rossi, D. Wallace, K. Haraki and R. Hoffmann, Forticon 8, Q.C.P.E. No. 344.
18. J. S. Binkley, J. A. Pople and W. J. Hehre, *J. Am. Chem. Soc.* 1980, **102**, 939.
19. J. Chandrasekhar, J. G. Andrade and P. K. Schleyer, *J. Am. Chem. Soc.* 1981, **103**, 5609.
20. A. Treinin, In *The Chemistry of the Azido Group* (Edited by S. Patin), p. 14. Interscience, New York (1971).
21. M. J. Frisch, J. A. Pople and J. S. Binkley, *J. Chem. Phys.* 1984, **80**, 3265.
22. P. C. Hariharan and J. A. Pople, *Theor. Chim. Acta* 1973, **28**, 213.
23. J. A. Pople, R. Krishnan, H. B. Schlegel and J. S. Binkley, *Int. J. Quantum Chem.* 1978, **14**, 545.
24. R. H. Nobes, W. J. Bouma and L. Radom, *Chem. Phys. Lett.* 1982, **89**, 497.
25. M. L. McKee and W. N. Lipscomb, *J. Am. Chem. Soc.* 1981, **103**, 4673.
26. R. L. Jackson, M. D. Pellerite and D. I. Brauman, *J. Am. Chem. Soc.* 1981, **103**, 1802.
27. R. Pettit and G. F. Emerson, *Adv. Organomet. Chem.* 1963, **1**, 1; M. S. Davis and C. S. Speed, *J. Organomet. Chem.* 1970, **21**, 401, and references therein.
28. T. H. Whitesides, D. L. Lichtenberger and R. A. Budnik, *Inorg. Chem.* 1975, **14**, 68.
29. T. A. Albright, P. Hofmann and R. Hoffmann, *J. Am. Chem. Soc.* 1977, **99**, 7546.
30. N. J. Fitzpatrick and G. H. Murphy, *Inorg. Chim. Acta* 1984, **81**, 41.
31. F. Herman and S. Skillman, *Atomic Structure Calculations*. Prentice-Hall, New Jersey (1963).
32. H. Basch, A. Viste and H. B. Gray, *Theor. Chim. Acta* 1965, **3**, 463.
33. J. H. Ammeter, H. B. Burgi, J. C. Thibeault and R. Hoffmann, *J. Am. Chem. Soc.* 1978, **100**, 3686.

APPENDIX

Semi-empirical parameters used in the EH calculations

Geometrical parameters. For the N_5^- ring, r(N–N) = 1.342 Å, and, in $(C_5H_5)^-$, r(C–C) = 1.418 Å and r(C–H) = 1.083 Å. The $M(CO)_3$ fragments were assumed to be octahedral with r(M–C) = 1.820 Å (Fe), 1.790 Å (Mn) and 1.840 Å (Cr) with r(C–O) = 1.150 Å in each case. The distance from the metal atom to the centroid of the ring was fixed at 1.712 Å for the Fe complexes, 1.821 Å for Mn and 1.686 Å for Cr.

Basis sets and diagonal coulomb terms. The basis set for the metal atoms consisted of valence Slater-type 3*d*, 4*s* and 4*p* atomic orbitals, and, for the first-row atoms, 2*s* and 2*p* AOs were used. 1*s* orbitals were included on the hydrogen atoms. The radial wave functions computed by Fitzpatrick and Murphy[30] as a least-squares fit to the SCF functions of Herman and Skillman[31] were chosen (double-zeta functions were used to represent the *d*-orbitals). A value of 1.3 was used as the exponent for the hydrogen 1*s* orbital. Valence orbital ionisation potentials for nine configurations of the metal atoms and two configurations of the first-row atoms were taken from the work of Basch *et al.*[32] as approximation to the diagonal terms of the coulomb matrix. Off-diagonal terms were calculated using the "weighted" Wolfsberg–Helmholz parameterisation.[33]

Polyhedron Vol. 4, No. 10, pp. 1727–1734, 1985
Printed in Great Britain

0277-5387/85 $3.00 + .00
© 1985 Pergamon Press Ltd

PREPARATION, STRUCTURES AND REACTIVITY OF TWO NEW ADDITION COMPOUNDS OF CARBODIIMIDES WITH DITUNGSTEN HEXA-*t*-BUTOXIDE

F. ALBERT COTTON* and EDWAR S. SHAMSHOUM
Department of Chemistry and Laboratory for Molecular Structure and Bonding, Texas A & M University, College Station, TX 77843, U.S.A.

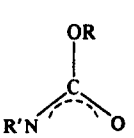
(*Received* 6 *February* 1985; *accepted* 19 *April* 1985)

Abstract—The reactions of ditungsten hexa-*t*-butoxide, $W_2(OCMe_3)_6$, with dicyclohexylcarbodiimide, $C_6H_{11}NCNC_6H_{11}$, and diisopropylcarbodiimide, $Me_2CHNCNCHMe_2$, afford the 1:1 adducts, $[W(OCMe_3)_3]_2(\mu\text{-}C_6H_{11}NCNC_6H_{11})$, **1**, and $[W(OCMe_3)_3]_2(\mu\text{-}C_3H_7NCNC_3H_7)$, **2**, respectively. These products were each shown by X-ray crystallography to be structurally homologous to the previously reported $[W(OCMe_3)_3]_2(\mu\text{-}CH_3C_6H_4NCNC_6H_4CH_3)$ and similar to $[W(OCMe_3)_3(\mu\text{-}C_6H_5NCO)$. It has been shown that the $[W(OCMe_3)_3]_2(\mu\text{-RNCNR})$ compounds fail to react with further RNCNR, with PhNCO, PMe_3, $LiOCMe_3$ or $LiOCHMe_2$, CO or CO_2, and also that $[W(OCMe_3)_3]_2(\mu\text{-PhNCO})$ does not afford any defined product when treated with $C_6H_{11}NCNC_6H_{11}$. Compounds **1** and **2** were fully characterized by IR and NMR spectroscopy and by X-ray crystallography. Compound **1** crystallizes in space group $C2/c$ with unit cell dimensions $a = 13.481(3)$ Å, $b = 18.129(4)$ Å, $c = 18.244(2)$ Å, $\beta = 97.54(1)°$, $V = 4420(2)$ Å^3, $Z = 4$. It was refined to $R = 0.0375$, $R_w = 0.0475$. Compound **2** crystallizes in space group $P2_1/c$ with unit cell dimensions $a = 14.752(2)$ Å, $b = 12.157(3)$ Å, $c = 22.189(3)$ Å, $\beta = 97.03(2)°$, $V = 3949(2)$ Å^3, $Z = 4$. The structure was refined to $R = 0.053$, $R_w = 0.059$. Each molecule has C_2-symmetry, with two $W(OCMe_3)$ units united by RNCNR bridges across W—W distances of 2.490(1) and 2.485(1) Å for **1** and **2**, respectively.

It has recently been reported[1] that $W_2(OCMe_3)_6$ as well as several $Mo_2(OR)_6$ compounds react with organic isocyanates to give products in which two RNCO molecules have been inserted into M—OR bonds, as shown in eqn (1):

$$W_2(OCMe_3)_6 + 2PhNCO \rightarrow W_2(OCMe_3)_4[\mu\text{-PhNC(OCMe}_3)O]_2. \quad (1)$$

The products have the molecular formulas $M_2(OR)_4[\mu\text{-R'NC(OR)O}]_2$, where R' originates from the R'NCO reactant. The bridging ligands are of type **a**. We then used a related "heterocumulene" molecule, R'N=C=NR', where R' = *p*-tolyl with $W_2(OCMe_3)_6$ and found that the only product is an adduct, $[W(OCMe_3)_3]_2(\mu\text{-}C_7H_7NCNC_7H_7)$, in which no insertion into W—O bonds has occurred.[2] We have also shown[3] that the reaction of $W_2(OCMe_3)_6$ with PhNCO proceeds by way of an initial 1:1 adduct much like that obtained as the only product with $C_7H_7NCNC_7H_7$. This has led us: (a) to examine the reactions of other carbodiimides with $W_2(OCMe_3)_6$; (b) to determine whether the $[W(OCMe_3)_3]_2(\mu\text{-RNCNR})$ adducts would react further with reagents such as excess RNCNR, RNCO, PMe_3, CO or CO_2; and (c) to see whether $[W(OCMe_3)_3]_2(\mu\text{-PhNCO})$ would react with RNCNR. The results of all of these studies, carried out to improve our understanding of the capacity of $W_2(OCMe_3)_6$ to react with heterocumulene type molecules in general, are reported here.



a

EXPERIMENTAL

Ditungsten hexa-*t*-butoxide was prepared[4] by reduction of WCl_4 with Na/Hg in THF at −10°C in

* Author to whom correspondence should be addressed.

the presence of $LiOCMe_3$. The product was recrystallized from hexane at $-10°C$. Dicyclohexylcarbodiimide was obtained from Aldrich Chemical Co. and diisopropyl carbodiimide was purchased from Pfaltz & Bauer Chemical Co.

IR spectra were measured on a Perkin–Elmer 783 spectrometer using KBr pellets. Proton NMR spectra were measured on C_6D_6 solutions at 25°C using a Varian XL-200 PFT spectrometer. Chemical shifts (δ) are specified in ppm downfield from TMS. The ^{13}C NMR spectrum of **2** was measured on a Varian FT-80 spectrometer in C_6D_6 solution. Chemical shifts are again given in ppm downfield from TMS.

Preparation of $[W(OCMe_3)_3]_2(\mu\text{-}C_6H_{11}NCNC_6H_{11})$ **(1)**

Under an argon atmosphere $W_2(OCMe_3)_6$ (0.41 g, 0.50 mmol) was dissolved in toluene and dicyclohexyl carbodiimide (0.206 g, 1.0 mmol) was added from a side-arm tube. After about 2 h a color change from red to brown had occurred, but the reaction mixture was stirred for a further 10 h. It was then filtered into a storage tube, concentrated by vacuum distillation to about 4 cm^3 volume and allowed to stand for about 12 h at $-10°C$. Blue crystals were obtained in 70–80% yield reproducibly, and the products always appeared to be homogeneous. The dry solid is stable in air for a few minutes.

IR. 2952(s), 2914(m), 2847(s), 1710(s), 1465(w), 1450(m), 1377(w), 1370(m), 1350(s), 1260(s), 1225(s), 1170(s), 1004(m), 985(m), 960(s), 925(s), 895(m), 840(w), 787(m), 765(m), 570(m), 550(w) and 524(w).

^1H *NMR* (*see Fig. 1A*). Singlets at δ 1.577 (a_6) and 1.805 (a_3) with relative intensities of 2:1. These signals are assigned to two types of $OCMe_3$ methyl groups, four which are *cis* and two which are *trans* to the carboximide ligand. Multiplets at δ 3.9 (not shown), δ 2.24 (a_1, a_2) and δ 1.18 (a_4, a_5) are assigned to the cyclohexyl groups. There was also an impurity peak ($LiOCMe_3$) at δ 1.034 (not shown).

Preparation of $[W(OCMe_3)_3]_2(\mu\text{-}C_3H_7NCNC_3H_7)$ **(2)**

Under argon $W_2(OCMe_3)_6$ (0.20 g, 0.25 mmol) was dissolved in toluene at room temperature and diisopropyl carbodiimide (0.15 cm^3, 1.0 mmol) was added by syringe. The solution was stirred for 4 h, although a color change from red to brown-purple appeared to be complete within the first 15 min. The solvent was completely removed under vacuum and the solid residue extracted with 10 cm^3 of hexane. This solution was concentrated by vacuum distillation to a volume of *ca* 3 cm^3 and *ca* 3 cm^3 of THF was added. During a period of 2 days at $-10°C$, blue crystals of **2** were deposited. This preparation was reproduced several times and found to give consistently yields of 60–70% of a homogeneous crystalline product. This compound is much more air-sensitive than compound **1** and must be protected at all times.

IR. 2950(m), 2905(s), 2822(w), 1687(m), 1450(s), 1375(m), 1352(m), 1259(s), 1227(w), 1167(m), 1100(m), 1020(m), 1310(w), 982(w), 965(w) and 800(s).

^1H *NMR* (*Fig. 1B*). Singlets at δ 1.519 (b_3) and 1.778 (b_2) with relative intensities of *ca* 2:1. These signals are assigned to two types of $OCMe_3$ methyl groups as for **1**. A doublet at δ 1.339 (J = 6.5 Hz) (b_4, b_5) assigned to the methyl protons of the isopropyl groups and a septet at δ 4.211 (b_1) assigned to the proton on the secondary carbon of the isopropyl group were also observed. There was an impurity peak at δ 1.033 ($LiOCMe_3$) (not shown).

^{13}C *NMR.* The following resonances, with their proposed assignments, were observed: δ 25.85 $[CH(\underline{C}H_3)_2]$, δ 32.14 $[OC(\underline{C}H_3)_3]$, δ 33.38 $[CH(\underline{C}H_3)_3]$, δ 79.22 $[O\underline{C}(CH_3)_3]$, δ 82.16 $[O\underline{C}CH_3)_3]$, and δ 160.32 ($C_3H_7N\underline{C}NC_3H_7$).

Reactions of **1** *and* **2** *with* PhNCO

A weighed amount of **1** or **2** was dissolved in 20 cm^3 of toluene and an excess (two-fold or greater) of

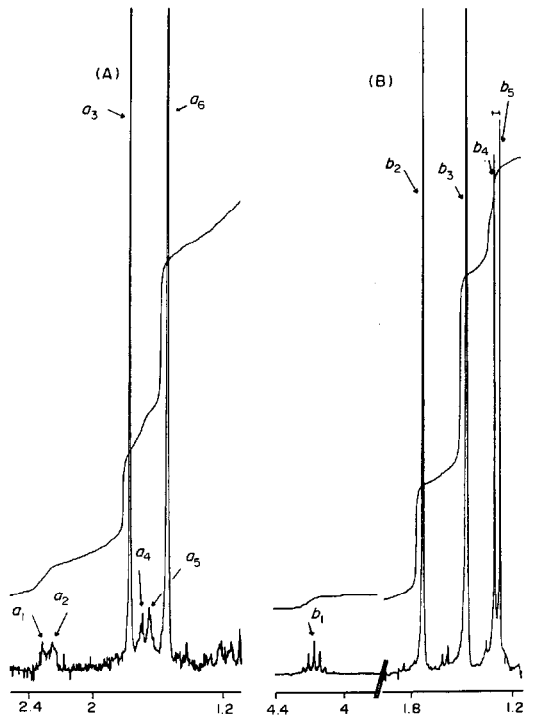


Fig. 1. ^1H NMR spectra of the $OCMe_3$ groups for: (A) $[W(OCMe_3)_3]_2(\mu\text{-}C_6H_{11}NCNC_6H_{11})$, and (B) $[W(OCMe_3)_3]_2(\mu\text{-}C_3H_7NCNC_3H_7)$ molecules.

PhNCO was added. These solutions were stirred at 27°C for 48 h, during which time little if any change was visible. It was possible to recover at least 85% of the starting materials, together with a small amount of a dark insoluble solid, presumably a decomposition product. Repetition of these reactions at 65°C for 15 h also allowed recovery of most of the starting materials (*ca* 70%), but somewhat more of the presumed decomposition products were also observed (but not identified).

Reaction of **2** *with* PMe_3

A weighed amount of **2** was dissolved in 20 cm^3 of toluene, and a 10-fold molar amount of PMe_3 was added. After the reaction mixture had been stirred for 24 h the color was unchanged and **2** was recovered essentially quantitatively upon evaporation of solvent and PMe_3.

Reactions of **1** *and* **2** *with lithium alkoxides*

To weighed amounts of **1** and **2** dissolved in 20 cm^3 of toluene were added 10-fold molar amounts of $LiOCMe_3$ or $LiOCHMe_2$. These mixtures were stirred at 27°C for 15 h. There was no visible evidence that reactions had occurred and starting material was recovered.

Reactions of **2** *with* CO_2 *and* CO

To a solution of **2** in toluene CO_2 was added at liquid nitrogen temperature. The mixture was allowed to warm to room temperature and then

Table 1. Crystallographic data

Formula	$W_2O_6N_2C_{37}H_{76}$	$W_2O_6N_2C_{31}H_{68}$
Formula weight	991.65	932.60
Space group	$C2/c$	$P2_1/c$
a (Å)	13.481(3)	14.752(2)
b (Å)	18.129(4)	12.157(3)
c (Å)	18.244(2)	22.189(3)
α (°)		
β (°)	97.54(1)	97.03(2)
γ (°)		
V (Å^3)	4420(2)	3949(2)
Z	4	4
d (g cm^{-3})	1.490	1.568
Crystal size (mm)	0.2 × 0.2 × 0.25	0.25 × 0.25 × 0.30
μ(Mo-K_α) (cm^{-1})	53.51	59.83
Data collection instrument	CAD-4	CAD-4
Radiation (monochromated in incident beam)	Mo-K_α	Mo-K_α
Orientation reflections, No., range (2θ) (°)	19, 8–29	25, 10–37
Temperature (°C)	25° ± 1	25° ± 1
Scan method	ω–2θ	ω–2θ
Data collection range (2θ) (°)	5–45	4–50
No. of unique data, total	2881	6645
with $F_o^2 > 3\sigma(F_o^2)$	2004	3027
No. of parameters refined	213	370
Transmission factors (max, min) (%)	99.98, 80.03	99.95, 77.56
R^a	0.0375	0.053
$R_w{}^b$	0.0474	0.059
Quality-of-fit indicator[c]	1.417	1.29
Largest shift/esd, final cycle	0.21	0.07
Largest peak (e Å^{-3})	1.1	0.7

[a] $R = \sum ||F_o| - |F_c|| / \sum |F_o|$.
[b] $R_w = [\sum w(|F_o| - |F_c|)^2 / \sum w|F_o|^2]^{1/2}$; $w = 1/\sigma^2(|F_o|)$.
[c] Quality of fit = $[\sum w(|F_o| - |F_c|)^2 / (N_{obs} - N_{parameters})]^{1/2}$.

Table 2. Selected bond distances and angles for $[W(OCMe_3)]_2(\mu\text{-}C_6H_{11}NCNC_6H_{11})$

	Bond distances (Å)		
W(1)—W(1)′	2.490(1)	O(1)—C(11)	1.488(12)
W(1)—O(1)	1.959(6)	O(2)—C(21)	1.425(13)
W(1)—O(2)	1.860(6)	O(3)—C(31)	1.444(13)
W(1)—O(3)	1.896(7)	N(1)—C(1)	1.264(9)
W(1)—N(1)	2.114(8)	N(1)—C(2)	1.482(13)
W(1)—C(1)	2.182(9)	N(1)—N(1)′	2.45(2)
	Bond angles (°)		
W(1)—W(1)′—O(1)	98.2(2)	O(1)—W(1)—C(1)	96.2(2)
W(1)—W(1)′—O(2)	104.9(2)	O(2)—W(1)—O(3)	90.2(3)
W(1)—W(1)′—O(3)	109.8(2)	O(2)—W(1)—N(1)	165.9(3)
W(1)—W(1)′—N(1)	89.2(3)	O(2)—W(1)—C(1)	159.9(3)
W(1)—W(1)′—C(1)	55.2(2)	O(3)—W(1)—N(1)	86.2(3)
W(1)—C(1)—W(1)′	69.6(4)	O(3)—W(1)—C(1)	94.8(2)
W(1)—C(1)—N(1)	138.9(8)	N(1)—W(1)—C(1)	34.2(3)
W(1)—C(1)—C(1)	75.9(6)	W(1)—O(1)—C(11)	129.0(7)
W(1)—C(1)—C(2)	150.4(7)	W(1)—O(2)—C(21)	151.3(9)
O(1)—W(1)—O(2)	88.5(3)	W(1)—O(3)—C(31)	154.4(7)
O(1)—W(1)—O(3)	151.3(3)	N(1)—C(1)—N(1)′	151.0(1)
O(1)—W(1)—N(1)	88.1(3)	C(1)—N(1)—C(2)	131.5(9)

stirred for 3 h. Essentially the same procedure was repeated with CO. In neither case was there any visible indication that a reaction had occurred.

Reaction of $[W(OCMe_3)_3]_2(\mu\text{-PhNCO})$ *with* $C_6H_{11}NCNC_6H_{11}$

One hundred milligrams of $[W(OCMe_3)_3]_2(\mu\text{-PhNCO})$ in 15 cm^3 of toluene was treated with a five-fold molar ratio of dicyclohexyl carbodiimide for 24 h at 25°C. About 15% of the starting ditungsten compound was recovered, but no other product could be isolated.

X-ray crystallographic procedures

The structures of single crystals of compounds **1** and **2** were determined by applying general procedures already described elsewhere.[5] Some details concerning each of the structure determinations are given below. The crystal parameters and basic information pertaining to data collection and structure refinement for both compounds are summarized in Table 1.

Crystal structure of **1**

Three standard reflections which were checked after every 100 measurements showed a 53% uniform drop in intensity over a period of 69.9 h of exposure to the X-ray beam. An appropriate linear, uniform correction was applied to the data. Absorption corrections were calculated based on azimuthal (ψ) scans of nine reflections with Eulerian angles (χ) near 90°. Systematic absences were consistent with space groups *Cc* and *C2/c*. The latter was provisionally assumed and proved to be correct according to the successful refinement. The position of the one independent tungsten atom was inferred from a three-dimensional Patterson function and the rest of the structure then developed by a succession of alternating cycles of least-squares refinements and difference electron density maps. All atoms were ultimately treated anisotropically and the refinement converged uneventfully.

Crystal structure of **2**

Three standard reflections showed an 11.6% uniform decay during 34.3 h of measurements, and a suitable correction was applied. Empirical absorption corrections, as for **1**, were also made. The space group was uniquely defined as $P2_1/c$ by the systematic absences. Positions for the tungsten atoms were derived from a Patterson function and the remaining non-hydrogen atoms then located as before. Carbon atoms (2), (4) and (6) did not refine well anisotropically, showing weak residual peaks (*ca* 0.7 *e* $Å^{-3}$) nearby, suggesting some disorder. However, no physically reasonable disorder model was found and these three atoms were simply refined isotropically while all others were treated anisotropically.

Tables 2 and 3 give important bond distances and angles for **1** and **2** respectively. Complete tables of anisotropic thermal parameters and structure factor

Table 3. Selected bond distances and angles for $W_2(OCMe_3)_6(\mu\text{-}C_3H_7NCNC_3H_7)$

	Bond distances (Å)		
W(1)—W(2)	2.485(1)	C(1)—N(1)	1.28(2)
W(1)—O(4)	1.943(12)	C(1)—N(2)	1.27(2)
W(1)—O(5)	1.871(11)	O(1)—C(11)	1.43(2)
W(1)—O(6)	1.891(14)	O(2)—C(21)	1.44(2)
W(1)—N(1)	2.071(14)	O(3)—C(31)	1.43(2)
W(1)—C(1)	2.20(2)	N(2)—C(3)	1.52(3)
W(2)—O(1)	1.946(12)	N(1)—C(2)	1.52(2)
W(2)—O(2)	1.891(12)	O(4)—C(41)	1.43(2)
W(2)—O(3)	1.839(13)	O(5)—C(51)	1.43(2)
W(2)—N(2)	2.096(15)	O(6)—C(61)	1.49(2)
W(2)—C(1)	2.20(2)	N(1)—N(2)	2.49(2)
	Bond angles (°)		
W(1)—W(2)—O(1)	98.0(4)	W(1)—C(1)—W(2)	68.7(5)
W(1)—W(2)—O(2)	106.2(4)	W(1)—N(1)—C(1)	78.0(1)
W(1)—W(2)—O(3)	109.7(4)	W(1)—C(1)—N(1)	67.0(1)
W(1)—W(2)—N(2)	89.7(5)	W(1)—C(1)—N(2)	136.0(1)
W(1)—W(2)—C(1)	55.7(6)	W(2)—C(1)—N(2)	68.0(1)
W(2)—W(1)—O(4)	97.6(4)	W(2)—C(1)—N(1)	135.0(2)
W(2)—W(1)—O(5)	105.2(4)	W(2)—N(2)—C(1)	78.0(1)
W(2)—W(1)—O(6)	110.3(4)	W(2)—N(2)—C(3)	150.0(1)
W(2)—W(1)—N(1)	90.1(4)	W(2)—O(1)—C(11)	130.0(1)
W(2)—W(1)—C(1)	55.7(5)	W(2)—O(2)—C(21)	150.0(1)
W(2)—O(2)—C(21)	150.0(1)	W(2)—O(3)—C(31)	155.0(1)
W(1)—O(4)—C(41)	129.0(1)	W(1)—O(5)—C(51)	151.0(1)
W(1)—O(6)—C(61)	152.0(1)	N(1)—C(1)—N(2)	157.0(2)
C(1)—N(1)—C(2)	127.0(2)	C(1)—N(2)—C(3)	129.0(2)
C(4)—C(2)—C(5)	114.0(2)	C(6)—C(3)—C(7)	108.0(2)
O(1)—W(2)—O(2)	89.0(5)	O(1)—W(2)—O(3)	151.5(5)
O(1)—W(2)—N(2)	86.1(6)	O(1)—W(2)—C(1)	94.6(6)
O(2)—W(2)—O(3)	89.4(5)	O(2)—W(2)—N(2)	163.9(6)
O(2)—W(2)—C(1)	161.8(7)	O(3)—W(2)—C(1)	161.8(7)
O(3)—W(2)—N(2)	87.6(6)	N(1)—W(2)—C(1)	34.2(6)
O(3)—W(2)—C(1)	95.6(6)	O(4)—W(1)—O(5)	89.8(5)
O(4)—W(1)—O(6)	151.3(5)	O(4)—W(1)—N(1)	86.8(5)
O(4)—W(1)—C(1)	95.1(6)	O(5)—W(1)—N(1)	164.7(6)
O(5)—W(1)—O(6)	89.1(5)	O(5)—W(1)—C(1)	160.7(6)
O(6)—W(1)—N(1)	86.8(6)	O(6)—W(1)—C(1)	95.3(6)
N(1)—W(1)—C(1)	34.6(6)		

data are available as supplementary material.* Figures 2 and 3 show the structures and atom numbering schemes.

RESULTS

The reactions of the two carbodiimides, RNCNR, R = cyclohexyl and isopropyl, with $W_2(OCMe_3)_6$ proceed just as did the reaction of di-*p*-tolyl carbodiimide. The formation of the 1:1 adduct appears to occur promptly but there is no apparent tendency to proceed further. Moreover, it appears to be generally true that these blue adducts, $[W(OCMe_3)_3]_2(\mu\text{-RNCNR})$, are not reactive toward any other ligands of interest, viz. CO, CO_2, PMe_3 and PhNCO.

The structures of the two new compounds, as shown in Figs 2 and 3, are quite analogous to those previously reported for $[W(OCMe_3)_3]_2(\mu\text{-}C_7H_7NCNC_7H_7)$[2] and $[W(OCMe_3)_3]_2(\mu\text{-PhNCO})$.[3] In compound **1** the molecule has rigorous crystallographic C_2-symmetry, with the symmetry axis passing through the carbodiimide carbon atom and the midpoint of the W=W bond. In compound **2**

* Supplementary material available: tables of structure factors, anisotropic thermal vibration parameters, complete tables of bond lengths and angles, and more detailed accounts of the crystallographic work for both structures (39 pp.) have been deposited with the Editor at Queen Mary College. Positional parameters and isotropic thermal parameters have been forwarded to the Director, Cambridge Crystallographic Data Centre.

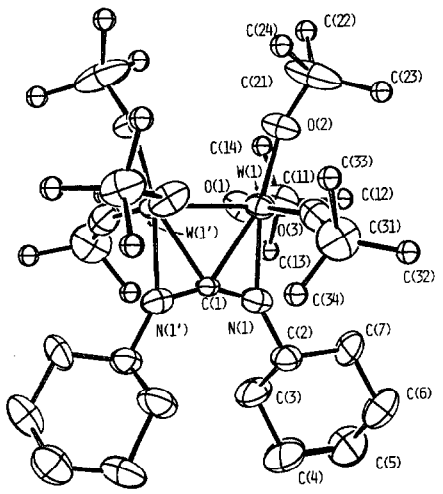


Fig. 2. An ORTEP drawing of the molecule $[W(OCMe_3)_3]_2(\mu\text{-}C_6H_{11}NCNC_6H_{11})$, giving the atomic labelling scheme. All methyl carbon atoms of $OCMe_3$ groups are represented by arbitrarily small spheres to avoid covering up other atoms. All other atoms are represented by their ellipsoids of thermal vibration at the 40% level.

there is no crystallographically rigorous symmetry, but the effective symmetry is again C_2.

DISCUSSION

We have shown that our previous observations[2] concerning the preparation, structure and reactivity of the di-*p*-tolyl carbodiimide adduct of $W_2(OCMe_3)_6$ apply to carbodiimides more generally, including those with alkyl rather than aryl groups on the nitrogen atoms. As before, the use of an excess of carbodiimide over the 1 : 1 mole ratio does not lead to any further reaction. In the two new compounds the mode of attachment is essentially identical to that previously observed in $[W(OR_3)_2]_2(\mu\text{-}C_7H_7NCNC_7H_7)$ and also, *mutatis mutandis*, to that in the 1:1 adduct of PhNCO with $W_2(OCMe_3)_6$.[3]

In all four molecules of this 1 : 1 adduct type the W=W distances are the same to within less than 0.01 Å and the bonding can be accounted for in the same way, as previously explained.[2] In the case of compound **2** we have, for the first time, been able to observe the ^{13}C NMR signal for the central carbon atom of the bound RNCNR (or RNCO) group. We find it at 160.32 ppm, which is within the general region where it might have been expected.

We have now established that not only are these carbodiimide adducts unreactive toward additional carbodiimide, they are unreactive towards a number of other reagents, specifically PnNCO, PMe_3, LiOR, CO_2 and CO. We have also shown that the PhNCO adduct, $[W(OCMe_3)]_2(\mu\text{-PhNCO})$, which reacts very readily with additional PhNCO, or with PMe_3, will not react with $C_6H_{11}NCNC_6H_{11}$. The relationship of these observations to our previously proposed[3] mechanism for reaction (1) must now be considered.

We proposed that the key, established features of the overall process represented by eqn (1) were the initial formation of the mono-adduct, of structure **b**, followed by a migratory insertion induced by the attack of a second molecule of PhNCO, or the nucleophile PMe_3 to form **c** or **d**. In the case of **d**, whose structure is known, no further reaction occurred, whereas **c**, the structure of which remains to be discussed, cannot be isolated (or even positively detected) because it immediately rearranges to afford the final product (**e**). Since the carbodiimide adducts (**f**) are very similar to **b**, why is it that they are not subject to further reaction so as to allow an overall process analogous to that described by eqn (1)?

Clearly, part of the problem is simply that a second molecule of RNCNR appears to be in itself an unsuitable reactant; it cannot act as a nucleophile, as can PhNCO or PMe_3. This is shown by the fact that **b** is unreactive toward $C_6H_{11}NCNC_6H_{11}$. This naturally prompts the thought that if PhNCO or PMe_3 were to be used the $[W(OCMe_3)_3]_2(\mu$-RNCNR) molecules might react, at least to the extent of forming analogs of **c** or **d**, if not further. Again, however, there is no reaction, and this poses an interesting question. While it is obvious that an

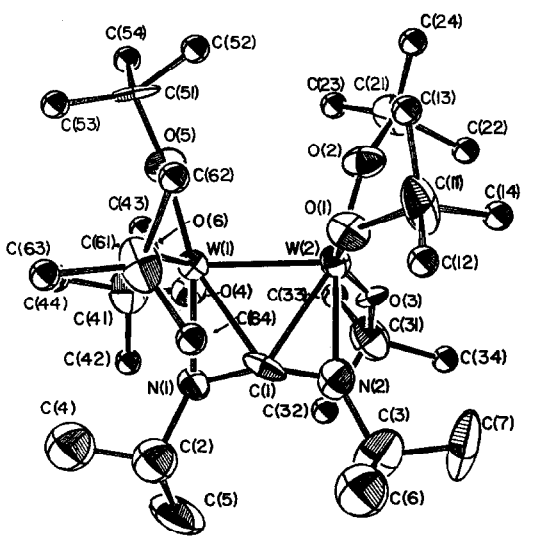
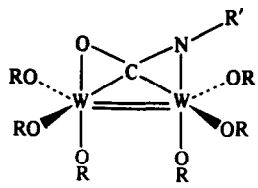
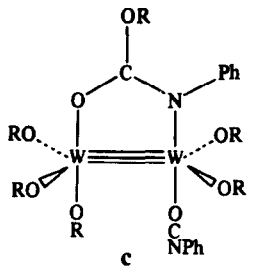


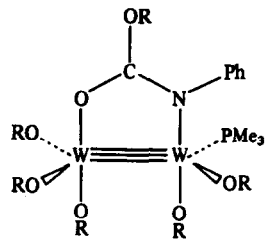
Fig. 3. An ORTEP drawing of the molecule $[W(OCMe_3)_3]_2(\mu\text{-}C_3H_7NCNC_3H_7)$, giving the atomic labelling scheme. All methyl carbon atoms of $OCMe_3$ groups are represented by arbitrarily small spheres to avoid covering up other atoms. All other atoms are represented by their ellipsoids of thermal vibration at the 40% level.



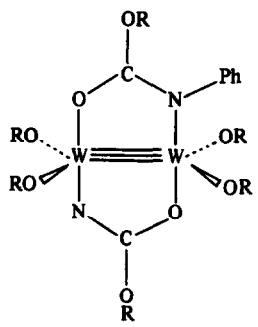
b



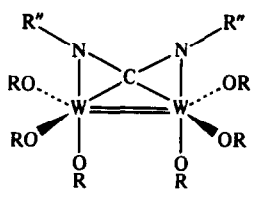
c



d

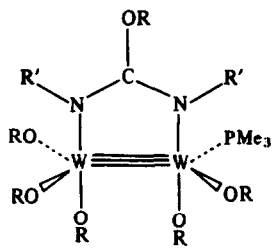


e



f

RNCNR molecule is much less suited than an RNCO or PMe_3 molecule, the present question is more subtle. It does not seem likely that a molecule such as **g**, the carbodiimide analog of **d**, or a carbodiimide analog of **c**, should be inherently unstable once formed. It thus seems more likely that we are dealing with a kinetic inhibition, i.e. there is a kinetic barrier to the process of getting from molecule **f** to molecule **g** that does not exist, or at least does not assume the same importance, in getting from **b** to **c** or **d**.



g

We believe that this barrier may be steric in nature. In the molecules of type **f** both ends of the attached molecule, R'NCNR', are sterically encumbered, whereas in **b** one end, the oxygen end, is relatively undemanding sterically. This could mean that a pathway close to the O atom, that is sterically open for migration of an $OCMe_3$ group in **b**, is not readily available in **f**. However, since it is also true that in **b** there is a type of polarity, due to the unsymmetrical nature of PhNCO, that does not exist in **f** with its symmetrical R'NCNR' ligand, we cannot rule out the possibility that polarity too is important.

Finally, we must say something about the possible structure of the posited intermediate, **c**, about which we have so far been silent. If we assume that the key difference between the reactive molecule **b** and the unreactive molecule **f** is the presence of O rather than R'N (for either steric or electronic reasons, but especially for steric reasons) we might tend to suppose that the transferred OR group would come from W(1), the W atom bonded to the isocyanate oxygen atom of **b**. This *might*, then, lead us to expect that **f**, and also **c**, would have the incoming nucleophilic ligand on that same tungsten atom, whereas in **d** it does not.

Does the actual structure of **d**, with its PMe_3 on the "wrong" metal atom refute our mechanistic reasoning? We think not. There is no logical need to believe that the added PMe_3 group must occupy the

very place vacated by the migrating OR group. It is entirely possible to imagine an OR group from one of the two closest positions on the W(1) atom of **b** moving to the carbon atom of PhNCO, either before, during or after an attack by PMe_3 (or PhNCO) on either of the W atoms, followed by migrations of PMe_3 and/or OR groups from one metal atom to the other to give **d**. It has been noted before in the chemistry of these multiply-bonded ditungsten and dimolybdenum alkoxide species that the alkoxide groups and other ligands are labile,[6] even to the point of making the molecules fluxional on the NMR time scale.[7] Thus, we have no right to conclude either that the observed structure of **d** is inconsistent with our proposal that **b** is transformed to **e** via a transient intermediate **c**, or that the stereochemistry (including the regiostereochemistry) of **c** is necessarily the same as that of **d**. After all, **d** is a kinetic dead end, whereas **c** is a very lively and unisolable kinetic intermediate.

Acknowledgements—We thank the Robert A. Welch Foundation for support. We are grateful to Drs L. Falvello and W. Schwotzer for advice and assistance with the X-ray crystallography.

REFERENCES

1. M. H. Chisholm, F. A. Cotton, K. Folting, J. C. Hoffman, A. R. Raterman and E. S. Shamshoum, *Inorg. Chem.* 1984, **23**, 4423.
2. F. A. Cotton, W. Schwotzer and E. S. Shamshoum, *Organometallics* 1985, **3**, 461.
3. F. A. Cotton and E. S. Shamshoum (in press).
4. R. R. Schrock, M. L. Listerman and L. G. Sturgeoff, *J. Am. Chem. Soc.* 1982, **104**, 4291.
5. A. Bino, F. A. Cotton and P. E. Fanwick, *Inorg. Chem.* 1979, **18**, 3558.
6. M. H. Chisholm, J. C. Huffman and R. J. Tatz, *J. Am. Chem. Soc.* 1984, **106**, 5385.
7. F. A. Cotton, M. W. Extine, D. A. Haitko, J. Leonelli and D. Little, *J. Am. Chem. Soc.* 1981, **103**, 779.

Polyhedron Vol. 4, No. 10, pp. 1735–1739, 1985
Printed in Great Britain

0277–5387/85 $3.00 + .00
© 1985 Pergamon Press Ltd

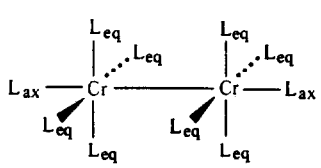
A DICHROMIUM(II) COMPOUND WITH AN ELONGATED METAL–METAL BOND: Cr_2(OXINDOLATE)$_4$(OXINDOLE)$_2$

F. ALBERT COTTON* and WENNING WANG
Department of Chemistry and Laboratory for Molecular Structure and Bonding,
Texas A & M University, College Station, TX 77843, U.S.A.

(*Received* 28 *January* 1985; *accepted* 26 *April* 1985)

Abstract—The title compound has been prepared by reaction of $(C_5H_5)_2Cr$ with oxindole (indole with C=O in place of CH_2 at the 2-position). Red single crystals belong to space group $P2_1/c$ with $a = 10.107(4)$ Å, $b = 22.496(7)$ Å, $c = 9.210(3)$ Å, $\beta = 93.26(3)°$, $V = 2091(2)$, and $Z = 2$. The centrosymmetric molecule has a Cr—Cr distance of 2.495(4) Å. The mean Cr—O and Cr—N distances for the bonds to bridging oxindolate anions are 2.024(7) and 2.065(8) Å, respectively. There is an oxindole molecule bound at each end with a Cr—O axial bond of length 2.341(8) Å and a hydrogen bond from the oxindole N—H group to an equatorial oxygen atom of length 2.83(1) Å. The significance of this compound with respect to Cr—Cr bonding is discussed.

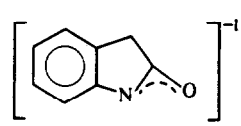
The enormous range of metal–metal distances (*ca* 1.83–2.54 Å) spanned by molecules containing two Cr(II) atoms interacting to give a singlet ground state has provoked considerable interest and activity, both experimental and theoretical.[1–9] The general structural situation is illustrated in **I**. In virtually all cases the adjacent pairs of L_{eq} ligands are parts of bridging bidentate ligands. Two factors are clearly pertinent: (1) the effect of the ligands that fill the eight "equatorial" positions, denoted in **I** as L_{eq}; and (2) the effect of the axial ligands, denoted in **I** as L_{ax}. While it is generally accepted that both play a significant role, views differ as to whether the L_{eq} or the L_{ax} influence is predominant.



I

It has been established unequivocally that when axial ligands are *entirely* absent the Cr—Cr distance is *always* short.[1] It has recently been shown that even when the eight L_{eq} atoms are derived from four acetate ions, if there are no axial ligands, the Cr—Cr distance is well under 2.00 Å.[9] There has, however, been the suggestion that, for an equatorial ligand set consisting of 4N + 4O or another combination not consisting exclusively of oxygen atoms, there would be a pronounced tendency to develop strong and short Cr—Cr bonding even in the presence of axial ligands.[6]

To test this suggestion, we have prepared and structurally characterized a compound in which the equatorial ligand set is of the 4N + 4O type, but two axial ligands are also present. This was done by employing the bridging bidentate ligand derived by deprotonation of oxindole, namely **II**. The conditions of preparation led to the crystallization of a crystalline product in which the Cr_2(oxindolate)$_4$ unit has two adjoined axial ligands, each of which is an oxindole molecule, coordinated to a chromium atom through its oxygen atom and also held in place by an N—H···O hydrogen bond to one of the equatorially coordinated oxygen atoms.



II

EXPERIMENTAL SECTION

Synthesis of $Cr_2(C_8H_6NO)_4(C_8H_7NO)_2$. 0.18 g $CrCp_2$ (1 mmol) and 0.27 g (2 mmol) of oxindole were dissolved in 20 cm^3 toluene. The mixture was stirred for 16 h at 25°C. The red filtrate was then stored at

* Author to whom correspondence should be addressed.

Table 1. Crystallographic parameters

Formula	$Cr_2(C_8H_6NO)_4 \cdot 2C_8H_7NO$
Formula weight	898.87
Space group	$P2_1/c$
a (Å)	10.107(4)
b (Å)	22.496(7)
c (Å)	9.210(3)
β (°)	93.26(3)
V (Å^3)	2091(2)
Z	2
d_c 'g cm^{-3})	1.286
Crystal size (mm)	0.2 × 0.3 × 0.3
μ(Mo-K_α) (cm^{-1})	11.252
Data collection instrument	CAD-4F
Radiation	Mo-K_α
Orientation reflections, No., range (2θ) (°)	20–30°
Temperature (°C)	26
Scan method	θ–2θ
Data collection range, 2θ (°)	4–50
No. of unique data, total with $F_o^2 > 3\sigma(F_o^2)$	3659, 1007
No. of parameters refined	280
R^a	0.0629
R_w^b	0.0660
Quality-of-fit indicator^c	1.627
Largest shift/esd, final cycle	0.01
Oargest peak (e Å^{-3})	0.378

$^a R = \sum ||F_o| - |F_c|| / \sum |F_o|$.
$^b R_w = [\sum w(|F_o| - |F_c|)^2 / \sum w|F_o|^2]^{1/2}$; $w = 1/\sigma^2(|F_o|)$.
^{c} Quality of fit $= [\sum w(|F_o| - |F_c|)^2 / (N_{obs} - N_{parameters})]^{1/2}$.

−20°C. After 1 week, large single crystals had formed in about 50% yield.

Structural solution of $Cr_2(C_8H_6NO)_4 \cdot 2C_8H_7NO$. X-ray data were collected in the monoclinic crystal system on a CAD-4F diffractometer. Systematic absences uniquely determined the space group as $P2_1/c$. The chromium atom position was obtained from a Patterson map. Alternate cycles of least-squares refinement and difference Fourier maps allowed location of all remaining non-hydrogen atoms. Refinement proceeded smoothly with all atoms finally treated anisotropically. General information concerning the crystallography is given in Table 1. No detectable diminution in the scattering by standard reflections was observed and, in view of the low absorption coefficient and the crystal dimensions, no absorption correction was made.

The atomic positional parameters and tables of thermal vibration parameters and structure factors are available as supplementary material.

RESULTS

The crystal consists of equivalent discrete centrosymmetric $Cr_2(C_8H_6NO)_4(C_8H_7NO)_2$ molecules. One such molecule is depicted in Fig. 1. It can be seen that the central portion consists of a Cr_2 unit bridged by four oxindolate anions arranged so that two mutually cisoid ones point in one direction and two in the other. This gives a *cis*-CrN_2O_2 coordination at each metal atom and gives the entire $Cr_2(C_8H_6NO)_4$ unit a virtual C_{2h}-symmetry. The addition of the axial C_8H_7NO ligands abolishes all but one of the symmetry operations of C_{2h} so that the complete molecule has as its highest possible symmetry the crystallographically rigorous inversion symmetry.

A list of bond distances and angles is given in Table 2, and Fig. 2 displays some of these that are important in discussing the arrangement of ligands about the Cr_2 core.

The way in which the axial oxindole molecules are

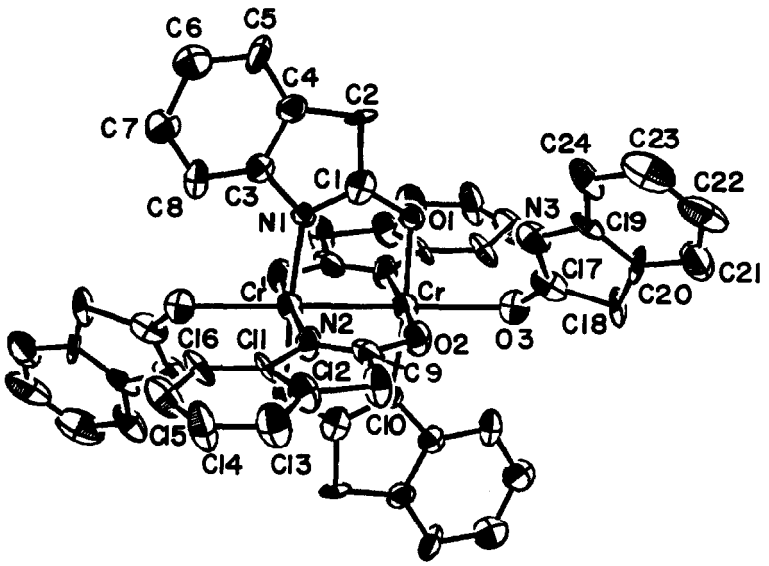


Fig. 1. An ORTEP drawing of the Cr_2(oxindolato)$_4$(oxindole)$_2$ molecule. Atoms are represented by thermal vibration ellipsoids drawn at the 40% level. Only the crystallographically independent ligand atoms are labelled in this centrosymmetric molecule.

held in place, by a combination of coordination from O to Cr as well as by N—H ··· O hydrogen bonding, is clearly displayed in Fig. 2. It is an efficient way to anchor axial ligands in place which might be usefully employed in a deliberate way in the future. It is not, however, unique to this structure. Previously, in $Rh_2(CH_3COS)_4(CH_3CSOH)_2$[10] and in $Ru(hp)_4Cl(Hhp)$,[11] where hp is the anion derived from 2-hydroxypyridine (Hhp), similar "two-prong" attachments have been observed.

DISCUSSION

In the structure reported here we have one of the longest Cr—Cr distances known within the general type of structure under consideration. This occurs despite the fact that the bridging ligands are of the N—C—O type, that is, the amidato type, that has been alleged to favor the shortest Cr—Cr bonds. Indeed, the Cr—Cr bond length here, 2.495(4) Å, is nearly as long as those found in three

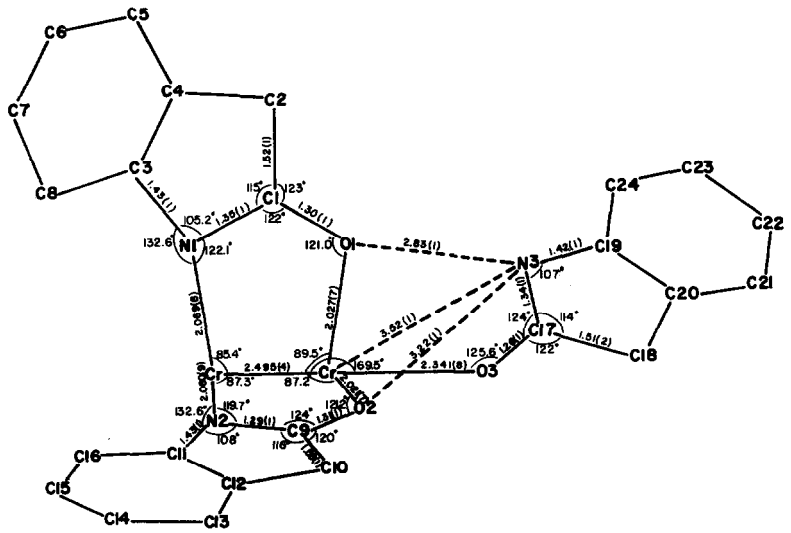


Fig. 2. A drawing featuring the distances and angles involved in ligand–metal bonding.

Table 2. Bond distances and bond angles for $Cr_2(C_8H_6NO)_4 \cdot 2C_8H_7NO$

	Bond distance (Å)		
Cr—Cr′	2.495(4)	C(6)—C(7)	1.43(2)
Cr—O(1)	2.027(7)	C(7)—C(8)	1.41(1)
Cr—O(2)	2.021(7)	C(9)—C(10)	1.55(1)
Cr—O(3)	2.341(8)	C(10)—C(12)	1.51(1)
Cr—N(1)	2.069(8)	C(11)—C(12)	1.40(1)
Cr—N(2)	2.060(9)	C(11)—C(16)	1.37(1)
O(1)—C(1)	1.30(1)	C(12)—C(13)	1.44(2)
O(2)—C(9)	1.31(1)	C(13)—C(14)	1.40(2)
O(3)—C(17)	1.26(1)	C(14)—C(15)	1.44(2)
N(1)—C(1)	1.35(1)	C(15)—C(16)	1.43(2)
N(1)—C(3)	1.43(1)	C(17)—C(18)	1.51(2)
N(2)—C(9)	1.29(1)	C(18)—C(20)	1.51(2)
N(2)—C(11)	1.43(1)	C(19)—C(20)	1.37(1)
N(3)—C(17)	1.34(1)	C(19)—C(24)	1.38(2)
N(3)—C(19)	1.42(1)	C(20)—C(21)	1.39(2)
C(1)—C(2)	1.52(1)	C(21)—C(22)	1.42(2)
C(2)—C(4)	1.51(1)	C(22)—C(23)	1.44(2)
C(3)—C(4)	1.42(1)	C(23)—C(24)	1.42(2)
C(3)—C(8)	1.38(1)	O(1)—N(3)	2.83(1)
C(4)—C(5)	1.36(1)	O(2)—N(3)	3.22(1)
C(5)—C(6)	1.41(2)		

carboxylato-bridged compounds, as the following comparison shows: $Cr_2(oxindolato)_4(oxindole)_2$ (**1**) 2.495(4) Å, $Cr_2(O_2CCF_3)_4(Et_2O)_2$ (**2**) 2.541(3) Å,[12] $[Cr_2(O_2CCH_2NH_3)_4Cl_2]^{2+}$ (**3**) 2.513(1) Å,[13] and $Cr_2(O_2CCH_2NH_3)_4Br_2]^{2+}$ (**4**) 2.524(1) Å.[13] These three carboxylato compounds are those containing the least basic carboxylato anions.

What our study of the structure of **1** shows is that if there is good axial coordination a long Cr—Cr distance will be obtained, without regard to whether the four bridging ligands are of the amidato ion (N—C—O$^-$) type or the carboxylato type.

It can even be argued that the reason why the Cr—Cr distance in **1** is a little shorter than those in **2**–**4** is because the axial donation is not as strong in **1** as in the others. If we take the Cr—L_{ax} distances in each of the four compounds and subtract the accepted single bond radii of the coordinated atom, we have the following results (Å): (**1**) 2.34 − 0.66 = 1.68, (**2**) 2.24 − 0.66 = 1.58, (**3**) 2.58 − 0.99 = 1.59, and (**4**) 2.74 − 1.14 = 1.60. Clearly, with due allowance for the inherently different atomic sizes, the axial ligands approach less closely in **1** than in the other three cases.

The idea that the basicity of the equatorial ligands has a dominant role and the presence or absence of axial ligands only a secondary role in determining Cr—Cr bond lengths in compounds of the class under consideration is flatly contradicted by the experimental results for compounds **1**–**4**, as well as by the experimental results recently obtained for the structure of $Cr_2(O_2CCH_3)_4$. There is evidently a need for new and reliable calculations concerning the electronic properties and resultant structures of molecules of this class.

Acknowledgements—We thank the National Science Foundation for financial support. We are grateful to M. B. Hall, M. Fink and T. R. Felthouse for prepublication copies of their manuscript.

REFERENCES

1. F. A. Cotton and R. A. Walton, *Multiple Bonds Between Metal Atoms*. Chap. 4. John Wiley, New York (1982).
2. F. A. Cotton and W. Wang, *Nouv. J. Chem.* 1984, **8**, 331.
3. P. M. Atha, I. H. Hillier and M. F. Guest, *Mol. Phys.* 1982, **46**, 437.
4. P. M. Atha, I. H. Hillier, A. A. MacDowell and M. F. Guest, *J. Chem. Phys.* 1982, **77**, 195.
5. P. Correa de Mello, W. D. Edwards and M. C. Zerner, *Int. J. Quantum Chem.* 1983, **23**, 425.
6. R. A. Kok and M. B. Hall, *J. Am. Chem. Soc.* 1983, **105**, 676.
7. P. M. Atha, J. C. Campbell, C. D. Garner, I. H. Hillier and A. A. MacDowell, *J. Chem. Soc., Dalton Trans.* 1983, 1085.
8. R. Wiest and M. Benard, *Chem. Phys. Lett.* 1983, **98**, 102.
9. S. N. Ketkar and M. Fink, *J. Am. Chem. Soc.* 1985, **107**, 338.

Table 2—*continued*

Bond angle (°)			
Cr′—Cr—O(1)	89.5(2)	C(17)—N(3)—C(19)	107(1)
Cr′—Cr—O(2)	87.2(2)	O(1)—C(1)—N(1)	122(1)
Cr′—Cr—O(3)	169.5(2)	O(1)—C(1)—C(2)	123(1)
Cr′—Cr—N(1)	85.4(3)	N(1)—C(1)—C(2)	115(1)
Cr′—Cr—N(2)	87.3(3)	C(1)—C(2)—C(4)	100(1)
O(1)—Cr—O(2)	88.9(3)	N(1)—C(3)—C(4)	112(1)
O(1)—Cr—O(3)	86.7(3)	N(1)—C(3)—C(8)	125(1)
O(1)—Cr—N(1)	174.9(3)	C(4)—C(3)—C(8)	123(1)
O(1)—Cr—N(2)	88.2(3)	C(2)—C(4)—C(3)	108(1)
O(2)—Cr—O(3)	82.9(3)	C(2)—C(4)—C(5)	130(1)
O(2)—Cr—N(1)	91.7(3)	C(3)—C(4)—C(5)	121(1)
O(2)—Cr—N(2)	173.8(4)	C(4)—C(5)—C(6)	117(1)
O(3)—Cr—N(1)	98.4(3)	C(5)—C(6)—C(7)	121(1)
O(3)—Cr—N(2)	102.3(3)	C(6)—C(7)—C(8)	122(1)
N(1)—Cr—N(2)	90.7(3)	C(3)—C(8)—C(7)	115(1)
Cr—O(1)—C(1)	121.0(8)	O(2)—C(9)—N(2)	124(1)
Cr—O(2)—C(9)	121.2(7)	O(2)—C(9)—C(10)	120(1)
Cr—O(3)—C(17)	125.6(8)	N(2)—C(9)—C(10)	116(1)
Cr—N(1)—C(1)	122.1(8)	C(9)—C(10)—C(12)	96.7(9)
Cr—N(1)—C(3)	132.6(8)	N(2)—C(11)—C(12)	109(1)
C(1)—N(1)—C(3)	105.2(9)	N(2)—C(11)—C(16)	127(1)
Cr—N(2)—C(9)	119.7(8)	C(12)—C(11)—C(16)	123(1)
Cr—N(2)—C(11)	132.6(8)	C(10)—C(12)—C(11)	111(1)
C(9)—N(2)—C(11)	108(1)	C(10)—C(12)—C(13)	128(1)
C(11)—C(12)—C(13)	121(1)	Cr′—Cr—N(3)	131.1(2)
C(12)—C(13)—C(14)	116(1)	Cr—O(1)—N(3)	91.6(3)
C(13)—C(14)—C(15)	123(1)	Cr—O(2)—N(3)	119.8(3)
C(14)—C(15)—C(16)	119(1)		
C(11)—C(16)—C(15)	118(1)		
O(3)—C(17)—N(3)	124(1)		
O(3)—C(17)—C(18)	122(1)		
N(3)—C(17)—C(18)	114(1)		
C(17)—C(18)—C(20)	98(1)		
N(3)—C(19)—C(20)	110(1)		
N(3)—C(19)—C(24)	122(1)		
C(20)—C(19)—C(24)	128(1)		
C(18)—C(20)—C(19)	111(1)		
C(18)—C(20)—C(21)	130(1)		
C(19)—C(20)—C(21)	119(1)		
C(20)—C(21)—C(22)	117(2)		
C(21)—C(22)—C(23)	122(2)		
C(22)—C(23)—C(24)	120(2)		
C(19)—C(24)—C(23)	114(1)		

10. L. M. Dikareva, M. A. Porai-Koshits, G. G. Sadikov, I. B. Baranovski, M. A. Golubnichaya and R. N. Shchelokov, *Zh. Neorg. Khim.* 1978, **23**, 1044.
11. A. R. Chakravarty, F. A. Cotton and D. A. Tocher, *Inorg. Chem.* 1985, **24**, 172.
12. F. A. Cotton, M. W. Extine and G. W. Rice, *Inorg. Chem.* 1978, **17**, 176.
13. M. Ardon, A. Bino, S. Cohen and T. R. Felthouse, *Inorg. Chem.* 1984, **23**, 3450.

Polyhedron Vol. 4, No. 10, pp. 1741–1743, 1985
Printed in Great Britain

0277–5387/85 $3.00 + .00
© 1985 Pergamon Press Ltd

DIRECT SYNTHESIS AND NMR SPECTRA OF $[(C_6H_5)_2PCH_2]_2CuB_5H_8$: COMMENTS ON THE SOLUTION STRUCTURE OF 2,3-μ-METALLOPENTABORANES

PAMELA K. RUSH and LAWRENCE BARTON*
Department of Chemistry, University of Missouri—St-Louis, St. Louis, MO 63121, U.S.A.

(*Received* 2 *January* 1985; *accepted after revision* 19 *April* 1985)

Abstract—The species $[(C_6H_5)_2PCH_2]_2CuB_5H_8$ has been prepared directly from $[(C_6H_5)_2PCH_2]_2CuI$ and $K[B_5H_8]$. NMR spectra unequivocally indicate that the species has a static structure in solution and an argument is presented that all 2,3-μ-metallopentaboranes have similarly static solution structures.

A recent study[1] described the synthesis of (dppe)CuB_5H_8 (**I**) by ligand exchange between solutions of $[(C_6H_5)_2PCH_2]_2$ and $[(C_6H_5)_3P]_2CuB_5H_8$ (**II**) [dppe = 1,2-bis(diphenylphosphino)ethane]. Apparently **I** is stabilized by the chelate effect. **I** is of comparable stability to **II** in the solid state but, in CH_2Cl_2 solution at 25°C, **II** decomposes completely after 4 days, whereas **I** is essentially unchanged under the same conditions. Since metalloboranes and metallocarboranes are useful in the synthesis of larger metalloboranes and borane clusters,[2] we decided to investigate the possibility of synthesizing directly the more stable species (**I**) from a dppe-ligated Cu(I) halide and $K[B_5H_8]$ as part of our continuing studies of dppe-ligated metalloboranes.[3] Furthermore, since we had access to high-field NMR, we though we might be able to provide some insight into some unresolved aspects of the solution dynamics of 2,3-μ-metallopentaboranes.

EXPERIMENTAL

Standard high-vacuum and inert-atmosphere techniques were employed in this work. B_5H_9 (Callery Chemical Co.) was distilled on the vacuum line before use, dppe (Pressure Chemicals Inc.) was used without purification and (dppe)CuI was prepared by literature methods.[4] KH (Alpha Products) was washed with pentane on the vacuum line until it was a free flowing white powder. Solvents were dried and distilled on the vacuum line before use. (dppe)CuB_5H_8 was prepared as follows. In the dry-box a two-neck 50-cm^3 reaction flask attached to an extractor was charged with KH (0.11 g, 2.6 mmol) and sealed with a rotatable solid addition tube containing (dppe)CuI (1.52 g, 2.61 mmol). After evacuation on the vacuum line B_5H_9 (0.27 cm^3, 2.61 mmol) and $(CH_3)_2O$ (10 cm^3) were condensed at −196°C. Stirring at −35°C for 45 min afforded H_2 (2.15 mmol) which was measured and removed using a Toepler pump. CH_2Cl_2 (20 cm^3) was condensed at −196°C and the (dppe)CuI was added. The solution was allowed to warm, stirred at −35°C for 1 h and at −78°C overnight. The solution was filtered at −78°C to remove KI, and the filtrate was frozen at −196°C and transferred to a clean extractor under a positive flow of N_2. $(CH_3)_2O$ was removed at −78°C, and the volume of CH_2Cl_2 was reduced by half at −35°C. The addition of $(C_2H_5)_2O$ (5 cm^3) and C_5H_{12} (5 cm^3) resulted in the isolation of (dppe)CuB_5H_8. The product was washed with $(C_2H_5)_2O$ followed by C_5H_{12} and identified by its IR and ^{11}B NMR spectra, which compared well with those reported previously. NMR spectra were run on a Nicolet NT 300 at 300.1 and 96.25 MHz for ^1H and ^{11}B observations respectively. IR spectra were run as KBr discs on a Perkin–Elmer 337 spectrometer.

RESULTS AND DISCUSSION

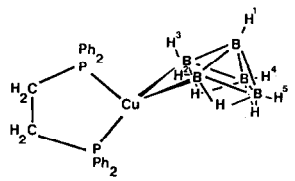
(dppe)CuB_5H_8 was prepared from the following series of reactions:

$$B_5H_9 + KH \xrightarrow[(CH_3)_2O]{-35°C} KB_5H_8 + H_2,$$

$$KB_5H_8 + [(C_6H_5)_2PCH_2]_2CuI \xrightarrow[CH_2Cl_2/(CH_3)_2O]{-35°C} [(C_6H_5)_2PCH_2]_2CuB_5H_8 + KI.$$

* Author to whom correspondence should be addressed.

Yields were in the same range as those reported earlier although our yields may be higher, based on B_5H_9 as the limiting reagent. The solid product was off-white in color and in the presence of traces of solvent and excess $[(C_6H_5)_2PCH_2]_2CuI$ at room temperature it turned bright orange yellow and specks of Cu(0) were observed, presumably due to reduction of the ligated Cu(I) iodide by borane complex. The species did not melt sharply but turned dark yellow at 145°C and decomposed at 156°C. The 96.25-MHz ^{11}B NMR spectra provided more information than those previously reported and are shown in Fig. 1 along with the proposed structure. The coupled spectrum indicates overlap of resonances due to the two sets of basal borons; however the $^{11}B\{^1H\}$ spectrum clearly resolves the spectrum into two resonances arising from two sets of two equivalent basal borons at $\delta = -11.33$ and -15.05 ppm and a single resonance arising from the apical boron at $\delta = -47.52$ ppm. The assignment of the basal resonances is based on that of Greenwood and Staves[5] for the analogous species $[(C_6H_5)_3P]Cd(Cl)B_5H_8$. The basal resonances are not resolved enough for the accurate measurement of the coupling constants, presumably due to quadrupolar broadening from the Cu atom; however, they are in the expected range. The value of $J_{^{11}B^1-^1H^1}$ is 161 Hz. These data confirm that this species has a static structure in solution and this is discussed later. The proton spectrum, which has not been reported previously, is complicated by the presence of ligand resonances. Thus resonances assigned to the phenyl Hs are seen at $\delta = 7.29$ and 7.13 ppm and the methylene Hs seen at $\delta = 2.4$ ppm show no significant splitting by the P atoms. This latter observation has been made for other dppe-ligated metallopentaboranes.[6,3] In addition, a resonance seen at $\delta = 1.2$ ppm is due presumably to the free dppe ligand which arises from dissociation. Such dissociation in solution has been observed[7] for other phosphine-ligated cuprioboranes. A broad resonance centered at 2.2 ppm, in the expected position for basal terminal Hs, is obscured by ligand resonances. The higher-field region of the spectrum is more informative and is repreduced in Fig. 2 along with that[8] for $[(C_6H_5)_3P]_2Cu\text{-}1\text{-}(CH_3)B_5H_7$. The small peak at $\delta = -0.8$ ppm in the spectrum of $(dppe)CuB_5H_8$ is the upfield member of a 1:1:1:1 quartet due to the apical hydrogen. The observed $^{11}B^{11}-^1H^1$ coupling constant is 163 Hz and, from the positions of the two upfield members of the quartet, the center of the multiplet is located at $\delta = -0.11$ ppm. The two resonances, in approximate area ratio 1:2, seen at $\delta = -2.7$ and -3.28 ppm respectively are assigned to the bridging hydrogens and compare well to those shown in Fig. 2b for $[(C_6H_5)_3P]_2Cu\text{-}1\text{-}(CH_3)B_5H$ which fall at $\delta = -2.45$ and -3.01 ppm



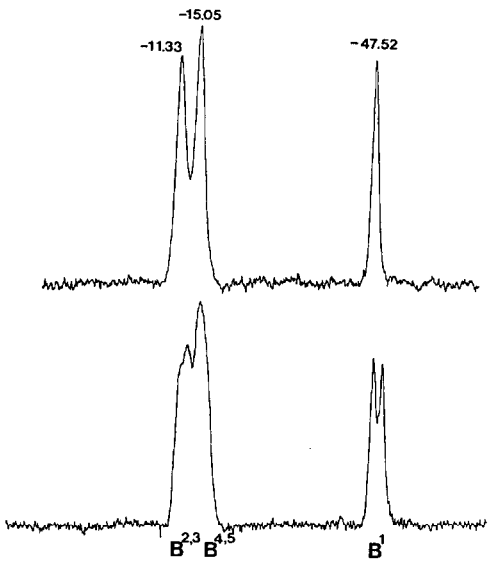


Fig. 1. 96.25-MHz ^{11}B NMR spectrum of $(dppe)CuB_5H_8$ in CD_2Cl_2 at -78°C. The upper trace is ^1H-decoupled and chemical shifts are in ppm.

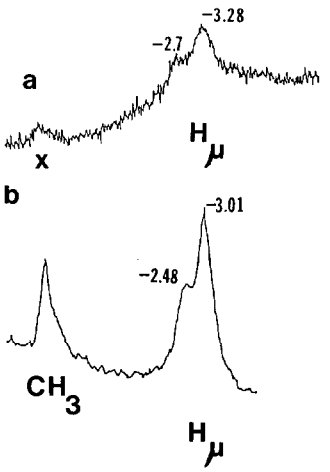


Fig. 2. (a) 300.1-MHz ^1H NMR spectrum of $(dppe)CuB_5H_8$ in the $H\mu$ region. (b) 100-MHz ^1H NMR spectrum of $[(C_6H_5)_3P]_2Cu\text{-}1\text{-}(CH_3)B_5H_7$ in the $H\mu$ region (from Ref. 8, reproduced with permission). (x) See text.

respectively. The observation of two resonances for the bridging hydrogens confirms that the species is not fluxional.

This work demonstrates the utility of the more direct method for the preparation of (dppe)Cu(I) complexes of boranes and confirms that the series of metalloboranes derived from insertion of ligated transition metal moieties into the boron–boron bond in the basal plane of $[B_5H_8]^-$ are not fluxional in solution. Previous attempts to resolve resonances due to basal B atoms in ^{11}B NMR spectra of cupriopentaboranes have been unsuccessful[1,8] and this has been attributed to the influence of the copper quadrupole. The related series of (dppe)NiX (X = Cl, Br or I) complexes of $[B_5H_8]^-$ were described[9] as fluxional based on the observation of a single broad ^{11}B resonance for the basal boron atoms in the ^{11}B NMR spectrum and single resonances for basal and bridging hydrogens in the ^1H NMR spectrum. Subsequently the same authors[10] concluded that the analogous Pd(II) and Pt(II) complexes were not fluxional on the basis of a more detailed NMR study and they surmised that all the complexes in the series (dppe)MXB_5H_8 (M = Ni, Pd or Pt) were probably[6,10] not fluxional. The data presented herein confirm that the cupriopentaboranes also have static structures as was originally suggested.[8] For such *nido*-pyramidal boranes and metalloboranes to be fluxional, it appears that it is necessary for there to be at least one formal B—B σ-bond which does not contain a bridging hydrogen in the basal plane of the species. This provides a site into which bridging hydrogens may move and also provides a mechanism whereby the borane cage in metalloboranes may move relative to the metal moiety. Thus species such as B_6H_{10},[11] $B_6H_9^-$,[12] $(THF)_2MgB_6H_9$,[13] $B_5H_8^-$[14] and $C_2B_4H_7^-$[15] are fluxional whereas $B_6H_{10}Fe(CO)_4$,[16] $[(C_6H_5)_3P]CdClB_5H_8$,[5] μ-$[\eta^5$-$C_5H_5)Fe(CO)_2]C_2B_4H_7$[17] and $[B_6H_{11}]^+$[18] are not. The former contain B—B bonds and the latter do not. Thus it is reasonable to expect that 2,3-μ-metallopentaboranes would have static structures.

Acknowledgements—We acknowledge the Weldon Spring Endowment Fund for financial support and PKR thanks the UMSL Graduate School and the Monsanto Fund for partial support. Finally we acknowledge the help of Dr V. Rutar of the University of Missouri—Columbia for assistance with the NMR spectra.

REFERENCES

1. N. N. Greenwood and J. Staves, *J. Chem. Soc., Dalton Trans.* 1978, 1144.
2. For example, see N. S. Hosmane and R. N. Grimes, *Inorg. Chem.* 1980, **19**, 3482.
3. L. Barton and P. K. Rush, *Inorg. Chem.* (in press).
4. N. Marsich, A. Camus and E. Cebulec, *J. Inorg. Nucl. Chem.* 1972, **34**, 933.
5. N. N. Greenwood and J. Staves, *J. Chem. Soc., Dalton Trans.* 1977, 1786.
6. J. D. Kennedy and J. Staves, *Z. Naturforsch.* 1979, **84B**, 808.
7. E. L. Muetterties, W. G. Peet, P. A. Wegner and C. W. Alegranti, *Inorg. Chem.* 1970, **9**, 2447; R. K. Hertz, R. Goetze and S. G. Shore, *Inorg. Chem.* 1979, **18**, 2813; P. A. Grutsch and C. W. Kutal, *J. Am. Chem. Soc.* 1977, **99**, 6466.
8. V. T. Brice and S. G. Shore, *J. Chem. Soc., Dalton Trans.* 1975, 334.
9. N. N. Greenwood and J. Staves, *J. Chem. Soc., Dalton Trans.* 1977, 1788.
10. N. N. Greenwood, J. D. Kennedy and J. Staves, *J. Chem. Soc., Dalton Trans.* 1978, 1146.
11. V. T. Brice, H. D. Johnson and S. G. Shore, *J. Am. Chem. Soc.* 1973, **95**, 6629.
12. G. L. Brubaker, M. L. Denniston, S. G. Shore, J. C. Carter and F. Swicker, *J. Am. Chem. Soc.* 1970, **92**, 7216.
13. D. L. Denton, W. R. Clayton, M. G. Mangion, S. G. Shore and E. A. Meyers, *Inorg. Chem.* 1976, **15**, 1546.
14. H. D. Johnson, R. A. Geanangel and S. G. Shore, *Inorg. Chem.* 1970, **4**, 908.
15. T. Onak, B. Lockman and G. Haran, *J. Chem. Soc., Dalton Trans.* 1973, 2115.
16. A. Davidson, D. D. Traficante and S. S. Wreford, *J. Chem. Soc., Chem. Commun.* 1972, 1155.
17. L. G. Sneddon, D. C. Beer and R. N. Grimes, *J. Am. Chem. Soc.* 1973, **95**, 6623.
18. H. D. Johnson, V. T. Brice, G. L. Brubaker and S. G. Shore, *J. Am. Chem. Soc.* 1972, **94**, 6711.

Polyhedron Vol. 4, No. 10, pp. 1745–1746, 1985
Printed in Great Britain

0277–5387/85 $3.00 + .00
© 1985 Pergamon Press Ltd

A CONVENIENT SYNTHESIS OF COPPER(I) CARBOXYLATES

THOMAS P. LOCKHART* and DEBORAH A. HAITKO
General Electric Corporate Research & Development Center, P.O. Box 8, Schenectady, NY 12301, U.S.A.

(*Received* 22 *February* 1985; *accepted* 19 *April* 1985)

Abstract—A simple procedure is described for the synthesis of aliphatic and aromatic copper(I) carboxylates by the reduction of copper(II) carboxylates with commercially available tin(II) 2-ethylhexanoate. In this way copper(I) acetate, benzoate and stearate have been prepared in good yield and purity from the corresponding copper(II) carboxylates.

Copper(I) carboxylates have found wide application as catalysts and stochiometric reagents in organic chemistry,[1] and have served as starting materials in the synthesis of novel copper(I) complexes.[2] These air- and moisture-sensitive compounds are usually prepared by one of the methods described by Edwards and Richards.[3] One procedure involves the reaction of copper(I) oxide with a carboxylic acid, with azeotropic removal of the water by-product. Reaction times are long (*ca* 12 h) and the several manipulations must be carried out under inert atmosphere. A second route involves treating a carboxylic acid solution of the copper(II) carboxylate with a reductant such as copper(0) or hydrazine hydrate. To employ this procedure, however, the acid must be a liquid at ambient conditions. Further, non-volatile carboxylic acids can be difficult to remove from the copper(I) product.

Recently several examples of the *in situ* generation of catalytically active copper(I) by the tin(II) reduction of copper(II) compounds have been reported.[4,5] In our study of the copper-catalyzed decomposition of diaryliodonium salts,[5] we employed tin(II) 2-ethylhexanoate to generate copper(I) carboxylate catalysts from the corresponding copper(II) carboxylates. The subject of this report is our development of the tin(II) reduction of simple copper(II) carboxylates as a convenient method for preparing copper(I) carboxylates of good purity in good isolated yield:

$$2\text{Cu(II)}(O_2CR)_2 + \text{Sn(II)}(O_2CR')_2 \xrightarrow[CH_2Cl_2]{25^\circ C} 2\text{Cu(I)}(O_2CR) + \text{Sn(IV)}(O_2CR')_2(O_2CR)_2.$$

RESULTS AND DISCUSSION

We have prepared three copper(I) carboxylates [copper(I) acetate, stearate and benzoate] in good yield (65–85%) from the corresponding commercially available copper(II) salts by reduction with tin(II) 2-ethylhexanoate in CH_2Cl_2 solution under an inert atmosphere. The occurrence of carboxylate exchange between copper and tin was ruled out by the IR spectrum of copper(I) benzoate which showed only strong absorbances due to aromatic C—H stretching; no absorbance due to aliphatic C—H stretching was observed. In addition, elemental and mass spectroscopic analyses indicated that the desired products were obtained in high purity.

Relative to the procedures of Edwards and Richards,[3] advantages of the method described here include the short reaction time and the simple apparatus and work up. Critical for some applications[5] is the fact that the reaction product produced by this method is obtained free of excess carboxylic acid or coordinating solvent. The tin(II) reductant, further, is inexpensive and readily available.

Isolation of a product of high purity requires the use of copper(II) carboxylates free of insoluble impurities such as copper oxides or halides.[6] Some commercially available copper(II) carboxylates are of modest purity; thus, the reduction of a commercial copper(II) caprylate gave the copper(I) salt (identified by FDMS and high-resolution EI mass spectroscopic experiments) in good yield, but elemental analysis revealed the presence of about 10% of a copper-containing impurity, presumably a copper(I) halide. The presence of small amounts of impurities may be of less concern in some application of the copper(I) carboxylates as a reaction catalyst.[4]

The method described here applies only to copper(II) carboxylates which have at least slight

* Current address: Central Research and Development Department, E. I. DePont de Nemours and Company, Experimental Station, Wilmington, DE 19898, U.S.A.

solubility in the organic solvent. Our attempts to reduce copper(II) gluconate and glycolate, which are extremely insoluble in CH_2Cl_2 and $CHCl_3$, were unsuccessful. Conversely, it appears that high solubility of the copper(I) carboxylate may result in over-reduction of the product [to copper(0)]. Therefore, in reactions involving substituted carboxylates it may be necessary in some instances to substitute other reaction solvents.

EXPERIMENTAL

Commercially available copper(II) carboxylates were dried in a vacuum oven at 80°C overnight and used without further purification. Tin(II) 2-ethylhexanoate (stannous "octoate") was used without purification (except for degassing) in the synthesis of copper(I) benzoate and stearate, but was distilled under vacuum (*ca* 0.005 torr, b.p. 155–165°C) through a short fractionating column for the synthesis of copper(I) acetate. A good commercial grade of CH_2Cl_2 was used after degassing on a vacuum line. We preferred to carry out the syntheses in an inert atmosphere glove box, but the reaction has also been carried out in a three-neck flask with a nitrogen blanket over the solution. Removal of the reaction and wash solvents from the copper(I) product can be accomplished with a cannula or a filtering side arm. Loss of the very fine copper(I) product through the fritted filter appears to be the major factor lowering the isolated yield. The representative synthesis of copper(I) benzoate is described below.

Copper(I) benzoate

In an inert atmosphere glove box, a mixture of copper(II) benzoate (0.016 mol) and tin(II) 2-ethylhexanoate (0.009 mol) in 25 cm^3 CH_2Cl_2 was prepared. While stirring at room temperature, the color of the solution changed from blue [due to copper(II)] to a faint grey-green color over about 4 h. The very fine whitish precipitate [copper(I) benzoate] was isolated by suction filtration [the tin(II) reagent and the tin(IV) product are very soluble in the organic solvent]. The product was washed 4 times with CH_2Cl_2, leaving a whitish-grey solid which was dried *in vacuo* for several hours. The moderately air-sensitive copper(I) benzoate was isolated in 84% yield and stored under nitrogen.

Found: Cu, 34.20; C, 45.30; H, 2.73. Calc. for $CuC_7H_5O_2$: Cu, 34.4; C, 45.5; H, 2.73%. IR (KBr) major bands at 3050(m), 1590(s), 1530(br, s), 1490(m), 1410(br, sh, 845(m), 710(s), 690(s) and 555(m) cm^{-1}.

Copper(I) acetate

Isolated as a very pale yellow solid in 75% yield. Found: Cu, 51.60; C, 19.59; H, 2.41. Calc. for $CuC_2H_3O_2$: Cu, 51.83; C, 19.60; H, 2.47%.

Copper(I) stearate

Isolated as a pale yellow solid in 65% yield: Found: Cu, 18.15; C, 62.08; H, 9.95. Calc. for $CuC_{18}H_{35}O_2$: Cu, 18.33; C, 62.33; H, 10.10%.

Acknowledgements—We gratefully acknowledge the expert assistance of Steven B. Dorn in carrying out mass spectroscopic experiments and thank James V. Crivello, Sandra L. Pratt and Diane V. Brezniak for their helpful comments.

REFERENCES

1. For example, see: T. Cohen and A. H. Lewis, *J. Am. Chem. Soc.* 1966, **88**, 4521; J. K. Kochi and A. Bemis, *Tetrahedron* 1968, **24**, 5099; G. W. Kumpp, H. Box, R. F. Schmitz and J. J. Vrielink, *Tetrahedron Lett.* 1975, 3429.
2. For recent examples, see: M. Pasquali, C. Floriani, G. Venturi, A. Gaetani-Manfredotti and A. Chiesi-Valla, *J. Am. Chem. Soc.* 1982, **104**, 4092; G. Doyle, K. A. Eriksen, M. Modrick and G. Ansell, *Organometallics* 1982, **1**, 1613.
3. D. A. Edwards and R. Richards, *J. Chem. Soc., Dalton Trans* 1973, 2463.
4. J. V. Crivello and J. L. Lee, *Macromol. Chem.* 1983, **184**, 463; C. Galli, *Tetrahedron Lett.* 1980, 4515.
5. T. P. Lockhart, *J. Am. Chem. Soc.* 1983, **105**, 1940.
6. Simple methods for preparing copper(II) carboxylates in high purity are described in: R. L. Martin and H. Waterman, *J. Chem. Soc.* 1957, 2545; D. P. Graddon, *J. Inorg. Nucl. Chem.* 1967, **17**, 222.

Polyhedron Vol. 4, No. 10, pp. 1747–1753, 1985
Printed in Great Britain

0277-5387/85 $3.00 + .00
© 1985 Pergamon Press Ltd

TETRAHEDRAL AND OCTAHEDRAL COORDINATION FOR COBALT(II) COMPLEXES OF *N*-ISOPROPYL-2-PYRROLIDINONE

BRUCE A. WILSON and STANLEY K. MADAN*
Department of Chemistry, State University of New York at Binghamton, Binghamton, NY 13901, U.S.A.

(*Received* 14 *February* 1985; *accepted* 19 *April* 1985)

Abstract—Complexes of the formulas $[Co(NIPP)_4](ClO_4)_2$ and $[Co(NIPP)_6](ClO_4)_2$ have been synthesized and isolated (NIPP = *N*-isopropyl-2-pyrrolidinone). IR spectra and conductance data are presented as proof that perchlorate coordination in $[Co(NIPP)_4](ClO_4)_2$ does not occur. Vibrational spectra indicate that coordination occurs through the NIPP carbonyl oxygen for both complexes. Spectral parameters obtained from the electronic spectra and magnetic moments indicate tetrahedral and octahedral coordination for $[Co(NIPP)_4](ClO_4)_2$ and $[Co(NIPP)_6](ClO_4)_2$, respectively. The powder X-ray diffraction data appear to support the assignments of these two geometries. The crystal-field prediction that $\Delta(T_d)/\Delta(O_h) = 0.44$ is in reasonably good agreement with the experimental results.

The best-known examples of mixed neutral ligand–anion complexes of a metal ion in two different symmetries are the four-coordinate $Co(py)_2X_2$ and the six-coordinate $Co(py)_4X_2$ (py = pyridine, X = halide).[1,2] Tetrahedral and octahedral symmetries for nickel(II)[3] and cobalt(II)[4] doped into ZnO and MgO lattices have also been investigated. The formation of octahedral and tetrahedral complexes from a single metal ion and anion has been reported by Foster and Goodgame.[5,6] Wayland *et al.*[7] were the first to report the synthesis and isolation of a transition-metal ion complex with different numbers of the same neutral ligand [*N*,*N*-dimethylacetamide (DMA)] as the only coordinated species. Madan[8] has provided a second example of this phenomenon by preparing and isolating perchlorate salts of *N*-methyl-2-pyrrolidinone (NMEP) (also known as *N*-methyl-γ-butyrolactam), in both tetrahedral and octahedral geometries.

This paper reports the third definite isolation of complexes of the form $[Co(NIPP)_4](ClO_4)_2$ and $[Co(NIPP)_6](ClO_4)_2$, where NIPP = *N*-isopropyl-2-pyrrolidinone is the only coordinated species and is a neutral ligand like DMA and NMEP. Magnetic susceptibility data, electronic spectra and powder X-ray diffraction data indicate the Co(II) possesses a tetrahedral field in $[Co(NIPP)_4](ClO_4)_2$, and an octahedral field in $[Co(NIPP)_6](ClO_4)_2$. For both complexes, the IR spectra show the NIPP ligand is coordinated to cobalt(II) through the carbonyl oxygen. Vibrational spectra and conductance measurements are utilized to demonstrate that the perchlorate ion is not coordinated in $[Co(NIPP)_4](ClO_4)_2$. Calculations made on the basis of regular symmetry for these complexes give $\Delta(T_d)/\Delta(O_h) = 0.52$, which compares favorably with the value of 0.44 predicted by the crystal-field theory.[9,10]

EXPERIMENTAL

Physical measurements

Electronic absorption spectra were determined using a Carey Model 14 recording spectrophotometer. IR spectra were obtained from a Perkin–Elmer Model 283B recording spectrophotometer. The conductance measurements were made on an Industrial Instrument Model RD 16B2 conductivity bridge, utilizing a conventional conductivity cell containing platinum electrodes. The magnetic susceptibilities were measured utilizing a Faraday magnetic balance. Mercury(II) tetrathiocyanate cobaltate(II) was used as the magnetic susceptibility standard. X-ray diffraction patterns were obtained on a Norelco (Phillips Electronics Instruments)

* Author to whom correspondence should be addressed.

Table 1. Analytical data

Compound	Theoretical				Found			
	% C	% H	% Co	% ClO_4	% C	% H	% Co	% ClO_4
$[Co(NIPP)_6](ClO_4)_2$	49.41	7.72	4.67	19.48	49.36	7.68	4.74	19.40
$[Co(NIPP)_4](ClO_4)_2$	43.87	6.85	7.69	25.95	43.85	6.61	7.69	25.76

wide-range gioniometer type 150-100-00 with a direct reading diffractometer. The *K*-alpha X-ray line from a nickel-filtered copper source was employed. The relative peak heights were determined by estimating the relative intensities.

Chemicals

The Co(II) perchlorate hexahydrate was of reagent grade. NIPP was obtained from GAF coporation in technical grade form and purified using vacuum distillation (84°C, 5 mm).

Synthesis

All syntheses were performed in a nitrogen atmosphere, utilizing glove box techniques.

$[Co(NIPP)_6](ClO_4)_2$ (*raspberry*). Cobalt(II) perchlorate hexahydrate, $Co(ClO_4)_2$ (0.3538 g), was added to a 500% excess of 2,2-dimethoxypropane (3.060 g). The resulting solution was stirred on a magnetic stirrer for 2 h at room temperature. A stoichiometric amount of NIPP (0.7475 g) was added to the resulting anhydrous solution dropwise while the solution was being stirred. This mixture was stirred for an additional 15 min. An equal volume of anhydrous ethyl ether was then added to the mixture with stirring. Vigorous trituration of the raspberry oil that formed upon the addition of NIPP did not result in the formation of crystals. Additional NIPP was added dropwise with continuous trituration until raspberry-colored crystals had formed. The crystals were then filtered, washed with anhydrous ethyl ether, and dried over P_4O_{10} for 48 h in a nitrogen atmosphere. The complex is extremely hygroscopic.

$[Co(NIPP)_4](ClO_4)_2$ (*violet*). The four-coordinate complex of NIPP coordinated to Co(II) was obtained by keeping the six-coordinate complex *in vacuo* at 80°C over P_4O_{10} in a drying pistol for 96 h. This complex is also extremely hygroscopic.

Analyses

Carbon and hydrogen analyses were performed by MicAnal Organic Microanalysis of Tucson, AZ. Metal ion analyses were performed by complexometric titration with EDTA, as described by Flaschka.[11] Perchlorate analyses were completed utilizing a gravimetric procedure based upon the precipitation of nitron perchlorate.[12]

RESULTS AND DISCUSSION

The analytical data for the complexes are summerized in Table 1. The electronic spectral data for the complexes are given in Table 2, with assignments for the transitions. The molar absorbtivity of $[Co(NIPP)_4](ClO_4)_2$ in CH_2Cl_2 is low for a tetrahedral complex. However, it was found that the

Table 2. Electronic spectral bands

Compound	Medium	ν_{max} (cm^{-1})	ε_{max} (cm^{-1} mol)	Band assignment
$[Co(NIPP)_6](ClO_4)_2$	Acetone +	7440	5.0	$^4T_{1g}(F) \rightarrow {}^4T_{2g}(F)$
	0.1 M NIPP	19,010	9.0	$^4T_{1g}(F) \rightarrow {}^4T_1(P)$
		21,100	5.0	
	Nujol	7170	(−)	$^4T_{1g}(F) \rightarrow {}^4T_{2g}(F)$
		19,080	(−)	$^4T_{1g}(F) \rightarrow {}^4T_1(P)$
		20,780	(−)	
$[Co(NIPP)_4](ClO_4)_2$	CH_2Cl_2	7560	15.0	$^4A_2(F) \rightarrow {}^4T_1(F)$
		18,180	94.0	$^4A_2(F) \rightarrow {}^4T_1(P)$
	Nujol	7340	(−)	$^4A_2(F) \rightarrow {}^4T_1(F)$
		17,110	(−)	$^4A_2(F) \rightarrow {}^4T_1(P)$

Table 3. Conductance data for various complexes in CH_2Cl_2

Compound	Type	Λ_{molar}	Concentration ($\times 10^3$ M)	Temperature (°C)
$[Ni(py)_4(ClO_4)_2]$[a]	Nonionic	1.72	0.292	22.4
$[Ni(py)_3(NO_3)_2]$[a]	Nonionic	0.194	0.324	22.6
$[Ni(py)_4(H_2O)_2](ClO_4)_2$[a]	2:1	8.74	1.04	24.0
$[Co(DMA)_4](ClO_4)_2$[a]	2:1	12.1	4.12	26.1
$[Co(NMEP)_4](ClO_4)_2$[b]	2:1	11.4	4.40	25.0
$[Co(NIPP)_4](ClO_4)_2$	2:1	9.27	5.00	25.0

[a] Data from Ref. 7.
[b] Data from Ref. 8.

spectra of the complex in Nujol and CH_2Cl_2 were not significantly different. Further, it was found that addition of NIPP to the complex in CH_2Cl_2 had no effect on the spectra. This indicates that the primary absorbing species in solution is $[Co(NIPP)_4]^{2+}$.

The conductance data are presented in Table 3 and magnetic susceptibility data are given in Table 4. X-ray data are displayed in Tables 5 and 6.

The IR spectrum of $[Co(NIPP)_4](ClO_4)_2$ may be used to determine if the perchlorate ion is coordinated to the cobalt(II) ion. It has been shown[13] that, for a unidentate coordinated perchlorate, the symmetry of the perchlorate ion is lowered from T_d to C_{3v} in the complex. This results in the splitting of the broad band into two intense peaks in the 1200–900 cm^{-1} region. However, the IR spectrum of $[Co(NIPP)_4](ClO_4)_2$ in the 1200–900 cm^{-1} region shows a broad band with a maximum at 1090 cm^{-1}, which is indicative of ionic perchlorate. The conductance data in Table 3 clearly indicate that $[Co(NIPP)_4](ClO_4)_2$ is an electrolyte. Hence, the perchlorate ion can not be coordinated.

The magnetic moments for crystalline $[Co(NIPP)_4](ClO_4)_2$ and $[Co(NIPP)_6](ClO_4)_2$ are within the acceptable ranges for tetrahedral and octahedral cobalt(II) complexes, respectively.[14] The magnetic moments for $[Co(DMA)_4](ClO_4)_2$, 4.62 B.M.,[7] and $[Co(NMEP)_4](ClO_4)_2$, 4.80 B.M.,[8] are considerably higher than the magnetic moment for $[Co(NIPP)_4](ClO_4)_2$, 4.42 B.M.

The electronic spectra for $[Co(NIPP)_4](ClO_4)_2$ and $[Co(NIPP)_6](ClO_4)_2$ compare favorably with spectra previously reported for tetrahedral[15] and octahedral[16] Co(II) complexes, respectively. For $[Co(NIPP)_6](ClO_4)_2$, the $^4T_1(F) \rightarrow {}^4A_2(F)$ transition, which is essentially a two-electron transition, is absent. The splitting of the ν_2 bands observed in the spectra of $[Co(DMA)_4](ClO_4)_2$[7] and $[Co(NMEP)_4](ClO_4)_2$[8] is not observed in the spectrum of $[Co(NIPP)_4](ClO_4)_2$.

It is expected that $[Co(NIPP)_4](ClO_4)_2$ is highly distorted, since it is formed from $[Co(NIPP)_6](ClO_4)_2$. Support for distortion from regular tetrahedral symmetry comes from consideration of the spin–orbit coupling constant, λ', for the tetrahedral complex. The λ' for the coordinated Co(II) are decreased in magnitude from that of the free ion value of -178 cm^{-1}. The λ' for a tetrahedral cobalt(II) complex can be calculated using the magnetic and spectral data, according to the relationship: $\mu_{obs} = \mu_{so} - 15.59\lambda'/10Dq = 3.89 - 15.19\lambda'/10Dq$.[7,8,15,17] Values of λ' for complexes of regular tetrahedral symmetry calculated from this relationship have been found to be in the range -130 to -160 cm^{-1}.[17] Wayland *et al.*[7] and Madan[8] have reported λ' for $[Co(DMA)_4](ClO_4)_2$ and $[Co(NMEP)_4](ClO_4)_2$ of -200 to -220 and -296 to -316 cm^{-1}, respectively. The authors have attributed these large negative λ' to the inappropriateness of the above equation in calculating the λ' for a distorted tetrahedral complex. For $[Co(NIPP)_4](ClO_4)_2$, the λ' has been found to be ir

Table 4. Magnetic susceptibility data

Compound	10^6 (χ_m)	10^6 (χ_m^{corr})	Temperature (°C)	μ_{eff}[a] (B.M.)	State
$[Co(NIPP)_6](ClO_4)_2$	10,488	11,093	299.9	5.18	Solid
$[Co(NIPP)_4](ClO_4)_2$	7798	8228	294.4	4.42	Solid

[a] Error ± 0.05 B.M.

Table 5. Powdered X-ray diffraction data of NIPP perchlorate complexes of Co(II), Cu(II) and Zn(II)

$[Cu(NIPP)_4](ClO_4)_2$		$[Cu(NIPP)_4](ClO_4)_2$		$[Zn(NIPP)_4](ClO_4)_2$	
d (Å)	I/I_{100} (%)	d (Å)	I/I_{100} (%)	d (Å)	I/I_{100} (%)
—	—	12.72	46.3	—	—
—	—	11.12	93.3	—	—
—	—	—	—	10.46	100.0
—	—	—	—	10.15	55.4
10.06	35.7	—	—	—	—
9.60	41.1	—	—	—	—
—	—	8.96	19.9	—	—
—	—	8.53	46.3	—	—
—	—	7.75	97.7	—	—
—	—	7.45	93.5	—	—
7.12	16.3	—	—	—	—
6.98	20.2	—	—	6.98	21.0
—	—	—	—	6.83	16.4
6.78	26.5	—	—	6.78	17.3
—	—	6.74	23.9	—	—
—	—	6.16	48.8	—	—
—	—	5.92	41.0	—	—
—	—	5.75	53.9	—	—
5.64	22.2	—	—	5.62	33.3
—	—	5.44	34.7	—	—
5.22	69.5	—	—	5.23	44.5
—	—	—	—	5.09	13.1
—	—	5.00	56.5	—	—
—	—	4.95	74.1	—	—
4.82	32.7	4.85	69.4	4.82	13.8
—	—	4.78	58.1	—	—
4.48	17.1	4.47	57.9	4.49	22.7
—	—	4.41	63.0	—	—
4.33	23.3	4.33	55.6	4.35	34.7
4.12	34.0	4.12	74.3	—	—
4.06	100.0	4.08	100.0	4.08	100.0
3.96	27.6	—	—	3.96	19.4
3.91	15.2	—	—	3.91	17.0
—	—	3.88	63.2	—	—
—	—	3.77	97.9	—	—
—	—	3.65	51.2	—	—
—	—	3.58	58.3	—	—
3.50	37.1	—	—	3.50	50.6
—	—	3.45	53.2	—	—
—	—	—	—	3.39	17.3
—	—	—	—	3.29	22.7
3.18	15.5	—	—	—	—
—	—	3.11	58.1	—	—
3.03	42.0	—	—	3.03	55.4
2.96	15.7	2.98	49.1	2.96	19.1

Table 6. Powdered X-ray diffraction data of NIPP perchlorate complexes of Co(II), Ni(II) and Cd(II)

$[Co(NIPP)_6](ClO_4)_2$		$[Ni(NIPP)_6](ClO_4)_2$		$[Cd(NIPP)_6](ClO_4)_2$	
d (Å)	I/I_{100} (%)	d (Å)	I/I_{100} (%)	d (Å)	I/I_{100} (%)
12.47	35.8	—	—	—	—
11.77	56.2	—	—	—	—
—	—	11.12	69.3	—	—
—	—	—	—	10.93	35.6
—	—	—	—	10.25	26.5
9.84	54.8	9.81	22.6	—	—
—	—	9.36	24.3	—	—
9.30	40.8	—	—	—	—
—	—	—	—	9.11	26.0
—	—	—	—	8.89	25.6
8.70	76.3	—	—	—	—
—	—	8.57	81.3	—	—
—	—	—	—	8.43	39.1
—	—	—	—	7.70	100.0
7.52	28.6	—	—	—	—
7.26	33.3	—	—	—	—
—	—	6.81	85.5	—	—
6.36	27.8	6.32	24.0	6.32	35.0
5.91	27.8	5.91	25.5	—	—
5.82	27.5	—	—	—	—
5.75	30.6	—	—	—	—
5.57	46.3	5.53	51.0	—	—
5.49	52.3	—	—	5.49	29.7
5.31	24.8	—	—	—	—
5.14	41.3	—	—	—	—
5.08	39.1	—	—	—	—
4.99	23.4	—	—	—	—
—	—	—	—	4.93	52.0
4.86	30.6	—	—	—	—
—	—	4.73	56.8	—	—
—	—	4.58	67.7	—	—
4.49	36.9	—	—	4.46	82.0
4.37	100.0	4.39	100.0	—	—
—	—	4.30	87.9	4.29	86.5
4.21	89.0	4.24	88.4	4.22	48.8
4.09	90.4	4.06	52.3	—	—
4.03	47.4	4.00	56.1	—	—
3.93	32.2	—	—	3.95	58.4
3.88	32.2	3.86	32.7	3.89	30.1
—	—	3.82	32.3	3.83	43.8
3.73	35.8	—	—	—	—
3.63	34.7	3.66	27.3	3.67	38.6
3.61	41.6	—	—	—	—
3.57	53.2	3.55	27.6	—	—
3.42	24.8	3.42	54.7	—	—
3.34	21.8	3.35	32.1	3.35	19.2
3.29	28.6	3.31	29.2	3.27	25.1
3.26	22.9	—	—	3.23	22.9
3.18	23.1	3.19	23.4	—	—
3.16	26.4	—	—	3.12	23.1
3.08	22.9	—	—	—	—
—	—	—	—	2.99	23.1

the range of -138 to $-158\ cm^{-1}$, which is in the range of Co(II) complexes exhibiting regular tetrahedral geometry. This is a rather surprising result, considering that the NIPP ligand has a bulkier alkyl substituent than either the DMA or NMEP ligands. However, Wayland *et al.*[7] and Madan[8] attribute the distortion from regular tetrahedral geometry to a weak bonding interaction between the nitrogen atom and the metal ion. It is possible that the isopropyl group prevents this interaction from occurring in $[Co(NIPP)_4](ClO_4)_2$.

The shift in the NIPP carbonyl stretching frequency to a lower frequency upon complexation is generally used to indicate coordination through the carbonyl oxygen.[18] The centers of intensity for the NIPP carbonyl stretching frequency in $[Co(NIPP)_4](ClO_4)_2$ and $[Co(NIPP)_6](ClO_4)_2$ are at 1610 and 1630 cm^{-1}, respectively. The carbonyl stretching frequency for neat NIPP is 1687 cm^{-1}. The carbonyl frequency shifts indicate that the carbonyl oxygen is the principal donor site.

Underhill and Billing[19] have shown that the calculations of the spectral parameters for the octahedral and tetrahedral d^7 Co(II) complexes can be determined using simplified quadratic equations for the Tanabe and Sugano energy expressions. The values for $[Co(NIPP)_6](ClO_4)_2$ and $[Co(NIPP)_4](ClO_4)_2$, in Nujol, are 8230 ± 100 and $4200 \pm 100\ cm^{-1}$, respectively. The ratio $\Delta(T_d)/\Delta(O_h)$ is 0.52 in Nujol for $[Co(NIPP)_{4,6}](ClO_4)_2$, compared to the value of 0.44 predicted by the crystal-field theory. There are several effects that should be considered in interpreting this slightly higher ratio for the Co(II) complexes of NIPP: (1) the steric interaction of the isopropyl group will lower the splitting energy of the octahedral complex, and (2) the increased covalency of the tetrahedral complex, as seen in the β values, should increase the crystal-field splitting energy of the tetrahedral complex. Foster and Goodgame[5,6] have determined $\Delta(T_d)/\Delta(O_h)$ for the pairs of complexes

$$Ni(NCS)_4^{2-}/Ni(NCS)_6^{4-}$$

and

$$Co(NCS)_4^{2-}/Co(NCS)_6^{4-},$$

to be 0.51 and 0.49, respectively. Wayland *et al.*[7] have determined $\Delta(T_d)/\Delta(O_h)$ for the pair $[Co(DMA)_4]^{2+}/[Co(DMA)_6]^{2+}$ to be 0.64, and Madan[8] found $\Delta(T_d)/\Delta(O_h)$ for the pair $[Co(NMEP)_4]^{2+}/[Co(NMEP)_6]^{2+}$ to be 0.60.

The powder X-ray diffraction patterns indicate that

$$[Co(NIPP)_4](ClO_4)_2$$

and

$$[Zn(NIPP)_4](ClO_4)_2{}^{20}$$

are isomorphous and that these patterns are significantly different from those for

$$[Cu(NIPP)_4](ClO_4)_2.{}^{20}$$

Although Co(II) and Zn(II) are known to form square-planar complexes with bidentate ligands, they predominantly form tetrahedral complexes with monodentate ligands. Conversely, Cu(II) is known to form a variety of square-planar complexes, as well as tetrahedral complexes. Therefore, it would be expected that the complexes of Co(II) and Zn(II) are tetrahedrally coordinated, whereas the Cu(II) complex is evidently a square-planar complex. A comparison of the X-ray diffraction patterns indicates that

$$[Co(NIPP)_6](ClO_4)_2$$

and

$$[Ni(NIPP)_6](ClO_4)_2{}^{20}$$

are isomorphous, whereas

$$[Cd(NIPP)_6](ClO_4)_2$$

is not isomorphous with either. A possible explanation of this may be that the steric interaction of the isopropyl group of NIPP results in the distortion of the complexes of Co(II) and Ni(II) from octahedral configuration. The larger ionic radius of Cd(II) may relieve some of these steric interactions, resulting in a "purer" octahedral geometry.

REFERENCES

1. C. H. King, E. Koros and S. M. Nelson, *J. Chem. Soc.* 1963, 5449.
2. S. M. Nelson, *Proc. Chem. Soc.* 1961, 372.
3. R. Pappalardo, D. L. Wood and R. C. Linares, *J. Chem. Phys.* 1961, **35**, 1460.
4. R. Pappalardo, D. L. Wood and R. C. Linares, *J. Chem. Phys.* 1961, **35**, 2041.
5. D. Foster and D. M. L. Goodgame, *Inorg. Chem.* 1965, **4**, 823.
6. D. Foster and D. M. L. Goodgame, *Inorg. Chem.* 1965, **4**, 1712.
7. B. B. Wayland, R. J. Fitzgerald and R. S. Drago, *J. Am. Chem. Soc.* 1966, **85**, 4600.
8. S. K. Madan, *J. Inorg. Nucl. Chem.* 1971, **33**, 1025.
9. L. E. Orgel, *An Introduction to Ligand Field Theory.* John Wiley, New York (1960).
10. C. J. Ballhausen, *Ligand Field Theory.* McGraw-Hill, New York (1962).
11. H. A. Flaschka, *EDTA Titrations.* Pergamon Press, New York (1959).
12. F. J. Welcher, *Organic Analytical Reagents.* D. Van Nostrand, New York (1946).

13. B. J. Hathaway and A. E. Underhill, *J. Chem. Soc.* 1961, 3091.
14. B. N. Figgis and J. Lewis, In *Modern Coordination Chemistry* (Edited by J. Lewis and R. G. Wilkins). Interscience, New York (1960).
15. F. A. Cotton, D. M. L. Goodgame and M. Goodgame, *J. Am. Chem. Soc.* 1961, **83**, 4690.
16. D. W. Meek, R. S. Drago and T. S. Piper, *Inorg. Chem.* 1962, **1**, 285.
17. F. A. Cotton, O. D. Faut, D. M. L. Goodgame and R. H. Holm, *J. Am. Chem. Soc.* 1961, **83**, 1780.
18. C. D. Schmalbach and R. S. Drago, *J. Am. Chem. Soc.* 1960, **82**, 4484.
19. A. E. Underhill and D. E. Billing, *Nature (London)* 1966, **210**, 834.
20. B. A. Wilson, Master of Arts Thesis, State University of New York, Binghamton, New York (1984).

Polyhedron Vol. 4, No. 10, pp. 1755–1760, 1985
Printed in Great Britain

0277–5387/85 $3.00 + .00
© 1985 Pergamon Press Ltd

CYCLIC AND OPEN-CHAIN TAUTOMERISM AND COMPLEX FORMATION BEHAVIOUR OF THE CONDENSATION PRODUCT OF 2-AMINO-3-AMINOMETHYL-4-METHOXYMETHYL-6-METHYLPYRIDINE WITH SALICYLALDEHYDE

Z. CIMERMAN and Z. ŠTEFANAC*
Laboratory of Analytical Chemistry, Faculty of Science, University of Zagreb, Strossmayerov trg 14, 41000 Zagreb, Yugoslavia

(*Received* 7 *November* 1984; *accepted* 19 *April* 1985)

Abstract—The crystalline product obtained by the condensation of 2-amino-3-aminomethyl-4-methoxymethyl-6-methylpyridine and salicylaldehyde was characterized by spectrometric methods (UV, IR, ^{1}H NMR and MS). It was shown that the dissolution of the crystalline cyclic diamine afforded its tautomeric conversion to the enolimine form of the Schiff base [2-amino-4-methoxymethyl-6-methyl-3-(salicylideneaminomethyl)pyridine] with a rate of the process and a ratio of both forms attained at equilibrium dependent upon the solvent. The presence of the ketoamine form was not evidenced. The behaviour of the condensation product as the ligand in formation of complexes with Cu(II), Ni(II), Co(II) and Cd(II) was investigated in methanolic solution. Coordination with Cu(II) and Ni(II) caused partial hydrolysis of the ligand and the formation of complexes of the bis Schiff base [4-methoxymethyl-6-methyl-2-(salicylideneamino)-3-(salicylideneaminomethyl)pyridine] characterized after their isolation by elemental analyses and spectrometric data.

Condensation of diamines with aldehydes or ketones yield products which form stable complexes with various metal ions with characteristic properties interesting from several points of view.[1,2]

The course of condensation depends on the reactants in question and on the reaction conditions, so that different intermediates, isomeric compounds or mixtures of tautomeric forms might be involved. Schiff bases are mostly obtained as mono and bis derivatives[1–3] but the presence in solution of cyclic diamines[4,5] and/or carbinolamines[5] has also been reported. Metal ions influence in some cases the course affording products unobtainable in their absence.[3,6]

Anticipating in the first place an improved analytical applicability of the product, the condensation of 2-amino-3-aminomethyl-4-methoxymethyl-6-methylpyridine with salicylaldehyde has been undertaken in the broadened frame of the study concerning the related amines.[7]

The behaviour of the condensation product and formation of some transition metal complexes have been pursued in solution and the structures of isolated solid species determined.

EXPERIMENTAL

Apparatus

Vibrational and electronic absorption spectra were recorded on Perkin–Elmer instruments. Models 598 with data station and 580B were used for recording IR spectra in solution ($CHCl_3$) and Model 283 for solid-state samples (KBr or CsBr pellets). UV/VIS spectra were recorded on Model 200. Mass spectra were recorded on an Hitachi Perkin–Elmer RMU-6M spectrometer. ^{1}H NMR spectra of saturated solutions [$CDCl_3$, CD_3OD and $(CD_3)_2SO$] were taken at various temperatures (20, 25, 40 and 50°C) on a JEOL JNM-FX-100FT instrument, using tetramethylsilane as internal standard.

Materials

2 - Amino - 3 - aminomethyl - 4 - methoxymethyl - 6 - methylpyridine was obtained as dihydrochloride by courtesy of Dr D. Korunčev, Pliva,

* Author to whom correspondence should be addressed.

Pharmaceutical and Chemical Works, Zagreb, Yugoslavia. Free amine was prepared and purified to analytical grade according to the procedure described in Ref. 8. Salicylaldehyde and metal salts of analytical purity grade, were purchased from Kemika, Zagreb, Yugoslavia. All solvents used were of analytical purity grade (E. Merck, Darmstadt, F.R.G.).

Procedures

Condensation of 2 - amino - 3 - aminomethyl - 4 - methoxymethyl - 6 - methylpyridine with salicylaldehyde. Equimolar amounts of amine and salicylaldehyde, both dissolved in ethanol ($\sim$ 1 mol dm^{-3} solution) were mixed and the resulting yellow solution was stirred thoroughly for 30 min at room temperature. The pale yellow precipitate which had formed during the stirring was separated and recrystallized from hot methanol.

Preparation of complexes with Cu(II) *and* Ni(II). Slow evaporation of a methanolic solution containing equimolar amounts of the condensation product and metal(II) sulphate resulted in the formation of white crystals of dibasic tetrasubstituted pyridine sulphate along with the coloured crystals of complexes, green with copper or dark brown with nickel. The water-soluble salt of the amine was removed by washing the crystals with large amounts of water after filtration. The remaining water-insoluble complex was recrystallized from a chloroform/methanol mixture.

The Cu(II) complex was also prepared by reaction of the condensation product with Cu(II) acetate and Cu(II) nitrate, respectively. The isolation procedure was the same as in the case of Cu(II) sulphate.

Characterization of solid compounds. Condensation product, $C_{16}H_{19}N_3O_2$, pale yellow crystals, m.p. 158–160°C, 80% yield.

Found (calc.): C, 67.26 (67.34); H, 6.85 (6.71); N, 14.74 (14.73)%.

IR spectrum, $\tilde{\nu}$ cm^{-1} relative intensity: (KBr) 3420 w, 3320 s, 3220 s, 3040 m, 2930 m, 2820 m, 1600 s, 1580 s, 1525 m, 1490 m, 1470 s, 1453 s, 1380 m, 1320 m, 1290 m, 1260 s, 1250 m, 1200 m, 1183 m, 1165 m, 1140 m, 1120 s, 1080 m, 980 m, 860 s, 750 s and 615 m; ($CHCl_3$, 15 min after dissolution) 3420 m, 3320 w, 3000 m, 2920 m, 1600 s, 1580 s, 1488 m, 1470 s, 1455 s, 1390 w, 1310 w, 1285 w, 1180 w, 1160 w, 1145 w, 1115 m, 1098 m, 1065 w and 845 m; ($CHCl_3$, 14 h after dissolution) 3500 w, 3420 m, 3390 m, 3320 w, 3000 m, 2920 m, 1630 s, 1600 s, 1580 s, 1488 m, 1470 s, 1455 s, 1400–1390 w, 1310 w, 1285 sh, 1275 m, 1180 w, 1160 w, 1145 w, 1115 sh, 1098 m, 1065 w and 840 m.

Mass spectrum, *m/z* [relative intensity (%)]: 285 (38), 270 (13), 269 (7), 268 (8), 253 (16), 238 (11), 237 (15), 192 (10), 165 (48), 149 (24), 135 (100), 134 (11), 122 (14), 121 (11), 120 (8), 118 (11), 108 (10), 107 (9), 106 (10), 91 (10) and 77 (18).

Cu(bis Schiff base), $C_{23}H_{21}N_3O_3Cu$, dark brown crystals after drying *in vacuo*, changing the colour to green after exposure to air ($C_{23}H_{21}N_3O_3Cu \cdot 1.5H_2O$), m.p. 260–265°C (decomp.), 18–20% yield.

Found (calc.): C, 61.13 (61.31); H, 4.69 (4.69); N, 9.32 (9.32); Cu, 14.32 (14.09)%.

IR spectrum, $\tilde{\nu}$ cm^{-1} relative intensity: (CsBr) 3055 vw, 3020 vw, 2920 w, 2820 w, 1628 s, 1610 vs, 1582 m, 1525 s, 1470 m, 1453 m, 1435 m, 1375 m, 1325 m, 1245 m, 1220 m, 1200 s, 1150 s, 1130 m, 1095 w, 960 w and 755 s.

Mass spectrum, *m/z* [relative intensity (%)]: 450 (100), 435 (2), 418 (3), 389 (18), 344 (10), 333 (12), 331 (24), 301 (8), 281 (6), 269 (10), 253 (5), 237 (28), 209 (14) and 182 (11).

Ni(bis Schiff base), $C_{23}H_{21}N_3O_3Ni$, dark brown crystals, m.p. 255–258°C (decomp.), 19% yield.

Found (calc.): C, 62.38 (61.92); H, 5.17 (4.74); N, 9.88 (9.41); Ni, 13.55 (13.15)%.

IR spectrum, $\tilde{\nu}$ cm^{-1} relative intensity: (CsBr) 3055 w, 3020 vw, 2920 w, 2820 vw, 1620 vs, 1610 vs, 1580 m, 1540 m, 1525 s, 1470 m, 1455 m, 1440 m, 1375 m, 1325 m, 1248 m, 1230 m, 1208 m, 1150 s, 1130 m, 1045 m, 950 m and 755 s.

Mass spectrum, *m/z* [relative intensity (%)]: 445 (100), 430 (2), 413 (2), 327 (5), 326 (5), 298 (6), 296 (4), 281 (6), 270 (13), 255 (3), 237 (4), 210 (12) and 181 (7).

Spectrophotometric determination of metal: ligand ratio in solution. The modified continuous-variation method of Job[9] was pursued throughout.

RESULTS AND DISCUSSION

Tautomeric equilibrium of the condensation product in solution

The investigation of the complexation ability in diluted solutions of the product obtained by condensation of 2-amino-3-aminomethyl-4-methoxymethyl-6-methylpyridine with salicylaldehyde afforded the evidence for very slow changes of UV/VIS spectrometric characteristics. For better understanding of the formation course of complex species we pursued also the behaviour of the ligand itself in solution. The more so, as in addition to the usual ketoenamine–enolimine tautomeric equilibria, some other resemblant systems have been considered.[4,5,10]

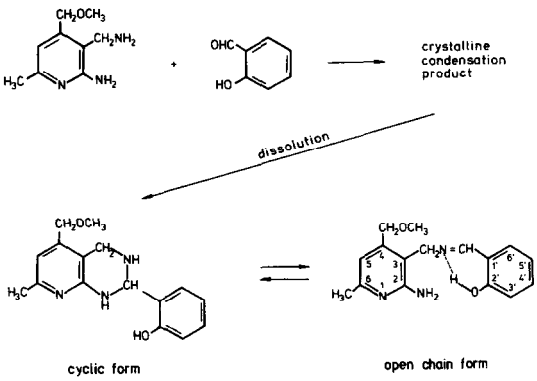
The absorption maxima (λ_{max}) (245, 283 and 312 nm) in the UV spectrum showed in methanolic solution an almost imperceptible incipient increase of absorbances which was more pronounced in chloroform and continued for 6 h. Nevertheless, this

information was a useful hint to prolong the measurement procedures with the other spectrometric methods.

The most striking new strong absorption band at 1630 cm^{-1} in the IR spectrum taken of the condensation product in chloroform solution after 14 h, corresponds by its position, intensity and feature to ν(C=N) vibration. Additional bands emerging at 3500 and 3390 cm^{-1} are joint with C_2—NH_2 asymmetric and symmetric stretching vibrations, respectively. This can be considered as an indication for the enolimine form of the Schiff base appearing only successively in solution, although the presence of a strong intramolecular hydrogen bond is not evident in the spectrum.

The fact that immediately after dissolution only the bands at 3420 and 3320 cm^{-1}—positions characteristic of Ar-NH-R and R-NH-R—are present in the spectrum points at the incipient absence of primary amino group on the pyridine ring.

Comparison of this latter spectrum with the one recorded with the crystalline product shows that the strongest absorption bands at 1600 and 1580 cm^{-1} as well as those in the range 1500–1450 cm^{-1} have analogous positions and features. Small differences in the positions of the bands at 1300–1200 and 1150–1100 cm^{-1}, as well as the fact that the range above 3000 cm^{-1} is better differentiated in solution while



Scheme 1.

this stands for the fingerprint region of the crystalline state spectrum, could be ascribed to intermolecular association and crystal lattice.

^{1}H NMR has been applied as more adequate for structure determinations of the involved species. The results are given in Scheme 1 and Tables 1 and 2. The assignments of the chemical shifts are based on a series of spectra recorded under different systematically varying conditions, on deuteration experiments, on the effect of different solvents and on the comparison with the literature data.[8,11,12]

The obtained information can logically be linked with the cyclic structure as the incipient tautomeric form (Table 1) attaining equilibrium with the

Table 1. ^{1}H NMR spectrometric data of the incipient tautomeric form: saturated $CDCl_3$ solution (~ 0.05 mol dm^{-3}), room temperature and TMS as internal standard

Chemical shift $\delta \pm$ SD (ppm) (number of spectra)	Protons included	Signal feature	Assignment
7.05–7.40 (4)	~ 2.7H	Multiplet	C'_4—H, C'_6—H, C'_2—OH
6.76–7.01 (4)	2H	Multiplet	C'_3—H, C'_5—H
6.558 ± 0.003 (14)	1H	Singlet	C_5—H
5.61 ± 0.01 (21)	2H	Broadened signal, mostly a singlet	C_2—NH—CH—C'_1
4.220 ± 0.003 (14)	2H	Singlet	C_4—CH_2—O—
δ_A = 4.030 ± 0.007 δ_B = 3.741 ± 0.008 (17)	2H	Two doublets, AB splitting pattern J = 17.4 ± 1.0 Hz	C_3—CH_2—N
3.355 ± 0.002 (14)	3H	Sharp singlet	CH_3O—
2.386 ± 0.005 (14)	3H	Sharp singlet	C_6—CH_3

Table 2. ^{1}H NMR spectrometric data of the consequent tautomeric form: saturated $CDCl_3$ solution (~ 0.05 mol dm^{-3}) with regard to the incipient tautomer, room temperature, TMS as internal standard[a]

Chemical shift $\delta \pm$SD (ppm) (number of spectra)	Protons included	Signal feature	Assignment
12.94±0.015 (10)	~0.5H	Singlet	C'_2—OH
8.370±0.002 (16)	1H	Triplet $J = 1.3 \pm 0.1$ Hz	C'_1—CH=
6.599±0.003 (15)	1H	Singlet	C_5—H
4.739±0.004 (16)	2H	Doublet $J = 1.3 \pm 0.1$ Hz	C_3—CH_2—N=
4.606±0.008 (15)	2H	Broad singlet	C_2—NH_2
4.415±0.003 (16)	2H	Singlet	C_4—CH_2O—

[a] ^{1}H NMR data for protons C'_3—H, C'_4—H, C'_5—H, C'_6—H, C_6—CH_3 and —OCH_3 are identical to those of the incipient tautomer (Table 1).

enolimino form after dissolution (Table 2). The rate of the attainment and the ratio of tautomeric forms at equilibrium depends on the solvent used as well as on the concentration and the temperature. Thus, a 1:1 ratio is reached after 24 h in saturated $CDCl_3$ solution at room temperature. Such slowly attaining equilibria but with an inverse course, i.e. conversion of the initially present Schiff base to the cyclic diamine form, have been reported for the condensation of pyridoxal with ornithine and two amino acids bearing an α and a terminal amino group.[4]

There is no evidence in the spectrum of any interaction with the proton bound to nitrogen and so only the presence of the enolimino form is obvious.[13,14] The absence of the ketoenamine form is evident also in the IR spectra taken in chloroform and in methanolic solution since the absorption band characteristic of the ν(C=O) vibration of the quinoid structure is missing.[15]

The hydroxyl proton sharing in a strong intramolecular hydrogen bond to imino nitrogen has a signal with a chemical shift conformable to the usual values.[13]

Complexes with Cu(II), Ni(II) *and* Co(II)

The complex formation behaviour of the condensation product (ligand) has been studied in methanolic solution and the solid species isolated from the methanolic medium have been characterized.

Preliminary spectrophotometric experiments with the series of metal ions comprising Cu(II), Ni(II), Co(II), Cd and Zn indicated complex formation of the ligand only in the cases of Cu(II), Ni(II) and Co(II).

UV/VIS spectra of complexes with these metals in methanolic solution are shown in Table 3.

Table 3. UV/VIS spectrometric characteristics of complexes with Cu(II), Ni(II) and Co(II) in methanolic medium 1 h after the preparation of solutions

M	$C_M = C_L$ (mol dm^{-3})	$\lambda_{max}(A)$ (nm)
Cu(II)	1.0×10^{-4}	238(1.226), 269(0.941), 356(0.582)
	7.1×10^{-2}	650(0.630)
Ni(II)	2.0×10^{-4}	236(1.130), 270sh(0.650), 278(0.720), 372(0.521)
	1.0×10^{-3}	430sh(0.140)
Co(II)	3.0×10^{-4}	236(1.052), 266(1.163), 285sh(0.800), 351sh(0.728), 370(0.672)
	6.6×10^{-2}	650(0.532)

The reaction of ligand with Co(II) proceeds very slowly. Continuous changes of the UV spectrum, including not only increases in but also variable shifts of maxima in the course of time, indicate the presence of unstable complex species which make detailed measurements uninterpretable.

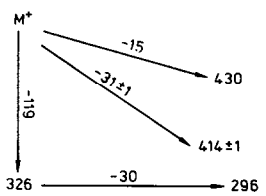
Complexes with Cu(II) and Ni(II) are formed immediately and their UV/VIS spectrometric characteristics do not change during 24 h in dilute solutions. The interacting molar ratio of the ligand with Cu(II) has been found to be 1 : 1, measured at all absorption maxima in the spectrum.

The metal : ligand ratio of 1 : 2 obtained for Ni(II) at 372 nm could not be confirmed by measurements at other wavelengths, thus indicating a more composed complex formation course.

The standing of a dilute (1×10^{-4} mol dm^{-3}) solution of the Cu(II) complex for more than 24 h is followed by formation of a new species evidenced through appearance of shoulders at 280 and 380 nm in the UV spectrum. Similarly, with the prolonged standing of a dilute methanolic solution of the Ni(II) complex hyper- and bathochromic shifts of the 430-nm shoulder accompanied by a hypsochromic shift of the 270-nm shoulder and the appearance of a new band at 348 nm have been noted. The arising of this last band, characteristic of the complex of the original aminopyridine with Ni(II), was linked with partial decomposition of the ligand. The structures of solid species obtained by isolation are in accordance with the mentioned changes proceeding very slowly in dilute but faster in concentrated methanolic solutions of Cu(II) and Ni(II) complexes.

One of the two solid compounds obtained during the isolation of the Ni(II) complex was characterized as a salt of 2-amino-3-aminomethyl-4-methoxymethyl-6-methylpyridine. Characterization of the other compound showed that Ni(II) is coordinatively bound in a 1 : 1 ratio to the bis Schiff base [4-methoxymethyl-6-methyl-2-(salicylideneamino)-3-(salicylideneaminomethyl)pyridine].

Fully conformable with such a structure are the elemental analyses and mass spectrometric data (Scheme 2). The most striking feature of the corresponding IR spectrum is the absence of absorption bands in the region 3100–3500 cm^{-1}, proving formation of two imino bonds. The assignment of absorption bands at 1620 and 1610 cm^{-1} to C=N stretching vibrations is based on the presumption that they are shifted to lower frequencies by coordination.[13] The UV spectrum of the solid complex solved in methanol shows λ_{max} of 440, 310 and 266 nm also appearing successively in a methanolic solution of the ligand in the presence of Ni(II) as mentioned before.



Scheme 2.

The same behaviour as in the case of Ni(II) was observed in the course of isolation of the Cu(II) complex formed in the methanolic medium containing incipient ligand and copper. In this case, the isolated species was characterized also by X-ray determination,[16] while IR and mass spectrometric data are in accordance with those obtained for the crude Ni(II) complex.

The features of the IR spectra of both isolated complexes, together with the values of C—N bond lengths at condensation sites determined by X-ray analysis[16] for the Cu(II) complex (1.277 and 1.282 Å) show unambiguously the enolimino character of the bis Schiff base.

The coordination sphere of Cu was found to be partially tetrahedral,[16] consisting of two N and two O atoms from two salicylaldimine moieties. On the basis of remarkable similarity of the IR spectra the same coordination mode can be presumed for the Ni(II) complex.

The formation of a tetradentate ligand has been reported previously[5] for the system comprising Zn(II) or Ni(II), ethylenediamine and glyoxylate in the ratio 1 : 1 : 2. The proposed course starts with the incipiently formed cyclic diamine, 2-carboxylate imidazolidine. In the presence of a complexing metal ion the ring opens up to form with the excess of glyoxylate for the complex species a tetradentate ligand, likely a carbinolamine. Analogously, in our case, the presence of the complexing metal ion plays the essential role.

Apart from different constitution of the ligand, added as the condensation product in the cyclic diamine form, there is no salicylaldehyde present in excess. Therefore the opening of the cyclic diamine ring is accompanied also by the decomposition to condensating components of a share of added ligand. Indeed, the salt of the 2-aminopyridine moiety has been separated during the preparation of the complexes. The free salicylaldehyde is condensed with the C_2 amino group to a bis Schiff base, affording simultaneously in the enolimine form the tetradentate ligand of the isolated complexes.

The formation of complexes with bis Schiff base proceeds in diluted solutions at an extremely slow rate as already mentioned.

Acknowledgements—We are indebted to Professor J. Seibl, ETH Zentrum, Zürich, for taking the mass spectra and

helping with interpretation. Thanks are also due to members of the Ruder Bošković Institute, Zagreb, and to Drs Z. Meić and N. Brničević for recording the ^{1}H NMR spectra and a part of IR spectra.

REFERENCES

1. U. Casellato, P. A. Vigato and M. Vidali, *Coord. Chem. Rev.* 1977, **23**, 31.
2. H. S. Maslen and T. N. Waters, *Coord. Chem. Rev.* 1975, **17**, 137.
3. T. Yano, T. Ushijima, M. Sasaki, H. Kobayashi and K. Ueno, *Bull. Chem. Soc. Jpn* 1972, **45**, 2452.
4. E. H. Abbott and A. E. Martell, *J. Am. Chem. Soc.* 1971, **93**, 5852.
5. A. Hilton and D. L. Leussing, *J. Am. Chem. Soc.* 1971, **93**, 6831.
6. D. E. Fenton and S. E. Gayda, *Inorg. Chim. Acta* 1975, **14**, L11.
7. Z. Cimerman and Z. Štefanac, *Polyhedron* 1985, **4**, 259.
8. D. Korunčev, A. Deljac and D. Cvek, Yugoslav Patent No. 35242 (Appl. 27.3.1973).
9. W. C. Vosburgh and G. R. Cooper, *J. Am. Chem. Soc.* 1941, **63**, 437.
10. P. S. Tobias and R. G. Kallen, *J. Am. Chem. Soc.* 1975, **97**, 6530.
11. S. Witek, A. Bielawska and J. Bielawski, *Pol. J. Chem.* 1981, **55**, 2025.
12. J. V. Paukstelis and R. M. Hammaker, *Tetrahedron Lett.* 1968, **32**, 3557.
13. G. C. Percy and D. A. Thornton, *J. Inorg. Nucl. Chem.* 1972, **34**, 3357; *idem ibid.* 3369.
14. H. Ranganathan, D. Ramaswamy and T. Ramasami, *Chem. Lett.* 1979, 1201.
15. G. Arnold, D. Staudacher, D. Hendriks and C. Schiele, *Spectrochim. Acta* 1968, **24A**, 1657.
16. N. Galešić, R. Trojko, Z. Cimerman and Z. Štefanac, *Acta Cryst.* 1984, **C40**, 232.

Polyhedron Vol. 4, No. 10, pp. 1761–1767, 1985
Printed in Great Britain

0277–5387/85 $3.00 + .00
© 1985 Pergamon Press Ltd

SYNTHESIS, X-RAY STRUCTURE AND SPECTROSCOPY OF Cu(II) COMPLEXES DERIVED FROM DIACETYLAZINE DIOXIME

F. ABRAHAM, J. M. CAPON, G. NOWOGROCKI and S. SUEUR
Laboratoire de Cristallochimie et Physicochimie du Solide, Bât. C7, Université de Lille, 59655 Villeneuve d'Ascq Cedex, France

and

C. BREMARD*
Laboratoire de Spectrochimie Infrarouge et Raman CNRS, Bât. C5, Université de Lille, 59655 Villeneuve d'Ascq Cedex, France

(*Received* 23 *November* 1984; *accepted* 26 *April* 1985)

Abstract—Complexes of Cu(II) with the polydentate diacetylazine dioxime ligand $C_8H_{14}N_4O_2$ have been synthesized by template and non-template reactions. The crystal structure of $[Cu(C_8H_{13}N_4O_2)]_2[ClO_4]_2(C_2H_5OH)_2$ has been determined to establish the conformation of the ligand and the coordination of the oxime function. The structural analysis shows that the nearly planar $[C_8H_{13}N_4O_2]^-$ group behaves as a bridging tetradentate ligand. The distorted square-pyramidal coordination about each Cu atom includes three N donors from two oxime and azine and one O donor from the other oxime, the ethanol molecule occupying the apical position. A perchlorate anion is loosely bonded to Cu. The intramolecular Cu...Cu separation is 3.725(2) Å. The compound crystallizes in the centrosymmetric space group $P\bar{1}$ triclinic lattice with refined lattice parameters of a = 11.963(8) Å, b = 9.784(7) Å, c = 7.501(6) Å, α = 90.69(4)°, β = 104.53(4)°, γ = 90.83(4)°, V = 849.7 Å^3 and Z = 2. Full-matrix least-squares refinement of 1490 independent reflexions led to final discrepancy indices, R = 0.059, and R_w = 0.065. The Cu centres are highly coupled as indicated by the ESR spectrum. There is no evidence that the $C_8H_{14}N_4O_2$ ligand stabilizes unusual oxidation states of Cu.

Macrocyclic ligands able to coordinate two or more metal ions offer the possibility of studying unusual electronic and chemical properties depending upon the proximity of the metal centres. An advantage of macrocyclic systems for this type of investigation is that the variation of ring size or other geometric constraints should allow the separation and disposition of the metal ions to be controlled in a systematic manner.[1,2]

The ketazine complexes are attractive systems[3] for structural and magnetic studies because the close proximity of the metal(II) ions implies a strong likelihood of magnetic coupling. During the investigation of new ketazine polymetallic compounds obtained by simple condensation between hydrazone and ketonato complexes,[4] the template reaction of 1,3-butanedione monoxime monohydrazone with 1,3-butanedione monoxime was studied. It should be noted that the non-template reaction produces diacetylazine dioxime,[4] which can be used as a dinucleating polyaza ligand in coordination chemistry.[5] Binuclear Cu(II) and Ni(II) complexes of the ketazine ligands have been known for several years;[6,7] unfortunately, to our knowledge, no X-ray structure has yet been published.

The ligand diacetylazine dioxime is likely to be sterically unstable and several stereoisomers are possible. In addition, oximes are widely recognized as versatile ligands that can be bound in different ways by O and/or N atoms.[8–10]

The compounds reported in this investigation result from the template reaction of 1,3-butanedione monoxime and 1,3-butanedione monoxime monohydrazone with copper perchlorate. We have

* Author to whom correspondence should be addressed.

undertaken an X-ray diffraction study of $[Cu(C_8H_{13}N_4O_2)]_2[ClO_4]_2(C_2H_5OH)_2$ to establish the nature of the oxime and azine coordination and the conformation of the polydentate ligand.

EXPERIMENTAL

Reagents

2,3-Butanedione monoxime, $C_4H_7NO_2$ (99%), was purchased from Merck. Hydrazine and hydrazine hydrate were purchased from Vendron. Copper perchlorate, $Cu(ClO_4)_2 \cdot 6H_2O$, was purchased from Fluka.

Syntheses

The 2,3-butanedione monoxime monohydrazone was obtained by mixing 2,3-butanedione monoxime (0.1 mol) and hydrazine hydrate (0.098 mol) in 100 cm^3 of ethanol. After 24 h, white needle crystals were obtained. The product was recrystallized by dissolving in ethanol, adding water and cooling. Found: C, 41.9; H, 7.9; N, 36.5; O, 14.0. Calc. for $C_4H_9N_3O$: C, 41.74; H, 7.82; N, 36.52; O, 13.91%.

The diacetylazine dioxime was obtained by the method of Stratton.[6] The product was recrystallized from hot ethanol yielding yellow needle crystals. Found: C, 48.3; H, 7.3; N, 27.9; O, 16.4. Calc. for $C_4H_9N_3O$: C, 48.48; H, 7.07; N, 28.28; O, 16.16%.

$[Cu(C_8H_{13}N_4O_2)]_2[ClO_4]_2$ (**A**). (1) Stoichiometric quantities of 2,3-butanedione monoxime monohydrazone (0.043 mol) and $Cu(ClO_4)_2 \cdot 6H_2O$ (0.043 mol) were dissolved in 50 cm^3 of ethanol, then 2,3-butanedione monoxime (0.043 mol) was added to the solution which was allowed to react at 60°C. The solution was filtered (removing a small amount of green precipitate) and allowed to stand in a covered beaker. The product crystallized as dark green crystals, which were separated by filtration, washed by cold ethanol and diethyl ether, and dried *in vacuo*. Found: Cu, 16.8; C, 27.8; H, 4.0; N, 13.8; O, 27.1; Cl, 9.4. Calc. for $C_8H_{13}ClCuN_4O_6$: Cu, 17.64; C, 26.67; H, 3.63; N, 15.55; O, 26.65; Cl, 9.84%. Single crystals suitable for crystal structure determination were obtained by mixing 2,3-butanedione monoxime monohydrazone (0.005 mol), 2,3-butanedione monoxime (0.005 mol) and $Cu(ClO_4)_2 \cdot 6H_2O$ (0.005 mol) in 50 cm^3 of ethanol. The solution was allowed to stand at 0°C. Well-developed dark green single crystals were obtained after several days.

(2) A stoichiometric amount of $Cu(ClO_4)_2 \cdot 6H_2O$ (0.043 mol) in ethanol was added to a refluxing solution of diacetylazine dioxime (0.043 mol) in ethanol and the solution was refluxed for several hours. After cooling the product crystallized immediately as a fine powder. The product was separated by filtration, washed by cold ethanol and ether, and dried *in vacuo*. Found: Cu, 16.3; C, 28.5; H, 4.4; N, 13.6; O, 27; Cl, 9.1. Calc. for $C_8H_{13}ClCuN_4O_6$: Cu, 17.64; C, 26.67; H, 3.63; N, 15.55; O, 26.65; Cl, 9.84%. The IR and UV–visible spectra are analogous for the products obtained by the template (1) and non-template (2) reactions.

$[Cu(C_8H_{13}N_4O_2)][ClO_4]$ (**B**). Five grams (0.043 mol) of diacetyl monohydrazone monoxime were dissolved in 50 cm^3 of hot ethanol with 8.055 g (0.0217 mol) of $Cu(ClO_4)_2 \cdot 6H_2O$. The dark red solution was refluxed for several hours, then the solution was allowed to stand at 0°C. The product crystallized as dark red crystals which were isolated by filtration, washed with cold ethanol and ethyl ether, and dried *in vacuo*. Found: Cu, 17.3; C, 28.0; H, 3.9; N, 15.1; O, 26.3; Cl, 9.4. Calc. for $C_8H_{13}ClCuN_4O_6$: Cu, 17.64; C, 26.67; H, 3.63; N, 15.55; O, 26.65; Cl, 9.84%.

Instrumentation

UV–visible spectra were run at room temperature in solution or in the solid state (Nujol mull) with a Jobin–Yvon DUOSPAC 203 spectrophotometer. IR spectra were recorded from Nujol mulls and KBr pressed discs (4000–400 cm^{-1}) and polyethylene discs (400–50 cm^{-1}) by use of a Bruker IFS 113 V Fourier-transform spectrometer. ESR spectra of solutions and powder samples were obtained on a Varian E-109 spectrometer operating at 9.315 GHz between 20 and −160°C. Electrochemistry was performed with a Tacussel PRT 20-10 potentiostat in combination with a Tacussel UAP4 universal programmer equipped with a current to voltage converter. Cyclic voltammograms were recorded on a Sefram TGM 164 X–Y recorder or a Tektronik R 5111 storage oscilloscope. The electrochemical experiments were carried out under argon with a conventional three-electrode system. The reference electrode used is the SCE (saturated calomel electrode). The solvent, $(CH_3)_2CO$, was distilled over a "molecular sieve" (4 Å) under argon prior to use. The supporting electrolyte, tetraethyl ammonium perchlorate, was purchased from Agfa and dried *in vacuo* at 50°C over P_4O_{10}.

CRYSTALLOGRAPHIC STUDIES

Cell dimensions were determined from the angular settings of 25 accurately centred reflections during diffractometer measurements.

Crystal data

$Cu_2C_{20}H_{38}N_8O_{14}Cl_2$; $M = 405.3$, triclinic space group $P\bar{1}$, $a = 11.963(8)$ Å, $b = 9.784(7)$ Å, $c = 7.501(6)$ Å, $\alpha = 90.69(4)°$, $\beta = 104.53(4)°$, $\gamma = 90.83(4)°$, $V = 849.7$ Å^3. $D_m = 1.56(3)$ g cm^{-3}, $D_c = 1.58$ g cm^{-3}, $Z = 4$, and μ(Mo-K_α) = 15.32 cm^{-1}.

Data collection

Data were obtained from a dark green crystal of dimensions $0.3 \times 0.2 \times 0.25$ mm^3 on a Philips PW 1100 diffractometer equipped with a graphite monochromator which isolates Mo-K_α radiation ($\lambda = 0.7107$ Å). The intensities of 1624 independent reflexions were collected for $2° < \theta < 30°$; 1499 reflexions were classified as observed with $I > 3\sigma(I)$. Background, Lorentz and polarization corrections were applied. No absorption corrections were applied.

Structure solution and refinement

The structure was solved by the heavy-atom method. Refinement and subsequent difference synthesis located the remaining non-H atoms. Three unexpected peaks were attributed to an ethanol solvate molecule which was not detected during elemental analysis of samples dried *in vacuo*. All atoms were refined anisotropically by a full-matrix least-squares program. Considerable difficulty was encountered in locating and refining the perchlorate O atoms: one of them is statistically disordered over two positions and all have abnormally high thermal motion.

Convergence was achieved with $R = 0.059$, and $R_w = 0.065$. The final Fourier difference function was featureless and does not permit the localisation of the H atoms. Unit weights were assumed for all reflections.

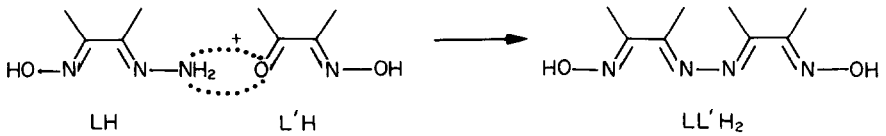
Scattering factors were taken from Cromer and Waber[11] for Cu^{2+}, C, N, O and Cl, and the anomalous dispersion corrections from Cromer and Liberman.[12] Final atomic coordinates, thermal parameters and F_o/F_c values have been deposited with the Editor as supplementary data.*

* Atomic coordinates have also been deposited with the Cambridge Crystallographic Data Centre for inclusion in their data base. Copies of all deposited data are available, on request, from the Editor at Queen Mary College.

RESULTS AND DISCUSSION

Syntheses

1,3-Butanedione monoxime monohydrazone, denoted LH, reacts with 1,3-butanedione monoxime, denoted L'H, in ethanol to give the diacetylazine dioxime ligand, denoted $LL'H_2$.[5,6]



LH L'H $LL'H_2$

The coordination of Cu(II) perchlorate with this ketazine ligand gives a dark green product corresponding to the $Cu(LL'H)ClO_4$ composition (compound **A**). If the reaction is performed under "template" conditions the same product is obtained, as evidenced by analytical, spectral and crystallographic results. If LH is mixed with Cu(II) perchlorate in refluxing ethanol a dark red compound (**B**) is isolated, which exhibits the same elemental analysis as **A**. We suspect that the elimination of one hydrazine molecule between the hydrazone function of two LH in the coordination sphere of Cu(II) can lead to the formation of the $LL'H_2$ ligand. The $LL'H_2$ ligand in compound **B** possesses a different conformation than that in compound **A**.

UV, visible and IR spectra

It is difficult to make an unequivocal assignment of the IR bands; nevertheless, some similarities exist in the IR absorptions of the free $LL'H_2$ ligand in compounds **A** and **B**. In particular, the broad absorption near 3400 cm^{-1} corresponds to the OH group of the oxime function involving inter- or intramolecular hydrogen bonding. Three bands corresponding to the ν(C=N) vibrations are found at 1658, 1598 and 1567 cm^{-1} for **A** whereas the IR spectrum of **B** exhibits two absorptions at 1640 and 1612 cm^{-1}; it should be noted that the spectrum of the free ligand possess two ν(C=N) bands at 1643 and 1602 cm^{-1}. However, several differences are observed near 1250 and 750 cm^{-1} particularly in the relative intensities of the IR absorption. The expected ν_3 and ν_4 IR bands of the ClO_4^- anion with T_d-symmetry are observed at 1108 and 628 cm^{-1} and 1092 and 632 cm^{-1} for **B** and **A** respectively. Nevertheless, the weak band observed at 932 cm^{-1} for **A** and the broadness of the ν_3-bands indicates that the symmetry may be lowered.

Compound **A** is sparingly soluble in ethanol and

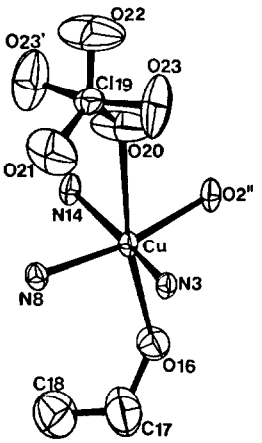


Fig. 1. View of the inner coordination sphere of Cu(II) showing the atom-labelling scheme.

its UV and visible absorption spectra exhibit a broad band centred at 360 nm and a shoulder at 460 nm. The electronic absorption spectra of **A** and **B** in the solid state exhibit an intense band centred at 360 and 340 nm, while the visible absorption peaks occur at 610 and 480 nm respectively.

Structure of $[Cu(LL'H)]_2[ClO_4]_2(C_2H_5OH)_2$ (**A**)

Since spectroscopic data could not decide the stereochemistry of complexes **A** and **B**, an X-ray investigation was necessary. While stable single crystals of **A** were easily obtained, attempts to crystallize product **B** by slow reaction or slow cooling led to well-shaped crystals which rapidly lose solvent when they are extracted from reaction mixture.

Coordination of the Cu(II) *ion*

Figure 1 shows the Cu atom coordination sphere along with the numbering scheme. The coordination polyhedron around Cu^{2+} comprises five atoms forming a square-pyramidal arrangement. The basal plane is formed by the N(3), N(8) and N(14) atoms of one LL'H ligand and the O(2) atom of the second $LL'H^-$ ligand. The apical position is occupied by the O(16) atom of ethanol. The "basal plane" is essentially planar with the largest deviation from the best least-squares planes being 0.03 Å. The Cu atom is displaced 0.165(1) Å from the basal plane in the direction of the O(16) atom of ethanol.

The Cu—N bond lengths are 2.008(8), 1.963(8) and 1.957(9) Å; the shortest corresponds to the N(4) azine atom, the intermediate to the N(3) atom (deprotonated oxime group) and the largest to the N(14) atom (non-deprotonated oxime function). The bond angles of the Cu atom coordination sphere (Table 1) are in the range of those found for the Cu complex derived from 2,6-diacetylpyridinedioxime (DAPDH).[13] An ethanol molecule is located above each Cu atom with a Cu—O(16) distance of 2.279(9) Å. This distance can be compared to the corresponding Cu—H_2O distances of 2.249(3) and 2.317(4) Å in the DAPDH complex.[13]

A distorted octahedral geometry around the Cu atom is obtained by a long Cu...O (perchlorate) contact. This interaction is clearly weak: the Cu—O(20) distance is 2.760(15) Å and may best be described as what Hathaway and coworkers[14] have called "semicoordination". The geometry of the ClO_4^- anion is not well defined because of the disorder. Two kinds of ClO_4^- anions are present with only half-occupancy, so that the interatomic angles and distances within a ClO_4^- tetrahedron are not significant.

Conformation of the LL'H ligand

As shown in Fig. 2, the complex is in fact a dimer, $[CuLL'H]_2^{2+}$; the two parts are related by the

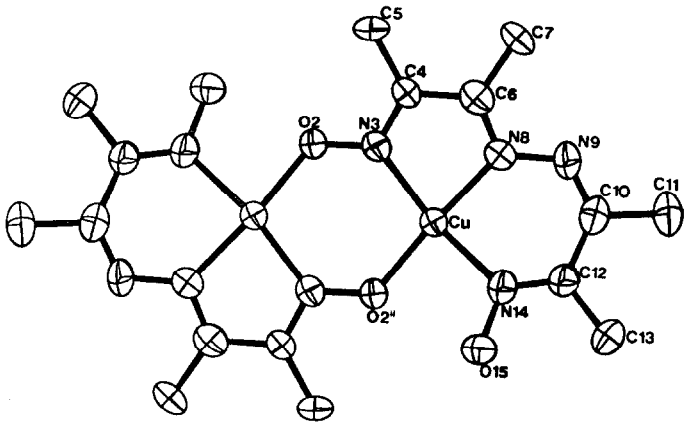


Fig. 2. View of the "basal plane" of the binuclear dication $[Cu(C_8H_{13}N_4O_2)]_2^{2+}$ showing the atom-labelling scheme.

Table 1. Interatomic distances (Å) and angles (°) in $[Cu(C_8H_{13}N_4O_2)]_2[ClO_4]_2(C_2H_5OH)_2$

Cu—O(2)[a]	1.937(8)	O(2)[a]—Cu—N(14)	85.7(5)
Cu—N(3)	1.963(8)	O(2)[a]—Cu—N(3)	103.2(7)
Cu—N(8)	1.957(9)	N(3)—Cu—N(8)	87.5(5)
Cu—N(14)	2.008(8)	N(8)—Cu—N(14)	87.9(6)
O(2)—N(3)	1.314(10)	O(2)—N(3)—Cu	128.9(11)
N(3)—C(4)	1.294(14)	O(2)—N(3)—C(4)	116.8(16)
C(4)—C(5)	1.499(15)	Cu—N(3)—C(4)	114.2(11)
C(4)—C(6)	1.466(14)	N(3)—C(4)—C(6)	114.9(17)
C(6)—C(7)	1.493(17)	N(3)—C(4)—C(5)	122.8(21)
C(6)—N(8)	1.300(14)	C(5)—C(4)—C(6)	122.3(19)
N(8)—N(9)	1.393(12)	C(4)—C(6)—C(7)	121.1(19)
N(9)—C(10)	1.268(14)	C(4)—C(6)—N(8)	115.0(16)
C(10)—C(11)	1.520(16)	C(7)—C(6)—N(8)	123.9(22)
C(10)—C(12)	1.491(17)	C(6)—N(8)—N(9)	116.2(17)
C(12)—C(13)	1.530(15)	C(6)—N(8)—Cu	114.0(13)
C(12)—N(14)	1.269(13)	Cu—N(8)—N(9)	129.7(13)
N(14)—O(15)	1.397(13)	N(8)—N(9)—C(10)	120.4(18)
ClO_4^- ion		N(9)—C(10)—C(11)	113.9(18)
Cu—O(20)	2.760(15)	N(9)—C(10)—C(12)	129.9(25)
Cl(19)—O(20)	1.320(17)	C(12)—C(10)—C(11)	116.2(19)
Cl(19)—O(21)	1.337(17)	C(10)—C(12)—C(13)	118.5(19)
Cl(19)—O(22)	1.269(19)	C(10)—C(12)—N(14)	120.3(20)
Cl(19)—O(23)	1.427(29)	N(14)—C(12)—C(13)	121.2(18)
Cl(19)—O(23)′	1.495(33)	O(15)—N(14)—C(12)	115.9(17)
O(20)—Cl(19)—O(21)	115.4(25)	O(15)—N(14)—Cu	114.0(9)
O(20)—Cl(19)—O(22)	120.5(29)	Cu—N(14)—C(12)	130.0(14)
O(20)—Cl(19)—O(23)	89.8(26)	Cu—O(20)—Cl(19)	143.3(2)
O(20)—Cl(19)—O(23)′	84.1(22)	Cu—O(16)—C(17)	136.9(39)
O(21)—Cl(19)—O(22)	124.1(31)	O(16)—C(17)—C(18)	117.7(43)
O(21)—Cl(19)—O(23)	98.0(28)	Ethanol molecule	
O(21)—Cl(19)—O(23)′	97.9(30)	Cu—O(16)	2.279(9)
O(22)—Cl(19)—O(23)	85.3(25)	C(17)—O(16)	1.382(32)
O(22)—Cl(19)—O(23)′	85.3(29)	C(17)—C(18)	1.325(39)
O(20)—Cu—O(2)[a]	86.0(8)	O(16)—C(17)—C(18)	117.7(43)
O(20)—Cu—N(3)	77.4(6)	O(16)—Cu—N(14)	97.1(6)
O(20)—Cu—N(8)	86.6(8)	O(16)—Cu—O(2)[a]	88.8(6)
O(20)—Cu—N(14)	91.1(8)	O(16)—Cu—N(3)	95.4(6)
		O(16)—Cu—N(8)	99.5(7)

[a] Generated by the symmetry operator $\bar{x}, \bar{y}, \bar{z}$.

inversion centre. The dimeric fragment composed of O(2), N(3), N(8), N(14), O′(2), N′(3), N′(8) and N′(14) is essentially planar with a largest deviation from the best least-squares plane of 0.014(8) Å (Table 2). This planarity was also observed in several dimeric copper complexes with μ-dihydroxo bridges[15,16] but not in the $[CuDAPDH]_2^{2+}$ dimer which contains a dihedral angle of 169.6° between pyramidal units.[13] The bond lengths and angles for this portion of the complex, as given in Table 1, are consistent with those found in similar complexes. The intramolecular Cu–Cu separation is 3.725(2) Å, longer than in the $DAPDH_2$ complex [3.5453(7) Å]. The tetradentate ligand gives two kinds of chelate rings with a Cu atom: a diaza five-membered ring and a triaza six-membered ring.

The $LL'H^-$ tetradentate ligand adopts the *cis–trans* conformation in the dimeric complex. The coordination of the Cu^{2+} ion induces appreciable deviations in the N—C—C, C—N—N, C—C—C and O—N—C angles. As noted in Ref. 14, deprotonation of the O oxime site is accompanied by a reduction in the N—O bond distance from 1.397(13) to 1.314(10) Å, and a lengthening of the Cu—N (oxime) distance.

Crystal structure

The unit cell contain only one dimer and the planes of dimeric ions, $[Cu(LL'H)]_2^{2+}$, related by lattice translations are of course parallel. The interdimer contacts are more than 3.4 Å, between the O atom of

Table 2. Equations of least-squares planes and perpendicular distances (Å) from these planes

Plane I: N(3), N(8), N(14), O(2)[a]
$P = 0.32591$ $Q = 0.78490$ $R = 0.52698$ $S = -0.01500$

N(3)	0.030(8)
N(8)	−0.031(9)
N(14)	0.033(9)
O(2)[a]	−0.032(8)
Cu	−0.170(1)

Plane II: N(3), N(8), N(14), O(2), N(3)[a], N(8)[a], N(14)[a], O(2)[a]
$P = 0.32162$ $Q = 0.78761$ $R = 0.52557$ $S = 0.00000$

N(3)	0.041(8)	N(3)[a]	−0.041(8)
N(8)	−0.033(9)	N(8)[a]	0.033(9)
N(14)	0.031(9)	N(14)[a]	−0.031(9)
O(2)	0.020(8)	O(2)[a]	−0.020(8)
Cu	−0.165(1)	Cu[a]	0.165(1)
O(16)	−2.433(10)	O(20)	2.576(15)

Plane III: O(2), N(3), C(4), C(5), C(6), C(7), N(8), N(9), C(10), C(11), C(12), C(13), N(14), O(15)
$P = 0.38743$ $Q = 0.74302$ $R = 0.54573$ $S = -0.34967$

O(2)	−0.382(8)	N(9)	−0.109(9)
N(3)	−0.254(8)	C(10)	−0.073(10)
C(4)	−0.009(10)	C(11)	−0.189(13)
C(5)	0.204(12)	C(12)	0.031(10)
C(6)	0.108(11)	C(13)	0.254(12)
C(7)	0.489(12)	N(14)	−0.046(9)
N(8)	−0.119(9)	O(15)	0.077(8)
Cu	−0.362(1)		

[a] Generated by the symmetry operator $\bar{x}, \bar{y}, \bar{z}$.

the ClO_4^- group and the C atom of the methyl group, and correspond to Van ver Waals' contacts.

Electrochemistry

The electrochemical study of the dimeric complex $[Cu(LL'H)]_2[ClO_4]_2$ was undertaken in dry acetone and under argon with the hope of obtaining Cu(III) and/or Cu(I) oxidation states. The reduction of the dinuclear Cu(II) complex occurs at +0.02 V vs SCE electrode. However, when measured by cyclic voltammetry, the Cu(II)/Cu(I) redox process is irreversible at all the scan rates used. The reason for this is not well understood, but could be due to chemical reaction or rearrangement subsequent to charge transfer. The oxidation of the two copper centres occurs nearly simultaneously at +0.84 V vs SCE (Fig. 3) and the two expected sequential oxidations are not clearly observed. In addition the cyclic voltammograms indicate the chemical decomposition of the Cu(III) species generated at the platinum electrode. There is no evidence that the $LL'H_2$ ligand stabilizes high or low oxidation states of Cu as occurs in the case of dinuclear macrocyclic ligands.[17]

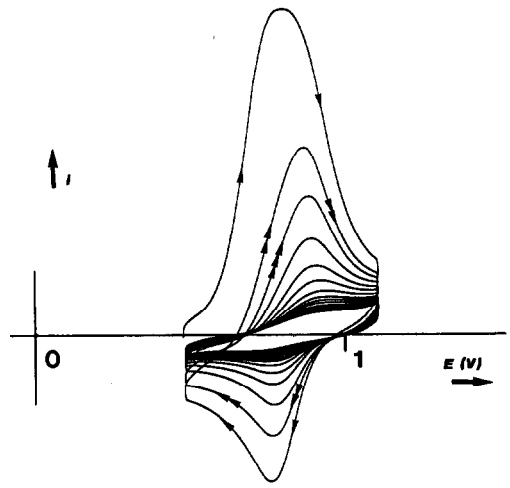


Fig. 3. Multiple scans of cyclic voltammetry of 10^{-3} M $[Cu(C_8H_{13}N_4O_2)]_2^{2+}$ in $(CH_3)_2CO$ with 0.1 M $[(C_2H_5)_4N][ClO_4]$ at 0.1 V s^{-1}.

ESR spectra

The dimeric structure of $[Cu(LL'H)]_2[ClO_4]_2$ is retained in nondonor solvents such as ethanol. Unfortunately, the red (**B**) and green (**A**) products are sparingly soluble in nondonor solvents and the ESR spectra obtained in ethanol at room temperature are poorly resolved with a bad signal: noise ratio. The ESR spectrum of compound **B** exhibits a signal centred at 3600 G with no obvious sign of coupling, whereas the spectrum of product **A** shows a more complicated signal near 2000 and 3600 G.

The difference between the ESR spectra of the two products is more evident with powder samples. The powder spectra of product **B** (Fig. 4) is typical of an isolated Cu(II) ion.[18] Lowering the sample temperature to 77 K produces no significant effect on

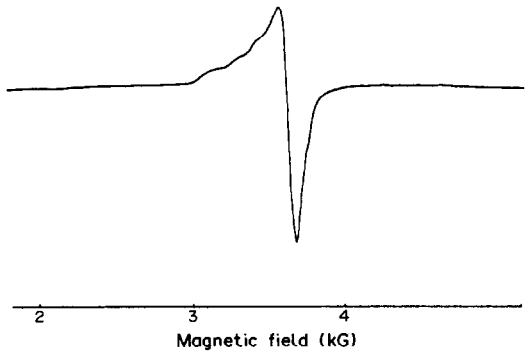


Fig. 4. Powder X-band ESR spectrum of **B** $[Cu(C_8H_{13}N_4O_2)(ClO_4)]$ at room temperature.

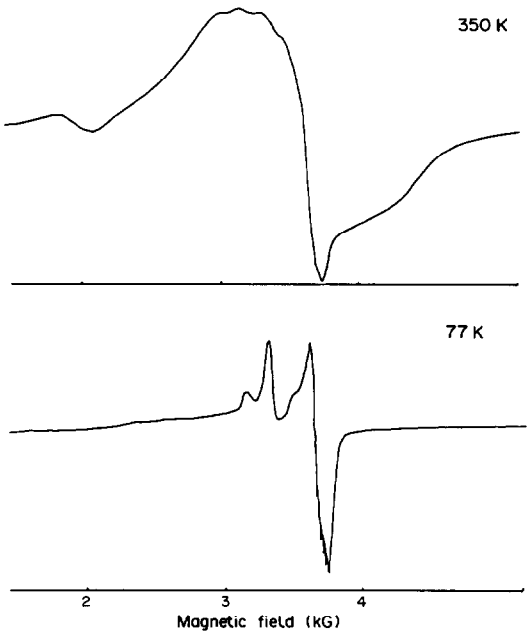


Fig. 5. Powder X-band ESR spectrum of binuclear A $\{[Cu(C_8H_{13}N_4O_2)]_2[ClO_4]_2\}$ compound at room temperature and 77 K.

the shape of the signal. The ESR spectra of powdered sample A are reported in Fig. 5: the spectra are typical of that shown by other highly coupled Cu dimers.[14,16,19,20] Lowering the temperature to 77 K produces a dramatic effect on the shape of the low-field signal. The usual Cu(II) and ^{14}N hyperfine couplings are observed in the spectrum recorded at 77 K.

The ESR spectra of the Cu(II) complexes derived from diacetylazine dioxime indicated a dramatic effect of the coordination mode of the ligand upon the magnetic properties.

In the light of the structure determination, it is apparent that electron exchange between the Cu(II) centres of the $[Cu(LL'H)]_2$ dimers is mediated through oximato bridges and gives a highly coupled system. The $LL'H_2$ appears to be a versatile polydentate ligand and confirmation of different stereoisomeric forms of the ligand coordinated to Cu(II) is under investigation. A detailed study of the magnetic properties in connection with the structural determination is currently being carried out.

REFERENCES

1. K. P. Danccy, K. Henrick, P. M. Judd, P. G. Owston, R. Peters and P. A. Tasker, *J. Am. Chem. Soc.* 1981, **103**, 4952.
2. O. Kahn, I. Morgenstein-Badarau, J. P. Audiere, J. M. Lehn and S. A. Sullivan, *J. Am. Chem. Soc.* 1980, **102**, 5936.
3. C. J. O'Connor, R. J. Ramananch, D. M. Robertson, E. E. Educk and F. R. Fronczek, *Inorg. Chem.* 1983, **22**, 449.
4. F. Abraham, J. M. Capon, G. Nowogrocki, S. Sueur and C. Bremard, *Acta Cryst.* 1984, **C40**, 1355.
5. A. Darapsky and H. Spannagel, *J. Prakt. Chem.* 1915, **92**, 272.
6. W. J. Stratton and P. J. Ogren, *Inorg. Chem.* 1970, **9**, 11.
7. S. Satpathy and B. Sahoo, *J. Inorg. Nucl. Chem.* 1971, **33**, 1312.
8. A. Chakravorty, *Coord. Chem. Rev.* 1974, **13**, 1.
9. R. J. Butcher, C. J. O'Connor and E. Sinn, *Inorg. Chem.* 1981, **20**, 537.
10. M. Sheung Ma and R. J. Angelici, *Inorg. Chem.* 1980, **19**, 924.
11. D. T. Cromer and J. T. Waber, *Acta Cryst.* 1965, **18**, 104.
12. D. T. Cromer and D. Liberman, *Chem. Phys.* 1970, **53**, 1891.
13. G. A. Nicholson, J. L. Pettersen and B. J. McCornick, *Inorg. Chem.* 1980, **19**, 195.
14. D. S. Brown, J. D. Lee, B. G. A. Melson, B. J. Hathaway, L. M. Procter and A. A. G. Tomlinson, *J. Chem. Soc., Chem. Commun.* 1967, 369.
15. D. L. Lewis, W. E. Hatfield and D. J. Hodgson, *Inorg. Chem.* 1974, **13**, 147.
16. D. L. Lewis, K. T. McGregor, W. E. Hatfield and D. J. Hodgson, *Inorg. Chem.* 1974, **13**, 1013.
17. R. R. Gagne, C. L. Spiro, T. J. Smith, C. A. Hamann, W. R. Thies and A. K. Shiemke, *J. Am. Chem. Soc.* 1981, **103**, 4073.
18. I. Morgenstern-Badarau, M. Rerat, O. Kahn, J. Jand and J. Galy, *Inorg. Chem.* 1982, **21**, 3050.
19. M. S. Haddad and D. N. Hendrickson, *Inorg. Chem.* 1978, **17**, 2622.
20. J. R. Wasson, C. I. Shyr and C. Trapp, *Inorg. Chem.* 1978, **7**, 469.

Polyhedron Vol. 4, No. 10, pp. 1769–1775, 1985
Printed in Great Britain

0277-5387/85 $3.00 + .00
© 1985 Pergamon Press Ltd

SPECTROSCOPIC AND MAGNETIC PROPERTIES OF A NEW CLASS OF TWO-DIMENSIONAL BITRIAZOLE COMPOUNDS: THE X-RAY STRUCTURE OF POLY-BIS(THIOCYANATO-*N*)-BIS-μ-(4,4'-BIS-1,2,4-TRIAZOLE-$N^1,N^{1'}$)-COBALT(II) MONOHYDRATE

W. VREUGDENHIL, S. GORTER, J. G. HAASNOOT* and J. REEDIJK
Department of Chemistry, Gorlaeus Laboratories, State University Leiden, P.O. Box 9502, 2300 RA Leiden, The Netherlands

(*Received* 2 *January* 1985; *accepted* 26 *April* 1985)

Abstract—The synthesis of a new class of two-dimensional triazole compounds is described, including the crystal structure of $[Co(NCS)_2(btr)_2]H_2O$ [btr stands for 4,4'-bis-1,2,4-triazole ($C_4H_4N_6$)]. Crystals are monoclinic, space group $C2/c$, $a = 11.159(1)$ Å, $b = 13.047(4)$ Å, $c = 12.993(3)$ Å, $\beta = 91.81(2)°$, $Z = 4$. The structure has been solved by Fourier and direct methods and refined by full-matrix least squares to $R = 0.0229$, $R_w = 0.0283$. The structure consists of layers of six-coordinated cobalt atoms, each having two *trans*-oriented *N*-bonded thiocyanate groups [Co—NCS 2.098(2) Å] and linked together in the equatorial plane by single bridges of btr to a two-dimensional network. The btr ligand coordinates through its N(1) and N(1') atoms [Co—N 2.128(1) and 2.142(1) Å]. The intralayer Co—Co distance is 9.207(2) Å, and the inter-layer Co—Co distance is 8.584(1) Å. The magnetic susceptibilities of the compound and of the isostructural nickel and iron compounds are discussed. The iron compound exhibits a high-spin–low-spin crossover at liquid-nitrogen temperatures, as shown by magnetic susceptibility.

Derivatives of 1,2,4-triazole are now well known to act as polynucleating ligands to first-row transition metals.[1,2] Unsubstituted 1,2,4-triazole has been demonstrated to coordinate in several ways: monodentate;[3] 1,2-bidentate,[4] leading to chains; and 2,4-bidentate,[5] leading to two-dimensional layer structures. 4-Substituted triazoles coordinate mainly via N(1) and N(2) producing again one-dimensional chains[6–8] of dimers, trimers and polymers (dinuclear etc.). These compounds show interesting magnetic properties,[1,2] not only by the fact that they are polynuclear, but also because this type of ligand coordinates rather strongly and may cause iron(II) compounds to become low-spin and spin transitions may occur above or below room temperature.[8,9] In a previous paper,[10] the preparation of the ligand 4,4'-bis-1,2,4-triazole (btr) and of two of its metal complexes were reported. One of the conclusions was that btr was a rather strong ligand among the triazoles and comparable in ligand-field strength to 1,2-diaminoethane, as deduced from ligand-field spectra. The free ligand btr has a remarkable structure, that was determining by Domiano.[11] The torsional angle around the N—N bond connecting the two triazole rings appeared to be 91.9°, and the two rings are, therefore, nearly perpendicular to each other. The four peripheral nitrogen atoms are chemically equivalent and in principle liable to coordinate to four metal ions which should afford three-dimensional coupled systems. Preliminary results showed the compounds $M(NCS)_2(btr)_2(H_2O)$ for M = Fe, Co and Ni to be mutually isomorphous, with interesting magnetic and spectroscopic properties. In order to investigate the mode of coordination of btr in the compound $[Co(NCS)_2(btr)_2]H_2O$ an X-ray crystal structure determination was done, the results of which are also reported in the present paper.

EXPERIMENTAL

Syntheses and X-ray structure determination. The ligand btr and its metal coordination compounds were prepared as described earlier.[10] Orange

* Author to whom correspondence should be addressed.

Table 1. Experimental data relevant to the structure determination of $[Co(NCS)_2(btr)_2]H_2O$

Empirical formula	$CoC_{10}H_{10}N_{14}S_2O$
Molecular weight (g mol^{-1})	465.346
Space group	$C2/c$
Cell dimensions	
a (Å)	11.159(1)
b (Å)	13.047(4)
c (Å)	12.993(3)
β (°)	91.82(2)
Cell volume (Å^3)	1890.75
Packing (Z)	4
Density	
D_c (Mg m^{-3})	1.635(1)
D_o (Mg m^{-3})	1.65(2)
Wavelength Mo-K_α, monochromated by graphite (Å)	0.71069
Crystal dimensions (mm^3)	$0.5 \times 0.3 \times 0.1$
Limits of data collection	$2 < \theta < 30°$
	$0 < h < 15$
	$0 < k < 18$
	$-18 < l < 18$
Number of reflections measured	2877
Agreement estimate of equivalent reflections	0.636
Number of independent reflections	2747
Number of significant independent reflections [$I > 2\sigma(I)$]	1860
$F(000)$	942
Final R	0.0264
Final R_w	0.0327

crystals of $[Co(NCS)_2(btr)_2]H_2O$ were grown by slowly cooling a hot (70°C) solution of the reactants to room temperature. The experimental density, determined in a mixture of 1,2-dibromoethane and trichloromethane, was 1.65 Mg m^{-3}. A rod-shaped single crystal suitable for analysis was mounted on an Enraf–Nonius CAD-4 diffractometer and data were measured at room temperature. Crystallographic and experimental data are tabulated in Table 1. The experimental intensities were corrected for Lorentz and polarisation effects and transmission coefficients ranged from 0.69 to 0.94. An absorption correction was calculated using the program ABSCOR[12] [μ(Mo-K_α) = 11.51 cm^{-1}]. After reduction to structure factors a Wilson plot afforded starting values for the scaling parameter and the overall isotropic thermal parameter. The position of the cobalt was located by means of a Patterson synthesis, the other non-hydrogens were found successively with the direct methods program MULTAN.[13] The hydrogen atoms could be located in a difference Fourier synthesis. Anisotropic refinement for the non-hydrogens and isotropic refinement for the hydrogens yielded $R = 0.0229$ and $R_w = 0.0283$, with omission of unobserved reflections. The scattering factors were taken from the *International Tables*.[14] All computer programs used were written or modified by Dr R. A. G. de Graaff and Mrs E. Rutten-Keulemans. The function minimized during the least-squares refinement was $\sum w(\Delta F)^2$, with $\Delta F = |F_o| - |F_c|$ and $w = (\sigma_F)^{-2}$. Reliability indices referred to in Table 1 are $R = \sum|\Delta|/|F_o|$ and $R_w = [\sum w(\Delta F)^2/\sum w|F_o|^2]^{1/2}$. Secondary extinction did not appear to be significant, therefore no correction for this effect was made. The thiocyanate sulphur atom and the water hydrogen atoms were found to be in disordered positions. Two positions with different occupancy numbers were refined. The occupancy numbers for S and S* are 0.82 and 0.18 respectively; the occupancy numbers for HW and HW* are 0.73 and 0.27 respectively.

Table of atomic coordinates, temperature factors and F_o/F_c values have been deposited with the Editor as supplementary materials and are available on request. Atomic coordinates have also been

deposited at the Cambridge Crystallographic Data Centre.

Magnetic measurements. The magnetic susceptibility measurements from 80 to 300 K were made by means of a Faraday balance.

$CoHg(SCN)_4$ was used as a calibrant.

RESULTS AND DISCUSSION

Description of the structure

Figure 1 gives an ORTEP[15] view of a part of the network structure of the compound. It also shows the thermal ellipsoids of the non-hydrogens at 50% probability and the numbering of the atoms as used in the structure determination. Table 2 gives the bond distances and bond angles of the compound. Some dihedral angles and information about the hydrogen bridging system are also given. As Fig. 1 shows, the coordination polyhedron around cobalt is a distorted octahedron with two thiocyanate N atoms *trans* to each other. Because the cobalt atoms are on centres of inversion the N—Co—N angles are 180°. The Co—NCS distance is 2.098(2) Å, in agreement with literature values.[16,17] The Co—N—C angle, 154.9(1)°, differs significantly from 180°; such a large deviation for an M—N—C angle in isothiocyanates is rare, but has been observed before.[1,2,7,17–20] The remaining four positions of the coordination polyhedron are occupied by ligand N atoms. Each ligand constitutes a bridge between two adjacent cobalt atoms by coordination through N(1) and N(1') [in the tables and Fig 1 named as N(11) and N(21) respectively]. In this way two-dimensional arrays of cobalt atoms are formed that are planar and nearly square: angles 89.76(2) and 90.24(2)°. These layers are parallel to the *bc* plane of the unit cell. Each cobalt atom of a layer is just between the centers of the "holes" of the two neighbouring layers, as imposed by the space group symmetry (see Fig. 2). The Co—Co distance in the layers is 9.207(2) Å, whereas between the layers the shortest Co—Co distance is 8.584(1) Å. The layers are connected to each other by means of Van der Waals' forces and weak hydrogen bridges through the water molecules. As there is only one water molecule on two ligands, each with two non-coordinating nitrogen atoms, only half of these nitrogen-free electron pairs can take part in hydrogen bonding. The disorder in the position of the water hydrogen atom is in agreement with this weak hydrogen bridge. The geometry of this bridge is detailed in Table 2 and illustrated in Fig. 2.

The H-bond interaction is rather weak indeed, as is illustrated by the comparatively narrow OH-stretching absorptions in the IR spectrum at 3500 cm^{-1}.[10] The position of the disordered hydrogens makes them unavailable for this hydrogen bond. The direction in which the disordering of this atom has taken place suggests instead that some additional H-bonding interaction may be present with the other

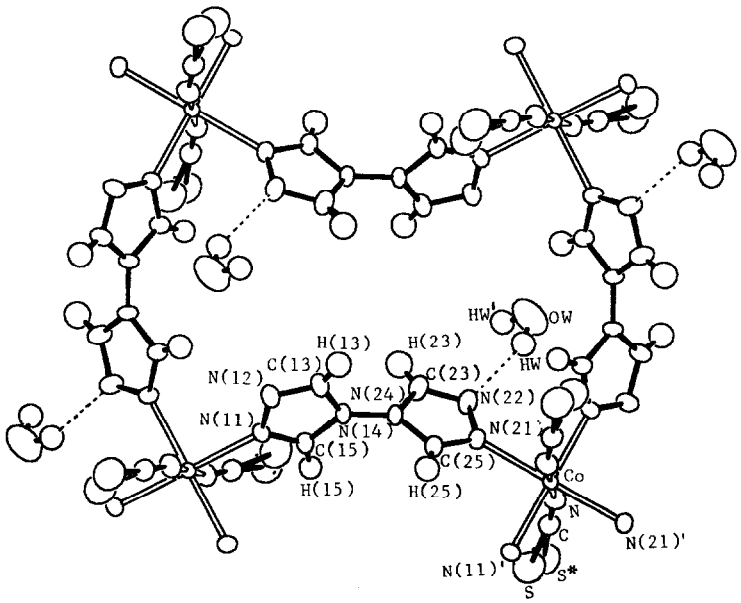


Fig. 1. Part of the two-dimensional layer structure of $[Co(NCS)_2(btr)_2]H_2O$ showing coordinating polyhedra, ligand bridging, part of hydrogen bonding (dotted lines) and numbering system used. ORTEP[15] drawing. HW' is related to HW by symmetry operation $-x, y, \frac{1}{2}-z$; N(11)' is related to N(11) by symmetry operation $x, 1-y, -\frac{1}{2}z$; N(12)' is related to N(12) by symmetry operation $1\frac{1}{2}-x, 1\frac{1}{2}-y, -z$.

Table 2. Intramolecular and relevant intermolecular distances and angles for $[Co(NCS)_2(btr)_2]H_2O$[a]

Distance (Å)			
Co—N	2.098(2)	N—C	1.151(2)
Co—N(11)‴	2.128(1)	C—S	1.635(2)
Co—N(21)	2.142(1)	C—S*	1.625(7)
Co...Co (intra)	9.207(2)		
Co...Co (inter)	8.584(1)		

	$p = 1$	$p = 2$
N(p1)[b]—N(p2)	1.388(2)	1.390(2)
N(p2)—C(p3)	1.296(2)	1.295(2)
C(p3)—N(p4)	1.355(2)	1.359(2)
N(p4)—C(p5)	1.354(2)	1.355(2)
C(p5)—N(p1)	1.294(2)	1.292(2)
C(p3)—H(p3)	0.88(2)	0.95(2)
C(p5)—H(p5)	0.94(2)	0.89(2)
N(14)—N(24)	1.377(2)	

Angle (°)			
N—Co—N(11)‴	88.48(5)	Co—N—C	154.9(1)
N—Co—N(21)	88.33(6)	N—C—S	164.5(5)
N(11)‴—Co—N(21)	89.12(2)	N—C—S*	176.5(2)
Co...Co...Co (intra)	90.24(2)	S—C—S*	18.8(4)

	$p = 1$	$p = 2$
Co—N(p1)—N(p2)	124.1(1)	123.9(1)
Co—N(p1)—C(p5)	127.1(1)	127.4(1)
C(p5)—N(p1)—N(p2)	108.6(1)	108.5(1)
N(p1)—N(p2)—C(p3)	106.5(1)	106.8(1)
N(p2—C(p3)—N(p4)	109.8(1)	109.6(2)
N(p2)—C(p3)—H(p3)	129(1)	127(1)
N(p4)—C(p3)—H(p3)	120(1)	123(1)
C(p3)—N(p4)—C(p5)	106.5(1)	106.3(1)
N(p4)—C(p5)—N(p1)	108.6(1)	108.9(1)
N(p4)—C(p5)—H(p5)	125(1)	122(1)
N(p1)—C(p5)—H(p5)	127(1)	129(1)
C(13)—N(14)—N(24)	128.1(1)	
C(15)—N(14)—N(24)	125.3(1)	
C(23)—N(24)—N(14)	127.6(1)	
C(25)—N(24)—N(14)	126.0(1)	

Hydrogen-bridging system

Distance (Å)		Angle (°)	
OW—HW	0.9(1)	HW—OW—HW′	92(12)
OW—HW*	0.8(2)	HW*—OW—HW*′	151(34)
OW—N(12)″	3.751(4)	OW—N(22)—N(21)	138.1(1)
OW—N(22)	3.130(4)	OW—N(22)—C(23)	110.5(1)
HW—N(22)	2.3(1)	OW—HW—N(22)	153(8)

Dihedral angle (°)

Least-squares plane ring 1–ring 2	93.60(8)

[a] * indicates the disordered atom with the lower occupancy number, 0.18 for S* and 0.27 for HW* respectively. A prime indicates symmetry operation $-x, y, \frac{1}{2}-z$. A double prime indicates symmetry operation $\frac{1}{2}-x, \frac{1}{2}-y, \frac{1}{2}+z$. A triple prime indicates symmetry operation $\frac{1}{2}-x, \frac{1}{2}+y, \frac{1}{2}-z$.

[b] $p = 1$ or 2.

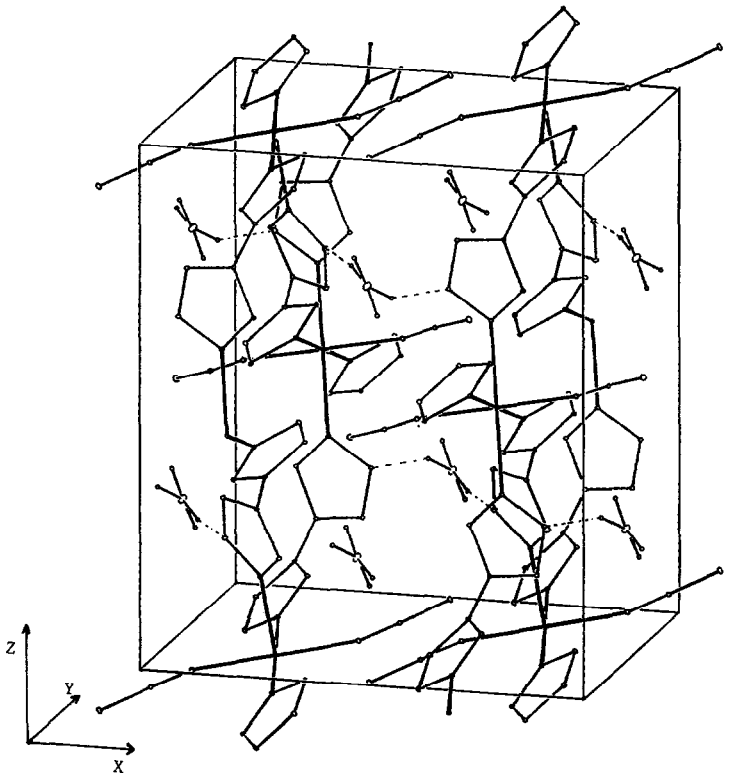


Fig. 2. Structure of $[Co(NCS)_2(btr)_2]H_2O$, showing relative positions of layers and unit cell. Hydrogen bondings are drawn with dotted lines. Both positions of the disordered hydrogen atoms of the water molecules are given. These hydrogen atoms are drawn with small temperature factors. The ligand hydrogen atoms have been omitted for clarity.

free electron pair on N(12), despite the long O...N bond of 3.75 Å. The disorder in the position of S is unusual for a nearly linear NCS geometry: angles N—C—S [176.5(2)°] and N—C—S* [164.5(5)°]. There was no disorder observed in the N or C positions. This sulphur disorder may be brought about by the fact that the NCS groups point to spaces between the layers where no active hydrogens are available to fix their position by means of hydrogen bonding.

Symmetry considerations do not give any support to a splitting of the ν(C—N) in the IR spectrum of $[Co(NCS)_2(btr)_2]H_2O$ and the isomorphous iron and nickel compounds.[21] Nevertheless, a splitting of about 18 cm^{-1} is observed.[10] This splitting can be attributed to the disorder in the position of the sulphur atoms. The splitting in the ν(C—S) (at 796 cm^{-1}) may also originate from this disorder. If this explanation is valid, the reported splitting of the NCS-bending mode into four absorptions could be ascribed to the deviation from linearity, as well as to the disorder in the sulphur atoms.

The geometry of the ligand btr, compared to that of the free molecule, shows a systematic decrease in all ligand bonds. Such an effect has been demonstrated before[5] for complexes of unsubstituted 1,2,4-triazole. The difference between the longest and the shortest endocyclic bonds, which is the largest found so far for 1,2,4-triazoles and their coordination compounds is quite remarkable. Domiano[11] inferred from this a more defined localisation of double-bond character between the N(1), C(5) and N(2), C(3) atoms. Apparently this localisation effect has been retained in the title compound. A comparable effect, although smaller, was observed in coordination compounds of 4-alkyl-substituted 1,2,4-triazoles.[2]

The torsional angle around the central N—N bond of the ligand is 93.60(8)°, which is almost equal to the angle in the free ligand (90.9°), allowing the conclusion that the molecular geometry of the ligand is retained in the complex.

Magnetic measurements

To investigate a possible magnetic interaction between the metal ions through the ligands, magnetic susceptibility measurements of the three isomorphous compounds were recorded. The results are summarised in Table 3. All compounds show

Table 3. Magnetic data for $[M(NCS)_2(btr)_2]H_2O$ (M = Fe, Co or Ni)

	M		
	Fe	Co	Ni
μ_{300K}	5.28	—	—
μ_{200K}	5.36	4.93	2.83
μ_{80K}	3.00	4.56	2.80
$\theta_{80-200K}$	—	−24.1	−2.5
$\theta_{80-150K}$	−9.5	—	—
$\theta_{150-300K}$	12.5	—	—

only small magnetic interactions, as could already be expected from the rather long metal–metal distances.

Much to our surprise, the iron(II) compound shows a high-spin–low-spin transition at 153 K, although a residual paramagnetic fraction of about 60% remains (Fig. 3). Preliminary analysis of this phenomenon indicates a relationship between crystal quality and magnitude of the residual paramagnetic fraction.

This effect, which has been observed before for several other compounds,[22–25] is the subject of further investigations, including magnetic susceptibility and Mössbauer measurements (to be published at a later stage[26]). Haasnoot and Groeneveld[10] have already reported a strengthening of the ligand field upon cooling to liquid-nitrogen temperature in the cobalt(II) and nickel(II) compounds.

The observed spin transition in

$$[Fe(NCS)_2(btr)_2]H_2O$$

is highly unusual and, in fact, has not been observed before in iron(II) compounds with *trans*-oriented thiocyanate groups. A variety of iron(II) compounds is known, showing an HS–LS transition; however, all have *cis*-oriented thiocyanate anions.[22–25] The very few iron(II) *trans*-thiocyanate compounds which are known[18,27–29] do not exhibit a spin transition upon cooling. It appears that $[Fe(NCS)_2(btr)_2]H_2O$ is the first compound with a spin transition in which the iron(II) is coupled weakly antiferromagnetically by ligand bridges, thus forming a two-dimensional network.

Concluding remarks

The structure of the title compound, which was proposed from analytical and spectroscopic data,[10] has been confirmed by the X-ray structure determination. The ligand indeed has *C*2 symmetry with 1,1′-coordination.

The splitting of the NCS IR vibrations have been explained mainly by the disorder found in the position of the sulphur atoms. This emphasizes that care must be taken in drawing conclusions about the coordination mode of thiocyanate from the positions of the NCS absorptions.

The conclusion that btr is a very strong ligand has been proven by the HS–LS transition in the X-ray isomorphous iron(II) compound. This makes it also worthwhile to continue the investigations on this ligand because of the fact that btr is a potentially tetradentate tetranucleating ligand.

Acknowledgements—We wish to thank W. G. Haije, R. C. M. de Groot and G. Renes for operating the Faraday balance. The present investigations have been carried

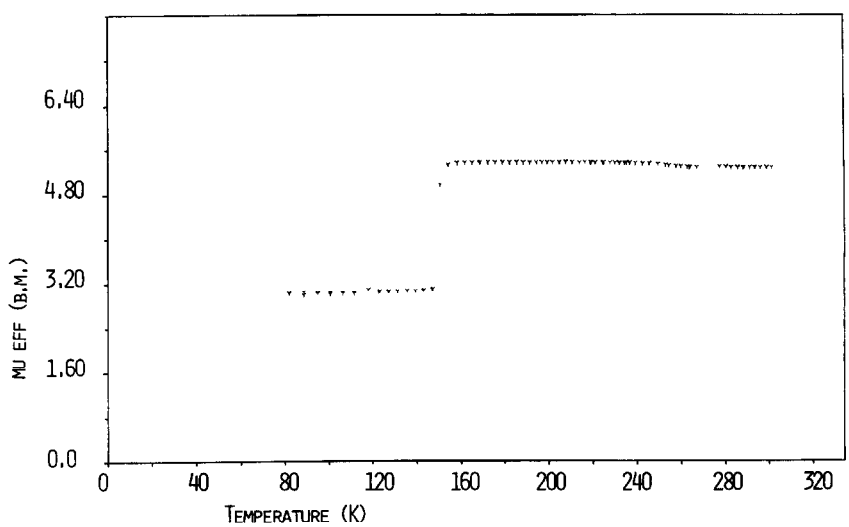


Fig. 3. Effective magnetic moment of $[Fe(NCS)_2(btr)_2]H_2O$ as a function of the temperature in the temperature region 80–300 K.

out with support from the Netherlands Foundation for Chemical Research (SON) and with financial aid from the Netherlands Organization for the Advancement of Pure Research (ZWO), through project 11-28-17.

REFERENCES

1. D. W. Engelfriet, Ph.D. thesis, Leiden (1980).
2. G. Vos, Ph.D. thesis, Leiden (1983).
3. J. G. Haasnoot, G. C. M. de Keyzer and G. C. Verschoor, *Acta Cryst.* 1983, **C39**, 1207.
4. C. W. Reimann and M. Zocchi, *Acta Cryst.* 1971, **B27**, 682.
5. D. W. Engelfriet, W. den Brinker, G. C. Verschoor and S. Gorter, *Acta Cryst.* 1979, **B35**, 2922.
6. G. Vos, J. G. Haasnoot and W. L. Groeneveld, *Z. Naturforsch.* 1981, **36B**, 802.
7. L. R. Groeneveld, G. Vos, G. C. Verschoor and J. Reedijk, *J. Chem. Soc., Chem. Commun.* 1982, 620.
8. G. Vos, R. A. le Fêbre, R. A. G. de Graaff, J. G. Haasnoot and J. Reedijk, *J. Am. Chem. Soc.* 1983, **105**, 1682.
9. J. G. Haasnoot, G. Vos and W. L. Groeneveld, *Z. Naturforsch.* 1977, **32b**, 1421.
10. J. G. Haasnoot and W. L. Groeneveld, *Z. Naturforsch.* 1979, **346**, 1500.
11. P. Domiano, *Cryst. Struct. Commun.* 1977, **6**, 503.
12. R. A. G. de Graaff, *Acta Cryst.* 1973, **A29**, 298.
13. P. Main, In *Crystallographic Computing Techniques* (Edited by F. R. Ahmed). Copenhagen (1976).
14. *International Tables for X-ray Crystallography*, Vol. 4. Kynoch Press, Birmingham (1974).
15. C. K. Johnson, Report ORNL-5138, Oak Ridge National Laboratory, Tennessee (1965).
16. H. Hartl and I. Brüdgam, *Acta Cryst.* 1980, **36B**, 162:
17. I. Søtofte and S. E. Rasmussen, *Acta Chem. Scand.* 1967, **21**, 2028.
18. K. Takahashi, Y. Nishida and S. Kida, *Bull. Chem. Soc. Jpn* 1984, **57**, 2628.
19. T. Ito, M. Kato and H. Ito, *Bull. Chem. Soc. Jpn* 1984, **57**, 2634.
20. T. Ito, M. Kato and H. Ito, *Bull. Chem. Soc. Jpn* 1984, **57**, 2641.
21. R. J. H. Clark and C. S. Williams, *Spectrochim. Acta* 1966, **22**, 1081.
22. P. Gütlich, *Struct. Bonding* 1981, **44**, 83.
23. E. König, G. Ritter and S. K. Kulshreshtha, *Inorg. Chem.* 1984, **23**, 1144.
24. E. W. Müller, H. Spiering and P. Gütlich, *J. Chem. Phys.* 1983, **79**, 1439.
25. E. W. Müller, H. Spiering and P. Gütlich, *Chem. Phys. Lett.* 1982, **93**, 567.
26. W. Vreugdenhil, A. M. van der Kraan, J. G. Haasnoot and J. Reedijk, in preparation.
27. G. Valle, U. Rosso and S. Calogero, *Transition Met. Chem.* 1980, **5**, 26.
28. M. G. B. Drew, Hamid bin Othman and S. M. Nelson, *J. Chem. Soc.* 1976, 1394.
29. G. J. Long, G. Galeazzi, U. Rosso, G. Vall and S. Calogero, *Inorg. Chem.* 1983, **22**, 506.

Polyhedron Vol. 4, No. 10, pp. 1777–1781, 1985
Printed in Great Britain

0277–5387/85 $3.00 + .00
© 1985 Pergamon Press Ltd

SPECTROSCOPIC AND STRUCTURAL PROPERTIES OF HOMONUCLEAR Fe(II) PYRAZINE-BRIDGED POLYMERIC COMPLEXES $[Fe(PYRAZINE)_2X_2]_n$ (X = Cl, Br OR I)

K. RACHLEWICZ,* J. PIETRZYK and K. DRABENT
Institute of Chemistry, University of Wrocław, 50-383 Wrocław, F. Joliot-Curie 14, Poland

(*Received* 23 *November* 1984; *accepted after revision* 26 *April* 1985)

Abstract—The reactions of FeX_2 (X = Cl, Br or I) with pyrazine (pyz) yield the $Fe(pyz)_2X_2$ compounds. Examination of IR and Raman spectra in the medium- and far-IR region as well as studies of electronic and Mössbauer spectra suggests that the complexes contain six-coordinate high-spin Fe(II) in the FeN_4X_2 chromophore. The complexes have a polymeric pseudo-octahedral pyz-bridged structure. The magnetic moments are independent of temperature and low-temperature magnetic measurements do not indicate any magnetic ordering above 4.2 K in these compounds. The π-acceptor properties of pyz are reflected both in the electronic spectra evaluated in terms of the angular overlap model and the Mössbauer parameters.

There are many papers dealing with the physico-chemical properties of transition metal compounds containing pyrazine (pyz) as one of the ligands. In most cases these studies refer to the compounds where pyz is a ligand bridging two metal ions,[1–4] although it also occurs as a unidentate ligand.[4–6]

Polymeric compounds with the formula FeL_2X_2 (where L = pyridine)[7,8] or $FeLX_2$ (where L = 2,2-bipyridyl or 1,10-phenanthroline, and X = halide or pseudo-halide ion)[9,10] containing halide or pseudo-halide bridges have been recently thoroughly studied because of their magnetic properties. These compounds were found to possess a pseudo-octahedral polymeric structure. A group of compounds of that composition with a monomeric pseudo-tetrahedral structure were reported.[7,11–14]

It seemed interesting to prepare and to investigate the structure and properties of the FeL_2X_2 compounds (X = Cl, Br or I), with the ligand L containing two coordination sites capable of bridge bond formation. The present paper shows the results obtained for compounds where the ligand L is pyz. The compound $Fe(pyz)_2Cl_2$ has been prepared previously[15,16] and on the basis of IR studies its structure was described as polymeric pseudo-octahedral, containing chloride bridges. The spectroscopic (IR, Raman, UV–Vis and Mössbauer) and magnetic results presented here do not confirm such a structure.

* Author to whom correspondence should be addressed.

EXPERIMENTAL

$Fe(pyz)_2Cl_2$ was prepared by the modified method of Bayer and Ferraro.[15] A solution of 2 mmol of $FeCl_2 \cdot 4H_2O$ in 10 cm^3 of water was added to a solution of 2 mmol of pyz in 10 cm^3 of water under a stream of nitrogen. A red precipitate formed immediately, which was filtered, washed with water, ethanol and ethyl ether, and dried in a desiccator over $CaCl_2$ in a nitrogen atmosphere. Found: Fe, 19.52; C, 33.56; H, 2.91; N, 19.44; Cl, 24.63. Calc. for $Fe(pyz)_2Cl_2$: Fe, 19.46; C, 33.48; H, 2.82; N, 19.53; Cl, 24.71%.

$Fe(pyz)_2Br_2$. An excess of iron powder was dissolved in 5 cm^3 of 40% HBr in a nitrogen atmosphere. After 12 h the solution was filtered to remove all traces of iron. A methanol solution of pyz was added to this solution (Fe : pyz = 1 : 1). A red precipitate formed immediately and was purified and dried as a chlorine derivative. Found: Fe, 14.92; C, 25.58; H, 2.24; N, 14.82; Br, 42.44. Calc. for $Fe(pyz)_2Br_2$: Fe, 14.86; C, 25.56; H, 2.15; N, 14.91; Br, 42.52%.

$Fe(pyz)_2I_2$ was prepared in a similar way to the bromine complex, except that 40% HI was used instead of HBr. Found: Fe, 11.88; C, 20.54; H, 1.86; N, 11.87; I, 53.93. Calc. for $Fe(pyz)_2I_2$: Fe, 11.89; C, 20.45; H, 1.72; N, 11.92; I, 54.02%.

Physical measurements. The X-ray powder patterns were obtained with a DRON-1 and Ni-filtered Cu radiation.

Diffuse reflectance electronic spectra in magnesium oxide were recorded on a Beckman 5240.

The IR spectra in the region 4000–20 cm^{-1} were obtained on a Perkin–Elmer 180 spectrometer in both KBr pressed pellets and Nujol mulls.

The Raman spectra were measured by means of a JEOL IRS-S1 Spectrophotometer using the 488 and 514.5 nm exciting lines of an Ar-ion laser. The magnetic measurements were made on either a Gouy or a Faraday balance calibrated with $HgCo(NCS)_4$.

The diamagnetic corrections were applied using Pascal's constants. The Mössbauer effect measurements of powders were done on a Mössbauer 2330 spectrometer (Polon, Poland). Measurements were made at 80 and 295 K. The isomer shift values were related to a sodium nitroprusside (SNP) standard. ^{57}Co in the Cr matrix of 20 mCi activity was used as the source. The source and SNP during all measurements were stored at room temperature. The spectra were processed numerically by distribution into Lorentz curves.

Carbon, hydrogen, nitrogen and halide analyses were performed by the Analytical Laboratory of the Institute of Chemistry, University of Wrocław.

Iron was determined by using dichromate titrimetry.[17]

RESULTS AND DISCUSSION

The reactions of FeX_2 (X = Cl, Br or I) with pyz in neutral or acid aqueous solutions at room temperature yield the $Fe(pyz)_2X_2$ compounds, irrespective of the metal : pyz concentration ratio. All compounds were prepared in the form of powders. The compounds were kept in a desiccator under nitrogen over $CaCl_2$. The compounds are stable under such conditions and no changes in their spectral characteristics were found to occur after several months.

Powder X-ray diffraction patterns of the chloride compounds were made. It was found that the compound is not isomorphous with $Co(pyz)_2Cl_2$, whose single-crystal structure is known[1] to be polymeric with pyz bridges. The pyz compound is also not isomorphous with the pyridine iron compounds $Fe(py)_2Cl_2$ and $Fe(py)_4Cl_2$.

Magnetic studies

The magnetic susceptibility was examined as a function of temperature over the 4.2–293 K range for the chloride compound and over 77–293 K for the bromide and iodide compounds. Over that temperature range the $Fe(pyz)_2X_2$ complexes obey the Curie–Weiss law.

The magnetic moment is independent of temperature over the temperature range studied. The magnitude of the magnetic moment is characteristic of the pseudo-octahedral high-spin Fe(II) complexes with the ground state $^5T_{2g}$, whose degeneracy is eliminated by the low ligand field symmetry. Low-temperature magnetic measurements of pyz complexes do not indicate any magnetic ordering above 4.2 K, which distinguishes these complexes with respect to pyridine compounds with the same composition, $Fe(py)_2X_2$.[7]

Electronic spectra

Diffuse reflectance spectra of the complexes examined were measured over the region from 4000 to 50,000 cm^{-1}. The electronic spectra of the chloride and bromide complexes over the NIR region exhibit one band with a shoulder in the low-frequency part of the spectrum. On the other hand, the spectrum of the iodide complex contains two well-resolved bands. The visible region shows one broad strong band corresponding to the charge-transfer transition at about 20,800 cm^{-1}, whose energy varies slightly depending on the ligand X (X = Cl, Br or I). One can also observe a band at 35,000 cm^{-1} which corresponds to the inner π–π^* transition of pyz. The bands found in the NIR region should be assigned to the *d–d* transitions for high-spin Fe(II) of the d^6-structure surrounded by a disturbed octahedron. These transitions are from the ground state $^7T_{2g}$ (with O_h-symmetry) to the excited level E_{2g}, which becomes split into the $^5A_{1g}$ and $^5B_{1g}$ levels in the field of lower symmetry. Characteristics of the *d–d* bands found in the NIR region are presented in Table 1.

The $\nu_1 - \nu_2$ parameter defines the magnitude of the *d–d* band splitting, whereas ν_{av} is the arithmetic mean of both *d–d* band energies.

Table 1. Experimental electronic spectral results[a]

Compound	$^5T_{2g} \xrightarrow{\nu^1} {}^5A_{1g}$	$^5T_{2g} \xrightarrow{\nu^2} {}^5B_{1g}$	$\nu_1 - \nu_2$	ν_{av}
$Fe(pyz)_2Cl_2$	9800	11,600	−1800	10,700
$Fe(pyz)_2Br_2$	8800	11,200	−2400	10,000
$Fe(pyz)_2I_2$	7200	11,200	−4000	9200

[a] All data in cm^{-1}.

The parameters presented in Table 1 are similar to those found for $Fe(py)_4X_2$[7] which indicates the presence of the FeN_4X_2 chromophore for iron(II) in the pyz complexes. For the compounds with the formula $Fe(pyz)_2X_2$ such an environment may be achieved only by bridge bonding. The splitting in the spectra may be related to the σ-bonding of the ligands by using the angular overlap model:[18,19]

$$\delta_{e\sigma} = E(d_{x^2-y^2}) - E(d_{z^2}) = -(\nu_1 - \nu_2) = 2(e_{\sigma pyz} - e_{\sigma X}).$$

The $\delta_{e\sigma}$ value for the chloride compound is, within experimental error, identical to that found for the pyridine complex ($-1800\ cm^{-1}$). On the other hand, for the pyz compounds with bromide and iodide this value is lower than that for the corresponding compounds with pyridine.

The differences in the splitting energy and e_σ values of ligand interactions should be interpreted with allowance for differences in π-acceptor interactions of pyridine and pyz. The π-acceptor properties of pyz modify the σ-donor properties of X, increasing them in the case of the bromide and iodide (with respect to the pyridine compounds), or, which is more probable, the interactions of both ligands mutually change their σ-donor properties. One could note that the difference between the σ-interactions of pyz and ligand X for bromide and iodide is smaller in the pyz compounds (compared to those of pyridine), which can also be observed in the Mössbauer spectral parameters.

Similar conclusions may apply to the magnitude of splitting in the σ- and π-orbitals of the metal. This splitting is measured by the ν_{av} parameter (equivalent to the $10Dq$ parameter in the crystal field approximation). The value of ν_{av} is higher for the pyz complexes. The formation of π-back bonding in pyz compounds results in a decrease in the t_{2g} orbital energy of the metal and, thus, an increase in the separation of the t_{2g}- and e_g-orbitals which is manifested by an increase in the ν_{av} parameter. ν_{av} decreases in the series Cl > Br > I according to the position of the ligand X in the spectrochemical series. However, the decrease in that parameter is lower in pyz than in pyridine compounds.[7] The increase in the σ-donor properties of bromide and iodide is responsible for increasing the e_g orbital energy and, as a result, the separation of the t_{2g}- and e_g-orbitals is larger compared to the pyridine counterparts.

IR and Raman spectra

Mid-IR and Raman spectra exhibit internal pyz fundamentals.[20–22]

In complexes where pyz is coordinated through a bridge with two identical acceptors, the symmetry centre is preserved and pyz bonded in this manner as well as that isolated has a D_{2h}-symmetry.[4,23,24] In effect there is no coincidence of bands in the IR and Raman spectra.

As shown in Table 2 a lack of coincidence is observed for the compounds under examination. This fact indicates that the assumed structure of the complexes is polymeric with pyz bridges. Most fundamental IR bands of pyrazine are slightly shifted (several by a dozen cm^{-1}) towards higher frequencies upon coordination. Exceptions are bands 19a and 9a (Table 2).

It is not possible to evaluate the σ- and π-interactions on the basis of those shifts since they are related above all with the interactions of rings in the lattice.

Far-IR spectra in the region from 400 to 50 cm^{-1} are characteristic of the D_{4h}-symmetry.[23,24] As predicted, there are two bands for such a symmetry of the metal environment. One of these bands should be assigned to the ν_{Fe-X} mode (X = Cl, Br or I) and one to $\nu_{Fe-N(pyz)}$ (see Table 3).

The ν_{Fe-N} frequency in the pyz complexes investigated is comparable with the ν_{Fe-N} frequency in monomeric pyridine complexes of formula $Fe(py)_4X_2$.[7] The ν_{Fe-X} frequency for the chloride and bromide compound is higher than that[7] for the monomeric compounds $Fe(py)_4Cl_2$ ($+37\ cm^{-1}$) and $Fe(py)_4Br_2$ ($+17\ cm^{-1}$) but is lower for the iodide compound with respect to $Fe(py)_4I_2$ ($-22\ cm^{-1}$). The high band frequency ν_{Fe-X} is more evidence that the halides occur in terminal positions in the compounds investigated by us. In the pyz compounds the Fe—X bond becomes stabilized in the chloride and bromide complex compared to the pyridine compounds. On the other hand, there is a certain destabilization of the Fe—I bond in the pyz compound which is manifested by a decrease in the ν_{Fe-I} frequency compared to the pyridine complex.

In terms of the hard and soft acids and bases principle[25–27] a shift of electron density from the metal ion as a result of π-acceptor interactions of pyz increases the hard nature of the metal ion and thus the bond with a hard base chloride becomes stabilized and that with a soft iodide becomes destabilized.

Mössbauer spectroscopy

The magnitude of the quadrupole splitting (QS), isomeric shift (IS) and line-width for the compounds measured at 80 and 295 K are presented in Table 4. The powder Mössbauer spectra for all the compounds under examination consist of a single quadrupole doublet with narrow resonance lines.

Table 2. Vibrational spectra of the complexes in the region of pyz fundamentals[a]

$Fe(pyz)_2Cl_2$		$Fe(pyz)_2Br_2$		$Fe(pyz)_2I_2$		Assignments	
Raman	IR	Raman	IR	Raman	IR	D_{4h}	Notation
	3100w		3110w		3110w	b_{1u}	20a
	3080m		3090m		3090m	b_{3u}	20b
3092s		3087s		3076s		a_g	2
1672w		1664w					
1604s		1604s		1604s		a_g	8a
	1480m		1485m		1485m	b_{1u}	19a
	1415s		1420s		1415s		
	1410		1412			b_{3u}	19b
	1380w		1385w		1375m	b_{3u}	14
1220s		1220s		1224s		a_g	9a
	1155m		1155m		1160s	b_{1u}	18a
	1120s		1120s		1120s	b_{3u}	15
	1055s		1055s		1055s	b_{1u}	12
1031s		1024s		1024s		a_g	1
	990w		985w		990m		
	815		815s		820s	b_{2u}	11
	810m						
	908						
640s		640s		640s		b_{3g}	4
	470m		470m		470m	b_{2u}	16b

[a] All data in cm^{-1}.

The values of QS and IS for the compounds examined are characteristic of high-spin iron(II) compounds with a distorted octahedron symmetry and for the chloride compound are close to the values observed for the $Fe(py)_4Cl_2$ complex and not $Fe(py)_2Cl_2$, which is further evidence that iron is bonded with four nitrogen atoms in the plane and with two chlorine atoms in the axial positions. The value of IS at room temperature does not depend on the type of X in the $Fe(pyz)_2X_2$ compounds, which indicates that *s*-electron density on the iron nucleus does not vary in these compounds. In addition, in the $Fe(py)_4X_2$ compounds no significant changes in the value of IS in the series (X = Cl, Br or I) are observed.

The value of QS reflects a change in substituent X in $Fe(pyz)_2X_2$ to a much less extent than in tetrakis(pyridine)[7,28–30] and tetrakis(isoquinoline)-iron(II)[28–30] complexes of general formula FeL_4X_2. However, significant differences occur in the QS values for the latter compounds. The value of QS as a measure of spherical charge distribution around the Mössbauer nucleus decreases in the series Cl > Br > I which is in agreement with expectations and reflects an increase in covalency of the Fe—X bond. In the case of the $Fe(pyz)_2X_2$ compounds the situation is different. No change in QS is found on transition from chloride to bromide and introduction of the iodide ion as X results in a much smaller change in QS than in the case of a similar substitution in the FeL_4X_2 complexes.

The absence of any differences in QS is consistent with the variations in the parameters of electronic spectra, $\nu_1 - \nu_2$ and ν_{av}. We believe that a slight change in QS results from the same reasons which were discussed in the description of the electronic spectra, that is, a decrease in the covalent nature of the Fe—X bond (X = Br and I) with respect to the analogues of formula FeL_4X_2. This effect results in the absence of significant changes in the electric field gradient on the nucleus in the bromide and iodide compound compared to the chloride compound. Therefore, no change in the QS parameter is found on passing from chloride to bromide and a slight decrease in this parameter (compared to the respective pyridine compound) for the iodide complex. A similar slight change in QS was observed

Table 3. Far-IR spectra of the complexes[a]

Compound	ν^b_{Fe-X}	ν^b_{Fe-N}	Other bands
$Fe(pyz)_2Cl_2$	274s	224m	154, 126, 114
$Fe(pyz)_2Br_2$	212s	221sh	148, 128, 98
$Fe(pyz)_2I_2$	174s	220m	136, 120, 88

[a] All data in cm^{-1}.

[b] Abbreviations: s, strong; m, medium; sh, shoulder.

Table 4. Mössbauer parameters and magnetic moments

Compound	T (K)	QS[a] (mm s^{-1})	IS[ab] (mm s^{-1})	Γ_-[a] (mm s^{-1})	Γ_+[a] (mm s^{-1})	μ_B[c]
$Fe(pyz)_2Cl_2$	295	3.24	1.27	0.29	0.29	5.40
	80	3.33	1.37	0.43	0.43	5.27
	4.2	—	—	—	—	4.94
$Fe(pyz)_2Br_2$	295	3.27	1.25	0.37	0.35	5.40
	80	3.38	1.30	0.40	0.35	5.33
$Fe(pyz)_2I_2$	295	2.02	1.25	0.26	0.25	5.80
	80	2.58	1.37	0.42	0.42	5.69
$Fe(py)_4Cl_2$[d]	295	3.08	1.32	0.31	0.31	
	78	3.49	1.44	0.30	0.30	
$Fe(py)_2Cl_2$[d]	295	0.57	1.34	0.25	0.25	
	78	1.25	1.47	0.34	0.32	

[a] Error in QS, IS and $\Gamma_\pm$ estimated as ± 0.01 mm s^{-1}.
[b] IS relative to SNP.
[c] Magnetic moments in Bohr magnetons.
[d] Data from Ref. 7.

for the $Fe(phen)_2X_2$ complexes.[28] However, in this case there is a symmetry effect apart from the π-back-bonding effect of phenanthroline donation since this compound is a *cis* isomer.

Acknowledgements—We thank Professor Dr S. Wajda for his interest in this work. Financial support from the Polish Academy of Science under Grant MR-I-9 is gratefully acknowledged.

REFERENCES

1. P. W. Carreck, M. Goldstein, E. M. McPartlin and W. D. Unsworth, *J. Chem. Soc., Chem. Commun.* 1971, 1635.
2. A. Yeh, A. Haim, M. Tanner and A. Ludi, *Inorg. Chim. Acta* 1979, **33**, 51.
3. K. Rachlewicz, J. Pietrzyk, K. Drabent and S. Wajda, *Inorg. Chim. Acta* 1983, **77**, L189.
4. M. Goldstein and W. D. Unsworth, *Spectrochim. Acta.* 1971, **27A**, 1055.
5. C. Cruetz and H. Taube, *J. Am. Chem. Soc.* 1969, **91**, 3988; *ibid.* 1973, **95**, 1086.
6. H. E. Toma and J. Malin, *Inorg. Chem.* 1973, **12**, 1039.
7. B. F. Little and G. J. Long, *Inorg. Chem.* 1978, **17**, 3401, and references therein.
8. W. M. Reiff, R. B. Frankel, B. F. Little and G. J. Long, *Inorg. Chem.* 1974, **13**, 2153.
9. W. M. Reiff, B. Dockum, M. A. Weber and R. B. Frankel, *Inorg. Chem.* 1975, **14**, 800.
10. W. M. Reiff and S. Foner, *J. Am. Chem. Soc.* 1973, **95**, 260.
11. R. C. Dickinson and G. J. Long, *Inorg. Chem.* 1974, **13**, 262.
12. J. T. Wroblewski and G. J. Long, *Inorg. Chim. Acta* 1978, **30**, 221.
13. T. Birchall and M. F. Morris, *Can. J. Chem.* 1972, **50**, 211.
14. F. Petillon, J. E. Guerchais and D. M. L. Goodgame, *J. Chem. Soc., Dalton Trans.* 1973, 1209.
15. R. Bayer and J. R. Ferraro, *Inorg. Chem.* 1969, **8**, 1654.
16. C. Beech and C. T. Mortimer, *J. Chem. Soc. (A)* 1967, 115.
17. J. Minczewski and Z. Marczenko, *Chemia Analityczna*, p. 468. P.W.N., Warszawa (1965).
18. C. E. Schäffer, *Struct. Bonding* 1968, **5**, 68.
19. M. Gerloch, and R. C. Slade, *Ligand-Field Parameters*, p. 173. Cambridge University Press, London (1973).
20. R. C. Lord, A. L. Marston and F. A. Miller, *Spectrochim. Acta* 1957, **9**, 113.
21. S. Califano, G. Adembri and G. Sbana, *Spectrochim. Acta* 1964, **20**, 385.
22. J. D. Simmons, K. K. Innes and G. M. Begum, *J. Mol. Spectrosc.* 1964, **14**, 190.
23. M. Goldstein and W. D. Unsworth, *Spectrochim. Acta* 1972, **28A**, 1297.
24. M. Goldstein, F. B. Taylor and W. D. Unsworth, *J. Chem. Soc., Dalton Trans.* 1972, 418.
25. S. Ahrland, J. Chatt and N. R. Davies, *Q. Rev.* 1958, **12**, 265.
26. S. Ahrland, *Struct. Bonding*, 1968, **5**, 118; *ibid.* 1973, **15**, 167.
27. R. G. Pearson, *J. Am. Chem. Soc.* 1963, **85**, 3533.
28. P. B. Merrithew, I. I. Guerrara and A. J. Modestino, *Inorg. Chem.* 1974, **13**, 644.
29. J. F. Duncan, R. M. Golding and K. F. Mok, *J. Inorg. Nucl. Chem.* 1966, **28**, 114.
30. C. D. Burbridge, D. M. L. Goodgame and M. Goodgame, *J. Chem. Soc. (A).* 1967, 349.

Polyhedron Vol. 4, No. 10, pp. 1783–1789, 1985
Printed in Great Britain

0277-5387/85 $3.00 + .00
© 1985 Pergamon Press Ltd

PREPARATION AND ELECTRICAL RESISTIVITIES OF TETRATHIAFULVALEN (TTF) AND TETRASELENAFULVALEN SALTS WITH THE $[SnR_2Cl_n]^{2-n}$ ANIONS ($n = 3$ OR 4: R = Et OR Ph) and X-RAY CRYSTAL STRUCTURE OF $[TTF]_3[SnEt_2Cl_4]$

KOSUKE UEYAMA, GEN-ETSU MATSUBAYASHI, RYUICHI SHIMIZU and TOSHIO TANAKA*

Department of Applied Chemistry, Faculty of Engineering, Osaka University, Yamada-oka, Suita, Osaka 565, Japan

(*Received* 1 *March* 1985; *accepted* 3 *May* 1985)

Abstract—Tetrathiafulvalen (TTF) and tetraselenafulvalen (TSF) salts with diorganochlorostannate anions, $[TTF][SnEt_2Cl_3]$ (**1**), $[TTF]_2[SnPh_2Cl_4]$ (**2**), $[TTF]_3[SnEt_2Cl_4]$ (**3**), $[TTF]_{3.3}[SnPh_2Cl_4]$ (**4**), $[TSF]_2[SnPh_2Cl_4]$ (**5**) and $[TSF]_{3.3}[SnPh_2Cl_4]$ (**6**), were prepared by the reactions of $[TTF \text{ or } TSF]_3[BF_4]_2$ with SnR_2Cl_2 (R = Et or Ph) in the presence of $[Ph_3PCH_2Ph]Cl$ and by electrocrystallization of TTF or TSF in acetonitrile containing SnR_2Cl_2 and $[Ph_3PCH_2Ph]Cl$. All the salts behave as semiconductors with electrical resistivities of the order of $10–10^8$ Ω cm as compacted samples at 25°C. Electronic reflectance spectra of the simple salts **1**, **2** and **5**, show a band due to the dimeric $(TTF^+)_2$ or $(TSF^+)_2$ unit in the 12,200–12,800-cm^{-1} region. The complex salt **3** exhibits a TTF^+/TTF^0 charge-transfer (CT) band at 8700 cm^{-1}, and the remaining complex salts, **4** and **6**, both display CT bands between the radical cations and between the radical cation and the neutral donor molecule. The crystal structure of **3** was determined by a single-crystal X-ray diffraction. The tetragonal crystal, space group *I4cm*, has cell dimensions $a = 11.710(3)$ Å, $c = 25.242(7)$ Å, and $Z = 4$. The structure was solved by the heavy-atom method and refined to a final R value of 0.082 for 479 independent reflections with $|F_o| > 3\sigma(F)$. TTF molecules exist as trimers, in which a slight lateral shift from the eclipsed TTF overlap occurs, although TTF molecules are arranged with equal spacing between them. The trimer units are located perpendicularly to each other, forming a two-dimensional layer. The $[SnEt_2Cl_4]^{2-}$ anion is disordered with respect to the two Sn—Et and two Sn—Cl bonds.

Tetrathiafulvalen (TTF) and tetraselenafulvalen (TSF) are known as good electron donors and can easily be oxidized to stable radical cations, forming electrically conductive salts with various anions.[1] Metal halide anions may be of much interest as the counterparts of TTF^+ or TSF^+ radical cation salts since they assume various geometries and different formal charges which can affect the packing of donor molecules in crystals. Recently, we reported the crystal structures and the electrical properties of $[TTF]_3[SnCl_6]$,[2] $[TTF]_3[SnMe_2Cl_4]$[3] and $[TTF][SnMe_2Cl_3]$.[3] Of those, $[TTF]_3[SnMe_2Cl_4]$ has a novel TTF packing, consisting of trimer units forming a two-dimensional layer, and exhibits a low electrical resistivity (16 Ω cm at 25°C as a compacted pellet).[3] Thus, we have undertaken an investigation of the TTF and TSF salts with more bulky diorganochlorostannate(IV) anions.

This paper reports the preparation and electrical resistivities of TTF and TSF salts with some diorganochlorostannate anions, $[SnEt_2Cl_n]^{2-n}$ ($n = 3$ or 4) and $[SnPh_2Cl_4]^{2-}$. The arrangements of TTF and TSF molecules in crystals are also discussed, based on electronic reflectance spectra of the salts, together with an X-ray crystallographic analysis of $[TTF]_3[SnEt_2Cl_4]$.

EXPERIMENTAL

Materials

TTF,[4] and TSF,[5] $[TTF]_3[BF_4]_2$,[6] $[TSF]_3[BF_4]_2$,[7] $SnEt_2Cl_2$[8] and $SnPh_2Cl_2$,[9] were prepared according to the literature. $[Ph_3PCH_2Ph]Cl$

* Author to whom correspondence should be addressed.

was obtained from an equimolar mixture of triphenylphosphine and benzylchloride in benzene.

Preparation of the TTF salts

To an acetonitrile (30 cm^3) solution of $[TTF]_3[BF_4]_2$ (50 mg, 0.064 mmol) was added an acetonitrile (20 cm^3) solution containing both $SnEt_2Cl_2$ (470 mg, 1.9 mmol) and $[Ph_3PCH_2Ph]Cl$ (50 mg, 0.13 mmol) under a nitrogen atmosphere. The mixture was allowed to stand in a refrigerator overnight to yield the simple salt $[TTF][SnEt_2Cl_3]$ (**1**), which was filtered and dried *in vacuo*, 44% yield based on the TTF^+ radical cation. A similar reaction, with $SnPh_2Cl_2$ in the place of $SnEt_2Cl_2$, afforded the simple salt $[TTF]_2[SnPh_2Cl_4]$ (**2**), 18% yield.

On the other hand, the reaction of an acetonitrile (5 cm^3) solution containing both $SnEt_2Cl_2$ (95 mg, 0.38 mmol) and $[Ph_3PCH_2Ph]Cl$ (30 mg, 0.077 mmol) with $[TTF]_3[BF_4]_2$ (30 mg, 0.038 mmol) in the same solvent (30 cm^3) in the presence of TTF (20 mg, 0.098 mmol) under a nitrogen atmosphere afforded the complex salt $[TTF]_3[SnEt_2Cl_4]$ (**3**), 16% yield. The same salt was also obtained by electrolysis of an acetonitrile (10 cm^3) solution containing TTF (51 mg, 0.25 mmol), $SnEt_2Cl_2$ (250 mg, 1.0 mmol) and $[Ph_3PCH_2Ph]Cl$ (190 mg, 0.50 mmol) for 11 days under conditions described elsewhere,[10] 8% yield based on TTF. By using $SnPh_2Cl_2$ in the place of $SnEt_2Cl_2$, electrocrystallization under the same conditions gave the complex salt $[TTF]_{3.3}[SnPh_2Cl_4]$ (**4**), 16% yield.

Preparation of the TSF salts

In contrast to the TTF salt electrocrystallization from an acetonitrile (10 cm^3) solution containing TSF (51 mg, 0.13 mmol), $SnPh_2Cl_2$ (340 mg, 1.0 mmol) and $[Ph_3PCH_2Ph]Cl$ (190 mg, 0.50 mmol) for 11 days afforded the simple salt $[TSF]_2[SnPh_2Cl_4]$ (**5**), 33% yield based on TSF. On the other hand, the reaction of an acetonitrile (5 cm^3) solution containing $SnPh_2Cl_2$ (190 mg, 0.56 mmol) and $[Ph_3PCH_2Ph]Cl$ (14 mg, 0.037 mmol) with $[TSF]_3[BF_4]_2$ (50 mg, 0.037 mmol) in the same solvent (30 cm^3) in the presence of TSF (20 mg, 0.51 mmol) under a nitrogen atmosphere gave the complex salt $[TSF]_{3.3}[SnPh_2Cl_4]$ (**6**), 36% yield.

Ratios of the TTF^+ radical cation to neutral TTF^0 in the salts were determined from electronic absorption spectra in acetonitrile. The involvement of diorganostannate groups in the salts obtained was confirmed from ^1H NMR spectra in conc. HNO_3. The analyses and properties of the salts are listed in Table 1.

Physical measurements

Electronic absorption spectra in acetonitrile and powder reflectance spectra were recorded as described elsewhere.[2] Electrical resistivities were measured as compacted samples by the conventional two-probe method.[11]

X-ray crystal structure determination of salt **3**

Crystal data for **3**. $C_{22}H_{22}Cl_4S_{12}Sn$, $M = 931.6$, tetragonal, space group *I4cm*, $a = 11.710(3)$ Å, $b = 25.242(7)$ Å, $U = 3461(2)$ Å^3, $Z = 4$, $D_c = 1.789(1)$ g cm^{-3}, μ(Mo-K_α) = 17.6 cm^{-1}.

A specimen (0.25 × 0.30 × 0.10 mm) was selected to collect intensities on a Rigaku four-circle diffractometer using graphite-monochromated Mo-K_α

Table 1. Analyses and physical properties of the salts

No.	Salt	Colour	M.p. (dec.) (°C)	Found (calc.) % C	% H
1	$[TTF][SnEt_2Cl_3]$	Brown plates	> 158	25.24 (24.64)	3.14 (2.89)
2	$[TTF]_2[SnPh_2Cl_4]$	Brown microcrystals	> 149	34.97 (35.01)	2.49 (2.20)
3	$[TTF]_3[SnEt_2Cl_4]$	Black plates	> 197	28.71 (28.37)	2.60 (2.38)
4	$[TTF]_{3.3}[SnPh_2Cl_4]$	Brown microcrystals	> 137	34.98 (35.08)	2.40 (2.15)
5	$[TSF]_2[SnPh_2Cl_4]$	Dark green microcrystals	> 134	24.27 (24.05)	1.69 (1.51)
6	$[TSF]_{3.3}[SnPh_2Cl_4]$	Dark green microcrystals	> 155	21.91 (22.33)	1.54 (1.37)

radiation ($\lambda = 0.71070$ Å) and employing the ω–2θ scan technique.[3]

The positions of the Sn atoms were determined by the heavy-atom method on the basis of 479 reflections of $|F_o| > 3\sigma(F)$ among the 926 independent reflections. Although three possible space groups, $I\bar{4}c2$, $I4cm$ and $I4/mcm$, were suggested on the basis of the extinction rule, $I4cm$ was proved to be correct by the successful analysis, and the positions of all non-hydrogen atoms except for the methyl-carbon atoms of ethyl groups were given by the Fourier maps. The positions of the methyl carbons were not found, due to a disorder between two chlorine and two methylene-carbon atoms. Structure refinement was performed by the block-diagonal least-squares method assuming anisotropic thermal parameters for the nonhydrogen atoms to give residual indices of

$$R = \sum ||F_o| - |F_c|| / \sum |F_o| = 0.082$$

and

$$R' = [\sum w(|F_o| - |F_c|)^2 / \sum w|F_o|^2]^{1/2} = 0.11.$$

The weighting scheme was $1/w = \sigma^2(F_o) + 0.01(F_o)^2$. Atomic scattering factors were taken from *International Tables*.[12] The final atomic co-ordinates, temperature factors, and observed and calculated structure factors have been deposited as supplementary data with the Editor, from whom copies are available on request.*

Crystallographic calculations were performed on an ACOS 900S computer at the Crystallographic Research Centre, Institute for Protein Research, Osaka University. Figures 1–3 were drawn by the local version of the ORTEP-II program.[13]

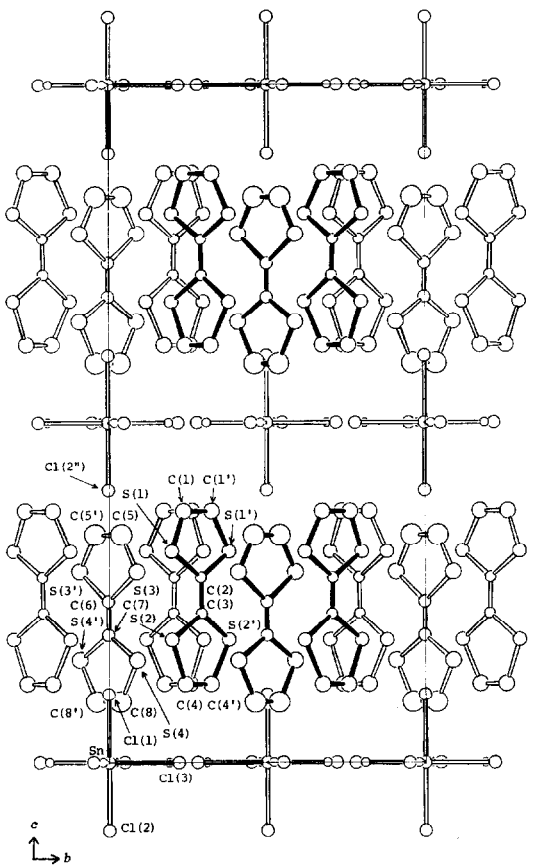


Fig. 1. Crystal structure of **3** projected along the *a*-axis. The atoms are drawn with arbitrary isotropic thermal factors for simplification.

RESULTS AND DISCUSSION

The crystal structure of **3**

The crystal structures of **3** projected along the *a*- and *c*-axes are shown in Figs 1 and 2, respectively, where the atoms are drawn by using arbitrary isotropic thermal parameters for simplification. Bond lengths and angles as well as relevant intermolecular atom–atom contacts are summarized in Table 2.

The tin atoms located in a distorted octahedral $[SnEt_2Cl_4]^{2-}$ anion occupy the positions (0, 0, 0), ($\frac{1}{2}$, $\frac{1}{2}$, 0), (0, 0, $\frac{1}{2}$) and ($\frac{1}{2}$, $\frac{1}{2}$, $\frac{1}{2}$), where four-fold axes exist parallel to the *c*-axis. Two chlorine atoms as well as two methylene-carbon atoms of the ethyl groups are almost on the (001) and (002) planes and they are

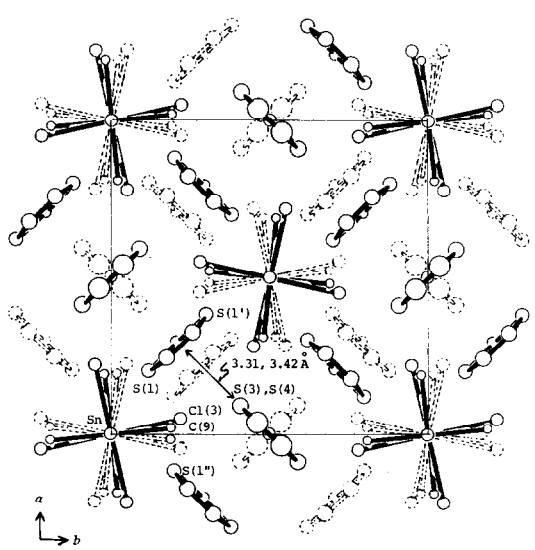


Fig. 2. Crystal structure of **3** projected along the *c*-axis. The atoms are drawn with arbitrary isotropic thermal factors for simplification.

* Atomic co-ordinates have also been deposited with the Cambridge Crystallographic Data Centre.

disordered on these planes. A similar disorder with respect to chlorine atoms and methyl groups has been reported for $[TTF]_3[SnMe_2Cl_4]$[3]. The positions of the methyl-carbon atoms of the ethyl groups have not been determined. The Sn—Cl distances [2.58(2), 2.62(2) and 2.67(1) Å are close to those of $[TTF]_3[SnMe_2Cl_4]$ [2.599(5) and 2.600(3) Å][3] and $[pyridinium]_2[SnMe_2Cl_4]$ [2.603(2) and 2.625(2) Å].[14] The Sn—C(9) bond [2.21(7) Å] is slightly longer than those reported for $[pyridinium]_2[SnMe_2Cl_4]$ [2.109(9) Å],[14] $[SnMe_2Cl(terpyridyl)][SnMe_2Cl_3]$ [2.11(5) and 2.12(4) Å for the anion moiety],[15] and $[Mo_3(h^5\text{-}C_5H_5)_3S_4][SnMe_3Cl_2]$ [2.12(1) Å],[16] whereas it is shorter than that for $[EtSn(OH)Cl_2 \cdot H_2O]_2$ [2.304(30) Å].[17]

TTF moieties exist as a trimer unit, where the co-facial molecular planes are located parallel to the *c*-axis, separated by the same distance. The molecular overlap of the TTF moieties within the trimer unit has a considerable lateral shift (0.79 Å) along the long molecular axis, as shown in Fig. 3. This is in marked contrast to the eclipsed overlap of the TTF moieties in $[TTF]_3[SnCl_6]$[2] and $[TTF]_3[SnMe_2Cl_4]$.[3]

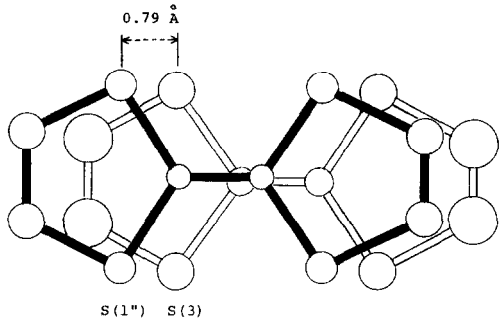


Fig. 3. Overlap scheme of the TTF moieties in the trimer unit.

Moreover, the TTF trimers are arranged perpendicularly to one another, the centres of terminal TTF molecules of the trimer unit being at $z = 0.245$ and 0.745 (Fig. 1). Thus, the two-dimensional TTF layers are constructed parallel to the *c*-plane, and are very similar to those of $[TTF]_3[SnCl_6]$ and $[TTF]_3[SnMe_2Cl_4]$, except for a significant shift of the TTF-eclipsed overlap within the trimer unit in **3**.

The intermolecular spacing [3.46(2) Å] within the TTF trimer units is close to those of $[TTF]_3[SnCl_6]$ [3.493(2) Å][2] and $[TTF]_3[SnMe_2Cl_4]$ [3.499(2)

Table 2. Selected bond distances (Å) and angles (°)[a] of **3** with the estimated standard deviations in parentheses

Sn—Cl(1)	2.67(1)	S(3)—C(6)	1.80(4)
Sn—Cl(2)	2.58(2)	S(4)—C(7)	1.73(3)
Sn—Cl(3)	2.62(2)	S(4)—C(8)	1.74(7)
Sn—C(9)[b]	2.21(7)	C(1)—C(1′)	1.46(13)
S(1)—C(1)	1.69(4)	C(2)—C(3)	1.34(7)
S(1)—C(2)	1.76(3)	C(4)—C(4′)	1.34(7)
S(2)—C(3)	1.75(4)	C(5)—C(5′)	1.37(16)
S(2)—C(4)	1.83(3)	C(6)—C(7)	1.26(8)
S(3)—C(5)	1.62(7)	C(8)—C(8′)	1.24(15)
Cl(1)—Sn—Cl(2)	180	C(3)—S(2)—C(4)	98(2)
Cl(1)—Sn—Cl(3)	87.8(6)	S(2)—C(4)—C(4′)	115(3)
Cl(2)—Sn—Cl(3)	92.2(6)	C(5′)—C(5)—S(3)	119(6)
Cl(1)—Sn—C(9)[b]	92(2)	C(5)—S(3)—C(6)	97(3)
Cl(2)—Sn—C(9)[b]	88(2)	S(3)—C(6)—S(3′)	109(2)
C(1′)—C(1)—S(1)	116(5)	S(3)—C(6)—C(7)	126(2)
C(1)—S(1)—C(2)	96(2)	S(6)—C(7)—S(4)	123(2)
S(1)—C(2)—S(1′)	115(2)	S(4)—C(7)—S(4′)	114(2)
S(1)—C(2)—C(3)	113(2)	C(7)—S(4)—C(8)	95(2)
C(2)—C(3)—S(2)	124(2)	S(4)—C(8)—C(8′)	118(6)
S(2)—C(3)—S(2′)	113(2)		
Non-bonded distances[c]			
S(1)–S(3)	3.69(3)	S(2)–Cl(1)	3.36(2)
S(1″)–S(3)	3.62(3)	S(1)–Cl(2″)	3.52(3)

[a] The atoms with a prime are in mirror symmetry with respect to the atoms with the same number (see Figs 1 and 2).

[b] Atom C(9) is the methylene-carbon atom of the ethyl group.

[c] See Figs 1 and 2.

Å].[3] The sulphur–sulphur distance [3.62(3) Å] within the trimer unit is somewhat longer than those of the $[SnCl_6]^{2-}$ and $[SnMe_2Cl_4]^{2-}$ analogues [3.493(2) and 3.498(3) Å, respectively],[2,3] owing to the considerable lateral shift of the TTF overlap in the present salt. The closest sulphur–sulphur contact between the TTF trimer units is 3.69(3) Å, which is almost equal to the sum of van der Waals' radii of sulphur atoms,[18] and is slightly longer than that of $[TTF]_3[SnMe_2Cl_4]$ [3.649(3) Å][3] and rather close to that of $[TTF]_3[SnCl_6]$ [3.705(2) Å].[2] On the other hand, the distances between the sulphur atoms [S(3) and S(4)] of the central TTF molecule and the neighbouring TTF molecular plane are 3.31(2) and 3.42(2) Å, respectively (see Fig. 2), which are similar to the corresponding sulphur–TTF plane distances in $[TTF]_3[SnCl_6]$ (3.40 Å)[2] and $[TTF]_3[SnMe_2Cl_4]$ (3.34 Å). Thus, **3** also forms a two-dimensional layer, consisting of the TTF trimer units, and a higher electrical conductance through the layer may appear, as mentioned later.

Although a weak interaction is observed between Cl(2) and S(1) atoms [3.52(3) Å], the Cl(1)–S(2) distance [3.36(2) Å][2] is appreciably shorter than the sum of the van der Waals' radii of sulphur and chlorine atoms (3.65 Å),[18] and is close to the shortest sulphur–chlorine distances reported for $[TTF]_3[SnCl_6]$ [3.367(2) Å][2] and $[TTF]_3[SnMe_2Cl_4]$ [3.344(2) Å].[3] This may be due to the electrostatic interaction between the rather positively polarized TTF sulphur and the negatively polarized chlorine atoms. In accordance with the short Cl(1)---S(2) distance, the Sn—Cl(1) bond [2.67(1) Å] is somewhat elongated in comparison with the Sn—Cl(2) bond [2.58(2) Å].

Electronic spectra

Figure 4 illustrates the powder electronic reflectance spectra of salts **1**, **3**, **4** and **5**. In the frequency region higher than 15,000 cm^{-1} local-excitation (LE) bands are observed for the TTF^{+} or TSF^{+} radical cations and the neutral TTF^{0} or TSF^{0} molecules.[19,20] Salt **1**, containing the TTF^{+} radical cation, exhibits a band around 12,500 cm^{-1}, which is assigned to the charge-transfer (CT) transition within the TTF^{+} radical cation dimer.[20,21] The same CT band was observed at 12,800 cm^{-1} in salt **2** (see Table 3). Analogously, salt **5** displays the band due to the $(TSF^{+})_2$ dimer, the frequency being lower than that of the $(TTF^{+})_2$ dimer. This is compatible with the fact that salt **5** has a considerably lower resistivity than the other simple salts, **1** and **2**, as described later.

Salt **3** in the solid state exhibits a broad band at 8700 cm^{-1} as well as LE bands with higher

Table 3. Powder electronic reflectance spectra of the salts

Salt	LE band (10^3 cm^{-1})			CT band (10^3 cm^{-1})	
				D^{+}/D^{+}[a]	D^{+}/D^{0}[a]
1	30.1	22.9	19.4	12.5	
2	26.6	[b]	19.1	12.8	
3	28.1	[b]	18.2		8.7
4	28.1	[b]	19.1	12.8	8.8
5	27.2	22.3	16.1	12.2	
6	27.8	21.6	16.0	12.2	8.8

[a] D = TTF or TSF.

[b] Not determined owing to being obscured by the high-frequency bands.

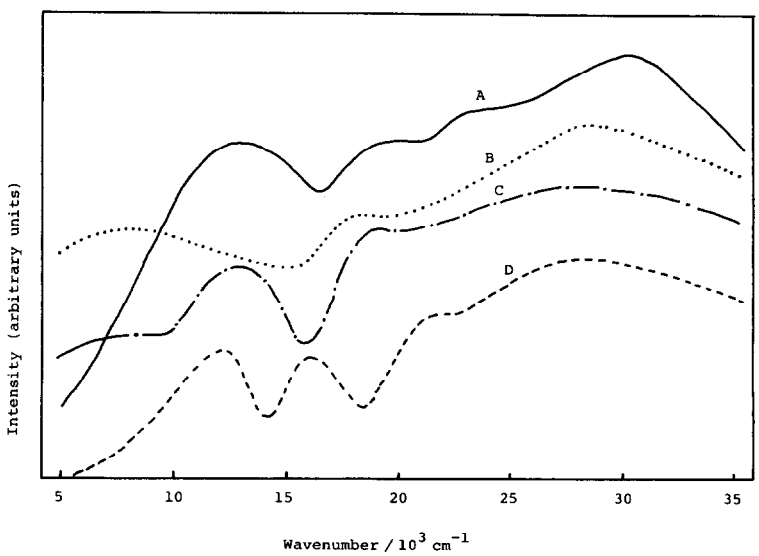


Fig. 4. Powder electronic reflectance spectra of **1** (A), **3** (B), **4** (C) and **5** (D).

Table 4. Electrical resistivities at 25°C ($\rho_{25°C}$) and activation energies (E_a) of the salts

Salt	$\rho_{25°C}$ (Ω cm)	E_a (eV)
1	2.1×10^8	0.53
2	9.0×10^8	0.60
3	4.2×10^1	0.13
4	2.9×10^3	0.28
5	7.1×10^3	0.10
6	3.0×10^3	0.18

frequencies. The low-frequency band is ascribed to the CT transition between the TTF^{+} radical cation and neutral TTF^0 within the TTF trimer, suggesting arrangement of the $TTF^{+}/TTF^0/TTF^{+}$ trimer. The same arrangement has been reported for $[TTF]_3[SnCl_6]$[2] and $[TTF]_3[SnMe_2Cl_4]$.[3] On the other hand, salt **4** displays two broad bands around 12,800 and 8800 cm^{-1} besides the LE bands in the higher-frequency region. These bands in the near-IR region can be ascribed to the CT transitions due to TTF^{+}/TTF^{+} and TTF^{+}/TTF^0, respectively. In view of this result, together with a relatively low resistivity, as described later, **4** may assume a columnar structure involving both TTF^{+}/TTF^{+} and TTF^{+}/TTF^0 interactions. A similar TSF columnar structure is suggested for salt **6**, based on the similarity between the spectra of these salts (Table 3).

Electrical resistivities

The temperature dependence of the the electrical resistivities of compacted samples has indicated that all the salts behave as typical semiconductors in the −20 to +30°C range.* Table 4 summarizes the resistivities at 25°C and activiation energies for electrical conduction. Salt **1** involving the TTF^{+} radical cation dimers exhibits a large resistivity and a high activation energy, indicating that each $(TTF^{+})_2$ dimer is located separately in the crystals, as was seen in $[TTF][SnMe_2Cl_3]$.[3] A large resistivity is also displayed in salt **2**, containing the TTF^{+} radical cation dimer, whereas the TSF^{+} radical cation analogue, **5**, exhibits a very small resistivity. A similar result has also been reported by us between the TTF and TSF salts with tris(oxalato)metallate anions (M = Si, Ge and Sn).[10]

Salt **3** displays a fairly small resistivity and a low activation energy. The electrical conduction in this salt may occur through the two-dimensional layer consisting of the TTF trimer units, as clarified by X-ray crystallographic analysis. On the other hand, the resistivity and the activation energy of **4** are larger than those of **3**, although **4** involves neutral TTF^0 as well as the TTF^{+} radical cation. This is indicative of the TTF stack not being suitable for the appearance of a high conductivity, while both the TTF^{+}/TTF^{+} and the TTF^{+}/TTF^0 CT bands have been observed. The TSF analogue, **6**, also displays electrical and spectroscopic properties similar to **4**.

* All the salts exhibit deviations of the log ρ–$1/T$ plots from a straight line above 40–60°C, due to some phase transitions.

REFERENCES

1. A. R. Siedle, G. A. Candela, T. F. Finnegan, R. P. van Duyne, T. Cape, G. F. Kokoszka, P. M. Woyciesjes, J. A. Hashmall, M. Glick and W. Ilsley, *Ann. N.Y. Acad. Soc.* 1978, **313**, 1; P. Kathirgamanathan, S. A. Mucklejohn and D. Rosseinsky, *J. Chem. Soc., Chem. Commun.* 1979, 86; A. R. Siedle, G. A. Candela, T. F. Finnegan, R. P. van Duyne, T. Cape, G. F. Kokoszka, P. M. Woyciejes and J. A. Hashmall, *Inorg. Chem.* 1981, **20**, 2635; P. Kathirgamanathan and D. R. Rosseinsky, *J. Chem. Soc., Chem. Commun.* 1980, 356; T. J. Kistenmacher, M. Rossi, C. C. Chiang, R. P. van Duyne and A. R. Siedle, *Inorg. Chem.* 1980, **19**, 3604; K. Yakushi, S. Nishimura, T. Sugano and H. Kuroda, *Acta Cryst.* 1980, **B36**, 358; R. C. Teitelbaum, T. J. Marks and C. K. Johnson, *J. Am. Chem. Soc.* 1980, **102**, 2986; G. C. Pavassiliou, *Mol. Cryst. Liq. Cryst.* 1982, **86**, 159; M. Bousseau, L. Valde, M. F. Bruniquel, P. Cassoux, M. Garbauskas, L. Interrante and J. Kasper, *Nouv. J. Chim.* 1984, **8**, 3.
2. K. Kondo, G. Matsubayashi, T. Tanaka, H. Yoshioka and K. Nakatsu, *J. Chem. Soc., Dalton Trans.* 1984, 379.
3. G. Matsubayashi, K. Ueyama and T. Tanaka, *J. Chem. Soc., Dalton Trans.* 1985, 465.
4. L. R. Melby, H. D. Hartzler and W. A. Sheppard, *J. Org. Chem.* 1974, **39**, 2456.
5. M. V. Lakshmikantham and M. P. Cava, *J. Org. Chem.* 1976, **41**, 882.
6. F. Wudl, *J. Am. Chem. Soc.* 1975, **97**, 1962.
7. W. M. Walsh, Jr, L. W. Rupp, Jr, F. Wudl, M. L. Kaplan, D. E. Schafer, G. A. Thomas and R. Gemmer, *Solid State Commun.* 1980, **33**, 413.
8. K. A. Kozeshkow, *Ber. Dtsch. Chem. Ges.* 1933, **66**, 1661.
9. R. K. Ingham, S. D. Rosenberg and H. Gilman, *Chem. Rev.* 1960, **60**, 459.
10. K. Ueyama, G. Matsubayashi and T. Tanaka, *Inorg. Chim. Acta* 1984, **87**, 143.
11. S. Araki, H. Ishida and T. Tanaka, *Bull. Chem. Soc. Jpn* 1978, **51**, 407.
12. *International Tables for X-ray Crystallography*, Vol. 4. Kynoch Press, Birmingham (1974).
13. C. K. Johnson, *ORTEP-II: A FORTRAN Thermal-Ellipsoid Plot Program for Crystal Structure Illustrations*, ORNL-5138. Oak Ridge National Laboratory, Oak Ridge, TN (1976).

14. L. E. Smart and M. Webster, *J. Chem. Soc., Dalton Trans.* 1976, 1924.
15. F. W. B. Einstein and B. R. Penfold, *J. Chem. Soc. (A)* 1968, 3019.
16. P. J. Vergammi, H. Vahrenkamp and L. F. Dahl, *J. Am. Chem. Soc.* 1971, **93**, 6327.
17. P. C. Lecomte, J. Protas and M. Devaud, *Acta Cryst.* 1976, **B32**, 923.
18. L. Pauling, *The Nature of the Chemical Bond*, 3rd edition, p. 246. Cornell University Press, Ithaca, NY (1960).
19. J. B. Torrance, B. A. Scott, B. B. Welba, F. B. Kaufman and P. E. Sieden, *Phys. Rev. B* 1979, **19**, 730.
20. T. Sugano, K. Yakushi and H. Kuroda, *Bull. Chem. Soc. Jpn* 1978, **51**, 1041.
21. K. Ueyama, A. Tanaka, G. Matsubayashi and T. Tanaka, *Inorg. Chim. Acta* 1985, **97**, 201.

Polyhedron Vol. 4, No. 10, pp. 1791–1792, 1985
Printed in Great Britain

0277–5387/85 $3.00 + .00
© 1985 Pergamon Press Ltd

REACTION OF A PHOSPHAKETENE WITH DIIRON ENNEACARBONYL: POSSIBLE INTERMEDIACY OF A TERMINAL PHOSPHINIDENE COMPLEX

DONALD H. CHAMPION and ALAN H. COWLEY*
Department of Chemistry, The University of Texas at Austin, Austin, TX 78712, U.S.A.

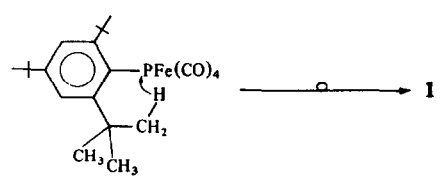
(*Received* 24 *April* 1985; *accepted* 28 *May* 1985)

Abstract—Evidence is presented for the intermediacy of a terminal phosphinidene complex, $[2,4,6\text{-}(t\text{-Bu})_3C_6H_2]PFe(CO)_4$, in the reaction of $[2,4,6\text{-}(t\text{-Bu})_3C_6H_2]P{=}C{=}O$ with $Fe_2(CO)_9$.

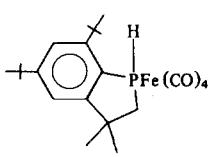
Compounds with phosphorus–phosphorus double bonds (diphosphenes, PR=RP) have received considerable attention recently.[1] Given the availability of species with metal–metal double bonds,[2,3] $L_nM{=}ML_n$ the obvious next step is to explore the chemistry of the phosphorus–metal double bond, viz. $RP{=}ML_n$. Elegant experiments by Mathey and co-workers[4] have established the intermediacy of $PhPW(CO)_5$, and recent reports by Bertrand, Gladysz *et al.*[5] and Roper *et al.*[6] have provided evidence for short-lived cationic phosphinidene complexes† of the type $[RPML_n]^+$. We report a potential route to neutral phosphinidene complexes starting with a phosphaketene.

Treatment of $ArP{=}C{=}O$[7] [Ar = 2,4,6-(*t*-Bu)$_3C_6H_2$] with $Fe_2(CO)_9$ in toluene at 25°C for 1–2 h, followed by chromatography (silica gel/*n*-hexane) resulted in a 39% yield of a yellow, crystalline product [m.p. 114°C (decomp.)] of empirical composition, $ArPFe(CO)_4$ (**1**). The 70 eV EI-MS of **1** revealed a low-intensity parent peak at *m/z* 444 and peaks corresponding to the sequential loss of 4 COs. However, the ^{31}P NMR spectrum of **1** (toluene, 32.2 MHz) featured a one-bond P—H coupling (δ + 14.8 ppm, $^1J_{PH}$ 360 Hz). The bicyclic structure of **1** was established by ^1H and ^{13}C–{^1H} NMR spectroscopy. ^1H NMR ($CDCl_3$, 90 MHz): δ 1.32 (s, 9H, *t*-Bu), δ 1.43 (s, 3H, 3-Me), δ 1.51 (s, 3H, 3-Me), δ 1.53 (s, 9H, *t*-Bu), δ 2.2–2.9 (m, 2H, 2-CH_2), δ 6.30 (d of m, 1H, P—H, $^1J_{PH}$ 360 Hz), δ 7.12 (br.s, 1H, aromatic), δ 7.47 (m, 1H, aromatic). ^{13}C–{^1H} NMR ($CDCl_3$, 20 MHz): δ 30.4 (s, 3-Me), δ 31.2 [s, $C(CH_3)_3$], δ 31.9 (s, 3-Me), δ 32.3 [s, $C(CH_3)_3$], δ 35.1 [s, $C(CH_3)_3$], δ 37.8 [s, $C(CH_3)_3$], δ 39.7 (d, C-2, $^1J_{PC}$ 35.8 Hz), δ 213.9 (d, CO, $^2J_{PC}$ 18.9 Hz). Confirmation of the above structure for **1** was provided by its independent synthesis from **2**[8] and $Fe_2(CO)_9$.

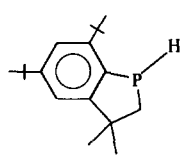
The most likely precursor to **1** is the terminal phosphinidiene complex, **3**, which rearranges to **1** via insertion of P into a C—H bond of an *ortho*-*t*-Bu group. We[8,9] and others[10] have reported ring closures of $[2,4,6\text{-}(t\text{-Bu})_3C_6H_2]$–phosphorus compounds. Reactions of this type occur when the phosphorus center is two- or three-coordinate and electropositive. In principle, **1** could be formed via a free radical pathway. However, this is unlikely because no P—D bond formation was detected when the reaction was conducted in toluene-d_8.



3



1



2

Attempts are underway to isolate terminal phosphinidene complexes by using more basic ML_n moieties.

* Author to whom correspondence should be addressed.

† Such complexes can also be regarded as metallophosphenium cations.

Acknowledgements—We thank the National Science Foundation and the Robert A. Welch Foundation for financial support.

REFERENCES

1. For reviews, see: A. H. Cowley, *Polyhedron* 1984, **3**, 389; A. H. Cowley, *Acc. Chem. Res.* 1984, **17**, 386.
2. F. A. Cotton and R. A. Walton, *Multiple Bonds Between Metal Atoms*. Wiley, New York (1982).
3. M. H. Chisholm, *Polyhedron* 1983, **2**, 681.
4. A. Marinetti, F. Mathey, J. Fischer and A. Mitschler, *J. Am. Chem. Soc.* 1982, **104**, 4484; A. Marinetti and F. Mathey, *Organometallics* 1982, **1**, 1488; *ibid.* 1984, **3**, 456.
5. H. Nakazawa, W. E. Buhro, G. Bertrand and J. A. Gladysz, *Inorg. Chem.* 1984, **23**, 3431.
6. G. R. Clark, W. R. Roper and A. H. Wright, *J. Organomet. Chem.* 1984, **273**, C17.
7. R. Appel and W. Paulen, *Angew. Chem., Int. Ed. Engl.* 1983, **22**, 785.
8. A. H. Cowley and M. Pakulski, *Tetrahedron Lett.* 1984, **25**, 2125.
9. A. H. Cowley, J. E. Kilduff, N. C. Norman, M. Pakulski, J. L. Atwood and W. E. Hunter, *J. Am. Chem. Soc.* 1983, **105**, 4845; J. I. G. Cadogan, A. H. Cowley, I. Gosney, M. Pakulski and S. Yaslak, *J. Chem. Soc., Chem. Commun.* 1983, 1408.
10. A. Baceiredo, G. Bertrand, P. Mazerolles and J.-P. Majoral, *J. Chem. Soc., Chem. Commun.* 1981, 1197; M. Yoshifuji, I. Shima, K. Ando and N. Inamoto, *Tetrahedron Lett.* 1983, **24**, 933.

Polyhedron Vol. 4, No. 10, pp. 1793–1795, 1985
Printed in Great Britain

0277–5387/85 $3.00 + .00
© 1985 Pergamon Press Ltd

COMMUNICATION

SPECTROCHEMICAL PROPERTIES OF MOLYBDO- AND TUNGSTO-HETEROPOLYANIONS CONTAINING Ce(IV) OR Ce(III) AS A HETEROATOM

KENJI NOMIYA, HIROYUKI MURASAKI and MAKOTO MIWA*
Department of Industrial Chemistry, Faculty of Engineering, Seikei University, Musashino, Tokyo 180, Japan

(*Received* 30 *January* 1985; *accepted* 1 *May* 1985)

Abstract—The absorption and MCD spectra in the VIS–UV region of the traditional Silverton-type polyanion $[Ce(IV)Mo_{12}O_{42}]^{8-}$ and Weakley-type polyanions, $[X(W_5O_{18})_2]^{n-}$ [X = Ce(IV) and Ce(III)], have been measured and two charge-transfer transitions, ligand-to-heteroatom and intra-ligand, are discussed.

In the chemistry of heteropoly compounds, 12- and 8-coordinations of rare-earth heteroatoms have been elucidated; the former is found in the Silverton-type molybdopolyanion $[XMo_{12}O_{42}]^{8-}$ [X(IV) = Ce, U, Th or Np] and the latter in the two Weakley-type polyanions, $[X(W_5O_{18})_2]^{n-}$ [$n = 9$ for X(III) = Y, La, Ce, Pr, Nd, Sm, Eu, Gd, Ho, Er or Yb; $n = 8$ for X(IV) = Ce, U or Th] and $[XL_2]^{n-}$ (L is lacunary derivatives of the Keggin and Dawson polyanions such as $[SiW_{11}O_{39}]^{8-}$ and $[P_2W_{17}O_{61}]^{10-}$).[1] The Silverton-type polyanion has been described as an XO_{12} icosahedron surrounded by six face-shared Mo_2O_9 units linked together by corner-sharing.[2] Two Weakley-type polyanions have been described as an XO_8 square antiprismatic complex, one is formed by two quadridentate W_5O_{18} groups viewed as "hypothetical" lacunary derivatives of the $[W_6O_{19}]^{2-}$ structure and the other by two quadridentate ligands.[3,4] As for spectrochemical characteristics of the skeleton structure of polyanions, we have paid attention to the MCD spectral pattern in the UV region due to the M ← O charge-transfer (CT) transition.[5–7] In this paper, we wish to report the optical and MCD spectra of the Silverton-type $[Ce(IV)Mo_{12}O_{42}]^{8-}$ and Weakley-type $[X(W_5O_{18})_2]^{n-}$ [X = Ce(IV) or Ce(III)] polyanions.

* Author to whom correspondence should be addressed.

EXPERIMENTAL

Spectral measurements were performed by previously reported methods.[5–7]

The Silverton-type polyanion of Ce(IV) was prepared according to the literature[8] and obtained as yellow crystals. Found: N, 3.49; H, 1.68. Calc. for $(NH_4)_6H_2[CeMo_{12}O_{42}] \cdot 8H_2O$: N, 3.78; H, 1.90%. The Weakley-type polyanions, $[Ce(IV)(W_5O_{18})_2]^{8-}$ and $[Ce(III)(W_5O_{18})_2]^{9-}$, were prepared according to the literature,[9] recrystallized many times from water, and obtained as yellow crystals for the Ce(IV) polyanion and as orange–yellow crystals for the Ce(III) one. All of the spectra were independent of concentration.

RESULTS AND DISCUSSION

The VIS–UV absorption and MCD spectra of the Silverton-type $[Ce(IV)Mo_{12}O_{42}]^{8-}$ and Weakley-type $[Ce(IV)(W_5O_{18})_2]^{8-}$ polyanions are presented in Figs 1 and 2, respectively. The former polyanion shows an intense band near 41,000 ($\varepsilon \sim 40{,}000$) and a very broad band near 30,000 cm^{-1} ($\varepsilon \sim 3000$) in the absorption spectrum, and a positive intense band near 41,000, and a positive broad band near 27,000, and a negative small band near 34,000 cm^{-1} in the MCD spectrum. The latter polyanion shows two absorption maxima at 38,000 ($\varepsilon \sim 19{,}000$) and 30,000 ($\varepsilon \sim 5600$), and an A-term shape MCD near

38,000, a positive broad MCD at 27,000 and a negative small MCD at 33,000 cm^{-1}. All of absorptions and MCD observed should be attributed to the CT transition in the polyanions. In the lower-frequency region, the MCD pattern of the former polyanion is very similar to that of the latter one. This fact indicates that there exist at least two types of CT transition. They are probably the ligand-to-Ce(IV) and the intra-ligand CT transitions. This stems from two empirical facts;[5-7] (1) the MCD pattern due to the intra-ligand CT is more influenced by exterior "homoatoms" such as Mo and W than by heteroatoms, and (2) the ligand-to-heteroatom CT in the polyanion is generally observed in the lower-frequency region rather than the intra-ligand CT. Thus, the absorption and MCD in the lower-frequency region are attributed to the ligand-to-Ce(IV) CT. The absorptions due to such a transition have been observed in other type of polyanions; at 27,000 cm^{-1} ($\varepsilon \sim 1000$) in the Evans–Showell-type $[Co(III)_2Mo_{10}O_{38}H_4]^{6-}$ polyanion[10] and at 25,000 cm^{-1} ($\varepsilon \sim 1180$) in the Keggin-type $[Co(III)W_{12}O_{40}]^{5-}$ polyanion,[5] and their MCD bands observed as a B-term shape with positive sign.[5,11] In the higher-frequency region, the absorption of the Silverton-type Ce(IV) molybdopolyanion is necessarily attributed to the CT within the $Mo_{12}O_{42}$ ligand. This is significantly more shifted to the high-frequency region than those of the usual Keggin-type dodecamolybdopolyanions, and,

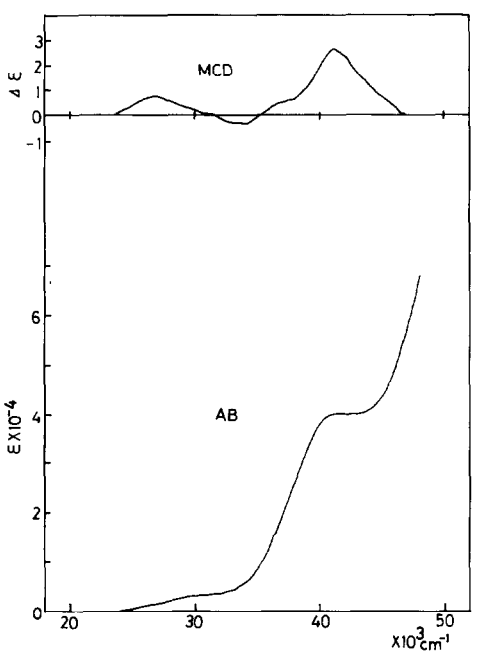


Fig. 1. VIS–UV absorption and MCD spectra of the Silverton-type $[Ce(IV)Mo_{12}O_{42}]^{8-}$ polyanion in aqueous solution.

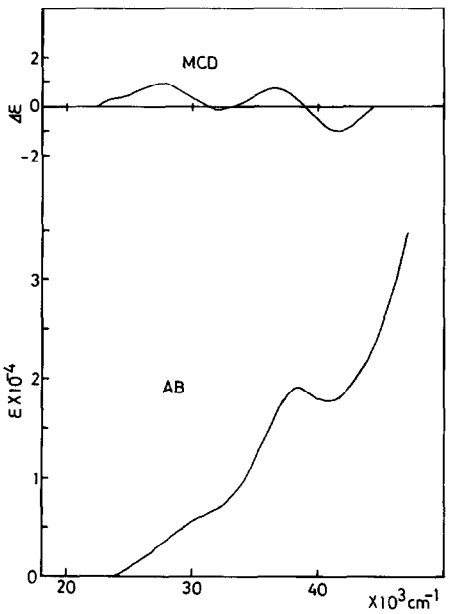


Fig. 2. VIS–UV absorption and MCD spectra of the Weakley-type $[Ce(IV)(W_5O_{18})_2]^{8-}$ polyanion in aqueous solution.

moreover, its MCD pattern is quite different from them. This is presumably caused by a participation of the face-sharing oxygen in a Mo ← O CT within the $Mo_{12}O_{42}$ ligand. On the other hand, the intra-ligand CT absorption of the Weakley-type Ce(IV) tungstopolyanion and the MCD with an apparent A-term shape seem consistent with those of the $[W_6O_{19}]^{2-}$ isopolyanion comprised only of edge-sharing WO_6 octahedra.

The absorption spectrum of the other Weakley-type polyanion, $[Ce(III)(W_5O_{18})_2]^{9-}$, is very similar to that of the Ce(IV) analogue, except that the intensities at 38,000 ($\varepsilon \sim 11{,}500$) and 30,000 cm^{-1} ($\varepsilon \sim 500$) decrease markedly (Fig. 3). However, the MCD is quite different, comprised only of positive bands. The electronic configurations of Ce(III) and Ce(IV) ions are $4f^1$ and $4f^0$, respectively. The only f–f transition of Ce(III) ion cannot contribute to the MCD and absorption in the VIS–UV region, because of its small energy difference. Rather, a contribution from an inter-shell ($5d \leftarrow 4f$) transition of Ce(III), besides the ligand-to-metal CT and intra-ligand CT transitions, should be taken into account in such a region. Recently, Okada *et al.*[12] have measured the absorption and MCD spectra due to the $5d \leftarrow 4f$ transition of the $[Ce(III)(H_2O)_8]^{3+}$ ion, which is formed by dissociation of one water molecule from $[Ce(III)(H_2O)_9]^{3+}$ in aqueous solution. They have found in the 34,000–51,000 cm^{-1} region five positive MCD bands in the crystals of the $[Ce(III)(H_2O)_9]^{3+}$ compound and six positive ones in the aqueous solution, in the latter the extra

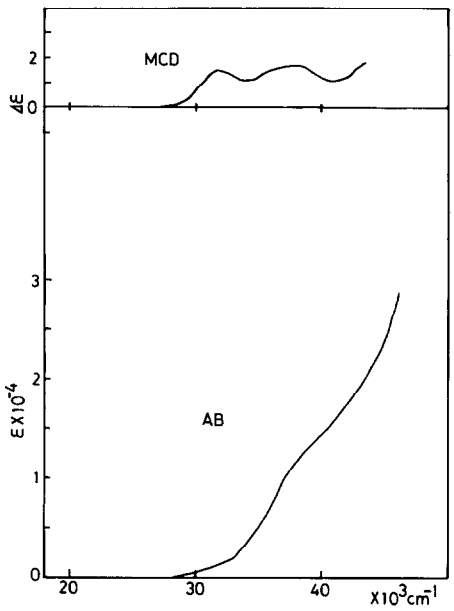


Fig. 3. VIS–UV absorption and MCD spectra of the Weakley-type $[Ce(III)(W_5O_{18})_2]^{9-}$ polyanion in aqueous solution.

band at 34,000 cm^{-1} being assigned to the lowest component of the $5d \leftarrow 4f$ transition of the $[Ce(III)(H_2O)_8]^{3+}$ species. This is consistent with the earlier assignment of the absorptions of the colourless Ce(III) aqua ion by Jørgensen and Brinen.[13] The intensity ratios of those MCD to absorptions ($\Delta\varepsilon \sim 10^{-3}$–$10^{-2}$) are sufficiently large. If this is the case for the $[Ce(III)(W_5O_{18})_2]^{9-}$ polyanion, the contribution of the $5d \leftarrow 4f$ transition should reflect markedly the MCD rather than the absorption. Thus, the MCD observed in the Weakley-type Ce(III) polyanion will be a superposition of such a contribution on the MCD due to the ligand-to-heteroatom CT and intra-ligand CT transitions as observed in the Ce(IV) analogue.

Acknowledgement. This work was partially supported by a Grant-in-Aid for scientific research, No. 59540402, from the Ministry of Education, Science and Culture of Japan.

REFERENCES

1. M. T. Pope, *Heteropoly and Isopoly Oxometalates.* Springer, New York (1983).
2. D. D. Dexter and J. V. Silverton, *J. Am. Chem. Soc.* 1968, **90**, 3589.
3. J. Iball, J. N. Low and T. J. R. Weakley, *J. Chem. Soc., Dalton Trans.* 1974, 2021.
4. V. N. Molchanov, L. P. Kazanskii, E. A. Torchenkova and V. I. Simonov, *Kristallografiya* 1979, **24**, 167; *Sov. Phys.—Cryst. (Engl. Trans.)* 1979, **24**, 96.
5. K. Nomiya, R. Kobayashi and M. Miwa, *Bull. Chem. Soc. Jpn* 1983, **56**, 2272.
6. K. Nomiya and M. Miwa, *Polyhedron* 1983, **2**, 955.
7. K. Nomiya, R. Kobayashi and M. Miwa, *Polyhedron* 1985, **4**, 149.
8. L. C. W. Baker, G. A. Gallagher and T. P. McCutcheon, *J. Am. Chem. Soc.* 1953, **75**, 2493.
9. R. D. Peacock and T. J. R. Weakley, *J. Chem. Soc. A* 1971, 1836.
10. T. Ama, J. Hidaka and Y. Shimura, *Bull. Chem. Soc. Jpn* 1970, **43**, 2654.
11. K. Nomiya, H. Murasaki and M. Miwa, to be submitted.
12. K. Okada, Y. Kaizu and H. Kobayashi, *J. Chem. Phys.* 1981, **75**, 1577.
13. C. K. Jørgensen and J. S. Brinen, *Mol. Phys.* 1963, **6**, 629.

Polyhedron Vol. 4, No. 10, pp. 1797–1798, 1985
Printed in Great Britain

0277-5387/85 $3.00 + .00
© 1985 Pergamon Press Ltd

COMMUNICATION

IMPROVED SYNTHESIS OF *ARACHNO*-6,9-$C_2B_8H_{14}$ AND ITS HALOGENATION UNDER ELECTROPHILIC CONDITIONS

ZBYNĚK JANOUŠEK, JAROMÍR PLEŠEK, STANISLAV HEŘMÁNEK and BOHUMIL ŠTÍBR*

Institute of Inorganic Chemistry, Czechoslovak Academy of Sciences, 250 68, Řež near Prague, Czechoslovakia

(*Received* 24 *April* 1985; *accepted* 20 *May* 1985)

Abstract—A convenient synthesis of *arachno*-6,9-$C_2B_8H_{14}$, based on the reduction of *nido*-5,6-$C_2B_8H_{12}$ with sodium tetrahydroborate, is reported. Electrophilic halogenation of the former carborane produced a series of 1-X-6,9-$C_2B_8H_{13}$ (X = Cl, Br and I) derivatives whose constitution was established on the basis of their ^1H and ^{11}B NMR spectra.

The first representative of the 10-vertex *arachno*-dicarbaborane family, 6,9-dicarba-*arachno*-decaborane(14), 6,9-$C_2B_8H_{14}$ (**I**), was prepared in our laboratory[1] by treatment of *nido*-5,6-$C_2B_8H_{12}$ (**II**)[2] with sodium amalgam in ethanol. For some still obscure reasons, this reaction sometimes fails and therefore we have searched for a more reliable method for preparing carborane **I**. We report herein a more convenient synthesis of the latter compound along with the preparation of its 1-halogenated derivatives.

Treatment of carborane **II** with sodium tetrahydroborate in an ethanolic solution of potassium hydroxide at higher temperatures, followed by the acidification of the reaction mixture, resulted in the isolation of 6,9-$C_2B_8H_{14}$ in higher than 35% yields. The product thus obtained is contaminated with less than 5% of 5-C_2H_5O-6,9-$C_2B_8H_{13}$ (**Ia**) {m.p. 48–50°C; *m/z* 166 (dehydrogenation); ^1H NMR (200 MHz, $CDCl_3$): δ 3.69 (2H, q, J = 7 Hz, CH_2), 1.16 (3H, t, J = 7 Hz, CH_3), 0.74 (2H, s, CH_{eq}), −0.61 (2H, s, CH_{ax}), −2.94 (2H, s, μH); ^{11}B NMR spectrum (64.18 MHz, $CDCl_3$): δ_B 5.45 [1B, s, B(5)], 2.10 [1B, d, 160, B(2)], 0.65 [1B, d, 166, B(4)], −20.60 [1B, d, 150(52), B(10)], −22.70 [1B, d, 144, B(8)], −24.10 [1B, d, 144, B(7)], −38.75 [1B, d, 147, B(1)], −40.85 [1B, d, 142, B(3)]}, which can be easily removed either by crystallization or by column chromatography on silica gel in benzene–hexane (1 : 2).

As proposed earlier,[1] formation of carborane **I** is consistent with a reductive cleavage of the

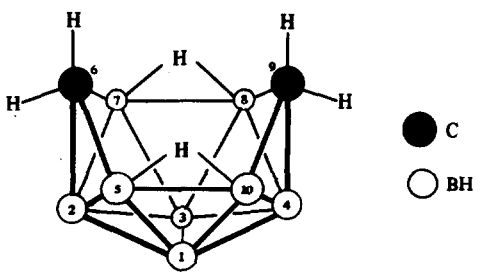


Fig. 1. Simplified structure and numbering system of *arachno*-6,9-$C_2B_8H_{14}$.

Table 1. Some properties of *arachno*-1-X-6,9-$C_2B_8H_{13}$ derivatives

X	M.p. (°C)	*m/z*	R_F[a]	δ (^1H NMR)[b] CH_{eq}	CH_{ax}	B–H–B
H[c]	146–147[1]	126[1]	0.32	0.86	−0.66	−2.84
Cl	155–158	162	0.11	1.11	−0.35	−2.10
Br	184–186	206	0.10	1.10	−0.38	−2.22
I	146–147	252	0.18	1.12	−0.38	−2.23

[a] TLC on Silufol [silica gel on aluminium foil, benzene–hexane (1 : 2)].

[b] Singlets of equal intensity, referenced to TMS internal standard (200 MHz, $CDCl_3$).

[c] Relevant data of parent 6,9-$C_2B_8H_{14}$ for comparison.

* Author to whom correspondence should be addressed.

Table 2. Assignments of the ^{11}B NMR spectra (64.18 MHz, $CDCl_3$) of *arachno*-1-X-6,9-$C_2B_8H_{13}$ derivatives

X	B(2, 4)	B(5, 10)	B(7, 8)	B(1)	B(3)
H	3.72(2)[a]	−17.50(4)		−37.65(2)	
	161[b]	155(52)		152	
Cl	4.35(2)	−16.50(2)	−16.80(2)	−18.10[c]	−35.90
	166	150	150		160
Br	4.50(2)	−15.90(2)	−16.65(2)	−25.45[c]	−35.20
	170	160(50)	158(50)		158
I	4.95	−15.10(2)	−16.20(2)	−43.00[c]	−34.25
	166	160(50)	160(50)		157

[a] Chemical shift in δ (ppm, referenced to $BF_3 \cdot OEt_2$ external standard, intensity higher than 1 in parentheses).
[b] $J_{^{11}B-^{1}H}$ ($J_{^{11}B-^{1}H}$) in Hz.
[c] Singlet.

C(5)—C(6) bond in the cage of 5,6-$C_2B_8H_{12}$, followed by moving the C(6) vertex into a new position. This type of rearrangement of the 10-vertex borane skeleton strongly parallels the mechanism proposed by Bould *et al.*[3] for the 6 → 5 rearrangement in the 6-irida-*nido*-decaborane series. The reduction of **II** to **I** represents a typical *nido*–*arachno* transformation and, in this respect, it is analogous to the well-known reduction[4] of $B_{10}H_{14}$ to $[B_{10}H_{14}]^{2-}$.

Halogenation of **I** with carbon tetrachloride, bromine in carbon disulphide, and iodine in benzene under reflux in the presence of anhydrous $AlCl_3$ produced a series of 1-halogenated derivatives, 1-X-6,9-$C_2B_8H_{13}$ (**Ib**, X = Cl; *Ic*, X = Br; and **Id**, X = I), as the main products. The explicit preference for electrophilic attack at the B(1) site fits well with the previously reported[1] results of the deuteration of carborane **I** in the DCl–$AlCl_3$–CS_2 system.

^1H NMR spectra of compounds **Ib–d** (Table 1) consist of two sharp singlets of intensity 1, assigned to two pairs of equatorial and axial CH groups, and one broad unresolved B–H–B singlet. ^{11}B NMR spectra of **Ib–d** (Table 2) exhibit one B(1) singlet along with four 2:2:2:1 patterns of doublets, while the corresponding spectrum of the ethoxoderivative **Ia** displays seven doublets and one low-field B(5) singlet of equal intensities. Besides the signals of the C_2H_5O group, the ^1H NMR spectrum of **Ia** shows three coincidentally overlapping singlets of two CH_{eq} and CH_{ax} groups and two bridging hydrogens.

The above NMR data for **Ib–d** are in agreement with the proposed 1-X-6,9-$C_2B_8H_{13}$ geometry and the relevant data for **Ia** are consistent with the asymmetrical structure[5] of 5-substituted derivatives of 6,9-$C_2B_8H_{14}$. We are presently engaged in the research aimed at preparing other substituted derivatives of **I**.

REFERENCES

1. B. Štíbr, J. Plešek and S. Heřmánek, *Collect. Czech. Chem. Commun.* 1973, **38**, 338.
2. J. Plešek and S. Heřmánek, *Collect Czech. Chem. Commun.* 1974, **39**, 821.
3. J. Bould, N. N. Greenwood, J. D. Kennedy and W. S. McDonald, *J. Chem. Soc., Chem. Commun.* 1982, 465.
4. E. L. Muetterties, *Inorg. Chem.* 1963, **2**, 647.
5. B. Štíbr, Z. Janoušek, J. Plešek, T. Jelinek and S. Heřmánek, *J. Chem. Soc., Chem. Commun.*, in press.

Polyhedron Vol. 4, No. 10, pp. 1799–1800, 1985
Printed in Great Britain

BOOK REVIEWS

Chemistry of the Elements. By N. N. Greenwood and A. Earnshaw, Pergamon Press, Oxford, 1984, over 3000 illustrations, 1542 pp., £53.00 (hardcover), £19.50 (flexicover).

The advent of a major new textbook on inorganic chemistry is an important event for all readers of this journal, more especially when it combines the virtues of scholarship, topicality and wide-ranging interest found here. The title evokes that of N. V. Sidgwick's magisterial volumes, *The Chemical Elements and Their Compounds*, published some 35 years ago, but still a fertile source of curious and fascinating information. This comparison is not a superficial one, as will appear later.

The book begins with two introductory chapters, the first being on the origin of the elements, isotopes and atomic weights, and the second dealing with chemical periodicity and the Periodic Table (37 pp.). Then follow 16 descriptive chapters on the *s*- and *p*-block or main-group elements (1021 pp.). After another general chapter on coordination compounds (41 pp.) come 12 further descriptive chapters on the *d*- and *f*-block metals (318 and 63 pp. respectively), and a series of appendices on such matters as orbital wave functions, point group symmetry, SI units, elemental abundances, ionic radii, and Nobel Prize winners in Chemistry and in Physics; nearly 1500 literature references are given throughout the text. Finally, there is a commendably full and detailed index of 36 pp.

Such a catalogue gives little idea of the distinctive flavour of this book, however. To begin with its most obvious characteristic, it is avowedly fact-based: there are no long sections on "general chemistry" or theoretical topics, no discussions of the niceties of electronegativity scales or atomic radii, and no entries in the index about hard/soft acids and bases or close-packing. So what kinds of facts are here? In essence, those of interest to inorganic chemists, construed in the broadest possible way. Besides the necessary information on preparations and properties and a good deal on structural aspects (illustrated by clear and attractive diagrams), there is also much on the human, social and industrial aspects of chemistry. People involved in the isolation of elements and the historical development of the subject, up-to-date and well-illustrated descriptions of important industrial processes, annual productions and costs, applications of inorganic materials (including both high-tonnage chemicals and such new developments as xerography, solid-state devices, non-asbestos fibres and high-performance ceramics), environmental factors in the manufacture and use of inorganic compounds, inorganic biochemistry, organometallic compounds and even cosmochemistry are all represented. Because of this wealth of interesting facts, it is possible to read this book as a voyage of discovery as well as a detailed reference work.

How about its use as a teaching text? It is not surprising, particularly in view of the senior author's long concern with chemical education and education through chemistry, that this has been taken carefully into account. Not so much explicitly—the student will find no ready-made list of 17 ways in which nitrogen differs from phosphorus—but implicitly in the wealth of factual

Table 1.[a]

	No. of pages (% of whole)			
	S.	H. & J.	C. & W. (IV)	G. & E.
Total length	1735	838	1412	1563
Main-group elements[b]	903 (52)	289 (34)	394 (28)	1021 (65)
Transition metals[b]	677 (39)	135 (16)	320+296[c] (44)	318 (20)
Hydrogen	48 (3)	40 (3)	38 (3)	37 (2)
Boron	78 (5)	10 (1)	37 (3)	88 (6)
Sulphur	73 (4)	10 (1)	~30 (2)	125 (8)
TiZrHf	24 (1)	11 (1)	23 (2)	27 (2)
FeRuOs	114 (7!)	11 (1)	39 (3)	48 (3)

[a] Abbreviations: S., N. V. Sidgwick, *The Chemical Elements and Their Compounds*. Oxford University Press, Oxford (1950). H. & J., R. B. Heslop and K. Jones, *Inorganic Chemistry*. Elsevier, Amsterdam (1976). C. & W. (IV), F. A. Cotton and G. Wilkinson, *Advanced Inorganic Chemistry*, 4th edition. Wiley, New York (1980). G. & E., book under review.

[b] Estimated for descriptive chemistry.

[c] Special topics (chiefly transition-metal chemistry).

material from which the student can make his own list. The clear style and organisation of the text, coupled with extensive cross-referencing and the good index, will make this book the natural first point of reference for a student writing an essay or a literature project. Equally one hopes that many lecturers' sets of notes will be enhanced from this source.

What about the balance of topics? Here it is interesting to compare the amount of space given to certain areas in some well-known texts (Table 1). It is clear that the present book gives proportionately far more coverage to main-group elements, particularly to non-metals such as boron and sulphur. This is certainly consistent with the present resurgence of interest in main-group chemistry, and compensates to some extent for the emphasis on transition-metal chemistry in some modern text-books. It suggests too that "Greenwood and Earnshaw" is complementary to the latest edition of "Cotton and Wilkinson", rather that directly overlapping with it, and that students will have to buy one or the other, while needing access to both.

To sum up, this is a notable and refreshingly different new text, which can significantly influence the future direction of the subject. In many ways, it is a new Sidgwick for the 1980s, which is high praise indeed.

Department of Chemistry **B. J. AYLETT**
Queen Mary College
Mile End Road
London E1 4NS
U.K.

Gmelin Handbook of Inorganic Chemistry. Uranium Supplement Vol. C4: Uranium Dioxide, Preparation and Crystallographic Properties. Published by the Gmelin Institute for Inorganic Chemistry of the Max Planck Society for the Advancement of Science, Springer, Berlin, 8th edition, 1984, xii + 140 pp., DM544.

This book on the preparation and crystallography of uranium dioxide is one of at least 27 supplementary volumes on uranium. The series, when completed in the near future, will comprise an authoritative and exhaustive account on all aspects of uranium chemistry. Uranium chemists with ready access to the series are in a particularly fortunate position and will be delighted by the excellent production qualities, the first-class use of English, and the outstanding scholarship.

Uranium dioxide is the most important compound in nuclear technology because it is the fuel of nearly all water nuclear power reactors. Volume C4 deals only with the preparation and crystallography while two others, C5 and C6, will deal with the physical and chemical properties. Two-thirds of volume C4 is devoted to the preparation of uranium dioxide and the production of pellets and other shapes. All of the well-characterised methods of preparation are included, the whole is well-illustrated, and contains 660 references. The crystallographic properties are also properly covered and no important results appear to be omitted. The literature is comprehensively covered to the end of 1982 and important results since then are also included.

One would normally expect a very large library to buy the entire Supplement but for specialised libraries, such as those covering nuclear technology, a selection from the many volumes would be well-worth considering, notwithstanding the high volume cost.

Department of Chemistry **J. I. BULLOCK**
University of Surrey
Guildford

material from which the student can make his own list. The clear style and organisation of the text, coupled with extensive cross-referencing and the good index, will make this book the natural first point of reference for a student writing an essay or a literature project. Equally one hopes that many lecturers' sets of notes will be enhanced from this source.

What about the balance of topics? Here it is interesting to compare the amount of space given to certain areas in some well-known texts (Table 1). It is clear that the present book gives proportionately far more coverage to main-group elements, particularly to non-metals such as boron and sulphur. This is certainly consistent with the present resurgence of interest in main-group chemistry, and compensates to some extent for the emphasis on transition-metal chemistry in some modern text-books. It suggests too that "Greenwood and Earnshaw" is complementary to the latest edition of "Cotton and Wilkinson", rather that directly overlapping with it, and that students will have to buy one or the other, while needing access to both.

To sum up, this is a notable and refreshingly different new text, which can significantly influence the future direction of the subject. In many ways, it is a new Sidgwick for the 1980s, which is high praise indeed.

Department of Chemistry **B. J. AYLETT**
Queen Mary College
Mile End Road
London E1 4NS
U.K.

Gmelin Handbook of Inorganic Chemistry. Uranium Supplement Vol. C4: Uranium Dioxide, Preparation and Crystallographic Properties. Published by the Gmelin Institute for Inorganic Chemistry of the Max Planck Society for the Advancement of Science, Springer, Berlin, 8th edition, 1984, xii + 140 pp., DM544.

This book on the preparation and crystallography of uranium dioxide is one of at least 27 supplementary volumes on uranium. The series, when completed in the near future, will comprise an authoritative and exhaustive account on all aspects of uranium chemistry. Uranium chemists with ready access to the series are in a particularly fortunate position and will be delighted by the excellent production qualities, the first-class use of English, and the outstanding scholarship.

Uranium dioxide is the most important compound in nuclear technology because it is the fuel of nearly all water nuclear power reactors. Volume C4 deals only with the preparation and crystallography while two others, C5 and C6, will deal with the physical and chemical properties. Two-thirds of volume C4 is devoted to the preparation of uranium dioxide and the production of pellets and other shapes. All of the well-characterised methods of preparation are included, the whole is well-illustrated, and contains 660 references. The crystallographic properties are also properly covered and no important results appear to be omitted. The literature is comprehensively covered to the end of 1982 and important results since then are also included.

One would normally expect a very large library to buy the entire Supplement but for specialised libraries, such as those covering nuclear technology, a selection from the many volumes would be well-worth considering, notwithstanding the high volume cost.

Department of Chemistry **J. I. BULLOCK**
University of Surrey
Guildford

Polyhedron Vol. 4, No. 11, pp. 1801–1846, 1985
Printed in Great Britain

0277–5387/85 $3.00 + .00
Pergamon Press Ltd

POLYHEDRON REPORT NUMBER 12

TRANSITION-METAL THIOCARBONYL COMPLEXES: PREPARATIVE METHODS, REACTIVITY AND THIOCARBONYL LIGAND BONDING PROPERTIES

PETER V. BROADHURST*
Union Carbide Corporation, Technical Center, P.O. Box 8361, South Charleston, WV 25303, U.S.A.

CONTENTS

I. INTRODUCTION . . . 1802
II.1. TERMINAL CS LIGANDS—PREPARATIVE METHODS . . . 1802
i. Direct reaction of CS . . . 1802
ii. Preparations using heteroallenes . . . 1802
iii. Preparations using [Cl(X)CS] (X = Cl or OR) and [$Cl_3C \cdot SR$] . . . 1810
iv. Preparations via dichlorocarbene or chlorocarbyne complexes . . . 1811
v. Modification of thiocarbonyl complexes . . . 1812
(a) Cr triad . . . 1812
(b) Mn triad . . . 1813
(c) Fe triad . . . 1814
(d) Co triad . . . 1816
II.2. BRIDGING CS LIGANDS—PREPARATIVE METHODS . . . 1818
i. Linear bridging (σ-C · σ-S) . . . 1818
ii. Thioketonic bridging (μ-CS) . . . 1819
(a) Formation from monometallic compounds . . . 1819
(b) Carbonyl substitution reactions of [{(η^5-C_5H_5)(CO)Fe}$_2$(μ-CS)(μ-CE)] (E = O or S) . . . 1820
II.3. CS LIGANDS COORDINATED TO THREE OR MORE METAL CENTERS—PREPARATIVE METHODS . . . 1820
i. (μ-C · σ-S) bonding . . . 1820
ii. (μ_3-CS) bonding and (μ_3-C · σ-S) derivatives . . . 1821
iii. Other M_4(CS) interactions . . . 1822
III.1. REACTIVITY OF THE CS LIGAND . . . 1822
III.2. SUBSTITUTION REACTIONS OF CS LIGANDS . . . 1822
III.3. ELECTROPHILIC ATTACK AT CS SULPHUR . . . 1823
i. Terminal CS ligands . . . 1823
ii. Bridging (μ-CS) ligands . . . 1824
iii. Triply-bridging (μ_3-CS) ligands . . . 1824
III.4. NUCLEOPHILIC ATTACK AT CS CARBON . . . 1825
i. Reactions with amines or amides . . . 1825
ii. Reactions with alcohols, alkoxides and water . . . 1826
iii. The use of NCO^-, NCS^-, N_3^- and N_2H_4 . . . 1826
iv. Reactions with EH^- (E = S or Se) . . . 1826
v. Reactions with other nucleophiles . . . 1826
III.5. INSERTION REACTIONS OF CS LIGANDS . . . 1826
III.6. OTHER REACTIONS AT CS LIGANDS . . . 1828
IV.1. BONDING, SPECTROSCOPIC AND STRUCTURAL PROPERTIES OF CS COMPLEXES . . . 1828
IV.2. THE NATURE OF CS COORDINATION—A SUMMARY . . . 1828

* Present address: Imperial Chemical Industries, Petrochemicals and Plastics Division, P.O. Box 90, Wilton, Middlesbrough, Cleveland TS6 8JE, U.K.

IV.3. THEORETICAL STUDIES 1829
IV.4. PHOTOELECTRON SPECTROSCOPY STUDIES 1830
IV.5. ELECTRONIC OR UV–VIS SPECTROSCOPY 1830
IV.6. MASS SPECTROSCOPIC STUDIES 1831
IV.7. MÖSSBAUER SPECTROSCOPY 1831
IV.8. ^{13}C NMR STUDIES 1831
IV.9. RAMAN SPECTROSCOPIC STUDIES 1832
IV.10. IR SPECTROSCOPIC STUDIES 1833
IV.11. X-RAY CRYSTALLOGRAPHIC DATA 1834
V. CONCLUSIONS 1836

I. INTRODUCTION

Although a very large number of examples occur of CO ligation of metal centers, relatively few exist of the isoelectronic CS. Undoubtedly this arises from the lack of stable molecular CS. Although CS can be prepared[1] by subjecting CS_2 to a high voltage a.c. discharge *in vacuo*, it polymerizes above $-160°C$. Syntheses of thiocarbonyl complexes have used necessarily indirect routes, mostly via CS_2.

However, examples of the thiocarbonyl ligand are not uncommon. In the last review of this area published in 1977,[2] Butler pointed out that "CS can be stabilized by coordination to many transition metals, and well over 100 thiocarbonyl complexes have been reported . . .". Since then, many more examples have been identified, displaying some novel coordination modes, showing an increased range of reactivity and using some different preparative methods. This article surveys the literature up to the end of 1984, classifying thiocarbonyl complexes by preparative method, followed by a discussion of the reactivity and of the bonding, spectroscopic and structural properties of such complexes.

Two other reviews should be noted, by Yaneff[3] and by Butler and Fenster,[4] which appeared in 1977 and 1974, respectively. In particular, these document thoroughly much of the spectroscopic data pertinent to the CS ligand in its then known complexes.

The nature of the transition-metal–thiocarbonyl interaction is considered below, especially in comparison to the carbonyl ligand. For now, it is sufficient to state that these interactions are largely analogous so that the CS ligand exhibits synergic bonding and has π-acid character. Differences in the chemistries of these ligands arise from the relative abilities for σ-donation of electrons to and π-acceptance of electrons from metal centers and from the relative strength of C—O and C—S π- and σ-bonding.

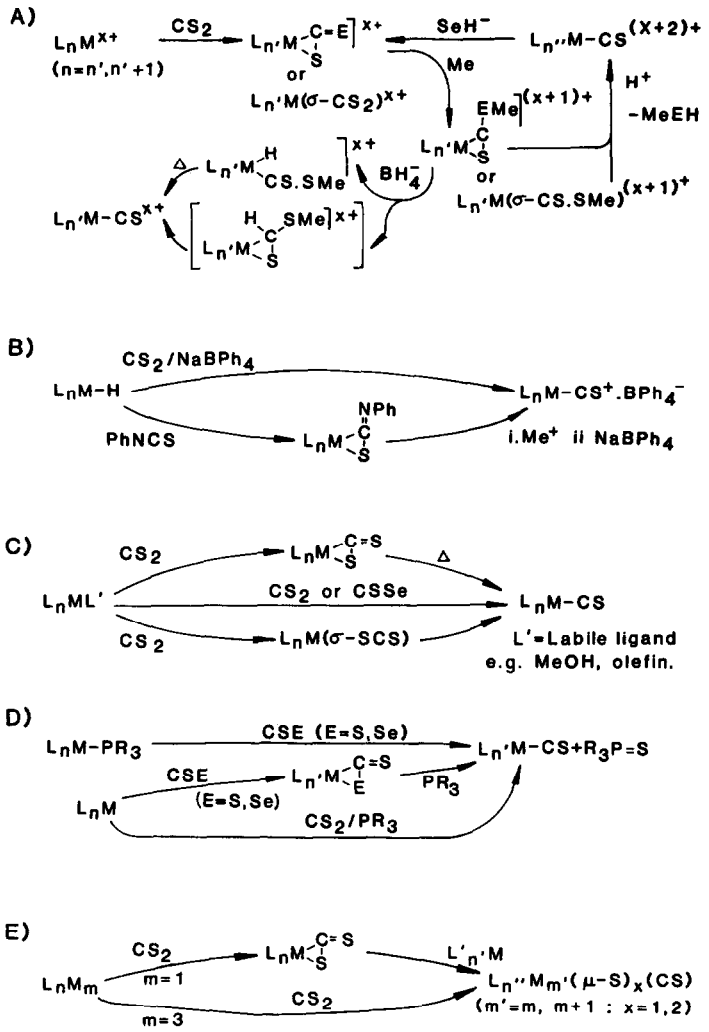
II.1. TERMINAL CS LIGANDS—PREPARATIVE METHODS

i. Direct reaction of CS

A single example of CS usage exists.[5] Microwave discharge through CS_2 vapour yields CS which is cocondensed with Ni atoms at 10 K in an argon matrix. The product was identified as $[Ni(CS)_4]$ by IR spectroscopy, assigning a ν(CS) mode to the 1305 cm^{-1} absorption, and by mass spectroscopy of the intractable black solid obtained at room temperature which displayed a $[Ni(CS)_4]$ molecular fragment and was proposed to be polymeric $[\{Ni(CS)_4\}_n]$.

ii. Preparations using heteroallenes

The use of CS_2 or its complexes comprises the most important means of generating thiocarbonyl ligands by far. In some cases, complexes of the heteroallenes CSSe and PhNCS may be used. When the coordination chemistry of the heteroallenes CSE (E = O, Se or NR) is investigated, the products often do not contain CS ligands. However, information can be gained on the mechanism in the derivation of CS ligands from CS_2. Aspects of this heteroallene work have been summarized recently.[6,7] Also, carbon



Scheme 1. Routes to CS ligands via CS_2.

diselenide is known to yield the selenocarbonyl ligand, CSe, by some routes that apply to CS_2 for the CS ligand.

The heteroallene-based preparations of the CS ligand, summarized in Scheme 1, are various. Many reactions give a number of other products and give only modest yields of the thiocarbonyl product. These methods are discussed in turn, as detailed in Scheme 1.

(A) Two related routes use the same initial steps. Coordination of CS_2 or CSSe to a metal center in either σ-dithiocarboxylate or η^2-fashion is followed by methylation, giving the corresponding σ- or η^2-chalcogen-methylated moiety. The two pathways differ hereon in that H^+ or H^- attack is employed, although both result in MeEH elimination (E = S or Se).

Protonation is used on the σ-dithiocarboxylate methyl ester examples. In work by Angelici and co-workers, $[\{(\eta^5\text{-}C_5H_5)M(CO)_2(CS)\}^+]$ (M = Fe[8] or Ru[9]) results from $[\{(\eta^5\text{-}C_5H_5)M(CO)_2\}^-]$ by using CS_2 to give $[\{(\eta^5\text{-}C_5H_5)M(CO)_2(CS_2)\}^-]$, then MeI, yielding a ($\sigma$-$CS_2Me$) unit, assigned by IR spectroscopy, and lastly H^+ attack (Fig. 1).

Analogous reagents were used by Roper and co-workers in conversions through (η^2-CSE)(E = S or Se) intermediates. Reaction of CS_2 with $[M(CO)_2(PPh_3)_3]$ (M = Ru or Os) yields $[M(CO)_2(PPh_3)_2(\eta^2\text{-}CS_2)]$ upon which attack by MeI, giving an η^2-CS_2Me ligand, and then HCl results in $[MCl_2(PPh_3)_2(CO)(CS)]$ (M = Ru or Os).[10] Starting from $[M(CO)(CS)(PPh_3)_3]$ (M = Os) allows $[MX_2(PPh_3)_2(CS)_2]$ (M = Os, X = Cl or Br) to be prepared analogously.[11] The same method is effective for the preparation of $[RuX_2(PPh_3)_2(CO)(CSe)]$ (X = Cl) from CSe_2 and $[Ru(CO)_2(PPh_3)_3]$.[12] These reactions are summarized in Fig. 2. The η^2-CSSe ligand in

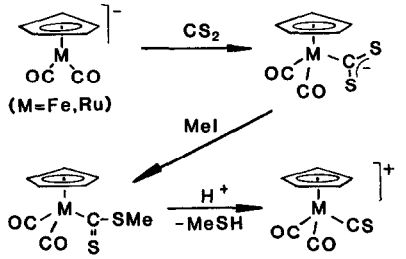
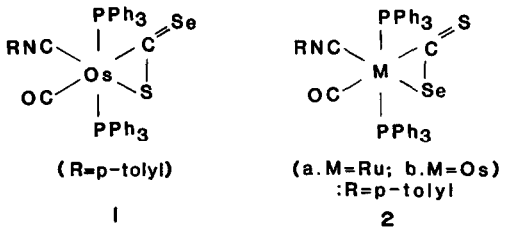


Fig. 1. σ-Dithiocarboxylate intermediates in CS ligand synthesis from CS_2.



$[Os(\eta^2\text{-}CSSe)(CO)(CNR)(PPh_3)_2]$ (R = *p*-tolyl) (**1**), although produced indirectly by SeH^- attack on $[\{OsCl(CS)(CO)(CNR)(PPh_3)_2\}^+]$, is reverted to this thiocarbonyl species by sequential attack of Me^+ (as MeI) at the uncoordinated Se atom and then HCl, eliminating MeSeH.[13] The analogous Ru compound $[\{RuCl(CS)(CO)(CNR)(PPh_3)_2\}^+]$ gives $[Ru(\eta^2\text{-}CSeS)(CO)(CNR)(PPh_3)_2]$ (**2a**) with SeH^- which MeI and HCl convert to $[RuCl_2(CSe)(CNR)(PPh_3)_2]$ in good yield.[13] Thus, the coordinated chalcogen of the η^2 ligand is retained in the chalcogenocarbonyl ligand but SeH^- attack on the CS ligand is able to give different η^2 connectivity in the $(\eta^2\text{-}CSSe)$ precursor depending on the individual case. However, this method is unable to convert $[Os(\eta^2\text{-}CSeS)(CO)(CNR)(PPh_3)_2]$ (**2b**) to a CSe species as HCl attack on the $(\eta^2\text{-}CSe \cdot SMe)^+$ methylation product is ineffective.[13]

Halide ligand coordination at the protonation step, sometimes displacing CO groups, causes a variable net charge on the product moiety but the metal has experienced a two-unit increase in its formal oxidation state through the CS ligand preparative sequence. This increased oxidation state coupled with an array of good π-acceptor ligands competing for metal electron density will render the CO more labile and promote its displacement by halide.

Hydride attack at $\eta^2\text{-}CS \cdot EMe$ (E = S or Se) ligands, prepared by methylation at η^2-CSE, can cause MeEH elimination resulting in CS groups. Overall, there is no change in the formal oxidation state of the metal. In two examples, the same $\eta^2\text{-}CS \cdot EMe$ compound may be used that gives a CS ligand through H^+ attack.[13,14] Thus, $[Os(\eta^2\text{-}CSSe)(CO)(CNR)(PPh_3)_2]$ (R = *p*-tolyl) (**1**) is methylated at Se upon which BH_4^- attack yields $[Os(CS)(CO)(CNR)(PPh_3)_2]$ and MeSeH,[13] and $[Os(CO)_2(PPh_3)_2(\eta^2\text{-}CS_2)]$ proceeds analogously to $[Os(CO)_2(PPh_3)_2(CS)]$ via $[\{Os(CO)_2(PPh_3)_2(\eta^2\text{-}CS_2Me)\}^+]$.[14] This

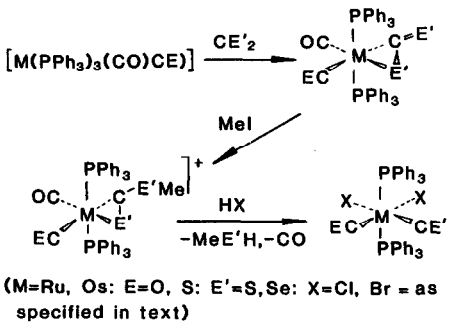


Fig. 2. η^2-Dichalcocarboxylate intermediates in CS ligand synthesis from CS_2.

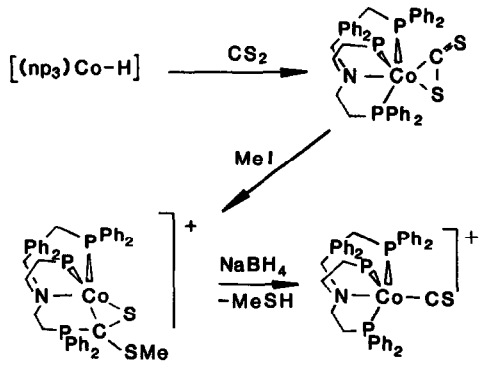


Fig. 3. A route to $[\{(np_3)Co(CS)\}^+]$.

method works on $[IrCl(CO)(PPh_3)_2(\eta^2\text{-}CS_2)]$ to give $[IrCl(PPh_3)_2(CS)]$ with additional CO loss[14] and can be applied directly to the analogous CSe_2 conversion.[15] In the last two cases an $[L_nM(H)(\sigma\text{-}CS_2Me)]$ intermediate (3) was isolated which is heated to induce MeSH elimination.[14]

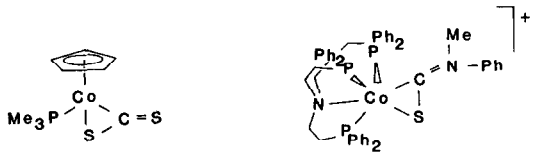


3 4

A different intermediate (4) has been proposed in a closely related system.[16,17] The η^2-CS_2 complex $[(np_3)Co(\eta^2\text{-}CS_2)]$, made by CS_2 attack upon $[(np_3)CoH]$, is methylated to give a phosphoniodithiomethyl ester moiety in $[\{Ph_2PCH_2CH_2N(CH_2CH_2PPh_2)_2Co(CS_2Me)\}^+]$. This undergoes hydride attack producing $[\{(np_3)Co(CS)\}^+]$ (Fig. 3).

The alteration in oxidation state between Co(0) and Co(I) in these reactions differs in pattern from the changes for the Os and Ir systems, and the modest yield of some steps suggests redox reactions occur with non-isolated cobalt species involved.

Sequential attack by Me^+ and H^- on an η^2-CSE ligand (E = S, Se or NR) resulting in a CS ligand is not a general reaction. For example, $[(\eta^5\text{-}C_5H_5)Co(PMe_3)(\eta^2\text{-}CS_2)]$ (5) does methylate with $[Me_3O\cdot BF_4]$ to an η^2-CS_2Me^+ ligand but reacts with NaH to give CH_4 and 5 rather than MeSH and $[(\eta^5\text{-}C_5H_5)Co(PMe_3)(CS)]$.[6]



5 6

(B) There are two related ways to make $[\{np_3)Co(CS)\}^+\cdot BPh_4^-]$, both via $[(np_3)CoH]$. The simultaneous use of CS_2 and $NaBPh_4$ gives[16] a low yield of $[\{(np_3)Co(CS)\}^+\cdot BPh_4^-]$ which equates to the formal loss of NaSH. Similarly, $[(np_3)CoH]$ reacts with PhNCS giving $[(np_3)Co(\eta^2\text{-}CS\cdot NPh)]$. Methylation is presumed to give $[\{(np_3)Co(\eta^2\text{-}CS\cdot NMePh)\}^+]$ (6) *in situ*, then $NaBPh_4$ addition produces $[\{(np_3)Co(CS)\}^+\cdot BPh_4^-]$.[17] Formally, NaNMePh is eliminated and the coordinated chalcogen of the η^2-ligand retained.

Both H^- and BPh_4^- addition to $[\{L_nM(\eta^2\text{-}CS\cdot EMe)\}^+]$ species result nominally in EMe^- elimination. Thus, other anions, X^-, may produce $[\{L_nM(CS)\}^+]$ similarly. Indeed, the use of HCl on the methylated ligand, discussed above, may be viewed as Cl^- acting in this role.

(C) These routes tend to give low yields of the CS complex either as the single isolated product or as one of a number of products. Also, the distinction in some cases from preparations involving phosphine ligands becomes tenuous [see Section II.1.ii(D)].

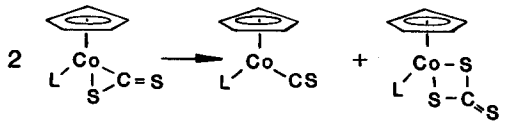


Fig. 4. The proposed disproportionation reaction of $[(\eta^5\text{-}C_5H_4R)CoL(\eta^2\text{-}CS_2)]$.

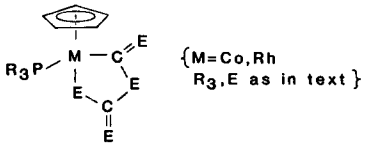
Cyclooctene loss from $[(\eta^5\text{-}C_5H_4R)Mn(CO)_2(C_8H_{14})]$ (R = H or Me) on reaction with CS_2 gives low yields of $[(\eta^5\text{-}C_5H_4R)Mn(CO)_2(CS)]$.[18,19] Cyclooctene was proposed to remove sulphur as cyclooctene sulphide but no evidence for this was found.[18] A $\eta^2\text{-}CS_2$ intermediate was proposed and the compound identified. Attack by CS_2 on $[(\eta^6\text{-}C_6H_5R)Cr(CO)_2(THF)^*]$ (R = H or CO_2Me) produces $[(\eta^6\text{-}C_6H_5R)Cr(CO)_2(CS)]$[20] and on [Os(OEP)$(N_2)$(THF)] in py gives [Os(OEP)(CS)py]:[21] both yields are fairly low and the sulphur's fate is unknown. These three CS complexes can be prepared in good yield by other routes (see below).

An intermediate in the reaction of CS_2 and $[RuBr_3(EPh_3)_2(MeOH)]$ (E = P or As) which produces $[RuBr_3(EPh_3)_2(CS)]$ is the σ-SCS compound $[RuBr_3(EPh_3)_2(\sigma\text{-SCS})]$. A mixture of these compounds occurs until a 30-min reflux has elapsed, when the former remains. The chloride analogue is stable at the σ-SCS stage.[22]

Reacting excess CS_2 with equimolar mixtures of $[(\eta^5\text{-}C_5H_5)Co(CO)_2]$ and L or with preformed $[(\eta^5\text{-}C_5H_5)Co(CO)L]$ (L = PR_3, *t*-BuNC; R_3 = Et_3, *n*-Pr_3, *n*-Bu_3, $PhMe_2$, Ph_2Me or Ph_3) gives four products, $[(\eta^5\text{-}C_5H_5)CoL(CS)]$, $[(\eta^5\text{-}C_5H_5)CoL(\eta^2\text{-}CS_2)]$, $[(\eta^5\text{-}C_5H_5)CoL(CS_3)]$ and $[(\eta^5\text{-}C_5H_5)_3Co_3(\mu_3\text{-}CS)(\mu_3\text{-}S)]$ in 5–25% yield each.[23] Refluxing $[(Cp)CoL(\eta^2\text{-}CS_2)]$ (L = PPh_3, Cp = $\eta^5\text{-}C_5H_5$ or $\eta^5\text{-}C_5H_4Me$; L = PPh_2Me, Cp = $\eta^5\text{-}C_5H_5$) in toluene mostly yields the Co_3 species with equal low yields of [CpCoL(CS)] and $[CpCoL(CS_3)]$. A disproportionation of the CS_2 ligand was proposed (Fig. 4). Involvement of dissociated PR_3 was ruled out as added PPh_3 did not have any effect.[23]

A closely related system of Werner's may proceed analogously in part. When $[(\eta^5\text{-}C_5H_5)Co(PR_3)_2]$ (R_3 = Me_3 or Me_2Ph) and excess CSSe react, $[(\eta^5\text{-}C_5H_5)Co(PR_3)(CS)]$ and $[(\eta^5\text{-}C_5H_5)Co(PR_3)(Se_2CS)]$ are isolated.[24] However, displaced or added phosphine abstracts Se from $[(\eta^5\text{-}C_5H_5)M(PR_3)(\eta^2\text{-}CSeS)]$ (M = Co or Rh) as discussed below. As yields of $[(\eta^5\text{-}C_5H_5)Co(PR_3)(Se_2CS)]$ are lower than for $[(\eta^5\text{-}C_5H_5)Co(PR_3)(CS)]$, a disportionation reaction between two molecules of $[(\eta^5\text{-}C_5H_5)Co(PR_3)(\eta^2\text{-}CSeS)]$ might account for equal yields of each, with displaced PR_3 abstracting Se to account for the remainder of the CS complex.

Both authors proposed the possible intermediacy of C_2S_4 or $C_2S_2Se_2$ groups in the rearrangement. Indeed, under certain conditions $[(\eta^5\text{-}C_5H_5)M(PR_3)_2]$ and CE_2 (E_2 = S_2, SSe or Se_2) gives $[(\eta^5\text{-}C_5H_5)M(PR_3)(C_2E_4)]$ (7) (M = Co, R_3 = Me_3, E_4 = Se_4;[24] M = Rh, R_3 = Me_3, E_4 = S;[25]



7

R_3 = Me_2Ph, E_4 = S_2Se_2).[24] Also, rearrangements via C_2S_4 groups have been proposed in routes to CS ligands involving phosphine ligands (see below).

(D) Three differing routes to CS ligands involve the abstraction of sulphur or selenium from CSE (E = S or Se) by PR_3 producing $R_3P{=}E$. Firstly, a CS_2–PR_3 mixture is used which is presumed to form an $\eta^2\text{-}CS_2$ complex which is attacked by PR_3. Secondly, coordinated PR_3 is displaced from a metal

* Abbreviations: bipy, 2,2′-bipyridine; Cy, cyclohexyl; diars, 1,2-bis(dimethylarsino)benzene; dppe, 1,2-bis(diphenylphosphine)ethane; phen, 1,10-phenanthroline; phthaln, phthalodinitrile; py, pyridine; pz, pyrazolate; THF, tetrahydrofuran; triphos, bis-(2-diphenylphosphinoethyl)phenyl phosphine; TPP, tetraphenylporphyrin; OEP, octaethylporphyrin; TTP, tetratolylporphyrin; morph, morpholine; Im, imidazole; pip, piperidine; tmeda, tetramethylethylenediamine; Idz, indazolate; cod, 1,5-cyclooctadiene.

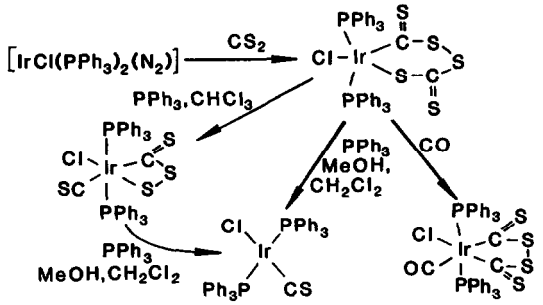


Fig. 5. Kubota and Carey's structural assignments of products derived from $[IrCl(PPh_3)_2(N_2)]$ and CS_2, and subsequent reactions.

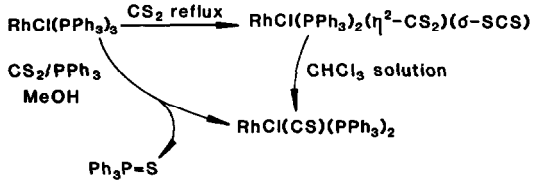


Fig. 6. The reaction of $[RhCl(PPh_3)_3]$ and CS_2. Products assigned by Wilkinson.

center and used as the abstracting molecule for the newly formed η^2-CES ligand or more complicated CSE-derived ligands. Thirdly, an isolated η^2-CES complex is attacked by added PR_3. Yields are variable, depending upon the exact system involved, and there is much overlap between these regimes.

The one-pot usage of excess CS_2 and PPh_3 converts $[MCl_2(PPh_3)_3]$ (M = Ru or Os) into *trans*-$[RuCl_2(CS)(H_2O)(PPh_3)_2]$[26] or $[OsCl_2(CS)(PPh_3)_3]$,[27] $[RhCl(PPh_3)_3]$ to $[RhCl(CS)(PPh_3)_2]$[28–30] and $[\{Ir(\mu\text{-}Cl)(cod)\}_2]$[31] or $[IrCl(PPh_3)_2(N_2)]$[32] into $[IrCl(CS)(PPh_3)_2]$. For these Rh and Ir cases, Wilkinson and co-workers[28,29,31] and Kubota and Carey[32] indicated that MeOH addition was needed with CS_2 and PPh_3 for good yields of the CS complex. Using CS_2, PPh_3 and MeOH individually allowed Kubota and Carey[32] to isolate intermediates and propose structures based on IR spectroscopy (Fig. 5). They suggested that these were unidentified compounds cited in Wilkinson's work.[31] Both groups identified $Ph_3P{=}S$ and inferred sulphur removal from CS_2 by PPh_3. Wilkinson observed[28,29] that without PPh_3 $[RhCl(PPh_3)_3]$ and CS_2 give a product assigned as $[RhCl(PPh_3)_2(\eta^2\text{-}CS_2)(\sigma\text{-}SCS)]$ which rearranges to $[RhCl(CS)(PPh_3)_2]$ in $CHCl_3$ solution. Figure 6 summarizes Wilkinson's work with $[RhCl(PPh_3)_3]$.

Reinvestigating this reaction, Thewissen proposes[30] that $[RhCl(PPh_3)_2(\eta^2\text{-}CS_2)]$ is formed first, identified spectroscopically, from which $[RhCl(CS)(PPh_3)_2]$ results on addition of excess PPh_3 in good yield *without* MeOH addition. With no added PPh_3, a slow reaction sequence occurs which was followed by IR and NMR spectroscopy and is shown in Fig. 7. The initially formed $[RhCl(PPh_3)_2(\eta^2\text{-}$

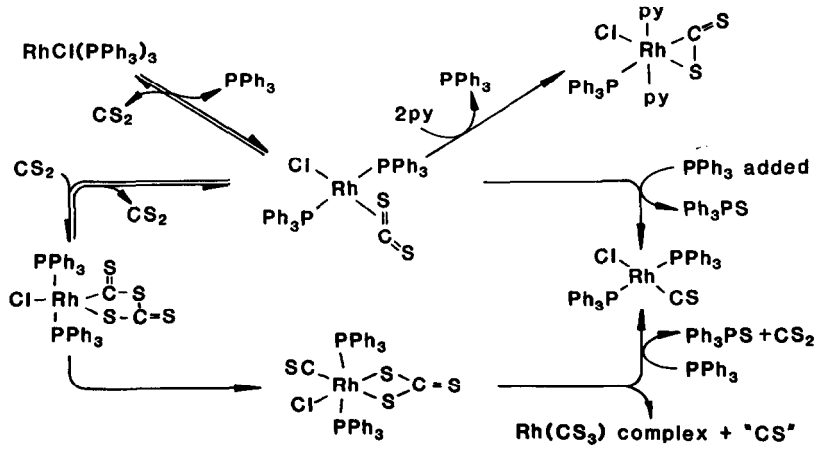
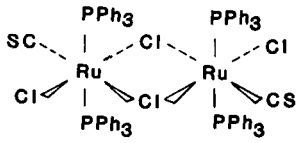
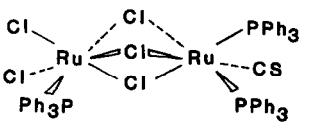


Fig. 7. The reaction of $[RhCl(PPh_3)_3]$ and CS_2 (py = pyridine). Products assigned by Thewissen.

CS_2)] reacts with CS_2 giving [$RhCl(PPh_3)_2(C_2S_4)$], which Thewissen suggests is the same compound as Wilkinson's [$RhCl(PPh_3)_2(\eta^2\text{-}CS_2)(\sigma\text{-}SCS)$]. This rearranges to [$RhCl(PPh_3)_2(CS)(S_2CS)$], which either loses "CS" to give unidentified $Rh(CS_3)$ products or loses CS_3 as CS_2 and $Ph_3P{=}S$ to give [$RhCl(CS)(PPh_3)_2$], the PPh_3 being derived from the original [$RhCl(PPh_3)_3$] reactant. This sequence is similar to Kubota and Carey's (Fig. 5) and the pathways are likely the same. Thewissen's later work gave him more literature IR data for his C_2S_4 and CS_3 assignments while Kubota and Carey's proposed C_2S_5 and CS_3 coordination modes remain unique. Also, Thewissen's work suggests *two routes* operate, excess PPh_3 directly abstracting sulphur from the η^2-CS_2 ligand but displaced PPh_3 eliminating the CS_3 group (as CS_2 and $Ph_3P{=}S$) after metal-centered CS_2 dimerization and disproportionation. The latter mechanism could operate in some of Werner's systems with [$(\eta^5\text{-}C_5H_5)Co(PR_3)_2$] and CSE (E = S or SE), although an attack of displaced PR_3 on an η^2-CES ligand is usually invoked,[6,24] as is discussed below.



8



9

Reacting [$RuCl_2(PPh_3)_3$] with excess CS_2 results in PPh_3 displacement and the isolation of three products, [$RuCl_2(S_2CPPh_3)(PPh_3)_2$], [$\{Ru(CS)Cl(PPh_3)_2\}_2(\mu\text{-}Cl)_2$] (**8**) and [$(PPh_3)_2ClRu(\mu\text{-}Cl)_3Ru(CS)(PPh_3)_2$] (**9**).[33–36] Mechanistic proposals suggested that [$RuCl_2(PPh_3)_2(CS)$] dimerizes to **8** or reacts with [$RuCl_2(PPh_3)_3$] giving **9**,[34,35] the latter by analogy with [$RuCl_2(PPh_3)_2(CO)$] behaviour.[35]

Another set of examples using either simultaneous or sequential use of CS_2 and PPh_3 are summarized in Fig. 8 and Table 1.[19,20,37–39] Generally, [(ring)$M(CO)_3$] (M = Mn, Re or Cr; ring = η^5- or η^6-ligand, as appropriate) is UV irradiated in the presence of a labile ligand L (L = THF or cyclooctene) producing [(ring)$M(CO)_2L$]. Then, CS_2 and PPh_3 are reacted with this, together or sequentially. The isolation of [(ring)$M(CO)_2(\eta^2\text{-}CS_2)$] in certain cases suggests the intermediacy of this in all cases, with PPh_3 abstracting sulphur as $Ph_3P{=}S$ to yield [(ring)$M(CO)_2(CS)$].

The same reaction sequence enables [$(\eta^5\text{-}C_5H_5)Cr(CO)_2(NO)$] to be converted to [$(\eta^5\text{-}C_5H_5)Cr(CO)(CS)(NO)$] using C_8H_{14} as labile ligand and CS_2–PPh_3 simultaneously.[40] This method applied twice over to [$(\eta^5\text{-}C_5H_5)Mn(CO)_2(CS)$] produces first [$(\eta^5\text{-}C_5H_5)Mn(CO)(CS)_2$] and finally [$(\eta^5\text{-}C_5H_5)Mn(CS)_3$].[19] Analogous usage of CSe_2–PPh_3 leads to the CSe analogues for the same Mn, Re and Cr reactants.[41,42]

The use of an excess of CS_2 and PPh_3 is *not* a general route to CS complexes. For instance, a wide range of analogues of [$Fe(CO)_2(PR_3)_2(\eta^2\text{-}CS_2)$] are made by reacting these reagents with appropriate Fe(0) precursors.[43,44]

Added P^nBu_3 is known to abstract sulphur from two η^2-CS_2 complexes. However, with [$W(CO)_3(R_2PC_2H_4PR_2)(\eta^2\text{-}CS_2)$] (R = Me or Ph), the reaction gives [$W(CO)_3(R_2PC_2H_4PR_2)(\sigma\text{-}SC(S)P^nBu_3)$] as well as [$W(CO)_3(R_2PC_2H_4PR_2)(CS)$][45] and, with [$Fe(CO)_2\{P(OPh)_3\}_2(\eta^2\text{-}CS_2)$], the yield of [$Fe(CO)_2\{P(OPh)_3\}_2(CS)$] proved variable.[46] The ready exchange of phosphine ligands in [$Fe(CO)_2(PR_3)_2(\eta^2\text{-}CS_2)$] indicates that the latter reaction is not general.[43,44]

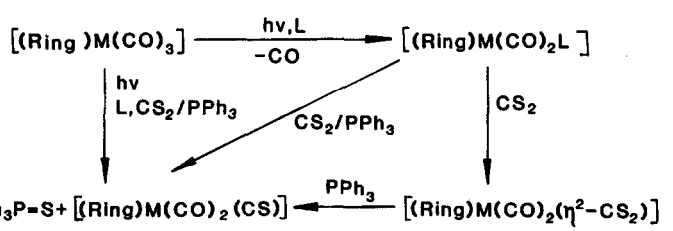


Fig. 8. The routes to prepare [(ring)$M(CO)_2(CS)$] using CS_2–PPh_3 (refer to Table 1).

Table 1.

M	L	Ring	η^2-CS_2 isolated	Reference
Mn	C_8H_{14}	η^5-C_5H_5	√	19, 37
Mn	C_8H_{14}	η^5-C_5H_4Me	√	19
Cr	C_8H_{14}	η^6-$C_6H_5CO_2Me$	×	38
Cr	C_8H_{14}	η^6-C_6Et_6	√	39
Mn	THF	η^5-C_5H_5	×	20
Mn	THF	η^5-C_5H_4Me	×	20
Re	THF	η^5-C_5H_5	×	20

Werner's work with $[(\eta^5\text{-}C_5H_5)M(PR_3)L]$ species (M = Co or Rh) involves the use of either displaced or added phosphine to give CS ligands by chalcogen abstraction from η^2-CES units. Sensitivity to the nature of M, PR_3 and CE_2 (E_2 = OS, S_2, SSe or Se_2) is indicated.[6,24,47] Reactions are summarized in Fig. 9. Reactions involving CS_2 give only $[(\eta^5\text{-}C_5H_5)M(PR_3)(\eta^2\text{-}CS_2)]$ [M = Co, R_3 = Me_3 or $(OMe)_3$; M = Rh, R_3 = Me_3 or Me_2Ph]. This was shown to be stable to added PPh_3 in some cases. Using COS, a near quantitative yield of $[(\eta^5\text{-}C_5H_5)Co(PMe_3)(CO)]$ results from $[(\eta^5\text{-}C_5H_5)Co(PMe_3)_2]$ when displaced PMe_3 was proposed to remove sulphur as $Me_3P{=}S$ from the unidentified intermediate $[(\eta^5\text{-}C_5H_5)Co(PMe_3)(\eta^2\text{-}CSO)]$. With CSSe or CSe_2, a variety of products result, the nature of which depends on the amount of this reagent used and the phosphine substituent. Stoichiometric quantities of CSSe with $[(\eta^5\text{-}C_5H_5)Co(PR_3)_2]$ (R_3 = Me_3) yield

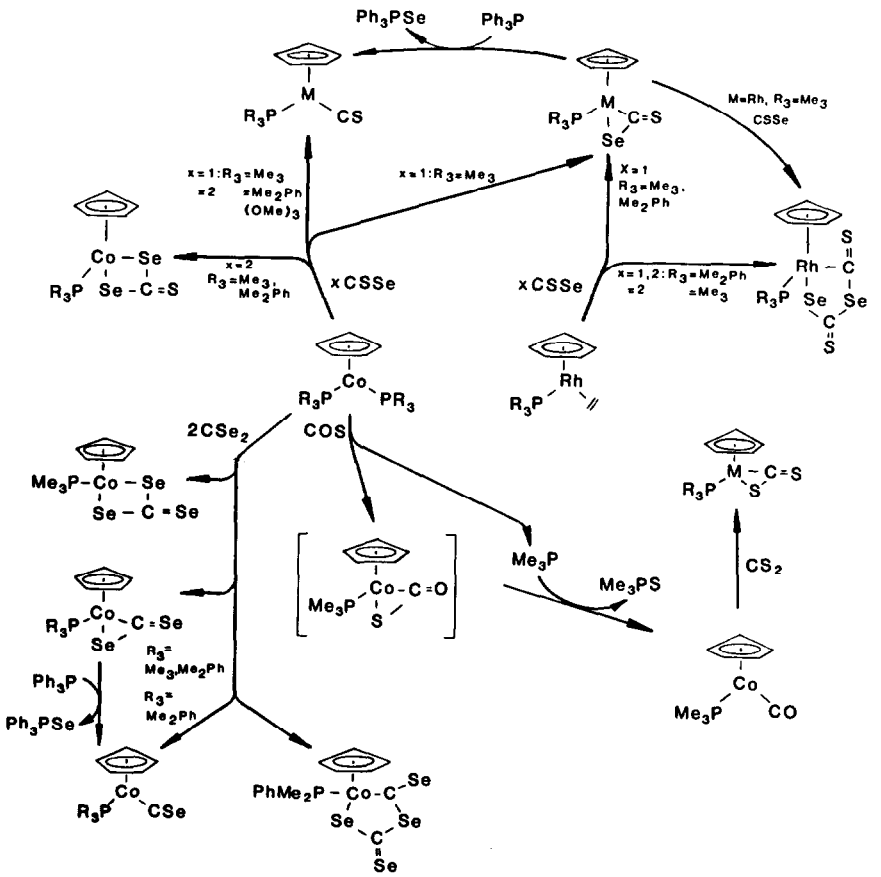


Fig. 9. Werner and co-workers results on the $[(\eta^5\text{-}C_5H_5)ML_2]$ (M = Co or Rh)–CEE′ (E and E′ = O, S or Se) system.

$[(\eta^5\text{-}C_5H_5)Co(PMe_3)(CS)]$ and $[(\eta^5\text{-}C_5H_5)Co(PMe_3)(\eta^2\text{-}CSeS)]$, the displaced PMe_3 being proposed to abstract selenium. Excess CSSe (two–three-fold) gives $[(\eta^5\text{-}C_5H_5)Co(PMe_3)(\eta^2\text{-}CSeS)]$ and $[(\eta^5\text{-}C_5H_5)Co(PMe_3)(Se_2CS)]$ but, when $R_3 = (OMe)_3$, results in $[(\eta^5\text{-}C_5H_5)Co\{P(OMe)_3\}(CS)]$ and $(MeO)_3P{=}SE$ or, for $R_3 = Me_2Ph$, yields $[(\eta^5\text{-}C_5H_5)Co(PMe_2Ph)(CS)]$ and $[(\eta^5\text{-}C_5H_5)Co(PMe_2Ph)(Se_2CS)]$. Using two equivalents of CSe_2 with $[(\eta^5\text{-}C_5H_5)Co(PR_3)_2]$ ($R_3 = Me_3$) is analogous to using CSSe, but, for $R_3 = Me_2Ph$, $[(\eta^5\text{-}C_5H_5)Co(PMe_2Ph)(C_2Se_4)]$ occurs in addition to the CSe and η^2-CSe_2 compounds. With one equivalent of CSSe, $[(\eta^5\text{-}C_5H_5)Rh(PR_3)(C_2H_4)]$ produces $[(\eta^5\text{-}C_5H_5)Rh(PR_3)(\eta^2\text{-}CSeS)]$ when $R_3 = Me_3$ but a mixture of this and $[(\eta^5\text{-}C_5H_5)Rh(PR_3)(C_2S_2Se_2)]$ when $R_3 = Me_2Ph$. Two equivalents give the $C_2S_2Se_2$ compound only for both $R_3 = Me_3$ and Me_2Ph. The lack of CS products in the rhodium cases coincides with the absence of displaced phosphine ligands, suggesting the intermediacy of these in the cobalt cases. All the above η^2-CSeS and η^2-CSe_2 products react with PPh_3, giving the respective CS and CSe complexes, with the identification of $Ph_3P{=}Se$ in some cases. In summary, these pathways are variable and do not reliably yield CS complexes.

In cases, where PR_3 abstracts a chalcogen from an η^2-CE_2 ligand, removal of the coordinated chalcogen atom is proposed.[6,24,46] This contrasts with reactions discussed in Section II.1.ii(A) whereby methylation at the uncoordinated chalcogen followed by H^+ or H^- attack eliminates this atom in MeEH (E = S or Se).

(E) A few examples exist whereby free or η^2-coordinated CS_2 is fragmented giving rise to terminal CS ligands and μ_2- or μ_3-sulphide groups. The metal core is bi- or trimetallic.

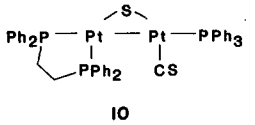
Reacting $[Pt(Ph_2PC_2H_4PPh_2)(\eta^2\text{-}CS_2)]$ and $[Pt(\eta^2\text{-}C_2H_4)(PPh_3)_2]$ gives

$$[(Ph_2PC_2H_4PPh_2)Pt(\mu\text{-}S)Pt(PPh_3)(CS)]$$

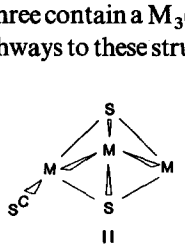
(**10**),[48] via a proposed $\overline{Pt\{S\text{-}C(S)\}Pt}$ intermediate. Free CS_2 interacts with $[Fe_3(CO)_{12}]$,[49,50] $[Os_3(CO)_{12}]$[50,51] or $[Os_3(CO)_8SH_2(MeCN)]$[52] to yield the clusters

$$[Fe_3(CO)_8(CS)S_2],\ [Os_3(CO)_8(CS)S_2] \quad \text{and} \quad [Os_3(CO)_7(CS)S_2(\mu\text{-}H)_2],$$

respectively, as one of a number of products in each case. All three contain a $M_3(\mu_3\text{-}S)_2(CS)$ core (**11**) for M = Os. Different CS positions give isomers in the iron case. Pathways to these structures were not proposed.



10



11

iii. Preparations using [Cl(X)CS] (X = Cl *or* OR) *and* $[Cl_3C\cdot SR]$

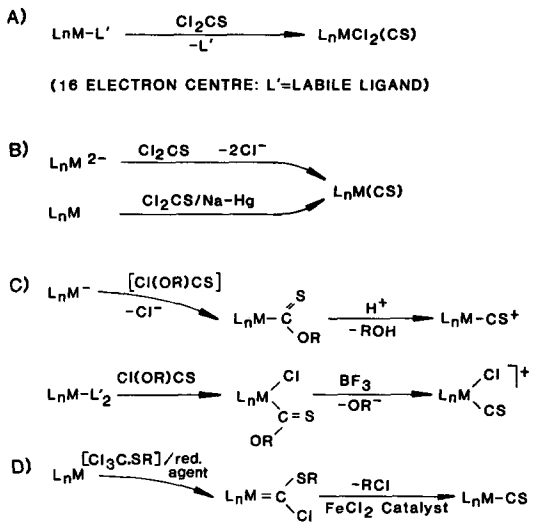
The uses of these reagents are summarized in Scheme 2 and are discussed in turn.

(A) Thiophosgene, Cl_2CS, reacts with the 16-electron Rh(I) and Ir(I) complexes $[RhCl(PPh_3)_3]$, $[IrCl(PPh_3)_2(N_2)]$ and $[\{Ir(PPh_3)_2(CO)(MeCN)\}^+]$. A neutral ligand is displaced (PPh_3, N_2 and MeCN, respectively) and Cl_2CS oxidatively adds to give the M(III) 18-electron complexes $[RhCl_3(PPh_3)_2(CS)]$, $[IrCl_3(PPh_3)_2(CS)]$ and $[\{IrCl_2(PPh_3)_2(CO)(CS)\}^+]$.[53] Similarly, $[Ru_3(CO)_{12}]$ fragments and loses one CO ligand from each Ru to give $[RuCl_2(CO)_3(CS)]$ with a two-unit increase in the formal metal oxidation state.[54]

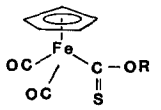
(B) Chlorine is removed from Cl_2CS in two differing ways. Two equivalents of chloride are eliminated in the reaction of Cl_2CS with $[\{Fe(CO)_4\}^{2-}]$[55] or $[\{M(CO)_5\}^{2-}]$ and $[\{M_2(CO)_{10}\}^{2-}]$ (M = Cr, Mo or W)[56] to produce $[Fe(CO)_4(CS)]$ and $[M(CO)_5(CS)]$ in low yield. A better preparation of $[Cr(CO)_5(CS)]$ is known,[57] as discussed in Section II.1.v.

Either Fe powder or Na–Hg is used to remove chlorine from Cl_2CS. The thiocarbonyl products are metal porphyrin species and [M(OEP)(CS)L] (M = Fe,[21] Ru,[58] or Os;[21] L = solvent EtOH, THF or py) are prepared as shown in Fig. 10. Both Na–Hg and Fe powder have been used to prepare [Fe(TPP)(CS)] from [Fe(TPP)Cl].[59]

(C) Two differing two-step routes to CS ligands have been noted using $[Cl(OR)\cdot CS]$. Using $[(\eta^5\text{-}C_5H_5)Fe(CO)_2\}^-]$ and $[Cl(OR)\cdot CS]$ (R = Me,[8] or Et[60]) produces $[(\eta^5\text{-}C_5H_5)Fe(CO)_2\{CS(OR)\}]$ (**12**) by chloride elimination. Attack by H^+ on this causes ROH loss, giving $[\{(\eta^5\text{-}C_5H_5)Fe(CO)_2(CS)\}^+]$.



Scheme 2. Routes to CS ligands from [Cl(X)CS] (X = Cl or OR) and [Cl_3CSR].



12

Alternatively, with [$Pt(PPh_3)_4$], [Cl(OMe)·CS] oxidatively adds to the Pt center to give [$PtCl(PPh_3)_2${CS(OMe)}]. Abstraction of OMe^- is achieved using BF_3 and *trans*-[{$PtCl(PPh_3)_2(CS)$}$^+BF_4^-$] is isolated. Addition of MeOH reverses the second step.[61]

(D) The reaction with [Cl_3C-SR] (R = Ph, CH_2Ph or NR'_2) is related to those with Cl(X)CS. With [Fe(II)(TPP)] in the presence of either sodium dithionite or Fe powder, [Fe(TPP){C(Cl)SR}] results. Elimination of RCl is caused by adding catalytic amounts of $CuCl_2$ or $FeCl_2$ to give [Fe(II)(TPP)(CS)].[62] Differing porphyrin ligands such as OEP, TTP and tetrakis(*p*-chlorophenyl)porphyrin were employed with [Cl_3C-SCH_2Ph].[62]

iv. Preparations via dichlorocarbene or chlorocarbyne complexes

These methods boast only one set of examples each, but yields are relatively high and these routes may prove more widely useful. Also, both routes lead not only to the CS complex but also to the CSe and CTe analogues.

Reacting [$OsCl_2(PPh_3)_2(CO)(CCl_2)$] with EH^- (E = S, Se or Te) caused the elimination of Cl^- and HCl to yield [$OsCl_2(PPh_3)_2(CO)(CE)$][63] (Fig. 11). Similarly, the chlorocarbyne ligand in [Mo(CCl)$(CO)_2$L] [L = $HB(3,5\text{-}Me_2\text{-}C_3HN_2)_3$] reacts with E^{2-} (E = S, Se or Te) giving [{Mo(CE)$(CO)_2$L}$^-$][64] (Fig. 12).

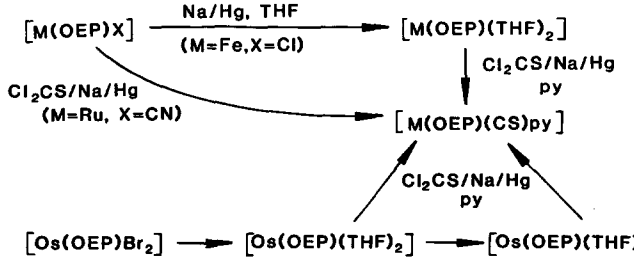


Fig. 10. [Cl_2CS]-based routes to [M(OEP)(CS)py] (M = Fe, Ru or Os: OEP = octaethylporphyrin).

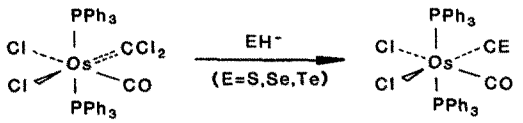


Fig. 11. The conversion of the dichlorocarbene ligand in $[OsCl_2(PPh_3)_2(CO)(CCl_2)]$ to CE using EH^- (E = S, Se or Te).

v. Modification of thiocarbonyl complexes

Novel thiocarbonyl complexes are often formed by ligand substitution or addition reactions of thiocarbonyl-containing species. Substitutions include those of neutral ligands (e.g. CO and PPh_3) often under the influence of heat or UV irradiation, anion exchange reactions and the displacement of a neutral ligand by an anion or vice versa. Addition reactions occur with sub-18-electron species which take on donor ligands (e.g. CO and PPh_3) or undergo oxidative addition of molecules such as H_2 or Cl_2. However, the discussion is not structured around reaction types but instead moves across the *d*-block, concentrating in turn on the major series of modification reactions which have been developed from certain thiocarbonyl complexes.

(a) Cr *triad*. UV irradiation of $[(\eta^5\text{-}C_5H_5)Cr(CO)(CS)(NO)]$ in the presence of cyclooctene eliminates CO to produce $[(\eta^5\text{-}C_5H_5)Cr(CS)(NO)(C_8H_{14})]$.[40] Both PMe_3 and NO^+ can displace the labile cyclooctene to give $[(\eta^5\text{-}C_5H_5)Cr(CS)(NO)(PMe_3)]$ and $[\{(\eta^5\text{-}C_5H_5)Cr(CS)(NO)_2\}^+]$.[40] Similarly, irradiation of $[\{\eta^6\text{-}o\text{-}C_6H_4(CO_2Me)R\}Cr(CS)(CO)_2]$ with PR'_3 in benzene leads to $[\{\eta^6\text{-}o\text{-}C_6H_4(CO_2Me)R\}Cr(CS)(CO)(PR'_3)]$ [R = H, $R'_3 = (OEt)_3$ or Me_2Ph: R = Me; R' = Ph, OEt or OPh][38,65–67] which when (R = Me, R' = OEt) can be reduced by $LiAlH_4$–$AlCl_3$ at the arene ligand to

$$[(\eta^6\text{-}o\text{-}C_6H_4Me_2)Cr(CS)(CO)\{P(OEt)_3\}].^{65,67}$$

These products are chiral, and optical isomers have been resolved in some cases.

At elevated temperature and pressure, CO displaces the arene ligand from $[(\eta^6\text{-}C_6H_5R)Cr(CO)_2(CE)]$ (R = H, E = S or Se; R = CO_2Me, E = S) to give $[Cr(CO)_5(CE)]$.[5] This is a higher-yield route than using $[\{Cr(CO)_5\}^{2-}]$ and Cl_2CS.[56]

The chemistry of $[M(CO)_5(CS)]$ (M = Cr or W) has been investigated and is mostly shown in Scheme 3. Spectroscopic investigation of the UV irradiation product of $[M(CO)_5(CS)]$ isolated in a gas matrix at 20 K indicates that *cis*-CO loss gives rise to C_{4v}- and C_s-isomers of $[M(CO)_4(CS)]$ (M = Cr or W).[68,69] Thermal ligand substitution results in $[M(CO)_4(CS)L]$ [M = Cr; L = PPh_3, *cis*- and *trans*-: M = W; L = PPh_3 (*cis*- and *trans*-), py (*trans*-)] and *mer*-$[M(CO)_3(CS)(dppe)]$ (M = Cr or W).[70–72] Further CO substitution in molten dppe produces *cis*-$[W(CO)(CS)(dppe)_2]$,[70–72] which is protonated by CF_3SO_3H at the metal giving $[\{WH(CO)(CS)(dppe)_2\}^+]$.[73,74] Halide substitution of CO in $[W(CO)_5(CS)]$ by using $^nBu_4NX$ gives [*trans*-$\{W(CO)_4(CS)X\}^- \cdot {}^nBu_4N^+$] (X = Cl, Br or I)[70,72,74] from which, when X = I, Ag^+ abstracts I^- and allows its replacement by a neutral ligand.[72,75] This gives a route other than thermal substitution of $[W(CO)_5(CS)]$ to a wider range of *trans*-$[W(CO)_4(CS)L]$ (L = ^{13}CO, CyNC, 4-Me-py or PR_3; R = Ph, tolyl, ^{n}Bu, OMe or OPh) without coproduction of the *cis*-isomer,[72,75] and also allows the preparation of *mer*-$[W(CO)_3(CS)(bipy)]$.[72] As I^- abstraction is performed in acetone solvent before ligand addition,[72,75] the intermediacy of *trans*-$[W(CO)_4(CS)(Me_2CO)]$ can be inferred. Heating *trans*-$[W(CO)_4(CS)L]$ (L = CyNC, 4-Me-py or PR_3) at 65°C in cyclohexane solution causes isomerization to a *cis–trans*-isomer mixture.[75] Anionic

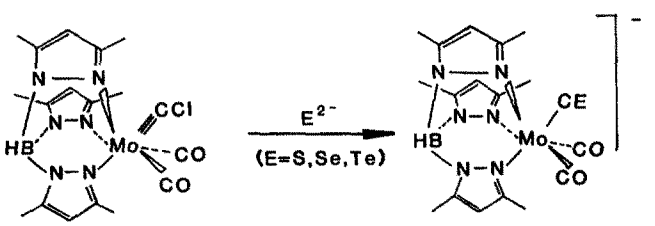
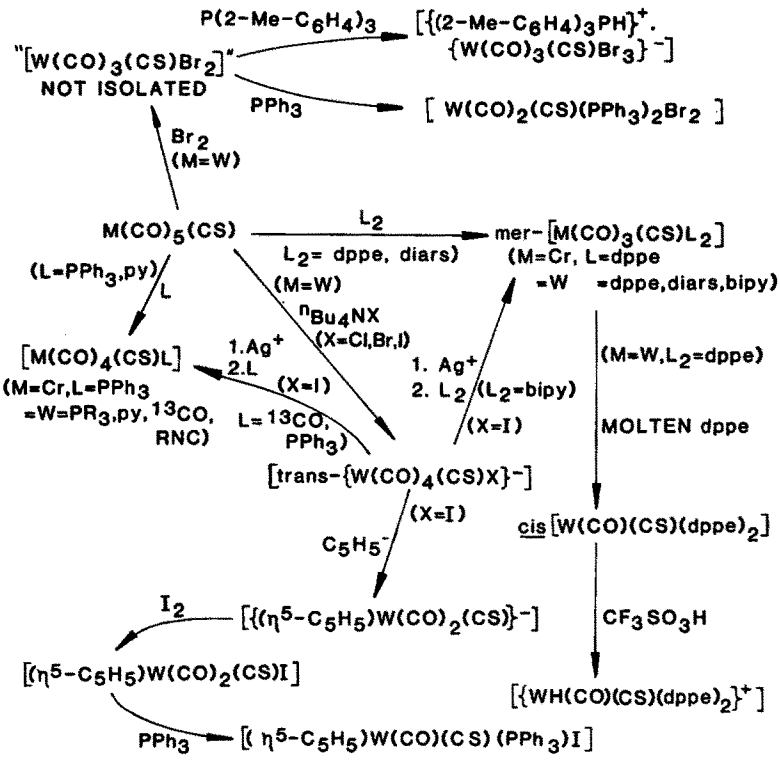


Fig. 12. Conversion of a chlorocarbyne ligand to CE by E^{2-} (E = S, Se or Te).



Scheme 3. CS complexes derived from $[M(CO)_5(CS)]$ (M = Cr or W) by ligand substitution.

substitution of I^- in [*trans*-$\{W(CO)_4(CS)I\}^-$] by $C_5H_5^-$ gives [$\{(\eta^5\text{-}C_5H_5)W(CO)_2(CS)\}^-$] to which I_2 nominally introduces I^+, yielding [$(\eta^5\text{-}C_5H_5)W(CO)_2(CS)I$] containing *trans*-CS and I ligands.[76,77] This stereochemistry is retained on CO substitution in refluxing toluene which produces [$(\eta^5\text{-}C_5H_5)W(CO)(CS)(L)I$] [L = PPh_3,[76] PMe_2Ph, $P(OPh)_3$, $P(NMe_2)_3$ or MeNC] although [$\{(\eta^5\text{-}C_5H_5)W(CO)(CS)L_2\}^+I^-$] (L = PMe_2Ph) is obtained using a lower reflux temperature.[77] Halide elimination between [$\{(\eta^5\text{-}C_5H_5)W(CO)_2(CS)\}^-$] and the substrates Ph_3SnCl, Ph_3PbCl, PhSeBr and HgI_2 gives [$(\eta^5\text{-}C_5H_5)W(CO)_2(CS)X$] {X = $SnPh_3$, $PbPh_3$ [*cis*-(CS)(X)], SePh or HgI [*cis*- and *trans*-(CS)(X)]}.[77] Reacting [$K\cdot\{HB(pz)_3\}$] and [*trans*-$\{W(CO)_4(CS)I\}^-$] eliminates I^- also to form [$\{W\{HB(pz)_3\}(CO)_2(CS)\}^-$] which, with I_2, yields [$W\{HB(pz)_3\}(CO)_2(CS)I$].[77] Other uses of halogen include Br_2 attack on $[W(CO)_5(CS)]$ when the formation of $[W(CO)_3(CS)Br_2]$ was inferred from the isolation of $[W(CO)_2(CS)(PPh_3)_2Br_2]$ and [$\{(2\text{-}Me\text{-}C_6H_4)_3PH\}^+\cdot\{W(CO)_3(CS)Br_3\}^-$] when the relevant phosphine is present.[73] Similarly, excess I_2 reacts with *mer*-$[W(CO)_3(CS)(dppe)]$ giving [$\{W(CO)_2(CS)(dppe)I\}^+\cdot I_3^-$], whereas stoichiometric amounts give a product assigned tentatively as $[W(CO)_2(CS)(dppe)I_2]$.[73]

(b) Mn *triad*. The substitution reactions of [$(\eta^5\text{-}C_5H_4R)Mn(CO)_2(CS)$] (R = H or Me) utilize UV irradiation extensively. The labile cyclooctene ligand is introduced thus into

$$[(\eta^5\text{-}C_5H_5)Mn(CO)(CS)(C_8H_{14})],$$

which reacts with CS_2–PPh_3 to form [$(\eta^5\text{-}C_5H_5)Mn(CO)(CS)_2$], on which the sequence of reactions can be repeated giving [$(\eta^5\text{-}C_5H_5)Mn(CS)_3$] via

$$[(\eta^5\text{-}C_5H_5)Mn(CS)_2(C_8H_{14})].^{19}$$

Cyclooctene may be displaced by PPh_3 or dppe also, producing

$$[(\eta^5\text{-}C_5H_5)Mn(CO)(CS)(PPh_3)]^{19,78} \quad \text{and} \quad [(\eta^5\text{-}C_5H_5)Mn(CS)(dppe)],^{79}$$

respectively. Irradiating [$(\eta^5\text{-}C_5H_5)Mn(CO)_2(CS)$] in THF leads to the *in situ* preparation of

$$[(\eta^5\text{-}C_5H_5)Mn(CO)(CS)(THF)].^{19,79,80}$$

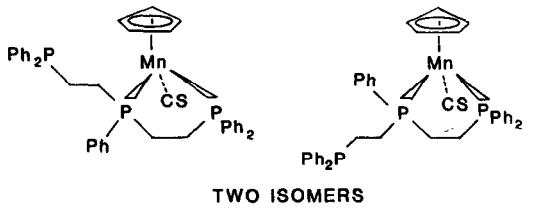


Fig. 13. The two isomeric forms of $[(\eta^5\text{-}C_5H_5)Mn(CS)(triphos)]$.

Production in the presence of or subsequent addition of a ligand displaces THF giving

$$[(\eta^5\text{-}C_5H_5)Mn(CO)(CS)L]$$

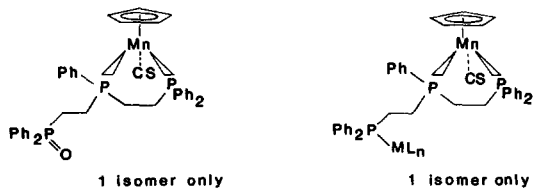
[L = PMe_2Ph, PCy_3, $P(OR)_3$, $AsPh_3$ or $SbPh_3$; R = Me, Et, Ph or CH_2CH_2Cl][80] and

$$[(\eta^5\text{-}C_5H_5)Mn(CS)(dppe)].^{19,79}$$

In benzene solvent with an excess of ligand, irradiation converts $[(\eta^5\text{-}C_5H_5)Mn(CO)_2(CS)]$ into $[(\eta^5\text{-}C_5H_5)Mn(CS)L_2]$ (L = PMe_2Ph or PR_3; R = Ph, OMe, OEt, OPh or OCH_2CH_2Cl; L_2 = triphos).[80] For $[(\eta^5\text{-}C_5H_5)Mn(CS)(triphos)]$, diastereomers exist through different orientations of the uncoordinated third phosphine functionality (Fig. 13). This functionality is converted to a phosphine oxide by ozone or coordinates to another metal center on reaction with

$$[ML_n(THF)]\ [ML_n = Cr(CO)_5 \text{ or } (\eta^5\text{-}C_5H_5)Mn(CO)_2]$$

(**13** and **14**), these compounds existing also in two diastereometric forms.[80]



Reaction of $[(\eta^5\text{-}C_5H_4R)Mn(CO)_2(CS)]$ (R = H or Me) with NO^+ gives

$$[\{(\eta^5\text{-}C_5H_4R)Mn(CO)(CS)(NO)\}^+].^{81}$$

In refluxing CH_2Cl_2, this readily produces

$$[\{(\eta^5\text{-}C_5H_4R)Mn(CS)(NO)L\}^+]$$

(R = H; L = PPh_3: R = Me; L = PPh_3, $AsPh_3$ or $SbPh_3$) and with KI in THF yields

$$[(\eta^5\text{-}C_5H_5)Mn(CS)(NO)I].^{82}$$

(c) Fe *triad*. For $[\{(\eta^5\text{-}C_5H_5)Fe(CO)_2(CS)\}^+ \cdot PF_6^-]$, which is isoelectronic to

$$[(\eta^5\text{-}C_5H_5)Mn(CO)_2(CS)],$$

CO substitution occurs without UV irradiation or heating using an excess of ligand in acetone to prepare

$$[\{(\eta^5\text{-}C_5H_5)Fe(CO)(CS)L\}^+ \cdot PF_6^-]$$

(L = PR_3, $AsPh_3$ or $SbPh_3$; R = Ph, Cy, C_6H_4F or C_6H_4OMe) or

$$[\{(\eta^5\text{-}C_5H_5)Fe(CS)(CNPh)_2\}^+ \cdot PF_6^-].^{83}$$

With irradiation,

$$[\{(\eta^5\text{-}C_5H_5)Fe(CS)(Me_2CO)\{MeC(CH_2As)_3\}\}^+]$$

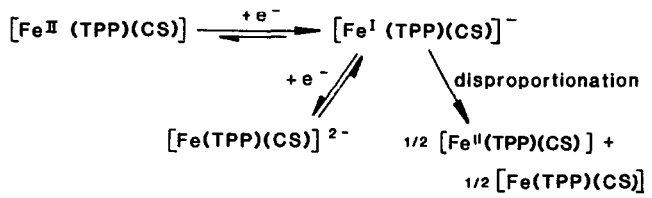
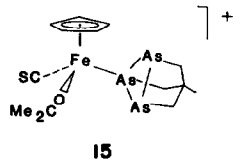


Fig. 14. The electrochemical behaviour of [Fe(II)(TPP)(CS)] (TPP = tetraphenylporphyrin).



15

(**15**) is prepared from the ligand and [{(η^5-C_5H_5)Fe(CO)$_2$(CS)}$^+$] in acetone.[84] For the related [{(η^5-C_5H_5)Fe(CO)(CS)}$^-$], reaction with Ph_3SnCl eliminates chloride, giving

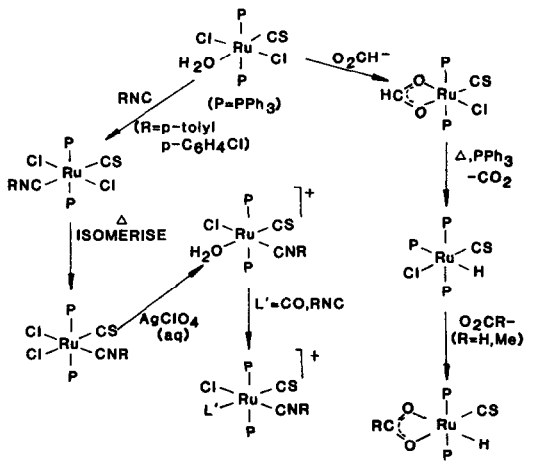
$$[(\eta^5\text{-}C_5H_5)Fe(CO)(CS)(SnPh_3)].^{85}$$

Petz has reacted [Fe(CO)$_4$(CS)] with $HgCl_2$ and Hg^{2+}(aq) to yield, respectively, [(CO)$_4$(CS)Fe → $HgCl_2$] containing an iron to mercury donor bond and polymeric [Hg{Fe(CO)$_3$(CS)}] in which Fe–Hg interactions are proposed to link the structure. The former is converted to the latter by H_2O.[86]

The porphyrin species [Fe(OEP)(CS)] is ligated *trans*- to CS by piperidine or 1-methyl-imidazole.[21] Addition of S^{n}Bu$^-$ to [Fe(TPP)(CS)] is reversible, the adduct stable only at low temperature,[87,88] and electrochemical modifications of [Fe(TPP)(CS)][87,88] are described in Fig. 14. A number of ligands form adducts of [Fe(TPP)(CS)] to give the six-coordinate [Fe(TPP)(CS)L] (L = py, ^{i}PrNH$_2$, *N*-methylimidazole, morpholine, PEt_3, MeOH or EtOH).[62]

Reacting PPh_3 with [Ru(CO)$_3$(CS)Cl$_2$] displaces CO to produce [Ru(CO)$_2$(CS)Cl$_2$(PPh$_3$)].[54] Chloride is also displaced by CyNC which yields [{Ru(CO)$_2$(CS)(CNCy)$_2$Cl}$^+$], as occurs on using [$Ph_2AsC_2H_4AsPh_2$] to yield [{Ru(CO)$_2$($Ph_2AsC_2H_4AsPh_2$)(CS)Cl}$^+$].[54] Both are isolated as BPh_4^- salts.

Much of the extensive work which Roper and co-workers have performed with *trans*-[M(PPh$_3$)$_2$(CS)L$_n$] (M = Ru or Os) species has been substitution chemistry with the L$_n$ ligands.[13,26,89–91] These reaction series begin with [MCl$_2$(CS)L(PPh$_3$)$_2$] (M = Ru, L = H_2O; M = Os, L = PPh_3) in which L is labile. Scheme 4 illustrates the reactions of [RuCl$_2$(CS)(H_2O)(PPh$_3$)$_2$],[13,26] to which the osmium cases are related. Conversion of [OsCl$_2$(CS)(PPh$_3$)$_3$] to [{OsCl(CS)(CO)(CNR)(PPh$_3$)$_2$}$^+$·ClO_4^-] (R = *p*-tolyl) is analogous to the ruthenium case[89] (refer to Scheme 4). Attack by RNC displaces PPh_3,



Scheme 4. CS complexes derived from [RuCl$_2$(CS)(H_2O)(PPh$_3$)$_2$] by ligand substitution.

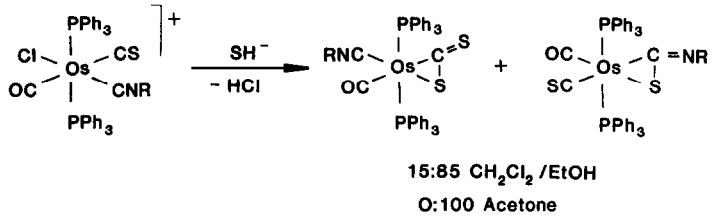


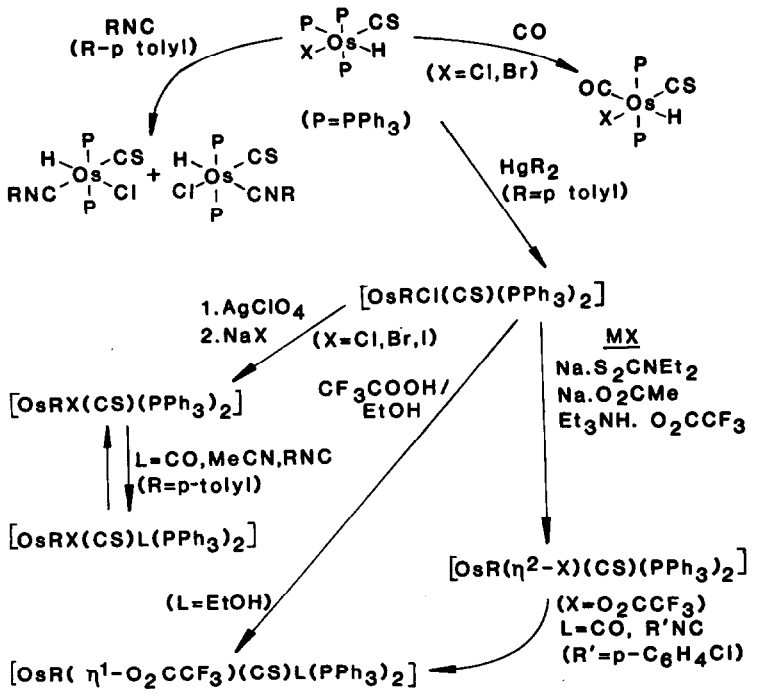
Fig. 15. The alternative sites of SH^- attack on $[\{OsCl(CS)(CO)(CNR)(PPh_3)_2\}^+]$ (R = *p*-tolyl).

giving $[OsCl_2(CS)(CNR)(PPh_3)_2]$ from which $AgClO_4$ removes Cl^- producing $[OsCl(CS)(CNR)(OClO_3)(PPh_3)_2]$; CO then displaces ClO_4^- to give the product. The analogous coordinated ClO_4^- species was proposed in the ruthenium system earlier[13] rather than H_2O ligation following $AgClO_4$ usage.

The osmium product, $[\{OsCl(CS)(CO)(CNR)(PPh_3)_2\}^+ \cdot ClO_4^-]$, reacts with SH^- at either the CS or CNR ligands to give $[Os(CS)(CO)(\eta^2\text{-}CS \cdot NR)(PPh_3)_2]$ or $[Os(CO)(CNR)(\eta^2\text{-}CS_2)(PPh_3)_2]$. The former is favoured, the ratio being solvent-dependent (Fig. 15).[89]

Other reactions of $[OsCl_2(CS)(PPh_3)_3]$ include the use of OH^- in EtOH which produces $[OsHCl(CS)(PPh_3)_3]$ or OH^- in $MeOCH_2CH_2OH$ with both of these to give $[OsH_2(CS)(PPh_3)_3]$.[90] The stepwise introduction of hydride can be reversed using HCl in stoichiometric or excess quantities for the mono- or dichloro species.[90] Also, $[OsH_2(CS)(PPh_3)_3]$ and HBr give $[OsHBr(CS)(PPh_3)_3]$.[90] The compounds $[OsHX(CS)(PPh_3)_3]$ (X = Cl or Br), containing *mer*-$(PPh_3)_3$ and *cis*-(H)(CS) groups, are a starting point for various reactions.[90,91] This substitution chemistry is shown in Scheme 5.

(d) Co *triad*. For Rh and Ir species, the reaction pathways begin with *trans*-$[MCl(CS)(PPh_3)_2]$ (M = Rh or Ir). In less polar solvents (e.g. $CHCl_3$) phosphine exchange occurs to give *trans*-$[MCl(CS)(PR_3)_2]$ (M = Rh; $R_3 = Me_2Ph$,[92] or Cy_3;[92,93] M = Ir; R = Cy[94]), while reaction with RLi or RMgX produces $[MR(CS)(PPh_3)_2]$ (M = Rh or Ir; R = C_6F_5 or C_6Cl_5).[95] For $[RhR(CS)(PPh_3)_2]$ (R = C_6F_5 or C_6Cl_5), HCl converts this back to $[RhCl(CS)(PPh_3)_2]$. However, the Ir analogues undergo a number of oxidative additions to form $[IrR(X)(Y)(CS)(PPh_3)_2]$ (R = C_6Cl_5; XY = HCl: R = C_6F_5; XY = HCl, Br_2, I_2 or $HgCl_2$), the addition of HCl being reversed by refluxing $[IrR(H)(Cl)(CS)(PPh_3)_2]$ in EtOH.[95]



Scheme 5. CS complexes derived from *mer*-$[OsHX(CS)(PPh_3)_3]$ (X = Cl or Br) by ligand substitution.

Substitution of Cl^- by $C_5H_5^-$ is achieved for $[MCl(CS)(PPh_3)_2]$ (M = Rh or Ir).[96] The resulting $[(\eta^5\text{-}C_5H_5)M(PPh_3)(CS)]$ react with halogens to form $[\{(\eta^5\text{-}C_5H_5)M(PPh_3)X(CS)\}^+ \cdot X^-]$ (X = Cl, Br or I).[96] For M = Rh, the reaction is performed at −78°C, the room-temperature reaction giving $[(\eta^5\text{-}C_5H_5)Rh(PPh_3)X_2]$, and $[\{(\eta^5\text{-}C_5H_5)Rh(PPh_3)X(CS)\}^+ \cdot X^-]$ is stable only at low temperature. Exchange of X^- by BPh_4^- increases stability somewhat. With dry HCl, $[(\eta^5\text{-}C_5H_5)Ir(PPh_3)(CS)]$ forms

$$[\{(\eta^5\text{-}C_5H_5)Ir(PPh_3)H(CS)\}^+ \cdot Cl^-],$$

but the Rh analogue eliminates the $\eta^5\text{-}C_5H_5$ ligand to give $[\{Rh(\mu\text{-}Cl)(CS)(PPh_3)\}_2]$, the dimeric nature indicated by its reaction with PPh_3 to regenerate $[RhCl(CS)(PPh_3)_2]$.[96] The sequential reaction of $ClCH_2CN$ and $NaBPh_4$ with $[(\eta^5\text{-}C_5H_5)Ir(PPh_3)(CS)]$ produces

$$[\{(\eta^5\text{-}C_5H_5)Ir(PPh_3)(CH_2CN)(CS)\}^+ \cdot BPh_4^-]$$

which indicated that $[\{(\eta^5\text{-}C_5H_5)Ir(PPh_3)Me(CS)\}^+ \cdot I^-]$ is the likely initial product of MeI addition which produces $[\{(\eta^5\text{-}C_5H_5)Ir(PPh_3)I\{C(S)SMe\}\}^+ \cdot I^-]$.[96]

In polar solvents which can ligate the metal center, ionization of $[RhCl(CS)(PPh_3)_2]$ occurs. Thus, $[RhCl(CS)(PPh_3)_2]$ in MeOH or Et_2O reacts with phosphorus-donor ligands to form $[\{Rh(CS)L_n\}^+]$ isolated as the BPh_4^- or PF_6^- salts [$n = 3$; L = PMe_2Ph, PEt_2Ph or $PPh(OPh)_2$: $n = 4$; L = $PMePh_2$, $PPh_2(OMe)$, $PPh(OMe)_2$, $PPh(OEt)_2$ or $\frac{1}{2}$dppe].[97] Similarly, $[\{Ir(CS)(dppe)_2\}^+]$ results from $[IrCl(CS)(PPh_3)_2]$.[94]

Uson and co-workers have furthered the chloride removal chemistry, using $AgClO_4$ to abstract AgCl. Earlier work in the presence of acetone indicated that $[\{Rh(CS)(PR_3)_2(Me_2CO)_n\}^+ \cdot ClO_4^-]$ (R = Ph or Cy) results from $[RhCl(CS)(PR_3)_2]$.[98,99] For R = Ph, donor ligands displace acetone to give

$$[\{Rh(CS)(PPh_3)_2L\}^+ \cdot ClO_4^-]$$

[monodentate L = py, 4-Et-py, 2-Et-py or PPh_3; bidentate L = bipy, phen or $o\text{-}C_6H_4(CN)_2$].[98] Without acetone, in CH_2Cl_2 solution,

$$[Rh(OClO_3)(CS)(PCy_3)_2]$$

is formed which converts to

$$[\{Rh(CS)(PCy_3)_2(Me_2CO)\}^+ \cdot ClO_4^-]$$

reversibly on addition and removal of acetone.[92] This coordinated ClO_4^- is displaced by donor ligands yielding $[\{Rh(CS)(PCy_3)_2L\}^+ \cdot ClO_4^-]$ [monodentate L = py, 4-Me-Py, phthaln, $p\text{-}(MeO)C_6H_4CN$ or $o\text{-}ClC_6H_4CN$; bidentate L = bipy or phen] or dppe giving a mixture of $[\{Rh(CS)(dppe)_2\}^+]$ and $[\{Rh(CS)(PCy_3)(dppe)\}^+]$.[92] The mixed-phosphine species $[Rh(OClO_3)(CS)(PPh_3)(PCy_3)]$ and $[\{Rh(CS)(PPh_3)_2(PCy_3)\}^+ \cdot ClO_4^-]$ result from reacting $[RhCl(CS)(PPh_3)_2]$ and $AgClO_4$ with PCy_3 present.[92] These form the donor ligand adducts

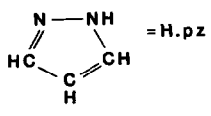
$$[\{Rh(CS)(PCy_3)(PPh_3)L\}^+ \cdot ClO_4^-]$$

[L = py, bipy, phen, phthaln or $P(OPh)_3$] and

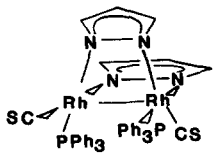
$$[\{Rh(CS)(PPh_3)_2L\}^+ \cdot ClO_4^-]$$

(L = py or bipy) respectively.

The pz ligands have been introduced to Rh-(CS) species by two routes (Fig. 16). The parent H · pz compound is illustrated (**16**). From $[RhCl(CS)(PR_3)_2]$ (R = Ph or Cy) and Na · L (L = pz or 3,5-Me_2-pz), $[Rh(CS)L(PR_3)_2]$ results, which is unstable when R = Ph and dimerizes to $[\{Rh(\mu\text{-}L)(CS)(PPh_3)\}_2]$ (**17**) with PPh_3 loss.[100] Using HL and $[\{Rh(CS)(PR_3)_2(Me_2CO)_n\}^+ \cdot ClO_4^-]$ gives



16



17

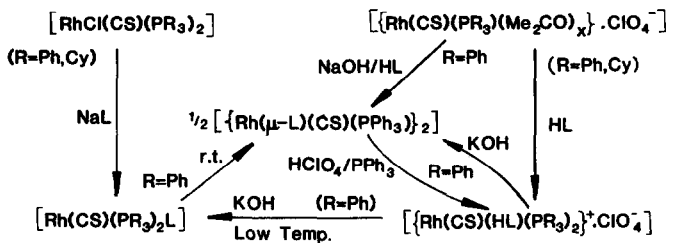


Fig. 16. Preparation and interconversions of Rh–CS–L systems (L = pyrazolate ligand).

$[\{Rh(CS)(HL)(PR_3)_2\}^+ \cdot ClO_4^-]$ (R = Ph; L = pz, 3-Me-pz or 3,5-Me_2-pz: R = Cy; L = pz or 3,5-Me_2-pz) whereas use of NaOH–HL when R = Ph proceeds to the dimer (**17**).[99] Base treatment of $[\{Rh(CS)(HL)(PPh_3)_2\}^+ \cdot ClO_4^-]$ causes the dimer (**17**) to form, this reaction being reversed by $HClO_4$ and PPh_3.[99] The py-bridged mixed bimetallic $[\{(R_3P)_2(CS)Rh(\mu\text{-}L)Au(PPh_3)\}^+ \cdot ClO_4^-]$ is formed from $[\{Rh(CS)(PPh_3)_2(Me_2CO)_n\}^+ \cdot ClO_4^-]$ and [Au(pz)(PPh_3)].[99]

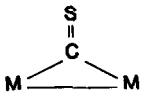
Turning to $[IrCl(CS)(PR_3)_2]$, other reactions include, when R = Ph, $[IrH(CS)(PPh_3)_3]$ formation using $NaBH_4$ and PPh_3,[31] 1 : 1 adducts with $[C_2(CN)_4]$ or fumaronitrile,[101] and 1 : *n* adducts with BX_3 (X = Cl or Br).[101] Attack by NO^+ yields $[\{IrCl(CS)(NO)(PR_3)_2\}^+]$ (R = Ph or Cy) and by CO gives $[\{Ir(CO)_2(CS)(PR_3)_2\}^+ \cdot Cl^-]$ (R = Ph or Cy), this product reacting with OMe^- forming [Ir(CO)(CS)$(PR_3)_2$(COOMe)] (R = Ph or Cy) or H_2 forming $[\{Ir(CO)_2(CS)(H)_2(PCy_3)_2\}^+ \cdot Cl^-]$.[94]

The only cobalt thiocarbonyl species which undergoes modification remote from the CS ligand is $[(\eta^5\text{-}C_5H_5)Co(PPh_3)(CS)]$. This forms adducts with HgX_2 (X = Cl or Br) in which there is a Co–Hg interaction.[23] Rhodium and iridium analogues are known.[96]

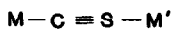
In summary, there are a large number of modification reactions of thiocarbonyl complexes. In a sense, it is the most prevalent synthetic method for terminal thiocarbonyl containing complexes. That other ligands are often substituted in preference to CS is indicative of its stability as a ligand. This point will be discussed further.

II.2. BRIDGING CS LIGANDS—PREPARATIVE METHODS

The thiocarbonyl ligand is known to bridge two metal centers in two ways, namely the thioketonic (μ-CS) (**18**) and linear (σ-C · σ-S) (**19**) bonding modes.



18



19

i. Linear bridging (σ-C · σ-S)

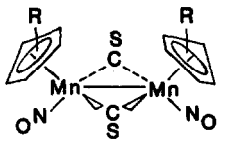
The few examples arise from reactions of *cis*-$[W(CO)(CS)(dppe)_2]$ with electrophilic metal compounds. The only case in which two transition-metal centers are linked is $[(dppe)_2(CO)W(\sigma\text{-}C \cdot \sigma\text{-}S)W(CO)_5]$ obtained by displacing acetone from $[W(CO)_5(Me_2CO)]$ on reaction with *cis*-$[W(CO)(CS)(dppe)_2]$.[70,73] This thiocarbonyl species also forms S-donor adducts to Ag^+ or HgX_2 (X = Cl or I) to give $[\{(dppe)_2(CO)W(\sigma\text{-}C \cdot \sigma\text{-}S)\}_2Ag^+]$ and $[(dppe)_2(CO)W(\sigma\text{-}C \cdot \sigma\text{-}S)HgX_2]$.[70,73] In all cases the sulphur donation is readily displaced by PPh_3 to regenerate *cis*-$[W(CO)(CS)(dppe)_2]$.[70,73] In the preceding section, it was noted that HgX_2 does not form adducts with other terminal CS complexes but rather shows M → HgX interactions,[23,86] oxidative addition giving (X)(HgX) ligands[95] or halide elimination forming an (HgX) ligand.[77]

From their work on these (σ-C · σ-S) species and on the reactivity of other $[L_nW(CS)]$ complexes with assorted electrophiles (see Section III.3.i),[70,73,74] Dombek and Angelici[70,73,74] suggested that a C—S stretching frequency, ν(CS), of below 1200 cm^{-1} is needed for sulphur donation to electrophiles. Thus, *cis*-$[W(CO)(CS)(dppe)_2]$, with ν(CS) at 1161 cm^{-1}, forms the linear bridging compounds, whereas *mer*-$[W(CO)_3(CS)(dppe)]$, with ν(CS) at 1215 cm^{-1}, does not. So, the ligand array must maintain a high electron density at the metal to encourage π-back donation to the CS ligand and make

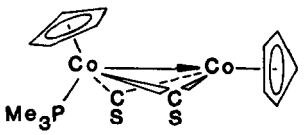
the sulphur more nucleophilic for donation to electrophiles, when ν(CS) will be below 1200 cm^{-1}. This criterion is upheld in the formation of other CS sulphur adducts (see Sections II.3 and III.2).

ii. Thioketonic bridging (μ-CS)

(a) *Formation from monometallic compounds.* Syntheses mostly use terminal CS complexes as a starting material. Some reactions are a dimerization of sorts, with $[(\eta^5\text{-}C_5H_4R)Mn(NO)(CS)I]$ (R = H or Me) reacting with Zn dust to remove iodine and give $[\{(\eta^5\text{-}C_5H_4R)Mn(NO)(\mu\text{-}CS)\}_2]$ (**20**),[82] reduction of $[\{(\eta^5\text{-}C_5H_5)M(CO)_2(CS)\}^+]$ (M = Fe or Ru) by NaH causing CO loss in forming $[\{(\eta^5\text{-}C_5H_5)(CO)M(\mu\text{-}CS)\}_2]$ (M = Fe[102] or Ru[9]), and $[(\eta^5\text{-}C_5H_5)Co(PMe_3)(CS)]$ and CH_2I_2 reacting to produce $[(\eta^5\text{-}C_5H_5)(PMe_3)Co(\mu\text{-}CS)_2Co(\eta^5\text{-}C_5H_5)]$ (**21**).[103] This cobalt compound results when $[(\eta^5\text{-}C_5H_5)Co(PMe_3)(\eta^2\text{-}CSeS)]$ is allowed to stand in toluene solution,[6] the mechanism of formation being unclear for either route. An X-ray diffraction study showed a non-planar $Co_2(\mu\text{-}CS)_2$ core in which a Co → Co donor bond allows both centers to achieve an 18-electron configuration.[103]



20



21

On reacting $[\{(\eta^5\text{-}C_5H_5)Ru(CO)_2(CS)\}^+]$ with NaH, a secondary product is

$$[\{(\eta^5\text{-}C_5H_5)(CO)Ru\}_2(\mu\text{-}CO)(\mu\text{-}CS)].^9$$

Its iron analogue results in good yield from

$$[\{(\eta^5\text{-}C_5H_5)Fe(CO)_2\}^-Na^+]$$

and $[(PhO)_2CS]$ in 2:1 ratio through OPh^- elimination, with $[(\eta^5\text{-}C_5H_5)Fe(CO)_2\{CS(OPh)\}]$ produced with a 1:1 ratio.[85,104] In solution $[\{(\eta^5\text{-}C_5H_5)(CO)M\}_2(\mu\text{-}CS)(\mu\text{-}CE)]$ (M = Fe or Ru, E = O or S) all exist as interconverting mixtures of *cis-* and *trans*-isomers of $(\eta^5\text{-}C_5H_5)$ ligands about the M—M bond,[9,85,102,104] although crystal structures of both iron cases show the *cis*-isomer.[102,105]

Examples of heterobimetallic (μ-CS) complexes are made by reacting a terminal CS species with a metal complex from which a labile ligand is readily lost. The interaction of $[(\eta^5\text{-}C_5H_5)M(CO)_2(CS)]$ (M = Mn or Re) with $[Pt(PR_3)_2(C_2H_4)]$ displaces C_2H_4 to produce

$$[(\eta^5\text{-}C_5H_5)(CO)_2M(\mu\text{-}CS)Pt(PR_3)_2]$$

(M = Mn, R_3 = Me_2Ph or $MePh_2$; M = Re, R_3 = Me_2Ph).[106,107] When M = Mn and R_3 = $MePh_2$, X-ray crystallography indicates a structure (**22**) with a semibridging CO which NMR spectroscopy indicates as the low-temperature solution structure for all cases. At higher temperatures, a fluxional process occurs involving bridge ⇌ terminal (CO)(CS) site exchange.[106,107]

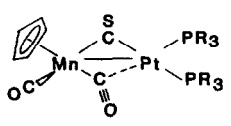
In an equimolar reaction, $[(\eta^5\text{-}C_5H_5)Co(PMe_3)(CS)]$ displaces THF from

$$[(\eta^5\text{-}C_5H_5)Mn(CO)_2THF)]$$

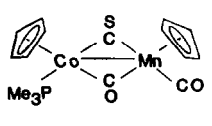
to give

$$[(\eta^5\text{-}C_5H_5)(PMe_3)Co(\mu\text{-}CS)(\mu\text{-}CO)Mn(CO)(\eta^5\text{-}C_5H_5)]$$ (**23**).[108]

Larger amounts of the Mn reagent lead to a sulphur-bound $(\eta^5\text{-}C_5H_5)Mn(CO)_2$ adduct of this product, which is displaced by PMe_3 to regenerate **23**.[108]



22



23

It is interesting to note that the terminal CS complexes used to form these heterobimetallic systems,[4,20] or some closely related analogues,[23] show ν(CS) above 1200 cm^{-1} and do not form stable linear (σ-C · σ-S) bridges, in line with the proposal of Dombek and Angelici[70,73,74] (see Section II.2.i). However, many of the bimetallic species with single (μ-CS) ligands do form sulphur-donor adducts to electrophilic centers and display ν(CS) below 1200 cm^{-1}, which is in agreement with the Dombek–Angelici proposal. This reactivity is discussed in Sections II.3.i and III.3.ii.

(b) *Carbonyl substitution reactions of* $[\{(\eta^5\text{-}C_5H_5)(CO)Fe\}_2(\mu\text{-}CS)(\mu\text{-}CE)]$ (E = O *or* S). Single carbonyl substitution in $[\{(\eta^5\text{-}C_5H_5)(CO)Fe\}_2(\mu\text{-}CO)(\mu\text{-}CS)]$ occurs under reflux conditions with 1–2 equivalents of certain ligands. In MeCN solvent, phosphine substitution yields

$$[\{(\eta^5\text{-}C_5H_5)Fe\}_2(CO)L(\mu\text{-}CO)(\mu\text{-}CS)]$$

[L = PEt_3, PMe_2Ph, $PMePh_2$ or $P(OMe)_3$] as a mixture of *cis-* and *trans-*(η^5-C_5H_5) isomers.[109] Isocyanide ligands substitute for CO and introduce the possibility of this ligand occupying a bridging position. Under benzene reflux, $[(\eta^5\text{-}C_5H_5)_2Fe_2(CO)_2(CS)(CNR)]$ (R = Me, Et, ^{i}Pr or ^{t}Bu) are formed which NMR spectroscopy shows to be present as interconverting (μ-CO)(μ-CS) and (μ-CNR)(μ-CS) isomers with both *cis-* and *trans-*(η^5-C_5H_5) ring orientations, the *cis-*$[\{(\eta^5\text{-}C_5H_5)Fe\}_2(CO)(CNR)(\mu\text{-}CO)(\mu\text{-}CS)]$ isomer being favoured increasingly as R becomes more bulky.[110] In refluxing THF, MeNC gives $[(\eta^5\text{-}C_5H_5)_2Fe_2(CO)_2(CS)(CNMe)]$, but in MeCN solvent the disubstituted product $[(\eta^5\text{-}C_5H_5)_2Fe_2(CO)(CS)(CNMe)_2]$ results, mostly as the (μ-CS)(μ-CNMe) isomer with a little of the (μ-CO)(μ-CS) isomer.[109] Introducing two MeNC ligands by UV irradiation is said to give only

$$[\{(\eta^5\text{-}C_5H_5)Fe\}_2(CO)(CNMe)(\mu\text{-}CS)(\mu\text{-}CNMe)].^{110}$$

Substitution of CO in $[\{(\eta^5\text{-}C_5H_5)(CO)Fe(\mu\text{-}CS)\}_2]$ by MeNC leads to the

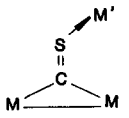
$$[\{(\eta^5\text{-}C_5H_5)Fe(\mu\text{-}CS)\}_2(CO)(CNR)]$$

isomer.[110]

II.3. CS LIGANDS COORDINATED TO THREE OR MORE METAL CENTERS—PREPARATIVE METHODS

i. (μ-C · σ-S) *bonding*

This bonding mode links three metal centers (**24**), wherein the sulphur of a (μ-CS) ligand forms a donor bond to another metal center.



24

Quick and Angelici[111] identified both transition- and non-transition-metal adducts at the sulphur of

$$[\{(\eta^5\text{-}C_5H_5)(CO)Fe\}_2(\mu\text{-}CO)(\mu\text{-}CS)].$$

From a *cis–trans* mixture, the *cis-*(η^5-C_5H_5) adduct is favoured in the products

$$[\{(\eta^5\text{-}C_5H_5)(CO)Fe\}_2(\mu\text{-}CO)\{\mu\text{-}C\cdot\sigma\text{-}SML_n\}]$$

[ML_n = $M'(CO)_5$ (M' = Cr or W), $\{(\eta^5\text{-}C_5H_5)Fe(CO)_2\}^+$, HgX_2 (X = Cl, Br or I), $HgMe^+$], the labile Me_2CO or THF ligands having been displaced from the transition-metal compounds $[M'(CO)_5(Me_2CO)]$ and $[\{(\eta^5\text{-}C_5H_5)Fe(CO)_2(THF)\}^+ \cdot BF_4^-]$. Spectroscopic evidence was obtained for analogous adducts on reaction with BX_3 (X = F, Cl or Br), $AlCl_3$,

$$[Fe(CO)_4(THF)],\quad [Mo(CO)_5(Me_2CO)],\quad [W(CO)_4(CS)(Me_2CO)]$$

and

$$[\{M(CO)_5(MeCN)\}^+ \cdot PF_6^-]$$

(M = Mn or Re).[111] An earlier report indicated that some

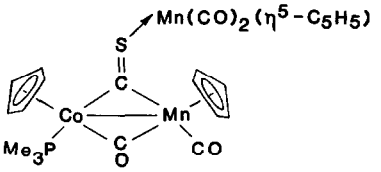
$$[\{\{(\eta^5\text{-}C_5H_5)(CO)Fe\}_2(\mu\text{-}CO)\{\mu\text{-}C\cdot\sigma\text{-}SFe(CO)_2(\eta^5\text{-}C_5H_5)\}\}^+\cdot BF_4^-]$$

results when

$$[\{(\eta^5\text{-}C_5H_5)(CO)Fe\}_2(\mu\text{-}CO)(\mu\text{-}CS)]$$

is exposed to O_2 and HBF_4.[85]

When $[(\eta^5\text{-}C_5H_5)Co(PMe_3)(CS)]$ and two equivalents of $[(\eta^5\text{-}C_5H_5)Mn(CO)_2(THF)]$ interact, the product is $[(\eta^5\text{-}C_5H_5)(PMe_3)Co(\mu\text{-}CO)\{\mu\text{-}C\cdot\sigma\text{-}SMn(CO)_2(\eta^5\text{-}C_5H_5)\}Mn(\eta^5\text{-}C_5H_5)(CO)]$ (**25**).[108] As



25

a 1:1 ratio yields $[(\eta^5\text{-}C_5H_5)(PMe_3)Co(\mu\text{-}CO)(\mu\text{-}CS)Mn(\eta^5\text{-}C_5H_5)(CO)]$ cleanly,[108] the 1:2 reaction seems likely to proceed via this compound.

ii. (μ_3-CS) *bonding and* (μ_3-C·σ-S) *derivatives*

One series of examples of the (μ_3-CS) ligand exists in $[(\eta^5\text{-}C_5H_5)_{3-x}(\eta^5\text{-}C_5H_4Me)_xCo_3(\mu_3\text{-}S)(\mu_3\text{-}CS)]$ (x = 0–3).[6,23,112,113] The various routes to $[\{(\eta^5\text{-}C_5H_5)Co\}_3(\mu\text{-}S)(\mu_3\text{-}CS)]$ are summarized in Fig. 17. The intermediacy of $[(\eta^5\text{-}C_5H_5)CoL(\eta^2\text{-}CS_2)]$ is indicated by its use as a starting material, and that in reactions between $[(\eta^5\text{-}C_5H_5)Co(CO)L]$ and CS_2 the yield of $[(\eta^5\text{-}C_5H_5)CoL(\eta^2\text{-}CS_2)]$ decreases and of the Co_3 species increases with reaction time.[23] The routes reported to

$$[(\eta^5\text{-}C_5H_5)_{3-x}(\eta^5\text{-}C_5H_4Me)_xCo_3(\mu_3\text{-}S)(\mu_3\text{-}CS)]$$

are the reflux in toluene of, for $x = 1$,

$$[(\eta^5\text{-}C_5H_4Me)Co(PMePh_2)(\eta^2\text{-}CS_2)] \quad \text{and} \quad [(\eta^5\text{-}C_5H_5)Co(CO)_2]$$

(1:2); for $x = 2$, use the reverse η^5 groups; and for $x = 3$, use $[(\eta^5\text{-}C_5H_4Me)Co(PPh_3)(\eta^2\text{-}CS_2)]$ alone.[23]

These (μ_3-CS) ligands can coordinate other metal centers via the sulphur. Thus,

$$[\{(\eta^5\text{-}C_5H_5)Co\}_3(\mu_3\text{-}S)(\mu_3\text{-}CS)] \quad \text{reacts with} \quad [Cr(CO)_5(THF)]$$

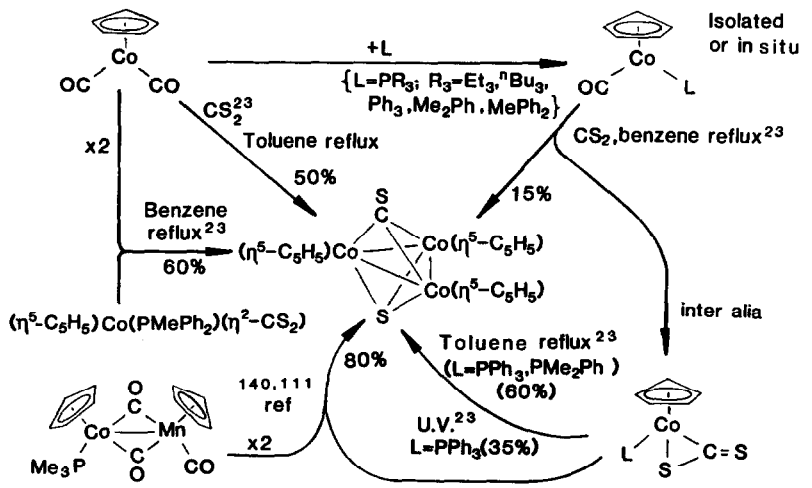
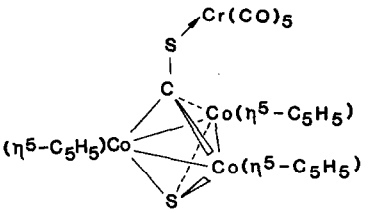


Fig. 17. The assorted reactions which give rise to $[\{(\eta^5\text{-}C_5H_5)Co\}_3(\mu_3\text{-}S)(\mu_3\text{-}CS)]$.

to give

$$[\{(\eta^5\text{-}C_5H_5)Co\}_3(\mu_3\text{-}S)\{\mu_3\text{-}C\cdot\sigma\text{-}SCr(CO)_5\}]$$

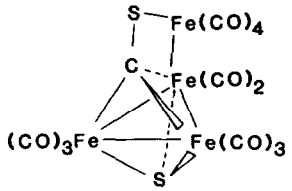
(**26**)[112,113] and forms Lewis acid–base pairs with $[ZnCl_2\cdot 2H_2O]$, $[CdI_2\cdot 2H_2O]$ or HgX_2 (X = Cl, Br or I)[23] as does Ag^+ with $[\{(\eta^5\text{-}C_5H_4Me)Co\}_3(\mu_3\text{-}S)(\mu_3\text{-}CS)]$.[23] Similar adducts to nonmetallic moieties are discussed in Section III.3.



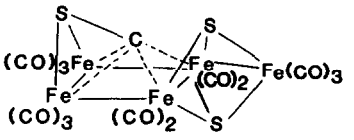
26

iii. Other $M_4(CS)$ *interactions*

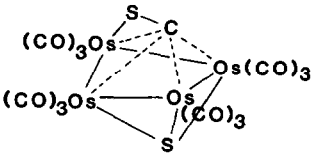
Three more ways are known for a CS ligand to interact with four metal atoms, the single examples of each characterized structurally by X-ray crystallography. The compounds are $[Fe_4(CO)_{12}(CS)S]$ (**27**)[50,114] containing a $(\mu_3\text{-}C\cdot\sigma\text{-}S)$ moiety, $[Fe_5(CO)_{13}(CS)S_2]$ (**28**)[50,115] with a $(\mu_4\text{-}C\cdot\mu_2\text{-}S)$ group and $[Os_4(CO)_{12}(CS)S]$ (**29**)[116] with a $(\mu_4\text{-}C\cdot\sigma\text{-}S)$ unit. The iron compounds are low-yield products of



27



28



29

the reaction of $[Fe_3(CO)_{12}]$ and excess CS_2 at elevated temperature under a modest CO–Ar pressure,[50,114,115] whereas an 8% yield of the osmium compound results from $[Os_6(CO)_{18}]$ and excess CS_2 at rather higher temperature and pressure.[116] For these clusters to be electron precise, the CS ligand formally donates four electrons in the Fe_4 and Os_4 cases but six in the Fe_5 example. This bonding is discussed more in Section IV.

III.1. REACTIVITY OF THE CS LIGAND

Modification reactions of CS complexes which do not involve the CS ligand were discussed in Sections II.1.v and II.2.ii. In this section, reactions occurring at the CS ligand are considered. This reactivity may be categorized into, firstly, CS substitution; secondly, attack by electrophiles at the CS sulphur; thirdly, nucleophilic attack at the CS carbon; fourthly, insertion reactions of the CS ligand; and lastly, the incidental reactions which do not correspond directly to these categories. Each category is discussed in turn.

III.2. SUBSTITUTION REACTIONS OF CS LIGANDS

There are few examples of displacement of a CS group from a metal center. The room-temperature reaction of $[(\eta^5\text{-}C_5H_5)Rh(PPh_3)(CS)]$ with the halogens X_2 (X = Cl, Br or I) causes CS elimination and $[(\eta^5\text{-}C_5H_5)Rh(PPh_3)X_2]$ is formed.[96] Addition of X_2 to $[\{Rh(CS)(PCy_3)_2(py)\}^+\cdot ClO_4^-]$ or $[RhCl(CS)(PCy_3)_2]$ gave spectroscopic evidence for CS ligand elimination, but the products were not characterized.[91] Treatment of $[\{(\eta^5\text{-}C_5H_5)(CO)Fe\}_2(\mu\text{-}CO)(\mu\text{-}CS)]$ with X_2 (X = Br or I) led to traces of $[(\eta^5\text{-}C_5H_5)Fe(CO)_2X]$, although a dimer cleavage is suggested rather than CS displacement as low amounts of $[(\eta^5\text{-}C_5H_5)Fe(CO)(CS)X]$ result also.[85] The porphyrin species [Fe(TPP)Cl] results from

[Fe(TPP)(CS)] and $FeCl_3$.[62] One nonhalogen substitution involves $[Os_3(CO)_7(CS)H_2S_2]$ and PEt_3 when CS is smoothly replaced, the PEt_3 ligand in $[Os_3(CO)_7(PEt_3)H_2S_2]$ occupying the same position on the $M_3(\mu\text{-}S)_2$ core as the CS ligand had done (**11**).[117]

The lack of CS substitution reactions is indicative of the strength of the M–CS interaction. This is discussed in Section IV.

III.3. ELECTROPHILIC ATTACK AT CS SULPHUR

A subset of these reactions, discussed in Sections II.2 and II.3, has another metal center as the electrophile, receiving electron donation from the nucleophilic sulphur. Thus, examples of (σ-C · σ-S), (μ-C · σ-S) and (μ_3-C · σ-S) thiocarbonyl bonding result from terminal, μ_2 and μ_3-CS ligands respectively. Interactions with other electrophiles are now considered for terminal, (μ-CS) and (μ_3-CS) compounds. In many cases, the same compounds react which display reactivity with metallic electrophiles.

i. Terminal CS *ligands*

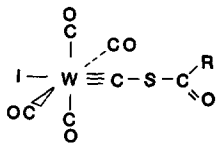
The electrophiles which interact with terminal CS ligands are R^+ (R = alkyl or acyl). Thus, $[\{Mo(CE)(CO)_2L\}^-]$ [E = S or Te, L = $HB(3,5\text{-}Me_2\text{-}C_3HN_2)_3$] with MeI gives

$$[Mo(\equiv CEMe)(CO)_2L].^{64}$$

Similarly, [*trans*-$\{W(CO)_4(CS)I\}^-$] and RX produces

$$\textit{trans}\text{-}[W(CO)_4(CSR)I] \ (RX = MeSO_3F \text{ or } Et_3O \cdot BF_4)$$

whereas acylation giving *trans*-$[W(CO)_4\{CSC(O)R\}I]$ (R = Me or CF_3) (**30**) is accomplished by acetic anhydride with BF_3 or trifluoroacetic anhydride alone.[73,74] Alkylation of *cis*-$[W(CO)(CS)(dppe)_2]$



30

produces [*cis*-$\{W(CO)(CSR)(dppe)_2\}^+X^-$] (R = Me or Et; X = SO_3F and BF_4, respectively), although CF_3SO_3H protonates at the tungsten.[73,74] With $MeSO_3F$,

$$[\{(\eta^5\text{-}C_5H_5)Co(PPh_3)(CSMe)\}^+]$$

results, although the weaker reagent MeI and the reactant $[(\eta^5\text{-}C_5H_5)Co(PPh_3)(CS)]$ do not react.[23] A double addition of MeI occurs to $[Ir(C_6F_5)(CS)(PPh_3)_2]$ producing

$$\textit{trans}\text{-}[Ir(C_6H_5)\{C(SMe)Me\}I_2(PPh_3)_2],$$

which was proposed to go through

$$[\{Ir(C_6H_5)(CSMe)(PPh_3)_2\}^+].^{95}$$

However,

$$[(\eta^5\text{-}C_5H_5)Ir(PPh_3)(CS)]$$

and MeI form

$$[\{(\eta^5\text{-}C_5H_5)Ir(PPh_3)I\{C(SMe)Me\}\}^+ \cdot I^-]$$

when the intermediates

$$[\{(\eta^5\text{-}C_5H_5)Ir(PPh_3)Me(CS)\}^+ \cdot I^-] \quad \text{and} \quad [(\eta^5\text{-}C_5H_5)Ir(PPh_3)I\{C(S)Me\}]$$

are proposed.[96]

Spectroscopic and structural data for the Mo and Co cases[23,64] indicate a large degree of carbyne character, M≡C-SR, to the metal–carbon interaction. In the Mo and W reactants, ν(CS) is below 1200 cm^{-1}, which Dombek and Angelici[70,73,74] suggested as a criterion for sufficient CS sulphur basicity to obtain electron pair donation. However, $[(\eta^5\text{-}C_5H_5)Co(PPh_3)(CS)]$ has ν(CS) at 1275 cm^{-1},[23] the only breakage of the suggested rule (including subsequent discussions).

ii. Bridging (μ-CS) *ligands*

Some bimetallic species with one (μ-CS) ligand are alkylated or arylated at this sulphur. Both

$$[(\eta^5\text{-}C_5H_5)(PMe_3)Co(\mu\text{-}CO)(\mu\text{-}CS)Mn(CO)(\eta^5\text{-}C_5H_5)]$$

(23) and

$$[(\eta^5\text{-}C_5H_5)(CO)_2Mn(\mu\text{-}CS)Pt(PMe_2Ph)_2]$$

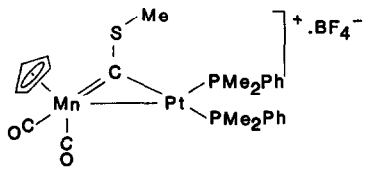
(22) are methylated, by $MeSO_3F$ and $Me_3O\cdot BF_4$, respectively, giving

$$[\{(\eta^5\text{-}C_5H_5)(PMe_3)Co(\mu\text{-}CO)(\mu\text{-}CSMe)Mn(\eta^5\text{-}C_5H_5)\}^+\cdot CF_3SO_3^-]^{108}$$

and

$$[\{(\eta^5\text{-}C_5H_5)(CO)_2Mn(\mu\text{-}CSMe)Pt(PMe_2Ph)_2\}^+\cdot BF_4^-]^{106,107}$$

(31). The (μ-CSMe) ligands are described as bridging methylthiocarbynes, although the CoMn case is drawn with delocalized bonding[108] and MnPt with localized [Mn=C(SMe)—Pt] bonding.[106,107] In



31

the latter, **31**, the CO ligands are terminal whereas one is semi-bridging in the reactant's limiting structure **(22)**.

A broader range of examples result from $[\{(\eta^5\text{-}C_5H_5)(CO)Fe\}_2(\mu\text{-}CO)(\mu\text{-}CS)]$ and organic halides, R.hal. The products

$$[\{\{(\eta^5\text{-}C_5H_5)(CO)Fe\}_2(\mu\text{-}CO)(\mu\text{-}CSR)\}^+]$$

were isolated, usually as PF_6^- salts, after using R.hal (R.hal = MeI, EtI, ^{n}PrI, ^{n}BuI, allyl.Br, $PhCH_2Br$ or EtO_2CCH_2Br), although $MeSO_3F$ or $Et_3O\cdot BF_4$ were also used.[104,109] Ligand exchange leads to

$$[\{(\eta^5\text{-}C_5H_5)_2Fe_2(CO)L(\mu\text{-}CO)(\mu\text{-}CSR)\}^+\cdot PF_6^-]$$

[L = PR'_3 or MeNC; R'_3 = Et_3, Me_2Ph, $MePh_2$ or $(OMe)_3$] which, for L = PEt_3 and R = $PhCH_2$, is accessible by $PhCH_2Br$ and PF_6^- treatment of

$$[(\eta^5\text{-}C_5H_5)_2Fe_2(CO)(PEt_3)(\mu\text{-}CO)(\mu\text{-}CS)].^{109}$$

Methylation of $[(\eta^5\text{-}C_5H_5)_2Fe_2(CO)(CS)(CNMe)_2]$ is reagent-dependent, an excess of MeI giving

$$[\{(\eta^5\text{-}C_5H_5)_2Fe_2(CNMe)(CO)(\mu\text{-}CNMe)(\mu\text{-}CSMe)\}^+]$$

but an excess of $MeSO_3F$ producing

$$[\{(\eta^5\text{-}C_5H_5)_2Fe_2(CNMe)(CO)(\mu\text{-}CNMe_2)(\mu\text{-}CSMe)\}^{2+}].^{109}$$

iii. Triply-bridging (μ_3-CS) *ligands*

The compounds $[\{(\eta^5\text{-}C_5H_4R)Co\}_3(\mu_3\text{-}S)(\mu_3\text{-}CS)]$ are alkylated by R'I to form

$$[\{\{(\eta^5\text{-}C_5H_4R)Co\}_3(\mu_3\text{-}S)(\mu_3\text{-}CSR')\}^+]$$

(R = H; R' = Me, Et or ^{i}Pr:[112,113] R = R' = Me[23]). Reacting $[\{(\eta^5\text{-}C_5H_5)Co\}_3(\mu_3\text{-}S)(\mu_3\text{-}CS)]$ with an equivalent of I_2 gives $[\{\{(\eta^5\text{-}C_5H_5)Co\}_3(\mu_3\text{-}S)(\mu_3\text{-}CSI)\}^+\cdot I^-]$.[23]

III.4. NUCLEOPHILIC ATTACK AT CS CARBON

Reactions have been reported only for terminal CS ligands which are classified by type of nucleophile.

i. Reactions with amines or amides

The reaction types observed are shown in Fig. 18. Primary amines, RNH_2, usually produce an isocyanide ligand through H_2S elimination. Examples, derived from the appropriate amine and terminal CS ligand, include $[W(CO)_5(CNR)]$ (R = Me, ^{n}Bu, ^{t}Bu, Cy, CH_2Ph or CH_2CO_2Et),[71] *cis*-$[W(CO)_4(PPh_3)(CNMe)]$,[71] $[Ir(C_6F_5)(CN\text{-}p\text{-tolyl})I_2(PPh_3)_2]$,[95] $[Fe(TPP)(^nBuNH_2)(CN^nBu)]$, which acquires an $^nBuNH_2$ ligand also,[62]

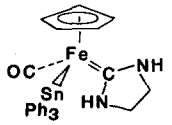
$$[(\eta^5\text{-}C_5H_5)Fe(CO)(CNMe)(SnPh_3)],^{85} \quad [\{(\eta^5\text{-}C_5H_5)Fe(CO)(CNR)(PR'_3)\}^+ \cdot PF_6^-]$$

(R = Me; R′ = Ph, Cy or C_6H_4F: R = Ph or Cy; R′ = Ph)[82] and $[Ru(CO)_2(CNR)Cl_2L]$ (L = CO; R = Ph, Cy or *p*-tolyl: L = PPh_3; R = Cy, *p*-tolyl or *p*-C_6H_4OMe).[54] Similarly,

$$[(\eta^5\text{-}C_5H_5)Fe(CO)(CS)(SnPh_3)]$$

and $H_2NCH_2CH_2NH_2$ eliminate H_2S, producing

$$[(\eta^5\text{-}C_5H_5)Fe(=\overline{CNHCH_2CH_2NH})(CO)(SnPh_3)] \ (\mathbf{32}).^{85}$$



32

The carbene {=C(SH)(NHR)} is a likely intermediate from which H_2S is eliminated. Evidence comes from the reaction of $[Fe(CO)_4(CS)]$ with $[C(NMe_2)_4]$ giving

$$[\{Fe(CO)_4\{C(S)NMe_2\}\}^- \cdot \{C(NMe_2)_3\}^+]$$

which then reacts with Me^+ forming the carbene-containing $[Fe(CO)_4\{C(SMe)NMe_2\}]$.[118]

Unlike its phosphine derivatives,[83] $[\{(\eta^5\text{-}C_5H_5)Fe(CO)_2(CS)\}^+]$ reacts with $MeNH_2$ eliminating H^+ and giving $[(\eta^5\text{-}C_5H_5)Fe(CO)_2\{C(S)NHMe\}]$, a reaction reversed by HCl.[119] Similarly, the secondary amine Me_2NH eliminates H^+ on reaction with $[\{PtCl(CS)(PPh_3)_2\}^+]$ and yields $[PtCl\{C(S)NMe_2\}(PPh_3)_2]$.[61]

Other reactions of secondary amines are $[W(CO)_5(CS)]$ with R_2NH [R = Me or $\frac{1}{2}(CH_2)_5$]. Here, the σ-thioaldehyde complexes $[W(CO)_5\{S{=}CH(NR_2)\}]$ result,[71] presumably through rearrangement of a $\{C(SH)(NR_2)\}$ carbene intermediate.

ii. Reactions with alcohols, alkoxides and water

Excepting the use of water, all examples display OR^- addition to the CS carbon. Thus, $[(\eta^5\text{-}C_5H_5)Fe(CO)_2\{C(S)OR\}]$ (R = Me or Et) results from $[\{(\eta^5\text{-}C_5H_5)Fe(CO)_2(CS)\}^+]$ and OR^-, a reaction reversed by HCl,[119] with the derivatives $[(\eta^5\text{-}C_5H_5)FeL_2\{C(S)OMe\}]$ [L_2 = (CO)(PPh_3) or $(CNMe)_2$] produced by OMe^- attack on the relevant precursors.[83] In EtOH solution, $[(CO)_4(CS)Fe$

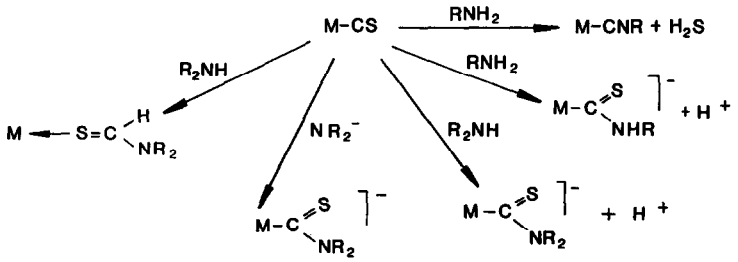


Fig. 18. The types of reaction known between terminal CS ligands and amines (1 and 2°) or amides (NR_2^-).

$\rightarrow HgCl_2$] liberates HCl to form [$(CO)_4Fe(HgCl)\{C(S)OEt\}$], which is obtained directly from [$Fe(CO)_4(CS)$] using $HgCl_2$ in EtOH.[86] Also, the cation [$\{PtCl(CS)(PPh_3)_2\}^+$] and MeOH react giving [$PtCl\{C(S)OMe\}(PPh_3)_2$].[61]

The conversion of a CS ligand to a CO ligand is achieved by H_2O in one case. When [$\{PtCl(CS)(PPh_3)_2\}^+$] and H_2O react, the product is [$\{PtCl(CO)(PPh_3)_2\}^+$]. The carbene group, $\{=C(SH)(OH)\}$, is proposed which eliminates H_2S to form the product.[61]

iii. The use of NCO^-, NCS^-, N_3^- *and* N_2H_4

Azide, N_3^-, converts CS ligands to NCS^- groups in five instances whereby [$\{(\eta^5\text{-}C_5H_5)M(CO)(CS)L\}^+$] (M = Fe[119] or Ru[9], L = CO; M = Fe,[83] L = PPh_3 or PCy_3) or [$W(CO)_5(CS)$][71] are transformed into [$(\eta^5\text{-}C_5H_5)M(CO)L(NCS)$] or [$\{W(CO)_5(NCS)\}^-$]. Initial formation of a $\{C(S)N_3\}^-$ group is proposed, losing N_2 and rearranging to the NCS^- unit.[117] The same iron reactants give [$(\eta^5\text{-}C_5H_5)Fe(CO)L(NCS)$] (L = CO,[117] PPh_3[83] or PCy_3[83]) on reaction with hydrazine when H^+ elimination is proposed to give a $\{C(S)\cdot NHNH_2\}$ intermediate which loses NH_3 and rearranges to the product.[119]

Although NCO^- might react like N_3^- with the elimination of CO rather than N_2, both NCO^- and NCS^- take a different path on reaction with [$\{(\eta^5\text{-}C_5H_5)M(CO)_2(CS)\}^+$] (M = Fe or Ru). The products, [$(\eta^5\text{-}C_5H_5)M(CO)_2(CN)$] (M = Fe[119] or Ru[9]), result by CSE (E = O or S) loss from the initially formed [$(\eta^5\text{-}C_5H_5)M(CO)_2\{C(S)\cdot NCE\}$].

iv. Reactions with EH^- (E = S *or* Se)

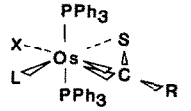
When [$\{MCl(CS)(CO)(CNR)(PPh_3)_2\}^+$] (M = Ru or Os, R = *p*-tolyl) and EH^- (E = S or Se) react, HCl is eliminated and (η^2-CS_2), (η^2-CSSe) or (η^2-CSNR) ligands are obtained. The products are dependent on M and E, so that SeH^- gives both (η^2-CS·Se) and (η^2-CSe·S) coordination isomers for M = Ru, but only (η^2-CSe·S) for M = Os in [$M(\eta^2\text{-}CSSe)(CO)(CNR)(PPh_3)_2$].[13] However, when M = Os, SH^- gives mostly [$Os(\eta^2\text{-}CS\cdot NR)(CO)(CS)(PPh_3)_2$] with some [$Os(\eta^2\text{-}CS_2)(CO)(CNR)(PPh_3)_2$].[89] These reactions are also discussed in Sections II.1.i and v. The mechanism may involve EH^- attack at the CS carbon followed by HCl elimination, although EH^- could substitute for Cl^- giving [$\{M(EH)(CS)(CO)(CNR)(PPh_3)_2\}^+$] which undergoes intramolecular rearrangement with H^+ loss. The former route could lead to all products but the latter could not give (η^2-CS·Se) connectivity from SeH^- attack without further rearrangement.

v. Reactions with other nucleophiles

Reaction of $NaBH_4$ with [$\{IrCl_2(CO)(CS)(PPh_3)_2\}^+$] gives [$IrCl_2(CO)(CHS)(PPh_3)_2$].[120] Formation of the thioformyl group by direct H^- attack at the CS carbon is likely as the Ir reactant has an 18-electron configuration and there is no other change in the ligand array.

III.5. INSERTION REACTIONS OF CS LIGANDS

Examples have been almost exclusive to osmium complexes. Insertion of CS into the Os—aryl bond of [$OsRX(CS)L(PPh_3)_2$] (R = *p*-tolyl: L = CO; X = Cl, Br, I or σ-O_2CCF_3: L = RNC; X = Cl: L = *p*-ClC_6H_4CN; X = O_2CCF_3) on warming produces an η^2-thioacyl ligand in [$OsXL(\eta^2\text{-}CS\cdot R)(PPh_3)_2$] (**33**).[91] Further reactivity of these compounds was demonstrated.[91]



(For L,X,R-see text)

33

On treatment of [$\{Os(CO)(CS)(\eta^2\text{-}CS\cdot NMeR)(PPh_3)_2\}^+$] (R = Me or *p*-tolyl) with $NaBH_4$,

[$Os(CO)(CS)H\{\sigma\text{-}C(S)\cdot NMeR\}(PPh_3)_2$]

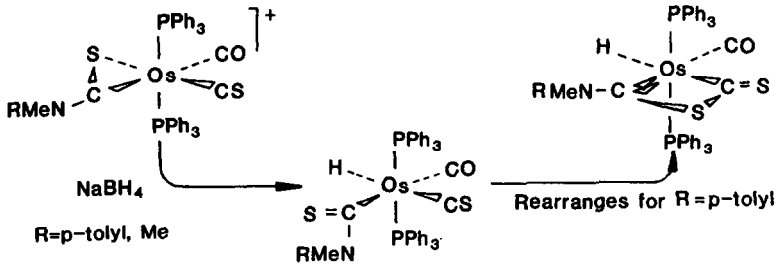


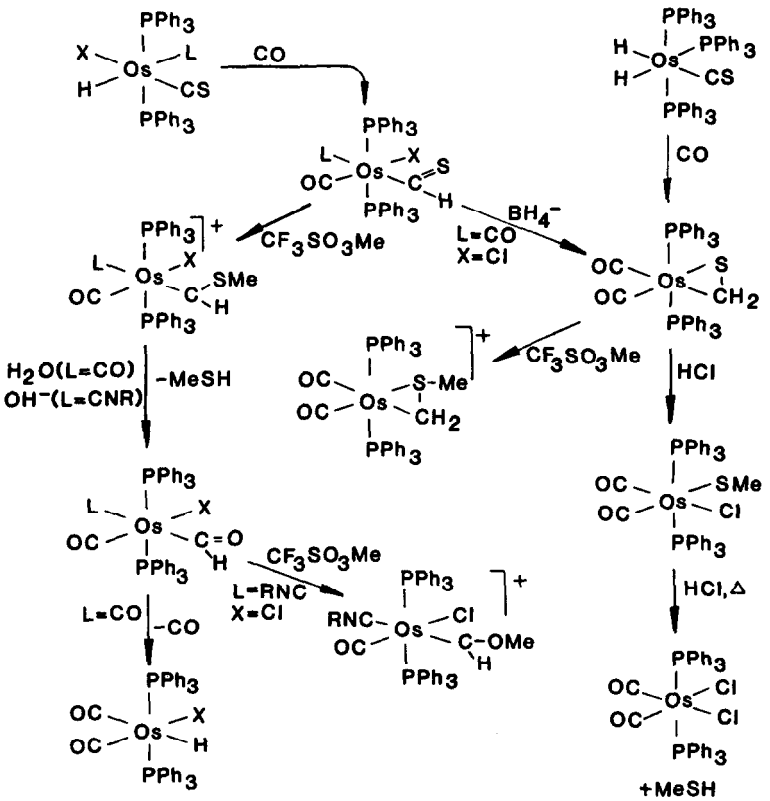
Fig. 19. The reaction of $[\{Os(CO)(CS)(\eta^2\text{-}CS\cdot NMeR)(PPh_3)_2\}^+]$ (R = Me or *p*-tolyl) with $NaBH_4$.

results. When R = *p*-tolyl, thermal rearrangement yields

$$[\overline{Os\{=C(NMeR)\cdot S\cdot C(S)\}}(CO)H(PPh_3)_2]$$

through CS insertion (Fig. 19).[89]

Elevated CO pressure induces CS insertion to the Os–H bond in various compounds. For $[Os(CS)L(H)X(PPh_3)_2]$ (X = Cl; L = PPh_3, CO or CN-*p*-tolyl: X = Br; L = PPh_3 or CO), 40 psig of CO gives $[Os(CHS)(CO)LX(PPh_3)_2]$ (L = CO or CN-*p*-tolyl: when L = PPh_3, CO substitutes).[90] When X = Cl and L = CO, BH_4^- converts the σ-thioformyl ligand to $(\eta^2\text{-}CH_2S)$ forming $[Os(CO)_2(\eta^2\text{-}CH_2S)(PPh_3)_2]$, but this product is accessible also by CO treatment (4 atm, 140°C) of $[Os(CS)H_2(PPh_3)_3]$ when a double insertion occurs.[90] Scheme 6 shows this and some subsequent chemistry, including the remaining steps in CS ligand conversion to MeSH. The cluster species $[Os_3(CO)_7(CS)H_2S_2]$ under CO pressure forms the thioformyl species $[Os_3(CO)_8H(CHS)S_2]$, which also displays reactivity at the (CHS) ligand.[117] The insertion reactions are especially relevant as these comprise thio-analogues of some of the first steps possible in the catalyzed reduction of CO by H_2, especially for MeOH production.



Scheme 6. Reaction pathways using CS insertion to Os–H bonds.

The one nonosmium system is an insertion reaction by inference when $[Ir(CS)H(PPh_3)_3]$ is converted into $[Ir(SMe)H_2(PPh_3)_3]$ under H_2 pressure.[120] Roper and Town[120] proposed that sequential insertion steps occur to Ir–H bonds derived by the oxidative addition of H_2 which are analogous to the characterized osmium sequence. Reaction of $[Ir(SMe)H_2(PPh_3)_3]$ with HCl forms $[IrCl(PPh_3)_3]$ and MeSH, completing the reduction of a CS ligand to MeSH.[120]

III.6. OTHER REACTIONS AT CS LIGANDS

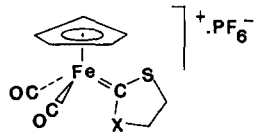
These reactions do not fit obviously into the preceding categories.

Sequential addition of MeLi and Me_3O^+ to $[W(CO)_5(CS)]$ results in low yields of $[W(CO)_5(SMe_2)]$ by an uncertain mechanism.[71] Also at tungsten, LiPh reacts with $[(\eta^5\text{-}C_5H_5)W(CO)(CS)(PPh_3)I]$ eliminating LiI to produce $[(\eta^5\text{-}C_5H_5)W(CO)(CSPh)(PPh_3)]$ in which a carbyne interaction $\{W{\equiv}CSPh\}$ is indicated.[76] Formally, this is nucleophilic attack by Ph^- at the CS sulphur, although a less simple mechanism may operate.

Electrochemical studies of $[Fe(TPP)(CS)]$ show spectroscopic evidence for the reversible conversion by H^+ of $[\{Fe(TPP)(CS)\}^-]$ and $[\{Fe(TPP)(CS)\}^{2-}]$ into $[Fe(TPP)(CHS)]$ and $[\{Fe(TPP)(CHS)\}^-]$.[87,88] The di-iron species, $[\{(\eta^5\text{-}C_5H_5)(CO)Fe\}_2(\mu\text{-}CO)(\mu\text{-}CS)]$, is cleaved by Na–Hg to give $[\{(\eta^5\text{-}C_5H_5)Fe(CO)_2\}^-]$ and $[\{(\eta^5\text{-}C_5H_5)Fe(CO)(CS)\}^-]$,[85] and less cleanly by X_2 (X = Br or I) when traces of $[(\eta^5\text{-}C_5H_5)Fe(CO)_2X]$ and $[(\eta^5\text{-}C_5H_5)Fe(CO)(CS)X]$ are obtained.[85]

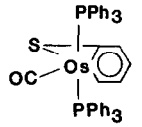
Interacting $[\{(\eta^5\text{-}C_5H_5)Fe(CO)_2(CS)\}^+ \cdot PF_6^-]$ with $[\overline{XCH_2CH_2}]$ (X = NH or S) in the presence of Br^- leads to $[\{(\eta^5\text{-}C_5H_5)Fe(=\overline{C \cdot S \cdot CH_2CH_2X})(CO)_2\}^+ \cdot PF_6^-]$ (**34**).[121] It was proposed that Br^- opens the aziridine or thiirane ring either before or after coordination of X at the CS carbon.[121] However, other mechanisms may operate such as a nucleophilic ring opening by CS sulphur.

An osmabenzene ring is derived from two C_2H_2 molecules, a CS ligand and an osmium atom when C_2H_2 reacts with $[Os(CO)(CS)(PPh_3)_3]$ to give $[\overline{Os\{CH(CH)_3CS\}}(CO)(PPh_3)_2]$ (**35**).[122]



(X=NH,S)

34



35

IV.1. BONDING, SPECTROSCOPIC AND STRUCTURAL PROPERTIES OF CS COMPLEXES

In most discussions of the physicochemical properties of the CS ligand comparisons are made to the carbonyl ligand. The deliberate spectroscopic studies have focussed upon the CS ligand when bonded terminally. For other bonding modes, some observations have been made from the available data which, although valid, are not as wide ranging as those for terminal CS coordination.

This section begins by summarizing the conclusions reached concerning CS bonding to metal centers. A discussion follows of the data derived by each analytical technique, of how these lead to the conclusions on CS bonding and of some other trends which may be noted. In the appendices, ν(CS) IR and ^{13}C NMR data are tabulated where they have not been compiled beforehand.

IV.2. THE NATURE OF CS COORDINATION—A SUMMARY

In broad terms, the terminal CS ligand interacts with a metal center analogously to CO. There is σ-donation of electrons from a filled non-bonding orbital located at the carbon to a vacant metal orbital of σ-symmetry and π-acceptance by a vacant π^* CS orbital from a filled metal orbital of π-symmetry. The M–C–S interaction is linear, the bonding synergic and the ligand π-acid in character.[3,123]

Detailed comparison of the M–CO and M–CS interactions reveals differences. The bonding orbitals of CS π-bonding are sufficiently unstable and high in energy that an appreciable π-donation to

the metal may occur.[124,125] The σ-donor and π-acceptor ability of CS are deemed better than those of CO,[126] but the contribution of the π-donor interaction in tying up metal *d*-orbital electron density should be noted.[125] Overall, this leads to a stronger M–C interaction for M–CS over M–CO.[123] These interactions allow CS to show a "charge-buffering effect" as it can donate and accept more or less electrons as the ligand sphere around the metal is altered.[75,123] As a result, the π-acceptor: $(\pi+\sigma)$-donor ratio is wider for CS than for CO and varies to either side of it, an effect manifested in the range of C–S bond lengths.[123] These effects should be more marked for CSe ligands, although the biggest difference is between CO and CS.[126]

The μ_2- and μ_3-CS ligands show increasingly weaker C–S bonding which, by analogy to CO, may be attributed to increasing back donation to the CS π^*-orbitals. In the μ_2-C · σ-S, μ_3-C · σ-S, μ_4-C · σ-S and μ_4-C · μ-S bonding modes when four or six electrons are donated formally, weaker C—S bonding is indicated. However, when the sulphur coordination is to metal atoms also attached to the carbon, a comparison to similar CO ligands suggests independent M_n–C, M_n–S and C–S interactions with a more extensive loss of the weaker $p\pi$–$p\pi$ bonding in CS.[116] For the CO cases, a retention of CO π-bonding and η^2-type interactions of this with metal centers is in evidence.[116]

IV.3. THEORETICAL STUDIES

Richards' *ab initio* calculations on CS and CO suggest that CS should be a more stable ligand.[127] The HOMO for CS, the 7σ orbital, constitutes the σ-donor lone pair at carbon and is largely antibonding and *C2p* in character. The corresponding orbital in CO, 5σ, is of lower energy and the electrons are less available for σ-donation, suggesting that CS should be the better σ-donor. Conversely, the CS LUMO, the 3π level, is the π-accepting π^* CS orbital and is of lower energy than the corresponding CO 2π level. This indicates that CS should be a more effective π-acceptor. Indeed, calculation at elongated equilibrium bond lengths for CS and CO, closer to those observed when the moieties are ligating, indicate little effect on donor ability but a marked drop in CS LUMO energy which would favour its π-accepting properties.

Lichtenberger and Fenske[124] performed MO calculations in conjunction with photoelectron spectroscopy (PES) studies on $[Cr(CO)_5(CS)]$ and $[(\eta^5\text{-}C_5H_5)Mn(CO)_2(CS)]$ and the tricarbonyl analogues. Although the absolute energy values for calculation and experiment do not agree, the ordering of occupied levels assigned is the same. Generally, results agree with those of Richards. The slightly better σ-donation of CS occurs because sulphur's lower electronegativity over oxygen leaves more charge at carbon and the better π-acceptor ability of CS. These destabilize the 7σ lone pair over the 5σ in CO. The better π-acceptance by CS results from the smaller metal *3d*-ligand π^* separation as the orbital overlap in both CO and CS cases is comparable. However, the *e* set of orbitals arising from this *3d*–π^* interaction is calculated at slightly higher energy than the non-interacting *3d*-derived b_2-orbital. This results from *3d* interaction with the filled CS 2π-orbitals offsetting the *e*-set stabilization, but the combined π-donor and π-acceptor interactions strengthen M–C and weaken C–S bonding.[124] This pair of effects explains both Raman and ^{13}C NMR observations (see Sections IV.8 and 9).[124] The metal (*d*)–CS (2π) interaction is mostly of *d*-orbital character in its filled antibonding combination and is more favourable than the *d*-orbital itself for interaction with the π^* set on CS, whereas the *d*-orbital electron density in the largely ligand character bonding combination is unavailable through this orbital's stability. These interactions cause a removal of metal *d*-orbital electron density to orbitals with much less *d*-character.[125] For CO the filled bonding π-orbitals are too stable to indulge in these interactions and, hence, none of the effects are manifested.[123,124]

Other *ab initio* calculations[126] agree with Richards' work. In $[(\eta^6\text{-}C_6H_5CO_2Me)Cr(CO)_2(CE)]$ (E = O, S or Se), the σ-donor and π-acceptor ability of CE increases from CO to CSe, the σ-donor and π-acceptor orbitals being calculated to increase and decrease in energy respectively. The increasing σ-donation is said to be mitigated by the decreasing localization of this orbital at the carbon. The calculations were rationalized against spectroscopic and structural data for the complexes.[126]

Lichtenberger and Fenske noted that, whereas nucleophiles react at the CS carbon, their calculations suggest an increasing electron density at this carbon over the less reactive CO ligand. They suggest that the attack is "lumophilic" and that the reaction is frontier orbital controlled, the HOMO being the nucleophile lone pair and the LUMO in the CS complex is an antibonding CS π^*-orbital.[124]

IV.4. PHOTOELECTRON SPECTROSCOPY STUDIES

Studies are limited to $[M(CO)_5(CS)]$ (M = Cr or W), $[(\eta^6\text{-}C_6H_6)Cr(CO)_2(CE)]$ (E = S or Se) and $[(\eta^5\text{-}C_5H_5)Mn(CO)_2(CS)]$, probably as these are relatively volatile and, therefore, lend themselves to the technique. Comparisons are made to the carbonyl analogues.

For $[M(CO)_5(CS)]$ (M = Cr or W),[128] the $C(1s)$ binding energy is some 2 eV lower than for $[M(CO)_6]$. This is attributed to the lower sulphur electronegativity, indicates a higher carbon electron density for CS and suggests a stronger σ-donation by CS. The lack of difference in the rest of the PES spectra of $[M(CO)_5(CE)]$ (E = O or S) indicated increased π-back donation to CS so that other electron distributions are unaffected. A suggestion that the CO O(1s) and CS $S(2p_{3/2})$ binding energies provide a measure of metal π-back donation is backed by the correlation of this value with the respective stretching force constant, k, for the CO or CS bond.[128]

The high-energy bonding orbital of $[M(CO)_5(CS)]$ (M = Cr or W) and $[(\eta^5\text{-}C_5H_5)Mn(CO)_2(CS)]$ were probed by He(I) photoelectron spectroscopy.[124] Binding energies at 8–9 eV derive from electrons in the largely metal d-character e- and b_2-levels, at about 11 eV from a CS (7σ) derived orbital, and at some 12 eV from a level derived largely from the CS (2π) level. From the relative ionization cross-sections of bands in $[M(CO)_5(CS)]$ (M = Cr or W) discrepancies between the 7σ and 2π-derived levels suggest different metal character of these orbitals, the 7σ derived having more. That the CS (2π) derived orbital has metal character indicates its interaction with metal orbitals. The many peaks at 13–17 eV derive from the σ- and π-levels of other ligands.

For $[(\eta^6\text{-}C_6H_6)Cr(CO)_2(CE)]$ (E = O, S or Se), the first ionization potential increases on going from CO to CSe[129] unlike $[Cr(CO)_5(CE)]$.[124,129] Also, the binding energies are some 1 eV lower for the $[(\eta^6\text{-}C_6H_6)Cr(CO)_2(CE)]$ series. A significant ring to chromium electron transfer is inferred.[129]

IV.5. ELECTRONIC OR UV–VIS SPECTROSCOPY

Only $[Cr(CO)_5(CE)]$ and $[(\eta^6\text{-}C_6H_6)Cr(CO)_2(CE)]$ (E = O, S or Se) have been studied, the data indicating more electron withdrawal by CE from CO to CSe.[130] An energy level diagram constructed for $[Cr(CO)_5(CE)]$ is shown (Fig. 20) and assignments of electronic transitions were made from the gas

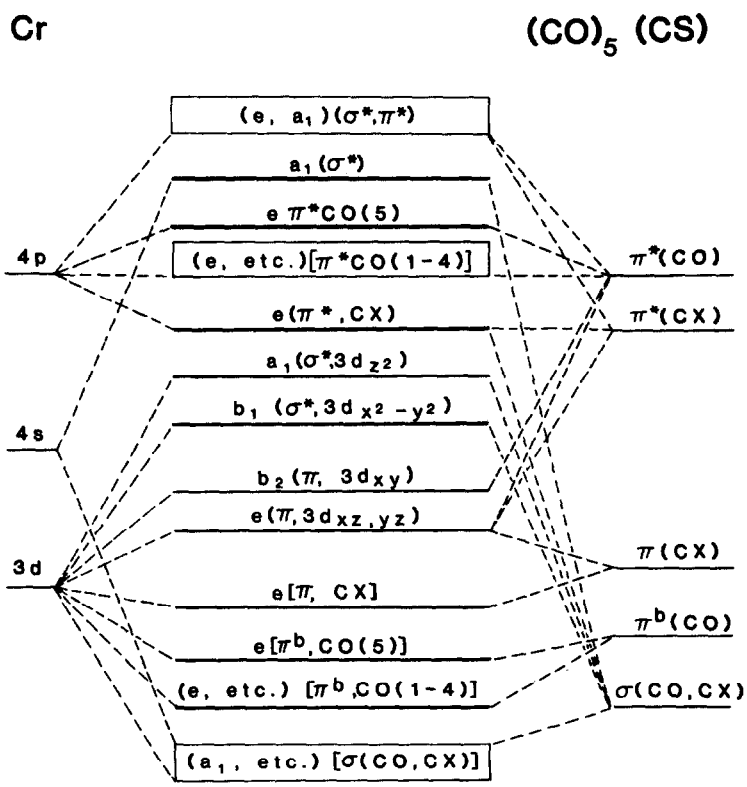


Fig. 20. A molecular orbital diagram for $[Cr(CO)_5(CS)]$.

phase or solution spectra. Increasing π-acceptor ability of CE from CO to CSe was deduced from the increasing energy of the lowest energy M → CO (π^*) charge-transfer band (36,000 → 36,600 cm^{-1}), although the high-energy bands do not adhere to this; from the increasing energy of the M → *trans*-CO (π^*) transition; and from the decreasing energy of the M → CE charge-transfer band ($b_2 \rightarrow e$ levels) backed by the greater intensity for CSe indicating a greater transition probability. However, a $[Cr(CO)_5(CS)]$ photoelectron spectrum indicates different energy differences for the M–CE charge transfer.[124] Two $d \rightarrow d$ transitions are observed ($b_2 \rightarrow b_1$, $e \rightarrow b_1$ or $e \rightarrow a_1$) out of the four possible ($b_2 \rightarrow b_1$, $b_2 \rightarrow a_1$, $e \rightarrow b_1$ or $e \rightarrow a_1$), at 27,000 and 24,000 cm^{-1}. Spectra of $[(\eta^6\text{-}C_6H_6)Cr(CO)_2(CE)]$ are comparable (with additional ring–Cr bands) although some discrepancy of the absolute energy of the HOMOs occurs from PES results.[129]

IV.6. MASS SPECTROSCOPIC STUDIES

As CO ligands are usually "lost" before CS in mass spectral fragmentation patterns, the M–CS linkage appears to be stronger. Some examples include $[(\eta^5\text{-}C_5H_4R)Mn(CO)_2(CS)]$ (R = H or Me),[131] $[Cr(CO)_5(CS)]$,[57] $[(\eta^6\text{-}C_6H_5CO_2Me)Cr(CO)(CS)L]$ [L = CO, $P(OEt)_3$ or $P(OPh)_3$],[2] $[Os_3(CO)_8(CS)S_2]$,[51] $[Os_3(CO)_7(CS)S_2(\mu\text{-}H)_2]$[52] and $[(\eta^5\text{-}C_5H_4Me)Mn(CO)(CS)L]$ (L = $AsPh_3$ or $SbPh_3$).[132] In the last case, the later loss of ligand L suggests that the Mn–As or Mn–Sb bonds are stronger.[132] The NO ligand is less enduring than CS in $[\{(\eta^5\text{-}C_5H_4R)Mn(NO)(\mu\text{-}CS)\}_2]$.[82]

Appearance potential data for $[(\eta^5\text{-}C_5H_4R)Mn(CO)_2(CS)]$ (R = H or Me) was used to suggest that CO is a better π-acceptor ligand and CS primarily a σ-donor,[131] an interpretation which has been questioned.[2,3] These arguments used only the σ-donor : π-acceptor ratio without reference to any π-donor effect of CS. Indeed, $[(\eta^6\text{-}C_6H_5CO_2Me)Cr(CO)(CS)L]$ [L = CO, $P(OEt)_3$ or $P(OPh)_3$] results were interpreted as showing better CS σ-donor and π-acceptor ability than CO.[2] Such differences may be explained by Andrews' "charge-buffering" concept.[123]

IV.7. MÖSSBAUER SPECTROSCOPY

In the compounds $[\{(\eta^5\text{-}C_5H_5)Fe(CO)_2L\}^+]$ (L = CO, CS, PPh_3, CN^-, NCO^-, NCS^- or Br^-), the electron density at iron increases in the order $Br^- < NCS^- < NCO^- < PPh_3 < CN^- < CO < CS$, suggesting CS as the best π-acceptor.[133] The iron electron density is augmented by σ-donation, increasing *s*-level electron density, and by π-acceptance, which decreases the shielding *d*-orbital electron density. As the π-accepting ligands increase iron's electron density most, π-acceptance is implied as the dominant effect.[133] The good σ-donor characteristics of CS over CO[123] and any Fe(3*d*)–CS(2π) interaction[125] will also contribute to these effects, the former in a σ-donor sense and the latter because this interaction augments the removal of *d*-orbital electron density by CS from the metal.

IV.8. ^{13}C NMR STUDIES

The ^{13}C NMR chemical shifts for CS ligands which have been reported are gathered in Appendix 1. These resonances occur at a lower field than their CO counterparts[2,3] generally in the range observed for metal–carbene species.[134] This suggests the importance of a carbenoid resonance form in the M–CS interaction in support of the proposal for a strong metal–carbon interaction,[124] although Yaneff suggested the importance of the polar resonance structure $M—C^+{=}S^-$.[3] Inspection of the appended data shows a range for terminal CS ligands of 286–442 ppm and for μ-CS ligands of 353–396 ppm. No data are reported for other bonding modes.

The effect of CS on other ^{13}C NMR chemical shifts has been considered. Bodner investigated the ^{13}C chemical shifts of two CO ligands in $[\{(\eta^5\text{-}C_5H_5)Cr(CO)_3\}^-]$, $[(\eta^5\text{-}C_5H_5)Mn(CO)_2L]$ [L = CS, CO, $P(OPh)_3$, $P(OMe)_3$, PPh_3, P^nBu_3, $C_5H_{10}NH$ or C_8H_{14}] and $[\{(\eta^5\text{-}C_5H_5)Fe(CO)_2L\}^+]$ (L = CS, CO, PPh_3 or NH_3).[135] The ^{13}C chemical shift of CO is deshielded more as π-acceptance by CO increases due to higher metal electron density. Deshielding is least when L = CS, indicating that, of the ligands L, CS most effectively reduces metal electron density. Hence, CS was deemed to have the highest π-acceptor : σ-donor ratio of these ligands.[135] For

$$[\{(\eta^5\text{-}C_5H_5)Fe(CO)(CS)L\}^+ \cdot PF_6^-] \text{ [L = CO, } PPh_3\text{, } P(C_6H_4F)_3 \text{ or } PCy_3\text{]},$$

$$[\{(\eta^5\text{-}C_5H_5)Fe(CS)(CNPh)_2\}^+ \cdot PF_6^-] \quad \text{and} \quad [\{(\eta^5\text{-}C_5H_5)Fe(CO)(PPh_3)_2\}^+ \cdot PF_6^-]$$

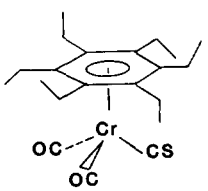
the CS ^{13}C chemical shift is similarly influenced as ligand L changes, indicating that iron electron density reduces in the order CNPh < PCy_3 < PPh_3 < $P(C_6H_4F)_3$ < CO.[83]

The very low field ^{13}C chemical shift of CS in [(η^5-C_5H_5)Mn(CO)$_2$(CS)] indicates a high positive charge at carbon and a prevalent M—$^{\delta+}$C=S$^{\delta-}$ resonance structure is suggested, which was related to Raman spectroscopy data.[136] The CE ^{13}C chemical shifts for [(η^6-C_6H_5R)Cr(CO)$_2$(CE)] (R = H or CO_2Me), [(η^5-C_5H_4R')Mn(CO)$_2$(CE)] (R' = H or Me) and [(η^5-C_5H_5)Re(CO)$_2$(CE)] (E = O, S or Se) suggest that the π-acceptor : σ-donor ratio increases from CO to CSe.[137] Downfield movement of ring resonances indicates decreased metal electron density, and increased carbonyl carbon shielding agrees with Bodner's arguments for increasing electron acceptance from CO to CS,[135] which continues with CSe. Changes in the metal or ring substituent affect the CO, CS and CSe ^{13}C resonance similarly, indicating related bonding criteria for these ligands.[137] Thus, substituting NO^+ for CO in [(η^5-C_5H_5)Mn(CO)$_2$(CE)] or going from manganese to rhenium analogues shows upfield chemical shift changes.[137]

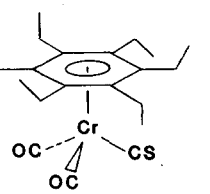
The downfield shift of CE from CO to CSe can be rationalized[137] by Pople's ^{13}C paramagnetic shielding expression.[138] Shielding is reciprocally related to the average electronic excitation energy, ΔE_{av}, which for CE is said to approximately equal the π–π^* energy difference which decreases from CO to CS, and probably also to CSe.[137]

The compounds *cis*- and *trans*-[W(CO)$_4$(CS)L] (*cis*- and *trans*-L = CO, 4-Me-py, CyNC or PR_3; R = Ph, ^{n}Bu, *p*-tolyl, OMe or OPh : *trans*-L = Cl^-, Br^- or I^-) have ^{13}C CS chemical shifts near 300 ppm which correlate well with CE (E = O or S) bond force constants, k_{CE}.[75] For *cis*-CO in *trans*-[W(CO)$_4$(CS)L] and CS in *cis*-[W(CO)$_4$(CS)L], k decreases linearly as $\delta(^{13}C)$ increases, and a method for calculating δ(CO) in other [W(CO)$_4$(CS)L] systems was proposed.[75] In *cis*-[W(CO)$_4$(CS)L], δ(CS) varies more than δ(CO) of the *trans*-CO ligand, suggesting that CS "buffers" CO against the electronic effects of altering the ligand L, with both δ(CS) and δ(CO) moved downfield by increased metal electron density.[75]

Controversy has arisen over the interpretation of the ^{13}C NMR spectrum of [(η^6-C_6Et_6)Cr(CO)$_2$(CS)]. McGlinchey *et al.*[39] infer slow tripodal rotation on the NMR time scale at low temperature with a 1,3,5-*distal*-2,4,6-*proximal* η^6-C_6Et_6 structure (**36**), as is observed in the solid state. Reinterpreting this data, Hunter and Mislow[139] prefer a 1,2,3,5-*distal*-4,6-*proximal* isomer (**37**), which



36



37

still undergoes rapid tripodal rotation, fluxional behaviour being explained by ethyl group *distal*, *proximal* exchange. Reaffirming their proposal, McGlinchey *et al.*[140] offered a more detailed spectral interpretation backed by a solid-state ^{13}C spectrum which is comparable to the limiting-solution spectrum, indicating that the same structure is present.

IV.9. RAMAN SPECTROSCOPIC STUDIES

As part of complete vibrational spectroscopic characterizations, Raman spectroscopy studies exist for [M(CO)$_5$(CE)] (M = Cr or W, E = S or Se), [(η^5-C_5H_5)Mn(CO)$_2$(CE)] (E = O or S) and [(η^6-C_6H_6)Cr(CO)$_2$(CE)] (E = O, S or Se).[136,141–143] The ν(CS) bands occur at 1250–1300 cm^{-1} but have very low intensity. In explanation, Lichtenberger and Fenske[124] argue that CS π- and π^*-levels (2π and 3π) are coupled as both interact with the same metal *d*-orbital set which reduces the polarizability change, and so Raman intensity, as the CS bond stretches. Both ν(M–CS) and δ(M–C–S) modes are Raman-active but tend to overlap with the equivalent M–CO modes. Tentative assignments have been made for ν(M–CS), 350–400 cm^{-1}, and δ(M–C–S), 300–500 cm^{-1}, which are more metal-dependent than ν(CS).

Table 2.

CS bonding type	Range of ν(CS)[a] (cm^{-1})
σ-CS	1135–1409
μ-CS	1100–1157
σ-C · σ-S	1049–1106
μ-C · σ-S	1017–1082
μ_3-CS[b]	1039–1075
μ_3-C · σ-S[b]	963
μ_4-C · σ-S[b]	843
μ_4-C · μ-S[b]	921

[a] IR-active.
[b] Single examples reported.

IV.10. IR SPECTROSCOPIC STUDIES

Assignment of the CS stretching vibration, ν(CS), is common although both ν(M–CS) and δ(M–C–S) IR-active modes have been reported.

In Table 2, the ν(CS) range for different CS coordination modes is noted.

Earlier reviewers[3,4] tabulated the known ν(CS) values. This listing has been updated (see Appendix 2) since the latter review.[3]

The ν(CS) value for "free" CS, trapped in a low-temperature matrix of CS_2, is 1274 cm^{-1}.[144] When ligating, ν(CS) falls to either side of this value. With the noted π-acceptor properties of CS an increase is unexpected but was rationalized from normal coordinate calculations on $[M(CO)_5(CE)]$ (M = Cr or W, E = O or S) which invoked a mixing of ν(CS) and ν(M–CS) stretching modes and showed that the ν(CE) force constant indeed decreases for E = S.[4,136] The MO calculations, which indicate both CS π- and π^*-orbitals overlap with metal d-orbitals,[124] lend support to the mixing of stretching modes. Also, correlating ν(CS) in $[ML_n(CS)]$ with k_{CO} for $[ML_n(CO)]$, Andrews[123] noted that other π-donor ligands cause a high ν(CS) with respect to a linear correlation and π-acceptor ligands a low value, again suggesting a complex interrelation of ν(CS) with M–CS interactions. As the d–π interaction tends to augment d-electron removal from the metal, increase M–C and decrease C–S bond strength,[125] π-donor ligands which will reduce this interaction will lead to stronger C–S bonding and higher ν(CS).

As carbon or sulphur becomes increasingly coordinated to metal centers, the ν(CS) ranges tend to decrease (see Table 2). The change from μ_4-C · σ-S at 843 cm^{-1} in $[Os_4(CO)_{12}(CS)S]$[116] to μ_4-C · μ-S at 921 cm^{-1} in $[Fe_5(CO)_{13}(CS)S_2]$[115] is an exception, but takes no account of ν(CS) and ν(M–CS) mixing nor of the change in metal.

Returning to terminal CS ligands, ν(CO) for the series of compounds $[\{(\eta^5\text{-}C_5H_5)Fe(CO)_2L\}^+]$ (L = CS, C_2H_4, PPh_3, MeCN or py) is greatest when L is CS which was taken to indicate that CS is the best π-acceptor amongst these ligands.[60] The largely analogous nature of metal–ligand interaction between CO and CS is shown by the similar direction of shift of ν(CO) and ν(CS) in $[\{(\eta^5\text{-}C_5H_5)Fe(CO)(CS)L\}^+]$ (L = CO, PR_3, $AsPh_3$ or $SbPh_3$; R = Ph, Cy, C_6H_4F or C_6H_4OMe), which both decrease as L has better σ-donor and worse π-acceptor properties.[83] However, ν(NO) and $\nu(CO)_{max}$ for $[\{(\eta^5\text{-}C_5H_5)Mn(CO)_2(NO)\}^+]$ are higher than for $[\{(\eta^5\text{-}C_5H_5)Mn(CO)(CS)(NO)\}^+]$, suggesting less π-acceptance by CS than CO, whereas replacing CO by CS in $[\{(\eta^5\text{-}C_5H_5)Mn(CE)(NO)L\}^+]$ (E = O or S; L = PPh_3, $AsPh_3$ or $SbPh_3$) causes slight increases in ν(NO), suggesting the opposite.[81]

Such conflicting data from various spectroscopic studies of CS complexes were rationalized by Andrews.[123] For numerous CS complexes, he compared ν(CS) in $[M(CO)_n(CS)]$ (M = metal with rest of ligand array) with k_{CO}, the stretching force constant for CO, in $[M(CO)_{n+1}]$ and k_{CO} in $[M(CO)_nL_1]$ and $[M(CO)_nL_2]$, where L_1 = CO and L_2 = CO, CS or PEt_3. Statistically significant correlations were found and some rationalization was made for deviation from exactitude of the correlations. He concluded that the basic interaction with metal of CO and CS is similar; σ-donor and π-acceptor. On correlating ν(CS) and k_{CO}, however, ν(CS) is lower than the ideal correlation when other good π-acceptor ligands are present but higher with good π-donor ligands, which will affect metal–ligand d–π

and d–π^* interactions. Estimation of ν(CS) of an unknown CS complex from k_{CO} of its CO analogue was suggested. The CS ligand was said to exhibit a "charge-buffering effect" as k_{CO} in $[M(CO)_n(CS)]$ varies less than in $[M(CO)_{n+1}]$, so that CS absorbs more of the charge differences between complexes. Hence, CS displays a wider donor : acceptor ratio range than CO, this ratio being higher than CO when k_{CO} in $[M(CO)_{n+1}]$ exceeds 17.1 mdyn $Å^{-1}$ and is lower below this value.[123]

In a similar vein, Dombek compared IR and ^{13}C NMR parameters for $[W(CO)_5L]$ and *cis*- and *trans*-$[W(CO)_4(CS)L]$ (*cis*- and *trans*-L = CyNC, 4-Me-py or PR_3; R = OMe, OPh, Ph, ^{n}Bu or tolyl : *trans*-L = Cl^-, Br^- or I^-).[75] For *trans*-$[W(CO)_4(CS)L]$, CS seems more effective at removing electron density from tungsten than CO in $[W(CO)_5L]$, with k_{CS} less variable than k_{CO} for the equivalent CO ligand. The availability of the opposing M–CS d–π and d–π^* interactions explains this. Also, decreasing k_{CS} correlates with decreasing CS ^{13}C shielding [increasing δ(CS)].[75]

The meticulous IR and Raman studies of Butler and co-workers are confined to $[(\eta^5\text{-}C_5H_5)Mn(CO)_x(CS)_y]$ ($x+y=3$, x and y = 1 or 2),[141,145] $[(\eta^6\text{-}C_6H_6)Cr(CO)_2(CE)]$ (E = O, S or Se)[143,146] and $[M(CO)_5(CE)]$ (M = Cr or W; E = O, S or Se).[136,142] Aided by isotopic labelling, detailed assignments have been made. The IR ν(CS) modes are strong, occurring at 1175–1300 cm^{-1}, although the Raman ν(CS) intensity is low, as discussed above. Both ν(M–CS) and δ(M–C–S) modes are IR- and Raman-active, varying significantly because of the changing metal atom. The manganese systems show ν(M–CS) modes at 359–404 cm^{-1} with δ(M–C–S) at the low end of 450–650 cm^{-1}, but undistinguishable from δ(M–C–O).[141] In $[(\eta^5\text{-}C_5H_5)Mn(CS)L_2]$ (L_2 = dppe or triphos), δ(M–C–O) IR-active modes occur from 530 to 555 cm^{-1}.[79] For the chromium complexes, ν(M–CS) occurs at 350–435 cm^{-1} with δ(M–C–S) assigned at 340 cm^{-1} for $[Cr(CO)_5(CS)]$, but at 490–520 cm^{-1} for $[(\eta^6\text{-}C_6H_6)Cr(CO)_2(CS)]$.[136,142,143] Values for $[W(CO)_5(CS)]$ are a little below the chromium analogue.[136,142,143]

Bond dipoles have been calculated from the absolute integrated IR intensity data for $[(\eta^5\text{-}C_5H_5)Mn(CO)_2(CS)]$[145] and $[(\eta^6\text{-}C_6H_6)Cr(CO)_2(CE)]$ (E = O, S or Se).[146] Increasing π-acceptor ability of CE in the order E = O < S < Se was assigned as the M–C–E dipole increases in this order also.

As noted already, no similarly detailed IR studies have been reported for CS ligands in bonding modes other than terminal.

IV.11. X-RAY CRYSTALLOGRAPHIC DATA

Data on the X-ray crystallographic studies of CS complexes is gathered in Table 3 with some related information on M–C bond lengths for comparable CO ligands and ν(CS) values.

Twelve cases contain terminal CS ligands and five μ-CS, the remainder being single examples of the μ_3-CS, the two μ_3-C · σ-S, μ_4-C · σ-S and μ_4-C · μ-S bonding modes. The shorter M–CS distance than M–CO in comparable structures indicates that the M–CS interaction is stronger.[3] Generally, this holds for the terminal CS complexes characterized structurally since (see Table 3), although in the cases of $[(\eta^5\text{-}C_5H_4Me)Mn(CO)(CS)I]$,[149] $[Os_3(CO)_8(CS)S_2]$[50,51] and $[Os_3(CO)_7(CS)S_2(\mu\text{-}H)_2]$[52] these distances are close to equal. However, in Andrews' correlation of IR data, the CS ligand in $[\{(\eta^5\text{-}C_5H_5)Mn(CO)(CS)(NO)\}^+]$ is determined to have a worse acceptor : donor ratio than CO in $[\{(\eta^5\text{-}C_5H_5)Mn(CO)_2(NO)\}^+]$.[123] Substituting CO by I^-, a good π-donor ligand, should reduce the Mn–CS d–π interaction, which itself augments the d–π^* interaction,[125] worsening the acceptor : donor ratio further and leading to a long Mn–CS bond due to the low π-component to this interaction. Examination of all M–CS bond lengths against the IR parameters used by Andrews might prove interesting. Where M–CS is shorter than M–CO, C–S bond elongation is greater. Notably, the cases where M–CS and M–CO are close display the three shortest C–S distances, indicative of relatively low CS π-acceptance.

In the few structural studies of μ-CS systems, the tendency for longer M–CS than M–CO of comparable μ-CO ligands is not marked, M–CS being both longer and shorter. In $[\{(\eta^5\text{-}C_5H_5)Fe\}_2(CO)(CN^iPr)(\mu\text{-}CO)(\mu\text{-}CS)]$ where M–CS is longer than M–CO, the C–S bond is short.[110] Carbonyl analogues are unknown for the compounds with other CS bonding modes so no judgment on M–C distances can be made.

The C–S bond length generally increases as more metal atoms are bonded to carbon with ν(CS) decreasing (Fig. 21). For the two electron donor σ-, μ- and μ_3-CS ligands increasing back donation to

Table 3.

Complex	M–CS (Å)	M–CO[a] (Å)	C–S (Å)	ν(CS) (cm^{-1})	Reference
Terminal					
$[(\eta^6\text{-}C_6H_5CO_2Me)Cr(CO)_2(CS)]$	1.80	1.85 (×2)	1.57	1205	126, 147
trans-$[W(CO)_4(CS)(CyNC)]$	1.94	2.06	1.54	1240	148
$[(\eta^5\text{-}C_5H_4Me)Mn(CS)(NO)I]$	1.80	1.80	1.51		149
[Fe(OEP)(CS)]	1.66	> 1.69	1.56		150
$[Fe(CO)_2(CS)\{P(OPh)_3\}_2]$	Disorder allows no accurate data				46
$[(Ph_3P)_2ClRu(\mu\text{-}Cl)_3Ru(PPh_3)_2(CS)]$					151
$[Os_3(CO)_8(CS)S_2]$	1.89	1.89	1.47	1324	50, 51
$[Os_3(CO)_7(CS)S_2(\mu\text{-}H)_2]$	1.90	1.91	1.43	1325	52
$[\{(np_3)Co(CS)\}^+ \cdot BPh_4^-]$	1.50	1.63	1.66, 1.78[b]		17
trans-$[RhCl(CS)(PPh_3)_2]$	1.80	1.86	1.54	1299	152
$[\{Rh(3,5\text{-}Me_2\text{-}pz)(CS)(PPh_3)\}_2]$	1.77	1.83	1.57		98, 99
$[\{Ir(CO)_2(CS)(PPh_3)_2\}^+ \cdot PF_6^-]$	1.87	1.92, 1.95	1.51	1391	153
Bridging					
$[\{(\eta^5\text{-}C_5H_5)(CO)Fe(\mu\text{-}CS)\}_2]$	1.90, 1.91		1.59	1131	102
$[\{(\eta^5\text{-}C_5H_5)Fe(CO)\}_2(\mu\text{-}CO)(\mu\text{-}CS)]$	1.89	1.91	1.60	1125	105
$[\{(\eta^5\text{-}C_5H_5)Fe\}_2(CO)(CN^iPr)(\mu\text{-}CO)(\mu\text{-}CS)]$	1.93	1.87	1.50	1121, 1115	110
$[(\eta^5\text{-}C_5H_5)(Me_3P)Co(\mu\text{-}CS)_2Co(\eta^5\text{-}C_5H_5)]$	1.81, 1.95		1.57		103
$[MnPt(\mu\text{-}CS)(CO)_2(\eta^5\text{-}C_5H_5)(PMePh_2)_2]$	Mn 1.88 Pt 2.02	1.80 2.22[c]	1.62		106, 107
Other					
$[\{(\eta^5\text{-}C_5H_5)Co\}_3(\mu_3\text{-}S)(\mu_3\text{-}CS)]$	1.83		1.78	1050	112, 113
$[\{(\eta^5\text{-}C_5H_5)Co\}_3(\mu_3\text{-}S)\{\mu_3\text{-}CS \cdot Cr(CO)_5\}]$	1.91		1.68		113
$[Fe_4(CO)_{12}(CS)S]$	1.97		1.70	963	114
$[Os_4(CO)_{12}(CS)S]$	2.16		1.76	843	116
$[Fe_5(CO)_{13}(CS)S_2]$	1.96		1.71	921	115

[a] Derived from either the CO ligands in the same complex or the CO analogue.
[b] 1.78 Å value seems anomalously high.
[c] Semi-bridging CO ligand.

the CS π^*-orbitals should weaken the C–S bond and lower ν(CS) like the behaviour of CO analogues.

When CO and CS donate more than two electrons, bonding differences have been noted.[116] For $[Fe_5(CO)_{13}(CS)S_2]$ (**28**) and $[Os_4(CO)_{12}(CS)S]$ (**29**), formal electron counting requires CS to donate six and four electrons respectively. However, for $[Os_4(CO)_{12}(CS)S]$, the C–S bond is longer and ν(CS) lower. In both cases, the M_n–CS distances are effectively equal with the sulphur bonded to metal atoms also involved in the M_n–C interaction. Considering CO ligands which donate four or six electrons and have shared metal atoms between C and O, the CO bond orders are slightly greater than for CS cases and M_n–CO is shorter for the "nearest-to-linear" M–CO interaction. These data suggested largely independent M_n–C, M_n–S and C–S bonding whereas CO retains more π-bonding and tends to have separate linear M–CO and Chatt–Dewar η^2-CO interactions with metal centers. That the C–S bond length does not increase nor ν(CS) decrease on increasing donation from four to six electrons suggests that the extra two electrons are nominally donated from a sulphur-localized lone pair and that at the four-electron donor stage C–S π-bonding is effectively sundered. This indicates the weaker CS $p\pi$–$p\pi$ bonding.[116]

When carbon and sulphur do not share metal atoms, these effects are not observed. In $[\{(\eta^5\text{-}C_5H_5)Co\}_3(\mu_3\text{-}S)\{\mu_3\text{-}CSCr(CO)_5\}]$ (**26**) the Co–C distances are equal[113] and in $[Fe_4(CO)_{12}(CS)S]$ (**27**)

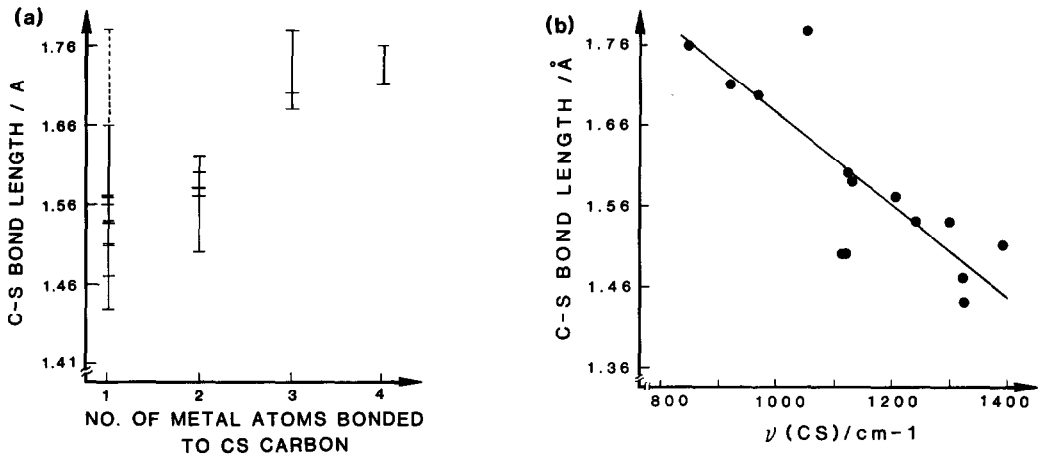
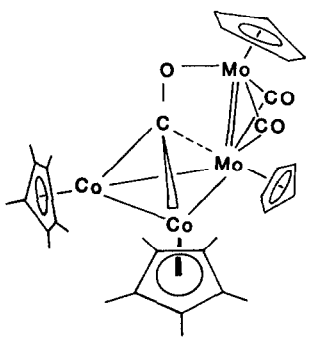


Fig. 21. Graphical comparison of the C–S bond length to : (a) the number of metal atoms bonded to the CS carbon, and (b) ν(CS).

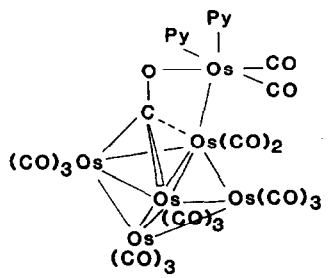
the μ_3-C · σ-S ligand is closer to the iron atom in the Fe_3 triangle which is attached to the $Fe(CO)_4$ group which is σ-bonded to the CS sulphur.[115,116] Two μ_3-C · σ-O analogues are known, in

$$[\{(\eta^5\text{-}C_5Me_5)Co\}_2\{(\eta^5\text{-}C_5H_5)Mo\}_2(\mu\text{-}CO)_3(\mu_3\text{-}C\cdot\sigma\text{-}O)]$$

(**38**)[154] and $[Os_6(CO)_{16}(\mu_3\text{-}C\cdot\sigma\text{-}O)(py)_2]$ (**39**).[155]



38



39

X-ray crystallography has proved vital in determining the structure of CS-containing complexes, especially those containing the more complex bonding modes.

In summary to this section, although CS displays a variety of two-, four- and six-electron donor bonding modes much like CO, differences do become apparent. The bonding of the terminal CS ligand has been studied in relative detail by a wide range of techniques and a reasonably good understanding of its bonding exists relative to that of CO.

In contrast, although the broad IR and ^{13}C NMR spectroscopic properties of μ-CS ligands are known, there is a paucity of data for the more complex bonding modes. This must arise, however, from the small number of such complexes which have been isolated.

V. CONCLUSIONS

This review encompasses the literature on thiocarbonyl complexes since the first identification in 1966, until approximately the end of 1984. The diversity of synthetic routes and the lack of general applicability of these become apparent, thus making the deliberate synthesis of thiocarbonyl complexes a fickle business.

Although there are a good number of terminal thiocarbonyl ligands of which a diverse reactivity has been demonstrated, there are rather few examples of other CS ligand bonding modes. Consequently,

the chemistry of these species remains uninvestigated to any extent. For the same reasons, detailed study of the bonding in such cases remains limited.

In 1977, Butler[2] concluded his account on this area by suggesting that "the chemistry of transition metal chalcocarbonyls will continue to be a fertile area of research... it is anticipated that the catalytic potential of these complexes will become an important research area." I suggest that the areas which remain fallow lie in the synthesis and study of the thiocarbonyl ligand in more complex bonding modes and in the consequent better understanding of the bonding in these species with respect to similarly coordinated carbonyl and selenocarbonyl ligands. It may also be noted that the catalytic potential of thiocarbonyl complexes remains an area lacking significant report.

Acknowledgements—This review was originally drafted while PVB was a research student at the University of Cambridge. Acknowledgement is made of Professor Sir J. Lewis and Dr B. F. G. Johnson for their support then and since towards the preparation of this review. The S.E.R.C. is acknowledged for a maintenance grant to PVB while at Cambridge. The Union Carbide Corporation is acknowledged for permission to update and publish this work and for providing the facilities necessary to research the material and to prepare the manuscript. The encouragement and interest of Drs G. L. O'Connor, S. W. Kaiser and J. R. Briggs is noted. I am indebted to Dr B. D. Dombek for his constructive criticism of draft manuscripts.

REFERENCES

1. K. J. Klabunde, C. M. White and H. F. Efner, *Inorg. Chem.* 1974, **13**, 1778.
2. I. S. Butler, *Acc. Chem. Res.* 1977, **10**, 359.
3. P. V. Yaneff, *Coord. Chem. Rev.* 1977, **23**, 183.
4. I. S. Butler and A. E. Fenster, *J. Organomet. Chem.* 1974, **66**, 161.
5. G. V. Calder, J. G. Verkade and L. W. Yarbrough, *J. Chem. Soc., Chem. Commun.* 1973, 705.
6. H. Werner, *Coord. Chem. Rev.* 1982, **43**, 165.
7. J. A. Ibers, *Chem. Soc. Rev.* 1982, **11**, 57.
8. L. Busetto, U. Belluco and R. J. Angelici, *J. Organomet. Chem.* 1969, **18**, 213.
9. T. A. Wnuk and R. J. Angelici, *Inorg. Chem.* 1977, **16**, 1173.
10. K. R. Grundy, R. O. Harris and W. R. Roper, *J. Organomet. Chem.* 1975, **90**, C34.
11. T. J. Collins and W. R. Roper, *J. Organomet. Chem.* 1977, **139**, C9.
12. G. R. Clark, K. R. Grundy, R. O. Harris, S. M. James and W. R. Roper, *J. Organomet. Chem.* 1975, **90**, C37.
13. P. J. Brothers, C. E. L. Headford and W. R. Roper, *J. Organomet. Chem.* 1980, **195**, C29.
14. T. J. Collins, W. R. Roper and K. G. Town, *J. Organomet. Chem.* 1976, **121**, C41.
15. W. R. Roper and K. G. Town, *J. Organomet. Chem.* 1983, **252**, C97.
16. C. Bianchini, A. Meli and G. Scapacci, *Organometallics* 1983, **2**, 1834.
17. C. Bianchini, D. Masi, C. Mealli, A. Meli, M. Sabat and G. Scapacci, *J. Organomet. Chem.* 1984, **273**, 91.
18. I. S. Butler and A. E. Fenster, *J. Chem. Soc., Chem. Commun.* 1970, 933.
19. A. E. Fenster and I. S. Butler, *Inorg. Chem.* 1974, **13**, 915.
20. I. S. Butler, N. J. Coville and D. Cozak, *J. Organomet. Chem.* 1977, **133**, 59.
21. J. W. Buchler, W. Kokisch, P. D. Smith and B. Tonn, *Z. Naturforsch.* 1978, **33B**, 1371.
22. L. Ruis-Ramirez, T. A. Stephenson and E. S. Switkes, *J. Chem. Soc., Dalton Trans.* 1973, 1770.
23. J. Fortune and A. R. Manning, *Organometallics* 1983, **2**, 1719.
24. O. Kolb and H. Werner, *J. Organomet. Chem.* 1984, **268**, 49.
25. H. Werner, O. Kolb, R. Feser and U. Schubert, *J. Organomet. Chem.* 1980, **191**, 283.
26. P. J. Brothers and W. R. Roper, *J. Organomet. Chem.* 1983, **258**, 73.
27. T. J. Collins and W. R. Roper, *J. Organomet. Chem.* 1978, **159**, 73.
28. M. C. Baird and G. Wilkinson, *J. Chem. Soc. A* 1967, 865.
29. M. C. Baird, G. Hartwell and G. Wilkinson, *J. Chem. Soc. A* 1967, 2037.
30. D. M. W. Thewissen, *J. Organomet. Chem.* 1980, **188**, 211.
31. M. P. Yagupsky and G. Wilkinson, *J. Chem. Soc. A* 1968, 2813.
32. M. Kubota and C. R. Carey, *J. Organomet. Chem.* 1970, **24**, 491.
33. P. W. Armit, T. A. Stephenson and E. S. Switkes, *Inorg. Synth.* 1982, **21**, 28.
34. T. A. Stephenson, E. S. Switkes and P. W. Armit, *J. Chem. Soc., Dalton Trans.* 1974, 1135.
35. P. W. Armit and T. A. Stephenson, *J. Organomet. Chem.* 1973, **74**, C33.
36. J. Gilbert, M. C. Baird and G. Wilkinson, *J. Chem. Soc. A* 1968, 2198.
37. A. E. Fenster and I. S. Butler, *Can. J. Chem.* 1972, **50**, 598.
38. G. Jaouen and R. Dabard, *J. Organomet. Chem.* 1974, **72**, 377.

39. M. J. McGlinchey, J. L. Fletcher, B. G. Sayer, P. Bougeard, R. Faggiani, C. J. L. Lock, A. D. Bain, C. Rodger, E. P. Kündig, D. Astruc, J. R. Haman, P. LeMaux, S. Top and G. Jaouen, *J. Chem. Soc., Chem Commun.* 1983, 634.
40. M. Herberhold and P. D. Smith, *Angew. Chem., Int. Ed. Engl.* 1979, **18**, 631.
41. I. S. Butler, D. Cozak and S. R. Stobart, *J. Chem. Soc., Chem. Commun.* 1975, 103.
42. I. S. Butler, D. Cozak and S. R. Stobart, *Inorg. Chem.* 1977, **16**, 1779.
43. P. Conway, S. M. Grant and A. R. Manning, *J. Chem. Soc., Dalton Trans.* 1979, 1920.
44. H. LeBozec, P. H. Dixneuf, A. J. Carty and N. J. Taylor, *Inorg. Chem.* 1978, **17**, 2568.
45. W. A. Schenk, T. Schwietzke and H. Müller, *J. Organomet. Chem.* 1982, **232**, C41.
46. P. Conway, A. R. Manning and F. S. Stephens, *J. Organomet. Chem.* 1980, **186**, C64.
47. H. Werner and O. Kolb, *Angew. Chem., Int. Ed. Engl.* 1979, **18**, 865.
48. W. M. Hawling, A. Walker and M. A. Woitzik, *J. Chem. Soc., Chem. Commun.* 1983, 11.
49. P. V. Broadhurst, B. F. G. Johnson, J. Lewis and P. R. Raithby, *J. Chem. Soc., Chem. Commun.* 1982, 140.
50. P. V. Broadhurst, B. F. G. Johnson, J. Lewis and P. R. Raithby, submitted for publication.
51. P. V. Broadhurst, B. F. G. Johnson, J. Lewis and P. R. Raithby, *J. Organomet. Chem.* 1980, **194**, C35.
52. P. V. Broadhurst, B. F. G. Johnson, J. Lewis, A. G. Orpen, P. R. Raithby and J. R. Thornback, *J. Organomet. Chem.* 1980, **187**, 141.
53. M. Kubota and C. J. Curtis, *Inorg. Chem.* 1974, **13**, 2277.
54. F. Faraone, P. Piraino, V. Marsala and S. Sergi, *J. Chem. Soc., Dalton Trans.* 1977, 859.
55. W. Petz, *J. Organomet. Chem.* 1978, **146**, C23.
56. B. D. Dombek and R. J. Angelici, *J. Am. Chem. Soc.* 1973, **95**, 7516.
57. A. M. English, K. R. Plowman, I. S. Butler, G. Jaouen, P. LeMaux and J. Y. Thepot, *J. Organomet. Chem.* 1977, **132**, C1.
58. P. D. Smith, D. Dolphin and B. R. James, *J. Organomet. Chem.* 1981, **208**, 239.
59. D. Mansuy, J. P. Battioni and J. C. Chottard, *J. Am. Chem. Soc.* 1978, **100**, 4311.
60. L. Busetto and R. J. Angelici, *J. Am. Chem. Soc.* 1968, **90**, 3283.
61. J. M. Lisy, E. D. Dobrzynski, R. J. Angelici and J. Clardy, *J. Am. Chem. Soc.* 1975, **97**, 656.
62. J. P. Battioni, J. C. Chottard and D. Mansuy, *Inorg. Chem.* 1982, **21**, 2056.
63. G. R. Clark, K. Marsden, W. R. Roper and L. J. Wright, *J. Am. Chem. Soc.* 1980, **102**, 1206.
64. T. Desmond, F. J. Lalor, G. Ferguson and M. Parvez, *J. Chem. Soc., Chem. Commun.* 1984, 75.
65. G. Jaouen, A. Meyer and G. Simmoneaux, *J. Chem. Soc., Chem. Commun.* 1975, 69.
66. G. Jaouen, *Tetrahedron Lett.* 1973, **52**, 5159.
67. G. Jaouen, A. Meyer and G. Simmoneaux, *Tetrahedron Lett.* 1973, **52**, 5163.
68. M. Poliakoff, *Inorg. Chem.* 1976, **15**, 2022.
69. M. Poliakoff, *Inorg. Chem.* 1976, **15**, 2892.
70. B. D. Dombek and R. J. Angelici, *J. Am. Chem. Soc.* 1974, **96**, 7568.
71. B. D. Dombek and R. J. Angelici, *Inorg. Chem.* 1976, **15**, 2403.
72. B. D. Dombek and R. J. Angelici, *Inorg. Chem.* 1976, **15**, 1089.
73. B. D. Dombek and R. J. Angelici, *Inorg. Chem.* 1976, **15**, 2397.
74. B. D. Dombek and R. J. Angelici, *J. Am. Chem. Soc.* 1975, **97**, 1261.
75. S. S. Woddard, R. J. Angelici and B. D. Dombek, *Inorg. Chem.* 1978, **17**, 1634.
76. W. W. Greaves, R. J. Angelici, B. J. Helland, R. Klima and R. A. Jacobson, *J. Am. Chem. Soc.* 1980, **101**, 7618.
77. W. W. Greaves and R. J. Angelici, *J. Organomet. Chem.* 1980, **191**, 49.
78. I. S. Butler and A. E. Fenster, *Inorg. Chim. Acta* 1973, **7**, 79.
79. I. S. Butler and N. J. Coville, *J. Organomet. Chem.* 1974, **80**, 235.
80. N. J. Coville and I. S. Butler, *J. Organomet. Chem.* 1974, **64**, 101.
81. A. Efraty, R. Arneri and J. Sikora, *J. Organomet. Chem.* 1975, **91**, 65.
82. A. Efraty, R. Arneri and M. H. A. Huang, *J. Am. Chem. Soc.* 1976, **98**, 639.
83. L. Busetto and A. Palazzi, *Inorg. Chim. Acta* 1976, **19**, 233.
84. J. Ellermann and M. Lietz, *J. Organomet. Chem.* 1981, **213**, C4.
85. M. H. Quick and R. J. Angelici, *J. Organomet. Chem.* 1978, **160**, 231.
86. W. Petz, *J. Organomet. Chem.* 1984, **270**, 81.
87. D. Lexa, J. M. Saveant, J. P. Battioni, M. Lange and D. Mansuy, *Angew. Chem., Int. Ed. Engl.* 1981, **20**, 578.
88. M. Lange, J. P. Battioni, D. Mansuy, D. Lexa and J. M. Saveant, *J. Chem. Soc., Chem. Commun.* 1981, 888.
89. G. R. Clark, T. J. Collins, D. Hall, S. M. James and W. R. Roper, *J. Organomet. Chem.* 1977, **141**, C5.
90. T. J. Collins and W. R. Roper, *J. Organomet. Chem.* 1978, **159**, 73.
91. G. R. Clark, T. J. Collins, K. Marsden and W. R. Roper, *J. Organomet. Chem.* 1983, **259**, 215.
92. R. Uson, P. Lahuerta, D. Carmona and L. A. Oro, *Transition Met. Chem.* 1980, **5**, 327.
93. H. L. M. van Gaal and J. P. J Verlaan, *J. Organomet. Chem.* 1977, **133**, 93.
94. M. J. Mays and F. P. Stefanini, *J. Chem. Soc. A* 1971, 2747.
95. G. Tresoldi, F. Faraone and P. Piraino, *J. Chem. Soc., Dalton Trans.* 1979, 1053.

96. F. Faraone, G. Tresoldi and G. A. Loprete, *J. Chem. Soc., Dalton Trans.* 1979, 933.
97. R. W. Matthews, L. Parkhill and M. J. Mays, *J. Organomet. Chem.* 1977, **139**, C77.
98. R. Uson, P. Lahuerta, D. Carmona, L. A. Oro and K. Hildenbrand, *J. Organomet. Chem.* 1978, **157**, 63.
99. R. Uson, L. A. Oro, M. A. Ciriano, D. Carmona, A. Tiripicchio and M. Tiripicchio-Camellini, *J. Organomet. Chem.* 1982, **224**, 69.
100. R. Uson, L. A. Oro, M. A. Ciriano, D. Carmona, A. Tiripicchio and M. Tiripicchio-Camellini, *J. Organomet. Chem.* 1981, **206**, C14.
101. R. J. Fitzgerald, N. Y. Sakkab, R. S. Strange and V. P. Naritis, *Inorg. Chem.* 1973, **12**, 1081.
102. J. W. Dunker, J. S. Finer, J. Clardy and R. J. Angelici, *J. Organomet. Chem.* 1976, **114**, C49.
103. H. Werner, O. Kolb, U. Schubert and K. Ackermann, *J. Organomet. Chem.* 1982, **240**, 421.
104. R. E. Wagner, R. A. Jacobson, R. J. Angelici and M. H. Quick, *J. Organomet. Chem.* 1978, **148**, C35.
105. D. E. Beckman and R. A. Jacobson, *J. Organomet. Chem.* 1979, **179**, 187.
106. J. C. Jeffery, H. Razay and F. G. A. Stone, *J. Chem. Soc., Chem. Commun.* 1981, 243.
107. J. C. Jeffery, H. Razay and F. G. A. Stone, *J. Chem. Soc., Dalton Trans.* 1982, 1733.
108. O. Kolb and H. Werner, *Angew. Chem., Int. Ed. Engl.* 1982, **21**, 202.
109. M. H. Quick and R. J. Angelici, *Inorg. Chem.* 1981, **20**, 1123.
110. J. A. S. Howell, P. Mathur, R. Kumar, A. R. Manning and F. S. Stephens, *J. Organomet. Chem.* 1984, **262**, 227.
111. M. H. Quick and R. J. Angelici, *Inorg. Chem.* 1982, **21**, 1674.
112. H. Werner and K. Leonhard, *Angew. Chem., Int. Ed. Engl.* 1979, **18**, 627.
113. H. Werner, K. Leonhard, O. Kolb, E. Röttinger and H. Vahrenkamp, *Chem. Ber.* 1980, **113**, 1654.
114. P. V. Broadhurst, B. F. G. Johnson, J. Lewis and P. R. Raithby, *J. Chem. Soc., Chem. Commun.* 1980, 812.
115. P. V. Broadhurst, B. F. G. Johnson, J. Lewis and P. R. Raithby, *J. Am. Chem. Soc.* 1981, **103**, 3198.
116. P. V. Broadhurst, B. F. G. Johnson, J. Lewis and P. R. Raithby, *J. Chem. Soc., Dalton Trans.* 1982, 1641.
117. P. V. Broadhurst, B. F. G. Johnson, J. Lewis and J. R. Thornback, submitted for publication.
118. W. Petz, *J. Organomet. Chem.* 1981, **205**, 203.
119. L. Busetto, M. Graziani and U. Belluco, *Inorg. Chem.* 1971, **10**, 78.
120. W. R. Roper and K. G. Town, *J. Chem. Soc., Chem. Commun.* 1977, 781.
121. M. M. Singh and R. J. Angelici, *Inorg. Chem.* 1984, **23**, 2691.
122. G. P. Elliott, W. R. Roper and J. M. Waters, *J. Chem. Soc., Chem. Commun.* 1982, 811.
123. M. A. Andrews, *Inorg. Chem.* 1977, **16**, 496.
124. D. Lichtenberger and R. F. Fenske, *Inorg. Chem.* 1976, **15**, 2015.
125. J. L. Hubbard and D. L. Lichtenberger, *Inorg. Chem.* 1980, **19**, 3865.
126. J. Y. Saillard, D. Grandjean, P. Caillet and A. L. Beuze, *J. Organomet. Chem.* 1980, **190**, 371.
127. W. G. Richards, *Trans. Faraday Soc.* 1967, **63**, 258.
128. H. W. Chen, W. L. Jolly, S. F. Xiang, I. S. Butler and J. Sedman, *J. Electron Spectrosc. Relat. Phenom.* 1981, **24**, 121.
129. A. M. English, K. R. Plowman, I. S. Butler, E. Diemann and A. Müller, *Inorg. Chim. Acta* 1979, **32**, 113.
130. I. M. Baibach and I. S. Butler, *Inorg. Chim. Acta* 1984, **89**, 73.
131. A. Efraty, M. H. A. Huang and C. A. Weston, *Inorg. Chem.* 1975, **14**, 2796.
132. A. Efraty, D. Liebman, M. H. A. Huang and C. A. Weston, *Inorg. Chim. Acta* 1980, **39**, 105.
133. K. Burger, L. Korecz, P. Mag, U. Belluco and L. Busetto, *Inorg. Chim. Acta* 1971, **5**, 362.
134. D. J. Cardin, B. Cetinkaja and M. F. Lappert, *Chem. Rev.* 1972, **72**, 545.
135. G. M. Bodner, *Inorg. Chem.* 1974, **13**, 2563.
136. I. S. Butler, A. Garcia-Rodriquez, K. R. Plowman and C. F. Shaw III, *Inorg. Chem.* 1976, **15**, 2602.
137. D. Cozak, I. S. Butler and I. M. Baibach, *J. Organomet. Chem.* 1979, **169**, 381.
138. J. A. Pople, *Mol. Phys.* 1964, **7**, 301.
139. G. Hunter and K. Mislow, *J. Chem. Soc., Chem. Commun.* 1984, 172.
140. M. J. McGlinchey, P. Bougeard, B. R. Sayer, R. Hofer and C. J. L. Lock, *J. Chem. Soc., Chem. Commun.* 1984, 789.
141. G. G. Barna, I. S. Butler and K. R. Plowman, *Can. J. Chem.* 1976, **54**, 110.
142. A. M. English, K. R. Plowman and I. S. Butler, *Inorg. Chem.* 1981, **20**, 2553.
143. A. M. English, K. R. Plowman and I. S. Butler, *Inorg. Chem.* 1982, **21**, 338.
144. R. Steudel, *Z. Naturforsch. B* 1966, **21b**, 1106.
145. I. S. Butler and D. A. Johanson, *Inorg. Chem.* 1975, **14**, 701.
146. I. M. Baibach, A. M. English and I. S. Butler, *Organometallics* 1984, **3**, 1786.
147. J. Saillard, C. LeBergne and D. Grandjean, *J. Organomet. Chem.* 1975, **94**, 409.
148. S. S. Woodard, R. A. Jacobson and R. J. Angelici, *J. Organomet. Chem.* 1976, **117**, C75.
149. J. A. Potenza, R. Johnson, S. Rudich and A. Efraty, *Acta Cryst. B* 1980, **36b**, 1933.
150. W. R. Scheidt and D. K. Geiger, *Inorg. Chem.* 1982, **21**, 1208.
151. A. J. Fraser and R. O. Gould, *J. Chem. Soc., Dalton Trans.* 1974, 1139.
152. J. L. DeBoer, D. Rogers, A. C. Skapski and P. G. H. Troughton, *J. Chem. Soc., Chem. Commun.* 1966, 756.

153. J. S. Field and P. Wheatley, *J. Chem. Soc., Dalton Trans.* 1972, 2269.
154. P. Brun, G. M. Dawkins, H. Green, A. D. Miles, A. G. Orpen and F. G. A. Stone, *J. Chem. Soc., Chem. Commun.* 1982, 926.
155. B. F. G. Johnson, J. Lewis, M. McPartlin, M. A. Pearsall and A. Sironi, *J. Chem. Soc., Chem. Commun.* 1984, 1089.

APPENDIX 1

Table A1. ^{13}C NMR chemical shifts of the CS ligand in its complexes

Compound	δ(CS)[a] (ppm)		Reference
$[(\eta^6\text{-}C_6H_6)Cr(CO)_2(CS)]$	364.4		137
$[(\eta^6\text{-}C_6H_5CO_2Me)Cr(CO)_2(CS)]$	347.6		137
$[(\eta^6\text{-}C_6Et_6)Cr(CO)_2(CS)]$	347.1		39
$[W(CO)_5(CS)]$	298.7		75
$[W(CO)_4(CS)L]$	*trans-*	*cis-*	
L = $P(OPh)_3$	301.4	301.5	75
L = $P(OMe)_3$	302.8	302.5	75
L = $P(p\text{-tolyl})_3$	299.8	306.5	75
L = PPh_3	299.6	306.0	75
L = P^nBu_3	300.0	305.1	75
L = 4-Me-py	302.7	—	75
L = CyNC	298.6	302.7	75
L = Cl^-	287.3	—	75
L = Br^-	287.4	—	75
L = I^-	285.7	—	75
$[(\eta^5\text{-}C_5H_5)W(CO)_2(CS)X]$			
X = I	310.5		76, 77
X = $SnPh_3$	283.3		77
X = $PbPh_3$	311.7		77
$[(\eta^5\text{-}C_5H_5)W(CO)(CS)I(L)]$			
L = PPh_3	353.1		76, 77
L = PMe_2Ph	352.8		77
L = $P(OPh)_3$	348.4		77
L = $P(NMe_2)_3$	355.9		77
L = CNMe	353.6		77
$[\{(\eta^5\text{-}C_5H_5)W(CO)(CS)(PMe_2Ph)_2\}^+ \cdot PF_6^-]$	338.1		77
$[\{HB(C_3N_2H_2)_3\}W(CO)_2(CS)I]$	300.0		77
$[(\eta^5\text{-}C_5H_5)Mn(CO)_2(CS)]$	442.9		135
	335.4		137
$[(\eta^5\text{-}C_5H_4Me)Mn(CO)_2(CS)]$	336.6		137
$[(\eta^5\text{-}C_5H_4Me)Mn(CO)(CS)_2]$	337.7		137
$[(\eta^5\text{-}C_5H_4Me)Mn(CO)(CS)(PPh_3)]$	340.2		137
$[\{(\eta^5\text{-}C_5H_4Me)Mn(CO)(CS)(NO)\}^+ \cdot PF_6^-]$	323.4		137
$[(\eta^5\text{-}C_5H_5)Re(CO)_2(CS)]$	288.7		137
$[Fe(CO)_4(CS)]$	327.5		55
$[\{(\eta^5\text{-}C_5H_5)Fe(CO)(CS)L\}^+ \cdot PF_6^-]$			
L = CO	307.9		83
L = PPh_3	317.4		83
L = PCy_3	320.0		83
L = $P(C_6H_4F)_3$	316.4		83
$[\{(\eta^5\text{-}C_5H_5)Fe(CS)(CNPh)_2\}^+ \cdot PF_6^-]$	320.1		83
[Fe(II)(TPP)(CS)(EtOH)]	313.5		59
$[\{(\eta^5\text{-}C_5H_5)Fe(CO)\}_2(\mu\text{-}CO)(\mu\text{-}CS)]$	380.8, 378.3		109, 110
$[\{(\eta^5\text{-}C_5H_5)Fe\}_2(CO)(PEt_3)(\mu\text{-}CO)(\mu\text{-}CS)]$	396.2		109
$[\{(\eta^5\text{-}C_5H_5)Fe(CO)(\mu\text{-}CS)\}_2]$	373.5		110
$[\{(\eta^5\text{-}C_5H_5)Fe(CO)\}_2(CS)(CNR)]$			
R = Me	391.4		110
R = Et	391.4		110

Table A1. (*Contd.*)

Compound	δ(CS)[a] (ppm)	Reference
R = ^{i}Pr	391.5	110
R = ^{i}Bu	391.0	110
[{(η^5-C_5H_5)Fe(μ-CS)}$_2$(CO)(CNMe)]	385.3	110
[{(η^5-C_5H_5)Fe}$_2$(CO)(CNMe)(μ-CS)(μ-CNMe)]	394.1	110
[(η^5-C_5H_5)(CO)$_2$M(μ-CS)Pt(PR_3)$_2$]		
M = Mn, R_3 = Me_2Ph	386.5	106, 107
M = Mn, R_3 = $MePh_2$	379.4	106, 107
M = Re, R_3 = Me_2Ph	353.4	106, 107

[a] Relative to TMS with downfield chemical shifts positive.

APPENDIX 2

Table A2. A collation of ν(CS) values for CS complexes isolated since 1976

Compound	ν(CS) (cm^{-1})	Medium	Reference
Terminal			
[(η^6-C_6H_6)Cr(CO)$_2$(CS)]	1220	CS_2	20
[(η^6-C_6H_6)Cr(CO)(CS)(PPh_3)]	1183	CS_2	20
[(η^5-C_5H_5)Cr(CO)(CS)(NO)]	1253	KBr	40
[(η^5-C_5H_5)Cr(CS)(NO)(PMe_3)]	1205	KBr	40
[{(η^5-C_5H_5)Cr(CS)(NO)$_2$}$^+$$PF_6^-$]	1352	KBr	40
[{{HB(3,5-Me_2-C_3HN_2)$_3$}Mo(CO)$_2$(CS)}$^-$]	1139	KBr	64
[W(CO)$_4$(CS)L]			
L = $P(OPh)_3$ *trans-*	1254	Hexane	75
cis-	1257	Hexane	75
L = $P(OMe)_3$ *trans-*	1248	Hexane	75
cis-	1247	Hexane	75
L = P(*p*-tolyl)$_3$ *trans-*	1238	Hexane	75
cis-	1238	Hexane	75
L = P^nBu_3 *trans-*	1236	Hexane	75
cis-	1238	Hexane	75
L = PPh_3 *cis-*	1241	Hexane	75
L = 4-Me-py *trans-*	1226	Hexane	75
cis-	1239	Hexane	75
L = CyNC *trans-*	1240	Hexane	75
cis-	1240	Hexane	75
[(η^5-C_5H_5)W(CO)(CS)I(L)]			
L = CO *trans-*	1267	CS_2	76, 77
L = PPh_3	1225	CS_2	76, 77
L = $P(OPh)_3$	1240	CS_2	77
L = $P(NMe_2)_3$	1221	CS_2	77
L = PMe_2Ph	1220	CS_2	77
L = CNMe	1241	CS_2	77
trans-[{(η^5-C_5H_5)W(CO)(CS)(PMe_2Ph)$_2$}$^+$ · PF_6^-]	1234	MeCN	77
[(η^5-C_5H_5)W(CO)$_2$(CS)(X)]			
X = $SnPh_3$ *cis-*	1238	CS_2	77
X = $PhPh_3$ *cis-*	1237	CS_2	77
X = HgI *cis/trans-*	1268, 1234	CS_2	77
X = SePh *cis/trans-*	1262	CS_2	77
[{{HB(3,5-Me_2-C_3NH_2)$_3$}W(CO)$_2$(CS)}$^-$]	1149	CH_2Cl_2	77
[{HB(3,5-Me_2-C_3NH_2)$_3$}W(CO)$_2$(CS)I]	1243	CS_2	77

Table A2. (*Contd.*)

Compound	ν(CS) (cm^{-1})	Medium	Reference
mer-[$W(CO)_3$(dmpe)(CS)]	1203	CH_2Cl_2	45
[$(\eta^5$-$C_5H_5)Re(CO)_2$(CS)]	1277	CS_2	20
[$(\eta^5$-$C_5H_5)$Re(CO)(CS)(PPh_3)]	1246	CS_2	20
[$Fe(CO)_4$(CS)]	1320, 1305	?	55
[$Fe(CO)_4$(CS){$HgCl_2$}$_3$]	1380	Nujol	86
[Hg{$Fe(CO)_3$(CS)}]	1280	Nujol	86
[$Fe(CO)_2${$P(OPh)_3$}$_2$(CS)]	1222	?	46
[{$(\eta^5$-$C_5H_5)$Fe(CS)(Me_2CO){$(AsCH_2)_3CMe$}}$^+ \cdot PF_6^-$]	1270	KBr	84
[Fe(TPP)(CS)]	1310	KBr	62
[Fe(TPP)(CS)L]			
L = MeOH	1295	KBr	62
L = EtOH	1295	KBr	62
L = morph	1285	KBr	62
L = py	1282	KBr	62
L = N-Me-Im	1278	KBr	62
L = PEt_3	1270	KBr	62
[Fe(OEP)(CS)]	1290, 1292	KBr	62, 21
[Fe(OEP)(CS)L]			
L = py	1282	KBr	21, 58
L = N-Me-Im	1275	KBr	21
L = pip	1278	KBr	21
[Fe(TTP)(CS)]	1300	KBr	62
[Fe{T(*p*-Cl)PP}(CS)]	1310	KBr	62
[{$(\eta^5$-$C_5H_5)Ru(CO)_2$(CS)}$^+$]	1364, 1352	CH_2Cl_2	9
[$(\eta^5$-$C_5H_5)$Ru(CO)(CS)I]	1308	CS_2	9
[$(\eta^5$-$C_5H_5)$Ru(CO)(CS){C(O)OMe}]	1304	Hexane	9
[$Ru(CO)_3(CS)Cl_2$]	1365	Nujol	54
[$Ru(CO)_2(CS)Cl_2(PPh_3)$]	1310	Nujol	54
[{$Ru(CNCy)_2(CO)_2$(CS)Cl}$^+ \cdot BPh_4^-$]	1325	Nujol	54
[{Ru(dpae)(CO)(CS)Cl}$^+BPh_4^-$]	1305	Nujol	54
[$RuCl_2(H_2O)(CS)(PPh_3)_2$]	1293	Nujol	13, 26
[$RuCl_2$(CS)(CNR)(PPh_3)$_2$] *trans*-	1270	Nujol	13, 26
(R = *p*-tolyl) *cis*-	1295	Nujol	13, 26
[{RuCl(CS)(CO)(CNR)(PPh_3)$_2$}$^+$]	1135	Nujol	13, 26
[$RuCl_2$(CS)(CNR′)(PPh_3)$_2$] *trans*-	1273	Nujol	26
(R′ = *p*-C_6H_4Cl) *cis*-	1292	Nujol	26
[Ru(η^2-O_2CH)Cl(CS)(PPh_3)$_2$]	1290	Nujol	26
[Ru(η^2-O_2CMe)H(CS)(PPh_3)$_2$]	1283	Nujol	26
[Ru(η^2-O_2CMe)H(CS)(PPh_3)$_2$]	1280	Nujol	26
[RuHCl(CS)(PPh_3)$_3$]	1256	Nujol	26
[{RuCl(CS)(PPh_3)$_2$(H_2O)(CNR)}$^+$]			
R = *p*-tolyl	1305	Nujol	26
R = *p*-C_6H_4Cl	1309	Nujol	26
[{RuCl(CS)(PPh_3)$_2$($CNR)_2$}$^+$]			
R = *p*-tolyl	1310	Nujol	26
R = *p*-C_6H_4Cl	1309	Nujol	26
[Ru(OEP)(CS)(py)]	1283	?	58
[$OsCl_2$(CS)(CO)(PPh_3)$_2$]	1315	Nujol	63
[OsH_2(CS)(PPh_3)$_3$]	1233	Nujol	90
[OsHCl(CS)(PPh_3)$_3$]	1280	Nujol	90
[OsHBr(CS)(PPh_3)$_3$]	1273	Nujol	90
[OsHCl(CS)(CNR)(PPh_3)$_2$] (R = *p*-tolyl)			
trans-(CS)(CNR)	1275	Nujol	90
trans-(CS)(Cl)	1282	Nujol	90
[OsHCl(CO)(CS)(PPh_3)$_2$]	1295	Nujol	90
[OsHBr(CO)(CS)(PPh_3)$_2$]	1300	Nujol	90

Table A2. (*Contd.*)

Compound	ν(CS) (cm^{-1})	Medium	Reference
$[Os(CS)(CO)(CNR)(PPh_3)_2]$ (R = *p*-tolyl)	1232, 1222	Nujol	13
$[\{OsCl(CS)(CO)(CNR)(PPh_3)_2\}^+]$ (R = *p*-tolyl)	1323	Nujol	13, 89
$[OsCl_2(CS)(CNR)(PPh_3)_2]$ (R = *p*-tolyl)	1305	Nujol	89
$[OsCl(OClO_3)(CS)(CNR)(PPh_3)_2]$ (R = *p*-tolyl)	1310	Nujol	89
$[Os(\eta^2\text{-}CS\cdot NR)(CS)(CO)(PPh_3)_2]$ (R = *p*-tolyl)	1285	Nujol	89
$[\{Os(\eta^2\text{-}CS\cdot NRMe)(CS)(CO)(PPh_3)_2\}^+]$ (R = *p*-tolyl)	1308	Nujol	89
$[Os(\eta^2\text{-}CS_2)(CS)(CO)(PPh_3)_2]$	1280	Nujol	11
$[\{Os(\eta^2\text{-}CS_2Me)(CS)(CO)(PPh_3)_2\}^+]$	1300	Nujol	11
$[OsCl_2(CS)_2(PPh_3)_2]$	1370, 1260	Nujol	11
$[OsBr_2(CS)_2(PPh_3)_2]$	1360, 1260	Nujol	11
$[Os(\sigma\text{-}S_2CNEt_2)(\sigma\text{-}CS_2Me)(CS)(CO)(PPh_3)_2]$	1290	Nujol	11
$[Os(\eta^2\text{-}S_2CNEt_2)(\sigma\text{-}CS_2Me)(CS)(PPh_3)_2]$	1268	Nujol	11
$[\{Os(\eta^2\text{-}S_2CNEt_2)(CS)_2(PPh_3)_2\}^+]$	1350, 1265	Nujol	11
$[Os(\eta^2\text{-}S_2CNEt_2)(CHS)(CS)(PPh_3)_2]$	1270	Nujol	11
$[Os(CS)(CO)_2(PPh_3)_2]$	1230	Nujol	14
$[OsR(CS)(PPh_3)_2X]$ (R = *p*-tolyl)			
X = Cl	1290	Nujol	91
X = Br	1285	Nujol	91
X = I	1281	Nujol	91
$X = \eta^2\text{-}S_2CNEt_2$	1270	Nujol	91
$X = \eta^2\text{-}O_2CMe$	1282	Nujol	91
$X = \eta^2\text{-}O_2CCF_3$	1290	Nujol	91
$[OsR(CS)(PPh_3)_2X(L)]$			
X = Cl, L = CO	1300	Nujol	91
X = Cl, L = MeCN	1282	Nujol	91
X = Cl, L = CNR (R = *p*-tolyl)	1290	Nujol	91
X = Br, L = CO	1292	Nujol	91
$X = \sigma\text{-}O_2CCF_3$, L = CO	1300	Nujol	91
$X = \sigma\text{-}O_2CCF_3$, L = CNR′ (R′ = *p*-$C_6H_4Cl$)	1291	Nujol	91
$[Os(CS)(PPh_3)_2(\sigma\text{-}O_2CCF_3)(EtOH)]$	1303	Nujol	91
[Os(OEP)(CS)(py)]	1284	KBr	21, 58
$[Os_3(CO)_8(CS)S_2]$	1324	CH_2Cl_2	50, 51
$[Os_3(CO)_7(CS)S_2(\mu\text{-}H)_2]$	1325	Nujol	52, 117
$[(\eta^5\text{-}C_5H_5)Co(CS)L]$			
$L = P^nBu_3$	1260	CS_2	23
$L = PPh_3$	1275	CS_2	23
$L = PMePh_2$	1267	CS_2	23
$L = PMe_2Ph$	1269	Nujol	24
$L = PMe_3$	1270	Nujol	24
$L = P(OMe)_3$	1289	Nujol	24
$[(\eta^5\text{-}C_5H_5)Co(CS)(PPh_3)(HgX_2)]$			
X = Cl	1310	KBr	23
X = Br	1310	KBr	23
$[\{(np_3)Co(CS)\}^+BPh_4^-]$	1270	Nujol	16
$[(\eta^5\text{-}C_5H_5)Rh(CS)L]$			
$L = PMe_3$	1279	CS_2	24
$L = PPh_3$	1268	Nujol	96
$[\{(\eta^5\text{-}C_5H_5)Rh(CS)(PPh_3)X\}^+\cdot BPh_4^-]$			
X = Cl	1370	Nujol	96
X = Br	1365	Nujol	96
X = I	1358	Nujol	96
$[(\eta^5\text{-}C_5H_5)RhCl_2(CS)(PPh_3)(HgCl_2)]$	1315	Nujol	96
$[\{RhCl(CS)(PPh_3)\}_2]$	1308	Nujol	96
trans-$[RhCl(CS)(PCy_3)_2]$	1283	?	93
trans-$[RhCl(CS)(PMePh_2)_2]$	1310	KBr	92

Table A2. (*Contd.*)

Compound	ν(CS) (cm^{-1})	Medium	Reference
$[Rh(CS)(PCy_3)_2(OClO_3)]$	1305	KBr	92
$[\{Rh(CS)(PCy_3)_2L\}^+ClO_4^-]$			
L = py	1285	KBr	92
L = 4-Me-py	1280	KBr	92
L = bipy	1259	KBr	92
L = phen	1260	KBr	92
L = phthaln	1280	KBr	92
L = *p*-(MeO)C_6H_4CN	1280	KBr	92
L = *p*-ClC_6H_4CN	1285	KBr	92
$[Rh(CS)(PPh_3)(PCy_3)(OClO_3)]$	1308	KBr	92
$[\{Rh(CS)(PPh_3)_2(PCy_3)\}^+ClO_4^-]$	1305	KBr	92
$[\{Rh(CS)(PPh_3)(PCy_3)L\}^+ClO_4^-]$			
L = py	1315	KBr	92
L = bipy	1270	KBr	92
L = phen	1275	KBr	92
L = phthaln	1325	KBr	92
L = $P(OPh)_3$	1310	KBr	92
$[\{Rh(CS)(PPh_3)(tmeda)\}^+ \cdot ClO_4^-]$	1313	Nujol	98
$[\{Rh(CS)(PPh_3)_2L\}^+ClO_4^-]$			
L = py	1320	Nujol	98
L = 2-Et-py	1315	Nujol	98
L = 4-Et-py	1310	Nujol	98
L = bipy	1290	Nujol	98
L = phen	1285	Nujol	98
L = *o*-$C_6H_4(CN)_2$	1327	Nujol	98
L = PPh_3	1312	KBr	98
$[\{Rh(CS)L_3\}^+ \cdot PF_6^-]$			
L = $PMePh_2$	1300	Nujol	97
L = PEt_2Ph	1281	Nujol	97
L = $PPh(OPh)_2$	1333	Nujol	97
$[\{Rh(CS)L_4\}^+ \cdot PF_6^-]$			
L = PMe_2Ph	1232	Nujol	97
L = $PPh_2(OMe)$	1278	Nujol	97
L = $PPh(OMe)_2$	1261	Nujol	97
L = $PPh(OEt)_2$	1260	Nujol	97
L = $P(OMe)_3$	1274	Nujol	97
L = $P(OEt)_3$	1269	Nujol	97
L = $\frac{1}{2}$dppc	1257	Nujol	97
$[Rh(CS)(PPh_3)_2R]$			
R = C_6F_5	1277	Nujol	95
R = C_6Cl_5	1278	Nujol	95
$[\{Rh(CS)(PPh_3)_2(HL)\}^+]$			
L = pz	1325	Nujol	99
L = 3-Me-pz	1317	Nujol	99
L = 3,5-Me_2-pz	1315	Nujol	99
$[\{Rh(CS)(PCy_3)_2(HL)\}^+]$			
L = pz	1285	KBr	99
L = 3,5-Me_2-pz	1285	KBr	99
$[Rh(CS)(PCy_3)_2(pz)]$	1285	Nujol	99
$[\{(R_3P)_2(CS)Rh(\mu\text{-pz})Au(PPh_3)\}^+]$			
R = Ph	1310	KBr	99
R = Cy	1285	Nujol	99
$[\{Rh(\mu\text{-L})(CS)(PPh_3)_2]$			
L = pz	1294, 1305	Nujol	99
L = 3-Me_2-pz	1288, 1302	Nujol	99
L = Idz	1290, 1300	Nujol	99

Table A2. (*Contd.*)

Compound	ν(CS) (cm^{-1})	Medium	Reference
$[(\eta^5\text{-}C_5H_5)Ir(CS)(PPh_3)]$	1292	Nujol	96
$[\{(\eta^5\text{-}C_5H_5)Ir(CS)(PPh_3)X\}^+ \cdot X^-]$			
X = Cl	1375	Nujol	96
X = Br	1373	Nujol	96
X = I	1370	Nujol	96
$[\{(\eta^5\text{-}C_5H_5)Ir(CS)(PPh_3)X\}^+ \cdot BPh_4^-]$			
X = H	1360	Nujol	96
$X = CH_2CN$	1365	Nujol	96
$[(\eta^5\text{-}C_5H_5)IrCl_2(CS)(PPh_3)(HgCl_2)]$	1338	Nujol	96
$[IrMeCl(CS)(PPh_3)_2]$	1376	Nujol	96
$[IrR(CS)(PPh_3)_2]$			
$R = C_6F_5$	1300	Nujol	95
$R = C_6Cl_5$	1302	Nujol	95
$[IrRCl(H)(CS)(PPh_3)_2]$			
$R = C_6F_5$	1358	Nujol	95
$R = C_6Cl_5$	1356	Nujol	95
$[IrBr_2(C_6F_5)(CS)(PPh_3)_2]$	1362	Nujol	95
$[IrI_2(C_6F_5)(CS)(PPh_3)_2]$	1355	Nujol	95
$[Ir(C_6F_5)Cl(CS)(HgCl)(PPh_3)_2]$	1335	Nujol	95
Bridging			
$[\{(\eta^5\text{-}C_5H_5)Fe(CO)\}_2(\mu\text{-}CO)(\mu\text{-}CS)]$	1130	CS_2	109
$[\{(\eta^5\text{-}C_5H_5)Fe\}_2(CO)L(\mu\text{-}CO)(\mu\text{-}CS)]$			
$L = PEt_3$	1102	CS_2	109
$L = PMe_2Ph$	1104	CS_2	109
$L = PMePh_2$	1100	CS_2	109
$L = P(OMe)_3$	1108	CS_2	109
$[\{(\eta^5\text{-}C_5H_5)Fe\}_2(CO)_2(CS)(CNMe)]^a$	1119, 1115	CS_2	109
$[\{(\eta^5\text{-}C_5H_5)Fe\}_2(CO)(CNMe)(\mu\text{-}CS)(\mu\text{-}CNMe)]^b$	1119, 1111	CS_2	109
$[\{(\eta^5\text{-}C_5H_5)Fe(CNMe)\}_2(\mu\text{-}CO)(\mu\text{-}CS)]$	1101	CS_2	109
$[\{(\eta^5\text{-}C_5H_5)Fe(CO)(\mu\text{-}CS)\}_2]^b$	1131, 1124	Hexane	110
$[\{(\eta^5\text{-}C_5H_5)Fe(CO)\}_2(\mu\text{-}CS)(\mu\text{-}CNR)]^+$			
R = Me			
$[\{(\eta^5\text{-}C_5H_5)Fe\}_2(CO)(CNR)(\mu\text{-}CO)(\mu\text{-}CS)]$	1119, 1113	Hexane	110
R = Et	1119, 1113	Hexane	110
R = ^{i}Pr	1121, 1115	Hexane	110
R = ^{t}Bu	1119, 1113	Hexane	110
$[\{(\eta^5\text{-}C_5H_5)Fe(\mu\text{-}CS)\}_2(CO)(CNMe)]$	1108	Hexane	110
$[\{(\eta^5\text{-}C_5H_5)Ru(CO)\}_2(\mu\text{-}CO)(\mu\text{-}CS)]$ *cis/trans*-	1125	CS_2	9
cis-$[\{(\eta^5\text{-}C_5H_5)Ru(CO)(\mu\text{-}CS)\}_2]$	1118	CS_2	9
trans-$[\{(\eta^5\text{-}C_5H_5)Ru(CO)(\mu\text{-}CS)\}_2]$	1128	CS_2	9
$[(\eta^5\text{-}C_5H_5)(Me_3P)Co(\mu\text{-}CS)_2Co(\eta^5\text{-}C_5H_5)]$	1157, 1121	CS_2	103
$[(\eta^5\text{-}C_5H_5)(Me_3P)Co(\mu\text{-}CO)(\mu\text{-}CS)Mn(\eta^5\text{-}C_5H_5)]$	1106	Nujol	108
μ-C · σ-S			
$[\{(\eta^5\text{-}C_5H_5)Fe(CO)\}_2(\mu\text{-}CO)(\mu\text{-}C \cdot \sigma\text{-}S \rightarrow A)]$			
$A = HgCl_2$	1020	CH_2Cl_2	111
$A = HgBr_2$	1020	CH_2Cl_2	111
$A = Cr(CO)_5$	1082	CS_2	111
$A = W(CO)_5$	1076	CS_2	111
$A = HgMe^+$	1017	CH_2Cl_2	111
$[(\eta^5\text{-}C_5H_5)(Me_3P)Co(\mu\text{-}CO)\{\mu\text{-}C \cdot \sigma\text{-}SMn(CO)(\eta^5\text{-}C_5H_5)\}$			
$Mn(CO)(\eta^5\text{-}C_5H_5)]$	1050	Nujol	108
Other bonding modes			
$[\{(\eta^5\text{-}C_5H_5)Co\}_3(\mu_3\text{-}S)(\mu_3\text{-}CS)]$	1039, 1075	KBr	23
$[\{(\eta^5\text{-}C_5H_4Me)Co\}_3(\mu\text{-}S)(\mu_3\text{-}CS)]$	1059, 1069	KBr	23

Table A2. (*Contd.*)

Compound	ν(CS) (cm^{-1})	Medium	Reference
$[Fe_4(CO)_{12}(CS)S](\mu_3\text{-}C \cdot \sigma\text{-}S)$	963	Nujol	50, 114
$[Os_4(CO)_{12}(CS)S](\mu_4\text{-}C \cdot \sigma\text{-}S)$	843	Nujol	116
$[Fe_5(CO)_{13}(CS)S_2](\mu_4\text{-}C \cdot \mu\text{-}S)$	921	Nujol	50, 115

[a] Two isomers due to terminal or bridging CNMe ligand.
[b] Two isomers due to *cis*- and *trans*-η^5-C_5H_5 orientations.

Polyhedron Vol. 4, No. 11, pp. 1847–1852, 1985
Printed in Great Britain

0277–5387/85 $3.00 + .00
© 1985 Pergamon Press Ltd

ESR AND ELECTRONIC ABSORPTION SPECTRA OF CHROMIUM ACETYLACETONATO NITROSYL COMPLEXES

A. KELLER* and B. JEŻOWSKA-TRZEBIATOWSKA
Institute of Chemistry, University of Wrocław, Poland

(*Received* 18 *September* 1984; *accepted* 27 *March* 1985)

Abstract—The *cis*- and *trans*-chromium nitrosyl complexes with formulae $[Cr(NO)(acac)_2L]$ ($L = H_2O$, NH_3, pyridine and imidazole) and $[Cr(NO)(acac)_2]_2(N\text{–}N)$ (N–N = bridge ligands, i.e. ethylenediamine and 4,4′-bipyridyl) were investigated by magnetic and spectroscopic (ESR and UV–VIS) methods. The character of metal–ligand bonding and the influence of the coordinated ligands on the electron density distribution within the molecular unit {CrNO} were determined.

Many papers concerning nitrosyl complexes of transition metals proved that the structure and properties of the coordinated NO group may be affected by a suitable choice of additionally coordinated ligands. Using acetylacetonate as the aditional ligand, nitrosyl *cis*-and *trans*-complexes of chromium of types $[Cr(NO)(acac)_2L]$ [where $L = H_2O$, NH_3, pyridine (py) and imidazole (imid)] and $[Cr(NO)(acac)_2]_2(N\text{–}N)$ [where N–N are bridge ligands ethylenediamine (en) and 4,4′-dipyridyl (bpy)] were obtained.[1] The structure of those complexes was determined on the grounds of X-ray powder diffractograms and IR spectra.

This paper concerns the electronic and ESR spectra of those complexes from which the nature of the metal–ligand bonding and the effect of the ligands on the electron density distribution within the {CrNO} molecular group were determined.

EXPERIMENTAL

Synthesis of trans-$[Cr(NO)(acac)_2(H_2O)]$ **(I)**

Ten grams of Na_2CO_3 was added to a solution of 7 g CrO_3 in 20 cm^3 H_2O previously cooled to 0°C. Then an aqueous solution of thiourea (5 g) and sodium carbonate (10 g) dissolved in water were added and subsequently 15 cm^3 of acetylacetone were added dropwise. This solution was then heated to room temperature and a solution containing 9 g of hydroxylamine hydrochloride in a minimum amount of water was added. After a few hours, the brown crystal precipitate was filtered off, washed with water and dried in a vacuum over P_4O_{10}.

Synthesis of trans-$[Cr(NO)(acac)_2(NH_3)]$ **(II)**

A solution of 7 g of CrO_3 in 15 cm^3 H_2O was cooled to about 0°C and neutralized with a concentrated sodium carbonate solution. Next, 10 cm^3 of a concentrated ammonia solution was added. To this solution 15 cm^3 of acetyloacetone and 9 g of hydroxylamine hydrochloride in a minimum amount of H_2O were added dropwise. The solution was left for 24 h at 0°C for crystallization. The orange precipitate was filtered off, washed with H_2O and dried over P_4O_{10}.

Synthesis of cis-$[Cr(NO)(acac)(NH_3)]$ **(IIa)**

To 7 g of CrO_3 dissolved in a small amount of H_2O and cooled to 0°C, 50 cm^3 of a 35% solution of KOH, 15 cm^3 of acetylacetone and 18 cm^3 of a concentrated NH_3 solution were added.

The solution was heated up to 70–80°C and then 9 g of hydroxylamine hydrochloride was added dropwise. The solution was cooled to room temperature. After 30 min, the light-brown non-crystalline precipitate was filtered off, washed with the H_2O–NH_3 mixture and with H_2O and dried over P_4O_{10}.

Synthesis of trans-$[Cr(NO)(acac)_2py]$ **(III)**

A known amount of the complex **I** was dissolved in methanol and treated with py, the molar ratio of the complex to py being 1:5. The red-brown crystal precipitate was next filtered off, washed with H_2O and dried over P_4O_{10}.

* Author to whom correspondence should be addressed.

Synthesis of cis-[Cr(NO)(acac)py] (**IIIa**)

A solution containing 7 g of CrO_3, 20 g of Na_2CO_3, 15 cm^3 of acetylacetone and 5 cm^3 of py dissolved in 50 cm^3 H_2O was heated to 70°C. Next, a solution of 10 g of hydroxylamine hydrochloride in a small amount of H_2O was added dropwise. After a dozen or so minutes of heating, the solution was cooled. The light-brown crystal precipitate was filtered off, washed with H_2O and dried over P_4O_{10}.

Synthesis of trans-{[Cr(NO)(acac)$_2$]$_2$en} (**IV**)

En was added to a methanol complex (**I**) solution, the molar ratio being 2:1. The solution was concentrated in a vacuum. The crystallized orange precipitate was washed with H_2O and dried over P_4O_{10}.

Synthesis of cis-{[Cr(NO)(acac)$_2$]$_2$en} (**IVa**)

Complex **IVa** was prepared similarly to complex **IIIa**, but 3 cm^3 of en was added instead of py. After reduction the solution was cooled and left for crystallization. The crystallized yellow-green precipitate was filtered off, washed with H_2O and dried over P_4O_{10}.

Synthesis of trans-{[Cr(NO)(acac)$_2$]$_2$(bipy)} (**V**) *and* trans-[Cr(NO)(acac)$_2$(imid)] (**VI**)

Complexes **V** and **VI** were prepared just like complex **III**, bipy and/or imid being added respectively, instead of py.

Instrumentation

Magnetic susceptibility measurements within the temperature range 77–295 K were made by the Gouy method. The ESR spectra were recorded with a JES-ME-3X X-band spectrometer at 125 and 295 K using Mn^{2+} in HgO and Fremi's salt as ESR standards and the JES-SH-3CX superheterodyne for microwave frequency measurement. The electronic absorption spectra were recorded within the range 50,000–10,000 cm^{-1} with a Cary 14 spectrophotometer.

RESULTS AND DISCUSSION

All the studied complexes are paramagnetic with magnetic moments corresponding to a single unpaired electron (Table 1). Typical ESR spectra are shown in Fig. 1. These spectra give no evidence of rhombic deformations and do not differ from those of complexes of $[Cr(NO)L_{5-n}X_n]^{m+}$ type.[1–4] In the spectra of complexes **II–VI**, in which the ligands are coordinated through nitrogen, no hyperfine interaction from the ^{14}N of the ligands is observed. A rather significant effect of the solvent on the ESR parameter values was noticed, particularly on the isotropic parameters. In Table 2 the spin Hamiltonian parameters of complex **I** in a few solvents are collected. For the other complexes under test those parameters depend on the solvent in the same way.

The spin Hamiltonian and bonding parameters of all the tested complexes, determined and calculated from the ESR spectra recorded for solutions in anhydrous ethanol, are given in Table 3. The ESR parameters indicate that the unpaired electron occupies the molecular orbital $\psi = c_{xy}d_{xy} - c\phi$ lig. For such an electronic configuration, the c_{xy}^2-coefficient and the isotropic contact term, K, were calculated from the McGarvey relationships.[5] The

Table 1. Analytical data and magnetic moments and ν(NO) frequencies of *cis*- and *trans*-[Cr(NO)(acac)$_2$L]

Complex	% Cr		% C		% N		% H		μ_{eff}[a] (MB)	θ (K)	ν(NO) (cm^{-1})
	Found	Calc.	Found	Calc.	Found	Calc.	Found	Calc.			
I	17.80	17.89	40.82	40.90	4.51	4.69	5.36	5.36	1.80	−11	1695
II	17.42	17.51	40.09	40.37	9.12	9.42	5.82	5.72	1.88	0	1677
IIa	17.48		40.22		9.60		5.59		1.99	−10	1670
III	14.51	14.48	50.08	50.14	7.59	7.79	5.30	5.29	1.89	−4	1672
IIIa	14.45		50.02		7.84		5.40		1.98	−12	1670
IV	16.70	16.76	42.48	42.54	8.92	9.02	5.51	5.85	1.85	−12	1668 1685 sh
IVa	16.80		42.46		8.93		5.97		1.99	−14	1674 1681
V	14.50	14.43	50.01	49.95	7.70	7.77	5.15	5.05	1.82	−11	1674
VI	14.82	14.94	44.71	44.80	11.92	12.07	5.36	5.21	1.89	−6	1670

[a] For complexes **IV**, **IVa** and **V** the μ_{eff} values were calculated for one atom of the metal.

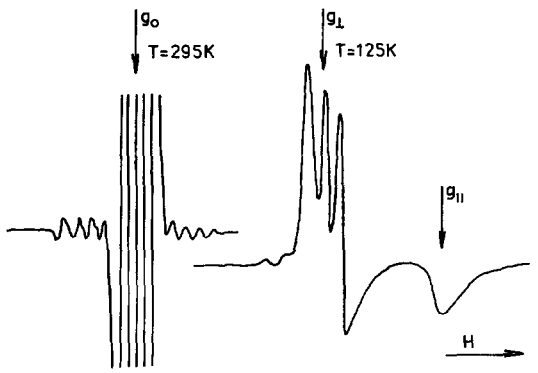


Fig. 1. The typical ESR spectrum for the chromium acetylacetonato nitrosyl complexes.

spin density of the *s*- and *p*-electrons of $^{14}N(NO)$ were estimated to be $c^2_{2s} = A_{iso}/A^o_{iso}$ and $c^2_{2p} = T_{zz}/T^o_{zz}$ (where A_{iso} is the isotropic part of the hyperfine interaction, and T_{zz} is the component of the anisotropic hyperfine tensor).[6] The signs of the hyperfine parameters of the complexes investigated were postulated from the general properties of those parameters[5] and from the results of zero-field spectroscopy investigations of similar complexes.[7] The $A_{iso}[^{14}N(NO)] < 0$ and $T_{zz}[^{14}N(NO)] > 0$ values are due to the negative spin density on the p_π-orbital of the nitrosyl nitrogen because of spin polarization of the nitrogen containing the $\pi^*(NO)$ orbital through the $\pi(d_{xz,yz})$ proper ligand system).[8,9]

The results indicate rather clearly the effect of the cordinated ligands L and N–N on the electron density distribution within the complex molecules. The variation of the K, T_{zz} and c^2_{xy} parameters (Table 3), the lowering of which may be considered to be a measure of the increase in the covalent character of the chemical bond, are consistent with the positions of those ligands in the nephelauxetic series. At the same time, those ligands exhibit their donor properties toward the strong acceptor NO. Those interactions are reflected in the variations of the c^2_{2s}- and c^2_{2p}-coefficients and of the c^2_{2p}/c^2_{2s} ratio (Table 3).

Acac as the ligand may exhibit both π-acceptor and π-donor properties toward the central ion since both the occupied bonding and the unoccupied antibonding π molecular orbitals are energetically suitable for overlap with the metal π-orbitals.[10] Which one of those interactions prevails depends on the population of the d_π-orbitals and on the relative orbital energies.[11,12] Therefore, those interactions will be considerably affected by the strongly π-acceptor properties of the NO group. A comparison of the experimental and calculated ESR parameter values of the *trans*- and *cis*-complexes (Table 3) indicates a stronger electron delocalization through π-bonding Cr → acac in the latter than in the *trans*-isomers. This is evidenced by the following sequences: $c^2_{2p}/c^2_{2s}(cis) < c^2_{2p}/c^2_{2s}(trans)$, $T_{zz}(cis) < T_{zz}(trans)$, $K(cis) < K(trans)$ and $g_\perp(cis) > g_\perp(trans)$ since the π M—L bonds contribute to the $g_\perp$ value due to the unpaired d_{xy}-electron interacting in the perpendicular orientation with the filled d_{xz}, d_{yz} orbitals, the positions of the latter depending on the donor–acceptor properties of the ligands.[13]

The above conclusions are consistent with the results of IR spectroscopic studies,[1] particularly when the frequencies of the Cr–O and NO vibrations are compared. For example, the ν(NO) frequency is lower for the *cis*-complexes than for the *trans*-isomers (Table 1). The correlation between ν(NO) and the structure of the M–NO group has been considered in many papers.[14–18] It is well known that the strength of the M–NO bond is related to the density of *s*- and *p*-electrons of the nitrogen of the NO group, the latter depending on the filling of the metal *d*-orbitals, on the character of the M–NO bonding and on the donor–acceptor abilities of the other coordinated ligands. Figure 2, in which the variation of the ν(NO) frequency is drawn as a function of the c^2_{2s}- and c^2_{2p}-coefficients, illustrates the global effect of donor–acceptor interactions of the coordinated ligands on the frequency ν(NO) in the complexes studied.

The diagram of molecular orbitals interpreting the ESR parameters of the complexes under test is shown in Fig. 3. The sequence of the δ^*-orbitals is determined by the δ-donor properties of the coordinated ligands. The diagram also explains the

Table 2. ESR parameters[a] for complex I in different solvents

Solvent	g_{iso}	$g_\perp$	$g_{||}$	$A_{iso}(^{14}N)$	$A_\perp(^{14}N)$	$A_{||}(^{14}N)$	$A_{iso}(^{53}Cr)$	$A_\perp(^{53}Cr)$	$A_{||}(^{53}Cr)$
Ethanol—anhydrous	1.974	1.994	1.940	6.76	8.42	3.44	24.11	16.66	39.01
Ethanol—96%	1.975	1.994	1.940	6.70	8.38	3.34	24.20	16.59	39.42
Methanol	1.966	1.993	1.940	7.53	8.60	5.39	23.76	16.70	37.88
Acetone + H_2O	1.970	1.993	1.940	7.01	8.29	4.45	23.32	16.47	37.02

[a] The A values are in G. The $A_{||}$ were calculated from the relation $A_{iso} = \frac{1}{3}(2A_\perp - A_{||})$.

Table 3. Experimental and calculated ESR parameters for chromium acetylacetonato nitrosyl complexes

Complex	g_{iso}	$g_\perp$	$g_\parallel$	10^4 cm $^{14}N(NO)$ A_{iso}	$A_\perp$	$A_\parallel$	^{53}Cr A_{iso}	$A_\perp$	$A_\parallel$	T_{zz} ±0.2	K ±0.2	100 c_{2s}^2	100 c_{2p}^2	c_{2p}^2/c_{2s}^2	c_{xy}^2
I	1.974	1.994	1.940	−6.23	−7.84	−3.15	22.22	15.51	35.33	13.42	−21.38	1.14	7.10	6.23	0.71
II	1.975	1.992	1.942	−5.92	−7.83	−2.21	21.77	15.45	34.10	12.64	−20.96	1.07	8.81	8.23	0.68
V	1.976	1.994	1.944	−5.83	−7.78	−1.97	21.48	15.31	33.53	12.34	−20.70	1.06	9.03	8.52	0.66
III	1.975	1.993	1.943	−5.75	−7.74	−1.93	21.34	15.25	33.23	12.18	−20.53	1.05	9.24	8.80	0.65
VI	1.975	1.993	1.943	−5.74	−7.72	−1.92	21.28	15.14	33.27	12.28	−20.47	1.05	9.30	8.94	0.66
IV	1.974	1.993	1.942	−5.73	−7.80	−1.68	21.57	15.35	33.75	12.44	−20.73	1.04	9.82	9.45	0.67
IIa	1.975	1.995	1.936	−6.13	−7.61	−3.26	21.49	15.19	34.09	12.58	−20.77	1.12	6.33	5.65	0.68
IIIa	1.975	1.995	1.940	−5.96	−7.51	−2.77	21.95	15.15	32.87	12.00	−20.34	1.08	6.75	6.22	0.64
IVa	1.974	1.994	1.941	−5.98	−7.78	−2.49	21.39	15.18	33.56	12.42	−20.55	1.09	8.24	7.56	0.66

Table 4. Electronic absorption spectra of chromium acetylacetonato nitrosyl complexes[a]

I		**II**		**IIa**		**III**		**IIIa**		**IV**		**IVa**	
(cm^{-1})	ε_{max}	(cm^{-1})	ε_{max}	(cm^{-1})	ε_{max}	(cm^{-1})	ε_{max}	(cm^{-1})	ε_{max}	(cm^{-1})	ε_{max}	(cm^{-1})	ε_{max}
				47,400	12,053			47,600	10,978			47,700	11,173
						40,700	8099	40,650	8207				
								39,550 sh	(9724)				
39,060	9767	39,290	7609	39,650	9895	39,250	9181	39,350	9931	39,400	7941	39,900	9993
								37,750	10,207				
				36,950	7493			36,700 sh	(10,138)			36,750 sh	(7678)
30,150	9400	30,250	5978	30,400	7867	30,300	6023	30,650	6483	30,500	6538	30,700	9464
25,350 sh	(505)	26,350 sh	(291)	25,800 sh	(520)	26,500 sh	(303)	25,850 sh	(559)	26,600 sh	(357)	26,000 sh	(504)
				24,200 sh	(480)			24,200 sh	(498)			24,200 sh	(478)
22,220 sh	(72.5)	22,300 sh	(41.3)	21,300 sh	(82)	22,500 sh	(59.0)	21,740 sh	(145)	22,000 sh	(47)	21,200 sh	(80.5)
17,550	37.1	17,500	33.7	17,600	47	17,350	40.5	17,650	45	17,600	27	17,700	33.0

[a] sh = shoulder.

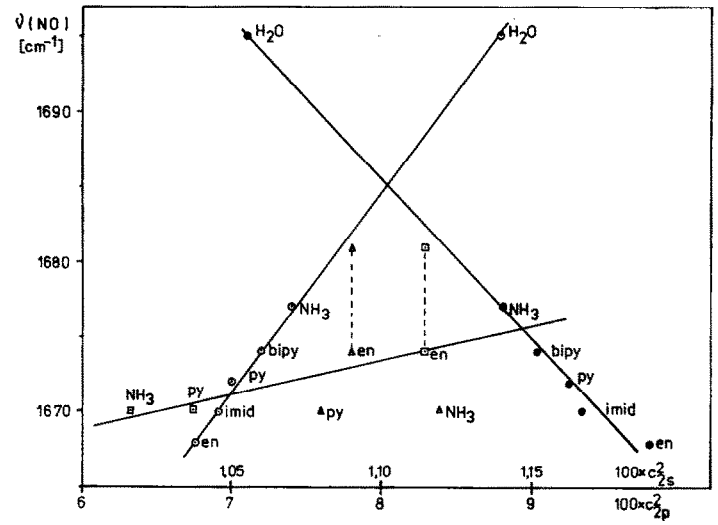


Fig. 2. The relationship between c^2_{2s}- and c^2_{2p}-coefficients and ν(NO) for the chromium acetylacetonato nitrosyl complexes. (○—○) $\nu(NO) = f(c^2_{2s})$ for *trans*-isomers, (●—●) $\nu(NO) = f(c^2_{2p})$ for *trans*-isomers, (△—△) $\nu(NO) = f(c^2_{2s})$ for *cis*-isomers, and (□—□) $\nu(NO) = f(c^2_{2p})$ for *cis*-isomers.

spectroscopic properties of the compounds discussed. Table 4 shows the electronic absorption spectra of complexes **I–IVa** in ethanol. The following electronic transitions were attributed to bands appearing in the spectra: the $^2B_2 \rightarrow {}^2E$ [$e(d_{xz,yz} + \pi^*NO) \rightarrow b_2(d_{xy})$] transition to the bands in the vicinity of 17,500 cm^{-1}, the $^2B_2 \rightarrow {}^2B_2$ [$e(d_{xz,yz} + \pi^*NO) \rightarrow e(\pi^*NO + d_{xz,yz})$] to the 22,000 cm^{-1} band (the energy of that transition is almost independent of the type of ligand in mononitrosyl complexes of chromium[2,19]), the $^2B_2 \rightarrow {}^2B_1$ [$b_2(d_{xy}) \rightarrow b_1(d_{x^2-y^2})$] transition to bands within 25,350–26,600 cm^{-1} and the $b_2(d_{xy}) \rightarrow [\pi^*_4(acac)]$ transition to bands within 30,150–30,700 cm^{-1}. The highest bands, i.e. those situated somewhat above 39,000 cm^{-1}, correspond to $\pi_3 \rightarrow \pi^*_4$ transitions of the coordinated acetylacetonates. For complexes **III** and **IIIa** (where L = py) $\pi \rightarrow \pi^*$(py) transitions are also observed at about 40,000 cm^{-1}. The above transitions were attributed to the bands assuming a C_{4v}-symmetry. This assumption is doubtless correct for the *trans*-isomers. In spectra of the *cis*-complexes, there are three additional bands at approximately 47,000, 36,000 and 24,000 cm^{-1} (Table 4). A $\pi_3 \rightarrow \pi^*_4$(acac) transition should be ascribed to the first one and a similar transition, or a transition of $d_\pi \rightarrow \pi^*_4$(acac) type, to the second one. The appearance of those bands is due to the coordination inequality of the acac ligands. The third band corresponds undoubtedly to a *d–d* type transition. Thus, it may be concluded that, because of the considerably lower symmetry of the central ion surroundings than in the *trans*-isomers with an unchanged degeneration of the d_{xz}, d_{yz} orbitals and sequence of molecular orbitals, the ground state of the *cis*-isomers is the ^2A-term (symmetry C_1). This means that all the electronic *d–d* type transitions ($^2A \rightarrow {}^2A$) are allowed. The relatively high energies of the $\pi_3 \rightarrow \pi^*_4$(acac) and $d_\pi \rightarrow \pi^*_4$(acac) transitions compared to those in M(acac)$_3$ type complexes,[12] confirm the previous considerations concerning π-interactions of {CrNO}—acac. A contribution to the high energy

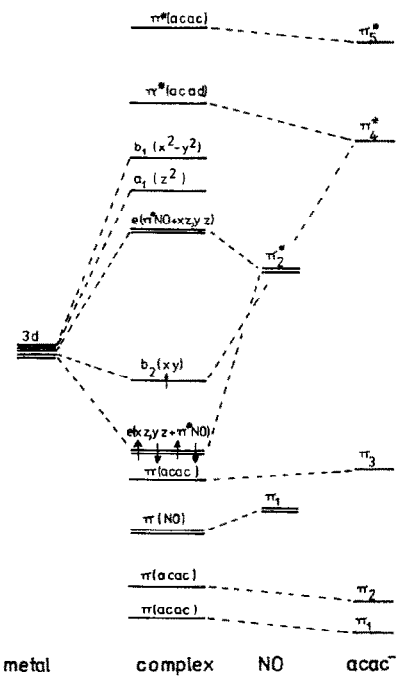


Fig. 3. Proposed molecular orbital scheme for *trans*-[Cr(NO)(acac)$_2$L].

of the $\pi_3 \rightarrow \pi_4^*$(acac) transitions may be caused by the M → L π-bonding (raising the π-antibonding level) as well as by L → M (lowering the π-bonding level). However the relatively high $d_\pi \rightarrow \pi_4^*$(acac) transition energy can result only from a significant contribution of πM → L bonding to the net π-interactions.

REFERENCES

1. A. Keller and B. Jeżowska-Trzebiatowska, *Bull. Acad. Pol. Sci. Ser. Chim.* 1980, **28**, 73.
2. B. A. Goodman, J. B. Raynor and M. C. R. Symons, *J. Chem. Soc.* 1968, 1973.
3. J. Burgess, B. A. Goodman and J. B. Raynor, *J. Chem. Soc.* 1968, 501.
4. B. Jeżowska-Trzebiatowska and A. Jezierski, *J. Mol. Struct.* 1978, **46**, 197.
5. B. R. McGarvey, *J. Phys. Chem.* 1967, **71**, 51.
6. M. C. R. Symons, In *Advances in Physical Organic Chemistry* (Edited by V. Gold). Academic Press, New York (1962).
7. B. Elschner and R. Neubert, *Hoch Frequenzspektroskopie*, p. 185. Akademisher, Berlin (1961).
8. J. J. Fortmen and R. G. Hayes, *J. Chem. Phys.* 1965, **43**, 15.
9. H. M. McConnel and D. B. Chesnut, *J. Chem. Phys.* 1958, **28**, 107.
10. D. W. Barnum, *J. Inorg. Nucl. Chem.* 1961, **21**, 221; 1961, **22**, 183.
11. D. R. Eaton, *J. Am. Chem. Soc.* 1965, **87**, 3097.
12. C. A. Fleming and D. A. Thornton, *J. Mol. Struct.* 1975, **25**, 271.
13. H. A. Kuska and M. T. Rogers, *J. Chem. Phys.* 1965, **42**, 3034.
14. W. P. Griffith, *Q. Rev.* 1962, 182; *Coord. Chem. Rev.* 1975, **17**, 177.
15. P. T. Manoharm and H. B. Gray, *Inorg. Chem.* 1966, **5**, 823.
16. J. J. Ziółkowski, B. Jeżowska-Trzebiatowska and B. Kędzia, *Bull. Acad. Pol. Sci.* 1972, **20**, 231.
17. R. F. Fenske and R. L. DeKock, *Inorg. Chem.* 1972, **11**, 437.
18. B. Jeżowska-Trzebiatowska and A. Keller, *Inorg. Chim. Acta* 1975, **13**, 201.
19. A. Keller and B. Jeżowska-Trzebiatowska, *Inorg. Chim. Acta* 1981, **51**, 123.

Polyhedron Vol. 4, No. 11, pp. 1853–1857, 1985
Printed in Great Britain

0277-5387/85 $3.00 + .00
© 1985 Pergamon Press Ltd

^{119m}Sn MÖSSBAUER SPECTROSCOPY AND ^{31}P AND ^{119}Sn NMR OF MIXED AQUEOUS 1-HYDROXY ETHYLIDENE-1,1-DISODIUM PHOSPHONATE (EHDP) AND TIN(II) CHLORIDE SOLUTIONS: EVIDENCE FOR EHDP–Sn COMPLEXES

N. ALBEROLA
Département de Radiologie Expérimentale, Hôpital Cardiologique, BP Lyon Montchat, 69394 Lyon Cedex 3, France

(*Received* 31 *October* 1984; *accepted after revision* 3 *May* 1985)

Abstract—1-Hydroxy ethylidene-1,1-disodium phosphonate (EHDP) labelled with ^{99m}Tc is well suited for human-bone scintigraphy. Before adding pertechnetate ions, the first step of the labelled-phosphorus procedure requires the preparation of a mixed aqueous EHDP and tin(II) solution. This mixture was investigated by both ^{119m}Sn Mössbauer spectroscopy and ^{31}P and ^{119}Sn NMR. ^{119m}Sn Mössbauer spectroscopy performed on mixed aqueous 0.1 M EHDP and 0.01 M $SnCl_2$ solutions at pH 6 and immediately frozen at −196°C after mixing showed the presence of an EHDP–Sn(II) complex. ^{31}P NMR spectra of freshly prepared solutions showed the weighted average of the signals of the free EHDP ligand and of the EHDP–Sn(II) complex. When the EHDP concentration was 10 times as large as the Sn(II) concentration, about 90% of the EHDP was present as the free ligand and the average NMR signal deviated little from the signal of the free ligand. ^{119m}Sn Mössbauer spectroscopy and ^{31}P NMR performed on these mixtures allowed to stand for 3 h at room temperature confirm the presence of a structure in which Sn(IV) atoms are included, in agreement with ^{119}Sn NMR results which show the presence of an $(EHDP)_2$–Sn(IV) complex.

1-Hydroxy ethylidene-1,1-disodium phosphonate (EHDP) labelled with ^{99m}Tc is used for human-bone scintigraphy.[1] A reducing agent such as tin(II) chloride is added to the aqueous compound before adding pertechnetate ions ($^{99m}TcO_4^-$). The reaction which occurs is unknown. However, in addition to ^{99m}Tc(Sn)–EHDP complexes, gel chromatography[2,3] of a mixed aqueous EHDP, tin(II) chloride and $^{99m}TcO_4^-$ solution has shown intermediates such as EHDP–Sn complexes. These observations suggest that an EHDP complexation with tin should occur in the intermediate EHDP and $SnCl_2$ solution. Moreover, the association constants of Sn(II) ions with EHDP and other diphosphonates have been measured by potentiometric titration.[4] Furthermore, ^{31}P NMR[5] and ^{119m}Sn Mössbauer[6] spectra obtained on analogous mixtures such as mixed aqueous pyrophosphate and tin(II) solutions only show a pyrophosphate–Sn(II) complex.

In the present work, ^{119m}Sn Mössbauer spectroscopy and ^{31}P and ^{119}Sn NMR were performed on mixed aqueous EHDP and tin(II) chloride solutions in order to confirm the presence of EHDP–Sn complexes and to get information on their molecular structures. EHDP and $SnCl_2$ molar concentrations and pH of the investigated mixtures, respectively, are very close to those used for bone tracer preparation: 0.1 M EHDP, 0.01 M $SnCl_2$ and pH 6.

EXPERIMENTAL

Chemicals

EHDP was provided by Procter & Gamble Co. (U.S.A.). $SnCl_2 \cdot 2H_2O$ and $SnCl_4 \cdot 5H_2O$ were purchased from Prolabo Co. (France). Deuterated solvents for NMR experiments and ^{119}Sn-enriched metallic tin (93% of ^{119}Sn) were from CEA-CEN Saclay (France). Distilled water was used as solvent for ^{119}Sn Mössbauer analyses. Other chemicals are commercial reagent grade materials.

Preparations of mixed aqueous 0.1 M *EHDP and* 0.01 M *tin(II) chloride solutions at pH* 6

$SnCl_2 \cdot 2H_2O$ (1.410 g) is dissolved in 12.5 M HCl (0.200 cm^3) and diluted (25 cm^3 H_2O and 25 cm^3 D_2O for Mössbauer and NMR experiments,

respectively). At this step, the $SnCl_2$ molar concentration is 0.12 M. EHDP (0.777 g) is solubilized in 25 cm^3 H_2O or D_2O. The EHDP molar concentration is 0.12 M. Some (0.200 cm^3) of the $SnCl_2$ solution is added to 4.167 cm^3 of the EHDP solution. The pH is adjusted to 6 with 1 and 0.1 M NaOH.

^{119}Sn NMR experiments require the use of ^{119}Sn-enriched tin. The preparation of the mixed aqueous solution with ^{119}Sn-enriched metal was as follows: ^{119}Sn-enriched metal (6 mg) was dissolved in 12.5 M HCl (0.400 cm^3) under nitrogen, then 0.391 cm^3 of this mixture was added to 0.12 M EHDP (4.167 cm^3) and the pH raised to 6 with NaOH.

For comparison purposes, reference solutions were prepared for Mössbauer and NMR experiments.

Reference aqueous solutions

0.01 M $SnCl_2$ *solution at pH* 1. 0.25 M $SnCl_2$ solution (0.200 cm^3) was added to distilled water (4.2 cm^3) and the pH raised to 1 with NaOH.

0.12 M *EHDP solution at pH* 6. EHDP (0.777 g) was dissolved in 25 cm^3 D_2O. In order to adjust the pH to 6, 12.5 M HCl (0.200 cm^3) was added to this aqueous EHDP solution (4.5 cm^3).

0.01 M $SnCl_4$ *solution at pH* 1. $SnCl_4 \cdot 5H_2O$ (2.191 g) was dissolved in 12.5 M HCl (0.200 cm^3) and diluted in distilled water (4.167 cm^3) and the pH adjusted to 1 with NaOH.

Mixed 0.1 M *EHDP and* 0.01 M $SnCl_4$ *solution at pH* 6. 0.01 M $SnCl_4$ (0.200 cm^3) was added to the 0.12 M EHDP solution (4.167 cm^3) and the pH adjusted to 6 with NaOH.

Instruments

Mössbauer spectroscopy was performed on the aqueous mixtures frozen at −196°C. The Mössbauer experiments were carried out using a constant-acceleration electromechanical drive system (Halder) together with a multichannel analyzer (Promeda, Inel) for collecting data. ^{119m}Sn in $CaSnO_3$ (Amersham Co.) was used as the gamma source. The velocity calibrations were done with a $CaSnO_3$ absorber. All the isomer shifts given in this paper refer to the Sn singlet of $CaSnO_3$ at −196°C.

NMR spectra were recorded on a Bruker WP 80 FT spectrometer equipped with a tunable multinuclear probe. ^{31}P and ^{119}Sn NMR experiments were carried out at observation frequencies of 32.38 and 29.85 MHz, respectively. Chemical shifts are given in ppm and are referred to external references: 85% H_3PO_4 and Me_4Sn for ^{31}P and ^{119}Sn NMR, respectively. Typical data acquisitions were as follows: 2500-Hz spectral width; 35-μs pulse width; 1–3-μs pulse repetition rate with complete proton decoupling. ^{31}P NMR spectrum recording requires 20 min vs 12 h for the ^{119}Sn NMR spectrum. NMR experiments were carried out at 23°C.

RESULTS

Mössbauer experiments

The following Mössbauer parameters are used: IS: isomer shift (mm · s^{-1}) relative to the reference Sn singlet ($CaSnO_3$); QS: quadrupole splitting (mm · s^{-1}); LW: experimental line width (mm · s^{-1}); I: relative intensity of line (%).

In the absence of EHDP, the ^{119m}Sn Mössbauer spectrum of the aqueous 0.01 M tin(II) chloride solution at pH 1 recorded immediately after the preparation displays a doublet (IS = 3.55 mm · s^{-1}, QS = 1.12 mm · s^{-1}, LW = 0.98 mm · s^{-1}). The ^{119m}Sn Mössbauer spectrum of the mixed aqueous 0.1 M EHDP and 0.01 M tin(II) chloride solution at pH 6 recorded at zero time exhibits a doublet (IS = 3.30 mm · s^{-1}, QS = 1.94 mm · s^{-1}, LW = 1.13 mm · s^{-1}). In addition to the doublets, the ^{119m}Sn Mössbauer spectra of the investigated solutions both allowed to stand for 3 h at room temperature display singlets: IS = −0.21 mm · s^{-1}, LW = 1.28 mm · s^{-1}, I = 15% for the EHDP and tin(II) chloride solution; IS = −0.09 mm · s^{-1}, LW = 1.06 mm · s^{-1}, I = 18% for the tin(II) chloride solution. The ^{119m}Sn Mössbauer spectrum of the aqueous 0.01 M tin(IV) chloride solution displays a single (IS = −0.11 mm · s^{-1}, LW = 1.12 mm · s^{-1}). The ^{119m}Sn Mössbauer spectrum of the mixed aqueous 0.1 M EHDP and tin(IV) chloride solution exhibits a singlet (IS = −0.19 mm · s^{-1}, LW = 0.96 mm · s^{-1}).

NMR experiments

The following NMR parameters are used: CS: chemical shift (ppm) relative to external reference; J: spin-coupling constant (Hz); I: relative intensity of line (%).

^{31}P NMR spectra. ^{31}P NMR spectra are recorded using the double-irradiation method in order to remove the spin-coupling interaction between 31P nuclei and protons of the methyl group of EHDP.

In the absence of tin(II) chloride, the decoupled ^{31}P NMR spectrum of the aqueous 0.1 M EHDP solution at pH 6 displays a unique line centered at 19.1 ppm. The ^{31}P NMR spectrum of the mixed aqueous 0.1 M EHDP and 0.01 M tin(II) chloride solution at pH 6 recorded immediately after compound mixing again displays one line centered at 19.1 ppm. Three hours later, in addition to the singlet A (CS = 19.0 ppm, I = 88%), a line, C (CS = 16.7

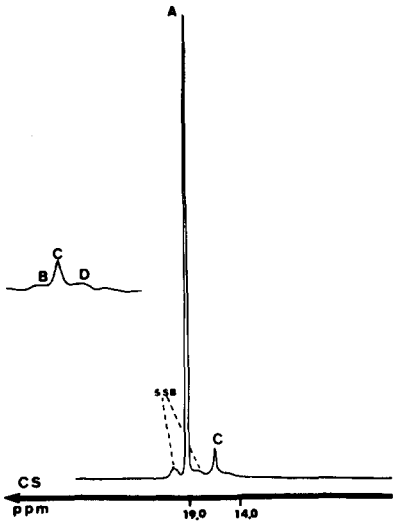


Fig. 1. ^{31}P NMR spectrum of a mixed aqueous 0.1 M EHDP and 0.01 M $SnCl_2$ solution at pH 6 and 25°C. The spectrum was recorded 3 h after mixing the two reactants. SSB represents the spinning side bands. In the left corner of the figure, scale expansion of the signal C reveals two weaker lines, B and D.

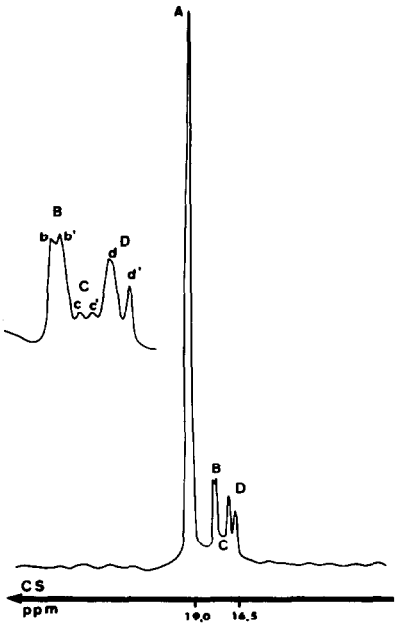


Fig. 2. ^{31}P NMR spectrum of a mixed aqueous 0.1 M EHDP and 0.01 M ^{119}Sn-enriched tin solution at pH 6 and 25°C. To the left, signal BCD is enlarged.

ppm, I = 8%), with two weaker signals, B (CS = 17.1 ppm, I = 2%) and D (CS = 16.4 ppm, I = 2%) on both sides, appears. Lines B and D are nearly symmetrical with respect to line C (J = 29 Hz) (Fig. 1). The ^{31}P NMR spectrum of the mixed aqueous 0.1 M EHDP and 0.01 M tin(IV) chloride solution at pH 6 recorded at zero time exhibits a high line A (CS = 19.0 ppm, I = 76%) and a line C (CS = 16.8 ppm, I = 15%). On both sides of line C two shoulders, B (CS = 17.1 ppm, I = 5%) and D (CS = 16.4 ppm, I = 4%), are observed and are roughly symmetrical with respect to C (J = 29 Hz). The ^{31}P NMR spectrum of the mixed aqueous 0.1 M EHDP and 0.01 M ^{119}Sn-enriched tin(II) chloride solution at pH 6 displays a main line A (CS = 19.2 ppm, I = 61%) and a group of three split lines, B–D, centered at 17.2 ppm (Fig. 2). Lines B and D are nearly symmetrical with respect to C (J is about 30 Hz). Lines B–D are greatly modified compared to that observed with natural tin. Thus, the central line C becomes the smallest and the two symmetrical signals become the highest.

^{119}Sn NMR spectra. The ^{119}Sn NMR spectrum of the mixed aqueous 0.1 M EHDP and 0.01 M ^{119}Sn-enriched tin solution at pH 6 displays five main lines, A–E (Fig. 3). Lines B, C and E are split, line A shows a shoulder on the downfield side and line D is enlarged. Lines A and E on the one hand and lines B and D on the other are roughly symmetrical with respect to line C. Each line is separated from the other by about 30 Hz.

DISCUSSION

IS (3.30 mm·s^{-1}) and QS (1.94 mm·s^{-1}) of the doublet observed in the mixed aqueous 0.1 M EHDP and 0.01 M tin(II) chloride solution was significantly different from those measured for the aqueous tin(II) chloride solution (IS = 3.55 mm·s^{-1}, QS = 1.12 mm·s^{-1}) whether Mössbauer analyses are per-

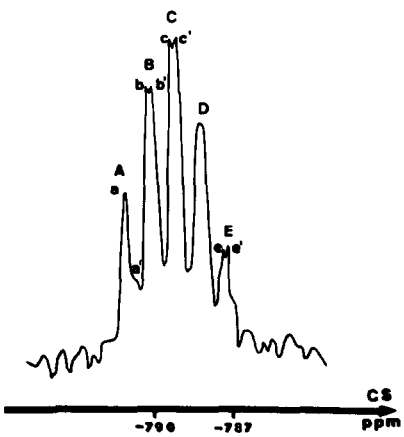


Fig. 3. ^{119}Sn NMR spectrum of a mixed aqueous 0.1 M EHDP and 0.01 M ^{119}Sn-enriched tin solution at pH 6 and 25°C.

formed on the solutions immediately after their preparation or 3 h later. Furthermore, the Mössbauer parameters of the investigated mixed aqueous EHDP and tin(II) solution are significantly different from those measured for $Sn(OH)_2$[7] (IS = 2.84 mm·s^{-1}, QS = 2.16 mm·s^{-1}). Thus, the doublet observed for the investigated mixture clearly indicates an EHDP complexation with tin. The IS value is located in the characteristic range of Sn(II).[8] Two possibilities could be suggested for the structure of the EHDP–Sn(II) complex: either Sn(II) could bridge two EHDP molecules forming a linear dimer or Sn(II) could form a ring structure with one EHDP molecule. In the same way, ^{119m}Sn Mössbauer spectroscopy performed on a mixed aqueous pyrophosphate and tin(II) chloride solution exhibited a pyrophosphate–Sn(II) complex. IS and QS values characterizing the EHDP–Sn(II) complex are significantly increased relative to those measured for the pyrophosphate–Sn(II) complex (IS = 3.19 mm·s^{-1}, QS = 1.76 mm·s^{-1}).[6] These results suggest that the ionic character of the bivalent Sn—O bonds is stronger within the EHDP–Sn(II) complex than within the pyrophosphate–Sn(II) complex.[9]

In addition to the doublets, ^{119m}Sn Mössbauer analyses performed on the EHDP and tin(II) mixture and on the tin(II) chloride solutions, both allowed to stand for 3 h at room temperature, exhibit singlets [IS = −0.21 mm·s^{-1} for the EHDP and tin(II) mixture; IS = −0.09 mm·s^{-1} for the tin(II) chloride solution], roughly identical, respectively, to singlets observed for the EHDP and tin(IV) mixture (IS = −0.19 mm·s^{-1}) and for the tin(IV) chloride solution (IS = −0.11 mm·s^{-1}). These results suggest that complexation between EHDP and tin(IV) should occur.[9]

The unique line of the ^{31}P NMR spectrum of the aqueous 0.1 M EHDP solution at pH 6 shows that the two ^{31}P nuclei of the EHDP molecule are present in the same electronic surroundings within the EHDP molecule. The ^{31}P NMR spectrum of the mixed aqueous 0.1 M EHDP and 0.01 M $SnCl_2$ solution recorded at zero time exhibits the same line and, thus, only indicates the presence of free EHDP. The appearance of three new lines, B–D, later indicates the formation of a new structure. Consequently, a reaction occurs that involves a probable EHDP complexation of EHDP with tin. The ^{31}P NMR spectrum of the mixed aqueous 0.1 M EHDP and 0.01 M $SnCl_4$ solution displays, in addition to the singlet related to free EHDP ions, three lines, B–D, with respective CSs equal to those of lines B–D reported for the EHDP and $SnCl_2$ mixture. Thus, tin included in the EHDP complex is Sn(IV). In the mixed EHDP and $SnCl_2$ solution allowed to stand for 3 h, oxidation of Sn(II) to Sn(IV) occurs. The symmetry of the group of lines B and D with respect to line C could be interpreted as a spin-coupling interaction between ^{31}P nuclei and ^{119}Sn and ^{117}Sn nuclei having a spin of $\frac{1}{2}$. This interpretation is confirmed by the change in the relative intensities of lines B–D observed for the mixed EHDP and ^{119}Sn-enriched tin solution. I_B/I_{B+C+D} and I_D/I_{B+C+D} ratios are 44 and 46% respectively and could be related to half of the ^{119}Sn isotropic enrichment (93%). Thus, the group of lines B and D originates when the coupling is present between ^{31}P and ^{119}Sn nuclei (and ^{117}Sn nuclei, too) and line C when coupling is absent (Sn nuclei having a spin of zero). On account of the high stability of the P—C—P bond in the EHDP molecule, P nuclei are expected to be associated in pairs in the complex. Thus, the presence of the B–D doublet ($J \sim 30$ Hz) is attributed to the signal of at least two equivalent ^{31}P nuclei split by one Sn nucleus. The splitting of each of the lines B–D observed for the mixed EHDP and ^{119}Sn-enriched tin solution is still unexplained. The two center peaks in the doublets have unequal separation (b–b′ and c–c′ peaks, $J = 4$ Hz; d–d′ peaks, $J = 10$ Hz). The EHDP complexation with Sn(IV) is confirmed by the ^{119}Sn NMR analysis of the EHDP and ^{119}Sn-enriched tin mixture. The quintuplet ($J \sim 30$ Hz) is attributed to the signal of one Sn nucleus having a spin of $\frac{1}{2}$ split by four equivalent P nuclei. Thus, the probable structure of the complex is $(EHDP)_2$–Sn(IV). One Sn atom and two EHDP molecules form a symmetrical spiro-structure (Fig. 4). The complexation of EHDP with tin(IV) exhibited by Mössbauer analyses is confirmed by NMR analyses. However, the splitting of lines B, C and E shown by the ^{119}Sn NMR spectrum is still unexplained (b–b′ peaks, $J = 3$ Hz; c–c′ peaks, $J = 5$ Hz; e–e′ peaks, $J = 4$ Hz). Furthermore, no NMR signal related to the presence of the EHDP–Sn(II) complex is exhibited. When the EHDP concentration is 10 times as large as the Sn(II) concentration, about 90% of the EHDP is present as the free ligand. It follows that the ^{31}P NMR spectrum of the freshly prepared EHDP and tin(II)

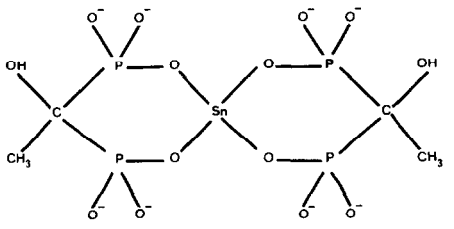


Fig. 4. Expected symmetrical spiro-structure of the $(EHDP)_2$–Sn(IV) complex consistent with ^{31}P and ^{119}Sn NMR results.

solution shows the weighted average of the signals of the free EHDP and of the EHDP–Sn(II) complex. ^{31}P NMR spectroscopy performed on mixed aqueous 0.1 M pyrophosphate and 0.01 M tin(II) chloride (or ^{119}Sn-enriched tin) solution at pH 6 displays a B–D doublet ($J = 40$ Hz),[5] for which lines B and D are not split. In agreement with ^{119m}Sn Mössbauer results, Mathieu *et al.*[5] have attributed this NMR doublet to the pyrophosphate–Sn(II) complex. However, according to the similarity of the experimental conditions used for the two NMR studies and according to the similarity of molecular structure between EHDP and pyrophosphate, the expected structure of the complex shown by Mathieu *et al.*[5] is probably (pyrophosphate)$_2$–Sn(IV). In addition to ^{31}P NMR spectroscopy performed on pyrophosphate and $SnCl_4$ mixture, ^{119}Sn NMR analysis should have avoided their earlier interpretation.

Acknowledgements—We thank Procter & Gamble Co. for providing EHDP. We are grateful to Dr Galy (Service de Radiopharmacie, Centre de Médecine Nucléaire, Lyon, France) and to Professor Marest (Institut de Physique Nucléaire, Lyon, France) for their helpful assistance.

REFERENCES

1. E. P. Castronovo and R. J. Callahan, *J. Nucl. Med.* 1972, **13**, 823.
2. J. A. G. M. Van Den Brand, H. A. Das, B. G. Dekker and C. L. Deligny, *Int. J. Appl. Radiat. Isot.* 1981, **32**, 637.
3. J. A. G. M. Van Den Brand, H. A. Das, B. G. Dekker and C. L. Deligny, *Int. J. Appl. Radiat. Isot.* 1982, **33**, 39.
4. R. A. M. J. Claessens, Technetium and tin diphosphonates; stability, bone uptake and redox behaviour. Dissertation, University of Nijmegen, The Netherlands (1982).
5. L. Mathieu, P. Thivolle, M. Delmau and M. Berger, *J. Magn. Reson.* 1982, **46**, 332.
6. L. Mathieu, P. Bussiere, D. Christofidis and M. Berger, *Radiochem. Radioanal. Lett.* 1979, **40**, 223.
7. D. Christofidis, Étude par effet Mössbauer de solutions aqueuses de pyrophosphate et de chlorure stanneux. Thèse, Université Cl. Bernard, Lyon, France (1978).
8. J. K. Lees and P. A. Flinn, *J. Chem. Phys.* 1968, **48**, 1982.
9. V. I. Goldanskii, *The Mössbauer Effect and Its Application to Chemistry*. D. Van Nostrand, Princeton, NJ (1966).

Polyhedron Vol. 4, No. 11, pp. 1859–1863, 1985
Printed in Great Britain

0277-5387/85 $3.00 + .00
© 1985 Pergamon Press Ltd

SYNTHESIS OF POLYMERIC LIGANDS HAVING A TETRAAZA MACROCYCLE SELECTIVE FOR COPPER(II)

MANABU FUJIWARA, YASUHIRO NAKAJIMA, TAKAYUKI MATSUSHITA* and TOSHIYUKI SHONO

Department of Applied Chemistry, Faculty of Engineering, Osaka University, Yamadaoka, Suita, Osaka 565, Japan

(*Received* 12 *March* 1985; *accepted* 3 *May* 1985)

Abstract—The novel polymeric ligands, poly-$(N_4)H_2$ (I) and poly-$(N_4)H_2$ (II), in which the tetraaza macrocycle was present as an integral part of the polymer backbone, were prepared by the reaction of 5,7,12,14-tetramethyl-1,4,8,11-tetraazacyclotetradeca-1,5,7,12-tetraene, $(N_4)H_2$, with diisocyanates [OCN-R-NCO, R = $(CH_2)_6$ (I) and $C_6H_4CH_2C_6H_4$ (II)]. These are insoluble in common organic solvents and water, suggesting that they have high molecular weights. The complexation of these polymeric ligands with copper(II) and nickel(II) in water under heterogeneous conditions showed that they can bind copper(II) selectively by complex formation with the tetraaza macrocycle. The percentage of copper(II) bound in II was found to depend on the concentration of copper(II), and the pH and ionic strength of the sample solutions. Moreover, the bound copper(II) in II could be desorbed by treatment with dilute hydrochloric acid.

Many tetraaza macrocycles and their metal complexes have been prepared and characterized.[1–4] However, the preparation and properties of polymeric ligands containing tetraaza macrocycles have been little studied so far.[5,6] In the previous work, we have found that the polymeric ligands containing 6,8,15,17-tetramethyl-dibenzo-5,9,14,18-tetraazacyclotetradecene, which are oligomers having a degree of polymerization of about 5, exhibit extraction rates of copper(II) faster than that of the corresponding monomeric ligand.[7,8] Moreover, we have described the preparation and characterization of novel tetraaza macrocycles with nitro[9] and carbamoyl[10] groups and their copper(II) and nickel(II) complexes.

In this paper, we describe the preparation of polymeric ligands containing the tetraaza macrocycle as an integral part of the polymer backbone and the complexing ability for copper(II) and nickel(II) under heterogeneous conditions.

EXPERIMENTAL

Materials

All reagents were of reagent grade. Chloroform was refluxed over P_4O_{10} and distilled. Benzene and *n*-hexane were refluxed over sodium and distilled. Other solvents were purified by common methods. Water was deionized.

Measurements

UV and visible reflectance spectra were recorded on a Hitachi 340 recording spectrophotometer attached with a Hitachi R-10A integrating sphere unit. IR spectra were recorded on a Hitachi 215 grating spectrophotometer. Atomic absorption spectra were obtained using a Nippon Jarrel Ash AA-1. The pH of a sample solution was measured with a Shibata 671 pH meter. Magnetic susceptibility was measured by the Gouy method at room temperature.

Procedure for binding and release of metal(II) ions

Binding of metal(II) ions by the polymeric ligands was carried out by using a 10-cm^3 test tube, with a stopper, which contained an aqueous solution (10 cm^3) of metal(II) acetate [copper(II) or nickel(II)] and the polymeric ligand powdered uniformly (2.0×10^{-5} unit mol). The test tube was shaken for an appropriate time, from 1 to 72 h, at room temperature by using a shaker. After shaking, the polymeric ligand was filtered off and washed with 10-cm^3 portions of water 3 times. The filtrate and

* Author to whom correspondence should be addressed.

washings were combined and diluted to 50 cm^3 with water, and the concentration of the metal(II) ion remaining in it was determined by atomic absorption spectrometry. For investigation of the effect of the ethanol content in the sample solution, filtration was carried out after shaking and the filtrate was evaporated very slowly at 80°C. The residual solution was added to dilute hydrochloric acid. The concentration of the copper(II) ion remaining in the sample solution was determined by atomic absorption spectrometry.

Release of copper(II) ion from the polymeric copper(II) complex was carried out by using a 25-cm^3 test tube, with a stopper, which contained a hydrochloric acid solution (25 cm^3) at an appropriate concentration and the copper(II) complex (25 mg, 4.46×10^{-5} unit mol). The mixture was stirred at constant revolution for an appropriate time, from 1 to 24 h. After stirring, it was filtered off and washed with 10-cm^3 portions of water several times. The filtrate and washings were combined and diluted to 100 cm^3 with water and the concentration of copper(II) ion was determined by atomic absorption spectrometry.

Preparation of poly-$(N_4)H_2$ **(I)**

To a chloroform solution (50 cm^3) of the parent tetraaza macrocycle[11] (1.0 g, 4.0 mmol) was added hexamethylene diisocyanate (0.67 g, 4.0 mmol). The mixture was stirred at room temperature for 48 h. After cooling, the resulting yellow precipitate was collected on a glass filter, washed with dry chloroform, *n*-hexane and ethanol and dried *in vacuo*. The yield was 85%. It was insoluble in water and ordinary organic solvents such as ethanol, benzene, chloroform and DMF. Found: C, 62.97; H, 9.04; N, 19.85. Calc. for $(C_{22}H_{36}N_6O_2)_n$: C, 63.42; H, 8.73; N, 20.18%. IR (in KBr disk): 3350, 1640, 1550, 1425, 1280, 1200, 1015, 820 and 760 cm^{-1}.

Preparation of poly-$(N_4)H_2$ **(II)**

To a chloroform solution (100 cm^3) of the parent macrocycle (1.0 g, 4.0 mmol) was added 4,4'-diphenylmethane diisocyanate (1.0 g, 4.0 mmol). The mixture was stirred at 30°C for 48 h. The resulting yellow precipitate was collected on a glass filter, washed with dry chloroform several times and dried *in vacuo*. The yield was 95%. It was insoluble in water and ordinary organic solvents. Found: C, 69.51; H, 6.79; N, 16.47. Calc. for $(C_{29}H_{34}N_6O_2)_n$: C, 69.84; H, 6.89; N, 16.86%. IR (in KBr disk): 3280, 1650, 1595, 1510, 1405, 1305, 1230, 810 and 750 cm^{-1}.

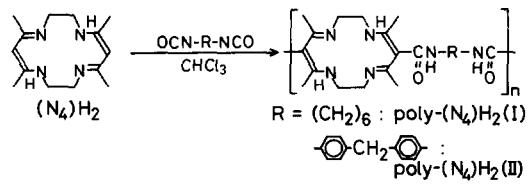


Fig. 1. Synthetic scheme for the polymeric tetraaza ligands studied.

Preparation of copper(II) complex with **II**, Cu[*poly*-(N_4)-**(II)**]

To a chloroform solution (100 cm^3) of the copper(II) complex with the parent tetraaza macrocycle (1.0 g, 3.2 mmol) was added 4,4'-diphenylmethane diisocyanate (0.8 g, 3.2 mmol). The mixture was stirred at room temperature for 48 h under a nitrogen atmosphere. The brownish green precipitate was collected on a glass filter, washed with dry benzene, chloroform and *n*-hexane, and dried *in vacuo*. The yield was 95%. Found: C, 61.85; H, 5.73; N, 14.82; Cu, 11.2 (by colorimetric determination). Calc. for $(CuC_{29}H_{32}N_6O_2)_n$: C, 62.17; H, 5.77; N, 15.00; Cu, 11.34%. IR (in KBr disk): 3250, 1640, 1590, 1405, 1310, 1235, 810 and 765 cm^{-1}. Magnetic moment (μ_{eff}) = 1.40 BM.

The preparative scheme for these polymeric ligands is shown in Fig. 1. In the reaction of the parent tetraaza macrocycle with monoisocyanates, carbamoyl derivatives substituted on the γ-carbon atoms were obtained exclusively,[10] which was confirmed by IR and ^1H NMR spectra. This is because of the high reactivity of the hydrogen atoms on them. Therefore, the present polymeric ligands may have the same unit structure as those for the carbamoyl derivatives. These polymeric ligands and the polymeric copper(II) complex were insoluble in ordinary organic solvents and water. Thus, their molecular weights could not be measured. Their poor solubilities, the analytical data and no absorption band due to isocyanate groups around 2280 cm^{-1} in the IR spectra suggest that their molecular weights are fairly high.

RESULTS AND DISCUSSION

Preliminarily, we have studied the binding abilities of the polymeric ligands for copper(II) and nickel(II) in batch systems under the following conditions: **I** (8.3 mg, 2.0×10^{-5} unit mol) and **II** (10.0 mg, 2.0×10^{-5} unit mol) were used, the concentration of aqueous solution (10 cm^3) of the metal(II) ions was 2.0×10^{-3} mol dm^{-3} (2.0×10^{-5} mol), and the pH of the sample solution was about 5.7 without using a buffer solution.

In the case of **I**, about 20% of the copper(II) was

bound after 24 h, and the percentage of bound copper(II) did not increase after additional shaking for 24 and 48 h. Moreover, the aqueous solution was wine red in color and the complex formed changed its color from brownish green to dark red, suggesting that some decomposition of the polymeric ligand occurred. This may be caused by a decrease in the pH of the aqueous phase by the complex formation. Under the same conditions binding of nickel (II) was not observed after shaking for 72 h, and thus coloration of the aqueous solution did not occur.

On the other hand, with **II** about 30% of the copper(II) was bound after shaking for 24 h and the percentage of bound copper(II) increased gradually with increasing shaking time. In this case, the polymeric complex formed was stable and its brownish color did not change after 72 h. Similarly, no binding of nickel(II) was observed after shaking for 72 h.

These results indicate that **II** is superior to **I** for application as a chelating resin selective for copper(II). Thus we studied the binding ability of the former for copper(II) in detail.

Effect of shaking time and concentration of copper(II) ion

Figure 2 shows the effects of shaking time and concentration of copper(II) ion on the percentage of copper(II) bound by **II**.

When the concentration of copper(II) ion was 2.0×10^{-3} mol dm^{-3} (equal to 1 unit mol of the polymeric ligand), the percentage of bound copper(II) reached 28% after shaking for 24 h and increased gradually with increase in shaking time. At a concentration of 2.0×10^{-4} mol dm^{-3} (0.1 unit mol of the polymeric ligand), the percentage of the bound copper(II) reached 55% after 24 h. This apparent value was larger than that at 2.0×10^{-3} mol dm^{-3}, but the amount of bound copper(II) per polymeric ligand was smaller compared to that at 2.0×10^{-3} mol dm^{-3}.

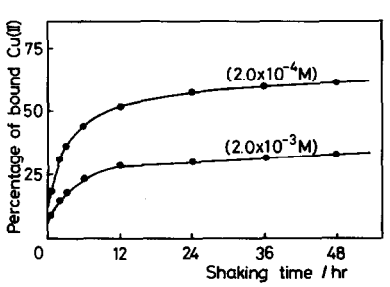


Fig. 2. Effects of shaking time and concentration of copper(II) ion on the percentage of copper(II) bound by **II**. **II**: 10 mg, copper(II) solution: 10 cm^3.

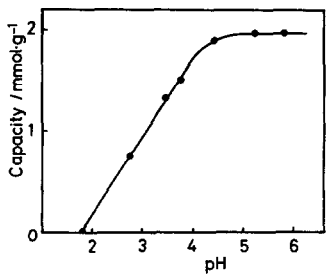


Fig. 3 Effect of pH on the binding capacity of poly-$(N_4)H_2$-(II) for the copper(II) ion. [copper(II)]: 2.0×10^{-2} mol dm^{-3}.

On the other hand, at a concentration of 2.0×10^{-2} mol dm^{-3} (10 unit mol of the polymeric ligand), the absorption equilibrium was attained within 24 h, where almost all the tetraaza macrocycles of the polymeric ligand were consumed by complex formation. The binding capacity of the polymeric ligand for copper(II) was estimated to be 2.0 mmol g^{-1}.

Effect of pH on the binding capacity

Figure 3 shows the effect of the pH of the sample solution on the binding capacity of the polymeric ligand for the copper(II) ion. The pH values were adjusted by using acetate buffer solutions (0.2 mol dm^{-3}) from 3.5 to 5.5 and by the addition of appropriate amounts of 1.0 mol dm^{-3} hydrochloric acid or sodium hydroxide below 3.5 or above 5.5, respectively.

Below pH 1.5 no copper(II) was bound by the polymeric ligand. The percentage of bound copper(II) increased linearly with increasing pH of the sample solution between 1.8 and 5.3, and was constant (2.0 mmol g^{-1}) above 5.8. This behavior agrees well with the pH effect observed in the solvent extraction of copper(II) by the corresponding monomeric ligand described in a previous paper.[10]

Effect of ionic strength

Figure 4 shows the effect of the ionic strength of the sample solution on the percentage of copper(II) bound by **II** under the following conditions: the concentration of the copper(II) ion was 2.0×10^{-3} mol dm^{-3}, shaking time was 24 h, and the pH of the sample solution was adjusted to 5.7. The ionic strength of the sample solution was varied from 0.0 to 3.0 by the addition of sodium nitrate.

The percentage of copper(II) bound by **II** increased with increasing ionic strength and approached a constant value (41%) above 1.0. The coexisting ionic salts in large amounts influence

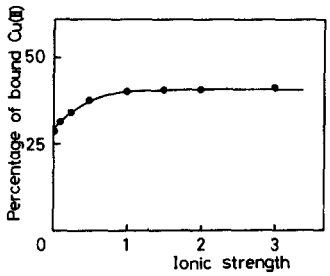


Fig. 4. Effect of ionic strength on the percentage of bound copper(II).

more or less the results for solvent extraction and adsorption on the resins: they exert a positive effect on the metal binding by desolvation around the metal ion to be captured, but spontaneously they exert a negative effect on it by weakening the interaction between the metal ion and the chelating agents. In the present system, the former process may operate effectively.

Effect of ethanol content in the sample solution

Figure 5 shows the effect of ethanol content in the sample solution on the percentage of bound copper(II). The concentration of the copper(II) ion was 2.0×10^{-3} mol dm^{-3} and ethanol content was varied from 0 to 80 vol %. Shaking time was 24 h.

The percentage of bound copper(II) after 24 h increased from 28 to 51% as ethanol content in the sample solutions increased from 0 to 80 vol %. It was noticeable at 30 vol % ethanol content. These results indicate that the complexation of the polymeric ligand with copper(II) is accelerated by the addition of ethanol.

It has already been pointed out that the addition of an appropriate organic solvent to an aqueous sample solution results in a strong retention of transition-metal ions on ion-exchange resins.[12–14] Such behavior has been ascribed to a decrease in the tendency for their hydration in a mixed solvent, in which the metal ions can interact easily with the

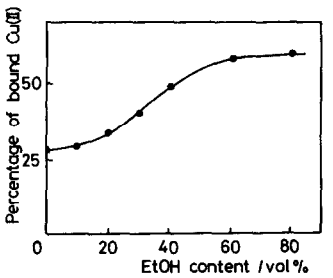


Fig. 5. Effect of ethanol content on the percentage of bound copper(II).

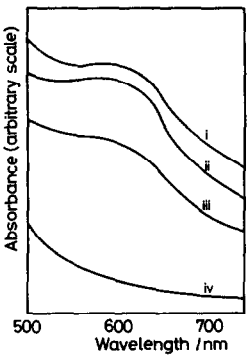


Fig. 6. Reflectance spectra: (i) Cu[poly-(N_4)-(II)], (ii) II loaded copper(II) ion (99%), (iii) II loaded copper(II) ion (30%), (iv) II.

binding sites. In the present study, a similar effect may operate and accelerate the complexation of copper(II) with tetraaza macrocycles of the polymeric ligand. Of course, other factors such as swelling of the polymeric ligand should preferably affect the increase in the percentage of bound copper(II).

Binding sites in Cu[*poly*-(N_4)-(II)]

Figure 6 shows the diffused reflectance spectra of II and its copper(II) complexes differing in the extent of their loadings; the absorption curves i–iii correspond to percentages of bound copper(II) in the polymeric ligand of 100, 99 and 30%, respectively. The first sample was Cu[poly-(N_4)-(II)] and the second and third samples were prepared by shaking the polymeric ligand with aqueous solutions of copper(II), followed by collection on a glass filter, washing thoroughly with water, and drying *in vacuo*. The polymeric ligand itself has no absorption band in the visible region. The copper(II) complex, Cu[poly-(N_4)-(II)] exhibits an absorption band centred at 600 nm, which may be assigned to ligand field transitions.[15] In fact, the absorption spectrum of the copper(II) complex with the corresponding monomeric ligand shows an absorption band at 609 nm in DMF.[10]

On the other hand, the spectra of the partially loaded polymeric complexes show an absorption band at a position similar to that of the polymeric copper(II) complex, and their intensities increase with increasing copper(II)-loaded percentage. These results suggest that the copper(II) ion is apparently bound to the tetraaza macrocycle of the polymeric ligand. Therefore, it can be said that the high selectivity of the present polymeric ligand for copper(II) results from the chelating ability of the tetraaza macrocycle itself.

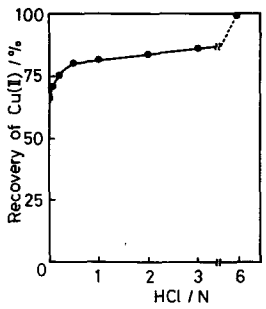


Fig. 7. Effect of concentration of hydrochloric acid on the recovery of copper(II).

Release of copper(II) from Cu[*poly*-(N_4)-**(II)**] *by hydrochloric acid*

We have examined the recovery of copper(II) bound in the polymeric ligand with hydrochloric acid, using Cu[poly-(N_4)-**(II)**]. When the polymeric complex was immersed in an acidic solution, it gradually turned from green to brownish yellow. In preliminary experiments, a constant recovery of copper(II) from the polymeric complex was obtained after stirring for 2 h with an aqueous solution of 1.0 mol dm^{-3} hydrochloric acid. Thus, this stirring time was adopted for the recovery of copper(II).

Figure 7 shows the effect of the concentration of hydrochloric acid on the recovery of copper(II). Seventy per cent of copper(II) was released with 0.1 mol dm^{-3} hydrochloric acid and the recovery of copper(II) increased to 87% when using 3.0 mol dm^{-3} hydrochloric acid. The loss of the polymeric ligand treated with 3.0 mol dm^{-3} hydrochloric acid was only 2–3%, indicating that little hydrolysis of the polymeric ligand occurred. By treating with 6.0 mol dm^{-3} hydrochloric acid, nearly 100% recovery of copper(II) was attained, but the solution turned faintly yellow and the loss of the polymeric ligand was about 13%. The polymeric ligand recovered from the polymeric copper(II) complex after release of copper(II) showed the same IR spectrum as the original polymeric ligand, indicating that the tetraaza macrocycle in the polymeric ligand was maintained after stirring in hydrochloric acid. The recovered polymeric ligand was found to be able to bind copper(II) effectively. Surprisingly, this polymeric ligand exhibits, even in concentrated hydrochloric acid, a strong resistance to hydrolysis, although imine double bonds are present in its polymer backbone. This may be caused by the hydrophobic effect of the linkage group, diphenylmethane. In fact, as described above, the polymeric ligand **I**, in which the tetraaza macrocycles are linked by a hexamethylene group, is easily hydrolysed by treatment with 1.0 mol dm^{-3} hydrochloric acid.

REFERENCES

1. T. J. Trux and R. H. Holm, *J. Am. Chem. Soc.* 1972, **94**, 4529.
2. S. C. Tang and R. H. Holm, *J. Am. Chem. Soc.* 1975, **97**, 3359.
3. A. M. Tait and D. H. Busch, *Inorg. Chem.* 1976, **15**, 197.
4. G. A. Melson, *Coordination Chemistry of Macrocyclic Compounds*. Plenum Press, New York (1979).
5. I. Tabushi, Japanese Patent 79,130,593.
6. V. Louvet, P. Appriou and H. Hemdél, *Tetrahedron Lett.* 1982, **23**, 2445.
7. T. Matsushita, N. Kubota, M. Fujiwara and T. Shono, *Chem. Lett.* 1984, 657.
8. N. Kubota, M. Fujiwara, T. Matsushita and T. Shono, *Polyhedron* 1985, **4**, 1059.
9. M. Fujiwara, T. Matsushita and T. Shono, *Polyhedron* 1984, **3**, 1357.
10. M. Fujiwara, Y. Nakajima, T. Matsushita and T. Shono, *Polyhedron* 1985, **4**, 1589.
11. T. Tokumitsu and T. Hayashi, *Bull. Chem. Soc. Jpn* 1981, **54**, 2348.
12. A. Iguchi, *Bull. Chem. Soc. Jpn* 1958, **31**, 600.
13. A. Iguchi, *Bull. Chem. Soc. Jpn* 1958, **31**, 746.
14. J. S. Fritz and D. J. Pietrzyk, *Talanta* 1961, **8**, 143.
15. J. A. Streeky, P. G. Pillsbury and D. H. Busch, *Inorg. Chem.* 1980, **19**, 3148.

Polyhedron Vol. 4, No. 11, pp. 1865–1868, 1985
Printed in Great Britain

0277–5387/85 $3.00 + .00
© 1985 Pergamon Press Ltd

THE THERMODYNAMICS OF SYNERGISTIC SOLVENT EXTRACTION OF Zn(II) WITH 1-PHENYL-3-METHYL-4-BENZOYL-PYRAZOLE-5-ONE

SOCK SUNG YUN*
Department of Chemistry, Chungnam National University, Daejon 300-31, Korea

and

HAN BEOM YANG and HYUN-SOO PARK
Korea Advanced Energy Research Institute, Daejon 300-31, Korea

(*Received* 21 *March* 1985; *accepted* 3 *May* 1985)

Abstract—The synergistic extraction of Zn(II) has been studied in the PMBP–TBP system (where PMBP = 1-phenyl-3-methyl-4-benzoyl-pyrazole-5-one and TBP = tri-*n*-butyl phosphate) at various temperatures using a radiochemical technique. The thermodynamic parameters for the reactions involved support the mechanism for the synergistic extraction in which the 5-coordinate monohydrated $Zn(PMBP)_2$ chelate exchanges a water molecule for TBP.

Several solvent extraction systems show a synergistic effect in their extractability of the metal ion. Among them, the chelating agent–neutral ligand group system has been the most extensively studied.[1–8] A representative example is the system with HTTA (thenoyltrifluoroacetone) as the chelating agent and TBP (tri-*n*-butyl phosphate) or TOPO (tri-*n*-octyl phosphine oxide) as the neutral ligand.

Synergism in solvent extraction has been explained in one of the following ways. In the case where the metal ion forms a partially neutralized and coordinatively unsaturated complex with its surrounding chelating agent, the hydrophilic complex formed is not very extractable from the organic solvent. With the addition of the neutral extractant as a secondary agent, however, a new organophilic complex is formed by the substitution of hydrated water molecules from the metal ion. This newly formed adduct posess a higher distribution coefficient than that of the hydrophilic hydrated complex.[4]

There are some examples that show a notable increase in extractability with the addition of a secondary agent in spite of the fact that the complex formed is completely neutralized and coordinatively saturated. In these cases, there are two different explanations to elucidate the mechanism of the synergism. One[9–11] is that the metal ion expands its coordination number and forms a more organophilic complex by the addition of a secondary ligand. The other is the opening of one of the chelate rings, thereby introducing the secondary extractant into the primary coordination sphere of the metal ion.[12,13]

It has been known that PMBP (1-phenyl-3-methyl-4-benzoyl-pyrazole-5-one) is one of the most interesting and promising reagents for the extraction of chelate compounds.[14] In this work, we have studied the extraction of Zn(II) with PMBP and TBP to identify the mechanism of the synergistic effect.

EXPERIMENTAL

Reagents

A solution of Zn(II) tracer in 0.1 M HCl was obtained from Korea Advanced Energy Research Institute. The HCl was boiled off from the Zn(II) tracer solution by heating it and adding 0.1 M $HClO_4$ repeatedly with an IR lamp. The stock solution was prepared by diluting the resulting Zn(II) tracer with 0.1 M $HClO_4$. TBP for extraction analysis was obtained from Merck Co. and used without further purification. PMBP was synthesized according to the method reported in the literature[15] and was 3 times recrystallized in *n*-heptane solvent. Benzene was used as the organic solvent.

* Author to whom correspondence should be addressed.

Procedure

The ionic strength of the aqueous phase was adjusted to 0.1 M with $NaClO_4$. The aqueous phase was buffered with 0.1 M sodium acetate. PMBP and TBP were dissolved in benzene.

All experiments were carried out in a 40 cm^3 glass reactor jacketed to circulate water from a constant-temperature bath which was maintained at the desired temperature. Volumes (10 cm^3 each) of the organic and aqueous solutions were placed in the reactor and agitated with a magnetic stirrer for more than 1 h to assure full extractive mixing. After that the phases were sampled for analysis by an NaI scintillation counter. Each experiment was repeated more than twice under the same experimental conditions to obtain reliable data.

RESULTS AND DISCUSSION

The results for the extraction of Zn(II) from 0.1 M $NaClO_4$ by PMBP–TBP mixtures of constant total molarity 0.1 M in benzene are shown in Fig. 1. It shows that there is a synergistic effect on the extraction of Zn(II) in the PMBP–TBP system and the distribution coefficient of Zn(II) increases with increasing pH value of the aqueous phase. Using the method of continuous variation[16] the complexes present in the organic phase have been determined. Table 1 shows the extraction of Zn(II) in the various compositions of PMBP–TBP in benzene. Detailed explanations of the extraction coefficients, q_x, Q_x and Q_{AB}, are given in Ref. 16. The maximum value of Q_x appears between $x = 0.6$ and $x = 0.7$, and agrees fairly well with the theoretical value of $x = 0.67$. This indicates that the species in the organic phase are $Zn(PMBP)_2$ and $Zn(PMBP)_2TBP$ in agreement with the result[17] obtained by the equilibrium shift method.

Table 1. Extraction of Zn(II) with PMBP+TBP in benzene[a]

x(PMBP)	q_x	Q_x	Log q_{AB}
0.00	0.007	—	—
0.10	4.264	4.032	2.651
0.20	12.970	12.044	2.575
0.30	30.39	28.30	2.652
0.40	40.01	36.29	2.577
0.50	48.63	42.84	2.534
0.60	60.01	51.66	2.555
0.70	61.70	50.35	2.535
0.80	47.97	33.15	2.413
0.90	35.62	16.86	2.318
1.00	23.16	—	—

[a] $[Zn]_{tot} = 1 \times 10^{-4}$ M. $\mu = 0.1$ M $Na(H)ClO_4$. [PMBP] + [TBP] = 0.1 M. Temperature = 23°C. pH = 4.284.

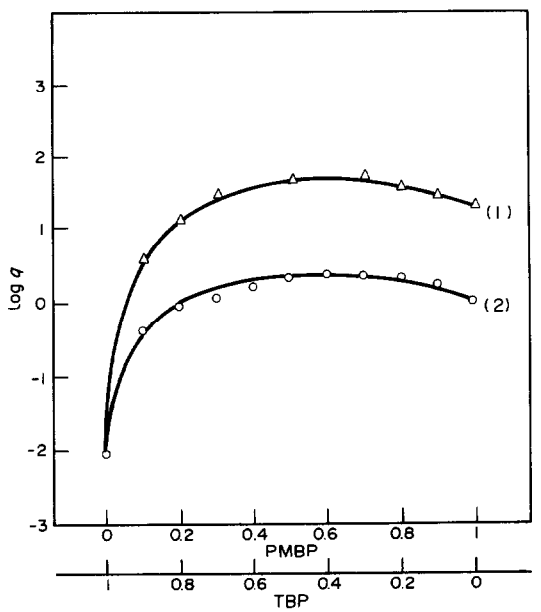


Fig. 1. Plot of log q, distribution ratio of Zn(II) vs [PMBP] (x M) and [TBP] (y M); $x + y = 0.1$ M. (1) PMBP–TBP, pH = 3.6; (2) PMBP–TBP, pH = 4.2.

The various equilibria of Zn(II) extraction by PMBP–TBP may be expressed as follows;

$$Zn^{2+}_{(aq)} + 2HPMBP_{(org)} \overset{K_1}{\rightleftharpoons} Zn(PMBP)_{2(org)} + 2H^+_{(aq)} \quad (1)$$

and

$$Zn^{2+}_{(aq)} + 2HPMBP_{(org)} + TBP_{(org)} \overset{K_2}{\rightleftharpoons} Zn(PMBP)_2TBP_{(org)} + 2H^+_{(aq)}. \quad (2)$$

In above equilibria, the equilibrium constants are:

$$K_1 = \frac{[Zn(PMBP)_2][H^+]^2}{[Zn^{2+}][HPMBP]^2} = q_o \frac{[H^+]^2}{[HPMBP]^2}$$

and

$$K_2 = \frac{[Zn(PMBP)_2TBP][H^+]^2}{[Zn^{2+}][HPMBP]^2[TBP]} = q \frac{[H^+]^2}{[HPMBP]^2[TBP]}.$$

The equilibrium for adduct formation in the organic phase is:

$$Zn(PMBP)_{2(org)} + TBP_{(org)} \overset{\beta_1}{\rightleftharpoons} Zn(PMBP)_2TBP_{(org)}, \quad (3)$$

where

$$\beta_1 = \frac{[Zn(PMBP)_2TBP]}{[Zn(PMBP)_2][TBP]} = K_2/K_1.$$

The equilibrium constants, K_1, K_2 and β_1, were determined at different temperatures. The enthalpy changes for reactions (1) and (2) were obtained through Gibbs–Helmholtz plots of the equilibrium constants against the reciprocal of the temperature. The values of enthalpy changes could be used to calculate the corresponding entropy changes. Figures 2 and 3 are Gibbs–Helmholtz plots for PMBP and PMBP–TBP systems, respectively. It was possible to calculate thermodynamic parameters for reaction (3) from the data for reactions (1) and (2). The results obtained at 23°C are given in Table 2. The errors estimated are less than 5% for ΔG and 10% for ΔS and ΔH.

There have been several suggestions for the structure of β-diketone complexes of Zn(II) and coordination numbers of 4, 5 and 6 are known.[18] An NMR study has shown that the hydration number of the Zn(II) ion in aqueous solution is 4.[19] Nash and Choppin[9] have proposed a mechanism for the synergistic extraction of Zn(II) in the TTA–TBP system, in which the increase in the coordination number of Zn(II) from 4 to 5 is caused by adduct formation with TBP. However, the thermodynamic parameters in Table 2 seem to indicate that the coordination number of the Zn(II) ion increases in the β-diketone complex formation of the hydrated Zn(II) ion in the PMBP–TBP system, i.e.:

$$[Zn(H_2O)_4]^{2+}_{(aq)} + 2HPMBP_{(org)} \rightleftharpoons Zn(PMBP)_2(H_2O)_{(org)} + 3H_2O_{(aq)} + 2H^+_{(aq)}. \quad (4)$$

Monohydrated bis(β-diketonato)Zn(II) complexes are also known.[20]

As Nash and Choppin[9] did, we could use similarly the argument that ΔH has only a unitary component and the cratic part of the entropy change is 7.9 Δn cal deg^{-1} where Δn is the change in the number of species. Assuming that the entropy change due to the hydrogen ion liberated in this buffer solution is nil, the cratic entropy change for reaction (4) is 7.9 cal deg^{-1}, since $n = 1$. If the chelation entropy for the formation of $Zn(PMBP)_2$ is approximately the same as that of $Zn(acac)_2$ (-17 cal deg^{-1}), as assumed for Zn(TTA),[9] the net entropy change for reaction (4)

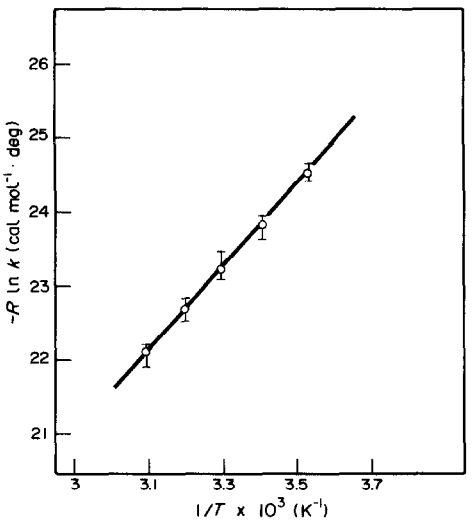


Fig. 2. Gibbs–Helmholtz plot for extraction of Zn(II) from 0.1 M $NaClO_4$ by PMBP in benzene.

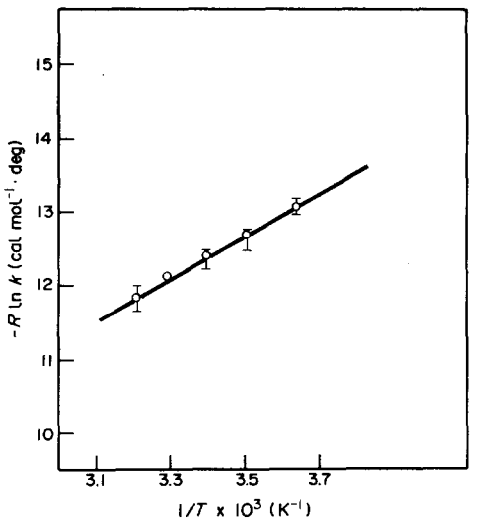


Fig. 3. Gibbs–Helmholtz plot for extraction of Zn(II) from 0.1 M $NaClO_4$ by PMBP–TBP mixtures in benzene.

Table 2. Thermodynamic values for reaction of Zn(II) with PMBP, and PMBP + TBP

Species	log K_1	log K_2	ΔG (kcal mol^{-1})	ΔH (kcal mol^{-1})	ΔS (cal deg^{-1} mol^{-1})
$Zn(PMBP)_2$	−5.203	—	+7.05	+5.51	−5.21
$Zn(PMBP)_2TBP$	—	−3.05	+4.13	+2.78	−4.51
	log β_1				
$Zn(PMBP)_2TBP$	+2.15		−2.92	−2.71	+0.70

would be -9 cal deg^{-1} mol^{-1}. The entropy change for this process was obtained experimentally to be -5.21 cal deg^{-1} mol^{-1}. This discrepancy may be due to the vibrational entropy of the PMBP ligand which is rather loosely bound in this five-coordinate as Nash and Choppin suggested for the TTA ligand.[9]

In the formation reaction of the mixed-ligand complex of Zn(II) with PMBP and TBP:

$$[Zn(H_2O)_4]^{2+}_{(aq)} + 2HPMBP_{(org)} + TBP_{(org)} \rightleftharpoons Zn(PMBP)_2TBP_{(org)} + 4H_2O_{(aq)} + 2H^+_{(aq)} \quad (5)$$

the net entropy change would be again -9 cal deg^{-1} mol^{-1}. The experimental value is about 4.5 cal deg^{-1} mol^{-1} larger, which would also be the vibrational entropy of rather loosely bound PMBP ligands.

From the above arguments, the reaction mechanism for the adduct formation of the $Zn(PMBP)_2$ chelate with TBP is deduced as follows:

$$\begin{array}{l} PMBP\text{-}Zn\text{-}PMBP_{(org)} + TBP_{(org)} \\ \quad | \\ \quad H_2O \end{array} \rightleftharpoons \begin{array}{l} PMBP\text{-}Zn\text{-}PMBP_{(org)} + H_2O. \\ \quad | \\ \quad TBP \end{array} \quad (6)$$

The rather small change in enthalpy, -2.71 kcal mol^{-1} for reaction (6) indicates the substitution of H_2O in the complex by TBP. The negligible value of the entropy change for this adduct formation, $+0.7$ cal deg^{-1} mol^{-1}, also supports this mechanism.

REFERENCES

1. H. Irving and D. N. Edgington, *J. Inorg. Nucl. Chem.* 1960, **15**, 1817.
2. H. Irving and D. N. Edgington, *J. Inorg. Nucl. Chem.* 1961, **21**, 169.
3. T. V. Healy and J. R. Ferraro, *J. Inorg. Nucl. Chem.* 1962, **24**, 1449.
4. T. V. Healy, *Nucl. Sci. Eng.* 1963, **16**, 413.
5. T. Sekine and D. Dyrssen, *J. Inorg. Nucl. Chem.* 1964, **26**, 1727.
6. L. Newman and P. Klotz, *Inorg. Chem.* 1966, **5**, 461.
7. T. Sekine and D. Dyrssen, *J. Inorg. Nucl. Chem.* 1967, **29**, 1457.
8. K. Batzar, D. E. Goldberg and L. Newman, *J. Inorg. Nucl. Chem.* 1967, **29**, 1511.
9. K. L. Nash and G. R. Choppin, *J. Inorg. Nucl. Chem.* 1977, **39**, 131.
10. D. P. Graddon and E. C. Watton, *J. Inorg. Nucl. Chem.* 1961, **21**, 49.
11. A. T. Kandil, H. E. Aly, M. Rahh and G. R. Choppin, *J. Inorg. Nucl. Chem.* 1975, **37**, 229.
12. J. R. Ferraro and T. V. Healy, *J. Inorg. Nucl. Chem.* 1962, **24**, 1463.
13. R. L. Scruggs, T. Kim and N. C. Li, *J. Phys. Chem.* 1963, **67**, 2194.
14. Yu. A. Zolotove, *Extraction of Chelate Compounds*, J. Schnorak (Trans.). Ann Arbor–Humphrey Science Publisher (1970).
15. B. S. Jensen, *Acta. Chem. Scand.* 1959, **13**, 1890.
16. I. J. Gal and R. M. Nikolic, *J. Inorg. Nucl. Chem.* 1966, **28**, 563.
17. Yu. A. Zolotove and L. G. Gavrillova, *J. Inorg. Nucl. Chem.* 1969, **31**, 3613.
18. Q. Fernando, *Sep. Sci.* 1966, **5**, 575.
19. T. J. Swift and W. G. Sayre, *J. Chem. Phys.* 1966, **44**, 3567.
20. D. P. Graddon, *Coord. Chem. Rev.* 1969, **4**, 1.

Polyhedron Vol. 4, No. 11, pp. 1869–1874, 1985
Printed in Great Britain

0277–5387/85 $3.00 + .00
© 1985 Pergamon Press Ltd

BIS(2,2′-BIPYRIDYL)DIISOPROPOXOMOLYBDENUM(II): A SPIN-STATE EQUILIBRIUM FOR A COMPLEX OF A SECOND-ROW TRANSITION ELEMENT

MALCOLM H. CHISHOLM† and EDWARD M. KOBER
Department of Chemistry, Indiana University, Bloomington, IN 47405, U.S.A.

and

DAVID J. IRONMONGER and PETER THORNTON†
Department of Chemistry, Queen Mary College, Mile End Road, London E1 4NS, U.K.

(*Received* 22 *April* 1985; *accepted* 10 *May* 1985)

Abstract—The variation of magnetic moment with temperature displayed by *cis*-$[Mo(OPr^i)_2(bipy)_2]$ shows that the complex exists in an equilibrium between singlet and triplet spin states, with the singlet lying lower in energy by 158 cm^{-1}. The magnetic data can be fitted to a Bleaney–Bowers equation with values of 1.96 for g and 2×10^{-4} cgs units for the second-order susceptibility N_α. The IR, resonance Raman and electronic absorption spectra together with electrochemical data establish that the spin-state equilibrium is principally metal-centred, arising from a splitting of the t_{2g}-orbitals, though there is substantial Mo d to bipy π^* bonding.

High-spin–low-spin equilibria occur in many transition-element complexes.[1] In most cases the metal ion has between four and seven d-electrons and the ligand field is near the so-called "crossover" point between the spin-free and spin-paired configurations for the stereochemistry involved, usually in the O_h point group. There are a few exceptions. A spin-state equilibrium occurs[2] in the d^8-configuration in the nickel(II) complex $[Ni(TAAB)X_2] \cdot H_2O$ (X = Cl or Br) of the macrocyclic tetradentate ligand TAAB derived from the self-condensation of 2-aminobenzaldehyde. The strong tetragonal ligand field of TAAB gives the complex D_{4h}- rather than O_h-symmetry and a singlet–triplet spin equilibrium can occur. On the other hand the singlet–triplet equilibrium in $[Ti(\eta^5\text{-}C_5H_5)_2(bipy)]$ was ascribed[3] to the diamagnetic molecule having a low-lying excited state in which one unpaired electron is located on the $Ti(C_5H_5)_2$ unit and the other is in a π^*-orbital of the bipy ligand.

All these examples occur in complexes of first-row transition elements. This paper reports the first observation of spin-state isomerism for a heavy transition element, in the complex *cis*-$[Mo(OPr^i)_2(bipy)_2]$, whose preparation we have already reported.[4] The weak and unquantified high-temperature paramagnetism found[5] for a ruthenium tris(α-diimine) complex which is diamagnetic at room temperature was suggested to be due to spin-state isomerism or some other effect, but this has not been verified by susceptibility studies over a range of temperatures. The only previous report of spin-state isomerism in the d^4-configuration is for a manganese(III) complex of a salen-type Schiff base,[6] but in another example[7] there seems to be a sharp change from an ^5E_g- to a $^3T_{2g}$-state at 40–50 K rather than an equilibrium.

There have been very few magnetic studies of mononuclear molybdenum(II) complexes over a range of temperature. Although the d^4-configuration can give rise to a spin quintet, this is unknown for molybdenum(II), and would not be expected in a complex such as ours, which contains two bipy groups, normally considered as strong ligands. A spin triplet occurs[8] in $[Mo(diars)_2X_2]$ [diars = bis-1,2-(dimethylarsino)benzene; X = Cl, Br or I]; for these complexes the magnetic moments are about 2.85 μ_B at room temperature, falling slightly as the temperature is lowered, in keeping with the occurrence of just a little spin–orbit coupling in these low-symmetry complexes. Other monomeric

† Authors to whom correspondence should be addressed.

molybdenum(II) complexes are diamagnetic, and many are seven-coordinate to achieve the 18-electron configuration.

EXPERIMENTAL

Standard procedures for the manipulation of air-sensitive materials were employed. All solvents were dried and deoxygenated prior to use.

IR spectra were obtained from Nujol mulls between KBr plates using a Perkin–Elmer 283 spectrophotometer. UV–visible spectra were recorded on a Hitachi 330 spectrophotometer using toluene as solvent. Magnetic measurements were obtained by the Faraday technique as described previously.[9]

The electrochemical measurements were made with a PAR 173 potentiostat, a PAR 175 programmer and a Houston 2000 XY recorder. The cyclic voltammetry was carried out in a one-compartment cell, while the coulometry used a three-compartment cell. The auxiliary electrode was of platinum gauze, the working electrode was either platinum wire or gauze and the reference electrode was 0.01 F $AgNO_3$ (CH_3CN)/Ag wire. Acetonitrile solutions were used with 0.1 M tetra-*n*-butylammonium hexafluorophosphate as the supporting electrolyte, using ferrocene as the internal standard.[10]

Preparation of cis[$Mo(OPr^i)_2(bipy)_2$]

To a stirred solution of [$Mo_2(OPr^i)_6$][11] (1.0 g, 1.84 mmol) in hexane (30 cm^3) was added 2,2′-bipy (0.6 g, 3.8 mmol). The initially yellow solution immediately changed to an intense purple. The solution was stirred for 1 h and allowed to stand overnight ($\simeq$ 12 h). Black crystals of [$Mo(OPr^i)_2(bipy)_2$] were collected by filtration and dried *in vacuo*. Yield 0.56 g, 60%. The compound may be recrystallised by addition of hexane to a solution in toluene. Found: C, 59.15; H, 5.68; N, 10.74. $C_{26}H_{30}MoN_4O_2$ requires C, 59.31; H, 5.74; N, 10.65%. IR data: 1583m, 1518m, 1304s, 1254m, 1158m, 1123s, 1023w, 991s, 973s, 954s, 839w, 741s, 735vs, 720s, 601m, 487w and 424w.

RESULTS AND DISCUSSION

Magnetic properties

The variations of the magnetic susceptibility and moment of *cis*-[$Mo(OPr^i)_2(bipy)_2$] with temperature are given in Table 1. The variation of moment with temperature is shown in Fig. 1. The error in the values of magnetic moment is ± 0.06 μ_B, which is higher than is often found in magnetochemical studies. This reflects the near cancellation of the paramagnetism of the complex by the diamagnetism of the ligands and the sample holder.

Table 1. Magnetic properties of *cis*-[$Mo(OPr^i)_2(bipy)_2$]

T (K)	10^3 χ_M (cgs)	μ (μ_B)
91	1.50	1.04
110	2.02	1.33
130	2.05	1.46
149	2.02	1.55
169	2.04	1.66
189	1.94	1.71
208	1.86	1.76
226	1.79	1.80
245	1.72	1.84
265	1.72	1.91
285	1.59	1.90
305	1.57	1.96

The magnetic behaviour is quite unlike that of the other Mo(II) complexes described in the introduction. The results are most easily explained by postulating a singlet–triplet spin-state equilibrium. The full curve in Fig. 1 represents the calculated variation of magnetic moment with temperature using the usual Bleaney–Bowers treatment[12] with values of $g = 1.96$, $J = -79 \pm 5$ cm^{-1} and $N_\alpha =$

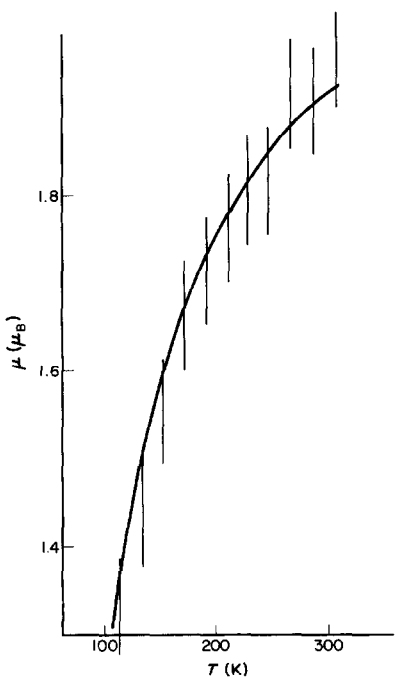


Fig. 1. Variation of magnetic moment (μ_B) of *cis*-[$Mo(OPr^i)_2(bipy)_2$] with temperature (K).

2×10^{-4} cgs units. The calculation assumed a spin-only value for the magnetic moment of the triplet state, which we think is reasonable in view of the low symmetry of the complex. The agreement with the experimental values is seen to be satisfactory.

The mol fractions of singlet and triplet spins at each temperature were also calculated to obtain the singlet–triplet equilibrium constants. An Arrhenius' plot of these gives a good straight line from which ΔH for the equilibrium was calculated as 145 ± 15 cm^{-1}. This compares favourably with the value of 158 ± 10 cm^{-1} ($= -2J$) for the singlet–triplet energy separation in the Bleaney–Bowers treatment.

Bleaney and Bowers[12] pioneered their method to interpret the behaviour of the antiferromagnetic dimer $[Cu_2(H_2O)_2(O_2CMe)_4]$, not a spin-state equilibrium in a mononuclear complex. However, their system is similar to ours in that there is a singlet ground state below a thermally accessible triplet state. This is not a common situation in spin-state isomerism; reduction in temperature usually gives a gradual or abrupt change in ground state from high spin to low spin, often accompanied by significant changes in molecular dimensions. As the evidence below shows, we believe our spin equilibrium arises from thermal population of two closely spaced orbitals which are essentially σ-nonbonding. We therefore do not expect much variation in molecular structure with temperature and conclude that there is virtually a constant energy difference between the spin states.

An alternative explanation, that the temperature dependence of the magnetic moment arises from spin–orbit coupling in a $^3T_{1g}$ ground state, can be excluded because our data do not fit any of the many combinations of parameters which describe[13] such a process.

IR and Raman spectra

The IR spectra of various metal–bipy complexes have been extensively studied, especially those with metal atoms in unusually low oxidation states where complexes of the type M^{n+}(bipy) might better be described as $M^{(n+1)+}$(bipy)$^-$, i.e. the bipy ligand is reduced.[14] On the basis of characteristic IR bands it was proposed[14] that complexes could be divided into three categories where the bipy ligands were in a normal, reduced or intermediate (partly reduced) state. The complexes with "normal" bipy ligands exhibited a strong band in the 1600–1610-cm^{-1} region and no bands in the 1500–1600- or 950–100-cm^{-1} regions. Complexes containing "reduced" bipy ligands did not have a band above 1600 cm^{-1}, but exhibited several strong bands in the 1490–1575-cm^{-1} region and a strong band in the 900–1000-cm^{-1} region. Complexes with "intermediate" bipy ligands exhibited bands in all three regions.

$[Mo(OPr^i)_2(bipy)_2]$ exhibits medium bands at 1583 and 1518 cm^{-1}, nothing above 1600 cm^{-1}, and three strong bands at 991, 972 and 954 cm^{-1}. It should be noted that O–C stretches in metal alkoxides typically occur in the 900–1000-cm^{-1} region.[15] Thus if two of the latter bands arise from O–C stretching modes, this still leaves one band assignable to a bipy mode. The IR data are therefore most consistent with a "reduced" bipy ligand on these criteria.

The resonance Raman (RR) spectrum of $[Mo(OPr^i)_2(bipy)_2]$ has previously been reported.[4] The seven A_1 framework stretches of the bipy ligand show RR enhancement and the frequencies of these modes shift to a lower energy as the electron density in the bipy π^*-orbitals is increased, either through reduction or metal $d \rightarrow$ bipy π^* back-bonding.[16] The RR frequencies of $[Mo(OPr^i)_2(bipy)_2]$ lie roughly halfway between the frequencies for a "normal" bipy ligand, such as in $[Ru(bipy)_2Cl_2]$ or $[Ru(bipy)_2(NH_3)_2]^{2+}$ and that of a fully reduced bipy as in Li^+bipy^-.[16] It was concluded that the bipy ligands in *cis*-$[Mo(OPr^i)_2(bipy)_2]$ have approximately 0.5 ε in their π^*-orbitals, i.e. they are partly but not fully reduced.

UV–visible data

The electronic absorption spectrum of *cis*-$[Mo(OPr^i)_2(bipy)_2]$ exhibits the following strong bands {[λ_{max} (nm)] [ε (M^{-1} cm^{-1})]}: 940sh, 745 (7800), 550 (17,000), 438 (5200), 380sh ($\simeq$ 6000) and 305 (27,000). No absorptions with $\varepsilon > 40$ M^{-1} cm^{-1} were found between 1300 and 2200 nm. This spectrum is not very similar to that of Na^+bipy^-: 850 (1900), 550 (4300), 380 (17,000).[17] For complexes where the $M^{(n+1)+}bipy^-$ formulation seems appropriate, spectra similar to that of Na^+bipy^- are often found.[18] The most distinguishing feature is that for "normal" bipy the intense $\pi \rightarrow \pi^*$ transition occurs[19] at $\lambda_{max} \simeq 300$ nm ($\varepsilon \simeq 15{,}000$ M^{-1} cm^{-1}) where for $bipy^-$ this transition moves to lower energy, $\lambda_{max} \simeq 380$ nm.[17] Therefore it seems more appropriate to refer to the present complex as

$$[Mo(OPr^i)_2(bipy)_2]$$

rather than

$$[Mo(IV)(OPr^i)_2(bipy^-)_2]$$

or

$$[Mo(III)(OPr^i)_2(bipy)(bipy^-)].$$

The observed transitions are then most readily assigned as metal d to bipy π^* charge-transfer

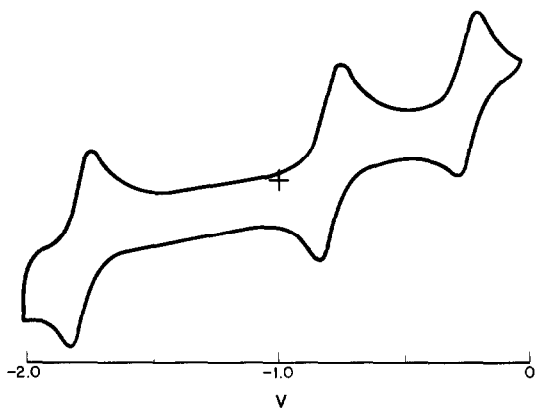


Fig. 2. Steady-state cyclic voltammogram of *cis*-[Mo(OPr^i)$_2$(bipy)$_2$]. Applied voltage is vs the SCE.

transitions. Their low energy can be ascribed to the great ease of oxidation of the metal (*vide infra*). The energy separation between the two lowest energy bands (745 and 550 nm) of $\simeq 5000\ cm^{-1}$ is typical for the separation of MLCT transitions to the lowest and second lowest π^*-orbitals of bipy.[19] The third transition (438 nm) is presumably MLCT to the third lowest π^*-orbital.

Electrochemistry

The electrochemical properties of the complex were examined in acetonitrile solutions (Fig. 2). Two oxidative couples were observed at −0.80 and −0.25 V vs the saturated calomel electrode (SCE). The anodic and cathodic peak currents of both couples were the same. Without compensation for internal resistance (ir), peak-to-peak separations of 70–80 mV were observed while separations of 60–65 mV were observed with ir compensation. Both couples are thereby implied to be reversible one-electron transfer processes. Oxidative coulometry at −0.5 V verified that the first first couple was indeed a one-electron process. A reversible reduction process was observed to occur at −1.80 V, and it also appears to be a one-electron couple.

The two oxidative couples can be assigned as Mo-centred since they do not occur at sufficiently negative potentials to be assigned as a bipy$^-$ → bipy + ε^- oxidation. Data for a wide variety of complexes have shown that bipy-based reductions occur at −1.2 V vs SCE.[20] Since the first oxidative couple occurs at a 0.3 V more positive potential than this, it can be assigned as predominantly metal-based, though substantial metal d → bipy π^* interactions are implied. Therefore the electrochemistry also supports the formulation as a neutral molecule, [Mo(II)(OPr^i)$_2$(bipy)$_2$], rather than a molybdenum(III) or (IV) species. The negative potentials for both oxidative couples show that the Mo centre is exceedingly electron-rich.

Molecular structure of cis-[Mo(OPr^i)$_2$(bipy)$_2$]

The crystal and molecular structures have previously been reported,[4] where it was emphasised that the C–C and C–N distances within the bipy ligands were substantially different from those normally seen in metal–bipy complexes. Similar distortions within the bipy ligands have subsequently been reported in the compound [Fe(η^6-toluene)(bipy)],[21] and this type of distortion has been demonstrated to result from the addition of substantial electron density to the lowest π^*-orbital of bipy.[22]

What is of particular interest in the present work is the orientation of the alkoxide ligands. This is shown in the stereoviews in Fig. 3. Assuming that the oxygen atoms are sp^2-hybridised (Mo–O–C angle is 130 ±2°), then the oxygen-filled p-orbitals lie roughly in the same plane such that they both (one on each O atom) will interact with the same Mo atomic orbital. The O–Mo–O angle of 105.3(1)° and the Mo–O distances (1.94 and 1.93 Å) are both consistent with some oxygen–Mo π-bond.[23]

Qualitative MO description

Two limiting situations may be invoked to account for the observed singlet–triplet spin-state

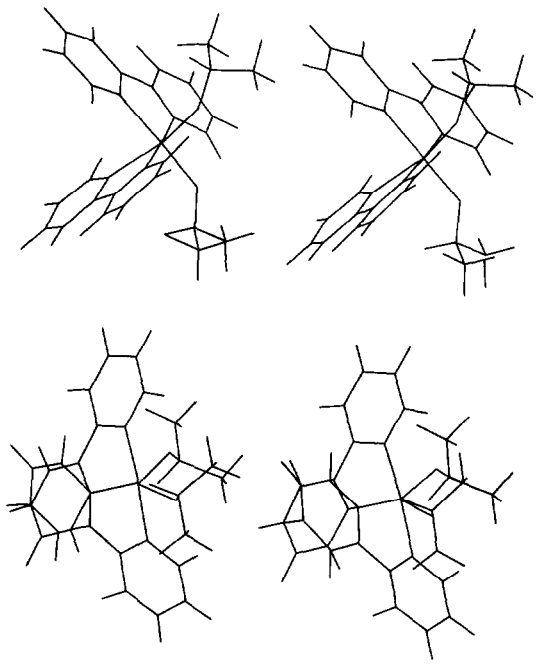


Fig. 3. Stereoviews of *cis*-[Mo(OPr^i)$_2$(bipy)$_2$] which emphasise the orientation of the alkoxide ligands.

equilibrium. (1) The electrons involved are in metal-centred orbitals and the spin equilibrium is between the configurations arising from t_{2g}^4. (2) The equilibrium is of a charge-transfer nature, Mo(II)(bipy)(singlet) $\rightleftharpoons$ Mo(III)(bipy)$^-$(triplet), similar to that previously found[3] for $[Cp_2Ti(bipy)]$. The observed electrochemical data and electronic spectrum argue against the presence of a fully reduced bipy ligand, bipy$^-$. It should be noted that these measurements were made at room temperature where the singlet : triplet ratio should be roughly 40 : 60, so that the presence of the bipy$^-$ species should be readily detectable. Although the IR data suggest the ligands belong to the "reduced" category, the more quantitative RR data showed them to be "reduced" by only $\simeq 0.5\,e$ each. The vibrational data may readily be accomodated by mixing of Mo *d*- and bipy π^*-orbitals, i.e. strong Mo *d* to bipy back-bonding. We therefore turn to a spin equilibrium involving the t_{2g}^4-configuration as a starting point for an understanding of this molecule.

The development of a simple molecular orbital scheme, based on the coordinate scheme shown in Fig. 4, can rationalise the observed results. In this axis system the t_{2g}-orbitals are d_{xz}, d_{xy} and $d_{z^2-y^2}$, which transform as *b*, *a* and *a* respectively in the C_2 point group.

First we turn to the metal–alkoxide interactions, since it is known that π-donor ligands can cause a "two below one" splitting of the t_{2g}-orbitals to give a diamagnetic d^4-configuration in an octahedral complex.[24] Both alkoxide ligands are oriented so that their filled $O(p\pi)$ orbitals essentially lie in the *yz* plane. In this situation the Mo $d_{z^2-y^2}$-orbital interacts with the oxygen *p*-orbitals. Formation of one RO–Mo π-bonding, one non-bonding (RO-centred) and one antibonding interaction may be anticipated. As noted previously the relatively short

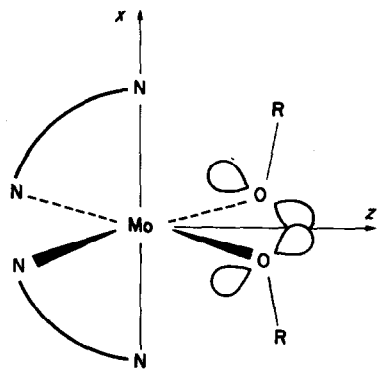


Fig. 4. Coordinate system for *cis*-$[Mo(OPr^i)_2(bipy)_2]$. The *z*-axis coincides with the C_2-axis of the molecule. The drawn $O(p\pi)$ orbitals essentially lie in the *yz* plane.

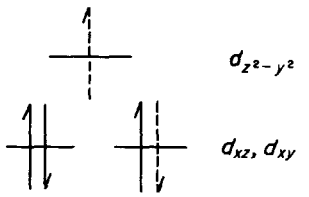


Fig. 5. Proposed orbital-ordering scheme. The dashed arrows indicate the two possible locations of the fourth metal electron for the singlet–triplet equilibrium.

Mo–O distances and enlarged (> 90°) O–Mo–O angle are all consistent with this picture. This leads to the orbital splitting shown in Fig. 5 wherein the $d_{z^2-y^2}$-orbital lies above the d_{xz}- and d_{yz}-orbitals, which are roughly equal in energy. It is also noteworthy that enlarging the O–Mo–O angle from 90° is predicted[25] to cause a further destabilisation of the Mo $d_{z^2-y^2}$-orbital as a result of a partial rehybridisation towards the alkoxide ligands which enhances π interaction. The singlet ground state corresponds to the $(d_{xy}, d_{xz})^4$ configuration, and the triplet excited state to $(d_{xy}, d_{xz})^3(d_{z^2-y^2})^1$.

Now the interactions with the bipy π^*-orbitals are considered. The lowest-energy π^*-orbital has the same phase at each N atom, i.e. it is antisymmetric with respect to rotation about the bipy C_2-axis.[3,16,21] The two combinations of these give MOs of *a*- and *b*-symmetry. Angular overlap considerations show that these have roughly equal overlaps with the $d_{xz}(b)$ and $d_{xy}(a)$ orbitals, though their overlaps with the $d_{z^2-y^2}(a)$ orbital is roughly twice as great. Thus the metal $d \rightarrow$ bipy π^* interactions should stabilise the $d_{z^2-y^2}$-orbital relative to the d_{xz}- and d_{xy}-orbitals, which is opposite to the effect of the RO ligands.

Which effect dominates? We feel the ordering with the $d_{z^2-y^2}$-orbital highest in energy is correct for the following reasons. (1) The orientation of the alkoxides implies that the $d_{z^2-y^2}$ is singled out for oxygen *p* interactions. (2) Alkoxides are strong π-donors whereas bipy ligands are relatively weak π-acceptors. The alkoxide interaction should thus be dominant. (3) If the $d_{z^2-y^2}$-orbital was beneath the d_{xy}- and d_{xz}-orbitals, then the energy splitting between the d_{xz}- and d_{xy}-orbitals would have to be responsible for the spin singlet–triplet equilibrium. There is no reason to believe that these orbitals should be split by an energy separation comparable to the pairing energy. However, the opposing influences of RO π-donor and bipy π^*-acceptor ligands could well result in the energy separation between the $d_{z^2-y^2}$ and (d_{xz}, d_{xy}) orbitals being sufficiently small (i.e. comparable to the spin-pairing energy) that the singlet–triplet spin-state equilibrium occurs.

A direct way of measuring the splitting of the t_{2g}-orbitals is to locate the $d\pi \rightarrow d\pi$ transitions. For example, many diamagnetic octahedral d^4 complexes have an absorption band in the region 500–700 nm with $\varepsilon \simeq 60$–$600\ M^{-1}\ cm^{-1}$, which has been assigned to the lowest energy $d\pi \rightarrow d\pi$ transition.[26] Unfortunately, for *cis*-$[Mo(OPr^i)_2(bipy)_2]$ this region of the spectrum is completely obscured by the strong MLCT transitions. Since no transitions with $\varepsilon > 40\ M^{-1}\ cm^{-1}$ are observed between 1300 and 2200 nm it is presumed that the energy separation is at least greater than $6000\ cm^{-1}$.

Concluding remarks

Normally, monomeric Mo(II) compounds are stabilised by strong π-acceptor ligands (CO, CNR etc.) or, when surrounded by hard or "classical"-type ligands (Cl^-, O_2CR^- etc.), are found with accompanying M–M bonds.[27] *Cis*-$[Mo(OPr^i)_2(bipy)_2]$ is unusual in being one of only a few octahedral Mo(II) complexes containing both π-donor and π-acceptor ligands.[25,26,28] It is unique, at least for the moment, in providing an example of a singlet–triplet spin-state equilibrium for a non-first-row transition element. The electrochemical data and electronic spectrum reliably establish the origin of the spin-state equilibrium to be metal centred while the IR and RR spectra and structural data provide evidence for extensive Mo *d* to bipy π^* back-bonding. This work emphasises the gradation of bipy reduction by back-bonding (analogous to the bond order reduction of C≡O) and the need to draw upon several techniques to establish a reasonable bonding description for low-valent metal–bipy complexes.

Acknowledgements—We thank Dr C. P. J. Vuik for experimental assistance, the Royal Society and Central Research Fund (University of London) for funds for the purchase of apparatus (at QMC) and the National Science Foundation for financial support (at IU).

REFERENCES

1. P. Day (Ed.) *Electronic Spectra and Magnetism of Inorganic Compounds.* Vols 1–6. Chemical Society Specialist Periodical Reports.
2. G. A. Melson and D. H. Busch, *J. Am. Chem. Soc.* 1964, **86**, 4830.
3. A. M. McPherson, B. F. Fieselmann, D. L. Lichtenberger, G. L. McPherson and G. D. Stucky, *J. Am. Chem. Soc.* 1979, **101**, 3425.
4. M. H. Chisholm, J. C. Huffman, I. P. Rothwell, P. G. Bradley, N. Kress and W. H. Woodruff, *J. Am. Chem. Soc.* 1981, **103**, 4945.
5. B. Chaudret, H. Koster and R. Poilblanc, *J. Chem. Soc., Chem. Commun.* 1981, 266.
6. V. V. Zelentsov and I. K. Somova, *Zh. Obshch. Khim.* 1974, **44**, 1309.
7. P. G. Sim and E. Sinn, *J. Am. Chem. Soc.* 1981, **103**, 241.
8. J. Lewis, R. S. Nyholm and P. W. Smith, *J. Chem. Soc.* 1962, 2592.
9. M. A. Laffey and P. Thornton, *J. Chem. Soc., Dalton Trans.* 1982, 313.
10. R. R. Gagne, C. A. Koval and G. C. Lesinsky, *Inorg. Chem.* 1980, **19**, 2854.
11. M. H. Chisholm, F. A. Cotton, C. A. Murillo and W. W. Reichert, *Inorg. Chem.* 1977, **16**, 1801.
12. B. Bleaney and K. D. Bowers, *Proc. R. Soc.* 1952, **A214**, 451.
13. B. N. Figgis, J. Lewis, F. E. Mabbs and G. A. Webb, *J. Chem. Soc. (A)* 1966, 1411.
14. Y. Saito, J. Takemoto, B. Hutchinson and K. Nakamoto, *Inorg. Chem.* 1972, **11**, 2003.
15. D. C. Bradley, R. C. Mehrotra and D. P. Gaur, *Metal Alkoxides*, p. 118. Academic Press, New York (1978).
16. P. G. Bradley, N. Kress, B. A. Hornberger, R. F. Dallinger and W. H. Woodruff, *J. Am. Chem. Soc.* 1981, **103**, 7441; G. H. Allen, J. V. Caspar, T. J. Meyer and W. H. Woodruff, submitted for publication.
17. E. Koenig and S. Kremer, *Chem. Phys. Lett.* 1970, **5**, 87; Y. Torii, T. Yazaki, Y. Kaizu, S. Murasato and H. Kobayashi, *Bull. Chem. Soc. Jpn* 1969, **42**, 2264.
18. I. Hanazaki and S. Nagakura, *Bull. Chem. Soc. Jpn* 1971, **44**, 2312; E. Koenig and S. Herzog, *J. Inorg. Nucl. Chem.* 1979, **32**, 585; R. Pappalardo, *Inorg. Chim. Acta* 1968, **2**, 209; G. A. Heath, L. J. Yellowlees and P. S. Braterman, *J. Chem. Soc., Chem. Commun.* 1981, 287.
19. G. M. Bryant, J. E. Fergusson and H. K. J. Powell, *Aust. J. Chem.* 1971, **24**, 257.
20. T. Sajim and S. Aoyagui, *J. Electroanal. Chem.* 1975, **63**, 405.
21. L. J. Radonovich, M. W. Eyring, T. J. Groshens and K. J. Klabunde, *J. Am. Chem. Soc.* 1982, **104**, 2816.
22. E. M. Kober and T. J. Meyer, submitted for publication.
23. M. H. Chisholm, *Polyhedron* 1983, **2**, 681.
24. L. J. Templeton, P. B. Winston and B. C. Ward, *J. Am. Chem. Soc.* 1981, **103**, 7713.
25. P. Kubacek and R. Hoffmann, *J. Am. Chem. Soc.* 1981, **103**, 4320.
26. P. B. Winston, S. J. Nieter Burgmayer and J. L. Templeton, *Organometallics* 1983, **3**, 167; C. M. Giandomenico, C. T. Lam and S. J. Lippard, *J. Am. Chem. Soc.* 1982, **104**, 1263; M. Kamata, K. Hirotsu, T. Higuchi, K. Tatsumi, R. Hoffman, T. Yoshida and S. Otsuka, *J. Am. Chem. Soc.* 1981, **103**, 5772.
27. F. A. Cotton and G. Wilkinson, *Advanced Inorganic Chemistry*, 4th edition. Wiley, New York (1980).
28. M. H. Chisholm, J. C. Huffman and R. L. Kelly, *J. Am. Chem. Soc.* 1979, **101**, 7615.

Polyhedron Vol. 4, No. 11, pp. 1875–1881, 1985
Printed in Great Britain

0277-5387/85 $3.00 + .00
© 1985 Pergamon Press Ltd

CLUSTER BONDING AND ENERGETICS OF THE BORANE ANIONS, $B_nH_n^{2-}$ ($n = 5$–12): A COMPARATIVE STUDY USING BOND LENGTH–BOND ENTHALPY RELATIONSHIPS AND MOLECULAR-ORBITAL BOND INDEX CALCULATIONS

CATHERINE E. HOUSECROFT

Chemistry Department, University of Notre Dame, Notre Dame, IN 46556, U.S.A.

RONALD SNAITH

Department of Pure and Applied Chemistry, Strathclyde University, 295 Cathedral St., Glasgow G1 1XL, U.K.

and

KAREN MOSS, ROBERT E. MULVEY, MARION E. O'NEILL and KENNETH WADE*

Chemistry Department, Durham University, South Road, Durham DH1 3LE, U.K.

(*Received* 11 *March* 1985; *accepted* 10 *May* 1985)

Abstract—Cluster bond enthalpies, E_L(B—B), and orders, $\bar{n}$(B—B), for the structurally characterised *closo* anions, $B_nH_n^{2-}$ ($n = 6$ and 8–12), have been estimated using the logarithmic length–enthalpy and enthalpy–order relationships E_L(B—B) (kJ mol^{-1}) = 1.766×10^{11} [L(B—B)]$^{-4.0}$ and E_L(B—B) (kJ mol^{-1}) = $318.8[\bar{n}$(B—B)]$^{0.697}$, respectively. In a parallel study, the molecular-orbital bond index CNDO-based calculation method has been used to give B—B and B—H bond indices, I(B—B) and I(B—H), from which bond index based bond enthalpies, E_I, have been calculated using the relationships E_I(B—B) = $297.9I$(B—B) and E_I(B—H) = $374.8I$(B—H) (enthalpies in kJ mol^{-1}; lengths in pm). From these, total skeletal bond enthalpies $\sum E$(B—B), and total bond enthalpies, $\sum E$(B—B) + $\sum E$(B—H), have been calculated. Although calculated values of E_L and $\sum E_L$ generally exceed those of E_I and $\sum E_I$ by some 8% and calculated values of I generally exceed those of $\bar{n}$ by a greater amount, the trends in these parameters for the series of $B_nH_n^{2-}$ anions are very similar, showing the greater efficiency with which the $n + 1$ skeletal electron pairs are used as n increases. However, the two approaches differ in that, whereas the $\sum E_I$ values suggest that the anions are all of comparable stability, the $\sum E_L$ values clearly show $B_6H_6^{2-}$, $B_{10}H_{10}^{2-}$ and $B_{12}H_{12}^{2-}$ to be more stable than $B_8H_8^{2-}$, $B_9H_9^{2-}$ and $B_{11}H_{11}^{2-}$. The interatomic distances in $B_7H_7^{2-}$ and in the unknown $B_5H_5^{2-}$ are estimated and used to assess their relative stabilities. The E_L values suggest that $B_7H_7^{2-}$ is of comparable stability to $B_8H_8^{2-}$ etc., but show $B_5H_5^{2-}$ as relatively unstable. The E_I values suggest that both of these anions should be relatively stable members of the series of *closo* anions.

In an earlier note,[1] we explored the assignment of bond length based bond enthalpies, E_L, to the skeletal bonds of the *closo* borane anions, $B_nH_n^{2-}$ ($n = 6$, 8, 9, 10 or 12) (Fig. 1), as a means of estimating their relative stabilities and electron distributions. Laurie and Perkins[2] subsequently used bond index based bond enthalpies, E_I, for the same purpose for the species $B_6H_6^{2-}$, $B_{10}H_{10}^{2-}$ and $B_{12}H_{12}^{2-}$. Here, we elaborate and extend these arguments to ascertain the extent of agreement between the two methods, and to include $B_{11}H_{11}^{2-}$ (a derivative of which, $B_{11}H_{10}SMe_2^-$, has been structurally characterised[3]

* Author to whom correspondence should be addressed.

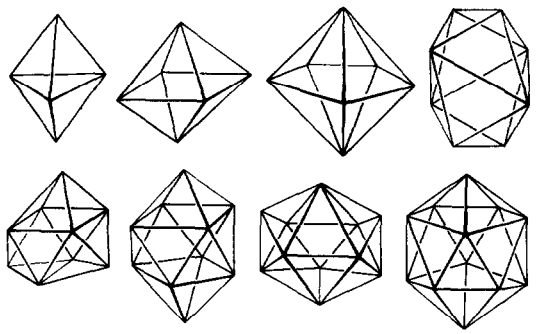


Fig. 1. Polyhedral skeletons of *closo* borane anions, $B_nH_n^{2-}$, considered in this paper (n = 5–12).

since the earlier work) and $B_7H_7^{2-}$ (for which we have estimated the interatomic distances). We also discuss briefly the probable interatomic distances and possible stability of the unknown species $B_5H_5^{2-}$.

Methods used to calculate E_L *and* E_I

The method of calculating *bond enthalpies from bond lengths* that we have used[1,4,5] employs relationships of the form $E_L(X—Y) = A[L(X—Y)]^{x-}$ to calculate bond enthalpies, E_L kJ mol^{-1}, of bonds of length L pm, where A and x are constants for the particular atom pair X—Y involved, their values being determined by fitting $\sum E_L(X—Y)$ to gas-phase atomisation enthalpies calculated from published values of ΔH_f^o for suitable molecules. The equations $E_L(B—B)$ (kJ mol^{-1}) $= 1.766 \times 10^{11}[L(B—B)]^{-4.0}$ and $E_L(B—H)$ (kJ mol^{-1}) $= 4.476 \times 10^{11}[L(B—H)]^{-4.4}$ were found[5] to give a good fit to published structural[6] and thermochemical[7] data for the *nido* and *arachno* boranes B_4H_{10}, B_5H_9, B_5H_{11}, B_6H_{10} and $B_{10}H_{14}$, using values of 560 and 218 kJ mol^{-1} for ΔH_f^o for gaseous boron and hydrogen atoms respectively. Both bridging and terminal B—H bonds were included, as were directly-bonded and hydrogen-bridged interactions, but longer-range interactions were assumed to be negligible.

These equations afforded values for $E_L(B—B)$ of 219 and 178 kJ mol^{-1} for the skeletal bonds in $B_6H_6^{2-}$ (length 168.6 pm)[8] and $B_{12}H_{12}^{2-}$ (length 177.5 pm)[9] respectively. Since the $n+1$ skeletal electron pairs in these two highly symmetrical anions can be assumed to be divided evenly between their $3n-6$ edges, these edges formally have bond orders, $\bar{n}$, of 7/12 and 13/30 respectively. This leads to the bond enthalpy–bond order relationship $E_L(B—B) = 318.8[\bar{n}(B—B)]^{0.697}$, whence a single bond between two boron atoms has a bond enthalpy of 318.8 kJ mol^{-1} and a length of 153.4 pm.

The *bond index method*[10–12] employs a CNDO–SCF calculation of molecular electronic structure, including all valence electrons and all possible orbital interactions, to obtain an electron density matrix. From this, bond indices, I, can be calculated and have been used to estimate E_I for numerous bonds, specifically for those in boranes[2] by means of the equations $E_I(B—B) = 297.9I(B—B)$ and $E_I(B—H) = 374.8I(B—H)$ (which gave a good fit to the published thermochemical data for B_4H_{10} and B_5H_9).[2] Since bond indices should correspond closely to bond orders for relatively non-polar bonds, these equations afford bond enthalpy terms, E_I, of 297.9 and 374.8 kJ mol^{-1} for single B—B and B—H bonds respectively.

The important differences between the bond length and bond index approaches to bond enthalpies are that the former assumes that the only bonding interactions of significance are those in the immediate coordination sphere of the atoms concerned, and relates their strength to their length, irrespective of the connectivities of the atoms concerned, whereas the latter relates bond enthalpies to a parameter (bond index) that is a measure of the electron density between the nuclei concerned, which may vary with atom connectivities as well as with internuclear distances, and includes all pair-wise interactions, whether involving first coordination sphere atoms or those further away, a factor which may be of importance when dealing with cluster compounds, for which neglect of cross-polyhedral interactions may not be justified.

RESULTS AND DISCUSSION

Closo *anions* $B_nH_n^{2-}$ *of known structure* (n = 6,[8] 8,[13] 9,[14] 10,[15] 11[3] *and* 12[9])

Table 1 lists the interatomic distances (L pm) for the various types of polyhedron edge in the *closo* borane anions, $B_nH_n^{2-}$ (n = 6 and 8–12), classified according to the skeletal atom connectivities, k and k', of the two boron atoms they link (k is the number of polyhedron edges that meet at the vertex occupied by the atom concerned). Table 1 also lists calculated bond indices, I, bond orders, $\bar{n}$, and bond enthalpies, E_I and E_L. Separate entries are made in cases where there are nonequivalent edges of a given connectivity—for example, for the two types of edge linking atoms of connectivities 4 and 5 in $B_8H_8^{2-}$, and for the two types of edge linking atoms of connectivities 5 and 5 in $B_9H_9^{2-}$. Average values are given in Table 2.

One structural feature of these *closo* anions $B_nH_n^{2-}$ is quite pronounced. Polyhedron edge lengths increase quite markedly with the connectivities of the atoms they link within a particular polyhedron. Clearly, the more atoms a particular boron atom

Table 1. Interatomic distances, L (pm), bond indices, I, orders, $\bar{n}$, and enthalpies, E_L and E_I, for *closo* borane anions, $B_nH_n^{2-}$

Species	L	k, k'[a]	I	$\bar{n}$	E_I	E_L
$B_5H_5^{2-}$[b]	164[c] × 6	3, 4	0.928	0.681	276	244
	183[c] × 3	4, 4	0.419	0.365	125	158
$B_6H_6^{2-}$	168.6 × 12	4, 4	0.681	0.583	203	219
$B_7H_7^{2-}$	163[c] × 5	4, 4	0.845	0.706	252	250
	179[c] × 10	4, 5	0.528	0.413	157	172
$B_8H_8^{2-}$	155.9 × 2	4, 4	0.926	0.912	276	299
	171.7 × 4	4, 5	0.700	0.523	209	203
	175.6 × 8	4, 5	0.529	0.462	158	186
	192.6 × 4	5, 5	0.463	0.270	138	128
$B_9H_9^{2-}$	170.8 × 12	4, 5	0.663	0.542	198	208
	183.7 × 3	5, 5	0.455	0.355	136	155
	190.6 × 6	5, 5	0.449	0.288	134	134
$B_{10}H_{10}^{2-}$	167.8 × 8	4, 5	0.674	0.599	201	223
	181.0 × 16	5, 5	0.501	0.389	149	165
$B_{11}H_{11}^{2-}$	165.5 × 4	4, 5	0.772	0.638	230	233
	174.5 × 2	4, 6	0.576	0.476	172	190
	177.1 × 2	4, 5	0.510	0.440	152	180
	178.8 × 15	5, 5	0.527	0.416	157	173
	201.2 × 4	5, 6	0.376	0.212	112	108
$B_{12}H_{12}^{2-}$	177.5 × 30	5, 5	0.539	0.433	161	178

[a] k and k' are the skeletal connectivities of the atoms concerned.
[b] Not yet prepared.
[c] Estimated distances—see later discussion.

bonds to, the weaker and so longer those bonds will be, since that atom's share of the $n+1$ skeletal bonding electrons has to be divided between more two-centre links. This structural trend is reflected in the trends in the calculated I, $\bar{n}$ and bond enthalpies, whether E_I or E_L. Although E_L exceeds E_I by some 8% on average, both E_L and E_I show the same general trends, with but few exceptions which are not considered to be significant in view of the variable quality of the structural data and the approximations inherent in our approach.

Another perhaps less recognised structural feature worth noting is the manner in which bonds of a particular connectivity type tend to get progressively *shorter* as n increases, the reverse of the trend that might have been expected as the number of skeletal electrons available per boron atom, $(n+1)/n$, or per polyhedron edge, $(n+1)/(3n-6)$ *decreases* as n increases. For example, bonds linking atoms of connectivity 4 have length 168.6 pm in $B_6H_6^{2-}$,[8] and 155.9 pm in $B_8H_8^{2-}$.[13] For bonds linking atoms of connectivities 4 and 5, average lengths are 174.3 pm ($B_8H_8^{2-}$),[13] 170.8 ppm ($B_9H_9^{2-}$),[14] 167.8 pm ($B_{10}H_{10}^{2-}$)[15] and 169.4 pm ($B_{11}H_{10}SMe_2$).[3] A similar trend is apparent in edges linking atoms of connectivity 5, which have average lengths 192.6, 186.0, 181.0, 178.8 and 177.5 pm for $n = 8$,[13] 9,[14] 10,[15] 11[3] and 12[9], respectively. These trends are believed to reflect more effective use of the skeletal bonding electrons as n increases.

Table 2. Mean bond distances, L^a, indices, I, orders, $\bar{n}$, and enthalpies, E_L and E_I, classified according to the skeletal connectivities, k, of the linked atoms for $B_nH_n^{2-}$ species

k, k'	L	I	$\bar{n}$	E_L	E_I
4, 4	166.8	0.716	0.630	230	213
4, 5	171.0	0.644	0.540	207	192
4, 6	174.5	0.576	0.476	190	172
5, 5	180.7	0.514	0.396	167	153
5, 6	201.2	0.376	0.212	108	112

[a] Data relate only to structurally characterised species, with $n = 6, 8, 9, 10, 11$ or 12.

The large discrepancy between the calculated I and $\bar{n}$ (Table 1) for the longer bonds in these polyhedra should not go unremarked, and may have its origin in two factors. On the one hand our method of calculating bond orders from bond enthalpies is crucially dependent on the interatomic distances in $B_6H_6^{2-}$[8] and $B_{12}H_{12}^{2-}$,[9] errors in which will necessarily be multiplied manifold in the considerable extrapolation involved. On the other hand,

Table 3. Total B—B bond indices, $\sum I$, and bond orders, $\sum \bar{n}$, compared with number of skeletal electron pairs for $B_nH_n^{2-}$

n	$\sum I$(B—B)	$\sum I$(B---B)	$\sum I$	$\sum I-(n+1)$	$\sum \bar{n}$	$\sum \bar{n}-(n+1)$
5[a]			6.90	0.90	5.18	−0.82
6	8.17	0.14	8.31	1.31	7.00	0.00
7[a]			9.59	1.59	7.66	−0.34
8	10.74	0.17	10.91	1.91	8.69	−0.31
9	12.02	0.25	12.27	2.27	9.30	−0.70
10	13.41	0.24	13.65	2.65	11.02	−0.53
11	14.67	0.33	15.00	3.00	11.47	−0.49
12	16.17	0.23	16.39	3.39	13.00	0.00

[a] Estimated interatomic distances used—see later discussion.

it is apparent that the bond indices calculated for these clusters when summed ($\sum I$) exceed the numbers of skeletal electron pairs available (Table 3). Although for simple molecules like hydrocarbons, calculated I correspond closely to $\bar{n}$,[10] the greater efficiency with which these polyhedral clusters use their relatively few skeletal electron pairs is believed to account for the difference between $\sum I$ and $n+1$ shown in column 5 of Table 3. In contrast, the total skeletal $\bar{n}$ for these clusters, $\sum \bar{n}$, listed in the penultimate column of Table 3, are, anyway, normalized against the number of skeletal bond pairs available in the cases of $B_6H_6^{2-}$ and $B_{12}H_{12}^{2-}$, and show only slight departures from the numbers of skeletal electron pairs, the extent of departure [$\sum \bar{n}-(n+1)$, listed in the final column of Table 3] reflecting the stability of $B_{10}H_{10}^{2-}$ and relative instability of $B_8H_8^{2-}$, $B_9H_9^{2-}$ and $B_{11}H_{11}^{2-}$, in keeping with their known chemistry.[6] The total I, $\sum I$, appear to vary with n or $n+1$ in a regular manner that gives no hint that $B_6H_6^{2-}$, $B_{10}H_{10}^{2-}$ and $B_{12}H_{12}^{2-}$ are more stable clusters than the other *closo* anions (which tend to disproportionate to generate these three species).

The second and third columns in Table 3 incidentally give a clear indication of the relative unimportance of the cross-polyhedral interactions in these clusters [$\sum I$(B---B), column 3] when compared with the nearest neighbour interactions [$\sum I$(B—B), column 2], in that the former represent only some 1–2% of the $\sum I$. This result, being in accord with most other treatments of these clusters which suggest that most of the skeletal electron density is close to the pseudo-spherical surfaces on which the boron atoms lie,[6] strengthens our view, made in an earlier paper,[16] that the approach developed by Fuller and Kepert,[17] in which cross-polyhedral interactions are assigned comparable energies to nearest neighbour interactions, grossly exaggerates the role of the former.

The trends apparent in the data in Table 3 are also discernible in the data in Table 4, which lists the total skeletal bond enthalpies, $\sum E_L$ and $\sum E_I$ (column 2), and the average skeletal bond enthalpy per boron atom (column 3), per electron pair (column 4) and per polyhedron edge (last column). Peaks of stability are indicated for $B_6H_6^{2-}$, $B_{10}H_{10}^{2-}$ and $B_{12}H_{12}^{2-}$ by the values of $\sum E_L$, whether expressed per boron atom, electron pair or polyhedron edge, whereas the bond index data show this to a much lesser extent, suggesting greater stability for $B_6H_6^{2-}$ than for the remainder, which all appear to be of comparable stability. This is shown in Fig. 2, which plots $\sum E/n$ and $\sum E/(n+1)$ against n. One respect in which both approaches concur is shown by the final column of Table 4, i.e. that the average enthalpy per polyhedron edge bond shows a decline after $B_6H_6^{2-}$, as the number of edges ($3n-6$) increases with n at too great a rate to be compensated by the greater efficiency with which the dwindling numbers of skeletal electrons per BH unit, $(2n+2)/n$, are used.

Puzzled that I(B—B) and the bond enthalpies derived therefrom did not show the relative stabilities of $B_6H_6^{2-}$, $B_{10}H_{10}^{2-}$ and $B_{12}H_{12}^{2-}$, and instabilities of $B_8H_8^{2-}$, $B_9H_9^{2-}$ and $B_{11}H_{11}^{2-}$, we summed I(B—H) for the whole series of anions, calculated $\sum E_I$(B—H) for each, and hence the total bond enthalpy, $\sum E_I$(B—B)+$\sum E_I$(B—H) for each anion. The data are given in Table 5. When expressed as a total bond enthalpy per boron atom, [$\sum E_I$(B—B)+$\sum E_I$(B—H)]/n (last column of Table 5), some hint of a marginally greater stability in the cases of $B_6H_6^{2-}$, $B_{10}H_{10}^{2-}$ and $B_{12}H_{12}^{2-}$ is apparent.

The anions $B_7H_7^{2-}$ *and* $B_5H_5^{2-}$

Although *closo* carboranes, $C_2B_{n-2}H_n$, with n ranging from 5 to 12 have long been known and structurally characterised, the related series of isoelectronic anions, $B_nH_n^{2-}$, lacks a pentanuclear

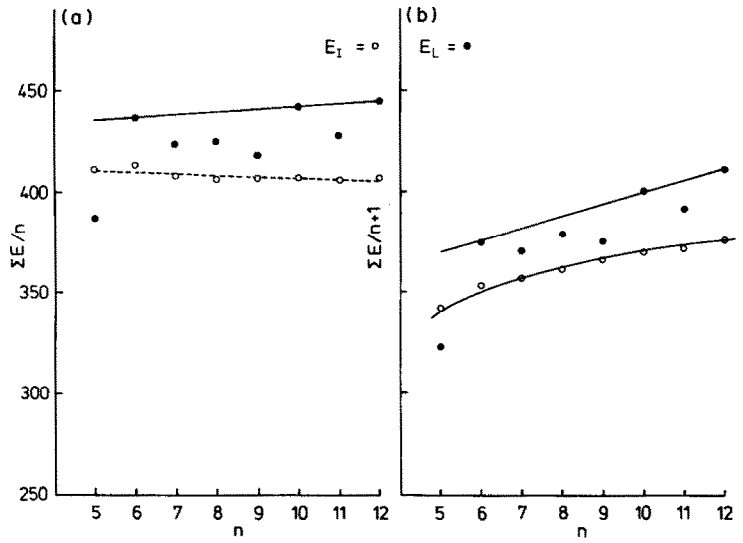


Fig. 2. (a) Average skeletal bond enthalpies (kJ mol^{-1}) per boron atom, $\sum E(B—B)/n$, plotted against the number of boron atoms, n, for $B_nH_n^{2-}$ anions. (b) Average skeletal bond enthalpies (kJ mol^{-1}) per skeletal electron pair, $\sum E(B—B)/(n+1)$, plotted against the number of boron atoms, n, for $B_nH_n^{2-}$ anions.

species $B_5H_5^{2-}$, and $B_7H_7^{2-}$, though believed on the basis of NMR solution studies[18] to be pentagonal bipyramidal, has not yet been the subject of X-ray crystallographic study. The probable interatomic distances in this anion were estimated as follows.

(i) The two distinct types of edge, which may be labelled equatorial and axial, connect atoms of connectivity 4 (equatorial) or 4 and 5 (axial). Tables 1 and 2 and our earlier discussion suggest that, for $B_7H_7^{2-}$, these will have lengths of 162 and 178 pm respectively.

(ii) For the regular polyhedral anions $B_6H_6^{2-}$[8] and $B_{12}H_{12}^{2-}$,[9] all the boron atoms are equivalent and so lie on spherical surfaces. This is not true for anions $B_nH_n^{2-}$ with n = 8–11, whose atoms of connectivity 4 lie on a sphere of radius *ca* 15% greater than that on which the atoms of connectivity 5 lie. If the same were true for $B_7H_7^{2-}$, edge lengths of *ca* 158 pm (equatorial) and 183 pm (axial) would be expected.

(iii) Comparison of anions $B_nH_n^{2-}$ with isoelectronic carboranes,[6,19] $C_2B_{n-2}H_n$, shows that the B—C distances in the latter are *ca* 8 pm shorter than B—B distances for comparable polyhedral edges in the former. From the structure of $C_2B_5H_7$,[20] we infer B—B bond distances of 163 pm (equatorial) and 179 pm (axial) for $B_7H_7^{2-}$.

Since these last figures were in good agreement with those obtained by method (i), and were obtained by comparison with a closely related compound, we decided to use them in our calculation of enthalpies

Table 4. Total skeletal bond enthalpies, $\sum E_L(B—B)$ and $\sum E_I(B—B)$, for species $B_nH_n^{2-}$, and average enthalpies per boron atom, per skeletal electron pair, and per B—B link (kJ mol^{-1} throughout)

n	$\sum E(B—B)^a$	$\sum E(B—B)/n^a$	$\sum E(B—B)/(n+1)^a$	$\sum E(B—B)/(3n-6)^a$
5[b]	1937 (2054)	387 (411)	323 (342)	215 (228)
6	2622 (2476)	437 (413)	375 (354)	219 (206)
7[b]	2971 (2859)	424 (408)	371 (357)	198 (191)
8	3410 (3250)	426 (406)	379 (361)	189 (181)
9	3758 (3655)	418 (406)	376 (366)	179 (174)
10	4415 (4067)	442 (407)	401 (370)	184 (170)
11	4705 (4468)	428 (406)	392 (372)	174 (165)
12	5337 (4884)	445 (407)	411 (376)	178 (163)

[a] Throughout the table, figures in parentheses relate to E_I. Remaining figures relate to E_L.
[b] Estimated interatomic distances used—see later discussion.

Table 5. Total bond index based bond enthalpies for species $B_nH_n^{2-}$, including E_I(B—H) (kJ mol^{-1})

n	$\sum E_I$(B—B)	$\sum E_I$(B—H)	Total[a]	Total/n[a]
5[b]	2054	1795	3849	770
6	2476	2148	4624	771
7[b]	2859	2526	5385	769
8	3250	2892	6142	768
9	3655	3272	6927	769
10	4067	3658	7725	773
11	4468	4013	8481	771
12	4884	4395	9279	773

[a] Total enthalpy, $\sum E_I$(B—B) + $\sum E_I$(B—H).
[b] Estimated interatomic distances used—see later discussion.

by the bond length and bond index methods. As a check, we also carried out molecular-orbital *I* (MOBI) calculations on four variations of this geometry, (a) expanded, (b) contracted, (c) compressed and (d) elongated on the five-fold axis; these changes resulted in edge length changes of 2–5 pm but gave no significant increase in bond index or enthalpy values, and therefore in stability.

Values of I, $\bar{n}$ and bond enthalpies calculated for the suggested structure have been included in Tables 1, 3, 4 and 5, and Fig. 2 without previous comment. Inspection of the data show that the known slight instability of $B_7H_7^{2-}$ to disproportionation into $B_6H_6^{2-}$ and $B_8H_8^{2-}$ is consistent with the figures obtained.

For the as yet unknown $B_5H_5^{2-}$, analogy with the known D_{3h} structure of 1,5-$C_2B_3H_5$[21] suggests axial bond lengths of 164 pm and equatorial bond lengths of 183 pm. Calculation of bond enthalpies using these interatomic distances affords the data given in Tables 1, 3 and 4. The values of E_L obtained suggest that, although the two-centre links in $B_5H_5^{2-}$ would be of comparable strength to those in $B_6H_6^{2-}$, the former would supply far less bond enthalpy per boron atom than the latter (Table 4), and so be expected to be far less stable. This may indeed be the reason why it has not yet been isolated. However, the enthalpies calculated by the I method present a different picture, that such a structure would generate a skeletal bond enthalpy per boron atom (column 3 of Table 4, figure in parentheses) very similar to that of $B_6H_6^{2-}$, and indeed greater than that of the higher borane anions. This is the only system for which there is major disagreement between the stabilities indicated by E_L and E_I.

Skeletal electron distribution

In our earlier discussion[1] of the bond length based bond enthalpies of selected borane anions, we argued that, comparing atoms of different connectivities within a particular anion, because the total enthalpy of the four bonds to a skeletal boron atom of connectivity 4 generally exceeded the total enthalpy of the five bonds to an atom with $k = 5$, one could infer that the former type of atom had a greater share of the skeletal electron density. An advantage of the MOBI method is that it calculates the charges on the various types of skeletal atom, allowing this feature to be checked directly. The charges on the boron atoms in the structures considered here were as follows: −0.254 a.u. for the two boron atoms with $k = 3$ in $B_5H_5^{2-}$; −0.146 a.u. averaged over the 25 atoms with $k = 4$ in the anions $B_5H_5^{2-}$–$B_{11}H_{11}^{2-}$; −0.027 a.u. for the 40 atoms with $k = 5$ in the anions $B_7H_7^{2-}$–$B_{12}H_{12}^{2-}$, and +0.094 a.u. for the unique atom with $k = 6$ in $B_{11}H_{11}^{2-}$. These charges substantiate in full the conclusions drawn from other treatments, and are intelligible in valence bond terms in that, if each boron atom is to participate in three skeletal bonds, whether two- or three-centre, then a progressively higher proportion of these will need to be three-centre bonds as the connectivity k increases. Since three-centre bonds shift charge away from skeletal atoms to a greater extent than two-centre bonds, then the lower electron density associated with the more highly coordinated skeletal atoms is readily understood.[22]

CONCLUSIONS

In this paper, we have used known structural data where available, and estimated interatomic distances otherwise, to calculate bond enthalpies for the series of *closo* borane anions, $B_nH_n^{2-}$ (n = 5–12). Using enthalpy data calculated from bond lengths using the empirical relationship E_L(B—B) = 1.766 × $10^{11}[L(\text{B—B})]^{-4.0}$ we find $B_6H_6^{2-}$, $B_{10}H_{10}^{2-}$ and $B_{12}H_{12}^{2-}$ to be of relatively high stability, and $B_5H_5^{2-}$ to be of particularly low stability compared to the

remainder. However, data calculated from bond indices suggest that all of these borane anions are of comparable stability, the variations with n being minor. Both approaches suggest that the higher anions use their skeletal electron pairs to progressively greater effect as n increases, though because of the rate at which the number of two-centre links $(3n-6)$ in these polyhedral clusters increases with n, the average enthalpy per two-centre link tends to decrease (with exceptions in the case of the E_L figures) as n increases. Cross-polyhedral bonding interactions, neglected in the bond length based method, are shown by the I calculations to be negligibly small in these clusters, accounting for at most *ca* 2.5% of the total bond enthalpy. The I calculations also show that the charges on the skeletal boron atoms become progressively less negative/more positive as the skeletal connectivity of those atoms increases.

Acknowledgements—We thank SERC for financial support and Professor P. G. Perkins for the use of his MOBI programs.

REFERENCES

1. C. E. Housecroft, R. Snaith and K. Wade, *Inorg. Nucl. Chem. Lett.* 1979, **15**, 343.
2. D. Laurie and P. G. Perkins, *Inorg. Chim. Acta* 1982, **63**, 53.
3. E. H. Wong, L. Prasad, E. J. Gabe and M. G. Gatter, *Inorg. Chem.* 1983, **22**, 1143.
4. C. E. Housecroft, K. Wade and B. C. Smith, *J. Chem. Soc., Chem. Commun.* 1978, 765; *J. Organomet. Chem.* 1981, **213**, 35.
5. C. E. Housecroft and K. Wade, *Inorg. Nucl. Chem. Lett.* 1979, **15**, 339.
6. E. L. Muetterties, *Boron Hydride Chemistry*. Academic Press, New York (1975).
7. D. D. Wagman *et al.*, Selected values of chemical thermodynamic properties. National Bureau of Standards (U.S.) Technical Note 270–3, Washington, D.C. (1968).
8. R. Schaeffer, Q. Johnson and G. S. Smith, *Inorg. Chem.* 1965, **4**, 917.
9. J. A. Wunderlich and W. N. Lipscomb, *J. Am. Chem. Soc.* 1960, **82**, 4427.
10. D. R. Armstrong, P. G. Perkins and J. J. P. Stewart, *J. Chem. Soc., Dalton Trans.* 1973, 838, 2273.
11. T. N. Bell and P. G. Perkins, *J. Phys. Chem.* 1977, **81**, 2002.
12. T. N. Bell, K. A. Perkins and P. G. Perkins, *J. Phys. Chem.*, 1977, **81**, 2610; 1979, **83**, 2321; *J. Chem. Soc., Faraday* I, 1981, **77**, 1779.
13. L. J. Guggenberger, *Inorg. Chem.* 1969, **8**, 2771.
14. L. J. Guggenberger, *Inorg. Chem.* 1968, **7**, 2260.
15. J. T. Gill and S. J. Lippard, *Inorg. Chem.* 1975, **14**, 751.
16. C. E. Housecroft and K. Wade, *Inorg. Chem.* 1983, **22**, 1391.
17. D. J. Fuller and D. L. Kepert, *Inorg. Chem.* 1982, **21**, 163.
18. F. Klanberg, D. R. Eaton, L. J. Guggenberger and E. L. Muetterties, *Inorg. Chem.* 1967, **6**, 1271.
19. R. N. Grimes, *Carboranes*. Academic Press, New York (1971).
20. T. Onak, G. B. Dunks, R. A. Beaudet and R. L. Poynter, *J. Am. Chem. Soc.* 1966, **88**, 4622.
21. I. A. McNeill, K. L. Gallaher, F. R. Scholer and S. H. Bauer, *Inorg. Chem.* 1973, **12**, 2108.
22. M. E. O'Neill and K. Wade, *Polyhedron* 1984, **3**, 199.

Polyhedron Vol. 4, No. 11, pp. 1883–1886, 1985
Printed in Great Britain

0277–5387/85 $3.00 + .00
© 1985 Pergamon Press Ltd

HAFNIUM(IV)–NITRILOTRIACETATE AND HAFNIUM(IV)–FLUORIDE COMPLEXES INVESTIGATED USING AN ION-SELECTIVE ELECTRODE

NICHOLAS E. IVORY and DAVID R. WILLIAMS*
Department of Applied Chemistry, University of Wales Institute of Science and Technology, PO Box 13, Cardiff CF1 3XF, U.K.

(*Received* 25 *April* 1985; *accepted* 10 *May* 1985)

Abstract—Models of plutonium solution chemistry *in vivo* require formation constants which are difficult to obtain but hafnium(IV) is biochemically similar to plutonium(IV) *in vivo*. This paper reports the use of fluoride as a competing ligand to suppress metal ion hydrolysis and formation constants, determined using a fluoride ion-selective electrode, for the following systems—fluoride–H^+, fluoride–hafnium(IV) and nitrilotriacetate–hafnium(IV) at 37°C, I = 150 mmol dm^{-3} sodium chloride.

Since the introduction of nuclear fission in the late 1930s, the element causing most public concern is undoubtedly plutonium, as it occurs in both weapons and energy production.[1,2] Many attempts have been made, and are still in progress, to determine the biochemistry of this man-made element.[2,3] A deeper understanding of the mechanisms of transport, tissue deposition, toxicity and excretion of complexes of plutonium would greatly assist toxicologists and clinicians. Hopefully, such an approach might lead to a range of therapeuticals that could be used to treat plutonium-intoxicated patients.[2]

The chemistry of plutonium has been widely reviewed.[3–7] The metal is unique in that it can exist simultaneously in all four of its oxidation states, (III), (IV), (V) and (VI). However, under physiological conditions it usually occurs as plutonium(IV). The human body is 70% water by weight and, when considering the biochemistry of plutonium, it is predominantly that of hydrolysis, polymerization and complex formation. The solubility product of plutonium(IV) hydroxide is of the order of 10^{-56} mol^5 dm^{-15} and so investigations into the sites of physiological attack of plutonium(IV) *in vivo* must, of necessity, have the plutonium firmly complexed in order to maintain it in solution. The ligand of choice is usually a polycarboxylic acid, such as nitrilotriacetate(NTA).

Various studies[8,9] concerning the physiological distribution of plutonium(IV) species predominating *in vivo* agree with our previous broad classification of metal distribution[2] into inert species, labile protein and low-molecular-weight complexes. The so-called inert plutonium species includes insoluble deposits of fluorides, hydroxides, oxides, and other polymeric aggregates in addition to protein complexes with ferritin and haemosiderin.[10–12] The second fraction is transferrin-bound and this β-globulin is responsible for transporting plutonium through the bloodstream.[13,14] Finally, there is some evidence that the third fraction, the low-molecular-weight complexes, is mainly plutonium citrate.[15] When soluble plutonium complexes are introduced into man, they initially complex with the iron transport protein transferrin and with citrate which carries the plutonium to the liver and bone marrow where it becomes associated with ferritin and haemosiderin.[12]

Clearly, any studies of this biochemistry and of competing complexes chosen to adapt such deposition mechanisms into excretion pathways, must be subject to the problems associated with the toxicity and radioactivity of the plutonium. Fortunately, Taylor *et al.*[16] have discovered that radiohafnium, when introduced into rats or hamsters, follows similar metabolic pathways to those for plutonium. In particular, it collects in the same target organs as plutonium(IV). Retention

* Author to whom correspondence should be addressed.

times of hafnium and plutonium in the plasma and in the liver are similar and the radiohafnium becomes bound to the iron transport protein transferrin in plasma and in liver cytosol in both the rat and the hamster. Indeed, these experiments using radiohafnium suggest that non-radioactive hafnium would be a good "surrogate" metal for studying the complexing of plutonium *in vivo*.

Chemically, plutonium and hafnium have many similarities which include relatively small sizes of the solvated ions, high charge densities, and a propensity towards hydrolysis and hydrolytic polymerization.[17,18] Even though hafnium does not display plutonium's range of valency states, it does have the important valence of 4 which is the physiologically-important state for plutonium *in vivo*. Thus, we use hafnium(IV) solutions as models of plutonium complexing with ligands of biological interest. These solutions can be used in the open laboratory without the necessity for radiation protection.

When plutonium model studies using hafnium are undertaken in animals, for example, the binding of hafnium to transferrin,[19] it is necessary to use a powerful ligand such as the NTA anion in order to keep the hafnium in solution and to permit it to transfer to transferrin binding. Thus, the main aim of this research is to produce formation constants for hafnium–NTA complexing under physiological conditions of 37°C and 150 mmol dm^{-3} sodium chloride appropriate to blood plasma.

EXPERIMENTAL

Our standard glass electrode–calomel electrode potentiometric approach proved inapplicable to the hafnium–NTA–proton system because metal–ligand binding was too powerful.[20] Rather, we found that it was necessary to introduce a competing ligand in order to moderate the hafnium ion's avidity for NTA. We chose fluoride as a second ligand capable of competing with the hydroxide ion for hafnium on the basis of speciation plots generated using literature values for the hafnium hydroxy species[21] and hafnium fluoride species.[22] In the absence of fluoride, hydroxy species are prevalent even at pH values below 1, whereas, in the presence of 30 mmol dm^{-3} fluoride, such hydrolysis can be suppressed right up to pH 6. As the fluoride ion-selective electrode has been used for two decades,[23] we decided to use this as an analytical tool rather than the glass electrode which is attacked by hydrofluoric acid, the silica in the glass being converted into fluorosilicic acid. This would have resulted in inaccurate readings from the glass electrode.[24,25]

The fluoride ion-selective electrode was supplied by Orion Research Inc., and was of classical design employing a lanthanium fluoride membrane doped with 0.05 mol % europium fluoride and a filling solution of 1 mol dm^{-3} potassium fluoride solution saturated with potassium chloride and sodium chloride.[26] This design of electrode is fairly free of interference effects other than those caused by the hydroxide, citrate and some other carboxylate ions. These were not found to be a problem in our studies as fairly low concentrations were used.

The electrode was calibrated using a range of concentrations of standard fluoride solution with a constant ionic background strength of 150 mmol dm^{-3} sodium chloride. Nernstian behaviour to within a 0.1-mV drift over 1 h was found. Any variation from reproducibility with time arising because of pitting or coating of the membrane, was easily polished off using a fine polishing powder.[27] The emf readings between this electrode and a calomel reference electrode was used as input for our standard potentiometric least-squares programmes.

Protonation of fluoride was measured using the fluoride ion-selective electrode and a calomel reference electrode. The titration data produced was fed into a modified version of MINIQUAD,[28,29] which considered the fluoride ion as equivalent to the acid in conventional acid-based titrations. The value for monoprotonated fluoride, HF, is in good agreement with the results from other works,[30–37] but the species HF_2^- [38] and H_2F^+ [39,40] in addition to H_2F_2,[22] were not found in this study. Our values and the appropriate statistics are shown in Table 1.

The hafnium fluoride interaction was quantified likewise and is reported in Table 1. Formation constants for the three higher complexes of 4:1, 5:1 and 6:1 fluoride:hafnium (the 410, 510 and 610 species, respectively) were apparently measurable but the 100, 210 and 310 species were not detectable because this would have involved fluoride concentrations below the detection limit of the electrode. (approximately 10^{-6} mol dm^{-3} F^-). However, constants for the lower species were taken from the literature[22] and these have been determined by solvent extraction and by the iron redox electrode approach to potentiometry. We had some difficulty establishing the existence of the 510 species and the value reported is that obtained using the Bjerrum's $Z_{1/2}$ method. The speciation plot in Fig. 1 shows a preponderance of 410 and 610 species and very low levels of the 510 intermediate. The values obtained from the MINIQUAD assessment for the 410 and 610 species are in reasonable agreement with those reported by other workers.[21,22,41,42]

Bearing in mind that we used the fluoride electrode in preference to the glass electrode, it is interesting to

Table 1. Log formation constants at 37°C and I = 150 mmol dm^{-3} sodium chloride for the following systems: (a) fluoride (p)–proton (r), (b) hafnium (q)–fluoride (p) and (c) hafnium (q)–nitrilotriacetate (p)

	Species								
	p	q	r	log β_{pqr}	Standard deviation	Sum of squares	R factor	No. of data points	No. of titrations
(a)	1	0	1	3.003	0.0011	9.9×10^{-7}	6.3×10^{-3}	325	8
(b)	(MINIQUAD)								
	4	1	0	30.158	0.8009				
	5	1	0	Negative	—	3.32×10^{-5}	1.53×10^{-2}	386	8
	6	1	0	40.481	0.3879				
(b)	(ESTA2)								
	4	1	0	24.533	0.0246				
	6	1	0	32.926	0.0260	—	2.08×10^{-2}	386	8
(c)	1	1	0	17.30	0.175		1.57×10^{-2}	268	7

note that the statistics found with the former method are not as good as those expected from the latter, the standard deviations being approximately an order of magnitude greater and the sum of the squares being two orders of magnitude larger than those for comparable glass electrode work. We must remember, however, that the glass electrode would not have worked in the presence of fluoride. The R factor obtained by both methods is of comparable magnitude and this value, along with the superimposability of the experimentally and theoretically produced formation curves, gives us confidence that these complexes are real and that the formation constant values are reliable. The data were also fed into the ESTA2 optimization program (see Table 1).[43,44] It is noteworthy that ESTA2 also failed to detect the existence of the 510 species.

Hafnium–NTA interaction

The literature values for this system suggest that the log β is approximately 20,[45,46] a magnitude beyond simple potentiometric determination. However, by using fluoride as a competing ligand, we were able to quantify the system in terms of a constant. A good competing ligand ought not to form mixed-ligand complexes with the metal and ligand under study and fluoride fitted this description. Additionally, it suppressed the hydrolysis of hafnium during the titrations, as mentioned previously. Experimentally, we titrated an acid solution of hafnium into mixtures of solutions of the trisodium salt of NTA and sodium fluoride. The double-ligand system was analyzable by the ESTA2 program and the results are shown in Table 1, the species detected being the 110 species. The log formation constant agrees reasonably well with values suggested from ion exchange methods.[47,48] Then *et al.*[49] have suggested that a second NTA ligand may be complexed as an eight-fold coordinated hafnium(IV) ion in a dodecahedral structure but this *bis* complex was not detected by our studies. Figure 2 shows the speciation for a

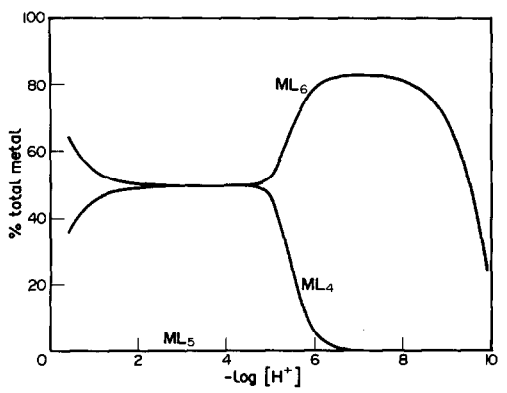


Fig. 1. Speciation plots of HfF_4, HfF_5^- and HfF_6^{2-} concentrations, pH = 0–10, calculated using the formation constants in Table 1. M = Hf(IV).

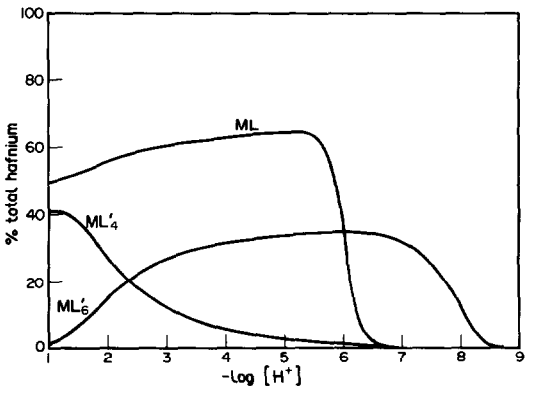


Fig. 2. Speciation plots of HfF_4, HfF_6^{2-} and $HfNTA^+$ complexes, pH 0–9, calculated using the formation constants in Table 1 for a typical fluoride and NTA competing-ligand titration. F^- = L′ and NTA^{3-} = L.

typical hafnium–NTA–fluoride system at various pHs.

CONCLUSIONS

It appears that fluoride ion-selective electrodes are a useful means of studying complexing between hafnium(IV) as a surrogate metal ion for plutonium(IV) in solution and they also permit computational studies to yield formation constants for hafnium with powerful ligands such as NTA. Furthermore, the presence of fluoride has successfully suppressed hydrolysis in this work. The fluoride electrode performed well at all times and the statistics produced for the formation constants are within an order of magnitude as good as those that could be expected from a non-glass-attacking ligand system studied using glass electrode potentiometry.

Acknowledgements—We acknowledge the assistance of Dr John Duffield, Dr Kevin Murray, Dr Peter May, Dr Gillian Christie and Professor David Taylor in this study and UWIST for a maintenance grant for one of us (NEI).

REFERENCES

1. N. E. Ivory, Ph.D. Thesis, University of Wales (1985).
2. J. R. Duffield, P. M. May and D. R. Williams, *J. Inorg. Biochem.* 1984, **20**, 199.
3. R. A. Bulman, *Struct. Bonding* 1978, **34**, 39.
4. W. J. Bair and R. C. Thompson, *Science* 1974, **183**, 715.
5. G. L. Voelz, L. H. Hempelmann, J. N. P. Lawrence and W. J. Moss, *Health Phys.* 1979, **37**, 445.
6. A. P. Nifatov, L. A. Buldakov and V. I. Matveev, *Health Phys.* 1972, **22**, 875.
7. R. Guillaumont and H. Metivier, *Radiochem. Radioanal. Lett.* 1972, **10**, 27.
8. D. M. Taylor, *Handbook Exp. Pharmacol.* 1973, **36**, 323.
9. K. G. Scott, D. J. Axelrod, H. Fisher, J. F. Crowley and J. G. Hamilton, *J. Biol. Chem.* 1948, **176**, 283.
10. G. Boocock, C. J. Danpure, D. S. Popplewell and D. M. Taylor, *Radiat. Res.* 1970, **42**, 381.
11. A. Lindenbaum and M. W. Rosenthal, *Health Phys.* 1972, **22**, 597.
12. P. W. Durbin, *Health Phys.* 1975, **29**, 495.
13. J. A. Hunts and E. S. G. Barron, Argonne National Laboratory (1947).
14. G. Boocock and D. S. Popplewell, *Nature* 1965, **208**, 282.
15. D. S. Popplewell, *IAE (Vienna)* 1976.
16. D. M. Taylor, M. Lehmann, F. Planas-Bohne and A. Seidel, *Radiat. Res.* 1983, **95**, 339.
17. J. S. Johnson and K. A. Kraus, *J. Am. Chem. Soc.* 1956, **78**, 3937.
18. J. S. Johnson, K. A. Kraus and R. W. Holmberg, *J. Am. Chem. Soc.* 1956, **78**, 26.
19. G. Then, H. Appel, I. Zell, W.-G. Thies, J. R. Duffield and D. M. Taylor, *Hyperfine Interact.* 1983, **15**, 893.
20. M. Filella and D. R. Williams, *Inorg. Chim. Acta* 1985, **106**, 49.
21. J. Kragten, *Atlas of Metal–Ligand Equilibria in Aqueous Solution.* Ellis Horwood, Chichester (1978).
22. B. Noren, *Acta Chim. Scand.* 1967, **21**, 2435.
23. M. S. Frant and J. W. Ross, *Science* 1944, **154**, 1553.
24. L. J. Warren, *Anal. Chim. Acta* 1971, **53**, 199.
25. M. Dole, R. M. Roberts and C. E. Holley, *J. Am. Chem. Soc.* 1941, **63**, 725.
26. M. S. Frant, US Patent No. 3,431,182 (4/3/69).
27. R. C. Hawkins, L. P. V. Corriveau, S. A. Kushnerjuk and P. Y. Wong, *Anal. Chim. Acta* 1978, **102**, 61.
28. A. Sabatini, A. Vacca and P. Gans, *Talanta* 1974, **21**, 53.
29. P. Gans, *Adv. Mol. Relaxation Interact. Processes* 1980, **18**, 136.
30. N. E. Vanderborgh, *Talanta* 1968, **15**, 1009.
31. G. T. Hefter, *Polyhedron* 1984, **3**, 75.
32. E. W. Baumann, *J. Inorg. Nucl. Chem.* 1969, **31**, 3155.
33. H. N. Farrer and F. J. C. Rossotti, *J. Inorg. Nucl. Chem.* 1964, **26**, 1959.
34. H. H. Broene and T. De Vries, *J. Am. Chem. Soc.* 1947, **69**, 1644.
35. A. J. Ellis, *J. Chem. Soc.* 1963, 4300.
36. P. R. Patel, E. C. Moreno and J. M. Patel, *J. Res. Nat. Bur. Stand.* 1971, **75A**, 205.
37. M. Salomon and R. K. Stevenson, *J. Chem. Eng. Data* 1974, **19**, 42.
38. A. M. Bond and G. T. Hefter, *IUPAC Chemical Data Series* No. 27. Pergamon Press, Oxford (1980).
39. O. Forero, J. I. Fernandez-Olonso and J. Bertran, *J. Chem. Soc., Dalton Trans.* 1979, 254.
40. T. A. O'Donnell, In *Comprehensive Inorganic Chemistry* (Edited by J. C. Bailar). Pergamon Press, Oxford (1973).
41. L. P. Varga and D. N. Hume, *Inorg. Chem.* 1964, **3**, 77.
42. L. P. Varga, *Anal. Chem.* 1969, **41**, 323.
43. K. Murray and P. M. May, *ESTA Users' Manual.* UWIST, Cardiff (1984).
44. P. M. May, K. Murray and D. R. Williams, *Talanta* 1985, **32**, 483.
45. R. M. Smith and A. E. Martell, *Critical Stability Constants. Vol.* 1: *Amino Acids.* Plenum Press, New York (1974).
46. G. Anderegg, *Pure Appl. Chem.* 1982, **54**, 2693.
47. A. N. Ermakov, I. N. Marov and G. A. Evtikova, *Russ. J. Inorg. Chem.* 1966, **11**, 618.
48. A. N. Ermakov, I. N. Marov and G. A. Evtikova, *Russ. J. Inorg. Chem.* 1964, **9**, 275.
49. G. Then, H. Appel, J. H. Raudies, J. Duffield and D. M. Taylor, *Hyperfine Interact.* 1983, **15**, 889.

Polyhedron Vol. 4, No. 11, pp. 1887–1890, 1985
Printed in Great Britain

0277–5387/85 $3.00 + .00
© 1985 Pergamon Press Ltd

PHOTOREDOX CHEMISTRY OF NITROSYLPENTACYANOFERRATE(II) IN METHANOLIC MEDIUM

GRAŻYNA STOCHEL and ZOFIA STASICKA*
Department of Inorganic Chemistry, Jagiellonian University, 30-060 Kraków, Poland

(*Received* 8 *February* 1985; *accepted* 10 *May* 1985)

Abstract—The solvent complexes $[Fe(CN)_5(CH_3OH]^{2-}$ and $[Fe(CN)_5CH_3O]^{3-}$ were found to be the main products of the photochemical reaction of nitrosylpentacyanoferrate(II) in MeOH at room temperature. Some minor production of iron(I) species was also detected. Quantum yields are dependent on the radiation energy. Prolonged irradiation leads to the generation of Prussian blue.

Photochemistry of the $[Fe(CN)_5NO]^{2-}$ complex in aqueous solution has attracted the interest of chemists for many years.[1–3] In contrast, the photochemical behaviour in non-aqueous solvents has received much less attention[4] up to recently, when two ESR studies have been published.[5,6] These papers, however, concern mainly the photolysis of glasses that could proceed through a different mechanism than that in the liquid state.

The most important difference consists in the production of $[Fe(III)(CN)_5L]^{n-}$ complexes that was found to proceed in liquid non-aqueous solvents[7–9] and was never observed in glasses.[5,6]

The aim of this work was to provide more detailed data on the photolysis of nitrosylpentacyanoferrate(II) in methanolic solution to establish the reaction mechanism in the liquid phase.

RESULTS

A methanolic solution of $[Fe(CN)_5NO]^{2-}$ is thermally stable at least for several days irrespective of atmosphere. Its spectrum resembles that of an aqueous solution with a bathochromic shift of the maxima. The spectrum (Fig. 1) shows three moderately weak bands at 18.9 ($\varepsilon = 9.3$), 24.8 ($\varepsilon = 25.1$) and $\sim 30 \times 10^3$ cm^{-1} ($\varepsilon \sim 55$) and three more intense bands at 36.6 ($\varepsilon = 1080$), ~ 42.6 ($\varepsilon \sim 2500$) and $\sim 47.7 \times 10^3$ cm^{-1} ($\varepsilon \sim 10{,}800$).

As in aqueous solutions,[10] radiation from the first band (I in Fig. 1) was also found to be inactive in methanolic medium. Radiation from more energetic bands (II–V) was photochemically active leading to the generation of three relatively stable products and one short lived species. The type of products was found to be independent of the radiation energy; only the quantum yield values were higher within the IV and V than in the II and III bands (Fig. 1, Table 1).

The main product of the photochemical reaction of nitrosylpentacyanoferrate(II) in methanolic solution appeared to be the iron(III) complex of formula $[Fe(CN)_5CH_3OH]^{2-}$ (Fig. 2), whereas in the presence of alkalis ($c \geqslant 10^{-4}$ M) its deprotonated form, $[Fe(CN)_5OCH_3]^{3-}$ was also generated. At higher alkali concentration ($c \sim 10^{-2}$ M) the only detected iron(III) complex was the alkoxo one (Fig. 3).†

The spectra of these complexes were also recorded upon flashing and no transient species were detected within the resolution time of our apparatus. Only in diluted deaerated solutions ($c \lesssim 10^{-5}$ M) did a diffuse transient absorption appear at $\tilde{\nu} > 32 \times 10^3$ cm^{-1} that decayed within microseconds without any definite influence on the absorption at lower wave numbers. This behaviour is similar to that found in aqueous solution,[2] although in methanolic medium the spectrum is shifted bathochromically. In both cases, the nature of the species is unknown but tentatively we assign this absorption to an unstable solvated form of the released NO ligand.

ESR detection has shown that, besides the iron(III) complexes, some iron(I) species are also generated photochemically in the methanolic solution. The ESR signals, $g_{av} = 2.026$ and $A(^{14}N) = 15.0$ G,

* Author to whom correspondence should be addressed.

† For the protonation equilibrium between these complexes see Ref. 8.

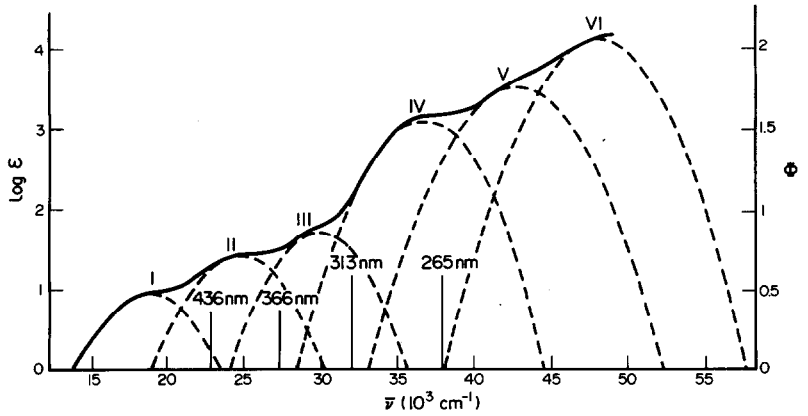


Fig. 1. Spectrum of the $[Fe(CN)_5(NO)]^{2-}$ complex in MeOH and quantum yields of $[Fe(CN)_5(CH_3OH)]^{2-}$ production. The broken lines represent the Gaussian analysis of the experimental curve made by a least-square procedure.[9]

recorded at room temperature, are consistent with those found earlier for the blue $[Fe(I)(CN)_4(NO)]^{2-}$ complex.[11,12]

Quantum yields of the Fe(I) complex formation could be only roughly assessed but doubtless they are about two orders lower than those of the iron(III) production (Table 1).

Prolonged irradiation (for minutes) of the $[Fe(CN)_5NO]^{2-}$ in methanol has led to generation of a blue precipitate that was analyzed by ESR and IR spectroscopy. In the ESR spectrum only one very broad line and no traces of the signal characteristic of $[Fe(CN)_4(NO)]^{2-}$ were detected. The IR spectrum showed a strong band due to a CN^- stretch at 2070 cm^{-1} and two weaker bands at 500 and 590 cm^{-1}. All of these features fit Prussian blue[13,14] and lead to the conclusion that prolonged irradiation of nitrosylpentacyanoferrate(II) in MeOH proceeds similarly to that in aqueous solution.[1]

Prussian blue precipitation was preceded by an increase in absorption and the appearance of a new strong band within $15.5–16.5 \times 10^3$ cm^{-1} (Fig. 4), that disappeared upon precipitation.

Both the shape and the intensity of the spectrum were affected by many factors leading to the conclusion that the absorption was due to different polymeric Fe(II)–Fe(III) precursors of Prussian blue.

Both flash and continuous-illumination experiments have shown that the Prussian blue precursors are generated in a secondary thermal reaction at the expense of the $[Fe(CN)_5(CH_3OH)]^{2-}$ complex, but the process is strongly photoaccelerated (Fig. 4).

In contrast to the iron(III) production (Table 1), the yields of $[Fe(CN)_4(NO)]^{2-}$ and the Prussian

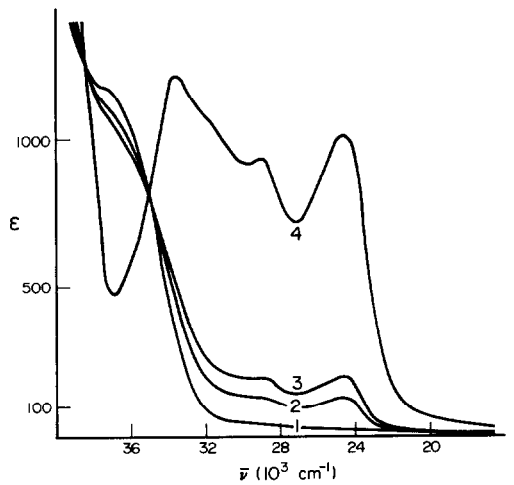


Fig. 2. Spectral changes recorded for 2×10^{-3} M methanolic solution of $[Fe(CN)_5(NO)]^{2-}$ (curve 1) upon irradiation for 2.5 (curve 2), and 4 (curve 3) s. The spectrum of the $[Fe(III)(CN)_5(CH_3OH)]^{2-}$ complex[8] is presented as curve 4.

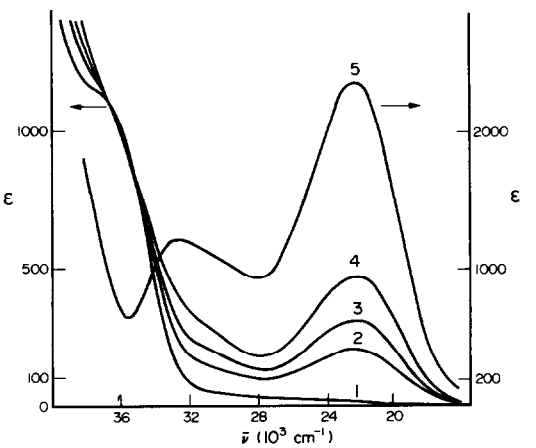


Fig. 3. As in Fig. 2 but in the presence of 1×10^{-2} M NaOH. Curve 1—nonirradiated solution, curve 2—3 s, curve 3—5 s, curve 4—8 s of exposure; curve 5—spectrum of the $[Fe(CN)_5(CH_3O)]^{3-}$ complex.[8]

Table 1. Photoredox quantum yields of $[Fe(CN)_5(NO)]^{2-}$ in MeOH

λ (nm)	$[Fe(III)(CN)_5(CH_3OH)]^{2-}$		$[Fe(III)(CN)_5(CH_3O)]^{3-}$		$[Fe(I)(CN)_4(NO)]^{2-}$
	N_2	O_2	N_2	O_2	N_2
265	0.61	0.62	0.54	0.54	—
313	0.63	0.61	0.50	0.53	6×10^{-3}
366	0.38	0.38	0.29	0.28	4×10^{-3}
436	0.37	0.38	0.30	0.29	4×10^{-3}

blue precursors were affected by oxygen: the former was decreased, whereas the latter was slightly increased in the presence of oxygen.

DISCUSSION

In the earlier photochemical study of the $[Fe(CN)_5NO]^{2-}$ complex in non-aqueous solvents, such as *N,N*-dimethylformamide (DMF), acetylacetone, benzaldehyde, *p*-nitrobenzaldehyde and dimethylaniline, photoreduction

$$[Fe(CN)_5(NO)]^{2-} \xrightarrow[S]{h\nu} [Fe(I)(CN)_5(NO)]^{3-} + {}^{\cdot}S^{+} \quad (1)$$

was the only process detected by EPR and UV–VIS spectroscopy.[4] This reaction was also reported to proceed as the major route in MeOH, DMF or hexamethylphosphoramide glasses.[6] On annealing, the release of one CN^- ligand

$$[Fe(CN)_5(NO)]^{3-} \rightarrow [Fe(I)(CN)_4(NO)]^{2-} + CN^- \quad (2)$$

and production of the pentacoordinated iron(I) species was detected.[6]

Our results have shown that, in methanolic liquid phases, the $[Fe(CN)_4(NO)]^{2-}$ ion is also photogenerated, but its yield is at least two orders lower than that for the photooxidation path (Table 1). The main mode detected in this medium may be summarized as follows:

$$[Fe(CN)_5(NO)]^{2-} \xrightarrow{h\nu} {}^{*}\{[Fe(CN)_5(NO)]^{2-}\} \begin{cases} \xrightarrow{CH_3OH} [Fe(III)(CN)_5(CH_3OH)]^{2-} + NO \\ \xrightarrow{CH_3O^-} [Fe(III)(CN)_5(CH_3O)]^{3-} + NO \end{cases} \quad (3)$$

The pathway is consistent with that reported earlier[2,10] for aqueous solutions. Moreover, this mode was found to be the major one in the photochemistry of nitrosylpentacyanoferrate(II) in some other solvents, such as ethylene glycol, DMF and dimethylsulphoxide.[9] In fact, the $[Fe(III)(CN)_5L]^{2-}$ complexes (where L = solvent molecule) were observed to be generated in all the liquid phases studied by us so far.[8] The lack of iron(III) complexes in the glassy phases[5,6] may be the result of the cage effect.

In the earlier liquid-phase study[4] the generation of iron(III) complexes was not detected due to analyzing the prolonged irradiated solutions, where

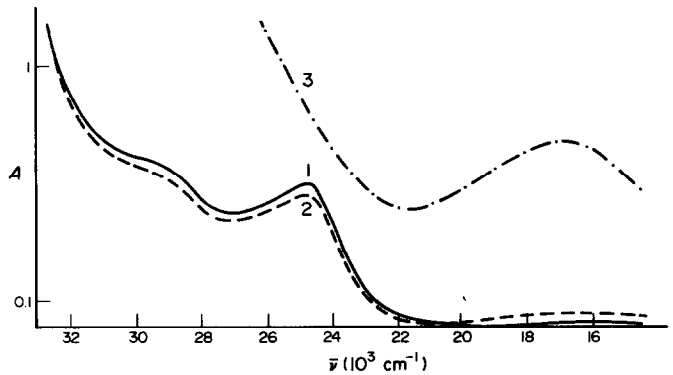


Fig. 4. Spectral changes due to secondary processes in the mixture of $[Fe(CN)_5(CH_3OH)]^{2-}$ ($c = 5\times10^{-4}$ M) and $[Fe(CN)_5(NO)]^{2-}$ ($c = 1.5\times10^{-3}$ M) (curve 1) upon thermal procedure (20 h, curve 2) and after 2 min of irradiation (curve 3).

a strong absorption of the Prussian blue precursors overlaps that of the $[Fe(CN)_5L]^{2-}$ complexes (Fig. 4). Moreover, absorption of the blue polymers occurs almost exactly within the same spectral region as that of the $[Fe(CN)_4NO]^{2-}$ complex[15] ($\tilde{\nu}_{max} = 16.5 \times 10^3$ cm^{-1}), which could lead to overestimation of the iron(I) yield.

The Fe(II)–Fe(III) polymers must be generated from the $[Fe(CN)_5(CH_3OH)]^{2-}$ complex in reaction with a Fe(II) species. When polymerization proceeds in a secondary thermal way the increase in absorption at $15.5–16.5 \times 10^3$ cm^{-1} is accompanied by decrease in absorption characteristic of the $[Fe(CN)_5(CH_3OH)]^{2-}$ complex (Fig. 4). Considerable acceleration of the reaction by light suggests that the iron(II) species is generated photochemically from the $[Fe(CN)_5NO]^{2-}$ or $[Fe(CN)_5(CH_3OH)]^{2-}$ ion.

The former would correspond to the ligand field route reported for an aqueous solution,[2] whereas the latter would be in agreement with the photoreduction of the $[Fe(CN)_5(H_2O)]^{2-}$ complex observed earlier by Moggi *et al.*[16]

The increase in the polymer concentration in the presence of oxygen also suggests that the iron(II) species may also be generated by oxygen oxidation of the $[Fe(CN)_4(NO)]^{2-}$ ion.

EXPERIMENTAL

Materials

Anhydrous sodium nitrosylpentacyanoferrate(II), $Na_2[Fe(CN)_5NO]$ was prepared by repeated recrystallization of a commercial dihydrate from aqueous solution in the dark and drying a pulverized sample at 440 K up to a constant weight. Alkalis were purified from carbonates, methanol of reagent grade was dried when it was necessary, and other chemicals were the best available commercial reagents used without further purification.

Apparatus and procedure

A high-pressure (HBO 200, Narva, G.D.R.) or a medium-pressure (ASH 400) mercury lamp was used for continuous irradiation of solutions placed in a thermostatted rectangular quartz cell ($d = 0.5$, 1.0 and 2.0 cm). Irradiations were performed at 295 ± 0.5 K with a continuous flow of nitrogen or oxygen. In some experiments cut-off filters (Schott, Jena, G.D.R.) were used to separate wave numbers: $\tilde{\nu} < 30 \times 10^3$ cm^{-1} (BG 9, 2 mm), $\tilde{\nu} < 23 \times 10^3$ cm^{-1} (OG 11, 2 mm), $\tilde{\nu} < 18 \times 10^3$ cm^{-1} (OG 2, 2 mm) and $28 \times 10^3 < \tilde{\nu} < 44 \times 10^3$ cm^{-1} (UG 5, 2 mm + 2 cm layer of saturated $NiSO_4$).

For quantum yield measurements glass filters (Schott), were used to isolate 436-, 366- and 313-nm wavelengths and an interference filter (KIF 265, C. Zeiss, Jena, G.D.R.) for 265-nm isolation. 10^{-1}–10^{-3} M solutions of $[Fe(CN)_5(NO)]^{2-}$ in MeOH or in MeOH containing additionally 10^{-2} M NaOH were irradiated up to less than 10% conversion. The light intensity was measured using trisoxalatoferrate(III) actinometry.[17] The reaction progress was followed spectrally by means of a Specord UV–VIS spectrophotometer (C. Zeiss). Flash photolysis apparatus was as described elsewhere;[2] its resolution time was not shorter than 20 μs.

ESR spectra were recorded using an ESR-220 (G.D.R.) spectrophotometer. DPPH and Mn^{2+} in MgO were used for g factor determination and magnetic field calibration. $CuSO_4$ in methanolic solution was used as a spin number standard.

Acknowledgement—We thank the Polish Academy of Sciences for support.

REFERENCES

1. V. Balzani and V. Carassiti, *Photochemistry of Coordination Compounds*. Academic Press, London (1970).
2. T. Jarzynowski, T. Senkowski and Z. Stasicka, *Pol. J. Chem.* 1981, **55**, 3, and references cited therein.
3. A. B. Nikolskii and A. M. Popov, *Dokl. Akad. Nauk SSSR* 1980, **250**, 902.
4. E. F. Hockings and I. Bernal, *J. Chem. Soc.* 1964, 5029.
5. R. B. Zhutkovskii and K. I. Zamarajev, *Chimia Wysokich Energii* 1976, **10**, 150.
6. M. C. R. Symons, J. G. Wilkinson and D. X. West, *J. Chem. Soc., Dalton Trans.* 1982, 2041.
7. G. Stochel and Z. Stasicka, In *Proceedings of the 3rd Symposium on Photochemical and Thermal Reactions of Coordination Compounds*, p. 107. Mogilany, Kraków, Poland (1980).
8. G. Stochel and Z. Stasicka, *Polyhedron* 1985, **4**, 481.
9. G. Stochel, Ph.D. dissertation, Jagiellonian University, Poland (1983).
10. S. K. Wolfe and J. H. Swinehart, *Inorg. Chem.* 1975, **14**, 1049.
11. J. Schmidt, H. Kühr, W. L. Dorn and J. Kopf, *Inorg. Nucl. Chem. Lett.* 1974, **10**, 55.
12. W. L. Bowden, P. Bonnar, D. B. Brown and W. E. Geiger, Jr, *Inorg. Chem.* 1977, **16**, 41.
13. R. E. Wilde, S. N. Ghosh and B. J. Marshall, *Inorg. Chem.* 1970, **9**, 2512.
14. J. C. Fanning, C. D. Elrod, B. S. Franke and J. D. Melnik, *J. Inorg. Nucl. Chem.* 1972, **34**, 139.
15. R. P. Cheney, M. G. Simic, M. Z. Hoffman, I. A. Taub and K. D. Asmus, *Inorg. Chem.* 1977, **16**, 2187.
16. L. Moggi, F. Bolletta, V. Balzani and F. Scandola, *J. Inorg. Nucl. Chem.* 1966, **28**, 2589.
17. C. A. Parker, *Proc. R. Soc. A* 1953, **220**, 104; C. G. Hatchard and C. A. Parker, *Proc. R. Soc. A* 1956, **235**, 518.

Polyhedron Vol. 4, No. 11, pp. 1891–1894, 1985
Printed in Great Britain

0277-5387/85 $3.00 + .00
© 1985 Pergamon Press Ltd

SYNTHESIS AND CHARACTERIZATION OF NICKEL(II) COMPLEXES WITH POTENTIALLY PENTADENTATE MACROCYCLIC LIGANDS HAVING N_3O_2 DONOR SET

KIKUO MIYOKAWA,*† HIDENORI HIRASHIMA and ISAO MASUDA

Department of Chemistry, Faculty of Science, Fukuoka University, Nanakuma, Jonan-ku, Fukuoka 814-01, Japan

(*Received* 17 *December* 1984; *accepted* 10 *May* 1985)

Abstract—Nickel(II) complexes of N_3O_2 donor macrocycles incorporating 17- to 19-membered macrocyclic rings have been prepared. Physical measurements indicate that the complexes are of the type Ni(macrocycle)$X_2 \cdot nH_2O$ (X = Cl, Br, I, NCS or NO_3; $n = 0, \frac{1}{2}$ or 1). The macrocycles behave as a tetradentate ligand when X = NCS and as a pentadentate ligand when X = I. The coordinating behavior of the macrocycles has been found to depend on the coordinating abilities of the coexisting anions.

In contrast to the metal ion chemistry of macrocyclic ligands incorporating all ether oxygen or all nitrogen donor atoms, the chemistry of mixed oxygen–nitrogen donor macrocycles has received less attention.[1] Lindoy *et al.* have extensively investigated synthetic, kinetic, thermodynamic and structural aspects of the interaction of macrocycles of type **I** in Fig. 1 with cobalt(II), nickel(II) and copper(II).[2–5] Recently they have investigated the interaction of copper(II) with N_3O_2 donor macrocycles of type **II**, and reported that $[CuL^2(H_2O)(ClO_4)_2] \cdot H_2O$ has a pseudo square planar coordination geometry with the coordination sphere consisting of three nitrogen atoms of the macrocycle together with an oxygen from water.[6] Such macrocycles containing an N_3O_2 donor set, however, have a potentially pentadentate property. In this study, nickel(II) complexes with 17-, 18- and 19-membered macrocycles, L^1, L^2 and L^3,‡ were isolated and the coordinating behavior of the macrocycles was investigated.

EXPERIMENTAL

The preparation of macrocycles L^1 and L^2 has been described in the literature.[6] The new macrocycle, L^3, was prepared as follows: 3,3′-diaminopropylamine (6.55 g) in methanol (20 cm^3) was added slowly to a stirred boiling solution of 1,4-bis(2′-formylphenyl)-1,4-dioxabutane[7] (13.5 g) in methanol (500 cm^3). The solution was then filtered and allowed to cool. Sodium tetrahydroborate (8.0 g) was added slowly and the volume was then reduced to 150 cm^3. Water (400 cm^3) was added and an oil separated, which was extracted with chloroform (3×100 cm^3). The chloroform extract was dried over anhydrous sodium sulfate and evaporated to 50 cm^3 and to it was added diethylether (200 cm^3). The solution was cooled below 0°C to yield a white solid. Yield 15%. The product was recrystallized from a chloroform–diethylether mixture. Found: C, 71.2; H, 8.2; N, 11.3. Calc. for $C_{22}H_{31}N_3O_2$: C, 71.5; H, 8.2; N, 11.3%.

The nickel(II) complexes were prepared in the following manner: nickel(II) salt (2 mmol) in methanol (20 cm^3) was slowly added to a stirred boiling ethanol or butanol solution (50 cm^3) of the ligand (2 mmol). While boiling, the solution separated blue or green crystals which were collected on a filter and washed with methanol and then diethylether and finally dried in an oven at 100°C.

Conductance measurements were performed by using Toa conduct meter CM-15A with a Toa

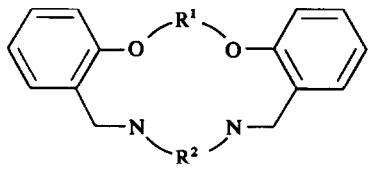
* Author to whom correspondence should be addressed.
† Present address: Radioisotope Center, Technological University of Nagaoka, Kamitomioka, Nagaoka 949-54, Japan.

‡ L^1, 1,12,15 - triaza - 3,4:9,10 - dibenzo - 5,8 - dioxacycloheptadecane; L^2, 1,12,15 - triaza - 3,4:9,10 - dibenzo - 5,8 - dioxacyclooctadecane; L^3, 1,12,16 - triaza - 3,4:9,10 - dibenzo - 5,8 - oxacyclononadecane.

Table 1. Characterization of $NiLX_2 \cdot nH_2O$ complexes

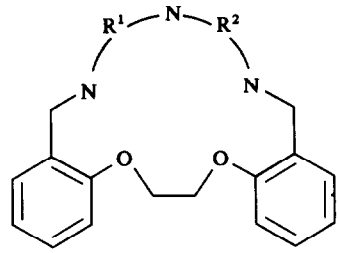
L	X	n	Elemental analysis[a] (%) Ni	C	H	N	Color[b]	μ_{eff}[c] (μ_B)	Reflectance spectra (10^3 cm^{-1})	IR band[d] ν(CN) (cm^{-1})	Conductivity[e] (Ω^{-1} cm^2 mol^{-1})
L^1	Cl	$\frac{1}{2}$	12.2 (12.13)	49.8 (50.04)	5.7 (5.88)	8.5 (8.76)	PG	3.12	15.8 25.8		26.3
	Br	1	10.3 (10.05)	41.2 (41.56)	4.9 (5.06)	7.2 (7.27)	YG	3.13	15.0 24.9		—
	I		9.0 (8.98)	36.7 (36.78)	4.2 (4.13)	6.4 (6.43)	DG	3.15	16.3 22.3 26.7		79.4
	NO_3		11.1 (11.20)	45.7 (45.83)	5.3 (5.19)	13.4 (13.36)	B	3.11	16.5 27.6		44.6
L^2	I		8.6 (8.79)	35.7 (37.76)	4.3 (4.37)	6.2 (6.29)	DG	3.14	16.4 27.3		75.8
	NO_3	$\frac{1}{2}$	10.6 (10.73)	46.1 (46.10)	5.5 (5.53)	13.1 (12.80)	B	3.16	16.2 27.4		26.0
	NCS		10.9 (11.07)	51.9 (52.09)	5.5 (5.51)	13.1 (13.21)	B	3.12	17.1 26.7	2075	5.0
L^3	Cl		11.5 (11.78)	52.6 (52.93)	6.3 (6.26)	8.2 (8.42)	PG	3.20	15.0 24.8		4.0
	Br		10.1 (9.97)	44.8 (44.93)	5.4 (5.31)	7.0 (7.14)	YG	3.17	14.7 24.3		13.1
	NO_3	$\frac{1}{2}$	10.4 (10.50)	47.2 (47.08)	5.8 (5.71)	12.4 (12.48)	B	3.14	16.3 26.8		20.6
	NCS	$\frac{1}{2}$	10.6 (10.62)	52.2 (52.11)	5.8 (5.79)	12.8 (12.66)	B	3.16	16.6 26.6	2070	6.1

[a] Calculated values are given in parentheses.
[b] PG, pale green; YG, yellowish green; DG, dark green; B, blue.
[c] Determined at 22–25°C.
[d] In KBr disk.
[e] In nitromethane.



Type I

R^1 and R^2 = CH_2CH_2 or $CH_2CH_2CH_2$



Type II

L^1: $R^1 = R^2 = CH_2CH_2$
L^2: $R^1 = CH_2CH_2$, $R^2 = CH_2CH_2CH_2$
L^3: $R^1 = R^2 = CH_2CH_2CH_2$

Fig. 1. Mixed oxygen–nitrogen donor macrocycles.

conductivity bridge CG-201PL. All measurements were recorded at 25°C on approximately 1×10^{-3} mol dm^{-3} solutions. Other physicochemical data were obtained by methods described elsewhere.[8]

RESULTS AND DISCUSSION

Reaction of L^1, L^2 and L^3 with the appropriate nickel(II) salts has led to the isolation of the green or blue complexes listed in Table 1. The elemental analyses indicate the formation of complexes with a nickel : ligand ratio of 1 : 1. All complexes have room-temperature magnetic moments in the range expected for nickel(II) with $S = 1$; these values are close to $\mu_{eff} = 3.1$–$3.3\ \mu_B$ for the nickel(II) complexes with macrocycles of type I.[2] These complexes have been reported to have an octahedral coordination geometry around the nickel atom.[2,5] The reflectance spectra exhibit two peaks in the visible region with maxima around 16 and 25×10^3 cm^{-1}; respective peaks are ascribed to the $^3A_{2g} \rightarrow {}^3T_{1g}(F)$ and the $^3A_{2g} \rightarrow {}^3T_{1g}(P)$ transitions of nickel(II) ion in an octahedral crystal field.[9] The magnetic and spectral characteristics indicate an octahedral coordination geometry for the present complexes. The IR spectra of the thiocyanato complexes show a single ν(CN) band around 2070 cm^{-1} which is in the expected range for N-bonded coordination.[10]

The conductivities in nitromethane of NiL^1I_2 and NiL^2I_2 are 75.9 and 76.3 Ω^{-1} cm^2 mol^{-1}, which fall in the range 75–95 Ω^{-1} cm^2 mol^{-1} reported for 1 : 1 electrolytes in nitromethane;[11] the macrocycles behave as pentadentate ligands in these complexes. On the other hand, $NiL^2(NCS)_2$, $NiL^3(NCS)_2$ and NiL^3Cl_2 are non-electrolytes and the macrocycles behave as tetradentate ligands. These facts seem to indicate that the coordinating behavior of the macrocycles depends on the nature of the coexisting anions. This differs from the coordinating behavior of the macrocycles of type I, which behave as tetradentate ligands in the Ni(II) complexes regardless of the sort of coexisting anions.[2] The spectrochemical series of the anions is

$$NCS > NO_3 > Cl > Br > I,$$

and the coordinating abilities of the anions are considered to decrease in this order.[12] The complexes with the isothiocyanate anion with the highest coordinating ability are non-electrolytes and the macrocycles are tetradentate, while the complexes of the iodide anion with the lowest coordinating ability are 1 : 1 electrolytes and the macrocycles are pentadentate. Other complexes which show intermediary conductivities between non- and 1 : 1 electrolytes are considered as a mixture of non- and 1 : 1 electrolytes since the nitromethane is such a weak coordinating solvent that the ionization of the complexes hardly occurred when the complexes were dissolved in this solvent.

REFERENCES

1. L. F. Lindoy, *Chem. Soc. Rev.* 1975, **4**, 421.
2. L. G. Armstrong, P. G. Grimsley, L. F. Lindoy, H. C. Lip, V. A. Norris and R. J. Smith, *Inorg. Chem.* 1978, **17**, 2350.
3. K. R. Adam, G. Anderegg, L. F. Lindoy, H. C. Lip, M. McPartlin, J. H. Rea, R. J. Smith and P. A. Tasker, *Inorg. Chem.* 1980, **19**, 2956; A. Ekstrom, L. F. Lindoy and R. J. Smith, *Inorg. Chem.* 1980, **19**, 724.
4. G. Anderegg, A. Ekstrom, L. F. Lindoy and J. P. Smith, *J. Am. Chem. Soc.* 1980, **102**, 2670; L. F. Lindoy, H. C. Lip, J. H. Rea, R. J. Smith, K. Henrick, M. McPartlin and P. A. Tasker, *Inorg. Chem.* 1980, **19**, 3360.
5. K. R. Adam, L. F. Lindoy, R. J. Smith, G. Anderegg, K. Henrick, M. McPartlin and P. A. Tasker, *J. Chem. Soc., Chem. Commun.* 1979, 812; A. Ekstrom, L. F.

Lindoy, H. C. Lip, R. J. Smith, H. Goodwin, M. McPartlin and P. Tasker, *J. Chem. Soc., Dalton Trans.* 1979, 1027.
6. K. R. Adam, L. F. Lindoy, H. C. Lip, J. H. Rea, B. W. Skelton and A. H. White, *J. Chem. Soc., Dalton Trans.*, 1981, 74.
7. L. G. Armstrong and L. F. Lindoy, *Inorg. Chem.* 1975, **14**, 1322.
8. K. Miyokawa, H. Hirashima and I. Masuda, *Bull. Chem. Soc. Jpn* 1981, **54**, 3361.
9. A. B. P. Lever, *Inorganic Electronic Spectroscopy*, p. 333. Elsevier, Amsterdam (1968).
10. J. L. Burmeister, *Coord. Chem. Rev.* 1968, **3**, 225.
11. W. J. Geary, *Coord. Chem. Rev.* 1971, **7**, 81.
12. F. Basolo and R. G. Peason, *Mechanisms of Inorganic Reactions*, 2nd edition, p. 67. Wiley, New York (1967).

Polyhedron Vol. 4, No. 11, pp. 1895–1900, 1985
Printed in Great Britain

0277-5387/85 $3.00 + .00
© 1985 Pergamon Press Ltd

REACTION OF DICHLOROMANGANESE(IV) SCHIFF-BASE COMPLEXES WITH WATER AS A MODEL FOR WATER OXIDATION IN PHOTOSYSTEM II

MANABU FUJIWARA, TAKAYUKI MATSUSHITA* and TOSHIYUKI SHONO*
Department of Applied Chemistry, Faculty of Engineering, Osaka University, Yamadaoka, Suita, Osaka 565, Japan

(*Received* 16 *April* 1985; *accepted* 10 *May* 1985)

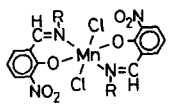
Abstract—The dichloromanganese(IV) Schiff-base complexes Mn(*N*-R-3-NO_2 sal)$_2Cl_2$ (R = *n*-C_3H_7, *n*-C_4H_9, *n*-C_6H_{13}, *n*-C_8H_{17}, *n*-$C_{12}H_{25}$ and $CH_2C_6H_5$) have been prepared and characterized by magnetic susceptibilities, electronic spectra and cyclic voltammograms. All the manganese(IV) complexes are found to react with water to liberate molecular oxygen (O_2). The maximal liberation of O_2 is observed at neutral pH. The following reaction scheme is proposed:

$$2Mn(IV)(L)_2Cl_2 + 2H_2O \rightarrow 2Mn(II)(L)_2 + O_2 + 4H^+ + 4Cl^-.$$

Manganese-containing proteins are believed to play an important role in the photosynthetic oxygen-evolving process from water by green algae and green plants.[1–3] Although much effort has been made to clarify their function,[4–7] the oxidation states of the manganese ions in the proteins, their structures, and the mechanism for water oxidation remain to be established.

Previously, we have reported the preparation and characterization of a series of novel dichloromanganese(IV) Schiff-base complexes.[8–10] Moreover, we have preliminarily shown that the manganese(IV) complex dichlorobis(*N*-propyl-3-nitrosalicylideneaminato)manganese(IV) reacts with water to liberate molecular oxygen (O_2).[11]

In this paper we describe the preparation and characterization of a series of dichloromanganese(IV) complexes with bidentate Schiff-base ligands derived from 3-nitrosalicylaldehyde and various monoamines (Fig. 1). All the manganese(IV) complexes are found to react with water to liberate O_2.



Mn(*N*-R-3-NO_2 sal)$_2Cl_2$
R = *n*-C_3H_7(Pr), *n*-C_4H_9(Bu), *n*-C_6H_{13}(Hx), *n*-C_8H_{17}(Oct), *n*-$C_{12}H_{25}$(Dod), $CH_2C_6H_5$(Bz).

Fig. 1. Manganese(IV) Schiff-base complexes studied.

EXPERIMENTAL

Materials

All reagents were of reagent grade. Methanol was refluxed over magnesium ribbon and distilled. Dichloromethane was refluxed over $CaCl_2$ and distilled. 2-Propanol was refluxed over CaO and distilled. Other solvents were purified by the usual methods.

Measurements

UV and visible absorption spectra were obtained from a Hitachi 340 recording spectrophotometer. IR spectra were recorded on a Hitachi EPI-215 and a Hitachi EPI-L grating spectrophotometer for the 4000–650- and 700–250-cm^{-1} regions, respectively. Mass spectra were measured with a Hitachi RMU-6E spectrometer. Magnetic susceptibilities were measured by the Gouy method at room temperature. Cyclic voltammograms were measured with a Yanaco P-8 polarograph connected with a Yanaco P8-PT potentiostat as described elsewhere.[10] Liberated O_2 in solution was determined by an EIL model 8012-1 oxygen electrode connected with a Yanaco PH 7-1913 voltmeter.

*Authors to whom correspondence should be addressed.

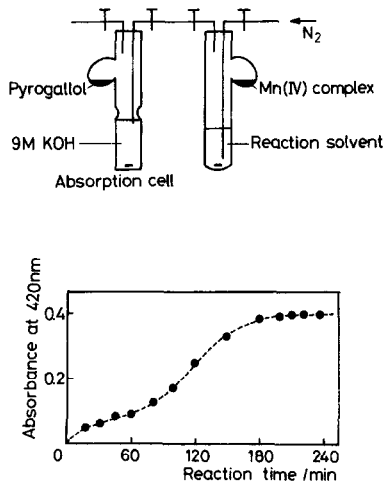


Fig. 2. Apparatus for spectrometric measurement, method 1, and changes in absorbance of pyrogallol solution in the reaction of Mn(IV)(*N*-Pr-3-NO_2 sal)$_2Cl_2$ (200 mg) with water (2 cm^3).

Procedure for detection and determination of liberated O_2

In the present work, the following two methods were employed to detect and determine O_2 liberated during the reaction of manganese(IV) complexes with water.

Method 1 is based on absorption spectrophotometry using an alkaline pyrogallol solution.[12] The apparatus is shown in Fig. 2. A reaction solvent [CH_3CN (8 cm^3)–H_2O (2 cm^3)] and a 9 M KOH solution placed in the apparatus were kept completely under a nitrogen atmosphere during all measurements. After nitrogen gas was passed through the reaction system for 1 h, pyrogallol (200 mg) was added to the alkaline solution and dissolved. The solution remained colorless and then the reaction system was sealed. A manganese(IV) complex was added to the reaction solvent, and its mixture was stirred vigorously at room temperature. Its color changed from deep green to yellowish brown, and the pyrogallol solution was colored gradually to dark brown. The color development of the pyrogallol solution was monitored by a spectrophotometer at 420 nm (Fig. 2).

Method 2 is based on the measurement of dissolved oxygen by an oxygen electrode. Dissolved oxygen in a reaction solvent [2-propanol (5 cm^3)–H_2O (20 cm^3)] was previously determined by the oxygen electrode at 10°C. After a manganese(IV) complex (10 mg) was added to the reaction solvent, the reaction system was sealed. Liberated O_2 was determined by the oxygen electrode as an increase in voltage while stirring the mixed solution at a constant revolution.

Preparation of bidentate Schiff-base ligands

3-Nitrosalicyladehyde was prepared by the method described in the literature.[13] The Schiff-base ligands were prepared by the condensation of 3-nitrosalicylaldehyde with various monoamines, R-NH_2 (R = Pr, Bu, Hx, Oct, Dod and Bz) (see Fig. 1) in tetrahydrofuran. They were recrystallized from appropriate organic solvents such as ethanol and ether. The yields were 65–85%.

Preparation of chloromanganese(III) Schiff-base complexes, Mn(N-R-3-NO_2 sal)$_2$Cl

A Schiff-base ligand [*N*-R-3-NO_2 salH (0.02 mol)], manganese(III) acetate dihydrate (0.01 mol) and lithium chloride (0.015 mol) were dissolved in a mixed solvent of methanol (100 cm^3) and dichloromethane (100 cm^3) and refluxed for 1 h. The mixture was evaporated under reduced pressure to give a dark brown solid. Upon recrystallization from a mixed solvent of dichloromethane and ether, the manganese(III) Schiff-base complex was obtained, washed with 2-propanol, and dried *in vacuo*. The yields were 70–80%. These complexes are soluble in dichloromethane, chloroform and 2-propanol, but insoluble in ether and water.

Preparation of dichloromanganese(IV) Schiff-base complexes, Mn(N-R-3-NO_2 sal)$_2Cl_2$

Mn(III)(*N*-R-3-NO_2 sal)$_2$Cl (2.0 mmol) was dissolved in 2-propanol (100 cm^3). A 2-propanol solution of hydrogen chloride (1.5-molar-fold excess over the complex) was added dropwise to the solution of the complex with stirring at room temperature. The mixture changed its color from brown to deep green immediately with a deep green precipitate. After stirring for 30 min, the resulting precipitate was collected on a glass filter, washed with 2-propanol and then ether, and dried *in vacuo*. Further purification was not carried out. The yields were 25–40%. These manganese(IV) complexes are soluble in dichloromethane, chloroform and acetonitrile, and slightly soluble in methanol and ethanol, but insoluble in ether and water. Their analytical data are given in Table 1.

RESULTS AND DISCUSSION

Electronic absorption spectra

Figure 3 shows the electronic absorption spectra of Mn(II)(*N*-Pr-3-NO_2 sal)$_2$(H_2O)$_2$, Mn(III)(*N*-Pr-3-NO_2 sal)$_2$Cl and Mn(IV)(*N*-Pr-3-NO_2 sal)$_2Cl_2$ measured in acetonitrile. The spectrum of the

Table 1. Analytical data for the manganese(IV) complexes, Mn(IV)(*N*-R-3-NO_2 sal)$_2Cl_2$

Complex R	Found (%) C	H	N	Cl	Mn	Calc. (%) C	H	N	Cl	Mn
Pr	45.0	4.5	10.2	13.7	10.3	44.46	4.11	10.37	13.13	10.17
Bu	46.7	4.8	9.8	13.2	9.8	46.49	4.62	9.86	12.84	9.67
Hx	49.9	5.4	8.7	11.6	8.9	50.00	5.50	8.97	11.35	8.80
Oct	52.2	6.3	8.4	10.8	8.1	52.93	6.23	8.23	10.42	8.07
Dod	57.7	7.5	7.0	8.8	6.9	57.56	7.39	7.07	8.94	6.93
Bz	52.2	3.8	8.8	11.6	8.6	52.84	3.49	8.81	11.14	8.63

manganese(III) complex possesses three absorption bands in the visible region at 16,100, 22,700 and 29,200 cm^{-1}. These bands can be assigned to the transitions due to $d_{xy} \rightarrow d_{x^2-y^2}$, $d_{xy} \rightarrow \pi^*$ (azomethine) involving d_{yz}, $d_{xz} \rightarrow d_{x^2-y^2}$, and d_{yz}, $d_{xz} \rightarrow \pi^*$ (azomethine) from lower energies.[8] Similarly, the spectrum of the manganese(IV) complex possesses three absorption bands, which are shifted to higher energies compared with those of the manganese(III) complex. The characteristic band for the manganese(IV) complex observed at 17,200 cm^{-1} may be assigned to the charge-transfer transition between manganese and chloride ions from its high intensity (log $\varepsilon = 3.4$).[8] The absorption bands due to *d–d* transitions for the manganese(IV) complex may be obscured by this intense band, so that the higher-energy bands cannot be assigned certainly, which may be associated with the charge-transfer transitions due to Mn($d\pi$) → π^* (azomethine). On the other hand, the spectrum of the manganese(II) complex has no absorption band in the region lower than 20,000 cm^{-1} and shows two absorption bands around 25,000 and 28,000 cm^{-1}. These results indicate that the oxidation states of the central manganese ions of the complexes can be easily discriminated from their electronic absorption spectra.

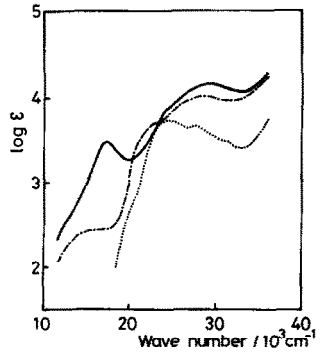


Fig. 3. Electronic spectra in CH_3CN. (——) Mn(IV)(*N*-Pr-3-NO_2 sal)$_2Cl_2$, (–·–·–) Mn(III)(*N*-Pr-3-NO_2 sal)$_2$Cl, and (·····) Mn(II) (*N*-Pr-3-NO_2 sal)$_2(H_2O)_2$.

The electronic spectra of the manganese(III) complexes with other alkyl groups are quite similar to that of Mn(III) (*N*-Pr-3-NO_2 sal)$_2$Cl, and those of the manganese(IV) complexes with other alkyl groups also possess absorption bands similar to those of Mn(IV)(*N*-Pr-3-NO_2 sal)$_2Cl_2$. The positions of the lowest-energy bands for the manganese(III) and manganese(IV) complexes are summarized in Table 2, together with their intensities. The band position of Mn(IV)(*N*-Pr-3-NO_2 sal)$_2Cl_2$ is blue-shifted about 900 cm^{-1} compared to that of Mn(IV)(*N*-Pr sal)$_2Cl_2$ obtained in a previous work.[8] This may be caused by the introduction of electron-withdrawing nitro groups on the aromatic rings.

Magnetic properties

The magnetic moments of the manganese(III) and manganese(IV) complexes determined at room temperature are summarized in Table 2. The magnetic moments of the manganese(III) complexes fall within the range 4.85–4.98 BM with the exception of Mn(III)(*N*-Bz-3-NO_2 sal)$_2$Cl. These values are consistent with the manganese(III) complexes adopting a d^4 high-spin electron configuration. The relatively low value (4.24 BM) observed for Mn(III)(*N*-Bz-3-NO_2 sal)$_2$Cl may be caused by magnetic exchange interaction due to the formation of a binuclear structure in the solid state like Mn(III)(*N*-Bz sal)$_2$Cl.[9] Further investigation on this complex was not made in this work.

On the other hand, the magnetic moments of the manganese(IV) complexes fall within the range 3.88–4.02 BM. These values are consistent with the manganese(IV) complexes adopting a d^3 high-spin electron configuration.

IR spectra

The IR spectra of the manganese(IV) complexes are almost the same as those of the corresponding manganese(III) complexes in the 4000–500-cm^{-1}

Table 2. Magnetic moments, absorption maxima and reduction potentials of the manganese(III) and manganese(IV) complexes, Mn(III)(*N*-R-3-NO_2 sal)$_2$Cl and Mn(IV)(*N*-R-3-NO_2 sal)$_2Cl_2$

	Complex R	μ_{eff}[a] (BM)	ν_{max}[b] (10^3 cm^{-1}) (log ε)	$E_{p/2}$ (vs SCE)[c] (V) Mn(IV) → Mn(III)	Mn(III) → Mn(II)	ν(Mn—Cl) (cm^{-1})
Mn(III)	Pr	4.93	16.13 (2.43)		0.25	
Mn(III)	Bu	4.98	16.03 (2.57)		0.28	
Mn(III)	Hx	4.94	16.23 (2.62)		0.21	
Mn(III)	Oct	4.85	16.10 (2.43)		0.14	
Mn(III)	Dod	4.95	16.18 (2.53)		0.02	
Mn(III)	Bz	4.24	16.18 (2.42)		0.27	
Mn(IV)	Pr	3.96	17.01 (3.46)	1.04	0.28	355
Mn(IV)	Bu	3.99	17.06 (3.42)	0.99	0.25	353
Mn(IV)	Hx	4.02	17.30 (3.43)	0.98	0.18	352
Mn(IV)	Oct	3.88	17.04 (3.73)	0.98	0.11	358
Mn(IV)	Dod	3.97	17.18 (3.47)	0.96	0.15	348
Mn(IV)	Bz	4.01	16.95 (3.41)	0.98	0.22	353

[a] Measured at room temperature.
[b] Measured in acetonitrile.
[c] Measured in acetonitrile containing 0.1 M Bu_4NClO_4 at 25°C.

region. However, in the 500–250-cm^{-1} region, the IR spectra of the manganese(III) and manganese(IV) complexes differ markedly, especially in the region sensitive to the vibration of ν(Mn—Cl). The manganese(III) complexes have weak absorption bands around 310 cm^{-1}, whereas the manganese(IV) complexes have one very sharp and strong absorption band around 350 cm^{-1} assignable to ν(Mn—Cl). The band positions listed in Table 2 are not affected so much by the alkyl groups of the Schiff-base ligands. These results indicate that all the manganese(IV) complexes adopt an octahedral configuration in which two chloride ions occupy a *trans* position about the central manganese ion as shown in Fig. 1.

Electrochemical properties

The current–potential curves of the manganese(IV) complexes measured in acetonitrile exhibit two-step cathodic waves around +1.0 and +0.25 V (vs SCE), which can be assigned to the reductions from Mn(IV) to Mn(III) and from Mn(III) to Mn(II) of the complex, respectively. The reduction potentials for the manganese(IV) complexes are given in Table 2, together with those for the manganese(III) complexes. The potentials for both reductions are not affected much by the alkyl groups of the Schiff-base ligands. These results are consistent with those obtained in the absorption spectra as described above.

It is noteworthy that the manganese(IV) complexes with *N*-alkyl-3-nitrosalicylideneamines have much more positive reduction potentials than those of the manganese(IV) complexes with *N*-alkylsalicylideneamines.[9] This is because the nitro group is one of the strongest electron-withdrawing substituents. Also, the manganese(IV) complexes with 5-nitro analogues have reduction potentials as high as the manganese(IV) complexes with 3-nitro analogues.[10] Such electrochemical properties are considered to be very important with regard to the effective generation of O_2 by oxidative decomposition of water.

Reactivity of the manganese(IV) complexes with water

All the manganese(IV) complexes investigated here are found to react with water based on their color changes from deep green to yellowish brown. These imply that the manganese(IV) species may be reduced to the manganese(III) or manganese(II) species. Thus, we have estimated the reactivity of the manganese(IV) complexes with water by measuring the absorption spectral changes of their acetonitrile solutions (5 cm^3, 2.5×10^{-4} M) caused by addition of water (0.1 cm^3). Figure 4 shows the time courses of the relative intensity of the absorbances at the maximal band positions near 17,000 cm^{-1} which are characteristic for the manganese(IV) species. It can be seen that the reactivity is affected by the alkyl groups of the complexes: the reaction with water is retarded in the order of *n*-C_3H_7 ≪ *n*-C_8H_{17} < *n*-$C_{12}H_{25}$). These results indicate that the long-chain alkyl groups such as *n*-C_8H_{17} and *n*-$C_{12}H_{25}$ can protect the central manganese(IV) ion from attack by

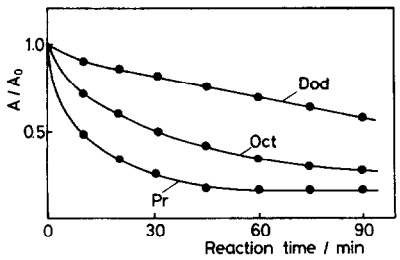


Fig. 4. Decreases in absorbance at λ_{max} after addition of water to acetonitrile solutions of Mn(IV)(*N*-R-3-NO_2 sal)$_2Cl_2$.

water molecules. This may arise from hydrophobicity of these groups. In other words, the reactivity of the manganese(IV) complexes with water can be controlled by the choice of alkyl groups.

Effect of pH of reaction media on quantities of liberated O_2

We have found that the pH values of reaction media decrease in the course of the reaction of the manganese(IV) complexes with water when without buffer solutions. Thus, the pH effect of reaction media on the quantity of liberated O_2 was examined by the use of Mn(IV)(*N*-Pr-3-NO_2 sal)$_2Cl_2$. The pH values were adjusted with 0.2 M acetate or 0.06 M phosphate buffer solutions. Figure 5(A) and (B) show the results obtained by methods 1 and 2, respectively. In both cases, the maximal liberation of O_2 was observed in the neutral pH region. This result is particularly interesting in connection with the photosynthetic oxygen evolution by green plants. The decrease in the liberated O_2 in acidic media may result from some decomposition of the manganese(IV) complex by hydrogen ions. On the other hand, the decrease in alkaline media cannot be explained clearly. However, it is supposed that the manganese(IV) complex may form Mn(IV)–OH species which further react with hydroxide ions to give relatively stable Mn(IV)=O species, which are not confirmed in this work.

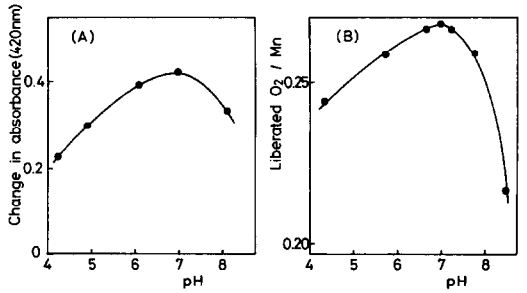


Fig. 5. Effect of pH on quantity of liberated O_2. (A) Method 1, and (B) method 2.

Table 3. Quantities of molecular oxygen (O_2) liberated during reaction of manganese(IV) complex (20 mg) with water in a mixed solvent of water (20 cm^3) and 2-propanol (5 cm^3) which was adjusted to pH = 7.0 with a phosphate buffer

Complex R	O_2 liberated/Mn
Pr	0.27
Bu	0.25
Hx	0.14
Oct	0.20
Dod	0.12
Bz	0.17

Oxygen liberation by various manganese(IV) complexes

Table 3 shows the quantities of O_2 liberated by the reactions of the manganese(IV) complexes with water at pH 7.0, which were determined by method 2. These values are presented as mol of liberated O_2 per mol of manganese(IV) complex. Among these complexes, Mn(IV)(*N*-Pr-3-NO_2 sal)$_2Cl_2$ exhibits the highest value and Mn(IV)(*N*-Dod-3-NO_2 sal)$_2Cl_2$ the lowest one. These results can be correlated with the reduction potentials and the reactivities of the manganese(IV) complexes as described above. Therefore, it can be said that the quantity of liberated O_2 depends on the oxidizing power of the manganese(IV) complexes.

Identification of reaction products of manganese(IV) complex with water

The acetonitrile or 2-propanol solution of Mn(IV)(*N*-Pr-3-NO_2 sal)$_2Cl_2$ changed its color from deep green to yellowish brown on the addition of water. This solution was evaporated under reduced pressure to yield a yellow solid, which was washed with water and dried *in vacuo*. The analytical data for this reaction product are consistent with the formula Mn(*N*-Pr-3-NO_2 sal)$_2(H_2O)_2$. Its magnetic moment determined at room temperature is 5.95 BM, indicating that the oxidation state of manganese ion in the reaction product is +II. The electronic spectrum of the product in acetonitrile is identical to that of Mn(II)(*N*-Pr-3-NO_2 sal)$_2(H_2O)_2$, which was prepared from manganese(II) acetate tetrahydrate and *N*-propyl-3-nitrosalicylideneamine. From these results, it is concluded that the manganese(IV) complexes are reduced to their corresponding manganese(II) complexes by reaction with water.

We now propose that the reaction of the manganese(IV) complexes with water proceeds

according to the following equation:

$$2Mn(IV)(L)_2Cl_2 + 2H_2O \rightarrow 2Mn(II)(L)_2 + O_2 + 4H^+ + 4Cl^-, \quad (1)$$

where L denotes the monoanion of *N*-alkyl-3-nitrosalicylideneamines. The concentration of chloride ions liberated into the reaction solvent was determined by a titration method using a silver nitrate solution. The value obtained was almost equal to that calculated from eqn (1). Moreover, the concentration of hydrogen ions liberated into the reaction solvent, when the reaction was carried out in a medium without buffer solution, was determined by measuring the decrease in the pH value. The value obtained from the pH drop was nearly equal to that calculated from eqn (1).

In order to prove that the liberated O_2 originated from water, isotopic labeled water, $H_2{}^{18}O$ (20.3 atom %), was used for the reaction solvent. Before reaction, the system and a solvent, 2-propanol (4 cm^3) and $H_2{}^{18}O$ (1 cm^3), were degassed under vacuum, and the manganese(IV) complex Mn(IV)(*N*-Pr-3-NO_2 sal)$_2Cl_2$ (10 mg) was added to it. After the reaction was complete, the generated gaseous components in the reaction system were analyzed by a mass spectrometer. The mass spectrum thus obtained shows relatively weak peaks at $m/z = 36$ and 34, in addition to an intense peak at $m/z = 32$. The former peaks can be assigned to ^{18}O–^{18}O and ^{16}O–^{18}O, respectively. Although quantitative determination of these species could not be made in this work, it is concluded that the liberated O_2 originated from the water.

REFERENCES

1. K. Sauer, *Acc. Chem. Res.* 1980, **13**, 249.
2. G. M. Cheniae, *Methods Enzymol.* 1980, **69**, 349.
3. J. Amesz, *Biochim. Biophys. Acta* 1983, **726**, 1.
4. D. V. Goodin, V. K. Yachandra, R. D. Britt, K. Sauer and M. P. Klein, *Biochim. Biophys. Acta* 1984, **767**, 209.
5. P. Mathur and G. C. Dismukes, *J. Am. Chem. Soc.* 1983, **105**, 7093.
6. B. Unni Nair and G. C. Dismukes, *J. Am. Chem. Soc.* 1983, **105**, 124.
7. G. C. Dismukes, K. Ferris and P. Watnick, *Photobiochem. Photobiophys.* 1982, **3**, 243.
8. T. Matsushita, H. Kono and T. Shono, *Bull. Chem. Soc. Jpn* 1981, **54**, 2646.
9. T. Matsushita, Y. Hirata and T. Shono, *Bull. Chem. Soc. Jpn* 1982, **55**, 108.
10. T. Matsushita and T. Shono, *Polyhedron* 1983, **2**, 613.
11. T. Matsushita, M. Fujiwara and T. Shono, *Chem. Lett.* 1981, 631.
12. I. A. Duncan, A. Harriman and G. Porter, *Anal. Chem.* 1979, **51**, 2206.
13. C. C. Hach, L. M. Liggett and H. Diehl, *Chem. Abstr.* 1948, **42**, 1240.

Polyhedron Vol. 4, No. 11, pp. 1901–1907, 1985
Printed in Great Britain

0277-5387/85 $3.00 + .00
© 1985 Pergamon Press Ltd

INTERACTION OF SOLVATED ELECTRONS WITH AN Mo(V) OXALATE COMPLEX IN A WATER–ETHYLENE GLYCOL SYSTEM

J. O. DZIĘGIELEWSKI

Department of Inorganic and Radiation Chemistry, Institute of Chemistry, Silesian University, Katowice, Szkolna 9 Street, Poland

(*Received* 1 *February* 1985; *accepted* 10 *May* 1985)

Abstract—The reactivity of metal ions towards e_s^- was studied to identify the stable and unstable reaction products by spectroscopic analysis of the observed absorption bands. The crystal field parameters Dq(2600 cm^{-1}), Ds(−5300 cm^{-1}) and $D\tau$(900 cm^{-1}) were determined from absorption spectra and the energy terms of the Mo(V) oxalate complex were calculated as functions of the crystal field parameters. On these grounds, the absorption bands at 22,200 and 26,670 cm^{-1} of an irradiated frozen solution of the Mo(V) complex were designated as the *d–d* transition of the "hot" Mo(IV) ion and charge transfer from π^*-orbital of $C_2O_4^{3-}$, toward the antibonding molecular orbital, respectively. The electronic structure of the "hot" Mo(IV) ion was determined as $(d_{xy})^1(d_{xz}, d_{yz})^1$. The decay of the "hot ion" results in a change in the fundamental level, i.e. (d_{xz}, d_{yz}).[2] Therefore, the ligand remains in the coordination sphere as proved by ^{13}C NMR studies (signal at 165.2 ppm) as well as an absorption band at 35,100 cm^{-1} ($n \rightarrow \pi^*$ transition in the $C_2O_4^{2-}$ ion). On the grounds of the spectrophotometric and NMR investigations the structure of the oxalate complex of Mo(IV) $\{[Mo_2O_2(C_2O_4)_2(OH_2)_4]\}$ was proposed. The rate constant of the reaction of e_s^- with $[Mo_2O_4(C_2O_4)_2(OH_2)_2]^{2-}$ ions was determined as 2.6×10^9 dm^3 mol^{-1} s^{-1}.

The reactivity of a considerable number of complexes towards solvated electrons and radicals has been determined by the method of pulse radiolysis. A comprehensive set of experimental data can be found.[1] Many studies have been aimed at the identification of unstable radiolysis products of the reactions of e_s^- with complexes.[2–6] Only a few authors have analysed the spectroscopic absorption bands or ESR signals of the reaction products.[6–8]

Such an analysis enables a more precise identification of the unstable radiolysis products and the determination of the relation between the observed radiation–chemical processes and such fundamental properties of the irradiated complex as its symmetry, the covalency of the coordination bond, the electronic configuration and the spin state of the central ion. From this point of view, the d^1-electron Mo(V) complex seems to be an interesting subject.

Earlier studies of oxalate complexes[9,10] brought to light differences in the reactivity of those compounds towards electrons, the reactivity depending on the type of central ion. The present study was aimed at the determination of the reactivity of an oxalate complex of Mo(V) towards e_s^- and the identification of the unstable and stable reaction products by spectroscopic analysis of the observed absorption bands. The water–ethylene glycol system was considered suitable for this purpose.

EXPERIMENTAL

The complex $(NH_4)_2[Mo_2O_4(C_2O_4)_2(OH_2)_2]$ was obtained according to Mitchell.[11] An alternative structure of this compound is given in Fig. 1(a).[11,12]

A solution of ethylene glycol of analytical grade in triply distilled water (mol ratio 1 : 3) was prepared for investigations at room temperature, while one with a mol ratio of 1 : 2 was prepared for investigations at liquid-nitrogen temperature.

The solutions of $[Mo_2O_4(C_2O_4)_2(OH_2)_2]^{2-}$ were prepared by dissolving a corresponding amount of the Mo(V) complex prepared as above in the solvent saturated with the appropriate gas for 15 min and

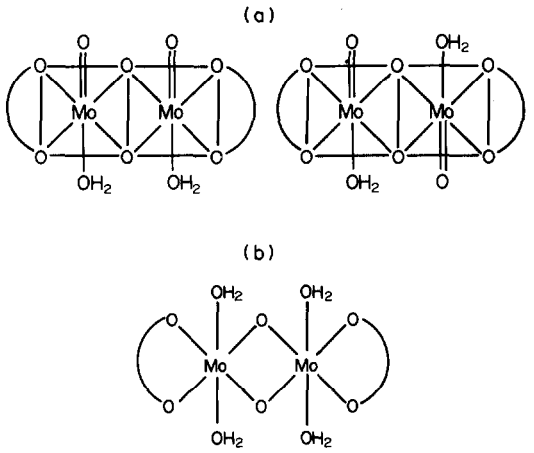


Fig. 1. Equivalent structures of the

$$[Mo_2O_4(C_2O_4)_2(OH_2)_2]^{2-}$$

ion (a) and the proposed structure of the Mo(IV) oxalate complex (b).

irradiated in the cobalt source "Issliedowatiel" with a dose rate of 2.4×10^{16} eV cm^{-3} s^{-1}.

The amount of compound modified by the radiation was determined from the intensity decrease in the 32,800-cm^{-1} band using a Beckman 5240 spectrophotometer. The low-temperature measurements were carried out in a cryostat by irradiating glassy matrices at 77 K and recording the absorption bands as functions of temperature.

The dose was determined with a Fricke's dosimeter and converted to the electron density of the water–ethylene glycol system.

The number of oxalate groups in the irradiated complex was monitored by ^{13}C NMR signals, applying external calibration by means of HMDSO.

The changes in the paramagnetic susceptibility resulting from irradiation of the oxalate Mo(V) complex in solution was determined by the ^1H NMR method described by Evans.[13,14]

Because of the low effective magnetic moment of the binuclear Mo(V) complex,[11,15] the concentration of the solution used for the measurements was 0.9 mol dm^{-3}. The variations in the magnetic susceptibility were determined from the ^1H NMR signal shift of acetone inserted into the solution after irradiation. For the NMR measurements an FT-80A multinuclear spectrometer was used.

RESULTS AND DISCUSSION

Absorption spectra of the

$$[Mo_2O_4(C_2O_4)_2(OH_2)_2]^{2-}$$

ion are presented in Table 1. The bands given in Table 1 were found for solutions of the oxalate complexes of Mo(V).[11] From the data given in Table 1, the crystal field parameters were determined: $Dq = 2600$ cm^{-1}, $Ds = -5300$ cm^{-1} and $D\tau = 900$ cm^{-1}. Assuming a C_{4v}-symmetry, the term energies of Mo(V) were calculated as functions of the crystal field parameters according to Ref. 16:

$$^2B_2 = (-4Dq + 2Ds - D\tau),$$

$$^2E = (-4Dq - Ds + D\tau),$$

$$^2B_1 = (6Dq + 2Ds - D\tau),$$

$$^2A_1 = (6Dq - 2Ds - 6D\tau).$$

The relative positions of the terms as well as the charge-transfer transitions are shown in Fig. 2.

The absorption bands resulting from irradiation of the Mo(V) complex in the frozen water–ethylene glycol system saturated with Ar are shown in Fig. 3 (line 1). Those bands do not practically appear in solutions saturated with N_2O.

As indicated by Fig. 3 (line 1), the irradiated matrix shows a very intense band at 26,670 cm^{-1} appearing

Table 1. Band positions, molar extinction coefficients and assignments

Band position (cm^{-1})	Molar extinction coefficient (dm^3 mol^{-1} cm^{-1})	Band assignment[11]
20,400	1	$(d_{xy})^1 \rightarrow (d_{xz}, d_{yz})^1$
26,000	170	$(d_{xy})^1 \rightarrow (d_{x^2-y^2})^1$
32,800	3520	$\pi \rightarrow (d_{xz}, d_{yz})$
		$\pi(C_2O_4^{2-}) \rightarrow (d_{xy})^a$
38,900	3520	$\pi \rightarrow (d_{x^2-y^2})$
		$\pi(O) \rightarrow (d_{xz}, d_{yz})^a$

[a] Corrected by the author of this paper with regard to the symmetry elements.

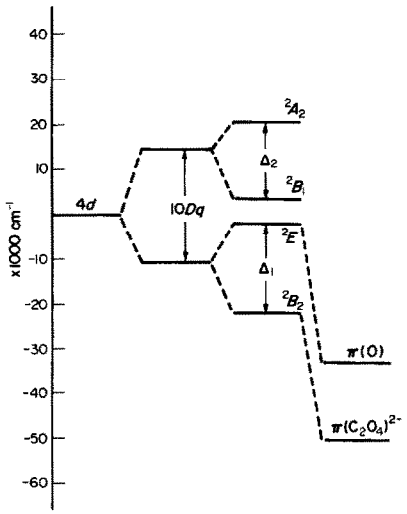


Fig. 2. Relative energies of the Mo(V) terms and the charge-transfer energies in the $[Mo_2O_4(C_2O_4)_2(OH_2)_2]^{2-}$ ion.

at 77 K and a band of low intensity at 22,200 cm^{-1} appearing at 173 K, both vanishing at about 210 K. The intense band cannot be attributed to a *d–d* inner-ligand transition because of its intensity and position. It is rather of the charge-transfer type, i.e. due to electron transfer from the π^*-orbital of $C_2O_4^{3-}$ ion, resulting from the electron capture by the oxalate ligand, toward the antibonding molecular orbital.[17,18] The disappearance of that high-energy state is connected with the transfer of electrons to the d_{xz}- or d_{yz}-orbitals of the central ion. The 22,200-cm^{-1} band may be attributed to the *d–d* transition because of its low intensity and position. The energy of this transition corresponds to the energy level difference of the terms $^2A_1 - {}^2E$. It may therefore be concluded that the trapping of an electron by Mo(V) results in the creation of the hot Mo(IV) ion with the following electronic structure, $(d_{xy})^1(d_{xz}, d_{yz})^1$. The vanishing of the 22,200-cm^{-1} transition is due to the transition of Mo(IV) from the excited to the ground state.

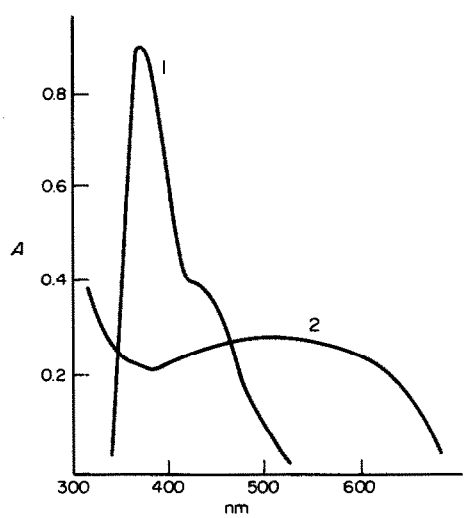


Fig. 3. Absorption bands arising after irradiation of the oxalate complex of Mo(V) at 175 K: $c = 10^{-2}$ mol dm^{-3} in the water–ethylene glycol system (2:1), dose = 7.8 kGy (line 1) and the differential spectrum of irradiated

$(NH_4)_2[Mo_2O_4(C_2O_4)_2(OH_2)_2]$

(dose = 1.9×10^{21} eV cm^{-3}) in the water–ethylene glycol system at room temperature. Solution (c = 1 mol dm^{-3}) saturated with Ar. Thickness of the absorption cell, d = 5 cm (line 2).

The reduction of Mo(V) to Mo(IV) is confirmed by the difference spectrum of the irradiated solution from the non-irradiated solution at room temperature shown in Fig. 3 (line 2). The single broad band of low intensity located at about 14,700 cm^{-1} may be attributed merely to a *d–d* transition. For Mo(IV) a band is indeed observed in the *d–d*-transition region.[19]

The distinctly lower Mo(IV) band compared to that of the crystal field of Mo(V) indicates a change in the ligand field of the reduced central ion. The variations occurring in the coordination sphere of the central ion are shown in Figs 4 and 5. From Fig. 4 it appears that the irradiation of $[Mo_2O_4(C_2O_4)_2(OH_2)_2]^{2-}$ results in a decrease in the intensity of the 32,800-cm^{-1} band and in the appearance of a new band at 38,900 cm^{-1}. The difference spectrum shown in Fig. 5 indicates that the irradiated compound also shows an additional band at about 35,100 cm^{-1}. The position of this band was determined by interpolation. The intensity decrease in the 32,800-cm^{-1} band is usually attributed to the decrease in the ligand or, at least, to its removal from the coordination sphere of the central ion.

Such an interpretation is at variance with the appearance of the new band at about 35,100 cm^{-1}, which indicates the presence of $C_2O_4^{2-}$ in the coordination sphere of Mo(IV).

As expected, the 35,100-cm^{-1} band is due to an inner transition within the $C_2O_4^{2-}$ ion.[11] In the oxalate complex of Mo(V), that band is not observed because of its low intensity and overlapping with the 32,800-cm^{-1} band. Taking into account the intensity and position of the 35,100-cm^{-1} band, it may be attributed, according to Ref. 20, to the $n \rightarrow \pi^*$ transition in the $C_2O_4^{2-}$ ion. The presence of $C_2O_4^{2-}$ ions in the coordination sphere of Mo(IV) is confirmed by the ^{13}C NMR signal of the irradiated solution at 165.2 ppm. The intensity and position of this signal are the same as for the non-irradiated solution of Mo(V).

The decrease in the intensity of the 32,800-cm^{-1}

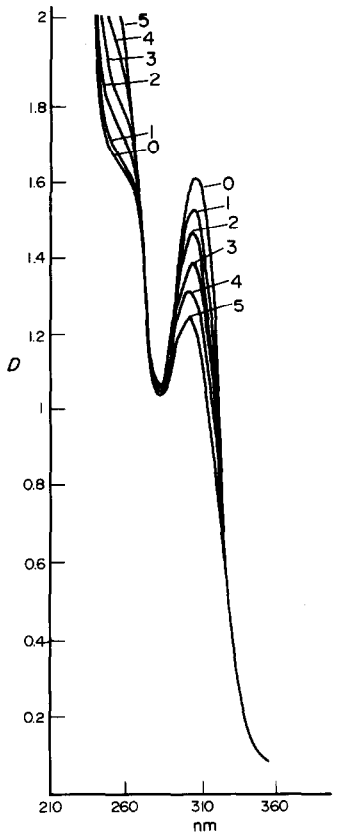


Fig. 4. Variations in the absorption spectrum (shortwave region) caused by the irradiation of the solution of

$$[Mo_2O_4(C_2O_4)_2(OH_2)_2]^{2-}$$

saturated with Ar (at room temperature) in the water–ethylene glycol system, $c = 5 \times 10^{-4}$ mol dm^{-3}, $d = 1$ cm. (0) non-irradiated solution, (1) 3.72×10^{18} eV cm^{-3}, (2) 8.68×10^{18} eV cm^{-3}, (3) 13.64×10^{18} eV cm^{-3}, (4) 15.60×10^{18} eV cm^{-3}, (5) 21.28×10^{18} eV cm^{-3}.

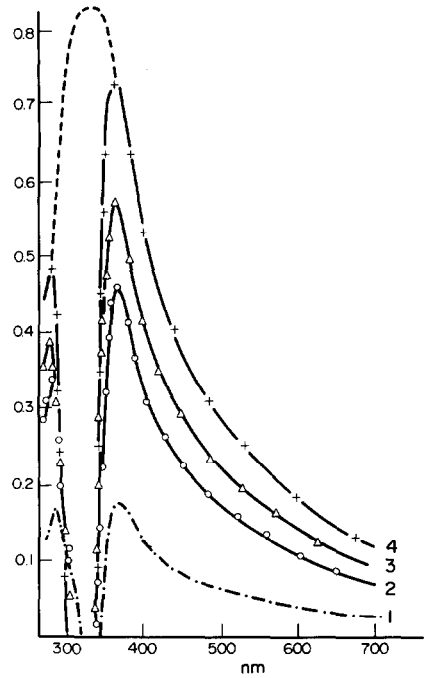


Fig. 5. Differential spectrum of the irradiated 10^{-2} mol dm^{-3} $[Mo_2O_4(C_2O_4)_2(OH_2)_2]^{2-}$ solution saturated with Ar in the water–ethylene glycol system, $c = 10^{-2}$ mol dm^{-3}, $d = 1$ cm (at room temperature): (1) 1.49×10^{20} eV cm^{-3}, (2) 2.98×10^{20} eV cm^{-3}, (3) 4.46×10^{20} eV cm^{-3}, (4) 5.95×10^{20} eV cm^{-3}.

band may, therefore, be due only to the change in the magnitude and symmetry of the crystal field around the reduced central ion. A decrease in the Dq parameter is indicated by the position of the band of the reduced Mo complex. The Dq decrease to 1470 cm^{-1} and the change in the crystal field symmetry are most probably caused by the vanishing of the Mo=O bond. The oxalate complex of Mo(IV) may, therefore, be depicted as in Fig. 1b. The presence of oxygen bridges in the Mo(IV) complex is corroborated by the weak paramagnetic properties of the irradiated solution.

The paramagnetic shift of the acetone signal is identified for both the non-irradiated and irradiated solutions and equals about 4 Hz in relation to the position of the signal of $(CH_3)_2C{=}O$ without the Mo complex. An oxalate complex of Mo(IV) with a similar structure was obtained by Wajda and Bezak,[21,22] who have also proved its weak paramagnetic properties. Thus, assuming a D_{4h}-symmetry for the Mo(IV) complex, the broad band shown in Fig. 3 can be attributed to the transitions $^3E_g \rightarrow {}^3B_{2g}$ and $^3E_g \rightarrow {}^3A_{1g}$.

The variation in the energy levels of the Mo(IV) orbitals in comparison with those of the Mo(V) orbitals explains the transfer band shift ($\pi C_2O_4^{2-} \rightarrow d_{xy}$) towards a higher frequency. In the irradiated compound, this band is shifted to 38,900 cm^{-1} (Fig. 3). The weak paramagnetism of the irradiated solution shown above confirms the fundamental term ^3E_g of Mo(IV). If there was no change in the position of the terms, the fundamental term of Mo(IV) would be $^1B_{2g}$ and the Mo(IV) complex would be diamagnetic.

The charge transfer $\pi(O) \rightarrow d_{xz}, d_{yz}$ is not observed in the irradiated solution, which indicates the vanishing of the Mo=O bond.

The quantity of the reduced Mo(V) complex was determined from the intensity decrease in the 32,800-cm^{-1} band. The quantity of reduced complex molecules depends non-linearly on the dose. The radiation yields from the conversion of the Mo(V) complex are listed in Table 2.

The yields for the solutions saturated with Ar,

higher than those for the solutions saturated with N_2O (Table 2), indicate interactions of the complex with e_s^-. The $[Mo_2O_4(C_2O_4)_2(OH_2)_2]^{2-}$ ions are most likely also reduced by hydrogen atoms produced during the radiolysis of glycol.[23] The OH radicals are not able to interact with the Mo(V) complex because of their high reactivity toward glycol.[24] From the results obtained we are led to assume the following mechanism for the radiolysis:

$$S \rightsquigarrow e_s^-, S^+, H, OH, R, \tag{1}$$

$$e_s^- + [Mo_2O_4(C_2O_4)_2(OH_2)_2]^{2-} \xrightarrow{\Sigma k_1} \begin{cases} \xrightarrow{k_1} Mo(IV)^* \\ \xrightarrow{k_1'} Mo_2O_4L_2(OH_2)_2]^{2-} \end{cases} \tag{2a}$$

$$\left[\begin{array}{l} O \\ \| \\ Mo(V)\!<\!L^- \\ | \\ OH_2 \end{array}\right]^- + 2H^+ \rightarrow \left[\begin{array}{l} OH_2 \\ | \\ Mo(IV)\!<\!L \\ | \\ OH_2 \end{array}\right]^{o}, \tag{2b}$$

$$N_2O + e_s^- \xrightarrow{H_2O} N_2 + OH + OH^-, \tag{3}$$

$$e_s^- + HOCH_2{-}CH_2OH \xrightarrow{k_3} HOCH_2{-}CH_2O^- + H, \tag{4}$$

$$(H), OH + HOCH_2{-}CH_2OH \rightarrow (H_2), H_2O + HOCH_2{-}\dot{C}HOH, \tag{5}$$

$$2HOCH{-}CH_2OH \rightarrow \begin{array}{l} HOCH{-}CH_2OH \\ | \\ HOCH{-}CH_2OH \end{array} \tag{6}$$

where S, R and L mean solvent, radical and ligand ($C_2O_4^{2-}$), respectively.

Applying the approximation of the steady state to reactions (2)–(4), the following relationship was derived:

$$\frac{1}{G_{[Mo(IV)]_{Ar}} - G_{[Mo(IV)]_{N_2O}}} = \frac{1}{G_{e_s^-}} + \frac{k_3[C_2H_6O_2]}{G_{e_s^-}[Mo(V)]\,\Sigma k_1}.$$

For $G_{[Mo(IV)]_{Ar}} - G_{[Mo(IV)]_{N_2O}}$ see Table 2. Figure 6 shows

$$\frac{1}{G_{[Mo(IV)]_{Ar}} - G_{[Mo(IV)]_{N_2O}}}$$

as a function of

$$\frac{1}{[Mo(V)]}.$$

From Fig. 6 the values $G_{e_s^-} = 0.74$ and

$$\frac{k_3[C_2H_6O_2]}{G_{e_s^-}\,\Sigma k_1} = 2.09 \times 10^{-3}$$

were found. Thus:

$$\frac{k_3}{k_1} = 1.73 \times 10^{-4},$$

assuming $k_3 = 4.5 \times 10^5$ dm^3 mol^{-1} s^{-1},[25] $k_1 = 2.6 \times 10^9$ dm^3 mol^{-1} s^{-1}.

The results obtained lead to the conclusion that the oxalate complex of Cr(III) of O_h-symmetry (lack of Jahn–Teller distortion for d^3) can react with e_s^- in a similar manner, i.e. forming the $C_2O_4^{3-}$ ion and reducing the central ion to Cr(II). However, due to the symmetry the transfer of e_s^- from $C_2O_4^{3-}$ to OM $\sigma_d^*(e_g)$ is forbidden. On the other hand, the transfer of e_s^- from $C_2O_4^{3-}$ to $\pi d(t_{2g})$ orbitals is symmetry-allowed but impossible because of the position of the oxalate ion in the spectrochemical series, which means that the ligand does not favour a $(t_{2g})^n$ low-spin configuration. Hence, the e_s^- interaction with ligand should lead to intermediate decomposition of the oxalate complex of Cr(III). The central ion reduction should decrease the oxalate σ $Cr(IV)\!<\!O_4C_2$ bond strength (e_g is an acceptor orbital) which can lead to the decomposition of Cr(III) oxalate. It may be predicted that the oxalate complex of Cr(III) of higher symmetry will be more reactive compared to the oxalate of Mo(V) of lower symmetry.

The rate constants of the reaction of e_{aq}^- with

Table 2. Yields from reduction of $(NH_4)_2[Mo_2O_4(C_2O_4)_2(OH_2)_2]$ in the water–ethylene glycol system as a function of concentration

Concentration (mol dm^{-3})	Number of reduced complex molecules per 100 eV: Solutions saturated with Ar $\{G_{[Mo(IV)]_{Ar}}\}$	Solutions saturated with N_2O $\{G_{[Mo(IV)]_{N_2O}}\}$	$G_{[Mo(IV)]_{Ar}} - G_{[Mo(IV)]_{N_2O}}$
2.5×10^{-4}	0.272	0.167	0.105
5.0×10^{-4}	0.367	0.137	0.180
7.5×10^{-4}	0.440	0.195	0.245
1.2×10^{-3}	0.620	0.293	0.327

Cr(III) oxalates determined by pulse radiolysis[9] are higher than k_1 and equal about 1.3×10^{10} dm^3 mol^{-1} s^{-1}. The lower value of Σk_1 for complex reactions seems to be comprehensible. In the light of our results, the higher symmetry (O_h) of the oxalate complexes of Cr(III) can also contribute to the increase in the probability of the decomposition of those complexes. The decomposition of the Cr(III) oxalates was proved experimentally.[9,10] The spin state of Cr(III) in oxalate complexes is $\frac{3}{2}$. In Cr(II) oxalate the spin state for the weak $C_2O_4^{2-}$ ligands should be 2 instead of 1.[26,27] According to our expectation the oxalate complex of Cr(III) has decomposed as a result of the reaction with e_s^-. The oxalate complex when undergoing an internal rearrangement (of the d-orbitals of the central ion) caused by the ligand field does not decompose if the resulting configuration (d_{xz}, d_{yz}) of d-electrons does not weaken the Mo$\langle$ O_4C_2 bond. The difference in the behaviour of the Mo(V) and Cr(III) compounds towards e_s^- is caused by differences in the electronic configuration of the central ions and in the symmetry of the oxalate complexes. Similarly, as was shown in a previous paper,[28] a different behaviour of the Mo(O) and Mo(IV) complexes with π-acceptor ligands, including lowering the complex symmetry from O_h to C_{4v}, was observed when they interact with e_s^-.

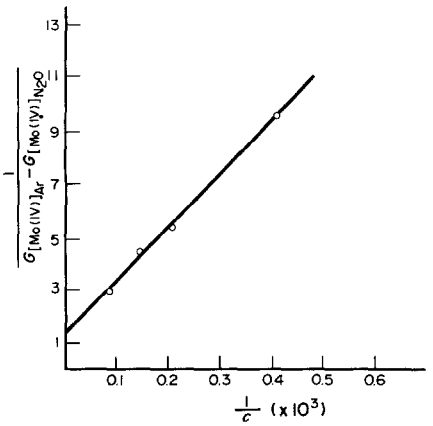


Fig. 6. Dependence of the reciprocal of $G_{[Mo(IV)]_{Ar}} - G_{[Mo(IV)]_{NO_2O}}$ on the reciprocal of the concentration of the Mo(V) complex.

REFERENCES

1. E. Hart and M. Anbar, *Gidratirowanyj Elektron, Atomizdat* (1973).
2. G. V. Buxton, F. S. Dainton and J. Kalecinsky, *Int. J. Radiat. Phys. Chem.* 1967, **1**, 87.
3. D. Zehavi and J. Rabani, *J. Phys. Chem.* 1974, **78**, 1368.
4. A. M. Tait, M. Z. Hoffman and E. Hayon, *Int. J. Radiat. Phys. Chem.* 1976, **8**, 691.
5. R. K. Broszkiewicz, *J. Chem. Soc., Dalton Trans.* 1973, 1799; *Int. J. Radiat. Phys. Chem.* 1974, **6**, 249.
6. A. Kumar and P. Neta, *J. Phys. Chem.* 1981, **25**, 2830.
7. J. Isoya and S. Fujivara, *Bull. Chem. Soc. Jpn* 1972, **45**, 2182.
8. S. Fujivara, T. Watanabe and H. Tadano, *J. Coord. Chem.* 1971, **1**, 195; E. Kalecińska and B. Jeżowska-Trzebiatowska, *Bull. Acad. Pol. Sci. Ser. Sci. Chim.* 1980, **28**, 577.
9. A. Schutka and K. Thomas, *J. Phys. Chem.* 1965, **69**, 284.
10. A. Sugimori and G. Tsuchihashi, *Bull. Chem. Soc. Jpn* 1961, **34**, 449.
11. P. C. H. Mitchell, *J. Inorg. Nucl. Chem.* 1963, **25**, 963; 1964, **26**, 1967.
12. S. Wajda and A. Zarzeczny, *Nukleonika* 1974, **19**, 33, 511.
13. D. P. Evans, *J. Chem. Soc.* 1959, 2003.
14. T. H. Crawford and J. Swanson, *J. Chem. Educ.* 1971, **48**, 382.
15. B. Jeżowska-Trzebiatowska and M. F. Rudolf, *Bull. Acad. Pol. Sci. Ser. Sci. Chim.* 1969, **17**, 419.
16. B. Jeżowska-Trzebiatowska and W. Wojciechowski,

Teoretyczne Problemy Chemii Koordynacyjnej, p. 73. PWN, Warsaw (1970).
17. A. Bartecki, *Spektroskopia Elektronowa Zwiazków Kompleksowych i Nieorganicznych*, p. 196. PWN, Warsaw (1971).
18. B. Jeżowska-Trzebiatowska, *Pure Appl. Chem.* 1971, 89.
19. C. A. McAuliffe and B. J. Sayle, *J. Chem. Soc., Dalton Trans.* 1977, 2055.
20. L. A. Kazicyna and N. B. Kupletska, *Metody Spektroskopowe Wyznaczania Struktury Zwiazków Organicznych*, p. 84. PWN, Warsaw (1976).
21. S. Wajda and E. Bezak, *Bull. Acad. Pol. Sci. Ser. Sci. Chim.* 1977, **25**, 45.
22. *Ibid.*, 1977, **25**, 109.
23. L. Kartaszewa and A. K. Pikajew, *Khim. Vys. Energ.* 1974, **7**, 434.
24. G. Adams and J. Boag, *Trans. Faraday Soc.* 1965, **61**, 492.
25. A. W. Rudniev, A. W. Vannikov and N. A. Bach, *Khim. Vys. Energ.* 1972, **6**, 473.
26. A. B. P. Lever, *Inorganic Electronic Spectroscopy*. Elsevier, Amsterdam (1968).
27. C. K. Jorgensen, *Modern Aspects of Ligand Field Theory*. North-Holland, Amsterdam (1971).
28. J. O. Dzięgielewski, *Polyhedron* 1984, **3**, 1131.

Polyhedron Vol. 4, No. 1, p. v, 1985
Pergamon Press Ltd. Printed in Great Britain

ERRATUM

M. J. Freeman, A. D. Miles, M. Murray, A. G. Orpen and F. G. A. Stone, The synthesis and X-ray crystal structure of the hexanuclear metal cluster complex $[Ir_3Pt_3(\mu\text{-}CO)_3(CO)_3(\eta\text{-}C_5Me_5)_3]$. *Polyhedron* 1984, **3**, 1093–1097.

The publishers regret that one line was omitted from and another repeated in the introductory paragraph on p. 1093 of the published version of the above paper. Lines 15–17 of that paragraph should read: "... the dimetal salts $[IrPt(H)(R)(\mu\text{-}H)_2(PEt_3)_4][BPh_4]$(R = H or Ph).[4] Recently we have employed $[Rh(CO)_2(\eta\text{-}C_5Me_5)]$ as a reagent for obtaining..." The corrected p. 1093 is reprinted overleaf.

Polyhedron Vol. 4, No. 11, pp. 1909–1913, 1985
Printed in Great Britain

0277–5387/85 $3.00 + .00
© 1985 Pergamon Press Ltd

COMPLEX FORMATION BETWEEN SILVER AND IODIDE IONS IN DIMETHYLSULPHOXIDE

F. GAIZER

Department of Inorganic and Analytical Chemistry, A. József University, Szeged, P.O. Box 440, Hungary

(*Received* 25 *April* 1985; *accepted* 22 *May* 1985)

Abstract—The interaction of silver and iodide ions in dimethylsulphoxide (DMSO) at 21–25°C has been investigated by spectrophotometry and potentiometric measurements over a wide concentration range. The stability constants of the complexes AgI, $Ag_6I_8^{2-}$, $Ag_5I_7^{2-}$, $Ag_4I_6^{2-}$, $Ag_2I_4^{2-}$, AgI_2^- and AgI_3^{2-} have been determined by systematic computer evaluation of the results. The IR spectrum shows that in the isolated compound $CdAg_6I_8 \cdot 8DMSO$ the DMSO is coordinated through oxygen.

In a previous paper[1] we presented the results of investigations on complex formation between silver and iodide ions in DMSO. On the basis of a systematic computer evaluation of measurements at constant silver concentrations in the range T_{Ag} = 0.5–7.5 mM, we presumed the formation of species (6, 8), (1, 2) and (1, 3).* Since the fit was not considered satisfactory and systematic deviations were observed as a function of silver concentration, we felt it necessary to perform further experiments differently planned and to supplement the potentiometric measurements with additional ones. The present paper gives an account of these investigations.

EXPERIMENTAL

Chemicals

Silver nitrate and potassium iodide were of analytical grade. Potassium nitrate was prepared from potassium hydrogen carbonate with nitric acid and was twice recrystallized. DMSO was twice distilled in vacuum.

Potentiometric measurements

A silver electrode was used as the measuring electrode and an Ag/AgCl electrode as the reference electrode.[2] During the titrations, potassium iodide solution was titrated with silver nitrate solution at 21 ± 0.5°C. Both solutions were adjusted to 0.5 M ionic strength with potassium nitrate. The solution concentration of silver was checked via the known iodide ion concentration by the Gran method, after the break appearing at I/Ag = 1 in the titration curves. The E^o value of the measuring cell was calculated from the measured points at I/Ag < 1, via the Nernst equation. The reference electrode was in contact with the reaction mixture through 0.5 mol dm^{-3} KNO_3 solution separated by sintered glass. The electromotive force of the cell was measured with an accuracy of 0.1 mV with an ORION 701/A potentiometer.

The joint evaluation of 136 experimental points from seven independent series of measurements was performed by the least-squares computer program published previously.[3]

The program calculated with the Nernst factor for the given temperature and the E^o values of the individual titration curves. The log β values yielding the minimum error square sum of the deviations between the measured and calculated emf were calculated by applying unit weighting factors. The standard deviation values given in the tables are $\sigma(\text{mV}) = \sqrt{\sum \Delta h^2/(\text{NMP} - \text{NP} - 1)}$, where NMP is the number of measured points and NP the number of parameters to be refined.

The *spectrophotometric measurements* revealed that the spectra of solutions with compositions $T_I/T_{Ag} < 1.8$ exhibit a maximum at 298 nm and a minimum at 282 nm. In the presence of an iodide ion excess, the spectrum is gradually transformed into a

* The complex Ag_qI_p is denoted by (q, p).

rising but not characteristic one, and after about $T_I/T_{Ag} = 2.4$ no further changes can be observed. Due to the strong interaction between iodide and silver ions, reliable stability constants could not be calculated from the spectrophotometric mole ratio curve.

Preparative work

A white solid complex with the composition $CdAg_6I_8 \cdot 8DMSO$ could be prepared; this precipitated from a concentrated solution of the components at 80°C (0.36 M CdI_2 + 2.13 M AgI + 8 cm^3 DMSO). The percentage analysis data (calculated values in parentheses) are as follows: Cd, 5.0 (4.68); Ag, 26.3 (26.96); I, 42.6 (42.3); DMSO (as difference), 26.3 (26.04).

Thermal examinations

Heating-stage microscopy showed that the crystals melted at 97–98°C and new crystal needles appeared before the old ones had disappeared. On further increasing the temperature, the crystals gradually decomposed and the substance became amorphous. In the course of the derivatographic studies, an endothermic peak appeared at 90°C in the DTA curve, which can be explained by the melting of the complex. Another endothermic peak appeared at 130°C, but this cannot be interpreted reliably and visual observation gives no reason for it. The endothermic peak appearing above 200°C alike in the DTA, DTG and TG curves is due to the cracking of DMSO. There are no signs of the stepwise removal of the solvent molecules.

The IR spectrum of the compound in KBr pellets revealed the S=O valence vibration of DMSO at 1000 cm^{-1}, which is definite proof of the coordination of the solvent molecules via oxygen. In the event of coordination via sulphur, the absorbance line should be at 1100 cm^{-1}.[4] The structural character of the spectrum in the range 1020–1050 cm^{-1} leads to the supposition of the presence also of crystal DMSO.

RESULTS AND EVALUATION OF POTENTIOMETRIC MEASUREMENTS

The potentiometric titration curves are presented in Fig. 1. Two breaks can be observed in the curves. The second one appears at I/Ag = 1, corresponding to the transformation of all the iodide ions into AgI. The first break, at the beginning of precipitation of AgI, is concentration-dependent. As can be seen in Fig. 2, in a solution containing about 2 mM silver it appears at I/Ag = 1.44, and in the presence of about

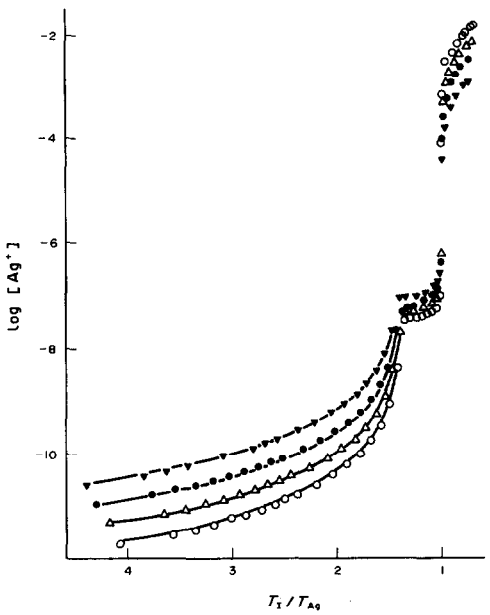


Fig. 1. Potentiometric titration of iodide ions with silver ions in DMSO. Initial iodide concentrations in mol dm^{-3}: (●) 0.00517, (+) and (▽) 0.0127, (▲) 0.0243 and (○) 0.048. The solid curves are those calculated using the constants of column 1 in Table 2.

30 mM silver at I/Ag = 1.36. Independent solubility measurements showed that in 1 mol dm^{-3} silver nitrate solution I/Ag = 1.32 ± 0.01.

Due to the complexity of the system, evaluation of the results of potentiometric measurements was carried out in several steps, different point groups being chosen. When the range I/Ag > 2 was evaluated it was found that complexes (1, 2) and (1, 3) and any polynuclear complexes with stoichiometry I/Ag < 2 were not sufficient to obtain a satisfactory fit. Evaluation with the normalized curves also excluded this supposition. We therefore attempted the introduction of polymers of the species (1, 2), $Ag_2I_4^{2-}$ giving the best fit. Inclusion of species (2, 4) besides (1, 2) reduced the standard deviation to almost two-thirds.

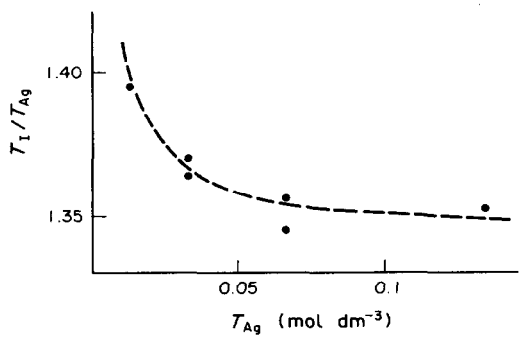


Fig. 2. I/Ag as a function of T_{Ag} at the precipitation of AgI.

Table 1. Results of least-squares refinements using points in the range I/Ag = 1.7–5

	log β values of complexes				σ
	(q, p)	(2, 4)	(1, 2)	(1, 3)	(mV)
(2, 3)	25.00	26.57	12.47	—	7.94
(3, 4)	37.20	26.93	12.79	—	5.49
(4, 6)	52.75	27.49	12.50	14.25	4.47
(5, 7)	64.85	27.33	12.71	—	2.65
(6, 8)	77.20	27.32	12.77	—	3.65
(7, 9)	89.57	27.32	12.80	—	4.76
(7, 10)	92.58	27.50	12.63	—	2.45
(8, 11)	104.94	27.42	12.73	—	3.18
(8, 12)	108.52	27.83	12.32	14.44	3.07

For substantiation of the composition of the potential polynuclear complex, systematic refinements were performed with the measured points in the range I/Ag > 1.7. The results are listed in Table 1. The formation of bi- and trinuclear species could definitely be excluded.

Extending the evaluation for the whole range freee of precipitate (I/Ag = 1.42–5), on the basis of stoichiometry the complex (4, 6) should have also been excluded as dominant species. However, refinements were made with the inclusion of the (4, 6) complex, too. Moreover, the (1, 1) complex was introduced in all evaluations on the assumption that, if its supposition is unnecessary, it will be eliminated through the decrease of its stability constant during the refinement cycles. The final results of this evaluation are presented in Table 2.

DISCUSSION

The potentiometric measurements in the range I/Ag > 2 revealed that this range could be described satisfactorily only by supposing the presence of the species $Ag_2I_4^{2-}$ besides AgI_2^-. The distribution curves in Fig. 3 show that this complex is formed in considerable amount. The presence of AgI_3^{2-} could not be substantiated, but our previous measurements,[1] where I/Ag reached 30–40, gave a reliable value for its stability constant and its formation reached about 40%. Our previous potentiometric measurements on silver bromide system[5] revealed only the predominant formation of $AgBr_2^-$ and $AgBr_3^-$ with log β values of 11.14 ± 0.04 and 12.02 ± 0.1, respectively.

To substantiate the complex(es) with I/Ag < 2, we considered the results of our liquid X-ray measurements[6] in solutions containing about 1 M silver. The differential radial distribution curves obtained (Fig. 4) did not substantiate the presence of complex(es) containing more than six silver atoms; nevertheless, curve A (I/Ag = 1.5) could be described by the supposition of $Ag_4I_6^{2}$, curve B (I/Ag = 2) by that of $Ag_4I_6^{2-}$ and a predominance of $Ag_2I_4^{2-}$, and curve C (I/Ag = 2.67) by that of $Ag_2I_4^{2-}$ and a small amount of AgI_3^{2-}. Sedimentation studies[7] did not point to the formation of species of large molecular weight either.

The data in Table 1 suggest that the supposition of species (5, 7) alone resulted in a satisfactory fit.

Table 2. Results of least-squares refinements using points in the range I/Ag = 1.42–5 (the probable errors in the last digits of the parameters are given in parentheses)

	log β values							
	Present work				Previous work[1]			
Composition of complexes	Without	With E^o correction			Without	With E^o correction		
(1, 1)	7.54	8.02	6.06 (?)	7.97 (15)	—	—	—	—
(6, 8)	76.21	76.14	76.63	76.31 (5)	74.06	74.72	75.12	75.02 (11)
(5, 7)	64.78	64.77	—	64.63 (3)	63.09	63.38	—	62.90 (37)
(4, 6)	—	—	52.36	51.83 (10)	—	—	51.27	51.13 (16)
(2, 4)	27.33	27.29	27.19	27.26 (4)	26.83	26.82	26.69	26.75 (8)
(1, 2)	12.72	12.74	12.70	12.72 (2)	12.34	12.47	12.47	12.47 (2)
(1, 3)	—	—	—	—	13.70	13.77	13.81	13.82 (5)
σ (mV)	2.69	1.07	2.03	0.89	2.7	1.47	1.35	1.22
t (°C)	21.0 ± 0.5				25.0 ± 0.1			

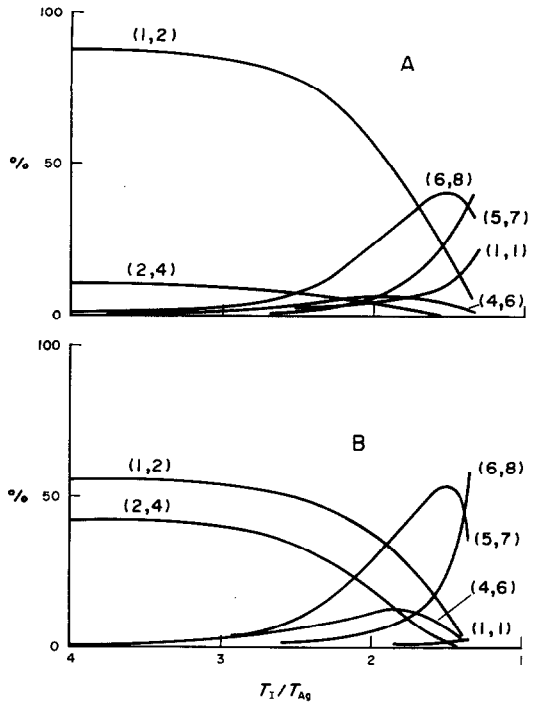


Fig. 3. Percentage distribution of silver in the individual complexes with the constants of column 4 in Table 2. T_{Ag} in mol dm^{-3}; (A) 0.001, and (B) 0.01.

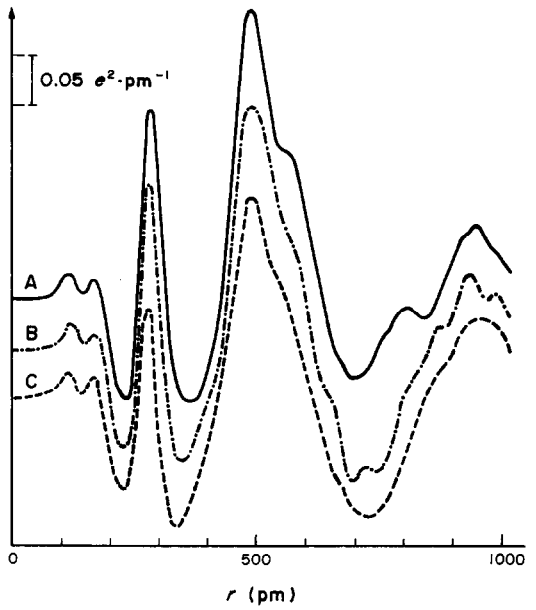


Fig. 4. Differential radial distribution curves. Compositions of solutions in mol dm^{-3}, in the sequence T_{Ag}, T_I and T_{DMSO}: (A) 1.0, 1.5 and 13.2; (B) 1.0, 2.0 and 12.9; and (C) 0.75, 2.0 and 13.0.

However with species (6, 8) as well, the fit improved and the assumption of the species (1, 1) led to a quite sufficient fit. In the course of the refinements, the (1, 1) complex was not eliminated by the program.

The inclusion of the species (1, 1) is disputable, but the concentration-dependence of the precipitation of AgI suggests that in these solutions the dissociation equilibrium of a soluble complex, e.g. $Ag_6I_8^{2-}$, should be considered:

$$Ag_6I_8^{2-} \rightleftarrows Ag_5I_7^{2-} + AgI;$$

$$K_D = [Ag_5I_7^{2-}] \times [AgI]/[Ag_6I_8^{2-}].$$

From the above expression the equilibrium concentration of AgI in solution is:

$$[AgI] = K_D \times \beta_{6,8} \times \beta_{5,7}^{-1} \times [Ag^+] \times [I^-]$$

$$= \beta_{1,1} \times [Ag^+] \times [I^-],$$

i.e. species (1, 1) can be included and K_D can be calculated.

Considering the above aspects, the stability constants obtained from the model (1, 1), (6, 8), (5, 7), (2, 4) and (1, 2) are substantiated in principle. The standard deviations of the measured and calculated values are shown in Table 2, while the calculated emf values are indicated in Fig. 1 with continuous lines. The fit is satisfactory, especially if one considers the measuring conditions, but the individual curves exhibit small systematic deviations. After the permissible and realistic correction of the E^o values for the individual titration curves by 0.5–2 mV these deviations disappeared and the fit can be considered fairly good. As can be seen from Table 2, evaluations were also performed with species (4, 6). The deviation then obtained proved a little better.

According to the models in Table 2, the previous measurements[1] have been re-evaluated. The fit obtained for 100 experimental points from five independent measurements at 25°C is satisfactory with the "rough" experimental data, too. Elimination of the systematic deviations through the E^o corrections resulted in a better fit than expected.

Evaluating our liquid X-ray measurements, we assumed the structure shown in Fig. 5 for the species (4, 6)[6] in a solution with I/Ag = 1.5. It is very likely that further AgI is bound to the two I′ and I″ atoms in the complex, and first $Ag_5I_7^{2-}$ is formed, then $Ag_6I_8^{2-}$. The formation of $Ag_2I_4^{2-}$ on the action of excess iodide ions can be explained if we assume splitting of the Ag--I--Ag bridges in (4, 6).

As a final conclusion of the present and previous

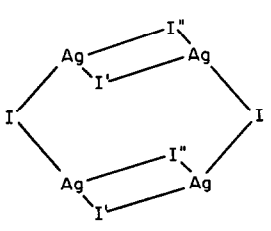


Fig. 5. Proposed structure of the species $Ag_4I_6^{2-}$.

studies, we do not consider the presence of $Ag_3I_4^-$ [8] and $Ag_2I_3^-$ [9] to be substantiated.

Acknowledgements—I express my gratitude to Mrs Mária Palotai for her valuable help in carrying out the experiments and to Dr Gy. Liptay for the thermal examinations.

REFERENCES

1. F. Gaizer, *Magy. Kém. Foly.* 1972, **78**, 54.
2. A. S. Brown, *J. Am. Chem. Soc.* 1934, **56**, 646.
3. F. Gaizer, *Acta Chim. Acad. Sci. Hung.* 1980, **103**, 397.
4. M. J. Bennet, F. A. Cotton and D. L. Weawer, *Nature* 1966, **212**, 286.
5. F. Gaizer and I. Szalay, *Magy. Kém. Foly.* 1972, **78**, 488.
6. F. Gaizer, G. Johansson and P. Sipos, *Collected Abstracts of Symposium on Structures of Liquids and Solutions*, p. 31. Veszprém, Hungary (1984).
7. I. Dékány, to be published.
8. M. Le Démézet, Ch. Madec and M. L'Her, *Bull. Soc. Chim. Fr.* 1970, 365.
9. N. A. Rumbaut and J. L. Peeters, *Bull. Soc. Chim. Belg.* 1967, **76**, 33.

Polyhedron Vol. 4, No. 11, pp. 1915–1923, 1985
Printed in Great Britain

0277–5387/85 $3.00 + .00
© 1985 Pergamon Press Ltd

FOUR- AND FIVE-COORDINATE PALLADIUM(II) COMPLEXES CONTAINING 1,10-PHENANTHROLINE AND ITS 2,9-DIMETHYL DERIVATIVE

SHINSAKU YAMAZAKI*
Chemistry Laboratory, Gakuen College Kochi, Kochi 780, Japan

(*Received* 2 *January* 1985; *accepted after revision* 22 *May* 1985)

Abstract—A series of potentially five-coordinate Pd(II) complexes, $[Pd(PMe_2Ph)_3(2,9\text{-}R_2\text{-}phen)][BF_4]_2$ (R = H or Me; phen = 1,10-phenanthroline), $[PdCl(PPh_3)_2(2,9\text{-}R_2\text{-}phen)]X$ (R = H or Me) and $[PdCl(2,9\text{-}Me_2\text{-}phen)_2]PF_6$ have been obtained from reactions of $[Pd(PMe_2Ph)_4][BF_4]_2$ and $[PdCl(PPh_3)_3]X$ (X = BF_4 or PF_6) with potentially bidentate phen and its 2,9-dimethyl derivative, respectively. By ^1H and $^{31}P\{^1H\}$FT NMR and electronic spectroscopy, these Pd(II) complexes have been characterized. Formally a three-coordinate complex of Pd(II), $[Pd(PR_2Ph)_3]BF_4$ (R = Et or Ph) has also been prepared by treating $[PdCl(PPh_3)_3]BF_4$ and $PdCl_2(PEt_2Ph)_3$ with $AgBF_4$.

Many studies concerning ligand substitution and isomerization of d^8 transition-metal complexes have been directed to monodentate phosphine ligands, especially to PMe_3 and $P(OMe)_3$. In some of these studies five-coordinate intermediates have been isolated and their crystal structures have been determined.[1–13] The systematic kinetics for MX_2L_3 [M = Ni,[1,2] X = CN, Cl or Br, L = PMe_3 or $P(OMe)_3$; M = Pd, Pt,[10] X = Cl, Br or I, L = PMe_3; M = Pt,[11] L = 1-R-3,4-dimethylphosphole, X = Cl, Br or I] have been established by ^{31}P NMR spectroscopy. However, five-coordinate Pd(II) complexes stabilized only by neutral ligands, especially by bulky PPh_3, are elusive. In addition, there have been only a few examples of five-coordinate Pd(II) complexes[5] containing potentially bidentate 1,10-phenanthroline (phen) or its 2,9-dimethyl derivative (2,9-Me_2-phen), and their solution behaviours have not been determined unambiguously compared with those of the corresponding Pt(II) complexes.[9]

The ligand substitution reactions of

$$[Pd(PPh_3)_4]X_2$$

(X = BF_4 or PF_6),[14] $[PdCl(PPh_3)_3]X$[15] and $[Pd(PMe_2Ph)_4][BF_4]_2$ may be expected to proceed comparatively readily due to the presence of bulky phosphines and the low coordination abilities of the anions. Several potentially five-coordinate Pd(II) complexes containing phen or 2,9-Me_2-phen have been prepared from these precursors.

In the five-coordinate Pt(II) complexes of phen so far isolated, it has been found that the crystal structures are mostly distorted square pyramid with elongation of the apical M—N bond length,[5,9] while no dissociation of the phen takes place in solution as evidenced by the observance of a ^{195}Pt satellite. Therefore, it seems that the apical M—N distance of the square-pyramid complex crystallographically determined is not the main factor in dominating its solution behaviour.

In this paper, the preparation and characterisation of potentially five-coordinate Pd(II) complexes are described. Some of the complexes that have been obtained have shown spectra sufficiently explicit to elucidate their dynamic structures. However, firm evidence by low-temperature NMR measurement, to freeze the dynamic motions of the complexes, has not been obtained on account of insufficient solubility. The preparation of the formally three-coordinate complexes of Pd(II), $[Pd(PR_2Ph)_3][BF_4]_2$ (R = Et or Ph), is also described.

EXPERIMENTAL

All the solvents were purified before use by distillation over $CaCl_2$ (CH_2Cl_2 or acetone) or Na (benzene or diethyl ether). Elemental analyses were performed by the Microanalytical Centre, Department of Pharmaceutical Science, Kyoto University. Spectrometers used for NMR studies are; ^1H NMR, JEOL-100; ^{13}C NMR, Hitachi R-900 (22.6 MHz); $^{31}P\{^1H\}$ NMR, JEOL FX-90Q (36.25 MHz) and FX-200 (100.14 MHz), whose measure-

ments were performed by the Applied Research Centre of NM, JEOL Ltd (Akishima). Electroconductivities were measured by a Denki Kagaku Keiki AO-6 instrument in dried acetone. Electronic spectra were obtained in a Hitachi 200-20 spectrometer. All reactions were carried out in air except for the preparation of $[Pd(PPh_3)_4]X_2$ (X = BF_4 or PF_6)[14] which was carried out *in vacuo* or under nitrogen. PMe_2Ph and PEt_2Ph were prepared by the literature procedure.[16]

Chlorotris(triphenylphosphine)palladium(II) complexes, $[PdCl(PPh_3)_3]X \cdot (CH_3)_2CO$ (X = BF_4[15] *or* PF_6)

$[Pd(PPh_3)_4][PF_6]_2 \cdot (CH_3)_2CO$ (0.3 g) was suspended in 30 cm^3 of acetone, and 0.2 g of *t*-BuCl in 3 cm^3 CH_2Cl_2 was added to the solution with vigorous stirring. The suspension dissolved in an hour, and a small amount of a canary yellow solid precipitated. After being stirred overnight, the solution was filtered and the filtrate was reduced in volume to about 10 cm^3 under reduced pressure. Addition of diethyl ether to the solution gave a yellow solid, which was recrystallized from acetone containing roughly an equimolar quantity of PPh_3 to give pale yellow needles of an acetone solvate (0.13 g, 57%). Found: C, 59.8; H, 4.5; Cl, 3.0. Calc. for the empirical formula: C, 60.48; H, 4.54; Cl, 3.14%. IR (Nujol mull): ν(CO) (acetone of solvation), 1707 cm^{-1} (vs). Conductance (in acetone): Λ_M 117 $\Omega^{-1} \cdot cm^2 \cdot mol^{-1}$. The BF_4^- salt was prepared analogously as an acetone or CH_2Cl_2 solvate (98%). Found: C, 60.8; H, 4.5. Calc. for the empirical formula: C, 60.12; H, 4.61%. IR (Nujol mull): ν(CO) (acetone of solvation), 1709 cm^{-1} (vs). ^1H NMR [in $(CD_3)_2SO$]: δ_{CH_2} (CH_2Cl_2 of solvation), 5.75 ppm (s). Conductance (acetone): Λ_M 144 $\Omega^{-1} \cdot cm^2 \cdot mol^{-1}$. The $^{31}P\{^1H\}$ NMR spectra ($CDCl_3$) show the AB_2 spin system at 32.52 (triplet, 1P) and 29.76 (doublet, 2P) ppm relative to 85% H_3PO_4 at 0.00: $J_{P,P}$ = 15.65 Hz.

Tetrakis(dimethylphenylphosphine)palladium(II) tetrafluoroborate, $[Pd(PMe_2Ph)_4][BF_4]_2$

$[Pd(PPh_3)_4][BF_4]_2 \cdot (CH_3)_2CO$ (2.0 g) was suspended in 30 cm^3 of acetone, and an acetone solution of PMe_2Ph (1.1 g) was added to the solution. The yellow mixture gradually dissolved to a pale orange homogeneous solution. The solvent was then removed under reduced pressure, giving an orange oil, which was washed with diethyl ether several times to remove liberated PPh_3 and residual PMe_2Ph. The oil was crystallized from methanol–diethyl ether to give pale yellow crystals (0.8 g, 65%). Found: C, 46.6; H, 5.1; P, 14.1. Calc. for the empirical formula: C, 46.16; H, 5.33; P, 14.88%. Conductance (acetone): Λ_M 224 $\Omega^{-1} \cdot cm^2 \cdot mol^{-1}$. $^{31}P\{^1H\}$ NMR [$(CD_3)_2CO$]: δ_P −5.96 ppm (s).

Tris(dimethylphenylphosphine)(1,10 - phenanthroline) palladium(II) tetrafluoroborate, $[Pd(PMe_2Ph_3(phen)][BF_4]_2$

$[Pd(PMe_2Ph)_4][BF_4]_2$ (0.27 g) was dissolved in acetone (25 cm^3) (partial suspension), and 0.14 g of phen monohydrate (phen · H_2O) was added to the suspension. The yellow mixture gradually dissolved, turning pale yellow, and a small amount of white solid precipitated. After 30 min, the solution was filtered and the solvent was removed under reduced pressure to give a yellow oil. The oil product was washed with 25 ml of diethyl ether to remove liberated PMe_2Ph and dissolved into 5 cm^3 of methanol. The solution was then dropped into 100 cm^3 of *n*-hexane with vigorous stirring, when a yellow crystalline solid was formed. The product was recrystallized from acetone–ethanol (0.13 g, 82%). Found: C, 49.2; H, 4.8; N, 3.1. Calc. for the empirical formula: C, 49.43; H, 4.73; N, 3.20%.

The corresponding 2,9-Me_2-phen complex, $[Pd(PMe_2Ph)_3(2,9\text{-}Me_2\text{-phen})][BF_4]_2$ was prepared analogously (54%). Found: C, 50.0; H, 5.2; N, 3.1. Calc. for the empirical formula: C, 50.56; H, 5.03; N, 3.10%.

Chlorobis(2,9 - dimethyl - 1,10 - phenanthroline)palladium(II) hexafluorophosphate, $[PdCl(2,9\text{-}Me_2Ph)_2]PF_6$

$[PdCl(PPh_3)_3]PF_6 \cdot (CH_3)_2CO$ (0.3 g) was dissolved in 3-pentanone (30 cm^3), and 0.085 g of 2,9-Me_2-phen · $\frac{1}{2}H_2O$ was added to the solution. The yellow mixture slowly became homogeneous and turned orange, giving a small amount of yellow solid. The solution was then filtered, and the filtrate was warmed at 100°C for a few minutes to give brown crystals in insoluble in 3-pentanone (0.06 g, 26%). Found: C, 48.6; H, 3.8; N, 7.5. Calc. for $[PdCl(2,9\text{-}Me_2\text{-phen})_2]PF_6 \cdot \frac{1}{3}(C_2H_5)_2CO$: C, 48.67; H, 3.76; N, 7.65%. IR (Nujol mull): ν(CO) (3-pentanone of solvation), 1710 cm^{-1} (s). ^1H NMR [in $(CD_3)_2SO$]: δ_{Me} (3-pentanone) 0.93 ppm (t); δ_{CH_2} (3-pentanone) 2.40 ppm (q); $J_{H,H'}$ = 7 Hz.

Bis(1,10 - phenanthroline)(triphenylphosphine)palladium(II) tetrafluoroborate, $[Pd(PPh_3)(phen)_2][BF_4]_2 \cdot (CH_3)_2CO$

The preparation of this complex and the PF_6^- salt have been described previously.[14]

Chlorobis(triphenylphosphine)(1,10 - phenantholine) palladium(II) tetrafluoroborate, $[PdCl(PPh_3)_2(phen)]BF_4 \cdot (CH_3)_2CO$

$[PdCl(PPh_3)_3]BF_4 \cdot (CH_3)_2CO$ (0.2 g) was suspended in acetone (20 cm^3), and 0.05 g of $phen \cdot H_2O$ was added to the mixture. The suspension gradually dissolved, turning orange. After 30 min, the solution was reduced in volume to about 5 cm^3 under reduced pressure, and addition of diethylether to the solution gave orange crystals of an acetone solvate (91%). Found: C, 61.5; H, 4.2; H, 2.6; Cl, 3.6. Calc. for the empirical formula: C, 61.77; H, 4.47; N, 2.82; Cl, 3.58%. IR (Nujol mull): ν(CO) (acetone of solvation), 1706 cm^{-1} (s). The PF_6^- salt was prepared analogously as orange crystals (96%). Found: C, 58.4; H, 3.8; N, 2.7; Cl, 3.3. Calc. for the empirical formula: C, 58.13; H, 3.86; N, 2.82; Cl, 3.58%.

Chloro(triphenylphosphine)(trimethylphosphite)(1,10-phenanthroline)palladium(II) tetrafluoroborate, $[PdCl(P(OMe)_3)(PPh_3)(phen)]BF_4$

$[PdCl(PPh_3)_2(phen)]BF_4 \cdot (CH_3)_2CO$ (0.19 g) was dissolved in 20 cm^3 of acetone, and 0.036 g of $P(OMe)_3$ was added to the solution. The orange solution turned pale yellow in a few minutes. The solution was then reduced in volume to 10 cm^3 under reduced pressure, and addition of diethyl ether to the solution gave yellow crystals (0.13 g, 84%). Found: C, 49.6; H, 3.9; N, 3.7. Calc. for the empirical formula: C, 49.84; H, 4.06; N, 3.52%.

Chlorobis(trimethylphosphite)(1,10 - phenanthroline) palladium(II) tetrafluoroborate, $[PdCl(P(OMe)_3)_2(phen)]BF_4$

$[PdCl(PPh_3)_2(phen)]BF_4 \cdot (CH_3)_2CO$ was suspended in 20 cm^3 of acetone containing 0.06 g of PPh_3, and to the solution 0.1 g of $P(OMe)_3$ was added with vigorous stirring, when the orange solution turned off white via pale yellow. The solution was then reduced in volume to about 5 cm^3 under reduced pressure. Addition of diethyl ether to the solution gave a white solid. Recrystallization from ethanol and ether gave off white crystals (0.8 g, 38%). Found: C, 33.6; H, 3.9; N, 4.5. Calc. for the empirical formula: C, 32.90; H, 3.99; N, 4.26%.

Chloro(1,10 - phenanthroline)(triphenylphosphine) palladium(II) hexafluorophosphate, $[PdCl(PPh_3)(phen)]PF_6$

0.3 g of $[PdCl(PPh_3)_3]PF_6 \cdot (CH_3)_2$ CO was suspended in 20 cm^3 of 3-pentanone and an acetone solution of $phen \cdot H_2O$ (0.08 g) was added to the suspension. The mixture slowly dissolved and a yellow solid gradually precipitated. The yellow powder obtained was then filtered and washed with acetone and diethyl ether (0.13 g, 66%). Found: C, 49.1; H, 3.3; N, 3.8. Calc. for the empirical formula: C, 49.40; H, 3.18; N, 3.84%.

Chlorobis(triphenylphosphine)(2,9 - dimethyl - 1,10 - phenanthroline)palladium(II) tetrafluoroborate, $[PdCl(PPh_3)_2(2,9\text{-}Me_2\text{-}phen)]BF_4 \cdot (CH_3)_2CO$

This complex was prepared by an analogous procedure to the corresponding 1,10-phen complex. Recrystallization from warm ethanol–acetone gave an orange crystal of an acetone solvate. Found: C, 62.5; H, 4.8; N, 2.8. Calc. for the empirical formula: C, 62.43; H, 4.75; N, 2.75%. IR (Nujol mol): ν(CO) (acetone of solvation), 1713 cm^{-1} (s). Yield 94%. The PF_6^- salt was prepared analogously (64%). Found: C, 59.3; H, 4.8; N, 2.4. Calc. for the empirical formula: C, 59.06; H, 4.49; N, 2.60%. IR (acetone of solvation): ν(CO) (acetone of solvation), 1709 cm^{-1}.

Tris(triphenylphosphine)palladium(II) tetrafluoroborate, $[Pd(PPh_3)_3][BF_4]_2$

$[PdCl(PPh_3)_3][BF_4] \cdot (CH_3)_2CO$ was dissolved in 30 cm^3 of CH_2Cl_2, and an acetone solution of $AgBF_4$ (0.14 g) was added to the solution. The yellow solution on addition of $AgBF_4$ turned canary yellow and AgCl precipitated. The solution was filtered after an hour and the filtrate was reduced in volume to about 10 cm^3 under reduced pressure. Addition of diethyl ether to the solution gave a canary yellow powder, which was recrystallized from CH_2Cl_2–diethyl ether giving canary yellow crystals (0.4 g, 56%). Found: C, 55.9; H, 4.0. Calc. for $[Pd(PPh_3)_3][BF_4]_2 \cdot \frac{3}{2}(CH_2Cl_2)$: C, 55.81; H, 4.05%. Conductance (acetone): Λ_M 234 $\Omega^{-1} \cdot cm^2 \cdot mol^{-1}$. $^{31}P\{^1H\}$ NMR ($CDCl_3$): δ 38.94 (1P) and 37.86 (2P) ppm. The structure of this complex is uncertain, but may resemble $[Rh(PPh_3)_3]BF_4$.

Tris(diethylphenylphosphine)palladium(II) tetrafluoroborate, $[Pd(PEt_2Ph)_3][BF_4]_2$

$PdCl_2(PEt_2Ph)_2$ (2 g) was suspended in 50 cm^3 of acetone, and 0.66 g of PEt_2Ph was added to the suspension as the yellow mixture dissolved to the deep orange of $PdCl_2(PEt_2Ph)_3$.[8] An acetone solution of $AgBF_4$ (1.57 g) was then added to the solution, when AgCl precipitated. After 10 min, a white precipitate AgCl was filtered, and the solvent was removed under reduced pressure to give a dark

yellow oil. The oil was dissolved in methanol (15 cm^3), and the solution was dropped into diethyl ether (150 cm^3) with vigorous stirring, giving a yellow solid. The product was recrystallized from CH_2Cl_2–diethyl ether to give deep yellow crystals (1.51 g, 43%). Found: C, 41.8; H, 5.4; P, 10.5. Calc. for $[Pd(PEt_2Ph)_3][BF_4]_2 \cdot \frac{3}{2}(CH_2Cl_2)$: C, 41.75; H, 5.34; P, 10.26%. Conductance (acetone): Λ_M 186 $\Omega^{-1} \cdot cm^2 \cdot mol^{-1}$. $^{31}P\{^1H\}$ NMR [$(CD_3)_2CO$)] of this complex shows three resonances at 36.30 (1P, broad singlet), 32.41 (1P, doublet) and 27.78 (1P, doublet) ppm with a formal $J_{P,P}$ of the latter two of 13.7 Hz ^{19}F NMR [$(CD_3)_2CO$]: δ −149.4 ppm (relative to $CFCl_3$ at 0.00). Further details about this complex are now under investigation.

Bis(diethylphenylphosphine)(1,10 - phenanthroline) palladium(II) tetrafluoroborate, $[Pd(PEt_2Ph)_2(phen)][BF_4]_2$

The deep yellow solution of

$$[Pd(PEt_2Ph)_3][BF_4]_2$$

[amount of the precursor, $PdCl_2(PEt_2Ph)_2$, 1.58 g], in acetone was bubbled through with CO for 30 min, while it turned orange. The solution was then added to phen·H_2O (0.62 g) to give grey crystals of $[Pd(phen)_2][BF_4]_2$. The solution was filtered and the solvent of the filtrate was removed under reduced pressure to give a deep green oil. The oil product was dissolved in ethanol, partially giving black Pd metal. After separation of the solid, addition of ethyl ether to the solution gave deep yellow prisms. Found: C, 48.4; H, 5.1; N, 3.3. Calc. for the empirical formula: C, 48.49; H, 4.83; N, 3.53%. Conductivity (acetone): Λ_M 294 $\Omega^{-1} \cdot cm^2 \cdot mol^{-1}$. $^{31}P\{^1H\}$ NMR [$(CD_3)_2CO$]: δ 33.00 ppm (s).

RESULTS AND DISCUSSION

$^{31}P\{^1H\}$ and ^1H NMR and conductivity data of $[Pd(PMe_2Ph)_3(2,9\text{-}R_2\text{-phen})][BF_4]_2$ (R = H or Me) are shown in Fig. 1 and Table 1. The ^{31}P NMR spectrum of the phen complex explicitly shows the typical AB_2 spin system: the ^{31}P doublet appears at a higher field than the ^{31}P triplet with $J_{P,P}$ = 22.79 Hz. In contrast, for the 2,9-Me_2-phen complex the relative positions are reversed and its ^{31}P–^{31}P coupling constant (20.34 Hz) is close to that of the phen complex.

In the five-coordinate Pd(II) and Pt(II) complexes so far studied, $PdX_2(PMe_3)_3$ (X = Br or I),[10] $[M(P(OMe)_3)_5]^{2+}$ (M = Pd or Pt)[1] and PtX_2L_3 (X = Cl, Br and I; L = 1-R-3,4-dimethylphosphole),[11]

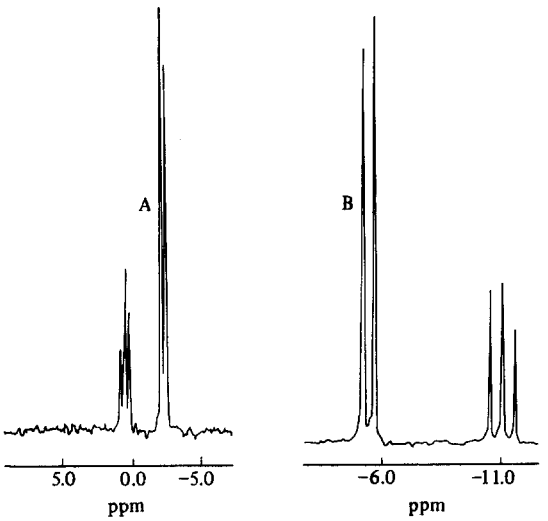


Fig. 1. ^{31}P NMR of: (A) $[Pd(PMe_2Ph)_3(phen)][BF_4]_2$, and (B) $[Pd[PMe_2Ph)_3(2,9\text{-}Me_2\text{-phen})][BF_4]_2$ in $(CD_3)_2CO$.

axial phosphines or phosphites always appear at a higher field than equatorial ones, whereas, in the corresponding Ni(II) complexes, $NiX_2(PMe_3)_3$ (X = CN or Br)[2] and $[Ni\{P(OMe)_3\}_5]^{2+}$,[1] the relative shifts are reversed. On the other hand, in the tetragonal pyramidal $PdCl_2(PMe_3)_3$[10] with one chloride atom in the axial position, the ^{31}P doublet appears at a higher field than the ^{31}P triplet with a larger $J_{P,P}$ than those of the corresponding bromide and iodide complexes.

These estimations for the previous works may be referred to the present case. The NMR spectrum of $[Pd(PMe_2Ph)_3(2,9\text{-}R_2\text{-phen})][BF_4]_2$ (R = H or Me) accordingly fits two idealized structures with one trigonal bipyramid (**A** or **C**) and one tetragonal pyramid (**B** or **D**) as shown in Fig. 2.

^1H NMR of $[Pd(PMe_2Ph)_3(2,9\text{-}Me_2\text{-phen})][BF_4]_2$ shows an equivalency of the two nitrogen atoms of the *N*-heterocyclic ligand, which corresponds to either fluxional motion of the ligand or a symmetrical environment around its halves. In addition, relatively large ^1H NMR downfield shifts for 2,9- and 3,8-protons of the *N*-heterocyclic ligand upon coordination have been observed: 0.84 and 0.45 ppm for the phen complex and 0.95 and 0.47 ppm for the 2,9-Me_2-phen complex, respectively. The coupling pattern of 3,4(7,8)-protons in the 2,9-Me_2-phen complex turns out to be an AB quartet $[J_{A,B}/(\delta_A - \delta_B) = 0.2]$. These downfield shifts for the corresponding protons of the *N*-heterocyclic ligand upon coordination are due to paramagnetic anisotropy of the metal.[17] It should also be noticed that in a seldom ion pair complex, $[Pd(PEt_2Ph)_2(phen)][BF_4]_2$, such a coordination shift of the phen has not been obtained but, rather, a higher field shift, particularly for its 2,9-protons.

Table 1. ^{1}H NMR[a] and conductivity data of $[Pd(PMe_2Ph)_3(2,9\text{-}R_2\text{-phen})][BF_4]_2$ (R = H or Me) and $[Pd(PEt_2Ph)_2(phen)][BF_4]_2$

Complex	Λ_M[b]	*N*-heterocyclic ring (δ)[c]				$J_{H,H}$			PR_2Ph (δ)[c,d] (R = Me or Et)			
		2,9-R	4,7-H	3,8-H	5,6-H	$J_{(8,9)}^{2,3}$	$J_{(7,9)}^{2,4}$	$J_{(7,8)}^{3,4}$	Ring proton	Methyl proton	Methylene proton	$\lvert^2J(P,H)\rvert$
Phen[e]		9.12	8.48	7.76	8.00	4.5	1.5	8.0				
2,9-Me_2-phen		2.80	8.33	7.58	7.83			7.5				
$[Pd(PMe_2Ph)_3(phen)][BF_4]_2$	300	9.96	8.78	8.21	8.08	5.5	2.0	8.0	7.75 (m) 7.03 (m)	2.18 (bd) 1.38 (bs)		
$[Pd(PMe_2Ph)_3(2,9\text{-}Me_2\text{-phen})][BF_4]_2$	278	3.75	8.45	8.05	7.68			8.0	7.80 (m) 6.46 (m)	2.47 (d) 1.63 (t)		9.0 5.0
$[Pd(PEt_2Ph)_2(phen)][BF_4]_2$	294	8.94	8.94	—	8.29				8.04 (m) 7.56	1.24 (m)	2.54 (m)	

[a] Satisfactory relative intensities for each complexes could be obtained: measured in $(CD_3)_2CO$.
[b] Conductivity ($\Omega^{-1} \cdot cm^2 \cdot mol^{-1}$) of *ca* 10^{-3} M acetone solutions.
[c] Chemical shifts are relative to Me_4Si at 0.00.
[d] m, multiplet; d, doublet; t, triplet due to $|J_{P,H}+J_{P',H}|$; s, singlet; bd, broad doublet; bs, broad singlet.
[e] Measured in $(CD_3)_2SO$.

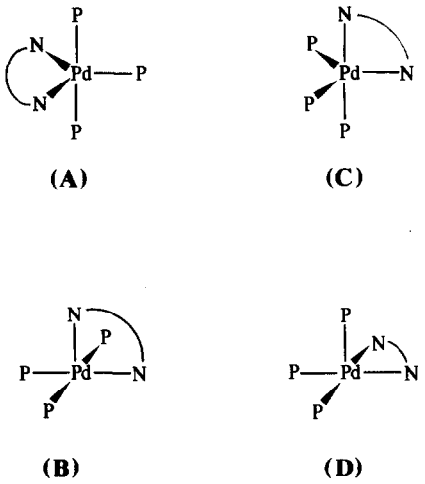


Fig. 2. Possible structures of $[Pd(PMe_2Ph)_3(2,9\text{-}R_2\text{-phen})][BF_4]_2$.

Some physical properties of $[PdCl(PPh_3)_2(2,9\text{-}R_2\text{-phen})]X$ (R = H or Me; X = BF_4 or PF_6) are given in Table 2.

The conductivity data of the complexes evidently indicate that dissociation of Cl or association of the anion does not occur in acetone solution.

^{31}P NMR spectral data of the complexes show a single resonance, which is consistent with an equivalency of the two PPh_3 ligands. ^1H NMR spectra of them also show an equivalency of the two nitrogen atoms of the *N*-heterocyclic ligand. These NMR data indicate either symmetrical environments around both the phosphines and the halves of the *N*-heterocyclic ligand or a rapid dynamic motion which may average the respective nuclei equivalently. Low-temperature NMR data could not be obtained on account of the insufficient solubility of the complexes. Any fluxional motion of $[PdCl(PPh_3)_2(2,9\text{-}Me_2\text{-phen})]X$ (X = BF_4 or PF_6), however it might occur, will be expected to be considerably restricted because of the steric crowdedness of the ligand compared to the corresponding phen complex.

The visible spectrum of $[PdCl(PPh_3)_2(phen)]PF_6$ is shown in Fig. 3, together with those of square-planar complexes, $[PdCl(PPh_3)(phen)]PF_6$ and $[Pd(PEt_2Ph)_2(phen)][BF_4]_2$. The spectrum of $[PdCl(PPh_3)_2(phen)]PF_6$ (quite analogous to that of the BF_4^- salt) with two electronic transitions at 355 and 338 nm unexpectedly shows a marked resemblance to those of the square-planar complexes, the absorptions of which may be concerned with charge-transfer bands (M → L or L → M)[8] possibly combined with a $d \rightarrow d$ transition.[18] Any characteristic absorption bands previously found for five-coordinate Pt(II) and Pd(II)[19] complexes have not been observed in the longer-wavelength region for the present case, and the $d \rightarrow d$ transition has not been resolved.

Direct evidence of the solution structure of $[PdCl(PPh_3)_2(phen)]PF_6$ has been minor. However, the electronic spectral data of the complex seem indicative that the geometry in solution is likely close to a square-planar conformation in which one nitrogen atom of the phen might be approaching to the coordination sphere from the fifth or sixth apical site of the coordination plane. The fluxional motion of the complex is accordingly explained as a rapid oscillation of the phen as observed in Pd(dmp)(2,9-Me_2-phen)(NO_3) (dmp = *N*,*N*-dimethylbenzylamine).[20]

On the other hand, the visible spectrum of $[PdCl(PPh_3)_2(2,9\text{-}Me_2\text{-phen})]PF_6$ is, as expected, different from that of the corresponding phen complex and it shows a broad and intensive electronic transition at 360 nm which is most probably caused by five coordination.

$[PdCl(PPh_3)_2(phen)]PF_6$ did not convert to $[PdCl(PPh_3)(phen)]PF_6$ but was recovered whether it had been warmed in acetone or in ethanol solution. The reaction of $[PdCl(PPh_3)_2(phen)]BF_4$ with $P(OMe)_3$ proceeds via a successive displacement of PPh_3 by $P(OMe)_3$ to give

$$[PdCl\{P(OMe)_3\}(PPh_3)(phen)]BF_4$$

and

$$[PdCl\{P(OMe)_3\}_2(phen)]BF_4.$$

The ^1H NMR spectra of both phosphite complexes similarly show an equivalency between the two nitrogen atoms of the phen. The ^1H NMR of the bis-phosphite complex shows two doublets due to Me-protons of the $P(OMe)_3$ ligand, which is consistent with two mutually *cis*-$P(OMe)_3$. The ^1H NMR coordination shifts for 2,9-protons of the phen have been obtained in these cases; 0.60 ppm for the bis-phosphite complex and 0.53 ppm for the mono-phosphite complex.

The visible spectral data for the phosphite complexes are shown in Table 3, together with the other complexes that I have obtained. The spectra of the phosphite complexes, analogously to the bis-phosphine complex, resemble considerably those of the square-planar complexes. Consequently, the solution structure of the bis-phosphite complex, in analogy with the bis-phosphine complex, is likely tetragonal pyramid, possibly approaching a square-planar conformation in which the two $P(OMe)_3$ are *cis*. The solution structure of the mono-phosphite complex (pale yellow) may be analogous to the bis-phosphite complex, while an enantiomer of this complex is uncertain.

Table 2. NMR and conductivity data

Complex	Λ_M[a]	^{1}H NMR[b] δ(*N*-heterocyclic ring proton) 2,9-R	4,7-H	5,6-H	3,8-H	$J_{2,3}$	$J_{2,4}$	$J_{3,4}$	P(OMe)$_3$ δ_{Me}	$J_{P,H}$	^{31}P{^{1}H} NMR[c] δ_{PPh_3}	δ_{PF_6}	^{19}F NMR[d] δ_F	$J_{P,F}$
$[PdCl(PPh_3)_2(phen)]BF_4$	167	9.20	8.73	8.12	7.84	4.8	1.3	8.4			16.56		−218.76	
$[PdCl(PPh_3)_2(phen)]PF_6$	152	9.41	8.60	7.99	7.80	5.3	2.0	8.8			17.63	−145	−67.69	708
$[PdCl(P(OMe)_3)(PPh_3)(phen)]BF_4$	152	9.65	8.65	8.05	7.94	6.0	2.0	8.8	3.78	10.0				
$[PdCl(P(OMe)_3)_2(phen)]BF_4$		9.72	8.96	8.25	8.05	5.0		9.0	4.08 3.74	11.0				
$[PdCl(PPh_3)_2(2,9\text{-}Me_2\text{-}phen)]BF_4$	159	2.95	8.25	7.78	—[e]			6.7			14.40			
$[PdCl(PPh_3)_2(2,9\text{-}Me_2\text{-}phen)]PF_6$	153	2.94	8.23	7.78	—[e]			7.0			11.04			
$[PdCl(2,9\text{-}Me_2\text{-}phen)_2]PF_6$		2.79	8.78	8.20	7.90			8.0						

[a] Conductivity ($\Omega^{-1} \cdot cm^2 \cdot mol^{-1}$) of *ca* 10^{-3} M acetone solution.
[b] Measured in $(CD_3)_2CO$. Chemical shifts are relative to Me_4Si at 0.00.
[c] Measured in $(CD_3)_2SO$. Chemical shifts are relative to H_3PO_4 at 0.00.
[d] Measured in $(CD_3)_2SO$. Chemical shifts are relative to $CFCl_3$ at 0.00.
[e] Obscured owing to overlapping with the resonances of PPh_3.
[f] Measured in $(CD_3)_2SO$.

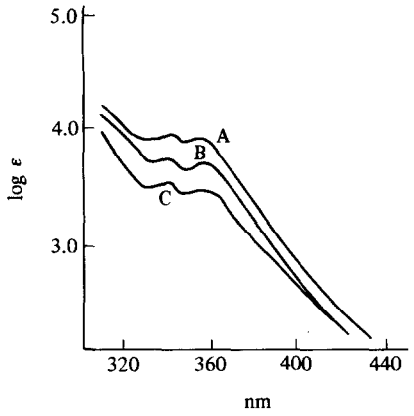
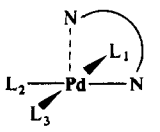


Fig. 3. Visible spectra of : (A) $[PdCl(PPh_3)(phen)]PF_6$, (B) $[PdCl(PPh_3)_2(phen)]PF_6$, and (C) $[Pd(PEt_2Ph)_2(phen)][BF_4]_2$.



$L_1 = L_3 = PPh_3$; $L_2 = Cl$
$L_2 = L_3 = P(OMe)_3$; $L_1 = Cl$
$L_2 = PPh_3$; $L_3 = P(OMe)_3$; $L_1 = Cl$

The ^1H NMR of $[Pd(PPh_3)(phen)_2][PF_6]_2$ and $[PdCl(2,9\text{-}Me_2\text{-}phen)_2]PF_6$ show that all four nitrogen atoms of the two *N*-heterocyclic ligands are equivalent, which corresponds to fluxional motion.

For $[Pd(PPh_3)(phen)_2][PF_6]_2$, there are ^1H NMR signals broadening below $-50°C$ and even at $-100°C$ no sharp limiting spectrum could be obtained, while, on addition of free phen to $[Pd(PPh_3)(phen)_2][PF_6]_2$ at room temperature, signal broadening is observed with a pattern similar to that obtained at lower temperatures and no separate signals could be obtained. These ^1H NMR spectral data of $[Pd(PPh_3)(phen)_2][PF_6]_2$ may suggest that inter- or intramolecular exchange of phen readily occurs.

An intramolecular ligand rearrangement system of this type of five-coordinate complexes has so far been proposed in which the fluxional motion of $[Pt(CN)(phen)_2]NO_3$ has been explained by pseudorotation with a trigonal-bipyramid transition state, while that of

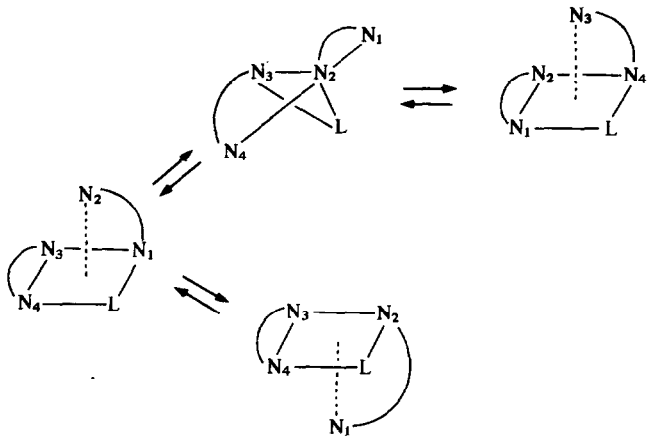
$[M(hfac)_2\{P(o\text{-tolyl})_3\}]$ (M = Pd or Pt; hfac = 1,1,1,5,5,5-hexafluoroacetylacetone)[21]

has been best rationalized by two rapid equilibria of twist motion and concurrent oscillation. For both cases, the mechanism of the fluxional motions has noticeably been proposed not to be dissociative, since the ^{195}Pt satellite has been observed.

The fluxional motion of the present complexes is sufficiently explained by two synchronous rearrangement systems as proposed for $[Pd(hfac)_2\{P(o\text{-tolyl})_3\}]$: one is a rapid oscillation of the apical phen which may result to average its two nitrogen atoms and the other is a twist motion of the square pyramid which may average the environments between the two *N*-heterocyclic ligands equivalently as shown in Scheme 1. The visible spectral data of $[Pd(PPh_3)(phen)_2][PF_6]_2$ and $[PdCl(2,9\text{-}Me_2\text{-}phen)_2]PF_6$ similarly show three absorption maxima, two of which are at 338–360 nm, with a resemblance to those of square-planar complexes, and the latter at 400–430 nm is now comparable with the characteristic absorptions of $PdX_2(PMe_2Ph)_3$ (X = Cl or Br)[8] at 410–444 nm. It is roughly indicated from these spectral data that the solution structure of $[PdY(2,9\text{-}R_2\text{-}phen)_2][PF_6]_{1\text{ or }2}$ (Y = PPh_3 or Cl; R = H or Me) is tetragonal pyramid with one nitrogen atom of the phen possibly at the

Table 3. Electronic spectral data in visible region

Complex	λ_{max} (ε)		
$[PdCl(PPh_3)_2(phen)]X$ (X = BF_4 or PF_6)	338 (4840)	355 (4560)	
$[PdCl(P(OMe)_3)(PPh_3)(phen)]BF_4$	338 (3750)	355 (2500)	
$[PdCl(P(OMe)_3)_2(phen)]BF_4$	338 (2210)	355 (1080)	
$[PdCl(PPh_3)_2(2,9\text{-}Me_2\text{-}phen)]X$ (X = BF_4 or PF_6)		360 (19,500, br)	
$[PdCl(PPh_3)(phen)]PF_6$	338 (8200)	355 (7290)	
$[Pd(PEt_2Ph)_2(phen)][BF_4]_2$	338 (3290)	355 (2840)	
$[Pd(PMe_2Ph)_3(phen)][BF_4]_2$	347 (3195, sh)	385 (841)	
$[Pd(PMe_2Ph)_3(2,9\text{-}Me_2\text{-}phen)][BF_4]_2$	325 (23,800, br sh)		412 (1060)
$[PdCl(2,9\text{-}Me_2\text{-}phen)_2]PF_6$	340 (3195, sh)	360 (2330)	400 (940)
$[Pd(PPh_3)(phen)_2]X_2$ (X = BF_4 or PF_6)	338 (5000, sh)	355 (3690)	430 (540)



Scheme 1.

apical position. Thus, the proposed fluxional behaviour of these complexes is based on the crystal structure of $[Pt(CN)(phen)_2]NO_3$[9] with a distorted square pyramid.

Acknowledgement—I am grateful to Dr K Hata (JEOL Ltd) for obtaining $^{31}P\{^1H\}FT$, ^{19}F and ^1HFT NMR spectra.

REFERENCES

1. P. Meakin and J. P. Jesson, *J. Am. Chem. Soc.* 1974, **96**, 5751.
2. P. F. Meier, A. E. Merbach, M. Dartiguenave and Y. Dartiguenave, *Inorg. Chem.* 1979, **18**, 610.
3. C. V. Senoff, *Inorg. Chem.* 1978, **17**, 2320.
4. A. D. Westland, *J. Chem. Soc.* 1965, 3036.
5. G. W. Bushnell, K. R. Dixon and M. A. Khan, *Can. J. Chem.* 1974, **52**, 1367.
6. B. A. Frenz and J. A. Ibers, *Inorg. Chem.* 1972, **11**, 1109; S. J. L. Placa and J. A. Ibers, *Acta Cryst.* 1965, **18**, 511.
7. P. E. Garrow, J. L. S. Curtis and G. E. Hartwell, *Inorg. Chem.* 1976, **12**, 3094.
8. W. J. Louw, D. J. A. Waal and G. J. Kruger, *J. Chem. Soc., Dalton Trans.* 1976, 2364.
9. O. Wernberg and A. J. Hazell, *J. Chem. Soc., Dalton Trans.* 1980, 973.
10. R. Favez and R. Roulet, *Inorg. Chem.* 1981, **20**, 1598; R. Favez, R. Roulet, A. A. Pinkerton and D. Schwarzenbach, *Inorg. Chem.* 1980, **19**, 1356.
11. J. J. MacDougall, J. H. Nelson and F. Mathey, *J. Am. Chem. Soc.* 1982, **21**, 2145.
12. P. Overbosch, G. van Koten, D. M. Grove and A. L. Spek, *Inorg. Chem.* 1982, **21**, 3253.
13. G. K. Anderson and R. J. Gross, *J. Chem. Soc., Dalton Trans.* 1980, 1988.
14. S. Yamazaki, *Inorg. Chem.* 1982, **21**, 1638.
15. K. R. Dixon and D. J. Hawke, *Can. J. Chem.* 1971, **49**, 3252.
16. M. A. Mathur, W. H. Myers, H. H. Sisler and G. E. Ryschkewitsch, *Inorg. Synth.* 1974, **XV**, 132; V. D. Bianco and S. Doronzo, *Inorg. Synth.* 1978, **XVIII**, 170.
17. R. G. Millar, R. D. Stauffer, D. R. Fahey and D. R. Parnell, *J. Am. Chem. Soc.* 1970, **92**, 1511.
18. K. R. Dixon and A. D. Rattray, *Can. J. Chem.* 1973, **51**, 618.
19. O. St. C. Headley, R. S. Nyholm, C. A. McAuliffe, L. Sindellari, M. L. Tobe and L. M. Venanzi, *Inorg. Chim. Acta* 1970, **5**, 93.
20. A. J. Deeming, I. P. Rothwell, M. B. Hursthouse and L. New, *J. Chem. Soc., Dalton Trans.* 1978, 1490.
21. S. Okeya, T. Miyamoto, S. Ooi, Y. Nakamura and S. Kawaguchi, *Bull. Chem. Soc. Jpn* 1984, **57**, 395.

Polyhedron Vol. 4, No. 11, pp. 1925–1928, 1985
Printed in Great Britain

0277–5387/85 $3.00 + .00
© 1985 Pergamon Press Ltd

X-RAY PHOTOELECTRON SPECTROSCOPIC AND MAGNETIC SUSCEPTIBILITY STUDY OF *CIS*-BIS ETHYLENEDIAMINOALKYLAMINO NITRITO COBALT(III) NITRATE

S. SRIVASTAVA
Coordination Group, C.S.M.C.R.I., Bhavnagar-364002, India

(*Received* 6 *March* 1985; *accepted after revision* 22 *May* 1985)

Abstract—X-ray photoelectron spectra of *cis*-$[Co(en)_2(RNH_2)(NO_2)](NO_3)_2$ complexes, where R = CH_2CHCH_2, CH_3, *n*-C_2H_5, *n*-C_4H_9, *n*-C_5H_{11} and C_6H_{13} have been recorded on a VG scientific ESCA-3MK II electron spectrometer to study the relative covalent bonding between the metal ion and the alkylamine group (RNH_2) and to study the degree of π-back bonding from metal to ligand nitrite. The magnetic susceptibility of all these complexes was also measured by the Faraday method at room temperature.

Since the advent of electron spectroscopy for chemical analysis (ESCA)[1,2] there has been considerable interest in studying transition-metal complexes using this technique.

Jolly *et al.*[3] studied the *trans*-$[Co(en)_2(NO_2)_2]NO_3$ complex and reported three peaks corresponding to the three different nitrogen environments. The complexes chosen for the present study contain a nitrogen atom in four different electronic environments. Such systems are being reported for first time. Moreover, the basicity of the substituent amine is likely to affect the energies of the nitrogen–metal bonds and also π-back bonding from the metal to the nitrite ligand. The present communication covers the above-mentioned cases.

EXPERIMENTAL

Preparation of complexes

Trans - dichloro - *bis* - (ethylenediamine)cobalt(III) chloride, *trans*-$[Co(en)_2Cl_2]Cl$, was prepared by the reported procedure.[4] It was converted to *cis*-chloro(alkylamine)-*bis*-(ethylenediamine)cobalt(III) chloride, *cis*-$[Co(en)_2RNH_2Cl]Cl$ and finally to the nitrate, *cis*-$[Co(en)_2RNH_2Cl]NO_3$, by the following general procedure.[5]

11.5 g of *trans*-$[Co(en)_2Cl_2]Cl$ in 5 cm^3 water was triturated with an equimolar amount of alkylamine. Ethanol was added to the deep red solution to precipitate the complex. The precipitate was dissolved in a small amount of water, cooled to 0°C and a few drops of conc. HCl was added. The product was washed with ethanol and ether and crystallised twice from a very dilute aqueous solution of HCl. The conversion to nitrate was carried out by dissolving the chloride complex in a small amount of water, and adding conc. HNO_3. On cooling to 0°C, fine red crystals of the nitrate separated out, which were washed with methanol and ether, and dried.

It was then converted to *cis*-nitro(alkylamine)-*bis*-(ethylenediamine)nitrate:

$$cis\text{-}[Co(en)_2RNH_2NO_2](NO_3)_2$$

by the following procedure:

7.4 g of the above product was dissolved in water and 1.4 g $NaNO_2$ was added. On trituration for 15 min an orange–red product was formed. It was filtered, washed with methanol and ether, and was recrystallised twice from water (50°C) containing a few drops of HNO_3. The estimation of cobalt and the nitro group conformed to the formula $[Co(en)_2(RNH_2)(NO_2)](NO_3)_2$. All the compounds in this show fairly similar physical and spectral characteristics.

The red complexes show two absorption bands at ~370 and ~445 nm with molar absorptivities of ~330 and 120 l mol^{-1} cm^{-1} respectively.

Recording of spectra

The X-ray photoelectron spectra (XPS) were recorded on a VG Scientific ESCA-3MK II electron

spectrometer. The Mg-K_α X-ray line (1253.6 eV) was used for photoelectron excitation.

The Cu($2p_{3/2}$) (Eb 932.8 ± 0.2) and Au($4f_{7/2}$) (Eb 83.3 ± 0.1) lines were used to calibrate the instrument and Ag($3d_{5/2}$) (Eb 368.2) was used for cross-checking.[6]

All spectra were recorded using the same spectrometer parameters of 50 eV pass energy and 4 mm slit width. The reduced full width at half maximum for Au($4f_{7/2}$) (Eb 84.0 eV) level under these conditions was 1.2 eV.

The powdered sample was mixed with high-purity silver powder to reduce the charging effect. A thin layer of such a sample was pressed on a gold metal gauze which was welded to a nickel sample holder. The Ag($3d_{5/2}$) level (Eb 368.2 eV) obtained from this sample was sharp and did not show any observable shift. Thus the charging of the samples, if at all present, was negligible.[7] The spectra were recorded in triplicate in the region of interest. In most cases the binding energies were reproducible within ± 0.1 eV. The usual least-squares fitting procedure of determining peak position, line widths and area was used.

Measurement of magnetic susceptibility

Magnetic susceptibility was measured by the Faraday method using a Cahn Magnetic susceptibility system. $Hg[Co(CNS)_4]$ was used as a standard for calibration.[8]

RESULTS AND DISCUSSION

The measured $Co2p_{1/2}$ and $Co2p_{1/2}$ binding energies in *cis*-$[Co(en)_2(RNH_2)(NO_2)](NO_3)_2$ are listed in Table 1 (Fig. 1). It may be seen that $Co2p_{1/2,3/2}$ binding energies are maximum for C_1 and minimum for C_6 when R is an alkyl group (CH_2CHCH_2 does not fall in this sequence). Using Siegbahn *et al.*s generalization[1,2] one may therefore conclude that the maximum effective positive charge on the cobalt ion is for C_1 and minimum in the case of C_6. The decreasing order of effective positive charge in these complexes is $C_1 > C_2 > C_4 > C_5 > C_6$. It is clear that the electron-donating ability of the RNH_2 group increases with increasing number of carbon atoms in "R". It is also clear that the presence of a double bond in R(CH_2CHCH_2) decreases its electron-donating capability. These XPS data may also be taken to suggest that bond between cobalt ion and RNH_2 is more covalent in C_6 and least in C_1. The decreasing order of covalent character in these complexes is $C_1 < C_2 < C_4 < C_5 < C_6$. In the case of $CH_2CHCH_2NH_2$ the presence of a double bond makes it even lower than C_1.

Table 1. Binding energies (eV) of cobalt ion, N1*s* in and magnetic susceptibilities of *cis*-$[Co(en)_2(RNH_2)(NO_2)](NO_3)_2$ complexes[a]

Complex *cis*-$[Co(en)_2(RNH_2)(NO_2)](NO_3)_2$ R	Cobalt ion		N1*s*			Magnetic susceptibility (cm g^{-1})
	$Co2p_{1/2}$	$Co2p_{3/2}$	(en + RNH_2)	NO_2	NO_3	
CH_2CHCH_2	800.4	785.0	404.2	408.6	411.0	-2.370×10^{-6}
	(2.0)	(4.0)	(3.0)	(2.8)	(2.4)	
CH_3	798.4	783.2	401.8	406.2	408.2	-2.229×10^{-6}
	(3.2)	(2.4)	(2.4)	(2.4)	(2.2)	
C_2H_5	798.0	783.0	401.3	405.8	407.9	-5.543×10^{-6}
	(3.2)	(2.24)	(2.24)	(2.4)	(2.2)	
n-C_4H_9	797.8	782.8	401.4	405.8	407.8	-1.829×10^{-6}
	(3.2)	(3.2)	(2.4)	(2.4)	(2.2)	
n-C_5H_{11}	797.6	782.6	401.2	405.6	407.6	-4.026×10^{-6}
	(3.2)	(2.4)	(2.4)	(2.4)	(2.2)	
n-C_6H_{13}	797.4	782.4	398.4	402.8	405.2	-2.550×10^{-6}
	(3.2)	(2.8)	(2.4)	(2.4)	(2.2)	

[a] Full width at half maximum is given in parentheses.

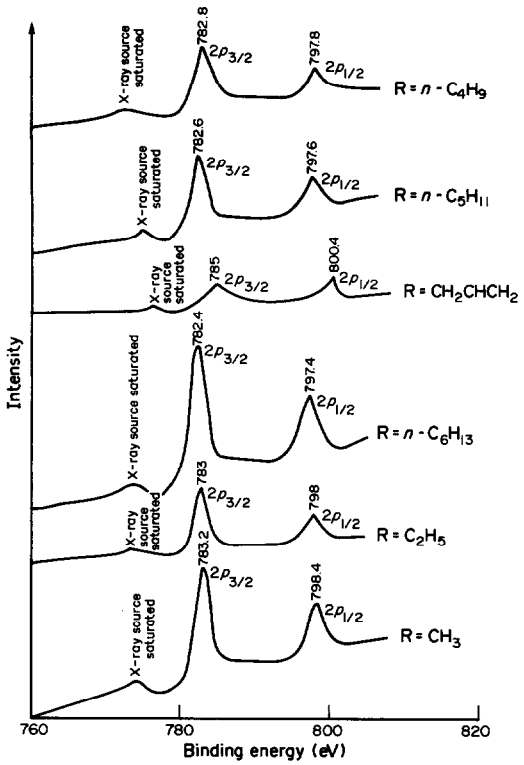


Fig. 1. $Co2p_{3/2}$ and $Co2p_{1/2}$ photoelectron peaks in *cis*-$[Co(en)_2RNH_2NO_2](NO_3)_2$.

Our magnetic susceptibility measurements (Table 1) show that all these complexes are diamagnetic.

Jolly *et al.*[3] found three N1*s* peaks for three nitrogen environments which are placed in different chemical environments in *trans*-$[Co(en)_2(NO_2)_2]NO_3$ complex at 401, 404 and 406.5 eV for ethylenediamine, nitrite and the nitro group respectively. In our study of N1*s* spectra of *cis*-$[Co(en)_2(RNH_2)(NO_2)](NO_3)_2$ complexes the nitrogen of ethylenediamine and the RNH_2 group coincide and give only three peaks with intensity ratio 5 : 1 : 2 (as shown in Fig. 2 for a few complexes). In the study of the N1*s* of the nitrite group, we observed the maximum binding energy value for C_1 and the minimum value for C_6 (see Table 1). From these XPS data we can conclude that π-back bonding from a filled metal ion orbital to a vacant antibonding ligand (NO_2) orbital is least for C_1 and increases towards C_6. The increasing order of π-back bonding in these complexes is $C_1 < C_2 \leqslant C_4 < C_5 < C_6$. When R is CH_2CHCH_2 the back bonding is minimal even lower than in the case of C_1. Thus one may conclude that, as the electron transfer from RNH_2 to the metal ion increases, the electron transfer from the metal ion to nitrogen (NO_2) through π-back bonding also increases.

Acknowledgements—I am thankful to CSIR, New Delhi, for the award of a fellowship. Thanks are also due to Dr A. P. B. Sinha, Head, Physical Chemistry Division, N.C.L., Poona-8, India, for the facilities given during this work.

REFERENCES

1. K. Siegbahn, C. Nordling, A. Fahlman, R. Nordberg, H. Hamrin, J. Hedman, G. Johnson, T. Bergmark, S. K. Karlsson, I. Lindgren and B. Lindberg, *ESCA, Atomic,*

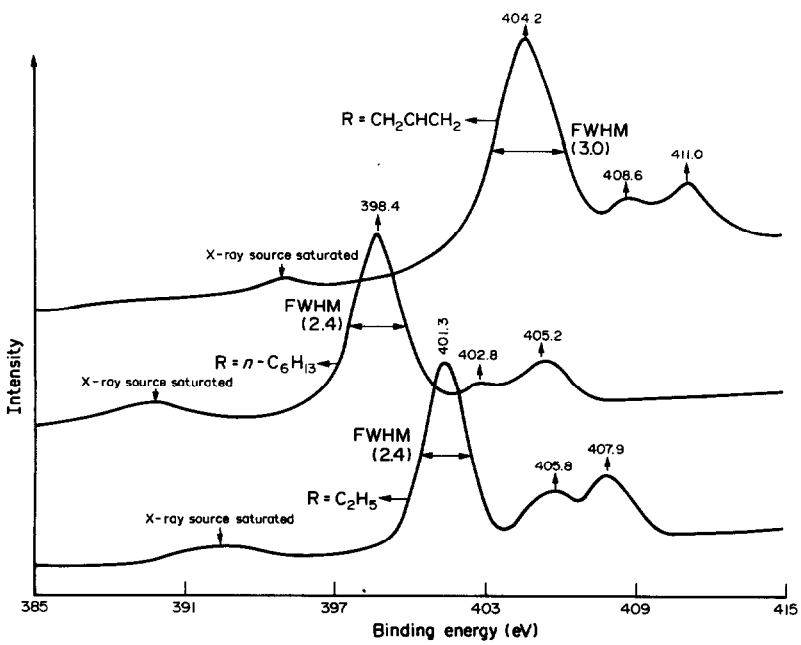


Fig. 2. XPS of *cis*-$[Co(en)_2RNH_2NO_2](NO_3)_2$(FHWM = full width at half maximum).

Molecular and Solid-State Structure by Means of Electron Spectroscopy. Almquist & Wiksell, Uppsala (1967).
2. K. Siegbahn, C. Nordling, G. Johnson, J. Hedman, P. Hedan, K. Hamrin, U. Gelius, T. Bergmark, L. Werme, R. Manne and Y. Baer, *ESCA, Applied to Free Molecules.* North-Holland, Amsterdam (1969).
3. W. L. Jolly, D. N. Hendrickson and J. M. Hollander, *Inorg. Chem.* 1969, **8**, 2642.
4. J. C. Bailar and L. B. Clapp, *J. Am. Chem. Soc.* 1945, **67**, 171.
5. J. C. Bailar, In *Inorganic Synthesis* (Edited by W. C. Fernelius), 1946, **2**, 222.
6. S. Evans, *Handbook of X-ray and Ultra-violet Photoelectron Spectroscopy* (Edited by Briggs), p. 128. Hayden, Rochelle Park, NJ (1975).
7. W. Jolly, *Coord. Chem. Rev.* 1974, **13**, 47.
8. Räde, *J. Phys. Chem.* 1973, **77**, 424.

Polyhedron Vol. 4, No. 11, pp. 1929–1939, 1985
Printed in Great Britain

0277–5387/85 $3.00 + .00
© 1985 Pergamon Press Ltd

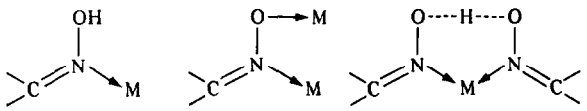
TRANSITION-METAL CHEMISTRY OF OXIME-CONTAINING LIGANDS—XXVII. FIVE- AND SIX-COORDINATE COMPLEXES OF IRON(II) AND IRON(III) WITH 2,6-DIACETYLPYRIDINE DIOXIME

MADAN MOHAN* and MUNESH KUMAR
Department of Chemistry, N.R.E.C. College, Khurja-203 131 (U.P.), India

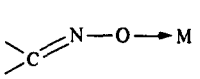
(*Received* 20 *June* 1984; *accepted after revision* 22 *May* 1985)

Abstract—Iron(II) and iron(III) complexes of 2,6-diacetylpyridine dioxime (H_2dapd) have been prepared and their electronic and structural properties investigated. The $[Fe(H_2dapd)X_2]$ (X = Cl, Br or I) are essentially monomeric five-coordinate complexes, whereas the $[Fe(H_2dapd)X_2]$ (X = NCS or NCSe) are polymeric, anion-bridged, six-coordinate complexes. The $[Fe(H_2dapd)_2](ClO_4)_2$ is a high-spin, distorted six-coordinate complex. The $[Fe_2(Hdapd)_2X_4]$ (Hdapd = anion of H_2dapd, X = Cl, Br, I, NCS or NCSe) are dimeric, high-spin, anion bridged, five-coordinate complexes, whereas $[Fe_2(Hdapd)_2O(NO_3)_2]$ is a dimeric, low-spin, oxygen-bridged five-coordinate complex. Intermolecular antiferromagnetic exchange interactions are present in these binuclear iron(III) complexes, where the exchange parameter varies from -9.7 to -7.0 cm^{-1} in $[Fe_2(Hdapd)_2X_4]$ complexes and is -102.0 cm^{-1} for the $[Fe_2(Hdapd)_2O(NO_3)_2]$ complex. The complexes exhibit asymmetric quadrupole-split doublets in their ^{57}Fe Mössbauer spectra. The asymmetries are found to be temperature-dependent with a relatively symmetric doublet seen at low temperatures.

Oximes are well known for their high coordinating abilities and versatile behaviour,[1] but much remains to be learned about the types of structures that are formed as well as the factors that dictate structure. In general, the oxime function coordinates to metal ions in four ways:



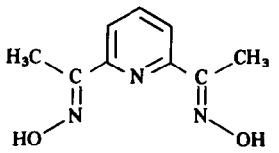
1 2 3



4

Coordination modes 1 and 3 are quite common among metal complexes but it should be noted that the oxime function is a poor donor unless it is part of a chelate ring.

2,6-Diacetylpyridine dioxime, H_2dapd (5), which possesses structural features in common with both the 2,2′,2″-terpyridyl (terpy) and the dimethylglyoxime ligand, is a particularly interesting chelating oxime ligand. H_2dapd was first investigated by Hanania *et al.*[2] who studied its Fe(II) complex in solution. They observed[2] that the pK_a for



H_2dapd

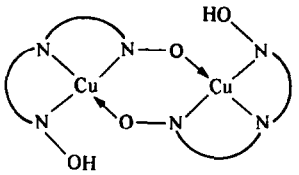
5

the ligand dropped markedly upon coordination, an effect that was attributed to resonance stabilization of anionic oxime conjugate base (=N—Ō). Following Hartkamp's report[3] that aqueous Ni(II) solutions of H_2dapd are oxidised by air, Baucum and Drago[4] isolated several complexes, including $[Ni(H_2dapd)_2](ClO_4)_2$, $Na_2[Ni(dapd)_2]$ and the oxidised complex, $[Ni(dapd)_2]$, believed to contain Ni(IV). It is argued[4] that the higher oxidation state of

* Author to whom correspondence should be addressed.

nickel is favoured by localized accumulation of negative charges on donor atoms and by the formation of strong metal–ligand σ-bonds. Subsequently Sproul and Stucky reported[5] the X-ray crystal structure of $[Ni(dapd)_2]$ and found that the ligand is a planar NNN donor chelating agent and that considerable strain is developed in the $dapd^{2-}$ moiety when it coordinates to nickel.

Recently Nicholson *et al.*[6] isolated the monomeric five-coordinate complex $[Cu(H_2dapd)Cl_2]$ which is remarkably acidic in aqueous solutions (the pK for proton dissociation being 2.8 ± 0.1 in H_2O at 25.1°C). The second proton is not removed by aqueous base. Deprotonation of $[Cu(H_2dapd)Cl_2]$ in alcoholic solution afforded the dimeric dication $[Cu(Hdapd)]_2^{2+}$, isolated as the chloride or tetrafluoroborate. In the dimer the copper centers are highly coupled and the fourth coordination position is occupied by an O^- donor derived from a deprotonated =N—OH group to give a bridged chromophore of type **6**.[7] The dimer structure is readily ruptured by coordinating solvents.



6

Because of these interesting properties, we have extended the previous work to several other metal ions. In this paper the synthesis and electronic and structural properties of Fe(II) and Fe(III) complexes with H_2dapd are reported.

EXPERIMENTAL

Materials

H_2dapd was prepared from 2,6-diacetylpyridine (Aldrich Chemical Co.) according to the method of Baucom and Drago.[4] The authenticity of the compound was established on the basis of elemental analysis (Table 1) and IR spectra. The anhydrous iron(II) halides, ferrous sulphate, potassium thiocyanate and selenocyanate, and other solvents were of reagent grade chemicals.

Dihalogeno - mono(2,6 - diacetylpyridine dioxime) iron(II), $[Fe(H_2dapd)X_2]$ (X = Cl, Br *or* I). A solution of ferrous halide (0.02 mol) in 50 cm^3 of anhydrous methanol was prepared and kept under an N_2 gas atmosphere. A solution of ligand (0.02 mol) in 50 cm^3 of anhydrous methanol was prepared by heating under reflux while bubbling a rapid stream of N_2 through the solution. The metal salt solution was then added very slowly under an N_2 gas atmosphere to the ligand solution. A red colour was developed immediately and a precipitate was formed within minutes. The mixture was allowed to stand for 30 min under N_2 and then heated to boil and filtered hot via suction through a sintered glass under N_2. The red crystalline solid was dried over P_4O_{10} *in vacuo*.

Bis(2,6-diacetylpyridine dioxime)iron(II) perchlorate, $[Fe(H_2dapd)_2](ClO_4)_2$. A hot solution of $FeSO_4 \cdot 7H_2O$ (0.02 mol) in 20 cm^3 of methanol was

Table 1. Analytical data of iron complexes

Compound[a]	Yield (%)	Found (calc.) (%) C	H	N	Fe	X[b]
H_2dapd	95	61.2 (59.95)	5.8 (5.69)	20.9 (21.76)	— —	— —
$[Fe(H_2dapd)Cl_2]$	85	33.7 (33.78)	3.7 (3.71)	13.1 (13.13)	17.4 (17.45)	22.2 (22.16)
$[Fe(H_2dapd)Br_2]$	70	26.4 (26.44)	2.6 (2.71)	10.2 (10.28)	13.7 (13.66)	39.1 (39.09)
$[Fe(H_2dapd)I_2]$	70	20.9 (21.15)	2.2 (2.20)	8.3 (8.36)	10.9 (11.11)	50.5 (50.47)
$[Fe(H_2dapd)(NCS)_2]$	80	29.4 (29.60)	2.9 (3.06)	11.6 (11.51)	15.3 (15.29)	31.8 (31.80)
$[Fe(H_2dapd)(NCSe)_2]$	75	28.8 (28.78)	2.4 (2.42)	15.2 (15.25)	12.2 (12.17)	34.4 (34.40)[c]
$[Fe(H_2dapd)_2](ClO_4)_2$	70	16.8 (16.88)	1.6 (1.72)	6.7 (6.56)	8.7 (8.72)	— —
$[Fe_2(Hdapd)_2Cl_4]$	75	33.9 (33.87)	3.1 (3.14)	13.2 (13.17)	17.4 (17.52)	22.2 (22.27)
$[Fe_2(Hdapd)_2Br_4]$	70	26.4 (26.49)	2.4 (2.40)	10.3 (10.30)	13.6 (13.70)	39.1 (39.20)
$[Fe_2(Hdapd)_2I_4]$	70	21.6 (21.53)	1.9 (1.99)	8.3 (8.37)	11.2 (11.13)	50.4 (50.59)
$[Fe_2(Hdapd)_2(NCS)_4]$	75	29.6 (29.68)	2.8 (2.75)	11.5 (11.54)	15.2 (15.35)	31.8 (31.88)
$[Fe_2(Hdapd)_2(NCSe)_4]$	70	28.8 (28.84)	2.1 (2.18)	15.3 (15.29)	12.1 (12.19)	34.5 (34.50)[c]
$[Fe_2(Hdapd)_2O(NO_3)_2]$	85	33.9 (33.98)	3.2 (3.15)	13.2 (13.21)	17.6 (17.57)	19.5 (19.51)

[a] H_2dapd, 2,6-diacetylpyridine dioxime ($C_9H_{11}N_3O_2$); Hdapd, anion of 2,6-diacetylpyridine dioxime ($C_9H_{10}N_3O_2$).
[b] Anion.
[c] Se.

added dropwise with constant stirring to a boiled solution of 5 (0.045 mol) in 20 cm^3 of methanol. A deep red solution was formed. Aqueous saturated solution of sodium perchlorate was added and the pH of the solution mixture was adjusted to *ca* 7.0 by adding a few drops of sodium hydroxide. The solution mixture was then heated under reflux for about 1 h. On cooling a dark red crystalline solid was formed which was filtered, washed with water, methanol and diethylether and dried over P_4O_{10} *in vacuo*.

Dihalogeno-di-μ-halogeno-di-hydrogen bis(2,6-diacetylpuridine dioxime)diiron(III),

$$[Fe_2(Hdapd)_2X_4] \ (X = Cl, Br \text{ or } I).$$

A solution of $FeSO_4 \cdot 7H_2O$ (0.01 mol) in 25 cm^3 of water was prepared by gently heating and added to a solution of **5** (0.015 mol) in 25 cm^3 of 1 : 1 acetone–18 M aqueous NH_3. To this solution, an excess of $(NH_4)_2S_2O_8$ in a minimum amount of water was added and the solution was mixed thoroughly until all traces of the red colour had disappeared leaving a blue–green solution. The solution was cooled in an ice-bath and 8–10 cm^3 of a saturated aqueous solution of NaCl, NaBr or NaI was added to effect precipitation. The dark red crystalline solid was filtered, washed with water and dried *in vacuo* over P_4O_{10}. The entire preparation was carried out in the dark to minimize the possibility of reduction.

Dithiocyanato-di-μ-thiocyanato and diseleno-cyanato-di-μ-selenocyanato-hydrogen bis(2,6-diacetyl-pyridine dioxime)diiron(III),

$$[Fe_2(Hdapd)_2X_4] \ (X = NCS \text{ or } NCSe).$$

A suspension of $[Fe_2(Hdapd)_2Cl_4]$ (0.01 mol) in 25 cm^3 of methanol was refluxed with an excess of solid KSCN or KSeCN (0.025 mol) for about 1 h. The dark red crystalline solid formed was filtered, washed with methanol and diethylether and dried *in vacuo* over P_4O_{10}.

Dinitrato-mono-μ-oxo-dihydrogen bis(2,6-diacetyl-pyridine dioxime)diiron(III),

$$[Fe_2(Hdapd)_2O(NO_3)_2].$$

The dark red crystalline solid,

$$[Fe_2(Hdapd)_2O(NO_3)_2],$$

was prepared by the similar procedure given above except that $NaNO_3$ was used to cause precipitation.

Analytical methods and physical measurements

Iron was determined[8] by EDTA titrimetry using Eriochrome Black T as an indicator after destroying the organic part first with aqua regia and then with conc. H_2SO_4. Halides were estimated by Volhard's method[9] and nitrate was determined[9] as its nitrone salt. The $[SCN]^-$ and $[SeCN]^-$ ions were estimated[9] as silver thiocyanate and selenium metal, respectively. Carbon, hydrogen and nitrogen were determined microanalytically at CDRI, Lucknow, India, and the data are given in Table 1.

Conductance measurements were made on a Toshniwal conductivity bridge type CL01/01. Magnetic measurements were made on a standard Gouy balance calibrated with $HgCo(NCS)_4$[10] from room temperature down to 78 K (Table 2). Diamagnetic corrections were applied using Pascal's constants.[11]

Diffuse reflectance spectra were recorded on a Cary-14 spectrophotometer equipped with a reflectance accessory, using MgO as the reference. The IR spectra of H_2dapd and its complexes were recorded in the 4000–200 cm^{-1} range on a Perkin–Elmer 337 spectrophotometer in CsI and far-IR spectra in the 400–100 cm^{-1} range were recorded on a Fourier spectrophotometer (FS-30).

^{57}Fe Mössbauer spectra were obtained on polycrystalline samples by using a constant-acceleration Mössbauer spectrometer which was calibrated with natural α-iron foil. The source was $^{57}Co(Pd)$ and was at room temperature for all experiments. The low-temperature results were measured in a vacuum cryostat with a sample holder which protected the sample from the cryostat vacuum. The Mössbauer results were determined by inspection with an accuracy of ± 0.01 mm s^{-1}.

RESULTS AND DISCUSSION

The interaction of iron(II) salts with H_2dapd in a 1 : 1 ratio in methanol afforded complexes of general formula $[Fe(H_2dapd)X_2]$ (X = Cl, Br, I, NCS or NCSe). Rapid isolation of these complexes was necessary to preserve the 1:1 (metal:ligand) stoichiometry. Longer reaction times, even with less than an equivalent amount of the ligand being present, result in the formation of $[Fe(H_2dapd)_2]X_2$ or products whose analyses suggested mixtures of 1 : 1 and 1 : 2 adducts. This type of rearrangement to a bis-ligand complex was previously observed for 1 : 1 terpyridyl complexes.[12] The bis-ligand complex $[Fe(H_2dapd)_2](ClO_4)_2$ was isolated by refluxing a solution of $FeSO_4 \cdot 7H_2O$ with H_2dapd in methanol, followed by the addition of a saturated solution of $NaClO_4$. The pH of the solution was maintained at *ca* 7.

Attempts to isolate pure iron(III)–H_2dapd complexes by direct addition of the ligand to iron(III) salts were unsuccessful and resulted in rapid

Table 2. Magnetic susceptibility data of iron complexes

Temperature (K)	χ_M (cgsu)	μ_{eff} (μ_B)	Temperature (K)	χ_M (cgsu)	μ_{eff} (μ_B)
[$Fe(H_2dapd)Cl_2$] $\theta = -6$ K			[$Fe(H_2dapd)Br_2$] $\theta = -6$ K		
298.5	11,589	5.26	298.8	11,578	5.26
264.2	13,094	5.26	262.5	13,079	5.24
210.0	16,001	5.20	207.0	16,333	5.20
192.5	17,429	5.18	185.0	17,996	5.16
140.6	23,770	5.17	132.7	24,604	5.11
108.8	30,481	5.15	112.0	28,697	5.05
95.6	33,753	5.08	98.5	32,373	5.04
78.0	41,044	5.06	78.0	40,720	5.04
[$Fe(H_2dapd)I_2$] $\theta = -1$ K			[$Fe(H_2dapd)(NCS)_2$] $\theta = -3$ K		
298.0	11,476	5.23	298.7	12,525	5.47
260.5	12,979	5.20	250.6	14,929	5.47
215.0	15,545	5.17	215.0	17,465	5.48
190.6	17,399	5.15	198.4	18,894	5.47
142.4	22,660	5.08	135.0	27,813	5.48
110.2	28,822	5.04	98.0	38,454	5.49
98.0	32,281	5.03	78.0	48,314	5.49
78.0	40,397	5.02			
[$Fe(H_2dapd)(NCSe)_2$] $\theta = -2$ K			[$Fe(H_2dapd)_2](ClO_4)_2$ $\theta = -6$ K		
298.5	12,486	5.46	298.5	11,767	5.30
250.7	14,868	5.46	230.0	14,927	5.24
210.5	17,642	5.45	195.6	17,285	5.20
195.6	18,986	5.45	150.2	22,337	5.18
140.2	26,586	5.46	112.4	25,619	5.16
95.6	39,132	5.47	95.0	34,908	5.15
78.0	47,962	5.47	78.0	42,023	5.12
[$Fe_2(Hdapd)_2Cl_4$] $J = -7.4$ cm^{-1}			[$Fe_2(Hdapd)_2Br_4$] $J = -7.0$ cm^{-1}		
298.0	11,662	5.27	298.5	11,747	5.30
252.0	13,171	5.15	253.5	12,120	4.95
192.6	15,682	4.91	185.5	16,401	4.93
150.2	17,921	4.63	148.3	18,525	4.68
112.5	19,377	4.18	128.5	19,674	4.50
92.6	20,809	3.93	90.4	22,271	4.01
78.0	21,346	3.65	78.0	22,660	3.80
[$Fe_2(Hdapd)_2I_4$] $J = -8.2$ cm^{-1}			[$Fe_2(Hdapd)_2(NCS)_4$] $J = -9.5$ cm^{-1}		
299.2	11,318	5.20	298.5	10,841	5.08
255.4	12,457	5.04	260.0	11,849	4.96
190.0	15,118	4.79	195.6	13,864	4.66
145.5	17,122	4.46	142.8	15,674	4.23
115.6	18,249	4.10	120.5	16,434	3.98
95.0	19,523	3.85	98.2	16,889	3.64
78.0	20,488	3.57	78.0	17,040	3.26

Table 2. (*Contd.*)

Temperature (K)	χ_M (cgsu)	μ_{eff} (μ_B)	Temperature (K)	χ_M (cgsu)	μ_{eff} (μ_B)
$[Fe_2(Hdapd)_2(NCSe)_4]$ $J = -9.7\ cm^{-1}$			$[Fe_2(Hdapd)_2O(NO_3)_2]$ $J = -102.0\ cm^{-1}$		
298.0	10,778	5.07	299.0	1414	1.80
258.2	11,803	4.94	260.4	1369	1.69
188.5	13,949	4.58	190.8	1235	1.37
135.5	15,676	4.12	130.5	963	1.00
115.8	16,218	3.88	110.0	800	0.84
95.0	16,598	3.55	85.0	513	0.59
78.0	16,644	3.22	78.0	418	0.51

reduction and formation of products whose analyses indicated mixtures of 1 : 1 and 1 : 2 iron(II) adducts. This is similar to the behaviour of terpyridyl which, upon direct reaction with iron(III) salts, results in the formation of bis-ligand iron(II) complexes.[13] Oxidation of $[Fe(terpy)_2]^{2+}$ followed by saturation of the solution with weakly reducing anions, Cl^-, ClO_4^- or NO_3^-, gave an iron(III)–terpy complex which is of a different nature in each case.[13] We applied this method to isolate iron(III)–H_2dapd complexes. It is interesting to note that the halide afforded binuclear red complexes of type $[Fe_2(Hdapd)_2X_4]$ (X = Cl, Br or I) and the nitrate a dark red binuclear oxo-complex of type $[Fe_2(Hdapd)O(NO_3)_2]$. Several attempts were made to isolate a bis-ligand iron(III) complex with perchlorate but failed. The $[Fe_2(Hdapd)_2X_4]$ (X = NCS or NCSe) were obtained by refluxing $[Fe_2(Hdapd)_2Cl_4]$ in methanol with an excess of KSCN or KSeCN.

All the complexes are quite stable at room temperature and do not show any sign of their decomposition after a long period of standing. They are insoluble in water and non-polar solvents and, except for iron(II) thiocyanato and selenocyanato, and iron(III) complexes, are soluble in polar solvents. The molar conductivities of $[Fe(H_2dapd)X_2]$ (X = Cl, Br or I) at 10^{-3} M in methanol are in the range expected for non-electrolytes while for the $[Fe(H_2dapd)_2](ClO_4)_2$ complex 1 : 2 electrolytes.[14]

Magnetic susceptibility results

The μ_{eff} values for iron(II) and iron(III) complexes have been measured as a function of temperature and are detailed in Table 2. The magnetic moments of $[Fe(H_2dapd)X_2]$ (X = Cl, Br or I) complexes are almost independent of temperature, ranging from 5.26–5.23 μ_B at *ca* 298 K to 5.06–5.02 μ_B at 78 K. These values are consistently lower than that of six-coordinate complexes ($\mu_{eff} = 5.50\ \mu_B$)[15] and are consistent with those reported for five-coordinate iron(II) complexes.[16] The presence of axial ligands in the five-coordination sphere would generate a great splitting of the $^5T_2$ state (of O_h origin), thereby reducing the orbital contribution to μ_{eff}. The magnitude and slight temperature dependence (*ca* 3% or less) of the magnetic moments strongly suggest a tetragonally distorted octahedral geometry for

$$[Fe(H_2dapd)X_2]\ (X = NCS^-\ \text{or}\ NCSe^-)$$

and

$$[Fe(H_2dapd)_2](ClO_4)_2$$

complexes.[17]

Compounds

$$[Fe_2(Hdapd)_2Cl_4],\ [Fe_2(Hdapd)_2Br_4],$$

$$[Fe_2(Hdapd)_2I_4],\ [Fe_2(Hdapd)_2(NCS)_4],$$

$$[Fe_2(Hdapd)_2(NCSe)_4]$$

and

$$[Fe_2(Hdapd)_2O(NO_3)_2]$$

have effective magnetic moments of 5.27, 5.30, 5.20, 5.08, 5.07 and 1.80 μ_B, respectively at *ca* 298 K. As the sample temperature is lowered, these μ_{eff} values decrease to 3.65, 3.80, 3.57, 3.26, 3.22 and 0.51 μ_B, respectively, at 78 K. Plots of the magnetic data for these complexes are illustrated in Fig. 1. This behaviour is a reflection of an intermolecular antiferromagnetic exchange interaction between the two $S = \frac{5}{2}$ ions in each of the six binuclear compounds.[18] Such an exchange interaction between two $S = \frac{5}{2}$ ions can be largely accounted for with an isotropic exchange spin Hamiltonian of the form $\hat{H} = -2J\hat{S}_1 \cdot \hat{S}_2$, where S_i is the spin operator on each of the two metal centers and J is the

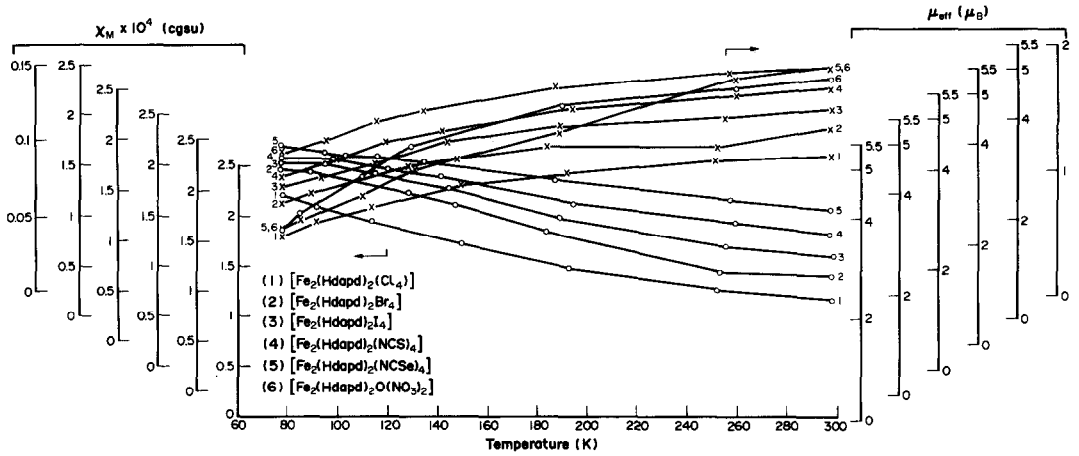


Fig. 1. Corrected molar paramagnetic susceptibility (χ_M in cgsu per mol of binuclear complex) and effective magnetic moment per mol of iron(III) ion (μ_{eff}/Fe) vs temperature curves for: (1) $[Fe_2(Hdapd)_2Cl_4]$, (2) $[Fe_2(Hdapd)_2Br_4]$, (3) $[Fe_2(Hdapd)_2I_4]$, (4) $[Fe_2(Hdapd)_2(NCS)_4]$, (5) $[Fe_2(Hdapd)_2(NCSe)_4]$, and (6) $[Fe_2(Hdapd)_2O(NO_3)_2]$. The solid lines result from the fitting of the data to theoretical equations.[19]

exchange parameter, which is a gauge of the magnitude of the interaction. An exchange-coupled, $S_1 = S_2 = \frac{5}{2}$, complex has electronic states with a total spin of $S' = 5$, 4, 3, 2, 1 and 0. It is the characteristic of such an interacting ferric dimer that, even for a weak interaction, the variation in Boltzmann distribution over the S' states as a function of temperature is gradual and has an effect even at high temperatures. Thus, even a weak antiferromagnetic exchange interaction can influence the μ_{eff} values at *ca* 298 K and this could partially explain why the observed values are below the spin-only value of 5.9 μ_B.

The variable-temperature magnetic susceptibility data for iron(III) complexes were fitted to the theoretical equations[19] to give

$$J = -7.4\ \{[Fe_2(Hdapd)_2Cl_4]\},$$
$$-7.0\ \{[Fe_2(Hdapd)_2Br_4]\},$$
$$-8.2\ \{[Fe_2(Hdapd)_2I_4]\},$$
$$-9.5\ \{[Fe_2(Hdapd)_2(NCS)_4]\},$$
$$-9.7\ \{[Fe_2(Hdapd)_2(NCSe)_4]\}$$

and

$$-102.0\ cm^{-1}\ \{[Fe_2(Hdapd)_2O(NO_3)_2]\}$$

and $g = 2.0$. The theoretical fits to both the μ_{eff} and χ_M vs temperature curves are indicated in Fig. 1 as solid lines. It can be seen that the fits are reasonable, which verifies the suggestion that there is an antiferomagnetic exchange interaction present in each of the binuclear complexes. It is interesting to note here that the J value for $[Fe_2(Hdapd)_2X_4]$ (X = Cl, Br, I, NCS or NCSe) is in the range of -7.0 to -9.5 cm^{-1} and for $[Fe_2(Hdapd)_2O(NO_3)_2]$ is -102.0 cm^{-1}. The magnitude of the latter interaction is very close to those found for μ-oxo-bridged iron(III) dimers.[13] Thus, the antiferromagnetic interaction is a reflection of the details of the electronic structure of bridged species and does not depend simply on metal–metal distance.

Mössbauer effect spectral data

^{57}Fe Mössbauer spectra of iron(II) complexes have been studied at room temperature and 78 K and the spectral parameters are listed in Table 3. The chemical isomer shift values, δ, relative to natural iron foil, which are sensitive to both the oxidation state and the spin-state of iron, are in agreement with the structural assignments made on the basis of magnetic, electronic and IR results (*vide infra*) for iron(II) complexes.[17,20,21] The small reduction in the chemical isomer shift in the $[Fe(H_2dapd)X_2]$ (X = NCS or NCSe) complexes as compared with reported nitrogen-containing octahedral iron(II) complexes[17] is believed to be due to the lower total electronegativity of the coordinated atoms. The lower sulphur electronegativity results in a higher *s*-electron density in the vicinity of the iron nucleus and, consequently, in a smaller chemical isomer shift in $[Fe(H_2dapd)X_2]$ (X = NCS or NCSe) complexes.

For $[Fe(H_2dapd)X_2]$ (X = Cl, Br or I), $[Fe(H_2dapd)X_2]$ (X = NCS or NCSe) and $[Fe(H_2dapd)_2](ClO_4)_2$ complexes characterization

Table 3. Mössbauer spectral data of iron(II) complexes

Complex	T (K)	ΔE_Q (mm s^{-1})	δ^a (mm s^{-1})	$\Gamma_1{}^b$ (mm s^{-1})	$\Gamma_2{}^b$ (mm s^{-1})
$[Fe(H_2dapd)Cl_2]$	78	4.00	1.14	0.30	0.34
	RT[c]	3.85	1.00	0.26	0.29
$[Fe(H_2dapd)Br_2]$	78	4.80	1.10	0.28	0.28
	RT	3.87	0.99	0.25	0.27
$[Fe(H_2dapd)I_2]$	78	3.98	1.12	0.28	0.29
	RT	3.88	1.04	0.24	0.26
$[Fe(H_2dapd)(NCS)_2]$	78	3.02	1.00	0.34	0.36
	RT	2.60	0.95	0.32	0.30
$[Fe(H_2dapd)(NCSe)_2]$	78	2.90	1.00	0.30	0.30
	RT	2.64	0.92	0.26	0.26

[a] Relative to natural iron foil.
[b] Full width at half-maximum for low-velocity line (Γ_1) and high-velocity line (Γ_2).
[c] Room temperature.

as five- and six-coordinate high-spin iron(II) derivatives is confirmed by the ΔE_Q values. These are in the ranges 3.85–3.88 and 2.60–2.64 mm s^{-1} at room temperature and 3.98–4.00 and 2.90–3.02 mm s^{-1} at 78 K which are characteristic of five- and six-coordinate high-spin iron(II), as demonstrated for a broad series of related complexes.[17,20,21] The large ΔE_Q values for the $[Fe(H_2dapd)X_2]$ (X = Cl, Br or I) complexes are most probably caused by large contributions of like sign from both the non-spherical electron density and the ligand field dissymmetry. The contribution to ΔE_Q from the nonspherical d-electron distribution will depend upon the nature of the ground state. Under a tetragonal distortion $^5T_2$-state (of O_h-symmetry) is split into $^5B_2$- and ^5E-states. The magnitude of contributions to ΔE_Q from a $3d$ electron in either a $^5B_2$ or a ^5E ground state are equal, but the electric field gradients associated with these two states are of opposite signs. The results of magnetically perturbed Mössbauer spectrum of a five-coordinate complex imply that the ground state is $^5B_2$ contrary to the ordering of the one-electron d-orbitals expected from crystal field theory for both the square pyramidal and the trigonal bipyramidal geometries.[22] From this result it is assumed that the ground state in $[Fe(H_2dapd)X_2]$ (X = Cl, Br or I) complexes is $^5B_2$.

The slightly large ΔE_Q values for $[Fe(H_2dapd)X_2]$ (X = NCS or NCSe) complexes are assumed to be caused by the larger ligand field dissymmetry which results in a larger electric field gradient. This ligand field dissymmetry may be a direct result of the lower total electronegativity of the coordinated atoms which comprise the coordination sphere of the complexes.

^{57}Fe Mössbauer spectra were obtained for all six iron(III) complexes; the spectral parameters are reported in Table 4. The spectra of $[Fe_2(Hdapd)_2Cl_4]$ and $[Fe_2(Hdapd)_2O(NO_3)_2]$ at 298, 78 and 4.2 K are illustrated in Figs 2 and 3, respectively. Essentially identical spectra to $[Fe_2(Hdapd)_2Cl_4]$ were observed for the remaining iron(III) complexes. The δ values are of the magnitude observed for high-spin binuclear five-coordinate iron(III) complexes and show, as expected, a slight increase with decreasing temperature.[23] These δ are surprisingly constant and do not significantly change with change in anion in $[Fe_2(Hdapd)_2X_4]$ complexes, indicating that varying electron-withdrawing effects of different anions have little effect upon the s-electron density at the surface of the iron nucleus. The magnitude of the quadrupole splitting ΔE_Q is also that which is observed for high-spin five-coordinate iron(III) complexes.[23]

The interesting aspect of the Mössbauer spectra of iron(III) complexes is the asymmetry observed in the intensity of the quadrupole-split lines. This asymmetry is apparent in Figs 2 and 3. The asymmetric quadrupole-split doublets may be explained in many ways. Partial orientation of sample crystallites in the sample container, as observed[24] for $Fe_2(CO)_9$, is one possible explanation. Because asymmetry was decreased with decreasing temperature, this explanation is not applicable.

Goldanski *et al.*[25] and Karyagin[26] suggested that anisotropy of the recoil-free fraction of the ^{57}Fe center should produce asymmetry in the $\frac{3}{2} \leftarrow \frac{1}{2}$ doublet, if a site distortion from octahedral geometry is present. The Goldanski–Karyagin effect leads to a change of relative peak areas of the two components of a doublet as a function of temperature while the

Table 4. Mössbauer spectral data of iron(III) complexes

Compound	δ^a (mm s^{-1})			ΔE_Q (mm s^{-1})			Γ (mm s^{-1})		
	RT[b]	78 K	4.2 K	RT	78 K	4.2 K	RT	78 K	4.2 K
$[Fe_2(Hdapd)_2Cl_4]$	0.36	0.44	0.47	1.22	1.27	1.28	0.20	0.20	0.16
							0.30	0.29	0.16
$[Fe_2(Hdapd)_2Br_4]$	0.36	0.45	0.48	1.10	1.15	1.16	0.24	0.24	0.17
							0.32	0.30	0.16
$[Fe_2(Hdapd)_2I_4]$	0.34	0.43	0.46	0.99	1.03	1.04	0.26	0.26	0.27
							0.32	0.30	0.27
$[Fe_2(Hdapd)_2(NCS)_4]$	0.40	0.51	0.53	1.25	1.30	1.31	0.24	0.26	0.20
							0.36	0.34	0.20
$[Fe_2(Hdapd)_2(NCS)_4]$	0.38	0.49	0.52	1.25	1.29	1.30	0.24	0.24	0.20
							0.38	0.36	0.19
$[Fe_2(Hdapd)_2O(NO_3)_2]$	0.43	0.52	0.55	1.90	2.30	2.32	0.25	0.20	0.20
							0.39	0.20	0.20

[a] Relative to natural iron foil.
[b] Room temperature.

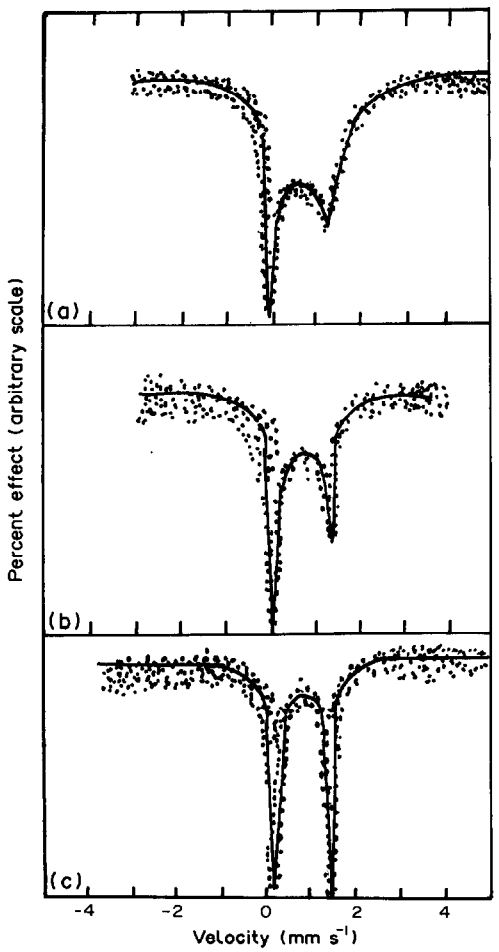


Fig. 2. Mössbauer spectra of $[Fe_2(Hdapd)_2Cl_4]$ at 298 (a), 78 (b) and 4.2 K (c).

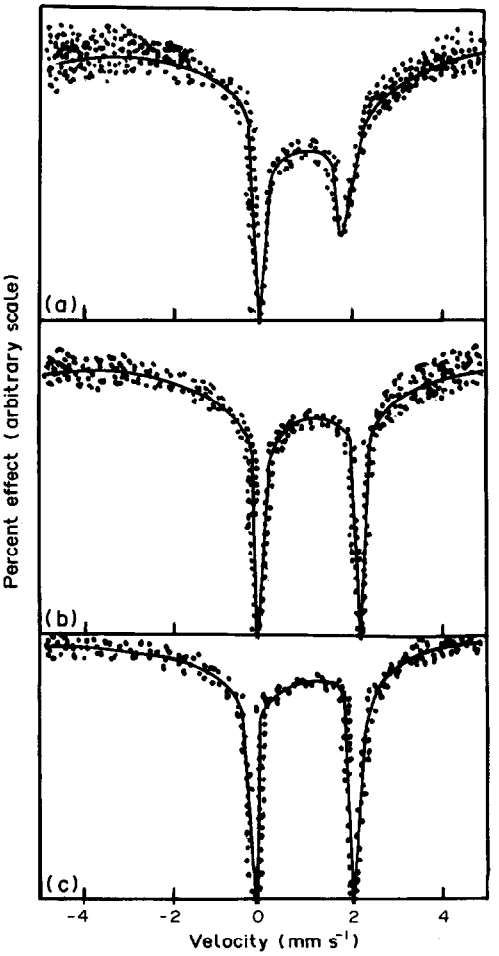


Fig. 3. Mössbauer spectra of $[Fe_2(Hdapd)_2O(NO_3)_2]$ at 298 (a), 78 (b) and 4.2 K (c).

line widths remain unchanged. This second explanation also does not appear to applicable, because the best fit of the spectral data is obtained when the areas of the high- and low-velocity peaks of one doublet are set equal. The best fit is illustrated in Figs 2 and 3 as solid lines.

The asymmetry of quadrupole-split doublet and broadening of lines in a Mössbauer spectrum may be attributed to paramagnetic relaxation of the Fe(III) ion. It has been shown[27] that such asymmetry is possible when the spin-relaxation rate is of the same magnitude as the Larmor precessional frequency of the Mössbauer nucleus in the internal hyperfine field generated by unpaired electron spins. For an exchange-interacting iron(III) dimer at 4.2 K, most of the molecules are in the diamagnetic $S' = 0$ state; there is no hyperfine field and the doublet is symmetric. At higher temperatures, other dimer states, where $S' \neq 0$, become populated and slow relaxation of the spins results a magnetic hyperfine broadening and an asymmetric doublet. That is why $[Fe(salen)Cl]_2$ [salen = *N*,*N*′-ethylene bis(salicylideneiminato)] ($J = -7.5\ cm^{-1}$)[28] gives a symmetric quadrupole-split doublet[29] at *ca* 6 K, whereas that for $[Fe(salen)]_2O$ ($J = -95\ cm^{-1}$)[30] is at 80 K.[31] Buckley *et al.*[32] have shown that the interactions in these types of molecules are intermolecular in nature. Hence, it appears that the asymmetric doublets and temperature dependence of asymmetry in our compounds is most likely due to the intermolecular spin–spin relaxation. In this regard, it is important to note that $[Fe_2(Hdapd)_2X_4]$ exhibit symmetric quadrupole-split doublets at 4.2 K whereas those for $[Fe_2(Hdapd)_2O(NO_3)_2]$ is at 78 K.

Electronic spectral results

The diffuse reflectance spectra of $[Fe(H_2dapd)X_2]$ (X = Cl, Br or I) exhibit two broad bands at *ca* 5.0 and *ca* 11.0 kK at room temperature. These two absorption bands are assigned[16] to the $^5A_1$- and $^5B_1$-states derived from the splitting of the ^5E spectroscopic term in the tetragonal ligand field. On the other hand, the spectra of $[Fe(H_2dapd)X_2]$ (X = NCS or NCSe) exhibit two well-resolved bands at *ca* 7.2 and 13.2 kK at room temperature. These spectral bands are assigned[33] to the $^5B_{1g}$- and $^5A_{1g}$-states which are components of the ^5E_g excited state in O_h-symmetry. It is apparent that in halogeno-iron(II) complexes the splitting of the ^5E excited state is of the order of *ca* 6 kK, while the separation of the $^5B_{1g}$- and $^5A_{1g}$-states in thiocyanato- and selenocyanato-iron(II) complexes is of the order of *ca* 3 kK. This indicates a much more highly distorted ligand field in the former complexes than in the latter and is certainly consistent with the two structure types of these complexes.

The diffuse reflectance spectrum of $[Fe(H_2dapd)_2](ClO_4)_2$ exhibits two bands at 8.7 and 11.2 kK at room temperature. These spectral bands are characteristic of distorted octahedral iron(II) and are assigned[34] to components of the $^5T_{2g} \rightarrow {}^5E_g$. The splitting of this band may be due to a pronounced reduction in the ligand field symmetry caused by the greater steric requirements of the two ligand molecules. The intense band observed at 18.5 kK in the spectrum is assigned to a charge-transfer band [$^1{2_g}$(Fe) → $\pi^*(H_2dapd)$].

The iron(III) complexes reported herein are dark red, as is common for iron(III) compounds of oxime-containing ligands. This colour is usually ascribed to the presence of one or more low-lying charge-transfer absorption bands. Because of these very intense bands, one does not usually observe *d–d* transitions in the visible spectra of such compounds. This unfortunate situation is found in the present iron(III) complexes and the positions and intensities of the spectral bands are affected little by the anions. A low-intensity band is however observed at *ca* 11.0 kK in $[Fe_2(Hdapd)_2X_4]$ (X = Cl, Br, I, NCS or NCSe) and $[Fe_2(Hdapd)_2O(NO_3)_2]$ complexes which can be assigned to a ligand field transition. A similar absorption has also been observed in the electronic spectrum of other five-coordinate iron(III) complexes.[13] Although the absorption observed at *ca* 11,000 cm^{-1} cannot be assigned properly, it appears to be a common feature of five-coordinate iron(III) complexes.[13,35]

IR spectral data

H_2dapd exhibits multiple bands between 3350 and 3000 cm^{-1} which are assigned[36] to the intermolecular H-bonded ν(OH) of the NOH groups. The $[Fe(H_2dapd)X_2]$ and $[Fe(H_2dapd)_2](ClO_4)_2$ complexes exhibit sharp bands at 3470–3460, 3370–3360, 3200–3150, 3050–3000 and 2840–2820 cm^{-1} which are assigned[36] to the free ν(OH), H-bonded ν(OH), ν(C—H), coupled ν(OH) and ν(C=N) (overtone), respectively. In $[Fe_2(Hdapd)_2X_4]$ and $[Fe_2(Hdapd)_2O(NO_3)_2]$ complexes, strong bands observed at 3510–3500, 3440–3430, 3110–3100, 3040–3000 and 2840–2830 cm^{-1} are assigned[36] to the free ν(OH), H-bonded ν(OH), ν(C—H) and ν(C=N) (overtone) modes of ligand molecules, respectively. None of these iron(III) complexes exhibit any band in the region 3400–3200 cm^{-1}, indicating ionization of one of the NOH groups of H_2dapd.

The free ligand H_2dapd exhibits ν(C=N)(acyclic) and ν(N—O) vibrations at 1560 and 970 cm^{-1},

respectively. In $[Fe(H_2dapd)X_2]$ and

$$[Fe(H_2dapd)_2](ClO_4)_2$$

complexes the ν(C=N)(acyclic) and ν(N—O) vibrations shift towards the higher-frequency side and appear at *ca* 1600 and *ca* 1050 cm^{-1}, respectively. The shift of bands towards the high-frequency side is an indication of the coordination of the nitrogen atom of the neutral oxime group,

$$\rangle C{=}N{-}OH,$$

to iron(II) ion.[36] In $[Fe_2(Hdapd)_2X_4]$ and

$$[Fe_2(Hdapd)_2O(NO_3)_2]$$

complexes the ν(C=N)(acyclic) is shifted towards the low-frequency side and is obscured by pyridine band-I stretching vibration. The ν(N—O) also appears at a lower frequency (*ca* 1010 cm^{-1}). This situation is certainly consistent with the heterolysis of one of the NOH group in H_2dapd and the coordination through the nitrogen of the

$$\rangle C{=}N{-}O$$

group to the iron(III) ion. The coordination of the pyridine nitrogen atom to iron (II) and iron(III) is indicated by the shifting and splitting of ring vibrations as is usually observed for pyridine coordination.[17]

The presence of bridging thiocyanato and selenocyanato groups in $[Fe(H_2dapd)X_2]$ (X = NCS or NCSe) is indicated[37] by the presence of almost equal intensity splitting ν_1 [ν(C—N stretch)] at 2110s and 2070s cm^{-1}, whereas the ν_1 bands at 2130s, 2090s and 2030m cm^{-1} suggest[38] the presence of both terminal and bridging thiocyanato and selenocyanato groups in $[Fe_2(Hdapd)_2X_4]$ complexes. The ν_2 [δ(NCS) or δ(NCSe) bending], and ν_3 [ν(C—S) or ν(C—Se) stretch] are obscured by ligand absorption bands. The appearance of bands at 1310m and 1450s cm^{-1} indicates[39] the monodentate coordination of nitrato groups in $[Fe_2(Hdapd)_2O(NO_3)_2]$ complex.

In the far-IR spectrum the $[Fe(H_2dapd)Cl_2]$ exhibits[16] bands at 288s [ν_{sym}(Fe-Cl)], 265m [ν_{asym}(Fe-Cl)], 250s [ν(Fe-py)], 236w [δ(Fe-Cl)] and 220m {ν[Fe-N(oxime)]} cm^{-1}, whereas the $[Fe(H_2dapd)Br_2]$ exhibits bands at 250w [ν(Fe-py)], 235s [ν_{sym}(Fe-Br)], 220m {ν[Fe-N(oxime)]}, 208s [ν_{asym}(Fe-Br)] and 196m [δ(Fe-Br)] cm^{-1}. No band in the spectrum of the $[Fe(H_2dapd)I_2]$ complex can be assigned to ν(Fe-I) vibration though such an absorption is expected near 200 cm^{-1}. The bands which appeared at 250s and 220m cm^{-1} are assigned to ν[Fe-N(py)] and ν[Fe-N(oxime)], respectively. The $[Fe(H_2dapd)X_2]$ (X = NCS or NCSe) complexes exhibit bands at *ca* 260s [ν(Fe-NCS) or ν(Fe-NCSe)], 220s {ν[Fe-N(oxime)]}, 208m {ν[Fe-N(py)]}, 185s [ν(Fe-SCN) or ν(Fe-SeCN)] and *ca* 160s [ν(Fe-NCS-Fe) or ν(Fe-NCSe-Fe)] cm^{-1}, again confirming the presence of bridging thiocyanato and selenocyanato groups in these complexes.[37] The ν[Fe-N(py)] and ν[Fe-N(oxime)] in the $[Fe(H_2dapd)_2](ClO_4)_2$ complex are observed at 250s and 220s cm^{-1}, respectively.

In the $[Fe_2(Hdapd)_2Cl_4]$ complex the bands are observed at 295s {ν[Fe-$Cl_{(terminal)}$]}, 250s {ν[Fe-N(py)]}, 240m {ν[Fe-$Cl_{(bridging)}$]}, and 220s {ν[Fe-N(oxime)]} cm^{-1}, whereas the spectrum of the $[Fe_2(Hdapd)_2Br_4]$ complex exhibits bands at 250s {ν[Fe-N(py)]}, 230s {ν[Fe-$Br_{(terminal)}$]}, 218 m {ν[Fe-N(oxime)]} and 185m {ν[Fe-$Br_{(bridging)}$]} cm^{-1}, respectively. The ratio of ν[Fe-$Cl_{(bridging)}$] to ν[Fe-$Cl_{(terminal)}$] and ν[Fe-$Br_{(bridging)}$] to ν[Fe-$Br_{(terminal)}$] is *ca* 0.80 and agrees well with the ratio observed in similar complexes.[16] In the $[Fe_2(H_2dapd)_2I_4]$ complex, the bands due to ν(Fe-I) vibrations are, as usual, weaker and in consequence less readily distinguishable from ligand vibrations, but the bands at 245m and 218w cm^{-1} are assigned to ν[Fe-N(py)] and ν[Fe-N(oxime)], respectively. The $[Fe_2(Hdapd)_2X_4]$ (X = NCS or NCSe) complexes exhibit bands at *ca* 280s, 270m, *ca* 245s, 220s and 186w cm^{-1}, which are assigned to ν[Fe-N(NCS or NCSe)$_{(terminal)}$], ν[Fe-N(NCS or NCSe)$_{(bridging)}$], ν[Fe-N(py)], ν[Fe-N(oxime)] and ν[Fe-S or Se(SCN or SeCN)$_{(bridging)}$], respectively. The bands observed at 245s and 220s cm^{-1} are assigned to ν[Fe-N(py)] and ν[Fe-N(oxime)] vibrations, respectively, in the $[Fe_2(Hdapd)_2O(NO_3)_2]$ complex. A sharp broad band at 845 cm^{-1} is assigned to ν(Fe-O-Fe) vibration.[13,40]

Acknowledgements—We are thankful to the authorities of RSIC, I.I.T., Madras, and C.D.R.I., Lucknow (U.P.) for recording electronic and IR spectra.

REFERENCES

1. A. Chakravorty, *Coord. Chem. Rev.* 1974, **13**, 1.
2. G. I. H. Hanania, D. H. Irvine and F. Schurauh, *J. Chem. Soc.* 1965, 1149.
3. H. Hartkamp, *Fresenius' Z. Anal. Chem.* 1960, **178**, 19.
4. E. I. Baucom and R. S. Drago, *J. Am. Chem. Soc.* 1979, **93**, 6469.
5. G. Sproul and G. D. Stucky, *Inorg. Chem.* 1973, **12**, 2898.
6. G. A. Nicholson, C. R. Lazarus and B. J. McCormick, *Inorg. Chem.* 1980, **19**, 192.
7. G. A. Nicholson, J. L. Petersen and B. J. McCormick, *Inorg. Chem.* 1980, **19**, 195.

8. F. J. Welcher, *The Analytical Uses of EDTA*. Van Nostrand, New York (1958).
9. A. I. Vogel, *A Textbook of Quantitative Inorganic Analysis*. Longmans, London (1961).
10. B. N. Figgis and R. S. Nyholm, *J. Chem. Soc.* 1958, 4190.
11. F. E. Mabbs and D. J. Machin, *Magnetism and Transition Metal Complexes*. Chapman & Hall, London (1961).
12. J. S. Judge and W. A. Baker, Jr, *Inorg. Chim. Acta* 1967, **1**, 239; C. M. Harris and T. N. Lockyer, *Aust. J. Chem.* 1970, **23**, 1703.
13. W. M. Reiff, W. A. Baker, Jr and N. E. Erickson, *J. Am. Chem. Soc.* 1968, **90**, 4794.
14. W. J. Geary, *Coord. Chem. Rev.* 1971, **7**, 81.
15. G. J. Long and W. A. Baker, Jr. *J. Chem. Soc. A* 1971, 2956.
16. M. Mohan, S. G. Mittal, H. C. Khera and A. K. Srivastava, *Gazz. Chim. Ital.* 1977, **107**, 393.
17. B. F. Little and G. J. Long, *Inorg. Chem.* 1978, **17**, 3401, and references therein.
18. J. Lewis, F. E. Mabbs and A. Richards, *J. Chem. Soc. A* 1967, 1014.
19. A. Earnshaw, *Introduction to Magnetochemistry*, p. 77. Academic Press, New York (1968).
20. W. M. Reiff, N. E. Erickson and W. A. Baker, Jr, *Inorg. Chem.* 1969, **8**, 2019.
21. D. P. Riley, P. H. Merrell, J. A. Stone and D. H. Busch, *Inorg. Chem.* 1975, **14**, 490.
22. W. M. Reiff, *Inorg. Chem.* 1974, **13**, 239.
23. N. N. Greenwood and T. C. Gibb, *Mössbauer Spectroscopy*, p. 161. Chapman & Hall, London (1971).
24. T. C. Gibb, R. Greatrex and N. N. Greenwood, *J. Chem. Soc. A* 1968, 890.
25. V. I. Goldanski, G. M. Gorodinskii, S.-V. Karyagin, L. A. Korytko, L. M. Krizhanskii, E. F. Makarov, I. P. Suzdalev and V. V. Khrapov, *Dokl. Akad. Nauk SSSR* 1962, **147**, 127.
26. S. V. Karyagin, *Dokl. Akad. Nauk SSSR* 1963, **148**, 1102.
27. M. Blume, *Phys. Rev. Lett.* 1965, **14**, 96.
28. M. Gerloch, J. Lewis, F. E. Mabbs and A. Richards, *J. Chem. Soc. A* 1968, 112.
29. A. N. Buckley, G. V. H. Wilson and K. S. Murray, *Solid State Commun.* 1969, **7**, 471.
30. J. Lewis, F. E. Mabbs and A. Richards, *J. Chem. Soc. A* 1967, 1014.
31. M. Cox, B. W. Fitzsimmons, A. W. Smith, L. F. Larkworthy and K. A. Rogers, *J. Chem. Soc., Chem. Commun.* 1969, 183.
32. A. N. Buckley, I. R. Herbert, B. D. Rumbold, G. V. H. Wilson and K. S. Murray, *J. Phys. Chem. Solids* 1970, **31**, 1423.
33. A. B. P. Lever, *Coord. Chem. Rev.* 1968, **3**, 119.
34. A. B. P. Lever, *Inorganic Electronic Spectroscopy*, p. 299. Elsevier, Amsterdam (1968).
35. J. T. Wrobleski and G. J. Long, *Inorg. Chim. Acta* 1979, **36**, 155.
36. M. Mohan and B. D. Paramhans, *Indian J. Chem.* 1980, **19A**, 759.
37. W. M. Reiff, R. B. Fankel, B. F. Little and G. J. Long, *Inorg. Chem.* 1974, **14**, 2153.
38. R. C. Dickinson and G. J. Long, *J. Inorg. Nucl. Chem.* 1974, **36**, 1235.
39. A. B. P. Lever, E. Mantovani and B. S. Ramaswamy, *Can. J. Chem.* 1971, **49**, 1957.
40. G. M. Bancroft, A. G. Maddock and R. P. Randl, *J. Chem. Soc. A* 1968, 2939.

Polyhedron Vol. 4, No. 11, pp. 1941–1945, 1985
Printed in Great Britain

0277–5387/85 $3.00 + .00
Pergamon Press Ltd

NITROSATION OF ALKENES BY NITRIC OXIDE: CRYSTAL STRUCTURES OF BIS-(1-NITROSO-2-NITRO-CYCLOHEXANE) AND BIS-(1-NITROSO-2-NITRO-1-PHENYLETHANE)

KWOK W. CHIU,* PAUL D. SAVAGE, GEOFFREY WILKINSON† and DAVID J. WILLIAMS†
Chemistry Department, Imperial College, London SW7 2AY, U.K.

(*Received* 27 *March* 1985; *accepted* 22 *May* 1985)

Abstract—The reaction of nitric oxide with alkenes has been studied. Crystal structures have been established by X-ray diffraction studies for bis-(1-nitroso-2-nitro-cyclohexane) and bis-(1-nitroso-2-nitro-1-phenylethane).

In a recent communication[1] it was reported that in certain solvents, e.g. dimethylformamide, styrene and nitric oxide in the presence of the cobaloxime, $[Co(DMGH)_2(py)Cl]$ (DMGH = monoanion of dimethylglyoxime, py = pyridine) and BH_4^- gave acetophenoneoxime in a slow catalytic reaction.

We had previously attempted an alkene nitrosation reaction analogous to hydroformylation [$CO + H_2$ + alkene + $RhH(CO)(PPh_3)_3$], namely that of $NO + H_2$ + alkene + $RuH(NO)(PPh_3)_3$. However, it was quickly apparent that: (a) the presence of the ruthenium complexes (or other similar metal species) did not affect the reaction pathway, and (b) no hydrogen was absorbed. Nitric oxide reacted with the alkene within an hour only at a pressure of 5 atm or above and yielded the well-known ψ-nitrosites (together with more complex unidentified materials). From cyclohexene and styrene we obtained the ψ-nitrosites[2] whose structures have been confirmed by X-ray crystallography (see below).

Such ψ-nitrosites commonly have been made by the interaction of alkenes with dinitrogen trioxide.[2,3] As pointed out by Brown[4] in his study of the reaction of nitric oxide with isobutylene, it was stated by N. V. Sidgwick as late as 1949 that pure nitric oxide did not react with olefins. However, pseudonitrites had already been obtained from cyclohexene and other olefins from nitric oxide (purity not specified) in 1944.[5]

Reactions of NO with fluoro-olefins were also established,[6] where it was assumed, like Brown,[4] that a trace of nitrogen dioxide is required as the initiator, either as an impurity or from traces of dioxygen. We have used purified nitric oxide at approximately 7 atm pressure. The exothermic reactions (carried out at 10°C) are much faster than those previously observed at 1 atm, although slower than when nitric oxide (which contains some NO_2) was used directly from the cylinder. We therefore suggest that the reaction involves the well-known[7] disproportionation

$$3NO = N_2O + NO_2,$$

although this reaction was studied at pressures much higher (200 atm) than those used here. As a product of the reaction we should expect to find N_2O rather than N_2,[4,5] and indeed we have confirmed (mass spectrometry) that the residual gas after complete absorption of nitric oxide by cyclohexene is only N_2O. The result is that the reaction with "pure NO" is tantamount to the reaction with dinitrogen trioxide or "nitrous fumes" as used in the older work. The initial rate of uptake of NO (% atm) by cyclohexene was measured semi-quantitatively at four temperatures between −10 and +22°C. An Arrhenius' plot gave a respectable straight line from which an activation energy (E_a) (=45.5 kJ mol^{-1}) was obtained. We assume that this is for the disproportionation reaction.

We have also studied the cobaloxime system[1] but were unable to reproduce the reported results. Styrene and NO in the presence of $NaBH_4$ or $[Co(DMGH)_2(py)Cl]$ in diethyl ether yield bis-(1-nitroso-2-nitro-1-phenylethane). Although reac-

* Present address: Department of Chemistry, University of Leicester, Leicester, U.K.
† Authors to whom correspondence should be addressed.

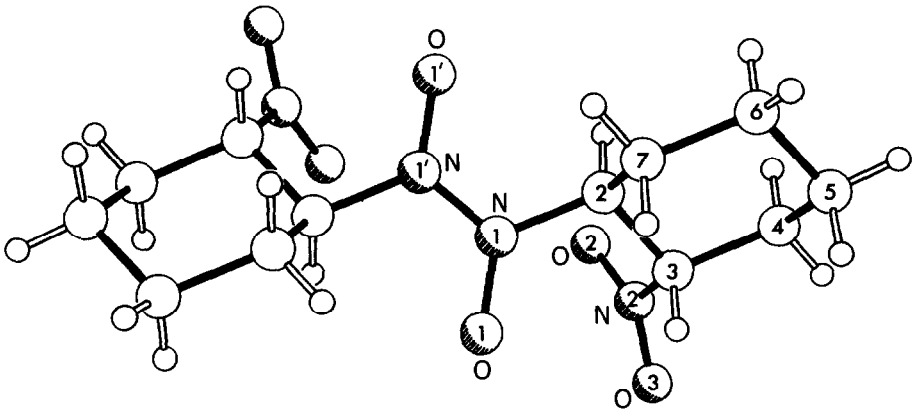


Fig. 1. Molecular structure of **1** giving the crystallographic numbering scheme. Selected torsion angles (°): N(1')N(1)C(2)H(2), −38; N(1')N(1)C(2)C(7), 81; C(2)C(3)N(2)O(2), 32.

tions involving alkenes, NO and cobalt nitrosyl complexes have been reported to yield species with C—N bonds[8] which may then be reduced by $LiAlH_4$ to amines, these reactions involved NO at 1 atm. In view of the present studies it seems unlikely that reactions with alkenes carried out under higher pressures of NO in order to achieve faster stoichiometric or catalytic reactions will prove useful, as competitive formation of ψ-nitrosites is likely to occur at a much faster rate.

CRYSTALLOGRAPHIC STUDIES

Figure 1 shows a perspective view of the molecule of the pseudonitrosite from cyclohexene (**1**) and bond lengths and angles are given in Tables 1 and 2. There is a crystallographic 2-fold axis passing through the centre of the N=N bond and normal to the plane of the *trans*-nitroso groups. The ONNO and CNNC torsion angles are 180.0(2) and 178.9(2)°, respectively, the latter angle reflecting a small out-of-plane distortion (0.004 Å) at the nitrogen atom. In nitrosocyclohexane[9] both the ONNO and CNNC torsion angles are 180° (there is a crystallographic centre of symmetry at the centre of the N=N bond); there is however a small rotation (0.7°) of the ONNO fragment with respect to that of the CNNC producing a 0.005 Å out-of-plane distortion at the nitrogen atom. The N=N, N=O and C—N bond lengths in **1** are all, within statistical significance, the same as those in nitrosocyclohexane.[9] These N=N and N—O bond distances are typical for a dimeric nitroso compound.[10] Clearly the addition of the *p*-nitro groups in **1** in no way significantly perturbs the geometry of the nitroso groups.

The bond lengths and valence angles for the compound from styrene (**2**) are given in Tables 3 and 4, while Fig. 2 shows a perspective view of the molecule. There is a crystallographic centre of symmetry at the centre of the N=N bond producing CNNC and ONNO torsion angles of 180°. The rotation about the N=N bond of the CNNC unit with respect to the ONNO (0.2°) and the consequent out-of-plane distortion at the nitrogen atom (0.002 Å) are both very small and probably not significant. The N=N, N—O and C—N bond lengths do not differ significantly from those of **1**.

Both **1** and **2** represent, in each case, one of three possible *trans* isomeric forms. **1** is chiral, though the presence of a glide plane in the crystal structure produces equal numbers of (*R*,*R*) and (*S*,*S*) molecules. For **2**, however, the crystal structure

Table 1. Bond lengths (Å) for bis-(1-nitroso-2-nitro-cyclohexane)

N(1)—O(1)	1.274(3)	N(1)—C(2)	1.487(2)
N(1)—N(1a)	1.302(4)	C(2)—C(3)	1.503(4)
C(2)—N(7)	1.525(3)	C(3)—C(4)	1.527(2)
C(3)—N(2)	1.507(3)	C(4)—C(5)	1.511(4)
C(5)—C(6)	1.514(5)	C(6)—C(7)	1.520(2)
N(2)—O(2)	1.212(4)	N(2)—O(3)	1.224(5)

Table 2. Bond angles (°) for bis-(1-nitroso-2-nitro-cyclohexane)

O(1)—N(1)—C(2)	121.4(2)	O(1)—N(1)—N(1a)	121.2(2)
C(2)—N(1)—N(1a)	117.4(3)	N(1)—C(2)—C(3)	109.1(2)
N(1)—C(2)—C(7)	110.2(1)	C(3)—C(2)—C(7)	109.8(2)
C(2)—C(3)—C(4)	109.7(2)	C(2)—C(3)—N(2)	111.3(2)
C(4)—C(3)—N(2)	109.1(2)	C(3)—C(4)—C(5)	109.4(2)
C(4)—C(5)—C(6)	112.3(2)	C(5)—C(6)—C(7)	111.1(3)
C(2)—C(7)—C(6)	109.2(2)	C(3)—N(2)—O(2)	118.7(3)
C(3)—N(2)—O(3)	117.2(2)	O(2)—N(2)—O(3)	124.1(2)

Table 3. Bond lengths (Å) for bis-(1-nitroso-2-nitro-1-phenylethane)

C(1)—C(2)	1.389(4)	C(1)—C(6)	1.361(5)
C(2)—C(3)	1.361(5)	C(3)—C(4)	1.366(6)
C(4)—C(5)	1.379(4)	C(5)—C(6)	1.376(3)
C(6)—C(7)	1.515(3)	C(7)—N(8)	1.479(3)
C(7)—C(10)	1.488(4)	N(8)—O(9)	1.269(3)
N(8)—N(8a)	1.301(4)	C(10)—N(11)	1.494(3)
N(11)—O(12)	1.213(3)	N(11)—O(13)	1.215(4)

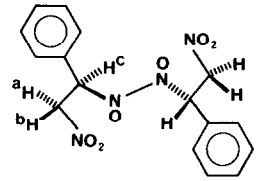
Table 4. Bond angles (°) for bis-(1-nitroso-2-nitro-1-phenylethane)

C(2)—C(1)—C(6)	120.0(3)	C(1)—C(2)—C(3)	120.5(4)
C(2)—C(3)—C(4)	119.7(3)	C(3)—C(4)—C(5)	119.9(3)
C(4)—C(5)—C(6)	120.6(3)	C(1)—C(6)—C(5)	119.3(2)
C(1)—C(6)—C(7)	118.8(2)	C(5)—C(6)—C(7)	121.9(3)
C(6)—C(7)—N(8)	110.0(2)	C(6)—C(7)—C(10)	111.1(2)
N(8)—C(7)—C(10)	109.6(2)	C(7)—N(8)—O(9)	120.9(2)
C(7)—N(8)—N(8a)	118.6(3)	O(9)—N(8)—N(8a)	120.5(3)
C(7)—C(10)—N(11)	113.7(2)	C(10)—N(11)—O(12)	119.0(3)
C(10)—N(11)—O(13)	117.0(2)	O(12)—N(11)—O(13)	124.0(2)

reveals only the *meso* form. Clearly in both instances there is the possibility that the other *trans* and *cis* isomers were formed in the chemical reaction. In both cases the alternative configurational or conformational geometries would change the crystal packing and probably also the crystal morphology. However, in neither case was there any noticeable inhomogeneity in the crystalline samples. We do not discount, however, the possibility that different crystalline isomers may have also been present.

In this respect it may be noted that the ^{1}H NMR spectrum of bis-(1-nitroso-2-nitro-1-phenylethane) (**2**) showed two distinct sets of peaks. These can be assigned to the (*R,S*) and the (*R,R*) and (*S,S*) stereoisomers. Due to the different chemical environments of the ethyl protons the spectrum exhibits an ABC character. As expected, 12 lines are observed in all, each proton signal being split into a doublet of doublets.

Handpicking of the crystal mass allowed separation of the clear *meso* (*R,S*) form and the opaque (*R,R* + *S,S*) form, whose conformation was confirmed by NMR (see Experimental and diagram **1**).



(1)

EXPERIMENTAL

Microanalysis was carried out by Imperial College Laboratories. Molecular weights were determined cryoscopically in benzene; m.ps are

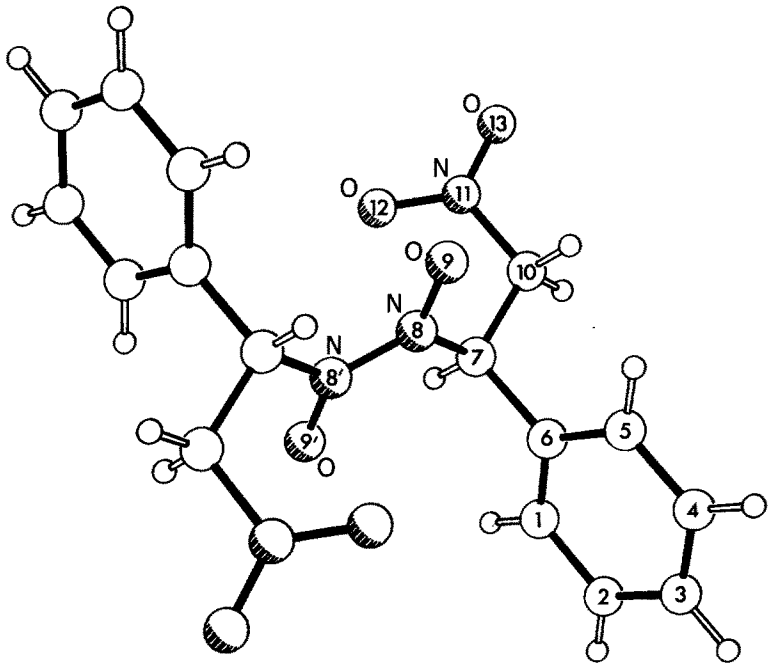


Fig. 2. Molecular structure of **2** giving the crystallographic numbering scheme. Selected torsion angles (°): N(8')N(8)C(7)H(7), 28; N(8')N(8)C(7)C(6), −91; N(8)C(7)C(6)C(5), −61; N(8)C(7)C(10)N(11), −62; C(7)C(10)N(11)O(12), −4.

uncorrected. All operations were carried out under nitrogen or in a vacuum. Solvents were dried over sodium–benzophenone and distilled before use. Alkenes were passed through alumina and distilled from sodium under reduced pressure. Nitric oxide (British Oxygen Co. cylinders, 0.35% NO_2) was passed through a steel cylinder packed with powdered sodium hydroxide, and then through a copper spiral coil at −78°C.

Spectrometers

NMR: JEOL FX 90Q and Bruker WM 250. Data are given in δ ppm referenced to Me_4Si (^1H) and d^6-acetone (^{13}C). IR: Perkin–Elmer 683, spectra (cm^{-1}) in Nujol mulls referenced to polystyrene. Mass spectra were obtained on a VG 7070 spectrometer.

Bis-(1-nitroso-2-nitro-cyclohexane) (**1**)

A typical reaction procedure is as follows. Cyclohexene (3 cm^3, 0.03 mol) in a 90-cm^3 pressure bottle was pressurized with nitric oxide (100 psi). The white solid formed after 1 h was collected, washed with diethylether, and recrystallised from dichloromethane and diethylether. Yield 3.4 g, 36% based on alkene. M.p. 136°C. [Analysis of $C_{12}H_{20}N_4O_6$: C, 45.6 (45.6); H, 6.4 (6.5); N, 17.7 (17.6)%. *M* 342 (320).] ^1H NMR ($CDCl_3$): 1.1–2.8 (16H), 4.80–5.18 (multiplet of six, 2H), 5.34–5.78 (multiplet of six, 2H). IR: 1556s, 1410sh, 1266, 1216s, 1133 and 910 cm^{-1}.

Bis-(1-nitroso-2-nitro-1-phenylethane) (**2**)

As above except that crystals were obtained from dichloromethane after 2 days at −20°C. Yield 2.9 g, 27% based on styrene. M.p. 108.4°C. [Analysis of $C_{16}H_{16}N_4O_6$: C, 53.1 (53.3); H, 4.4(4.5); N, 15.4 (15.5)%. *M* 340(360).] Two distinct types of crystals were separated manually. NMR: (a) clear (*R,S*). ^1H (C_6D_6): 3.29, d of d, (2H), H^b, J_{AB} = 16 Hz, J_{BC} = 11.4 Hz; 4.82, d of d, (2H), H^a; 6.57, d of d, (2H), H^c, J_{AC} = 2.9 Hz; 7.0–7.16, (10H), Ph. (b) Opaque crystals, (*R,R*) and (*S,S*) forms. ^1H: 3.21, d of d, (2H), H^b, J_{AB} = 14.9 Hz; 3.79, d of d, (2H), H^a, J_{AC} = 3.6 Hz; 6.06, d of d, (2H), H^c, J_{BC} = 10.1 Hz; 6.9–7.09, (10H), Ph. ^{13}C–{^1H} (d^6-acetone): 139.5s (CH_2NO_2); 138.7s (*C*HPhNO); 132.7s (*para* ring C); 131.6s (quaternary C); 130.3s (*meta* ring C); 130.1s (*ortho* ring C). IR: 1568s, 1502, 1415, 1267, 1210s and 984 cm^{-1}.

Bis-(1-nitroso-2-nitro-norbornane)

As for **2** but using norbornylene (2 g) and ether (5 cm^3) as solvent in pressure bottle. Yield 2.5 g, 34%. M.p. 118.4°C. [Analysis: C, 49.7 (49.4); H, 5.9 (5.9);

N, 16.3(16.5)%.] Mass spectrum (130°C, 70 eV): *m/z*: 170 ($\frac{1}{2}M^+$, 8%); 140 ($\frac{1}{2}M^+ - NO$, 86%); 124 ($\frac{1}{2}M^+ - NO_2$, 89%); 96 ($\frac{1}{2}M^+ - NO_2 - C_2H_4$, 56%), 94 ($C_7H_{10}$, 51%). IR: 1545s, 1410, 1370sh, 1330, 1305, 1265, 1240s, 1190, 1050, 890 and 780 cm^{-1}.

X-RAY STRUCTURAL ANALYSES OF 1 AND 2

Crystal data

(**1**) $C_{12}H_{20}N_4O_6$, monoclinic, $a = 14.438(2)$, $b = 12.382(1)$, $c = 11.706(2)$ Å, $\beta = 131.38(1)°$, $U = 1570$ Å^3, space group $C2/c$, $Z = 4$, $M = 316.3$, $D_c = 1.34$ g cm^{-3}. (**2**) $C_{16}H_{16}N_4O_6$, triclinic, $a = 5.494(3)$, $b = 8.742(8)$, $c = 9.507(4)$ Å, $\alpha = 70.20(6)$, $\beta = 78.28(4)$, $\gamma = 89.60(6)°$, $U = 420$ Å^3, space group $P\bar{1}$, $Z = 1$, $M = 360.3$, $D_c = 1.43$ g cm^{-3}.

Measurements

Refined unit cell parameters were obtained by centering 16 (**1**) and 12 (**2**) reflections on a Nicolet R3m diffractometer. 971 and 1029 independent observed reflections [$|F_o| > 3\sigma(|F_o|)$] were measured for **1** and **2** respectively. The data were corrected for Lorentz and polarisation factors; no absorption corrections were performed.

Both structures were solved by direct methods and the non-hydrogen atoms refined anisotropically. All hydrogen atoms were placed at idealised positions (C—H = 0.96 Å), assigned isotropic thermal parameters, $U(H) = 1.2U_{eq}(C)$, and allowed to ride on their parent carbons. Refinement was by block-cascade, full-matrix least-squares to $R = 0.038$, $R_w = 0.048$ [$w^{-1} = \sigma^2(F) + 0.0003F^2$] for **1** and $R = 0.053$, $R_w = 0.063$ [$w^{-1} = \sigma^2(F) + 0.0005F^2$] for **2**. Computations were carried out on an Eclipse S140 computer using the SHELXTL program system.[11]

Final atomic coordinates for both compounds, including those of the hydrogen atoms, and thermal parameters have been deposited with the Editor as supplementary data.*

Acknowledgements—We thank the SERC for support (K.W.C.) and for provision of the diffractometer. We also thank Mr R. Jones for his assistance with the X-ray analyses.

REFERENCES

1. T. Okamoto and S. Oka, *J. Chem. Soc., Chem. Commun.* 1984, 289.
2. D. Klamann, W. Koser, P. Weyerstahl and M. Fligge, *Chem. Ber.* 1965, **98**, 1831.
3. J. H. Boyer, In *The Chemistry of the Nitro and Nitroso Groups* (Edited by H. Feuer), Part 1, Chap. 5. Interscience, New York (1969); P. A. S. Smith, *Open Chain Nitrogen Compounds*, Vol. 2. Benjamin, New York (1966). A. Gasco and A. J. Bouton, In *Advances in Heterocyclic Chemistry* (Edited by A. R. Katritzky and A. J. Boulton), Section 4, p. 251. Academic Press, New York (1981).
4. J. F. Brown, *J. Am. Chem. Soc.* 1957, **79**, 2480.
5. G. F. Bloomfield and G. A. Jeffrey, *J. Chem. Soc.* 1944, 120.
6. J. D. Park, A. P. Stefani, G. H. Crawford and J. R. Lacher, *J. Org. Chem.* 1961, **26**, 3316.
7. T. P. Melia, *J. Inorg. Nucl. Chem.* 1965, **27**, 95.
8. P. N. Becker, M. A. White and R. G. Bergman, *J. Am. Chem. Soc.* 1980, **102**, 5676; P. N. Becker and R. G. Bergman, *J. Am. Chem. Soc.* 1983, **105**, 2985; P. N. Becker and R. G. Bergman, *Organometallics* 1983, **2**, 787.
9. M. Tanimura, K. Kobori, M. Kashiwagi and Y. Kinoshita, *Bull. Chem. Soc., Jpn* 1970, **43**, 1962.
10. D. A. Dieterich, I. C. Paul and D. Y. Curtin, *J. Am. Chem. Soc.* 1974, **96**, 6372, and references therein.
11. G. M. Sheldrick, *SHELXTL, An Integrated System for Solving, Refining and Displaying Crystal Structures from Diffraction Data.* University of Göttingen, F.R.G. (1978), Revision 4.1 (1983).

* Atomic coordinates have also been deposited with the Cambridge Crystallographic Data Centre.

Polyhedron Vol. 4, No. 11, pp. 1947–1950, 1985
Printed in Great Britain

0277-5387/85 $3.00 + .00
© 1985 Pergamon Press Ltd

THE PREPARATION AND X-RAY STRUCTURE OF (DISULPHURDINITRIDO)BIS(TRIPHENYLPHOSPHINE)PLATINUM(II)—TETRACHLOROFORM SOLVATE, $Pt(S_2N_2)(PPh_3)_2 \cdot 4CHCl_3$

RAY JONES, PAUL F. KELLY, DAVID J. WILLIAMS and J. DEREK WOOLLINS*

Department of Chemistry, Imperial College of Science and Technology, South Kensington, London SW7 2AY, U.K.

(*Received* 25 *April* 1985; *accepted* 10 *June* 1985)

Abstract—Reaction of $Pt(PPh_3)_3$ with $S_4N_4H_4$ gives *cis*-$Pt(S_2N_2)(PPh_3)_2$ (**1**) in 45% yield. **1** was characterised by IR, ^{31}P NMR and X-ray crystallography as the tetrachloroform solvate (**2**), which crystallises in the monoclinic system, space group $P2_1$ with $a = 14.635(7)$ Å, $b = 12.758(4)$ Å, $c = 15.405(8)$ Å, $\beta = 117.77(3)°$. The $S_2N_2^{2-}$ ligand coordinates in a bidentate fashion with Pt—N = 2.018(14) Å, Pt—S = 2.288(5) Å and contains two short [1.546(16) and 1.567(19) Å] and one long [1.682(16) Å] S—N bond.

The preparation of transition-metal complexes containing simple sulphur–nitrogen ligands is currently an area of interest both from the point of view of establishing new structural types and as a result of the unusual electrical properties of polymeric sulphur nitride, $(SN)_x$. Reactions between higher oxidation state transition-metal halides/complexes and tetrasulphurtetranitride, S_4N_4, or, more recently, S_7NH have been reported by us,[1,2] whilst Dehnicke and co-workers have studied reactions of $S_3N_3Cl_3$ with group V and VI metal halides.[3,4] Although there are examples of reactions between $S_3N_3Cl_3$ and low oxidation state metal–phosphine complexes[5] very few reactions between metal(0) complexes and S_4N_4 or $S_4N_4H_4$ have been reported. Bhattacharyya *et al.* have carried out some work on reactions between $Pt(PPh_3)_4$ and $S_4N_4/S_4N_4H_4$. In their first paper[6] they claimed the preparation of $Pt(S_2N_2H_2)(PPh_3)_2$ and $Pt(S_2N_2)(PPh_3)_2$ (**1**) on the basis of microanalytical data and UV–Vis spectroscopy. More recently[7,8] they have changed the formulation of the disulphurdiimide complex to $Pt(OSNH)_2(PPh_3)_2$ as a result of X-ray crystallographic studies, although, in a later paper,[9] they again postulated the existence of a complex containing an $S_2N_2H_2$ ligand.

As part of a wider study of the interactions between sulphur–nitrogen species and transition-metal centres we are investigating the usefulness of Pt(0) complexes in the synthesis of metalla-sulphur–nitrogen complexes and clusters and we have recently been successful[10] in the reaction of $Pt(C_2H_4)(PPh_3)_2$ with $(Me_3Si)_2N_2S$ to form $Pt(NSNSiMe_3)_2(PPh_3)_2$. Here we report on our studies on the reaction between $S_4N_4H_4$, $Pt(PPh_3)_3$ and $Pt(PPh_3)_4$, together with the X-ray crystal structure of the major product from these reactions, **1**. We also report NMR studies of the reaction between S_4N_4 and the above Pt(0) phosphines.

EXPERIMENTAL

All chemicals were of reagent grade. K_2PtCl_4 was from Johnson–Matthey Chemicals. Solvents were dried before use; hexane and toluene were distilled from sodium–benzophenone, dichloromethane was distilled from calcium hydride, and acetone was dried over 4 Å molecular sieves. $^{31}P-\{^1H\}$ NMR spectra were recorded on a JEOL FX90Q F.T. NMR spectrometer and are referred to external 85% H_3PO_4, and IR spectra were recorded as KBr discs on a Perkin–Elmer 683 spectrophotometer. Elemental analyses were performed by the microanalytical department of the chemistry department of Imperial College.

Tetrasulphurtetraimide, tetrasulphurtetranitride, $Pt(PPh_3)_4$, $Pt(PPh_3)_3$ and $Pt(C_2H_4)(PPh_3)_2$ were prepared as described in the literature.[11–14]

* Author to whom correspondence should be addressed.

Preparation of $Pt(S_2N_2)(PPh_3)_2$ (1)

Tetrasulphurtetraimide (0.019 g, 1.0 mmol) in acetone (5 cm^3) was treated with tris(triphenylphosphine)platinum (0.1 g, 0.1 mmol) in toluene (5 cm^3). The reaction mixture was stirred for 1.5 h whereupon hexane (*ca* 30 cm^3) was added to precipitate the crude product which was dried *in vacuo*, extracted with cold toluene and reprecipitated with hexane to give a fine yellow powder (yield 36 mg, 45%). Found: C, 52.3; H, 3.9; N, 3.6. Calc. for $C_{36}H_{30}N_2P_2S_2Pt$: C, 53.26; H, 3.72; N, 3.45%. $^{31}P-\{^1H\}$ ($CDCl_3$): $\delta = 23.57$ [*d*, $^2J(^{31}P-^{31}P)$ 22 Hz, $^1J(^{31}P-^{195}Pt)$ 2827 Hz]; $\delta = 11.42$ (d, ^2J 22 Hz, ^1J 2994 Hz). IR (KBr disc): 1045(s) [ν(NS)], 610(sh, m) [ν(NS)], 445(w) [ν(PtN)], 360(m) [δ(NS)] and 352(sh) [ν(PtS)]. Crystals suitable for X-ray crystallography were obtained by slow diffusion of hexane into a chloroform solution of **1**.

X-ray structural analysis of $Pt(S_2N_2)(PPh_3)_2 \cdot 4CHCl_3$ (2)

Crystal data. $C_{36}H_{30}N_2P_2PtS_2 \cdot 4CHCl_3$, yellow plates, monoclinic, $a = 14.635(7)$ Å, $b = 12.758(4)$ Å, $c = 15.405(8)$ Å, $\beta = 117.77(3)°$, $U = 2545$ Å^3, space group $P2_1$, $Z = 2$, $M = 1289.3$, $D_c = 1.68$ g cm^{-3}, μ(Cu-K_α) = 128 cm^{-1}.

Measurements. Crystal dimensions $0.29 \times 0.34 \times 0.12$ mm. Refined unit cell parameters were obtained by centering 14 reflections on a Nicolet R3m diffractometer, 3603 independent reflections ($\theta \leqslant 58°$) were measured with Cu-K_α radiation (graphite monochromator) using the ω-scan measuring routine. Of these 3423 had $|F_o| > 3\sigma(|F_o|)$ and were considered to be observed. Lorentz polarisation and an empirical absorption correction based upon 360 azimuthal measurements (maximum and minimum transmission factors 0.95 and 0.15) were applied.

Structure analysis. The structure was solved by the heavy-atom method. The positions of the platinum and one of the phosphorus atoms were determined from a Patterson map. The positions of the remaining atoms were found from a succession of ΔF maps which also revealed the presence of four solvent chloroform molecules. The non-hydrogen atoms were refined anisotropically. The hydrogen atom positions were idealised (C—H = 0.96 Å) assigned isotropic thermal parameters [U(H) = $1.2U_{eq}$(C)] and allowed to ride on their parent carbon atoms.

Refinement was by block cascade full-matrix least squares to $R = 0.052$, $R_w = 0.054$ [$w^{-1} = \sigma^2(F) + 0.0014F^2$]. The polarity of the structure was established by an R factor test. Computations were carried out on an Eclipse S140 computer using the SHELXTL program system.[15] Scattering factors were taken from the *International Tables for X-ray Crystallography*.[16]

Final atomic coordinates, including those of the hydrogen atoms, and thermal parameters have been deposited with the Editor as supplementary data.*

RESULTS AND DISCUSSION

Reaction of tetrasulphurtetraimide with tris(triphenylphosphine)platinum(0) proceeds at room temperature to give **1** as a pale yellow solid, in good (45%) yield. **1** was characterised by microanalysis, IR and NMR and its structure [as the tetrachloroform solvate (**2**)] determined by X-ray crystallography.

The IR spectrum of **1** shows the expected absorptions due to triphenylphosphine together with bands due to ν(NS) at 1045 and 610 cm^{-1} and δ(NS) at 360 cm^{-1}; the ν(PtN) and ν(PtS) vibrations (445 and 352 cm^{-1}) are assigned by analogy with previous work[17] on $M(S_2N_2H)_2$ complexes.

The $^{31}P-\{^1H\}$ NMR of **1** is an **AX** spectrum with satellites due to $^{31}P-^{195}Pt$ couplings. The $^2J(^{31}P-^{31}P)$ coupling constant (22 Hz) and the $^1J(^{31}P-^{195}Pt)$ couplings (2827 and 2994 Hz) are as expected for a Pt(II) compound with *cis* phosphine ligands. It is possible to assign the individual phosphorus resonances since the larger ^1J coupling is expected to be associated with the shorter Pt—P bond,[18] i.e. P(2) *trans* to nitrogen, $\delta = 11.42$. The chemical shift of P(2) in **1** is very close to that observed[10] for the phosphorus nuclei in $Pt(NSNSiMe_3)_2(PPh_3)_2$ ($\delta = 11.76$ ppm) consistent with the triphenylphosphine groups in these two compounds being in similar environments, i.e. both having phosphines *trans* to sulphur diimide groups.

The crystal structure of **2** (Fig. 1 and Table 1) reveals planar coordination of the platinum by two

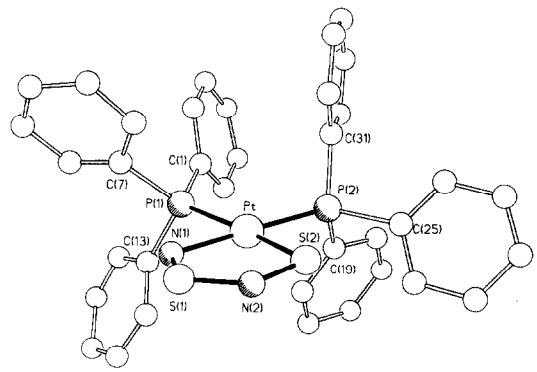


Fig. 1. Crystal structure of $Pt(S_2N_2)(PPh_3)_2 \cdot 4CHCl_3$.

* Atomic coordinates have also been deposited with the Cambridge Crystallographic Data Centre.

Table 1. Selected bond distances (Å) and angles (°) for $Pt(S_2N_2)(PPh_3)_2 \cdot 4CHCl_3$

Pt—S(2)	2.288(5)	Pt—P(1)	2.317(4)
Pt—P(2)	2.263(4)	Pt—N(1)	2.018(14)
S(1)—N(1)	1.546(16)	S(1)—N(2)	1.567(19)
S(2)—N(2)	1.682(16)	P(1)—C(1)	1.806(17)
P(1)—C(7)	1.847(14)	P(1)—C(13)	1.791(13)
P(2)—C(19)	1.803(12)	P(2)—C(25)	1.836(19)
P(2)—C(31)	1.813(13)		
S(2)—Pt—P(1)	170.0(1)	S(2)—Pt—P(2)	91.1(2)
P(1)—Pt—P(2)	98.4(1)	S(2)—Pt—N(1)	87.6(5)
P(1)—Pt—N(1)	82.8(5)	P(2)—Pt—N(1)	178.7(5)
N(1)—S(1)—N(2)	116.0(9)	Pt—S(2)—N(2)	104.0(7)
S(1)—N(2)—S(2)	116.1(11)	Pt—N(1)—S(1)	116.2(9)
Pt—P(1)—C(1)	122.9(6)	Pt—P(1)—C(7)	109.2(5)
Pt—P(1)—C(13)	112.6(5)	Pt—P(2)—C(19)	115.0(5)
Pt—P(2)—C(25)	117.3(5)	Pt—P(2)—C(31)	111.6(5)

cis-triphenylphosphine groups and a bidentate $S_2N_2^{2-}$ ligand, with a maximum deviation from the least-square plane comprising Pt, P(1), and P(2) and the S_2N_2 ring of 0.049 Å. The PtS_2N_2 plane is even closer to planar with a maximum deviation of 0.008 Å. As is often the case steric effects open up the PPtP angle [98.4(1)°] whilst the NPtS angle is slightly less than 90 at 87.6(5)°. The Pt—P distances [2.317(4) and 2.263(4) Å] are normal for a Pt(II) complex, the slight difference in the two bond lengths being attributable to the differences in π-acceptor and σ-donor ability of the sulphur and nitrogen atoms. The S—N distances in the $S_2N_2^{2-}$ ligand are unequal with two short [1.546(16) and 1.567(19) Å] and one long [1.681(16) Å] bond as is the case for previous examples of complexes containing this ligand[19–21] and its protonated analogue.[22,23] The longer S—N distance indicates a bond order of close to one whilst the two shorter distances are reasonable for double bonds in the sulphur di-imide (N_2S) like part of the ring. The bond angles within the PtS_2N_2 ring correspond well with previous studies[19–22] with N(1), S(1) and N(2) having ring angles of close to 116° and Pt—S(2)—N(2) being 104.0(7)°. These angles are consistent with the description of the ring as being made up of a delocalised N_2S group with S(2) being sp^3-hybridised. Complete delocalisation of the six π-electrons formally present is thus not apparent.

The formation of **1** from the reaction described above is somewhat surprising in the light of the reports[8] that treatment of $Pt(PPh_3)_4$ with $S_4N_4H_4$ gives $Pt(OSNH)_2(PPh_3)_2$ (**3**) in 94% yield. We have carried out the reaction, as reported here, several times, both under N_2 and in air and always observed (by ^{31}P NMR) the formation of **1** as the only platinum phosphine. Reaction under N_2 was found to be preferable to avoid sulphate impurities (from IR) but **1**, once obtained, is not air-sensitive and so does not appear to be the source of **3**. Attempts to prepare **3** by the published route[6] have, in our hands, been unsuccessful. The crude toluene solution from the published reaction contains approximately (by ^{31}P NMR) 10% Ph_3PS, 30% Ph_3PO, 20% Ph_3P and 40% **1**. We suspect that the formation of **3** may have come about as a result of the presence of catalytic quantities of impurities in previous workers' reactions.

Other routes to **1** have also been studied. Reaction of $Pt(PPh_3)_4$ with S_4N_4 has been reported as giving rise to **1** as a brown solid in 73% yield. Since **1** is yellow the previously reported product[6] obviously contained impurities and our ^{31}P NMR studies indicate several other compounds with **1** (*ca* 25%) when we repeated the published procedure. Reaction of $Pt(O_2)(PPh_3)_2$, $Pt(C_2H_4)(PPh_3)_2$ or $Pt(PPh_3)_3$ with S_4N_4 all give **1** (*ca* 20% by ^{31}P NMR) together with other platinum phosphines which we hope to report on later.

The mechanism of formation of **1** is not clear; however, it is interesting to note that reactions of the S_3N^- anion with metal halides result in the formation of compounds containing $S_2N_2H^-$ ligands.[24] It seems possible that the currently unknown $S_2N_2^{2-}$ anion is involved as an intermediate in many of the solution equilibria of sulphur imides.

Acknowledgements—We are grateful to Johnson–Matthey Chemicals for loans of precious metals and to Dr C. P. Warrens for useful discussions on ^{31}P NMR.

REFERENCES

1. J. D. Woollins, R. Grinter, M. K. Johnson and A. J. Thomson, *J. Chem. Soc., Dalton Trans.* 1980, 1910.
2. J. D. Woollins, *Polyhedron* 1984, **3**, 1365.
3. U. Kynast, E. Conradi, U. Muller and K. Dehnicke, *Z. Naturforsch.* 1984, **39B**, 1680.
4. J. Hanich, M. Krestel, U. Muller, K. Dehnicke and D. Rehder, *Z. Naturforsch.* 1984, **39B**, 1686.
5. M. B. Hursthouse, N. P. C. Walker, C. P. Warrens and J. D. Woollins, *J. Chem. Soc., Dalton Trans.* 1985, 1043.
6. A. A. Bhattacharyya, J. A. McLean, Jr and A. G. Turner, *Inorg. Chim. Acta* 1979, **34**, L199.
7. A. A. Bhattacharyya, A. G. Turner, E. M. Holt and N. W. Alcock, *Inorg. Chim. Acta* 1980, **44**, L185.
8. E. M. Holt, N. W. Alcock, A. A. Bhattacharyya and A. G. Turner, *Inorg. Chim. Acta* 1981, **47**, 255.
9. A. A. Bhattacharyya and A. G. Turner, *Inorg. Chim. Acta* 1981, **53**, L89.
10. N. P. C. Walker, M. B. Hursthouse, C. P. Warrens and J. D. Woollins, *J. Chem. Soc., Chem. Commun.* 1985, 227.
11. F. Feher, In *Handbook of Preparative Inorganic Chemistry* (Edited by G. Brauer), Vol. 1, p. 411. Academic Press, New York (1965).
12. M. Villena-Blanco and W. L. Jolly, *Inorg. Synth.* 1967, **9**, 99.
13. R. Ugo, F. Cariata and G. LaMonica, *Inorg. Synth.* 1968, **11**, 105.
14. C. D. Cook and G. S. Jauhal, *J. Am. Chem. Soc.* 1968, **90**, 1464.
15. G. M. Sheldrick, *SHELXTL, An Integrated System for Solving, Refining, and Displaying Crystal Structures from Diffraction Data.* University of Göttingen, Göttingen, F.R.G. (1978), Revision 4.1 (August 1983).
16. *International Tables for X-ray Crystallography*, Vol. 4, pp. 99–149. Kynoch Press, Birmingham (1974).
17. D. B. Powell and J. D. Woollins, *Spectrochim. Acta* 1980, **A36**, 447.
18. P. S. Pregosin and R. W. Kunz, ^{31}P *and* ^{13}C *NMR of Transition Metal Phosphine Complexes.* Springer, New York (1979). Number 16 in the series *NMR Basic Principles and Progress.*
19. F. Edelmann, *J. Organomet. Chem.* 1982, **228**, C47.
20. H. Martan and J. Weiss, *Z. Anorg. Allg. Chem.* 1984, **514**, 107.
21. J. Weiss, *Z. Anorg. Allg. Chem.* 1983, **502**, 165.
22. J. Weiss and U. Thewalt, *Z. Anorg. Allg. Chem.* 1968, **363**, 159.
23. K. F. Mayer and J. Weiss, *Acta Cryst.* 1978, **B34**, 1999.
24. J. Bojes, T. Chivers, W. G. Laidlaw and M. Trsic, *J. Am. Chem. Soc.* 1982, **104**, 4841.

Polyhedron Vol. 4, No. 11, pp. 1951–1956, 1985
Printed in Great Britain

0277–5387/85 $3.00 + .00
© 1985 Pergamon Press Ltd

A POTENTIOMETRIC STUDY ON THE COMPLEX EQUILIBRIA BETWEEN NICKEL(II) AND 2-MERCAPTO-2-PHENYLACETIC ACID

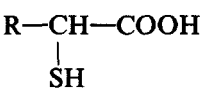
ENRIC CASASSAS,* MONTSERRAT FILELLA, ALVARO IZQUIERDO, DOLORS PRAT and ROSA RODRÍGUEZ

Departament de Química Analítica, Universitat de Barcelona, 08028 Barcelona, Spain

(*Received* 29 *April* 1985; *accepted* 26 *May* 1985)

Abstract—Complex formation between nickel(II) and 2-mercapto-2-phenylacetic acid (H_2MPA) has been studied at 25°C and 1 mol dm^{-3} ClO_4^- in 50% (v/v) ethanol–water using glass electrode potentiometry. The emf data obtained have been analyzed using the ESTA programs. Protonation constants for the ligand and formation constants for the complexes $Ni_3(MPA)_4^{2-}$, $Ni_2(MPA)_3^{2-}$ and $Ni(MPA)_2^{2-}$ are reported.

2-Mercaptoacids are compounds with the general structure



which act as complexing agents for metal ions. They have many applications in analytical chemistry and they are also of interest in relation to various biological systems.

Nickel(II) is one of the metal ions whose complexation by 2-mercaptoacids has been most widely studied. After an initial investigation of the complex formation between nickel(II) and mercaptoacetic acid (R = H),[1] where only the existence of mononuclear complexes was found, Leussing *et al.*[2] established that polynuclear complexes of the type $M[ML_2]_n^{2-2n}$ were commonly formed in this system. The main species were $M_4L_6^{4-}$ and ML_2^{2-}. The same system has been studied by Perrin and Sayce,[3] who also found that $M_4L_6^{4-}$ and ML_2^{2-} were the major species but that $M_3L_4^{2-}$, $M_2L_3^{2-}$, MLH^+ and ML_3^{4-} did occur simultaneously. These results were largely confirmed in a subsequent study by De Brabander *et al.*,[4] although these authors could not find any evidence for the formation of $M_2L_3^{2-}$, MLH^+ and ML_3^{4-}.

Fewer studies have been conducted on the complexation of nickel(II) with 2-mercaptopropanoic acid (R = CH_3). However, De Brabander *et al.*[5] have reported that only $M_3L_4^{2-}$ and ML_2^{2-} are formed; they attributed the lack of formation of the complex $M_4L_6^{4-}$ to the steric hindrance caused by the 2-methyl group.

As has already been pointed out by Perrin and Sayce,[3] many published values of formation constants for the nickel(II) complexes of these ligands must be considered unreliable because they have been calculated on the assumption that the monomeric species are the only ones formed.

No studies on the complexation of 2-mercapto-2-phenylacetic acid (R = Ph) with metal ions appear in the literature. This is probably because it is not commercially available and it is not soluble in water. In order to compare the influence of an arylic substituent on the complexing ability of 2-mercaptoacids with nickel(II) we undertook the study of the system between nickel(II) and 2-mercapto-2-phenylacetic acid.

EXPERIMENTAL

Materials

2-Mercapto-2-phenylacetic acid was prepared by the action of potassium *O*-ethyldithiocarbonate on 2-bromo-2-phenylacetic acid.[6] The product obtained, a yellow oil which crystallizes rapidly, was hydrolyzed with concentrated ammonium hydroxide.[7] The crude product is again an oil which only crystallizes gradually. By recrystallization from petroleum ether 40–60°C, 2-mercapto-2-phenylacetic acid is obtained as white crystals (m.p. 60–61°C). *Analysis.* Found: C, 57.0; H, 4.8; S, 18.9.

* Author to whom correspondence should be addressed.

Calc. for $C_8H_8O_2S$: C, 57.1; H, 4.8; S, 19.1%. Its purity was tested periodically by iodometric titrations.[8] Although the compound was found to be quite stable, a freshly prepared solution was used for each titration.

A standard stock solution of nickel was prepared as its perchlorate salt (K&K) and standardized gravimetrically as bis(dimethylglyoximato)nickel for metal concentration[9] and by Gran plots for hydrogen ion concentration.[10]

Sodium hydroxide solution was prepared frequently from sodium hydroxide pellets (Merck) and standardized by titration against standard grade potassium hydrogen phtalate (Merck).

To maintain ionic strength, all solutions were made up to a perchlorate concentration of 1 mol dm^{-3} by the addition of sodium perchlorate prepared as described in Ref. 11.

All solutions were prepared using deionized double distilled water boiled and cooled under nitrogen and absolute ethanol (Merck), so that all solutions were 50% (v/v) ethanol–water.

High-grade nitrogen (S.E.O.) was passed through a vanadate solution,[12] concentrated sodium hydroxide, sulphuric acid and ionic background thermostatted at 25°C. A purified nitrogen atmosphere was maintained in the vessel during the titrations and all solutions were thoroughly flushed with nitrogen before use.

Method

Protonation constants for the ligand and formation constants for the nickel complexes were determined by potentiometric titrations in a double walled vessel, thermostatted at 25.0±0.05°C by circulating water. The free hydrogen ion concentration was measured using Radiometer PHM 84 Research pH Meter equipped with a wide-range glass electrode (Radiometer G202B) and a silver–silver chloride electrode prepared as described by Brown.[13] The following cell, which includes a Wilhelm bridge,[14] was employed:

Ag, AgCl(s)	10 mmol dm^{-3} NaCl 990 mmol dm^{-3} $NaClO_4$ [50% (v/v) ethanol–water]	1 mol dm^{-3} $NaClO_4$ [50% (v/v) ethanol–water]	TS	glass electrode.

The electrode system was calibrated in terms of hydrogen ion concentration by performing strong acid vs strong base titrations.[15]

Experimental solutions containing ligand, metal (when appropriate) and perchloric acid were titrated, the hydrogen ion concentration being varied by adding sodium hydroxide. Total metal ion concentrations were kept constant by adding, after each addition of sodium hydroxide, an equal volume of metal ion solution with a concentration twice that of the total metal ion in the cell.

Protonation curves for the ligand were obtained at a variety of different ligand concentrations and, similarly, the metal complex formation curves were obtained at different ligand:metal ratios and for different ligand and metal concentrations.

The number of the titration points, the compositions of the starting solutions and the $-\log [H]$ ranges used in the calculations are shown in Table 1. The upper limits of the reactants were largely determined by the insolubility of the ligand or by the formation of metal complex precipitates. The upper limits of the $-\log [H]$ ranges were determined by a sudden drop in the rate at which equilibrium was attained, as evidenced by a slow drift in the potentiometric readings.

Data treatment

In evaluating the equilibrium constants, metal M^{2+}, ligand L^{2-} [i.e. deprotonated 2-mercapto-2-phenylacetic acid (MPA)] and H^+ were chosen as components. The general three-component equilibrium can be written as:

$$pM + qL + rH \rightleftharpoons M_pL_qH_r. \quad (1)$$

The overall formation constants are defined as:

$$\beta_{pqr} = \frac{[M_pL_qH_r]}{[M]^p[L]^q[H]^r}, \quad (2)$$

where the square brackets indicate the concentration of the free-metal, ligand and hydrogen ions. Charges are omitted for simplicity.

The initial model, initial estimates of the values of the formation constants and the final selection of species were obtained as described in Ref. 16.

Formation constant refinement was performed using the ESTA[17] optimization module with a weighted least-squares objective function based on emf residuals:

$$U = \frac{\sum_n w(\text{emf}^o - \text{emf}^c)^2}{N - n_p}, \quad (3)$$

where N = total number of experimental titration points and n_p = total number of optimized parameters. The weight at each titration point was

Table 1. Summary of the titration data used for calculating formation constants: number of titration points, initial concentrations of nickel (C_{Ni}) and ligand (C_{MPA}), and rough $-\log$ [H] ranges (concentrations expressed in mol dm^{-3})

System	Titration	No. of points	C_{Ni}	C_{MPA}	$-\log$ [H] range
MPA–H$^+$	1	54		3.280	3.7–10.7
	2	59		3.433	3.7–10.7
	3	56		3.595	3.6–10.6
	4	52		3.662	3.6–10.8
	5	67		3.772	3.7–10.8
	6	51		5.229	3.7–10.7
	7	51		7.957	3.7–10.7
	8	57		8.044	3.7–10.8
	9	51		12.047	3.7–10.6
Ni^{2+}–MPA–H$^+$	1	39	0.465	1.718	3.5–5.4
	2	44	0.465	3.559	3.2–4.9
	3	57	0.929	7.489	3.0–5.5
	4	41	1.071	1.422	2.8–4.8
	5	48	1.071	2.781	2.9–5.4
	6	32	1.071	5.015	2.9–4.7
	7	36	2.142	2.414	2.9–4.9
	8	48	2.142	4.690	2.9–5.7
	9	37	2.142	10.876	2.8–4.8
	10	33	2.324	4.985	3.2–4.5
	11	33	2.324	9.595	3.1–5.0
	12	47	2.324	17.575	2.9–6.0
	13	50	4.647	20.303	2.9–4.7
	14	32	6.428	11.132	2.9–4.2
	15	38	6.428	17.596	2.9–4.8

based on standard deviations in titre of 0.001 cm^3 and in emf of 0.05 mV. The sum of squares of residuals is based on total electrode ion concentrations.

All calculations were performed on a VAX 11/780 computer at UWIST (Cardiff, U.K.).

RESULTS AND DISCUSSION

2-Mercapto-2-phenylacetate shows two protonation constants (Table 2), that can be assigned to the carboxylate and thiol group. The values found are quite similar to those reported for mercaptoacetic and 2-mercaptopropanoic acids[18] as might be expected from the inductive, electrostatic and mesomeric effects that usually modify protonation constant values.

An analysis of the formation curves (Fig. 1) and the deprotonation curves (Fig. 2) clearly suggests the presence of polynuclear complex species in the Ni^{2+}–MPA–H$^+$ system. The formation of polynuclear species is favoured by the tendency of ligands

Table 2. Formation constants determined in this study at 25°C and I = 1 mol dm^{-3} ClO_4^- [50% (v/v) ethanol–water]

	pqr	$\log \beta_{pqr}$	U	Sum of squares of residuals	No. of data points	No. of titrations
H$^+$	011	10.366 ± 0.001	521.5	3.365E-06	498	9
	012	14.420 ± 0.002				
Ni^{2+}	340	40.437 ± 0.013	131.7	3.892E-06	615	15
	230	28.819 ± 0.008				
	120	16.717 ± 0.003				

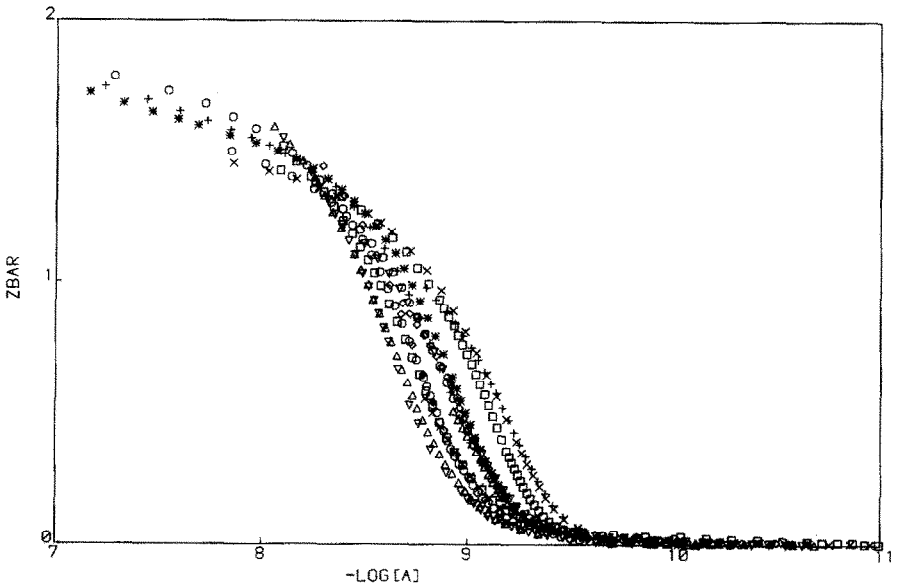


Fig. 1. Ni^{2}–MPA–H^{+} experimental formation curves. Different symbols refer to different titrations having different ligand : metal ratios and different ligand and metal concentrations.

containing a mercapto group to form complexes with sulphur bridges between two or more metal ions as well as by the ability of metal ions containing filled or almost filled *d*-electron shells to form bonds with the vacant 3*d* orbitals of the sulphur atom.

The best model was found to contain the species 340, 230 and 120. The lack of formation of the 460 complex, reported for mercaptoacetic acid, is probably caused by steric hindrance due to the presence of bulky phenyl group in the molecule. The complexes 340 and 230 would probably have the same structure as the corresponding complexes for mercaptoacetic acid proposed by Leussing *et al.*[2]

Table 3 contains some literature values of formation constants of nickel complexes of related 2-mercaptoacids. The comparison of those values with

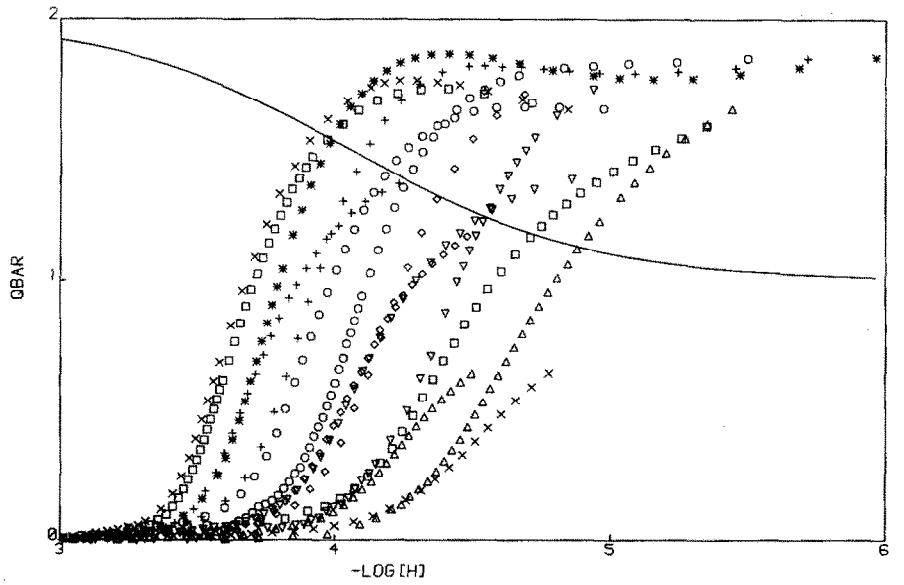


Fig. 2. Ni^{2+}–MPA–H^{+} experimental deprotonation curves. The different symbols have the same meaning as in Fig. 1. A plot of $\bar{n}$ vs $-\log[H]$ appears as a solid line.

Table 3. Literature potentiometric formation constants of nickel complexes of similar ligands

Ligand	*pqr*	log β_{pqr}	Conditions	Reference
Mercaptoacetic acid	110	6.98	25°C	1
	120	13.53	100 mmol dm^{-3} KCl	
	460	51.83, 50.67, 49.84, 49.23, 48.48	0°C, 15°C, 25°C, 35°C, 40°C	2
	120	13.15, 13.04, 13.04, 12.90, 12.70	100 mmol dm^{-3} KCl	
	110	6.2	20°C	3
	340	33.267	100 mmol dm^{-3} $NaClO_4$	
	230	22.68		
	460	49.849		
	120	13.009		
	130	14,987		
	110	6.63	35°C	19
	120	13.10	200 mmol dm^{-3} $NaClO_4$	
	110	7.04	20°C	20
	120	13.51	100 mmol dm^{-3} KCl	
	340	32.219	25°C	4
	460	49.157	500 mmol dm^{-3} KNO_3	
	120	12.759		
2-Mercaptopropanoic acid	110	7.23, 7.08, 6.93	35°C, 45°C, 55°C	21
	120	13.93, 13.62, 13.30	200 mmol dm^{-3} $NaClO_4$	
	110	6.97	20°C	20
	120	13.47	100 mmol dm^{-3} KCl	
	110	5.66, 6.03, 6.28	20°C, 30°C, 40°C	22
	120	13.35, 13.68, 13.80	100 mmol dm^{-3} $NaClO_4$	
	110	6.052	25°C	5
	340	30.709	500 mmol dm^{-3} KNO_3	
	120	13.144		

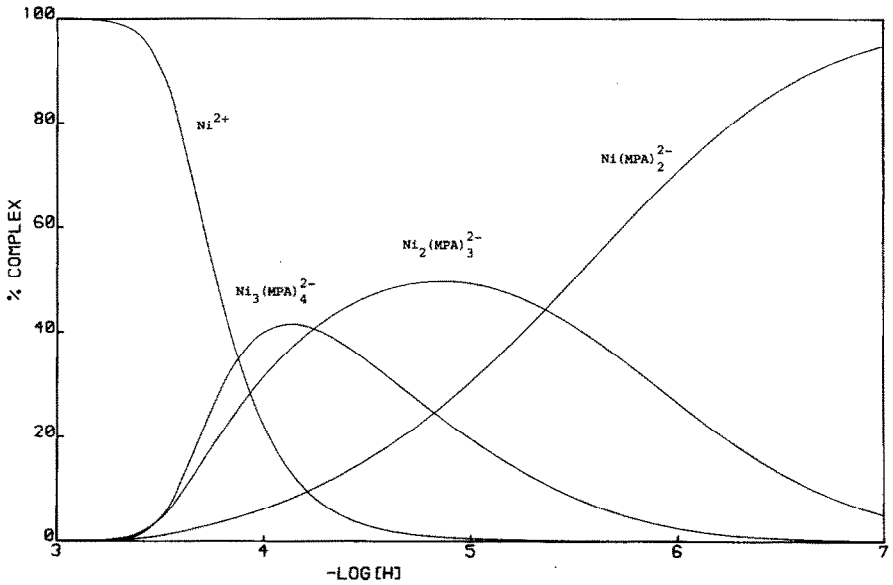


Fig. 3. Species distribution as a function of $-\log[H]$. Ligand concentration = 16.0 mmol dm^{-3}; metal concentration = 4.0 mmol dm^{-3}.

the ones obtained in the present work shows that the presence of a phenyl group seems to confer greater stability on the complexes formed.

Figure 3 shows the species distribution for the Ni^{+}–MPA–H^{+} system, computed from the constants in Table 2 for total concentrations of ligand (16 mmol dm^{-3}) and metal (4 mmol dm^{-3}).

Acknowledgements—We gratefully acknowledge Dr P. M. May (UWIST, Cardiff, U.K.) for helpful discussions. One of us (M. Filella) thanks the C.I.R.I.T. (Generalitat de Catalunya) for a maintenance grant tenable at UWIST (Cardiff, U.K.).

REFERENCES

1. D. L. Leussing, *J. Am. Chem. Soc.* 1958, **80**, 4180.
2. D. L. Leussing, R. E. Laramy and G. S. Alberts, *J. Am. Chem. Soc.* 1960, **82**, 4826.
3. D. D. Perrin and I. G. Sayce, *J. Chem. Soc.* (*A*) 1967, 82.
4. H. F. De Brabander, L. C. Van Poucke and Z. Eeckhaut, *Anal. Chim. Acta* 1974, **70**, 401.
5. H. F. De Brabander, A. M. Goeminne and L. C. Van Poucke, *J. Inorg. Nucl. Chem.* 1975, **37**, 799.
6. J. M. Bruce and F. K. Sutcliffe, *J. Chem. Soc.* 1957, 4789.
7. W. A. Bonner, *J. Org. Chem.* 1968, **33**, 1831.
8. D. L. Leussing and I. M. Kolthoff, *J. Electrochem. Soc.* 1953, **100**, 334.
9. A. I. Vogel, *A Textbook of Quantitative Inorganic Analysis*. Longman, London (1978).
10. D. Dyrssen, D. Jagner and F. Wengelin, *Computer Calculation of Ionic Equilibria and Titration Procedures*. Wiley, London (1968).
11. *Some Laboratory Methods in Current Use at the Department of Inorganic Chemistry*. KTH, Stockholm (1959).
12. L. Meites, *Polarographic Techniques*. Interscience, New York (1965).
13. A. S. Brown, *J. Am. Chem. Soc.* 1934, **56**, 646.
14. W. Forsling, S. Hietanen and L. G. Sillén, *Acta Chem. Scand.* 1952, **6**, 901.
15. P. M. May, D. R. Williams, P. W. Linder and R. G. Torrington, *Talanta* 1982, **29**, 249.
16. M. Filella and D. R. Williams, *Inorg. Chim. Acta* 1985, **106**, 49.
17. K. Murray and P. M. May, *ESTA. Equilibrium Simulation for Titration Analysis*. UWIST, Cardiff (1984).
18. R. M. Smith and A. E. Martell, *Critical Stability Constants*. Plenum Press, New York (1974–1982).
19. M. V. Reddy and P. K. Bhattacharya, *J. Prakt. Chem.* 1970, **312**, 69.
20. E. Casassas, *Estudi sobre la reactivitat envers els ions metàl.lics d'alguns reactius quelatants amb grups-SHi sobre la formació de complexos per alguns mercaptans alifàtics*. Institut d'Estudis Catalans, Arxius de la Secció de Ciències XLV, Barcelona (1971).
21. M. V. Reddy and P. K. Bhattacharya, *Indian J. Chem.* 1969, **7**, 282.
22. R. S. Saxena and P. Singh, *J. Indian Chem. Soc.* 1972, **49**, 325.

Polyhedron Vol. 4, No. 11, pp. 1957–1958, 1985
Printed in Great Britain

0277–5387/85 $3.00 + .00
© 1985 Pergamon Press Ltd

STRUCTURE OF A DIRUTHENIUM(II,III) COMPLEX WITH BENZAMIDATO BRIDGING LIGANDS

AKHIL R. CHAKRAVARTY and F. ALBERT COTTON*
Department of Chemistry and Laboratory for Molecular Structure and Bonding, Texas A&M University, College Station, TX 77843, U.S.A.

(*Received* 4 *April* 1985; *accepted* 28 *May* 1985)

Abstract—The compound $Ru_2Cl(C_6H_5CONH)_4$ has now been obtained in crystalline form and the crystal and molecular structure determined by X-ray methods. The crystals are triclinic, $P\bar{1}$, with the following unit cell dimensions: $a = 11.666(4)$ Å, $b = 12.721(4)$ Å; $c = 10.754(6)$ Å, $\alpha = 90.62(4)°$; $\beta = 111.10(5)°$; $\gamma = 83.21(2)°$; $V = 1478(2)$ Å^3; $Z = 2$. The $[Ru_2(C_6H_5CONH)_4]^+$ ions are linked by Cl^- ions into infinite, zigzag chains with Ru—Cl—Ru angles of 116.2(1)° and a mean Ru—Cl distance of 2.592(3) Å. The benzamidato ligands are arranged in a cisoid 2:2 fashion about the Ru_2^{5+} units, in which the average Ru—Ru distance is 2.293(2) Å.

Recent reports[1,2] from this laboratory on the reactivity of amidato-bridged diruthenium(II,III) complexes towards triarylphosphines have shown that $P(Ar)_3$ when reacted with $Ru_2Cl(ArCONH)_4$ undergoes a metal assisted P—C bond cleavage leading to transfer of an aryl group from $P(Ar)_3$ to Ru, thus giving an edge-sharing bioctahedral diruthenium(III,III) species,

$$Ru_2(Ar)_2(ArCONH)_2[Ar_2POC(Ar)N]_2.$$

Transfer of a *p*-tolyl group from $P(p\text{-tol})_3$ onto the metal reveals[2] the fact that there is indeed a simple migration of a C—P bond from P to Ru, rather than an orthometallated intermediate, or other more complex process.

Discussions of the reaction processes, as presented in our earlier reports,[1,2] were based on the assumption that the arrangement of ligands in tetra-amidato species are of the cisoid 2:2 type as observed[3] in $Ru_2Cl(4\text{-}Cl\text{-}C_6H_4CONH)_4 \cdot MeOH$. However, this assumption was unproven for $Ru_2Cl(PhCONH)_4$ since earlier attempts to prepare single crystals of this compound had been unsuccessful.

Recently, in an investigation of the generality of the migratory processes we attempted to react diphenylphosphinobutane (dppb) with $Ru_2Cl(PhCONH)_4$ following procedures similar to those described in our previous reports.[1,2] It was found that dppb is unreactive towards $Ru_2Cl(PhCONH)_4$, but from the reaction mixture we were able to isolate a homogeneous crystalline mass of $Ru_2Cl(PhCONH)_4 \cdot MeOH$. We report here the results of structural investigations on this compound.

The structure which has been obtained by X-ray crystallography† is shown in Fig. 1. The asymmetric unit consists of two half dimers linked by a Cl atom, and one methanol molecule as solvent of crystallization. The dinuclear units,

$$[Ru_2(PhCONH)_4]^+,$$

form infinite zigzag chains through Cl bridges. Similar sorts of arrangements are known to occur among tetracarboxylates[4–8] and in

$$Ru_2Cl(4\text{-}Cl\text{-}C_6H_4CONH)_4 \cdot MeOH.^3$$

* Author to whom correspondence should be addressed.

† The triclinic crystals belong to the space group $P\bar{1}$. Cell dimensions: $a = 11.666(4)$ Å, $b = 12.721(4)$ Å, $c = 10.754(6)$ Å, $\alpha = 90.62(4)°$, $\beta = 111.10(5)°$, $\gamma = 83.21(2)°$, $V = 1478(2)$ Å^3, $Z = 2$, $d_c = 1.616$ g cm^{-3}, μ(Mo-K_α) = 11.33 cm^{-1}. Instrument: Enraf–Nonius CAD-4; radiation: Mo-K_α ($\lambda = 0.71073$ Å); scan method = ω–2θ; total data = 5172 in the range $4° < 2\theta < 50°$ with 2406 having $F_o^2 > 3\sigma(F_o^2)$; residuals: $R_1 = 0.062$ ($R_2 = 0.069$); quality-of-fit = 1.55; largest shift/esd = 0.06. Empirical absorption corrections were made. No decay of the crystal was seen during 68.7 h exposure time. Complete tables of structure factors, anisotropic thermal parameters and complete lists of bond distances and angles (22 pp.) have been deposited with the Editor at Queen Mary College. Positional parameters and isotropic thermal parameters have been forwarded to the Director, Cambridge Crystallographic Data Centre.

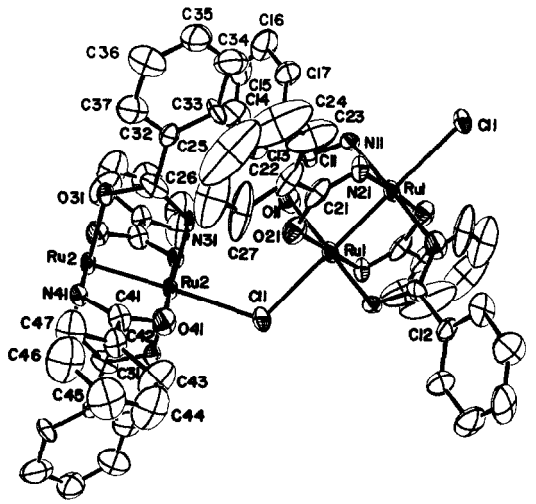


Fig. 1. An ORTEP drawing of the complex in $Ru_2Cl(PhCONH)_4 \cdot MeOH$ with atom-labelling scheme. Selected bond lengths and bond angles are: Ru(1)—Ru(1), 2.295(2), Ru(2)—Ru(2), 2.290(2), Ru(1)—Cl(1), 2.572(3), Ru(2)—Cl(1), 2.612(3), Ru(1)—O(11), 2.049(8), Ru(1)—O(21), 2.018(9), Ru(1)—N(11), 2.034(9), Ru(1)—N(21), 2.006(10), Ru(2)—O(31), 2.042(7), Ru(2)—O(41), 2.043(9), Ru(2)—N(31), 2.001(9), Ru(2)—N(41), 2.058(9) Å; Ru(1)—Cl(1)—Ru(2), 116.2(1), av. Ru(1)—Ru(1)—O, 89.9(3), av. Ru(1)—Ru(1)—N, 89.4(3), av. Ru(2)—Ru(2)—O, 90.6(3), av. Ru(2)—Ru(2)—N, 89.4(3)°. The C(1)—O(1) distance in MeOH is 1.36(3) Å.

The average Ru—Ru distance in $Ru_2Cl(PhCONH)_4$ is 2.293(2) Å and each ruthenium center has an $RuClN_2O_2$ coordination sphere where the Ru—Ru—Cl angles are essentially linear. The formal oxidation state of Ru is +2.5 and the Ru—Ru bond order is 2.5. The Ru—Cl—Ru bridge angle is 116.2(1)°. The average Ru—N, Ru—O and Ru—Cl distances are 2.025(9), 2.038(8) and 2.592(3) Å, respectively. The axial Ru—Cl distance is similar to those in other diruthenium(II,III) complexes[3–10] having axial coordination at both metal atoms, but considerably longer than the Ru—Cl distances in polar[9–13] diruthenium(II,III) species. Physicochemical studies reported[1] on $Ru_2Cl(PhCONH)_4$ and other amidato species[14,15] show that the Ru—Cl bonds are weak and can be easily cleaved by strongly polar solvents like Me_2SO. The reaction between $Ru_2Cl(PhCONH)_4$ and PPh_3 in Me_2SO–MeOH mixture is known[1] to give $Ru_2(Ph)_2(PhCONH)_2[Ph_2POC(Ph)N]_2$. Our proposed mechanism in an earlier report[2] suggested that the arrangement of bridging ligands in $Ru_2Cl(PhCONH)_4$ should be of the cisoid 2:2 type. The structure of this compound confirms that assumption and thus supports the proposed[2] mechanism.

Acknowledgements—We are grateful to the National Science Foundation for support and to Dr W. Schwotzer for his help in solving the structure.

REFERENCES

1. A. R. Chakravarty, F. A. Cotton and D. A. Tocher, *J. Am. Chem. Soc.* 1984, **106**, 6409.
2. A. R. Chakravarty and F. A. Cotton, *Inorg. Chem.*, in press.
3. A. R. Chakravarty, F. A. Cotton and D. A. Tocher, *Polyhedron* 1985, **4**, 1097.
4. F. A. Cotton and R. A. Walton, *Multiple Bonds Between Metal Atoms*. John Wiley, New York (1982).
5. M. J. Bennett, K. G. Caulton and F. A. Cotton, *Inorg. Chem.* 1969, **8**, 1.
6. A. Bino, F. A. Cotton and T. R. Felthouse, *Inorg. Chem.* 1979, **18**, 2559.
7. T. Togano, M. Mukaida and T. Nomura, *Bull. Chem. Soc. Jpn* 1980, **53**, 2085; *ibid.* 1972, **45**, 2143.
8. D. S. Martin, R. A. Newman and L. M. Vlasnik, *Inorg. Chem.* 1980, **19**, 3404.
9. A. R. Chakravarty, F. A. Cotton and D. A. Tocher, *Inorg. Chem.* 1985, **24**, 172.
10. A. R. Chakravarty and F. A. Cotton, *Inorg. Chim. Acta*, in press.
11. A. R. Chakravarty and F. A. Cotton, *Inorg. Chem.*, in press.
12. A. R. Chakravarty and F. A. Cotton, *Inorg. Chem.*, in press.
13. A. R. Chakravarty, F. A. Cotton and W. Schwotzer, *Polyhedron* in press.
14. T. Malinski, D. Chang, F. N. Feldman, J. L. Bear and K. M. Kadish, *Inorg. Chem.* 1983, **22**, 3225.
15. M. Y. Chavan, F. N. Feldmann, X. Q. Lin, J. L. Bear and K. M. Kadish, *Inorg. Chem.* 1984, **23**, 2373.

Polyhedron Vol. 4, No. 11, pp. 1959–1964, 1985
Printed in Great Britain

0277–5387/85 $3.00 + .00
© 1985 Pergamon Press Ltd

SYNTHESIS AND CHARACTERIZATION OF NEW COMPLEXES BETWEEN SODIUM MONOALKYL BENZENEAZOPHOSPHONATES AND DIBENZO-18-CROWN-6

LJ. TUŠEK-BOŽIĆ* and D. SEVDIĆ

Department of Physical Chemistry, Institute Rudjer Bošković, Zagreb, Yugoslavia

(*Received* 1 *May* 1985; *accepted* 26 *May* 1985)

Abstract—A new series of crystalline complexes of sodium monoethyl ester and sodium monobutyl ester of [α-(4-benzeneazoanilino)-*N*-benzyl]phosphonic acid, [α-(4-benzeneazoanilino)-*N*-4-hydroxybenzyl]phosphonic acid and [α-(4-benzeneazoanilino)-*N*-4-methoxybenzyl]phosphonic acid with dibenzo-18-crown-6 have been synthesized. The complexes obtained were identified and characterized by elemental and thermogravimetric analysis, conductivity measurements and UV, IR and ^{1}H NMR spectra. The molecular structure and the electronic configuration of the anion are important factors in a salt–ligand system with influence on ease of solubilization, charge separation and the formation of crystalline complex in alcoholic and acetonitrile solutions.

Macrocyclic polyethers as polydentate ligands of flexible conformation can form complexes with alkali and other metal salts providing increased salt solubility and increased anion reactivity in aprotic organic solvents.[1,2] In recent years macrocyclic polyethers and their complexes have therefore been extensively employed in studies of mediated ion transport, solute separations, and anion-activated catalysis.[3,4] Besides the complexes with simple salts of inorganic acids, great interest has developed in obtaining information on macrocyclic polyether complexes with salts of organic anions. The chelating organic anions mostly used were those obtained by the deprotonation of nitrophenols and hydroxy-, nitro- or aminobenzoic acids.[5–9]

In continuation of our systematic study of the macrocyclic polyether complexes with various alkali metal salts,[9–11] this paper describes for the first time the preparation and the properties of complexes with sodium salts of some benzeneazophosphonates (NaA_1–NaA_6). The various factors, including the dimensions of the polyether hole and the metal cation, size and charge density of anion as well as solvent used, have been found to play a fundamental role on the formation of the salt complexes.

EXPERIMENTAL

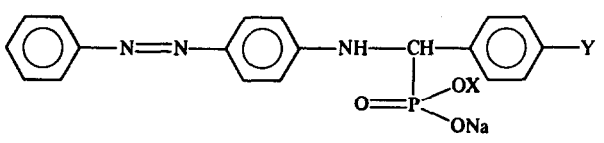
Materials

The preparation of the sodium salt of the monoethyl ester and the sodium salt of the monobutyl ester of [α-(4-benzeneazoanilino)-*N*-benzyl] phosphonic acid (NaA_1 and NaA_2), [α-(4-benzeneazoanilino) - *N* - 4 - hydroxybenzyl]phosphonic acid (NaA_3 and NaA_4) and [α-(4-benzeneazoanilino) - *N* - 4 - methoxybenzyl]phosphonic acid (NaA_5 and NaA_6) has been described earlier.[12,13] Sodium salts were purified by repeated recrystallization from absolute ethanol and dried by heating to about 50°C under high vacuum.

Dibenzo-18-crown-6 (DBC) (the trivial name for 6,7,9,10,17,18,20,21 - octahydrodibenzo[b,k] [1,4,7,10,13,16]hexaoxacyclooctadecin) prepared as previously described[14] was recrystallized twice from acetone.

The purification of methanol[15] and acetonitrile[16] was carried out by published methods in order to obtain solvents suitable for conductance measurements.

* Author to whom correspondence should be addressed.



X	Y	Salt
Et	H	NaA_1
n-Bu	H	NaA_2
Et	OH	NaA_3
n-Bu	OH	NaA_4
Et	OMe	NaA_5
n-Bu	OMe	NaA_6

Preparation of complexes

An equimolar amount of macrocyclic polyether and sodium salt of monoalkyl ester of benzeneazophosphonic acids was dissolved in ethanol or acetonitrile and refluxed for 2–6 h with vigorous stirring. The clear hot solution was filtered and the solvent was slowly evaporated at room temperature. Complexes of sodium monoethyl esters were gradually formed by removal of solvent. The crystalline precipitate was filtered off, washed with cold reaction solvent and dried. The filtrate was again subjected to evaporation in order to achieve further crystallization of the complex. Complexes of sodium monobutyl esters were isolated after the whole of the solvent was driven off. The homogeneity of the crystals was ascertained under the microscope. The majority of the complexes obtained were hygroscopic compounds as were the free sodium salts.[12,13] After drying under high vacuum for several hours at room temperature the complexes of sodium salts of methoxy-substituted benzeneazophosphonates became anhydrous, while the others were obtained as monohydrated complexes.

We tried to prepare all complexes in methanol, ethanol and acetonitrile solutions. Complexes of sodium salts of hydroxy-substituted benzeneazophosphonates were isolated only from ethanol, while all the other complexes were precipitated from acetonitrile solutions. It was shown that free macrocyclic polyether gradually precipitated from methanolic solutions, and no complex could be isolated.

Physical measurements and analyses

Melting points were recorded using hot-stage (0–360°C) microscopy and are uncorrected. UV spectra were obtained in methanolic solutions with a Perkin–Elmer 124 spectrophotometer. IR spectra were recorded on KBr pellets and Nujol mulls using a Perkin–Elmer 580 B spectrophotometer in the region 4000–200 cm^{-1}. NMR spectra were determined on JEOL FX90Q Fourier transform NMR spectrometer in deuterochloroform solutions with tetramethylsilane as the internal standard using a sweep width of 1200 Hz. Thermogravimetric measurements were performed with a Cahn RG electromicro balance applying a heating rate of 2° min^{-1} in an atmosphere of static air.

Conductivity measurements were performed in methanol and acetonitrile using a Tacussel conductivity bridge, type CD 7A. The solutions were thermostatted at 25 ± 0.02°C by a double water bath and stirred by means of a magnetic stirrer. The procedure of measuring and calculation of equivalent conductance at infinite dilution and ion-pair dissociation constants of free sodium salts and their complexes was the same as described previously.[17] The conductance data were analysed by the Fuoss–Onsager theory in the usual form, through an iterative machine calculation procedure using the expanded form of the Fuoss–Hsia conductance equation.

Elemental analyses were performed in the Microanalytical Laboratory of the Rudjer Bošković Institute.

RESULTS AND DISCUSSION

The complexes isolated between sodium monoalkyl benzeneazophosphonates (NaA_1–NaA_6) and DBC with the analytical data and the other physical properties are listed in Table 1, the UV and IR data in Table 2, the summarized ^1H NMR spectra are shown

Table 1. Analytical and physical data of complexes between sodium monoalkyl benzeneazophosphonates (NaA) and dibenzo-18-crown-6

	Complex	Reaction solvent	M.p. (°C)	Found (calc.) (%) C	H	N	P	Na	H_2O
I	$NaA_1 \cdot DBC \cdot H_2O$	Acetonitrile	139–140	61.7 (61.86)	6.0 (5.96)	5.3 (5.28)	3.9 (3.89)	2.7 (2.89)	2.2 (2.27)
II	$NaA_2 \cdot DBC \cdot H_2O$	Acetonitrile	126–127	62.8 (62.67)	6.0 (6.24)	5.2 (5.10)	3.7 (3.76)	2.8 (2.79)	1.8 (2.19)
III	$NaA_3 \cdot DBC \cdot H_2O$	Ethanol	121–122	60.8 (60.64)	5.9 (5.84)	5.1 (5.18)	3.9 (3.82)	2.6 (2,83)	2.4 (2.22)
IV	$NaA_4 \cdot DBC \cdot H_2O$	Ethanol	127–128	61.4 (61.47)	5.9 (6.12)	5.0 (5.01)	3.7 (3.69)	2.6 (2.74)	2.1 (2.15)
V	$NaA_5 \cdot DBC$	Acetonitrile	132–134	62.7 (62.43)	5.9 (5.87)	5.3 (5.21)	3.9 (3.82)	2.7 (2.85)	—
VI	$NaA_6 \cdot DBC$	Acetonitrile	130–131	63.3 (63.20)	6.0 (6.15)	5.2 (5.03)	3.5 (3.71)	2.8 (2.75)	—

Table 2. Selected UV and IR data of the novel complexes

Complex	UV data[a] λ_{max} (log ε)	IR data[b] (cm^{-1}) ν(OH), ν(NH) $\nu(H_2O)$	ν_{as}(Ar—O—CH_2) $\nu_{as}(PO_2^-)$	ν_{as}(CH_2—O—CH_2)	$\nu_{sym}(PO_2^-)$ ν[P—O—(C)]	ω, $\tau(CH_2)$ $\nu_{aliph.}$(C—C)
I	271 (4.12)	3620w	1250vs	1126vs	1088s	961m
	278sh (4.03)	3370w	1220vs	1105s	1062vs br	952s
		3230m				
II	272 (4.18)	3615 w	1253vs	1125vs	1080sh	948m
	279sh (4.11)	3365m br	1220s		1065s br	
III	272 (4.10)	3610w	1252vs	1126vs br	1070vs	948s
		3370m br	1220s		1050vs	
IV	272 (4.19)	3600w	1250vs	1125vs br	1060vs	972w
	278sh (4.13)	3372m br	1220vs		1050vs	950s
V	272 (4.17)	3370m br	1254vs	1125vs	1070sh	947m
			1220s		1052s	
VI	272 (4.15)	3360m br	1252vs	1126vs	1978 sh	975w
	279sh (4.09)		1220s		1065s	950m

[a] In methanol: 250–300-cm^{-1} region.

[b] vs, very strong; s, strong; m, medium; w. weak; br, broad; as, asymmetric; sym, symmetric; sh, shoulder.

in Table 3, and the conductance data are given in Table 4.

DBC forms 1 : 1 complexes with sodium salts. The sodium ion (ionic diameter 1.94 Å) easily fits into the hole of the 18-membered polyether ring (2.6–3.2 Å diameter),[18] and the anion and water molecules are able to interact with it from the vacant axial directions. The low melting points of the complexes as against the high melting points of the corresponding sodium salts (above 220°C), indicate that the charge of the sodium ion in the complexes is extensively delocalized. On the other hand some degree of charge-transfer between the cation and anion can take place, increasing the stability of the complex.

The great similarity in the properties and the spectral data of all the sodium salt complexes indicates that metal–polyether interactions are essentially the same. Differences which are observed in their preparation can be attributed partially to the different solubility of sodium salts in the solvent of reaction. Sodium salts of monobutyl esters are more soluble than the corresponding monoethyl esters, as are also the sodium methoxy-substituted benzeneazophosphonates compared to those of non-substituted or hydroxy-substituted analogues,

Table 3. ^{1}H NMR data of the salt complexes

Complex	Chemical shift (δ) (ppm) (J in Hz)[a]
I	1.03 (t, 3H, J = 7, CH_3); 3.44–3.80 (m, 2H, $POCH_2$); 4.06 (s, 16H, four OCH_2CH_2O); 4.63 (dd, 1H, J = 22 and 8, PCH); 5.96 (s br, 1H, NH); 6.30–7.86 (m, 22H, aromatic H)
II	0.63–1.60 (m, 7H, $CH_2CH_2CH_3$); 3.45–3.86 (m, 2H, $POCH_2$); 4.06 (s, 16H, four OCH_2CH_2O); 4.52 (dd, 1H, J = 23 and 8, PCH); 6.02 (s br, 1H, NH); 6.33–7.89 (m, 22H, aromatic H)
III	1.03 (t, 3H, J = 6.5, CH_3); 3.41–3.75 (m, 2H, $POCH_2$); 3.95 (s, 16H, four OCH_2CH_2O); 4.54 (d br, 1H, J = 23, PCH); 5.94 (s br, 1H, NH); 6.31–7.86 (m, 22H, aromatic H + OH)
IV	0.61–1.62 (m, 7H, $CH_2CH_2CH_3$); 3.40–3.79 (m, 2H, $POCH_2$); 3.90 (s, 16H, four OCH_2CH_2O); 4.52 (d br, 1H, J = 22, PCH); 5.90 (s br, 1H, NH); 6.34–7.93 (m, 22H, aromatic H + OH)
V	1.03 (t, 3H, J = 7, CH_3); 3.41–3.83 (m, 2H, $POCH_2$); 3.63 (s, 3H, OCH_3); 4.06 (s, 16H, four OCH_2CH_2O); 4.65 (dd, 1H, J = 23 and 8, PCH); 6.01 (s br, 1H, NH); 6.30–7.90 (m, 21H, aromatic H)
VI	0.62–1.57 (m, 7H, $CH_2CH_2CH_3$); 3.45–3.78 (m, 1H, $POCH_2$); 3.64 (s, 3H, OCH_3); 4.07 (s, 16H, four OCH_2CH_2O); 4.55 (dd, 1H, J = 22 and 7.5, PCH); 5.90 (s br, 1H, NH); 6.26–7.86 (m, 21H, aromatic H)

[a] s, singlet; d, doublet; dd, doublet of doublets; t, triplet; m, multiplet; br, broad signal.

Table 4. Conductance data for sodium monoalkyl benzeneazophosphonates and their complexes with dibenzo-18-crown-6[a]

Complex	Methanol	Acetonitrile[b]	
	Λ_o	Λ_o	$K_D \times 10^4$
I	65.8 (97.7)	105.3	7.08
II	64.2 (91.6)	104.0	7.27
III	64.8 (96.4)	104.2	6.98
IV	63.2 (90.8)	103.5	7.14
V	63.7 (95.6)	102.5 (113.6)	7.12 (6.72)
VI	62.0 (89.9)	99.7 (106.1)	7.67 (6.69)

[a] Λ values in Ω^{-1} cm^2 mol^{-1}; K_D in 1 mol^{-1} at 25°C. Data for salts NaA_1–NaA_6 are given in parentheses.

[b] Salts NaA_1–NaA_4 are too insoluble for measurement.

respectively. Although all the salts form complexes with DBC in alcoholic solutions, they cannot be isolated always in the solid state. The uncomplexed polyether precipitates when the solution is concentrated. Generally, it was shown that the failures to isolate the metal salt complexes can be attributed either to the strong M^+A^- ion association as a consequence of which M^+ fails to cause necessary polarization of the polyether molecule, to the high lattice energy of the salt, or to the strong hydrogen bonding between the cation or anion and the synthesis media.

UV spectra

DBC has, in methanol, a characteristic absorption maximum at 274 nm (log ε 3.72).[14] Complexing with a cation brings about distinctive changes in this band. When salts themselves do not absorb too strongly in the region of 270–290 nm, a hypsochromic shift, variations in absorbance or the appearance of a second peak to the longer wavelength side of the major peak can be attributed to complex formation.[1] In the spectra of complexes of sodium monoalkyl benzeneazophosphonates a slight hypsochromic shift, and in some cases a new peak not clearly separated from the main one, is evident. Interaction between polyether and the sodium salt can take place in alcoholic solution even when it was not possible to isolate the complex in a crystalline form.[9]

Sodium salts give an absorption maximum at 397 nm (log ε 4.45) which corresponds to conjugation of the azo group with aromatic rings (π–π^* transition). It remains unchanged upon complex formation, suggesting non-coordinated ionic monoakyl benzeneazophosphonato groups.

IR spectra

IR spectra of macrocyclic polyether complexes with sodium monoalkyl benzeneazophosphonates are very complex and a complete assignment of the absorption bands is not possible. Only the frequencies associated with the characteristic functional groups are presented in Table 2. Generally, significant differences between the spectra of macrocyclic polyether and its complexes may be noticed in the region 1250–900 cm^{-1} where bands arising from various modes of vibration of ether and methylene groups are present.[9] In every case the spectrum of the solid complex distinctly differed from that of the physical mixture of the constituents.

Since all the sodium salts alone give a series of complex bands between 1250 and 1165 cm^{-1}, characteristic of asymmetric stretching of the ionised PO_2^- group,[13,19] it is not possible to determine the exact position of the ν_{as}(Ar—O—CH_2) bands in their complexes (free polyether exhibits these bands at 1256 and 1230 cm^{-1}). The complexes are characterized by the very intense bands near 1250 and 1220 cm^{-1}, respectively. The ν_{as}(CH_2—O—CH_2) band, present in the polyether at 1130 cm^{-1}, upon complexing is slightly shifted to lower energy. Considerable differences are observed in the 1000–900-cm^{-1} region which contains bands attributed to wagging, twisting and rocking modes of vibration of the methylene groups. DBC shows two bands arising from these vibrations at 997 and 932 cm^{-1}. In the spectra of its complexes they are missing, and a rather intense band appears around 950 cm^{-1}. Less restriction on the coupling of these vibrational modes in the complexes is probably due to some bonding between the oxygen atoms of the polyether ring and the metal cation.

All the salt complexes which contain water have one peak at about 3600 cm^{-1}, indicating metal-coordinated water. A water molecule in the complex is considered metal-coordinated if relatively sharp absorption bands appear over 3400 cm^{-1}, especially above 3500 cm^{-1}, but anion-bonded if the latter is missing and the broad peaks or humps appear around and below 3400 cm^{-1}.[6]

^{1}H NMR spectra

The ^{1}H NMR spectrum of DBC in $CDCl_3$ has two multiplets at about δ 4.11 ppm for methylene protons of the polyether ring, and a singlet at δ 6.92 ppm due to the aromatic protons.[14] The ether multiplet is typical of what is observed for a XCH_2CH_2Y fragment undergoing rapid rotamer conversion.[20] In the complexes the polyether ring protons show

only one singlet at about δ 4.06 ppm. The slight broadening observed is a reflection of the slower dissociation rate for the ion-pair complexes in the solvent system. The overlapping of the polyether aromatic protons by the signals of the anion aromatic protons results in an unresolved multiplet. Comparison of the spectra of sodium monoalkyl benzeneazophosphonates with the spectra of their polyether complexes indicates some chemical shift differences for the anion protons. In the complexes of sodium salts of monoethyl esters a triplet (J = 8 Hz) for the CH_3 part of the $POCH_2CH_3$ group is shifted slightly upfield by 10 cps. The absorption of the methylene protons of the ethoxy group is complex. In addition to the coupling between the CH_2 and CH_3 protons, there is a spin–spin splitting of the CH_2 protons by the phosphorus. Butyl derivatives give too complex spectra to allow analysis. The proton of the benzylic CH group usually appears as a doublet of doublets, because of the spin–spin interaction with the phosphorus (J = 22 Hz) and with the NH proton (J = 8 Hz).[13,21] D_2O exchange eliminates the smaller splitting and retains the larger one. In the *p*-hydroxy substituted derivatives the doublet observed is broad and blurred. Shaking with D_2O produces a sharp doublet. The NH proton is found as a broad singlet (δ 5–6 ppm), while the phenolic OH group is hidden by the aromatic protons.

Conductivity measurements

The conductance of sodium monoalkyl benzeneazophosphonates and their complexes with DBC was investigated in methanol and acetonitrile at 25°C. The values of the equivalent conductance at infinite dilution (Λ_o) and the ion-pair dissociation constants (K_D) of the complexes are compared with those obtained for the free sodium salts, and the results are summarized in Table 4.

It was shown that the sodium salts and their complexes are completely dissociated in a methanolic solution. With all complexes the difference Λ_o(NaA) − Λ_o(NaA · DBC) is substantial, implying that the average cross-section of the complexed sodium ion is larger than that of the solvated one. Some additional interaction of the complex cation with solvent molecules, which becomes possible after the anion is removed, causes a further decrease in the mobility of the cation complex. The gradation in Λ_o values of the complexes reflects the increase in their bulkiness.

Sodium monoalkyl benzeneazophosphonates are slightly soluble in acetonitrile at room temperature, and only for the *p*-methoxy-substituted derivatives could the conductance measurements be performed. Our studies indicate very small K_D values for free salts and their macrocyclic polyether complexes. The low symmetry of monoalkyl benzeneazophosphonato anions with sites of charge localization may account for the increased association observed in these compounds. A similar behaviour was found in acetonitrile solutions for picrate complexes of some macrocyclic polyethers.[17] The fact that the total drop in the equivalent conductance for the complexes is remarkably smaller in acetonitrile than in methanol, can be explained by the weaker solvation and the great ion-pair association in acetonitrile solutions.

The results of the present investigation corroborate the results obtained in the recently published conductometric studies of the complexes of various alkali metal salts with macrocyclic polyethers in methanol[11,22] and acetonitrile.[17,23]

The conduction process is not only conditioned by the size of the complexes which are formed, but also by competitive interactions with the cation caused by the solvent and the macrocyclic polyether. The anion in a salt–ligand system is important for the ease of solubilization and the resulting charge separation in solution. Applications involving phase-transfer catalysis often restrict variables to a choice of ligand, cation and its counterion.

Acknowledgement—We thank the Foundation for Scientific Research of SR Croatia, Zagreb, for financial support.

REFERENCES

1. C. J. Pedersen and H. K. Frensdorf, *Angew. Chem., Int. Ed. Engl.* 1972, **11**, 16.
2. C. L. Liotta and H. P. Harris, *J. Am. Chem. Soc.* 1974, **96**, 2250; P. E. Stott, J. S. Bradshaw and W. W. Parish, *J. Am. Chem. Soc.* 1980, **102**, 4810.
3. R. M. Izatt and J. J. Christensen, *Progress in Macrocyclic Chemistry*. Wiley–Interscience, New York; Vol. 1 (1981) Vol. 2 (1982).
4. W. P. Weber and G. W. Gokel, *Phase Transfer Catalysis in Organic Synthesis*. Springer, Berlin (1977); C. M. Stark and C. L. Liotta, *Phase Transfer Catalysis—Principles and Techniques*. Academic Press, New York (1978).
5. N. S. Poonia and M. R. Truter, *J. Chem. Soc., Dalton Trans.* 1973, 2062; N. S. Poonia, B. P. Yaday and V. W. Bhaywart, *Inorg. Nucl. Chem. Lett.* 1977, **13**, 119.
6. N. S. Poonia, *J. Am. Chem. Soc.* 1974, **94**, 1012.
7. M. Bourgoin, K. H. Wong, J. Y. Hui and J. Smid, *J. Am. Chem. Soc.* 1975, **97**, 3462; R. Sinta, P. S. Rose and J. Smid, *J. Am. Chem. Soc.* 1983, **105**, 4337.
8. E. Buncel, H. S. Shin, R. A. B. Bannard, J. G. Purdon and B. G. Cox, *Talanta* 1984, **31**, 585.
9. Lj. Tušek, H. Meider-Goričan and P. R. Danesi, *Z. Naturforsch.* 1976, **31B**, 330.

10. Lj. Tušek, P. R. Danesi and R. Chiarizia, *J. Inorg. Nucl. Chem.* 1975, **37**, 1538; Lj. Tušek-Božić and P. R. Danesi, *J. Inorg. Nucl. Chem.* 1979, **41**, 833.
11. Lj. Tušek-Božić and B. Božić, *Croat. Chem. Acta* 1984, **57**, 119.
12. V. Jagodić and Lj. Tušek, *J. Org. Chem.* 1972, **37**, 1222.
13. Lj. Tušek and V. Jagodić, *Croat. Chem. Acta* 1977, **49**, 829.
14. C. J. Pedersen, *J. Am. Chem. Soc.* 1967, **89**, 7017.
15. R. E. Kay, C. Zawoyyski and D. F. Evans, *J. Phys. Chem.* 1965, **69**, 4208.
16. J. F. Coetzee, G. P. Cunningham, D. K. McGuire and G. R. Padmanabban, *Anal. Chem.* 1962, **34**, 1139.
17. Lj. Tušek-Božić and B. Božić, *Electrochim. Acta* 1985, **30**, 789.
18. C. J. Pedersen, *J. Am. Chem. Soc.* 1970, **92**, 386.
19. V. Jagodić and Lj. Tušek, *Croat. Chem. Acta* 1972, **44**, 445.
20. D. Live and S. I. Chan, *J. Am. Chem.* Soc. 1976, **98**, 3769.
21. V. Jagodić, *Croat. Chem. Acta* 1976, **48**, 325.
22. D. F. Evans, S. L. Wellington, J. A. Nadis and E. L. Cussler, *J. Solution Chem.* 1972, **1**, 499.
23. H. P. Hopkins and A. B. Norman, *J. Phys. Chem.* 1980, **84**, 309; M. Della Monica, A. Ceglie and A. Agostino, *Electrochim. Acta* 1983, **28**, 529; 1984, **29**, 161.

Polyhedron Vol. 4, No. 11, pp. 1965–1967, 1985
Printed in Great Britain

0277-5387/85 $3.00 + .00
© 1985 Pergamon Press Ltd

PREPARATION AND STUDY OF SILVER MALEONITRILEDITHIOLATE COMPLEXES

F. ESTEVAN, P. LAHUERTA* and I. SOLANA

Departamento de Química Inorgánica, Facultad de Químicas, Universidad de Valencia, Burjasot, Valencia, Spain

(*Received* 15 *May* 1985; *accepted* 26 *May* 1985)

Abstract—This paper reports the reaction of $Ag_2(mnt)$ and $[(NEt_4)Ag(mnt)]$ (mnt^{2-} = maleonitriledithiolate) with PPh_3 and 1,2-bis(diphenylphosphino)ethane. In the first case, compounds of formulation $[Ag_2(mnt)(PPh_3)_4]$ and $[(NEt_4)Ag(mnt)(PPh_3)_2]$ were isolated. ^{31}P NMR and conductivity measurements suggest that the complex $[Ag_2(mnt)(PPh_3)_4]$ has an ionic structure in solution, $[Ag(PPh_3)_2]^+[Ag(mnt)(PPh_3)_2]^-$, with an anion–cation interaction via a sulfur atom from the mnt ligand.

The transition-metal complexes with 1,2-dithiolene ligands have attracted considerable interest over the last decades because of their special properties, like the ability to undergo reversible oxidation–reduction processes. This produces series of structurally similar molecules apparently differing in the formal oxidation state for the metal.[1,2]

Many complexes with the ligand 1,2-maleonitrile dithiolate (mnt^{2-}) are known,[3] but only a few references are found in the literature for silver mnt^{2-} complexes.[4,5]

The preparation of $Ag_2(mnt)$ by reacting $AgNO_3$ with $Na_2(mnt)$ in water–chloroform,[4] has been reported previously but without describing any reactivity. The same compound has been prepared by an indirect reaction from $[(NEt_4)Cu(mnt)_2]$.[6] A related complex of stoichiometry $[Ag_2(mnt)(PPh_3)_4]$ has been briefly described by Caffery and Coucouvanis[5] through reaction of $Na_2Ni(mnt)_2$ with $Ag(PPh_3)_2Cl$.

We report in this paper the preparation of complexes of Ag(I) with mnt^{2-} and their reactivity with PPh_3 and diphosphines, as well as some ^{31}P NMR data on some of the most representative compounds.

EXPERIMENTAL

$Na_2(mnt)$ was recrystallized by dissolving it in ethanol–isopropanol (1 : 1) and precipitating it with diethyl ether. It is unstable and decomposes even in an inert atmosphere. The solvents were deoxygenated prior to use. All the reactions were carried out in an inert atmosphere using the Schlenck technique.

Preparation of the compounds

$Ag_2(mnt)$ (I). This compound was prepared by a modified version of the previously described method.[4]

A solution of $AgNO_3$ (459 mg, 2.7 mmol) in water (10 cm^3) was added to a solution of $Na_2(mnt)$ (168 mg, 0.9 mmol) in acetone (50 cm^3). The precipitation was completed in 10 min. The precipitate was filtered, washed with acetone–water (5 : 1) and then with acetone. The compound was dried *in vacuo* over P_4O_{10}. (Found: C, 13.4; N, 7.8. $C_4Ag_2N_2S_2$ requires: C, 13.5; N, 7.5%.) Melting point 170°C (decomposes).

$(NEt_4)Ag(mnt)$ (II). A solution of $AgNO_3$ (155 mg, 0.9 mmol) in water (8 cm^3) was added to a solution of $Na_2(mnt)$ (166 mg, 0.9 mmol) in acetone (60 cm^3). Then a solution of $NEt_4Cl \cdot H_2O$ (164 mg, 0.9 mmol) in water (6 cm^3) was added. The solvent was evaporated under reduced pressure until the volume was approximately 20 cm^3, precipitating a red–orange compound which was filtered, washed with water and dried *in vacuo* over P_4O_{10}. (Found: C, 38.4; H, 6.0; N, 10.0. $C_{12}H_{20}AgN_3S_2$ requires: C, 38.1; H, 5.3; N, 11.1%.) Melting point 160°C (decomposes).

$Ag_2(mnt)(PPh_3)_4$ (III). PPh_3 (223 mg, 0.85 mmol) was added slowly to a suspension of $Ag_2(mnt)$ (61 mg,

* Author to whom correspondence should be addressed.

0.17 mmol) in DMF (15 cm^3). The silver compound was dissolved giving a yellow solution from which yellow crystals separated by standing at room temperature. The crystals were filtered, washed with diethyl ether and dried *in vacuo*. The compound can be recrystallized from CH_2Cl_2–acetone. (Found: C, 64.4; H, 4.4; N, 2.0. $C_{76}H_{60}Ag_2N_2P_4S_2$ requires: C, 65.0; H, 4.3; N, 2.0%.) Melting point 185°C.

Other solvents, like acetone, CH_2Cl_2 or $CHCl_3$, can be used for this preparation, but the best-quality crystals are obtained from DMF.

The same compound is obtained by direct reaction of stoichiometric amounts of $Na_2(mnt)$, $AgNO_3$ and PPh_3 in the solvents previously mentioned.

When 1,2-bis(diphenylphosphino)ethane (dppe) (181 mg, 0.45 mmol) was used in the previous procedure, a compound of stoichiometry $[Ag_2(mnt)(dppe)_2]$ was obtained. (Found: C, 58.7; H, 4.4; N, 2.2. $C_{56}H_{48}Ag_2N_2P_4S_2$ requires: C, 58.3; H, 4.2; N, 2.4%.) Melting point 148°C.

$NEt_4Ag(mnt)(PPh_3)_2$ (**IV**). PPh_3 (81 mg, 0.3 mmol) was added to a suspension of $(NEt_4)Ag(mnt)$ (58 mg, 0.15 mmol) in acetone (10 cm^3). The mixture was stirred until a yellow solution was formed. The solvent was removed under reduced pressure and diethyl ether was added. The yellow precipitate was filtered, washed with diethyl ether and dried *in vacuo*. (Found: C, 64.1; H, 4.2; N, 5.3. $C_{48}H_{50}AgN_3P_2S_2$ requires: C, 63.9; H, 4.6; N, 5.5%.) Melting point 194°C.

The same compound was obtained by direct reaction of stoichiometric amounts of $Na_2(mnt)$, $Ag(PPh_3)_2NO_3$ and $NEt_4Cl \cdot H_2O$ in the same solvent.

When dppe (60 mg, 0.15 mmol) was used in the previous procedure a yellow compound of stoichiometry $[(NEt_4)Ag(mnt)(dppe)]$ was obtained. (Found: C, 58.4. $C_{38}H_{44}AgN_3P_2S_2$ requires: C, 58.7%.) Melting point 158°C.

RESULTS AND DISCUSSION

I was obtained by reacting $Na_2(mnt)$ with $AgNO_3$ in acetone–water. The insolubility of **I** in all the common solvents suggests a polymeric nature. Its amorphous structure was confirmed by X-ray diffraction.

This product reacts with basic phosphines or diphosphines in almost any solvent. No reaction was observed with more π-acid P-donating ligands like $P(OMe)_3$ or $P(OPh)_3$, or with N-donating ligands. The resulting compounds can only be isolated in the crystalline state when PPh_3 or dppe are used.

The product of the reaction of **I** with PPh_3 gives an analysis of **III**. It behaves as a 1:1 electrolyte in acetone, but the values of molar conductivity in this solvent are low. The representation of $(\Lambda_0 - \Lambda)$ vs $\sqrt{c}$ according to Feltham and Hayter[7] is a straight line with a slope similar to the 1:1 electrolytes. An increase in the molar conductivity is observed by addition of an excess of PPh_3 to the solution of compound **III** in acetone.

The reaction of **II** with PPh_3 yields a yellow compound (**IV**). This compound behaves as a 1:1 electrolyte in acetone.

The ^{31}P NMR spectrum of **III** in CD_2Cl_2 at room temperature shows a broad signal at $\delta = 7.0$ ppm (reference $\delta = 0$ for 85% H_3PO_4 in D_2O). When some PPh_3 was added to the sample, the signal shifted towards a higher field.

This result indicates the existence of a fast dissociative process for the phosphine ligand, already reported for other silver–phosphine complexes.[8]

The low-temperature spectrum (−96°C) shows eight signals corresponding to two doublets of doublets centered at $\delta_1 = 6.0$ ppm and $\delta_2 = 4.6$ ppm, indicating the presence of two different silver moieties in solution with different values of ^1J(Ag—P) coupling constants.

Muetterties and Alegranti[9] have established a direct relationship between the *s* character in the Ag—P bond and the values of ^1J(Ag—P) valid for several silver–phosphine complexes. According to these values we can fix the signal at 4.6 ppm [$^1J(^{107}Ag—P) = 223$ Hz] to the phosphine ligands bonded to a tetracoordinated silver atom, and the signal at 6.0 ppm [$^1J(^{107}Ag—P) = 309$ Hz] to phosphine bonded to a tricoordinated silver atom.

The ratio $^1J(^{109}Ag—P)$: $^1J(^{107}Ag—P)$ is equal to 1.15, approximating the theoretical value (1.149).[10]

The ^{31}P NMR spectrum of compound **IV** at −96°C shows two doublets centered at $\delta = 4.6$ ppm with $^1J(^{107}Ag—P) = 223$ Hz. This coupling constant value is in good agreement with that calculated for tetracoordinated silver atoms. The δ (ppm) and $^1J(^{107}Ag—P)$ values are identical to the signals observed for compound **III**.

These spectroscopic results indicate that the tetracoordinated anionic species

$$[Ag(mnt)(PPh_3)_2]^-$$

is present in solution in compounds **III** and **IV**.

The conductivity values for compounds **III** and **IV** indicate the existence of an ionic equilibrium at room temperature as follows:

$$[Ag_2(mnt)(PPh_3)_4] \rightarrow [Ag(PPh_3)_2]^+ + [Ag(mnt)(PPh_3)_2]^-,$$

$$[(NEt_4)Ag(mnt)(PPh_3)_2] \rightarrow [NEt_4]^+ + [Ag(mnt)(PPh_3)_2]^-.$$

Table 1. ^{31}P NMR parameters for the complexes

	$^1J(^{107}Ag—P)$ (Hz)	$^1J(^{109}Ag—P)$ (Hz)
$[Ag_2(mnt)(PPh_3)_4]$	309 223	354 257
$[(NEt_4)Ag(mnt)(PPh_3)_2]$	223	258
$[Ag\{P(C_7H_7)_3\}_4PF_6]$[a]	224	
$[Ag\{P(C_7H_7)_3\}_3PF_6]$[a]	321	
$[Ag\{P(C_7H_7)_3\}_2PF_6]$[a]	496	

[a] Values obtained from Ref. 9.

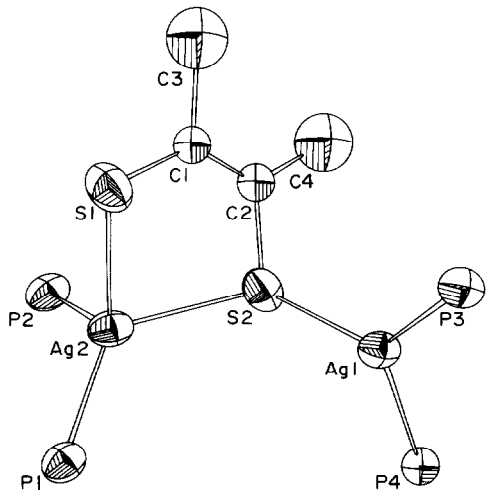


Fig. 1.

The low value of $^1J(^{107}Ag—P)$ observed at −96°C for the second signal in the spectrum of compound **III** is more consistent with the existence of an sp^2 hybridisation in the cationic silver species, indicating the existence at this temperature of an anion–cation interaction via S—Ag bonds. This result is in accordance with the low values for molar conductivity found for this compound and with the increase in molar conductivity by addition of PPh_3 to a solution of compound **III** in acetone.

An S—Ag interaction is observed in the molecular structure of **III** in the solid state[11] (see Fig. 1).

A similar interaction is found in the complex $[Ag(PPh_3)_2]_2[Ni(mnt)_2]$.[12]

The ^{31}P NMR spectra of compounds

$[Ag_2(mnt)(dppe)_2]$

and

$[(NEt_4)Ag(mnt)(dppe)]$

at low temperature are more complex than for compounds **III** and **IV**, suggesting the existence of more equilibria in solution.

Acknowledgement—We thank Mrs B. Ulbrich for technical assistance in the preparation of the ligand.

REFERENCES

1. D. Coucouvanis, *Prog. Inorg. Chem.* 1970, **11**, 233.
2. J. A. McCleverty, *Prog. Inorg. Chem.* 1968, **10**, 49.
3. R. P. Burns and C. A. MacAuliffe, *Adv. Inorg. Chem. Radiochem.* 1979, **22**, 303.
4. G. Bahr and G. Schleitzer, *Chem. Ber.* 1957, **90**, 431.
5. M. L. Caffery and D. Coucouvanis, *J. Inorg. Nucl. Chem.* 1975, **37**, 2081.
6. T. Yoshimura, W. Storck and G. Maneke, *Makromol. Chem.* 1977, **178**, 75.
7. R. D. Feltham and R. G. Hayter, *J. Chem. Soc.* 1964, 4587.
8. R. G. Goel and P. Pilon, *Inorg. Chem.* 1978, **17**, 2876.
9. E. L. Muetterties and C. W. Alegranti, *J. Am. Chem. Soc.* 1972, **94**, 6386.
10. R. C. Weast (Ed.) *CRC Handbook of Chemistry and Physics*, p. E-71 (1980).
11. E. Gutierrez Puebla and M. A. Monge, private communication.
12. D. Coucouvanis, N. C. Baezinger and S. M. Johnson, *Inorg. Chem.* 1974, **13**, 1191.

Polyhedron Vol. 4, No. 11, pp. 1969–1974, 1985
Printed in Great Britain

0277-5387/85 $3.00 + .00
© 1985 Pergamon Press Ltd

VARIABLE-TEMPERATURE FOURIER TRANSFORM IR AS A PROBE OF INTERMOLECULAR FORCES: APPLICATION TO ORGANOTIN COMPOUNDS

R. H. HERBER

Department of Chemistry, Rutgers, The State University of New Jersey, New Brunswick, NJ 08903, U.S.A.

(*Received* 21 *February* 1985; *accepted after revision* 29 *May* 1985)

Abstract—The medium and strong IR absorptions of a number of organometallic complexes of Sn(IV) have been studied as a function of temperature over the range $78 \leqslant T \leqslant 300$ K and $4800 \geqslant \omega \geqslant 400$ cm^{-1}, using variable-temperature Fourier transform IR techniques. The positions of the IR bands are essentially temperature-independent (± 1 cm^{-1}) for $(C_6H_5)_4Sn$ and $(C_6H_5)_3SnCl$, which are aggregates of monomeric units in the solid state, whereas the IR bands of $(CH_3)_2SnF_2$, $(CH_3)_3SnF$ and $(CH_3)_2SnCl_2$, which form polymeric network solids, are observed to have appreciable frequency shifts with temperature. In particular, for the organotin polymers, both $\nu_{as}(SnC_2)$ and $\nu_s(SnC_2)$ shift to lower frequency as the temperature is raised, whereas the symmetric and antisymmetric CH modes shift in the opposite direction. A plausible origin for these temperature-dependent frequency shifts is suggested.

Modern techniques of Fourier transform IR (FTIR) spectroscopy have provided the experimentalist with a powerful new tool for the study of vibrations of molecular systems. Among the major strengths of this methodology is the digitization of the spectral data (intensity and band profile) and reference of the wavelength scale to a laser-locked frequency standard which permits the determination of absorption band positions with high accuracy and with replicability from spectrum to spectrum.

Because the IR power deposition[1] on the sample in an FTIR spectrometer is of the order of two magnitudes smaller than it is in a typical dispersive IR spectrometer, it has become possible to carry out vibrational spectroscopic studies over the cryogenic-temperature range (4.2–300 K) using relatively simple cooling techniques, and to gather such IR data conveniently and rapidly. This method of variable-temperature Fourier transform IR (VTFTIR) spectroscopy has opened up a new area of investigation of the temperature dependence of IR absorptions, and in particular of the study of the effect of inter-molecular forces on the band positions of IR active modes in solids. At the present time, there are very few data in the literature concerning the temperature dependence of IR modes in solids and what kind of information can potentially be extracted from such measurements.

SOME FUNDAMENTALS

In the following discussion a very simple phenomenological approach will be used to account in a qualitative manner for the temperature dependence of the IR band line positions in monomeric and polymeric covalent solids.[2] As a starting point we consider the relationship between the frequency, ν, of a vibration in a diatomic molecule, and the force constant, K, arising from the chemical bonding interaction between the two atoms; that is:

$$\nu = \frac{1}{2\pi}\left(\frac{K}{\mu}\right)^{1/2}, \tag{1}$$

where μ is the reduced mass of the diatomic system. K, in turn, is given by the second derivative of the interatomic potential and coordinate:

$$K = \left(\frac{\partial^2 V}{\partial q^2}\right) \tag{2}$$

and is thus related to the shape of the potential energy surface in the vicinity of the two quantized vibrational levels involved in the spectroscopically detected transition. For a diatomic molecule in the gas phase, the potential energy surface for a given set of vibrational states is insensitive to temperature, and hence the energy difference between the two

states will be temperature-insensitive. By extension, in covalent solids with small or negligible intermolecular forces, the frequency of a given vibrational transition will be temperature-insensitive, since the shape of the potential energy surface does not change significantly with temperature. The cubic expansion coefficient for such solids reflects the increase in vibrational amplitudes as the temperature is raised, but such effects do not change significantly the frequency of the transition between a given set of vibrational states, nor—to a first approximation—the equilibrium internuclear distances and electron densities at a given lattice site in the solid.

When intermolecular forces are not negligible, as in polymeric compounds, or where there are significant hydrogen bonding forces between adjacent molecules, the temperature dependence of K becomes significant, and hence some (or all) of the spectroscopically active transitions will show a non-negligible temperature dependence. If one considers a linear polymer of the form ... ABAB ..., the cubic expansion (thermal) of the solid will influence the internuclear distances of all the atoms in the chain, and hence the shape of the potential energy surface and the overlap of the electronic (molecular) wave functions which obtain in the condensed matter matrix. In the presence of such intermolecular forces, $V = V(T)$, and hence $K = K(T)$, so that $\nu = \nu(T)$. A similar situation is expected to arise in solids in which the monomer units are tied together by strong intermolecular interactions in two and three dimensions, since, in principle, the cubic expansion of such solids should result in a change in the electron density at each atomic lattice point.

In this connection, two points need to be kept in mind: the IR-active modes considered (experimentally) in the discussion below are—in general—not fundamental normal modes, but involve a variety of combination modes in which several motional symmetries may be coupled to give rise to the absorption being measured. Secondly, it is likely that thermal expansion—and the concomitant change in K in molecular solids—will result in both positive and negative shifts in IR band positions, and in some instances, mutual cancellation of opposing effects may, in fact, result in a temperature invariance of *some* of the bands observed in the spectra. Thus it is appropriate to consider *all* of the IR-active modes which can be observed in such solids.

It is the purpose of the present study to demonstrate that $\nu(T)$ reflects the presence (or absence) of strong intermolecular interactions in solids, and to suggest the utility of such temperature dependencies of vibrational mode frequencies in the study of polymer interaction in solids.

EXPERIMENTAL

All of the compounds examined in the present study were obtained commercially,[3] and purified by recrystallization [e.g. $(C_6H_5)_3SnCl$ from hexane and $(C_6H_5)_4Sn$ from 1,1,2-trichloroethane] as necessary. Dimethyltindichloride was resublimed twice at ~ 1 torr and 50–60°C prior to use. Pellets were prepared by pulverizing the subject compound with spectroscopic grade KBr in a plastic ball mill ("wiggle bug") arrangement and pressing the resultant powders at 20,000 lb in^{-2} in an evacuated die, using a concentration of 0.5–1% by weight.

These pellets were clamped into an Invar cell (chosen because of the exceptionally low thermal expansion coefficient of this material to prevent breakage of the sample pellet on thermal cycling) which in turn was mounted on the copper cold finger of a Heli-tran cryostat[4] whose temperature was monitored via thermocouples attached to the copper block adjacent to the sample space. The thermal lag between the temperature registered by the thermocouple and that of the KBr disc was determined experimentally, using the well-defined first-order phase transitions in adamantane,[5] NH_4Br[6] and benzil.[7] This thermal lag was determined to be less than 0.5° in the range $78 \leqslant T \leqslant 300$ K.[8]

IR spectral data were obtained using a nitrogen purged IBM 32 FTIR spectrometer. In a typical scan, the sample was allowed to reach thermal equilibrium (usually 15–20 min, although ancillary data suggested that a steady-state value was reached in less than 5 min under the prevailing conditions), after which time 100 interferometer scans were co-added and ratioed to a background obtained with a comparable KBr blank in the sample compartment. The peak positions of the relevant (medium- or strong-intensity) IR bands were determined using the IBM IR software in the manual (cursor) mode or by using the PEAKPICK software. Replicate scans, using different samples, and acquired several days apart, showed that line positions of a given band at a given temperature were reproducible within an error of ± 0.5 cm^{-1} or less at a resolution of 2 cm^{-1}.

RESULTS AND DISCUSSION

Tetraphenyltin(IV)

The crystal structure of this molecule has been reported by Chieh and Trotter[9] who concluded that the solid is composed of discrete molecular units, despite the fact that it has a relatively high melting point (229°C) and exhibits an observable ^{119}Sn

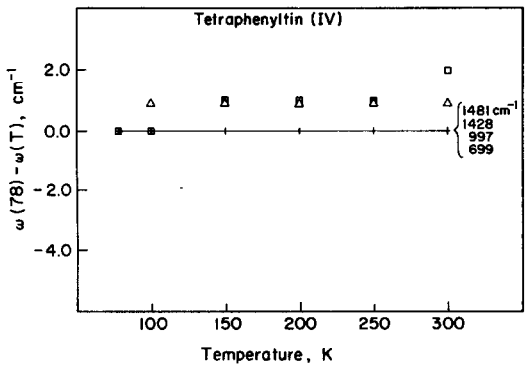


Fig. 1. Temperature dependence of the most prominent mid-range IR modes of tetraphenyltin(IV). The shift is taken with respect to the band position observed at 78 K. The horizontal axis indicates the sample temperature in K. The crosses pertain to four temperature-invariant modes at 699, 997, 1428 and 1481 cm^{-1}.

Mössbauer resonance at room temperature.* The effect of temperature change on the angle of rotation of the molecule about the $\bar{4}$ axis, the z-axis of the crystal, is not known, especially in a KBr matrix. Nonetheless, for the purposes of the present discussion this compound is taken to be representative of a covalent solid with negligible intermolecular forces. The vibrational spectrum shows nine medium or strong IR active bands in the range $400 \leqslant \omega \leqslant 1600$ cm^{-1}. The temperature dependence of the band positions is summarized graphically in Fig. 1, from which it is noted that the maximum frequency shift, $\Delta\omega$, defined by:

$$\Delta\omega(T) = \omega(78\text{ K}) - \omega(T),$$

is 2 cm^{-1} for the y'-mode, identified either as the symmetric Sn—C stretch[10] or an out-of-plane ring bending mode.[11,12] For all of the other bands, over the entire temperature range, the band position is either temperature-invariant or within the experimental uncertainty cited above. This temperature invariance of the band positions over a 200° temperature interval is taken to be characteristic of covalent monomeric solids. With two exceptions, the observed band positions are in good agreement with the data cited in the literature. The CH out-of-plane bending mode (ν_{11b}, ν_{10b}) reported[13] as a strong absorption at 710 cm^{-1} is observed in the present study at 699 cm^{-1}, while the comparable mode (ν_4) reported earlier[13] at 745, and 736 cm^{-1},[14] is seen at 731 cm^{-1} in the present work.

Triphenyltin(IV) chloride

Although there has been some speculation in the literature concerning the possible penta-coordination of the metal atom in this molecule at low temperature,[15,16] detailed variable-temperature ^{119m}Sn Mössbauer effect studies[17] in the range $4.2 \leqslant T \leqslant 300$ K have failed to support a transition from the tetracoordination at room temperature which can be inferred from the crystallographic data of Bokii *et al.*[18] and the IR data of Kriegsmann and Geissler,[10] and which argues against the presence of bridging chlorine ligands at room temperature. The temperature independence of the IR modes of this solid support this conclusion, since none of the nine medium- or strong-intensity bands reported by Kriegsmann and Geissler[10] and Griffiths and Derwish[13] show a temperature dependence outside the resolution limit of the present study. The temperature dependence of $\Delta\omega$ for the nine modes observed in the frequency range $400 \leqslant \omega \leqslant 1600$ cm^{-1} are summarized graphically in Fig. 2. The combination band $\nu_5{}^1$ at 1156 cm^{-1}, which involves the Sn—C asymmetric stretch, and the weak band ν_5 at 1064 cm^{-1}, which involves the Sn—C symmetric stretch [reported at 1156 and 1072 cm^{-1}, respectively, in tetraphenyltin(IV) by Randle and Whiffen[19]] are apparently completely temperature-invariant under the conditions of the present study.

Dimethyltin(IV) difluoride

In contrast to the two monomeric solids considered above, this compound is a well-characterized polymeric material in which fluorine bridges join adjacent six-coordinate metal centers in an infinite lattice. A detailed X-ray diffraction structural study has been reported by Schlemper and

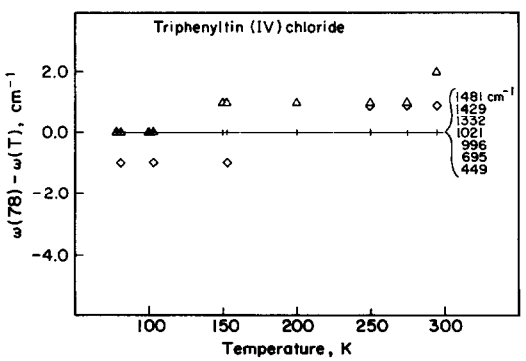


Fig. 2. Temperature dependence of the most prominent IR modes of triphenyltin(IV) chloride. The crosses pertain to seven temperature invariant modes at 449, 695, 996, 1021, 1332, 1429 and 1481 cm^{-1}. For axes, see caption to Fig. 1.

* It has been pointed out by one of the reviewers that "... a convincing case can be made that this material acts as a 'virtual polymer', even though the closest carbon–carbon approach is 3.54 Å—a van der Waals' interaction".

Hamilton[20] and the IR spectrum has been examined by Hobbs and Tobias[21] and Goldstein and Unsworth,[22] *inter alia*. The latter authors have also reported the IR spectrum of $(CH_3)_2SnF_2$ at ~120 K and note a 1-cm^{-1} shift in the symmetric SnC_2 stretch over their temperature range. The rotational barrier of the methyl group is calculated to be ~1 kJ mol^{-1} at 296 K. Hobbs and Tobias[21] have carried out a complete normal coordinate analysis of this compound, making the assumption that the constituent moieties are $(CH_3)_2Sn^{2+}$ cations and F^- anions, and make use of a Urey–Bradley force field equation to calculate K_{C-H} (4.63 ± 0.02 mdyne $Å^{-1}$), K_{C-Sn} (1.53 ± 0.06 mdyne $Å^{-1}$) and K_{Sn-F} (0.99 ± 0.04 mdyne $Å^{-1}$).

The temperature dependence of the IR band positions for this compound are summarized in Fig. 3, from which it is seen that there are gradual and significant shifts in the line positions of all of the medium and strong bands observed in the spectrum. In particular, both the symmetric and asymmetric SnC_2 stretches (526 and 599 cm^{-1} at 295 K, respectively) show a similar decrease in frequency with an increase in temperature, and this is also comparable to the symmetric $\delta(CH_3)$ mode at 1206 cm^{-1}. On the other hand the CH_3Sn rocking mode at 780 cm^{-1} and both the symmetric and asymmetric methyl group CH stretches at 2930 and 3015 cm^{-1} show a similar frequency increase over the same temperature interval.

Of the seven assigned modes in the interval $3100 \geq \omega \geq 400$ cm^{-1}, with the exception of the weak band at 1408 cm^{-1} assigned to the asymmetric bending mode of the methyl group, all show a temperature dependence of the line position to be expected if the electron density at *each* atomic lattice

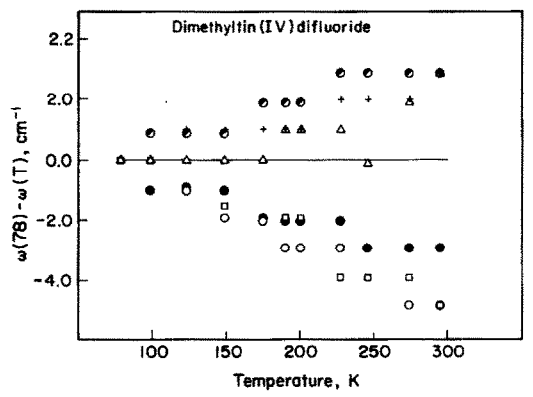


Fig. 3. Temperature dependence of the most prominent IR modes of dimethyltin(IV) difluoride. The following symbols are used: (○) $\rho(CH_3Sn)$, (□) $\nu_{as}(CH_3)$, (●) $\nu_s(CH_3)$, (+) $\delta_s(CH_3)$, (△) $\nu_s(SnC_2)$, and (◑) $\nu_{as}(SnC_2)$. For axes, see caption to Fig. 1.

point is influenced by the thermal expansion of the solid as the temperature is increased. In contrast to the observations noted for the two monomeric aryl tin compounds, none of the significant IR absorptions remain temperature-invariant. To ensure that the temperature-dependent frequency shifts observed in the IR spectra of $(CH_3)_2SnF_2$ are not matrix-dependent, a replicate set of experiments was carried out, using TlBr as a dispersant, instead of KBr, since the heavier bromide crystallizes in the CsCl structure, while KBr has the NaCl structure. However, using TlBr as above, the results are completely identical (within experimental error) to those observed using the KBr matrix samples—both $\nu_s(SnC_2)$ and $\nu_{as}(SnC_2)$ move to lower frequencies as T is increased, whereas $\nu_s(CH_3)$, $\nu_{as}(CH_3)$ and $\rho(CH_3Sn)$ all move to higher frequencies. These results confirm the assumption that the temperature-dependent frequency shifts observed in this polymeric solid reflect the electron distribution in the molecule rather than being an artifact of the dispersing medium, although the possibility of halogen exchange within the matrix is not directly addressed by this procedure.

Trimethyltin(IV) flouride

The structure of this polymeric solid was determined by Clark *et al.*[23] and discussed in detail in the review by Ho and Zuckerman.[16] A fundamental disorder of the fluorine atoms and the F—Sn—F chains in the crystal at room temperature prevents the structure of trimethyltin fluoride from being solved to the usual R factors.[23] The solid is composed of non-planar $(CH_3)_3Sn$ units bridged by fluorine atoms to give rise to a zig-zag chain with non-linear Sn—F—Sn units. IR assignments for this compound have been reported by Kriegsmann and Pischtschan[24] and Yasuda.[25] The presence of strong inter-monomer unit forces is inferred both from the optical and chemical properties of this material, as well as from the observation by Licht *et al.*[26] of a 239-cm^{-1} shift of the Sn—F vibration in going from the polymeric solid- (349 cm^{-1}) to the gas-phase monomer (588 cm^{-1}), which may be ascribed to a change from five to four coordination around the metal atom.

The temperature dependence of the four prominent modes in the $1600 \geq \omega \geq 400$ cm^{-1} range is summarized in Fig. 4. The symmetric SnC_3 mode at 619 cm^{-1} is too weak in the IR spectrum to be used in the present analysis, although the non-planar $Sn(CH_3)_3$ configuration should make this band (which is observed as a strong absorption at ~520 cm^{-1} in the Raman spectrum) extractable from the spectra. As noted from Fig. 4 the three CH_3

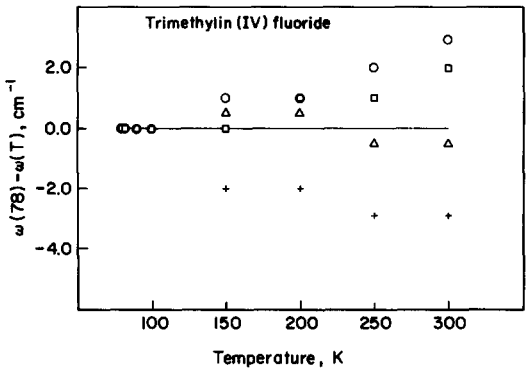


Fig. 4. Temperature dependence of the most prominent IR modes of trimethyltin(IV) fluoride. The following symbols are used: (△) $\rho(CH_3)$, (+) $\rho(CH_3)$, (□) $\nu_{as}(SnC_3)$, and (○) $\delta_s(CH_3)$. For axes, see caption to Fig. 1.

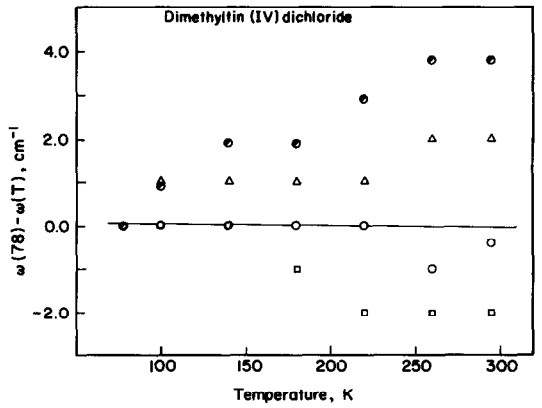


Fig. 5. Temperature dependence of the most prominent IR modes of dimethyltin(IV) dichloride. The following symbols are used: (○) $\nu_{as}(CH_3)$, $\delta_s(CH_3)$ and $\rho(CH_3)$, (◑) $\nu_{as}(SnC_2)$, (△) $\nu_s(SnC_2)$, and (□) $\delta_{as}(CH_3)$.

modes at 782, 1189 and 1210 cm^{-1}, as well as the asymmetric SnC_3 stretch show a progressive shift as the temperature is raised from 78 to 300 K. As in the case of the two-dimensionally polymeric $(CH_3)_2SnF_2$, the one-dimensionally polymeric $(CH_3)_3SnF$ shows the temperature-dependent IR band shifts discussed above. For these solids with one or more strong intermolecular bonding interactions, the present data suggest a small but real change in the electron density around the central metal atom as thermal expansion effects a change in the internuclear distance of the atoms involved in this bonding mode.

Dimethyltin(IV) dichloride

The structure of this solid has been discussed by Davies *et al.*[27] who were able to show that adjacent $(CH_3)_2Sn$ units are bridged by four chlorine atoms, two of which have Sn—Cl distances of 2.40 Å and the other two (in an approximately *trans* position) of 3.54 Å. The C—Sn—C bond angle is found to be 123.5° so that the local environment around the metal atom is that of a symmetry strongly distorted away from tetrahedral. Such large distortions from ideal T_d-geometry—even in the absence of bridging interactions of the chloride ligands—appear to be more common than has been assumed, but are usually associated with sterically demanding (i.e. bulky) organic moieties attached to the metal atom. As Baxter *et al.*[28] have recently pointed out in connection with their structural study of bis(biphenylyl-2) tin(IV) dichloride, compression of the Cl—Sn—Cl bond angle to 99.71°, and expansion of the C—Sn—C bond angle to 130.8°, can be traced to steric demands of the organic group rather than to any involvement of the halogen atom in bridging behavior. Such steric demands are, however, minimal in $(CH_3)_2SnCl_2$. The absence of an inversion center at the metal atom leads to the ready observation of both $\nu_{as}(Sn—C_2)$ and $\nu_{as}(Sn—C_2)$ at 566 and 516 cm^{-1}, respectively, as sharp intense bands in the IR spectrum. The most prominent band in the spectrum is a broad intense band at 799 cm^{-1} assigned by Edgell and Ward[29] to a CH_3 rocking mode. Other IR assignments for this compound have been reported by Taimsalu and Wood[30] and Okawara *et al.*[31] The only mode which is too weak to be used in the present analysis is the $\nu_s(CH_3)$ band at ~2925 cm^{-1}, although this band has been reported[29] to be of strong intensity in the IR spectrum of the liquid.

The temperature dependence of the six most prominent IR active bands of $(CH_3)_2SnCl_2$ is shown in Fig. 5. Of these, $\nu_{as}(CH_3)$, $\delta_s(CH_3)$ and $\rho(CH_3)$ at 3013, 1201 and 799 cm^{-1}, respectively, are essentially temperature-independent over the range $78 \leqslant T \leqslant 300$ K, while the mode at 566 cm^{-1}, due to the asymmetric SnC_2 stretch, shows the most pronounced variation with temperature, being red shifted by 3.8 cm^{-1} between 78 K and room temperature. In addition, both the $\delta_{as}(CH_3)$ mode at 1404 cm^{-1} and the symmetric SnC_2 stretch at 516 cm^{-1} show a small temperature dependence, as expected from the polymeric structure of this compound.

CONCLUSIONS

In the present study of the IR spectra of a number of organotin(IV) compounds, it has been observed that, for those solids which are comprised of non-interacting monomeric molecular entities, the location of the most prominent absorption bands is essentially temperature-independent over the range

$79 \leqslant T \leqslant 300$ K within an experimental resolution limit of $\sim \pm 1$ cm^{-1}. In contrast, the spectra of associated solids which form one- or two-dimensional polymeric structures, all of the prominent absorption bands show temperature-dependent frequency shifts. On the basis of currently available data it is inferred that these frequency shifts originate from bond distance changes resulting from thermal expansion of the solid. These changes in the internuclear distances of some of the bonded atom pairs in the structure result in principle—by virtue of electron-following effects—in a change in the electron density in all of the bonding overlaps in the molecule.

The magnitudes of the effects observed in the present study are not large enough to answer the question of whether the temperature dependence of $\Delta\nu$, as defined above, is a linear function of temperature (as implied in the figures) or not. This question, as well as development of a more detailed theoretical treatment of the observed effects, is currently under study in these laboratories. Notwithstanding the paucity of the present results, it is clear that the experimental demonstration of temperature-dependent IR band positions has provided the spectroscopist with a new, sensitive and powerful tool for the study of intermolecular associations in covalent solids.

Acknowledgements—I am indebted to my colleagues, Professors K. Krogh-Jespersen and L. Goodman, for stimulating discussions of this problem. This research has been made possible by a grant from the National Science Foundation (DMR 810 2940) which also provided support for the acquisition of the FTIR Spectrometer.

REFERENCES

1. J. M. Casper, IBM Instruments Co., private communication.
2. For a more detailed introduction to IR fundamentals, see, for example, K. Nakamoto, *Infrared Spectra of Inorganic and Coordination Compounds*, Wiley–Interscience, New York (1970), and references therein. For a discussion of FTIR methods, see, for example, J. R. Ferraro and L. J. Basile (Eds), *Fourier Transform Infrared Spectroscopy*, Academic Press, New York (1978); P. R. Griffiths, *Chemical Infrared Fourier Transform Spectroscopy*, Wiley, New York (1975); J. R. Durig (Ed.), *Analytical Applications of Fourier Transform Infrared Spectroscopy*, D. Reidel, Boston (1980).
3. Alfa Products, P.O. Box 299, Danvers, MA 01923, U.S.A.; and Aldrich Chemical Co., P.O. Box 355, Milwaukee, WI 53201, U.S.A.
4. Air Products Corp., Allentown, PA 18103, U.S.A.
5. S. S. Chang and E. F. Westrum, *J. Phys. Chem.* 1960, **64**, 1547; R. C. Fort and P. von R. Schleyer, *Chem. Rev.* 1965, **64**, 277; P. J. Wu, L. Hsu and D. A. Dows, *J. Chem. Phys.* 1971, **54**, 2714.
6. N. E. Schumaker and C. W. Garland, *J. Chem. Phys.* 1970, **53**, 392; C. W. Garland and N. E. Schumaker, *J. Phys. Chem. Solids* 1967, **28**, 799; H. A. Levy and S. W. Peterson, *Phys. Rev.* 1951, **83**, 1270; *ibid.*, 1952, **86**, 766; *J. Am. Chem. Soc.* 1953, **75**, 1536.
7. P. Esherick and B. Kohler, *J. Chem. Phys.* 1973, **59**, 6681; P. Figuiere and H. Szwarc, *Mol. Cryst. Liq. Cryst.* 1976, **35**, 1.
8. L. M. Casson and R. H. Herber, *Rev. Sci. Instrum.* 1985, **56**, 1593.
9. P. C. Chieh and J. Trotter, *J. Chem. Soc. A* 1970, 911; see also N. A. Akhmed and G. G. Aleksandrov, *J. Struct. Chem., Engl. Transl.* 1970, **11**, 824.
10. H. Kriegsmann and H. Geissler, *Z. Anorg. Allg. Chem.* 1963, **323**, 170.
11. L. A. Harrah, M. T. Ryan and C. Tamborski, *Spectrochim. Acta* 1962, **18**, 21; see also the discussion in R. C. Poller, *Spectrochim. Acta* 1966, **22**, 935; as well as M. E. Bishop, *Spectrochim. Acta* 1976, **A32**, 1519.
12. A. L. Smith, *Spectrochim. Acta* 1968, **A24**, 695.
13. V. S. Griffiths and G. A. W. Derwish, *J. Mol. Spectrosc.* 1960, **5**, 148.
14. R. C. Poller, *J. Inorg. Nucl. Chem.* 1962, **24**, 593.
15. T. S. Srivastava, *J. Organomet. Chem.* 1967, **10**, 373.
16. B. Y. K. Ho and J. J. Zuckerman, *J. Organomet. Chem.* 1973, **49**, 1; see also J. A. Zubieta, *Prog. Inorg. Chem.* 1978, **24**, 251.
17. B. King, H. Eckert, D. Z. Denney and R. H. Herber, to be published.
18. N. T. Bokii, G. N. Zakharova and Yu. T. Structkov, *J. Struct. Chem., Engl. Transl.* 1970, **11**, 828.
19. R. R. Randle and D. H. Wiffen, cited in ref. 13.
20. E. O. Schlemper and W. C. Hamilton, *Inorg. Chem.* 1966, **5**, 955.
21. C. W. Hobbs and R. S. Tobias, *Inorg. Chem.* 1970, **9**, 1037.
22. M. Goldstein and W. D. Unsworth, *J. Chem. Soc. A* 1971, 2121.
23. H. C. Clark, R. J. O'Brien and J. Trotter, *J. Chem. Soc.* 1964, 2332; H. C. Clark, R. J. O'Brien and J. Trotter, *Proc. Chem. Soc.* 1963, 85.
24. H. Kriegsmann and S. Pischtschan, *Z. Anorg. Allg. Chem.* 1961, **308**, 212.
25. K. Yasuda, *Bull. Chem. Soc. Jpn* 1965, **38**, 1216.
26. K. Licht, H. Geissler, P. Koehler, H. Schnorr and H. Kriegsmann, *Z. Anorg. Allg. Chem.* 1971, **385**, 271.
27. A. G. Davies, H. J. Milledge, D. C. Puxley and P. J. Smith, *J. Chem. Soc. A* 1970, 2862; see also J. D. Graybeal and D. A. Berta, *Nat. Bur. Stand. (U.S.), Spec. Publ.* 1969, **301**, 393.
28. J. L. Baxter, E. M. Holt and J. J. Zuckermann, *Organometallics* 1985, **4**, 255.
29. W. F. Edgell and C. H. Ward, *J. Mol. Spectrosc.* 1962, **8**, 343.
30. P. Taimsalu and J. L. Wood, *Spectrochim. Acta* 1964, **20**, 1043.
31. R. Okawara, D. E. Webster and E. G. Rochow, *J. Am. Chem. Soc.* 1960, **82**, 3287.

Polyhedron Vol. 4, No. 11, pp. 1975–1979, 1985
Printed in Great Britain

0277-5387/85 $3.00 + .00
© 1985 Pergamon Press Ltd

CYANATO-COPPER(II) COMPLEXES WITH ORGANIC LIGANDS—XXIV.* DIISOCYANATO-BIS(3,5-DIMETHYLPYRAZOLE)COPPER(II)—THE CYANATE MEMBER OF THE COLIGAND ISOMER PAIR FROM THE Cu(II)–NCO^-–3,5-DIMETHYLPYRAZOLE SYSTEM

JIŘÍ KOHOUT,† JERZY MROZIŃSKI‡ and MÁRIA HVASTIJOVÁ

Department of Inorganic Chemistry, Slovak Technical University, 812 37 Bratislava, Czechoslovakia; and ‡Institute of Chemistry, Wrocław University, 50 383 Wrocław, Poland

(*Received* 18 *December* 1984; *accepted* 4 *June* 1985)

Abstract—The title compound was prepared, and found to be isomeric with the known bis(1-carbamoyl-3,5-dimethylpyrazolato)copper(II). Its IR, far-IR, electronic and ESR spectra were recorded and its magnetic susceptibilities down to 4.2 K were measured. A five-coordinate binuclear or polymeric chain structure is assumed with *N*-bridging as well as terminal NCO groups. The ESR spectrum shows zero-field splitting in the triplet state. The temperature-dependent magnetic behaviour is characteristic of an intramolecular ferromagnet. The exchange parameters were determined on the basis of a dimeric model and three various linear-chain models, and the fits were compared.

In 1979 we reported[2] the crystal and molecular structures of α-bis(1-carbamoyl-3,5-dimethylpyrazolato)copper(II), $Cu(dmpz \cdot NCO)_2$ (dmpz = 3,5-dimethylpyrazole), and the physical properties of this compound, as well as of its isomeric (β) form. The anionic chelate ligands in these complexes were formed by nucleophilic addition between dmpz and NCO in the Cu(II) coordination sphere. The isomeric cyanato complex, $Cu(NCO)_2(dmpz)_2$, which should form with $Cu(dmpz \cdot NCO)_2$ a pair of coligand isomers,[3] was not isolated at that time. However, in the course of further attempts we succeeded in preparing this complex. Therefore we report the preparation of $Cu(NCO)_2(dmpz)_2$ and its characterization by chemical analysis, spectroscopy and magnetochemistry. We used indirect structural methods, as we had not been able to obtain single crystals suitable for X-ray study.

EXPERIMENTAL

Preparation

A solution of 12.5 mmol of $Cu(NO_3)_2 \cdot 3H_2O$ in 10 cm^3 of water, cooled in a refrigerator, was mixed with a cooled solution of 26.5 mmol of KOCN in 10 cm^3 of water. The mixture was poured into a cooled solution of 23.7 mmol of dmpz in a mixture of 25 cm^3 of water and 15 cm^3 of methanol. From the resulting solution a green suspension has been separated, which changed into a blue, crystalline substance. This was washed with ice-cold water, dried in a desiccator with KOH, and put in a refrigerator. Found: C, 42.2; H, 4.7; N, 24.6; Cu, 18.8. Calc. for $C_{12}H_{16}N_6O_2Cu$: C, 42.4; H, 4.75; N, 24.7; Cu, 18.7%.

Physical measurements

Magnetic susceptibilities have been measured in the range of 4.2–300 K using a Faraday balance, calibrated using $HgCo(NCS)_4$.[4] Magnetic susceptibilities calculated per Cu(II) were corrected for diamagnetism of -180×10^{-6} cm^3 mol^{-1} and for temperature-independent paramagnetism of 60×10^{-6} cm^3 mol^{-1} to obtain χ_M^{corr} values. The effective magnetic moments, μ_{eff}, in Bohr magnetons, μ_B,§ were calculated from the formula $\mu_{eff} = 2.83(\chi_M^{corr}T)^{1/2}$. The exchange parameter, J, was obtained by fitting the susceptibility data to the respective theoretical model on an Odra 1204 computer. The spectroscopic splitting factor, g_{av}, obtained from the ESR spectrum, was used as a constant in the fitting process. The minimization of

* For Part XXIII, see Ref. 1.

† Author to whom correspondence should be addressed.

§ 1 $\mu_B = 9.274 \times 10^{-24}$ J T^{-1}.

Table 1. Characteristic IR data for $Cu(NCO)_2(dmpz)_2$

ν (cm^{-1})	Assignment	ν (cm^{-1})	Assignment
3337s	ν(NH)	668s	δ(NCO)
3204m,br		657s	
2227vs	ν_{as}(NCO)	645s	
2185vs		625w[a]	
2133sh		614s	
1345m	ν_s(NCO)	607s	
1191m	δ(NH)	591s[b]	
1167m			
1148m			
1138m			

[a] Probably belongs to the dmpz vibration.

[b] Unresolved splitting occurs; the average frequency is given.

Table 2. Far-IR data for $Cu(NCO)_2(dmpz)_2$

ν[a] (cm^{-1})
354s,[b] 298sh, 295s, 258s, 186s, 138m,[c] 126m,[c] 84m, 79sh, 62sh, 57w

[a] Only the skeletal modes are included.

[b] Weak splitting appears; the average frequency is given.

[c] The component of the double maximum with an unresolved complex splitting.

the sum, defined as $ERR = \sum_{i=1}^{n} [\chi_M(calc.)_i - \chi_M(expt)_i]^2$, was the criterion used to determine the best fit.

The ESR spectrum was recorded using a JES-ME-3X spectrometer. The magnetic field was calibrated with Mn^{2+} ion doped in MgO ($\Delta H_{3-4} = 86.9$ G*).

The IR (3800–400 cm^{-1}),[5] far-IR (400–50 cm^{-1})[6] and electronic spectrum (4.0–0.4 μm^{-1})[7] were obtained as described in the cited papers.

The results of the physical measurements are listed in Tables 1–3.

RESULTS AND DISCUSSION

General

The analytical results of $Cu(NCO)_2(dmpz)_2$ are satisfactory for a chemical individual. The IR spectrum shows that the majority of the bands belonging to free dmpz[8] can be identified in the complex. Some of these bands, however, are perceptibly shifted, apparently as a consequence of coordination and possibly also the hydrogen bonding of dmpz (see IR section).

The blue compound $Cu(NCO)_2(dmpz)_2$ is sufficiently stable only in the cool. At ambient temperature it is gradually converted to a gray and finally a gray–black product. It is interesting that $Cu(NCO)_2(dmpz)_2$ does not change to the already investigated[2] α- or β-form of $Cu(dmpz \cdot NCO)_2$.

IR spectrum

The IR spectrum of $Cu(NCO)_2(dmpz)_2$ was compared with that of free dmpz published by Zecchina *et al.*[8] as well as of $CuCl_2(dmpz)_2$ and, thus, the bands of cyanate vibrations were picked out. These bands are indicative of the cyanate groups coordinated through nitrogens.[9] There are six absorptions between *ca* 670 and 590 cm^{-1}, which can be assigned only to the δ(NCO) mode. Such an extensive splitting indicates N-bridged NCO groups[9] and with respect to the number of bands, even two kinds of NCO groups (bridged and terminal) can be supposed.[10] The two well-separated bands in the region of 2200 cm^{-1} belonging to the ν_{as}(NCO) mode are consistent with the latter assumption.

For the NH stretching vibration two bands were found separated by ≈ 130 cm^{-1}, that of the higher frequency being shifted with respect to the band of free dmpz (in CCl_4 solution)[8] lower by ≈ 145 cm^{-1}. These facts suggest the occurrence of two NH···OCN hydrogen bonds of unequal strength formed from one structure unit. The behaviour of the NH deformation is still stranger, apparently involving four absorptions between *ca* 1190 and 1140 cm^{-1}.

The IR spectrum of the gray sample formed by the aging of blue $Cu(NCO)_2(dmpz)_2$ contains also bands characteristic of the species with chelate ligands of the carbamoylpyrazolate type.[2,3] In this substance apparently a fraction of the original ligands underwent a linking into the dmpz·NCO ligand system. Since all the cyanate bands remain present (somewhere with an additional splitting), probably only the terminal NCO groups are involved in the nucleophilic addition, the bridging ones being substantially unchanged.

Electronic spectrum

The electronic spectrum shows a broad ligand field band with the maximum at 1.56 μm^{-1} and a pronounced shoulder at about 1.28 μm^{-1}. Such a band accords with a planar nitrogen environment of Cu(II), being completed in one axial position by the

* 1 G = 10^{-4} T.

Table 3. Magnetic susceptibility data for $Cu(NCO)_2(dmpz)_2$[a]

T (K)	$\chi_M^{corr} \times 10^5$ (cm^3 mol^{-1})	μ_{eff} (B.M.)	T (K)	$\chi_M^{corr} \times 10^5$ (cm^3 mol^{-1})	μ_{eff} (B.M.)
295	139	1.81	16	2920	1.93
255	163	1.82	10	4930	1.99
200	210	1.83	7.0	7410	2.04
140	302	1.84	6.0	8990	2.08
80	528	1.84	5.0	11,100	2.10
35	1230	1.86	4.2	12,200	2.03
20	2180	1.87			

[a] Some values selected from among 60 experimental points are presented.

bridging cyanate nitrogen to a tetragonal pyramid.[11] In such a case the presence of bridging as well as of terminal NCO groups, indicated by the IR spectrum, is understandable and a binuclear (A) or polymeric chain (B) structure may be postulated (Fig. 1).

Far-IR spectrum

An approximate symmetry around Cu(II) in the proposed coordination environment is C_{2v}. Based on this local symmetry, we can expect 11 IR-active skeletal modes, five A_1 + three B_1 + three B_2. From those, two A_1 + two B_1 species are Cu—N(dmpz) as well as two in-plane Cu—NCO stretchings, and one B_2 species is the out-of-plane Cu—NCO stretching. The remaining species, three A_1 + one B_1 + two B_2, are Cu—N deformations.

An inspection of Table 2 reveals that three strong bands appear in the region allowable for stretchings involving the equatorial donors, viz. at 354, 295 and 258 cm^{-1}. We assign the first band to the in-plane Cu—NCO stretch[9] and the two bands below 300 cm^{-1} to the Cu—N(dmpz) stretch.[12] Thus, there is only a single in-plane Cu—NCO stretching band, but the relevant two modes may be accidentally degenerate or close to each other in energy.

The assignment of the lower-frequency bands is less warranted. By analogy with the region of the Cu—OCN stretches for the Cu(II) cyanate having long axial Cu—OCN bonding[6] we suppose that the medium band near 80 cm^{-1} might belong to the out-of-plane Cu—NCO stretch. Further bands occurring below 200 cm^{-1} are probably Cu—N deformations or torsions[13] and the $\approx$60 cm^{-1} band might also be a lattice vibration.

ESR spectrum

The ESR spectrum of $Cu(NCO)_2(dmpz)_2$ measured at two temperatures is presented in Fig. 2.

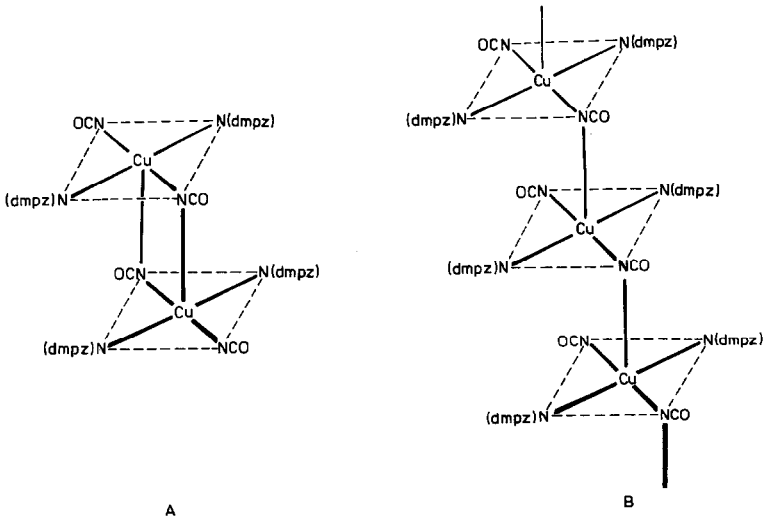


Fig. 1. Possible structure variants for $Cu(NCO)_2(dmpz)_2$.

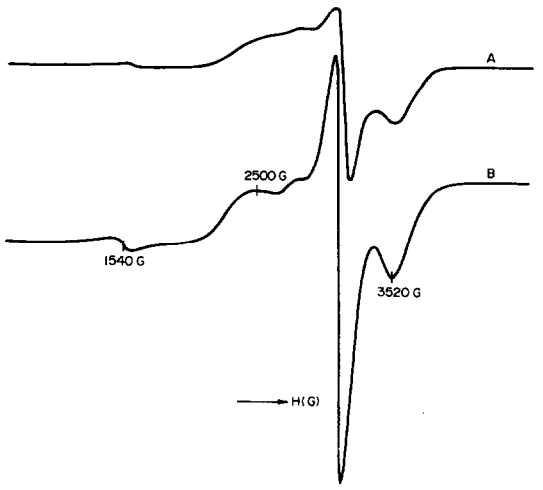


Fig. 2. ESR spectrum of $Cu(NCO)_2(dmpz)_2$ at 293 (A) and 193 K (B).

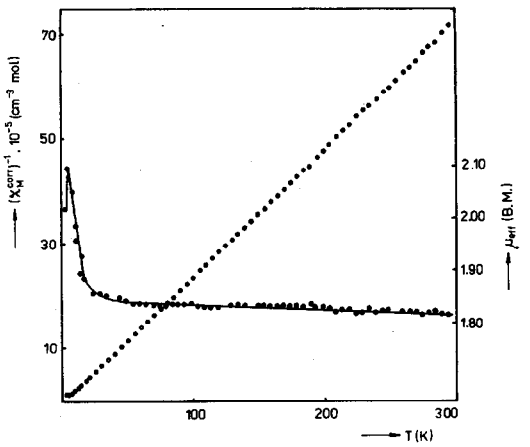


Fig. 3. Temperature dependence of inverse molar susceptibility (○) and magnetic moment (●) for $Cu(NCO)_2(dmpz)_2$.

At 293 K the spectrum consists of a very broad line spreading over ≈1600 G, with bulges at low and high fields. An improved resolution appears at 193 K when the spectrum shows distinct evidence of triplet state transitions.[14] Therefore, it has been interpreted on the basis of the usual spin Hamiltonian for $S = 1$. The bands at 2500 and 3520 G can be assigned to the low- and high-field parallel $\Delta M_S = 1$ transitions and this assignment leads to the values of $g_{\parallel} = 2.206$ and $D = 0.0526$ cm^{-1} (D = zero-field splitting parameter). In this calculation it was assumed that the orthorhombic splitting, E, is zero.

Since $h\nu > D$ ($h\nu$ is the microwave quantum of 0.310 cm^{-1}), the forbidden $\Delta M_S = 2$ transition was observed, viz. at 1540 G (see Fig. 2). From this resonance field position, H_{min}, and from the use of the following equation:[15]

$$g_{av} = \frac{(\omega_o^2 - \frac{4}{3}D^2)^{1/2}}{H_{min}},$$

where $\omega_o = h\nu$, a value of $g_{av} = 2.115$ is calculated.

The value of $g_{\perp}$ can now be obtained using the formula $g_{av} = \frac{1}{3}(2g_{\perp} + g_{\parallel})$; this value amounts to 2.070. Thus, the positions of the perpendicular $\Delta M_S = 1$ resonances would be predicted at *ca* 3410 and 3470 G, where they are superimposed by the high-field parallel absorption. The strong line centered at 3130 G cannot be reliably identified, but it might originate in monomeric paramagnetic impurities contaminating our compound.

Magnetic susceptibilities

The temperature dependence of the inverse molar magnetic susceptibility (Fig. 3) exhibits a Curie–Weiss behaviour over practically the whole temperature range of the measurements, with deviations only beginning to appear at the lowest temperatures. A least-squares analysis of the $(\chi_M^{corr})^{-1}$ vs T function with use of the Curie–Weiss law yields Curie–Weiss constant values for three temperature ranges (Table 4). In the region of 25–295 K, completely beyond the area of deviations, the C value is practically unchanged, but the θ value is somewhat higher.

The variation of the magnetic moment with temperature (Fig. 3) is characteristic of an intramolecular ferromagnet. With decreasing temperature the magnetic moment increases from 1.81 B.M. at room temperature to the maximum value of 2.10 B.M. at 5 K. Below this temperature, the decrease of μ_{eff} (2.03 B.M. at 4.2 K) was observed, probably due to the intermolecular antiferromagnetic interaction between the molecular units.

For the dimer (Fig. 1A) the magnetic susceptibility data were least-squares fitted to the Bleaney–Bowers equation[16] to give a J of $+3.23$ cm^{-1}.

For the polymeric system (Fig. 1B) the fitting was accomplished by the use of three different models for exchange coupling: the Heisenberg model for ferromagnetically coupled $S = \frac{1}{2}$ centres,[17] the Ising

Table 4. Parameters from the Curie–Weiss law

Temperature range (K)	C (cm^3 K mol^{-1})	θ (K)
4.2–295	0.413	1.89
6–295	0.413	1.97
25–295	0.412	2.26

Table 5. Estimated exchange parameters

Model	J (cm^{-1})	ERR $\times 10^4$
Binuclear Bleaney–Bowers	+3.23	0.817
Heisenberg model for ferromagnetically coupled $S = \frac{1}{2}$ ions	+0.93	1.53
Ising model for isolated regular chain	+0.80	1.83
One-dimensional zero-field Heisenberg model ($N+1$ spins)	+0.80	1.82

model for an isolated regular chain,[18] and the one-dimensional zero-field Heisenberg model ($N+1$ spins).[19] The exchange parameter values determined on the basis of these models (Table 5) are around +0.9 cm^{-1} and are much lower than those calculated from the binuclear model.

A comparison of the magnetic data fits for the two possible structures of the complex indicates that the binuclear model describes the susceptibility data more accurately than the linear chain models do, but this difference is not definitive.

The exchange coupling is realized most likely by a σ-orbital mechanism[20] using the orbitals of the bridging cyanate nitrogens for electron transfer and intraatomic direct exchange.

Conclusions

The compound $Cu(NCO)_2(dmpz)_2$, forming with $Cu(dmpz \cdot NCO)_2$ previously studied[2] a coligand isomer pair, shows in the family of $Cu(NCO)_2L_2$ complexes[9] a unique structure, as well as spectroscopic and magnetic properties. Its five-coordinate dimeric or polymeric chain structure with half of the NCO groups N-bridging the Cu(II) atoms has consequences in ferromagnetic exchange coupling and zero-field splitting in the triplet ground state. These interesting features are surely caused by the dmpz ligand and its structural properties, which also demonstrate the relatively difficult formation of the complex.

REFERENCES

1. J. Kohout, M. Hvastijová and L. Omelka, *Transition Met. Chem.* 1985, **10**, 155.
2. F. Valach, J. Kohout, M. Dunaj-Jurčo, M. Hvastijová and J. Gažo, *J. Chem. Soc., Dalton Trans.* 1979, 1867.
3. M. Hvastijová, J. Kohout and J. Gažo, *J. Coord. Chem.* 1982, **12**, 27.
4. B. N. Figgis and R. S. Nyholm, *J. Chem. Soc.* 1958, 4190.
5. J. Kohout, M. Hvastijová, A. Mašlejová, J. Gažo and L. Omelka, *Z. Anorg. Allg. Chem.* 1977, **434**, 29.
6. J. Kohout, M. Hvastijová and J. Mroziński, *J. Mol. Struct.* 1984, **116**, 211.
7. M. Hvastijová, J. Kohout, H. Wusterhausen and H. Köhler, *Z. Anorg. Allg. Chem.* 1984, **510**, 37.
8. A. Zecchina, L. Cerutti, S. Coluccia and E. Borello, *J. Chem. Soc. B* 1967, 1363.
9. J. Kohout, M. Hvastijová and J. Gažo, *Coord. Chem. Rev.* 1978, **27**, 141.
10. J. Kohout, M. Liška and M. Hvastijová, *Inorg. Chim. Acta* 1977, **25**, L71.
11. B. J. Hathaway, *J. Chem. Soc., Dalton Trans.* 1972, 1196.
12. J. Reedijk, J. C. A. Windhorst, N. H. M. van Ham and W. L. Groeneveld, *Recl Trav. Chim.* 1971, **111**, 234.
13. D. M. Adams and W. R. Trumble, *J. Chem. Soc., Dalton Trans.* 1975, 30.
14. E. Wassermann, L. C. Snyder and W. A. Yager, *J. Chem. Phys.* 1964, **41**, 1763; T. R. Felthouse and D. N. Hendrickson, *Inorg. Chem.* 1978, **17**, 444.
15. M. S. de Groot and J. H. van der Waals, *Mol. Phys.* 1963, **6**, 545; J. F. Villa and W. E. Hatfield, *J. Chem. Phys.* 1971, **55**, 4758.
16. B. Bleaney and K. D. Bowers, *Proc. R. Soc. London A* 1952, **214**, 451.
17. G. A. Baker, Jr, G. S. Rushbrooke and H. E. Gilbert, *Phys. Rev. A* 1964, **135**, 1372.
18. J. W. Stout and R. C. Chisholm, *J. Chem. Phys.* 1962, **36**, 979; B. C. Gerstein, F. D. Gehring and R. D. Willett, *J. Appl. Phys.* 1972, **43**, 1932.
19. T. Smith and S. A. Friedberg, *Phys. Rev.* 1968, **176**, 660.
20. W. E. Hatfield, J. A. Barnes, D. Y. Jeter, R. Whyman and E. R. Jones, Jr, *J. Am. Chem. Soc.* 1970, **92**, 4982.

Polyhedron Vol. 4, No. 11, pp. 1981–1984, 1985
Printed in Great Britain

0277–5387/85 $3.00 + .00
© 1985 Pergamon Press Ltd

THE CHEMISTRY OF ISOMERS OF ICOSABORANE(26): CRYSTAL AND MOLECULAR STRUCTURE OF 1,2′-BI(*NIDO*-DECABORANYL)

SIMON A. BARRETT, NORMAN N. GREENWOOD,* JOHN D. KENNEDY and MARK THORNTON-PETT

Department of Inorganic and Structural Chemistry, University of Leeds, Leeds LS2 9JT, U.K.

(*Received* 8 *May* 1985; *accepted* 7 *June* 1985)

Abstract—The crystal and molecular structure of 1,2′-(*nido*-$B_{10}H_{13}$)$_2$ has been determined by single-crystal X-ray diffraction analysis, thus confirming the results of an earlier characterisation of this species by multi-element multiple-resonance NMR spectroscopy. Crystals were monoclinic, space group $P2_1/n$ with $a = 1099.7(2)$, $b = 1144.6(3)$, $c = 1409.4(3)$ pm, $\beta = 111.80(1)°$; final R factors were $R = 0.0467$ and $R_\omega = 0.0557$ for 3491 observed reflections. The intercluster boron–boron *conjuncto* linkage is 169.6(4) pm, and there appears to be a slight lengthening of intracluster boron–boron distances associated with the two atoms in the *conjuncto* linkage.

Since its initial characterization as an impurity in technical-grade *nido*-decaborane,[1] a number of routes have been used for the synthesis of icosaborane(26),[2–4] so that it is now the largest neutral binary borane that can be reliably synthesized (though in small yield).[5] Its constitution is that of bi(*nido*-decaboranyl), $[B_{10}H_{13}]_2$, and 11 distinct geometrical isomers are possible.[4] Of these the (1,2′), (1,5′), (2,2′), (2,5′), (2,6′), (5,5′) and (6,6′) isomers have been separated and structurally identified by NMR spectroscopy,[4,6] and the (1,5′), (2,2′) and (2,6′) isomers characterized by single-crystal X-ray diffraction analysis.[3,7,8] We now report the results of single-crystal X-ray diffraction analysis of 1,2′-bi(*nido*-decaboranyl), which has previously been characterized only by NMR spectroscopy. It was prepared by the photolysis of *nido*-decaborane in cyclohexane solution.

EXPERIMENTAL

$B_{10}H_{14}$ was photolysed in cyclohexane solution under N_2 as described previously.[2,4,8] After removal of the solvent (rotary evaporator, $T \leqslant ca$ 70°C), the unreacted decaborane was sublimed off under reduced pressure (*ca* 70°C/<1 mmHg, *ca* 95% recovery). The residue was taken up in CH_2Cl_2, filtered through silica, evaporated to dryness under reduced pressure, dissolved in CH_2Cl_2–hexane (1:10), and subjected to chromatographic separation using a Perkin–Elmer Series 2 HPLC chromatograph with a 16 × 250 mm Knauer preparative column packed with Si60 7 μm silica and 10% CH_2Cl_2 in AnalaR light petroleum (40–60°C) as eluting medium, flow-rate 20 cm^3 min^{-1}. Eluted components were detected by changes in the UV absorption of the eluted fluid at 315 nm. Best separations were obtained using aliquots of *ca* 25 mg reaction product in *ca* 1 cm^3 of solvent, and repeated injections were required to gather sufficient pure product for further work. Under these conditions traces of residual decaborane had a retention time of *ca* 4 min, and 2,2′-($B_{10}H_{13}$)$_2$ and 1,2′-($B_{10}H_{13}$)$_2$ were readily separable as pure products with retention times of *ca* 6.7 and 7.4 min respectively; the other $B_{20}H_{26}$ isomers present did not mutually separate. Removal of the solvent from the 1,2′-($B_{10}H_{13}$)$_2$ fraction, followed by recrystallization from CH_2Cl_2–hexane (50:50) at 4°C gave crystals suitable for single-crystal X-ray diffraction analysis.

CRYSTALLOGRAPHIC STUDIES

Unit cell and intensity data were obtained using a Syntex $P2_1$ diffractometer operating in the ω–2θ scan mode and using graphite monochromatized Mo-K_α radiation ($\lambda = 71.069$ pm) following a procedure described elsewhere in detail.[9]

* Author to whom correspondence should be addressed.

Crystal data

$B_{20}H_{26}$, $M = 242.41$, monoclinic, $a = 1099.7(2)$, $b = 1144.6(3)$, $c = 1409.4(3)$ pm, $\beta = 110.80(1)°$, $U = 1.659$ nm^3, space group $P2_1/n$ (= $P2_1/c$, No. 14), $Z = 4$, $D_c = 0.97$ g cm^{-3}, μ(Mo-K_α) = 0.18 cm^{-1}, $F(000) = 504$, $T = 290$ K. Scan speeds 2.0–29.3° min^{-1}, $4.0 < 2\theta < 45.0°$, scans running from 1° below $K_{\alpha 1}$ to 1° above $K_{\alpha 2}$. 4372 data were collected, and 3491 were considered observed [$I > 2\sigma(I)$].

Structure solution and refinement

The structure was solved by direct methods using the SHELXS program system[10] and refined by full-matrix least-squares using the SHELX76 program system.[11] All boron atoms were assigned anisotropic thermal parameters. All hydrogen atoms were located experimentally and were freely refined with individual isotropic thermal parameters. The weighting scheme $\omega = 1/[\sigma^2(F_o) + 0.00045(F_o)^2]$ was used at the end of refinement to give acceptable agreement analyses. Final R values were $R = 0.0467$ and $R_\omega = 0.0557$ (285 parameters).

RESULTS AND DISCUSSION

The molecular structure of the compound is shown in Fig. 1. Interatomic distances are given in Table 1 and selected angles about atoms B(1) and B(2′) are in Table 2. (Tables of atomic coordinates and other crystallographic data have been deposited with the Editor.*) The structure is clearly 1,2′-$(B_{10}H_{13})_2$, consistent with earlier conclusions based upon multi-element multiple-resonance NMR spectroscopy.[4] The molecule conforms approximately to an idealized mirror-plane symmetry; the twist-angle about the intercluster B(1)—B(2′) bond [as defined by planes passing through: (a) B(2′)B(4′)B(9′)B(6′), and (b) B(1)B(3) and the mid-points of B(5)B(10) and B(7)B(8)] being *ca* 5.4°. It should be noted that in solution there is free rotation about this bond, giving time-averaged mirror-plane symmetry in terms of interpretation of NMR properties.[4]

The intercluster B(1)—B(2′) bond distance of 169.6(4) pm is very close to those determined for the (1,5′), (2,2′) and (2,6′) isomers, which have values of 169.8(2),[3] 169.2(3)[7,8] and 167.9(3)[8] pm respectively. These values are similar to other interboron two-electron two-centre σ-bonds, e.g. 169.3(9) pm in $(\overline{NMeCH_2CH_2NMeB}\text{-})_2$[12] and 171.1(6) pm in $(\overline{OCMe_2CMe_2OB}\text{-})_2$.[13] The values within the $(B_{10}H_{13})_2$ isomers themselves show a small but probably significant variation, which may well reflect differences in boron electron character available for *exo*-polyhedral bonding at the various *nido*-decaboranyl cluster sites. This should also be manifested in the intercluster boron–boron ^{11}B NMR spin–spin coupling constant $^1J(^{11}B\text{–}^{11}B)$, which will be strongly dependent, *inter alia*, on the boron electron *s*-character available for bonding.[14] For 1,2′-$(B_{10}H_{13})_2$ this coupling constant takes a value of *ca* 105 Hz,[4] but comparative data are not available for the other isomers. In the related series of *conjuncto*-bi(*nido*-pentaboranyl) compounds, $(B_5H_8)_2$, however, the corresponding values of $^1J(^{11}B\text{–}^{11}B)$ vary by the large factor of almost 2 among the (1,1′), (1,2′) and (2,2′) isomers, indicating a considerable variation in *exo*-polyhedral bond character among these three intercluster linkages.[15] In these $(B_5H_8)_2$ compounds, however, only one intercluster boron–boron distance is available, that for the (1,1′) isomer at 174(6) pm,[16] but the estimated standard deviation on this is too large for meaningful comparison with the $(B_{10}H_{13})_2$ species.

* They have also been deposited with the Cambridge Crystallographic Data Centre.

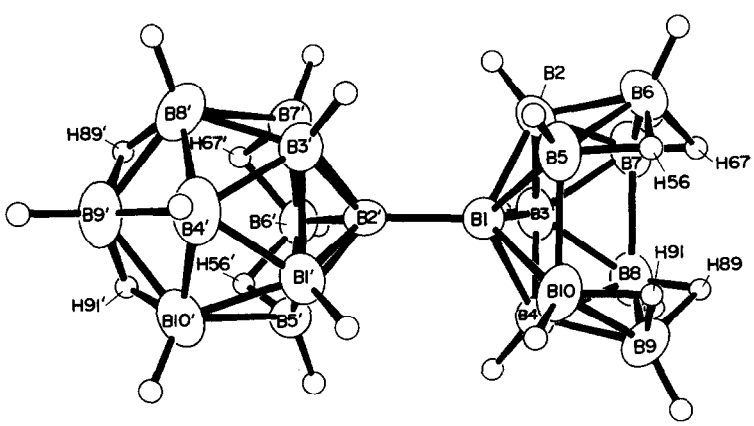


Fig. 1. Molecular structure diagram and numbering system for 1,2′-bi(*nido*-decaboranyl), $B_{20}H_{26}$.

Table 1. Interatomic distances (pm) for 1,2′-(*nido*-$B_{10}H_{13}$)$_2$ with estimated standard deviations in parentheses

				Boron–boron			
B(1)—B(2′)	169.6(4)						
B(1)—B(2)	177.8(4)	B(2)—B(3)	175.8(4)	B(1′)—B(2′)	178.2(4)	B(2′)—B(3′)	179.6(4)
B(1)—B(3)	178.9(4)			B(1′)—B(3′)	176.5(4)		
B(1)—B(4)	178.9(4)	B(3)—B(4)	176.3(4)	B(1′)—B(4′)	177.1(4)	B(3′)—B(4′)	177.4(4)
B(1)—B(5)	175.2(4)	B(3)—B(7)	174.0(4)	B(1′)—B(5′)	173.8(4)	B(3′)—B(7′)	173.8(4)
B(1)—B(10)	175.1(4)	B(3)—B(8)	173.9(4)	B(1′)—B(10′)	174.4(4)	B(3′)—B(8′)	173.7(4)
B(2)—B(5)	176.3(4)	B(2)—B(7)	178.3(4)	B(2′)—B(5′)	179.3(4)	B(2′)—B(7′)	180.2(4)
B(2)—B(6)	170.7(4)	B(4)—B(9)	171.7(4)	B(2′)—B(6′)	172.7(4)	B(4′)—B(9′)	171.5(4)
B(4)—B(8)	178.2(4)	B(4)—B(10)	177.1(4)	B(4′)—B(8′)	176.9(4)	B(4′)—B(10′)	177.6(4)
B(5)—B(6)	177.8(4)	B(6)—B(7)	176.7(4)	B(5′)—B(6′)	177.3(4)	B(6′)—B(7′)	177.7(4)
B(5)—B(10)	195.3(4)	B(7)—B(8)	196.5(4)	B(5′)—B(10′)	197.6(4)	B(7′)—B(8′)	196.8(4)
B(8)—B(9)	177.9(4)	B(9)—B(10)	178.0(4)	B(8′)—B(9′)	177.1(4)	B(9′)—B(10′)	177.7(4)
				Boron–hydrogen			
		B(3)—H(3)	108(1)	B(1′)—H(1′)	108(1)	B(3′)—H(3′)	109(1)
B(2)—H(2)	108(2)	B(4)—H(4)	107(1)			B(4′)—H(4′)	108(2)
B(5)—H(5)	109(2)	B(7)—H(7)	110(2)	B(5′)—H(5′)	109(1)	B(7′)—H(7′)	112(1)
B(6)—H(6)	106(2)	B(9)—H(9)	108(1)	B(6′)—H(6′)	110(1)	B(9′)—H(9′)	108(2)
B(8)—H(8)	109(2)	B(10)—H(10)	110(1)	B(8′)—H(8′)	109(2)	B(10′)—H(10′)	110(2)
B(5)—H(56)	125(2)	B(7)—H(67)	125(1)	B(5′)—H(5′6′)	119(1)	B(7′)—H(6′7′)	125(1)
B(6)—H(56)	125(2)	B(6)—H(67)	130(2)	B(6′)—H(5′6′)	124(1)	B(6′)—H(6′7′)	129(1)
B(8)—H(89)	132(2)	B(10)—H(910)	126(1)	B(8′)—H(8′9′)	131(1)	B(10′)—H(9′10′)	124(1)
B(9)—H(89)	129(2)	B(9)—H(910)	132(1)	B(9′)—H(8′9′)	129(1)	B(9′)—H(9′10′)	130(1)

Table 2. Selected angles (°) about atoms B(1) and B(2'), with estimated standard deviations in parentheses

B(2')—B(1)—B(2)	118.6(2)	B(1)—B(2')—B(1')	124.1(2)
B(2')—B(1)—B(3)	127.1(2)	B(1)—B(2')—B(3')	123.9(2)
B(2')—B(1)—B(4)	119.6(2)	B(1)—B(2')—B(5')	124.3(2)
B(2')—B(1)—B(5)	117.7(2)	B(1)—B(2')—B(6')	118.1(2)
B(2')—B(1)—B(10)	118.2(2)	B(1)—B(2')—B(7')	124.4(2)

The individual clusters themselves have very similar geometries to the individual *nido*-decaboranyl clusters of the other isomers examined by X-ray diffraction analysis,[3,7,8] and also to the cluster geometry of *nido*-decaborane itself.[17] In particular the characteristically long open-face distances B(5)B(10), B(7)B(8), B(5')B(10') and B(7')B(8') of 195.3(4)–197.6(4) pm are readily apparent. Compared to otherwise equivalent distances in the molecule, there appears to be a lengthening of about 1–3 pm in the intracluster B—B distances associated with the B(1) and B(2') atoms in the intercluster linkage. This again is also characteristic of the other isomers examined, and may be indicative of an increased electron demand for the intercluster B—B bond formation vs bond formation of an *exo*-terminal B—H bond.

Acknowledgements—We thank the SERC for support, and Yvonne Cheek for some assistance in the initial stages of this project.

REFERENCES

1. N. N. Greenwood, J. D. Kennedy and D. Taylorson, *J. Phys. Chem.* 1978, **82**, 623.
2. N. N. Greenwood, J. D. Kennedy, T. R. Spalding and D. Taylorson, *J. Chem. Soc., Dalton Trans.* 1979, 840.
3. J. W. Pinson, G. M. Brown and L. L. Ingram, *Inorg. Chem.* 1979, **18**, 1951.
4. S. K. Boocock, Y. M. Cheek, N. N. Greenwood and J. D. Kennedy, *J. Chem. Soc., Dalton Trans.* 1981, 1430.
5. S. K. Boocock, N. N. Greenwood, J. D. Kennedy, W. S. McDonald and J. Staves, *J. Chem. Soc., Dalton Trans.* 1981, 2573.
6. S. K. Boocock, N. N. Greenwood, J. D. Kennedy and D. Taylorson, *J. Chem. Soc., Chem. Commun.* 1979, 16.
7. N. N. Greenwood, J. D. Kennedy, W. S. McDonald, D. Taylorson and J. Staves, *J. Chem. Soc., Chem. Commun.* 1979, 17.
8. S. K. Boocock, N. N. Greenwood, J. D. Kennedy, W. S. McDonald and J. Staves, *J. Chem. Soc., Dalton Trans.* 1980, 790.
9. A. Modinos and P. Woodward, *J. Chem. Soc., Dalton Trans.* 1974, 2065.
10. G. M. Sheldrick, *SHELXS, Program System for X-ray Structure Solution.* Universität Göttingen (1984).
11. G. M. Sheldrick, *SHELX76, Program System for X-ray Structure Determination.* University of Cambridge (1976).
12. H. Fusstetter, J. C. Huffman, H. Nöth and R. Schaeffer, *Z. Naturforsch.* 1976, **31B**, 1441.
13. H. Nöth, *Z. Naturforsch.* 1984, **39B**, 1463.
14. J. D. Kennedy, In *Multinuclear NMR* (Edited by J. Mason), Chap. 8. Plenum, New York (in press).
15. J. A. Anderson, R. J. Astheimer, J. D. Odom and L. G. Sneddon, *J. Am. Chem. Soc.* 1984, **106**, 2275.
16. R. N. Grimes, F. E. Wang, R. Lewin and W. N. Lipscomb, *Proc. Nat. Acad. Sci. U.S.A.* 1961, **47**, 996.
17. A. Tippe and W. C. Hamilton, *Inorg. Chem.* 1969, **8**, 464.

Polyhedron Vol. 4, No. 11, pp. 1985–1988, 1985
Printed in Great Britain

0277–5387/85 $3.00 + .00
© 1985 Pergamon Press Ltd

NEW NICKEL(II) CHLORIDE–MORPHOLINE COMPLEXES

JOSÉ PALAZÓN, JOSÉ GÁLVEZ, GABRIEL GARCÍA and GREGORIO LÓPEZ*

Department of Inorganic Chemistry, University of Murcia, Murcia, Spain

(*Received* 15 *January* 1985; *accepted after revision* 10 *June* 1985)

Abstract—The compounds $[NiCl_2(Morph)_3(H_2O)_2]$ and $[NiCl_2(Morph)_3]$ have been prepared by treating $NiCl_2 \cdot 6H_2O$ with morpholine (Morph) in the presence of 2,2-dimethoxypropane or 2,2-dimethoxypropane–ethanol, respectively. The thermal treatment of both compounds leads to the formation of $[NiCl_2(Morph)_2]$ and $[NiCl_2(Morph)]$. The thermal study also includes the determination of reaction enthalpies and kinetic parameters such as activation energies and reaction orders. Magnetic and spectral data can be interpreted assuming a pseudo-octahedral environment around the nickel atom.

Two recent articles have been published on the preparation[1] and thermal behaviour[2] of some adducts of morpholine (Morph) with nickel salts. The thermal treatment of some of these complexes has been shown to be a useful method for the preparation of intermediates which cannot be isolated directly by reaction of the nickel salts with Morph.[2]

As a continuation of our study on nickel(II)–Morph complexes, we have investigated the $NiCl_2$–Morph system. The compounds $[NiCl_2(Morph)_3]$ and $[NiCl_2(Morph)_3(H_2O)_2]$ have been prepared and the thermal treatment of both compounds has led to the isolation of the new adducts $[NiCl_2(Morph)_2]$ and $[NiCl_2(Morph)]$.

EXPERIMENTAL

Materials and methods

Morph, 2,2-dimethoxypropane and nickel(II) chloride were commercial products and used as such. Diethyl ether was distilled over sodium in the presence of benzophenone and ethyl alcohol was dried with calcium oxide and distilled over magnesium.

The C, H and N analyses were performed with a Perkin–Elmer 240 C microanalyzer. Nickel was determined by titration with EDTA.[3]

IR spectra were recorded in the 4000–250 cm^{-1} range on a Perkin–Elmer 457 spectrophotometer as Nujol mulls. The diffuse reflectance spectra were recorded in Nujol mulls on a Beckman DK-2A spectrophotometer; the mulls were smeared between two glass plates on filter paper and run against a reference consisting of similar plates containing Nujol only. Thermal decomposition studies were carried out on a Netzsch STA-429 thermobalance. The thermograms were recorded with a heating rate of 5°C min^{-1}, but those used for the determination of reaction orders and activation energies were recorded with a heating rate of 2°C min^{-1} in order to achieve greater accuracy. Magnetic susceptibilities were measured at 20°C by the Faraday method using a Cahn RG 2102 electrobalance and a Systron Conner 6001 electromagnet calibrated with $Co[Hg(SCN)_4]$.[4]

Preparation of the complexes

$[NiCl_2(Morph)_3]$. A solution of $NiCl_2 \cdot 6H_2O$ (0.9 g, 3.8 mmol) in ethanol–2,2-dimethoxypropane (15 and 5 cm^3, respectively) was refluxed for 45 min. After cooling, Morph (8 cm^3) was added and the colour of the solution changed from yellow to green. On stirring, a yellow solid precipitated from the solution which was filtered off under nitrogen, washed with diethyl ether and dried *in vacuo*. Yield = 84%. The compound is hygroscopic and was kept in a P_4O_{10} desiccator.

IR (cm^{-1}): 3240m, 3200s, 1325m, 1310s, 1295m, 1265s, 1245s, 1200m, 1185s, 1165m, 1110vs, 1095vs, 1050s, 1035vs, 1025vs, 890vs, 870vs, 835m, 820m, 645m, 635m, 435w and 415w.

$[NiCl_2(Morph)_3(H_2O)_2]$. A suspension of $NiCl_2 \cdot 6H_2O$ (0.82 g, 3.4 mmol) in 2,2-dimethoxypropane (10 cm^3) was refluxed for 45 min. After

* Author to whom correspondence should be addressed.

Table 1. Colours and analytical data of nickel compounds

Compound	Colour	Analyses (%) [found (calc.)]			
		Ni	C	H	N
$[NiCl_2(Morph)_3(H_2O)_2]$	Pale green	13.9 (13.8)	33.2 (33.7)	6.9 (7.3)	9.9 (9.8)
$[NiCl_2(Morph)_3]$	Yellow	15.3 (15.0)	36.9 (36.9)	7.0 (6.9)	11.2 (10.7)
$[NiCl_2(Morph)_2]$	Pale yellow		31.7 (31.6)	6.1 (5.9)	9.0 (9.2)
$[NiCl_2(Morph)]$	Brown		22.1 (22.1)	4.2 (4.1)	7.0 (6.5)

cooling, Morph was added (8 cm^3) and the yellow solid turned green. The solid was filtered off under nitrogen, washed with diethyl ether and dried *in vacuo*. Yield = 94%. The compound was kept in a P_4O_{10} desiccator.

IR (cm^{-1}): 3300s(br), 3200s, 1325m, 1315m, 1310m, 1260s, 1250s, 1200sh, 1190m, 1180m, 1120sh, 1115s, 1100vs, 1055s, 1040s, 1030vs, 895s, 880vs, 850m, 640m, 610w, 445w, 415w and 280w.

$[NiCl_2(Morph)_2]$ *and* $[NiCl_2(Morph)]$. Both compounds were obtained by heating either $[NiCl_2(Morph)_3]$ or $[NiCl_2(Morph)_3(H_2O)_2]$ as described below.

IR $[NiCl_2(Morph)_2]$ (cm^{-1}): 3200s, 1310s, 1305s, 1250s, 1205s, 1190s, 1110s, 1095s, 1060s, 1030s, 895s, 880vs, 835w, 825w, 640m and 445w.

IR $[NiCl_2(Morph)]$ (cm^{-1}): 3200s, 1315m, 1305m, 1255sh, 1250s, 1200s, 1115vs, 1085s, 1065s, 1030s, 1015m, 895s, 885vs, 830w, 645m, 445w.

RESULTS AND DISCUSSION

Partial or complete elimination of the H_2O molecules from $NiCl_2 \cdot 6H_2O$ is accomplished by the use of the dehydrating agent 2,2-dimethoxypropane,[5] which is hydrolyzed according to eqn (1):

$$CH_3C(OCH_3)_2CH_3 + H_2O \rightarrow CH_3COCH_3 + 2CH_3OH. \quad (1)$$

The presence of Morph in the reaction medium determines the formation of either

$$[NiCl_2(Morph)_3(H_2O)_2]$$

or

$$[NiCl_2(Morph)_3],$$

depending on whether 2,2-dimethoxypropane is used alone or together with ethanol, respectively. The analytical data of both compounds (Table 1) fit quite well the respective stoichiometries.

Figures 1 and 2 illustrate simultaneous TG and DTA curves for $[NiCl_2(Morph)_3]$ and $[NiCl_2(Morph)_3(H_2O)_2]$. The results of TG and DTA are summarized in Table 2.

Under an N_2 atmosphere $[NiCl_2(Morph)_3]$ is stable up to 140°C and then decomposes through three stages discernible in the TG curve within the

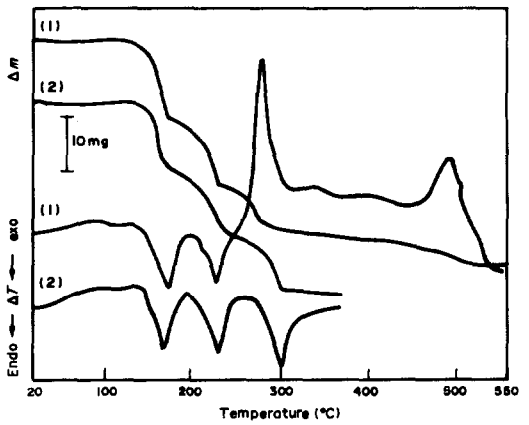


Fig. 1. Simultaneous TG and DTA curves for thermal decomposition of $[NiCl_2(Morph)_3]$ in: (1) air, 60.0 mg; and (2) N_2, 55.6 mg.

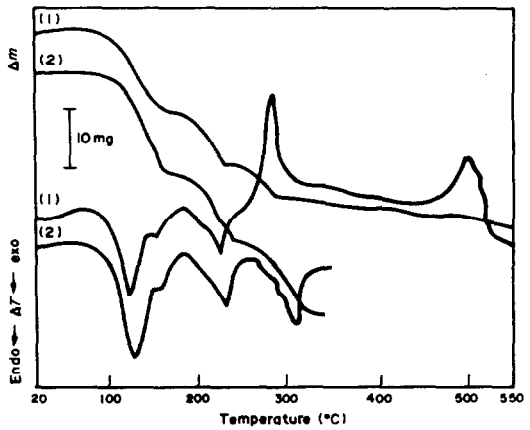


Fig. 2. Simultaneous TG and DTA curves for thermal decomposition of $[NiCl_2(Morph)_3(H_2O)_2]$ in: (1) air, 49.4 mg; and (2) N_2, 62.8 mg.

Table 2. Data on thermal decomposition of nickel complexes in N_2

Decomposition reaction	Weight loss[a] (%)	Temperature range [°C (TG)]	DTA peaks	ΔH (kJ mol^{-1})	Activation energy (kJ mol^{-1})	Reaction order	Mechanism suggested[b]
(1) $[NiCl_2(Morph)_3](s) \rightarrow [NiCl_2(Morph)_2](s) + Morph(g)$	23.8 (22.3)	140–175	170	53.32	214.6[c] 225.7[d]	1	F_1
(2) $[NiCl_2(Morph)_2](s) \rightarrow [NiCl_2(Morph)](s) + Morph(g)$	21.5 (22.3)	175–233	230	56.43	134.6[c] 137.9[d]	0.5	R_2
(3) $[NiCl_2(Morph)](s) \rightarrow NiCl_2(s) + Morph(g)$	21.0 (22.3)	233–305	300	66.68	163.1[c] 167.2[d]	0.5	R_2
(4) $[NiCl_2(Morph)_3(H_2O)_2](s) \rightarrow [NiCl_2(Morph)_2](s) + Morph\ (g) + 2H_2O(g)$	29.5 (28.8)	90–162	130	165.67	—	—	—

[a] Calculated values are given in parentheses.
[b] See Ref. 9.
[c] Coats–Redfern method.
[d] Satava method.

temperature ranges 140–175, 175–233 and 233–305°C. The stages lead to the formation of $[NiCl_2(Morph)_2]$, $[NiCl_2(Morph)]$ and $NiCl_2$, respectively. The transformations are endothermic with DTA peaks at 170, 230 and 300°C. The behaviour under an air atmosphere is the same as in N_2 up to 233°C but above this temperature $[NiCl_2(Morph)]$ decomposes through two exothermic stages (in the 233–280 and 280–540°C ranges; DTA peaks at 278 and 540°C). The difference between experimental (24.32%) and theoretical (22.3%) weight losses may be attributed to partial transformation of $NiCl_2$ into NiO.[6]

$[NiCl_2(Morph)_3(H_2O)_2]$ gives $[NiCl_2(Morph)_2]$ in two overlapped stages, between 90 and 162°C (in nitrogen), or 90 and 155°C (in air). Once $[NiCl_2(Morph)_2]$ is formed, the thermal behaviour is identical with that observed for the same intermediate from $[NiCl_2(Morph)_3]$.

Reaction enthalpies are collected in Table 2. They have been derived from the DTA curves as described in Ref. 2. As expected, enthalpy values increase as the Morph content decreases across the series

$$[NiCl_2(Morph)_3] \rightarrow [NiCl_2(Morph)_2] \rightarrow [NiCl_2(Morph)] \rightarrow NiCl_2.$$

This result is in agreement with our previous observations[2] and the study of Van Dam *et al.*[7] on complexes of nickel halides with imidazole. The rather high value of ΔH for the reaction

$$[NiCl_2(Morph)_3(H_2O)_2](s) \rightarrow [NiCl_2(Morph)_2](s) + (Morph)(g) + 2H_2O(g)$$

is roughly the sum of the ΔHs for the liberation of one Morph molecule and two water molecules (according to Ref. 7 a value of 60 kJ mol^{-1} H_2O may be assumed).

Activation energies and reaction orders for the processes (1)–(3) have been evaluated by the Coats–Redfern method,[8] and, furthermore, activation energies and reaction mechanisms have been determined by the Satava[9] method (Table 2). According to Ref. 9, process (1) should be controlled by a random nucleation mechanism and processes (2) and (3) by a phase boundary reaction with cylindrical symmetry.

The room-temperature magnetic moments (Table 3) are typical for the paramagnetic d^8-species. Electronic spectra (Table 3) are all compatible with a pseudo-octahedral geometry for the nickel compounds.[10] Two or three bands are observed, which can be assigned to the transitions from the ground state $^3A_{2g}(F)$ to the excited states $^3T_{2g}(F)$, $^3T_{1g}(F)$ and $^3T_{1g}(P)$; moreover, the frequencies of maxima are quite similar to those observed for related nickel

Table 3. Magnetic moments and electronic spectra of nickel compounds

Compound	μ_{eff} (BM)	Electronic bands (cm^{-1})
$[NiCl_2(Morph)_3(H_2O)_2]$	3.48	8695, 14,925
$[NiCl_2(Morph)_3]$	3.46	14,085, 22,470
$[NiCl_2(Morph)_2]$	3.57	8200, 13,425, 22,370
$[NiCl_2(Morph)]$	3.05	7550, 13,245, 21,280

amine halocomplexes in which a distorted octahedral configuration has been proposed.[10]

The IR spectra of the nickel compounds show that coordination of Morph to nickel is through the nitrogen atom, since in all cases a drop of $\sim 100\,cm^{-1}$ is observed for the N—H stretching frequency (Table 4). The fundamentals ν_{13} and ν_{14}, which in free Morph have the largest contributions from the C—N and C—O stretches,[11] appear in the spectra of $[NiCl_2(Morph)_3(H_2O)_2]$, $[NiCl_2(Morph)_3]$ and $[NiCl_2(Morph)_2]$ as single bands. However, the presence of two bands at 1030 and 1015 cm^{-1} (see Table 4) in the spectrum of $[NiCl_2(Morph)]$ could be indicative of a nickel–oxygen interaction, i.e. of bidentate Morph. On this basis, and assuming an octahedral environment about the nickel atom, the polymeric structures

$$[NiCl_{4/2}(Morph)_2]$$

and

$$[NiCl_{4/2}(Morph)_{2/2}]$$

may be proposed for

$$[NiCl_2(Morph)_2]$$

and

$$[NiCl_2(Morph)],$$

respectively.

From previous results and those reported herein, it is now possible to compare $[NiCl_2(Morph)_3]$ with $[NiBr_2(Morph)_3]$. Whereas the enthalpy change in the process

$$[NiX_2(Morph)_3](s) \xrightarrow{\Delta} [NiX_2(Morph)_2](s) + (Morph)(g)$$

is nearly the same for both compounds,[2] the structures of the resulting halocomplexes are different. In $[NiCl_2(Morph)_2]$ the nickel atom is in an octahedral environment, but in the deep blue $[NiBr_2(Morph)_2]$ the stereochemistry around the metal atom was shown to be tetrahedral.[1] This difference is attributed to the different size of the halogen. A similar reason may be adduced for the fact that nickel iodide forms the adduct $[NiI_2(Morph)_4]$,[1] in contrast to the above-mentioned halides where the highest adduct is $[NiX_2(Morph)_3]$.

REFERENCES

1. J. Palazón, J. Gálvez, G. García and G. López, *Polyhedron* 1983, **2**, 1353.
2. J. Gálvez, J. Palazón, G. López and G. García, *J. Therm. Anal.* 1984, **29**, 465.
3. G. Schwarzenbach and H. Flashka, *Complexometric Titrations*, p. 248. Methuen, London (1969).
4. B. N. Figgis and J. Lewis, In *Modern Coordination Chemistry* (Edited by J. Lewis and R. G. Wilkins), p. 415. Interscience, New York (1960).
5. F. A. Cotton and G. Wilkinson, *Advanced Inorganic Chemistry*, p. 550. Wiley, New York (1980).
6. P. Lumme and O. Vuokila, *Suom. Kemistil.* 1969, **B42**, 306.
7. J. C. Van Dam, G. Hakvoort, J. C. Jansen and J. Reedijk, *J. Inorg. Nucl. Chem.* 1975, **37**, 713.
8. A. W. Coats and J. P. Redfern, *Nature* 1964, **201**, 68.
9. V. Satava, *Thermochim. Acta* 1971, **2**, 423.
10. L. Sacconi, In *Transition Metal Chemistry* (Edited by R. L. Carlin), Vol. 4, p. 210. Marcel Dekker, New York (1968).
11. D. Vedal, O. H. Ellestad and P. Klaboe, *Spectrochim. Acta* 1976, **32A**, 877.

Table 4. Relevant IR data of the nickel complexes

Free Morph[11]	$[NiCl_2(Morph)_3(H_2O)_2]$	$[NiCl_2(Morph)_3]$	$[NiCl_2(Morph)_2]$	$[NiCl_2(Morph)]$
ν_1[a] 3298s (N—H stretch)	3200s	3240m 3200s	3200s	3200vs
ν_{13} 1097vs (C—N stretch)	1100vs	1095vs	1095vs	1085s
ν_{14} 1031s (C—O stretch)	1030vs	1025vs	1030s	1030s 1015m

[a] This value is for the axial conformer; in the equatorial one it appears at 3336 cm^{-1}.[11]

Polyhedron Vol. 4, No. 11, pp. 1989–1992, 1985
Printed in Great Britain

0277–5387/85 $3.00 + .00
© 1985 Pergamon Press Ltd

PALLADIUM(II) MALONATO COMPLEXES WITH SOME HETEROCYCLIC LIGANDS

M. MASSACESI, R. PINNA and G. PONTICELLI*

Istituto di Chimica Generale, Inorganica ed Analitica, Università di Cagliari, Via Ospedale 72, 09100 Cagliari, Italy

G. DEVOTO

Cattedra di Chimica A, Facoltà di Medicina, Istituto Medicina del Lavoro, Università di Cagliari, Via S. Giorgio, 09100 Cagliari, Italy

and

I. A. ZAKHAROVA

N. S. Kurnakov Institute of General and Inorganic Chemistry, Academy of Sciences, Moscow, U.S.S.R.

(*Received* 7 *June* 1984; *accepted after revision* 10 *June* 1985)

Abstract—Palladium(II) malonato complexes with heterocyclic ligands have been synthesized and characterized by spectroscopic and biological studies. The compounds are of the general formula $Pd(mal)(L)_n$, where mal = malonato; and L = *N*-methylimidazole, *N*-ethylimidazole, *N*-propylimidazole and 2-methylbenzoxazole for $n = 2$; L = benzoxazole and ethylenediamine for $n = 1$. Our results have shown that the four $Pd(mal)(L)_2$ derivatives are soluble in water and are monomeric square planar. The two Pd(mal)(L) derivatives have poor solubility in water: the benzoxazole compound is dimeric square planar with bridging bidentate ligands, while the ethylenediamine derivative is monomeric square planar with a chelating ligand.

In previous studies[1] we prepared and studied the palladium(II) oxalato complexes with some heterocyclic ligands. The oxalato compounds are soluble in water and important in biological systems, but they present a relatively high toxicity.

Because malonate complexes have a good biological activity but a lower toxicity than oxalate derivatives, for the present paper we prepared the malonato complexes with the heterocyclic ligands *N*-methylimidazole (*N*-MeIm), *N*-ethylimidazole (*N*-EtIm), *N*-propylimidazole (*N*-PropIm), benzoxazole (Benzox), 2-methylbenzoxazole (2-MeBenzox) and ethylendiamine (en), in order to establish the stereochemistry of the compounds and to compare their biological effects with respect to the oxalato compounds.

EXPERIMENTAL

N-MeIm, en and 2-MeBenzox purum were supplied by Fluka, Benzox purum by EGA-Chemie, and *N*-EtIm and *N*-PropIm were kindly presented by BASF.

Palladium(II) malonate was prepared mixing the aqueous solution of potassium tetrachloro palladate(II) and potassium malonate in a 1:1 ratio at room temperature, and then heated in a water bath.

Pd(mal) was purified by washing with ethyl alcohol and dried over P_4O_{10}.

All the complexes were prepared by refluxing

* Author to whom correspondence should be addressed.

Pd(mal) with the ligand in excess for about 48 h. The compounds were washed in petroleum ether and dried over P_4O_{10}.

Analyses

The percentage values of carbon, hydrogen and nitrogen were determined with a Perkin–Elmer 240 elemental analyzer.

IR spectra

The IR spectra were recorded in the 4000–200-cm^{-1} range on a Perkin–Elmer 325 spectrophotometer with CsI discs in a Nujol mull.

Electronic spectra

The reflectance spectra were recorded on a Varian Cary 219 spectrophotometer in the range 40,000–10,000 cm^{-1}.

Biological activity

The method of extraction of the sarcoplasmatic reticulum containing Ca, Mg-dependent ATP-ase was performed according to a previous paper.[2] Inhibitory activity of the complexes towards the substrate in aqueous solution was obtained by determining the number of the SH groups by means of amperometric titrations.[2] When the complexes were insoluble in water we proceeded as follows: the complexes were dissolved in $CHCl_3$ or in C_2H_5OH and, after the solvent had completely evaporated and a thin film had formed, ATP-ase in aqueous solution was added, in order to evaluate the inhibitory activity of the complexes.

RESULTS AND DISCUSSION

The isolated complexes are reported in Table 1 together with analytical data and other physical properties.

The compounds are of two types: Pd(mal)$(L)_2$, where L = *N*-MeIm, *N*-EtIm, *N*-PropIm and 2-MeBenzox; and Pd(mal)L where L = Benzox and en.

All the complexes are powder-like, diamagnetic and non-conductors. The Pd(mal)$(L)_2$ derivatives are soluble in water and in the usual solvents, while the Pd(mal)L derivatives have a poor solubility in water and a good solubility in EtOH, $CHCl_3$ and DMF.

The IR spectra of the ligands in the 4000–400-cm^{-1} range are interpreted on the basis of previously reported data.[3,4]

In Table 2 the principal IR bands of the complexes in the 4000–200 cm^{-1} range are reported.

The medium absorption band within the 3440–3380-cm^{-1} range for ν(OH), and that within the 1650–1630-cm^{-1} range for δ(HOH), are present in all the complexes which lose water completely at 110°C before decomposing. From a detailed analysis of the IR spectra we have found that the rocking, twisting and wagging modes, ascribable to coordinated water according to Nakamoto,[5] are absent. However, the above bands are absent in Pd(mal)(Benzox), since it does not contain water molecules.

The IR spectra of the complexes are more difficult to interpret and the ν_{sym}(COO) and ν_{asym}(COO) are often ambiguously assigned as can be seen in the literature.[6,7] On our part, we have decided to follow a recent article[8] by O'Brien, where the (COO) vibrations are attributed differently, as regards the oxalate complexes.

In fact, in the IR spectra the vibrations present in the 1630–1580- and 1575–1540-cm^{-1} ranges are assigned to ν_{sym}(COO), and the vibrations in the 1450–1402- and 1370–1340-cm^{-1} ranges to ν_{asym}(COO). These values are in agreement with the fact that the carboxyl groups are unidentate and therefore that the bridging malonato groups[8] are absent.

Table 1. Analytical and physical data

Compound	Colour	Melting point (°C)	Found (calc.) (%) C	H	N
Pd(mal)·H_2O	Ivory	—	16.1(15.9)	1.8(1.9)	—
Pd(mal)(*N*-MeIm)$_2$·$2H_2O$	Beige	140–148 dec.[a]	32.6(32.3)	4.3(4.4)	13.7(14.2)
Pd(mal)(*N*-EtIm)$_2$·$2H_2O$	Ivory	140	33.7(33.4)	5.0(4.9)	11.8(11.5)
Pd(mal)(*N*-PropIm)$_2$·$2H_2O$	Beige	165–178 dec.	38.4(38.7)	5.4(5.6)	11.9(12.0)
Pd(mal)(Benzox)	Brown	150	36.5(36.6)	2.5(2.1)	4.9(4.3)
Pd(mal)(2-MeBenzox)$_2$·$2H_2O$	Pale beige	175	47.0(46.5)	3.5(3.7)	6.1(5.7)
Pd(mal)(en)·H_2O	Beige	160–170 dec.	20.9(20.9)	4.2(4.2)	9.2(9.7)

[a] Decomposition-temperature range.

Table 2. Principal IR bands (4000–200 cm^{-1})

Compound	ν_{sym}(COO)	ν_{asym}(COO)	ν(Pd—O)[a]	ν(Pd—O)[b]	ν(Pd—N)
Pd(mal)(*N*-MeIm)$_2 \cdot 2H_2O$	1580 vs, 1540 vs	1405 m, 1350 s	465 m		240 msh, 220 ssh
Pd(mal)(*N*-EtIm)$_2 \cdot 2H_2O$	1640 ms, 1560 vs	1402 s, 1352 sh	530 m		248 sh, 228 sh
Pd(mal)(*N*-PropIm)$_2 \cdot 2H_2O$	1610 sh, 1570 m	1450 m, 1370 m	585 w		248 m, 228 m
Pd(mal)(Benzox)	1605 s, 1560 m	1400 m, 1350 s		325 m	241 m
Pd(mal)(2-MeBenzox)$_2 \cdot 2H_2O$	1630 vs, 1560 m	1450 sh, 1360 vs	545 sh	304 m	
Pd(mal)(en)$\cdot H_2O$	1620 sh, 1575 m	1430 sh, 1340 sh	585 m		565 m
Pd(mal)$\cdot H_2O$	1600 s, 1570 s	1410 w, 1370 vs			
K_2(mal)	1570–1550 sh	1370 s			

[a] Stetching vibration of the malonate.
[b] Stretching vibration of the heterocyclic ligand.

In the far-IR region a stretching band appears at 585–465 cm^{-1}, and it is attributed to ν(Pd—O), due to the coordinated malonato group.

The Pd(mal)$(L)_2 \cdot 2H_2O$ derivatives, where L = *N*-MeIm, *N*-EtIm or *N*-PropIm, show two bands in the 248–228-cm^{-1} range, due to ν(Pd—N) for the square-planar stereochemistry[9] in a *cis* configuration.

In the Pd(mal)(2-MeBenzox)$_2 \cdot 2H_2O$ derivate, we observe a band at 304 cm^{-1}, due to the metal–oxygen vibrations; therefore we may say that the ligand is oxygen-bonded.[10]

Pd(mal)(Benzox) is a dimeric square-planar compound.

In fact the absorption band at 325 cm^{-1}, due to ν(Pd—O), and the band at 241 cm^{-1}, due to (Pd—N), confirm that Benzox acts as a bridging bidentate ligand.[9,10] Pd(mal)(en)$\cdot H_2O$ shows a band at 565 cm^{-1} assigned to ν(Pd—N) according to literature data.[11]

In Table 3 the reflectance electronic spectra and the Δ_1 values are reported.

In the solid state these spectra are indicative of a square-planar geometry.[12] The band in the 28,170–25,640-cm^{-1} range was assigned to the $^1A_{1g} \rightarrow {}^1B_{1g}$ transition. In the UV region, the strong absorption vibrations in the 37,740–29,410-cm^{-1} range are due to charge-transfer transitions mal → Pd and L → Pd.

By assuming a value of $F_2 = 10F_4 = 600$ cm^{-1} for the Slater–Condon interelectronic repulsion parameters,[12] we were able to derive the value $\Delta_1 = \nu_1 + 3.5F_2$ from the first spin-allowed *d–d* transition. The values lie in the 30,270–27,740-cm^{-1} range.

Biological activity

Inhibitory activity towards the Ca, Mg-dependent ATP-ase was obtained only with some of the Pd(mal)$(L)_n$ complexes, since the others were reduced in solution.

We have compared the results of these palladium malonate complexes with respect to the analogous oxalato complexes.[1]

The inhibitory effect of Pd(mal)(*N*-EtIm)$_2 \cdot 2H_2O$ is twice as great as that of Pd(ox)(*N*-EtIm)$_2$. The malonate anion is more basic than the oxalate, so the *N*-EtIm is less strongly bonded to the Pd(II) ion and is easier to substitute with the thiol groups of the enzyme.

The Pd(mal)(Benzox) have 12% inhibitory activity, which value is smaller than that of the *cis*-Pd(Benzox)$_2$Br$_2$ derivative,[4] because in the former

Table 3. Electronic reflectance spectra

Compound	Bands (cm^{-1})	Δ_1
Pd(mal)(*N*-MeIm)$_2 \cdot 2H_2O$	37,740, 33,330, 26,670, 25,640	27,740
Pd(mal)(*N*-EtIm)$_2 \cdot 2H_2O$	37,740, 30,770, 33,330, 27,300	29,400
Pd(mal)(*N*-PropIm)$_2 \cdot 2H_2O$	37,740, 33,330, 26,100	28,200
Pd(mal)(Benzox)	37,740, 33,330, 31,750, 27,030	29,130
Pd(mal)(2-MeBenzox)$_2 \cdot 2H_2O$	37,740, 33,330, 26,320	28,420
Pd(mal)(en)$\cdot H_2O$	37,450, 33,330, 29,410, 28,170	30,270

Table 4. Inhibitory activity of some malonato complexes with respect to the analogous oxalato

Compound	% (±2)[a] at 10^{-4} M	Solvent
Pd(mal)(*N*-EtIm)$_2 \cdot 2H_2O$	46	Water
Pd(ox)(*N*-EtIm)$_2$	23	Water
Pd(mal)(Benzox)	12	$CHCl_3$
cis-Pd(Benzox)$_2Br_2$	16	$CHCl_3$
Pd(mal)(en)$\cdot H_2O$	0	C_2H_5OH
Pd(ox)(en)	0	C_2H_5OH

[a] % is the percentage of the inhibitory activity.

the bridging ligand with weaker bonds is more easily replaced by the S^- of the ATP-ase mash.

In Pd(mal)(en)$\cdot H_2O$, as in Pd(ox)(en), this effect is zero, because the en is a strong chelating agent and it is difficult to substitute one or two positions with the thiol group(s) of the enzyme.

As far as regards the inhibitory mechanism, the irreversible interaction of the enzyme on the complexes occurs with the sulphur anion of the SH groups of the ATP-ase, which replaces the ligands in the square-planar complexes.

REFERENCES

1. G. Devoto, M. Biddau, M. Massacesi, R. Pinna, G. Ponticelli, L. V. Tatjanenko and I. A. Zakharova, *J. Inorg. Biochem.* 1983, **19**, 311.
2. E. Benesch, H. A. Lardy and R. Benesch, *J. Biol. Chem.* 1965, **216**, 663.
3. M. Biddau, G. Devoto, M. Massacesi, G. Ponticelli and I. A. Zakharova, *Polyhedron* 1983, **12**, 1261.
4. M. Massacesi, R. Pinna, M. Biddau, G. Ponticelli and I. A. Zakharova, *Inorg. Chim. Acta* (*Bioinorg. Sect.*) 1983, **80**, 151.
5. K. Nakamoto, *Infrared Spectra of Inorganic and Coordination Compounds.* Wiley–Interscience, New York (1963).
6. M. J. Schmelz, I. Nakagawa, San-J. Mizushima and J. V. Quagliano, *J. Am. Chem. Soc.* 1959, **81**, 287.
7. J. R. Ferraro, *Low Frequency Vibrations of Inorganic and Coordination Compounds.* Plenum Press, New York (1971).
8. P. O'Brien, *J. Chem. Soc., Dalton Trans.* 1981, 1540.
9. M. N. Hughes and K. J. Rutt, *J. Chem. Soc. A* 1970, 3015.
10. E. J. Duff and M. N. Hughes, *J. Chem. Soc. A* 1969, 477.
11. G. W. Watt and D. S. Klett, *Inorg. Chem.* 1966, **5**, 1278.
12. P. L. Goggin, R. J. Goodfellow and F. J. S. Reed, *J. Chem. Soc., Dalton Trans.* 1972, 1298.

Polyhedron Vol. 4, No. 11, pp. 1993–1994, 1985
Printed in Great Britain

0277-5387/85 $3.00 + .00
© 1985 Pergamon Press Ltd

COMMUNICATION

A 2,3-NAPHTHOQUINODIMETHANE COMPLEX OF RUTHENIUM

WILLIAM FAULKNER, DAVID S. BARRATT, DOMENICO C. CUPERTINO and DAVID J. COLE-HAMILTON*
School of Chemistry, University of Liverpool, P.O. Box 147, Liverpool L69 3BX, U.K.

(*Received* 24 *May* 1985; *accepted* 26 *May* 1985)

Abstract—Treatment of 2,3-dimethylnaphthalene with BuLi·TMED (TMED = tetramethylethylenediamine) gives 2-lithiomethyl-3-methyl-naphthalene·TMED, which in turn reacts with $[RuCl_2(PMePh_2)_4]$ to give the 2,3-naphthoquinodimethane complex.

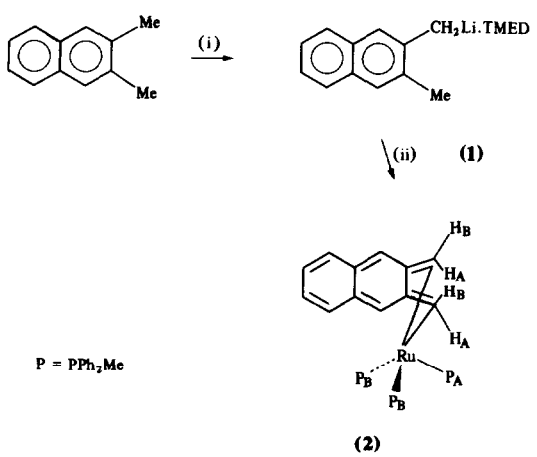
The stabilisation of otherwise unstable organic compounds by coordination to transition elements is an area of particular interest, especially if the organic moiety can be released and undergo subsequent reactions.

A number of reports has recently appeared[1–6] on the stabilisation of *o*-quinodimethane (*o*-xylylene), which is an important intermediate in the synthesis of a range of organic products.[7] Most of these syntheses involve deprotonation[2,4] (or oxidation)[6] of coordinated hexamethylbenzene complexes or reactions of *o*-bis(bromomethyl)benzene derivatives.[1,3] Since these types of precursor are not always readily available for more complex aromatic systems, complexes of more elaborate analogues of *o*-quinodimethane have not been prepared.

In contrast, we have reported[5] that *o*-quinodimethane complexes of ruthenium can be obtained directly from *o*-xylene by deprotonation with BuLi·TMED (TMED = tetramethylethylenediamine) and reaction of the resulting lithium salt with, for example, $[RuCl_2(PMe_3)_4]$. Since *o*-dimethylaromatic compounds are often readily available, this reaction should be of more general applicability. We now report the preparation of a 2,3-naphthoquinodimethane complex by this method.

Reaction of 2,3-dimethylnaphthalene with BuLi·TMED in light petroleum affords a red oil, presumed to be **1** (see Scheme 1). Reaction of excess of this oil with $[RuCl_2(PMePh_2)_4]$ in diethylether affords a red solution from which **2** can be crystallised in 70% yield. Although large crystals of **2** can be obtained, they are soft and do not diffract X-rays, the identification of **2** as the 2,3-naphthoquinodimethane complex therefore relies on spectroscopic data.

Table 1 shows a comparison of certain features of the ^1H and ^{31}P NMR spectra of **2** and the related η^4-*o*-quinodimethane complex, $[Ru(CH_2C_6H_4CH_2)(PMePh_2)_3]$ (**3**).[5] The similarity between the spectra of the two complexes confirms the η^4-binding of the 2,3-naphthoquinodimethane complexes, in particular the high field shift of the H_A protons is indica-



Scheme 1. Preparation of **2** from 2,3-dimethylnaphthalene, BuLi and $[RuCl_2(PMePh_2)_4]$. (i) BuLi, TMED, petroleum, 25°C, 6 h. (ii) $[RuCl_2(PMePh_2)_4]$, Et_2O, 25°C, 48 h.

* Author to whom correspondence should be addressed. Present address: Chemistry Department, University of St. Andrews, St. Andrews, Fife KY16 9ST, U.K.

Table 1. Selected ^1H and ^{31}P NMR parameters for **2** and **3** in CD_2Cl_2

	Chemical shift (ppm)[a]						Coupling constant (Hz)			
	H_A	H_B	$Me(P_A)$	$Me(P_B)$	P_A[b]	P_B[b]	H_AH_B	H_AP	H_BP	P_AP_B
2	0.73dd	1.74dd	2.16d (7.8)[c]	1.50 (4.1)[d]	41.4t	19.5d	4.5	4.5	5.5	4.0
3	0.16dd	1.47dd	2.16d (7.0)[c]	1.53 (4.2)[d]	35.7s	19.7s	3.8	6.8	5.0	0

[a] ^1H relative to tetramethylsilane at 0 ppm.
[b] In C_6H_6, to high frequency of external 85% H_3PO_4.
[c] J_{P_AH}.
[d] $J_{P_BH}+J_{P_BH'}$.

tive of a butadiene-like coordination.[5] Furthermore, the very low value of $J_{P_AP_B}$ rules out the alternative structure involving a five-coordinate complex of a substituted ruthenacyclopentene, but similar low values of $J_{P_AP_B}$ have been noted for a range of complexes of the general form [Ru(diene)P_2L] (P = PPh_3, L = PPh_3[8] or styrene,[9] diene = buta-1,3-diene or hexa-1,3-diene; P = L = PMe_2-Ph, $PMePh_2$, PMe_3 or PEt_3, diene = *o*-quinodimethane[5]).

The red colour of **2** is somewhat surprising since 18e complexes of ruthenium(0) or (II) are generally yellow, whilst 16e complexes are red.[10] However, the red colour of **2** arises from an absorption in the visible spectrum at 510 nm (ε = 2410), which is close to the position of the major absorption of matrix isolated 2,3-naphthoquinodimethane (541 nm), which is also reported to be red.[11]

The isolation of this 2,3-naphthoqinodimethane complex is somewhat surprising since η^4-binding leads to localisation of the bonding in the aromatic system.[5] Assuming that this occurs in the naphthoquinodimethane complex, a much larger resonance energy will be lost (resonance energies for benzene and naphthalene are 164 and 315 kJ mol^{-1}, respectively). This demonstrates the very high affinity of ruthenium for diene-like coordination.

Acknowledgements—We thank the SERC for a fellowship (D.S.B.) and studentship (D.C.C.) and Johnson–Matthey Ltd for loans of ruthenium. D.J.C.-H. is the Sir Edward Frankland Fellow of the Royal Society of Chemistry, 1984–1985.

REFERENCES

1. W. R. Roth and J. D. Meier, *Tetrahedron Lett.* 1967, 2053.
2. M. A. Bennett, I. J. McMahon and T. W. Turney, *Angew. Chem., Int. Ed. Engl.* 1982, **21**, 379.
3. W. H. Hersh and R. G. Bergman, *J. Am. Chem. Soc.* 1981, **103**, 6992.
4. J. W. Hull and W. L. Gladfelter, *Organometallics* 1982, **1**, 1716.
5. S. D. Chappell, D. J. Cole-Hamilton, A. M. R. Galas and M. B. Hursthouse, *J. Chem. Soc., Dalton Trans.* 1982, 1867.
6. D. Astruc, private communication.
7. W. Oppoltzer, *Angew. Chem., Int. Ed. Engl.* 1977, **16**, 10 and references therein.
8. D. J. Cole-Hamilton and G. Wilkinson, *Nouv. J. Chim.* 1977, **1**, 141.
9. B. N. Chandret, D. J. Cole-Hamilton and G. Wilkinson, *J. Chem. Soc., Dalton Trans.* 1979, 1739.
10. B. N. Chaudret, D. J. Cole-Hamilton, R. S. Nohr and G. Wilkinson, *J. Chem. Soc., Dalton Trans.* 1977, 1546.
11. M. Gisin and J. Wirz, *Helv. Chim. Acta* 1976, **59**, 2273.

Polyhedron Vol. 4, No. 11, pp. 1995–1996, 1985
Printed in Great Britain

0277–5387/85 $3.00 + .00
© 1985 Pergamon Press Ltd

COMMUNICATION

ESR STUDIES ON THE PREPARATION OF THE SULPHITE RADICAL ANION, $SO_3^{\dot{-}}$, IN AQUEOUS SOLUTION

T. OZAWA*

National Institute of Radiological Sciences, 9-1, Anagawa-4-chome, Chiba-shi 260, Japan

and

T. KWAN

Faculty of Pharmaceutical Sciences, Teikyo University, Sagamiko-cho, Tsukui-gun, Kanagawa 199-01, Japan

(*Received* 1 *March* 1985; *accepted* 4 *June* 1985)

Abstract—The sulphite radical anion, $SO_3^{\dot{-}}$, was generated from the redox reactions between the bisulphite ion, HSO_3^-, and transition-metal ions such as VO_2^+, CrO_4^{2-} and MnO_4^-, as well as the reaction of Ce^{4+} with HSO_3^-. The formation of the $SO_3^{\dot{-}}$ radical was determined by ESR spectroscopy coupled with a rapid-mixing flow technique.

It is well known that the rapid-mixing flow technique coupled with ESR is very useful in detecting short-lived radicals having lifetimes longer than a few milliseconds. By using this technique we have reported in previous papers that the sulphite radical anion, $SO_3^{\dot{-}}$, which is generated from a Ce^{4+}–$NaHSO_3$ system in acidic aqueous solutions[1] can add to compounds having C=C,[2,3] C≡C[4] and C=S[5] bonds to give the corresponding secondary radicals. Also, in alkaline aqueous solutions at pH 9, the same radical species, $SO_3^{\dot{-}}$, which is obtained from a Ti^{3+}(ethylenediaminetetraacetic acid)–H_2O_2–Na_2SO_3 system,[6] can add to uracil derivatives having a C=S bond.[7]

Since the $SO_3^{\dot{-}}$ radical is generated by the redox reaction between Ce^{4+} and the bisulphite ion,[1] HSO_3^-, we have further examined the reactions of many kind of metal ions having the redox ability and HSO_3^- in acidic aqueous solutions by the use of an ESR method coupled with the rapid-mixing flow technique to detect the $SO_3^{\dot{-}}$ radical.

We report these results in this paper.

EXPERIMENTAL

The ESR measurements were carried out on a JEOL-PE-lX ESR spectrometer (X-band) with 100-kHz field modulation in conjunction with a JEOL mixing chamber. This apparatus enabled us to detect radicals having lifetimes of 5–100 ms. The ESR parameters were calibrated by comparison with an aqueous solution of Fremy's salt ($g = 2.0055$, $a^N = 1.30$ mT)[8] kept in a capillary tube attached to the sample. The concentrations of the spins were approximated to the peak-to-peak height of a given signal.

To detect the formation of the $SO_3^{\dot{-}}$ radical, the following metal salts were used without further purification: $CuSO_4 \cdot 5H_2O$ (Wako), $Fe_2(SO_4)_3 \cdot nH_2O$ (Wako), NH_4VO_3 (Wako), $K_2Cr_2O_7$ (Wako), $KMnO_4$ (Wako) and $Ce(NO_4)_4 \cdot 2(NH_4NO_3)$ (Wako). Sodium bisulphite ($NaHSO_3$) was obtained from Wako and used without further purification.

Two solutions were prepared, containing: (a) 0.01 M metal ions acidified to pH 2 with sulphuric acid, and (b) 0.1 M $NaHSO_3$. Details of the experimental procedure have been reported previously.[9]

* Author to whom correspondence should be addressed.

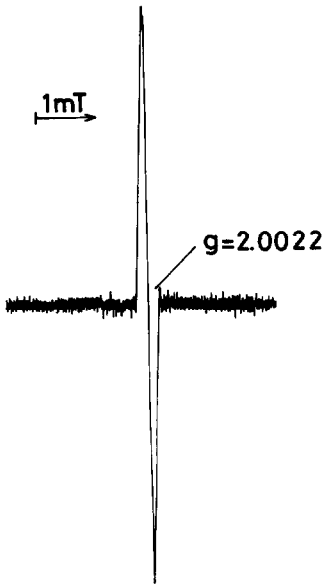


Fig. 1. ESR spectrum observed during the reaction of VO_2^+ with HSO_3^- in an acidic aqueous solution (pH 2) at room temperature.

RESULTS AND DISCUSSION

When two solutions [(a) (metal ion is Ce^{4+}) and (b)] were mixed in the cavity of the ESR spectrometer, a singlet line was observed, as expected ($g = 2.0022$), which has been assigned by us to the $SO_3^{\dot{-}}$ radical.[1] The same singlet signal was observed upon mixing HSO_3^- with the following metal ions: VO_2^+, CrO_4^{2-} and MnO_4^-. Figure 1 shows the ESR spectrum of the $SO_3^{\dot{-}}$ radical observed during the reaction of VO_2^+ with HSO_3^-. However, the signal intensity of the $SO_3^{\dot{-}}$ radical obtained from a VO_2^+–, CrO_4^{2-}– or MnO_4^-–$NaHSO_3$ system is smaller than that obtained from Ce^{4+}. No ESR signal could be observed during the reaction of Cu^{2+} or Fe^{3+} with HSO_3^-.

These results are summarized in Table 1, along with the reduction potentials of metal ions used here.[10]

In view of the strong one-electron oxidizing capability of Ce^{4+}, the $SO_3^{\dot{-}}$ radical must be formed according to reaction (1):

$$HSO_3^- + Ce^{4+} \rightarrow SO_3^{\dot{-}} + H^+ + Ce^{3+}. \quad (1)$$

Table 1. Abilities of metal ions to oxidize HSO_3^- and their reduction potentials

Metal ion	Valence change	Generation of $SO_3^{\dot{-}}$	Reduction potential (V)
Cu^{2+}	$Cu^{2+} \rightarrow Cu^+$	No	0.153
Fe^{3+}	$Fe^{3+} \rightarrow Fe^{2+}$	No	0.77
VO_2^+	$VO_2^+ \rightarrow VO^{2+}$	Yes	1.00
CrO_4^-	$Cr^{6+} \rightarrow Cr^{3+}$	Yes	1.36
MnO_4^-	$Mn^{7+} \rightarrow Mn^{2+}$	Yes	1.52
Ce^{4+}	$Ce^{4+} \rightarrow Ce^{3+}$	Yes	1.61

On using VO_2^+, the same reaction as shown in eqn (1) may occur to give the $SO_3^{\dot{-}}$ radical. Although, when CrO_4^{2-} or MnO_4^- is used, the stoichiometry of the reaction is not clear, these ion can oxidize HSO_3^- to yield the $SO_3^{\dot{-}}$ radical.

From Table 1, it is reasonable to consider that, because of the low reduction potentials of Fe^{3+} or Cu^{2+}, these ions cannot oxidize HSO_3^- and so no ESR signal could be observed.

In conclusion, the formation of the $SO_3^{\dot{-}}$ radical is dependent on the reduction potentials of the oxidizing metal ions.

REFERENCES

1. T. Ozawa, M. Setaka and T. Kwan, *Bull. Chem. Soc. Jpn* 1971, **44**, 3473.
2. T. Ozawa, M. Sato and T. Kwan, *Chem. Lett.* 1972, 591.
3. T. Ozawa and T. Kwan, *Polyhedron* 1983, **2**, 1019.
4. T. Ozawa and T. Kwan, *J. Chem. Soc., Chem. Commun.* 1983, 1295.
5. T. Ozawa, M. Setaka, H. Yamamoto and T. Kwan, *Chem. Pharm. Bull.* 1974, **22**, 962.
6. R. O. C. Norman and P. M. Storey, *J. Chem. Soc. (B)* 1971, 1009.
7. T. Ozawa and T. Kwan, *J. Chem. Soc., Chem. Commun.* 1983, 1295.
8. J. Q. Adams, S. W. Nicksick and J. R. Thomas, *J. Chem. Phys.* 1966, **45**, 654.
9. T. Ozawa, Y. Kirino, M. Setaka and T. Kwan, *Nippon Kagaku Zasshi* 1971, **92**, 304.
10. W. M. Latimer, *Oxidation Potentials*, 2nd edition. Prentice-Hall, Englewood Cliffs, NJ (1952).

Polyhedron Vol. 4, No. 11, pp. 1997–1999, 1985
Printed in Great Britain

0277–5387/85 $3.00 + .00
© 1985 Pergamon Press Ltd

COMMUNICATION

SYNTHESIS, ^{31}P AND ^{199}Hg NMR SPECTROSCOPY OF THE CATIONIC HETERODIMETALLACYCLE $[HgAg\{\mu\text{-}[BIS(DIPHENYLPHOSPHINO)METHANE]\}_2]^{3+}$

MARIA LUSSER and PAUL PERINGER*

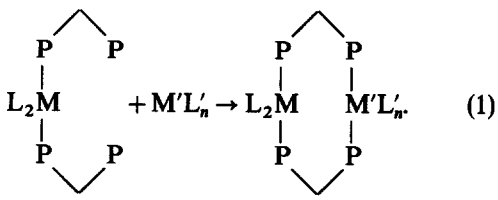
Institut für Anorganische und Analytische Chemie der Universität Innsbruck, Innrain 52a, A-6020 Innsbruck, Austria

(*Received* 20 *May* 1985; *accepted* 11 *June* 1985)

Abstract—The complex $[Hg(\eta^1\text{-dppm})_2](O_3SCF_3)_2$ [dppm = bis(diphenylphosphino) methane] reacts with AgO_3SCF_3 to give the new eight-membered ring compound $[HgAg(\mu\text{-dppm})_2](O_3SCF_3)_3$ (**1**) in high yield. **1** is also formed in a redistribution reaction of the respective homobimetallic mercury and silver rings, and was characterized by ^{31}P and ^{199}Hg NMR spectroscopy. The magnitude of the coupling constant $J(^{199}Hg, ^{107}Ag)$ amounts to 60 Hz.

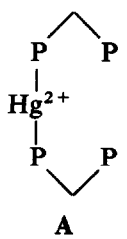
Bis(diphenylphosphino)methane (dppm) is an excellent ligand for grouping two metal centres in close proximity in complexes of the form of eight-membered rings $[M_2(\mu\text{-dppm})_2]$.[1] The synthetic methods suited to the formation of homonuclear complexes are not generally adaptable for the generation of heterobimetallic compounds.

Shaw *et al.*[2] recently described a systematic high-yield synthesis for heterobimetallic compounds involving M = Pt or Pd [eqn (1)]:



(1)

We found very recently that $[Hg(dppm)_2](O_3SCF_3)_2$ adopted structure **A**,[3]



A

which was expected to have a corresponding synthetic potential for heterobimetallic eight-membered metallacycles involving mercury.

EXPERIMENTAL

Chemical analyses were obtained on a Heraeus EA-415, and NMR spectra were recorded on a multinuclear Bruker WP-80 spectrometer operating in the FT mode. The chemical shifts are referred to 85% H_3PO_4 or aqueous $Hg(ClO_4)_2$ (2 mmol HgO cm^{-3} 60% $HClO_4$), and positive shifts are to high frequency of the reference. Coupling constants are in Hz. The program PANIC on a Bruker Aspect 2000 computer was used for the simulation of the spectra and for the refinement of the parameters by iteration.

Preparation of bis[sulfinylbis[methane]]silverbis[μ-methylenebis[diphenylphosphine]-P : P']bis[sulfinylbis[methane]] mercury(3+)tris[trifluoromethanesulfonate] (**1**)

0.125 mmol $[Hg_2(\mu\text{-dppm})_2](O_3SCF_3)_4$[4] {prepared *in situ* from 242 mg (0.25 mmol) $[Hg(Me_2SO)_6](O_3SCF_3)_2$ and 96 mg (0.25 mmol) dppm} in 1 cm^3 CH_2Cl_2 and 160 mg (0.125 mmol) $[Ag_2(\mu\text{-dppm})_2](O_3SCF_3)_2$ in 1 cm^3 CH_2Cl_2 are mixed together and concentrated to *ca* 1 cm^3. The product crystallizes upon standing overnight as

* Author to whom correspondence should be addressed.

colorless air-stable crystals in 70% yield. M.p. 220°C (dec.).

Found: C, 40.0; H, 3.7. Calc. for

$C_{61}H_{68}AgF_9HgO_{13}P_4S_7$: C, 39.9; H, 3.7%.

The complex is sparingly soluble in CH_2Cl_2, MeOH or acetone, and readily soluble in Me_2SO or DMF.

1 is also obtained from equivalent amounts $[Hg(\eta^1\text{-dppm})_2](O_3SCF_3)_2$[3] {prepared *in situ* from $[Hg(Me_2SO)_6](O_3SCF_3)$ and two equivalents dppm} and AgO_3SCF_3 in CH_2Cl_2, followed by a similar work-up procedure.

Preparation of bis[μ-methylene[diphenylphosphine]-P:P']disilver(2+)bis[trifluoromethanesulfonate]

96 mg (0.25 mmol) dppm and 64 mg (0.25 mmol) AgO_3SCF_3 are mixed together in 1 cm^3 of MeOH and stirred for 10 min. The product crystallizes upon evaporation of the solvent *in vacuo* in the form of colorless crystals in almost quantitative yield. M.p. 110–118°C.

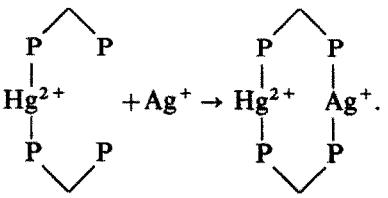
Found: C, 48.1; H, 3.3. Calc. for

$C_{52}H_{44}Ag_2F_6O_6P_4S_2$: C, 48.7; H, 3.5%.

Corresponding carboxylato and tetrafluoroborato complexes were obtained by Van der Ploeg and Van Koten.[5]

RESULTS AND DISCUSSION

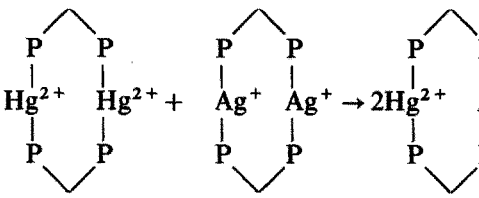
The reaction of $[Hg(\eta^1\text{-dppm})_2](O_3SCF_3)_2$ and AgO_3SCF_3 leads to the heterobimetallacyclic compound **1** according to eqn (2):



(2)

1

This compound is also accessible from the respective homobimetallic mercury and silver rings [eqn (3)]:



(3)

Remarkably, the redistribution equilibrium positions are far on the side of the heterobimetallic compound **1**, as evidenced by the absence of signals of the homobimetallic species in the ^{31}P NMR spectrum. The redistribution proceeds within 20 min at ambient temperature in methanol solution. The product was isolated in the form of colorless air-stable crystals in almost quantitative yield as Me_2SO solvate.

The mixed Ag–Hg–dppm complex has been characterized by $^{31}P\{^1H\}$ and $^{199}Hg\{^1H\}$ NMR spectroscopy.

The $^{31}P\{^1H\}$ NMR spectrum of **1** recorded in DMF at 253 K as shown in Fig. 1 is a superposition of the four NMR relevant isotopomers

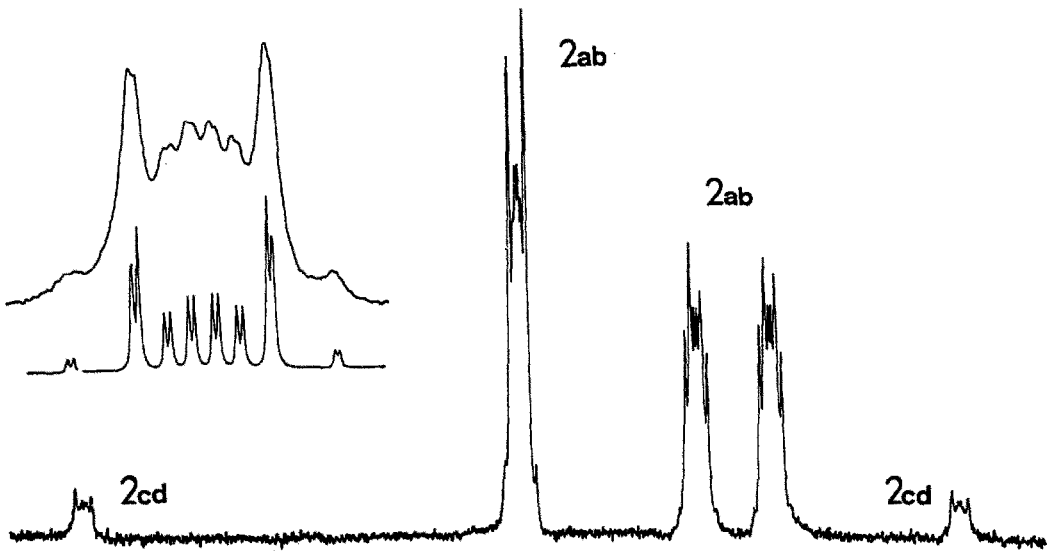


Fig. 1. $^{31}P\{^1H\}$ NMR spectrum of **1** in DMF at 253 K. The part of the phosphorus atoms coordinated to mercury is enlarged together with the corresponding computer-simulated pattern (the parameters are shown in Table 1).

Table 1. NMR parameters[a]

	$[AgHg(dppm)_2]^{3+}$	$[Ag_2(dppm)_2]^{2+}$	$[Hg_2(dppm)_2]^{4+}$ [b]
$\delta(^{31}P)Hg$	26.1	—	36.8
$\delta(^{31}P)Ag$	−0.9	4.8	—
$\delta(^{199}Hg)$	1358	—	1361
$^1J(^{199}Hg, ^{31}P)$	5899	—	5675
$^3J(^{199}Hg, ^{31}P)$	19	—	147
$^1J(^{107}Ag, ^{31}P)$	470	482	—
$^3J(^{107}Ag, ^{31}P)$	4	4	—
$^2J(^{31}PC^{31}P)$	111	160	32
$J(M, M)$	60	—	959
T (K)	253	233	—

[a] Ambient temperature unless otherwise stated; solvent is DMF.
[b] Taken from Ref. 4.

$[Hg^{107}Ag(dppm)_2]$ (**2a**, 43.09%), $[Hg^{109}Ag(dppm)_2]$ (**2b**, 40.07%), $[^{199}Hg^{107}Ag(dppm)_2]$ (**2c**, 8.73%) and $[^{199}Hg^{109}Ag(dppm)_2]$ (**2d**, 8.11%). The high-frequency part of the spectrum of **2a** and **b** (Fig. 1) originates from the phosphorus atoms bound to mercury, whereas the low-frequency part is attributed to the phosphorus atoms bound to silver in keeping with greater coordination chemical shifts of tertiary phosphines usually observed for mercury complexes compared with that of silver.[6] The part of the phosphorus atoms coordinated to mercury is enlarged together with the corresponding computer-simulated pattern. The parameters, refined by iteration, are shown in Table 1 together with the data of the homobimetallic mercury and silver rings. Major differences between data of the homo- and heterometallic rings, e.g. $\delta(^{31}P)$, $^3J(^{199}Hg, ^{31}P)$ and $^2J(^{31}PC^{31}P)$, may be caused by different geometries of the rings. The form of the patterns turned out to be rather insensitive to the value of the couplings $^2J(^{31}PHg^{31}P)$ and $^2J(^{31}PAg^{31}P)$.

The coupling between the ^{199}Hg and ^{107}Ag nuclei amounts to 60 Hz compared with a value of 900 Hz for $J(^{199}Hg, ^{199}Hg)$ in the homobimetallic mercury ring.[4]

REFERENCES

1. R. J. Puddephatt, *Chem. Soc. Rev.* 1983, 99.
2. P. G. Pringle and B. L. Shaw, *J. Chem. Soc., Chem. Commun.* 1982, 956; D. M. McEwan, P. G. Pringle and B. L. Shaw, *J. Chem. Soc., Chem. Commun.* 1982, 859; G. R. Cooper, A. T. Hutton, C. R. Langrick, D. M. McEwan, P. G. Pringle and B. L. Shaw, *J. Chem. Soc., Dalton Trans.* 1984, 855; C. R. Langrick, P. G. Pringle and B. L. Shaw, *J. Chem. Soc., Dalton Trans.* 1984, 1233.
3. P. Peringer and M. Lusser, *Inorg. Chem.* 1985, **24**, 109.
4. M. Lusser and P. Peringer, *Chem. Ber.* 1985, **118**, 2140.
5. A. F. M. J. Van der Ploeg and G. Van Koten, *Inorg. Chim. Acta* 1981, **51**, 225.
6. P. S. Pregosin and R. W. Kunz, ^{31}P *and* ^{13}C *NMR of Transition Metal Phosphine Complexes.* Springer, Berlin (1979).

Polyhedron Vol. 4, No. 11, p. 2001, 1985
Pergamon Press Ltd. Printed in Great Britain

BOOK REVIEW

Gmelin Handbook of Inorganic Chemistry, 8th Edition. Sn—Organic Compounds, Part 11, Trimethyltin- and Triethyltin–Oxygen Compounds. H. Schumann and I. Schumann, Springer, Berlin, 1985, ISBN 3-540-93501-0, x + 292 pp., DM995.

In this eleventh volume of their Herculean effort, the Schumanns deal with the mononuclear trimethyl- and triethyltin–oxygen compounds, Me_3SnOX and Et_3SnOX, covering the literature up to the end of 1982. Much of the space is devoted to the hydroxides, alkoxides and carboxylates, but the derivatives of the oxyacids of sulphur, nitrogen, phosphorus and so on, are included.

The presentation follows that with which has been established in the previous volumes.

The book begins with a list (43 pp.) of general references, and ends with a formula index (20 pp.). The text is nowadays wholly in English. Much of the material is presented in tabular form, and molecular structures obtained by X-ray diffraction are reproduced. For example, more than 7 pp. and 111 references are devoted to the description of triethyltin hydroxide. Eleven references are given to various preparations, and contradictory reports of the melting point and boiling point are discussed. Physical properties such as the chromatographic behaviour, and the IR and Mössbauer spectra are given; the reactions are presented mainly in tabular form, and there is more than a page on its biological properties and industrial applications.

This volume carries the stamp of authority which characterises this series by the Schumanns; all organotin chemists will want to have access to it.

Department of Chemistry **A. G. DAVIES**
University College London
20 *Gordon Street*
London WC1H 0AJ

Polyhedron Vol. 4, No. 12, pp. 2003–2025, 1985
Printed in Great Britain

0277–5387/85 $3.00 + .00
© 1985 Pergamon Press Ltd

POLYHEDRON REPORT NUMBER 13

THE SYNTHESIS, STRUCTURES, BONDING AND UNUSUAL REACTIVITY OF SULFIDO OSMIUM CARBONYL CLUSTER COMPOUNDS

RICHARD D. ADAMS
Department of Chemistry, University of South Carolina, Columbia, SC 29208, U.S.A.

CONTENTS

I. INTRODUCTION 2003

II. SYNTHESES AND STRUCTURES 2004
1. Reagents and reactions 2004
2. Cluster condensation reactions 2010
(a) Homonuclear clusters 2010
(b) Mixed-metal clusters 2016

III. BONDING AND UNUSUAL REACTIVITY 2020
1. M_4S_2 clusters 2021
2. M_4S clusters 2022

I. INTRODUCTION

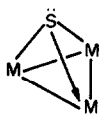
The class of low-valent polynuclear metal complexes that contain metal–metal bonds are known as cluster compounds. These compounds have attracted a great deal of attention with the idea they might serve as models for metal surfaces and heterogeneous catalysts.[1–3] More recently, interest has been focused on the chemical properties that may make them distinct from both heterogeneous and mononuclear metal homogeneous catalysts.[4]

A major problem in the use of cluster compounds as catalysts is their tendency to undergo degradative fragmentation when subjected to forcing reaction conditions. In an effort to prevent this a number of workers have chosen to employ bridging ligands.[5,6] The bridging ligands are usually derived from elements of the main groups and may be suitably modified with alkenyl and aryl substituents (e.g. NR, PR, PR_2, As, AsR, AsR_2, S, SR etc.). In this report attention will be focused on compounds that contain the bridging sulfido ligand and the transition element osmium.

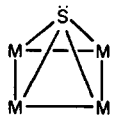
In cluster complexes containing three metal atoms, the sulfido ligand invariably serves as a triple bridge, **1**.[6] It contains a lone pair of electrons and, when viewed as an uncharged ligand, it serves as a four-electron donor. Thus, within the framework of the valence-bond description one of the three M—S bonds would be viewed as a two-electron S to M donor bond. It is not a requirement that the M_3 group contain three M—M bonds and there are many documented examples where triply bridging sulfido ligands span M_3 units which have two or less metal–metal bonds.[6]

In the presence of four metal atoms the sulfido ligand frequently serves as a quadruply bridging ligand, **2** or **3**. If all the metal atoms lie on the same side of a plane that passes through the sulfido ligand, it is regarded as a four-electron donor and it contains a lone pair of electrons (**2**).* Interestingly, the ligand then has only three orbitals for use in bonding to the four metal atoms. Although the bonding is difficult to describe in terms of valence-bond theory, it fits naturally into the framework of the delocalized bonding scheme of the polyhedral skeletal electron pair (PSEP) theory. In most, if not all cases, the structural type **2** contains an M_4 cluster with four metal–metal bonds.

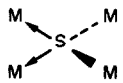
* There may be one exception to this definition. This occurs in the complex $[HPtOs_3(CO)_8(\mu_4\text{-}S)(\mu_3\text{-}S)(PPh_2C_6H_4)]_2$ which is described later in this section.



1



2



3

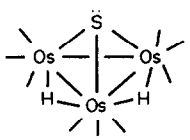
The structural type **3** contains four metal atoms arranged in a tetrahedral or distorted tetrahedral array about a centralized sulfido ligand. This sulfido ligand, viewed as an uncharged atom, serves as a six-electron donor and two of the four M—S bonds can be viewed as donor–acceptor bonds. There are no examples of type **3** sulfido ligands in the presence of six metal–metal bonds. The sulfido ligand appears to be very flexible and able to adapt to conditions imposed upon it by the arrangements of the metal atoms. For example, in the presence of M—M bonding, M—S—M bond angles as low as 65–75° are common. In the absence of M—M bonding these angles may range from 125 to 140°.[9] A compound which imposes an unprecedented degree of distortion upon a quadruply bridging sulfido ligand is $[HPtOs_3(CO)_8(\mu_4\text{-}S)(\mu_3\text{-}S)(PPh_2C_6H_4)]_2$.[7] The heavy-atom framework of the structure of this molecule is shown in Fig. 1. The quadruply bridging sulfido ligands, S_1 and S_2, are believed to serve as six-electron donors of type **3**. However, due to the highly strained polycyclic network of M_nS rings, all the metal atoms are drawn to one side of a plane which passes through the sulfido ligand. Similar highly strained geometries have been observed for carbon atoms in certain polycyclic hydrocarbon compounds, and these geometries have been described as "inverted" tetrahedral.[10]

II. SYNTHESES AND STRUCTURES

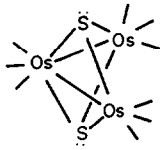
1. *Reagents and reactions*

Although a number of sulfur-containing compounds have been used in the synthesis of sulfido-transition-metal cluster compounds,[6] surprisingly few of these have been used for the synthesis of sulfido osmium carbonyl clusters.

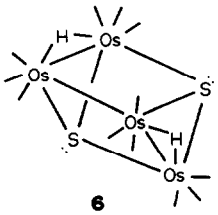
Hydrogen sulfide (H_2S) would seem to be an ideal source of sulfide, but it has not yet been used with wide success. H_2S does react with $Os_3(CO)_{12}$ at 125°C to form the cluster $Os_3(\mu\text{-}H)_2(\mu_3\text{-}S)(CO)_9$ (**4**) in nearly quantitative yields.[11] Both hydrogen atoms are transferred from the sulfur atom to the metal atoms where they bridge adjacent metal–metal bonds. The sulfido ligand serves as a triple bridge.



4



5



6

The reaction of $Os_3(CO)_{12}$ with elemental sulfur at 125°C yields compound **4** plus the compounds $Os_3(\mu_3\text{-}S)_2(CO)_9$ (**5**) and $Os_4(\mu\text{-}H)_2(\mu_3\text{-}S)_2(CO)_{12}$ (**6**).[12] Compound **5** and the selenium homologue of **6** have been characterized crystallographically. Compound **5** contains triply bridging sulfido ligands on each side of an open triangular cluster of three metal atoms.[13] The Os_4S_2 framework of **6** has the shape of a trigonal prism with only three osmium–osmium bonds, two of which contain bridging hydride ligands.[12] At temperatures greater than 200°C, the reaction yields the higher-nuclearity sulfido osmium carbonyl clusters, $Os_5(\mu_4\text{-}S)(CO)_{15}$ (**7**), $Os_7(\mu_4\text{-}S)_2(CO)_{20}$ (**8**) and $Os_{10}(\mu_4\text{-}S)_2(CO)_{23}$ (**9**).[14] These have been characterized structurally by X-ray diffraction methods. ORTEP diagrams of **7** and **8** are shown in Figs 2 and 3, respectively. Compound **7** consists of a square pyramid of five osmium atoms with a quadruply bridging sulfido ligand spanning the square base.[15] Compound **8** consists of an Os_5S_2 cluster core in the shape of a pentagonal bipyramid and has two $Os(CO)_4$ units bridging adjacent apical–equatorial edges of the cluster.[16] To date, compound **9** is the highest-nuclearity sulfido osmium carbonyl cluster that has been characterized. Its structure has been described as two square pyramids fused to two trigonal bipyramids that have one Os—Os edge in common.[14] Quadruply bridging sulfido

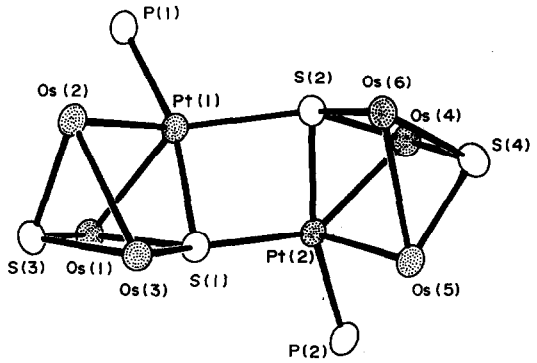
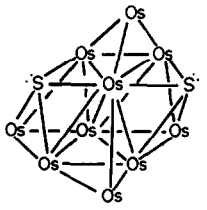


Fig. 1. An ORTEP drawing of the heavy-atom structure for the compound $[HPtOs_3(CO)_8(\mu_4\text{-}S)(\mu_3\text{-}S)(PPh_2C_6H_4)]_2$ showing the inverted tetrahedral geometry of the sulfido ligands S(1) and S(2). Pt(1)–S(1)–Os(1) = 68.3(2)°, Pt(1)–S(1)–Os(3) = 102.86(2)°, Os(1)–S(1)–Os(3) = 97.8(2)°, Pt(1)–S(1)–Pt(2) = 85.0(2), Pt(2)–S(1)–Os(1) = 116.2(2)°, Pt(2)–S(1)–Os(3) = 145.3(3)°, Pt(2)–S(2)–Os(4) = 67.3(2)°, Pt(2)–S(2)–Os(6) = 101.2(2)°, Os(4)–S(2)–Os(6) = 97.6(2)°, Pt(2)–S(2)–Pt(1) = 83.8(2)°, Pt(1)–S(2)–Os(4) = 135.0(3)°, Pt(1)–S(2)–Os(6) = 122.2(2)°.

ligands span the square bases of the two square pyramidal units.



9

Carbon disulfide (CS_2) reacts with $Os_3(CO)_{12}$ to form the compound $Os_3(\mu_3\text{-}S)_2(CO)_8(CS)$ (**10**) which is structurally analogous to **5** but contains a terminally coordinated thiocarbonyl ligand in place of one of the carbonyl ligands.[17] CS_2 reacts with the lightly-stabilized cluster $Os_3(\mu\text{-}H)_2(\mu_3\text{-}S)(CO)_8(NCMe)$ to form the compound $Os_3(\mu\text{-}H)_2(\mu_3\text{-}S)_2(CO)_8(CS)$ (**11**).[18] Compound **11** is an open cluster with two triply bridging sulfido ligands, a bridging hydride ligand across

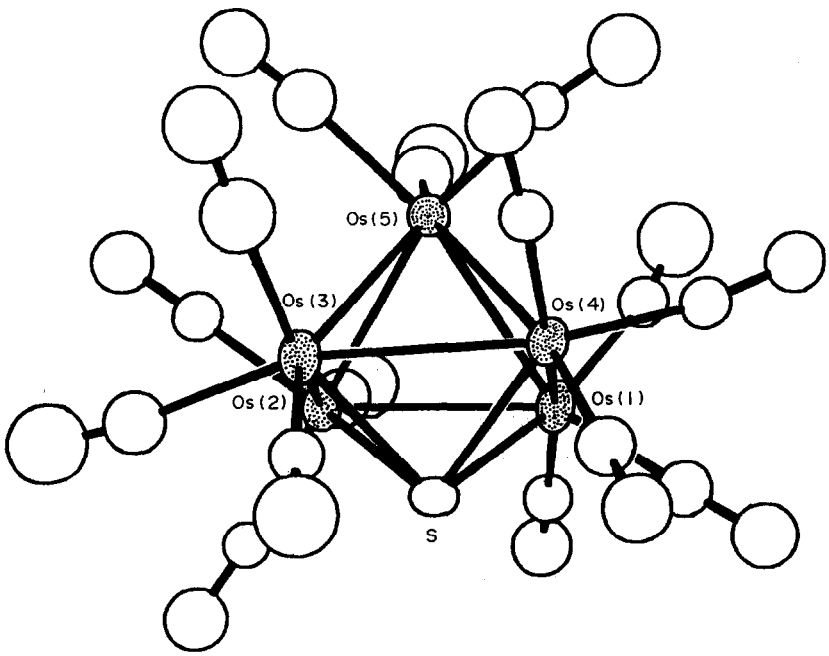


Fig. 2. An ORTEP diagram of $Os_5(\mu_4\text{-}S)(CO)_{15}$ (**7**) showing 50% probability thermal ellipsoids.

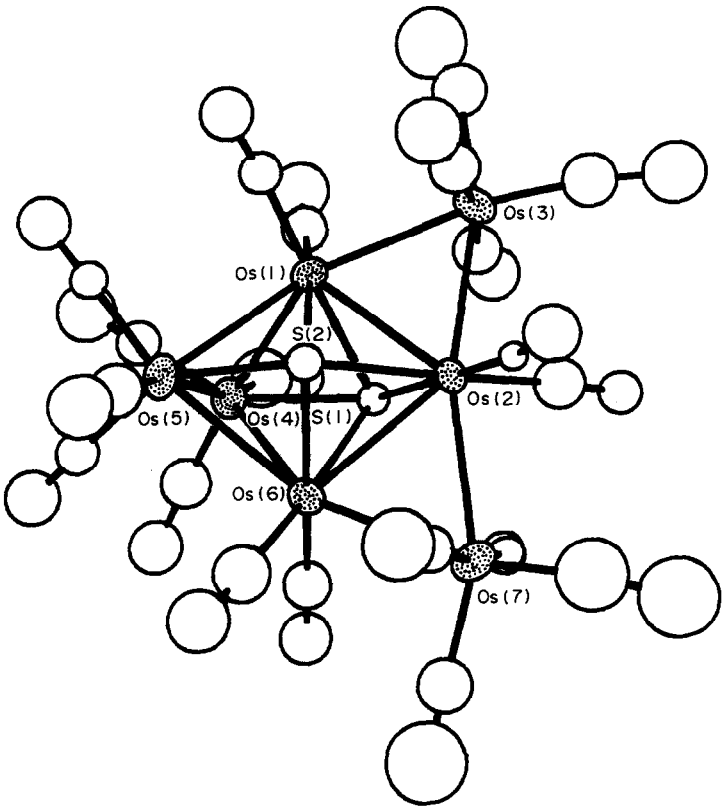
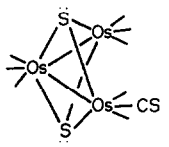
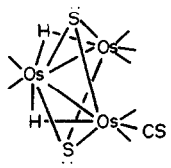


Fig. 3. An ORTEP diagram of $Os_7(\mu_4\text{-}S)_2(CO)_{20}$ (**8**) showing 50% probability thermal ellipsoids.

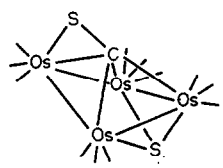
each of the two metal–metal bonds and one linear terminal thiocarbonyl ligand. The reaction of $Os_6(CO)_{18}$ with CS_2 at 165°C under CO pressure yields compounds **5**, **10** and the new compound $Os_4(\mu_3\text{-}S)(\mu_4\text{-}CS)(CO)_{12}$ (**12**) in 8% yield.[19] The structure of **12** consists of four osmium atoms arranged in the form of a puckered square. Three of the osmium atoms are bridged by a triply bridging sulfido ligand. The thiocarbonyl ligand serves as a quadruple bridge with the carbon atom bonded to all four osmium atoms and the sulfur bonded to only one. The C—S bond length, 1.757(18) Å, is slightly shorter than a C—S single bond length (i.e. 1.81 Å).



10

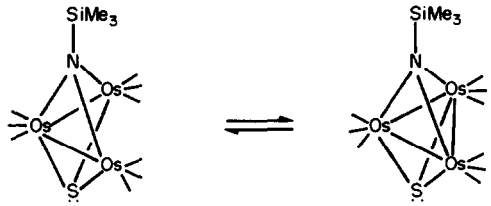


11



12

Süss-Fink *et al.*[20] have reported that the sulfurdimide, $Me_3SiN{=}S{=}NSiMe_3$, reacts with $Os_3(CO)_{12}$ at 125°C to give the compound $Os_3(\mu_3\text{-}S)(\mu_3\text{-}NSiMe_3)(CO)_9$ (**13**) in 13% yield. The crystal structure analysis of **13** reveals an open triangular structure similar to that of **5** but it contains a triply bridging amido ligand, Me_3SiN, and one triply bridging sulfido ligand. The temperature-dependent ^{13}C NMR spectrum of **13** in solution reveals the reversible formation of a second species at high temperature in which all the carbonyl ligands are either equivalent or are rapidly averaged. This was interpreted in terms of an isomeric species, **14**, which contains three metal–metal bonds. Although the structure **14** could explain the spectral observations, it should be pointed out that this structure does not adhere to currently accepted cluster bonding theories. Thus, until further evidence is presented it should be regarded as tentative.



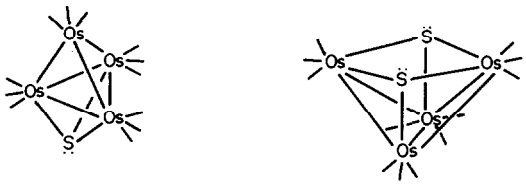
13 14

Of all the routes to sulfido osmium carbonyl clusters, perhaps the most productive, are those which involve the desulfurization of organosulfur ligands. For example, the arylthiolatotriosmium-decarbonylhydride clusters readily eliminate arene when heated to 150°C to yield a variety of sulfido osmium carbonyl clusters [i.e. eqn (1)]:[21]

$$\underset{\mathbf{15}}{Os_3(\mu\text{-H})(\mu\text{-SPh})(CO)_{10}} \xrightarrow[-C_6H_6]{150^\circ C} \underset{\mathbf{5}}{Os_3(\mu_3\text{-S})_2(CO)_9} + \underset{\mathbf{16}}{Os_4(\mu_3\text{-S})(CO)_{12}}$$

$$+ \underset{\mathbf{17}}{Os_4(\mu_3\text{-S})_2(CO)_{12}} + \underset{\mathbf{7}}{Os_5(\mu_4\text{-S})(CO)_{15}} + \underset{\mathbf{18}}{Os_6(\mu_4\text{-S})(\mu_3\text{-S})(CO)_{16}} + \underset{\mathbf{8}}{Os_7(\mu_4\text{-S})_2(CO)_{20}}. \quad (1)$$

The yields of the various products are very sensitive to the reaction conditions. For example, when pyrolyzed in the absence of solvent at temperatures greater than 200°C, only compounds **5**, **16**, **7** and **8** are obtained.[16] When pyrolyzed at 160°C under 100 bar CO pressure, only compound **5** plus three equivalents of $Os(CO)_5$ is obtained.[15] Compounds **16**–**18** have been characterized by X-ray diffraction methods. Compound **16** consists of a tetrahedral cluster of four osmium atoms with a triply bridging sulfido ligand on one of the Os_3 faces.[22] Compound **17** consists of a "butterfly" tetrahedral cluster of



16 17

four osmium atoms with triply bridging sulfido ligands across the two open triangular faces.[21] The structures and bonding of **16** and **17** will be described further in Section III. An ORTEP diagram of compound **18** is shown in Fig. 4.[21] The molecule consists of a square pyramid of five osmium atoms with a quadruply bridging sulfido ligand spanning the square base and an $Os(CO)_3$ group and a triply

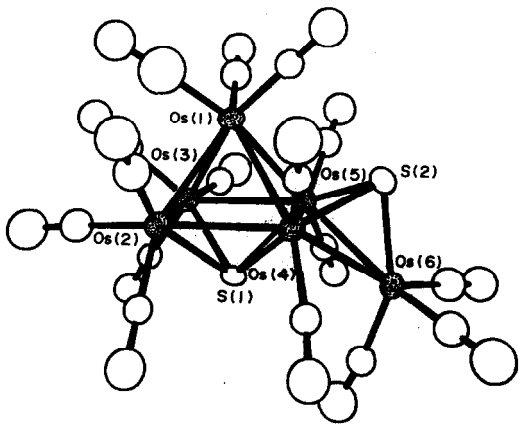


Fig. 4. An ORTEP diagram of $Os_6(\mu_4\text{-S})(\mu_3\text{-S})(CO)_{16}$ (**18**) showing 50% probability thermal ellipsoids.

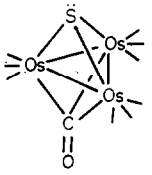
bridging sulfido ligand bridging an edge of the square base. The independent syntheses of compounds **7**, **8** and **16–18**, as well as related compounds suggest mechanisms for their formation. These are described in Section II.2(a).

When irradiated under a rapid purge of CO, compound **15** loses benzene and yields the compound $Os_3(\mu_3\text{-}S)(\mu_3\text{-}CO)(CO)_9$ (**19**) [eqn (2)]:[23]

$$Os_3(\mu\text{-}H)(\mu\text{-}SPh)(CO)_{10} \xrightarrow[-C_6H_6]{h\nu/CO} Os_3(\mu_3\text{-}S)(\mu_3\text{-}CO)(CO)_9. \quad (2)$$

19

Compound **19** consists of a triangular cluster of three osmium atoms with a triply bridging sulfido ligand one side of the Os_3 plane and a triply bridging carbonyl ligand on the other side.



19

Thermal degradation of the benzylthiolato cluster, $Os_3(\mu\text{-}H)(\mu\text{-}SBz)(CO)_{10}$ (**20**) occurs apparently by two competing mechanisms.[24] One which is analogous to that found for **15** results in the elimination of toluene and the formation of compounds **5**, **16** and **8**. The other mechanism results in formation of dibenzyl and the two isomeric hexaosmium dihydro clusters $Os_6(\mu\text{-}H)_2(\mu_4\text{-}S)(\mu_3\text{-}S)(CO)_{17}$ (**21** and **22**). ORTEP diagrams of **21** and **22** are shown in Figs 5 and 6. The red isomer **21** contains a quadruply bridging sulfido ligand of type **3** while the green isomer **22** contains a quadruply bridging sulfido ligand of type **2** and an extended planar array of six osmium atoms. The formation of dibenzyl and dihydrido hexaosmium species suggests a radical mechanism involving an initial homolysis of the sulfur–carbon bond in **20**.

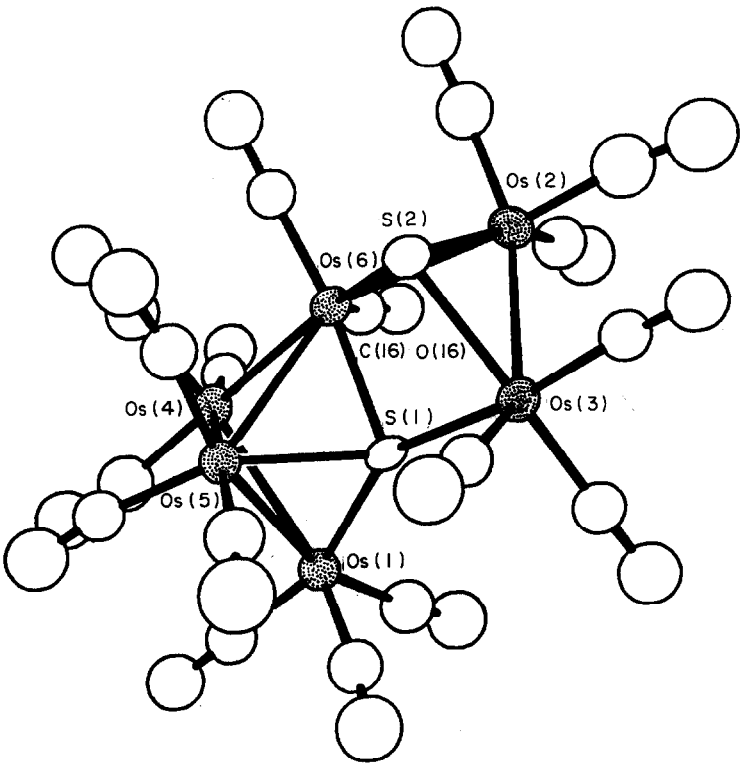


Fig. 5. An ORTEP diagram of the red isomer of $Os_6(\mu\text{-}H)_2(\mu_4\text{-}S)(\mu_3\text{-}S)(CO)_{17}$ (**21**) showing the quadruply bridging sulfido ligand S(1) of type **3**.

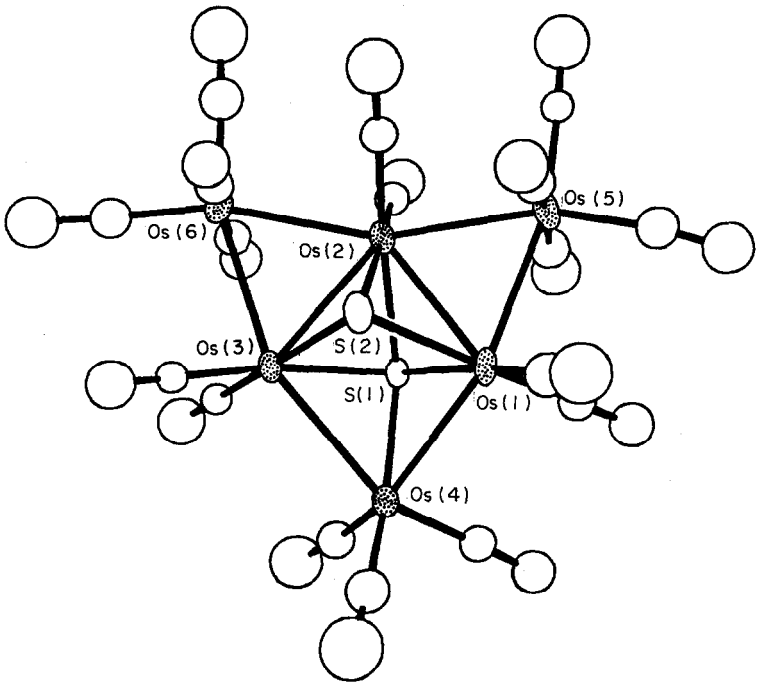


Fig. 6. An ORTEP diagram of the green isomer of $Os_6(\mu\text{-}H)_2(\mu_4\text{-}S)(\mu_3\text{-}S)(CO)_{17}$ (**22**) showing the quadruply bridging sulfido ligand S(1) of type **2**.

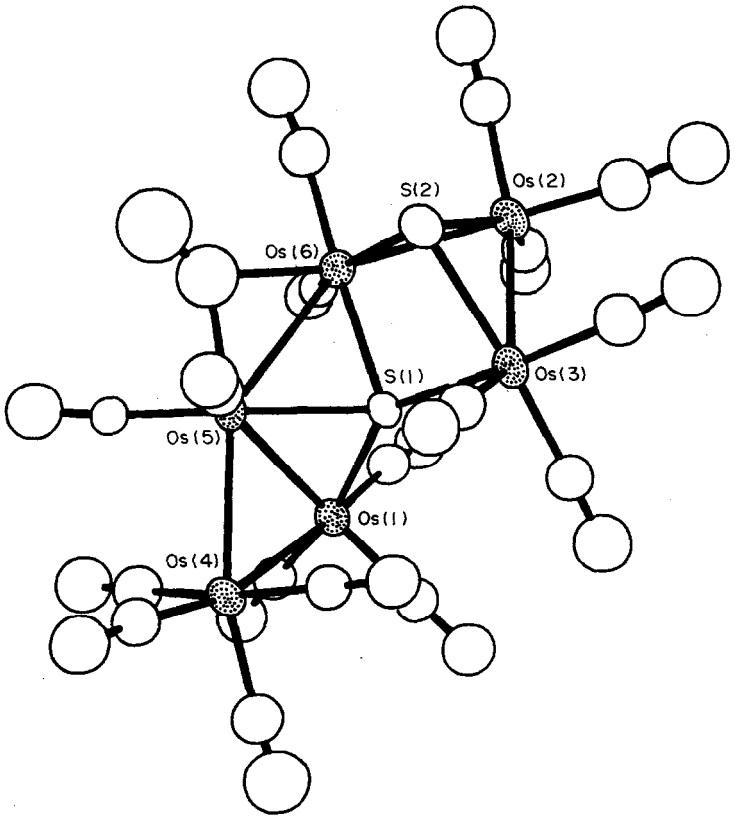
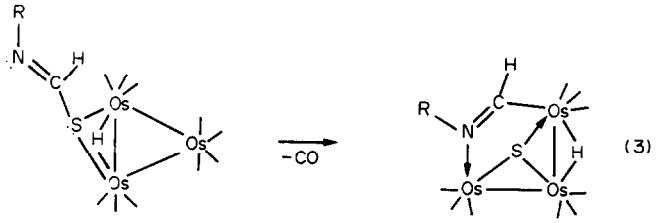


Fig. 7. An ORTEP diagram of $Os_6(\mu\text{-}H)_2(\mu_4\text{-}S)(\mu_3\text{-}S)(CO)_{18}$ (**23**) which is a precursor to $Os_6(\mu\text{-}H)_2(\mu_4\text{-}S)(\mu_3\text{-}S)(CO)_{17}$ (**21**).

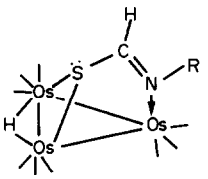
The principal product formed when compound **20** is irradiated at 25°C is the compound $Os_6(\mu\text{-}H)_2(\mu_4\text{-}S)(\mu_3\text{-}S)(CO)_{18}$ (**23**). An ORTEP diagram of **23** is shown in Fig. 7. It is similar to **21**, and was shown to be a precursor to **21** by its thermal decarbonylation.

Thioformamido and dithioformato ligands can serve as precursors for sulfido ligands [eqns (3)[25] and (4)[26]]:

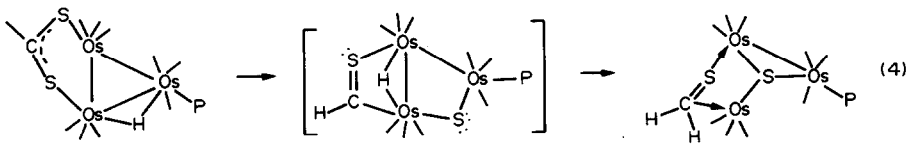


(3)

24 **25**



26



(4)

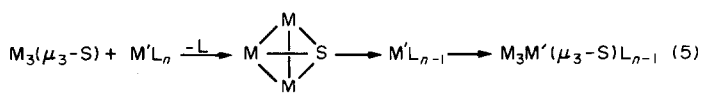
27 **A** **28**

The desulfurization of the thioformamido complex in **24** was found to proceed via a decarbonylated intermediate **26** which was isolated and shown to contain a triply bridging thioformamido ligand. Structural analyses of **24** and **26** showed that the C—S bond length was significantly longer than the C—S bond length of thioformamido ligands in complexes where the sulfur atom was not in a bridging position. Thus, it was inferred that *the bridging environment induced a weakening of the* C—S *bond and this facilitated the bond cleavage.* In ligand-splitting reactions such as these both fragments of the ligand usually remain coordinated to the cluster.

The desulfurization of the dithioformato ligand in **27** probably proceeds via an intermediate species such as **A** containing a thioformyl ligand, but this was not observed. The species **28** which contains a bridging thioformaldehyde ligand was isolated. This could be formed by a reductive elimination of C—H from the proposed intermediate.

2. *Cluster condensation reactions*

(a) *Homonuclear clusters.* The triply bridging sulfido ligand with its lone pair of electrons would seem to be an ideal species for use in cluster size-expansion reactions. By using the lone pair of electrons to form coordinative interactions to electron-deficient metal groupings, the sulfido ligand could facilitate the entry of metal-containing units into the cluster [eqn (5)]:



(5)

B **C**

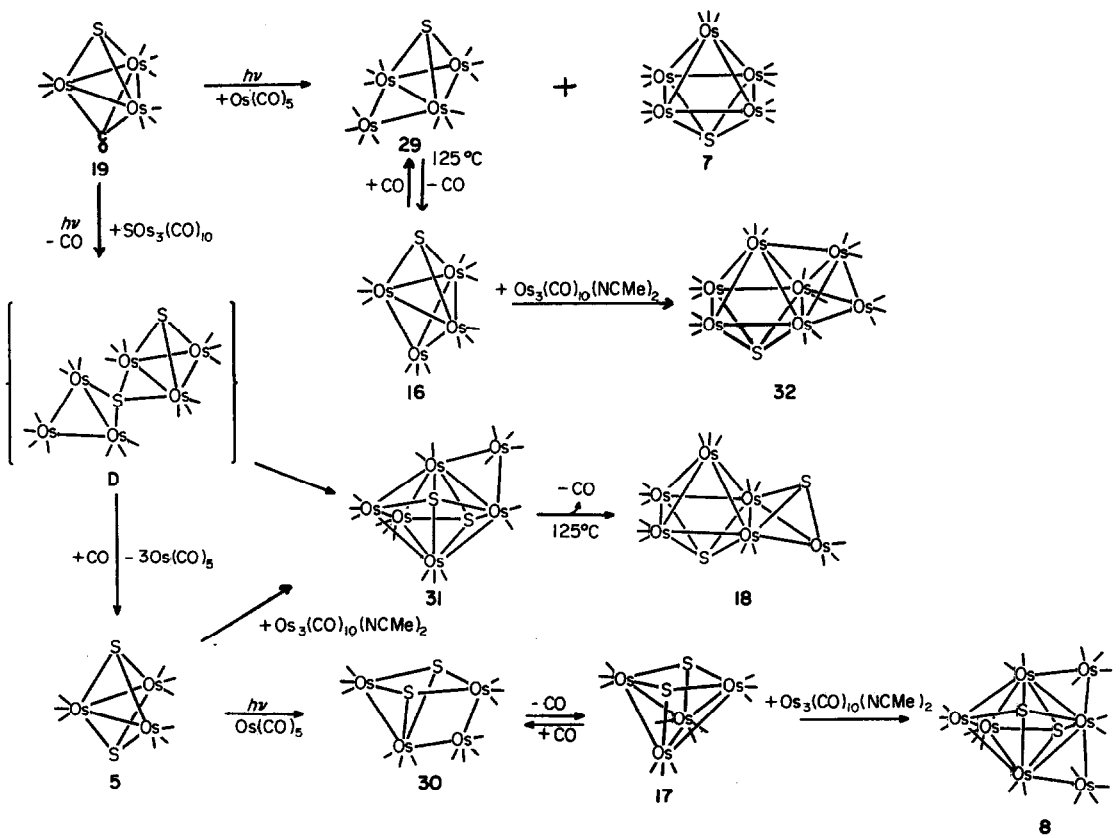
The paucity of isolated intermediates such as **B** suggests that these species are less stable than their rearrangement products **C**.

The low-nuclearity sulfido clusters **5** and **19** have served as starting points for these aggregation or *condensation* reactions. Osmium pentacarbonyl which is readily decarbonylated to the reactive intermediate $Os(CO)_4$ when irradiated has been used as a source of monoosmium fragments. The lightly stabilized complex $Os_3(CO)_{10}(NCMe)_2$ has been found to serve as a reagent for the addition of triosmium groupings. By using this methodology most of the cluster complexes synthesized in low yields in the pyrolysis reactions described in Section II.1 have now been made in much higher yields. In addition, a number of new complexes that were not observed in the pyrolysis reactions have been isolated. Some of these can be converted into the pyrolysis products and thus suggest mechanisms for their formation.

The irradiation of solutions of **19** and $Os(CO)_5$ has resulted in the formation of the higher-nuclearity clusters, **29** and **7** in 40 and 3% yields, respectively (see Scheme 1). The structure of **29** consists of a nearly planar butterfly cluster of four osmium atoms with a triply bridging sulfido ligand on one triangular face.[15] When heated to 125°C, **29** loses 1 mol of CO and condenses to **16** quantitatively.

When solutions of **5** and $Os(CO)_5$ are irradiated the compound $Os_4(\mu_3\text{-}S)_2(CO)_{13}$ (**30**) is formed in 40% yield[16] (see Scheme 1). The structure **30** consists of a planar group of four osmium atoms connected by three Os—Os bonds.[27] Triply bridging sulfido ligands are symmetrically disposed about the Os_4 plane. When heated to 68°C, **30** loses 1 mol of CO quantitatively and the cluster closes to form **17**.

The reaction of **5** with $Os_3(CO)_{10}(NCMe)_2$ yields the new hexaosmium cluster $Os_6(\mu_4\text{-}S)_2(CO)_{17}$ (**31**) in 29% yield.[28] The structure of **31** is shown in Fig. 8. The molecule is very similar to **8** and contains an Os_5S_2 cluster in the form of a pentagonal bipyramid but has only one $Os(CO)_4$ group bridging an apical–equatorial edge.[28] This compound was also prepared in good yield by the UV irradiation of **19** in an inert solvent. The condensation of 2 mol of **19** via the unobserved intermediate **D** is shown in Scheme 1. An intermediate such as **D** is probably also traversed in the formation of **5** as observed in the pyrolysis of **15** under CO pressure.[15] When heated to 125°C compound **31** quantitatively loses 1 mol of CO to yield **18**. The CO ligand that is lost probably comes from th CO-rich bridging $Os(CO)_4$ grouping. A rearrangement that would readily produce condensation of **31** to **18** is shown in Scheme 2.[28]



Scheme 1.

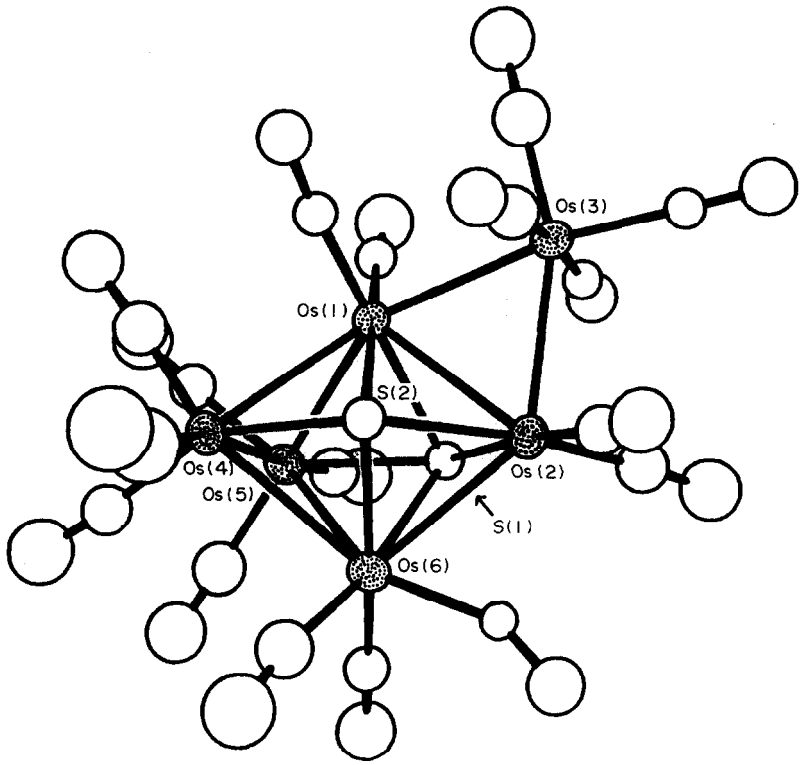
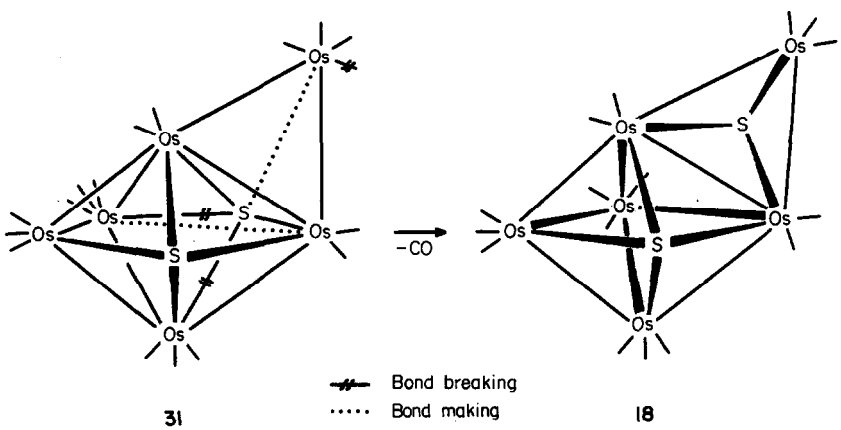


Fig. 8. An ORTEP diagram of $Os_6(\mu_4\text{-}S)_2(CO)_{17}$ (**31**) which is a precursor to $Os_6(\mu_4\text{-}S)(\mu_3\text{-}S)(CO)_{16}$ (**18**).

The reaction of **16** with $Os_3(CO)_{10}(NCMe)_2$ in refluxing octane yields the highly condensed heptanuclear cluster $Os_7(\mu_4\text{-}S)(CO)_{19}$ (**32**) in 23% yield.[22] No intermediates have been isolated. The structure of **32** is shown in Fig. 9. The structure is best described as a fused combination of a square pyramid of five osmium atoms and a trigonal bipyramid of five osmium atoms with one triangular face [Os(1)–Os(2)–Os(4)] in common. The base of the square pyramid is spanned by a quadruply bridging sulfido ligand of type **2**.

The addition of $Os_3(CO)_{10}(NCMe)_2$ to **17** leads to the formation of **8** in 16% yield.[16] Curiously, it was found that compound **8** could not be prepared by the irradiation of solutions of **31** and $Os(CO)_5$.

It has been found that $Os_3(CO)_{10}(NCMe)_2$ will add to **19** to form the sequence of products $Os_6(\mu_3\text{-}S)(CO)_{19}$ (**33**) and $Os_6(\mu_4\text{-}S)(CO)_{17}$ (**34**). Compound **33** is converted into **34** in 23% yield at



Scheme 2.

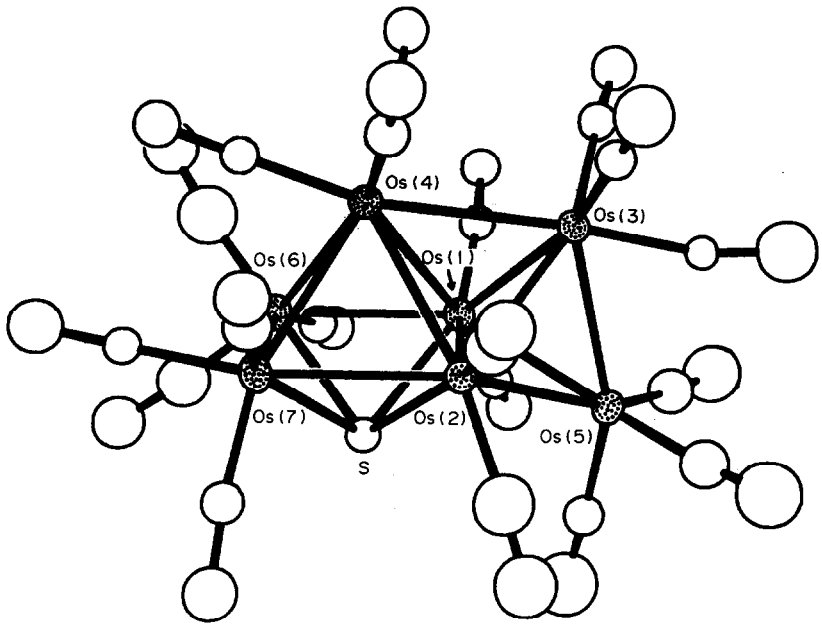


Fig. 9. An ORTEP diagram of the fused cluster $Os_7(\mu_4\text{-}S)(CO)_{19}$ (**32**) showing 50% probability thermal ellipsoids.

110°C.[29] The molecular structure of **33** is shown in Fig. 10. The molecule consists of a butterfly tetrahedral cluster of four osmium atoms with a triply bridging sulfido ligand across one of the open triangular faces. $Os(CO)_4$ groupings bridge the two edges of that same open triangular face. The structure of **34** is shown in Fig. 11. This molecule consists of a square pyramid of five osmium atoms with a quadruply bridging sulfido ligand over the square base and a capping $Os(CO)_3$ group on one of the triangular faces. The transformation of **33** into **34** involves the loss of 2 mol of CO. A proposed rearrangement which involves the loss of one CO from each of the bridging $Os(CO)_4$ units is shown in Scheme 3.

When irradiated under a rapid purge with nitrogen, compound **5** undergoes a self-condensation and forms the green dimer $[Os_3(\mu_3\text{-}S)_2(CO)_8]_2$ (**35**). Compound **35** has a most unusual structure which is shown in Fig. 12. The central portion of the molecule consists of a butterfly tetrahedron of four osmium atoms [Os(1)–Os(2)–Os(3)–Os(4)] with a dihedral angle of 136°. Exterior $Os(CO)_3$ groups are attached to the hinge atoms Os(1) and Os(2). Pairs of triply bridging sulfido ligands bridge opposite edges of the butterfly tetrahedron and extended to the exterior $Os(CO)_3$ groups. The formation of **35**

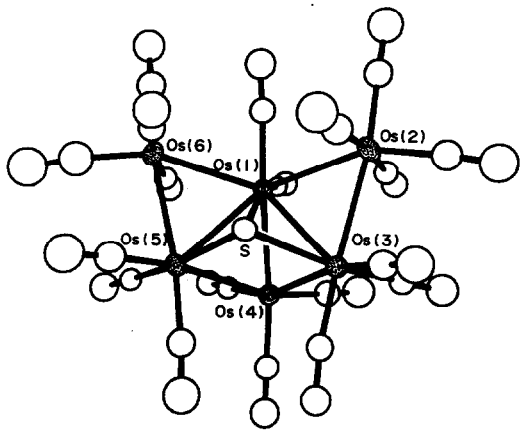


Fig. 10. An ORTEP diagram of $Os_6(\mu_3\text{-}S)(CO)_{19}$ (**33**) showing 50% probability thermal ellipsoids.

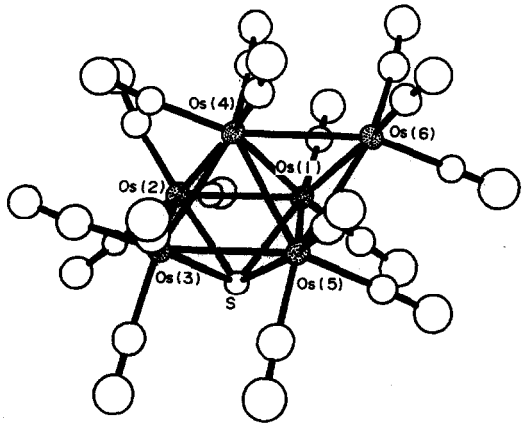
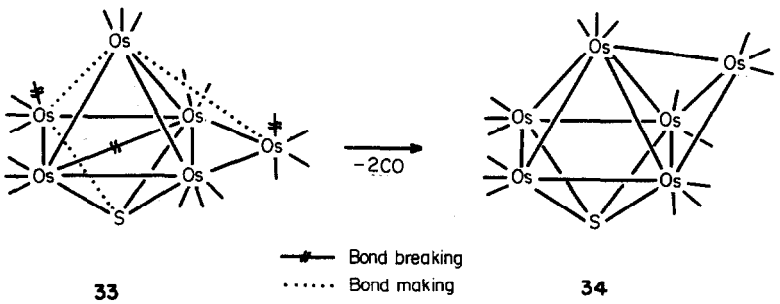


Fig. 11. An ORTEP diagram of the condensed cluster $Os_6(\mu_4\text{-}S)(CO)_{17}$ (34).



Scheme 3.

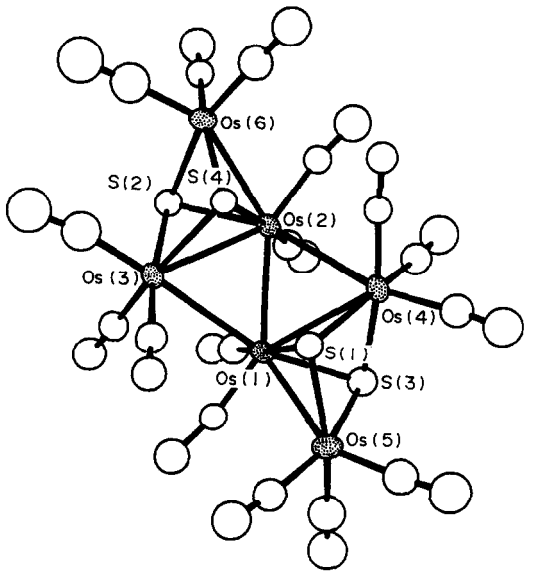
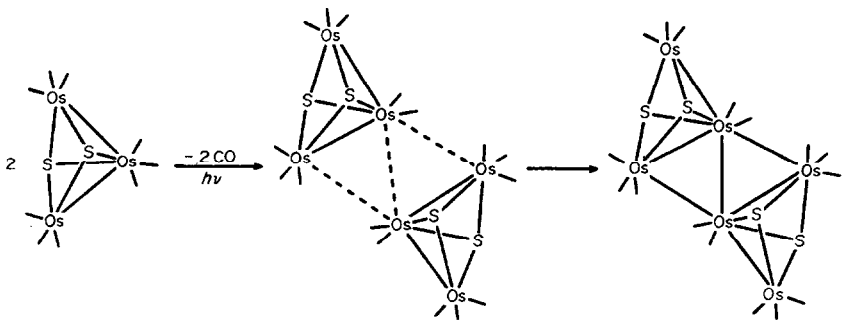


Fig. 12. An ORTEP diagram of the dimer $[Os_3(\mu_3\text{-}S)_2(CO)_8]_2$ (35). Os(1)–Os(2) = 2.834(1) Å, Os(1)–Os(3) = 2.973(1) Å, Os(1)–Os(4) = 2.941(1) Å, Os(2)–Os(3) = 2.957(1) Å, Os(2)–Os(4) = 2.971(1) Å, Os(1)–Os(5) = 2.789(1) Å, Os(2)–Os(6) = 2.792(1) Å.



Scheme 4.

can be viewed as a back-to-back coupling of two $Os_3(\mu_3\text{-}S)_2(CO)_8$ units derived from **5** by the loss of one CO ligand from the central osmium atom (see Scheme 4).

The self-condensation of compound **25** provides an interesting sequence of products that reveals in great detail the importance of the bridging sulfido ligand to the cluster growth process. When heated to 125°C compound **25** is decarbonylated and yields a mixture of several hexaosmium compounds.[30] Of particular importance are the compounds of formula $Os_6(\mu\text{-}H)_2(\mu_4\text{-}S)(\mu_3\text{-}S)(\mu\text{-}HC{=}NR)_2(CO)_{17}$ (**36**) and $Os_6(\mu\text{-}H)_2(\mu_4\text{-}S)(\mu_3\text{-}S)(\mu\text{-}HC{=}NR)_2(CO)_{16}$ (**37**) (R=C_6H_5 and *p*-C_6H_5F). The former exists in two separable isomeric forms. The latter exists in three separable isomeric forms. Compounds **36** can be converted into **37** by further heating at 125°C. An ORTEP diagram of one of the isomers of **36** is shown in Fig. 13. The molecule consists of two open triosmium clusters linked by a quadruply bridging sulfido ligand of type **3**. The Os(1)–Os(2)–Os(3) grouping contains 10 CO ligands which is one more than it contained in the form **25**. The Os(4)–Os(5)–Os(6) grouping contains only seven CO ligands. It is not known if the CO ligand acquired by the Os(1)–Os(2)–Os(3) group was transferred intramolecularly or intermolecularly from the Os(4)–Os(5)–Os(6) group. The most important feature of the molecule is the quadruply bridging sulfido ligand S(1) which has brought the two triosmium groups into an

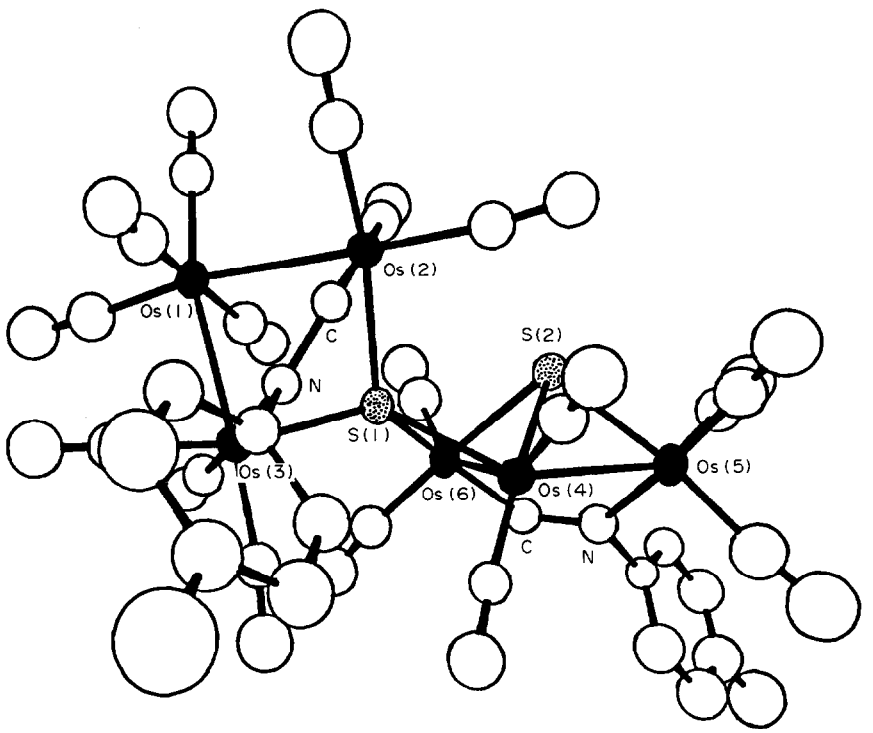


Fig. 13. An ORTEP diagram of one of the isomers of $Os_6(\mu\text{-}H)_2(\mu_4\text{-}S)(\mu_3\text{-}S)(\mu\text{-}HC{=}NC_6H_4F)_2(CO)_{17}$ (**36**). The metal atoms are blackened completely.

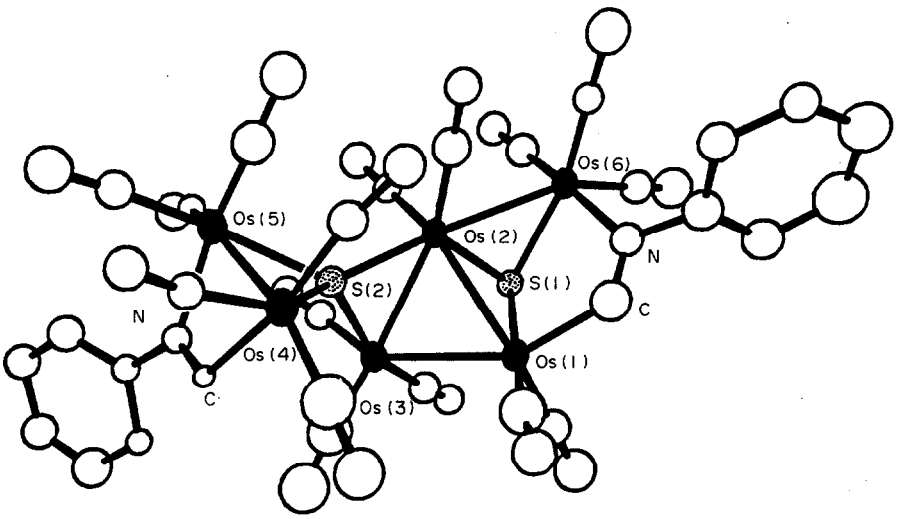


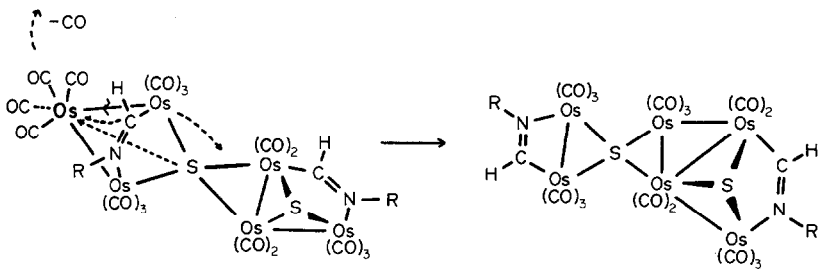
Fig. 14. An ORTEP diagram of one of the isomers of $Os_6(\mu\text{-}H)_2(\mu\text{-}HC{=}NC_6H_5)_2(CO)_{16}$ (**37**). The metal atoms are blackened completely.

inseparable relationship. No metal–metal bonds were made and none were broken in the conversion of **25** into **36**.

An ORTEP diagram of **37** is shown in Fig. 14. This molecule consists of groups of four and two osmium atoms. A quadruply bridging sulfido ligand S(2) joins these two groups. The formation of **37** from **36** has occurred by the transfer of one osmium atom from one group of three metal atoms to the other group of three. In this transformation there is a loss of one CO ligand and a net increase by one in the number of metal–metal bonds. The transformation of **36** into **37** must have involved several steps. A mechanism that shows the essential atomic and ligand shifts is shown in Scheme 5.

When heated to 150°C, compound **37** loses another CO ligand plus an equivalent of H_2 and forms the compound $Os_6(\mu_4\text{-}S)_2(\mu\text{-}HC{=}NR)_2(CO)_{15}$ (**38**). An ORTEP diagram of the molecular structure of **38** is shown in Fig. 15. This molecule consists of a butterfly tetrahedron of four osmium atoms with external $Os(CO)_3$ groups attached to each of the "hinge" atoms of the butterfly tetrahedron. Quadruply bridging sulfido ligands bridge the open triangular faces of the butterfly tetrahedron and extend to the external $Os(CO)_3$ groups. These sulfido ligands are highly strained and conform to the definition of "inverted" tetrahedra (see Section I). There is a bridging carbonyl ligand across the Os(2)–Os(3) hinge bond. A transformation that shows the rearrangements implicit in the conversion of **37** into **38** is given in Scheme 6. The most important feature is that the condensation process has progressed further and at this stage a new cluster grouping (the butterfly tetrahedron) that is quite distinct from the two original triosmium units has assembled and has become a focal point of the molecule.

(b) *Mixed-metal clusters.* Some efforts have been made to investigate the potential for the synthesis of mixed-metal cluster compounds by adding groupings with transition elements other than osmium to



36 **37**

Scheme 5.

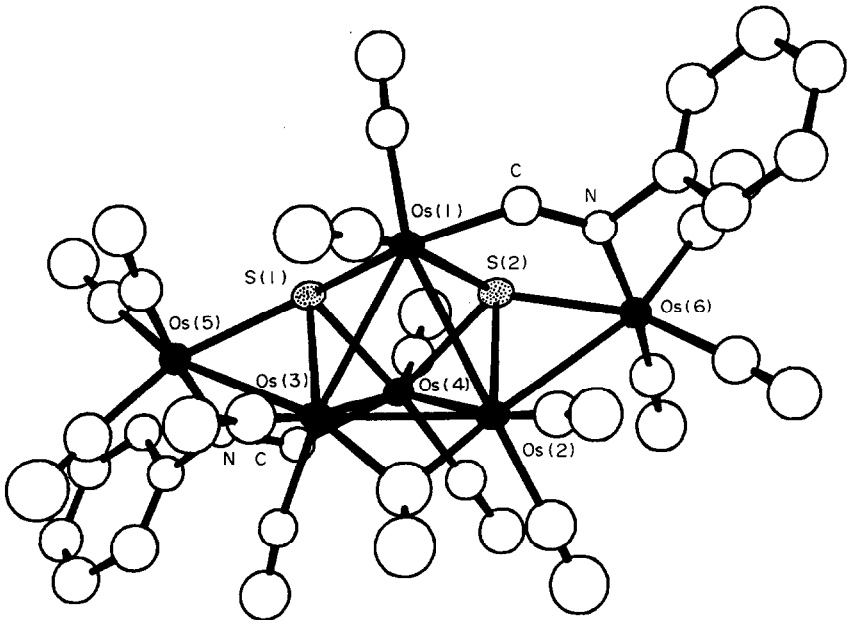
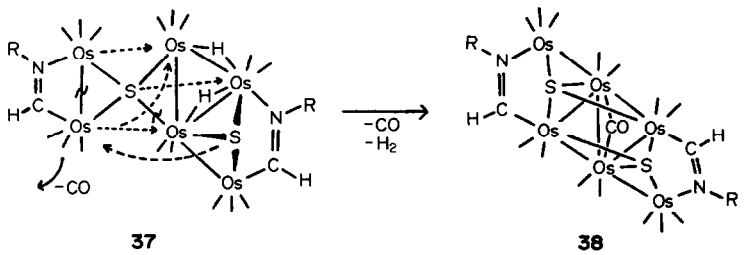


Fig. 15. An ORTEP diagram of $Os_6(\mu_4\text{-}S)_2(\mu\text{-}HC{=}NC_6H_5)_2(CO)_{15}$ (**38**). The metal atoms are blackened completely.

the sulfido osmium clusters described above. These preliminary studies have been quite successful. The groupings that have received the most attention are platinum phosphine species and tungsten carbonyl complexes. Platinum phosphine complexes are labile and usually add to the sulfido osmium clusters smoothly at room temperature. The tungsten carbonyl complexes are less reactive and usually require application of UV irradiation to initiate the reactions. The reactions of mononuclear metal species with the clusters results usually in the addition of only one metal unit.

The reactions of **19** with $Pt(PMe_2Ph)_4$ yields four tetranuclear products. These are $PtOs_3(\mu_3\text{-}S)(CO)_{10}(PMe_2Ph)_2$ (**39**), $PtOs_3(\mu_3\text{-}S)(CO)_9(PMe_2Ph)_3$ (**40**), $PtOs_3(\mu_3\text{-}S)(CO)_9(PMe_2Ph)_2$ (**41**) and $PtOs_3(\mu_3\text{-}S)(CO)_8(PMe_2Ph)_3$ (**42**).[31] The last two can be prepared from the first two, in order, by thermal decarbonylation. An ORTEP diagram of **39** is shown in Fig. 16. The molecule consists of a planar butterfly tetrahedron (dihedral angle = 177°) of three osmium and one platinum atoms. The platinum atom contains only two phosphine ligands and the sulfido ligand bridges a $PtOs_2$ triangular group instead of an Os_3 group as it did in **19**. Compound **40** is structurally analogous but contains an $Os(CO)_3(PMe_2Ph)$ group instead of the $Os(CO)_4$ group in **39**.[31] Of the two decarbonylation products, only compound **42** has been characterized structurally.[31] An ORTEP diagram of **42** is shown in Fig. 17. This molecule consists of a closed tetrahedral cluster of three osmium and one platinum atoms, but in this case the sulfido ligand bridges an Os_3 triangle. Compound **41** is believed to be structurally analogous to **42**. A mechanism that accounts for the formation of this sequence of products is shown in Scheme 7. It is believed that an interaction of the sulfido ligand



37 **38**

Scheme 6.

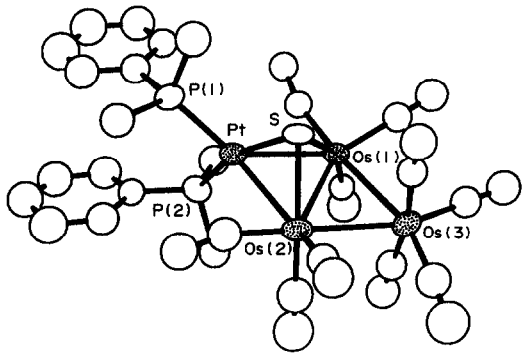


Fig. 16. An ORTEP diagram of $PtOs_3(\mu_3\text{-}S)(CO)_{10}(PMe_2Ph)_2$ (**39**) showing 50% probability thermal ellipsoids.

with the platinum moiety is an important first step in the reaction. It should be noted that the facile synthesis of the mixed-metal clusters **39–42** contrasts sharply with similar reactions in which no sulfido ligands are present. For example, the reaction of $Os_3(CO)_{12}$ with $Pt(PR_3)_4$ yields only phosphine-substituted derivatives of $Os_3(CO)_{12}$.[32]

The irradiation of solutions of **19** and $W(CO)_5(PMe_2Ph)$ in hexane solvent leads to formation of the

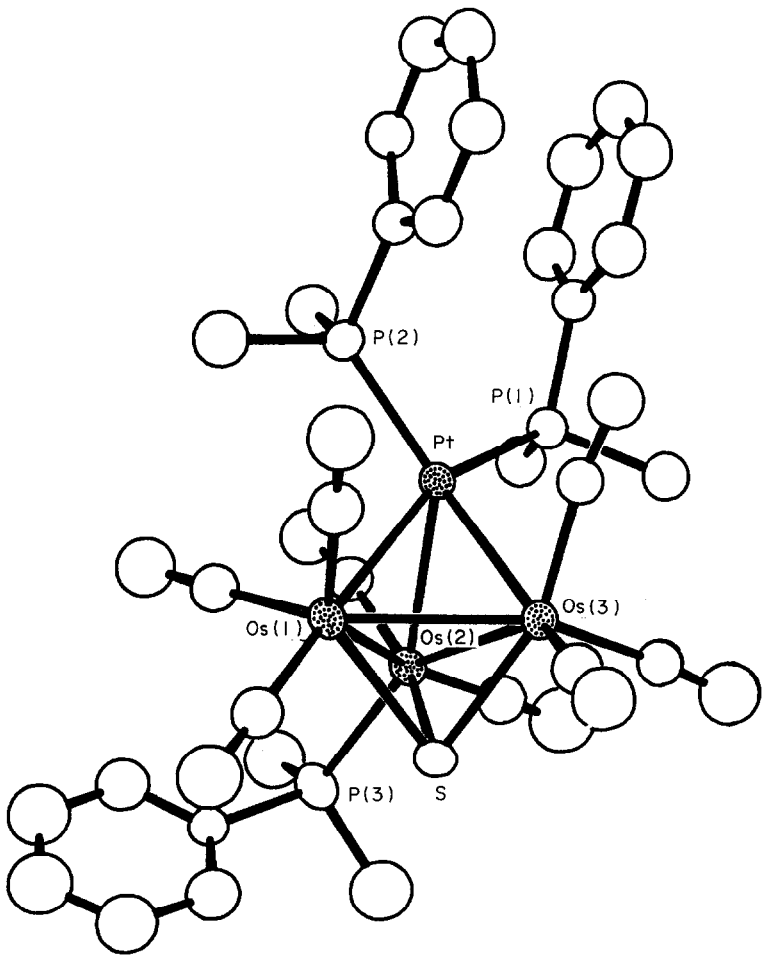
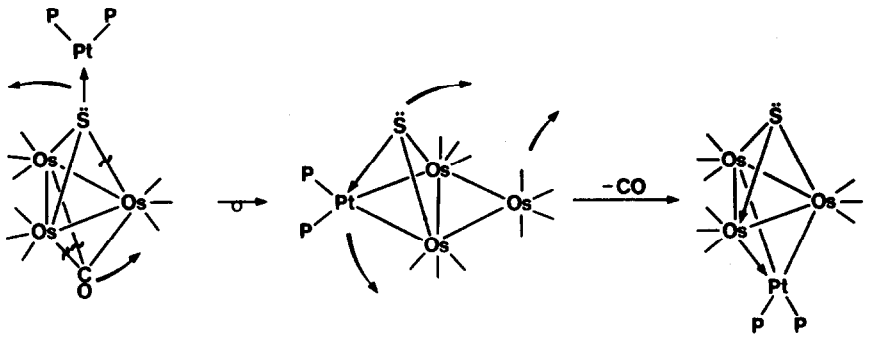
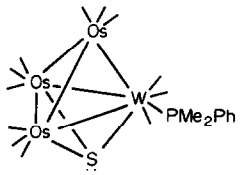


Fig. 17. An ORTEP diagram of $PtOs_3(\mu_3\text{-}S)(CO)_8(PMe_2Ph)_3$ (**42**) showing 50% probability thermal ellipsoids. Os(1)–Pt = 2.853(1) Å, Os(2)–Pt = 2.740(1) Å, Os(3)–Pt = 2.766(1) Å, Os(1)–Os(2) = 2.816(1) Å, Os(1)–Os(3) = 2.770(1) Å, Os(2)–Os(3) = 3.064(1) Å.



Scheme 7.

mixed tungsten–osmium cluster $Os_3W(\mu_3\text{-}S)(CO)_{11}(PMe_2Ph)_2$ (**43**) in 27% yield. The molecule consists of a closed tetrahedral cluster with the sulfido ligand bridging an Os_2W triangular face.[33] The mechanism of formation of **43** has not been established yet.



43

Compound **5** reacts with $Pt(PPh_3)_2C_2H_4$ to give two tetranuclear products $PtOs_3(\mu_3\text{-}S)_2(CO)_9(PPh_3)L$ (**44**) (L = CO) and **45** (L = PPh_3) and a PPh_3 substitution product of **5**. Compound **44** has acquired one CO ligand, and its yield is significantly increased when the reaction is performed under a CO atmosphere. The structure of **44** is shown in Fig. 18. The molecule contains four metal–metal bonds. Three of these exist in a triangular $PtOs_2$ group. The fourth links an $Os(CO)_3$ group to

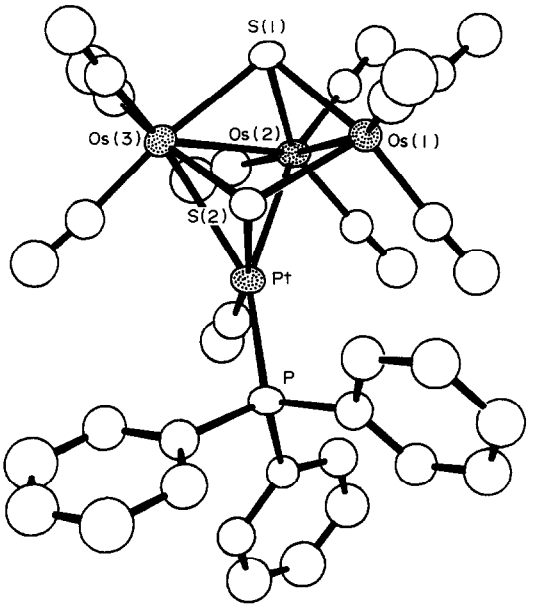
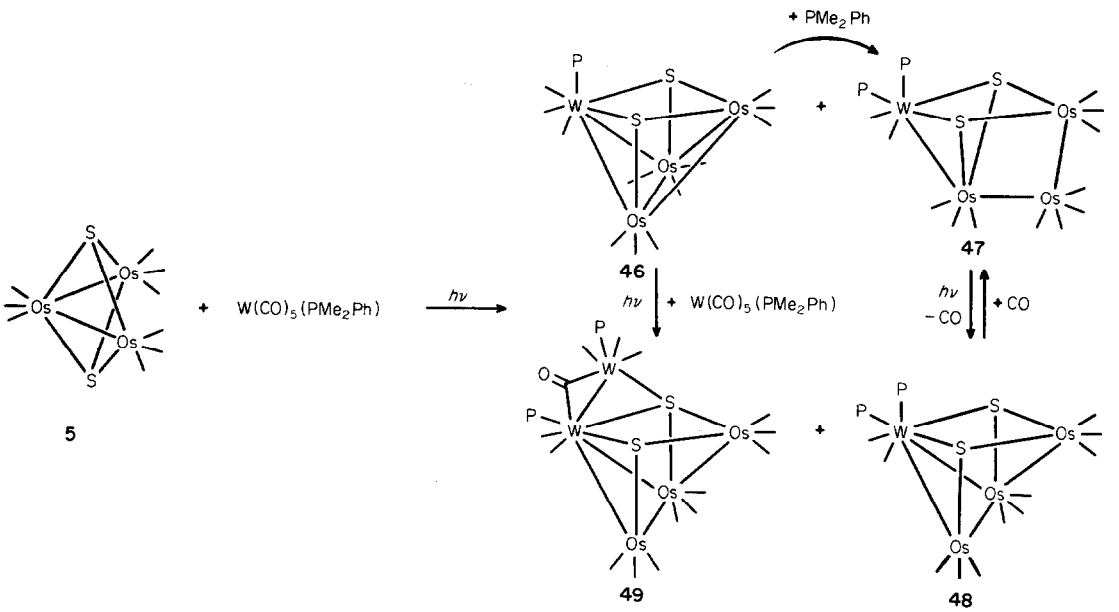


Fig. 18. An ORTEP diagram of $PtOs_3(\mu_3\text{-}S)_2(CO)_{10}(PPh_3)$ (**44**) showing 50% probability thermal ellipsoids. Os(1)–Os(2) = 2.826(1) Å, Os(2)–Os(3) = 2.990(1) Å, Pt–Os(2) = 2.858(1) Å, Pt–Os(3) = 2.905(1) Å, Os(1)...Os(3) = 3.585(1) Å, Os(1)...Pt = 3.401(1) Å.

the triangular group at one of the osmium atoms. The distance of this external osmium atom to the platinum atom is 3.401(1) Å, which seems to be too long for a significant bonding interaction. The $PtOs_2$ group contains triply bridging sulfido ligands that bridge a Pt—Os and the Os—Os edges and extend to the third osmium atom. The compound appears to have been formed by the insertion of a Pt-containing group into two adjacent Os—S bonds of **5**. Compound **45** has a similar structure. Unlike compound **17** (see below) compounds **44** and **45** are electron-precise [i.e. all the metal atoms obey the effective atomic number (EAN) rule].

When irradiated in the presence of $W(CO)_5PMe_2Ph$, compound **5** yields four new products: $Os_3W(\mu_3\text{-}S)_2(CO)_{12}(PMe_2Ph)$ (**46**), $Os_3W(\mu_3\text{-}S)_2(CO)_{12}(PMe_2Ph)_2$ (**47**), $Os_3W(\mu_3\text{-}S)_2(CO)_{11}(PMe_2Ph)_2$ (**48**) and $Os_3W_2(\mu_4\text{-}S)(\mu_3\text{-}S)(CO)_{14}(PMe_2Ph)_2$ (**49**).[34] The structures and relationships between these molecules are shown schematically in Scheme 8. Compound **46** has a butterfly tetrahedral cluster of four metal atoms with triply bridging sulfido ligands on the two open triangular faces. It is structurally analogous to the homonuclear compound **17**. Compound **47** consists of a planar cluster of four metal atoms with triply bridging sulfido ligands on opposite sides of the Os_3W plane. Compound **47** can be made from **46** by adding one equivalent of PMe_2Ph. Compound **48** is isoelectronic with **46** but it adopts a structure similar to **44** and **45**, consisting of triangular group of three metal atoms with an external $Os(CO)_3$ group linked to the triangle by one metal–metal bond and the bridging sulfido ligands. Compound **48** can be made independently by the irradiation-induced decarbonylation of **47**. The pentanuclear Os_3W_2 compound **49** contains an Os_3W cluster analogous to **48** but has a $W(CO)_4(PMe_2Ph)$ group bridging a W—S edge of the cluster. Compound **49** can be made by the irradiation-induced addition of a $W(CO)_4(PMe_2Ph)$ moiety to **46**.

In all of the tungsten–osmium complexes there are bonds between the tungsten atoms and the sulfido ligands. As discussed earlier [cf. eqn (5)], it is believed that preliminary metal–sulfur interactions may be important to the condensation process. The photo-induced reaction of $W(CO)_6$ with **5** yields the product $Os_3(\mu_4\text{-}S)(\mu_3\text{-}S)(CO)_9[W(CO)_5]$ (**50**), which shows such an interaction in its most fundamental form.[35] The structure of **50** is shown in Fig. 19. Most simply, the molecule contains a $W(CO)_5$ group attached to one of the triply bridging sulfido ligands of a molecule of **5**. The connection involves a simple donor–acceptor bond formed by donation of the lone pair of electrons on the sulfido ligand into an empty orbital on the tungsten atom.



Scheme 8.

III. BONDING AND UNUSUAL REACTIVITY

The nature of the metal–metal bonding in polynuclear metal complexes is still not well understood. Localized 2*c*–2*e* bonding and application of the EAN rule works well for small clusters (i.e. four metal

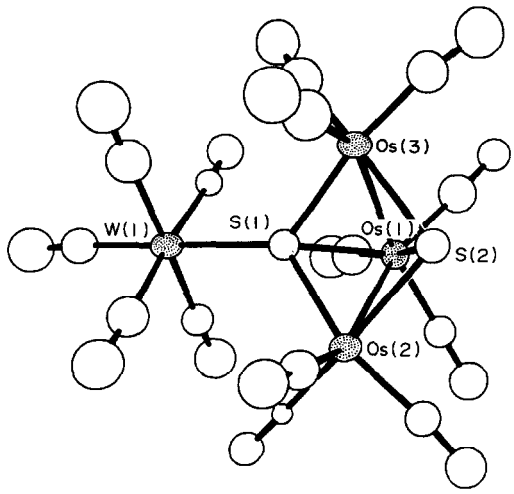


Fig. 19. An ORTEP diagram of $Os_3(\mu_4\text{-}S)(\mu_3\text{-}S)(CO)_9[W(CO)_5]$ (**50**) showing 50% probability thermal ellipsoids.

atoms or less) while the PSEP theory,[36] which employs a delocalized bonding, works better for the larger clusters (i.e. five atoms or more). Recently, Teo has described the topological electron counting theory which incorporates the essential features of both the EAN and the PSEP theories.[37] It should be pointed out, however, that in many cases the EAN rule and the PSEP theory predict the same connectivities for the metal atoms in both the large and small clusters.

1. M_4S_2 *clusters*

Recent studies have revealed a small number of tetranuclear clusters that conform to the PSEP theory but show unusually high reactivities.[27,38] In reactions they convert to products that obey the EAN rule. One of these clusters is the sulfido osmium cluster $Os_4(\mu_3\text{-}S)_2(CO)_{12}$ (**17**).[27] An ORTEP diagram of **17** is shown in Fig. 20. The molecule consists of a butterfly tetrahedron of four metal atoms and has sulfido ligands bridging the two open triangular faces. There are five osmium–osmium distances that are short enough (less than 3.10 Å) to imply significant bonding interactions. Each metal

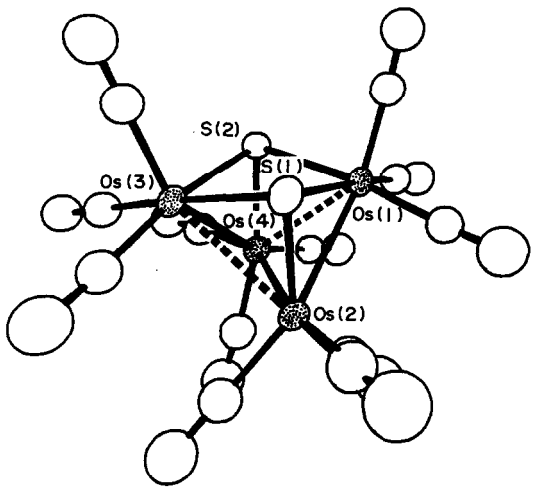
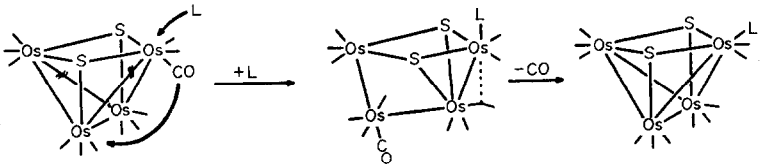


Fig. 20. An ORTEP diagram of $Os_4(\mu_3\text{-}S)_2(CO)_{12}$ (**17**) showing 50% probability thermal ellipsoids. Os(1)–Os(2) = 2.914(1) Å, Os(1)–Os(4) = 3.091(1) Å, Os(2)–Os(4) = 2.935(1) Å, Os(2)–Os(3) = 3.002(1) Å, Os(3)–Os(4) = 2.940(1) Å, Os(1)...Os(3) = 3.551(1) Å.

atom contains three carbonyl ligands and, if the sulfido ligands serve as four-electron donors, then the cluster contains 64 valence electrons. This is two in excess of the requirements of the EAN rule. For this reason we have chosen to describe the molecules as *electron-rich*. If the molecule simply eliminated one metal–metal bond, then all the metal atoms could be made to adhere to the EAN rule. Curiously enough, the isoelectronic compounds **44**, **45** and **47** do have only four metal–metal bonds, but **46** has five. The reason for this is not clear, but steric effects could be important. Intuitively, it seems that compound **47** is more sterically crowded than **46** and this could mitigate against the formation of the fifth bond. The structures of **17** and **46** are, however, in accord with the PSEP theory. According to the PSEP theory $Os(CO)_3$ groups contribute two electrons to cluster bonding and triply bridging sulfido ligands contribute four. There are thus 16 or 8 pairs of cluster valence electrons present in **17**. The PSEP theory predicts a cluster shape based on a polyhedron with seven vertices. This is the pentagonal bipyramid. The structure of **17** can be regarded as a pentagonal bipyramid with one vertex missing (i.e. a *nido*-pentagonal bipyramid). Thus, the observed structure with five metal–metal bonds is the expected one. However, upon close examination of the metal–metal bonding, it is observed that two of the metal–metal bonds, indicated by the dashed connections in Fig. 20, are significantly longer (greater than 3.00 Å) than the other metal–metal bonds in **17** and also the metal–metal distances in $Os_3(CO)_{12}$ [2.877(3) Å]. The latter might best be regarded as Os—Os single bonds. It has not been established if these bond lengthenings are a result of incomplete delocalization or are caused by distortions in the ligand structure.

Studies were undertaken to try to establish if compounds **17** and **46**, which show similar distortions, might exhibit any unusual reactivity. These studies showed the compounds to be remarkably reactive and most surprisingly, toward the addition of Lewis donors, L. For example, compound **17** adds 1 mol of CO at room temperature under 1 bar pressure to form compound **30**.[27] The addition of phosphines and isocyanides proceeds similarly to yield the derivatives $Os_4(\mu_3\text{-}S)_2(CO)_{12}L$ (**51**) (L = PMe_2Ph) and (**52**) (L = $CNBu^t$).[39] The structures of **51** and **52** (see Scheme 9) show that a shift of a carbonyl ligand between the metal atoms must have occurred since each molecule contains an $Os(CO)_4$ group. Also since phosphine ligands do not engage in intramolecular shifts, it implies that the site of addition was one of the "wing-tip" metal atoms of the cluster of **17**. Compounds **30**, **51** and **52** each contain only three metal–metal bonds. They are thus "electron-precise" and all the metal atoms obey the EAN rule. The formation of these compounds can be achieved most easily by cleaving the two elongated bonds in **17**, transferring one CO ligand between a pair of metal atoms, and shifting the attachment of one of the bonds of one of the sulfido ligands to a different metal atom. The reason for the nucleophilic addition at the wing-tip metal atom in **17** could be steric. The wing-tip metal atoms are less crowded being only 6-coordinate while the hinge atoms are 7-coordinate. Compounds **51** and **52** lose CO when heated to form substitution derivatives of **17**. Compound **46** reacts similarly to **17**, but the electron-precise analogs, especially **44** and **45**, are considerably less reactive and undergo cluster degradation when subjected to forcing conditions. Surprisingly, none of these compounds will add alkenes or alkynes.

Another interesting and important reaction is the addition of hydrogen to **17**.[40] The reaction requires a temperature of 100°C and cluster degradation due to further reaction occurs but the initial product is compound **6**. The mechanism of the reaction is not known, but it involves the addition of 1 mol of H_2 and the cleavage of the two elongated metal–metal bonds in **17**. The end product of the reaction is $H_2Os_3(\mu_3\text{-}S)(CO)_9$.

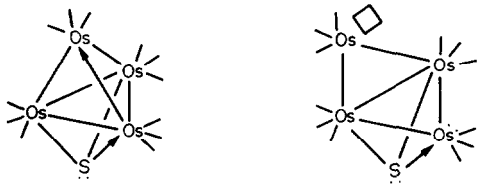


Scheme 9.

2. M_4S *clusters*

The archetypical molecule of this series is compound **16** which is a 60-electron cluster that consists of a closed tetrahedral cluster of metal atoms with a triply bridging sulfido ligand on one triangular face.

The molecule is electron-precise and all the metal atoms obey the EAN rule, but careful consideration reveals a feature about the bonding that could be important to its reactivity. Specifically, one of the metal–metal bonds to the unique osmium atom can be viewed as a heteropolar (donor–acceptor) bond.[41] In addition, since the sulfido ligand is a four-electron donor, one of the Os—S bonds can be



16 16A

regarded similarly. Of course, in its resonance stabilized state all the metal–metal bonds to the unique osmium atom and all the metal–sulfur bonds will be chemically equivalent. However, the notion of the heteropolar bond suggests something about its potential reactivity that may distinguish it from the homopolar bond. Namely, one of these bonds can be opened **16A** without producing a charge separation and a ligand can be added to the vacant site on the unique metal atom. In compound **16** reactions of this type are remarkably facile.[42] For example, **16** adds 1 mol of CO at room temperature under 1 bar pressure to form compound **29**. The reaction is quantitative and complete in approximately 3 h. A similar reaction occurs with phosphines and even with amines, and with amines the reaction is complete in a matter of seconds. These additions are also reversible.

Compound **16** activates hydrogen, and this reaction proceeds albeit slowly even at room temperature/1 bar pressure. The product is $Os_4(\mu\text{-}H)_2(\mu_3\text{-}S)(CO)_{12}$ (**53**) and the ORTEP diagram of structure of **53** is shown in Fig. 21. The molecule consists of a butterfly tetrahedral cluster with the sulfido ligand bridging one of the open triangular faces. The hydride ligands were not located in the structural analysis, but the two metal–metal bonds opposite the sulfido ligand are elongated and this suggests that each may contain one bridging hydride ligand. The formation of **53** has involved the cleavage of one of the homopolar sulfur-bridged metal–metal bonds in **16** and not the "heteropolar" bond. This may be related to the fact that the addition of hydrogen *results* in a homolytic cleavage of the H_2 molecule.

The reaction of **16** with alkynes is especially interesting, but to date only reactions with terminal alkynes have been investigated.[43] The reaction of **16** with PhC≡CH yields two noninterconvertible products. These have been identified as $Os_4(\mu_3\text{-}S)[\mu_4\text{-}C{=}C(H)Ph](CO)_{12}$ (**54**) and $Os_4[\mu_4\text{-}SC(Ph)CH](CO)_{12}$ (**55**). The structure of **54** is shown in Fig. 22. The molecule consists of a puckered rhombus of four osmium atoms connected by four metal–metal bonds. A sulfido ligand bridges three of the metal atoms while a phenylvinylidene ligand bridges all four metal atoms on the opposite side of the

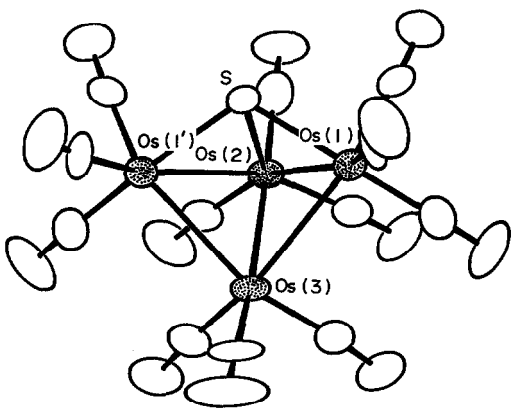


Fig. 21. An ORTEP diagram of $Os_4(\mu\text{-}H)_2(\mu_3\text{-}S)(CO)_{12}$ (**53**). The molecule contains a crystallographic plane of symmetry passing through the atoms S, Os(2) and Os(3). Os(1)–Os(2) = 2.8149(6) Å, Os(1)–Os(3) = 2.9699(9) Å, Os(2)–Os(3) = 2.8578(10) Å, Os(1)...Os(1') = 3.9295(9) Å.

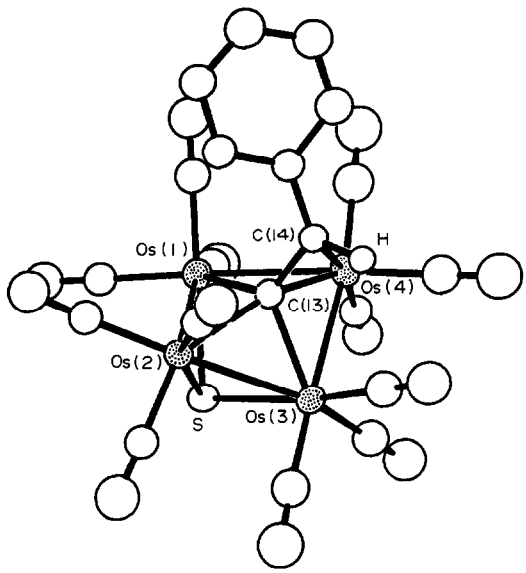


Fig. 22. An ORTEP diagram of $Os_4(\mu_3\text{-}S)[\mu_4\text{-}C{=}C(H)Ph](CO)_{12}$ (**54**) showing 50% thermal ellipsoids. Os(1)–Os(2) = 2.850(1) Å, Os(1)–Os(4) = 2.859(1) Å, Os(2)–Os(3) = 2.787(1) Å, Os(3)–Os(4) = 2.866(1) Å, C(13)–C(14) = 1.446(16) Å.

rhombus. The formation of the vinylidene has obviously occurred by a 1,2-shift of the acetylenic hydrogen atom. These rearrangements have been observed previously in a number of cases in reactions of metal complexes with terminal alkynes.[44] The structure of **55** is shown in Fig. 23. The molecule consists of a butterfly tetrahedral cluster of four metal atoms with a quadruply bridging S—CPh=CH thiolato ligand. The sulfur atom of this unusual ligand bridges two osmium atoms while the alkenyl group is σ,π-bonded to the other two. The ligand was formed by the formation of a carbon–sulfur bond between the phenyl-substituted carbon of the alkyne and the sulfido ligand and a cleavage of one osmium–sulfur and one osmium–osmium bond in the cluster. Curiously, the hydrogen shift that occurred in the formation of **54** did not occur in the formation of **55**. Although the mechanism of this hydrogen shift is not yet known, it is tempting to speculate that the absence of a hydrogen shift in the formation of **55** may somehow be related to the formation of the bonding interaction between the

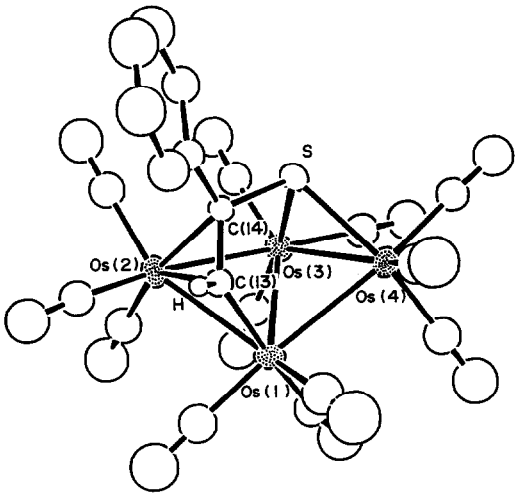


Fig. 23. An ORTEP diagram of $Os_4[\mu_4\text{-}SC(Ph){=}CH](CO)_{12}$ (**55**) showing 50% probability thermal ellipsoids. Os(1)–Os(2) = 2.7840(7) Å, Os(1)–Os(3) = 2.8490(7) Å, Os(1)–Os(4) = 2.8442(7) Å, Os(2)–Os(3) = 2.8132(7) Å, Os(3)–Os(4) = 2.764(1) Å, S–C(14) = 1.817(11) Å, C(13)–C(14) = 1.400(15) Å.

alkyne and the sulfido ligand. Such effects might also occur in the sulfur-inhibited reactions of certain heterogeneous transition metal catalysts. In fact a variety of sulfur–ligand interactions similar to those found in **55** could be responsible for and explain a range of the sulfur-poisoning effects that exist for heterogeneous catalysts.[45,46]

Acknowledgements—Our research on this subject has been supported by the Office of Basic Energy Sciences of the U.S. Department of Energy, and the National Science Foundation.

REFERENCES

1. E. L. Muetterties, *Science* 1977, **196**, 839.
2. E. L. Muetteries, *Bull. Soc. Chim. Belg.* 1975, **84**, 959.
3. R. Ugo, *Catal. Rev.* 1975, **11**, 225.
4. (a) E. L. Muetterties, *Catal. Rev.—Sci. Eng.* 1981, **23**, 69; (b) R. D. Adams and I. T. Horvath, *Prog. Inorg. Chem.* 1985, **33**, 127.
5. H. Vahrenkamp, *Adv. Organomet. Chem.* 1983, **22**, 169.
6. H. Vahrenkamp, *Angew. Chem., Int. Ed. Engl.* 1975, **14**, 322.
7. R. D. Adams and T. S. A. Hor, *Organometallics* 1984, **3**, 1915.
8. K. Wade, In *Transition Metal Clusters* (Edited by B. F. G. Johnson), John Wiley, New York (1980).
9. R. D. Adams and D. F. Foust, *Organometallics* 1983, **2**, 323.
10. K. B. Wiberg, *Acc. Chem. Res.* 1984, **17**, 379.
11. A. J. Deeming and M. Underhill, *J. Organomet. Chem.* 1972, **42**, C60.
12. B. F. G. Johnson, J. Lewis, P. G. Lodge and P. R. Raithby, *J. Chem. Soc., Chem. Commun.* 1979, 719.
13. R. D. Adams, I. T. Horvath, B. E. Segmuller and L. W. Yang, *Organometallics* 1983, **2**, 144.
14. J. P. Attard, B. F. G. Johnson, J. Lewis, J. M. Mace, M. McPartlin and A. Sironi, *J. Chem. Soc., Chem. Commun.* 1984, 595.
15. R. D. Adams, I. T. Horvath, B. E. Segmuller and L. W. Yang, *Organometallics* 1983, **2**, 1301.
16. R. D. Adams, I. T. Horvath, P. Mathur, B. E. Segmuller and L. W. Yang, *Organometallics* 1983, **2**, 1078.
17. P. V. Broadhurst, B. F. G. Johnson, J. Lewis and P. R. Raithby, *J. Organomet. Chem.* 1980, **194**, C35.
18. P. V. Broadhurst, B. F. G. Johnson, J. Lewis, A. G. Orpen, P. R. Raithby and J. R. Thornback, *J. Organomet. Chem.* 1980, **187**, 141.
19. P. V. Broadhurst, B. F. G. Johnson, J. Lewis and P. R. Raithby, *J. Chem. Soc., Dalton Trans.* 1982, 1641.
20. G. Süss-Fink, U. Thewalt and H. P. Klein, *J. Organomet. Chem.* 1982, **224**, 59.
21. R. D. Adams and L. W. Yang, *J. Am. Chem. Soc.* 1982, **104**, 4115.
22. R. D. Adams, D. F. Foust and P. Mathur, *Organometallics* 1983, **2**, 990.
23. R. D. Adams, I. T. Horvath and H. S. Kim, *Organometallics* 1984, **3**, 548.
24. R. D. Adams, I. T. Horvath, P. Mathur and B. E. Segmuller, *Organometallics* 1983, **2**, 996.
25. R. D. Adams, Z. Dawoodi, D. F. Foust and B. E. Segmuller, *Organometallics* 1983, **2**, 315.
26. R. D. Adams, N. M. Golembeski and J. P. Selegue, *J. Am. Chem. Soc.* 1981, **103**, 546.
27. R. D. Adams and L. W. Yang, *J. Am. Chem. Soc.* 1983, **105**, 235.
28. R. D. Adams, I. T. Horvath and L. W. Yang, *J. Am. Chem. Soc.* 1983, **105**, 1533.
29. R. D. Adams, I. T. Horvath and P. Mathur, *Organometallics* 1984, **3**, 623.
30. R. D. Adams, Z. Dawoodi, D. F. Foust and B. E. Segmuller, *J. Am. Chem. Soc.* 1983, **105**, 831.
31. R. D. Adams and T. S. A. Hor, *Inorg. Chem.* 1984, **23**, 4723.
32. M. I. Bruce, G. Shaw and F. G. A. Stone, *Chem. Commun.* 1971, 1288.
33. R. D. Adams, T. S. A. Hor and P. Mathur, *Organometallics* 1984, **3**, 634.
34. R. D. Adams, I. T. Horvath and P. Mathur, *J. Am. Chem. Soc.* 1984, **106**, 6296.
35. R. D. Adams, I. T. Horvath and S. Wang, *Inorg. Chem.* 1985, **22**, 1728.
36. K. Wade, In *Transition Metal Clusters* (Edited by B. F. G. Johnson), Chap. 3. John Wiley, Chichester (1980).
37. B. K. Teo, *Inorg. Chem.* 1984, **23**, 1251, 1257.
38. H. Vahrenkamp and D. Wolters, *Organometallics* 1982, **1**, 874.
39. R. D. Adams, I. T. Horvath and K. Natarajan, *Organometallics* 1984, **3**, 1540.
40. R. D. Adams, Z. Dawoodi, D. F. Foust and L. W. Yang, *Ann. N. Y. Acad. Sci.* 1984, **415**, 47.
41. G. R. John, B. F. G. Johnson and J. Lewis, *J. Organomet. Chem.* 1979, **181**, 143.
42. R. D. Adams and S. Wang, report in preparation.
43. R. D. Adams and S. Wang, *Organometallics* (in press).
44. M. I. Bruce, *Adv. Organomet. Chem.* 1983, **22**, 60.
45. C. H. Bartholomew, P. K. Agrawal and J. R. Katzer, *Adv. Catal.* 1982, **31**, 135.
46. J. Oudar, *Catal. Rev.—Sci. Eng.* 1980, **22**, 171.

Polyhedron Vol. 4, No. 12, pp. 2027–2030, 1985
Printed in Great Britain

0277–5387/85 $3.00 + .00
© 1985 Pergamon Press Ltd

SYNTHESIS, CRYSTAL STRUCTURE, AND SPECTROSCOPIC CHARACTERIZATION OF af-DICHLORO-bd,ec-BIS{μ-[2-(1-METHYL-2-PIPERIDINYL)ETHANETHIOLATO]-*S*,*N*,μ-*S*} DIPALLADIUM(II)

H. BARRERA and J. M. VIÑAS*

Departament de Química Inorgànica, Universitat Autònoma de Barcelona, Bellaterra, 080 Barcelona, Spain

and

M. FONT-ALTABA and X. SOLANS

Departament de Cristal.lografia i Mineralogia, Universitat de Barcelona, Gran Via 585, 08007 Barcelona, Spain

(*Received* 29 *March* 1985; *accepted* 10 *June* 1985)

Abstract—The reaction of 2-(1-methyl-2-piperidinyl)ethanethiol with sodium tetrachloropalladate(II) at pH = 8 yields a yellow precipitate of formula $[Pd_2(C_8H_{16}NS)_2Cl_2]$ which crystallized in the orthorhombic space group *Pcab* with $a = 22.050(4)$ Å, $b = 14.644(3)$ Å, $c = 13.834(3)$ Å, $V = 4467(3)$ Å^3, and $Z = 8$. The organic ligands chelate to one Pd atom through the S and N atoms and bridges to another Pd atom through the S atom to form a dimer in which each molecule of the organic ligand has the same chirality. IR, UV–Vis and ^{1}H NMR spectra are presented for this compound.

The study of complexes with aliphatic γ-mercaptoamines has been undertaken in our Department and several results have been published elsewhere.[1–4] 3-Amino-1-propanethiol has been revealed as a chelating agent while *N*,*N*-dimethyl-3-amino-1-propanethiol behaves as a unidentate ligand with first-row transition metals, and as a bidentate one with second-row transition metals. In order to investigate the influence of substituents on the nitrogen atom upon the coordination through this atom we have studied the ligand 2-(1-methyl-2-piperidinyl)ethanethiol. This ligand resembles *N*,*N*-dimethyl-3-amino-1-propanethiol but with a crowded substituent around the nitrogen atom and the possibility of optical isomerism.

EXPERIMENTAL

To a solution of 0.150 g of ligand (0.964 mmol) in 5 cm^3 of a water–methanol mixture [8 : 2 (v/v)] 0.284 g of $Na_2(PdCl_4)$ (0.964 mmol) in 5 cm^3 of water were slowly added with stirring. The precipitate that formed was allowed to redissolve and the resulting yellow solution was treated with dilute NaOH to pH = 8. The solid that precipitated was stirred for 15 min, filtered, washed with a water–methanol mixture [8 : 2 (v/v)] several times and dried *in vacuo* over silica gel. The dry product was recrystallized by slow diffusion of ether into a dichloromethane solution of the complex. Elemental analyses agreed with a stoichiometry of $PdC_8H_{16}NSCl$. Found : C, 32.1 ; H, 5.2 ; N, 4.7. Calc. for $[Pd_2(C_8H_{16}NS)_2Cl_2]$: C, 32.0 ; H, 5.37; N, 4.67%. Elemental analyses were performed on a Perkin–Elmer 240 elemental analyzer.

The electronic spectrum of the complex was analyzed by the fourth-derivative method[5] and the following bands were found : 23.2 (sh), 27.5 (sh), 35.5, 43.9 (sh) and 45.7 kK. The first two can be assigned to *d*–*d* transitions but they are strongly overlapped with charge-transfer bands.

IR spectra were recorded on a Beckman IR-20 A

* Author to whom correspondence should be addressed.

spectrophotometer as KBr (4000–600 cm^{-1}) or polyethylene (600–250 cm^{-1}) pellets. UV–Vis spectrum was recorded on a Shimadzu 240 spectrophotometer in dichloromethane solution.

The IR spectrum of the complex shows two bands at 2927 and 2857 cm^{-1} instead of the four bands at 2930, 2850, 2780, and 2705 cm^{-1} in the ligand. The bands at 2780 and 2705 cm^{-1} in the latter have been assigned to the ν(C—H) vibrations of a methyl group when bonded to a nitrogen atom having a lone electron pair on it[6] and disappear upon coordination. The bands at 475, 322 and 278 cm^{-1} have been assigned to ν(Pd—N), ν(Pd—S) and ν(Pd—Cl) respectively according to reported data.[7]

The ^{1}H NMR spectrum was recorded on a Varian XL-200 spectrometer in $CDCl_3$ solution.

In the ^{1}H NMR spectrum the signal assigned in the ligand to the methyl group shifts to lower fields (δ = 2.75 and 2.26 in the ligand), and the signal assigned to the proton bonded to the sulphur atom disappears. These facts revealed a bidentate behaviour of the ligand in the complex.

The above-mentioned results were confirmed by X-ray diffraction methods. An orange prism (0.1 × 0.1 × 0.2 mm) was selected and mounted on a Philips PW-1100 four-circle diffractometer. The unit cell parameters were determined from the automatic centering of 25 reflections ($4 \leqslant \theta \leqslant 9°$) and refining the cell parameters by least squares. Intensities were collected with Mo-K_α radiation and the ω scan mode. A summary of the main crystal data are shown in Table 1. Lorentz polarization, but not absorption, corrections were made.

The palladium atoms were located from a Patterson synthesis while the remaining non-hydrogen atoms were located with the DIRDIF system.[8] The structure was isotropically and anisotropically refined by full-matrix least-squares method using the SHELX 76 computer program.[9] The function minimized was $\sum w\|F_o|-|F_c\|^2$, where $w = [\sigma^2(F_o)+0.0108|F_o|^2]^{-1}$: f, f' and f'' were taken from the *International Tables of X-ray Crystallography*.[10] Hydrogen atoms were refined with an overall isotropic temperature coefficients from computed positions. The final R value was 0.068 (R_w = 0.091) for all observed reflections. Atomic coordinates, thermal parameters and lists of F_o and F_c values have been deposited as supplementary material with the Editor. Atomic coordinates have also been deposited with the Cambridge Crystallographic Data Centre.

DISCUSSION

Figure 1 is a perspective view of the molecule showing the atom numbering. Hydrogen atoms have been omitted for clarity. Table 2 lists the principal intramolecular distances and angles. The structure consists of discrete molecules linked by Van der Waals' forces. Each palladium atom is linked to two sulphur atoms, a nitrogen atom and a chlorine atom in a nearly planar fashion [largest deviation of atom from mean plane is −0.079(4) Å for Pd(1) and −0.084(4) for Pd(2), respectively]. The ring formed by Pd and S atoms is hinged Å dihedral angle between S,Pd,S planes (θ) = 142.8(1)°] with a *syn–endo* conformation. The Pd—S distance is shorter than the sum of their covalent radii (2.36 Å according to

Table 1. Experimental data for the X-ray diffraction study of $[Pd_2(C_8H_{16}NS)_2Cl_2]$

(A) Crystal data

Crystal system: orthorhombic	Molecular weight = 600.3
Space group: *Pcab*	$F(000)$ = 2400
a = 22.050(4) Å	μ(Mo-K_α) = 19.89 cm^{-1}
b = 14.644(3) Å	D_c = 1.78 cm^{-3}
c = 13.834(3) Å	
V = 4467(3) Å^3	

(B) Measurements of intensity data

Crystal size: 0.1 × 0.1 × 0.2 mm
Diffractometer: Philips PW-1100
Radiation: Mo-K_α(λ = 0.71069 Å)
Monochromator: graphite crystal
Scan type: ω scan
Scan speed: 0.03° s^{-1}
θ scan range: $2 \leqslant \theta \leqslant 30°$
Measured intensities: 3748
Observed intensities: 3584 [$I \geqslant 2.5\sigma(I)$]

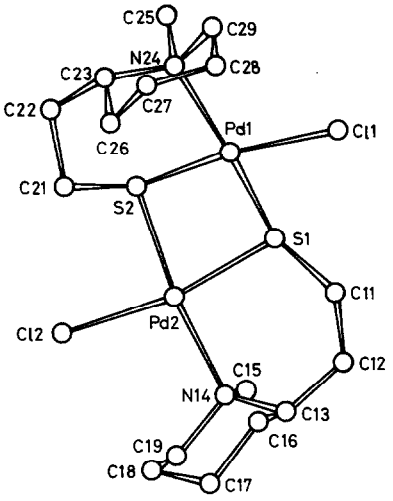


Fig. 1.

Pauling[11]) and also shorter than others reported in the literature.[12] The S—S distance is shorter than the sum of the Van der Waals' radii (3.70 Å), suggesting the existence of weak interactions between the two sulphur atoms according to Fackler.[12(f)] The six-membered chelate rings have chair conformation as well as the piperidine rings. Both piperidine rings lie on the same side of the coordination planes of the palladium atoms. In each molecule only one of the optical isomers of the ligand is found. The centre of inversion relates four molecules of the *R*,*R* isomer with the other four of the *S*,*S* isomer.

The structure of the molecule as a whole resembles that of af-dichloro-bd,ec-bis[μ-(*N*,*N*-dimethyl-3-amino - 1 - propanethiolato) - *S*,*N*,μ - S]dipalladium(II). A comparison of the salient dimensions of the molecules is presented in Table 3. The major observation is that $[Pd_2(C_5H_{12}NS)_2Cl_2]$ more

Table 2. Principal intramolecular distances (Å) and angles (°) (standard deviation in parentheses)

Distance		Angle	
Cl(1)—Pd(1)	2.368(3)	Pd(1)—S(1)—Pd(2)	95.2(1)
S(1)—Pd(1)	2.282(2)	Pd(1)—S(2)—Pd(2)	95.3(1)
S(2)—Pd(1)	2.281(2)	S(1)—Pd(1)—S(2)	77.6(1)
N(24)—Pd(1)	2.163(8)	S(1)—Pd(2)—S(2)	77.5(1)
Cl(2)—Pd(2)	2.359(2)	S(1)—Pd(1)—Cl(1)	91.6(1)
S(1)—Pd(2)	2.283(2)	S(2)—Pd(1)—N(24)	93.1(2)
S(2)—Pd(2)	2.287(2)	N(24)—Pd(1)—Cl(1)	97.3(2)
N(14)—Pd(2)	2.197(7)	S(2)—Pd(2)—Cl(2)	91.1(1)
Pd(1)...Pd(2)	3.374(1)	S(1)—Pd(2)—N(14)	94.1(2)
S(1)...S(2)	2.859(3)	N(14)—Pd(2)—Cl(2)	96.9(2)

Table 3. Comparison of principal crystallographic features of $[Pd_2(C_8H_{16}NS)_2Cl_2]$ and $[Pd_2(C_5H_{12}NS)_2Cl_2]$

	$[Pd_2(C_8H_{16}NS)_2Cl_2]^a$	$[Pd_2(C_5H_{12}NS)_2Cl_2]^b$
Crystal system	Orthorhombic	Monoclinic
Space group	*Pcab*	$P2_1/n$
Conformation of S,Pd,S ring	*syn–endo*	*syn–endo*[c]
Pd—S range (Å) (esd)	2.281(2)–2.282(2)	2.270(3)–2.294(3)
Pd—S mean value (Å) (esd)	2.283(2)	2.279(6)
S—Pd—S range (°) (esd)	77.6(1)–77.5(1)	79.8(1)–80.1(1)
θ (°) (esd)	142.8(1)	154.4(2)
S...S mean value (Å) (esd)	2.859(3)	2.929(4)
Pd...Pd mean value (Å) (esd)	3.374(1)	3.305(1)

[a] This work.
[b] Reference 2.
[c] Misstated as *syn–exo* in Ref. 2.

closely approximates to the square planar symmetry, probably owing to the presence of a piperidine ring in $[Pd_2(C_8H_{16}NS)_2Cl_2]$. The opening of the Pd—S—Pd angles makes shorter the S—S distance in the former, but also in the latter this is shorter than the sum of the Van der Waals' radii. The dihedral angle is larger in $[Pd_2(C_5H_{12}NS)_2Cl_2]$ but the disorder observed in this molecule may account for this feature.

Acknowledgement—The crystallographic work was sponsored by a grant from the Universitat de Barcelona.

REFERENCES

1. H. Barrera, J. Suades, M. C. Perucaud and J. L. Briansó, *Polyhedron* 1984, **3**, 839.
2. X. Solans, M. Font-Altaba, J. L. Briansó, J. Sola, J. Suades and H. Barrera, *Acta Cryst.* 1983, **C39**, 1653.
3. H. Barrera, J. C. Bayón, J. Suades, G. Germain and J. P. Declerq, *Polyhedron* 1984, **3**, 969.
4. J. Suades, X. Solans and M. Font-Altaba, *Polyhedron* 1984, **3**, 1227.
5. J. R. Dickinson, T. R. Griffith and Ph. J. Potts, *J. Inorg. Nucl. Chem.* 1975, **37**, 511.
6. J. T. Braunholtz, E. A. V. Ebsworth, T. G. Mann and N. Sheppard, *J. Chem. Soc.* 1958, 2780.
7. K. Nakamoto, *Infrared Spectra of Inorganic and Coordination Compounds*, 2nd edn. Wiley, New York (1972).
8. P. T. Beurskens, W. P. Bosman, H. N. Doesburg, R. D. Gould, Th. E. Van den Hark, P. A. J. Prick, J. H. Noordik, G. Beurskens and V. Parthasarathi, DIRDIF, an automatic procedure for phase extension and refinement of difference structure factors. Technical Report 1981/2, Crystallographic Laboratory, Toernoiveld, Nijmegen, The Netherlands (1981).
9. G. M. Sheldrick, *SHELX, A Computer Program for Crystal Structure Determination.* University of Cambridge, England (1976).
10. *International Tables of X-ray Crystallography*, Vol. 4, pp. 149–152 and 99–104. Kynoch Press, Birmingham (1974).
11. L. Pauling, *The Nature of the Chemical Bond*, 3rd edn. Cornell University Press, Ithaca, NY (1973).
12. (a) J. Ahmed, K. Itoh, I. Matsuda, F. Ueda, Y. Ishii and J. A. Ibers, *Inorg. Chem.* 1977, **16**, 620; (b) M. Bonamico, G. Dessy and V. J. Fares, *J. Chem. Soc., Dalton Trans.* 1977, 2315; (c) H. W. Chen and J. P. Fackler, *Inorg. Chem.* 1978, **17**, 22; (d) R. H. Fen and G. R. Sergott, *J. Chem. Soc., Dalton Trans.* 1972, 330; (e) R. L. Girling and E. L. Amma, *Acta Cryst.* 1976, **B32**, 2903; (f) J. P. Fackler, *Prog. Inorg. Chem.* 1976, **21**, 55.

Polyhedron Vol. 4, No. 12, pp. 2031–2038, 1985
Printed in Great Britain

0277–5387/85 $3.00 + .00
© 1985 Pergamon Press Ltd

CATALYTIC ACTIVITY OF ETHYLENE-BRIDGED AMINOACID–COPPER(II) COMPLEXES FOR THE DISMUTATION OF SUPEROXIDE

B. M. KATZ and V. I. STENBERG*

Department of Chemistry, University of North Dakota, Grand Forks, ND 58202, U.S.A.

(*Received* 2 *February* 1985; *accepted after revision* 10 *June* 1985)

Abstract—Copper complexes of bridged ethylene derivatives of the aminoacids leucine, isoleucine, valine, alanine, glycine and 2-methylalanine showed marked differences in their ability to quench superoxide. Leucine, alanine and 2-methylalanine ethylene-bridged copper complexes displayed the highest activity, the glycine complex was the least active, and valine had low and isoleucine intermediate activities. A study of differences in speciation, chelation, electronic and steric factors with the aid of molecular models led to a tentative hypothesis that the methyl groups of isoleucine and valine, when distorted toward tetrahedral, are able to block the axial site of copper from binding to superoxide. The glycine-bridged copper complex is believed to form a dimer at the axial copper site which completely blocks the attachment of superoxide.

Copper is an essential trace element required by several enzymes of the body. One of these is superoxide dismutase which has the function of inhibiting the superoxide anion (O_2^-). The production of the latter has been associated with oxygen toxicity.[1] The active site of the enzyme is copper and the mechanism of catalytic activity of copper towards superoxide appears to involve open-coordination positions of copper for reaction with superoxide.[2]

Kinetic studies of superoxide dismutation by copper histidine,[3] *o*-phenanthroline[4] and an ESR study of copper salicylate[5] indicate that superoxide initially binds to the axial copper site. When the open-coordination site of copper is bound by a polypeptide nitrogen, the activity of the metal complex is markedly reduced.[6] Aminoacid–copper complexes were found to exhibit a wide range of activities with superoxide, but mechanistic studies to elucidate structure–activity relationships were not done.[7]

The objectives of this study were to synthesize various substituted ethylenediaminediacetic acid complexes and examine their ability to react with the superoxide ion. The ethylene bridge is for the purpose of attaining compounds that possess enhanced chelation properties compared to the unbridged amino acids.[8] In catabolism, the organic ligand is expected to yield the corresponding ketoacids and ethylenediamine by transamination. The ethylenediamine ligands are derivatives of the aliphatic aminoacids: valine, isoleucine, leucine, alanine, 2-methylalanine and glycine.

EXPERIMENTAL

Aminoacids and ethylenediamine-*N*,*N*′-diacetic acid were supplied by Sigma Chemical Co., Eastman Co. and Fisher Scientific Co. NMR spectra were recorded on a Varian EM 390 spectrometer. The aminoacid derivatives were dissolved in NaOD. The internal standard was 3-(trimethylsilyl)-1-propanesulfonic acid, sodium salt hydrate.

General procedure for the preparation of ethylene derivatives of aminoacids

The appropriate aminoacid (0.1 mol) was dissolved in 100 cm^3 of water containing 0.1 mol NaOH and 0.05 mol sodium carbonate. To this solution was added 0.05 mol ethylene bromide in 100 cm^3 95% ethanol. The solution was heated for approximately 3 h under reflux or until a homogeneous solution was attained. This solution was cooled and acidified to pH 3 with 6 M HCl. The resultant precipitate was filtered, washed with

* Author to whom correspondence should be addressed.

distilled, deionized water and 95% ethanol. The aminoacid derivatives were air-dried. Solutions that did not precipitate with acid were concentrated until a precipitate formed. The compounds were purified by dissolving in aqueous solution, pH 10, and reprecipitating by adding HCl to pH 3.

D,L-leucine–ethylene. Yield 18.3%, m.p. (°C) 237–239 decomposed (d), molecular weight (MW) 288.22. Found: C, 58.2; H, 9.4; N, 9.4. Calc. for $C_{14}H_{28}O_4N_2$: C, 58.3; H, 9.7; N, 9.7%. NMR spectra: δ 0.9 (*d*, 6, $J = 2$ Hz) $(CH_3)_2CH$; 1.4 (*m*, 3) CH_2CH; 2.6 (*s*, 2) CH_2CH_2; 3.1 (*t*, 1, $J = 4$ Hz) $CHCOO^-$.

D,L-isoleucine–ethylene. Yield 21%, m.p. (°C) 260–262 d, MW 288.22. Found: C, 58.3; H, 10.0; N, 9.8. Calc. for $C_{14}H_{28}O_4N_2$: C, 58.3; H, 9.7; N, 9.7. NMR: δ 0.08 (*t*, 6) CH_3CH_2, CH_3CH; 1.1 (*m*, 2) CH_2CH; 1.5 (*m*, 1) CH_2CH; 2.5 (*s*, 2) CH_2CH_2; 2.8 (*d*, *d*, 1, $J = 3$ Hz, 6 Hz) $CHCOO^-$.

L-valine–ethylene. M.p. (°C) 301–302 d, reported 270–310 d.[9] NMR: δ 0.9 (*d*, *d*, 6, $J = 1$ Hz), $(CH_3)_2CH$; 1.8 (*m*, 1, $J = 4$ Hz) $CHCH_2$; 2.7 (*s*, 2) CH_2CH_2; 2.9 (*d*, 1, $J = 6$ Hz) $CHCOO^-$.

D,L-alanine–ethylene. M.p. (°C) 260–262 d, reported 264–266.[10] NMR: δ 1.4 (*d*, 3, $J = 4.5$ Hz), CH_3CH; 2.9 (*s*, 2) CH_2CH_2; 3.3 (*q*, 1, $J = 5$ Hz) $CHCOO^-$. The method of Schlesinger[11] was used for the preparation of 2-methylalanine.

Test solutions

Solutions for superoxide-quenching assays, ESR and photometric studies were prepared by weighing an appropriate amount of the ligand to obtain 1×10^{-2} M aminoacid–ethylene derivatives. A 10^{-2} M solution of $Cu(NO_3)_2$ was also prepared. Dilutions of 1×10^{-3} and 1×10^{-4} M copper complexes were attained by mixing equal volumes of the 1×10^{-2} M solution of the ligand and 1×10^{-2} M solution of the copper ion and diluting with a pH-7.6 aqueous buffer. Only a metal : ligand ratio of 1 : 1 was prepared.

Superoxide assays

KO_2 method.[12] To a series of test tubes were added 3.0 cm^3 buffer solution followed by 0.05, 0.1, 0.3 and 0.5 cm^3 of 1×10^{-4} M solution of the compound to be tested and brought to the same volume with 0.45, 0.4, 0.2 and 0 cm^3 of distilled deionized water. The final concentration varies from 1×10^{-6} to 1×10^{-5} M. To each tube was then added 0.1 cm^3 of a nitroblue tetrazolium (NBT) solution (4 mg cm^{-3}) in dimethylsulfoxide (DMSO) (Aldrich Gold Label), 0.1 cm^3 of a solution containing 20 mg KO_2 with 0.1056 g/10 cm^3 18-crown-6 (Aldrich) in DMSO. The tubes were shaken thoroughly after the addition of each reagent. The absorbance was read immediately at 540 mμ using a Bausch & Lomb Spectronic 20. All readings were taken against a blank containing everything except the potassium superoxide solution. A standard curve of increasing concentrations of KO_2 with absorbance gave a straight line with a correlation coefficient of 0.999. Three repetitive assays for one concentration were conducted for most of the test compounds in order to assure reproducibility. The average error did not exceed 5%.

β-Nicotinamide–adeninedinucleotide (NADH) method.[13] The assay was identical to the KO_2 method except for the following. After the addition of the NBT solution, 0.1 cm^3 phenazine methosulfate (PMS, 10 mg/100 cm^3 in buffer) was added. The reaction was then started by the addition of 0.3 cm^3 of NADH (1.5 mM in buffer) solution. The NADH solutions were made fresh before each assay. After standing in the dark for 10 min the readings were taken as described above. Preweighed vials purchased from Sigma Chemical Co. were the source of NADH. The results of three successive determinations with NADH from the same vial did not vary over 1%. The phosphate buffer was prepared by mixing 4.24 cm^3 of solution A (22.6 g $NaH_2PO_4 \cdot H_2O$ in 1 l) and 45.75 cm^3 of solution B (71.7 g $Na_2HPO_4 \cdot 12H_2O$ in 1 l) and diluting to 200 cm^3. Distilled, deionized water was used for all preparations and assays.

Potentiometric and spectrophotometric measurements

Potentiometric titrations were performed on the valine–, leucine– and isoleucine–copper complexes with metal : ligand ratio of 1 : 1, 10^{-2} M concentration, 25°C and 0.1 M KNO_3.[14] The dissociation constants were calculated from the inflection points. With the copper complexes of valine, leucine and isoleucine ethylene-bridged compounds, dissolution does not occur until a slightly basic pH is reached. Rapid back-titration with HCl provided a means for titration to an acid pH before bulk precipitation occurred. The values obtained with the back-titration were used in the calculations. Titration of copper with the basic ligands for determination of stability constants were done as outlined for nickel glycine.[14] The calculation of association constants was adapted to a dibasic acid system as described by Courtney *et al.*[15]

Equations (1)–(5) were assumed for the calculation of the dissociation constants where $[L^{2-}]$ is the concentration of completely deprotonated ligand, $[LH^-]$ is the concentration of monopronated ligand, $[LH_2]$ is the concentration of protonated

ligand, and α_L^{2-} is the fraction of the deprotonated ligand:

$$LH_2 \rightleftarrows LH^- + H^+, \quad (1)$$

$$LH^- \rightleftarrows L^{2-} + H^+, \quad (2)$$

$$k_1 = \frac{[LH^-][H^+]}{[LH_2]}, \quad (3)$$

$$k_2 = \frac{[L^{2-}][H+]}{[LH^-]}, \quad (4)$$

$$\alpha_L^{2-} = \frac{k_1 k_2}{[H^+]^2 + k_1[H^+] + k_1 k_2}. \quad (5)$$

The calculation of the metal–ligand speciation was done using eqns (6)–(8), where $[L^{2-}] = L_T \times \alpha_L^{2-}$, $[L_T]$ is the original concentration and K_1 and K_2 are the association constants of metal and ligand:

$$\beta_{Cu^{2+}} = \frac{1}{1 + K_2[L^{2-}] + K_1 K_2[L^{2-}]^2},$$

fraction of free Cu^{2+}; (6)

$$\beta_{CuLH^+} = \frac{K_1[L^{2-}]}{1 + K_1[L^{2-}] + K_1 K_2[L^{2-}]^2},$$

fraction of $CuHL^+$; (7)

$$\beta_{CuL} = \frac{K_1 K_2[L^{2-}]^2}{1 + K_1[L^{2-}] + K_1 K_2[L^{2-}]^2},$$

fraction of CuL. (8)

Calculations for speciation were made for a ligand concentration of 1×10^{-5} M similar to that for the superoxide-quenching assays. Calculations made for the alanine- and glycine-bridged copper complexes from the constants given by Chaberek and Martell[16] indicate that both compounds contained less than 0.1% of the free Cu(II). Calculations of metal–ligand association constants followed the procedure of Courtney *et al.*[15] for dibasic acids. All absorbance measurements were made with a Beckman 25 recording spectrophotometer at a pH of 7.6.

ESR spectroscopy

Copper complexes in aqueous solution buffered at pH 7 and ambient temperature were taken in capillaries with the concentration of the metal and ligand each at 10^{-3} M. Superoxide was prepared immediately before use as described above. Ratios of 1:1, 1:2, 1:4, 1:6 and 1:8 (metal complex : superoxide) were prepared. Measurements were taken on a Model ER-420 JOEL X band ESR spectrometer.

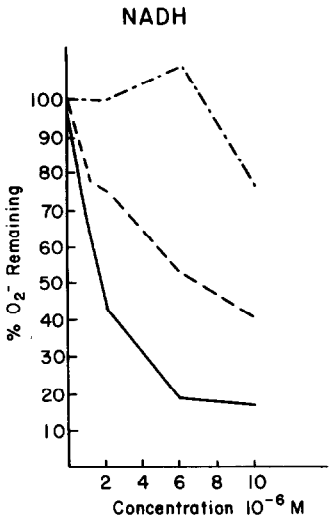


Fig. 1. The quenching of superoxide by the copper complexes using the NADH assay. (——) Ethylene–dileucine, (– – –) ethylene–di-isoleucine, and (–·–) ethylene–divaline.

RESULTS

The rates of reaction of the complexes with superoxide ion *in vitro* were leucine ≅ alanine ≅ 2-methylalanine > isoleucine > valine ≫ glycine (cf. Figs 1–4). The ligands without copper had no reactivity with the superoxide anion. Copper(II) ion in the absence of the synthesized aminoacid ligands quenched superoxide at rates comparable to that of the leucine complex. The activity to quench the superoxide ion was examined at four different

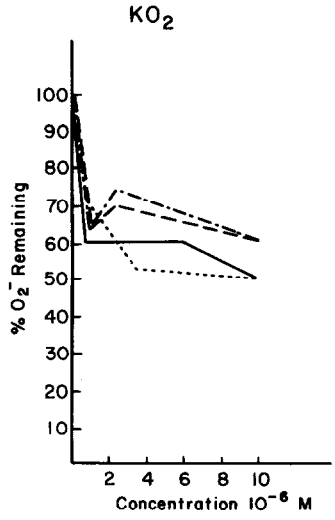


Fig. 2. The quenching of superoxide by the copper complexes using the KO_2 assay. (——) Ethylene–dileucine, (– – –) ethylene–di-isoleucine, (–·–) ethylene–divaline, and (···) Cu^{2+}.

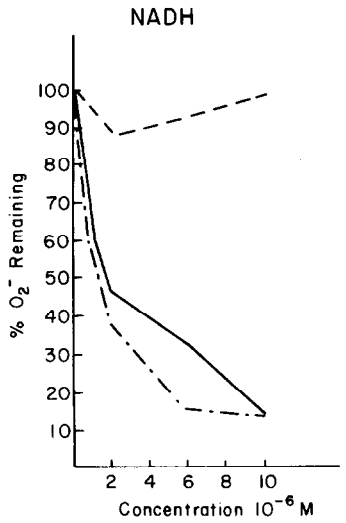


Fig. 3. The quenching of superoxide by the copper complexes using the NADH assay. (——) Ethylene–dialanine, (---) ethylene–diglycine, and (-·-) ethylene–2-methylalanine.

concentrations of the copper complexes. Although the reactivity order of the copper complexes were the same for the two independent assays, the potassium superoxide assay sensitivity decreased markedly at higher concentrations of the complexes.

The results in Figs 5–7 indicate the speciation is the same for the three different copper complexes. The main species in the region of pH 7–8 for the valine–, leucine– and isoleucine–ethylene–copper complexes ia a copper complex with a net plus one charge. The titration curves of the ethylene-bridged amino acids (unprocessed data for Figs 5–7) shows two inflection points.

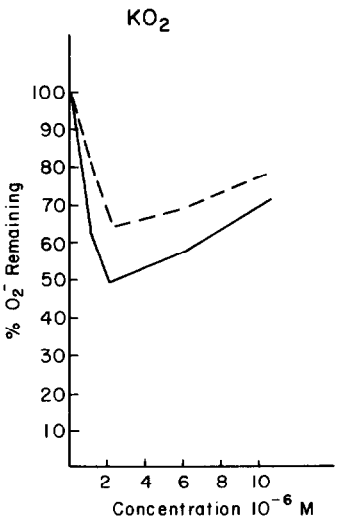


Fig. 4. The quenching of superoxide by the copper complexes using the KO_2 assay. (——) Ethylene–dialanine, and (---) ethylene–diglycine.

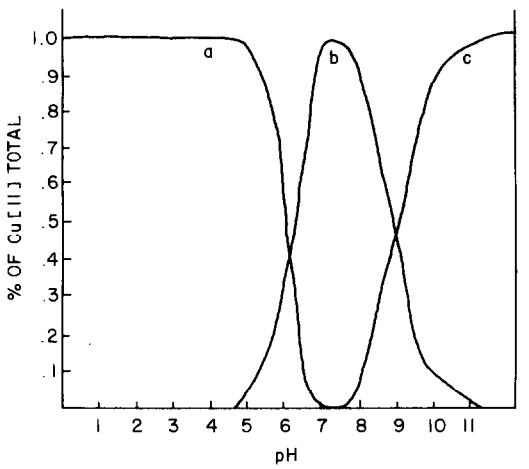


Fig. 5. Species distribution for the 1:1 copper(II)–ethylene–dileucine complex as a function of pH. (a) Cu^{2+}, (b) $CuHL^+$, and (c) CuL.

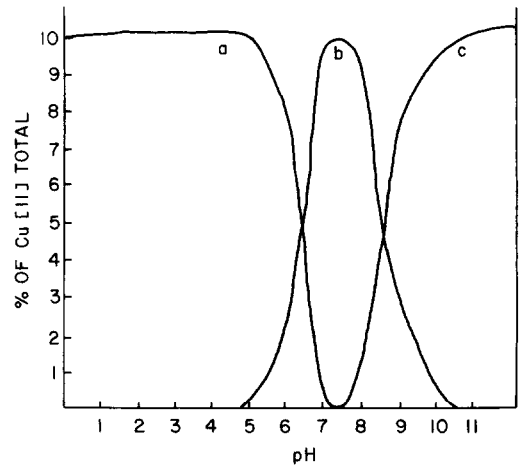


Fig. 6. Species distribution for the 1:1 copper(II)–ethylene–di-isoleucine complex as a function of pH. (a) Cu^{2+}, (b) $CuHL^+$, and (c) CUL.

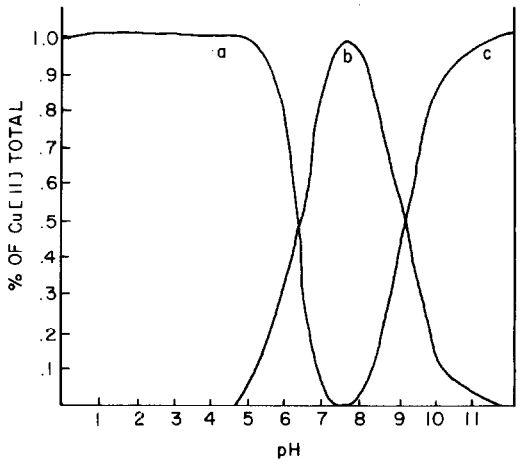


Fig. 7. Species distribution for the 1:1 copper(II)–ethylene–divaline complex as a function of pH. (a) Cu^{2+}, (b) $CuHL^+$, and (c) CuL.

Table 1. The UV and visible spectra of substituted ethylenediaminediacetic acid–copper complexes in aqueous solution

Copper–ethylene complex	Visible λ_{max} (nm)	Visible ε_{max}	UV λ_{max} (nm)	UV ε_{max}
Valine	635–665	39	254	4465
Isoleucine	630–665	31	250	4135
Leucine	640–665	27	250	3750
Alanine	660–700	30	250	4000
Glycine	600–615	16	nd[a]	
2-Methylalanine	580–620	19	—[b]	

[a] Not detected.
[b] Not determined.

The visible and UV spectra from aqueous solutions of the bridged aminoacid–copper complexes were determined in order to observe possible differences in configuration. The λ_{max} and ε_{max} are summarized in Table 1. The visible region of the spectra consists of broad absorption bands for all complexes. They are very close in energy but differ in intensity. The latter increase in the series: leucine– < isoleucine– < valine–copper complexes. The λ_{max} for the copper–alanine complex was slightly higher than the other copper complexes in the series. In the UV region of the spectra, very intense peaks at low concentrations were observed at the 250-nm region for all complexes but the glycine–copper complex. This peak was absent with copper(II) and the ligands without copper.

The ESR spectra of the copper–aminoacid bridged complexes were obtained in the presence and absence of superoxide. All complexes except the glycine had four hyperfine peaks. The glycine one had seven peaks. Figure 8 shows the spectra of alanine–, glycine–, isoleucine– and leucine–copper complexes before superoxide was added. The spectrum of the copper–alanine complex was poorly resolved compared to the other copper complexes. After the first addition of superoxide anion, another type of spectra occurs which represents a paramagnetic species but differs from the spectrum without superoxide by an increase in hyperfine structure. This occurs before further reduction to a species where all absorption bands disappear with further addition of superoxide.

The spectra for the copper–valine complex before and after addition of two increments of superoxide is illustrated in Fig. 9. The copper–valine complex prior to superoxide addition did not have a pronounced hyperfine structure compared to the leucine one (Figs 8 and 9).

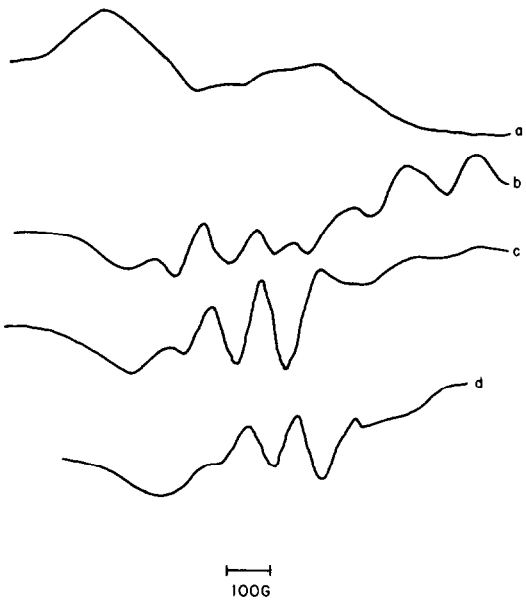


Fig. 8. ESR spectra of ambient aqueous solutions of copper(II) complexes. (a) Ethylene–*N*,*N*′-dialanine, (b) ethylene–diglycine; (c) ethylene–*N*,*N*′-di-isoleucine, and (d) ethylene–dileucine.

DISCUSSION

The substituted ethylenediaminediacetic acid–copper complexes formed from leucine, alanine and 2-methylalanine display the highest rate of reactivity with the superoxide ion of the derivatives synthesized (Figs 1–4). The copper–glycine derivative did not show any activity. In these complexes, the presence of the copper ion is essential to the complexes in order for them to react with the superoxide anion. A superoxide intermediate is believed to account for observations in kinetic studies of superoxide reacting with copper complexes.[4,17] The site proposed for superoxide attachment is the axial site of Cu(II), and the mechanism of the interaction is represented by eqns (9)–(11):

$$Cu(II) + O_2^- \rightleftharpoons Cu(II)O_2^-, \quad (9)$$

$$Cu(II)O_2^- \rightleftharpoons Cu(I)O_2, \quad (10)$$

$$Cu(I)O_2 \rightleftharpoons Cu(I) + O_2. \quad (11)$$

$Cu(II)O_2$ and $Cu(I)O_2$ are the oxygen adducts.

The ESR spectra of solutions in which these complexes are reacted with various concentrations of the superoxide anion give evidence for the initial bonding of the anion with the copper(II) cation and its subsequent reduction to copper(I). The buffered, aqueous, ambient-temperature ESR spectra of all copper complexes show an initial increase in the hyperfine structure of copper with increasing

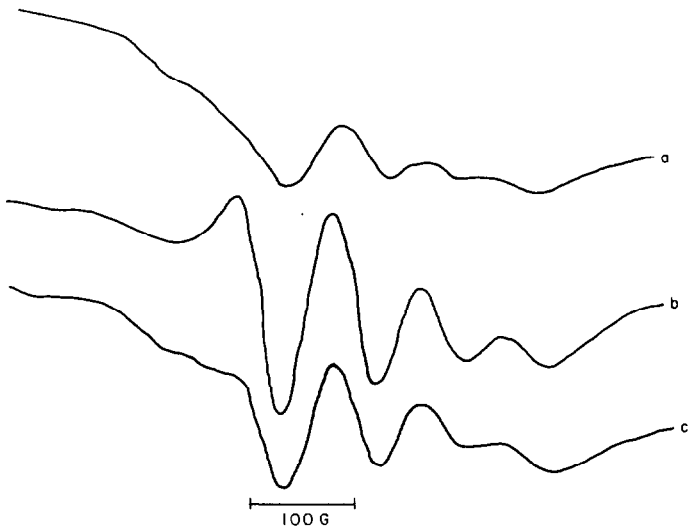


Fig. 9. ESR spectra of ambient aqueous solutions of ethylene–*N,N'*-divaline with increments of superoxide. (a) No equivalent superoxide, (b) one equivalent superoxide, and (c) three equivalents of superoxide.

increments of superoxide followed by loss of the hyperfine structure as reduction to Cu(I) occurs. As an example, the ESR spectra of the valine derivative copper(II) complex interaction with three different concentrations of superoxide are given in Fig. 9. In a study of copper salicylate, DeAlvare *et al.*[5] previously interpreted such spectra as superoxide complexing to copper with subsequent reduction.

All five complexes examined herein have two nitrogen atoms complexed with the copper(II) ion. Agarwal and Perrin[18] have shown that the number of nitrogen atoms bound to copper can be distinguished by the visible spectra. If an absorption occurs below 600 nm, the copper ion is bound to three nitrogen atoms, but above 600 nm to two nitrogen atoms. The compounds in the present study all have absorption maxima above 600 nm (Table 1).

The intense peaks in the UV spectra of the copper complexes are charge-transfer bands of the N—Cu—N bonds as verified by their absence in the spectra of copper(II) solutions and the ligands without copper. By comparison with the bis(diamine)copper complexes, the bands are assigned to a σ–σ^* (R_1N–Cu–NR_2) transition.[19] Only the glycine complex does not show the charge-transfer band. This indicates it has a different structure from the other four aminoacid complexes.

Since the concentration of copper is identical for all the complexes, the data of Figs 1–4 demonstrate that the copper ligand nature influences the rate of reaction with the superoxide anion. The coordination number of the copper ion does not change within the series: isoleucine, leucine, and valine ethylene-bridged copper complexes. The speciation curves illustrated in Figs 5–7, calculated from the experimentally derived association constants for these three complexes, are virtually identical. Consequently, the diverse reactivities of these three complexes towards the superoxide ion are caused by factors other than speciation.

Steric hindrance to the approach of the superoxide ion to the copper(II) is believed to account for the decreased reactivity of the valine- and isoleucine-bridged derivatives. Both have branching of the hydrocarbon chain at C-3, whereas the most reactive three complexes do not. Hence there is steric hindrance in close proximity to the active site. The 2-methylalanine-bridged complex ability to quench superoxide approximates that of the leucine complex in spite of the extra methyl group at C-2. Therefore, the important steric interactions appear to be at C-3. By using conformational analysis, Raos and Simeon[20] presented evidence that a methyl group which extends over copper reduces hydration of the axial copper site. This, together with the known tendency of copper complexes to distort toward tetrahedral, provides the possibility of the two C-3 alkyl groups of isoleucine and valine to extend over the axial site of copper to block this site and lessen its catalytic activity.[21–26] This was examined with the aid of molecular models. The C-3 alkyl groups of the isoleucine and valine complexes are unlikely to extend over copper in a square planar conformation. However, with an incease in distortion toward tetrahedral, these alkyl groups can readily be positioned over the copper(II).

There is evidence for tetrahedral distortion among the six ethylenediamineacetic acid complexes of

copper studied herein. Red shifts and intensity enhancements of *d–d* electronic absorption bands accompany changes from square planar toward tetrahedral geometry.[21] The λ_{max} of the aminoacid bridged complexes (Table 1) have broad bands and are close in energy, but the intensities increase markedly from leucine- to valine-bridged copper complexes. With the exception of alanine, the degree of tetrahedral distortion roughly corresponds to the extent of superoxide quenching by these complexes. It appears that both the presence of two alkyl blocking groups at C-3 and tetrahedral distortion are necessary and act synergistically to block the axial site of copper(II) to superoxide.

Bereman *et al.*[27] concluded that tetrahedral distortion is the single most important dominating factor which changes $E_{1/2}$ for their copper complexes and ESR parameters which reflect the degree of tetrahedral distortion varied linearly with $E_{1/2}$.[27] Yokoi and Addison[28] also showed that ESR parameters varied linearly with $E_{1/2}$. It is therefore probable that the reduction potential varies in the series studied here. However, it appears that the resultant potential is a function of the structure which determines the availability of the axial copper site for the redox reaction with superoxide.

The lack of activity of the copper glycine-bridged complex is attributed to formation of a dimer on the axial copper site. The complex is the smallest of the series, and small copper compounds have been found to dimerize.[29] In an analogous study of copper–aminoacid complexes, only with glycine did a third group add to the axial site of copper.[30] Although dimeric copper compounds are antiferromagnetically coupled, resulting in an absence of an ESR spectra,[31] the ESR of the copper–glycine–ethylene complex had seven peaks, indicating a weaker interaction of two copper nuclei (cf. Fig. 8). Although it was recognized that dimerization had occurred from a frozen ESR spectra of a 1 : 1 copper-bridged glycine complex, the nature of the structure was not forwarded.[32] The significance of seven lines for a copper dimer was attributed to out-of-plane interactions for the *N,N'*-ethylene-bis(salicyldeneiminato) copper complex.[33] Based on the ESR spectrum and the absence of a charge-transfer band which indicates a change of symmetry (Table 1), a tentative structure is proposed (Fig. 10). The axial copper site in this structure is occupied by another bridged glycine so that it is inaccessible to superoxide, resulting in deactivation of the catalytic activity of copper to quench superoxide.

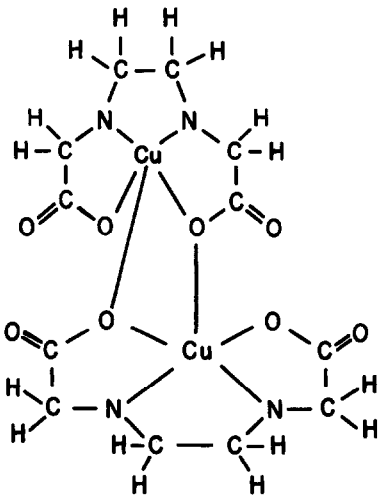


Fig. 10. Proposed structure for Cu(II)–ethylene–diglycine.

REFERENCES

1. I. Fridovich, *Science* 1978, **201**, 875.
2. G. Rotilio, A. Rigo and L. Calabrese, *Frontiers in Physicochemical Biology*, p. 357. Academic Press, New York (1978).
3. J. Weinstein and B. M. Bielski, *J. Am. Chem. Soc.* 1980, **120**, 4916.
4. S. Goldstein and G. Czapski, *J. Am. Chem. Soc.* 1983, **105**, 7276.
5. L. R. DeAlvare, K. Goda and T. Kimura, *Biochem. Biophys. Res. Commun.* 1976, **69**, 687.
6. C. Amar, E. Vilkas and J. Foos, *J. Inorg. Biochem.* 1982, **17**, 313.
7. K. E. Joester, G. Jung, U. Weber and U. Weser, *FEBS Lett.* 1972, **25**, 25.
8. F. Bell and K. A. K. Lott, *Modern Approaches to Inorganic Chemistry*, p. 150. Butterworths, London (1963).
9. R. J. Magee, W. Mazurek, M. J. O'Conner and A. T. Phillip, *Aust. J. Chem.* 1974, **27**, 1885.
10. P. Blondeau, C. Berse and D. Gravel, *Can. J. Chem.* 1967, **45**, 49.
11. N. Schlesinger, *Ber. Chem. Dtsch. Ges.* 1911, **44**, 1135.
12. M. Younes and U. Weser, *FEBS Lett.* 1976, **61**, 209.
13. R. Fried, *Biochemie* 1975, **57**, 657.
14. R. J. Angelici, *Synthesis and Technique in Inorganic Chemistry*, p. 115. W. B. Saunders, Philadelphia (1977).
15. R. C. Courtney, S. Chaberek, Jr and A. E. Martell, *J. Am. Chem. Soc.* 1953, **75**, 4814.
16. S. Chaberek, Jr and A. E. Martell, *J. Am. Chem. Soc.* 1952, **74**, 5052.
17. J. Rabini, D. Klug-Roth and J. Lillie, *J. Phys. Chem.* 1973, **77**, 1169.
18. R. P. Agarwal and D. D. Perrin, *J. Chem. Soc., Dalton Trans.* 1976, 89.
19. B. P. Kennedy and A. B. P. Lever, *J. Am. Chem. Soc.* 1973, **95**, 6907.
20. N. Raos and V. I. Simeon, *J. Inorg. Biochem.* 1983, **18**, 133.

21. K. F. Purcell and J. C. Kotz, *Inorganic Chemistry*, p. 761. W. B. Saunders, Philadelphia (1977).
22. R. C. Rosenberg, C. A. Root, R. K. Bernstein and H. B. Gray, *J. Am. Chem. Soc.* 1975, **97**, 2092.
23. L. Sacconi and M. Ciampolini, *J. Chem. Soc.* 1964, 276.
24. M. J. Adam and L. D. Hall, *Can. J. Chem.* 1982, **60**, 2229.
25. H. Yokoi, *Bull. Chem. Soc. Jpn* 1974, **47**, 3037.
26. S. Yamada and A. Tokeuchi, *Coord. Chem. Rev.* 1982, **43**, 187.
27. R. D. Bereman, J. R. Dorfman, J. Bordner, P. D. Rillema, P. McCarthy and G. D. Shields, *J. Inorg. Biochem.* 1982, **16**, 47.
28. H. Yokoi and A. W. Addison, *Inorg. Chem.* 1977, **16**, 1341.
29. R. Österberg, *Coord. Chem. Rev.* 1974, **12**, 309.
30. I. Nagypál, E. Farkas and A. Gergely, *J. Inorg. Nucl. Chem.* 1975, **37**, 2145.
31. U. Weser, K. H. Sellinger, E. Lengfelder, W. Werner and J. Strähle, *Biochim. Biophys. Acta* 1980, **631**, 232.
32. N. Yokoi and M. Chikera, *J. Chem. Soc., Chem. Commun.* 1982, 1125.
33. G. O. Carlisle and W. E. Hatfield, *Inorg. Nucl. Chem. Lett.* 1970, **6**, 633.

Polyhedron Vol. 4, No. 12, pp. 2039–2042, 1985
Printed in Great Britain

0277–5387/85 $3.00 + .00
© 1985 Pergamon Press Ltd

NONIONIC SURFACTANTS AS LIGANDS FOR THE COMPLEXATION OF ALKALI AND ALKALINE-EARTH CATIONS IN METHANOL

HANS-JÜRGEN BUSCHMANN

Universität-GH Siegen, Physikalische Chemie, Postfach 101240, D-5900 Siegen, F.R.G.

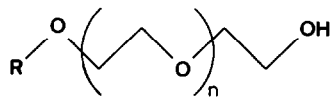
(*Received* 15 *May* 1985; *accepted* 10 *June* 1985)

Abstract—The stability constants and thermodynamic values of complex formation of nonionic surfactants with alkali and alkaline-earth cations were determined by calorimetric titration in methanol. The purity of the ligands examined was checked by calorimetric end point titration. This method gives good results only if 1:1 complexes are formed. For the smallest ligands a ligand:cation ratio of x:1 is found. In contrast the surfactant with the longest oligoethylene glycol chain forms 1:x complexes. With increasing number of donor atoms the reaction enthalpies become more negative but the stability constants do not change very much due to compensating changes in entropies. Compared with the monocyclic ligand 18-crown-6 it is possible to obtain higher values of the reaction enthalpies and the high stability constants for crown complexes are caused mainly by favourable entropic factors.

The complexing properties of oxygen-containing noncyclic ligands have not hitherto been much investigated because they are not able to compete with crown ethers[1] and cryptands.[2] Only in a few cases were the complex stabilities of noncyclic polyethers determined for comparison with the cyclic analogues.[3] Favretto[4] reported data for the complexation of alkali metal ions with polyoxyethylene glycol derivatives in methanol where the number of ether atoms varies from 4 to 11. Stability constants and thermodynamic values for the reaction of alkali and alkaline-earth cation with short-chain glycols and glymes have also been published.[5] The publications mentioned above show that, with increasing chain length, the stability of the formed complexes is enhanced. So far no measurements have been performed to answer the question whether it is possible or not to obtain stability constants with linear polyethers of the same order of magnitude as for crown ethers. The synthesis and purification of well-defined long-chain polyethers is rather difficult and this is probably the main reason why no data for complex formation are available. We found that the purity of some nonionic surfactants was high enough to use them as noncyclic ligands for the complexation of mono- and bivalent cations in methanol. The complexing properties of these ligands were examined by calorimetric titrations.

EXPERIMENTAL

All ligands examined (see Fig. 1) are commercially available samples and were used without further purification. Only 2,5,8,11,14-pentaoxapentadecanol (PEGM, Janssen) was distilled *in vacuo* prior to use. The names of the nonionic surfactants, with abbreviations, are given in Fig. 1. All are registered trade marks so the letter B stands for Brij (ICI Americas Inc.) and I for Igepal (GAF Corp.).



$R=CH_3$	n= 4 : PEGM
$R=C_{12}H_{25}$	n= 3 : B30
	n=22 : B35
$R=C_{16}H_{33}$	n=19 : B58
$R=C_{18}H_{35}$	n=19 : B99
$R=C_9H_{19}$-C$_6$H$_4$-	n=11 : JCO-720
	n=39 : JCO-890

Fig. 1. Nonionic surfactants studied in this work.

Table 1. Theoretical molecular weights (MWs) and experimental molecular weights ($\overline{MW}$s) of nonionic surfactants calculated from calorimetric end point titrations

Ligand	MW	$\overline{MW}$
PEGM	251.31	380
B30	362.56	1357
B35	1199.57	1191
B58	1123.52	1101
B99	1149.56	1102
JCO-720	749.00	884
JCO-890	1982.50	1254

The salts $NaNO_3$ (Merck), KNO_3 (Merck), $RbNO_3$ (Ventron), CsF (Ventron), $Ca(NO_3)_2$ (BDH), $Sr(NO_3)_2$ (Merck) and $Ba(ClO_4)_2$ (Merck) were anhydrous and of the highest purity commercial available. All solutions were prepared by dissolving the dried salt in anhydrous methanol (Merck, H_2O content less than 0.01%).

All calorimetric titrations were performed using a Tronac calorimeter (Modell 450). The purity of all ligands was checked by calorimetric end-point titrations. The values of Table 1 were estimated by titrating a solution of $Ba(ClO_4)_2$ ($1.0–1.5 \times 10^{-3}$ N). A typical thermogram is given in Fig. 2. No sharp end-point of the titration is found. To test the accuracy of this method the molecular weight (MW) of Kryptofix-5 (Merck, MW = 448.52) which also gives no well-defined end point at the titration with cations was estimated. A value of 448.8 ± 0.1 was found.

To measure thermograms for the calculation of stability constants and reaction enthalpies a ligand solution (0.08 N) was titrated to a solution of a metal ion (5×10^{-3} N). A typical thermogram is given in Fig. 3. After correction for all nonchemical heat effects the heat produced during the reaction is related to the reaction enthalpy by:

$$Q_t = \Delta H \cdot \Delta n_t. \quad (1)$$

The number of mols of complex formed at the time t, Δn_t, is a function of the stability constant. The reactions observed can be described by the following equation:

$$M^{n+} + L \rightleftharpoons ML^{n+}, \quad K = \frac{[ML^{n+}]}{[M^+][L]}. \quad (2)$$

An iterative procedure was used to calculate stability constants and reaction enthalpies from the thermograms.[6] The temperature increase during the titration is very small so the stability constant is not affected.

RESULTS AND DISCUSSION

The calorimetric end-point titration gives information about the composition of the complex (see Table 1). If the measured MW of the ligand is higher than expected a complex of composition ML_x^{n+} is formed. A 1:1 complex is present in the case when given and estimated MW are nearly identical. If the MW calculated from the end-point is smaller than the theoretical value the ratio of ligand to cation changes to M_xL^{xn+}. This happens with ICO-890 and no effort was made to calculate any data from the

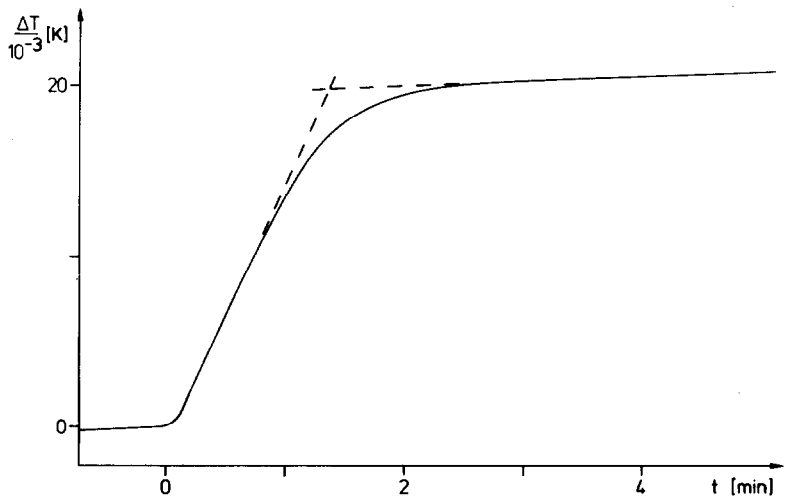


Fig. 2. Thermogram for the evaluation of the molecular weight. At time $t = 0$ the addition of a solution of B99 to a solution of $Ba(ClO_4)$ (1.5×10^{-3} M) starts.

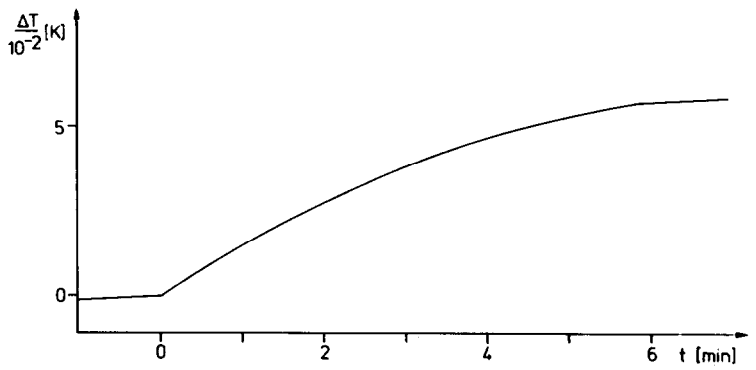


Fig. 3. Thermogram for the titration of K^+ with B99. The titration starts at $t = 0$ and ends at $t = 6$ min.

thermogram. This problem will be treated in more detail in another publication.[7]

All measured values for the 1:1 complexes of PEGM and nonionic surfactants with alkali and alkaline-earth cations are given in Table 2. The complexation behaviour of PEGM is very similar to that of PG. These ligands and PEG possess the same numbers of oxygen atoms as 18-crown-6 and they are

Table 2. Log K (K in M^{-1}), ΔH (kJ M^{-1}) and ΔS (J M^{-1} K^{-1}) for the complexation of nonionic surfactants with cations in methanol at 25°C.

Ligand	Value	Na^+	K^+	Rb^+	Cs^+	Ca^{2+}	Sr^{2+}	Ba^{2+}
PEG[a]	Log K[b]	—	2.01	1.92	1.29	3.79	3.58	3.71
	ΔH		−24.9	−24.7	−44.2	−3.7	−24.5	−28.4
	ΔS		−45	−46	−124	60	−14	−25
PEGM	Log K	—[c]	1.98	1.77	1.68	—[c]	3.38	3.35
	ΔH		−43.2	−55.8	−35.1		−11.4	−27.0
	ΔS		−107	−153	−86		26	−27
PG[d]	Log K[b]	1.54	2.07	1.98	1.76	—[c]	—[c]	2.59
	ΔH	−19.7	−44.7	−46.7	−38.6			−20.2
	ΔS	−37	−110	−119	−96			−18
B30	Log K	—[c]	3.76	4.29	3.88	—[c]	3.84	4.40
	ΔH		−9.7	−9.2	−7.6		−3.6	−10.6
	ΔS		39	51	48		61	48
JCO-720	Log K	1.52	2.72	2.77	2.98	—[c]	3.17	3.68
	ΔH	−36.8	−52.9	−55.3	−42.4		−13.7	−37.1
	ΔS	−94	−126	−133	−85		14	−54
B58	Log K	1.98	2.59	2.59	2.42	—[c]	2.51	2.76
	ΔH	−29.9	−79.3	−90.3	−91.4		−24.8	−60.3
	ΔS	−63	−217	−254	−260		−35	−150
B99	Log K	2.00	2.62	2.64	2.47	—[c]	2.66	2.69
	ΔH	−22.1	−72.6	−77.5	−85.7		−19.3	−65.3
	ΔS	−36	−193	−210	−240		−14	−168
B35	Log K	2.07	2.50	2.56	2.57	2.48	3.29	2.57
	ΔH	−26.8	−88.0	−88.8	−74.4	−1.5	−14.1	−76.1
	ΔS	−50	−248	−249	−201	42	15	−206
18C6[e]	Log K[f]	4.32	>5	>5	4.44	3.87	>5	>5
	ΔH	−34.0	−54.6	−49.6	−49.9	−11.2	−37.2	−48.5
	ΔS	−32			−83	36		

[a] $HOCH_2CH_2(OCH_2CH_2)_4OH$.
[b] From Ref. 5.
[c] No detectable heat produced during the titration; log K very small or $\Delta H = 0$.
[d] $CH_3OCH_2CH_2(OCH_2CH_2)_4OCH_3$.
[e] 18-Crown-6.
[f] From Ref. 8.

able to surround Na^+, K^+, Rb^+, Ca^{2+} and Sr^{2+}. The bulky methyl groups hinder the complex formation more than the small protons of the OH groups do. This is reflected in the values of the reaction entropies. On the other hand the higher dipole moment of the hydroxyl end-groups compared with the ether groups leads to a stronger repulsion of the opposing parts of the ligand. Thus, the reaction enthalpies of the complex formation with PEG are lowered. These factors do not influence the reaction with the biggest cations, Cs^+ and Ba^{2+}. The ligands are too small to wrap around the cations and the different end-groups are not able to reach each other. Therefore reaction enthalpies and entropies for the complexation of Cs^+ by PEG, PEGM and PG are very similar. The same situation is found for the reactions of Ba^{2+}.

Although the number of oxygen atoms is only reduced by one the nonionic surfactant B30 shows a behaviour quite different from PEGM. The values of the reaction enthalpies for the complexation of alkali and alkaline-earth cations by B30 are much smaller compared to PEGM. This indicates that the number of donor atoms participating in the reaction is small. On the other hand the reactions of B30 are favored by the reaction entropies. The long nonpolar chain of B30 possibly produces a conformation of the uncomplexed ligand which facilitates complex formation. A similar behaviour was found for the reactions of a ligand with the same number of oxygen atoms containing chinoline end-groups.[5]

With increasing number of donor atoms the nonpolar chain becomes unimportant for the complexation. Reaction enthalpies and entropies for ICO-720 and PEGM are nearly identical. The same is found for the reactions of B58 and B99. B35, the ligand with the longest oligoethylene glycol chain which forms 1 : 1 complexes, acts nearly like the smaller ligands. Generally with increasing number of donor atoms in the nonionic surfactants the reaction enthalpies with all cations favor the complex formation. In contrast the reaction entropies become more negative with chain length. As a result the stability constants for all complexes do not increase. Log K reaches a very similar value for all cations examined.

It is not surprising that no selectivity for cations is found as in the case of crown ethers. The ligands are so flexible as to get optimal interactions with the different cations. The reaction enthalpies of the noncyclic ligands reach much higher values than 18-crown-6 (see Table 2). The monocyclic ligand is not able to surround the complexed cation completely. Some solvent molecules are still coordinated to the cation. Only steric requirements are responsible for the low stability constants of the noncyclic ligands examined. Crown ethers already possess an ordered conformation with a fixed position of the donor atoms. This leads to less negative values of the reaction entropy.

In water an interesting effect is possible. The nonionic surfactants are able to form micelles with a more regular conformation compared to the monomeric form of the molecules. Therefore these micelles should act as ligands and form complex ions. Further investigations are in progress and the results will be reported later.

REFERENCES

1. R. M. Izatt and J. J. Christensen (Eds), *Synthetic Multidentate Macrocyclic Compounds.* Academic Press, New York (1978).
2. J. M. Lehn, *Struct. Bonding* 1973 **16**, 1.
3. (a) C. J. Pedersen and H. K. Frensdorff, *Angew. Chem., Int. Ed. Engl.* 1972, **11**, 16; (b) M. Kodawa and E. Kimura, *Bull. Chem. Soc. Jpn* 1976, **49**, 2465; (c) B. L. Haymore, J. D. Lamb, R. M. Izatt and J. J. Christensen, *Inorg. Chem.* 1982, **21**, 1548.
4. (a) L. Favretto, *Ann. Chim.* 1976, **66**, 621; (b) L. Favretto, *Ann. Chim.* 1981, **71**, 163.
5. H.-J. Buschmann, *Z. Phys. Chem.* 1984, **139**, 113.
6. R. M. Izatt, R. E. Terry, D. P. Nelson, Y. Chan, D. J. Eatough, J. S. Bradshaw, L. D. Hausen and J. J. Christensen, *J. Am. Chem. Soc.* 1976, **98**, 7626.
7. H.-J. Buschmann, *Makromol. Chem.* (in press).
8. H.-J. Buschmann, *Chem. Ber.* 1985, **118**, 2746.

Polyhedron Vol. 4, No. 12, pp. 2043–2050, 1985
Printed in Great Britain

0277–5387/85 $3.00+.00
© 1985 Pergamon Press Ltd

SPECTROPHOTOMETRIC AND POTENTIOMETRIC STUDY OF THE COBALT(II)–THIOCYANATE SYSTEM IN AQUEOUS MEDIUM

NINA COICHEV FERREIRA VELLOSO, EDUARDO ALMEIDA NEVES* and IVANO G. R. GUTZ

Instituto de Química da Universidade de São Paulo, Caixa Postal 20.780—CEP 01498, São Paulo—SP, Brasil

(*Received* 18 *March* 1985; *accepted* 19 *June* 1985)

Abstract—The cobalt(II)–thiocyanate system was spectrophotometrically studied at 2.0 M ionic strength ($NaClO_4$) and 25°C. The following formation constants were obtained: $\beta_1 = 6.9\ M^{-1}$, $\beta_2 = 28.9\ M^{-2}$, $\beta_3 = 12.1\ M^{-3}$ and $\beta_4 = 1.30\ M^{-4}$. Three wavelengths were considered, 515, 590 and 615 nm, and the molar absorptivities of each species were calculated. Linear relationships were obtained for $\bar{\varepsilon}$ vs $\bar{n}$ and α_i. There is strong evidence that the tetrahedral $[Co(SCN)_4]^{2-}$ is virtually the only species absorbing at 590 and 615 nm. An indirect potentiometric method led to comparable equilibrium constants. The cadmium(II)–thiocyanate formation constants used in the indirect method, under the same conditions, were found to be $\beta_1 = 21.51 \pm 0.09\ M^{-1}$, $\beta_2 = 123 \pm 1\ M^{-2}$, $\beta_3 = 130 \pm 3\ M^{-3}$ and $\beta_4 = 173 \pm 1.2\ M^{-4}$, in good agreement with earlier literature data.

The cobalt(II)–thiocyanate reaction is an old analytical test[1] known as Vogel's reaction. The bluish colour obtained, enhanced in acetone medium, is well accepted as being caused by the formation of the tetrahedral $[Co(SCN)_4]^{2-}$ species.[2–8]

In spite of theoretical and practical concerns about this reaction, the equilibrium studies in aqueous medium are incomplete, most of them referring only to the $[Co(SCN)]^+$ species, and showing inconsistencies. There are very few equilibrium data referring to the stepwise complexes up to four thiocyanate ligands.[9,10]

This paper reports a spectrophotometric study of this system by the corresponding solutions method,[11] with the main purpose of obtaining the overall stepwise formation constants of this system in aqueous medium of 2.0 M ionic strength, at 25°C. An indirect potentiometric method, using an indicator cadmium(II)–thiocyanate system, provided comparable results in a fairly limited ligand concentration range.

EXPERIMENTAL

All spectrophotometric measurements were carried out with a Zeiss DMR 10 instrument with the cell compartment thermostatted at 25.0±0.1°C. A recorder was used to obtain the full spectra. It was substituted by a digital voltmeter with $4\frac{1}{2}$ digits for the precise measurement of the absorbance (±0.002) at fixed wavelengths. Cells with 1.000-cm pathlength were normally used. However, with highly absorbing solutions, a calibrated 0.1000-cm pathlength pair of cells was used. The wavelengths of 515, 590 and 615 nm were conveniently selected for the determination of the stability constants. Three series of solutions with 0.01000, 0.05000 and 0.1000 M cobalt(II) were measured at several thiocyanate concentrations, all of them with the ionic strength adjusted to 2.0 M with sodium perchlorate.

The potentiometric measurements were performed with a hanging cadmium amalgam drop electrode using the same experimental arrangement as previously described.[12] The precision was ±0.02 mV.

The cadmium(II)–thiocyanate system was accurately studied to be used as an indicator for the cobalt(II)–thiocyanate system. The working solutions for potential measurements were prepared by adding increasing volumes of 1.700 M sodium thiocyanate with 0.1000 M cobalt(II) perchlorate, 1.000 mM cadmium perchlorate and 1.000 mM perchloric acid to 10.00 ml of a similar solution in which sodium perchlorate changes the thiocyanate, at 25.0±0.1°C.

* Author to whom correspondence should be addressed.

Data of the cadmium(II)–thiocyanate system were analysed with a previously described programme[13–15] on an HP-9825 desk-top computer. The same computer was used in the other calculations described in this paper.

Chemicals were of A.R. or C.P. specifications from Merck, Carlo–Erba and Baker.

Cobalt(II) perchlorate was prepared by treatment of 1 M perchloric acid with excess cobalt(II) carbonate for 2 days, at room temperature. The filtered solution was boiled. Perchloric acid was added to a pH of 2. Standardization was performed by electrogravimetry.[16]

Sodium thiocyanate was potentiometrically titrated with silver nitrate.

Sodium perchlorate solution was gravimetrically standardized by slow evaporation of 3.00 ml and heating in an oven at 120°C.

RESULTS AND DISCUSSION

Spectrophotometric determination of the equilibrium constants

Figure 1 shows the spectra for a wide ligand concentration range, at 2.0 M constant ionic strength. $\bar{\varepsilon}$ is the average molar absorptivity at a given wavelength and free ligand concentration:

$$\bar{\varepsilon} = \frac{A}{C_{Co} \cdot b}, \tag{1}$$

where A is the absorbance of the solution with C_{Co} (M), the analytical concentration of cobalt(II), and b is the pathlength (cm).

It can be seen that the band at 615 nm begins to be defined only above 0.6 M thiocyanate. Conversely the band at 515 nm begins to develop even at low thiocyanate concentrations. Thus it is more appropriate for equilibrium studies at smaller ligand concentrations. Measurements were taken at these two wavelengths and also at the minimum at 590 nm.

The data obtained at the two absorption peaks can be seen in Figs 2 and 3, and were used to calculate the average ligand number, $\bar{n}$, and the free ligand concentration, [SCN^-]. This is possible because the corresponding solutions, with the same $\bar{\varepsilon}$, have the same $\bar{n}$ and [SCN^-]. The three C_{SCN^-} collected for each group of corresponding solutions in Figs 2 and 3, plotted vs C_{Co}, yield a straight line with the free ligand concentration as the intercept and $\bar{n}$ as the

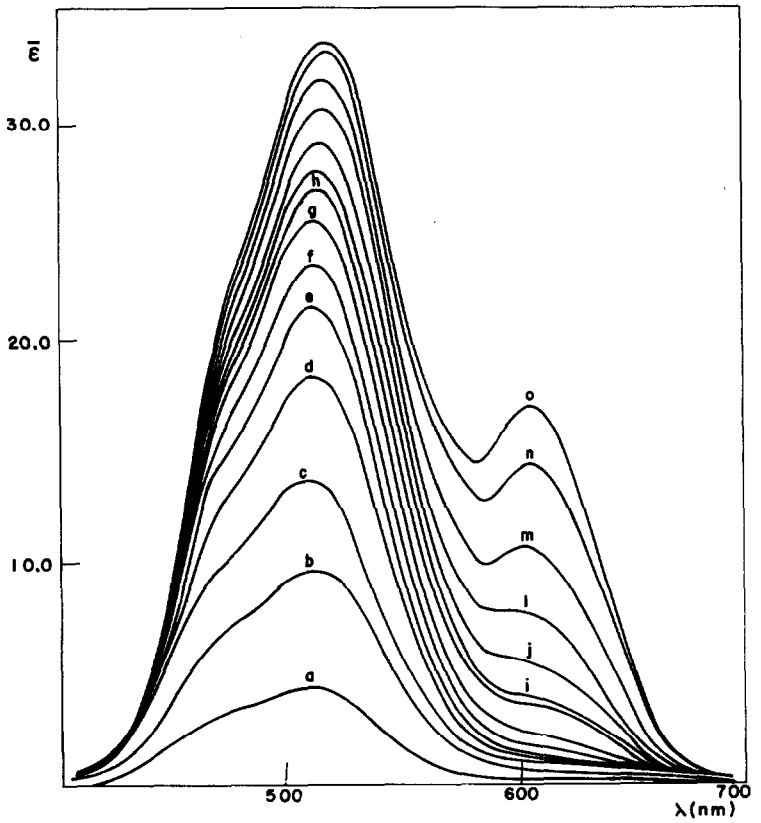


Fig. 1. Spectra for the cobalt(II)–thiocyanate system. b = 1.000 cm, C_{Co} = 0.05000 M, T = 25.0°C, and C_{SCN^-} = (a) zero, (b) 0.05000 M, (c) 0.1000 M, (d) 0.2000 M, (e) 0.3000 M, (f) 0.4000 M, (g) 0.5000 M, (h) 0.6000 M, (i) 0.7000 M, (j) 0.8000 M, (l) 1.000 M, (m) 1.200 M, (n) 1.400 M, and (o) 1.600 M.

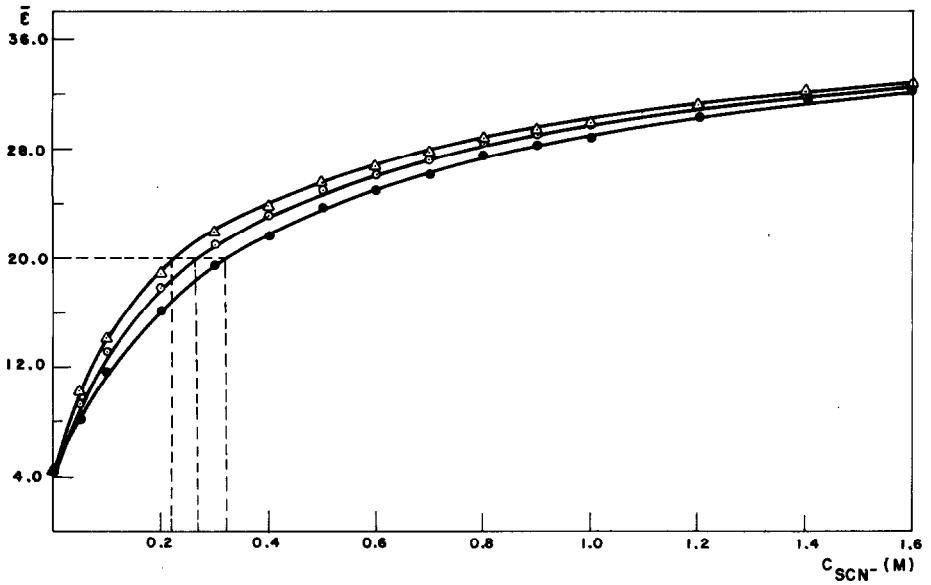


Fig. 2. Calculated curves traced from the experimental data, with: $\beta_1 = 6.9\ M^{-1}$, $\beta_2 = 28.9\ M^{-2}$, $\beta_3 = 12.1\,M^{-3}$ and $\beta_4 = 1.3\,M^{-4}$. $\lambda = 515$ nm. $C_{Co} = (\triangle)0.01000$ M, $(\bigcirc)0.05000$ M, and $(\bullet)0.1000$ M. An example of three corresponding solutions is indicated by the dashed lines.

slope:[17]

$$C_{SCN^-} = [SCN^-] + \bar{n} \cdot C_{Co}. \qquad (2)$$

The resulting formation curve is presented in Fig. 4, which contains data for the three wavelengths. The average curve was found by smoothing the experimental data by least-squares fitting of moving polynomials.

The data at 515 nm become inconsistent above 0.4 M thiocyanate and were rejected. The contributions of the data at 590 and 615 nm become more significant in this region of the formation curve.

Integration of the $\bar{n}$ vs log $[SCN^-]$ curve leads to the well-known Fronaeus[18] function:

$$F_0(SCN) = 1 + \sum_{i=1}^{N} \beta_i [SCN^-]^i. \qquad (3)$$

The analysis of subsidiary functions[18] (Fig. 5) indicates the existence of four stepwise complexes. The following overall constants were obtained

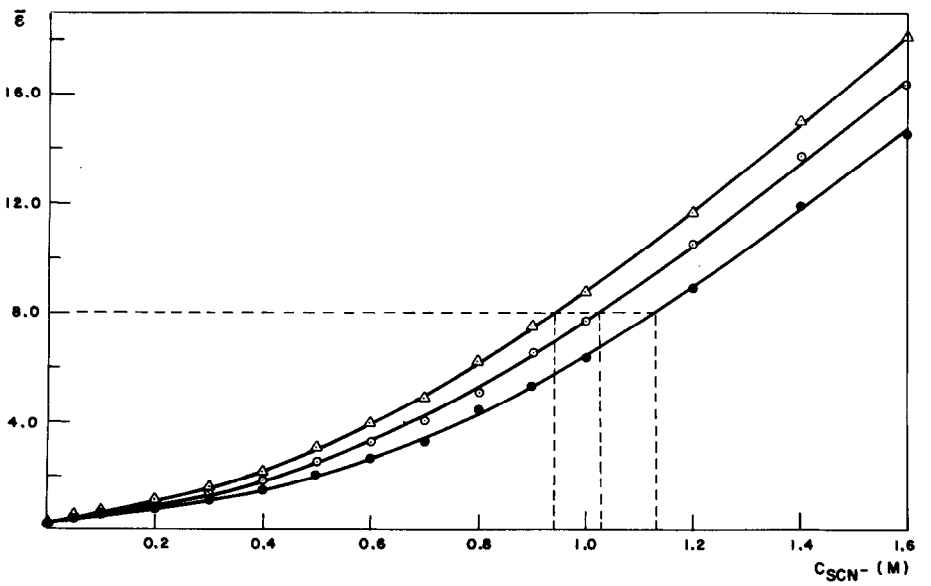


Fig. 3. Calculated curves traced from the experimental data. Same conditions as in Fig. 2. $\lambda = 615$ nm.

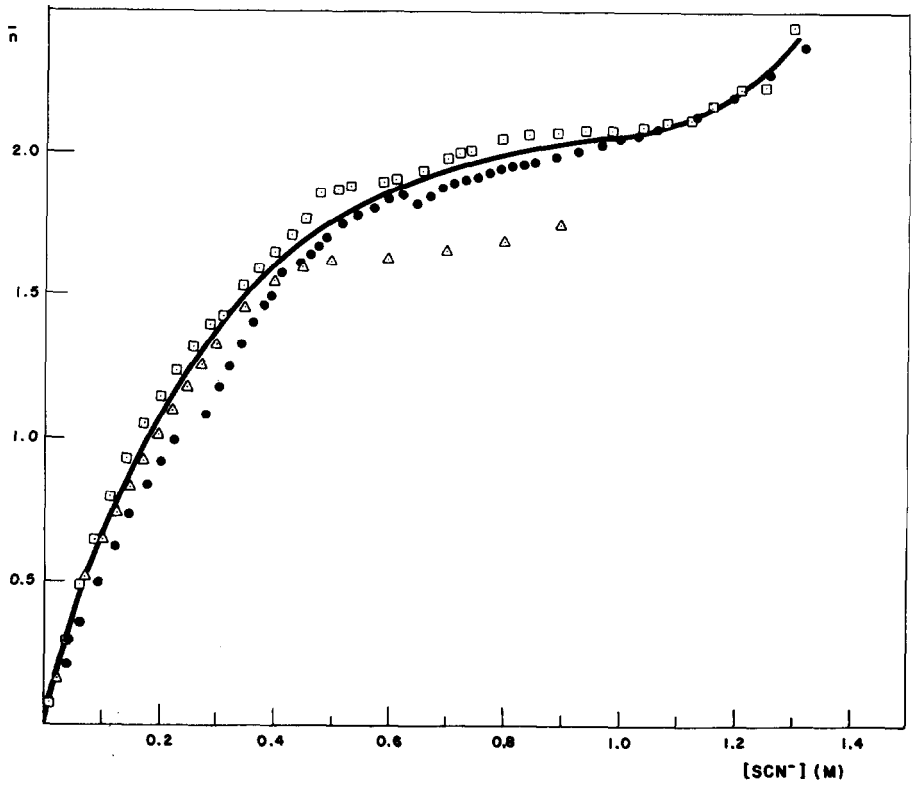


Fig. 4. Medium curve traced on basis of the data obtained from measurements at: (△) 515 (□) 590, and (●) 615 nm.

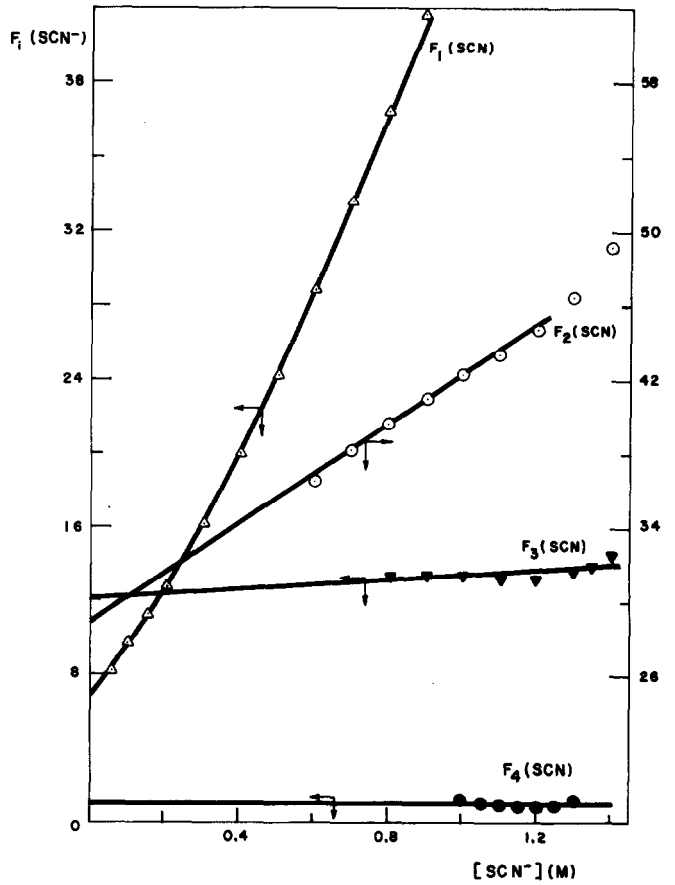


Fig. 5. Graphical extrapolation of the F_i data to obtain β_i.

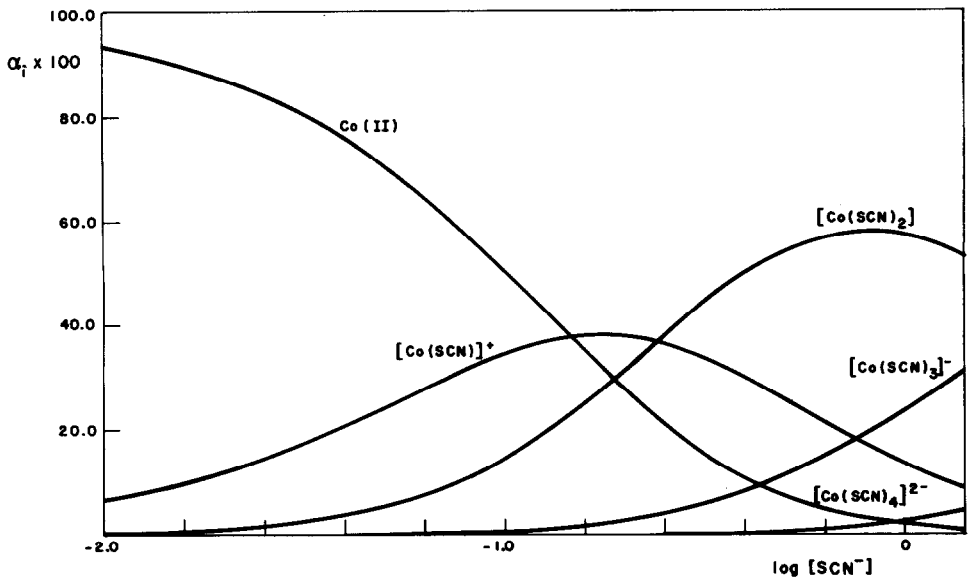


Fig. 6. Distribution diagram for the cobalt(II)–thiocyanate system. Ionic strength 2.0 M ($NaClO_4$) and $T = 25°C$.

by a previously described weighted least-squares procedure:[15] $\beta_1 = 6.9\ M^{-1}$, $\beta_2 = 28.9\ M^{-2}$, $\beta_3 = 12.1\ M^{-3}$ and $\beta_4 = 1.30\ M^{-4}$.

It can be inferred that the complexes are weak and that it is difficult to introduce more than two ligands, as can be seen in a distribution diagram (Fig. 6).

Dependence of $\bar{\varepsilon}$ on equilibrium data: evolution of ε_i

Interesting information was obtained from plots of $\bar{\varepsilon}$ vs equilibrium data calculated from the formation constants. A linear relationship is found at 515 nm (but not at 590 and 615 nm) for $\bar{\varepsilon}$ vs the calculated $\bar{n}$ (spectrophotometric constants) (from 0.4 to 2.4), corresponding to a wide ligand range (Fig. 7). This suggests a regular increase in the individual molar absorptivity of each complex as the number of ligands attached increases. On this basis the extrapolation of $\bar{\varepsilon}$ to $\bar{n} = 4$ leads to the estimation of ε_4, referred to $[Co(SCN)_4]^{2-}$. This also means that all species absorb at this wavelength whether tetrahedral or not.

At 590 and 615 nm a linear plot is observed for $\bar{\varepsilon}$ vs α_4 (see Fig. 8) with an intercept at a low value in the ordinate axis. This indicates that only the highly symmetrical tetrahedral fourth species absorbs. The contribution of the lower members of the series is very small. The limit of $\bar{\varepsilon}$ for α_4 tending to 1 is ε_4, which can be obtained by linear extrapolation.

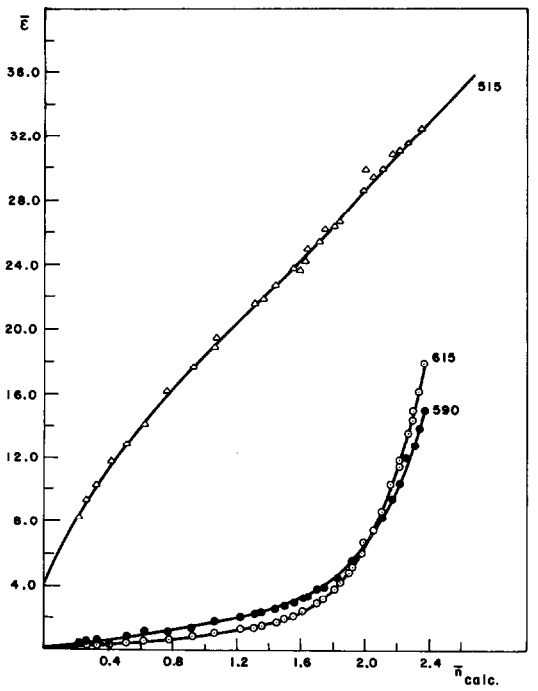


Fig. 7. Variation of $\bar{\varepsilon}$ with $\bar{n}$ at 515, 590 and 615 nm.

The following equation relates $\bar{\varepsilon}$ with the molar absorptivities and the corresponding β_i formation constants:[17]

$$\bar{\varepsilon} = \frac{\varepsilon_0 + \varepsilon_1\beta_1[SCN^-] + \varepsilon_2\beta_2[SCN^-]^2 + \varepsilon_3\beta_3[SCN^-]^3 + \varepsilon_4\beta_4[SCN^-]^4}{1 + \beta_1[SCN^-] + \beta_2[SCN^-]^2 + \beta_3[SCN^-]^3 + \beta_4[SCN^-]^4}. \quad (4)$$

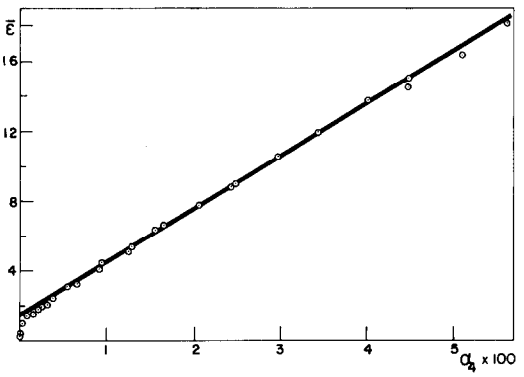


Fig. 8. Verification of the linearity of $\bar{\varepsilon}$ vs α_4 at 615 nm.

Combination with eqn (3) gives:

$$\bar{\varepsilon}\cdot F_0(SCN) = \varepsilon_0+\varepsilon_1\beta_1[SCN^-] +\varepsilon_2\beta_2[SCN^-]^2+\varepsilon_3\beta_3[SCN^-]^3 +\varepsilon_4\beta_4[SCN^-]^4. \quad (5)$$

The number of unknowns is decreased from nine to five by introducing the previously determined formation constants. In addition, ε_0 is found by direct measurement in uncomplexed medium and ε_4 from linear extrapolation. A simpler system of simultaneous equations can be used for calculation of ε_1, ε_2 and ε_3:

$$\phi_0 = \bar{\varepsilon}F_0(SCN)-\varepsilon_0-\varepsilon_4\beta_4[SCN^-]^4 \quad (6A)$$

$$= \varepsilon_1\beta_1[SCN^-]+\varepsilon_2\beta_2[SCN^-]^2 +\varepsilon_3\beta_3[SCN^-]^3 \quad (6B)$$

and

$$\phi_1 = \frac{\phi_0}{[SCN^-]} = \varepsilon_1\beta_1+\varepsilon_2\beta_2[SCN^-] +\varepsilon_3\beta_3[SCN^-]^2. \quad (7)$$

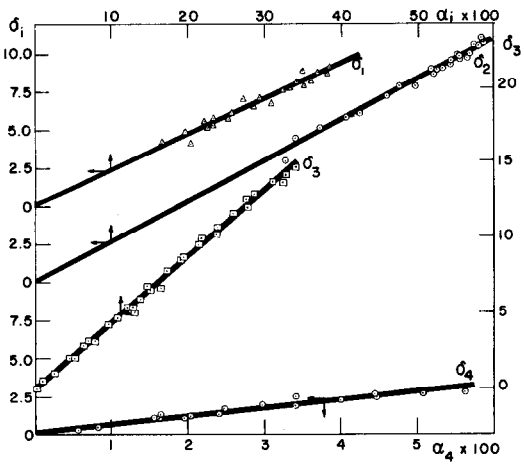


Fig. 9. Verification of the linearity of δ_i [eqn (10)] vs α_i at 515 nm.

Simultaneous equations were taken for ϕ_1 vs $[SCN^-]$. As the magnitude of ϕ_1 terms changes markedly with the concentration of the ligand, a weighting factor:

$$\omega_j = \frac{1}{\bar{\varepsilon}_j} \quad (8)$$

was used in order to place all $\bar{\varepsilon}$ data to a same magnitude. The reason of that is the adjustment of the magnitude of the relative error of absorbance measurements to a same level, in order to provide a consistent system of simultaneous equations. This kind of procedure has been successfully used with other experimental data of equilibrium studies.[15,19]

Table 1 presents the molar absorptivities of the individual species at the three wavelengths, as found from a combination of strategies.

At 515 nm, a verification of the compatibility of the β_i and ε_i values with the experimental $\bar{\varepsilon}$ data was obtained by considering the isolated contribution of each species. At a determined free ligand concentration:

$$\bar{\varepsilon} = \sum_{i=0}^{4} \varepsilon_i\cdot\alpha_i. \quad (9)$$

The contribution of the first species is:

$$\delta_1 = \bar{\varepsilon}-(\varepsilon_0\alpha_0+\varepsilon_2\alpha_2+\varepsilon_3\alpha_3+\varepsilon_4\alpha_4) = \varepsilon_1\cdot\alpha_1. \quad (10)$$

As expected, the plot of δ_1 as a function of the α_1 calculated for each datum point can be fitted by a straight line with zero intercept and slope ε_1. The same agreement was observed for ε_2, ε_3 and ε_4 (Fig. 9).

The ε_1–ε_4 values at 515 nm have a linear relationship to the number of ligands, but ε_0 is too low to be fitted in this series. The behavior at 590 and 615 nm suggests (see Figs 7 and 8) that the fourth species is virtually tetrahedral with a fairly high molar absorptivity. Very little of this complex is present in the equilibrium in the explored concentration range but its molar absorptivity is fairly high at 590 and 615 nm, compared to the other ε_i. A situation of ambiguity exists with regard to the other lower species. They can be octahedral with a very low molar absorptivity, or the observed data are averages of highly absorbing tetrahedral complexes, but present in a very low concentration, in equilibrium with the octahedral ones, which do not absorb at 590 and 615 nm.

The use of the determined paramaters (ε_i and β_i) in eqn (4) for the several thiocyanate concentrations led to the calculated $\bar{\varepsilon}$ for the three cobalt(II) concentrations used in the measurements. The comparison between calculated and experimental $\bar{\varepsilon}$ data led to relative standard deviations of 1.8% at 515 nm, 1.9% at 590 nm and 2.6% at 615 nm.

It should be pointed out that the assumption of a

Table 1. Molar absorptivities calculated at the three wavelengths, with $\beta_1 = 6.9\ M^{-1}$, $\beta_2 = 28.9\ M^{-2}$, $\beta_3 = 12.1\ M^{-3}$ and $\beta_4 = 1.3\ M^{-4}$

ε_i ($M \cdot cm^{-1}$)	λ(nm) 515	590	615
ε_0[a]	4.31	0.29	0.20
ε_1	22.6	1.3	0.90
ε_2	26.3	3.2	1.5
ε_3	42.8	3.9	2.2
ε_4[b]	50.3	215	294

[a] Direct measurement in perchlorate medium.
[b] Extrapolated to $\bar{n} = 4$ or $\alpha_4 = 1$.

system with only three stepwise complexes led to a very inconsistent fit between calculated and experimental measurements.

Indirect potentiometric determination of the equilibrium constants

Another set of constants was obtained by an indirect method.[14] Firstly the formation constants of cadmium(II)–thiocyanate were redetermined under very reliable conditions with a cadmium amalgam electrode, leading to the following values: $\beta_1 = 21.51 \pm 0.09\ M^{-1}$, $\beta_2 = 123 \pm 1\ M^{-2}$; $\beta_3 = 130 \pm 3\ M^{-3}$ and $\beta_4 = 173 \pm 1\ M^{-4}$, in good agreement with published data.[20]

Substituting these constants in eqn (3) and remembering that the change in the potential of the amalgam electrode is related to $F_0(SCN)$, at 25°C, by:

$$\Delta E = \frac{-0.05916}{2} \log F_0(SCN), \qquad (11)$$

and that the free ligand concentration must satisfy the equilibria involving both metal ions, it is possible to calculate $[SCN^-]$ in the presence of added cobalt(II). The calculation of $[SCN^-]$ and the $\bar{n}$ of the cobalt(II) complexes was done with an appropriate computer programme. The smoothed curve in the range 0–2.2 for $\bar{n}$ was integrated and analysed by the same procedure as used for the spectrophotometric data. The stability constants obtained are $\beta_1 = 11.0\ M^{-1}$, $\beta_2 = 22.0\ M^{-2}$, $\beta_3 = 11.2\ M^{-3}$ and $\beta_4 = 1.63\ M^{-4}$.

Table 2. Values of stability constants obtained by different authors for the Co(II)–SCN^- system

Method	Ionic strength	T (°C)	β_1 (M^{-1})	β_2 (M^{-2})	β_3 (M^{-3})	β_4 (M^{-4})	Reference
Potentiometry	0.1 M (KNO_3)		24				21
(Ag–AgSCN	Ionic strength → 0		73.5				22
electrode)							
Polarography	0.7 M	25.0	8.8				23
[kinetic wave							
of Ti(IV)]	1.5 M ($NaClO_4$)	25.0	9.6				24
Spectrophotometry	0.6 M ($NaClO_4$)	20.0	12.7±0.4				25
[Fe(III)–SCN^-	0.3 M ($NaClO_4$)	20.0	15.3±0.5				25
as indicator]	0.15 M ($NaClO_4$)	20.0	18.9±0.45				25
	0.54–0.71 M		Between 12 and 21				26
Kinetics	1.0 M ($NaClO_4$)	25.0	8.23				27
Spectrophotometry	0.5 M ($NaClO_4$)	1.5	16				28
	1.0 M ($NaClO_4$)	25.0	10.09				29
	1.0 M ($NaClO_4$)	25.0	10.38				29
	1.5 M ($NaClO_4$)	20.0	7.5				10
	1.5 M ($NaClO_4$)		9.9				30
	Variable	20.0	10^3	10^3	200	184	9
	1.0 M	20.0	2.5				31
	1.5 M	25.0	9.0	40±15[a]	60±20[a]	0.5±0.3[a]	10
	0.16 M	25.0	52.4				32
	Variable		8.9				33
	0.3 M ($NaClO_4$)	20.0	15.3				25
	Ionic strength → 0		75.8				22
Potentiometry							
[Cd(Hg) electrode]	2.0 M ($NaClO_4$)	25.0	11	22.0	11.2	1.63	Present work
Spectrophotometry	2.0 M ($NaClO_4$)	25.0	6.9	28.9	12.1	1.3	Present work

[a] Extraction with methyl isobutyl ketone.

The formation curve is very close to that obtained from spectrophotometric data up to $\bar{n} = 0.9$. A speculative explanation for the disagreement after this point is an interaction of the anionic $[Cd(SCN)_3]^-$ and $[Cd(SCN)_4]^{2-}$ with $Co(SCN)_2$ to form binuclear species at higher thiocyanate concentration. This point deserves further investigation.

The potentiometric method provides more accurate equilibrium data when the free metal cation is directly measurable. In the cobalt(II)–thiocyanate system an indirect potentiometric method was used. The spectrophotometric $\bar{n}$ data are probably more reliable because they come from a direct method. In fact the linear plot involving experimental $\bar{\varepsilon}$ data vs calculated $\bar{n}$ looks more consistent when β_i values from a spectrophotometric origin are considered in calculations.

Table 2 is a survey of several equilibrium constants determined by a variety of methods and background electrolytes.

There is a reasonable agreement in the β_1 values, situated in the range from 7 to 11 in the majority of cases. Only one study with the estimation of four stepwise equilibrium constants was found for an aqueous medium, but obtained by a solvent extraction method,[10] with severe disagreement with the present results for β_2, β_3 and β_4. Only the first constant falls in the previously mentioned range, certainly because it was separately determined by a spectrophotometric method.[10] However, the solvent extraction method can be much more critical for such a complex study, because the distribution function can be affected by other factors such as the change in the activity of extracted species in the organic phase with a wide range of ligand concentration in the aqueous phase.

REFERENCES

1. H. W. Vogel, *Ber.* 1875, **8**, 1533.
2. W. Libus, *Rocz. Chem.* 1957, **31**, 1075.
3. W. Libus, *Rocz. Chem.* 1959, **33**, 951.
4. W. Libus, *Rocz. Chem.* 1961, **35**, 411.
5. V. P. Vasil'ev, V. N. Vasil'eva, F. I. Ivanova and O. N. Morozova, *Izv. Vyssh. Uchebn. Zaved. Khim. Khim. Tekhnol.* 1963, **6**, 712.
6. M. S. Barvinok, *Izv. Akad. Nauk SSSR, Ser. Fiz.* 1948, **12**, 636.
7. G. Sitaramaiah and C. L. Sanghi, *Proc. Natl Acad. Sci. India* 1958, **A27**, 103.
8. F. A. Cotton and G. Wilkinson, *Advanced Inorganic Chemistry*, 3rd edn, p. 880. Interscience, New York (1962).
9. M. Lehné, *Bull. Soc. Chim. Fr.* 1951, 76.
10. S. Tribalat and C. Zeller, *Bull. Soc. Chim. Fr.* 1962, 2041.
11. J. Bjerrum, *K. Dan. Vidensk. Selsk. Mat.-Fys. Medd.* 1944, **4**, 21.
12. I. G. R. Gutz and E. A. Neves, *J. Electroanal. Chem.* 1985, **183**, 123.
13. P. Senise and E. A. Neves, *J. Am. Chem. Soc.* 1961, **83**, 4146.
14. N. C. F. Velloso, E. A. Neves and I. G. R. Gutz, *III Simpósio Brasileiro de Eletroquímica e Eletroanalítica (Universidade de São Paulo—S. Carlos—SP, Brazil)*, 1982, 307.
15. E. A. Neves, N. Milcken and D. W. Franco, *J. Inorg. Nucl. Chem.* 1981, **43**, 2081.
16. A. I. Vogel, *A Textbook of Quantitative Inorganic Analysis*, 2nd edn, pp. 358, 613. Longmans Green, London (1961).
17. M. T. Beck, *Chemistry of Complex Equilibria.* pp. 96, 97. Van Nostrand, London (1969).
18. F. J. C. Rossotti and H. Rossotti, *The Determination of Stability Constants*, p. 108. McGraw-Hill, New York (1961).
19. E. A. Neves, I. G. R. Gutz and R. G. Tavares, *J. Electroanal. Chem.* 1984, **179**, 91.
20. P. Gerding, *Acta. Chem. Scand.* 1968, **22**, 1283.
21. M. Polasek and M. Bartusek, *Scr. Fac. Sci. Nat. Univ. Purkynianae Brun.* 1971, **1**, 109.
22. R. C. Das, A. C. Dash, D. Satyanarayan and U. N. Dash, *Thermochim. Acta* 1971, **2**, 435.
23. S. Tribalat, D. Delafosse, C. Piolet and D. Zeller, *J. Electroanal. Chem.* 1959/1960, **1**, 443.
24. S. Tribalat and J. M. Caldero, *J. Electroanal. Chem.* 1963, **5**, 1976.
25. V. N. Kumok and V. V. Serebrennikov, *Russ. J. Inorg. Chem.* 1964, **9**, 1160.
26. G. Saini and C. Sapetti, *Atti Accad. Sci. Torino* 1951, **86**, 247.
27. M. H. Hutchinson and W. C. E. Higginson, *J. Chem. Soc., Dalton Trans.* 1973, **12**, 1247.
28. A. G. Davies and W. M. Smith, *Proc. Chem. Soc., London* 1961, 380.
29. P. Senise and M. Perrier, *J. Am. Chem. Soc.* 1958, **80**, 4194.
30. S. Tribalat and J. M. Caldero, *C. R. Seances. Acad. Sci.* 1962, **255**, 925.
31. J. M. Smithson and R. J. P. Williams, *J. Chem. Soc.* 1958, 457.
32. T. Williams, *J. Inorg. Nucl. Chem.* 1962, **24**, 1215.
33. S. Fronaeus and R. Larsson, *Acta Chem. Scand.* 1962, **16**, 1433.

Polyhedron Vol. 4, No. 12, pp. 2051–2057, 1985
Printed in Great Britain

0277–5387/85 $3.00 + .00
© 1985 Pergamon Press Ltd

THE PAIRING PRINCIPLE IN TENSOR SURFACE HARMONIC THEORY: ELECTRON COUNTS OF LARGE *CLOSO* BORANES

P. W. FOWLER*

Department of Theoretical Chemistry, University Chemical Laboratory, Lensfield Road, Cambridge CB2 1EW, U.K.

(*Received* 8 *May* 1985; *accepted* 19 *June* 1985)

Abstract—Tetratomic tetrahedral main-group clusters have four or six (but not five) skeletal pairs, an exception to the $(n+1)$ rule for *closo* clusters. A general group-theoretical criterion, based on the pairing principle in Stone's tensor surface harmonic (TSH) theory, is presented for symmetry-induced departures from the $(n+1)$ rule. A count of $(n+2)$ or n skeletal pairs is *forced by symmetry* for: (i) T- or T_d-clusters with an odd number of sets of four equivalent cage atoms, and (ii) C_m or C_{mv} ($m \geqslant 3$) clusters with an odd number of cage atoms on the C_m-axis. Three such cases, B_nH_n or $B_nH_n^{4-}$, are found among the hypothetical supraicosahedral *closo* boranes proposed by Brown and Lipscomb (n = 16, 19 or 22). Extended Hückel calculations show that the TSH pattern applies to the whole series of *closo* boranes ($n \leqslant 24$). Charges of +4, −8 and −2 are discussed for a very large $B_{32}H_{32}^{q}$ cluster.

Polyhedral boranes have a special significance in the theory of cluster compounds, because they give the simplest example of the link between molecular structure and electron count.[1] The *closo* series $B_nH_n^{2-}$ consists of molecules that are deltahedral in shape (for $5 \leqslant n \leqslant 12$), and held together by $(n+1)$ skeletal electron pairs. If we regard linear $B_2H_2^{2-}$ and triangular $B_3H_3^{2-}$ as trivally deltahedral, the only exception to the $(n+1)$ rule is the tetrahedral cluster which needs either four (represented in B_4Cl_4) or six skeletal pairs, but not five. The MO diagram for B_4H_4 has a nonbonding doubly degenerate level, as a well-understood consequence of T_d-symmetry, and we may regard the $n = 4$ tetrahedron as an "*intrinsic*" exception to the $(n+1)$ rule.

A second class of departures from the $(n+1)$ rule is found for boron halides, B_nCl_n (e.g. $n = 8$ or 9), where clusters which are geometrically *closo* are held together by only n skeletal pairs.[2] These electron counts are rationalised by noting that the $(n+1)$th skeletal pair would occupy a nondegenerate, not very bonding MO for these clusters, and supposing that the cluster geometry is not sensitive to loss of this pair.[2] It is also possible that back-donation from the *exo* halides may be a significant factor in the stabilisation of B_nX_n relative to $B_nX_n^{2-}$.[3] Insofar as the electron count is determined by numerical values of the MO energies, we may regard these exceptions to the $(n+1)$ rule as "*accidental*" in contrast to the tetrahedral case.

Related to the *closo* boranes are the *nido* (formally $B_nH_n^{4-}$) and *arachno* (formally $B_nH_n^{6-}$) compounds with skeletons corresponding to the *closo* polyhedra minus one and two vertices, respectively.

There have been various attempts to explain these regularities and to derive the electron-counting rules from first principles.[4–6] One, which is based on a simple assumption that borane skeletons are roughly spherical clusters of B atoms, was put forward by Stone.[7] This is the tensor surface harmonic (TSH) theory. It accounts for the $(n+1)$ rule for *closo* boranes and the special stability of the deltahedral shapes. When combined with point group symmetry arguments, it explains the electron counts of tetrahedral clusters. In an extended Hückel (EH) formulation of TSH[8] the derived MO energies can be used to rationalise the "accidental" departures from the $(n+1)$ rule for B_nX_n.

Although the experimental series of *closo* boranes ends at $n = 12$, there is interest in the possibility that supra-icosahedral clusters may be stable. Brown and Lipscomb[9] invented plausible structures for the hypothetical 13- to 24-atom clusters, and speculated on clusters of even higher nuclearity such as the 32-boron omnicapped dodecahedron. The proposed structures were deltahedral, very roughly spherical

* Present address: Department of Chemistry, University of Exeter, Stocker Road, Exeter EX4 4QD, U.K.

in overall shape, with bond lengths estimated from known molecules. Approximate PRDDO calculations on these structures[10] verified the appropriateness of the -2 charge for all but three clusters. For $n = 16$, 19 or 22 it was found, "surprisingly", that the *neutral* molecule had a closed shell. It is shown in the present work how Stone's TSH theory can be used to predict, without calculation, that precisely these three clusters have an "*intrinsic*" departure from the $(n+1)$ rule.

In this paper we present an analysis of "*intrinsic*" exceptions to the $(n+1)$ rule and establish a general criterion for their existence based on the pairing principle in TSH theory. Energy level diagrams for the whole series $B_nH_n^q$ $(13 \leqslant n \leqslant 24)$ are obtained by EH calculation and found to conform to the TSH pattern. *Nido* structures are also studied. Finally, EH energy levels are calculated for $B_{32}H_{32}^q$ and it is found that the HOMO–LUMO gap predicts a charge of $+4$ or -8 on this deltahedral cluster.

AN OUTLINE OF TSH THEORY

Stone's theory of clusters starts from a very simple picture and uses the power of angular momentum and group theory to give a general analysis of cluster bonding. The polyhedral boranes $B_nH_n^q$ consist, to a first approximation, of a set of B atoms distributed on the surface of a sphere, each participating in an *exo* radial BH bond. After subtraction of localised BH bonds, the basis left for skeletal bonding consists of an inward-pointing (σ) hybrid and two tangential (π) orbitals on each boron. In TSH we construct a set of approximate molecular orbitals from the solution of a model problem—the free electron on a sphere.[7]

The analytical solutions to the model problem are known; they are the scalar spherical harmonics (σ), the even (π) and odd ($\bar{\pi}$) vector surface harmonics, and higher functions not needed here. In common with other free-electron MO models, TSH uses the analytical forms to set the coefficients of the basis functions in the MOs. Thus the amplitude of the spherical harmonic at the boron vertex gives the contribution of the σ-hybrid on that atom to a σ MO of the cluster. Similarly, π and $\bar{\pi}$ MOs are formed from atomic tangential p-functions, weighted according to the vector surface harmonics. For the infinite, spherical cluster there are three infinite series of MOs (S^σ, P^σ, D^σ, ... L^σ ...; P^π, D^π, ... L^π...; $\bar{P}^\pi$, $\bar{D}^\pi$,... $\bar{L}^\pi$...) but for a finite cluster we count only the first n independent functions of the σ, π and $\bar{\pi}$ type, respectively.[7] In spherical symmetry both L^σ and L^π belong to the same representation of the spherical group, Γ_g^L (for even L) or Γ_u^L (for odd L). Thus, even within the spherical model, they can mix. In contrast, the $\bar{\pi}$-orbitals $\bar{L}^\pi$ have Γ_u^L-symmetry (for even L) or Γ_g^L-symmetry (for odd L) and cannot mix with σ- or π-orbitals within the TSH model.

The lowest MO, S^σ, consists of an in-phase combination of σ-hybrids on all atoms and is always bonding. More detailed reasoning[7] shows that σ–π interaction of the remaining σ-orbitals and their equisymmetric π counterparts produces n bonding and n antibonding orbitals for a deltahedral cluster. The $\bar{\pi}$-orbitals are intrinsically antibonding; thus the total number of skeletal bonding MOs is $(n+1)$ in agreement with Wade's rules.

The detailed order of orbital energies is also predicted rather well by a TSH calculation with σ–π interaction,[8] even though the MOs are based on such a simple model. As in other situations where free-electron models work well, e.g. conjugated hydrocarbons, the energy order in clusters is determined by the nodal pattern of the orbitals rather than their detailed form. TSH uses MOs with the correct nodal characteristics, though derived from a different Schrödinger equation, and therefore achieves the correct ordering. This is also the reason for the success of semiempirical schemes like EH[11] or MNDO[12] in predicting electron counts and orbital patterns.

THE PAIRING PRINCIPLE IN TSH THEORY

Although the π and $\bar{\pi}$ MOs are of different spherical symmetries, there is a pairing principle or one-to-one correspondence between them.[7] A component of a π-set L^π is converted to a component of the $\bar{\pi}$-set $\bar{L}^\pi$ by the "parity operation"—a twist of each p-orbital in the cluster through 90°, all in the same clockwise or counterclockwise sense. A second application of the operation recovers the original π-orbital but with all signs reversed (Fig. 1). Stone has shown how every bonding overlap is converted to antibonding by the parity operation, and vice versa. Thus in the absence of σ–π interaction, there would be a mirror relationship between π (bonding) orbital energies and $\bar{\pi}$ (antibonding) energies. Even after σ–π interaction an approximate mirror relationship persists near the bonding/antibonding frontier.[8]

In terms of representations, the symmetry of an L^π-set is converted to that of the $\bar{L}^\pi$-set by multiplication by the odd-parity, pseudoscalar representation:

$$\left.\begin{aligned} \Gamma(L^\pi) &= \Gamma(\bar{L}^\pi) \times \Gamma_u^o, \\ \Gamma_u^o \times \Gamma(L^\pi) &= \Gamma(\bar{L}^\pi). \end{aligned}\right\} \qquad (1)$$

Γ_u^o is a one-dimensional representation with character $+1$ under proper operations and -1 under improper ones. Its effect here is to switch g and

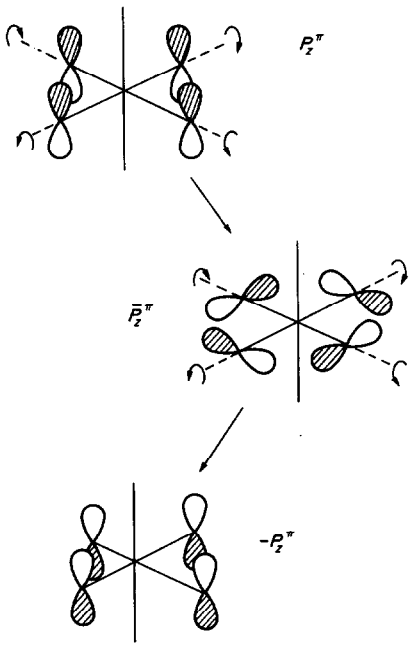


Fig. 1. Effect of the parity operation on P_z^π-orbitals of an octahedral cluster. Each atomic p-orbital is rotated by 90° about the line joining the vertex to the centre of the cluster.

u labels. A formal proof that the parity operator itself transforms as Γ_u^o is given by Ceulemans.[13]

The labels σ, π and $\bar{\pi}$ apply to infinite spherical clusters. In finite clusters the MOs are labelled by their point group representations, which follow from the splittings of the $(2L+1)$-degenerate sets of harmonics on descent in symmetry. A detailed discussion of the relation between fragment and cluster orbitals is given in Ref. 13. Table 1 shows how the harmonics transform in the point groups O_h, T_d, C_{3v} and D_3. Notice that because O_h retains the inversion symmetry g/u, the mixing of orbitals L^π and $\bar{L}^\pi$ is still forbidden. In finite groups the parity operation still interconverts π and $\bar{\pi}$ and eqn (1) applies to the symmetries in the point group, e.g. in O_h:

$$\Gamma(P^\pi) = T_{1u}, \quad \Gamma_u^o = A_{1u}, \quad \Gamma(\bar{P}^\pi) = T_{1g} = A_{1u} \times T_{1u}.$$

If we define representations as *conjugate* when they are related by the parity operation, i.e. Γ_A and Γ_B are conjugate when:

$$\Gamma_A = \Gamma_B \times \Gamma_u^o, \quad \Gamma_B = \Gamma_A \times \Gamma_u^o,$$

then the L^π and $\bar{L}^\pi$ representations are always conjugate. In the spherical group R_{3h}, Γ_A and Γ_B are distinct. However, for the finite point groups there are three possibilities (illustrated by Table 1).

(i) Γ_A is always distinct from its conjugate Γ_B, e.g. in O_h Γ_A and Γ_B are of opposite parity since $\Gamma_u^o = A_{1u}$, so $\Gamma_A \neq \Gamma_B$. Groups of this type include C_i, C_s, C_{2v}, $D_{(2n+1)d}$, C_{nh}, $S_{(4n-2)}$, D_{nh}, T_h, O_h, I_h and R_{3h}, and contain the inversion and/or a σ_h mirror plane.

(ii) Γ_A is always *self-conjugate*, e.g. in D_3 Γ_u^o is A_1, so $\Gamma_A = \Gamma_B \times A_1 = \Gamma_B$. Groups of this type describe optically active molecules, e.g. C_n, D_n, T, O and I. In these groups $\Gamma(L^\pi) = \Gamma(\bar{L}^\pi)$ with two exceptions (see below).

(iii) Some Γ_A are self-conjugate and some are not, e.g. in T_d Γ_u^o is A_2 and thus E is self-conjugate ($E \times A_2 = E$), whereas T_1 and T_2 are conjugate to each other ($T_1 \times A_2 = T_2$). The self-conjugate representations are those with zero character under all improper operations, and must be doubly degenerate. Groups of this type are C_{nv} ($n \geqslant 3$), S_{4n}, D_{2nd} and T_d.

These considerations become relevant to the theory of bonding in clusters when we remember that TSH assigns essentially bonding character to L^π-orbitals (really to L^σ–L^π combinations) and essentially antibonding character to $\bar{L}^\pi$.[7] The total representation of all tangential p-orbitals, $\Gamma_{\pi+\bar{\pi}}$ splits into two distinct subshells for cases (i) and (ii).[13] In case (ii) it is particularly easy to assign π and $\bar{\pi}$ just by counting half of each symmetry species in π and half in $\bar{\pi}$. It is when the molecule belongs to a group of

Table 1. Symmetries of the spherical harmonics in some finite point groups

	O_h	T_d	C_{3v}	D_3
S^σ	A_{1g}	A_1	A_1	A_1
P^σ, P^π	T_{1u}	T_2	A_1+E	A_2+E
D^σ, D^π	E_g+T_{2g}	$E+T_2$	A_1+2E	A_1+2E
F^σ, F^π	$A_{2u}+T_{1u}+T_{2u}$	$A_1+T_1+T_2$	$2A_1+A_2+2E$	A_1+2A_2+2E
G^σ, G^π	$A_{1g}+E_g+T_{1g}+T_{2g}$	$A_1+E+T_1+T_2$	$2A_1+A_2+3E$	$2A_1+A_2+3E$
Γ_u^o	A_{1u}	A_2	A_2	A_1
$\bar{P}^\pi$	T_{1g}	T_1	A_2+E	A_2+E
$\bar{D}^\pi$	E_u+T_{2u}	$E+T_1$	A_2+2E	A_1+2E
$\bar{F}^\pi$	$A_{2g}+T_{1g}+T_{2g}$	$A_2+T_1+T_2$	A_1+2A_2+2E	A_1+2A_2+2E
$\bar{G}^\pi$	$A_{1u}+E_u+T_{1u}+T_{2u}$	$A_2+E+T_1+T_2$	A_1+2A_2+3E	$2A_1+A_2+3E$

type (iii) that things are more interesting. If the representation $\Gamma_{\pi+\bar{\pi}}$ contains an *odd* number of a self-conjugate E-type symmetry species, the cluster is *forced* by symmetry *to show a non-Wade electron count.*

To see why this is, consider the example of the tetrahedral cluster.[7] The four σ-orbitals transform as $A_1 + T_2$ ($= S^\sigma + P^\sigma$). The eight tangential p-orbitals transform as $E + T_1 + T_2$. From Table 1 we can assign T_2 to P^π and T_1 to $\bar{P}^\pi$, which leaves the E pair. If one component of the pair is π, then the other must be $\bar{\pi}$ since E is self-conjugate, but the two components are degenerate and so the pair must be *nonbonding.* Thus TSH and symmetry arguments lead to the correct picture of the bonding–bonding orbitals and a nonbonding level that may contain zero or four electrons for a closed shell. Intermediate occupations would give rise to Jahn–Teller distortion and loss of tetrahedral symmetry. The departure from the $(n+1)$ rule is an "intrinsic" consequence of the cluster symmetry.

We can generalise this reasoning: If the total $(\pi + \bar{\pi})$ representation contains an *odd* number $(2m+1)$ of a self-conjugate species, then, when we have assigned m to π and m to $\bar{\pi}$ there is left a pair of $(\pi, \bar{\pi})$ character that must be nonbonding. An electron count of n or $(n+2)$ but not $(n+1)$ skeletal pairs is then predicted.

Stone and Alderton[7] used this argument to deduce the electron count for *nido* boranes, supposing that the nonbonding doubly degenerate frontier orbital is stabilised by protonation and therefore occupied, to give the $B_nH_n^{4-}$ electron count. Removal of a vertex from a *closo* cluster in high-symmetry cases, is often accompanied by descent in symmetry from our case (i) to case (iii) and the appearance of self-conjugate representations, e.g. E in C_{4v} and T_d and E_1 and E_2 in C_{5v}:

$$\underset{O_h}{B_6H_6^{2-}} \xrightarrow[-\text{vertex}]{} \underset{C_{4v}}{B_5H_5^{4-}},$$

$$\underset{D_{3h}}{B_5H_5^{2-}} \xrightarrow[-\text{axial vertex}]{} \underset{T_d}{B_4H_4^{4-}},$$

$$\underset{I_h}{B_{12}H_{12}^{2-}} \xrightarrow[-\text{vertex}]{} \underset{C_{5v}}{B_{11}H_{11}^{4-}}.$$

The pairing principle is also useful in explaining the bonding in electron-precise polyhedral hydrocarbons, C_nH_n, which have three-connected skeletons. TSH calculations reproduce the correct total of $3n/2$[8] skeletal pairs. Mingos and Johnson[14] show how this is related to the weakly bonding character of $(n/2-1)$ L^π MOs, and thus by the pairing principle an equal number of weakly antibonding $\bar{L}^\pi$ MOs exist. In these polyhedra the π–$\bar{\pi}$ pairs are not exactly degenerate, but if we suppose $(n/2-1)$ $\bar{\pi}$ MOs are occupied the correct electron count is found. ETSH calculations[8] confirm that the extra π–$\bar{\pi}$ pairs are all bonding for C_nH_n clusters.

APPLICATION TO LARGE *CLOSO* BORANES

The ideas in the previous section were applied to the list of preferred structures for *closo* $B_nH_n^q$ $(13 \leqslant n \leqslant 24)$ postulated by Brown and Lipscomb.[9] Table 2 lists the point groups of the polyhedra; the structures themselves are illustrated in Ref. 9. They divide neatly into four each of cases (i), (ii) and (iii). Thus four structures are optically active and four others are candidates for non-Wade electron counts.

In order to apply the pairing principle we need to find the symmetry of the basis atomic orbitals. The representation of the σ-hybrids, Γ_σ, is easily found: for any operation it has the character χ_σ, equal to the number of atoms unshifted by that operation. Γ_σ is also called the positional or permutational representation. A very neat way of deriving the representation of the remaining $2n$ tangential p-orbitals, $\Gamma_{\pi+\bar{\pi}}$, has been described recently.[15] If Γ_{xyz} is the vector representation, i.e. the symmetry of the translations (x, y, z), then the symmetry of the tangential orbitals is derived from Γ_σ by:

$$\Gamma_{\pi+\bar{\pi}} = \Gamma_\sigma \times \Gamma_{xyz} - \Gamma_\sigma.$$

Another way to find $\Gamma_{\pi+\bar{\pi}}$ is to note that the full basis $n(\sigma+\pi+\bar{\pi})$ transforms as the set of vibrational, rotational and translational displacements of the skeleton:

$$\Gamma_\sigma + \Gamma_{\pi+\bar{\pi}} = \Gamma_{\text{vib}} + \Gamma_{\text{rot}} + \Gamma_{xyz}.$$

Standard tables for Γ_{vib} are available for many point groups.[16]

In Table 3 are shown the MO symmetries for the optically active clusters in the series. As pointed out in the previous section, the representation of the tangential orbitals contains an even number of each symmetry present when the molecule is optically active and is easily assigned to π- and $\bar{\pi}$-subspaces.

Table 2. Symmetry groups of the hypothetical *closo* clusters $(13 \leqslant n \leqslant 24)$

n	Group	n	Group	n	Group
13	C_{2v}	17	C_{2v}	21	D_3
14	D_{6d}	18	D_3	22	T_d
15	D_{3h}	19	C_{3v}	23	D_3
16	T_d	20	D_{6h}	24	T

Table 3. Representations of the skeletal MOs of optically active structures

n	Group	Γ_σ	$\Gamma_{\pi+\bar{\pi}}$
18	D_3	$3A_1+3A_2+6E$	$6A_1+6A_2+12E$
21	D_3	$4A_1+3A_2+7E$	$6A_1+8A_2+14E$
23	D_3	$5A_1+4A_2+7E$	$6A_1+8A_2+16E$
24	T	$2A+2E+6T$	$4A+4E+12T$

For example, for $n = 21$:

$$\Gamma_\pi = 3A_1+4A_2+7E,$$

$$\Gamma_{\bar{\pi}} = 3A_1+4A_2+7E,$$

and the occupied MOs span $\Gamma_\pi+A_1$, i.e. $(n+1)$ skeletal pairs. The more interesting case is shown in Table 4. Groups D_{6d}, T_d and C_{3v} contain a single self-conjugate representation (E_3, E and E, respectively). For $n = 14$ the tangential representation contains $2E_3$, which may be assigned separately to F^π and $\bar{F}^\pi$, giving a TSH picture of $(n+1)$ occupied orbitals

$$(S^\sigma)^2(P^{\sigma/\pi})^6(D^{\sigma/\pi})^{10}(F^{\sigma/\pi})^{12}$$

in this cluster. However for each of $n = 16$, 19 and 22 there is an *odd* number of E representations in $\Gamma_{\pi+\bar{\pi}}$ and consequently a nonbonding E pair is predicted. Inspection of Table 1 shows that one component of the pair is G^π, the other $\bar{G}^\pi$, where the corresponding pair for the $n = 4$ tetrahedron is $D^\pi/\bar{D}^\pi$. Thus, of the proposed *closo* structures, those for $n = 16$, 19 and 22 have closed shells as neutral (or 4−) systems. This purely group theoretical use of the pairing principle gives results in agreement with the PRDDO calculations of Bicerano *et al.*[10]

It might be supposed that *all* T_d-clusters would show an odd number of E MOs. That this is not true can be seen from the Brester table of Γ_{vib} for T_d molecules.[16] From it we can deduce that the number of E pairs in $\Gamma_{\pi+\bar{\pi}}$ is $(4m+2m_d+m_3)$, where the cluster has m sets of 24, m_d sets of 12 and m_3 sets of four equivalent atoms. Thus the non-Wade electron count occurs only if m_3 is odd; in all cases so far encountered $m_3 = 1$ but it is possible to envisage larger T_d-clusters with atoms at the four vertices *and* over the centroids of the four faces of a tetrahedron, giving $m_3 = 2$ and obeying the $(n+1)$ rule.

The tables[16] also show that for C_{nv}-clusters the $(\pi+\bar{\pi})$ representation contains an odd number of the self-conjugate representation if there is an odd number of cage atoms on the n-fold axis. However it can be shown that, for the remaining point groups of type (iii), i.e. D_{2nd} and S_{4n}, that the $(\pi+\bar{\pi})$ representation *never* contains an odd number of the self-conjugate E species. Thus we can state the group-theoretical criterion for symmetry-induced departures from the $(n+1)$ electron count. A count of $(n+2)$ or n, but not $(n+1)$ skeletal pairs is predicted for geometrically *closo* clusters in just two cases:

(i) T- or T_d-clusters with an odd number of sets of four equivalent cage atoms,

(ii) C_m or C_{mv} $(m \geqslant 3)$ clusters with an odd number of cage atoms on the C_m-axis.

In order to check these qualitative considerations, and to see how well TSH describes bonding in these large clusters, EH calculations[17] were performed for the full set of *closo* structures. The Cartesian coordinates were generated by a symmetry-adapted iterative procedure, using the B—B bond lengths from Ref. 9. All BH bonds were taken to be radial and of length 1.19 Å. Figure 2 shows the resulting orbital energies, grouped in $L^{\sigma/\pi}$ shells using the TSH classification. As was found for the smaller *closo* boranes,[8] the energies occur in quite well-defined bands corresponding to different L values. Some crossing of F and D, and F and G bands occurs, but the general picture is as one would predict from TSH theory. The three non-Wade clusters are found to have a doubly degenerate level within 0.15 eV of the nonbonding energy. In Fig. 2 the lowest virtual and the highest occupied MOs conform to the mirror pattern about the nonbonding energy. The terminal BH bonds also follow a set of L^σ bands, giving an approximate order:

$$S^\sigma(\text{skel}) < P^\sigma \ldots G^\sigma(\text{BH}) < P^{\sigma/\pi} \ldots G^{\sigma/\pi}(\text{skel}),$$

though there is strong mixing of terminal and skeletal P, and to a smaller extent of D.

For comparison, Fig. 3 shows the equivalent energy bands for $2 \leqslant n \leqslant 12$ *closo* boranes. These

Table 4. Symmetries of skeletal MOs of clusters belonging to groups with *some* self-conjugate representations

n	Group	Γ_σ	$\Gamma_{\pi+\bar{\pi}}$
14	D_{6d}	$2A_1+2B_2+E_1+E_2+E_3+E_4+E_5$	$A_1+A_2+B_1+B_2+3E_1+2E_2+2E_3+2E_4+3E_5$
16	T_d	$2A_1+E+T_1+3T_2$	$A_1+A_2+3E+4T_1+4T_2$
19	C_{3v}	$6A_1+A_2+6E$	$6A_1+6A_2+13E$
22	T_d	$3A_1+2E+T_1+4T_2$	$A_1+A_2+3E+6T_1+6T_2$

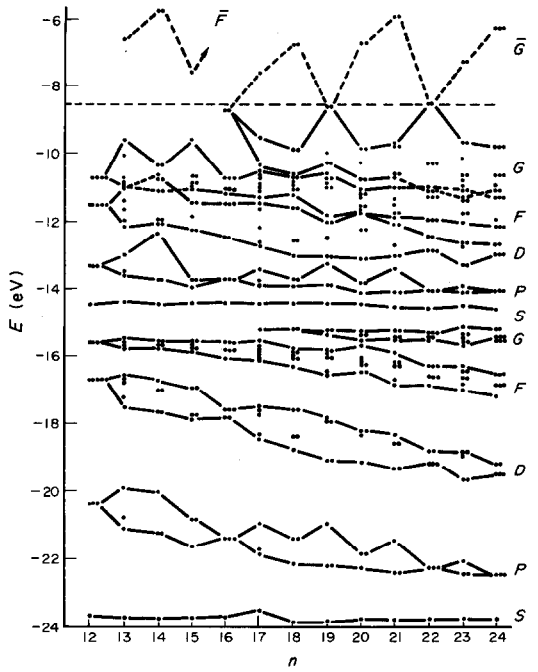


Fig. 2. Orbital energies of the supraicosahedral *closo* boranes calculated by the EH method.

calculations[8] used equilateral deltahedra with r(BB) = 1.70 Å and therefore there is some mismatch of energies between Figs 2 and 3. Figure 2 includes the icosahedral $B_{12}H_{12}^{2-}$ levels for r(BB) = 1.77 Å. It can be seen that the qualitative features of the TSH description apply for the whole range of clusters $2 \leqslant n \leqslant 24$, confirming Brown and Lipscomb's suggestion as very plausible guesses for supra-icosahedral *closo* boranes.

For $n > 13$ the clusters all have 12 boron atoms of coordination number 6 (including the terminal H) and $(n-12)$ of coordination number 7. EH calculations on all possible *nido* structures obtained by abstracting a vertex from the *closo* clusters showed, as expected, that removal of the HCV was always favoured. This is consistent with the TSH explanation[7] that the open face of a *nido* cluster is analogous to a conjugated ring system and the frontier orbital is more stable for larger rings, i.e. for removal of the HCV. The favoured *nido* structures formally derived from those *closo* clusters obeying the $(n+1)$ rule have a $B_nH_n^{4-}$ electron count. Removal of a vertex from the $n = 16, 19$ or 22 clusters leads to (-2) or (-6) species.

Returning to the distinction made in the introduction between "*intrinsic*" and "*accidental*" depatures from the $(n+1)$ electron count, it appears from Fig. 2 that clusters with 13, 15 and 17 boron atoms *might* retain their *closo* structures with only n skeletal pairs as B_nCl_n because they have nondegenerate orbitals near the nonbonding line.

The simple calculations described here do not, of course, rule out other structures as the most stable arrangements of large groups of boron atoms. Bicerano *et al.*[10] were able to find low-symmetry structures for $n = 16$, 19 and 22 obeying the $(n+1)$ electron count. The only clusters of more than 12 boron atoms known so far contain more open arrangements of subicosahedral fragments.[18]

Finally, some deltahedra of even higher nuclearity have been proposed as possible borane structures.[10,18] One example is $B_{32}H_{32}^{q}$, the omnicapped I_h dodecahedron (I). It has 20 seven-coordinate borons on a dodecahedron, capped by an icosahedral array of 12 six-coordinate borons. The structure is deltahedral but what charge would it carry? The basic I_h dodecahedron is an electron-precise structure, adopted by $C_{20}H_{20}$, and has 30

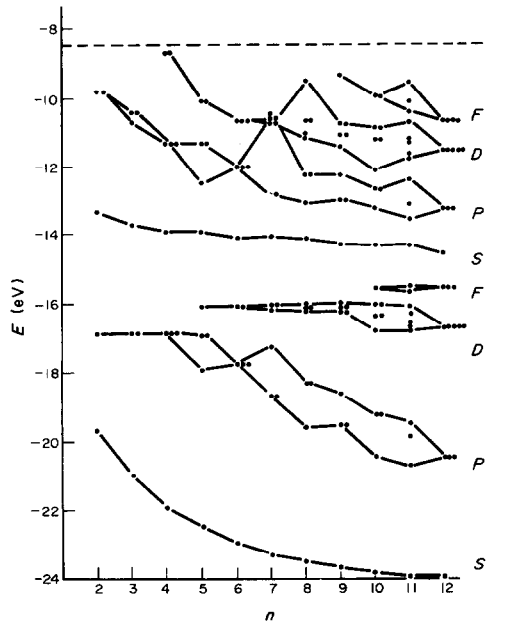
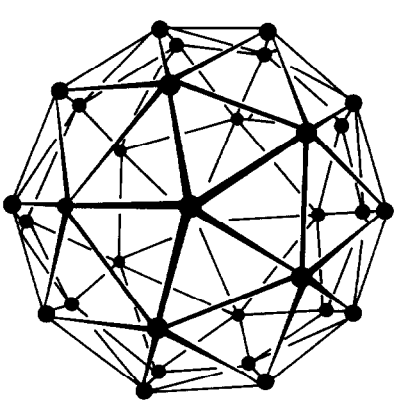


Fig. 3. Orbital energies of the small *closo* boranes calculated for equilateral deltahedra by the EH method.



I

Table 5. Symmetries of the spherical harmonics in the icosahedral group I_h

	σ, π	$\bar{\pi}$
S	A_g	
P	T_{1u}	T_{1g}
D	H_g	H_u
F	$T_{2u}+G_u$	$T_{2g}+G_g$
G	G_g+H_g	G_u+H_u
H	$T_{1u}+T_{2u}+H_u$	$T_{1g}+T_{2g}+H_g$

skeletal pairs in MOs spanning:

$$\Gamma_{30} = A_g+T_{1u}+T_{2u}+G_g+G_u+2H_g+H_u.$$

An icosahedral set of capping BH units has frontier orbitals spanning:

$$\Gamma_{cap} = A_g+T_{1g}+2T_{1u}+T_{2u}+G_g+G_u+2H_g+H_u,$$

so the 30 skeletal pairs will be stabilised by capping but also some new MOs will appear. Γ_{cap} contains T_{1g}, not present in Γ_{30}, that may be stabilised by interaction with an antibonding orbital of the dodecahedron, and in addition Γ_{cap} has one more T_{1u} set than Γ_{30}. Inspection of Table 5 shows that a weakly-bonding T_{1g} set would come from $\bar{H}^{\pi}$, paired to a T_{1u} set in H^{π}. Thus symmetry predicts a maximum count of 36 skeletal pairs, $B_{32}H_{32}^{8-}$.

Figure 4 shows EH orbital energies calculated with an expanded version of Ref. 17 for $B_{20}H_{20}$, $(BH)_{12}$ and $B_{32}H_{32}^{q}$. Lying ~2.5 V above the $B_{32}H_{32}^{4+}$ ($\equiv C_{20}H_{20}$) closed shell is a $(T_{1g}+T_{1u})$ set separated by only 0.12 eV and with a centre of gravity bonding by 0.06 eV. A gap of 7.2 eV separates these from the antibonding orbitals. Thus the most likely charges on $B_{32}H_{32}$, according to EH theory, would be +4 or −8 rather than the conventional *closo* count. However it is possible that the T_{1g} and T_{1u} orbital energies may split in a more sophisticated calculation, i.e. one that includes electron–electron repulsions, and that the −2 electron count would be restored, albeit with a low-lying unoccupied set of 3 MOs.

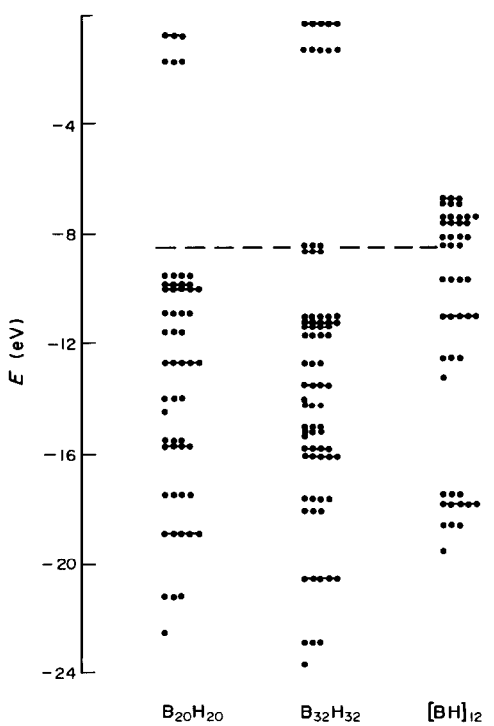


Fig. 4. Orbital energy diagrams for the capping of a pentagonal dodecahedron by 12 BH units, calculated by the EH method. g levels (●—●); u levels (● ●). All nondegenerate levels shown are A_g.

Acknowledgements—I would like to thank A. J. Stone and A. Ceulemans for useful comments on this work.

REFERENCES

1. K. Wade, *J. Chem. Soc. D* 1971, 792; *Adv. Inorg. Chem. Radiochem.* 1976, **18**, 1.
2. M. E. O'Neill and K. Wade, *Inorg. Chem.* 1982, **21**, 461; *J. Mol. Struct. (Theochem.)* 1983, **103**, 259; *Polyhedron* 1984, **3**, 199.
3. R. P. Brint, to be published.
4. R. B. King and D. H. Rouvray, *J. Am. Chem. Soc.* 1977, **99**, 7834; *Theor. Chim. Acta* 1978, **48**, 207; R. B. King, *ibid.* 1977, **44**, 223; *Inorg. Chem.* 1977, **16**, 1822.
5. S. F. A. Kettle and V. Tomlinson, *J. Chem. Soc. A* 1969, 2002, 2007; *Theor. Chim. Acta* 1969, **14**, 175.
6. W. N. Lipscomb, *Boron Hydrides*. W. A. Benjamin, New York (1963).
7. A. J. Stone, *Mol. Phys.* 1980, **41**, 1339; *Inorg. Chem.* 1981, **20**, 563; *Polyhedron* 1984, **3**, 1299; A. J. Stone and M. Alderton, *Inorg. Chem.* 1982, **21**, 2297.
8. P. W. Fowler and W. W. Porterfield, *Inorg. Chem.* 1985 (in press).
9. L. D. Brown and W. N. Lipscomb, *Inorg. Chem.* 1977, **16**, 2989.
10. J. Bicerano, D. S. Marynick and W. N. Lipscomb, *Inorg. Chem.* 1978, **17**, 2041, 3443.
11. W. W. Porterfield, M. E. O'Neill and K. Wade, to be published.
12. R. P. Brint, J. P. Cronin, E. Seward and J. Whelan, *J. Chem. Soc., Dalton Trans.* 1983, 975.
13. A. Ceulemans, *Mol. Phys.* 1985, **54**, 161.
14. D. M. P. Mingos and R. L. Johnson, to be published.
15. D. B. Redmond, C. M. Quinn and J. G. R. McKiernan, *J. Chem. Soc., Faraday II* 1983, **79**, 1791.
16. G. Herzberg, *Infrared and Raman Spectra of Polyatomic Molecules*. Van Nostrand, New York (1945).
17. J. Howell, A. Rossi, D. Wallace, K. Haraki and R. Hoffman, QCPE Program No. 344.
18. N. N. Greenwood, *Chem. Soc. Rev.* 1984, **13**, 353.

Polyhedron Vol. 4, No. 12, pp. 2059–2062, 1985
Printed in Great Britain

0277–5387/85 $3.00 + .00
© 1985 Pergamon Press Ltd

PALLADIUM(II) AND PLATINUM(II) COMPLEXES IN MN_2X_2 CHROMOPHORES

A. BENEDETTI

Centro Strumenti, University of Modena, 41100 Modena, Italy

and

A. C. FABRETTI* and G. C. FRANCHINI

Department of Chemistry, University of Modena, 41100 Modena, Italy

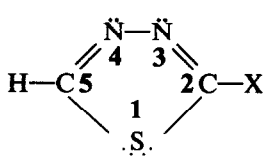
(*Received* 19 *April* 1985; *accepted* 19 *June* 1985)

Abstract—Some Pd(II) and Pt(II) halide complexes with 2-bromo- and 2-chloro-1,3,4-thiadiazoles have been prepared and characterized by electronic, NMR, Raman and IR spectroscopy, and by thermogravimetric analysis and conductivity measurements. All of the complexes appear to have square-planar stereochemistry with MN_2X_2 (X = Cl or Br) chromophores. Two of them are present in the *cis* configuration while for all the others unambiguous *trans* configurations are observed.

As a part of a series of investigations on the behaviour of heterocyclic ligands showing interesting biological[1,2] and pharmaceutical[3] properties, with some transition-metal ions, we have considered the 1,3,4-thiadiazole ring, which is the main framework of a very important class of diuretic drugs, the sulphonamide inhibitors of the zinc metallo-enzyme carbonic anhydrase.[4]

In this paper we have taken into account the coordination behaviour of 2-chloro-1,3,4-thiadiazole (ctz) and 2-bromo-1,3,4-thiadiazole (btz) with Pd(II) and Pt(II).

We have already theoretically investigated the nucleophilic ability of the nitrogen and sulphur atoms in the ring.[5] It was pointed out that the sulphur atom has the lowest chance of coordination, whereas the N(4) atom has the greatest chance, as the halogen atom X hinders the nitrogen in the 3-position.



* Author to whom correspondence should be addressed.

EXPERIMENTAL

Preparation of the complexes

Two methods of preparation have been followed:

(a) PtL_2Br_2 (L = ctz or btz). One millimole of solid $PtBr_2$ and 2.3 mmol of solid L were mixed and heated at 80°C in 5 cm^3 of DMF solution for 5 min. The yellow precipitate was filtered and washed with EtOH and dried.

(b) PdL_2X_2 and PtL_2Cl_2 (M = Pd or Pt, X = Cl or Br). One millimole of MX_4^- was solubilized in a minimum amount of water and then MeOH was added, avoiding any insolubilization. To the above solution, 2.3 mmol of L dissolved in the same mixture solution (water–MeOH) were added. The precipitate obtained was washed with MeOH and dried.

Analysis

Carbon, nitrogen, sulphur and hydrogen were determined using a Carlo–Erba 1106 analyser.

The electrical conductances of the complexes were measured in DMF. The IR spectra were recorded with a Perkin–Elmer 180 spectrophotometer as KBr disks or Nujol mulls on polyethylene. The electronic spectra were recorded with a Shimadzu MPS 50L spectrometer either in DMF or in the solid state.

NMR measurements of the ligand btz (0.06 M in DMF-d_7) and of the $Pt(btz)_2Cl_2$ complex (0.06 M in DMF-d_7) were registered at 293 and 350 K on a Varian XL-200 spectrometer. The external reference for ^{195}Pt is related to the signal of the $PtCl_4^{2-}$ ion in a 0.036 M solution of K_2PtCl_4 in D_2O. The aquospecies $PtCl_3(D_2O)^-$ signal is 437 ppm at a lower field than $PtCl_4^{2-}$, in good agreement with other authors.[6]

Thermal gravimetric analysis (t.g. and d.t.g.) were made in air on a Mettler TG50 thermobalance equipped with a Mettler TC10 TA processor; a scan rate of 10° min^{-1} was used.

RESULTS AND DISCUSSION

The new compounds prepared in the present investigation are listed in Table 1. Analytical data agree very well with the formula ML_2X_2.

The molar conductances in DMF are in the 20–30 Ω^{-1} mol^{-1} cm^2 range in 10^{-3} M, indicating the nonelectrolytic nature of the compounds. This is consistent with the stoichiometry assumed for the complexes on the basis of analytical data.

All the compound are diamagnetic, as would be expected for planar coordination around the Pd(II) and Pt(II) ions in the complexes.

Electronic spectra

The relative pale colour of the derivatives indicate that 2-X-1,3,4-thiadiazoles have low ligand field strength in forming the complexes in which the *d–d* bands can easily be found.

Two ligand field bands at *ca* 24.5 and 31.0 and 26.5 and 35.0 kK in solution or in the solid state, for Pd(II) and Pt(II) respectively, are detected. Considering a square-planar configuration they can be assigned to $^1A_{1g} \rightarrow {}^1B_{1g}$ and $^1A_{1g} \rightarrow {}^1E_g$ transitions, respectively (Table 2). A strong charge-transfer band has been found at *ca* 38.0 kK in all the complexes. The crystal field stabilization energies for Pd(II) and Pt(II) complexes obtained from the relation: $E(\nu) = \Delta_1 - 35F_4$[7] [$F = 60$ cm^{-1} for both Pd(II) and Pt(II)] are summarized in Table 2. For the Pd(II) complexes the Δ_1 values are close in value to those of PdN_2Cl_2 and PdN_2Br_2 chromophores.[8] In the case of Pt(II) the observed values are somewhat lower than those of the PtN_2X_2 (X = Cl or Br) chromophores,[7] probably due to a stronger interaction of the X atoms than the N atoms with respect to the metal ion.

IR and Raman spectra

In the 2-X-1,3,4-thiadiazoles (X = Cl or Br) the halogen atom lower the symmetry of the ring molecule, a decoupling of the C=N stretching vibration and a large modification of the ring spectra are expected.

Because of the rigidity of the penta-atomic ring containing the three potentially coordinating atoms, the IR bands of the ligands arising from the vibration of several atoms of the ring cannot be related to definite bonds and supply direct and unambiguous informations on the coordination of the ligand molecules. Only the strong and well-isolated band at 650 cm^{-1} for ctz and at 642 cm^{-1} for btz can be easily identified in the complexes without any possibility of confusion with other neighbouring bands. Its frequency lies in the range characteristic for C—S stretching frequencies (750–570 cm^{-1}) and may be attributed principally to ν(CS) vibrations. An effective increase of about 10–20 cm^{-1} to higher frequencies for all the complexes is attributable to the shift produced by the coordination of the ligands to the metal ions.

Table 1. Analytical and other physical properties for the Pd(II) and Pt(II) complexes

Compound	Colour	Found (calc.) (%)				Λ_M^a
		N	C	H	S	
$Pd(ctz)_2Cl_2$	Pale yellow	13.3 (13.4)	11.5 (11.5)	0.5 (0.5)	15.3 (15.3)	20
$Pd(ctz)_2Br_2$	Orange yellow	11.0 (11.0)	9.9 (9.5)	0.5 (0.4)	12.6 (12.6)	25
$Pd(btz)_2Cl_2$	Pale yellow	11.0 (11.0)	9.6 (9.5)	0.4 (0.4)	12.6 (12.6)	21
$Pd(btz)_2Br_2$	Orange yellow	9.4 (9.4)	8.1 (8.1)	0.3 (0.3)	10.9 (10.8)	28
$Pt(ctz)_2Cl_2$	Pale yellow	11.0 (11.0)	9.5 (9.5)	0.4 (0.4)	12.5 (12.6)	25
$Pt(ctz)_2Br_2$	Yellow	9.6 (9.4)	8.3 (8.1)	0.3 (0.3)	10.7 (10.8)	30
$Pt(btz)_2Cl_2$	Pale yellow	9.4 (9.4)	8.1 (8.1)	0.4 (0.3)	10.8 (10.8)	24
$Pt(btz)_2Br_2$	Yellow	8.1 (8.2)	7.2 (7.0)	0.2 (0.3)	9.2 (9.4)	27

[a] Ω^{-1} mol^{-1} cm^2 in DMF.

Table 2. Electronic spectra (kK), Δ_1[c] and more significant IR and Raman bands (cm^{-1})

Compound	$^1A_{1g} \rightarrow {}^1B_{1g}$		$^1A_{1g} \rightarrow {}^1E_g$		Δ_1	M—X		M—N		ν(CS)
	[a]	[b]	[a]	[b]		IR	Raman	IR	Raman	IR
$Pd(ctz)_2Cl_2$	24.0	24.1	—	31.0	26.1	365vs	309vs	270ms	267vw	674m
$Pd(ctz)_2Br_2$	23.4	24.0	—	—	25.5	249s	199vs	271m	268vw	673m
$Pd(btz)_2Cl_2$	24.0	24.4	—	30.8	26.1	349vs	295vs	278m	267vw	660m
$Pd(btz)_2Br_2$	23.7	24.0	—	31.0	25.8	236vs	196vs	277w	250vw	662m
$Pt(ctz)_2Cl_2$	25.6	24.7	—	35.0	27.7	349vs, 340vs	340vs, 336sh	269mw, 257w	267w, 253mw	673m
$Pt(ctz)_2Br_2$	24.4	24.1	—	35.7	26.5	243vs	214vs	282ms	253vw	670m
$Pt(btz)_2Cl_2$	26.3	26.3	—	35.0	28.4	352vs, 341s	351s, 343vs	264mw, 257sh	267w, 258m	664m
$Pt(btz)_2Br_2$	26.7	26.0	—	35.7	28.8	237vs	210vs	282s	251m	663m

[a] Solid state.
[b] DMF solution.
[c] Ligand field splitting energy.

The bands at *ca* 350 and 240 cm^{-1} in the IR spectra are halogen-sensitive and hence attributable to the M—Cl and M—Br stretching vibration modes. Also those at *ca* 300 and 200 cm^{-1} for Pd(II) derivatives and at 210 cm^{-1} for Pt(II) derivatives in the Raman spectra are attributable to the same modes. The general lack of coincidence between IR and Raman spectra suggests a centrosymmetric structure in all the complexes with the exception of PtL_2Cl_2. A *trans*-square-planar symmetry can be proposed in agreement with the principal features included in Table 3.

In the PtL_2Cl_2 complexes four almost coincident bands in the far-IR and Raman spectra, two of them attributable to ν(Pt—Cl) (the values are some cm^{-1} higher than those found in the literature[9]), and the others to ν(Pt—N) are observed. For these last complexes a *cis*-configuration can be formulated.

The steric hindrance of the two ligands and two halogens atoms seems to be always critical in the Pd(II) complexes, while in the case of Pt(II) complexes the steric hindrance will be critical passing from chlorine to bromine. In conclusion the IR and Raman spectra are not particularly useful, in this case, for a precise identification of the ligand nitrogen atom involved in the coordination; moreover the band shifts found cannot be correlated either to the monodentate or the bidentate behaviour of the hetero-ring.

NMR spectra

The only complex suitable for structural investigations by NMR spectroscopy is $Pt(btz)_2Cl_2$.

This complex exhibits, just like the btz ligand, a good solubility and stability in DMF.

All NMR data are consistent with the hypothesis that the ligand is *N*-bonded to the Pt(II) atom, and in particular through the N_4 atom of the 1,3,4-thiadiazole ring. In fact the ^1H spectrum of $Pt(btz)_2Cl_2$ shows a downfield shift for the ligand proton: δ_H (free ligand) = 8.04 ppm and δ_H $Pt(btz)_2Cl_2$ = 9.85 ppm, and a Pt–H coupling constant of 25.5 Hz. This coupling constant is in agreement with other $^3J_{Pt-H}$ values found for system containing the Pt—N=C—H fragment.[9]

Table 3.

Compound	Structure	Point group	Active zone	Tension M—X	Tension M—L
cis	Square plane	C_{2v}	IR	A_1, B_2	A_1, B_2
			Raman	A_1, B_2	A_1, B_2
trans	Square plane	D_{2h}	IR	B_{3v}	B_{2v}
			Raman	A_g	A_g

The ^{13}C spectrum shows a different deshielding of the two carbon atoms:

	δ_{C_2} (ppm)	δ_{C_5} (ppm)
Free ligand	140.78	158.90
$Pt(btz)_2Cl_2$	143.33	165.82
$\Delta\delta$ (ppm)	+2.55	+6.92

At first sight the carbon nearest to the coordination centre should be the most sensitive, so the most important changes in δ value generally affect the C nucleus directly bonded to the N atom coordinated to the metal ion.

The $\{^1H\}$–^{195}Pt spectrum performed at 298 K exhibits an unresolved broad signal ($\Delta\nu_{1/2} \cong 400$ Hz) at −335 ppm (the minus sign means upfield with respect to the external reference). The large ^{195}Pt linewidth in the complex due to spin–spin interactions with ^{14}N quadrupolar nuclei suggests a Pt—N bond; the spectrum recorded at 350 K shows a fine structure, a typical multiplet (quintet) clearly attributable to Pt—^{14}N coupling ($^1J_{Pt-^{14}N} = 230 \pm 5$ Hz). In addition, a chemical shift variation ($\Delta\delta_{Pt} = +14$ ppm) due to the increased temperature is visible according with other authors.[10]

Thermal behaviour of the complexes

The t.g. studies of the compounds show that all the present compounds start decomposing at *ca* 160–200°C, in a first step, losing a great part of the ligand atoms. In a second step the halogens and the remaining part of the ligand are lost. All the compounds attain constant weight at *ca* 600–800°C.

The dark-grey residue in each complex has been characterised as Pd(II) oxide or platinum metal sponge.

Acknowledgements—We thank the M.P.I. for the financial support (60%), Mr. Gianni Goldoni for the elemental analyses and the Centro Strumenti of the University of Modena for IR, Raman and NMR spectra.

REFERENCES

1. S. Lindskog, *Advances in Inorganic Biochemistry*, Vol. 4, p. 115. Elsevier Biomedical, Amsterdam (1982).
2. I. Bertini and C. Luchinat, *Acc. Chem. Res.* 1983, **16**, 272.
3. E. J. Crague, Jr, *Diuretics Chemistry, Pharmacology and Medicine*, p. 49. Wiley Interscience, New York (1983).
4. P. G. DeBenedetti, C. Frassineti and M. C. Menziani, *Quant. Struct.–Act. Relat.* 1985, **4**, 23.
5. A. Benedetti, P. G. DeBenedetti, A. C. Fabretti, G. C. Franchini and C. Gatti, *Transition Met. Chem.* 1984, **9**, 457.
6. W. Freeman, P. S. Pregosin, S. N. Sze and L. M. Venanzi, *J. Magn. Reson.* 1976, **22**, 473.
7. H. B. Gray and C. J. Ballhausen, *J. Am. Chem. Soc.* 1963, **85**, 260.
8. A. R. Latham, V. C. Hascall and H. B. Gray, *Inorg. Chem.* 1965, **4**, 788.
9. C. G. VanKralingen, J. K. DeRidder and J. Reedijk, *Inorg. Chim. Acta* 1979, **36**, 69.
10. I. M. Ismail, S. John, S. Kerrison and P. J. Sadler, *Polyhedron* 1982, **1**, 57.

Polyhedron Vol. 4, No. 12, pp. 2063–2066, 1985
Printed in Great Britain

0277-5387/85 $3.00 + .00
© 1985 Pergamon Press Ltd

REDUCTIVE ISOMERIZATION OF ICOSAHEDRAL METALLOCARBABORANES

TIMOTHY P. HANUSA and LEE J. TODD*

Department of Chemistry, Indiana University, Bloomington, IN 47405, U.S.A.

(*Received* 19 *April* 1985; *accepted* 26 *June* 1985)

Abstract—When reduced over a sodium amalgam, a variety of icosahedral metallocarbaboranes are found to isomerize under mild experimental conditions. Complexes containing second-row transition metals (Ru and Rh) rearrange rapidly at room temperature, but even cobaltacarbaboranes will isomerize in refluxing 1,2-dimethoxyethane (85°C) or diethylene glycol dimethyl ether (162°C). The direction of rearrangement is that found in straight thermally-induced isomerizations.

Thermal polyhedral rearrangements of *closo* borane anions[1] and isoelectronic carbaborane,[2] and metallocarborane species[3–5] have been known for some time. Depending upon the experimental conditions involved, the skeletal rearrangements induced in a given compound may give one or several isomeric products.

We wish to report our initial findings concerning a rather low temperature reductive isomerization procedure which gives rearranged products in the thermally-expected order. Reductive polyhderal isomerization may offer access to selected rearrangement products under comparatively mild experimental conditions.

EXPERIMENTAL

Physical measurements

Boron (^{11}B) NMR spectra were obtained at 115.8 MHz with a Nicolet NT-360 spectrometer and were externally referenced to $BF_3 \cdot O(C_2H_5)_2$ (positive values downfield). Proton NMR spectra were recorded at 361 MHz on the Nicolet instrument and were referenced to internal Me_4Si. Melting points were determined in sealed, evacuated capillaries and are uncorrected.

Materials

All reactions were performed under an atmosphere of prepurified dinitrogen. Tetrahydrofuran (THF), 1,2-dimethoxyethane (DME) and diethylene glycol dimethyl ether (diglyme) were distilled from sodium benzophenone ketyl. (Cyclopentadienyl)diiodorhodium

$([(C_5H_5)RhI_2]_n)$,[6] 3,1,2-$(C_5H_5)CoC_2B_9H_{11}$,[7]

3,6,1,2-$[(C_5H_5)Co]_2C_2B_8H_{10}$,[7]

3,1,2-$(\eta$-$C_6H_6)RuC_2B_9H_{11}$,[8]

and $Tl[3,1,2\text{-}TlC_2B_9H_{11}]$[9] were prepared according to literature methods.

Preparation of 3,1,2-$(C_5H_5)RhC_2B_9H_{11}$

To a slurry of $[(C_5H_5)RhI_2]_n$ (0.62 g) in dry THF (50 cm^3) was added $Tl[3,1,2\text{-}TlC_2B_9H_{11}]$ (0.42 g, 0.77 mmol) while stirring. Stirring under nitrogen was continued for 24 h, after which the dark brown mixture was opened to air and silica gel (1 g, 100–200 mesh) added. After the solvent was removed *in vacuo*, the solids were transferred to a silica gel column (2 × 30 cm) packed with toluene–hexane [2:1 (v/v)]. Elution was begun with the same solvent mixture; enrichment of the eluent with toluene and finally CH_2Cl_2 produced a pale yellow band. Stripping of the solvent from the eluate yielded 3,1,2-$(C_5H_5)RhC_2B_9H_{11}$. The product was redissolved in CH_2Cl_2 and treated with decolorizing carbon. Hexane was added to the filtered solution, and slow evaporation produced apple-green plates (69 mg, 30% yield), m.p. 225–228°C (dec.). ^{11}B NMR (115.8 MHz, $CDCl_3$): δ 6.5 (d, 1, J = 145 Hz), 4.5 (d, 1, J = 151 Hz), −4.9 (d, 2, J = 156 Hz), −7.1 (d,

* Author to whom correspondence should be addressed.

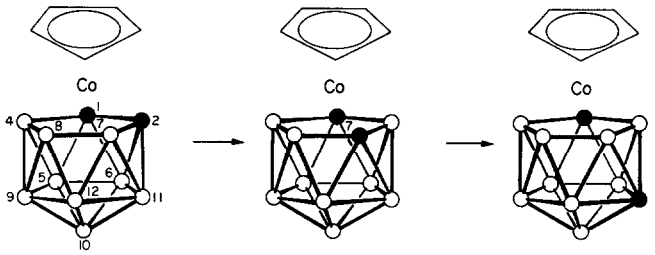


Fig. 1. Rearrangement of 3,1,2-$(C_5H_5)CoC_2B_9H_{11}$ to its 2,1,7 and 4,1,7 isomers.

2, J = 144 Hz), −17.3 (d, 1, J = 158 Hz), −23.3 (d, 1, J = 170 Hz). ^{1}H NMR (361 MHz, $CDCl_3$): δ 5.90 (s, 5), 4.2 (br s, 2). Mass spectrum, m/z 302.1170 (calc. for $^{12}C_7{}^1H_{16}{}^{103}Rh^{11}B_9$; 302.1172).

Reductions: general procedures

A sodium amalgam ranging from 0.4 to 0.6% (0.24–0.41 g Na in 68 g Hg) was prepared under nitrogen and *ca* 40 cm^3 of the designated solvent were added. The metallocarbaborane (0.08–0.78 mmol) was dissolved with stirring in the liquid, and the reaction then maintained over the amalgam at room temperature (24°C in THF) or under reflux (85 and 162°C in DME and diglyme, respectively). Samples (*ca* 1 cm^3) were withdrawn at measured intervals and dioxygen bubbled through the solution for 1 min to quench the reaction. The products were then analyzed by ^{11}B and/or ^{1}H NMR spectroscopy.

RESULTS AND DISCUSSION

The four icosahedral metallocarbaboranes,

3,1,2-(η-C_6H_6)$RuC_2B_9H_{11}$,

3,1,2-$(C_5H_5)CoC_2B_9H_{11}$,

3,1,2-$(C_5H_5)RhC_2B_9H_{11}$

and 3,6,1,2-$[(C_5H_5)Co]_2C_2B_8H_{10}$, were reduced in various solvents over sodium amalgam, and then maintained over the amalgam either at room temperature or under reflux. Samples were withdrawn periodically from the reactions, oxidized and analyzed by NMR spectroscopy. The ratios of observed products at each measured time and temperature are expressed as percentage conversions in the Table. All isomerized complexes were those either known or expected from thermally-induced rearrangements (i.e. involved a migration of the carbon atoms away from each other and the metal)[3–5] but several results were obtained which are not typical of thermal isomerizations of icosahedral metallocarbaboranes at the higher temperatures reported previously. Figures 1 and 2 illustrate the structures of the starting materials and products of these isomerization processes.

Temperature

The most striking feature of the isomerizations is the temperature at which the onset of isomerization occurs; the rhodium and ruthernium complexes undergo over 90% conversion while at room temperature, and even the two cobalt species have begun to isomerize at 85°C. Such mild conditions do not normally effect the rearrangement of monocage icosahedral metallocarbaboranes;* the lowest reported temperatures for the thermal isomerization of 3,1,2-$(C_5H_5)CoC_2B_9H_{11}$ and 3,6,1,2-$[(C_5H_5)Co]_2C_2B_8H_{10}$, for example, are 380 and 340°C, respectively.[4,5]

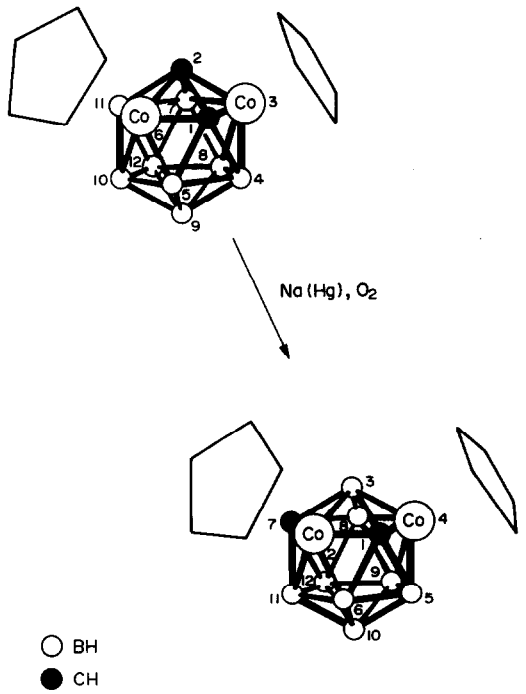


Fig. 2. Reductive isomerization of 3,6,1,2-$[(C_5H_5)Co]_2C_2B_8H_{10}$ to the 2,4,1,7 configuration.

* Several *bis*-cage complexes of the form $[(RC)_2B_9H_9]_2M^{n-}$ (R = H or CH_3; M = Ni or Pd; n = 0, 1 or 2) are known which rearrange at or below room temperature.[10]

Selectivity

The specificity of the reactions distinguishes them from the gas-phase isomerization of transition-metal metallocarbaboranes,[4] but is similar to that observed with thermal isomerizations in solution.[5] All of the reactions described here generally yielded only one isomer in addition to the starting material; the exception was $(C_5H_5)CoC_2B_9H_{11}$, for which none of the starting isomer was present after 3 h at 162°C, and instead a mixture of the 2,1,7 and 4,1,7 complexes was present. Evidently the thermodynamically-favored products are able to accumulate during the comparatively long reaction times involved. The approach to an equilibrium state of isomerized products is evident with $(C_5H_5)CoC_2B_9H_{11}$ at 85 and 162°C, as the 3,1,2:2,1,7 and 2,1,7:4,1,7 isomer ratios, respectively, eventually converge to *ca* 1:5.

Conversion of $3,6,1,2\text{-}[(C_5H_5)Co]_2C_2B_8H_{10}$

The extraordinary slowness of the isomerization of the bimetallocarbaborane differentiates it from the isoelectronic monometallic species, as only under 162°C reflux is an appreciable rate of transformation noticed. In contrast, the thermal rearrangement of $3,6,1,2\text{-}[(C_5H_5)Co]_2C_2B_8H_{10}$ requires a temperature no greater than that for $3,1,2\text{-}(C_5H_5)CoC_2B_9H_{11}$.[4,5]

Rate dependence on metal

The rapidity of isomerization of $3,1,2\text{-}(\eta\text{-}C_6H_6)RuC_2B_9H_{11}$ under reducing conditions is remarkable: in 3 h at room temperature, 50% is converted to the 2,1,7 isomer,* whereas the isoelectronic complex incorporating $(C_5H_5)Co(III)$ undergoes only a 6% change during a reaction period over 30 times as long.

In order to determine the extent to which the change in rate was due solely to the effect of the second-row transition metal (rather than the difference in the metal oxidation state or the ligand), the new metallocarbaborane, $3,1,2\text{-}(C_5H_5)RhC_2B_9H_{11}$, was synthesized from $[(C_5H_5)RhI_2]_n$ and $Tl[3,1,2\text{-}TlC_2B_9H_{11}]$ in THF, and isolated as yellow-green plates in moderate yield. Its ^{11}B NMR spectrum indicates that the molecule possesses a *closo* icosahedral geometry exactly analogous to that of its cobalt counterpart.[4] Under reducing conditions, the rhodium complex undergoes over 90% conversion in 3 h at room temperature to the 2,1,7 isomer.† Thus its rate of isomerization is well over an order of magnitude faster than the cobalt homologue under identical conditions and nearly twice as rapid as for the (π-benzene) ruthenium metallocarbaborane. Clearly, the presence of a second-row transition metal exerts a major influence on the rearrangement process.

Sodium amalgam reduction of $(C_5H_5)CoC_2B_9H_{11}$ is known to produce the $(C_5H_5)CoC_2B_9H_{11}^-$ ion,[11] and, since the ruthenium complex, and probably the rhodium species as well, are even more difficult to reduce,‡ it is likely that only one-electron reductions occur in all the cases. Some *nido* 12-atom metallocarbaboranes are known to undergo thermal rearrangement at relatively low temperature.[13] Although the resulting $27e^-$ compounds would presumably not possess the open geometry observed for 12-membered $28e^-$ *nido* metallocarbaboranes,[14] the extra electron might relax the rigidity of the polyhedron producing a more-flexible cage with a lowered E_{act} for rearrangement. If this is the case, then the enhanced overlap between the cage orbitals and those of the 4*d* relative to the 3*d* elements might promote more effective electron delocalization and hence more rapid isomerization.[15]§

Recently it was reported that *closo*-3,3-$(Ph_3P)_2$-3-H-1-C_6H_5-3,1,2-$IrC_2B_9H_{10}$ will undergo polytopal rearrangement to the 2,1,8 isomer under toluene reflux in 30 h.[16] Compounds of this type are known to undergo conversion, in an equilibrium process, to an "*exo–nido*" structure.[17,18] It may well be that the *exo–nido* intermediate provides the facile pathway for this lower-temperature polyhedral isomerization.

---

*2,1,7-$(\eta\text{-}C_6H_6)RuC_2B_9H_{11}$. ^{11}B NMR (115.8 MHz, $Me_2SO\text{-}d_6$): δ −0.9 (1, J = 126 Hz), −6.3 (2, J = 144 Hz), −11.7 (1, J = 159 Hz), −14.9 (2, J = 139 Hz), −16.0 (1, J = 130 Hz), −20.4 (2, J = 146 Hz); ^1H NMR (361 MHz, $Me_2SO\text{-}d_6$): δ 6.38 (s, 6, C_6H_6), 3.0 (br, 2, C_{cage}—H); mass spectrum, m/z 316.1230 (calc. for $^{11}B_9{}^{12}C_8{}^1H_{17}{}^{104}Ru$ = 316.1223); light yellow crystals, m.p. 310–312°C (dec.).

†2,1,7-$(C_5H_5)RhC_2B_9H_{11}$. ^{11}B NMR (115.8 MHz, $CDCl_3$): δ 3.4 (1, J = 142 Hz), −1.9 (2, J = 153 Hz), −8.2 (1, J = 164 Hz), −13.4 (3, J = 152 Hz), −18.6 (2, J = 157 Hz); ^1H NMR (361 MHz, $CDCl_3$); δ 5.89 (s, 5, C_5H_5), 3.2 (br, s, 2, C_{cage}—H); yellow needles, m.p. 220–222°C (dec.). The low-resolution mass spectrum cut off at m/z 302 corresponds to $^{12}C_6{}^{13}C_1{}^1H_{16}{}^{103}Rh{}^{11}B_9$.

‡Cyclic voltammetry of $3,1,2\text{-}(\eta\text{-}C_6H_6)RuC_2B_9H_{11}$ [THF, 0.2 M $(n\text{-}Bu)_4N^+OH^-$ as supporting electroyte, Ag–AgCl reference electrode, Pt bead working electrode, 100 μA, 200 mV sec^{-1}] indicates irreversible reduction occurs at −1.83 eV. Under identical conditions in CH_3CN, $3,1,2\text{-}(C_5H_5)CoC_2B_9H_{11}$ displays a reversible reduction wave at −1.16 eV.[12]

§A similar argument based on the "diffuseness' of 5*d* relative to 4*d* orbitals has been invoked in connection with the more rapid thermal isomerization of $(C_2B_{10}H_{12})_2Hf^{2-}$ compared to the isoelectronic $(C_2B_{10}H_{12})_2Zr^{2-}$ ion.[15]

Table 1. Isomer conversions from reductive isomerization[a]

	$(C_5H_5)CoC_2B_9H_{11}$ (3,1,2/2,1,7/4,1,7)%	$(C_5H_5)RhC_2B_9H_{11}$ (3,1,2/2,1,7)%	$(\eta\text{-}C_6H_6)RuC_2B_9H_{11}$ (3,1,2/2,1,7)%	$[(C_5H_5)Co]_2C_2B_8H_{10}$ (3,6,1,2/2,4,1,7)%
3 h, 24°C	[b]	6/94	47/53	[b]
50 h, 24°C	—	4/96	8/92	[b]
93 h, 24°C	94/6/[b]			
9 h, 85°C	28/72/[b]			[b]
90 h, 85°C	16/84/[b]			94/4[c]
120 h, 85°C	17/83/[b]			89/11
3 h, 162°C	[b]/35/65			35/65
9 h, 162°C	[b]/20/80			—
15 h, 162°C	—			26/74[e]
50 h, 162°C	[b]/16/84			
90 h, 162°C	[d]			

[a] Estimated measuring error is ±3%.
[b] Percent conversion or amount present is below reliable detection limit (<4%).
[c] 92 h.
[d] Decomposition evident.
[e] Additional small peaks present.

CONCLUSIONS

Reductive polyhedral isomerization offers access to various isomers of icosahedral metallocarbaboranes under comparatively mild experimental conditions, and its full scope remains to be explored. Applied to other icosahedral and non-icosahedral systems, such isomerizations could be a valuable probe of the relative thermodynamic stabilities of metallocarbaboranes, and perhaps of the many structurally and electronically-related metal atom clusters as well.[19]

Acknowledgements—We would like to thank Professor Sheldon G. Shore (Ohio State University) and Dr Allen R. Siedle (3M Central Research Labs) for obtaining the high-resolution mass spectral data, and James F. Corning (Indiana University) for conducting the cyclic-voltammetry experiments.

REFERENCES

1. E. L. Muetterties and W. H. Knoth, *Polyhedral Boranes*. Marcel Dekker, New York (1968), and references therein.
2. R. N. Grimes, *Carboranes*. Academic Press, New York (1970).
3. D. F. Dustin, W. J. Evans, C. J. Jones, R. J. Wiersema, H. Gong, S. Chan and M. F. Hawthorne, *J. Am. Chem. Soc.* 1974, **96**, 3085.
4. M. K. Kaloustian, R. J. Wiersema and M. F. Hawthrone, *J. Am. Chem. Soc.* 1972, **94**, 6679.
5. W. J. Evans, C. J. Jones, B. Stibr, R. A. Grey and M. F. Hawthorne, *J. Am. Chem. Soc.* 1974, **96**, 7405.
6. A. Kasahara, T. Izumi and K. Tanaka, *Bull. Chem. Soc. Jpn* 1967, **40**, 699.
7. C. J. Jones and M. F. Hawthorne, *Inorg. Chem.* 1973, **12**, 608.
8. T. P. Hanusa, J. C. Huffman and L. J. Todd, *Polyhedron* 1982, **1**, 77.
9. H. D. Smith, Jr and M. F. Hawthorne, *Inorg. Chem.* 1974, **13**, 2312.
10. L. F. Warren and M. F. Hawthorne, *J. Am. Chem. Soc.* 1970, **92**, 1157; and T. E. Paxson, M. K. Kaloustian, G. M. Tom, R. J. Wiersema and M. F. Hawthorne, *J. Am. Chem. Soc.* 1972, **94**, 4882.
11. R. G. Wiersema and M. F. Hawthorne, *J. Am. Chem. Soc.* 1974, **96**, 761.
12. W. E. Geiger and D. E. Brennan, *Inorg. Chem.* 1982, **21**, 1963.
13. R. B. Maynard, E. Sinn and R. N. Grimes, *Inorg. Chem.* 1981, **20**, 1201.
14. J. R. Bowser and R. N. Grimes, *J. Am. Chem. Soc.* 1978, **100**, 4623.
15. C. G. Salentine and M. F. Hawthorne, *Inorg. Chem.* 1976, **15**, 2872.
16. J. A. Doi, E. A. Mizusawa, C. B. Knobler and M. F. Hawthorne, *Inorg. Chem.* 1984, **23**, 1482.
17. J. A. Doi, R. G. Teller and M. F. Hawthorne, *J. Chem. Soc., Chem. Commun.* 1980, 80.
18. C. B. Knobler, T. B. Marder, E. A. Mizusawa, R. G. Teller, J. A. Long, P. E. Behnken and M. F. Hawthorne, *J. Am. Chem. Soc.* 1984, **106**, 2990.
19. (a) M. E. O'Neill and K. Wade, In *Metal Interactions with Boron Clusters* (Edited by R. N. Grimes), Chap. 1. Plenum, New York (1982); (b) K. Wade, In *Transition Metal Clusters* (Edited by B. F. G. Johnson), Chap. 3. John Wiley, New York (1980).

Polyhedron Vol. 4, No. 12, pp. 2067–2068, 1985
Printed in Great Britain

0277-5387/85 $3.00+.00
© 1985 Pergamon Press Ltd

DECOMPOSITION OF SILANE ON SOLID P_4O_{10}

B. S. SURESH and D. K. PADMA*

Department of Inorganic and Physical Chemistry, Indian Institute of Science, Bangalore 560 012, India

(*Received* 15 *April* 1985; *accepted* 25 *June* 1985)

Abstract—Silane undergoes thermal decomposition on the surface of "phosphorus pentoxide" (P_4O_{10}) into its elements around 200–400°C. The hydrogen formed partially reduces the P_4O_{10} forming lower oxides of phosphorus and water. Elemental silicon is precipitated as reddish-brown solid, which is separated by dissolving out the phosphorus oxides. Silica and disiloxane are not formed in the reaction.

In the course of our study on the reaction of silicon compounds with "phosphorus pentoxide" (P_4O_{10}), an interesting observation was the decomposition of silane into silicon and hydrogen over a bed of P_4O_{10} held around 200–400°C, a temperature much lower than the decomposition temperature of silane in glass vessels.[1] The details of such a study are presented in this paper.

EXPERIMENTAL

Materials and methods

Silane was prepared by the standard method of reduction of SiF_4 with $LiAlH_4$.[2] P_4O_{10} (BDH) was purified by sublimation in a stream of dry oxygen.[3] IR spectra of gaseous compounds were recorded in a 10-cm cell with KBr windows and those of the solids in a KBr pellet on a Perkin–Elmer (599) spectrophotometer.

Reaction of silane with P_4O_{10}

Procedure: P_4O_{10} (1.7 g, ~6.0 mmol) and silane (~96 mg, ~3.0 mmol) were placed in an evacuated reaction vessel and heated at 200°C. After about an hour, a reddish-brown solid began to deposit on the surface of the P_4O_{10}. The heating was continued for 12 h. IR spectra of the gaseous component indicated the presence of unreacted silane. The temperature of the reaction vessel was raised to 400°C and it was heated at this temperature for 12 h. On cooling, the gaseous component indicated the absence of silane but the presence of an uncondensable gas. Mass spectral data indicated the presence of hydrogen. The solid was treated with water and slightly warmed, when a gas with a characteristic odour of phosphine was evolved which turned moist silver nitrate paper black. The aqueous solution decolourized a dilute potassium permanganate solution. The tests indicated that the solid contained lower oxides of phosphorus such as P_4O_6.[4] The bulk solid was treated with water and well stirred. Excess P_4O_{10} as well as the lower oxides of phosphorus formed were dissolved and the remaining reddish-brown solid was filtered, washed thoroughly with water and dried *in vacuo* and analysed.

This dried solid did not exhibit any IR absorption bands. It remained unchanged in both dilute hydrofluoric acid and dilute alkaline solutions indicating the absence of Si—H and Si—O bonds. When the solid was heated in an air oven it turned white. The white solid was characterised to be silica by elemental analysis and IR spectral data.

The effect of relative proportions of reactants on the nature of the products formed was studied by conducting the experiment with silane in excess (~4.0 mmol), (P_4O_{10} ~ 1.0 mmol) at 200 (12 h) or 400°C (12 h). The products were found to be the same as in the previous case. Possible products such as silica and disiloxane were not observed.

Pure silane (~96 mg, ~3.0 mmol) was heated alone in a reaction vessel between 200 and 400°C for 24 h, but no decomposition was observed.

* Author to whom correspondence should be addressed.

RESULTS AND DISCUSSIONS

The experimental results indicate that the reaction of silane with P_4O_{10} is one of decomposition, the products being an orange red solid, hydrogen and lower oxides of phosphorus. The analytical results indicate that the red solid is amorphous silicon. The fact that other expected products such as silica and disiloxane were not formed in the reaction even when the relative proportions of the reactants were changed, indicates that no other reaction has taken place other than decomposition. This is in contrast to the reported reactions of tetrahalosilanes[1] with P_4O_{10} where the reaction products are phosphoryl halides and silica.

The overall decomposition reaction could be represented as follows:

$$SiH_4 \xrightarrow{200\text{–}400^\circ C} Si + 4[H],$$

$$P_4O_{10} + 8[H] \xrightarrow{200\text{–}400^\circ C} P_4O_6 + 4H_2O.$$

An interesting aspect of the present study is that P_4O_{10} lowers the decomposition temperature of silane. Similar decomposition of silane around 200°C have been noted on silica gel or charcoal.[5] An added advantage in the present case is the easy separation of silicon formed by the addition of water.

Acknowledgement—One of us (BSS) wishes to thank the Department of Atomic Energy, India for financial support.

REFERENCES

1. B. S. Suresh and D. K. Padma, *J. Fluorine Chem.* 1984, **24**, 399.
2. D. K. Padma, B. S. Suresh and A. R. Vasudeva Murthy, *J. Fluorine Chem.* 1979, **14**, 327.
3. R. Klement, In *Handbook of Preprative Inorganic Chemistry* (Edited by G. Brauer), 2nd edn, p. 541. Academic Press, New York (1963).
4. J. R. Van Wazer, *Phosphorus Chemistry*, Vol. 1, pp. 268 and 363. Interscience, New York (1958).
5. E. G. Rochow, *Comprehensive Inorganic Chemistry* (Edited by J. C. Bailar, Jr, H. J. Emeleus, Sir Ronald Nyholm and A. F. Trotman-Dickenson), Vol. 1, p. 1364. Pergamon Press, Oxford (1973).

Polyhedron Vol. 4, No. 12, pp. 2069–2072, 1985
Printed in Great Britain

0277–5387/85 $3.00 + .00
© 1985 Pergamon Press Ltd

PREPARATION AND CHARACTERIZATION OF TETRAHALODIMOLYBDENUM(II) COMPLEXES WITH ALKYL-SUBSTITUTED PYRIDINES

K. J. EWING* and S. I. SHUPACK

Department of Chemistry, Villanova University, Villanova, PA 19085, U.S.A.

(*Received* 29 *March* 1985; *accepted* 27 *June* 1985)

Abstract—The preparation and characterization of new tetrahalodimolybdenum(II) complexes with alkyl-substituted pyridines is described. IR and visible data are used to infer structural information with respect to previously prepared complexes of this type.

Many dimolybdenum complexes of the types $Mo_2X_4L_4$ and $Mo_2X_4(LL)_2$, where X = Cl or Br, L = C_5H_5N, 4-$CH_3C_5H_4N$, $P(C_4H_{10})_3$ or $P\{S(CH_3)\}_3$, and LL = bipy, dppe, arphos or dpae, have been prepared and characterized.[1–3] These complexes characteristically have two Mo—Cl stretching bands in the IR; complexes with monodentate ligands exhibit these bands[2] at 337 ± 15 and 285 ± 10 cm^{-1}, the complex α-$Mo_2Cl_4(dppe)_2$ exhibits these bands at 307 and 290 cm^{-1}, while complexes with arphos and dpae exhibit these bands[3] at 350 ± 10 and 295 ± 5 cm^{-1}. The existence of a *trans* arrangement of chlorine atoms about each molybdenum in complexes with monodentate ligands, a *cis* arrangement in the α-$Mo_2Cl_4(dppe)_2$ complex, and a unique staggered structure in complexes with arphos and dpae have been proposed from these data. The X-ray structures of $Mo_2Br_4(arphos)_2$[4] and β-$Mo_2Cl_4(dppe)_2$[5] agree with the proposed structure of each complex. The position of the δ–δ^* transition has also been shown to reflect a complex geometry.[3]

The structure of Mo_2X_4(4-methylpyridine)$_4 \cdot CHCl_3$ (X = Cl or Br) as determined by X-ray is shown in Fig. 1(a). Changes in its low-frequency IR spectrum may indicate rotation about the quadruple bond to the structure in Fig. 1(b).[6]

We report here the synthesis and characterization of the complexes $Mo_2X_4L_4$, where X = Cl or Br, and L = 3-methylpyridine (3PIC), 3,4-dimethylpyridine (34LUT), 3,5-dimethylpyridine (35LUT) and 4-*t*-butylpyridine (4TBP). These complexes were prepared to study the effect that different substituents on pyridine would have on the electronic and structural properties of the complex. A more comprehensive report will be forthcoming.

EXPERIMENTAL

All solvents and ligands were dried via literature methods and kept under dry nitrogen prior to use.[7] All reactions, filtrations and recrystallizations were also carried under a dry nitrogen atmosphere using Schlenk equipment. IR and visible spectra of Nujol mulls of the complexes were taken using the Perkin–Elmer 229 and Cary 219 spectrophotometers, respectively. NMR spectra of the complexes in $CDCl_3$ or C_6D_6 were obtained from the Varian XL-200 spectrometer in sealed tubes. Raman spectra were obtained as described elsewhere.[8]

Tricesium hydridooctachlorodimolybdate(II) and tricesium hydridooctabromodimolybdate(II) were prepared via literature methods.[2,9,10] Dimolybdenum tetraacetate was purchased from Aldrich and used without further purification. The ligands 3-picoline and 4-picoline were purchased

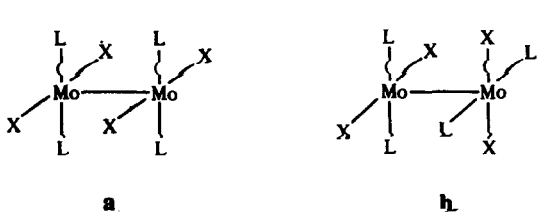


Fig. 1.

* Author to whom correspondence should be addressed.

from the Eastman Kodak Co.; 3,4-lutidine, 3,5-lutidine and 4 TBP were purchased from Aldrich. The general synthesis for the complexes is similar to the synthesis of the tetrahalodimolybdenum tetrapyridine complex.[2] Microanalyses were performed by Galbraith Laboratories Inc., Knoxville, TN.

Found: C, 35.7; H, 3.5; N, 6.6; Cl, 30.2. Calc. for $Mo_2Cl_4C_{25}H_{29}N_4$ (4PIC): C, 36.3; H, 3.5; N, 6.8; Cl, 30.1%.

Found: C, 39.3; H, 4.1; N, 7.5; Cl, 19.1. Calc. for $Mo_2Cl_4C_{24}H_{28}N_4$ (3PIC): C, 40.8; H, 4.0; N, 7.9; Cl, 20.1%.

Found: C, 41.4; H, 4.6; N, 7.0; Cl, 18.9. Calc. for $Mo_2Cl_4C_{28}H_{36}N_4$ (35LUT): C, 44.1; H, 4.1; N, 7.3; Cl, 18.6%.

Found: C, 47.6; H, 5.2; N, 7.9; Cl, 17.8. Calc. for $Mo_2Cl_4C_{28}H_{36}N_4$ (34LUT): C, 44.1; H, 4.8; N, 7.3; Cl, 18.6%.

Found: C, 50.3; H, 6.3; N, 6.2; Cl, 17.0. Calc. for $Mo_2Cl_4C_{36}H_{52}N_4$ (4TBP): C, 49.4; H, 5.9; N, 6.4; Cl, 16.2%.

Found: C, 35.7; H, 4.1; N, 6.8; Br, 29.7. Calc. for $Mo_2Br_4C_{30}H_{34}N_4$ (4PIC): C, 37.4; H, 3.5; N, 5.8; Br, 33.2%.

Found: C, 35.3; H, 3.7; N, 6.1; Br, 35.7. Calc. for $Mo_2Br_4C_{24}H_{28}N_4$ (3PIC): C, 32.6; H, 3.2; N, 6.3; Br, 36.2%.

Found: C, 37.6; H, 4.3; N, 6.2; Br, 35.3. Calc. for $Mo_2Br_4C_{28}H_{36}N_4$ (34LUT): C, 35.6; H, 3.8; N, 5.9; Br, 33.9%.

Found: C, 45.5; H, 5.7; N, 5.5; Br, 31.2. Calc. for $Mo_2Br_4C_{36}H_{52}N_4$ (4TBP), green cubes and blue needles: C, 41.1; H, 5.0; N, 5.3; Br, 30.4%.

RESULTS AND DISCUSSION

The visible, IR, NMR and Raman spectra of the complexes $Mo_2X_4L_4$, where X = Cl or Br and L = py, 4PIC, 3PIC, 4TBP, 34LUT and 35LUT, are given in Table 1. Complexes with 4PIC, py, 3PIC and 34LUT have similar IR and visible spectra, with two Mo—Cl stretching bands in the ranges 320–340 and 270–280 cm^{-1}; the proposed δ–δ^* transition energy increases in the order py $\cong$ 4PIC < 3PIC $\cong$ 34LUT. This transition for the 3PIC and 34LUT complexes ranges from 585 to 725 cm^{-1} higher in energy than those of the py and 4PIC complexes. The similarity in the IR spectra of these complexes leads us to propose that the 3PIC and 34LUT complexes have the same structure as that of the 4PIC complex determined by Brencic *et al.*[6] The Raman shows a single intense band for these complexes in the vicinity of 350 cm^{-1}, indicative of the Mo≡Mo quadruple bond. Proton NMR spectra of these complexes show a downfield shift for the *ortho* protons of approximately 0.8 ppm. The deshielding of these protons is due to their close proximity to the quadruple bond.[11]

The 35LUT complex has the proposed δ–δ^* transition higher in energy than any of the other complexes; it is also the most sterically restrictive ligand. The proposed δ–δ^* transition occurs 1179 cm^{-1} higher in energy than that of the 4PIC complex, with three Mo—Cl bands in the IR. The Raman spectrum of this complex shows a very intense band at 349 cm^{-1}, indicative of the Mo≡Mo quadruple bond. The NMR spectrum of this

Table 1.

$Mo_2X_4L_4$		Visible[a]	IR[ab]	Raman[bc]	NMR (ppm)	
L	X	(cm^{-1})	(cm^{-1})	(cm^{-1})	Complex[d]	Ligand
Py	Cl	16,667[e]	342[f](s)	343(s)		
			280[f](m)			
4PIC	Cl	16,807[e]	362(m)	348(s)	2.42	2.35
		24,331	321[f](s)		7.14	7.10
			276[f](s)		7.17	7.13
					9.32	8.46
					9.35	8.48
3PIC	Cl	17,331[e]	373(m)	346(s)	2.27	2.34
		25,641	323[f](s)		7.08	7.16
			278[f](s)		7.12	7.18
					7.14	7.22
					7.43	7.48
					7.46	7.51
					9.24	8.46
					9.27	

Table 1. (*Contd.*)

34LUT	Cl	17,391[e]		321[f](s)	350(s)	2.16	2.25
		25,641		288(m)		2.24	2.27
				273[f](s)		6.96	7.04
						6.99	7.06
						9.09	8.30
						9.12	8.33
35LUT	Cl	17,986[e]		343[f](s)	349(s)	2.19	2.62
		25,974		319[f](s)		7.19	2.63
				290(s)		7.23	7.63
				280[f](m)		9.04	8.59
4TBP	Cl	Green	Blue	Green	Blue		
		17,182[e]	17,544[e]	342[f](m)	333[f](s)		
		26,247	23,923	313[f](s)	314[f](s)		
				277(m)	277(s)		
4PIC	Br			276(w)			
				260(w)			
				228(w)			
3PIC	Br	15,198[e]		366(m)			
		21,008		261(s)			
				241(sh)			
34LUT	Br	17,094[e]		255(s)			
		27,027		247(sh)			
35LUT	Br			287(m)			
				279(m)			
				262(s)			
4TBP[g]	Br	15,038[e]	15,129	399(w)		0.78	1.07
		20,492	16,584[e]	369(vw)		6.37	6.86
			20,619	340(vw)		6.40	6.87
						9.73	6.88
						9.76	6.89
						8.48	
						8.49	
						8.50	
						8.51	

[a] Nujol mull.
[b] s = strong, m = medium, w = weak, vw = very weak.
[c] Mo≡Mo bond.
[d] $CDCl_3$.
[e] Proposed δ–δ^* transition.
[f] Mo—Cl stretch.
[g] C_6D_6.

complex shows a downfield shift for all ligand protons. However, the *ortho* protons are not shifted as far downfield as in the 4PIC, 3PIC and 34LUT complexes. The data suggest that $Mo_2Cl_4(35LUT)_4$ has a different geometry from any of the latter complexes. Further work is necessary to be conclusive.

The complex $Mo_2Cl_4(4TBP)_4$ precipitates from a pentane–4 TBP mixture as a green powder, while precipitation from a pentane–benzene mixture yields a blue powder. The green material has the proposed δ–δ^* transition at 17,182 cm^{-1} and is the material reported on in this paper. The blue material has not been analyzed, but possesses visible and IR spectral characteristics of $Mo_2X_4L_4$ type complexes (see Table 1). When $Mo_2Br_4(4TBP)_4$ was slowly recrystallized from a benzene–pentane mixture at 0°C, a mixture of dark blue needles and dark green

cubic crystals were obtained. The analysis of these crystals gave the stoichiometry of both crystalline forms as $Mo_2Br_4(4TBP)_4$. The separated crystals gave identical IR spectra down to 200 cm^{-1}, but different visible spectra (see Table 1). This indicates that $Mo_2X_4(4TBP)_4$ (X = Cl or Br) may exist as geometric isomers similar to structures **a** and **b**. We are currently growing crystals of these complexes for X-ray analysis.

Acknowledgements—We wish to thank Drs T. Spiro and R. Czernuszewicz for their generous help in obtaining Raman spectra.

REFERENCES

1. F. A. Cotton and R. A. Walton, *Multiple Bonds Between Metal Atoms*. Wiley Interscience, New York (1982).
2. J. San Filippo, Jr, H. J. Snaidoch and R. L. Grayson, *Inorg. Chem.* 1974, **13**, 2121.
3. S. A. Best, T. J. Smith and R. A. Walton, *Inorg. Chem.* 1978, **17**, 99.
4. F. A. Cotton, P. E. Fanwick, J. W. Fitch, H. D. Glicksman and R. A. Walton, *J. Am.. Chem. Soc.* 1979, **101**, 1752.
5. P. A. Agaskar and F. A. Cotton, *Inorg. Chem.* 1984, **23**, 3383.
6. J. V. Brencic, D. Dobcnik and P. Segedin, *Monatsh. Chem.* 1976, **107**, 395.
7. Gordon and Ford, *The Chemists Companion*. Wiley Interscience, New York (1972).
8. R. S. Czernuszewicz and M. K. Johnson, *Appl. Spectrosc.* 1983, **37**, 297.
9. M. J. Bennett, J. V. Brencic and F. A. Cotton, *Inorg. Chem.* 1969, **8**, 1060.
10. J. San Filippo, Jr and M. A. Schaefer King, *Inorg. Chem.* 1976, **15**, 1228.
11. J. San Filippo, Jr, *Inorg. Chem.* 1972, **11**, 3140.

Polyhedron Vol. 4, No. 12, pp. 2073–2081, 1985
Printed in Great Britain

0277–5387/85 $3.00 + .00
© 1985 Pergamon Press Ltd

SELF-CONSISTENT-FIELD-Xα-SCATTERED-WAVE MOLECULAR ORBITAL CALCULATION OF [CpMoS(μ-S)]$_2$, A MOLECULE THAT UNDERGOES A PHOTOCHEMICALLY INDUCED ISOMERIZATION

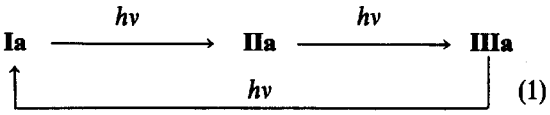
MITCHELL R. M. BRUCE, ALICE E. BRUCE and DAVID R. TYLER*

Department of Chemistry, Columbia University, New York, NY 10027, U.S.A.

(*Received* 3 *April* 1985; *accepted* 27 *June* 1985)

Abstract—A self-consistent-field-Xα-scattered-wave molecular orbital calculation was carried out on the [CpMoS(μ-S)]$_2$ (Cp = η^5-C_5H_5) complex. The calculated results were used to rationalize the observed photochemical isomerization of the title complex to [CpMo(μ-S)][μ-S_2]. It is proposed that a terminal sulfur (S_t) → Mo charge-transfer excitation is responsible for the isomerization, which is an intramolecular redox; i.e. Mo(V) is reduced to Mo(IV) and S^{2-} is oxidized to S_2^{2-}, a result consistent with the charge-transfer character of the excitation. Specifically, the transition responsible for the isomerization is proposed to be $16b_u \rightarrow 18a_g$ ($^1A_g \rightarrow {}^1B_u$). The $18a_g$ orbital is primarily Mo in character but it is also Mo—S_t π-antibonding; cleavage of the Mo—S_t π-bond facilitates the isomerization.

As part of our continuing study[1–5] of the ligand-to-metal charge-transfer (LMCT) photochemistry of organometallic complexes, we investigated the photochemical reactivity of the [Cp*MoS(μ-S)]$_2$ [Cp* = η^5-$C_5(CH_3)_5$] and [(MeCp)MoS(μ-S)]$_2$ (MeCp = η^5-$CH_3C_5H_4$) complexes, **Ia** and **Ib**, respectively (Fig. 1).[5] When **Ia** is irradiated, isomer **IIa** forms and then isomer **IIa** undergoes a photochemical isomerization to **IIIa**. This sequence of reactions is best described by the cyclic photoisomerization process shown in eqn (1):[5]

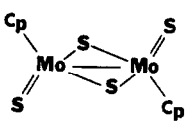


(1)

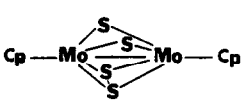
A similar photochemistry is observed for the **b** isomers.[5] In order to gain insight into the electronic structures of **Ia** and **Ib**, we carried out a self - consistent - field - Xα - scattered - wave (SCF-Xα-SW) molecular orbital calculation on [CpMoS(μ-S)]$_2$ (Cp = η^5-C_5H_5) (**Ic**). The results of the calculation are presented here and discussed in relation to the isomerization process, **I** → **II**.

EXPERIMENTAL

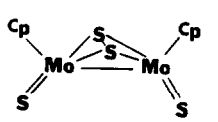
Calculations were carried out by the SCF-Xα-SW molecular orbital method.[6–9] Current versions of



Ia, Cp = η^5-$(CH_3)_5C_5$
Ib, Cp = η^5-$(CH_3)C_5H_4$
Ic, Cp = η^5-C_5H_5



IIa, Cp = η^5-$(CH_3)_5C_5$
IIb, Cp = η^5-$(CH_3)C_5H_4$
IIc, Cp = η^5-C_5H_5



IIIa, Cp = η^5-$(CH_3)_5C_5$
IIIb, Cp = η^5-$(CH_3)C_5H_4$
IIIc, Cp = η^5-C_5H_5

Fig. 1. Photoisomerization products [eqn (1)]: (**I**) [CpMoS(μ-S)]$_2$, (**II**) [CpMo(μ-S)]$_2$(μ-S_2), and (**III**) [CpMoS]$_2$(μ-S_2).

* Address correspondence to this author at: Department of Chemistry, University of Oregon, Eugene, OR 97403, U.S.A.

the programs were used* and they were run on the Columbia chemistry department's DEC VAX 11/780 computer. Norman's procedure for interpolation of overlapping sphere sizes was used to optimize the virial coefficient at one.[10,11]† Schwarz's α_{HF} values[12,13] were used for the atomic exchange parameters. The α values for the intersphere and outersphere regions were a weighted average of the atomic α values, where the weights are the number of valence electrons on the different neutral free atoms. A minimal basis set in partial wave expansion was used.‡ The coordinates used for **Ic** were based on the crystal structure data of Rakowski DuBois *et al.*[14]§ for **Ib** and adjusted to idealized C_{2h}-symmetry (Table 1). The coordinate axis and atomic labels used in the calculation are shown in Fig. 2. The outersphere was centered at the origin. The exact coordinates are listed in Table 2.

Table 1. Structural data for $[(\eta^5\text{-}C_5H_5)MoS(\mu\text{-}S)]_2$

Distance (Å)	
Mo—Mo	2.89[a]
C—C	1.43[a]
C—H	0.91[b]
Mo—C	2.38[a]
Mo—S_t	2.14[a]
Mo—S_b	2.29[a]
Angle (°)	
Cp—Mo—S_t	129[c]
C—C—C	108[d]
Mo—Mo—S_t	113[a]
S_t—Mo—S_b	104[a]
S_b—Mo—S_b	102[a]

[a] Based on the structural data of $[(\eta^5\text{-}CH_3C_5H_4)MoS(\mu\text{-}S)_2$.[14]

[b] Based on the structural data of $(\eta^5\text{-}C_5H_5)_2TiCl_2$.[4]

[c] The placement of the cyclopentadienyl ligand was estimated based on analogous Cp—Mo—Cp and Cp—Mo—S bond angles.[16–18]

[d] Idealized C—C—C angle in the cyclopentadienyl ring.

RESULTS

The SCF-Xα-SW molecular orbital calculation was performed on **Ic** rather than the analogs **Ia** and **Ib** in order to simplify the calculation.[14] This simplification is justified for two reasons. First, the initial photochemical isomerization of **I** to **II** is identical for the Cp* and MeCp complexes.[5] Second, the electronic absorption spectra for **Ia** and **Ib** are identical in the photochemically active region 400–600 nm. Because the substitution of five methyl groups on the Cp ring causes a small perturbation relative to MeCp (in terms of the photochemical reactivity and the electronic spectra), it is reasonable that the perturbation between MeCp and Cp will also be small.

The groundstate eigenvalues and symmetries of the upper occupied and lower unoccupied molecular orbitals are shown in Table 3. Of special interest to us are the charge distributions of the upper occupied and lower unoccupied molecular orbitals which are predicted to be involved in the low-energy electronic transitions. The charge distributions of these molecular orbitals can be most clearly seen by inspection of contour plots of the wave function density.

Figure 3 shows the contour plots of the wave function density for the three highest occupied molecular orbitals, $9b_g$, $16b_u$ and $17a_g$. Figure 4 shows the plots for the four lowest unoccupied molecular orbitals, $17b_u$, $10b_g$, $18a_g$ and $10a_u$. Four types of contour plots are shown: (1) the *xz*, *yz* and *xy* planes; (2) a plane parallel to the *yz* plane but containing Mo [this is labeled *yz* (Mo)]; (3) a plane that contains a Mo and a terminal S (S_t) and is perpendicular to the *xy* plane (this plane is labeled MoS_t); and (4) a plane that contains an Mo and a bridging S (S_b) and is perpendicular to the *xz* plane (this plane is labeled MoS_b).

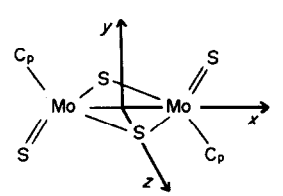


Fig. 2. Coordinate system used in the SCF-Xα-SW calculation of $[CpMoS(\mu\text{-}S)]_2$.

* The programs were received from K. H. Johnson in 1981 and converted for use on a DEC VAX 11/780 by W. H. Klemperer and M. R. M. Bruce.

† In practice, the program calculates the ratio of atomic radii and varies the percent of the calculated atomic radii while holding the ratio fixed to be used in the molecular potential. Limited computer time necessitates close but non-one virial coefficients. For **Ic** the percent value of 89% produced a virial coefficient of 1.000190 at convergence.

‡ Minimal basis set: Mo, $l = 2$; C, $l = 1$; H, $l = 1$; S, $l = 1$. For the outersphere region the value of $1 = 2$ was sufficient to generate basis function components in all representations. (The use of a minimal basis set was justified based on previous work.[4])

§ The complex with unsubstituted cyclopentadienyl ligands is suggested to be a polymer composed of dimeric units connected by sulfide or polysulfide bridges.

Table 2. Coordinates,[a] sphere radii[a] and Xα values for $[CpMoS(\mu\text{-}S)]_2$

Number	Atom	x	y	z	Radius	Xα
1	Out	0.0000	0.0000	0.0000	9.1597	0.74394
2	Mo	−2.7222	0.0000	0.0000	2.4822	0.70341
3	S_b	0.0000	0.0000	3.3873	2.4940	0.72475
4	S_t	−4.3122	−3.7080	0.0000	2.5365	0.72475
5	C_a	−2.5308	4.5005	0.0000	1.6881	0.75928
6	C_b	−3.9300	3.7487	2.1862	1.6760	0.75928
7	C_c	−6.1940	2.5323	1.3512	1.6860	0.75928
8	H_a	−1.0161	5.3145	0.0000	1.1499	0.77725
9	H_b	−3.4619	4.0003	3.8216	1.1485	0.77725
10	H_c	−7.4194	1.8738	2.3619	1.1511	0.77725
11	Mo	2.7222	0.0000	0.0000	2.4822	0.70341
12	S_b	0.0000	0.0000	−3.3873	2.4940	0.72475
13	S_t	4.3122	3.7080	0.0000	2.5365	0.72475
14	C_a	2.5308	−4.5005	0.0000	1.6881	0.75928
15	C_b	−3.9300	3.7487	−2.1862	1.6760	0.75928
16	C_b	3.9300	−3.7487	2.1862	1.6760	0.75928
17	C_b	3.9300	−3.7487	−2.1862	1.6760	0.75928
18	C_c	−6.1940	2.5323	−1.3512	1.6860	0.75928
19	C_c	6.1940	−2.5323	1.3512	1.6860	0.75928
20	C_c	6.1940	−2.5323	−1.3512	1.6860	0.75928
21	H_a	1.0161	−5.3145	0.0000	1.1499	0.77725
22	H_b	−3.4619	4.0003	−3.8216	1.1485	0.77725
23	H_b	3.4619	−4.0003	3.8216	1.1485	0.77725
24	H_b	3.4619	−4.0003	−3.8216	1.1485	0.77725
25	H_c	−7.4194	1.8738	−2.3619	1.1511	0.77725
26	H_c	7.4194	−1.8738	2.3619	1.1511	0.77725
27	H_c	7.4194	−1.8738	−2.3619	1.1511	0.77725

[a] In bohrs.

Table 3. Symmetries, energies, % character and metal–metal interactions for the molecular orbitals of $[CpMoS(\mu\text{-}S)]_2$

Symmetry	Energy (eV)	% Character				Metal–metal interactions	Figure
		S_b	S_t	Cp	Mo		
$19b_u$	−2.738	12	19	17	43	$d_{x^2-y^2}$, $d_{x^2-y^2}$ antibonding	
$19a_g$	−2.771	6	15	14	33	d_{z^2}, d_{z^2} bonding	
$11a_u$	−2.893	20	0	14	44	d_{yz}, d_{yz} antibonding	
$11b_g$	−3.873	13	0	30	36	d_{xz}, d_{xz} antibonding	
$18b_u$	−4.090	19	0	10	58	d_{z^2}, d_{z^2} antibonding	
$10a_u$	−4.724	5	17	18	38	d_{xz}, d_{xz} bonding	4
$18a_g$	−4.855	4	22	3	54	d_{xy}, d_{xy} antibonding	4, 6
$10b_g$	−5.076	16	20	0	43	d_{yz}, d_{yz} bonding	4
$17b_u$	−5.173	10	21	4	44	d_{xy}, d_{xy} bonding	(LUMO) 4, 6
$17a_g$	−6.238	1	11	40	17		(HOMO) 3
$16b_u$	−6.406	16	18	32	8		3
$9b_g$	−6.769	36	5	22	14		3
$9a_u$	−7.093	6	24	29	11		
$16a_g$	−7.443	6	14	7	56	$d_{x^2-y^2}$, $d_{x^2-y^2}$ bonding	
$8b_g$	−7.745	14	38	11	10		
$15b_u$	−7.980	21	32	10	14		
$15a_g$	−8.301	17	36	7	17		

Table 3. (*Cont.*)

Symmetry	Energy (eV)	% Character				Metal–metal interactions	Figure
		S_b	S_t	Cp	Mo		
$8a_u$	−8.790	2	33	8	38		
$14b_u$	−9.186	28	29	5	18		
$14a_g$	−9.695	10	23	23	30		
$13b_u$	−9.737	16	7	26	33		
$7b_g$	−9.797	37	9	4	31		
$6b_g$	−9.869	47	4	2	39		
$13a_g$	−10.278	24	4	32	16		
$12b_u$	−10.445	20	10	31	14		
$7a_u$	−10.639	53	1	2	35		
$12a_g$	−10.683	14	37	6	39		
$11b_u$	−10.860	21	31	3	43		
$6a_u$	−13.030	0	0	96	0		
$5b_g$	−13.036	0	0	97	0		
$10b_u$	−13.075	0	0	96	0		
$11a_g$	−13.077	0	0	98	0		
$5a_u$	−15.033	0	0	98	1		
$4b_g$	−15.043	0	0	99	1		
$9b_u$	−15.051	0	1	99	1		
$10a_g$	−15.064	0	0	98	1		
$8a_g$	−18.104	0	85	0	11		
$8b_u$	−18.119	0	85	0	11		
$9a_g$	−18.796	82	0	4	7		
$4a_u$	−18.841	83	0	3	9		
$7b_u$	−19.823	0	0	99	1		
$7a_g$	−19.831	1	0	97	1		
$6b_u$	−20.035	0	0	99	0		
$6a_g$	−20.042	1	0	98	0		
$3b_g$	−20.256	0	0	100	0		
$3a_u$	−20.280	1	0	98	0		
$2b_g$	−22.671	0	0	99	0		
$2a_u$	−22.676	0	0	99	0		
$5a_g$	−22.697	0	0	0	0		
$5b_u$	−22.702	0	0	99	0		
$4b_u$	−25.079	0	0	99	1		
$4a_g$	−25.084	0	0	99	1		
$3b_u$	−41.024	1	0	0	99		
$1b_g$	−41.204	1	0	0	98		
$1a_u$	−41.262	2	0	0	98		
$3a_g$	−41.286	1	1	0	98		
$2b_u$	−41.522	0	5	0	95		
$2a_g$	−41.586	1	4	0	95		
$1b_u$	−64.003	0	1	0	99		
$1a_g$	−64.046	0	1	0	99		

The contour plots show that the $9b_g$ orbital (Fig. 3) is primarily S_b in character. The contour plots of the $16b_u$ orbital (Fig. 3) show it to be a highly delocalized molecular orbital with Cp, S_t and S_b character. The $16b_u$ orbital is essentially Cp–S_t–S_b nonbonding. The $17a_g$ orbital (Fig. 3) is primarily Cp in character with a small amount of Mo character. The interaction is only slightly Cp–Mo bonding. As expected, there is a significant amount of wave function density in the planes above and below the Cp ring, parallel to the carbon skeleton. However, these planes are not shown (see Table 3).

The contour plots of the unoccupied molecular orbitals (Fig. 4) show that the $17b_u$, $10b_g$, $18a_g$ and

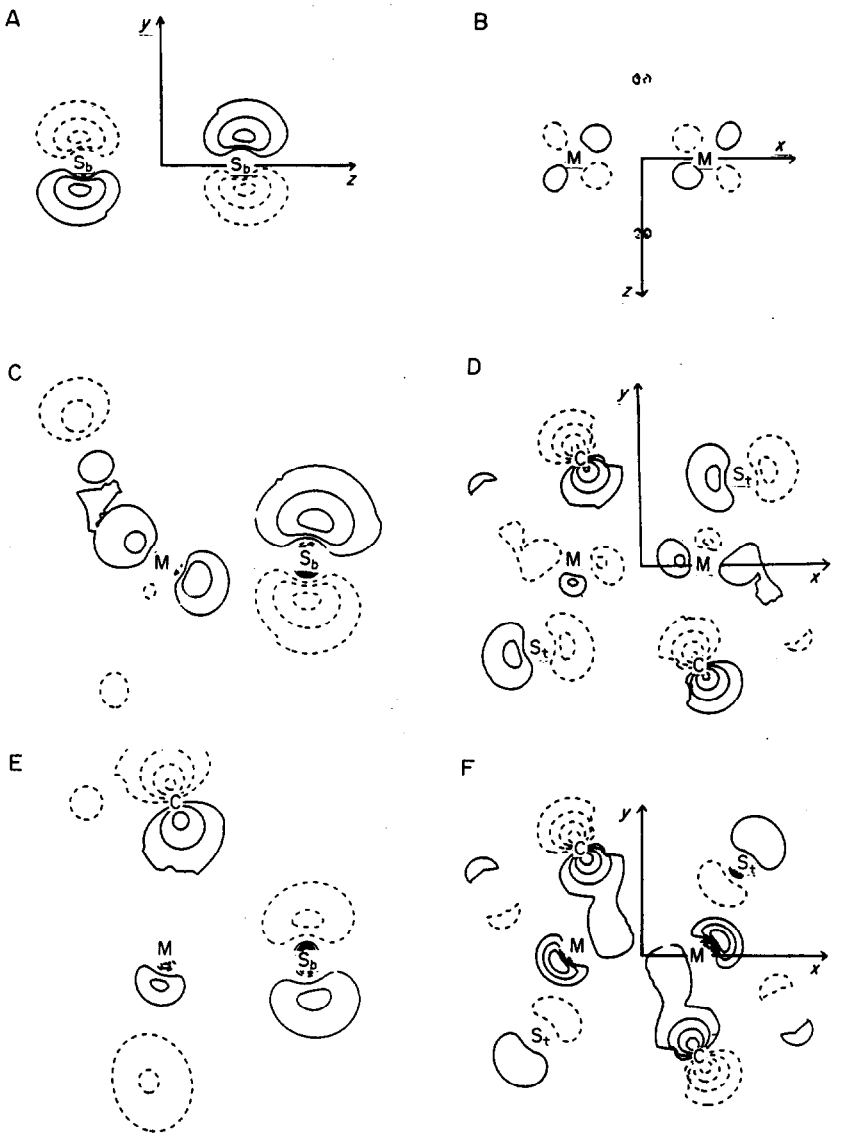


Fig. 3. Wave function contour plots for $[CpMoS(\mu\text{-}S)]_2$: (A) $9b_g$, yz plane; (B) $9b_g$, xz plane; (C) $9b_g$, MoS_b plane; (D) $16b_u$, xy plane; (E) $16b_u$, MoS_b plane; and (F) $17a_g$, xy plane. See Fig. 2 for coordinate system. Solid lines denote contours at values of 0.04–0.32 $e^{1/2}$ bohr$^{-3/2}$, while broken lines denote values of -0.04 to -0.32 $e^{1/2}$ bohr$^{-3/2}$. Those atoms that are in the plane are labeled as follows: M = molybdenum, S_b = bridging sulfur, S_t = terminal sulfur, and C = carbon.

$10a_u$ molecular orbitals are all primarily Mo in character with significant S_t content. In addition, there is some S_b character in the $17b_u$ and $10b_g$ orbitals. The Mo–S_t interaction is antibonding in all four molecular orbitals with the strongest interaction in the $17b_u$ and $18a_g$ orbitals. The Mo–S_b interactions are essentially nonbonding in these four unoccupied orbitals.

The eigenvalues can be used to predict unrelaxed transition state energies by taking the difference between occupied and unoccupied energy levels (see Table 4).* Assignments are then made by comparing the overall experimental pattern with that predicted by the SCF-Xα-SW calculation. Figure 5 compares the overall pattern of experimental optical transition energies to the calculated transition energies. Only

* Unrelaxed transition-state energies do not take into account electron–electron repulsion effects. In order to account for the effects of orbital relaxation, a relaxed transition-state procedure was developed by Slater (see Ref. 6, pp. 49–53). However, as Johnson and Slater have pointed out, close agreement between the unrelaxed and relaxed transition-state energies is expected where the perturbation to the potential energy is small when optical transitions occur between valence orbitals and empty orbitals lying immediately above (see Ref. 7, pp. 168–169, and references therein).

Table 4. Calculated and experimental[a] electronic transition energies[b] for $[CpMoS(\mu\text{-}S)]_2$

Transition	A/F[c]	Primary transition type[d]	Transition energy		
				Experimental	
			Calculated[e]	**Ia**	**Ib**
$17a_g \rightarrow 17b_u$ ($^1A_g \rightarrow {}^1B_u$)	A	Cp → Mo–S_t	1.1	1.4 (900)	1.5 (840)
$17a_g \rightarrow 10b_g$ ($^1A_g \rightarrow {}^1B_g$)	F		1.2		
$16b_u \rightarrow 17b_u$ ($^1A_g \rightarrow {}^1A_g$)	F		1.2		
$16b_u \rightarrow 10b_g$ ($^1A_g \rightarrow {}^1B_u$)	A	Cp–S_t–S_b → Mo	1.3	1.7 (740)	1.8 (700)
$17a_g \rightarrow 18a_g$ ($^1A_g \rightarrow {}^1A_g$)	F		1.4		
$17a_g \rightarrow 10a_u$ ($^1A_g \rightarrow {}^1A_u$)	A	Cp → Mo	1.5		
$16b_u \rightarrow 18a_g$ ($^1A_g \rightarrow {}^1B_u$)	A	Cp–S_t–S_b → Mo–S_t	1.5	2.1 (600)	2.1 (600)
$9b_g \rightarrow 17b_u$ ($^1A_g \rightarrow {}^1A_u$)	A	S_b → Mo–S_t	1.6		
$16b_u \rightarrow 10a_u$ ($^1A_g \rightarrow {}^1B_g$)	F		1.7		
$9b_g \rightarrow 10b_g$ ($^1A_g \rightarrow {}^1A_g$)	F		1.7		
$9b_g \rightarrow 18b_g$ ($^1A_g \rightarrow {}^1A_g$)	F		1.9		
$9a_u \rightarrow 17b_u$ ($^1A_g \rightarrow {}^1B_g$)	F		1.9		
$9a_u \rightarrow 10b_g$ ($^1A_g \rightarrow {}^1B_u$)	A	Cp–S_t → Mo	2.0		
$9b_g \rightarrow 10a_u$ ($^1A_g \rightarrow {}^1B_u$)	A	S_b → Mo	2.0	2.5 (485sh)	2.5 (490sh)
$17a_g \rightarrow 18b_u$ ($^1A_g \rightarrow {}^1B_u$)	A	Cp → Mo	2.1		
$9b_u \rightarrow 18a_g$ ($^1A_g \rightarrow {}^1B_u$)	A	Cp–S_t → Mo–S_t	2.2	2.8 (446)	2.8 (440)
$16a_g \rightarrow 17b_u$ ($^1A_g \rightarrow {}^1B_u$)	A	Mo → Mo–S_t	2.3		

[a] Reference 5 and A. Bruce and D. Tyler, unpublished results.
[b] Energies in eV except for those in parentheses which are in nm.
[c] Symmetry allowed or forbidden.
[d] Shown only for allowed transitions. See text for discussion of how transition type assignments are made.
[e] Unrelaxed transition-state calculation.

symmetry-allowed transitions are considered. The top two lines show the experimental transition energeis for **Ia** and **Ib** respectively, and the bottom line shows the calculated transition energies for **Ic**. It is apparent that the SCF-Xα-SW calculated transition energies are red shifted with respect to the experimental values, but the pattern of the transitions (i.e. the energy spacings between the peaks) predicted by the calculation is in excellent agreement with the experimental pattern.*

The two lowest energy allowed electronic transitions are predicted to be the $17a_g \rightarrow 17b_u$ ($^1A_g \rightarrow {}^1B_u$) and $16b_u \rightarrow 10b_g$ ($^1A_g \rightarrow {}^1A_u$) transitions, respectively. When **Ia** and **Ib** are irradiated into their two low-energy absorption bands ($\lambda > 700$ nm, 1.8 eV), there is no apparent photochemistry. The next transition is predicted to be composed of the following group of transitions: $17a_g \rightarrow 10a_u$ ($^1A_g \rightarrow {}^1A_u$), $16b_u \rightarrow 18a_g$ ($^1A_g \rightarrow {}^1B_u$) and $9b_g \rightarrow 17b_u$ ($^1A_g \rightarrow {}^1A_u$). The isomerization occurs when the complexes are irradiated into this absorption band ($\lambda \approx 600$ nm, 2.1 eV).

The transitions at higher energy ($\lambda < 500$ nm, 2.5 eV) are predicted to be composed of two sets of transitions: a set of three transitions at ≈500 nm (2.5 eV), $9a_u \rightarrow 10b_g$ ($^1A_g \rightarrow {}^1B_u$), $9b_g \rightarrow 10a_u$ ($^1A_g \rightarrow {}^1B_g$) and $17a_g \rightarrow 18b_u$ ($^1A_g \rightarrow {}^1B_u$); and another set of two transitions at ≈445 nm (2.8 eV), $9a_u \rightarrow 18a_g$ ($^1A_g \rightarrow {}^1A_u$) and $16a_g \rightarrow 17b_u$ ($^1A_g \rightarrow {}^1B_u$). Isomerization also occurs when the complex is irradiated in these absorption bands.

* It should be noted that the procedure as outlined in Experimental will generate one "best" calculated answer, i.e. one that optimizes the viral coefficient at one while holding the ratio of the overlapping sphere sizes fixed. When making electronic spectral assignments, there are other approaches which can be used to fit the calculation to experiment, including the use of variable overlapping sphere sizes.

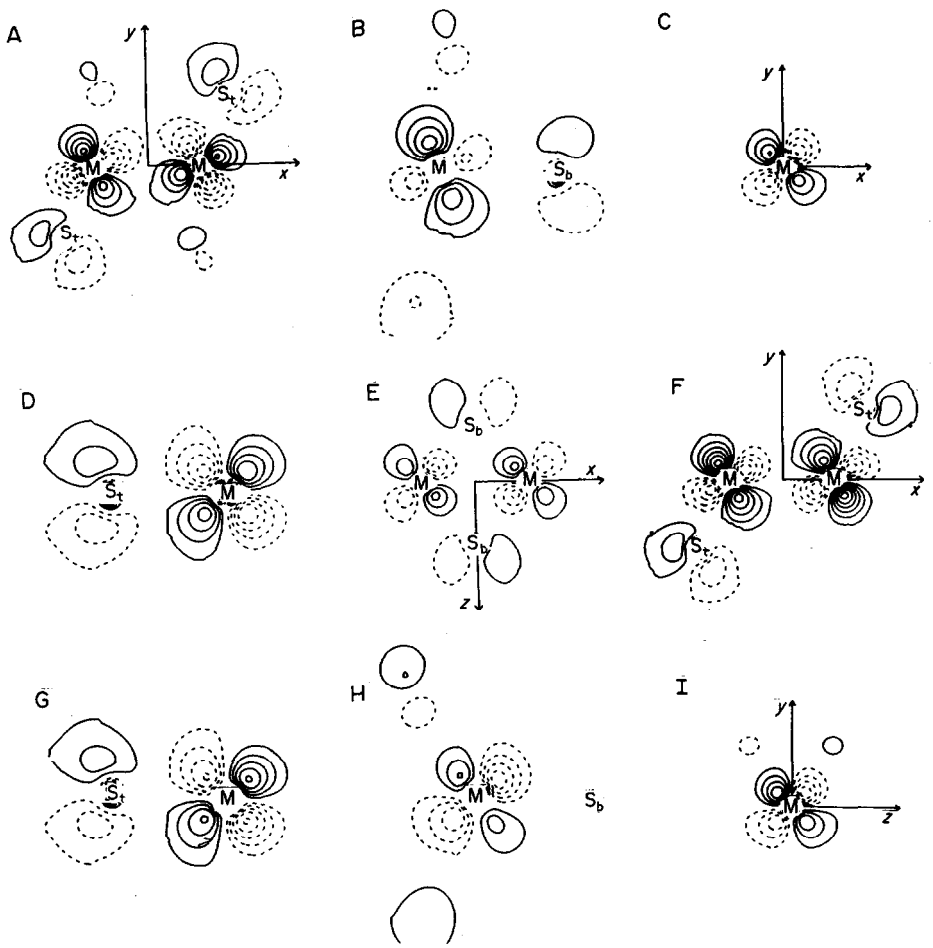


Fig. 4. Wave function contour plots for $[CpMoS(\mu\text{-}S)]_2$: (A) $17b_u$, xy plane; (B) $17b_u$, MoS_b plane; (C) $10b_g$, yz plane; (D) $10b_g$, MoS_t plane; (E) $10b_g$, xz plane; (F) $18a_g$, xy plane; (G) $10a_u$, MoS_t plane; (H) $10a_u$, MoS_b plane; and (I) $10a_u$, yz plane. See Fig. 2 for coordinate system. Solid lines denote contours at values of 0.04–0.32 $e^{1/2}$ bohr$^{-3/2}$, while broken lines denote values of -0.04 to -0.32 $e^{1/2}$ bohr$^{-3/2}$. Those atoms that are in the plane are labeled as follows: M = molybdenum, S_b = bridging sulfur, S_t = terminal sulfur, and C = carbon.

Because **Ic** is a dinuclear complex the orbitals on the two metals can interact with each other to form σ, π, and δ bonding and antibonding orbitals. The Mo–Mo interactions are indicated on the right-hand side of Table 3. Of special interest is the $16a_g$ orbital which is the Mo–Mo σ-bonding interaction, and the $19b_u$ orbital which is the antibonding interaction.

DISCUSSION

Lack of photofragmentation

When **Ic** is irradiated, there is no photofragmentation. We explain the lack of Mo–Cp cleavage by reasoning that no Mo–Cp antibonding orbitals are populated in the excited states for $\lambda > 300$ nm (see Fig. 4). Using the same logic, the Mo—S_b bonds are also not expected to be broken. However, low-energy transitions are predicted to weaken the Mo—S_t π-bond by a population of molecular orbitals which show Mo–S_t antibonding interactions. This is especially true for excitations that populate the $17b_u$ or $18a_g$ orbital. Note, however, that while cleavage of the Mo—S_t π-bond may occur, cleavage of the Mo—S_t σ-bond is very unlikely. The calculation shows that the Mo—S_t σ-bond is low in energy (≈ -10.8 eV vs -6.2 eV for the HOMO) and therefore transitions originating in the S_t–Mo σ-orbital, or terminating in the S_t–Mo σ^*-orbital (> -2.7 eV) will not occur at any of the wavelengths used in our experiments. Thus, even if the Mo—S_t π-bond breaks completely, the Mo—S_t σ-bond will remain intact and prevent fragmentation of the complex. The calculation also demonstrates why no photochemistry involving the Mo—Mo bond is observed. As the right-hand side of Table 3 shows, the $16a_g$

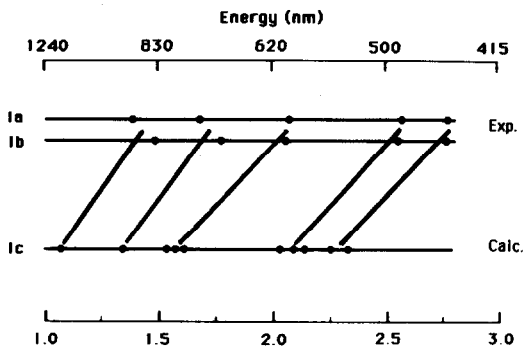


Fig. 5. SCF-Xα-SW transition state vs experimental transition energies for $[CpMoS(\mu\text{-}S)]_2$. **(Ia)** $[(\eta^5\text{-}(CH_3)_5C_5)MoS(\mu\text{-}S)]_2$, experimental transition energies;[5] **(Ib)** $[(\eta^5\text{-}(CH_3)C_5H_4)MoS(\mu\text{-}S)]_2$, experimental transition energies;[5] and **(Ic)** $[(\eta^5\text{-}C_5H_5)MoS(\mu\text{-}S)]_2$, unrelaxed SCF-Xα-SW transition state calculation. Only allowed transitions are shown.

molecular orbital is primarily Mo–Mo bonding.* Because of its low energy, it is not expected to be depopulated upon irradiation with $\lambda > 600$ nm (2.1 eV). The $19b_u$ molecular orbital which is Mo–Mo σ^* is also not involved in any low-energy excitations ($\lambda > 600$ nm). Thus, cleavage of the metal–metal bond is not expected. In conclusion, the results of the SCF-Xα-SW calculation are consistent with the experimental results with regard to the lack of photofragmentation.

Photoisomerization

Analysis of the calculations for **Ic** in conjunction with the observed photochemistry leads to the conclusion that the most significant aspect of the electronic transitions responsible for the photochemistry is the population of an Mo–S_t π^* molecular orbital. As mentioned above, the $17b_u$ and $18a_g$ orbitals show the strongest Mo–S_t π^* interaction. In order to show this interaction more clearly, the low-density contour plots for these two orbitals are shown in Fig. 6. The $17b_u$ orbital is populated in the lowest-energy transition but no photochemistry is observed by irradiating into this weak ($\varepsilon \sim 50$), low energy ($\lambda \approx 900$ nm, 1.4 eV) absorption band. The absence of photochemistry demonstrates that occupation of an Mo–S_t π^*-orbital is not sufficient to photoisomerize the complex. As explained below, the excited state must also have considerable $S_t \rightarrow$ Mo charge-transfer character. Note that the next to lowest energy transition $[16b_u \rightarrow 10b_g\ (^1A_g \rightarrow {}^1B_u)]$ is also photochemically inactive; no Mo–S_t π^*-orbital is populated in this transition.

Recall that the photochemical isomerization occurs when complex **I** is irradiated at wavelengths shorter than 600 nm. Two of the three transitions which are predicted to occur at 600 nm (≈ 50 kcal mol^{-1}) involve the $17b_u$ and $18a_g$ orbitals; these are $16b_u \rightarrow 18a_g$ and $9b_g \rightarrow 17b_u$. Each of these transitions is an LMCT transition (see Table 4), and both result in a formal reduction of the molybdenum, oxidation of the ligand (S_t in the $16b_u \rightarrow 18a_g$ and S_b in the $9b_g \rightarrow 17b_u$), and weakening of the Mo–S_t π-bond. The photoisomerization of **I** to **II** is logical when viewed as a redox process involving cleavage of the Mo–S_t π-bond. The molybdenum is reduced from oxidation state +5 to +4 and the terminal sulfides (S^{2-}) are oxidized to a disulfide (S_2^{2-}). We suggest that the $16b_u \rightarrow 18a_g$ transition is responsible for the observed photochemistry because the $16b_u$ orbital has S_t character. [The $9b_g$ orbital is assigned as primarily S_b in character (see Table 4 and Fig. 3)]. It is logical to propose that the two oxidized S_t ligands couple to form the bridging S_2^{2-} ligand. This coupling may occur by twisting the two halves of the molecule so as to bring the S_t ligands together.

Alternatively, we can speculate that the LMCT excitation initiates a coupling of the oxidized sulfido (S·) ligand on one Mo atom with the other Mo atom. The resulting $CpMo(\mu\text{-}S)_4MoCp$ complex would then rearrange to give **II**. Hoffmann *et al.*[19] used theoretical calculations in an analogous system to analyze the interconversion of doubly-bridged and quadruply-bridged structures of $Cp_2M_2(CO)_4$. They showed that the Cp—M—M angle in the doubly-bridged structure can open up to accommodate two more bridging CO ligands to form the quadruply-bridged structure with very little change in energy. The isomerization of **I** to **II** is expected to be a more facile process than the interconversion of doubly-bridged to quadruply-bridged isomers of $Cp_2M_2(CO)_4$. There is less constraint on the geometry in the sulfur-bridged structure, **II**, because the sulfur atoms need not be kept from interacting, i.e. sulfur–sulfur bonds readily form.

In summary, the SCF-Xα-SW calculation predicts that the photoisomerization of **I** to **II** is initiated by population of the Mo–S_t π^* molecular orbital. The driving force for the isomerization may be due to the redox nature of the LMCT excited state.

Acknowledgements—We thank Procter & Gamble Co. for a University Exploratory Research Grant and American Cyanamid for a fellowship to A. E. B.

* Enemark *et al.* performed extended Hückel and Fenske–Hall molecular orbital calculations on three isomers of $Mo_2S_4(dme)_2^{2-}$, one of which has the anti-Mo_2S_4 core as in complex **I**. They found that the HOMO orbital in each isomer was the Mo–Mo σ-bonding orbital.[19]

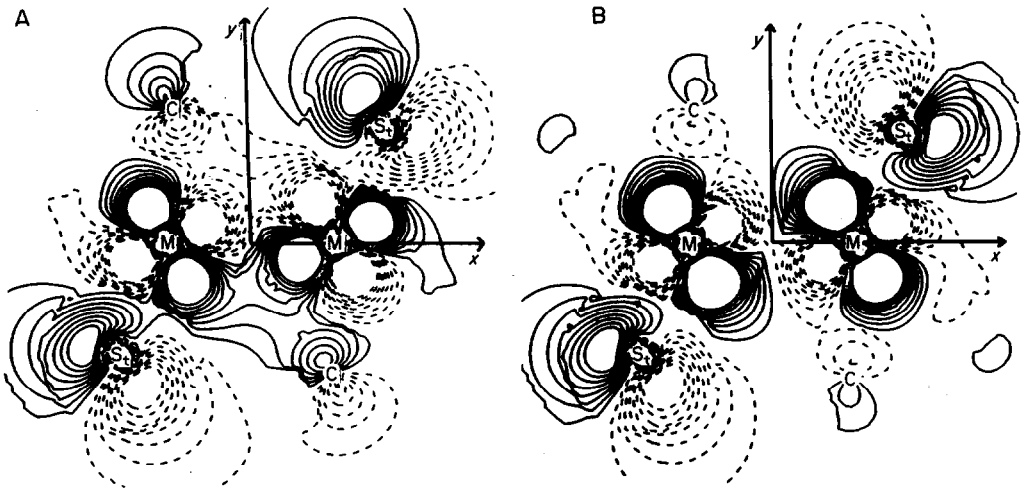


Fig. 6. Wave function contour plot for $[CpMoS(\mu\text{-}S)]_2$: (A) $17b_u$, xy plane; and (B) $18a_g$, xy plane. See Fig. 2 for coordinate system. Solid lines denote contours at values of 0.01–0.08 $e^{1/2}$ bohr$^{-3/2}$, while broken lines denote values of -0.01 to -0.08 $e^{1/2}$ bohr$^{-3/2}$. Those atoms that are in the plane are labeled as follows: M = molybdenum, S_t = terminal sulfur, and C = carbon.

REFERENCES

1. M. R. M. Bruce, A. Kenter and D. R. Tyler, *J. Am. Chem. Soc.* 1984, **106**, 639.
2. A. E. Bruce, M. R. M. Bruce, A. Sclafani and D. R. Tyler, *Organometallics* 1984, **3**, 1610.
3. M. R. M. Bruce and D. R. Tyler, *Organometallics* 1985, **3**, 528.
4. A. E. Bruce, M. R. M. Bruce and D. R. Tyler, *J. Am. Chem. Soc.* 1984, **106**, 6660.
5. A. E. Bruce and D. R. Tyler, *Inorg. Chem.* 1984, **23**, 3433.
6. J. C. Slater, *The Calculation of Molecular Orbitals*, and references therein. Wiley, New York (1979).
7. K. H. Johnson, *Adv. Quantum Chem.* 1973, **7**, 143, and references therein.
8. N. Rosch, W. G. Klemperer and K. H. Johnson, *Chem. Phys. Lett.* 1973, **23**, 149.
9. K. H. Johnson and F. C. Smith, *Phys. Rev. B* 1972, **5**, 831.
10. J. G. Norman, Jr, *J. Chem. Phys.* 1974, **61**, 4630.
11. J. G. Norman, Jr, *Mol. Phys.* 1976, **31**, 1191.
12. K. Shwarz, *Phys. Rev. B* 1972, 2466.
13. K. Schwarz, *Theor. Chim. Acta* 1974, **34**, 225.
14. M. Rakowski BuBois, D. L. DuBois, M. C. Van Derveer and R. C. Haltiwanger, *Inorg. Chem.* 1981, **20**, 3064.
15. H. D. Block and R. Allman, *Cryst. Struct. Commun.* 1975, **4**, 53.
16. D. L. Stevenson and L. F. Dahl, *J. Am. Chem. Soc.* 1967, **89**, 3721.
17. K. Prout, *Acta Cryst.* 1974, **B30**, 2290.
18. T. Chandler, D. L. Lichtenberger and J. H. Enemark, *Inorg. Chem.* 1981, **20**, 75.
19. E. D. Jemmis, A. P. Pinhas and R. Hoffmann, *J. Am. Chem. Soc.* 1978, **102**, 2576.

Polyhedron Vol. 4, No. 12, pp. 2083–2087, 1985
Printed in Great Britain

0277–5387/85 $3.00 + .00
© 1985 Pergamon Press Ltd

SYNTHESIS AND CHARACTERIZATION OF TRIORGANOANTIMONY(V) COMPLEXES WITH BIDENTATE LIGANDS

NARENDRA K. JHA* and DHIRENDRA M. JOSHI

Department of Chemistry, Indian Institute of Technology, New Delhi 110 016, India

(*Received* 9 *July* 1984; *accepted after revision* 29 *June* 1985)

Abstract—Monochelated organoantimony(V) complexes of the type $R_3Sb(OMe)L$, where R = Me or Ph, and L is the anion of acetylacetone, 8-hydroxyquinoline, salicylaldehyde, *o*-hydroxyacetophenone or 2-hydroxy-1-naphthaldehyde have been obtained from triorganoantimony(V) dibromide and the sodium derivative of the ligands in a benzene–methanol mixture. Molecular weight determination in benzene reveals the monomeric nature of these complexes. IR and NMR data suggest that L acts as a bidentate ligand giving an octahedral environment for the antimony atom.

Triorganoantimony(V) complexes with potentially chelating organic ligands are interesting from the synthetic and structural points of view. Some such complexes have been reported in the literature containing bi- and tridentate ligands.[1–7] We have also reported such complexes containing tetradentate ligands.[8] In the complexes of the type R_3SbXL, where R = alkyl or aryl group, X = simple anion like Cl^-, Br^- or OH^-, and L = anion of bidentate ligand, the antimony atom has a choice between penta- and hexa-coordination, depending upon the monodentate or bidentate nature of the ligand L. Recently hexa-coordination of antimony has been observed in a number of complexes having a β-diketone as chelating ligand.[5] For some of the complexes a change in geometry has also been reported, e.g. $Ph_3SbCl(ox)$, ox = 8-hydroxyquinolinate ion, has a trigonal bipyramidal geometry in solution but is octahedral in the solid state.[1]

Gopinathan and coworkers, without assigning any structure, have reported replacement of both the bromine atoms of Ph_3SbBr_2 with monobasic bidentate ligands (HL).[9] Complexes formed are of the type Ph_3SbL_2. If L^- is behaving as a bidentate ligand, the coordination number of antimony in these complexes ought to be seven. Other workers have also used similar bidentate ligands but they have not been able to get Ph_3SbL_2 but found that only one X was replaced by L even though the Ph_3SbBr_2 : ligand ratio was 1 : 2.[5] It is because of these conflicting reports that we took up the present investigation. The potential bidentate ligands used in this investigation are the anions of acetylacetone (acac), 8-hydroxyquinoline (ox), salicylaldehyde (sal), *o*-hydroxyacetophenone (hap) and 2-hydroxy-1-naphthaldehyde (hna).

RESULTS AND DISCUSSION

The complexes have been prepared by the treatment of R_3SbBr_2 (R = Me or Ph) with the sodium salt of the ligand in 1 : 3 molar ratio in a dry benzene–methanol mixture:

$$R_3SbBr_2 + 2NaL \xrightarrow{\text{benzene + methanol}} R_3Sb(OMe)L + 2NaBr.$$

All the complexes are white in colour, except for the ox complexes, which are yellow. $Me_3Sb(OMe)(acac)$ was obtained as a brown coloured viscous liquid which is highly sensitive to moisture. All the complexes were recrystallised either from a benzene–hexane or a benzene–petroleum ether (b.p. 40–60°C) mixture. Physical and analytical data of the complexes prepared are given in Table 1. Molecular weight determination of the complexes soluble in benzene show that they are non-dissociating monomers in benzene.

* Author to whom correspondence should be addressed.

Table 1. Analytical data for complexes

Complex	M.p.	% Yield	% C found (calc.)	% H found (calc.)	% N found (calc.)	% Sb found (calc.)	Molecular weight found (calc.)
$Ph_3Sb(OMe)(acac)$	145–148	60.0	59.9 (59.6)	5.2 (5.2)	—	25.8 (25.3)	478 (469)
$Ph_3Sb(OMe)(ox)$	248[a]	80.4	63.6 (63.6)	4.5 (4.5)	2.6 (2.6)	23.7 (23.1)	523 (528)
$Me_3Sb(OMe)(ox)$	120[a]	52.4	45.3 (45.6)	5.1 (5.3)	4.1 (4.1)	35.2 (35.7)	—
$Ph_3Sb(OMe)(sal)$	150[a]	63.6	61.2 (61.8)	4.3 (4.5)	—	24.8 (24.2)	498 (505)
$Me_3Sb(OMe)(sal)$	167[a]	55.5	41.8 (41.4)	5.3 (5.3)	—	38.5 (38.2)	315 (319)
$Ph_3Sb(OMe)(hap)$	210–212	70.2	63.1 (62.4)	4.5 (4.8)	—	23.9 (23.5)	526 (519)
$Me_3Sb(OMe)(hap)$	140[a]	48.6	43.3 (43.2)	5.6 (5.7)	—	36.5 (36.6)	—
$Ph_3Sb(OMe)(hna)$	180[a]	68.4	65.1 (64.9)	4.5 (4.5)	—	22.3 (22.0)	567 (555)
$Me_3Sb(OMe)(hna)$	136[a]	56.0	48.5 (48.8)	5.2 (5.1)	—	33.4 (33.1)	365 (369)

[a] Decomposed.

IR spectra

The main IR frequencies of the ligands and their complexes are given in Table 2 with their assignment.

A broad band in the region 2800–2700 cm^{-1} in the ligands, which may be assigned to the intramolecularly hydrogen bonded OH[10] is not observed in the IR spectra of the complexes, indicating Sb—O bond formation.

The absence of a free carbonyl band at 1620 cm^{-1} and the presence of a ν(C···O) absorption band at 1565–1590 cm^{-1} in the IR spectrum of $Ph_3Sb(OMe)(acac)$ suggests that the ligand moiety is bonded to the antimony atom through the carbonyl oxygen.[2,4]

Similar shifts in the ν(C···O) are observed in the other complexes, except for those of ox (Table 2). In the IR spectrum of $Ph_3Sb(OMe)(ox)$ the presence of two bands at 1605 and 1575 cm^{-1}, in place of only one band at 1590 cm^{-1} attributed to ν(C=N)[11] in the ligand, indicates coordination of nitrogen with the antimony. This is further confirmed by the

Table 2. Main IR frequencies (cm^{-1}) and their assignment

S. No.	Ligand/complex	ν(C—O)	ν(C=N)	ν(Sb—OMe)	ν(Sb—O)
1.	acacH	1620	—	—	—
2.	$Ph_3Sb(OMe)(acac)$	1565–1590	—	1060	405
3.	oxH	—	1580	—	—
4.	$Ph_3Sb(OMe)(ox)$	—	1605, 1575	1070	415
5.	$Me_3Sb(OMe)(ox)$	—	1565	1070	400
6.	salH	1660, 1640	—	—	—
7.	$Ph_3Sb(OMe)(sal)$	1600	—	1070	405
8.	$Me_3Sb(OMe)(sal)$	1630	—	1065	410
9.	hapH	1580	—	—	—
10.	$Ph_3Sb(OMe)(hap)$	1600, 1575	—	1060	410
11.	$Me_3Sb(OMe)(hap)$	1565	—	1065	410
12.	hnaH	1640	—	—	—
13.	$Ph_3Sb(OMe)(hna)$	1600	—	1075	400
14.	$Me_3Sb(OMe)(hna)$	1620	—	1070	405

Table 3. PMR spectral data for ligands and complexes (δ ppm)

S. No.	Ligand/complex	OH	=CH—/—CH=O	Aromatic H	Sb—OMe	C—Me	Sb—Me
1.	acacH	14.92	5.50	—	—	1.97	—
2.	$Ph_3Sb(OMe)(acac)$	—	5.21	7.56–7.24	2.14	1.80	—
3.	oxH	8.42	—	8.78–7.14	—	—	—
4.	$Ph_3Sb(OMe)(ox)$	—	—	8.64–6.71	2.13	—	—
5.	salH	11.01	9.84	7.55–6.90	—	—	—
6.	$Me_3Sb(OMe)(sal)$	—	10.81	7.77–6.70	2.16	—	1.81
7.	hapH	12.05	—	7.61–6.68	—	2.45	—
8.	$Ph_3Sb(OMe)(hap)$	—	—	8.29–6.80	2.08	2.51	—
9.	$Me_3Sb(OMe)(hap)$	—	—	7.65–6.51	2.15	2.53	1.62
10.	hnaH	13.10	10.67	8.25–7.01	—	—	—
11.	$Me_3Sb(OMe)(hna)$	—	10.70	9.01–6.69	2.15	—	1.71

presence of a band at 270 cm^{-1} which is assigned to the ν(Sb—N).[12] A sharp band at $\sim$1070 cm^{-1} in all the complexes might be due to the Sb—OMe streching mode.[4]

A band at $\sim$400 cm^{-1} is assigned to the Sb—O stretching frequency in all the complexes.[4,13]

PMR spectra

PMR spectra of all the complexes (Table 3) recorded in $CDCl_3$ or DMSO-d_6 do not show the presence of hydroxyl protons originally present in the free ligands in the hydrogen-bonded state. This indicates the replacement of hydroxyl protons by antimony, thus confirming Sb—O bond formation.

The PMR spectrum of $Ph_3Sb(OMe)(acac)$ in $CDCl_3$ at room temperature showed a quartet (δ 7.56–7.47 ppm) due to the *ortho*-protons of three equivalent phenyl groups, a triplet (δ 7.30–7.24 ppm) due to the *meta*- and *para*-protons of the phenyl group, a sharp singlet each for methine (δ 5.21 ppm), methoxy (δ 2.14 ppm) and methyl (δ 1.80 ppm) protons. Integrated intensities due to the phenyl, methine, methoxy and methyl protons were in a 15 : 1 : 3 : 6 ratio, confirming the coordination of only one ligand moiety with the antimony atom in the complex formation.

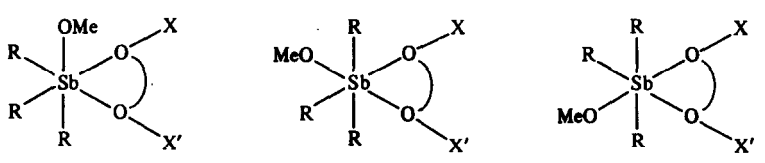
In the PMR spectra of $R_3Sb(OMe)(sal)$ and $R_3Sb(hna)$ a downfield shift of the aldehydic proton on coordination confirms strong interaction of antimony atom with the carbonyl oxygen of the ligand ring. Such a downfield shift was also observed for the $COCH_3$ protons in $R_3Sb(OMe)(hap)$, although the shift is smaller than expected, because the protons are attached to an adjacent carbon atom in this case.

Tentatively an octahedral structure is proposed for all the complexes. Such complexes having bidentate ligands may exist in three possible configurations as shown in the Fig. 1.

For $Ph_3Sb(OMe)(acac)$ (Fig. 1; R = Ph, and X = X′ = Me; structures **ii** and **iii** are the same) only two isomers are possible. Structure **i** will give rise to single peaks due to the methyl and methine protons of the acac group whereas two peaks are expected for the methyl protons of structure **ii** or **iii**. Since only single peaks were observed, structure **i** is suggested at first sight in which the methoxy group is *trans* to a phenyl group. However, at room temperature the possibility of a configuration in which the methoxy group is *cis* to a phenyl group (structures **ii** and **iii**) cannot be ruled out completely. Since structures **ii** and **iii** will also give single peaks if the molecule has a stereochemically non-rigid configuration. An X-ray single crystal study would be required for assignment of an unambiguous structure for these molecules.

The single peak for the methyl group may also arise if the acac acts as a labile unidentate ligand, but the IR spectrum indicates that acac is bidentate.

For complexes with sal, hap and hna three



i **ii** **iii**

Fig. 1. *fac*-R (**i**), *mer*-R (**ii**), and *mer*-R (**iii**).

geometrical isomers are possible (Fig. 1, $X \neq X'$). Since singlets were observed for aldehydic protons in the complexes $R_3Sb(OMe)(sal)$ and $R_3Sb(OMe)(hna)$ and for methyl protons of the $COCH_3$ group in $R_3Sb(OMe)(hap)$ structure **i** is again suggested in the first instance in this case as well. However, structures **ii** and **iii** cannot be ruled out for the same reasons as discussed for the acac complex.

In the complex $Ph_3Sb(OMe)(ox)$ the downfield shift of the aromatic protons of the ox group to δ 8.86–6.71 is attributed to strong interaction of the metal atom with the nitrogen of the ligand ring in the complex.

The ^{13}C NMR spectra of acetylacetone (acacH) and the complex $Ph_3Sb(OMe)(acac)$ were also recorded. The ^{13}C signals of acacH agreed with those reported in the literature.[14] In acacH different signals were obtained due to $\diagdown C{=}O$ (201 ppm) and $\diagdown C{-}OH$ (190 ppm), but in the complex only one signal was obtained at 191 ppm. Similarly two signals due to the methyl groups at 30 and 22 ppm for acacH were replaced by only one signal at 28 ppm in the complex. Further a slight shift was also observed in the $-CH\diagdown$ signal of the ligand which changes from 99 to 102 ppm on complexation. Aromatic ^{13}C signals were observed from 151 to 127 ppm in the complex. A signal at 47 ppm in the complex is assigned to the methoxo carbon. The complex $Ph_3Sb(OMe)(acac)$ has also been reported by Jain *et al.*[5] Their preparative route was slightly different from ours. PMR data for the complex indicates two peaks for methine, three for methoxy and three for methyl protons. On this basis they have suggested both of the geometrical isomeric forms (*fac*-Ph and *mer*-Ph) at room temperature. In our case, however, we believe that we have obtained only the *fac*-Ph form of this complex.

EXPERIMENTAL

Ph_3SbBr_2[15] and Me_3SbBr_2[16] were prepared and purified by the methods given in the literature. Ligands and solvents were purified and dried before use. All the reactions were performed in an atmosphere of dry nitrogen.

Antimony was determined volumetrically by a reported method.[17] Carbon, hydrogen and nitrogen were analysed in semi-micro scale at CDRI, Lucknow. Molecular weights of the complexes soluble in benzene were determined cryoscopically using a Beckmann thermometer of $\pm 0.01°C$ accuracy.

IR spectra in the range 4000–400 cm^{-1} were recorded in KBr pellets using an SP-1200 spectrophotometer. The far-IR spectra of some of the complexes were recorded in the range 500–100 cm^{-1} on a Fourier transform spectrophotometer, Polytech FIR 30. NMR spectra were recorded in $CDCl_3$ solution on a JEOL JNM 100 NMR spectrometer using TMS as an internal standard.

Preparation

Methanolic solution of the sodium salt of the ligand (15 mmol in 50 cm^3) (prepared from 15 mmol each of sodium and ligand in dry methanol) was added to the benzene solution of triorganoantimony(V) dibromide (5 mmol in 50 cm^3). The mixture was refluxed for 4 h. The volume of the solvent was reduced to 50 cm^3 by distilling under reduced pressure. The sodium bromide and unreacted sodium salt of the ligand were filtered. The benzene–methanol mixture was removed from this filtrate under reduced pressure. Recrystallisation from a benzene–hexane or a benzene–petroleum ether (b.p. 40–60°C) mixture gave crystalline products. The yields of the various complexes are reported in the Table 1.

Acknowledgements—One of us (DMJ) is grateful to the UGC, India, and to Garhwal University, Srinagar (U.P.), for the award of a Teacher fellowship. We thank the referees for helpful comments.

REFERENCES

1. H. A. Meinema, E. Rivarola and J. G. Noltes, *J. Organomet. Chem.* 1969, **17**, 71.
2. H. A. Meinema, A. Mackar and J. G. Noltes, *J. Organomet. Chem.* 1972, **37**, 285.
3. F. DiBianca, E. Rivarola, A. L. Speak, H. A. Meinema and J. G. Noltes, *J. Organomet. Chem.* 1973, **63**, 293.
4. R. G. Goel and D. R. Ridley, *J. Organomet. Chem.* 1979, **182**, 207.
5. V. K. Jain, R. Bohra and R. C. Mehrotra, *J. Organomet. Chem.* 1980, **184**, 57.
6. G. Wilkinson, F. G. A. Stone and E. W. Abel (Eds) *Comprehensive Organometallic Chemistry*, Vol. 2, p. 681. Pergamon Press, Oxford (1982).
7. B. J. Aylett (Ed.) *MTP International Review of Science*, Inorganic Chemistry Series One and Two, Butterworths, London Vol. 4, p. 355 (1972), and Vol 4, p. 319 (1975).
8. N. K. Jha and D. M. Joshi, *Synth. React. Inorg. Met–Org. Chem.* 1984, **14**, 455.
9. S. Gopinathan and C. Gopinathan, *Indian J. Chem.* 1977, **15A**, 660.
10. A. W. Baker and A. T. Sulgin, *J. Am. Chem. Soc.* 1959, **81**, 1523.
11. N. S. Gill, R. H. Nuttal, D. E. Escaife and D. W. A. Sharpe, *J. Inorg. Nucl. Chem.* 1961, **18**, 79.

12. R. G. Goel, E. Maslowsky, Jr and C. V. Senoff, *Inorg. Chem.* 1971, **10**, 2572.
13. R. G. Goel and H. S. Prasad, *Inorg. Chem.* 1972, **11**, 2141.
14. R. M. Silverstein, G. C. Bassler and T. C. Morril, *Spectrometric Identification of Organic Compounds*, 4th edn. p. 270. John Wiley, New York (1981).
15. W. J. Bile and R. C. Menzies, *J. Chem. Soc.* 1970, 617.
16. G. T. Morgan and G. R. Davies, *Proc. R. Soc., London* 1926, **A110**, 523.
17. A. Ouchi, M. Nakatani, Y. Takahashi, S. Kitazima, T. Sugihara, M. Tatsumoto, T. Uehiro, K. Kitano, K. Kawashima and H. Honda, *Sci. Pap. Coll. Gen. Educ., Univ. Tokyo* 1975, **25**, 73.

Polyhedron Vol. 4, No. 12, pp. 2089–2096, 1985
Printed in Great Britain

0277–5387/85 $3.00 + .00
© 1985 Pergamon Press Ltd

^{15}N, ^{13}C AND ^{119}Sn NMR AND OTHER SPECTROSCOPIC STUDIES OF 8-QUINOLINOL, ITS *O*- AND *N*-METHYL DERIVATIVES, AND CHELATE DI- AND TRI-ORGANOTIN(IV) COMPLEXES

VIMAL K. JAIN

Department of Chemistry, University of Guelph, Ontario, Canada N1G 2W1

JOAN MASON* and BHIM SEN SARASWAT

Department of Chemistry, The Open University, Milton Keynes MK7 6AA, U.K.

and

RAM C. MEHROTRA

Department of Chemistry, University of Rajasthan, Jaipur 302004, India

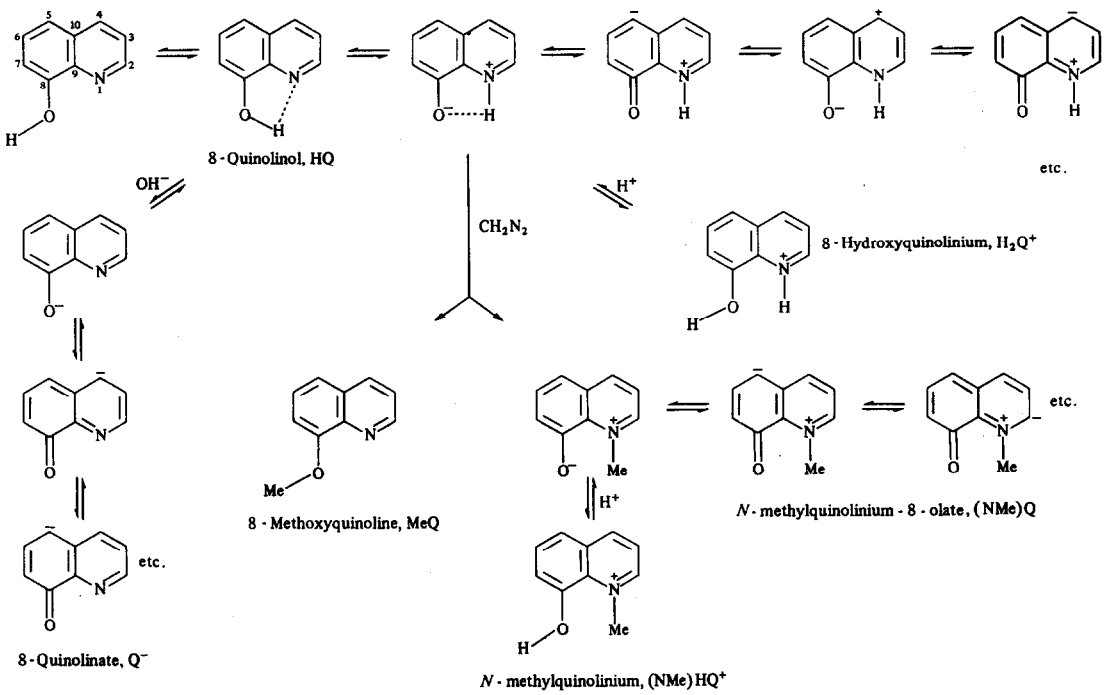
(*Received* 29 *April* 1985; *accepted* 29 *July* 1985)

Abstract—The nature of the 8-quinolinato ligand in various forms has been examined by ^{15}N, ^{13}C and ^{119}Sn NMR spectroscopy, with evidence also from electronic spectroscopy. These forms include 8-quinolinol (HQ), 8-quinolinate, the 8-hydroxyquinolinium ion, *O*- and *N*-methyl derivatives, 8-methoxyquinoline (MeQ), the zwitterionic *N*-methylquinolinium-8-olate and the *N*-methylquinolinium ion, and the chelating ligand in organotin(IV) complexes. The ^{15}N shift from MeQ to HQ affords a measure of the intramolecular hydrogen bonding in HQ. The ^{15}N shifts and $^{2}J(^{15}N^{1}H)$ couplings afford criteria of chelation, and the *O*- and *N*-methyl compounds provide useful reference points for its assessment. Evidence for chelation is demonstrated in three groups of compounds, $[SnR_2Q_2]$ (R = Me, Et, Bu^n, Oct^n or Ph), $[SnR_3Q]$ (R = Me, Et, Bu^n or Ph) and $[SnR_2ClQ]$ (R = Me, Et, Bu^n or Oct^n), the ^{15}N and ^{119}Sn shielding increasing from the $[SnR_3Q]$ to the $[SnR_2Q_2]$ compounds.

8-Quinolinol (HQ or oxine) coordinates to a large number of metal ions. It has long been used as an analytical and sequestering agent, and as an "unnatural" chelate it is also a bactericide and fungicide.[1] The molecule is particularly versatile because of its amphoteric, tautomeric, and zwitterionic capabilities, shown in Scheme 1. It can also coordinate in monodentate or bidentate fashion. Both possibilities arise in organoderivatives of metals such as tin or antimony[2] which form strong bonds to oxygen and weaker bonds to nitrogen, and can expand their coordination sphere with electronegative substituents and with chelating ligands such as 8-quinolinol which have a small bite. Various physical methods have been used to indicate the mode of coordination, and differing results reported which may reflect the differing conditions appropriate to the method. The observed degree of chelation may decrease from the solid state, monitored by X-ray crystallography or Mössbauer or IR spectroscopy, to concentrated solutions as used to increase NMR sensitivity, and decrease further in the dilute solutions studied by UV spectroscopy, particularly if the solvent competes with the metal in bonding or hydrogen-bonding to nitrogen. Intermolecular association is found in many tin compounds but various measurements have shown the 8-quinolinates to be monomolecular in solution and in the solid state.

Nitrogen NMR spectroscopy has obvious potential[3,4] for detecting the chelation, or dynamic

* Author to whom correspondence should be addressed.



Scheme 1.

equilibrium, but poses technical problems, such as quadrupolar broadening for the abundant nucleus ^{14}N, particularly for uncoordinated nitrogen (carrying a lone pair of electrons) and larger molecules. The spin-$\frac{1}{2}$ nucleus ^{15}N has a low natural abundance (0.36%) and relaxation is slow in the absence of nearby protons. Both ^{14}N and ^{15}N have relatively low NMR sensitivity, and ^{15}N has a negative magnetogyric ratio and nuclear Overhauser effect. In the absence of inexpensive routes to ^{15}N-enriched 8-quinolinol we have measured ^{15}N spectra in natural abundance in saturated solutions in a wide-bore spectrometer at 4.228 T, normally with added $[Cr(pd)_3]$ as relaxation reagent and without proton decoupling. A further problem in the NMR study of 8-quinolinates is their limited solubility in many solvents, which limited the range we could measure.

A useful criterion of chelation of 8-quinolinol is the $^2J(^{15}N^1H)$ coupling, which decreases sharply on coordination or protonation of the nitrogen, and so is diagnostic of chelation on the time-scale given by the coupling constant. On this score the organotin 8-quinolinates that we have studied appear to contain the chelating ligand whereas the organoantimony compounds[2] appear to contain the monodentate and some bidentate ligand, conclusions which we could check against the evidence from ^{13}C, ^{119}Sn and UV spectroscopy. A further criterion is the chemical shift. Protonation of aza-arenes, which removes the long-wavelength $n_N \rightarrow \pi^*$ band from the electronic spectrum, is well-known to increase the nitrogen shielding by 100 ppm or more, by removal of this low-energy paramagnetic contribution. Hydrogen-bonding acts in the same sense to a lesser degree, by stabilising the ground state relative to the excited state, the shielding increasing as the $n_N \rightarrow \pi^*$ band moves to shorter wavelengths.[3,5]

The difference in shielding from the free ligand to the complex can therefore be diagnostic of the mode of coordination. These results we found puzzling: the ^{15}N coordination shifts ($\Delta\delta$) relative to 8-quinolinol in $CDCl_3$ were only -5 to -35 ppm for di- and tri-organotin complexes of the apparently chelating ligand, and formed a continuous range with the smaller (or positive) coordination shifts in the related organoantimony complexes.[2] This raised the question of what should be taken as the "free ligand" for this purpose. In 8-quinolinol strong intramolecular hydrogen-bonding persists even in strongly hydrogen-bonding solvents or basic solvents such as DMSO,[6] and such hydrogen-bonding can be taken to model the chelation of a metal ion.

We therefore undertook ^{15}N and ^{13}C and further UV spectroscopic studies of different species in Scheme 1 in which selective methylation models the *O*- or *N*-coordination separately. This has the added interest of the comparison of the chemical shifts with the electronic absorption of the changing chromo-

phore, including the coordinated ligand, for which there is additional information from ^{119}Sn NMR and other physical methods. Whereas the electronic absorption (which also affords a criterion of chelation) is a property of the chromophore as a whole, the NMR method can monitor the changes at each atom.

RESULTS AND DISCUSSION

Metamorphoses of 8-quinolinol

Table 1 shows that the largest coupling constant, $^2J(^{15}N^1H)$, is nearly 11 Hz for pyridine or quinoline[7] and slightly smaller in 8-quinolinol. It decreases to 3 Hz or less in pyridinium or quinolinium ion[7] and was not resolved by us in the protonated, *N*-methylated or chelated forms of 8-quinolinol. The large increase in reduced two-bond coupling constant when one of the atoms carries a *cis* lone pair is general, and can be traced to the lone pair's Fermi contact contribution, which is large because of the high *s* character and small energy denominator;[8] any decrease from pyridine or quinoline to 8-quinolinol could then be linked with the internal hydrogen bonding.

The increase in ^{15}N shielding on protonation or *N*-methylation of 8-quinolinol (as measured in $CDCl_3$ solution) is somewhat smaller than for pyridine or quinoline. That the decrement can be related to the internal hydrogen bonding in 8-quinolinol is suggested by the decrease in nitrogen shielding, by 11.7 ppm, on *O*-methylation. In pyridine, for comparison, the nitrogen is shielded by 10 ppm in $CHCl_3$ and 20 ppm in aqueous solution relative to solution in CCl_4.[5] We have therefore used

Table 1. Spectroscopic properties of 8-quinolinol and related compounds[a]

		^{15}N NMR[b]				Electronic absorption[c]			
Compound	Solvent	δ (ppm)	$\Delta\delta$[d] (ppm)	^2J(NH) (Hz)	^3J(NH) (Hz)	Solvent	λ_{max} (nm)	$\log \varepsilon_{max}$	Ref. (UV)
$H_2Q^+Cl^-$	1 M HCl	−200.3	−104.6	—	—				
	0.1 M HCl	−192.6	−96.9	—	—	0.1 M HCl	358	3.22	10
(NMe)HQ^+Cl^-	1 M HCl					aq acid	440	0.75	—
						aq	443	2.5	—
	$CDCl_3$	[e]				aq base	445	3.07	—
(NMe)Q	CD_3OD	−187.7	−92.0			EtOH	484	2.7	12
	$CDCl_3$			—	—	$CHCl_3$	554	2.5	12
						EtOH/H^+	370	2.75	12
$H_2Q^+HSO_4^-$	DMSO	−138.3	−42.6						
HQ	aq	[e]				aq	305	3.30	—
							430	1.72	—
	$CDCl_3$	−95.7	0	(−)8.9	—	C_6H_{12}	320	3.39	28
						$CHCl_3$	318	3.36	10
Na^+Q^-	0.1 M NaOH	−89.0	6.7	—	—	0.1 M NaOH	353	3.43	10
	CD_3OD	−89.0	6.7	—	—				
MeQ	$CDCl_3$	−84.0	11.7	*ca* (−)9	—		297		30
(NMe)py^+Cl^-	aq	−180.2	−109.2						
(PyridineH$^+$)[f]	2 M in tfa	−179.0	−109.0	−3.0	−4.0				
Pyridine[f]	$CDCl_3$	−70.0	0	−10.9	−1.5	C_6H_{12}	270	2.65	
(QuinolineH$^+$)[f]	H_2SO_4	−193.1	−126.2	−2.0[g]	−4.5[g]				
Quinoline[f]	Acetone	−66.9	0	−10.8	−1.3	C_6H_{12}	313	3.37	

[a] HQ is 8-quinolinol, MeQ is 8-methoxyquinoline, (NMe)Q is *N*-methylquinolium-8-olate (cf. Scheme 1).

[b] Spectra were run at 293 K. ^{15}N shifts are referenced to neat $CH_3^{15}NO_2$, high frequency positive, and corrected for differences in susceptiblity due to the addition of $[Cr(pd)_3]$ to promote relaxation. Digital resolution is 3 Hz in our measurements; unresolved $^{2,3}J(^{15}NH)$ coupling constants are therefore <3 Hz.

[c] Longest-wavelength bands; concentration typically 10^{-4} M.

[d] $\Delta\delta$ is the coordination shift from the free base HQ in $CDCl_3$.

[e] Insufficiently soluble.

[f] NMR.[7]

[g] In tfa.

the *O*-methylated compound as a reference for nitrogen coordination shifts in the 8-quinolinates in Table 2. We were unable to observe a signal for 8-quinolinol in water, in which the solubility is low.

The nitrogen-shielding sequence has no simple relationship with the longest wavelength of absorption given in Table 1. The $n_N \rightarrow \pi^*$ band is observable for pyridine, but for more extended π systems as in quinoline the stronger $\pi \rightarrow \pi^*$ bands move to longer wavelengths and obscure the $n_N \rightarrow \pi^*$ band.[9] With incorporation of oxygen into the delocalised system in the quinonoid forms the $\pi \rightarrow \pi^*$ bands move into the visible region, as in the 8-quinolinol zwitterion present in tautomeric equilibrium in water (Scheme 1). These bands are blue-shifted by hydrogen-bonding solvents or acids which protonate oxygen and nitrogen, so to that extent blue-shifting may correlate with increased shielding of nitrogen, and carbon adjacent to oxygen or nitrogen. Although these $\pi \rightarrow \pi^*$ excitations are magnetic dipole forbidden,[3] the LUMOs are of course related to those of $n \rightarrow \pi^*$ excitations in the same system.

Moeller[10] and Sone[11] noted that the absorption near 310 nm of 8-quinolinol in neutral solution shifted to 350–360 nm in acid or alkaline solution, and to 370–430 nm or so in chelates. The longer-wavelength absorption was therefore proposed as a criterion of chelation; according to Sone,[11] the longer the wavelength of absorption the more stable the chelate. In fact neutral aqueous solution shows a weaker band at 430 nm due to the zwitterion, and it

Table 2. Spectroscopic properties of organotin(IV) 8-quinolinates

	^{15}N NMR[bc]		^{119}Sn NMR[d]		Electronic absorption[e]		
Compound[a]	δ^{15}N (ppm)	$\Delta\delta$ (ppm)	δ^{119}Sn (ppm)	$^1J(^{119}\text{SnC})$ (Hz)	Solvent	λ_{max} (nm)	$\log \varepsilon_{max}$
$[SnPh_2Q_2]$	−125.4	−41.4	−397[f]	—	bz	380	3.06
$[SnBu^n_2Q_2]$	−123.7	−39.7	−262.0[f]	614	$CHCl_3$	372	3.66
$[SnEt_2Q_2]$	−121.0	−37.0	−261.0[g]	633	$CHCl_3$	375	3.71
$[SnOct^n_2Q_2]$	−120.2	−36.2	−263.1	611	$CHCl_3$	372	3.71
$[SnMe_2Q_2]$	−120.0	−36.0	−236[h]	618	EtOH	372[i]	
			−237.0[f]	632	bz	380[i]	3.69
					Dioxan	378[i]	3.70
$[SnPh_3Q]$	−118.6	−34.6	−190.1[f]	663	C_6H_{12}	362[i]	3.39
$[SnMe_3Q]$	−103.0[j]	−19.0	50.9[h]	418	C_6H_{12}	362[i]	3.40
			47.8[j]		$CHCl_3$	347	3.49
$[SnEt_3Q]$	−103.1	−19.1	28.5	391	$CHCl_3$	356	3.21
$[SnBu^n_3Q]$	−100.6	−16.6	36[h]	391	C_6H_{12}	362[i]	3.31
			29[jk]				
$[SnPh_2ClQ]$			−245[f]				
$[SnEt_2ClQ]$	[l]		−114.7[m]	619			
$[SnBu^n_2ClQ]$	[l]		−112.0[f]	598	$CHCl_3$	370	3.32
$[SnOct^n_2ClQ]$	[l]		−111.0[m]	605	$CHCl_3$	370	3.37
$[SnMe_2ClQ]$	[l]		−92.0[f]	646	Dioxan	378[i]	3.34
MeQ	−84.0	0				297	

[ab] As for Table 1. $\Delta\delta$ is the coordination shift from 8-methoxyquinoline (MeQ) in $CDCl_3$.

[c] Near-saturated solutions in $CDCl_3$. No spin–spin splitting was resolved, i.e. $^2J(NH) < 3$ Hz.

[d] $CDCl_3$ solutions, concentrations 0.5–1 M unless otherwise specified. Linewidths typically 10 Hz, except for the SnR_2ClQ compounds. $^1J(^{119}Sn^{13}C)$ values from Table 2.

[e] Concentrations typically 10^{-4} M.

[f] Reference 20.

[g] Reference 23.

[h] Reference 22.

[i] Reference 28.

[j] Neat liquid.

[k] J. D. Kennedy and W. McFarlane, reported in Ref. 16, p. 353.

[l] No ^{15}N signal could be observed (with or without the addition of $[Cr(pd)_3]$).

[m] Broad resonance.

can be isolated as the *N*-methyl derivative, *N*-methylquinolinium-8-olate [(NMe)Q], called an "anhydro-salt"[12] or "diazoxine",[13] as it is the ether-insoluble product of reaction of diazomethane with "oxine". This zwitterion is a red solid which gives violet solutions in non-polar solvents, the long-wavelength band blue-shifting with hydrogen-bonding. Our ^{15}N NMR studies with this interesting compound were limited by the low solubility in non-polar solvents. In methanol, however, the nitrogen is deshielded relative to the 8-hydroxyquinolinium ion (H_2Q^+) in aqueous acid, consistent with lowering of the excitation energies in the zwitterion. It is shielded relative to H_2Q^+ in DMSO, a rather basic solvent.

The evidence as to the nature of the 8-quinolinol ligand that is available from the ^{13}C shifts was shown by measurements on Zn(II) and Mo(VI) chelate complexes of 4-methyl-8-quinolinol (4MQ), chosen for greater solubility, and comparisons with $4MQ^-$, 4MQH and $4MQH_2^+$.[14] Our measurements in Table 2 follow these assignments, the $4MQ^-$ shifts affording an estimate of the values for Q^-, as in Table 3. The largest spread of aromatic carbon shifts, 60 ppm, is given by the zwitterion (NMe)Q and the anions, and the next largest (55 ppm) by the zinc chelate, in which the bonding to the metal is relatively ionic. In the more covalent molybdyl and tin complexes the spread is 45 ppm or less. In the tin complexes, however, the carbon bonded to oxygen (C-8) is still relatively deshielded (though 4 ppm more

Table 3. ^{13}C NMR data for 8-quinolinol and derivatives[a]

Compound	C-2	C-3	C-4	C-5	C-6	C-7	C-8	C-9	C-10	C-1	C-2	C-3	C-4
Q^-[b]	146.9	121.6	137.5	111.3	130.3	115.9	165.2	144.2	131.5				
HQ[b]	147.8	121.5	136.1	117.8	127.6	110.4	152.3	138.1	128.5				
(NMe)Q	145.7	124.0	141.9	106.2	132.8	118.0	166.3	135.9	134.1	NMe, 50.6			
MeQ	149.2	121.7	135.9	107.5	126.7	119.6	155.4	140.0	127.7	OMe, 55.9			
$[SnMe_2Q_2]$	142.2	121.2	136.2	113.4	129.7	112.8	157.5	138.4	130.9	6.9 (618)			
$[SnMe_2ClQ]$	144.3	121.7	140.5	114.8	130.7	114.4	156.5	137.3	129.5	7.9 (646)			
$[SnEt_2Q_2]$	142.4	121.0	138.3	113.5	130.2	112.7	158.3	136.7	129.7	17.4 (633)	9.9 (32)		
$[SnEt_2ClQ]$	144.8	121.8	140.5	114.8	130.6	114.3	157.3	137.9	129.5	20.2 (619)	9.7 (42)		
$[SnBu^n_2Q_2]$	142.4	121.0	138.2	113.4	130.1	112.6	158.1	136.6	129.7	25.6 (614)	27.8 (26)	26.8 (102)	13.7
$[SnBu^n_2ClQ]$	144.6	121.8	140.5	114.8	129.5	114.2	157.1	137.7	129.5	27.9 (598)	27.1	26.4	13.5
$[SnOct^n_2Q_2]$	142.3	120.9	138.2	113.5	130.2	112.5	158.2	136.7	129.7	26.0 (611)			
$[SnOct^n_2ClQ]$	144.6	121.8	140.5	114.9	130.6	114.2	157.2	137.9	129.5	28.3 (605)			
$[SnPh_2Q_2]$[c]	142.7	121.2	138.8	113.9	130.3	113.2	157.5	142.7?	129.7	149.4	135.0 (35)	128.0 (85)	128.1
$[SnPh_3Q]$[cd]	144.2	121.2	138.3	114.0	128.0	113.5	156.0	137.9	129.5	145.0 (663)	136.0 (47.8)	128.2 (62.5)	128.7 (12.7)
$[SnMe_3Q]$	143.4	121.3	136.8	113.7	128.6	112.3	156.1	138.3	128.6	2.1 (418)			
$[SnEt_3Q]$	143.7	120.9	136.9	113.8	128.9	113.6	157.6	139.7	128.9	11.3 (391)	10.1		
$[SnBu^n_3Q]$	143.8	120.9	136.8	113.9	128.9	113.9	157.7	139.9	129.3	20.0 (391)	28.2 (20)	27.2	13.7

[a] All values are chemical shifts in ppm, except those in parentheses which are $^{119}Sn^{13}C$ coupling constants in Hz. The C-2–C-10 series refers to the 8-quinolinol ligand and the C-1–C-4 series to the alkyl or phenyl group.

[b] DMSO solution: similar values were reported in Ref. 14.

[c] Assignments tentative as the phenyl resonances are in the same region.

[d] Reference 21.

shielded than in the zinc complex), suggesting that the oxygen is still quite negative.

Protonation, methylation and coordination of the oxygen all increase the *ipso* carbon (C-8) shielding. They deshield the *para*-carbon (C-5), as commonly observed with electron-withdrawing substituents,[14] and also C-2, *ortho* to nitrogen. Similarly, protonation or methylation of nitrogen deshields the *para*-carbon C-4, e.g. by 4–5 ppm from 8-quinolinate to (NMe)Q, cf. 2 ppm in the zinc complex, 10 ppm on methylation of pyridine,[4] and 14 ppm in the molybdyl complex. C-4 is deshielded by 3 ppm in the organohalogenotin complexes, in which bonding to tin is relatively strong, and by about 0.5 ppm in the $[SnR_2Q_2]$ complexes and $[SnPh_3Q]$, but very slightly shielded (by 1 ppm or less) in the $[SnR_3Q]$ compounds. For C-2 and C-9 (*ortho* to nitrogen) the shielding increases from 8-quinolinate to (NMe)Q, and with protonation, or coordination of the nitrogen to tin, zinc or molybdenum, cf. increases of 3 or 7 ppm on *N*-methylation or protonation of pyridine.[4]

Evidently protonation or methylation can model the coordination of oxygen or nitrogen to a metal, in its effect on the carbon shifts. It is likely therefore that *N*-methylation can distinguish the additional effects of chelation. The carbon shifts thus provide evidence of zwitterionic character in the ligand, the more ionic the complex, and of increasing strength of chelation from the $[SnR_3Q]$ to the $[SnR_2Q_2]$ and $[SnR_2ClQ]$ complexes.

The nature of the 8-quinolinato ligand in organotin(IV) complexes

Further criteria of the coordination number in solution are available in the ^{119}Sn shift and in the $^1J(^{119}Sn^{13}C)$ couplings to the organo ligands, since the tin shielding and the reduced coupling constant both increase with coordination number. They increase also with electronegative substituents, as in the chloro complexes, and with π-delocalisation, as in the phenyltin complexes.[15–22] This is evident in Table 2, which compares ^{15}N and ^{119}Sn NMR and electronic spectral measurements for $[SnR_2Q_2]$, $[SnR_3Q]$ and $[SnR_2ClQ]$ complexes. We were unable to see an ^{15}N signal for any halogeno derivative, despite many attempts using $CDCl_3$ or CD_3OD as solvent, with and without added $[Cr(pd)_3]$. The problem is not one of solubility, as the dioctyl and dibutyl complexes in particular are highly soluble. If some kind of fluxionality is responsible, there was no evidence for this in the ^{13}C spectra, though linewidths of 50–55 Hz were observed in ^{119}Sn resonance, as against *ca* 10 Hz for the $[SnR_2Q_2]$ and $[SnR_3Q]$ compounds. Little or no concentration-dependence is observed in these spectra.

^{119}Sn shifts, but not coupling constants, have been reported for most of the compounds in Table 3.[20–23] The relatively high shielding was considered to reflect six-coordination in $[SnEt_2Q_2]$,[23] cf. the X-ray crystallographic evidence of a distorted six-coordinate structure for $[SnMe_2Q_2]$, with NSnO angles of 74° in the chelate ring.[24] Typical ranges of tin shifts have been proposed[20] for coordination numbers five (−90 to −330 ppm) and six (−125 to −515 ppm) for organotin chelates in $CHCl_3$ solution, this description being applied to the $[SnR_2Q_2]$ and $[SnR_2ClQ]$ compounds and $[SnPh_3Q]$, but not $[SnR_3Q]$ with R = alkyl. According to proposed ranges of $^1J(^{119}Sn^{13}C)$ coupling constants,[19] the $[SnR_3Q]$ compounds could be four- or five-coordinate. Mössbauer work has demonstrated five-coordinate (trigonal bipyramidal) structures in the solid state for $[SnPh_3Q]$ and $[SnR_2ClQ]$ and confirms six-coordination for $[SnR_2Q_2]$ compounds.[25] Following Bent's rule[26] (and Walsh) the electronegative substituents occupy axial positions preferentially. This gives equatorial–axial chelation of 8-quinolinate in trigonal bipyramidal structures, the small equatorial–axial angle being suited to a ligand with a small bite. Dependence of the tin shifts and $^1J(^{119}Sn^{13}C)$ coupling constants on the geometry of the coordination sphere has been pointed out,[21] with lower shielding and coupling constants for equatorial–axial chelation and equatorial and axial phenyl groups in $[SnPh_3(LL')]$ compounds, compared with all phenyls equatorial. Lower shielding is observed also for ligating carbon in phenyl groups in five-coordinate compared with four-coordinate compounds.[21]

The $[SnR_2Q_2]$ and $[SnR_2ClQ]$ compounds and $[SnPh_3Q]$ may thus be characterised as chelates in $CHCl_3$ solution, with the $[SnR_3Q]$ compounds apparently marginal. They have been described as four-coordinate, on the ^{119}Sn NMR evidence.[22] If five-coordinate, a possible explanation for low tin shielding is that this is observed when tin forms part of a five-membered ring. Tin is deshielded by 50 ppm in $[SnMe_2C_4H_8]$ compared to $[SnMe_2Et_2]$,[27] and by 130 ppm in $SnMe_2Q_2]$ compared to $[SnMe_2(pd)_2]$[20] (the shielding being enhanced in a six-membered ring).[27] Comparable ^{31}P deshielding is observed in five-membered rings formed by chelating diphosphines, relative to equivalent monophosphine complexes.

On Moeller's criterion[10] all three compound types in Table 2 contain chelating 8-quinolinate, since all show the longer-wavelength absorption in several

solvents.[28] An earlier report of four-coordination in $[SnPh_3Q]$ was explained in terms of displacement of nitrogen by a polar solvent, in aqueous alcohol solution.[29] This criterion does not however exclude the presence of some monodentate ligand (depending on the absorptivity observed).

Proton NMR criteria of the denticity have been formulated. On the evidence of the H-2 shifts, the 8-quinolinato ligand was considered to be monodentate in CH_2Cl_2 solutions of $[SnR_2Q_2]$ and $[SnR_3Q]$ compounds. This proton, like C-2, is deshielded (with respect to 8-methoxyquinoline in the same solvent) when the interaction with nitrogen is strong, as in the halogeno derivatives, though shielded when it is weak. The shielding of H-4 (like C-4) decreases with increasing interaction.[6,30] Another proposed criterion is the benzene-induced shift of H-2 of the 8-quinolinate ligand. Such shifts (in benzene relative to a chloro solvent) are to lower frequency near positively charged sites, and vice versa. The 2-proton shows a large shift of this type (0.5–0.7 ppm) in the chelating or protonated ligand, compared with a small shift (0–0.3 ppm) in the free or *O*-methylated ligand. $[SnMe_3Q]$ passes this test of chelation.[31]

The last word for the present remains with the ^{15}N NMR evidence so far obtained. The singlet ^{15}N resonance observed for the $[SnR_2Q_2]$ and $[SnR_3Q]$ compounds alike is consistent with chelation, or perhaps with exchange involving a proportion of the monodentate ligand. Any such exchange, however, must be very fast, since no signs were observed in the ^{13}C or ^{119}Sn spectra, nor in the proton spectrum at 400 MHz of $[SnMe_3Q]$ at $-85°C$ in CH_2Cl_2 solution. The exchange would then be expected to average the $^2J(^{15}N^1H)$ couplings for ligating and non-ligating nitrogen as well as the nitrogen shifts.

As to the chemical shifts, few measurements on compounds containing Sn—N bonds are available for comparison. In stannylamines[32] the tin is relatively deshielded but the nitrogen highly shielded, as in other amines; in stannatranes both the tin (bound to three oxygens) and the (amino) nitrogen are highly shielded.[33]

A particularly interesting feature of Table 2 is the tendency for the ^{15}N and ^{119}Sn shielding to increase together, as might be expected with increase in strength of the tin–nitrogen bond, from $[SnR_3Q]$ to $[SnR_2Q_2]$. Interestingly, there is some red-shifting of the long-wavelength bands, from $[SnR_3Q]$ to $[SnR_2ClQ]$ and to the $[SnR_2Q_2]$ compounds. It seems reasonable to ascribe the rather low shielding of tin and nitrogen, particularly in the $[SnR_3Q]$ compounds, to the influence of low-lying π^* LUMOs for magnetically active excitations of the *p*-electrons in the bonds to the 8-quinolinato ligand.[3]

Conclusions

Selective methylation of oxygen or nitrogen in amphoteric compounds such as 8-quinoline can provide new insights as to the nature of the protonated, hydrogen-bonded or ligating compound, in conjunction with NMR spectroscopy, as earlier by the use of electronic spectroscopy. With the NMR method, we have three or more sensitive probes of the sites of interaction.

EXPERIMENTAL

8-Quinolinol was methylated by CH_2N_2 to give (NMe)Q as ether-insoluble and 8-methoxyquinoline as ether-soluble portions.[12,13] *N*-methylquinolinium hydrochloride was made by methylation of 8-quinoline with methyl iodide, followed by anion exchange. The organotin(IV) 8-quinolinates were made from the corresponding chlorides by published methods.

The ^{13}C, ^{119}Sn and ^1H spectra were measured on Bruker WH180 and WH400 and JEOL FX90Q spectrometers. The ^{15}N spectra were measured in natural abundance on 15-cm^3 samples in a Bruker WH180 spectrometer taking 25-mm tubes. The $^1J(^{119}Sn^{13}C)$ coupling constants were obtained from satellites in the ^{13}C spectra, but sensitivity was insufficient for satellites to be observed in ^{15}N resonance.

Acknowledgements—We thank Dr R. E. Lenkinski of the South Western Ontario High Field NMR Centre for high-field measurements, Mr Maurice Cooper of the Physico-Chemical Measurements Unit for ^{15}N measurements (also the S.E.R.C. for the widebore spectrometer facilities) and Dr P. J. Smith of the International Tin Research Institute for organotin(IV) chlorides. V.K.J. and B.S.S. thank the Council of Scientific and Industrial Research (New Delhi) and the Open University respectively for post-doctoral fellowships.

REFERENCES

1. A. E. Martell and M. Calvin, *Chemistry of the Metal Chelate Compounds*, Prentice-Hall, New York (1952); J. P. Phillips, *Chem. Rev.* 1956, **56**, 271; R. G. W. Hollingshead, *Oxine and its Derivatives*, part 1. Butterworths, London (1954).
2. V. K. Jain, J. Mason, R. C. Mehrotra and B. S. Saraswat, unpublished work.
3. J. Mason, *Chem. Rev.* 1981, **81**, 205; *Chem. Br.* 1983, 654.
4. G. J. Martin, M. L. Martin and J.-P. Gouesnard, *^{15}N-NMR Spectroscopy*, Springer, Berlin (1981); M. Witanowski, L. Stefaniak and G. A. Webb, *Annu. Rep.*

NMR Spectrosc. 1981, **11B**. G. C. Levy and R. L. Lichter, ^{15}N *NMR Spectroscopy*, Wiley, New York (1979).
5. R. Duthaler and J. D. Roberts, *J. Am. Chem. Soc.* 1978, **100**, 4969.
6. B. C. Baker and D. T. Sawyer, *Anal. Chem.* 1968, **40**, 1945.
7. R. L. Lichter and J. D. Roberts, *J. Am. Chem. Soc.* 1971, **93**, 5218; T. Bundgard and H. J. Jakobsen, *Tetrahedron Lett.* 1976, 1621.
8. J. M. Schulman and T. Venanzi, *J. Am. Chem. Soc.* 1976, **98**, 4701, 6739.
9. H. H. Jaffe and M. Orchin, *Theory and Applications of Ultraviolet Spectroscopy*, Wiley, New York (1962); J. N. Murrell, *The Theory of the Electronic Spectra of Organic Molecules*, Methuen, London (1963).
10. T. Moeller and A. J. Cohen, *J. Am. Chem. Soc.* 1950, **72**, 5346; T. Moeller and F. L. Pundsack, *J. Am. Chem. Soc.* 1954, **76**, 617.
11. K. Sone, *J. Am. Chem. Soc.* 1953, **75**, 5207.
12. J. P. Saxena, W. H. Stafford and W. L. Stafford, *J. Chem. Soc.* 1959, 1579.
13. J. P. Phillips and R. W. Keown, *J. Am. Chem. Soc.* 1951, **73**, 5483.
14. J. K. Howie, P. Bosserman and D. R. Sawyer, *Inorg. Chem.* 1980, **19**, 2293.
15. A. G. Davies and P. J. Smith, In *Comprehensive Organometallic Chemistry* (Edited by G. Wilkinson, F. G. A. Stone and E. W. Abel), Vol. 11, p. 527. Pergamon Press, Oxford (1982).
16. J. D. Kennedy and W. McFarlane, In *NMR and the Periodic Table* (Edited by R. K. Harris and B. E. Mann), p. 342. Academic Press, London (1978).
17. P. J. Smith and A. P. Tupčiauskas, *Annu. Rev. NMR Spectrosc.* 1978, **8**, 291.
18. V. S. Petrosyan, *Prog. Nucl. Magn. Reson. Spectrosc.* 1977, **11**, 115.
19. T. N. Mitchell, *J. Organomet. Chem.* 1973, **59**, 189.
20. J. Otera, *J. Organomet. Chem.* 1981, **221**, 57.
21. J. Holeček, M. Nádvorník, K. Handlíř and A. Lyčka, *J. Organomet. Chem.* 1983, **241**, 177.
22. H. C. Clark, V. K. Jain, I. J. McMahon and R. C. Mehrotra, *J. Organomet. Chem.* 1983, **243**, 299.
23. W. McFarlane, J. C. Maire and M. Delmas, *J. Chem. Soc., Dalton Trans.* 1972, 1863.
24. E. O. Schlemper, *Inorg. Chem.* 1967, **6**, 2012.
25. J. N. R. Ruddick and J. R. Sams, *J. Chem. Soc., Dalton Trans.* 1974, 470; R. C. Poller and J. N. R. Ruddick, *J. Chem. Soc. (A)* 1969, 2273.
26. H. A. Bent, *Chem. Rev.* 1961, **61**, 275.
27. J. D. Kennedy, W. McFarlane and G. S. Pyne, *Bull. Soc. Chim. Belg.* 1975, **84**, 289.
28. K. Kawakami and R. Okawara, *J. Organomet. Chem.* 1966, **6**, 249.
29. M. Wada, K. Kawakami and R. Okawara, *J. Organomet. Chem.* 1965, **4**, 159.
30. Y. Kawasaki, *Inorg. Nucl. Chem. Lett.* 1969, **5**, 805.
31. Y. Kawasaki, *Org. Magn. Reson.* 1970, **2**, 165.
32. J. D. Kennedy, W. McFarlane, G. S. Pyne and B. Wrackmeyer, *J. Organomet. Chem.* 1980, **195**, 285; K. Barlos, G. Hübler, H. Nöth, P. Wanninger, N. Wiberg and B. Wrackmeyer, *J. Magn. Reson.* 1978, **31**, 363.
33. K. Jurkschat, C. Mugge, A. Tzschach, A. Zschunke, G. Engelhardt, E. Lippmaa, M. Mägi, M. F. Larin, V. A. Pestunovich and M. G. Voronkov, *J. Organomet. Chem.* 1979, **171**, 301.

Polyhedron Vol. 4, No. 12, pp. 2097–2101, 1985
Printed in Great Britain

0277–5387/85 $3.00 + .00
© 1985 Pergamon Press Ltd

EXTRACTION OF Ni(II) BY *n*-DODECANOIC ACID DISSOLVED IN TOLUENE

M. P. ELIZALDE,* J. M. CASTRESANA and M. C. ALONSO

Departamento de Química, Universidad del País Vasco, Apartado 644, Bilbao, Spain

and

M. AGUILAR

Department de Química, ETSIIB, Universidad Politécnica de Catalunya, Diagonal 647, Barcelona 08028, Spain

(*Received* 20 *May* 1985; *accepted* 10 *June* 1985)

Abstract—The extraction of Ni(II) from nitrate medium of ionic strength 2.0 mol · dm^{-3} by *n*-dodecanoic acid (HA) dissolved in toluene has been studied at 293 K. Distribution measurements of the metal ion in a wide range of pH and carboxylic acid concentration have been performed. Experimental data, treated by different graphical methods as well as numerically by the LETAGROP-DISTR program, have been explained assuming the presence in the organic phase of the species NiA_2, $NiA_2(HA)_2$, $[NiA_2(HA)_2]_2$ and $[NiA_2(HA)_2]_3$. Equilibrium constants for the different extraction reactions are given.

The extraction of metal ions by long-chain carboxylic acids has been widely investigated under a great variety of experimental conditions. Most of the early work was directed to explore industrial applications whereas less emphasis was given to equilibrium studies. Later on, many authors published detailed series of studies concerning the extraction equilibria of different metal ions with carboxylic acids, reporting the composition of the extracted species and their extraction constants.

Literature on the subject, reviewed by Fletcher and Flett,[1] Flett and Jaycock,[2] Miller[3] and Rice[4] basically agree on the existence in the organic phase of monomer–polymer equilibria between solvated metal carboxylates. In the case of Ni(II) extraction many authors agree on the existence of dimeric species, although some discrepancies concerning the solvation number of the nickel carboxylates have been found.[5–14]

In the present work the study of the extraction of Ni(II) in nitrate medium by *n*-dodecanoic acid dissolved in toluene has been undertaken as a necessary intermediate step in the interpretation of the distribution data in the system Ni(II)–LIX 63–*n*-dodecanoic acid. The object of the work was to determine the composition of the metallic extracted species as well as their extraction constants.

EXPERIMENTAL

Reagents

$Ni(NO_3)_2 \cdot 6H_2O$ (C, Erba, p.a.) was purified by recrystallization from doubly distilled water. *n*-Dodecanoic acid (Merck, p.a.) was purified twice by recrystallization from ethanol and acetone.[15] Sodium nitrate, nitric acid, sodium hydroxide and toluene (Merck, p.a.) were used as supplied.

Experimental technique

The distribution coefficient of Ni(II) was determined for several *n*-dodecanoic acid concentrations as a function of pH. Organic solutions of *n*-dodecanoic acid (HA) in the concentration range of 0.050–0.300 mol · dm^{-3} were mixed with the aqueous solutions consisted of 0.5 mmol · dm^{-3} Ni(II), 2.0 mol · dm^{-3} $NaNO_3$ and variable pH from approximately 5 to 8. The pH was measured using a

* Author to whom correspondence should be addressed.

Radiometer pHM 64 meter, fitted with a GK2322C Radiometer combined glass electrode standardized with buffer solutions of pH 4.00 and 7.00 at 293 K.

Equal volumes (10 cm^3) of organic and aqueous phases were mechanically shaken in special stoppered tubes until equilibrium was attained (less than 15 min). Nickel concentration in both phases was measured by atomic absorption spectroscopy (Perkin–Elmer 560). In order to determine the organic metal concentration, the stripping of nickel from the organic phases with 1.0 mol·dm^{-3} nitric acid was carried out.

RESULTS

Figure 1 shows the experimental results in the form log D vs pH, at several total n-dodecanoic acid concentrations. The non-linear dependence on the aqueous phase acidity seems to indicate the formation of polynuclear metallic species in the organic phase.

The extraction of Ni(II) by the carboxylic acid can be described by the following general equation:

$$j\mathrm{Ni}^{2+} + \tfrac{1}{2}(2+m)j(\mathrm{HA})_{2\,\mathrm{org}} \rightleftharpoons [\mathrm{NiA_2(HA)}_m]_{j\,\mathrm{org}} + 2j\mathrm{H}^+, \quad (1)$$

where HA represents n-dodecanoic acid, which behaves as a dimer in the organic diluent.[16]

Assuming an ideal behaviour in both phases, the stoichiometric equilibrium constant for this reaction may be written as:

$$k_{mj} = \frac{[(\mathrm{NiA_2(HA)}_m)_j]_{\mathrm{org}}[\mathrm{H}^+]^{2j}}{[\mathrm{Ni}^{2+}]^j[(\mathrm{HA})_2]_{\mathrm{org}}^{[(2+m)/2]j}}. \quad (2)$$

Considering eqn (2), the distribution coefficient of Ni(II), defined by:

$$D = C_{\mathrm{Ni,org}} \cdot C_{\mathrm{Ni,aq}}^{-1} \quad (3)$$

can be easily transformed into:

$$D = \sum_j \sum_m j k_{mj} \alpha_{\mathrm{Ni}}^{-1} [\mathrm{Ni}^{2+}]^{j-1} \times [(\mathrm{HA})_2]_{\mathrm{org}}^{[(2+m)/2]j} [\mathrm{H}^+]^{-2j}, \quad (4)$$

α_{Ni} being the side-reaction coefficient of Ni(II) in the aqueous phase due to the formation of hydroxo[17] and nitrate[18] complexes.

From eqn (4), values of the stoichiometric coefficient for the extracted species as well as their extraction constants were determined using both graphical and numerical methods.

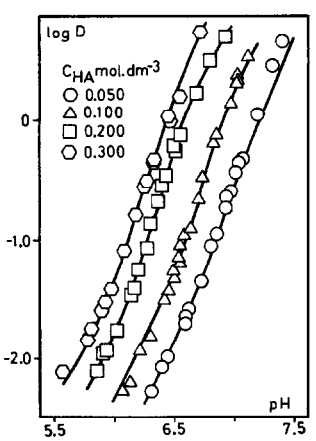


Fig. 1. Variation of the nickel distribution coefficient as a function of pH at several total n-dodecanoic acid concentrations. Continuous lines have been drawn using the proposed extraction constants.

Graphical treatment of the data

In order to estimate the degree of polymerization of the metal species extracted in the organic phase, a preliminary curve-fitting analysis assuming the formation of monomers and polymers of general composition $\mathrm{NiA_2(HA)}_x$ and $[\mathrm{NiA_2(HA)}_z]_j$, respectively, was carried out. Under this hypothesis, eqn (4) may be written as:

$$D = k_{x1}\alpha_{\mathrm{Ni}}^{-1}[(\mathrm{HA})_2]_{\mathrm{org}}^{(x+2)/2}[\mathrm{H}^+]^{-2} + jk_{zj}\alpha_{\mathrm{Ni}}^{-1} \times [\mathrm{Ni}^{2+}]^{j-1}[(\mathrm{HA})_2]_{\mathrm{org}}^{(j/2)(2+z)}[\mathrm{H}^+]^{-2j}. \quad (5)$$

Defining the new variables:

$$V = D[\mathrm{H}^+]^2\alpha_{\mathrm{Ni}}k_{x1}^{-1}[(\mathrm{HA})_2]_{\mathrm{org}}^{-(2+x)/2}, \quad (6)$$

$$W = (jk_{x1}^{-1}k_{zj}[(\mathrm{HA})_2]_{\mathrm{org}}^{-1-x/2+j(1+z/2)})^{1/(j-1)} \times [\mathrm{Ni}^{2+}][\mathrm{H}^+]^{-2}, \quad (7)$$

and the parameter:

$$i = j - 1, \quad (8)$$

eqn (5) can be rearranged to give:

$$\log V = \log (1 + W^i). \quad (9)$$

By comparison between the model functions defined by eqn (8) plotted at different i values with the experimental function $\log D + \log \alpha_{\mathrm{Ni}} - 2\mathrm{pH}$ vs $\log [\mathrm{Ni}^{2+}] + 2\mathrm{pH}$ at constant reagent concentration, values of the coefficient j were estimated. As an example of the treatment, Fig. 2 shows the fit between the experimental data at $C_{\mathrm{HA}} = 0.200$ mol·dm^{-3} with the theoretical functions. The best agreement for all the reagent concentrations was found for $i = 2$, which, according to eqn (8), indicates the extraction of a trimeric metal species, whereas the poor fit obtained for higher i values seems to exclude the formation of polymers of higher aggregation degrees.

The results of the above treatment indicate the

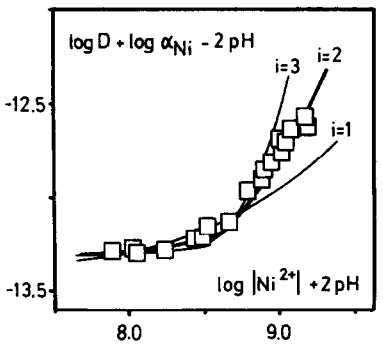


Fig. 2. Determination of the degree of polymerization of the extracted species.

predominance in organic solution of metallic monomer–trimer equilibria. Taking into account that intermediate dimer species may be also formed in the organic phase, the formation of the species $NiA_2(HA)_x$, $[NiA_2(HA)_y]_2$ and $[NiA_2(HA)_z]_3$ has been assumed.

With k_{x1}, k_{y2} and k_{z3}as the respective equilibrium constants for the above species, the nickel distribution coefficient can be written as follows:

$$D = k_{x1}\alpha_{Ni}^{-1}[(HA)_2]_{org}^{(2+x)/2}[H^+]^{-2} + 2k_{y2}\alpha_{Ni}^{-1}[Ni^{2+}][(HA)_2]_{org}^{2+y}[H^+]^{-4} + 3k_{z3}\alpha_{Ni}^{-1}[Ni^{2+}]^2[(HA)_2]_{org}^{[3(z+2)]/2}[H^+]^{-6}. \quad (10)$$

Equation (10) can be rearranged to give:

$$\frac{D\alpha_{Ni}[H^+]^2}{k_{x1}[(HA)_2]_{org}^{(2+x)/2}} = 1 + \frac{2k_{y2}[Ni^{2+}][(HA)_2]_{org}^{1+y-1/2x}}{k_{x1}[H^+]^2} + \frac{3k_{z3}[Ni^{2+}]^2[(HA)_2]_{org}^{(4+3z-x)/2}}{k_{x1}[H^+]^4}. \quad (11)$$

Defining the new normalized variables:

$$Y = \frac{D\alpha_{Ni}[H^+]^2}{k_{x1}[(HA)_2]_{org}^{(2+x)/2}}, \quad (12)$$

and

$$X = \frac{2k_{y2}[Ni^{2+}][(HA)_2]_{org}^{1+y-1/2x}}{k_{x1}[H^+]^2}, \quad (13)$$

the following family of theoretical curves is obtained:

$$Y = 1 + X + aX^2, \quad (14)$$

where a is a parameter defined by:

$$a = 3k_{z3}(4k_{y2}^2)^{-1}k_{x1}[(HA)_2]_{org}^{(3z+x)/2-2y}. \quad (15)$$

The experimental functions $\log D + \log \alpha_{Ni} - 2pH = f(\log [Ni^{2+}] + 2pH)$ and the model function $\log Y = f(\log X)$ for given values of the parameter a, will have the same shape since its variables differ only in constant values:

$$\Delta Y = \log Y - (\log D + \log \alpha_{Ni} - 2pH) = -\log k_{x1} - \tfrac{1}{2}(2+x)\log [(HA)_2]_{org}, \quad (16)$$

$$\Delta X = \log X - (\log [Ni^{2+}] + 2pH) = \log 2k_{y2}k_{x1}^{-1} + (1 + y - \tfrac{1}{2}x)\log [(HA)_2]_{org}. \quad (17)$$

Superimposing both functions by translation in the two axes, a position was found where both sets coincide, being $a = 10$ the best parameter value for all the reagent concentrations studied (Fig. 3).

In order to obtain x, y, k_{x1} and k_{y2} values, plots of ΔY and ΔX vs $\log [(HA)_2]_{org}$ were made, yielding two straight lines of slope values -2 and 2 respectively (Fig. 4). According to eqns (16) and (17), values of the stoichiometric coefficients $x = 2$ and $y = 2$ were deduced. From the intercepts of the plots on the Y-axis, values of the extraction constants $\log k_{21} = -11.52$ and $\log k_{22} = -19.10$ were determined.

Finally, according to eqn (15), the constant value of the parameter a for all the experimental curves indicates that $z = 2$ and, consequently, the extraction constant of the species $[NiA_2(HA)_2]_3$ could be determined from eqn (15), yielding $\log k_{23} = -25.55$.

Numerical treatment of the data

Computer calculations were undertaken both in order to refine the values of the extraction constants graphically obtained as well as to search for additional species which could contribute to improve the fit to the experimental data. Numerical

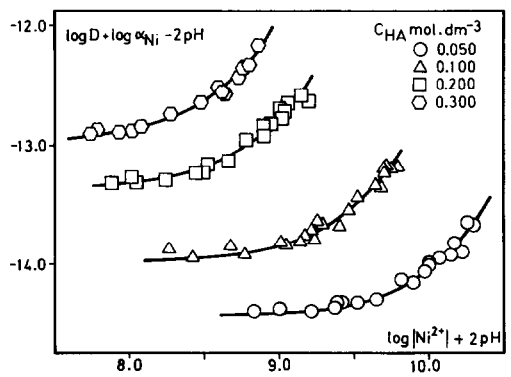


Fig. 3. Superimposition of the experimental functions $\log D + \log \alpha_{Ni} - 2pH = f(\log [Ni^{2+}] + 2pH$ and the theoreticals $\log Y = f(\log X)_a$ in the position of best fit.

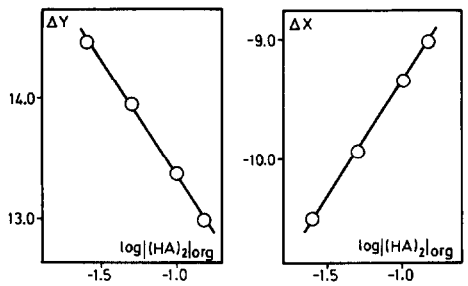


Fig. 4. Values of the differences in Y-axis (ΔY) and X-axis (ΔX) from Fig. 3 plotted as a function of log $[(HA)_2]_{org}$.

calculations were performed by using the program LETAGROP-DISTR,[19] which searches for the best set of species which would minimize the error square sum, U, defined by:

$$U = \sum_{N_p} (\log D_{calc} - \log D_{exp})^2, \qquad (18)$$

where D_{exp} represents the experimental distribution coefficient and D_{calc} the corresponding magnitude calculated by the program assuming a certain set of species and constants. N_p is the number of experimental data. For each combination of species tried the program calculates both U_o and $\sigma \log D$, the mean standard deviation defined by:

$$\sigma \log D = (U/N_p)^{1/2}. \qquad (19)$$

The results of the calculations are summarized in Table 1, and indicate that the combination of the species graphically determined, $NiA_2(HA)_2$, $[NiA_2(HA)_2]_2$ and $[NiA_2(HA)_2]_3$, as well as the monomer NiA_2, provides the best fit to the data. In Table 2 the values of the extraction constants for these species are given. The fit to the data is illustrated in Fig. 1, where the theoretical log D vs pH curves calculated with the extraction constants in Table 2 have been represented.

Table 1. Values of U_o and $\sigma \log D$ for the different combinations of complexes tried

Species (m, j)	U_o	$\sigma \log D$
(2,1), (2,3)	0.580	0.105
(2,1), (2,2)	0.648	0.111
(2,1), (2,2), (2,3)	0.570	0.105
(4,1), (2,2)	2.988	0.237
(0,1), (2,1), (2,2)	0.212	0.064
(0,1), (2,2), (2,3)	0.363	0.082
(0,1), (2,2)	0.363	0.083
(2,1), (2,2), (2,4)	1.230	0.153
(0,1), (2,1), (2,2), (2,3)	0.162	0.056

Table 2. Values of the extraction constants for the different species extracted into the organic phase

Species	Log k_{mj}
NiA_2	-12.92 ± 0.12
$NiA_2(HA)_2$	-11.52 ± 0.18
$[NiA_2(HA)_2]_2$	-18.96 max -18.67
$[NiA_2(HA)_2]_3$	-26.57 max -26.30

CONCLUSIONS

The results of this work, summarized in Table 2, indicate that a sequence of monomer–polymer equilibria may explain the extraction of Ni(II) in nitrate medium by *n*-dodecanoic acid dissolved in toluene. With the constants in Table 2 the mole fraction of Ni(II) in the different species has been computed as a function of the total extractant concentration and plotted in Fig. 5. From this plot it can be seen that the unsolvated monomer NiA_2 predominates in the low reagent concentration range, whereas at higher *n*-dodecanoic acid concentrations the polymerization of the solvated metal carboxylate is almost complete. This type of distribution diagram suggests that nickel extraction proceeds by a stepwise process in which the solvation of the metal carboxylate is followed by self-association reactions of the solvated monomer.

Several monomeric species ranging from NiA_2[10] to $NiA_2(HA)_4$[7] in equilibrium with the dimeric nickel carboxylate $[NiA_2(HA)_2]_2$[5–7,10,14] have been proposed for the extraction of the metal ion with different carboxylic acids in a wide range of conditions. This pattern is partially in agreement with the results obtained in our work, suggesting that the formation of the dimeric $[NiA_2(HA)_2]_2$ is

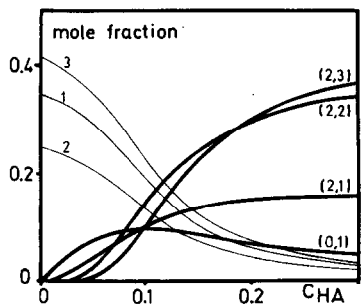


Fig. 5. Nickel distribution diagram as a function of the total *n*-dodecanoic acid concentration at pH = 7.00. Lines 1–3 represent, respectively, Ni^{2+}, $NiNO_3^+$ and $Ni(NO_3)_2$ species in the aqueous phase.

strongly favoured whereas the solvation number of the monomer seems to be highly dependent on the characteristics of the system and experimental conditions.

In addition to the monomer–dimer equilibrium, both graphical and numerical calculations support the formation in our system of trimeric species but exclude the presence of metal carboxylates with aggregation number higher than three. A monomer–dimer–trimer equilibrium of this type has been proposed by Nakasuka *et al.*[20] in a similar system involving the extraction of Cd(II) by *n*-decanoic acid dissolved in benzene.

REFERENCES

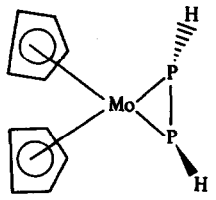
1. A. W. Fletcher and D. S. Flett, *Solvent Extraction Chemistry of Metals*. Macmillan, London (1966).
2. D. S. Flett and M. J. Jaycock, *Ion Exchange and Solvent Extraction*, Vol. 3, Chap. 1. Marcel Dekker, New York (1973).
3. F. Miller, *Talanta* 1974, **21**, 685.
4. N. M. Rice, *Hydrometallurgy* 1978, **3**, 111.
5. I. Satake and R. Matsuura, *Kolloid Z.* 1961, **31**, 176.
6. A. W. Fletcher and D. S. Flett, *J. Appl. Chem.* 1964, **14**, 250.
7. M. Tanaka, N. Nakasuka and S. Sasane, *J. Inorg. Nucl. Chem.* 1969, **31**, 2591.
8. A. W. Ashbrook, *J. Inorg. Nucl. Chem.* 1972, **34**, 3243.
9. A. D. Jones and C. Robinson, *J. Inorg. Nucl. Chem.* 1974, **36**, 1871.
10. M. J. Jaycock, A. D. Jones and C. Robinson, *J. Inorg. Nucl. Chem.* 1974, **36**, 887.
11. S. Jiménez, J. Pérez and N. Hurtado, *20th Biennial Meeting of the Royal Spanish Society of Chemistry, Castellón*, Vol. 8, No. 1 (1984).
12. G. J. Lawson and B. J. Pridden, *Proc. ISEC '74, Lyon*, p. 711 (1974).
13. M. Nakasuka, H. Yamada and M. Tanaka, *Proc. ISEC '74, Lyon*, p. 823 (1974).
14. A. J. Van der Zeeuw, *Hydrometallurgy* 1979, **4**, 21.
15. D. D. Perrin, W. L. F. Armarego and D. R. Perrin, *Purification of Laboratory Chemicals*. Pergamon Press, Oxford (1980).
16. G. K. Schweitzer and D. K. Morris, *Anal. Chim. Acta* 1969, **45**, 65.
17. E. Högfeldt, *Stability Constants of Metal-ion Complexes. Part A: Inorganic Ligands*. Pergamon Press, Oxford (1982).
18. V. A. Fedorov, I. I. Shmyd'ko, A. M. Robov, L. S. Simaeva, V. A. Kukhtina and V. E. Mironov, *Russ. J. Inorg. Chem.* 1973, **18**, 673.
19. D. H. Liem, *Acta Chem. Scand.* 1971, **25**, 1521.
20. N. Nakasuka, Y. Mitsuoka and M. Tanaka, *J. Inorg. Nucl. Chem.* 1974, **36**, 431.

Polyhedron Vol. 4, No. 12, p. 2103, 1985
Pergamon Press Ltd. Printed in Great Britain

ERRATA

A. H. Cowley, Double bonding between the heavier main-group elements: from reactive intermediates to isolable molecules. *Polyhedron* 1984, **3**, 389–432.

The publishers regret that the structure of compound **87** on p. 412 of the above article is incorrect. The correct structure is shown below.



87

P. R. Reddy and V. B. M. Rao, Role of secondary ligands in the structure and stability of metal–cytidine complexes in solution. *Polyhedron* 1985, **4**, 1603–1609.

The authors regret that it was omitted from Table 2 on p. 1406 of the above article that the 1 : 1 metal : cytidine data were from B. T. Khan and R. M. Raju, *Indian J. Chem.* 1981, **20**, 860. The corrected table is shown below.

Table 2. Stability constants[a] of the binary and ternary complexes of cytidine (HL) with glycine (H_2A) and oxalic acid (H_2A): temperature = 35°C, μ = 0.10 mol dm^{-3} (KNO_3)

Metal ion	Metal : cytidine[b] (1 : 1)	Metal : glycine (1 : 1)	Metal : cytidine : glycine (1 : 1 : 1)			Metal : oxalic acid (1 : 1)	Metal : cytidine : oxalic acid (1 : 1 : 1)
	K^{M}_{ML}	K^{M}_{MA}	$K^{M}_{M(HA)L}$	$K^{M(HA)L}_{MLA}$	K^{M}_{MLA}	K^{M}_{MA}	K^{M}_{MLA}
Cu(II)	3.19	8.61			13.85	6.16	9.93
Ni(II)	2.94	5.92	8.56	5.72		5.23	9.31
Zn(II)	2.60	5.22	8.23	5.54		5.31	9.40
Co(II)	2.74	5.50	8.03	5.10		4.97	9.17
Mn(II)	2.51	3.85	8.16	3.79		5.14	9.53
Mg	2.42	3.40	8.19	3.59		4.65	8.81
Ca	2.47	3.58	8.24	3.63		4.85	8.80

[a] Deviations are omitted for clarity.
[b] Data from B. T. Khan and R. M. Raju, *Indian J. Chem.* 1981, **20**, 860.